AIRPLANE DESIGN

PART I: PRELIMINARY SIZING OF AIRPLANES

by

Dr. Jan Roskam
Ackers Distinguished Professor
of Aerospace Engineering
The University of Kansas
Lawrence, Kansas

NO PART OF THIS BOOK MAY BE REPRODUCED WITHOUT
PERMISSION FROM THE AUTHOR

Copyright: Roskam Aviation and Engineering Corporation
Rt4, Box 274, Ottawa, Kansas, 66067
Tel. 913-2421624
First Printing: 1985

TABLE OF CONTENTS

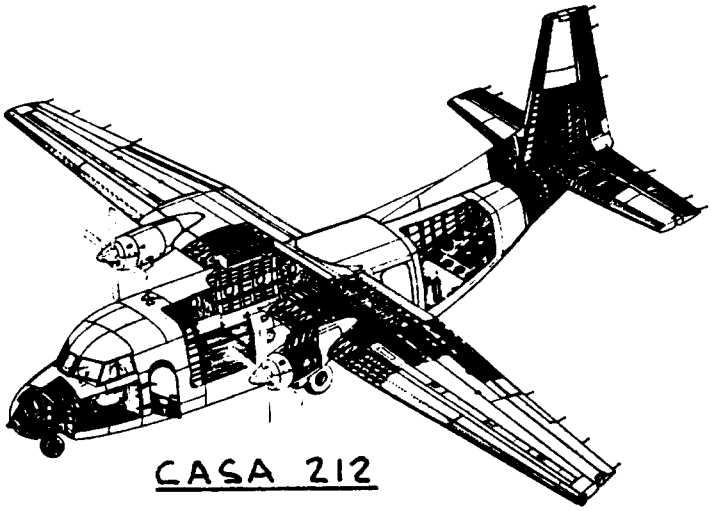

CASA 212

TABLE OF SYMBOLS

Symbol	Definition	Dimension
A	Aspect ratio	-----
a,b	Regression line constants defined by Eqn.(3.21)	-----
A, B	Regression line constants defined by Eqn.(2.16)	-----
c,d	Regression line constants defined by Eqn.(3.22)	-----
C	Fuel fraction parameter defined by Eqn.(2.31)	-----
c_f	Equivalent skin friction coefficient	-----
c_j	Specific fuel consumption	lbs/lbs/hr
c_p	Specific fuel consumption	lbs/hp/hr
C_D	Drag coefficient	-----
C_{D_o}	Zero lift drag coefficient	-----
CGR	Climb gradient, defined by Eqn.(3.28)	rad
CGRP	Climb gradient parameter, defined by Eqn.(3.30)	rad
C_L	Lift coefficient	-----
D	Drag	lbs
D(Alternate meaning)	$W_{PL} + W_{crew}$	lbs
D_p	Propeller diameter	ft
e	Oswald's efficiency factor	-----
E	Endurance	hours
$\bar{E}$	$\ln(W_i/W_{i+1})$, Eqns.(2.37 and 2.39)	-----
f	equivalent parasite area	ft^2
F	Weight sensitivity parameter, Eqn.(2.44)	lbs
FAR	Federal Air Regulation	-----
g	acceleration of gravity	ft/sec^2
h	altitude	ft

I_p	Power index, Eqn.(3.51)	$(hp/ft^2)^{1/3}$
k	number between 0 and 1	-----
k_1	constant in Eqn.(3.9)	sec^2/ft
k_2	constant in Eqn.(3.9)	-----
l_p	factor in k_2, see p.102	
L	Lift	lbs
L/D	Lift-to-drag ratio	-----
M_{ff}	Mission fuel fraction (M_{ff}= End weight/Begin weight)	none
n	Load factor	-----
nm	Nautical mile(6,076 ft)	nm
N	Number of engines	-----
P	Power, Horse-power (1hp = 550 ft.lbs/sec)	hp
P_{dl}	Parameter in $\sin\gamma$, Eqns.(3.38) and (3.39)	-----
P_s	Specific excess power	ft/sec
$\bar{q}$	dynamic pressure	psf
R	Range	nm or m
$\bar{R}$	$\ln(W_i/W_{i+1})$, Eqns.(2.36 and 2.38)	-----
RC	Rate of climb	fpm or fps
RCP	Rate-of-climb parameter, Eqns.(3.24) and (3.25)	hp/lbs
s	distance, used in take-off and landing equations with subscripts	ft
sm	Statute mile(5,280 ft)	sm
S	Wing area	ft^2
SHP	Shaft horsepower	hp_2
S_{wet}	Wetted area	ft^2
t	time	sec, min, hr
T	Thrust	lbs
TOP_{23}	FAR 23 Take-off parameter	lbs^2/ft^2hp
TOP_{25}	FAR 25 Take-off parameter	lbs/ft^2

V	True airspeed	mph, fps, kts
wod, WOD	Wind over the deck	kts
W	Weight	lbs
X	T(hrust) or P(ower)	lbs or hp

Greek Symbols
==========

η_p	propeller efficiency	-----
π	product, or 3.142	-----
ρ	air density	slugs/ft^3
σ	air density ratio	-----
μ_G	ground friction coefficient	-----
δ	pressure ratio	-----
γ	flight path angle	deg or rad
$\dot{\Psi}$	turn rate	rad/sec
θ	temperature ratio	-----
λ	bypass ratio	-----

Subscripts
==========

A	Approach
abs	absolute
cat	catapult
cl	climb
cr	cruise
crew	crew
E	Empty
f	flaps
ff	fuel fraction (see M_{ff})
F	Mission fuel
FEQ	Fixed equipment
FL	Field length
guess	guessed
h	altitude
L	Landing
LG	Landing, ground
LO	Lift-off
ltr	loiter
max	maximum
ME	Manufacturer's empty
MIF	Maximum internal fuel
OE	Operating empty
PA	Powered approach
PL	Payload
RC	Rate-of-climb

res	reserve, as in fuel reserve
reqd	required
s	stall
TO	Take-off
TOFL	Take-off field length
TOG	Take-off, ground
tent	tentative
tfo	trapped fuel and oil
used	used, as in fuel used
wet	wetted
wod	wind over the deck

Acronyms
========

AEO	All engines operating
APU	Auxiliary power unit
C^3I	Communication, Control, Command, Intelligence
OEI	One engine inoperative
OWE	Operating weight empty
RFP	Request for proposal
sls	Sealevel standard
TBP	Turboprop

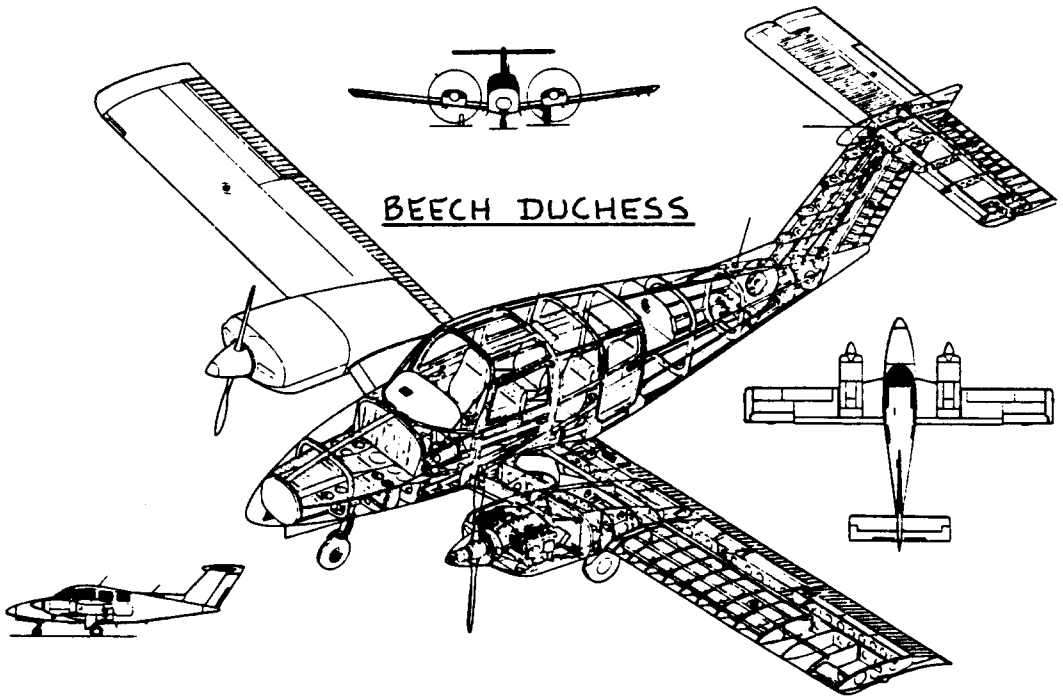

ACKNOWLEDGEMENT

Writing a book on airplane design is impossible without the supply of a large amount of data. The author is grateful to the following companies for supplying the raw data, manuals, sketches and drawings which made the book what it is:

Beech Aircraft Corporation
Boeing Commercial Airplane Company
Canadair
Cessna Aircraft Company
DeHavilland Aircraft Company of Canada
Gates Learjet Corporation
Lockheed Aircraft Corporation
McDonnell Douglas Corporation
Rinaldo Piaggio S.p.A.
Royal Netherlands Aircraft Factory, Fokker
SIAI Marchetti S.p.A.

A significant amount of airplane design information has been accumulated by the author over many years from the following magazines:

Interavia (Swiss, monthly)
Flight International (British, weekly)
Business and Commercial Aviation (USA, monthly)
Aviation Week and Space Technology (USA, weekly)
Journal of Aircraft (USA, AIAA, monthly)

The author wishes to acknowledge the important role played by these magazines in his own development as an aeronautical engineer. Aeronautical engineering students and graduates should read these magazines regularly.

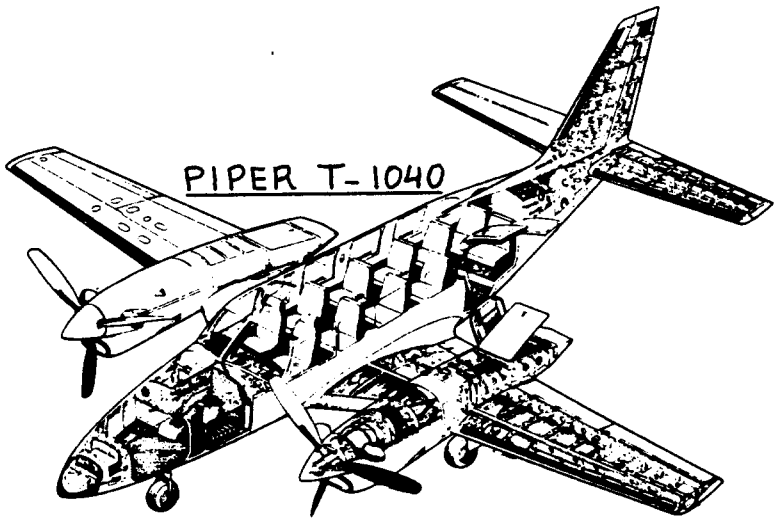

Cessna

MODEL 441 CONQUEST

AIRFOILS

WING
CENTER WING-NACA 23018
CONSTRUCTION TIP-NACA 23019

TAIL (VERTICAL
ROOT-NACA 0012
TIP-NACA 0009 MODIFIED

TAIL (HORIZONTAL
ROOT-NACA 0012
TIP-NACA 0010

INCIDENCE
CENTER WING +2°
CONSTRUCTION TIP —1°
HORIZONTAL TAIL 0°

DIHEDRAL
CENTER WING 3°30'
OUTER WING 4°55'
HORIZONTAL TAIL 12°

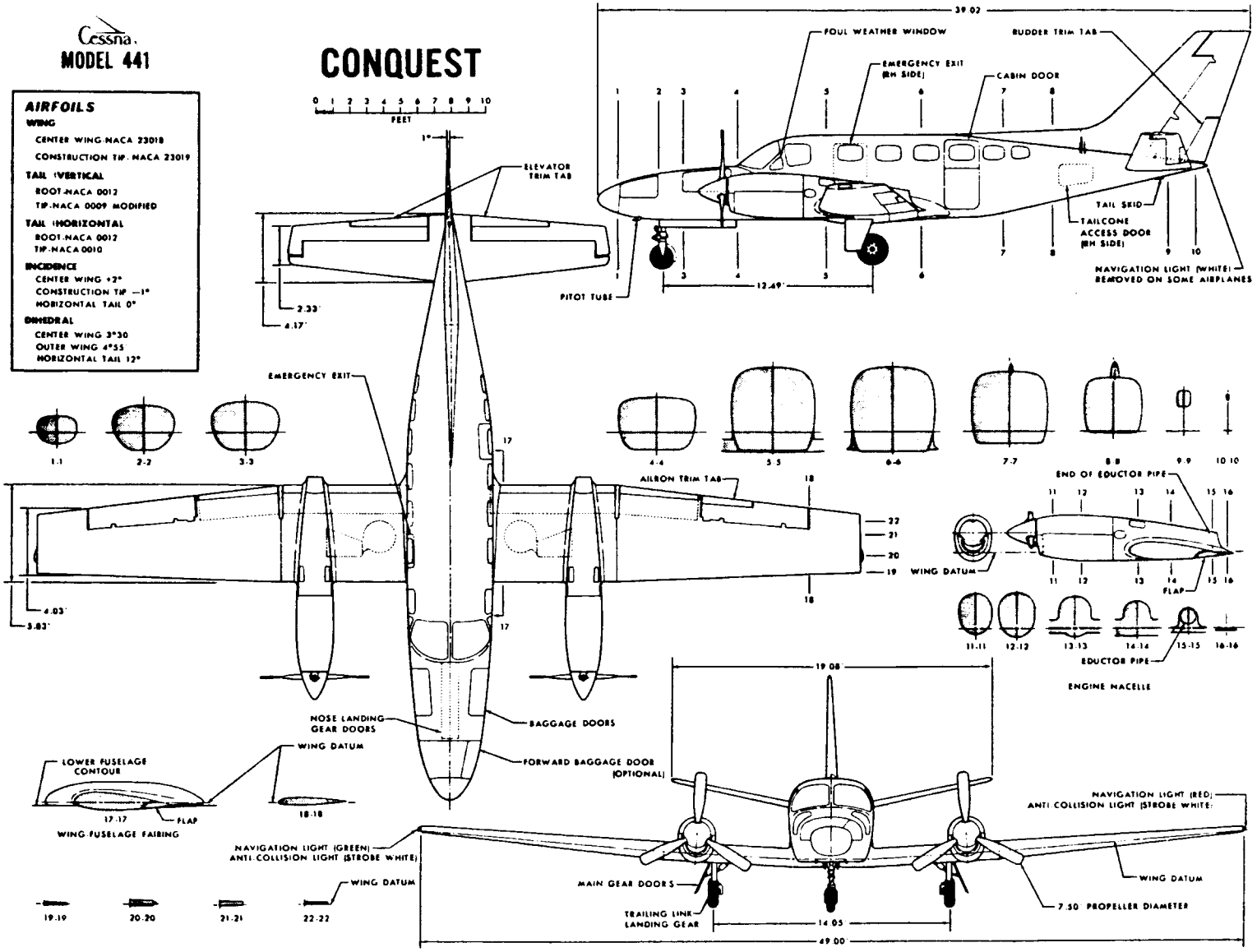

1. INTRODUCTION

The purpose of this series of books on Airplane Design is to familiarize aerospace engineering students with the methodology and decision making involved in the process of designing airplanes.

To design an airplane it is necessary that a mission specification for the airplane is available. Airplane mission specifications come about in different ways, depending on the type of airplane and sometimes depending on the customer.

Figure 1.1 illustrates several paths along which mission specifications can evolve. The reader will note, that the words preliminary sizing and preliminary design appear in Figure 1.1. This series of books concentrates on these phases of airplane design.

Many airplanes never make it beyond the initial or preliminary design phase. In fact, most don't. What happens beyond the preliminary design phase depends to a large extent on the results obtained during preliminary design and on the real or perceived market interest afterward.

If, as a result of the preliminary design studies a specific need can be met, then full scale development of the airplane can follow. If, as a result of the preliminary design studies certain problem areas are discovered (such as specific technological deficiencies which need development to be corrected, or such as a lacking data base) then a research and development program can be initiated aimed at overcoming these problems. Eventually, with the problems solved, a final mission specification is evolved which then can lead to full scale development.

If it becomes evident during the research program, that the problems cannot be solved in a reasonable time frame or at a reasonable cost, the subject design can be dropped or modified.

Figure 1.2 illustrates the preliminary design process as it is covered in this series of books.

The series of books is organized as follows:

PART I:	PRELIMINARY SIZING OF AIRPLANES
PART II:	PRELIMINARY CONFIGURATION DESIGN AND INTEGRATION OF THE PROPULSION SYSTEM
PART III:	LAYOUT DESIGN OF COCKPIT, FUSELAGE, WING AND EMPENNAGE: CUTAWAYS AND INBOARD PROFILES
PART IV:	LAYOUT DESIGN OF LANDING GEAR AND SYSTEMS
PART V:	COMPONENT WEIGHT ESTIMATION

PART VI: PRELIMINARY CALCULATION OF AERODYNAMIC, THRUST AND POWER CHARACTERISTICS
PART VII: DETERMINATION OF STABILITY, CONTROL AND PERFORMANCE CHARACTERISTICS: FAR AND MILITARY REQUIREMENTS
PART VIII: AIRPLANE COST ESTIMATION: DESIGN, DEVELOPMENT, MANUFACTURING AND OPERATING

The purpose of PART I is to present a rapid method for the preliminary sizing of an airplane to a given mission specification.

Preliminary sizing is defined as the process which results in the numerical definition of the following airplane design parameters:

*Gross Take-off Weight, W_{TO}

*Empty Weight, W_E

*Mission Fuel Weight, W_F

*Maximum Required Take-off Thrust, T_{TO} or Take-off Power, P_{TO}

*Wing Area, S and Wing Aspect Ratio, A

*Maximum Required Lift Coefficient (Clean), $C_{L_{max}}$

*Maximum Required Lift Coefficient for Take-off, $C_{L_{max_{TO}}}$

*Maximum Required Lift Coefficient for Landing, $C_{L_{max_L}}$ or $C_{L_{max_{PA}}}$

It is assumed in this book that a mission specification for the airplane is available. Typical parameters which are numerically defined in a mission specification are:

*Payload and type of payload
*Range and/or loiter requirements
*Cruise speed and altitude
*Field length for take-off and for landing
*Fuel reserves
*Climb requirements
*Maneuvering requirements
*Certification base (For example: Experimental, FAR 23, FAR 25 or Military)

Some mission specifications will contain much more detail than others. This depends on the customer who wrote the specification and on the amount of design flexibility this customer wants the airplane designer to have.

The sizing methods presented in this book appear in the following sequence:

Chapter 2: Estimating take-off gross weight, W_{TO}, empty weight, W_E and mission fuel weight, W_F.

Chapter 3: Estimating wing area, S, wing aspect ratio, A, take-off thrust, T_{TO} and maximum lift coefficients, $C_{L_{max}}$, $C_{L_{max_{TO}}}$ and $C_{L_{max_L}}$.

Chapter 4 provides a user's guide through the preliminary sizing process.

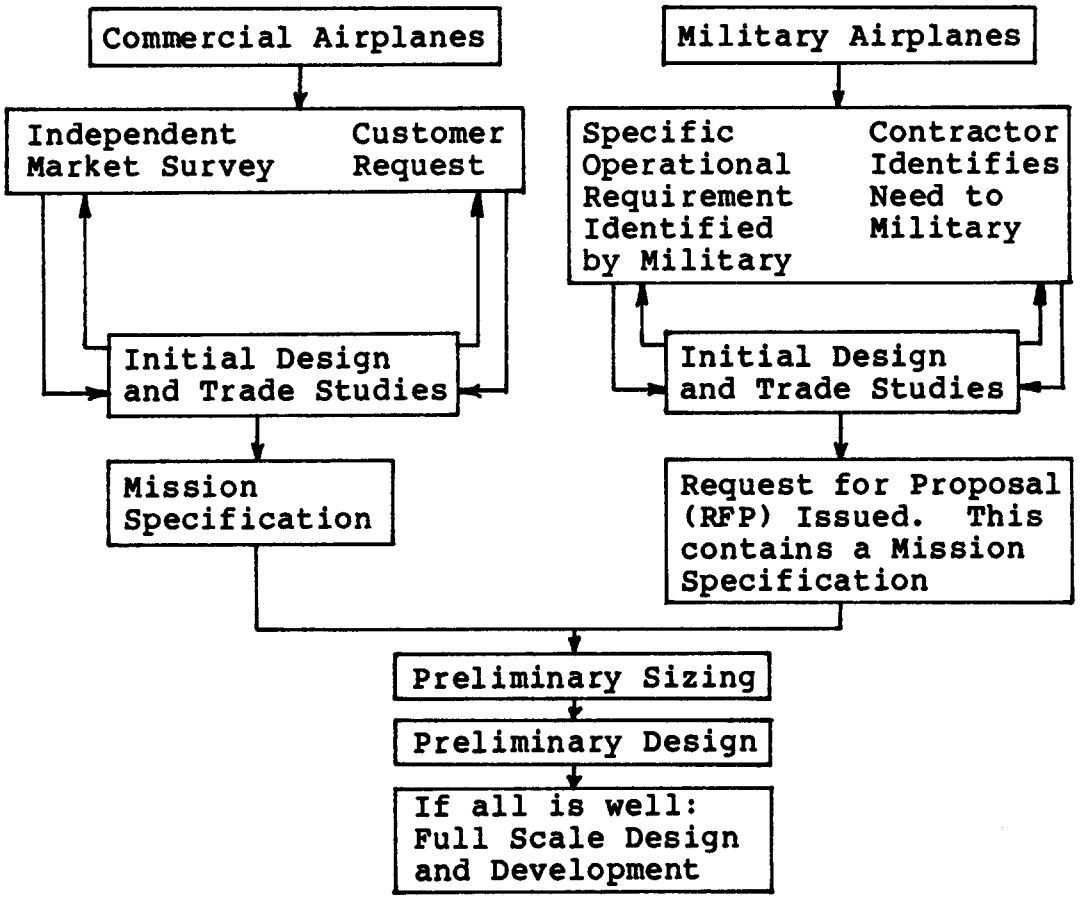

Figure 1.1 Example of Evolution of a Mission Specification and its Relation to Preliminary Sizing and Design

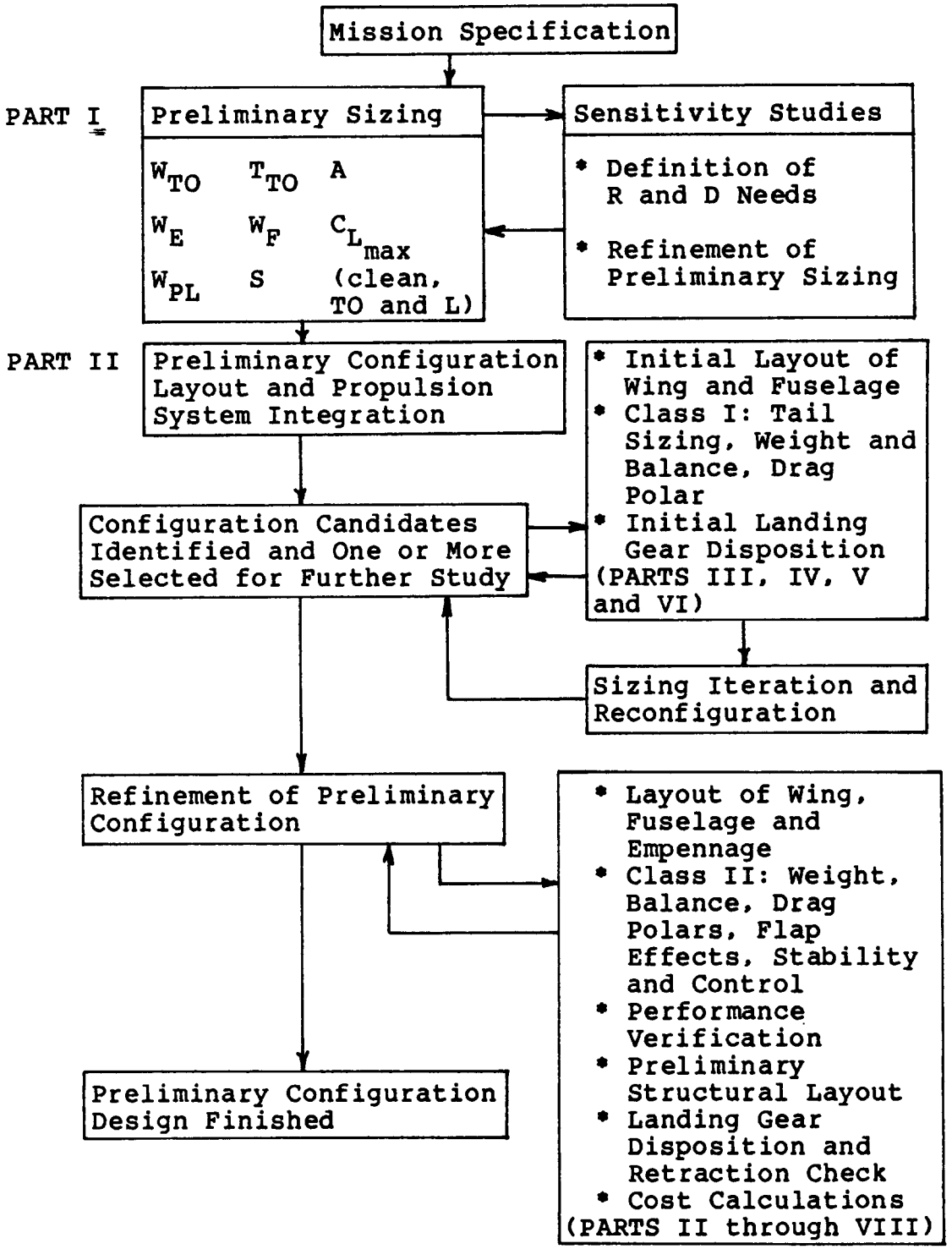

Figure 1.2 The Preliminary Design Process As Covered In Parts I Through VIII Of 'AIRPLANE DESIGN'

2. ESTIMATING TAKE-OFF GROSS WEIGHT, W_{TO}, EMPTY WEIGHT, W_E, AND MISSION FUEL WEIGHT, W_F

Airplanes must normally meet very stringent range, endurance, speed and cruise speed objectives while carrying a given payload. It is important, to be able to predict the minimum airplane weight and fuel weight needed to accomplish a given mission.

For a given mission specification, this chapter presents a rapid method for estimating:

- *Take-off gross weight, W_{TO}
- *Empty weight, W_E
- *Mission fuel weight, W_F

The method applies to the following twelve types of airplanes:

1. Homebuilt Propeller Driven Airplanes
2. Single Engine Propeller Driven Airplanes
3. Twin Engine Propeller Driven Airplanes
4. Agricultural Airplanes
5. Business Jets
6. Regional Turbopropeller Driven Airplanes
7. Transport Jets
8. Military Trainers
9. Fighters
10. Military Patrol, Bomb and Transport Airplanes
11. Flying Boats, Amphibious and Float Airplanes
12. Supersonic Cruise Airplanes

2.1 GENERAL OUTLINE OF THE METHOD

A convenient way to break down W_{TO} is as follows:

$$W_{TO} = W_{OE} + W_F + W_{PL} \qquad (2.1)$$

where:

W_{OE} is the airplane operating weight empty,

W_F is the mission fuel weight,

W_{PL} is the payload weight.

The operating weight empty, W_{OE} (also called OWE),

is frequently written as follows:

$$W_{OE} = W_E + W_{tfo} + W_{crew} \qquad (2.2)$$

where:

W_E is the empty weight,

W_{tfo} is the weight of all trapped (=unusable) fuel and oil,

W_{crew} is the weight of the crew required to operate the airplane.

It must be kept in mind, that the empty weight, W_E is sometimes broken down in the following manner:

$$W_E = W_{ME} + W_{FEQ} \qquad (2.3)$$

where:

W_{ME} is the manufacturers empty weight, sometimes referred to as the green weight,

W_{FEQ} is the fixed equipment weight.

Fixed equipment weight can include such items as:

- *avionics equipment
- *airconditioning equipment
- *special radar equipment
- *auxiliary power unit (APU)
- *furnishings and interiors
- *other equipment needed to operate the airplane during its intended mission

At this junction, two key points must be made:

Point 1: It is not difficult to estimate the required mission fuel weight W_F from very basic considerations. This will be shown in Section 2.4.

Point 2: There exists a linear relationship between $\log_{10} W_{TO}$ and $\log_{10} W_E$ for the twelve types of airplanes mentioned before. Graphical evidence for this will be shown in Section 2.5.

Based on these two points, the process of estimating

values for W_{TO}, W_E and W_F consists of the following steps:

Step 1. Determine the mission payload weight, W_{PL} (Section 2.2). → puede ser cualquiera

Step 2. Guess a likely value of take-off weight, $W_{TO_{guess}}$ (Section 2.3).

Step 3. Determine the mission fuel weight, W_F (Section 2.4).

Step 4. Calculate a tentative value for W_{OE} from:

$$W_{OE_{tent}} = W_{TO_{guess}} - W_F - W_{PL} \qquad (2.4)$$

Step 5. Calculate a tentative value for W_E from:

$$W_{E_{tent}} = W_{OE_{tent}} - W_{tfo} - W_{crew} \qquad (2.5)$$

Although W_{tfo} can amount to as much as 0.5% or more of W_{TO} for some airplanes, it is often neglected at this stage in the design process.
How to determine the numerical value for W_{crew} is discussed in Section 2.2.

Step 6. Find the allowable value of W_E from Section 2.5.

Step 7. Compare the values for $W_{E_{tent}}$ and for W_E as obtained from Steps 5 and 6. Next, make an adjustment to the value of $W_{TO_{guess}}$ and repeat Steps 3 through 6. Continue this process until the values of $W_{E_{tent}}$ and W_E agree with each other to within some pre-selected tolerance. A tolerance of 0.5% is usually sufficient at this stage in the design process.

Sections 2.2 through 2.5 contain detailed methods for estimating W_{PL}, W_{TO} and W_F. Section 2.6 applies the stepwise methodology to three types of airplanes.

2.2 DETERMINATION OF MISSION PAYLOAD WEIGHT, W_{PL}, AND CREW WEIGHT, W_{crew}

Mission payload weight, W_{PL} is normally specified in the mission specification. This payload weight usually consists of one or more of the following:

1. Passengers and baggage
2. Cargo
3. Military loads such as ammunition, bombs, missiles and a variety of stores or pods which are usually carried externally and therefore affect the airplane drag

For passengers in a commercial airplane an average weight of 175 lbs per person and 30 lbs of baggage is a reasonable assumption for short to medium distance flights. For long distance flights, the baggage weight should be assumed to be 40 lbs. per person.

The crew weight, W_{crew} is found from the following considerations:

Commercial:

The crew consists of the cockpit crew and the cabin crew. The number of people in each crew depends on the airplane and its mission. It depends also on the total number of passengers carried. Reference 8, FAR 91.215 specifies the minimum number of cabin crew members required.

For crew members an average weight of 175 lbs plus 30 lbs of baggage is a reasonable assumption.

Military:

For military crew members a weight of 200 lbs should be assumed because of extra gear carried.

Caution:

Because FAR 23 certified airplanes (Types 2 and 3) are frequently operated by owner/pilots it is not unusual to define the crew weight as part of the payload in these cases.

2.3 GUESSING A LIKELY VALUE OF TAKE-OFF WEIGHT, $W_{TO_{guess}}$

An initial 'guess' of the value of take-off weight, $W_{TO_{guess}}$ is usually obtained by comparing the mission specification of the airplane with the mission capabilities of similar airplanes listed in Reference 9. If no reasonable comparison can be made (perhaps because

the specification calls for a type of airplane never before conceived) then it will be necessary to make an arbitrary 'guess'.

2.4 DETERMINATION OF MISSION FUEL WEIGHT, W_F

In Section 2.1, Point 1 indicated that it is not difficult to estimate a value for W_F from basic considerations. This section presents a method for doing just that.

Mission fuel weight, W_F can be written as:

$$W_F = W_{F_{used}} + W_{F_{res}} \qquad (2.6)$$

where:

$W_{F_{used}}$ is the fuel actually used during the mission,

$W_{F_{res}}$ are the fuel reserves required for the mission.

Fuel reserves are normally specified in the mission specification. They are also specified in those FAR's which regulate the operation of passenger transports. Fuel reserves are generally specified in one or more of the following types:

1. as a fraction of $W_{F_{used}}$
2. as a requirement for additional range so that an alternate airport can be reached
3. as a requirement for (additional) loiter time

To determine $W_{F_{used}}$, the fuel weight actually used during the mission, the so-called fuel-fraction method will be used. In this method the airplane mission is broken down into a number of mission phases. The fuel used during each phase is found from a simple calculation or estimated on the basis of experience.

The fuel-fraction method will be illustrated by applying it to an arbitrary airplane. Figure 2.1 defines the mission profile for this airplane.

It will be observed that the mission profile is broken down into a number of mission phases. Each phase has a number. Each phase also has a begin weight and an end weight associated with it.

La fracción $\frac{W_{ramp}}{W_{TO}}$ suele ser practicamente 1

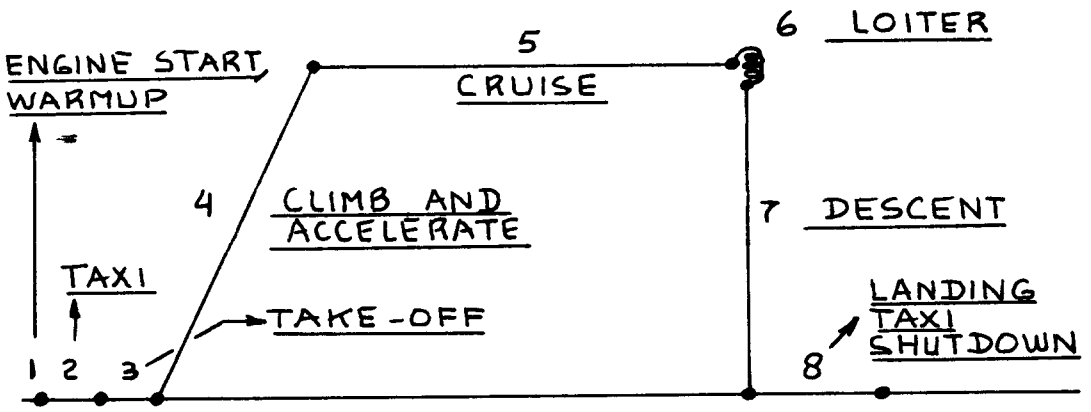

Figure 2.1 Mission Profile for an Arbitrary Airplane

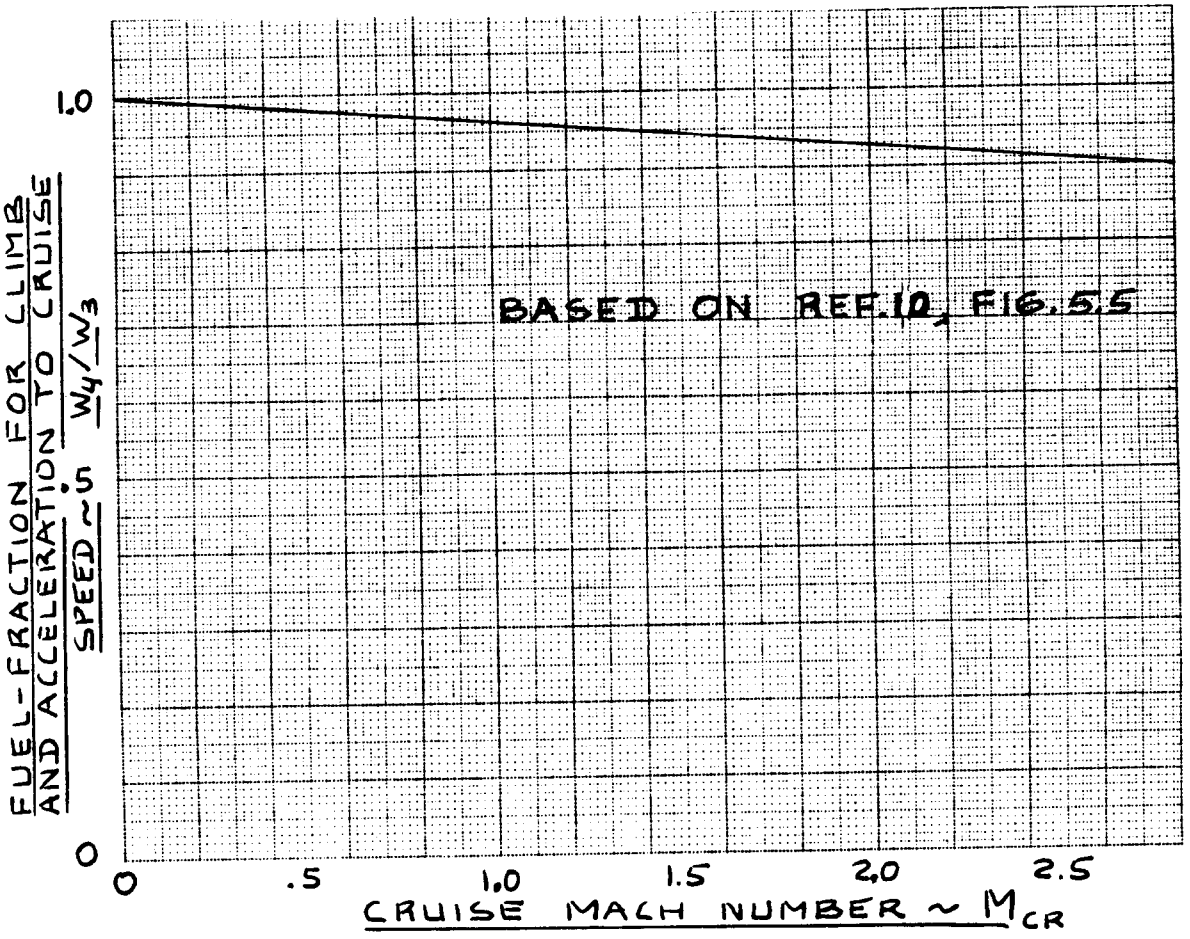

Figure 2.2 Fuel Fraction for Phase 4 of Figure 2.1

The following definition is important:

Definition: The fuel-fraction for each phase is defined as the ratio of end weight to begin weight.

The next step is to assign a numerical value to the fuel-fraction corresponding to each mission phase. This is done as follows:

Phase 1: Engine start and warm-up.
Begin weight is W_{TO}. End weight is W_1.

The fuel-fraction for this phase is by previous definition given by: W_1/W_{TO}.

Table 2.1 provides a guide for determining this fraction for twelve types of airplanes.

Phase 2: Taxi.
Begin weight is W_1. End weight is W_2.

The fuel-fraction for this phase is W_2/W_1.

Table 2.1 provides a guide for determining this fraction for twelve types of airplanes.

Phase 3: Take-off.
Begin weight is W_2. End weight is W_3.

The fuel-fraction for this phase is W_3/W_2.

Table 2.1 provides a guide for determining this fraction for twelve types of airplanes.

Phase 4: Climb to cruise altitude and accelerate to cruise speed.
Begin weight is W_3. End weight is W_4.

The fuel fraction for this phase, W_4/W_3 may be determined directly from

Figure 2.2.
However, in some cases it is desirable to calculate this fraction from Breguet's equation for endurance (Ref.14):

Table 2.1 Suggested Fuel-Fractions For Several Mission Phases

Mission Phase No.(See Fig.2.1) / Airplane Type:	Engine Start, Warm-up 1	Taxi 2	Take-off 3	Climb 4	Descent 7	Landing Taxi, Shutdown 8
1. Homebuilt	0.998	0.998	0.998	0.995	0.995	0.995
2. Single Engine	0.995	0.997	0.998	0.992	0.993	0.993
3. Twin Engine	0.992	0.996	0.996	0.990	0.992	0.992
4. Agricultural	0.996	0.995	0.996	0.998	0.999	0.998
5. Business Jets	0.990	0.995	0.995	0.980	0.990	0.992
6. Regional TBP's	0.990	0.995	0.995	0.985	0.985	0.995
7. Transport Jets	0.990	0.990	0.995	0.980	0.990	0.992
8. Military Trainers	0.990	0.990	0.990	0.980	0.990	0.995
9. Fighters	0.990	0.990	0.990	0.96-0.90	0.990	0.995
10. Mil.Patrol, Bomb, Transport	0.990	0.990	0.995	0.980	0.990	0.992
11. Flying Boats, Amphibious, Float Airplanes	0.992	0.990	0.996	0.985	0.990	0.990
12. Supersonic Cruise	0.990	0.995	0.995	0.92-0.87	0.985	0.992

Notes: 1. The numbers in this table are based on experience or on judgment.
2. There is no substitute for common sense! If and when common sense so dictates, the reader should substitute other values for the fractions suggested in this table.

for propeller-driven airplanes:

$$E_{cl} = 375(1/V_{cl})(\eta_p/c_p)_{cl}(L/D)_{cl}\ln(W_3/W_4) \qquad (2.7)$$

Note: V_{cl} in Eqn.(2.7) is in mph.

If the fuel-fraction for the climb phase is to be calculated in this manner then it is necessary to estimate average values during the climb for V_{cl}, for $(\eta_p/c_p)_{cl}$ and for $(L/D)_{cl}$. Table 2.2 provides a guide from which these quantities can be found.

for jet airplanes:

$$E_{cl} = (1/c_j)_{cl}(L/D)_{cl}\ln(W_3/W_4) \qquad (2.8)$$

If the fuel-fraction for the climb phase is to be calculated in this manner then it is necessary to estimate average values during the climb for $c_{j_{cl}}$, and for $(L/D)_{cl}$. Table 2.2 provides a guide from which it is possible to find these quantities.

E_{cl} in Eqn.(2.8) is equal to the time to climb, usually expressed as a fraction of an hour. This can be found in turn by assuming a value for the average rate-of-climb. The altitude at the end of the climb (usually referred to as the cruise or loiter altitude) is normally provided in the airplane mission specification. Methods for rapid evaluation of climb performance are discussed in Chapter 3.

Phase 5: Cruise.
Begin weight is W_4. End weight is W_5.

The ratio W_5/W_4 can be estimated from Breguet's range equation (Ref.14), which can be written as follows:

Table 2.2 Suggested Values For L/D, c_j, η_p, And For c_p For Several Mission Phases

	Cruise				Loiter			
	L/D	c_j	c_p	η_p	L/D	c_j	c_p	η_p
Mission Phase No. (See Fig. 2.1)		lbs/lbs/hr	lbs/hp/hr			lbs/lbs/hr	lbs/hp/hr	
		5				6		
Airplane Type								
1. Homebuilt	8-10*		0.6-0.8	0.7	10-12		0.5-0.7	0.6
2. Single Engine	8-10		0.5-0.7	0.8	10-12		0.5-0.7	0.7
3. Twin Engine	8-10		0.5-0.7	0.82	9-11		0.5-0.7	0.72
4. Agricultural	5-7		0.5-0.7	0.82	8-10		0.5-0.7	0.72
5. Business Jets	10-12	0.5-0.9			12-14	0.4-0.6		
6. Regional TBP's	11-13		0.4-0.6	0.85	14-16		0.5-0.7	0.77
7. Transport Jets	13-15	0.5-0.9			14-18	0.4-0.6		
8. Military Trainers	8-10	0.5-1.0	0.4-0.6	0.82	10-14	0.4-0.6	0.5-0.7	0.77
9. Fighters	4-7	0.6-1.4	0.5-0.7	0.82	6-9	0.6-0.8	0.5-0.7	0.77
10. Mil. Patrol, Bomb, Transport	13-15	0.5-0.9	0.4-0.7	0.82	14-18	0.4-0.6	0.5-0.7	0.77
11. Flying Boats, Amphibious, Float Airplanes	10-12	0.5-0.9	0.5-0.7	0.82	13-15	0.4-0.6	0.5-0.7	0.77
12. Supersonic Cruise	4-6	0.7-1.5			7-9	0.6-0.8		

Notes: 1. The numbers in this table represent ranges based on existing engines.
2. There is no substitute for common sense! If and when actual data are available, these should be used.
3. A good estimate for L/D can be made with the drag polar method of Sub-section 3.4.1.
* Homebuilts with smooth exteriors and/or high wing loadings can have L/D values which are considerably higher.

for propeller-driven airplanes:

$$R_{cr} = 375(\eta_p/c_p)_{cr}(L/D)_{cr}\ln(W_4/W_5) \qquad (2.9)$$

Note: R_{cr} in Eqn.(2.9) is in stat. miles.

for jet airplanes:

$$R_{cr} = (V/c_j)_{cr}(L/D)_{cr}\ln(W_4/W_5) \qquad (2.10)$$

Note, that R_{cr} is usually expressed in n.m. Values for $(\eta_p/c_p)_{cr}$, for $c_{j_{cr}}$ and for $(L/D)_{cr}$ may again be obtained from Table 2.2. Values for R_{cr} and for V_{cr} are usually given in the mission specification.

Phase 6: Loiter.
Begin weight is W_5. End weight is W_6. The fuel-fraction W_6/W_5 can be found with the help of Breguet's endurance equation:

for propeller-driven airplanes:

$$E_{ltr} = 375(1/V_{ltr})(\eta_p/c_p)_{ltr}(L/D)_{ltr}\ln(W_5/W_6) \qquad (2.11)$$

Note: V_{ltr} in Eqn.(2.11) is in mph.

for jet airplanes:

$$E_{ltr} = (1/c_{j_{ltr}})(L/D)_{ltr}\ln(W_5/W_6) \qquad (2.12)$$

Note, that E_{ltr} is usually expressed in hours. Values for $(\eta_p/c_p)_{ltr}$, for $c_{j_{ltr}}$ and for $(L/D)_{ltr}$ can be obtained again from Table 2.2. Values for V_{ltr} and for E are often given in the mission specification.

Phase 7: Descent.

Begin weight is W_6. End weight is W_7.

The fuel-fraction W_7/W_6 may be found from Table 2.1.

Phase 8: Landing, taxi and shut-down.

Begin weight is W_7. End weight is W_8.

The fuel-fraction W_8/W_7 may be found from Table 2.1.

It is now possible to calculate the mission fuel-fraction, M_{ff} from:

$$M_{ff} = (W_1/W_{TO})\prod_{i=1}^{i=7}(W_{i+1}/W_i) \qquad (2.13)$$

producto

The fuel used during the mission, $W_{F_{used}}$ can be found from:

$$W_{F_{used}} = (1 - M_{ff})W_{TO} \qquad (2.14)$$

The value for mission fuel weight, W_F can finally be determined from:

$$W_F = (1 - M_{ff})W_{TO} + W_{F_{res}} \qquad (2.15)$$

Specific examples of how this fuel-fraction method can be applied to airplanes are presented in section 2.6.

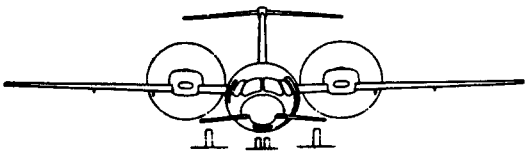

$W_{Freservas}$: dependería de la regulación o tipo de operación a aplicar

2.5 FINDING THE ALLOWABLE VALUE FOR W_E

In Section 2.1, Point 2 raised the issue of the existence of a linear relationship between $\log_{10}W_E$ and $\log_{10}W_{TO}$. Once such a relationship is established, it should be easy to obtain W_E from W_{TO}.

Figures 2.3 through 2.14 demonstrate that such relationships indeed exist. The data presented in Figures 2.3 through 2.14 are based on Tables 2.3 through 2.14. These tables in turn are based on data found in Reference 9 or on data obtained directly from airplane manufacturers.

The trend lines in Figures 2.3 through 2.14 were established with the help of a regression analysis. The reader should consider these trend lines to be a fair representation of the 'state-of-the-art' of airplane design. It is desirable to have as small a value for W_E for any given value of W_{TO}. Therefore, it is reasonable to assume, that a manufacturer will always try to make W_E as small as possible for any given take-off weight, W_{TO}.

For that reason, at any value of W_{TO} in Figures 2.3 through 2.14, the corresponding value of W_E should be viewed as the 'minimum allowable' value at the current 'state-of-the-art' of airplane design.

Several ways for finding W_E from W_{TO} present themselves:

1. For a given value of W_{TO} as obtained from Step 2 in Section 2.1, the allowable value for W_E can be read from Figures 2.3 through 2.14.

2. For a given value of W_{TO} as obtained from Step 2 in Section 2.1, the allowable value for W_E can be found by interpolation from Tables 2.3 through 2.14.

3. For a given value of W_{TO} as obtained from Step 2 in Section 2.1, the allowable value for W_E can be found from the following equation:

$$W_E = \text{inv.log}_{10}\{(\log_{10}W_{TO} - A)/B\} \qquad (2.16)$$

This equation represents the regression lines shown in Figures 2.3 through 2.14. Numerical values for the quantities A and B are listed in Table 2.15.

An important note of caution:

The primary structures of most of the airplanes listed in Figures 2.3 through 2.14 and Tables 2.3 through 2.14 are manufactured primarily of metallic materials. Exceptions are indicated. If the reader wishes to obtain an estimate of W_E for an airplane which is to be made of composite materials, the following guidelines should be observed:

1.) Determine which airplane components are to be made from composite materials.

2.) Determine an average value for W_{comp}/W_{metal} for the new airplane from Table 2.16. The allowable value of W_E as found from Figures 2.3 through 2.14 must now be multiplied by W_{comp}/W_{metal}, listed in Table 2.16.

The reader should keep in mind, that non-primary structures, such as floors, fairings, flaps, control surfaces and interior furnishings, have been manufactured from composites for several years. Claims of weight reductions relative to the airplanes in Figures 2.3 through 2.14 should therefore be made with great caution.

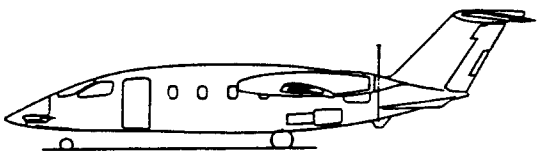

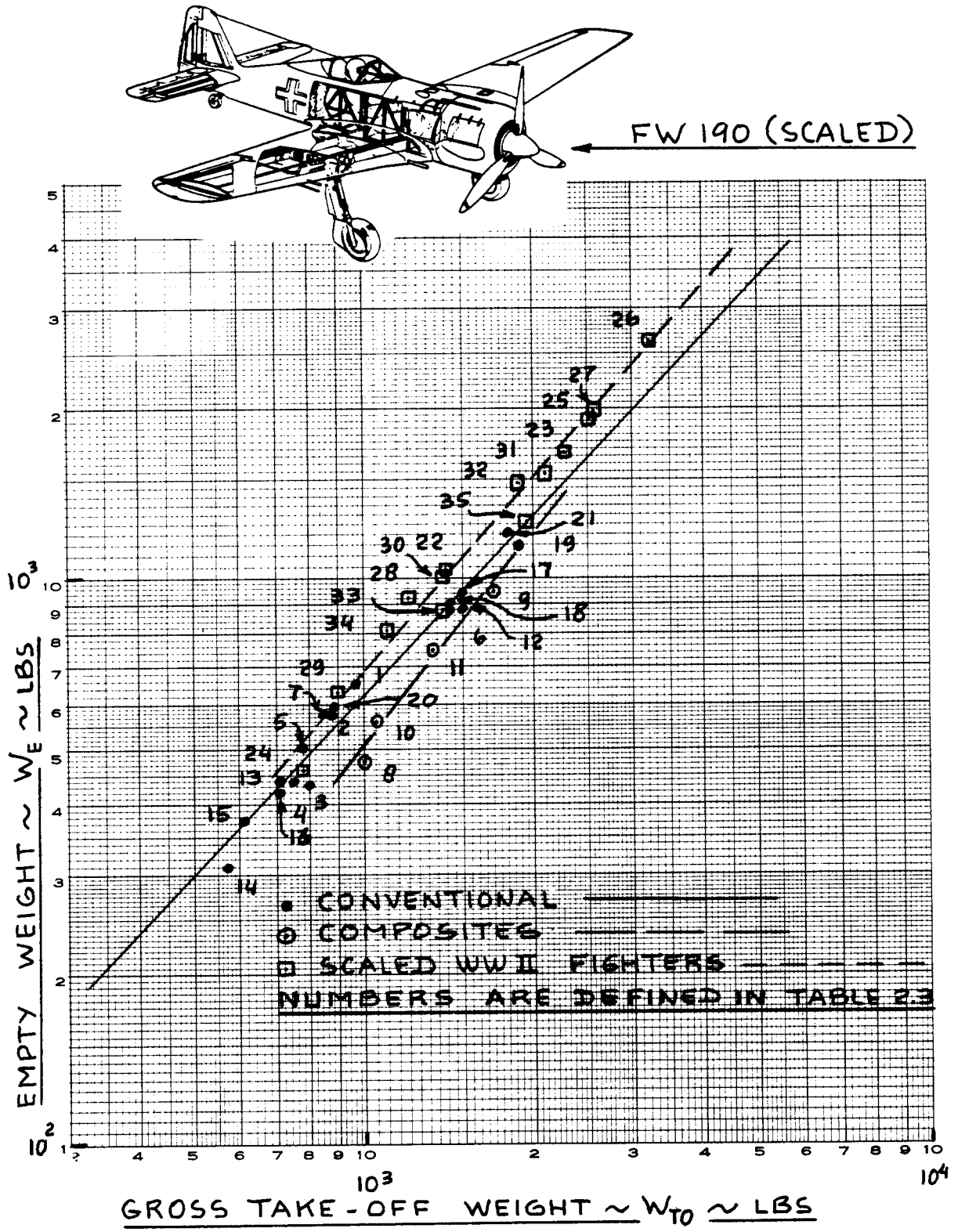

Figure 2.3 Weight Trends for Homebuilt Propeller Driven Airplanes

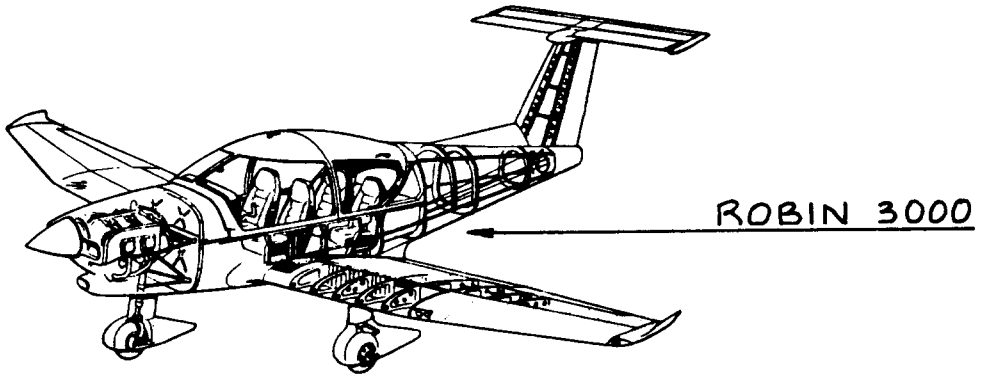

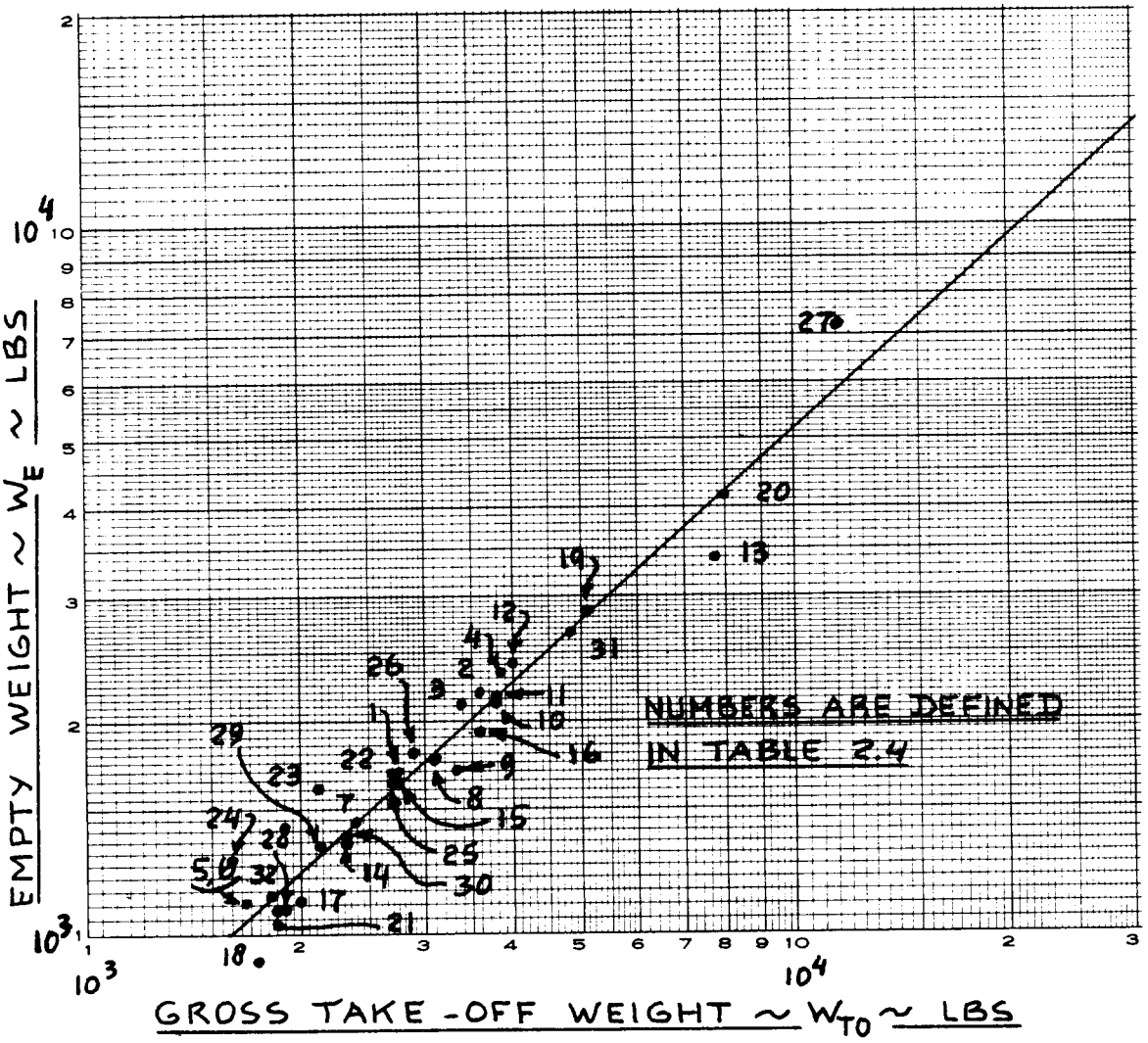

Figure 2.4 Weight Trends for Single Engine Propeller Driven Airplanes

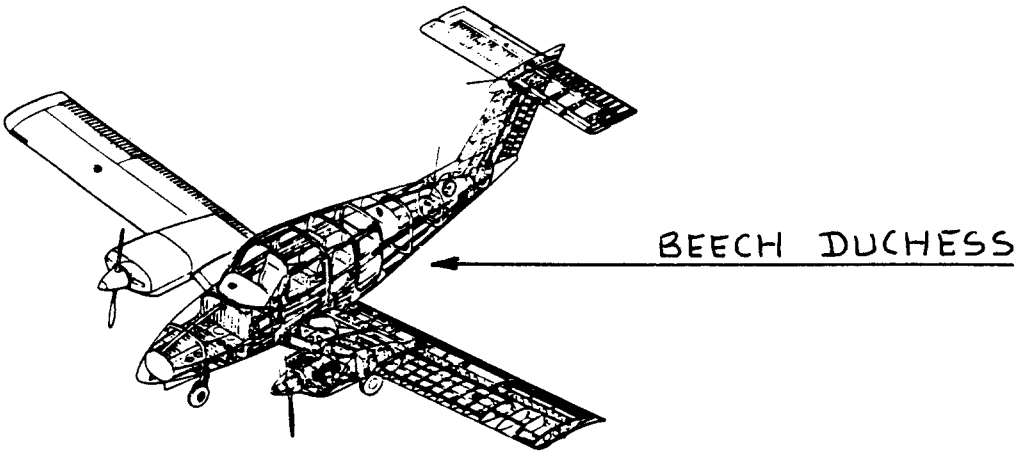

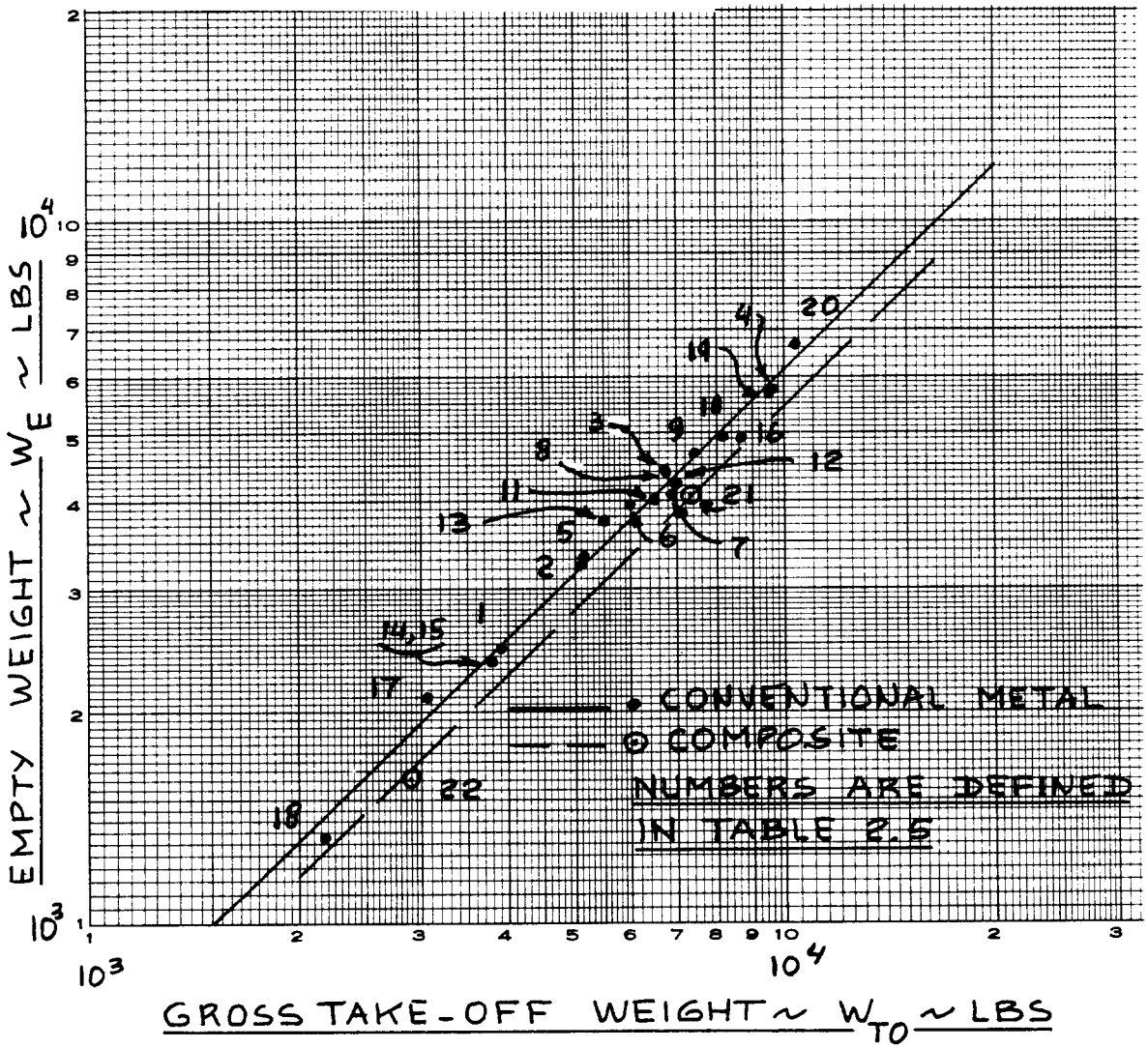

Figure 2.5 Weight Trends for Twin Engine Propeller Driven Airplanes

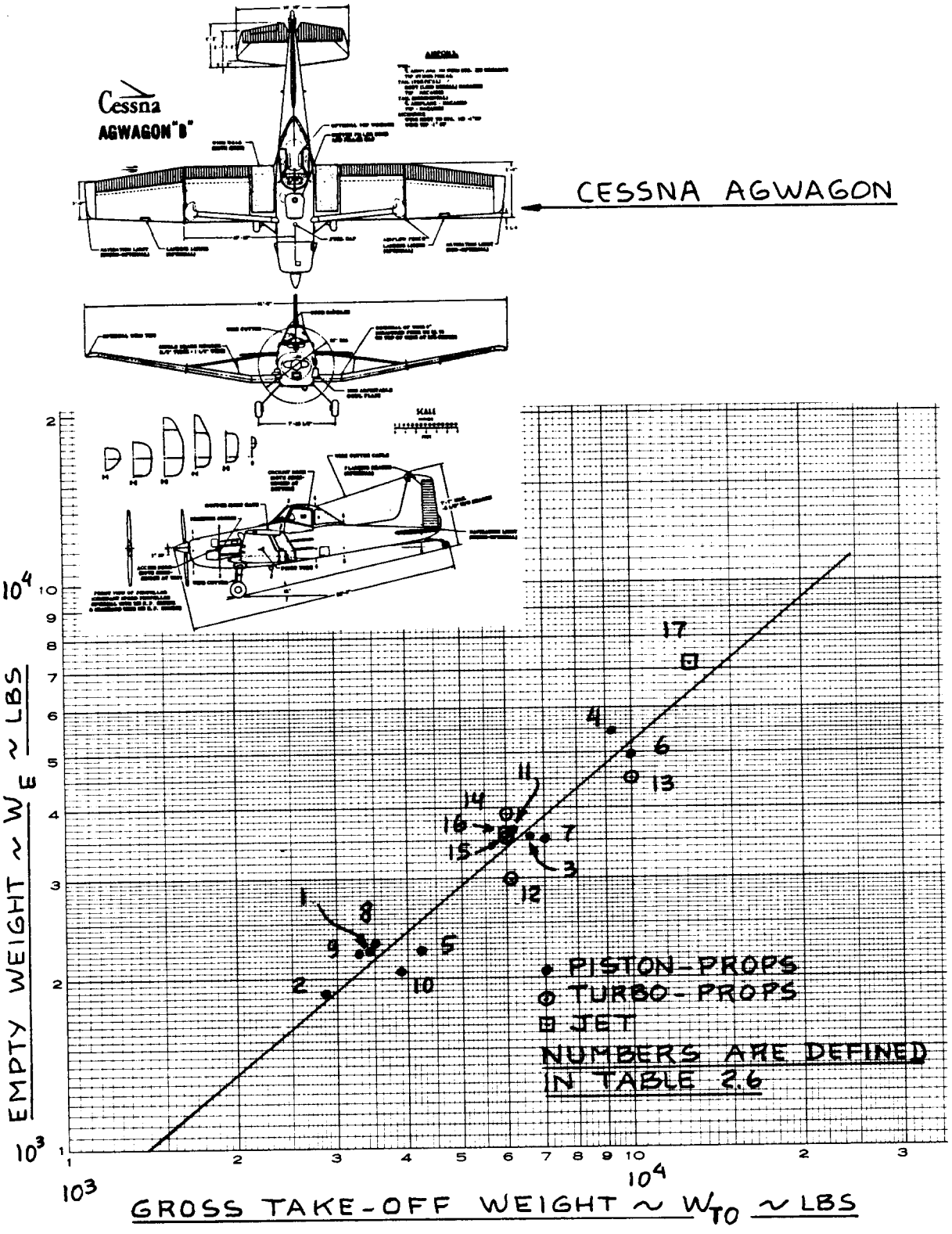

Figure 2.6 Weight Trends for Agricultural Airplanes

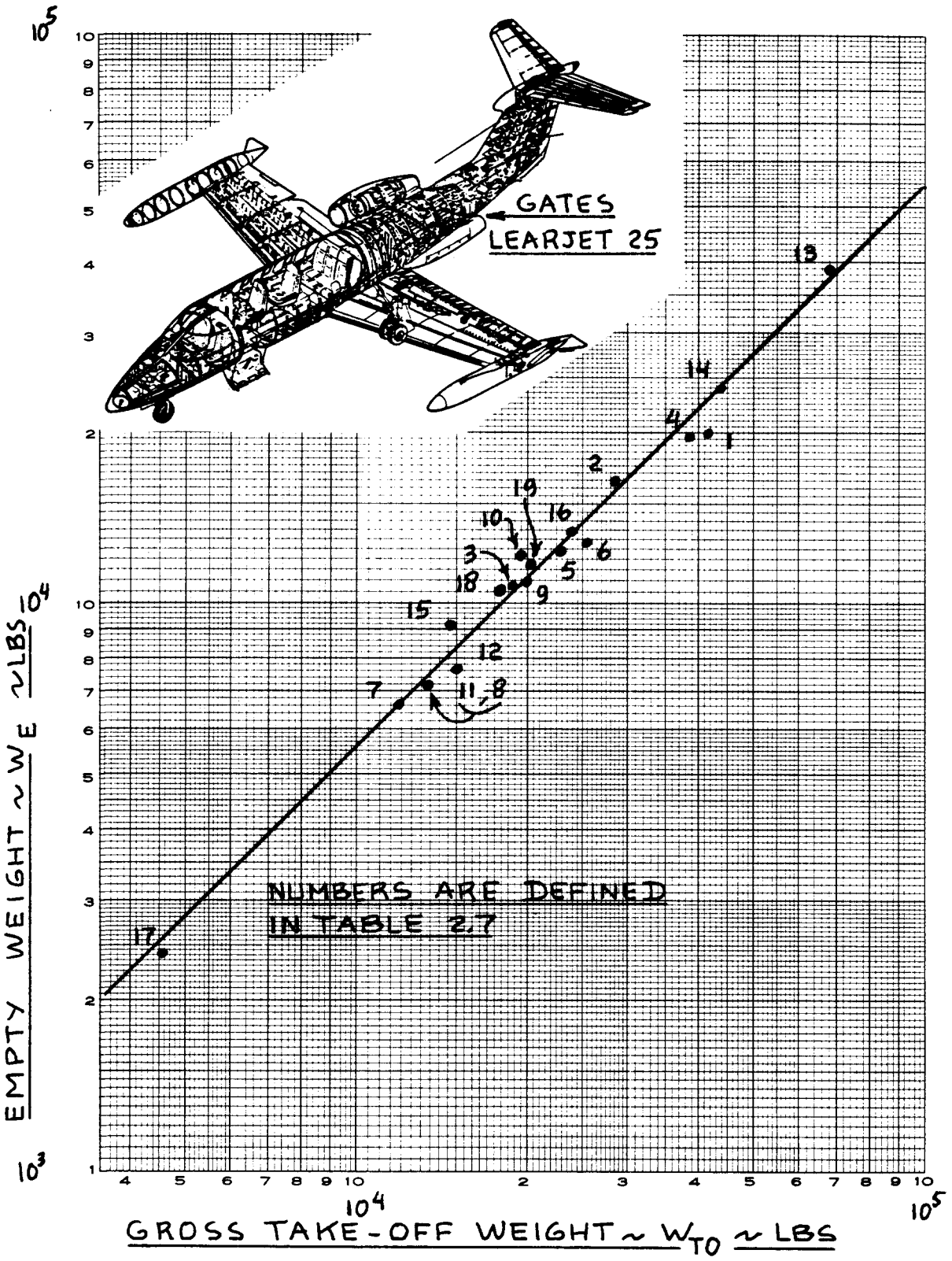

Figure 2.7 Weight Trends for Business Jets

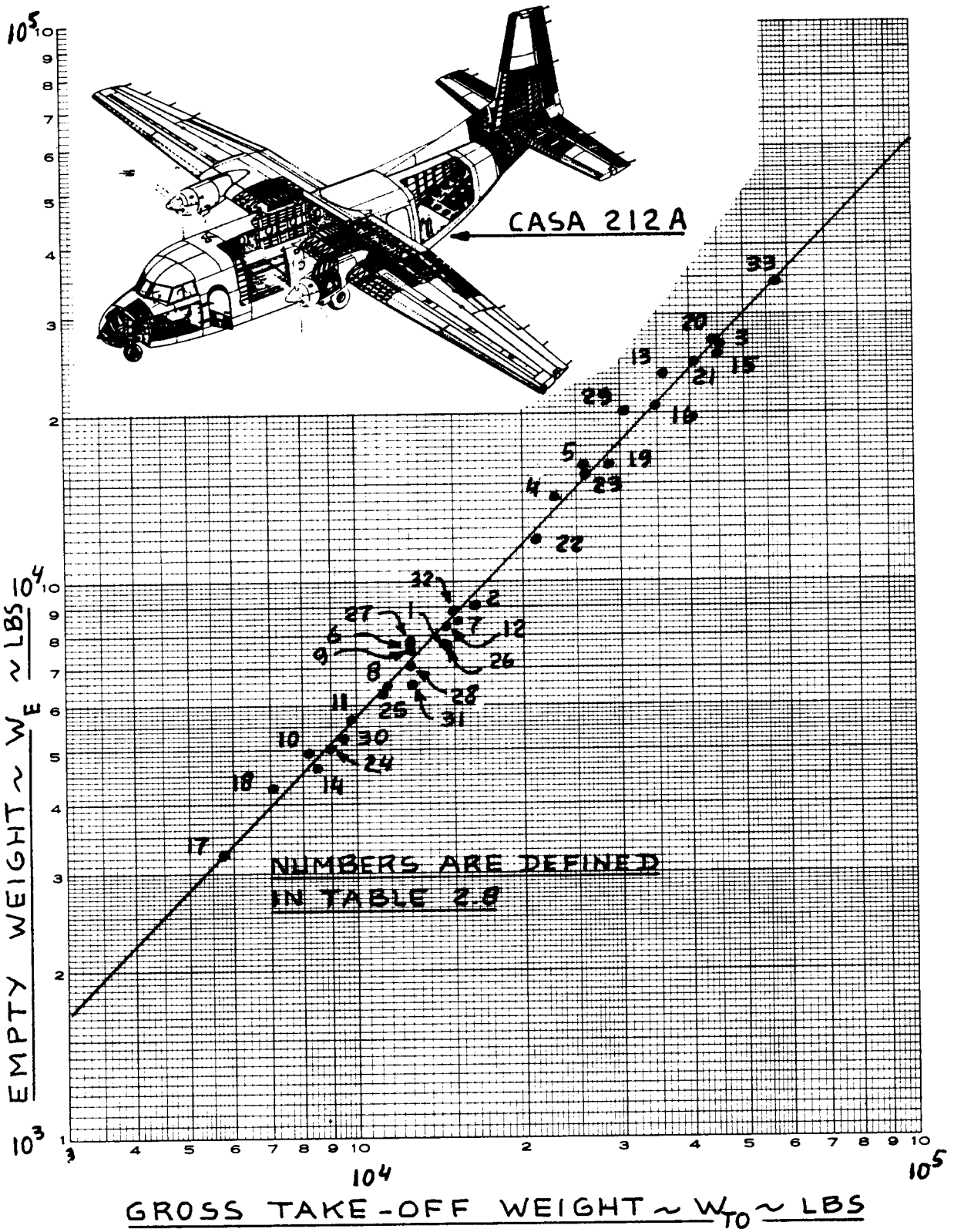

Figure 2.8 Weight Trends for Regional Turbo-Propeller Driven Airplanes

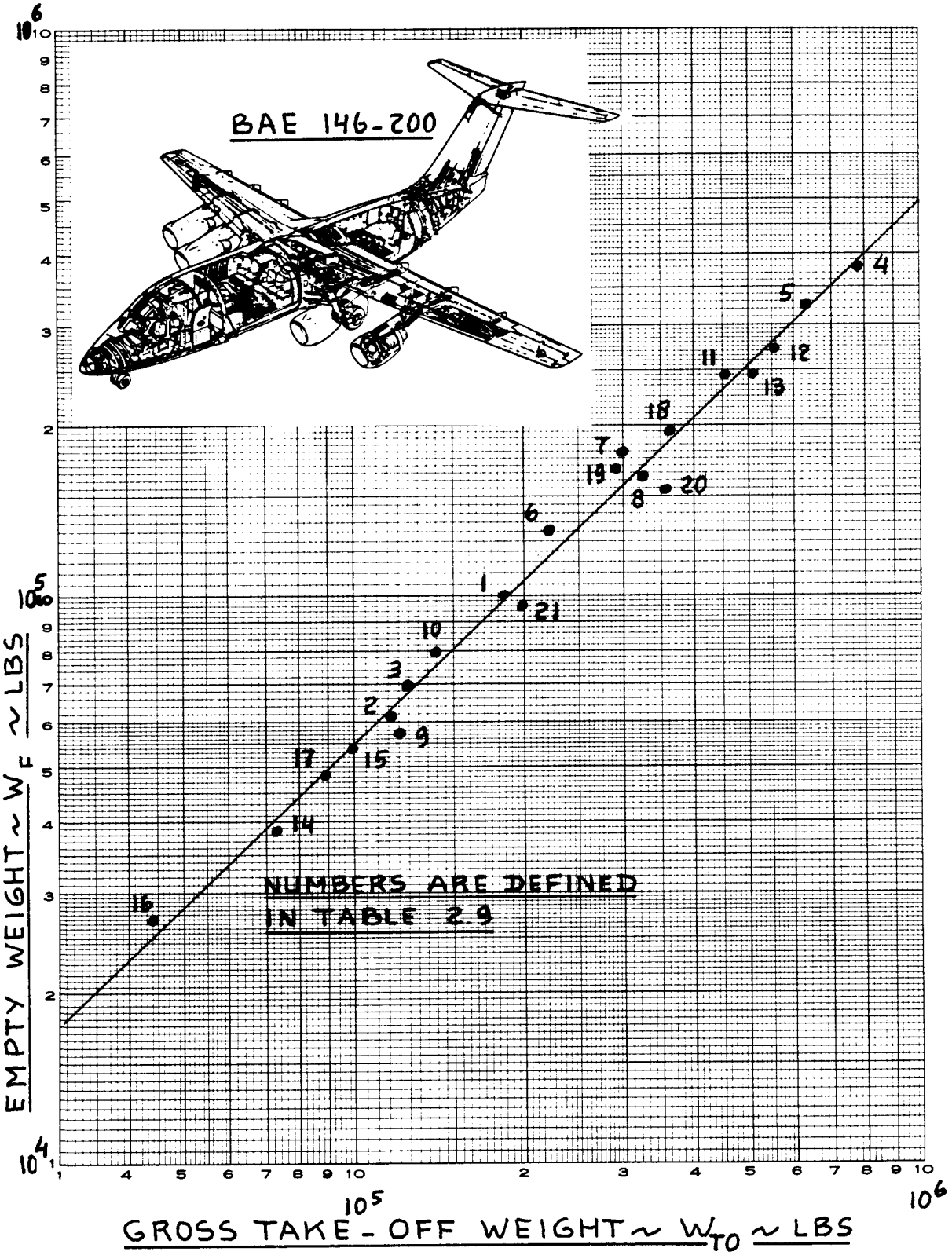

Figure 2.9 Weight Trends for Transport Jets

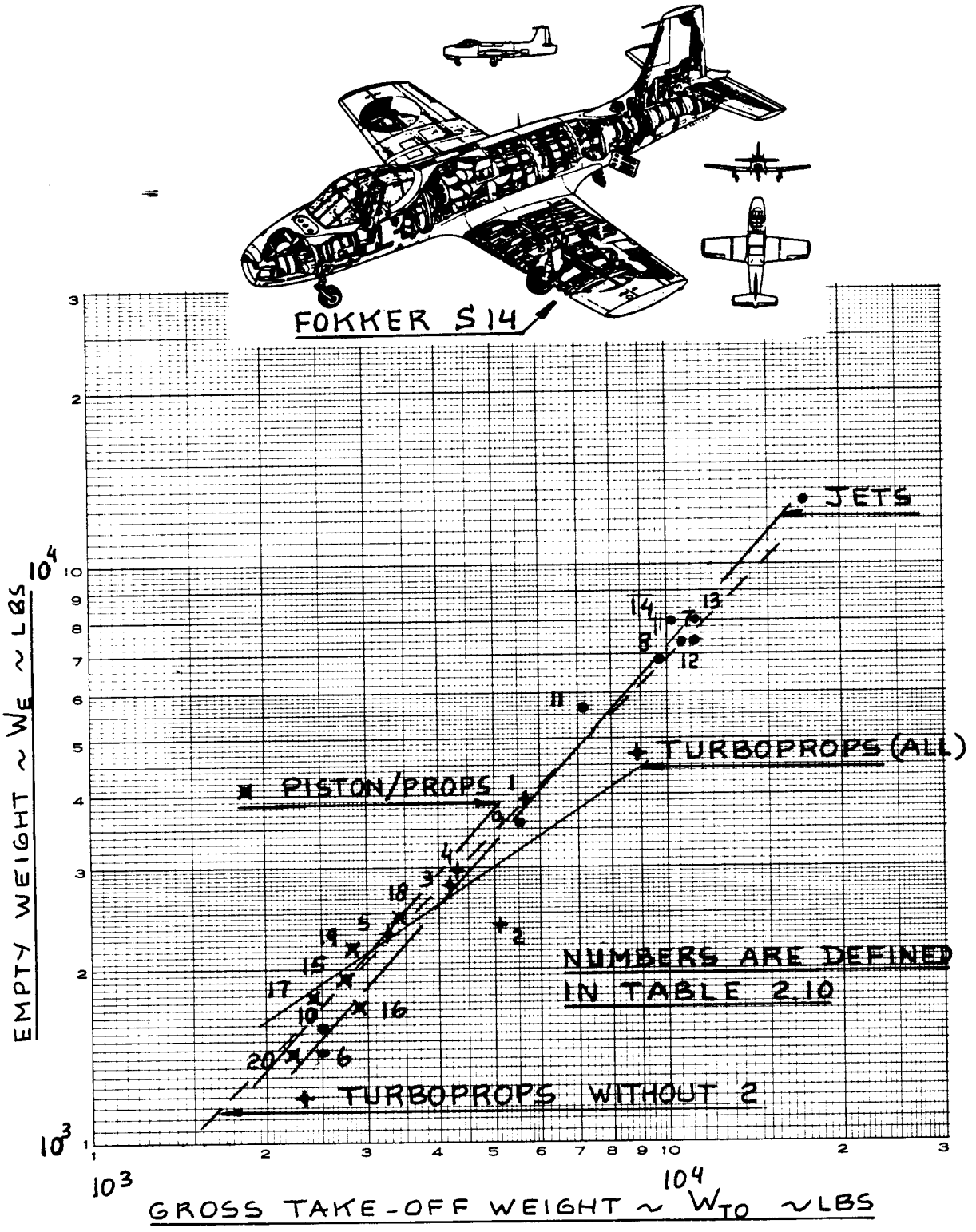

Figure 2.10 Weight Trends for Military Trainers

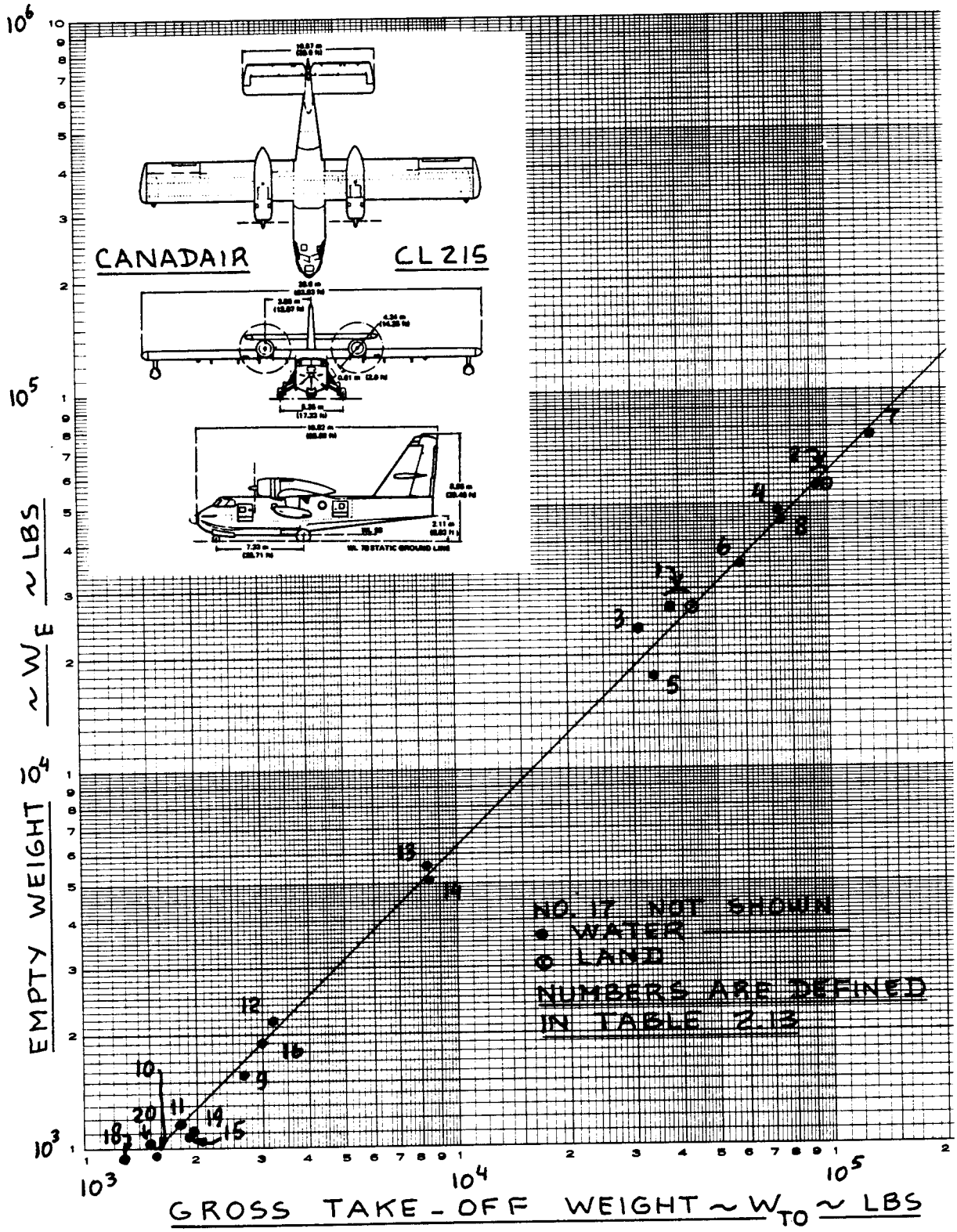

Figure 2.13 Weight Trends for Flying Boats and Amphibious and Float Airplanes

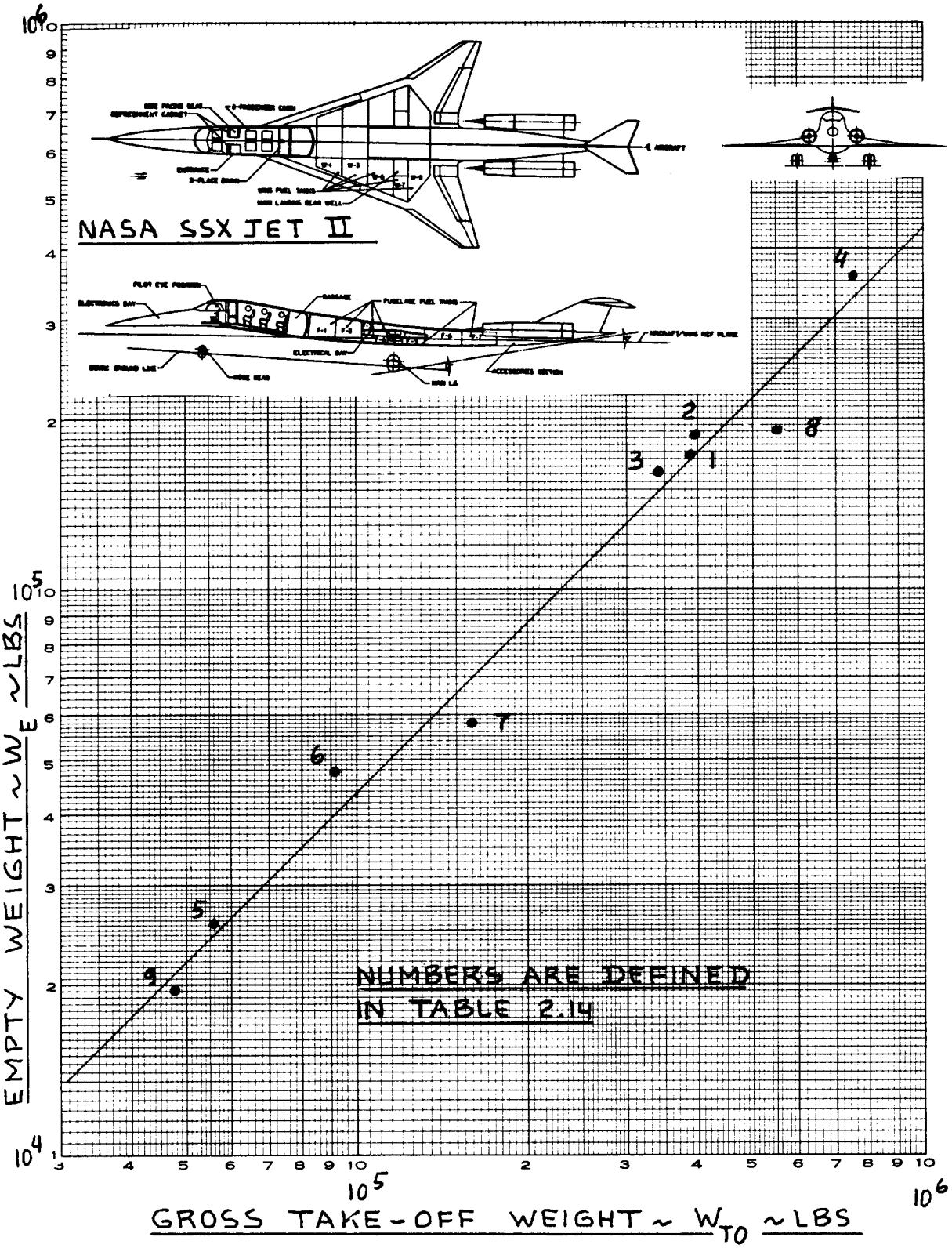

Figure 2.14 Weight Trends for Supersonic Cruise Airplanes

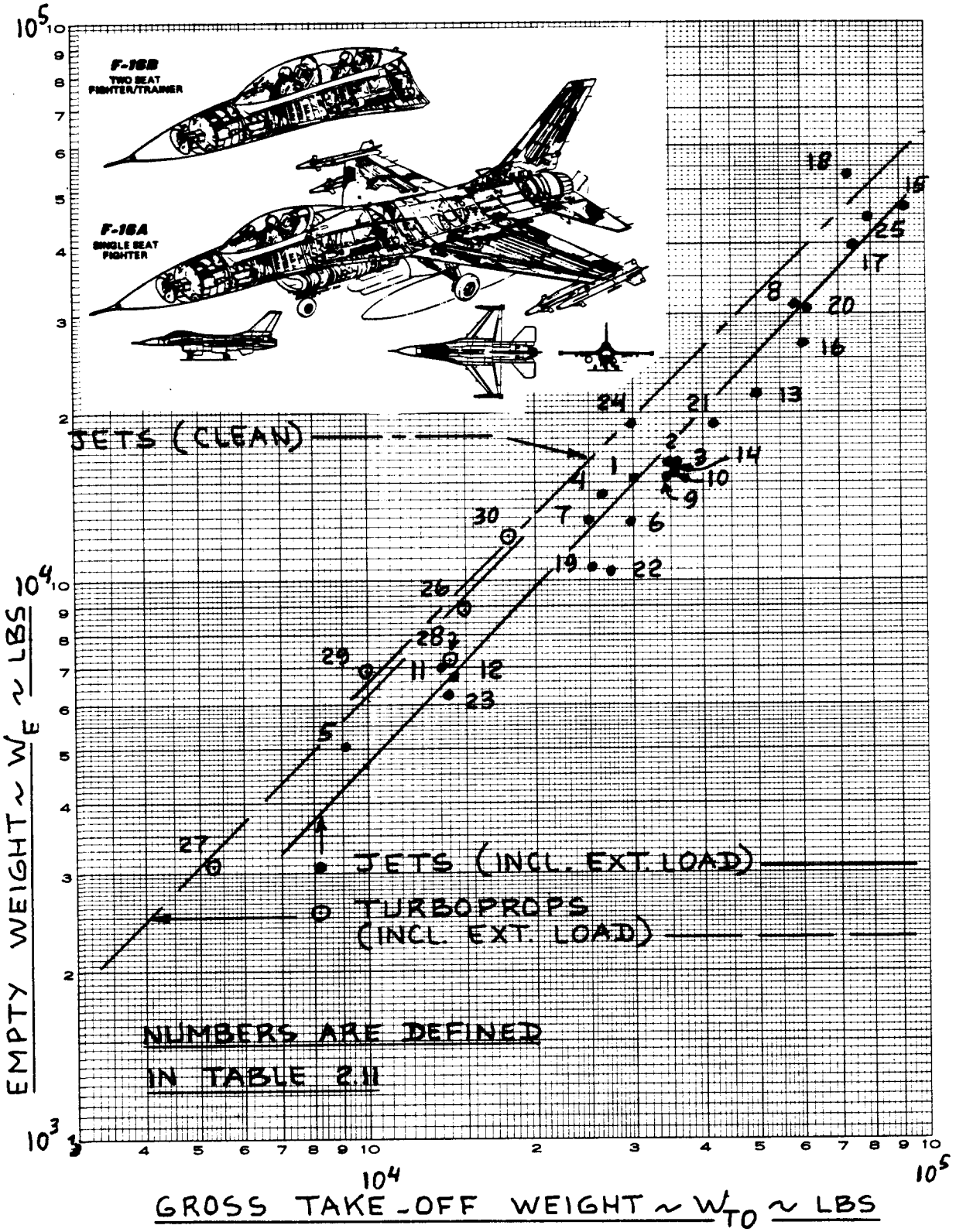

Figure 2.11 Weight Trends for Fighters

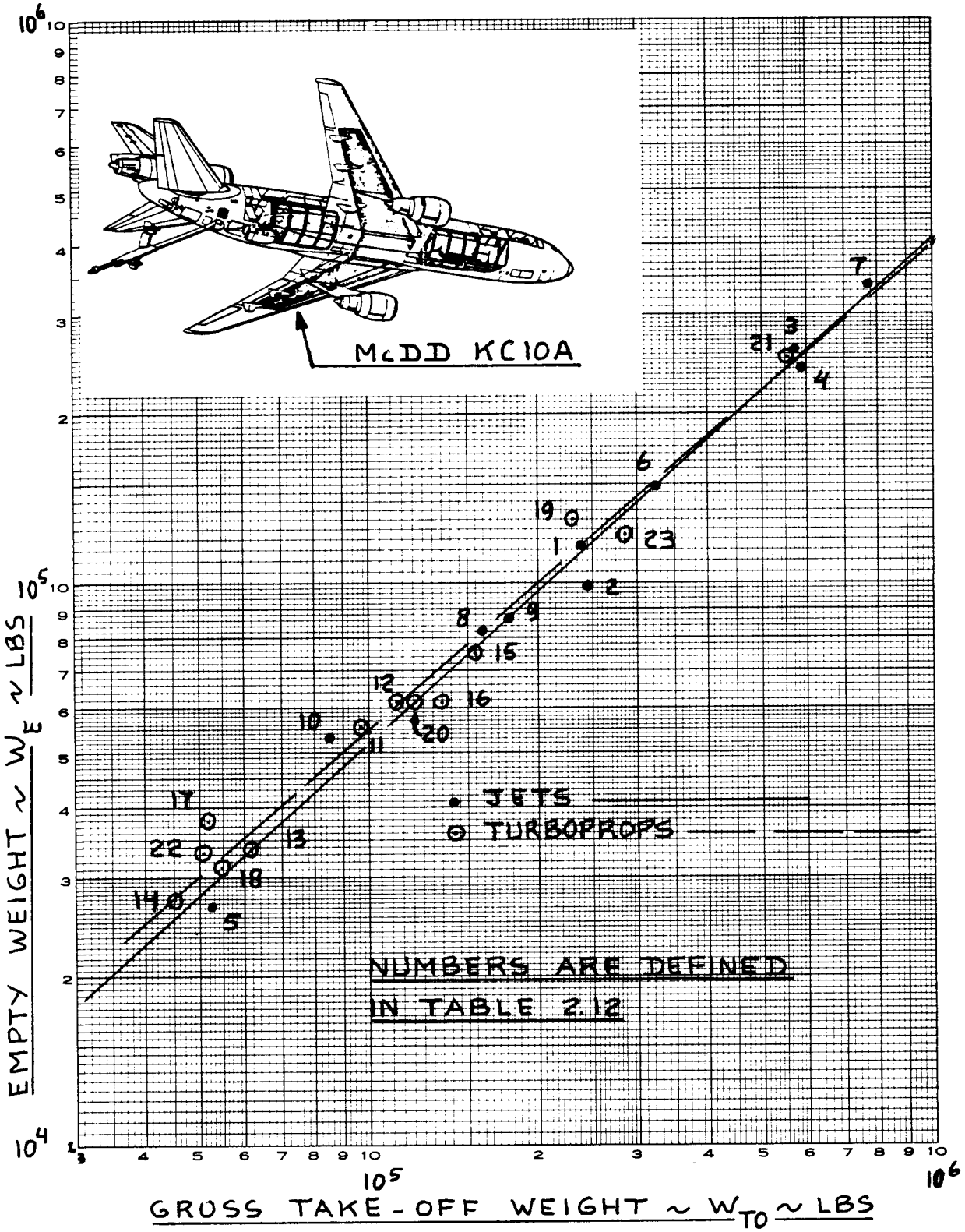

Figure 2.12 Weight Trends for Military Patrol, Bomb and Transport Airplanes

Table 2.3 Weight Data for Homebuilt Propeller Driven Airplanes

No.	Type	Gross Take-off Weight, W_{TO} (lbs)	Empty Weight, W_E (lbs)	Maximum Landing Weight, W_{Land} (lbs)	Max. Internal Fuel Weight, W_{MIF} (lbs)
	PERSONAL FUN OR TRANSPORTATION				
	USA				
1	Bowers Fly Baby 1-B	972	651	972	94
2	Bushby MM-1-85	875	575	875	88
3	Cassutt II	800	433	800	85
4	Monnett Sonerai I	750	440	750	59
5	Mooney Mite	780	505	780	64
6	Pazmany PL-2A	1,416	875	1,416	147
7	Pazmany PL-4A	850	578	850	70
8	Quickie Q2	1,000*	475	1,000	117
9	Rutan Variviggen	1,700*	950	1,700	205
10	Rutan Varieze	1,050*	560	1,050	141
11	Rutan Longeze	1,325*	750	1,325	305
	CANADA				
12	Zenith-CH 200	1,499	881	1,433	139
	FINLAND				
13	PIK-21	705	438	705	62
	FRANCE				
14	Croses EAC-3	573	310	573	15
15	Gatard AG02	617	375	617	46
16	Jodel D92	705	420	705	39
17	Jurca M.J.5EA2	1,499	947	1,499	180
18	Piel Emeraude CP320	1,433	903	1,433	124
19	Piel Super Diamant	1,873	1,146	1,873	248
20	Pottier P50	882	595	882	93
	ITALY				
21	Stelio Frati Falco F8L	1,808	1,212	1,808	183

*Constructed from composites

Table 2.3 (Cont'd) Weight Data for Homebuilt Propeller Driven Airplanes

No.	Type	Gross Take-off Weight, W_{TO} and Maximum Landing Weight, W_{Land} (lbs)	Empty Weight, W_E (lbs)	Max. Internal Fuel Weight, W_{MIF} (lbs)	Builder
	SCALED WWII FIGHTERS				
	USA				
22	2/3 Westland Whirlwind	1,400	1,042	117	Butterworth
23	7/10 Ju87B-2 Stuka	2,275	1,680	182	Langhurst
24	2/3 NAA P 51	780	460	135	Meyer
25	8/10 Spitfire IX	2,505	1,905	382	Thunder Wings
26	8/10 Curtiss P-40	3,204	2,630	264	N.A.
27	8/10 FW 190A	2,575	1,978	294	N.A.
28	1/2 F4U Corsair	1,200	921	N.A.	WAR
29	1/2 FW 190A	900	630	70	WAR
30	5/8 Hurricane IIC	1,375	1,005	176	Sindlinger
31	4/5 Boeing F4B/P12	2,100	1,530	235	Aero-Tech
	FRANCE				
32	2/3 P 51	1,875	1,485	N.A.	Jurca MJ7
33	3/4 FW 190A	1,380	880	N.A.	Jurca MJ8
	ENGLAND				
34	6/10 Spitfire	1,100	805	71	Isaacs
	CANADA				
35	3/4 Reggiane 2000 Falco 1	1,950	1,260	N.A.	Tesori

Table 2.4 Weight Data for Single Engine Propeller Driven Airplanes

No.	Type	Gross Take-off Weight, W_{TO} (lbs)	Empty Weight, W_E (lbs)	Maximum Landing Weight, W_{Land} (lbs)	Max. Internal Fuel Weight, W_{MIF} (lbs)
	BEECH				
1	Sierra 200	2,750	1,694	2,750	335
2	Bonanza A36	3,600	2,195	3,600	434
3	Bonanza V35B	3,400	2,106	3,400	434
4	Turbo Bonanza	3,850	2,338	3,850	599
5	Skipper 77	1,675	1,100	1,675	170
	CESSNA				
6	152	1,670	1,112	1,670	229
7	Skyhawk II	2,400	1,427	2,400	252
8	Skylane RG	3,100	1,757	3,100	517
9	Skywagon 185	3,350	1,700	3,350	517
10	Stationair 8	3,800	2,123	3,800	358
11	Centurion II	3,800	2,153	3,800	511
12	Centurion Press.	4,000	2,426	3,800	511
13	Caravan 208 (TBP)	7,750	3,385	7,000	2,194
	PIPER				
14	Warrior II	2,325	1,348	2,325	282
15	Arrow IV	2,750	1,637	2,750	452
16	Saratoga	3,600	1,935	3,600	628
17	Tripacer PA22	2,000	1,110	2,000	211
18	Super Cub PA18-150	1,750	930	1,750	211
	DeHAVILLAND				
19	DHC-2 Beaver (land)	5,100	2,850	5,100	556
20	DHC-3 Otter (land)	8,000	4,168	8,000	1,286
	SOCATA				
21	Rallye 125	1,852	1,125	1,852	149
22	Diplomate ST-10	2,690	1,594	2,690	310

Table 2.4 (Cont'd) Weight Data for Single Engine Propeller Driven Airplanes

No.	Type	Gross Take-off Weight, W_{TO} (lbs)	Empty Weight, W_E (lbs)	Maximum Landing Weight, W_{Land} (lbs)	Max. Internal Fuel Weight, W_{MIF} (lbs)
	ZLIN				
23	142	2,138	1,609	2,138	194
24	Z50L	1,587	1,256	1,587	93
	MOONEY				
25	201(M20J)	2,740	1,640	2,740	376
26	231 Turbo(M20K)	2,900	1,800	2,900	462
27	Antonov AN-2	11,574	7,275	N.A.	1,984
28	Beagle B.121-2 Pup	1,900	1,090	1,900	169
29	Partenavia P66C	2,183	1,322	2,183	251
30	Fuji FA-200	2,335	1,366	2,335	317
31	Pilatus PC-6(TBP)	4,850	2,685	4,850	832
32	Varga 2150A Kachina	1,817	1,125	1,817	205

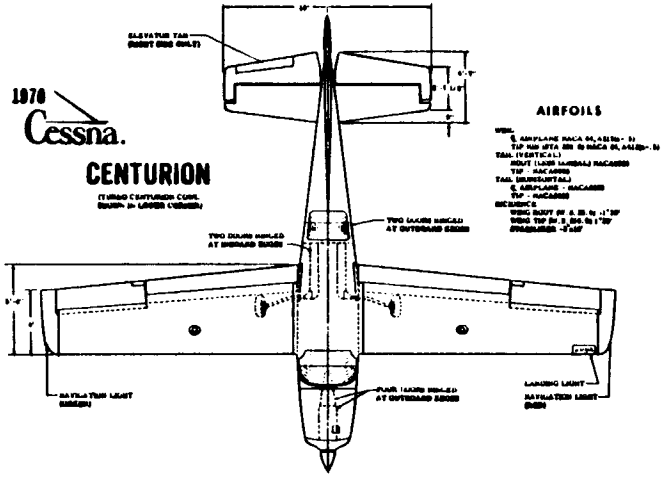

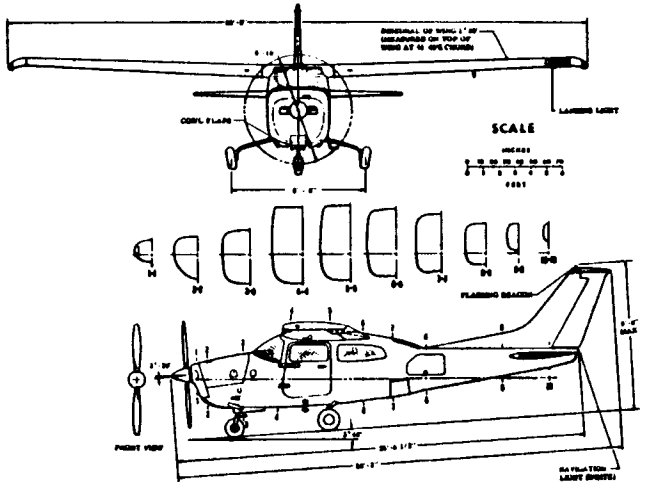

Table 2.5 Weight Data for Twin Engine Propeller Driven Airplanes

No.	Type	Gross Take-off Weight, W_{TO} (lbs)	Empty Weight, W_E (lbs)	Maximum Landing Weight, W_{Land} (lbs)	Max. Internal Fuel Weight, W_{MIF} (lbs)
	BEECH				
1	Duchess 76	3,900	2,466	3,900	587
2	Baron 95-B55	5,100	3,236	5,100	587
3	Duke B60	6,775	4,423	6,775	834
4	King Air C90 (TBP)	9,650	5,765	9,168	2,515
	CESSNA				
5	Crusader T303	5,150	3,305	5,000	898
6	340A	5,990	3,948	5,990	1,192
7	402C Businessliner	6,850	4,077	6,850	1,250
8	414A Chancellor	6,750	4,368	6,750	1,250
9	421 Golden Eagle	7,450	4,668	7,450	1,250
10	Conquest I (TBP)	8,200	4,915	8,000	2,443
	PIPER				
11	Navajo	6,500	4,003	6,500	1,127
12	Chieftain	7,000	4,221	7,000	1,127
13	Aerostar 600A	5,500	3,737	5,500	1,018
14	Seminole PA-44-180	3,800	2,354	3,800	646
15	Seminole PA-44-180T	3,800	2,430	3,800	646
16	Cheyenne I (TBP)	8,700	4,910	8,700	2,017
17	Wing Derringer D-1	3,050	2,100	2,900	511
18	Partenavia P66C-160	2,183	1,322	2,183	251
19	Piaggio P166-DL3 (TBP)	9,480	5,732	8,377	1,850
20	Gulf-Am 840A (TBP)	10,325	6,629	10,325	2,784
21	Learfan 2100 (TBP)	7,350*	4,100	7,000	1,572
22	Rutan 40 Defiant	2,900*	1,610	2,900	528

* 21 and 22 are composite built airplanes

Table 2.6 Weight Data for Agricultural Airplanes

No.	Type	Gross Take-off Weight, W_{TO} (lbs)	Empty Weight, W_E (lbs)	Maximum Landing Weight, W_{Land} (lbs)	Max. Internal Fuel Weight, W_{MIF} (lbs)
	PISTON-PROPS				
1	EMB-201A (N)	3,417	2,229	3,417	1,714
2	PZL-104	2,866	1,880	2,866	1,145
3	PZL-106	6,614	3,550	6,614	1,761
4	PZL-M18A	9,259	5,445	9,259	2,348
5	Transavia T-300	4,244	2,242	3,800	293
6	Ayres S2R-R1820	10,000	4,990	N.A.	1,115
7	Schweizer AG-CATB	7,020	3,525	7,020 470	
8	Cessna AG Husky*	3,500	2,306	3,300	317
9	Cessna AG Truck	3,300	2,229	3,300	317
10	Piper PA-36 Brave	3,900	2,050	3,900	528
11	IAR-827A	6,173	3,660	N.A.	713
	TURBO-PROPS				
12	Pilatus PC-6	6,100	2,995	4,850	837
13	NDN 6	10,000	4,500	N.A.	1,524
14	Ayres Turbo-Thrush	6,000	3,900	N.A.	1,245
15	Air Tractor AT400	6,000	3,550	N.A.	825
16	Marsh S2R-T	6,000	3,600	N.A.	694
	JETS				
17	PZL M-15	12,675	7,120	8,815	2,525

* Turbocharged

Note: Weights listed are for the 'normal category'.

Table 2.7 Weight Data for Business Jets

No.	Type	Gross Take-off Weight, W_{TO} (lbs)	Empty Weight, W_E(lbs)	Maximum Landing Weight, W_{Land} (lbs)	Max. Internal Fuel Weight, W_{MIF}(lbs)
1	Canadair Cl-601	41,650	19,960	36,000	16,725
	DASSAULT-BREGUET				
2	Falcon 20F	28,660	16,600	19,685	9,170
3	Falcon 10	18,740	10,760	17,640	5,910
4	Falcon 50	38,800	19,840	35,715	15,520
5	IAI Westwind 2	22,850	12,300	19,000	8,515
6	BAe-700	25,500	12,845	22,000	9,288
	CESSNA				
7	Citation I	11,850	6,605	11,350	3,780
8	Citation II	13,300	7,196	12,700	5,009
9	Citation III	20,000	10,951	16,500	7,155
	GATES LEARJET				
10	Learjet 55	19,500	12,130	17,000	6,707
11	Learjet 24	13,500	7,064	11,880	5,628
12	Learjet 25	15,000	7,650	13,300	6,098
13	Gulfstream IIB	68,200	38,750	58,500	28,300
14	Lockheed Jetstar	43,750	23,828	36,000	14,253
15	Mitsub. Diamond I	14,630	9,100	13,200	4,260
16	Rockw. Sabrel. 65	24,000	13,400	21,755	8,626
17	Foxjet(not built)	4,550	2,408	N.A.	N.A.
18	Piaggio PD-808	18,000	10,650	16,000	6,445
19	HFB320 Hansa	20,280	11,775	19,400	6,084

Table 2.8 Weight Data for Regional Turbo-Propeller Driven Airplanes

No.	Type	Gross Take-off Weight, W_{TO} (lbs)	Empty Weight, W_E(lbs)	Maximum Landing Weight, W_{Land} (lbs)	Max. Internal Fuel Weight, W_{MIF}(lbs)
1	Antonov 28	14,330	7,716	14,330	3,483
2	Casa C212-200	16,424	9,072	16,204	3,527
3	BAe 748 2B(A)	46,500	26,560	43,000	11,326
4	Shorts 330	22,900	14,175	22,600	3,840
5	Shorts 360	25,700	16,075	25,400	3,840
6	Shorts SC7-3	12,500	7,750	12,500	2,303
7	Beech 1900	15,245	8,500	15,245	2,855
8	Beech C99	11,300	6,494	11,300	2,466
9	Beech King Air B200	12,500	7,538	12,500	3,645
10	Cessna Conquest I	8,200	4,915	8,000	2,459
11	Cessna Conquest II	9,850	5,682	9,360	3,183
12	FS Metro III	14,500	8,387	14,000	4,342
13	Gulfstream IC	36,000	23,693	34,285	10,460
14	GAF Nomad N22B	8,500	4,613	8,500	1,770
15	Fokker F27 Mk200	45,000	25,525	41,000	9,090
16	ATR-42-200	34,720	20,580	33,730	9,920
17	Aeritalia AP68TP -200	5,732	3,245	5,445	1,340
18	SM SF600 Canguro	7,054	4,299	7,054	1,902
19	Airtec CN235	28,660	16,094	28,220	8,818
20	DeHavilland DHC-7	44,000	27,000	42,000	9,925
21	DeHavilland DHC-5D Buffalo (A)	41,000	24,635	39,100	13,696
22	EMB-120 Brasilia	21,165	11,945	21,165	5,624
23	Saab-Fairchild 340	26,000	15,510	25,500	5,900
24	Piper PA-31T Cheyenne II	9,000	5,018	9,000	2,555

Table 2.8 (Cont'd) Weight Data for Regional Turbo-Propeller Driven Airplanes

No.	Type	Gross Take-off Weight, W_{TO} (lbs)	Empty Weight W_E(lbs)	Maximum Landing Weight, W_{Land} (lbs)	Max. Internal Fuel Weight, W_{MIF}(lbs)
25	Piper PA-42 Cheyenne III	11,200	6,389	10,330	2,686
26	BAe 31 Jetstream	14,550	7,606	14,550	3,017
27	Embraer EMB-110 Bandeirante	12,500	7,837	12,500	2,974
28	DeHavilland DHC-6 Twin Otter-300	12,500	7,065	12,500	2,500
29	DeHavilland DHC-8	30,500	20,176	30,000	5,875
30	Dornier 128-6	9,590	5,230	9,127	1,544
31	Dornier 228-200	12,566	6,495	See '84 Janes	See '84 Janes
32	Arava 202	15,000	8,816	15,000	2,876
33	DeHavilland DHC-7, Series 300	57,250	34,250	55,600	10,000

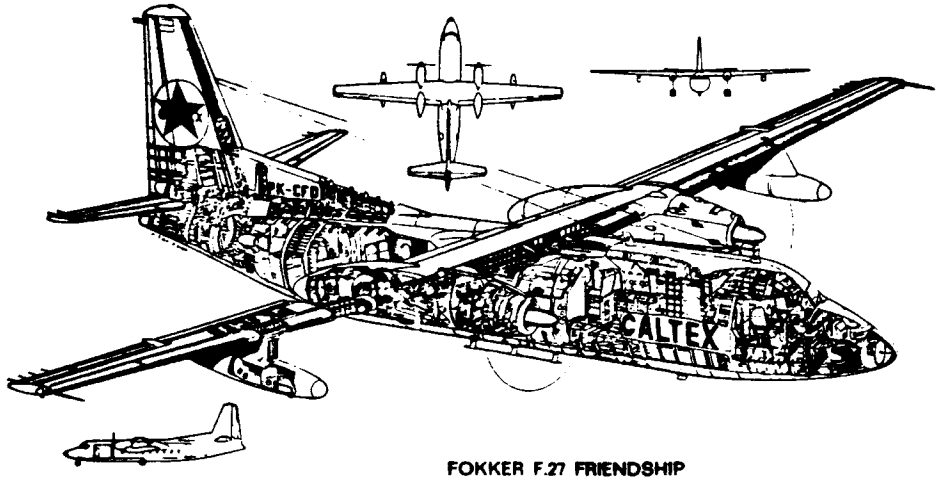

FOKKER F.27 FRIENDSHIP

Table 2.9 Weight Data for Transport Jets

No.	Type	Gross Take-off Weight, W_{TO} (lbs)	Empty Weight*, W_E(lbs)	Maximum Landing Weight, W_{Land} (lbs)	Max. Internal Fuel Weight, W_{MIF}(lbs)
	BOEING				
1	727-200	184,800	100,000	154,500	52,990
2	737-200	115,500	61,630	103,000	39,104
3	737-300	124,500	69,930	114,000	35,108
4	747-200B	775,000	380,000	564,000	343,279
5	747-SP	630,000	325,000	450,000	329,851
6	757-200	220,000	130,420	198,000	73,229
7	767-200	300,000	179,082	270,000	109,385
	McDONNELL-DOUGLAS				
8	DC8-Super 71	325,000	162,700	240,000	156,733
9	DC9-30	121,000	57,190	110,000	24,117
10	DC9-80	140,000	79,757	128,000	37,852
11	DC10-10	455,000	244,903	363,500	142,135
12	DC10-40	555,000	271,062	403,000	239,075
13	Lockheed L1011-500	510,000	245,500	368,000	155,982
14	Fokker F28-4000	73,000	38,683	69,500	16,842
15	Rombac-111-560	99,650	53,762	87,000	24,549
16	VFW-Fokker 614	44,000	26,850	44,000	10,928
17	BAe 146-200	89,500	48,500	77,500	22,324
	AIRBUS				
18	A300-B4-200	363,760	195,109	295,420	195,109
19	A310-202	291,000	168,910	261,250	94,798
20	Ilyushin-Il-62M	357,150	153,000	231,500	183,700
21	Tupolev-154	198,416	95,900	176,370	73,085

* W_E here means typical airline operating weight empty, W_{OE}

Table 2.10 Weight Data for Military Trainers

No.	Type	Gross Take-off Weight, W_{TO} (lbs)	Empty Weight, W_E (lbs)	Maximum Landing Weight, W_{Land} (lbs)	Max. Internal Fuel Weight, W_{MIF} (lbs)
	TURBO-PROPS				
1	EMB-312 Tucano	5,622	3,946	6,173	1,193
2	RFB Fantrainer 600B	5,070	2,337	4,409	750
3	Pilatus PC7/CH	4,188	2,800	4,188	820
4	Beech T34C	4,300	2,960	4,300	852
5	NDN1T Firecracker	3,250	2,300	3,250	738
	JETS				
6	Microjet 200	2,535	1,433	2,491	688
7	MDB Alpha Jet	11,023	7,374	11,023	3,351
8	MB339A	9,700	6,889	N.A.	2,425
9	SM S211	5,511	3,560	5,511	2,491
10	Caproni C22J	2,502	1,587	2,502	540
11	PZL TS-11	7,150	5,644	7,150	2,421
12	CASA C-101	10,692 (13889)	7,385	10,361	4,078 (2866 Normal)
13	BAe Hawk Mk1	11,100	8,040	10,250	2,497
14	Aero Albatros L39	10,028	7,859	9,480	2,170
	PISTON-PROPS				
15	Aerosp. Epsilon	2,755	1,936	2,755	325
16	Chincul Arrow	2,900	1,730	2,900	421
17	SM-SF260M	2,425	1,797	2,425	377
18	Fuji KM-2B T-3	3,400	2,469	3,329	411
19	Yakovlev-52	2,844	2,205	2,844	189
20	BAe Bulldog 121	2,238	1,430	2,238	226

Note: Weights listed are for the airplanes in a clean configuration. With external loads most weights will increase significantly.

Table 2.11 Weight Data for Fighters

No.	Type	Gross Take-off Weight, W_{TO} (lbs) CLEAN	Gross Take-off Weight, W_{TO} (lbs) WITH EXT. LOAD	Empty Weight, W_E (lbs)	Maximum Landing Weight, W_{Land} (lbs)	Max. Internal Fuel Weight, W_{MIF} (lbs)
	JETS					
1	MD Mirage III	21,165	30,200	15,540	N.A.	5,188
2	MD Mirage F-1	24,030	35,715	16,314	N.A.	5,188
3	MD Mirage 2000N	N.A.	36,375	16,315	N.A.	6,571
4	MD Etendard*	20,833	26,455	14,330	N.A.	5,654
5	HAL Ajeet**	7,803	9,200	5,086	6,100	2,334
6	McDD AV8B**	N.A.	29,750	12,750	19,400	7,500
7	BAe Harrier**	N.A.	25,000	12,800	N.A.	4,954
8	Tornado F.Mk2	45,000	58,400	31,065	N.A.	N.A.
9	Sepecat Jaguar	24,149	34,612	15,432	N.A.	7,263
10	IAI Kfir	20,700	35,715	16,060	N.A.	5,670
11	MB339 Veltro 2	10,974	13,558	6,997	N.A.	3,487
12	SAAB 105G	10,714	14,330	6,757	N.A.	3,458
13	F.R. A10A	32,771	50,000	21,541	N.A.	10,700
14	G.D. F16A	23,810	35,400	15,586	N.A.	6,972
15	G.D. F111A*	N.A.	91,500	46,172	N.A.	N.A.
16	Grumman A6*	N.A.	60,400	26,660	45,000	15,939
17	Grumman F14A*	N.A.	74,348	39,762	51,830	16,200
18	Grumman EF111A	N.A.	72,750	53,418	80,000	32,894
19	Northrop F5F	N.A.	25,225	10,567	25,147	4,434
20	McDD F4E	N.A.	61,795	30,328	46,000	12,150
21	Vought A7E	N.A.	42,000	19,111	N.A.	9,825

* Carrier suitable fighter. ** V/STOL fighter.

Table 2.11 (Cont'd) Weight Data for Fighters

No.	Type	Gross Take-off Weight, W_{TO} (lbs) CLEAN	Gross Take-off Weight, W_{TO} (lbs) WITH EXT. LOAD	Empty Weight, W_E (lbs)	Maximum Landing Weight, W_{Land} (lbs)	Max. Internal Fuel Weight, W_{MIF} (lbs)
	JETS					
22	McDD A4F	N.A.	27,420	10,448	N.A.	11,790
23	Cessna A37B	N.A.	14,000	6,211	14,000	3,321
24	Sukhoi Su 7BM	N.A.	29,750	19,000	N.A.	7,000
25	MiG 25A	N.A.	79,800	44,100	N.A.	30,865
	TURBOPROPS					
26	FMA IA58B Pucara	N.A.	14,991	8,884	12,345	2,215
27	GA F20TP Condor	N.A.	5,291	3,086	5,291	1,038
28	Piper PA-48 Enforcer		14,000	7,200	8,000	2,777
29	Rockwell OV10A	N.A.	9,908	6,893	N.A.	1,651
30	Grumman OV-1D Mohawk	N.A.	17,912	12,054	N.A.	1,808

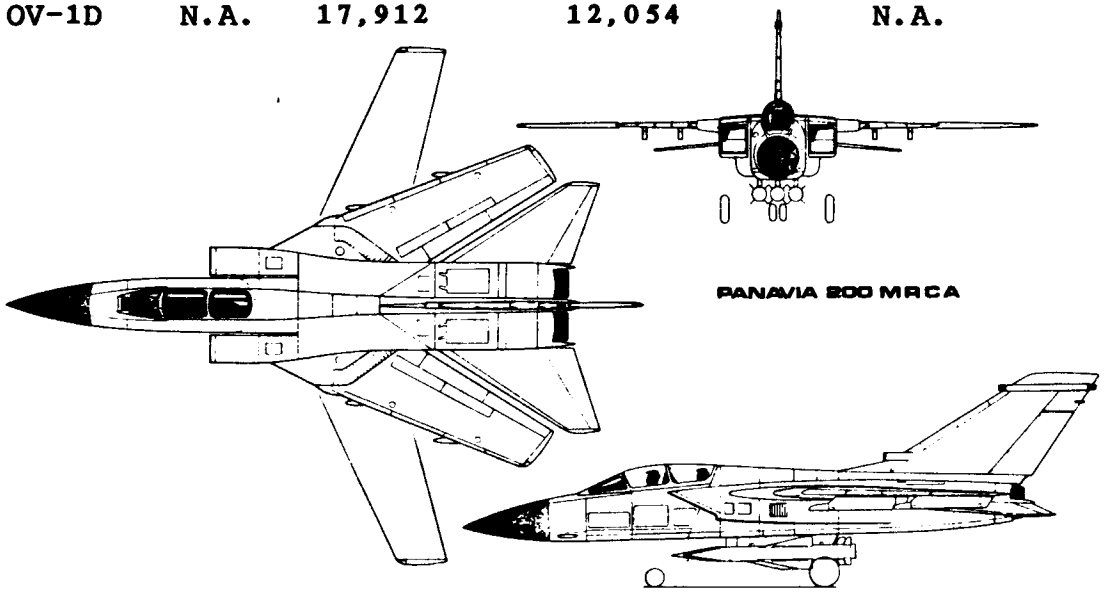

Table 2.12 Weight Data for Military Patrol, Bomb and Transport Airplanes

No.	Type	Gross Take-off Weight, W_{TO} (lbs)	Empty Weight, W_E (lbs)	Maximum Landing Weight, W_{Land} (lbs)	Max. Internal Fuel Weight, W_{MIF} (lbs)
	JETS				
1	Boeing YC-14**	237,000	117,500	N.A.	66,400
2	Boeing KC-135A	245,000	98,466	185,000	N.A.
3	McDD C17	572,000	259,000	N.A.	N.A.
4	McDD KC-10A	590,000	240,065	403,000	228,975
5	Lockheed S3A	52,539***	26,650*	45,914	12,445
6	Lockheed C141B	323,100	148,120*	343,000	154,527
7	Lockheed C5A	769,000	337,937	635,850	320,950
8	Tupolev Tu-16	158,730	82,000	N.A.	78,592
9	BAe Nimrod Mk2	177,500	86,000	120,000	84,350
10	NAMC XC-1	85,320	53,130	N.A.	26,284
	TURBOPROPS				
11	DB Atlantic-II	96,780	55,775	79,365	40,785
12	Transall C-160	112,435	61,730	103,615	38,480
13	Aeritalia G222	61,730	33,950	58,420	20,725
14	Fokker F27 Maritime	45,000	27,600*	41,000	16,000
15	Lockheed C130E	155,000	75,331	130,000	63,404
16	Lockheed P3C	135,000	61,491	103,880	60,260
17	Grumman E2C	51,817	37,945	N.A.	12,400
18	Grumman C2A	54,830	31,154	47,372	11,947
19	Shorts Belfast	230,000	130,000	215,000	82,400
20	Antonov AN12	121,475	61,730	N.A.	31,299
21	Antonov AN22	551,160	251,325	N.A.	94,800
22	Antonov AN26	50,706	33,113	50,706	12,125
23	Douglas C133B	286,000	120,363	N.A.	118,634

* These weights are typical W_{OE} values. ** This is a STOL airplane.
*** for 2.50g only. W_{TO} = 343,000 lbs for 2.25g.

Table 2.13 Weight Data for Flying Boats and Amphibious and Float Airplanes

No.	Type	Gross Take-off Weight, W_{TO} (lbs)	Empty Weight, W_E (lbs)	Maximum Landing Weight, W_{Land} (lbs)	Max. Internal Fuel Weight, W_{MIF} (lbs)
1	Canadair CL-215	43,500(L)	26,810	34,400(L)	9,159
		37,700(W)	26,810	37,000(W)	9,159
2	Shin Meiwa US-1(TBP)	99,200(L)	56,218	N.A.	38,620
		94,800(W)	56,218	N.A.	38,620
3	Grumman Albatros	30,800(L)	23,500	29,160(L)	6,438
		31,150(W)	23,500	31,150(W)	6,438
4	Martin P5M2	74,000	48,000	N.A.	23,333
5	Consol.V PBY-5	34,000	17,564	N.A.	10,273
	SHORTS				
6	Sunderland III	58,000	34,500	N.A.	15,540
7	Shetland	130,000	74,985	N.A.	45,000
8	Seaford	75,000	45,000	N.A.	N.A.
9	Lake 200 Buccaneer	2,690	1,555	2,690	323
10	Osprey II	1,560	970	1,560	153
11	Spencer Air Car Jr	1,800	1,150	1,800	317
12	Spencer Air Car Sr	3,200	2,190	3,200	552
13	GAF N22B(Amph)(TBP)	8,300	5,560	N.A.	1,770
14	GAF N22B(Float)(TBP)	8,500	5,050	N.A.	1,770
15	AAC S1B2(Float)	1,900	1,073	1,900	235
16	IAC TA16	3,000	1,900	3,000	540
17	Militi MB3 Leonardo	683	452	683	N.A.
18	Mukai Olive SM6 III	1,268	948	1,268	46
19	Aerocar Sooper-Coot	1,950	1,100	1,950	294
20	Anderson Kingfisher	1,500	1,032	1,500	117

Notes: 1. (L) indicates Land, (W) indicates Water.
2. (Float) indicates a float equipped airplane.
3. (Amph) indicates an amphibious airplane, (TBP) indicates turboprop. All others are Piston-Propeller equipped.

Table 2.14 Weight Data for Supersonic Cruise Airplanes

No.	Type	Gross Take-off Weight, W_{TO} (lbs)	Empty Weight, W_E(lbs)	Maximum Landing Weight, W_{Land} (lbs)	Max.Internal Fuel Weight, W_{MIF}(lbs)
1	Concorde	389,000	172,000*	245,000	202,809
2	TU144	396,830	187,400*	264,500	209,440
3	Boeing 969-512BA	340,194	162,510	N.A.	155,501
4	Boeing 969-512BB	750,000	358,270	N.A.	342,824
5	SM-SST	56,200	25,200	45,000	29,800
6	GD-F111A	91,500	47,500	N.A.	N.A.
7	GD-B58A	160,000	58,000	N.A.	98,250
8	NAA B70A	550,000	190,000	N.A.	300,000
9	NASA Supersonic Cruise Fighter (n=4)	47,900	19,620	N.A.	N.A.
10	Rockwell B1B	477,000	N.A.	422,000	N.A.

Notes:
1. Airplanes 1 through 5 are commercial transports.
2. Airplanes 3 through 5 are study projects only.
3. Remaining airplanes are military.
* Indicates W_{OE} in these cases.

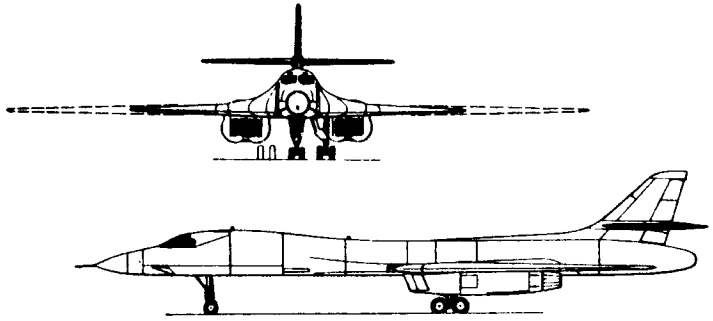

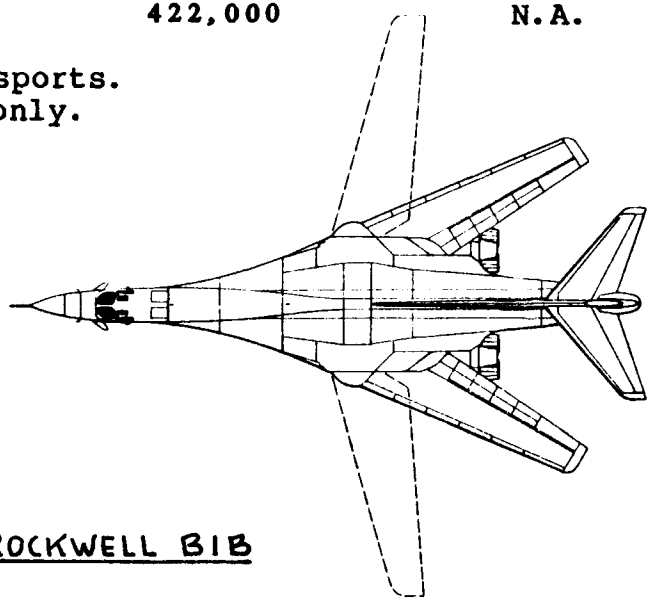

ROCKWELL B1B

Table 2.15 Regression Line Constants A and B of Equation (2.16)

Airplane Type	A	B
1. Homebuilts		
Pers. fun and transportation	0.3411	0.9519
Scaled Fighters	0.5542	0.8654
Composites	0.8222	0.8050
2. Single Engine Propeller Driven	-0.1440	1.1162
3. Twin Engine		
Propeller Driven	0.0966	1.0298
Composites	0.1130	1.0403
4. Agricultural	-0.4398	1.1946
5. Business Jets	0.2678	0.9979
6. Regional TBP	0.3774	0.9647
7. Transport Jets	0.0833	1.0383
8. Military Trainers		
Jets	0.6632	0.8640
Turboprops	-1.4041	1.4660
Turboprops without No.2	0.1677	0.9978
Piston/Props	0.5627	0.8761
9. Fighters		
Jets(+ ext.load)	0.5091	0.9505
Jets(clean)	0.1362	1.0116
Turboprops(+ ext.load)	0.2705	0.9830
10. Mil. Patrol, Bomb and Transport		
Jets	-0.2009	1.1037
Turboprops	-0.4179	1.1446
11. Flying Boats, Amphibious and Float Airplanes	0.1703	1.0083
12. Supersonic Cruise	0.4221	0.9876

Equation (2.16) is repeated here for convenience:

$$W_E = \text{invlog}_{10}\{(\log_{10} W_{TO} - A)/B\}$$

A y B HAN CAMBIADO MUY POCO CON EL TIEMPO DESDE LOS AÑOS 1950

Table 2.16 Weight Reduction Data for Composite

Structural Component	Construction W_{comp}/W_{metal}
Primary Structure	
Fuselage	0.85
Wing, Vertical Tail, Canard or Horizontal Tail	0.75
Landing Gear	0.88
Secondary Structure	
Flaps, Slats, Access Panels, Fairings	0.60
Interior Furnishings	0.50
Air Induction System	0.70 - 0.80

Notes: 1) These weight reduction factors should be used with great caution. They are intended to apply when changing from 100% conventional aluminum alloys to 100% composite construction.

2) For Lithium-aluminum alloys used in the fuselage, wing or empennage structure, a weight reduction of 5 to 10 percent may be claimed relative to conventional aluminum alloys.

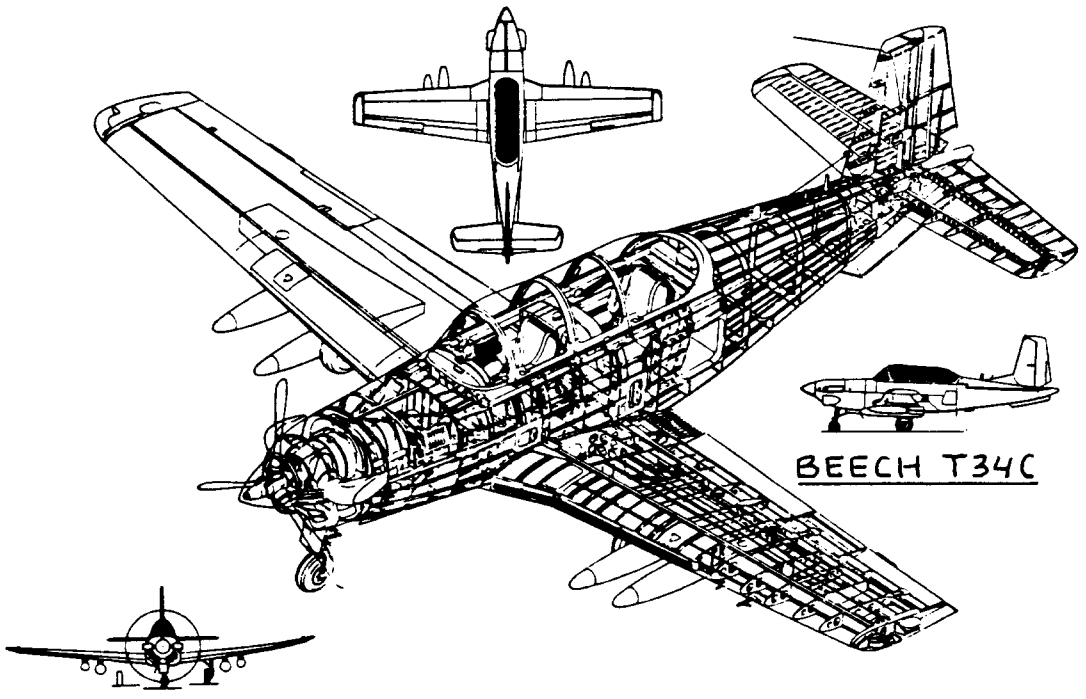

2.6 THREE EXAMPLE APPLICATIONS

The method for estimating W_{TO}, W_E and W_F will now be illustrated with three examples:

2.6.1 Example 1: Twin Engine Propeller Driven Propeller Driven Airplane
2.6.2 Example 2: Jet Transport
2.6.3 Example 3: Fighter

2.6.1 Example 1: Twin Engine Propeller Driven Airplane

Table 2.17 gives an example mission specification for a twin engine propeller driven airplane. Note that the various mission phases have been numbered. The example follows the step-by-step procedure outlined in Section 2.1.

Step 1. From Table 2.17, the payload weight, W_{PL} is:

$$W_{PL} = 6x175 + 200 = 1,250 \text{ lbs}$$

Step 2. A likely value for W_{TO} is obtained by looking at data for similar airplanes. In Reference 9, the following information can be found:

Airplane Type	W_{PL} (lbs)	W_{TO} (lbs)	$V_{cr_{max}}$ (kts)	Range (nm)
Beech Duke B60	1,300	6,775	239	1,080
Beech Baron M58	1,500	5,400	200	1,200
Cessna T303	1,650	5,150	196	1,000
Piper PA-44-180	1,250	3,800	168	725

From these data a value for W_{TO} of 7,000 lbs seems reasonable, so:

$$W_{TO_{guess}} = 7,000 \text{ lbs}$$

Step 3. To determine a value for W_F, the procedure indicated in Section 2.4 will be followed. Mission phases are defined in Table 2.17.

Table 2.17 Mission Specification For A Twin Engine Propeller Driven Airplane

Payload:	Six passengers at 175 lbs each (this includes the pilot) and 200 lbs total baggage.
Range:	1,000 sm with max. payload. Reserves equal to 25% of required mission fuel.
Altitude:	10,000 ft (for the design range).
Cruise Speed:	250 kts at 75% power at 10,000 ft.
Climb:	10 minutes to 10,000 feet at max. W_{TO}.
Take-off and Landing:	1,500 ft groundrun at sealevel, std. day. Landing performance at $W_L = 0.95W_{TO}$.
Powerplants:	Piston/Propeller
Pressurization:	None
Certification Base:	FAR 23

Mission Profile:

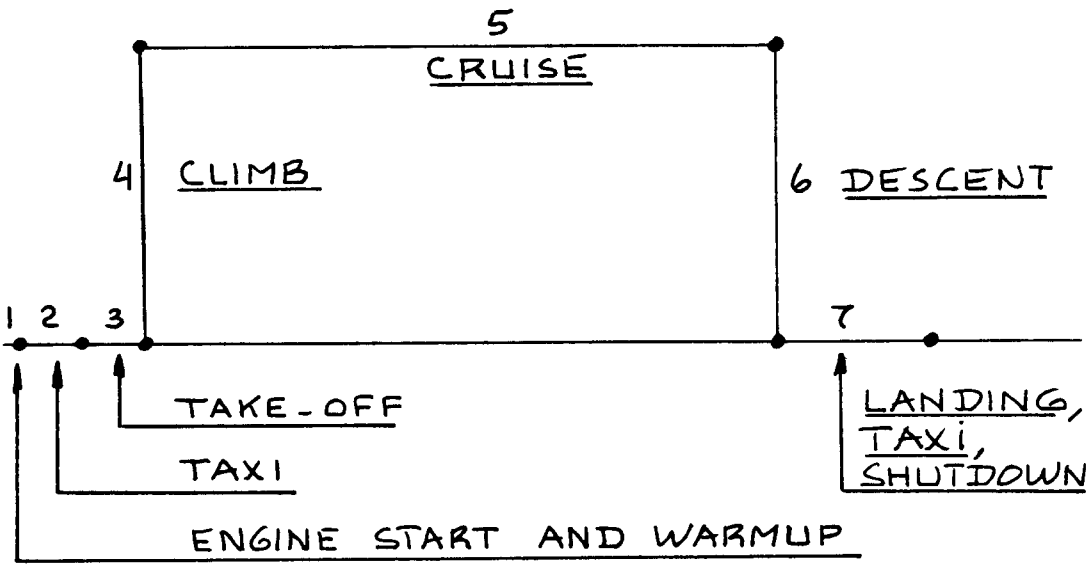

Phase 1: Engine start and warm-up.
Begin weight is W_{TO}. End weight is W_1.

The ratio W_1/W_{TO} is typically 0.992 as indicated in Table 2.1.

Phase 2: Taxi.
Begin weight is W_1. End weight is W_2.

The ratio W_2/W_1 is typically 0.996 as indicated in Table 2.1.

Phase 3: Take-off.
Begin weight is W_2. End weight is W_3.

The ratio W_3/W_2 is typically 0.996 as indicated in Table 2.1.

Phase 4: Climb to cruise altitude.
Begin weight is W_3. End weight is W_4.

The ratio W_4/W_3 depends on the climb performance of the airplane which is being designed and on the specified cruise altitude. A reasonable value for this ratio is 0.990 as indicated in Table 2.1.

Phase 5: Cruise.
Begin weight is W_4. End weight is W_5.

The ratio W_5/W_4 can be estimated from Breguet's range equation which for propeller-driven airplanes is:

$$R_{cr} = 375(\eta_p/c_p)_{cr}(L/D)_{cr}\ln(W_4/W_5) \qquad (2.9)$$

From Table 2.17 the range, R is 1,000 nm.

During cruise, $c_p = 0.5$ lbs/hp/hr and $\eta_p = 0.82$ are reasonable choices, according to Table 2.2. With good aerodynamic design a value of L/D=11 should be attainable, even though Table 2.2

suggests that a value of 10 is high. With these numbers, Eqn.(2.9) yields:

$$1{,}000 = 375(0.82/0.5)(11)\ln(W_4/W_5)$$

from which is found:

$$W_5/W_4 = 0.863.$$

Phase 6: Descent.
Begin weight is W_5. End weight is W_6.

The fuel-fraction follows from Table 2.1:

$$W_6/W_5 = 0.992.$$

Phase 7: Landing, Taxi, Shutdown.
Begin weight is W_6. End weight is W_7.

The ratio W_7/W_6 is assumed to be 0.992, based again on Table 2.1.

The overall mission fuel fraction, M_{ff} can be computed with the help of Eqn.(2.13):

$$M_{ff} = \left\{\frac{W_7W_6W_5W_4W_3W_2W_1}{W_6W_5W_4W_3W_2W_1W_{TO}}\right\} =$$

$$= (0.992)(0.992)(0.863)(0.990)(0.996)(0.996)x$$
$$x(0.992) = 0.827$$

The fuel used during phases 1 through 7 is given by Eqn.(2.14). This yields here:

$$W_{F_{used}} = (1 - 0.827)W_{TO} = 0.173W_{TO}.$$

The value for W_F needed for the mission is equal to the fuel used plus fuel reserves. The latter are defined in Table 2.17 as 25% of the fuel used. Thus:

$$W_F = 0.173x1.25xW_{TO} = 0.216W_{TO}$$

Step 4. A tentative value for W_{OE} is found from Eqn.(2.4) as:

$W_{OE_{tent}}$ = 7,000 - 0.216x7,000 - 1,250 =
= 4,238 lbs

Step 5. A tentative value for W_E is found from Eqn.(2.5) as:

$W_{E_{tent}}$ = 4,238 - 0.005x7,000 = 4,203 lbs.
The crew is counted here as part of the payload.

Step 6. The allowable value for W_E is found from

Figure 2.5 as: W_E= 4,300 lbs.

Step 7. The difference between W_E and $W_{E_{tent}}$

is 97 lbs. This difference is too large. An iteration will therefore be necessary. The reader is asked to show, that when W_{TO}= 7,900 lbs, the following values for

empty weight are obtained:

$W_{E_{tent}}$ = 4,904 lbs and:
W_E= 4,900 lbs. These numbers are within

0.5% of each other.

To summarize, the following preliminary numbers define the airplane with the mission specification of Table 2.17:

W_{TO}= 7,900 lbs,

W_E = 4,900 lbs,

W_F = 1,706 lbs.

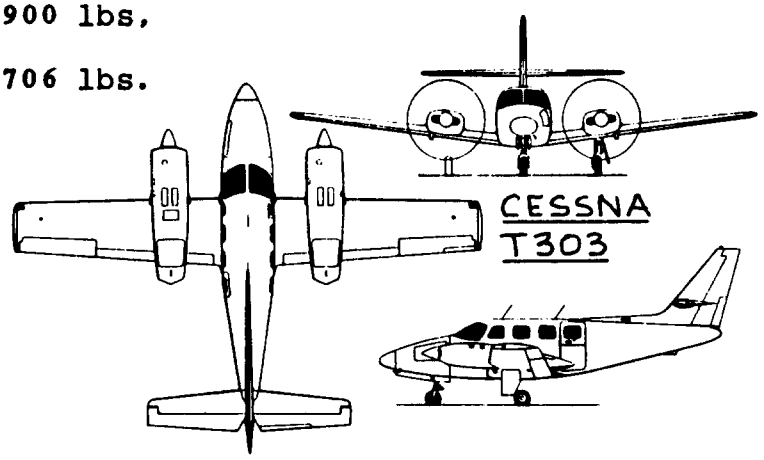

2.6.2 Example 2: Jet Transport

Table 2.18 gives an example mission specification for a jet transport. Note that the various mission phases have been numbered. The example follows the step-by-step procedure outlined in Section 2.1.

Step 1. From Table 2.18, the payload weight, W_{PL} is:

$$W_{PL} = 150x(175 + 30) = 30,750 \text{ lbs}$$

Step 2. A likely value for W_{TO} is obtained by examining data for similar airplanes. In Reference 9, the following information can be found:

Airplane Type	W_{PL} (lbs)	W_{TO} (lbs)	$V_{cr_{max}}$ (kts)	Range (nm)
Boeing 737-300	35,000	135,000	460	1,620
McDD DC9-80	38,000	140,000	M=.8	2,000
Airbus A320	42,000	145,000	450	2,700

From these data a value for W_{TO} of 130,000 lbs seems reasonable, so:

$$W_{TO_{guess}} = 130,000 \text{ lbs.}$$

Step 3. To determine a value for W_F, the procedure indicated in Section 2.4 will be followed. Mission phases are defined in Table 2.18.

Phase 1: Engine Start and Warmup.
Begin weight is W_{TO}. End weight is W_1.
The ratio W_1/W_{TO} is typically 0.990 as indicated in Table 2.1.

Phase 2: Taxi.
Begin weight is W_1. End weight is W_2.
The ratio W_2/W_1 is typically 0.990 as indicated in Table 2.1.

Table 2.18 Mission Specification For A Jet Transport

Payload:	150 Passengers at 175 lbs each and 30 lbs of baggage each.
Crew:	Two pilots and three cabin attendants at 175 lbs each and 30 lbs baggage each.
Range:	1,500 nm, followed by 1 hour loiter, followed by a 100 nm flight to alternate.
Altitude:	35,000 ft (for the design range).
Cruise Speed:	M = 0.82 at 35,000 ft.
Climb:	Direct climb to 35,000 ft. at max. W_{TO} is desired.
Take-off and Landing:	FAR 25 fieldlength, 5,000 ft. at an altitude of 5,000 ft and a 95°F day. Landing performance at $W_L = 0.85W_{TO}$.
Powerplants:	Two turbofans.
Pressurization:	5,000 ft. cabin at 35,000 ft.
Certification Base:	FAR 25

Mission Profile:

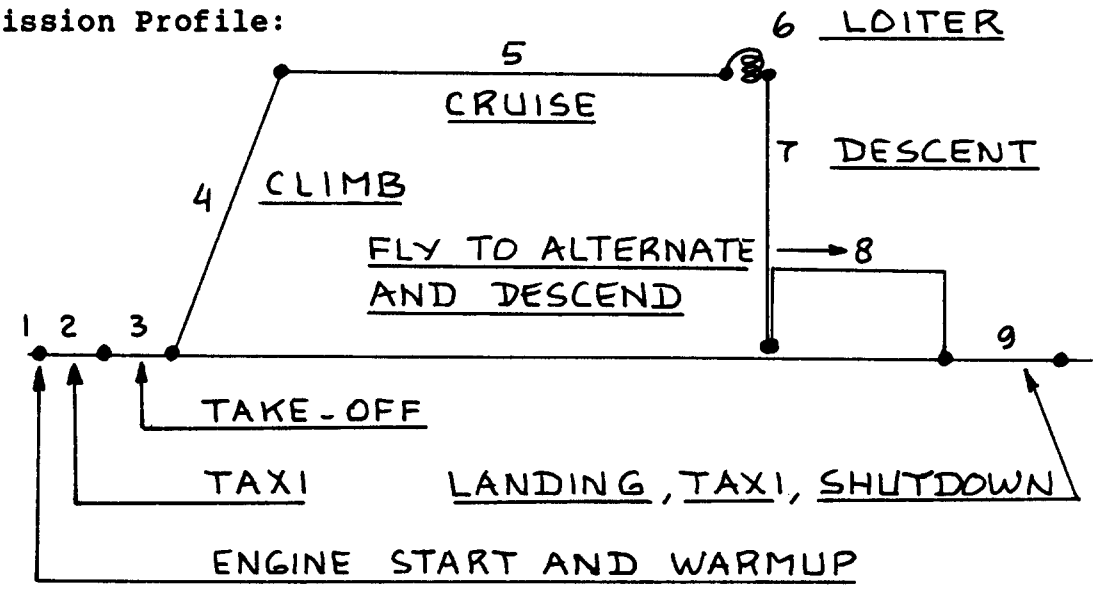

Phase 3: Take-off.
Begin weight is W_2. End weight is W_3.

The ratio W_3/W_2 is typically 0.995 as indicated by Table 2.1.

Phase 4: Climb to cruise altitude and accelerate to cruise speed.
Begin weight is W_3. End weight is W_4.

The ratio W_4/W_3 is typically 0.980 as indicated by Table 2.1.
As suggested by the mission profile of Table 2.18, range credit is to be taken for the climb. It will be assumed, that climb is performed at an average speed of 275 kts and with an average climb-rate of 2500 fpm. To 35,000 ft, it takes 14 min. and this covers a range of (14/60)x275 = 64 nm.

Phase 5: Cruise.
Begin weight is W_4. End weight is W_5.

The specification of Table 2.18 calls for a cruise Mach number of 0.82 at an altitude of 35,000 ft. This amounts to a cruise speed of 473 kts.
The amount of fuel used during cruise can be found from Breguet's range equation which for jet transports is:

$$R_{cr} = (V/c_j)_{cr}(L/D)_{cr}\ln(W_4/W_5) \qquad (2.10)$$

It will be assumed, that the transport will be able to cruise at a L/D value of 16 and an (optimistic) value of $c_j = 0.5$ lbs/lbs/hr. Table 2.2 shows these numbers to be reasonable.
Substitution of these numbers in Eqn.(2.10) with a range of 1,500 - 64 = 1436 nm, yields:

$$W_5/W_4 = 0.909$$

Phase 6: Loiter.
Begin weight is W_5. End weight is W_6.

The ratio W_6/W_5 can be estimated from

Breguet's endurance equation which for a jet transport is:

$$E_{ltr} = (1/c_j)_{ltr}(L/D)_{ltr}\ln(W_5/W_6) \qquad (2.12)$$

It will be assumed, that the transport be able to loiter at a L/D value of 18 and a value of c_j = 0.6 lbs/lbs/hr.

Table 2.2 shows these to be reasonable numbers. Note from Table 2.18, that the mission profile assumes no range credit during loiter. Loiter time is 1 hour. Substitution of the afore mentioned numbers into Eqn.(12) yields:

$W_6/W_5 = 0.967$.

Phase 7: Descent.
Begin weight is W_6. End weight is W_7.

No credit is taken for range. However, a penalty for fuel used during descents from high altitudes needs to be assessed. Typically the ratio $W_7/W_6 = 0.990$, as

seen from Table 2.1.

Phase 8: Fly to alternate and descend.
Begin weight is W_7. End weight is W_8.

The ratio W_8/W_7 can be estimated from

Eqn.(2.10). This time however, because of the short distance to fly, it will not be possible to reach an economical cruise altitude. It will be assumed, that for the cruise to alternate a value for L/D of only 10 can be achieved. For c_j a value

of only 0.9 will be used. Because the flight to alternate will probably be carried out at or below 10,000 ft, the cruise speed can be no more than 250 kts in accordance with FAA regulations. With these data and with Eqn.(2.10) it is found

that:

$W_8/W_7 = 0.965$.

No credit or penalty was taken for the descent into the alternate airport.

Phase 9: Landing, Taxi, Shutdown.
Begin weight is W_8. End weight is W_9.

For a jet transport the ratio W_9/W_8

can be assumed to be 0.992, in accordance with Table 2.1.

The overall mission fuel-fraction, M_{ff} can now be computed from Eqn.(2.13) as:

$$M_{ff} = \{\frac{W_9W_8W_7W_6W_5W_4W_3W_2W_1}{W_8W_7W_6W_5W_4W_3W_2W_1W_{TO}}\} =$$

$$= (0.992)(0.965)(0.990)(0.967)(0.909)(0.980)x$$
$$(0.995)(0.990)(0.990) = 0.796$$

The fuel used during phases 1 through 9 is given by Eqn.(2.14) as:

$$W_{F_{used}} = (1 - 0.796)W_{TO} = 0.204W_{TO}$$

Since the fuel reserves are already accounted for, it is seen that in this case also:

$$W_F = 0.204W_{TO}$$

Step 4. A tentative value for W_{OE} is found from Eqn.(2.4) as:

$$W_{OE_{tent}} = 130,000 - 0.204x130,000 - 30,750 =$$
$$= 72,730 \text{ lbs}$$

Step 5. The crew weight, $W_{crew} = 1,025$ lbs is found from the mission specification, Table 2.18.
A tentative value for W_E is found from Eqn.(2.5) as:

$$W_{E_{tent}} = 72,730 - 0.005x130,000 - 1,025 =$$
$$= 71,055 \text{ lbs.}$$

Step 6. The allowable value for W_E is found from Figure 2.9 (or from Eqn.(2.16) as: W_E= 70,000 lbs. It is seen that the difference between W_E and $W_{e_{tent}}$ is 1,055 lbs. This difference is too large. An iteration is thus needed.

Step 7. Note that the iteration in this example will have to drive the estimate for W_{TO} down. It is left to the reader to show, that a value of W_{TO}= 127,000 lbs does satisfy the iteration criterion as stated in Section 2.1, Step 7.

To summarize, the following preliminary numbers define the airplane with the mission specification of Table 2.18:

W_{TO}= 127,000 lbs

W_E = 68,450 lbs

W_F = 25,850 lbs

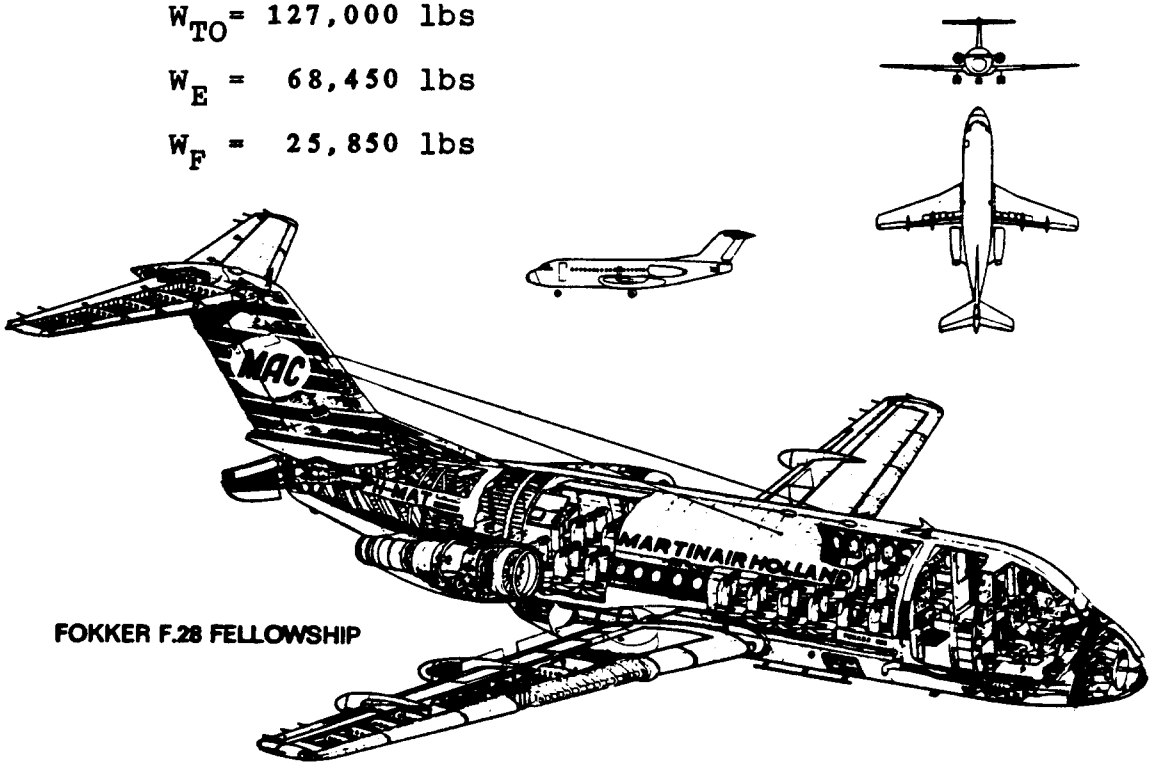

FOKKER F.28 FELLOWSHIP

2.6.3 Example 3: Fighter

Table 2.19 gives an example mission specification for a ground attack fighter airplane. Note that the various mission phases have been numbered. The example follows the step-by-step method outlined in Section 2.1.

Step 1. From Table 2.19, the payload weight, W_{PL} is: 2,000 + 20x500 = 12,000 lbs

Step 2. A likely value for W_{TO} is obtained by examining data for similar airplanes. In Reference 9, the following information is found:

Airplane Type	W_{PL} (lbs)	W_{TO} (lbs)	V_{max} (kts)	Range (nm)
F.R. A10A	15,000	50,000	450	540
Grumman A6	17,000	60,400	689	1,700
Tornado F.Mk2	16,000	58,400	600*	750

* with ext. stores, 1,106 clean!

From these data, an initial guess for W_{TO} is: $W_{TO_{guess}}$ = 60,000 lbs.

Step3. To determine a value for W_F, the procedure of Section 2.4 will be followed. Mission phases are defined in Table 2.19.

Phase 1: Engine Start and Warm-up.
Begin weight is W_{TO}. End weight is W_1.
The ratio W_1/W_{TO} is typically 0.990 as indicated in Table 2.1.

Phase 2: Taxi.
Begin weight is W_1. End weight is W_2.
The ratio W_2/W_1 is typically 0.990 as indicated by Table 2.1.

Table 2.19 Mission Specification For A Fighter

Payload:	20x500 lbs bombs, carried externally and 2,000 lbs of ammunition for the GAU-81A multi-barrel cannon. The cannon weight of 4,000 lbs, is part of W_E.
Crew:	One pilot (200 lbs).
Range and Altitude:	See mission profile. No reserves.
Cruise Speed:	400 kts at sealevel with external load. 450 kts at sealevel, clean. M = 0.80 at 40,000 ft with external load. M = 0.85 at 40,000 ft, clean.
Climb:	Direct climb to 40,000 ft. at max. W_{TO} in 8 minutes is desired. Climb rate on one engine, at max. W_{TO} should exceed 500 fpm on a 95°F day.
Take-off and Landing:	groundrun of less than 2,000 ft at sealevel and a 95°F day.
Powerplants:	Two turbofans.
Pressurization:	5,000 ft. cockpit at 50,000 ft.
Certification Base:	Military.

Mission Profile:

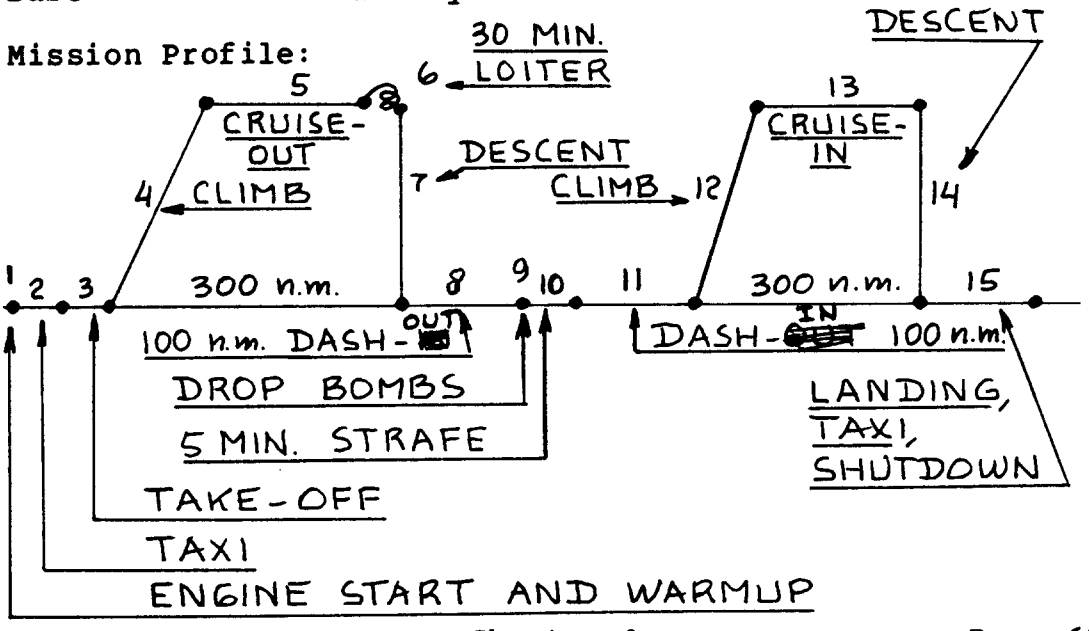

Phase 3. Take-off.
Begin weight is W_2. End weight is W_3.

The ratio W_3/W_2 is typically 0.990 as seen in Table 2.1.

Phase 4. Climb to cruise altitude and accelerate to cruise speed.
Begin weight is W_3. End weight is W_4.

The ratio W_4/W_3 is 0.971 as seen from Figure 2.2, with V_{cruise}= 459 kts, which corresponds to M = 0.8 at 40,000 ft. Range credit needs to be taken, according to the mission profile of Table 2.19. It will be assumed, that the climb is performed at an average speed of 350 kts and with an average climb-rate of 5,000 fpm. To 40,000 ft this takes 8 min. The range covered is (8/60)x350 = 47 nm.

Phase 5. Cruise-out.
Begin weight is W_4. End weight is W_5.

The cruise phase is to be carried out at 40,000 ft and with a speed corresponding to M=0.80 (with ext. load). This means V_{cruise}=459 kts. Fuel used during this part of the mission can be estimated from Breguet's range equation:

$$R_{cr} = (V/c_j)_{cr}(L/D)_{cr}\ln(W_4/W_5) \qquad (2.10)$$

The range is 300 - 47 = 253 nm. Because this fighter carries its bomb load externally and because it cruises at a rather high cruise speed, the L/D value during cruise-out is not likely to be very high. A value of 7.0 seems reasonable. For c_j, Table 2.2 indicates that 0.6 might be an optimistic choice. With these numbers the fuel-fraction for this phase follows from Eqn.(2.10) as: W_5/W_4= 0.954.

Phase 6. Loiter.
Begin weight is W_5. End weight is W_6.

During loiter, the lift-to-drag ratio will be significantly better than during high speed cruise-out. A value of 9.0 for $(L/D)_{ltr}$ will be used. For c_j,

Table 2.2 indicates that 0.6 is o.k. Loiter time is specified at 30 min. The fuel-fraction for this phase follows from Breguet's endurance equation:

$$E_{ltr} = (1/c_j)(L/D)_{ltr} \ln(W_5/W_6) \qquad (2.12)$$

This yields: $W_6/W_5 = 0.967$

Phase 7. Descent.
Begin weight is W_6. End weight is W_7.

Table 2.1 suggests that W_7/W_6 is 0.99

No range credit is to be taken, as seen from the mission profile of Table 2.19.

Phase 8. Dash-out.
Begin weight is W_7. End weight is W_8.

The speed during dash-out is specified as 400 kts in the ext.load configuration. This means a poor lift-to-drag ratio: a value of 4.5 will be assumed. With a range of 100 nm, $c_j = 0.9$ and puede incluso ser menor para los aviones actua

L/D = 4.5, the fuel fraction can be found again with Eqn.(2.10): $W_8/W_7 = 0.951$.

Phase 9. Drop Bombs.
Begin weight is W_8. End weight is W_9.

No fuel penalty is assessed and no range credit is taken. The ratio $W_9/W_8 = 1.0$.

CAUTION:
The bomb load which is dropped is given in Table 2.19 as 10,000 lbs.
The total fuel fraction up to this point in the mission is found as:
$M_{ff_{1-9}} = 0.818$. Therefore, (1 - 0.818) = 0.182 is the fuel used as a fraction of W_{TO}. The latter was guessed to be:

60,000 lbs. Therefore, just prior to the bomb-drop:
W = 60,000x(1- 0.182) = 49,080 lbs.
Immediately after the bomb-drop:
W = 49,080 - 10,000 = 39,080 lbs.
Since the next weight ratio is predicated on the weight after bomb-drop, it will be necessary to correct the following fuel-fraction of Phase 10.

Phase 10. Strafe.
Begin weight is W_9. End weight is W_{10}.

Strafing time is defined as 5 min. Assuming that during the strafing phase maximum military thrust is used, c_j is

probably high: a value of 0.9 will be assumed. The lift-to-drag ratio will also be poor during this phase. A value of 4.5 will be assumed. Using the loiter equation (2.12), the ratio W_{10}/W_9 can

be calculated to be 0.983. This ratio needs to be corrected for the weight change which occurred during bomb-drop. The bomb-drop weight ratio is found as:
39,080/49,080 = 0.796.
The corrected ratio W_{10}/W_9 is now

found as: {1- (1 - 0.983)x0.796} = 0.986.

<u>CAUTION:</u>
During the strafing run 2,000 lbs of ammunition is expended. The weight at the end of the strafing run due to fuel consumed is found as:

39,080 - (1 - 0.983)x39,080 = 38,416 lbs.

After ammo firing this becomes: 36,416 lbs
Again, the following fuel-fraction for Phase 11 will have to be corrected.

Phase 11. Dash-in.
Begin weight is W_{10}. End weight is W_{11}.

During this dash, the fighter is back in a clean configuration. For L/D, a value of 5.5 will be used, while for c_j

0.9 seems reasonable here. The dash-out speed is 450 kts according to the specification in Table 2.19. The range is 100 nm. With Eqn.(2.10) the fuel-fraction is computed as:

$W_{11}/W_{10} = 0.964.$

This ratio needs to be corrected again. The weight ratio due to ammo firing is: 36,416/38,416 = 0.948.
The corrected weight ratio, W_{11}/W_{10} is found as:
{1- (1- 0.964)x 0.948} = .966.

Phase 12. Climb to cruise altitude and accelerate to cruise speed.
Begin weight is W_{11}. End weight is W_{12}.

The mission specification in this case calls for a cruise speed of M = 0.85. It will be assumed, that this phase is executed in the same manner as Phase 4. Therefore: $W_{12}/W_{11} = 0.969$ and the

range covered is taken to be 47 nm.

Phase 13. Cruise-in.
Begin weight is W_{12}. End weight is W_{13}.

Cruise-out speed in Table 2.19 is given as M = 0.85 at 40,000 ft or 488 kts The fighter is now lighter than it was during Phase 5. This makes L/D lower. The fighter is also aerodynamically cleaner, because the external load has been dropped. For L/D a value of 7.5 will be assumed. The range is 253 nm and c_j will be assumed to be 0.6, as for

Phase 5. It is found that:

$W_{13}/W_{12} = 0.959.$

Phase 14. Descent.
Begin weight is W_{13}. End weight is W_{14}.

No credit for range is taken. From Table 2.1: $W_{14}/W_{13}= 0.99$.

Phase 15. Landing, Taxi and Shutdown.
Begin weight is W_{14}. End weight is W_{15}.

Table 2.1 suggests: $W_{15}/W_{14}= 0.995$.

The overall mission fuel-fraction follows from Eqn.(2.13) as:

$$M_{ff}= \{\frac{W_{15}W_{14}W_{13}\cdot\cdot\cdot\cdot W_3W_2W_1}{W_{14}W_{13}W_{12}\cdot\cdot\cdot\cdot W_2W_1W_{TO}}\} =$$

$$= (0.995)(0.99)(0.959)(0.969)(0.966)(0.986)(1.0)x$$
$$x(0.951)(0.99)(0.967)(0.954)(0.971)(0.99)(0.99)x$$
$$x(0.99) = 0.713.$$

It must be observed that this value for M_{ff} is already the corrected fuel-fraction.
For mission fuel, W_F it is found that:

$$W_F= (1-0.713)x60,000 = 17,220 \text{ lbs.}$$

Step 4. The value for $W_{OE_{tent}}$ follows with the help of Eqn.(2.4) as:

$$W_{OE_{tent}} = 60,000 - 17,220 - 12,000 =$$
$$= 30,780 \text{ lbs.}$$

Step 5. A tentative value for W_E follows with the help of Eqn.(2.5) as:

$$W_{E_{tent}} = 30,780 - 0.005x60,000 - 200=$$
$$= 30,280.$$

Step 6. The allowable value for W_E is found in Figure 2.11 as: $W_E= 31,000$ lbs.

Step 7. The difference between W_E and $W_{E_{tent}}$ is

seen to be 720 lbs. This difference is too large. An iteration is therefore needed. The reader is asked to show, that after iteration, W_{TO}= 64,500 lbs.

To summarize, the ground attack fighter airplane with the mission specification of Table 2.19 is defined by the following initial weight estimates:

W_{TO}= 64,500 lbs (with external stores)

W_{TO}= 54,500 lbs (without external stores)

W_E = 33,500 lbs

W_F = 18,500 lbs

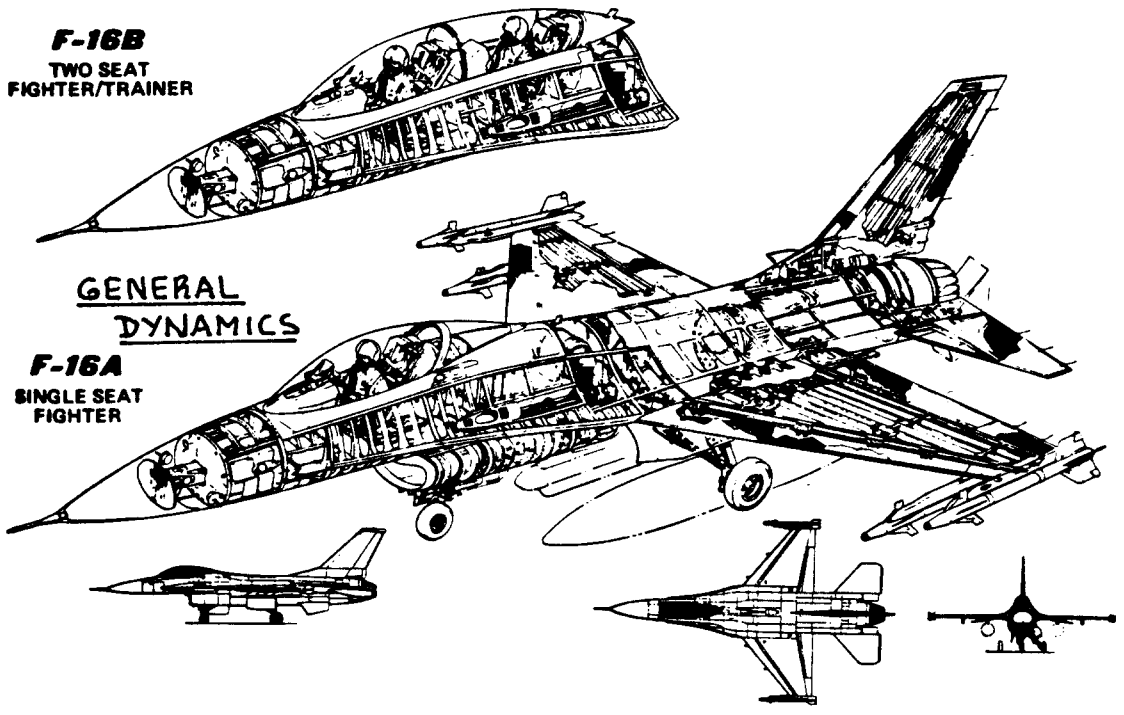

Coste actual "fighters", EEUU ~ 500 $/lb

2.7 SENSITIVITY STUDIES AND GROWTH FACTORS

It is evident from the way the results in Section 2.6 were obtained, that their outcome depends on the values selected for the various parameters in the range and endurance equations.

This section will show with some examples, how airplane take-off weight, W_{TO} varies with:

1. Payload, W_{PL}
2. Empty weight, W_E
3. Range, R
4. Endurance, E
5. Lift-to-drag ratio, L/D
6. Specific fuel consumption, c_p or c_j
7. Propeller efficiency, η_p

After preliminary sizing of a new airplane with the methods outlined in Section 2.4, it is mandatory to conduct sensitivity studies on the parameters 1-7 listed before.

The reasons for doing this are:

A. To find out which parameters 'drive' the design
B. To determine which areas of technological change must be pursued, if some new mission capability must be achieved.
C. If parameters 5,6 or 7 were selected optimistically (or pessimistically), the sensitivity studies provide a quick estimate of the impact of such optimism (or pessimism) on the design.

2.7.1 An Analytical Method For Computing Take-off Weight Sensitivities

With the help of Eqns. (2.4) and (2.5), it is possible to write:

$$W_E = W_{TO} - W_F - W_{PL} - W_{tfo} - W_{crew} \tag{2.17}$$

Equation (2.6) can also be written as:

$$W_F = (1 - M_{ff})W_{TO} + W_{F_{res}} \tag{2.18}$$

Reserve fuel, $W_{F_{res}}$ can in turn be written as:

$$W_{F_{res}} = M_{res}(1 - M_{ff})W_{TO}, \qquad (2.19)$$

where:

M_{res} is the reserve fuel fraction expressed in terms of mission fuel used.

If M_{tfo} is introduced as the trapped fuel and oil fraction expressed in terms of the take-off gross weight, W_{TO}, then it follows that:

$$W_E = W_{TO}\{1 - (1 + M_{res})(1 - M_{ff}) - M_{tfo}\} + \\ - (W_{PL} + W_{crew}) \qquad (2.20)$$

The latter can in turn be written as:

$$W_E = CW_{TO} - D, \qquad (2.21)$$

where:

$$C = \{1 - (1 + M_{res})(1 - M_{ff}) - M_{tfo}\} \qquad (2.22)$$

and:

$$D = (W_{PL} + W_{crew}) \qquad (2.23)$$

The reader is asked to show, that W_E can be eliminated from Eqns.(2.21) and (2.16) to yield:

$$\log_{10}W_{TO} = A + B\log_{10}(CW_{TO} - D) \qquad (2.24)$$

The parameters A and B are the regression line constants of Table 2.15. The parameters C and D are those of Eqns.(2.22) and (2.23).

It is observed, that Eqn.(2.24) also offers the opportunity for a numerical solution to the iteration process discussed in Section 2.4.

If the sensitivity of W_{TO} to some parameter y is desired, it is possible to obtain that sensitivity by partial differentiation of W_{TO} in Eqn.(2.24). This results in:

$$(1/W_{TO})\partial W_{TO}/\partial y =$$

$$B(W_{TO}\partial C/\partial y + C\partial W_{TO}/\partial y - \partial D/\partial y)/(CW_{TO}-D) \qquad (2.25)$$

Since the regression line constants A and B vary only with airplane type, the partial derivatives $\partial A/\partial y$ and $\partial B/\partial y$ are zero.

From Eqn.(2.25) it is possible to solve for $\partial W_{TO}/\partial y$ as:

$$\partial W_{TO}/\partial y =$$

$$\{B(W_{TO})^2\partial C/\partial y - BW_{TO}\partial D/\partial y\}/\{C(1-B)W_{TO}-D\} \qquad (2.26)$$

The parameter y can be any one of those listed as 1-7 at the beginning of this section.

The following sensitivities will now be derived:

2.7.2 Sensitivity of Take-off Weight to Payload Weight

2.7.3 Sensitivity of Take-off Weight to Empty Weight

2.7.4 Sensitivity of Take-off Weight to Range, Endurance, Speed, Specific Fuel Consumption, Propeller Efficiency and Lift-to-Drag Ratio.

2.7.2 Sensitivity of Take-off Weight to Payload Weight

If $y=W_{PL}$, then $\partial D/\partial W_{PL} = 1.0$ by Eqn.(2.23). Also, $\partial C/\partial W_{PL} = 0$ by Eqn.(2.22).

Therefore:

$$\partial W_{TO}/\partial W_{PL} = BW_{TO}\{D - C(1-B)W_{TO}\}^{-1} \qquad (2.27)$$

The derivative $\partial W_{TO}/\partial y$ is called the airplane growth factor due to payload. Some examples will now be discussed. The examples utilize the airplanes which were discussed in Section 2.6.

2.7.2.1 Example 1: Twin engine propeller driven airplane

For this twin, the following data can be found:

A = 0.0966(Table 2.15)
B = 1.0298(Table 2.15)

C = {1 - 1.25(1 - 0.827) - 0.005} = 0.779
(See SubSection 2.6.1)
D = 1,250 lbs(Table 2.17)

Note that substitution of A, B, C and D in Eqn.(2.24) yields:

W_{TO}= 7,935 lbs, which agrees quite well with the iterative solution found in Par.2.6.1.

With this value for W_{TO}, it is possible to compute the sensitivity of W_{TO} to W_{PL} from Eqn.(2.27) as:

$\partial W_{TO}/\partial W_{PL}$= 5.7.

This means, that for each pound of payload added, the airplane take-off weight will have to be increased by 5.7 lbs. This assumes, that the mission performance stays the same. The factor 5.7 is called the growth factor due to payload for this twin.

2.7.2.2 Example 2: Jet transport

For this jet transport, the following data can be found:

A = 0.0833(Table 2.15)
B = 1.0383(Table 2.15)
C = {1 - (1 - 0.796) - 0.005} = 0.791
(See SubSection 2.6.2)
D = 31,775 lbs (Table 2.18)

Note that substitution of A, B, C and D in Eqn.(2.24) yields:

W_{TO}= 126,100 lbs, which agrees very well with the iterative solution found in SubSection 2.6.2.

With this value for W_{TO} it is possible to compute the sensitivity of W_{TO} to W_{PL} from Eqn.(2.27) as:

$\partial W_{TO}/\partial W_{PL}$= 3.7

This means that for each pound of payload added, the airplane take-off gross weight will have to be increased by 3.7 lbs. This assumes, that the mission performance stays the same. In this case the factor 3.7 is called the growth factor due to payload for this jet transport.

2.7.2.3 Example 3: Fighter

For this fighter, the following data can be found:

A = 0.5091(Table 2.15)
B = 0.9505(Table 2.15)
C = {1 - (1 - 0.713) - 0.005} = 0.708
(See SubSection 2.6.3)
D = 12,200 lbs(Table 2.18)

Note, that substitution of A, B, C and D into Eqn.(2.24) yields:

W_{TO}= 64,000 lbs, which agrees quite well with the iterative solution found in SubSection 2.6.3.

With this value of W_{TO} it is possible to compute the sensitivity of W_{TO} to W_{PL} from Eqn.(2.27) as:

$$\partial W_{TO}/\partial W_{PL} = 6.1$$

This means that for each pound of payload added, the airplane take-off gross weight will have to be increased by 6.1 lbs. This assumes, that mission performance is kept the same. The factor 6.1 is called the growth factor due to payload for this fighter.

2.7.3 Sensitivity of Take-off Weight to Empty Weight

From Eqn.(2.16) it follows that:

$$\log_{10} W_{TO} = A + B\log_{10} W_E \qquad (2.28)$$

By partial differentiation of W_{TO} with respect to W_E the take-off weight to empty weight sensitivity is expressed as:

$$\partial W_{TO}/\partial W_E = BW_{TO}[\text{invlog}_{10}\{(\log_{10} W_{TO} - A)/B\}]^{-1} \qquad (2.29)$$

To illustrate the meaning of Eqn.(2.29), three examples will be discussed. The airplanes used are those of Section 2.6.

2.7.3.1 Example 1: Twin engine propeller driven airplane

For this airplane, the following values were previously found:

A = 0.0966(Table 2.15)
B = 1.0298(Table 2.15)
W_{TO}= 7,935 lbs(See 2.7.2.1)

Eqn.(2.29) yields with these data:

$\partial W_{TO}/\partial W_E$= 1.66

For each lbs of increase in empty weight, the take-off weight must be increased by 1.66 lbs, to keep the mission performance the same. The factor 1.66 is the growth factor due to empty weight for this twin.

2.7.3.2 Example 2: Jet transport

For the jet tranport, the following data were previously found:

A = 0.0833(Table 2.15)
B = 1.0383(Table 2.15)
W_{TO}= 126,100 lbs(See 2.7.2.2)

Eqn.(2.29) produces with these data:

$\partial W_{TO}/\partial W_E$= 1.93

For each pound of increase in empty weight, the take-off weight must be increased by 1.93 lbs, to keep the mission performance the same. The factor 1.93 is the growth factor due to empty weight for this jet transport.

2.7.3.3 Example 3: Fighter

For this fighter airplane, the following data were previously determined:

A = 0.5091(Table 2.15)
B = 0.9505(Table 2.15)
W_{TO}= 64,000 lbs(See 2.7.2.3)

It is found with Eqn.(2.29) and these data that:

$\partial W_{TO}/\partial W_E$= 1.83

For each pound of increase in empty weight, the take-off weight must be increased by 1.83 lbs, to keep the mission performance the same. The factor 1.83 is the growth factor due to empty weight for this fighter.

2.7.4 Sensitivity of Take-off Weight to Range, Endurance, Speed, Specific Fuel Consumption, Propeller Efficiency and Lift-to-Drag Ratio

In this sub-section the parameters Range, R, Endurance, E, Speed, V, Specific Fuel Consumption, c_p and c_j, Propeller Efficiency, η_p and Lift-to-Drag Ratio, L/D are represented by the symbol y.

The sensitivity of W_{TO} to any parameter y, which is not payload, W_{PL} is found from Eqn.(2.26) as:

$$\partial W_{TO}/\partial y = \{CW_{TO}(1 - B) - D\}^{-1} BW_{TO}^{2} \partial C/\partial y \qquad (2.30)$$

where C is defined by Eqn.(2.22) which can also be written as:

$$C = \{M_{ff}(1 + M_{res}) - M_{tfo} - M_{res}\} \qquad (2.31)$$

Partial differentiation with respect to y gives:

$$\partial C/\partial y = (1 + M_{res})\partial M_{ff}/\partial y \qquad (2.32)$$

As was seen in the examples of the fighter and the jet transport, the reserve fraction M_{res} is often zero, because the reserves were included in the mission profile.

For the twin propeller, this was not the case and the value for M_{res} was 0.25. The reader should carefully inspect the mission specification, before assigning a value to M_{res}.

The differential $\partial M_{ff}/\partial y$ can be found from Eqn.(2.13) as:

$$\partial M_{ff}/\partial y = M_{ff}(W_i/W_{i+1})\partial(W_{i+1}/W_i)/\partial y \qquad (2.33)$$

At this point, it is recalled that the ratio W_i/W_{i+1} can be determined from Breguet's equations. These Breguet equations take on two different forms, depending on whether range or endurance is sought. Breguet's equations can be generalized as:

$$\bar{R} = \ln(W_i/W_{i+1}) \qquad (2.34)$$

or as:

$$\bar{E} = \ln(W_i/W_{i+1}) \tag{2.35}$$

The quantities $\bar{R}$ and $\bar{E}$ in turn are found as follows:

For propeller driven airplanes:

$$\bar{R} = Rc_p(375\eta_p L/D)^{-1} \tag{2.36}$$

$$\bar{E} = EVc_p(375\eta_p L/D)^{-1} \tag{2.37}$$

For jet airplanes:

$$\bar{R} = Rc_j(VL/D)^{-1} \tag{2.38}$$

$$\bar{E} = Ec_j(L/D)^{-1} \tag{2.39}$$

The reader is asked to show that equations (2.34) and (2.35) can be differentiated to yield:

$$\partial(W_{i+1}/W_i)/\partial y = -(W_{i+1}/W_i)\partial\bar{R}/\partial y \tag{2.40}$$

and:

$$\partial(W_{i+1}/W_i)/\partial y = -(W_{i+1}/W_i)\partial\bar{E}/\partial y \tag{2.41}$$

respectively.

By combining Eqns.(2.30), (2.32), and (2.33) with (2.40) or (2.41), the sensitivity of W_{TO} with respect to y can be written as:

$$\partial W_{TO}/\partial y = F\partial\bar{R}/\partial y \tag{2.42}$$

for the case involving a ratio (W_{i+1}/W_i) dependent on range, and:

$$\partial W_{TO}/\partial y = F\partial\bar{E}/\partial y \tag{2.43}$$

for the case involving a ratio (W_{i+1}/W_i) dependent on endurance.

The factor F in these equations is defined as:

$$F = -BW_{TO}^2\{CW_{TO}(1 - B) - D\}^{-1}(1 + M_{res})M_{ff} \tag{2.44}$$

The form taken by the so-called Breguet partials

$\partial\bar{R}/\partial y$ and $\partial\bar{E}/\partial y$ depends on whether the particular weight ratio being differentiated is defined by Eqn.(2.34) or by Eqn.(2.35). Table 2.20 gives the forms for the Breguet partials. These partials are derived by partially differentiating Eqns. (2.36) through (2.39) with respect to R, E, V, c_p, c_j, η_p or L/D.

2.7.5 Examples of Sensitivities to Range, Endurance and Speed

Range, R, endurance, E and speed, V are all items which are normally specified in the mission specification. Since mission specifications are often open to negotiation, it is of great interest to be able to determine how these items affect the design gross weight, W_{TO} of an airplane.

This sub-section will show with examples, how the sensitivity of W_{TO} to changes in R, E and V can be found.

Implications for the design of the airplane will be indicated.

By setting R, E and V sequentially equal to y it is possible to calculate the sensitivity of W_{TO} to these parameters from Eqns.(2.42) and (2.43). The corresponding Breguet Partials $\partial\bar{R}/\partial y$ and $\partial\bar{E}/\partial y$ can be found from Table 2.20.

2.7.5.1 Example 1: Twin engine propeller driven airplane

First it is noted from the mission specification of Table 2.17 that no value for E was specified. Also, it is observed, that R, for a propeller driven airplane does not depend on V. Therefore, the only sensitivity to be computed here is $\partial W_{TO}/\partial R$.

The reader is asked to show, that the take-off weight to range sensitivity in this case can be found from:

$$\partial W_{TO}/\partial R = Fc_p(375\eta_p L/D)^{-1}, \qquad (2.45)$$

where F is defined by Eqn.(2.44).

For this twin, the following data are found:

B = 1.0298 (Table 2.15) $\quad M_{res} = 0.25$ (incl. in M_{ff})
C = 0.779 (2.7.2.1)

Table 2.20 Breguet Partials for Propeller Driven and for Jet Airplanes

		Propeller Driven		Jet
Range Case	$y = R$	$\partial\bar{R}/\partial y = c_p(375\eta_p L/D)^{-1}$		$\partial\bar{R}/\partial y = c_j(VL/D)^{-1}$
Endurance Case	$y = E$	$\partial\bar{E}/\partial y = Vc_p(375\eta_p L/D)^{-1}$		$\partial\bar{E}/\partial y = c_j(L/D)^{-1}$
Range Case	$y = c_p$	$\partial\bar{R}/\partial y = R(375\eta_p L/D)^{-1}$	$y = c_j$	$\partial\bar{R}/\partial y = R(VL/D)^{-1}$
Endurance Case	$y = c_p$	$\partial\bar{E}/\partial y = EV(375\eta_p L/D)^{-1}$	$y = c_j$	$\partial\bar{E}/\partial y = E(L/D)^{-1}$
Range Case	$y = \eta_p$	$\partial\bar{R}/\partial y = -Rc_p(375\eta_p{}^2 L/D)^{-1}$		Not Applicable
Endurance Case	$y = \eta_p$	$\partial\bar{E}/\partial y = -EVc_p(375\eta_p{}^2 L/D)^{-1}$		Not Applicable
Range Case	$y = V$	Not Applicable		$\partial\bar{R}/\partial y = -Rc_j(V^2 L/D)^{-1}$
Endurance Case	$y = V$	$\partial\bar{E}/\partial y = Ec_p(375\eta_p L/D)^{-1}$		Not Applicable
Range Case	$y = L/D$	$\partial\bar{R}/\partial y = -Rc_p(375\eta_p(L/D)^2)^{-1}$		$\partial\bar{R}/\partial y = -Rc_j(V(L/D)^2)^{-1}$
Endurance Case	$y = L/D$	$\partial\bar{E}/\partial y = -EVc_p(375\eta_p(L/D)^2)^{-1}$		$\partial\bar{E}/\partial y = -Ec_j(L/D)^{-2}$
		Note: R in sm V in mph		Note: R in nm or sm V in kts or mph

D = 1,250 lbs (Table 2.17) M_{ff}= 0.827 (2.6.1)
W_{TO}= 7,935 lbs (2.7.2.1)

c_p= 0.5, η_p= 0.82, L/D = 11 as given in 2.7.2.1.

With these data substituted into Eqn.(2.44) it is found that:

F = 46,736 lbs.

From Eqn.(2.45) it now follows that:

$\partial W_{TO}/\partial R$ = 6.9 lbs/nm.

The significance of this partial is as follows. Suppose that the range in the mission specification of Table 2.17 is changed from 1,000 nm to 1,100 nm. The result just found indicates that this would require an increase in gross weight at take-off of 100x6.9 = 690 lbs.

2.7.5.2 Example 2: Jet transport

The mission specification for the jet transport is given in Table 2.18. It is seen that both range and endurance are specified. Therefore the sensitivities of W_{TO} to both R and to E need to be calculated.

For the jet transport, the following data are found:

B = 1.0383 (Table 2.15) M_{res}= 0 (incl in M_{ff})
C = 0.791 (2.7.2.2)
D = 31,775 lbs (Table 2.18) M_{ff}= 0.796 (2.6.2)

W_{TO}= 126,100 lbs (2.7.2.2) F = 369,211 lbs (Eqn.(2.44))

for cruise:
c_j= 0.5, L/D = 16 and V = 473 kts as given in Sub-section 2.6.2.

for endurance:
c_j= 0.6, L/D = 18 as given in Sub-section 2.6.2.

The reader is asked to verify, that the sensitivities of take-off gross weight to range and to endurance can be written as:

$$\partial W_{TO}/\partial R = Fc_j(VL/D)^{-1} \qquad (2.46)$$

and:

$$\partial W_{TO}/\partial E = Fc_j(L/D)^{-1}, \qquad (2.47)$$

where F is again given by Eqn.(2.44).

When the jet transport data are substituted into Eqns. (2.46) and (2.47), the following sensitivities are found:

$$\partial W_{TO}/\partial R = 24.4 \text{ lbs/nm, and:}$$

$$\partial W_{TO}/\partial E = 12{,}307 \text{ lbs/hr.}$$

The significance of these sensitivities is as follows. If the range in the mission specification of Table 2.18 is decreased from 1,500 nm to 1,400 nm, the take-off gross weight can be decreased by 100x24.4 = 2,440 lbs. Similarly, if the loiter requirement of Table 2.18 is increased from 1 hour to 1.5 hours, the take-off gross weight will be increased by 1/2x12,307 = 6,154 lbs.

The transport is also sensitive to the specification of cruise speed. Since cruise speed has a major impact on block-speed, it will be necessary to compute the sensitivity of take-off gross weight to cruise speed. The reader is asked to verify that:

$$\partial W_{TO}/\partial V = -FRc_j(V^2L/D)^{-1}, \qquad (2.48)$$

where F is defined in Eqn.(2.44).

With the data at the beginning of this example substituted into Eqn.(2.48) it is found that:

$$\partial W_{TO}/\partial V = -74.1 \text{ lbs/kt.}$$

What this means, is that if the cruise speed could be increased without changing any of the other parameters, the gross weight would actually come down. From a mathematical viewpoint, this result is correct. From a practical viewpoint it is not. There are several reasons for this. When the cruise speed is increased, the cruise lift coefficient is decreased. This usually means a decrease in L/D. It also usually means a change in c_j. Finally, there is the effect of increased Mach number on L/D. This also tends to decrease L/D.

2.7.5.3 Example 3: Fighter

From the mission specification of Table 2.19 it is seen, that the fighter has range, endurance and speed sensitivity. Because the mission profile consists of

several range phases and an endurance phase, it will be necessary to calculate the sensitivities with respect to these phases separately.

The reader is asked to verify, that the sensitivities of fighter take-off gross weight to changes in range and endurance can be computed also from Eqns. (2.46) and (2.47). For the fighter, the following data can be found:

B = 0.9505 (Table 2.15)
C = 0.708 (2.7.2.3)
D = 12,200 lbs (Table 2.19)
M_{res} = 0 (mission spec. shows no reserves)
M_{ff} = 0.713 (2.7.2.3)
W_{TO} = 64,000 (2.7.2.3)
F = 278,786 lbs (Eqn.(2.44))

Values for c_j, V and L/D vary with each mission phase. The following tabulation shows these numbers as found in (2.7.2.3) and also shows the corresponding sensitivities.

	Cruise-out	Dash-out	Dash-in	Cruise-in	Loiter
c_j	0.6	0.9	0.9	0.6	0.6
V	459	400	450	488	N.A.
L/D	7.0	4.5	5.5	7.5	9.0
$\partial W_{TO}/\partial R$	52.1	139	101	45.7	N.A.
$\partial W_{TO}/\partial E$	N.A.	N.A.	N.A.	N.A.	18,586

It is clear from these data, that the dash-out part of the mission has the greatest sensitivity of W_{TO} to range. If there is a military need to increase the dash-out range from 100 nm to 200 nm, the consequence is an increase of take-off gross weight of 100x139 = 13,900 lbs. At the current fighter cost of 500 dollars/lbs, that would increase the unit cost of the fighter by 7.0 million dollars! It will be clear to the reader, that military need and affordability must be traded against each other in the final definition of the mission specification.

It is also clear from the data, that if the loiter time of 30 min could be cut to 15 min. (such as by improved C^3I), the take-off gross weight would decrease by 0.25x18,586 = 4,645 lbs. This would result in a decrease in unit cost of 2.3 million dollars!

2.7.6 Examples of Sensitivities to Specific Fuel Consumption, Propeller Efficiency and Lift-to-Drag Ratio

Specific fuel consumption, c_p or c_j, propeller efficiency, η_p and lift-to-drag ratio, L/D are all items which the designer has under his control to the extent of the existing state of technology. The fuel consumption is dependent on the state of engine technology. Propeller efficiency depends on the state of propeller technology. Airplane lift-to-drag ratio depends on the aerodynamic configuration, the method used to integrate the propulsion system into the configuration and on the state of aerodynamic technology (for example laminar versus turbulent boundary layers).

Sensitivities of gross weight at take-off to these factors must be evaluated for the following reasons:

1. A large sensitivity may force a different configuration design approach. Higher wing loading, different schemes of propulsion system integration or different engine choices may result.

2. It is quite possible that the sensitivity results lead to the establishment of improvement targets in these factors. Sometimes such improvements can be brought about by a directed research and development program.

The purpose of this sub-section is to illustrate, with examples, how the sensitivity of W_{TO} to these factors can be computed.

2.7.6.1 Example 1: Twin engine propeller driven airplane

For this airplane, the sensitivity of W_{TO} to the parameters c_p, η_p and L/D needs to be determined.

Because the mission specification for this twin (Table 2.17) does not specify a requirement for endurance, only the range dependent Breguet Partials in Table 2.20 are needed.

The reader is asked to show that the sensitivity of take-off gross weight to specific fuel consumption can be obtained from:

$$\partial W_{TO}/\partial c_p = FR(375\eta_p L/D)^{-1}, \qquad (2.49)$$

where F is defined by Eqn.(2.44).

The required data for the twin were already given in (2.7.5.1). The value for range, R is 1000 nm, according to Table 2.18.

Eqn.(2.49) yields in this case:

$$\partial W_{TO}/\partial c_p = 13,817 \text{ lbs/lbs/hp/hr.}$$

The significance of this finding is as follows. Suppose an engine could be found with a c_p of 0.45 instead of 0.50. The take-off gross weight of this twin could then be decreased by 0.05x13,817 = 691 lbs.

The sensitivity of take-off gross weight to propeller efficiency can be calculated from:

$$\partial W_{TO}/\partial \eta_p = -FRc_p(375\eta_p^2 L/D)^{-1}, \qquad (2.50)$$

where F is given by Eqn.(2.44)

Using the previous data in Eqn.(2.50) yields:

$$\partial W_{TO}/\partial \eta_p = - 8,425 \text{ lbs.}$$

The meaning of this finding is as follows. If the propeller efficiency could be increased from 0.82 to 0.84, the take-off gross weight would decrease by 0.02x8,425 = 168 lbs.

The sensitivity of take-off gross weight to lift-to-drag ratio can be computed from:

$$\partial W_{TO}/\partial (L/D) = -FRc_p\{375\eta_p (L/D)^2\}^{-1}, \qquad (2.51)$$

where F is again given by Eqn.(2.44).

Substituting the previous data into Eqn.(2.51) results in:

$$\partial W_{TO}/\partial (L/D) = - 628 \text{ lbs.}$$

This result means, that if L/D could be increased from 11 to 12, the take-off gross weight would come down by 628 lbs. It comes as no surprise, that L/D in a range dominated airplane has a powerful effect on gross weight.

2.7.6.2 Example 2: Jet transport

In the case of the jet transport, the sensitivities of take-off gross weight to specific fuel consumption and

to L/D need to be determined. Since the mission specification calls for both range and loiter, two sensitivities need to be looked at for each parameter.

The reader is asked to verify that:

With respect to the range requirement:

$$\partial W_{TO}/\partial c_j = FR(VL/D)^{-1} \quad (2.52)$$

$$\partial W_{TO}/\partial (L/D) = - FRc_j(V(L/D)^2)^{-1} \quad (2.53)$$

With respect to the loiter requirement:

$$\partial W_{TO}/\partial c_j = FE(L/D)^{-1} \quad (2.54)$$

$$\partial W_{TO}/\partial (L/D) = - FEc_j(L/D)^{-2} \quad (2.55)$$

From previous data in (2.7.5.2) it is found that F = 369,211 lbs in this instance.

For the range case, this yields the following sensitivities:

$\partial W_{TO}/\partial c_j =$

369,211x0.190 = 70,056 lbs/lbs/lbs/hr.

and:

$\partial W_{TO}/\partial (L/D)$ = 369,211x(- 0.00593) = - 2,189 lbs.

These numbers have the following implications:

1. If specific fuel consumption was incorrectly assumed to be 0.5 and in reality turns out to be 0.8, the design take-off gross weight will increase by 0.3x70,056 = 21,017 lbs.

2. If the lift-to-drag ratio of the airplane were 17 instead of the assumed 16, the design take-off gross weight would decrease by 2,189 lbs.

For the loiter case, the following sensitivities are found:

$\partial W_{TO}/\partial c_j =$

369,211x0.0556 = 20,512 lbs/lbs/lbs/hr.

and:

$\partial W_{TO}/\partial (L/D)$ = 369,211x(- 0.001852) = - 684 lbs.

These numbers have the following significance:

1. If the specific fuel consumption during loiter could be improved from the assumed value of 0.6 to 0.5, the take-off gross weight would decrease by 0.1x20,512 = 2,051 lbs.

2. If the lift-to-drag ratio during loiter could be improved from the assumed value of 18 to 19, the take-off gross weight would be reduced by 684 lbs.

These sensitivity data show again how sensitive the take-off gross weight of a range-dominated airplane is to L/D and to specific fuel consumption.

2.7.6.3 Example 3: Fighter

For the fighter, with four range type mission phases and one endurance type mission phase, a range of sensitivities need to be computed. Equations (2.52), (2.53), (2.54) and (2.55) also apply to this fighter.

The value of F in these equations was previously determined to be 278,786 lbs. The following tabulation shows the sensitivities for the five important mission phases.

	Cruise-out	Dash-out	Dash-in	Cruise-in	Loiter
c_j	0.6	0.9	0.9	0.6	0.6
V(kts)	459	400	450	488	N.A.
L/D	7.0	4.5	5.5	7.5	9.0
R(nm)	253	100	100	253	N.A.
E(hr)	N.A.	N.A.	N.A.	N.A.	0.5
$\partial W_{TO}/\partial c_j$	21,952	15,488	11,264	19,271	15,488
	<	Eqn.(2.52)		>	<Eqn.(2.54)>
$\partial W_{TO}/\partial(L/D)$	-1,882	-3,098	-1,843	-1,542	-1,033
	<	Eqn.(2.53)		>	<Eqn.(2.55)>

Implications of these results will now be discussed. An improvement in sfc by 0.1 in the dash-out part of the mission would save 0.1x15,488 = 1,549 lbs in take-off gross weight. An increase in L/D by 0.5 in the cruise-out part of the mission would result in a decrease in take-off gross weight of 0.5x1,882 = 941 lbs.

2.8 PROBLEMS

1.) For the jet transport example of 2.6.2 redo the mission fuel-fraction analysis by splitting the cruise phase (Phase 5) into five equal distances. Account for the estimated weight changes due to fuel consumption by adjusting the L/D to the average weight which prevails during each sub-phase. Keep the cruise Mach number and the cruise altitude as in Table 2.18. Assume that the drag polar of the airplane is:

$$C_D = 0.0200 + 0.0333C_L^2.$$

Compute the sensitivities of W_{TO} to C_{D_o}.

2.) A regional transport has the following mission specification:

Payload:	34 passengers at 175 lbs each and 30 lbs of baggage each.
Crew:	two pilots and one cabin attendant.
Range:	four consecutive trips of 250 nm: R_1 through R_4, with max. payload.
	Reserves for flight to an alternate airport, 100 nm. away, followed by 45 min. loiter.
Altitude:	25,000 ft for design mission.
Cruise speed:	250 kts.
Climb:	Climb to 25,000 ft in 10 min.
Take-off and landing:	FAR 25 fieldlength, 5,000 ft at an altitude of 5,000 ft and a 95°F day. Assume that $W_L = 0.9W_{TO}$.
Powerplants:	Two turboprops or propfans.
Pressurization:	5,000 ft cabin at 35,000 ft.
Certification Base:	FAR 25.

Determine W_{TO}, W_E and W_F for this airplane.

Compute the sensitivities of W_{TO} to c_p, η_p, and to L/D. Find how W_{TO} varies if the range segment is changed from 250 nm to 200 nm and to 300 nm.

3.) A high altitude loiter and reconnaissance airplane has the following mission specification:

Payload:	3,000 lbs of avionics equipment and a rotating external antenna (equivalent to that on the Grumman E2C) with a weight of 3,500 lbs.
Crew:	Two pilots, one avionics systems operator plus a relief crew of three. Use 200 lbs per crewmember.
Range:	1500 nm from a coastal base, followed by 48 hours of loiter on station, followed by return to base. No reserves.
Altitude:	Loiter altitude: 45,000 ft. Must be able to maintain station with 120 kts wind.
Cruise speed:	Larger than 250 kts desired.
Climb:	Must be able to climb to 45,000 ft at arrival on loiter station.
Take-off and Landing:	5,000 ft groundrun, standard day, sea-level at maximum take-off weight and at maximum landing weight respectively. Assume that $W_L = 0.75 W_{TO}$.
Powerplants:	Propfans. At least two engines.
Pressurization:	5,000 ft cabin at 45,000 ft.
Certification Base:	Military.
Note:	To save weight, it is acceptable to set the limit loadfactor at 2.0 instead of the usual 2.5, for the outgoing leg of the mission. Upon arrival at the loiter station, limit loadfactor should be the standard 2.5.

Determine W_{TO}, W_E and W_F for this airplane.

Calculate the sensitivities of W_{TO} to R, E, L/D and to c_p and η_p.

Determine how W_{TO} changes, if the loiter station is 2000 nm and 1000 nm from base. Also find W_{TO} for loiter times of 24, 36 and 50 hours. How would W_{TO} change, if L/D could be improved by 30 percent?

4.) A homebuilt composite airplane has the following mission specification:

Payload:	Two pilots at 175 lbs each and 30 lbs of baggage each.
Range:	800 nm, reserves for 200 nm flight to alternate airport.
Altitude:	10,000 ft for the design range.
Cruise Speed:	250 kts at 10,000 ft.
Climb:	10 min. to 10,000 ft.
Take-off and Landing:	2,500 ft fieldlength.
Powerplant:	Piston-propeller, single engine.
Pressurization:	None.
Certification Base:	Experimental. Use FAR 23 for Take-off and landing.

Determine W_{TO}, W_E and W_F for this airplane.

Calculate the sensitivity of W_{TO} to R, c_p and η_p.

5.) A supersonic cruise airplane has the following mission specification:

Payload:	300 passengers at 175 lbs each and 30 lbs of baggage each.
Crew:	Two pilots and ten cabin attendants at 175 lbs each and 30 lbs baggage each.
Range:	3,500 nm, followed by 1 hour loiter, followed by a 100 nm flight to an alternate airport.
Altitude:	75,000 ft (for the design range).
Cruise Speed:	Mach 2.7.
Climb:	Direct to 75,000 ft at W_{TO}.
Take-off and Landing:	10,000 ft FAR fieldlength, 95° day, at sealevel. Assume that $W_L = 0.8W_{TO}$.
Powerplants:	At least three turbofans. These could be fitted for afterburning, if needed.
Pressurization:	7,500 ft cabin at 75,000 ft.
Certification Base:	FAR 25.

Determine W_{TO}, W_E and W_F for this airplane.

Find the sensitivities of W_{TO} to cruise range and to specific fuel consumption.

6.) A high altitude, unmanned communications airplane has the following mission specification:

Payload:	2,000 lbs.
Crew:	Not applicable.
Range:	1,000 nm out and 1,000 nm in. No reserves.
Endurance:	168 hours (= 7 days) on station.
Cruise Speed:	250 kts is desired.
Loiter Altitude:	85,000 ft.
Loiter Speed:	At least 35 kts, to cope with prevailing winds.
Take-off and Landing:	8,000 ft groundrun is acceptable. Assume that $W_L = 0.65W_{TO}$.
Powerplants:	Up to designer. Fuel must be JP4 or 5.

Determine W_{TO}, W_E and W_F for this vehicle.

Show how sensitive the vehicle is to changes in L/D, E and c_j or to c_p and η_p.

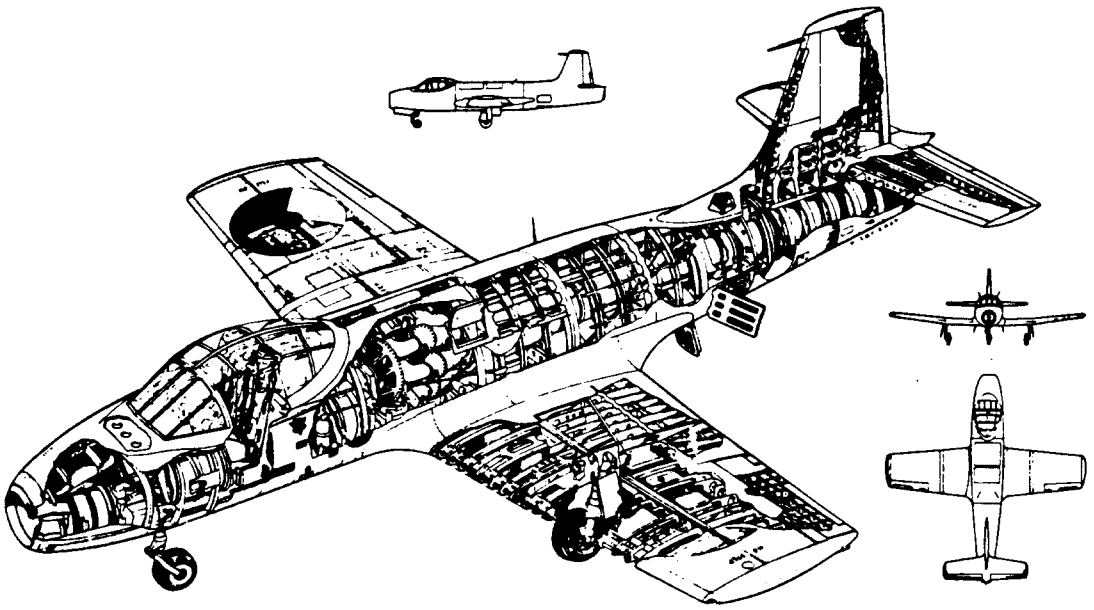

FOKKER S.14 'MACH TRAINER'

3. ESTIMATING WING AREA, S, TAKE-OFF THRUST, T_{TO} (OR TAKE-OFF POWER, P_{TO}) AND MAXIMUM LIFT COEFFICIENT, $C_{L_{max}}$: CLEAN, TAKE-OFF AND LANDING

In addition to meeting range, endurance and cruise speed objectives, airplanes are usually designed to meet performance objectives in the following categories:

a. Stall speed
b. Take-off field length
c. Landing field length
d. Cruise speed (sometimes maximum speed)
e. Climb rate (all engines operating, AEO and one engine inoperative, OEI)
f. Time to climb to some altitude
g. Maneuvering

In this chapter, methods will be presented which allow the rapid estimation of those airplane design parameters which have a major impact on the performance categories a) through f). The airplane design parameters are:

1. Wing Area, S
2. Take-off Thrust, T_{TO} or Take-off Power, P_{TO}
3. Maximum Required Take-off Lift Coefficient with flaps up: $C_{L_{max}}$ (clean)
4. Maximum Required Lift Coefficient for Take-off, $C_{L_{max_{TO}}}$
5. Maximum Required Lift Coefficient for Landing, $C_{L_{max_L}}$, or $C_{L_{max_{PA}}}$

The methods will result in the determination of a range of values of wing loading, W/S, thrust loading, T/W (or power loading, W/P) and maximum lift coefficient, $C_{L_{max}}$, within which certain performance requirements are met. From these data it usually follows that the combination of the highest possible wing loading and the

lowest possible thrust loading (or power loading) which still meets all performance requirements results in an airplane with the lowest weight and the lowest cost.

Since W_{TO} was already determined with the methods of Chapter 2, it is clear that now S and T_{TO} can also be determined.

3.1 SIZING TO STALL SPEED REQUIREMENTS

For some airplanes the mission task demands a stall speed not higher than some minimum value. In such a case, the mission specification will include a requirement for a minimum stall speed.

FAR 23 certified single engine airplanes may not have a stall speed greater than 61 kts at W_{TO}.

In addition, FAR 23 certified multiengine airplanes with $W_{TO} < 6{,}000$ lbs must also have a stall speed of no more than 61 kts, unless they meet certain climb gradient criteria (Ref. 8, Par. 23.49).

These stall speed requirements can be met flaps-up or flaps-down at the option of the designer.

There are no requirements for minimum stall speed in the case of FAR 25 certified airplanes.

The power-off stall speed of an airplane may be determined from:

$$V_s = \{2(W/S)/\rho C_{L_{max}}\}^{1/2} \longrightarrow \text{Clean aircraft} \qquad (3.1)$$

By specifying a maximum allowable stall speed at some altitude, Eqn. (3.1) defines a maximum allowable wing loading W/S for a given value of $C_{L_{max}}$.

Table 3.1 presents typical values of $C_{L_{max}}$ for different types of airplanes with associated flap settings.

The reader should recognize the fact that $C_{L_{max}}$ is strongly influenced by such factors as:

1. Wing and airfoil design
2. Flap type and flap size
3. Center of gravity location

Table 3.1 Typical Values For Maximum Lift Coefficient

Airplane Type	$C_{L_{max}}$	$C_{L_{max_{TO}}}$	$C_{L_{max_L}}$
1. Homebuilts	1.2 - 1.8	1.2 - 1.8	1.2 - 2.0*
2. Single Engine Propeller Driven	1.3 - 1.9	1.3 - 1.9	1.6 - 2.3
3. Twin Engine Propeller Driven	1.2 - 1.8	1.4 - 2.0	1.6 - 2.5
4. Agricultural	1.3 - 1.9	1.3 - 1.9	1.3 - 1.9
5. Business Jets	1.4 - 1.8	1.6 - 2.2	1.6 - 2.6
6. Regional TBP	1.5 - 1.9	1.7 - 2.1	1.9 - 3.3
7. Transport Jets	1.2 - 1.8	1.6 - 2.2	1.8 - 2.8
8. Military Trainers	1.2 - 1.8	1.4 - 2.0	1.6 - 2.2
9. Fighters	1.2 - 1.8	1.4 - 2.0	1.6 - 2.6
10. Mil. Patrol, Bomb and Transports	1.2 - 1.8	1.6 - 2.2	1.8 - 3.0
11. Flying Boats, Amphibious and Float Airplanes	1.2 - 1.8	1.6 - 2.2	1.8 - 3.4
12. Supersonic Cruise Airplanes	1.2 - 1.8	1.6 - 2.0	1.8 - 2.2

* The Rutan Varieze reaches 2.5, based on stall speed data from Ref.9.

Notes: 1. The data in this table reflect existing (1984) flap design practice.

2. Considerably higher values for maximum lift coefficient are possible with more sophisticated flap designs and/or with some form of circulation control.

3. Methods for computing $C_{L_{max}}$ values are contained in Ref.6.

Reference 5 presents methods for computing $C_{L_{max}}$ while accounting for these three factors.

During the preliminary sizing process it suffices to 'select' a value for $C_{L_{max}}$ consistent with the mission requirements and consistent with the type of flaps to be employed.

An example of stall speed sizing will now be discussed.

3.1.1 Example of Stall Speed Sizing

Assume that the following marketing requirement must be met:

A propeller driven airplane must have a power-off stall speed of no more than 50 kts at sealevel with flaps full down (i.e. landing flaps). With flaps up the stall speed is to be less than 60 kts. Both requirements are to be met at take-off gross weight, W_{TO}.

From Table 3.1 it is seen that the following maximum lift coefficient values are within the 'state-of-the-art':

$$C_{L_{max}} = 1.60 \text{ and } C_{L_{max_L}} = 2.00$$

With the help of Eqn.(3.1) it now follows that:

To meet the flaps down requirement:
$(W/S)_{TO} < 17.0$ psf.

To meet the flaps up requirement:
$(W/S)_{TO} < 19.5$ psf.

Therefore, to meet both requirements, the take-off wing loading, $(W/S)_{TO}$ must be less than 17.0 psf.

Figure 3.1 illustrates this. Because the stall speed requirement was formulated as a power-off requirement, neither power loading nor thrust loading are important in this case.

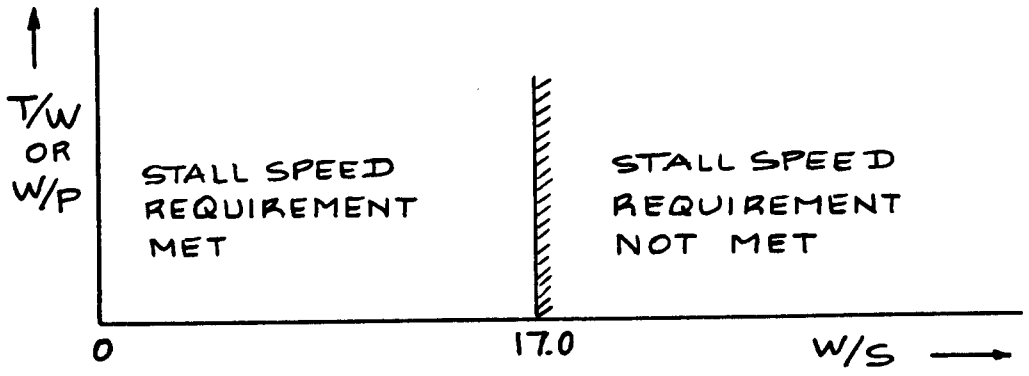

Figure 3.1 Example of Stall Speed Sizing

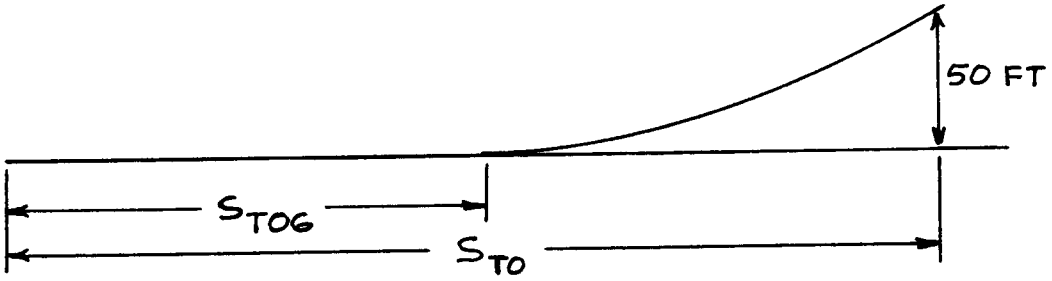

Figure 3.2 Definition of FAR 23 Take-off Distances

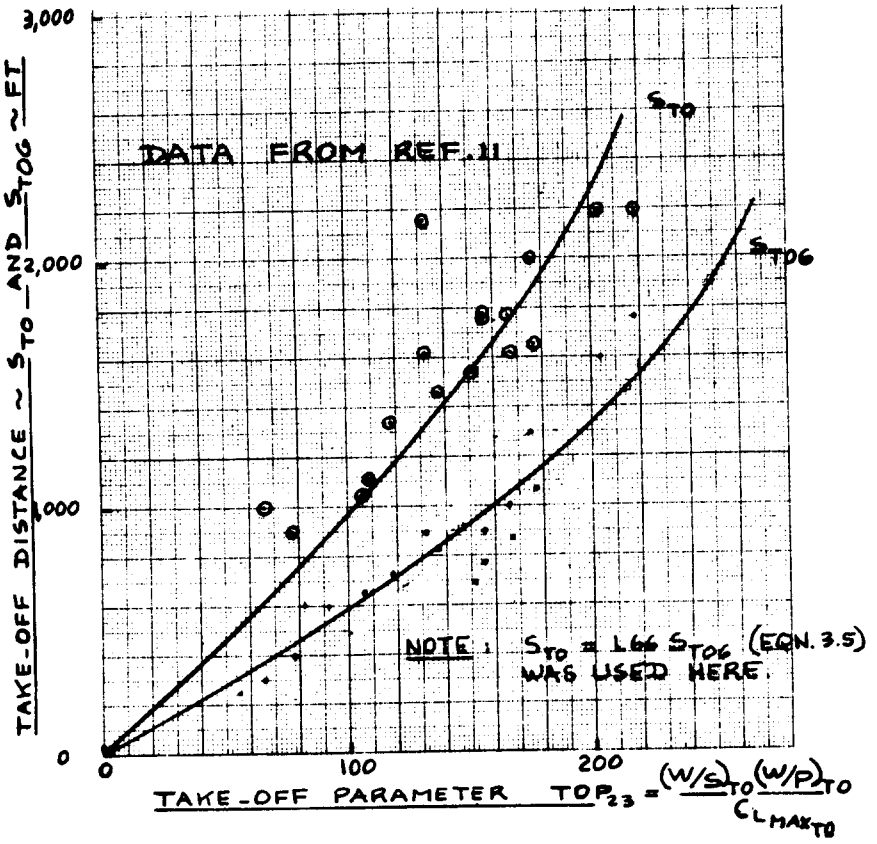

Figure 3.3 Effect of Take-off Parameter, TOP_{23} on Take-off Distances

3.2 SIZING TO TAKE-OFF DISTANCE REQUIREMENTS

Take-off distances of airplanes are determined by the following factors:

1. Take-off weight, W_{TO}
2. Take-off speed, V_{TO} (also called lift-off speed)
3. Thrust-to-weight ratio at take-off, $(T/W)_{TO}$ (or weight-to-power ratio, $(W/P)_{TO}$ and the corresponding propeller characteristics)
4. Aerodynamic drag coefficient, C_{D_G} and ground friction coefficient, μ_G
5. Pilot technique

In this section it will be assumed, that take-offs take place from hardened surfaces (concrete or asphalt) unless otherwise stated.

Take-off requirements are normally given in terms of take-off field length requirements. These requirements differ widely and depend on the type of airplane under consideration.

For civil airplanes, the requirements of FAR 23 and FAR 25 must be adhered to. In the case of homebuilt airplanes it is not necessary to design to the FAR's. In that case, the individual designer may set his own take-off requirements.

For military airplanes the requirements are usually set forth in the so-called Request-for-Proposal or RFP. All take-off calculations for military airplanes must be done with the definitions of Reference 15.

Depending on the type of mission, the take-off requirements are frequently spelled out in terms of minimum ground run requirements in combination with some minimum climb capability. For Navy airplanes with carrier capability, the limitations of the catapult system on the carrier must be accounted for.

Sub-sections (3.2.1) through (3.2.6) address the sizing to take-off requirements for airplanes with essentially mechanical flap systems. For airplanes with 'augmented' flaps systems or for vectored thrust airplanes the reader should consult Refs. 12 and 13.

3.2.1 Sizing to FAR 23 Take-off Distance Requirements

Figure 3.2 presents a definition of take-off distances used in the process of sizing an airplane to FAR 23 requirements. FAR 23 airplanes usually are propeller driven airplanes.

In Reference 11 it is shown, that the take-off ground run, s_{TOG} of an airplane is proportional to take-off wing loading $(W/S)_{TO}$, take-off power loading, $(W/P)_{TO}$ and to the maximum take-off lift coefficient, $C_{L_{max_{TO}}}$:

$$s_{TOG} \propto (W/S)_{TO}(W/P)_{TO}/\sigma C_{L_{max_{TO}}} = TOP_{23}, \qquad (3.2)$$

where TOP_{23} is the so-called take-off parameter for FAR 23 airplanes. Its dimension is lbs^2/ft^2hp.

The reader should keep in mind, that the lift coefficient at lift-off, $C_{L_{TO}}$ is related to the maximum take-off lift coefficient, $C_{L_{max_{TO}}}$ by:

$$C_{L_{TO}} = C_{L_{max_{TO}}}/1.21 \qquad (3.3)$$

Figure 3.3 relates s_{TOG} to the take-off parameter, TOP_{23} for a range of range of single and twin engine FAR 23 certified airplanes. Figure 3.4 relates s_{TO} and s_{TOG} to each other. There is a lot of scatter in the data. One reason is, that take-off procedures vary widely. Another is that take-off thrust depends strongly on propeller characteristics. Finally, take-off rotation to lift-off attitude depends on control power, control feel and on airplane inertia. Nevertheless, it is useful to employ the correlation lines of Figures 3.3 and 3.4 in the preliminary sizing process. The correlation lines drawn suggest the following relationships:

$$s_{TOG} = 4.9TOP_{23} + 0.009TOP_{23}^2 \qquad (3.4)$$

and, since Figure 3.4 implies:

$$s_{TO} = 1.66s_{TOG} \qquad (3.5)$$

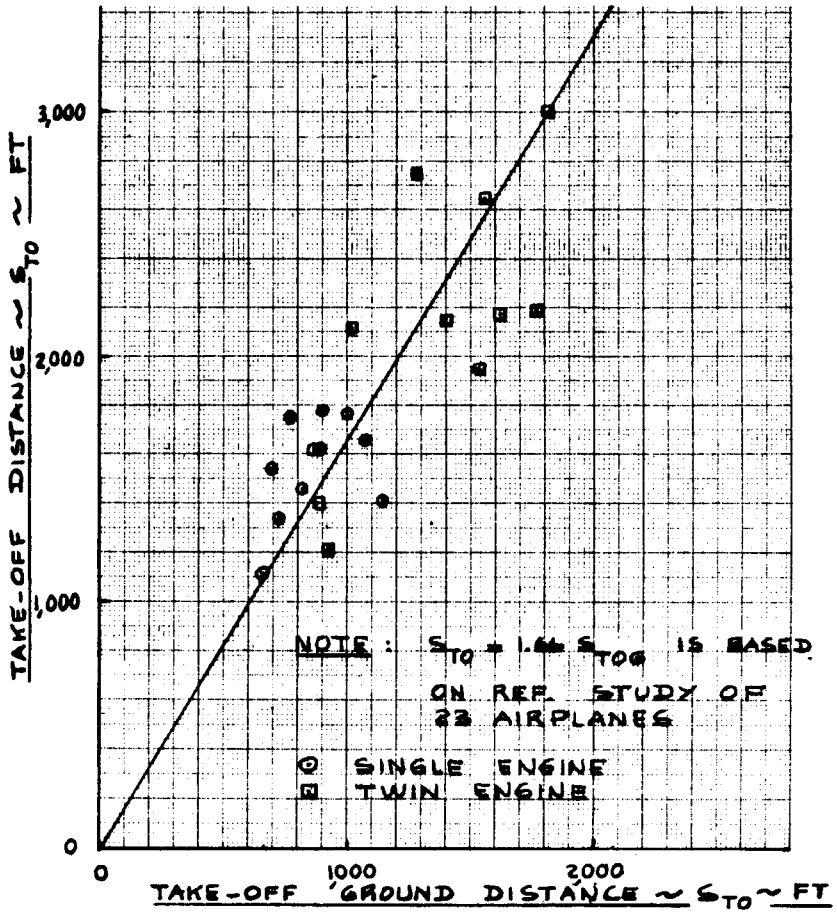

Figure 3.4 Correlation of Ground Distance and Total Distance for Take-off (FAR 23)

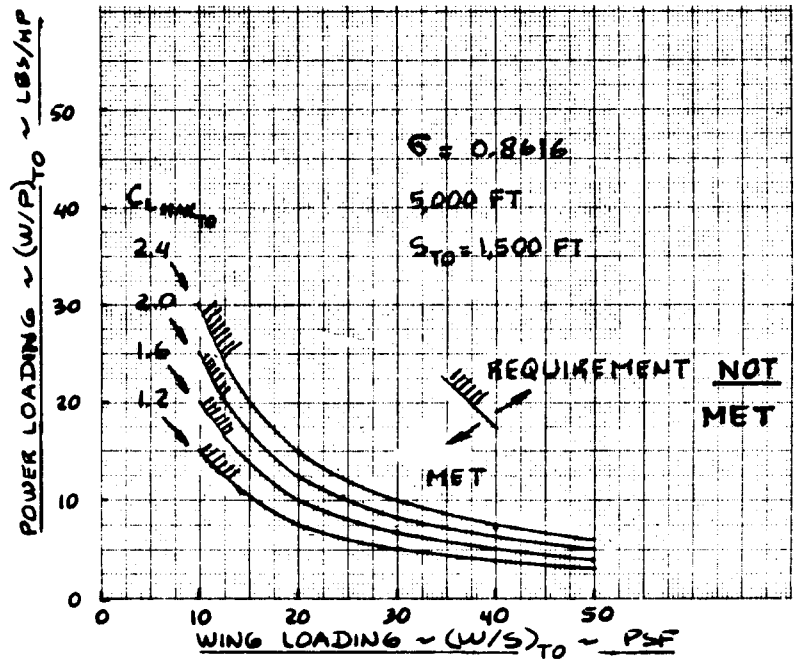

Figure 3.5 Effect of Take-off Wing Loading and Maximum Take-off Lift Coefficient on Take-off Power Loading

it follows that:

$$s_{TO} = 8.134TOP_{23} + 0.0149TOP_{23}^2 \qquad (3.6)$$

The assumption was made that FAR 23 airplanes are nearly always propeller driven airplanes. For jet airplanes the parameter W/P in Eqn.(3.2) should be replaced by W/T. The reader is advised to use the sizing procedure of 3.2.3 for FAR 23 jet airplanes.

An example of FAR 23 take-off sizing will now be discussed.

3.2.2 Example of FAR 23 Take-off Distance Sizing

Assume that it is required to size a propeller-driven airplane to the following take-off criteria:

$s_{TOG} < 1,000$ ft and $s_{TO} < 1,500$ ft at an altitude of 5,000 ft in standard atmosphere.

Since Eqn.(3.5) stipulates that s_{TOG} and s_{TO} are related to each other, the first requirement translates into:

$$s_{TO} < 1,660 \text{ ft.}$$

This clearly violates the second requirement. Therefore the second requirement dominates. From Eqn.(3.5) it follows that for both take-off requirements to be met, it is necessary that:

$$1,500 = 8.134TOP_{23} + 0.0149TOP_{23}^2$$

From this in turn it follows that:

$$TOP_{23} = 145.6 \text{ lbs}^2/\text{ft}^2\text{hp}$$

Since $\sigma = 0.8616$ at 5,000 ft, this result when combined with Eqn.(3.2) translates into:

$$(W/S)_{TO}(W/P)_{TO}/C_{L_{max_{TO}}} < 145.6 \times 0.8616 = 125.4 \text{ lbs}^2/\text{ft}^2\text{hp}$$

The following tabulation can now be made for the required values of $(W/P)_{TO}$:

$(W/S)_{TO}$ psf	$C_{L_{max_{TO}}}$ =	1.2	1.6	2.0	2.4
10	$(W/P)_{TO}$ =	15.0	20.1	25.1	30.1
~~30~~		5.0	6.7	8.4	10.0
50		3.0	4.0	5.0	6.0

Figure 3.5 translates this tabulation into regions of $(W/S)_{TO}$ and $(W/P)_{TO}$ for given values of $C_{L_{max_{TO}}}$ so that the take-off distance requirement is satisfied.

3.2.3 Sizing to FAR 25 Take-off Distance Requirements

Figure 3.6 defines those quantities important to FAR 25 take-off field length requirements.

In Reference 11 it is shown that the take-off field length, s_{TOFL} is proportional to take-off wing loading, $(W/S)_{TO}$, take-off thrust-to-weight ratio, $(T/W)_{TO}$ and to maximum take-off lift coefficient, $C_{L_{max_{TO}}}$:

$$s_{TOFL} \propto (W/S)_{TO}/\{\sigma C_{L_{max_{TO}}} (T/W)_{TO}\} = TOP_{25}, \qquad (3.7)$$

where TOP_{25} is the take-off parameter for FAR 25 certified airplanes. Its dimension is lbs/ft^2.

Figure 3.7 shows that the relationship expressed by Eqn.(3.7) can be written as:

$$s_{TOFL} = 37.5(W/S)_{TO}/\{\sigma C_{L_{max_{TO}}} (T/W)_{TO}\} = 37.5TOP_{25} \qquad (3.8)$$

Typical values for $C_{L_{TO_{max}}}$ can be found in Table 3.1.

FAR 25 certified airplanes can be both jet-driven or propeller-driven (for example prop-fans or turboprops). In the case of propeller-driven airplanes it is necessary to convert the value of T/W required in take-off to the corresponding value of W/P. Figure 3.8 shows how this can be done, depending on the assumed propeller characteristics.

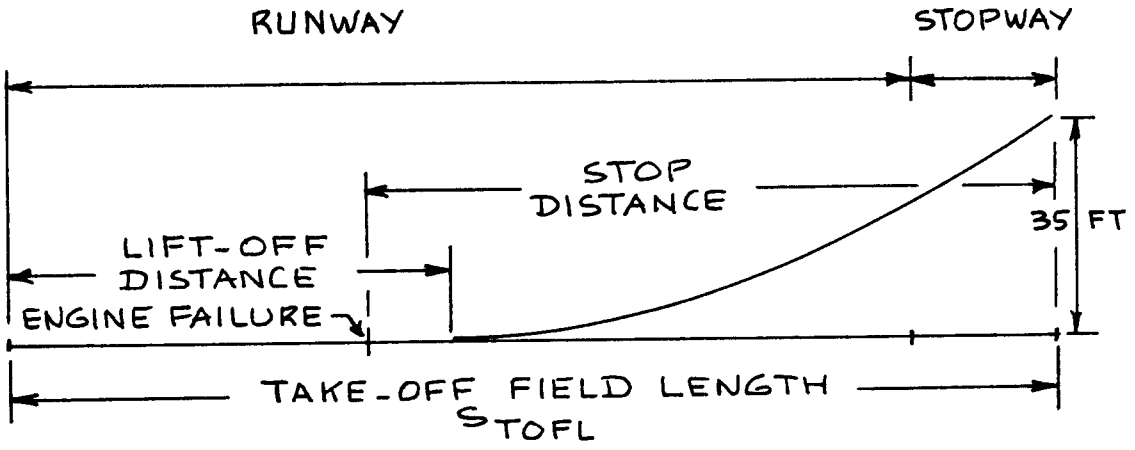

Figure 3.6 Definition of FAR 25 Take-off Distances

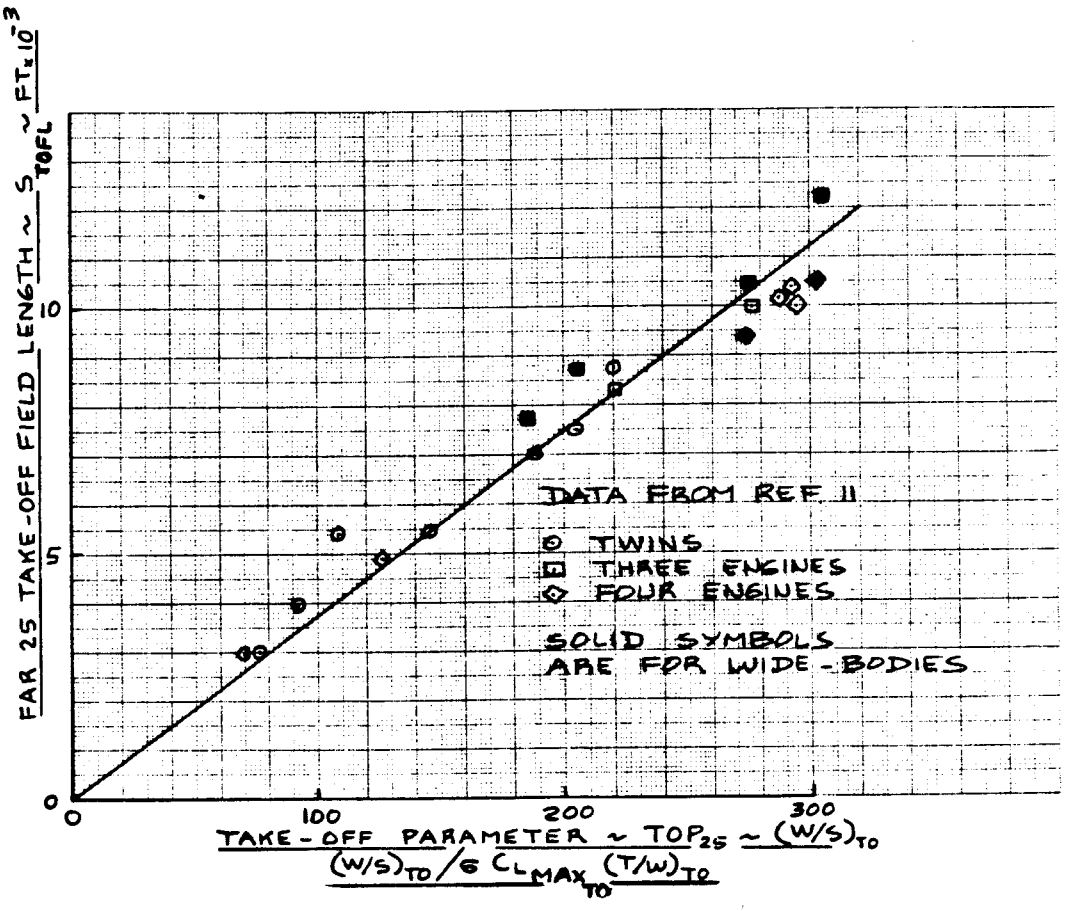

Figure 3.7 Effect of Take-off Parameter, TOP_{25} on FAR 25 Take-off Field Length

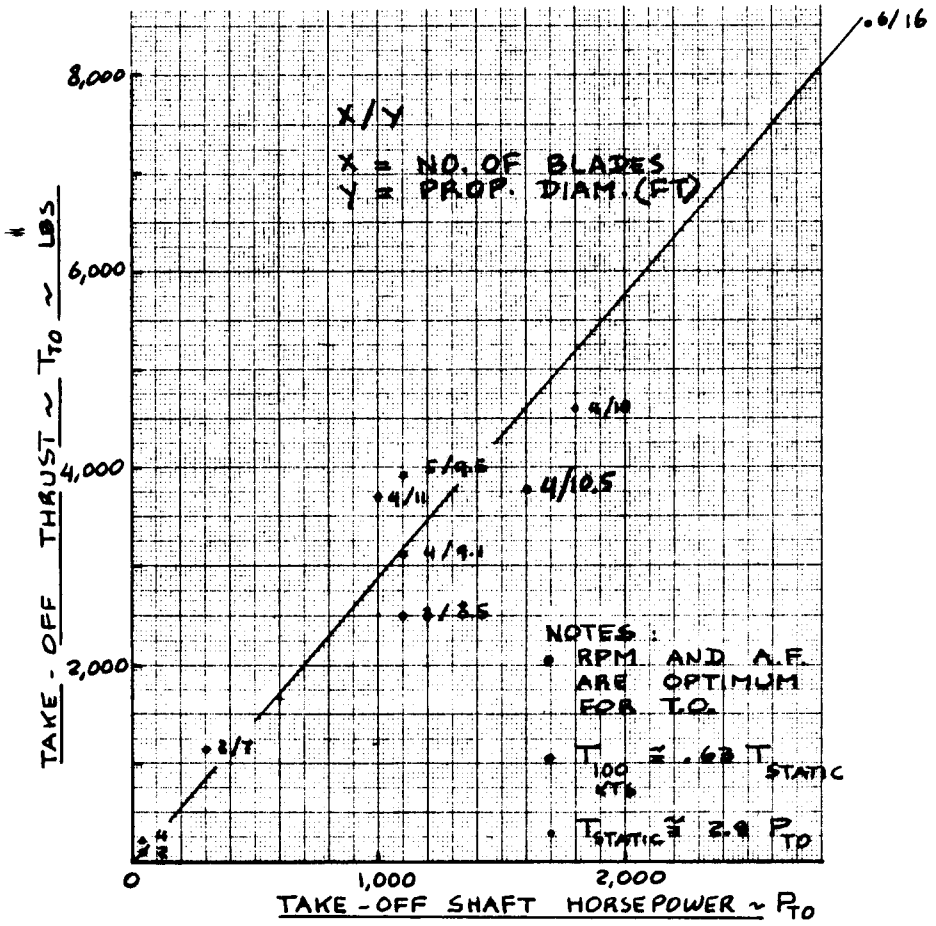

Figure 3.8 Effect of Shaft Horsepower on Take-off Thrust

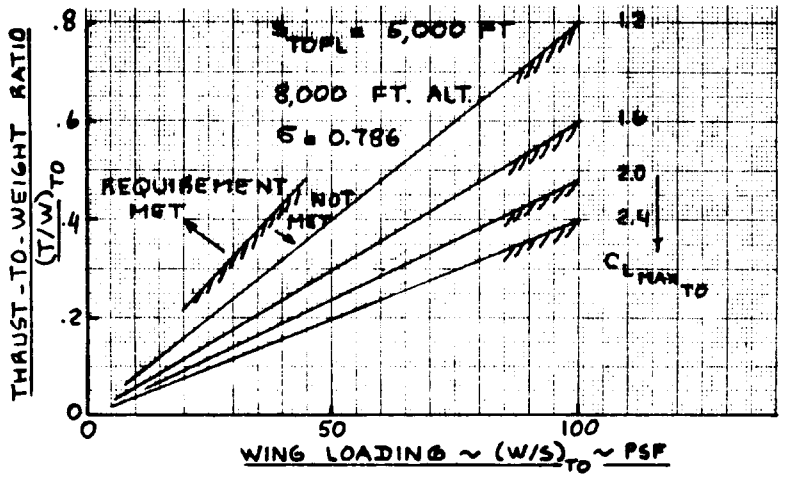

Figure 3.9 Effect of Take-off Wing Loading and Maximum Take-off Lift Coefficient on Take-off Thrust-to-Weight Ratio

3.2.4 Example of FAR 25 Take-off Distance Sizing

It is required to size a passenger airplane so that the FAR 25 fieldlength is given by:

s_{TOFL} < 5,000 ft at 8,000 ft standard atmosphere

From Eqn.(3.8) it is seen, that the fieldlength requirement will be satisfied as long as:

TOP_{25} = 5,000/37.5 = 133.3 lbs/ft^2

At 8,000 ft, σ = 0.786. Therefore with Eqn.(3.7):

$(W/S)_{TO}/\{C_{L_{max_{TO}}} (T/W)_{TO}\}$ = 133.3x0.786 = 104.8 lbs/ft^2

The following tabulation can now be made for the required values of $(T/W)_{TO}$:

$(W/S)_{TO}$ psf	$C_{L_{max_{TO}}}$ =	1.2	1.6	2.0	2.4
40	$(T/W)_{TO}$ =	0.32	0.24	0.19	0.16
60		0.48	0.36	0.29	0.24
80		0.64	0.48	0.38	0.32
100		0.80	0.60	0.48	0.40

Figure 3.9 illustrates the range of values of $(W/S)_{TO}$, $(T/W)_{TO}$ and $C_{L_{max_{TO}}}$ for which the fieldlength requirement is satisfied.

3.2.5 Sizing to Military Take-off Distance Requirements

3.2.5.1 Land based airplanes

Reference 15 defines the military take-off field length as that in Figure 3.6 except for the obstacle height, which is 50 ft instead of 35 ft.

Military take-off requirements are frequently specified in terms of maximum allowable groundrun, s_{TOG}.

The groundrun may be estimated from:

$$s_{TOG} = \frac{k_1 (W/S)_{TO}}{\rho [C_{L_{max_{TO}}} \{k_2 (X/W)_{TO} - \mu_G\} - 0.72 C_{D_o}]} \qquad (3.9)$$

This equation is a variation of Eqn.(5-75) in Ref.16. It assumes that the following conditions prevail:

a. no wind
b. level runway

The quantities k_1, k_2 and X, are defined as follows:

for jets:	for props:
$X = T$	$X = P$
$k_1 = 0.0447$	$k_1 = 0.0376$
$k_2 = 0.75 \frac{(5 + \lambda)}{(4 + \lambda)}$	$k_2 = l_p (\sigma N D_p^2 / P_{TO})^{1/3}$
λ = engine bypass ratio	for constant speed props: $l_p = 5.75$
	for fixed pitch props: $l_p = 4.60$

The term P_{TO}/ND_p^2 is the propeller disk loading. Note, that P_{TO} stands for the total take-off power with all engines operating. N is the number of engines. Typical values for propeller disk loading can be deduced from the data in Ref.9. Lacking such data it is suggested to use the following ranges:

Typical Propeller Disk Loadings in hp/ft^2

Singles	Light Twins	Heavy Twins	Turboprops
3-8	6-10	8-14	10-30

Equation (3.9) applies whenever power or thrust effects on lift can be neglected. If this is not the case the reader is referred to Refs. 12 and 13.

Table 3.2 gives typical values for the ground friction coefficient, μ_G for different surfaces.

Table 3.2 Ground Friction Coefficient, μ_G

Surface Type	μ_G	
Concrete	0.02 - 0.03	(0.025 per Ref.15)
Asphalt	0.02 - 0.03	
Hard Turf	0.05	
Short Grass	0.05	
Long Grass	0.10	
Soft Ground	0.10 - 0.30	

3.2.5.2 Carrier based airplanes

For carrier based airplanes, the limitations of the catapult system need to be accounted for. These limitations are usually stated in terms of relations between take-off weight and launch speed at the end of the catapult, V_{cat}. Figure 3.10 provides some data for existing catapult systems used by the USNavy.

At the end of the catapult stroke, the following relationship must be satisfied:

$$0.5\rho(V_{wod} + V_{cat})^2 SC_{L_{max_{TO}}} / 1.21 = W_{TO} \qquad (3.10)$$

From Eqn.(3.10) it is possible to determine the range of values for W/S, T/W and $C_{L_{max_{TO}}}$ which ensure staying within catapult capabilities.

3.2.6 Example of Sizing to Military Take-off Distance Requirements

It is required to size a Navy attack airplane such that:

a) for land based take-offs: $s_{TOG} < 2{,}500$ ft at sealevel, standard atmosphere, concrete runways.

b) for carrier take-offs: with $V_{wod} = 25$ kts the airplane is to be compatible with the Mark C13 catapult system.

Figure 3.11 shows the range of values of W_{TO}/S,

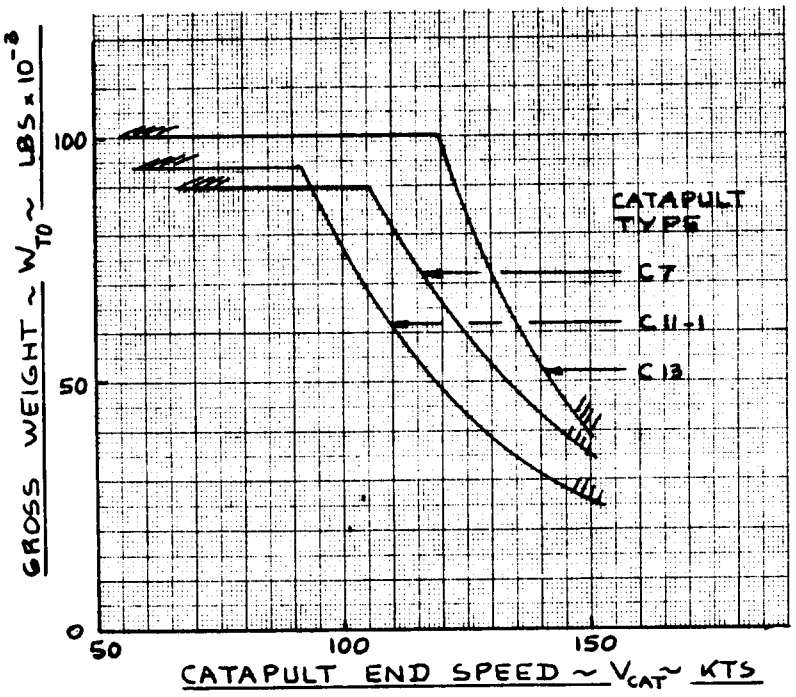

Figure 3.10 Effect of Take-off Weight on Catapult End Speed for Three Types of Catapult

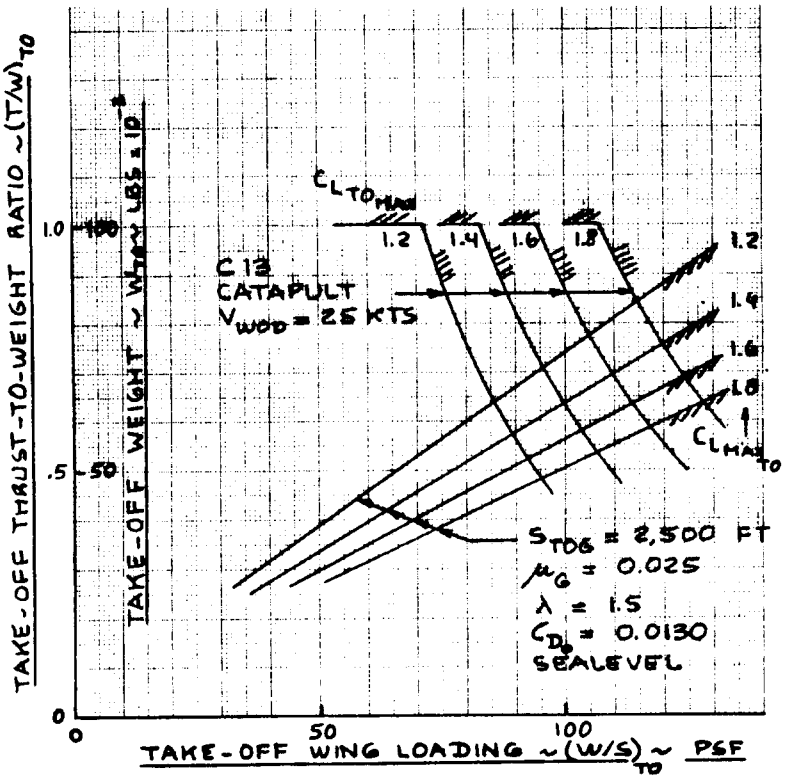

Figure 3.11 Effect of Maximum Take-off Lift Coefficient and Catapult Limitations on Weight, Wing Loading and Thrust-to-Weight Ratio at Take-off

$(T/W)_{TO}$ and $C_{L_{max_{TO}}}$, which satisfy the land based groundrun requirement for $\mu_G = 0.025$, for an assumed bypass ratio of $\lambda = 1.5$ and for an assumed zero-lift drag coefficient of $C_{D_o} = 0.0130$.

The C13 catapult data of Figure 3.10 indicate that $W_{TO} < 100{,}000$ lbs must always be satisfied. Below that weight, Figure 3.10 shows the following relationship between weight and catapult speed:

Take-off Weight, W_{TO} (lbs)	Catapult Speed, V_{cat} (kts)
100,000	120
72,000	130
53,000	140
39,000	150

Eqn.(3.10) can be used to relate values of take-off weight, W_{TO} to allowable take-off wing loadings, $(W/S)_{TO}$ for different take-off lift coefficients, $C_{L_{max_{TO}}}$

Figure 3.11 shows the results for a WOD of 25 kts.

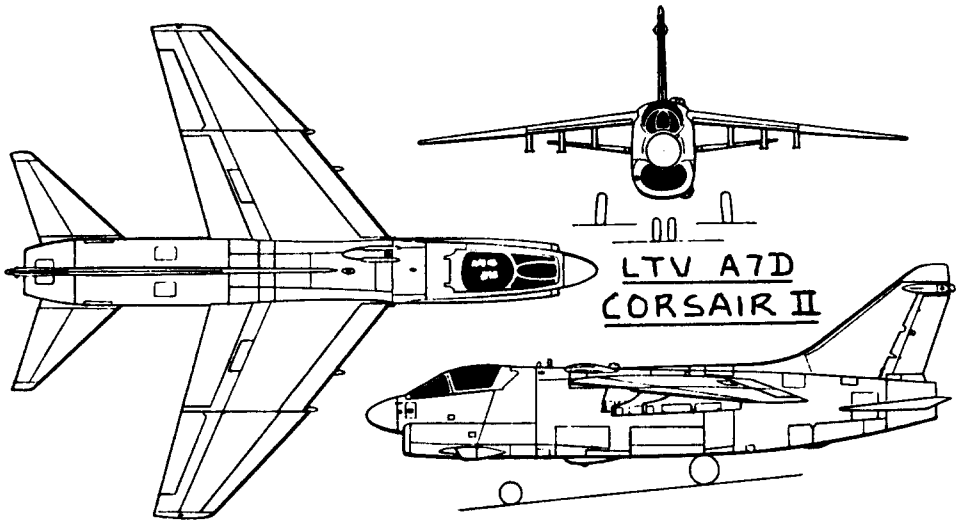

3.3. SIZING TO LANDING DISTANCE REQUIREMENTS

Landing distances of airplanes are determined by four factors:

1. Landing Weight, W_L
2. Approach speed, V_A
3. Deceleration method used
4. Flying qualities of the airplane
5. Pilot technique

Landing distance requirements are nearly always formulated at the design landing weight, W_L of an airplane. Table 3.3 shows how W_L is related to W_{TO} for twelve types of airplanes.

Kinetic energy considerations suggest that the approach speed should have a'square' effect on the total landing distance. After an airplane has touched down, the following deceleration methods can be used:

a. Brakes
b. Thrust reversers
c. Parachutes
d. Arresting systems (field-based or carrier-based)
e. Crash barriers

Data presented in this section are based on existing industry practice in decelerating airplanes after touchdown.

For civil airplanes, the requirements of FAR 23 and FAR 25 are in force. In the case of homebuilt airplanes, it is not necessary to design to FAR landing distance requirements.

For military airplanes the requirements are usually laid down in the RFP. Ground runs are sometimes specified without their accompanying air distances.

In the case of Navy airplanes the capabilities of the on deck arresting system need to be taken into consideration.

Table 3.3 Typical Values For Landing Weight to Take-off Weight Ratio

Airplane Type	W_L/W_{TO} Minimum	Average	Maximum
1. Homebuilts	0.96	1.0	1.0
2. Single Engine Propeller Driven	0.95	0.997	1.0
3. Twin Engine Propeller Driven	0.88	0.99	1.0
4. Agricultural	0.7	0.94	1.0
5. Business Jets	0.69	0.88	0.96
6. Regional TBP	0.92	0.98	1.0
7. Transport Jets	0.65	0.84	1.0
8. Military Trainers	0.87	0.99	1.1
9. Fighters (jets)	0.78	insufficient	1.0
(tbp's)	0.57	data	1.0
10. Mil. Patrol, Bomb and Transports (jets)	0.68	0.76	0.83
(tbp's)	0.77	0.84	1.0
11. Flying Boats, Amphibious and Float Airplanes (land)	0.79	insufficient	0.95
(water)	0.98	data	1.0
12. Supersonic Cruise Airplanes	0.63	0.75	0.88

Note: These data are based on Tables 2.3 through 2.14.

Sub-sections 3.3.1 through 3.3.6 address the sizing to landing requirements for airplanes with essentially mechanical flap systems. For airplanes with 'augmented' flaps or for vectored thrust airplanes the reader should consult Refs. 12 and 13.

3.3.1 Sizing to FAR 23 Landing Distance Requirements

Figure 3.12 presents a definition of landing distances used in the process of sizing an airplane to FAR 23 requirements.

The reader should note that the approach speed is specified as:

$$V_A = 1.3V_{s_L} \tag{3.11}$$

Figure 3.13 shows how the landing ground run, s_{LG} is related to the square of the stall speed, V_{s_L}. The stall speed here is that in the landing configuration: gear down, landing flaps and power-off.

The data in Figure 3.13 suggest the following relation:

$$s_{LG} = 0.265V_{s_L}^2 \tag{3.12}$$

Note, that the distance is in ft and the stall speed is in kts.

Figure 3.14 shows how the total landing distance, s_L is related to s_{LG}. This figure suggests the following relationship:

$$s_L = 1.938s_{LG} \tag{3.13}$$

By specifying the maximum allowable total landing distance, s_L, it is possible to find the corresponding landing groundrun, s_{LG}. From the latter the maximum allowable stall speed can be found. It was already shown in section 3.1 that this in turn can be translated into a relation between wing-loading $(W/S)_L$ and $C_{L_{max_L}}$.

It is often useful to combine Eqns.(3.12) and (3.13) into:

$$s_L = 0.5136V_{s_L}^2 \tag{3.14}$$

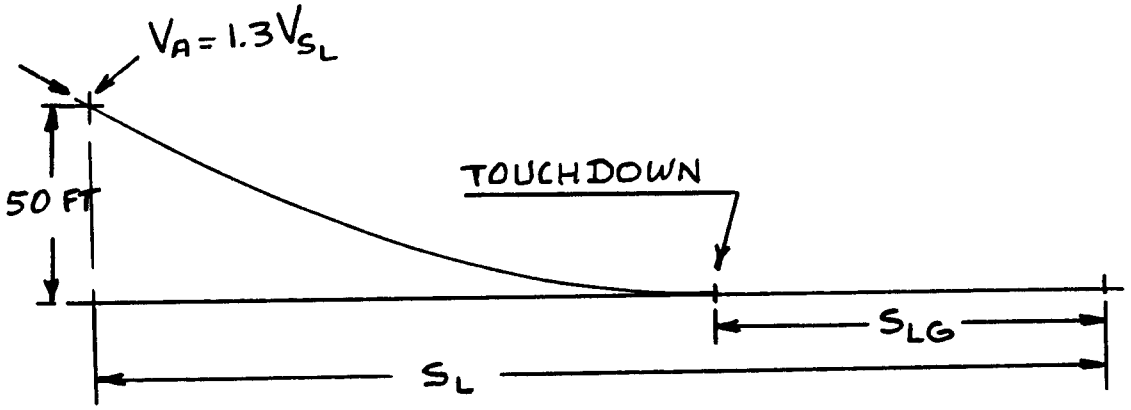

Figure 3.12 Definition of FAR 23 Landing Distances

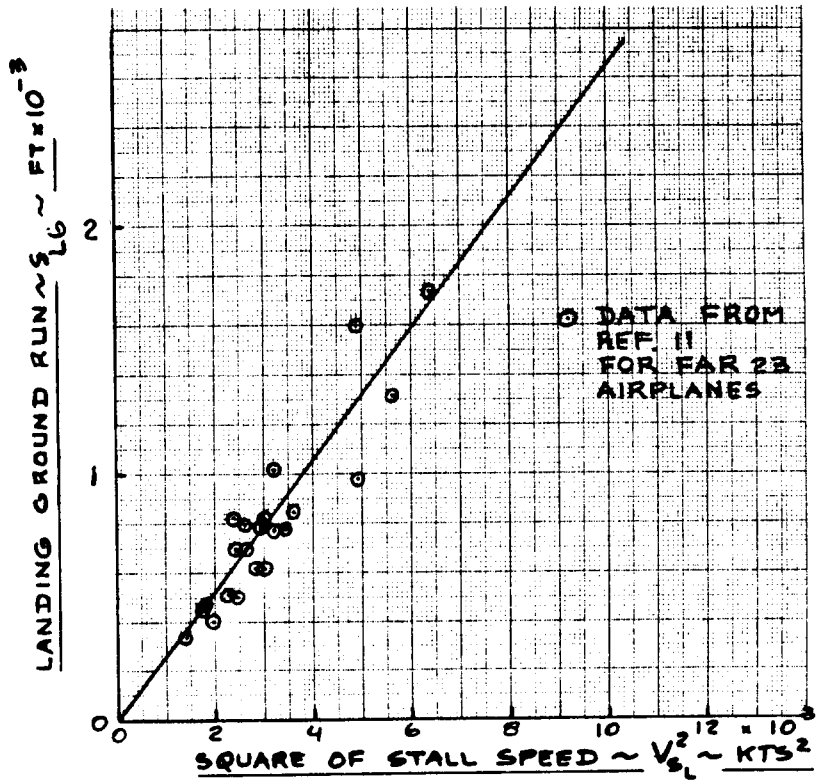

Figure 3.13 Effect of Square of Stall Speed on Landing Groundrun

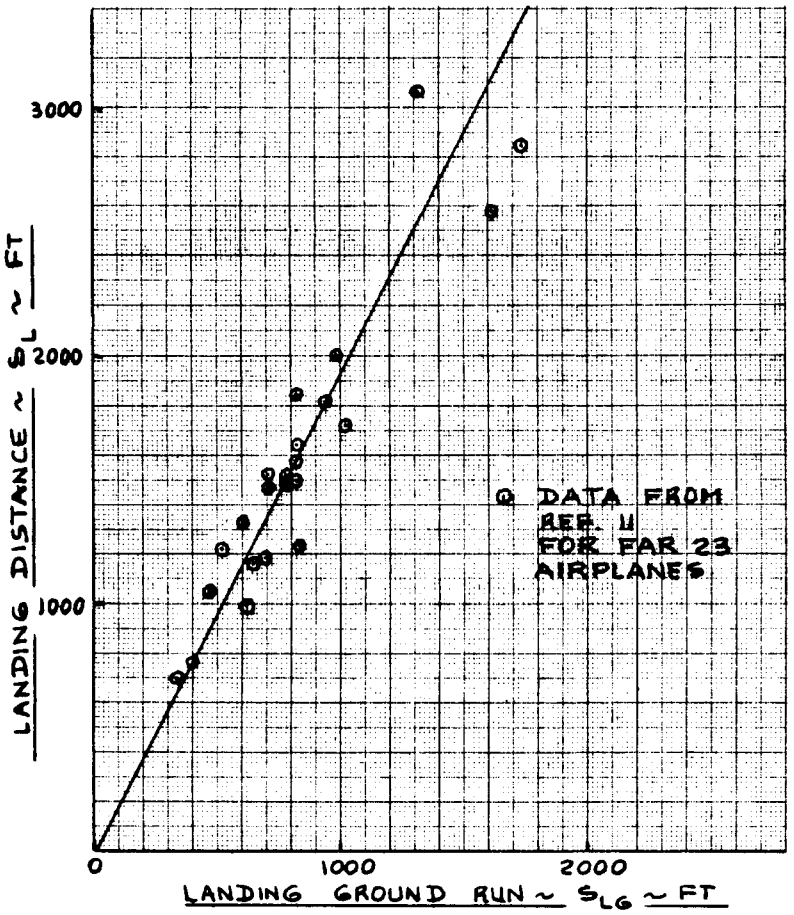

Figure 3.14 Correlation Between Groundrun and Landing Distance

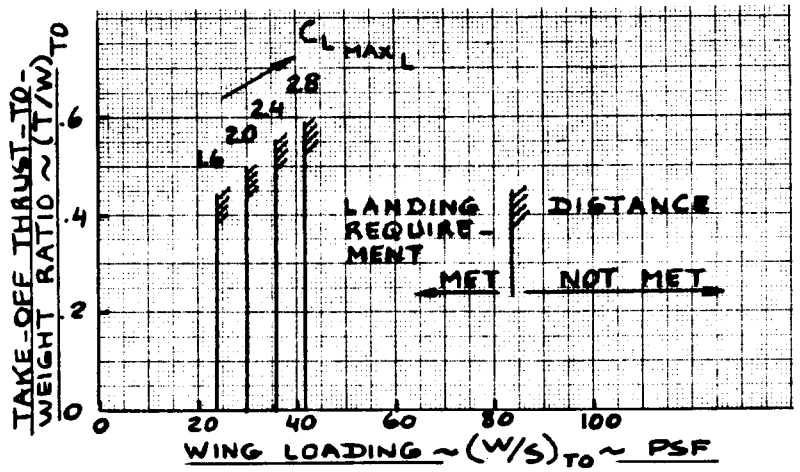

Figure 3.15 Allowable Wing Loadings to Meet a Landing Distance Requirement

3.3.2 Example of FAR 23 Landing Distance Sizing

It is required to size a propeller driven twin to a landing field length of 2,500 ft. at 5,000 ft altitude. The design landing weight is specified as: $W_L = 0.95W_{TO}$.

From Eqn.(3.14) it follows that:

$$V_{s_L} = \{2,500/0.5136\}^{1/2} = 69.8 \text{ kts}$$

With the help of Eqn.(3.1) this translates into the following requirement:

$$2(W/S)_L/0.002049C_{L_{max_L}} = (69.8x1.688)^2 = 13,869 \text{ ft}^2/\text{sec}^2$$

From this it follows that:

$$(W/S)_L = 14.2C_{L_{max_L}}$$

With $W_L = 0.95W_{TO}$, this yields:

$$(W/S)_{TO} = 14.9C_{L_{max_L}}$$

Figure 3.15 presents the range of values of $(W/S)_{TO}$ and $C_{L_{max_L}}$ which meet the landing distance requirement.

3.3.3 Sizing to FAR 25 Landing Distance Requirements

Figure 3.16 defines the quantities which are important in the FAR 25 field length requirements.

The FAR landing field length is defined as the total landing distance (Figure 3.16) divided by 0.6. This factor of safety is included to account for variations in pilot technique and other conditions beyond the control of FAA.

Note that the approach speed is always defined as:

$$V_A = 1.3V_{s_L} \tag{3.15}$$

Figure 3.17 relates the FAR field length to V_A^2:

$$s_{FL} = 0.3V_A^2, \tag{3.16}$$

where s_{FL} is in ft and V_A is in kts.

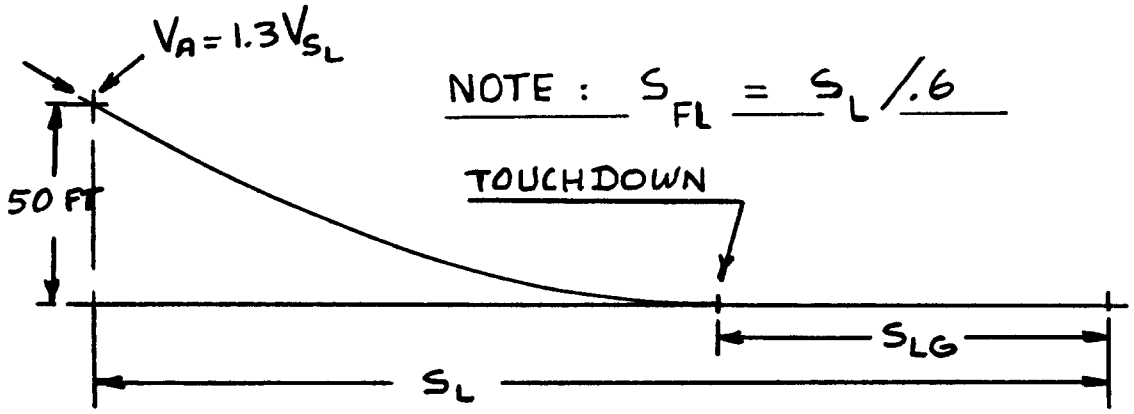

Figure 3.16 Definition of FAR 25 Landing Distances

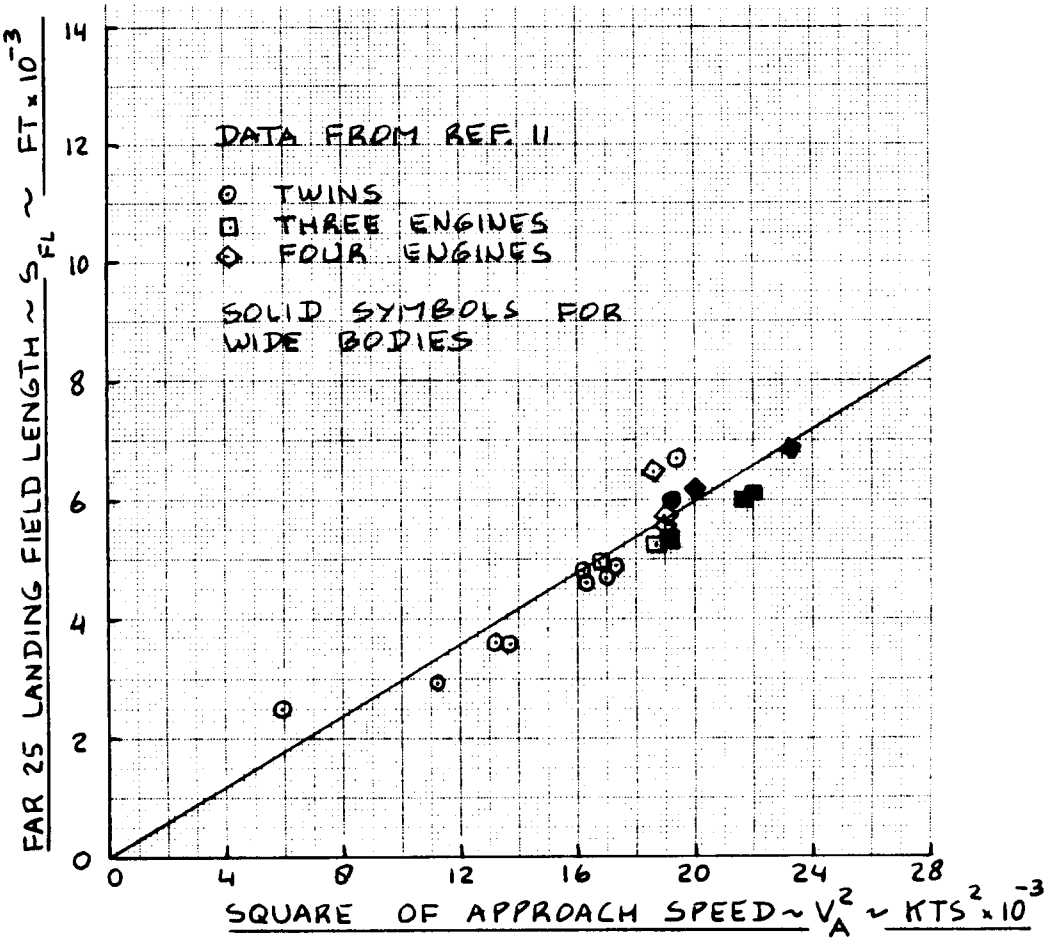

Figure 3.17 Effect of Square of Approach Speed on FAR 25 Field Length

With the help of Eqn.(3.1) and a requirement for a maximum acceptable landing field length it is again possible to relate $(W/S)_L$ (and thus $(W/S)_{TO}$) to $C_{L_{max_L}}$.

The reader will have observed that under FAR 23 the fieldlength is correlated with V_{S_L} while under FAR 25 it is correlated with V_A. The reason is that data available in the literature (such as Ref.9) tends to be presented in such a way as to force this type of correlation.

3.3.4 Example of FAR 25 Landing Distance Sizing

It is required to size a jet transport for a landing field length of 5,000 ft at sealevel on a standard day. It may be assumed, that: $W_L = 0.85W_{TO}$.

From Eqn.(3.16) it follows that:

$$V_A = (5{,}000/0.3)^{1/2} = 129.1 \text{ kts}$$

With Eqn.(3.15):

$$V_{S_L} = 129.1/1.3 = 99.3 \text{ kts.}$$

With Eqn.(3.1) this in turn yields:

$$2(W/S)_L/0.002378C_{L_{max_L}} = (99.3 \times 1.688)^2 = 28{,}100 \text{ ft}^2/\text{sec}^2$$

Therefore:

$$(W/S)_L = 33.4C_{L_{max_L}}, \text{ so that:}$$

$$(W/S)_{TO} = (33.4/0.85)C_{L_{max_L}} = 39.3C_{L_{max_L}}$$

Figure 3.18 illustrates how $(W/S)_{TO}$ and $C_{L_{max_L}}$ are related to satisfy the stated field length requirement.

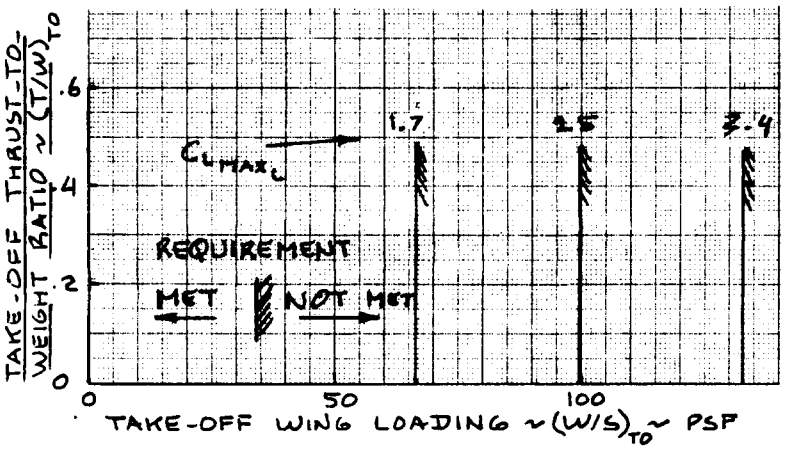

Figure 3.18 Allowable Wing Loadings to Meet a Field Length Requirement

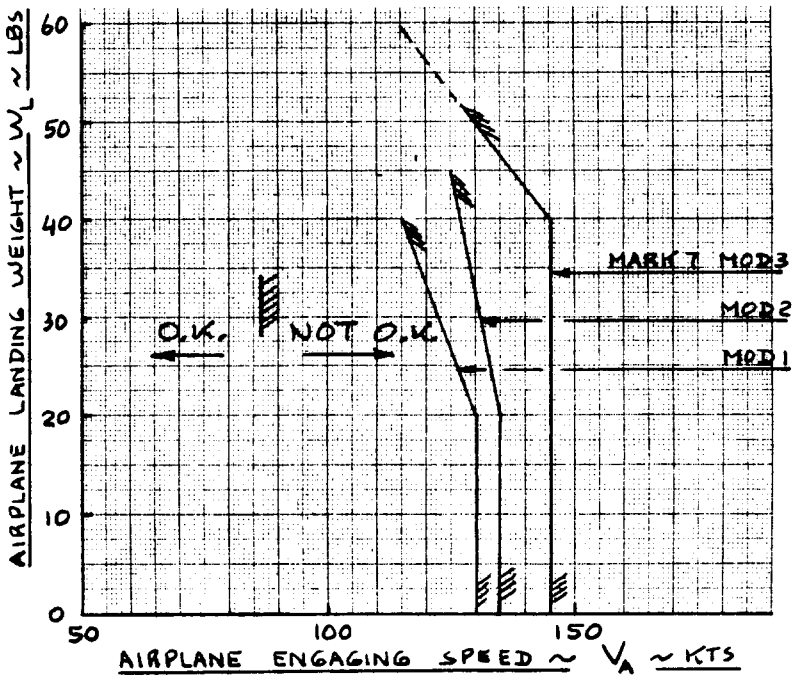

Figure 3.19 Performance Limitations of Three Types of Arresting Gears

3.3.5 Sizing to Military Landing Distance Requirements

3.3.5.1 Land based airplanes

Military requirements for landing distances are normally defined in the RFP. The sizing methods for FAR 25 can be employed with one proviso: military approach speeds are usually less than those of commercial airplanes. From Reference 15:

$$V_A = 1.2V_{s_L} \tag{3.17}$$

The effect of this is to decrease the landing distance by the square of the approach speed ratio.

3.3.5.2 Carrier based airplanes

For carrier based airplanes, the approach speed is usually given by:

$$V_A = 1.15V_{s_{PA}} \tag{3.18}$$

In addition, the limitations of the arresting system need to be accounted for. Figure 3.19 illustrates typical arresting gear limitations.

3.3.6 Example of Sizing to Military Landing Distance Requirements

For the same Navy attack airplane of Sub-section 3.2.6, it is requested to perform the sizing to landing requirements such that:

a) for shore based landings: s_{FL} = 3,500 ft at sea-level, standard atmosphere, concrete runways.

b) for carrier landings the airplane is to be compatible with the Mark7 Mod3 arresting gear.

c) landing weight, W_L is equal to 0.80 times the take-off weight, W_{TO}

First item a) will be discussed. The FAR 25 data of Figure 3.17 are used to establish the fact, that for a fieldlength of s_{FL} = 3,500 ft, the corresponding approach speed is $(11,800)^{1/2}$ = 108.6 kts.

However, for military airplanes this implies an approach stall speed of 108.6/1.2 = 90.5 kts.

From Eqn.(3.1) it now follows that:

$$2(W/S)_L \times 0.002378 C_{L_{max_L}} = (90.5 \times 1.688)^2 = 23,337 \text{ ft}^2/\text{sec}^2$$

Therefore:

$$(W/S)_L = 27.7 C_{L_{max_L}}$$

From item c) it follows that:

$$(W/S)_{TO} = 34.7 C_{L_{max_L}}$$

Figure 3.20 shows the allowable wing loadings at take-off, to meet this landing requirement.

To satisfy item b), it is observed from Figure 3.19 that for the Mark7 Mod3 arresting gear, V_A = 145 kts, as long as the landing weight is under 40,000 lbs. That implies a take-off weight of less than 50,000 lbs.

From Eqn.(3.18) it follows that:

$$V_{S_{PA}} = 145/1.15 = 126.1 \text{ kts}$$

With Eqn.(3.1) this in turn yields:

$$(W/S)_A = 0.5 \times 0.002378 \times (126.1 \times 1.688)^2 \times C_{L_{max_{PA}}} =$$

$$= 53.9 C_{L_{max_{PA}}}$$

This implies a take-off wing loading of:

$$(W/S)_{TO} = (53.9/0.8) C_{L_{max_{PA}}} = 67.3 C_{L_{max_{PA}}}$$

Figure 3.20 shows how this requirement compares with the shore based field length requirement. It is seen that at least in this example, the latter is the more critical.

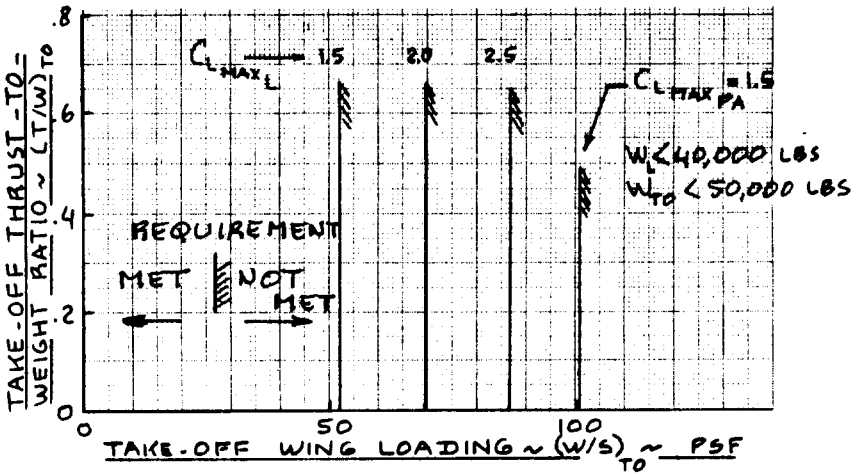

Figure 3.20 Allowable Wing Loadings to meet Military Field and Carrier Landing Requirements

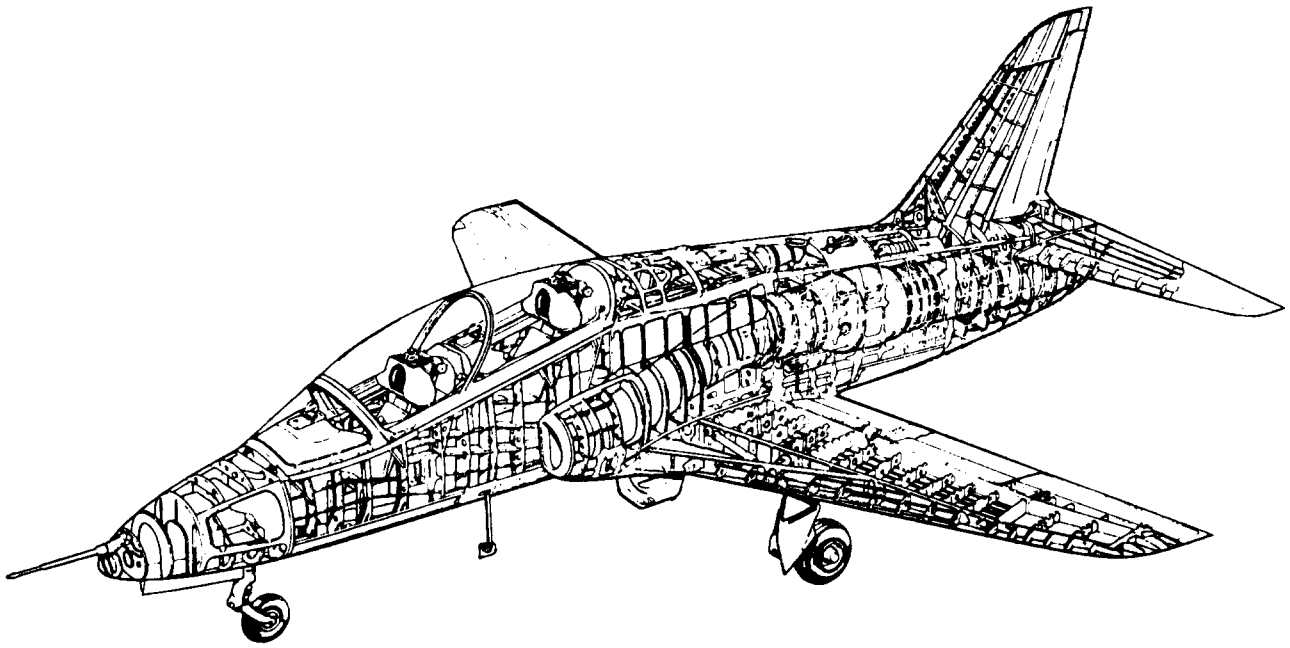

BRITISH AEROSPACE HAWK

3.4 SIZING TO CLIMB REQUIREMENTS

All airplanes must meet certain climb rate or climb gradient requirements. To size an airplane for climb requirements, it is necessary to have an estimate for the airplane drag polar. Sub-section 3.4.1 presents a rapid method for estimating drag polars for low speed flight conditions. Sub-section 3.4.2 applies this method to an example airplane.

For civil airplanes, the climb requirements of either FAR 23 or FAR 25 must be met. Sub-sections 3.4.3 and 3.4.6 summarize these requirements. Sub-sections 3.4.4 and 3.4.7 present rapid methods for sizing airplanes to these requirements. Example applications are presented in Sub-sections 3.4.5 and 3.4.8.

For military airplanes either the requirements of Reference 15 or, whatever climb requirements are specified in the RFP must be met. The military climb requirements of Reference 15 are summarized in Sub-section 3.4.9.

The methods of Sub-sections 3.4.3 and 3.4.6 can also be used to size military airplanes to low speed climb requirements. For sizing to: very high climb rates, time-to-climb to altitude and ceiling requirements, the reader is referred to Sub-section 3.4.10. Sizing to specific excess power requirements is discussed in Sub-section 3.4.11. An application of these military requirements is presented in Sub-section 3.4.12.

3.4.1 A Method for Estimating Drag Polars at Low Speed

Assuming a parabolic drag polar, the drag coefficient of an airplane can be written as:

$$C_D = C_{D_o} + C_L^2/\pi Ae \qquad (3.19)$$

The zero-lift drag coefficient, C_{D_o} can be expressed as:

$$C_{D_o} = f/S, \qquad (3.20)$$

where f is the equivalent parasite area and S is the wing area.

It is possible to relate equivalent parasite area, f to wetted area S_{wet}. This is shown in Figures (3.21a and b).

It is possible to represent Figures (3.21) with the following empirically obtained equation:

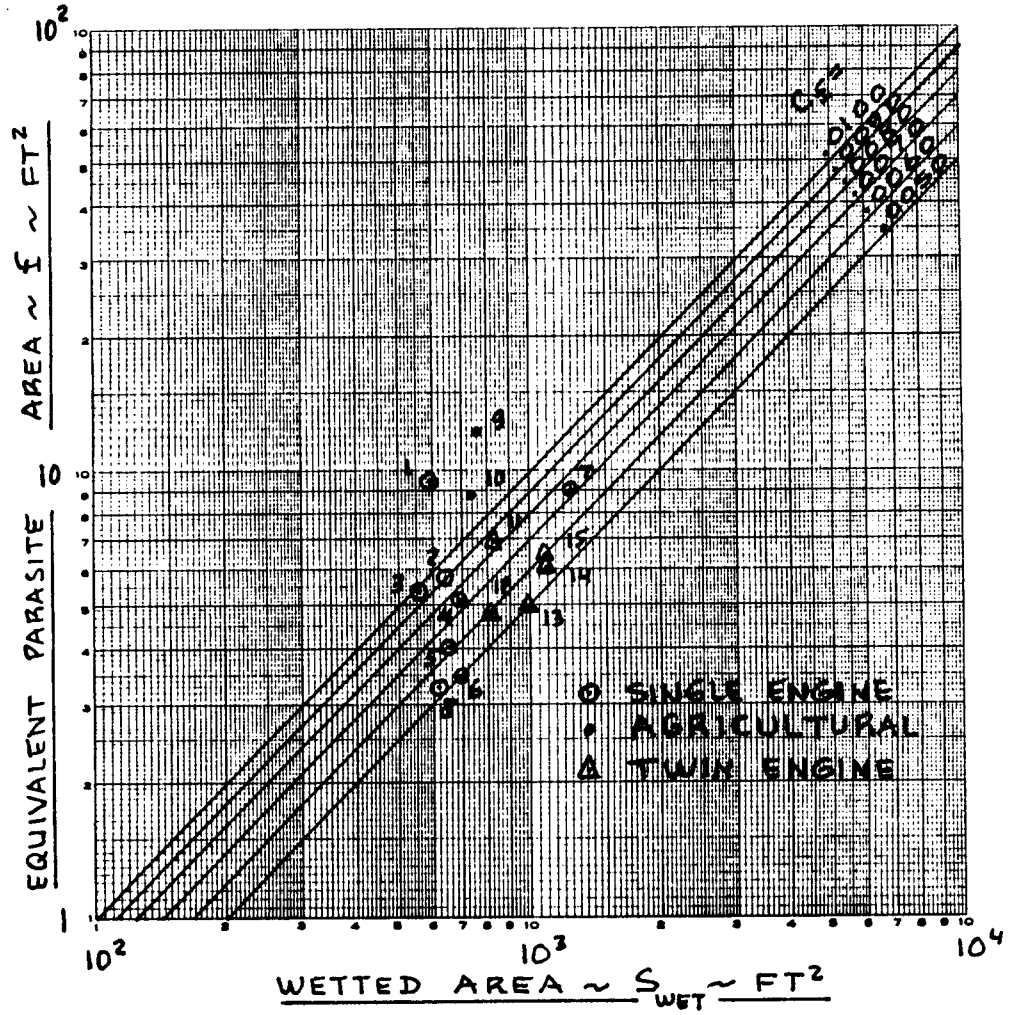

1	CESSNA	L-5	9	CESSNA	AG-HUSKY T188C SPRAY BAR ON
2	✓	172			
3	✓	152	10	✓	AG-HUSKY T188C SPRAY BAR OFF
4	✓	182	11	✓	303*
5	✓	180	12	✓	310*
6	✓	210*	13	✓	310* (PROTOTYPE)
7	✓	208	14	✓	402*
8	BEECH	35*	15	✓	421*

* GEAR-UP

OTHERS GEAR DOWN

Figure 3.21a) Effect of Equivalent Skin Friction on Parasite and Wetted Areas

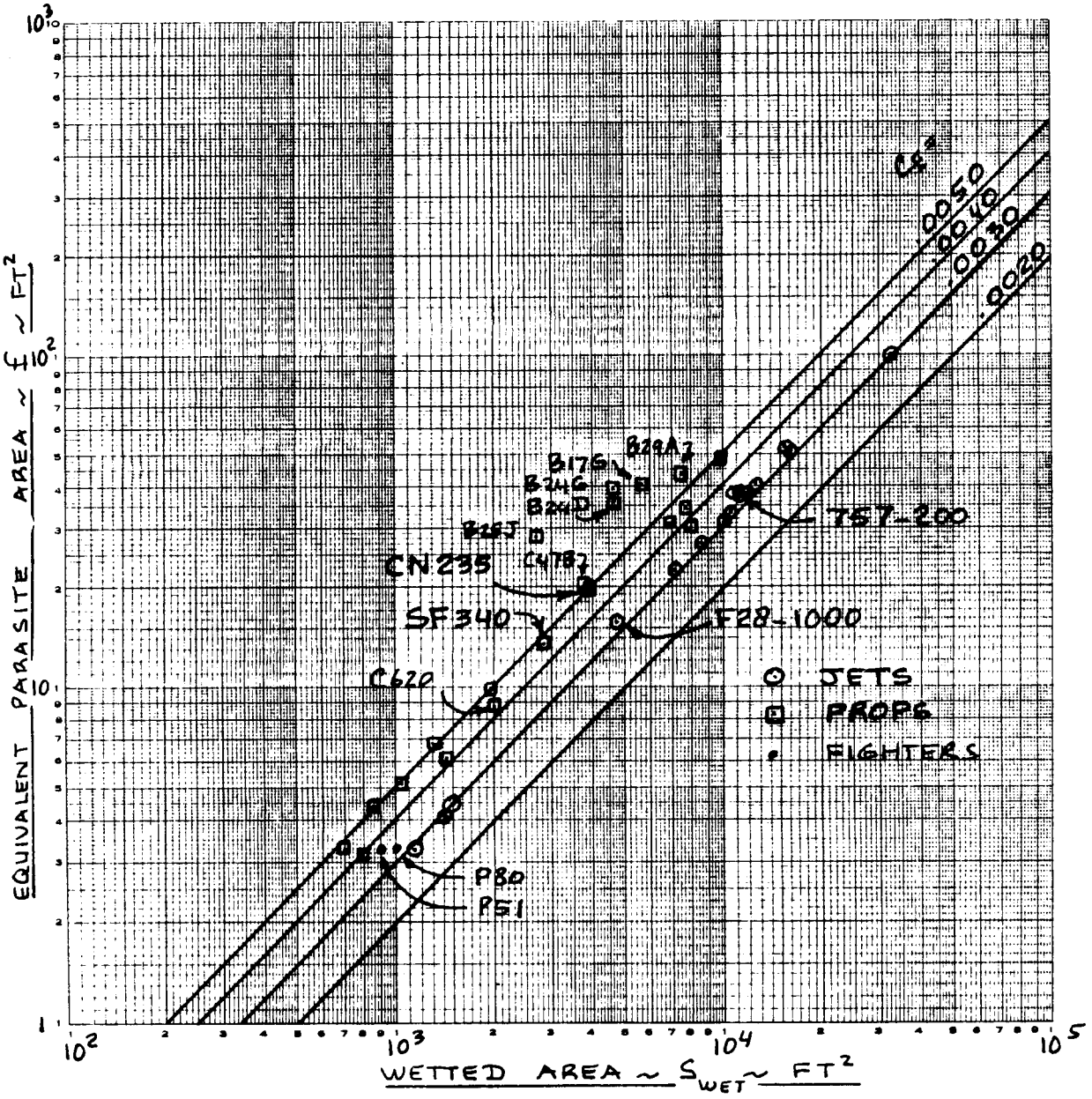

Figure 3.21b) Effect of Equivalent Skin Friction on Parasite and Wetted Areas

$$\log_{10} f = a + b\log_{10} S_{wet} \qquad (3.21)$$

The correlation coefficients a and b are themselves a function of the equivalent skin friction coefficient of an airplane, c_f. The latter is determined by the smoothness and streamlining designed into the airplane. Table (3.4) shows typical values for a and for b for a range of c_f- values. Figures (3.21) in turn allow the reader to quickly estimate a realistic value for c_f.

It is evident, that the method for estimating drag boils down to the ability to predict a realistic value for S_{wet}. It turns out, that S_{wet} correlates well with W_{TO} for a wide range of airplanes. Figures (3.22a-d) show this. The scatter in these figures is mainly due to differences in wing loading, cabin sizes and nacelle design. Most airplanes fall in the ten percent band.

With the help of Figures 3.22 it is possible to obtain an initial estimate for airplane wetted area without knowing what the airplanes actually looks like.

Figures (3.22) also imply the following:

$$\log_{10} S_{wet} = c + d\log_{10} W_{TO} \qquad (3.22)$$

The constants c and d are regression line coefficients. Values for c and d were obtained by correlating wetted area and take-off weight data for 230 airplanes. These airplanes were categorized in the same types used in Chapter 2. Table 3.5 lists the values of the regression line coefficients c and d for twelve types of airplanes.

Since an estimate for W_{TO} was already obtained in Chapter 2, the drag polar for the clean airplane can now be determined.

For take-off and for landing, the effect of flaps and of the landing gear need to be accounted for. The additional zero-lift drag coefficients due to flaps and due to landing gear are strongly dependent on the size and type of these items.

Typical values for ΔC_{D_0} are given in Table 3.6.

Table 3.4 Correlation Coefficients for Parasite Area Versus Wetted Area (Eqn.(3.21))

Equivalent Skin Friction Coefficient, c_f	a	b
0.0090	-2.0458	1.0000
0.0080	-2.0969	1.0000
0.0070	-2.1549	1.0000
0.0060	-2.2218	1.0000
0.0050	-2.3010	1.0000
0.0040	-2.3979	1.0000
0.0030	-2.5229	1.0000
0.0020	-2.6990	1.0000

Table 3.5 Regression Line Coefficients for Take-off Weight Versus Wetted Area (Eqn.(3.22))

Airplane Type	c	d
1. Homebuilts	1.2362	0.4319
2. Single Engine Propeller Driven	1.0892	0.5147
3. Twin Engine Propeller Driven	0.8635	0.5632
4. Agricultural	1.0447	0.5326
5. Business Jets	0.2263	0.6977
6. Regional Turboprops	-0.0866	0.8099
7. Transport Jets	0.0199	0.7531
8. Military Trainers*	0.8565	0.5423
9. Fighters*	-0.1289	0.7506
10. Mil. Patrol, Bomb and Transport	0.1628	0.7316
11. Flying Boats, Amph. and Float	0.6295	0.6708
12. Supersonic Cruise Airplanes	-1.1868	0.9609

* For these airplanes, wetted areas were correlated with 'clean', maximum take-off weights. No stores were accounted for.

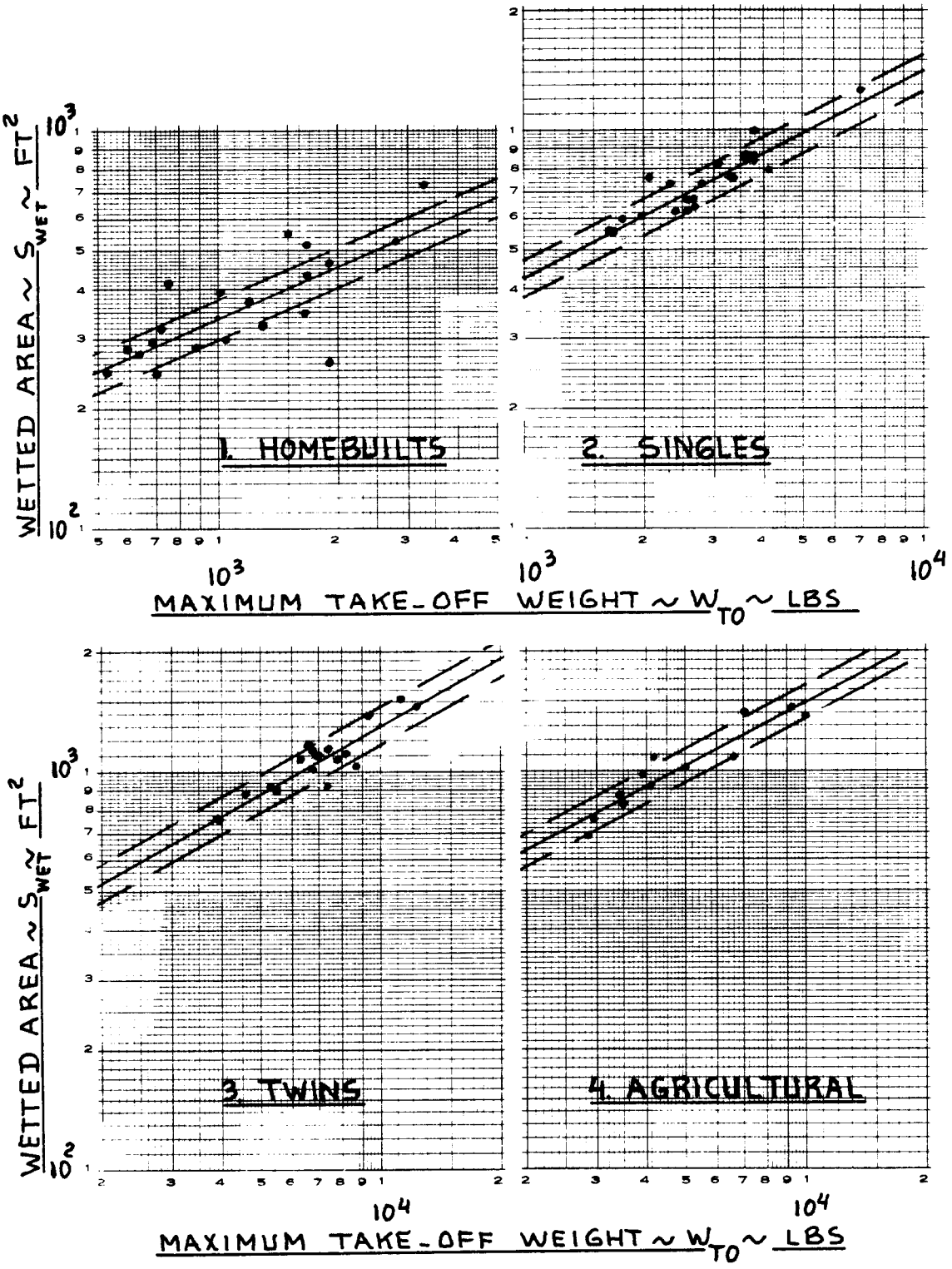

Figure 3.22a) Correlation Between Wetted Area and Take-off Weight

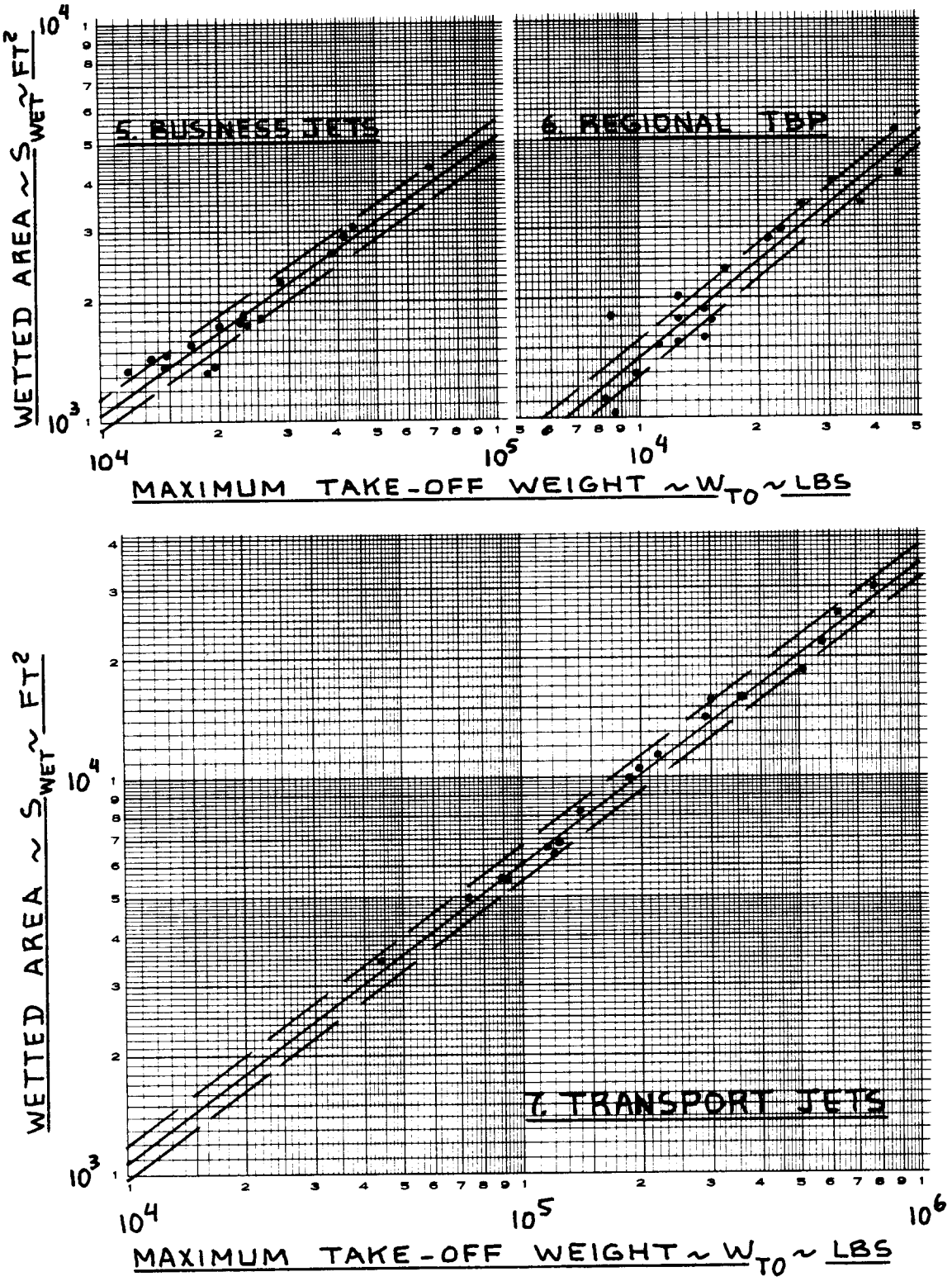

Figure 3.22b) Correlation Between Wetted Area and Take-off Weight

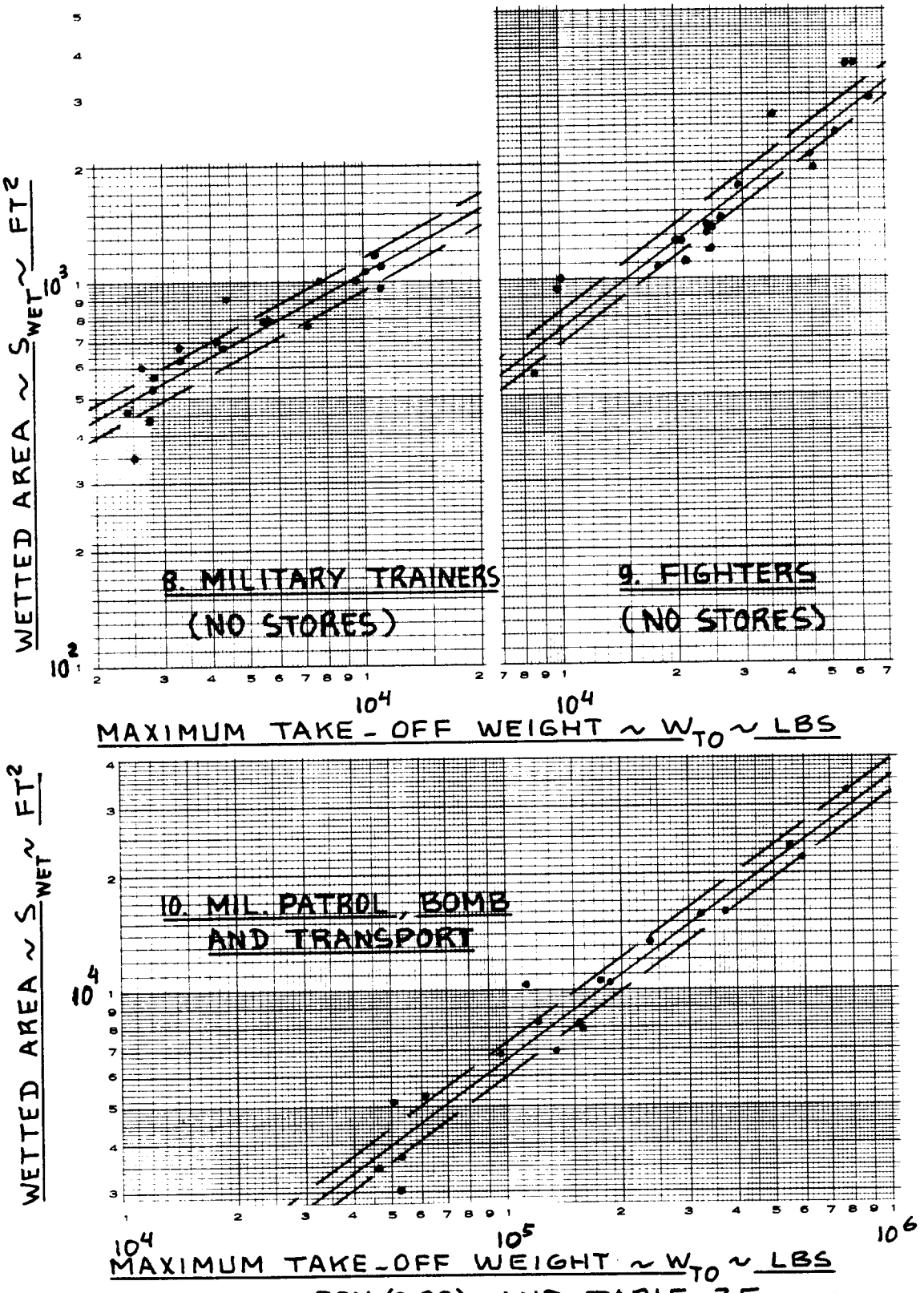

Figure 3.22c) Correlation Between Wetted Area and Take-off Weight

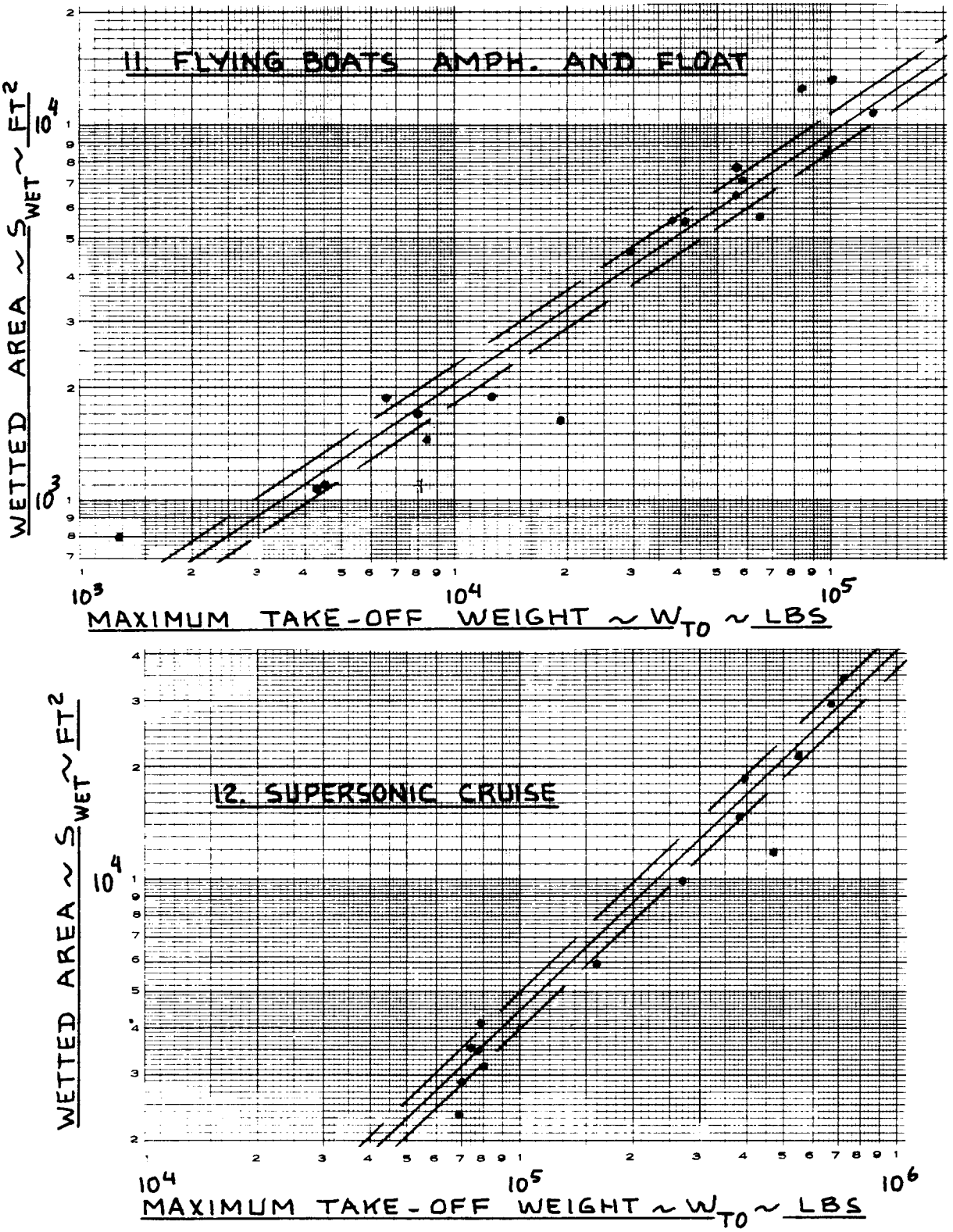

Figure 3.22d) Correlation Between Wetted Area and Take-off Weight

Table 3.6 First Estimates for ΔC_{D_o} and 'e'

With Flaps and Gear Down		
Configuration	ΔC_{D_o}	e
Clean	0	0.80 - 0.85
Take-off flaps	0.010 - 0.020	0.75 - 0.80
Landing Flaps	0.055 - 0.075	0.70 - 0.75
Landing Gear	0.015 - 0.025	no effect

Which values are selected depends on flap and gear type. Split flaps are more 'draggy' than Fowler flaps. Full span flaps are more 'draggy' than partial span flaps. Wing mounted landing gears on high wing airplanes are more 'draggy' than those on low wing airplanes. Reference 5 provides detailed information on how to estimate these drag items.

3.4.2 Example of Drag Polar Determination

It is required to find the clean, take-off and landing drag polars for a jet airplane with W_{TO}= 10,000 lbs.

Figure (3.22), or Eqn.(3.22) shows that for this airplane, S_{wet}= 1,050 ft^2. From Figure (3.21) it is apparent, that a c_f value of 0.0030 is reasonable. The reader is asked to show, that use of Eqn.(3.21) gives the same result. From Figure (3.21) or from Eqn.(3.21) it now follows that:

$$f = 3.15\ ft^2.$$

For a jet airplane in this category, typical wing loadings will range from 50 psf to 100 psf. It will be assumed, that an average wing loading for this category airplane is 75 psf. With the weight of W_{TO} = 10,000 lbs, the following data are now obtained:

W_{TO}	$(W/S)_{TO}$	S	S_{wet}	f	C_{D_o}
10,000	75	133	1,050	3.15	0.0237

The reader will note, that when wing area is varied at constant weight, the wetted area will change.

If it is now assumed, that A = 10 and e = 0.85 then it is possible to find the 'clean' drag polars at low speed as:

$$C_D = 0.0237 + 0.0374C_L^2$$

The additional zero-lift drag coefficients due to flaps and due to gear are assumed from Sub-section 3.4.1 as:

ΔC_{D_0} due to:

take-off flaps = 0.015, with e = 0.8

landing flaps = 0.060, with e = 0.75

Landing gear = 0.017

To summarize, the airplane drag polars are:

Low speed, clean: $C_D = 0.0237 + 0.0374C_L^2$

Take-off, gear up $C_D = 0.0387 + 0.0398C_L^2$

Take-off, gear down $C_D = 0.0557 + 0.0398C_L^2$

Landing, gear up $C_D = 0.0837 + 0.0424C_L^2$

Landing, gear down $C_D = 0.1007 + 0.0424C_L^2$

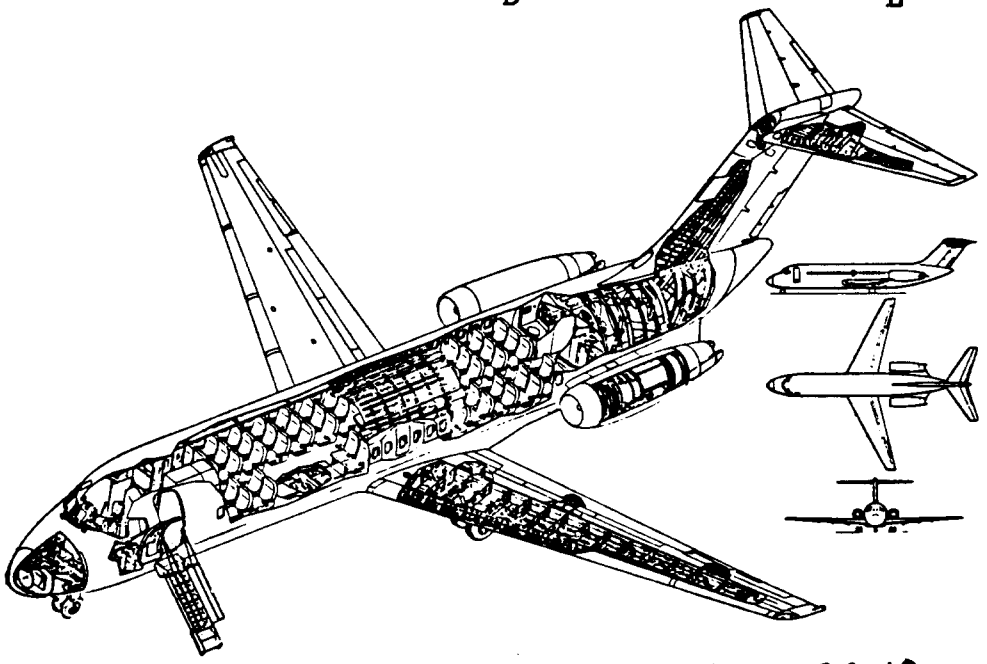

Mc DONNELL-DOUGLAS DC9-10

3.4.3 Summary of FAR 23 Climb Requirements

The FAR 23 climb requirements are contained in Ref. 8. The climb requirements are given for two flight conditions: take-off and balked landing.

These requirements must be met with the power (or thrust) available minus installation losses and minus losses caused by accessory operation. For reciprocating engine powered airplanes, the engine power must be that for 80 percent humidity at and below standard temperature. For turbine powered airplanes, the engine thrust (or power) must be that for 34 percent humidity and standard temperature plus 50°F. FAR 23.45 provides more details.

The take-off climb requirements of FAR 23.65 (AEO = All Engines Operating) and FAR 23.67 (OEI = One Engine Inoperative) can be summarized as follows:

3.4.3.1 FAR 23.65 (AEO) → ALL ENGINES OPERATING

All airplanes must have a minimum climb rate at sealevel of 300 fpm and a steady climb angle of at least 1:12 for landplanes and 1:15 for seaplanes, in the following configuration:

1) Not more than maximum continuous power on all engines
2) Landing gear retracted
3) Flaps in the take-off position
4) Cowl flaps as required for proper engine cooling (FAR 23.1041-1047).

For turbine powered airplanes, there is an additional requirement for a steady climb gradient of at least 4 percent at a pressure altitude of 5,000 ft and at 81°F, under the same configuration conditions 1-4.

3.4.3.2 FAR 23.67 (OEI)

For multiengine (reciprocating engines) airplanes with $W_{TO} > 6{,}000$ lbs, the steady climb rate must be at least $0.027V_{s_o}^2$ fpm, at 5,000 ft altitude, where V_{s_o} is in kts.

This requirement applies with the airplane in the

following configuration:

1) Critical engine inoperative and its propeller in the minimum drag position
2) Remaining engines at no more than maximum continuous power
3) Landing gear retracted
4) Wing flaps in the most favorable position
5) Cowl flaps as required for proper engine cooling (FAR 23.1041-1047)

For multiengine (reciprocating engines) airplanes with W_{TO} < 6,000 lbs, and with V_{s_o} > 61 kts the previous requirements also apply.

For multiengine (reciprocating engines) airplanes with W_{TO} < 6,000 lbs, and with V_{s_o} < 61 kts the requirement is that the steady climb rate at 5,000 ft altitude must be determined. Note, that this implies that a negative climb rate with one engine inoperative is allowed.

For turbine powered airplanes, the following requirements apply regardless of the weight:

a) minimum climb gradient of 1.2 percent or minimum climb rate of $0.027V_{s_o}^2$ at 5,000 ft, standard atmosphere, whichever is the most critical.

b) minimum climb gradient of 0.6 percent or minimum climb rate of $0.014V_{s_o}^2$ at 5,000 ft pressure altitude and 81°F, whichever is the most critical.

These requirements apply in the configurations previously given.

The balked landing climb requirements of FAR 23.77 can be summarized as follows:

3.4.3.3 FAR 23.77 (AEO)

The steady climb angle shall be at least 1:30 with the airplane in the following configuration:

a) Take-off power on all engines

b) Landing gear down

c) Flaps in landing position, unless they can be safely retracted in two seconds without loss of altitude and without requiring exceptional pilot skills

For turbine powered airplanes it is also necessary to show, that a zero steady climb rate can be maintained at a pressure altitude of 5,000 ft and 81°F in the aforementioned configuration.

The reader should note that positive engine-out climb performance, for FAR 23 certified airplanes in the landing configuration, is not required!

3.4.4 Sizing Method for FAR 23 Climb Requirements

Reference 11 contains rapid methods for estimating rate-of-climb (RC) and climb gradient (CGR) of an airplane.

3.4.4.1 Sizing to FAR 23 rate-of-climb requirements

Equations 6.15 and 6.16 of Reference 11 contain all ingredients needed for sizing to rate-of-climb criteria:

$$RC = \text{Rate of climb} = dh/dt = 33{,}000 \times RCP \qquad (3.23)$$

where:

$$RCP = \text{Rate of climb Parameter} = \left[\eta_p/(W/P) - \{(W/S)^{1/2}/19(C_L^{3/2}/C_D)\sigma^{1/2}\}\right] \qquad (3.24)$$

The reader should note that RC in Eqn.(3.23) is given in fpm.

To maximize RC, it is evidently necessary to make $C_L^{3/2}/C_D$ as large as possible. This is achieved when:

$$C_{L_{RC_{max}}} = (3C_{D_o}\pi Ae)^{1/2} \qquad (3.25)$$

and:

$$C_{D_{RC_{max}}} = 4C_{D_o} \qquad (3.26)$$

which yields:

$$(C_L^{3/2}/C_D)_{max} = 1.345(Ae)^{3/4}/C_{D_o}^{1/4} \qquad (3.27)$$

Figure 3.23 shows how A and C_{D_o} affect the value of $(C_L^{3/2}/C_D)_{max}$ for an an example case. Observe, that Figure 3.23 also shows the corresponding lift coefficient, $C_{L_{RC_{max}}}$.

3.4.4.2 Sizing to FAR 23 climb gradient requirements

Equations (6.29) and (6.30) of Reference 11 contain all ingredients needed for sizing to climb gradient criteria:

$$CGR = \text{Climb gradient} = (dh/dt)/V \qquad (3.28)$$

and:

$$CGRP = \text{Climb gradient parameter} = \{CGR + (L/D)^{-1}\}/C_L^{1/2}, \qquad (3.29)$$

where:

$$CGRP = 18.97\eta_p\sigma^{1/2}/(W/P)(W/S)^{1/2} \qquad (3.30)$$

To find the best possible climb gradient, it is necessary to find the minimum value of CGRP. This minimum value depends on the lift coefficient and on the corresponding lift-to-drag ratio. A problem is, that the minimum value of CGRP is usually found at a value of C_L very close to $C_{L_{max}}$.

Some margin relative to stall speed is always desired. FAR 23 does not specify this margin. Instead, FAR 23 demands, that the manufacturer clearly identify to the operator, what the speed for best rate of climb is. There is no requirement to identify the speed for best climb gradient. It is suggested to the reader, to ensure that a margin of 0.2 exists between $C_{L_{max}}$ and $C_{L_{climb}}$.

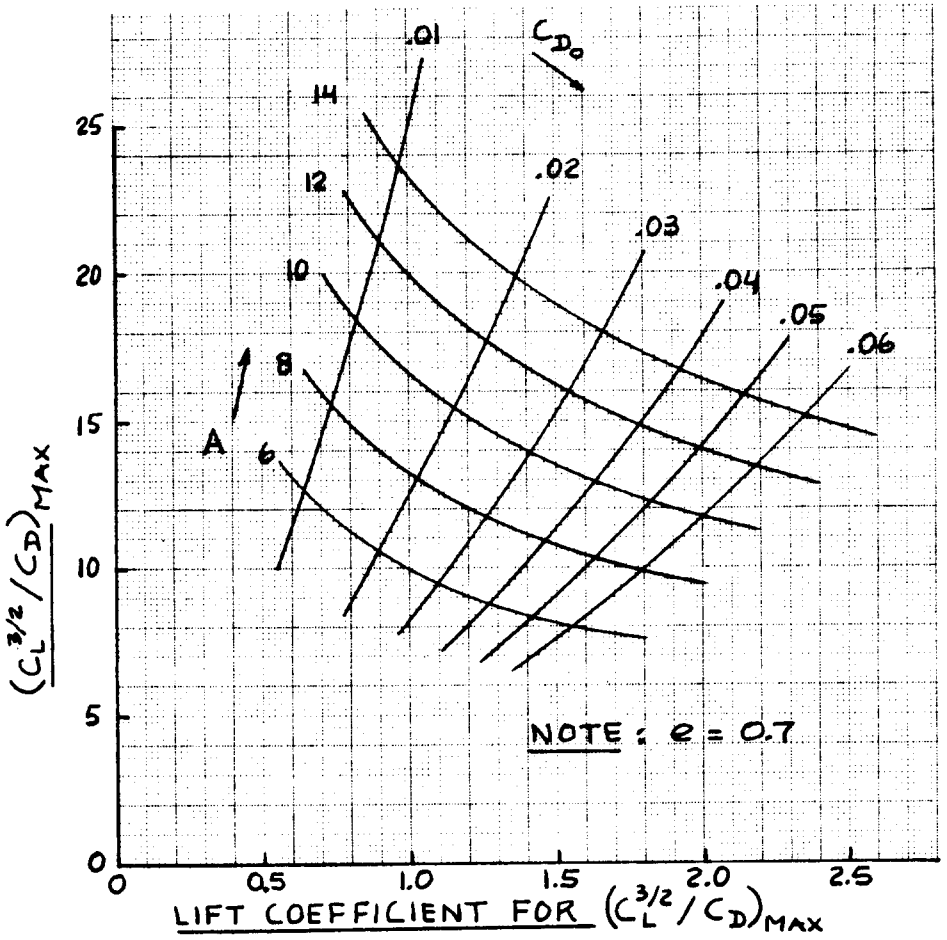

Figure 3.23 Effect of Aspect Ratio and Zero-lift Drag on $(C_L^{3/2}/C_D)_{max}$ and the Lift Coefficient Where This Occurs

3.4.5 Example of FAR 23 Climb Sizing

It is required to size a twin engine propeller driven airplane with a take-off weight of 7,000 lbs and a landing weight of 7,000 lbs, to the FAR 23 climb requirements.

Referring to sub-section 3.4.3 it is seen that this airplane must meet the following requirements:

FAR 23.65 (AEO): RC $\geq$ 300 fpm
CGR $\geq$ 1/12 rad
Configuration: gear up, take-off flaps, max. cont. power on all engines.

FAR 23.67 (OEI): RC $\geq 0.027V_{s_e}^2$ fpm at 5,000 ft
Configuration: gear up, flaps most favorable, stopped propeller feathered, take-off power on operating engine.

FAR 23.77 (AEO): CGR $\geq$ 1/30 rad
Configuration: gear down, landing flaps, take-off power on all engines.

The climb sizing calculations proceed as follows:

3.4.5.1 Sizing to rate-of-climb requirements

From Eqn.(3.23):

$$RCP = (33{,}000)^{-1}dh/dt = (33{,}000)^{-1}RC$$

For FAR 23.65: $RCP = (33{,}000)^{-1} \times 300 = 0.0091$ hp/lbs.

For FAR 23.67: V_{s_e} needs to be computed first.

Assuming that flaps-up represents the most favorable case (this has to be checked later!) and that $C_{L_{max}} = 1.7$ (consistent with Table 3.1, flaps-up), the value of V_{s_e} at 5,000 ft is found from:

$$W = C_{L_{max}}(1/2)\rho V_{s_e}^2 S,$$

or:

$$V_{s_e} = \{(2W/S)/\rho C_{L_{max}}\}^{1/2}$$

For W/S a range of 20-50 psf will be investigated. The density of the atmosphere at 5,000 ft is

0.002049 slugs/ft^3. The following table can now be constructed:

$(W/S)_{TO}$	V_{s_o}		RC	RCP
psf	fps	kts	fpm	hp/lbs
20	107	63	107	0.0032
30	131	78	164	0.0050
40	152	90	219	0.0066
50	169	100	270	0.0082

Next, the drag polars of this airplane need to be estimated. This will be done using the method discussed in Sub-section 3.4.1.

From Figure 3.22 the wetted area of this airplane is seen to be in the neighbourhood of 1,060 ft^2. From Figure 3.21 this yields f = 5 ft^2 if c_f is taken to be 0.0050.

The effect of wing loading on the zero lift drag will be neglected. An average wing loading of 35 psf will be assumed. This yields: C_{D_o} = 5/200 = 0.0250.

For 'e', a value of 0.80 will be assumed. For aspect ratio, A a value of 8 will be used.

The following additional assumptions will also be made:

For take-off flaps: ΔC_{D_o} = 0.0150

For landing flaps: ΔC_{D_o} = 0.0600

For landing gear: ΔC_{D_o} = 0.0200

The drag polar for the FAR 23.65 requirement is now:

$$C_D = 0.0250 + 0.0150 + C_L^2/20.1$$

$$C_D = 0.0400 + C_L^2/20.1$$

With this drag polar the value of $\{C_L^{3/2}/C_D\}_{max}$ = 12.1.

From Eqn.(3.24) it now follows that:

$$[0.8/(W/P) - \{(W/S)^{1/2}/19x12.1x1.0\}] = 0.0091,$$

where it was assumed that η_p = 0.8.

This relationship translates into the following tabular results:

$(W/S)_{TO}$ psf	W/P cont. lbs/hp	W/P take-off lbs/hp	
20	28.1	25.5	On the bais of typical
30	24.3	22.1	piston engine data, the
40	21.9	19.9	ratio $P_{to}/P_{max.cont.}$
50	20.1	18.3	
	:1.1		was taken to be 1.1

Figure 3.24 shows the range of W/S and W/P values for which the FAR 23.65 climb requirement is satisfied.

For the FAR 23.67 requirement the drag polar is:

$$C_D = 0.0250 + \underset{\text{stopped propeller}}{0.0050} + C_L^2/20.1$$

$$= 0.0300 + C_L^2/20.1$$

In this case, the value of $\{C_L^{3/2}/C_D\}_{max}$ is: 13.0.

Using Eqn.(3.24) again, but now at 5,000 ft:

$[0.8/(W/P) - (W/S)^{1/2}/19x13x0.8617^{1/2}] = RCP$, or:

$[0.8/(W/P) - (W/S)^{1/2}/229] = RCP$,

where RCP is the previously determined function of wing loading, since in FAR 23.67 the climb performance is a function of V_{s_o}.

The following tabular relationship can now be constructed:

$(W/S)_{TO}$ psf	W/P take-off one engine 5,000 ft lbs/hp	W/P take-off two engines 5,000 ft lbs/hp	W/P take-off two engines sealevel lbs/hp
20	35.2	17.6	15.0
30	27.7	13.9	11.8
40	23.4	11.7	9.9
50	20.5	10.3	8.8
	:2	x0.85	

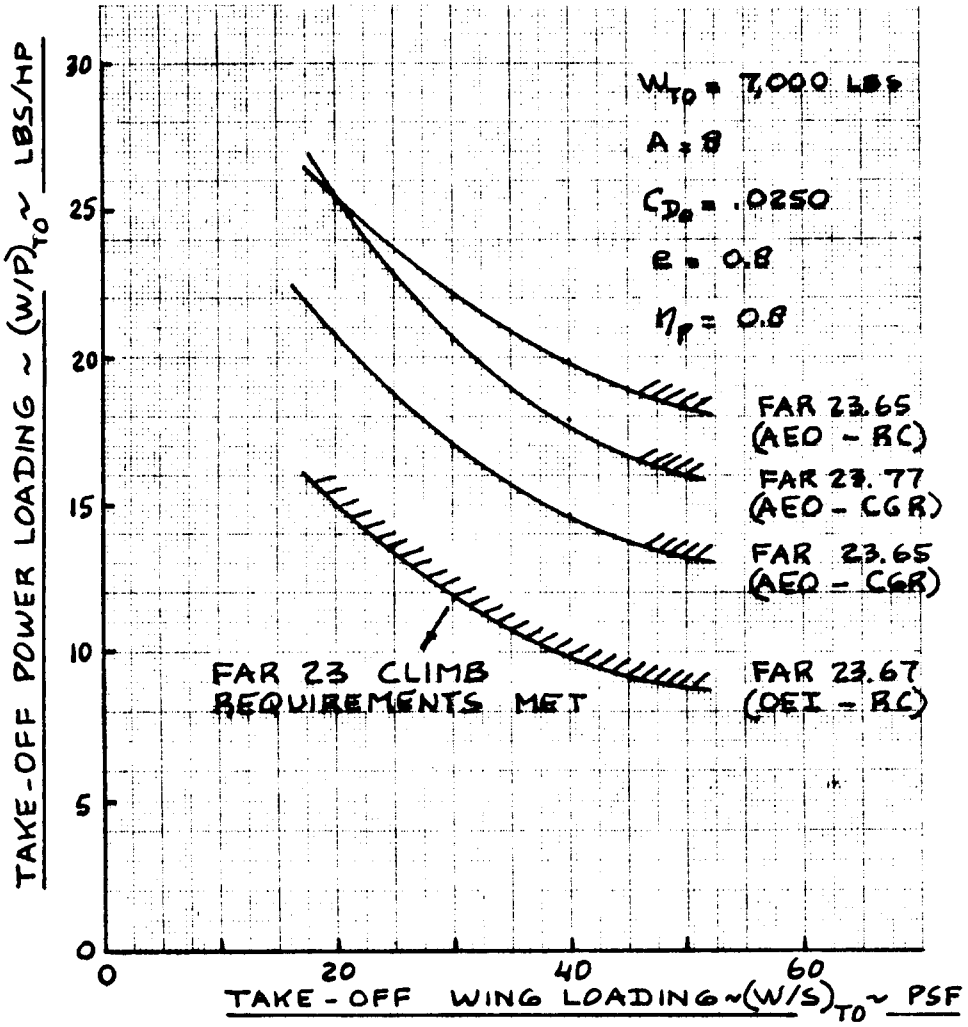

Figure 3.24 Effect of FAR 23 Climb Requirements on the Allowable Values of Take-off Thrust-to-Weight Ratio and Take-off Wing Loading

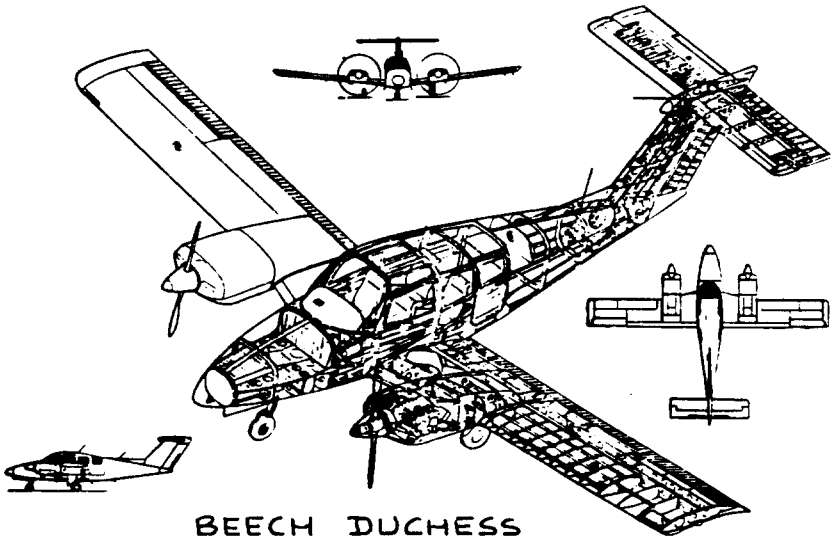

BEECH DUCHESS

The take-off power ratio between 5,000 ft and sealevel was assumed to be 0.85. This ratio is fairly typical for normally aspirated piston engines.

Figure 3.24 also shows how this requirement compares to that of FAR 23.65.

3.4.5.2 Sizing to climb gradient requirements

Climb gradient requirements are computed with the help of Eqn.(3.29):

$$CGRP = 18.97\eta_p\sigma^{1/2}/(W/P)(W/S)^{1/2} = \{CGR + (L/D)^{-1}\}/C_L^{1/2}$$

For the FAR 23.65 requirement: CGR = 1/12 = 0.0833. The drag polar for this case was already found to be:

$$C_D = 0.0400 + C_L^2/20.1$$

It will be assumed now, that with take-off flaps the value of $C_{L_{max}} = 1.8$. Observing a margin of $\Delta C_L = 0.2$:

$$C_{L_{climb}} = 1.6$$

This yields $(L/D)_{climb} = 9.6$

Therefore:

$$CGRP = (0.0833 + 1/9.6)/1.6^{1/2} = 0.1482$$

This requirement now yields:

$$(W/P)(W/S)^{1/2} = 18.97x0.8/0.1482 = 102.4$$

The following tabular relationship can now be constructed:

$(W/S)_{TO}$	W/P max. cont.	W/P max. take-off
psf	lbs/hp	lbs/hp
20	22.9	20.8
30	18.7	17.0
40	16.2	14.7
50	14.5	13.2
	x0.85	

Figure 3.24 also shows how this requirement compares with the previous two.

In the case of the FAR 23.77 requirement:

CGR = 1/30 = 0.0333

It will be assumed, that with the gear down and landing flaps, a value of $C_{L_{max_L}} = 2.0$ can be achieved.

The drag polar in this case is:

$$C_D = 0.1050 + C_L^2/20.1$$

Assuming that the climb is carried out with the same margin as before:

$$C_{L_{climb}} = 2.0 - 0.2 = 1.8$$

The corresponding value of L/D is found to be 6.8.

This in turn means:

$$CGRP = (0.0333 + 1/6.8)/1.8^{12} = 0.1345$$

Therefore:

$$(W/P)(W/S)^{1/2} = 18.97 \times 0.8/0.1345 = 113$$

This results in the following tabular relationship:

$(W/S)_{TO}$ psf	W/P take-off lbs/hp
20	25.3
30	20.6
40	17.9
50	16.0

Figure 3.24 compares this requirement with the other three. It is clear that the FAR 23.67 (OEI) requirement is the most critical one in this case.

The reader is asked to study the effect of aspect ratio, $C_{L_{max}}$ and C_{D_o} on these results.

3.4.6 Summary of FAR 25 Climb Requirements

The FAR 25 climb requirements are contained in Ref. 8. The climb requirements are given for two flight conditions: take-off and balked landing.

These requirements must be met with the thrust (or power) available minus installation losses and minus losses caused by accessory operation. For turbine powered airplanes, the engine thrust or power must be that for 34 percent humidity and standard temperature plus 50° F. For reciprocating engine powered airplanes, the engine power must be that for 80 percent humidity at and below standard temperature. FAR 25.101 provides more details.

The take-off climb requirements of FAR 25.111 (OEI) and FAR 25.121 (OEI) can be summarized as follows:

3.4.6.1 FAR 25.111 (OEI)

The climb gradient with the critical engine inoperative must be at least:

a) 1.2 percent for two-engine airplanes
b) 1.5 percent for three-engine airplanes
c) 1.7 percent for four-engine airplanes,

in the following configuration:

1) Take-off flaps
2) Landing gear retracted
3) Speed is $V_2 (= 1.2V_{S_{TO}})$
4) Remaining engines at take-off thrust or power
5) Between 35 ft and 400 ft altitude, ground effect must be accounted for
6) Ambient atmospheric conditions
7) At maximum take-off weight

This is referred to as the initial climb segment requirement.

3.4.6.2 FAR 25.121 (OEI)

The climb gradient with the critical engine inoperative must be at least:

a) positive for two-engine airplanes
b) 0.3 percent for three-engine airplanes
c) 0.5 percent for four-engine airplanes,

in the following configuration:

1) Take-off flaps
2) Landing gear down
3) Remaining engines at take-off thrust or power
4) Between V_{LOF} and V_2
5) In ground effect
6) Ambient atmospheric conditions
7) At maximum take-off weight

This requirement is also referred to as the transition segment climb requirement.

The so-called second segment climb requirement demands a climb gradient with one engine inoperative of no less than:

a) 2.4 percent for two-engine airplanes
b) 2.7 percent for three-engine airplanes
c) 3.0 percent for four-engine airplanes,

in the following configuration:

1) Take-off flaps
2) Landing gear retracted
3) Remaining engines at take-off thrust or power
4) At $V_2 (= 1.2V_{S_{TO}})$
5) Out of ground effect
6) Ambient atmospheric conditions
7) At maximum take-off weight

The en-route climb requirement with one engine inoperative demands that the climb gradient be no less than:

a) 1.2 percent for two-engine airplanes
b) 1.5 percent for three-engine airplanes
c) 1.7 percent for four-engine airplanes,

in the following configuration:

1) Flaps retracted
2) Landing gear retracted
3) Remaining engines at maximum continuous thrust or power
4) At $1.25V_S$
5) Ambient atmospheric conditions
6) At maximum take-off weight

The reader will have observed, that there is no AEO take-off climb requirement. The reason is that the OEI requirements are so severe, that climb with AEO is not a problem in FAR 25 airplanes.

The landing climb requirements of FAR 25.119 (AEO) and FAR 25.121 (OEI) can be summarized as follows:

3.4.6.3 FAR 25.119 (AEO)

The climb gradient may not be less than 3.2 percent at a thrust or power level corresponding to that obtained eight seconds after moving the throttles from minimum flight idle to the take-off position. This requirement applies in the following configuration:

1) Landing flaps
2) Landing gear down
3) At $1.3V_s$

4) Ambient atmospheric conditions
5) At maximum design landing weight

3.4.6.4 FAR 25.121 (OEI)

The climb gradient with the critical engine inoperative may not be less than:

a) 2.1 percent for two-engine airplanes
b) 2.4 percent for three-engine airplanes
c) 2.7 percent for four-engine airplanes,

in the following configuration:

1) Approach flaps
2) Landing gear as defined by normal AEO operating procedures
3) At no more than $1.5V_{s_A}$
4) V_{s_A} must not be more than $1.1V_{s_L}$
5) Remaining engines at take-off thrust or power
6) Ambient atmospheric conditions
7) At maximum design landing weight

These last two requirements are known as the go-around or balked landing requirements.

3.4.7 Sizing Method For FAR 25 Climb Requirements

To size an airplane, so that it can meet the FAR 25 climb requirements it is suggested to use:

1) for propeller driven airplanes: Eqns.(3.23) and (3.28) of Sub-section 3.4.3

2) for jet powered airplanes:

with one engine inoperative (OEI):

$$(T/W) = \{N/(N - 1)\}\{(L/D)^{-1} + CGR\} \qquad (3.31a)$$

with all engines operating (AEO):

$$(T/W) = \{(L/D)^{-1} + CGR\} \qquad (3.31b)$$

where:

CGR is the required climb gradient (this is the same as the flight path angle γ),

N is the number of engines,

L/D is the lift-to-drag ratio in the flight condition being analyzed, and

T/W is the thrust-to-weight ratio in the flight condition being analyzed.

The reader note carefully, that (T/W) and (L/D) are those for take-off or for landing, depending on the requirement being analyzed.

The process of sizing for climb requirements amounts to finding relations between $(W/S)_{TO}$, $(T/W)_{TO}$ or $(W/P)_{TO}$ and A for a given value of W_{TO}.

3.4.8 Example of FAR 25 Climb Sizing

It is required to size a twin engine jet transport with: W_{TO} = 125,000 lbs and W_L = 115,000 lbs to FAR 25 climb requirements.

From the climb requirements in Sub-section 3.4.6 it follows that this airplane must be sized to the following requirements:

For Take-off climb:

FAR 25.111 (OEI): CGR > 0.012
Configuration: gear up, take-off flaps, take-off thrust on remaining engines, ground effect, $1.2V_{S_{TO}}$.

FAR 25.121 (OEI): CGR > 0
Configuration: gear down, take-off flaps, take-off thrust on remaining engines, ground effect, speed between V_{LOF} and $1.2V_{S_{TO}}$.

FAR 25.121 (OEI): CGR > 0.024
Configuration: gear up, take-off flaps, no ground effect, take-off thrust on remaining engines, $1.2V_{S_{TO}}$.

FAR 25.121 (OEI): CGR > 0.012
Configuration: gear up, flaps up, en route climb altitude, maximum continuous thrust on remaining engines, $1.25V_S$.

For Landing Climb:

FAR 25.119 (AEO): CGR > 0.032
Configuration: gear down, landing flaps, take-off thrust on all engines, maximum design landing weight, $1.3V_{S_L}$.

FAR 25.121 (OEI): CGR > 0.021
Configuration: gear down, approach flaps, take-off thrust on remaining engines, $1.5V_{S_A}$.

All FAR 25 climb criteria involve the climb gradient, CGR and the lift-to-drag ratio of the airplane in some configuration, as seen from Eqn.(3.31a and b). It is therefore necessary to obtain an initial estimate of the drag polar of this airplane. The method of Sub-section 3.4.1 will be used to find this drag polar.

From Figure 3.22b the wetted area of this airplane is about 8,000 ft^2 for the 125,000 lbs take-off weight. From Figure 3.21 this yields f = 23 ft^2 if c_f is taken to be 0.0030. Assuming an average wing loading of 100 psf it is found that S = 1,250 ft^2. From this it follows: C_{D_o} = 0.0184.

The following drag polar data will now be assumed:

Configuration	C_{D_o}	A	e	C_{D_i}	$C_{L_{max}}$
Clean	0.0184	10	0.85	$C_L^2/26.7$	1.4
Take-off flaps	0.0334	10	0.80	$C_L^2/25.1$	2.0
Landing flaps	0.0784	10	0.75	$C_L^2/23.6$	2.8
Gear down	0.0150 for incremental zero-lift drag coefficient				no effect

The climb sizing calculations can now proceed as follows:

<u>FAR 25.111 (OEI)</u>:

$(T/W)_{TO} = 2\{ 1/(L/D) + 0.012\}$, at $1.2V_{s_{TO}}$.

Since the value assumed for $C_{L_{TO_{max}}}$ = 2.0, the actual lift coefficient in this flight condition is 2.0/1.44 = 1.4.

The drag polar is: $C_D = 0.0334 + C_L^2/25.1$.

This yields L/D = 12.6. Therefore:

$(T/W)_{TO} = 2\{1/12.6 + 0.012\} = 0.182$.

However, this does not account for the 50°F temperature effect. Typical turbofan data indicate that at sealevel, the ratio of maximum thrust at standard

temperature to that at a 50°F higher temperature is 0.80. Thus, for sizing purposes: $(T/W)_{TO} = 0.182/0.8 = 0.23$.

FAR 25.121 (OEI) (gear down, t.o. flaps):

$(T/W)_{TO} = 2\{ 1/(L/D) + 0\}$, between V_{LOF} and V_2.

It will be assumed, that $V_{LOF} = 1.1V_{S_{TO}}$.

Because $C_{L_{TO_{max}}} = 2.0$, $C_{L_{LOF}} = 2.0/1.1^2 = 1.65$.

The drag polar is: $C_D = 0.0484 + C_L^2/25.1$.

This yields L/D = 10.5. Therefore:

$(T/W)_{TO} = 2\{1/10.5\} = 0.19$.

At V_2, the value of the lift coefficient is:

$2.0/1.44 = 1.4$.

Therefore L/D = 11.1 and $(T/W)_{TO} = 2\{1/11.1\} = 0.18$.

It is seen that the requirement at V_{LOF} is the more critical. Correcting for temperature this requirement now becomes: $(T/W)_{TO} = 0.19/0.8 = 0.24$.

FAR 25.121 (OEI) (gear up, t.o.flaps):

$(T/W)_{TO} = 2\{1/(L/D) + 0.024\}$ at $1.2\ V_{S_{TO}}$.

The lift coefficient is $2.0/1.44 = 1.4$.

The drag polar is: $C_D = 0.0334 + C_L^2/25.1$.

This yields L/D = 12.6. Therefore:

$(T/W)_{TO} = 2\{1/12.6 + 0.024\} = 0.21$.

With the temperature correction this becomes: $(T/W)_{TO} = 0.21/0.8 = 0.26$.

FAR 25.121 (OEI) (gear up, flaps up):

$(T/W)_{TO} = 2\{1/L/D + 0.012\}$ at $1.25V_S$.

Since in the clean configuration $C_{L_{max}} = 1.4$,

$C_L = 1.4/1.25^2 = 0.9.$

The drag polar is: $C_D = 0.0184 + C_L^2/26.7.$

This yields: L/D = 18.5. Therefore:

$(T/W)_{TO} = 2\{1/18.5 + 0.012\} = 0.136.$

However, this is for maximum continuous thrust. A typical value for the ratio of maximum continuous thrust to maximum take-off thrust is 0.94 for turbofan engines. With this correction and with the temperature correction, the requirement is: $(T/W)_{TO} = 0.136/0.94/0.8 = 0.18.$

FAR 25.119 (AEO) (balked landing):

$(T/W)_L = \{1/L/D + 0.032\}$ at $1.3V_{s_L}$.

In the landing configuration it was assumed that $C_{L_{max_L}} = 2.8$, the lift coefficient in this case is:

$2.8/1.3^2 = 1.66.$

The drag polar now is: $C_D = 0.0934 + C_L^2/23.6.$

This yields: L/D = 7.9. Therefore:

$(T/W)_L = \{1/7.9 + 0.032\} = 0.16.$

Since the design landing weight is 115,000 lbs, this translates into the following take-off requirement, after also applying the temperature correction:

$(T/W)_{TO} = 0.16(115{,}000/125{,}000)/0.8 = 0.19.$

FAR 25.121 (OEI) (balked landing):

$(T/W)_L = 2\{1/(L/D) + 0.021\}$ at $1.5\ V_{s_A}$.

It will be assumed, that in the approach configuration, $C_{L_{max_A}} = 2.4$. This results in the following value for approach lift coefficient:

$C_{L_A} = 2.4/1.5^2 = 1.07$

With approach flaps, the drag increment due to flaps will be assumed to be halfway between landing and

take-off flaps. This yields for the drag polar:

$$C_D = 0.0709 + C_L^2/23.6.$$

Therefore: L/D = 9.0 and:

$$(T/W)_L = 2\{1/9.0 + 0.021\} = 0.26.$$

With the weight and temperature corrections as before, it follows that:

$$(T/W)_{TO} = 0.26(115{,}000/125{,}000)/0.8 = 0.30.$$

It appears that this last requirement is the most critical one for this airplane. Figure 3.25 shows how the six climb requirements compare with each other.

The reader is asked to investigate the effect of aspect ratio, $C_{L_{max}}$ and C_{D_o} on these results.

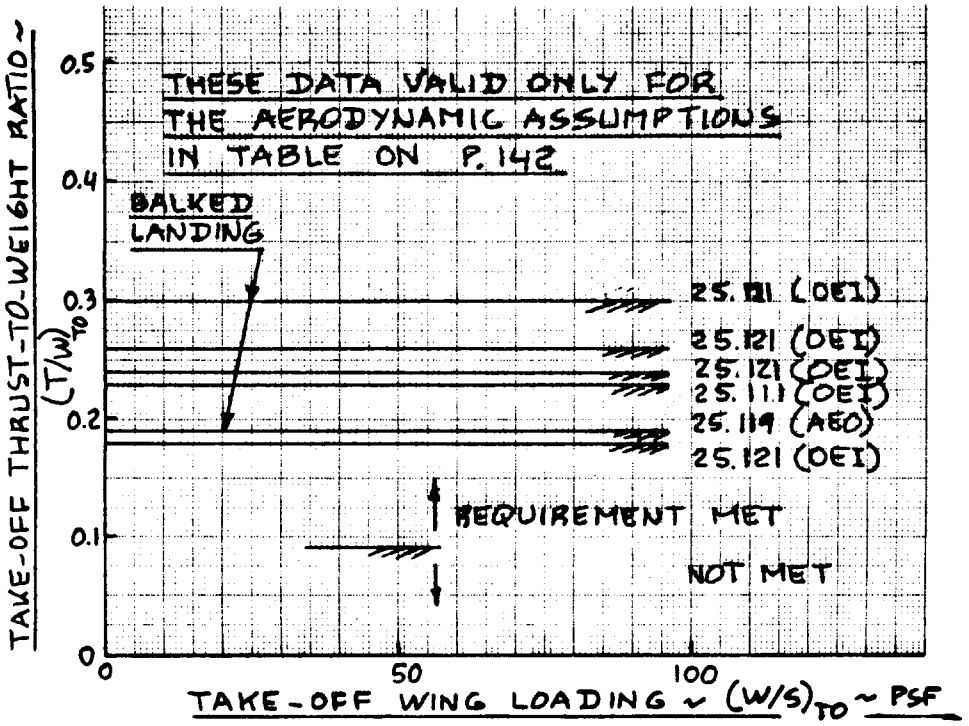

Figure 3.25 Effect of FAR 25 Climb Requirements on the Allowable Values of Take-off Thrust-to-Weight Ratio and Take-off Wing Loading

3.4.9 Summary of Military Climb Requirements

Military requirements for climb characteristics are usually specific to an RFP. Those requirements that deal with climb rate or climb gradient minima are given in Reference 15: MIL-C-005011B.

The requirements apply to single engine airplanes and to multi engine airplanes with the most critical engine inoperative.

The requirements must be met at W_{TO} and with applicable external stores.

A summary of these requirements now follows:

1) Take-off climb requirements

a) Ref. 15, par.3.4.2.4.1:

At take-off speed, $V_{TO} = 1.1V_{s_{TO}}$, the climb gradient must be at least 0.005.

Configuration: gear down, flaps take-off, maximum power.

b) Ref. 15, par.3.4.2.5:

At the 50 ft obstacle and at $1.15V_{s_{TO}}$, the climb gradient must be at least 0.025.

Configuration: gear up, flaps take-off, maximum power.

2) Landing climb requirements

a) Ref. 15, par.3.4.2.11:

At the 50 ft obstacle and at $1.2V_{s_{PA}}$ the climb gradient must be at least 0.025.

Configuration: gear up, flaps approach, maximum dry power.

NOTE: these climb requirements can be analyzed with the methods of Sub-section 3.4.7.

Frequently, military airplanes have to meet certain time-to-climb and ceiling requirements. A method for rapid sizing to these requirements is presented in Sub-section 3.4.10.

Particularly for fighter airplanes, where combat maneuverability plays an important role, there frequently exist requirements for a certain amount of specific excess power, P_s. Sub-section 3.4.11 presents a method for sizing to specific excess power requirements.

3.4.10 Sizing for Time-to-climb and Ceiling Requirements

3.4.10.1 Sizing to time-to-climb requirements

Figure 3.26 shows an assumed linear relationship between rate-of-climb and altitude. Whether or not this relation in reality is linear depends on the engine and on the airplane characteristics as well as on the flight speed at which the climb is carried out.

Figure 3.26 introduces the following quantities:

RC_e = rate of climb at sealevel in fpm

RC_h = rate of climb at altitude, h in fpm

The reader is asked to show, that the rate-of-climb at a given altitude can be written as:

$$RC = RC_e(1 - h/h_{abs}) \tag{3.32}$$

Typical values for h_{abs} are given in Table 3.7 for different propulsive installations.

When sizing an airplane to a given time-to-climb requirement, the time-to-climb, t_{cl} will be specified.

A value for h_{abs} can be selected from Table 3.7 unless it is specified in the mission specification. The rate-of-climb at sealevel, RC_e can be calculated from:

$$RC_e = (h_{abs}/t_{cl})\ln(1 - h/h_{abs})^{-1} \tag{3.33}$$

Having determined RC_e, it is possible to find the required power loading or thrust-to-weight ratio as follows:

For shallow flight path angles: $\gamma < 15$ deg.

a) For propeller driven airplanes:
   from Eqns.(3.23) and (3.24)

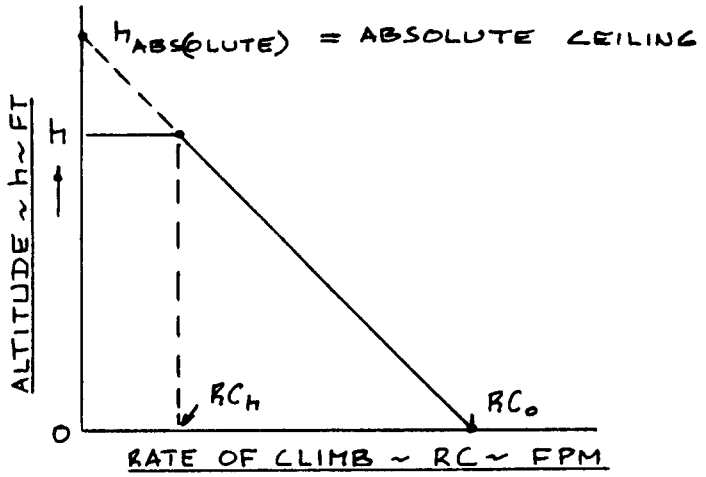

Figure 3.26 Linearized Rate-of-climb With Altitude

Table 3.7 Typical Values for the Absolute Ceiling, h_{abs}

Airplane Type	h_{abs} (ft)x10^{-3}
Airplanes with piston-propeller combinations:	
normally aspirated	12-18
supercharged	15-25
Airplanes with turbojet or turbofan engines:	
Commercial	40-50
Military	40-55
Fighters	55-75
Military Trainers	35-45
Airplanes with turbopropeller or propfan engines:	
Commercial	30-45
Military	30-50
Supersonic Cruise Airplanes (jets)	55-80

b) For jet driven airplanes:
from Eqn.(3.34):

$$RC = V\{(T/W) - 1/(L/D)\} \tag{3.34}$$

If the climb rate is to be maximized, Ref.14 shows that L/D needs to be maximized. In that case:

$$V = [2(W/S)/\{\rho(C_{D_o}\pi Ae)^{1/2}\}]^{1/2} \tag{3.35}$$

and:

$$(L/D)_{max} = 0.5(\pi Ae/C_{D_o})^{1/2} \tag{3.36}$$

From Eqns.(3.23) and (3.24) or from Eqns.(3.34) through (3.36) it is possible to find regions of $(T/W)_{TO}$ and $(W/S)_{TO}$ for which the climb requirements are satisfied.

For steep flight path angles: $\gamma > 15$ deg.

The reader should note that this case applies to fighter type airplanes only.

$$RC = V\sin\gamma, \tag{3.37}$$

where:

$$\sin\gamma = (T/W)[P_{dl} - [P_{dl}^{2} - P_{dl} + \{1 + (L/D)^{2}\}^{-1}]^{1/2}], \tag{3.38}$$

and where:

$$P_{dl} = (L/D)^{2}/\{1 + (L/D)^{2}\} \tag{3.39}$$

For best climb performance, the value of L/D in Eqn.(3.39) can be taken to be $(L/D)_{max}$.

3.4.10.2 Sizing to ceiling requirements

When sizing to a given ceiling requirement, the minimum required rate of climb at the ceiling altitude is specified. Table 3.8 defines the minimum climb rates for different ceilings.

The rate of climb at any altitude is given by:

Table 3.8 Definition of Airplane Ceilings

Ceiling Type	Minimum Required Climb Rate
Absolute ceiling	0 fpm
Service ceiling	
Commercial/Piston-propeller	100 fpm
Commercial/jet	500 fpm
Military at maximum power	100 fpm
Combat ceiling	
Military/Subsonic/maximum power	500 fpm at M<1
Military/Supersonic/maximum power	1,000 fpm at M>1
Cruise ceiling	
Military/Subsonic/max.cont. power	300 fpm at M<1
Military/Supersonic/max.cont. power	1,000 fpm at M>1

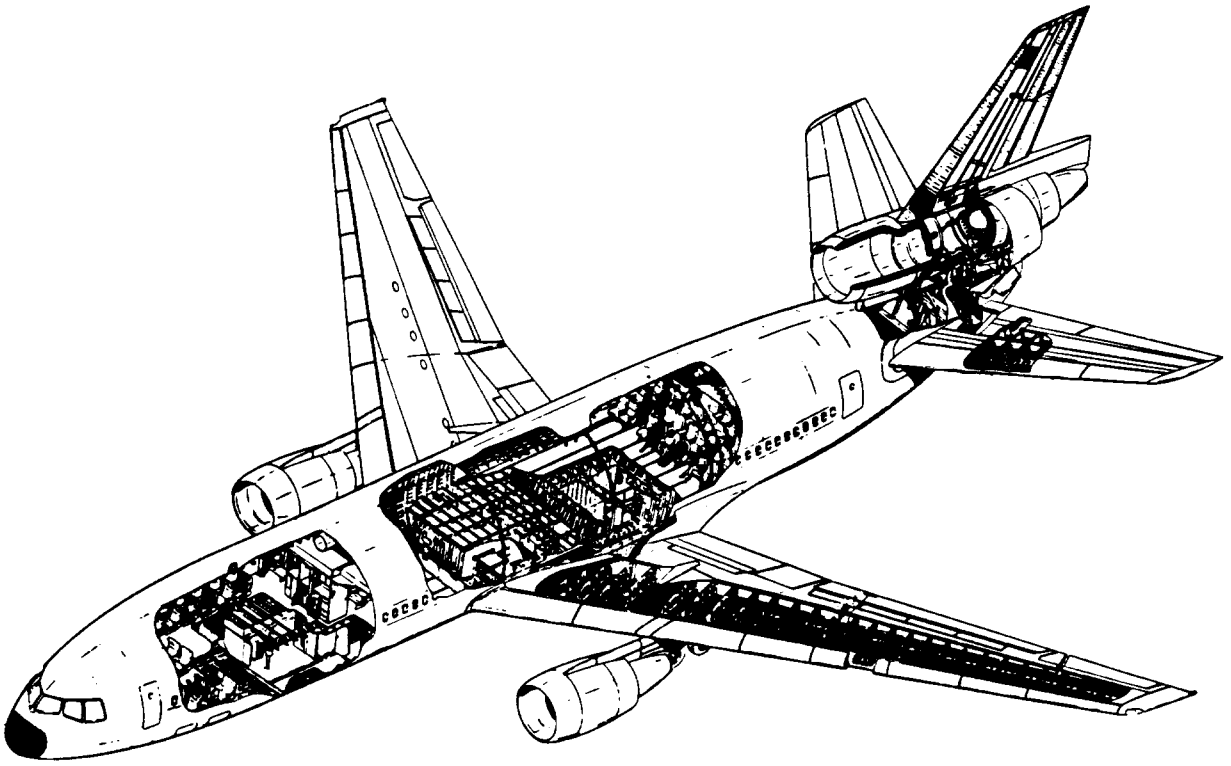

McDonnell Douglas

DC-10

a) For propeller driven airplanes:
   from Eqns.(3.23) and (3.24)

b) For jet driven airplanes:
   from Eqns.(3.34) through (3.36)

From these equations it is again possible to derive ranges of values for $(T/W)_{TO}$ and $(W/S)_{TO}$ for which the ceiling requirement is met.

3.4.11 Sizing to Specific Excess Power Requirements

Specific excess power is defined as follows:

$$P_s = dh_e/dt = (T - D)V/W, \qquad (3.40)$$

where:

$$h_e = \text{specific energy} = V^2/2g + h \qquad (3.41)$$

For certain fighter airplanes the value of P_s can be specified at a given combination of Mach number, M, weight, W and altitude, h. The reason for this is to assure combat superiority over some known or perceived threat.

To obtain the best possible P_s, Eqn.(3.40) suggests to:

a) install a high value of T/W and,
b) design for a high value of L/D.

For preliminary sizing purposes it is suggested that a range of realistic values are assumed for L/D. From Eqn.(3.40) it is then possible to determine the required value of T/W for a given value of P_s. The thus obtained value for T/W needs to be transferred to a corresponding value for $(T/W)_{TO}$ using engine data.

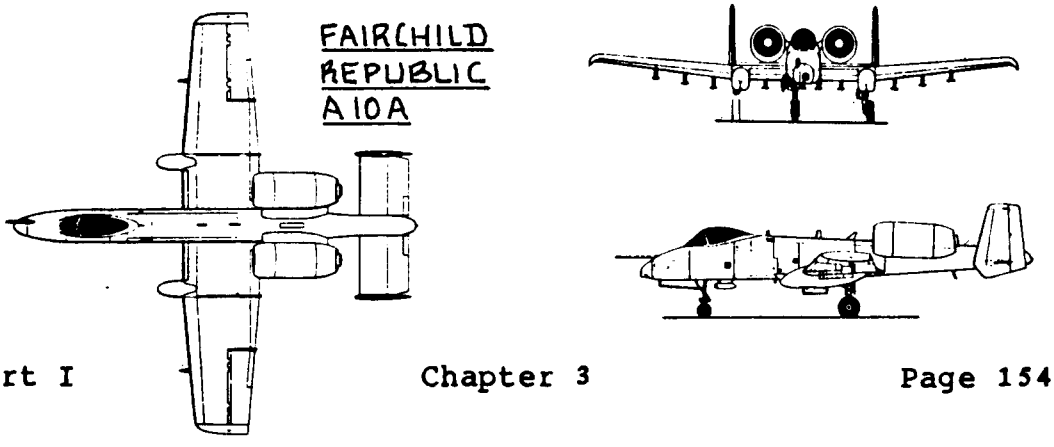

3.4.12 Example of Sizing to Military Climb Requirements

An attack fighter with the mission specification of Table 2.19 needs to be sized such that its climb performance meets that specified in Table 2.19.

The specification consists of two requirements:

1) RC > 500 fpm with one engine out, sealevel 95°F and at maximum take-off weight. This includes external stores.

The mission specification does not specify the airplane configuration. It is assumed, that this is gear up and flaps take-off.

2) T_{cl} = 8 min. to 40,000 ft at maximum (clean) take-off weight.

In addition, it is assumed, that the following P_s requirement must also be met:

3) P_s = 80 fps at 40,000 ft and M = 0.8, in the clean configuration and at maximum (clean) take-off weight.

First, the drag polar must be estimated. To do this, the procedure of Sub-section 3.4.1 will be used.

From p.67, it follows that W_{TO} = 64,500 lbs. This weight includes external stores! The effect of external stores is not included in the wetted area correlation of Figure 3.22b. The clean maximum take-off weight for this fighter is 64,500 - 10,000 = 54,500 lbs.

From Figure 3.22c it is found that the corresponding S_{wet} = 3,500 ft^2. This value is taken to Figure 3.21b and, assuming C_f = 0.0030, it follows that f = 10.5 ft^2.

A reasonable average wing loading for this type of attack fighter is 50 psf. This yields S_w = 1,090 ft^2. Therefore:

$$C_{D_o} = 10.5/1,090 = 0.0096$$

It will be assumed that the external stores cause an

increase in equivalent flat plate area of: $\Delta f = 3.2$ ft^2.
This yields:

$$\Delta C_{D_o} = 3.2/1,090 = 0.0030$$

The following additional assumptions are made:

Wing aspect ratio, A = 4
Oswald's efficiency factor, e = 0.8 clean and
e = 0.7 flaps take-off
Incremental value for flaps take-off zero lift drag coefficient:

$$\Delta C_{D_o} = 0.0200.$$

Compressibility drag increment, clean, at M = 0.8:

$$\Delta C_{D_o} = 0.0020.$$

The drag polars may be summarized as follows:

Clean, low speed: $C_D = 0.0096 + 0.0995C_L^2$

Clean, M = 0.8: $C_D = 0.0116 + 0.0995C_L^2$

Take-off, gear up: $C_D = 0.0296 + 0.1137C_L^2$

The three climb requirements will now be analyzed one by one.

Climb requirement 1): Engine out, t.o., gear up

With the help of Eqns.(3.34) through (3.36) it is now possible to determine the relation between W/S and T/W so that this climb rate is satisfied.
It will be assumed that the climb can be performed at $(L/D)_{max}$. From Eqn.(3.36) it is found that:

$$(L/D)_{max} = 8.6$$

From Eqn.(3.35) it is seen that the corresponding speed depends on wing loading and on density. The latter is to be taken on a 95°F day. In that case the corresponding temperature ratio is: 554.7/518.7 = 1.069.
The density ratio at sealevel now is:

$\sigma = 1/1.069 = 0.935$, so that $\rho = 0.002224$ slugs/ft^3.

With the help of Eqns. (3.34) and (3.35) it is now

possible to construct the following tabulation:

$(W/S)_{TO}$	V	RC/V	1/L/D	$(T/W)_{TO}$	$(T/W)_{TO}$	$(T/W)_{TO}$
psf	fps			one eng.	two eng.	two eng.
				95°F	95°F	sls
	(3.35)			(3.34)		
40	265	0.031	0.116	0.147	0.294	0.346
60	325	0.026	0.116	0.142	0.284	0.334
80	375	0.022	0.116	0.138	0.276	0.325
100	420	0.020	0.116	0.136	0.272	0.320
				x2	:0.85	

To obtain the numbers in the last column, it was assumed that for the 95°F day, the thrust is 0.85 times that at sealevel standard (sls).

Figure 3.27 shows the region of $(W/S)_{TO}$ and $(T/W)_{TO}$ for which this climb requirement is met.

Climb Requirement 2: Clean, without stores

The time-to-climb to 40,000 ft is to be 8 min. in the clean configuration. It will be assumed that the absolute ceiling is 45,000 ft. From Eqn.(3.33) it follows that:

$$RC_o = (45{,}000/8)\ln(1 - 40/45) = 12{,}359 \text{ fpm} = 206 \text{ fps}$$

Because this is a fighter airplane, the climb angle is probably steep. Therefore, the method of Eqns.(3.37) through (3.39) will be used in the sizing process.

It is assumed, that the climb will take place at $(L/D)_{max}$.

Since $C_{D_o} = 0.0096$, it follows from Eqn.(3.36) that: $(L/D)_{max} = 16.2$. The corresponding speed follows again from Eqn.(3.35).

The value for P_{dl} may be found from Eqn.(3.39) as: 0.996. With Eqns.(3.37) and (3.38) it also follows that:

$$RC_o = 0.996V(T/W)$$

It is now possible to construct the following tabulation:

$(W/S)_{TO}$ clean (without stores) psf	$(W/S)_{TO}$ maximum (with stores) psf	V (3.35) fps	$(T/W)_{TO}$ clean (without stores)	$(T/W)_{TO}$ maximum (with stores)
40	47	329	0.629	0.531
60	71	403	0.514	0.434
80	95	465	0.445	0.376
100	118	520	0.398	0.336
:1.18			:1.18	

The factor 1.18 represents the ratio of take-off weight with stores (64,500 lbs) to that without stores (54,500 lbs).

Figure 3.27 shows regions of $(W/S)_{TO}$ and $(T/W)_{TO}$ where this requirement is met.

Climb Requirement 3: Clean, without stores

With P_s = 80 fps, Eqn.(3.40) can be rearranged to yield:

$$(T/W) = 80/V + 1/(L/D)$$

At M = 0.8 and 40,000 ft, the dynamic pressure is:

$$\bar{q} = 1482 \times 0.1851 \times M^2 = 176 \text{ psf}$$

The clean drag polar at M = 0.8 was previously given. The clean maximum weight is 54,500 lbs. The following tabulation can now be constructed:

$(W/S)_{TO}$ clean (without stores) psf	$\bar{q}$ psf	C_L	C_D	L/D	1/(L/D)	V fps
40	176	0.23	0.0169	13.6	0.074	774
60	176	0.34	0.0231	14.7	0.068	774
80	176	0.45	0.0317	14.2	0.070	774
100	176	0.57	0.0439	13.0	0.077	774

$(W/S)_{TO}$ maximum (with stores) psf	80/V	(T/W) at 40K M = 0.8	$(T/W)_{TO}$ sls
47	0.103	0.177	0.96
71	0.103	0.171	0.92
95	0.103	0.173	0.93
118	0.103	0.180	0.97

x5.4

The last column was obtained by multiplying (T/W) at 40,000 ft and M = 0,8 by 5.4, which is the pressure ratio for that altitude. This corresponds roughly to the thrust ratio for these two conditions.

From typical engine data it can be observed that at high altitude and subsonic flight no significant change in thrust occurs between M = 0 and M = 0.8.

Figure 3.27 shows the region of $(W/S)_{TO}$ and $(T/W)_{TO}$ where this specific excess power requirement is met. It is clear that this requirement is by far the more critical one in this case.

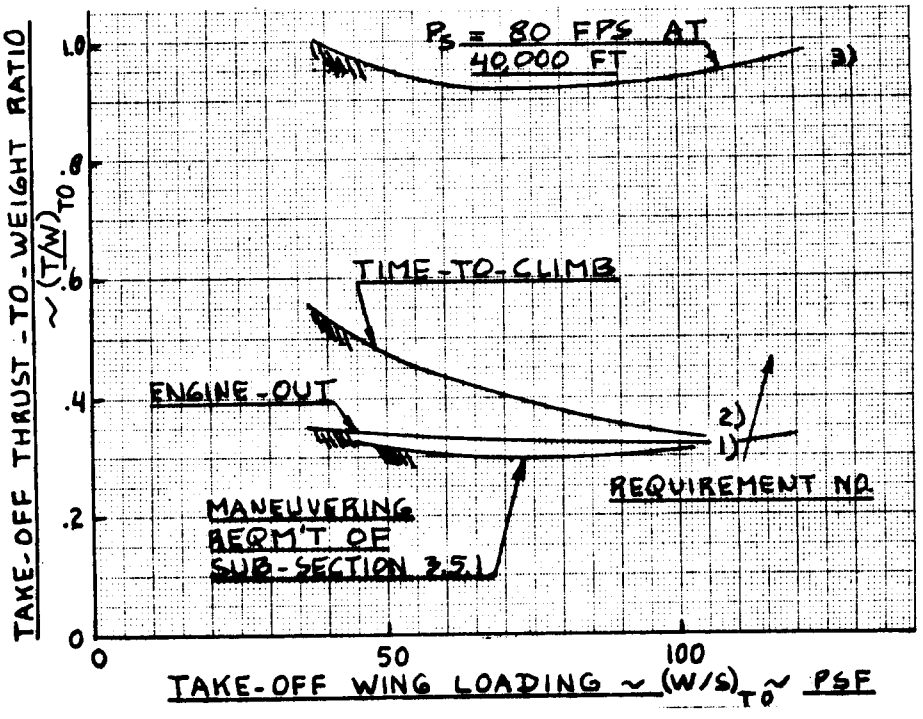

Figure 3.27 Effect of Military Climb Requirements on the Allowable Values of Take-off Thrust-to-Weight Ratio and Take-off Wing Loading

3.5 SIZING TO MANEUVERING REQUIREMENTS

Specific requirements for sustained maneuvering capability (including sometimes specific turn rate) are often contained in the mission specification for utility, agricultural, aerobatic or for military airplanes.

Sustained maneuvering requirements are usually formulated in terms of a combination of sustained load factor (g's) to be pulled at some combination of speed and altitude.

The sustained maneuvering capability of an airplane depends strongly on its maximum lift coefficient and on its installed thrust.

For equilibrium perpendicular to the flight path, it is necessary that:

$$nW = C_L \bar{q} S = 1,482 \delta M^2 C_L S \qquad (3.42)$$

The maximum load factor capability of an airplane, n_{max} can be found from Eqn.(3.42) as:

$$n_{max} = (1,482 C_{L_{max}} \delta M^2)/(W/S) \qquad (3.43)$$

This load factor can be sustained as long as there is sufficient thrust. Since:

$$T = C_{D_o} \bar{q} S + (C_L^2/\pi Ae) \bar{q} S \qquad (3.44)$$

After dividing Eqn.(3.44) by W and rearranging:

$$(T/W) =$$

$$\bar{q} C_{D_o}/(W/S) + (W/S)(n_{max})^2/(\pi Ae\bar{q}) \qquad (3.45)$$

If some maximum load factor, n_{max} is desired on a sustained basis at a given combination of Mach number, M and altitude (δ), then Eqn.(3.45) can be used to find the relation between T/W and W/S, for a given value of C_{D_o}. The latter can be found with the methods discussed in Sub-section 3.4.1.

If a requirement is included for a specific minimum turn rate, the following equation may be used:

$$\dot{\psi} = (g/V)(n^2 - 1)^{1/2} \qquad (3.46)$$

This equation is derived in Ref.14, p.493.

If turn rate is specified at a given speed, the required sustained load factor, n may be found from:

$$n_{reqd} = \{(V\dot{\psi}/g)^2 + 1\}^{1/2} \qquad (3.47)$$

Equation (3.45) can then be used to find the relation between (T/W) and (W/S) for which the turn rate requirement is satisfied.

3.5.1 Example of Sizing to a Maneuvering Requirement

The fighter with the mission specification of Table 2.19 must also meet the following maneuvering requirement: a sustained steady turn corresponding to 3.5g at sealevel, 450 kts and with a clean weight of 54,500 lbs.

It is assumed, that the clean C_{D_o} of the airplane at M =450/661.2 = 0.68 and sealevel is 0.0096. With A =4 and e = 0.8 it follows from Eqn.(3.45) that:

$$(T/W)_{reqd} = 6.6/(W/S) + 0.00178(W/S)$$

The following tabulation can now be made:

→ peso al que se requiere el factor de carga

(W/S) actual psf	$(W/S)_{TO}$ max psf	First Term	Second Term	(T/W) clean	$(T/W)_{TO}$ max M = 0.68	$(T/W)_{TO}$ max static
40	47	0.165	0.071	0.236	0.200	0.320
60	71	0.110	0.107	0.217	0.184	0.294
80	95	0.083	0.142	0.225	0.191	0.305
100	118	0.066	0.178	0.244	0.207	0.331
x1.18					:1.18 x1.6	

The value of $(T/W)_{TO}$ in the last column is obtained from that at M = 0.68 by multiplying by 1.6. This number is representative of the thrust ratio between M = 0 and M = 0.68 at sealevel. Such a number comes from typical engine data.

Figure 3.27 also shows the regions of $(W/S)_{TO}$ and $(W/S)_{TO}$ for which the maneuvering requirement is met.

3.6 SIZING TO CRUISE SPEED REQUIREMENTS

3.6.1 Cruise Speed Sizing of Propeller Driven Airplanes

The power required to fly at some speed and altitude is given by:

$$P_{reqd} = TV = C_D qSV \qquad (3.48)$$

This can also be written as:

$$550SHP\eta_p = 0.5\rho V^3 SC_D \qquad (3.49)$$

Cruise speeds for propeller driven airplanes are usually calculated at 75 to 80 percent power. In that case it can be shown that the induced drag is small compared to the profile drag. Frequently, the assumption:

$$C_{D_i} = 0.1C_{D_o} \qquad (3.50)$$

is made.

Loftin (ref.11) showed, that because of this fact, cruise speed turns out to be proportional to the following factor:

$$V_{cr} \propto [\{(W/S)/(W/P)\}(\eta_p/\sigma C_{D_o})^{-1}]^{1/3} \qquad (3.51)$$

From this, Loftin derived the fact that:

$$V_{cr} \propto I_p \qquad (3.52)$$

where:

$$I_p = \{(W/S)/\sigma(W/P)\}^{1/3} \qquad (3.53)$$

The parameter I_p is called the power index.

Figures 3.28, 3.29 and 3.30 show how V_{cr} is related to I_p for a range of example airplanes. These figures can therefore be used as a first estimate for I_p for a given desired cruise speed. From that in turn it is possible to determine the relationship between (W/S) and (W/P) needed to meet a given cruise speed requirement.

It is possible to use this method to reconstruct C_{D_o} from measured speed and power data.

The next Sub-section presents an application.

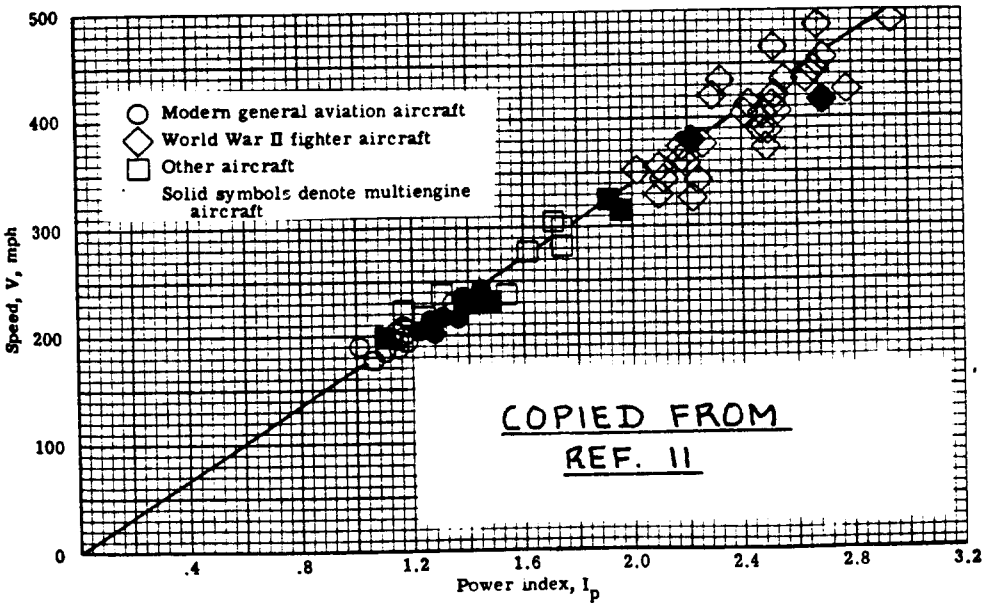

Figure 3.28 Correlation of Airplane Speed with Power Index for Retractable Gear, Cantilevered Wing Configurations

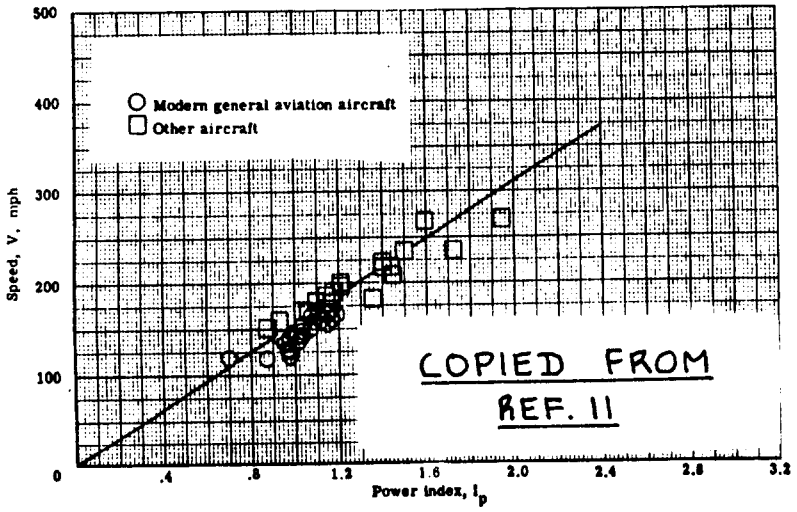

Figure 3.29 Correlation of Airplane Speed with Power Index for Fixed Gear, Cantilevered Configurations

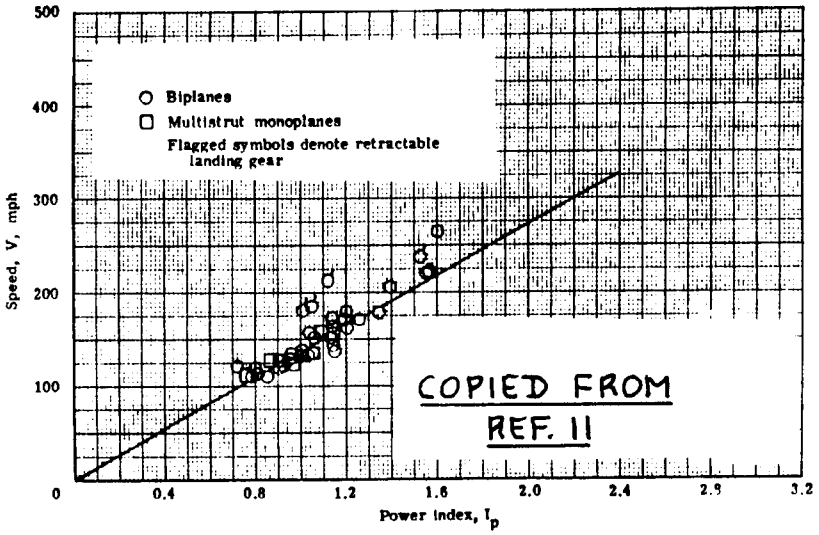

Figure 3.30 Correlation of Airplane Speed with Power Index for Biplanes and Strutted Monoplanes with Fixed Gear

Table 3.9 Typical Values for Zero-lift Drag Coefficient and Maximum Lift-to-drag Ratio

Airplane Type	C_{D_0}	A	e	$(L/D)_{max}$
Boeing 247D	0.0212	6.55	0.75	13.5
Douglas DC-3	0.0249	9.14	0.75	14.7
Boeing B-17G	0.0236	7.58	0.75	13.8
Seversky P-35	0.0251	5.89	0.62	10.7
Piper J-3 Cub	0.0373	5.81	0.75	9.6
Beechcraft D17S	0.0348	6.84	0.76	10.8
Consolidated B-24J	0.0406	11.55	0.74	12.9
Martin B-26F	0.0314	7.66	0.75	12.0
North American P-51D	0.0161	5.86	0.69	14.0
Lockheed L.1049G	0.0211	9.17	0.75	16.0
Piper Cherokee	0.0358	6.02	0.76	10.0
Cessna Skyhawk	0.0319	7.32	0.75	11.6
Beech Bonanza V-35	0.0192	6.20	0.75	13.8
Cessna Cardinal RG	0.0223	7.66	0.63	13.0

Note: These data are copied from Ref.11, Table 5.I.

3.6.2 A Method for Finding C_{D_o} from Speed and Power Data.

Loftin, in Ref.11, Eqn.(6.3) derives the following equation:

$$V = 77.3\{\eta_p(W/S)/\sigma C_D(W/P)\}^{1/3} \qquad (3.54)$$

With Eqn.(3.53) it is possible to rewrite this as:

$$C_D = \eta_p 77.3^3 (I_p/V)^3 \qquad (3.55)$$

By now assuming that in a high speed cruise condition $\eta_p = 0.85$ and that $C_{D_o} = 0.9C_D$, Eqn.(3.55) becomes:

$$C_{D_o} = 1.114x10^5 (I_p/V)^3 \qquad (3.56)$$

It must be noted that V in Eqn.(3.56) is in mph!

If for a given airplane the maximum power and speed at some altitude are given, it is possible to use Eqn.(3.56) to estimate C_{D_o}. Table 3.9 shows some results as obtained by Loftin in Ref.11.

3.6.3 Example of Cruise Speed Sizing for a Propeller Driven Airplane

The airplane of Table 2.17 must achieve a cruise speed of 250 kts at 85 percent power at 10,000 ft and at take-off weight. Size the airplane so it can do that.

Observe, that 250 kts is equivalent to 288 mph. From Figure 3.28 it follows that: $I_p = 1.7$.

At 10,000 ft, $\sigma = 0.7386$. Therefore, with Eqn.(3.53) it is found that:

$$(W/S) = 3.63(W/P)$$

Figure 3.31 shows the range of combinations of W/S and W/P for which the cruise speed requirement is met.

Note that (W/P) is at 10,000 ft. To transfer that ratio to sealevel it is necessary to multiply by the power ratio for cruise power at 10,000 ft to that at sealevel. This ratio is typically 0.7 for reciprocating engines without supercharging.

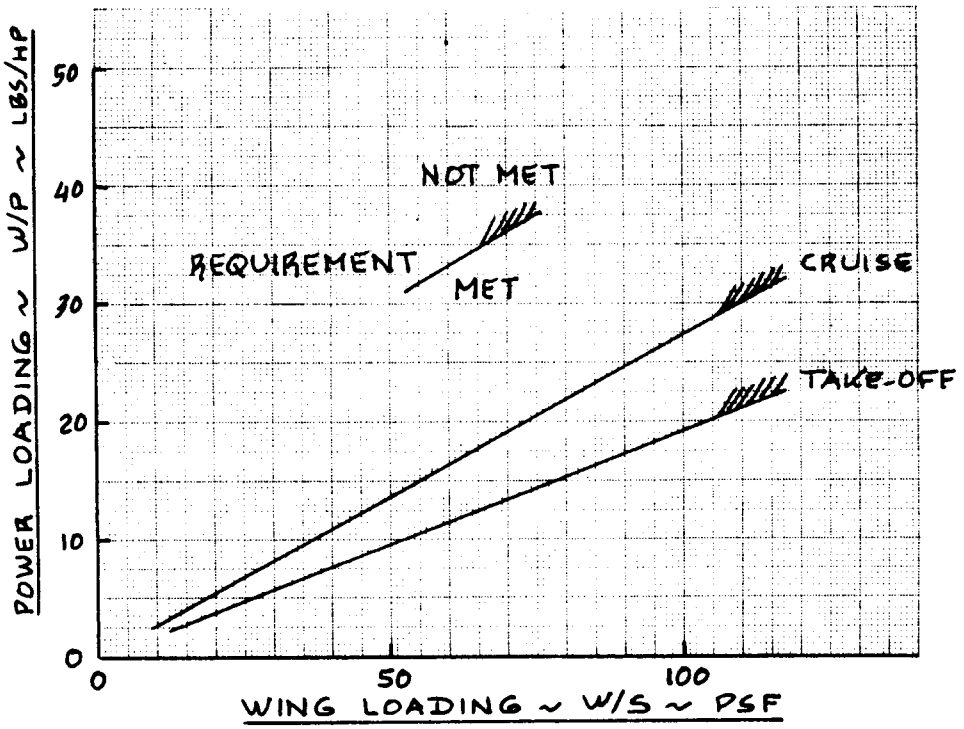

Figure 3.31 Allowable Values of Wing Loading and Thrust-to-Weight Ratio to Meet a Given Cruise Speed

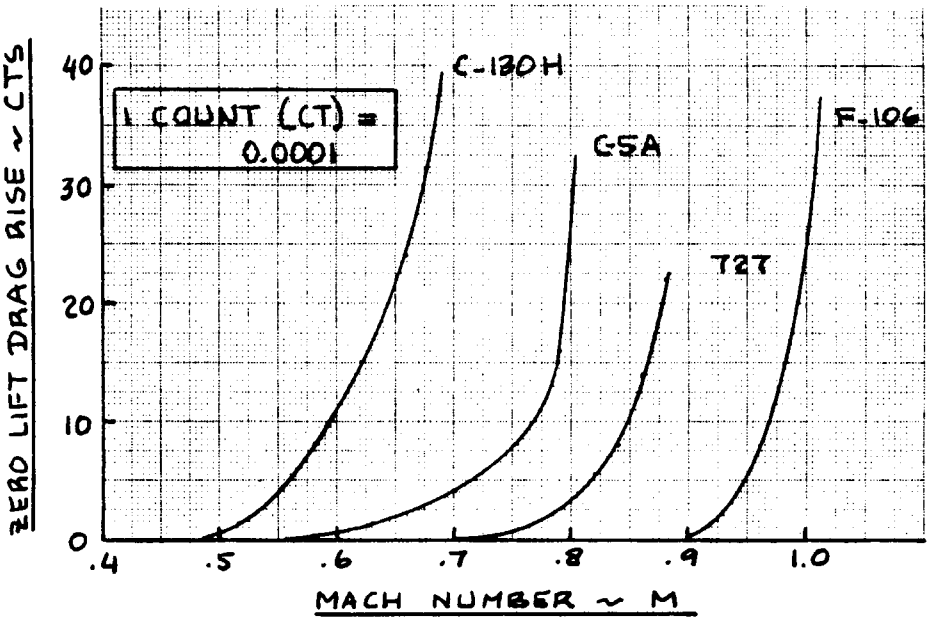

Figure 3.32 Rapid Method for Estimating Drag Rise

3.6.4 Cruise Speed Sizing of Jet Airplanes

At maximum level speed the following equations are simultaneously satisfied:

$$T_{reqd} = C_D \bar{q} S \tag{3.57}$$

$$W = C_L \bar{q} S \tag{3.58}$$

If a parabolic drag polar is assumed, Eqn.(3.57) can be written as:

$$T_{reqd} = C_{D_o} \bar{q} S + C_L^2 \bar{q} S / \pi A e \tag{3.59}$$

Dividing by weight:

$$(T/W)_{reqd} = C_{D_o} \bar{q} S / W + W / \bar{q} S \pi A e \tag{3.60}$$

If the maximum speed is specified at some combination of Mach number and altitude, then the dynamic pressure, $\bar{q}$ is known. For a given value of zero lift drag coefficient, C_{D_o}, it is possible to use Eqn.(3.60) to construct relations between T/W and W/S which satisfy the maximum speed requirements.

The maximum speed tends to be specified at a value of weight, below take-off weight, that is at:

$$W = kW_{TO}, \tag{3.61}$$

where k is a number $0 < k < 1.0$. The required take-off wing loading must therefore be obtained from:

$$(W/S)_{TO} = k^{-1} (W/S)_{Eqn.(3.60)} \tag{3.62}$$

Similarly, the required thrust-to-weight ratio at take-off must be reconstructed from the thrust-to-weight ratio found from Eqn.(3.60). To do this requires knowledge of how the installed thrust of the airplane varies with Mach number and with altitude.

The methodology just discussed works fine for speeds at Mach numbers below that where compressibility effects play a role. If compressibility is important (and generally above M=0.5 it is), a modification of C_{D_o} will be required. Figure (3.32) shows how ΔC_{D_o} can be quickly found.

3.6.5 Example of Sizing to Maximum Speed for a Jet

It is desired to size an airplane with W_{TO} = 10,000 lbs so that it has a maximum speed of M = 0.9 at sealevel.

At this high Mach Number, the effects of drag rise need to be accounted for.

From Figure 3.22b, at 10,000 lbs, a wetted area estimate for this airplane is: S_{wet} = 1,050 ft^2.

From Figure 3.21b, assuming a C_f = 0.0030, it is seen that: f = 3.2 ft^2.

A typical value for wing loading is taken to be 60 ft^2. This implies S = 167 ft^2 and therefore:

$$C_{D_o} = 0.0192$$

The compressibility drag increment is assumed to be 0.0030. Assuming A = 5 and e = 0.8, Eqn.(3.60) can be written as:

$$T/W = 26.6/(W/S) + (W/S)/15,080$$

The following tabulation can now be made:

$(W/S)_{TO}$ psf	Profile Drag Term	Induced Drag Term	T/W M = 0.9	$(T/W)_{TO}$ static
40	0.665	0.003	0.668	1.07
60	0.443	0.004	0.447	0.72
80	0.333	0.005	0.338	0.54
100	0.266	0.007	0.273	0.44

Figure 3.33 shows the region of W/S and T/W for which the speed requirement is met. Note the advantage of high wing loading at high speed and at sealevel.

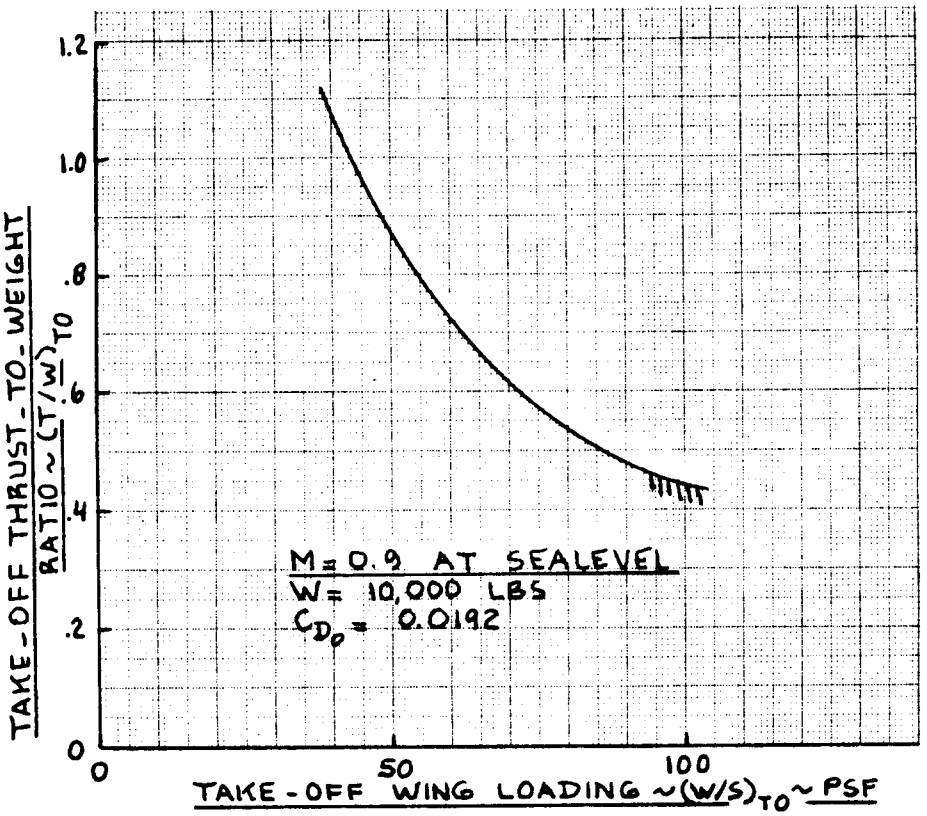

Figure 3.33 Allowable Values of Wing Loading and Thrust-to-Weight Ratio to Meet a Given Maximum Speed at Sealevel

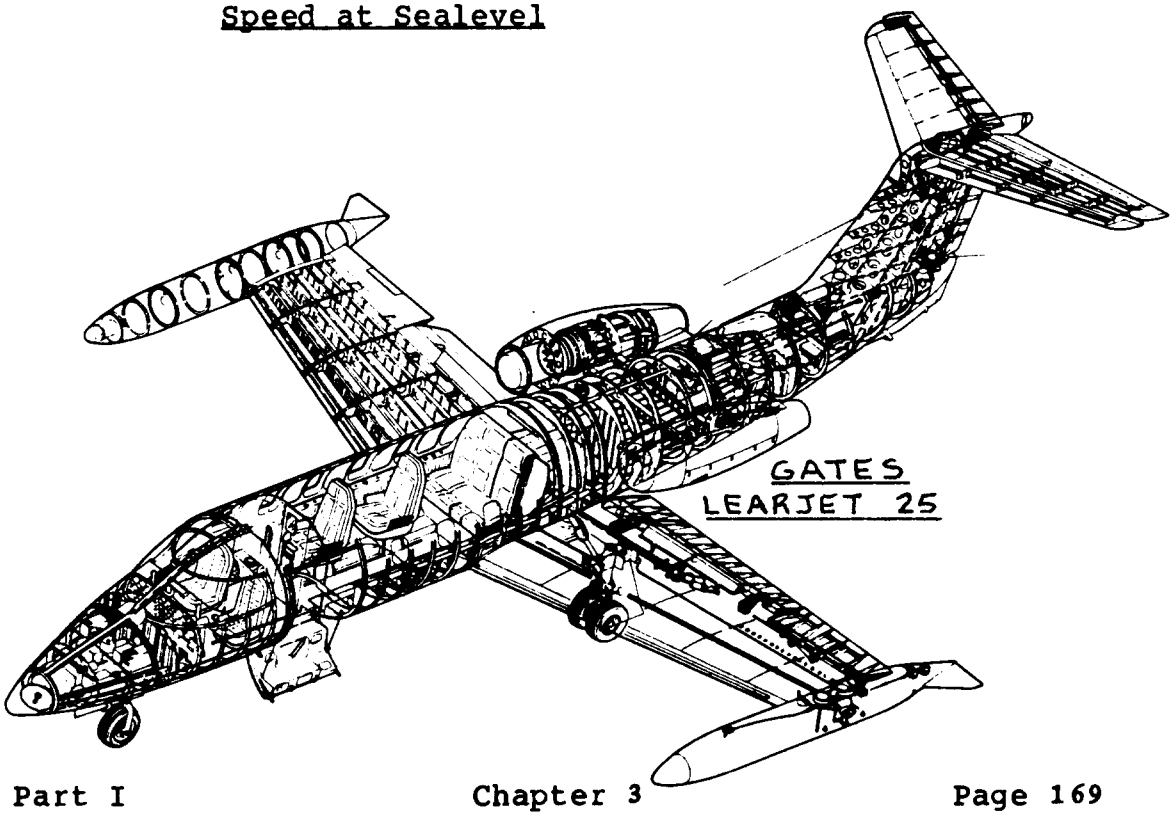

3.7 MATCHING OF ALL SIZING REQUIREMENTS AND THE APPLICATION TO THREE EXAMPLE AIRPLANES

3.7.1 Matching of all Sizing Requirements

Having established a series of relations between:

Take-off thrust-to-weight ratio,

Take-off wing loading,

Maximum required lift coefficients,

and Aspect ratio,

it is now possible to determine the 'best' combination of these quantities for the design at hand. The word 'best' is used rather than 'optimum' because the latter implies a certain mathematical precision. What is usually done at this point is to overlay all requirements and select the lowest possible thrust-to-weight ratio and the highest possible wing loading which are consistent with all requirements. This process is also known as the matching process.

Typical matching diagrams resulting from this matching process are discussed in Sub-sections 3.7.2 through 3.7.4.

3.7.2 Matching Example 1: Twin Engine Propeller Driven Airplane

Table 2.17 contains the mission specification for this airplane. To determine the allowable power and wing loadings, the landing, take-off, climb and cruise speed requirements will all be translated into ranges of allowable values for (W/S), (W/P) and $C_{L_{max}}$.

3.7.2.1 Take-off distance sizing

Table 2.17 requires $s_{G_{TO}}$ = 1,500 ft under FAR 23 rules at sealevel and for a standard day. From Eqn.(3.4) it is found that:

$$1{,}500 = 4.9\ TOP_{SL} + 0.009 TOP_{SL}^{2}$$

This yields:

$$TOP_{SL} = 218\ hp/ft^2$$

Because $\sigma = 1.0$ in this case, Eqn.(3.2) yields:

$$(W/S)(W/P) = 218 C_{L_{max_{TO}}}$$

Typical values for $C_{L_{max_{TO}}}$ for a twin propeller driven airplane are seen to be 1.4 - 2.0 from Table 3.1.

For this airplane values of 1.4, 1.7 and 2.0 will be considered. The following tabulation can now be made:

$C_{L_{max_{TO}}}$ =	1.4	1.7	2.0
$(W/S)_{TO}$	$(W/P)_{TO}$	$(W/P)_{TO}$	$(W/P)_{TO}$
psf	lbs/hp	lbs/hp	lbs/hp
20	15.3	18.5	21.8
30	10.2	12.4	14.5
40	7.6	9.3	10.9
50	6.1	7.4	8.7
60	5.1	6.2	7.3

Figure 3.34 shows a graphical presentation of these results.

3.7.2.2 Landing distance sizing

Table 2.17 requires that s_{G_L} = 1,500 ft under FAR 23 rules at sealevel and a standard day. From Eqn.(3.12):

$$V_{s_L}^2 = 1,500/0.265 = 5,660 \text{ kts}^2$$

Therefore:

$$V_{s_L} = 75.2 \text{ kts} = 127 \text{ fps}$$

With Eqn.(3.1) this now requires that:

$$(W/S)_L = \{(127^2 \times 0.002378)/2\} C_{L_{max_L}} = 19.2 C_{L_{max_L}}$$

Table 2.17 also specified:

$$W_L = 0.95 W_{TO}$$

The wing loading requirement therefore changes to:

$$(W/S)_{TO} = (19.2/0.95) C_{L_{max_L}} = 20.2 C_{L_{max_L}}$$

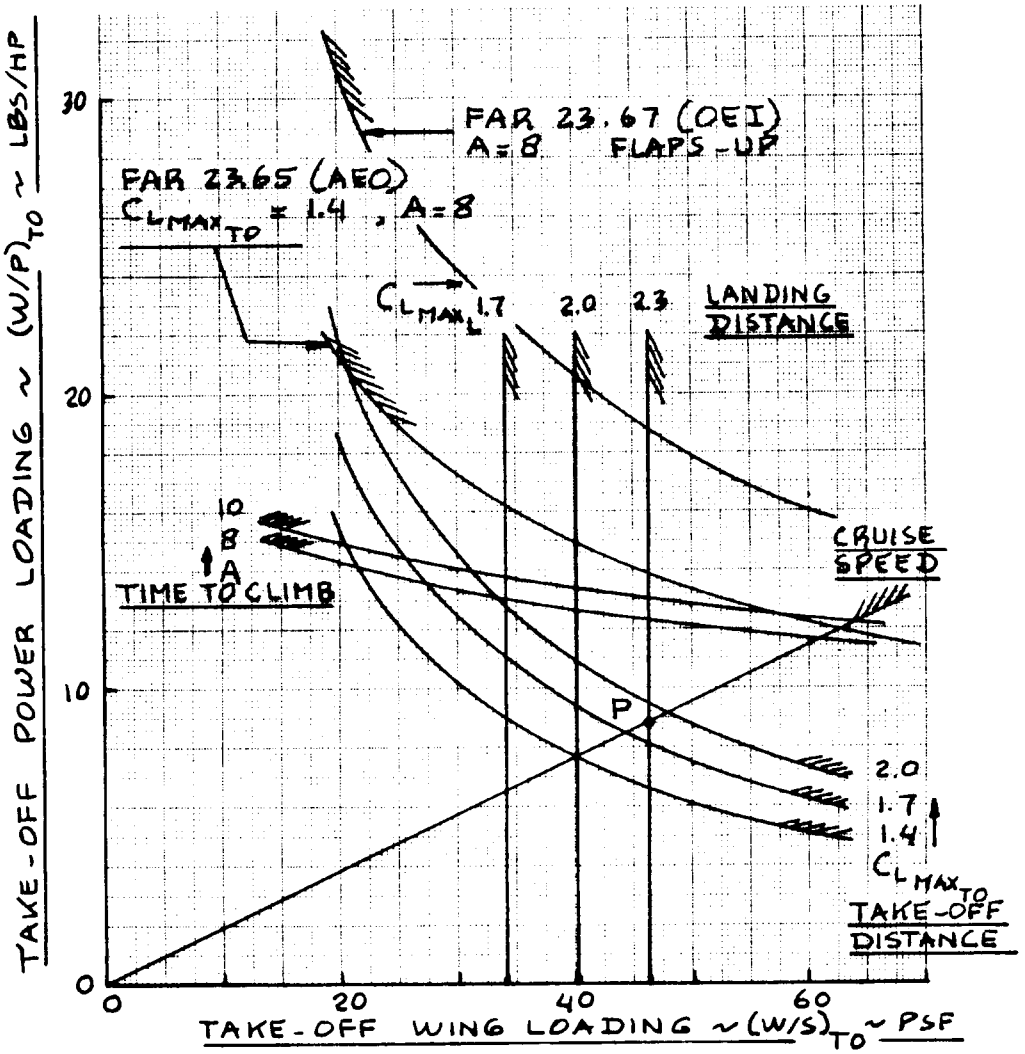

Figure 3.34 Matching Results for Sizing of a Twin Engine Propeller Driven Airplane

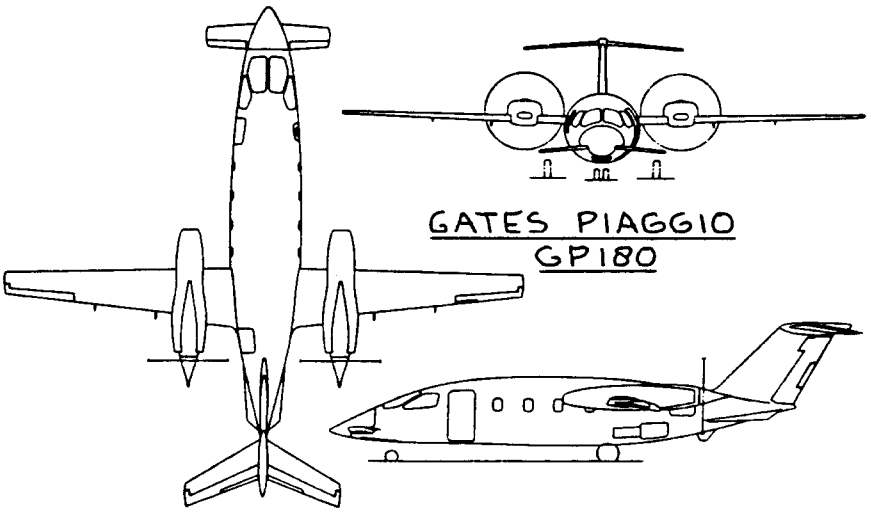

From Table 3.1 it follows that typical values for $C_{L_{max_L}}$ for this type airplane are: 1.6 - 2.5.

In this case a range of values of 1.7, 2.0 and 2.3 will be considered, leading to maximum allowable wing loadings of 34.3, 40.4 and 46.5 psf respectively.

Figure 3.34 shows how this further restricts the useful range of combinations of $(W/S)_{TO}$ and $(W/P)_{TO}$.

3.7.2.3 FAR 23 climb sizing

The example in Sub-section 3.4.4 showed that for this type of airplane, the requirements of FAR 23.65 and 23.67 were the most critical. Therefore only these requirements will be considered in this example calculation.

The inexperienced reader is warned not to always take this outcome for granted. When in doubt: check all requirements!

FAR 23.65 (AEO)

As shown in Sub-section 3.4.4 the climb gradient component of this requirement was more critical than the climb rate component.

From Eqn.(3.30):

$$(18.97\eta_p\sigma^{1/2})/(W/P)(W/S)^{1/2} = \{0.0833 + (L/D)^{-1}\}/C_L^{1/2}$$

The drag polar for this airplane in the gear-up, take-off flaps configuration is found with the procedure of Sub-section 3.4.1.

From p.53, W_{TO} = 7,900 lbs. With Figure 3.22a, this yields: S_{wet} = 1,400 ft^2. Figure 3.21a shows that f = 7 ft^2 is a reasonable value for equivalent parasite area.

Using an average wing loading of 30 psf, S = 263 ft^2 and thus:

C_{D_o} = 0.0266. For take-off flaps an incremental drag coefficient of 0.0134 will be assumed. The drag polars for this airplane can be summarized as follows:

for the clean configuration: $C_D = 0.0266 + C_L^2/\pi Ae$, with e = 0.8

for take-off:
gear up $C_D = 0.0400 + C_L^2/\pi Ae$, with $e = 0.8$

For this airplane, aspect ratios of 8 and 10 will be considered. Values for $C_{L_{max_{TO}}}$ were taken as 1.4, 1.7 and 2.0. The corresponding 'safe' values of C_L for this flight condition are: 1.2, 1.5 and 1.8. This yields a 'margin' of $\Delta C_L = 0.2$. With this information the following table of L/D values can now be determined:

		A = 8		A=10	
$C_{L_{max_{TO}}}$	$C_{L_{TO}}$	(L/D)	$(L/D)^{-1}$	(L/D)	$(L/D)^{-1}$
1.4	1.2	10.8	0.093	12.3	0.081
1.7	1.5	9.9	0.101	11.6	0.086
2.0	1.8	8.9	0.112	10.7	0.094

Assuming $\eta_p = 0.0$, while $\sigma = 1.0$ it is possible to tabulate values for W/P as follows:

	A=8			A=10		
$C_{L_{max_{TO}}}$	1.4	1.7	2.0	1.4	1.7	2.0
$(W/S)_{TO}$			$(W/P)_{TO}$			
psf			lbs/hp			
20	21.1	22.6	23.3	22.6	24.6	25.7
30	17.2	18.4	19.0	18.5	20.1	21.0
40	14.9	15.9	16.5	16.0	17.4	18.2
50	13.3	14.3	14.7	14.3	15.5	16.2
60	12.2	13.0	13.5	13.1	14.2	14.8

The reader will note that for increasing A and for increasing $C_{L_{max_{TO}}}$ less power is required!

Figure 3.34 superimposes the FAR 23.65 results on results obtained from previous sizing criteria.

FAR 23.67 (OEI)

To meet this requirement the flaps may be in the most favorable position. Most favorable in this case means that position of the flaps which yields the highest value of $(C_L^{3/2})/C_D)_{max}$. The drag polars for this case are estimated as follows:

Flaps up, gear up, one propeller feathered: $C_D = 0.0266 + 0.0034_{prop.} + C_L^2/\pi Ae$

Flaps take-off, gear up, one propeller feathered:

$$C_D = 0.0266 + 0.0034_{prop.} + 0.0134_{flaps} + C_L^2/\pi Ae$$

The following results are now obtained:

	flaps up		flaps t.o.	
	e = 0.85		e = 0.80	
A=	8	10	8	10
$(C_L^{3/2}/C_D)_{max}$ (Eqn.(3.27))	13.6	16.1	11.8	13.9
$C_{L_{RC_{max}}}$ (Eqn.(3.25))	1.39	1.55	1.65	1.84

It is clear that the flaps up case is the more favorable one. For flaps up it was already assumed that $C_{L_{max}} = 1.7$. The lift coefficient values of 1.4 and 1.6 are reasonably compatible with this.

Next, V_{s_o} at 5,000 ft needs to be determined as a function of wing loading.

This yields: $V_{s_o} = 23.96\ (W/S)^{1/2}$. The required value of rate of climb parameter, RCP can now be computed as follows:

$(W/S)_{TO}$	V_{s_o}	V_{s_o}	RC $=.027V_{s_o}^2$	RCP Eqn.(3.23)
psf	fps	kts	fpm	
20	107.2	63.5	109	0.00330
30	131.2	77.7	163	0.00494
40	151.5	89.8	218	0.00661
50	169.4	100.4	272	0.00824
60	185.6	110.0	327	0.00991

Equation 3.24 relates the required value of RCP to those of allowable values for W/S and W/P. For the two values of aspect ratio it can now be shown that Eqn.(3.24) yields:

For A = 8:

$RCP = 0.8/(W/P) - (W/S)^{1/2}/239.9$ and,

For A = 10:

$RCP = 0.8/(W/P) - (W/S)^{1/2}/284$

The following tabulation can now be made:

A = 8

$(W/S)_{TO}$ psf	$(W/S)^{1/2}/239.9$	RCP	(W/P) 5,000 ft lbs/hp	$(W/P)_{TO}$ sealevel lbs/hp
20	0.01864	0.00330	36.5	30.7
30	0.02283	0.00494	28.8	24.2
40	0.02636	0.00661	24.3	20.4
50	0.02948	0.00824	21.2	17.8
60	0.03229	0.00991	19.0	16.0

A = 10

$(W/S)_{TO}$ psf	$(W/S)^{1/2}/284$	RCP	(W/P) 5,000 ft lbs/hp	$(W/P)_{TO}$ sealevel lbs/hp
20	0.01575	0.00330	42.0	35.3
30	0.01929	0.00494	33.0	27.7
40	0.02227	0.00661	27.7	23.3
50	0.02490	0.00824	24.1	20.2
60	0.02727	0.00991	21.5	18.1

Only the A = 8 requirement is shown in Figure 3.34.

It is clear, that for this airplane, the AEO climb requirement is the more critical one. Since this finding is strongly dependent on the values used for the drag polars, it should be checked as soon as more accurate estimates of the drag polars are available. Such an estimate is available as soon as the first configuration threeview of the airplane has been generated. How this can be done is the subject of Part II in this series (Ref.1).

3.7.2.4 Cruise speed sizing

The 250 kts speed requirement at 10,000 ft (Table 2.17) was used in Sub-section 3.6.3 and the results plotted in Figure 3.31. These results are now superimposed on Figure 3.34. It is seen, that this a rather critical requirement.

3.7.2.5 Time-to-climb sizing

Table 2.17 requires a 10 min. time-to-climb to 10,000 ft. It will be assumed, that h_{abs} = 25,000, which is compatible with a normally aspirated piston engine installation.

From Eqn.(3.33) it now follows that:

RC_o = 1,277 fpm, in the clean configuration.

From Eqn.(3.23) a value for RCP is found as: 0.0387.

With Eqn.(3.27), and C_{D_o} = 0.0266 it is found that:

For A = 8: $(C_L^{3/2})/C_D = 13.4$

For A = 10: $(C_L^{3/2})/C_D = 15.8$

Eqn.(3.24) now yields the following results:

For A = 8 : $0.0387 = 0.8/(W/P) - (W/S)^{1/2}/255$

For A = 10: $0.0387 = 0.8/(W/P) - (W/S)^{1/2}/300$

The following tabulation can now be made:

$(W/S)_{TO}$	RCP	$(W/S)^{1/2}/255$	$(W/P)_{TO}$	$(W/S)^{1/2}/300$	$(W/P)_{TO}$
psf			lbs/hp		lbs/hp
20	0.0387	0.0175	14.2	0.0149	14.9
30	0.0387	0.0215	13.3	0.0183	14.0
40	0.0387	0.0248	12.6	0.0211	13.4
50	0.0387	0.0277	12.1	0.0236	12.8
60	0.0387	0.0304	11.6	0.0258	12.4

These time-to-climb results are also plotted in Figure 3.34.

3.7.2.6 Summary of matching results

Examining the matching requirements of Figure 3.34, Point P seems a reasonable choice. With this choice, the twin propeller driven airplane is now characterized by the following design parameters:

Take-off weight: 7,900 lbs
Empty weight: 4,900 lbs
Fuel weight: 1,706 lbs

These data were already known on p.53.

Maximum lift coefficients:

Clean: $C_{L_{max}} = 1.7$

Take-off: $C_{L_{max_{TO}}} = 1.85$ (Point P in Figure 3.34)

Landing: $C_{L_{max_L}} = 2.3$ (Point P in Figure 3.34)

Aspect ratio: A = 8 is sufficient by Figure 3.34.

Take-off wing loading: 46 psf (Point P in Fig. 3.34)

Wing area: 172 ft^2

Power loading at take-off: 8.8 lbs/hp

Take-off power: 898 hp

In Part II of this text an example is given showing how a configuration can be developed on the basis of this information.

3.7.3 Matching Example 2: Jet Transport

Table 2.18 defines the mission for this airplane. Note, that the fieldlength is 5,000 ft at 5,000 ft altitude and for a 95°F day.

3.7.3.1 Take-off distance sizing

For take-off flaps a corresponding range of values of $C_{L_{max_{TO}}}$ = 1.6 to 2.2 is found from Table 3.1. For this example values of 1.6, 2.0 and 2.4 will be investigated.

Next, it is observed that at 5,000 ft, the pressure ratio $\delta = 0.8320$. With a temperature of 95°F, the temperature ratio $\theta = (95 + 459.7)/518.7 = 1.0694$. This yields $\sigma = 0.8320/1.0694 = 0.7780$.

From Eqn.(3.8):

$$5{,}000 = 37.5(W/S)\{0.7780 C_{L_{max_{TO}}} (T/W)\}^{-1}$$

After rearrangement this yields:

$$(T/W) = \{0.009640(W/S)\}/C_{L_{max_{TO}}}$$

In the latter equation, (T/W) is the same as $(T/W)_{TO}$ for the 5,000 ft, hot day condition.

The following table can now be constructed:

		$(T/W)_{TO}$			$(T/W)_{TO}$		
		5,000 ft, hot			sealevel std.		
(W/S) psf	$C_{L_{max_{TO}}}$ =	1.6	2.0	2.4	1.6	2.0	2.4
60		0.36	0.29	0.24	0.42	0.34	0.28
80		0.48	0.39	0.32	0.56	0.45	0.37
100		0.60	0.48	0.40	0.70	0.56	0.47
120		0.72	0.58	0.48	0.84	0.67	0.56
				x1.17			

A factor of 1.17 was used to translate the 5,000 ft, hot day thrust requirement into a sealevel, standard day thrust requirement. This factor was obtained from typical turbofan data for this type of airplane.

Figure 3.35 shows the allowable combination of $(W/S)_{TO}$, $(T/W)_{TO}$ and $C_{L_{max_{TO}}}$ for which the take-off requirement is satisfied.

3.7.3.2 Landing distance sizing

From Eqns.(3.15) and (3.16) it is found that:

$$5,000 = 0.3 \times 1.69 V_{s_L}^2 = 0.507 V_{s_L}^2$$

Therefore:

$$V_{s_L}^2 = 9,862, \text{ or: } V_{s_L} = 99.3 \text{ kts.}$$

From Eqn.(3.1) this now yields:

$$V_{s_L}^2 = 2(W/S)/\rho C_{L_{max_L}}$$

At the 5,000 ft hot day condition, this results in:

$$(W/S)_L = 26.0 C_{L_{max_L}}$$

From Table 3.1 it follows that a suitable range of maximum lift coefficients in the landing configuration is: 1.8 to 2.8. For this example the values 1.8, 2.2, 2.6 and 3.0 will be investigated.

The following table can now be constructed:

$C_{L_{max_L}}$	$(W/S)_L$	$(W/S)_{TO}$	
1.8	46.8	55.1	It must be remembered
2.2	57.2	67.3	from Table 2.18 that
2.6	67.6	79.5	landing weight is 0.85x
3.0	78.0	91.8	the take-off weight.
	:0.85		

Figure 3.35 shows these results graphically.

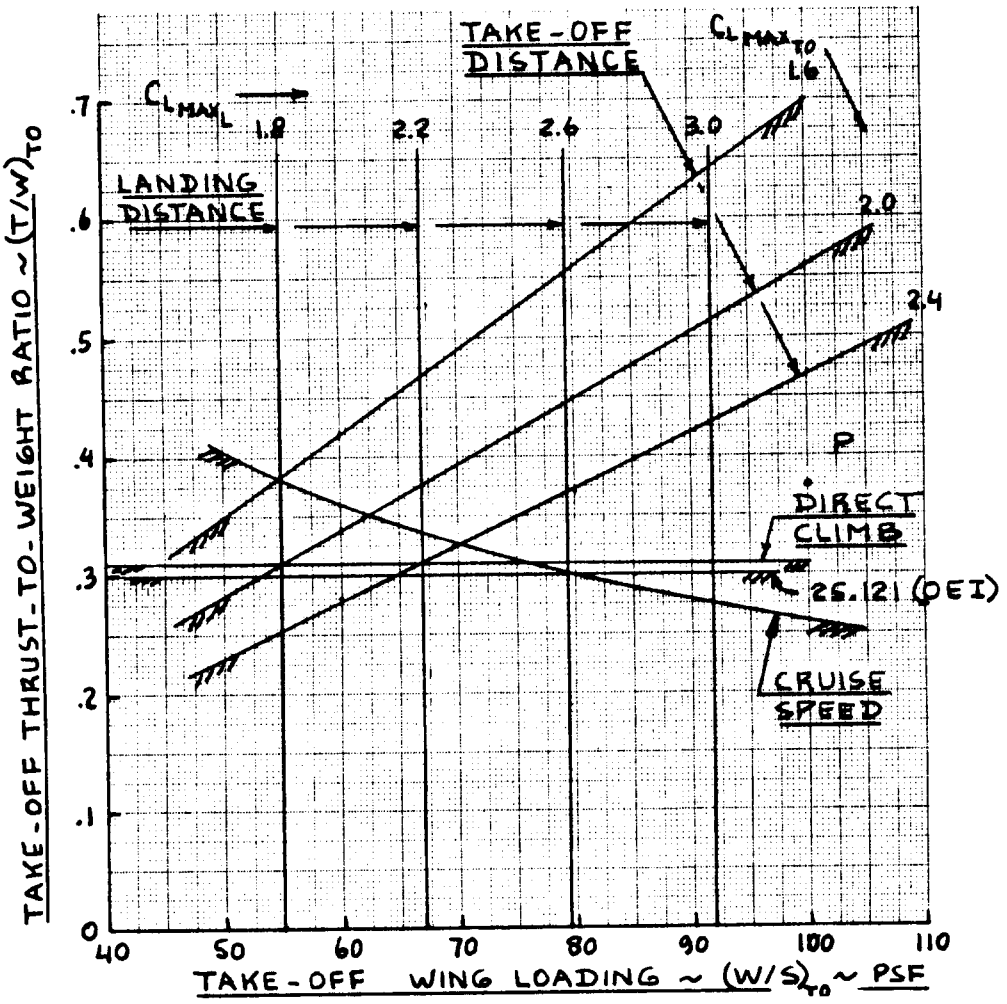

Figure 3.35 Matching Results for Sizing of a Jet Transport

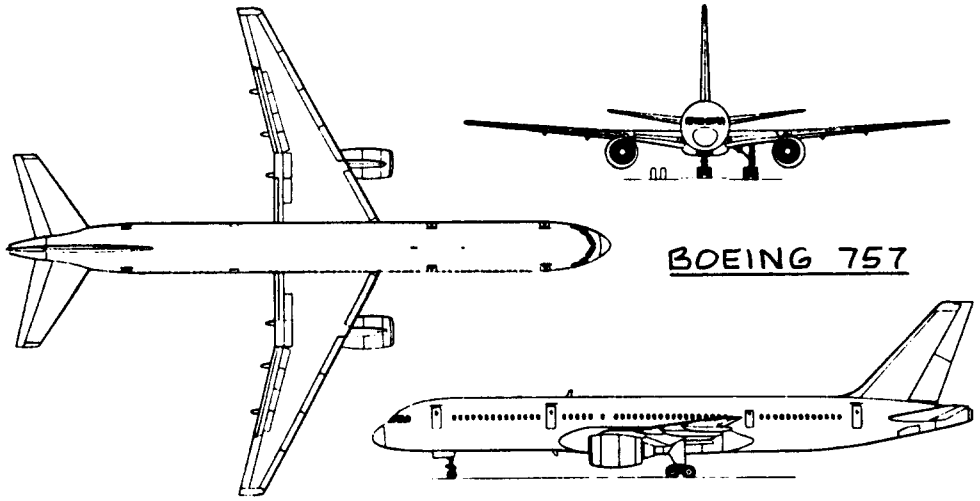

3.7.3.3 FAR 25 climb sizing

For a similar transport, it was already shown in Sub-section 3.4.8, that the most critical requirement was that of FAR 25.121 (OEI). For that reason, only this requirement will be accounted for. The example in Sub-section 3.4.8 dealt with a jet transport with W_{TO} = 125,000 lbs. The airplane resulting from the specification of Table 2.18 has W_{TO} = 127,000 lbs.

This is judged to be sufficiently similar, so that the numerical results of Figure 3.25 apply. Figure 3.35 shows the FAR 25.121 (OEI) line from Figure 3.25.

3.7.3.4 Cruise speed sizing

Table 2.18 specifies a cruise speed of M = 0.82 at 35,000 ft. The low speed, clean drag polar for this airplane is roughly that of page 145:

$$C_D = 0.0184 + C_L^2/26.7, \text{ for } A = 10 \text{ and } e = 0.85.$$

From Figure 3.32 the compressibility drag increment at M = 0.82 is assumed to be 0.0005. At 35,000 ft,

$$\bar{q} = 1482 \times 0.2353 \times M^2 = 234 \text{ psf.}$$

Eqn.(3.60) now yields:

$$(T/W)_{reqd} = 4.42/(W/S) + (W/S)/6,249$$

The following tabulation results from the speed sizing process:

$(W/S)_{TO}$	(T/W)	$(T/W)_{TO}$	
psf	cruise	take-off	
60	0.083	0.36	The ratio of thrust at M = 0.82 at 35,000 ft to that at sealevel, static is roughly 0.23. This is based on typical turbofan data for this type of airplane.
80	0.068	0.30	
100	0.060	0.26	
120	0.056	0.24	
	:0.23		

Figure 3.35 shows these results graphically.

3.7.3.5 Direct climb sizing

Table 2.18 specifies that direct climb to 35,000 ft at take-off gross weight must be possible. It will be assumed here, that this means that the airplane service ceiling at gross take-off weight is to be 35,000 ft. From Table 3.8 this means a climb rate of 500 fpm at 35,000 ft and in this case at M = 0.82

Eqn.(3.34) will be used in the climb sizing to this requirement. In Eqn.(3.34):

$RC = 500/60 = 8.33$ fps $\qquad V = 798$ fps

$S = 127{,}000/100 = 1{,}270\ ft^2 \qquad \bar{q} = 234$ psf

$C_L = 0.43 \qquad C_D = 0.0257$

$L/D = 16.7$, so that:

$$(T/W)_{reqd} = 8.33/798 + 1/16.7 = 0.07 \text{ at } 35{,}000 \text{ ft}$$

and at M = 0.82. Therefore, the sealevel, static value for T/W is:

$$(T/W)_{TO} = 0.07/0.23 = 0.31.$$

Figure 3.35 shows this result also.

3.7.3.6 Summary of matching results

Figure 3.35 shows that there is an interesting problem with this airplane. The take-off requirement from the relatively short field on a hot day dominates the (T/W) requirements. It will therefore be of utmost importance to develop a low drag high lift system for the take-off configuration. Trimmed values for $C_{L_{max_{TO}}}$ with existing mechanical flaps are limited to about 2.4 with a conventional configuration. With a canard or three-surface configuration it may be possible to get up to 2.8. The corresponding landing value of trimmed maximum lift coefficient is 3.2. If these numbers are selected, the matching process yields an airplane defined by point P in Figure 3.35.

It is clear, that a considerable amount of high lift development will be needed, to make this airplane viable.

If point P is accepted as a satisfactory match point, the airplane characteristics can be summarized as follows:

Take-off weight: W_{TO} = 127,000 lbs

Empty weight: W_E = 68,450 lbs

Fuel weight: W_F = 25,850 lbs

These data were already known on p.59.

Maximum lift coefficients:

Clean: $C_{L_{max}}$ = 1.4 (p.145)

Take-off: $C_{L_{max_{TO}}}$ = 2.8

Landing: $C_{L_{max_L}}$ = 3.2

Aspect ratio: 10. (Note: the reader should investigate the beneficial effect of designing toward a higher aspect ratio.)

Take-off wing loading: $(W/S)_{TO}$ = 98 psf (PointP)

Wing area: S = 127,000/98 = 1,296 ft^2

Take-off thrust-to-weight ratio:
$(T/W)_{TO}$ = 0.375 (Point P)

Take-off thrust: T_{TO} = 47,625 lbs

In Part II of this text an example is given of how the configuration design for this jet transport can be started with the help of the information generated in the preliminary sizing process.

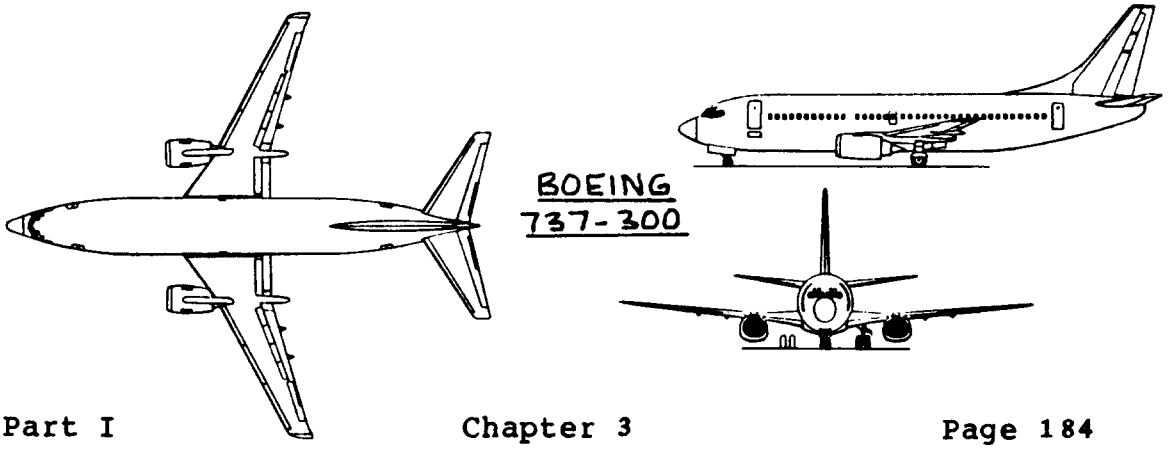

3.7.4 Matching Example 3: Fighter

Table 2.19 defines the mission of this airplane. To determine the allowable range of wing loadings and thrust-to-weight ratios, the take-off, landing, climb and cruise speed requirements will all be translated into ranges of allowable values for $(W/S)_{TO}$, $(T/W)_{TO}$ and the various values of $C_{L_{max}}$.

3.7.4.1 Take-off distance sizing

Table 2.19 stipulates a groundrun of 2,000 ft at sealevel and for a 95°F day. It will be assumed that this take-off is from a hard surface. Ref.15 specifies: $\mu_G = 0.025$ in that case.

On page 155 it was determined that for a 95°F day the density is: $\rho = 0.002224$ slugs/ft^3

Eqn.(3.9) yields:

$$2{,}000 = \frac{0.0447(W/S)_{TO}}{0.002224\left[C_{L_{max_{TO}}}\{k_2(T/W)_{TO} - 0.025\} - 0.72C_{D_o}\right]}$$

From p.102, with an assumed bypass ratio of $\lambda = 3{:}1$, $k_2 = 0.75 \times 8/7 = 0.857$. From pages 154 and 155, the value of C_{D_o} without stores is:

$$C_{D_o} = 0.0096 + 0.0030 = 0.0126.$$

Therefore, the take-off distance requirement can be reduced to:

$$C_{L_{max_{TO}}}\{85.3(T/W)_{TO} - 2.49\} - 0.905 = (W/S)_{TO}$$

The following tabulation can now be made:

$(T/W)_{TO}$ 95°F	$C_{L_{max_{TO}}}$ = 1.6	1.8	2.0	$(T/W)_{TO}$ std. day
	$(W/S)_{TO}$			
0.4	50	56	62	0.47
0.6	77	87	96	0.71
0.8	104	117	131	0.94
1.0	132	148	165	1.18

A factor of 1.18 was used to translate the hot day thrust data into standard day thrust data. This factor comes from typical turbofan data for this type of airplane.

Figure 3.36 shows the graphical results.

3.7.4.2 Landing distance sizing

According to 3.3.5.1 the FAR 25 method can be used except that a correction for approach speed must be made.

Table 2.19 specifies the groundrun as < 2,000 ft. The ratio of groundrun to total distance during landing is roughly 1.9 unless special retardation precedures are used:

$$s_L = 1.9 s_{LG}$$

For this fighter therefore: $s_L = 1.9 \times 2{,}000 = 3{,}800$ ft.

From Figure 3.16, $s_L = 3{,}800/0.6 = 6{,}333$ ft.

From Figure 3.17 this yields: $V_A^2 = 21{,}200$ kts^2.

However, since for a fighter $V_A = 1.2V_{S_L}$ instead of $1.3V_{S_L}$ it follows that:

$$V_A = \{21{,}200(1.3/1.2)^2\}^{1/2} = 158 \text{ kts}$$

Therefore, $V_{S_L} = 158/1.2 = 132$ kts $= 222$ fps.

From Eqn.(3.1):

$$222^2 = (2/0.002224)(W/S)_L / C_{L_{max_L}}, \text{ or:}$$

$$(W/S)_L = 54.8 C_{L_{max_L}}$$

If it is assumed, that $W_L = 0.85 W_{TO}$ (not specified in Table 2.19), the following tabulation can now be made:

$C_{L_{max_L}}$	$(W/S)_L$ psf	$(W/S)_{TO}$ psf
1.8	98.6	116
2.0	109.6	129
2.2	120.6	142

:0.85

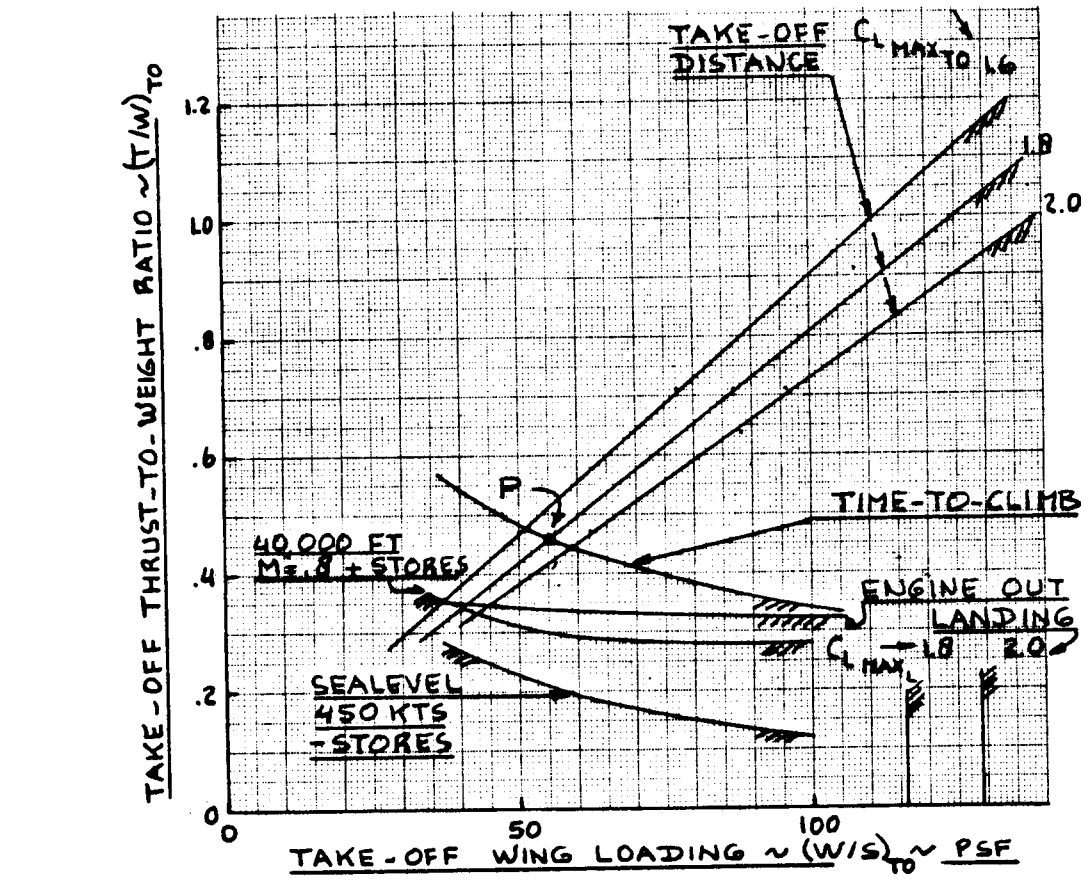

Figure 3.36 Matching Results for Sizing of a Fighter

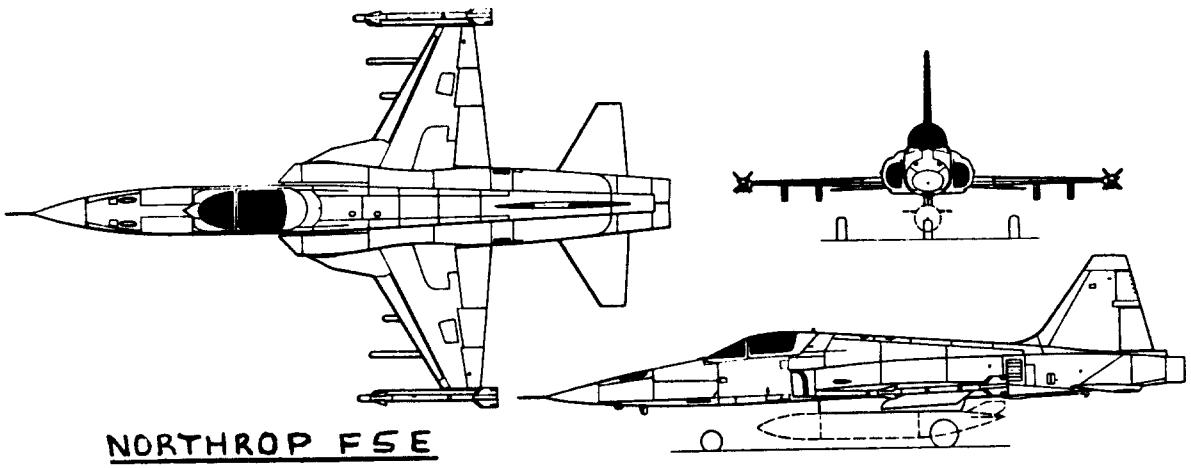

Figure 3.36 shows that the landing requirement is not critical in the selection of wing loading. The reason is that a 2,000 ft groundrun is very liberal for this type of a fighter.

3.7.4.3 Climb sizing

The climb performance specifications are given in Table 2.19. Examples were alreay computed in Sub-section 3.4.12 and graphically shown as requirements 1) and 2) in Figure 3.27. These lines are repeated in Figure 3.36. The reader will note that requirement 3) of Figure 3.27 is not shown in Figure 3.36 because this requirement was not a part of those listed in Table 2.19.

3.7.4.4 Cruise speed sizing

According to Table 2.19 the airplane must satisfy four different speed requirements:

At sealevel: 450 kts 'clean' and
400 kts with external stores

At 40,000 ft: M = 0.85 'clean and
M = 0.80 with external stores

These requirements will be subjected to the speed sizing process of Sub-section 3.6.4.

Sealevel speed sizing

The Mach numbers at these speeds are 0.68 and 0.6 respectively. It will be assumed that there are no compressibility effects at these Mach numbers. The drag polars of Sub-section 3.4.12 can therefore be used:

Low speed 'clean: $C_D = 0.0096 + 0.0995C_L^2$

Low speed + stores: $C_D = 0.0126 + 0.0995C_L^2$

Eqn.(3.60) will be used for the speed sizing. The following is found:

For 450 kts 'clean':

$$(T/W) = 6.58/(W/S) + (W/S)/6,886$$

This results in the following tabulation:

$(W/S)_{TO}$ with stores (psf)	(W/S) clean (psf)	(T/W) M=0.68 clean	$(T/W)_{TO}$ static clean	$(T/W)_{TO}$ with stores
40	33.8	0.20	0.32	0.27
60	50.7	0.14	0.22	0.19
80	67.6	0.11	0.17	0.15
100	84.5	0.09	0.15	0.12
x0.85			x1.65	x0.85

For 400 kts with stores:

$(T/W) = 6.73/(W/S) + (W/S)/5,368$

This results in the following tabulation:

$(W/S)_{TO}$ with stores (psf)	(W/S) clean (psf)	(T/W) M=0.60 clean	$(T/W)_{TO}$ static clean	$(T/W)_{TO}$ with stores
40	33.8	0.21	0.32	0.27
60	50.7	0.14	0.22	0.18
80	67.6	0.11	0.17	0.15
100	84.5	0.10	0.15	0.12
x0.85			x1.54	x0.85

Figure 3.36 shows the graphical results of the sealevel speed sizing.

<u>40,000 ft speed sizing</u>

At M = 0.8 a compressibility drag increment of 0.0020 was assumed for this airplane on p.152. At M = 0.85 a compressibility drag increment of 0.0030 will be assumed. The compressibility drag due to the stores will be neglected. This is a reasonable assumption because slender stores show no drag rise until about M = 0.9.

The following drag polars are therefore used:

at M = 0.85 'clean': $C_D = 0.0126 + 0.0995C_L^2$

at M = 0.80, + stores: $C_D = 0.0146 + 0.0995C_L^2$

Eqn.(3.60) will again be used in the speed sizing. It is found that:

For M = 0.85 'clean':

$(T/W) = 2.5/(W/S) + (W/S)/1,991$

This results in the following tabulation:

$(W/S)_{TO}$ with stores (psf)	(W/S) clean (psf)	(T/W) M=0.85 clean	$(T/W)_{TO}$ static clean	$(T/W)_{TO}$ with stores
40	33.8	0.09	0.40	0.33
60	50.7	0.07	0.33	0.27
80	67.6	0.07	0.31	0.26
100	84.5	0.07	0.31	0.26
x0.85		:0.23	x0.85	

For M = 0.8 with stores:

$(T/W) = 2.5/(W/S) + (W/S)/1,769$

This results in the following tabulation:

$(W/S)_{TO}$ with stores (psf)	(W/S) clean (psf)	(T/W) M=0.8 clean	$(T/W)_{TO}$ static clean	$(T/W)_{TO}$ with stores
40	33.8	0.09	0.40	0.34
60	50.7	0.08	0.34	0.29
80	67.6	0.08	0.33	0.28
100	84.5	0.08	0.34	0.28
x0.85		:0.23	x0.85	

Figure 3.36 shows the graphical results of the 40,000 ft speed sizing.

3.7.4.5 Summary of matching results

It can be seen from Figure 3.36 that the take-off requirement and the time-to-climb requirement are the critical ones. Assuming a take-off lift coefficient of $C_{L_{max_{TO}}} = 1.8$, point P is selected as the matching point for this fighter. Therefore, by selecting:

$(T/W)_{TO} = 0.46,$

$(W/S)_{TO} = 55$ psf,

$C_{L_{max_{TO}}} = 1.8,$

all requirements are met. The landing lift coefficient is seen to be not critical. Therefore it would be possible <u>not</u> to put a separate landing flap setting in the airplane.

The fighter airplane is now determined by the following characteristics:

Take-off weight with stores:	64,500 lbs
Take-off weight 'clean':	54,500 lbs
Empty weight:	33,500 lbs
Fuel weight:	18,500 lbs

These data were already known on p.67.

Maximum lift coefficients:

Clean: $C_{L_{max}}$ not determined

Take-off: $C_{L_{max_{TO}}} = 1.8$

Landing: $C_{L_{max_{L}}}$ not critical

Aspect ratio: 4 (The reader should carry out an analysis to see what the effect is of aspect ratios of 3.5 and 4.5).

Wing area: $64,500/55 = 1,173$ ft^2

Thrust at take-off: $T_{TO} = 64,500 \times 0.46 = 29,670$ lbs

In part II of this text an example is given of how the configuration design for this fighter airplane can be started with this information.

3.8. PROBLEMS

1) For the regional transport of Section 2.8, problem 2, do the take-off, climb and landing sizing according to FAR 25 requirements.

2) For the high altitude loiter and reconnaissance airplane of Section 2.8, problem 3, perform the take-off, climb and landing sizing to FAR 25 requirements.

3) For the homebuilt airplane of Section 2.8, problem 4, carry out the take-off, climb and landing sizing to FAR 23 requirements.

4) For the supersonic cruise airplane of Section 2.8, problem 5, do the take-off, climb and landing sizing to FAR 25 requirements.

5) Do the FAR 23 sizing for an agricultural airplane with the following (sealevel only) mission requirements:

* spray or dust load of 4,000 lbs.
* ferry distance is 10 miles.
* ferry speed should be 160 mph.
* swath turn-around must be less than 20 sec.
* load dispersal rate is 45 lbs per acre.
* swath width must be 80 ft.
* speed while spraying should be 100 mph.
* take-off distance to a 50 ft obstacle must be less than 1,500 ft.
* fuel reserves after emptying the hopper must be sufficient for 20 min. at 160 mph.

6) Do the FAR 25 sizing for a 90 passenger, twin engine turboprop with the following mission:

* range 1,500 n.m. at M = 0.7 and 30,000 ft.
* crew: two pilots and three flight attendants.
* assume 200 lbs per person, including baggage.
* fieldlength 7,000 ft. for a standard day at 9,000 ft altitude.
* engine-out service ceiling: 16,000 ft.
* maximum approach speed less than 130 kts.
* fuel reserves per FAR Part 121.

7) For the fighter of Table 2.19, determine the relation between T/W and W/S at take-off if the airplane must pull sustained level turns with load factors of 4, 6 and 8. Do a trade study of the effect of maximum lift coefficient values of 1.0, 1.2 and 1.4. All this at sealevel and M = 0.8.

4. A USER'S GUIDE TO PRELIMINARY AIRPLANE SIZING

The process of preliminary airplane sizing to a variety of mission and certification requirements was discussed in detail in chapters 2 and 3.

In this chapter a step-by-step guide is provided to help guide the reader through the maze of sizing methods.

Step 1. Obtain a mission specification and construct from it a mission profile. Example mission profiles are given in Tables 2.17, 2.18 and 2.19.

Step 2. Number the mission phases in sequence, as shown in the examples of Tables 2.17 through 2.19.

Step 3. For certain mission phases the fuel fraction can be estimated directly from Table 2.1. For other mission phases, estimate the corresponding L/D and sfc values. Table 2.2 can be used as a guide.

Step 4. Determine the overall mission fuel fraction, M_{ff} with the method of Section 2.4: Eqn.(2.13).

Step 5. From the mission specification determine the fuel reserves, $W_{F_{res}}$ or the fuel reserve fraction, M_{res}.

Step 6. Follow the step-by-step procedures outlined as steps 1-7 of page 7.

Note: if the mission demands dropping of weights (such as in many military missions) some of the fuel fractions need to be corrected for this. The procedure for doing this is illustrated in Sub-section 2.6.3.

At the termination of Step 6, the following information is available for the airplane:

Take-off weight, W_{TO}

Empty weight, W_E

Fuel weight, W_F

Payload and crew weights, W_{PL} and W_{crew}, follow from the mission specification.

Step 7. Note from the mission specification what the certification base is for the airplane: homebuilt, FAR 23, FAR 25 or military. If a homebuilt is being considered, FAR 23 should be used for further preliminary sizing.

Step 8. Make a list of performance parameters to which the airplane must be sized. Such a list can be put together from the mission specification and from the certification base. The following examples are discussed in Chapter 3:

3.1 Sizing to stall speed requirements.
3.2 Sizing to take-off distance requirements.
3.3 Sizing to landing distance requirements.
3.4 Sizing to climb requirements.
3.5 Sizing to maneuvering requirements.
3.6 Sizing to cruise speed requirements.

Step 9. Perform the sizing calculations in accordance with the methods of Sections 3.1 through 3.6. This involves estimating a drag polar. This can be done rapidly with the method of Sub-section 3.4.1.

Step 10. Construct a sizing matching graph for all performance sizing requirements. Examples for constructing such matching graphs are presented in Section 3.7.

Step 11. From the matching graph select:

1) Take-off power loading: $(W/P)_{TO}$ or

   Take-off thrust-to-weight ratio: $(T/W)_{TO}$

2) Take-off wing loading: $(W/S)_{TO}$

3) Maximum (clean) lift coefficient: $C_{L_{max}}$

4) Maximum take-off lift coefficient: $C_{L_{max_{TO}}}$

5) Maximum landing lift coefficient: $C_{L_{max_L}}$

6) Wing aspect ratio: A

Step 12. Determine the take-off power, P_{TO} or the take-off thrust, T_{TO} from:

$$P_{TO} = W_{TO}/(W/P)_{TO} \text{ or from:}$$

$$T_{TO} = W_{TO}(T/W)_{TO}$$

Step 11. Determine the wing area, S from:

$$S = W_{TO}/(W/S)_{TO}$$

All airplane parameters needed to begin the development of a configuration are now defined. Part II of this book, (Ref.1) presents a methodology for the selection and layout of a preliminary airplane configuration.

GATES
LEARJET
MODEL 55

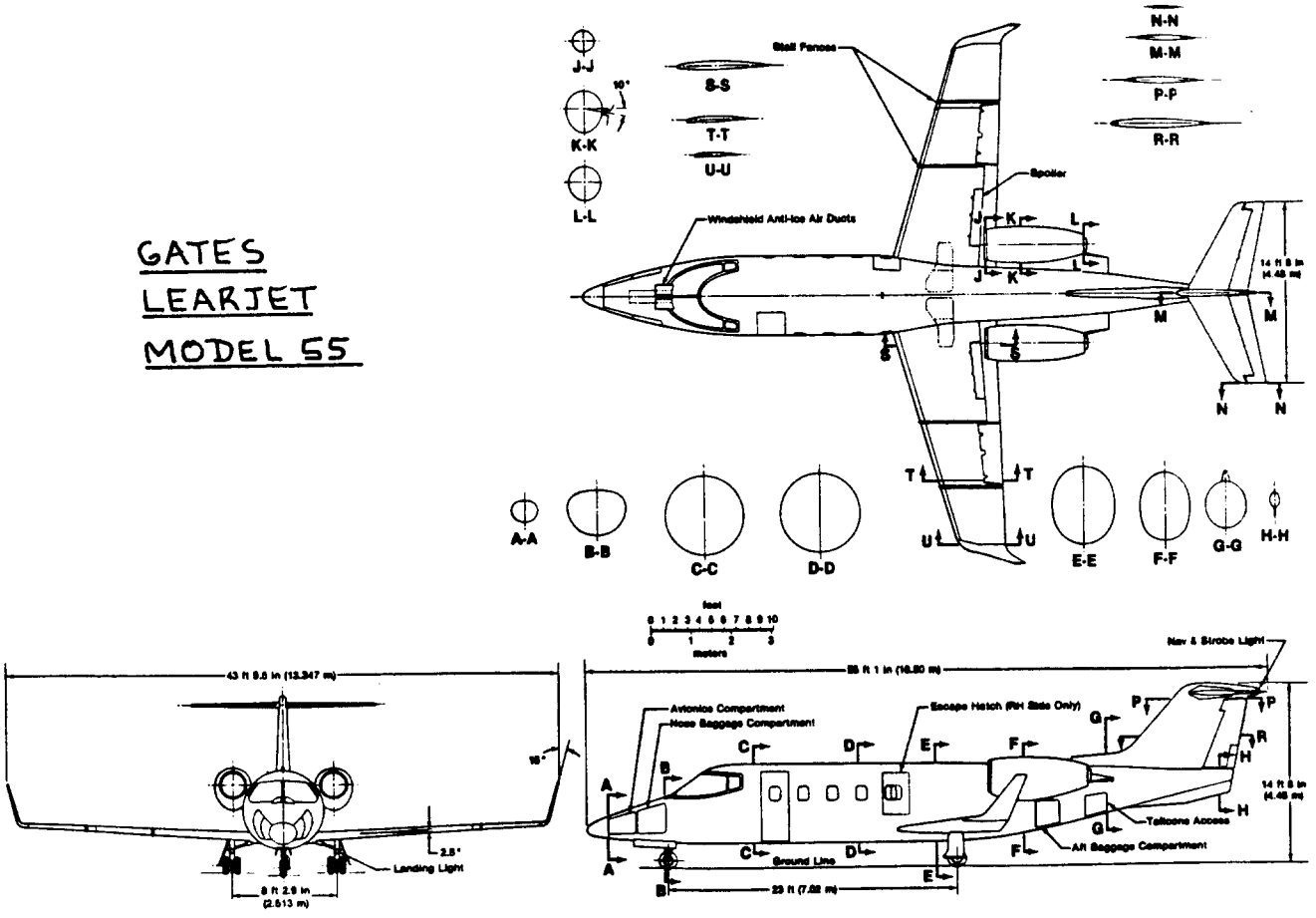

CESSNA 310Q

AIRFOILS
WING
- ℄ AIRPLANE - NACA 23018
- ℄ NACELLE - NACA 23015
- TIP - NACA 23009

TAIL (VERTICAL)
- ROOT (LESS DORSAL) - NACA 0009
- TIP - NACA 0006

TAIL (HORIZONTAL)
- ℄ AIRPLANE - 0009
- TIP - 0006

INCIDENCE
- WING ROOT +2°30'
- WING TIP -0°30'
- STABILIZER 0°

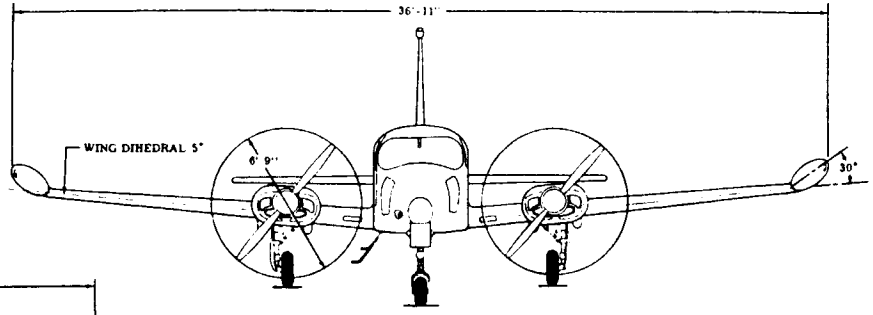

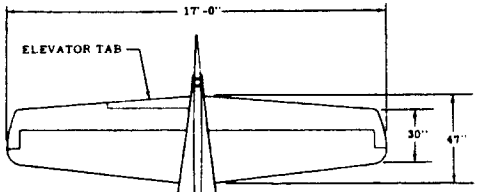

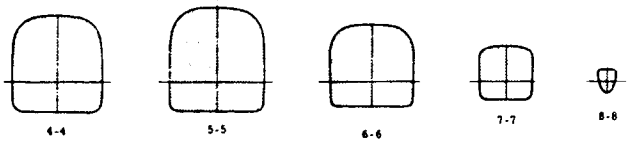

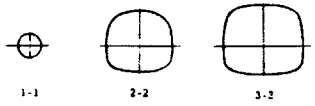

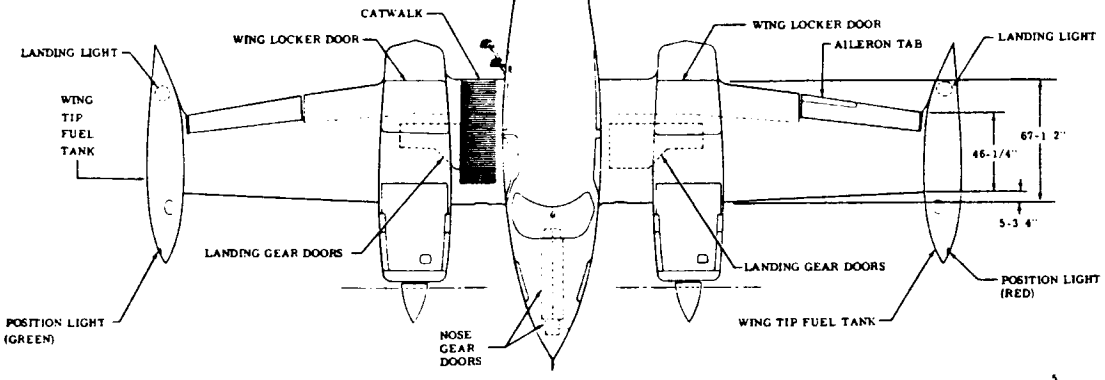

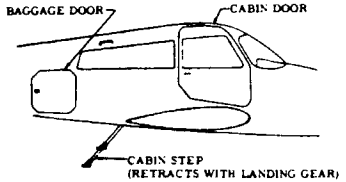

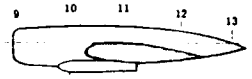

SECTION THRU ℄ OF ENGINE NACELLE

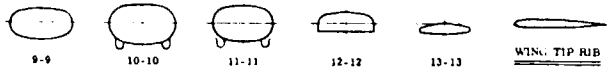

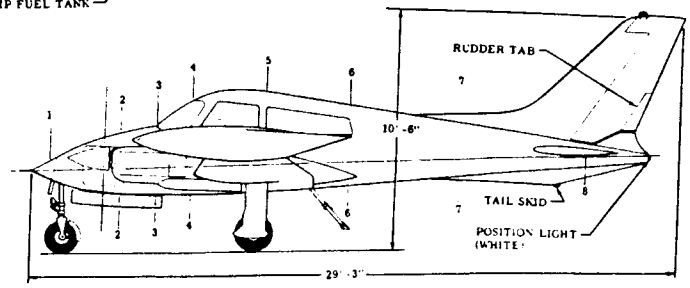

5. REFERENCES

1. Roskam, J., Airplane Design: Part II, Preliminary Configuration Design and Integration of the Propulsion System.

2. Roskam, J., Airplane Design: Part III, Layout Design of Cockpit, Fuselage, Wing and Empennage: Cutaways and Inboard Profiles.

3. Roskam, J., Airplane Design: Part IV, Layout Design of Landing Gear and Systems.

4. Roskam, J., Airplane Design: Part V, Component Weight Estimation.

5. Roskam, J., Airplane Design: Part VI, Preliminary Calculation of Aerodynamic, Thrust and Power Characteristics.

6. Roskam, J., Airplane Design: Part VII, Determination of Stability, Control and Performance Characteristics: FAR and Military Requirements.

7. Roskam, J., Airplane Design: Part VIII, Airplane Cost Estimation and Optimization: Design, Development Manufacturing and Operating.

Note: These books are all published by: Roskam Aviation and Engineering Corporation, Rt4, Box 274, Ottawa, Kansas, 66067, Tel. 913-2421624.

8. Anon., Federal Aviation Regulations, Department of Transportation, Federal Aviation Administration, Distribution Requirements Section, M-482.2, Washington, D.C., 20590.

9. Taylor, J.W.R., Jane's All The World Aircraft, Published Annually by: Jane's Publishing Company, 238 City Road, London EC1V 2PU, England. (Issues used: 1945/46, 1968/84)

10. Nicolai, L.M., Fundamentals of Aircraft Design, METS, Inc., 6520 Kingsland Court, CA, 95120.

11. Loftin, Jr., L.K., Subsonic Aircraft: Evolution and the Matching of Size to Performance, NASA Reference Publication 1060, 1980.

12. Kohlman, D.L., Introduction to V/STOL Airplanes, Iowa State University Press, Ames, Iowa, 50010, 1981.

13. McCormick, B.W., Aerodynamics of V/STOL Flight, Academic Press, New York, 1967.

14. Lan, C.E. and Roskam, J., Airplane Aerodynamics and Performance, Roskam Aviation and Engineering Corp., Rt4, Box 274, Ottawa, KS, 66067, 1981.

15. MIL-C-005011B(USAF), Military Specification, Charts: Standard Aircraft Characteristics and Performance, Piloted Aircraft (Fixed Wing), June 1977.

16. Torenbeek, E., Synthesis of Subsonic Airplane Design, Kluwer Boston Inc., Hingham, Maine, 1982.

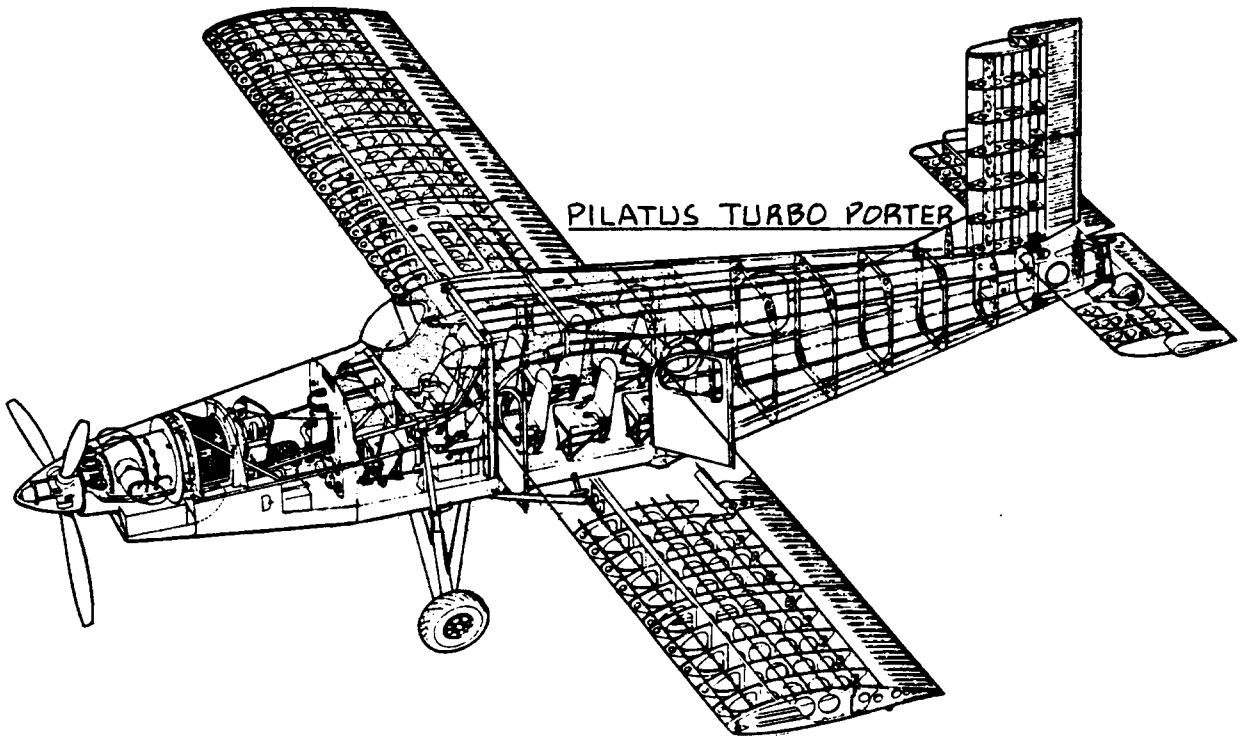

6. INDEX

AIRPLANE DESIGN

PART II: PRELIMINARY CONFIGURATION DESIGN AND INTEGRATION OF THE PROPULSION SYSTEM

by

Dr. Jan Roskam
Ackers Distinguished Professor
of Aerospace Engineering
The University of Kansas
Lawrence, Kansas

NO PART OF THIS BOOK MAY BE REPRODUCED WITHOUT
PERMISSION OF THE AUTHOR

Copyright: Roskam Aviation and Engineering Corporation
Rt4, Box 274, Ottawa, Kansas, 66067
Tel. 913-2421624
First Printing: 1985

TABLE OF CONTENTS

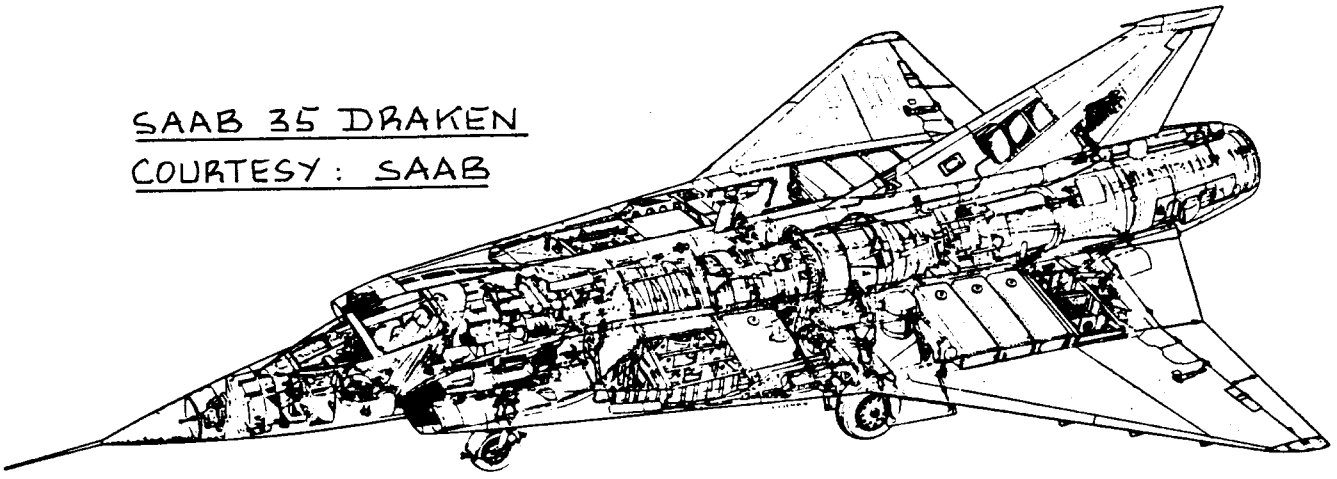

SAAB 35 DRAKEN
COURTESY: SAAB

TABLE OF SYMBOLS

Symbol	Definition	Dimension
A	Wing aspect ratio	-----
b	Wing span	ft
b_a	Aileron span	ft
b_f	Flap span	ft
b_t	Tire width	ft
c	Wing chord	ft
c'	Wing chord with t.e. flaps down	ft
c''	Wing chord with l.e. flaps down	ft
$\bar{c}$	Wing mean geometric chord	ft
c_f	Flap chord	ft
c_f (second use)	Equivalent skin friction coefficient	-----
C_D	Drag coefficient	-----
C_{D_o}	Zero lift drag coefficient	-----
c_l	Section lift coefficient	-----
c_{l_α}	Section liftcurve slope	1/rad
$c_{l_{\alpha_f}}$	Section liftcurve slope with flaps down	1/rad
$c_{l_{\delta_f}}$	Derivative of section lift coefficient with flap deflection	1/rad
C_L	Lift coefficient	-----
C_m	Pitching moment coeff.	-----
D	Drag	lbs
D_p	Propeller diameter	ft
D_t	Tire diameter	ft
d_f, D_f	fuselage diameter	ft

e	Oswald's efficiency factor	-----
E	Endurance	hours
f	equivalent parasite area	ft^2
FAR	Federal Air Regulation	-----
g	acceleration of gravity	ft/sec^2
h	altitude	ft
i_w	wing incidence angle	deg
k_Λ	Sweep angle corr. factor	-----
k_f	Corr. factor for split flaps	--
k_λ	Taper ratio corr. factor	-----
K'	Corr. factor for plain flaps	--
L	Lift	lbs
L/D	Lift-to-drag ratio	-----
l_f	fuselage length	ft
l_{fc}	fuselage cone length	ft
l_m	Dist. c.g. to main gear	ft
l_n	Dist. c.g. to nose gear	ft
M	Mach number	-----
n	Load factor	-----
nm	Nautical mile (6,076 ft)	nm
n_p	number of propeller blades	----
n_s	Number of struts	-----
N	No. of engines, Yaw. mom.	-----
P	Power, Horse-power (1hp = 550 ft.lbs/sec)	hp
P_{bl}	Blade power loading	hp/ft^2
P_{ef}	Probability of engine failure	-
P_n	Load on nosewheel strut	lbs
P_m	Load on main gear strut	lbs
$\bar{q}$	dynamic pressure	psf

R	Range	nm or m
R_n	Reynold's number	-----
S	Wing area	ft^2
SHP	Shaft horsepower	hp_2
S_{wet}	Wetted area	ft^2
S_{wf}	Flapped wing area	-----
t	time	sec, min, hr
t/c	thickness ratio	-----
T	Thrust	lbs
V	True airspeed	mph, fps, kts
$\bar{V}$	Volume coefficient	-----
W	Weight	lbs
X	T(hrust) or P(ower)	lbs or hp
$\bar{X}_{ac}$	Distance from l.e. $\bar{c}$ to aerodynamic center	
x,y,z	Distance from reference to a component c.g.	ft
x_v, x_h, x_c	Dist. from c.g. to a.c. of a surface	ft
y_t	Engine-out moment arm	ft

Greek Symbols
==========

α	Angle of attack	-----
β	Sideslip angle	-----
δ	Control surface defl.	-----
λ	Taper ratio	-----
Λ	Sweep angle	-----
π	Product, or 3.142	-----
Γ	Dihedral angle	-----
σ	Air density ratio	-----
θ_{fc}	Fuselage cone angle	deg.
ϕ	Lateral ground clearance angle	
θ	Longitudinal ground clearance angle	
θ_{lof}	Lift-off angle	
ε	Downwash angle	-----
ε_t	Twist angle	-----
η	Spanwise station, fr. span	----
Ψ	Lateral tip-over angle	deg.

Subscripts

a	aileron	ME	Manufacturer's empty
A	Approach	mc	Minimum control speed
abs	absolute	OE	Operating empty
c	canard	PL	Payload
cat	catapult	RC	Rate-of-climb
cl	climb	r	root, or rudder
cr	cruise	res	reserve (fuel)
crew	crew	reqd	required
crit	critical	s	stall
c/2	semi chord	TO	Take-off
c/4	quarter chord	t	tip
des	design	te	trailing edge
dry	without fluids or afterburner	tent	tentative
		tfo	trapped fuel and oil
e	elevator	used	used (fuel)
E	Empty	v	vertical tail
f	flaps	w	wing
ff	fuel fraction (see M_{ff})	wet	wetted
		wb	wing-body
F	Mission fuel		
h	altitude		
h	horizontal tail		
le	leading edge		
max	maximum		
L	Landing		

Acronyms

AEO	All engines operating	LCC	Life cycle cost
APU	Auxiliary power unit	p.d.	preliminary design
B.L.	Buttock line	RFP	Request for proposal
c.g.	center of gravity	ROI	Return on investment
DOC	Direct operating cost	R.S.	Rear spar
FOD	Foreign object damage	sls	Sealevel standard
F.S.	Fus.sta., Front spar	TBP	Turboprop
OEI	One engine inoperat.	W.L.	Waterline
OWE	Oper. weight empty		

ACKNOWLEDGEMENT

Writing a book on airplane design is impossible without the supply of a large amount of data. The author is grateful to the following companies for supplying the raw data, manuals, sketches and drawings which made the book what it is:

Beech Aircraft Corporation
Boeing Commercial Airplane Company
Canadair
Cessna Aircraft Company
DeHavilland Aircraft Company of Canada
Gates Learjet Corporation
Lockheed Aircraft Corporation
McDonnell Douglas Corporation
Rinaldo Piaggio S.p.A.
Royal Netherlands Aircraft Factory, Fokker
SIAI Marchetti S.p.A.

A significant amount of airplane design information has been accumulated by the author over many years from the following magazines:

Interavia (Swiss, monthly)
Flight International (British, weekly)
Business and Commercial Aviation (USA, monthly)
Aviation Week and Space Technology (USA, weekly)
Journal of Aircraft (USA, AIAA, monthly)

The author wishes to acknowledge the important role played by these magazines in his own development as an aeronautical engineer. Aeronautical engineering students and graduates should read these magazines regularly.

Most of the threeviews in this part of the book were prepared by Mr. G.Tukker of Molenaarsgraaf, The Netherlands. The author wishes to thank Mr. Tukker for his patience and for his painstaking attention to detail.

BEECH STARSHIP I
COURTESY : BEECH

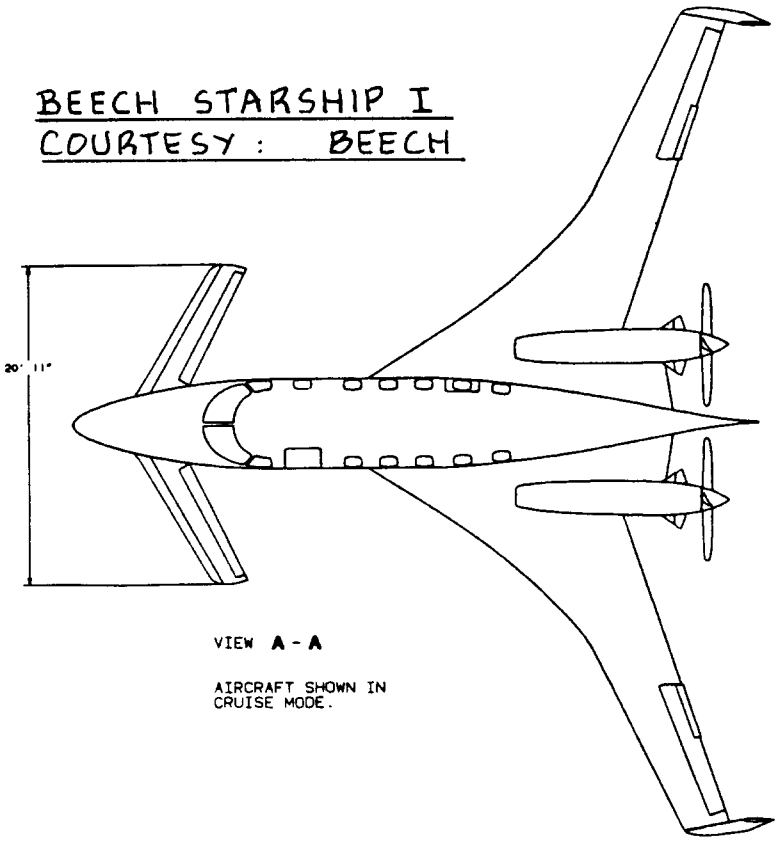

VIEW **A - A**

AIRCRAFT SHOWN IN
CRUISE MODE.

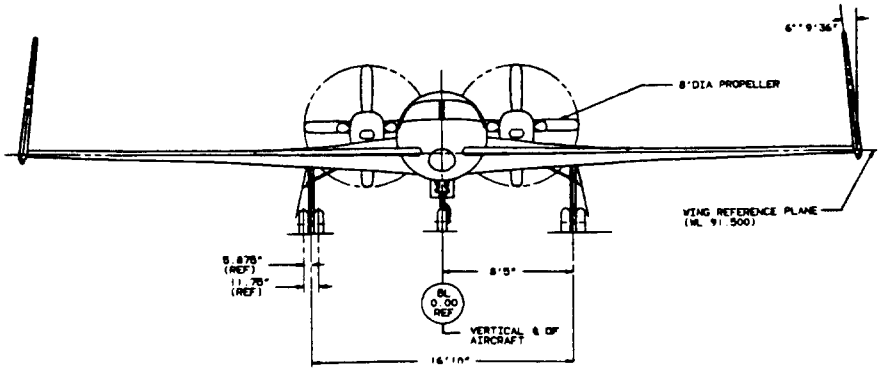

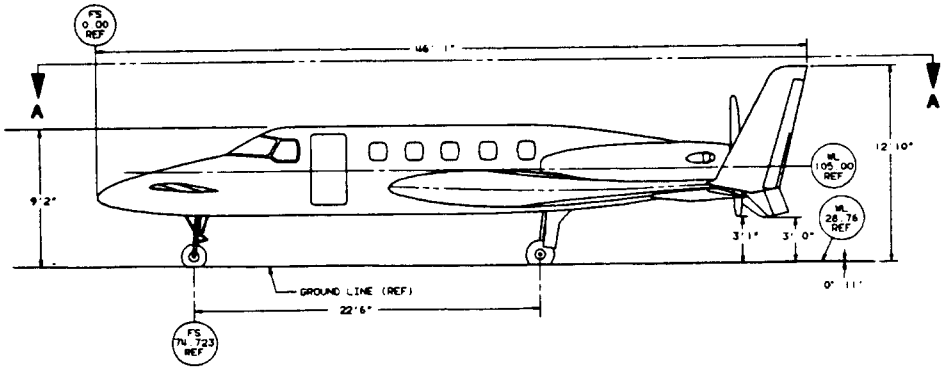

1. INTRODUCTION

The purpose of this series of books on Airplane Design is to familiarize aerospace engineering students with the design methodology and design decision making involved in the process of designing airplanes.

The series of books is organized as follows:

PART I:	PRELIMINARY SIZING OF AIRPLANES
PART II:	PRELIMINARY CONFIGURATION DESIGN AND INTEGRATION OF THE PROPULSION SYSTEM
PART III:	LAYOUT DESIGN OF COCKPIT, FUSELAGE, WING AND EMPENNAGE: CUTAWAYS AND INBOARD PROFILES
PART IV:	LAYOUT DESIGN OF LANDING GEAR AND SYSTEMS
PART V:	COMPONENT WEIGHT ESTIMATION
PART VI:	PRELIMINARY CALCULATION OF AERODYNAMIC, THRUST AND POWER CHARACTERISTICS
PART VII:	DETERMINATION OF STABILITY, CONTROL AND PERFORMANCE CHARACTERISTICS: FAR AND MILITARY REQUIREMENTS
PART VIII:	AIRPLANE COST ESTIMATION: DESIGN, DEVELOPMENT, MANUFACTURING AND OPERATING

The purpose of PART II is to present a systematic approach to the problem of configuration design, including the integration of the propulsion system.

Configuration design amounts to making the following decisions:

1. Selection of the overall configuration:

   * Conventional (that means tail aft)
   * Flying wing (that means no horizontal tail and no canard)
   * Tandem wing
   * Canard
   * Three Surface
   * Joined Wing

2. Selection of the fuselage layout:

   * Arrangement of crew, passengers, baggage, fuel, cargo and other payloads
   * Cockpit or flightdeck layout
   * Cabin layout
   * Window, door and emergency exit layout

* Check of fuel, baggage and cargo volume
* Weapons and stores arrangement
* Access for loading and unloading
* Access for maintenance and for servicing

In the case of a flying wing design all these items must be arranged to fit in the wing.

3. Selection of propulsion system type(s):

   * Piston/propeller with or without super-charging
   * Turbo/propeller or prop-fan
   * Propfan or unducted fan
   * Turbojet or turbofan
   * Ramjet or rocket
   * Rotary/diesel
   * Electric (solar, microwave, lithium fuel cell)

4. Selection of the number of engines and/or propellers

5. Integration of the propulsion system:

   * Propellers: pusher or tractor
   * Engines buried in the fuselage or in the wing
   * Engines in nacelles on the fuselage or on the wing
   * Disposition of engines and nacelles

6. Selection of planform design parameters for the wing and for the empennage (tails and/or canard:

   * Size (i.e. area) of wing
   * Aspect ratio
   * Sweep angle (fixed or variable)
   * Thickness ratio
   * Airfoil type
   * Taper ratio
   * Control surface size and disposition
   * Incidence angle (fixed or variable)
   * Dihedral angle

7. Selection of type, size and disposition of high lift devices:

   * Mechanical or powered (blown) flaps
   * Trailing edge and/or leading edge devices

8. Selection of landing gear type and disposition:

   * Fixed or retractable
   * Tail dragger, tricycle or tandem
   * Number of struts and tires
   * Wheel location up and down
   * Feasibility of gear retraction

9. Selection of major systems to be employed by the airplane:

   * Flight control system, primary and secondary
   * Auxiliary power unit (APU)
   * Fuel system
   * Hydraulic System
   * Pneumatic system
   * Electrical system
   * Oxygen system
   * Environmental control system (this includes the cabin pressurization system)
   * Anti-icing and de-icing system
   * Spray system (i.e. for agricultural airplanes)
   * Navigation and guidance system
   * Fire control system

10. Selection of structural arrangement, type of structure and manufacturing breakdown:

   * Metallic, composite or mixture
   * Arrangement of primary structure of major airplane components
   * Attachment structure for landing gear
   * Manufacturing and assembly sequence

11. Determination of the cost of research, development, manufacturing and operation:

   * Assessment of profit potential (civil)
   * Assessment of mission effectiveness = (availability)x(survivability)x(accuracy) for military airplanes
   * Assessment of life cycle cost (civil and military)

Decisions 1-11 are <u>not</u> listed in an implied order of importance.

<u>IMPORTANT NOTES:</u>

<u>1.) Configuration design is a non-unique and iterative process</u>

2.) During the early phases of configuration design 90 percent of the life cycle cost of an airplane gets locked in

There are many different methodologies which can lead to a satisfactory design. It is quite possible that more than one and sometimes radically different configurations can be found to satisfy a given mission specification. Classical illustrations of this fact are the Boeing B47 and the AVRO Vulcan jet bombers. These airplanes while differing radically in their configurations were designed to very similar mission specifications. Figure 1.1 shows threeviews of these airplanes. The tabulated data in Figure 1.1 serve to illustrate the differences in geometry and the similarity in performance between these two airplanes.

Chapter 2 provides a step-by-step guide through the process of configuration design.

Configuration design as presented in Chapter 2 is broken down into two preliminary design (p.d.) sequences:

1. p.d. sequence I which involves 16 design steps.

The objective of p.d. sequence I is to decide on the feasibility of a given configuration with a minimum amount of engineering work.

2. p.d. sequence II which involves 30 design steps.

The objective of p.d. sequence II is to arrive at a reasonably detailed layout of a given configuration so that its mission capabilities can be compared to those of other competing concepts with confidence.

During each p.d. sequence estimates must be made for drag, for stability and control, for weight and balance and for other factors involved in making the 11 decisions listed before. The depth to which these estimates are made should match the depth required in each p.d. sequence.

Engineering methods used in conjunction with p.d. sequence I are referred to as Class I methods. These methods have limited accuracy but require only a small amount of engineering manhours. This part (Part II) concentrates on the so-called Class I methods only.

Engineering methods used in conjunction with p.d.

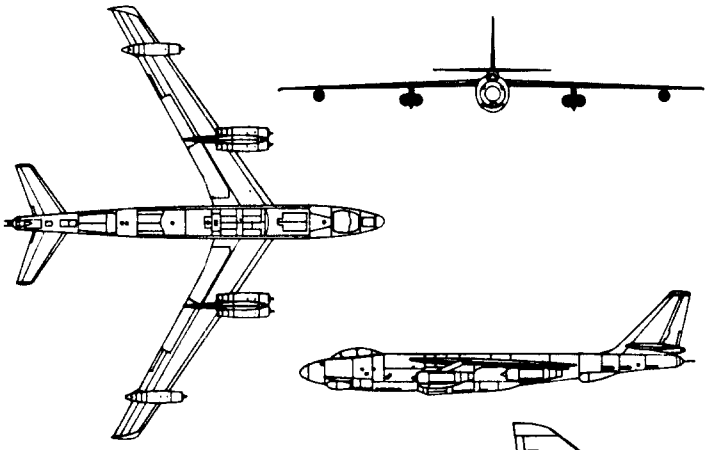

Boeing B-47H

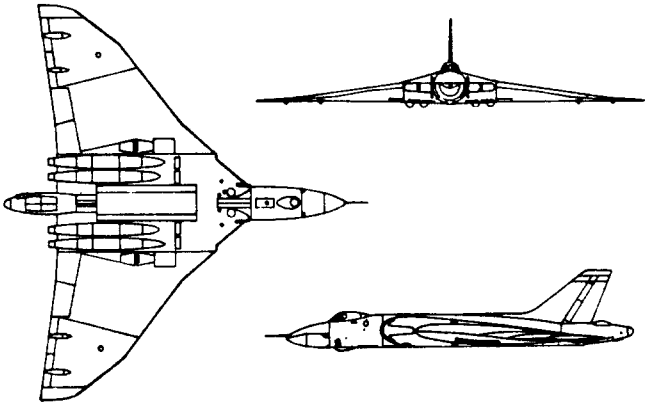

AVRO Vulcan B2

		B-47H	Vulcan B2
W_{TO}	(lbs)	202,000	200,000
S	(ft^2)	1,400	3,964
S_{wet}	(ft^2)	11,300	9,600
b	(ft)	116	111
$(W/S)_{TO}$	(psf)	144	50.5
$(W/b)_{TO}$	(lbs/ft)	1,741	1,801
A		9.6	3.1
C_f (assumed)		0.0030	0.0030
f	(ft^2)	34.0	29.0
dC_D/dC_L^2	(e = 0.8 assumed)	0.041	0.128
$(L/D)_{max}$		15.8	16.4
$C_{L_{(L/D)_{max}}}$		0.77	0.24

Figure 1.1 Example of Radically Different Configurations with Similar Mission Performance

sequence II are referred to as Class II methods. These methods have fairly good accuracy but require a significant expenditure of engineering manhours. Parts III through VIII of this series of books deal with the so-called Class II methods.

Chapter 3 presents a discussion of factors which play a role in the process of selecting an overall configuration.

Chapter 4 gives guidelines for the design of the fuselage and the cockpit or flightdeck.

Chapter 5 provides a methodology for deciding on the type of propulsion system to be used. In addition, the problem of deciding on the number of engines and their disposition over the airplane is discussed.

Chapter 6 presents a discussion of the problem of selection of planform design parameters for the wing. Included also is a method for sizing wing mounted lateral control surfaces.

Chapter 7 contains a method for determining the maximum clean lift coefficient capability of an airplane. A rapid method for preliminary sizing of the required high lift devices is also presented.

Chapter 8 contains a step-by-step procedure for selecting empennage sizes (areas) and empennage planform geometries and disposition. Included also is a method for sizing longitudinal and directional control surfaces.

Chapter 9 presents a method for landing gear sizing and for deciding on the landing gear disposition.

Chapter 10 presents a method for checking the weight and balance characteristics of an airplane.

Chapter 11 contains a method for determining the essential stability and control characteristics of a new design.

Chapter 12 presents a rapid method for estimating the drag polar(s) of an airplane.

Chapter 13 presents three example Class I threeviews which result from the work outlined in Chapters 2 - 12. Tables with geometric characteristics for these example threeviews are also presented.

2. STEP-BY-STEP GUIDE TO CONFIGURATION DESIGN

The purpose of this chapter is to provide a step-by step guide through the process of airplane configuration design.

Figure 2.1 shows a schematic of the preliminary design (p.d.) process. As can be seen from Figure 2.1, the p.d. process is broken down into the following parts:

1.) Preliminary sizing

2.) Preliminary configuration layout and integration of the propulsion system

It will be assumed here, that the preliminary sizing part of this p.d. process has been completed. Part I (Ref.1) presents a systematic methodology for the preliminary sizing of airplanes. The preliminary sizing started by assuming that a mission specification for the airplane to be designed is available. Example mission specifications were given in Part I (Ref.1) as Tables 2.17 through 2.19.

As a result of the preliminary sizing of Part I, the following data are available for the airplane:

Weights: Take-off weight, W_{TO}

Operating weight empty, W_E

Payload weight, W_{PL}

Mission fuel weight, W_F

Wing area: S

Wing aspect ratio: A

Take-off power: P_{TO} or take-off thrust, T_{TO}

Required lift coefficients: clean, $C_{L_{max}}$

take-off, $C_{L_{max_{TO}}}$

landing, $C_{L_{max_L}}$

These data are the 'input' data for the airplane

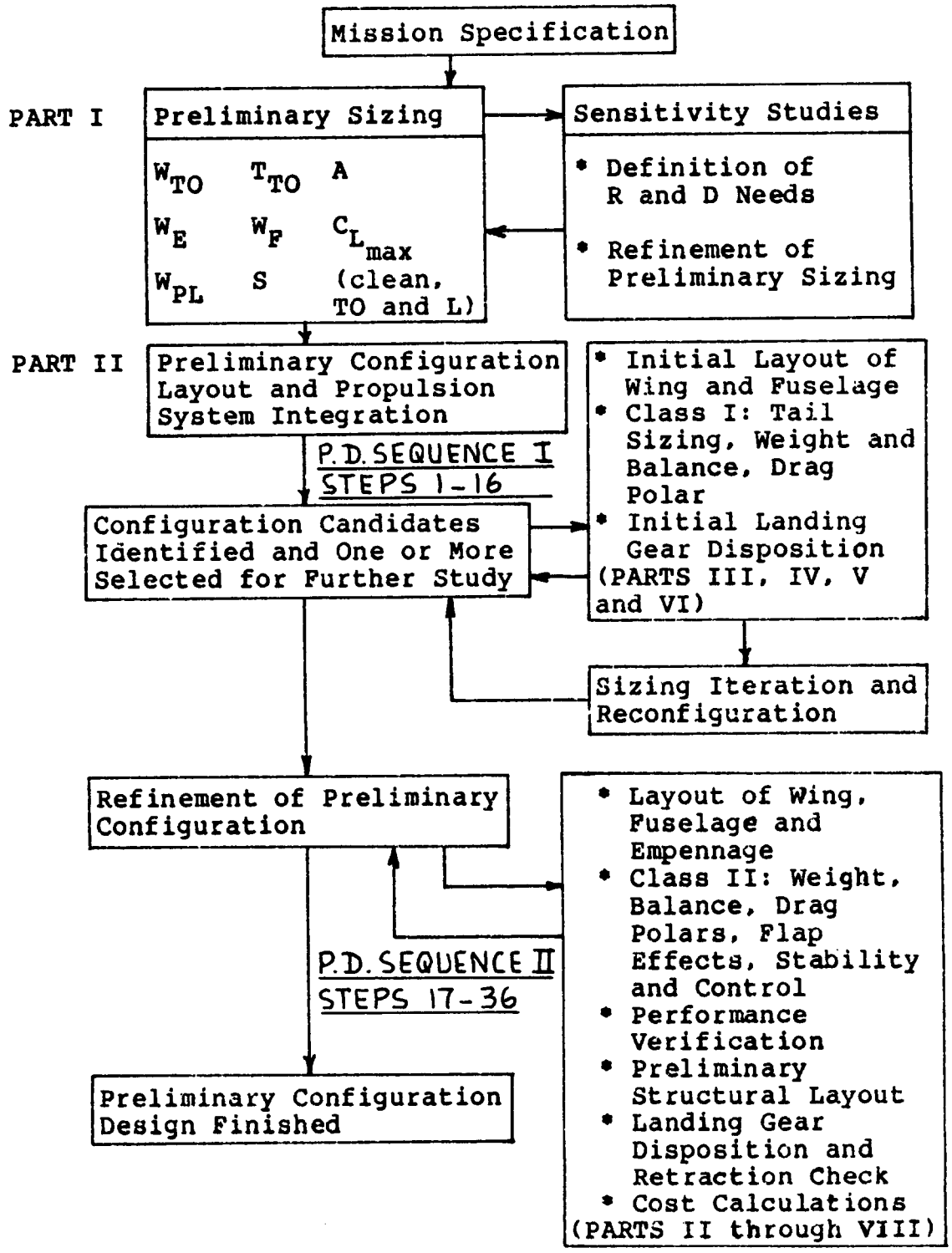

Figure 2.1 The Preliminary Design Process as Covered in Parts I Through VIII of Airplane Design

configuration design process. This process includes overall layout design as well as the integration of the propulsion system.

Figure 2.1 divides the process of preliminary configuration layout and propulsion system integration into two iterative p.d. sequences:

1.) Preliminary Design Sequence I:

The objective here is to arrive at a decision about the feasibility of a certain configuration with a minimum amount of engineering work. Engineering methods employed in this first p.d. sequence are preliminary in nature: they are referred to as Class I methods. Chapters 3 - 13 in this book concentrate on these Class I methods.

Section 2.1 presents an outline of the work which needs to be done during p.d. sequence I. The outline of work is presented in the form of a step-by-step guide: Steps 1 - 16. After completing these steps, it should be evident to the designer, whether or not the proposed configuration is workable. If indeed it is, then there is reason to proceed with the second p.d. sequence:

2.) Preliminary Design Sequence II:

The objective here is to arrive at a realistic, reasonably detailed layout of an airplane configuration. The feasibility of this configuration was already determined in p.d. sequence I. The goal now is to 'fine tune' this configuration. That means to determine whether or not the configuration indeed meets all requirements laid down in its mission specification.

Engineering methods employed during p.d. sequence II are referred to as Class II methods. As the reader will see, these class II methods require considerably more engineering manhours. However, they also are more accurate. Parts III - VIII (Refs 2-7) concentrate on these Class II methods.

Section 2.2 presents an outline of the work which needs to be done during p.d. sequence II. The outline of work is presented in the form of a step-by-step guide: Steps 17 - 36. After completing these steps it will be evident to the designer whether or not the proposed design can meet all requirements of the mission specification.

The end result of p.d. sequence II is sometimes referred to as a 'point' or 'baseline' design. This point design should now be compared with other competing concepts. Depending on the outcome of this comparison, further studies may be called for. In particular studies involving the optimization of the point design in terms of a number of cost criteria may be required. Typical cost criteria can be: (L/D), (nm/lbs), (fuel burn per seat mile), DOC, ROI, and LCC. Methods for cost determination and optimization are the subject of Part VIII (Ref.7).

ADVICE TO STUDENTS:

1.) Students in their first semester of a course on airplane design are urged to follow the design guide of Sections 2.1 and 2.2 as closely as possible. The author has seen many students waste a large amount of calendar time by aimlessly floundering about while trying to come up with a satisfactory configuration.

2.) In the process of going through Steps 1 - 36 a sizable number of engineering calculations will have to be made. These calculations should be recorded in a professional manner, so that other people can follow them without undue effort. All engineering calculations should be:

a) neatly and logically organized according to subject. A table of contents should be provided.
b) dated, with the name of the originator appearing on each page.
c) cross-referenced throughout so that it is obvious where input numbers come from.
d) assumptions made must be carefully stated and identified as such.
e) page numbered

3.) Don't carry more significant figures in any calculations than are justified by the accuracy of the methods used. In preliminary design it is generally not justified to carry more than three significant figures. Round off all computer outputs accordingly!

2.1 PRELIMINARY DESIGN SEQUENCE I

Step 1: Carefully review the mission specification and prepare a list of those items which have a major impact on the design.

Examples of items which can have a major impact on the design are:

a) very short and soft field requirements
b) hot and high field requirements
c) water based or amphibious requirements
d) requirements for carrying large vehicles
e) requirements for extreme range or endurance
f) requirements for large search radars

Make it a habit to review the mission specification at each step in the p.d. sequences. Not doing so will result in a design which is only partially responsive to the mission specification.

Step 2: Perform a comparative study of airplanes with similar mission performance.

This can usually be accomplished by referring to one or more issues of Ref. 8: Jane's All the World Aircraft. A collection of data on five to ten similar airplanes should be included in this comparative study. Results of this study should include:

1. A discussion of major differences in mission capability and configuration.

2. A tabulated comparison of significant airplane sizing parameters and planform design parameters.

3. A critical discussion of the configurations of these airplanes, as seen from their threeviews in Ref. 8.

THE OBJECTIVE IS: FAMILIARIZE YOURSELF WITH THE COMPETITION AND WITH WORK DONE BY OTHERS!

Step 3: Select the type of configuration to be designed.

Chapter 3, Section 3.1 contains a discussion of existing configurations for twelve categories of airplanes. A discussion of 'unusual' configurations is included in Section 3.2. An outline of configuration possibilities is presented in Section 3.3.

In selecting a configuration type, the required characteristics of the propulsion system, including its disposition, should be kept in mind. Step 5 deals with the propulsion system more specifically.

Section 3.4 presents a step-by-step procedure for selecting a configuration.

For a student who is just getting started in the study of airplane design it is important to:

MAKE A DECISION TO GO WITH A CERTAIN TYPE OF CONFIGURATION AND MOVE ON

At this point in the p.d. process, many airframe manufacturers follow the so-called red, white and blue team approach. Different design teams are assigned the task to evolve and study different types of configurations. The idea is to find the most suitable configuration for the mission task at hand.

Step 4: Prepare a preliminary (scaled) drawing of the fuselage and cockpit layout.

Chapter 4 contains a step-by-step guide for preparing fuselage and cockpit layouts.

Step 5: Decide which type of propulsion system is to be used and how the propulsion system will be arranged.

This step has a major impact on the design. Selection of engine type(s), number of engines and overall engine arrangement will affect the layout of the fuselage (sometimes the cockpit), the wing and/or other components of the airplane.

The reader is reminded of the fact that the total required thrust or power level (at take-off) is already known: this was determined during the preliminary sizing work outlined in Part I (Ref.1).

Chapter 5 contains a step-by-step outline of the process used in deciding on the type, the number and the disposition of the engines.

Step 6: Decide which wing planform design parameters are to be used. Also decide on the size and location of wing mounted lateral controls.

The reader is reminded of the fact that wing area, S

and wing aspect ratio, A are already known: these were determined during the preliminary sizing work outlined in Part I (Ref. 1).

The following additional parameters must now be selected:

*Wing taper ratio, λ_w

*Wing sweep angle, Λ_w

*Wing thickness ratio, $(t/c)_w$

*Wing airfoil(s)

*Wing incidence angle, i_w

*Wing dihedral angle, Γ_w

If the mission calls for a variable geometry wing (such as variable sweep), the effect of this on the planform must also be determined.

Another result of the preliminary sizing process was the numerical determination of the required maximum lift coefficients: clean, take-off and landing. The planform parameters of the wing must be compatible with the required maximum lift coefficients. As will be seen in Step 7, the maximum lift coefficient requirements may limit the available choice of wing planform parameters.

Chapter 6 contains a step-by-step procedure for determining the wing planform geometry as well as the size and the disposition of wing mounted lateral controls.

Step 7: Decide on the type, the size and the disposition of high lift devices.

The reader is again reminded of the fact that numerical values for the required maximum lift coefficients (clean and flaps down) are already known. These were the result of the preliminary sizing process described in Part I (Ref.1).

Chapter 7 contains a step-by-step methodology for defining the required high lift devices.

Step 8: Decide on the layout of the empennage: size, planform geometry and disposition. Also select the size and location of longitudinal and directional controls.

The word 'empennage' is used here to indicate tails, canards and other additional stabilizing or control surfaces to be used in the configuration.

From Step 3 it is known whether the overall configuration is:

a) conventional (i.e. tail aft)
b) flying wing (i.e. no horizontal tail and no canard)
c) tandem wing
d) canard
e) three surface
f) joined wing

In either case it will now be necessary to decide on the following empennage design parameters:

*Area and location,
*Aspect ratio,
*Taper ratio,
*Sweep angle,
*Thickness ratio
*Airfoil(s)
*Incidence angle
*Dihedral angle

In addition, the preliminary size and disposition of the longitudinal and directional controls need to be selected.

Chapter 8 contains a step-by-step method for arriving at these design decisions.

Step 9: Decide which type of landing gear is to be used. Also: decide on the landing gear disposition and determine the required number and size of tires.

The following questions need to be answered:

1. What type of landing gear is required?

2. How many and what size tires are required?

3. How are the landing gear wheels to be arranged?

4. Is the space designated for the retracted landing gear sufficient?

5. Does the landing gear retraction cause the gear to interfere with other airplane components or airplane structure?

6. Do the landing gear attachment points require major additional structural provisions?

WARNING: Students should not underestimate the importance of preliminary landing gear design. The answers to questions 1-6 may well determine the ultimate feasibility of the proposed configuration.

Questions 4 and 5 are mute in the case of fixed landing gears.

Chapter 9 contains a step-by-step procedure for making these landing gear design decisions.

Step 10: Prepare a scaled preliminary arrangement drawing of the proposed configuration and perform a Class I weight and balance analysis.

Chapter 10 provides a step-by-step method for performing a Class I weight and balance analysis. Examples of the required preliminary arrangement drawings are also presented.

Step 11: Perform a Class I stability and control analysis of the proposed configuration.

Chapter 11 contains a step-by-step method for performing a Class I stability and control analysis.

Step 12: Perform a Class I drag polar analysis.

Chapter 12 presents a step-by-step method for computing Class I drag polars.

Step 13: Analyze the results of Steps 10 and 11.

By inspecting the results obtained under Steps 10 and 11, it is possible to draw one or more of the following conclusions:

1. The weight and balance results (Step 10) as well as the stability and control results (Step 11) are satisfactory:

   Proceed to Step 14.

2. The results of Step 10 show that the airplane has a 'tip-over' problem. This means that the c.g. is incorrectly located relative to the landing gear.

   Try making minor adjustments to wing and landing gear locations and see if the problem can be solved that way. If it can, make the change(s) and go on to Step 14. If the problem cannot be solved with minor adjustments, consider a change in the configuration. That may imply going back to Step 2.

3. The airplane has too much travel between forward and aft c.g.

   The suggestions made under 2. apply here also.

   This problem tends to disappear if the payload c.g., the fuel c.g. and the OWE c.g. are close together. Try to achieve this.

   Sometimes the problem can be solved by relocation of a particularly 'heavy' component.

4. The results of Step 11 show that the airplane has too much or too little longitudinal and/or directional stability, or that a V_{mc} problem exists.

   Make the required adjustments to tail or canard sizes and when necessary redo Steps 10 and 12.

   Proceed to Step 14.

Chapters 10 and 11 provide the information needed to arrive at one or more of these four conclusions.

Step 14: From the drag polars of Step 12, compute those L/D values which correspond to the mission phases and to the sizing requirements considered in the prelimininary sizing process of Part I (Ref.1).

14.1) Tabulate the new and the old L/D values.

14.2) Determine the impact of any changes in L/D on W_{TO}, W_E and W_F. This can be done using

the results of the sensitivity analyses carried out during the preliminary sizing process described in Part I (Ref.1).

The following cases should be considered:

1. Weight changes are less than 5 percent.
2. Weight changes are more than 5 percent but less than 15 percent.
3. Weight changes are more than 15 percent.

Case 1. Resizing of the airplane is not necessary. Proceed to Step 15.

Case 2. Resize the airplane using the results of the sensitivity analyses carried out during the preliminary sizing process described in Part I (Ref.1).

Go back to Step 3.

Case 3. Resize the airplane with the methods of Part I.

Go back to Step 3.

While working on Steps 13 and 14 the discovery may be made that the configuration choice made in Step 3 was a bad one. Don't be discouraged. This is precisely the reason for p.d. sequence I: to weed out the bad ideas from the good ones.

From the work done up to this point it is possible to distill clues for any configuration changes which need to be made.

Step 15: Prepare a dimensioned threeview which reflects all the changes which were made as a result of the iterations involved in Steps 10 through 14.

On the threeview or as an addendum to the threeview, include a tabulation af all essential dimensional and dimensionless design parameters. Chapter 13 shows examples of such tabulations.

Step 16: Prepare a report which documents the results obtained during p.d. sequence I. Include recommendations for change, for further study or for research and development work which needs to be carried out.

At this point the first preliminary design sequence is complete. The second preliminary design sequence can now be started. Section 2.2 presents an outline of work to be done during p.d. sequence II: Steps 17 - 36.

2.2 PRELIMINARY DESIGN SEQUENCE II

This p.d. sequence starts with the threeview of Step 15 and with the report of Step 16.

The reader will quickly discover, that the amount of work to be done in p.d. sequence II is considerable. For that reason, p.d. sequence II is usually carried out by a team of engineers. Such a team may number anywhere from 3-15 engineers depending on the complexity of the airplane.

Step 17: List the major systems needed in the airplane. Also: prepare 'ghost' views indicating the general system arrangements and their location in the airframe.

Part IV (Ref.4) addresses this problem. There are two reasons for identifying the required airplane systems at this point:

1. Airplane systems have a significant impact on empty weight. In Step 21 a detailed weight estimate must be made.

2. To determine any obvious conflicts which would arise by having two or more systems occupy the same space in the airplane. The so-called 'ghost' views help identify such conflicts early in the design.

Step 18: Size the landing gear tires and struts using Class II methods. Also: verify the validity of the proposed landing gear disposition and of the proposed retraction scheme.

Part IV contains the Class II landing gear sizing methods as well as detailed examples of landing gear design practice.

epare drawings showing that the landing gear can be ... cted into the designated volume. These drawings should include a so-called 'stick-diagram' of the retraction kinematics to be employed. The force-stroke diagram for the retraction actuator should be determined and its feasibility verified.

Part IV (Ref.4) addresses these problems.

Step 19: Prepare an initial structural arrangement drawing.

A step-by-step method by which a structural arrangement can be put together is contained in Part III (Ref.2).

There are two reasons for preparing the structural arrangement at this point:

1. The structural arrangement has a major impact on the Class II weight predictions of Step 21.

2. The structural arrangement will influence the manufacturing breakdown of Step 34 and in turn the cost estimates of Step 36.

Important Note: Frequently it is possible to achieve a synergistic effect by cleverly combining major structural components to take advantage of mutually supporting functions. Whenever structural synergism can be achieved, the empty weight of the proposed airplane will be reduced.

Step 20: Construct a V-n diagram.

Part V (Ref.3) addresses the problem of how to construct a V-n diagram for a given type airplane.

Step 21: Perform a Class II weight and balance analysis. This includes the calculation of moments and product(s) of inertia.

Part V (Ref.3) addresses this problem.

Step 22: Analyze the results of Step 21. This step is similar to Step 13, points 1-3.

Step 23: Redraw the threeview obtained at the end of p.d. sequence I, as required.

Step 24: Perform a Class II stability and control analysis using the threeview of Step 23.

As part of the Class II stability and control analysis, the following items need to be considered:

1. Trim diagram (power-on and power-off)
2. Take-off rotation
3. Minimum control speed with engine out including the effect of bank angle
4. Roll performance
5. Crosswind control during final approach and on the runway
6. Open loop dynamic handling
7. Gain sizing of any required SAS-loops
8. For airplanes with reversible flight control systems the slopes $\partial F/\partial V$ (stick-force versus speed) and $\partial F/\partial n$ (stick-force versus load factor) need to be determined and checked against the certification base
9. Actuator size and rate requirements

The necessary Class II stability and control analysis methods are presented in Part VII (Ref.6).

The important outcome of the Class II stability and control analysis is that 'final' sizes of stabilizing and control surfaces are established. If necessary, the threeview of Step 23 should be adjusted. Any other required iterations should also be performed. An example of a required iteration would be the case where the tail sizes change by more than 10 percent in area and/or in weight, in going from Class I to Class II results. Both drag (thrust and fuel) and weight may be significantly affected, requiring another iteration in the design.

For airplanes which lack inherent static and/or dynamic stability, the Class II analysis should also result in the preliminary definition of any required stability augmentation system and its required gains. This includes the initial determination of actuator size and rate requirements. Part VII contains a methodology for arriving at a preliminary definition of the SAS and of the required actuator performance.

Step 25: Recompute the drag polars using Class II methods.

In recomputing the drag polars the tail and surface

sizes of Step 23 should be used.

Class II drag polar methods, also called component build-up methods are presented in Part VI (Ref.5).

Step 26: Compute the installed power and/or thrust characteristics of the propulsion system.

Nota bene: Account for all essential installation losses as well as for losses caused by the operation of all 'flight essential' airplane systems.

Methods for computing installed power and/or thrust characteristics are presented in Part VI(Ref.5).

Step 27: List all performance requirements which the airplane must meet. This includes FAR as well as mission requirements. Identify those requirements found to be critical in the preliminary sizing of the airplane.

Step 28: Compute the critical performance capabilities of the airplane and compare them with the requirements of Step 27.

All calculations of critical performance capabilities must be carried out with the Class II drag polars of Step 25 and with the Class II installed engine characteristics of Step 26.

The Class II performance methods of Part VII (Ref.6) must be used in this case. Depending on the results of these performance calculations further design iterations may be needed.

Step 29: Iterate through Steps 17 - 28 as needed and adjust the configuration.

The reader will now appreciate why configuration design was referred to as a non-unique, iterative process in the introduction (Chapter 1).

Step 30: Finalize the threeview and tabulate the essential airplane geometry.

Examples of threeviews and of geometric tabulations are presented in Part III (Ref.2).

Step 31: Finalize the inboard profile(s).

Examples are shown in Part III (Ref.2).

Step 32: Prepare a preliminary layout drawing for all essential airplane systems, in particular the primary and secondary flight control systems.

Part IV contains examples of layout drawings for various airplane systems.

Check for any conflicts and go through the 'WHAT IF' safety and maintenance checklist given in Part IV (Ref.3).

It is of particular importance to insure that no undue fire hazards and no obstacles to crash survivability have been 'built in'.

Step 33: Finalize the structural arrangement.

Step 19 asked for an initial structural arrangement. As a result of any modifications imposed by the work done in Steps 20-32 this initial structural arrangement may have to be modified.

Step 34: Prepare a preliminary manufacturing breakdown.

Part III (Ref.3) addresses the problem of deciding on manufacturing breakdowns.

Step 35: Make a study of maintenance and accessibility requirements.

As part of this study the following schematics are needed:

1. A schematic showing all essential access requirements for inspection and for maintenance. Compatibility with the structural arrangement should be ensured.

2. For transports and for military airplanes, a schematic demonstrating the accessibility of standard service, loading and unloading vehicles is required.

3. Prepare a schematic showing that the engine(s) and the APU can be easily inspected and removed.

Part IV contains useful hints with regard to maintenance requirements of various airplane systems.

Step 36: Perform a preliminary cost analysis for the airplane.

This generally includes an estimation of the following cost items:

1. Design and development cost
2. Manufacturing cost
3. Operating cost

Part VIII (Ref.7) presents methods for estimating these cost items.

On the basis of these estimates a judgement can be made as to whether or not the proposed airplane will allow the manufacturer as well as the operator to make a profit.

In the case of a military airplane, the cost analysis should include a comparison of the military utility or the 'bang-per-buck' obtainable with the proposed new airplane as compared to alternate solutions. A rationale for the selected design in view of expected enemy threats must be included.

At this point it often makes sense to study the possible benefits of design optimization relative to cost criteria. Typical of such cost criteria are: DOC, ROI and LCC. Part VIII (Ref.7) addresses this problem also.

A final report documenting the results obtained during p.d. sequence II should be prepared. This rounds off all p.d. sequence II work.

IMPORTANT COMMENT:

Experience has shown that the decisions made during preliminary configuration design 'lock in' 90 percent of the life-cycle-cost (LCC) of the airplane.

This is of staggering importance, because the total investment made in the airplane at the end of the preliminary design phase is negligible when compared even with the total full scale development cost.

Clearly, it is penny-wise and dollar-foolish not to invest heavily in supportive research work during the early design work on a new airplane.

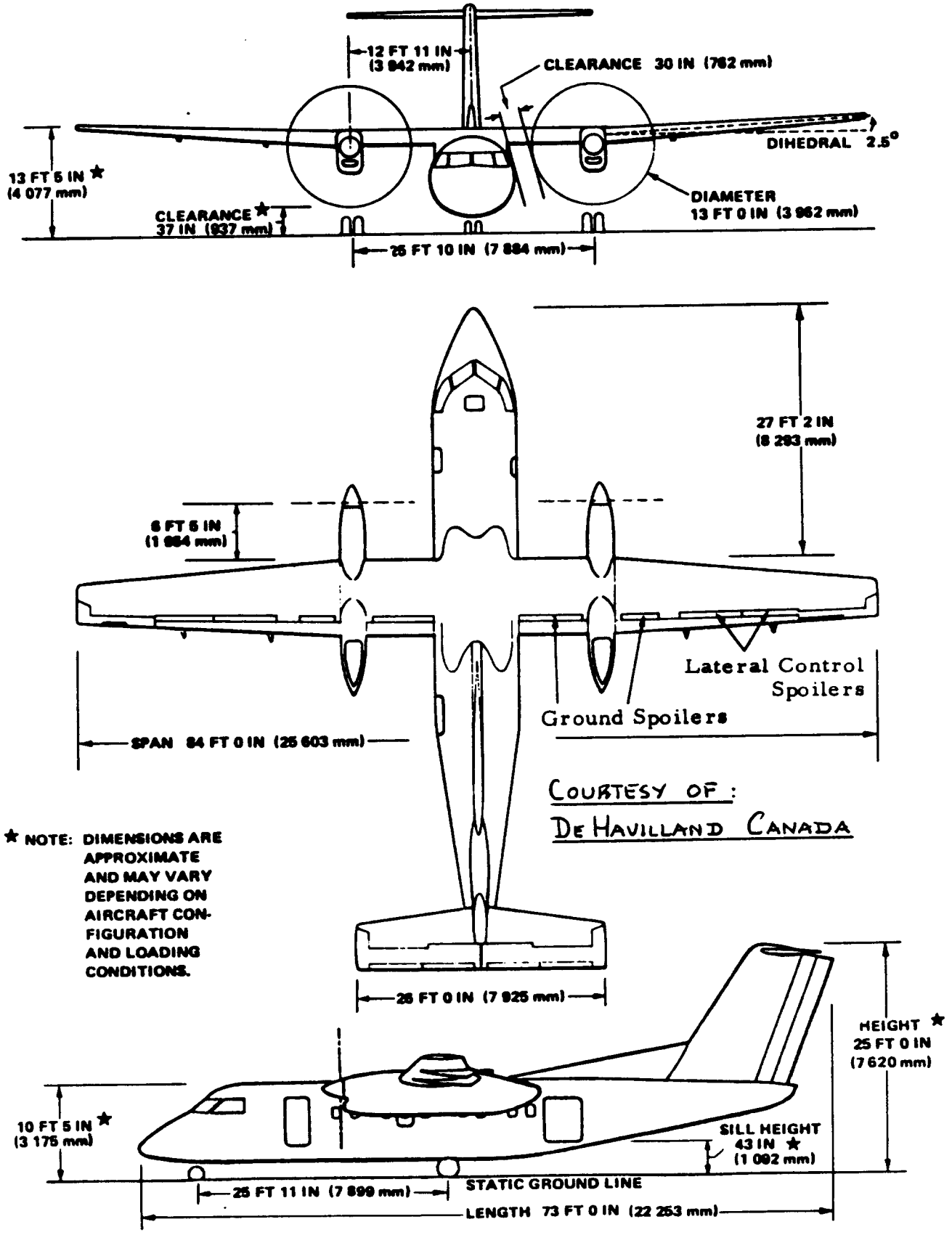

DASH 8 General Arrangement

3. SELECTION OF THE OVERALL CONFIGURATION

In addition to a large number of technical considerations, configuration design is also influenced by marketing, emotional and styling considerations. Only technical considerations are discussed in this chapter.

The following technical considerations play a role in the selection of the overall configuration:

1. It is nearly always desirable to place the fuel c.g., the payload c.g. and the empty weight c.g. at the same longitudinal location. Doing this limits c.g. travel. Limiting c.g. travel results in a configuration with less wetted area due to less need for trim control power.

   This consideration has a major influence on the relative placement of those airplane components, which primarily affect the overall c.g. location.

2. The critical Mach number of the wing of a subsonic airplane should be selected such that the airplane does not cruise too far into the drag rise.

   This requirement means that wing sweep angle, airfoil type and airfoil thickness ratio must be choosen in such a way as to avoid excessive drag rise at cruise Mach numbers.

3. The critical Mach number of the wing should always be lower than the critical Mach number of stabilizing or control surfaces.

   This requirement means that the thickness ratio, sweep angle and aspect ratio of stabilizing and of control surfaces must be selected to yield critical Mach numbers greater than that of the wing.

4. The integration of major components such as: nacelle on wing, nacelle on fuselage, wing on fuselage and so on needs to be done so that interference drag is minimized.

   Ideally this means that any connecting, intersecting items should intersect at as close as possible to 90 degrees. If it is not possible to do this, extensive fairings are needed to avoid

interference drag penalties.

At high subsonic speeds it is frequently found necessary to apply local area ruling to reduce subsonic wave drag. Subsonic area ruling is discussed in Part VI (Ref.5).

5. In fighter aircraft with requirements for supersonic cruise performance or supersonic maneuvering performance the wave drag becomes an essential design consideration.

To minimize supersonic wave drag the configuration must be arranged such that the shape of the cross-sectional area distribution (arranged as an equivalent body of revolution) is smooth. Ideally this should approximate the so-called Sears-Haack shape. Supersonic area ruling is discussed in Part VI (Ref.5).

6. Major intersecting structural components should be arranged to avoid duplication of special heavy structure.

Low weight airplane structures come about only by judiciously combining multiple functions into major structural elements. This is referred to as structural synergism.

For example: in a high wing transport with fuselage mounted main landing gear, it is desirable to attach the landing gear to the same fuselage frames which are used to attach the wing. This is referred to as structural synergism.

7. In deciding on the location of the major airplane components:

<u>THINK LIGHT, THINK SIMPLE, THINK ACCESSIBILITY, THINK MAINTAINABILITY AND THINK COST.</u>

Remember that above certain cost levels no airplanes will be sold. Another way of putting this is: <u>Your job depends on it!</u>

Configurations are often selected as an outgrowth of an existing configuration. This is particularly true in the large airplane companies. Examples are: 707, 727, 737 and 757. These airplanes all use the same fuselage cross section. The same is true for the DC-9 and MD-80 and -82 series.

When a new configuration evolves, it is often the result of a large number of trade studies done by different teams trying to come up with the most economical solution to some mission requirement. In the large companies two or more teams may be working toward the same mission objective, each folowing a different configuration approach. It may be safely assumed, that the companies would not do this, if configurations could be selected on a direct rational basis.

It is not yet possible to present straightforward, unique procedures by which an airplane configuration can be selected so that it 'best' satisfies customer requirements. There are too many variables involved in this process, most of which defy mathematical modelling.

For the beginning design student it is difficult to get started on the selection of a configuration. To assist the student in that process, a number of existing configurations will be presented in the form of airplane threeviews for twelve different airplane categories. These configurations are discussed in Section 3.1.

Section 3.2 presents a discussion of what are called unusual configurations.

Section 3.3 provides an outline of configuration possibilities. This section should be consulted before 'freezing' a configuration.

A step-by-step process for selecting a configuration is presented in Section 3.4.

Section 3.5 contains three example applications.

3.1 EXAMPLES OF EXISTING CONFIGURATIONS

The purpose of this section is to review a number of existing configurations. The review is presented for the following airplane categories.

3.1.1 Homebuilts
3.1.2 Single engine propeller driven airplanes
3.1.3 Twin engine propeller driven airplanes
3.1.4 Agricultural airplanes
3.1.5 Business jets
3.1.6 Regional turbopropeller driven airplanes
3.1.7 Jet transports
3.1.8 Military trainers
3.1.9 Fighters
3.1.10 Military patrol, bomb and transport airplanes
3.1.11 Flying boats, amphibious and float airplanes
3.1.12 Supersonic cruise airplanes

The reader is encouraged to also consult Jane's All the World's Aircraft (Ref.8) for further information on these and other airplane configurations. Jane's has been published annually since 1909 and contains a wealth of data. The author believes that a historical perspective is vitally important to any aeronautical engineer. An easy way to acquire such a perspective is to study earlier versions of Jane's. In addition to reading Jane's, the author recommends that students of airplane design read the books listed under 'historical references' in Section 14.2.

CAUTION: In the following discussions the author presents a number of pros and cons for various configuration aspects. After reading the remainder of this section the reader should keep the following points in mind:

1. In airplane configuration design there are no absolute pros and cons, only relative pros and cons.

2. During configuration design many pros and cons are traded against each other and a compromise is struck.

3. Unless one has been involved in the decision making process leading to a given configuration, it is very hard to know how the pros and cons were compromised.

4. In discussing pros and cons it is almost impossible not to reflect a certain amount of personal biasses. Therefore: reader beware!

3.1.1 Homebuilts

Figures 3.1-3.3 illustrate twelve fairly typical homebuilt configurations. The following observations are offered:

1. These airplanes range from simple, basic, low performance machines (such as the Sizer Sapphire of Fig.3.2b) to rather sophisticated high performance machines (such as the Sequoia Model 300 of Fig.3.1c).

2. Except for the tandem wing Piel C.P.500 (Fig.3.3d) all of the homebuilts shown have rather conventional configurations.

3. To some homebuilders the ability to store the airplane at home is a necessity. This sometimes leads to the incorporation of wing-fold mechanisms. Examples are shown in Figures 3.1a, 3.2a and 3.3a.

4. There seems to be no preference amongst homebuilders for tri-cycle or for tail-dragging landing gear designs. Both types are widely used. However: note the preference for fixed landing gears (cost and simplicity!).

5. The homebuilts shown have tractor, piston-propeller type of propulsion. The Coot of Fig.3.3a is the only exception. It is also the only amphibious layout shown.

6. Observe that except for the airplanes of Figures 3.2b, 3.2d and 3.3d all wings are of the cantilever type.

7. Of interest is the wide variety in wing planforms, ranging from bi-plane to mono-plane and from straight untapered to elliptical. Cost and hours spent in construction are important considerations to the homebuilder. If a homebuilder wants an efficient, elliptical wing, he will have to spend the time required to build such a wing.

8. It is interesting to note the preference for low wing designs. This is probably caused by the desire to attach the landing gear to the wing and to keep the gear as short (and thus light) as possible.

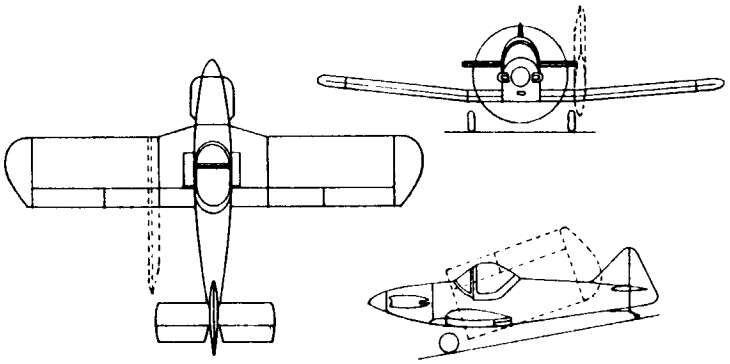

a) CLUTTON- TABENOR E.C.2 EASY TOO

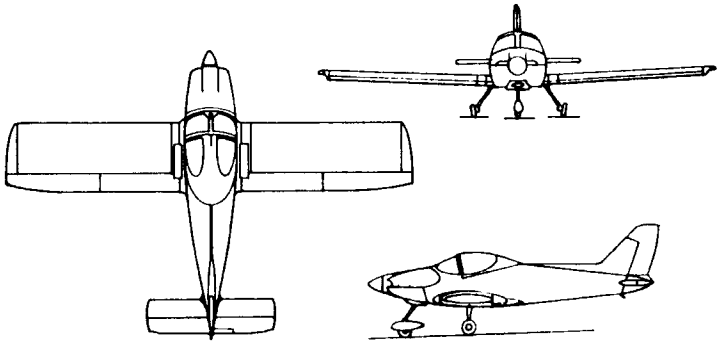

b) COATES S.A.III SWALESONG

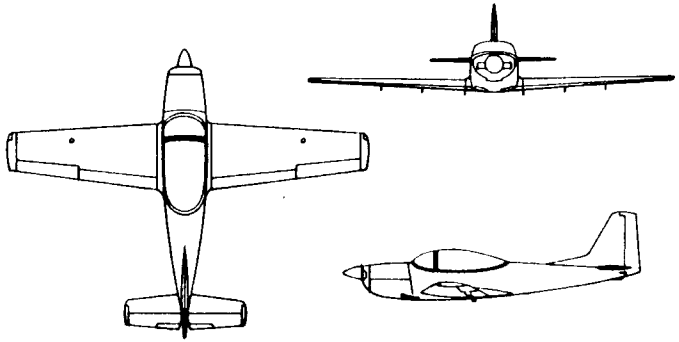

c) SEQUOIA MODEL 300

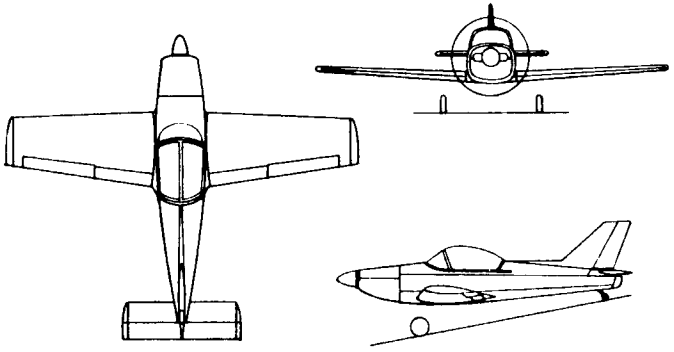

d) PIEL C.P. 1320

Figure 3.1 Homebuilt Propeller Driven Airplanes

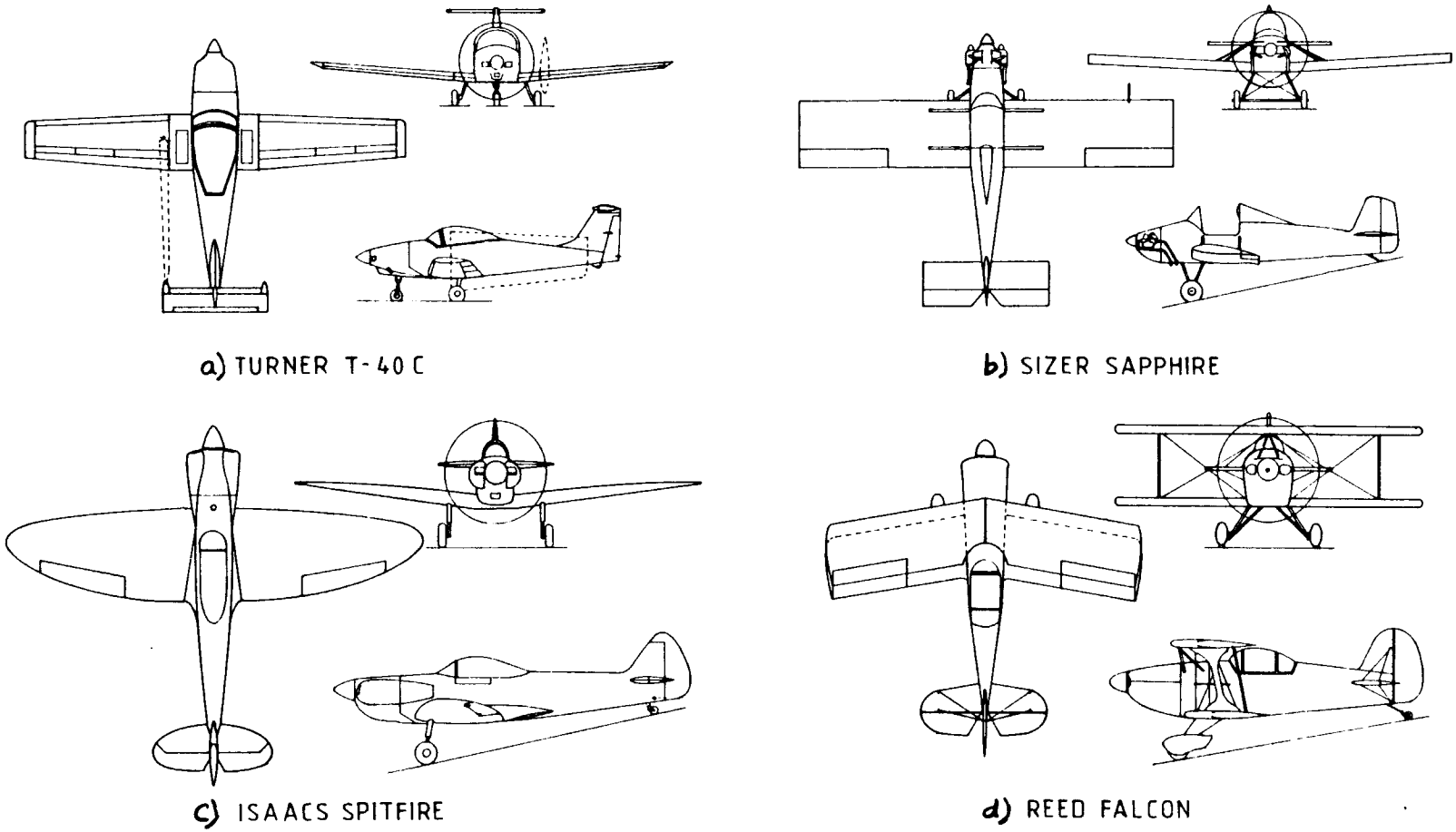

Figure 3.2 Homebuilt Propeller Driven Airplanes

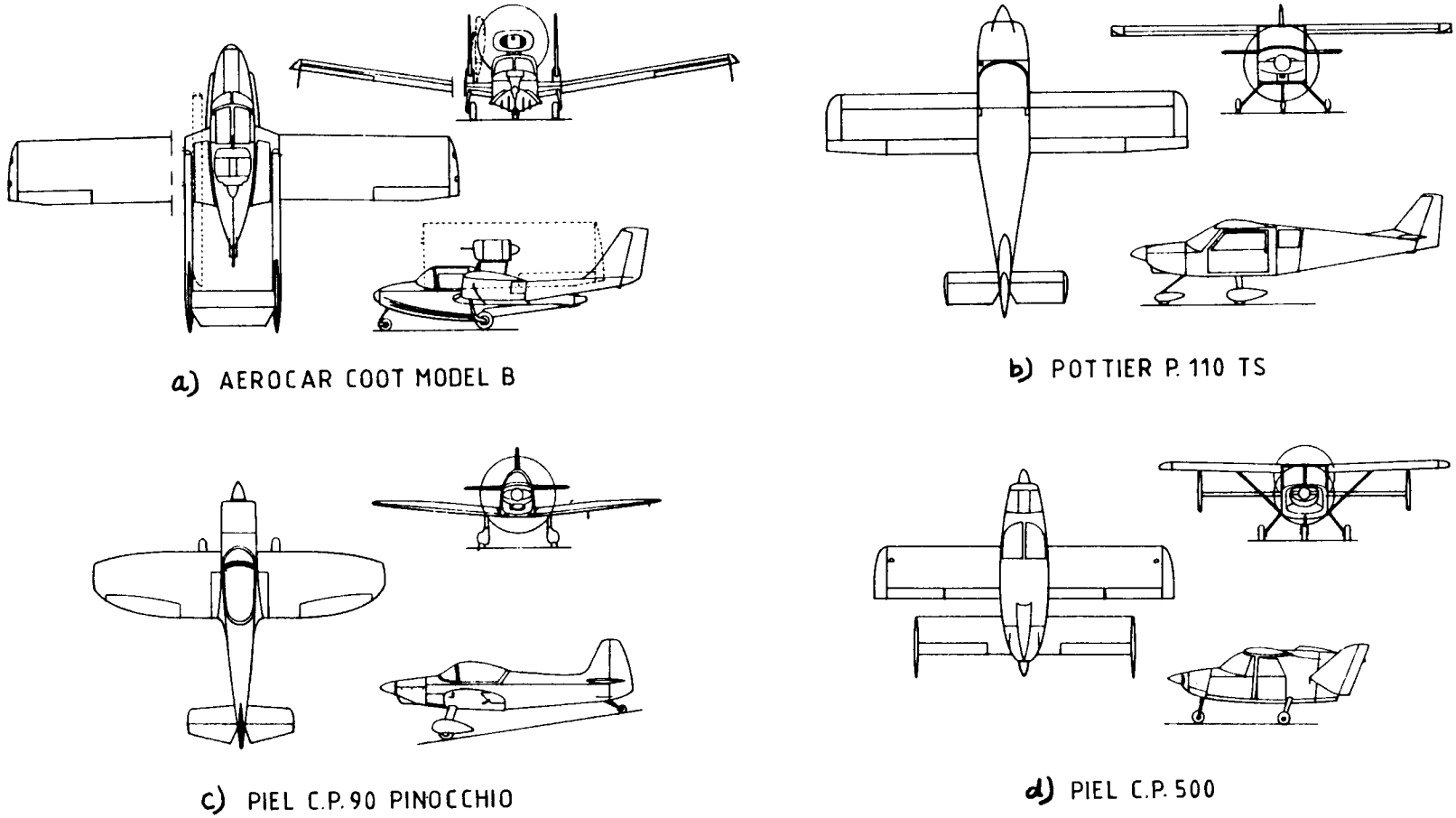

Figure 3.3 Homebuilt Propeller Driven Airplanes

3.1.2 Single Engine Propeller Driven Airplanes

Figures 3.4-3.6 show twelve typical configurations for airplanes in this category. The following observations are offered:

1. Nine of these airplanes have low wings, three have high wings. Except for the Cessna's of Fig.3.5 which have externally braced wings, all employ cantilever wings.

2. All configurations are of the tractor type, except for the Pöschel P-300 Equator of Figure 3.5.

3. Observe the vertical placement of the horizontal tail on these airplanes: three have T-tails, while nine have the horizontal tail placed roughly at the root of the vertical tail. T-tail airplanes in this category share some problems which need to be weighed before deciding to incorporate a T-tail:

a) because of the height of the T-tail, they are difficult to inspect without a ladder.
b) having the horizontal tail away from the propeller slipstream makes rotation during take-off more difficult. That results in longer take-off runs. Note that the Pöschel P-300 gets around that problem by having the propeller installed at the T-tail junction.

4. Also observe the longitudinal placement of the horizontal tails on these airplanes. On several, the horizontal tail is placed aft of the rudder hinge line. This is done to keep the rudder away from the separated horizontal tail wake, when the airplane has stalled and may be entering a spin. Keeping the rudder away from this wake allows for easier recovery from a spin. This does not imply however, that the other types cannot be recovered from a spin.

5. Only four of these airplanes have retractable landing gear. A retractable gear reduces cruise drag but increases cost: both acquisition cost and maintenance cost. In this type of airplane a retractable gear also tempts the pilot to forget lowering the gear before landing.

6. Except for one airplane, all have swept aft vertical tails. For low sweep angles, this improves the product of tail moment arm and tail lift curve slope. This in turn improves vertical tail effectiveness. Vertical tails are also swept for reasons of styling.

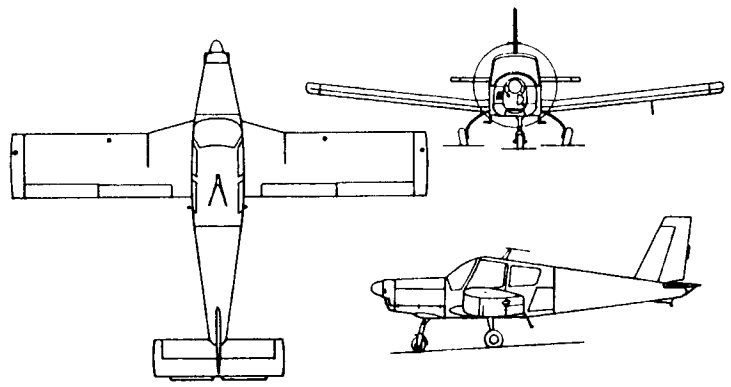

a) ZLIN 43

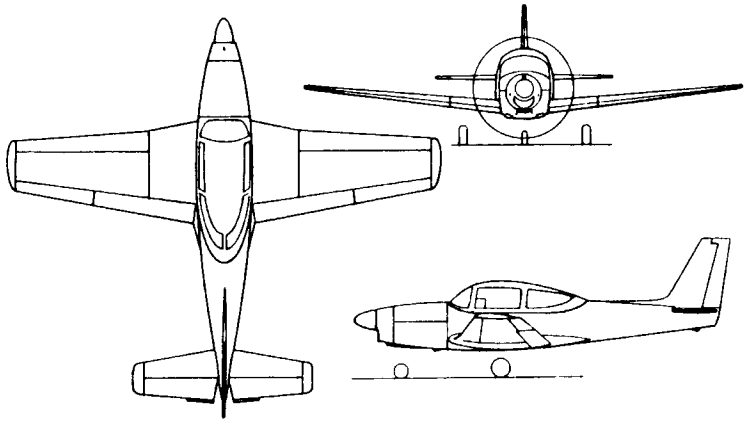

b) INTERCEPTOR 400

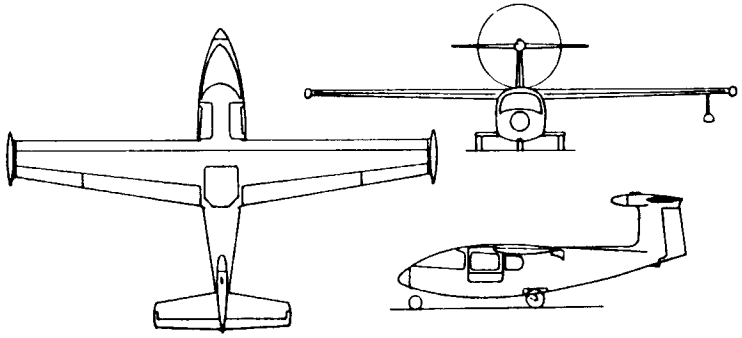

c) PÖSCHEL P-300 EQUATOR

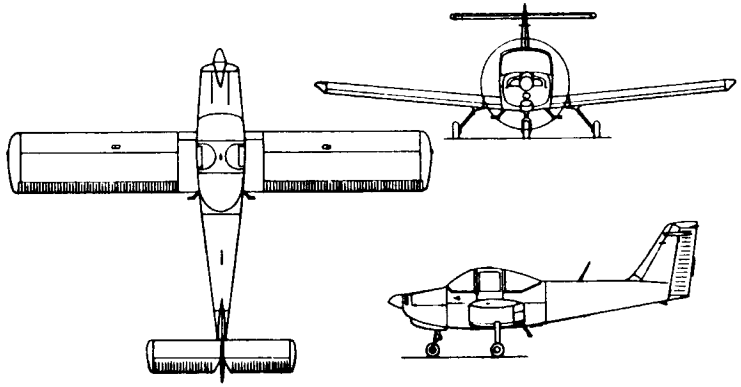

d) PIPER TOMAHAWK II

Figure 3.4 Single Engine Propeller Driven Airplanes

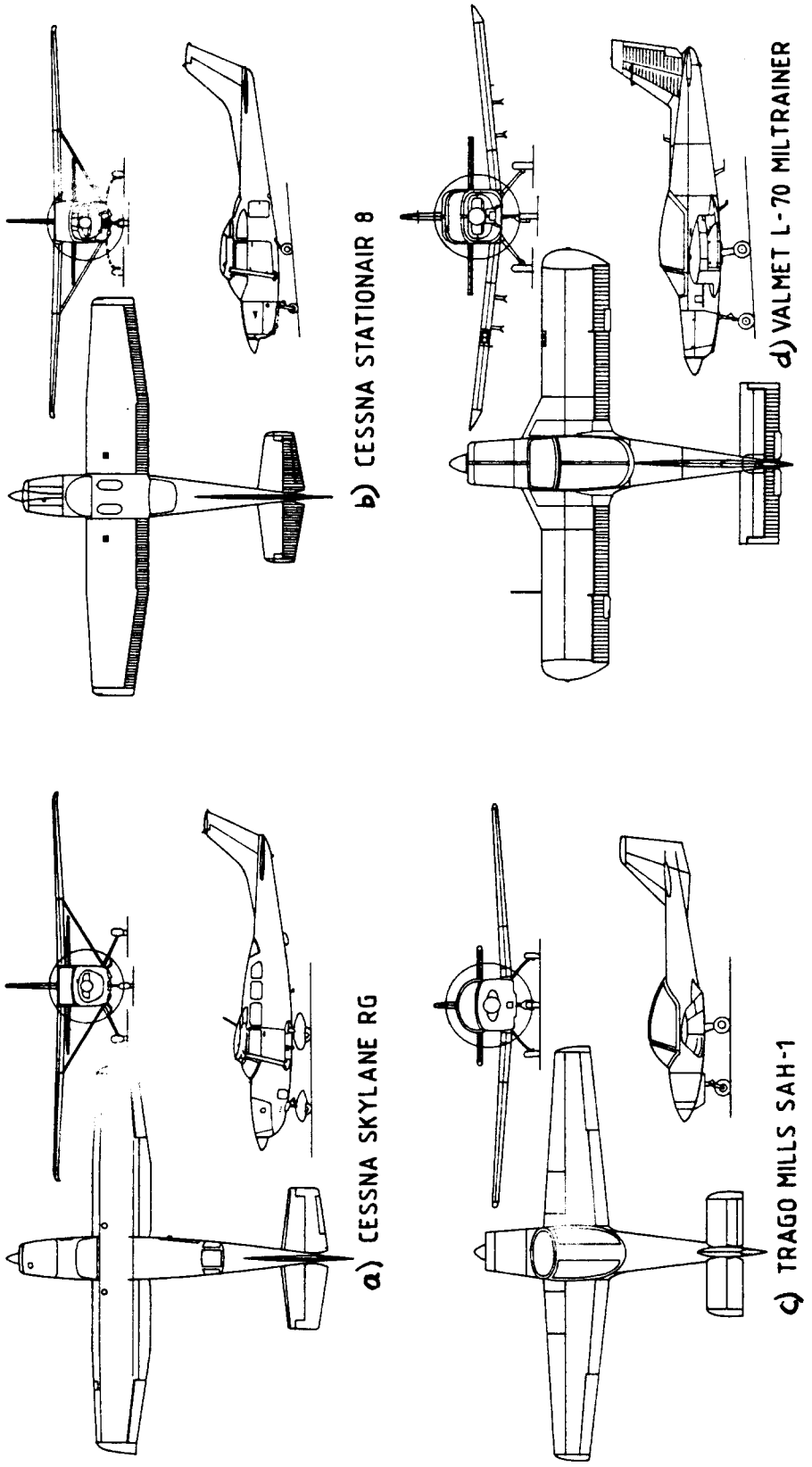

Figure 3.5 Single Engine Propeller Driven Airplanes

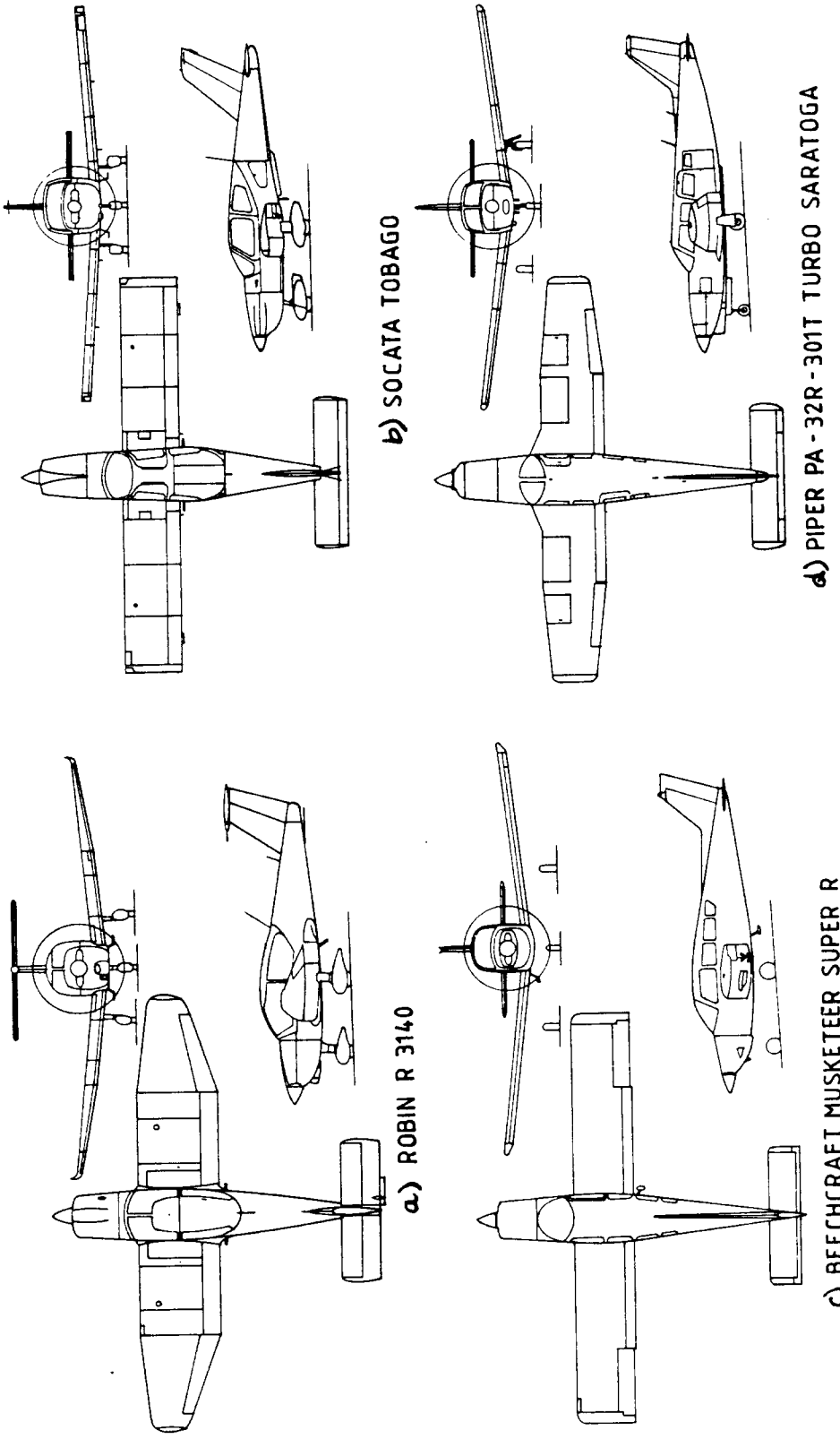

Figure 3.6 Single Engine Propeller Driven Airplanes

3.1.3 Twin Engine Propeller Driven Airplanes

Figures 3.7-3.9 show twelve examples of twin engine propeller driven airplanes. The following observations are offered:

1. Note that some of these were listed in Part I (Ref.1) as regional propeller driven airplanes. This is an indication that any categorization of airplanes is an arbitrary one. At the 'high' weight end of twins and at the 'low' weight end of the 'regionals' there is a considerable overlap.

2. Note that four of the twins are high wing airplanes while the other eight have low wings.

3. The only pure pusher configuration is the Piaggio P166. The Cessna 336 is a pusher-tractor combination. This is also referred to as 'centerline' thrust. Clearly in an engine out situation, this type will be much easier to control. Engine-out control problems are a major design consideration in conventional twins.

4. Observe the horizontal tail locations in Figures 3.7-3.9. Several twins have the horizontal tail directly in the propeller slipstream. The effect of that is to make controllability a function of engine power. There can be advantages to that. However, particularly for twins with low power loadings (that means very powerful engines), propeller slipstream can cause significant tail fatigue problems.

5. Another factor which has to be weighed before deciding on horizontal tail location is controllability in a 'go-around' situation. In a low power approach, with the airplane trimmed for that flight situation, the sudden application of power can result in a large increase in control force required from the pilot. A physically not so strong pilot may have problems with longitudinal control in that case. By keeping the tail away from the slipstream, this problem is diminished. An interim solution sometimes is to give the horizontal tail enough geometric dihedral.

6. Note that nine of the twins have retractable landing gears. Most twins retract the gear into the wings. This is not the lightest solution! However, from a weight and balance viewpoint there sometimes is no choice.

7. Except for the Islander of Fig.3.9a all twins have single wheel main gears.

8. Several of the twins are seen to have 'sharp-edged' dorsal fins. These help to increase directional stability as well as to eliminate 'rudder-lock'.

9. Observe the widely differing nacelle/wing integration methods in use. There is no unanimity about the nacelle/wing shape with the lowest interference effects. One problem with low wing twins is the fact that propeller/ground clearance may dictate the nacelle location.

10. Several twins have the outboard aileron stations inboard relative to the wing tip. This comes about when additional wing span is added to a 'growth' version of an airplane. In that case it is often found that the tooling expense associated with extending the ailerons outboard is not worth it. This is particularly true if the airplane does not need the additional lateral control power.

11. A potential disadvantage of a twin boom pusher configuration such as the Cessna 336 (Fig.3.9c) is that failure of an aft propeller blade can result in structural failure of one of the tailbooms.

12. The gull wing of the Piaggio P166-DL3 of Fig.3.7b came about because this airplane was derived from an amphibious airplane. Gull wings are often used in amphibious airplanes to keep the propeller out of the water spray from the hull. An advantage of the gull wing is that it provides a low interference intersection with the fuselage. A disadvantage is the structural discontinuity which adds weight to the wing.

13. Note that many twins have baggage space in the rear of the nacelles.

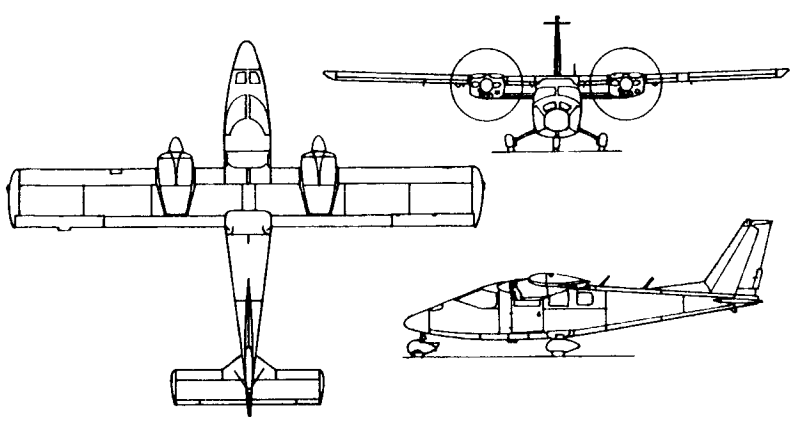

a) PARTENAVIA P. 68C VICTOR

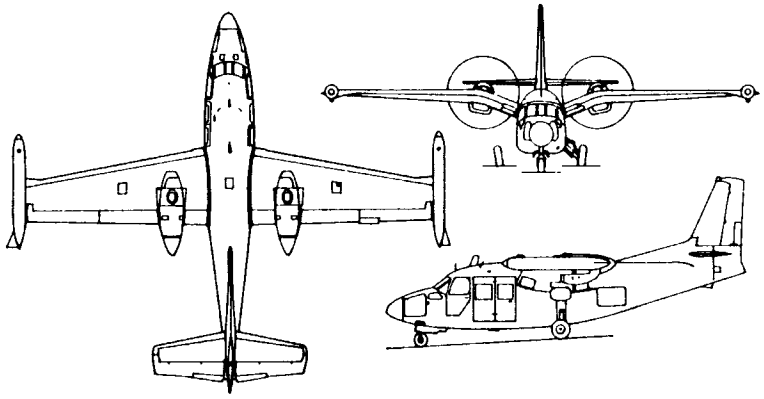

b) PIAGGIO P. 166-DL 3

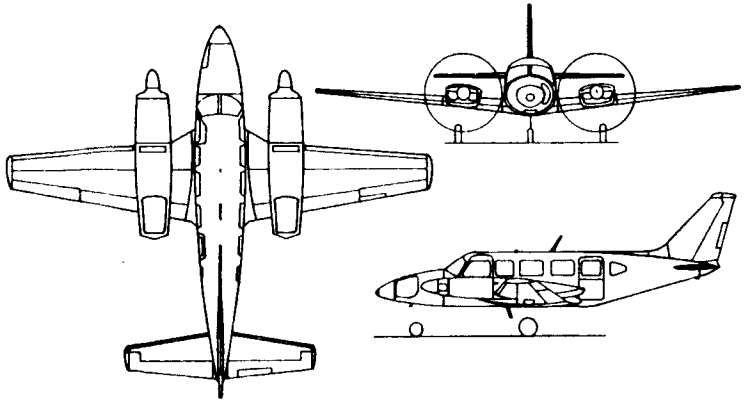

c) PIPER PA-31-350 CHIEFTAIN

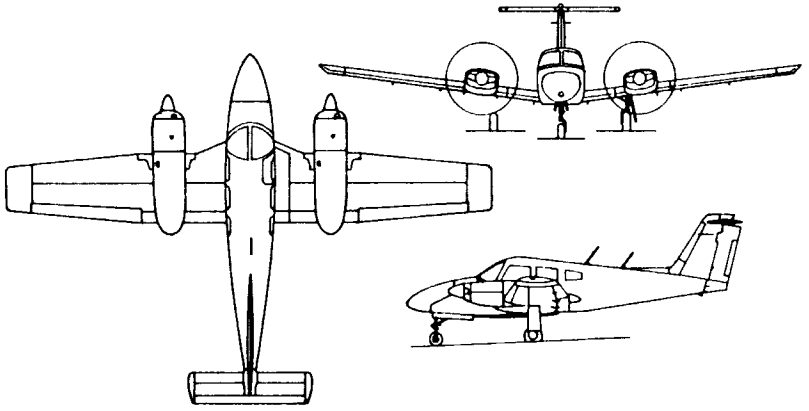

d) PIPER PA-44-180T TURBO SEMINOLE

Figure 3.7 Twin Engine Propeller Driven Airplanes

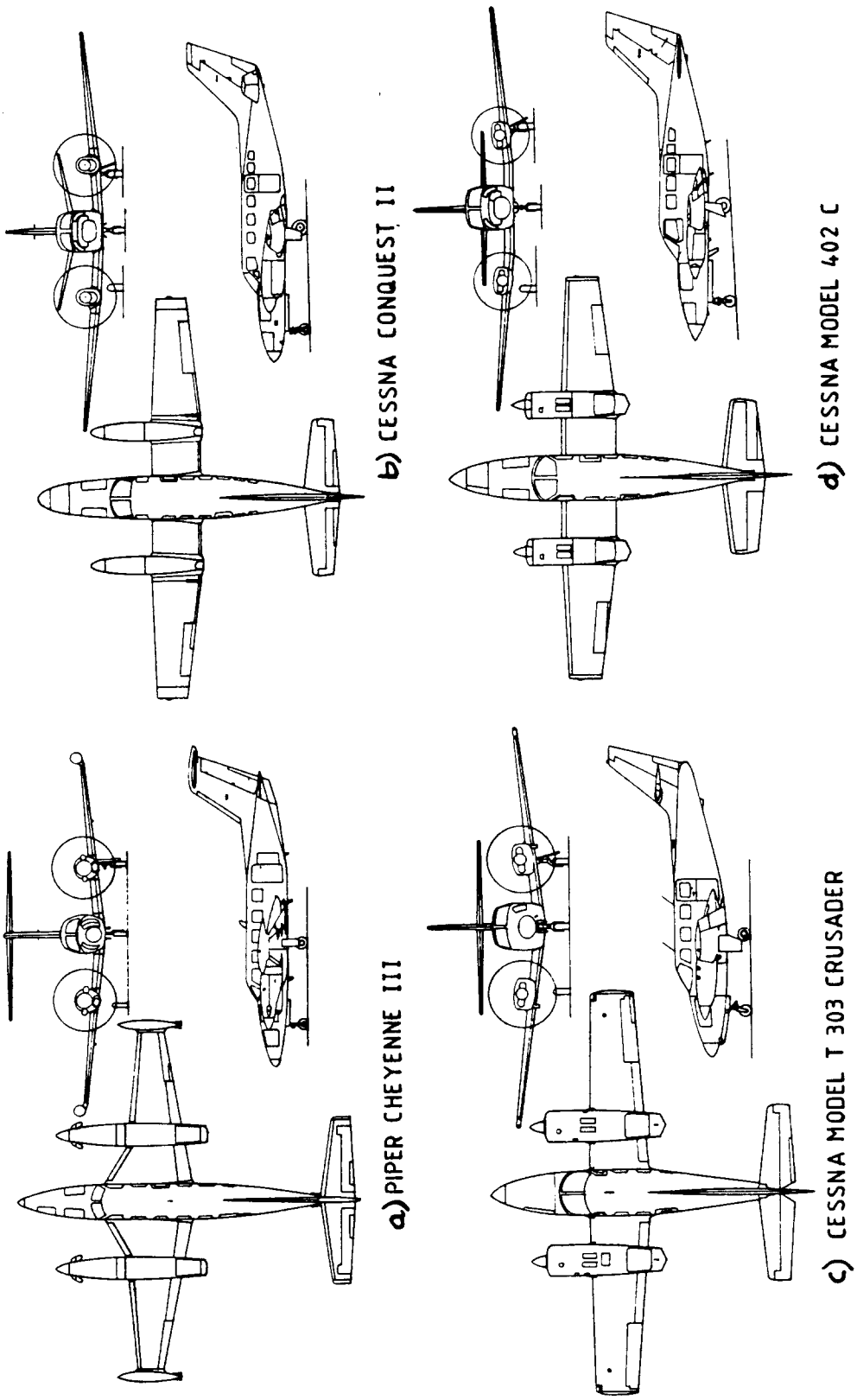

Figure 3.8 Twin Engine Propeller Driven Airplanes

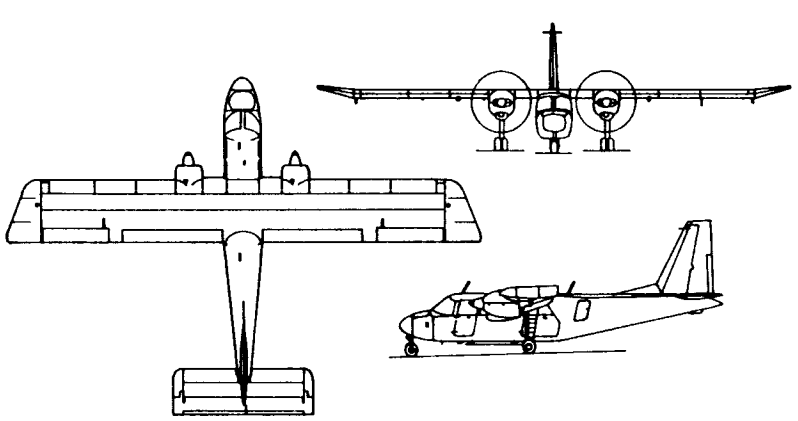

a) BRITTEN-NORMAN BN-2A ISLANDER

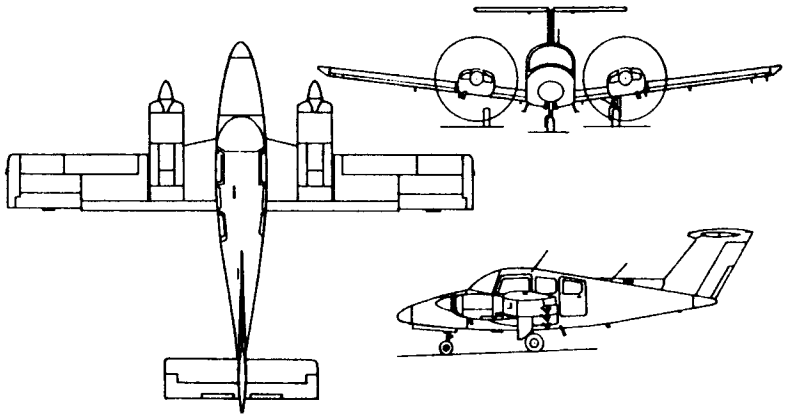

b) BEECHCRAFT DUCHESS 76

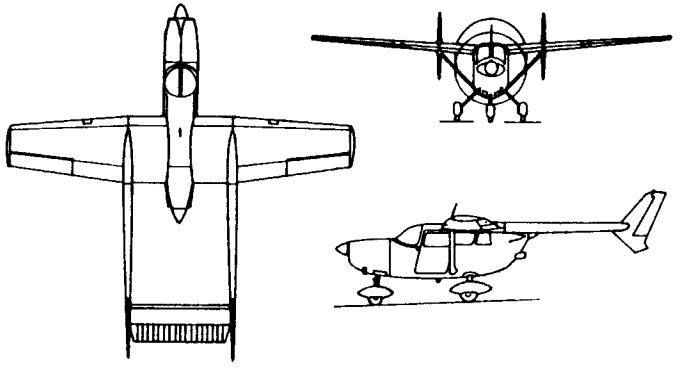

c) CESSNA MODEL 336 SKYMASTER

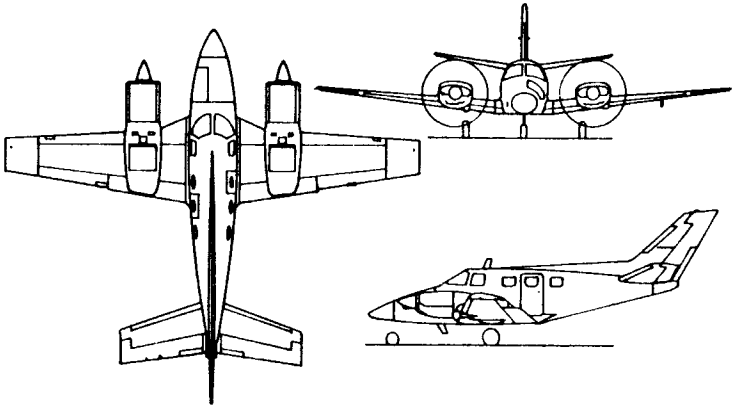

d) BEECHCRAFT DUKE A 60

Figure 3.9 Twin Engine Propeller Driven Airplanes

3.1.4 Agricultural Airplanes

Figures 3.10-3.12 show twelve configurations of recently built agricultural airplanes. The following observations are offered:

1. Nine are low wing and three are bi-plane configurations. The biplanes are all externally braced, even the jet powered airplane of Fig.3.11c. Of the monoplanes, four have cantilever wings, the others also have external bracing on the wing. Note, that most of these ag-airplanes also have external bracing of the horizontal tail. The reason for all this is to keep the structural weight down as much as possible.

2. Eleven are tractor-propeller driven, while one is jet driven. Of the propeller driven configurations only two have turbo-propeller installations. The author predicts that this will be the future trend for these airplanes. The reason is the greater inherent reliability of the turboprop when compared with the piston engine. The high acquisition cost of the turboprop has been responsible for its slow market penetration.

3. All configurations, except for the jet, suffer to some extent from a classical problem of ag-airplanes: the propeller slipstream and the wing tip vortices have a 'swirling' effect on the material which is being deposited from the spray bar system. The reader will note, that the spraybar systems are not shown in the threeviews. However, these systems are mounted close to the wing trailing edge on all airplanes shown in Figures 3.10-3.13. Part IV of this text (Ref. 3) contains some information on the location, sizing and design of such spraybar systems.

4. All, except for the jet, have 'raised' cockpits. The reason for this is to get good visibility. Pilot visibility is absolutely essential in an agricultural airplane. These airplanes have to maneuver in and out of some very tough spots with obstacles everywhere. An extreme variation on the visibility theme is the HAL HA-31 of Fig.3.10b. The reader should understand that the price for so-called '360-degree' visibility is high drag.

5. All are designed with crash survivability in mind. This is not directly obvious from the configurations. However, all contain some form of support structure above the pilot's head, in case of an

inverted crash. The jet of Fig.3.11c seems to have a problem in terms of pilot survivability in case of a head-on collision with an obstacle.

6. Except for two, all are configured as 'taildraggers'. Most ag operators feel, that because they operate from some very rough fields, the weight penalty associated with a nose gear is not worth the improvement in ground handling.

7. The 'hoppers' in most ag-planes are mounted ahead of the pilot. The concensus is that this improves crash survivability. On the other hand, in case of a leaky hopper, the pilot can be exposed to chemicals. On the IA 53 (Fig.3.11a) and on the HAL HA-31(Fig.3.10b), the hoppers are mounted beneath the pilot. On the WSK-Mielec M-15(Fig.3.11c) the hoppers are mounted in the fuselage behind the pilot and in the wing-strut containers. On the Antonov An-2M (which was not specifically designed for ag-duties), shown in Fig.3.10a, the hoppers are mounted in the cabin behind the cockpit.

A method used in a number of ag airplanes to positively evacuate chemicals from the cockpit is to apply a slight amount of pressurization with suitably installed escape vents. Such a 'directed' leakage path can keep most of the undesirable compounds away from the human operator.

8. Bird-proof windshields, wire cutters and wire deflectors are necessary features in all ag-planes. The birdproof windshields imply some weight penalty, particularly when the windshield is large. Wire cutters are usually mounted ahead of the windscreen. Wire deflectors generally run from the top of the canopy or cockpit roof to the top of the vertical tail.

9. Note that most ag-planes have non-retractable landing gears. Several arguments can be made against a retractable landing gear in the case of an ag-airplane:

a.) complexity and maintenance
b.) pilots tend to forget lowering the landing gear
c.) the drag advantage is small in an airplane which has very large drag increments due to bracing, spray-bar and raised windshield.

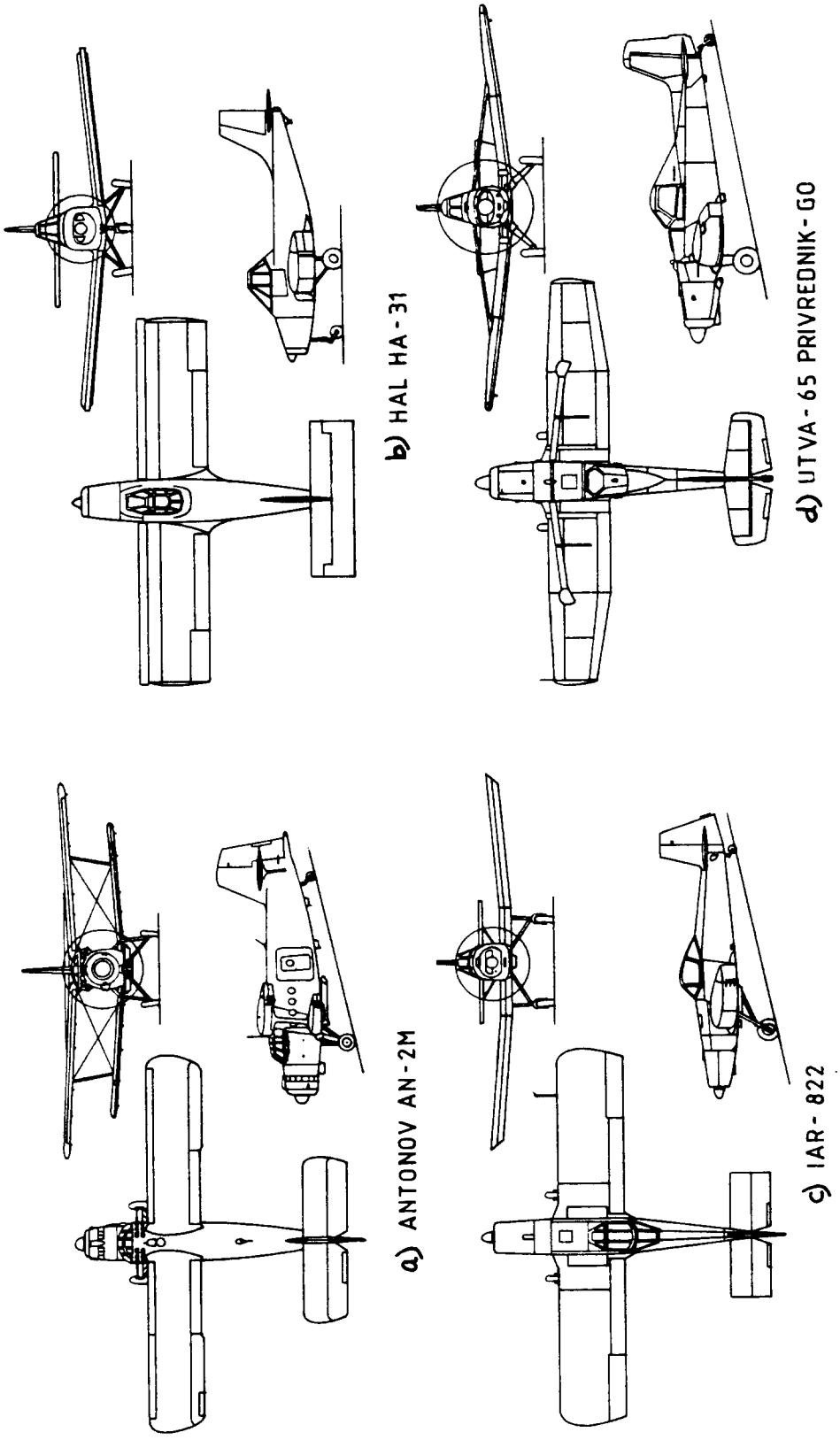

Figure 3.10 Agricultural Airplanes

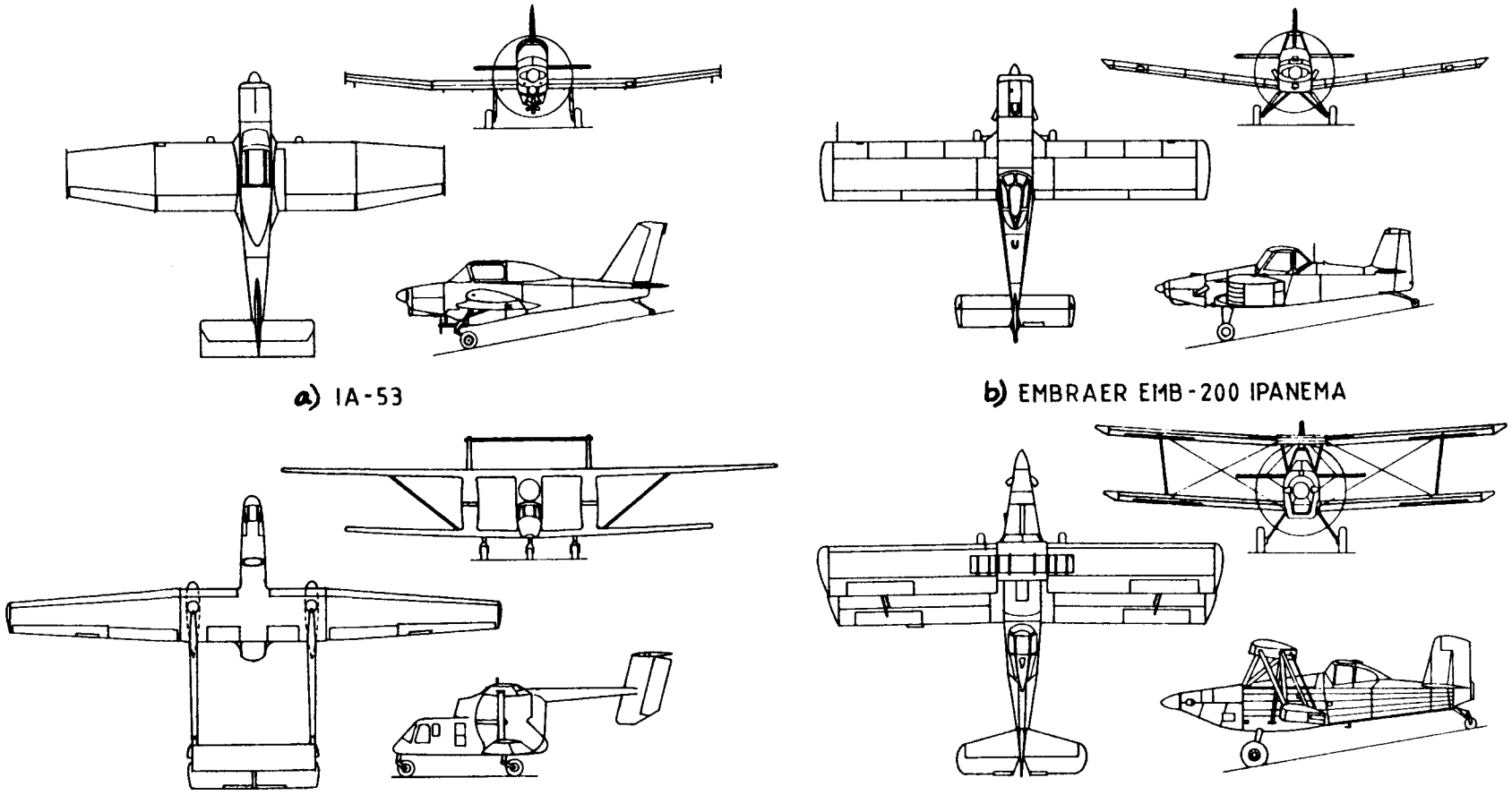

Figure 3.11 Agricultural Airplanes

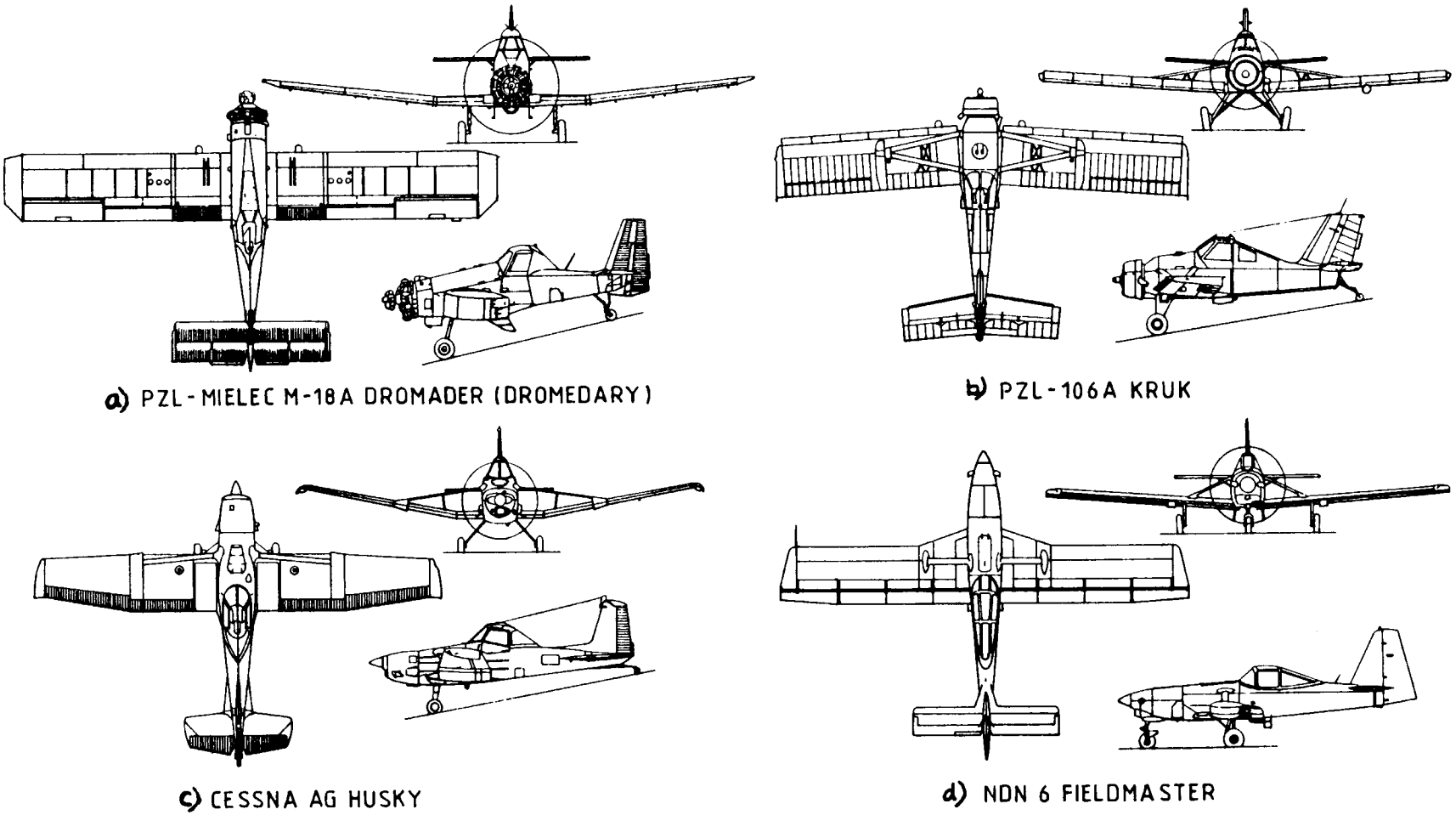

Figure 3.12 Agricultural Airplanes

3.1.5 Business Jets

Figures 3.13-3.15 present twelve configurations of business jets. The following observations are offered:

1. Ten of the twelve are twins, one is a tri-jet (Fig.3.13d) and one has four jet engines (Fig.3.13a)

2. All have the engines installed in nacelles on the rear fuselage. This configuration was pioneered by the French on the Sud Caravelle jet transport. The middle engine of the Falcon 50 is an exception, it is installed like the center engine on the Boeing 727.

3. The early business jets had severe problems with fuel volume. This is evidenced by the use of tiptanks and slipper tanks as seen in Figs. 3.13a, 3.13b, 3.14b & 3.15c. The reason for this was the very high specific fuel consumption of the early jet engines.

4. Business jets were among the first airplane types to use winglets for lower induced drag. Examples are shown in Figs. 3.13c and 3.14c.

5. Designers of several recent business jets have opted for a so-called supercritical wing. This provides improved dragrise behavior. Examples are shown in Figs. 3.13c, 3.14a, 3.15a and 3.15d.

6. All business jets retract the landing gear into the wing or into the wing/fuselage intersection.

7. Except for the Westwind (Fig.3.15c) all business jets have a low wing configuration. It is observed that the Westwind was originally developed from the propeller driven Aero Commander which had a mid wing configuration.

8. Observe that only four of the business jets have T-tail configurations. The rest have cruciform or low tail arrangements.

9. All landing gears are of the tricycle type. Single and double wheels are used.

10. Observe that three of the business jets have essentially no sweep angle. This implies a thin wing at high speed (Learjet of Fig.3.13b) or a thick wing at somewhat lower speed (Citation of Fig.3.14c).

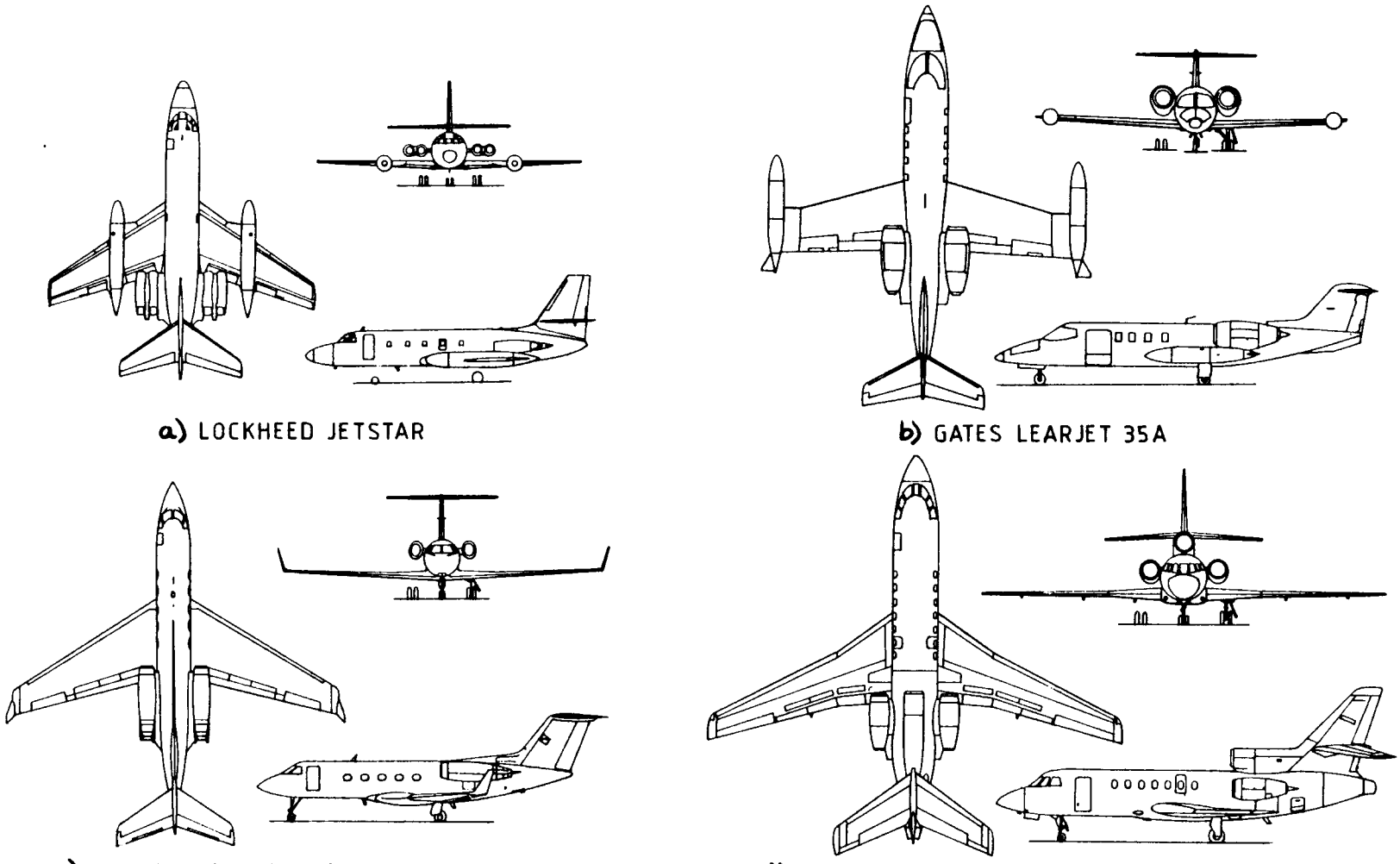

Figure 3.13 Business Jets

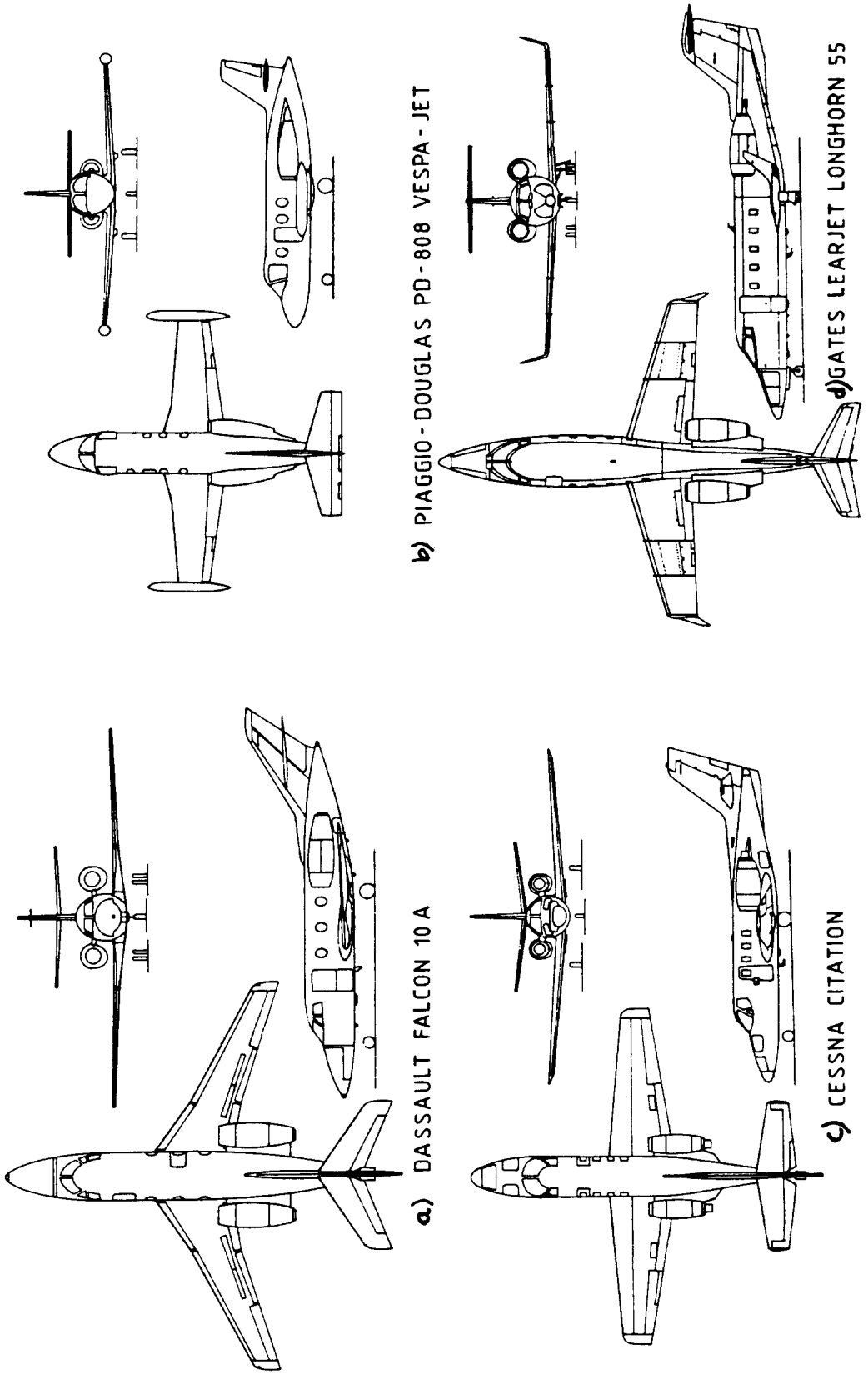

Figure 3.14 Business Jets

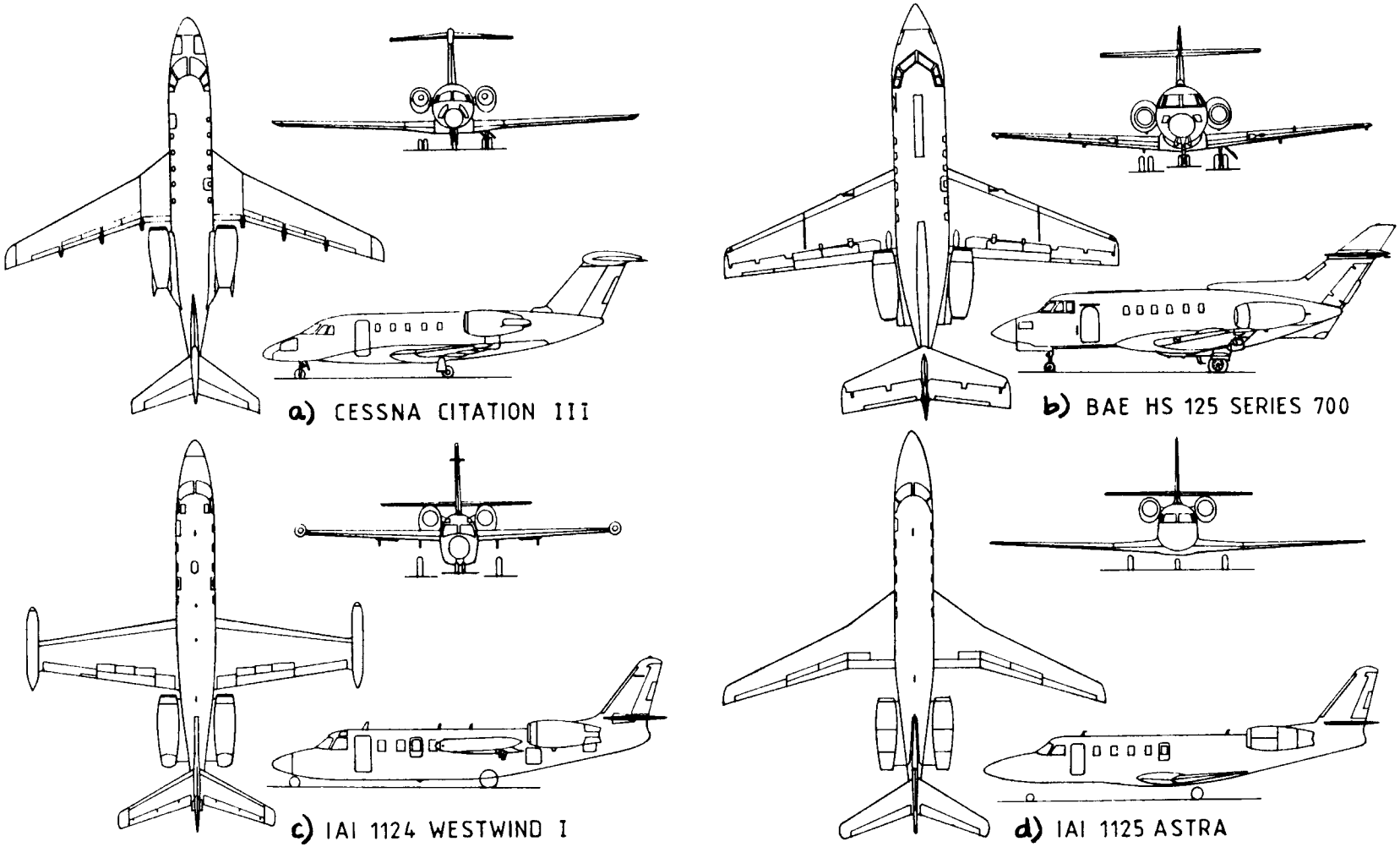

Figure 3.15 Business Jets

3.1.6 Regional Turbopropeller Driven Airplanes

Figures 3.16-3.18 show twelve configurations of regional turbopropeller driven airplanes. The following observations are offered:

1. Five are high wing and seven are low wing configurations.

2. Only one (the Shorts 330 of Fig.3.18d) has external bracing, all others are of cantilever construction. For cruise type vehicles, the drag penalty associated with external bracing is usually not acceptable, despite the weight advantage. Note that several of the configurations have wings with very large aspect ratios: A = 12.7 for the BAe 748 of Fig.3.18c is the highest.

3. Four have T-tail empennages, one a twin vertical tail empennage while the others have conventional horizontal and vertical tails. The position of the horizontal tail relative to the slipstream of the propeller is important from a handling quality point of view and from a tail fatigue point of view. The comments made for the twins in sub-section 3.1.4 apply here as well. Note that the Beech 1900 has an extra horizontal stabilizing surface as well as 'taillets'.

4. All have the nacelles installed in the wings. Note also that all are of the tractor configuration.

Wing-nacelle integration is important from an interference drag and from an induced drag point of view. Propeller distance to the ground and associated landing gear length all play a role in deciding how to integrate a nacelle into a wing. The fact, that significant differences exist between the twelve designs are indicative of the fact that nacelle integration continues to be a significant design problem.

5. Most retract the landing gear into a nacelle. Two of the high wing airplanes use a 'blister' fairing on the fuselage for gear retraction. The Jetstream retracts the gear into the wing itself. Landing gear retraction is an important design aspect of these airplanes. Blister fairings tend to be very draggy. On the other hand, they lead to short gear legs and thus save weight. Retracting a gear into the wing is potentially a bad idea: major cut-outs in the primary structure are usually the result. This leads to a substantial weight increase for the wing structure.

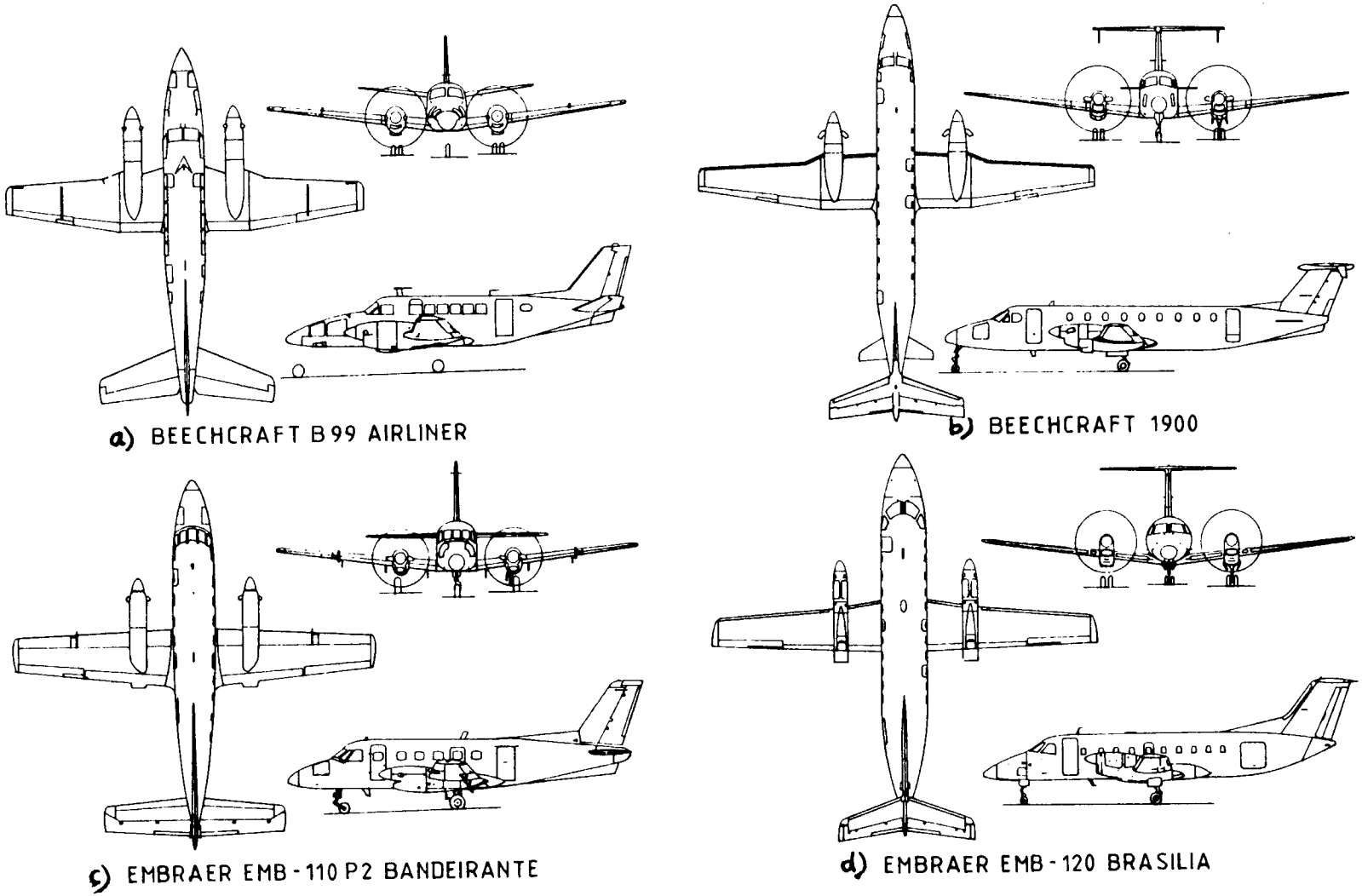

Figure 3.16 Regional Turbo-Propeller Driven Airplanes

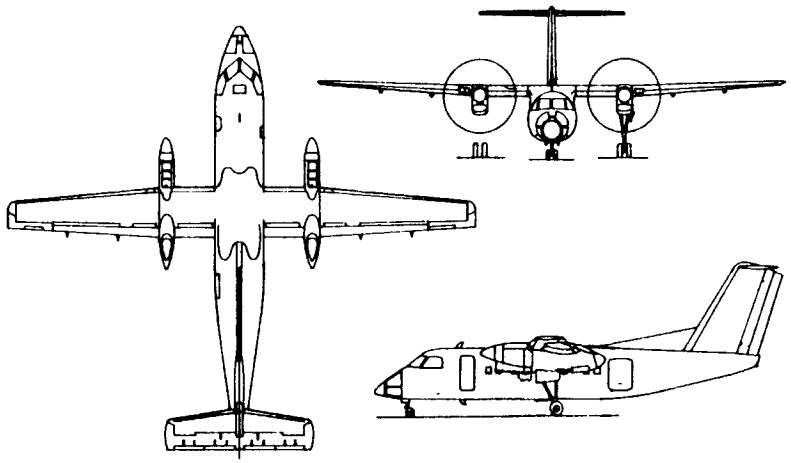

a) DE HAVILLAND CANADA DHC-8 DASH 8

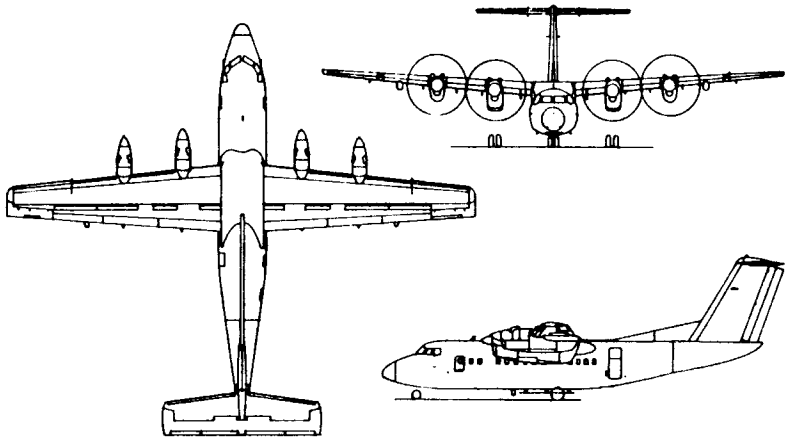

b) DE HAVILLAND CANADA DHC-7 DASH 7

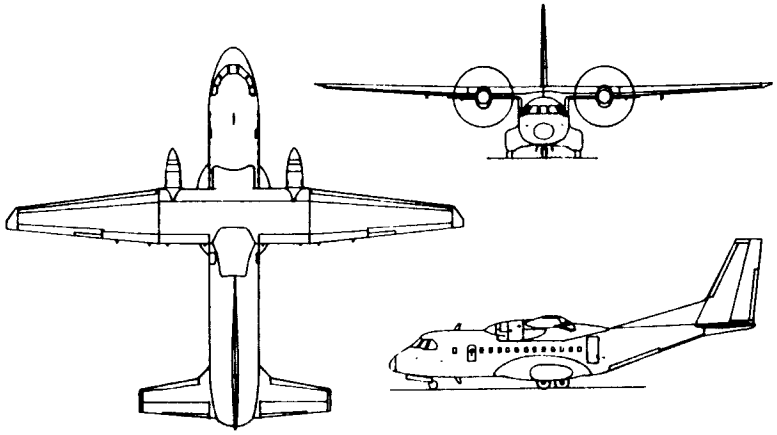

c) AIRTECH (CASA/NURTANIO) CN-235

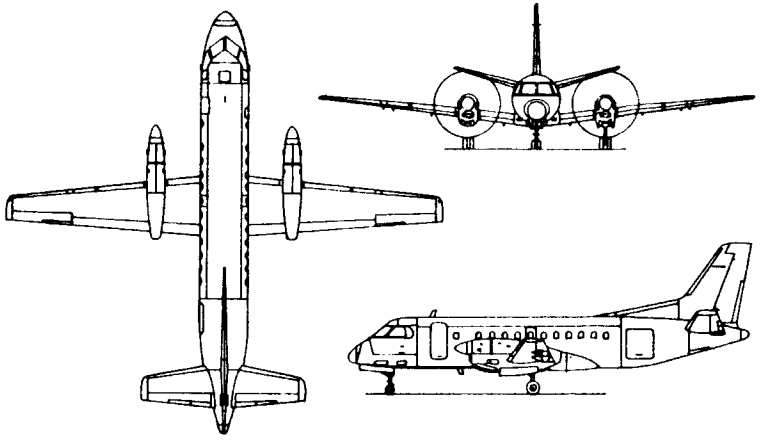

d) SAAB-FAIRCHILD 340

Figure 3.17 Regional Turbo-Propeller Driven Airplanes

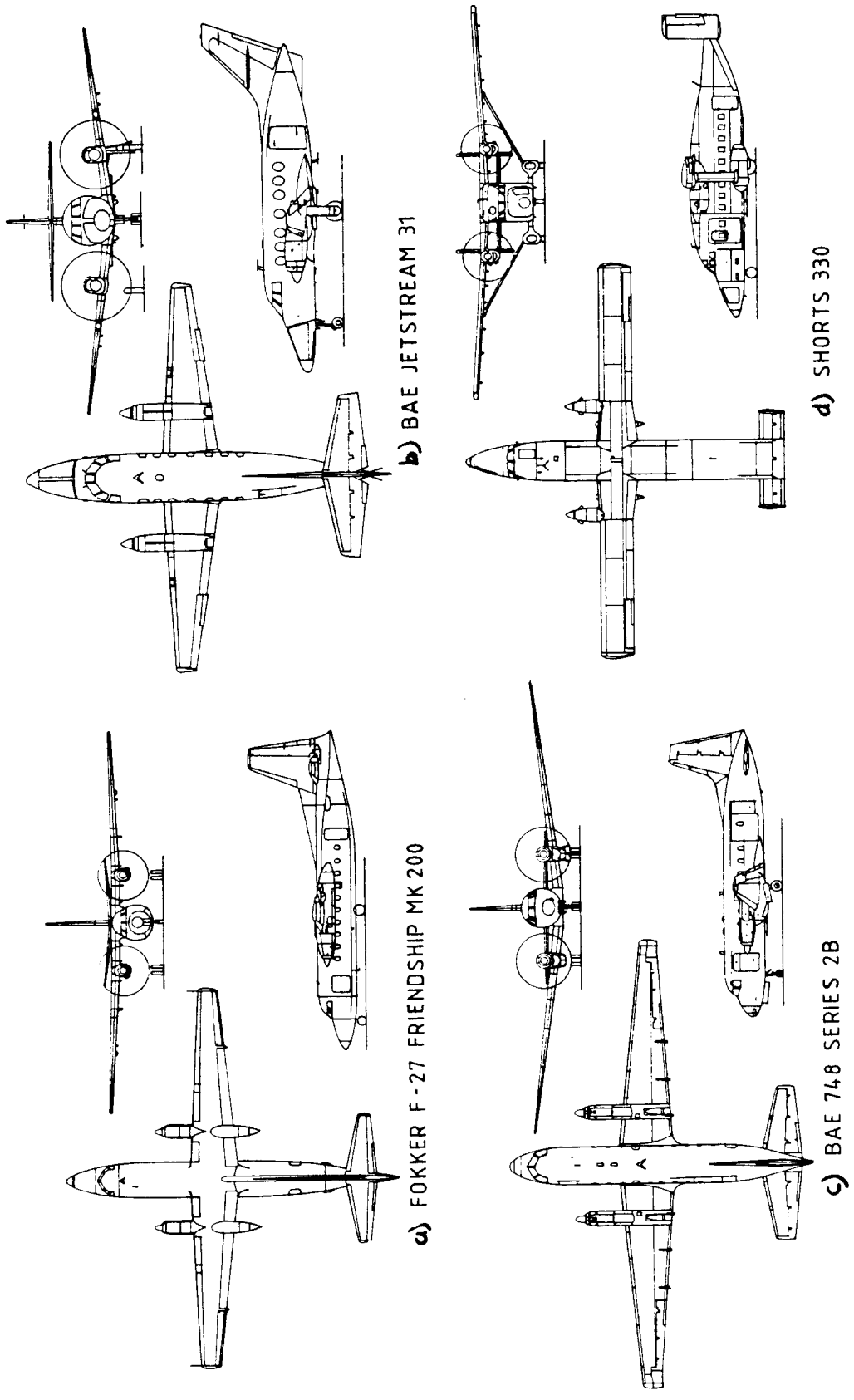

Figure 3.18 Regional Turbo-Propeller Driven Airplanes

3.1.7 Jet Transports

Figures 3.19-3.21 present twelve configurations of jet transports. The following observations are offered:

1. Except for the BAe 146 of Fig.3.21d, all jet transports have a low wing configuration.

2. All have the engines installed in nacelles on the rear fuselage or under the wing. The Tristar of Fig.3.20a has its center engine buried in the fuselage with an inlet in the form of an S-duct. Jet engines podded below the wing were pioneered by Boeing on the B47 bomber and before that by Arado in Germany during WWII. Jet engines on fuselage mounted nacelles were pioneered by the French on the Sud Caravelle.

Not shown in Figs. 3.19-3.21 are jet engines buried in the wing. These were pioneered by the British and used on many jet bombers and transports. Examples are the DH Comet, the HP Victor, The AVRO Vulcan (Fig.1.1) and the Vickers Valiant. The BAe Nimrod of Fig.3.28b which was derived from the Comet also sports this type of engine arrangement.

3. Note that except for the BAe 146 all jet transports retract the landing gear into the wing/fuselage intersection. The fuselage mounted gear of the BAe 146 is a very clean installation (aerodynamically speaking). However it does limit lateral stability on the ground due to the small distance between the main gears.

4. Many jet transports follow the Boeing wing/fuselage arrangement with a wing glove and a wing yehudi. The glove/yehudi arrangement (pioneered on the 707) provides for favorable drag, a thick wingroot and a way to get the landing gear retracted without interfering with either the inboard flaps or the rear spars. It also offers very good lateral stability on the ground.

5. Most jet transports use a tricycle landing gear layout. The Boeing 747 uses four main gear struts, while the DC 10-30 uses three main gear struts.

6. Observe that three jet transports use T-tails, the remainder using low horizontal tails.

7. For in-flight speedbrakes, ten of the jet transports use wing mounted spoilers. However, the Fokker F-28 and the BAe 146 (Figs. 3.21c and d) use rear fuselage mounted clamshell doors.

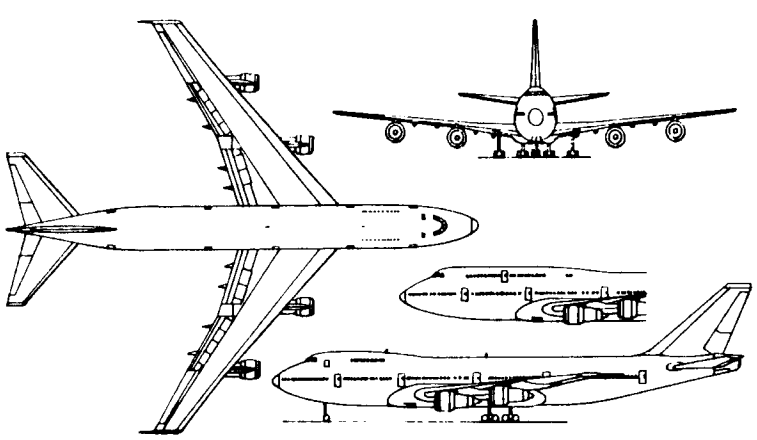

a) BOEING 747-200B (SCRAP VIEW: 747-300)

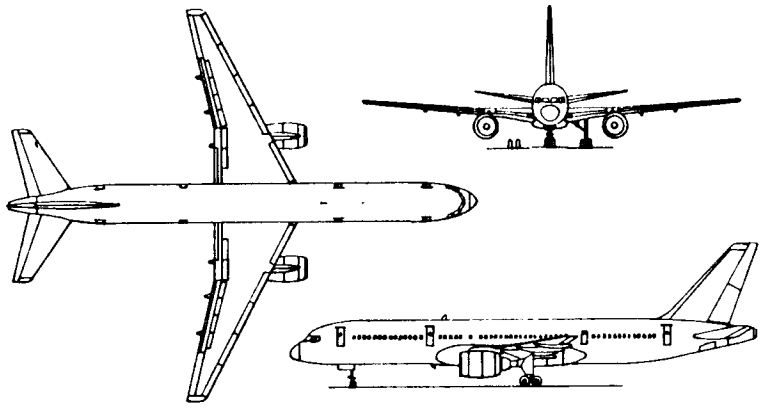

b) BOEING MODEL 757-200

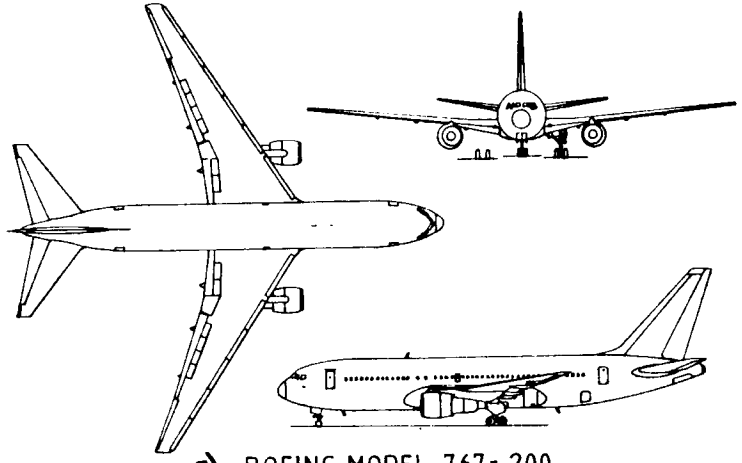

c) BOEING MODEL 767-200

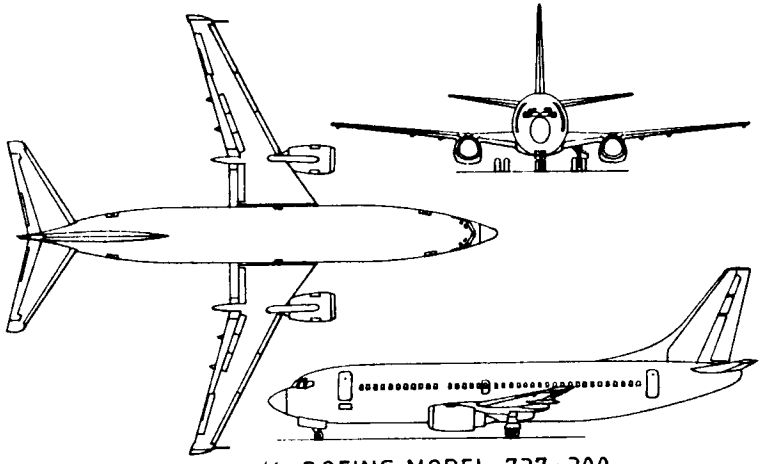

d) BOEING MODEL 737-300

Figure 3.19 Jet Transports

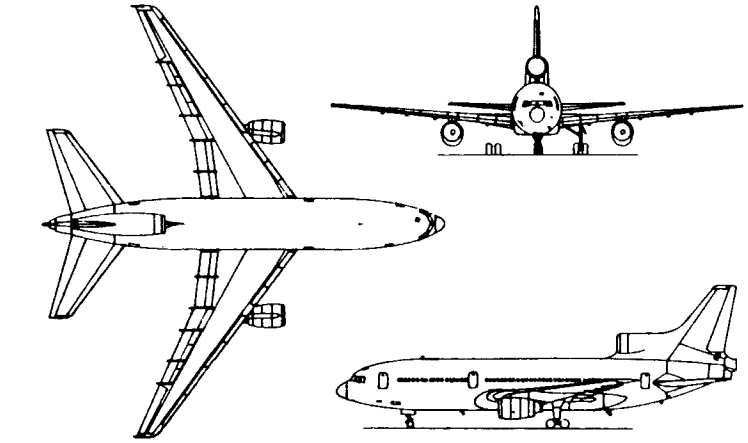

a) LOCKHEED L-1011-500 TRISTAR

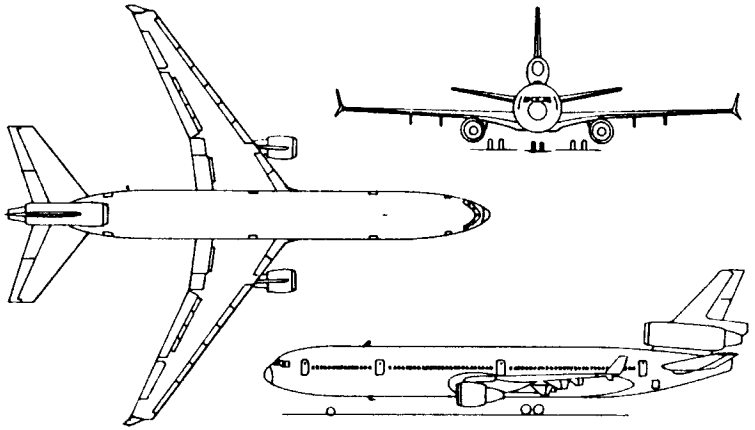

b) MCDONNELL DOUGLAS MD-100

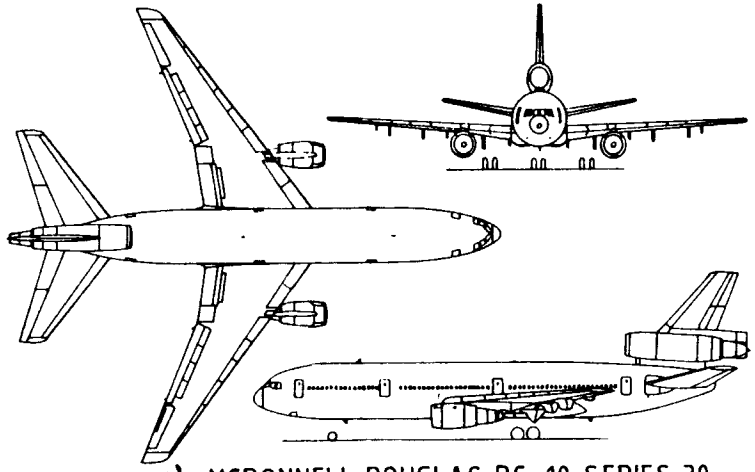

c) MCDONNELL DOUGLAS DC-10 SERIES 30

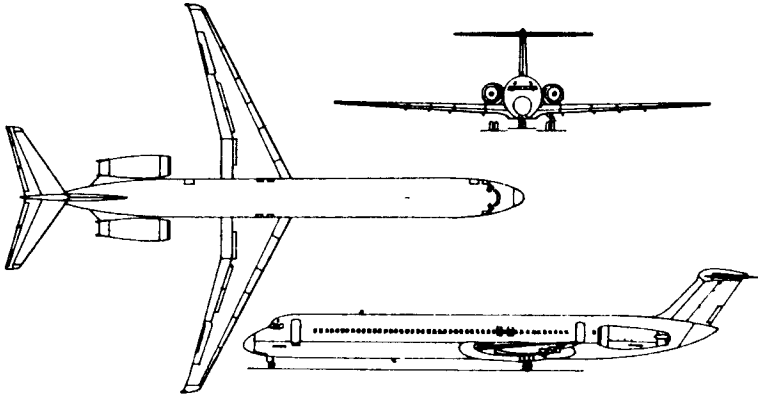

a) MCDONNELL DOUGLAS MD-80

Figure 3.20 Jet Transports

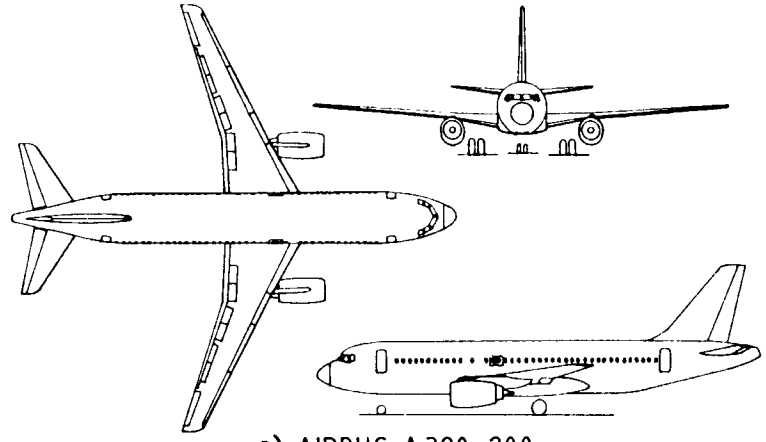

a) AIRBUS A 320-200

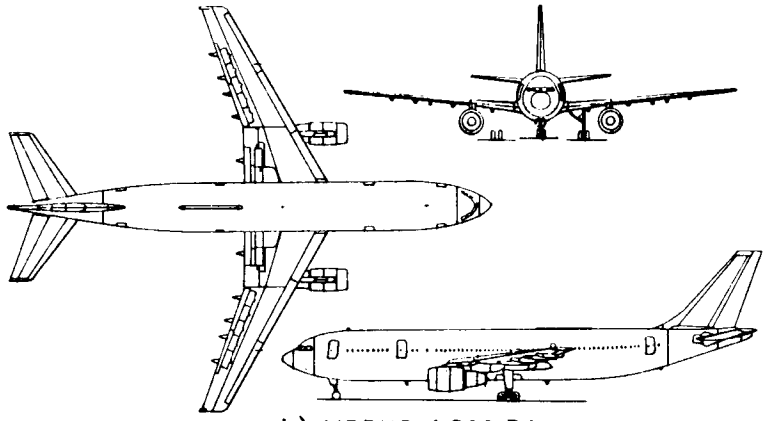

b) AIRBUS A 300 B4

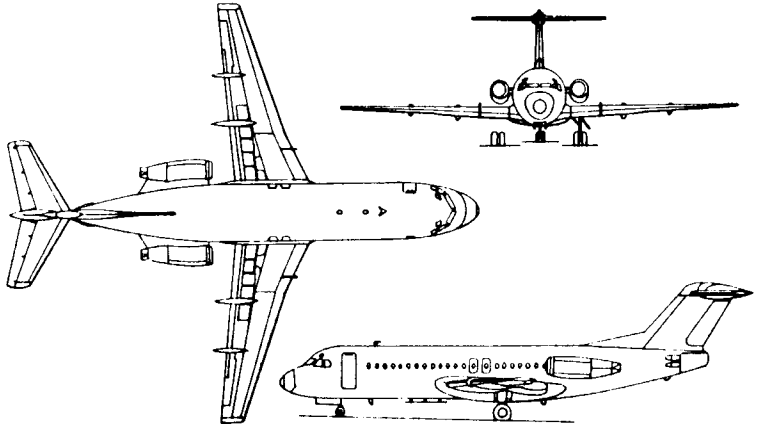

c) FOKKER F 28 MK 4000 FELLOWSHIP

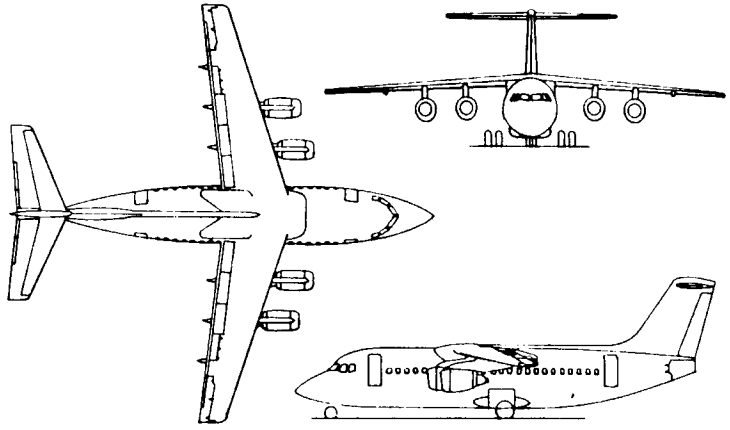

d) BAE 146 SERIES 200

Figure 3.21 Jet Transports

3.1.8 Military Trainers

Figure 3.22 shows four propeller driven military trainers. Figures 3.23 and 3.24 present eight jet driven military trainers. The following observations are offered:

1. The propeller driven trainers are primarily used for initial or basic training. The jet driven trainers are used for advanced training.

2. All are capable of being equipped with gun and bomb racks.

3. Note the RFB Fantrainer of Fig.3.22d. It uses a ducted fan (5 blades) with the fan shaft and duct structure used as an integral part of the fuselage. The forward sweep angle on the wing was selected for reasons of weight and balance, not for aerodynamic reasons. The Fantrainer is the only pusher, the others are tractors.

4. Observe the extensive use of strakes and fins on most trainers. These were probably added during flight test as 'aerodynamic afterthoughts' to fix stall and/or spin problems.

5. Note that two of the eight jet trainers have high wings, the rest have low wings.

6. All jet trainers shown use buried engines in the fuselage. A major drag problem with all these configurations is to fair the relatively large inlets into the wing root or into the fuselage with a minimum of flow distortion. With the single engine configurations, another design problem is the bifurcated s-ducts leading to the engine. These ducts are very critical to the successful operation of the engine and require a lot of detail design attention early on.

7. Observe that the inboard part of the engine inlets are located a good distance away from the fuselage. The reason is to prevent 'tired' boundary layers from getting into the inlet duct.

8. All trainers use the tricycle landing gear layout.

9. The tail configurations range from one T-tail to several cruciform and low tail layouts. The T-46A of Fig.3.23b uses a twin vertical tail, an unusual feature for this type of airplane.

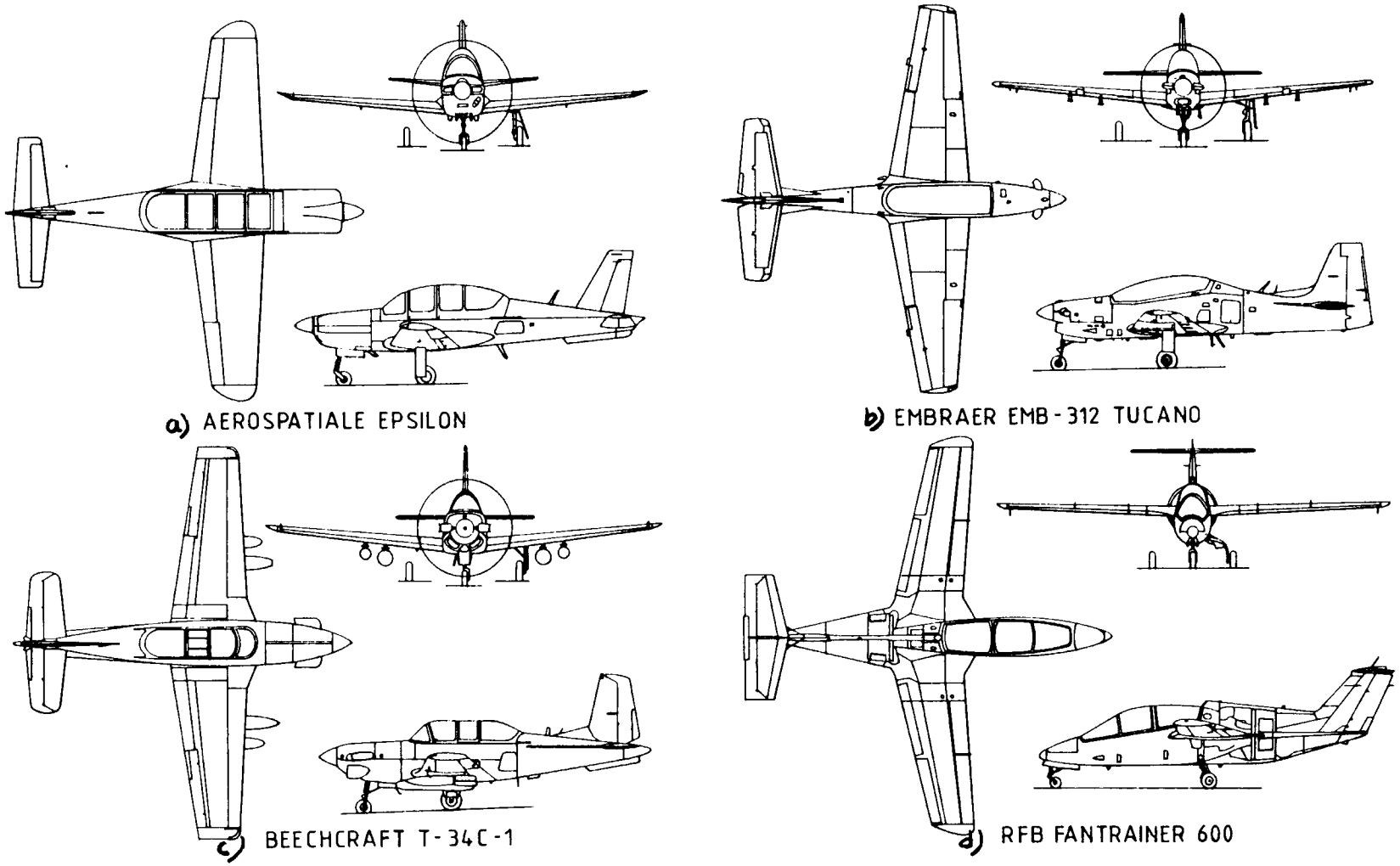

Figure 3.22 Military Trainers

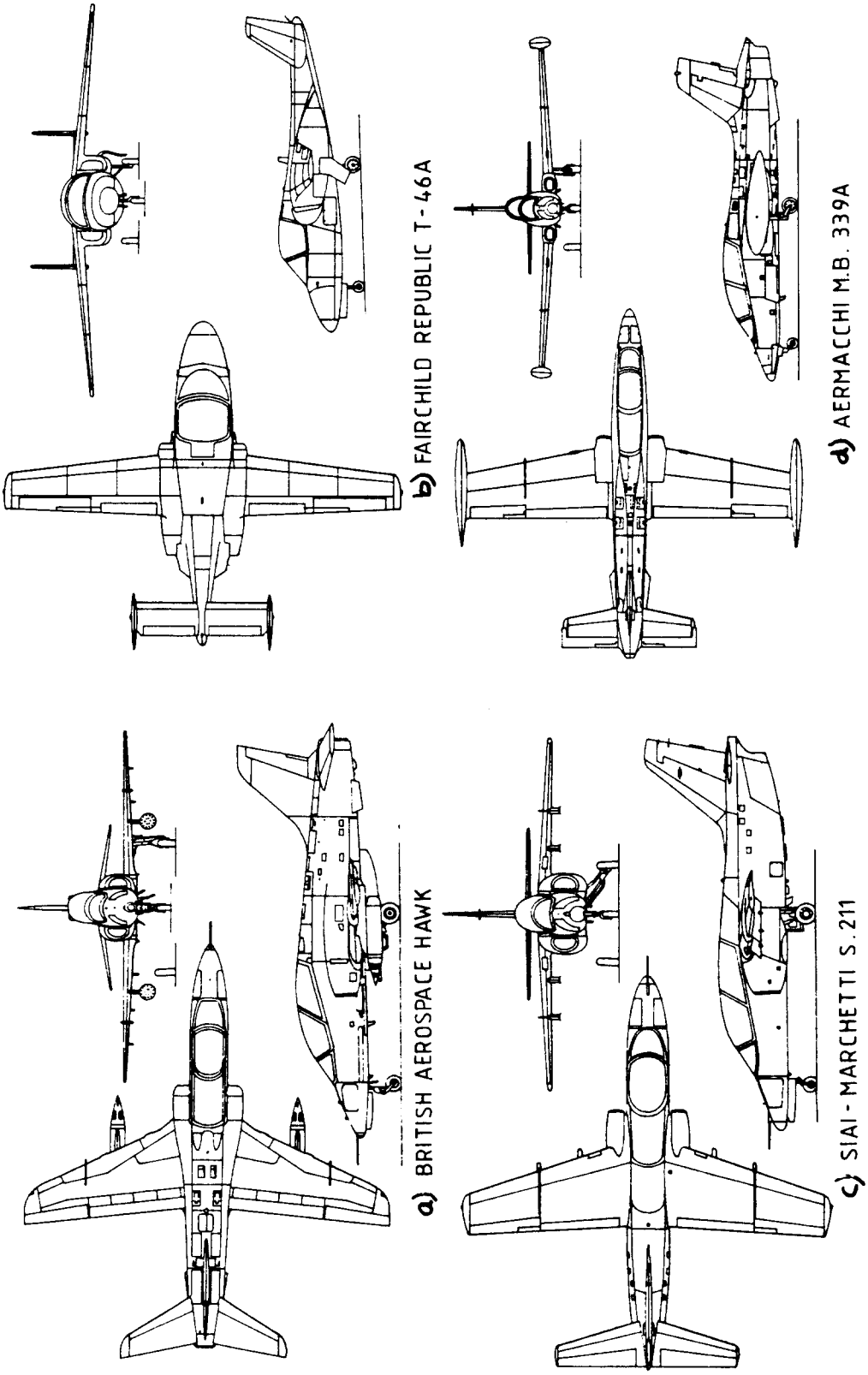

Figure 3.23 Military Trainers

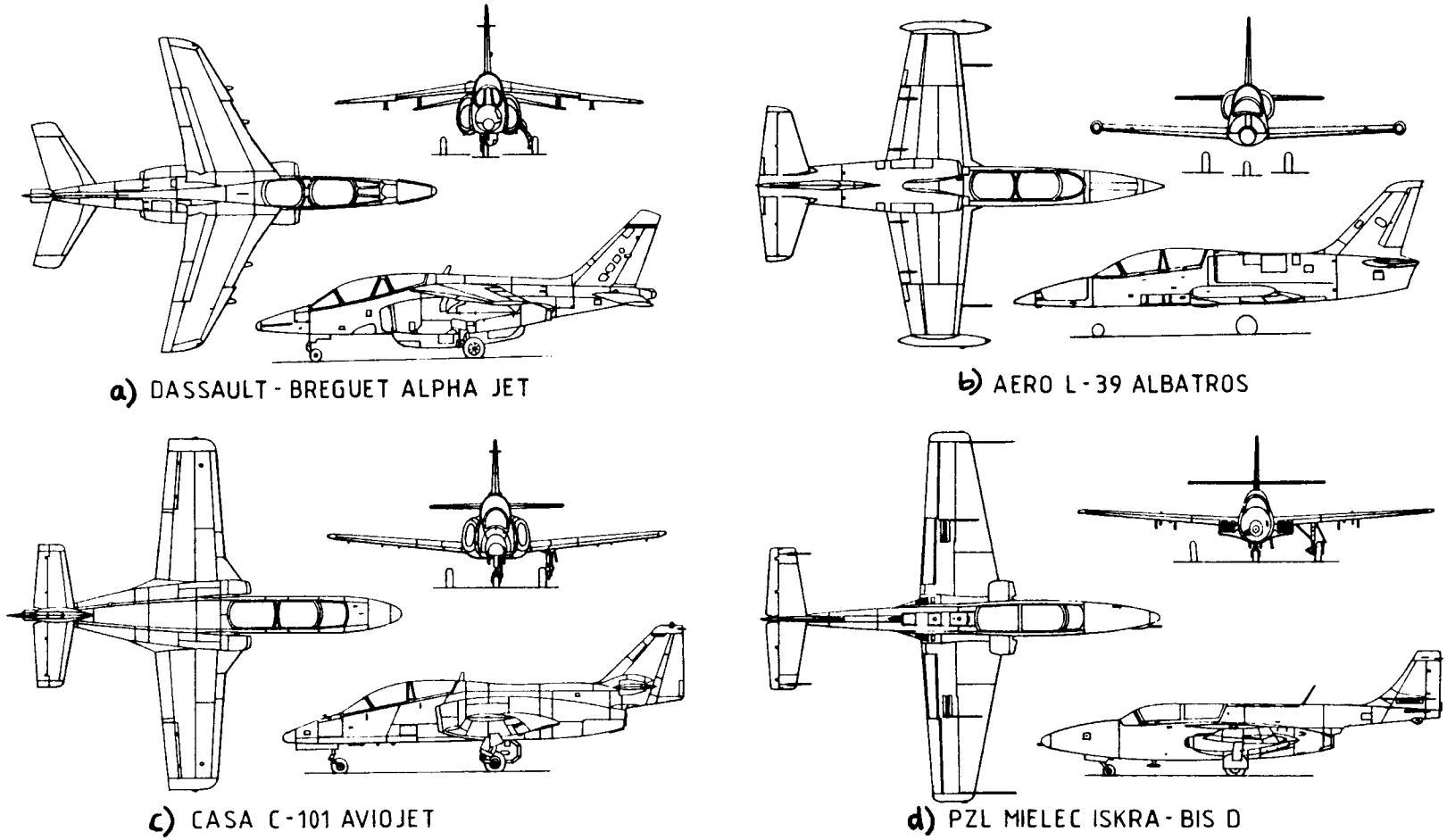

Figure 3.24 Military Trainers

3.1.9 Fighters

Figures 3.25-3.27 present twelve fighter configurations. The following observations are offered:

1. Except for the Pucara of Fig.3.26c all fighters are jet driven. Unless there is a requirement for high dash speeds, the turboprop offers a cost and a take-off performance advantage over jets.

2. Note that six of the fighters are singles and six are twins.

3. All fighters shown have a tri-cycle landing gear. Note the tandem wheel arrangement on the Viggen of Fig.3.27d. That arrangement was selected to allow the gear to be retracted into the thin wing.

4. Observe that most of the fighters shown employ only one wheel per main strut. However four of them have two nosewheel tires.

5. Two of the fighters shown use a variable sweep wing. This is a very expensive feature (in terms of weight and cost) and is justified only in cases where supersonic range, subsonic range and low speed performance are all critical to the mission of the airplane.

6. Note the preference for conventional configurations. The Mirage IIIE of Fig.3.26c employs a delta wing configuration. This is a very efficient form if the dominating mission requirement is for rapid acceleration to supersonic attack or cruise. The blended wing-body of the GD F-16XL (Fig.3.25c) is a modern variation on the delta theme.

7. The coupled canard/delta planform (Fig.3.27c) of the Viggen was pioneered by SAAB (Sweden). By proper relative arrangement of the canard above and forward of the wing it is possible to achieve very favorable interference between the canard lifting vortex and the flow over the following delta wing.

8. A major design problem with a high speed, highly maneuverable fighter is the achievement of sufficient directional stability at high angles of attack. Vortices shed from the forebody tend to interfere with the vertical tail. This leads some designers to use two large vertical tails. Figures 3.25a and 3.27b are typical examples.

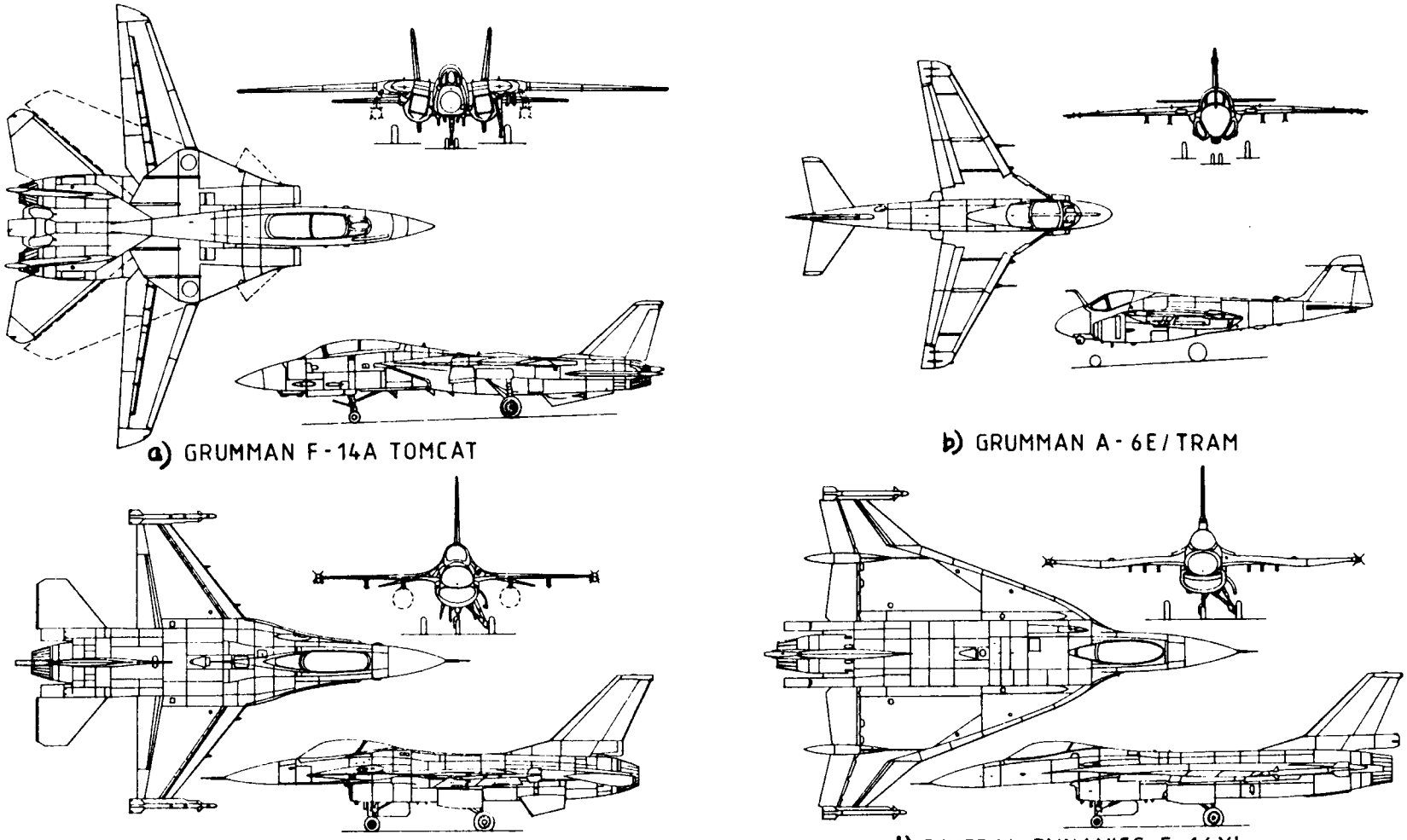

Figure 3.25 Fighters

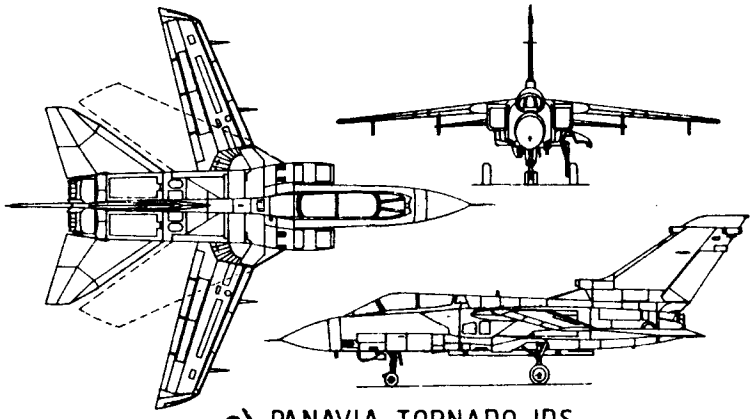

a) PANAVIA TORNADO IDS

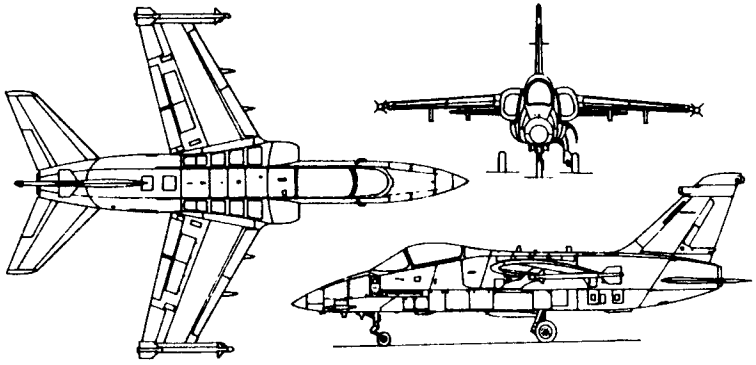

b) AERITALIA/AERMACCHI/EMBRAER AM-X

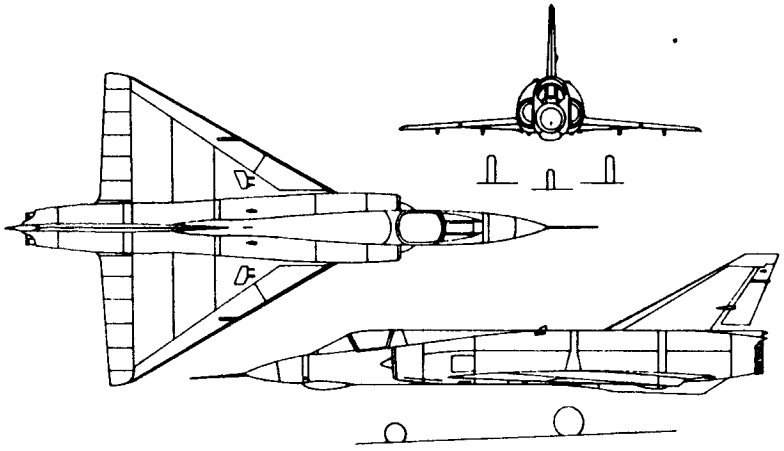

c) DASSAULT-BREGUET MIRAGE III-E

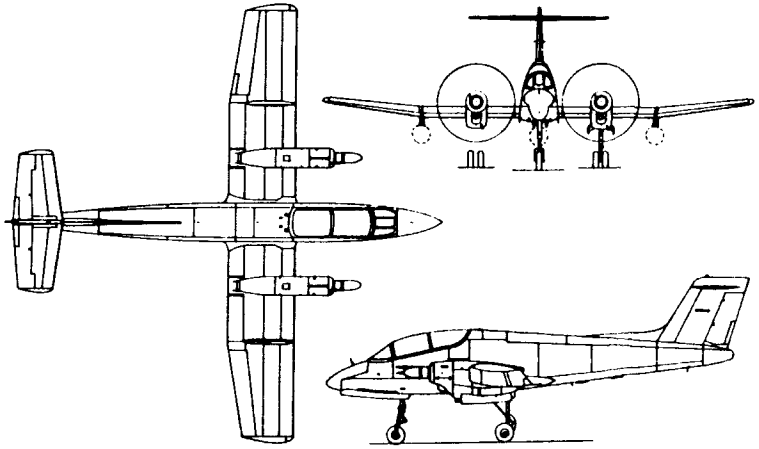

d) FMA IA 58A PUCARA

Figure 3.26 Fighters

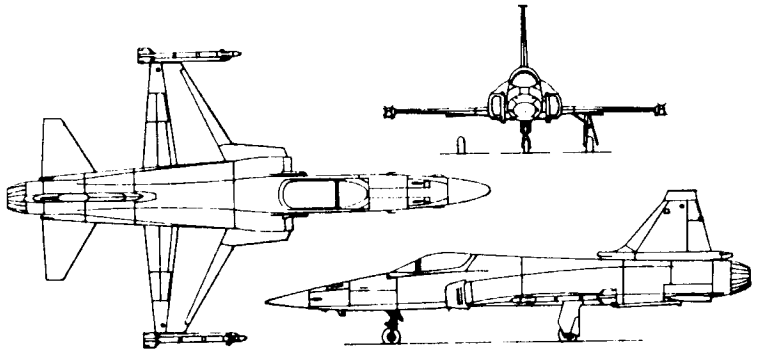

a) NORTHROP F-20 TIGERSHARK

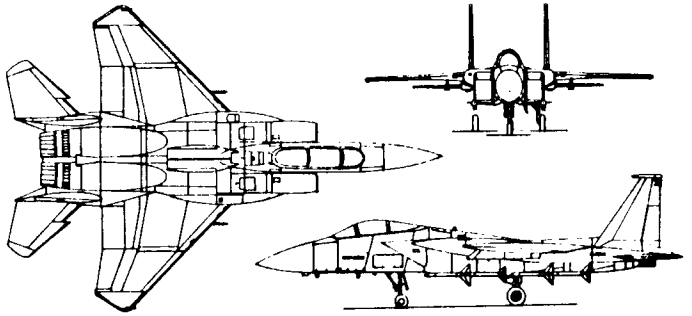

b) MCDONNELL DOUGLAS F-15C EAGLE

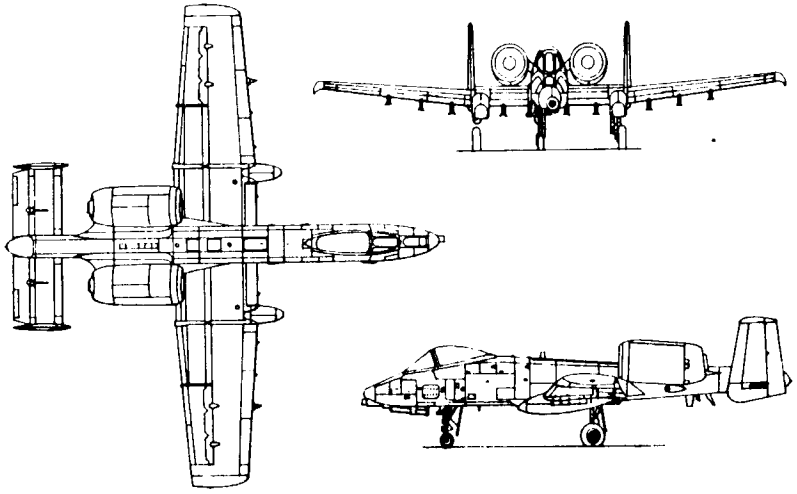

c) FAIRCHILD REPUBLIC A-10A THUNDERBOLT II

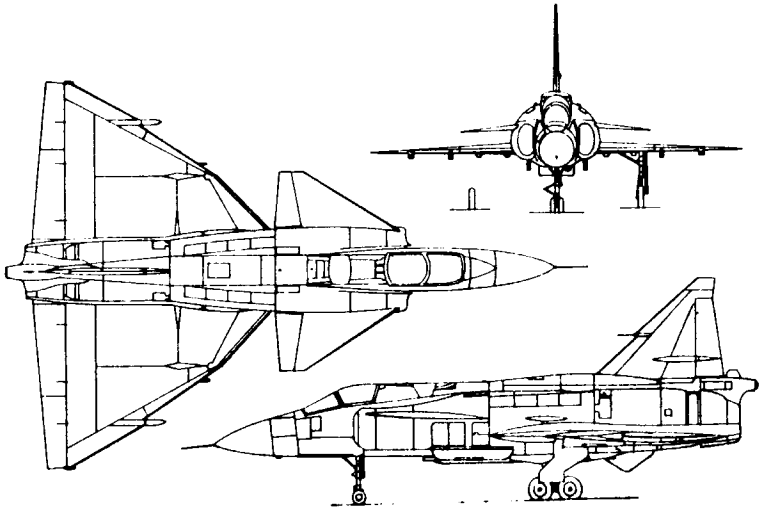

d) SAAB JA 37 VIGGEN

Figure 3.27 Fighters

3.1.10 Military Patrol, Bomb and Transport Airplanes

Figures 3.28-3.30 present twelve configurations for airplanes in this category. The following observations are offered:

1. The B52H of Fig.3.28a is a long range bomber designed around a long bomb bay. This forced the high wing layout and the tandem landing gear. Because of the tandem gear layout, rotation during take-off is not possible: the airplane 'flies off'. This in turn results in longer take-off distances. It also forces a rather large wing incidence angle. In turn this causes the airplane to cruise 'nose down' which is not the best attitude from a drag viewpoint. The point of these comments is: a seemingly innocent and logical mission requirement such as a long bomb bay can dominate the configuration design of an airplane.

2. Note thet the transports of Figures 3.28c, d, 3.29b, d and 3.30a all have high wing layouts with body mounted landing gears. This configuration feature is forced by the requirement to load and unload heavy equipment without external help.

3. The tanker/transports of Figures 3.29b and d and the patrol airplane of Fig.3.28b were developed from civil transports. That is the main reason for their low wing configurations.

4. Note that the configurations are conventional.

5. Note the large search radars in Fig.3.30c and 3.30d. These radars are designed for 'look-up' as well as 'look-down' capability. The fuselage and the empennage of both airplanes hinder the look-down' capability to some extent. The empennage of the Hawkeye is made of composites for that reason.

6. All jets in this category have significant wing sweep while the turboprops do not. The reason is the difference in design cruise speed.

7. Note the four vertical tails on the Hawkeye. This is a carrier based airplane with commensurate restrictions on length, width and height. In turn this leads to 'short-coupled' configurations. When a large radome is added, directional stability suffers, leading to the requirement for more vertical tail area. Since the height is also restricted, one solution is to put on more vertical tails.

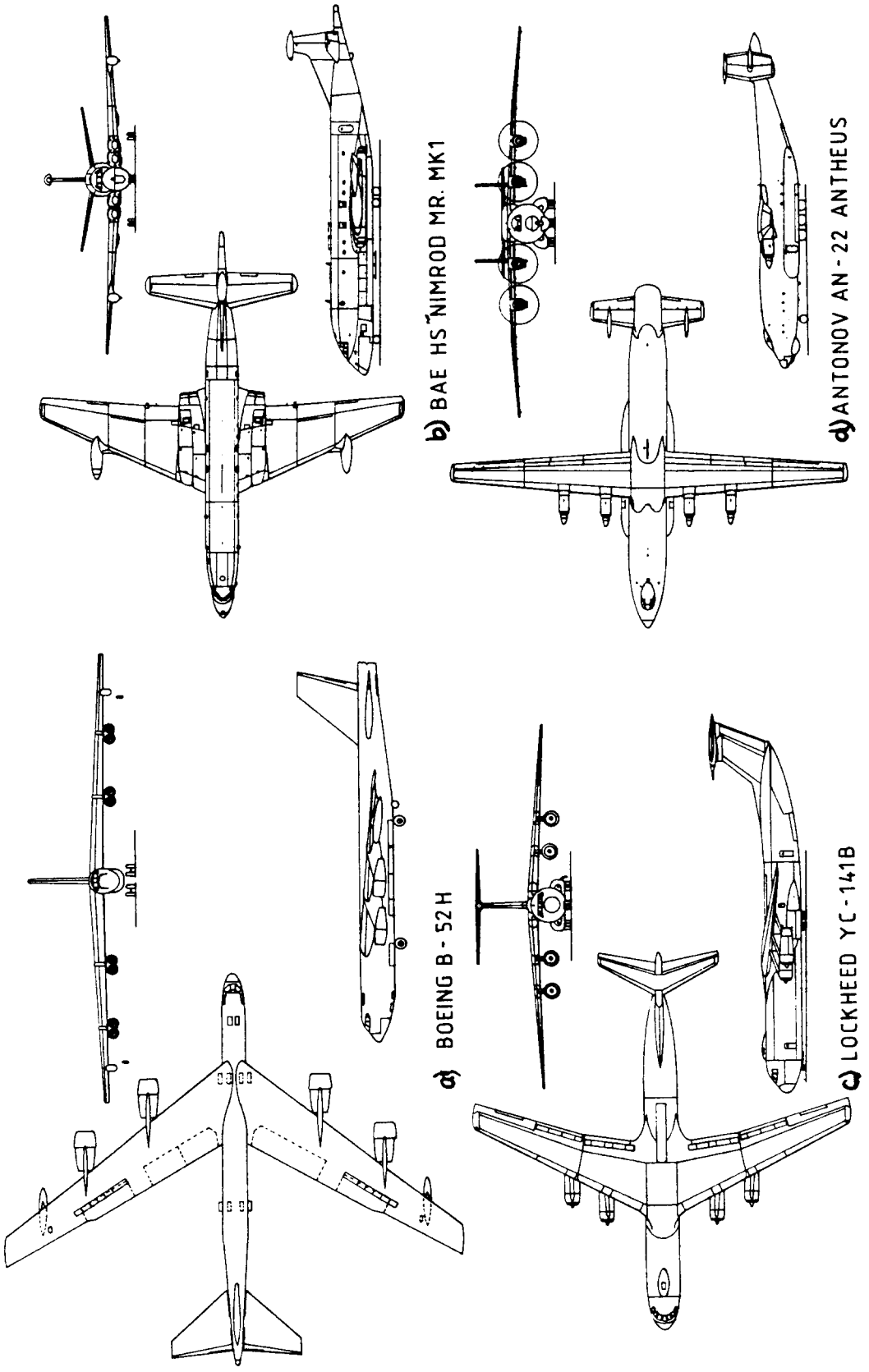

Figure 3.28 Military Patrol, Bomb and Transport Airplanes

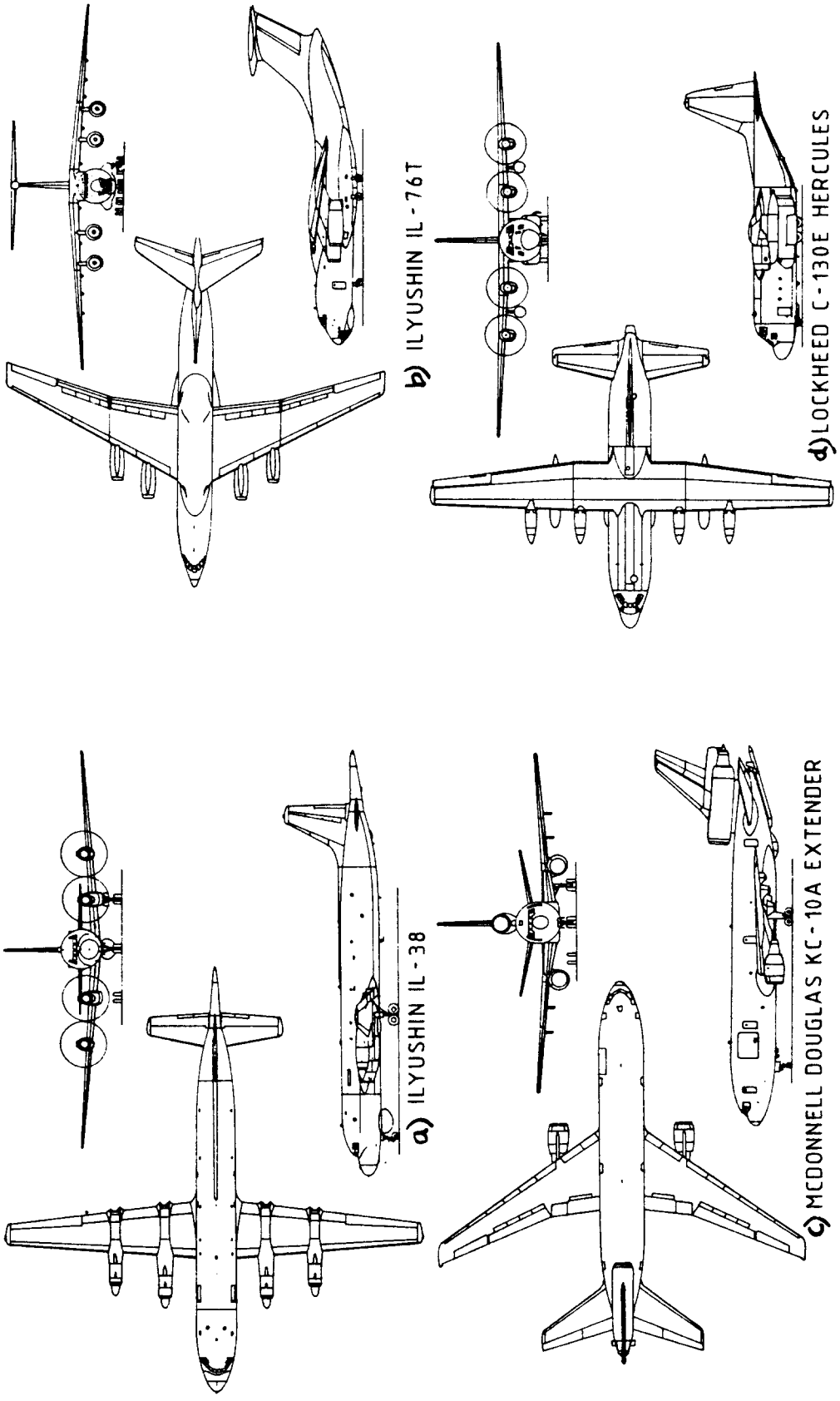

Figure 3.29 Military Patrol, Bomb and Transport Airplanes

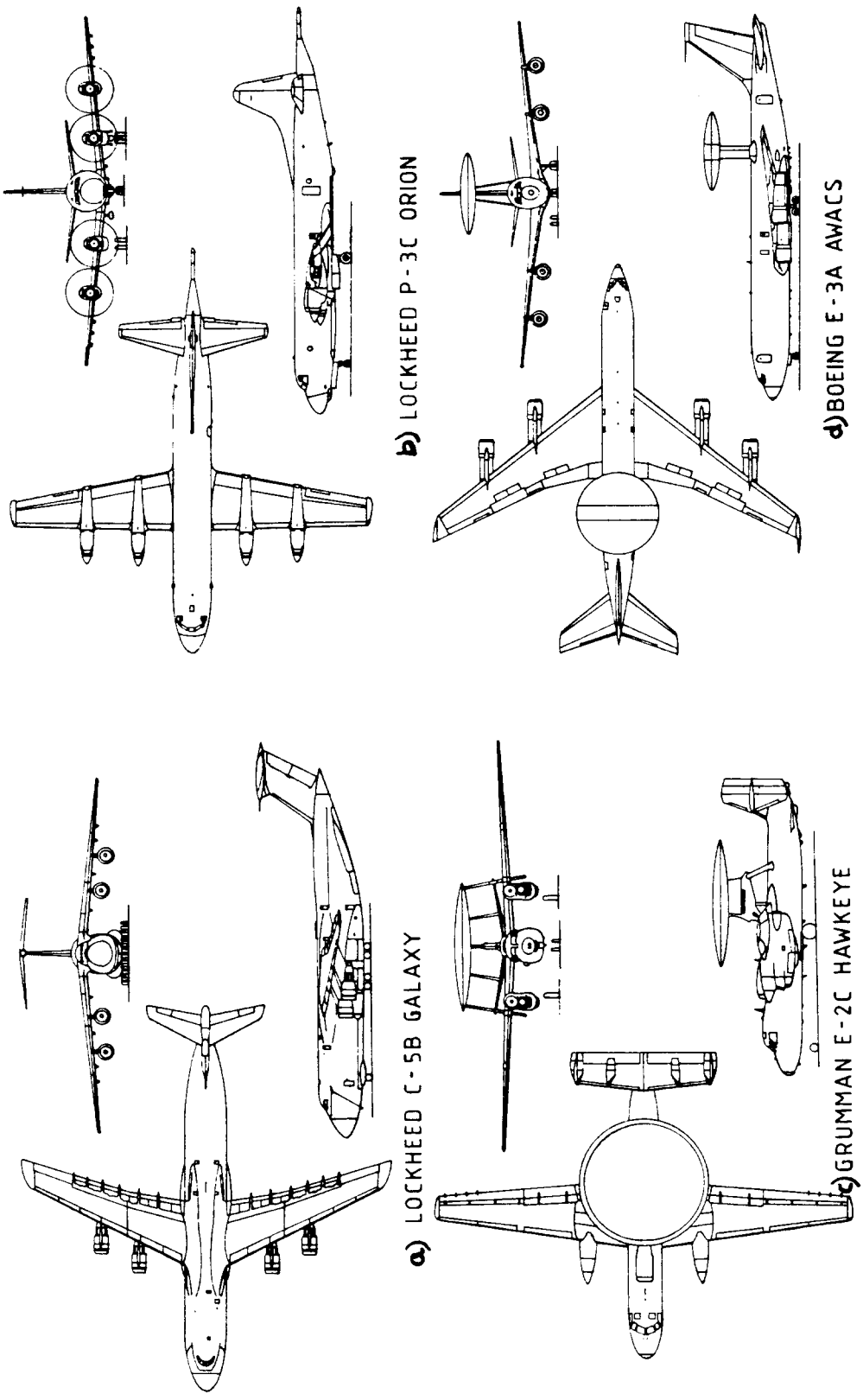

Figure 3.30 Military Patrol, Bomb and Transport Airplanes

3.1.11 Flying Boats, Amphibious and Float Airplanes

Figures 3.31-33 present twelve configurations in the flying boat and amphibious category. The following observations are offered:

1. These airplanes are dominated by the requirement for a large, hydrodynamically shaped hull. This requirement results in much larger wetted area and profile drag than is the case in land based airplanes. On the other hand it gives these airplanes a unique capability: landing and take-off from water.

2. The airplanes in Figures 3.31-3.32c are 'modern era' types, the others date from just before and during WWII. Observe the preference for conventional configurations.

3. A major design problem with water based airplanes is to keep the water spray from the hull away from engine components: salt water does not agree very well with most metals.

4. A consequence of item 3 is that the thrust lines in some flying boats end up rather high above the c.g. This has significant consequences to the flying characteristics of these airplanes in going from power-on to power-off.

5. Note that turboprops are used in most modern flying boats.

6. The Martin Seamaster of Fig.3.32b was an attempt to develop a very high speed flying boat for the USNavy. Ref.22 in Section 14.2 gives the reasons for its failure.

7. The huge, ten-engine, turboprop Princess of Fig.3.32c was an attempt just after WWII to capture the transatlantic passenger market. It failed because of the introduction of passenger jets such as the 707, the DC8 and the Comet.

8. Most of the amphibians have a tri-cycle landing gear configuration. The Beriev M12 of Fig.3.31d is an interesting exception.

9. Landing gear wells in water based airplanes have to be sealed to prevent water from entering the hull. The hulls themselves must have a number of sealed, watertight compartments. This is to prevent damage to a small area from causing the entire machine to sink.

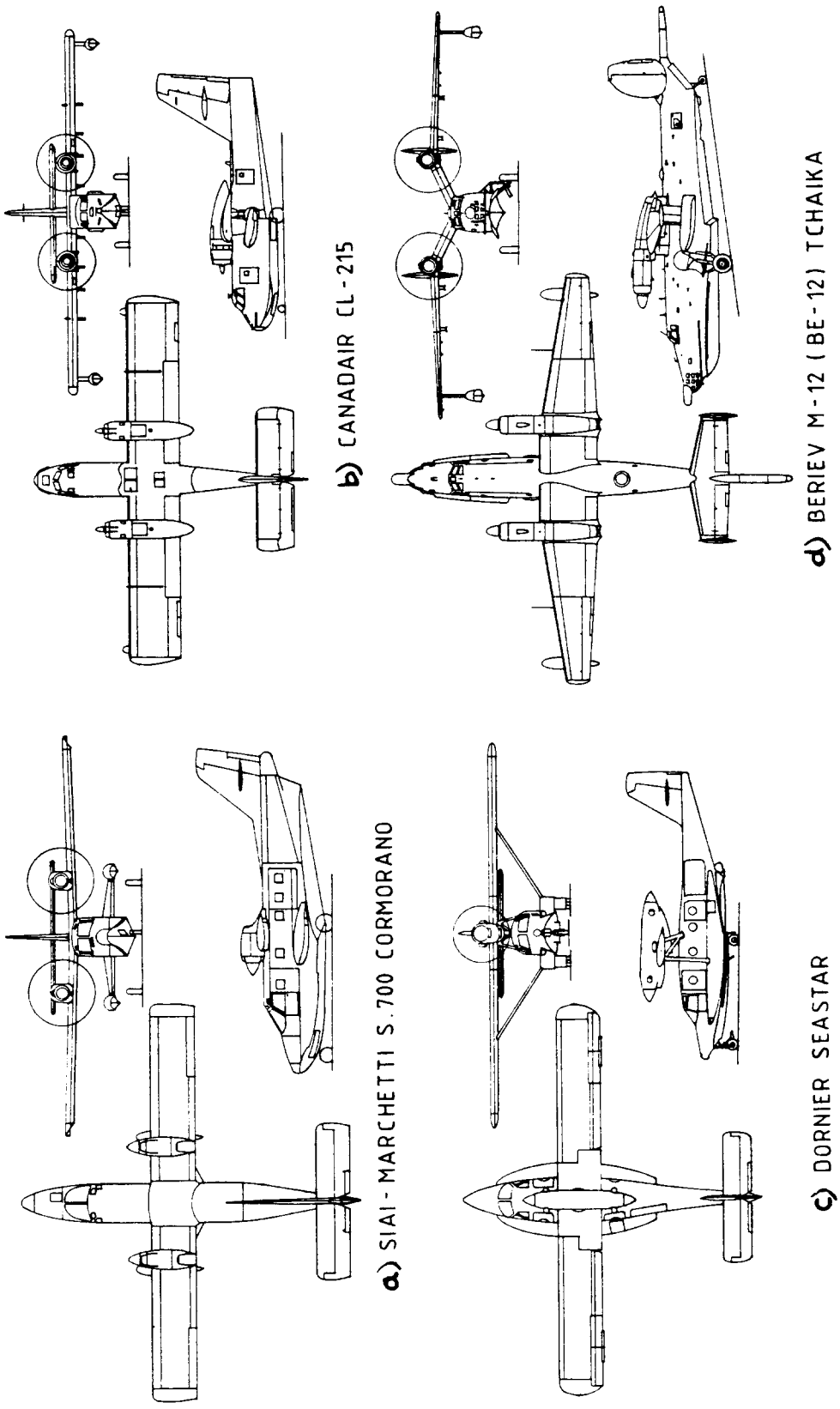

Figure 3.31 Flying Boats, Amphibious and Float Airplanes

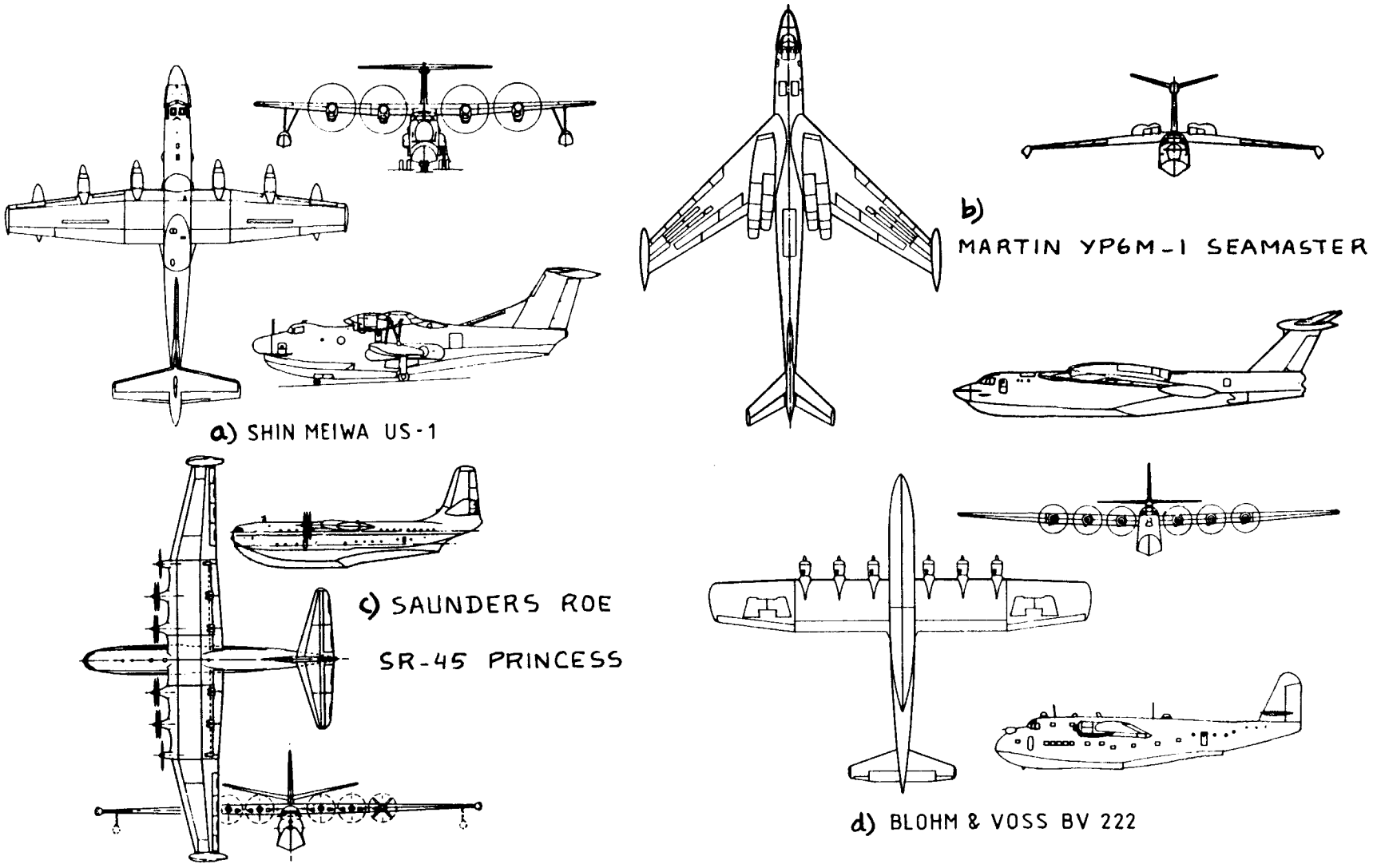

Figure 3.32 Flying Boats, Amphibious and Float Airplanes

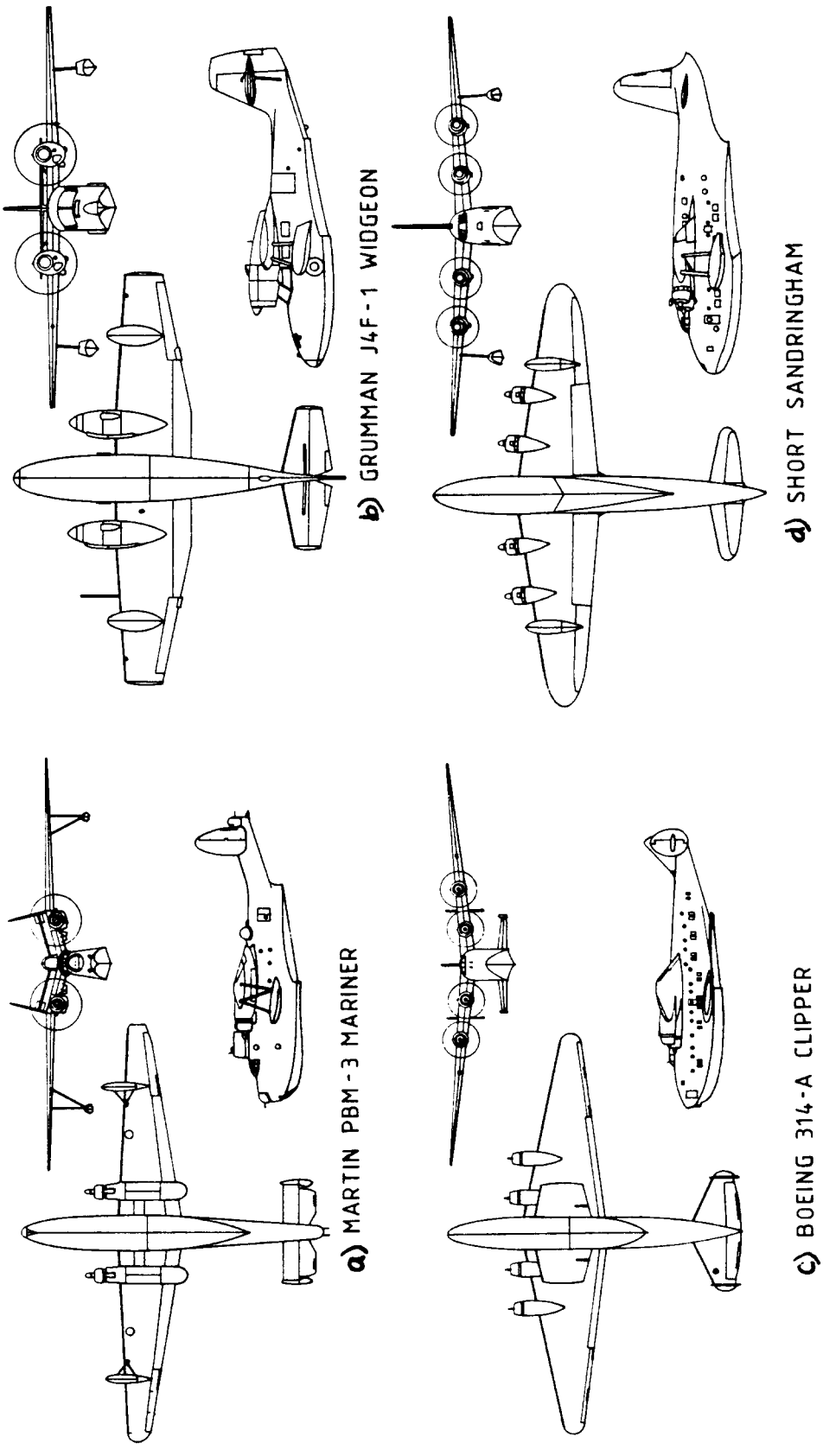

Figure 3.33 Flying Boats, Amphibious and Float Airplanes

3.1.1. Supersonic Cruise Airplanes

Figures 3.34-36 present twelve configurations of supersonic cruise airplanes. The following observations are offered:

1. The airplanes of Figures 3.34 and 3.35 have flown and except for the XB-70 have been or still are operational. The airplanes of Figure 3.36 are design studies only in the sense that they have not been built.

2. Note the large sweep angles on all supersonic airplanes. The airplanes shown all have 'subsonic' leading edges in supersonic cruise. That means the leading edge of the wing is behind the Mach cone. Supersonic cruise vehicles are dominated by the requirement to minimize wave drag. The cross sectional area distribution of these airplanes is therefore very critical.

3. Because of the large l.e. sweep, the lift-curve slope of these airplanes is low. At approach speeds this results in a high angle of attack which makes visibility over the nose a major problem. In the airplanes of Figs. 3.35c, d and 3.36a, b this problem was solved by a 'drooped nose'. In the B1-B of Fig.3.35b a variable sweep wing is used to allow the airplane to cruise with reasonable efficiency at subsonic speeds. This VSW feature can make it unnecessary to use a drooped nose. Note that in the Boeing SST proposal of Fig.3.36a both features are employed.

4. A major design problem with commercial supersonic transports is the sonic boom. It is very difficult to design an SST with acceptable sonic boom characteristics during overland flight. That is the reason why sofar most countries (including the USA) prohibit supersonic flight overland. Military airplanes are exempted from this requirement as long as they stay within certain corridors.

5. Inlet placement in supersonic airplanes is another critical design consideration. Note that most have the inlet far aft under the wing. Such an arrangement results in favorable pressure interference.

6. Trimmed cruise lift-to-drag ratios at supersonic speeds are typically 7 to 9. For the subsonic transports these values are 14 to 18. Here lies an aerodynamic design problem with serious implications for economic feasibility.

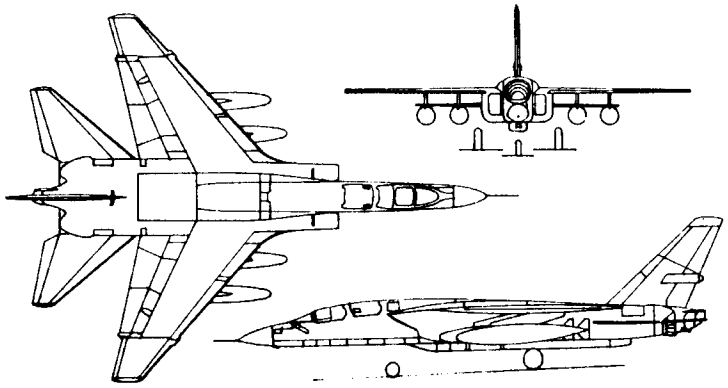

a) NORTH AMERICAN RA-50 VIGILANTE

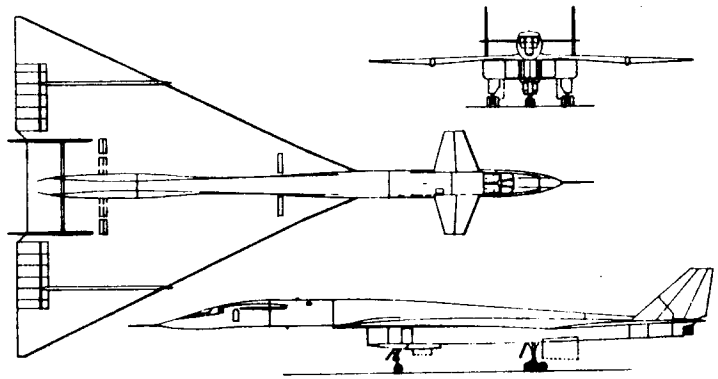

b) NORTH AMERICAN XB-70A VALKYRIE

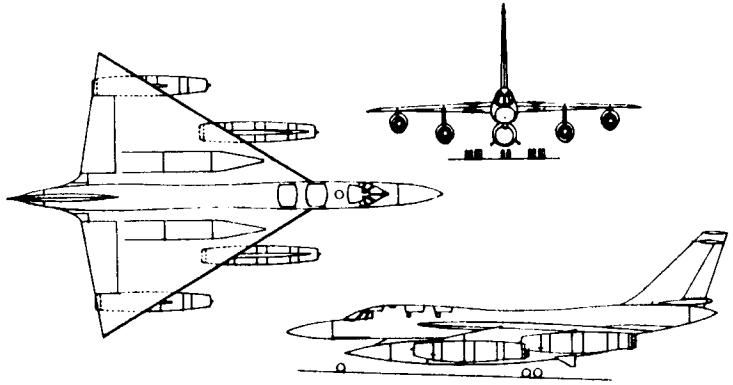

c) CONVAIR B-58A HUSTLER

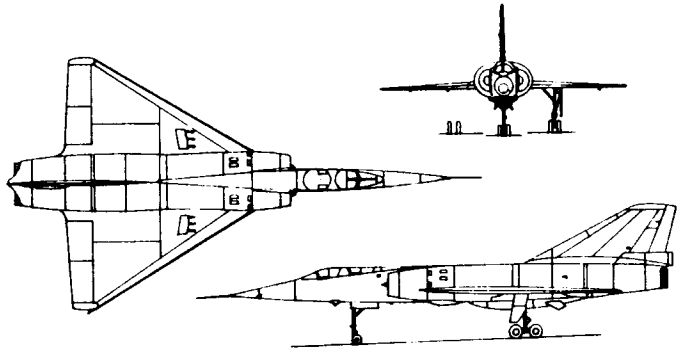

d) DASSAULT MIRAGE IV-A

Figure 3.34 Supersonic Cruise Airplanes

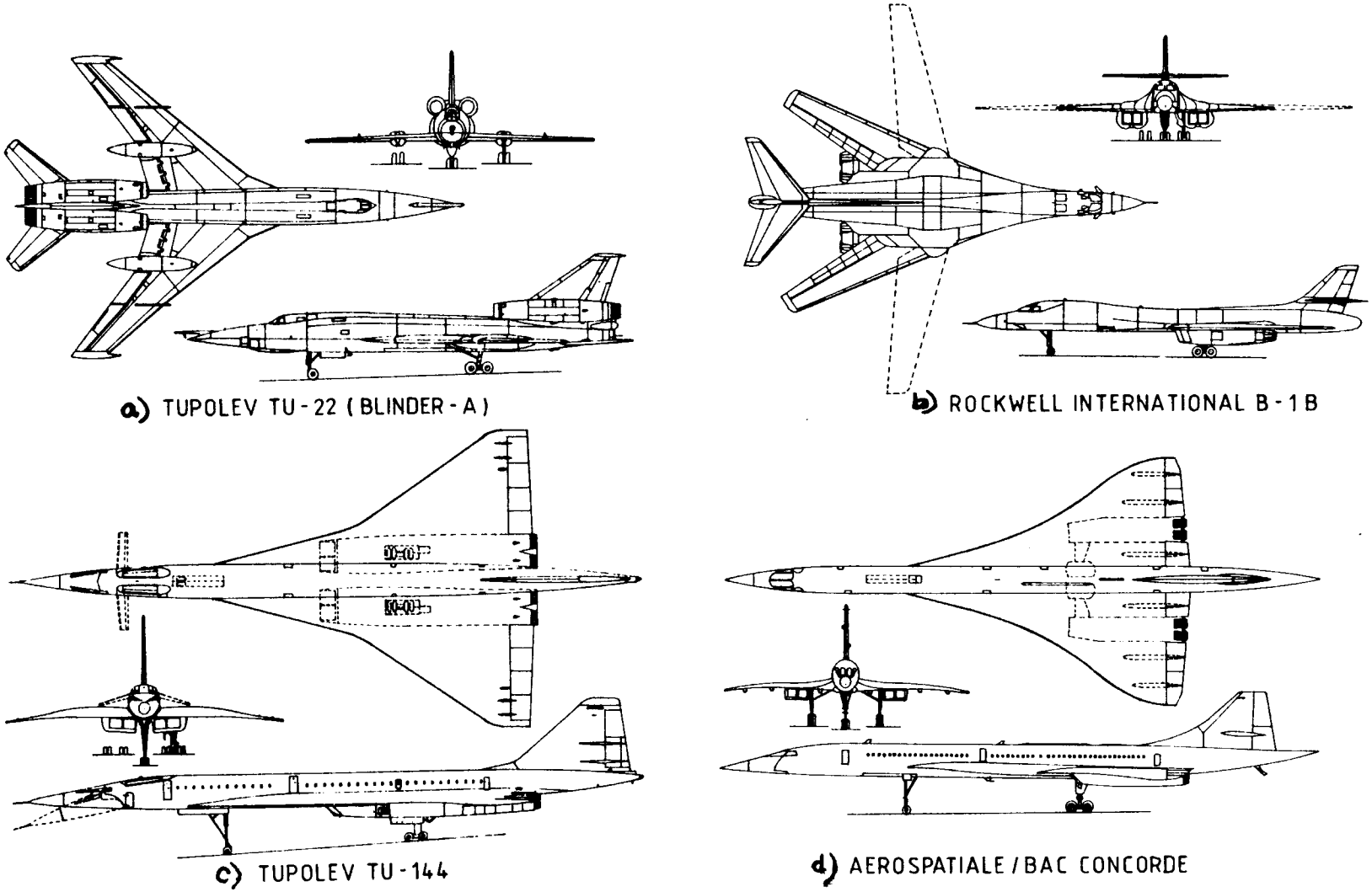

Figure 3.35 Supersonic Cruise Airplanes

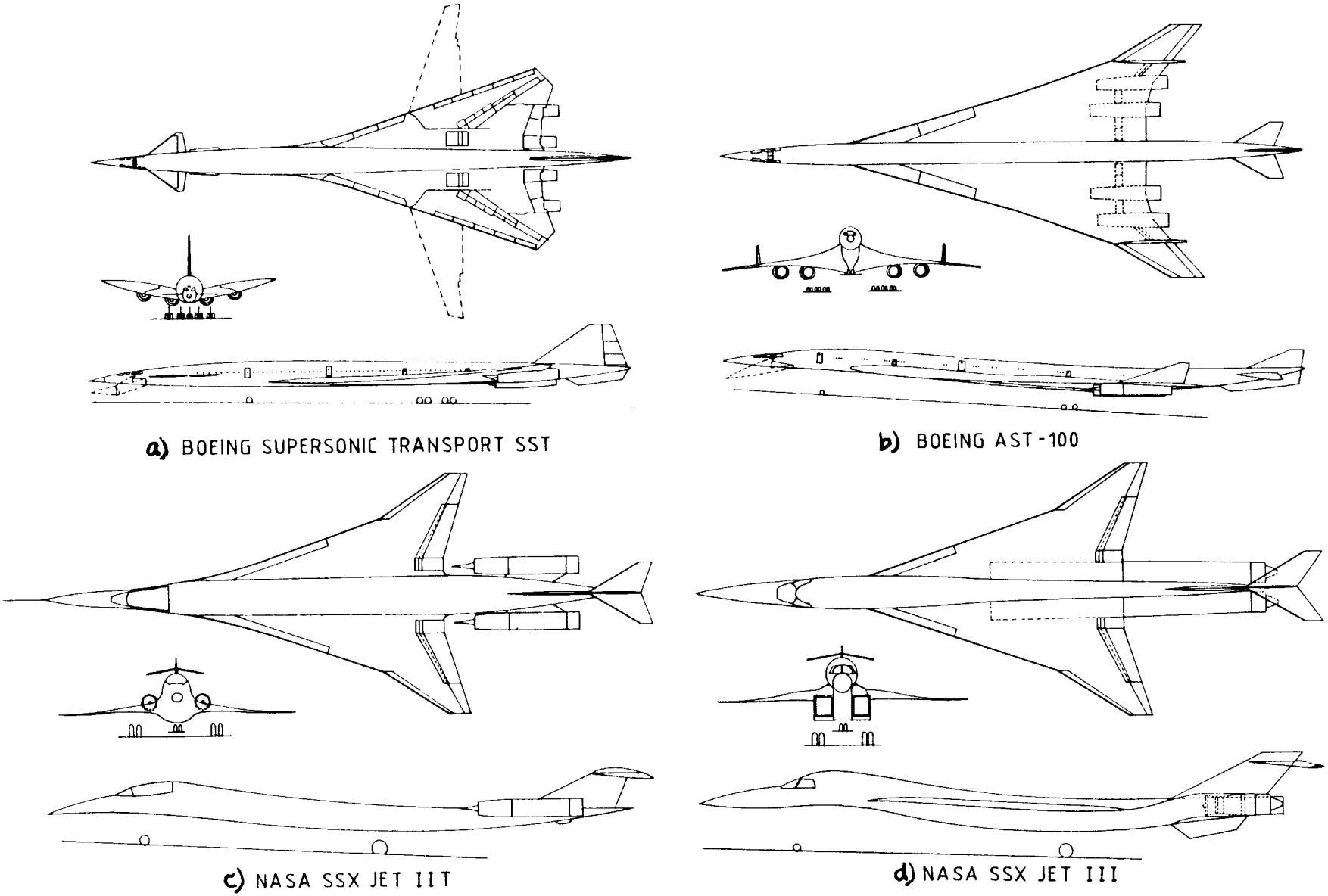

Figure 3.36 Supersonic Cruise Airplanes

3.2 UNUSUAL CONFIGURATIONS

The reader will find that while studying the historical references listed in Section 14.2 a large number of 'unusual' configurations have actually been built and flown. Some of these were successful, others were not. Therefore, when trying to innovate in the area of configuration design the reader will also find that it is very difficult indeed to come up with something which has not (in one form or other) been tried before.

The purpose of this section is to discuss a number of such unusual configurations. The discussion is organized as follows:

3.2.1 Canard and tandem wing configurations.
3.2.2 Joined wing configurations
3.2.3 Three-surface configurations
3.2.4 Double fuselage configurations
3.2.5 Flying wings
3.2.6 Burnelli configurations
3.2.7 Oblique wing configurations
3.2.8 Roadable airplanes

3.2.1 Canard and Tandem Wing Configurations

The world's first powered, controllable airplane was the Wright Flyer. Its configuration was that of a twin-propeller (single engine), pusher, pure canard design. Figure 3.37 shows a threeview of the Wright Flyer.

It is difficult to pinpoint the reason why canard designs were dropped shortly after the Wright Flyer. The main reason probably was a lack of aerodynamic understanding of the subtleties of canard design as known today.

Just before and during WWII a number of canard designs were evolved, the most notable probably were the Miles M39B Libellula, the Curtiss XP-55 Ascender and the Kyushu J7W1 Shinden. Figures 3.38 through 3.40 show three views of these airplanes.

Observe that the Libellula was in fact a tractor: the propeller disks are forward of the center of gravity. The Ascender and the Shinden were pushers.

Note that the Ascender is very similar in layout to the Rutan Varieze of Figure 3.41. The inboard strake and the winglets are the primary features which make the

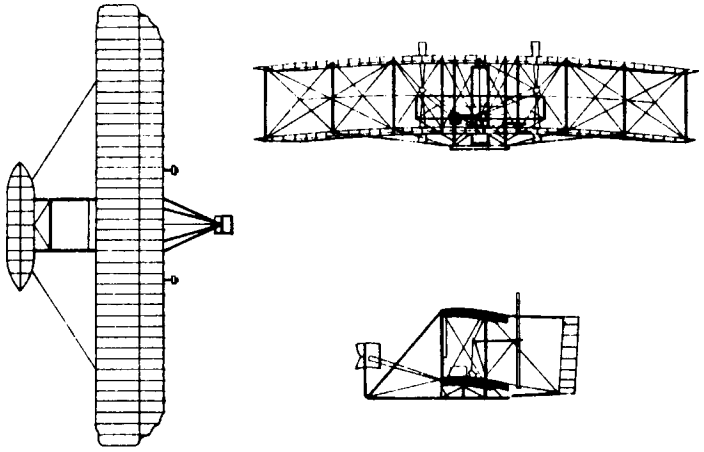

Figure 3.37 The Wright Flyer

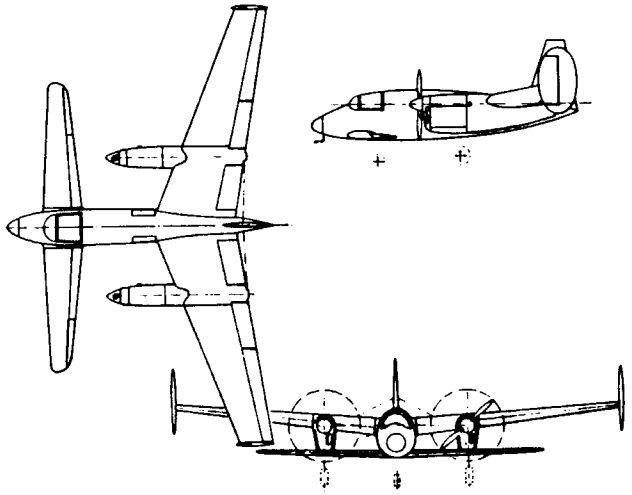

Figure 3.38 Miles M39B Libellula

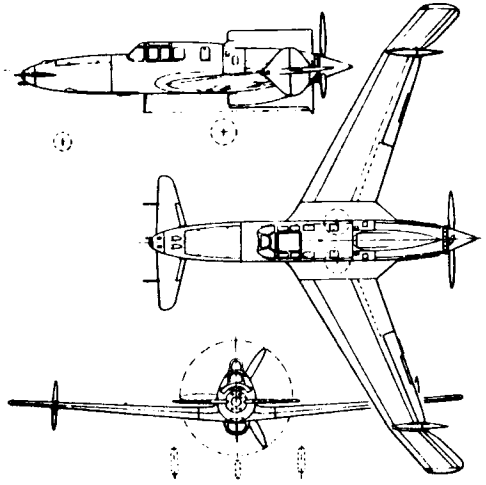

Figure 3.39 Curtiss XP-55 Ascender

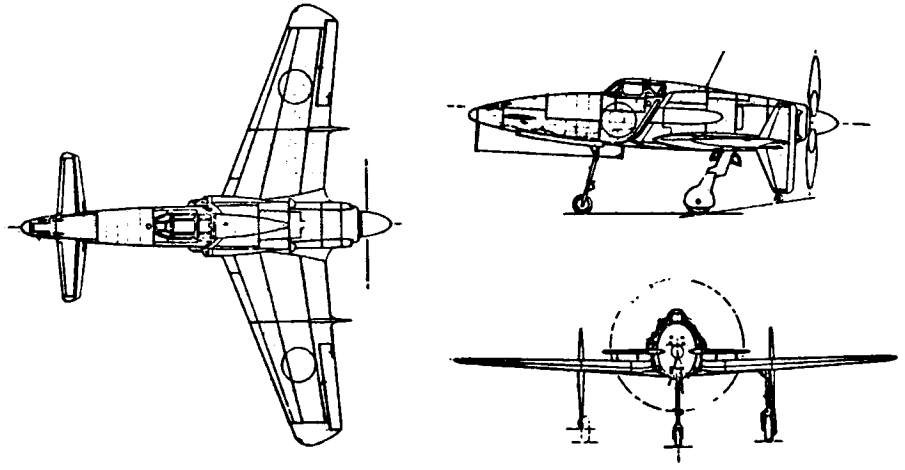

Figure 3.40 Kyushu J7W1 Shinden

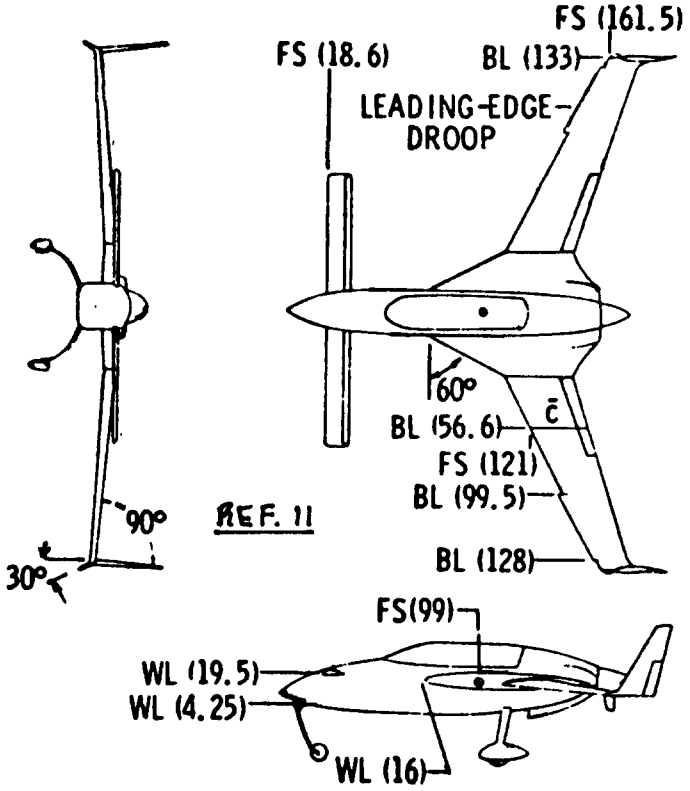

Figure 3.41 Rutan Varieze

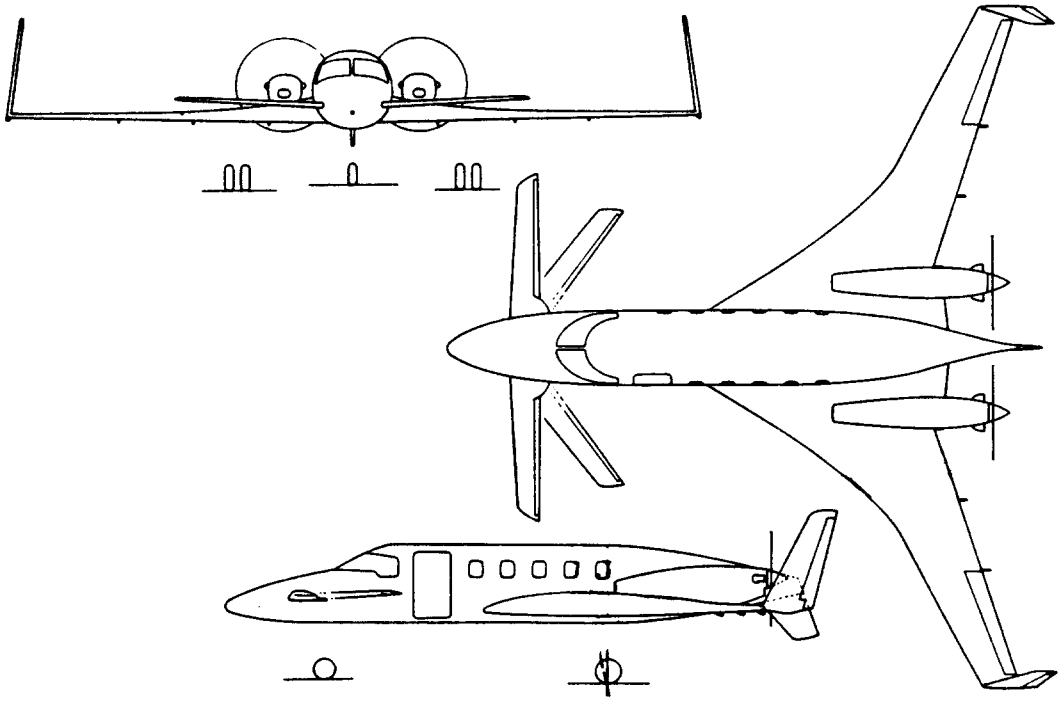

Figure 3.42 Beech Starship I (Tentative Threeview)

Varieze layout different from the Ascender.

A logical development from the Varieze configuration into an executive airplane is the twin turboprop pusher now being developed by Beech Aircraft Corp., Starship I, shown in Figure 3.42.

Why this rekindling of interest in canard configurations? The reason is that canards do have certain inherent advantages. Some of these advantages are presented here on the assumption that 'everything else is the same':

1. Trimmed maximum lift coefficient for a canard is higher than that for a conventional airplane.

2. By proper canard/wing layout design it is possible to achieve better trimmed lift-to-drag ratios with a canard design.

A problem with canard airplanes is that the canard must be designed so that it stalls before the wing. This way a stable 'pitch-break' is obtained. If this is not done, and the wing is allowed to stall before the canard, an uncontrollable and sometimes violent pitch-up can occur.

Obviously, the canard must stall before the wing with wing flaps up as well as down. To trim out the negative pitching moment associated with deployment of wing flaps, the canard must be able to develop rather large lift coefficients itself. This can be handled by putting flaps on the canard, by varying the sweep angle of the canard or by varying the incidence of the canard. All these 'approaches' have been tried.

Note that in Figures 3.41 and 3.42 the wing is given a very high inboard sweep angle: in a fighter airplane this would be called a 'strake'. The strake serves two purposes:

1. It provides volume for fuel to be carried close to the 'empty weight c.g.', and:

2. It serves to delay wing stall.

The Beech Starship I, shown in Figure 3.42 also features a variable sweep canard. This is used to trim out the negative pitching moment of the wing flaps.

Arranging the propulsion system so that it is

'pushing' instead of 'pulling' the airplane through the air is a feature which seems to be increasing in popularity. It is shown in Ref.9 that pusher configurations exhibit a stabilizing tendency in both pitch and yaw when compared to a tractor configuration. This feature can be capitalized upon by a slight reduction in tail surface requirements.

Another potential advantage of a pusher propeller configuration is that it can serve to lower cabin interior noise. This is a major problem in conventional propeller driven airplanes. Many of these have cabin noise levels well into the decibel regime where permanent hearing damage occurs.

An example of a tandem wing configuration is shown in Figure 3.43. The reader will recognize that it can be a matter of semantics whether a configuration is called a pure canard or a tandem wing layout. This is one reason why some designers prefer to refer to the canard as a front wing.

Reference 10 shows that the particular configuration of Fig.3.43 has some serious handling quality problems. In a high angle of attack flight condition with power off, the result of rapidly adding power is to:

1. Increase the lift on the front wing.

2. Decrease the lift on the rear wing due to the downwash from the front wing.

Both effects cause a large positive (nose-up) pitching moment which may be impossible to control.

Reference 11 contains more discussions of the handling characteristics of 'unusual' configurations.

A major design problem with any canard or tandem wing layout is the aerodynamic induction effect of the front wing on the rear wing. The vortex system generated by the front wing will influence the rear wing in a manner strongly dependent on:

1. Relative wing area and wing span sizes

2. Longitudinal and vertical separation between the wings

3. Angle of attack

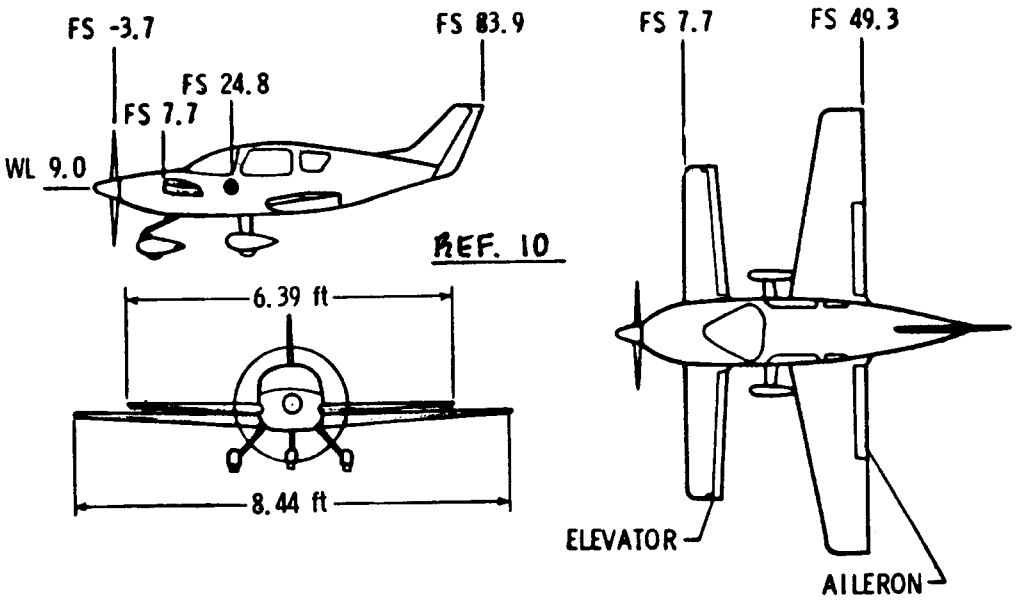

Figure 3.43 Tandem Wing Configuration

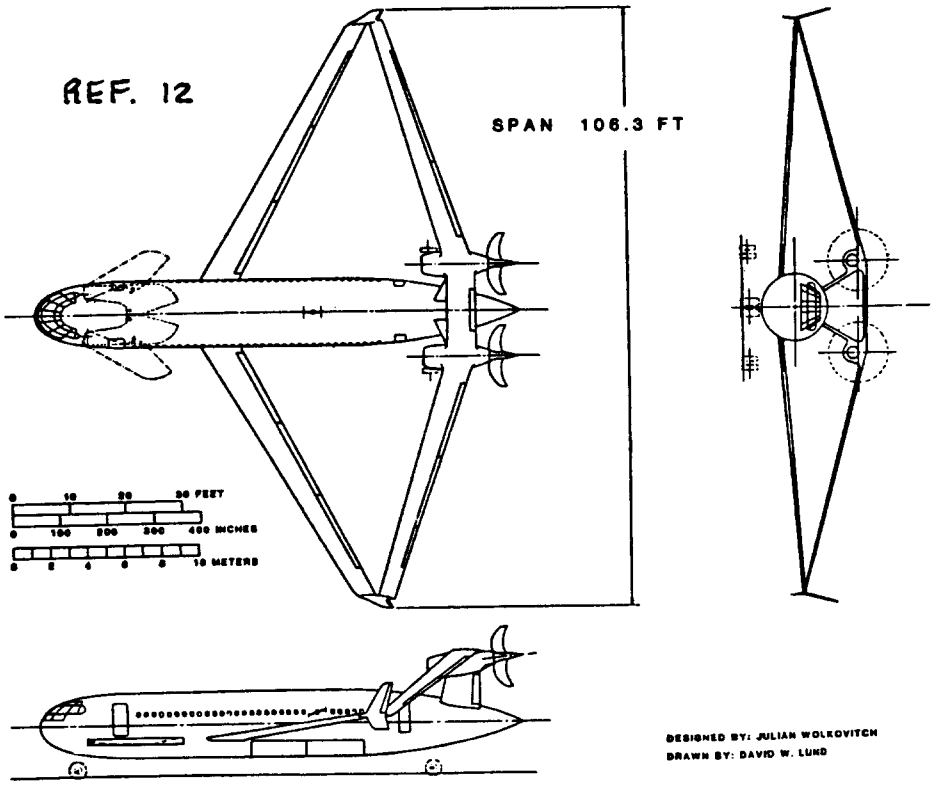

Figure 3.44 Joined Wing Transport Configuration

The canard (or front wing) tip vortex will induce an upwash on the wing outboard of the canard span. At the same time this canard tip vortex will induce a downwash on the wing inboard of the canard span. This results in poor induced drag behavior of the wing and also increases the root bending moment of the wing.

These effects can be deminished by:

1. Locating the canard far forward and below the wing.

2. Applying opposite camber and twist to the wing at the wing station corresponding to the canard span.

By closely coupling the canard to the wing (as has been done in the fighter configurations of Figures 3.27d and 3.46) it is possible to use the canard wash to enhance wing lift and reduce induced drag.

3.2.2 Joined Wing Configurations

Figures 3.44 and 3.45 show examples of projected joined wing configurations. Based on work done by J.Wolkovitch (Refs.12 and 13) the following advantages are claimed for the joined wing when compared to a conventional configuration:

1. Lower structural weight because of improved stiffness in torsion as well as in bending. ($\Delta \approx 30\%$)

2. Built-in direct lift and direct side-force capability

3. Reduced induced drag.

4. Reduced transonic and supersonic wave drag as well as improved area ruling.

3.2.3 Three Surface Configurations

Figures 3.46 and 3.47 show examples of recent three surface layouts: the Grumman X-29 and the Gates-Piaggio GP180.

The three surface layout for these widely differing airplanes came about for the following reasons:

For the X-29:

1. In a transonic fighter configuration with a

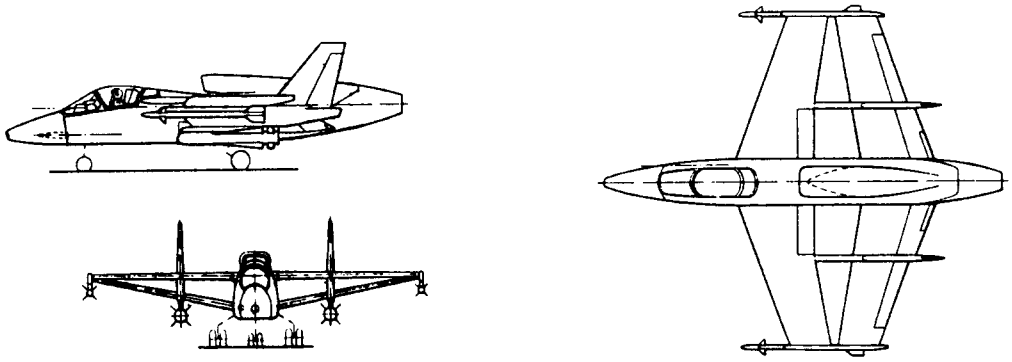

Figure 3.45 Joined Wing Fighter Configuration

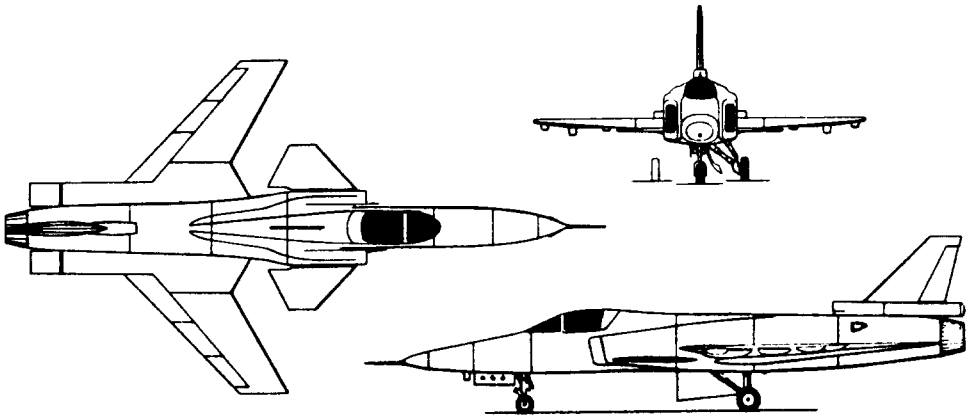

Figure 3.46 Grumman X-29A FSW Demonstrator

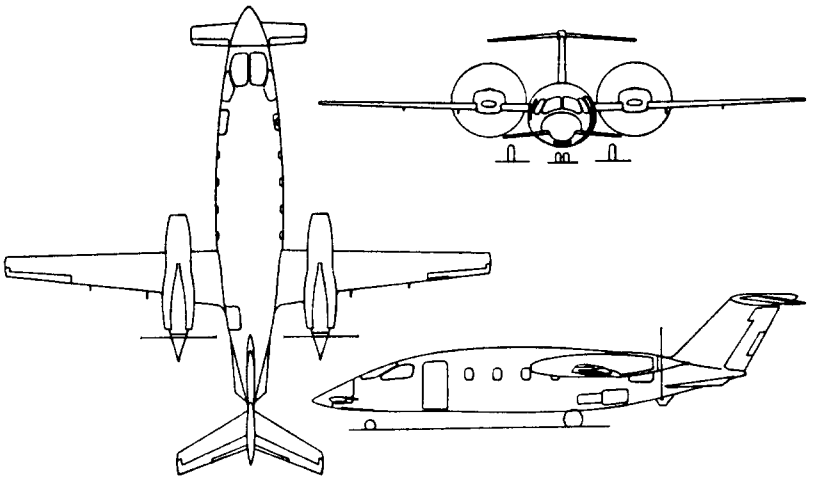

Figure 3.47 Gates Piaggio GP-180

requirement for very high sustained maneuvering at high subsonic speeds, a closely coupled canard with a forward swept wing results in reduced trim drag and in reduced wave drag.

2. An additional aft surface for trim in off-c.g. conditions results in less trim drag than by employing the canard for this purpose.

It is noteworthy to point out that the X-29 is designed to a level of inherent static longitudinal instability of 35 percent. The all-digital flight control system assures the de-facto stability of this airplane.

For the GP-180:

1. The three surface layout allows for minimization of induced trimmed drag over a wider range of center of gravity than do two surface layouts.

2. The longitudinal primary and trim controls are incorporated in the horizontal tail as in a conventional configuration.

3. Trim of flap induced pitching moments is done by a geared flap on the canard (front wing). This canard flap is mechanically geared to the wing flaps.

4. The wing torque box, the aft pressure bulkhead and the main landing gear share the same primary structure in the fuselage. This results in structural weight savings.

3.2.4 Double Fuselage Configurations

Figures 3.48 and 3.49 show examples of double fuselage airplanes.

There appear to be wetted area advantages to the double fuselage layout in subsonic as well as in supersonic applications. In addition, there may be significant development cost savings involved in 'growing' an airplane from one existing fuselage to two such fuselages.

3.2.5 Flying Wings

Flying wing configurations were pioneered by designers like Northrop, DeHavilland, Handley Page and Lippisch.

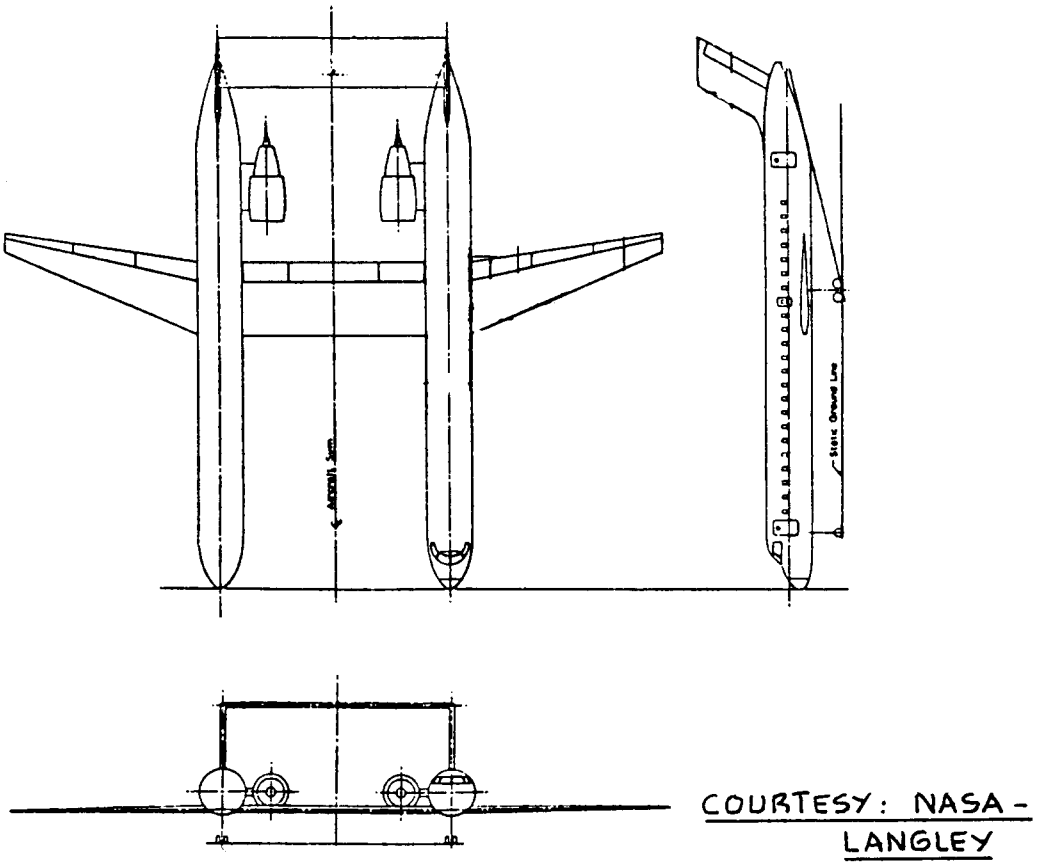

Figure 3.48 Double Fuselage Configuration: Example 1

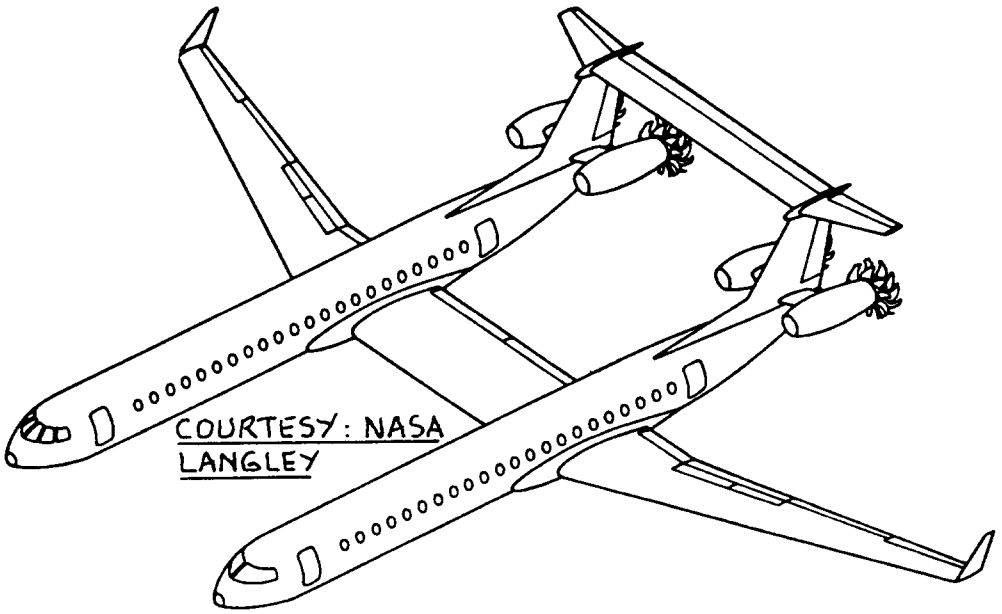

Figure 3.49 Double Fuselage Configuration: Example 2

References 12,17, 21 and 27 in sub-section 14.2 provide detailed information on some of the flying wing designs built and flown by these designers.

Reference 14 defines a flying wing as an airplane without an empennage. In this text a vertical tail is allowed.

Figures 3.50 through 3.54 are examples of several flying wing projects. Except for the configuration of Figure 3.52 all of these have flown and some even became operational.

An interesting variation on the flying wing theme is the so-called double-delta shape exhibited by the SAAB Draken of Figure 3.55. More extensively tailored versions of this wing shape are those of the Concorde (Fig.3.35d) and the F-16XL (Fig.3.25d).

Another variation on the flying wing concept is the so-called span-loader design by Lockheed as shown in Figure 3.56.

Pure flying wings tend to have higher trimmed L/D values compared with other configurations. They also have favorable payload weight fractions. With a conventional flight control system a flying wing can have serious dynamic handling deficiencies due to low inherent pitch damping. With today's highly reliable digital flight control and feedback systems these deficiencies are no longer a detriment.

For military applications a major advantage of the flying wing is its very small radar cross section (stealth).

3.2.6 Burnelli Configurations

Figure 3.57 shows an example of a so-called Burnelli airplane. Here the idea is to make the fuselage participate in the production of lift. A problem is that such a fuselage shape becomes heavy when used in a pressurized airplane. For certain large freighter applications the Burnelli configuration may warrant further consideration.

3.2.7 Oblique Wing Configurations

Figure 3.58 shows two oblique wing configurations. Note that one is also a double fuselage arrangement.

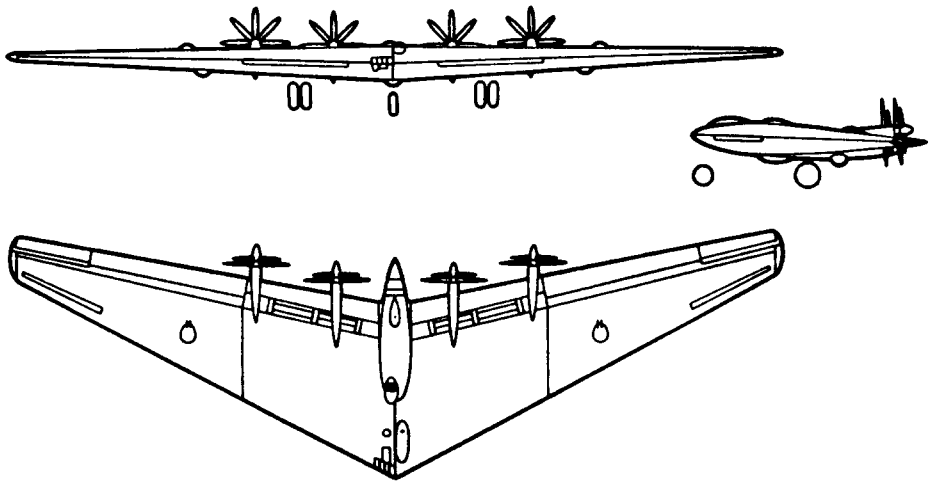

Figure 3.50 Northrop XB-35

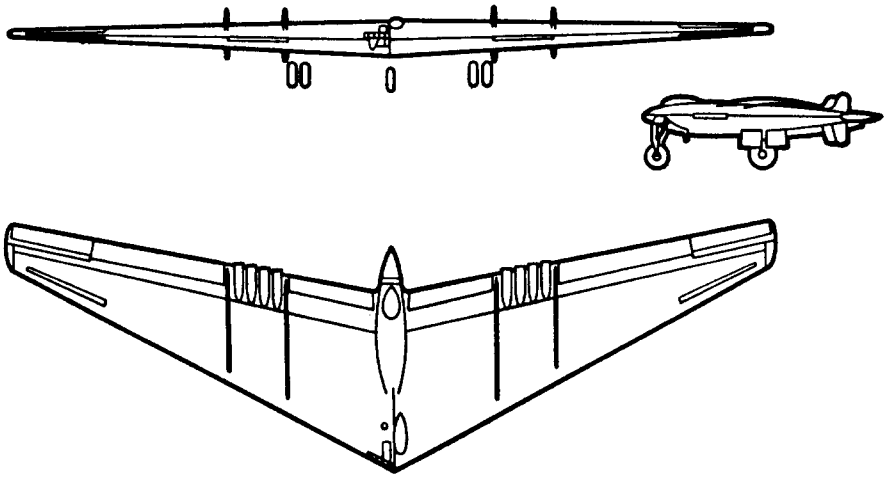

Figure 3.51 Northrop YB-49

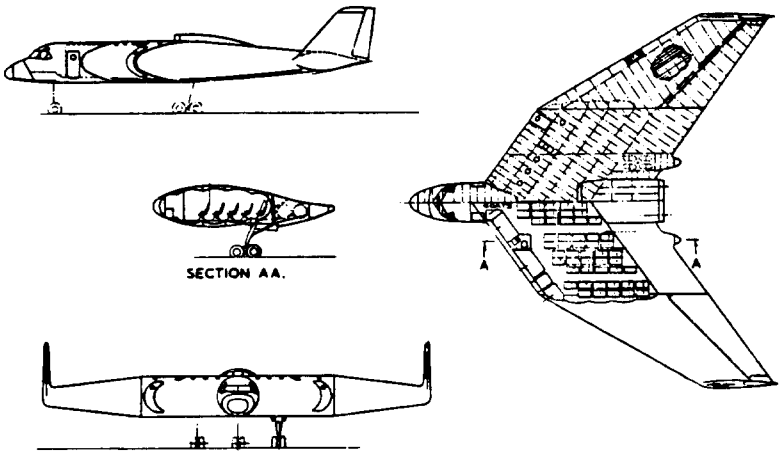

Figure 3.52 Handley Page 126 Aerobus Design

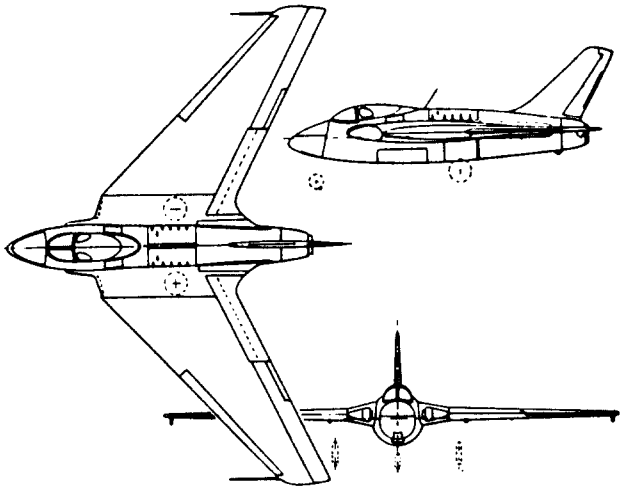

Figure 3.53 DeHavilland DH 108

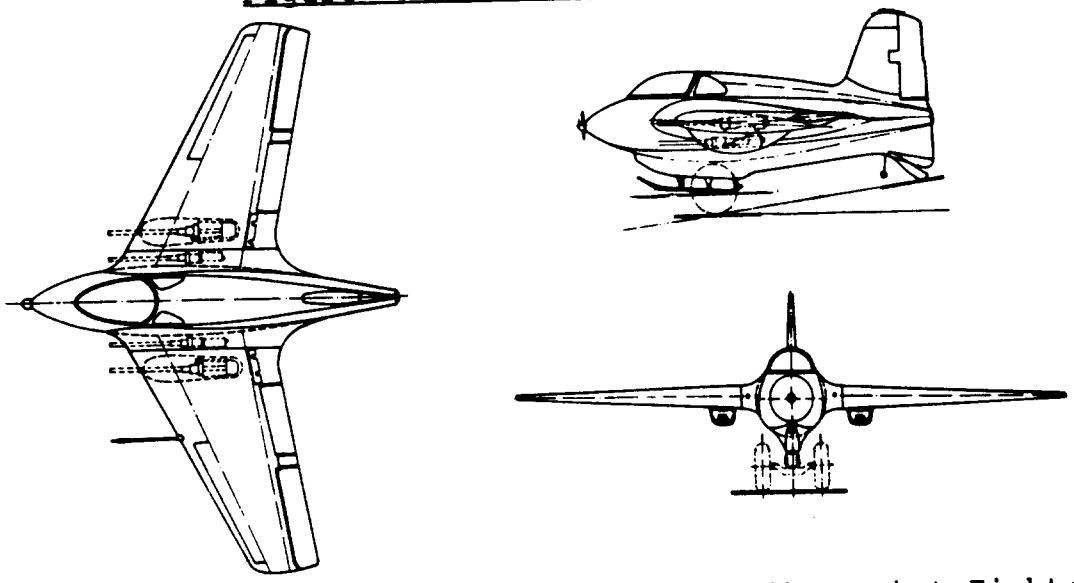

Figure 3.54 Messerschmitt (Lippisch) 163B Rocket Fighter

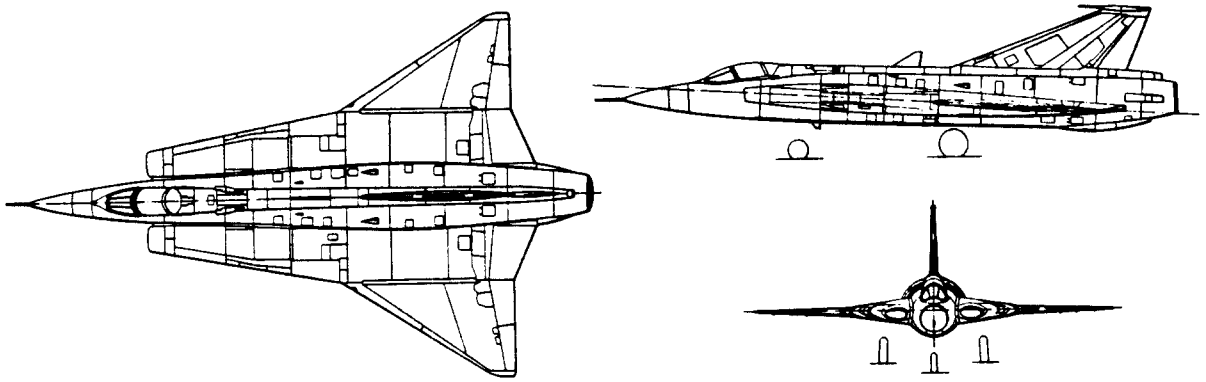

Figure 3.55 SAAB 35 Draken

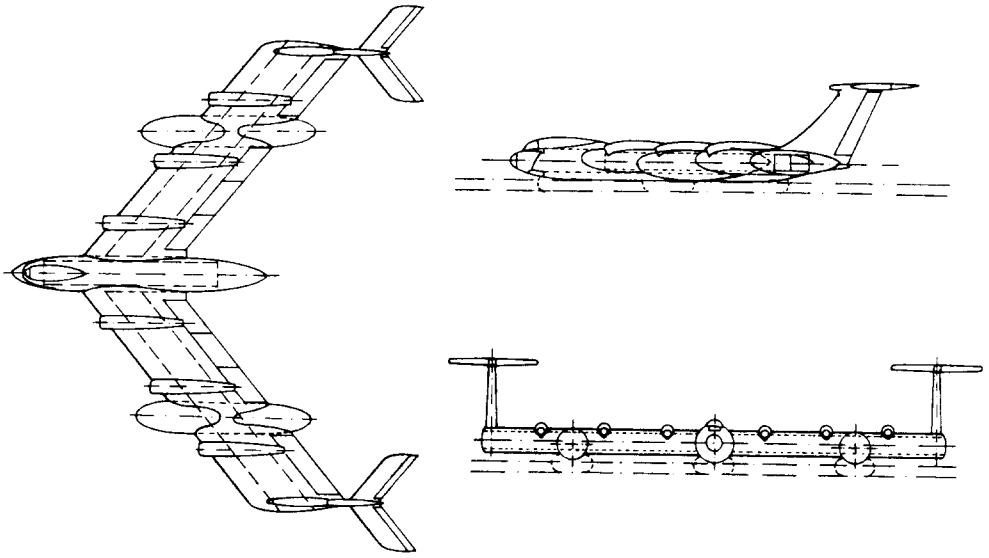

Figure 3.56 Lockheed Span-Loader Concept

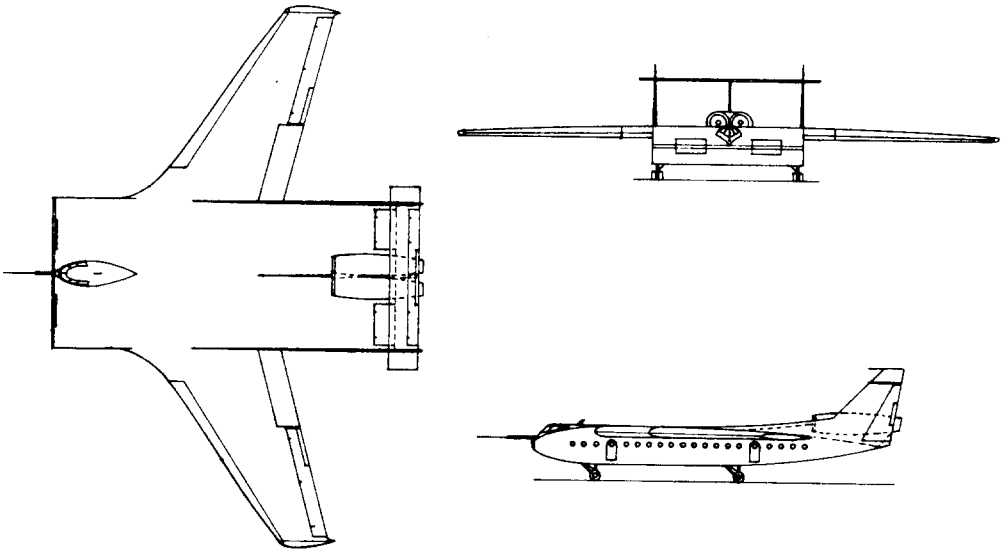

Figure 3.57 Burnelli Configuration

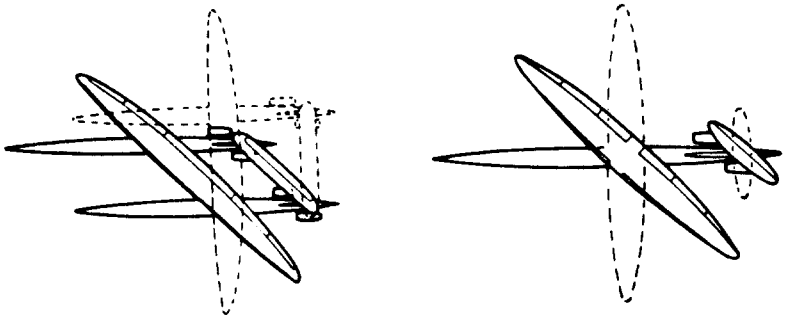

Figure 3.58 Oblique Wing Configurations

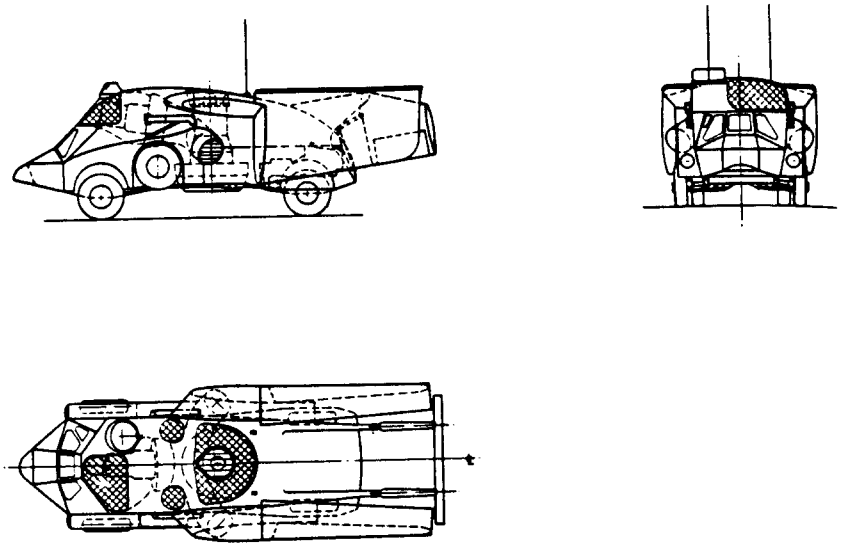

Figure 3.59 Handley Page 120 Roadable V/STOL Design

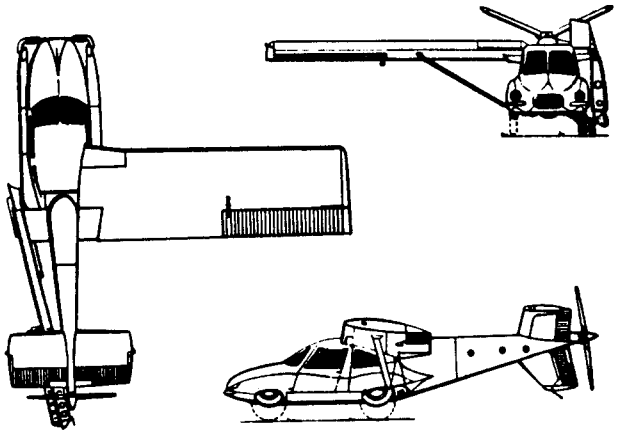

Figure 3.60 Taylor Aeroçar III

Oblique wings have significantly lower drag than conventional fixed sweep or variable sweep wings in the transonic speed range. In addition there is only one instead of two pivots as is the case with a conventional variable sweep wing.

3.2.8 The Roadable Airplane

The idea of combining a roadworthy vehicle and an airworthy vehicle into one is an old idea which sofar has not been translated into commercial or military reality. Several attempts at realizing this idea have been made. Examples are shown in Figures 3.59 and 3.60. Molt Taylor's Aerocar of Figure 3.60 has actually been flown and certified to FAR 23 standards. Sofar the reaction of the market has been cool.

A major problem is the large number of design compromises which must be made to create a vehicle which can fulfill both roles. These design compromises result in performance penalties which apparently have been too large to offset the flexibility which such vehicles would offer.

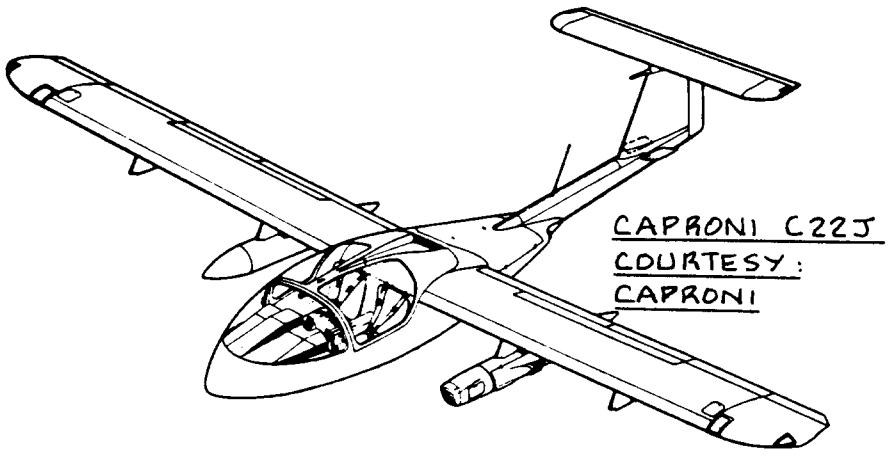

3.3 OUTLINE OF CONFIGURATION POSSIBILITIES

The purpose of this section is to present an outline of configuration possibilities. This outline is addressed to aerospace engineering students and not to experienced configuration designers.

The outline covers the following aspects of configuration design choices:

3.3.1. Overall configuration
3.3.2 Fuselage configuration
3.3.3 Engine type, number of engines and engine disposition
3.3.4 Wing configuration
3.3.5 Empennage configuration
3.3.6 Landing gear type and disposition

3.3.1 Overall Configuration

From a basing point of view airplanes can be classified as follows:

1. Land based
2. Water based
3. Amphibious

Within these basing modes the following overall configurations are possible:

1. Conventional (that means tail aft)
2. Flying wing (that means no horizontal tail or canard
3. Canard or Tandem wing
4. Three surface
5. Joined wing

Most airplanes which have been built or are being built today are of a conventional configuration. With certain exceptions, designers have not felt compelling reasons to deviate from the conventional configuration. One reason is that the data base and the experience base dealing with conventional configurations is very large. This data base is narrow and even non-existent in some of the other configurations.

Section 3.4 presents a step-by-step guide which should be useful to aeronautical engineering students in selecting the overall configuration of an airplane.

Within each overall configuration (1-5), it is

possible to utilize a wide variety of choices for the arrangement of the major airplane components. These choices are discussed in the following sub-sections:

3.3.2 Fuselage configuration
3.3.3 Engine type, number of engines and engine disposition
3.3.4 Wing type and placement
3.3.5 Empennage type and placement
3.3.6 Landing gear type and placement

Most airplanes have the XZ plane as a plane of symmetry. In some instances there may be a good reason to deviate from a symmetrical configuration. The oblique wings of Figure 3.58 are examples of this.

3.3.2 Fuselage Configuration

Fuselage configurations can be broadly classified as follows:

1. Conventional (Example: virtually all airplanes in Figures 3.1 - 3.36 have a conventional fuselage.)
2. Twin fuselage (Example: Figures 3.48 and 3.49)
3. Twin boom with center fuselage (Example: Figures 3.9c and 3.11c)
4. Burnelli (Example: Figure 3.57)

Chapter 4 presents a step-by-step guide to cockpit and fuselage layout design. Part III (Ref.2) contains detailed discussions and data useful in the design of cockpit and fuselage layouts.

3.3.3 Engine Type, Number of Engines and Engine Disposition

3.3.3.1 Engine type

The selection of engine type depends mostly on the matching of desired airplane performance to the inherent performance of an engine type. From a pragmatic (cost and certification) viewpoint, the choice of engine type for the next 10 years is probably limited to:

1. Piston/propeller combinations
2. Turbo/propeller combinations
3. Propfans
4. Unducted fans
5. Turbojets
6. Turbofans

7. Rockets
8. Ramjets

Any combination 1 through 8 which makes sense in a given application also presents a viable choice of engine type.

Several engine types are under research and development. Examples of such types are:

9. Diesel and turbo/diesel engines
10. Rotary engines for a variety of fuels
11. Variable cycle jet engines (primarily for supersonic cruise applications)
12. Electrical propulsion using Lithium fuel cells (these latter have as an interesting but important feature the fact that airplane weight will increase in flight due to the formation of certain chemical compounds: see Ref.15.)
13. Electrical propoulsion with photo-voltaic cells
14. Electrical propulsion with microwave beams

Items 13 and 14 are probably of interest primarily in very high altitude long endurance platforms.

Whether or not any of these propulsion types will materialize will depend on a combination of need, fuel prices and fuel availability. It will take a minimum of five to ten years to bring anyone of these types to maturity.

Section 5.1 contains a step-by-step procedure for selecting the engine type(s) to be used.

3.3.3.2 Number of engines

Selection of the number of engines depends on a combination of the following factors:

1. Total power or thrust required and availability of engines in a given power or thrust class.

2. Relationship between critical field and climb performance and the probability of engine failure

3. Other safety considerations

4. Cost of acquisition and of maintenance

Historically the number of engines used on any given airplane type has ranged from 1 to 10. The B36D (Ref.28,

Section 14.2) was an example of the latter. The range of 1 to 4 engines has proven to be the most practical for many airplanes.

Section 5.2 presents a step-by-step procedure for determining the number of engines to be used.

3.3.3.3 Engine disposition

Broadly speaking, engines can be arranged as:

1. Tractors (point of thrust application ahead of the center of gravity)
2. Pushers (point of thrust application behind the center of gravity)
3. Combination tractor and pusher

Within these three basic arrangements, engines can be installed in the following manner:

1. In pods or nacelles
2. Buried

Whether podded or buried, engines can be dispositioned on or in:

1. The wing: below, above or in-line
2. The fuselage
3. The empennage

The disposition of engines has major consequences for:

* airplane weight
* airplane vibration and noise
* engine efficiency
* handling characteristics from a pilot viewpoint
* maintenance

Section 5.3 presents a step-by-step procedure for determining the disposition of the engines. Part III (Ref.2) contains many examples of propulsion system integration.

3.3.4 Wing Configuration

From a structural viewpoint wing configurations can be classified as follows:

1. Cantilever wing
2. Braced (or strutted) wing

Note that joined and tandem wing arrangements were already accounted for under the overall airplane configuration possibilities discussed in sub-section 3.3.1.

In terms of wing/fuselage arrangement, wings can be classified as follows:

1. High wing
2. Mid wing
3. Low wing

From a sweep angle viewpoint, wings can be classified in the following manner:

1. Zero or negligible sweep
2. Aft sweep (also called positive sweep)
3. Forward sweep (also called negative sweep)
4. Variable sweep (meaning symmetrically variable sweep)
5. Oblique sweep (meaning asymmetrically variable sweep)

Most wings are given a fixed wing incidence angle on the fuselage. In certain cases however, the wing is given a variable incidence angle. An example of the latter is the Vought F8U naval fighter (See Ref. 8, 1969-1970 issue).

In addition to these overall wing configuration possibilities, the following wing design characteristics are important to the weight, the performance and the stability and control characteristics of an airplane:

1. Aspect ratio
2. Thickness ratio
3. Airfoil(s)
4. Taper ratio
5. Twist
6. Incidence angle
7. Dihedral angle
8. High lift and control surface requirements
9. Winglets

Chapter 6 presents a step-by-step procedure for the selection of all major wing configuration design characteristics.

Chapter 7 contains a step-by-step method for selecting the high lift devices which may be required.

Part III (Ref.2) contains more detailed information on the subject of wing and high lift layout design.

3.3.5 Empennage Configuration

The word empennage as used here can mean:

1. Horizontal tail(s)
2. Vertical tail(s)
3. Canard(s): horizontal and/or vertical

The empennage configuration is intimately tied up with the selection of the overall configuration.

In principle, all that has been said about the wing configuration, applies to the empennage.

In addition, the following configurational choices must be made:

For the horizontal tail:

1. Fuselage mounted, usually far aft on the fuselage
2. Boom mounted, such as in twin boom designs
3. Vertical tail mounted as either a cruciform or a T-tail installation
4. Butterfly or V-tail (Examples are the Beech V35 Bonanza and the Potez CM570 Magister of Ref.8, 1963-1964 edition)

For the vertical tail:

1. Fuselage mounted
2. Boom mounted, such as in twin boom designs
3. Single or multiple vertical tail(s)
4. Butterfly or V-tail

For the canard:

For horizontal and for vertical canards the configurational choices are essentially those of the horizontal and/or the vertical tail.

In many airplanes it is found necessary to add strakes, ventral fins and/or dorsal fins to the empennage. Examples of these may be seen in many of the airplane configurations presented in Section 3.1.

Chapter 8 provides a step-by-step method for determining the size and location of the empennage. Parts III and VII (Refs 2 and 6) contain more detailed

information on the layout design and sizing of the empennage.

3.3.6 Landing Gear Type And Disposition

From a systems viewpoint landing gears can be classified as:

1. Fixed or non-retractable (Many single engine, propeller driven types of Section 3.1)
2. Retractable (Most airplanes in Section 3.1)

According to their layout, landing gears can be classified as:

1. Taildraggers (See Figs 3.10a,c,d)
2. Conventional or tricycle (Most airplanes in Section 3.1)
3. Tandem (See Fig.3.28a)
4. Outrigger (See Fig.3.28a)

Landing gears can be mounted in or on:

1. Wing and/or nacelle
2. Fuselage

Many flying boats employ outrigger floats for lateral stability on the water. Sometimes these outrigger floats are retractable. Figs 3.33a,b,d are examples of fixed outrigger floats while Figs 3.32 c,d are examples of retracting outrigger floats.

Retracting water skis have also been tried. The water based Convair Seadart (See Ref.22 in Section 14.2) was an example.

The following landing gear design aspects have a major impact on the ultimate configuration of the landing gear:

* Number of main gear struts
* Number of tires per strut
* Retraction kinematics and available volume to receive the gear

Selection of the number of struts and tires is intimately tied to the type of surface the airplane needs to operate from.

Chapter 9 presents a step-by-step procedure for deciding on the type of gear, the disposition of the gear

and the size of struts and tires. Part IV contains more detailed information on the problem of designing landing gears, assuring their satisfactory disposition and designing the retraction system.

3.4 A PROCEDURE FOR SELECTING THE OVERALL CONFIGURATION

The following step-by-step procedure is offered to assist in arriving at the decision which overall configuration to use:

Step 3.1: Determine whether or not the airplane to be designed falls into one of the twelve categories described in Section 3.2.

If it does, read the appropriate sub-section. This will help in familiarizing yourself with what the competition has been doing.

If it does not, proceed to Step 3.2.

Step 3.2: Review the study results of Step 1, Section 2.1.

Step 3.3: Obtain a historical perspective by reviewing the appropriate references listed under 'historical bibliography' in Section 14.2. Consult older versions of Ref. 8.

Step 3.4: Review Section 3.3 and write down which overall configuration candidates are considered suitable. List the reasons why.

Step 3.5: If time and/or available manpower don't allow for the red, white and blue team approach, select one configuration and go with it.

Step 3.6: Document the decisions made in selecting the configuration.

3.5 EXAMPLE APPLICATIONS

Three example applications will now be presented:

3.5.1 Twin Engine Propeller Driven Airplane
3.5.2 Jet Transport
3.5.3 Fighter

The applications are all presented in the Step 3.1 through 3.5 sequence of Section 3.4.

3.5.1 Twin Engine Propeller Driven Airplane

For easy future reference the twin engine propeller driven airplane will be given the name 'Selene'. Selene is the goddess of the moon in Greek mythology.

Step 3.1: As a propeller driven twin the Selene belongs to category 3 of the categories listed on p.28. Figures 3.7-3.9 contain twelve 3-views of airplanes in this category.

Steps 3.2 and 3.3: To save space these steps are not presented in detail.

The following tabulation compares the Selene with several potential competitors. All data are from Part I, sub-section 2.6.1.

Airplane Type	W_{PL} (lbs)	W_{TO} (lbs)	$V_{cr_{max}}$ (kts)	Range (nm)
Beech Duke B60	1,300	6,775	239	1,080
Beech Baron M58	1,500	5,400	200	1,200
Cessna T303	1,650	5,150	196	1,000
Piper PA-44-180	1,250	3,800	168	725
Selene	1,250	7,900	250	1,000

Step 3.4: The following configurations are suitable candidates for the Selene:

*conventional *canard or tandem *three surface

The flying wing is not considered a suitable candidate: it would cause problems in packaging passengers and payload. It would also suffer from poor pitch damping which can besolved only with a SAS. This is thought to be unacceptable from a cost viewpoint in this type of airplane.

The joined wing is not considered a suitable candidate primarily because of lack of a data base. Fear of adverse market reactions to such a 'radical' configuration also plays a role in rejecting this configuration.

The Beech Starship I and the Gates-Piaggio GP180 employ the canard and the three surface layout respectively. Figures 3.42 and 3.47 give threeviews of these airplanes.

Step 3.5: For the Selene a conventional configuration will be selected, but with a twist: a high wing layout combined with a pusher layout will be used. This proposed layout is similar to that of the Piaggio P166 of Figure 3.7b. Two advantages of a pusher configuration are:

1. Less cabin noise because the propellers are behind the cabin.
2. Pusher propellers are stabilizing in longitudinal and directional stability: this can lead to savings in tail area and thus in drag and weight.

3.5.2 Jet Transport

For easy future reference this jet transport will be named the 'Ourania', after the Greek muse of astronomy.

Step 3.1: By definition, the Ourania falls in category 7 of those listed on p.28. Figures 3.19 - 3.21 present twelve 3-views of airplanes in this category.

Steps 3.2 and 3.3: To save space, these steps are not presented in detail.

The following tabulation compares the Ourania with several competitors. These data are taken from sub-section 2.6.2 in Part I.

Airplane Type	W_{TO} (lbs)	W_{TO} (lbs)	$V_{cr_{max}}$ (kts)	Range (nm)
Boeing 737-200	35,000	135,000	460	1,620
McDD DC9-80	38,000	140,000	M=.8	2,000
Airbus A320	42,000	145,000	450	2,700
Ourania	30,750	127,000	473	1,500

Step 3.4: The following configurations are suitable candidates for the Ourania:

*conventional *canard or tandem *three surface
*joined wing

The flying wing is not considered suitable because of packaging problems with passengers and baggage. Access would have to be from the leading edge or via stairways from below. Sealing access door on the leading edge might be a problem. Servicing access from below is not compatible with existing servicing equipment.

The other configuration candidates should be evaluated against each other. The red, white and blue team approach would have to be employed.

Step 3.5: For reasons of conservatism a conventional configuration will be selected for the Ourania. However, the airplane will be designed for relaxed static stability and will employ a digital fly-by-wire primary flight control system. This, to save weight and wetted area.

3.5.3 Fighter

For easy future reference the fighter will be given the name of Eris, goddess of war in greek mythology.

Step 3.1: The Eris belongs to category 9 of the airplane categories listed on p.28. Figures 3.25 - 3.27 present twelve 3-views of airplanes in this category.

Steps 3.2 and 3.3: To save space these steps are not presented in detail.

The following tabulation compares the Eris with several competitors. All data are those from Part I, sub-section 2.6.3.

Airplane Type	W_{PL} (lbs)	W_{TO} (lbs)	V_{max} (kts)	Range (nm)
F.R. A10A	15,000	50,000	450	540
Grumman A6	17,000	60,400	689	1,700
Tornado F.Mk2	16,000	58,400	600*	750
Eris	12,000	64,500	400*	800*

*with external stores

Step 3.4: The following configurations are suitable for the Eris:

*conventional *flying wing *canard or tandem
*three surface *joined wing

None of these configurations can be ruled out.

The flying wing is attractive because of its obvious stealth qualities. Experience with the B35 and YB49 flying wing bombers (See Figures 3.50 and 3.51) indicated that these airplanes were very difficult to detect on the radars of their era.

The joined wing may present a problem in this regard. However, by making the joined wing out of composites a very small radar cross section should be obtainable. The proposed joined wing configuration of Figure 3.45 does represent an attractive possibility for an attack fighter.

Since there is no requirement for transonic/supersonic performance, a three surface layout like that of the X29 (See Fig.3.46) may not be appropriate.

That leaves the canard and the conventional layout. Because an attack fighter must have excellent forward visibility a canard configuration could present some problems. This would have to be verified before accepting or rejecting the canard in this case.

Step 3.5: The conventional layout with engines buried in the fuselage, a triangular fuselage cross section (for stealth) and a twin boom tail arrangement will be selected for the Eris. Figure 3.61 shows an example of a british fighter which employed this type of layout.

The airplane will be designed for negative inherent stability. It will employ a digital FBW flight control system. This should save on wetted area as well as on trim drag.

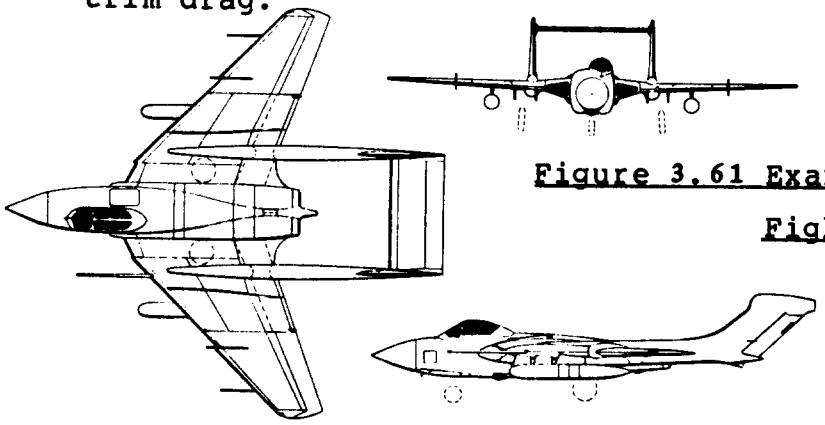

Figure 3.61 Example of a Twin Boom Fighter Airplane

4. DESIGN OF COCKPIT AND FUSELAGE LAYOUTS

The purpose of this chapter is to provide a step-by-step guide to the preparation of cockpit and fuselage layouts so that the mission requirements in terms of crew, passengers and payload are met.

For military airplanes this includes the necessary weapons and stores layouts on the fuselage.

The method is presented as part of Step 4 in p.d. sequence I as outlined in Chapter 2.

Section 4.1 presents the step-by-step guide. Example applications are contained in Section 4.2.

4.1 A PROCEDURE FOR THE DESIGN OF COCKPIT AND FUSELAGE LAYOUTS

Step 4.1: Referring to the mission specification, make a list of crew, payload and operational items which need to be located in the fuselage.

Note that this step assumes that the overall configuration is not a flying wing.

Typical items to be included on this list are:

1. number and weight of cockpit crew members
2. number and weight of cabin crew members
3. number and weight of 'special duty' crew members (such as radar and systems operators
4. number and weight of passengers
5. weight and volume of 'carry-on' baggage
6. weight and volume of 'check-in' baggage
7. weight and volume of cargo
8. number, weight and size of cargo containers
9. weight and volume of 'special operational equipment' (such as sensor and computer equipment required by patrol airplanes)
10. weight and volume of military payload (such as: guns, stores, bombs, torpedoes, missiles etc.)
11. weight and volume of fuel carried in fuselage
12. radar equipment
13. auxiliary power unit (APU)
14. beaching requirements such as in the case of flying boats

Step 4.2: Translate the list obtained in Step 4.1 into a dimensioned drawing of a proposed cabin interior layout.

This step includes making a decision on the size and shape of the fuselage cross section to be used, the location of the cabin floor in that cross section and a check of volumetric requirements imposed by any of the items 1-14 in Step 4.1. Part III (Ref.2) contains detailed information on cabin and fuselage layouts used by a number of existing airplanes.

This step involves the definition of access doors, hatches and emergency exits. Depending on the certification base of the airplane, there are very definite minimum requirements for size, placement and number of exits which need to be provided. Part III contains detailed information on these important items.

In passenger/troop transport airplanes and in business airplanes it is important to consider carefully the following choices:

1. Number of persons abreast
2. Number and size of aisles
3. Type of seating to be employed: first class, business class, tourist class or economy class
4. Cabin provisions required in terms of: closets, toilets, overhead storage compartments, galleys
5. Seating provisions for the cabin crew

Part III contains data on all these items.

In certain cargo airplanes there may be a requirement for loading and off-loading from both ends of the fuselage. This usually requires large doors and ramps. These items can dominate the fuselage design of such airplanes and need detailed attention in terms of the structural layout. How to prepare an initial structural layout is discussed in Part III.

In many military applications it is necessary to account for the installation of guns, ammo containers, missiles and other weapons. Data on sizes and volumes for such military items are also included in Part III.

Step 4.3: Add the appropriate distances to the cabin interior layout of Step 4.2, to allow for the required structural depth for fuselage frames, fuselage bulkheads and fuselage skins.

Typical distances which allow for sufficient structural depth are:

for small commercial airplanes: 1.5 inches
for fighters and trainers: 2 inches
for large transports: $0.02d_f$ + 1 inch

Step 4.4: Finish the exterior lines which define the cabin part of the fuselage.

Step 4.5: Translate the cockpit crew requirement into a dimensioned drawing of the cockpit.

Part III (Ref.2) contains detailed data with which civil and military cockpits can be laid out while observing typical requirements for pilot visibility and for pilot ability to reach the essential cockpit controls.

Make certain that the aerodynamic 'fairing' of the cockpit exterior into the fuselage exterior causes as little extra drag as possible.

Step 4.6: Prepare a dimensioned drawing of the entire fuselage, including the rear fuselage cone.

Figure 4.1 defines several important geometric parameters for the fuselage. Table 4.1 shows ranges of these parameters which are currently employed. Unless there is a good reason, these ranges should not be exceeded.

The fuselage cone is normally a smooth transition from the maximum fuselage cross section to the 'end' of the fuselage. When the 'fineness ratio' of this cone is too low, there will be a large base drag penalty although the fuselage weight may be reduced. When the 'fineness ratio' of this cone is too large, there will be a large friction drag penalty as well as a large weight penalty.

It will be obvious to the reader, that a long fuselage cone tends to increase the tail moment arm thereby reducing required tail area and vice versa.

The decision on the fuselage cone fineness ratio is therefore one that involves a number of trade-offs.

Caution 1. The geometry of the fuselage cone can also have an impact on the ability of the airplane to

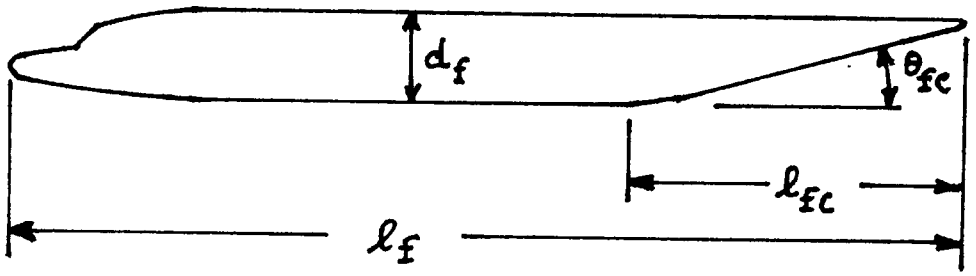

Figure 4.1 Definition of Geometric Fuselage Parameters

Table 4.1 Currently Used Geometric Fuselage Parameters

Airplane Type	l_f/d_f	l_{fc}/d_f	θ_{fc} (deg)
Homebuilts	4 - 8	3*	2 - 9
Single Engine	5 - 8	3 - 4	3 - 9
Twins	3.6** - 8	2.6 - 4	6 - 13
Agricultural	5 - 8	3 - 4	1 - 7
Business Jets	7 - 9.5	2.5 - 5	6 - 11
Regionals	5.6 - 10	2 - 4	15 - 19***
Jet Transports	6.8 - 11.5	2.6 - 4	11 - 16
Mil. Trainers	5.4 - 7.5	3*	up to 14
Fighters	7 - 11	3 - 5*	0 - 8
Mil. Transports, Bombers and Patrol Airplanes	6 - 13	2.5 - 6	7 - 25****
Flying Boats	6 - 11	3 - 6	8 - 14
Supersonics	12 - 25	6 - 8	2 - 9

*Tailcone as defined by Figure 4.1 not easily defined
**Cessna 336 (Fig.3.9c) ***Embraer Brasilia (Fig.3.16d)
****Lockheed Hercules (Fig.3.29d)

rotate about its rear gear during take-off. Make sure that the selected cone geometry does not interfere with take-off rotation.

Table 4.1 shows ranges of rear fuselage angles used on existing airplanes.

Caution 2. In the case of twin boom configurations, the fuselage tends to have a rather small fineness ratio. Examples are the AW Argosy (Ref.14, Section 14.2) and the Fairchild C-119 (Ref.29, Section 14.2). These airplanes all experienced high drag due to the fuselage configuration. The obvious trade-off between a larger fineness ratio for the fuselage to reduce drag and the greater weight caused by such a larger fineness ratio will have to be established and a decision made.

Caution 3. In the case of flying boats it is essential that the lower part of the fuselage (called hull) has the 'correct' hydrodynamic lines. The reader should refer to Part III for data on these shapes.

Step 4.7: Document the decisions made under steps 4.1 - 4.6 in a brief descriptive report including clear, dimensioned drawings.

One of these drawings should be a so-called 'inboard profile'. Examples of inboard profiles may be found in Part III.

4.2 EXAMPLE APPLICATIONS

Three example applications will be presented:

4.2.1 Twin Engine Propeller Driven Airplane: Selene
4.2.2 Jet Transport: Ourania
4.2.3 Fighter: Eris

The applications are all presented in accordance with the Step 4.1 through Step 4.7 sequence presented in Section 4.1.

4.2.1 Twin Engine Propeller Driven Airplane

Step 4.1: Table 2.17 of Part I defines the mission of the Selene. The following items from Table 2.17 need to be carried in the fuselage:

1. Six passengers (this includes the pilot)
2. 200 lbs of luggage

The mission specification does not stipulate the required baggage volume. Comparison with competitive airplanes (Ref.8) shows that a baggage volume of 40 cubic would be acceptable.

Step 4.2: A two abreast layout is selected for the Selene. This type of layout is common to most airplanes in this category. Two cockpit seats and four cabin seats are therefore required, for a total of three rows.

The selection of cabin cross section is critical to passenger comfort and to weight and wetted area. Looking at the fuselage cross sections for this type of airplane in Part III shows most of them to be rather flat sided. For an unpressurized fuselage that is acceptable. It also is easy to manufacture. For a pressurized fuselage the perfect cross section would be circular. The reader should try and prepare a layout of a circular cross section for the Selene. Because of the human anatomy it will be discovered that the fuselage will become rather bulky. This is another reason why the fuselage cross section of most smaller general aviation airplanes is more or less rectangular.

Since it is forseen that future versions of the Selene will have to be pressurized, the double circle cross section of Figure 4.2a was selected. Note the slab sides which connect the two circles. The internal cabin dimensions of the Selene were selected after comparison with four competitors:

Airplane Type	Internal cabin dimensions in ft		
	Length	Max. Width	Max. Height
Beech Duke	11.8	4.2	4.3
Beech Baron M58	12.6	3.5	4.2
Cessna T303	13.6	4.0	4.0
Piper PA-44-180	8.0	3.5	4.0
Selene	18.5	4.25	4.4

Most cabin type twins have an access door in the rear. Because Selene will be configured as a high wing pusher with the propellers behind the wing trailing edge, a rear access door would be awkward: the propellers are to close to the door. Therefore, the cabin access door will be located directly behind the pilot on the left side. This arrangement is also used in several business jets. Figure 4.2b shows the proposed interior arrangement of the cabin.

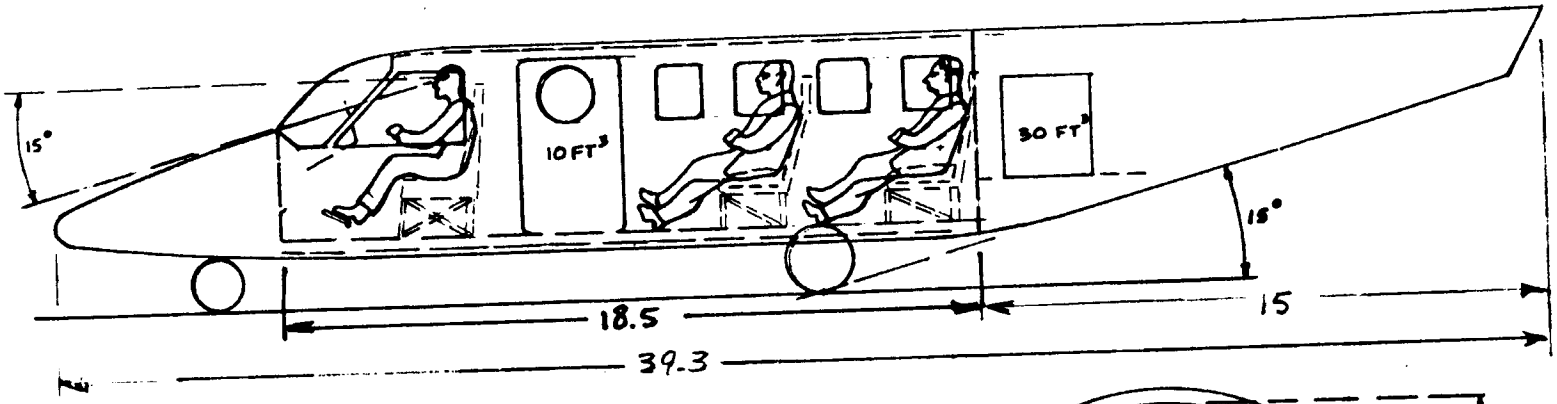

Figure 4.2b Selene: General Arrangement of the Fuselage

ALL DIMENSIONS IN FT.
DO NOT SCALE

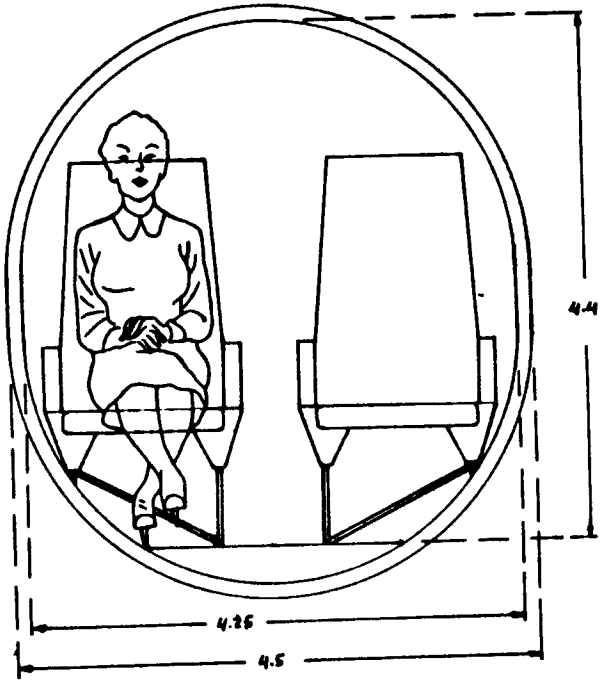

Figure 4.2a Selene: Cabin Cross Section

Step 4.3: Figure 4.2a also shows the proposed structural depth of 1.5 inches.

Steps 4.4 and 4.5: Figure 4.2b shows the general arrangement of the cockpit and the fairing into the exterior lines of the cabin. Note the 15 degree 'over the nose' visibility.

Step 4.6: Figure 4.2b shows the rear fuselage cone. The up-slope of the bottom of the cone is 15 degrees. This is consistent with attached flow and with the requirement for take-off rotation. The length of the cone was selected so that a fineness ratio of 2.7 resulted. The overall fuselage fineness ratio is 7.2. These numbers are consistent with those of Table 4.1.

Step 4.7: To save space this step is omitted. Example inboard profiles for several airplanes are presented in Part III.

4.2.2 Jet Transport

Step 4.1: Table 2.18 of Part I defines the mission of the Ourania. The following items from Table 2.18 must be carried in the fuselage:

1. 150 passengers
2. 150x30 = 4,500 lbs of luggage
3. flight deck crew of two + three cabin attendants
4. 5x30 = 150 lbs of luggage for the crew

There is no specific requirement for cargo containers. It will be assumed, that the total of 4,650 lbs of luggage will be carried in containers located below the cabin floor. Typical luggage density is 12.5 lbs/ft^3. This yields a requirement for 372 ft^3 of baggage volume. Because of the large number of 727's and 737's which are in airline service, interchangeability of cargo containers with these airplanes is felt to be desirable. Typical Boeing 727 belly containers have a volumetric capacity of about 80 ft^3. Therefore five such containers will be necessary.

Data on cargo and luggage containers may be found in Part III.

Step 4.2: According to Ref.8, comparable airplanes to the Ourania have five or six abreast seating. A

circular fuselage cross section is required to keep the weight of the pressurized shell down.

Five abreast seating results in 30 seat rows.
Six abreast seating results in 25 seat rows.

A future problem with a 5-abreast arrangement may be that any growth version will end up with a very long fuselage. This is one reason to opt for 6-abreast seating for the Ourania.

The next question to be decided is the seat and aisle width to be used. Part III contains detailed data on this subject. It is decided here to opt for the seats shown in Figure 4.3 with an aisle of 22 inches. Figure 4.4 shows the proposed seating/aisle arrangement. At this point a circle needs to be drawn such that the aisle height is reasonable and such that the shoulders of passengers seated in window seats do not touch the interior side wall. Figure 4.3 also shows the proposed interior circle.

Airline experience shows that an item high on the list of passenger preferences is easy to reach and liberally sized overhead storage. Figure 4.3 also shows the overhead storage.

The seat pitch needs to be selected next. Part III shows that a 34 inch seat pitch is reasonable for this type airplane. The cabin floor arrangement can now be drawn. Figure 4.5 shows the proposed floor arrangement. Note that provisions are made for door and emergency exits. Part III also contains data on the required number and size of doors and emergency exits in passenger airplanes.

Figure 4.5 also shows the proposed arrangement of galleys, toilets and wardrobes. Part III contains data on the dimensions of these items also.

The following data compare the cabin interior dimensions of the Ourania with those of three competitors:

Airplane Type	Seats Abreast	Internal cabin dimensions in ft Length	Max.Width	Max.Height
Boeing 737-300	6	68.5	11.5	7.2
McDD DC9-80	5	101	10.1	6.8
Airbus 320	6	NA	12.2	7.3
Ourania	6	76.6	12.4	7.5

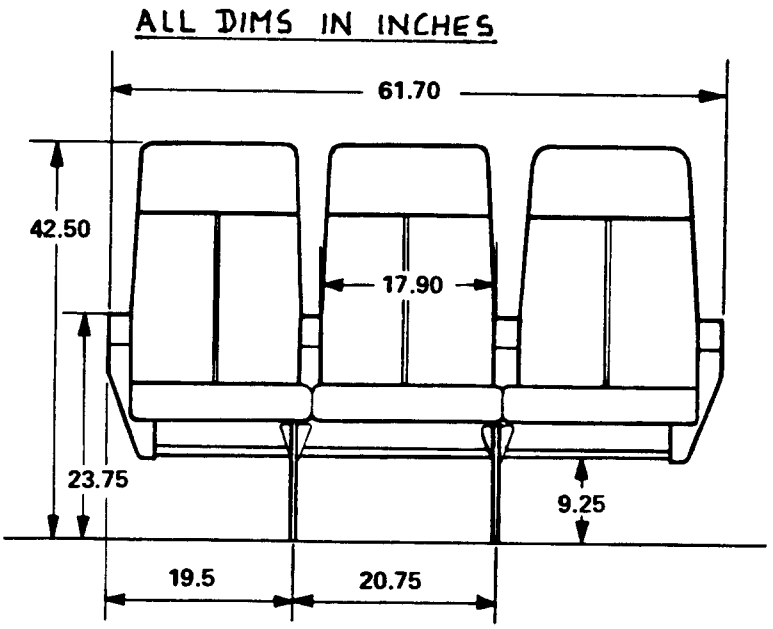

Figure 4.3 Ourania: Proposed Triple Seats

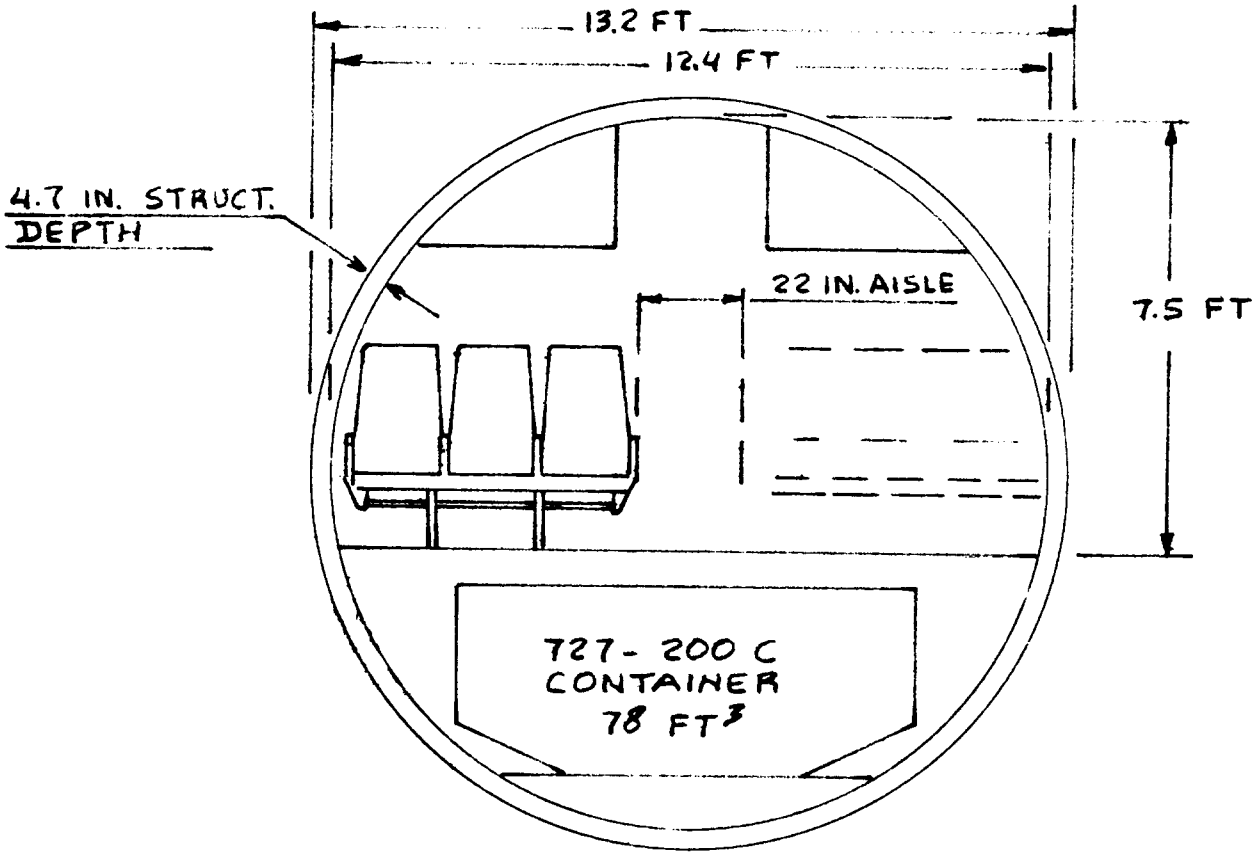

Figure 4.4 Ourania: Cabin Cross Section

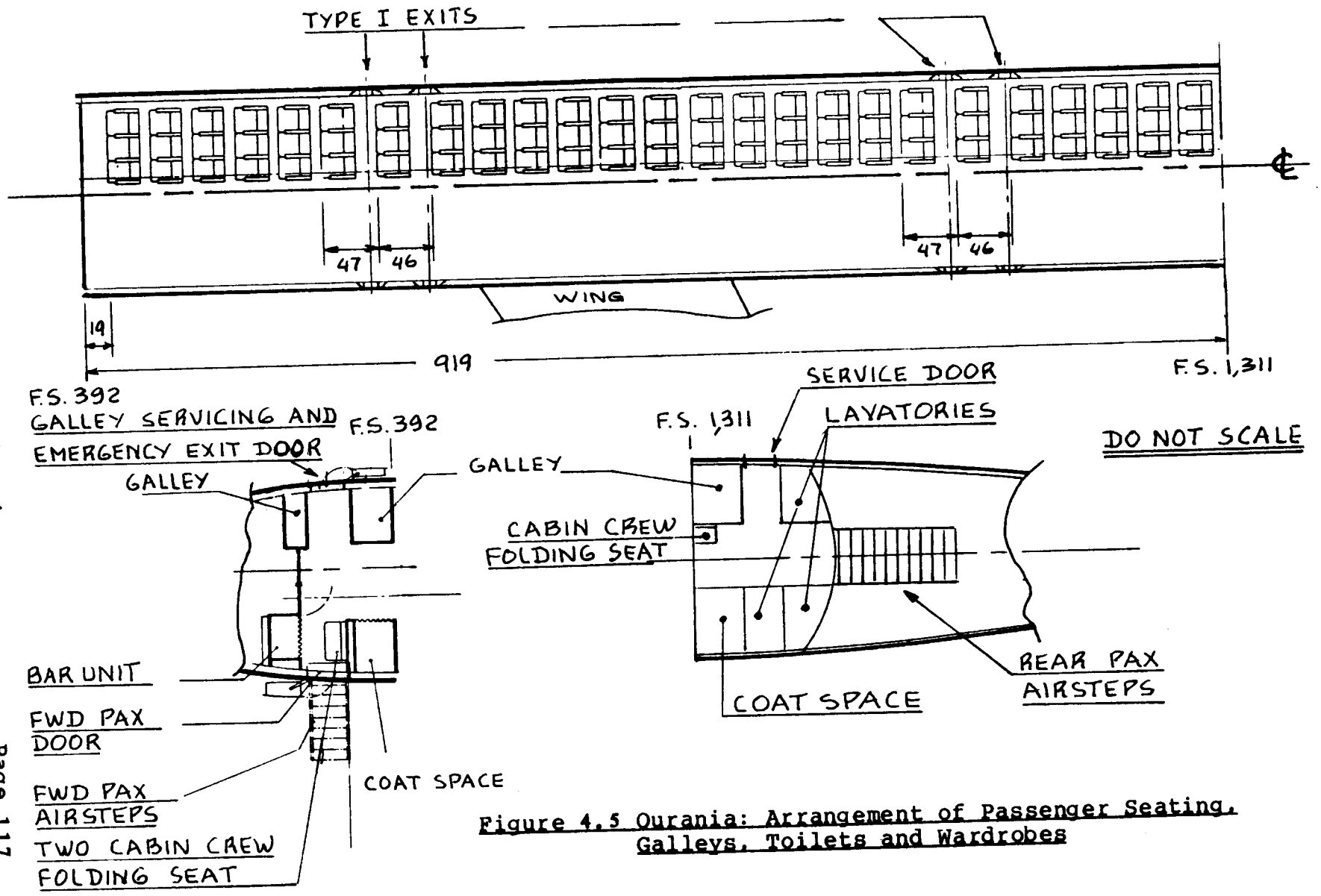

Figure 4.5 Ourania: Arrangement of Passenger Seating, Galleys, Toilets and Wardrobes

Step 4.3: Figure 4.4 also shows the exterior cross section. Note that the structural depth is 4.7 inches. This is consistent with the recommendation of Section 4.1, Step 4.3.

Step 4.4: Figure 4.5 also shows the exterior lines of the cabin.

Step 4.5: Figure 4.6 presents the proposed interior arrangement of the flight deck. Note the added seats for carrying 'check' pilots.

Figure 4.6 also shows that visibility from the cockpit is probably acceptable. To make sure a visibility pattern drawing needs to be made. Part III shows how to prepare such a visibility pattern.

Step 4.6: Figure 4.7 presents a dimensioned drawing of the entire fuselage. The rear fuselage cone has a fineness ratio of 3.5. The entire fuselage has a fineness ratio of 10.1. Note that these numbers are consistent with Table 4.1.

Step 4.7: To save space this step has been omitted. Part III contains example inboard profiles of several airplanes.

4.2.3 Fighter

Step 4.1: Table 2.19 of Part I defines the mission of the Eris. The following items need to be carried in the fuselage:

1. Pilot with ejection seat
2. GAU 8/A multi barrel cannon
3. Two engines

Item three is a result not of the mission specification but of the configuration choice made in sub-section 3.5.3.

Step 4.2 - 4.7: Because a fighter airplane needs to be tightly 'packed' to save weight, wetted area and volume it is not feasible to take these steps individually. Following is a description of how the proposed fuselage arrangement of the Eris was arrived at.

Figure 4.8 shows a dimensioned sketch of the GAU 8/A cannon and its ammunition container. Note the large size of this weapon. It is currently installed also in the

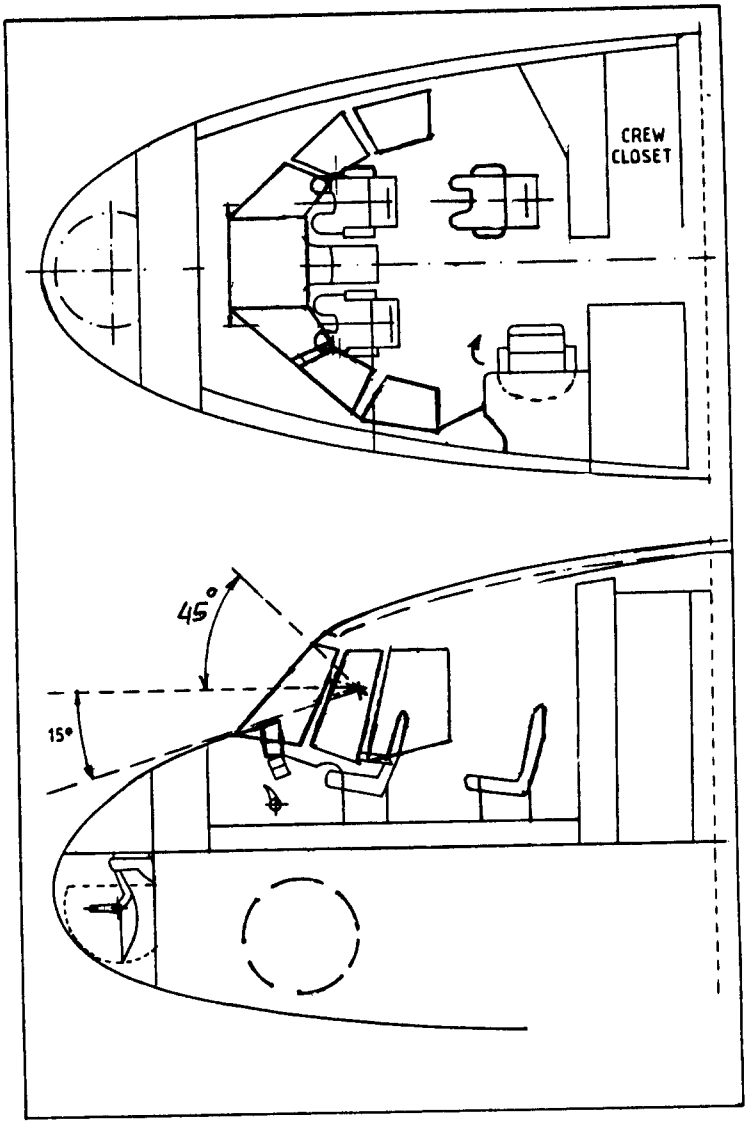

Figure 4.6 Ourania: Flight Deck Arrangement

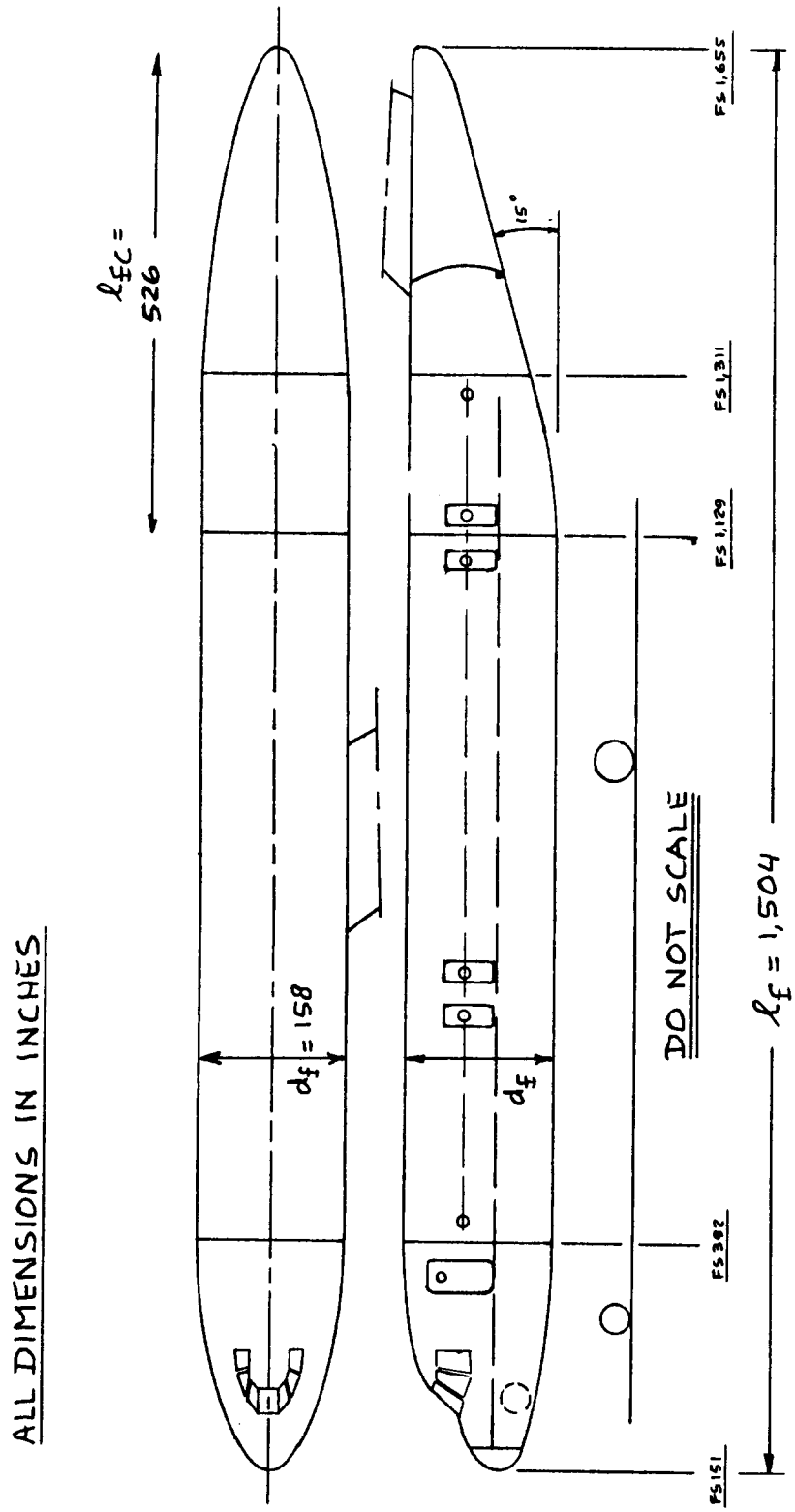

Figure 4.7 Ourania: General Arrangement of the Fuselage

Fairchild Republic A10 attack airplane.

Figure 3.61 shows the threeview of the DeHavilland DH110 SeaVixen. The overall configuration of this airplane is the one selected for the Eris. It can therefore be used as a guide.

To keep the length of the fuselage within reasonable bounds, the large ammo container will be placed behind the pilot. The cannon itself will be placed forward of and below the pilot. The nose gear will be retracted forward into the nose. Because nosegear and cannon compete for the same space, they will be separated laterally. This results in the cannon being on the right side and the nose gear on the left side.

The engines will be mounted as closely behind the ammo container as possible.

The wing torque box must pass through the fuselage above or below the ammo container. To reduce fuselage depth as much as possible it was decided to mount the wing on the fuselage above the ammo container. This results in a high wing configuration. In turn this forces the inlet ducts to be of the so-called 'armpit' type. A potential problem is that the exhaust gasses from the cannon can enter the inlets. To prevent this a special exhaust gas deflector is installed on the nose of the fuselage.

Figure 4.9 shows the proposed fuselage arrangement. Note the 15 degree downward visibility over the nose.

The mission specification of the Eris also calls for twenty 500 lbs bombs to be carried externally. It is decided to try the following arrangement:

8 bombs mounted conformally under the fuselage
12 bombs mounted in racks under the wings at the same spanwise station which carries the tail-booms.

Example inboard profiles for fighters and trainers are contained in Part III.

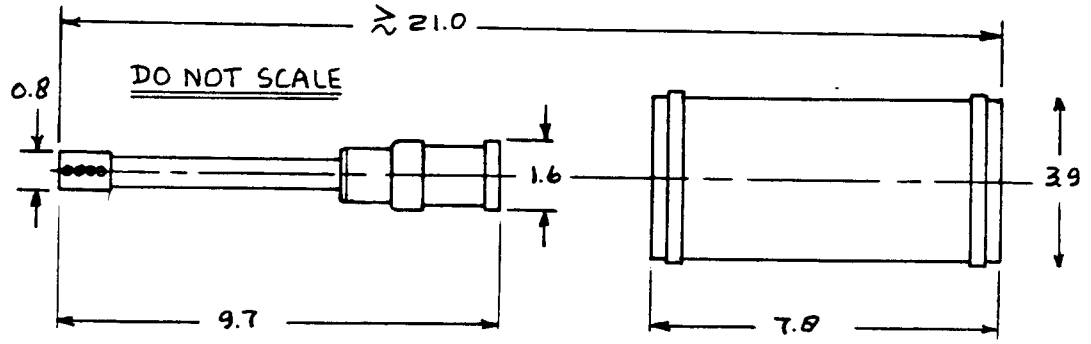

Figure 4.8 Eris: GAU 8/A Cannon Dimensions

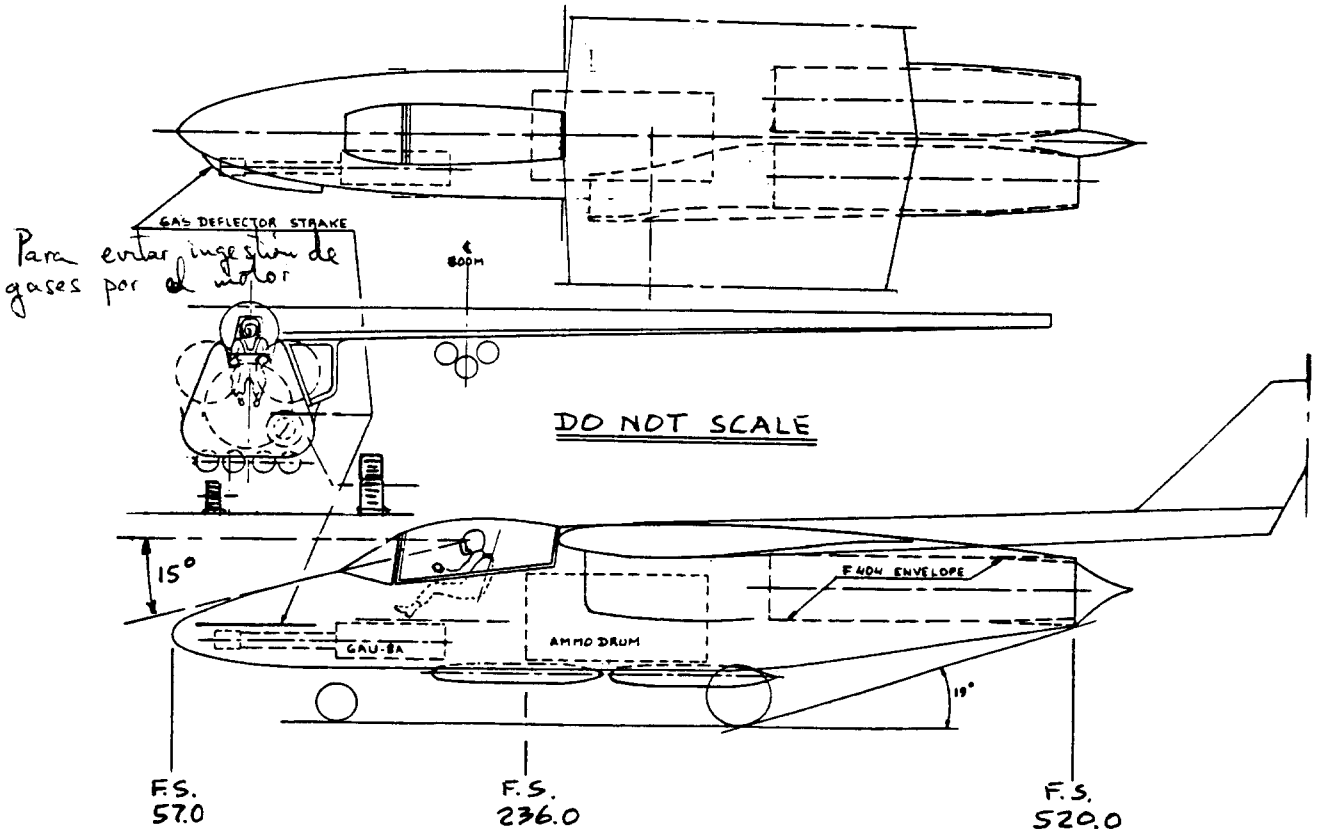

Figure 4.9 Eris: General Arrangement of the Fuselage

5. SELECTION AND INTEGRATION OF THE PROPULSION SYSTEM

The purpose of this chapter is to provide a guide to the selection and to the integration of the propulsion system. The method is presented as part of Step 5 in p.d. sequence I as outlined in Chapter 2.

Selection and integration of the propulsion system involves the following three decisons:

1. Selection of the propulsion system type or types.

2. Determination of the number of engines to be used and the power (or thrust) level of each.

3. Disposition of these engines, i.e. integration of these engines into the configuration.

Sections 5.1 through 5.3 address these decisions in a step-by-step manner. Example applications are discussed in Section 5.4

5.1 SELECTION OF PROPULSION SYSTEM TYPE

The following factors play a role in selecting the type of propulsion system to be used:

1. Required cruise speed and/or maximum speed
2. Required maximum operating altitude
3. Required range and range economy
4. FAR 36 noise regulations (applies to civil airplanes only)
5. Installed weight
6. Reliability and maintainability
7. Fuel amount needed
8. Fuel cost
9. Fuel availability
10. Specific customer or market demands
11. Timely certification

Overall fuel efficiency and installed weight often dominate the arguments pro and con a certain type of propulsion system. Figure 5.1 provides an overview of trends in propulsion system application as it relates to the flight envelope of airplanes. The data are based on 1985+ technology.

It is clear from Figure 5.1 that the flight envelope (speed-altitude envelope) of an airplane has an important bearing on the choice of the type of propulsion system.

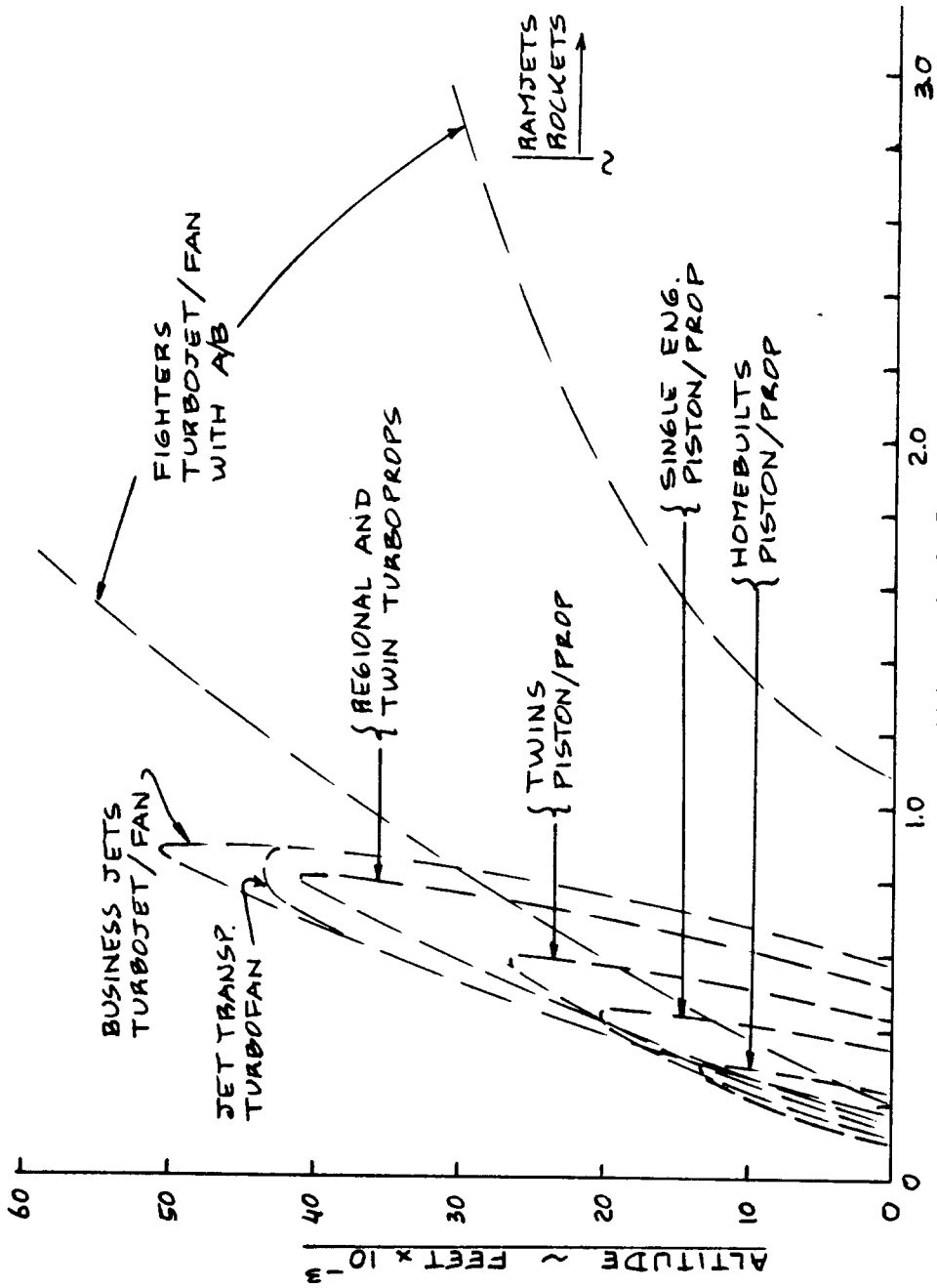

Figure 5.1 Engine Types Used in Relation to the Speed-Altitude Envelope of Airplanes

From a certification point of view (civil and military), only the following propulsion system types will be viable for application during the next 5-10 years:

1. Piston/propeller with or without supercharging
2. Turbo/propeller
3. Propfan
4. Unducted fan
5. Turbojet
6. Turbofan
7. Rocket
8. Ramjet

Propulsion types 1-4 can be expected to be offered with single as well as with contra rotating propellers and/or fans.

References 16 - 18 contain excellent discussions on the characteristics of these propulsion systems.

The following step-by-step procedure is suggested to arrive at a decision on the type(s) of propulsion system to be used:

Step 5.1: Check the mission specification for any definition of the type of powerplant required. Frequently the type of powerplant is specified in the mission specification. If so, proceed to Step 5.4. If not, proceed to Step 5.2.

Step 5.2: Draw a preliminary Speed (or Mach) versus Altitude envelope for the airplane.

This can usually be done from the preliminary sizing work described in Part I (Ref.1).

Step 5.3: Compare the airplane speed-altitude envelope with those of Figure 5.1 and decide which type of powerplant provides the best overall match.

Conventional wisdom says that it is undesirable to 'mix' different types of powerplant in one airplane. An important argument in favor of this standpoint is that different types of propulsion system call for different operating procedures. This certainly increases the crew workload which is not desirable.

Another argument if favor of this standpoint is that

maintenance will become more costly when different types of propulsion system are used in the same airplane.

While these arguments are certainly correct, there have been several successful deviations from this rule. Examples of such deviations are:

1. The Convair B36 bomber, which used six piston/propeller engines and four turbojet engines.

2. The DeHavilland Comet, which used rockets in addition to its four turbojet engines to improve the field performance at 'hot-and-high' airports.

3. The Lockheed P2V Neptune, which used two piston/propeller engines and two turbojet engines.

5.2 SELECTION OF THE NUMBER OF ENGINES AND THE POWER OR THRUST LEVEL PER ENGINE

The reader is reminded of the fact, that the total required power or thrust level required for take-off is already known from the preliminary sizing work done in Section 3.7 of Part I (Ref.1). The type of propulsion system was decided upon in Section 5.1, Step 5.3. What is needed now is a decision on the number of engines.

There are two possibilities at this point:

1. A new engine will be developed for the proposed design.

In this case, the engine(s) can be tailored to the existing design. The reader must be aware of the fact that the development and certification of a new powerplant is expensive and takes a long lead time. For new jet engines a typical lead time is 7-10 years.

2. An existing engine must be used.

Reference 8 provides data on existing aircraft engines. Because the power or thrust level of existing engines is basically 'frozen', the number of engines is determined by dividing the required take-off power or thrust level by an integer: usually 1,2,3 or 4. In the past more than four engines have been employed on a number of airplanes. The concensus today is that beyond four engines the problems of maintenance, rigging and failure probabilities become unacceptable. If in the future there is a requirement for very large airplanes, it may be that the cost of developing new, large engines

becomes prohibitive. Design studies performed by Lockheed and Boeing for such airplanes indicate thet in such cases more than four engines is again a reasonable solution.

Table 5.1 relates the numerical engine failure probability to the number of engines used.

Table 5.1 Relation Between Engine Failure Probability and the Number of Engines Used

Failure of:	1 Engine	2 Engines	3 Engines
Airplane with:			
two engines	$^{2}P_{ef}$	P_{ef}^{2}	not appl.
three engines	$^{3}P_{ef}$	$^{3}P_{ef}^{2}$	P_{ef}^{3}
four engines	$^{4}P_{ef}$	$^{6}P_{ef}^{2}$	$^{4}P_{ef}^{3}$

Conventional wisdom says that it is not desirable to use engines of differing power (or thrust) levels in one airplane. The main arguments for this position are the same arguments advanced in Section 5.1 for not using more than one type of powerplant.

While these arguments are generally correct, there have been several instances of successful deviations from this rule as well. Examples of such deviations are:

1. The DeHavilland 121 Trident IIIE which uses four jet engines, three large, one small. The fourth smaller engine was added to allow for higher take-off weights and to do so with minimum development and production cost.

2. Rutan's Voyager, which uses two piston/propeller engines of different power output. Because of the extreme range requirement placed on this airplane it was important to match best fuel consumption to power required. In this application, the solution of two different power levels was a sensible one.

In many instances the mission specification will define how many power plants are to be used. If this is not the case, the following step-by-step procedure may be followed:

Step 5.4: Determine the maximum power (or thrust) requirement for the airplane.

The reader is reminded of the fact that the maximum

power, P_{TO} (or thrust, T_{TO}) requirement was already established from the preliminary sizing work outlined in Section 3.7, Part I (Ref.1).

Step 5.5: Decide on the number of engines and on the specific engine model to be used.

The number of engines to be used in an airplane is often specified in the mission specification. If this is not the case, make a list of candidate engines which are available on the market. This information can be found in Reference 8 or in brochures from engine manufacturers.

The power (or thrust) levels of the candidate engine should be as close as possible to the take-off power (or thrust) levels divided by an integer. Don't worry about being off the mark by +/- 10 percent: the sizing calculations of Part I have the same accuracy.

Step 5.6: If the airplane being designed is a propeller driven airplane, determine the required propeller diameter and the number of propeller blades with the following Class I method:

Tables 5.2, 5.3 and 5.4 list typical take-off power and propeller data for six types of airplanes. Note that the so-called 'blade-power-loading' number, P_{bl} is within a certain range for these four types of airplanes.

By assuming a suitable value for P_{bl} and for the number of blades, n_p, it is possible to determine the propeller diameter from:

$$D_p = \{4P_{max}/(\pi n_p P_{bl})\}^{1/2} \qquad (5.1)$$

5.3 INTEGRATION OF THE PROPULSION SYSTEM

Having decided on the type and the number of engines to be employed, the next decision is: where should these engines be located?

As may be seen from the configurations presented in Chapter 3, the number of possible arrangements is very large indeed. The following factors play a role in deciding on the engine disposition:

Table 5.2 Relation Between Max. Engine Power, Propeller Diameter and Number of Propeller Blades for Homebuilts and for Single Engine FAR23 Certified Airplanes

Airplane Type	Prop. Pitch	Max. Power per Engine, P_{max}, hp	Prop. Diam., D_p, ft	Number of Prop. Blades, n_p,	Power Loading per Blade, P_{bl}, hp/ft^2
Homebuilts					
Jurca MJ5	Fixed	115	6.1	2	2.0
Piel CP1320	Fixed	160	5.9	2	2.9
Piel CP80	Fixed	90	5.0	2	2.3
Pottier P70S	Fixed	60	4.3	2	2.1
Pazmany PL4A	Fixed	50	5.7	2	1.0
Variviggen	Fixed	150	5.8	2	2.8
Rand/R KR-1	2-pos.	90	4.4	2	3.0
Van's RV-3	Fixed	125	5.7	2	2.5
Sequoia F8L	Fixed	135	6.2	2	2.2
Per. Osprey II	Fixed	150	5.5	2	3.2
				P_{bl} range:	1.0-3.2
Single Engine FAR23 Certified					
CESSNA					
152	Fixed	108	5.8	2	2.0
Skyhawk	Fixed	160	6.3	2	2.6
Skylane	C.Spd	230	6.8	2	3.2
Skywagon (185)	C.Spd	300	6.7	3	2.8
Caravan I	C.Spd	600	8.3	3	3.7
BEECH					
V35B Bonanza	C.Spd	285	7.0	2	3.7
38P Lightning	C.Spd	550	7.7	3	3.9
PIPER					
PA28 Warrior II	Fixed	160	6.2	2	2.6
Mooney 201	C.Spd	200	6.2	2	3.3
Mooney 301	C.Spd	360	6.5	3	3.6
				P_{bl} range:	2.0-3.9

Note: $P_{bl} = 4P_{max}/\pi n_p D_p^2$

Table 5.3 Relation Between Max. Engine Power, Propeller Diameter and Number of Propeller Blades for Agricultural Airplanes and for Military Propeller Driven Trainers

Airplane Type	Prop. Pitch	Max. Power per Engine, P_{max}, hp	Prop. Diam., D_p, ft	Number of Prop. Blades, n_p,	Power Loading per Blade, P_{bl}, hp/ft^2
Agricultural Airplanes					
Schweiz. AgCat	C.Spd	750	9.0	2	5.9
Airtruk PL12	C.Spd	300	7.3	2	3.6
EMB 201A	C.Spd	300	7.0	2	3.9
PZL-104	C.Spd	260	8.7	2	2.2
PZL-106A	C.Spd	592	8.6	4	2.5
PZL-M18A	C.Spd	1,000	10.8	4	2.7
NDN Fieldmaster	C.Spd	750	8.8	3	4.1
Cessna AgTruck	C.Spd	300	7.2	2	3.7
Air Tr. AT-301A	C.Spd	600	9.1	2	4.6
Ayr. Thrush S2R	C.Spd	600	9.0	2	4.7
				P_{bl} range:	2.2-5.9
Military Propeller Driven Trainers					
EMB 312 Tucano	C.Spd	750	7.8	3	5.2
Indaer Pillan	C.Spd	300	6.3	3	3.2
Aerosp. Epsilon	C.Spd	300	6.5	2	4.5
RFB 600 Fantr.	C.Spd	420	4.0	5*	6.7
SM SF-260	C.Spd	260	6.3	2	4.2
FFA AS32T	C.Spd	420	7.2	3	3.4
Pilatus PC-7	C.Spd	650	7.8	3	4.5
NDN-1 Firecr.	C.Spd	260	6.3	3	2.8
NDN-1T Firecr.	C.Spd	715	7.0	3	6.2
Beech T34C	C.Spd	715	7.5	3	5.4
				P_{bl} range:	2.8-6.7

Note: $P_{bl} = 4P_{max}/\pi n_p D_p^2$

*This airplane has a ducted fan instead of a propeller

Table 5.4 Relation Between Max. Engine Power, Propeller Diameter and Number of Propeller Blades for Twin Engine FAR23 and for Regional Turbopropeller Driven Airplanes

Airplane Type	Prop. Pitch	Max. Power per Engine, P_{max}, hp	Prop. Diam., D_p, ft	Number of Prop. Blades, n_p,	Power Loading per Blade, P_{bl}, hp/ft^2
Twin Engine FAR23 Certified Airplanes					
PIPER					
PA-31 Navajo	C.Spd	325	6.7	3	3.1
PA-31T Chey. II	C.Spd	620	7.8	3	4.3
CESSNA					
T303	C.Spd	250	6.2	3	2.8
340A	C.Spd	310	6.4	3	3.2
Conquest I	C.Spd	450	7.8	3	3.1
Conquest II	C.Spd	636	7.5	3	4.8
BEECH					
Baron 95-B55	C.Spd	260	6.5	2	3.9
Duke B60	C.Spd	380	6.2	3	4.2
King Air C90-1	C.Spd	550	7.8	3	3.8
BN2B Islander	C.Spd	260	6.5	2	3.9
				P_{bl} range:	2.8-4.8
Regional Turbopropeller Driven Airplanes					
EMB-110 Bandar.	C.Spd	750	7.8	3	5.2
EMB-120 Brasil.	C.Spd	1,500	10.5	4	4.3
SF-340	C.Spd	1,630	10.5	4	4.7
Fokker F27-200	C.Spd	2,140	11.5	4	5.2
Brit.Aer. 748	C.Spd	2,280	12.0	4	5.0
Casa Nurt. 235	C.Spd	1,700	10.8	4	4.6
Beech C99	C.Spd	715	7.8	3	5.0
Beech 1900	C.Spd	1,100	9.1	4	4.2
ATR-42	C.Spd	1,800	13.0	4	3.4
IAI Arava 201	C.Spd	750	8.5	3	4.4
				P_{bl} range:	3.4-5.2

Note: $P_{bl} = 4P_{max}/\pi n_p D_p^2$

1. Effect of power changes or power failures on stability and control: longitudinal, lateral and directional. The vertical and/or lateral location of the thrustline(s) are critically important in this respect.

2. Drag of the proposed installation.

3. Weight and balance consequences of the proposed installation.

4. Inlet requirements and resulting effect on 'installed' power and efficiciency.

5. Accessibility and maintainability.

The following step-by-step procedure is offered as a guide in deciding on the integration of the propulsion system:

Step 5.7: Decide on a pusher, a tractor or a mixed installation.

As a general rule, when the propeller or inlet plane is forward of the c.g., the installation is referred to as a tractor installation. When the propeller or the inlet plane is located behind the c.g. the installation is referred to as a pusher installation.

Tractor installations tend to be destabilizing while pusher installations tend to be stabilizing in both static longitudinal and static directional stability. This feature can be used to save some empennage area in pusher installations.

Methods for computing these effects are discussed in Parts VI and VII (Refs 5 and 6).

If it is decided to go with a pusher propeller installation with the propeller behind the trailing edge of the wing (such as the airplanes of Figures 3.42 and 3.47), make certain that the distance between the wing trailing edge and the propeller plane is at least one half the local wing chord. This is to alleviate dynamic excitation of the propeller blades by the wing vortex system.

Step 5.8: Decide on mounting the engines on:

a. the wing
b. the fuselage
c. the empennage
d. any combination of a through c.

The reader should again refer to the configuration discussions in Sections 3.1 and 3.2.

Before deciding where to mount the engines, refer to the factors 1-5 listed at the beginning of this section and carefully consider the various trade-offs involved. Document all decisions and list the reasons for and/or against.

In the case of propeller installations it is highly desirable to maintain a clearance between the propeller tips and the fuselage of 20 - 40 inches, depending on the blade power loading and on the propeller tipspeed. This clearance is necessary to avoid acoustic fatigue of the adjacent structure and to avoid excessive noise entering the cabin.

In the case of jet engines, make sure that no primary structure is placed too close to exhaust gases.

Step 5.9: Obtain the necessary information on:

1. engine geometry and clearance envelope
2. engine mounting (attachment) points
3. engine air-ducting requirements
4. engine thrust reversing requirements
5. engine exhaust system requirements
6. engine accessory requirements
7. engine c.g. location
8. engine firewall requirements
9. in the case of a propeller/pusher installation, verify that the propeller thrust bearings are suitable for a pusher installation.
10. engine inlet requirements can play a major role in the layout of those jet engine installations where long inlets are needed. This is the case in many 'buried' installations.
11. for supersonic airplanes a variable geometry inlet duct is often required.

The reader should refer to Part III for more details on engine installations.

Items 1 - 9 are normally obtained directly from the engine manufacturer.

Step 5.10: Make dimensioned drawings of all engine installations required by your airplane.

These drawings should identify the engine envelope, nacelle envelope and any required inlet ducts. Example engine installations are shown in Part III.

Step 5.11: Make certain that the proposed engine installations are compatible with such requirements as:

1. acceptable FOD characteristics
2. geometric clearance when static on the ramp: no nacelle or propeller tip may touch the ground with deflated landing gear struts and tires
3. geometric clearance during take-off rotation: no scraping of nacelles or of propeller tips is allowed, with deflated landing gear struts and tires
4. geometric clearance during a low speed approach with a five degree bank angle
5. no gun exhaust gasses may enter the inlet a jet engine. Such gun exhaust gasses are highly corrosive to fan, compressor and turbine blades.

Step 5.12: Draw the engine installation in the threeview. The amount of detail here depends on the type of threeview being drawn.

The reader should refer to Part III for more details on engine installations.

Step 5.13: Document the decisions made in Steps 5.1 through 5.11 in a brief, descriptive report. Include clear, dimensioned drawings where applicable.

5.4 EXAMPLE APPLICATIONS

Three example applications will be presented:

5.4.1 Twin Engine Propeller Driven Airplane: Selene
5.4.2 Jet Transport: Ourania
5.4.3 Fighter: Eris

The applications are all presented in accordance with the Step 5.1 through Step 5.13 sequence as presented in Sections 5.1 through 5.3.

5.4.1 Twin Engine Propeller Driven Airplane

Step 5.1: The mission specification of Table 2.17 in Part I specifies that two piston engine/propeller combinations are to be used.

Note: Steps 5.2 and 5.3 can be omitted. They are presented here as a help to the reader.

Step 5.2: Figure 5.2 shows the preliminary speed-altitude envelope of the Selene. All necessary data were taken from Part I.

Step 5.3: Comparison of Figure 5.2 with Figure 5.1 shows that the piston/propeller combination is an acceptable choice for the Selene.

Step 5.4: The maximum take-off power required for the Selene was determined to be P_{TO} = 898 hp, according to the matching results of page 178, Part I.

Step 5.5: The number of engines was specified as: two, in Table 2.17, Part I. Per engine, a maximum power level of 898/2 = 449 hp is therefore required.
Consulting with Ref.8 (1983-84), the following engines are available with roughly this power level:

1. AVCO-Lycoming TIGO-541-E1A, with 425 maximum hp output from sealevel to 15,000 ft (supercharged) and a dry weight of 700 lbs.
2. Teledyne-Continental GTSIO-520-F,K with 435 maximum hp output from sealevel to 11,000 ft (supercharged) and a dry weight of 502 lbs.

An arbitrary decision was made to use the AVCO-Lycoming engine. This engine is 24 hp short of the required power. However, the accuracy of the sizing calculations in Part I is such that this difference can

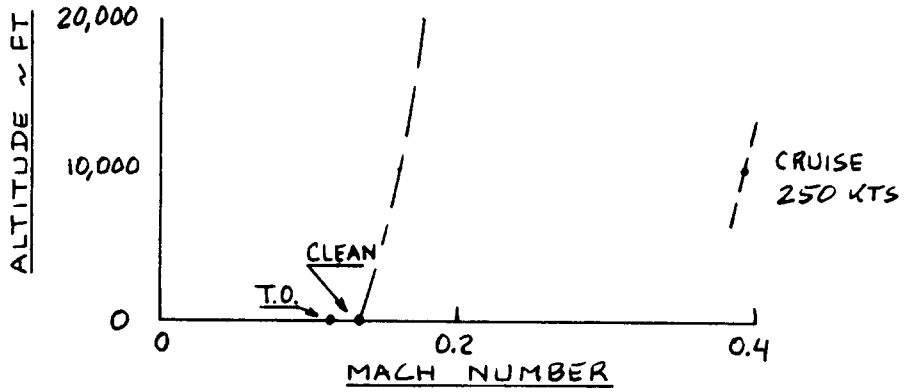

Figure 5.2 Selene: Preliminary Speed-Altitude Envelope

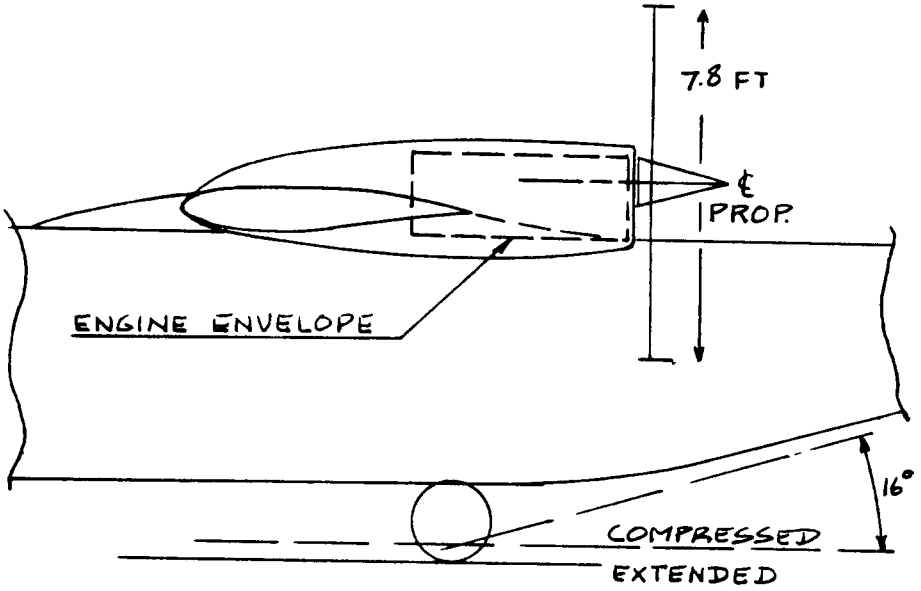

Cuidar el flujo de aire para refrig. del mot Puede imponer resistencia ali

Figure 5.3 Selene: Preliminary Engine Installation

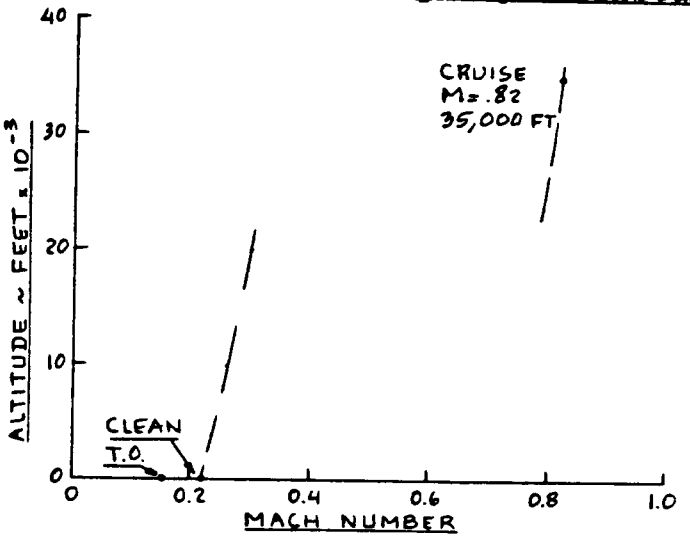

Figure 5.4 Qurania: Preliminary Speed-Altitude Envelope

be safely disregarded at this stage of the design process.

Step 5.6: Table 5.3 shows that for twins three blades per propeller are normal: therefore $n_p = 3$. For the power loading per blade a value of $P_{bl} = 3.0$ will be selected. With Eqn.(5.1) it is found that $D_p = 7.8$ ft.

Step 5.7: It was already decided in Step 3.5, that a pusher configuration was to be selected.

Step 5.8: In Step 3.5 it was decided to mount the engines in the wing. The propellers are located behind the wing trailing edge.

Step 5.9: The necessary engine information was obtained from AVCO-Lycoming as Specification No.2397-C.

Step 5.10: Figure 5.3 shows the preliminary engine installation.

Step 5.11: Figure 5.3 also shows that the installation satisfies requirements 2, 3 and 4 of this step. Requirements 1 and 5 do not apply.

Step 5.12: The threeview of Figure 13.1 shows the proposed installation.

Step 5.13: To save space this step is omitted.

5.4.2 Jet Transport

Step 5.1: The mission specification of Table 2.18 of Part I specifies that two turbofan engines are to be used.

Note: Steps 5.2 and 5.3 can be omitted. They are presented here as a help to the reader.

Step 5.2: Figure 5.4 shows the preliminary speed-altitude envelope of the Ourania. The necessary data were obtained from Part I.

Step 5.3: Comparison of Figure 5.4 with Figure 5.1 shows that the turbofan is an appropriate choice.

Step 5.4: The preliminary matching results for the Ourania as presented on pages 183-184 of Part I show that: $T_{TO} = 47,625$ lbs.

Step 5.5: Two engines are required, according to Table 2.18, Part I. The maximum required thrust per engine is therefore: 23,813 lbs.

Consultation with Ref.8 (1983-84) shows that the CFM56-2 turbofan is the only engine which satisfies this thrust requirement: T_{max} = 24,000 lbs with a dry weight of 4,612 lbs.

Step 5.6: Not applicable.

Step 5.7: It is decided to mount the engines under the wing, forward of the center of gravity. This makes the airplane a tractor.

Step 5.8: See Step 5.7.

Step 5.9: The engine envelope information was obtained from Ref.8 (1983-84).

Step 5.10: Figure 5.5 shows the proposed engine installation.

Step 5.11: In terms of FOD characteristics, the engine installation of the Ourania is very similar to that of the Boeing 737-300. The latter satisfies FOD requirements. It will be assumed that these requirements are also satisfied for the Ourania.

Figure 5.5 shows that requirements 2-4 are also satisfied.

Requirement 5 is not applicable.

Step 5.12: Figure 13.2 shows the proposed engine installation in the threeview.

Step 5.13: To save space this step is omitted.

5.4.3 Fighter

Step 5.1: Table 2.19 of Part I specifies the use of two turbofans.

Step 5.2: Figure 5.6 shows a preliminary speed-altitude envelope for the Eris. All necessary data were obtained from Part I.

Step 5.3: Comparison of Figure 5.6 with Figure 5.1 shows that the choice of turbofans is an appropriate one.

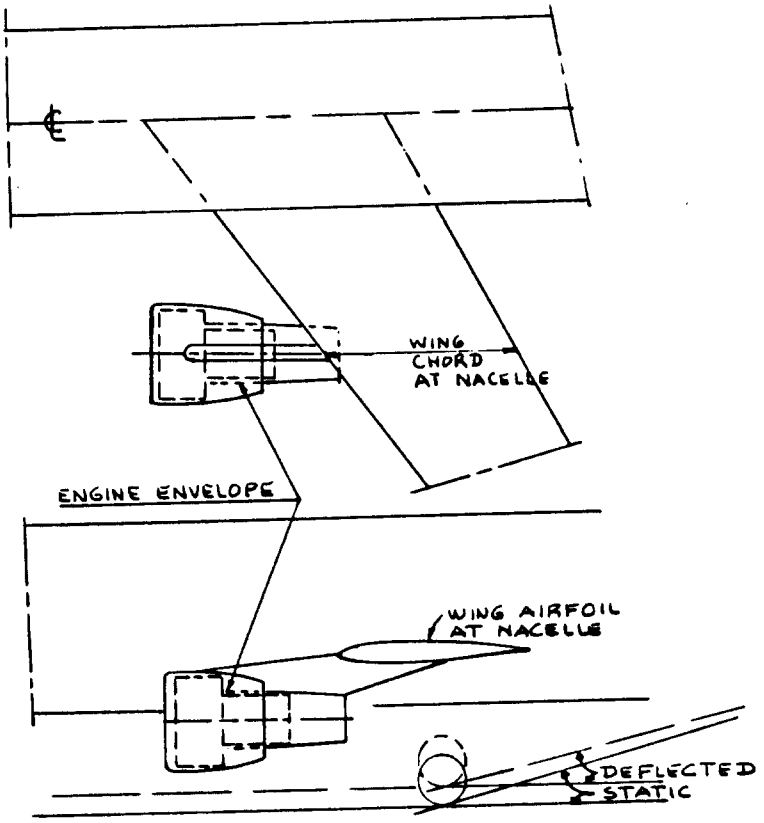

Figure 5.5 Ourania: Preliminary Engine Installation

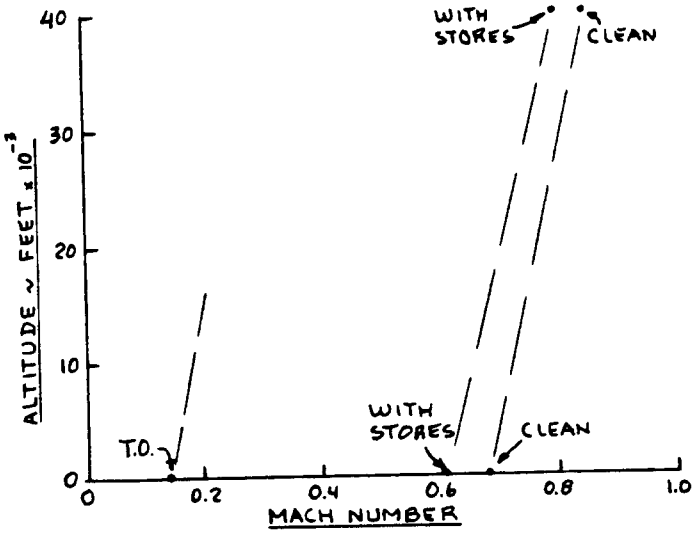

Figure 5.6 Eris: Preliminary Speed-Altitude Envelope

Step 5.4: From the preliminary matching results of pages 190-191 of Part I it follows that T_{TO} = 29,670 lbs.

Step 5.5: Since two engines are required, the maximum rated thrust per engine is: 14,835 lbs.
Consultation with Ref.8 (1983-84) shows that the following engine candidates are available:

1. Pratt and Whitney JT3D(TF33) with T_{max} = 18,000 lbs, dry and W_{dry} = 4,340 lbs.

2. Pratt and Whitney JTF22(F100) with T_{max} = 14,670 lbs, dry and W_{dry} = 3,033 lbs.

3. General Electric F404 with T_{max} = 16,000 lbs in afterburner and W_{dry} = 2,000 lbs.

Since the F404 is a relatively light weight engine with operational use in the F17, F18 and X29 it is selected here for the Eris.

Step 5.6: Not applicable.

Step 5.7: It was decided in Step 3.5, page 106 that the engines are to be mounted in the fuselage as in the DH110 of page 106. From an installation viewpoit that makes the Eris a tractor since the inlets are ahead of the c.g.

Step 5.8: See Step 5.7.

Step 5.9: The geometric envelope of the F404 was obtained from Ref.8(1983-84).

Step 5.10: Figure 4.9(p.122) shows the proposed engine installation.

Step 5.11: The Eris is similar to the DH110 of p.106. It is therefore assumed, that requirement1 is satisfied. Figure 4.9(p.122) indicates that requirements 2-4 are satisfied. To accomodate requirement 5 a gun-gas deflector plate will be installed on the fuselage nose. Figure 4.9(p.122) shows this deflector plate.

Step 5.12: Figure 13.3 shows the proposed installation in a threeview.

Step 5.13: To save space this step is omitted.

6. CLASS I METHOD FOR WING PLANFORM DESIGN AND FOR SIZING AND LOCATING LATERAL CONTROL SURFACES

The purpose of this chapter is to present a step-by-step methodology for determining the following planform design characteristics of the wing:

1. Size (i.e. area), S
2. Aspect ratio, A
3. Sweep angle, Λ
4. Thickness ratio, t/c
5. Airfoils
6. Taper ratio, λ
7. Incidence angle, i_w and twist angle, ε_t
8. Dihedral angle, Γ_w
9. Lateral control surface size and layout

The method is presented as part of Step 6 in p.d. sequence I as outlined in Chapter 2.

The reader will recall that items 1 and 2 for the wing are already known: these were determined by the preliminary sizing process of Part I. Items 3 through 9 for the wing remain to be determined.

As a result of Step 3 in p.d. sequence I (Chapter 2, p.11) it has already been decided whether the overall configuration of the airplane is one of the following:

1. Conventional (that means tail aft)
2. Flying wing (that means no horizontal tail or canard)
3. Tandem Wing
4. Canard
5. Three surface
6. Joined wing

Section 6.1 presents a step-by-step procedure for determining the wing design characteristics listed as 3-9 at the beginning of this chapter. Example applications are discussed in Section 6.2.

6.1 A PROCEDURE FOR WING PLANFORM DESIGN AND FOR SIZING AND LOCATING LATERAL CONTROL SURFACES

Step 6.1: If the airplane is a flying wing, all items discussed in Chapter 4 must somehow be integrated into the wing. This will have a major impact on the wing layout and therefore needs to be looked into first.

If the airplane is not a flying wing, proceed to Step 6.2.

Step 6.2: Decide on the overall structural wing configuration.

The choices here are between:

1. Cantilever wing
2. Braced (or strutted wing)

→ puede salvar ~ 30% peso, a costa de más resistencia

Tables 6.1 through 6.12 provide an initial guide to this choice. The reader will note that braced wings are used primarily on relatively low speed airplanes. The reason is: the trade between profile and interference drag increments (due to the struts) and wing weight is generally unfavorable to strutted arrangements above a speed of around 200 kts.

Step 6.3: Decide on the overall wing/fuselage arrangement.

The choices here are:

1. High wing 2. Mid wing 3. Low wing

Tables 6.1 through 6.12 provide an initial guide to this choice. The reader should also review the pertinent configurations presented in Chapter 3.

The following ratings of overall wing/fuselage configurations are correct only if 'everything else' is the same. The number 1 means 'preferred' and the number 3 means 'least preferred'.

	High wing	Mid Wing	Low Wing
Interference Drag	2	1	3
Lateral Stability	1	2	3
Visibility from Cabin*	1	2	3
Landing Gear Weight	3**	2	1

* strongly dependent on where the wing passes through the fuselage

** if the gear is retracted into the fuselage, gear weight is not necessarily a factor. In that case the landing gear often requires a 'bump fairing' which causes additional drag.

Table 6.1 Homebuilt Airplanes: Wing Geometric Data

Type	Dihedral Angle, Γ_w, deg.	Incidence Angle, i_w, root/tip deg.	Aspect Ratio, A	Sweep Angle, $\Lambda_{c/4}$, deg.	Taper Ratio, λ_w	Max. Speed, V_{max}, kts	Wing Type
PIK-21	0	0	3.8	0	1.0	NA	ctl/low
Duruble RD-03C	6.5	3/0	7.0	0	0.51	182	ctl/mid
PIEL							
CP-750	5.7	4.2	5.9	0	0.55	183	ctl/low
CP-90	5.7	3	5.4	0	0.44	171	ctl/low
POTTIER							
P-50R	4.4	NA	5.1	2	0.54	167	ctl/low
P-70S	0	2	4.8	0	1.0	129	ctl/mid
O-O Aerosport	2.5	NA	5.7	0	1.0	76	ctl/low
Aerocar Micro-Imp	0	4	4.7	0	1.0	260	ctl/high
Coats SA-III	4	1.5	5.6	0	1.0	165	ctl/low
Sequoia 300	3	3.5/1.5	6.9	0	0.55	243	ctl/low
Ord-Hume OH-4B	3	3	5	5.0	1.0	95	brcd/parasol
Procter Petrel	5	0	6.6	0	1.0	113	ctl/low
Bede BD-8	0	3	3.9	0	1.0	238	ctl/low

ctl = cantilever brcd = braced (strutted)

Table 6.2 Single Engine Propeller Driven Airplanes: Wing Geometric Data

Type	Dihedral Angle, Γ_w, deg.	Incidence Angle, i_w, root/tip deg.	Aspect Ratio, A	Sweep Angle, $\Lambda_{c/4}$, deg.	Taper Ratio, λ_w	Max. Speed, V_{max}, kts	Wing Type
CESSNA							
Skywagon 207	1.7	1.5/-1.5	7.4	0	0.69	182	brcd/high
Cardinal RG	1.5	4.1/0.7	7.3	0	0.73	156	ctl/high
Skylane RG	1.7	0.8/-2.8	7.4	0	0.67	187	brcd/high
PIPER							
Cherokee Lance	7.0	2/-1	6.2	0	1.0	188	ctl/low
Cher. Warrior	7.0	2/-1	7.2	5	0.67	152	ctl/low
Turbo Sarat.SP	6.8	NA	7.3	0	0.68	195	ctl/low
Bellanca Skyrocket	2	2	6.7	0	0.57	287	ctl/low
Grumman Am. Tiger	5	1.4	7.1	0	1.0	148	ctl/low
Rockwell Commander 112A	7	2	7.0	-2.5	0.50	180	ctl/low
Trago Mills SAB-1	5	3/1	7.5	0	0.54	202	ctl/low
Scottish Aviation							
Bullfinch	6.5	1.2	8.4	0	0.57	150	ctl/low
Robin HR100/4	6.3	4.7	5.4	0	1.0	180	ctl/low
Socata Rallye 235E	7	4	7.6	0	1.0	148	ctl/low
Fuji FA-200	7	2.5	6.3	0	1.0	123	ctl/low
Gen Avia F15F	6	4	7.7	0	0.49	167	ctl/low

ctl = cantilever brcd = braced (strutted)

Table 6.3 Twin Engine Propeller Driven Airplanes: Wing Geometric Data

Type	Dihedral Angle, Γ_w, deg.	Incidence Angle, i_w, root/tip deg.	Aspect Ratio, A	Sweep Angle, $\Lambda_{c/4}$, deg.	Taper Ratio, λ_w	Max. Speed, V_{max}, kts	Wing Type
CESSNA							
310R	5	2.5/-.5	7.3	0	0.67	236	ctl/low
402B	5 (outer)	2/-.5	7.5	0 L.E.	0.67	227	ctl/low
414A	5	2.5/-.5	8.6	0 L.E.	0.60	232	ctl/low
T303	7	3/0	8.1	0 L.E.	0.71	216	ctl/low
PIPER							
PA-31P	6	1/-1.5	7.2	0	0.39	243	ctl/low
PA-44-180T	7.2	NA	8.1	0	0.63	196	ctl/low
Chieftain	5	1/-1.5	7.2	1.9	0.40	231	ctl/low
Cheyenne I	5	1.5/-1	7.4	0	0.37	249	ctl/low
Cheyenne III	5	1.5	7.8	0	0.31	296	ctl/low
BEECH							
Duchess 76	6.5	3/.6	8.0	0	0.80	194	ctl/low
Duke B60	6	4/0	7.2	0	0.32	246	ctl/low
Learfan 2100	4	1.5	9.5	0	0.45	369	ctl/low
Rockwell Commander							
700	7	NA	9.0	0	0.43	231	ctl/low
Piaggio P166-							
DL3	21.5/2.5*	2.7	7.3	7.5	0.35	215	ctl/gull
EMB-121	7	3	7.2	0.33	0.61	316	ctl/low

ctl = cantilever brcd = braced (strutted)
*21.5 inboard, 2.5 outboard on this gull wing configuration

Table 6.4 Agricultural Airplanes: Wing Geometric Data

Type	Dihedral Angle, Γ_w, deg.	Incidence Angle, i_w, root/tip deg.	Aspect Ratio, A	Sweep Angle, $\Lambda_{c/4}$, deg.	Taper Ratio, λ_w	Max. Speed, V_{max}, kts	Wing Type
IAR-822	5 (outer)	5	6.3	0	1.0	92	ctl/low
UTVA-65	2	2.5	7.2	0	0.7	95	brcd/low
IA-53	7.5 (out)	4.3	6.3	0	0.7	116	ctl/low
EMB-200	7	3	7.0	0	1.0	116	ctl/low
Ag-cat	3	6	8.7	0	1.0	113	brcd/bipl
WSK M-15	NA	NA	NA	0	NA	146	brcd/bipl
PZL M-18A	1.3	3	7.8	0	1.0	128 138*	ctl/low
PZL 106A	4	6.5	7.8	4	1.0	114*	brcd/low
NDN-6	4.3	4.5	7.5	0	0.7	135	brcd/low
Cessna AgHusky	9	1.5/-1.5	8.5	0	0.7	106	brcd/low
Antonov AN-2M	2.5 both wings	NA	NA	0	1.0	136	brcd/bipl
HAL-31	6	0	6.0	0	1.0	108	ctl/low

*speed without spray equipment installed
ctl = cantilever brcd = braced (strutted) bipl = biplane

Table 6.5 Business Jets: Wing Geometric Data

Type	Dihedral Angle, Γ_w,	Incidence Angle, i_w,	Aspect Ratio, A	Sweep Angle, $\Lambda_{c/4}$,	Taper Ratio, λ_w	Max. Speed, V_{max},	Wing Type
	deg.	root/tip deg.		deg.		kts	
DASSAULT/BREGUET							
Falcon 10	1.5	NA	7.1	27	0.36	492(25K)	ctl/low
Falcon 20F	2	1.5	6.4	30	0.31	465(25K)	ctl/low
Falcon 50	0	NA	7.6	24	0.32	475	ctl/low
CESSNA							
Citation I 500	4	2.5/-0.5	7.8	0	0.39	277(28K)	ctl/low
Citation II	4.7	NA	8.3	2	0.32	277(28K)	ctl/low
Citation III	2.8	NA	8.9	25	0.35	472(33K)	ctl/low
GATES LEARJET							
24	2.5	1	5.0	13	0.50	473(31K)	ctl/low
35A	2.5	1	5.7	13	0.50	464	ctl/low
55	2.9	NA	7.3	13	0.42	470(30K)	ctl/low
IAI							
1124 Westw. I	2	1/-1	6.5	5	0.33	471	ctl/mid
1125 Astra	2.6 (out)	NA	8.8	34/25 at LE	0.30	472(35K)	ctl/low
Canadair CL601	2.3	3	8.5	25	0.26	450	ctl/low
BAe 125-700	2	2.1/-0.3	6.3	20	0.28	436(28K)	ctl/low
GA Gulfst. III	3	3.5/-0.5	6.5	28	0.31	487	ctl/low
Mu Diamond I	2.7	3/-3.5	7.5	20	0.35	431(30K)	ctl/low
L. Jetstar II	2	1/-1	5.3	30	0.37	475(30K)	ctl/low

ctl = cantilever (30K) = 30,000 ft altitude

Table 6.6 Regional Turbopropeller Driven Airplanes: Wing Geometric Data

Type	Dihedral Angle, Γ_w,	Incidence Angle, i_w,	Aspect Ratio, A	Sweep Angle, $\Lambda_{c/4}$,	Taper Ratio, λ_w	Max. Speed, V_{max},	Wing Type
	deg.	root/tip deg.		deg.		kts	
CASA C-212-200							
SHORTS							
330	3 (outer)	NA	12.3	0	1.0	190(10K)	brcd/high
360							
BEECH							
1900	6	3.5/-1.1	9.8	0	0.42	263(8K)	ctl/low
B99	7	4.8	7.5	0	0.5	247(12K)	ctl/low
CESSNA CONQUEST							
I							
II							
GA Gulfstr. Ic							
GAF N22B							
Fokker F27-200	2.5	3.5	12.0	0	0.41	259(20K)	ctl/high
DeHAVILLAND CANADA							
DHC-6-300							
DHC-7	4.5	3	10.0	0	0.44	231(8K)	ctl/high
DHC-8	2.5 (out)	NA	12.3	0	0.45	270(15K)	ctl/high
EMB 110	7	3	9.9	0	0.50	248(8K))	ctl/low
EMB 120	6.5	2	9.9	0	0.50	NA	ctl/low
BRITISH AEROSPACE							
Jetstream 31	7	2	10.0	0.5	0.37	263(20K)	ctl/low
748	7	3	12.7	2.9	0.36	244(15K)	ctl/low

ctl = cantilever (30K) = 30,000 ft altitude

Table 6.7 Jet Transports: Wing Geometric Data

Type	Dihedral Angle, Γ_w, deg.	Incidence Angle, i_w, root/tip deg.	Aspect Ratio, A	Sweep Angle, $\Lambda_{c/4}$, deg.	Taper Ratio, λ_w	Max. Speed, V_{max}, kts	Wing Type
BOEING							
727-200	3	2	7.1	32	0.30	549(22K)	ctl/low
737-200	6	1	8.8	25	0.34	462(33K)	ctl/low
737-300	6	1	8.0	25	0.28	462(33K)	ctl/low
747-200B	7	2	7.0	37.5	0.25	523(30K)	ctl/low
747SP	7	2	7.0	37.5	0.25	529(30K)	ctl/low
757-200	5	3.2	7.9	25	0.26		ctl/low
767-200	6	4.3	7.9	31.5	0.27		ctl/low
McDONNELL DOUGLAS							
DC-9 Super 80	3	1.3	9.6	24.5	0.16	500	ctl/low
DC-9-50	1.5	NA	8.7	24	0.18	537	ctl/low
DC-10-30	5.3/3	+/-	7.5	35	0.25	530(25K)	ctl/low
AIRBUS							
A300-B4	5	NA	7.7	28	0.35	492(25K)	ctl/low
A310	11.1/4.1	5.3	8.8	28	0.26	483(30K)	ctl/low
Lockh.1011-500	7.5/5.5	NA	7.0	35	0.30	525(30K)	ctl/low
Fkr F28-4000	2.5	NA	8.0	16	0.31	390	ctl/low
Rombac 111-495	2	2.5	8.5	20	0.32	470(21K)	ctl/low
BAe 146-200	-3	3.1/0	9.0	15	0.36	420(26K)	ctl/high
Tupolev Tu154	0	NA	7.0	35	0.27	526(31K)	ctl/low

ctl = cantilever (30K) = 30,000 ft altitude

Table 6.8 Military Trainers: Wing Geometric Data

Type	Dihedral Angle, Γ_w, deg.	Incidence Angle, i_w, root/tip deg.	Aspect Ratio, A	Sweep Angle, $\Lambda_{c/4}$, deg.	Taper Ratio, λ_w	Max. Speed, V_{max}, kts	Wing Type
Propeller Driven							
EMB-312 Tucano	5.5	1.4/-0.8	6.4	0.7	0.47	292	ctl/low
Pilatus PC-7	7 (outer)	NA	6.5	1	0.55	270	ctl/low
NDN-1	5 (outer)	3	5.4	0	0.79	247	ctl/low
Beech T-34C	7	4/1	6.2	0	0.41	280	ctl/low
Aerosp.Epsilon	5	2	7.0	0	0.63	281	ctl/low
SM SP-260M	6.3	2.8/0	6.3	0	0.49	235	ctl/low
Yak-52	2	2	5.8	0	0.54	194	ctl/low
Neiva T-25	6	2	7.1	0	0.54	269	ctl/low
Jet Driven							
Aero L-39C	2.5	2	4.4	2	0.52	491	ctl/low
Microjet 200B	5	3	8	0	0.39	300	ctl/low
DB/D Alphajet	-6	NA	4.8	28	0.36	495(33K)	ctl/shldr
Aermac. MB339A	2.6	NA	5.3	9	0.58	500	ctl/low
SM S-211	-2	2.2/-1.3	5.1	16	0.46	400	ctl/shldr
PZL TS-11	2.7	NA	5.7	7	0.51	404	ctl/mid
CASA C-1-1	5	1	5.6	2	0.60	428(25K)	ctl/low
Bae Hawk Mk1	2	NA	5.3	22	0.34	572	ctl/low
Tupolev Tu154	0	NA	7.0	35	0.27	526(31K)	ctl/low

ctl = cantilever shldr = shoulder (30K) = 30,000 ft altitude

Table 6.9 Fighters: Wing Geometric Data

Type	Dihedral Angle, Γ_w, deg.	Incidence Angle, i_w, root/tip deg.	Aspect Ratio, A	Sweep Angle, $\Lambda_{c/4}$, deg.	Taper Ratio, λ_w	Max. Speed, V_{max}, kts	Wing Type
DASSAULT BREGUET							
Mirage III-E	-1	0	1.9	61(LE)	0	1,268(39K)	ctl/low
Mirage F1-C	-4.5	NA	2.8	48(LE)	0.29	1,260	ctl/shldr
Mirage 2000	-1	NA	2.0	58(LE)	0	1,260	ctl/low
Super Etendard	-3.5	NA	3.2	45	0.50	573	ctl/mid
Fairch.R.A-10A	7 (outer)	-1	6.5	0	0.66	450	ctl/low
Grumman A-6E	0	NA	5.3	25	0.30	700	ctl/mid
Grumman F14A	-1.5(out)	NA	7.3*	20/68(LE)	0.40	M = 2.4	vsw/high
Northrop F-5E	0	0	3.8	24	0.19	710	ctl/low
Vought A-7E	-5	-1	4	35	0.25	595(5K)	ctl/high
McDONNELL DOUGLAS							
F-4E	0/12	NA	2.8	45(LE)	0.18	1,146	ctl/low
F-15	-1	0	3.0	39	0.25	M =2.5	ctl/high
AV-8B	-12	1.8	4.0	24	0.28	585(0K)	ctl/shldr
GD FB-111A	0	NA	7.6*	16/73(LE)	0.33	1,260	ctl/shldr
GD F-16	0	0	3.0	40(LE)	0.22	495(33K)	ctl/mid
Cessna A37B	3	3.6/1	6.2	0	0.68	455	ctl/low
Aerm. MB339K	2.6	NA	5.3	8.5	0.58	500	ctl/low
Sukhoi Su-7BMK	0	NA	2.6	62(LE)	0.26	730(0K)	ctl/mid

ctl = cantilever shldr = shoulder (30K) = 30,000 ft altitude
* taken at lowest sweep angle

Table 6.10 Military Patrol, Bomb and Transport Airplanes: Wing Geometric Data

Type	Dihedral Angle, Γ_w, deg.	Incidence Angle, i_w, root/tip deg.	Aspect Ratio, A	Sweep Angle, $\Lambda_{c/4}$, deg.	Taper Ratio, λ_w	Max. Speed, V_{max}, kts	Wing Type
Turbopropeller Driven							
Lockh'd C130E	2.5	3/0	10.1	0	0.49	325	ctl/high
Lockheed P3C	6	0/0.5	7.5	0	0.40	411(15K)	ctl/low
Antonov 12BP	-3.8(out)	NA	11.9	7.4	0.34	419	ctl/high
Antonov 22	-3.5	NA	12.0	3	0.36	399	ctl/high
Antonov 26	-2(out)	3	11.7	7	0.34	NA	ctl/high
Grumman E2C	3.1	NA	9.3	5.3	0.34	325	ctl/high
DB Atlantic 2	6 (outer)	3	11.6	9 (LE)	0.39	348	ctl/low
Aerital.G222	2.5 (out)	NA	9.2	2.1	0.50	291	ctl/high
Transall C-160	3.5 (out)	NA	10.0	1.9	0.50	320	ctl/high
Jet Driven							
Lockheed S3A	0	3/-3.5	7.9	15	0.25	450	ctl/high
Lockh'd C-141B	-3.5	NA	7.5	25.5	0.41	492	ctl/high
Lockheed C-5A	-5.1	NA	7.8	25.6	0.34	496(25K)	ctl/high
BAe Nimrod Mk2	2.7	NA	6.2	20	0.23	500	ctl/low
Boeing YC-14	0	NA	9.4	4.6	0.30	438	ctl/high
McDD KC-10A	5/3	+/-	7.5	35	0.25	530(25K)	ctl/low
Tupolev Tu-16	-3.7	NA	6.6	43(LE)	0.44	535(6K)	ctl/high
Tupolev Tu-22	0	NA	4.0	51(LE)	0.31	800(40K)	ctl/mid
Ilyushin Il76T	-3.6	NA	11.7	25	0.37	459	ctl/high

ctl = cantilever shldr = shoulder (30K) = 30,000 ft altitude

Table 6.11 Flying Boats, Amphibious and Float Airplanes: Wing Geometric Data

Type	Dihedral Angle, Γ_w, deg.	Incidence Angle, i_w, root/tip deg.	Aspect Ratio, A	Sweep Angle, $\Lambda_{c/4}$, deg.	Taper Ratio, λ_w	Max. Speed, V_{max}, kts	Wing Type
SHORTS							
Sandringham	2.1	NA	8.6	3.6	0.38	188	ctl/high
Shetland	4.1	NA	8.6	7.7	0.34	232(8K)	ctl/high
DORNIER							semi ctl
Do 24	0	NA	6.8	7	0.36	165	brcd/high
Do 24/72	0	NA	7.5	2	0.71	224	brcd/par.
Do Seastar	0	NA	9.1	0	1.0	220	brcd/par.
Grumman JRF-6B	2	NA	6.4	-1	0.46	175(5K)	ctl/high
Grumman J4F-1	NA	NA	6.5	0	0.48	133	ctl/high
SM S-700	2.1	NA	9.4	0	1.0	180(10K)	ctl/high
Canadair CL215	0	NA	8.2	0	1.0	158	ctl/high
BV-222	3.2	NA	8.0	0	0.72	183	ctl/high
Shin Meiwa US1	2.1	NA	8.0	2.1	0.50	260	ctl/high
Boeing 314-A	5.3	NA	7.7	7.9	0.23	183	ctl/high
Martin PBM-3	19/0	NA	10.1	-1.5	0.33	174	ctl/high
Beriev M-12	26/-2	NA	8.4	6.0	0.41	328	ctl/high
Partenav. P68B*	1	1.5	7.7	0	1.0	173	ctl/high
McKinnon G-21G	2.5	NA	6.1	0	0.50	211	ctl/high

ctl = cantilever shldr = shoulder (30K) = 30,000 ft altitude
par. = parasol * float airplane

Table 6.12 Supersonic Cruise Airplanes: Wing Geometric Data

Type	Dihedral Angle, Γ_w, deg.	Incidence Angle, i_w, root/tip deg.	Aspect Ratio, A	Sweep Angle, $\Lambda_{c/4}$, deg.	Taper Ratio, λ_w	Max. Speed, V_{max}, kts	Wing Type
NORTH AMERICAN AVIATION (ROCKWELL)							
XB-70A	-3	NA	1.8	65.6(LE)	0.02	M = 2+	ctl/low
RA-5C	0	NA	4.0	37.5	0.19	1,204(40K)	ctl/high
B-1B	0	NA	??	??	0.32	M = 2+	ctl/low
BOEING							
SST	NA	NA	3.4*	30-72	0.21	1,565(75K)	ctl/low
AST-100	get data from NASA reports						
NASA							
SSXJet I	0	NA	1.84	72(LE)	0.08	M =	ctl/
SSXJet II	0	NA	1.84	72(LE)	0.08	M =	ctl/
SSXJet III	0	NA	1.84	72(LE)	0.08	M =	ctl/
TUPOLEV							
Tu-144	8.3 (out)	NA	1.9	76/57	0.13	1,350(50K)	ctl/low
Tu-22M	0	NA	8.0*	20-65	0.28	1,446	ctl/mid
Dassault MIVA	-1.5	NA	1.8	60(LE)	0.11	1,261(36K)	ctl/low
GD F-111A	0	NA	7.5*	16-72	0.33	1,432	ctl/high
GD B-58	0	NA	2.2	59(LE)	0	M = 2+	ctl/low
Aerospatiale/British Aerospace							
Concorde	0	NA	1.7	ogive	0.12	1,259(55K)	ctl/low

ctl = cantilever (30K) = 30,000 ft altitude
* taken at lowest sweep angle

Step 6.4: Select the wing quarter chord sweep angle, $\Lambda_{c/4}$ and the wing thickness ratio, t/c.

The choices for type of sweep were listed in sub-section 3.3.4 as:

1. Zero or negligible sweep
2. Aft sweep (also called positive sweep)
3. Forward sweep (also called negative sweep)
4. Variable sweep (meaning symmetrically variable sweep)
5. Oblique sweep (meaning asymmetrically variable sweep)

Sweep types 4 and 5 are appropriate choices only for missions where there is a combined requirement for supersonic and for subsonic cruise and/or for high 'g' maneuvering. If in addition the mission calls for short field lengths, variable or oblique sweep could be an appropriate choice. Keep in mind that a severe weight penalty is associated with the wing pivot structure needed in the mechanization of variable sweep or oblique sweep wings.

For most airplanes the sweep choice is restricted to items 1-3.

Tables 6.1 through 6.12 provide an initial guide to the selection of sweep angle. For some guidance to the selection of thickness ratio refer to Tables 8.1 through 8.12.

While computing the Class II drag polars of the airplane as part of the work in p.d.sequence II, the reader will discover that sweep angle and thickness ratio have a major influence on the dragrise characteristics of an airplane. For airplanes with a requirement for high subsonic cruise and/or a requirement for supersonic cruise, the trade between thickness ratio and sweep angle turns out to be a deciding factor in the design of the wing.

Figures 6.1 and 6.2 show the effect of sweep angle and thickness ratio on critical Mach number. Note that the cruise lift coefficient $C_{L_{cr}}$ is an important factor.

This cruise lift coefficient may be estimated from:

$$C_{L_{cr}} = (W_{TO} - 0.4W_F)/\bar{q}S \qquad (6.1)$$

In many designs it is possible by sweeping the wing

NOTE: FOR SUPERCRITICAL AIRFOILS USE $\Delta M_{CR} = 0.05$

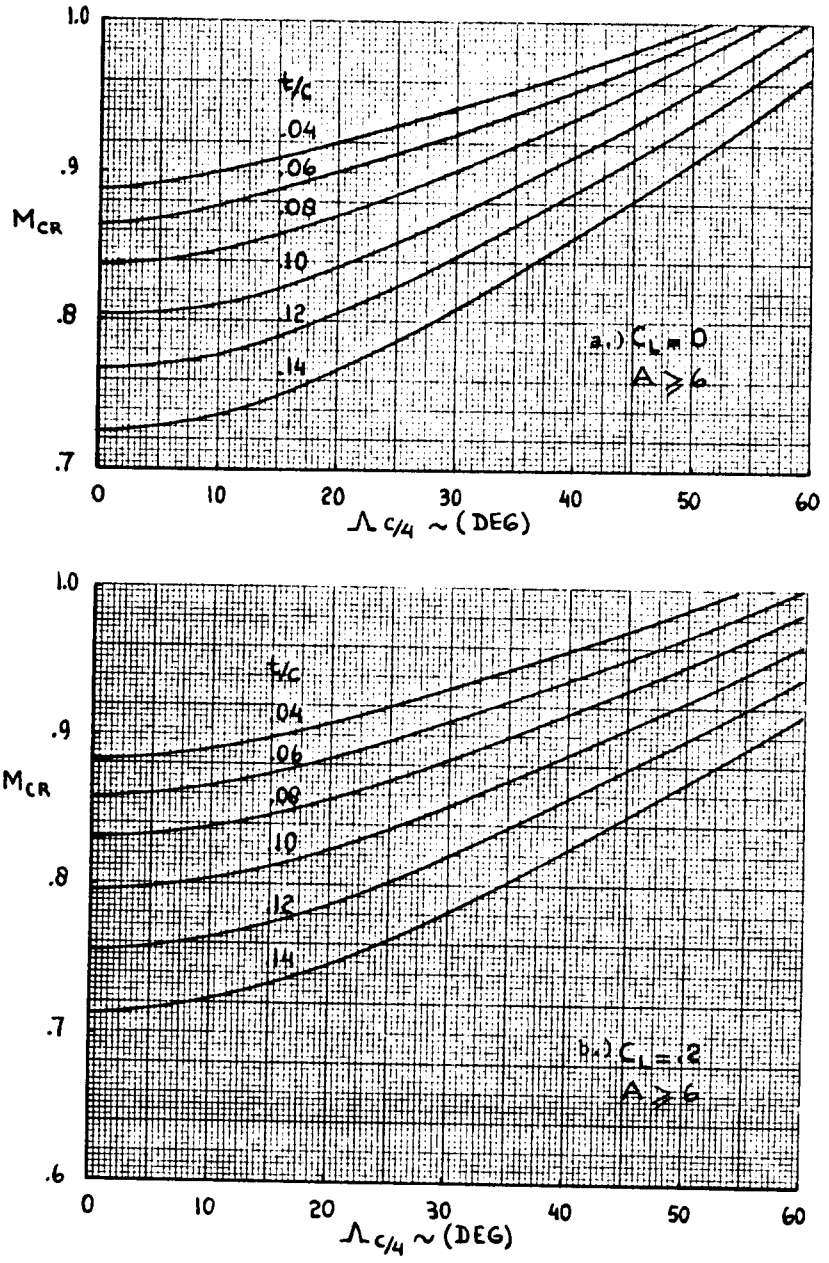

Figure 6.1a Effect of Thickness Ratio and Sweep Angle on Critical Mach Number

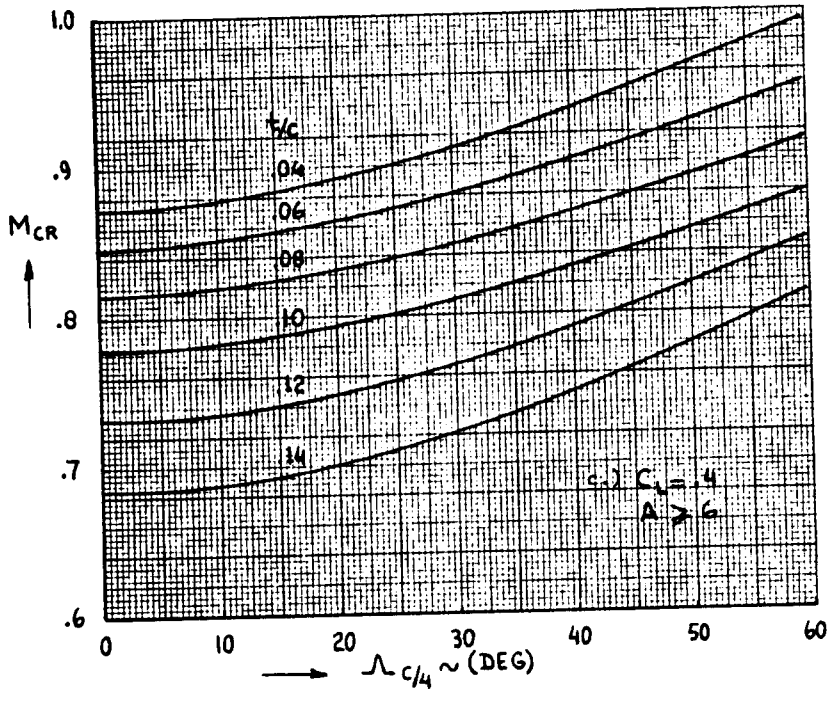

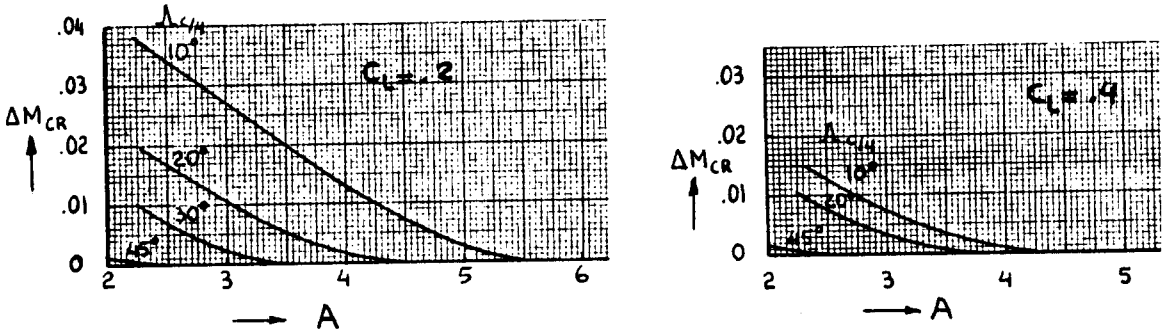

Figure 6.1b Effect of Thickness Ratio and Sweep Angle on Critical Mach Number

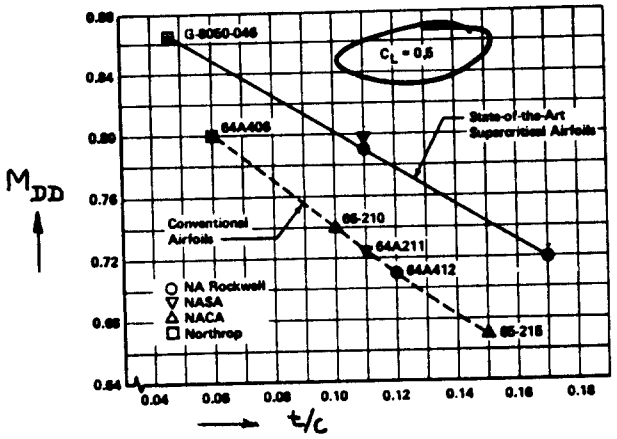

VERY ROUGHLY:

$M_{DD} = M_{CR} + 0.1$

Supercritical — Conventional

Figure 6.2 Effect of Thickness Ratio on Drag Divergence Mach Number for NACA and Supercrit. Airfoils

forward or aft to achieve a reduction in c.g. travel. In addition, a slight change in sweep angle (away from zero) can have a significant influence on the location of the wing/fuselage a.c. The importance of the latter is discussed in Chapter 11.

Step 6.5: Decide which wing airfoil to use.

Tables 8.1 through 8.12 (Chapter 8) provide an initial guide to the selection of airfoils. Ref.20 contains a detailed review of NACA airfoils. When consulting recent issues of Ref.8, the reader will discover that most airplanes which are in production in 1985 still use NACA airfoils. This, despite the fact that modern computational airfoil design technology makes it possible to tailor airfoils to a specific mission.

In selecting or designing an airfoil, the following important section characteristics must be kept in mind:

section drag coefficient, C_d at the:

section design lift coefficient, $C_{l_{des.}}$

section critical Mach number, M_{crit}

section pitching moment coefficient, $C_{m_{c/4}}$

Part VI, References 16 - 18 and Ref.21 contain data on recently developed airfoils.

Step 6.6: Decide on the wing taper ratio, λ_w and prepare a dimensioned drawing of the wing planform to be used.

Tables 6.1 through 6.12 provide some guidance relative to the choice of wing taper ratio, λ_w. It will become clear in Chapter 7 and in Part V that the choice of taper ratio has important consequences to wing stall behavior as well as to wing weight.

Step 6.7: Proceed to Step 7.1, Chapter 7.

Step 6.8: Decide on the type, size and location of lateral control devices.

Tables 8.1b through 8.12b (chapter 8) provide an initial guide to this decision. Compatibility with the required high lift devices is a major factor in laying out the lateral control surfaces.

Step 6.9: Draw the front and rear spar lines in the wing planform drawing of Step 6.6.

The data developed under Steps 6.7 and 6.8 are required before the spar lines can be located. A clearance of roughly 0.005c should be observed between the spar lines and the outlines of the high lift devices and/or ailerons. Any spoiler hingelines should be just aft of the rear spar line.

Step 6.10: Compute the wing fuel volume.

It will be assumed here that the wing fuel is carried in what is called a 'wet wing'. That means there are no separate fuel tanks. The wing torque box (that is the part of the wing structure between the front and the rear spar) is sealed and forms the fuel tank.

Check in Part IV for rules of where 'dry bays' need to be to suppress fires in the case of a crash. Don't count the 'dry bay' volume as fuel volume.

Assume that no fuel can be carried beyond the 85 percent span point. This is to prevent lightning strikes (which are most likely to hit the airplane extremities) from starting an in-flight fire.

Note: fuel may be carried in wingtips or in tiptanks, provided the skin is locally 'beefed up' to assure that lightning strikes have enough metal to disperse. This solution costs a lot of weight but is sometimes used.

Compare the computed wing fuel volume with the total fuel volume required for the mission. The latter was determined from the preliminary sizing in Part I.

Torenbeek (Ref.17, Eqn.B-12) suggests the following equation for estimating wing fuel volume in preliminary design:

$$V_{WF} =$$

$$0.54(S^2/b)(t/c)_r\{(1 + \lambda_w\tau_w^{1/2} + \lambda_w^2\tau_w)/(1 + \lambda_w)^2\}, \quad (6.2)$$

where:

$$\tau_w = (t/c)_t/(t/c)_r \quad (6.3)$$

This equation is based on statistical data and presumably accounts for any required dry bays as well as for the lightning strike problem.

If there is sufficient fuel volume, proceed to Step 6.11. If not, decide on where to incorporate the additional fuel volume which is required.

Additional fuel volume can sometimes be included in tiptanks, slipper tanks, fuselage tanks and even empennage tanks.

Keep in mind that the accuracy of Eqn.(6.2) is perhaps +/- 10 percent.

In some airplanes, if the fuel volume discrepancy is significant (larger than 20 percent) it may be necessary to enlarge the wing beyond the size determined from the preliminary sizing process of Part I.

Step 6.11: Decide on the wing dihedral angle, Γ_w.

This choice is tied to a trade between lateral stability and dutch roll stability. A detailed discussion of this trade problem is found in Ref.9. Part VI also contains information on this design trade.

Geometric ground clearance (such as for wingtips and wing mounted nacelles and propellers) during flare attitude with a five degree bank angle can also be a deciding factor in selecting wing dihedral.

At this poin in the p.d. process it suffices to consult Tables 6.1 through 6.12 for initial guidance to this choice.

Step 6.12: Decide on the wing incidence angle, i_w and on the wing angle, ε_t.

The choice of wing incidence angle has important consequences for:

1. Cruise drag
2. Take-off distance (particularly in the case of airplanes with tandem landing gears)
3. Attitude of the fuselage floor in cruise and the ability of flight attendants to push liqour carts up and down the isles: This is not a trivial requirement!

For specific equations which may be used to determine the wing incidence angle for airplanes dominated by a cruise requirement, the reader is referred to Part VI.

At this stage in the p.d. process, Tables 6.1 through 6.12 should be consulted for the initial choice of wing incidence angle.

Wing twist has important consequences to wing stall characteristics. A method for accounting for this is contained in Part VI.

In terms of wing twist, the following possibilities present themselves:

1. Wash-out (negative twist consisting of decreasing airfoil incidence angles outboard along the span): this tends to suppress tip stall.

2. Wash-in (positive twist: the opposite of 1.): this tends to promote tip stall.

3. Aerodynamic twist (consisting of varying the airfoils along the span): this can suppress or promote tipstall, depending on how the airfoils are changed along the span.

Most airplanes have wash-out. Aerodynamic twist is also found but is more expensive to manufacture.

Some guidance to the selection of twist angles may be found in the second column of Tables 6.1 through 6.12.

Step 6.13: Document the decisions made under Steps 6.1 through 6.12 in a brief, descriptive report including clear dimensioned drawings.

6.2 EXAMPLE APPLICATIONS

The following three example applications will be presented:

6.2.1 Twin Engine Propeller Driven Airplane: Selene
6.2.2 Jet Transport: Ourania
6.2.3 Fighter: Eris

All applications are presented in accordance with Steps 6.1 through 6.12 in Section 6.1.

6.2.1 Twin Engine Propeller Driven Airplane

The following information is already available for the wing of the Selene:

$S = 172\ ft^2$, A = 8 and therefore b = 37.1 ft. These data follow from the preliminary sizing work of sub-section 3.7.2 in Part I.

Step 6.1: Not applicable: the Selene is not a flying wing.

Step 6.2: The cruise speed of the Selene is required to be 250 kts at 75 percent power at 10,000 ft (Table 2.17, Part I). This speed requirement is consistent only with a cantilever wing.

Step 6.3: In sub-section 3.5.1 it was already decided to go with a high wing. Such a wing configuration does have the appeal of good downward visibility for the passengers.

Step 6.4: In the speed range of the Selene only very low sweep angles are appropriate from an aerodynamic and weight viewpoint. The data of Table 6.3 confirm this. For the Selene a sweep angle of $\Lambda_{c/4} = 0$ deg. is selected.

Selection of thickness ratio for a low speed wing involves a trade-off between clean maximum lift requirement and structural weight. Table 8.3 shows that airplanes in this category have wing root thickness values as high as 18 percent. It is shown in Figure 7.1 (Chapter 7) that values for airfoil maximum lift coefficient deteriorate very rapidly beyond 13 percent thickness. The following airfoil thickness ratios are selected for the Selene:

at the wing centerline: $(t/c)_r = 0.17$

at the wing tip: $(t/c)_t = 0.13$

Step 6.5: Because of its excellent maximum lift characteristic, NASA MS(1)-0317 is selected for the root airfoil. This airfoil is 'thinned out' to NASA(1)-0313 at the tip in a spanwise linear manner. Reference 22 provides the required aerodynamic and geometric data for these airfoils.

Step 6.6: Table 6.3 shows that a wing taper ratio of $\lambda_w = 0.4$ is an appropriate choice. Figure 6.3a shows a dimensioned drawing of the proposed wing planform. The planform is defined by the following parameters:

$S = 172\ ft^2$, A = 8, b = 37.1 ft

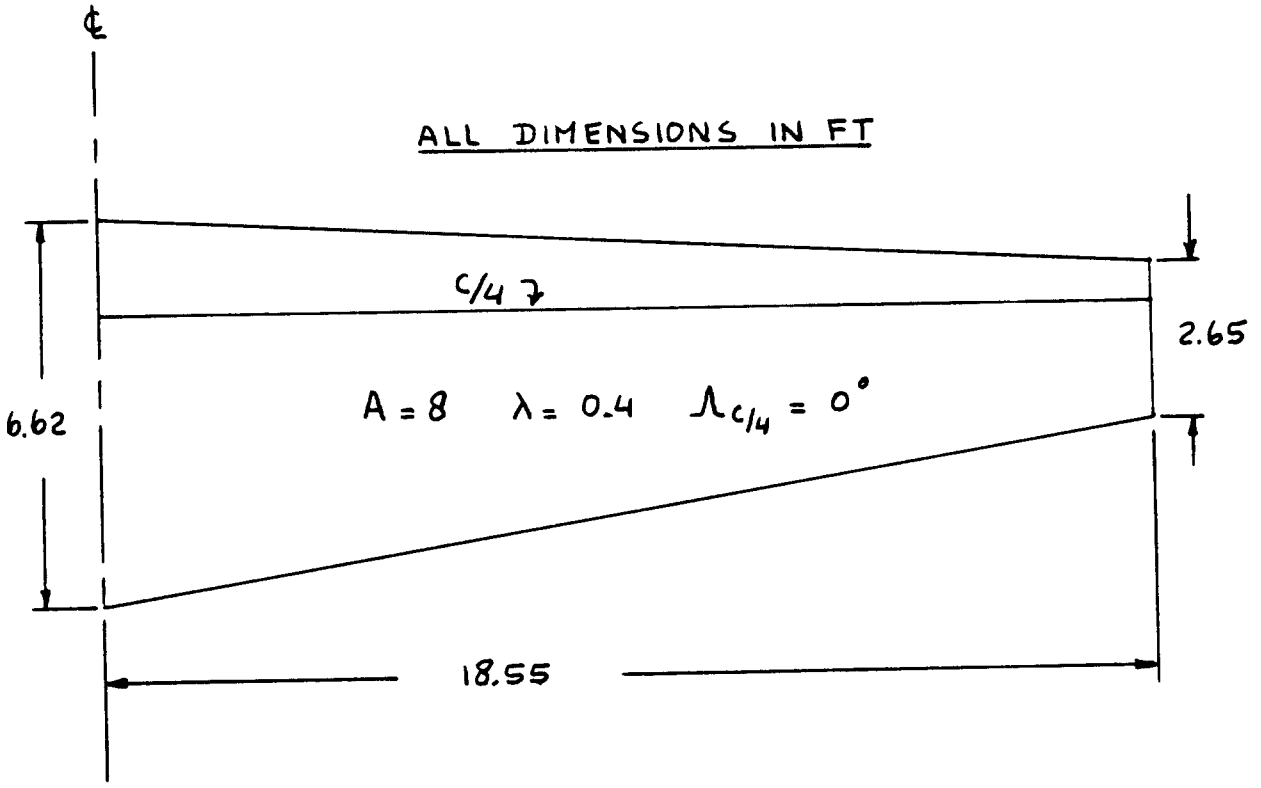

Figure 6.3a Selene: Wing Planform

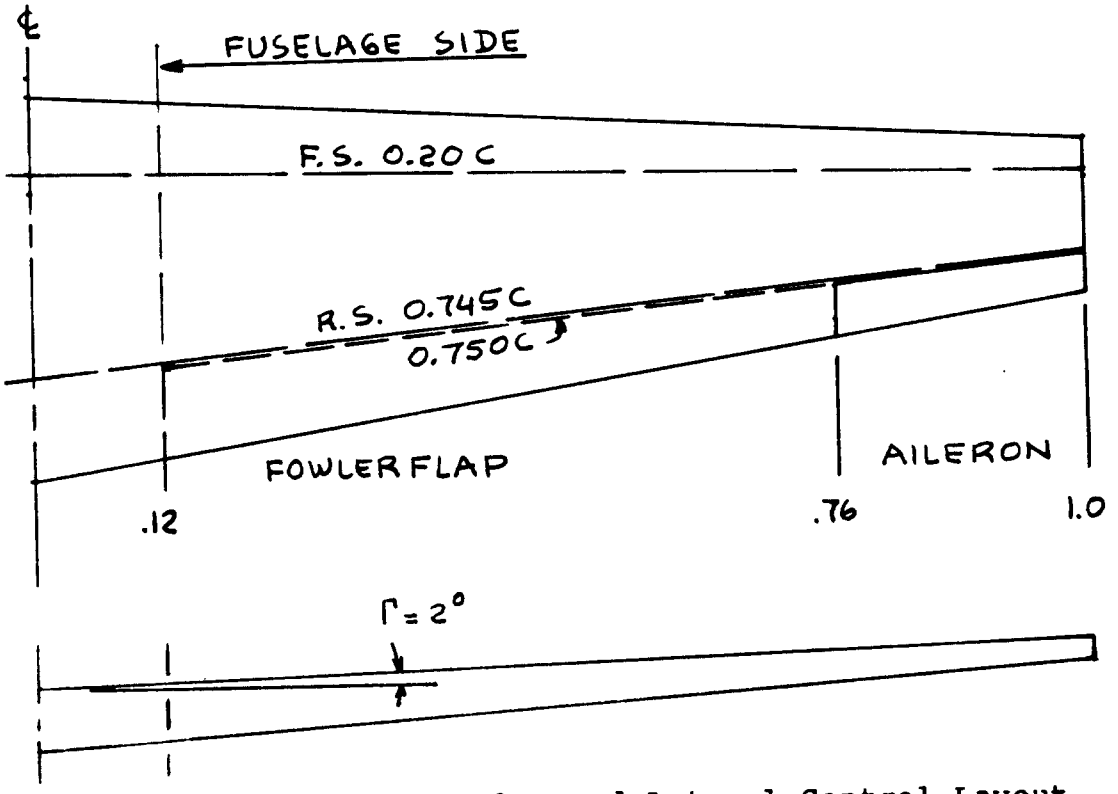

Figure 6.3b Selene: Flap and Lateral Control Layout

$\Lambda_{c/4} = 0^{\circ}$, $\lambda_w = 0.4$

From these data: $c_r = 6.62$ ft and $c_t = 2.65$ ft.

Step 6.7: See sub-section 7.2.1.

Step 6.8: The data in Table 8.3b suggest that the following aileron dimensions are appropriate:

aileron chord ratio: 0.22 - 0.30
aileron span ratio: 0.60 - 1.00

The flap sizing for the Selene in sub-section 7.2.1 shows that an aileron span of 0.76 to 1.00 is available without conflicting with high lift needs. The aileron chord ratio is set at 0.25c to be consistent with the flaps.

These ailerons are drawn into the planform of Figure 6.3b. These ailerons appear to be too small. This can be 'fixed' by using a larger flap chord ratio (say 0.30 instead of 0.25), by adding roll control spoilers or by using smaller span Fowler flaps. To save space, this was not investigated further.

Step 6.9: With an aileron and flap chord ratio of 0.25 the rear spar will be at (1 - 0.25 - 0.005)c = 0.745c. The front spar will be assumed to be at 0.20c. Figure 6.3b shows these spar locations.

Step 6.10: Using Eqn.(6.1), with $\tau = 0.13/0.16 = 0.81$, $\lambda_w = 0.4$, $S = 172$ ft^2 and $b = 37.1$ ft:

$V_{WF} = 52.4$ ft^3.

The required amount of fuel is 1,706 lbs. This follows from p.53 of Pt.I. This amounts to 1,706/44.9 = 38 ft^3 of required fuel volume. The wing therefore has a sufficient amount of fuel volume.

Step 6.11: From Table 6.3 it is observed that wing dihedral angles are about 6 degrees for most twins. However, except for the P166, all twins in Table 6.3 are essentially low wing configurations. Because of the inherent dihedral effect caused by a high wing (Ch.4, Ref.9), a dihedral angle of $\Gamma_w = 2$ degrees should be sufficient.

This choice agrees with the dihedral angles found in high wing single engine airplanes as shown in Table 6.2.

Step 6.12: From Table 6.3 it is seen that a wing incidence angle of i_w = 2.5 degrees with a linear twist of ε_t = -3 degrees toward the tip is fairly common. The NASA MS(1)-0317 airfoil has a value of C_{l_o} = 0.35. This compares to a cruise lift coefficient of:

$$C_L = 7,100/(172x156) = 0.26$$

Therefore an incidence at the root of roughly i_w=0 degrees is appropriate. At the wing tip, the effect of lower airfoil thickness is to increase section maximum lift coefficient. However, the smaller tipchord reduces local Reynold's number which offsets this favorable effect. Therefore, a certain amount of twist will probably be required. A value of ε_t = -3 degrees will be used.

Step 6.13: This step has been omitted to save space.

6.2.2 Jet Transport

The following information is already available for the wing of the Ourania:

S = 1,296 ft^2, A = 10 and therefore b = 113.8 ft. These data follow from the preliminary sizing work of sub-section 3.7.3 in Part I.

Step 6.1: Not applicable: the Ourania is not a flying wing.

Step 6.2: The cruise speed of the Selene is required to be M = 0.82 at 35,000 ft (Table 2.18, Part I). This speed requirement is consistent only with a cantilever wing.

Step 6.3: A low wing is considered the most appropriate choice for this airplane.

Step 6.4: The sweep angle for the Ourania wing must be selected on the basis of a critical Mach number of at least 0.82. The cruise lift coefficient of the Ourania may be estimated from Eqn.(6.1) as:

$$C_{L_{cr}} = (127,000 - 0.4x25,850)/1,482x0.2353x0.82^2x1,296 = 0.38$$

If a supercritical airfoil is used, a value of $\Delta M_{crit} = 0.05$ can be used in Figure 6.2. It is seen that with a sweep angle of 35 deg. a thickness ratio of 0.13 is acceptable. Therefore:

$\Lambda_{c/4} = 35$ deg., $(t/c)_r = 0.13$, $(t/c)_t = 0.11$ appear to be reasonable choices at this point.

Step 6.5: A supercritical derivative of NACA 64A413/411 will be used. The airfoil geometry would have to be derived with the help of a transonic airfoil code.

Step 6.6: Table 6.7 shows that a wing taper ratio of $\lambda_w = 0.32$ is an appropriate choice. Figure 6.4a shows a dimensioned drawing of the proposed wing planform. The planform is defined by the following parameters:

$S = 1{,}296\ ft^2$, $A = 10$, $b = 113.8$ ft

$\Lambda_{c/4} = 35^\circ$, $\lambda_w = 0.32$

From these data: $c_r = 17.4$ ft and $c_t = 5.6$ ft.

Step 6.7: See sub-section 7.2.2.

Step 6.8: Tables 8.7b and c provide typical aileron dimensions for jet transports.

The inboard ailerons for the Ourania will run from 0.23b/2 to 0.34b/2 along the wing span. This takes care of the required flap cut-out because of the engine exhaust. A chord ratio of 0.30 will be selected for the inboard ailerons. The inboard ailerons are used for trim and by the autopilot.

The flap sizing data of sub-section 7.2.2 suggest that the flaps need to be full span. Therefore spoilers will be used for additional lateral control. Table 8.7c shows that the following spoiler geometry is a reasonable choice:

inb'd span fraction: 0.50, inb'd chord fraction 0.20
outb'd span fraction: 0.80, outb'd chord fraction 0.20

The spoiler hinge line will be placed at 0.70c.

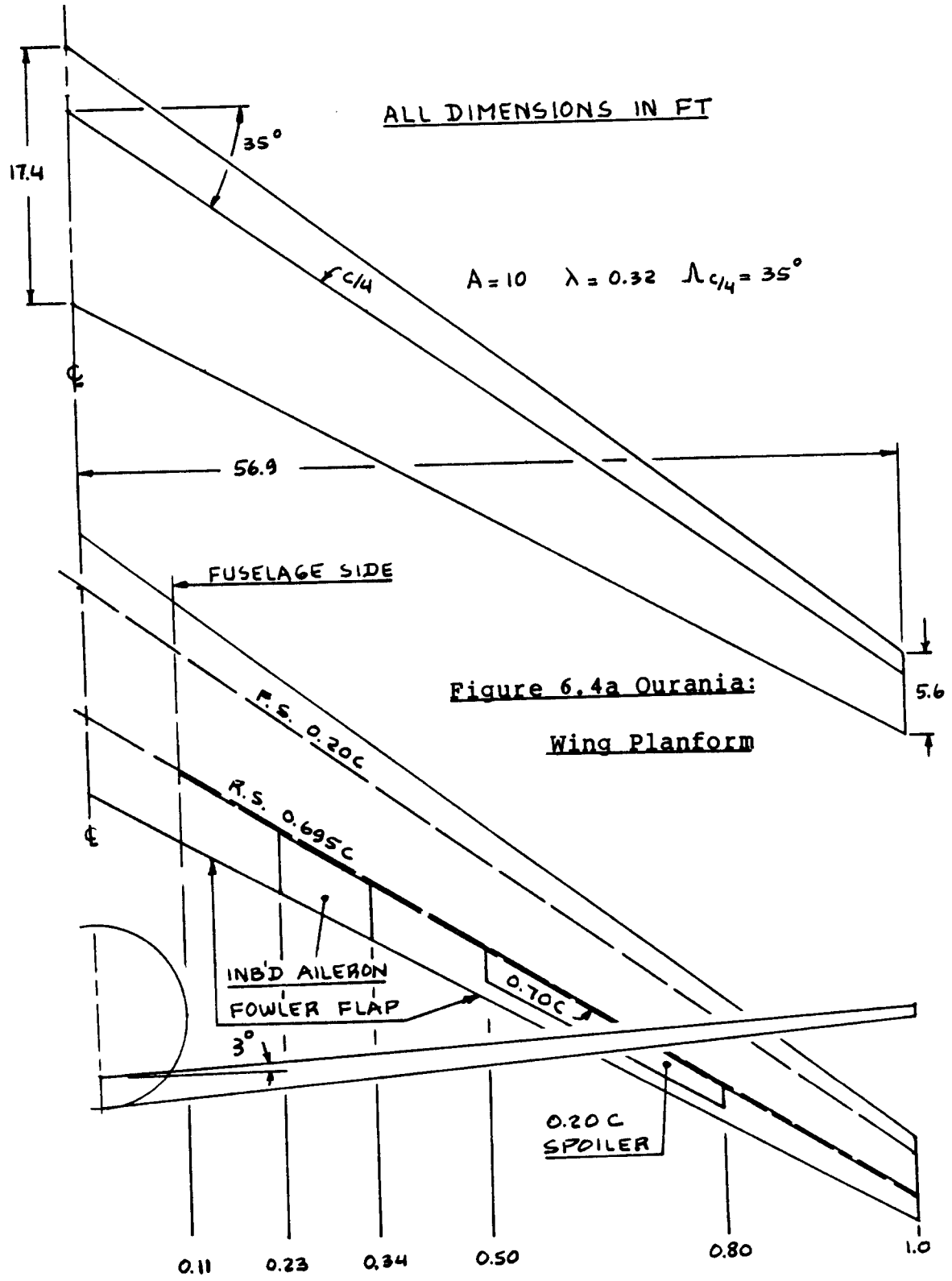

Figure 6.4a Ourania: Wing Planform

Figure 6.4b Ourania: Flap and Lateral Control Layout

Step 6.9: With an aileron and flap chord ratio of 0.30 the rear spar will be at (1 - 0.30 - 0.005)c = 0.695c. The front spar will be assumed to be at 0.20c. Figure 6.4b shows these spar locations.

Step 6.10: Using Eqn.(6.1), with τ = 0.11/0.13 = 0.85, λ_w = 0.32, S = 1,296 ft^2 and b = 113.8 ft:

V_{WF} = 821 ft^3.

The required amount of fuel is 25,850 lbs. This follows from p.59 of Pt.I. This amounts to 25,850/50.4 = ft^3 of required fuel volume. The wing therefore has a sufficient amount of fuel volume.

Step 6.11: From Table 6.7 it is observed that a wing dihedral angle of 3 degrees is an acceptable choice.

Step 6.12: From Table 6.7 it is seen that a wing incidence angle of i_w = 1.5 degrees may be o.k. A twist angle of ε_t = -2 deg. at the tip with a linear distribution from root to tip will be assumed for now.

Step 6.13: To save space this step has been omitted.

6.2.3 Fighter

The following information is already available for the wing of the Eris:

S = 1,173 ft^2, A = 4 and therefore b = 68.5 ft.

These data follow from the preliminary sizing work of sub-section 3.7.4 in Part I.

Comparing the wing area of this fighter with that of the transport example indicates that the fighter wing is very large indeed. If a taper ratio of 0.4 were used, a root chord of 24.5 ft would result. This represents almost the length of the fuselage of the Eris as drawn in Figure 4.9! This is probably not acceptable. It is therefore proposed to take another look at the matching results of Figure 3.36 in Part I(p.187). It is observed from Figure 3.36 that higher wing loadings could be accepted, provided higher values of $C_{L_{max_{TO}}}$ are allow-

able. Extrapolating to $C_{L_{max_{TO}}} = 2.8$ while maintaining the same value of $(T/W)_{TO} = 0.46$ yields a wing loading of 84 psf. This in turn leads to the much more reasonable value for wing area of 787 ft^2.

While reexamining the wing geometry it becomes evident that the previously selected value for aspect ratio of 4 is probably too low for this type of fighter. Table 6.9 shows that A = 6 is a more reasonable choice when compared to similar attack fighters.

The reader should redo the performance sizing calculations of sub-section 3.7.4 (pt.I) with A = 6 to verify that this is indeed a better choice.

The Eris wing geometry is now defined by:

S = 787 ft^2, A = 6, and therefore b = 68.7 ft.

Step 6.1: Not applicable: the Eris is not a flying wing.

Step 6.2: The cruise speed of the Eris is required to be M = 0.85 at 40,000 ft (Table 2.19, Part I). This speed requirement is consistent only with a cantilever wing.

Step 6.3: A high wing was already decided on in the selection of the overall configuration in sub-section 3.5.3.

Step 6.4: The sweep angle for the Eris wing must be selected on the basis of a critical Mach number of at least 0.85. The cruise lift coefficient of the Eris may be estimated from Eqn.(6.1) as:

At 40,000 ft: $C_{L_{cr}} =$

$(54,500 - 0.4x18,500)/1,482x0.1851x0.85^2x0.185x787 = 0.30$

At sealevel:

$C_{L_{cr}} = (54,500 - 0.4x18,500)/1,482x(450/662)^2x787 = 0.09$

Figures 6.1 and 6.2 show that with (t/c) = 0.10 and no sweep, a critical Mach number of 0.83 may be achievable. Since the wing will actually be thinner at

the wing/fuselage intersection, this choice may be acceptable.

The following choices are therefore made:

$\Lambda_{c/4}$ = 0 deg., $(t/c)_r$ = 0.10, $(t/c)_t$ = 0.08

There exists a trade between wing critical Mach number, wing weight, wing sweep and wing thickness ratio. A more detailed stude of this trade relation will be required before making a final choice.

Step 6.5: A supercritical derivative of NACA 64A210/208 will be used. The airfoil geometry would have to be derived with the help of a transonic airfoil code.

Step 6.6: Table 6.8 shows that a wing taper ratio of λ_w = 0.50 is an appropriate choice. Figure 6.5a shows a dimensioned drawing of the proposed wing planform. The planform is defined by the following parameters:

$S = 787\ ft^2$, A = 6, b = 68.7 ft

$\Lambda_{c/4} = 0^\circ$, λ_w = 0.50

From these data: c_r = 15.3 ft and c_t = 7.6 ft.

Step 6.7: See sub-section 7.2.3.

Step 6.8: The flap sizing analysis of sub-section 7.2.3 shows that a full span flap is needed. That means no aileron can be used. Therefore spoilers will have to be employed. The following spoiler geometry is guessed at for now:

inb'd spoiler span fraction: 0.40, chord fraction: 0.20
outb'd spoiler span fraction: 1.00, chord fraction: 0.20

The spoiler hingeline will be placed at 0.70c.

Step 6.9: With a spoiler and flap chord ratio of 0.30 the rear spar will be at (1 - 0.30 - 0.005)c = 0.695c. The front spar will be assumed to be at 0.20c. Figure 6.5b shows these spar locations.

Step 6.10: Using Eqn.(6.1), with τ = 0.08/0.10 = 0.80, λ_w = 0.50, $S = 787\ ft^2$ and b = 68.7 ft:

$V_{WF} = 357\ ft^3$.

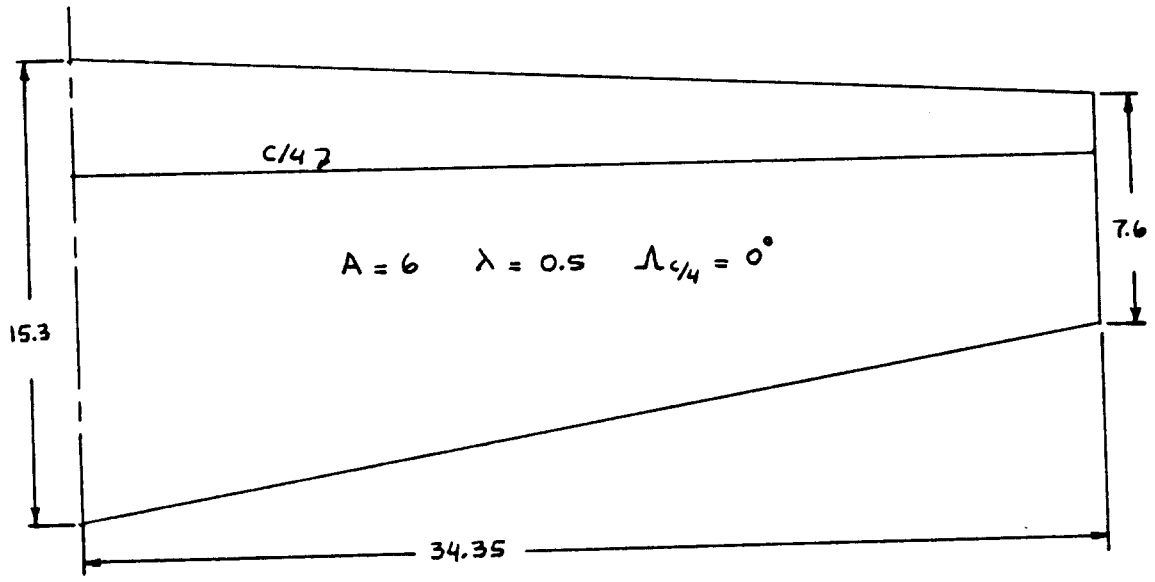

Figure 6.5a Eris: Wing Planform

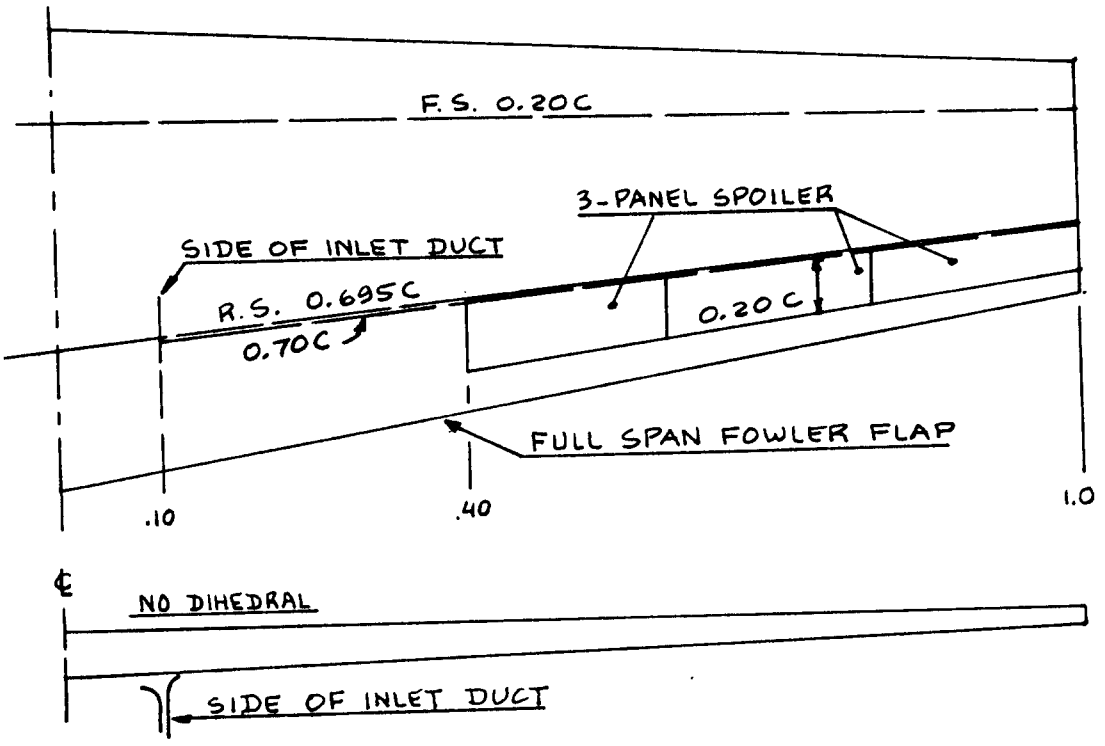

Figure 6.5b Eris: Flap and Lateral Control Layout

The required amount of fuel is 18,500 lbs. This follows from p.67 of Pt.I. This amounts to 18,500/49 = ft^3 of required fuel volume. The wing therefore is slightly deficient in fuel volume. However, the difference is so small that at this stage in the design process no change in wing area needs to be contemplated. Besides, there appears to be a reasonable amount of fuselage volume available for additional tankage if required: Figure 4.9 shows this.

Step 6.11: From Table 6.9 it is observed that a wing dihedral angle of Γ_w= 0 deg. is probably acceptable. The Eris is a high wing airplane and therefore has some inherent lateral stability.

Step 6.12: From Table 6.7 it is seen that a wing incidence angle of i_w = 0 degrees may be o.k. A twist angle of ε_t= -2 deg. at the tip with a linear distribution from root to tip will be assumed for now.

Step 6.13: To save space this step has been omitted.

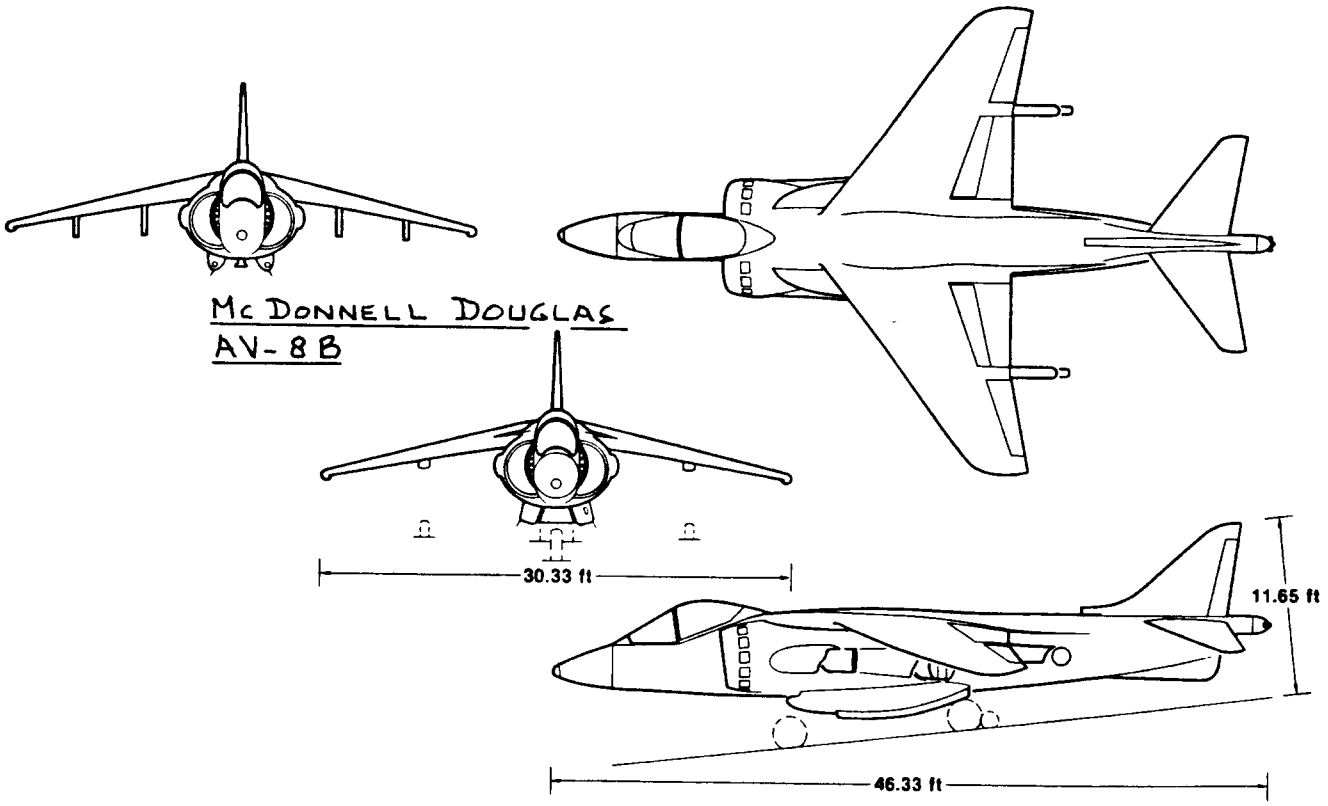

7. CLASS I METHOD FOR VERIFYING CLEAN AIRPLANE $C_{L_{max}}$ AND FOR SIZING HIGH LIFT DEVICES

The purpose of this chapter is to present a Class I methodology for determining:

1. Whether or not the wing geometry selected in Chapter 6 is consistent with the required value of clean airplane $C_{L_{max}}$.

2. The type and size of high lift devices needed by the airplane to meet the requirements for $C_{L_{max_{TO}}}$ and for $C_{L_{max_L}}$.

The method presented is part of Step 7 in p.d. sequence I as outlined in Chapter 2.

Section 7.1 contains the method as an 8-step procedure. Example applications to three types of airplanes are contained in Section 7.2.

7.1 A PROCEDURE FOR DETERMINING CLEAN AIRPLANE $C_{L_{max}}$ AND FOR SIZING HIGH LIFT DEVICES

Important note: The method presented here should not be used for wing sweep angles larger than about +/- 35 degrees. For larger sweep angles the reader should refer to Part VI(Ref.5).

Step 7.1: List the values for the following maximum lift coefficients:

Clean: $C_{L_{max}}$ Take-off: $C_{L_{max_{TO}}}$ Landing: $C_{L_{max_L}}$

The reader will recall that these values followed from the preliminary sizing process of Part I.

Step 7.2: Verify that the existing wing planform can produce a value of $C_{L_{max_W}}$, which is consistent with the required value of clean airplane $C_{L_{max}}$.

First it must be realized that any value for total airplane $C_{L_{max}}$ must be assumed to be a 'trimmed' value.

For most airplane configurations (conventional as well as canard) it is conservative in the early phases of preliminary design to assume:

$$C_{L_{max_w}} = 1.05 \text{ to } 1.1 C_{L_{max}} \qquad (7.1)$$

The factor 1.05 to 1.1 accounts for the 'tail down-load to trim' or for the interference of the 'canard up-load to trim' on the wing. For 'short-coupled' airplanes, use 1.1. For 'long-coupled' airplanes use 1.05.

A 'short-coupled' airplane is one with $l_h/\bar{c} < 3.0$.

A 'long-coupled' airplane is one with $l_h/\bar{c} > 5.0$.

If the wing sweep angle is between 0 and 35 degrees it will be necessary to 'correct' for the effect of sweep by using the so-called cosine-rule:

$$C_{L_{max_{unswept_w}}} = C_{L_{max_{swept_w}}} / \cos\Lambda_{c/4} \qquad (7.2)$$

To verify whether or not the wing can produce its required value of unswept $C_{L_{max_w}}$ as determined from Eqn.(7.2) the following approximation may be used:

$$C_{L_{max_w}} = k_\lambda (C_{l_{max_r}} + C_{l_{max_t}})/2 \qquad (7.3)$$

where: $k_\lambda = 0.88$ for $\lambda = 1.0$

and: $k_\lambda = 0.95$ for $\lambda = 0.4$

NOTE: Eqn.(7.3) does not account for wing twist!

Values for section maximum lift coefficients may be determined from Ref.20 and from Ref.23. In the absence of these references, values for section maximum lift coefficients at the root and at the tip may be determined from Figure 7.1. Note that before Fig. 7.1 can be used, the Reynolds numbers for the root and tip sections must be computed. This can be done with Equations (7.4) and (7.5):

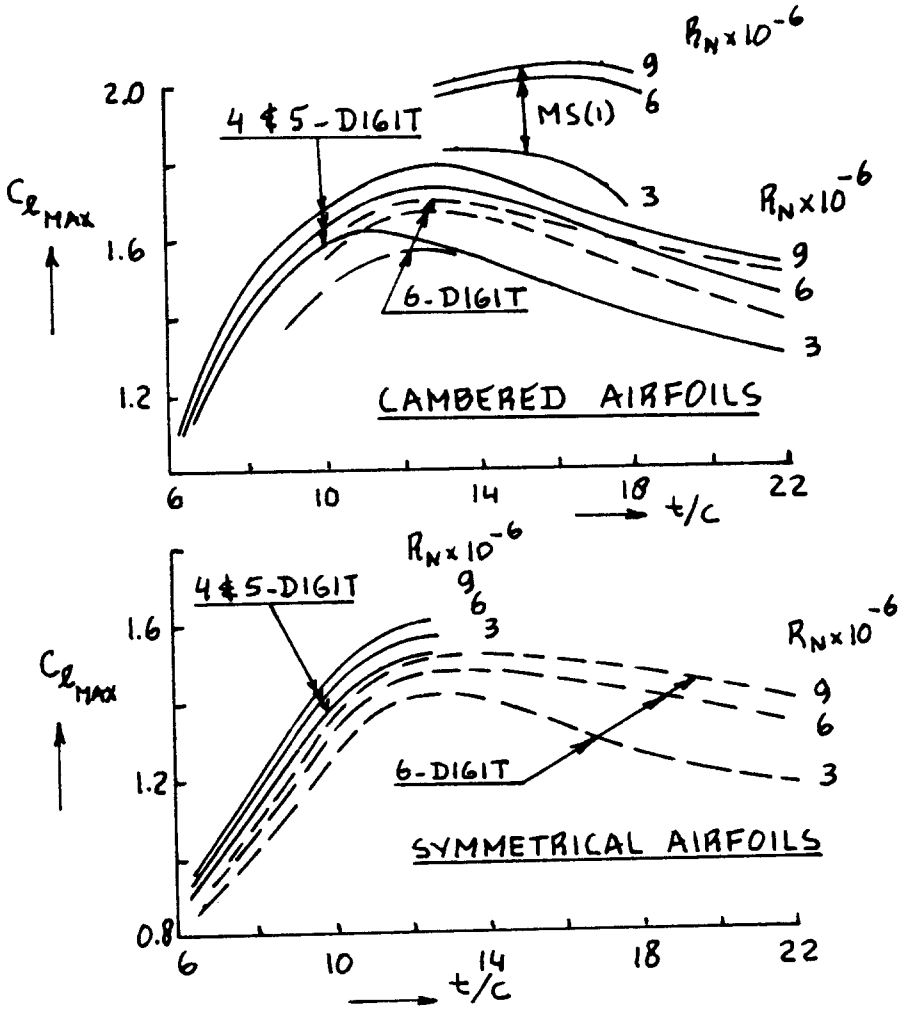

Figure 7.1 Effect of Thickness Ratio and Reynold's Number on Section Maximum Lift Coefficient

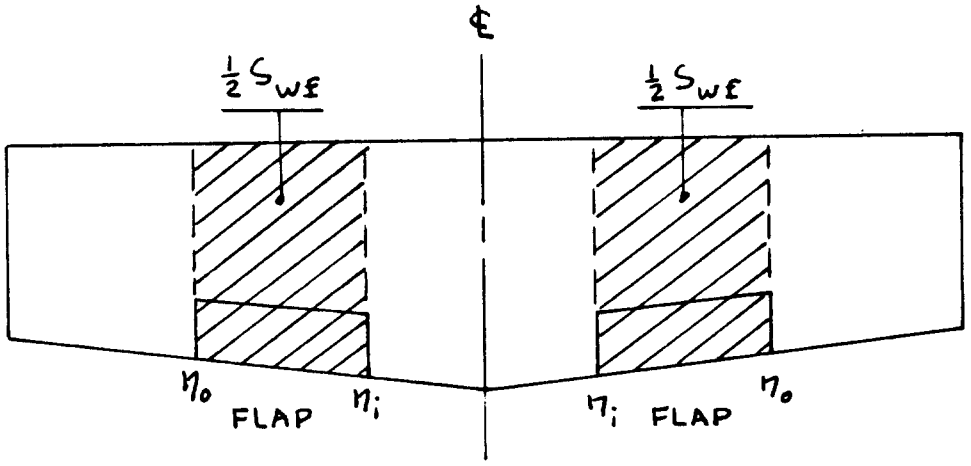

Figure 7.2 Definition of Flapped Wing Area

at the root: $R_{n_r} = \rho V c_r / \mu$ (7.4)

at the tip: $R_{n_t} = \rho V c_t / \mu$ (7.5)

If the wing planform under consideration cannot meet the required value of $C_{L_{max}}$ within 5 percent it will be necessary to redesign the wing planform and/or to select different airfoils until it does. It makes very little sense to proceed with a wing design which cannot deliver the required value of clean maximum lift coefficient.

Step 7.3: Determine the incremental values of maximum lift coefficient which need to be produced by the high lift devices:

Take-off: $\Delta C_{L_{max_{TO}}} = 1.05(C_{L_{max_{TO}}} - C_{L_{max}})$ (7.6)

Landing: $\Delta C_{L_{max_L}} = 1.05(C_{L_{max_L}} - C_{L_{max}})$ (7.7)

The factor 1.05 in Eqns.(7.6) and (7.7) accounts for the additional trim penalties incurred by the use of flaps. These penalties exist for conventional as well as for canard configurations.

Step 7.4: Compute the required incremental section maximum lift coefficient with the flaps down from:

$$\Delta C_{l_{max}} = \Delta C_{L_{max}} (S/S_{wf}) K_{\Lambda}, \quad (7.8)$$

where S_{wf} is defined in Figure 7.2 and where K_{Λ} is found from:

$$K_{\Lambda} = (1 - 0.08\cos^2\Lambda_{c/4})\cos^{3/4}\Lambda_{c/4} \quad (7.9)$$

The factor K_{Λ} accounts for the effect of sweep angle in the flaps down case.

For straight, tapered wings the ratio S_{wf}/S can be computed from:

$$S_{wf}/S = (\eta_o - \eta_i)\{2 - (1 - \lambda)(\eta_i + \eta_o)\}/(1 + \lambda), \quad (7.10)$$

where the span stations η_i and η_o are defined in Fig.7.2.

Step 7.5: Compute the required value of incremental section lift coefficient, ΔC_l, which the flaps must generate and relate this value to flap type, flap angle and flap chord.

The incremental section lift coefficient due to flaps, ΔC_l is related to its counterpart $\Delta C_{l_{max}}$ as defined in Figure 7.3.

In preliminary design it is conservative to use:

$$\Delta C_l = (1/K)\Delta C_{l_{max}}, \tag{7.11}$$

where the factor K is found from Figure 7.4.

The magnitude of incremental section lift coefficient due to flaps depends on the following factors:

1. the flap-to-chord ratio c_f/c of the flaps
2. the type of flaps used
3. the flap deflection angle used

Equations for computing obtainable values for ΔC_l are now given for four types of flaps:

Plain flaps: $$\Delta C_l = C_{l_{\delta_f}} \delta_f K', \tag{7.12}$$

where $C_{l_{\delta_f}}$ and K' may be found from Figure 7.5 and from Figure 7.6 respectively.

Split flaps: $$\Delta C_l = k_f (\Delta C_l)_{c_f/c = 0.2}, \tag{7.13}$$

where k_f and $(\Delta C_l)_{c_f/c = 0.2}$ can be found from Fig.7.7.

Single slotted flaps: $$\Delta C_l = C_{l_{\alpha_f}} \alpha_{\delta_f} \delta_f, \tag{7.14}$$

where α_{δ_f} may be found from Figure 7.8 and where $C_{l_{\alpha_f}}$ is the flapped section lift curve slope which can be

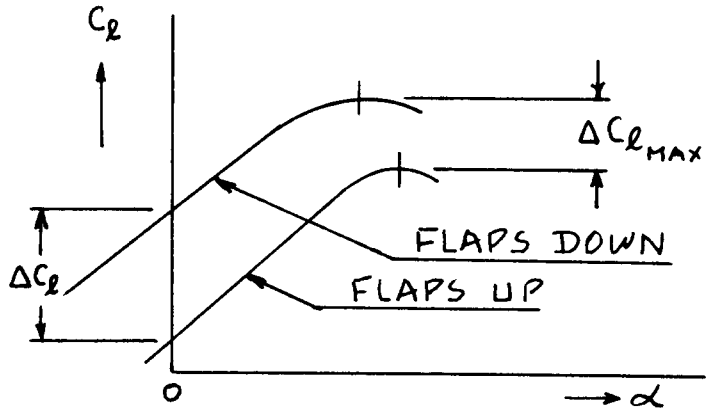

Figure 7.3 Relation Between ΔC_l and $\Delta C_{l_{max}}$

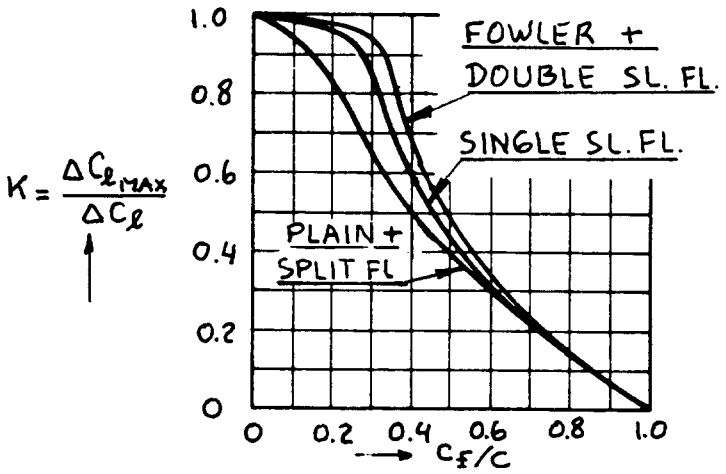

Figure 7.4 Effect of Flap Chord Ratio and Flap Type on $K = \Delta C_{l_{max}} / \Delta C_l$

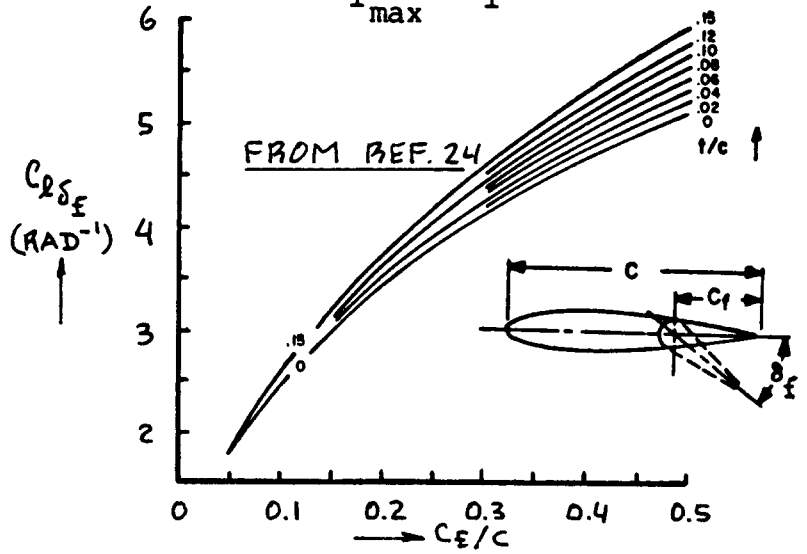

Figure 7.5 Effect of Thickness Ratio and Flap Chord Ratio on $C_{l_{\delta_f}}$

Figure 7.6 Effect of Flap Chord Ratio and Flap Deflection on K'

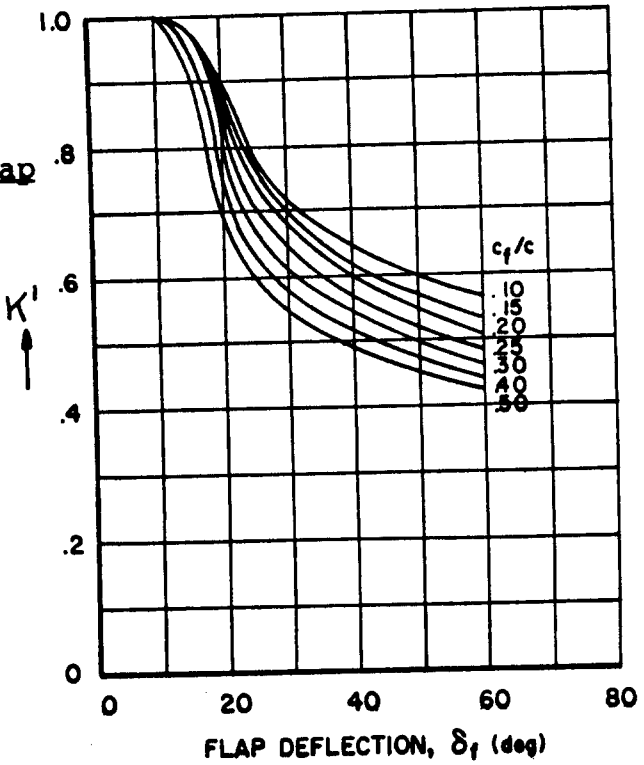

COPIED FROM REF. 24

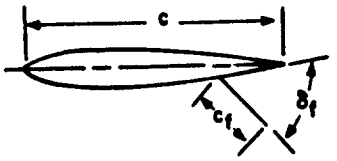

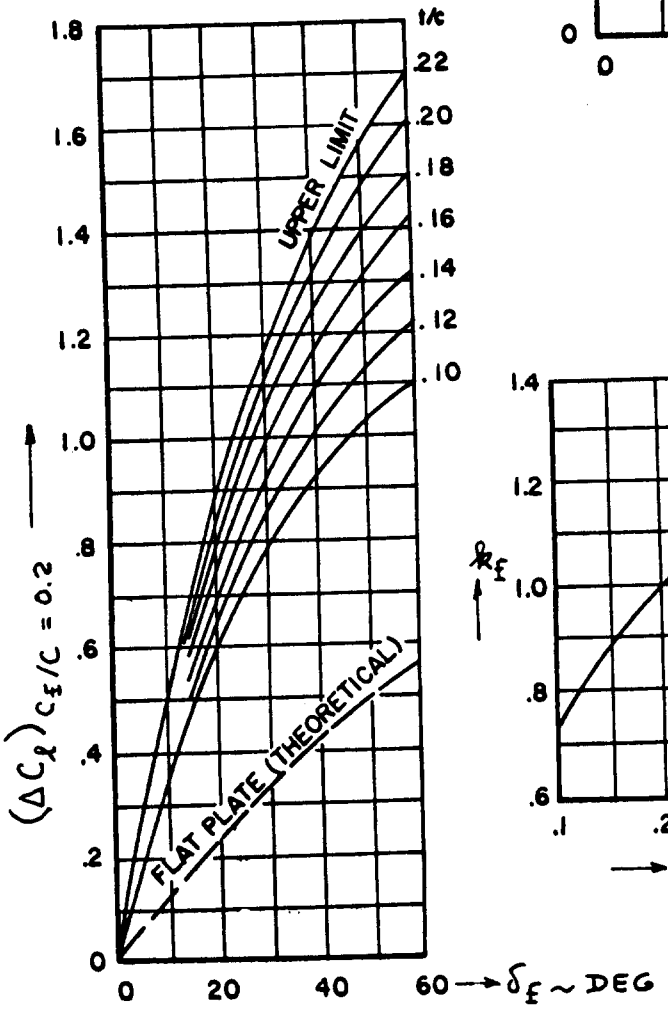

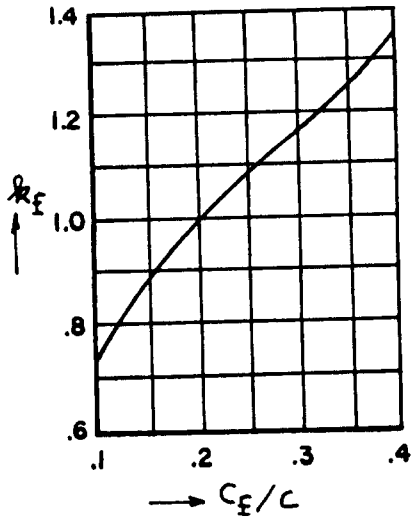

Figure 7.7 Empirical Constants for Split Flap Analysis

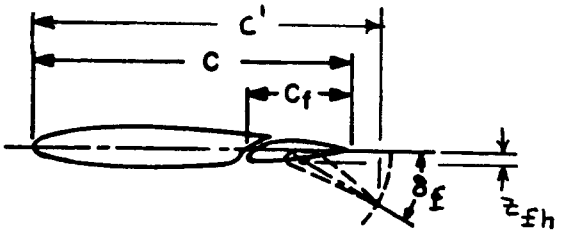

COPIED FROM REF. 24

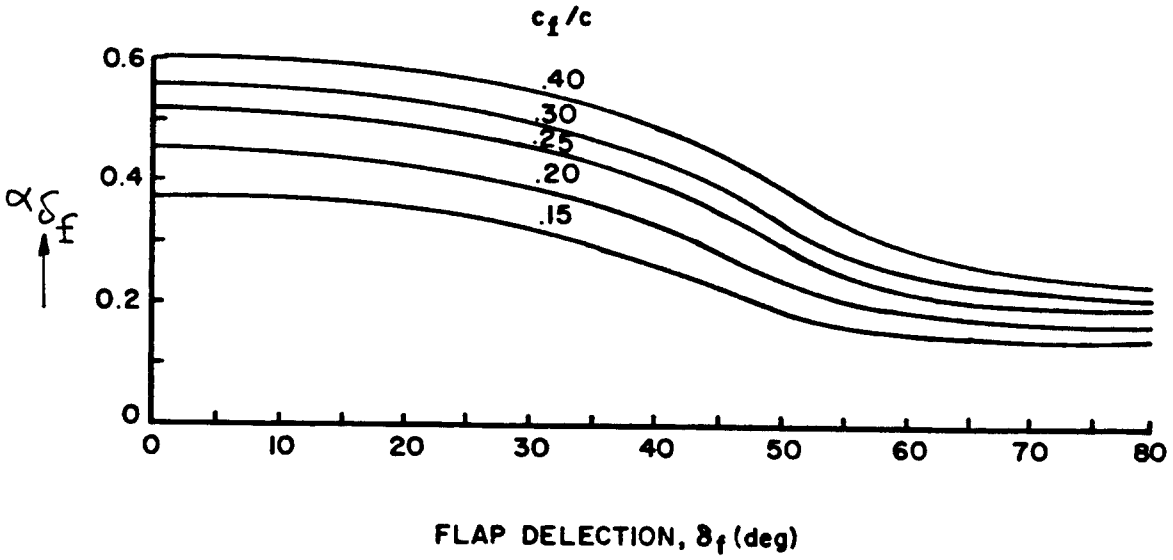

Figure 7.8 Section Lift Effectiveness Parameter for Single Slotted Flaps

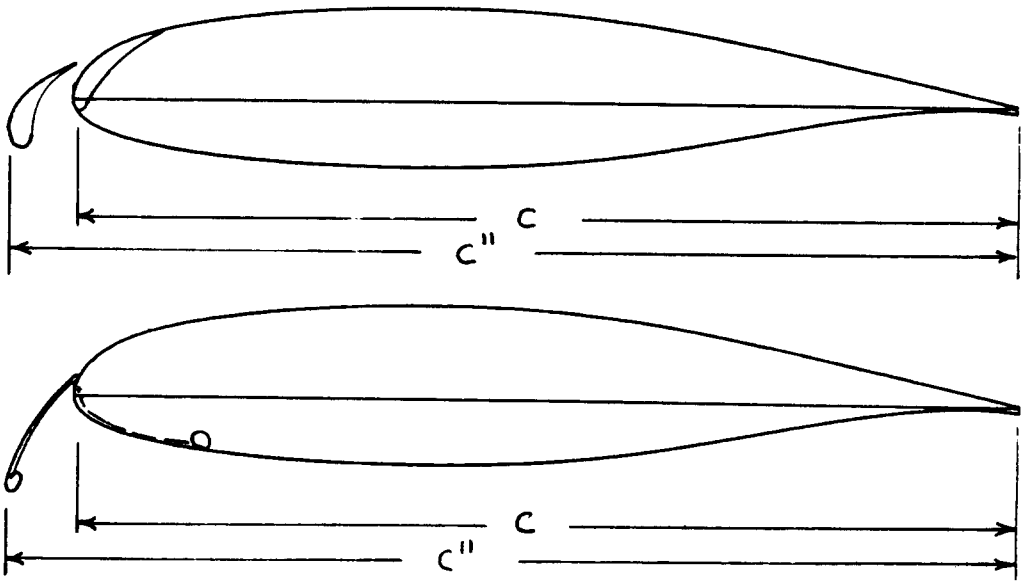

Figure 7.9 Definition of Section Chords With Deployed Leading Edge Devices

obtained from:

$$C_{l_{\alpha_f}} = C_{l_\alpha}(c'/c) \tag{7.15}$$

$$\text{with: } c'/c = 1 + 2(z_{fh}/c)\tan(\delta_f/2) \tag{7.16}$$

Geometric definitions for c' and for z_{fh} are given in Figure 7.8.

The value of unflapped section lift curve slope, C_{l_α} in Eqn.(7.15) may be found from section data as in Ref.20 or may be assumed to be 2π.

<u>Fowler flaps:</u> use Eqn.(7.14), however with:

$$C_{l_{\alpha_f}} = C_{l_\alpha}(1 + c_f/c), \tag{7.17}$$

which applies to a fully aft translating Fowler flap.

The four flap types discussed sofar are all trailing edge devices.

In many cases it will be necessary to also employ leading edge devices. The reader should preferably use experimental data to estimate the effect of leading edge devices on maximum section lift. In the absence of such data the following equation may be used in the early phase of preliminary design:

$$C_{l_{max}}{}_{\text{with l.e. flap}} = C_{l_{max}}{}_{\text{no l.e. flap}}(c''/c), \tag{7.18}$$

where c'' is defined in Figure 7.9 for slats and for Krueger flaps.

References 20 and 23 contain a significant amount of data on maximum lift coefficient capability for a wide variety of high lift devices.

With the methods of Step 7.5 it is possible to determine that combination of items 1 through 4:

1. Flap angle δ_f
2. Flap chord ratio c_f/c
3. S_{wf}/S and thus flap span ratio b_f/b
4. Flap type (trailing and leading edge)

which satisfies the flaps down lift coefficient requirements as listed in Step 7.1.

Step 7.6: Draw the required flap geometries in the wing planform drawing of Step 6, Ch.6.

Make sure that the required flaps are compatible with:

1. required lateral controls (as defined in Step 6.7 in Chapter 6.
2. fuselage width at the inboard flap station.
3. engine nacelles placed on the wing: it is not desirable to have hot exhaust gasses impinge on the flaps unless these are made of steel or titanium.

Step 7.7: Document the decisions made under Steps 7.1 - 7.6 in a brief, descriptive report including clear dimensioned drawings.

Step 7.8: Return to Step 6.9 in Chapter 6.

7.2 EXAMPLE APPLICATIONS

The following three example applications will be presented:

7.2.1 Twin Engine Propeller Driven Airplane: Selene
7.2.2 Jet Transport: Ourania
7.2.3 Fighter: Eris

7.2.1 Twin Engine Propeller Driven Airplane

Step 7.1: The values of the required maximum lift coefficients are found from Part I, p.178 as:

$$C_{L_{max}} = 1.7 \qquad C_{L_{max_{TO}}} = 1.85 \qquad C_{L_{max_L}} = 2.3$$

Step 7.2: The wing planform selected for this airplane is described in Chapter 6, sub-section 6.2.1. It was found that:

$A = 8$, $S = 172$ ft^2, $b = 37.1$ ft, $\Lambda_{c/4} = 0$ deg.

$\lambda = 0.4$, $c_r = 6.62$ ft and $c_t = 2.65$ ft.

It may be judged from the fuselage arrangement drawing of Figure 4.2b that the Selene is a moderately

short-coupled airplane. Therefore, from Eqn.(7.1):

$$C_{L_{max_w}} = 1.06 \times 1.7 = 1.80.$$

Because the Selene has no sweep, it follows from Eqn.(7.3) that: $(C_{l_{max_r}} + C_{l_{max_t}}) = 2 \times 1.80/0.95 = 3.79.$

Section maximum lift coefficients of the order of 2.0 are therefore required. Consultation of Figure 7.1 shows that NACA airfoils are not able to deliver the required section maximum lift coefficients. The data in Ref.22, on the NASA MS(1)-0317/0313 airfoils suggest that these airfoils may meet the required maximum lift value. To check this, the Reynold's numbers of root and tip are computed from Eqns.(7.4) and (7.5):

$$R_{n_r} = (0.002378 \times 151 \times 6.62)/3.737 \times 10^{-7} = 6.4 \times 10^6$$

$$R_{n_t} = 0.4 \times 6.4 \times 10^6 = 2.5 \times 10^6$$

From Figure 6 of Ref.22 it follows that for this airfoil:

$C_{l_{max_r}} + C_{l_{max_t}} = 2.0 + 1.7 = 3.7$, which is close enough to the required value of 3.79.

The selected wing geometry will therefore result in the required value of clean airplane maximum lift coefficient as long as NASA MS(1)-0317/0313 are used.

Step 7.3: From Step 7.1 and with Eqn.(7.6) and with Eqn.(7.7):

$$\Delta C_{L_{max_{TO}}} = 1.07(1.85 - 1.7) = 0.16.$$

$$\Delta C_{L_{max_L}} = 1.07(2.3 - 1.7) = 0.64.$$

It is observed that the required flap lift increments are not very high. It is therefore conjectured that a relatively small single slotted flap will probably be sufficient.

Step 7.4: Equation (7.8) which depends on the flap size parameter S_{wf}/S will be used. This flap size para-

meter is not yet known.

At this point it is possible to proceed with two or three arbitrary values for S_{wf}/S. Example values selected are: 0.3 and 0.6.

The sweep correction factor K_Δ from Eqn.(7.9) is 0.92. Eqn.(7.8) now yields:

	Landing flaps		Take-off flaps	
S_{wf}/S =	0.3	0.6	0.3	0.6
$\Delta C_{l_{max}}$ =	0.49	0.25	1.96	0.98

Step 7.5: It was observed earlier that a simple single slotted flap might be sufficient for this airplane. The following 'educated' guesses are made for the flap geometry:

$z_{fh}=0.1$ $c_f/c = 0.25$ $\delta_{f_{TO}} = 15$ deg. $\delta_{f_L} = 40$ deg.

Take-off: From Eqn.(7.15): $c'/c = 1.03$

From Eqn.(7.14): $C_{l_{\alpha_f}} = 1.03x2x3.14 = 6.45$

From Eqn.(7.13) and from Figure 7.7:

$\Delta C_l = 6.45x(15/57.3)x0.5 = 0.84$

The factor K from Figure 7.3b is: K = 0.93 and thus:

From Eqn.(7.10): $\Delta C_{l_{max}} = (0.93)x0.84 = 0.78$

It is seen that this is much more than needed with the previously assumed values of S_{wf}/s. The take-off flaps are thus not critical.

Landing: From Eqn.(7.15): $c'/c = 1.06$

From Eqn.(7.14): $C_{l_{\alpha_f}} = 1.06x2x3.14 = 6.66$

From Eqn.(7.13) and from Figure 7.7:

$\Delta C_l = 6.66x(40/57.3)x0.43 = 2.0$

From Eqn.(7.10): $\Delta C_{l_{max}} = (0.93)x2.0 = 1.86$

Interpolating for the ratio S_{wf}/S yields the following value:

$S_{wf}/S = 0.33$

Step 7.6: The following summarizes the flap geometry:

$S_{wf}/S = 0.33$ $c_f/c = 0.25$ Single slotted flap with hinge at:

Take-off $\delta_f = 10$ deg. $z_{fh} = 0.10$

Landing $\delta_f = 40$ deg.

The ratio of flapped wing area to wing area, $S_{wf}/S = 0.33$ needs to be translated into the required spanwise flap stations. This is done with the help of Eqn.7.10. For the Selene, the value of $\eta_i = 4.5/37.1 = 0.12$.

It follows that: $\eta_o = 0.76$

The take-off flap deflection of 10 deg. is an arbitrary choice at this point.

Figure 6.3b shows a dimensioned sketch of the proposed flap, spar and aileron layout. The body width of 4.5 ft was selected in sub-section 4.2.1, the aileron geometry required in subsection 6.2.1.

Since it was decided in sub-section 3.6.1 to retract the landing gear into the fuselage, the flap/spar geometry has no effect on the landing gear.

The flaps are seen to be compatible with the lateral control size requirement described in sub-section 6.2.1.

Step 6.7: To save space, this step is omitted.

7.2.2 Jet Transport

Step 7.1: The values of the required maximum lift coefficients are found from Part I, p.184 as:

$C_{L_{max}} = 1.4^*$ $C_{L_{max_{TO}}} = 2.8$ $C_{L_{max_L}} = 3.2$

* This value was assumed for purposes of climb sizing calculations only. It is not essential that this value be met.

Step 7.2: The wing planform selected for this airplane is described in Chapter 6, sub-section 6.2.2. It was found that:

$$A = 10,\ S = 1{,}296\ ft^2,\ b = 113.8\ ft,\ \Lambda_{c/4} = 35\ deg.$$

$$\lambda = 0.32,\ c_r = 17.4\ ft \text{ and } c_t = 5.60\ ft.$$

To determine the maximum lift coefficient capability of the Ourania wing, the Reynold's numbers of root and tip are computed from Eqns.(7.4) and (7.5):

$$R_{n_r} = (0.002378 \times 243 \times 17.4)/3.737 \times 10^{-7} = 26.9 \times 10^6$$

$$R_{n_t} = 0.32 \times 26.9 \times 10^6 = 8.6 \times 10^6$$

The speed of 243 fps was computed for the take-off weight and by assuming the clean maximum lift coefficient to be 1.4.

From Figure 7.1 it is seen that the root airfoil with t/c = 0.13 could yield a section maximum lift coefficient of 1.9. For the tip airfoil with t/c = 0.11 the corresponding value is 1.7. Therefore, with Eqn.(7.3):

$$C_{L_{max_w}} = 0.95(1.9 + 1.7)/2 = 1.71.$$

This in turn yields with Eqn.(7.2):

$$C_{L_{max_w}} = 1.71\cos 35 = 1.4.$$

Since the Ourania is seen from Fig.4.7 to be a moderately short coupled airplane, Eqn.(7.1) yields:

$$C_{L_{max}} = 1.4/1.06 = 1.32.$$

This is judged to be close enough to the assumed value of 1.4. The latter will be used in the flap sizing calculations.

Step 7.3: From Step 7.1 and with Eqns.(7.6) and (7.7):

$$\Delta C_{L_{max_{TO}}} = 1.05(2.8 - 1.4) = 1.47.$$

$$\Delta C_{L_{max_L}} = 1.05(3.2 - 1.4) = 1.89.$$

It is observed that the required flap lift increments are high. It is therefore conjectured that Fowler flaps will be needed to meet the required lift increments. This is entirely in line with the type of flaps employed on existing Boeing transports.

Step 7.4: Equation (7.8) which depends on the flap size parameter S_{wf}/S will be used. This flap size parameter is not yet known.

At this point it is possible to proceed with two or three arbitrary values for S_{wf}/S. Example values selected are: 0.6 and 0.8.

The sweep correction factor K_Λ from Eqn.(7.9) is 0.82. Eqn.(7.8) now yields:

	Take-off flaps		Landing flaps	
S_{wf}/S =	0.6	0.8	0.6	0.8
$\Delta C_{l_{max}}$ =	2.00	1.51	2.58	1.94

Step 7.5: It was observed earlier that a Fowler flap will probably be required. The following 'educated' guesses are made for the flap geometry:

$c_f/c = 0.30 \quad \delta_{f_{TO}} = 20$ deg. $\quad \delta_{f_L} = 40$ deg.

The necessary values of ΔC_l are found from Eqn.(7.10) and with Figure 7.3b (K = 0.94) as follows:

	Take-off flaps		Landing flaps	
S_{wf}/S =	0.6	0.8	0.6	0.8
ΔC_l =	2.13	1.61	2.74	2.06

Take-off: From Eqn.(7.16): $C_{l_{\alpha_f}} = 2\pi \times 1.3 = 8.17$

From Eqn.(7.13) and from Figure 7.7:

$\Delta C_l = 8.17 \times 0.53 \times (20/57.3) = 1.51$

It is seen that leading edge devices will be needed to produce the required lift increments or that the flap span will have to be carried all the way to the tip. Assuming that the flaps run from the fuselage side (at $\eta_i = 0.11$) to the tip ($\eta_o = 1.0$), a value of $S_{wf}/s = 0.84$ is found with Eqn.7.10. Extrapolating the values of available ΔC_l versus S_{wf}/S, it is found that $\Delta C_l = 1.1$ is needed. Since a value of 1.51 is available, full span flaps will be more than adequate.

The reader should note that the interruption of the flap span by the high speed aileron has been ignored in this calculation. That interruption will cause some loss in flap lift but not as much as a linear analysis would predict. For purposes of preliminary design it will therefore be assumed that full span Fowler flaps with a chord ratio of 0.30 are required. Instead of outboard ailerons, there will have to be outboard spoilers.

Step 7.6: The following summarizes the flap geometry:

$S_{wf}/S = 0.86$ $c_f/c = 0.30$ Fowler flap.

Take-off $\delta_f = 10$ deg.

Landing $\delta_f = 40$ deg.

The take-off flap deflection of 10 deg. is an arbitrary choice at this point.

Figure 6.4b shows a dimensioned sketch of the proposed flap, spar and aileron layout. The body width of 13.2 ft was selected in sub-section 4.2.2, the lateral control geometry required in subsection 6.2.2.

Since it was decided in sub-section 3.6.2 to retract the landing gear into the fuselage, the flap/spar geometry has no effect on the landing gear.

Step 6.7: To save space, this step is omitted.

7.2.3 Fighter

Step 7.1: The values of the required maximum lift coefficients are found from Part I, p.184 as:

$C_{L_{max}}$ and $C_{L_{max_L}}$ are not critical, $C_{L_{max_{TO}}} = 2.8$

Step 7.2: The wing planform selected for this airplane is described in Chapter 6, sub-section 6.2.3. It was found that:

$$A = 6,\ S = 787\ ft^2,\ b = 68.7\ ft,\ \Lambda_{c/4} = 0\ deg.$$

$$\lambda_w = 0.50,\ c_r = 15.3\ ft \text{ and } c_t = 7.6\ ft.$$

To determine the maximum lift coefficient capability of the Eris wing, the Reynold's numbers of root and tip are computed from Eqns.(7.4) and (7.5):

$$R_{n_r} = (0.002378 \times 157 \times 15.3)/3.737 \times 10^{-7} = 15.3 \times 10^6$$

$$R_{n_t} = 0.50 \times 15.3 \times 10^6 = 7.7 \times 10^6$$

The speed of 157 fps was computed for the take-off weight and by assuming the clean maximum lift coefficient to be 2.8.

From Figure 7.1 it is seen that the root airfoil with t/c = 0.10 could yield a section maximum lift coefficient of 1.65. For the tip airfoil with t/c = 0.08 the corresponding value is 1.55. Therefore, with Eqn.(7.3):

$$C_{L_{max_w}} = 0.95(1.65 + 1.55)/2 = 1.52.$$

This in turn yields with Eqn.(7.2):

$$C_{L_{max_w}} = 1.52\cos 0 = 1.52$$

Since the Eris is seen from Fig.4.7 to be a short coupled airplane, Eqn.(7.1) yields:

$$C_{L_{max}} = 1.52/1.10 = 1.38.$$

This is judged to be close enough to the assumed value of 1.4. The latter will be used in the flap sizing calculations.

Step 7.3: From Step 7.1 and with Eqns.(7.6) and (7.7):

$$\Delta C_{L_{max_{TO}}} = 1.05(2.8 - 1.4) = 1.47.$$

It is observed that the required flap lift increments are high. It is therefore conjectured that Fowler flaps will be needed to meet the required lift increments.

Step 7.4: Equation (7.8) which depends on the flap size parameter S_{wf}/S will be used. This flap size parameter is not yet known.

At this point it is possible to proceed with two or three arbitrary values for S_{wf}/S. Example values selected are: 0.4, 0.8 and 1.0

The sweep correction factor K_Δ from Eqn.(7.9) is 0.92. Eqn.(7.8) now yields:

Take-off flaps

S_{wf}/S =	0.4	0.8	1.0
$\Delta C_{l_{max}}$ =	3.38	1.69	1.35

Step 7.5: It was observed earlier that a Fowler flap will probably be required. The following 'educated' guesses are made for the flap geometry:

$c_f/c = 0.30 \quad \delta_{f_{TO}} = 20$ deg.

The necessary values of ΔC_l are found from Eqn.(7.10) and with Figure 7.3b (K = 0.94) as follows:

Take-off flaps

S_{wf}/S =	0.4	0.8	1.0
ΔC_l =	3.60	1.80	1.44

From Eqn.(7.16): $C_{l_{\alpha_f}} = 2\pi \times 1.3 = 8.17$

From Eqn.(7.13) and from Figure 7.7:

$\Delta C_l = 8.17 \times 0.53 \times (20/57.3) = 1.51$

It is seen that a full span Fowler flap will be required. This in turn makes it necessary to use

spoilers for lateral control. Since a fighter is operated without an autopilot, an aileron surface is not really needed.

Step 7.6: The following summarizes the flap geometry:

$S_{wf}/S = 1.0$ $c_f/c = 0.30$ Fowler flap.

Take-off $\delta_f = 20$ deg.

Landing $\delta_f = 40$ deg.

The landing flap deflection of 40 deg. is an arbitrary choice at this point.

Figure 6.5b shows a dimensioned sketch of the proposed flap, spar and spoiler layout. The body width of 8 ft was selected in sub-section 4.2.3, the lateral control geometry required in subsection 6.2.3.

Since it was decided in sub-section 3.6.2 to retract the landing gear into the fuselage, the flap/spar geometry has no effect on the landing gear.

Step 6.7: To save space, this step is omitted.

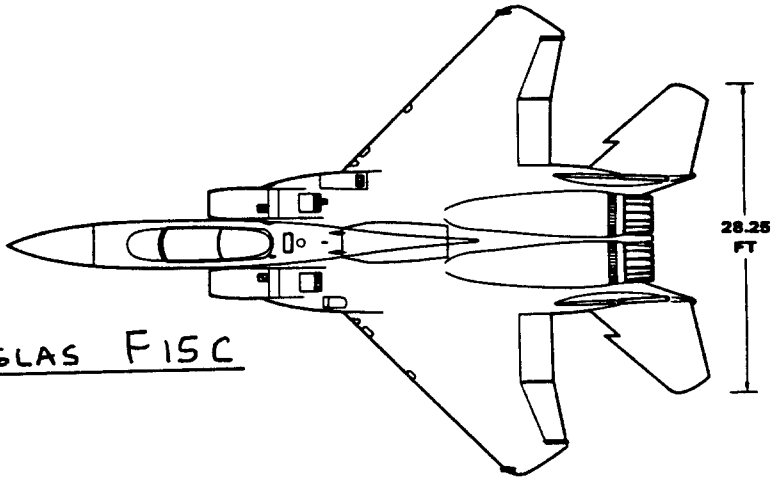

Mc Donnell Douglas F15C

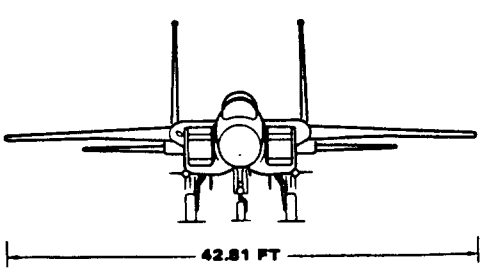

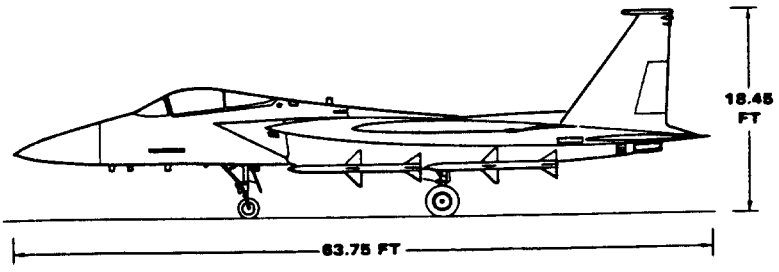

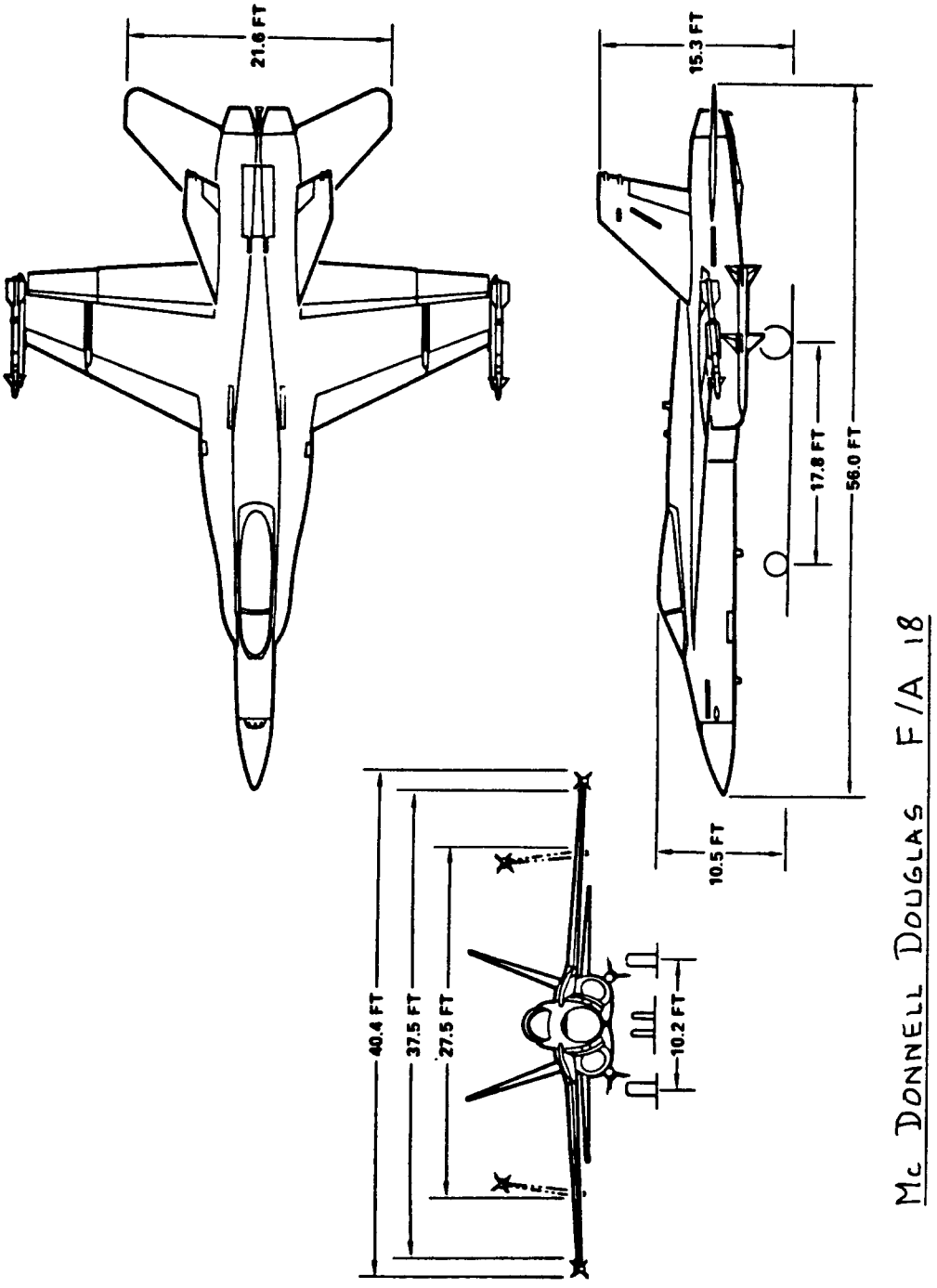

Mc Donnell Douglas F/A 18

8. CLASS I METHOD FOR EMPENNAGE SIZING AND DISPOSITION AND FOR CONTROL SURFACE SIZING AND DISPOSITION

The purpose of this chapter is to present a step-by-step method for deciding on the size and disposition of the empennage as well as on the size and disposition of the longitudinal and directional control surfaces. The method is presented as part of Step 8 in p.d. sequence I as outlined in Chapter 2.

Section 8.1 presents the method while Section 8.2 contains three example applications.

8.1 STEP-BY-STEP METHOD FOR EMPENNAGE SIZING AND DISPOSITION AND FOR CONTROL SURFACE SIZING AND DISPOSITION

Step 8.1: Decide on the overall empennage configuration to be used.

The possibilities which present themselves were already discussed in sub-section 3.3.5. The reader should consult that sub-section and make a decision.

As a general rule, the horizontal tail should not be placed directly in the propeller slipstream. By referring to section 3.1 the reader will observe that many airplanes in fact do have the horizontal tail in the slipstream. The reasons against this arrangement are:

a.) The slipstream will usually cause the tail to buffet which leads to structure-borne cabin noise. Tail buffet can also lead to early structural fatigue.

b.) Rapid power increases or decreases called for by the pilot can result in undesirably large trim changes.

These comments also apply to canards. There is not usually a problem with a vertical tail mounted in the slipstream at the aft end of a fuselage.

Note: Single engine propeller driven airplanes usually do have the empennage mounted in the slipstream. This does enhance elevator effectiveness and rudder effectiveness during the take-off roll. On the other hand, it also causes considerable tail buffet during the take-off roll in some airplanes.

Step 8.2: Determine the disposition of the empennage.

Having decided on the overall empennage configuration in Step 8.1 the location of the empennage components on the airplane should now be decided. This amounts to deciding on the empennage moment arms x_h, x_v and x_c as defined in Figure 8.1. These empennage moment arms can be determined from the general arrangement drawing of the fuselage which was prepared in Chapter 4.

To keep the airplane weight and drag down as much as possible it is obviously desirable to keep the empennage area as small as possible. This in turn can be achieved by locating the empennage components at as large a moment arm as possible relative to the critical center of gravity (aft c.g. for conventional layouts and forward c.g. for a canard).

Note: in some airplanes (carrier based airplanes are one example) severe restrictions are place on the allowable length, height and width!

Step 8.3: Determine the size of the empennage.

Three types of configurations will be considered:

a. Conventional configurations

b. Canard configurations

c. Three-surface configurations

d. Butterfly empennage configurations

a. Conventional configurations.

Sizing the empennage for a conventional configuration means deciding on the magnitude of S_h and S_v.

For a first 'cut' at the size of either the vertical or the horizontal tail, the so-called $\bar{V}$-method is often used. The tail volume coefficients are defined as follows:

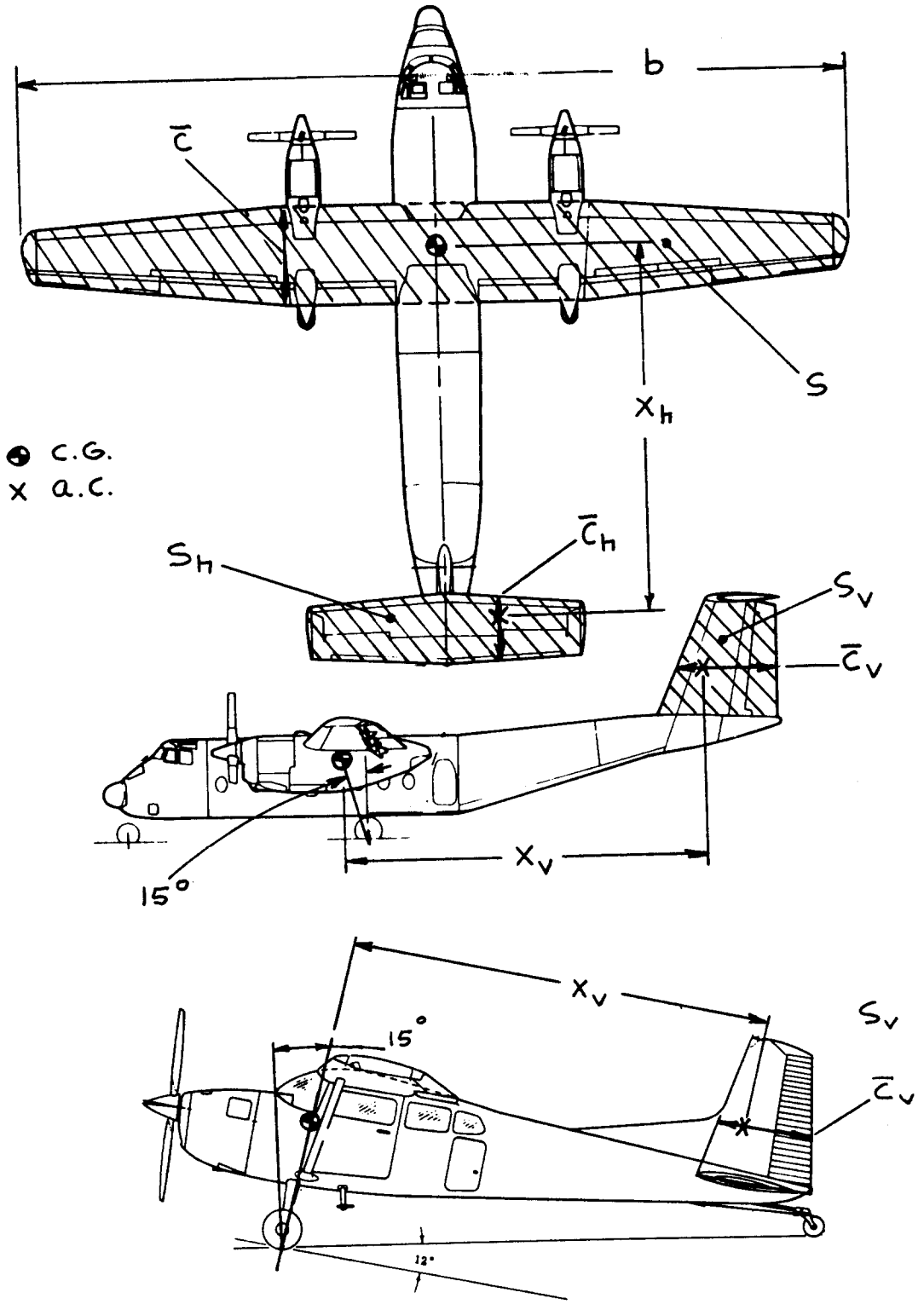

Figure 8.1 Definition of Volume Coefficient Quantities

$$\bar{V}_h = x_h S_h / S\bar{c} \qquad (8.1)$$

$$\bar{V}_v = x_v S_v / Sb \qquad (8.2)$$

Figure 8.1 defines the various quantities in Equations (8.1) and (8.2).

Tables 8.1 through 8.12 present the values of tail volume coefficients for twelve types of airplanes.

Having determined which type airplane best fits the airplane being designed, suitable values for $\bar{V}_h$ and $\bar{V}_v$ are selected. This can be done by averaging or by comparison to specific types. In deciding which value for $\bar{V}_v$ to use, care must be taken that the lateral disposition of the engines is not too dissimilar. Note that vertical tail sizes are often dictated by the engine-out (i.e. V_{mc}) condition. Section 11.3 contains a vertical tail sizing procedure for V_{mc}.

Having selected the volume coefficients, and having determined the moment arms x_h and x_v from the fuselage arrangement sketches mentioned in Step 8.2, the tail areas can be computed from:

$$S_h = \bar{V}_h S\bar{c} / x_h \qquad (8.3)$$

$$S_v = \bar{V}_v Sb / x_v \qquad (8.4)$$

The reader will have noted from the supersonic fighter configurations of Figures 3.25a and 3.27b that twin vertical tails are sometimes used. This is often done to avoid a very large single fin. The lateral placement of these twin verticals is a critical problem because of vortex shedding from the fuselage. These vortices can cause structural fatigue as well as a reduction in tail effectiveness.

b. Canard configurations.

The concept of volume coefficients can in principle be extended to a canard configuration. The problem is

Table 8.1a) Homebuilt Airplanes: Horizontal Tail Volume and Elevator Data

Type	Wing Area	Wing mgc	Wing Airfoil	Hor. Tail Area	S_e/S_h	x_h	$\bar{V}_h$	Elevator Chord
	S	$\bar{c}$	root/tip	S_h				root/tip
	ft^2	ft	NACA*	ft^2		ft		fr.c_h
PIK-21	76.4	4.50	64212	10.4	0.45	10.1	0.30	0.45
Duruble RD-03C	119	4.30	23018/23012	22.2	0.33	11.3	0.49	.47/.32
PIEL								
CP-750	118	3.82	23012	23.5	0.51	12.6	0.66	.55/.47
CP-90	104	3.81	NA	22.3	0.50	11.8	0.66	.56/.38
POTTIER								
P-50R	80.7	3.74	23015/23012	13.4	0.52	10.6	0.47	.50/.55
P-70S	77.5	4.10	4415	14.5	0.60	9.68	0.44	0.60
O-O Aerosport	80.7	3.77	23012	15.4	0.48	10.6	0.54	0.48
Aerocar Micro-Imp	81.0	3.00	GA(Pc)-1	11.7	0.25	6.27	0.30	.28/.33
Coats SA-III	112	4.50	63415	16.5	0.46	10.9	0.36	0.46
Sequoia 300	130	4.37	64$_3$A215/64A210	25.5	0.43	13.2	0.59	0.43
Ord-Hume OH-4B	125	5.25	RAF48	25.4	0.49	11.1	0.43	0.49
Procter Petrel	135	4.54	3415	26.0	0.52	12.2	0.52	0.52
Bede BD-8	96.7	5.0	63$_3$015	19.4	0.14	7.64	0.31	0.17

* Unless otherwise indicated.

Table 8.1b) Homebuilt Airplanes: Vertical Tail Volume, Rudder and Aileron Data

Type	Wing Area	Wing Span	Vert. Tail Area	S_r/S_v	x_v	$\bar{V}_v$	Rudder Chord	S_a/S	Ail. Span Loc.	Ail. Chord
	S	b	S_v				root/tip		in/out	in/out
	ft^2	ft	ft^2		ft		fr.c_v		fr.b/2	fr.c_w
PIK-21	76.4	17.0	3.49	0.33	10.5	0.028	.24/.49	0.130	0/1.0	0.13
Duruble RD-03C	119	28.7	8.35	0.30	12.5	0.031	.38/.32	0.063	.63/.93	.22/.24
PIEL										
CP-750	118	26.4	9.49	0.55	12.9	0.039	.50/.64	0.077	.44/.96	.19/.14
CP-90	104	23.6	7.64	0.50	11.9	0.037	.47/.54	0.092	.42/.91	.22/.18
POTTIER										
P-50R	80.7	20.3	11.3	0.42	10.4	0.072	.34/.61	0.067	.60/.98	.24/.22
P-70S	77.5	19.4	4.36	0.67	10.5	0.031	.59/.76	0.082	.52/.88	0.20
O-O Aerosport	80.7	21.3	6.86	0.38	10.0	0.040	.34/.44	0.080	.54/.97	0.19
Aerocar Micro-Imp	81.0	27.0	7.15	0.31	6.27	0.020	.33/.43	0.140	.07/.95	0.16
Coats SA-III	112	25.0	7.53	0.44	10.6	0.028	.35/.68	0.130	.55/1.0	0.26
Sequoia 300	130	30.0	16.5	0.31	13.2	0.055	.27/.43	0.085	.60/.95	0.29
Ord-Hume OH-4B	125	25.0	6.73	0.71	12.5	0.027	.57/1.0	0.110	.35/.91	0.20
Procter Petrel	135	30.0	11.7	0.35	11.4	0.033	.31/.57	0.097	.62/.98	0.26
Bede BD-8	96.7	19.3	6.89	0.24	8.65	0.032	.20/.34	0.083	.53/.92	0.22

Table 8.2a) Single Engine Propeller Driven Airplanes: Horizontal Tail Volume and Elevator Data

Type	Wing Area S ft^2	Wing mgc $\bar{c}$ ft	Wing Airfoil root/tip NACA*	Hor. Tail Area S_h ft^2	S_e/S_h	x_h ft	$\bar{V}_h$	Elevator Chord root/tip fr.c_h
CESSNA Skywagon 207	174	4.55	2412	44.9	0.45	16.2	0.92	.48/.47
Cardinal RG	174	4.79	64A215/64A412	35.0	1.00	14.3	0.60	stabilator
Skylane RG	174	4.52	2412	38.8	0.41	14.3	0.71	.47/.39
PIPER Cherokee Lance	175	5.25	$65_3$415	34.6	1.00	16.1	0.61	stabilator
Warrior	170	4.44	$65_3$415	26.5	1.00	13.5	0.48	stabilator
Turbo Saratoga SP	178	4.71	NA	36.2	1.00	16.2	0.70	stabilator
Bellanca Skyrocket	183	5.30	$63_3$215	42.6	0.38	13.8	0.61	.36/.42
Grumman Tiger	140	4.44	NA	37.6	0.28	12.6	0.76	0.39
Rockwell Commander	152	4.58	63415	31.2	0.34	10.9	0.49	.33/.44
Trago Mills SAH-1	120	3.94	2413.6	22.0	0.46	17.8	0.83	0.46
Scottish Aviation Bullfinch	129	3.97	$63_3$615	27.5	0.58	11.9	0.63	0.45

* Unless otherwise indicated.

Table 8.2b) Single Engine Propeller Driven Airplanes: Vertical Tail Volume, Rudder and Aileron Data

Type	Wing Area S ft^2	Wing Span b ft	Vert. Tail Area S_v ft^2	S_r/S_v	x_v ft	$\bar{V}_v$	Rudder Chord root/tip fr.c_v	S_a/S	Ail. Span Loc. in/out fr.b/2	Ail. Chord in/out fr.c_w
CESSNA Skywagon 207	174	35.8	16.0	0.44	18.0	0.046	.46/.46	0.10	.61/.94	.25/.22
Cardinal RG	174	35.5	17.4	0.37	13.5	0.038	.35/.43	0.11	.65/.97	.38/.37
Skylane RG	174	35.8	18.6	0.37	15.8	0.047	.41/.42	0.11	.47/.96	.17/.24
PIPER Cherokee Lance	175	32.8	13.8	0.31	15.3	0.037	.26/.50	0.064	.56/.88	0.20
Warrior	170	35.0	11.5	0.36	13.2	0.026	.29/.52	0.078	.48/.96	.27/.24
Turbo Saratoga SP	178	36.2	15.9	0.29	15.2	0.038	.23/.58	0.057	.52/.84	0.19
Bellanca Skyrocket	183	35.0	18.1	0.33	13.2	0.037	.28/.40	0.076	.60/1.0	.25/.22
Grumman Tiger	140	31.5	8.4	0.43	12.6	0.024	.36/.46	0.055	.56/.92	0.24
Rockwell Commander	152	32.8	17.0	0.28	11.4	0.039	.30/.46	0.072	.64/.97	.27/.36
Trago Mills SAH-1	120	30.7	17.1	0.40	18.6	0.086	.35/.54	0.080	.58/.97	.25/.29
Scottish Aviation Bullfinch	129	33.8	22.7	0.39	11.9	0.062	.35/.56	0.073	.61/.95	.23/.30

Table 8.3a) Twin Engine Propeller Driven Airplanes: Horizontal Tail Volume and Elevator Data

Type	Wing Area S ft^2	Wing mgc $\bar{c}$ ft	Wing Airfoil root/tip NACA*	Hor. Tail Area S_h ft^2	S_e/S_h	x_h ft	$\bar{V}_h$	Elevator Chord root/tip fr.c_h
CESSNA								
310R	179	4.77	23018/23009	54.3	0.41	14.9	0.95	.42/.39
402B	196	4.77	23018/23009	60.7	0.29	16.5	1.07	.41/.39
414A	226	4.73	23018/23009	60.7	0.27	16.4	0.93	.37/.38
T303	189	4.9	23017/23012	48.1	0.42	14.9	0.78	.41/.44
PIPER								
PA-31P	229	5.79	$63_3$415/$63_1$212	68.7	0.44	16.2	0.84	.41/.51
PA-44-180T	184	4.34	NA	23.4	1.0	15.7	0.46	stabilator
Chieftain	229	6.00	63_3A415/63_1A212	61.4	0.38	16.1	0.72	0.38
Cheyenne I	229	5.69	63_3A415/63_1A212	70.5	0.40	15.7	0.85	.40/.41
Cheyen.III	293	7.33	63_3A415/63_1A212	61.8	0.39	23.7	0.68	.35/.44
BEECH								
Duchess	181	5.08	63_3A415	39.4	0.35	15.6	0.67	0.40
Duke B60	213	6.60	23016.5/23010.5	62.0	0.27	14.5	0.64	0.39
Lear Fan 2100	163	4.36	NA	55.0	0.23	13.1	1.01	.36/.31
Rockwell Comdr 700	200	5.28	NA	55.4	0.37	19.7	1.03	0.37
Piaggio								
P166-DL3	286	6.06	230 series	51.6	0.27	17.2	0.51	.40/.50
EMB-121	296	6.62	NA	62.9	0.43	20.3	0.65	.39/.46

* Unless otherwise indicated

Table 8.3b) Twin Engine Propeller Driven Airplanes: Vertical Tail, Rudder and Aileron Data

Type	Wing Area S ft^2	Wing Span b ft	Vert. Tail Area S_v ft^2	S_r/S_v	x_v ft	$\bar{V}_v$	Rudder Chord root/tip fr.c_v	S_a/S	Ail. Span Loc. in/out fr.$b/2$	Ail. Chord in/out fr.c_w
CESSNA										
310R	179	36.9	26.1	0.45	15.9	0.063	.48/.41	0.064	.60/.90	.30/.29
402B	196	39.9	37.9	0.47	16.5	0.080	.48/.40	0.058	.64/.91	.29/.27
414A	226	44.1	41.3	0.38	17.0	0.071	.49/.37	0.061	.62/.87	.30/.28
T303	189	39.0	23.2	0.44	16.5	0.052	.46/.39	0.087	.64/.97	.31/.30
ConquestI	225	44.1	41.3	0.38	17.1	0.071	.47/.34	0.060	.61/.86	0.29
PIPER										
PA-31P	229	40.7	30.1	0.38	17.2	0.056	.37/.40	0.056	.59/.97	.24/.29
PA44-180T	184	38.6	21.5	0.37	14.4	0.044	.30/.50	0.077	.45/.90	.19/.18
Chieftain	229	40.7	29.5	0.40	17.3	0.055	.40/.38	0.060	.66/.98	.24/.30
Cheyen. I	229	42.7	26.5	0.40	16.5	0.045	.37/.42	0.057	.62/.93	.24/.29
Cheye.III	293	47.7	43.6	0.46	20.8	0.065	0.33	0.046	.66/.94	.23/.26
BEECH										
Duchess	181	38.0	25.6	0.29	14.2	0.053	.34/.42	0.059	.67/.97	0.28
Duke B60	213	39.3	28.8	0.43	17.4	0.060	.44/.46	0.054	.50/.84	.24/.26
Lear Fan 2100	163	39.3	44.4	0.17	14.0	0.097	.32/.34	0.044	.72/.98	.31/.24
Rockwell Comdr 700	200	42.5	39.9	0.38	20.5	0.096	.37/.38	0.087	.58/.99	.28/.24
Piaggio										
P166-DL3	286	48.2	30.7	0.43	18.3	0.041	.38/.43	0.073	.61/.94	.19/.22
EMB-121	296	46.4	42.6	0.45	17.8	0.055	.42/.41	0.052	.71/.97	0.22

Table 8.4a) Agricultural Airplanes: Horizontal Tail Volume and Elevator Data

Type	Wing Area S ft^2	Wing mgc $\bar{c}$ ft	Wing Airfoil root/tip NACA*	Hor. Tail Area S_h ft^2	S_e/S_h	x_h ft	$\bar{V}_h$	Elevator Chord root/tip fr.c_h
PZL-104	167	4.60	2415	34.0	0.60	17.3	0.77	0.51
PZL-106A	306	6.23	Clark Y	81.4	0.56	18.6	0.79	.30/.50
PZL-M18	431	7.50	4416/4412	70.0	0.49	17.4	0.38	0.49
NDN-6	338	6.71	NA	60.4	0.36	17.4	0.46	0.36
EMB201A	215	5.63	23015	50.3	0.32	13.6	0.56	0.56
Cessna Ag Husky	205	4.55	2412	40.7	0.41	15.6	0.68	.43/.37
Schweizer Ag-Cat B	392	4.83	4412	45.0	0.49	12.9	0.31	.38/.60
Aero Boero 260Ag	189	5.29	23012	25.5	0.41	14.1	0.36	0.44
Let Z-37A	256	5.91	23015/43012A	54.1	0.41	16.8	0.60	.44/.42
Hal HA-31	251	6.54	USA35B	45.6	0.43	17.9	0.50	0.46
IAR-822	280	6.90	23014	48.4	0.44	17.4	0.44	0.46
Piper PA-36	226	6.22	63$_3$618	43.3	0.48	15.0	0.46	.38/.62

* Unless otherwise indicated.

Table 8.4b) Agricultural Airplanes: Vertical Tail Volume, Rudder and Aileron Data

Type	Wing Area S ft^2	Wing Span b ft	Vert. Tail Area S_v ft^2	S_r/S_v	x_v ft	$\bar{V}_v$	Rudder Chord root/tip fr.c_v	S_a/S	Ail. Span Loc. in/out fr.b/2	Ail. Chord in/out fr.c_w
PZL-104	167	36.5	20.3	0.49	16.1	0.054	.41/.50	0.10	.58/.94	0.25
PZL-106A	306	48.5	31.0	0.56	17.1	0.036	.45/.51	0.087	.53/.96	0.22
PZL-M18	431	58.1	28.5	0.65	18.5	0.021	.50/.46	0.11	.59/.92	0.32
NDN-6	338	50.3	31.0	0.54	18.4	0.034	.50/.64	0.047	.73/1.0	.19/.14
EMB201A	215	38.4	13.0	0.52	14.1	0.022	.39/.36	0.08	.57/.90	0.19
Cessna Ag Husky	205	41.7	18.0	0.38	16.2	0.034	.32/.39	0.11	.53/.94	.27/.28
Schweizer Ag-Cat B	392	42.3	30.0	0.40	13.5	0.024	.25/.31	0.08	.53/.86	0.29
Aero Boero 260Ag	189	35.8	9.94	0.39	15.1	0.022	.32/.51	0.11	.52/.94	.20/.19
Let Z-37A	256	40.1	22.1	0.52	15.3	0.033	.59/.65	0.086	.64/1.0	0.32
HAL HA-31	251	39.4	20.7	0.45	16.6	0.035	.50/.46	0.092	.55/.89	0.28
IAR-822	280	42.0	22.9	0.69	17.9	0.035	.56/.64	0.11	.63/.98	0.27
Piper PA-36	226	38.8	19.9	0.49	16.5	0.038	.59/.21	0.096	.52/.92	0.28

Table 8.5a) Business Jets: Horizontal Tail Volume and Elevator Data

Type	Wing Area	Wing mgc	Wing Airfoil	Bor. Tail Area	S_e/S_h	x_h	$\bar{V}_h$	Elevator Chord
	S	$\bar{c}$	root/tip	S_h				root/tip
	ft^2	ft	NACA*	ft^2		ft		fr.c_h
DASSAULT-BREGUET								
Falcon 10	259	6.71	NA	72.7	0.20	16.5	0.69	.31/.29
Falcon 20	440	9.33	NA	122	0.22	21.9	0.65	.28/.31
Falcon 50	495	9.31	NA	144	0.23	21.7	0.68	.31/.34
CESSNA CITATION								
500	260	6.44	23014/23012	70.6	0.29	17.3	0.73	.32/.23
II	323	6.77	NA	73.1	0.36	19.2	0.64	.37/.35
III	312	6.07	NASA Sprcrt	69.6	0.34	26.9	0.99	.39/.42
GATES LEARJET								
24	232	7.03	64A109	54.0	0.26	20.2	0.67	.36/.26
35A	253	7.22	64A109	54.0	0.33	21.9	0.65	.33
55	265	6.88	NA	57.8	0.32	23.8	0.76	.31/.35
Canadair Challenger								
CL-601	450	11.3	NA	105	0.28	32.2	0.67	.30/.31
Aerospatiale								
SN-601	237	5.60	NA	58.9	0.42	16.7	0.74	.40/.44
ISRAEL AIRCRAFT IND.								
Astra	317	5.62	Sigma 2	77.1	0.25	22.8	0.99	.30/.32
Westwind	308	7.58	64A212	70.1	0.25	19.8	0.59	.29/.26
British Aerospace HS								
125-700	353	7.52	NA	100	0.48	19.1	0.72	.37/.67
G.A.-III	935	13.8	NA	184	0.33	35.6	0.51	0.33
MU Diam.I	241	6.23	NA	57.2	0.37	22.4	0.85	0.37

• Unless otherwise indicated.

Table 8.5b) Business Jets: Vertical Tail Volume, Rudder and Aileron Data

Type	Wing Area	Wing Span	Vert. Tail Area	S_r/S_v	x_v	$\bar{V}_v$	Rudder Chord	S_a/S	Ail. Span Loc.	Ail. Chord
	S	b	S_v				root/tip		in/out	in/out
	ft^2	ft	ft^2		ft		fr.c_v		fr.b/2	fr.c_w
DASSAULT BREGUET										
Falcon 10	259	42.9	48.9	0.32	14.4	0.063	.34/.49	0.051	.67/.95	.27/.31
Falcon 20	440	53.5	81.8	0.23	18.1	0.063	.25/.39	0.057	.62/.92	0.25
Falcon 50	495	61.9	106	0.12	18.7	0.064	.21/.32	0.049	.68/.97	0.27
CESSNA CITATION										
500	260	43.9	50.9	0.36	18.2	0.081	0.36	0.096	.55/.94	.32/.30
II	323	51.7	53.0	0.34	19.36	0.062	.35/.31	0.078	.56/.89	.32/.30
III	312	53.5	70.2	0.30	20.5	0.086	.37/.38	NA*	.70/.86	.21/.17
GATES LEARJET										
24	232	35.6	38.4	0.17	16.6	0.077	.23/.22	0.050	.63/.89	.25/.23
35A	253	38.1	38.4	0.17	16.6	0.066	.26/.25	0.066	.55/.79	.30/.27
55	265	43.8	52.4	0.17	19.2	0.086	.26/.25	0.062	.49/.71	0.30
Can.CL601	450	64.3	96.0	0.26	24.9	0.083	.29/.31	0.033	.73/.91	.23/.26
Aerospatiale										
SN-601	237	42.2	45.4	0.30	15.7	0.071	.36/.32	0.033	.68/.91	.22/.20
ISRAEL AIRCRAFT IND.										
Astra	317	52.7	48.3	0.21	22.0	0.064	.33/.32	0.040	.67/.95	.26/.25
Westwind	308	44.8	59.7	0.18	20.1	0.087	.34/.44	0.050	.59/.90	.21/.31
British Aerospace HS										
125-700	353	47.0	63.8	0.22	15.9	0.061	.31/.37	0.084	.66/1.0	.33/.46
G.A. III	935	77.8	159	0.24	26.9	0.059	0.28	0.038	.66/.86	.24/.27
MU Diam.I	241	43.4	55.9	0.25	17.4	0.093	.33/.28	0.012	.86/.94	.20/.22

• Also uses spoilers for lateral control

Table 8.6a) Regional Turboprop Airplanes: Horizontal Tail Volume and Elevator Data

Type	Wing Area S ft^2	Wing mgc $\bar{c}$ ft	Wing Airfoil root/tip NACA*	Hor. Tail Area S_h ft^2	S_e/S_h	x_h ft	$\bar{V}_h$	Elevator Chord root/tip fr.c_h
CASA C-212-200								
	431	6.68	653-218	135	0.35	24.9	1.17	.49/.53
SHORTS								
330	453	6.06	NA	83.6	0.33	27.3	0.83	0.50
360	453	6.06	NA	106	0.39	33.0	1.28	0.48
BEECH								
1900	303	5.35	23018/23015	71.3	0.43	30.3	1.33**	.43/.48
B200	303	5.35	23018.5/23011.3	68.0	0.28	24.6	0.91	0.42
CESSNA CONQUEST			*** I airfoils carry -63 mod.					
I***	225	4.73	23018/23009	62.0	0.33	16.4	0.95	.36/.43
II	254	4.98	23018/23009	63.4	0.29	18.0	0.90	.43/.40
GA Ic	610	8.28	NA	134	0.26	36.5	0.97	.29/.32
GAF N22B	324	5.94	23018	78.0	1.00	20.6	0.83	stabilator
Fokker F27-200								
	754	8.43	64-421/64-415	172	0.27	36.0	0.98	.29/.34
DeHAVILLAND CANADA								
DHC-6-300	420	6.50	NA	100	0.35	24.8	0.91	0.47
DHC-7	860	9.45	63A418/63A415	217	0.46	41.6	1.11	.42/.47
DHC-8	585	6.51	NA	154	0.42	36.3	1.47	.41/.43
EMB-120	409	6.57	23018/23012	108	0.39	31.7	1.27	.38/.44
BAe 31	270	5.27	63A418/63A412	84.0	0.46	20.7	1.22	.43/.48
Metro III	309	6.03	65$_3$A215/64$_3$A415	76.0	0.28	26.1	1.07	.31/.48

* Unless otherwise indicated. ** 1900 also has a small fixed stabilizer.

Table 8.6b) Regional Turboprop Airplanes: Vertical Tail Volume, Rudder and Aileron Data

Type	Wing Area S ft^2	Wing Span b ft	Vert. Tail Area S_v ft^2	S_r/S_v	x_v ft	$\bar{V}_v$	Rudder Chord root/tip fr.c_v	S_a/S	Ail. Span Loc. in/out fr.b/2	Ail. Chord in/out fr.c_w
CASA C-212-200										
	431	62.3	77.5	0.41	24.8	0.072	0.41	0.061	.69/1.0	.24/.26
SHORTS										
330	453	74.7	93.1	0.26	27.3	0.075	0.41	0.061	.70/.95	0.27
360	453	74.7	91.4	0.37	33.9	0.091	.39/.36	0.074	.69/.98	0.27
BEECH										
1900*	303	54.5	47.5	0.35	26.5	0.076	.40/.38	0.064	.60/1.0	0.21
B200	303	54.5	52.3	0.29	20.5	0.065	.47/.41	0.059	.60/1.0	0.21
CESSNA CONQUEST										
I	225	44.1	41.3	0.38	17.1	0.071	.46/.38	0.060	.61/.86	.29/.28
II	254	49.3	43.5	0.37	18.7	0.065	.48/.33	0.058	.62/.89	.30/.32
GA Ic	610	78.3	117	0.25	35.4	0.087	.29/.33	0.061	.65/.98	.27/.22
GAF N22B	324	54.2	70.2	0.44	21.6	0.086	.49/.43	0.085	.54/1.0	0.24
Fokker F27-200										
	754	95.2	153	0.30	36.0	0.077	.33/.29	0.050	.69/.98	.31/.29
DeHAVILLAND CANADA										
DHC-6-300	420	65.0	82.0	0.42	25.7	0.077	.35/.44	0.079	.44/.97	0.20
DHC-7	860	93.0	170	0.28	35.7	0.076	.25/.30	0.027	.81/1.0	.27/.31
DHC-8	585	84.0	190	0.26	31.4	0.121	.27/.35	0.031	.80/1.0	.23/.22
EMB-120	409	64.9	74.3	0.38	27.3	0.076	.32/.31	0.084	.63/.97	0.24
BAe 31	270	52.0	83.1	0.26	20.7	0.120	.34/.39	0.061	.59/.97	.28/.30
Metro III	309	57.0	56.0	0.35	27.9	0.089	.37/.56	0.046	.61/.98	.31/.36

* 1900 also has taillets on horizontal tail.

Table 8.7a) Jet Transports: Horizontal Tail Volume and Elevator Data

Type	Wing Area S ft^2	Wing mgc $\bar{c}$ ft	Wing Airfoil root/tip	Hor. Tail Area S_h ft^2	S_e/S_h	x_h ft	$\bar{V}_h$	Elevator Chord root/tip fr.c_h
BOEING								
727-200	1,700	18.0	BAC	376	0.25	67.0	0.82	.29/.31
737-200	980	11.2	BAC	321	0.27	43.8	1.28	.30/.32
737-300	1,117	10.9	BAC	330	0.24	49.7	1.95	.24/.34
747-200B	5,500	38.0	BAC	1,470	0.24	104.5	0.74	0.29
747SP	5,500	38.0	BAC	1,534	0.21	72.9	0.54	.32/.20
757-200	1,951	14.9	BAC	585	0.25	56.9	1.15	.29/.38
767-200	3,050	19.8	BAC	856	0.23	67.6	0.94	.30/.25
McDONNELL-DOUGLAS								
DC-9 S80	1,270	15.7	N.A.	314	0.34	61.4	0.96	.39/.38
DC-9-50	1,001	11.8	N.A.	276	0.38	56.8	1.92	.41/.47
DC-10-30	3,958	24.7	N.A.	1,338	0.22	65.9	0.90	.25/.30
AIRBUS								
A300-B4	2,799	19.2	N.A.	748	0.26	80.4	1.12	0.35
A310	2,357	19.3	N.A.	689	0.26	72.0	1.09	.33/.30
Lockheed L1011				geared elevator				
-500	3,541	24.5	N.A.	1,282	0.19	55.9	0.83	stabilator
Fokker F-28								
-4000	850	10.9	N.A.	210	0.20	47.2	1.07	.34/.33
Rombac/British Aerospace								
1-11 495	1,031	11.8	N.A.	258	0.27	40.7	0.86	.41/.35
British Aerospace								
146-200	832	10.2	N.A.	276	0.39	45.3	1.48	.42/.44
Tu-154	2,169	16.8	N.A.	436	0.18	58.9	0.71	.27/.25

Table 8.7b) Jet Transports: Vert. Tail Volume, Rudder, Aileron and Spoiler Data

Type	Wing Area S ft^2	Wing Span b ft	Vert. Tail Area S_v ft^2	S_r/S_v	x_v ft	$\bar{V}_v$	Rudder Chord root/tip fr.c_v	S_a/S	Inb'd Ail. Span in/out fr.$b/2$	Inb'd Ail. Chord in/out fr.c_w
BOEING										
727-200	1,700	108	422	0.16	47.4	0.110	.29/.28	0.034	.38/.46	.17/.24
737-200	980	93.0	233	0.24	40.7	0.100	.25/.22	0.024	none	none
737-300	1,117	94.8	239	0.31	45.7	0.100	.26/.50	0.021	none	none
747-200B	5,500	196	830	0.30	102	0.079	0.30	0.040	.38/.44	.17/.25
747-SP	5,500	196	885	0.27	69.5	0.057	.31/.34	0.040	.38/.44	.17/.25
757-200	1,951	125	384	0.34	54.2	0.086	.35/.33	0.027	none	none
767-200	3,050	156	497	0.35	64.6	0.067	.33/.36	0.041	.31/.40	.23/.20
McDONNELL-DOUGLAS										
DC-9 S80	1,270	108	168	0.39	50.5	0.062	.49/.46	0.030	none	none
DC-9-50	1,001	93.4	161	0.41	46.2	0.079	.45/.44	0.038	none	none
DC-10-30	3,958	165	605	0.18	64.6	0.060	0.35	0.047	.32/.39	.20/.25
AIRBUS										
A300-B4	2,799	147	487	0.30	79.5	0.094	.35/.36	0.049	.29/.39	.23/.27
A310	2,357	144	487	0.35	68.5	0.098	.33/.35	0.027	.32/.40	.23/.27
Lockheed L1011										
-500	3,541	164	550	0.23	58.2	0.055	.29/.26	0.051	.40/.49	.22/.23
Fokker F-28										
-4000	850	82.3	157	0.16	37.9	0.085	.29/.31	0.034	none	none
Rombac/British Aerospace										
1-11 495	1,031	93.5	117	0.28	31.6	0.038	.39/.37	0.030	none	none
British Aerospace										
146-200	832	86.4	224	0.44	38.9	0.12	0.29	0.046	none	none
Tu-154	2,169	123	341	0.27	43.3	0.055	0.37	0.036	none	none

Table 8.7c) Jet Transports: Vert. Tail Volume, Rudder, Aileron and Spoiler Data

Type	Outb'd Ail. Span in/out fr.b/2	Outb'd Ail. Chord in/out fr.c_w	Inb'd Spoiler Span Loc. in/out fr.b/2	Inb'd Spoiler Chord in/out fr.c_w	Inb'd Spoiler Hinge Loc. in/out fr.c_w	Outb'd Spoiler Span Loc. in/out fr.c_w	Outb'd Spoiler Chord in/out fr.c_w	Outb'd Spoiler Hinge Loc. in/out fr.c_w
BOEING								
727-200	.76/.93	.23/.30	.14/.37	.09/.14	.79/.69	.48/.72	.16/.20	.65/.63
737-200	.74/.94	.20/.28	.40/.66	.14/.18	.66/.67	none	none	none
737-300	.72/.91	.23/.30	.38/.64	0.14	.64/.70	none	none	none
747-200B	.70/.95	.11/.17	.46/.67	.12/.16	0.71	none	none	none
747-SP	.70/.95	.11/.17	.46/.67	.12/.16	0.71	none	none	none
757-200	.76/.97	.22/.36	.41/.74	.12/.13	.73/.69	none	none	none
767-200	.76/.98	.16/.15	.16/.31	.09/.11	.85/.78	.44/.67	.12/.17	.74/.71
McDONNELL-DOUGLAS								
DC-9 S80	.64/.85	.31/.36	.35/.60	.10/.08	.69/.65	none	none	none
DC-9-50	.78/.95	.30/.35	.35/.60	.10/.08	.69/.65	none	none	none
DC-10-30	.75/.93	.29/.27	.17/.30	.05/.06	.78/.74	.43/.72	.11/.16	.75/.70
AIRBUS								
A300-B4	.83/.99	.32/.30	.57/.79	.16/.22	.73/.72	none	none	none
A310	none	none	.62/.83	.16/.22	.69/.66	none	none	none
Lockheed L1011								
-500	.77/.98	.26/.22	.13/.39	.08/.12	.82/.73	.50/.74	.14/.14	.67/.67
Fokker F-28								
-4000	.66/.91	.29/.28	no lateral control spoilers					
Rombac/British Aerospace								
1-11 495	.72/.92	0.26	.37/.68	.06/.11	.68/.63	none	none	none
British Aerospace								
146-200	.78/1.0	.33/.31	.14/.70	.22/.27	.76/.68	none	none	none
Tu-154	.76/.98	.34/.27	.43/.70	.14/.20	.62/.60	none	none	none

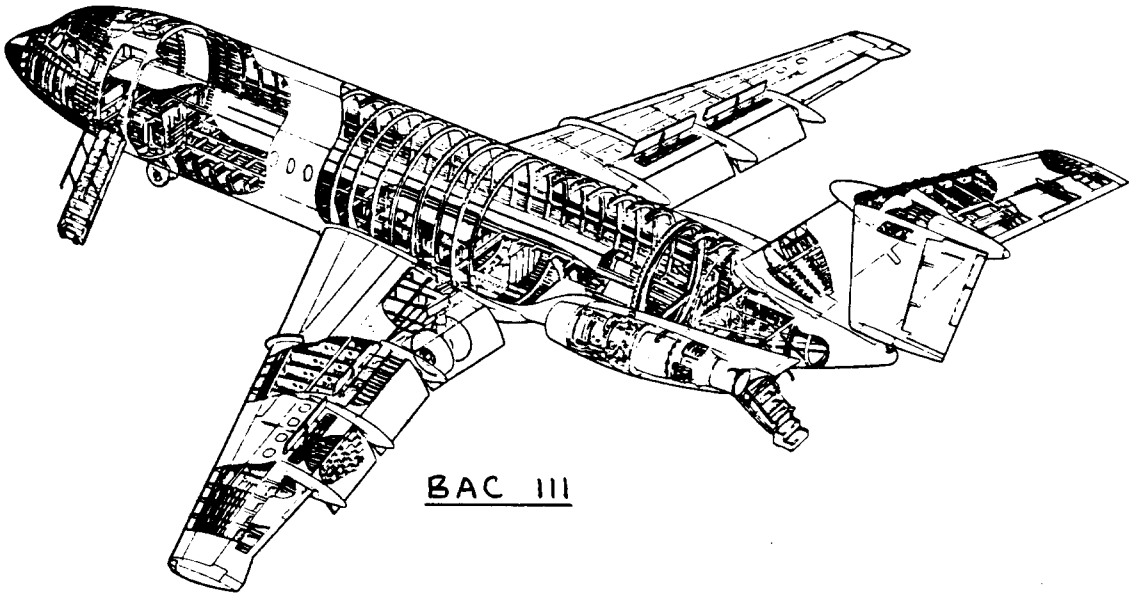

BAC 111

Table 8.8a) Military Trainers: Horizontal Tail Volume and Elevator Data

Type	Wing Area	Wing mgc	Wing Airfoil	Hor. Tail Area	S_e/S_h	x_h	$\bar{V}_h$	Elevator Chord
	S	$\bar{c}$	root/tip	S_h				root/tip
	ft^2	ft	NACA*	ft^2		ft		fr.c_h
Turbopropeller Driven								
EMB-312	209	5.77	63_1A415/63_1A212	49.2	0.44	16.9	0.69	.42/.44
Pil. PC-7	179	5.23	64_1A415/64_1A612	36.9	0.49	16.2	0.64	.49/.50
NDN 1T	126	5.4	23012	25.8	0.47	14.0	0.53	0.44
T-34C	180	4.01	23016.5/23012	37.2	0.37	14.8	0.76	.43/.44
Epsilon	96.9	3.97	RA1643/RA1243	21.5	0.48	13.8	0.77	.49/.54
SF-260M	109	4.35	$64_1$212/$64_1$210	26.0	0.40	12.7	0.70	.55/.56
Yak-52	162	5.20	Clark YN	30.8	0.54	13.3	0.49	.54/.60
Neiva T25	185	5.19	63_1A315/63_1A212	33.0	0.44	15.0	0.52	.46/.40
Jet Driven								
Aero L39C	202	7.04	64A012	54.6	0.23	15.2	0.58	.35/.44
Microturbo Microjet 200B	65.9	2.79	RA16.3C3	22.9	0.32	8.98	1.12	.37/.34
Dassault-Breguet/Dornier Alphajet	188	7.37	N.A.	42.4	1.0	14.1	0.43	stabilator
Aermacchi MB-339A	208	6.34	64A114/64A212	46.9	0.23	14.6	0.52	.26/.36
SM S-211	136	5.40	KU .17 sprcrt.	36.4	0.40	15.2	0.75	.41/.40
PZL TS-11	188	5.80	64209/64009	38.1	0.33	16.3	0.57	.31/.32
CASA C101	215	6.32	Norcasa 15	47.8	0.23	15.2	0.54	.33/.46
British Aerospace Hawk Mk1	180	6.30	N.A.	46.6	1.0	14.8	0.61	stabilator

* Unless otherwise indicated.

Table 8.8b) Military Trainers: Vertical Tail Volume, Rudder and Aileron Data

Type	Wing Area	Wing Span	Vert. Tail Area	S_r/S_v	x_v	$\bar{V}_v$	Rudder Chord	S_a/S	Ail. Span Loc.	Ail. Chord
	S	b	S_v				root/tip		in/out	in/out
	ft^2	ft	ft^2		ft		fr.c_v		fr.b/2	fr.c_w
Turbopropeller Driven										
EMB-312	209	36.5	22.4	0.70	16.6	0.049	.37/1.0*	0.100	.56/.99	.21/.31
Pil. PC-7	179	34.1	20.2	0.47	14.4	0.048	.52/.49	0.082	.56/.97	.23/.27
NDN 1T	126	26.0	13.5	0.52	11.8	0.049	.38/.57	0.110	.50/.87	0.26
T-34C	180	33.3	19.8	0.35	14.4	0.048	.41/.40	0.063	.55/.95	.22/.23
Epsilon	96.9	26.0	11.0	0.39	13.4	0.058	.48/.45	0.090	.58/.91	.30/.29
SF-260M	109	27.4	16.4	0.40	12.5	0.069	.35/.63	0.075	.61/.92	.23/.30
Yak-52	162	30.5	15.9	0.59	13.9	0.045	.46/.51	0.130	.47/.98	.27/.26
Neiva T25	185	36.1	18.5	0.52	15.7	0.043	.53/.52	0.085	.51/.96	.16/.22
Jet Driven										
Aero L39C	202	31.0	37.8	0.28	13.9	0.083	.36/.33	0.066	.62/.93	.36/.34
Microturbo Microjet 200B	65.9	24.8	14.5	0.39	10.0	0.089	.37/.43	0.073	.64/.96	.29/.32
Dassault-Breguet/Dornier Alphajet	188	29.9	32.0	0.21	14.8	0.084	.32/.36	0.059	.68/1.0	.23/.27
Aermacchi MB-339A	208	35.6	25.5	0.26	12.6	0.043	.30/.38	0.069	.60/.92	0.25
SM S-211	136	27.7	21.6	0.33	13.5	0.078	.37/.36	0.100	.58/.97	.22/.21
PZL TS-11	188	33.0	24.2	0.31	16.8	0.066	.24/.47	0.085	.55/.95	.23/.27
CASA C101	215	34.8	34.4	0.41	15.8	0.072	.37/.36	0.080	.61/.93	.26/.27
British Aerospace Hawk Mk1	180	30.8	27.0	0.23	12.1	0.059	.28/.31	0.063	.65/1.0	.26/.32

* Large hornbalance at tip.

Table 8.9a) Fighters: Horizontal Tail Volume and Elevator Data

Type	Wing Area	Wing mgc	Wing Airfoil	Hor. Tail Area	S_e/S_h	x_h	$\bar{V}_h$	Elevator Chord
	S	$\bar{c}$	root/tip	S_h				root/tip
	ft^2	ft	NACA*	ft^2		ft		fr.c_h
DASSAULT-BREGUET								
Mir. IIIE	377	17.7	NA	0	0	0	0	elevons
Mir. F1C	269	10.4	NA	96.9	1.0	14.9	0.51	stabilator
Mir. 2000	441	18.2	NA	0	0	0	0	elevons
Super Et.	306	10.5	NA	59.7	1.0	15.5	0.29	stabilator
FR A-10A	506	8.94	6716/6713	89.4	0.32	20.6	0.41	0.33
Grum.A6A	529	10.9	NA	109.8	1.0	24.2	0.46	stabilator
Grum.F14A	565	10.2	NA	140	1.0	16.4	0.40	stabilator
North.F5E	186	8.05	65A004.8	59.0	1.0	15.0	0.51	stabilator
Vht A7A	375	10.8	65A007	56.2	1.0	16.2	0.22	stabilator
McDONNELL DOUGLAS								
F-4E	530	15.5	64A005.9	96.9	1.0	22.2	0.26	stabilator
F-15	608	17.8	McD .003	104	1.0	20.7	0.20	stabilator
GENERAL DYNAMICS								
FB-111A	476	8.22	63(NA)	168	1.0	17.6	0.75	stabilator
F-16	300	11.4	64A204	66.6	1.0	15.4	0.30	stabilator
Cessna								
A37B	184	5.61	2418/2412	46.7	0.25	15.1	0.68	.34/.31
Aermacchi								
MB339K	208	6.30	64A114/64A212	36.4	0.29	14.5	0.40	.26/.37
MIG-25	612	17.3	NA	236	1.0	16.0	0.36	stabilator
Su-7BMK	329	12.5	0.008 thick	92.7	1.0	17.9	0.40	stabilator

* Unless otherwise indicated.

Table 8.9b) Fighters: Vertical Tail Volume, Rudder and Aileron Data

Type	Wing Area	Wing Span	Vert. Tail Area	S_r/S_v	x_v	$\bar{V}_v$	Rudder Chord	S_a/S	Ail. Span Loc.	Ail. Chord
	S	b	S_v				root/tip		in/out	in/out
	ft^2	ft	ft^2		ft		fr.c_v		fr.b/2	fr.c_w
DASSAULT BREGUET										
Mir. IIIE	377	27.0	48.4	0.20	13.9	0.066	.22/.29	0.14	.18/1.0	.13/1.0
Mir. F1C	269	27.6	53.9	0.16	13.5	0.098	.21/.35	0.031	.77/1.0	.23/.25
Mir. 2000	441	29.5	71.8	0.16	13.6	0.075	.21/.34	0.13	.19/1.0	.13/1.0
Super Et.	306	31.5	48.3	0.18	12.4	0.062	.25/.49	0.053	.57/.81	.23/.27
FR A-10A	506	57.5	84.0	0.28	20.9	0.060	.31/.34	0.094	.58/.91	.42/.40
Grum.A6A	529	53.0	79.3	0.21	24.6	0.069	.28/.21	see Jane's 81-81		
Grum.F14A	565	64.1	118	0.29	18.4	0.060	.29/.33	see Jane's 81-82		
North.F5E	186	26.7	41.4	0.15	11.7	0.098	.26/.30	0.050	.76/.99	.34/.33
Vht A7A	375	38.8	115	0.13	16.1	0.13	.21/.29	0.053	.59/.90	.20/.24
McDONNELL DOUGLAS										
F-4E	530	38.4	59.6	0.20	18.3	0.054	.20/.29	0.040	.63/.98	.23/.28
F-15	608	42.8	143	0.25	17.8	0.098	.30/.50	0.053	.60/.86	.25/.27
GENERAL DYNAMICS								look under Grumman		
FB-111A	476	63.0	96.1	0.21	17.0	0.054	.25/.26	see Jane's 82-83		
F-16	300	31.8	62.2	0.25	14.4	0.094	.34/.33	0.13*	.30/.73	.21/.23
Cessna										
A37B	184	35.9	17.8	0.35	15.1	0.041	.37/.39	0.061	.56/.91	.27/.32
Aermacchi										
MB339K	208	36.2	25.5	0.26	12.6	0.043	.26/.41	0.069	.58/.90	.24/.26
MIG-25	612	45.8	174	0.15	16.8	0.10	0.24	0.053	.54/.79	.22/.21
Su-7BMK	329	29.3	58.2	0.26	16.9	0.10	.28/.25	0.11	.62/.97	.29/.35

* Flaperon

Table 8.10a) Military Patrol, Bomb and Transport Airplanes: Horizontal Tail Volume and Elevator Data

Type	Wing Area S ft^2	Wing mgc $\bar{c}$ ft	Wing Airfoil root/tip NACA*	Hor. Tail Area S_h ft^2	S_e/S_h	x_h ft	$\bar{V}_h$	Elevator Chord root/tip fr.c_h
Turbopropeller Driven								
LOCKHEED								
C-130E	1,745	13.7	64A318/64A412	536	0.29	42.1	0.94	.34/.44
P3C	1,300	14.1	0014/0012	322	0.25	48.5	0.85	.29/.37
ANTONOV								
An-12BP	1,310	11.3	NA	319	0.24	52.5	1.13	.33/.36
An-22	3,713	18.8	NA	846	0.28	87.4	1.06	.34/.53
An-26	807	8.79	NA	213	0.28	43.5	1.31	.34/.38
Grum.E2C	700	9.73	NA	174	0.29	26.9	0.69	.29/.36
D/B Atlant.2	1,295	11.5	NA	355	0.25	43.4	1.04	.35/.36
Aerital.G222	883	8.65	NA	255	0.20	37.0	1.24	.39/.30
Jet Driven								
LOCKHEED								
S-3A Viking	598	9.85	NA	176	0.28	20.0	0.60	.35/.25
C-141B	3,406	21.4	NA	545	0.26	82.5	0.62	.28/.29
C-5A	6,200	32.9	NA	966	0.27	130.4	0.62	0.30
BA Nimrod 2	2,121	20.5	NA	435	0.31	50.5	0.51	.32/.40
Boeing YC-14	1,762	16.8	NA	690	0.40	61.5	1.43	0.46
McDD KC-10A	3,958	24.7	NA	1,338	0.22	65.1	0.89	0.27
Tu-16	1,772	15.9	NA	360	0.27	50.6	0.65	.26/.41
Il-76T	3,229	20.7	NA	639	0.25	71.2	0.68	.31/.30

* Unless otherwise indicated.

Table 8.10b) Military Patrol, Bomb and Transport Airplanes: Vertical Tail Volume, Rudder, Aileron and Spoiler Data

Type	Wing Area S ft^2	Wing Span b ft	Vert. Tail Area S_v ft^2	S_r/S_v	x_v ft	$\bar{V}_v$	Rudder Chord root/tip fr.c_v	S_a/S	Inb'd Ail. Span in/out fr.b/2	Inb'd Ail. Chord in/out fr.c_w
Turbopropeller Driven										
LOCKHEED										
C-130E	1,745	133	300	0.25	40.5	0.053	.26/.31	0.063	none	none
P3C	1,300	99.7	176	0.34	46.1	0.063	.32/.39	0.069	none	none
ANTONOV										
An-12BP	1,310	125	205	0.28	48.9	0.061	.42/.44	0.064	none	none
An-22	3,713	211	700	0.44	82.6	0.074	.54/.40	0.040	none	none
An-26	807	95.8	171	0.40	39.9	0.088	.41/.43	0.071	none	none
Grum.E2C	700	80.6	199	0.52	27.7	0.098	.44/.64	0.077	none	none
D/B Atl.2	1,295	123	179	0.36	44.3	0.050	.37/.42	0.044	none	none
Aer.G222	883	94.2	207	0.37	36.7	0.091	.39/.47	0.045	none	none
Jet Driven										
LOCKHEED										
S-3A Viking	598	68.7	129	0.29	20.0	0.063	.37/.35	0.022	none	none
C-141B	3,406	160	455	0.21	72.1	0.060	.24/.28	0.056	none	none
C-5A	6,200	223	961	0.24	113	0.079	.27/.31	0.041	none	none
BA Nimr.2	2,121	115	118	0.35	50.4	0.024	.45/.37	0.058	none	none
B. YC-14	1,762	129	650	0.26	55.7	0.160	0.40	0.048	none	none
MDD KC10A	3,958	165	605	0.18	62.9	0.058	.39/.40	0.047	.32/.39	.20/.25
Tu-16	1,772	108	276	0.24	48.5	0.070	.35/.29	0.057	none	none
Il-76T	3,229	166	596	0.26	60.7	0.068	.46/.38	0.040	none	none

Table 8.10c) Military Patrol, Bomb and Transport Airplanes: Vertical Tail Volume, Rudder, Aileron and Spoiler Data

Type	Outb'd Ail. Span in/out fr.b/2	Outb'd Ail. Chord in/out $fr.c_w$	Inb'd Spoiler Span Loc. in/out fr.b/2	Inb'd Spoiler Chord in/out $fr.c_w$	Inb'd Spoiler Hinge Loc. in/out $fr.c_w$	Outb'd Spoiler Span Loc. in/out $fr.c_w$	Outb'd Spoiler Chord in/out $fr.c_w$	Outb'd Spoiler Hinge Loc. in/out $fr.c_w$
Turbopropeller Driven								
LOCKHEED								
C-130E	.70/.99	0.29	no lateral control spoilers					
P3C	.63/.96	.22/.25	no lateral control spoilers					
ANTONOV								
An-12BP	.68/.98	.31/.33	no lateral control spoilers					
An-22	.63/.98	.27/.32	no lateral control spoilers					
An-26	.66/.98	.32/.26	no lateral control spoilers					
Grum.E2C	.57/.98	.22/.33	no lateral control spoilers					
D/B Atl.2	.70/.95	.24/.25	.37/.65	.06/.08	.74/.68	none	none	none
Aer.G222	.72/1.0	.35/.45	.48/.70	.07/.08	.70/.66	none	none	none
Jet Driven								
LOCKHEED								
S-3A Vik.	.79/.96	.23/.25	.24/.79	.12/.15	.67/.56	none	none	none
C-141B	.67/1.0	.26/.23	.15/.41	.09/.12	.85/.80	.43/.66	.10/.13	.83/.83
C-5A	.72/.93	.28/.30	.36/.70	.13/.12	0.80	none	none	none
BA Nimr.2	.61/.96	.26/.27	no lateral control spoilers					
B. YC-14	.78/1.0	.37/.33	none	none	none	.53/.78	0.16	.74/.64
MDD KC10A	.75/.93	.29/.27	.17/.30	.05/.06	.78/.74	.43/.72	.11/.16	.75/.70
Tu-16	.66/.97	.25/.29	no lateral control spoilers					
Il-76T	.74/.98	.25/.26	.17/.71	.10/.13	.80/.69	none	none	none

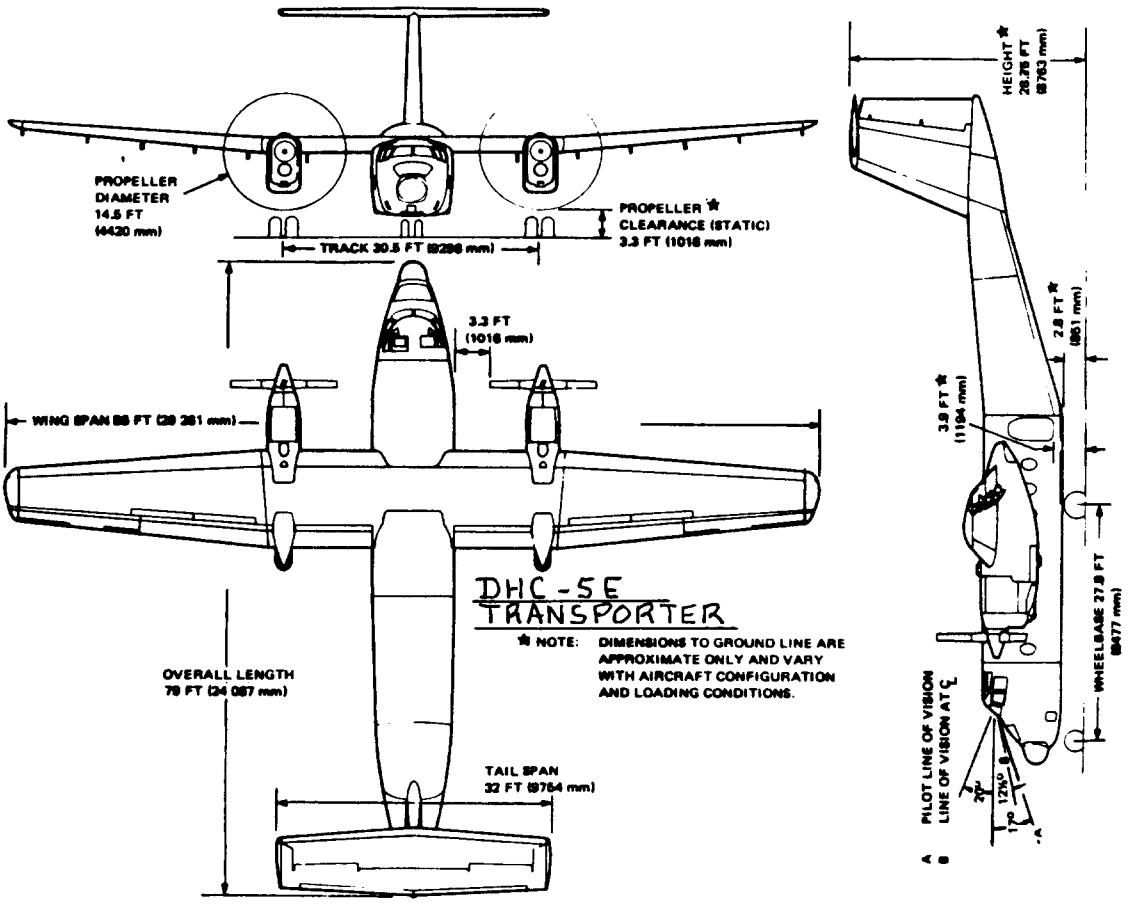

Table 8.11a) Flying Boats, Amphibious and Float Airplanes: Horizontal Tail Volume and Elevator Data (Piston/Prop. Except as Indicated)

Type	Wing Area S ft^2	Wing mgc $\bar{c}$ ft	Wing Airfoil root/tip NACA*	Hor. Tail Area S_h ft^2	S_e/S_h	x_h ft	$\bar{V}_h$	Elevator Chord root/tip fr.c_h
SHORTS								
Sandringham	1,487	16.6	NA	259	0.35	44.1	0.46	.53/.35
Shetland	2,773	20.0	Gott. 436	388	0.32	55.8	0.39	.45/.41
DORNIER								
Do 24	1,162	13.8	NA	202	0.35	33.6	0.42	0.42
Do 24/72	1,129	12.4	NA	262	0.25	40.2	0.75	.25/.31
Do Seastar**	258	5.27	23018	52.6	0.41	18.7	0.72	0.41
GRUMMAN								
JRF-6B	375	8.33	NA	79.9	0.38	21.8	0.56	0.42
J4F-1	245	5.85	NA	50.4	0.43	16.8	0.56	.45/.48
SM S-700	258	5.31	NASA GAW-1	76.1	0.47	18.5	1.03	0.47
Can. CL-215	1,080	11.5	NA	306	0.28	28.2	0.70	0.40
BV-222	3,077	18.1	NA	413	0.23	59.0	0.44	.31/.17
SM US-1**	1,462	12.6	NA	343	0.28	51.3	0.95	.33/.34
Boeing 314-A	3,001	22.3	BAC	580	0.26	52.8	0.46	.31/.39
Martin PBM-3	1,385	12.8	NA	257	0.42	39.8	0.58	0.50
Beriev M-12***	1,130	10.2	NA	244	0.40	39.9	0.85	.37/.57
Part.P6B****	200	5.08	NA	47.5	1.00	15.7	0.74	stabilator
McK G-21G	378	7.78	23000	84.5	0.53	22.1	0.64	.49/.69

* Unless otherwise indicated. ** Turbopropeller driven *** Jet Driven
**** Float Airplane

Table 8.11b) Flying Boats, Amphibious and Float Airplanes: Vertical Tail Volume. Rudder and Aileron Data

Type	Wing Area S ft^2	Wing Span b ft	Vert. Tail Area S_v ft^2	S_r/S_v	x_v ft	$\bar{V}_v$	Rudder Chord root/tip fr.c_v	S_a/S	Ail. Span Loc. in/out fr.b/2	Ail. Chord in/out fr.c_w
SHORTS										
Sandr'ham	1,487	113	157	0.31	43.5	0.041	.43/.36	0.089	.52/.93	.26/.20
Shetland	2,773	150	247	0.28	53.6	0.032	.33/.30	0.069	.51/.92	.22/.23
DORNIER										
Do 24	1,162	88.6	98.4	0.46	33.6	0.032	.41/.56	0.090	.32/.94	.15/.21
Do 24/72	1,129	91.8	200	0.38	42.2	0.081	.28/1.0	0.088	.63/.97	.29/.27
Do Seastar*	258	48.6	31.3	0.35	18.5	0.046	.33/.41	0.098	.60/.96	0.28
GRUMMAN										
JRF-6B	375	49.0	45.3	0.44	20.7	0.051	.41/.57	0.077	.56/.92	.27/.21
J4F-1	245	40.0	26.8	0.43	16.5	0.045	.35/.59	0.063	.57/.94	.20/.23
SM S-700	258	49.2	47.8	0.34	17.9	0.067	.29/.44	0.058	.63/.94	0.19
Can.CL215	1,080	93.8	186	0.35	29.2	0.053	.41/.57	0.080	.64/.95	0.26
BV-222	3,077	157	255	0.40	60.6	0.032	.36/.64	0.052	.56/.97	.12/.16
SM US-1*	1,462	109	265	0.29	46.4	0.077	.17/.30	0.047	.72/.98	.23/.21
B 314A	3,001	152	252	0.41	54.8	0.030	0.41	0.033	.58/.95	.09/.23
M PBM-3	1,385	118	196	0.44	39.7	0.048	.48/.39	0.053	.66/.96	.25/.28
Beriev M-12**	1,130	97.5	203	0.38	41.9	0.077	.36/.38	0.076	.58/.98	.29/.30
P6B***	200	39.4	21.9	0.22	15.5	0.043	.36/.40	0.096	.62/.96	0.21
McK G21-G	378	50.8	40.1	0.56	22.3	0.047	.39/.71	0.078	.55/.89	.23/.21

* Turbopropeller driven ** Jet Driven *** Float Airplane

Table 8.12a) Supersonic Cruise Airplanes: Horiz. Tail Volume and Elevator Data

Type	Wing Area	Wing mgc	Wing Airfoil	Hor. Tail Area	S_e/S_h	x_h	$\bar{V}_h$	Elevator Chord
	S	$\bar{c}$	root/tip	S_h				root/tip
	ft^2	ft		ft^2		ft		fr.c_h
NORTH AMERICAN AVIATION (Now Rockwell)								
XB-70A	6,297	78.5	NA	delta with elevons and small canard				
RA-5C	700	15.7	NA	356	1.0	17.1	0.56	stabilator
BOEING								
SST*	9,000	29.0**	NA	592	0.16	161	0.36	.24/.74
AST-100*	11,630	96.2	NA	547	1.0	107	0.052	stabilator
NASA*								
SSXjet I	965	30.6	.002/.003	65.0	1.0	47.2	0.10	stabilator
SSXjet II	965	30.6	.002/.003	80.0	1.0	41.2	0.09	stabilator
SSXjet III	1,128	33.1	.002/.003	80.0	1.0	41.9	0.09	stabilator
TUPOLEV								
Tu-144	4,715	58.3		delta with elevons and folding canard				
Tu-22M	1,585	15.4**	NA	727	1.0	37.2	1.11	stabilator
Tu-22	2,062	23.7***	NA	620	0.12	34.7	0.44	.29/.30
Dassault								
Mirage IVA	840	24.7	NA	delta with elevons				
GD F-111A	530	9.12**	NA	352	1.0	17.6	1.28	stabilator
Concorde	3,856	61.7	NA	ogive with elevons				
Rockwell B1B	1,950	15.8**	NA	494	1.0	49.9	0.80	stabilator
Convair B58	1,481	34.6	NA	delta with elevons				

* Study projects only ** Measured at forward sweep *** Fixed sweep airplane
See Refs. xx - yy

Table 8.12b) Supersonic Cruise Airplanes: Vertical Tail Volume, Rudder, Aileron and Spoiler Data

Type	Wing Area	Wing Span	Vert. Tail Area	S_r/S_v	x_v	$\bar{V}_v$	Rudder Chord	S_a/S	Ail. Span Loc.	Ail. Chord
	S	b	S_v				root/tip		in/out	in/out
	ft^2	ft	ft^2		ft		fr.c_v		fr.b/2	fr.c_w
NORTH AMERICAN AVIATION (Now Rockwell)										
XB-70A	6,297	105	468	0.75	48.5	0.034	****	0.067	.33/.72	.13/.31*
RA-5C	700	53.0	102	1.0**	21.8	0.060	1.0**	no ailerons		
BOEING***										
SST	9,000	174	866	0.26	88.5	0.049	.23/.46	0.014	.78/.96	.32/.43
AST-100	11,630	138	890	1.0**	121	0.067	1.0**	0.017	.72/1.0	.15/.29
NASA***										
SSXjet I	965	42.1	75.0	1.0**	38.3	0.071	1.0**	0.018	.76/1.0	.21/.26
SSXjet II	965	42.1	75.0	1.0**	35.5	0.066	1.0**	0.018	.76/1.0	.21/.26
SSXjt III	1,128	45.6	97.0	1.0**	32.1	0.061	1.0**	0.017	.74/1.0	.19/.26
TUPOLEV										
Tu-144	4,715	94.5	648	0.19	55.6	0.081	.20/.35	0.100	.31/.97	.11/.51*
Tu-22M	1,585	113	437	0.17	35.6	0.087	.39/.36	NA	.80/.95	.24/.28
Tu-22	2,062	90.9	376	0.14	29.6	0.059	.25/.33	0.051	.66/.95	.29/.31
Dassault										
Mirage IVA	840	38.9	129	0.12	14.1	0.056	.14/.24	0.120	.30/.96	.17/.63*
GD F-111A	530	63.0	115	0.25	18.6	0.064	.27/.29	no ailerons		
Concorde	3,856	84.0	477	0.24	54.1	0.080	.18/.47	0.089	.51/1.0	.15/.27*
Rockw.B1B	1,950	137	230	0.30	45.8	0.039	.29/.38	no ailerons		
Conv. B58	1,481	57.0	153	0.24	31.8	0.057	.32/.31	0.120	.18/.69	.16/.28*

* Elevon equipped ** Slab vertical tail ***Study projects only
**** Rudder hingeline skewed

Table 8.12c) Supersonic Cruise Airplanes: Vertical Tail Volume, Rudder, Aileron and Spoiler Data

Type	Inb'd Ail. Span	Inb'd Ail. Chord	Inb'd Spoiler Span Loc.	Inb'd Spoiler Chord	Inb'd Spoiler Hinge Loc.	Outb'd Spoiler Span Loc.	Outb'd Spoiler Chord	Outb'd Spoiler Hinge Loc.
	in/out	in/out	in/out	in/out	in/out	in/out	in/out	in/out
	fr.b/2	fr.c_w	fr.b/2	fr.c_w	fr.c_w	fr.c_w	fr.c_w	fr.c_w
NORTH AMERICAN AVIATION (Now Rockwell)								
XB-70A	none	none	no lateral control spoilers					
RA-5C	none	none	none	none	none	.25/.73	.14/.19	.60/.65
BOEING*								
SST	none	none	none	none	none	.36/.78	.17/.15	.69/.67
AST-100	none	none	none	none	none	.60/.70	.08/.11	.73/.65
NASA*								
SSXjet I	none	none	none	none	none	.38/.75	.04/.07	.88/.78
SSXjet II	none	none	none	none	none	.31/.75	.04/.07	.85/.78
SSXjt III	none	none	none	none	none	.31/.74	.04/.06	.86/.78
TUPOLEV								
Tu-144	none	none	no lateral control spoilers					
Tu-22M	none	none	none	none	none	.32/.80	.08/.13	.69/.66
Dassault								
Mir. IVA	none	none	no lateral control spoilers					
GD F111A	none	none	none	none	none	.25/.79	0.17	.65/.66
Concorde	none	none	no lateral control spoilers					
Rockw.B1B	none	none	none	none	none	.47/.81	.36/.35	.64/.65
Conv. B58	none	none	no lateral control spoilers					

* Study projects only

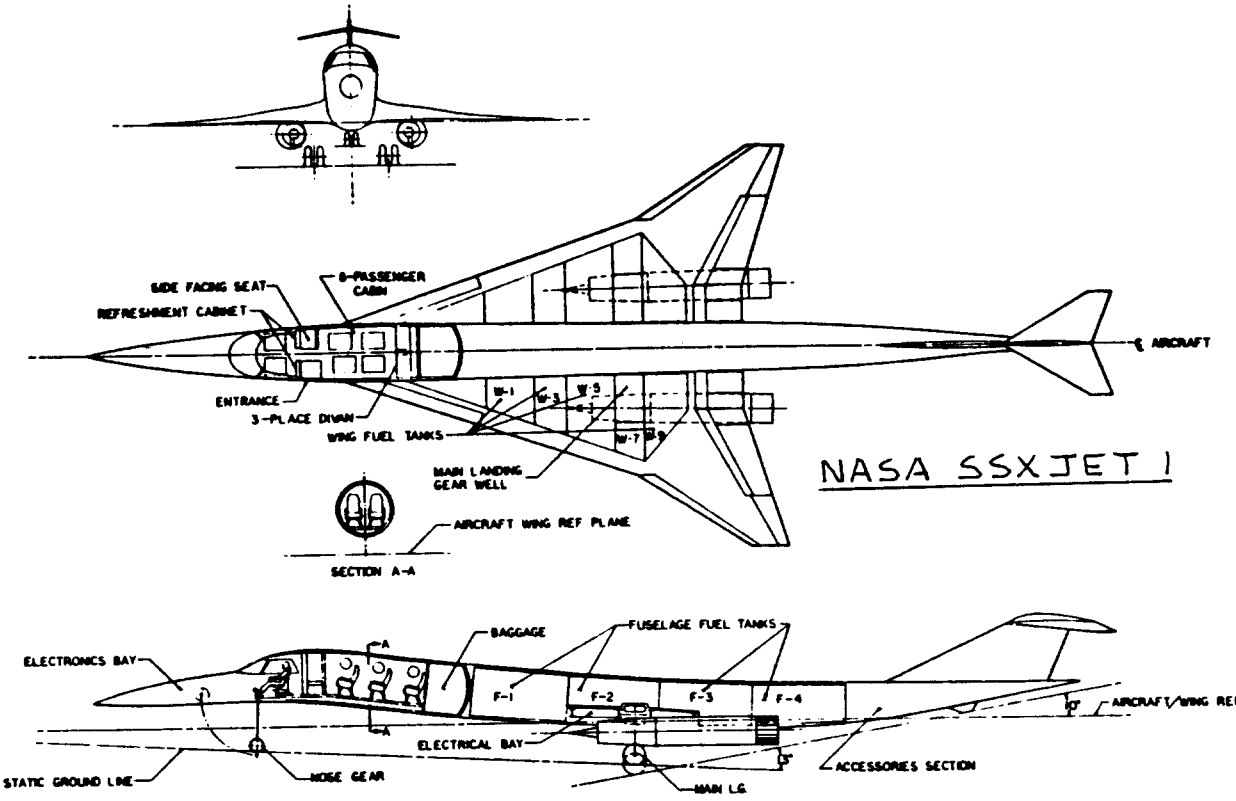

that not enough different canard configurations have been built for a reliable data base.

For this reason it is suggested that the reader use the so-called X-plot method for the sizing of a canard. This method is explained in Chapter 11.

c. Three-surface configurations.

The comments made under b. also apply here. The reader should use the X-plot method of Chapter 11 to size the canard and the horizontal tail of a three-surface airplane.

d. Butterfly empennage configurations.

For a butterfly arrangement, the first step is to apply the sizing method as if the tail were conventional. The surface areas S_h and S_v obtained in this manner must now be considered to be equal to the projections of the butterfly arrangement onto the horizontal and vertical reference planes. The required 'butterfly angle', Γ_h follows from this projection analogy:

$$\Gamma_h = \arctan(S_v/S_h) \qquad (8.5)$$

Step 8.4: Decide on the planform geometry of the empennage.

This involves making the following choices:

1. aspect ratio
2. sweep angle
3. taper ratio
4. thickness ratio
5. airfoil
6. dihedral
7. incidence angle

Tables 8.13 and 8.14 provide some guidance in making these choices. The selection of items 1-7 follow some of the same reasoning used in selecting these items for the wing in Chapter 6.

In selecting sweep angle/thickness ratio combinations for tail aft configurations it is important to ensure that the critical Mach number for the tails is higher than that of the wing. An increment of $\Delta M = 0.05$ is usually sufficient.

Table 8.13 Planform Design Parameters for Horizontal Tails

Type	Dihedral Angle, Γ_h deg.	Incidence Angle, i_h deg.	Aspect Ratio, A_h	Sweep Angle, $\Lambda_{c/4_h}$ deg.	Taper Ratio, λ_h
Homebuilts	+5 - -10	0 fixed to variable	1.8 - 4.5	0 - 20	0.29 - 1.0
Single Engine Prop. Driven	0	-5 - 0 or variable	4.0 - 6.3	0 - 10	0.45 - 1.0
Twin Engine Prop Driven	0 - +12	0 fixed to variable	3.7 - 7.7	0 - 17	0.48 - 1.0
Agricultural	0 - +3	0	2.7 - 5.4	0 - 10	0.59 - 1.0
Business Jets	-4 - +9	-3.5 fixed	3.2 - 6.3	0 - 35	0.32 - 0.57
Regional Turbo-Props.	0 - +12	0 - 3 fixed to variable	3.4 - 7.7	0 - 35	0.39 - 1.0
Jet Transports	0 - +11	variable	3.4 - 6.1	18 - 37	0.27 - 0.62
Military Trainers	-11 - +6	0 fixed to	3.0 - 5.1	0 - 30	0.36 - 1.0
Fighters	-23 - +5	0 fixed to variable	2.3 - 5.8	0 - 55	0.16 - 1.0
Mil. Patrol, Bomb and Transports	-5 - +11	0 fixed to variable	1.3 - 6.9	5 - 35	0.31 - 0.8
Flying Boats, Amph. and Float Airplanes	0 - +25	0 fixed	2.2 - 5.1	0 - 17	0.33 - 1.0
Supersonic Cruise Airplanes	-15 - 0	0 fixed to variable	1.8 - 2.6	32 - 60	0.14 - 0.39

Table 8.14 Planform Design Parameters for Vertical Tails

Type	Dihedral Angle, Γ_v deg.	Incidence Angle, i_v deg.	Aspect Ratio, A_v	Sweep Angle, $\Lambda_{c/4_v}$ deg.	Taper Ratio, λ_v
Homebuilts	90	0	0.4 - 1.4	0 - 47	0.26 - 0.71
Single Engine Prop. Driven	90	0	0.9 - 2.2	12 - 42	0.32 - 0.58
Twin Engine Prop Driven	90	0	0.7 - 1.8	18 - 45	0.33 - 0.74
Agricultural	90	0	0.6 - 1.4	0 - 32	0.43 - 0.74
Business Jets	90	0	0.8 - 1.6	28 - 55	0.30 - 0.74
Regional Turbo-Props.	90	0	0.8 - 1.7	0 - 45	0.32 - 1.0
Jet Transports	90	0	0.7 - 2.0	33 - 53	0.26 - 0.73
Military Trainers	90	0	1.0 - 2.9	0 - 45	0.32 - 0.74
Fighters	75 - 90	0	0.4 - 2.0	9 - 60	0.19 - 0.57
Mil. Patrol, Bomb and Transports	90	0	0.9 - 1.9	0 - 37	0.28 - 1.0
Flying Boats, Amph. and Float Airplanes	90	0	1.2 - 2.4	0 - 32	0.37 - 1.0
Supersonic Cruise Airplanes	75 - 90	0	0.5 - 1.8	37 - 65	0.20 - 0.43

For most horizontal tails and vertical tails NACA symmetrical airfoils are in use. Typical of such airfoils are NACA 0009/0018. Ref.20 provides data on these airfoils.

For canards the choice of airfoil is particularly critical. The required maximum lift coeffficient capability at the canard Reynold's number must be determined so that the canard always stalls first. If a laminar flow airfoil is selected for the canard it will be necessary to verify that the canard lift is not altered drastically when the flow becomes turbulent such as may happen when suddenly encountering rain.

Step 8.5: Prepare dimensioned drawings of the selected empennage planforms.

Step 8.6: Decide on the sizes and disposition of the longitudinal and directional control surfaces.

Tables 8.1 through 8.12 provide data for twelve types of airplanes on the size and location of:

1. elevators and stabilators 2. rudders

After deciding which type of airplane best 'fits' the type being designed, initial control surface sizes can be determined directly from Tables 8.1 through 8.12.

The control surfaces should now be sketched into the planform drawings of Step 8.5. Watch out for a possible conflict between rudder and elevator deflections. Such conflicts often arise in conventional arrangements and lead to inboard cut-outs of one of these surfaces. Typical examples are shown in Figures 3.4b and 3.4d.

Step 8.7: Document the decisions made under Steps 8.1 through 8.6 in a brief, descriptive report including clear dimensioned drawings.

8.2 EXAMPLE APPLICATIONS

Three examples applications will now be discussed:

8.2.1 Twin Engine Propeller Driven Airplane: Selene
8.2.2 Jet Transport: Ourania
8.2.3 Fighter: Eris

8.2.1 Twin Engine Propeller Driven Airplane

Step 8.1: It was decided in sub-section 3.5.1 to employ a conventional configuration. That implies a tail aft arrangement.

Step 8.2: From the general arrangement drawing of the fuselage in Figure 4.2b (p.113) the following moment arms are 'guestimated':

x_h = 21.4 ft. and x_v = 16.8 ft.

Step 8.3: The following table summarizes volume coefficient and control surface size data for comparable airplanes. The data are taken from Tables 8.3a and b:

Airplane Type	$\bar{V}_h$	S_e/S_h	$\bar{V}_v$	S_r/S^v
Cessna 310R	0.95	0.41	0.063	0.45
Cessna 402B	1.07	0.29	0.080	0.47
Cessna 414A	0.93	0.27	0.071	0.38
Cessna T303	0.78	0.42	0.052	0.44
Beech Duke B60	0.64	0.27	0.060	0.43
Piaggio P166-DL3	0.51	0.27	0.041	0.43
Averages:	0.81	0.32	0.061	0.43

For the Selene the following values are selected:

$\bar{V}_h$ = 0.94, S_e/S_h = 0.32, $\bar{V}_v$ = 0.10, S_r/S_v = 0.43

The reason for selecting higher volume coefficients is the higher wing loading of the Selene. With a relatively smaller wing this could lead to tail surfaces which are too small.

For the Selene, S = 172 ft^2, $\bar{c}$ = 4.92 ft and b = 37.1 ft. With Eqns (8.3) and (8.4) this leads to the following tail sizes:

S_h = 37 ft^2 and S_v = 38 ft^2.

Step 8.4: The following table summarizes the geometric parameters for the horizontal and for the vertical tail of the Selene. These quantities are in overall agreement with those listed in Tables 8.13 and 8.14 for twin engine propeller driven airplanes:

Parameter	Hor. Tail	Vert. Tail
Aspect ratio, A	3.85	1.0
Leading edge sweep angle	30 deg.	50 deg.
Taper ratio	0.40	0.56
Thickness ratio	0.12	0.15
Airfoil	NACA 0012	NACA 0015
Dihedral angle	0 deg.	not appl.
Incidence angle	variable	0 deg.

Step 8.5: Figure 8.2 presents dimensioned drawings of the proposed empennage arrangement for the Selene.

Step 8.6: Using the control surface ratios selected in Step 8.3, the elevator and rudder outlines are drawn into the planforms of Figure 8.2.

Step 8.7: This step has been omitted to save space.

8.2.2 Jet Transport

Step 8.1: It was decided in sub-section 3.5.2 to employ a conventional configuration. That implies a tail aft arrangement.

Step 8.2: From the general arrangement drawing of the fuselage in Figure 4.7 (p.120) the following moment arms are 'guestimated':

x_h = 51.0 ft. and x_v = 54.0 ft.

Step 8.3: The following table summarizes volume coefficient and control surface size data for comparable airplanes. The data are taken from Tables 8.7a and b:

Airplane Type	$\bar{V}_h$	S_e/S_h	$\bar{V}_v$	S_{r/S^v}
Boeing 737-200	1.28	0.27	0.100	0.24
Boeing 737-300	1.35	0.24	0.100	0.31
McDD DC-9-S80	0.96	0.34	0.062	0.39
McDD DC-9-50	1.32	0.38	0.079	0.41
Fokker F-28-4000	1.07	0.20	0.085	0.16
Rombac/BAe 1-11-495	0.86	0.27	0.038	0.28
Averages:	1.14	0.28	0.077	0.30

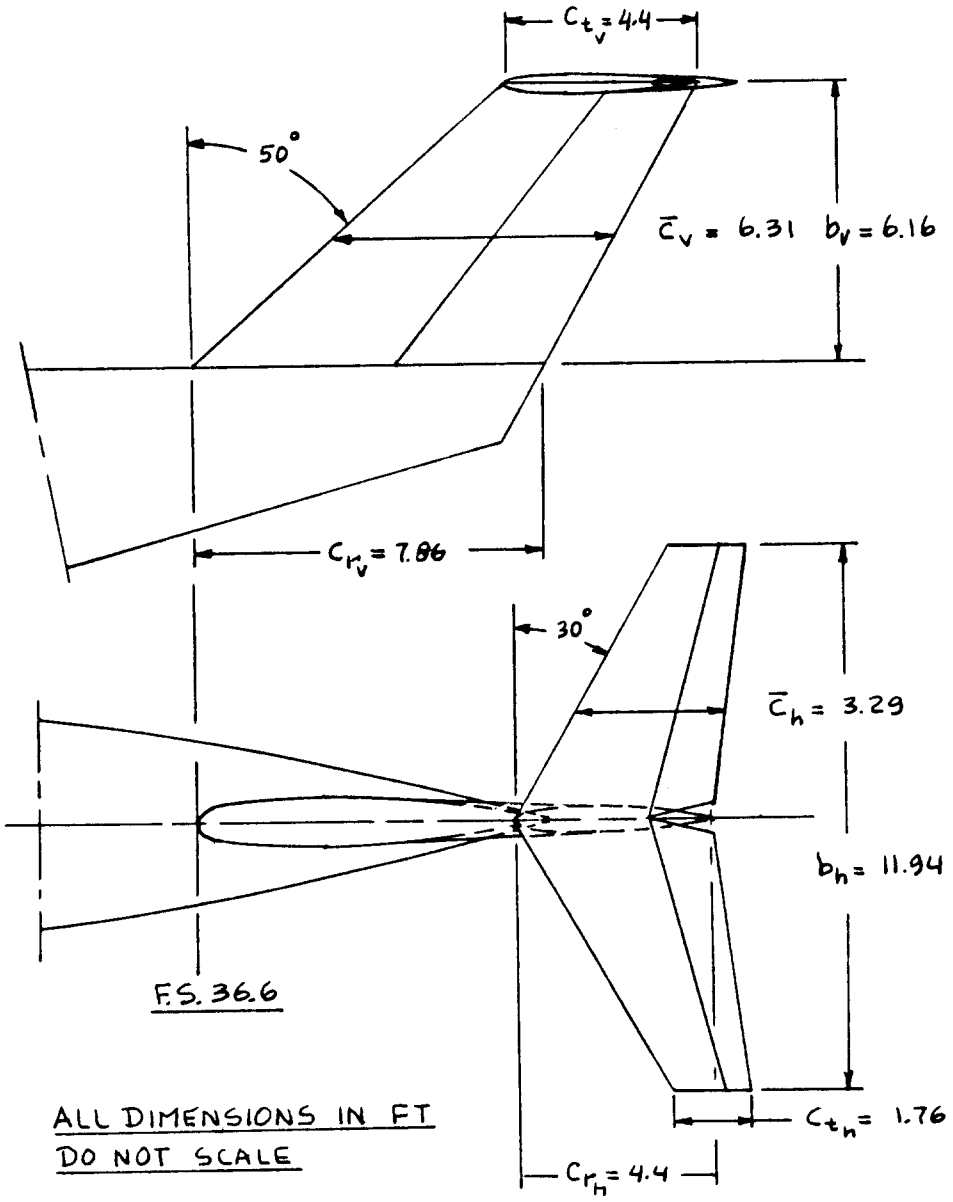

Figure 8.2 Selene: Empennage Configuration

For the Ourania the following values are selected:

$\bar{V}_h = 0.80$, $S_e/S_h = 0.30$, $\bar{V}_v = 0.06$, $S_r/S_v = 0.35$

The reason for selecting lower volume coefficients is the fact that it was decided in sub-section 3.5.2 to employ 'relaxed' static stability combined with a digital 'fly-by-wire' flight control system.

For the Ourania, $S = 1{,}296$ ft^2, $\bar{c} = 12.5$ ft and $b = 113.8$ ft. Using Eqns (8.3) and (8.4) this leads to the following tail sizes:

$S_h = 254$ ft^2 and $S_v = 164$ ft^2.

Step 8.4: The following table summarizes the geometric parameters for the horizontal and for the vertical tail of the Ourania. These quantities are in overall agreement with those listed in Tables 8.13 and 8.14 for jet transports.

Parameter	Hor. Tail	Vert. Tail
Aspect ratio, A	5.0	1.8
Leading edge sweep angle	35 deg.	45 deg.
Taper ratio	0.32	0.32
Thickness ratio	0.12	0.15
Airfoil	NACA 0012	NACA 0015
Dihedral angle	0 deg.	not appl.
Incidence angle	variable	0 deg.

The reader should verify with the help of Figure 6.1a (p.150) that the critical Mach number of both tail surfaces is higher than that of the wing.

Step 8.5: Figure 8.3 presents dimensioned drawings of the proposed empennage arrangement for the Selene.

Step 8.6: Using the control surface ratios selected in Step 8.3, the elevator and rudder outlines are drawn into the planforms of Figure 8.3.

Step 8.7: This step has been omitted to save space.

8.2.3 Fighter

Step 8.1: It was decided in sub-section 3.5.3 to employ a conventional, twin boom configuration. That implies a tail aft arrangement.

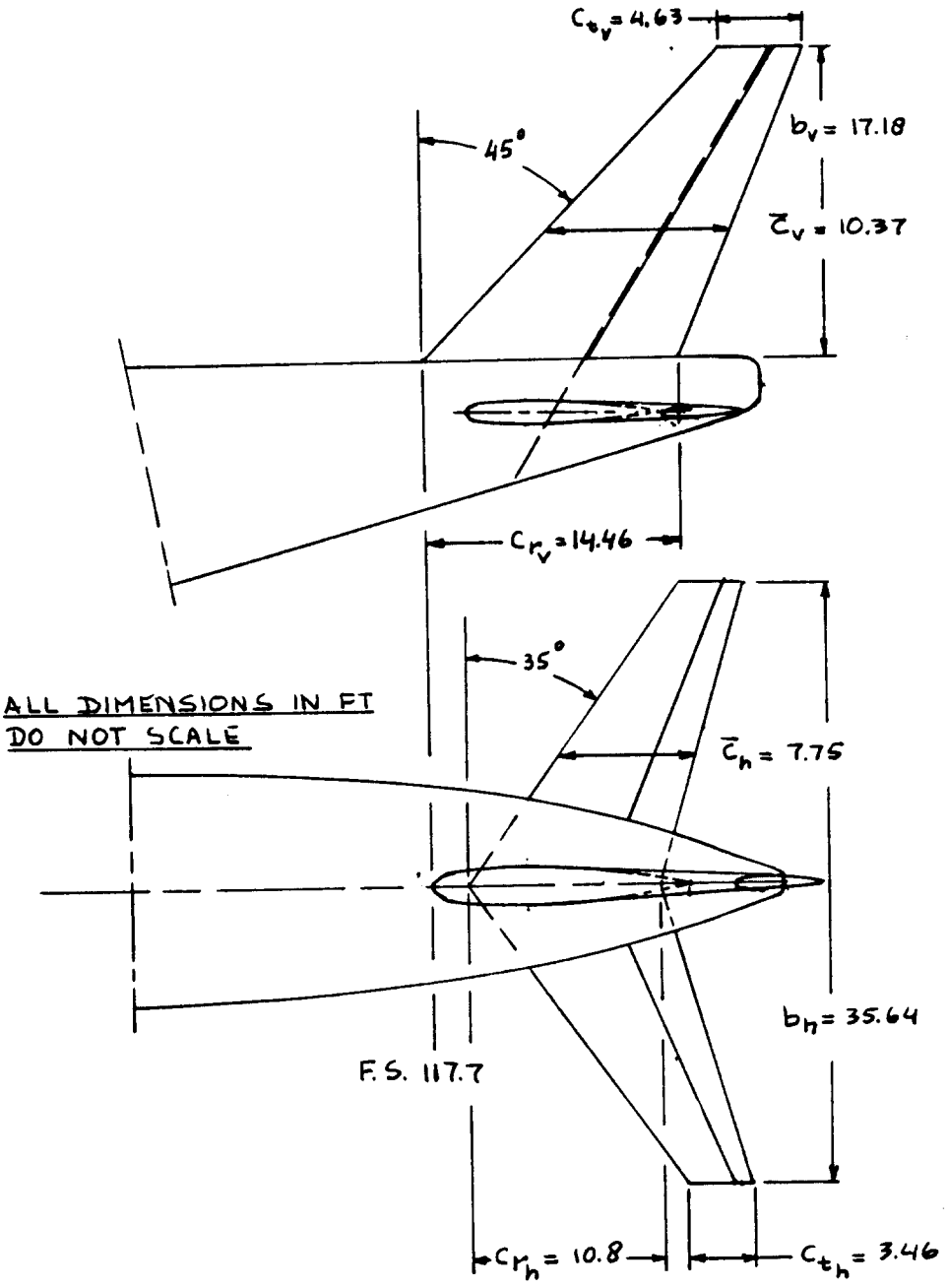

Figure 8.3 Ourania: Empennage Configuration

Step 8.2: From the general arrangement drawing of the fuselage in Figure 4.9 (p.122) the following moment arms are 'guestimated':

x_h = 25.3 ft. and x_v = 22.0 ft.

Step 8.3: The following table summarizes volume coefficient and control surface size data for comparable airplanes. The data are taken from Tables 8.9a and b:

Airplane Type	$\bar{V}_h$	S_e/S_h	$\bar{V}_v$	S_r/S^v
Fairchild Rep. A-10A	0.41	0.32	0.060	0.28
Grumman A6A	0.46	1.00*	0.069	0.21
Aermacchi MB339K**	0.40	0.29	0.043	0.26
Vought A7A**	0.22	1.00*	0.130	0.13
Averages:	0.37	0.31	0.076	0.22

*stabilator **single engine fighter

For the Eris the following values are selected:

$\bar{V}_h$ = 0.25, S_e/S_h = 0.31, $\bar{V}_v$ = 0.06, S_r/S_v = 0.22

The reason for selecting lower volume coefficients is the fact that it was decided in sub-section 3.5.3 to employ 'relaxed' static stability combined with a digital 'fly-by-wire' flight control system.

For the Eris, S = 787 ft^2, $\bar{c}$ = 11.9 ft and b = 68.7 ft. Using Eqns (8.3) and (8.4) this leads to the following tail sizes:

S_h = 93 ft^2 and S_v = 147 ft^2.

Step 8.4: The following table summarizes the geometric parameters for the horizontal and for the vertical tail of the Eris. These quantities are in overall agreement with those listed in Tables 8.13 and 8.14 for fighters.

Parameter	Hor. Tail	Vert. Tail
Aspect ratio, A	3.6	1.2
Leading edge sweep angle	0 deg.	45 deg.
Taper ratio	1.0	0.55
Thickness ratio	0.10	0.15
Airfoil	NACA 0010	NACA 0015
Dihedral angle	0 deg.	not appl.
Incidence angle	0 deg.	0 deg.

The reader should verify with the help of Figure 6.1a (p.150) that the critical Mach number of both tail surfaces is higher than that of the wing.

Step 8.5: Figure 8.4 presents dimensioned drawings of the proposed empennage arrangement for the Eris.

Step 8.6: Using the control surface ratios selected in Step 8.3, the elevator and rudder outlines are drawn into the planforms of Figure 8.4.

Step 8.7: This step has been omitted to save space.

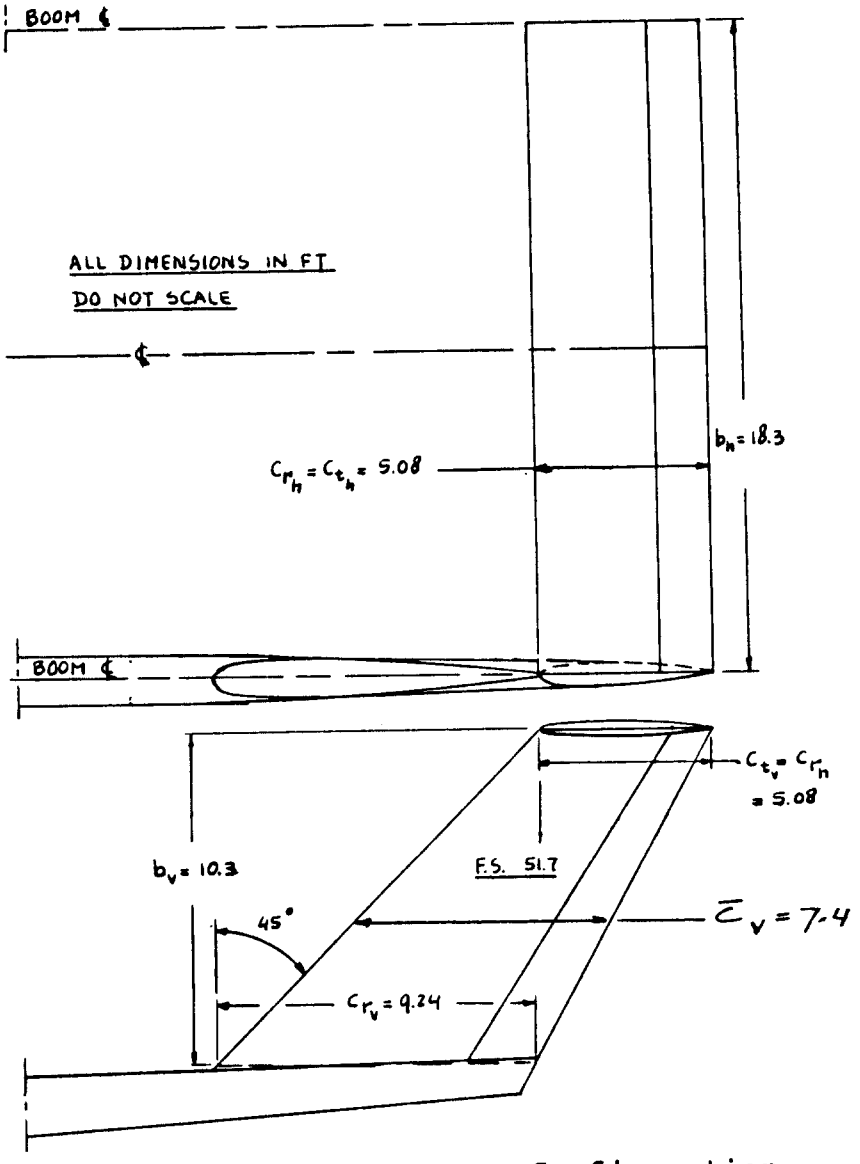

Figure 8.4 Eris: Empennage Configuration

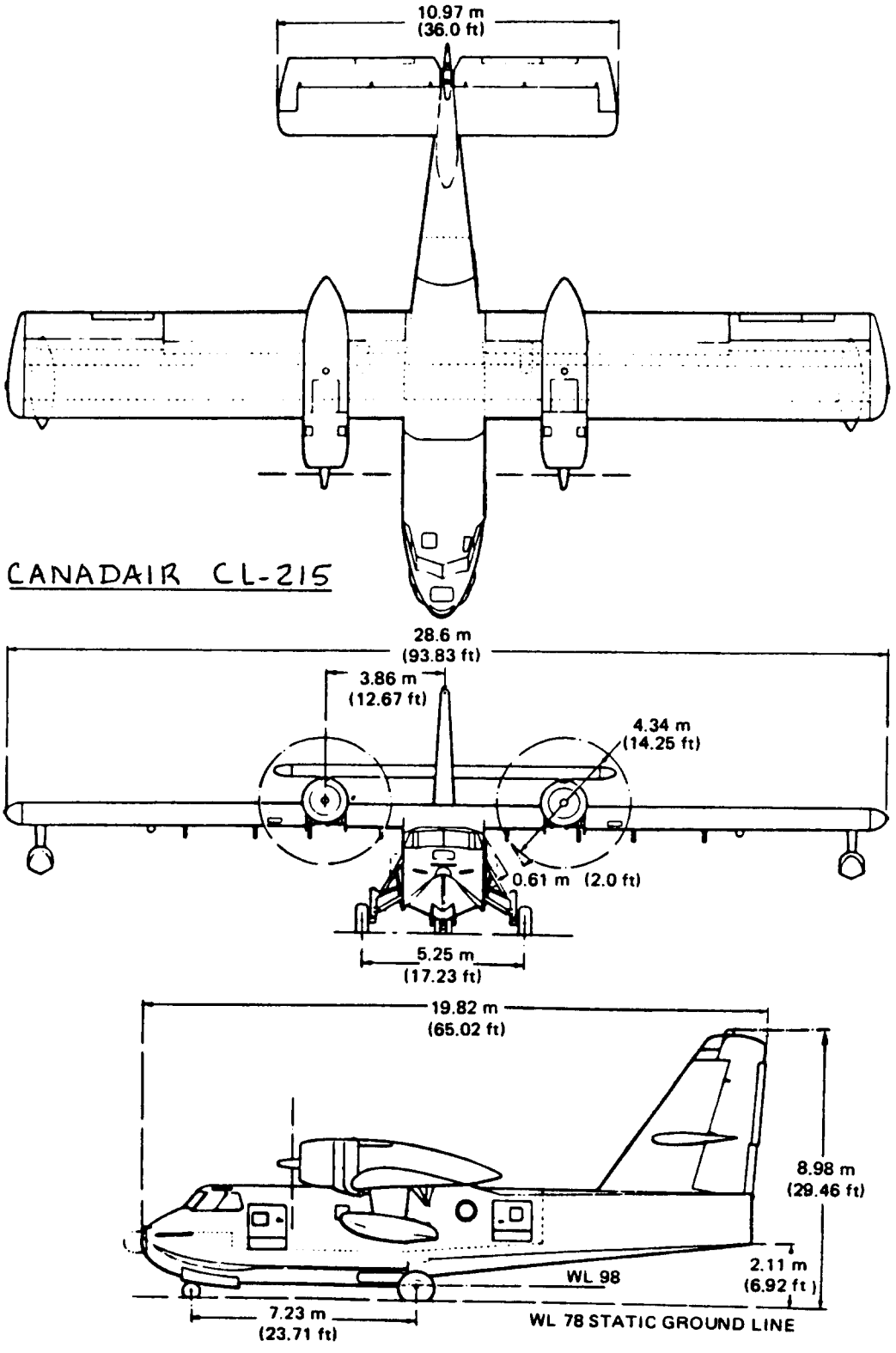
10.97 m
(36.0 ft)
CANADAIR CL-215
28.6 m
(93.83 ft)
3.86 m
(12.67 ft)
4.34 m
(14.25 ft)
0.61 m (2.0 ft)
5.25 m
(17.23 ft)
19.82 m
(65.02 ft)
8.98 m
(29.46 ft)
2.11 m
(6.92 ft)
WL 98
7.23 m
(23.71 ft)
WL 78 STATIC GROUND LINE

9. CLASS I METHOD FOR LANDING GEAR SIZING AND DISPOSITION

The purpose of this chapter is to provide a rapid, step-by-step method to determine the following landing gear characteristics:

1. Number, type and size of tires
2. Length and diameter of strut(s)
3. Preliminary disposition
4. Retraction feasibility

The method is presented as part of Step 9 of p.d. sequence I as outlined in Chapter 2. Section 9.1 presents the step-by-step method. Example applications are given in Section 9.2.

9.1 CLASS I METHOD FOR LANDING GEAR SIZING AND DISPOSITION

Step 9.1: Decide which landing gear system to use.

The choices here are:

1. Fixed or non-retractable
2. Retractable

In the past several airplanes have used droppable and/or skid type landing gears. One such example is the Me163. Such landing gears will not be considered here.

Another type of landing gear is the so-called air-cushion (or ground effect) type gear. This type of gear will not be considered either.

As a general rule, if the cruise speed of the airplane is above 150 kts, a fixed landing gear imposes an unacceptably high drag penalty.

Step 9.2: Decide on the overall landing gear configuration.

The choices here are as follows:

1. Tailwheel or taildragger
2. Conventional (i.e. nosewheel or tricycle)
3. Tandem
4. Outrigger
5. Beaching gear (for flying boats)

Tandem and outrigger gears are often combined: the Boeing B52 (Fig.3.28a) and the McDonnell Douglas AV8B (Page 221) are typical examples.

For ground operations on soft and/or unprepared fields taildraggers offer a minor weight advantage.

From an ease of ground maneuvering viewpoint as well as a groundlooping viewpoint the nosewheel configuration is to be preferred. Most airplanes today are equipped with nosewheel (tricycle) type landing gears.

Part V contains more detailed discussions of landing gears.

IMPORTANT NOTE: Before embarking on the next steps, it will be necessary to determine the c.g. range of the airplane:

Step 9.3: Proceed to Chapter 10 and prepare a rough weight and balance statement for an assumed disposition of the landing gear.

Step 9.4: Decide on a preliminary landing gear strut disposition and sketch the proposed strut disposition in the general arrangement drawing of Step 10.2, Chapter 10.

There are two geometric criteria which need to be considered in deciding the disposition of the landing gear struts:

1.) Tip-over Criteria.

2.) Ground Clearance Criteria.

1. Tip-over Criteria:

Figure 9.1a presents the tip-over criteria A and B:

A) Longitudinal Tip-over Criterion:

a. For tricycle gears: The main landing gear must be behind the aft c.g. location. The 15 deg. angle shown in Figure 9.1a represents the 'usual' relation between main gear and the aft c.g.

b. For taildraggers: The main landing gear must be forward of the aft c.g. location. The 15 deg. angle shown in Figure 9.1a represents the 'usual' relation between main gear and aft c.g.

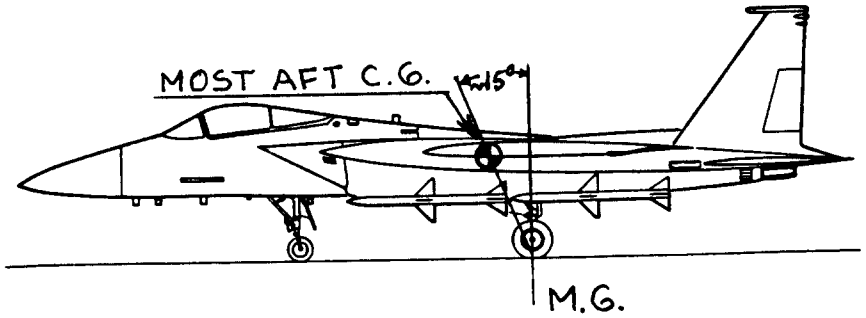

Longitudinal Tip-over Criterion for Tricycle Gears

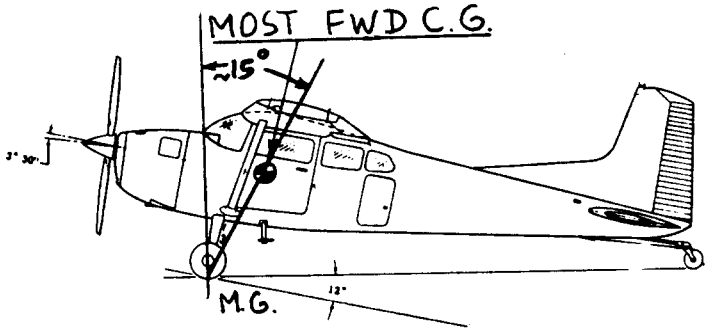

Longitudinal Tip-over Criterion for Taildraggers

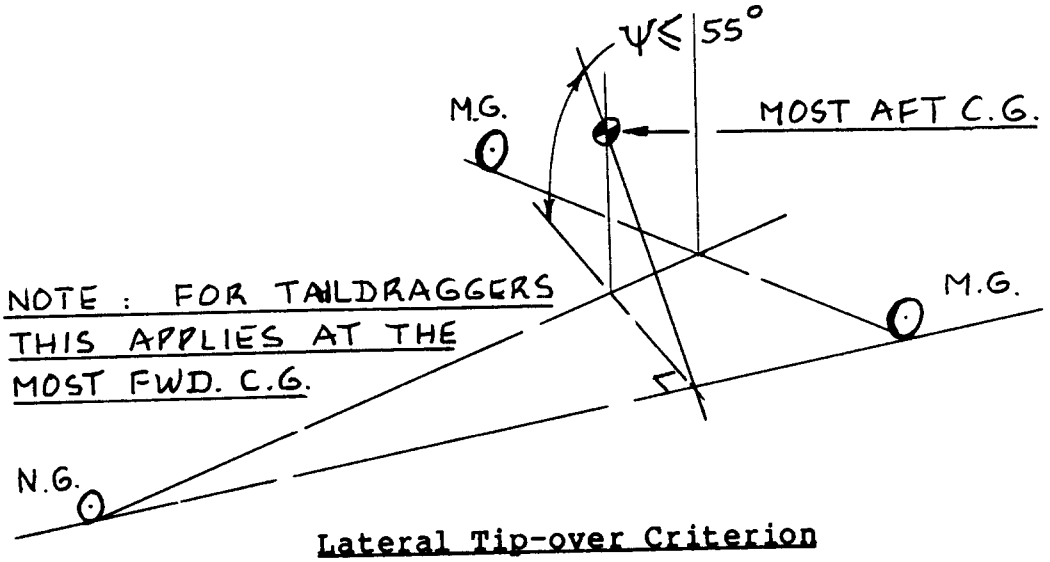

Lateral Tip-over Criterion

Figure 9.1a Tip-over Criteria for Landing Gear Placement

B) Lateral Tip-over Criterion:

The lateral tip-over is dictated by the angle ψ, in Figure 9.1a. The lateral tip-over situation in Figure 9.1a is drawn for a tricycle gear. Note that this criterion applies in a similar fashion to taildraggers.

Approximate forward and aft c.g. locations were be obtained in Step 9.3.

2. Ground Clearance Criteria:

Figure 9.1b summarizes the required ground clearance angles.

The lateral ground clearance angle applies to tricycles and to taildraggers. The longitudinal ground clearance angle applies to tricycles only.

Keeping in mind the geometric criteria, the following decisions must now be made:

1. Number, location and length of main gear struts:

   a.) under the wing
   b.) under the fuselage
   c.) both (as in the 747 and DC 10-30)

2. Number, location and length of nose gear struts:

   usually only one strut, located at the forward end of the fuselage.

This decision should initially be made by referring to competitive concepts. The configurations presented in Chapter 3 should be reviewed.

To summarize, the selection of strut length has a major impact on:

* the weight of the landing gear
* the ground clearance of the airplane with deflated tires and struts
* the tip-over characteristics
* Overall airplane stability during ground operation

Part V (Ref.4) contains detailed discussions on these factors.

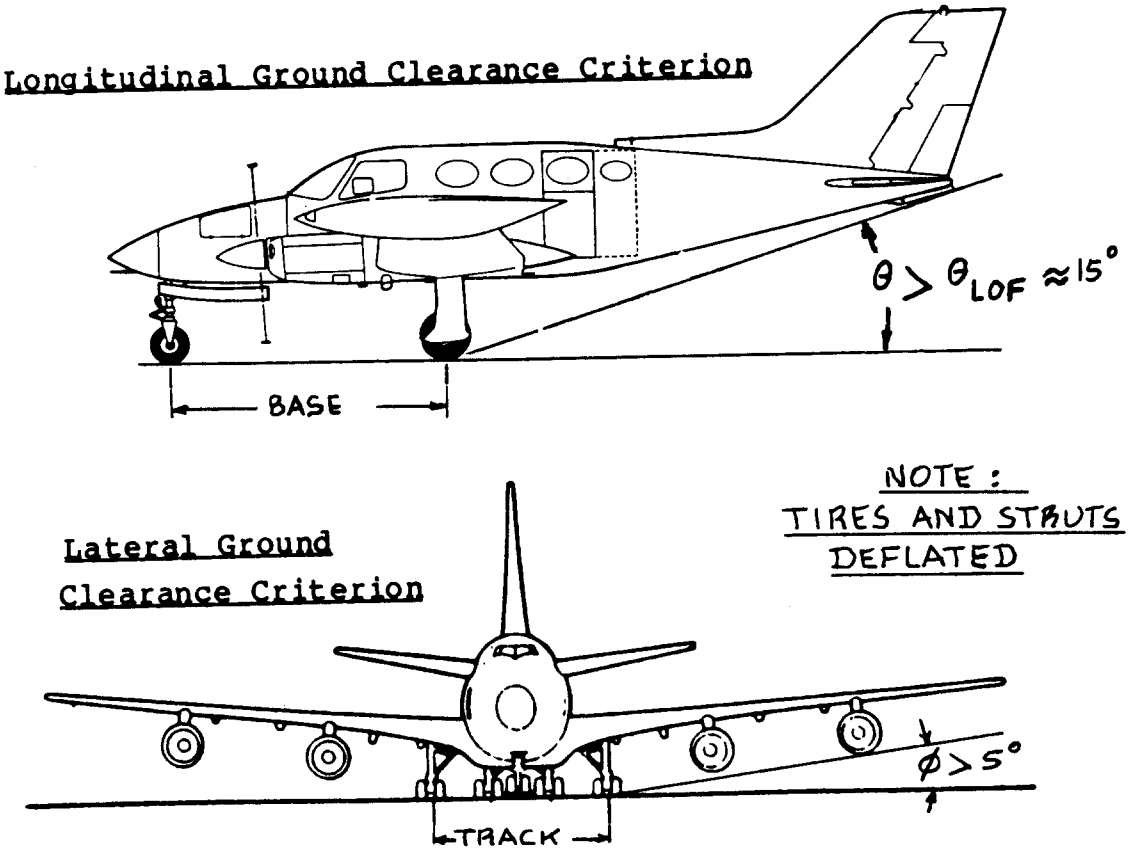

Figure 9.1b Ground Clearance Criteria for Gear Placement

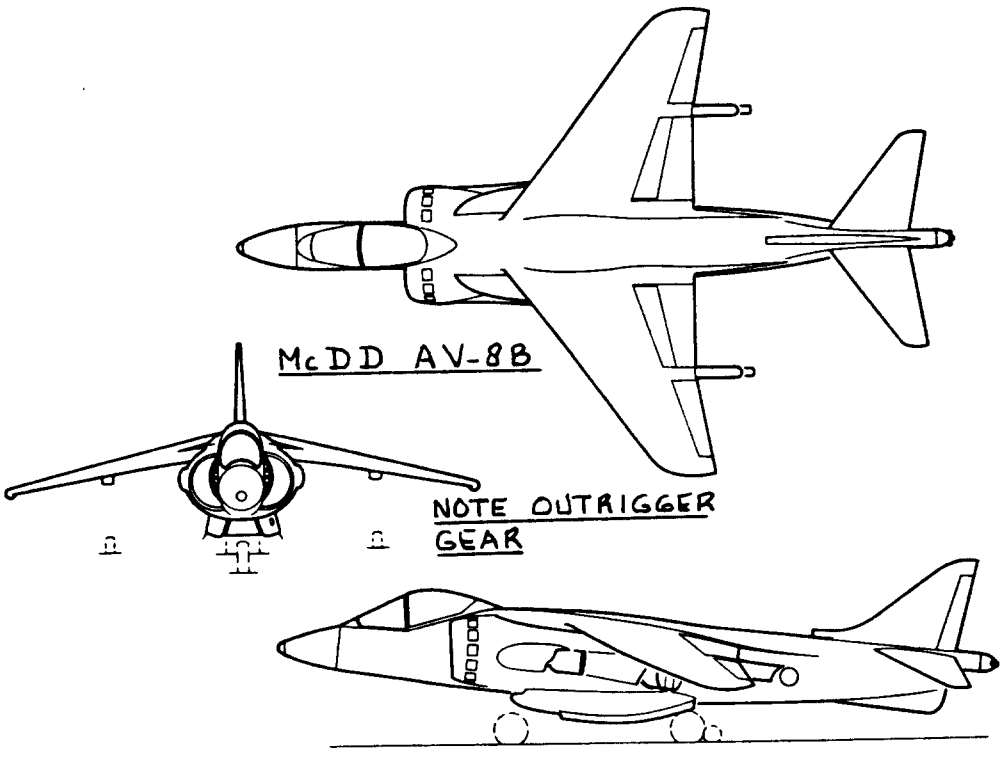

Step 9.5: Calculate the maximum static load per strut.

The following Class I equations can be used to compute the maximum static load per strut:

1. For tricycle landing gears:

Nose wheel strut: $P_n = (W_{TO} l_m)/(l_m + l_n)$ (9.1) $\leq 8\%$

Main gear strut: $P_m = (W_{TO} l_n)/n_s(l_m + l_n)$ (9.2)

Figure 9.2a defines the quantities which are used in Eqns (9.1) and (9.2).

2. For taildragging landing gears:

Replace 'n' by 't' in Eqns (9.1) and (9.2) and refer to Figure 9.2b.

Step 9.6: Decide on the number of wheels to be used.

The usual number of wheels is as follows:

* for tailwheels: one * for nosewheels: one or two

* for main gears the number of wheels depends on the following considerations:

1. Load per tire and the associated surface bearing strength
2. Consequences of a tire blow-out
3. Cost.

Tables 9.1 and 9.2 provide some guidance in making this decision.

Step 9.7: Compute the ratios P_n/W_{TO} and $n_s P_m/W_{TO}$ and select the approximate tire size from Tables 9.1 or 9.2.

Step 9.8: Locate the tires in the general arrangement of Step 10, Chapter 2.

It is important to draw the tires to the proper scale!

Step 9.9: Make sure that the gear as now configured can be retracted into the designated retraction volume(s).

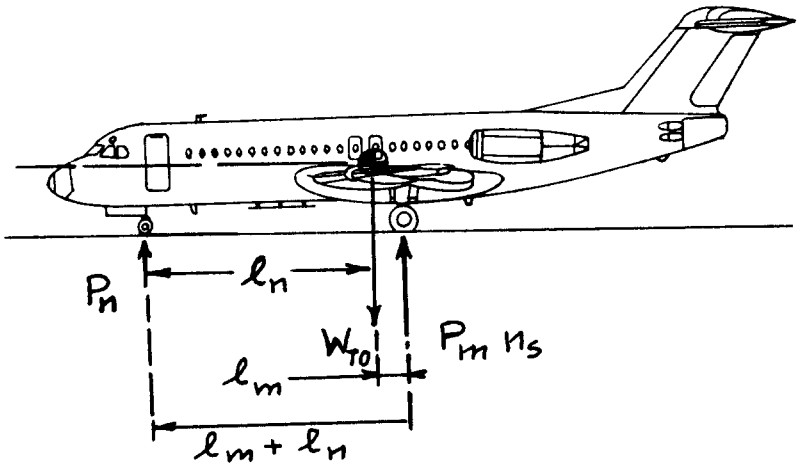

Figure 9.2a Geometry for Static Load Calculation for Tricycle Gears

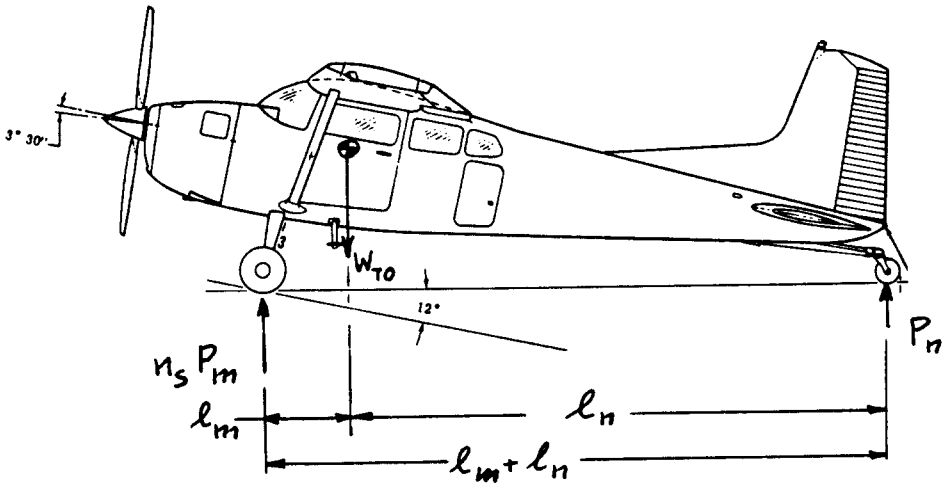

Figure 9.2b Geometry for Static Load Calculation for Taildraggers

Table 9.1 Typical Landing Gear Wheel Data (n_s = 2)

Type	W_{TO}	Main Gear				Nose Gear			
		$D_t x b_t$	$2P_m/W_{TO}$	PSI	n_{mt}	$D_t x b_t$	P_n/W_{TO}	PSI	n_{nt}
	lbs	in.xin.				in.xin.			
Homebuilts	600	13x5	0.80	25	1	9x3.4	0.17	25	1
	1,200	12x5	0.78	45	1	12x5	0.22	45	1
	3,300	16x6	0.87	45	1	16x6	0.13	45	1
Single Engine Prop. Driven	1,600	15x6	0.80	18	1	15x5	0.20	28	1
	2,400	17x6	0.84	19	1	12.5x5	0.16	22	1
	3,800	16.5x6	0.84	55	1	14x5	0.16	49	1
Twin Engine Prop. Driven	5,000	16x6	0.83	55	1	16x6	0.17	40	1
	8,000	22x6.5	0.88	75	1	17x6	0.12	40	1
	12,000	26.6x7	0.84	82	1	19.3x6.6	0.16	82	1
Agricultural	3,000	22x8	0.95	35	1	9x3.5*	0.05*	55*	1*
	7,000	24x8.5	0.92	35	1	12.4x4.5*	0.08*	50*	1*
						*Note: these are tailwheel data			
	10,000	29x7.5	0.85	35	1	25x7	0.15	35	1
Regional Turbo-propeller Driven Airplanes	12,500	18x5.5	0.89	105	2	22x6.75	0.11	57	1
	21,000	24x7.25	0.90	85	2	18x5.5	0.10	65	2
	26,000	36x11	0.92	40	1	20x7.5	0.08	40	1
	44,000	30x9	0.93	107	2	23.4x6.5	0.07	77	2
Business Jets	12,000	22x6.3	0.93	90	1	18x5.7	0.07	120	1
	23,000	27.6x9.3	0.95	155	1	17x5.5	0.05	50	2
	39,000	26x6.6	0.92	208	2	14.5x5.5	0.08	130	2
	68,000	34x9.25	0.93	174	2	21x7.25	0.07	113	2

Table 9.2 Typical Landing Gear Wheel Data (n_s = 2 unless otherwise noted)

Type	W_{TO}	Main Gear				Nose Gear			
		$D_t x b_t$	$n_s P_m/W_{TO}$	PSI	n_{mt}	$D_t x b_t$	P_n/W_{TO}	PSI	n_{nt}
	lbs	in.xin.				in.xin.			
Transport Jets	44,000	34x12	0.89	75	2	24x7.7	0.11	68	2
	73,000	40x14	0.92	77	2	29.5x6.75	0.08	68	2
	116,000	40x14	0.94	170	2	24x7.7	0.06	150	2
	220,000	40x14	0.94	180	4	29x7.7	0.06	180	2
	330,000	46x16	0.93	206	4	40x14	0.07	131	2
	572,000	52x20.5	0.93	200	4*	40x15.5	0.07	190	2
	775,000	49x17	0.94	205	4**	46x16	0.06	190	2
Military Trainers	2,500	17x6	0.82	36	1	13.5x5	0.18	28	1
	5,500	20.3x6.5	0.91	60	1	14x5	0.09	40	1
	7,500	20.25x6	0.92	65	1	17.2x5.0	0.08	45	1
	11,000	23.3x6.5	0.90	143	1	17x4.4	0.10	120	1
Fighters	9,000	20x5.25	0.86	135	1	17x3.25	0.14	82	1
	14,000	18.5x7	0.87	110	1	18x6	0.13	37	1
	25,000	24x8	0.91	210	1	18x6.5	0.09	120	1
	35,000	24x8	0.90	85	2	21.5x9.8	0.10	57	1
	60,000	35.3x9.3	0.88	210	1	21.6x7.5	0.12	120	2
	92,000	42x13	0.93	150	1	20x6.5	0.07	120	2

For Flying Boats, Amphibious and Float Airplanes as well as for Supersonic cruise airplanes, use jet transport data.

*three main gear struts: n_s = 3 ** four main gear struts: n_s = 4

Note: all other airplanes have n_s = 2: two main gear struts.

At this stage of the preliminary design process it is useful to verify the retraction capability with the help of a so-called 'stick diagram'. Examples of such stick diagrams are given in Figure 9.3.

Step 9.10: With the gear layout defined, proceed to Chapter 10, perform the weight and balance calculations and if necessary, iterate back to Step 9.3 until the gear location satisfies all criteria.

Step 9.11: Document the decisions made under Steps 9.1 through 9.10 in a brief, descriptive report with clear dimensioned drawings.

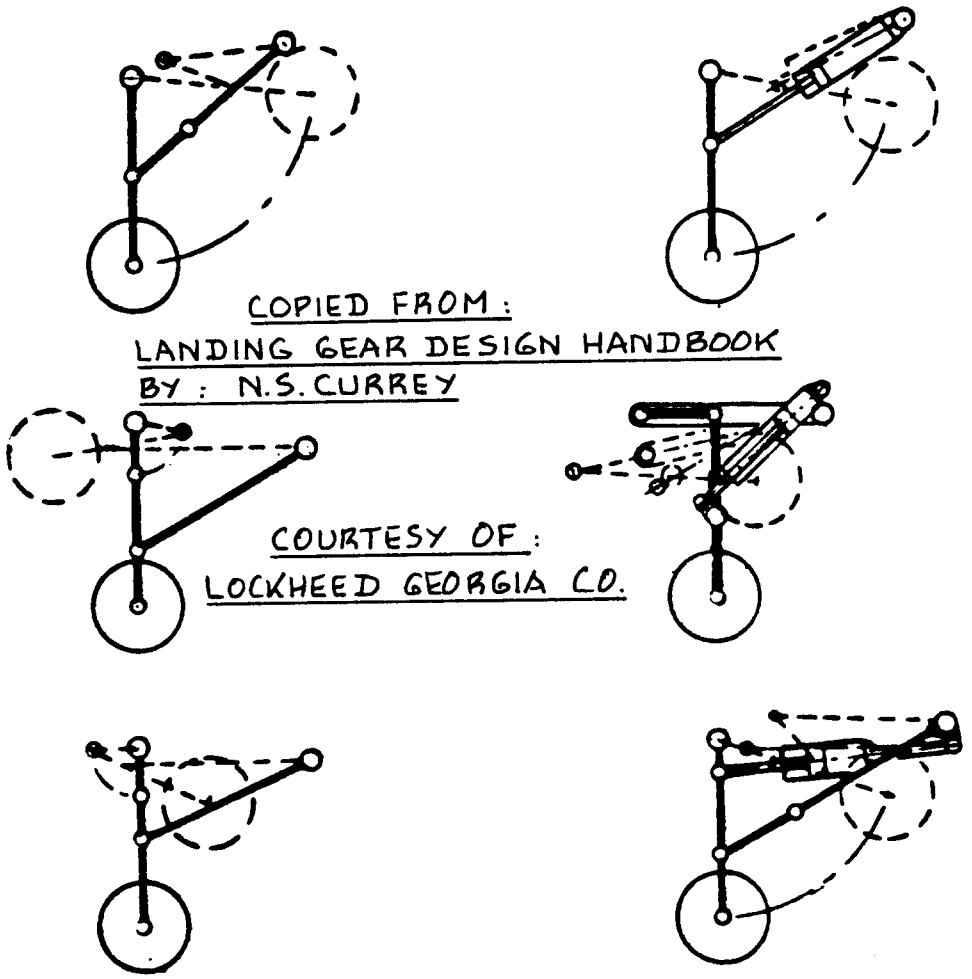

Figure 9.3 Typical Gear Retraction Stick Diagrams

9.2 EXAMPLE APPLICATIONS

Three example applications will now be discussed:

9.2.1 Twin Engine Propeller Driven Airplane: Selene
9.2.2 Jet Transport: Ourania
9.2.3 Fighter: Eris

9.2.1 Twin Engine Propeller Driven Airplane

Step 9.1: Because of the 250 kts cruise speed requirement of Table 2.17 (Part I) a retractable landing gear will be selected.

Step 9.2: A conventional, tricycle type landing gear will be selected.

Step 9.3: See Sub-section 10.2.1, Chapter 10.

Step 9.4: For the Selene there appear to be three options for positioning of the main landing gear:

Option 1 (Figure 9.4) is wing/nacelle mounted.

Options 2 and 3 (Figures 9.5 and 9.6) are fuselage mounted.

The wing/nacelle mounted option would result in long main struts. Retraction will probably have to be done forward and under the wing into a lower wing/nacelle fairing. For this solution the gear track will be wide and lateral stability would not be a problem. On the other hand the gear would probably be fairly heavy.

The fuselage mounted options requires a 'fighter' type gear retracting into the fuselage. Two options were laid out for the fuselage mounted gear. Figures 9.5 and 9.6 shows these options. Option 3 results in better lateral stability as shown by Figure 9.5. Option 3 is very similar to the MiG 23 landing gear.

Figure 9.7 shows the proposed nosewheel arrangement.

Figure 9.8 presents the layout of the strut locations. It is seen that the Selene meets the tip-over criteria of Figure 9.1a.

The strut disposition is shown also in the general arrangement drawing of Figure 10.3 (Chapter 10). It will be seen that the Selene meets the ground clearance criteria of Figure 9.1b.

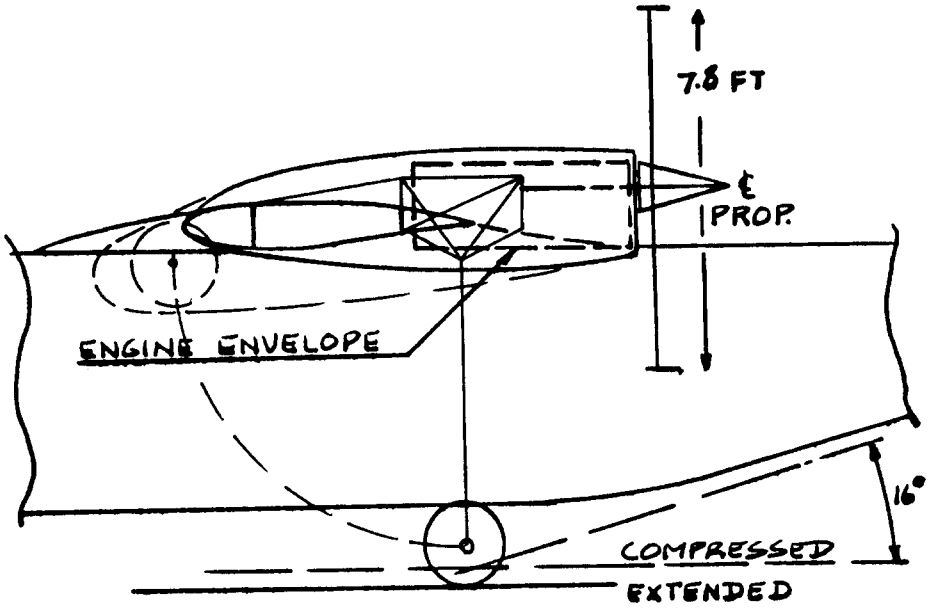

Figure 9.4 Selene: Main Gear Arrangement: Option 1

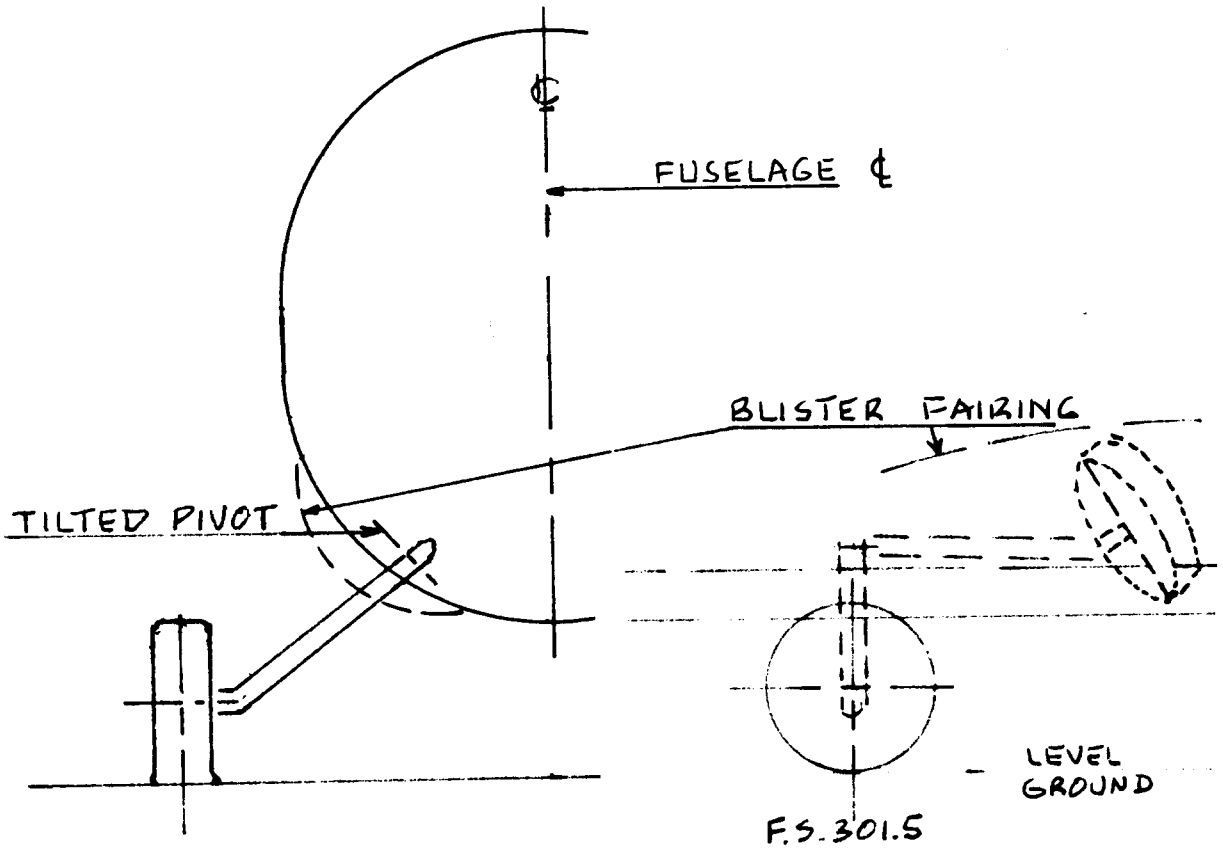

Figure 9.5 Selene: Main Gear Arrangement: Option 2

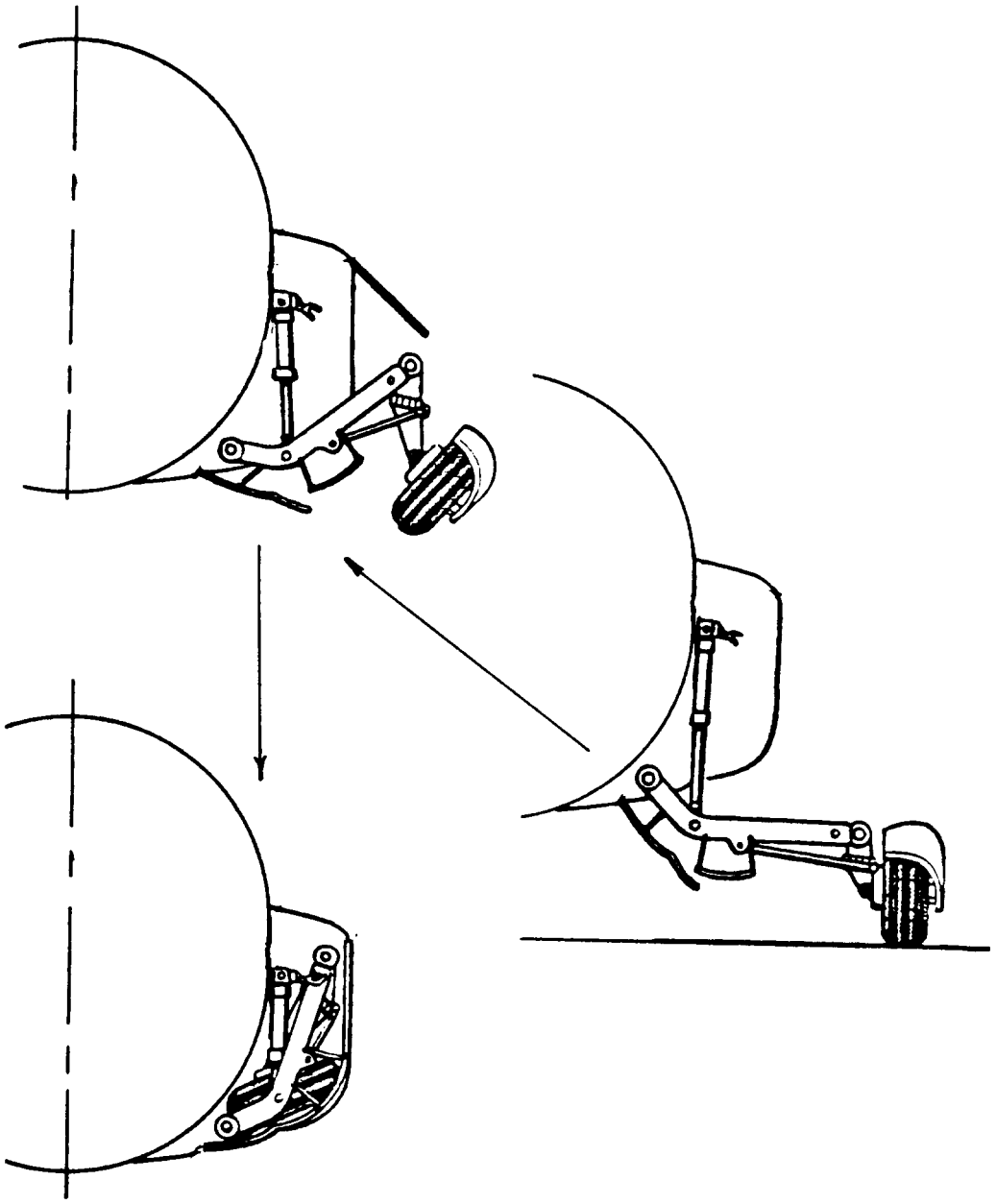

Figure 9.6 Selene: Main Gear Arrangement: Option 3

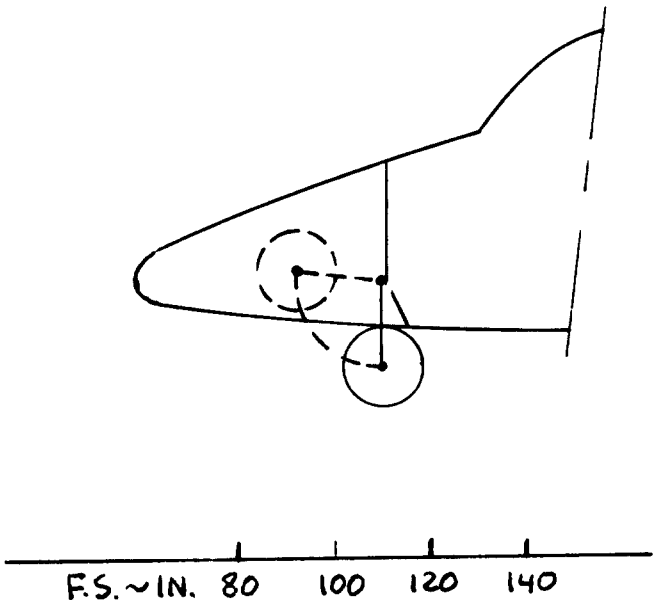

Figure 9.7 Selene: Nose Gear arrangement

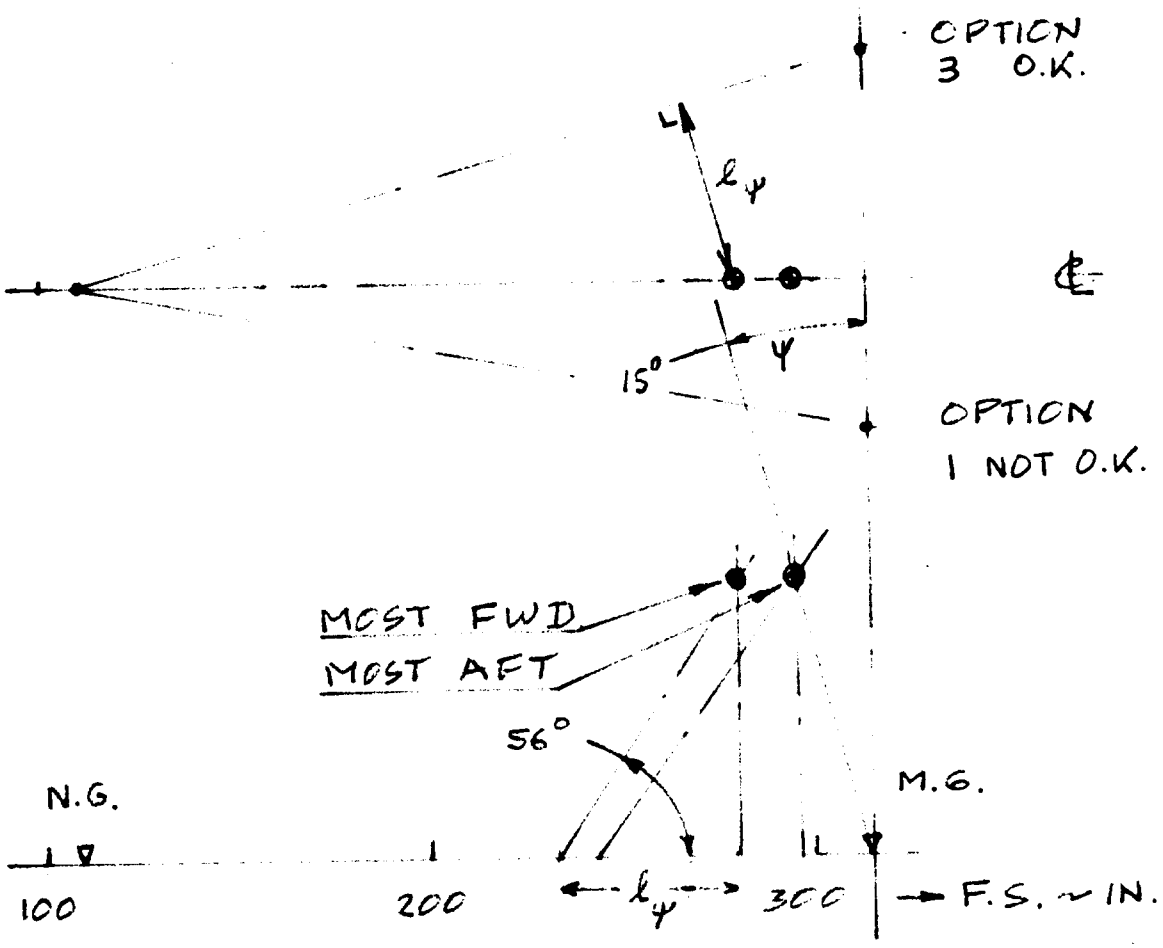

Figure 9.8 Selene: Tip-over Criteria

Step 9.5: From the strut disposition in Figure 10.3 the following data are found:

l_m = 34 in., l_n = 171 in., n_s = 2.

With these data and with Eqns (9.1) and (9.2) it is found that:

P_n = 1,310 lbs and P_m = 3,295 lbs.

The following gear load ratios are found:

P_n/W_{TO} = 0.17 and $2P_m/W_{TO}$ = 0.83

Step 9.6: For airplanes in this category Table 9.1 shows that one nose wheel tire and one main gear tire per strut are acceptable choices.

Step 9.7: From Table 9.1 it follows that the following tire sizes are acceptable choices:

Nosewheel tire: $D_t x b_t$ = 17x6 with 40 psi.

Main gear tire: $D_t x b_T$ = 22x6.5 with 85 psi.

Step 9.8: The tires are drawn into the c.g. sideview of Figure 10.3, Chapter 10.

Step 9.9: Figure 9.6 and 9.7 show the proposed stick diagrams for the Selene.

It appears that nose gear retraction will not present a conflict with any primary structure. Fig.9.7 indicates that for option 3 a blister fairing will be needed on the fuselage.

Step 9.10: From the Class I weight and balance analysis in Chapter 10 it appears that the gear configuration will be satisfactory from a weight and balance viewpoint. The only potential problem which needs to be verified is the take-off rotation. This is part of Class II stability and control analyses as outlined in Part VII (Ref.6).

Step 9.11: This step has been omitted to save space.

9.2.2 Jet Transport

Step 9.1: Because of the high cruise speed requirement of Table 2.18 (Part I) a retractable landing gear will be selected.

Step 9.2: A conventional, tricycle type landing gear will be selected.

Step 9.3: See Sub-section 10.2.2, Chapter 10.

Step 9.4: For the Ourania there appears to be only one option for integrating the main landing gear into the airplane: under the rear spar and retracting into the fuselage. This type of arrangement is very similar to that found on the B737. Figure 9.9 shows the proposed landing gear arrangement. Note that the nosegear retracts forward into the nose.

Figure 9.10 shows the proposed strut layout. It is clear that the Ourania meets the tip-over criteria of Figure 9.1a.

The strut disposition is also shown in the general arrangement drawing of Figure 10.5. It will be seen that the Ourania also meets the geometric ground clearance criteria of Figure 9.1b.

Step 9.5: From the strut disposition in Figure 10.5 the following data are found:

l_m = 60 in., l_n = 520 in., n_s = 2.

The take-off weight is: 127,000 lbs.

With these data and with Eqns (9.1) and (9.2) it is found that:

P_n = 13,138 lbs and P_m = 56,931 lbs.

The following gear load ratios are found:

P_n/W_{TO} = 0.10 and $2P_m/W_{TO}$ = 0.90

Step 9.6: For airplanes in this category Table 9.2 shows that two nose wheel tires and two main gear tires per strut are acceptable choices.

Step 9.7: From Table 9.2 it follows that the following tire sizes are acceptable choices:

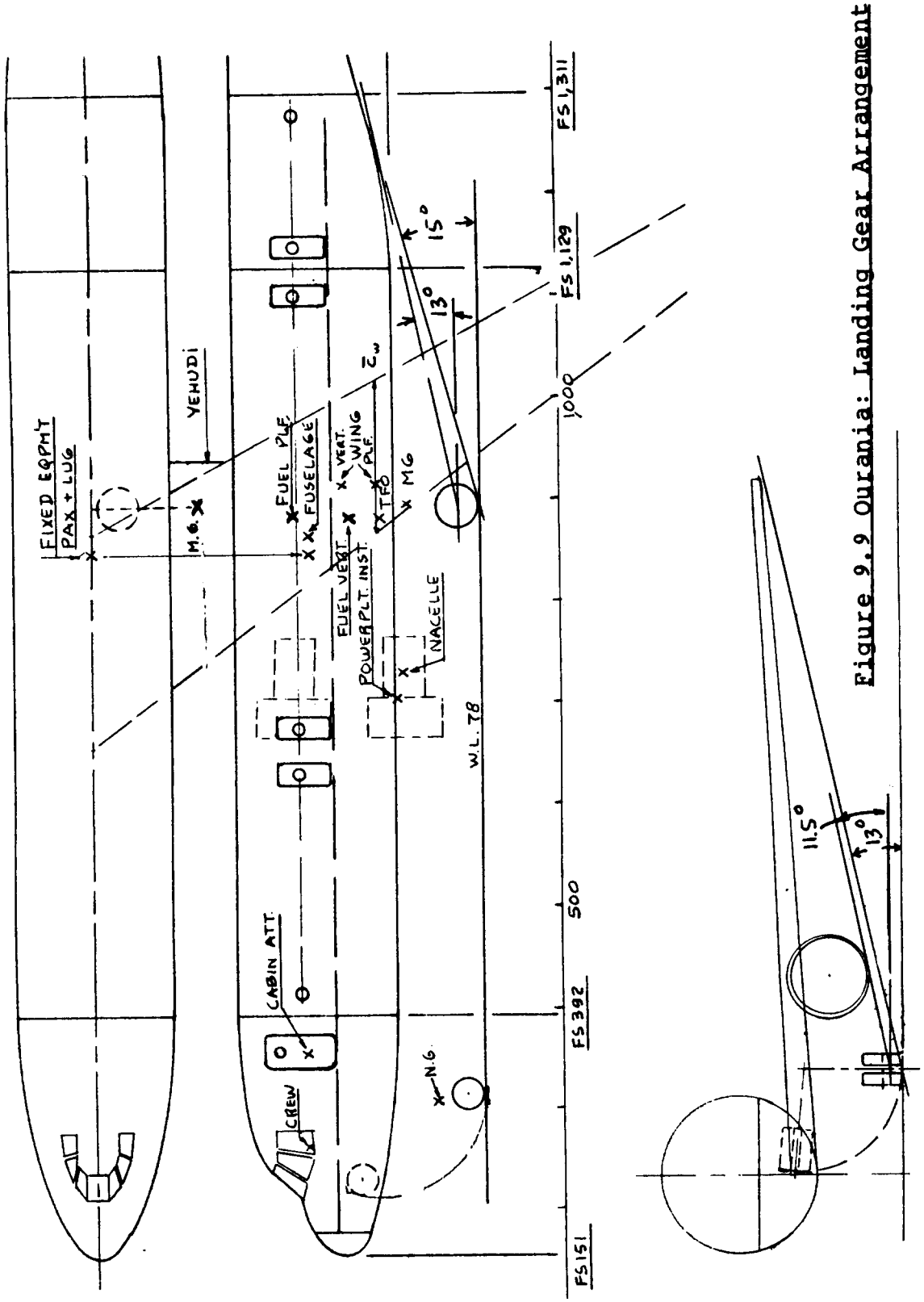

Figure 9.9 Ourania: Landing Gear Arrangement

Nosewheel tire: $D_t x b_t$ = 24x7.7 with 180 psi.

Main gear tire: $D_t x b_T$ = 40x14 with 180 psi.

Step 9.8: The tires are drawn into the c.g. sideview of Figure 10.5 and into the landing gear arrangement of Figure 9.9.

Step 9.9: Figure 9.9 also shows the stick diagrams. These indicate that landing gear retraction does not conflict with any primary structure or with the flaps. Note that to accomodate the main gear a so-called 'yehudi' had to be added to the wing planform. This yehudi carries the inboard flaps. Such an arrangement was pioneered by Boeing on the 707 and is still frequently used in jet transports.

Step 9.10: From the Class I weight and balance analysis in Sub-section 10.2.2 it appears that the gear configuration will be satisfactory from a weight and balance viewpoint. The only potential problem which needs to be verified is the take-off rotation. This is part of Class II stability and control analyses as outlined in Part VII (Ref.6).

Step 9.11: This step has been omitted to save space.

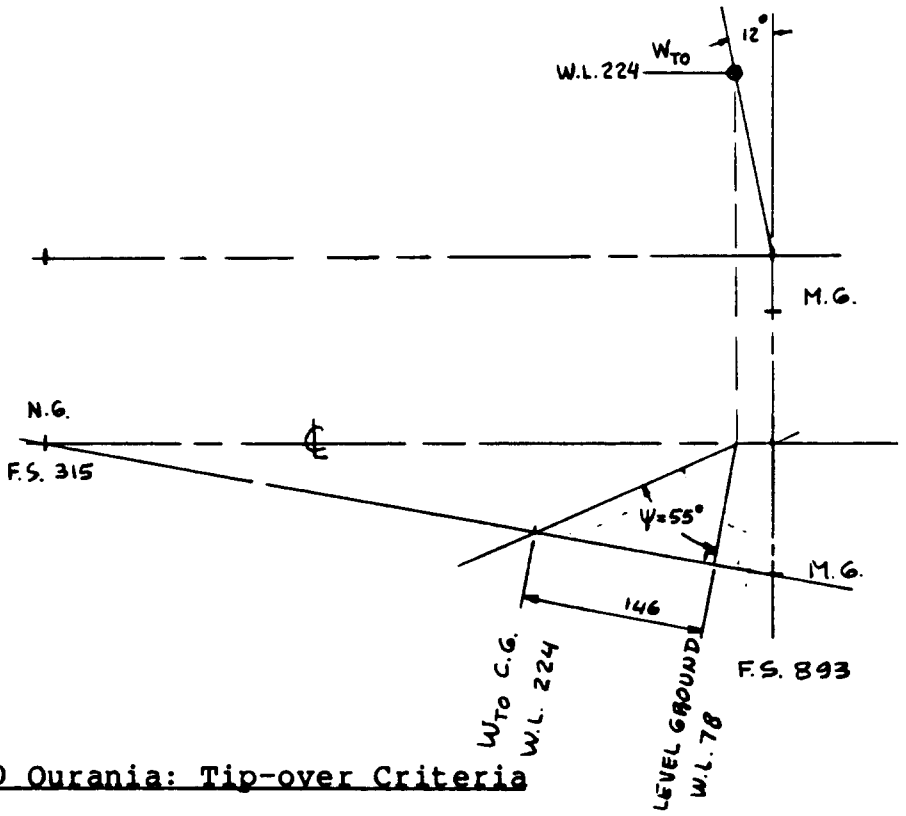

Figure 9.10 Ourania: Tip-over Criteria

9.2.3 Fighter

Step 9.1: Because of the high cruise speed requirement of Table 2.19 (Part I) a retractable landing gear will be selected.

Step 9.2: A conventional, tricycle type landing gear will be selected.

Step 9.3: See Sub-section 10.2.3, Chapter 10.

Step 9.4: For the Eris there appears to be only one option for integrating the main landing gear into the airplane: under the fuselage and retracting into the fuselage underneath the engine bays. This arrangement is fairly typical for modern jet fighters. Figure 9.11 shows the proposed landing gear arrangement.

Figure 9.12 shows the proposed strut layout. It may be seen that the Eris meets the tip-over criteria of Figure 9.1a.

The strut disposition is also indicated in the general arrangement drawing of Figure 10.7. As seen, the Eris also meets the ground clearance criteria of Figure 9.1b.

Step 9.5: From the strut disposition in Figure 10.7 the following data are found:

l_m = 20 in., l_n = 185 in., n_s = 2.

The take-off weight is: 64,905 lbs.

With these data and with Eqns (9.1) and (9.2) it is found that:

P_n = 6,332 lbs and P_m = 29,286 lbs.

The following gear load ratios are found:

P_n/W_{TO} = 0.10 and $2P_m/W_{TO}$ = 0.90

Step 9.6: For airplanes in this category Table 9.2 shows that two nose wheel tires and one main gear tires per strut are acceptable choices.

Step 9.7: From Table 9.2 it follows that the following tire sizes are acceptable choices:

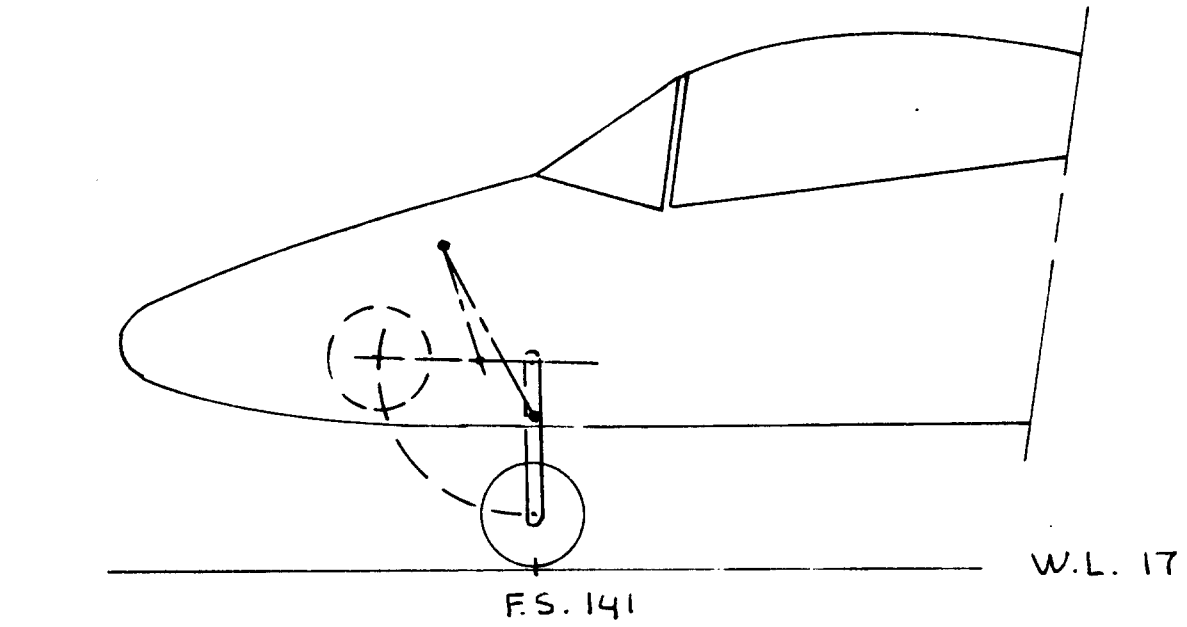

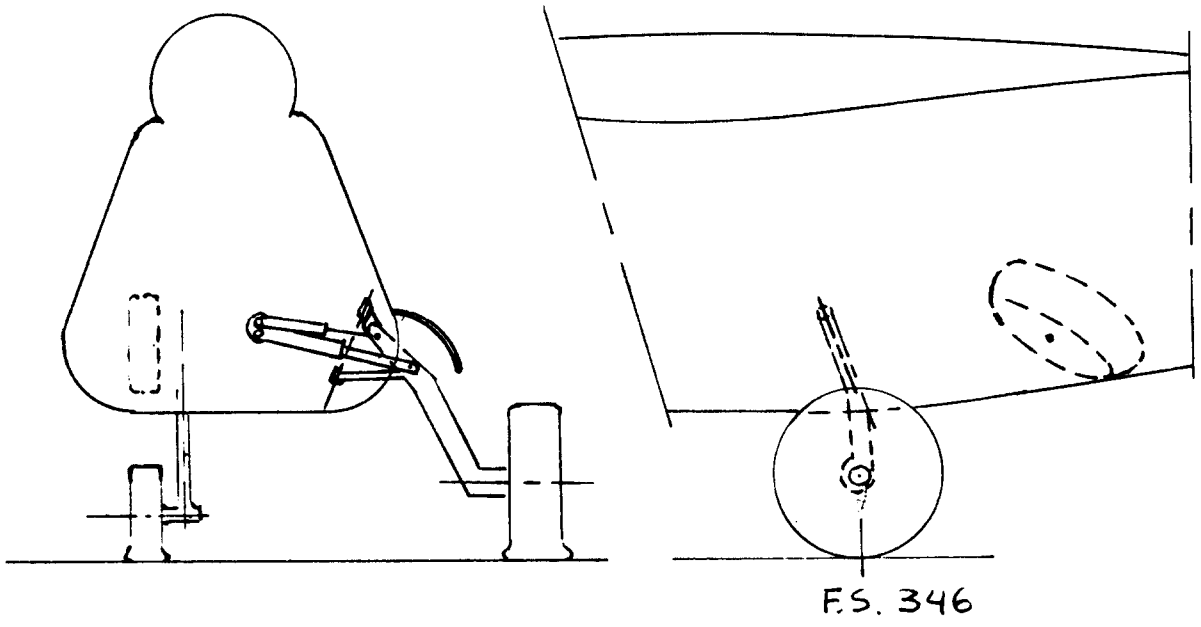

Figure 9.11 Eris: Landing Gear Arrangement

Nosewheel tire: $D_t x b_t$ = 21.6x7.5 with 120 psi.

Main gear tire: $D_t x b_T$ = 35.3x9.3 with 210 psi.

Step 9.8: The tires are drawn into the c.g. sideview of Figure 10.7 and into the landing gear arrangement of Figure 9.11.

Step 9.9: Figure 9.11 also shows the stick diagrams. These indicate that landing gear retraction does not conflict with any primary structure.

Step 9.10: From the Class I weight and balance analysis in Sub-section 10.2.3 it appears that the gear configuration will be satisfactory from a weight and balance viewpoint. The only potential problem which needs to be verified is the take-off rotation. This is part of Class II stability and control analyses as outlined in Part VII (Ref.6).

Step 9.11: This step has been omitted to save space.

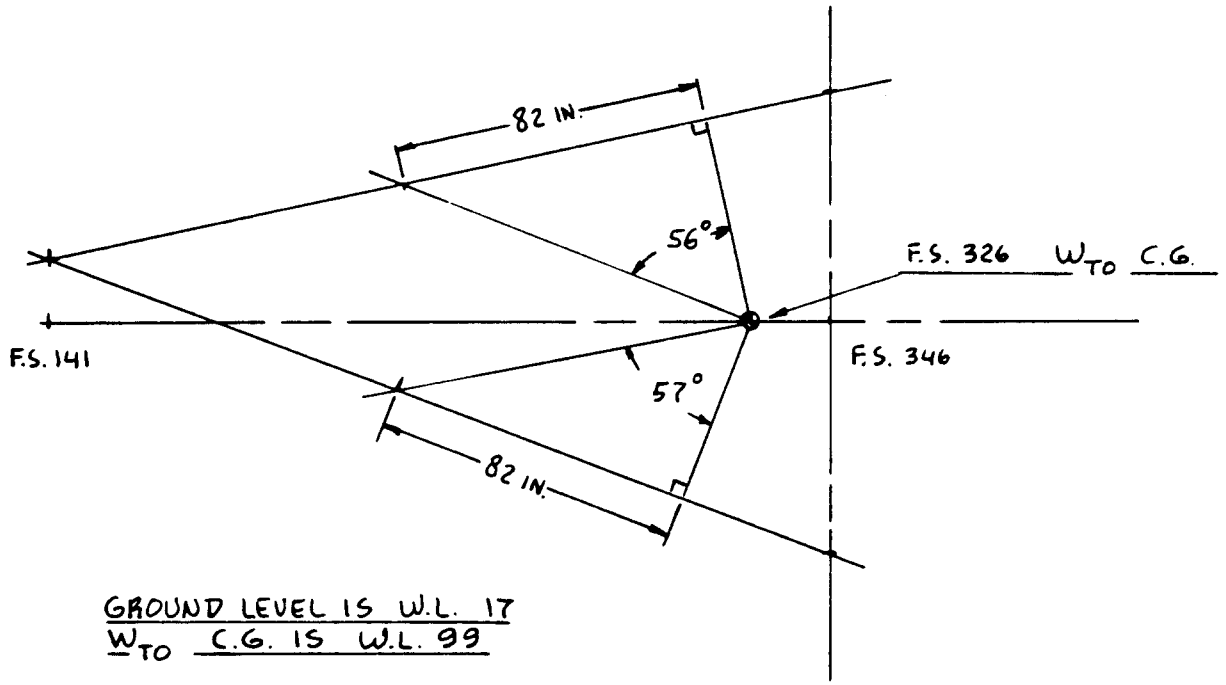

Figure 9.12 Eris: Tip-over Criteria

10. CLASS I WEIGHT AND BALANCE ANALYSIS

The purpose of this chapter is to familiarize the reader with a rapid method to determine whether or not the center of gravity of the proposed airplane design is in 'the right place' for different loading scenarios.

The method is referred to as a Class I weight and balance method and is to be used in conjunction with Step 10 of p.d. sequence I as outlined in Chapter 2.

Section 10.1 presents the method as a 9-step procedure. Example applications are given in Section 10.2.

10.1 CLASS I WEIGHT AND BALANCE METHOD

Step 10.1: Using Class I component weight prediction methods, determine the initial component weight breakdown of the airplane.

Part V (Ref.4), Chapter 2 shows how a Class I component weight breakdown can be prepared. Table 10.1a shows a list of weight components which are typically found in a Class I weight breakdown. Three numerical examples of Class I component weight breakdowns are presented in Section 10.2.

Table 10.1a Typical Class I Component Weight Breakdown

1. Fuselage group
2. Wing group
3. Empennage group
4. Engine group
5. Landing gear group
6. Fixed equipm't group
7. Trapped fuel and oil
8. Crew
9. Fuel
10. Passengers
11. Baggage
12. Cargo
13. Military load

Empty weight: $W_E = \text{Sum}_{i=1}^{i=6} W_i$

Take-off weight: $W_{TO} = \text{Sum}_{i=1}^{i=13} W_i$

Operating weight empty: $W_{OE} = \text{Sum}_{i=1}^{i=8} W_i$

Step 10.2: Prepare a preliminary arrangement drawing of the airplane using the drawings developed in Chapters 5-9.

Figure 10.1 shows a conceptual preliminary arrangement drawing as used in a typical weight and balance analysis. Figure 10.1 is drawn as a threeview because of the asymmetry of that configuration. For many symmetrical airplanes a sideview is sufficient.

Step 10.3: Locate the centers of gravity of all Class I weight components in Figure 10.1.

Note: some airplanes have severe asymmetries in their weight distribution. In that case it will also be necessary to locate the y locations of the component c.g.'s.

At this point, Figure 10.1 is also referred to as a 'c.g. threeview'.

Step 10.4: Enter the appropriate x,y and z coordinates of each component c.g. in a table such as Table 10.1b.

Table 10.2 provides some guidance for locating component c.g.'s of major weight groups. Further guidance to finding the location of component c.g.'s can be found in Chapter 2 of Part V (Ref.4).

CAUTION: Make absolutely certain that the zero reference point as shown in Figures 10.1 is always selected so that all coordinates are positive. To assure that this will be so even for future growth versions of the airplane, 'pick' the zero reference point well to the left and well below the nose of the airplane.

The author has seen both engineers in industry and aeronautical engineering design students make the most awful 'sign' errors as a result of not selecting the zero reference point as suggested here.

The following nomenclature is widely used in the aircraft industry:

x-coordinates as defined in Figure 10.1 are referred to as fuselage stations (F.S.).

y-coordinates as defined in Figure 10.1 are referred to as wing buttock lines (B.L. or W.B.L.).

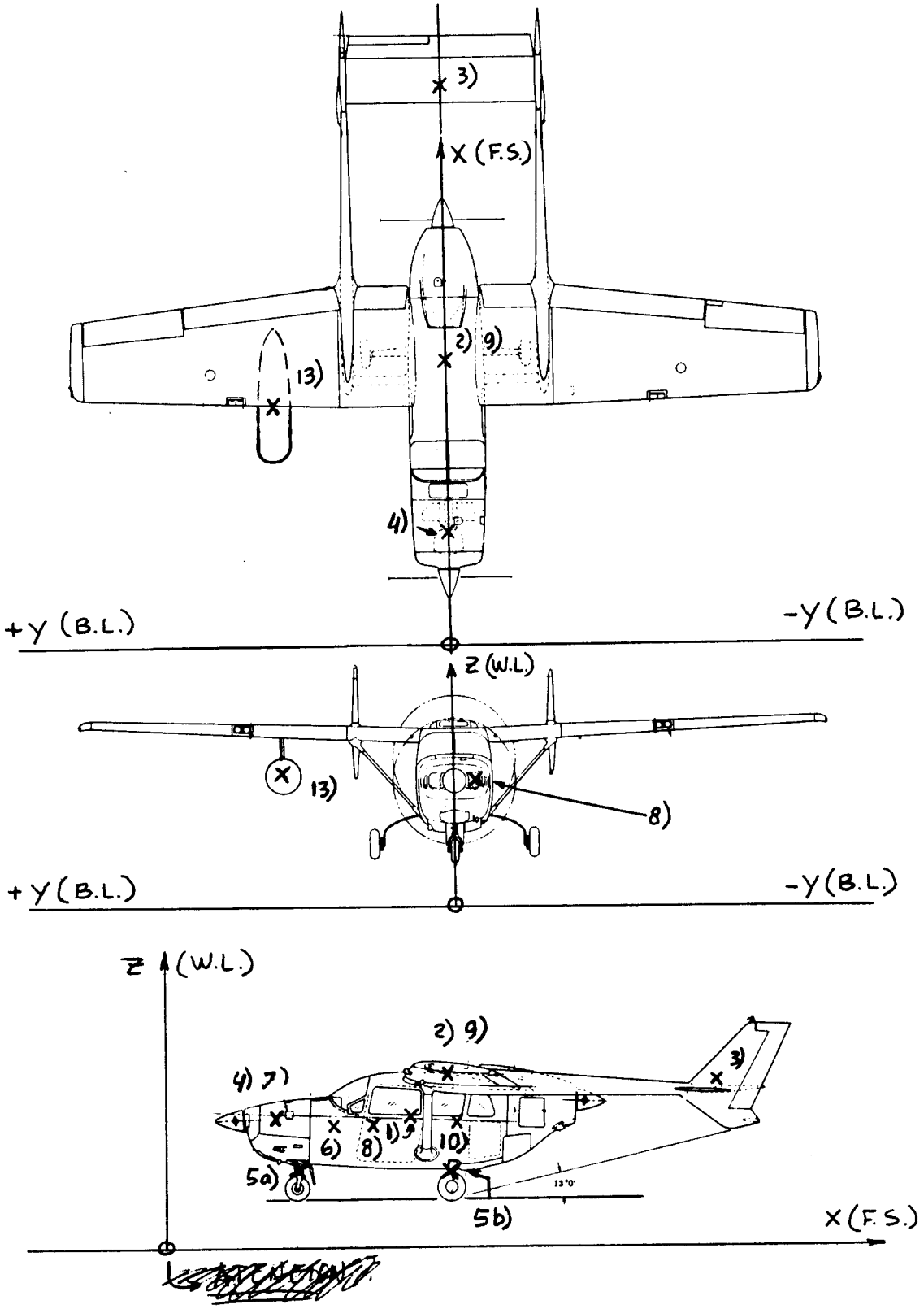

Figure 10.1 Preliminary Configuration Arrangement

Table 10.1b Class I Weight and Balance Calculation

No.	Type of Component	W_i lbs	x_i in.	$W_i x_i$ inlbs	y_i in.	$W_i y_i$ inlbs	z_i in.	$W_i z_i$ inlbs
1.	Fuselage group	W_1	x_1	$W_1 x_1$	y_1	$W_1 y_1$	z_1	$W_1 z_1$
2.	Wing group							
3.	Empennage group							
4.	Engine group							
5.	Landing gear group							
6.	Fixed equipm't group							
	Empty weight: $W_E = \text{Sum}_{i=1}^{i=6} W_i$					$x_{cg_{W_E}} = (\text{Sum}_{i=1}^{i=6} W_i x_i)/W_E$		
7.	Trapped fuel and oil							
8.	Crew							
	Operating weight empty: $W_{OE} = \text{Sum}_{i=1}^{i=8} W_i$					$x_{cg_{W_{OE}}} = (\text{Sum}_{i=1}^{i=8} W_i x_i)/W_{OE}$		
9.	Fuel							
10.	Passengers							
11.	Baggage							
12.	Cargo							
13.	Military load							
	Take-off weight: $W_{TO} = \text{Sum}_{i=1}^{i=13} W_i$					$x_{cg_{W_{TO}}} = (\text{Sum}_{i=1}^{i=13} W_i x_i)/W_{TO}$		

Note: Locations for y_{cg} and for z_{cg} are found from similar equations.

Table 10.2 Location of C.G.'s of Major Components

WINGS

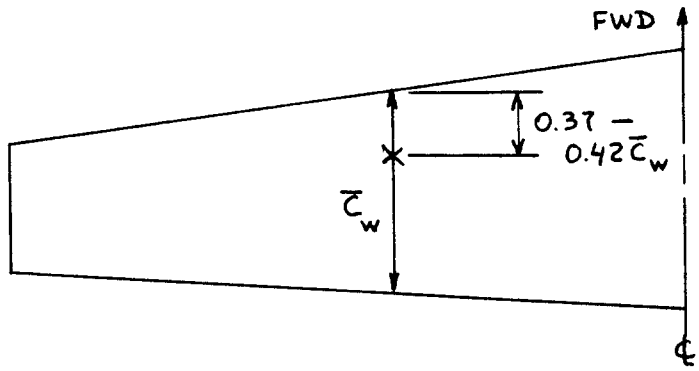

STABILIZERS

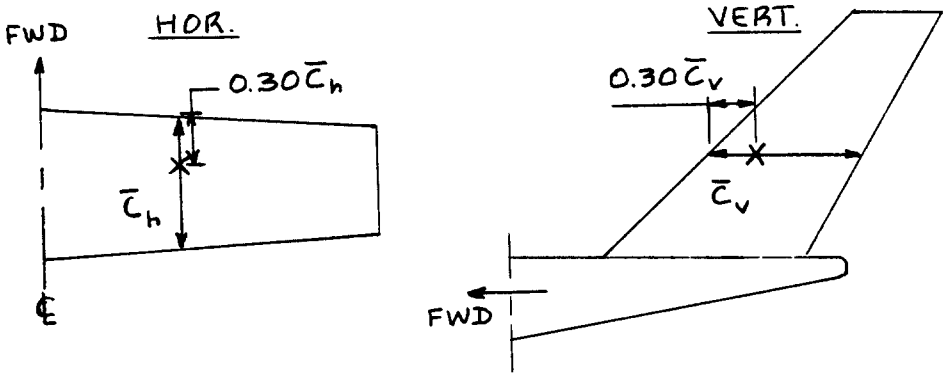

NACELLES

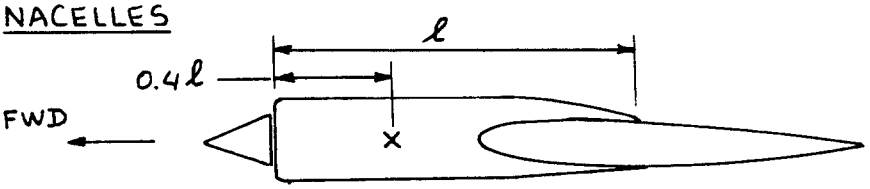

FUSELAGES

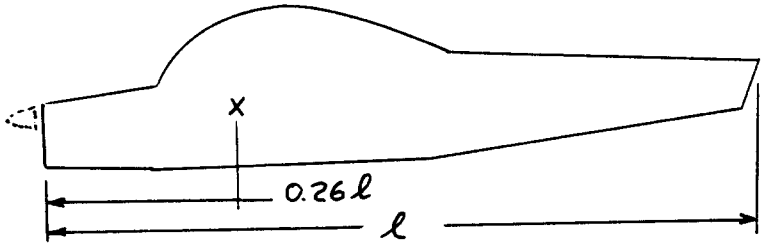

CANOPY TYPE

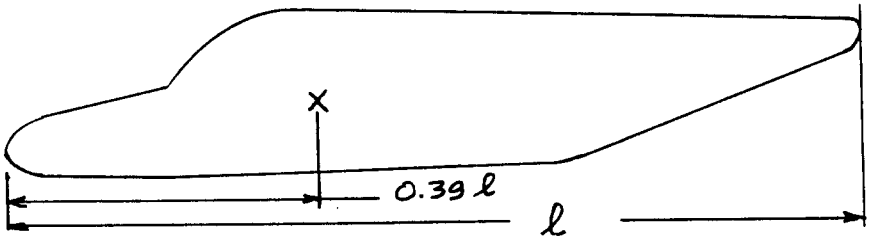

CABIN TYPE

AIRLINERS: 0.45 - 0.50 ℓ

z-coordinates as defined in Figure 10.1 are referred to as water lines (W.L.). This term is a carry-over from the ship building industry.

Step 10.5: Calculate the x_{cg}, y_{cg} and z_{cg} of the airplane with the help of Table 10.1b.

These c.g. locations must be calculated for all feasible loading scenarios. These loading scenarios depend to a large extent on the mission of the airplane. Typical loading combinations are:

1. Empty weight
2. Empty weight + crew
3. Empty weight + crew + fuel
4. Empty weight + crew + fuel + payload = Take-off weight

The reader will realize that these four loading combinations give rise to the following six loading scenarios:

1 2 3 4	1 3 2 4	1 4 2 3
1 2 4 3	1 3 4 2	1 4 3 2

In reality there can be many more depending on:

1. the type of payload and the way it can be stowed: (for example passengers piling into a Boeing 747)

2. the way the fuel tankage is arranged and how the fuel can be sequenced in and out.

Examples of typical loading scenarios are given in Section 10.2.

Step 10.6: Construct a weight-c.g. excursion diagram for the proposed airplane.

Figure 10.2 shows an example of a typical c.g. excursion diagram. It is important to identify in this diagram the loading sequences as well as the critical weights such as W_E and W_{TO}. Note also in Figure 10.2 that the c.g. locations are plotted as follows:

1. in terms of fuselage station (F.S.)

and:

2. in terms of a fraction of the wing mean geometric chord, $\bar{c}_w$.

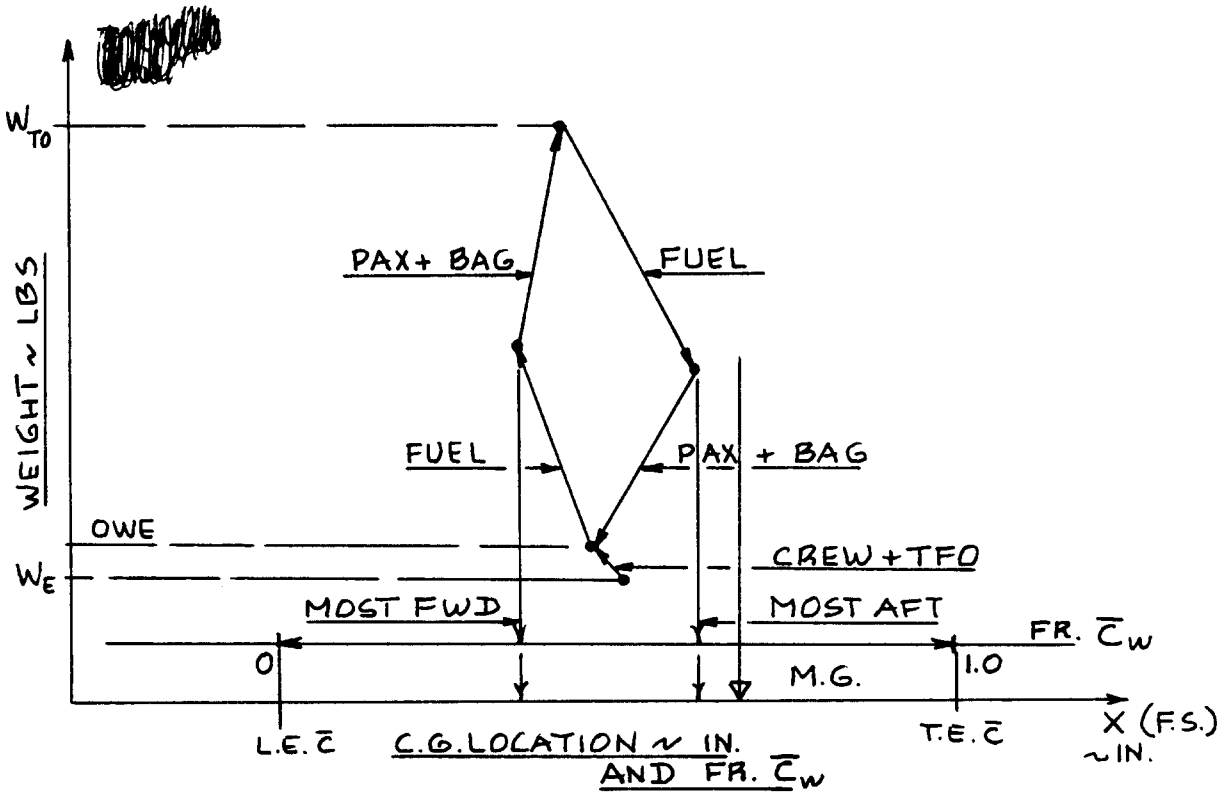

Figure 10.2 Weight-C.G. Excursion Diagram

Table 10.3 Examples of Center of Gravity Ranges

Type	C.G. Range (in.)	C.G. Range fr.$\bar{c}_w$	Type	C.G. Range (in.)	C.G. Range fr.$\bar{c}_w$
Homebuilts	5	0.10	Military Trainers	8	0.10
Single Engine Prop. Driven	7-18	0.06-0.27	Fighters	15	0.20
Twin Engine Prop. Driven	9-15	0.12-0.22	Mil.Patr. Bomb and Transp.	26-90	0.30
Ag. Airpl.	5	0.10	Fl.Boats,	7-28	0.25
Business Jets	8-17	0.10-0.21	Amph. and Float		
Regional TBP	12-20	0.14-0.27	Amph. and		
Jet Transp.	26-91	0.12-0.32	Supersonic Cruise	20-100	0.30

Note also in Figure 10.2 that the main landing gear location is identified. This is important to determine if there is a longitudinal 'tip-over' problem.

For some airplanes it may be important to also draw c.g. excursion diagrams which reflect the vertical and lateral c.g. situations. These c.g. situations may have an impact on the landing gear disposition because of lateral tip-over potential.

Step 10.7: Determine the most forward and the most aft c.g. location of the airplane. Compare the resulting c.g. range with the c.g. ranges of other airplanes in the same category.

Figure 10.2 is used to determine where the most forward and most aft c.g. locations are. The reader will now understand why it is vital to have 'smoked' out the most adverse loading scenarios which are consistent with the mission of the airplane.

Table 10.3 presents data for comparing the resulting c.g. range with the c.g. ranges of other airplanes.

Step 10.8: Draw conclusions about the feasibility of the proposed airplane arrangement and if necessary make changes.

In judging the feasibility of the proposed airplane arrangement the following principles must be kept in mind:

Principle 1:

Where possible, the ideal c.g. arrangement is one for which the OWE-c.g., the fuel-c.g. and the payload-c.g. are in the same vertical location.

The reader will find that in most airplane designs it is not possible to reach this ideal situation. One should try to come as close as possible.

Principle 2:

Try to position the landing gear so that no major structural cutouts are needed to retract the gear. Also: make sure that there is a sufficient amount of volume available to retract the gear into.

Principle 3:

Keep in mind that the airplane also has to satisfy certain basic stability and control requirements. Step 12 in p.d. sequence I (Chapter 2) deals with this problem. In this regard there are two types of airplanes:

1. Airplanes which must have inherent static longitudinal and static directional stability. The so-called X-plot method of Step 12 is used in conjunction with the Class I weight and balance analysis to assure inherent static stability. Keep in mind that without minimum static stability levels the proposed airplane design is invalid.

2. Airplanes which can have inherent static longitudinal and/or static directional instability. These airplanes must now have a flight control system which through the correct feedback loops signal control surface actuators to in turn move flight control surfaces in such a way that 'de-facto' stability is insured. This implies a relationship between the 'design' level of inherent instability, control power, feedback gains and actuator rate requirements. A Class I method to account for this during p.d. sequence I is discussed in Chapter 11.

Pricple 4:

If an airplane design turns out to have major balance problems it is often possible to 'fix' these problems by moving the wing. If the gear needs to be attached to the wing, the entire wing/gear combination must be moved.

Step 10.9: Document the decisions made under Steps 10.1 - 10.8 in a brief descriptive report including clear, dimensioned drawings.

10.2 EXAMPLE APPLICATIONS

Three examples will now be discussed:

10.2.1 Twin Engine Propeller Driven Airplane: Selene
10.2.2 Jet Transport: Ourania
10.2.3 Fighter: Eris

10.2.1 Twin Engine Propeller Driven Airplane

Step 10.1: Table 10.4 shows the component weight breakdown for the Selene. This breakdown is the result of applying a Class I component weight estimation method to the airplane. This method is discussed in detail in Chapter 2 of Part V (Ref.4).

Step 10.2: Figure 10.3 shows the preliminary arrangement drawing for the Selene. This drawing is the result of combining Figures 4.2, 5.3, 6.3, 8.2 and 9.3. For the Selene only the sideview is important in establishing its weight and balance characteristics.

Step 10.3: Figure 10.3 also shows the component centers of gravity.

Step 10.4: Table 10.4 also lists the x, y and z coordinates of all Selene weight components.

Step 10.5: Table 10.4 also lists the centers of gravity for several important loading configurations.

Step 10.6: Figure 10.4 shows the weight-c.g. excursion diagram for the Selene.

Step 10.7: From Figure 10.4 it follows that the c.g. limits are:

most forward c.g. occurs at W = 7,000 lbs,

F.S.= 280 in. and $0.62\bar{c}_w$

most aft c.g. occurs at W = 5,500 lbs, F.S.= 295 in.

and $0.78\bar{c}_w$

The c.g. range of the Selene is 15 inches or $0.16\bar{c}_w$.

Note that this compares favorably with the data of Table 10.3.

Table 10.4 Component Weight and Coordinate Data: Selene

Component	Weight	x	Wx	y	Wy	z	Wz
	lbs	in.	in.lbs	in.	in.lbs	in.	in.lbs
Wing	738	269	198,522	0	0	118	87,084
Empennage H.T.	120	559	67,080	0	0	189	22,680
V.T.	59	504	29,736	0	0	146	8,614
Fuselage	621	220	136,620	0	0	76	47,196
Nacelles	249	315	78,435	0	0	126	31,374
Landing Gear N.G.	76	110	8,360	0	0	47	3,572
M.G.	304	315	95,760	0	0	55	16,720
Engines + inst.	1,508	331	499,148	0	0	126	190,008
Propellers	200	362	72,400	0	0	129	25,800
Fixed Equipment	1,025	220	225,500	0	0	76	77,900
Empty weight, W_E	4,900	288	1,411,561	0	0	104	510,948
TFO	44	315	13,860	0	0	118	5,192
Fuel	1,706	276	470,856	0	0	118	201,308
2 Pax.	350	184	64,400	0	0	76	26,600
2 Pax.	350	282	98,700	0	0	76	26,600
2 Pax.	350	337	117,950	0	0	76	26,600
Baggage	200	220	44,000	14	2,800	76	15,200
Take-off wht, W_{TO}	7,900	281	2,221,327	0	2,800	103	812,448

Note: other loading conditions shown in Figure 10.4.

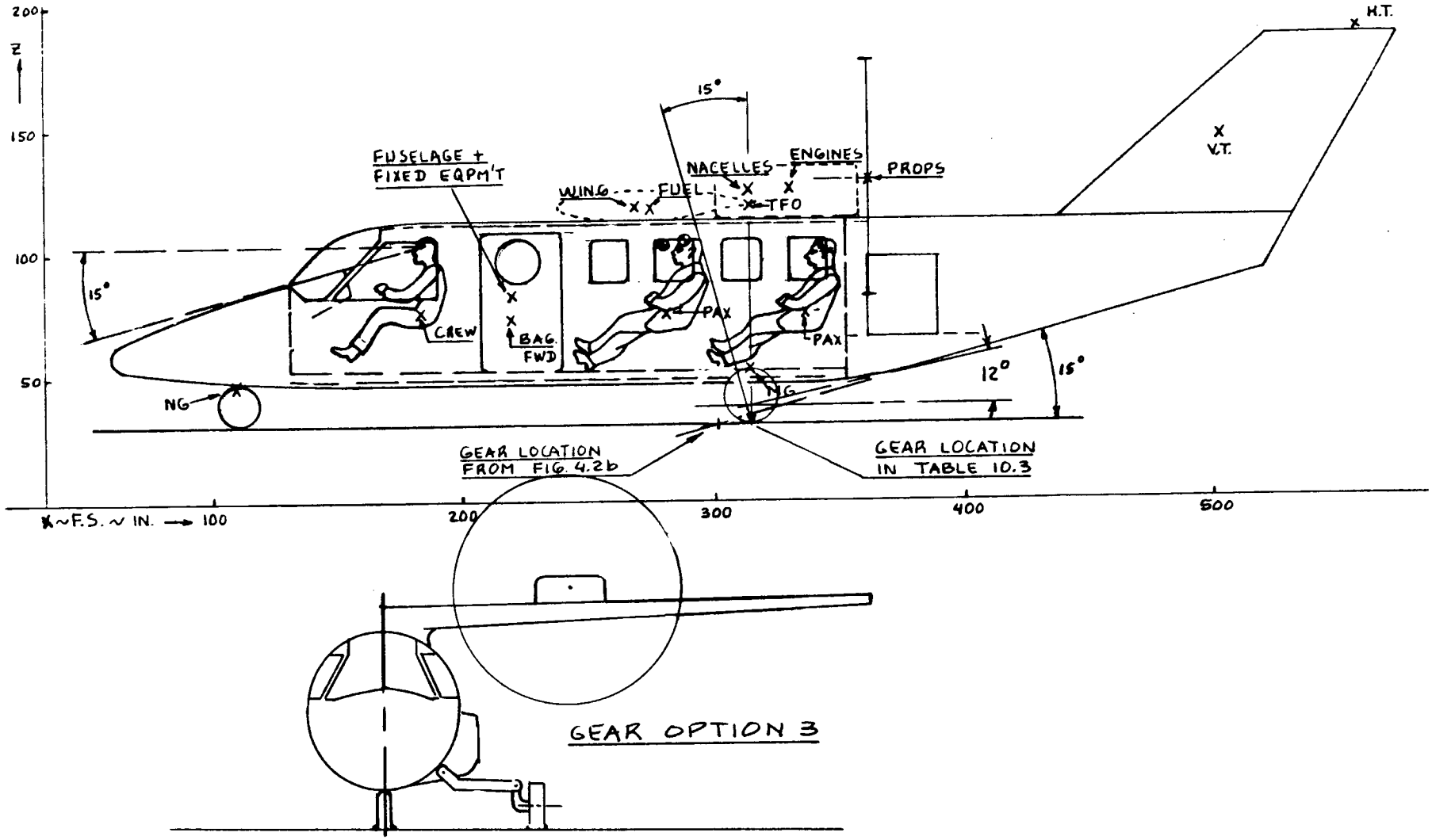

Figure 10.3 Selene: General Arrangement

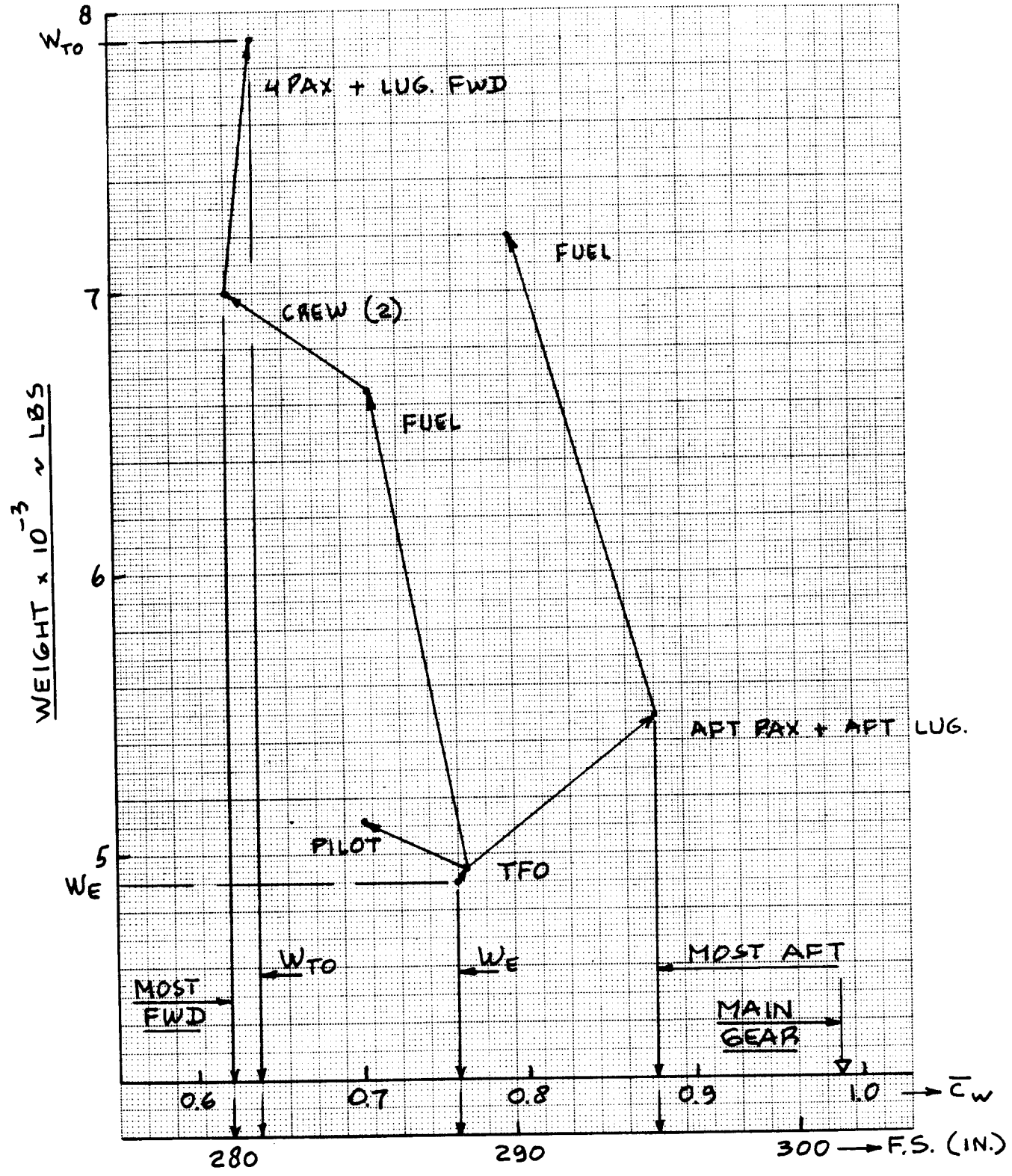

Figure 10.4 Selene: Weight-C.G. Excursion Diagram

Step 10.8: The most aft c.g. is well forward of the main landing gear contact point. The overall landing gear disposition problem relative to the c.g. range is discussed in Chapter 9, Sub-section 9.2.1.

The suitability of the aft c.g. location from a static longitudinal and static directional stability viewpoint is discussed in Chapter 11, Sub-section 11.2.1.

Step 10.9: To save space this step has been omitted.

10.2.2 Jet Transport

Step 10.1: Table 10.5 shows the component weight breakdown for the Ourania. This breakdown is the result of applying a Class I component weight estimation method to the airplane. This method is discused in detail in Chapter 2 of Part V (Ref.4).

Step 10.2: Figure 10.5 shows the preliminary arrangement for the Ourania. This drawing is the result of combining Figures 4.7, 5.5, 6.4, 8.3 and 9.5. For the Ourania only the sideview and the topview are needed to establish its weight and balance characteristics.

Step 10.3: Figure 10.5 also shows the component centers of gravity.

Step 10.4: Table 10.5 also lists the x, y and z coordinates of all Ourania weight components.

Step 10.5: Table 10.5 also lists the centers of gravity for several important loading configurations.

Step 10.6: Figure 10.6 shows the weight-c.g. excursion diagram for the Ourania.

Step 10.7: From Figure 10.6 it follows that the c.g. limits are:

most forward c.g. occurs at W = 100,000 lbs,

F.S. = 861 in. and $-0.04\bar{c}_w$.

most aft c.g. occurs at W = 100,000 lbs,

F.S. = 884 in. and $0.12\bar{c}_w$.

The c.g. range of the Ourania is seen to be 23 in.

This is equivalent to $0.16\bar{c}_w$.

Table 10.5 Component Weight and Coordinate Data: Ourania

Component	Weight	x	Wx	y	Wy	z	Wz
	lbs	in.	in.lbs	in.	in.lbs	in.	in.lbs
Wing	13,664	913	12,475,232	0	0	213	2,910,432
Empennage	3,253	1,535	4,993,355	0	0	343	1,115,779
Fuselage	14,184	866	12,283,344	0	0	248	3,517,632
Nacelles	2,082	728	1,515,696	0	0	150	312,300
Landing Gear N.G.	573	307	175,911	0	0	122	69,906
M.G.	4,632	894	4,141,008	0	0	146	676,272
Powerplant inst.	9,891	705	6,973,155	0	0	157	1,552,887
Fixed Equipment	20,171	846	17,064,666	0	0	248	5,002,408
Empty weight, W_E	68,450	871	59,622,367	0	0	221	15,157,616
TFO	925	882	815,850	0	0	173	160,025
Fuel	25,850	882	22,799,700	0	0	205	5,299,250
Crew flight deck	410	260	106,600	0	0	248	101,680
cabin att.	205	1,339	274,495	0	0	248	50,840
cabin att.	410	354	145,140	0	0	248	101,680
Pax + luggage	30,750	846	26,014,500	0	0	248	7,626,000
Take-off wht, W_{TO}	127,000	864	109,778,652	0	0	224	28,497,091

Note: other loading conditions shown in Figure 10.6.

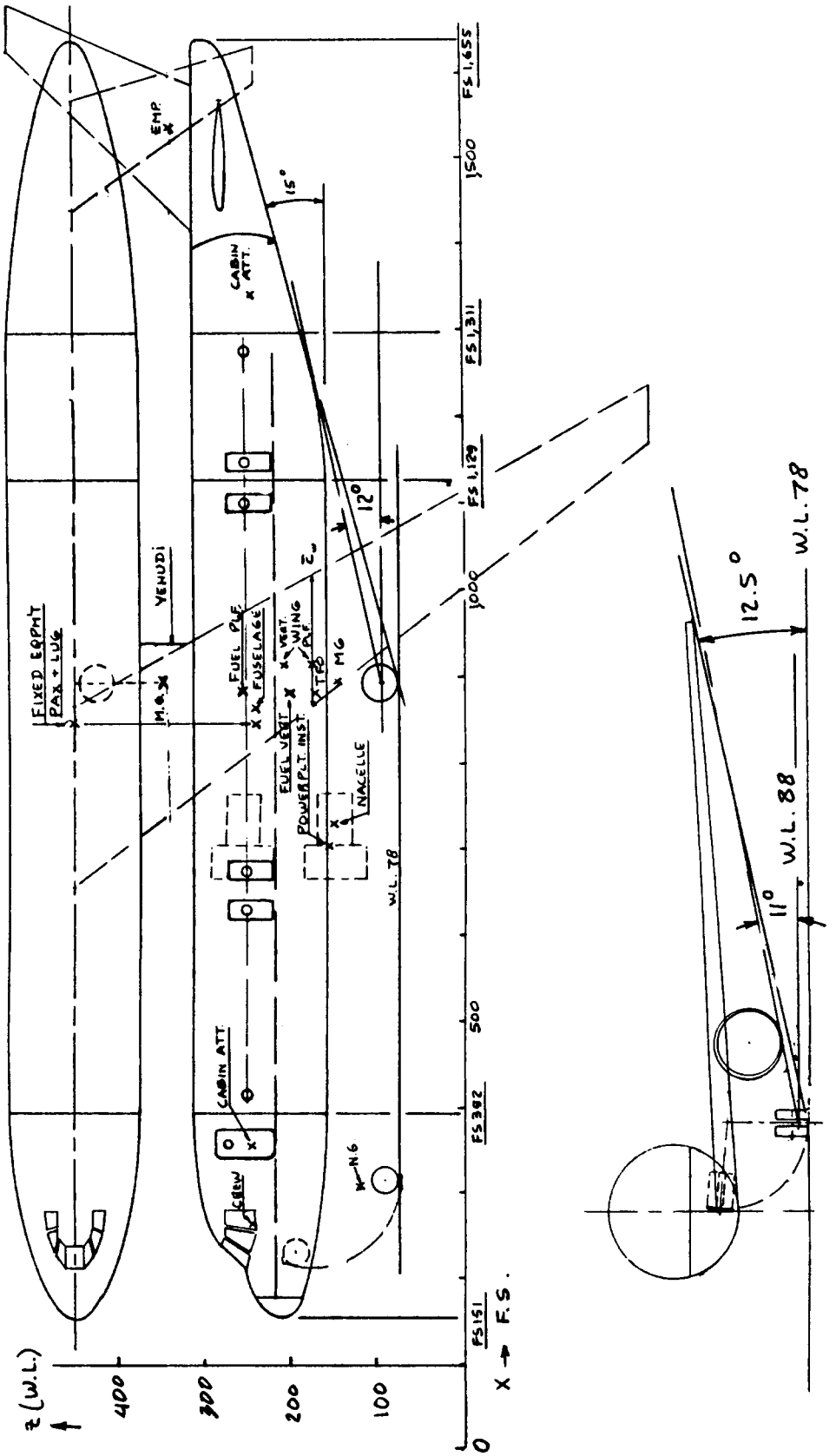

Figure 10.5 Ourania: General Arrangement

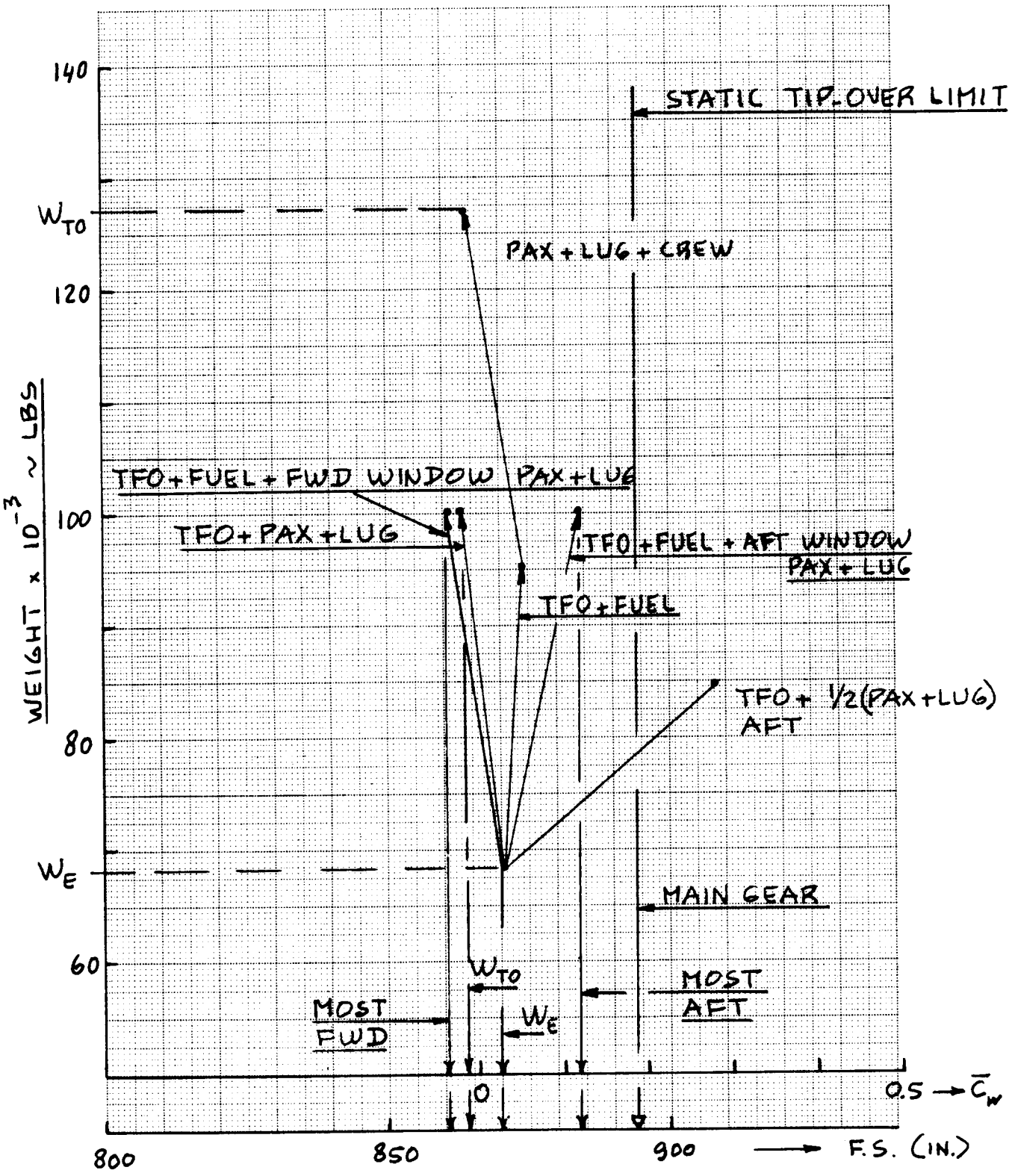

Figure 10.6 Ourania: Weight-C.G. Excursion Diagram

Note that this compares favorably with the data of Table 10.3.

Step 10.8: The most aft c.g. of the Ourania is well forward of the main gear contact point. The overall gear disposition relative to the c.g. range is discussed in Chapter 9, Sub-section 9.2.2.

The suitability of the aft c.g. location from a viewpoint of static longitudinal and static directional stability is discussed in Chapter 11, Sub-section 11.2.2.

Step 10.9: To save space this step has been omitted.

10.2.3 Fighter

Step 10.1: Table 10.6 shows the component weight breakdown for the Eris. This breakdown is the result of applying a Class I component weight estimation method to the airplane. This method is discussed in detail in Chapter 2 of Part V (Ref.4).

Step 10.2: Figure 10.7 shows the preliminary arrangement drawing for the Eris. This drawing is the result of combining Figures 4.9, 6.5, 8.4 and 9.7. Because of the asymmetries involved in the gun and nose gear placement, a front view and a top view are included in Figure 10.7.

Step 10.3: Figure 10.7 also shows the component centers of gravity.

Step 10.4: Table 10.6 also lists the x, y and z coordinates of all Eris weight components.

Step 10.5: Table 10.6 also lists the centers of gravity for several important loading configurations.

Step 10.6: Figure 10.8 shows the weight-c.g. excursion diagram for the Eris.

Step 10.7: From Figure 10.8, the c.g. limits are:

most forward c.g. occurs at W = 46,400 lbs,

F.S.= 324 in. and $0.43\bar{c}_w$.

most aft c.g. occurs at W = 33,500 lbs,

F.S.= 334 in. and $0.50\bar{c}_w$.

Table 10.6 Component Weight and Coordinate Data: Eris

Component	Weight	x	Wx	y	Wy	z	Wz
	lbs	in.	in.lbs	in.	in.lbs	in.	in.lbs
Wing	6,762	331	2,238,222	0	0	118	797,916
Empennage	1,597	614	980,558	0	0	173	276,281
Fuselage + booms	7,347	323	2,373,081	0	0	94	690,618
Engine section	160	417	66,720	0	0	91	14,560
Landing Gear N.G.	554	137	75,898	+16	8,864	44	24,376
M.G.	2,214	350	774,900	0	0	58	128,412
Engines	6,000	417	2,502,000	0	0	91	546,000
Engine inst.	2,834	370	1,048,580	0	0	102	289,068
GAU-8A Gun	2,014	180	362,520	-20	-40,280	60	120,840
Fixed Eq.(- gun)	4,018	189	759,402	0	0	85	341,530
Empty weight, W_E	33,500	334	11,181,881	-1	-31,416	96	3,229,601
TFO	300	370	111,000	0	0	85	25,500
Fuel	18,500	331	6,123,500	0	0	118	2,183,000
Pilot	200	209	41,800	0	0	91	18,200
Ammunition	1,785	283	505,155	0	0	73	130,305
Bombs (fuselage)	4,248	277	1,176,696	0	0	44	186,912
Bombs (wings)	6,372	315	2,007,180	0	0	100	637,200
Take-off wht, W_{TO}	64,905	326	21,147,212	0	-31,416	99	6,410,718

Note: other loading conditions shown in Figure 10.8.

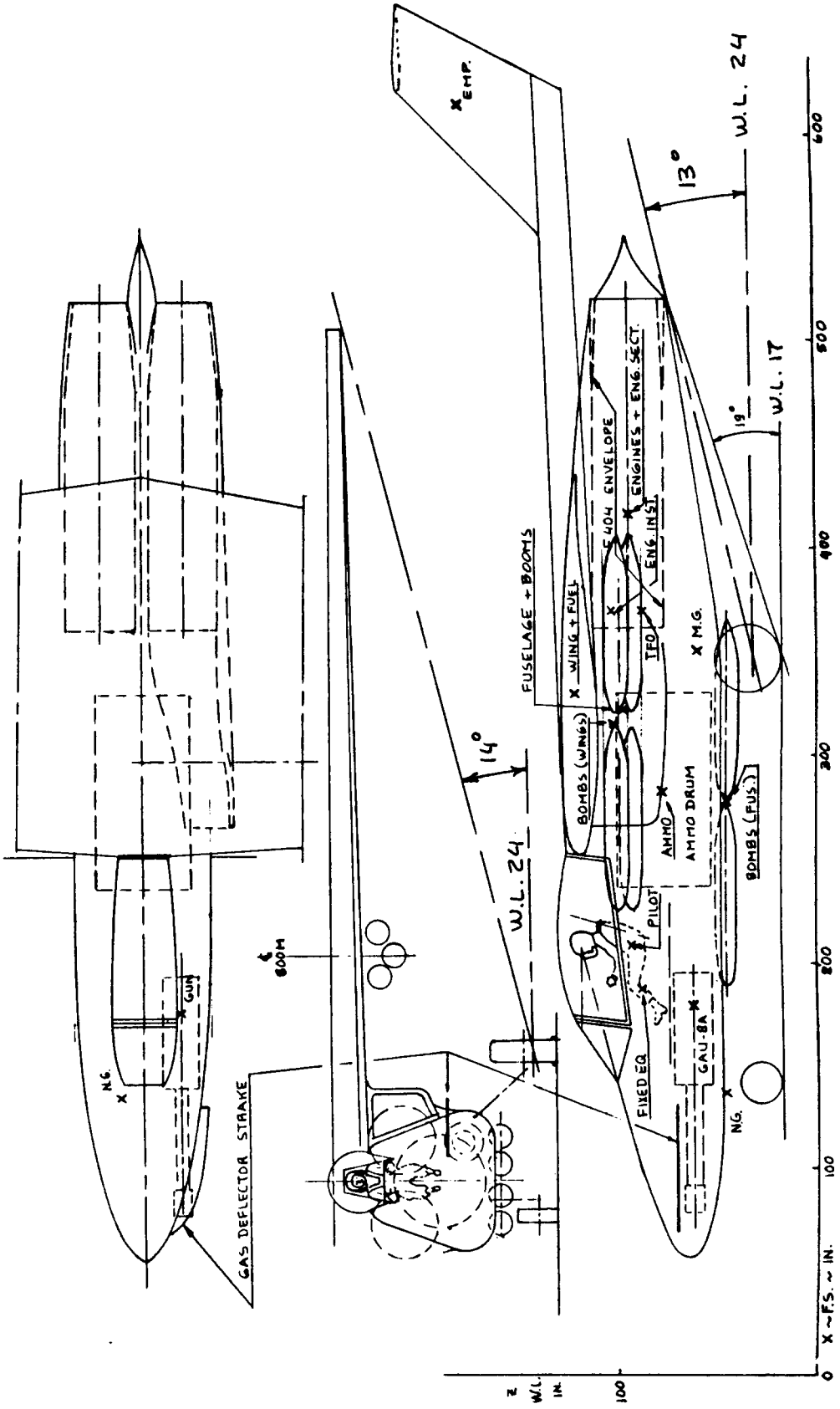

Figure 10.7 Eris: General Arrangement

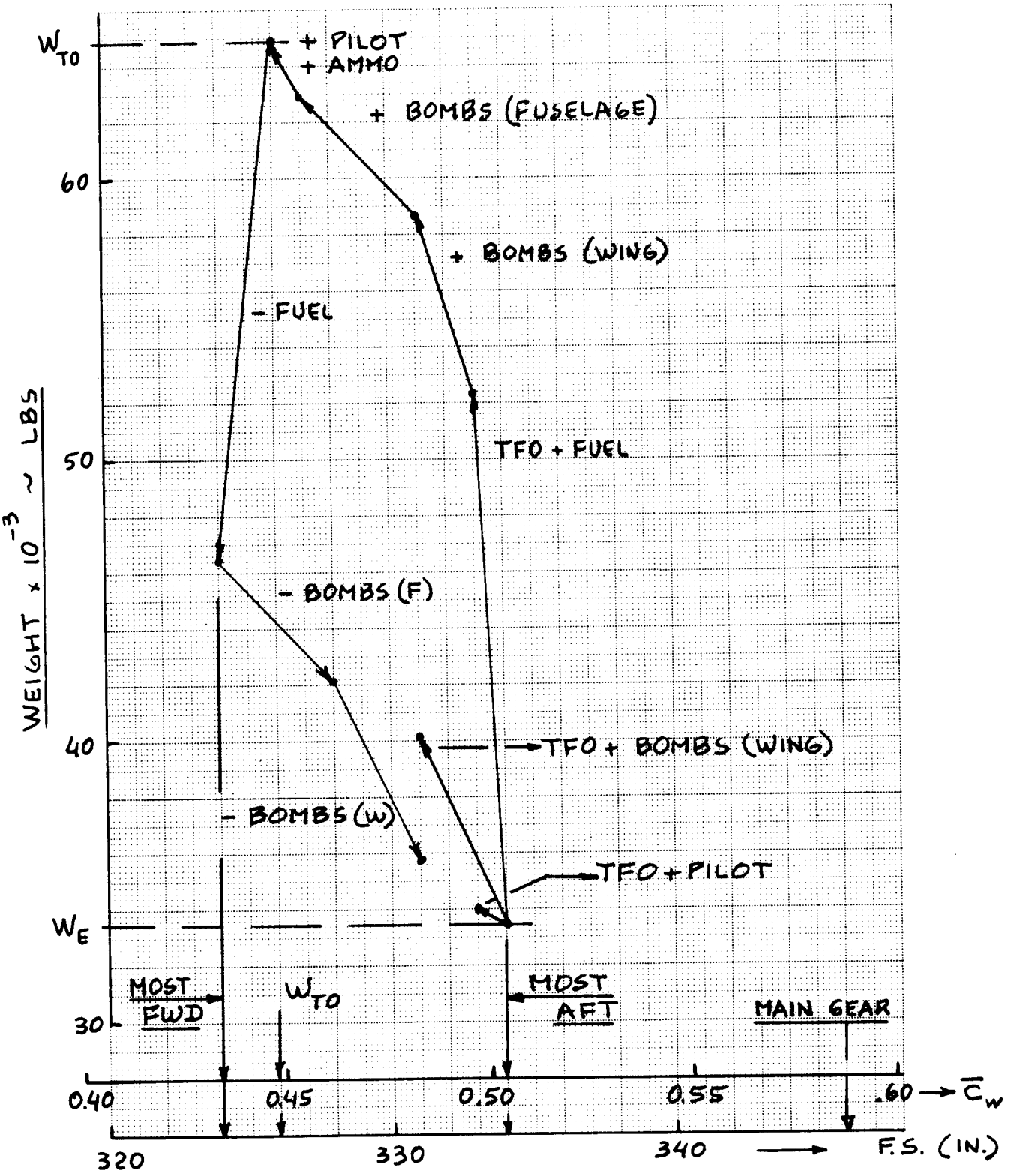

Figure 10.8 Eris: Weight C.G. Excursion Diagram

The c.g. range of the Eris is 10 inches or $0.07\bar{c}_w$.

Note that this compares favorably with the data of Table 10.3.

Step 10.8: The most aft c.g. is well forward of the main landing gear. The overall disposition of the landing gear relative to the c.g. range is discussed in Chapter 9, Sub-section 9.2.3.

The suitability of the aft c.g. location in terms of static longitudinal and static directional stability is discussed in Chapter 11, Sub-section 11.2.3.

Step 10.9: To save space this step has been omitted.

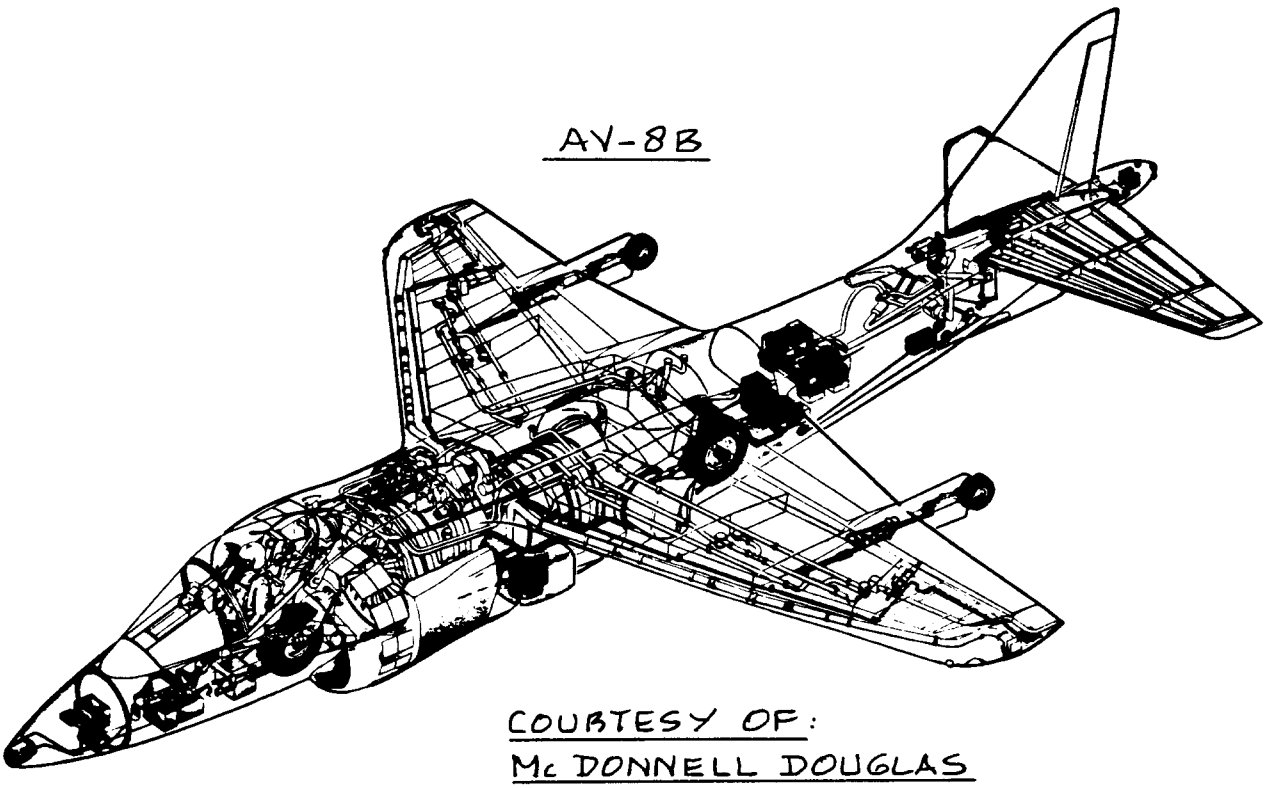

AV-8B

COURTESY OF:
Mc DONNELL DOUGLAS

11. CLASS I METHOD FOR STABILITY AND CONTROL ANALYSIS

The purpose of this chapter is to present a method for rapidly determining whether or not the proposed configuration will have satisfactory stability and control characteristics. The method is presented as part of Step 11, p.d. sequence I as outlined in Chapter 2. Because the method is limited in scope as well as in accuracy, it should be used only in conjunction with preliminary design sequence I.

The method consists of 16 steps and deals with the following stability and control characteristics:

1. Static longitudinal stability (Longitudinal X-plot), see steps 11.1 through 11.7 in Section 11.1.

2. Static directional stability (Directional X-plot), see steps 11.8 through 11.11 in Section 11.2.

3. Minimum control speed with one engine out, see steps 11.12 through 11.16 in Section 11.3.

Example applications are given in Section 11.4.

Other important stability and control characteristics such as take-off rotation, cross-wind controllability, trim through the c.g. range and a variety of dynamic stability considerations are not covered by this Class I method. The reader should refer to Part VII (Ref.6) for a detailed discussion of these characteristics.

11.1 STATIC LONGITUDINAL STABILITY (LONGITUDINAL X-PLOT)

Step 11.1: Prepare a longitudinal X-plot for the airplane.

Figure 11.1 presents examples of longitudinal X-plots. Note that the two legs of the X are representative of:

1. The c.g. leg represents the rate at which the c.g. moves aft (fwd) as a function of horizontal tail (canard) area.

2. The a.c. leg represents the rate at which the a.c. moves aft (fwd) as a function of horizontal tail (canard) area.

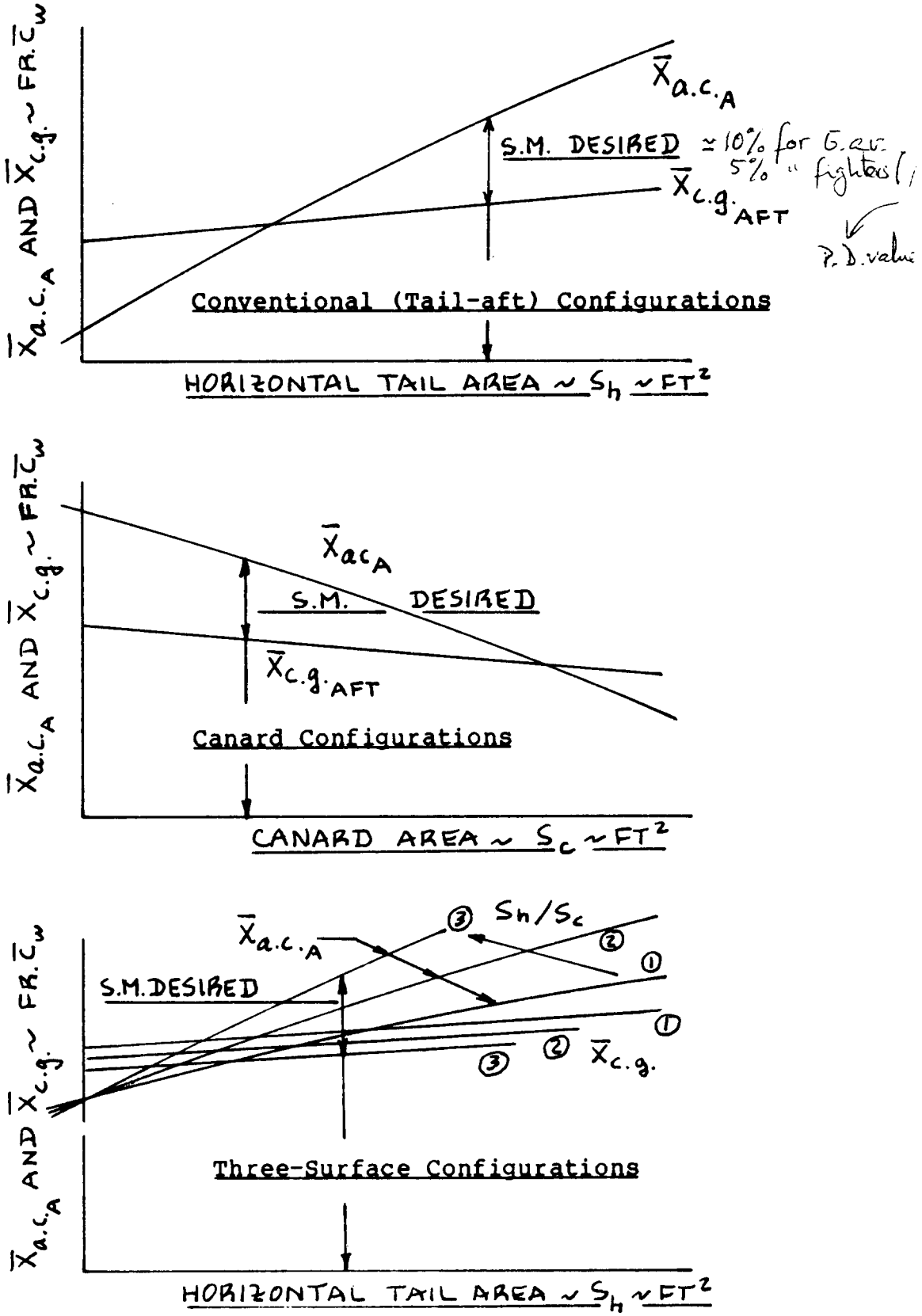

Figure 11.1 Examples of Longitudinal X-Plots

The c.g. leg is easily calculated with the help of the Class I weight and balance analysis of Step 10. From the Class I weight analysis the weight of the horizontal tail (canard) is known on a per ft^2 basis. Assuming this quantity to be independent of surface area, the c.g. can be found for any area of the horizontal tail (or canard).

The a.c. leg is calculated with the following equations:

$$\bar{X}_{ac_A} = [\bar{X}_{ac_{wb}} + \{C_{L_{\alpha_h}}(1 - d\varepsilon_h/d\alpha)(S_h/S)\bar{X}_{ac_h} - C_{L_{\alpha_c}}(1 + d\varepsilon_c/d\alpha)\bar{X}_{ac_c}(S_c/S)\}/C_{L_{\alpha_{wb}}}]/F, \quad (11.1)$$

where:

$$F = [1 + \{C_{L_{\alpha_h}}(1 - d\varepsilon_h/d\alpha)(S_h/S) + C_{L_{\alpha_c}}(1 + d\varepsilon_c/d\alpha)(S_c/S)\}/C_{L_{\alpha_{wb}}}] \quad (11.2)$$

Figure 11.2 defines the required geometric quantities in these equations. The aerodynamic quantities can be computed with methods presented in Part VI (Ref.5).

Note that Eqns.(11.1) and (11.2) apply to three types of airplanes in the following manner:

<u>For a tail-aft airplane:</u> set $S_c = 0$ and consider S_h as the independent variable.

<u>For a canard airplane:</u> set $S_h = 0$ and consider S_c as the independent variable.

<u>For a three-surface airplane:</u> freeze the ratio S_h/S_c and consider S_h as the independent variable.

For a three-surface airplane, the X-plot should be made for different ratios of S_h/S_c.

Both the c.g. leg and the a.c. leg of the 'X' can now be plotted as a function of area (hor.tail or canard). This completes the longitudinal X-plot.

Figure 11.1 presents conceptual X-plots for three types of airplanes.

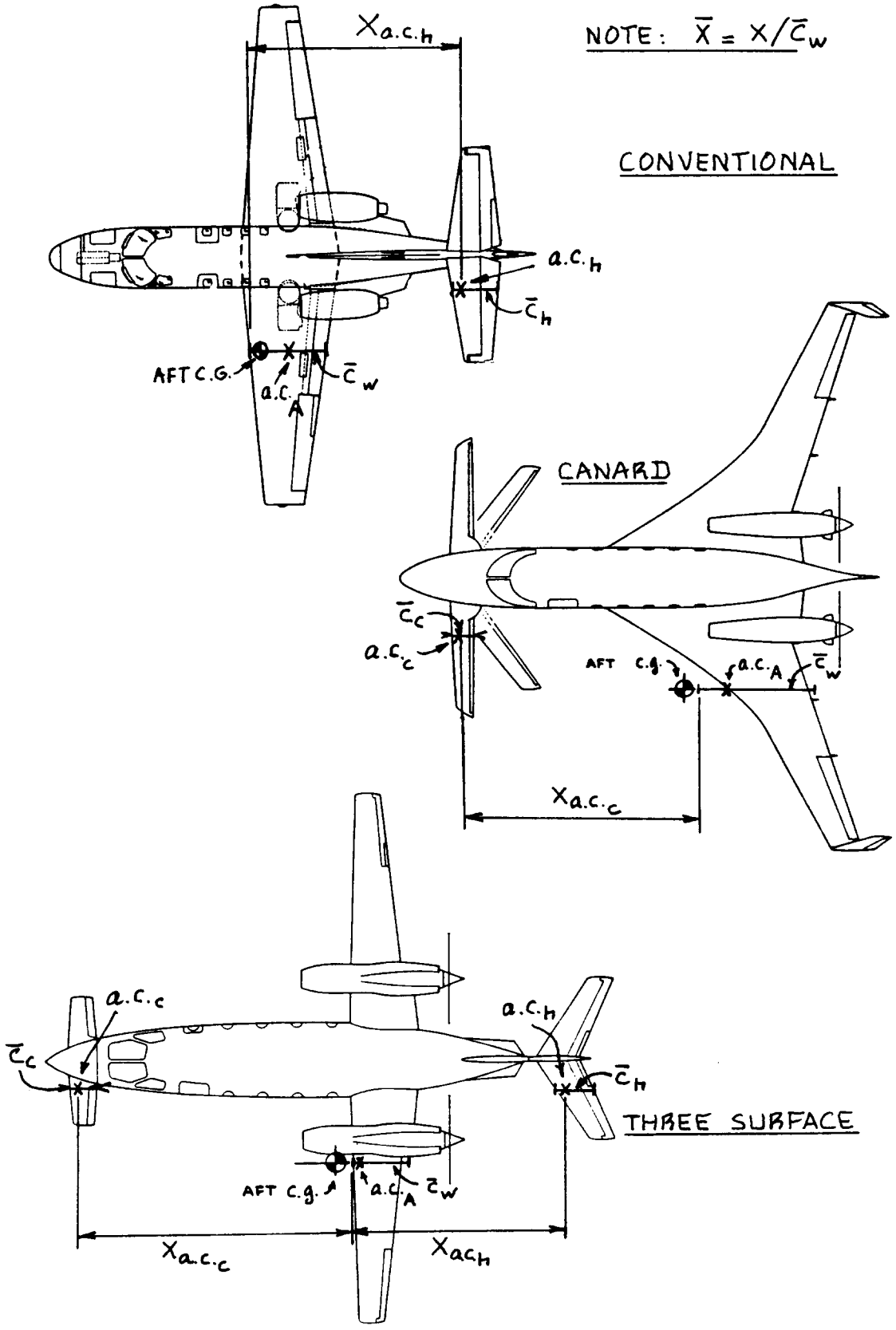

Figure 11.2 Geometric Quantities for A.C. Calculations

Step 11.2: Determine whether or not the airplane being designed needs to be 'inherently stable' or 'de facto stable.

Inherent stability is required of all airplanes which do not rely for their stability on a feedback augmentation system. If the airplane falls in this category proceed to Step 11.3.

De facto stability is required of all airplanes which are stable only with a feedback augmentation system in place. If the airplane falls in this category proceed to Step 11.6.

Step 11.3: Determine whether the airplane being designed fits in any of the twelve categories listed on p.28 in Chapter 2.

If the airplane fits in categories 1-4, proceed to Step 11.4.

If the airplane fits in categories 5-12, proceed to Step 11.5.

Step 11.4: Using the 'aft' c.g. leg in Figure 11.1 find the empennage area required for a minimum static margin of 10 percent.

Reference 9 (Chapter 5) shows that for a static margin of 10 percent:

$$dC_m/dC_L = \bar{X}_{ac} - \bar{X}_{cg} = -0.10 \qquad (11.3)$$

Figure 11.1 shows how the empennage area follows from this. The required empennage area should be recorded.

Step 11.5: Using the 'aft' c.g. leg in Figure 11.1 find the empennage area required for a minimum static margin of 5 percent.

Reference 9 (Chapter 5) shows that for a static margin of 5 percent:

$$dC_m/dC_L = \bar{X}_{ac} - \bar{X}_{cg} = -0.05 \qquad (11.4)$$

Figure 11.1 shows how the empennage area follows from this. The required empennage area should be recorded.

Step 11.6: Using the 'aft' c.g. leg in Figure 11.1 find the SAS feedback gain required as a function of negative static margin.

This feedback gain is estimated from:

$$k_\alpha = (\Delta SM) C_{L_\alpha} / C_{m_{\delta_e}}, \qquad (11.5)$$

where: ΔSM → Δ Static Margin

$$C_{L_\alpha} = C_{L_{\alpha_{wb}}} + C_{L_{\alpha_h}} (1 - d\varepsilon/d\alpha)(S_h/S) + C_{L_{\alpha_c}} (1 + d\varepsilon/d\alpha) S_c/S \qquad (11.6)$$

The value of k_α thus computed should not exceed 5 deg. of elevator per degree of angle of attack.

Equation (11.5) is 'set up' in terms of angle of attack feedback to the elevator. If angle of attack is fed back to the stabilizer (in some fighters) or to the canard (as in the X29), the limit of 5 deg/deg also applies.

The value of incremental static margin, ΔSM in Eqn.(11.5) itself is obtained from the following 'de-facto' stability requirement:

$$\Delta SM + \bar{X}_{cg} - \bar{X}_{ac} = -0.05 \qquad (11.7)$$

Values for $\bar{X}_{cg}$ and for $\bar{X}_{ac}$ follow from the X-plot in Figure 11.1 at any value of empennage area.

The highest level of static instability which is practical from a stability augmentation viewpoint is that which drives k_α to above 5 deg/deg. The corresponding empennage area is the smallest one allowable. This value should be recorded.

Step 11.7: The empennage area obtained from either Eqn.(11.4), (11.5) or (11.6) is the area to be used instead of that obtained from the $\bar{V}$-method, Eqn.(8.3).

If there is more than 10 percent difference between

the empennage areas predicted from the V-method and the method just described, the airplane weight and balance calculations of Chapter 10 should be reviewed and any necessary adjustments made.

11.2 STATIC DIRECTIONAL STABILITY (DIRECTIONAL X-PLOT)

Step 11.8: Prepare a directional X-plot for the airplane.

Figure 11.3 shows an example of such an X-plot. The c.g. leg is again determined with the help of the Class I weight analysis of Step 10. The weight per ft^2 of the vertical tail is known from this weight analysis.

The C_{n_β} leg of the X-plot follows from:

$$C_{n_\beta} = C_{n_{\beta_{wb}}} + C_{L_{\alpha_v}} (S_v/S)(x_v/b) \qquad (11.8)$$

The geometric quantities in Eqn.(11.8) are defined in Figure 11.4. The aerodynamic quantities on the right hand side of Eqn.(11.8) can be computed with the methods of Part VI (Ref.5).

Step 11.9: Determine whether or not the airplane being designed needs to have 'inherent' or 'de facto' directional stability.

If the airplane needs to be 'inherently' directionally stable, proceed to Step 11.10.

If the airplane needs to have 'de facto' directional stability proceed to Step 11.11.

Step 11.10: Assume that the overall level of directional stability must be:

$$C_{n_\beta} = 0.0010 \text{ per deg.} \qquad (11.9)$$

Proceed to the X-plot of Figure 11.3 and find the value of S_v which produces this level of directional stability.

Step 11.11: Compute the required sideslip to rudder feedback gain from:

$$k_\beta = (\Delta C_{n_\beta})/C_{n_{\delta_r}} \qquad (11.10)$$

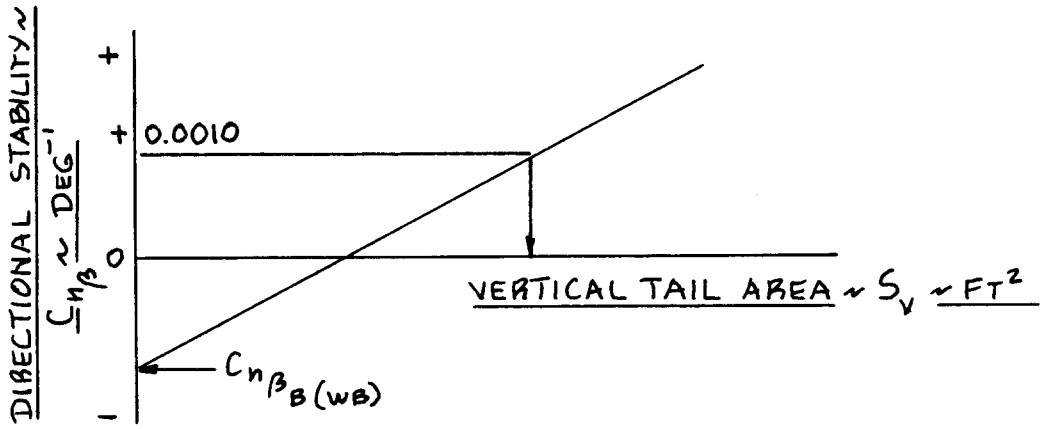

Figure 11.3 Example of Directional X-Plot

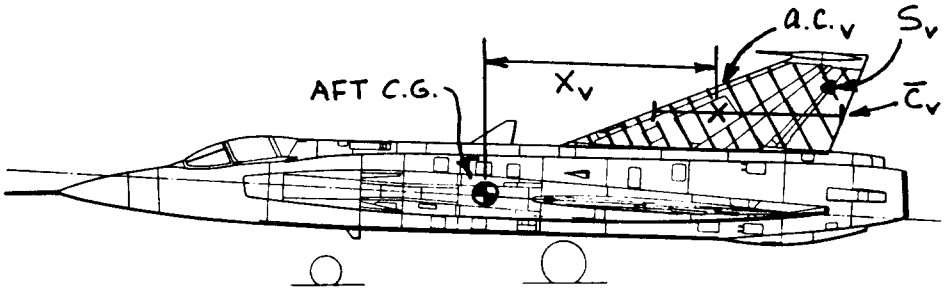

Figure 11.4 Geometric Quantities for Directional X-Plot

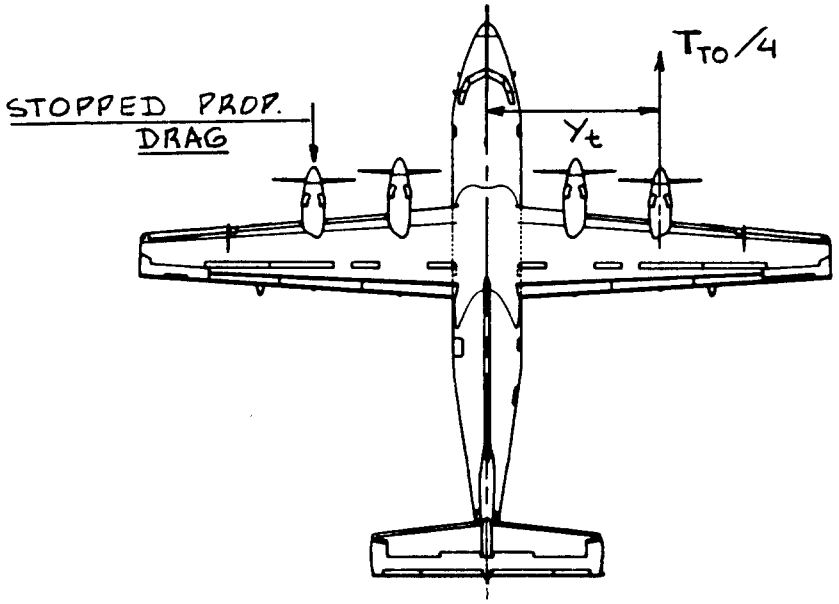

Figure 11.5 Geometry for Engine-out V_{mc} Calculation

The required value of ΔC_{n_β} follows from:

$$\Delta C_{n_\beta} = 0.0010 - C_{n_\beta} \qquad (11.11)$$

The value of k_β thus computed should not exceed 5 deg/deg.

The vertical tail area resulting in the lowest value of inherent C_{n_β} which is consistent with Eqn.(11.11) is the smallest allowable vertical tail area. This empennage area should be recorded.

11.3 MINIMUM CONTROL SPEED WITH ONE ENGINE INOPERATIVE

Step 11.12: Determine the critical engine-out yawing moment from:

$$N_{t_{crit}} = T_{TO_e} y_t \qquad (11.12)$$

The value of y_t corresponds to the lateral thrust moment arm of the most critical engine. Figure 11.5 illustrates y_t.

For a propeller driven airplane the known value of P_{TO} must be changed to the corresponding value of T_{TO}. Figure 3.8 of Part I (p.100) can be used to do this.

Step 11.13: Determine the value of drag induced yawing moment due to the inoperative engine from:

For a propeller driven airplane with fixed pitch propellers:

$$N_D = 0.75 N_{t_{crit}} \qquad (11.13)$$

For a propeller driven airplane with variable pitch propellers:

$$N_D = 0.25 N_{t_{crit}} \qquad (11.14)$$

For a jet driven airplane with a windmilling engine with low b.p.r.:

$$N_D = 0.15N_{t_{crit}} \quad (11.15)$$

For a jet driven airplane with a windmilling engine with high b.p.r.:

$$N_D = 0.25N_{t_{crit}} \quad (11.16)$$

Step 11.14: Calculate the maximum allowable V_{mc} from:

$$V_{mc} = 1.2V_s, \quad (11.17)$$

where V_s is the lowest stall speed of the airplane. This is usually the landing stall speed.

Step 11.15: Calculate the rudder deflection required to hold the engine out condition at V_{mc} from:

$$\delta_r = (N_D + N_{t_{crit}})/\bar{q}_{mc}SbC_{n_{\delta_r}} \quad (11.18)$$

The value of the control power derivative $C_{n_{\delta_r}}$ may be computed with the methods of Part VI (Ref.5).

The rudder deflection resulting from Eqn.(11.18) should be no more than 25 degrees. If it is more, adjust the rudder size and/or the vertical tail size until this is satisfied. Record this vertical tail area.

Step 11.16: The largest vertical tail area which results from Steps 11.10, 11.11 or 11.15 is the vertical tail area required for the airplane. Determine this area.

If this vertical tail area differs by more than 10 percent from the one computed with the $\bar{V}$-method of Eqn.(8.4) it will be necessary to adjust the weight and balance calculations of Chapter 10.

11.4 EXAMPLE APPLICATIONS

Three example applications will now be discussed:

11.4.1 Twin Engine Propeller Driven Airplane: Selene
11.4.2 Jet Transport: Ourania
11.4.3 Fighter: Eris

11.4.1 Twin Engine Propeller Driven Airplane

Step 11.1: Figure 11.6 presents the longitudinal X-plot for the Selene.

Observe, that for the airplane to be 0.10 stable at its operating weight empty, a horizontal tail area of 58 ft^2 is required. This represents an increase of 58 - 37 = 21 ft^2. This larger horizontal tail has the effect of shifting the aft c.g. to $0.9\bar{c}_w$. This is still forward of the main landing gear. However, it may be necessary to move the main gear aft a bit to accomodate the longitudinal tip-over criterion of Chapter 9.

Note also from the X-plot, that the Selene will have to be restricted from flying at W_{OE} plus two aft passengers plus aft luggage. The airplane would become unstable in this flight condition. This is a rather common occurrence in this type of airplane.

Observe also from the X-plot, that with power-on the stability of the airplane is much better. This is a typical characteristic of pusher-propeller airplanes.

Step 11.2: The Selene must be an inherently stable airplane. Full time stability augmentation in this type of airplane is probably not affordable.

Step 11.3: The Selene fits into category 3: twin engine propeller driven airplanes.

Step 11.4: It was already decided in Step 11.1 that the horizontal tail area needs to be increased from 37 to 58 ft^2.

Steps 11.5 - 11.7: Not applicable.

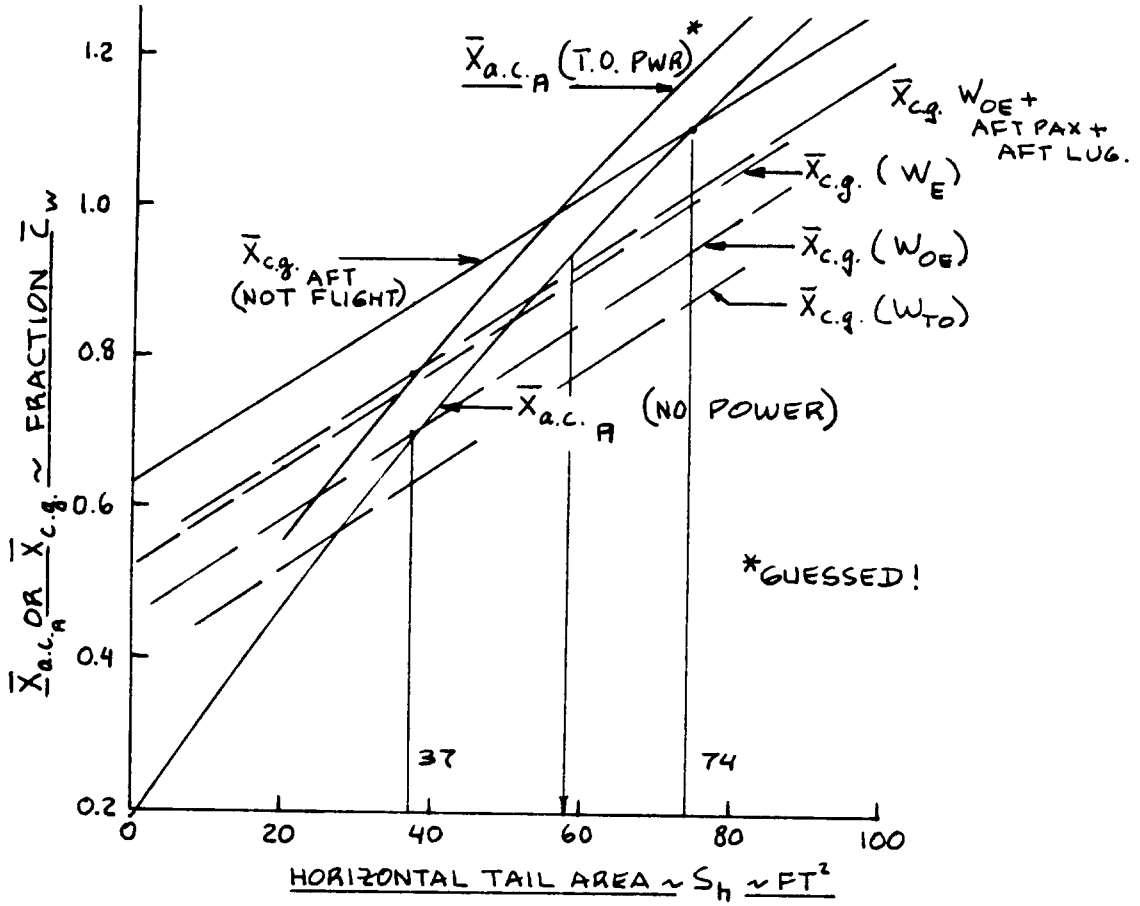

Figure 11.6 Selene: Longitudinal X-Plot

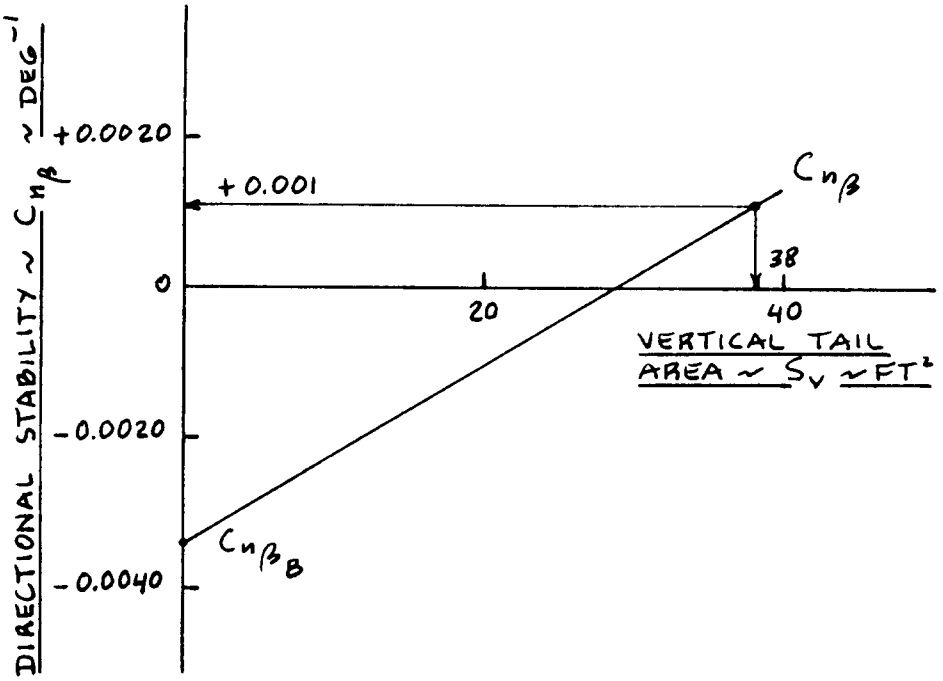

Figure 11.7 Selene: Directional X-Plot

Step 11.8: Figure 11.7 presents the directional X-plot for the Selene.

Step 11.9: The Selene needs to have inherent directional stability: full time stability augmentation in this type of airplane is probably not affordable.

Step 11.10: Note from Figure 11.7 that the vertical tail of the Selene is slightly too large: an area of 36 ft^2 would be sufficient from a directional stability viewpoint.

Step 11.11: Not applicable.

Step 11.12: From the general arrangement drawing of the Selene (Fig.10.3) it follows that y_t= 6.3 ft. The maximum take-off power, P_{TO} was determined in Chapter 5 (p.135) as 449 hp. per engine. From Figure 3.8 in Part I (p.100) it is seen that at this power level, the take-off thrust is: T_{TO}= 1,200 lbs per engine.

The critical engine-out yawing moment it therefore: 1,200x6.3 = 7,560 ftlbs.

Step 11.13: The Selene will have variable pitch propellers. The value for N_D therefore is: 0.25x7,560 = 1,890 ftlbs.

Step 11.14: The landing stall speed is the lowest stall speed for the Selene. At the landing weight this is found to be: 99.3 kts.

The maximum allowable value for V_{mc} is therefore: 1.2x99.3 = 119 kts.

Step 11.15: From the vertical tail and rudder geometry definitions in Chapter 8 (p.210-211) and from the methods of Part VI the following value for rudder control power derivative is computed:

$$C_{n_{\delta_r}} = -0.0027 \text{ deg}^{-1}$$

With Eqn.(11.18) this yields for the rudder deflection required at V_{mc} a value of 16.4 deg. This is well within the allowable value of 25 deg.

Step 11.16: The vertical tail size of the Selene is thus 'critical' from a directional stability viewpoint. As seen in Step 11.10 the existing tail size of 38 ft^2 is sufficient.

11.4.2 Jet Transport

Step 11.1: Figure 11.8 presents the longitudinal X-plot for the Ourania.

Observe, that the Ourania is longitudinally stable without a horizontal tail. The cause for this is the too forward position of the wing on the fuselage. By moving the wing, together with the main landing gear 200 inches aft a more reasonable result is obtained. Note that now, at the nominal tail area of 254 ft^2 the Ourania has a level of instability of $0.085\bar{c}_w$. The reader will remember that the Ourania was to be configured as a 'relaxed' stability airplane.

Figure 11.9 shows how 'wing + main gear' movement affects the c.g. location on the mean geometric chord of the wing, $\bar{c}_w$.

Step 11.2: The Ourania must be a 'relaxed stability' airplane. The level of instability at aft c.g. should be the subject of a detailed study of the benefits in 'trimmed lift-to-drag ratio' which this confers on the airplane. For purposes of this p.d. study a level of instability of $0.085\bar{c}_w$ is arbitrarily selected.

Step 11.3: The Selene fits into category 7: jet transports.

Step 11.4: Not applicable.

Step 11.5: Not applicable.

Step 11.6: Using the 'aft' c.g. leg corresponding the 200 in. aft shift of the wing (Figure 11.8) it is found that the longitudinal stability augmentation system must generate a value of incremental static margin of:

$$\Delta SM = 0.085 + 0.05 = 0.135.$$

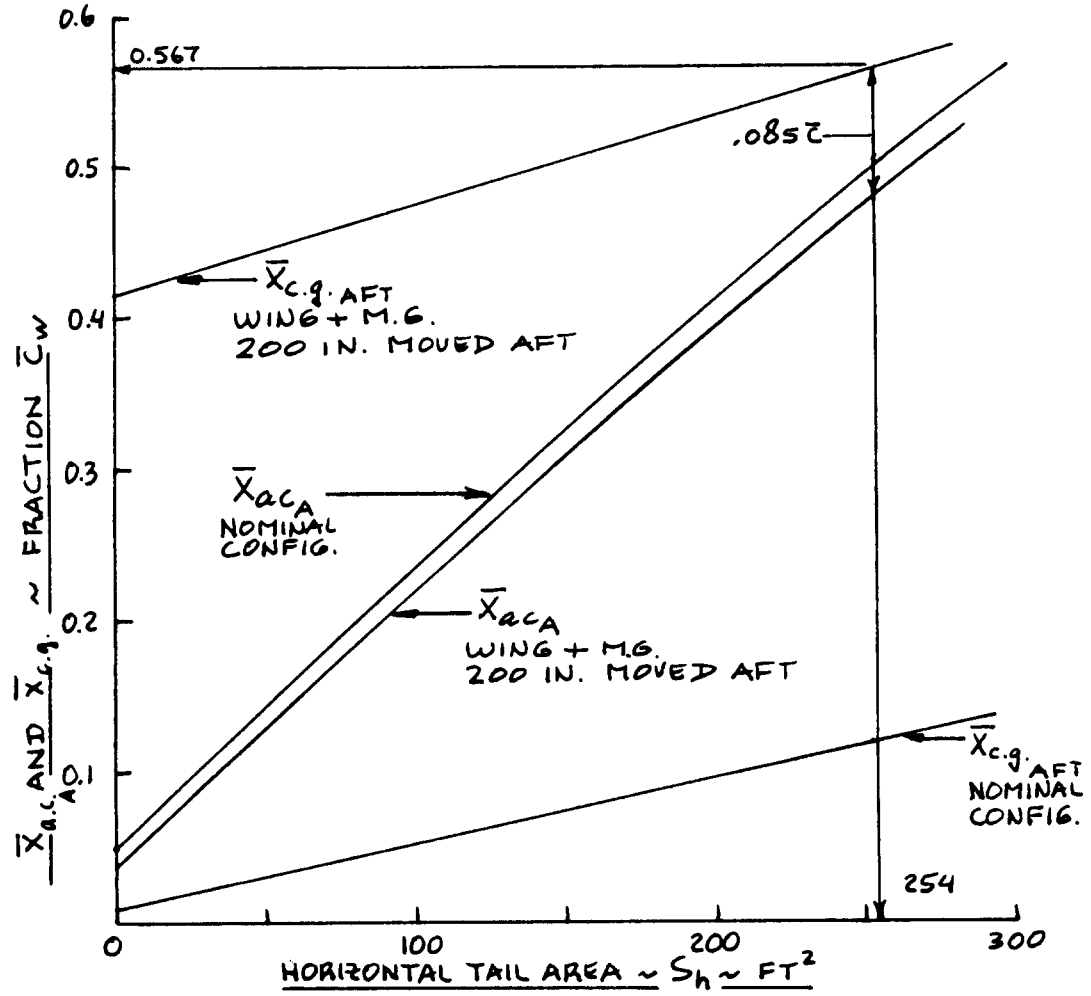

Figure 11.8 Ourania: Longitudinal X-Plot

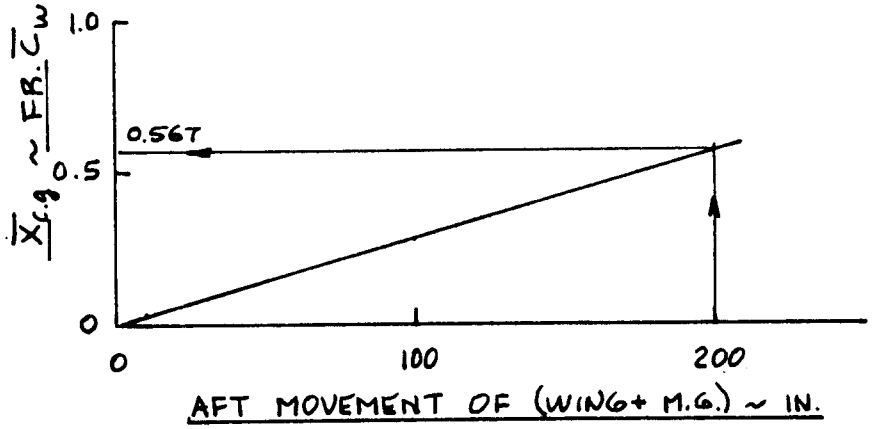

Figure 11.9 Ourania: Effect of 'Wing + Main Gear' Aft Movement on Airplane Center of Gravity

The total airplane lift curve slope was computed to be: $C_{L_\alpha} = 0.081\ deg^{-1}$. The value of the elevator control power derivative was found to be: $C_{m_{\delta_e}} = -0.0251\ deg^{-1}$.

With these values and with Eqn.(11.5) it follows that: $k_\alpha = 0.44$ which is an acceptable value of feedback gain. It would appear that from this viewpoint the horizontal tail could be made smaller. At this point it is prudent not to do this. Class II methods may show that take-off rotation and trim at forward c.g. with the flaps down are more restrictive in tailplane design.

Step 11.7: The horizontal tail area will be maintained at 254 ft^2.

Step 11.8: Figure 11.10 presents the directional X-plot for the Ourania.

Step 11.9: The Ourania is to be a 'relaxed' stability airplane.

Step 11.10: Not applicable.

Step 11.11: Note from Figure 11.10 that the vertical tail of the Ourania already results in a level of directional instability of $C_{n_\beta} = -0.0016$. Desired is a 'de-facto' level of 0.0010. The decrement of 0.0026 must be provided by the sideslip feedback system.

The rudder control power derivative of the Ourania was computed to be: $C_{n_{\delta_r}} = -0.0012\ deg^{-1}$.

With the help of Eqn.(11.10) the feedback gain can be computed to be:

$$k_\beta = 0.0026/0.0012 = 2.2\ deg/deg.$$

This is acceptable. From this viewpoint then the vertical tail of the Ourania is not critical.

Step 11.12: From the general arrangement drawing of the Ourania (Fig.10.4) it follows that $y_t = 16.7$ ft. The

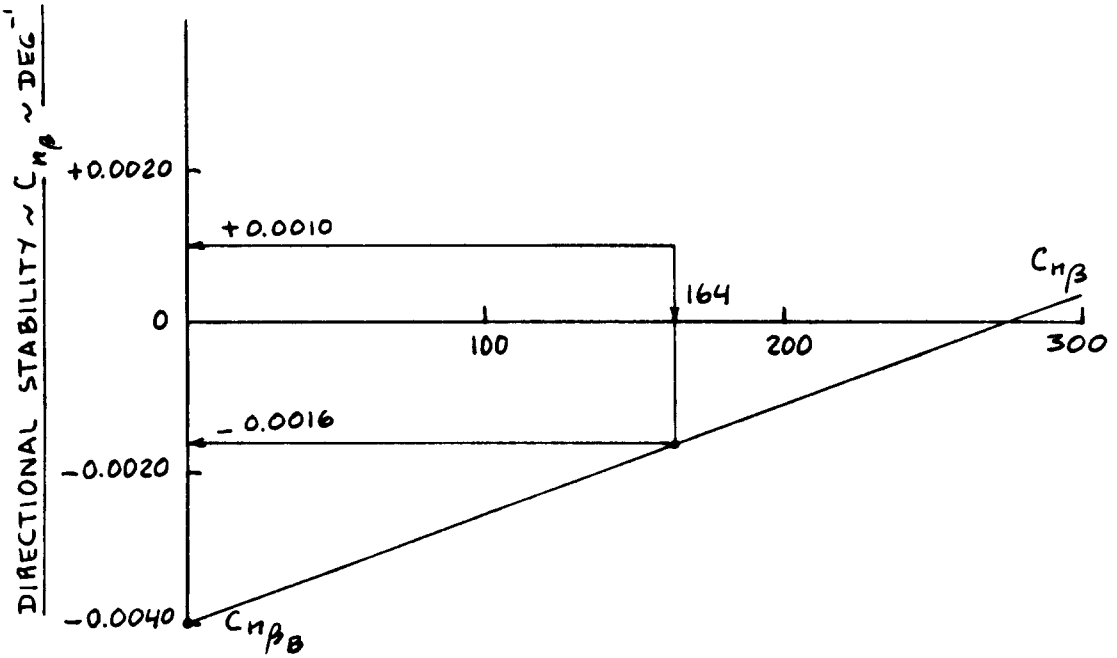

Figure 11.10 Qurania: Directional X-Plot

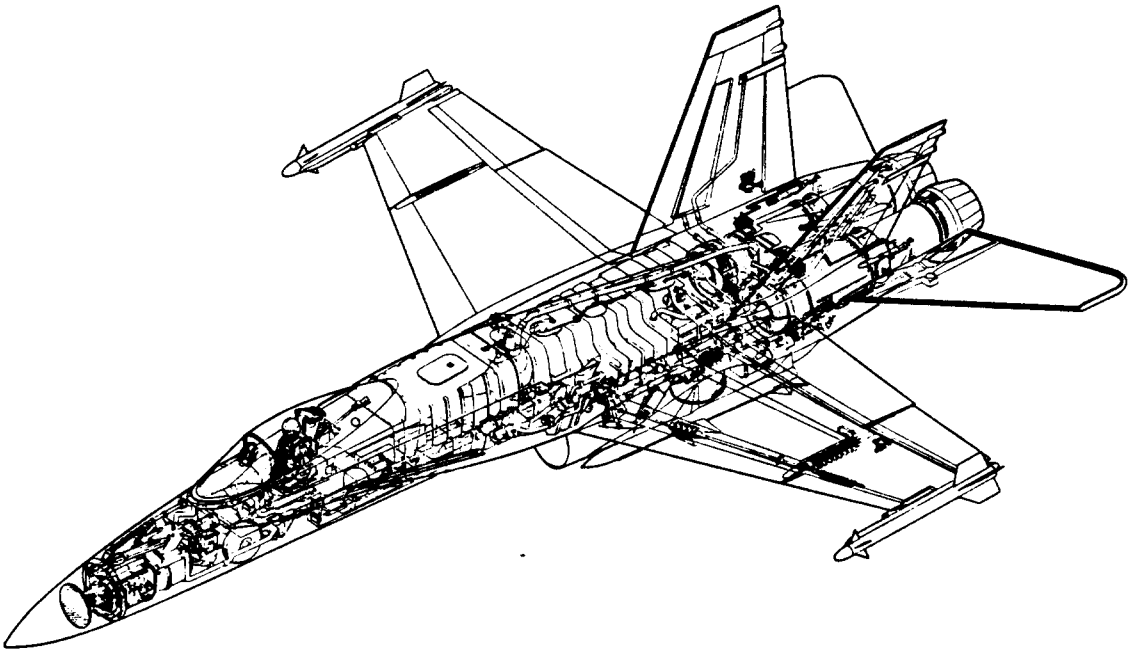

F/A - 18A HORNET
COURTESY OF:
McDONNELL DOUGLAS

maximum take-off thrust, T_{TO} was determined in Chapter 5 (p.138) as 24,000 lbs per engine.

The critical engine-out yawing moment it therefore: 24,000x16.7 = 400,800 ftlbs.

Step 11.13: The Ourania has high b.p.r engines. Eqn.(11.16) therefore applies in determining the windmilling drag induced yawing moment. The total yawing moment to be 'held' at V_{mc} is therefore 1.25x400,800 = 501,000 ftlbs.

Step 11.14: The landing stall speed is the lowest stall speed for the Ourania. At the landing weight it is found that V_{s_L} = 87 kts. This yields a V_{mc} = 105 kts.

Step 11.15: From the vertical tail and rudder geometry definitions in Chapter 8 (p.210-211) and from the methods of Part VI the following value for rudder control power derivative is computed:

$$C_{n_{\delta_r}} = -0.0012 \text{ deg}^{-1}$$

With Eqn.(11.18) this yields for the rudder deflection required at V_{mc} a value of 61 deg. This is clearly too much. The vertical tail of the Ourania is therefore too small.

If the vertical tail size is increased to 200 ft^2 while at the same time the rudder area ratio S_r/S_v is increased from 0.35 to 0.45 and the rudder is given a double hinge line (variable camber) so the rudder can be driven to 40 deg., a satisfactory solution can be obtained. The reader will realize that this will have to be verified with more detailed analyses and possibly a windtunnel test before the final decision on the vertical tail size can be made. However, for p.d. purposes it will be assumed that the vertical tail will have to be increased to 200 ft^2.

Step 11.16: It was already decided in the previous step to increase the vertical tail from 164 to 200 ft^2.

11.4.3 Fighter

Step 11.1: Figure 11.11 presents the longitudinal X-plot for the Eris.

Observe, that the Eris is longitudinally unstable without a horizontal tail. At the horizontal tail area of 93 ft^2 (determined from the V-method in Chapter 8) the level of instability is $0.133\bar{c}_w$. The reader should realize that the X-29 was designed to a level of instability of $0.350\bar{c}_w$ at its aft c.g!

Step 11.2: The Eris must be a negative stability airplane. The level of instability at aft c.g. and at forward c.g. should be the subject of a detailed study of the benefits in 'trimmed lift-to-drag ratio' and maneuvering performance which are conferred upon the airplane. For purposes of this p.d. study a level of instability of $0.133\bar{c}_w$ is arbitrarily selected.

Step 11.3: The Selene fits into category 9: fighters.

Step 11.4: Not applicable.

Step 11.5: Not applicable.

Step 11.6: Using the 'aft' c.g. leg of Figure 11.11 it is found that the longitudinal stability augmentation system must generate a value of incremental static margin of:

$$\Delta SM = 0.133 + 0.05 = 0.185.$$

The total airplane lift curve slope was computed to be: $C_{L_\alpha} = 0.078\ deg^{-1}$. The value of the elevator control power derivative was found to be: $C_{m_{\delta_e}} = -0.0182\ deg^{-1}$.

With these values and with Eqn.(11.5) it follows that: $k_\alpha = 0.80$ which is an acceptable value of feedback gain. It would appear that from this viewpoint the horizontal tail could be made smaller. At this point it

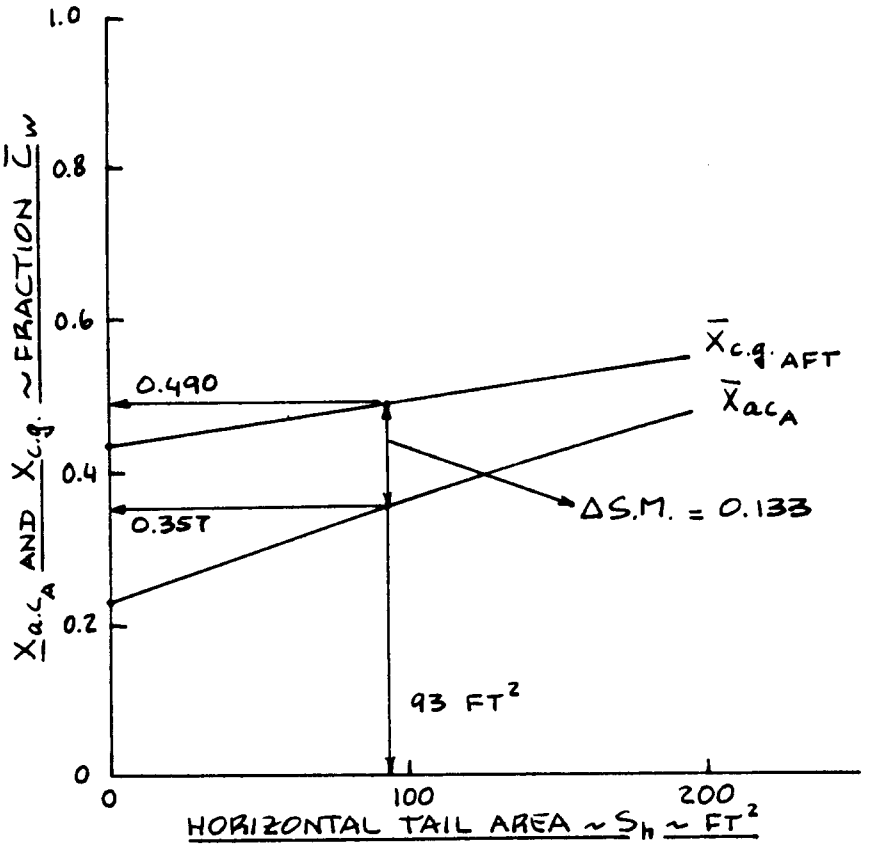

Figure 11.11 Eris: Longitudinal X-Plot

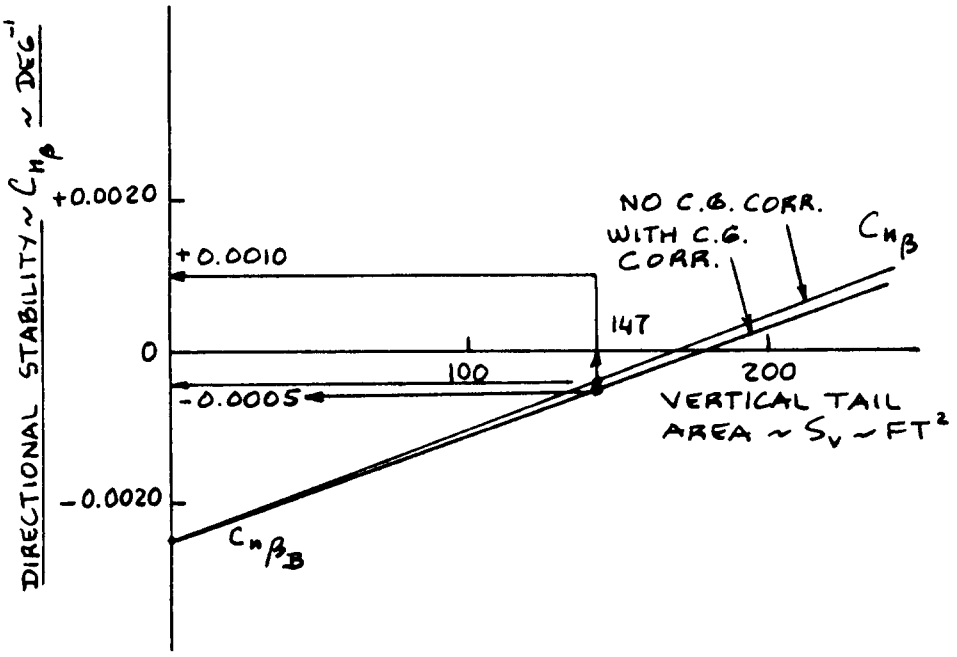

Figure 11.12 Eris: Directional X-Plot

is prudent not to do this. Class II methods may show that take-off rotation and trim at forward c.g. with the flaps down are more restrictive in tailplane design.

Step 11.7: The horizontal tail area of 93 ft^2 will be kept.

Step 11.8: Figure 11.12 presents the directional X-plot for the Eris.

Step 11.9: The Eris is to be a 'negative' stability airplane.

Step 11.10: Not applicable.

Step 11.11: Note from Figure 11.12 that the vertical tail of the Eris renders the airplane directionally unstable at a level of C_{n_β} = - 0.0005. Desired is a 'de-facto' level of 0.0010. The decrement of 0.0015 must be provided by the sideslip feedback system.

The rudder control power derivative of the Eris was computed to be: $C_{n_{\delta_r}}$ = - 0.0007 deg^{-1}.

With the help of Eqn.(11.10) the feedback gain can be computed to be:

k_β = 0.0015/0.0007 = 2.1 deg/deg.

This is acceptable. From this viewpoint then the vertical tail of the Eris is not critical.

Step 11.12: From the general arrangement drawing of the Eris (Fig.10.5) it follows that y_t= 1.7 ft. The maximum take-off thrust, T_{TO} was determined in Chapter 5 (p.140) as 16,000 lbs per engine.

The critical engine-out yawing moment it therefore: 12,000x1.7 = 20,400 ftlbs.

Step 11.13: The Eris has low b.p.r engines. Eqn.(11.16) therefore applies in determining the windmilling drag induced yawing moment. The total yawing moment to be 'held' at V_{mc} is therefore 1.15x20,400 = 23,460 ftlbs.

Step 11.14: The landing stall speed is the lowest stall speed for the Eris. At the landing weight this is 131 kts. This yields a V_{mc} = 158 kts.

Step 11.15: From the vertical tail and rudder geometry definitions in Chapter 8 (p.214-215) and from the methods of Part VI the following value for rudder control power derivative is computed:

$$C_{n_{\delta_r}} = -0.00074 \text{ deg}^{-1}$$

With Eqn.(11.18) this yields for the rudder deflection required at V_{mc} a value of 9.3 deg. This is acceptable. The vertical tail of the Eris is therefore not critical from a viewpoint of engine-out control.

Step 11.16: It was already decided in the previous step to keep the vertical tail size at 147 ft^2.

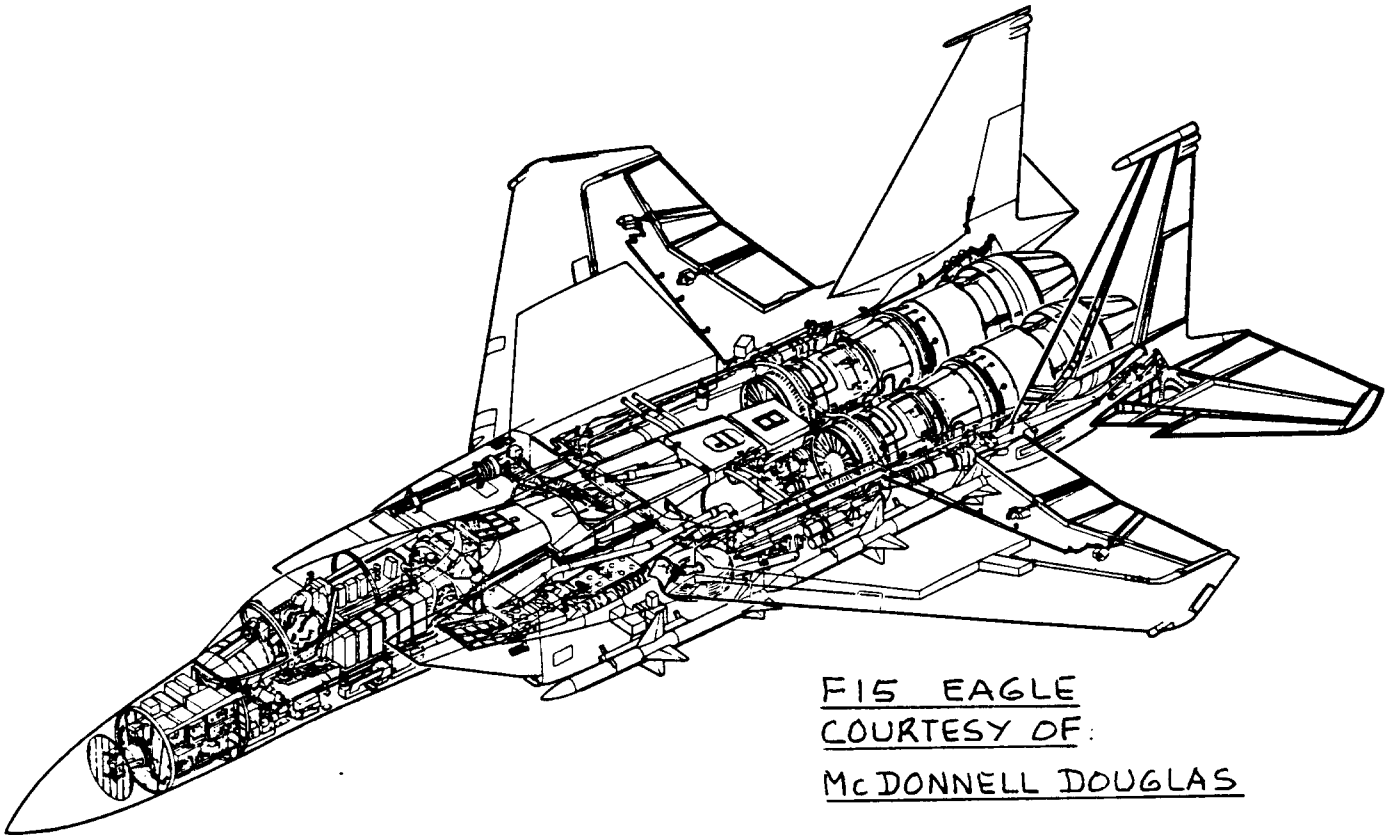

F15 EAGLE
COURTESY OF:
McDONNELL DOUGLAS

12. CLASS I METHOD FOR DRAG POLAR DETERMINATION

The purpose of this chapter is to present a method for rapidly computing the drag polars for airplanes in the first preliminary design sequence. The method is presented as part of Step 12 in p.d. sequence I as outlined in Chapter 2. Section 12.1 presents the method. Example applications are given in Section 12.2.

12.1 STEP-BY-STEP METHOD FOR DRAG POLAR DETERMINATION

Step 12.1: List all airplane components which contribute to wetted area, compute the wetted area of these components. Find the sum, S_{wet}.

It is assumed here. that a threeview with appropriate cross sections is available for the airplane. Figure 12.1 shows an example threeview.

The wetted area of the airplane is the integral of airplane perimeter versus distance from nose to tail.

A convenient way to find the wetted area is to split the airplane into components such as:

1. fuselage and or tailbooms
2. wing(s)
3. empennage
4. nacelles
5. other components which contribute to wetted area

For fuselages, booms and for nacelles the perimeter method is usually the most efficient way to find the wetted area. Figure 12.2 shows an example of a perimeter plot. Note that the perimeter needs to be known only at certain fuselage stations. Where-ever a significant change in perimeter (or cross section)occurs, there should be a fuselage station defining the local perimeter.

At each fuselage, boom or nacelle station the local perimeter can be determined from:

1. A CAD-program

2. Calculation, provided the cross section has a simple geometry.

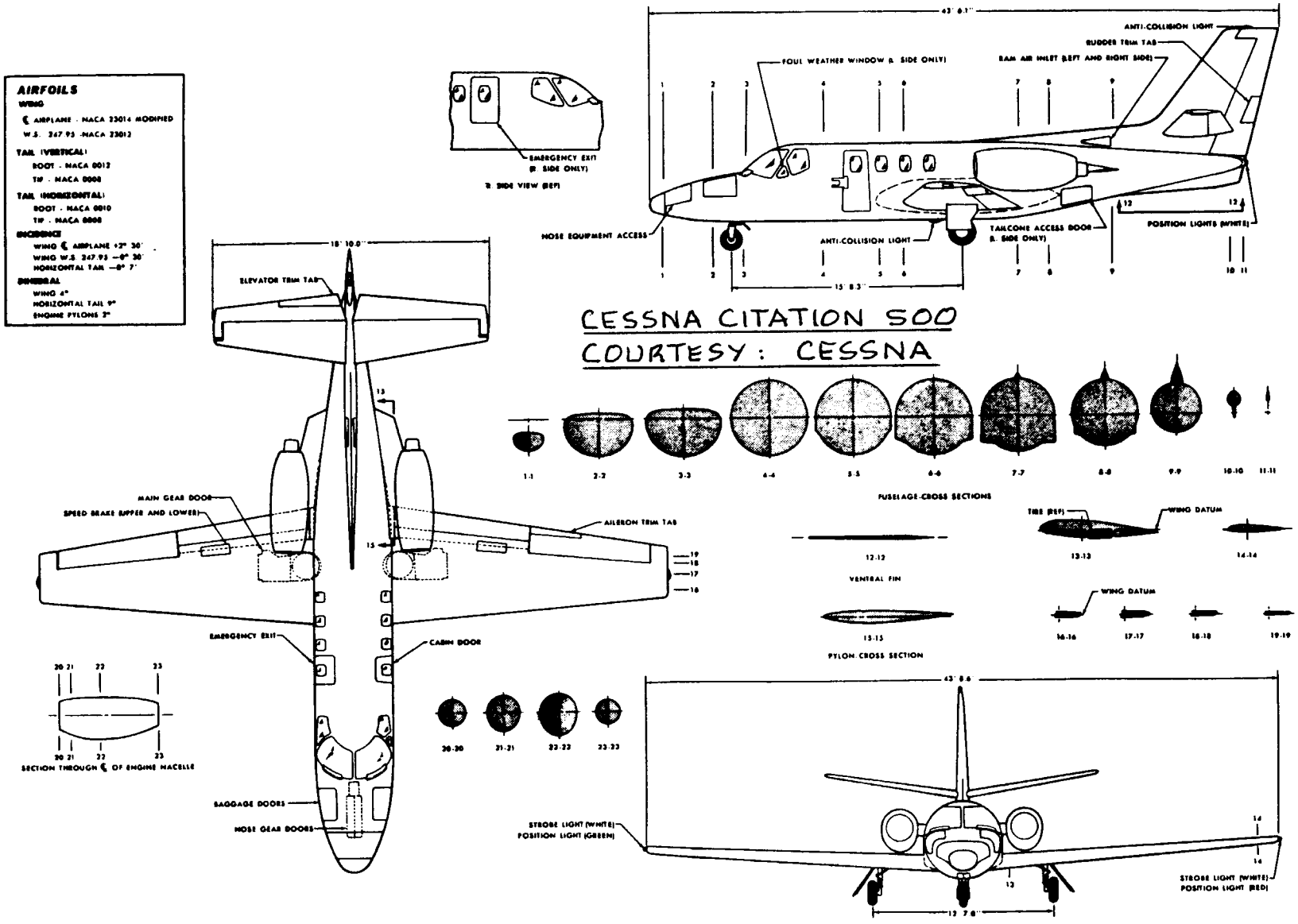

Figure 12.1 Example Threeview with Cross Sections

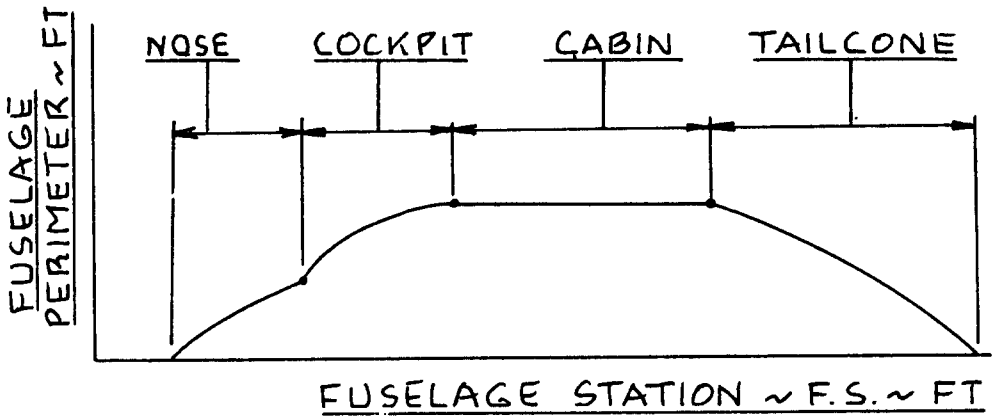

Figure 12.2 Example of a Perimeter Plot

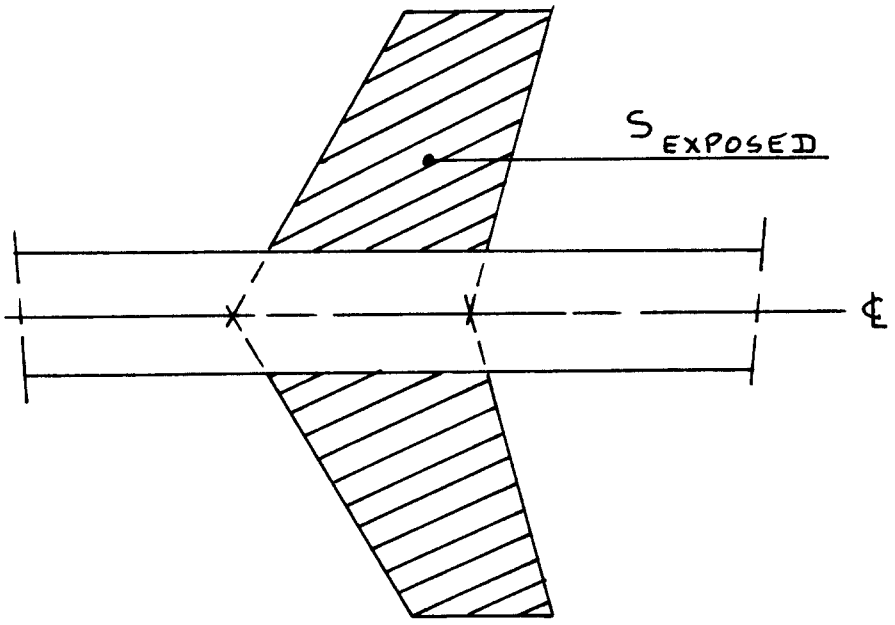

Figure 12.3 Definition of Exposed Planform

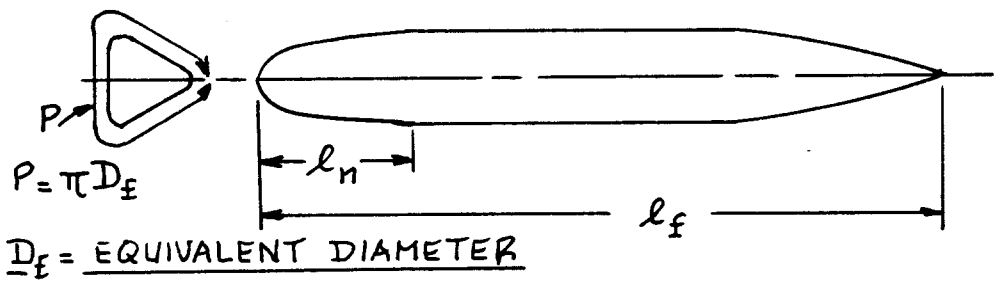

Figure 12.4 Definition of Fuselage Quantities Used in Equation (12.4)

3. A planimeter trace, provided a planimeter is available.

4. The 'pin/string' method: by placing pins along the outside of each cross section and measuring the length of a string wrapped around the outside of the pins.

In the following, a number of simple equations are presented for finding wetted areas of major components.

Wetted Areas for Planforms

For straight tapered planforms (wing, tail, canard, fin and pylon) the wetted area is most easily found from:

$$S_{wet_{plf}} = 2S_{exp.plf}\{1 + 0.25(t/c)_r(1 + \tau\lambda)/(1 + \lambda)\}, \quad (12.1)$$

where $\tau = (t/c)_r/(t/c)_t$ and $\lambda = c_t/c_r$.

Figure 12.3 shows how $S_{exposed}$ is defined.

If a planform has broken or curved leading and/or trailing edges, the wetted area must be obtained from a spanwise integration of the planform perimeter at each planform station. This planform perimeter may be estimated from:

$$p_{plf} = 2c(1 + 0.25t/c) \quad (12.2)$$

Wetted Areas for Fuselages

For fuselages with cylindrical mid-sections:

$$S_{wet_{fus}} = \pi D_f l_f (1 - 2/\lambda_f)^{2/3}(1 + 1/\lambda_f^2), \quad (12.3)$$

where $\lambda_f = l_f/D_f$, the fuselage finess ratio.

For streamlined fuselages without a cylindrical mid-section:

$$S_{wet_{fus}} = \pi D_f l_f (0.50 + 0.135 l_n/l_f)^{2/3}(1.015 + 0.3/\lambda_f^{1.5}) \quad (12.4)$$

Figure 12.4 defines the quantities D_f, l_n and l_f.

Wetted Areas for Externally Mounted Nacelles

Figure 12.5 shows the geometry of an externally mounted nacelle. The following components of the nacelle contribute to wetted area: fan cowling, gas generator cowling and the plug. For these components, Ref.17, p.449 gives:

$$S_{wet_{\substack{fan\\cowl.}}} = l_n D_n \{2 + 0.35 l_1/l_n + 0.8 l_1 D_{hl}/l_n D_n + 1.15(1 - l_1/l_n) D_{ef}/D_n\} \quad (12.5)$$

$$S_{wet_{\substack{gas\\gen.}}} = \pi l_g D_g [1 - (1/3)(1 - D_{eg}/D_g)\{1 - 0.18(D_g/l_g)^{5/3}\}] \quad (12.6)$$

$$S_{wet_{plug}} = 0.7\pi l_p D_p \quad (12.7)$$

Since wings, empennage and nacelle pylons usually intersect a fuselage or a nacelle it is usually necessary to subtract the areas of intersection from the wetted area of a fuselage or of a nacelle. Figure 12.6 shows some examples of these 'to be subtracted' areas.

Make a list of all wetted area contributions and determine the total wetted area. Compare this number with the statistical correlations of Figures 3.22 in Part I. The difference should not be larger than 10 percent. If the difference is larger, an explanation should be sought.

Step 12.2: Using Figures 3.21 of Part I find the equivalent parasite area, 'f' of the airplane.

Step 12.3: Determine the 'clean zero lift drag coefficient at low speed from:

$$C_{D_o} = f/S \quad (12.3)$$

Step 12.4: Find the compressibility drag increment of the airplane from Figure 12.7.

Important note 1: The data of Figure 12.7 do not apply to airplanes with cruise Mach numbers above 0.90.

Important note 2: For airplanes with cruise Mach numbers above 0.90 (this includes supersonic cruise airplanes) it will be necessary to prepare a cross sectional area plot. Such a plot is used to determine

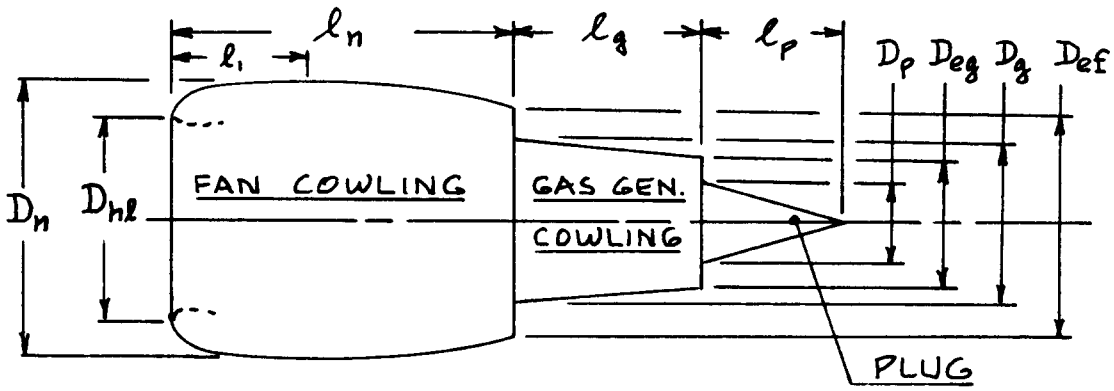

Figure 12.5 Nacelle Geometry for Use in Eqns. (12.5-12.7)

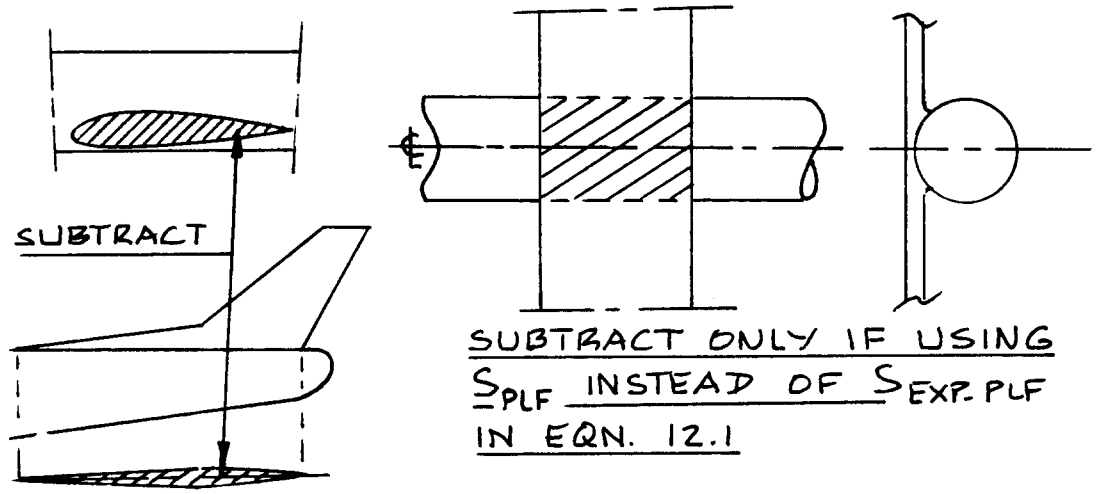

Figure 12.6 Examples of 'Areas to be Subtracted' in a Wetted Area Calculation

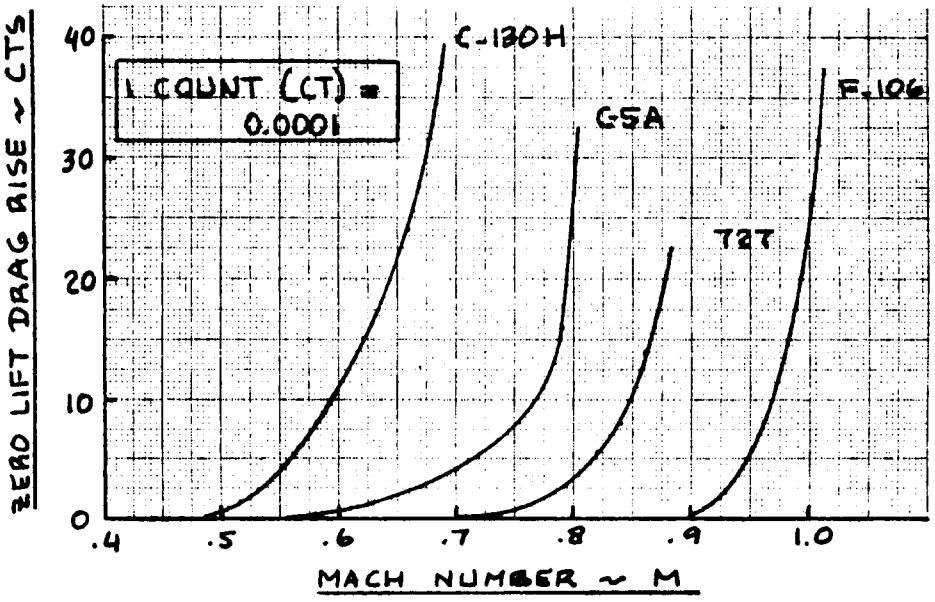

Figure 12.7 Typical Compressibility Drag Behavior

any requirements for area ruling. The area ruling process is described in Part VI (Ref.5).

Step 12.5: Find the flap drag increment(s) from Table 3.6, p.127, Part I.

Step 12.6: Find the landing gear drag increment from Table 3.6, p.127, Part I.

Step 12.7: Construct the cruise, take-off and landing drag polars of the airplane.

Step 12.8: Find the critical L/D values from these drag polars as defined by Step 14 in Chapter 2. Proceed to Step 14 in Ch.2.

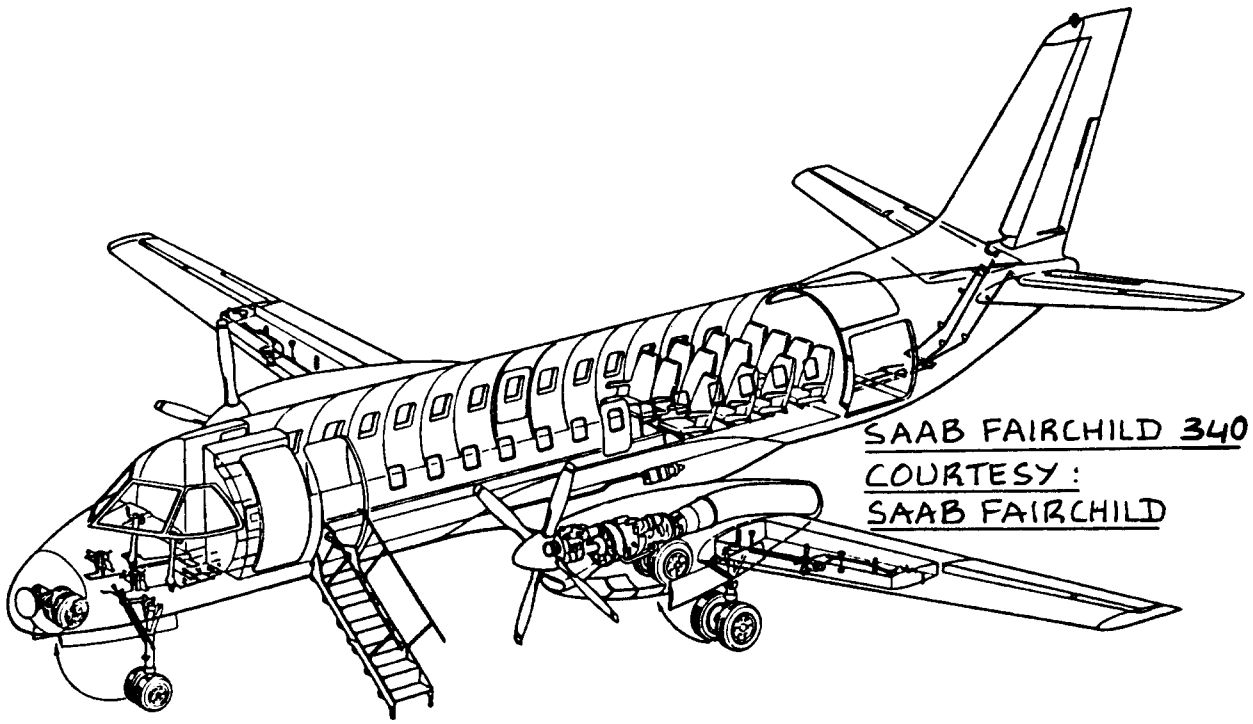

12.2 EXAMPLE APPLICATIONS

Three example applications will be presented:

12.2.1 Twin Engine Propeller Driven Airplane: Selene
12.2.2 Jet Transport: Ourania
12.2.3 Fighter: Eris

12.2.1 Twin Engine Propeller Driven Airplane

Step 12.1: The following tabulation lists all items which contribute to the wetted area of the Selene. Equation numbers used in the calculations are also given.

Component	Equation No.	Wetted Area (ft^2)
Wing	(12.1) with $S=172\ ft^2$, $(t/c)_r=0.17$, $(t/c)_t=0.13$, $\tau=1.3$, $\lambda=0.4$	360
Subtract intersection of wing and fuselage:	$-6.62x4.5=$	-30
Vertical Tail	(12.1) with $S_v=38\ ft^2$, $(t/c)=0.15$, $\lambda=0.56$	79
Horizontal Tail* *increased, see p.269, Ch.11.	(12.1) with $S_h=58\ ft^2$, $(t/c)=0.12$, $\lambda=0.4$	119
Nacelles	perimeter method	105
Fuselage	(12.3), with $D_f=0.5x(4.5+5.5)=5$ ft, $l_f=38.3$ ft	500
Increment due to blister fairings		20
Total wetted area		1,153

Comparison with Figure 3.22a, (Pt.I) shows that for twins with a take-off gross weight of 7,900 lbs the wetted area is predicted to be 1,130 ft^2. This compares very well with the 1,153 ft^2 value computed from the actual configuration!

Steps 12.2-12.8: Because of the excellent agreement in wetted areas just noted there is no need to recompute the Selene drag polars. Those of Part I, Sub-section 3.7.2 should still be valid.

12.2.2 Jet Transport

Step 12.1: The following tabulation lists all items which contribute to the wetted area of the Ourania. Equation numbers used in the calculations are also given.

Component	Equation No.	Wetted Area (ft^2)
Wing	(12.1) with S=1,296 ft^2, $(t/c)_r$=0.13, $(t/c)_t$=0.11, τ=1.18, λ=0.32	2,795
Subtract intersection of wing and fuselage:	-12.9x17.5=	-226
Vertical Tail*	(12.1) with S_v=200 ft^2, (t/c)=0.15, λ=0.32	415
Horizontal Tail	(12.1) with S_h= 254 ft^2, (t/c)=0.12, λ=0.32	523
Nacelles	perimeter method	455
Fuselage	(12.3), with D_f= 12.9 ft, l_f= 123.3 ft	4,320
Total wetted area		8,282

*increased, see p.276, Ch. 8.

Comparison with Figure 3.22b, (Pt.I) shows that for transport jets with a take-off gross weight, W_{TO} of 127,000 the wetted area is predicted to be 7,400 ft^2. This is within the 10 percent expected in the wetted area correlations. However, since it is a significant increase, the impact of any change in cruise L/D needs to be evaluated.

Step 12.2: From Figure 3.21b, p.120, Part I it is seen that for an advanced jet transport a value of

c_f = 0.0030 should be attainable. With the wetted area of 8,282 ft^2 this implies a value of f = 25 ft^2.

Step 12.3: The zero lift drag coefficient of the Ourania at low subsonic speed now follows from Eqn.(12.3): C_{D_o} = 25/1,296 = 0.0193.

Step 12.4: The compressibility drag increment for the Ourania is seen from Figure 12.7 to be roughly 0.0005.

Steps 12.5 - 12.6: Because the slight change in cruise drag has a negligible effect on the take-off and landing polars, these do not have to be re-evaluated.

Step 12.7 and 12.8: The cruise value of zero lift drag coefficient is now:

$$C_{D_o} = 0.0005 + 0.0193 = 0.0198$$

In Part I, p.182 it was determined that:

$$C_{D_o} = 0.0005 + 0.0184 = 0.0189$$

The maximum value of lift-to-drag ratio, $(L/D)_{max}$ is the critical measure of cruise fuel consumption in any comparative study of jet transports, assuming all other factors stay constant. For the Ourania it is found that:

$$\text{Before: } (L/D)_{max} = (\pi x 10 x 0.85/4 x 0.0189)^{1/2} = 18.8$$

$$\text{Now: } (L/D)_{max} = (\pi x 10 x 0.85/4 x 0.0198)^{1/2} = 18.4$$

From the sensitivity analysis data in Part I, p.78 it can be found that:

$$\partial W_{TO}/\partial(L/D) = -2287 \text{ lbs.}$$

This means that because of the effectice decrease in L/D from 18.8 to 18.4 the take-off weight of the Ourania needs to be increased by 2287x0.4 = 915 lbs.

This weight increase will not result in any drastic changes to the airplane. In fact, it is quite possible to absorb this by the use of more advanced structural materials. The structural weight of the Ourania can be computed from Table 10.5 (Ch.10) as $W_{struct.}$ = 33,183 lbs.

The 915 lbs represents only 2.8 percent of this structural weight. Structural weight savings of up to 10 percent are probably 'in the cards'.

It is concluded that the Ourania design is now 'ready' for preliminary design sequence II.

12.2.3 Fighter

Step 12.1: The following tabulation lists all items which contribute to the wetted area of the Eris. Equation numbers used in the calculations are also given.

Component	Equation No.	Wetted Area (ft^2)
Wing	(12.1) with $S=787 ft^2$, $(t/c)_r=0.10$, $(t/c)_t=0.08$, $\tau=1.25$, $\lambda=0.50$	1,617
Subtract intersection of wing and fuselage:	$-15x7.7=$	-115
Vertical Tail	(12.1) with $S_v=147 ft^2$, $(t/c)=0.15$, $\lambda=0.55$	305
Horizontal Tail	(12.1) with $S_h= 93 ft^2$, $(t/c)=0.10$, $\lambda=1.0$	191
Penalty for inlet bulges	perimeter method	50
Fuselage	(12.3), with $D_f= 5.5$ ft, $l_f= 38.3$ ft	540
Tail booms	assume cylinder shape	229
Total wetted area		2,817

Comparison with Figure 3.22c,(Pt.I) shows that for fighters with a take-off gross weight of 64,905 lbs the wetted area is predicted to be 3,500 ft^2. This number is obtained from Fig.3.22c (Pt.I) by accounting for the fact that a number of high weight fighters have wetted areas

actually aboven the correlation line.

The Eris appears to have an actual wetted area which is significantly below that of fighters with similar gross weights. This does not seem reasonable. One reason is the fact that the 'base-drag' due to the Eris engine configuration is not accounted for in this 'wetted area' method. This base drag is estimated from the general arrangement drawing of Figure 10.7 (Ch.10) to result in an additional parasite area of 2 ft^2.

Step 12.2: From Figure 3.21b, p.120, Part I it is seen that for a fighter a value of $c_f = 0.0030$ should be attainable. With the wetted area of 2,817 ft^2 this implies a value of f = 8.7 ft^2.

Add to this the estimated base drag value of 2 ft^2 results in a total f = 10.7 ft^2.

Step 12.3: The zero lift drag coefficient of the Eris at low subsonic speed now follows from Eqn.(12.3): $C_{D_o} = 10.7/787 = 0.0135$.

Step 12.4: The compressibility drag increment for the Eris is seen from Figure 12.7 to be roughly 0.0020 at M=0.80 and 0.0030 at M=0.85.

Steps 12.5 - 12.6: Because the change in cruise drag has a negligible effect on the take-off and landing polars, these do not have to be re-evaluated.

Step 12.7: The following tabulation summarizes the drag polars of the Eris and compares them with those obtained in Part I (p.188 and 189) on the basis of very rough estimates.

Flight Condition	Part I	Part II
	A = 4, e = 0.8	A = 5, e = 0.75
Low speed, clean	$0.0096 + 0.0995C_L^2$	$0.0135 + 0.0707C_L^2$
Low speed, stores	0.0126 + ''	0.0165 + ''
M = 0.8, stores	0.0146 + ''	0.0185 + ''
M = 0.85, clean	0.0126 + ''	0.0165 + ''

Step 12.8: The following tabulation lists the lift and drag coefficients for the critical mission legs of the Eris. The resulting values of L/D are also shown.

The data are shown for both Part I and Part II drag polars

Part I				Part II			
W lbs	C_L	C_D	L/D	W lbs	C_L	C_D	L/D
sealevel, 400 kts, stores							
64,500	0.101	0.0136	7.4	64,905	0.152	0.0181	8.4
sealevel, 450 kts, clean							
54,500	0.068	0.0101	6.7	54,905	0.102	0.0142	7.2
40,000 ft, M=0.8, stores							
64,500	0.312	0.0243	12.8	64,905	0.469	0.0341	13.8
40,000 ft, M=0.85, clean							
54,500	0.235	0.0181	13.0	54,905	0.352	0.0253	13.9

These data indicate that the Eris has slightly better L/D values than predicted during the performance sizing in Part I. However, when comparing these values of L/D with those used in the preliminary weight sizing of Sub-section 2.6.3 in Part I considerably larger differences are seen to exist:

Mission Leg	Preliminary Weight Sizing Part I, Sub-section 2.6.3 L/D	P.D. Sequence I Step 12.8, Part II L/D
s.l., 400 kts, stores	4.5	8.4
s.l., 450 kts, clean	5.5	7.2
40,000 ft, M=0.8, stores	7.0	13.8
40,000 ft, M=0.85, clean	7.5	13.9

What this implies is that the weight sizing process should be repeated at this point. The reader is encouraged to do this. Actual engine sfc data should be

used in this process. Preliminary data indicate that the engine sfs values are significantly higher than those assumed in Part I. The overall effect on the weight of the Eris is therefore expected to be rather minor.

Caution: The reader should not attempt to use the 'sensitivity slopes' of Part I, p.84. These slopes apply only for weight extrapolations dus to small changes in the independent parameters. The L/D changes which have occurred here are too large for the sensitivity slopes to be valid!

To summarize, it is expected that, after doing the weight resizing the Eris will come out relatively unchanged. It can then be taken into the design process of p.d. sequence II.

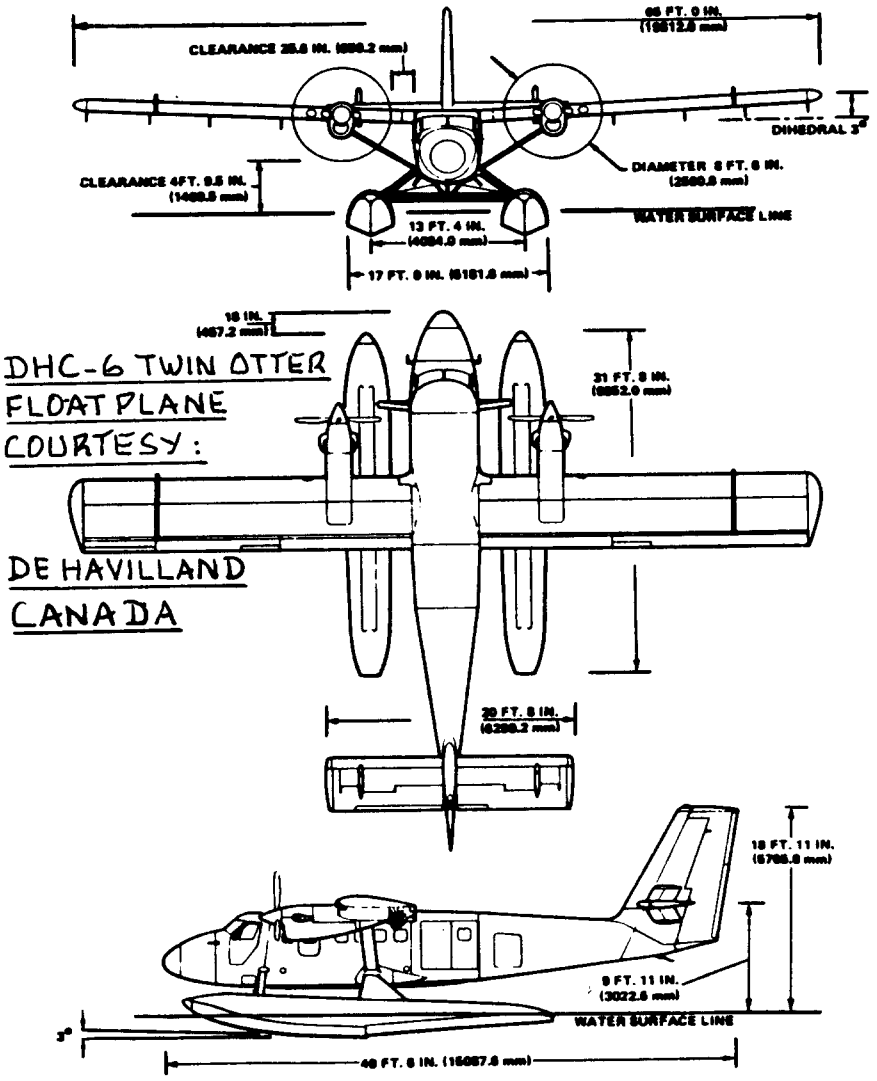

13. THE RESULT OF PRELIMINARY DESIGN SEQUENCE I: THE PRELIMINARY THREEVIEW

The purpose of this chapter is to combine the work done in Chapters 3 - 12 into a preliminary threeview of the configuration. The reader must understand the fact that such a preliminary threeview (also called Class I threeview) is just that: PRELIMINARY. This threeview combines all necessary corrections to the configuration which needed to be made as a result of the work outlined in Chapters 3 - 12. It forms the basis for the work which needs to be done in p.d. sequence II. That work starts with Step 17 in Chapter 2.

During p.d. sequence II the reader will have to use more sophisticated approaches to further configuration development. These approaches form the subject of Parts III through VIII.

The remaining part of this chapter presents the Class I threeviews for three example airplanes. The geometric characteristics of these airplanes are all summarized in tables.

13.1 CLASS I THREEVIEW AND GEOMETRIC SUMMARY FOR A TWIN ENGINE PROPELLER DRIVEN AIRPLANE

Figure 13.1 presents the Class I threeview for the Selene. The geometric characteristics are contained in Table 13.1.

13.2 CLASS I THREEVIEW AND GEOMETRIC SUMMARY FOR A JET TRANSPORT

Figure 13.2 presents the Class I threeview for the Ourania. The geometric characteristics are given in Table 13.2.

13.3 CLASS I THREEVIEW AND GEOMETRIC SUMMARY FOR A FIGHTER

Figure 13.3 presents the Class I threeview for the Eris. The geometric characteristics are contained in Table 13.3.

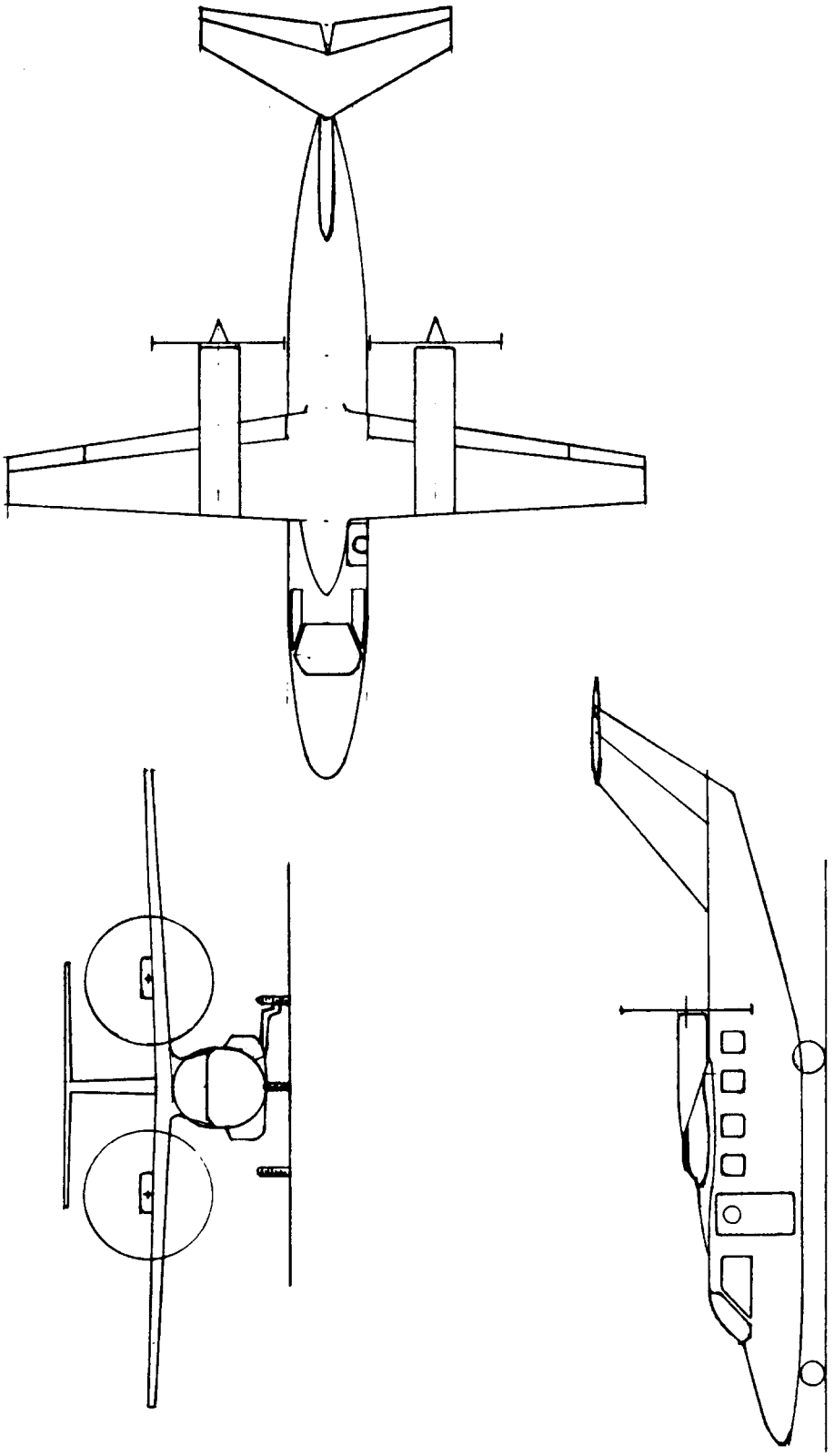

Figure 13.1 Selene: Class I Threeview

Table 13.1 Selene: Geometric Characteristics

	Wing	Horizontal Tail	Vertical Tail
Area	172 ft^2	58 ft^2	38 ft^2
Span	37.1 ft	14.9 ft	6.16 ft
MGC	4.92 ft	4.12 ft	6.31 ft
MGC L.E.: F.S.	20.3 ft	45.1 ft	40.0 ft
Aspect Ratio	8	3.85	1.0
Sweep Angle	0 deg.(c/4)	30 deg.(L.E.)	50 deg.(L.E.)
Taper ratio	0.4	0.4	0.56
Thickness Ratio	0.17 root 0.13 tip	0.12	0.15
Airfoil: root tip	NASA(1)-0317 NASA(1)-0313	NACA0012	NACA 0015
Dihedral angle	2 deg.	0 deg.	not appl.
Incidence angle	+2.5 deg. root -0.5 deg. tip	variable	0 deg.
Aileron chord ratio	0.25	Elevator chord	Rudder chord
Aileron span ratio	0.76 - 1.00	ratio 0.32	ratio 0.43
Flap chord ratio	0.25		
Flap span ratio	0.12 - 0.76		

	Fuselage	Cabin Interior	Overall
Length	39.3 ft	18.5 ft	43.0 ft
Maximum height	5.5 ft	4.4 ft	12.8 ft
Maximum width	4.5 ft	4.25 ft	37.1 ft

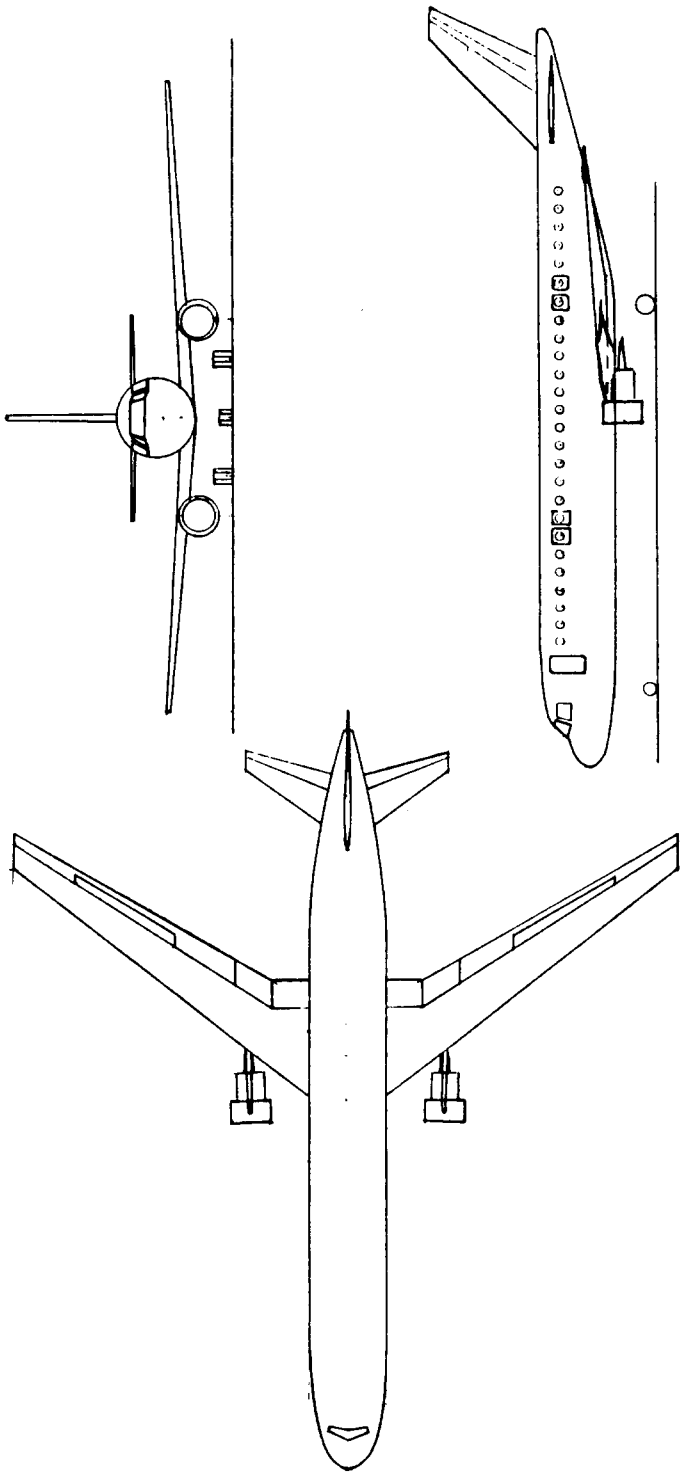

Figure 13.2 Ourania: Class I Threeview

Table 13.2 Ourania: Geometric Characteristics

	Wing	Horizontal Tail	Vertical Tail
Area	1,296 ft^2	254 ft^2	200 ft^2
Span	113.8 ft	35.6 ft	19.0 ft
MGC	12.5 ft	7.75 ft	11.5 ft
MGC L.E.: F.S.	88.8 ft	124.9 ft	123.5 ft
Aspect Ratio	10	5	1.8
Sweep Angle	35 deg.(c/4)	35 deg.(L.E.)	45 deg.(L.E.)
Taper ratio	0.32	0.32	0.32
Thickness Ratio	0.13 root 0.11 tip	0.12	0.15
Airfoil: root	NACA 64A413(mod.)	NACA0012	NACA 0015
tip	NACA 64A411(mod.)		
Dihedral angle	3 deg.	0 deg.	not appl.
Incidence angle	+1.5 deg. root -0.5 deg. tip	variable	0 deg.
Aileron chord ratio	0.30	Elevator chord	Rudder chord
Aileron span ratio	0.23 - 0.34	ratio 0.30	ratio 0.45
Spoiler chord ratio	0.20 hinge line at 0.70c		(Double hinge rudder)
Spoiler span ratio	0.50 - 0.80		
Flap chord ratio	0.30		
Flap span ratio	0.11 - 0.23 and 0.34 - 1.00		

	Fuselage	Cabin Interior	Overall
Length	1243 ft	90.8 ft	1270 ft
Maximum height	13.2 ft	7.5 ft	38.3 ft
Maximum width	13.2 ft	12.4 ft	113.8 ft

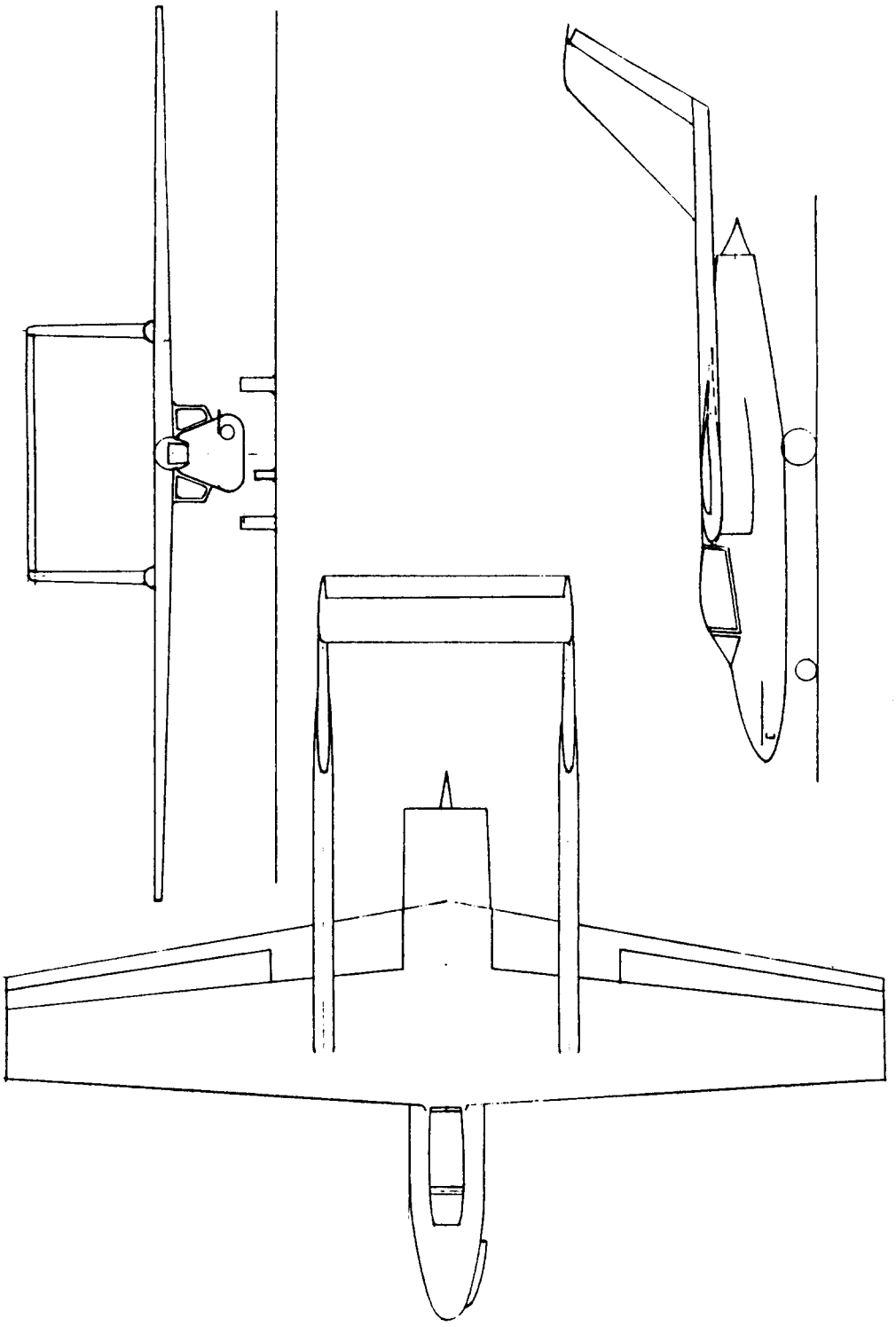

Figure 13.3 Eris: Class I Threeview

Table 13.3 Eris: Geometric Characteristics

	Wing	Horizontal Tail	Vertical Tail
Area	787 ft^2	93 ft^2	147 ft^2
Span	68.7 ft	18.3 ft	10.3 ft
MGC	11.9 ft	5.08 ft	7.4 ft
MGC L.E.: F.S.	21.8 ft	51.7 ft	46.4 ft
Aspect Ratio	6	3.6	1.2
Sweep Angle	0 deg.(c/4)	0 deg.(L.E.)	45 deg.(L.E.)
Taper ratio	0.5	1.0	0.55
Thickness Ratio	0.10 root 0.08 tip	0.10	0.15
Airfoil: root	NACA 64A210(mod.)	NACA0010	NACA 0015
tip	NACA 64A208(mod.)		
Dihedral angle	0 deg.	0 deg.	not appl.
Incidence angle	0 deg. root -2 deg. tip	variable	0 deg.
Spoiler chord ratio	0.20	Elevator chord ratio 0.31	Rudder chord ratio 0.22
Spoiler span ratio	0.40 - 1.00		
Spoiler hinge line at 0.70c			
Flap chord ratio	0.30		
Flap span ratio	0.12 - 1.0		

	Fuselage	Overall
Length	41.3 ft	50.7 ft
Maximum height	6.83 ft	15.7 ft
Maximum width	7.47 ft	68.7 ft

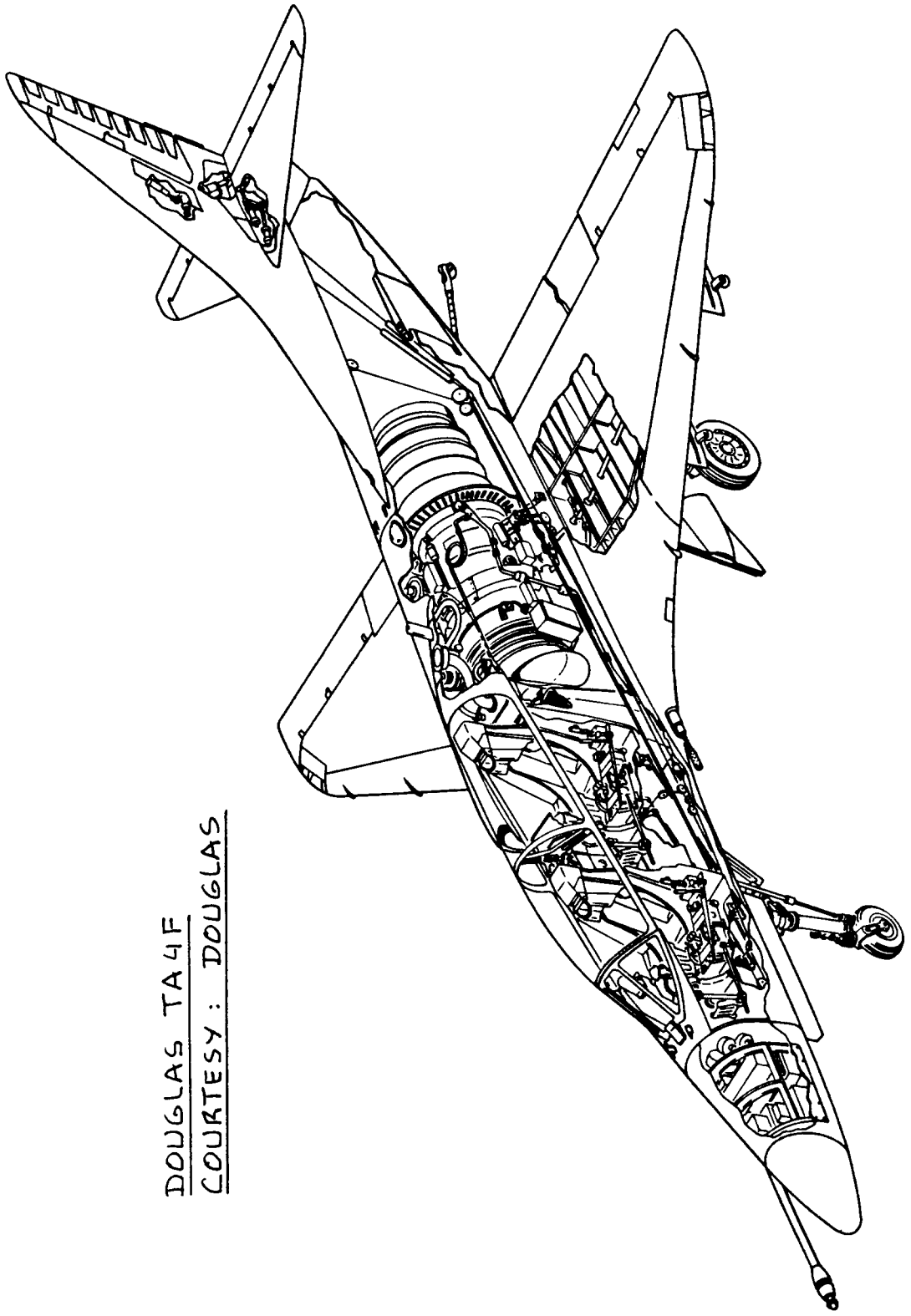

DOUGLAS TA4F
COURTESY: DOUGLAS

14. REFERENCES

14.1 TECHNICAL REFERENCES CITED IN THIS TEXT

1. Roskam, J., Airplane Design: Part I, Preliminary Sizing of Airplanes.

2. Roskam, J., Airplane Design: Part III, Layout Design of Cockpit, Fuselage, Wing and Empennage: Cutaways and Inboard Profiles.

3. Roskam, J., Airplane Design: Part IV, Layout Design of Landing Gear and Systems.

4. Roskam, J., Airplane Design: Part V, Component Weight Estimation.

5. Roskam, J., Airplane Design: Part VI, Preliminary Calculation of Aerodynamic, Thrust and Power Characteristics.

6. Roskam, J., Airplane Design: Part VII, Determination of Stability, Control and Performance Characteristics: FAR and Military Requirements.

7. Roskam, J., Airplane Design: Part VIII, Airplane Cost Estimation: Design, Development, Manufacturing and Operating.

Note: These books are all published by: Roskam Aviation and Engineering Corporation, Rt4, Box 274, Ottawa, Kansas, 66067, Tel. 913-2421624.

8. Taylor, J.W.R., Jane's All The World Aircraft, Published Annually by: Jane's Publishing Company, 238 City Road, London EC1V 2PU, England. (Issues used: 1945/46, 1968/84)

9. Roskam, J., Airplane Flight Dynamics and Automatic Flight Controls, Part I, Fourth Printing, 1984. For publisher see note after ref.7.

10. Chambers, J.R. and Yip, L.P., Wind-Tunnel Investigation of an Advanced General Aviation Canard Configuration, NASA TM 85760, April 1984.

11. Anderson, S.B., Handling Qualities of Canards, Tandem Wings, and Other Unconventional Configurations, SAE Paper 830763, April 12-15, 1983.

12. Wolkovitch, J., Principles of the Joined Wing, Engel Engineering Report No. 80-1, 28603 Trailriders Drive, Rancho Palos Verdes, CA, 90274.

13. Clyde, J.A., Bonner, E., Goebel, T.P. and Spacht, L., Joined Wing Transonic Test Validation, NA-84-1434, Rockwell International, North American Aircraft Ops., P.O. Box 92098, L.A., CA, 90009.

14. Adams, F.D., Aeronautical Dictionary, NASA, US Government Printing Office, Washington D.C., 1959.

15. Kohlman, D.L. and Hammer, J., Design Study of Technology Requirements for High Performance Single-Propeller-Driven Business Airplanes, NASA Contractor Report 3863, January, 1985.

16. Nicolai, L.M., Fundamentals of Aircraft Design, METS, Inc., 6520 Kingsland Court, CA, 95120.

17. Torenbeek, E., Synthesis of Subsonic Airplane Design, Kluwer Boston Inc., Hingham, Maine, 1982.

18. Stinton, D., The Design of the Aeroplane, Granada Publishing, London, England, 1983.

19. Küchemann, F.R.S., The Aerodynamic Design of Aircraft, Pergamon Press, London, England, 1978.

20. Abbott, I.H. and Von Doenhoff, A.E., Theory of Wing Sections, Dover Publications, Inc., N.Y., 1959.

21. Shevell, R.S., Fundamentals of Flight, Prentice Hall, Englewood Cliffs, N.J., 1983.

22. McGhee, R.J. and Beasley, W.D., Low-Speed Aerodynamic Characteristics of a 17-Percent-Thick Medium-Speed Airfoil Designed for General Aviation Applications, NASA Technical Paper 1786, December 1980.

23. Hoerner, S.F. and Borst, H.V., Fluid Dynamic Lift, Hoerner Fluid Dynamics, P.O. Box 342, Brick Town, N.J., 08723, 1975.

24. Hoak, D.E., Ellison, D.E. et al., USAF Datcom, Air Force Flight Dynamics Laboratory, WPAFB, Ohio.

14.2 HISTORICAL REFERENCES

1. Mansfield, H., Vision, A Saga of the Sky, Duell, Sloan and Pierce, N.Y., 1956.

2. Mansfield, H., Billion Dollar Battle, David McKay Company, Inc., N.Y., 1965.

3. James, D.N., Gloster Aircraft Since 1917, Putnam, London, 1971.

4. Bowers, P.M., Boeing Aircraft Since 1916, Putnam, London, 1966.

5. Jackson, A.J., Blackburn Aircraft Since 1909, Putnam, London, 1968.

6. Barnes, C.H., Bristol Aircraft Since 1910, Putnam, London, 1970.

7. Mason, F.K., Hawker Aircraft Since 1920, Putnam, London, 1961.

8. Andrews, C.F., Vickers Aircraft Since 1908, Putnam, London, 1969.

9. Taylor, H.A., Fairey Aircraft Since 1915, Putnam, London, 1974.

10. Francillon, R.J., McDonnell Douglas Aircraft Since 1920, Putnam, London, 1979.

11. Francillon, R.J., Lockheed Aircraft Since 1913, Putnam, London, 1982.

12. Barnes, C.H., Handley Page Aircraft Since 1907, Putnam, London, 1976.

13. Tapper, O., Armstrong Whitworth Aircraft Since 1913, Putnam, London, 1973.

14. Taylor, H.A., Airspeed Aircraft Since 1931, Putnam, London, 1970.

15. Andrews, C.F. and Morgan, E.B., Supermarine Aircraft Since 1914, Putnam, 1981.

16. Bowers, P.M., Curtiss Aircraft 1907-1947, Putnam, London, 1979.

17. Jackson, A.J., De Havilland Aircraft Since 1909, Putnam, London, 1962.

18. Brown, D.L., Miles Aircraft Since 1925, Putnam, London, 1970.

19. AIAA Professional Study Series, Case Study in Aircraft Design: The Boeing 727, September 14, 1978.

20. Duval, G.R., British Flying Boats and Amphibians, 1909-1952, Putnam, London, 1966.

21. Lippisch, A., The Delta Wing, Iowa State University Press, Ames, Iowa, 1961.

22. Knott, R.C., The American Flying Boat, U.S. Naval Institute, 1979.

23. Heinemann, E.H. and Rausa, R., Ed Heinemann: Combat Aircraft Designer, U.S. Naval Institute, 1980.

24. Hegener, H., Fokker: The Man and the Aircraft, Aero Publishers, Inc., Fallbrook, CA, 1961.

25. Van Ishoven, A., Messerschmitt: Aircraft Designer, Gentry Books Ltd., London, 1975.

26. Ingells, D.J., L-1011 Tristar and The Lockheed Story, Aero Publishers, Inc, Fallbrook, CA, 1973.

27. Anderson, F., Northrop, an Aeronautical History, Published by Northrop Corporation, Century City, CA, 90067, 1976.

28. Jones, L.S., U.S. Bombers, Aero Publishers, L.A., CA, 1962.

29. Angelucci, E., The Rand McNally Encyclopedia of Military Aircraft 1914-1980, The Military Press, NY, '83.

15. INDEX

AIRPLANE DESIGN

PART III: LAYOUT DESIGN OF COCKPIT, FUSELAGE, WING AND EMPENNAGE: CUTAWAYS AND INBOARD PROFILES

by

Dr. Jan Roskam
Ackers Distinguished Professor
of Aerospace Engineering
The University of Kansas
Lawrence, Kansas

NO PART OF THIS BOOK MAY BE REPRODUCED WITHOUT
PERMISSION FROM THE AUTHOR

Copyright: Roskam Aviation and Engineering Corporation
Rt4, Box 274, Ottawa, Kansas, 66067
Tel. 913-2421624
First Printing: 1986

TABLE OF CONTENTS

TABLE OF SYMBOLS

Symbol	Definition	Dimension

The symbols for flying boat hull geometry are defined in Figure 3.9.

All other symbols used in this part are identical to the symbols used in Parts I, II, V, VI and VII.

Symbols used in Chapter 2 are defined in the text.

Symbols used in Chapter 3 are defined in Part II.

Symbols used in Chapter 4 are defined in Part I.

Symbols used in Chapter 5 are defined in Part II, in Part VI and in Part VII.

Symbols used in Chapter 6 are defined in Part II.

ACKNOWLEDGEMENT
==========

Writing a book on airplane design is impossible without the supply of a large amount of data. The author is grateful to the following companies for supplying the raw data, manuals, sketches and drawings which made the book what it is:

Aerospatiale
Beech Aircraft Corp.
The Boeing Company
British Aerospace Corp.
Cessna Aircraft Company
Fairchild Republic Co.
Gates Learjet Corporation
General Electric Corp.
Pratt and Whitney
Avco Lycoming
Detroit Diesel Allison
The Garrett Corporation
Fairchild Republic
Gates Learjet Corporation
Grumman Aerospace Corp.
Gulfstream Aerospace Corp.
Lockheed Aircraft Corp.
McDonnell Douglas Corp.
Royal Netherlands Aircraft Factory: Fokker
SIAI Marchetti S.p.A.
Teledyne Continental
Hamilton Standard
NASA

A significant amount of airplane design information has been accumulated by the author over many years from the following magazines:

Interavia (Swiss, monthly)
Flight International (British, weekly)
Business and Commercial Aviation (USA, monthly)
Aviation Week and Space Technology (USA, weekly)
Journal of Aircraft (USA, AIAA, monthly)

The author wishes to acknowledge the important role played by these magazines in his own development as an aeronautical engineer. Aeronautical engineering students and graduates should read these magazines regularly.

Nearly all cockpit and fuselage design data as well as most inboard profiles in this book were drawn by Mr. Govert Tukker of Molenaarsgraaf, The Netherlands. The author is grateful to Mr. Tukker for his skill and patience in carrying out this most difficult assignment.

A number of drawings in this book are credited to companies which merged into other companies or ceased operation.

1. INTRODUCTION

The purpose of this series of books on Airplane Design is to familiarize aerospace engineering students with the methodology and decision making involved in the process of designing airplanes.

The series of books is organized as follows:

PART I:	PRELIMINARY SIZING OF AIRPLANES
PART II:	PRELIMINARY CONFIGURATION DESIGN AND INTEGRATION OF THE PROPULSION SYSTEM
PART III:	LAYOUT DESIGN OF COCKPIT, FUSELAGE, WING AND EMPENNAGE: CUTAWAYS AND INBOARD PROFILES
PART IV:	LAYOUT DESIGN OF LANDING GEAR AND SYSTEMS
PART V:	COMPONENT WEIGHT ESTIMATION
PART VI:	PRELIMINARY CALCULATION OF AERODYNAMIC, THRUST AND POWER CHARACTERISTICS
PART VII:	DETERMINATION OF STABILITY, CONTROL AND PERFORMANCE CHARACTERISTICS: FAR AND MILITARY REQUIREMENTS
PART VIII:	AIRPLANE COST ESTIMATION: DESIGN, DEVELOPMENT, MANUFACTURING AND OPERATING

The purpose of PART III is to assist the aeronautical engineering student in making realistic layouts for the following airplane components:

1. Cockpit (also called flightdeck)
2. Fuselage (including tailbooms)
3. Wing
4. Empennage (tails and or canards)
5. Installation of the propulsion system

Chapter 2 provides the necessary data needed to assure realistic design of the cockpit. Included in this material are guidelines for visibility, human factors in terms of control and instrument placement and crew seats. The data provided are for civil and for military applications.

Chapter 3 gives guidelines for fuselage design. The effect of fuselage shape on drag is discussed. Consideration is given to passenger seating arrangements, seats, window and exit placement, cargo and baggage requirements, loading, unloading, and servicing. Examples of typical structural arrangements are given.

Chapter 4 provides information on the layout design of wings. The effects of wing planform design on drag, on lift and on stability and control are discussed. Examples of structural arrangements are given.

Chapter 5 contains guidelines for the layout design of the empennage. The effects of empennage planform design on drag and on stability and control are discussed. Examples of a variety of empennage layouts are given, including example structural layouts.

Chapter 6 presents information helpful in the layout design of the propulsion installation. For propeller installations the effects of propeller type and propeller placement on propulsive efficiency are discussed.

Performance and geometric data are included for piston engines, turbo-propeller engines, jet engines and propfans.

For jet engine installations examples of the layout of inlets are presented.

Many examples are given of the way engines are mounted inside the airframe.

The effect of the propulsive installation on external and internal noise is briefly discussed.

Chapter 7 discusses the problem of preparing an overall structural arrangement, material selection and deciding on the manufacturing breakdown.

Chapter 8 contains a collection of airplane cutaway drawings for both old and recent designs.

The design and integration of the landing gear into an airframe as well as the layout design of most of the necessary systems in an airplane are covered in Part IV.

Discussions of weapon system integration, design for low radar cross sections and examples of typical military loads such as bombs, missiles, external fuel tanks, pods and armored vehicles are also presented in Part IV.

Much of the work involved in arriving at satisfactory airplane layouts is done through drawings and sketches. In industry the bulk of this work is done through 'Computer Aided Design' (CAD) although in many instances a combination of CAD and hand drawing is still being used.

2. COCKPIT (OR FLIGHT DECK) LAYOUT DESIGN

The following considerations play an important role in the layout of a cockpit or a flight deck:

1. The pilot(s) and other crew members must be positioned so that they can reach all controls comfortably, from some reference position.

2. The pilot(s) and other crew members must be able to see all 'flight essential' instruments without undue effort.

3. Communication by voice or by touch must be possible without undue effort.

4. Visibility from the cockpit must adhere to certain minimum standards.

This chapter provides the information, necessary to make realistic layouts of cockpits and/or flightdecks for civil and for military airplanes.

The word 'cockpit' is usually associated with small to medium sized airplanes. The word 'flightdeck' is usually associated with large airplanes. In this textbook these words are used interchangeably.

Section 2.1 contains baseline data on the dimensions and weights of crew members. In laying out cockpit arrangements it is essential that these data are accounted for.

Section 2.2 contains data needed to prepare realistic layouts for cockpit seating and for cockpit controls. Civilian as well as military arrangements are covered.

Section 2.3 presents methods for assuring that minimum standards of visibility from the cockpit are met.

Section 2.4 shows example cockpit layouts for several airplane types.

2.1 DIMENSIONS AND WEIGHTS FOR CREW MEMBERS

Figure 2.1 and Table 2.1 provide baseline data for weights and for dimensions of 'standing' (male) crew members. Notice that the center of gravity of a 'standing' crew member is roughly at the hip joint.

Figure 2.2 and Table 2.2 provide baseline data for dimensions of 'sitting' (male) crew members. Observe, that the center of gravity of a 'sitting' crew member is roughly at the forward intersection of the lower torso and the upper legs.

Note: For female crew members it is suggested to multiply all weight and dimension data by 0.85.

With this information the designer can ensure that all crew members 'fit' into their assigned positions.

Particularly when developing new cockpit or flight deck arrangements it is essential (before going into the mock-up stage) to validate the proposed arrangement. This is done by constructing a 'puppet'. Figure 2.1 can serve as the model for such a puppet. The puppet must be made to the same scale as the drawings of the proposed cockpit. The puppet should be made with rotating joints, using the joint rotation points shown in Figure 2.1. This way it is possible to position the puppet on the drawing board or on the CAD screen in relationship to the proposed interior cockpit contours. Checks for conflicts can then be easily made.

Once the puppet has been positioned in its reference position, a check should be made to ensure that arm and leg motions needed to carry out control manipulation of throttles, stick or wheel, side-arm controller and rudder pedals are indeed feasible. Data for such required control manipulations are given in Section 2.2. Figure 2.3 shows which areas are easy and which areas are difficult to reach for the 'average' crew member.

Figure 2.4 shows scaled views for 'standing' military crew members in typical military gear. Figures 2.5 and 2.6 present scaled views for 'sitting' military crew members. The sizes reflected in Figures 2.4 through 2.6 are for the '90-percentile, male' crew member. For females, the factor 0.85 previously suggested may be used.

References 8 and 9 provide more detailed information about the human body.

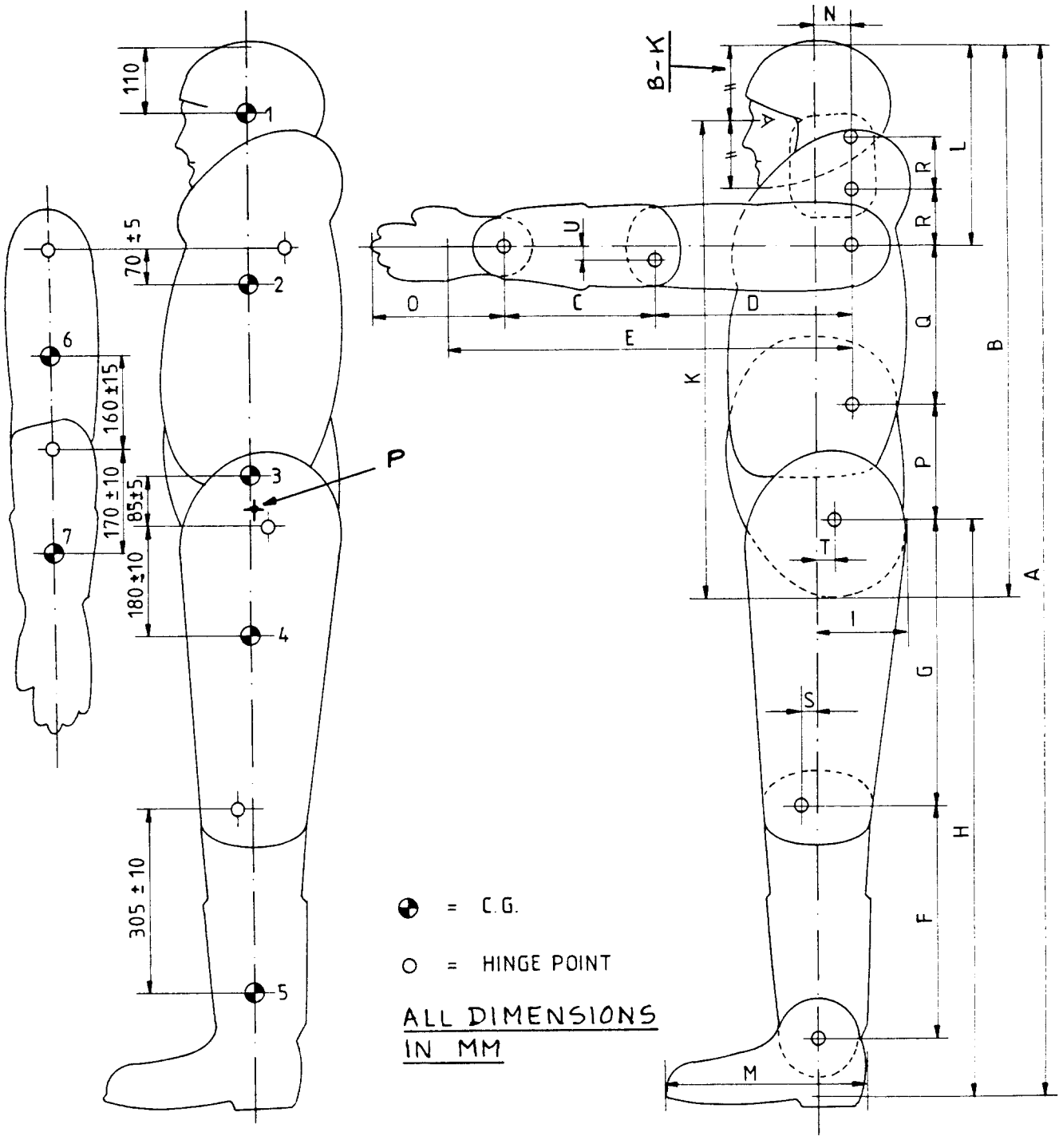

Figure 2.1 Dimensions of Standing, Male Crew Member, Winter Clothing and Light Helmet Included

Table 2.1 Dimensions and Weights for Male Crew Members as Shown in Figure 2.1

A	B	C	D	E	F	G	H	I	K	L
1,600	870	230	300	620	350	435	850	140	760	300
1,750	920	255	335	685	390	475	950	150	805	330
1,900	990	280	370	750	430	515	1,050	160	875	360

A	M	N	O	P	Q	R	S	T	U
1,600	300	50	200	190	260	80	25	20	20
1,750	325	60	220	200	270	90	30	30	20
1,900	350	70	240	210	280	100	30	30	20

Body width across shoulders: 533 mm, across elbows: 561 mm and across hips: 457 mm.

Body component weights are for a male pilot with a weight of 179.3 lbs.

Body Component	Number in Figure 2.1	Weight in lbs.
Head and neck	1	15.0
Upper torso	2	49.0
Lower torso	3	28.0
Upper legs	4	39.9
Lower legs and feet	5	29.8
Upper arms	6	9.9
Lower arms and hands	7	7.7
Total		179.3

Notes:
1. All dimensions in mm. (1 in.=25.4 mm.)
2. The c.g. of the 'upright' pilot of Figure 2.1 is at point P.
3. For pilot positions differing from the upright, the new c.g. can be computed with the help of the table to the left.
4. All weights include helmet and flight clothing.
5. For a female pilot multiply all weight data by 0.81.
6. Data source: Design Requirements for the RAF and RN (England).

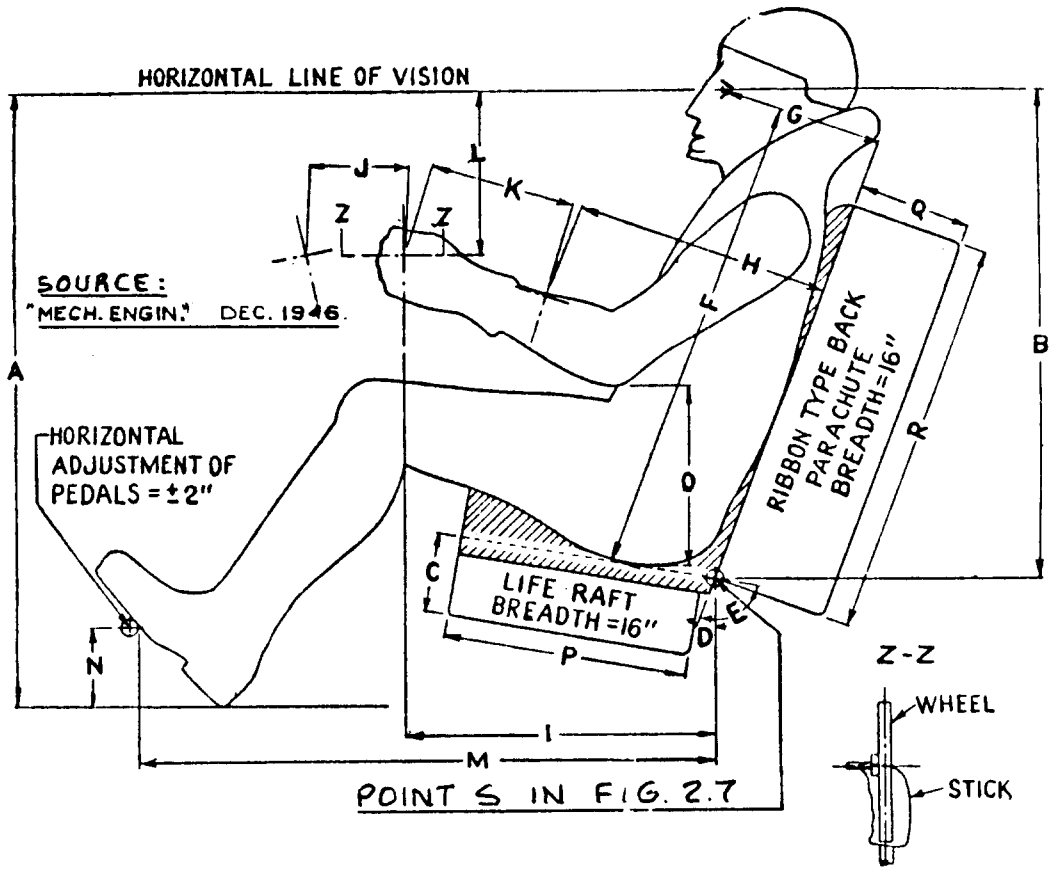

Figure 2.2 Dimensions of Sitting, Male Crew Member, Winter Clothing and Light Helmet Included

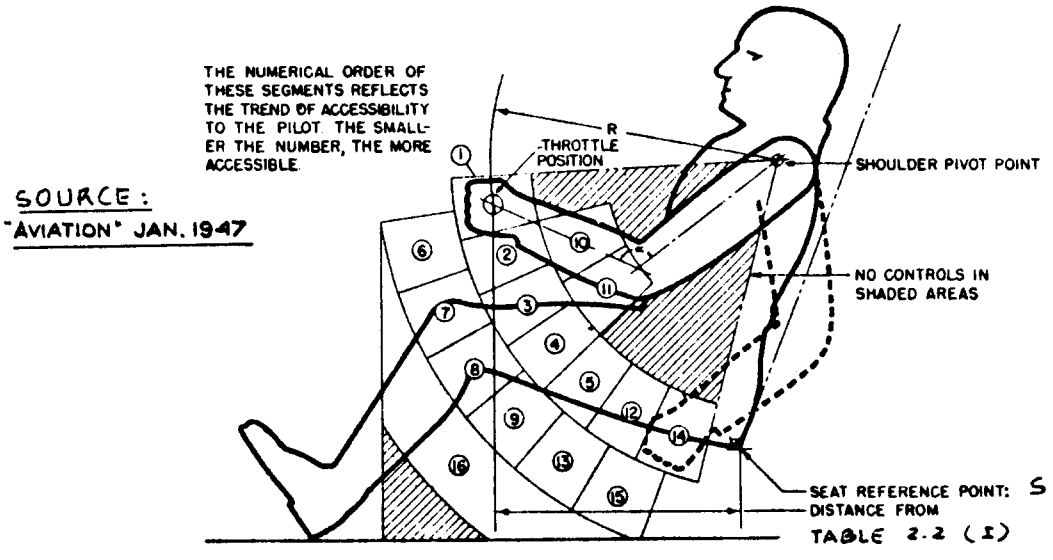

Figure 2.3 Areas of Good and Poor Accessibility

Table 2.2 Dimensions and Weights for Male Crew Members as Shown in Figure 2.2

For Wheel Type Controllers:

A	B	C	D deg.	E deg.	F	G	H	I	J	K
37	30.25	5	21	101	29.75	10.00	16.63	19	6	9
39	30.75	5	19	101	30.25	9.75	15.75	19	6	9
41	31.50	5	16	101	31.00	9.75	15.13	19	6	9
43	31.75	5	16	101	31.25	10.00	15.13	19	6	9

A	L	M	N	O	P	Q	R
37	10.00	36.0	5	9.25	15	7	25
39	10.50	35.0	5	9.25	15	7	25
41	10.75	34.5	5	9.25	15	7	25
43	11.00	34.5	5	9.25	15	7	25

For Stick Type Controllers:

A	B	C	D deg.	E deg.	F	G	H	I	J	K
37	30.25	5	21	101	29.75	10.00	14.50	19	6	9
39	30.75	5	19	101	30.25	9.75	13.75	19	6	9
41	31.50	5	16	101	31.00	9.75	13.50	19	6	9
43	31.75	5	16	101	31.25	10.00	13.00	19	6	9

A	L	M	N	O	P	Q	R
37	11.50	36.0	5	9.25	15	7	25
39	13.75	35.0	5	9.25	15	7	25
41	15.50	34.5	5	9.25	15	7	25
43	17.50	34.5	5	9.25	15	7	25

Seat adjustment: Horizontal: +/- 1.5 in. and Vertical: +/- 3.5 in.

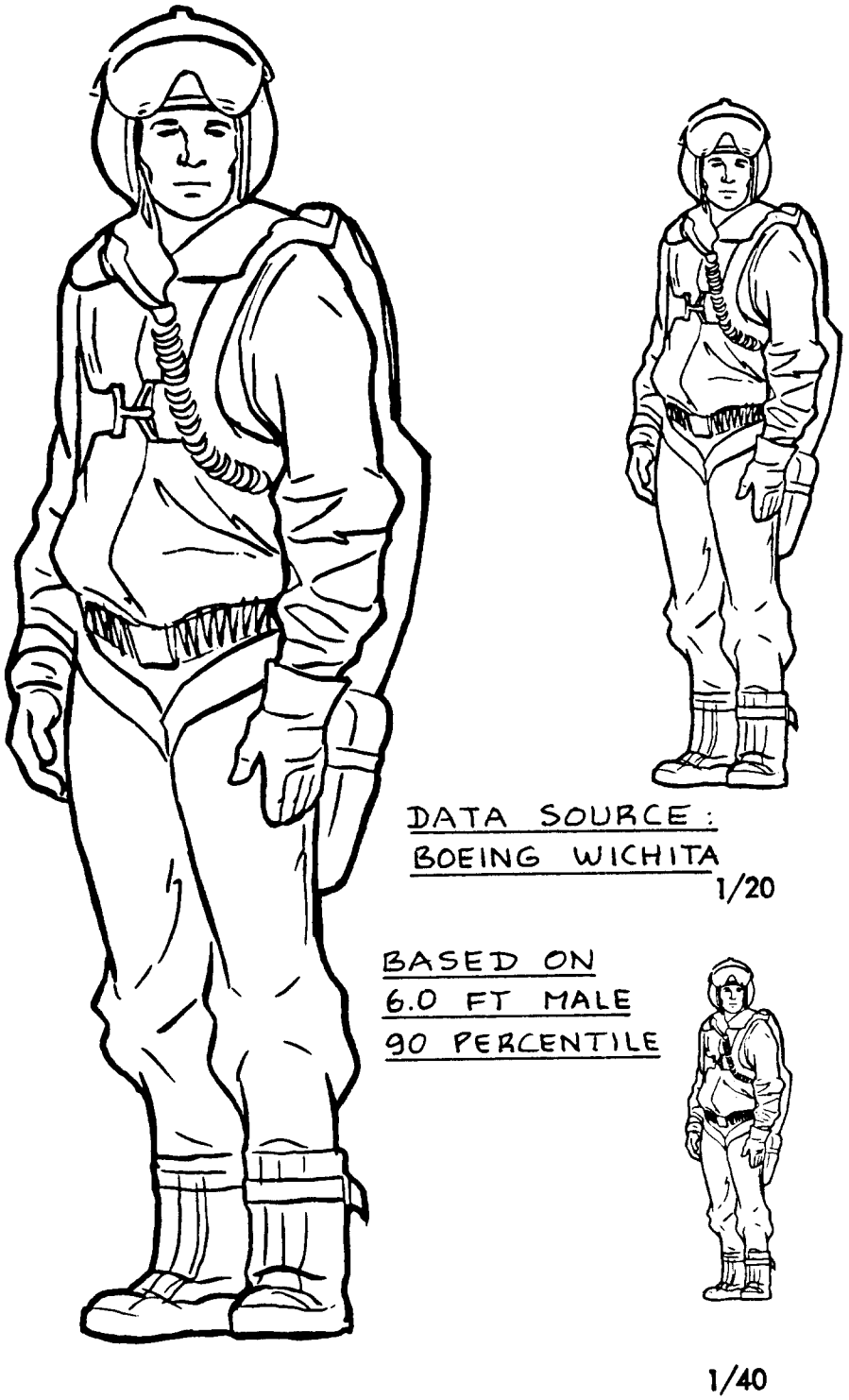

Figure 2.4 Scaled Views of Standing, Male Crew Member in Military Gear

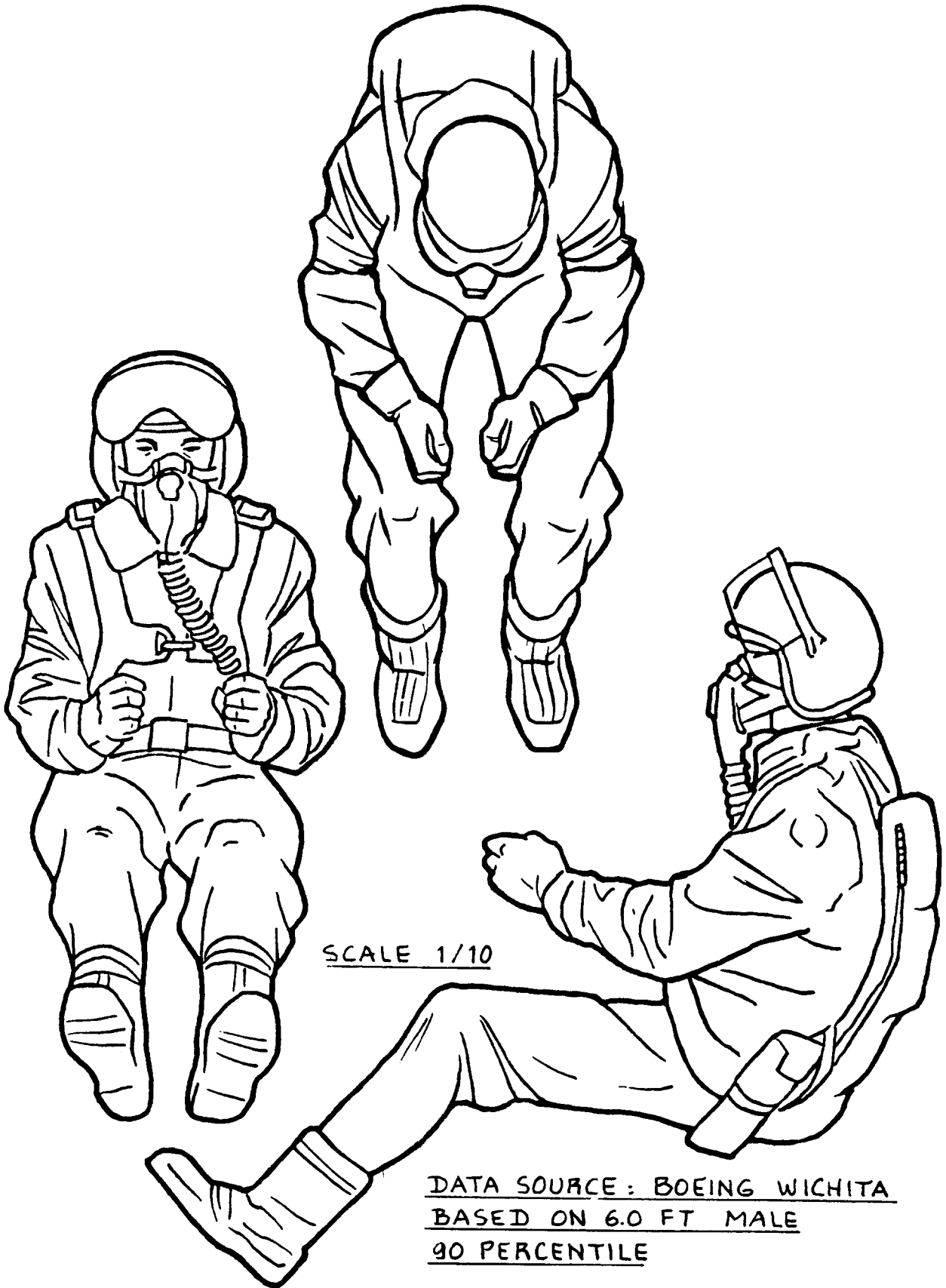

Figure 2.5 Scaled Views of Sitting Male Crew Member in Military Gear

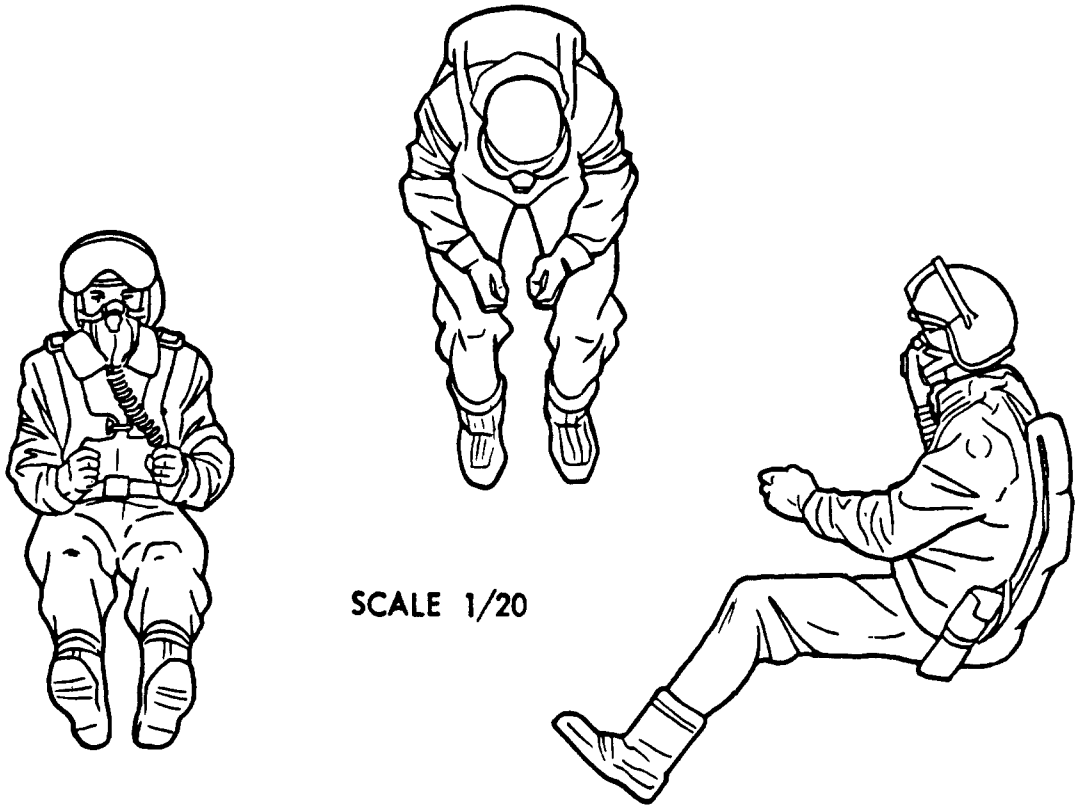

SCALE 1/20

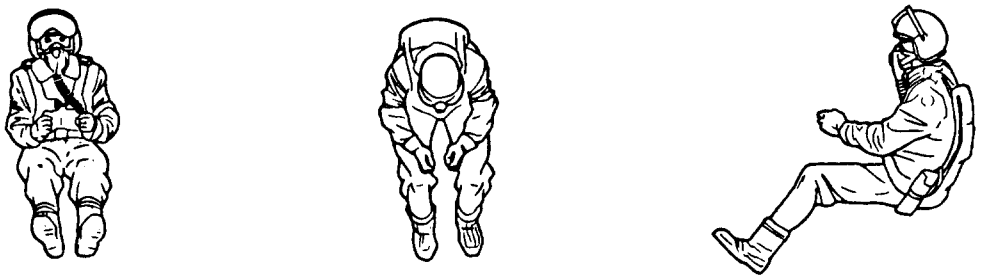

SCALE 1/40

DATA SOURCE : BOEING WICHITA
BASED ON 6.0 FT MALE, 90 PERCENTILE

Figure 2.6 Scaled Views of Sitting, Male Crew Member in Military Gear

2.2 LAYOUT OF COCKPIT SEATING AND COCKPIT CONTROLS

. Two types of cockpit (or flight deck) layout will be considered:

2.2.1 Civil Cockpit Layouts
2.2.2 Military Cockpit Layouts

All cockpit layouts must account for dimensional limitations of the human body. Since humans come in widely differing sizes, the design of cockpits must, to some extent, allow for these variations. This is accomplished by arranging for seat position adjustment and, where needed also for rudder pedal adjustment.

2.2.1 Civil Cockpit Layouts

Figure 2.7 shows a typical arrangement of pilot seat and pilot controls for civil airplanes. The geometric quantities in Figure 2.7 are defined in Table 2.3.

It is not practical to employ a fixed relationship between pilot seating and pilot controls. The reason is that human bodies vary greatly in geometrical dimensions. Typical of the variations that have been measured in adults are:

variation in armlength (C+D+O in Fig.2.1): +/- 15 cm
variation in leglength (H in Fig.2.1): +/- 20 cm
variation in seat-eye distance (c in Fig.2.7): +/- 12 cm

It is of interest to note that no systematic relationship between (C+D+O), H and c has been observed by human factors researchers. This implies that a considerable amount of adjustment must be designed into cockpits. Table 2.3 defines the most important adjustment requirements.

Figure 2.7 applies to wheel controlled and to center-stick controlled airplanes. Adjustment requirements are listed in Table 2.3. Note that a wheel rotation of more than 85 deg. is not acceptable!

For homebuilt, center-stick controlled airplanes the layout of Figure 2.8 can be used. The adjustment requirements previously suggested, apply here also.

In several airplanes, side-stick controllers are now being used. Figure 2.9 shows a typical side-stick controller. In a transport cockpit (such as the Airbus 320) the side-stick controllers are arranged to the left

for the captain (port side) and to the right for the co-pilot (starboard side).

In a side-stick controller layout the pilot's arm must rest on a flat surface. It may be assumed that this 'arm-rest' surface is a distance (L-(B-K)+D) below the pilot's eye position (point C in Figure 2.7).

2.2.2 Military Cockpit Layouts

Guidelines for military cockpit layouts are given in Ref.10. Figure 2.10 shows the recommended layout for center-stick controllers.

Figure 2.11 presents the recommended layout for wheel controllers. Although Figure 2.11 shows that wheel rotation should not exceed 90 deg., MIL-STD-1472B indicates that a limit of 120 deg. is acceptable.

Figure 2.10 applies primarily to fighter and trainer type airplanes, while Figure 2.11 applies primarily to cargo (including transport) and bomber (including patrol) type airplanes.

Many military airplanes are equipped with ejection seats. In that case it is essential that certain minimum clearances are provided, to facilitate ejection. Fig.2.12 shows what these minimum clearance requirements are. Observe that Figure 2.12 also defines the clearance requirements for tandem seat arrangements.

Figure 2.13 gives typical dimensions for an ejection seat.

CAUTIONARY NOTES:

1) Flight essential crew members and their primary cockpit controls should not be located within the 5 degree arcs shown in Figure 2.14.

2) In civil airplanes (FAR 23.771 and FAR 25.771, Ref.11) this 'arc' requirement must be met for propeller driven airplanes only.

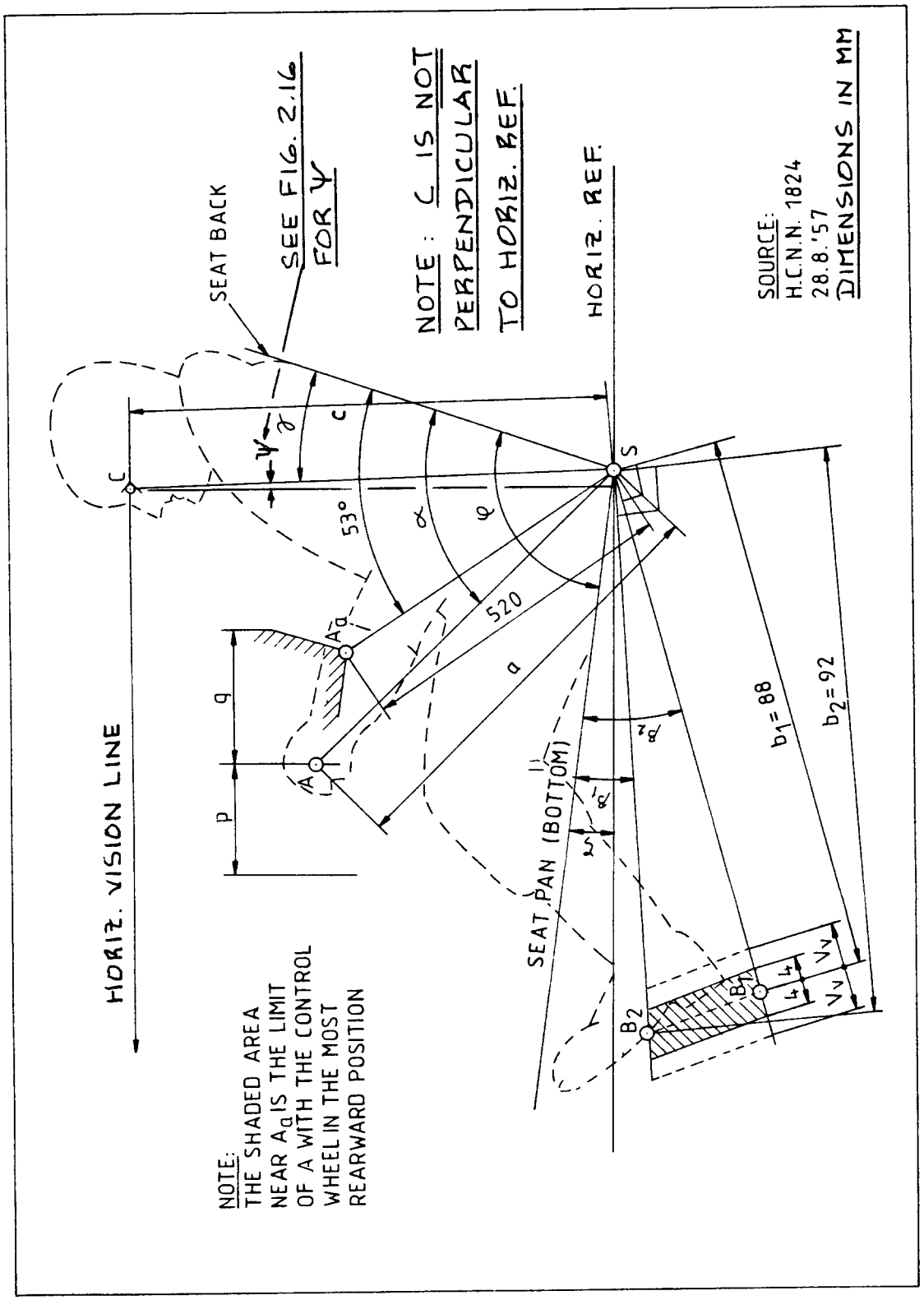

Figure 2.7 Recommended Seat Arrangement for Civil Wheel and Center-stick Controlled Airplanes

Table 2.3 Dimensions for Civil Cockpit Controls and for Seat Adjustments

Notes: 1) See Figure 2.7 for explanation of symbols.
2) All linear dimensions are in cm.
3) All angular dimensions are in deg.

Symbol	Wheel Control	Stick Control
a	67 (+/- 4)	63 (+/- 4)
ξ	7° ($+/- 2^\circ$)	7° ($+/- 2^\circ$)
p = Forward motion of point A:	18 (+/- 2)	16 (+/- 2)
q = Rearward motion of point A:	22 (+/- 2)	20 (+/- 2)
r = Sidewise motion of point A from center*:	-----	15 (+/- 2)
d = Distance between handgrips of wheel*:	38 (+/- 5)	-----
ε = Wheel rotation from center*:	85° (max.)	-----
v = Distance between rudder pedal center lines*:	38 (+/- 12)	45 (+/- 5)
α	64° ($+/- 3^\circ$)	70° ($+/- 3^\circ$)
β_1	22°	same
β_2	10°	same
c	77 (+/- 2)	same
γ	21° ($+/- 1^\circ$)	same
φ	102° ($+/- 2^\circ$)	same
V_v = Adjustment range of pedals from center position B:	7 (+/- 2)	same
U_v = Forward and aft pedal motion from center position B*:	10 (+/- 2)	same
S_h = Horizontal adjustment range of S from center position*:	< 10	same
S_v = Vertical adjustment range of S from center position*:	8 (+/- 1)	same

* Not shown in Figure 2.7.

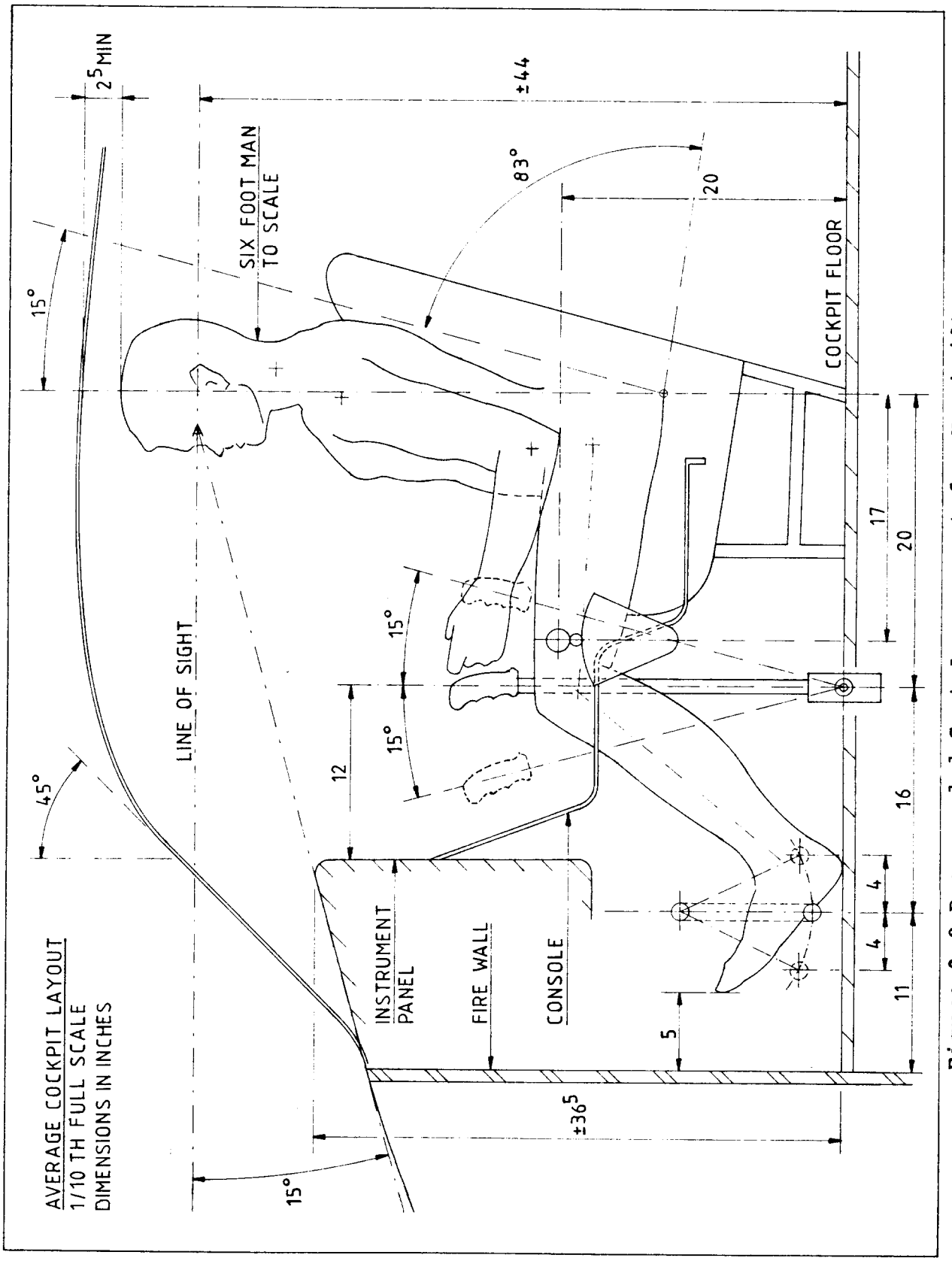

Figure 2.8 Recommended Seat Arrangement for Homebuilt Center-stick Controlled airplanes

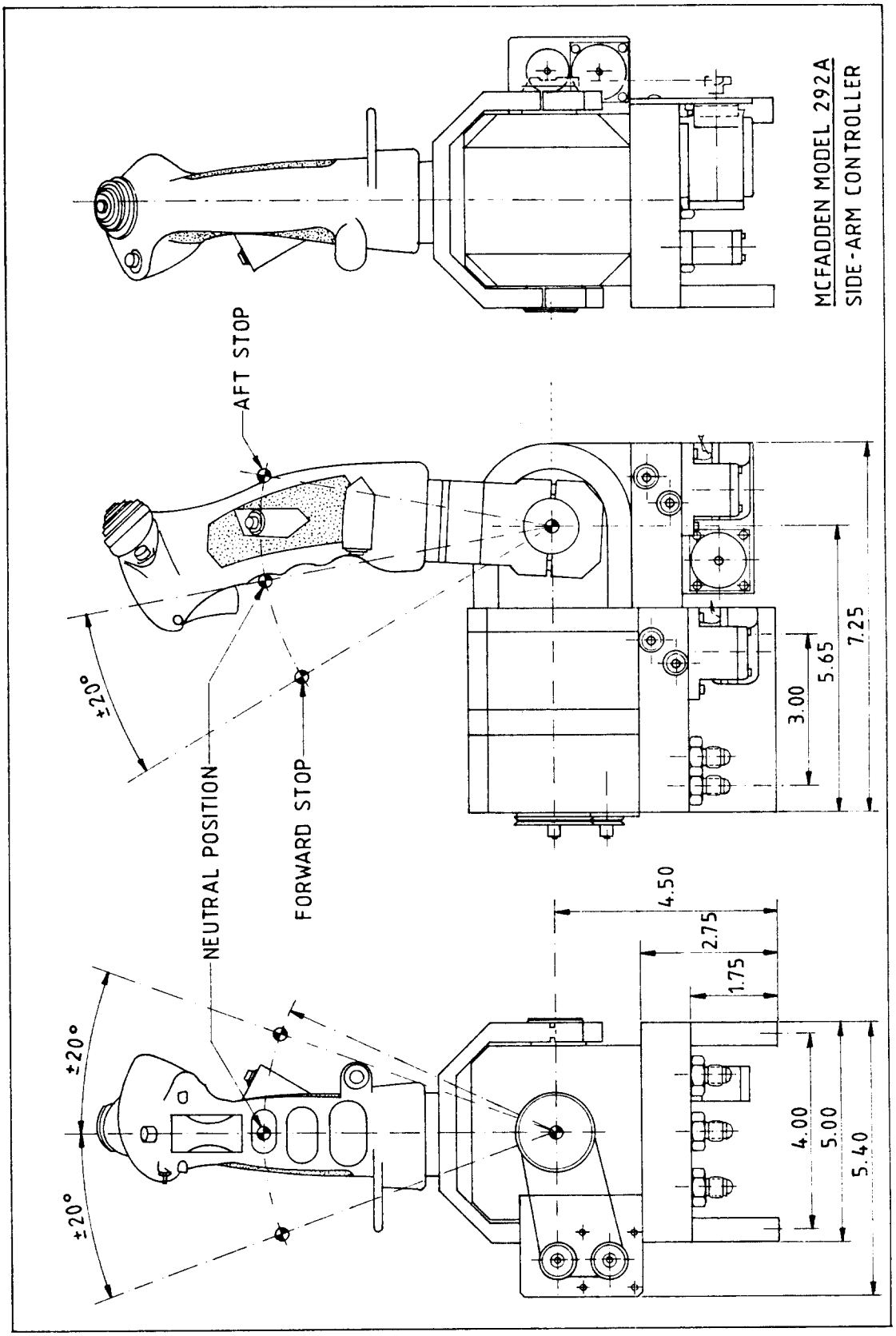

Figure 2.9 Typical Side-stick Dimensions

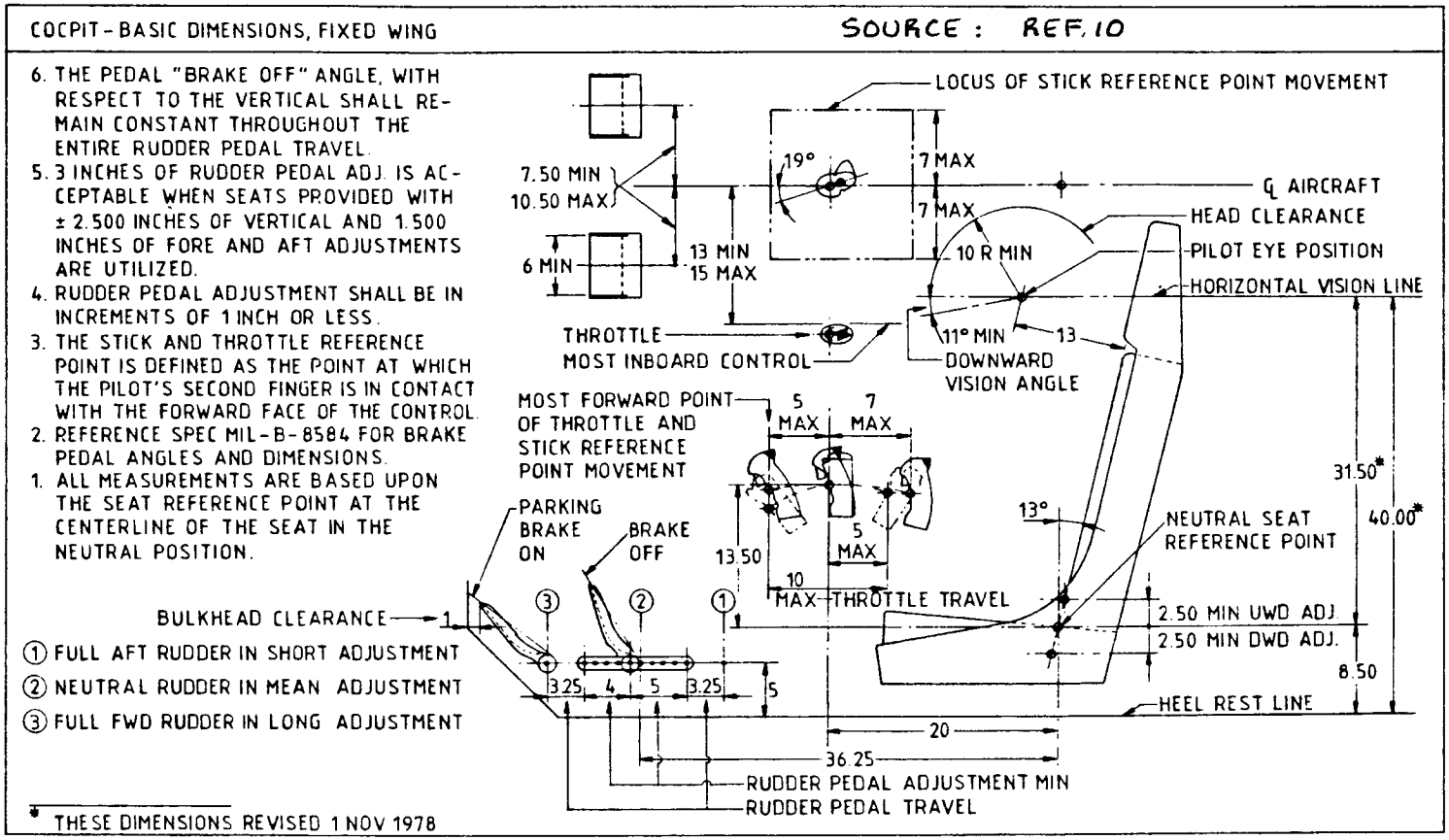

Figure 2.10 Recommended Seat Arrangement for Military, Center-stick Controlled Airplanes

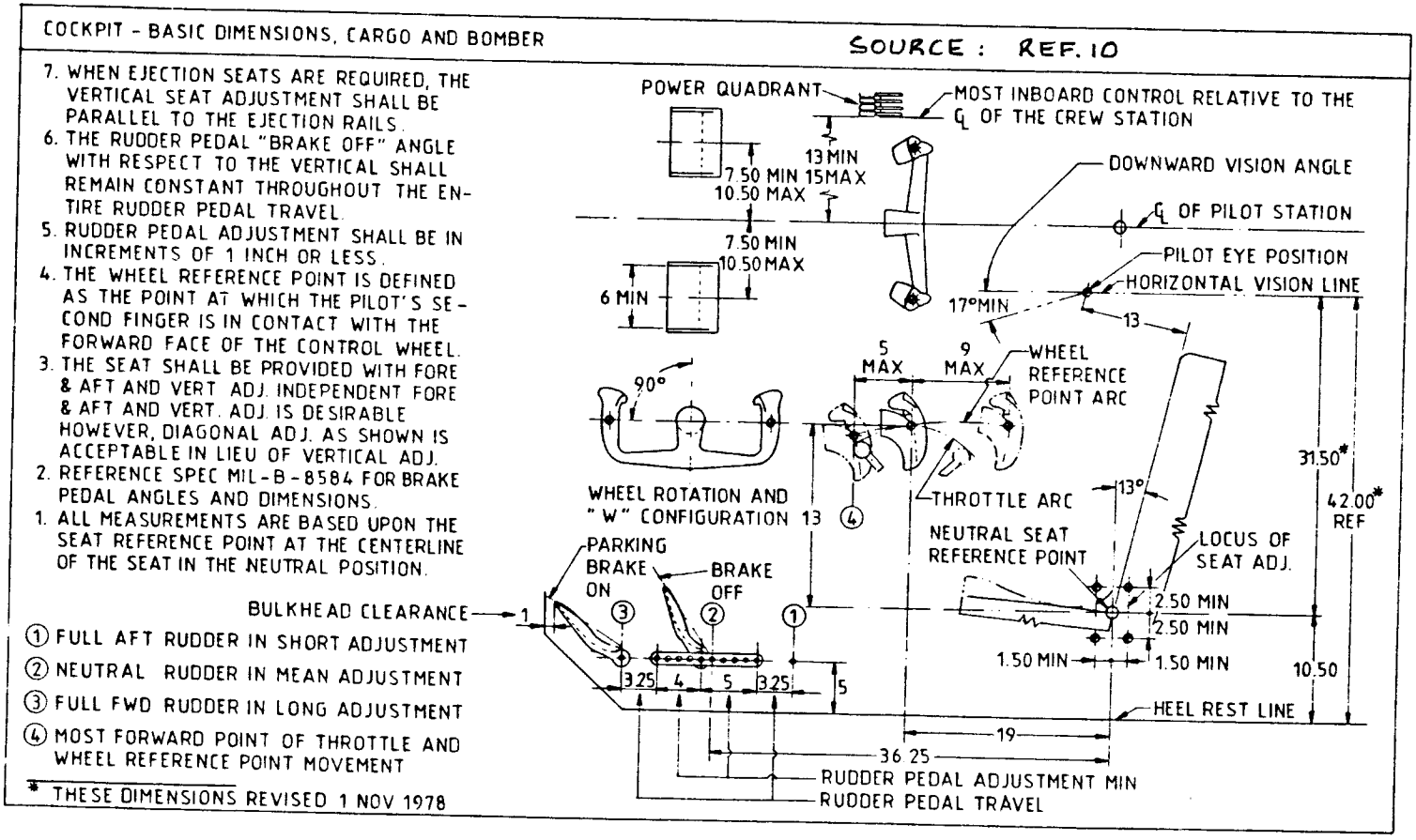

Figure 2.11 Recommended Seat Arrangement for Military, Wheel Controlled Airplanes

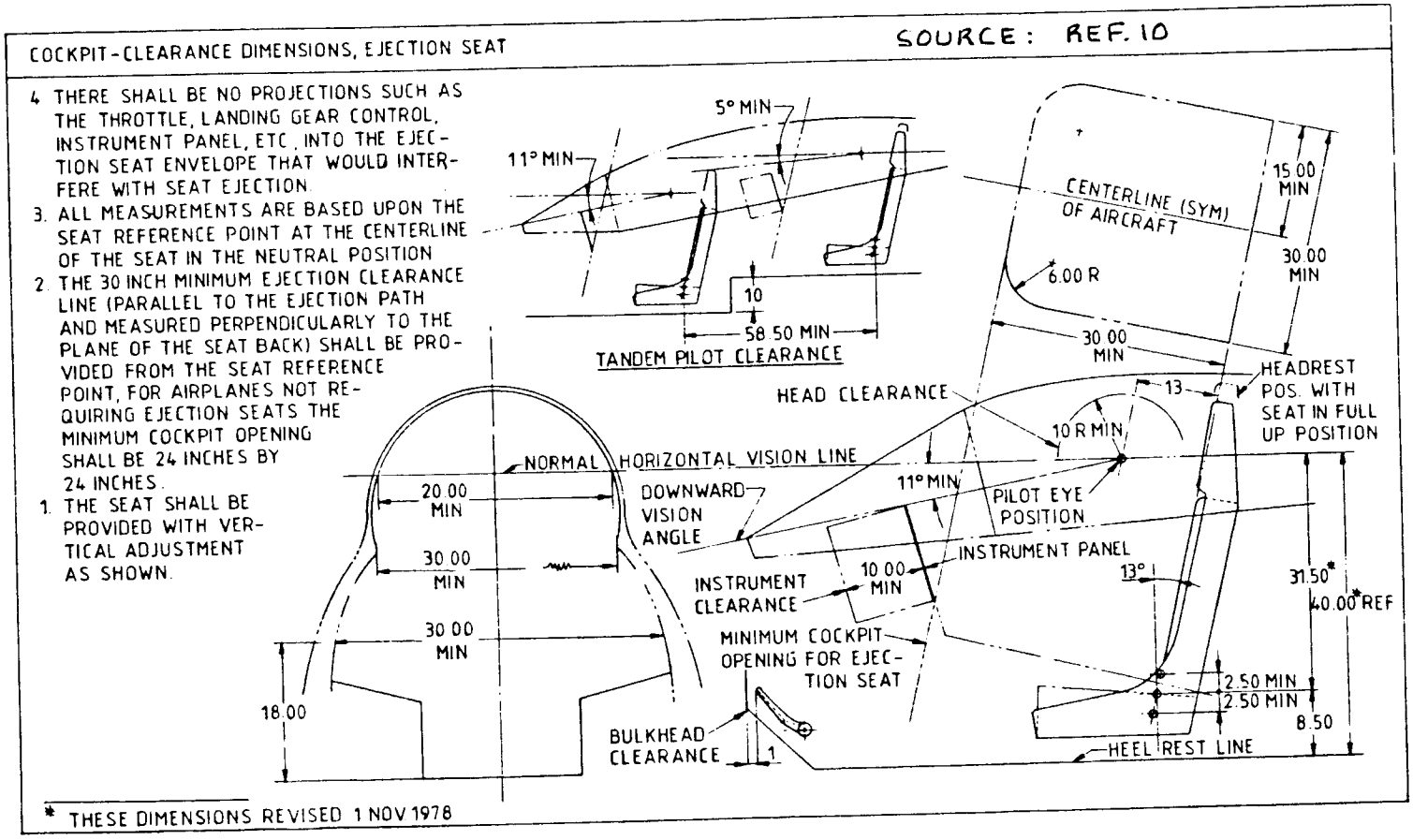

Figure 2.12 Recommended Clearances for Ejection Seats

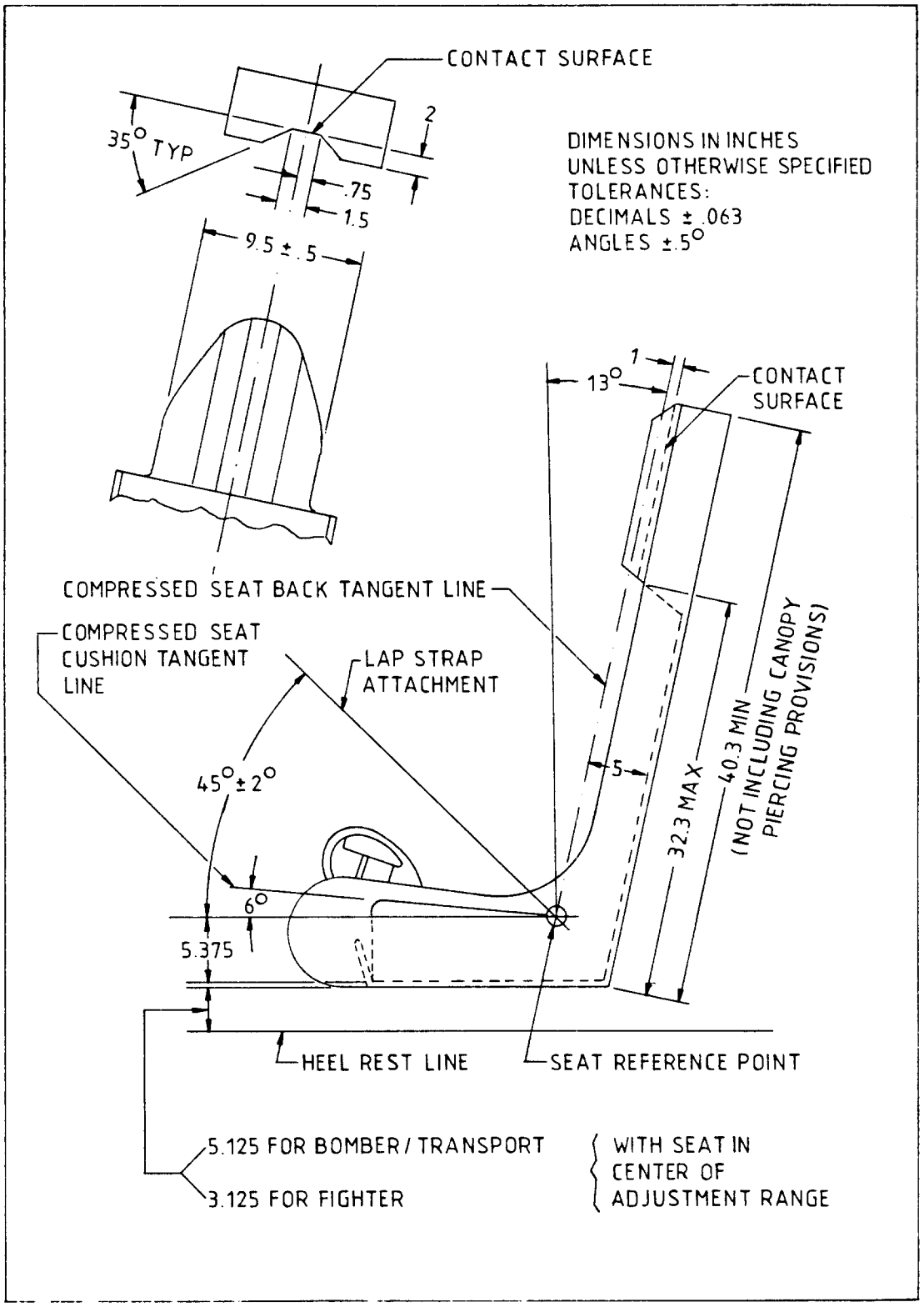

Figure 2.13 Typical Ejection Seat Dimensions

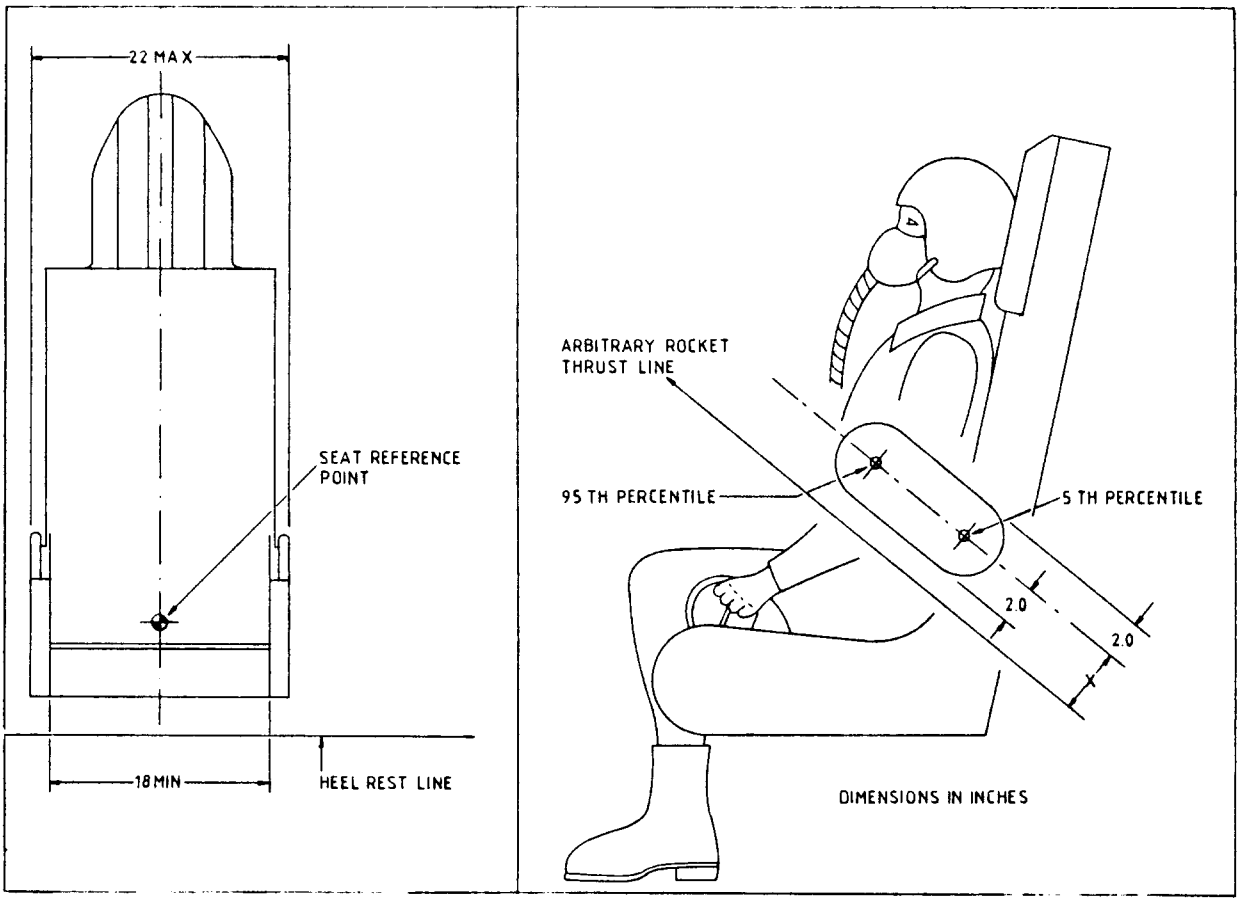

Figure 2.13 (Cont'd) Typical Ejection Seat Dimensions

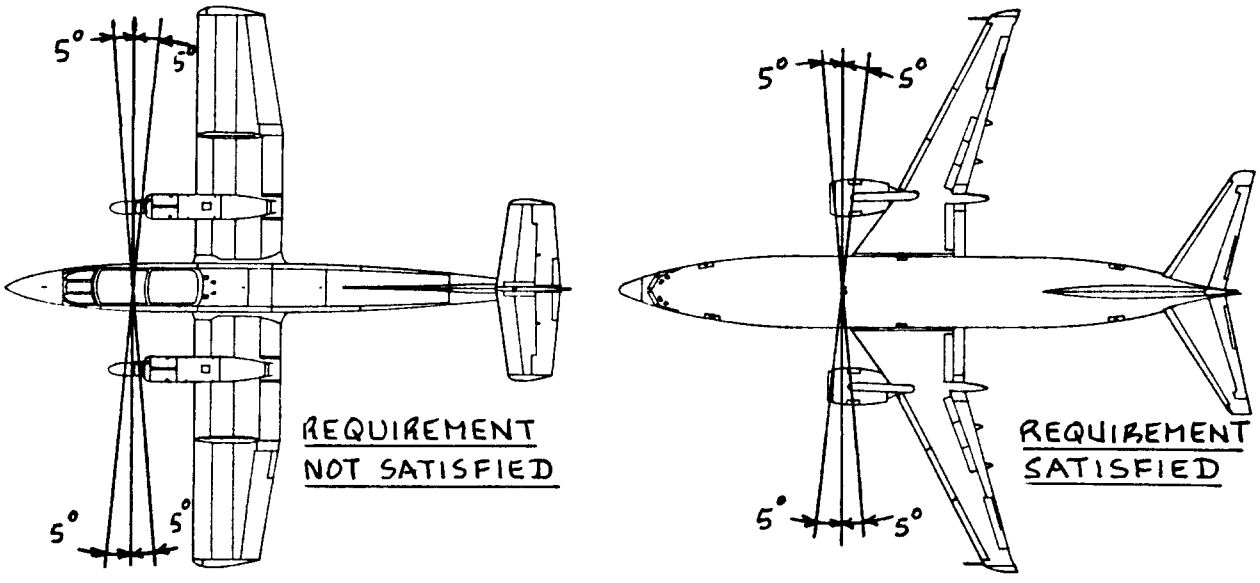

Figure 2.14 Areas Where Pilots and Their Primary Flight Controls Should NOT be Located

2.3 DETERMINATION OF VISIBILITY FROM THE COCKPIT

Good visibility from the cockpit is essential for a number of reasons:

1. During take-off and landing operations a pilot must have a good view of the immediate surroundings.

2. During en-route operations the pilot must be able to observe conflicting traffic.

3. In fighters, success in combat may depend on good visibility. Formation flying is impossible without it.

Minimum cockpit visibility rules are in force for civil as well as for military airplanes. The following definition and visibility design procedure applies to civil and to military transport airplanes. For fighters, trainers and aerobatic airplanes much more stringent visibility requirements are used. The customer defines the minimum required visibility in each specific case.

Visibility from the cockpit is defined as the angular area obtained by intersecting the airplane cockpit with radial vectors emanating from the eyes of the pilot. These radial vectors are assumed to be centered on the pilot's head. Fig.2.15 illustrates a typical situation.

Reference 11 contains rules for minimum visibility of civil airplanes. In implementing these rules, use is made of a horizontal reference plane H, defined in Fig.2.15a. The azimuth and vertical inclination of unobstructed eye vectors are determined as shown in Figure 2.15b. Note in Figure 2.15a that the pilot's eye center is assumed to move on a circle with a radius of 84 mm about the axis of rotation of the pilot's head.

Although pilots generally see through both eyes, it is customary to construct the visibility pattern by assuming that point C (Figure 2.15) is the center of vision.

In laying out a cockpit for acceptable visibility it is important to locate Point C as shown in Figure 2.15b. Point C can then be used to locate the pilot seat. The seat itself must be located relative to the floor and relative to the cockpit controls using the dimensions discussed in Section 2.2. The process is shown in Fig.2.16. It can be broken down into the following steps:

Step 1: Locate point C on the horizontal vision axis as shown in Figure 2.16.

Step 2: Make sure that the distance labelled L_c in Figure 2.15b is within the indicated range.

Step 3: Draw the angle ψ = 8.75 degrees.

Step 4: Locate point S with the help of the distance 'c' as defined in Fig. 2.7 and in Table 2.3. The maximum allowable value for c is 80 cm.

Step 5: Orient the pilot seat in accordance with the dimensions of Figure 2.7.

Step 6: Draw in the areas required for cockpit control and for seat motions and adjustments.

Step 7: Check the minimum required visibility with the visibility rules of Figs 2.15 and 2.16.

1. In transports with side-by-side pilot seating there shall be no obstructing window frames in the area from 30° starboard to 20° port: See Figure 2.17.

2. In the area from 20° port to 60° port, window frames may not be wider than 2.5 inches.

3. Figure 2.17 illustrates the combined azimuth and vertical inclination areas where cockpit visibility cannot be obstructed.

Figure 2.18 shows the 'ideal' visibility pattern.

In reality it is very difficult to achieve the 'ideal' visibility pattern. Large windows require very stiff frames. Both windows and frames must meet the 'birdstrike' requirement (Ref.11, FAR 25.775). The larger the windows and the stiffer the frames, the more weight this means.

Another problem is drag. Large flat windows result in large drag increments. Curved windows on the other hand offer low drag but may lead to image distortions.

In reality it is therefore necessary to strike a compromise. Figure 2.19 illustrates typical visibility patterns in certified transports. These patterns illustrate that compromises are indeed accepted.

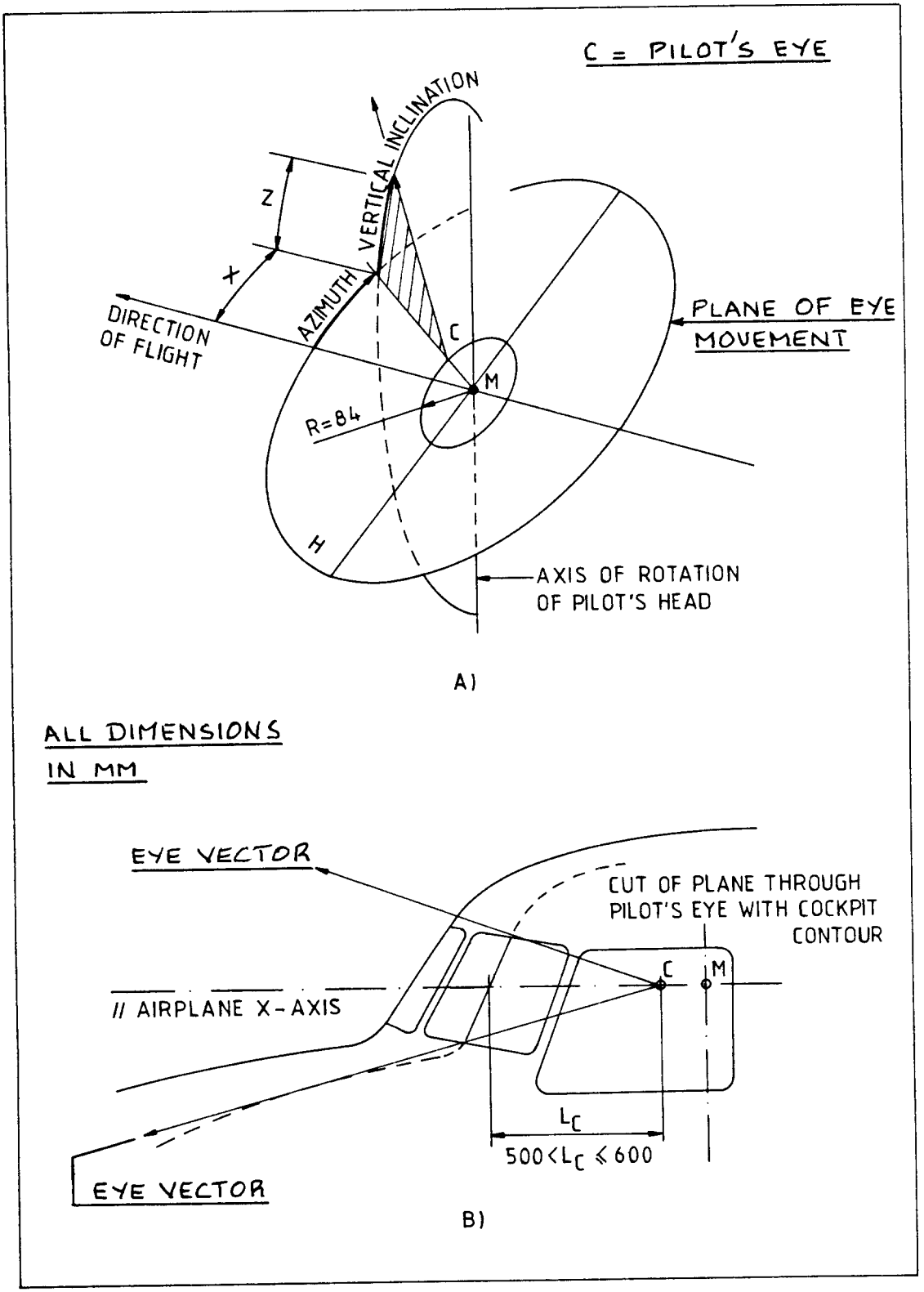

Figure 2.15 Definition of Radial Eye Vectors

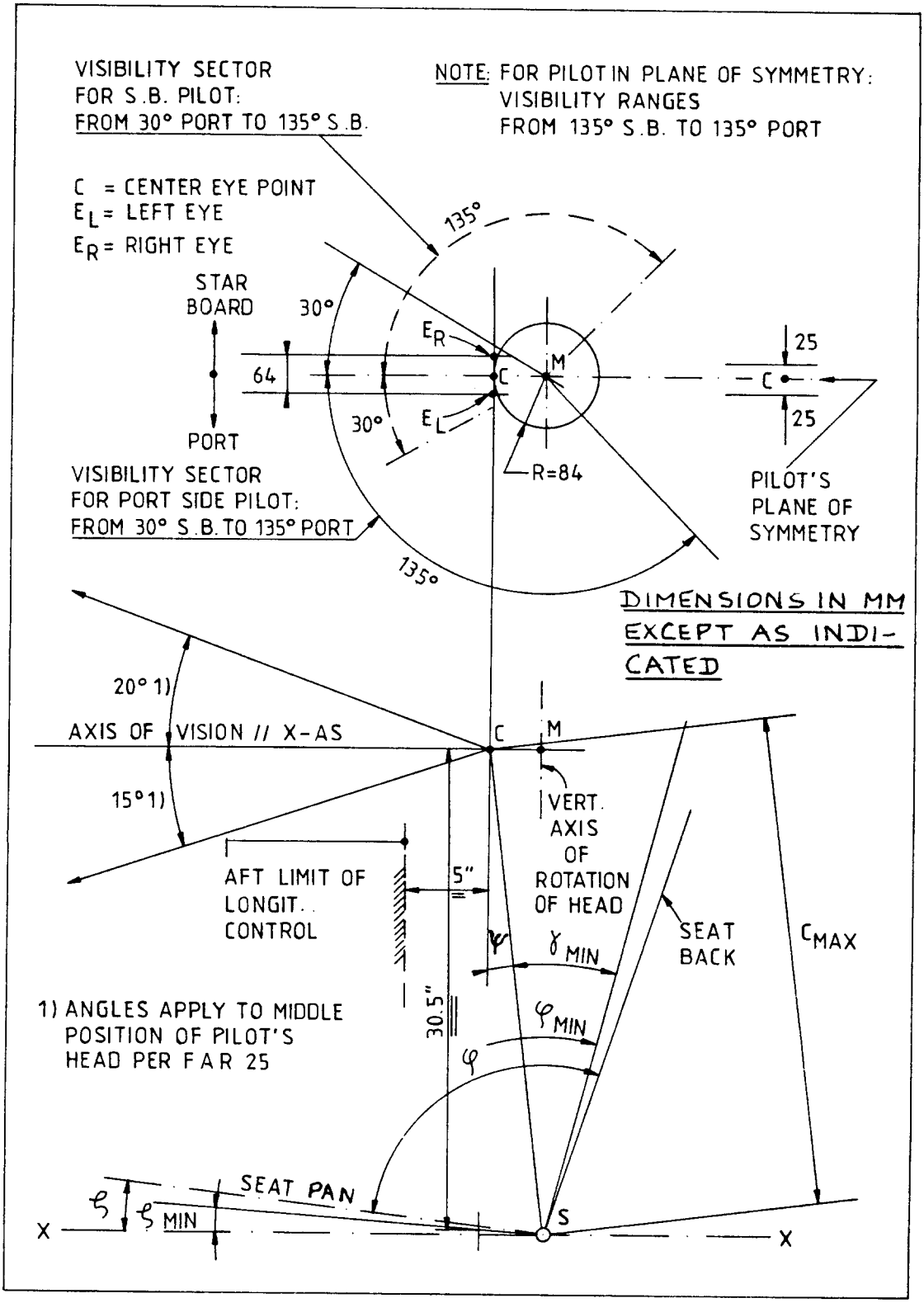

Figure 2.16 Visibility Requirements for the Port and for the Starboard Side and the Connection with Acceptable Seat Arrangements

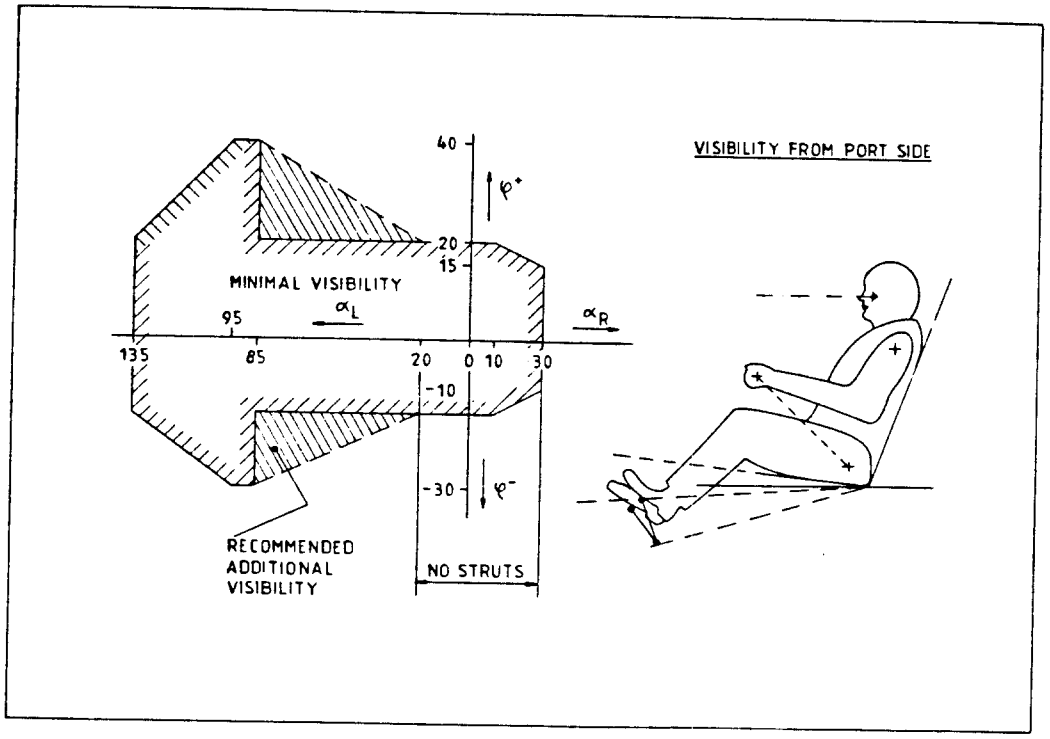

Figure 2.17 Minimum Recommended Visibility Pattern for for the Port Side

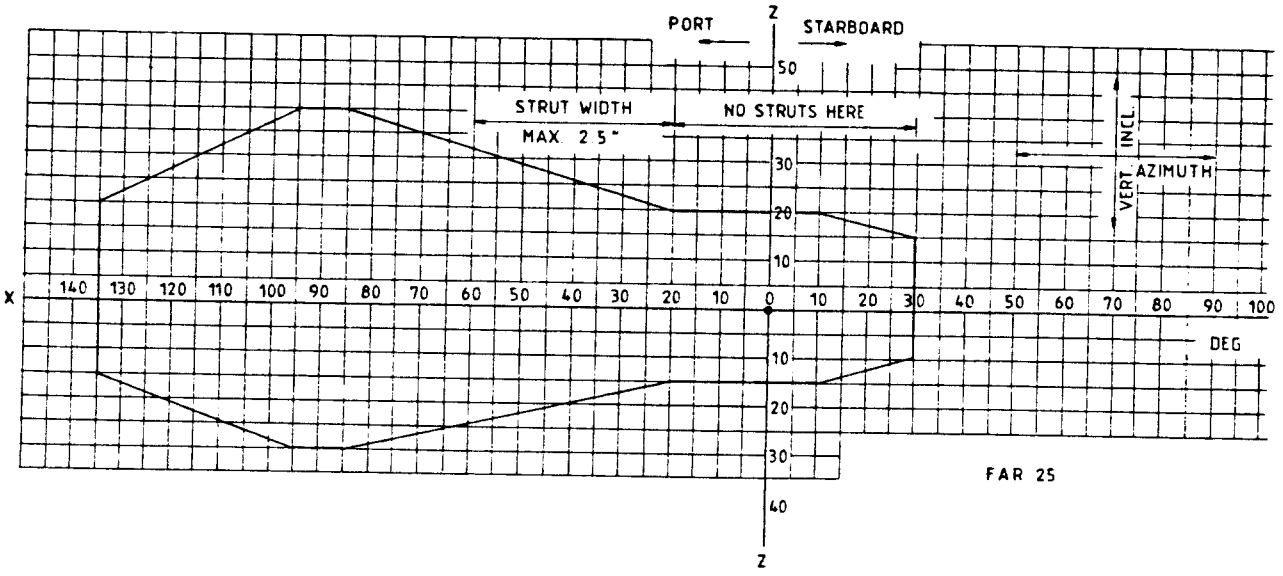

Figure 2.18 Ideal Minimum Visibility Pattern for Transport Airplanes

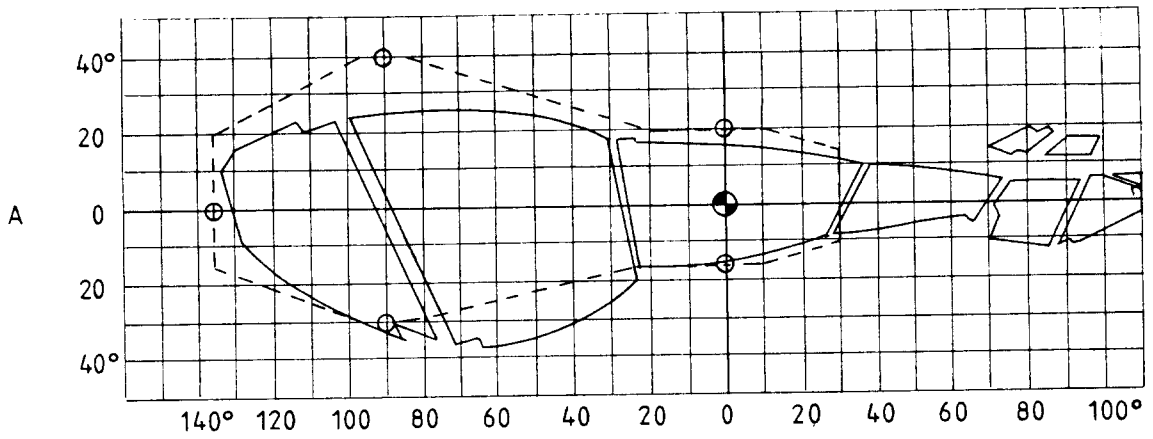

A) VISIBILITY PATTERN BOEING 727
POINT C IS 43" ABOVE HEEL REST AND 5" BEHIND THE MOST AFT POSITION OF THE LONGITUDINAL CONTROLS

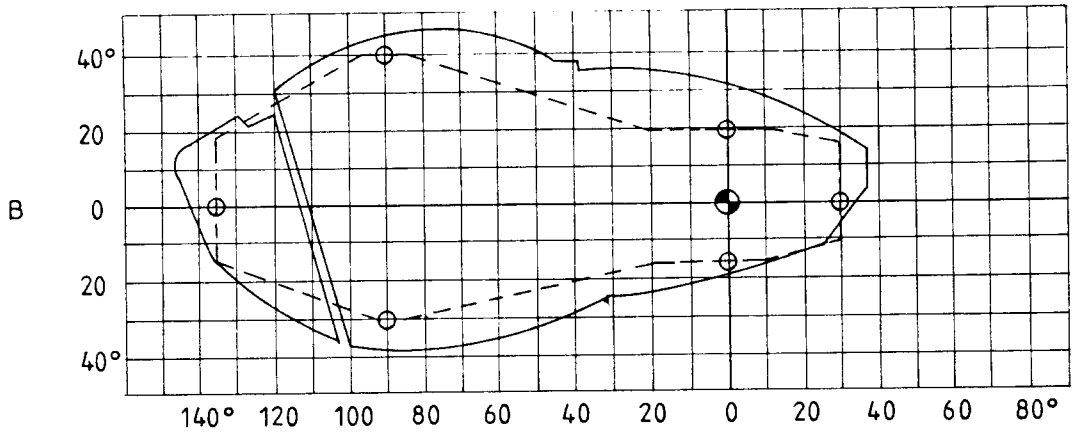

B) VISIBILITY PATTERN BOEING 727
POINT C IS 43" ABOVE HEEL REST AND IMMEDIATELY ABOVE THE MOST AFT POSITION OF THE LONGITUDINAL CONTROLS

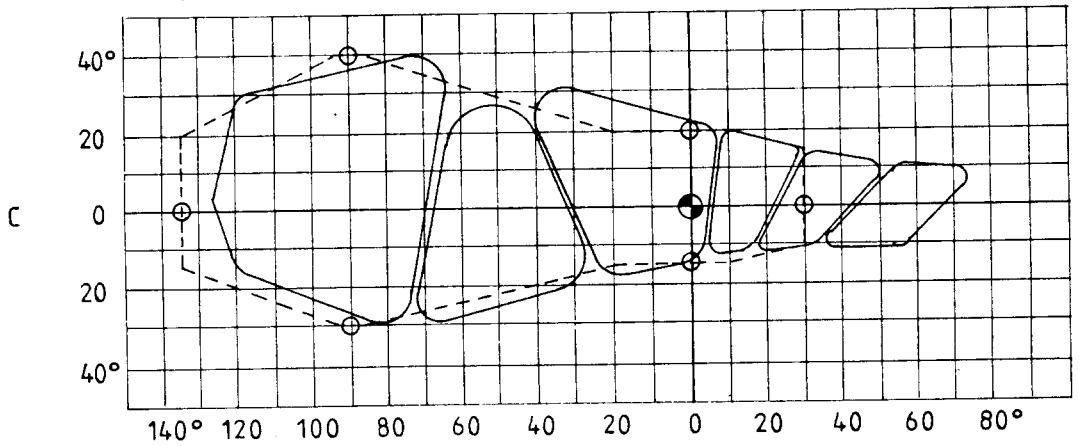

C) VISIBILITY PATTERN SUD-CARAVELLE

SOURCES: A), B) FROM BOEING
C) FROM TECHNIQUE ET SCIENCE "AERONAUTIQUES ET SPATIALES" MAY-JUNE 1962

– – – – – REQUIRED BY FAR 25
——— MEASURED

Figure 2.19 Typical Visibility Patterns for Three Transport Airplanes

2.4 EXAMPLES OF COCKPIT LAYOUTS

Figures 2.20 through 2.27 present examples of cockpit layouts for FAR 25 certified transports and for fighters. For typical cockpit layouts of FAR 23 certified airplanes the reader should refer to the examples of cabin arrangements for these airplanes as presented in Chapter 3.

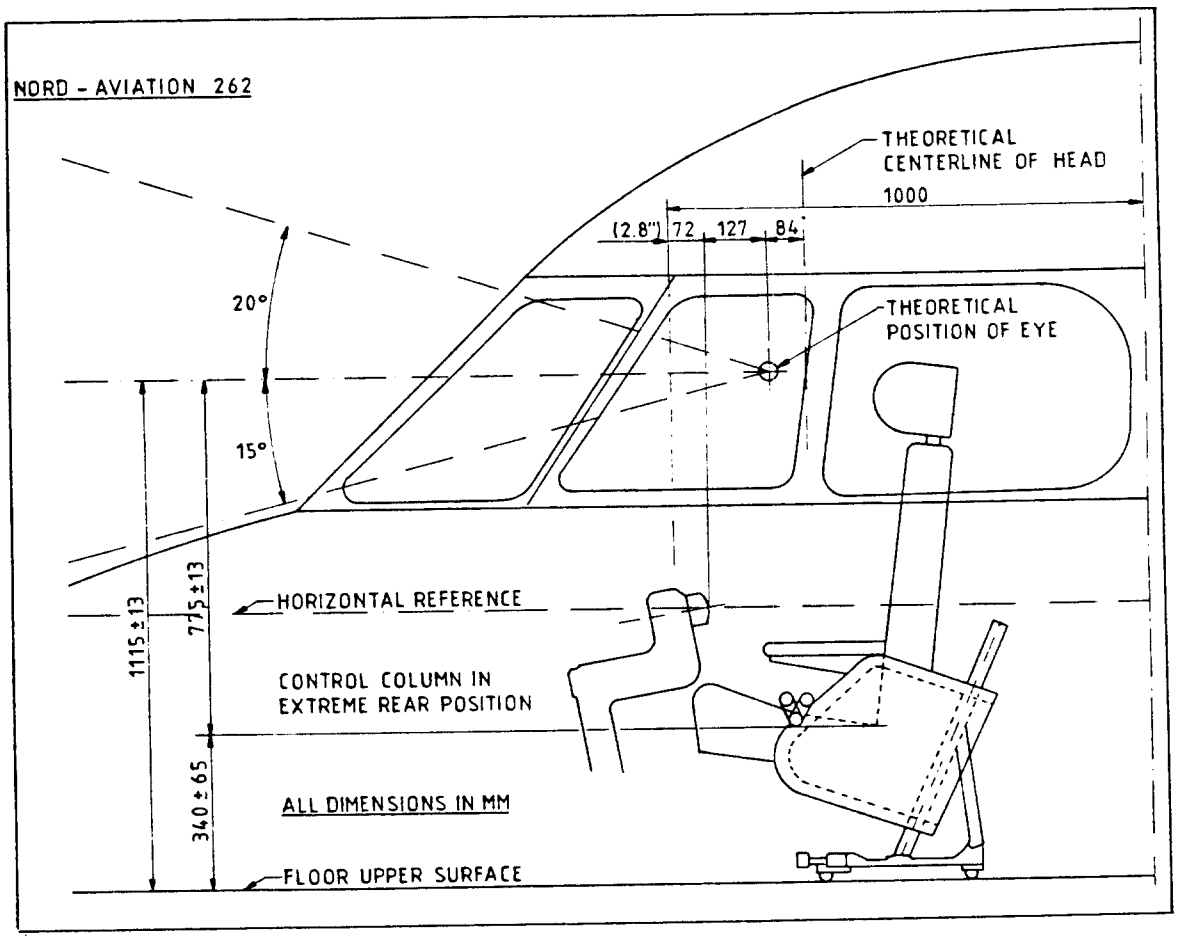

Figure 2.20 Cockpit Layout: Nord 262

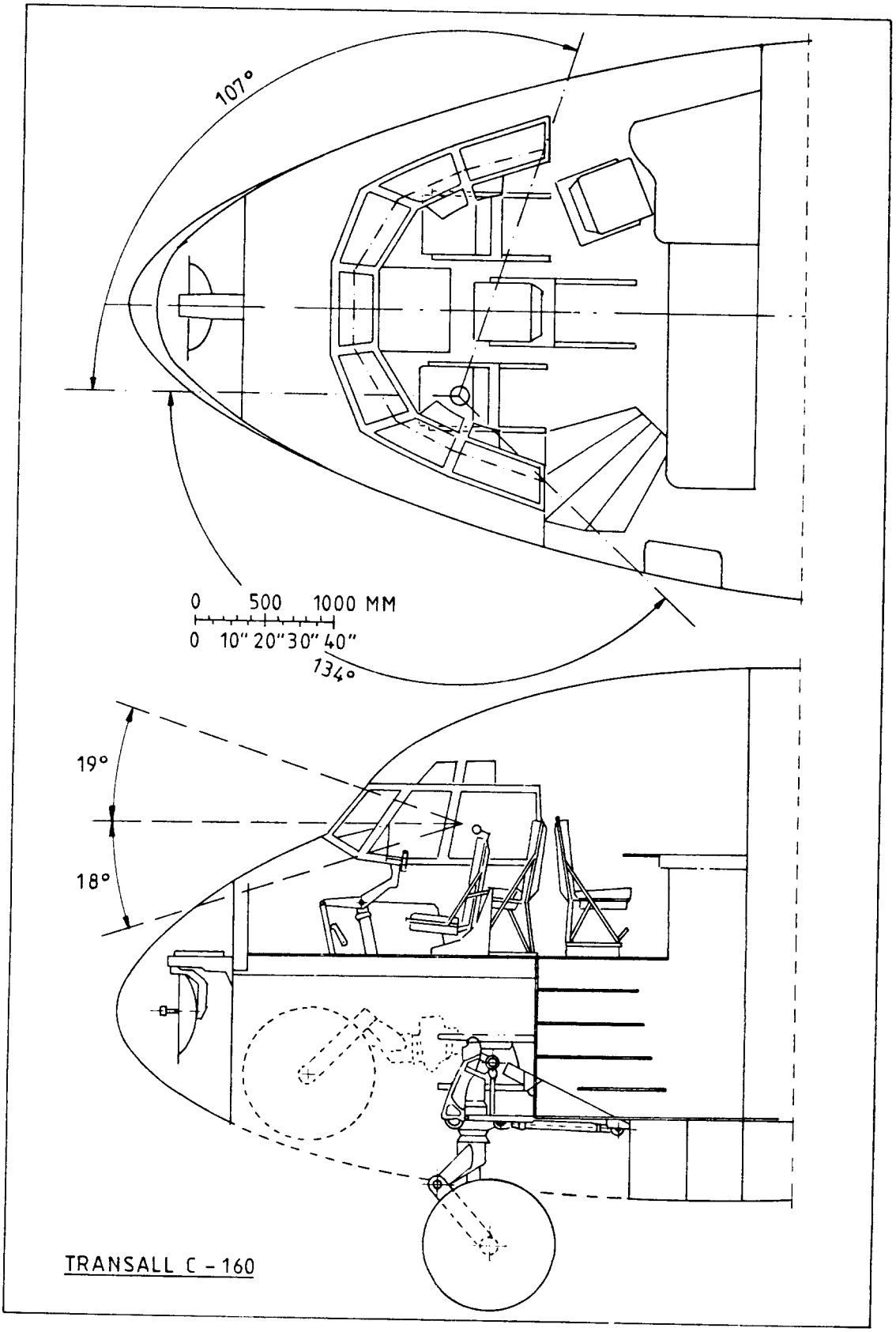

Figure 2.21 Cockpit Layout: Transall C-160

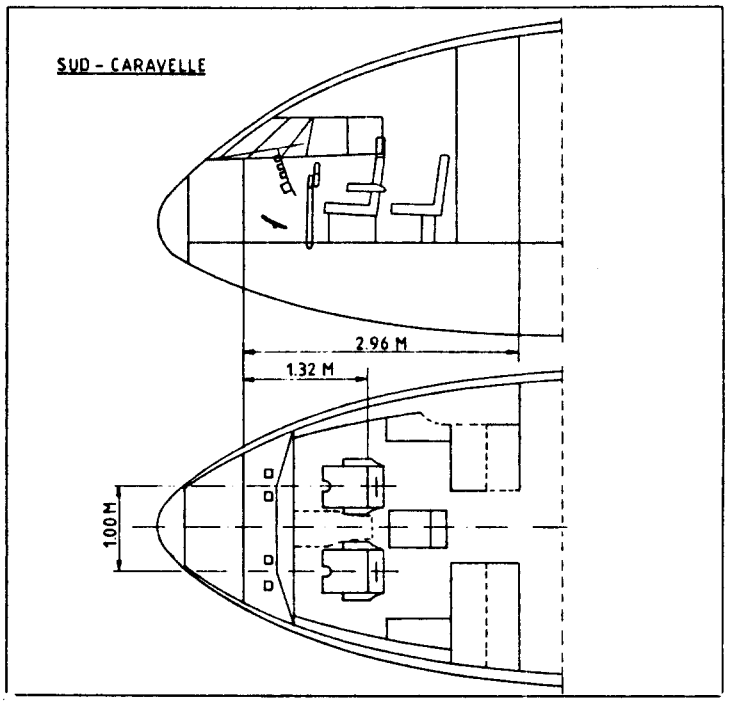

Figure 2.22 Cockpit Layout: Sud Caravelle

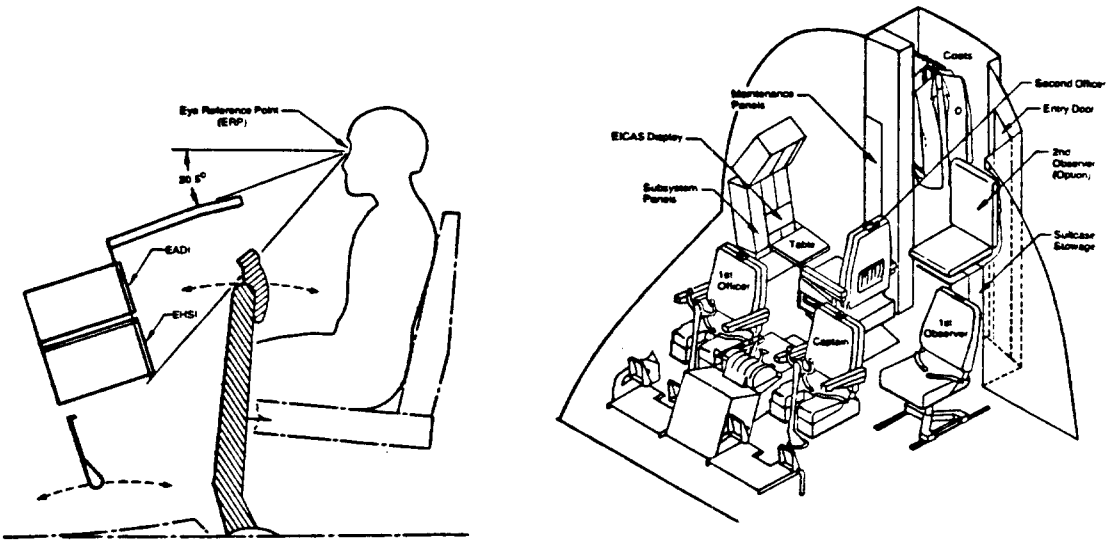

Figure 2.23 Cockpit Layout: Boeing 767 (Three Crew Alt.)

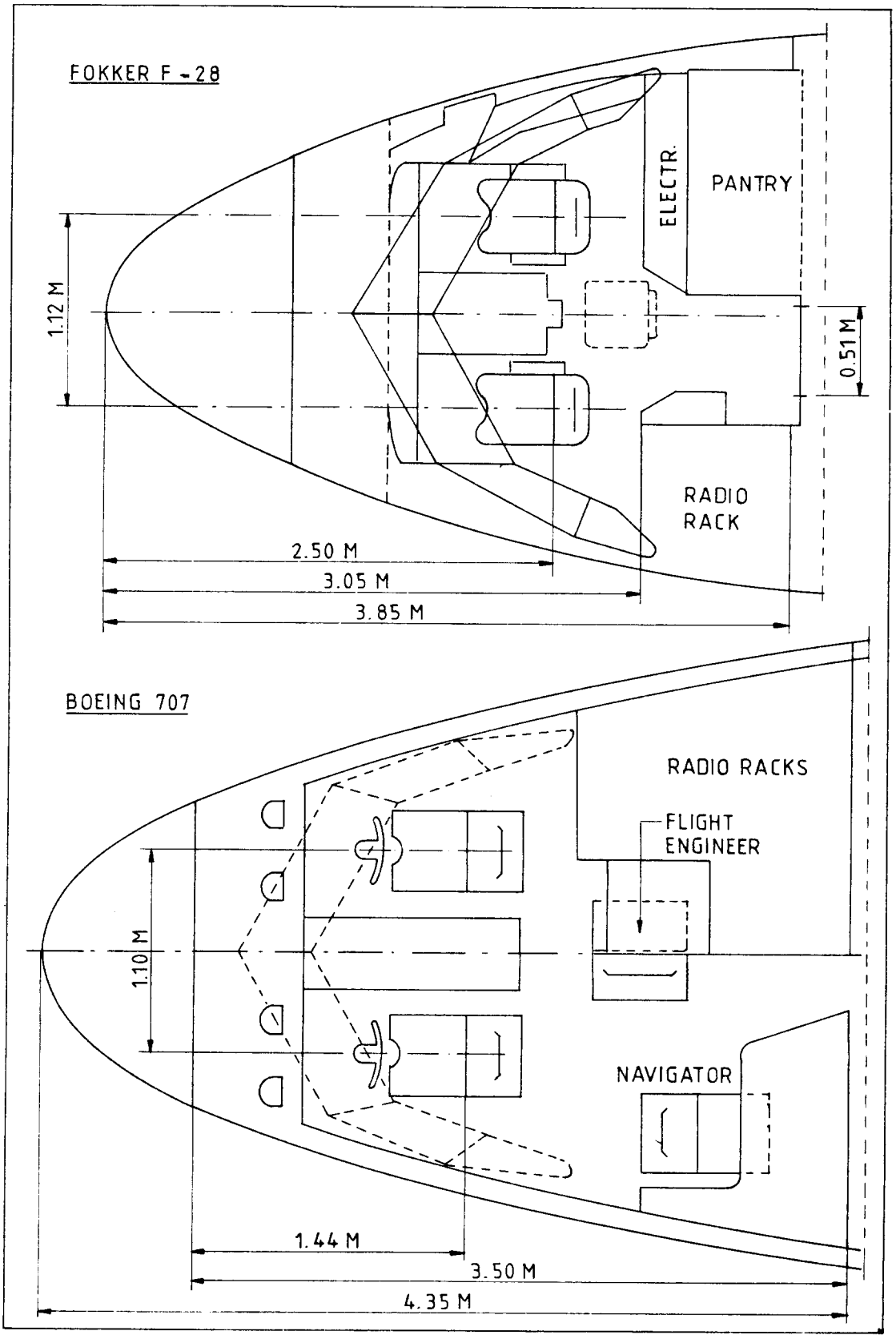

Figure 2.24 Cockpit Layout: Fokker F28 and Boeing 707

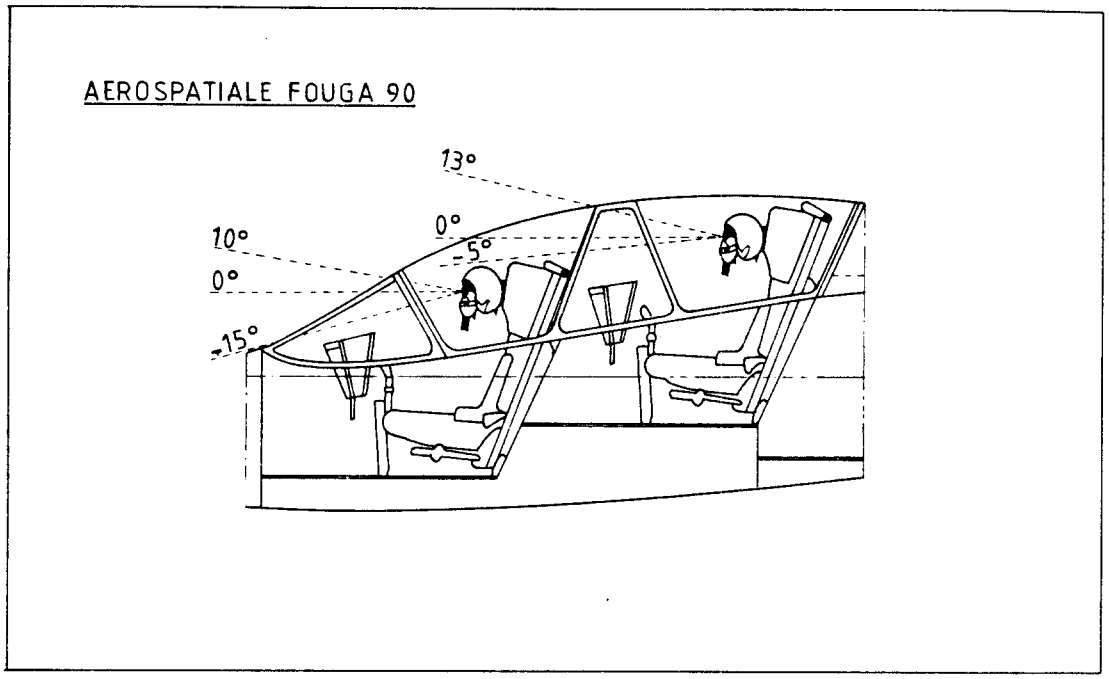

Figure 2.24 Cockpit Visibility and Layout: Fouga 90

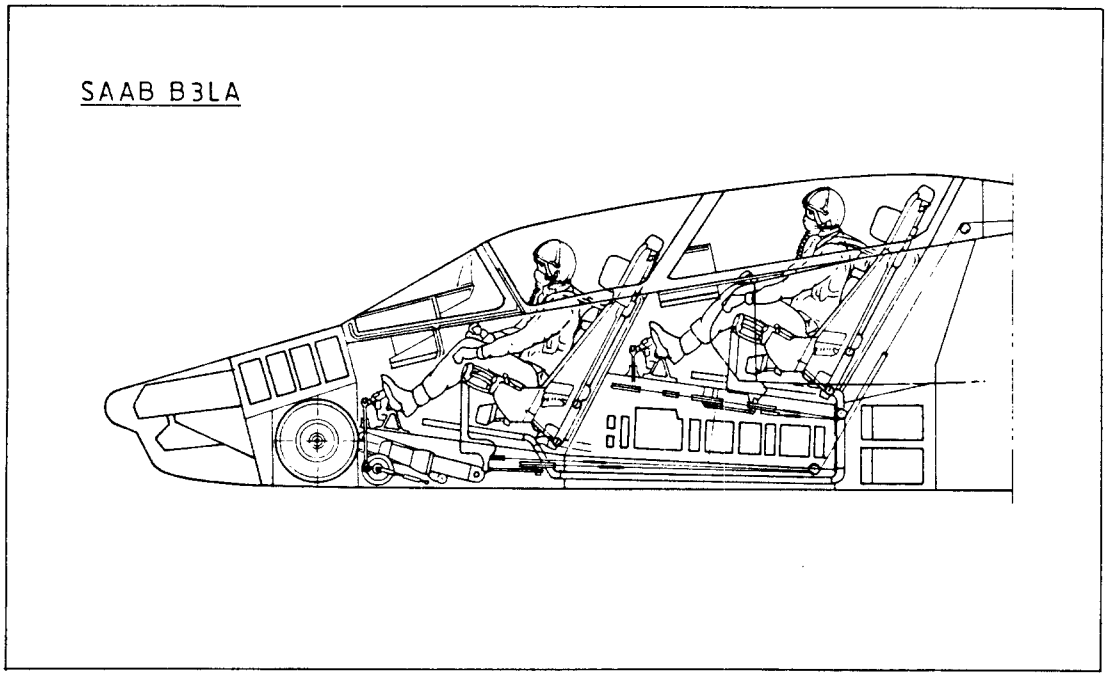

Figure 2.25 Cockpit Layout and Inboard Profile: SAAB B3LA

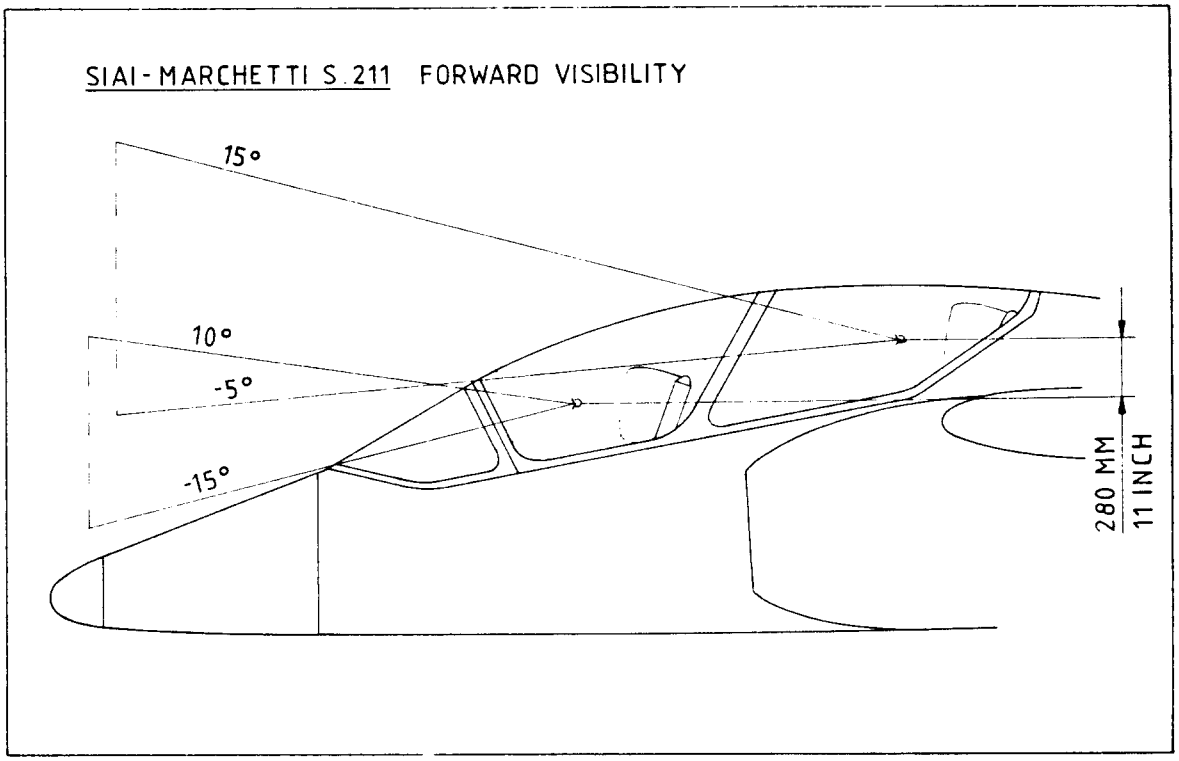

Figure 2.26 Visibility Pattern: SIAI-Marchetti S211

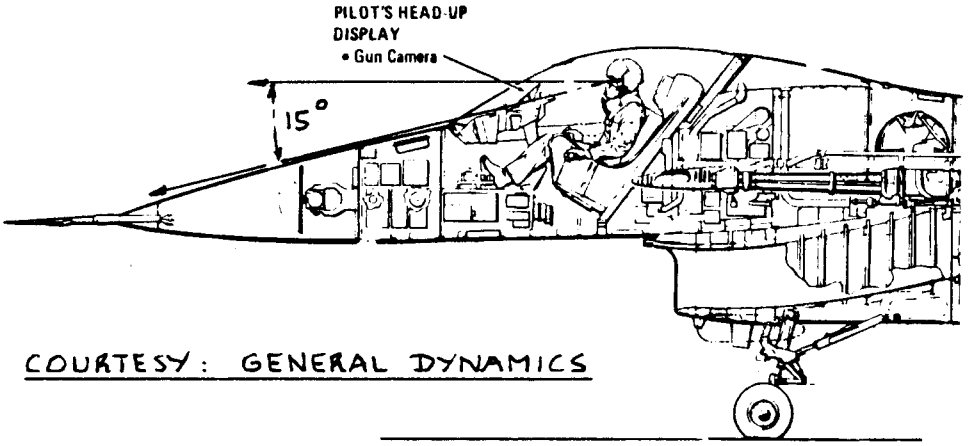

Figure 2.27 Cockpit Layout and Inboard Profile: GD F-16

3. FUSELAGE LAYOUT DESIGN

The purpose of this chapter is to provide the rationale behind the selection of fuselage size, shape, interior and structural arrangement of airplane fuselages.

A step-by-step procedure for arriving at a satisfactory fuselage layout is presented in Chapter 4 of Part II. It is recommended that the reader use that procedure together with the broad range of data on fuselage design given in this chapter.

The reader should also review the configurations presented in Chapter 3 of Part II. It is always useful to find out what has been done by various manufacturers!

Section 3.1 contains a discussion of aerodynamic design considerations.

Section 3.2 contains some guidelines for the exterior layout of flying boat hulls and floats.

Section 3.3 considers the problem of interior fuselage layout design. Data on seat dimensions, exit and door dimensions, galleys, lavatories, wardrobes, cargo containers, maintenance and servicing provisions are provided.

Section 3.4 contains design data on fuselage cross sections, cabin and cargo hold layouts, door and window layouts, as used in a wide range of airplanes.

Section 3.5 presents a number of structural design considerations. Examples of structural layouts of important fuselage details such as: frame and longeron layout, cross section, skin splices, doors, stairs, windows, pressure bulkheads and floors are included.

The fuselage contains not only the payload in most airplanes but also the crew and an assortment of systems needed to operate the airplane. It is not difficult to envision that conflicts for available space will arise. To help visualize the relative arrangement of crew, payload, systems and structure an inboard profile is usually prepared. Section 3.6 presents several example inboard profiles.

For additional information and study references 12 through 15 are highly recommended.

3.1 AERODYNAMIC DESIGN CONSIDERATIONS

The fuselage is responsible for a large percentage of the overall drag of most airplanes: 25 - 50 percent. Since it is desirable to have as little drag as possible, the fuselage should be sized and shaped accordingly.

Fuselages generate the following types of drag:

1. Friction drag
2. Profile drag
3. Base drag
4. Compressibility drag
5. Induced drag

For more detailed data on the relationship between fuselage drag and fuselage shape the reader should consult References 13 and 15. Methods for estimating fuselage drag are presented in Part VI.

3.1.1 Friction Drag

Friction drag is directly proportional to wetted area. Wetted area itself is directly related to fuselage length and to the perimeters of fuselage cross sections. To reduce friction drag, two options are available:

1. Shape the fuselage so that laminar flow is possible.

2. Reduce the length and perimeter as much as possible.

A significant amount of research is being conducted by NASA to determine the conditions for and the extent of laminar flow which can be achieved on a fuselage. Exterior roughness and nose shape are the primary factors which determine the extent of laminar flow which can be achieved at any given combination of Mach Number and Reynold's Number. Without the use of direct boundary layer control it appears that no more than 20 to 30 percent laminar flow (based on fuselage length) can be achieved. A smooth, cambered nose shape (See Figure 3.47, Part II) is required to achieve this.

Most fuselages today have a turbulent boundary layer with correspondingly high friction coefficients. It is shown in Figure 3.1 that the fuselage fineness ratio parameter, l_f/d_f plays an important role in determining fuselage friction drag. A 'weak' minimum occurs for a fineness ratio of around 6.0. Table 4.1 in Part II shows ranges of fineness ratio employed in fuselages of twelve types of airplanes. Note the trend toward very high fineness ratios as the cruise speed increases.

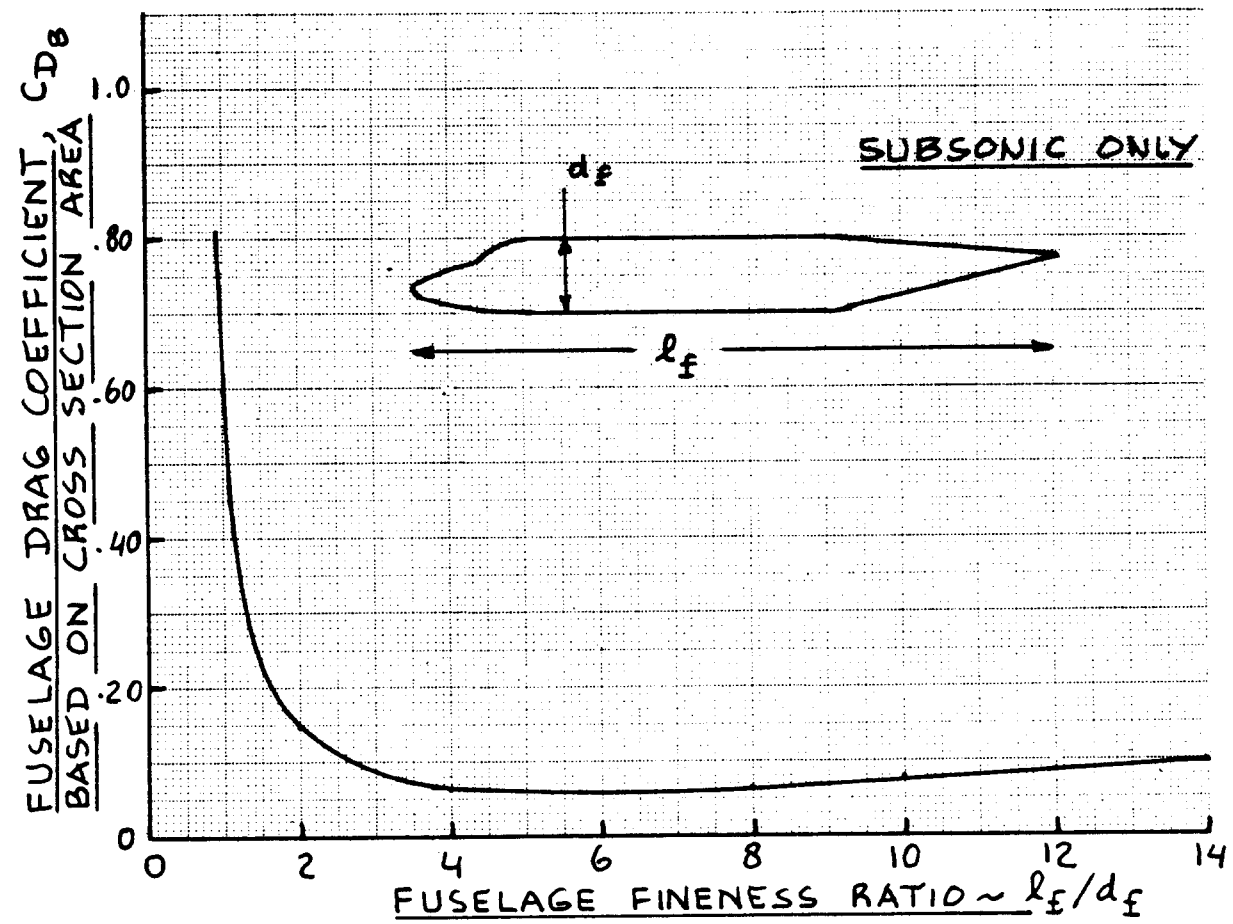

Figure 3.1 Effect of Fineness Ratio on Fuselage Drag

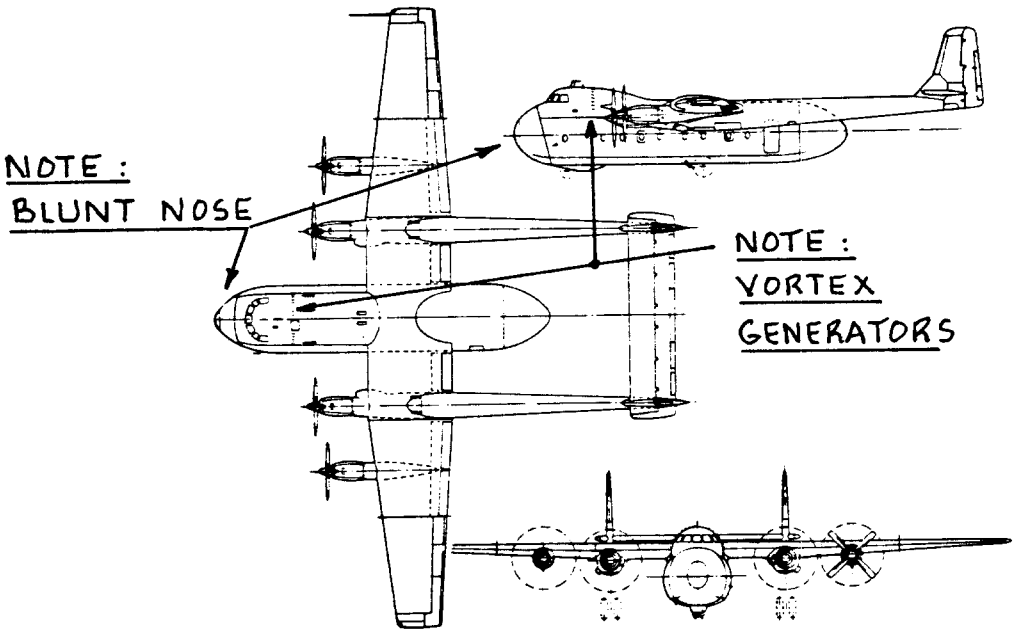

Figure 3.2 Armstrong Whitworth 650 Argosy Freighter

Reference 16 shows that if fuselage length is increased for the same level of static stability, the tail sizes can be decreased thereby reducing overall friction drag. If this factor is accounted for, the optimum fuselage finess ratio from a viewpoint of friction drag (at subsonic speeds) is around 8.0.

In many airplanes design constraints of non-aerodynamic nature will prevent the application of high fineness ratios. Examples are cargo airplanes with rear loading capability, twin boom configurations and carrier based airplanes which must fit on the carrier elevators.

3.1.2 Profile and Base Drag

Profile and base drag are a strong function of front and aft body shape. Blunt fore-bodies and blunt aft-bodies promote flow separations which lead to high profile and base drag.

Fore-body bluntness can be caused by:

1. Poor cockpit window or canopy shaping

2. Requirement for front end loading

The ideal 'streamline' nose shape can be achieved only if the windshields are integrated smoothly into the surface of the fuselage. The DH Comet and the Sud Caravelle (which used the Comet nose and cockpit) are early examples of such a configuration. Recently, the GP180 (Fig.3.47, Part II) uses this concept. Although drag can be considerably reduced by these types of windshield fairing, image distortions may be introduced if the 'fairing angle' becomes too acute.

Figure 3.2 (AW 650 Argosy) illustrates what can happen to the shape of a fuselage nose if front loading is a requirement. It must be remembered that all design decisions are based on a compromise. It would have been possible to streamline the Argosy nose. That would have made it longer, increasing wetted area and thereby friction drag and structural weight. In the case of the Lockheed Galaxy (Fig.3.30, Part II) and the Antonov AN124 (See Jane's, 1985 edition) the longer streamlined nose option was exercised. Reference 15 contains detailed data on the effect of fore-body shape on profile drag.

In the case of fighters and trainers the requirement for good visibility from the cockpit becomes a dominant design criterion. This calls for a large canopy. Canopy

drag then becomes an important factor in the design of the fuselage. Part VI contains data with which canopy drag can be related to canopy size.

Figure 3.3 illustrates the effect of aft body bluntness on drag.

Even with a large fuselage fineness ratio, it is possible to increase fuselage drag by using too much 'upsweep' in the aft-body. Figure 3.4 shows what is meant by 'upsweep'. Figure 3.4 also shows how 'upsweep' affects drag.

Upsweep of the aft-body can lead to vortex induced separations. Figure 3.5 illustrates such a vortex flow situation. These separated vortices not only increase drag but can cause lateral oscillation problems. The vortex flow can be stabilized by the use of 'sharp' corners. These 'sharp' corners have been shown to reduce the lateral oscillation problem and also to reduce drag. Figure 3.6 shows an example.

Upsweep is applied to airplanes for the following reasons:

1. to facilitate take-off rotation

2. to facilitate rear cargo loading

Sometimes it becomes necessary to add a 'bulge' to the upper rear fuselage if a large upsweep angle was dictated by rear loading considerations. This bulge is needed to create sufficient structural depth in the fuselage to resist tailloads. Examples of such 'bulged' fuselages are seen in Figures 3.29a and 3.30a in Part II.

3.1.3 Compressibility Drag

A fuselage alone does not experience compressibility drag effects until very high subsonic Mach numbers. Compressibility drag arises from the existence of shocks on the fuselage. The appearance of shocks is strongly coupled to the sweep and thickness of the wing in the area of wing/fuselage juncture. The area rule concept must be used to minimize compressibility drag. The area rule is discussed in Ref.13 and in Part VI. Figure 3.7 shows an area ruled fuselage for a high subsonic transport. Figures 3.34 through 3.36 (Part II) show area ruled fuselages for supersonic applications.

3.1.4 Induced Drag

A fuselage contributes to induced drag primarily because of its adverse effect on wing spanload distribution. Figure 3.8 illustrates a typical effect.

When a fuselage is equipped with leading edge strakes (lexes) and/or the fuselage is sharply blended into the wing (such as is the trend in modern fighter design), there will be significant effects of the fuselage on induced drag.

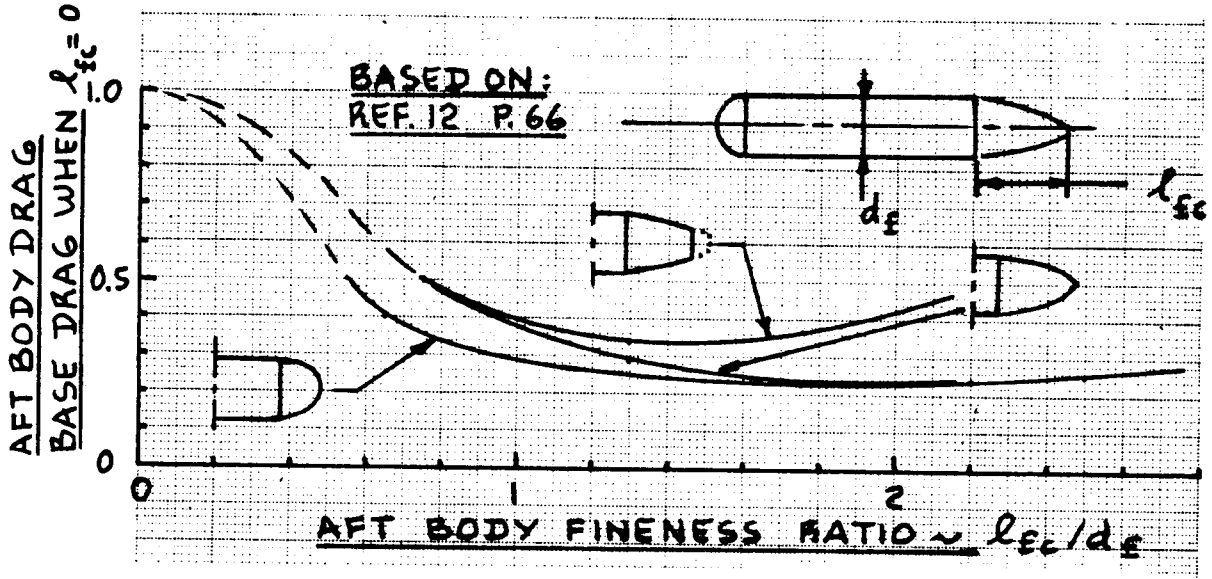

Figure 3.3 Effect of Aft Body Bluntness on Drag

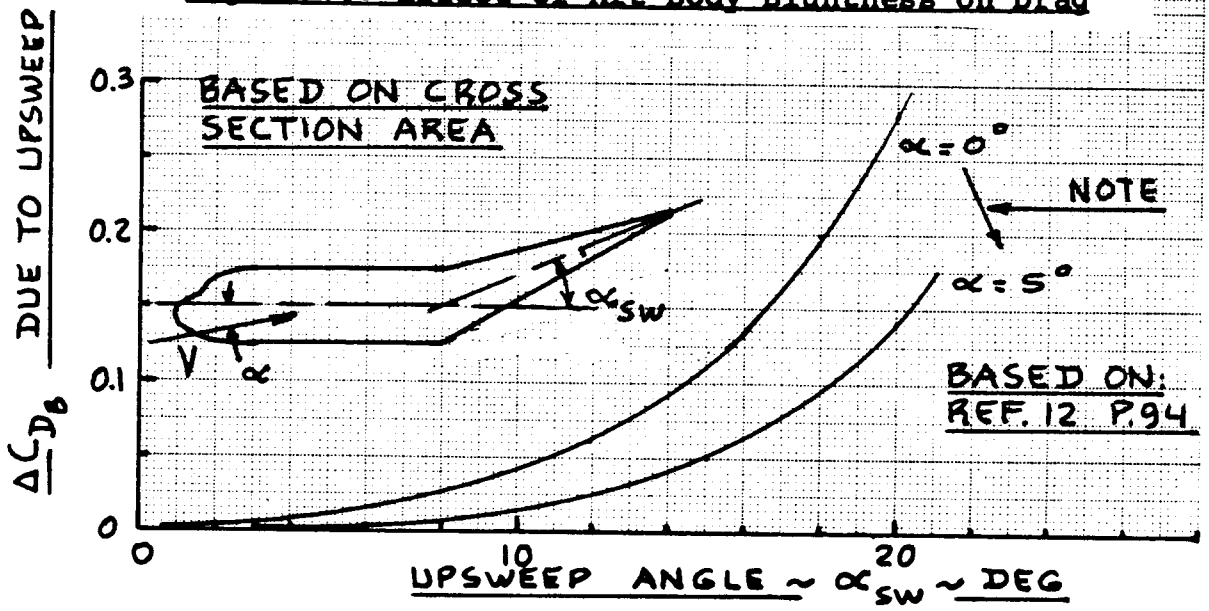

Figure 3.4 Definition of Upsweep and Its Effect on Drag

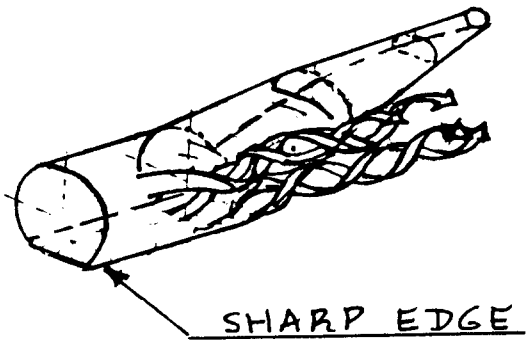

Figure 3.5 Vortex Separation from a Fuselage

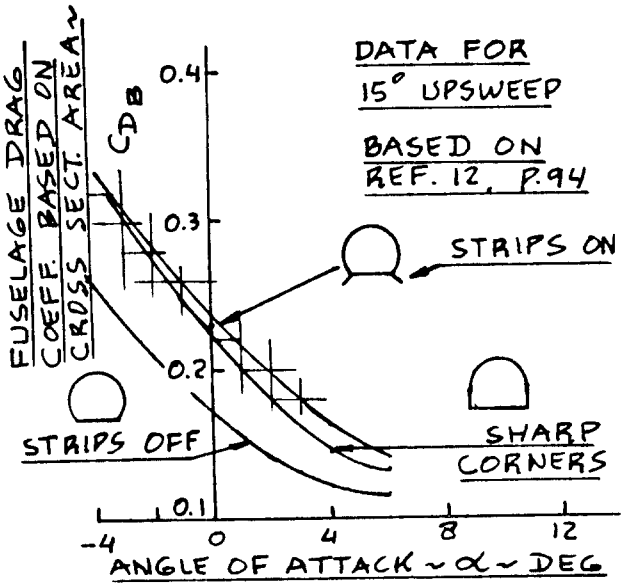

Figure 3.6 Effect of Cross Section Shape on Drag

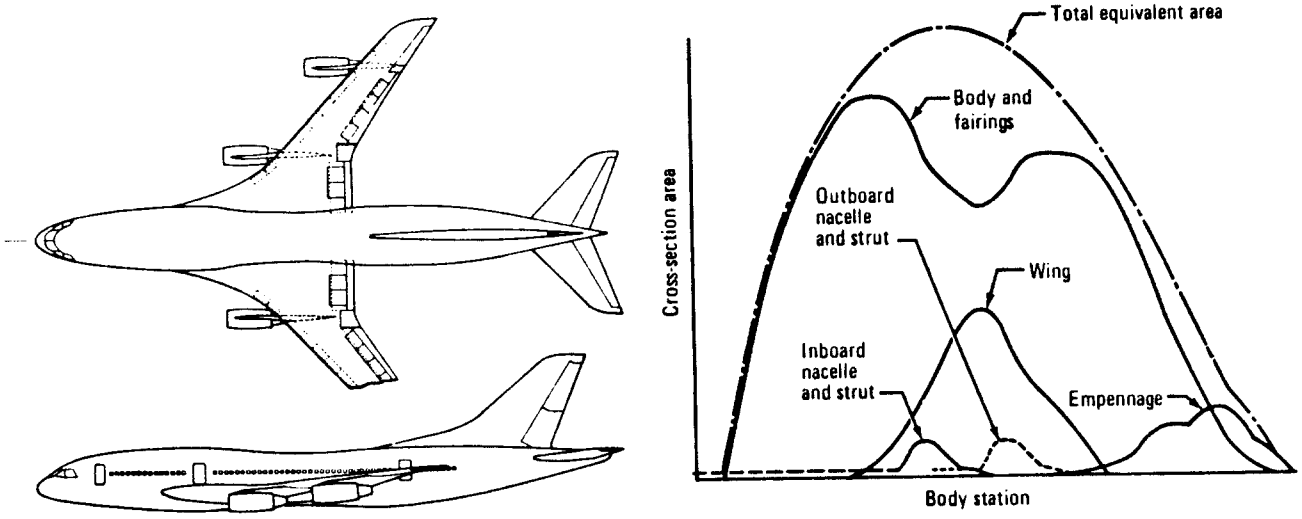

Figure 3.7 Example of an Area Ruled Fuselage

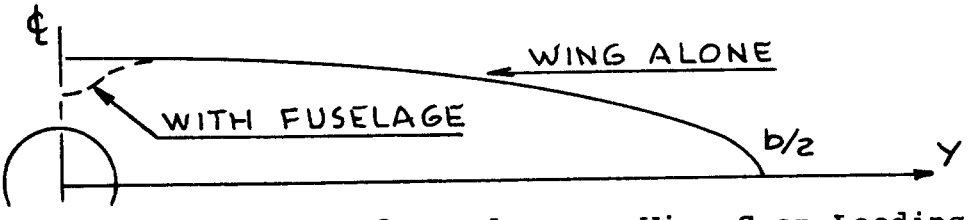

Figure 3.8 Effect of Fuselage on Wing Span Loading

3.2 GUIDELINES FOR FLYING BOAT HULL AND FLOAT DESIGN

Figure 3.9 shows the typical hull geometry employed in flying boats as well as in floats. The following design considerations are important:

1. Buoyancy. 2. Hydrodynamic drag and aerodynamic drag.
3. Effect of hull shape on directional stability.
4. Effect of hull shape on landing and take-off characteristics (air and water).
5. Effect of hull shape on water spray and on where the spray goes: salt water sprays into engines are bad.
6. Effect of hull shape and hull size on ability to operate in certain sea states.
7. It is essential that the hull bottom be designed with enough watertight compartments so that the flooding of one does not result in the sinking of the airplane.
8. Special attention needs to be given to the selection of hull materials: particularly sea water is a very corrosive environment!

The reader should consult references 14, 15 and 17 for information on aerodynamic and hydrodynamic hull and float design. A wealth of design and analysis information on flying boats and on floats may be found in NACA Technical Reports issued as 'annual bound volumes' in the 1920-1958 era. Ref.18 is an example of such data.

Flying boats and float equipped airplanes all have 'built-in' drag and weigt penalties associated with the need for boyuancy and acceptable handling characteristics in the water. Part VI shows that the drag penalties due to wetted area compared to land based airplanes are rather large.

Reference 17 contains data showing the effect of stall speed on hull loading for water landings. This effect needs to be accounted for in the early weight estimates of any new water based airplane.

Figures 3.10 through 3.12 contain design guidelines for the exterior shape of the hull. The nomenclature is explained in Figure 3.9.

Figure 3.13 shows that the ability of a flying boat

to operate in given sea state conditions is directly related to the displacement (i.e. take-off weight, i.e. airplane size).

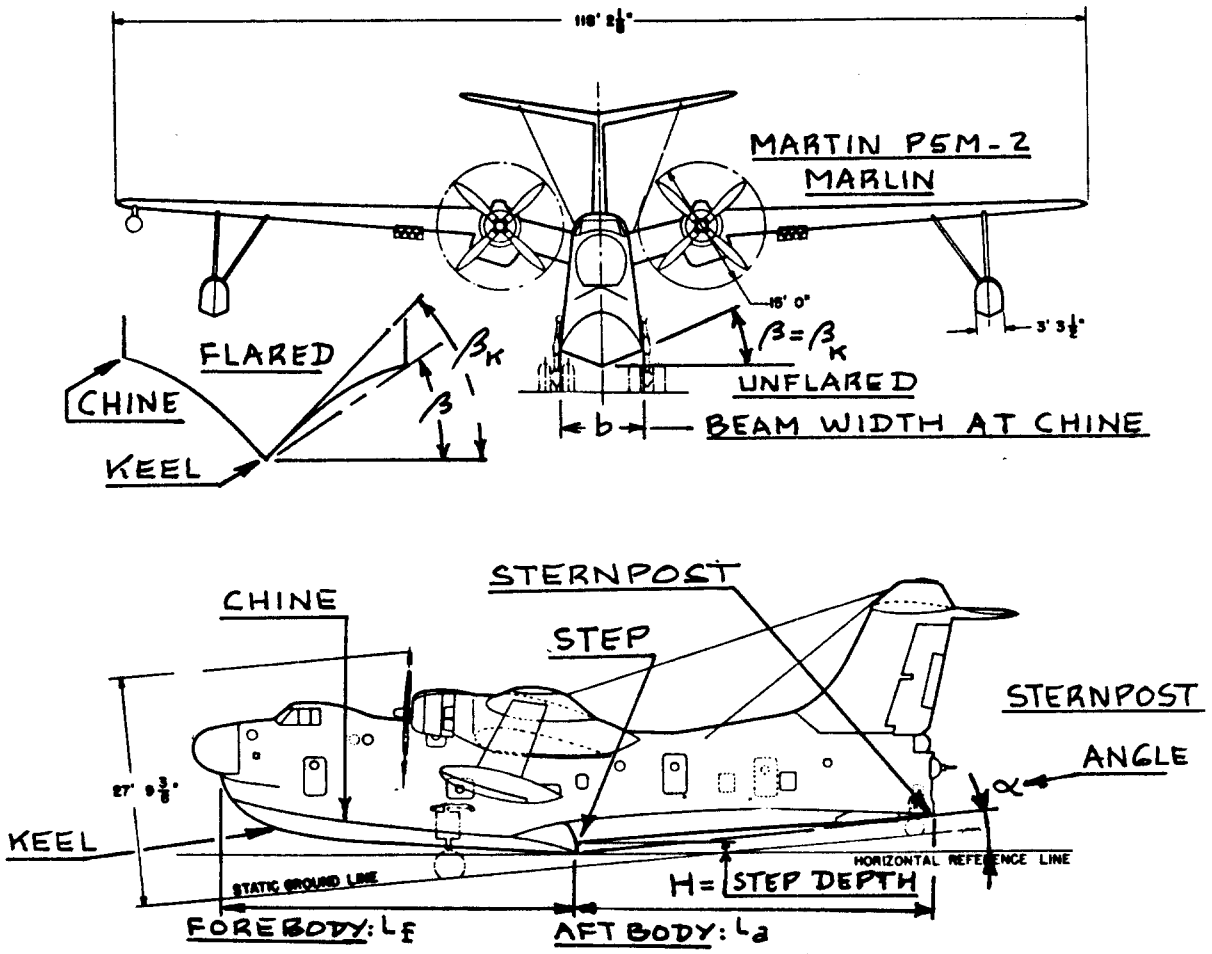

Figure 3.9 Typical Flying Boat and Float Hull Geometry

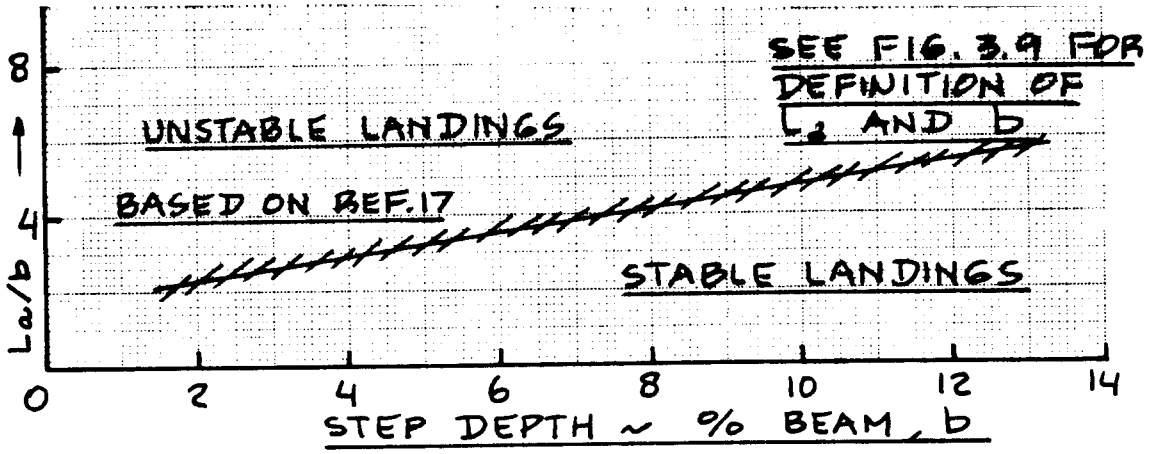

Figure 3.10 Effect of Hull Geometry on Stability of Water Landings: I

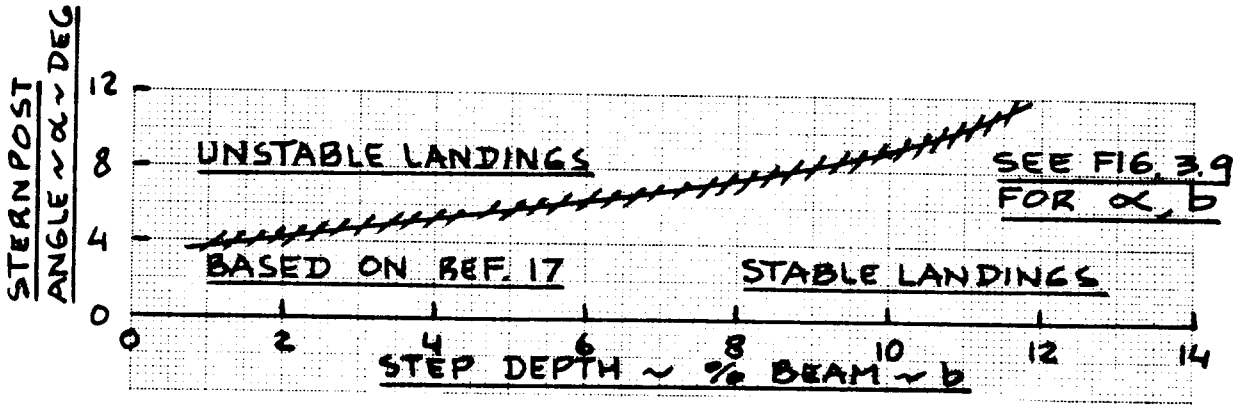

Figure 3.11 Effect of Hull Geometry on Stability of Water Landings: II

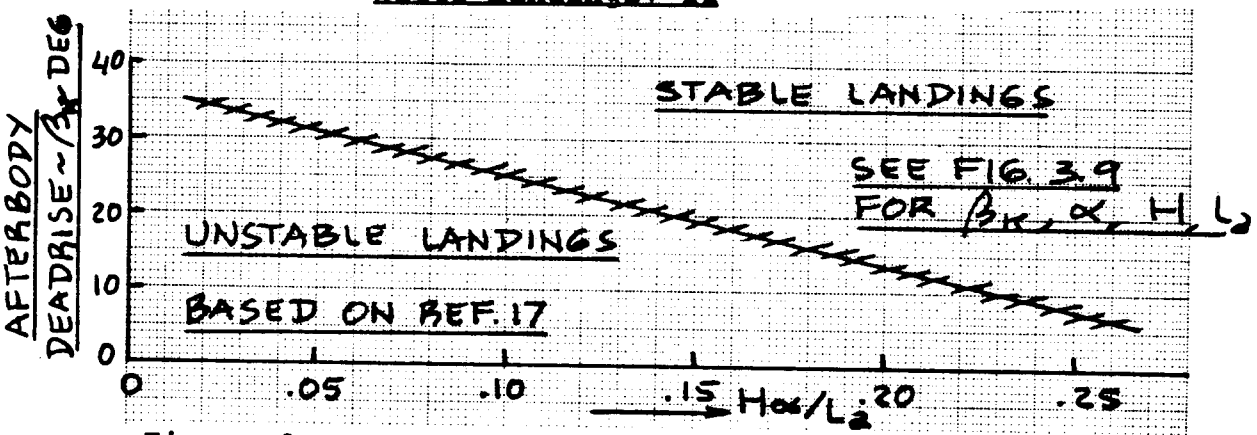

Figure 3.12 Effect of Hull Geometry on Stability of Water Landings: III

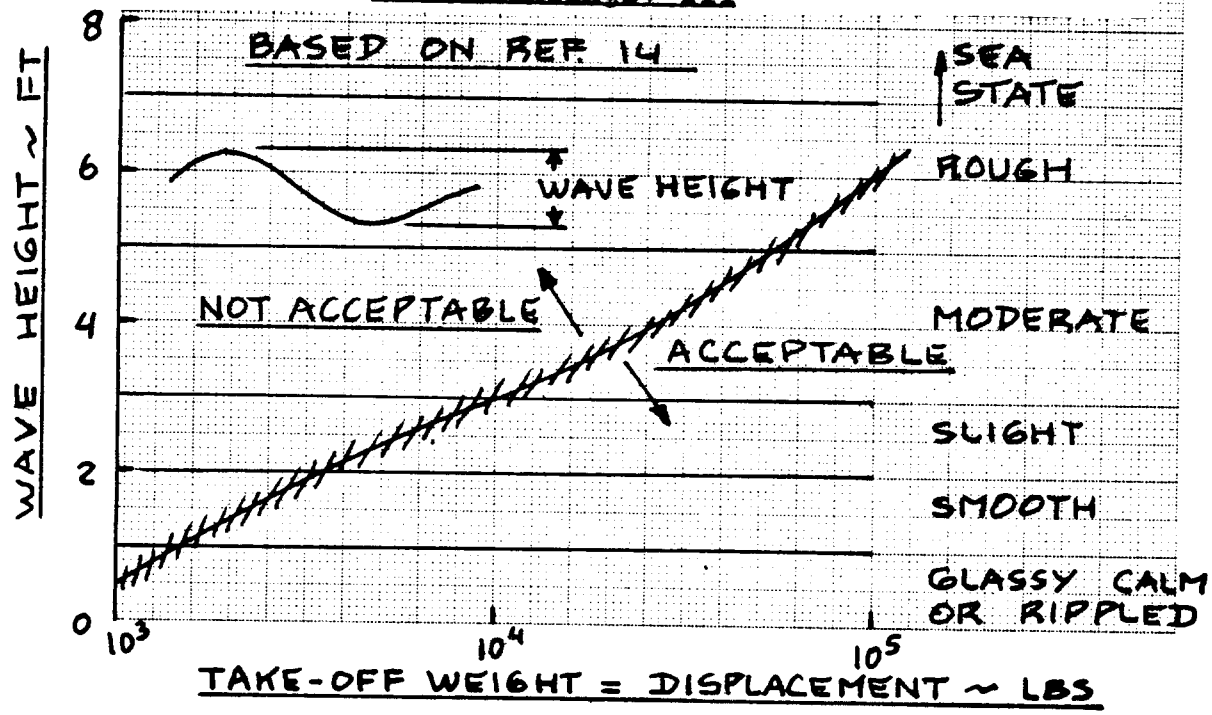

Figure 3.13 Effect of Hull Displacement on Ability to Operate in Sea States

3.3 INTERIOR LAYOUT DESIGN OF THE FUSELAGE

The fuselage in most airplanes carries the crew, the payload (passengers and/or cargo and weapons) and many of the systems needed for the operation of an airplane.

In commercial passenger operations the interior design reflects a compromise between level of creature comforts and the weights and sizes required to create the creature comforts.

In cargo operations the ability to efficiently load and unload cargo plays an important role.

In fighter design a major problem is that of 'packaging' of all required systems so that they operate satisfactorily, don't interfere with another (particularly important with avionics) and can be easily accessed.

In commercial as well as military operations the problems associated with servicing and maintenance dictate where access must be designed into the fuselage. Design for good access, maintenance and inspectability usually conflicts directly with design for low structural weight, low complexity and low drag.

The fuselage normally also houses the cockpit (or flight deck). Design requirements for satisfactory cockpit layouts are provided in Chapter 2. This chapter contains design information for the following aspects of fuselage interior layout design:

3.3.1 Layout of the cross section
3.3.2 Seating layouts, seats and restraint systems
3.3.3 Layout of doors and emergency exits
3.3.4 Galley, lavatory and wardrobe layouts
3.3.5 Layout of cargo/baggage holds, including data on cargo containers
3.3.6 Maintenance and servicing considerations

3.3.1 Layout of the Cross Section

Fuselage cross sections, for commercial airplanes are the result of compromises between weight, drag, systems and creature comfort considerations. In military applications, additional considerations may be those of radar observability and weapons system integration.

For pressurized airplanes the most efficient cross section from a structural viewpoint is the cirle. However, for small airplanes a circular cross section is

wasteful in terms of volume. To verify this, draw a circle around the human body in a sitting position.

From a manufacturing viewpoint a flat sided fuselage is the cheapest to build. The Shorts 330 of Fig.3.18d, Part II is an example of such an approach.

3.3.1.1 Passenger cabin

The dimensions of the human body dictate the minimum cabin size that will 'fit around' the occupant(s) after a decision has been made whether the cabin cross section allows for 'stand-up' room or for 'crawl-to-your-seat' room.

Figures 3.14 through 3.18 provide scaled drawings of males and females in a variety of postures.

In small civil airplanes (such as homebuilts, single engine airplanes and most twin engine airplanes) it is usually not practical to design for 'stand-up' room. The added weight, drag and cost are judged not to be acceptable. Figures 3.45 and 3.48-3.52 in Section 3.4 provide dimensioned cross sections for 'small' civil airplanes.

Sailplanes and the BD-5J represent extremes of cabin comfort at the 'low' end of the scale. The inboard profile of Figure 3.87 in Section 3.6 shows the tight fit of the BD-5J around the human body.

For transport airplanes, Figure 3.19 shows a statistical relationship between fuselage width and the number of seats abreast. The minimum allowable width of aisles between seats is dictated by emergency evacuation considerations. Figure 3.20 summarizes the allowable dimensions based on FAR 25.815.

FAR 25.817 states that on each side of an aisle, no more than three seats may be placed abreast.

In passenger transports a critical choice which affects the design of the cross section is the number of seats abreast. The fewer seats abreast, the longer the fuselage and the more difficult 'growing' the airplane becomes. The more seats abreast, the shorter the fuselage and the easier it becomes to 'grow' the airplane.

Important note: In passenger transports it is undesirable to interrupt the fuselage cross section locally by a wing torque box. This can be a real problem in the case of high wing transports.

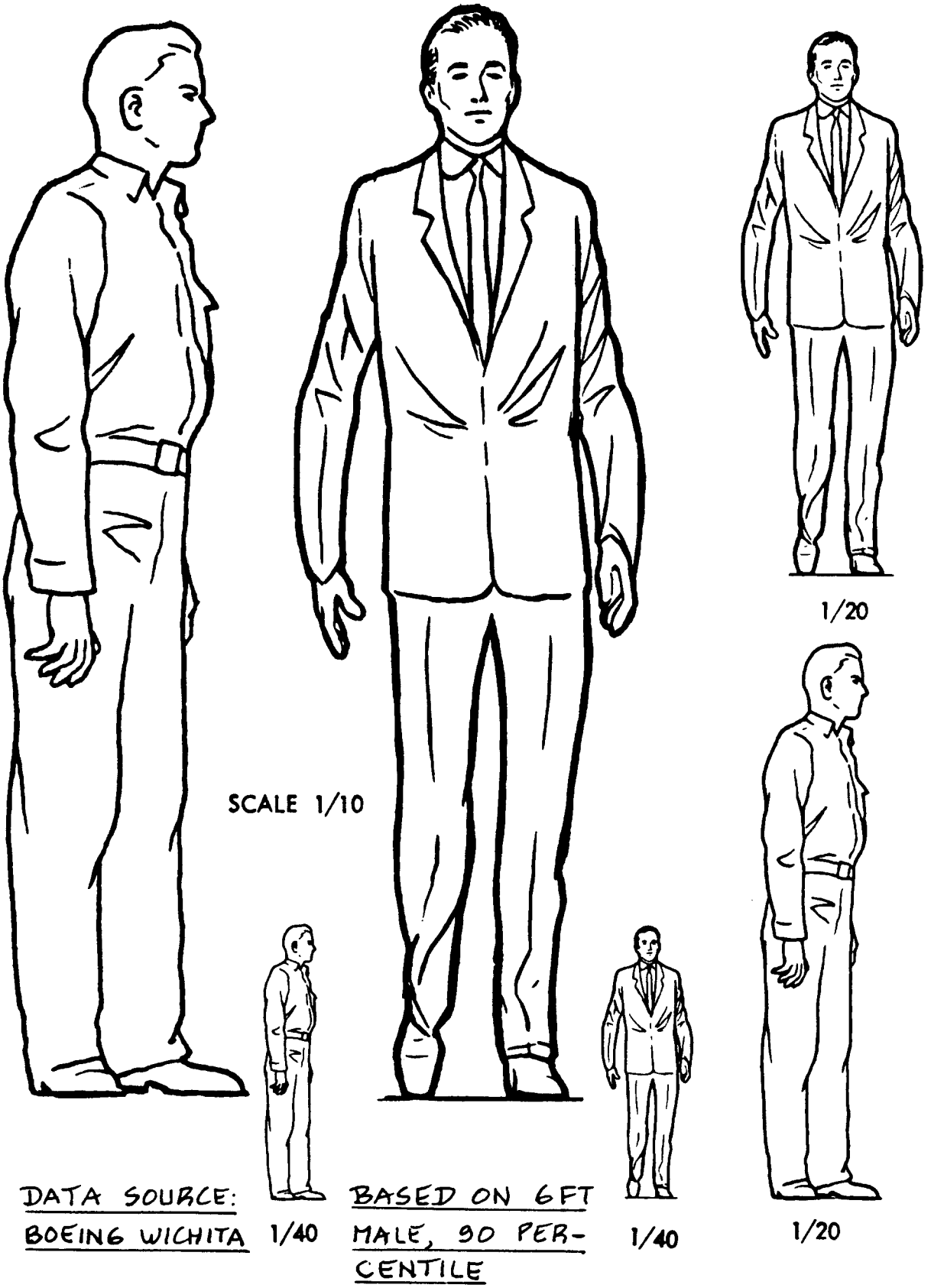

Figure 3.14 Scaled Views of Standing, Male Passengers

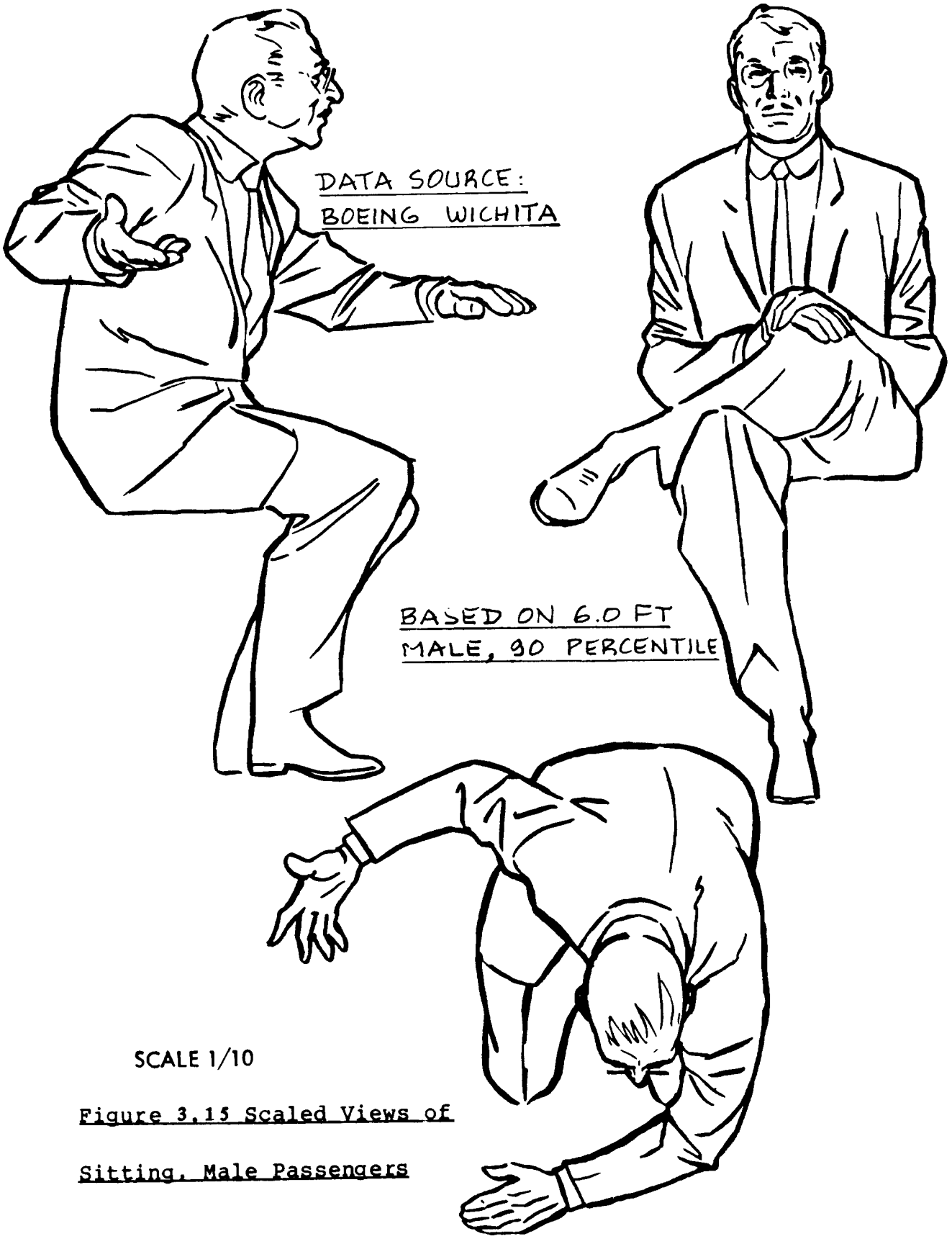

SCALE 1/10

Figure 3.15 Scaled Views of Sitting, Male Passengers

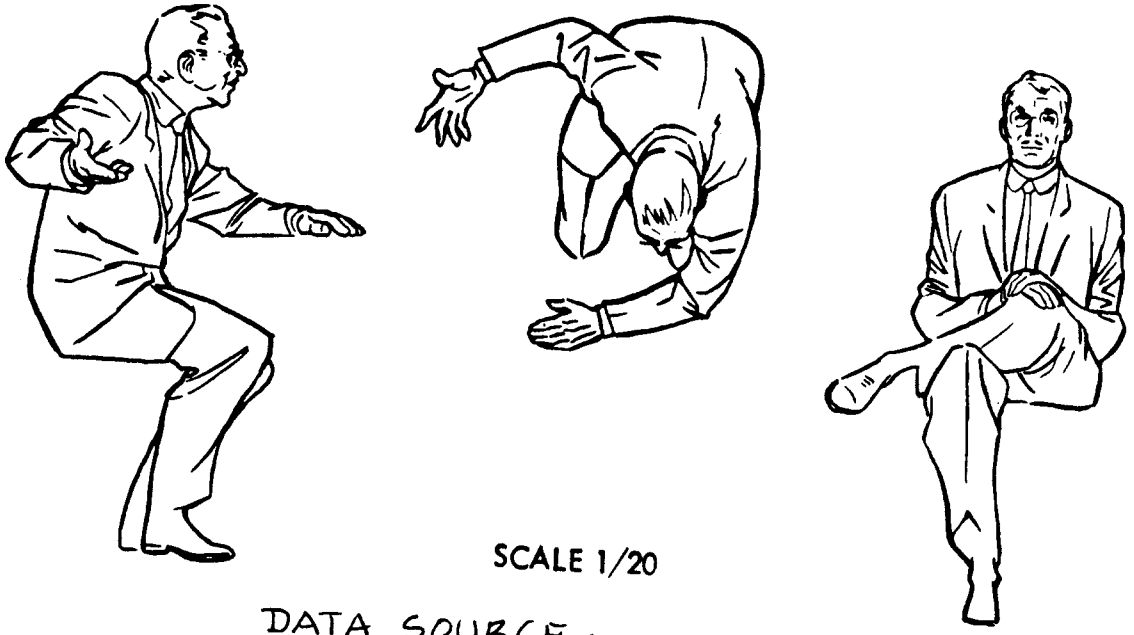

SCALE 1/20

DATA SOURCE:
BOEING WICHITA
BASED ON 6.0 FT MALE
90 PERCENTILE

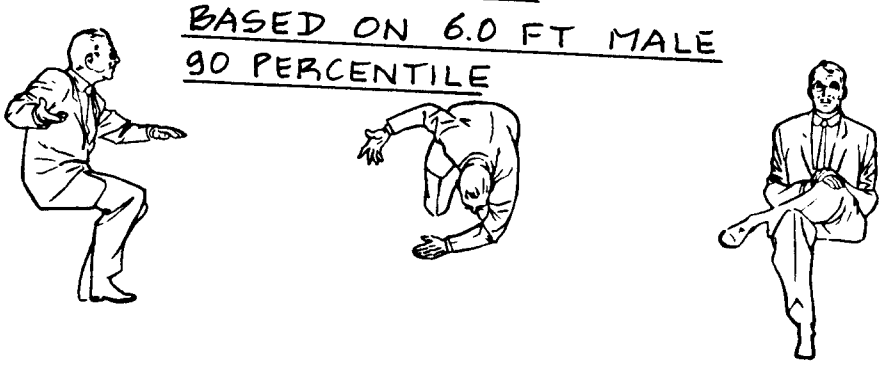

SCALE 1/40

Figure 3.16 Scaled Views of Sitting, Male Passengers

1/20

DATA SOURCE :
BOEING WICHITA

1/40

SCALE 1/10

Figure 3.17 Scaled Views of Standing, Female Passengers

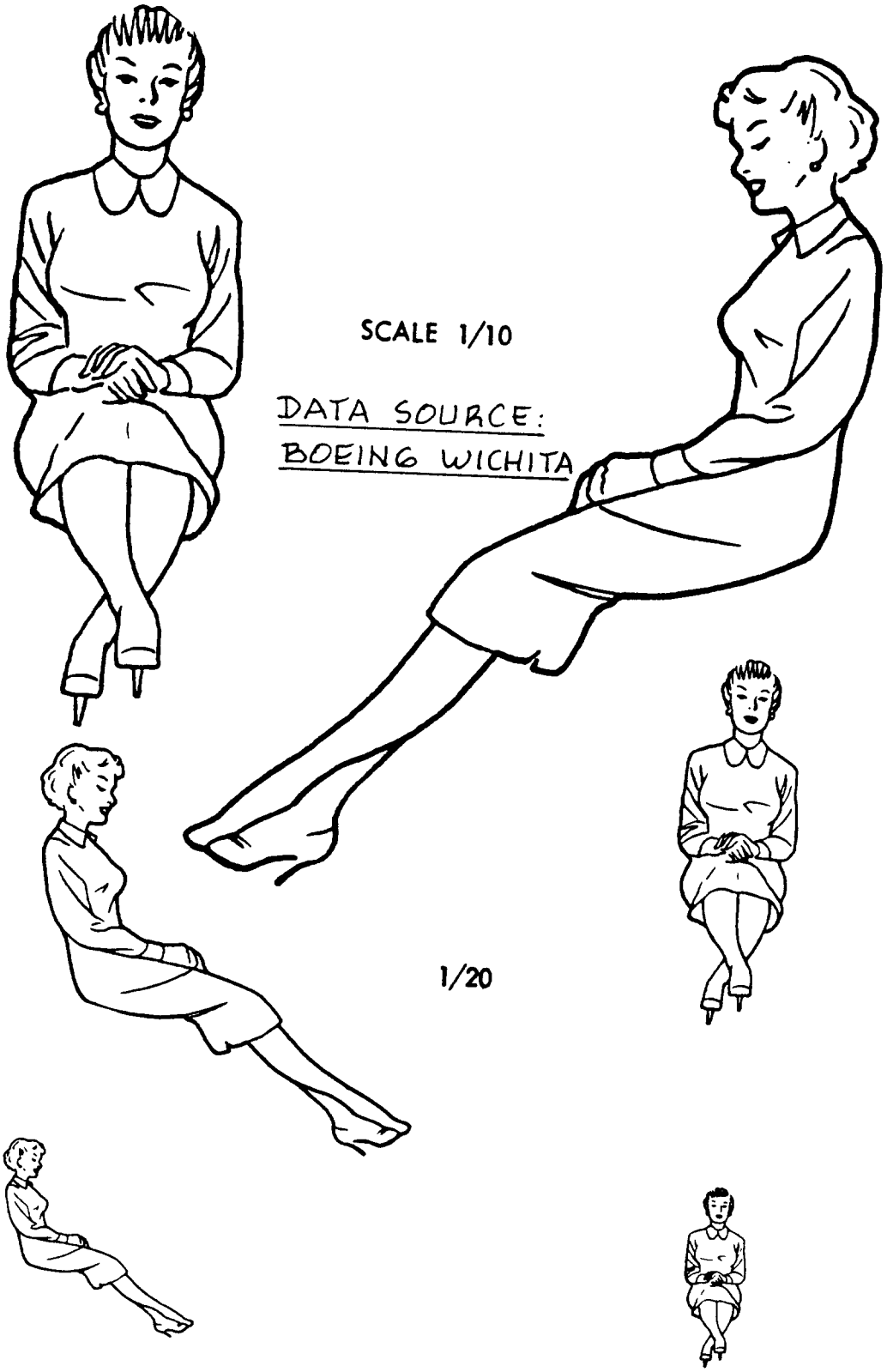

Figure 3.18 Scaled Views of Sitting, Female Passengers

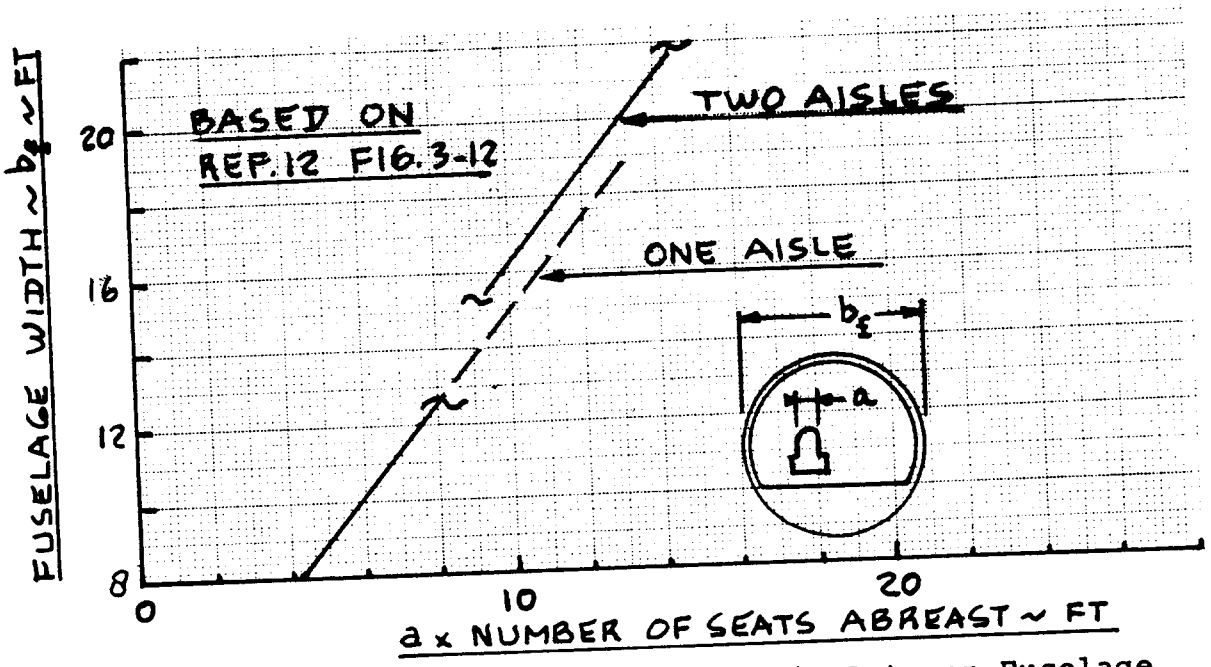

Figure 3.19 Statistical Relationship Between Fuselage Width and Total Seat Width

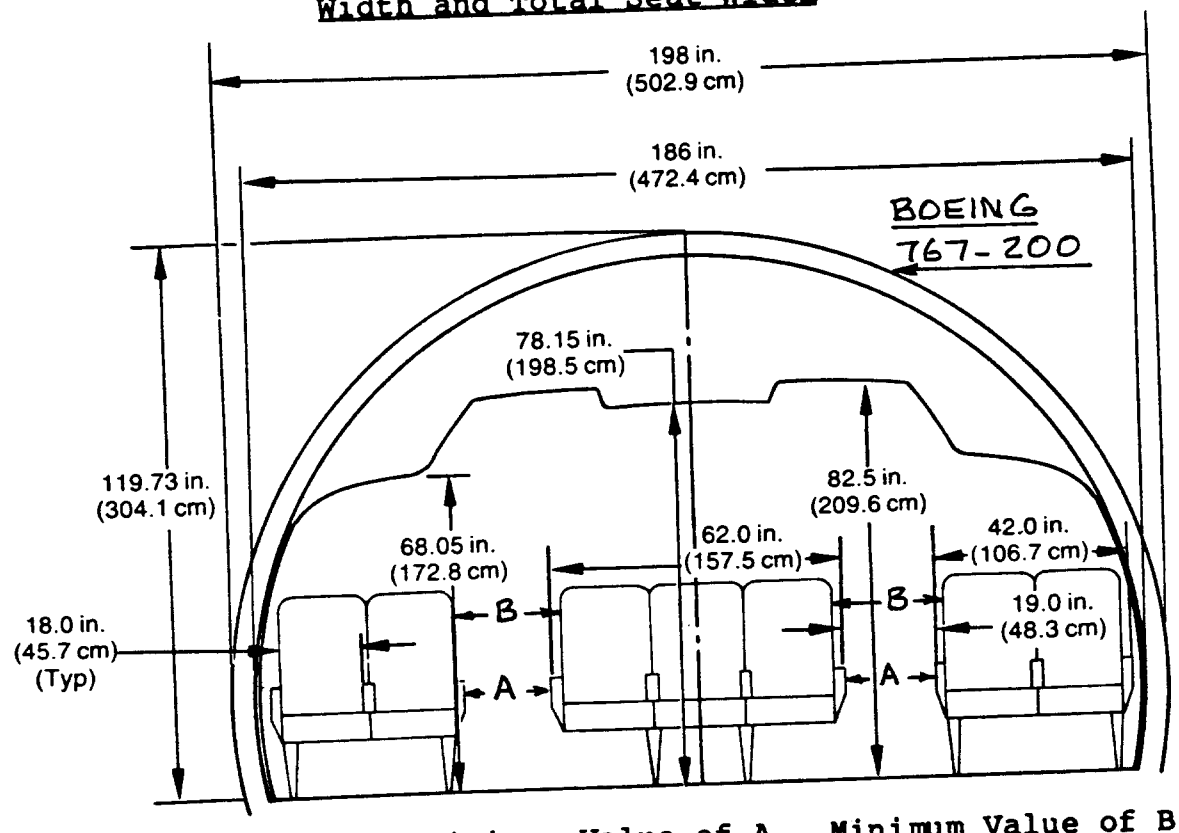

Number of Seats	Minimum Value of A	Minimum Value of B
10 or less	12 inches	15 inches
11 - 19	12 inches	20 inches
20 or more	15 inches	20 inches

Figure 3.20 Minimum Aisle Width Requirements

3.3.1.2 Cargo hold

In most passenger airplanes baggage and cargo is carried in 'standard' containers. From a competitive viewpoint it is important to be able to carry as many different types of containers as possible. This represents a very difficult design problem. The problem needs to be solved as part of the overall cross section and fuselage layout process. To accomplish this, baseline data on cargo/baggage containers are needed. Sub-section 3.3.5 provides these data.

The location of the wing on the fuselage as well as the amount of space needed for landing gear retraction can help dictate the amount of cargo containers that can be carried in a given volume. If from a competitive viewpoint it becomes desirable to carry one or two more containers, the fuselage length, the cross section or the wing location on the fuselage may have to be reexamined.

3.3.1.3 Military

In laying out the cross section of troop transports it is necessary to account for the dimensions of 'combat-ready' troops. Figures 3.21 - 3.23 provide scaled drawings of combat ready troops in a variety of postures.

In military airplanes the additional problems of pilot visibility (as in fighters) and radar observability influence the design of the cross section. Design rules for achieving a low radar cross section are given in Chapter 7.

Dimensions of a number of military vehicles which may have to be carried in military transports are given in Chapter 7.

Weapons integration needs may further complicate the choice of cross section design. Chapter 7 also deals with weapons integration problems.

3.3.1.4 Supersonic airplanes

In the case of supersonic airplanes the need for area ruling places further constraints on cross section design. Part VI contains a discussion of the area ruling concept. An example of a fuselage with subsonic area ruling can be found in Figure 3.7.

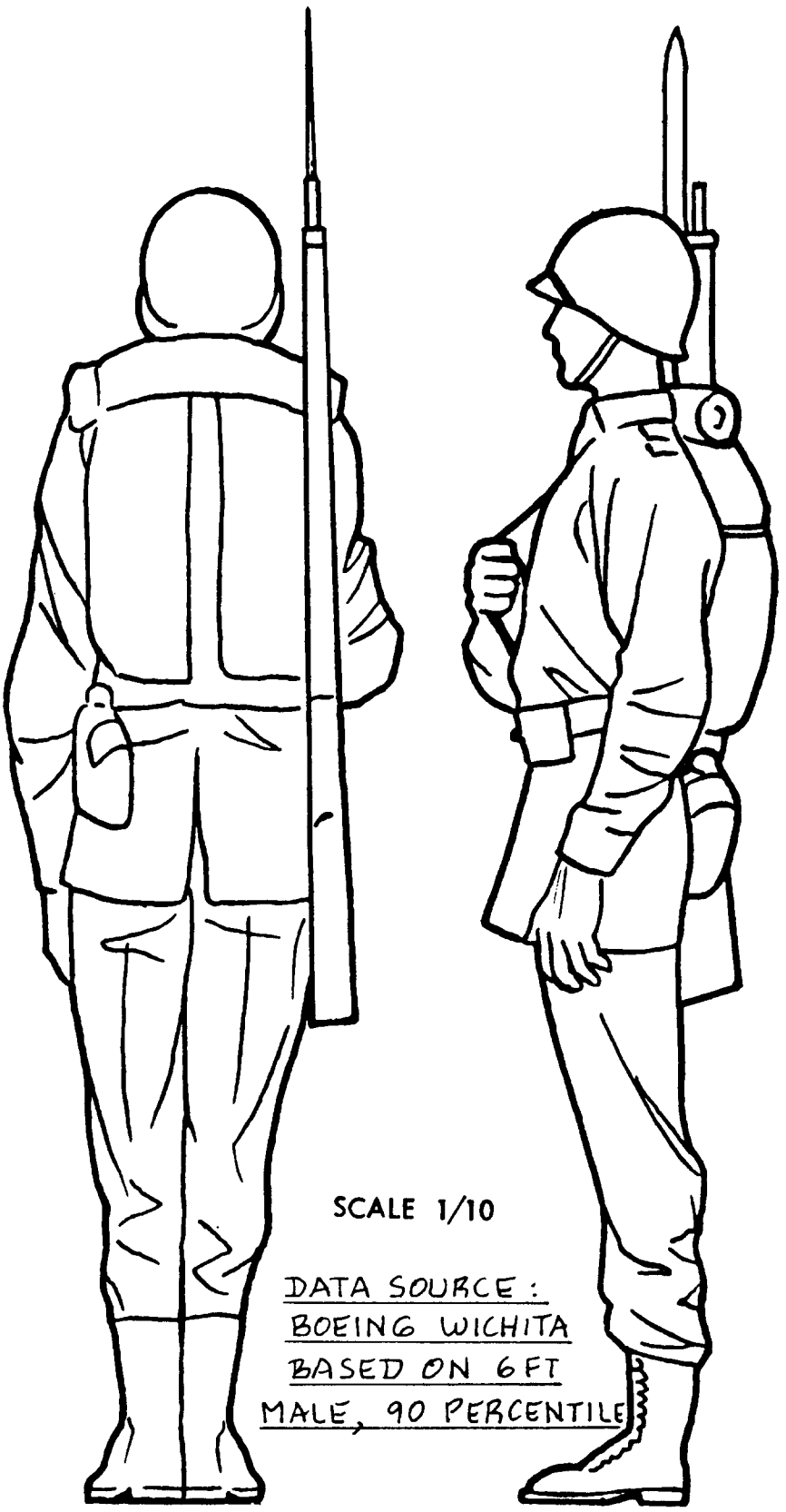

Figure 3.21 Scaled Views of Standing, Combat Ready Troops

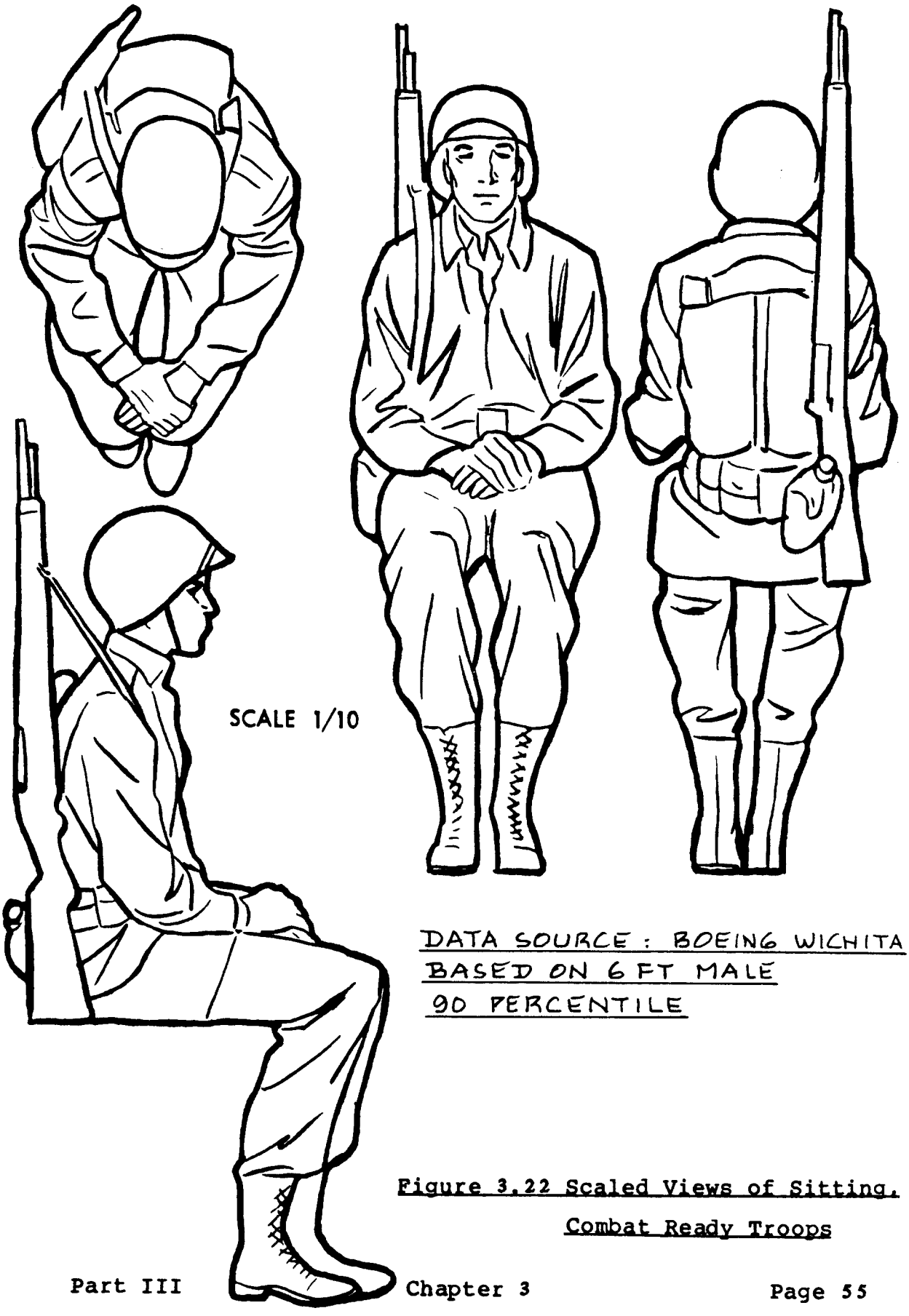

DATA SOURCE : BOEING WICHITA
BASED ON 6 FT MALE
90 PERCENTILE

Figure 3.22 Scaled Views of Sitting, Combat Ready Troops

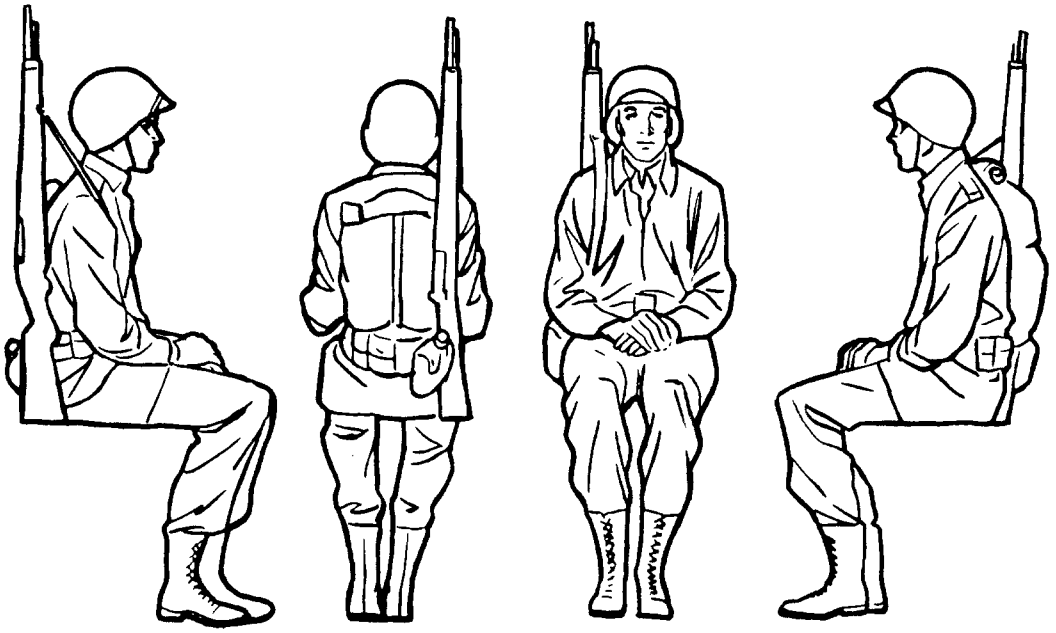

SCALE 1/20

DATA SOURCE : BOEING WICHITA

BASED ON 6 FT MALE, 90 PERCENTILE

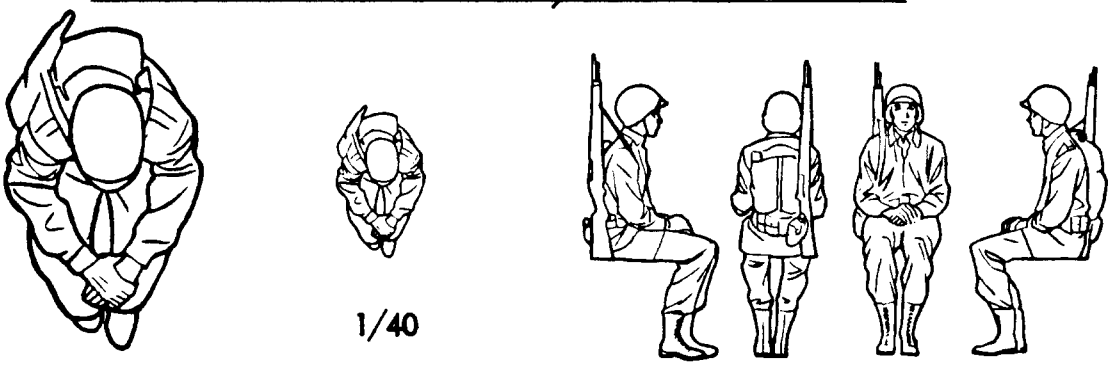

1/20

1/40

SCALE 1/40

Figure 3.23 Scaled Views of Sitting, Combat Ready Troops

3.3.2 Seating Layouts, Seats and Restraint Systems

An important decision in laying out the overall seating arrangement in passenger airplanes is that of x-seats-abreast versus y-seat-rows. This choice has a significant impact on:

1. cabin length and cabin width
2. fuselage weight and drag
3. future growth potential for the airplane
4. passenger appeal and therefore market acceptance

Sub-sub-section 3.3.2.1 provides information on seating arrangements and seats for general aviation airplanes. Sub-sub-section 3.3.2.2 gives similar data for transport airplanes.

In many airplanes it is desirable and/or necessary to have restraint systems built in, to prevent injury in the case of a crash. Sub-sub-section 3.3.2.3 deals with the layout of restraint systems.

3.3.2.1 Seating arrangements and seats for general aviation airplanes

Figures 3.48 through 3.52 in Section 3.4 provide dimensioned data on cabins and on seating layouts of existing general aviation airplanes.

In some types of general aviation airplanes it is necessary to carry a parachute. Parachutes can be worn as a back-pack or as a seat-pack. Figure 3.24 illustrates the two types with typical dimensions and weights. In the layout of seats, these dimensions need to be accounted for.

3.3.2.2 Seating arrangements and seats for transports

The passenger cabin should be laid out so that in cruise flight the cabin floor is level. If this criterion is not satisfied, cabin service and moving about in the cabin are made much more difficult. The level cabin floor requirement is linked directly to the choice of wing incidence. This is expained further in Chapter 4.

Figure 3.25 shows a statistical correlation between cabin length, seat pitch, total number of seats and seats abreast. As long as the right number and size exits are provided (See sub-section 3.3.3) the seating arrangement is up to the designer. However, the seat pitch near

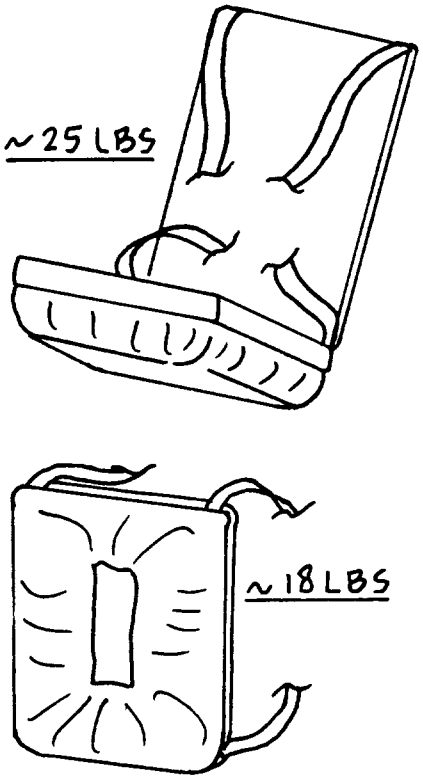

Seatpack parachute:

length 13 in.
width 15.5 in.
depth 8 in.
(These dimensions include a 2 in. thick cushion)

Backpack parachute:

length 23 in.
width 14.5 in.
depth 6 in.
(These dimensions include the back pad)

(Data from Ref.14, p.349)

Figure 3.24 Typical Parachute Dimensions

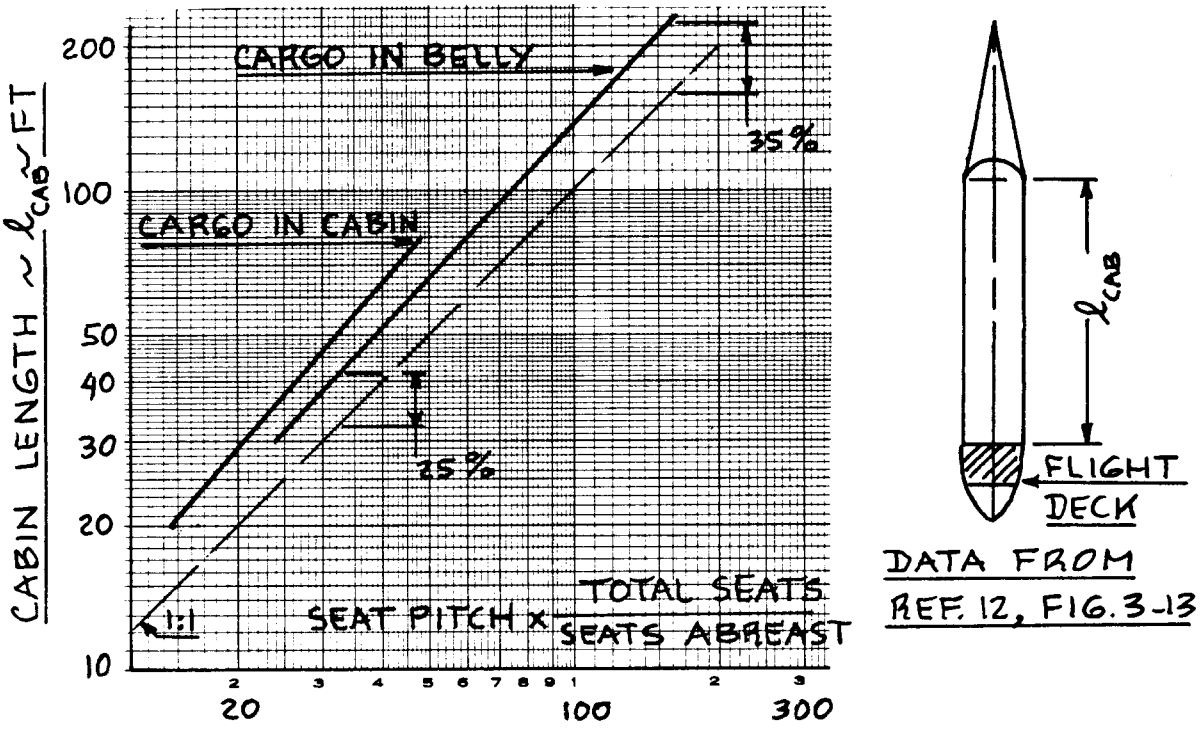

Figure 3.25 Statistical Relationship Between Cabin Length, Seat Pitch, Number of Seats and Number of Seats Abreast

emergency exits must meet the requirement stated in sub-section 3.3.3.

In laying out a proposed seating arrangement, remember that passengers (when given an equal choice) do not like three seats in a row. Nevertheless, many narrow body airplanes are configured in precisely this manner. Also remember that the FAR's prohibit more than three seats in a row, unless an extra aisle is included. The four-seat rows in the center of a B-747, flanked by two aisles are acceptable.

The following seat pitch values reflect industry practice:

seat pitch for: first class seating, 38 - 40 inches
tourist/coach/econ., 34 - 36 inches
high density, 30 - 32 inches

Examples of transport seating arrangements are shown in Figures 3.26 and 3.27.

Note the cabin attendant (cabin crew) seats in the seating layouts of Figures 3.26 and 3.27. Requirements for cabin attendants as a function of the number of passengers carried are given in FAR 91. These requirements are summarized as follows:

Light transports: 1 attendant per 20 passengers (minimum)

Large transports: 1 attendant per 50 passengers (minimum)
1 attendant per 35 passengers (this reflects industry practice)

Table 3.1 relates seat classification (in terms of class of service) to seat dimensions. The seat dimension symbols are defined in Figure 3.28.

Finally, data on a number of seats available on the market are given in Figures 3.29a-c.

All seats must meet the requirements of FAR 23 and 25, parts 561 and 785. Table 3.2 presents the design limit load factors for seats with a nominal 170 lbs passenger according to FAR 25.785.

When preparing a Class II weight and balance statement (Step 21, page 19, Part II) it is useful to have actual data on seat weights. Table 3.3 provides these data for six seat types. Figures 3.29a-c contain additional seat weight data.

475 SERIES 74 PASSENGERS - TOURIST CLASS

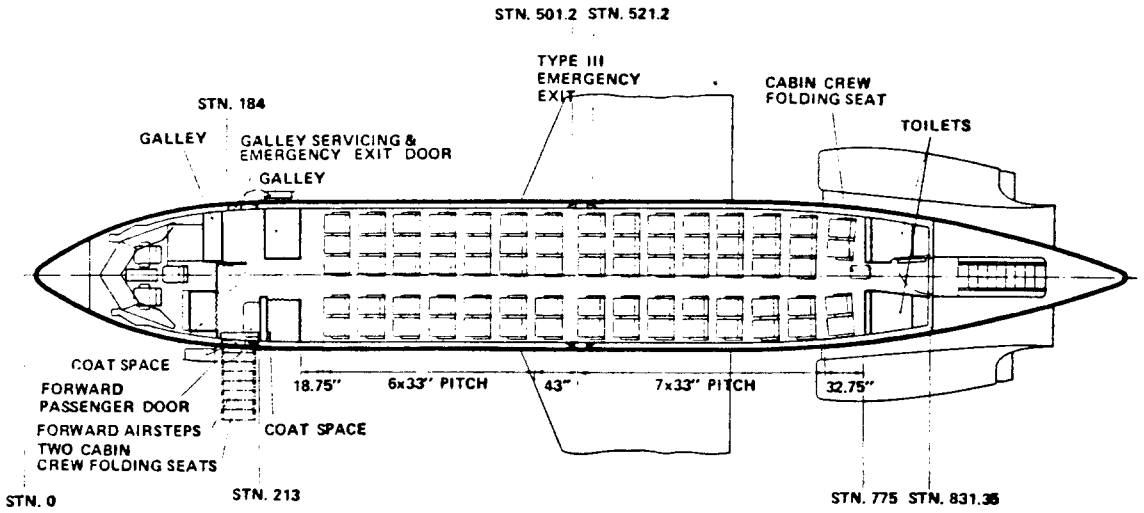

475 SERIES 65 PASSENGERS - MIXED CLASS

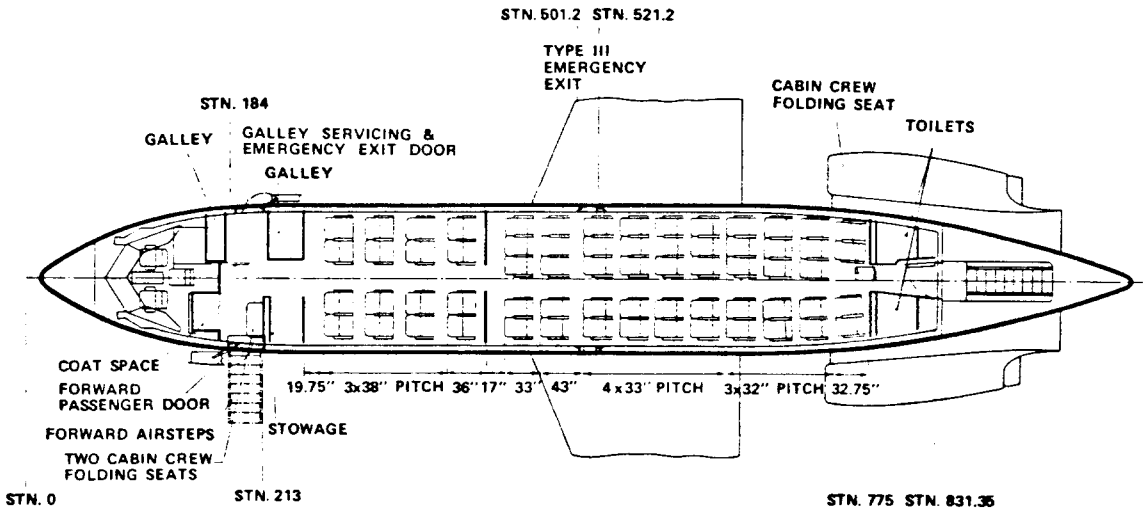

NARROW BODY

COURTESY: BAC

Figure 3.26 Example Seating Arrangements: BAC 111

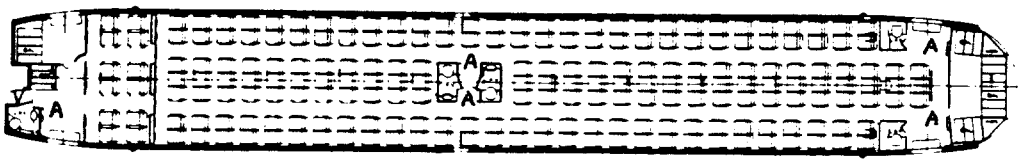

12 First Class (Total 212 Passengers)

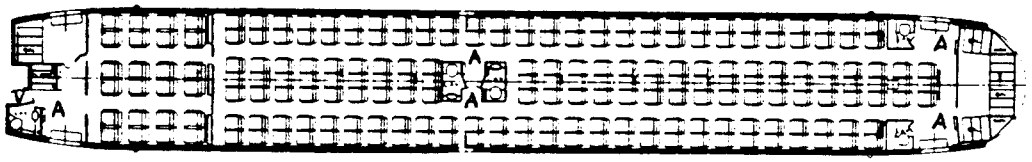

24 First Class (Total 210 Passengers)

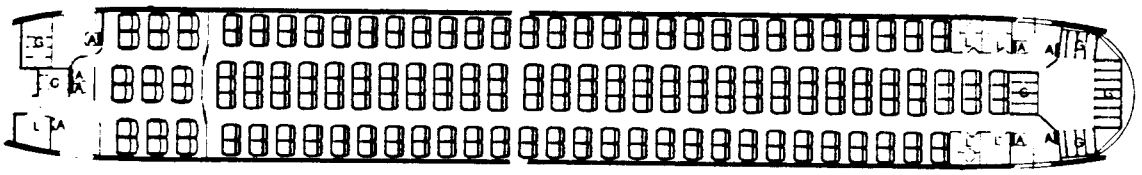

18 First Class-38 in. Pitch

213 Passengers

195 Tourist-34 in. Pitch

One and
One Half
Meal Service

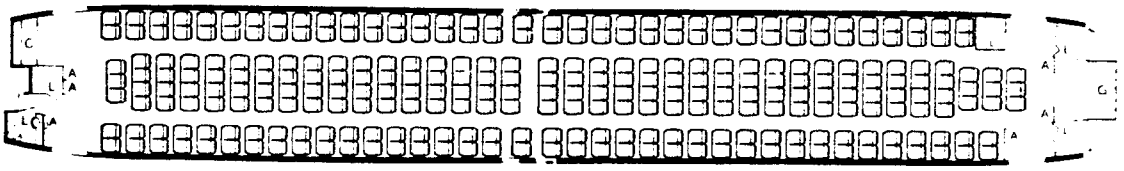

290 Passengers-31/30 in. Pitch

Very High
Density
Inclusive Tour
Two Overwing
Exits Per Side

A = ATTENDANT L = LAVATORY

G = GALLEY

WIDE BODY

COURTESY: BOEING

Figure 3.27 Example Seating Arrangements: Boeing 767-200

Table 3.1 Seat Classification and Seat Dimensions

Note: see Figure 3.28 for definition of seat dimensions.

Symbol	Unit	Seat Classification De Luxe	Normal	Economy
a	in.	20(18.5-21)	17(16.5-17.5)	16.5(16-17)
b	in.	47(46-48.5) for two seats per block	40(39-41)	39(38-40)
b	in.	---	60(59-63) for three seats per block	57
l	in.	2.75	2.25	2.0
h	in.	42(41-44)	42(41-44)	39(36-41)
k	in.	17	17.75	17.75
m	in.	7.75	8.5	8.5
n	in.	32(24-34)	32(24-34)	32(24-34)
p/p_{max}	in./in.	28/40	27/37.5	26/35.5
α/α_{max}	deg/deg	15/45	15/38	15/38

The data in brackets indicate the range of numbers found.

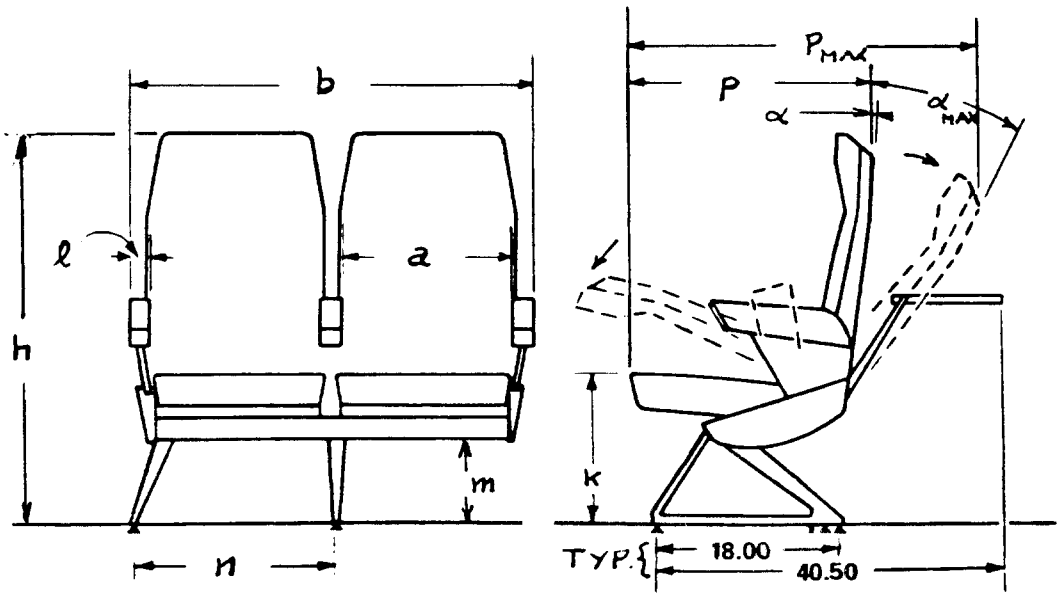

Figure 3.28 Definition of Seat Dimensions in Table 3.1

L. A. RUMBOLD AND CO. LTD.
LONDON, N. W. 10. ENGLAND

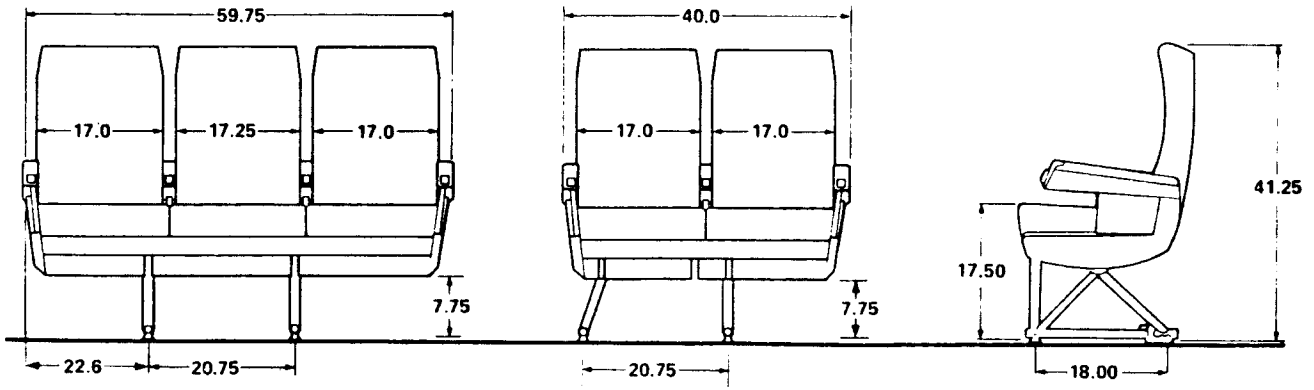

WEIGHT TRIPLE 62.5 lb. HYDRAULIC RECLINE

WEIGHT DOUBLE 43.5 lb. HYDRAULIC RECLINE

TYPE 1600 ('PACEMAKER')

BURNS AERO SEAT COMPANY, INC.
BURBANK, CALIFORNIA, USA

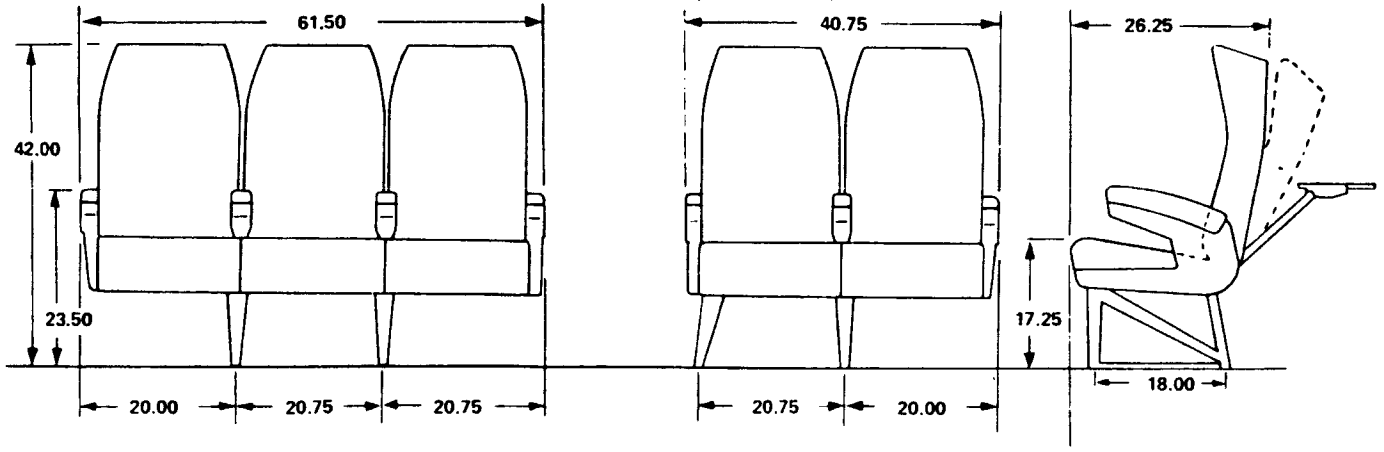

WEIGHT TRIPLE 69.3 lb. DOUBLE 49.7 lb.

TYPE 811

All measurements in inches

Figure 3.29a Example Airline Seats

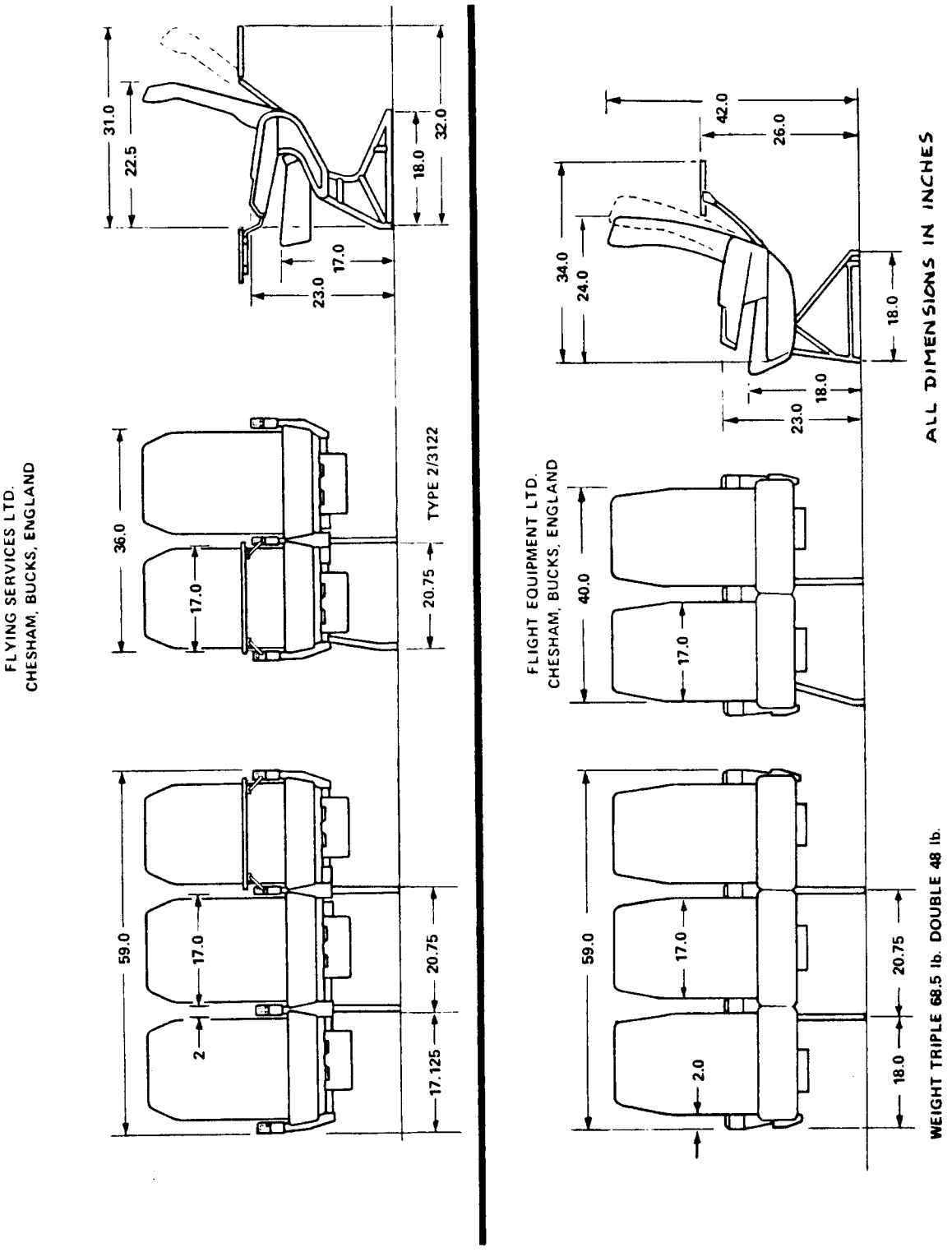

Figure 3.29b Example Airline Seats

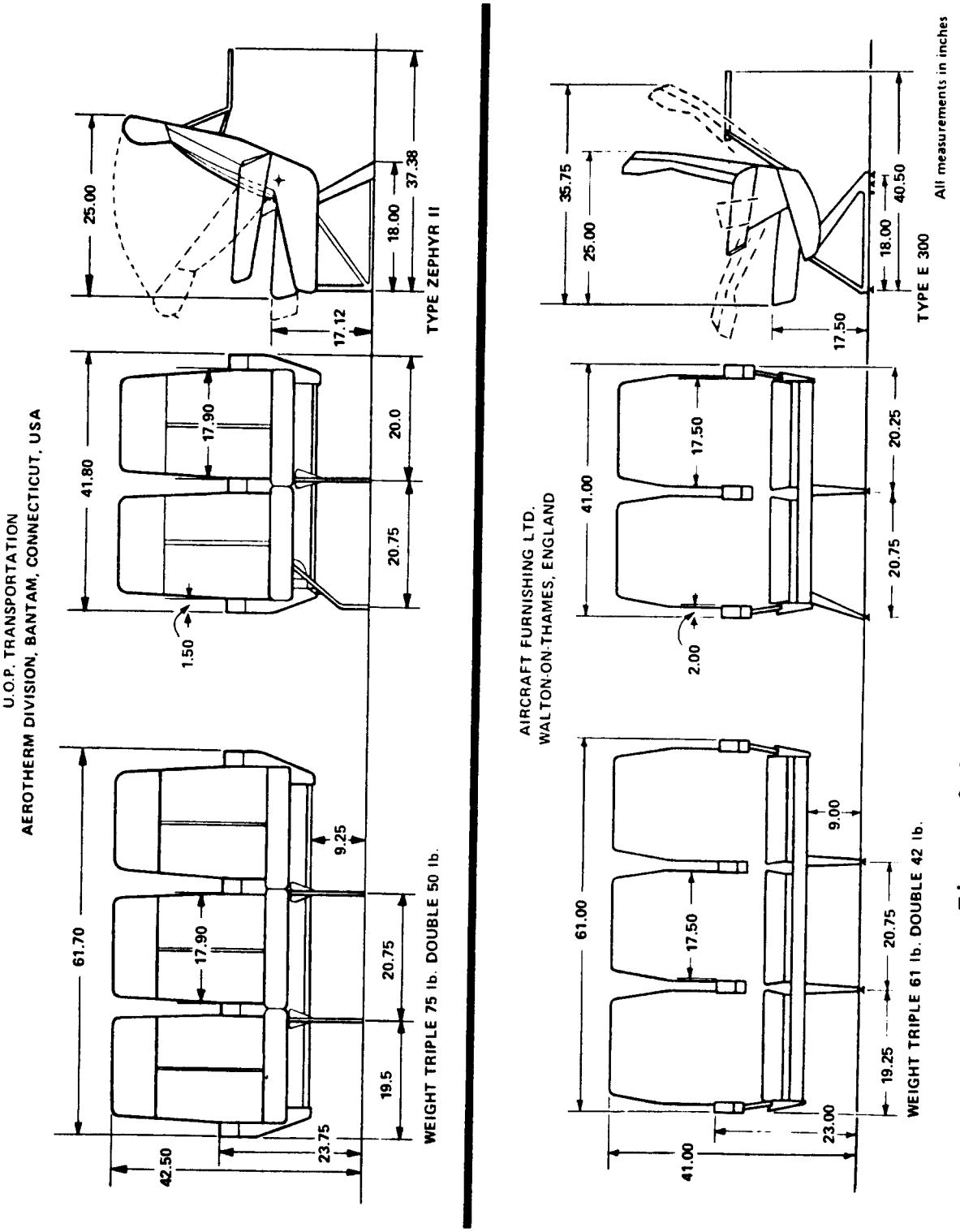

Figure 3.29c Example Airline Seats

Table 3.2 Design Limit Load Factors for Airplane Seats

Certif. Base	Forward	Rearward	Upward	Downward	Sideward
FAR 25.561	9.0	-	2.0	4.5	1.5
BCAR D3-8	9.0	1.5	4.5	4.0	2.25

The numbers reflect the amount of g's the seat must be able to withstand with a nominal 170 lbs passenger. Seat attachment fittings must be able to withstand an additional factor 1.33 according to FAR 25.785.

Table 3.3 Seat Weights for Commercial Airplanes

Seat Classification	Medium/Long Haul (lbs)	Short Haul (lbs)
De Luxe Single	47	40
Double	70	60
Normal Single	30	22
Double	56	42
Triple	78	64
Economy Single	24	20
Double	47	39
Triple	66	60
Commuter Single	--	17
Double	--	29
Light weight seats (civil and military)		14
Attendants seats	18	14
Executive seats	32 - 50	
Ejection seats (installed)	150	

3.3.2.3 Restraint systems

For protection of passengers and crew members in the case of flight through turbulence as well as in the case of a crash, restraint systems are required.

Reference 11, FAR 23 and 25 parts 561 and 785 define the design requirements for restraint systems. Seat belts are required for all seats. In addition, shoulder harnesses are required for crew members.

Reference 22 contains useful hints to airplane designers in the area of occupant injury prevention. Figure 3.30 shows the preferred geometry for shoulder harness installations according to Ref.23.

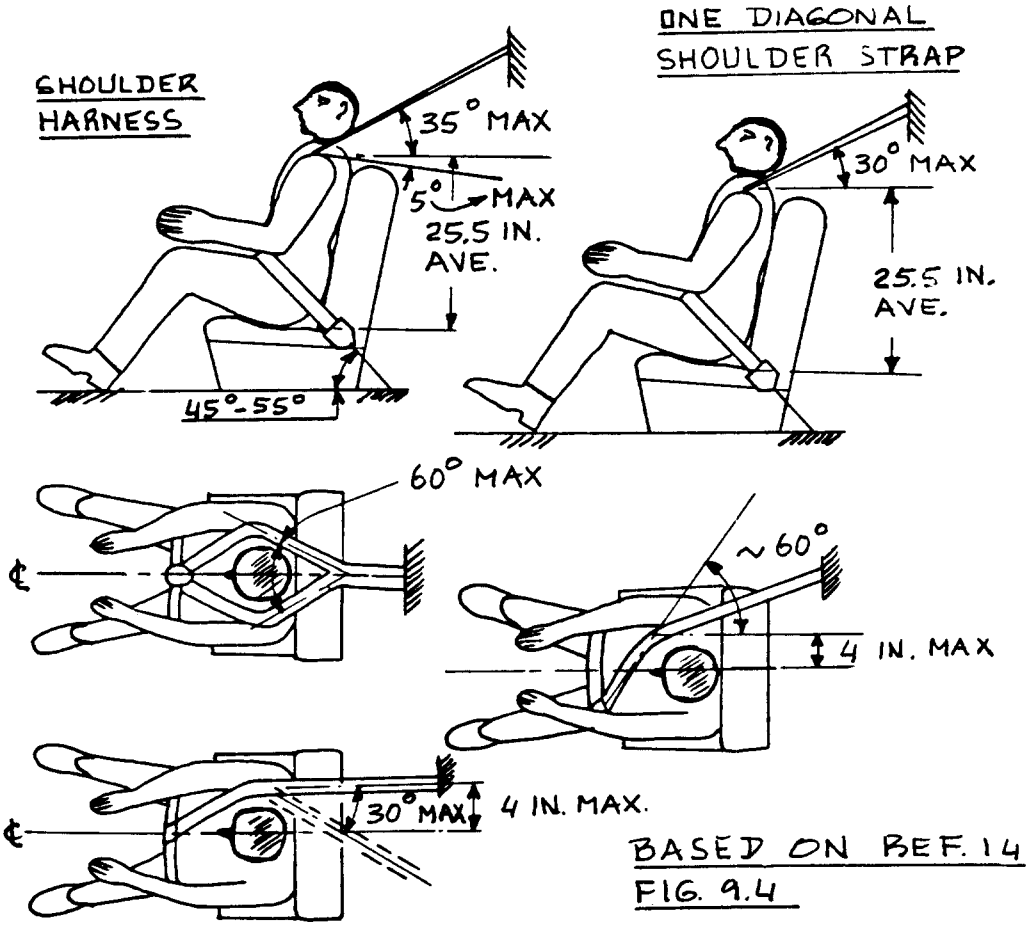

Figure 3.30 Geometry for Shoulder Harness Installation

3.3.3 Layout of Doors, Emergency Exits and Windows

All doors, exits and windows are potential sources for leaks, noise, drag and excess weight. Passenger comfort and emergency evacuation requirements demand a minimum number of as well as a minimum size for doors, exits and windows. Here is a clear conflict between requirements of safety, comfort and economics.

3.3.3.1 General aviation airplanes

FAR 23.807 (Ref.11) lists the requirements for emergency exits which apply to this airplane category. Consult this FAR before finalizing any door and exit layout.

Window layout is normally dictated by the seating arrangement in this type of airplane. The reader should look at the door and window layouts shown in the threeviews of Chapter 3, Part II.

Figures 3.48 through 3.52 contain information about door and exit layouts used in general aviation airplanes.

In many general aviation airplanes the wing attaches to the fuselage via two or more fuselage frames. In such cases the window spacing and sizing is dictated by structural considerations.

Refer to sub-sub-section 3.3.3.2 for more information about window location and window design.

3.3.3.2 Transport airplanes

Transport airplanes normally are required to have three types of doors/exits:

1. Passenger access doors 2. Service access doors
3. Emergency exits

Passenger access doors are normally located on the port side. Servicing access doors are normally located on the starboard side.

For airplanes carrying less than 80 passengers one passenger access door is normally sufficient. For airplanes carrying between 80 and 200 passengers at least two such doors should be provided. For airplanes carrying more than 200 passengers, the number of doors depends on the envisioned boarding scenarios.

Comfortably sized passenger access doors should be

6x3 ft. These dimensions are very difficult to achieve in smaller airplanes and a compromise is needed.

The reader must bear in mind that any door or exit represents a potential pressurization leak, a potential drag cause (because of seal deterioration) and a significant increment in weight. From a weight as well as from an economics viewpoint it makes sense to have as few doors and exits as possible. From an emergency evacuation viewpoint the opposite is true.

The number and the size of doors and emergency exits required in civil airplanes are defined in FAR 23 and 25 parts 807-813. The reader should consult these FAR's before starting the door layout process.

Table 3.4 defines the number and the type of required exits as a function of the number of passengers carried. Table 3.5 provides the minimum required dimensions for each type of exit. Figure 3.31 shows what the various exit types look like and where they are located.

Important notes:

1. FAR 25.807 also demands ventral and/or tailcone exits.

2. All emergency exits and doors must meet the 'unobstructed access' requirement. To satisfy this requirement the following dimensions are used:

   For Type I exits: 36 inches of access width
   For Type II exits: 20 inches of access width
   For Type III and IV exits: 18 inches of access width.

3. The unobstructed access width requirement affects the allowable seat pitch near emergency exits! Account for this in preparing a seating layout.

4. FAR 25.807 also requires escape chutes in some cases. Figure 3.32 shows an example for the Boeing 767-200.

5. Additional requirements apply to airplanes which are operated over water, to cope with emergency evacuation following a ditching.

The window pitch in a passenger transport is normally dictated by the 'frame spacing' requirement and not by the seating layout. Fuselage frames are typically spaced about 20 inches apart.

Windows should be shaped as circles, ovals or rec-

Table 3.4 Required Number of Exits per FAR 25

Number of Passenger Seats	Number of Required Exits on Each Side of the Fuselage			
	Type I	Type II	Type II	Type IV
1 - 10	none	none	none	1
11 - 19	none	none	1	none
20 - 39	none	1	none	1
40 - 59	1	none	none	1
60 - 79	1	none	1	none
80 - 109	1	none	1	1
110 - 139	2	none	1	none
140 - 179	2	none	2	none
more than 179	The FAA imposes special conditions			

Notes: 1. The BCAR requirements of Ref.23 are different.
2. Exits do not have to be located diametrically opposed to each other.
3. Instead of one Type III exit it is permissible to use two Type IV exits.
4. See Table 3.5 for dimensions of each exit Type.

Table 3.5 Minimum Dimensions for Exits of Table 3.4

Exit Type and Location	Dim. B	Dim. H	Dim. R	Maximum Step Height	
				Dim. h_1 inside	Dim. h_2 outside
I Floor level	24	48	8.0	not applicable	
II Floor level Above wing	20	44	6.7	not applicable 10	17
III Above wing	20	36	6.7	20	27
IV Above wing	19	26	6.3	29	36

Notes: 1. See Figure 3.31 for explanation of dimensions.
2. All dimensions are in inches.

tangles with liberally rounded corners. This is to avoid unneccessary stress concentrations in the pressure shell.

Window tops should be located at eye level of a 90 percentile passenger.

Many dedicated cargo transports do not have windows to save weight!

In supersonic airplanes which fly at very high altitudes cabin windows should be as small as possible. The large pressure differentials encountered by such airplanes may dictate the elimination of passenger windows.

Examples of door and window layouts of passenger and cargo airplanes are given in Section 3.4.

3.3.3.3 Military airplanes

The door and exit requirements for military airplanes varies with the type of mission. The military RFP will normally include references from which the door and exit requirements can be distilled.

Figures 3.53 (AN-26 and Hercules) show examples of door and window layouts of typical military transports.

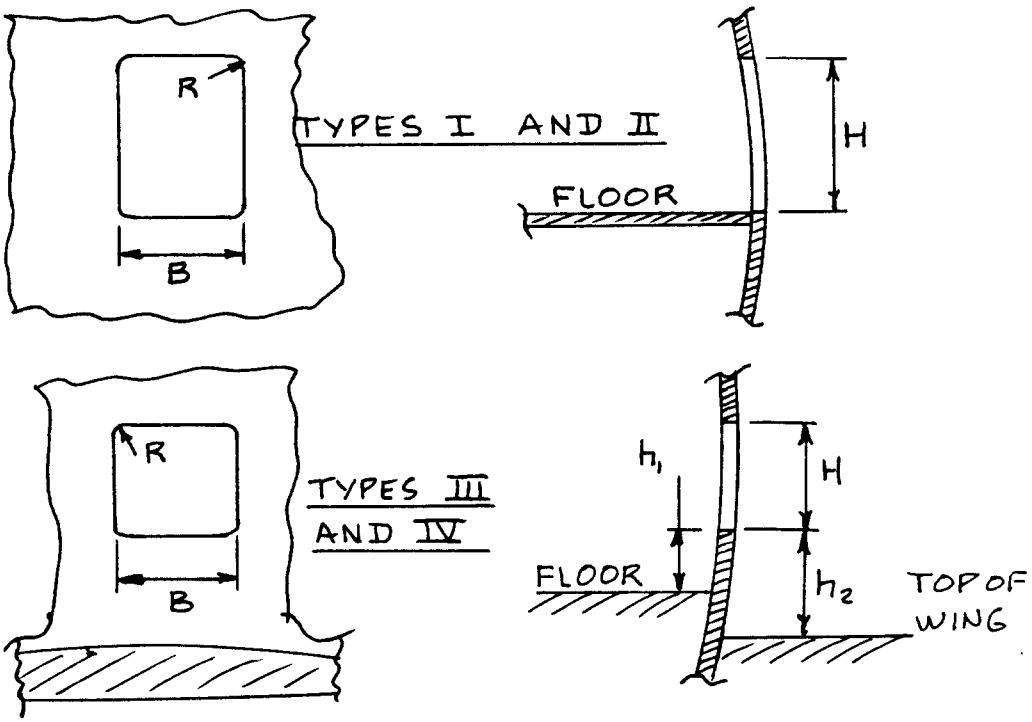

Figure 3.31 Definition of Exit Geometry

Emergency Evacuation Slides

- Inflatable slides automatically deploy upon opening each exit
- Inflation by stored gas
- Escape system disarmed when door opened from outside airplane
- Slides usable in all landing gear conditions
- Optional slide/rafts available at type "A" doors.*

BOEING 767-200
COURTESY: BOEING

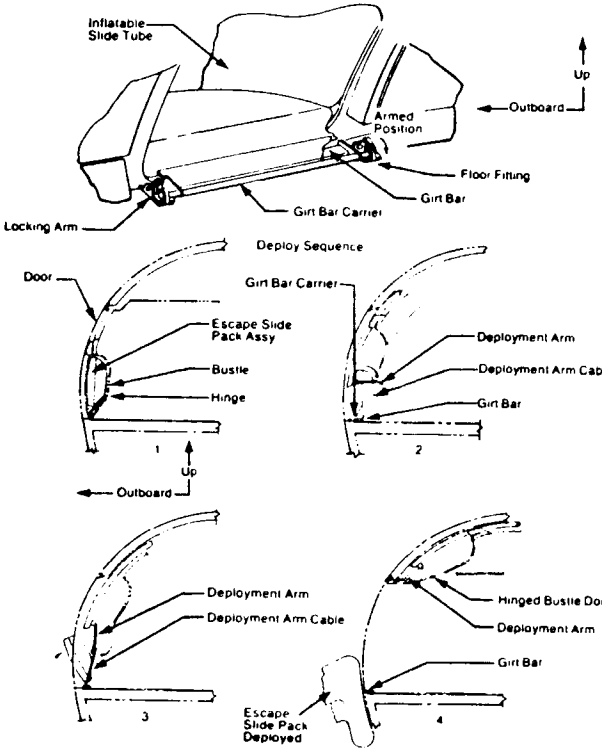

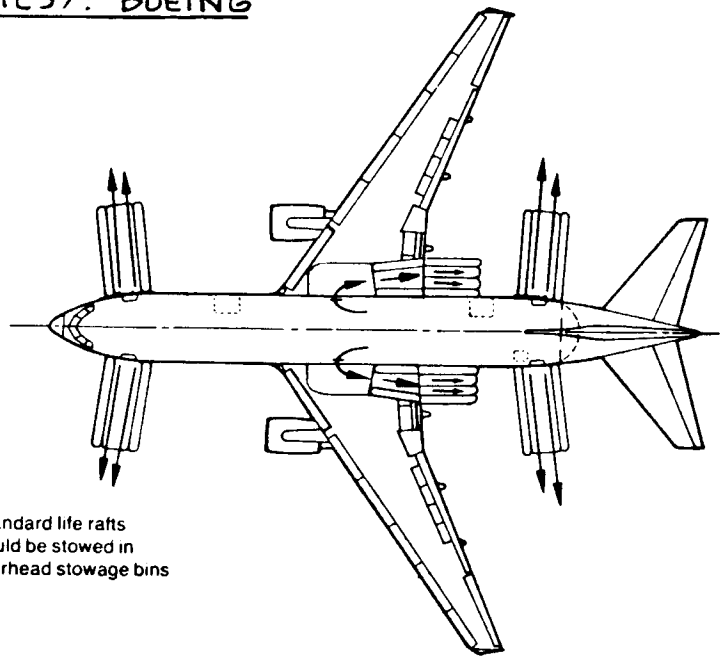

*Standard life rafts would be stowed in overhead stowage bins

Slides Deployed

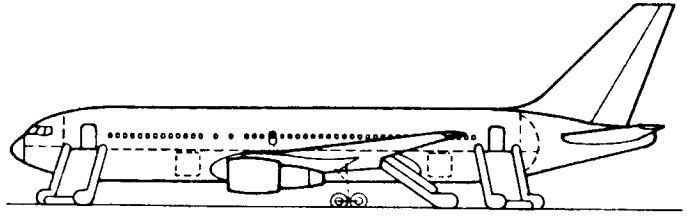

Figure 3.32 Example of Escape Chute Deployment

3.3.4 Galley, Lavatory and Wardrobe Layouts

Table 3.6 presents typical dimensions of galleys, lavatories and wardrobes as they are found in a number of airplane types. For smaller general aviation airplanes Figures 3.51 and 3.52 provide an indication of typical dimensions associated with these items.

Figures 3.33 and 3.34 show typical installations used in a narrow-body and in a wide-body transport.

Table 3.6 Typical Dimensions of Galleys, Lavatories and Wardrobes Used in Several Airplanes

Airplane Type	N_{pax}	Range	Galleys No.	Galleys Dim.	Lavatories No.	Lavatories Dim.	Wardrobes No.	Wardrobes Dim.
Business Jets								
HFB 320	7	1,000	1	24x24	1	30x26	1	24x15
Falcon 20F	10	1,500	1	27x18	1	44x30	1	51x25
BAe HS 125	8	1,450	none		1	35x28	1	24x12
Regional Turboprops								
Nord 262	29	400	1	23x20	1	41x28	1	40x24
Gulfstr. I	19	2,100	1	34x25	1	67x37	1	36x32
Bae HS 748	44	1,000	1	37x14	1	53x35	none	
Fokker F27	48	1,100	1	43x35	1	47x46	1	31x16
DHC-7	44	800	1	26x24	1	46x30	1	26x24
Electra	95	2,300	2	46x26	4	46x41	2	46x34
Jet Transports								
VFW 614	40	700	1	35x28	1	55x32	1	65x40
Fokker F28	60	1,025	1	44x25	1	58x25	1	25x21
BAC 111	74	900	2	49x22	2	65x35	1	49x22
McDD DC9-10	80	1,100	1	48x33	2	48x48	2	48x21
B 737-200	115	1,800	1	55x43	2	43x34	1	55x43
Caravelle	118	1,000	1	51x43	2	55x43	2	24x17
D Mercure	140	800	none		2	47x34	2	49x16
B 727-200	163	1,150	2	51x32	3	43x39	Overhead	
A 300 B4	295	1,600	3	?	5	59x35	Overhead	
L 1011	330	2,700	1	240x162*	7	45x36	Overhead	
McDD DC10	380	3,000	1	240x162*	9	40x40	2	76x22
B 747	490	5,000	4	79x25	12	40x40	2	71x28

*under floor galley

All dimensions in inches. Data based on Ref.12, page 80.

AFT GALLEY

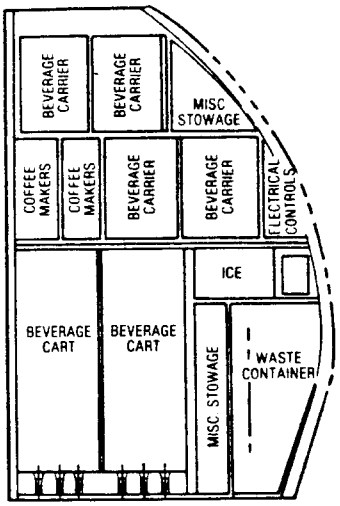

- Tourist class capacity
  - 2 beverage carts
  - 4 beverage carriers

AFT GALLEY

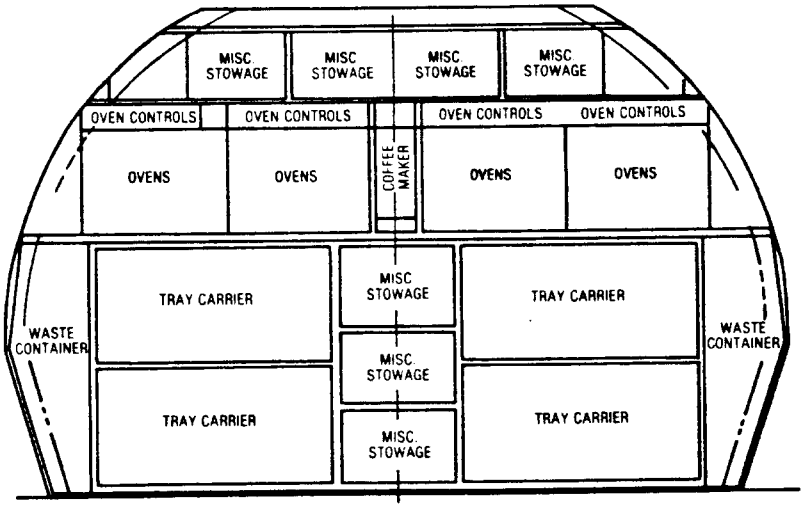

- Tourist class capacity
  - 12 tray carriers-168 trays
  - 8 ovens-168 entrees

- Main deck galleys
- Aft tray carrier service complexes
  - Galley complexes located at the aft end of the passenger cabin
  - Recessed floor gutter and door periphery connected to sump drain

FWD GALLEY

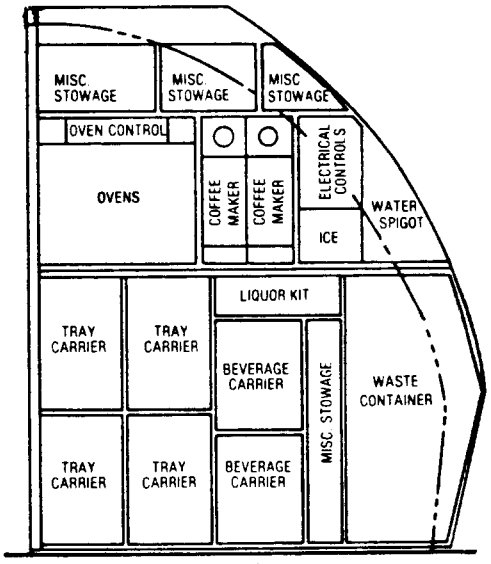

BOEING 757

COURTESY : BOEING

- First class capacity
  - 2 ovens-42 entrees
  - 4 tray carriers-56 trays

- Main deck galley
- Forward tray carrier service galley complex
  - Galley complex located at forward end of passenger cabin
  - Recessed gutters around galleys and periphery connected to overboard drain

Figure 3.33 Example of Narrow Body Galley Layout

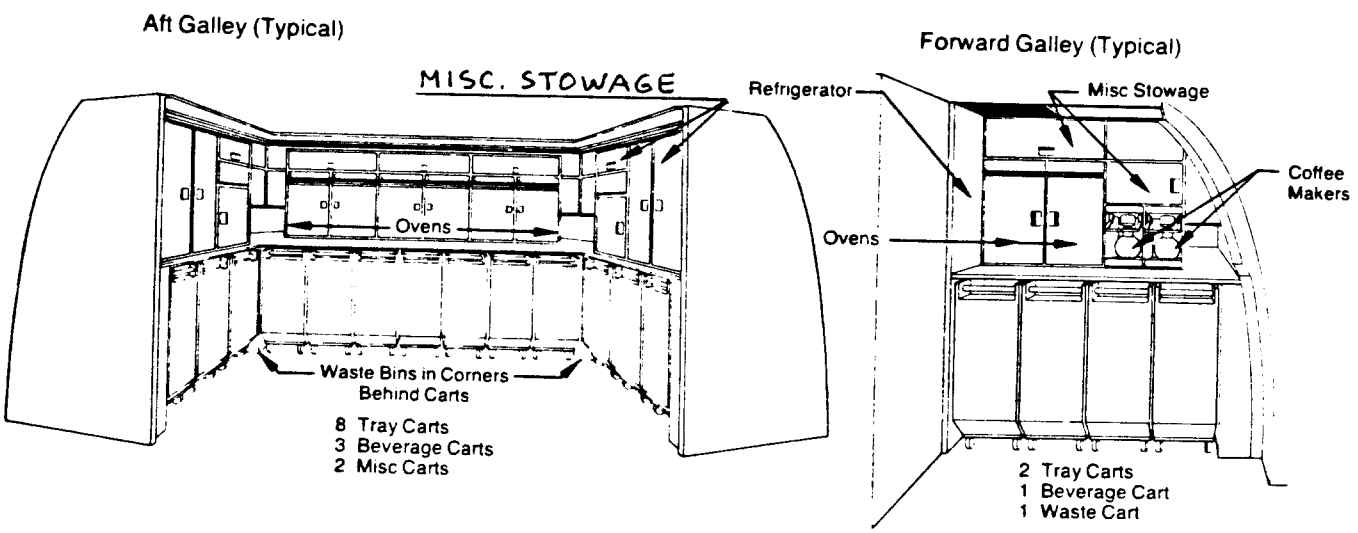

Passenger Services

Interior	Lavatory Ratio – Pass/Lav		Galley Volume – ft^3/Pass (m^3/Pass)		Coat Rod – in./Pass (cm/Pass)	Attendants
	F/C	T/C	F/C	T/C		
208 Mixed Class	18	48	7.72 (0.20)	2.10 (0.06)	0.16 (0.41)	6
211 Mixed Class	18	48	5.11 (0.14)	1.61 (0.05)	0.33 (0.84)	6
213 Mixed Class	18	49	5.11 (0.14)	2.04 (0.06)	0.33 (0.84)	6
216 Mixed Class	18	50	5.11 (0.14)	1.57 (0.04)	0.32 (0.81)	6
230 All Tourist		46		1.47 (0.04)		6
241 All Tourist		60		1.67 (0.05)		6
255 (7) All Tourist		64		1.85 (0.03)		6
255 (8) All Tourist		51		1.85 (0.03)	0.49 (1.24)	6
289(8) All Tourist		58		1.39 (0.03)		6

One Meal Service – 211 Passenger Arrangement (Typical)

Item	Total
Tray Carts 12 in. Wide (14 or 28 Tray Capacity)	10 *(252 Meals)
Bev Carts	4
Misc Carts	2
Waste Carts	1
Waste Bins	2
Coffee Makers	6
Ovens	7
Refrig Compt	5
Misc Stowage	7 ft^3

* 211 Meals Plus 19% Overage for Crew and Spare Meals

BOEING 767-200
COURTESY: BOEING
SEE P.61 FOR TYPICAL LOCATION OF PASSENGER SERVICES

Figure 3.34 Example of Wide Body Galley Layout

3.3.5 Layout of Cargo/Baggage Holds Including Data on Cargo Containers and Pallets

The amount of cargo which needs to be carried by a particular airplane depends strongly on the operator and his route system. Cargo is carried in passenger transports as well as in dedicated freighter type airplanes. In passenger transports the cargo is usually carried below the cabin floor. In dedicated freighter airplanes cargo is carried above the cabin floor as well as below the cabin floor. In addition there exist so-called 'quick-change' and 'combi' configurations of passenger transports where any mix of cargo and/or passengers can be carried.

Data on cargo and baggage volume requirements are presented in sub-sub-section 3.3.5.1. Shapes, sizes and weights of 'standard' containers and pallets are given in sub-sub-section 3.3.5.2.

Sub-sub-section 3.3.5.3 presents severel airplane configurations which have been used to allow for easy loading and unloading of cargo and luggage.

3.3.5.1 Cargo and baggage volume requirements

For cargo a workable average density is: 10 lbs/ft^3.

Loading efficiency for cargo varies from 75 to 100 percent depending on the method used in carrying the cargo.

For passenger baggage (luggage) the following numbers represent typical averages:

Baggage weight per passenger is:

30-35 lbs for short haul flights
40-45 lbs for long haul flights

Baggage density averages to: 12.5 lbs/ft^3.

Loading efficiency for baggage is 85 percent. This means that 15 percent of the design baggage volume is in fact lost!

Many passengers (particularly business people) insist on carrying their own luggage on board. Although the airlines have established limits on the amount of 'carry-on' luggage, they also have provided convenient overhead storage bins in most larger transport airplanes.

Figure 3.35 shows an example of such overhead storage facilities.

The cargo/baggage hold in the belly of transport airplanes should have an effective (i.e. usable) height of at least 35 inches if loading personnel are required to move about the belly holds. If no personnel need to be in the belly holds, a height of 20 inches may suffice. The need for a workable height in belly holds may force a non-circular cross section on the designer, such as a so-called 'double-bubble' cross section (See Fig. 3.36).

In laying out the belly hold it is essential that the impact of all possible loading scenarios on center of gravity location be accounted for. Chapter 10 of Part II contains a method for determining the 'weight and balance' consequences of different loading scenarios.

Many airplanes have belly holds forward of the wing as well as behind the wing for precisely this reason.

3.3.5.2 Data on standard containers and pallets

The use of pallets and containers greatly reduces the loading time of baggage and cargo. On nearly all medium to long haul operations, cargo as well as luggage is preloaded in containers and/or on pallets. The industry has developed a range of so-called standard containers and pallets as shown in Figure 3.37. Ref.12, p.85 contains data on dedicated freight containers and pallets.

3.3.5.3 Typical loading/unloading configurations

Figures 3.47 and 3.54 show typical dimensions of belly holds and freight floor layouts used in different airplane types. Examples of the door and ramp configurations which have been used in a number of airplanes are given in Figures 3.38 through 3.42.

It is essential that a certain amount of clearance be 'designed into' any freight/cargo door. Adequate clearance means a minimum of five inches in height and a minimum of nine inches in width.

To facilitate loading and unloading many floors are equipped with roller systems. The 747F of Figure 3.38 is a typical example.

Freight floors need to be equipped with tie-down provisions to prevent the cargo from sliding and thereby

changing the c.g. It is also necessary to build in provisions to prevent cargo from sliding into passengers or crew in the case of a crash. A 9g limit load requirement is therefore imposed on all tie-down or catch-net restraint systems.

Typical structural arrangements of freight floors are given in Section 3.5.

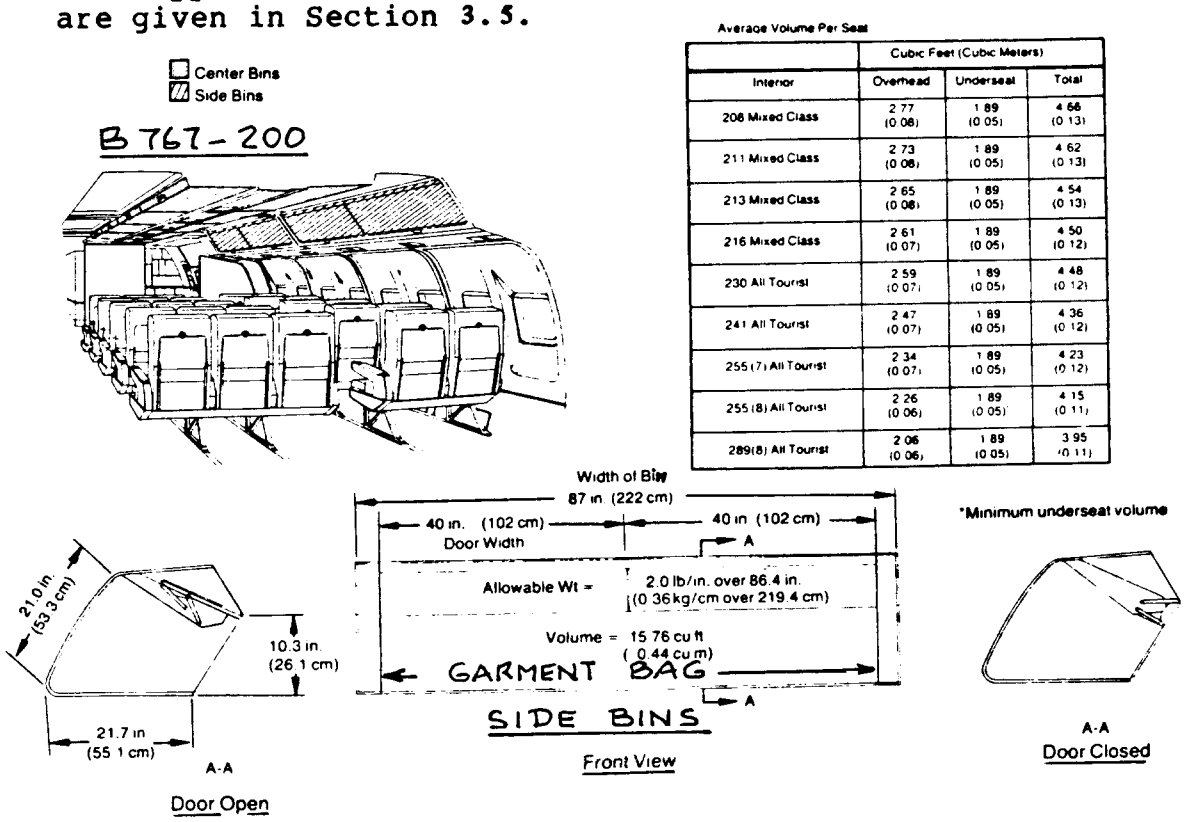

Figure 3.35 Example of Overhead Storage

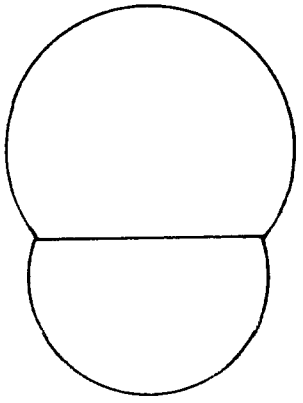

BOEING STRATOCRUISER

Figure 3.36 Example of a Double-Bubble Cross Section

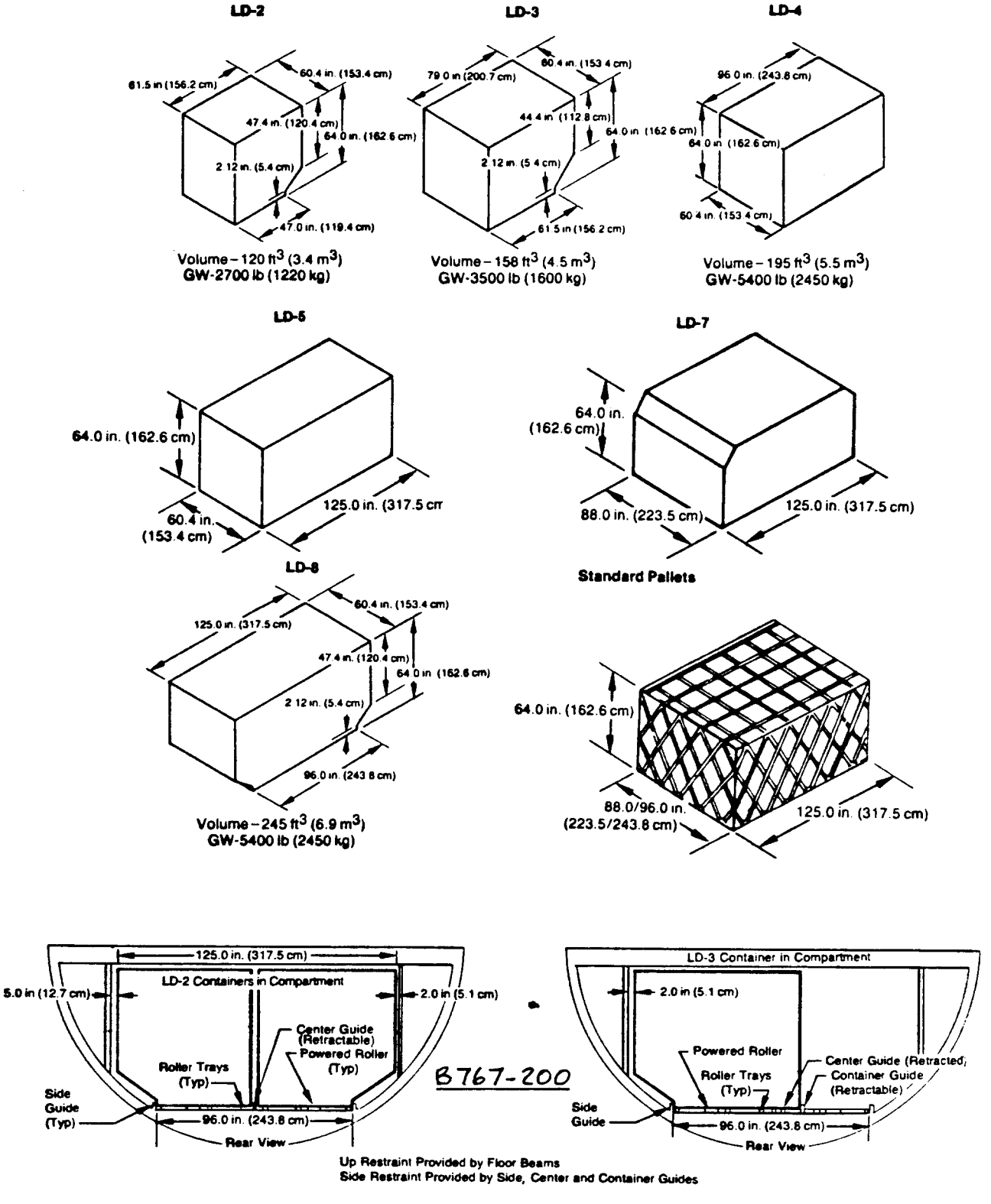

Figure 3.37 Typical Pallet and Container Sizes

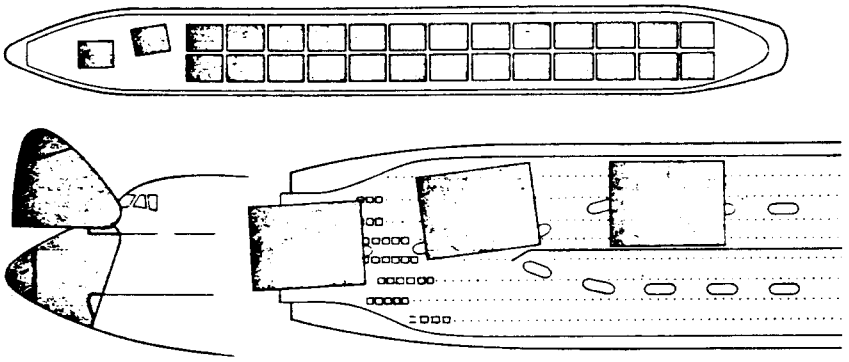

Figure 3.38 Cargo Deck Arrangement for the Boeing 747F

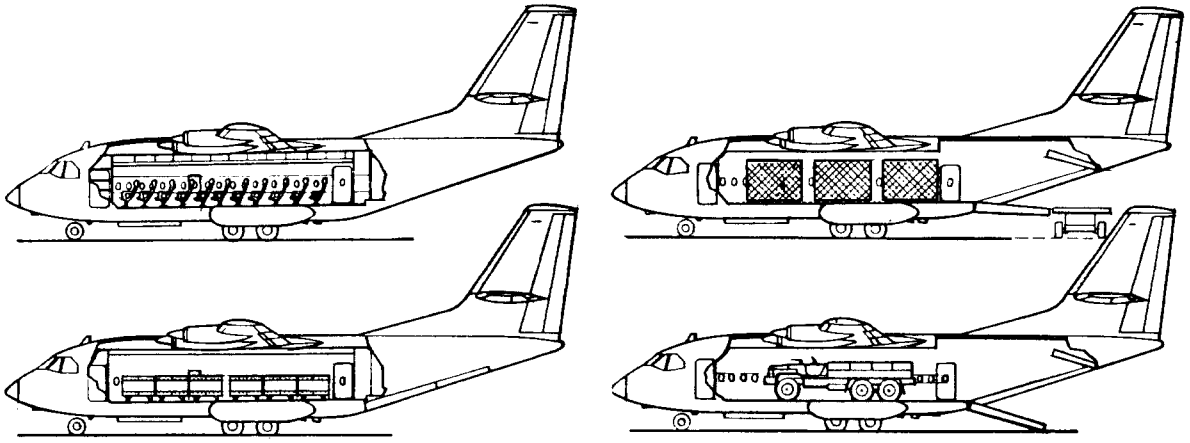

Figure 3.39 Passenger or Cargo Arrangement CASA 401

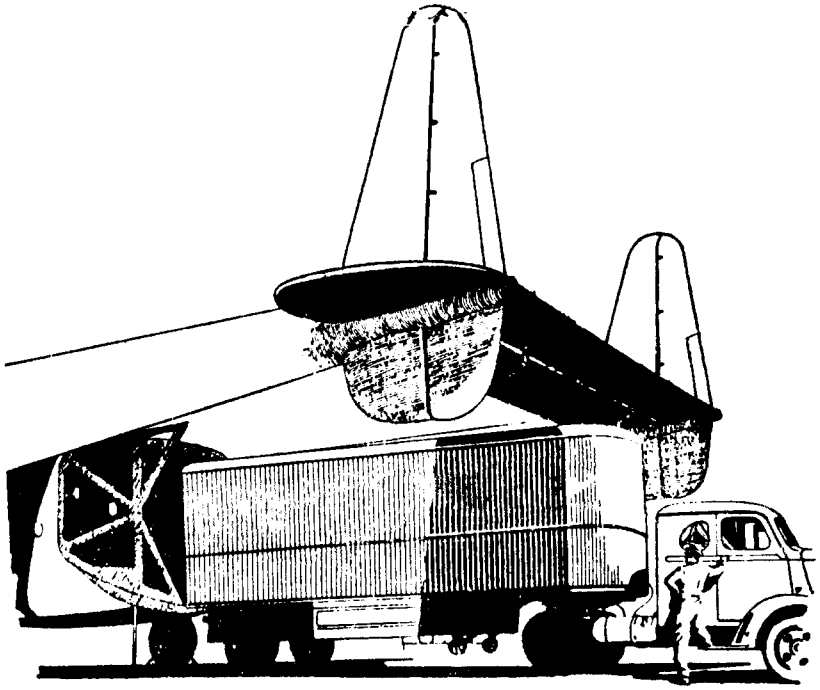

Figure 3.40 Loading/Unloading of a Fairchild C119

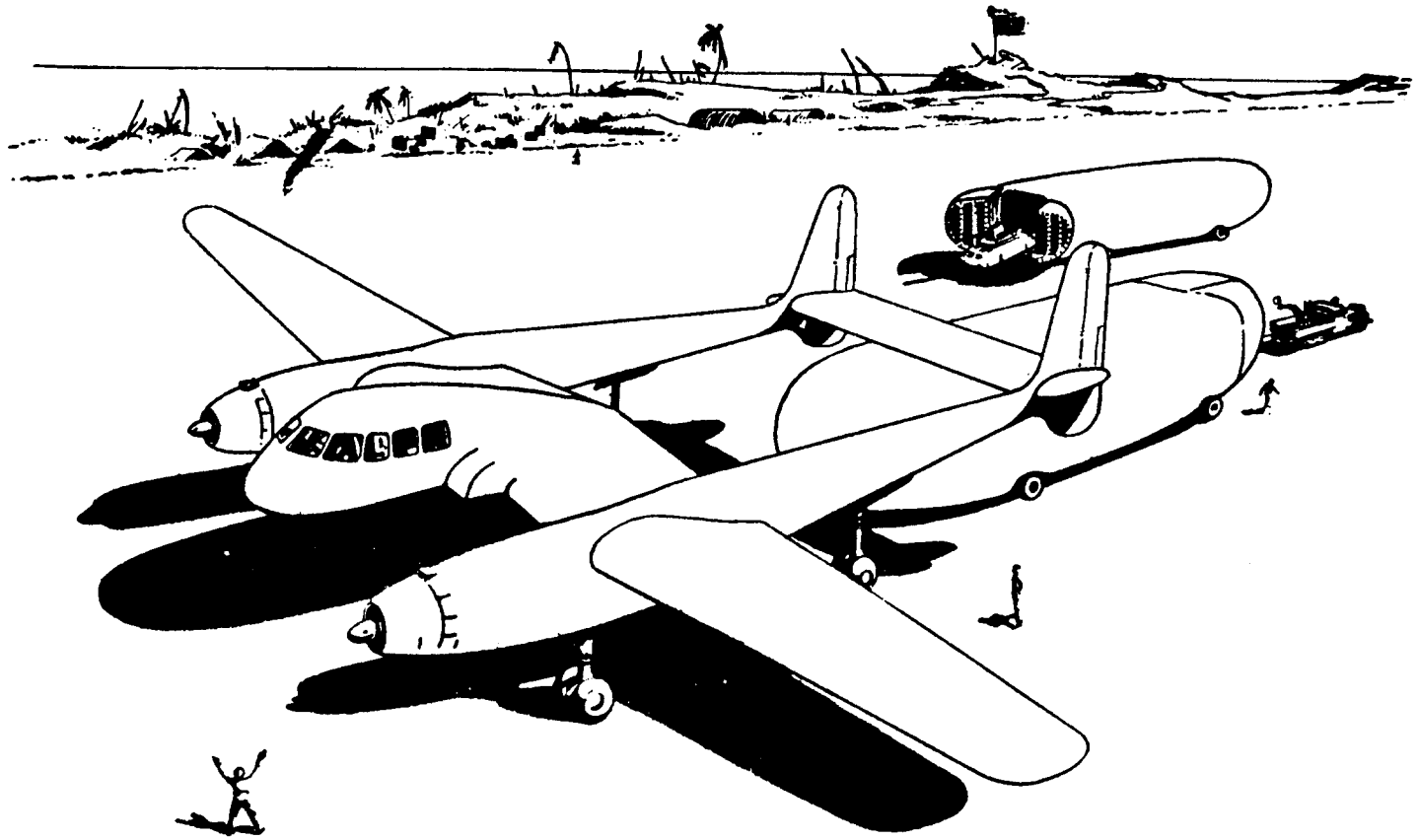

Figure 3.41 Example of a Detachable Pod Concept

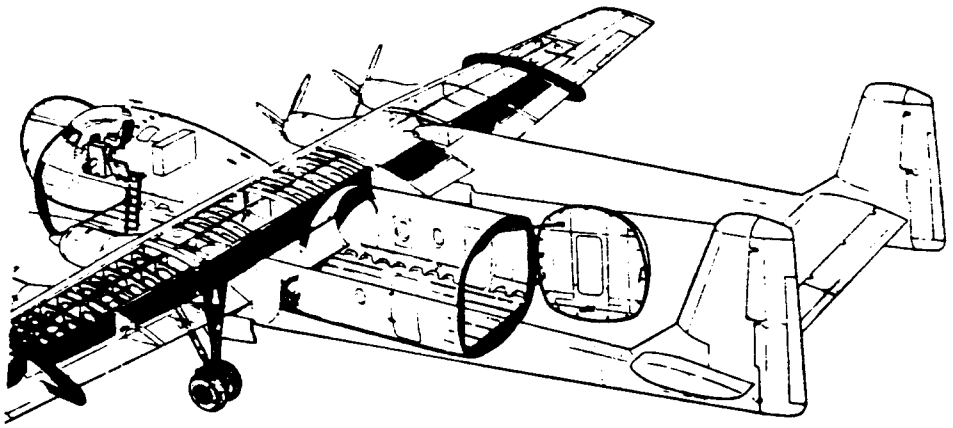

Figure 3.42 Rear and Front Loading Doors: AW650 Argosy

3.3.6 Inspection, Maintenance and Servicing Considerations

It is essential that those areas of the fuselage which require frequent access for inspection, replacement of parts or repairs be easily accessible. Design engineers need to work with airplane mechanics to find out the conditions under which typical inspection, maintenance and servicing procedures are being carried out!

The author has witnessed mechanics in freezing conditions trying to open an undersized access cover. Having finally achieved this after having to take off their gloves (!) they discovered that it was impossible to look inside without putting down their parka top, exposing their faces to sub-zero conditions.

ENGINEERS: design for maintenance and inspectability under climatic conditions which can be expected to prevail.

In transport operations it is essential that the 'turn-around' time be minimized as much as possible. This means that a large number of vehicles need to have simultaneous access to the airplane when parked at the gate. Typical of the services which need to be performed on an airplane simultaneously are:

1. load and unload passengers
2. refuel and reoil
3. replenish potable water
4. clean airplane cabin
5. remove food and beverage left-overs and load fresh food and beverage supplies
6. service lavatories

The required trucks and other servicing vehicles, loading and unloading ramps, stairs etc. must not interfere with each other or with protruding components of the airplane (for example: wing tip booms are an invitation to collisions). Careful attention needs to be given to the layout of all service doors, cargo doors and access covers.

Figures 3.43 and 3.44 present diagrams used to demonstrate to potential customers that an airplane design satisfies these requirements.

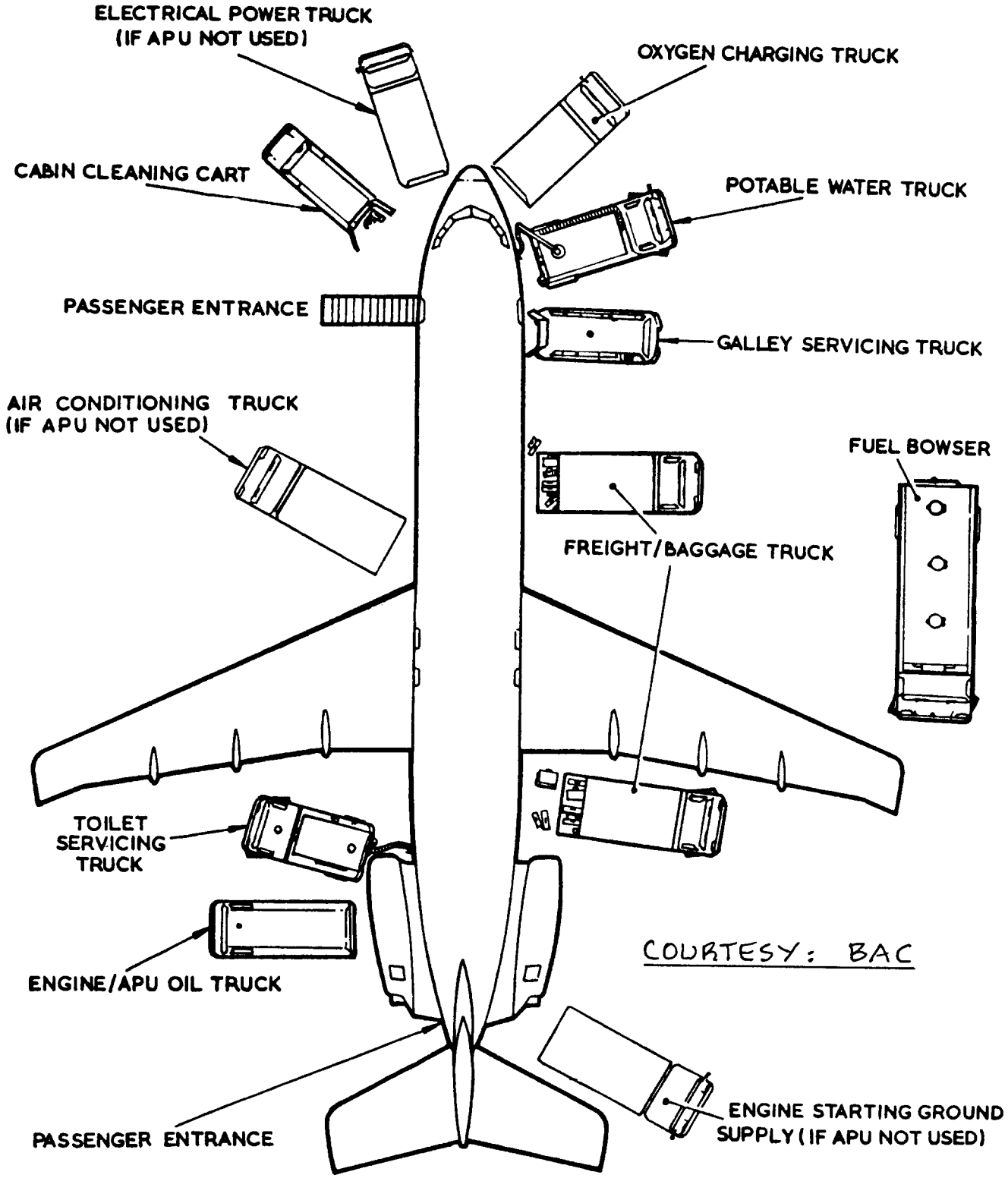

Figure 3.43 Terminal Servicing of a BAC 111

1. Radar Antenna, Glide Scope
2. Nose Gear Hinge Attach Bolt
3. Air Conditioner Condenser Blower and Relay
4. Avionics Compartment
5. Rudder Bell Crank
6. Rudder Tab Actuator
7. Elevator Bell Crank
8. Rudder Control Horn, Rudder Stops
9. Landing Gear Doors
10. Control Cables and Pulleys below Pedestal
11. Aft Fuselage Access, Outflow and Safety Valves
12. Oxygen Filler Gage and Service Valve
13. Air Conditioner Condenser
14. Horizontal Stabilizer Attachment
15. Elevator Push Rods, Pulleys, Tab Cables
16. Horizontal Stabilizer Attachment
17. Elevator Tab Actuators and Stops

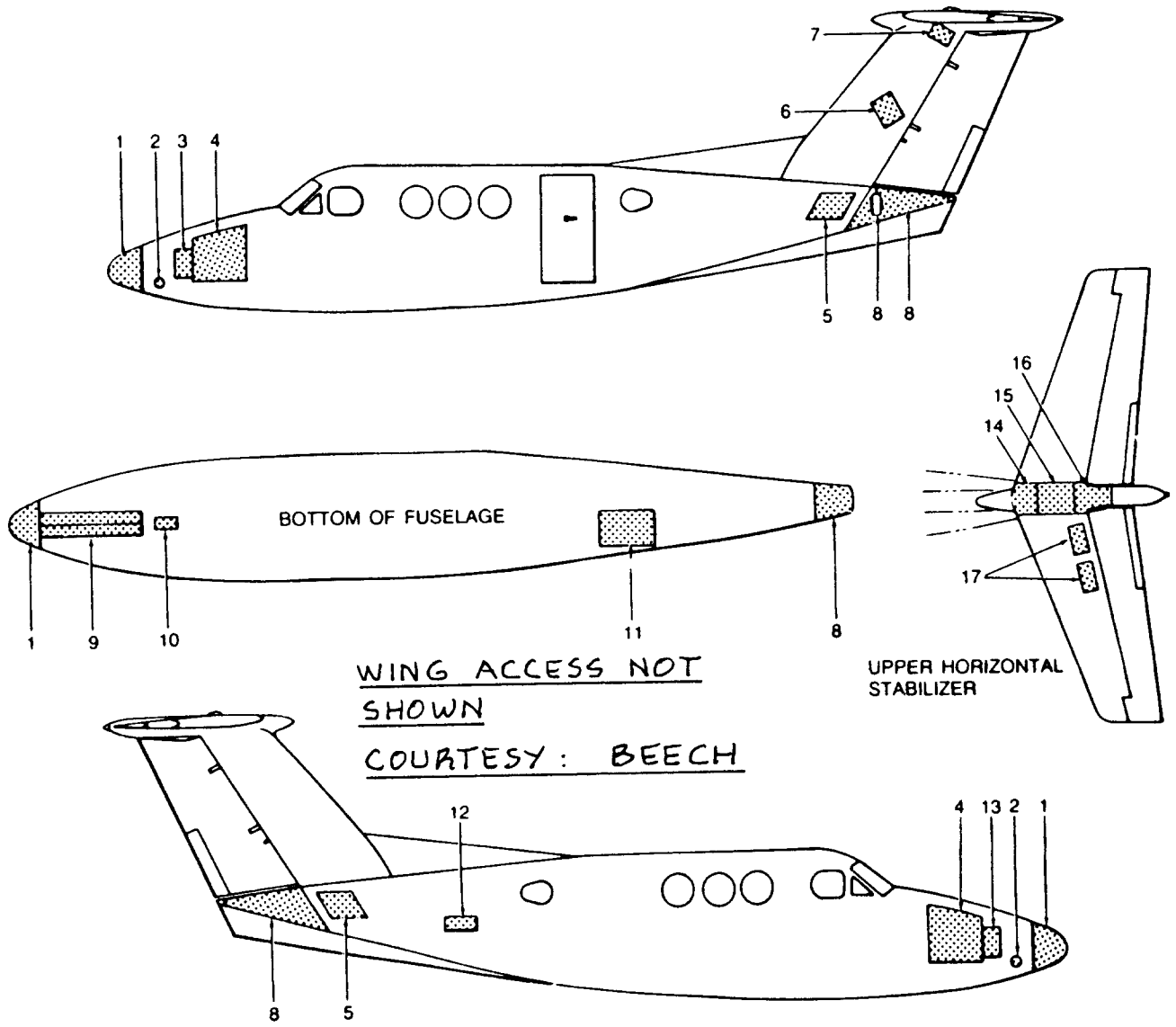

Figure 3.44 Access Diagram for the Beech King Air F90

3.4 DESIGN DATA FOR FUSELAGE CROSS SECTIONS, CABIN AND CARGO HOLD LAYOUTS, WINDOW AND DOOR LAYOUTS

During the fuselage layout design process decisions need to be made regarding the basic fuselage cross section, the overall cabin and cargo hold arrangement, and the window and door layout. Steps 4.1, through 4.6 of Chapter 4, Part II deal with these decisions. To arrive at these decisions it is desirable to have available a set of design data showing solutions arrived at by various airframe manufacturers. The purpose of this section is to provide these design data.

The data are organized as follows:

For fuselage cross sections:

Figure 3.45:	Fuselage Cross Sections for Business Jets
Figure 3.46:	Fuselage Cross Sections for Regional Turboprops
Figures 3.47a-c:	Fuselage Cross Sections for Jet Transports

For cabin and cargo hold layouts:

Figures 3.48a-d:	Cabin and baggage hold dimensions for single engine prop. driven airplanes
Figure 3.49:	Cabin dimensions for single engine piston/propeller driven airplanes
Figure 3.50:	Cabin dimensions for twin engine piston/propeller driven airplanes
Figures 3.51a-f:	Cabin dimensions for twin engine turbo-propeller driven airplanes
Figures 3.52a-e:	Cabin dimensions for business jets
Figures 3.53a-c:	Fuselage and cargo hold dimensions for turbopropeller driven transports
Figures 3.54a-l:	Fuselage and cargo hold dimensions for jet transports

For window and door layouts:

Figures 3.45 through 3.54 all show window, door (and emergency exit) arrangements.

NOTE: The design information in this section is based on data accumulated over several years from the following magazines:

1. Flight International (British weekly)
2. Business and Commercial Aviation (US monthly)

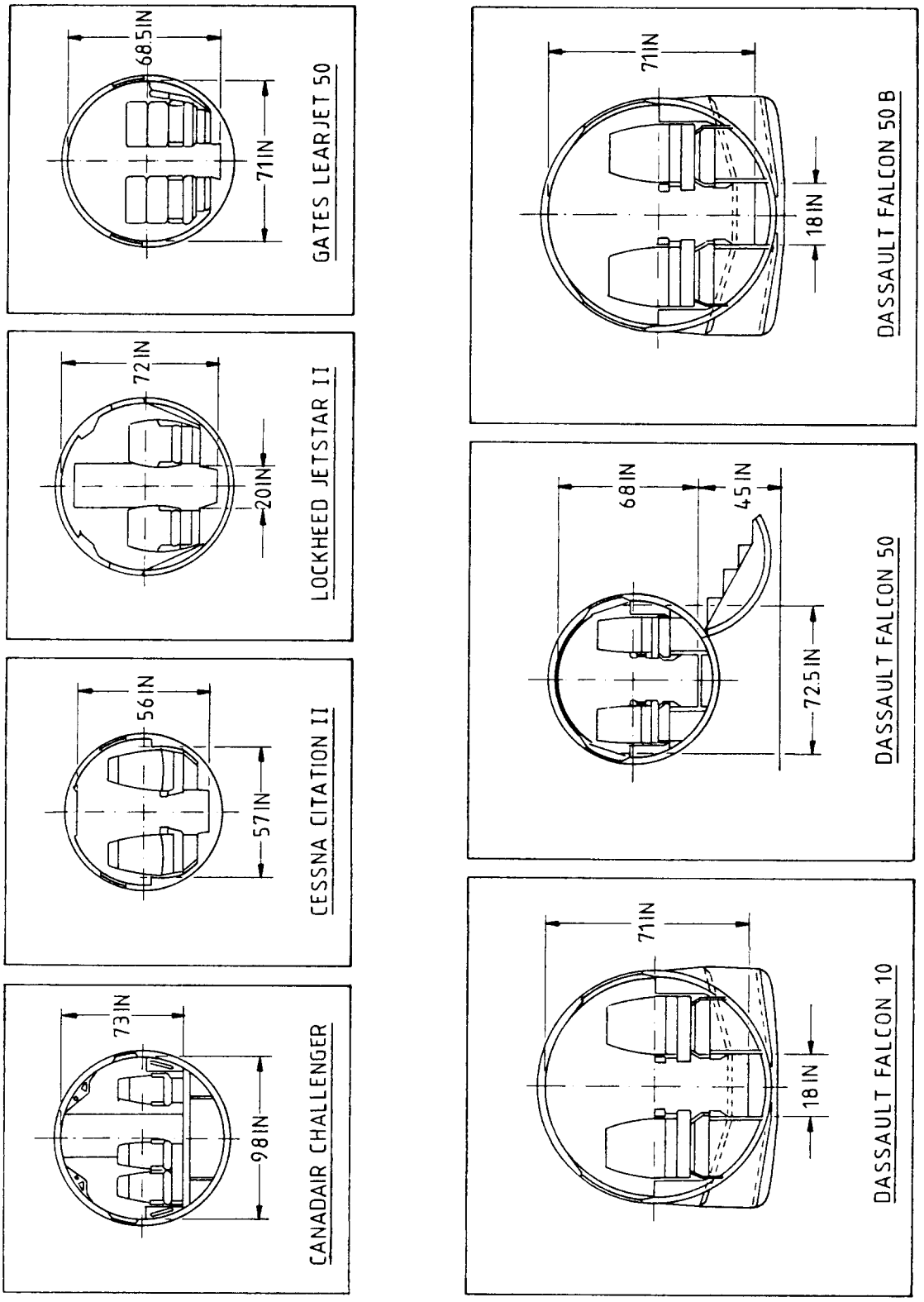

Figure 3.45 Fuselage Cross Sections for Business Jets

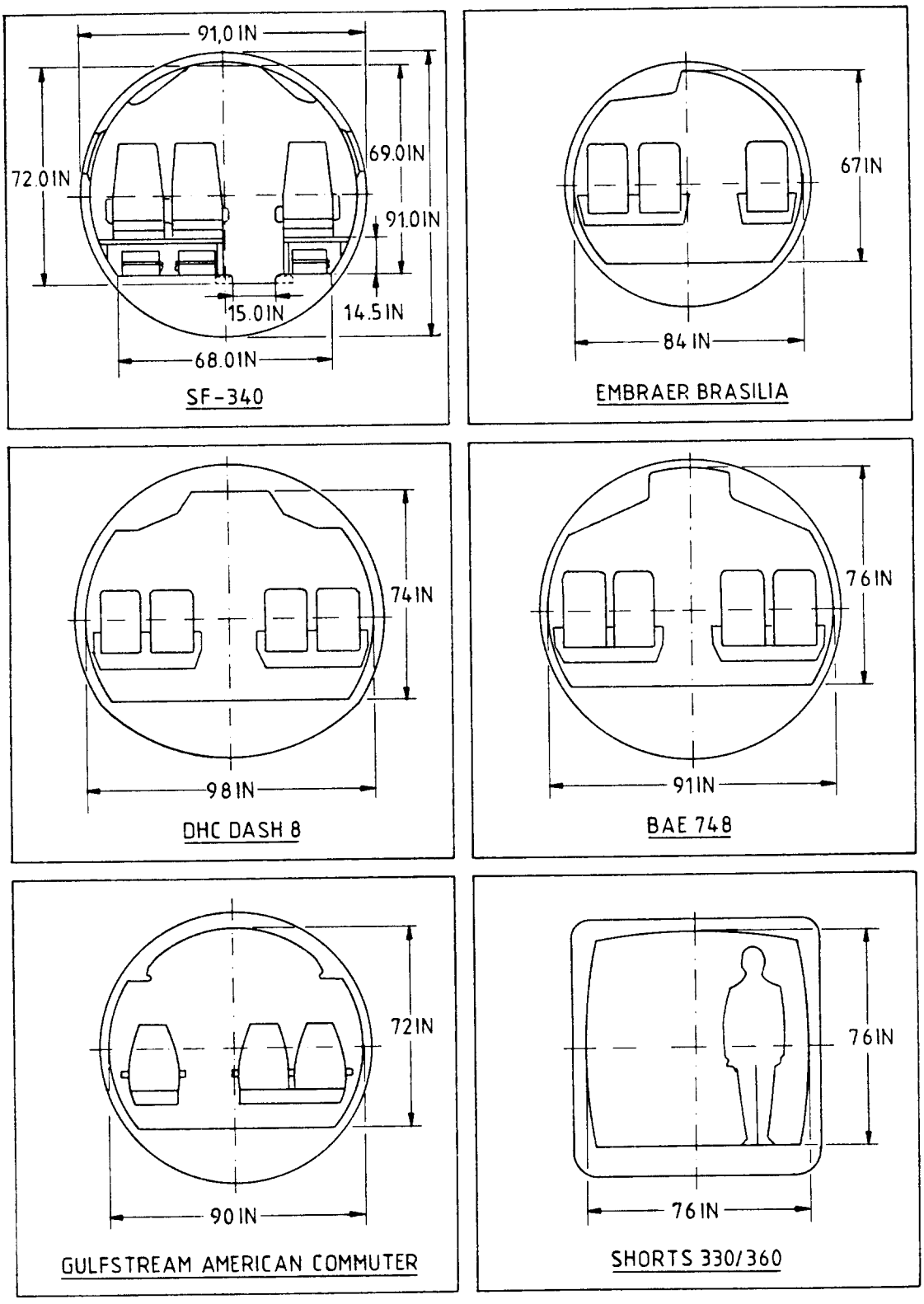

Figure 3.46 Fuselage Cross Sections for Regional Turboprops

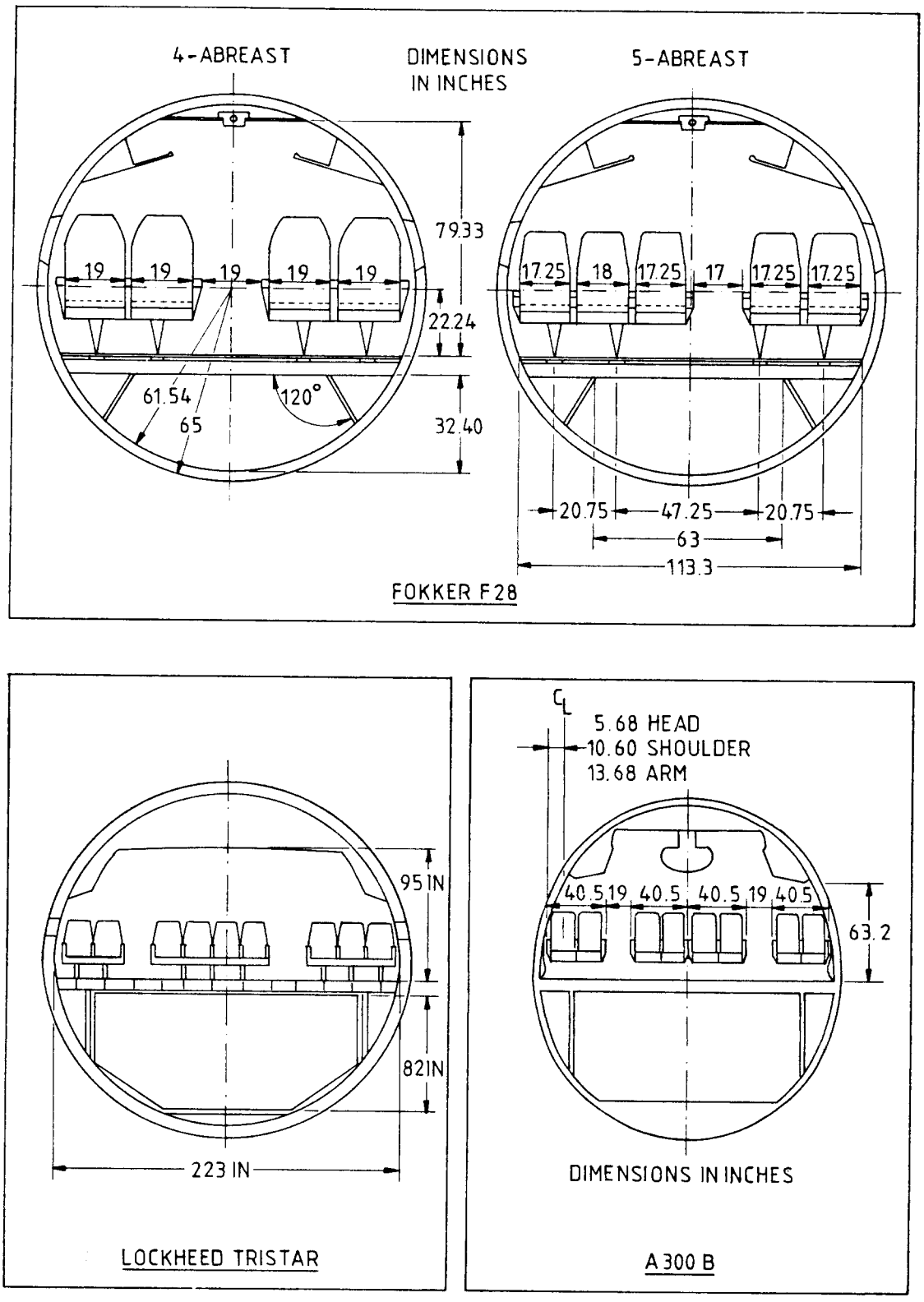

Figure 3.47a Fuselage Cross Sections for Jet Transports

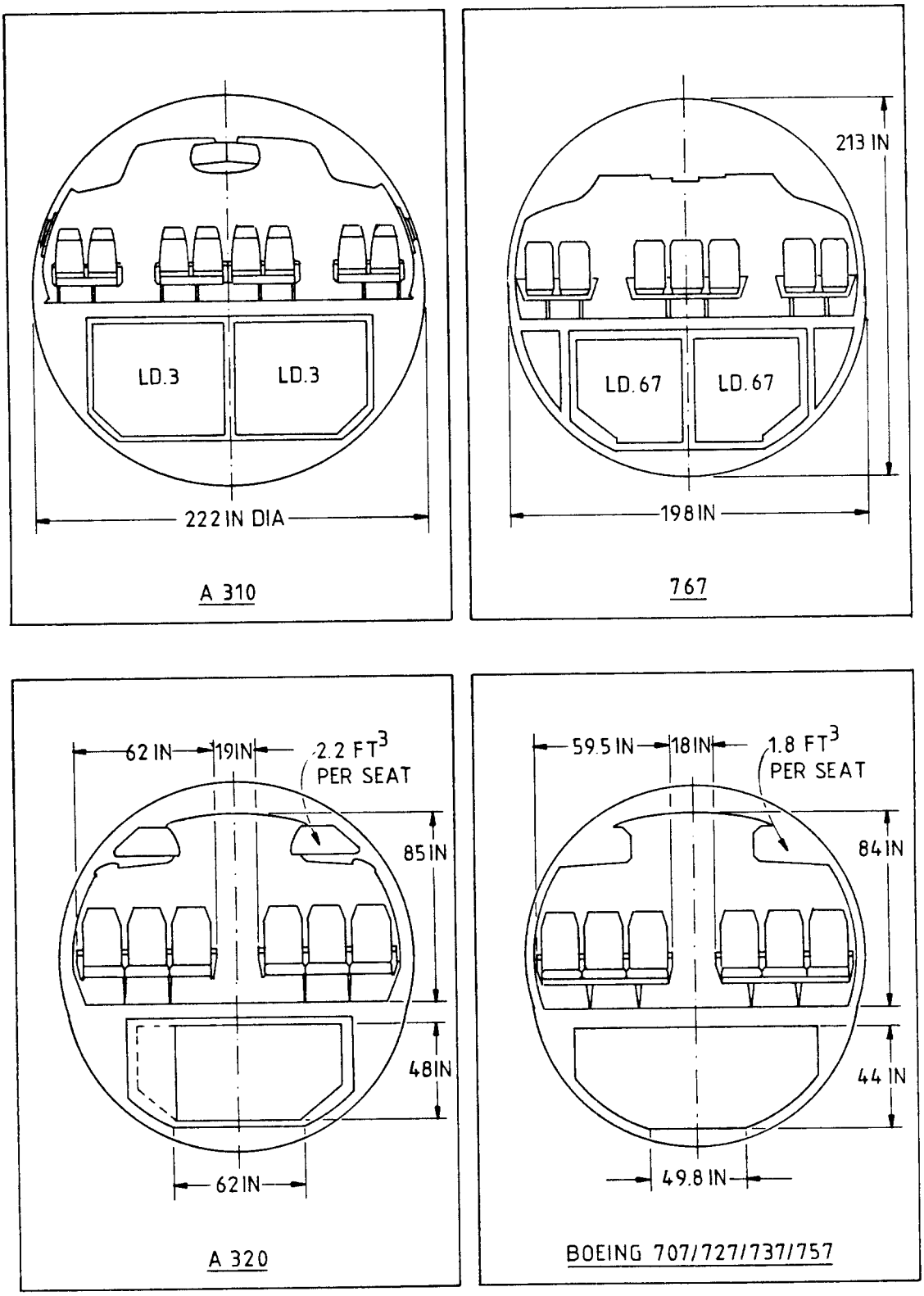

Figure 3.47b Fuselage Cross Sections for Jet Transports

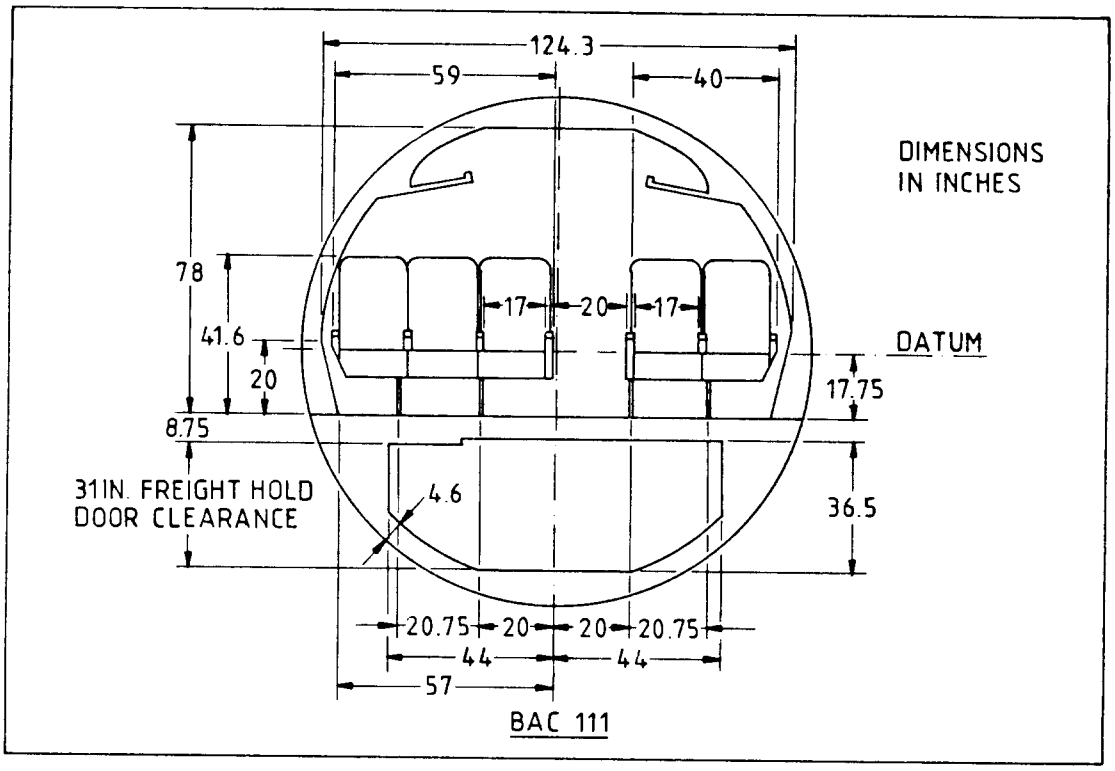

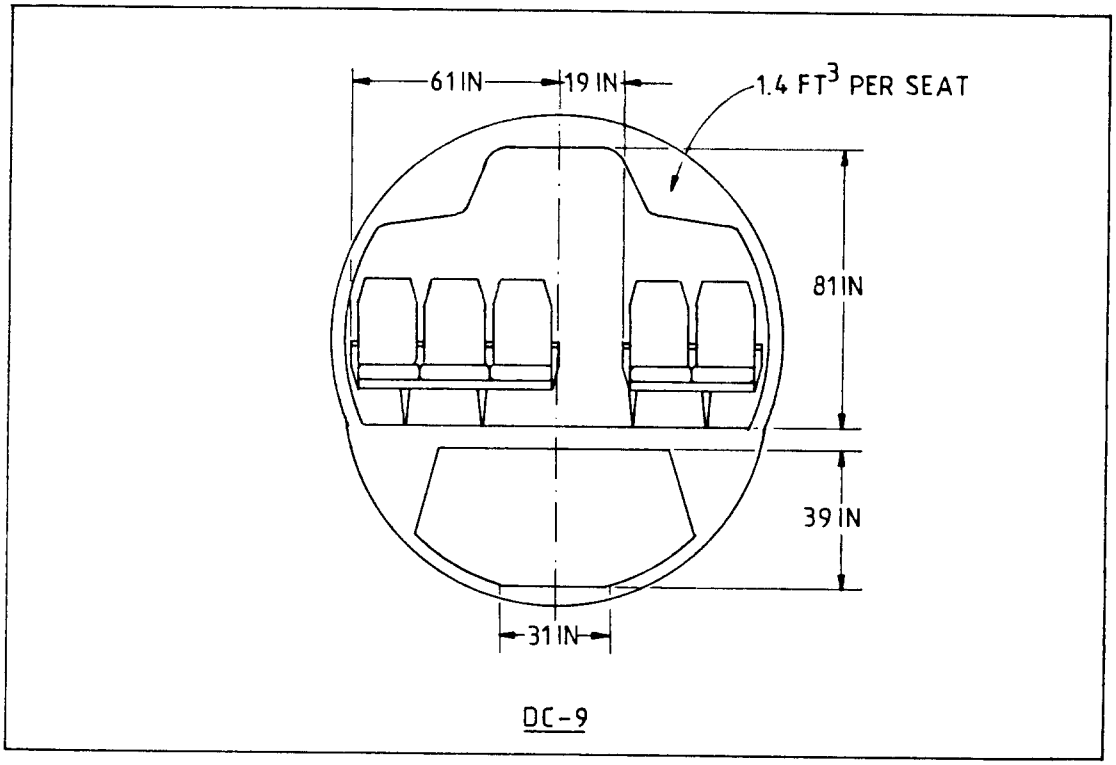

Figure 3.47c Fuselage Cross Sections for Jet transports

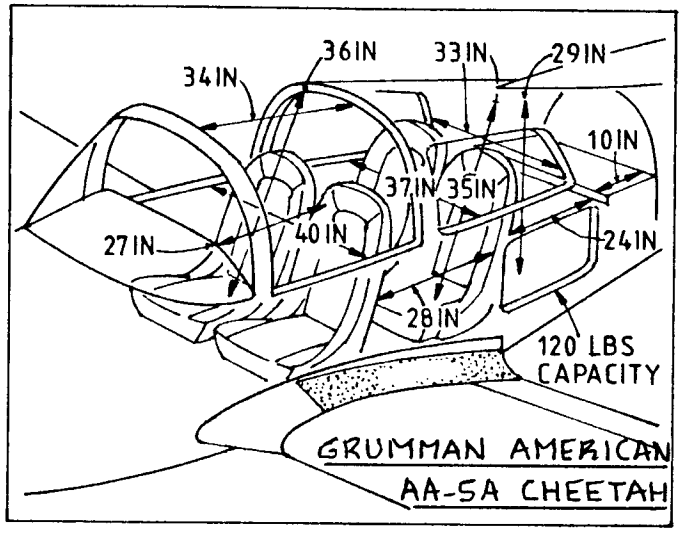

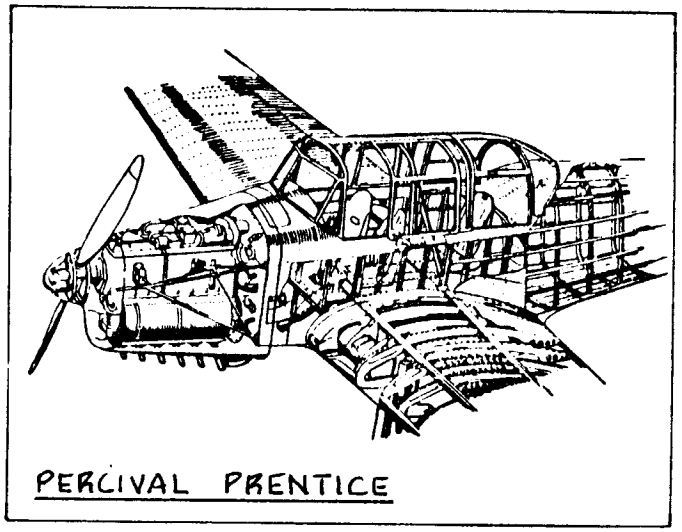

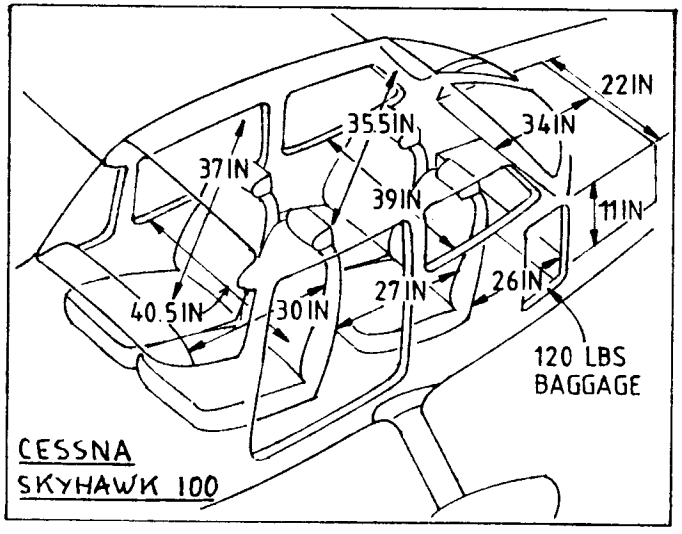

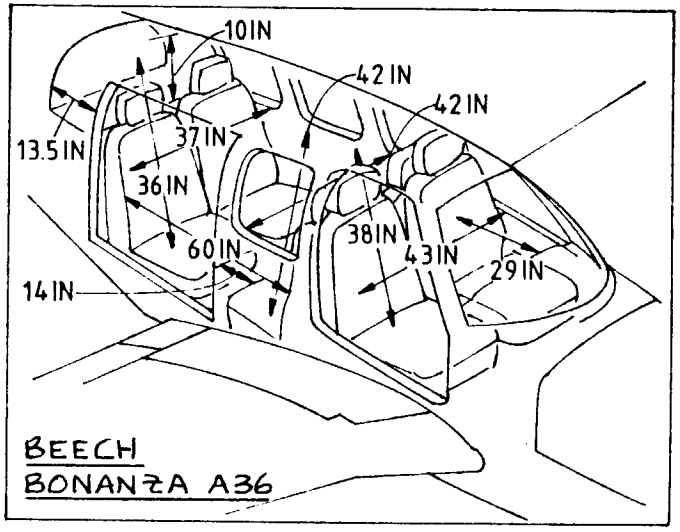

Figure 3.48a Cabin and Baggage Hold Dimensions for Single Engine Piston/Propeller Driven Airplanes

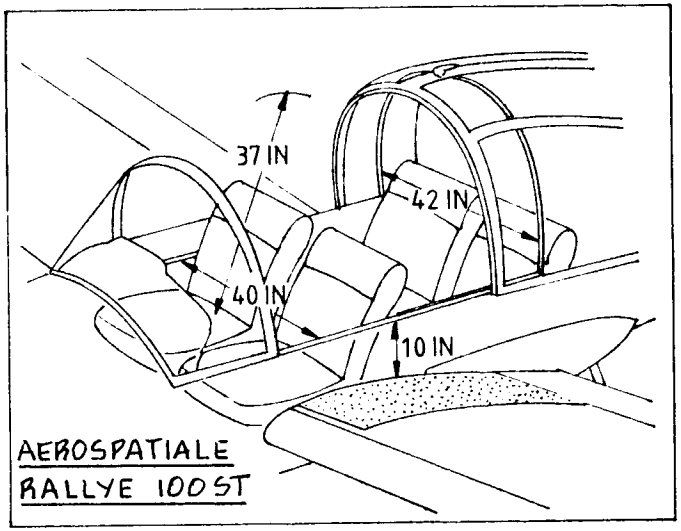

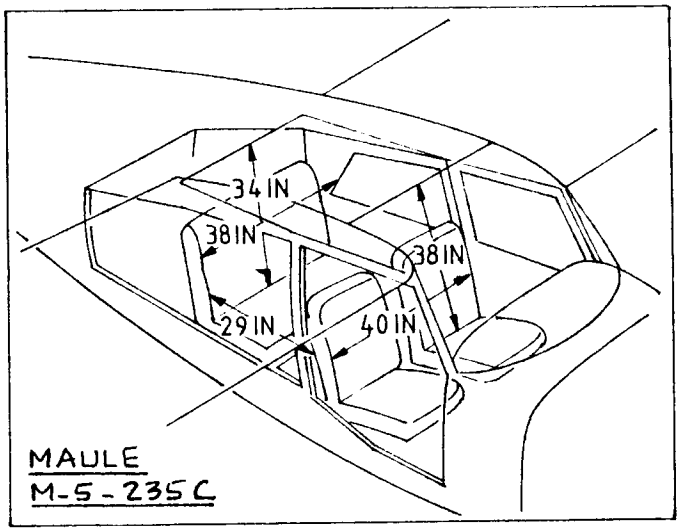

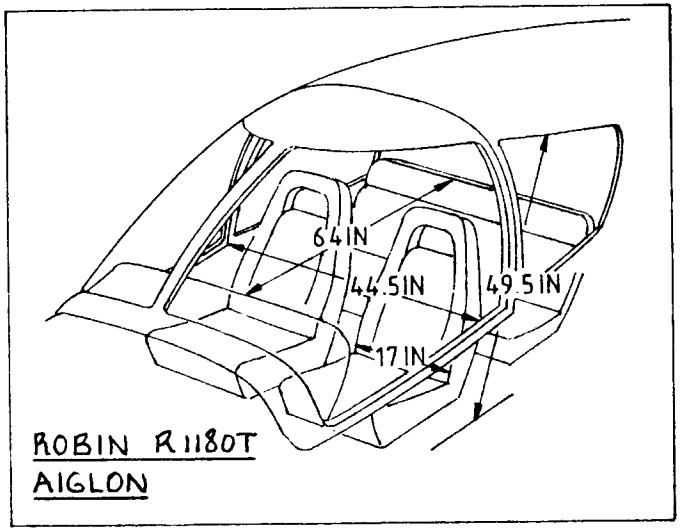

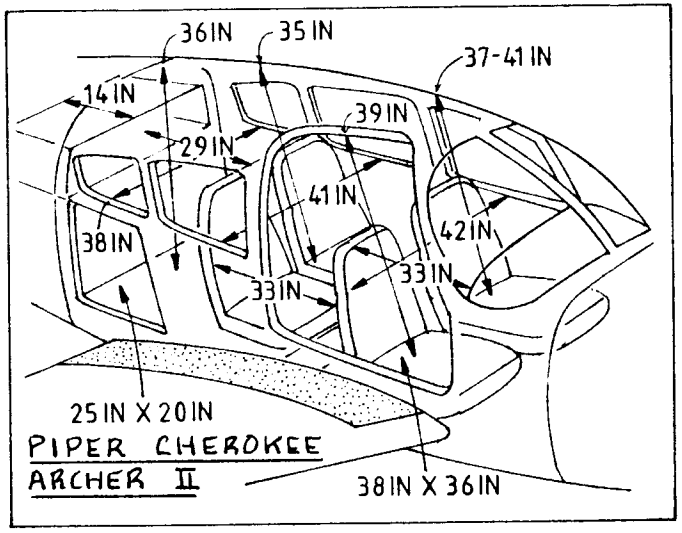

Figure 3.48b Cabin and Baggage Hold Dimensions for Single Engine Piston/Propeller Driven Airplanes

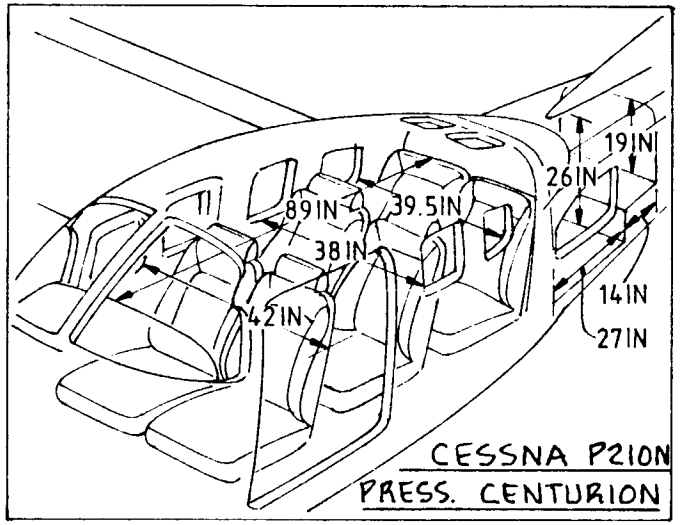

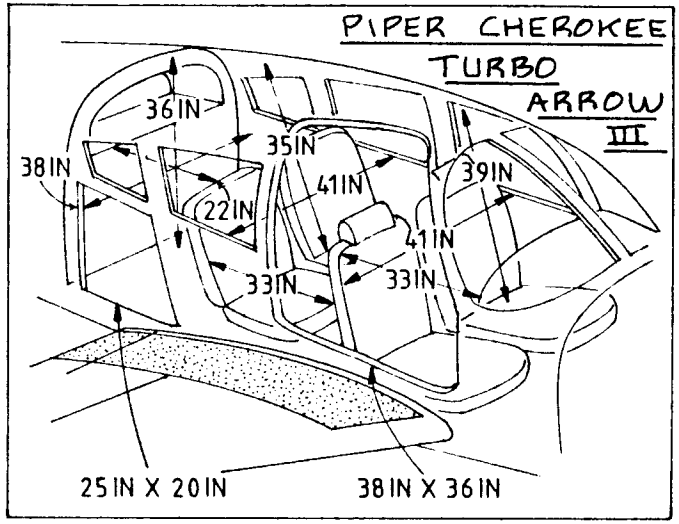

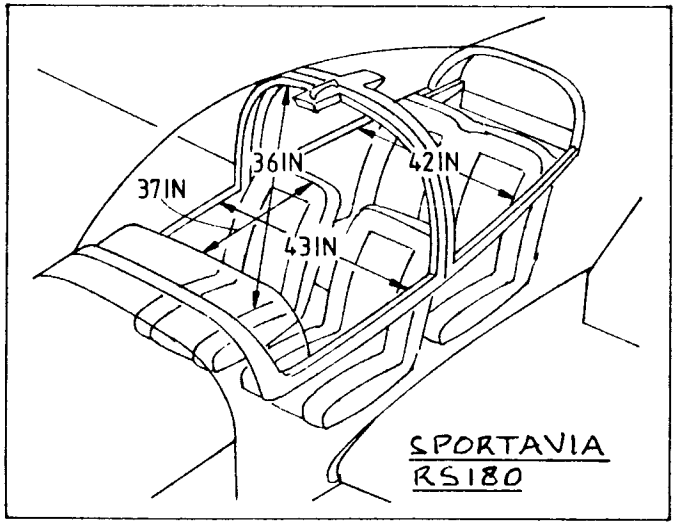

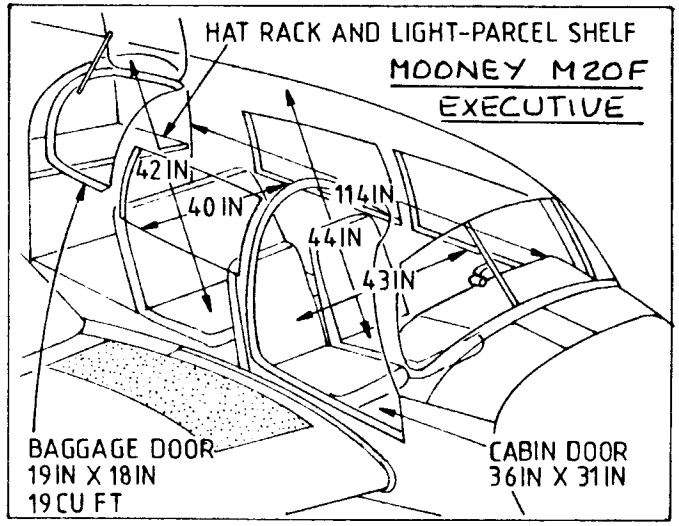

Figure 3.48c Cabin and Baggage Hold Dimensions for Single Engine Piston/Propeller Driven Airplanes

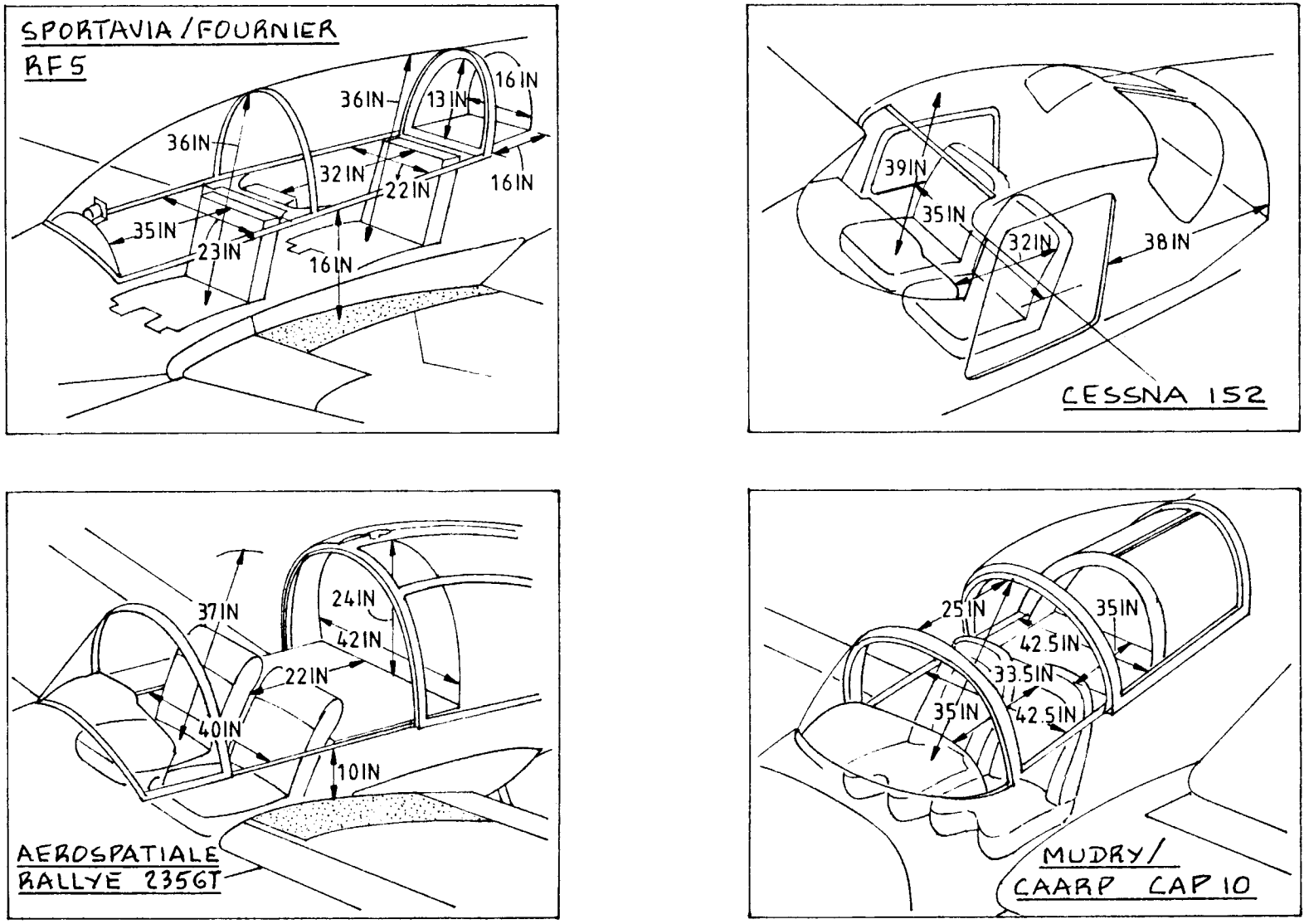

Figure 3.48d Cabin and Baggage Hold Dimensions for Single Engine Piston/Propeller Driven Airplanes

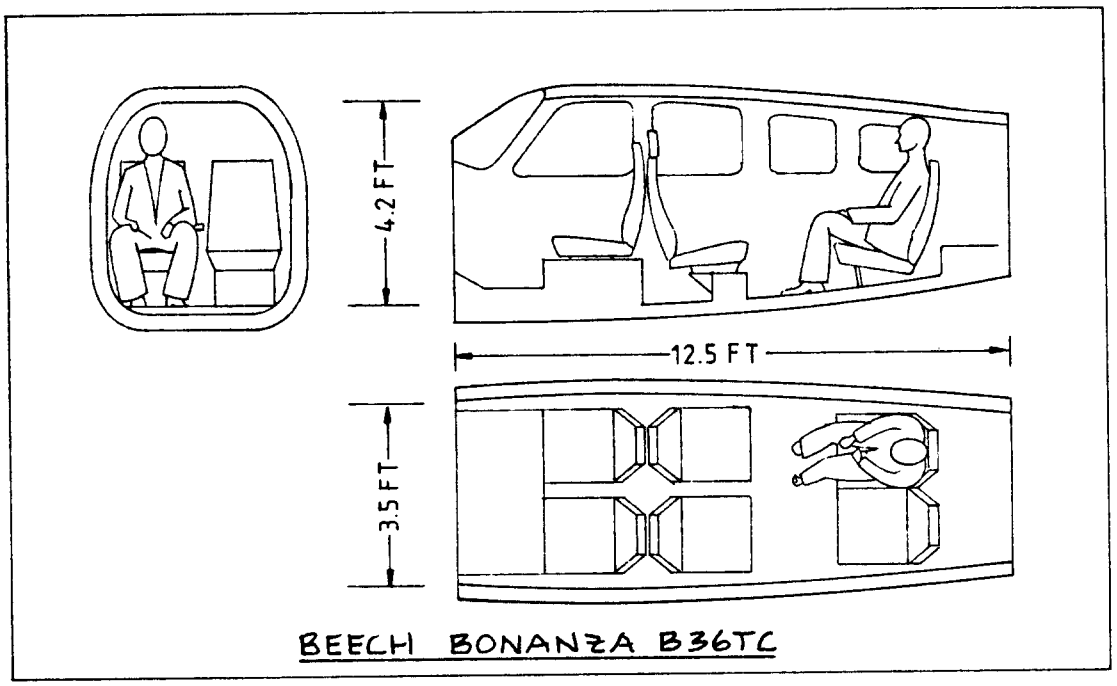

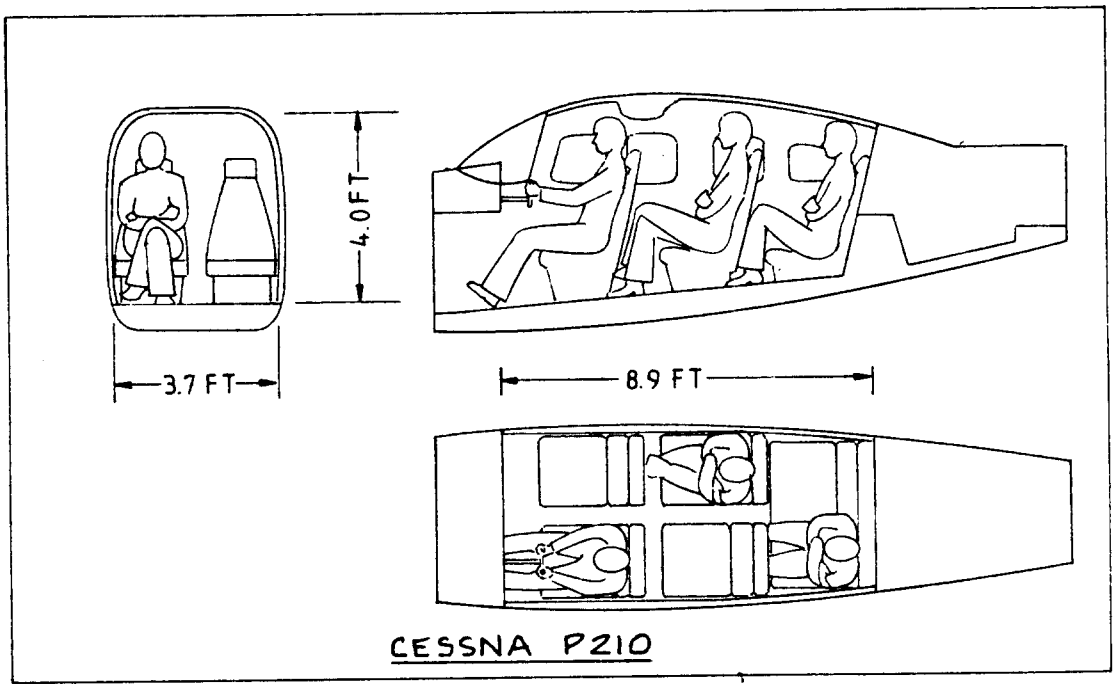

Figure 3.49 Cabin Dimensions for Single Engine Piston/ Propeller Driven Airplanes

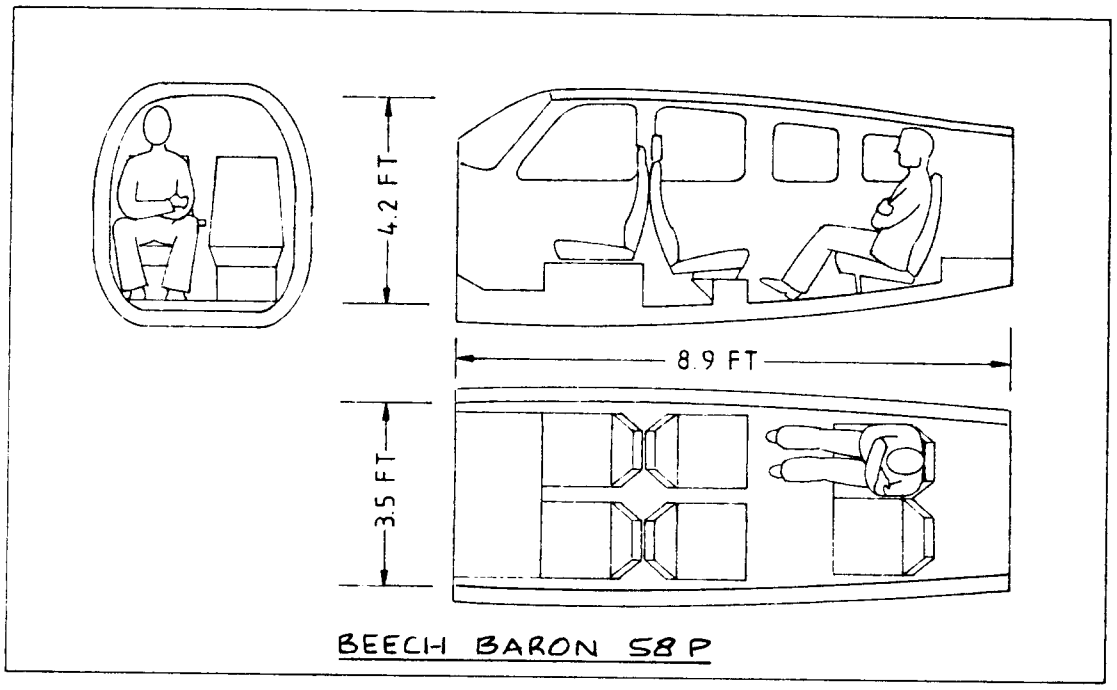

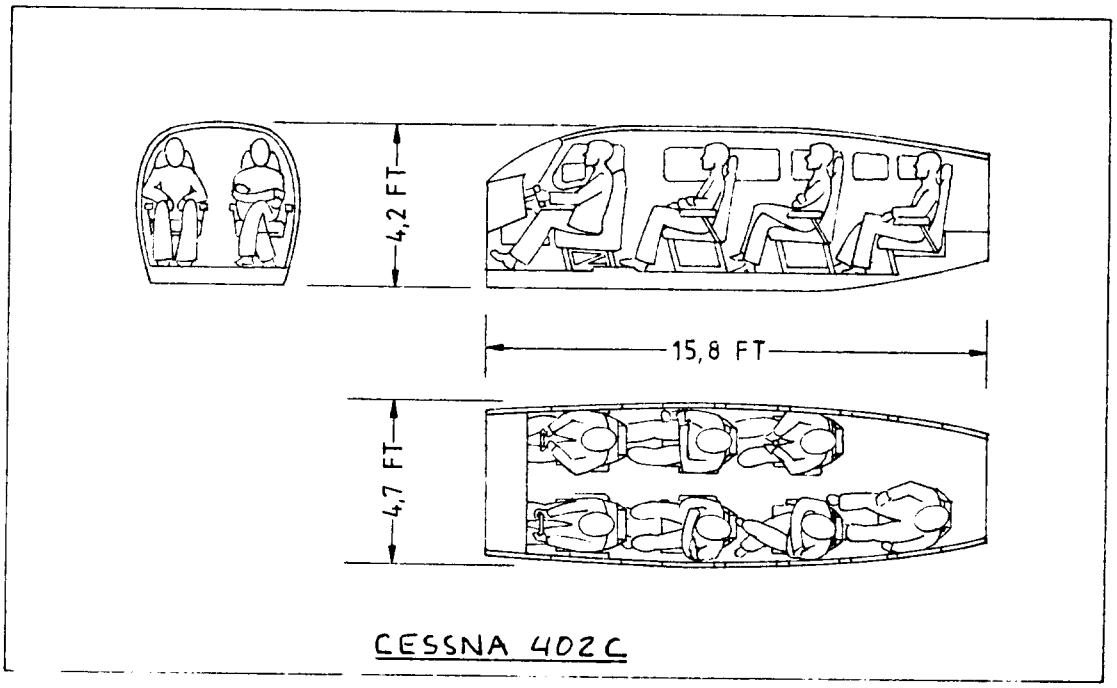

Figure 3.50 Cabin Dimensions for Twin Engine Piston/ Propeller Driven Airplanes

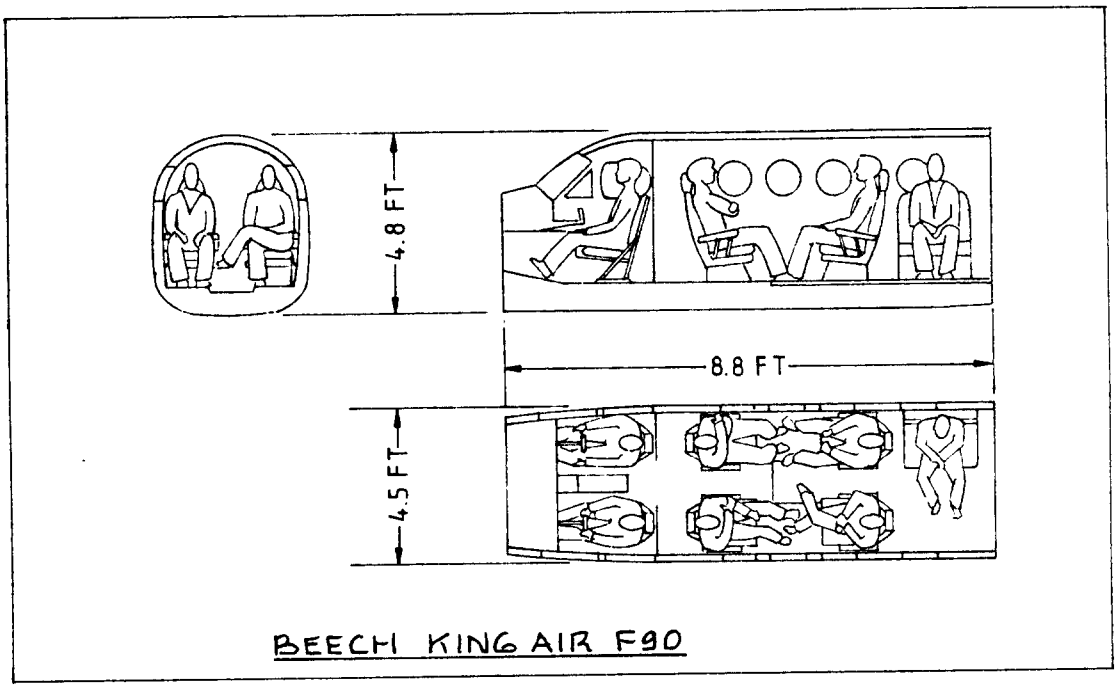

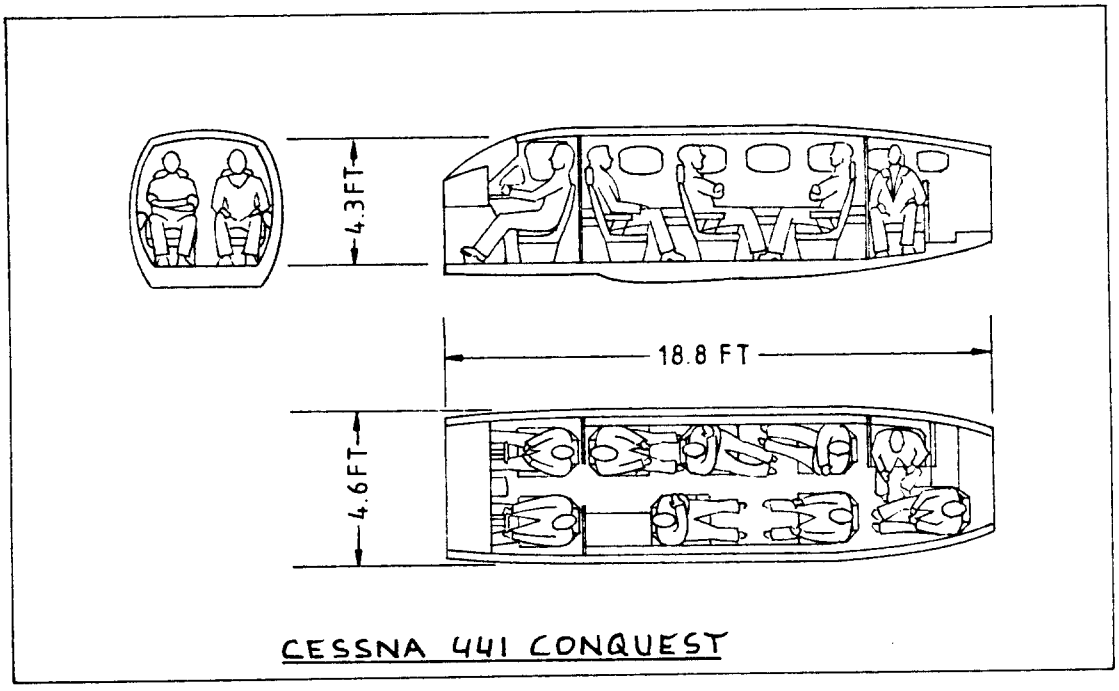

Figure 3.51a Cabin Dimensions for Twin Engine Turbo-Propeller Driven Airplanes

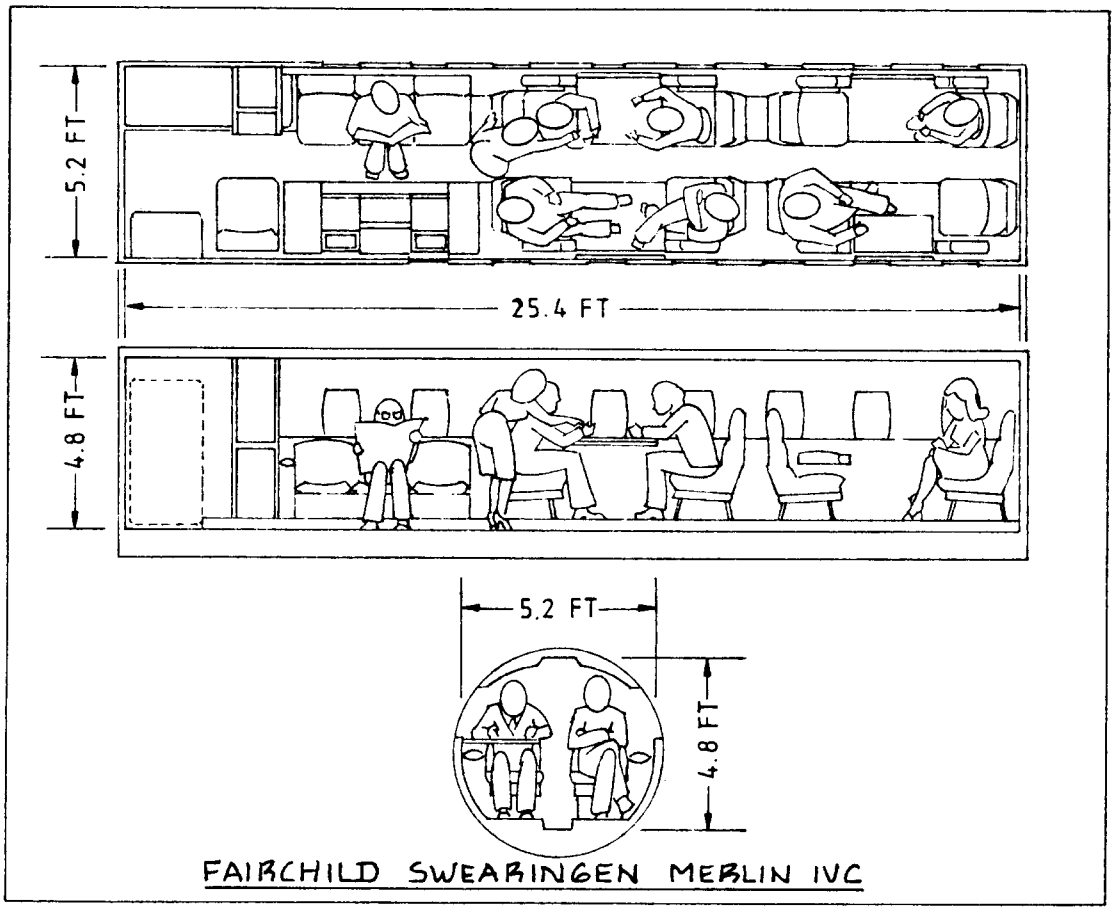

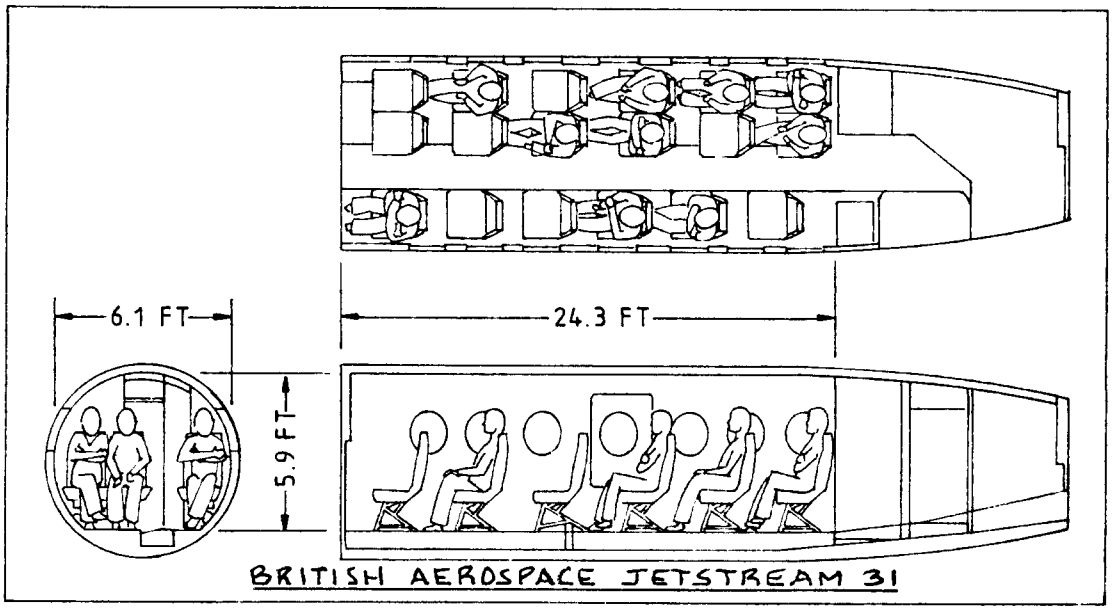

Figure 3.51b Cabin Dimensions for Twin Engine Turbo-Propeller Driven Airplanes

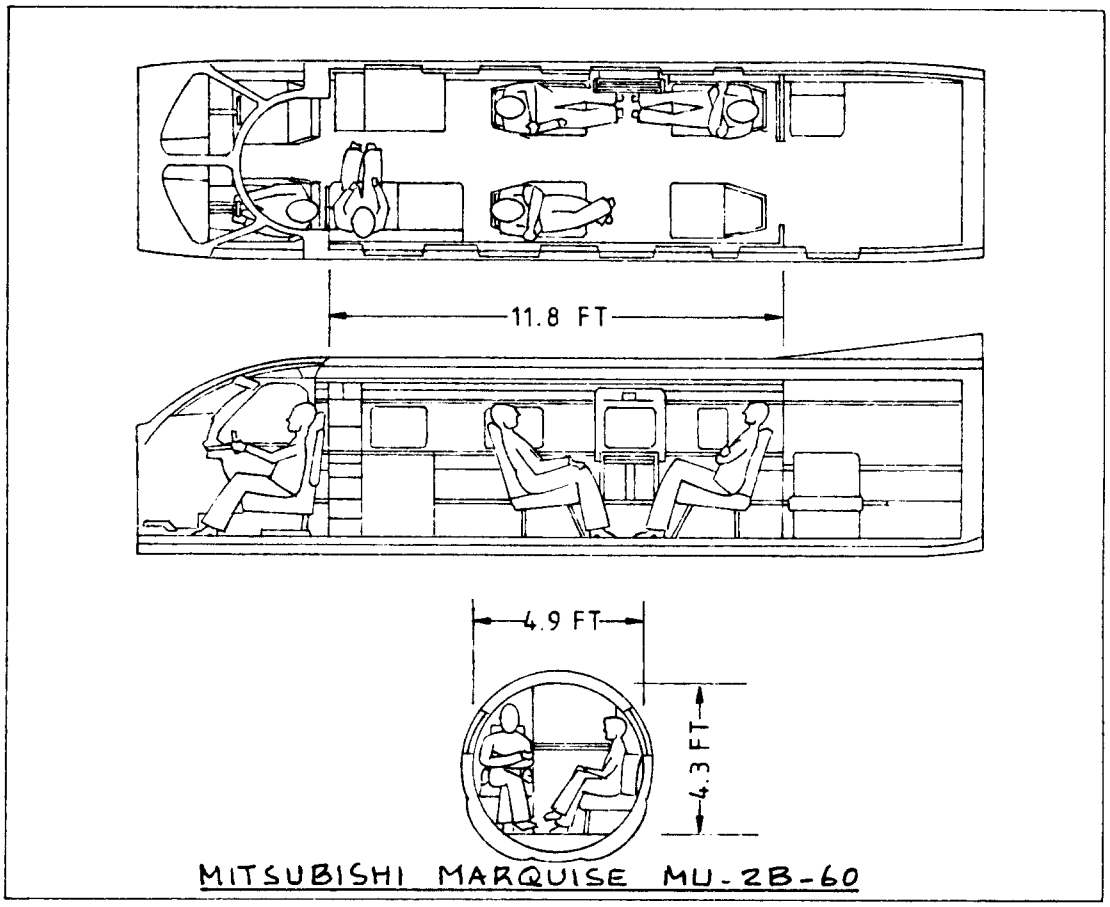

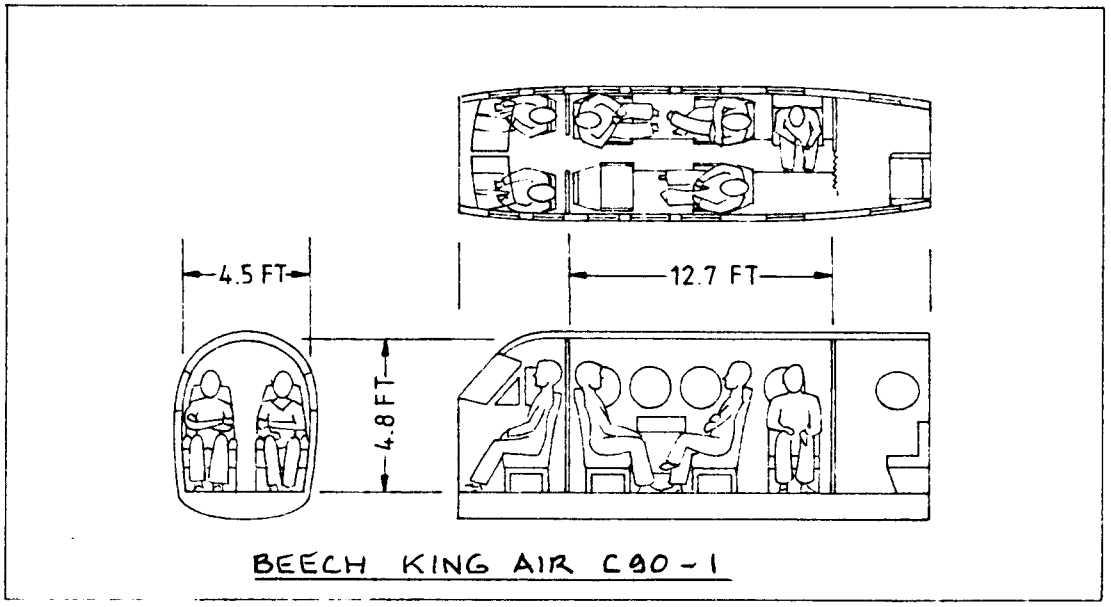

Figure 3.51c Cabin Dimensions for Twin Engine Turbo-Propeller Driven Airplanes

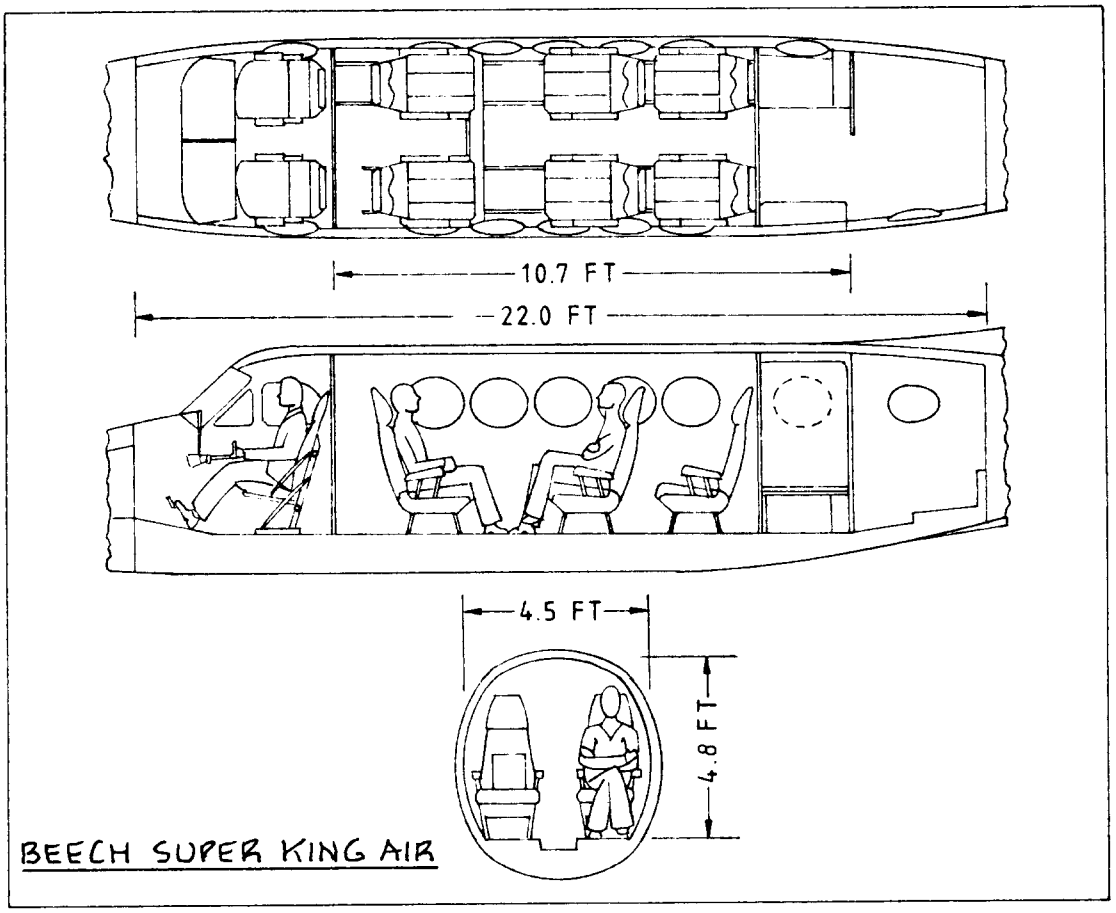

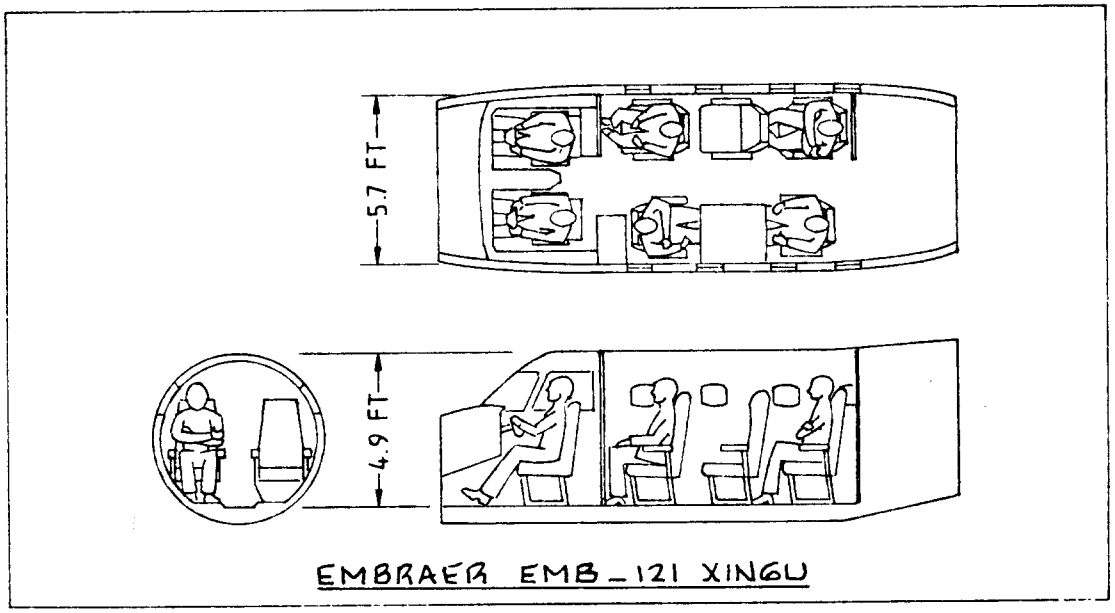

Figure 3.51d Cabin Dimensions for Twin Engine Turbo-Propeller Driven Airplanes

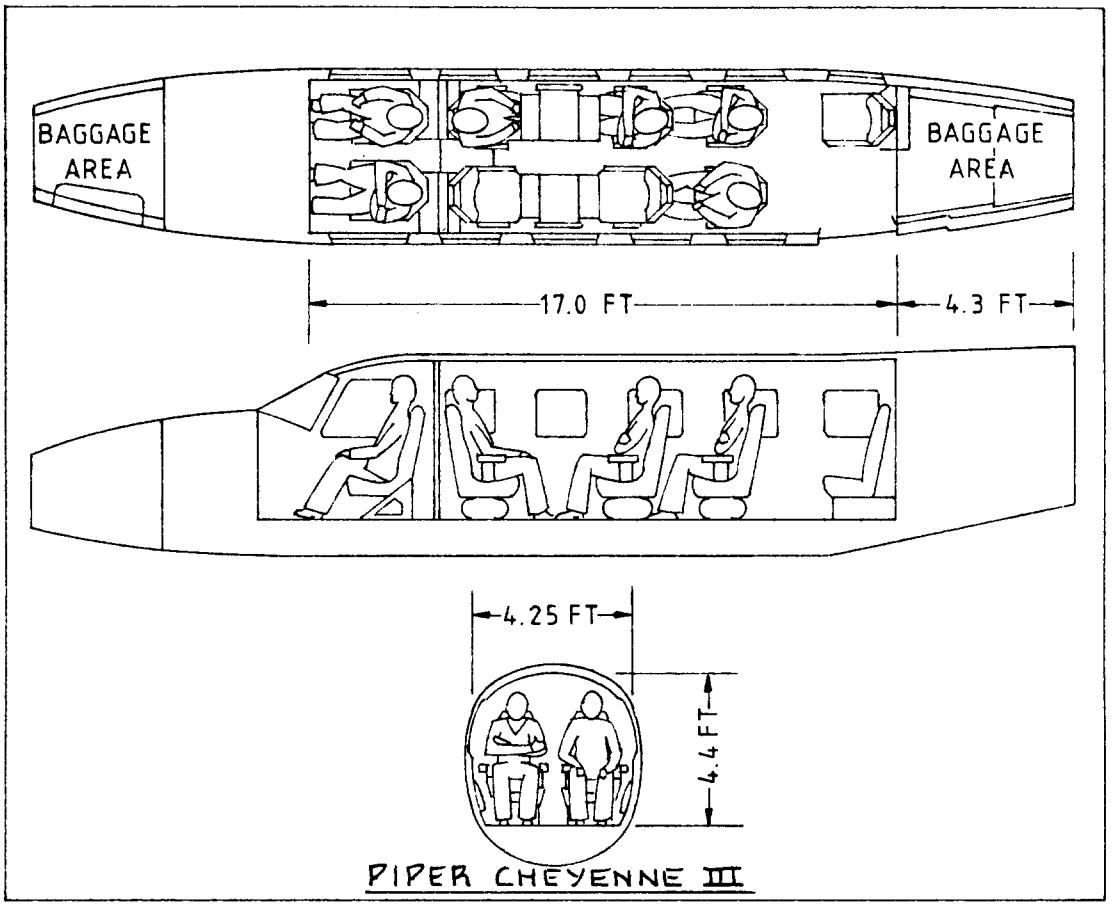

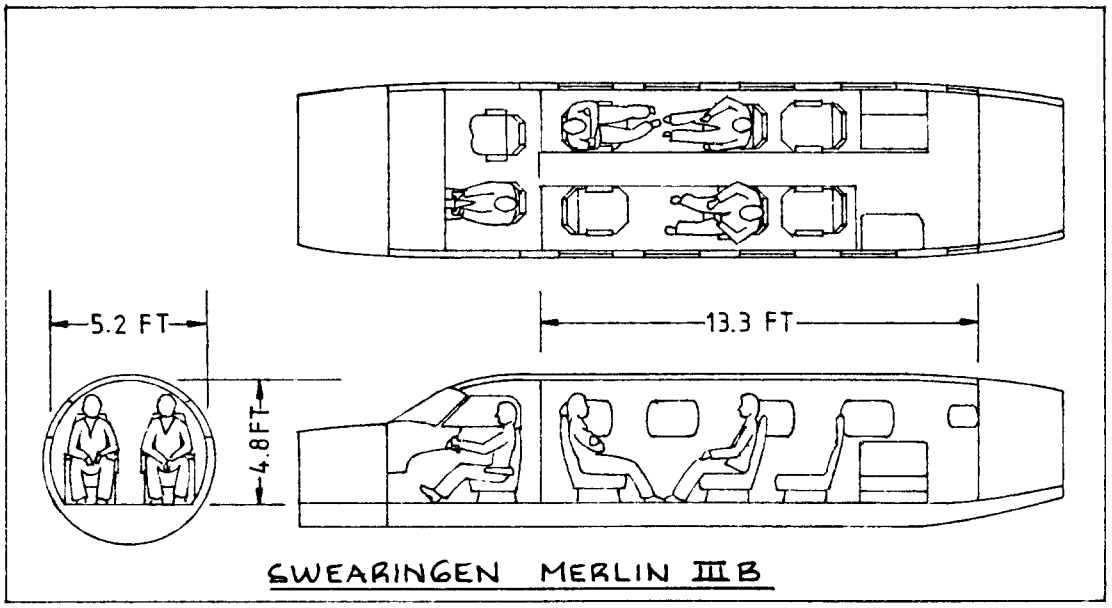

Figure 3.51e Cabin Dimensions for Twin Engine Turbo-Propeller Driven Airplaes

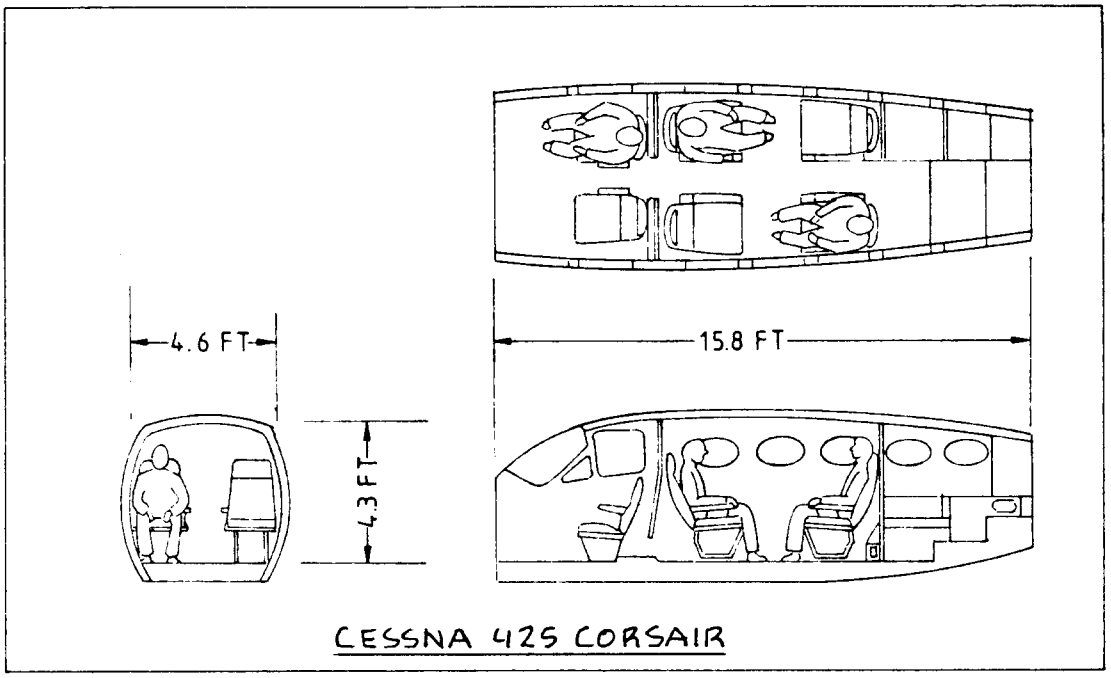

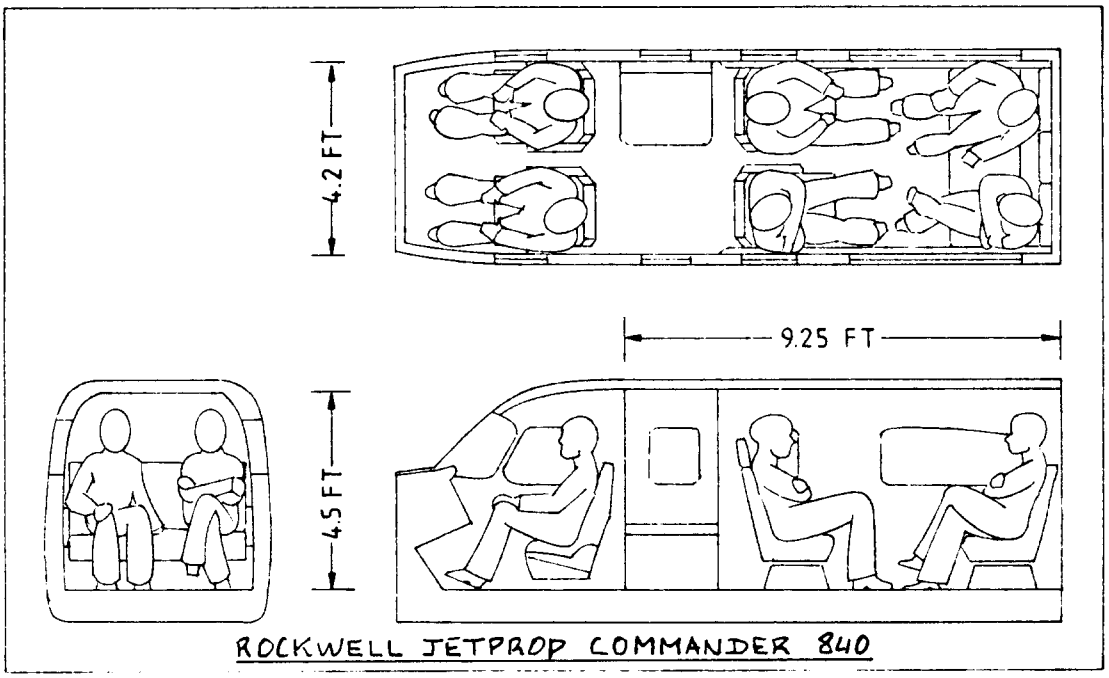

Figure 3.51f Cabin Dimensions for Twin Engine Turbo-Propeller Driven Airplanes

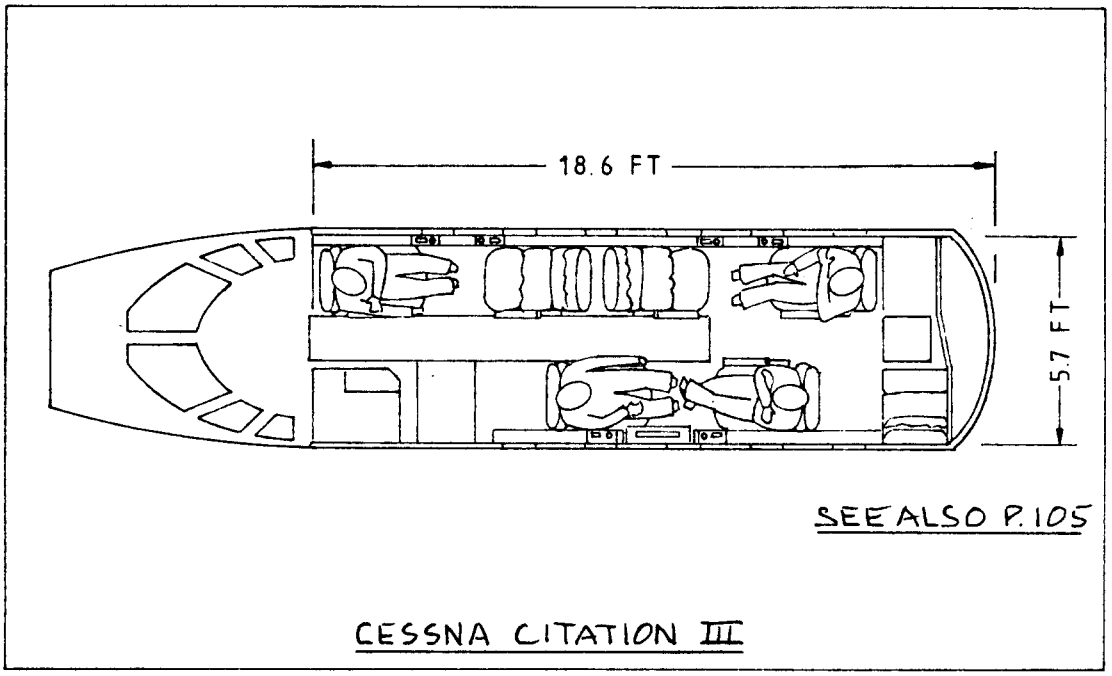

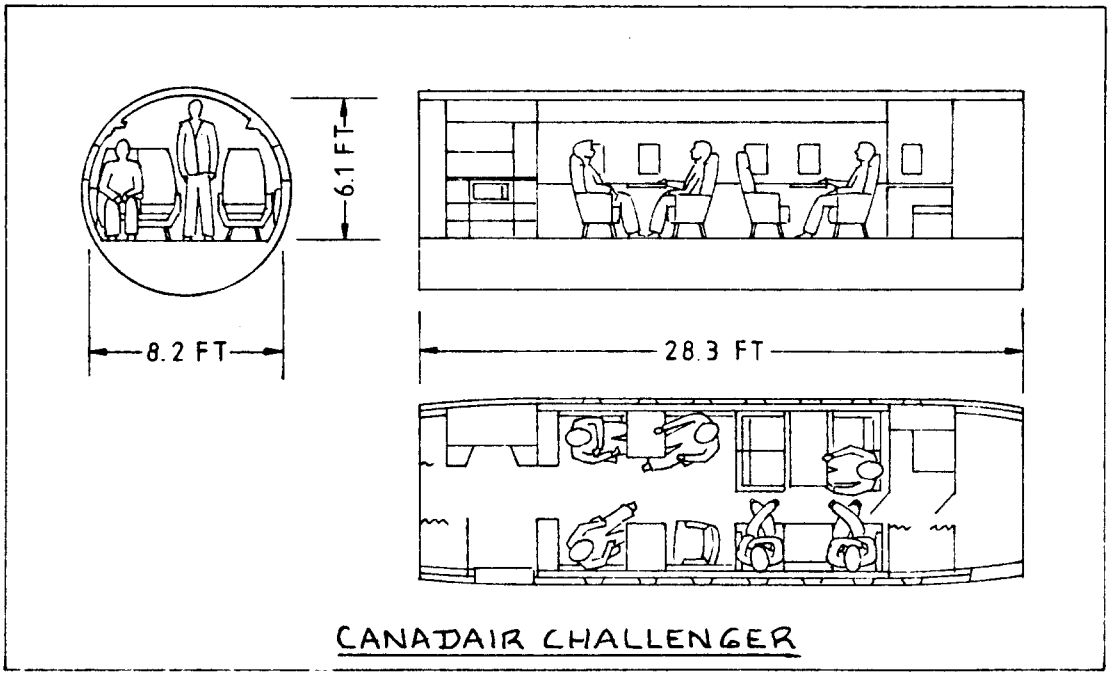

Figure 3.52a Cabin Dimensions for Business Jets

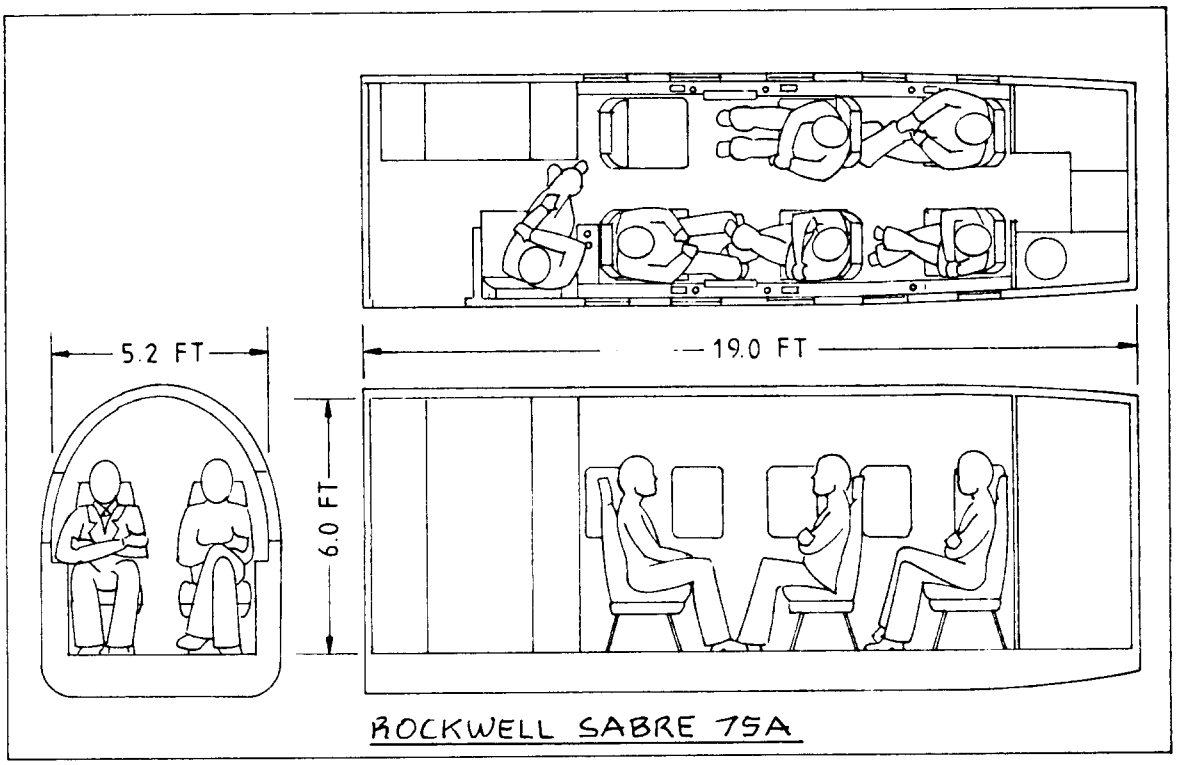

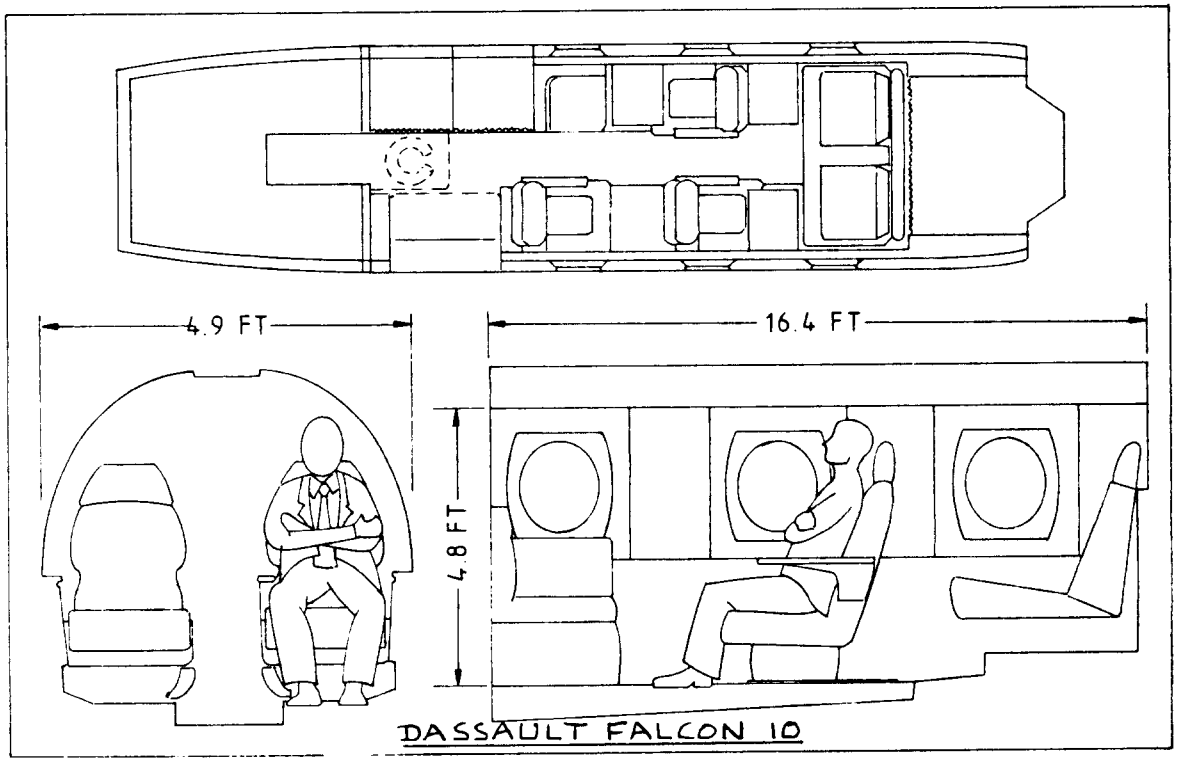

Figure 3.52b Cabin Dimensions for Business Jets

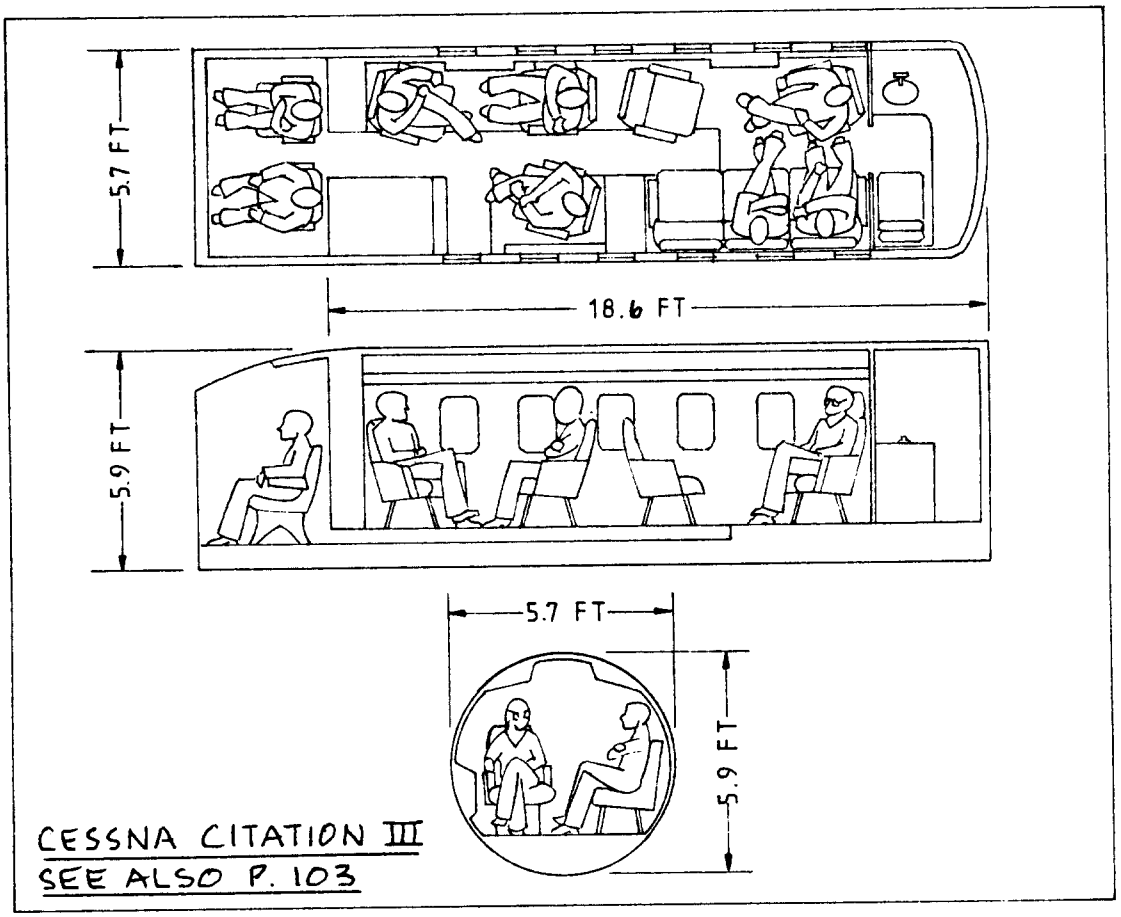

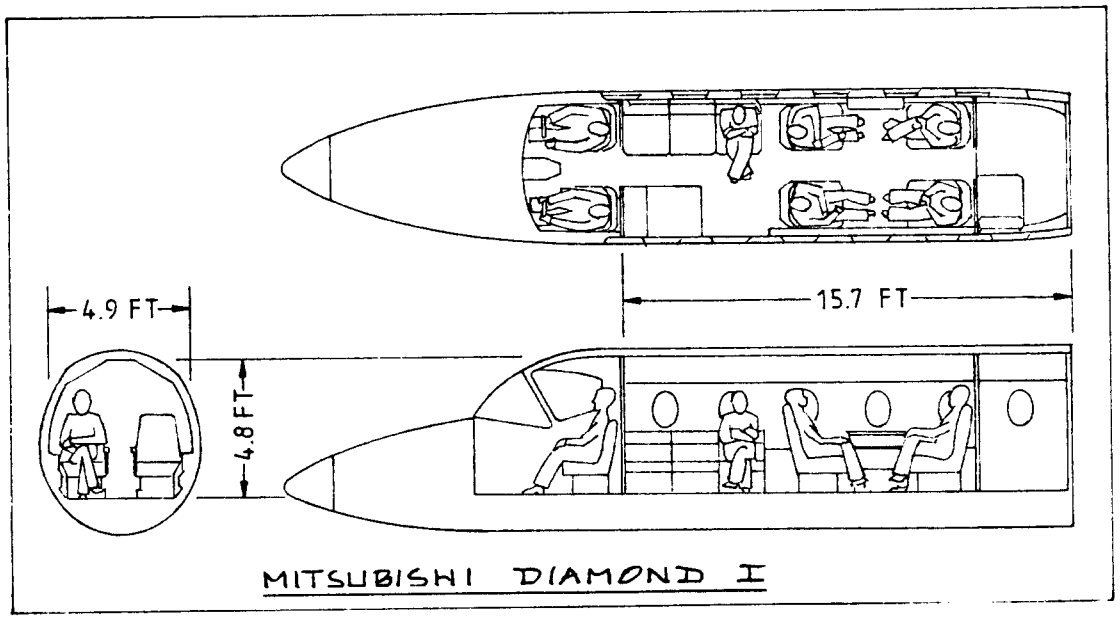

Figure 3.52c Cabin Dimensions for Business Jets

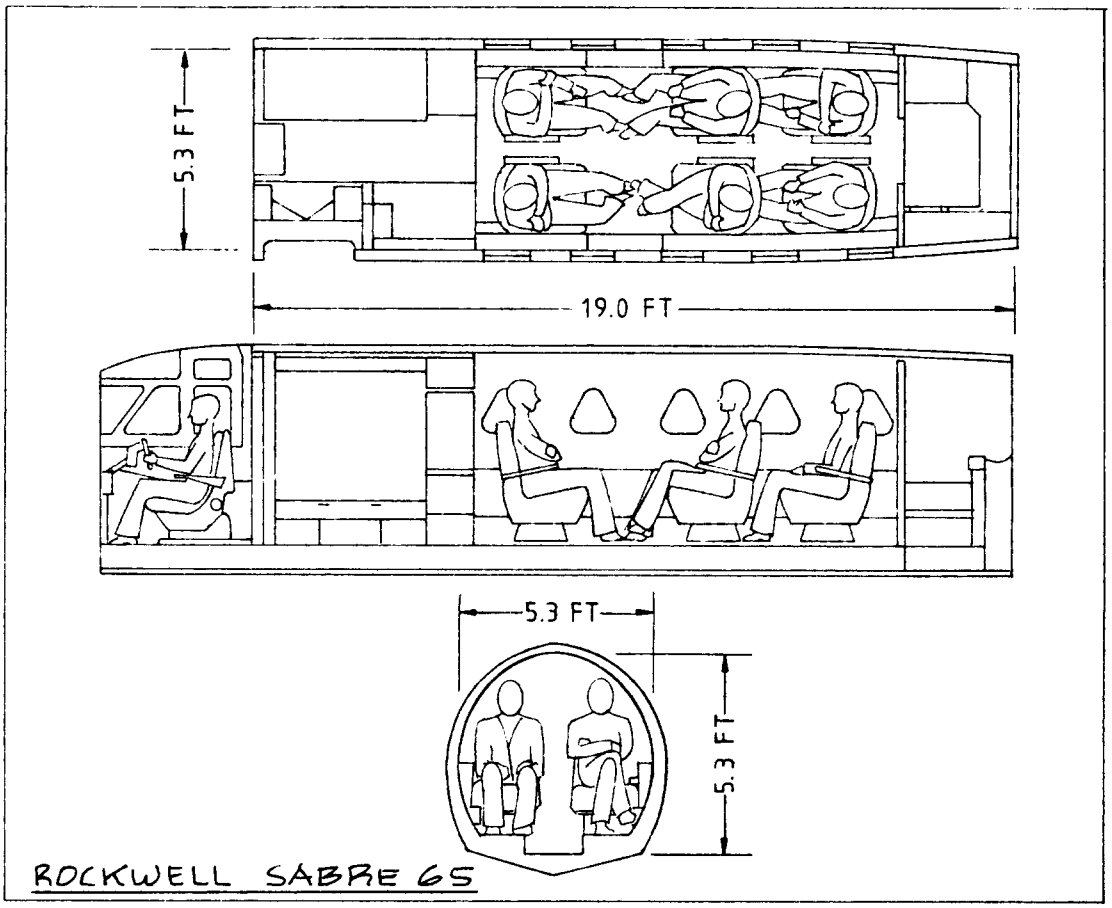

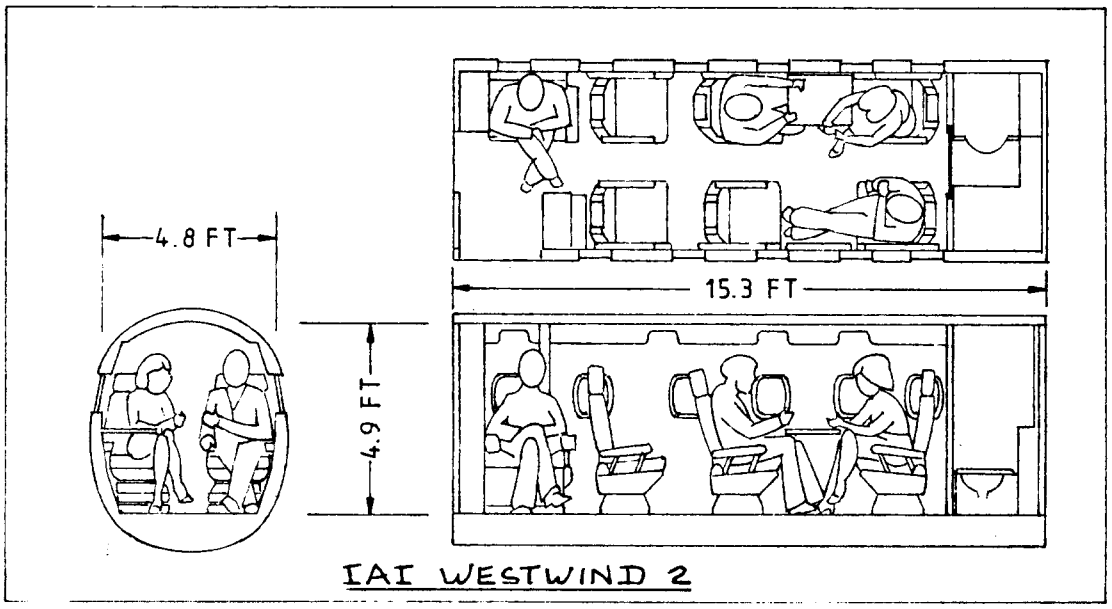

Figure 3.52d Cabin Dimensions for Business Jets

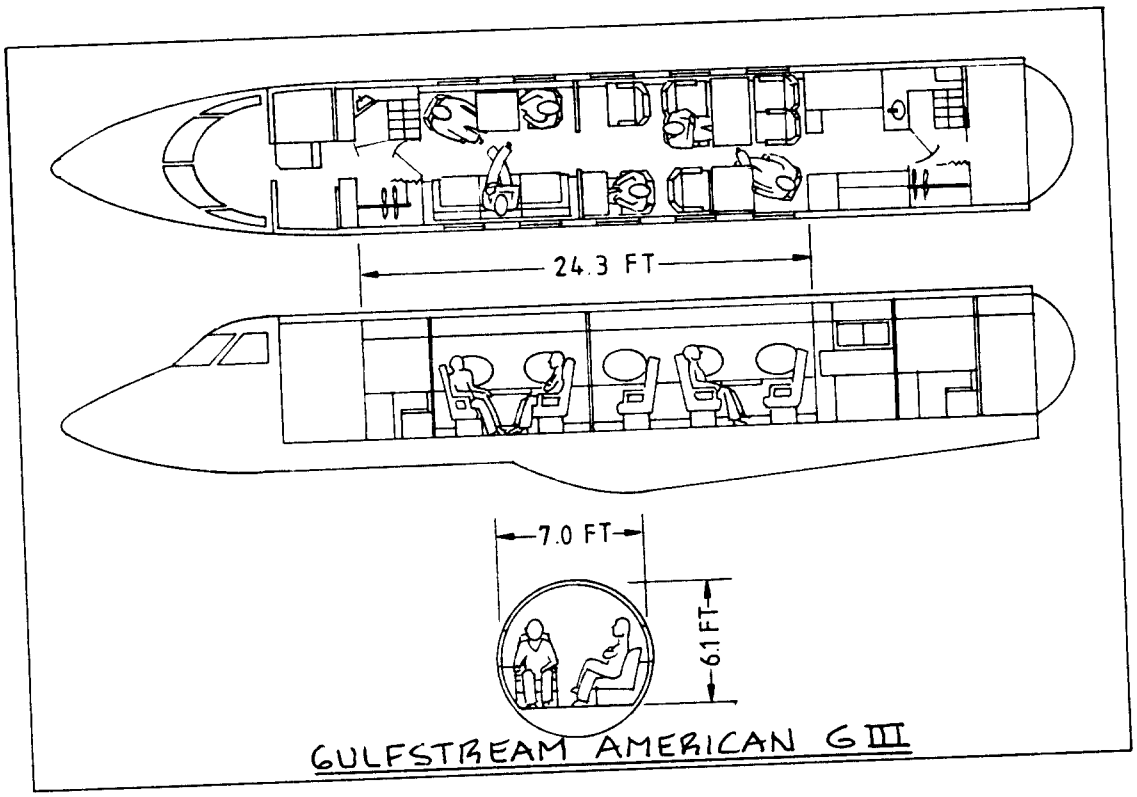

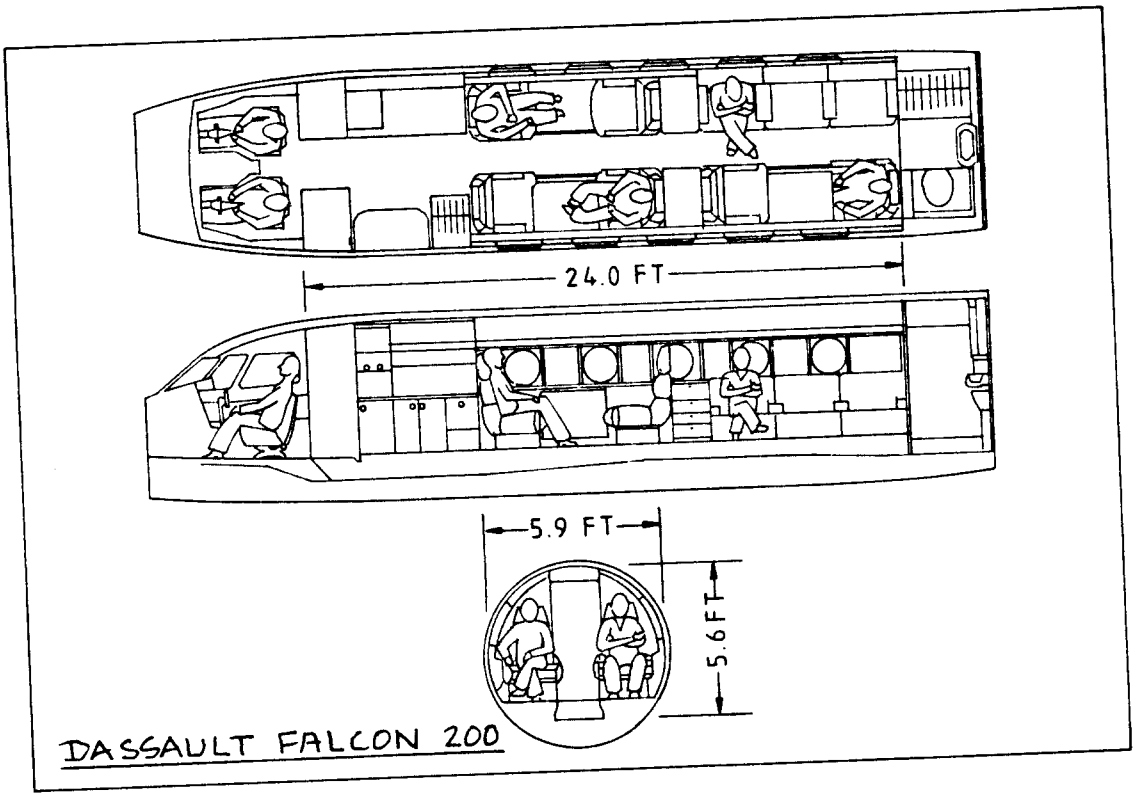

Figure 3.52e Cabin Dimensions for Business Jets

ANTONOV AN-26/32

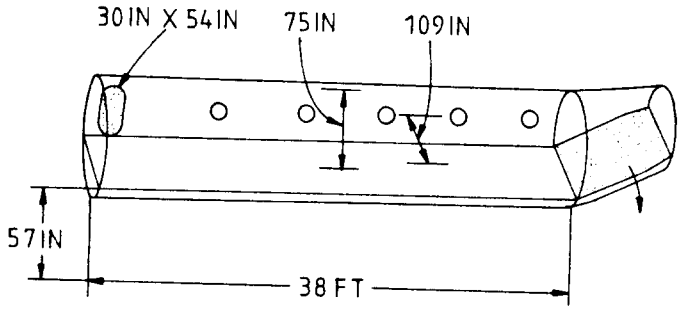

DE HAVILLAND CANADA DHC DASH 7

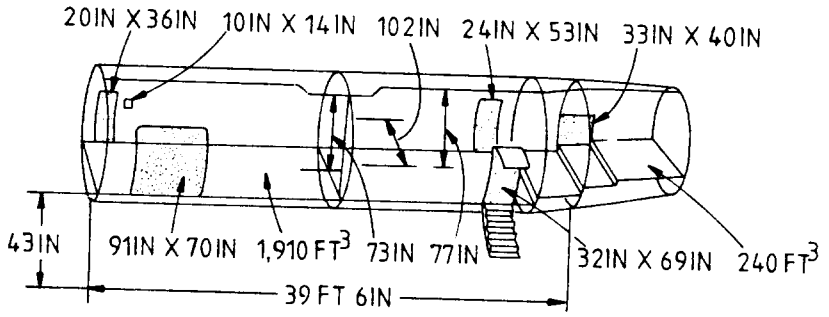

BRITISH AEROSPACE 748

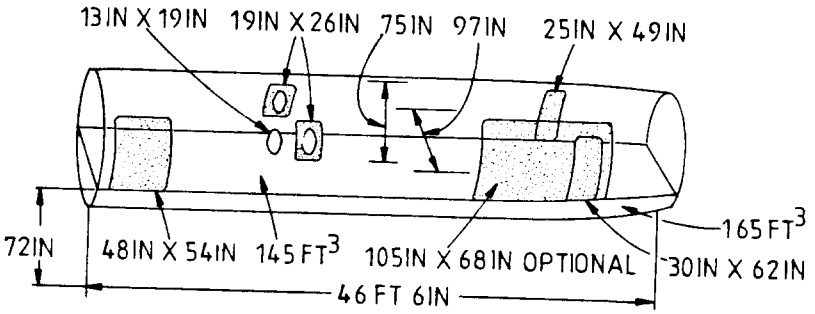

Figure 3.53a Fuselage and Cargo Hold Dimensions for Turbopropeller Driven Transports

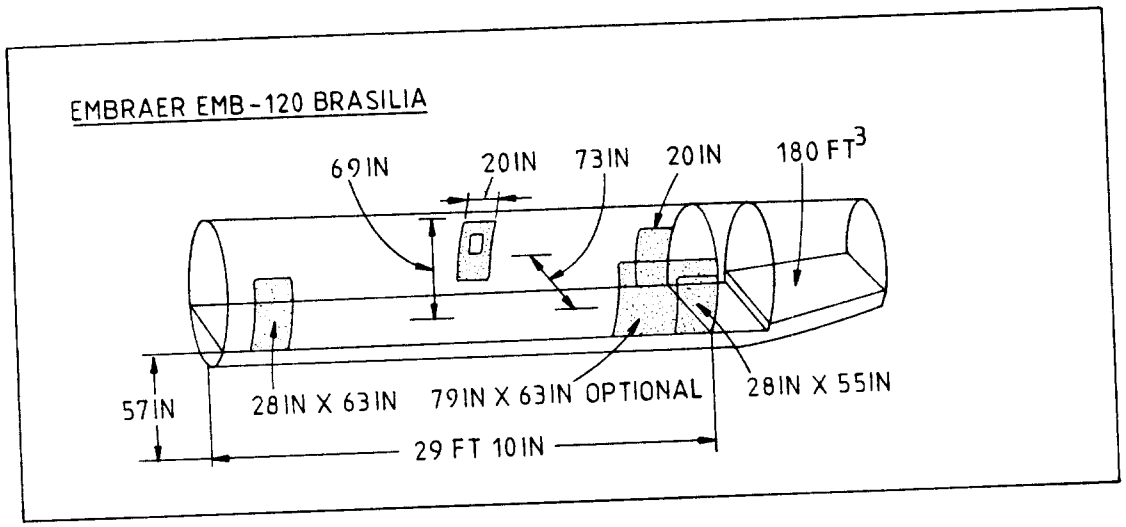

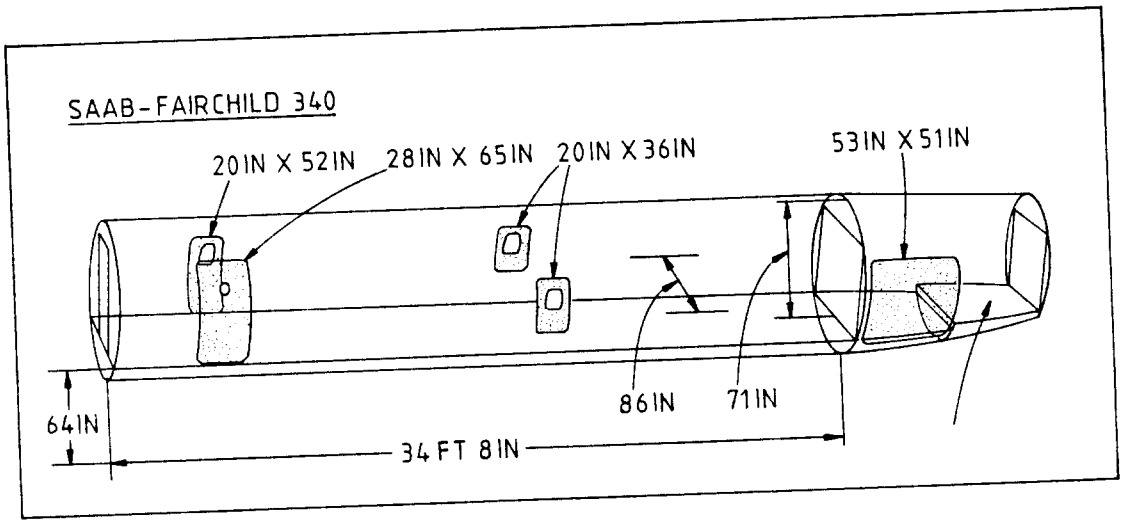

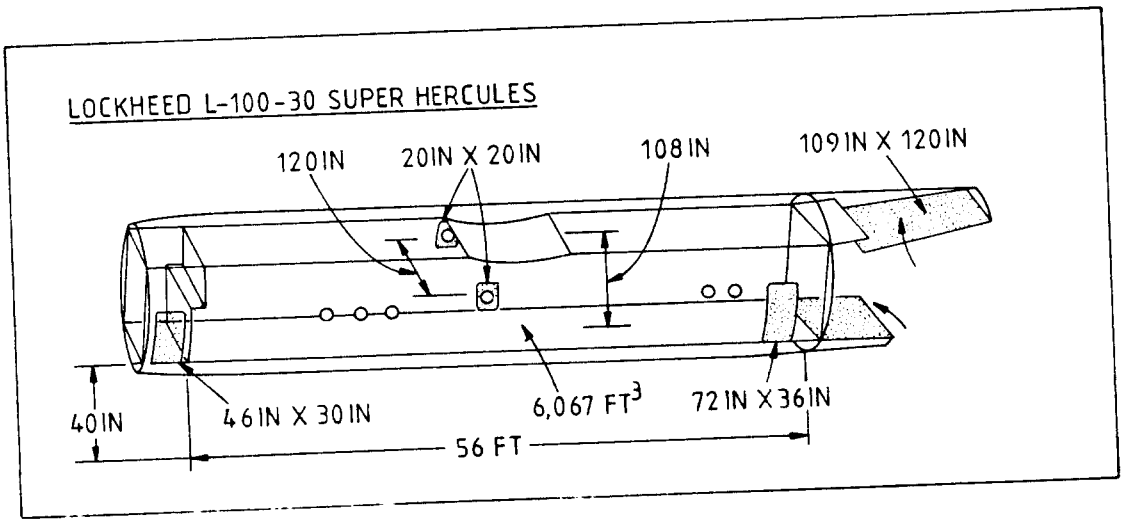

Figure 3.53b Fuselage and Cargo Hold Dimensions for Turbopropeller Driven Transports

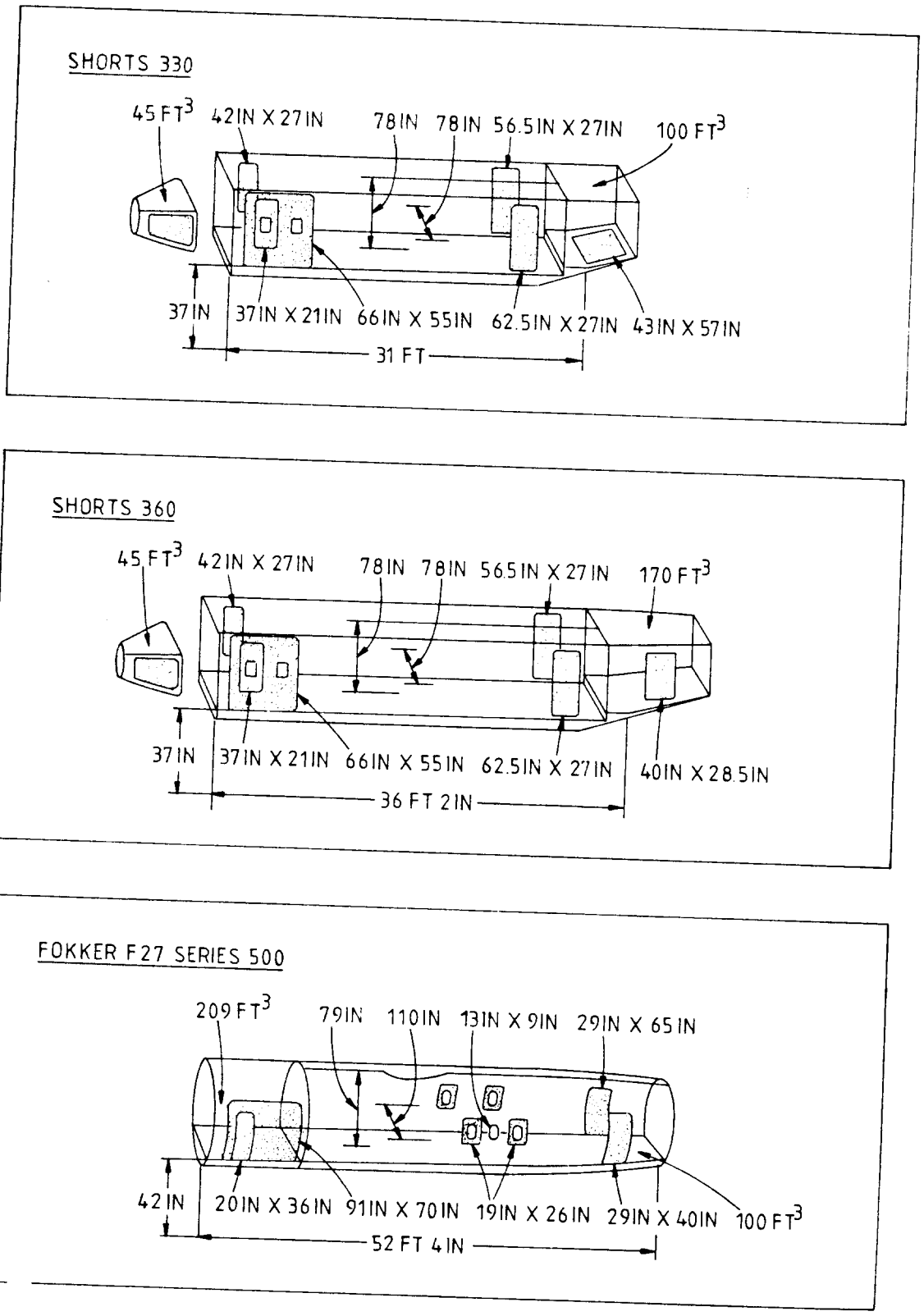

Figure 3.53c Fuselage and Cargo Hold Dimensions for Turbopropeller Driven Transports

YAKOVLEV YAK-40

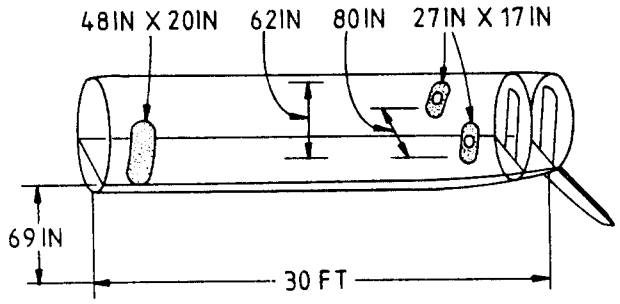

BRITISH AEROSPACE 146-100 (ALSO 146-200 WITH 58 FT 5IN CABIN)

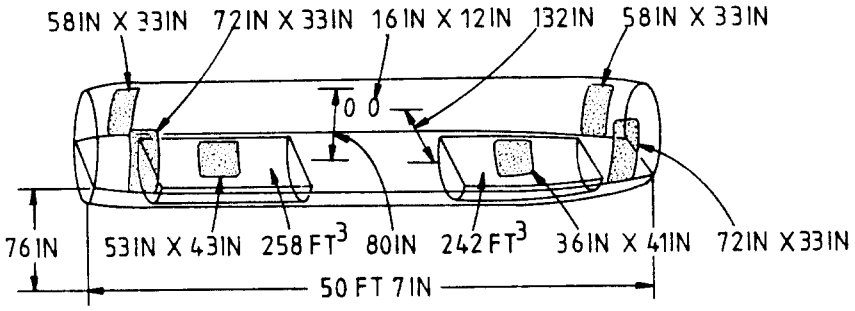

YAKOVLEV YAK-42

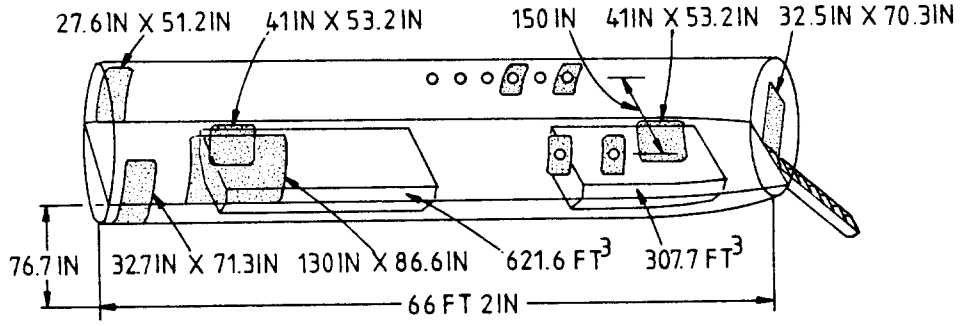

Figure 3.54a Fuselage and Cargo Hold Dimensions for Jet Transports

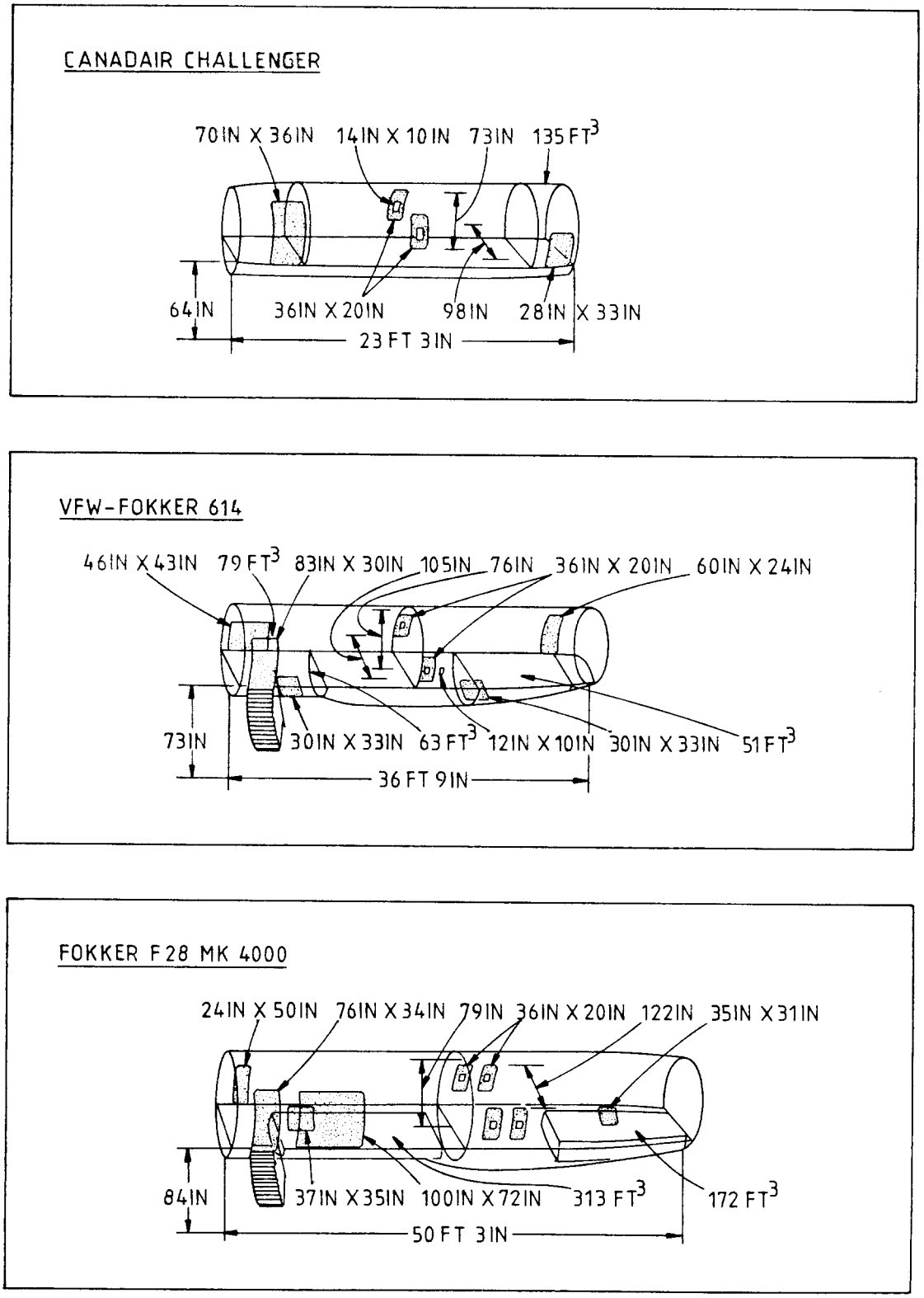

Figure 3.54b Fuselage and Cargo Hold Dimensions for Jet Transports

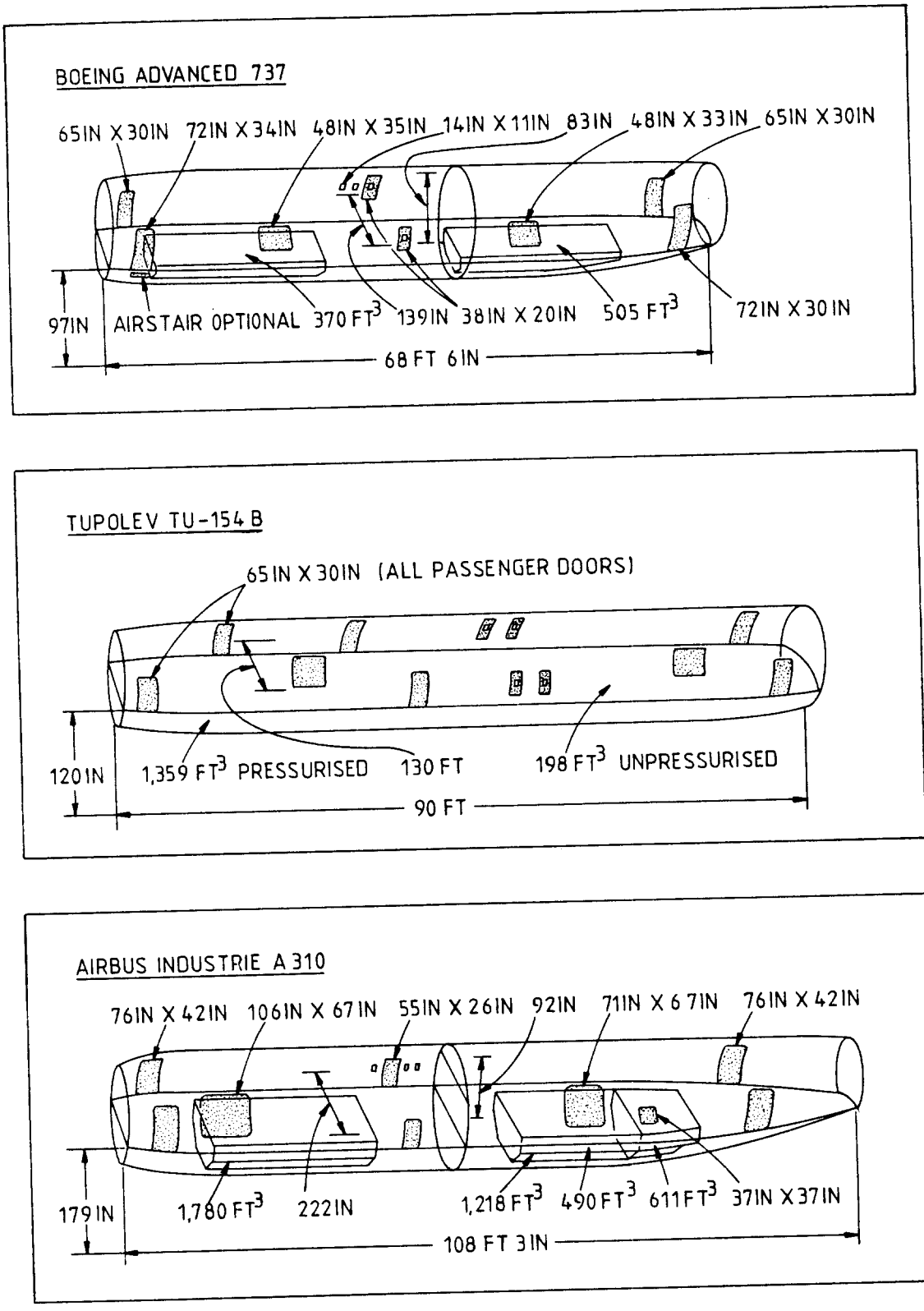

Figure 3.54c Fuselage and Cargo Hold Dimensions for Jet Transports

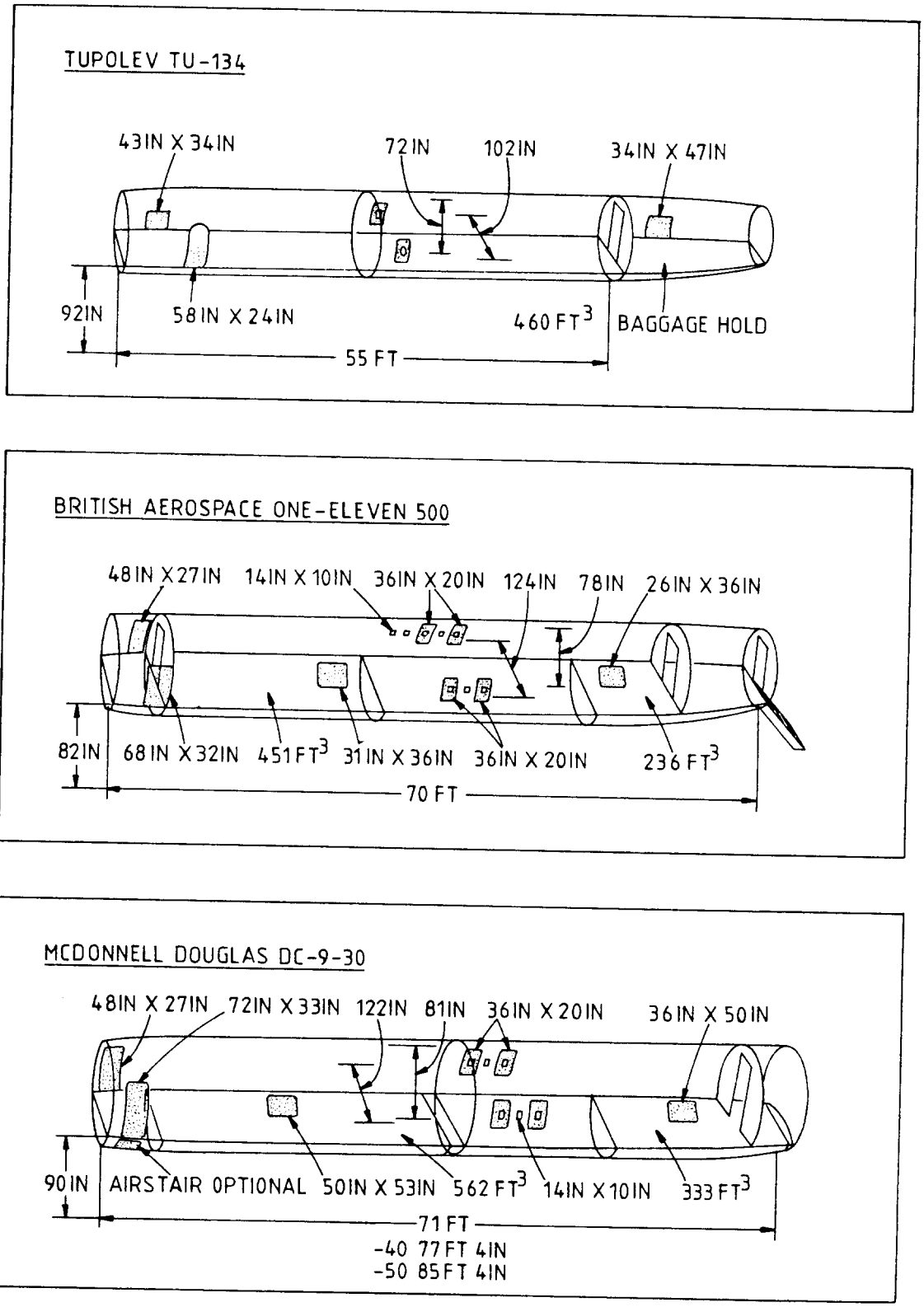

Figure 3.54d Fuselage and Cargo Hold Dimensions for Jet Transports

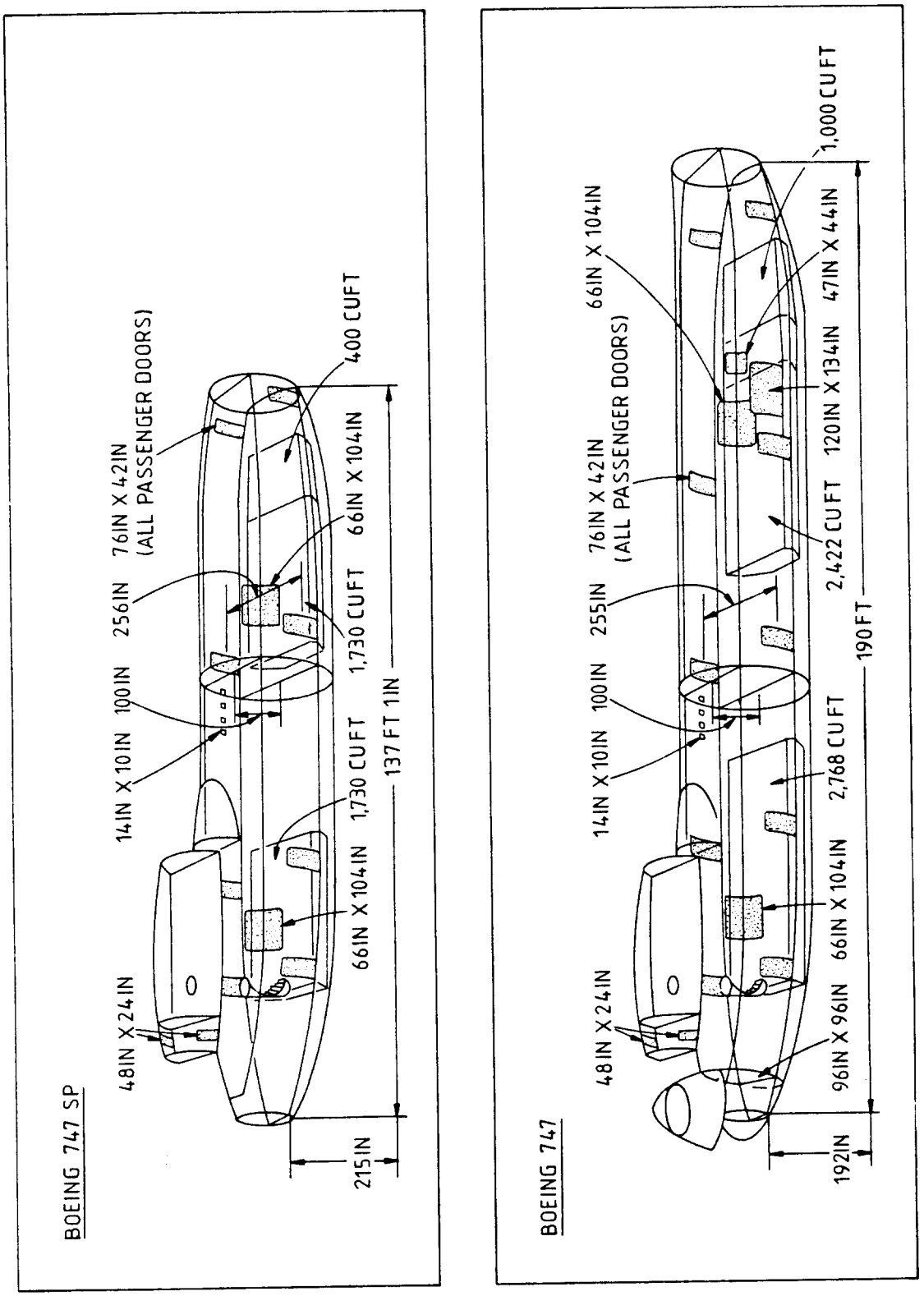

Figure 3.54e Fuselage and Cargo Hold Dimensions for Jet Transports

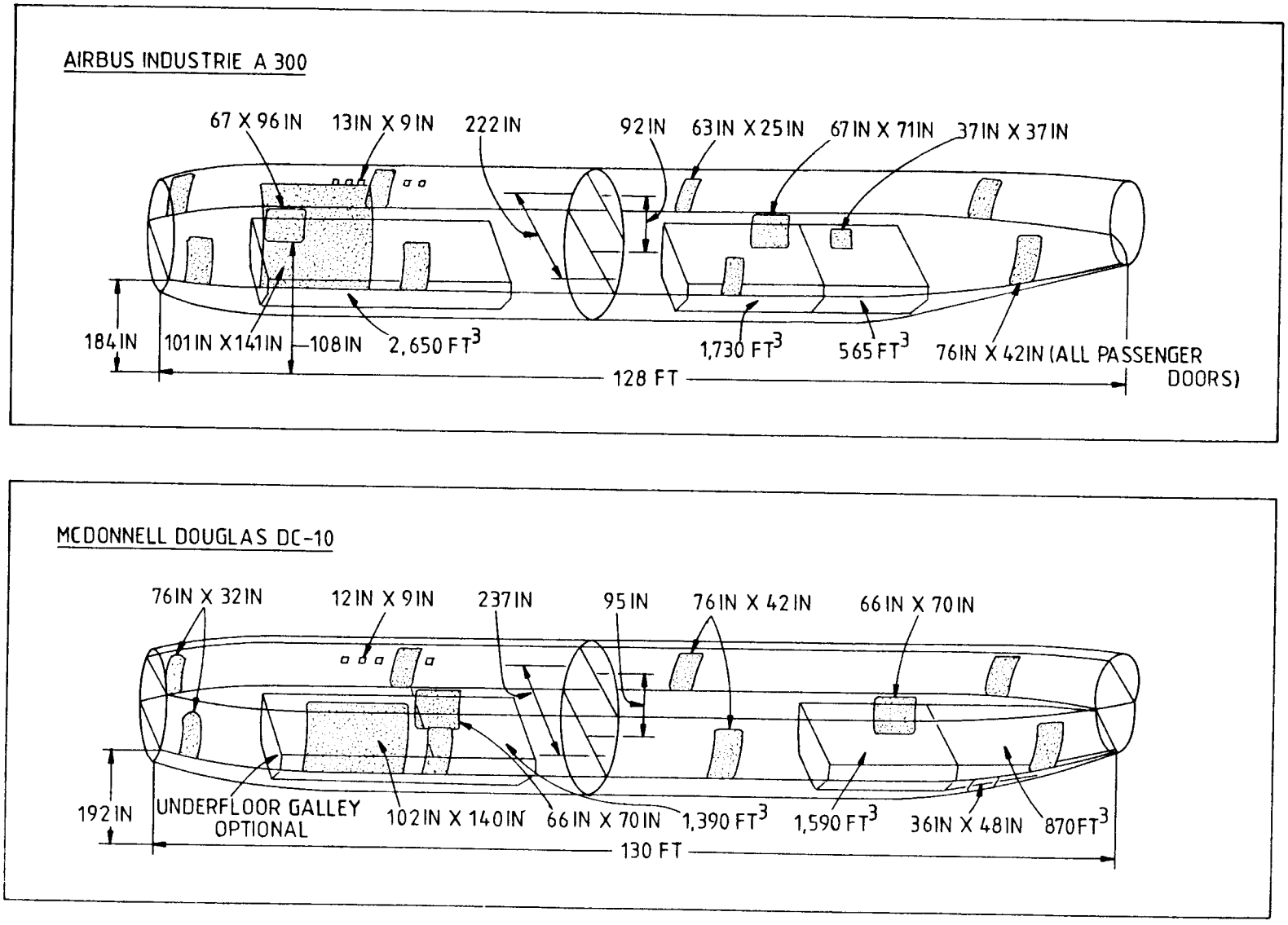

Figure 3.54f Fuselage and Cargo Hold Dimensions for Jet Transports

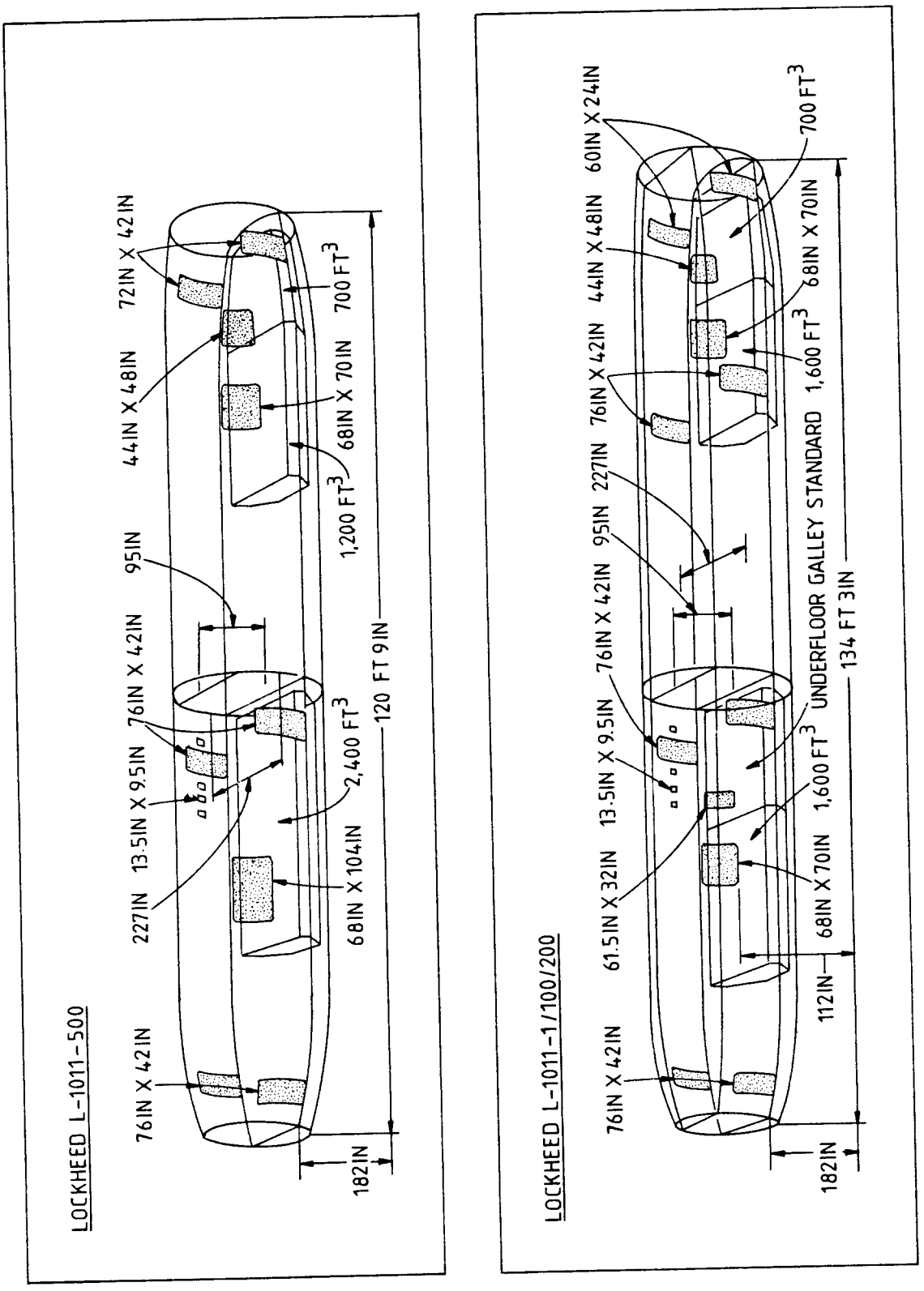

Figure 3.54g Fuselage and Cargo Hold Dimensions for Jet Transports

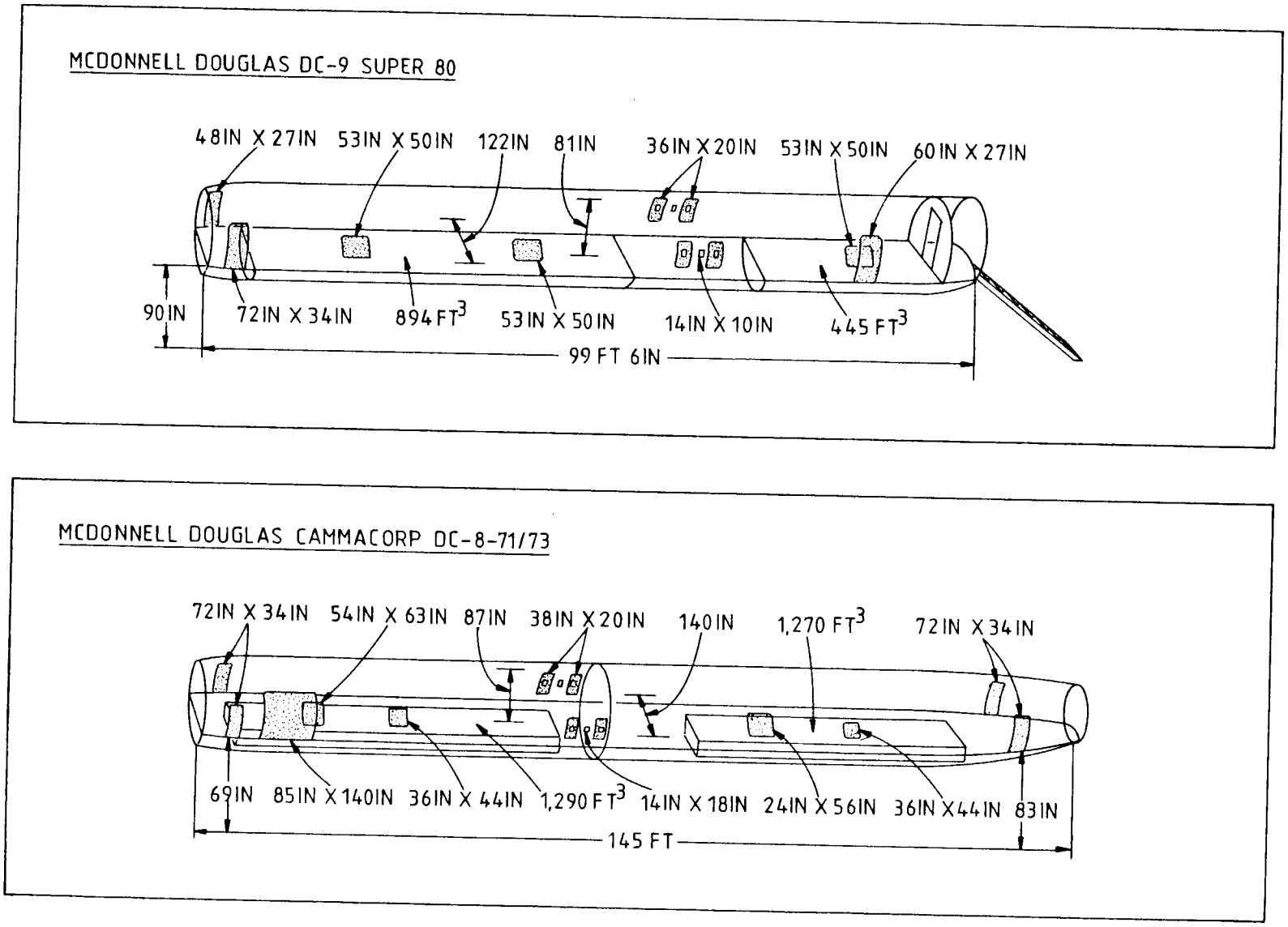

Figure 3.54h Fuselage and Cargo Hold Dimensions for Jet Transports

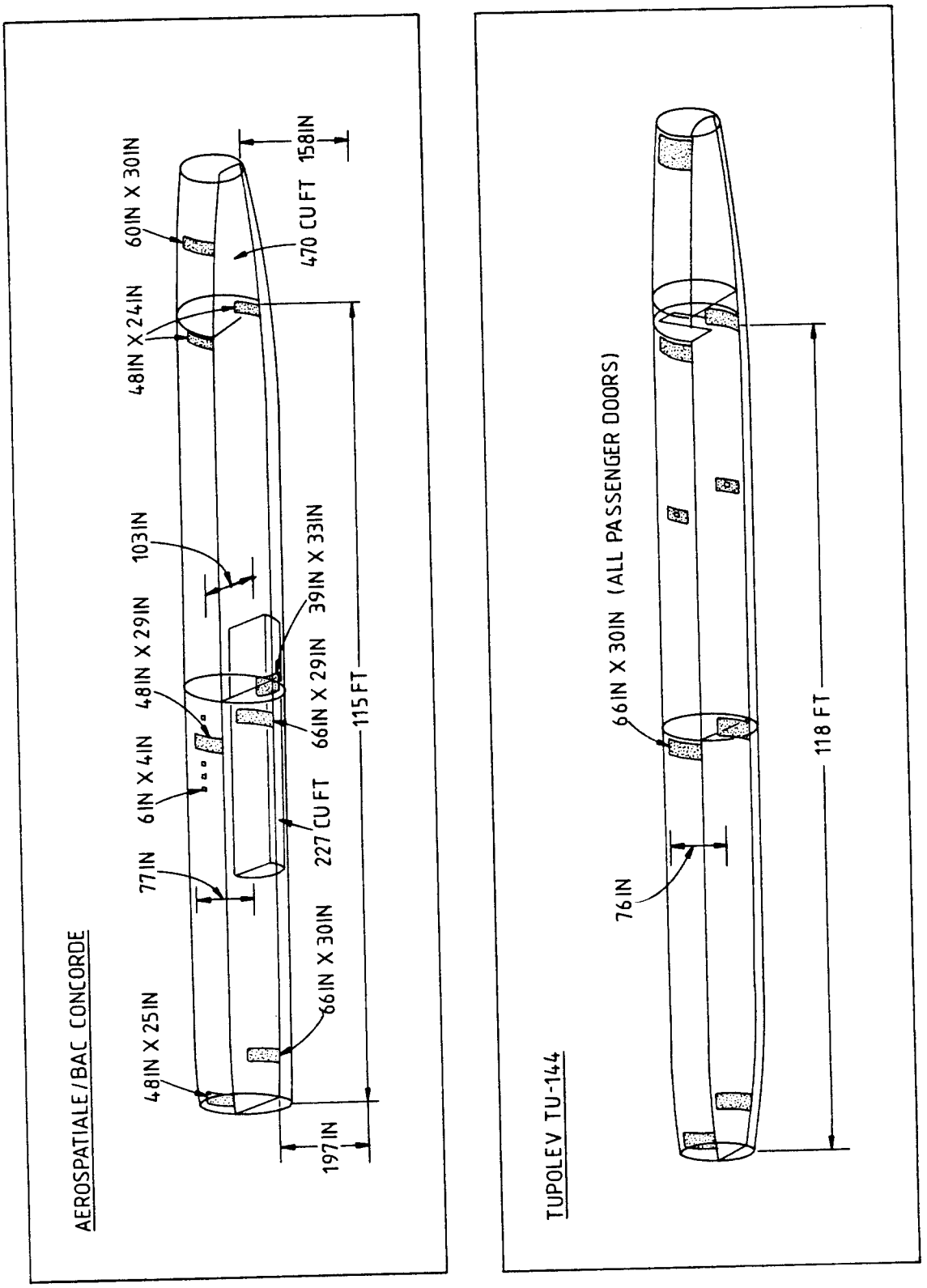

Figure 3.54i Fuselage and Cargo Hold Dimensions for Jet Transports

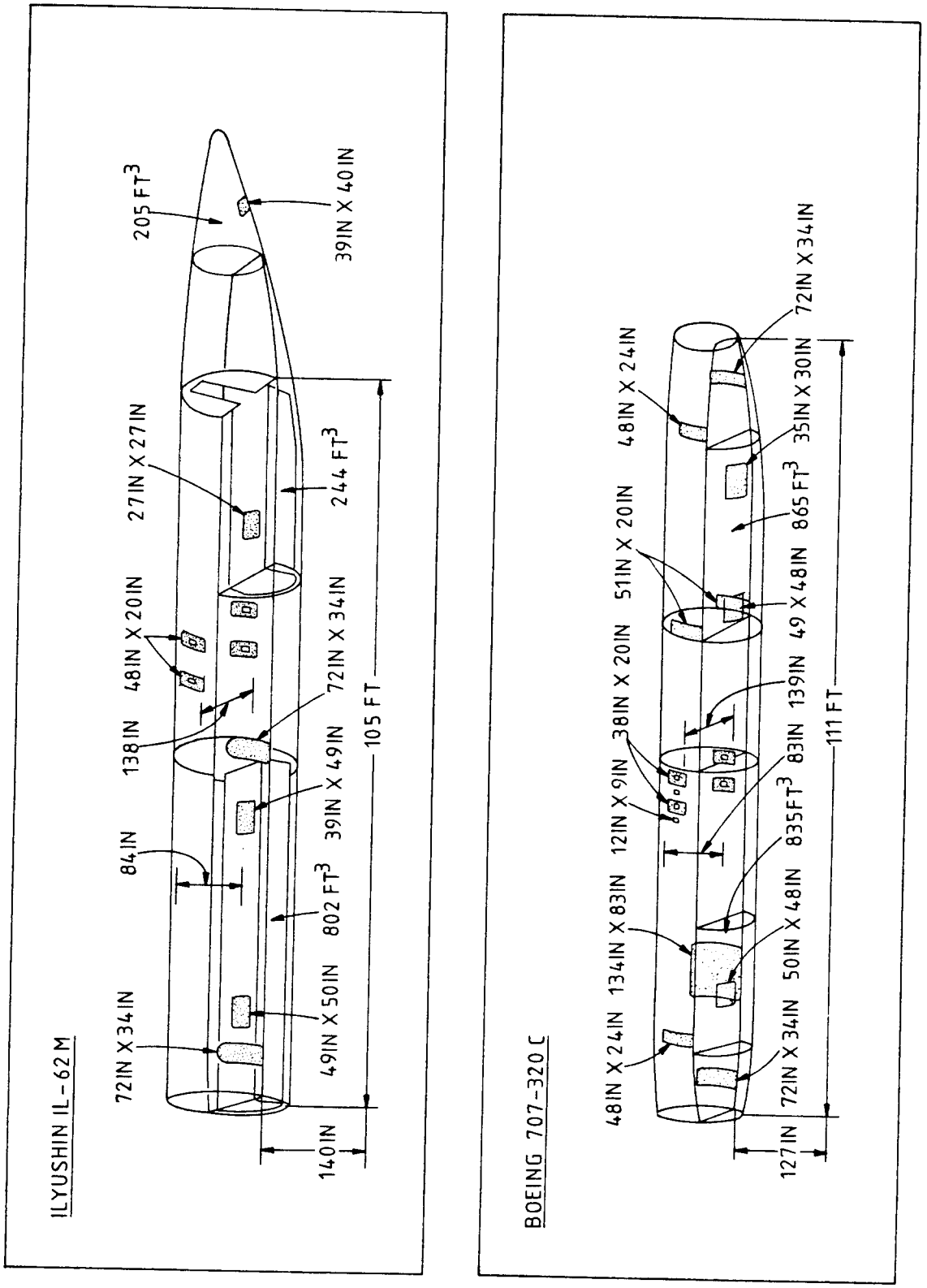

Figure 3.54j Fuselage and Cargo Hold Dimensions for Jet Transports

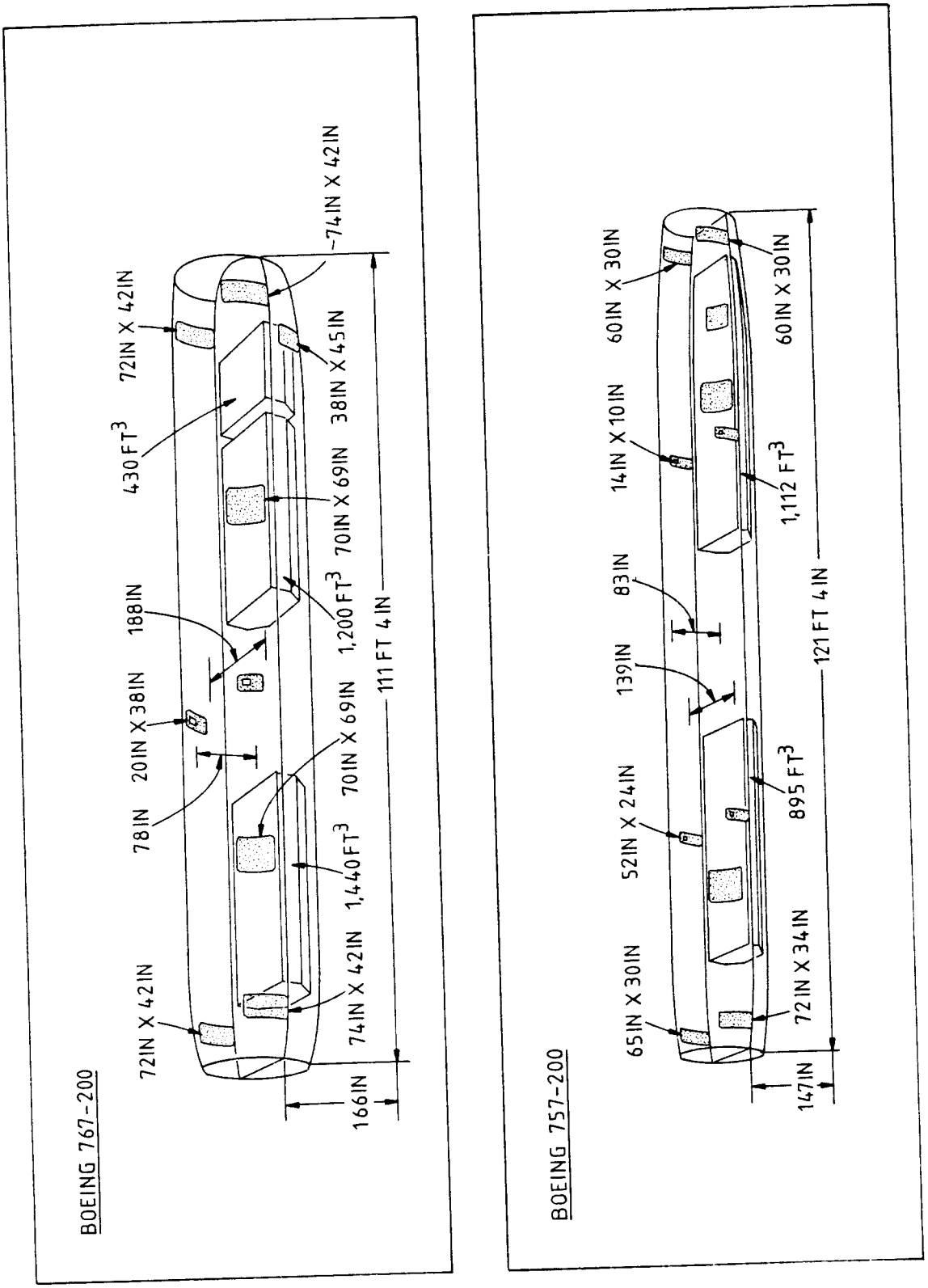

Figure 3.54k Fuselage and Cargo Hold Dimensions for Jet Transports

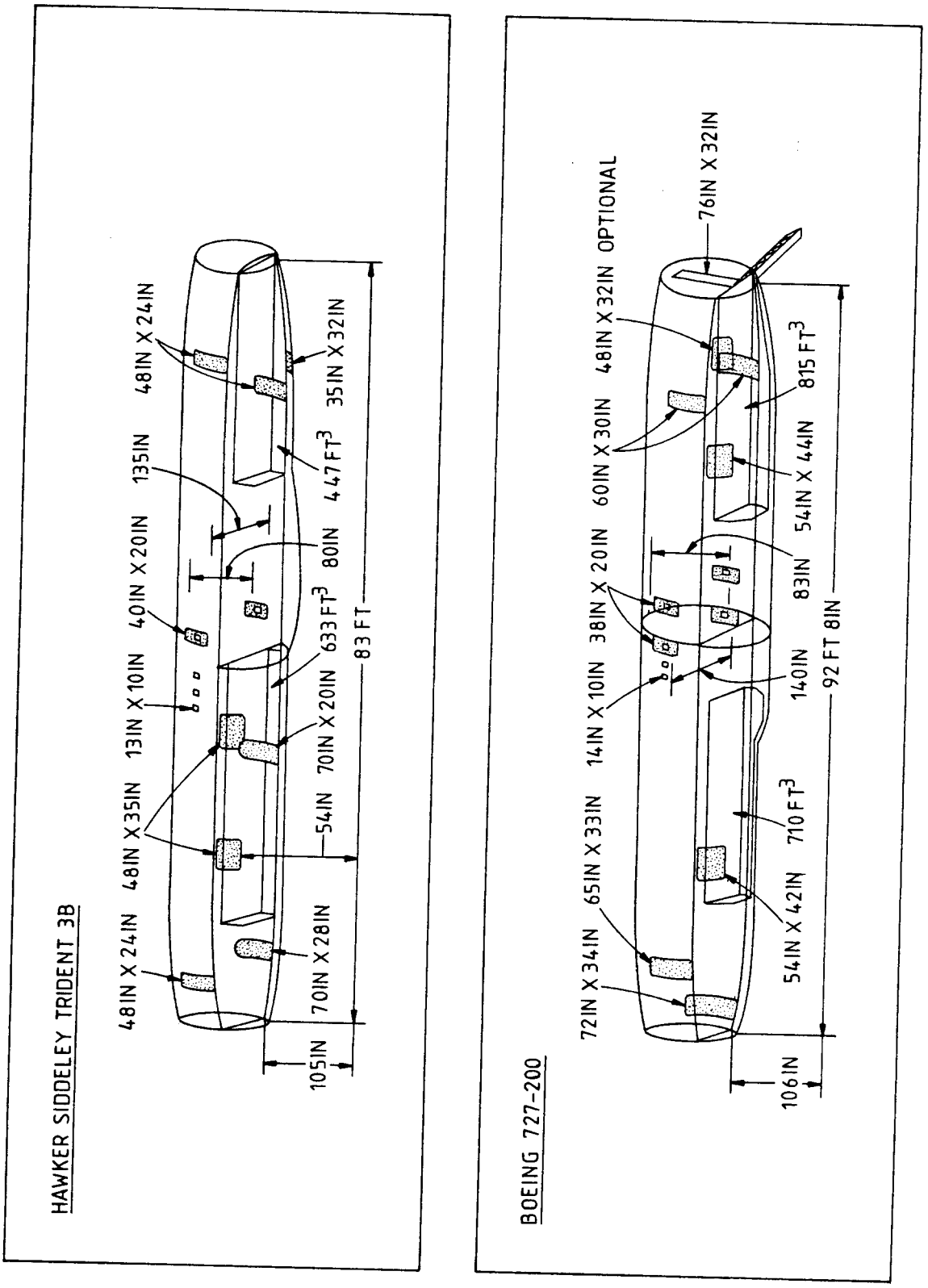

Figure 3.541 Fuselage and Cargo Hold Dimensions for Jet Transports

3.5 STRUCTURAL DESIGN CONSIDERATIONS AND EXAMPLES OF STRUCTURAL LAYOUT DESIGN OF FUSELAGES

From a structural design viewpoint the fuselage of most airplanes can be viewed as that component to which the wing, the empennage and in some instance the landing gear and the nacelles are attached.

The fuselage structure therefore must be designed so that the following types of load can be taken without major structural failures and without major structural fatigue problems:

1. Empennage loads due to trim, maneuvering, turbulence and gusts.

2. Pressure loads due to cabin pressurization.

3. Landing gear loads due to landing impact, taxiing and ground maneuvering.

4. Loads induced by the propulsion installation when the latter is attached to the fuselage.

References 11 and 19 define the loads for which airplanes must be designed. References 20 and 21 contain methods for structural sizing of structural components.

In 'survivable' crashes the fuselage must provide sufficient protection to prevent injuries to its occupants. References 22 and 24 through 27 contain information on the subject of 'design for reasonable crashworthiness'.

Cabin materials used for sound-proofing, decorative panels, seats, trays and carpets must not generate toxic fumes when exposed to fire. Ref.11 contains the regulations which must be observed in this regard.

Once the initial fuselage layout is completed (Chapter 4, Part II) and the dimensioned threeview of Step 15 (Part II) has been drawn up, it is possible to prepare an initial structural arrangement for the fuselage. Chapter 7 gives a step-by-step method for preparing the overall preliminary structural arrangement for an airplane.

The purpose of this section is to provide the reader with some ground rules for and some examples of typical structural arrangements employed in airplane fuselages.

The material is organized as follows:

3.5.1 Typical Frame Depths, Frame Spacings and Longeron Spacings

In laying out an initial structural arrangement for a fuselage the following design 'groundrules' are useful:

Frame Depths:

For small commercial airplanes:	1.5 inches.
For fighters and trainers:	2.0 inches.
For large transports:	$0.02d_f$ + 1.0 inches.

Frame Spacings:

For small commercial airplanes:	24 - 30 inches.
For fighters and trainers:	15 - 20 inches.
For large transports:	18 - 22 inches.

Longeron Spacings:

For small commercial airplanes:	10 - 15 inches.
For fighters and trainers:	8 - 12 inches.
For large transports:	6 - 12 inches.

Figure 3.55 defines these structural parameters. The actual numbers used for these structural design parameters depend on the skin thickness. In the case of composite structures these guidelines are not valid.

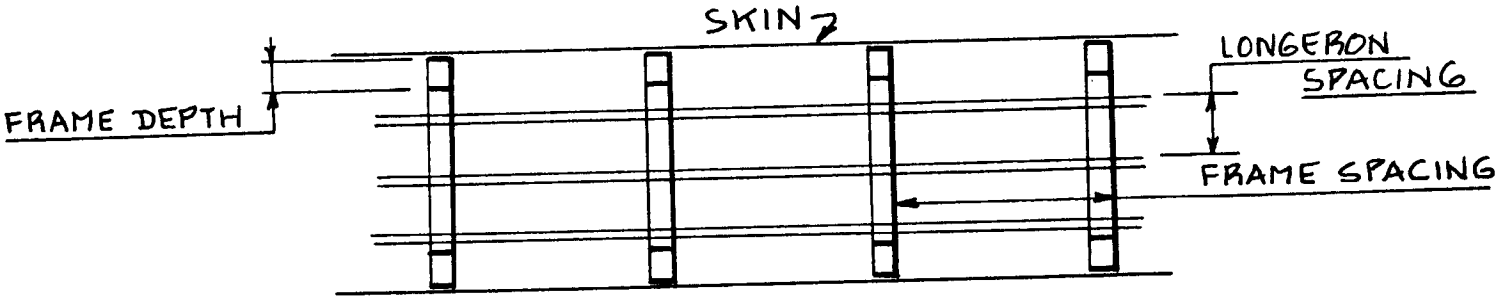

Figure 3.55 Definition of Frame Depth, Frame Spacing and Longeron Spacing

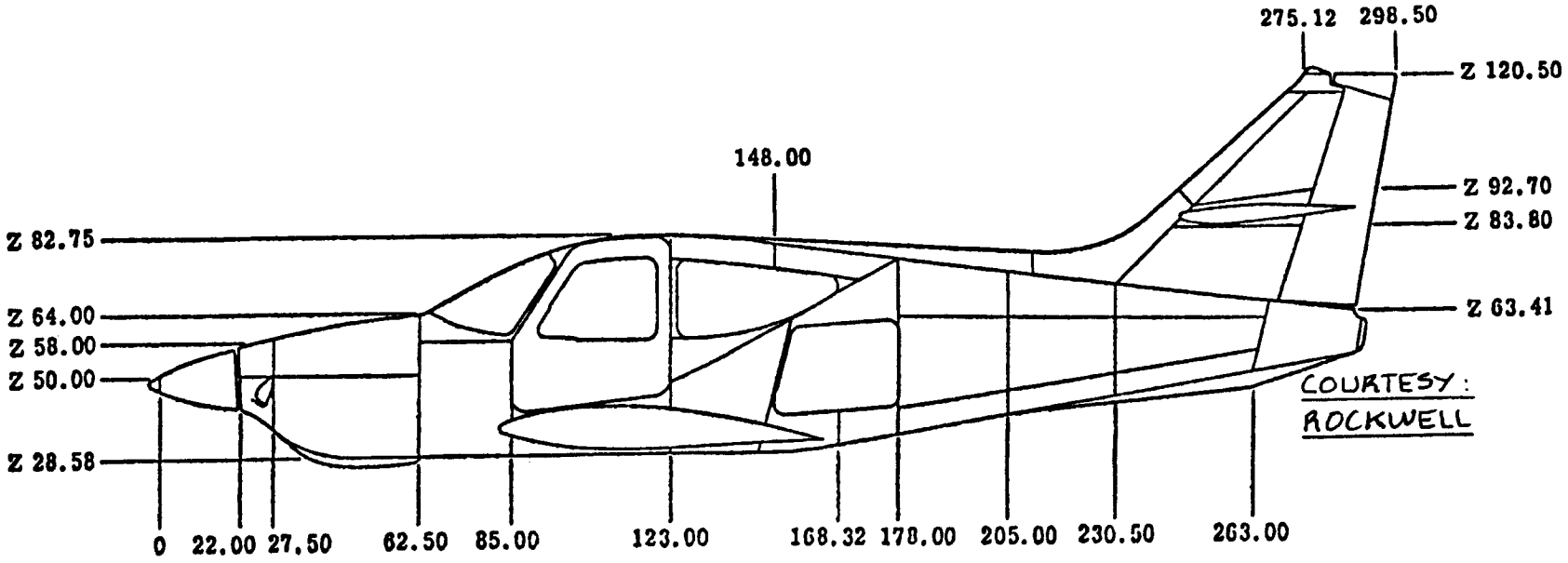

Figure 3.56 Fuselage Structural Arrangement for the Rockwell Model 112

3.5.2 Examples of Fuselage Structural Arrangements

Figures 3.56 through 3.60 show examples of structural arrangements for the fuselages of several airplanes.

Figure 3.56 represents a small, unpressurized, general aviation airplane. Note the wide spacing between frames and between longerons.

Figure 3.57 represents a small, unpressurized, twin engine turbopropeller airplane. There are no fuselage longerons. Their function has been take over by bonded, corrugated skin panels.

Figure 3.58 represents a pressurized business jet. Note the tight spacing between fuselage frames and longerons. Also note that both pressure bulkheads are flat. Forward pressure bulkheads are normally small enough for the weight penalty due to flatness to be negligible. The nose gear is often attached to stiffeners placed on the forward pressure bulkhead. In that case any weight penalty due to flatness may disappear.

The rear pressure bulkheads are normally large. A significant weight penalty is incurred by making these flat. However, sometimes it is desirable to gain useful cabin volume by making the rear pressure bulkhead flat.

Figures 3.59 and 3.60 show the fuselage structural arrangements of typical jet transports. Both airplanes have flat forward pressure bulkheads which are also used to mount the weather radar disks.

Note that the 767 has a spherical aft pressure bulkhead while the DC10 has a flat one. In the latter, the aft pressure bulkhead is also used to mount the front spar of the vertical tail.

Figure 3.61 shows a typical structural arrangement for the fuselage of a fighter airplane. The irregular fuselage structure is mandated by the requirements for:

1. engine removal
2. speed brakes
3. nose wheel retraction
4. canopy

Note the tail hook attachment.

Important observation: The airplanes in Figures 3.56-3.58 violate the principle of p.238, Part II which requires the zero reference point to be well ahead of the nose! Don't fall into this trap!

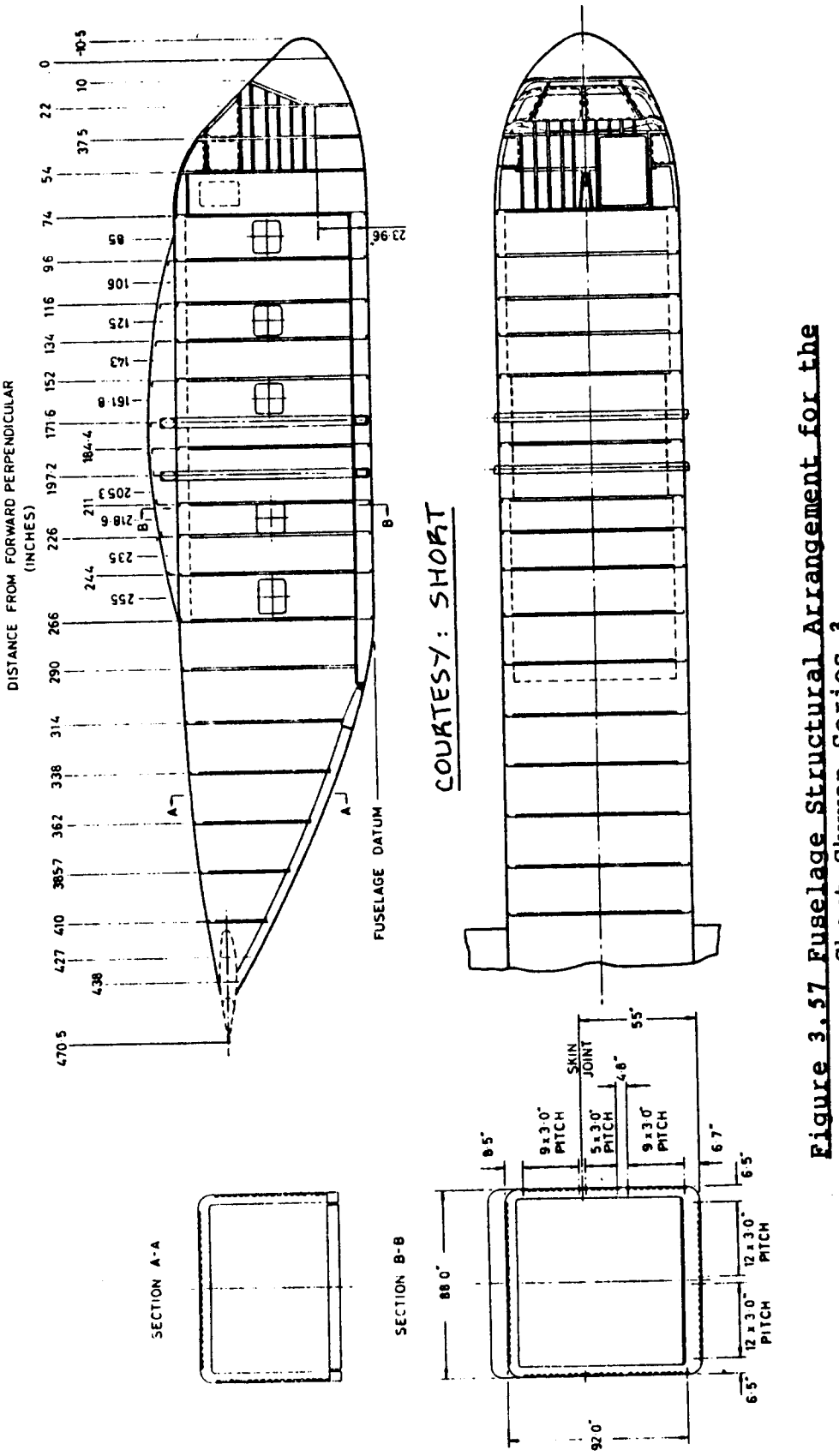

Figure 3.57 Fuselage Structural Arrangement for the Short Skyvan Series 3

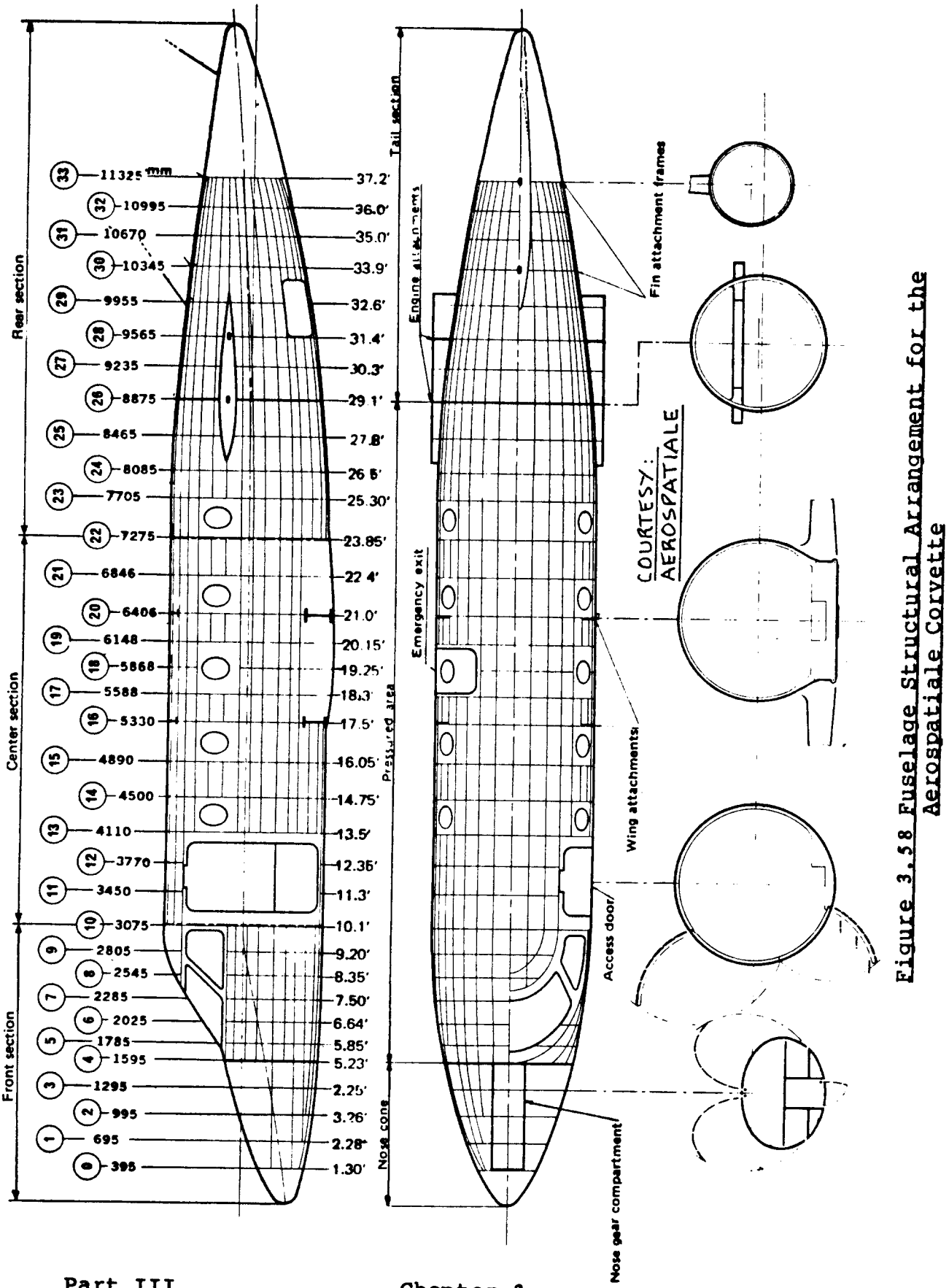

COURTESY: AEROSPATIALE

Figure 3.58 Fuselage Structural Arrangement for the Aerospatiale Corvette

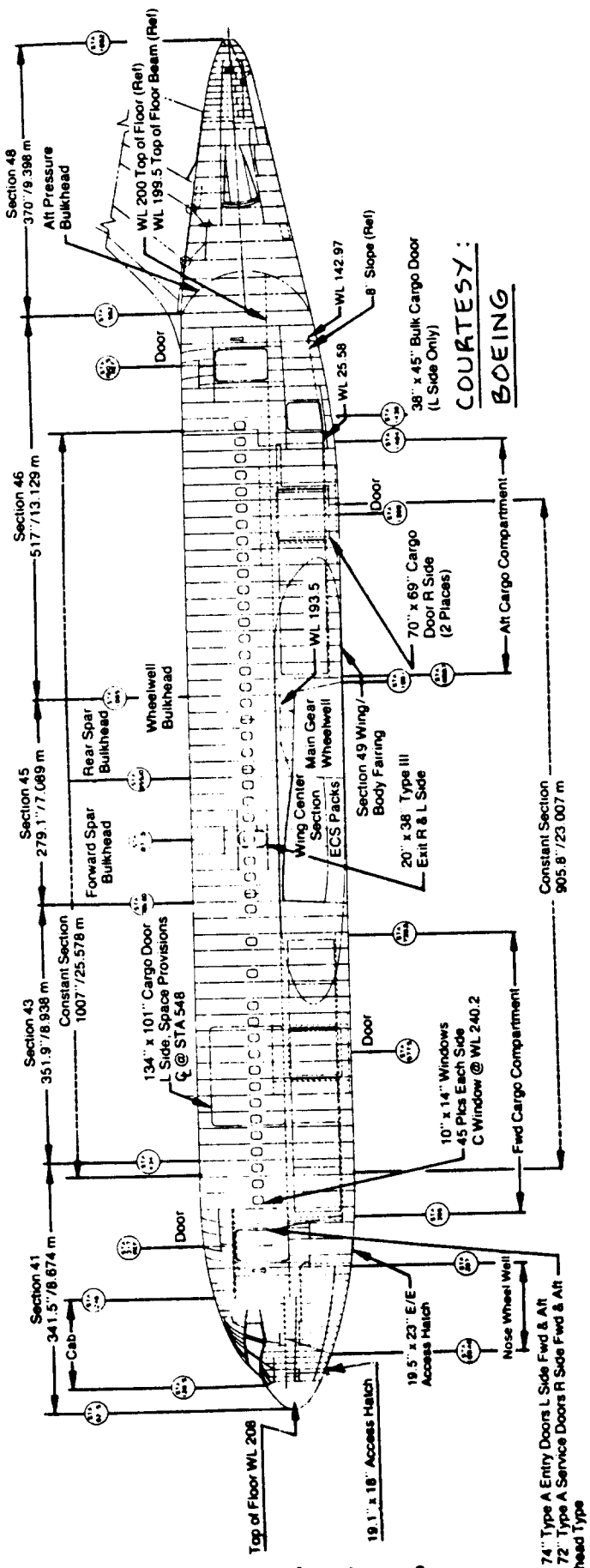

Figure 3.59 Fuselage Structural Arrangement for the Boeing 767-200

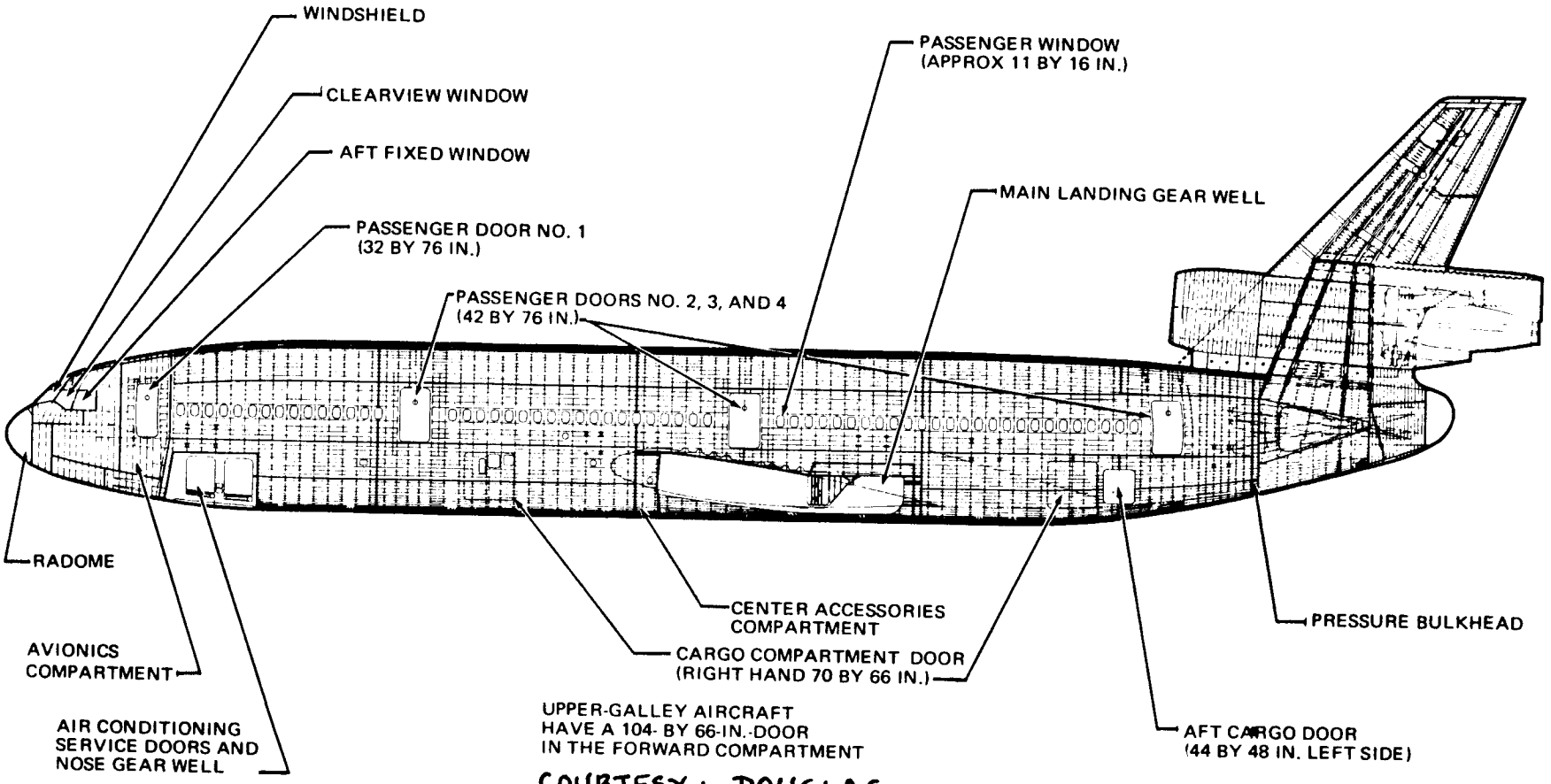

COURTESY : DOUGLAS

Figure 3.60 Fuselage Structural Arrangement for the McDonnell Douglas DC10

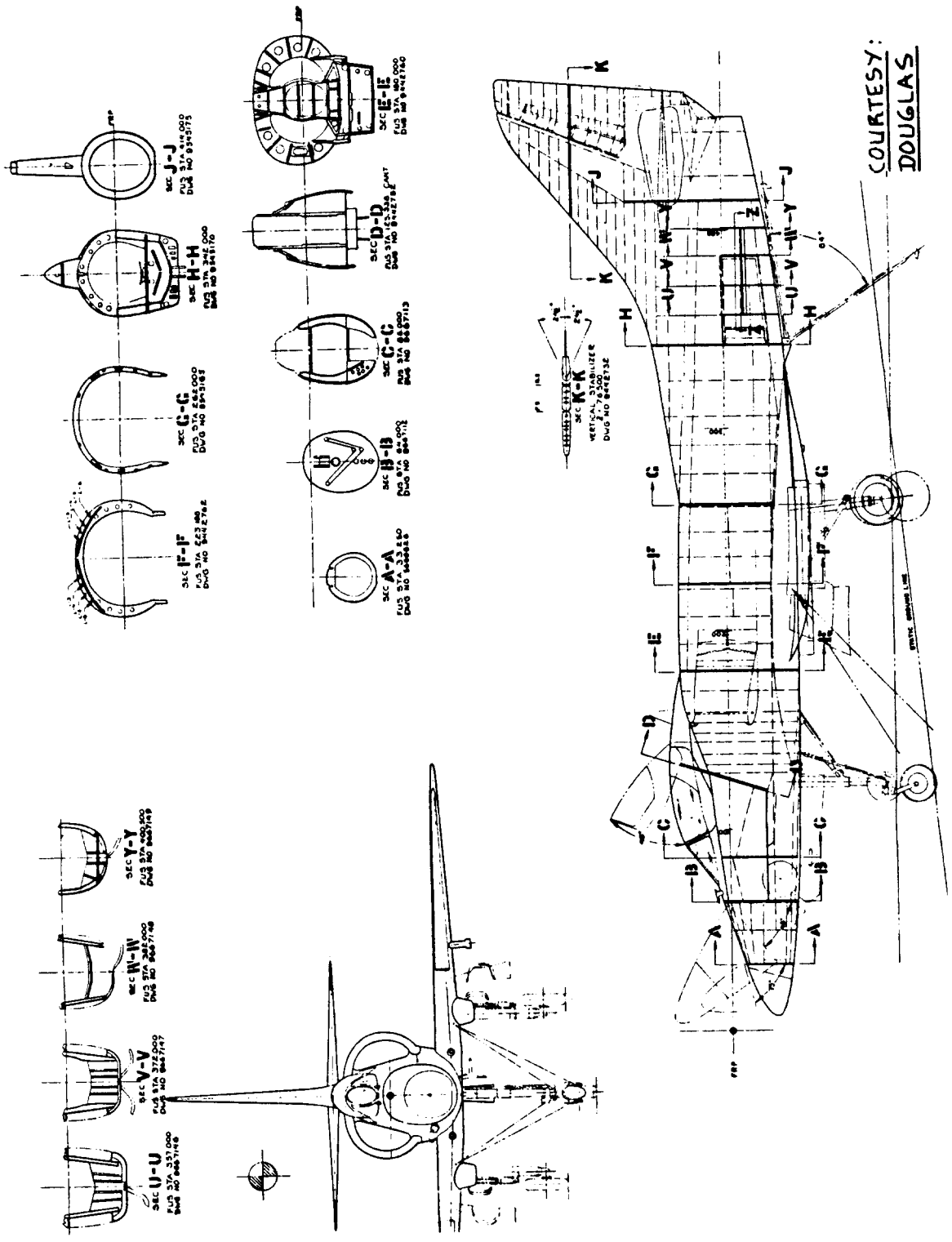

Figure 3.61 Fuselage Structural Arrangement for the Douglas A4D-2N Skyhawk

3.5.3 Examples of Fuselage Shell Layout

Figures 3.62 and 3.63 provide typical shell and skin layouts for general aviation airplanes. Note that relatively thin skin gauges are sufficient.

Figures 3.64 and 3.65 illustrate the shell layout used in a typical large jet transport. To facilitate manufacturing and final assembly, the fuselage and the skin are made in varying sections. This necessitates skin splicing. Figures 3.66 and 3.67 show typical skin splices used in such transports.

When using honeycomb panels for the fuselage skin, most frames and longerons are no longer needed. Fig.3.68 shows an example concept of such a shell layout, applied to a short haul airplane design.

SKIN NO.	MATERIAL	THICKNESS (IN.)
1	2024-T3	.016
2	2024-0*	.032
3	2024-T3	.020
4	2024-T3	.025
5	2024-T3	.032
6	2024-T3	.040
7	2024-0*	.040
8	FIBERGLASS	
9	THERMOPLASTIC	

COURTESY : PIPER

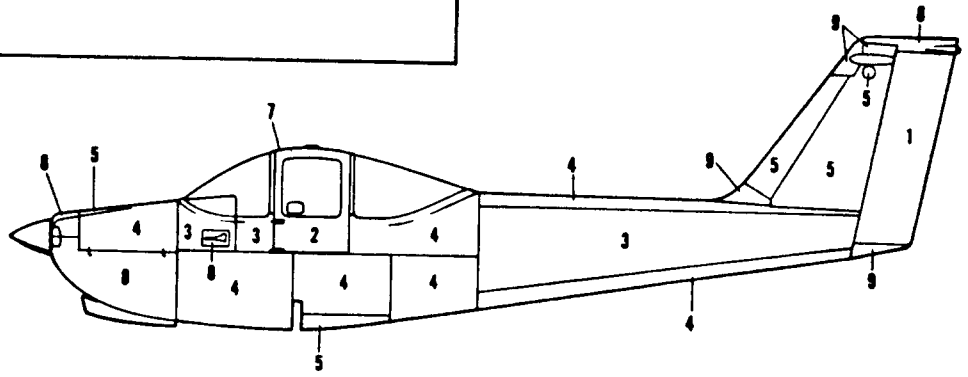

Figure 3.62 Fuselage Shell and Skin Layout for the Piper PA-38-112 Tomahawk

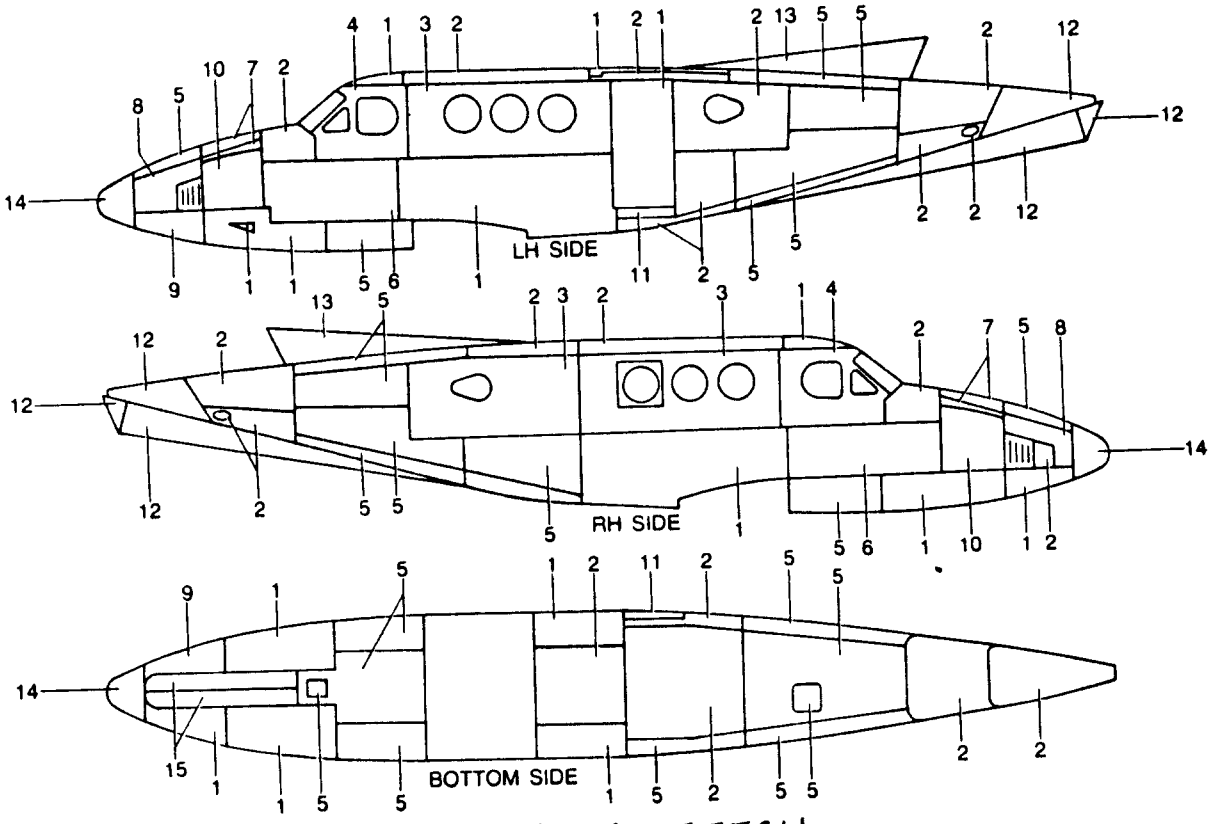

COURTESY: BEECH

ITEM	MATERIAL	THICKNESS IN INCHES
1	2024T3	.040
2	2024T3	.050
3	2024T3	.063
4	2024T3	.071
5	2024T3	.025
6	2024T42	.040
7	2024T4	.025
8	2024T4	.050
9	2024T4	.032
10	6061T4	.040
11	2024T3	.080
12	6061T6	.025
13	Laminated No. 181 Glass Cloth per MIL-C-9084	.030
14	Laminated No. 181 Glass Cloth per MIL-C-9084	.035-.050
15	2024T3	.032

Figure 3.63 Fuselage Shell and Skin Layout for the Beech King Air F90

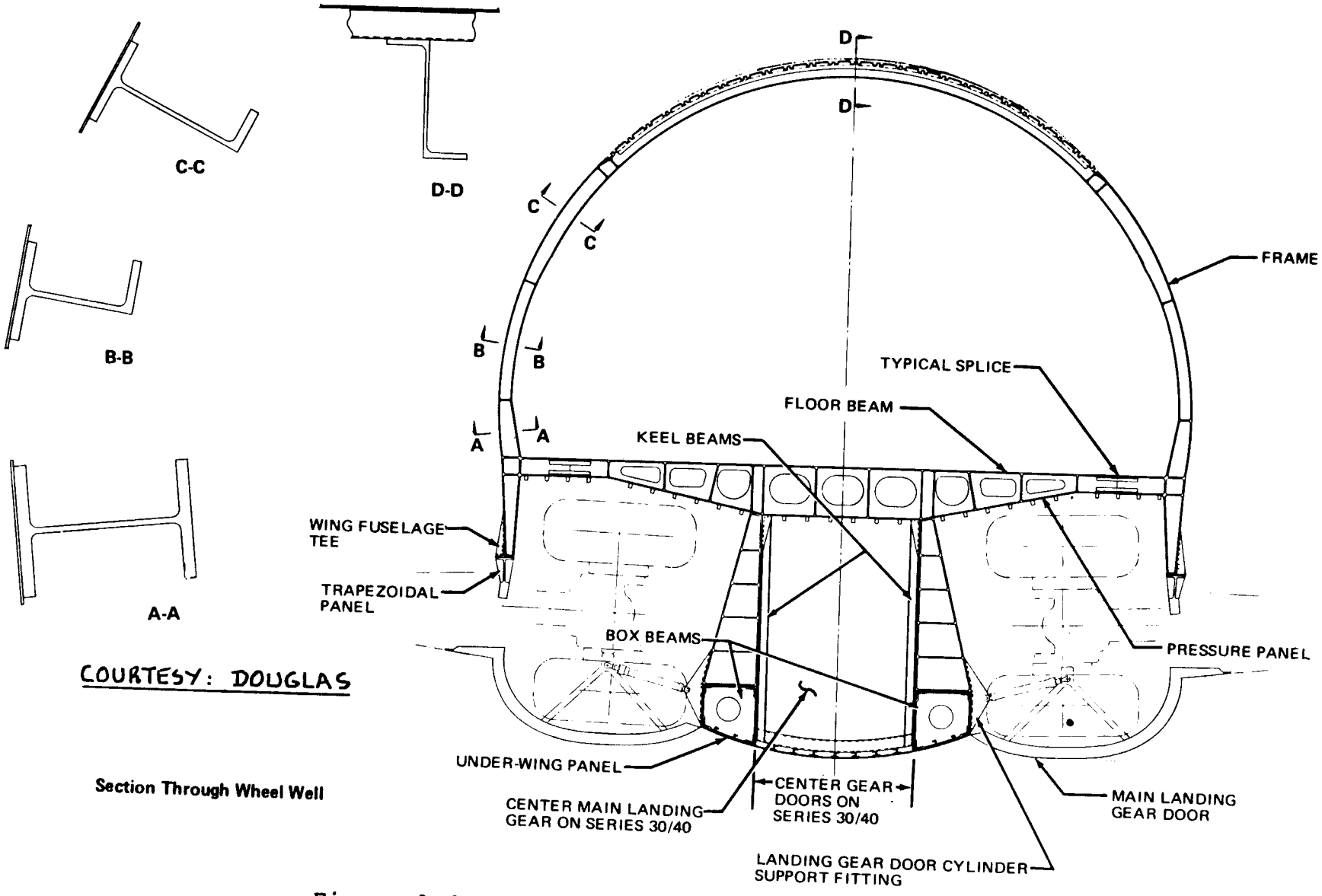

COURTESY: DOUGLAS

Section Through Wheel Well

Figure 3.64 Fuselage Shell and Skin Layout for the McDonnell Douglas DC10

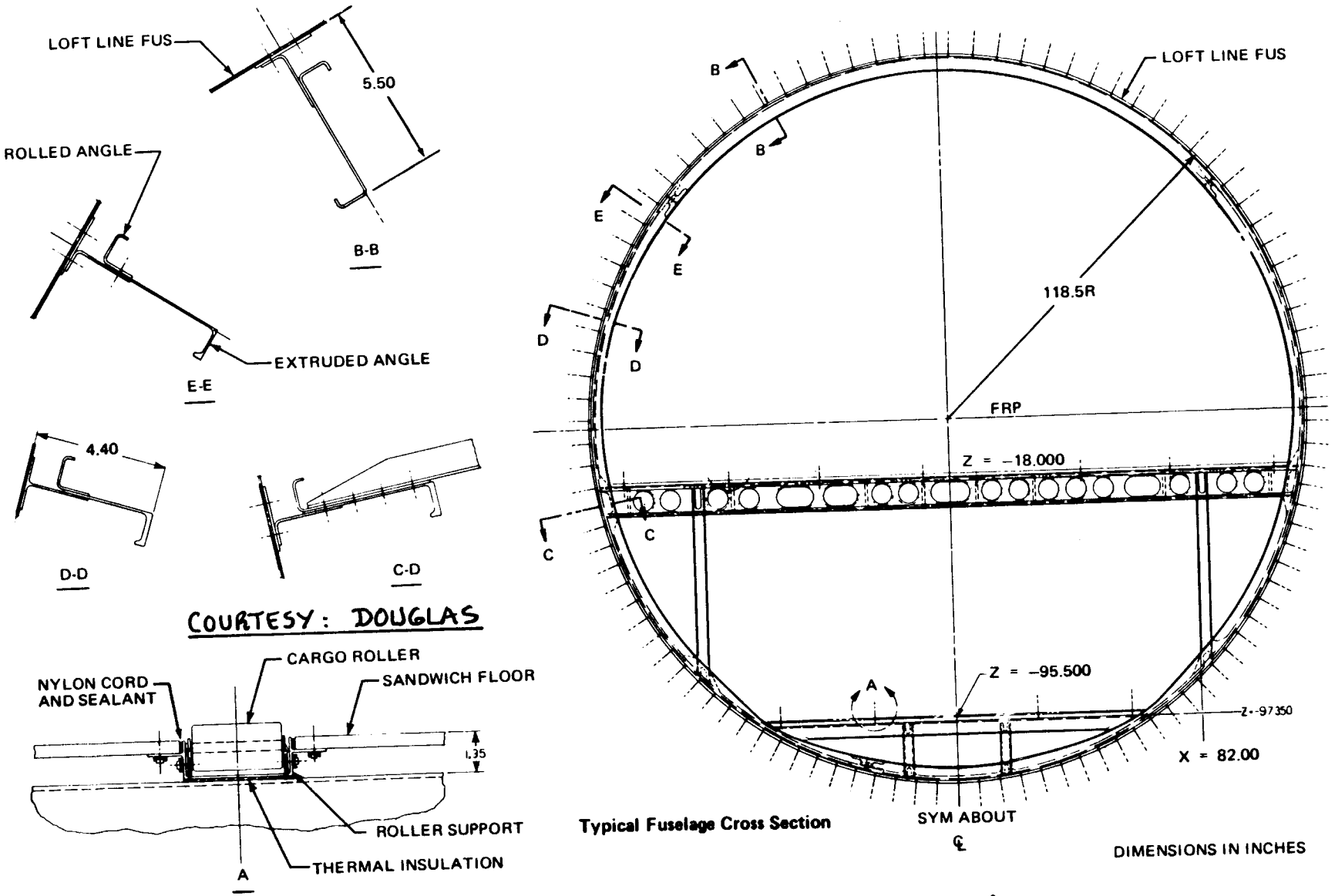

Figure 3.65 Fuselage Shell and Skin Layout for the McDonnell Douglas DC10

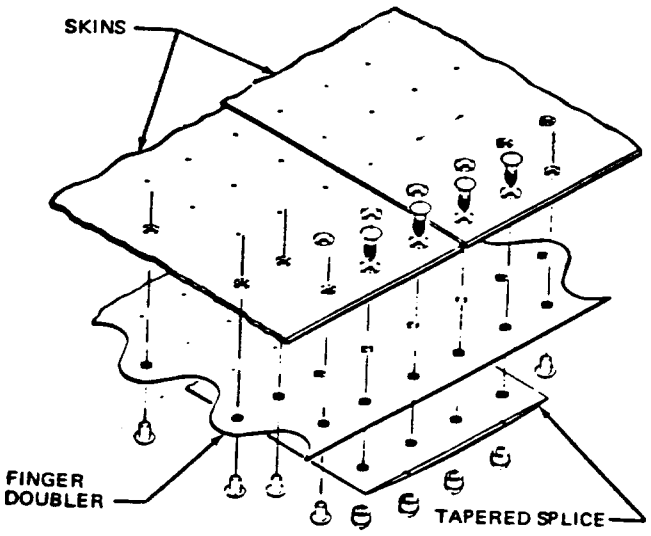

Figure 3.66 Typical Transverse Fuselage Skin Splice for the McDonnell Douglas DC10

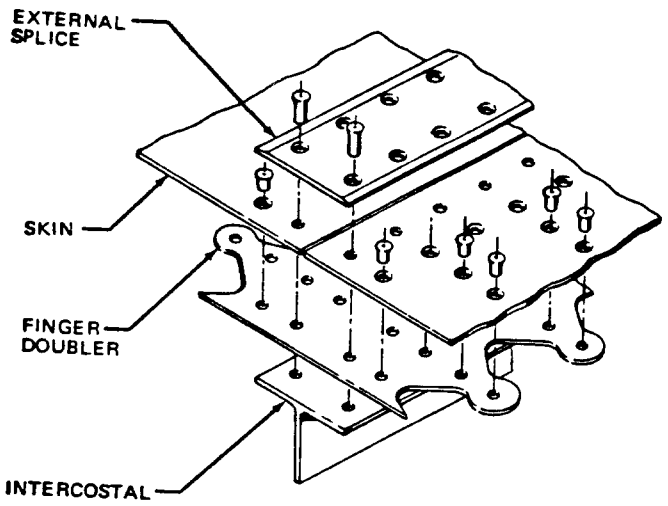

Figure 3.67 Typical Longitudinal Fuselage Skin Splice for the McDonnell Douglas DC10

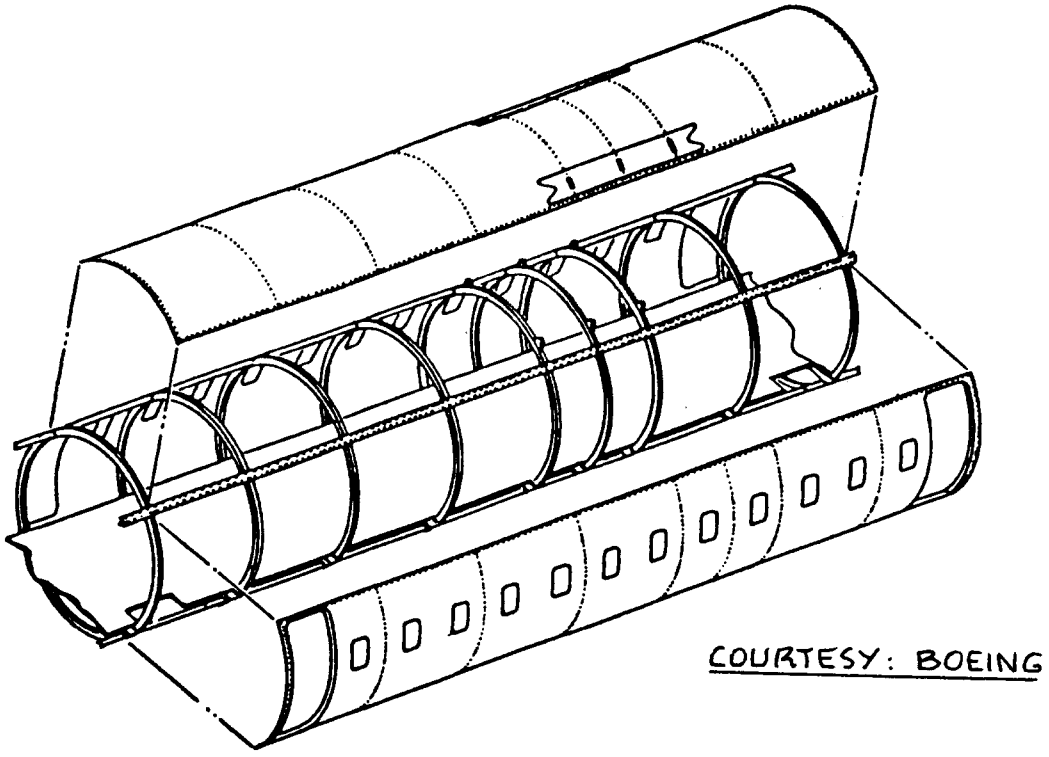

Figure 3.68 Example of a Fuselage with Honeycomb Skin Panels According to a Boeing Proposal

3.5.4 Examples of Door and Stair Design

Figure 3.69 shows a typical door installation used in a light, unpressurized airplane. Contrast this with the forward passenger door of Figure 3.70 for a jet transport! Many transports also have doors in their rear pressure bulkheads. Figure 3.71 shows an example of such a design.

When operating from fields without passenger loading ramps, transports need to carry 'built-in', retractable stairways. Figures 3.72 show an example of a ventral stairway mounted outside the pressure vessel.

Cargo compartments in pressurized transports must have special doors to allow for easy loading/unloading. These doors must be easy to open and close. They also must be able to hold the cabin pressure differential. Figure 3.73 shows an example of such a cargo door.

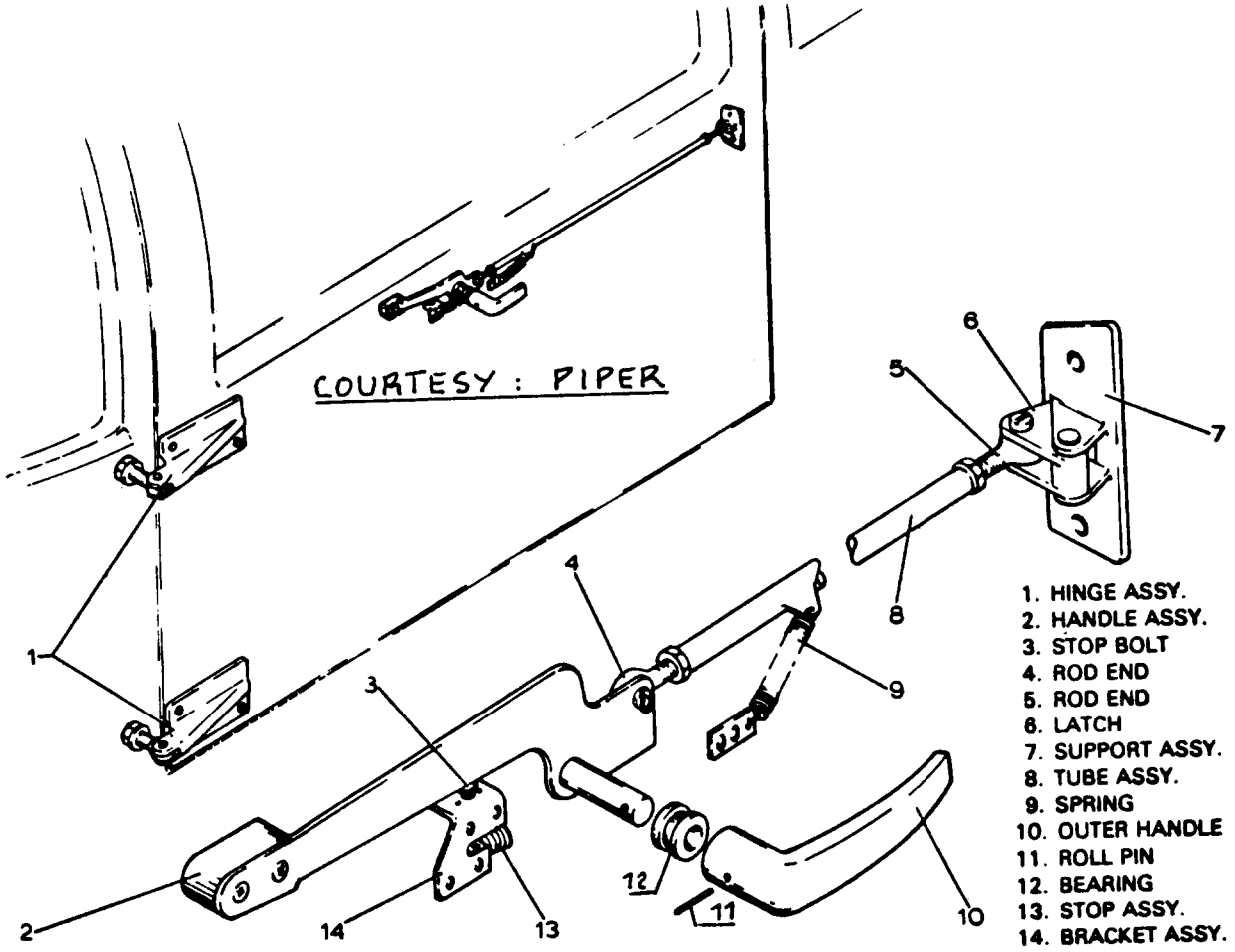

Figure 3.69 Cabin Door Installation for the Piper PA-38-112 Tomahawk

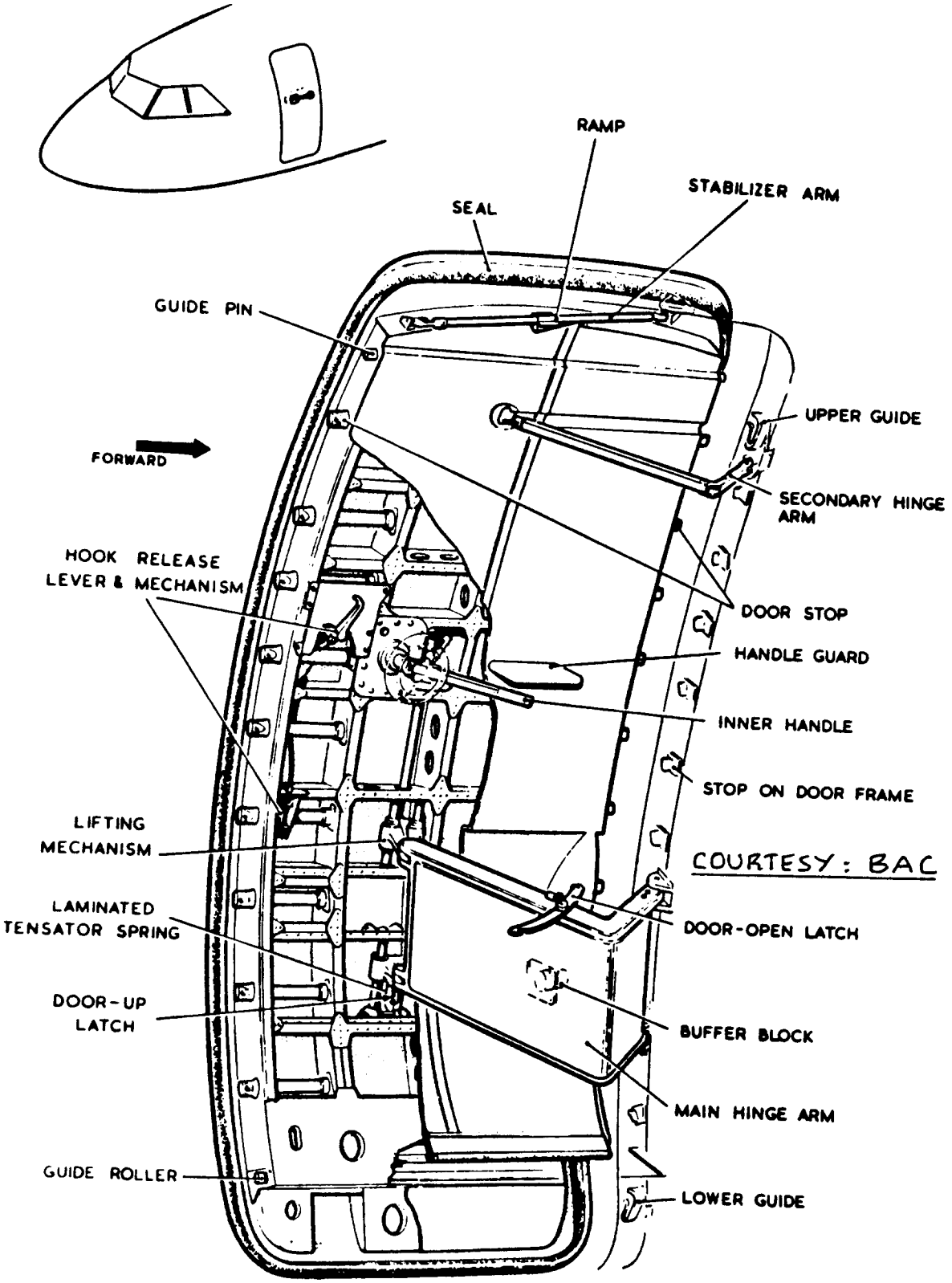

Figure 3.70 Passenger Door Installation for the BAC 111

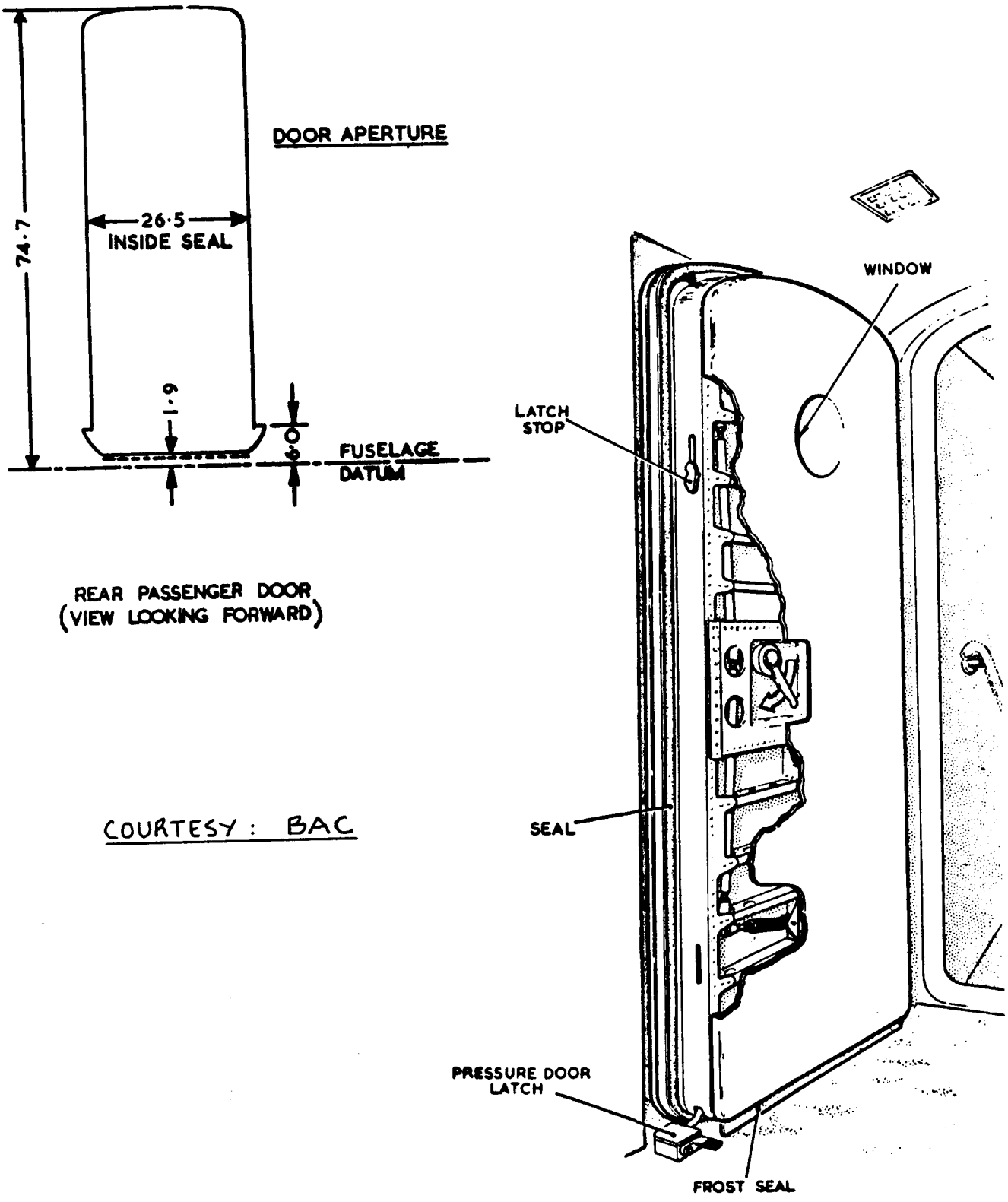

COURTESY : BAC

Figure 3.71 Pressure Bulkhead Door Installation for the BAC 111

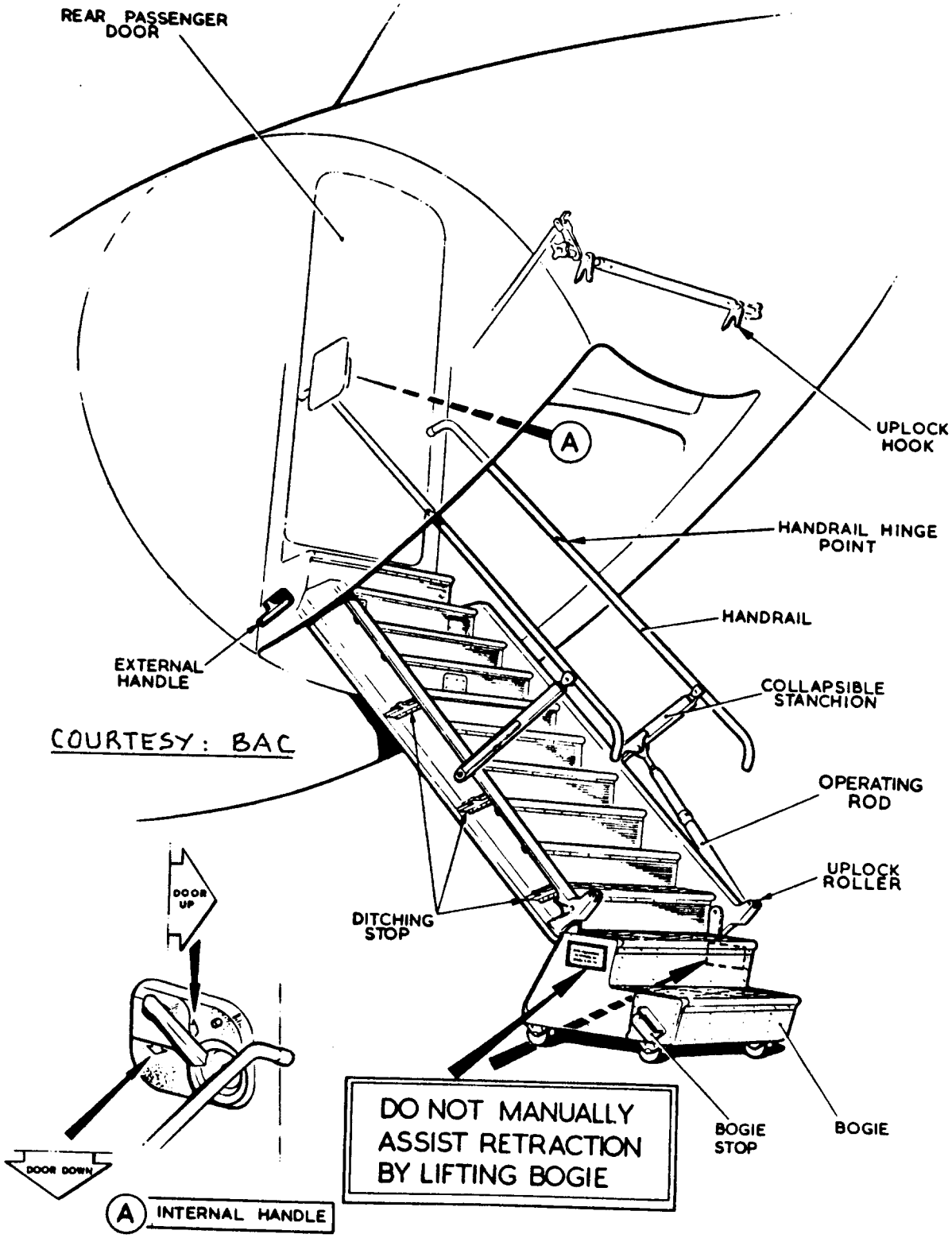

Figure 3.72a Ventral Stair Installation for the BAC 111

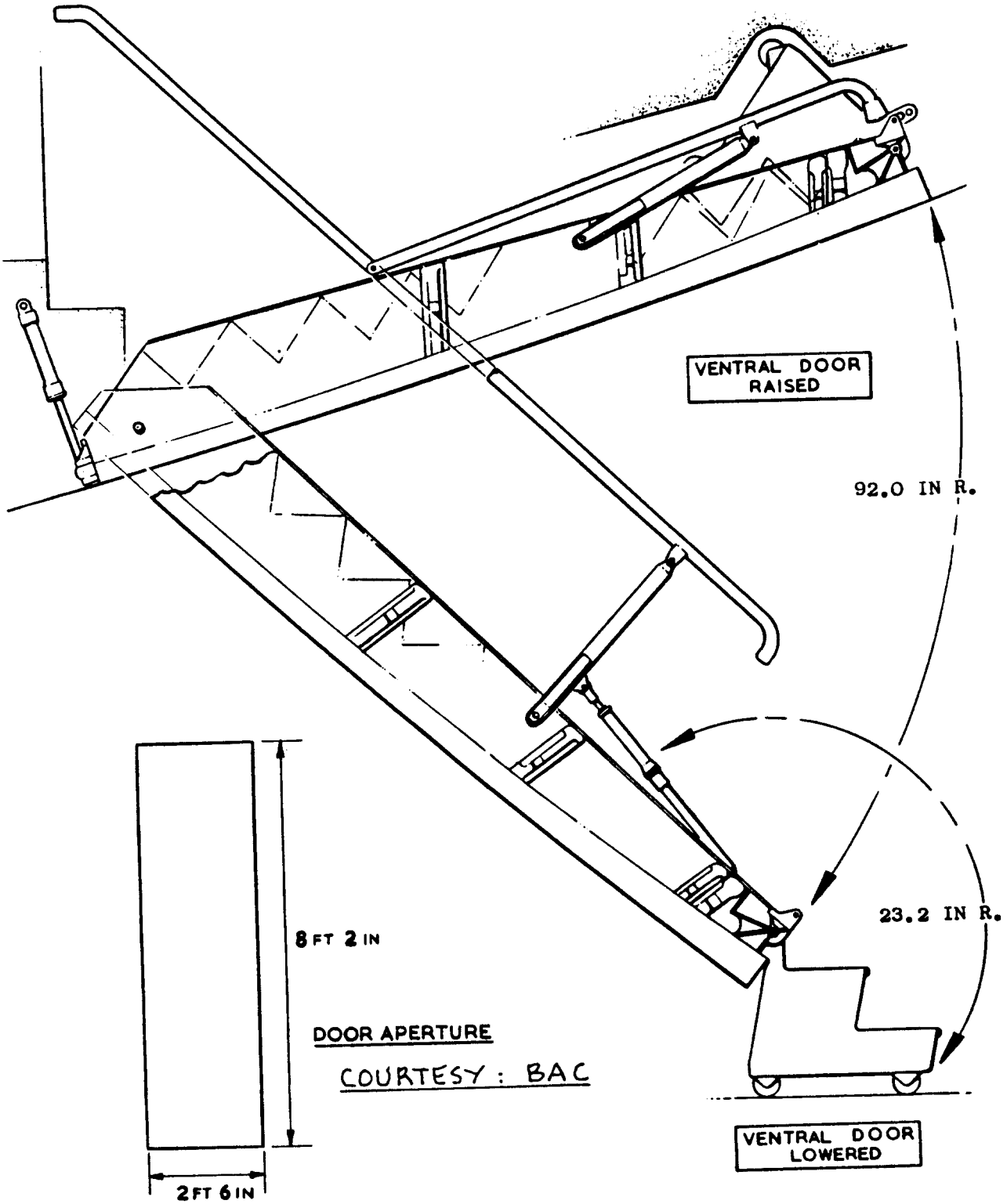

Figure 3.72b Ventral Stair Installation for the BAC 111

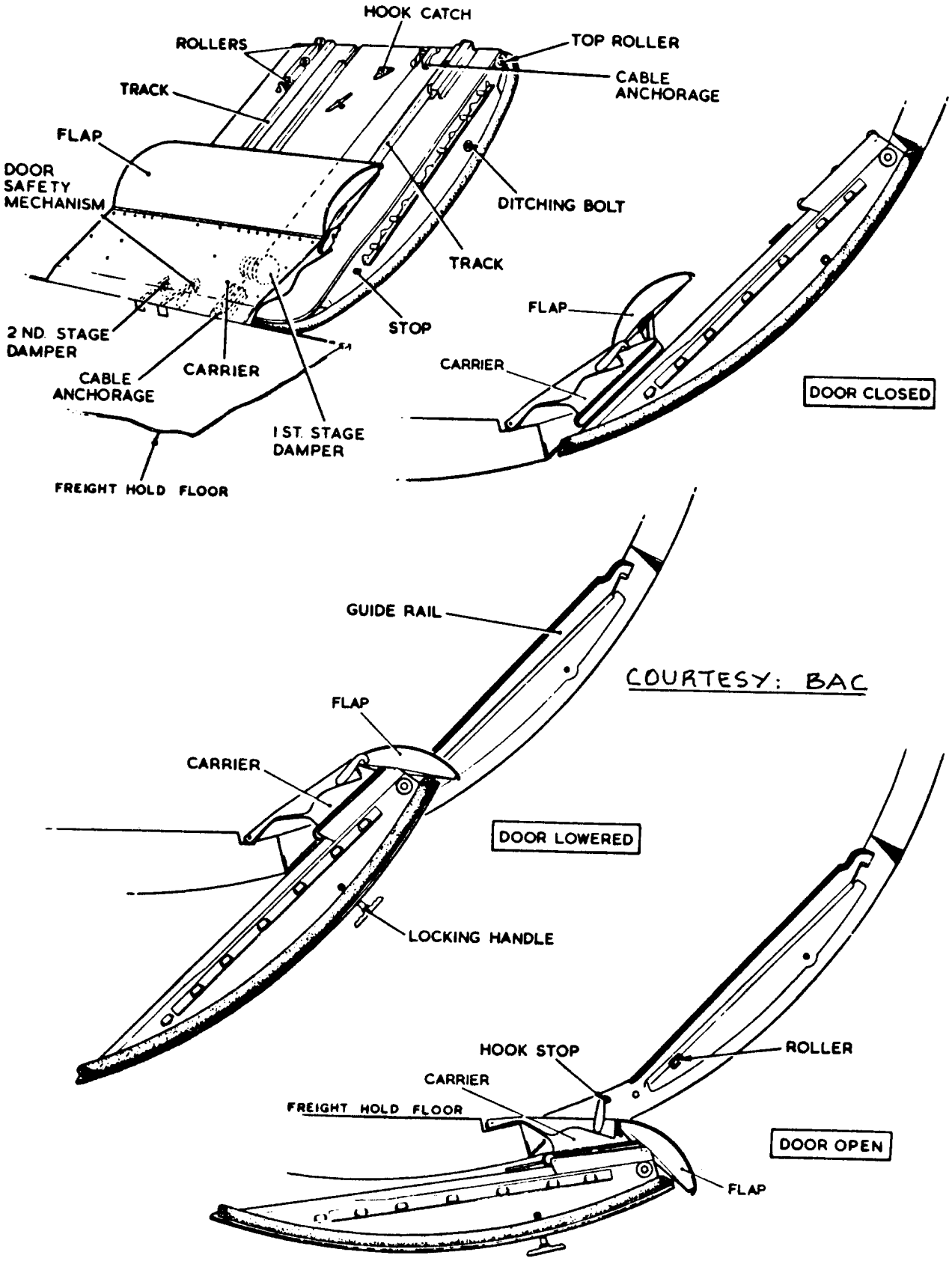

Figure 3.73 Cargo Compartment Door Installation for the BAC 111

3.5.5 Examples of Cockpit and Cabin Window Design

Cockpit windows must satisfy a number of conflicting design criteria:

1. they must be large enough to provide good visibility
2. they must have good optical qualities
3. they must be resistant to rain, hail and dust induced abrasion
4. they must cause little extra drag
5. for airplanes faster than 250 kts, they must meet the bird-strike requirement
6. they must be light

It is not easy to find a design solution which represents an acceptable compromise beteween these criteria.

Figure 3.74 shows an example of a typical light airplane windshield and window installation. Contrast the windshield of Figure 3.74 with that of Figure 3.75 for a business jet which must meet the bird-strike requirement. Note the complicated and heavy structure needed to meet this requirement.

In many business airplanes the cabin windows are arranged to polarize the incoming light. This is to prevent glare and still allow the passengers to look out the window. Figure 3.76 shows an example of such a polarized installation.

In jet transports the cabin windows are a potential source for leaks and for structural fatigue problems. The structure surrounding the windows is usually reenforced to prevent fatigue cracks from developing. Figure 3.77 shows an approach to this design problem: a forged (or cast) sub-frame is used to install each window. The window itself normally consists of three layers: two are redundant panes, each of which can hold the cabin pressure differential and an inner pane to protect the actual panes from passenger vandalism.

Figure 3.78 shows an example of a cabin window installation including the cabin wall trim. A cross section through the structure at the window is shown in Figure 3.79.

To cut noise coming through the wall, to provide thermal protection and to present a pleasant looking

interior a series of provisions are made to the cabin inside. Figure 3.78 shows a typical trim installation. A cross section through a cabin wall is depicted in Figure 3.80.

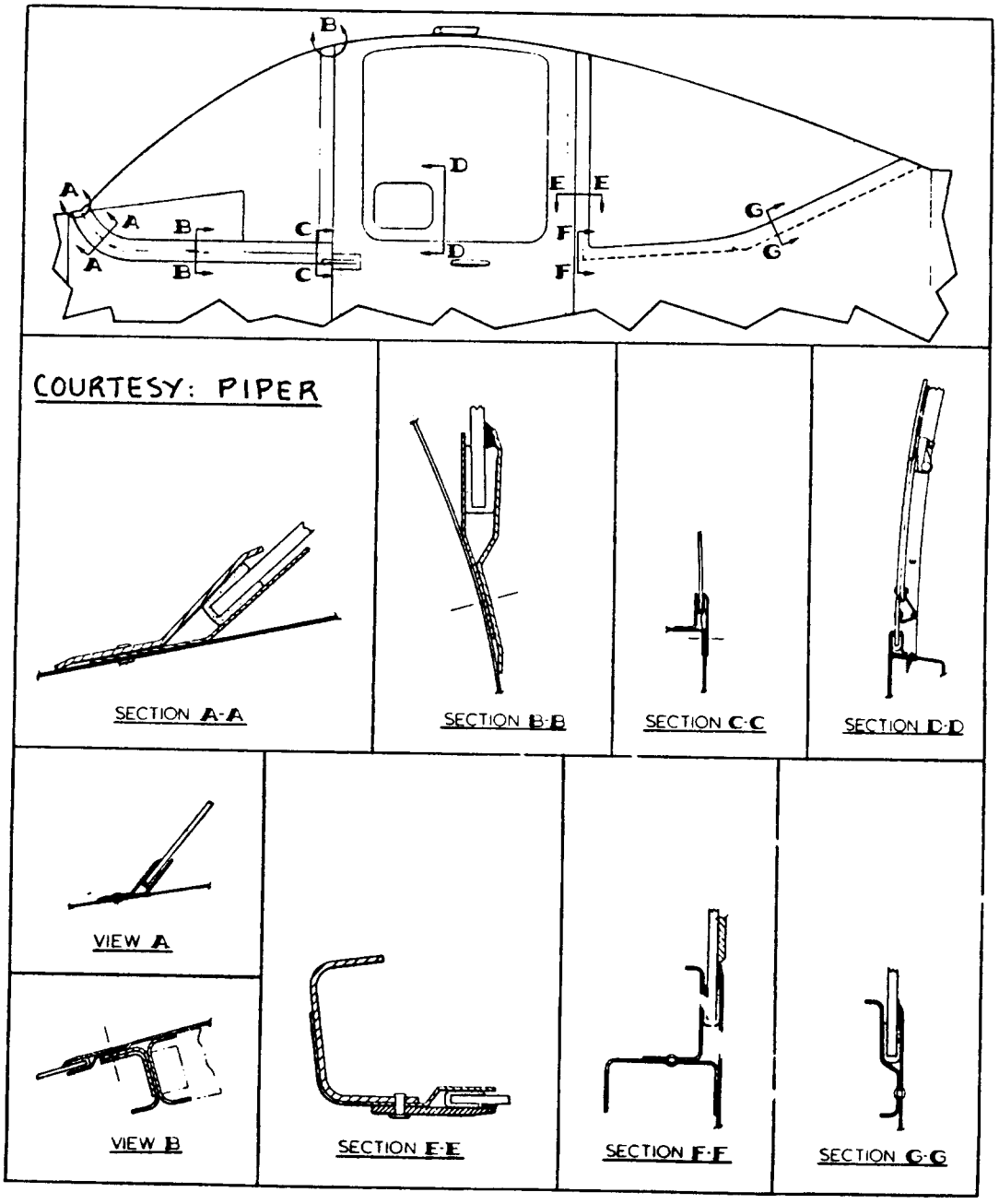

Figure 3.74 Windshield Installation for the Piper PA-38-112 Tomahawk

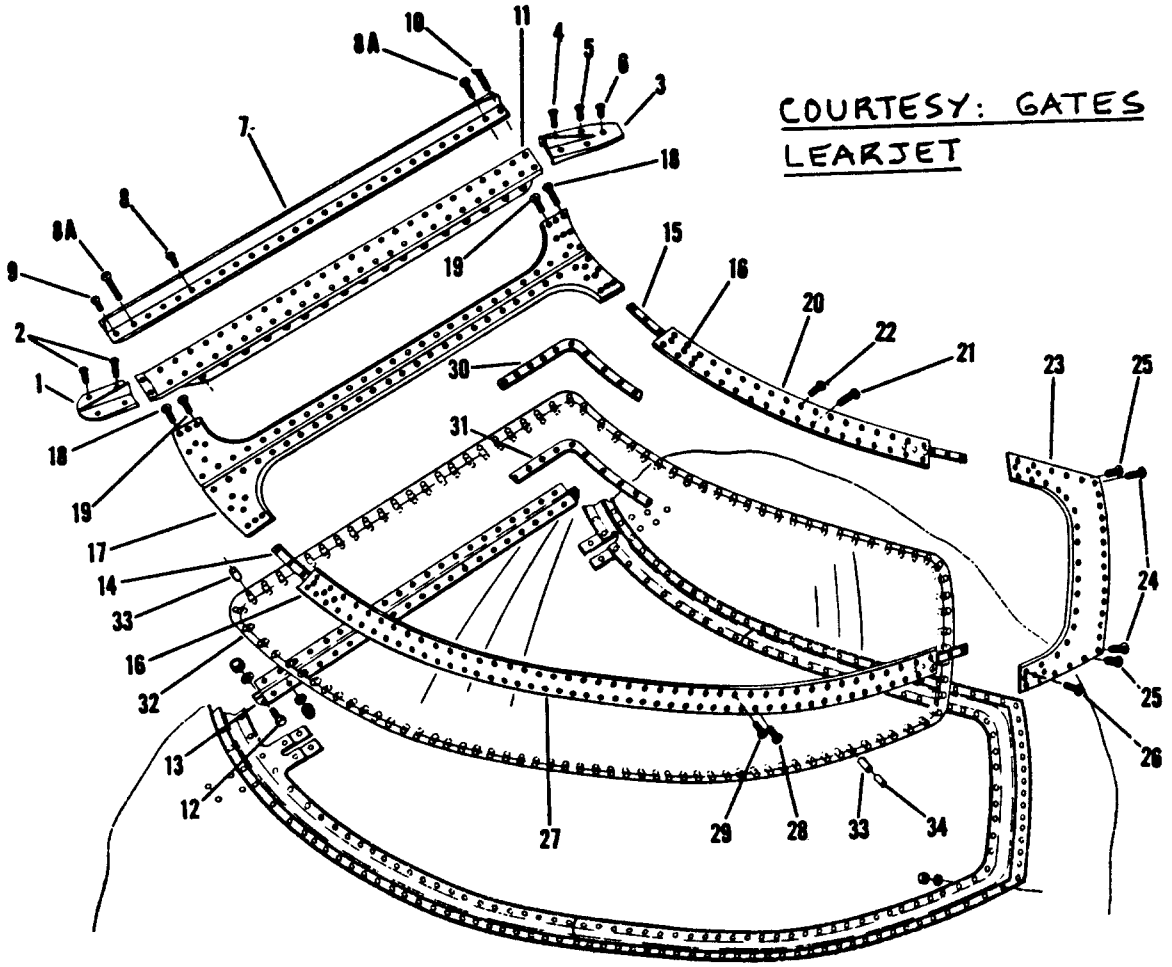

Figure 3.75 Windshield Installation for the Learjet 23

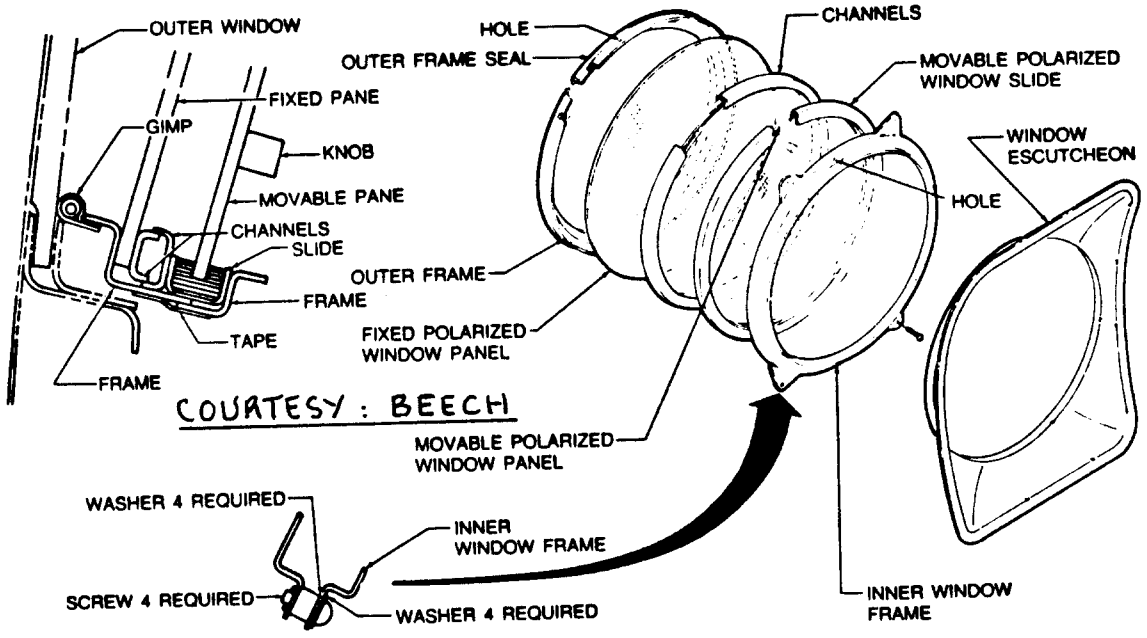

Figure 3.76 Polarized Window Installation for the Beech King Air F90

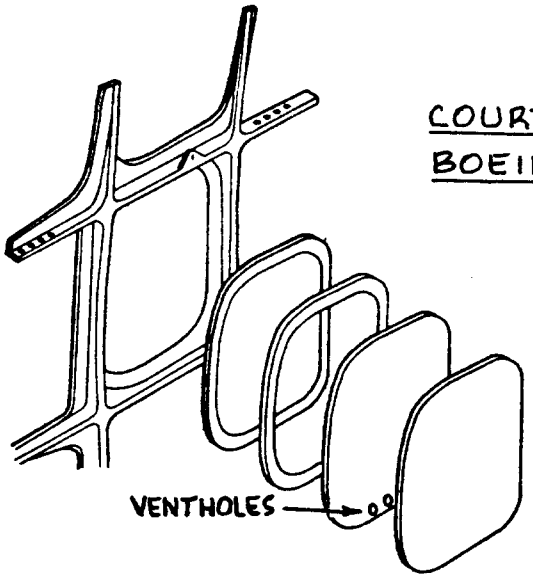

COURTESY:
BOEING

Figure 3.77 Typical Window and Window Frame Installation for a Jet Transport

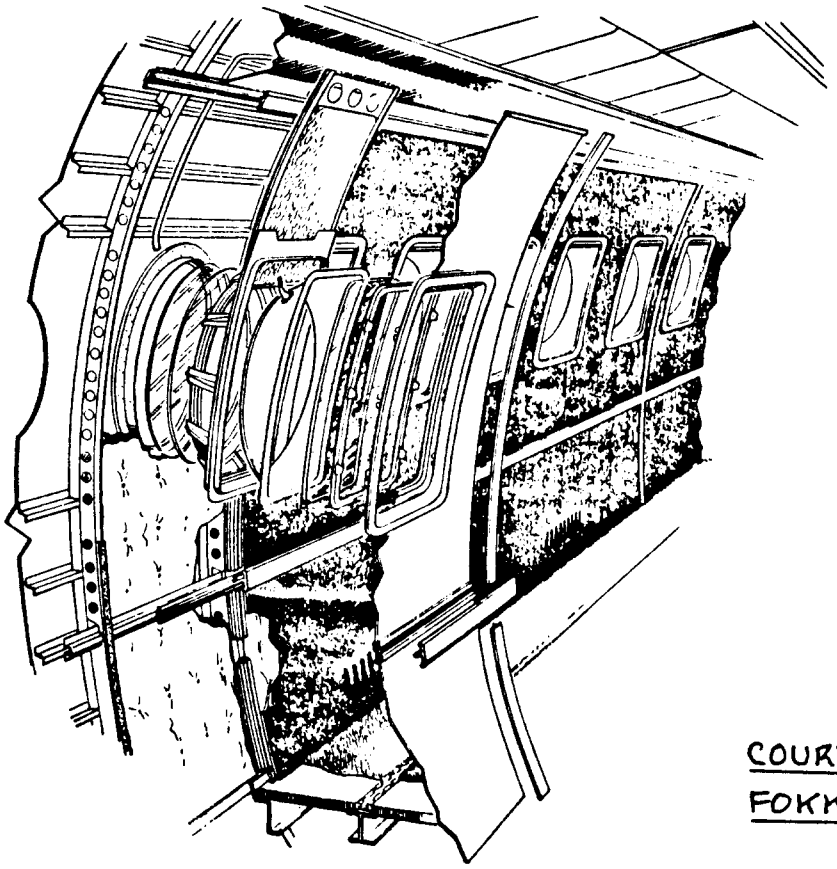

COURTESY:
FOKKER

Figure 3.78 Cabin Window and Cabin Wall Trim Installation for the Fokker F28

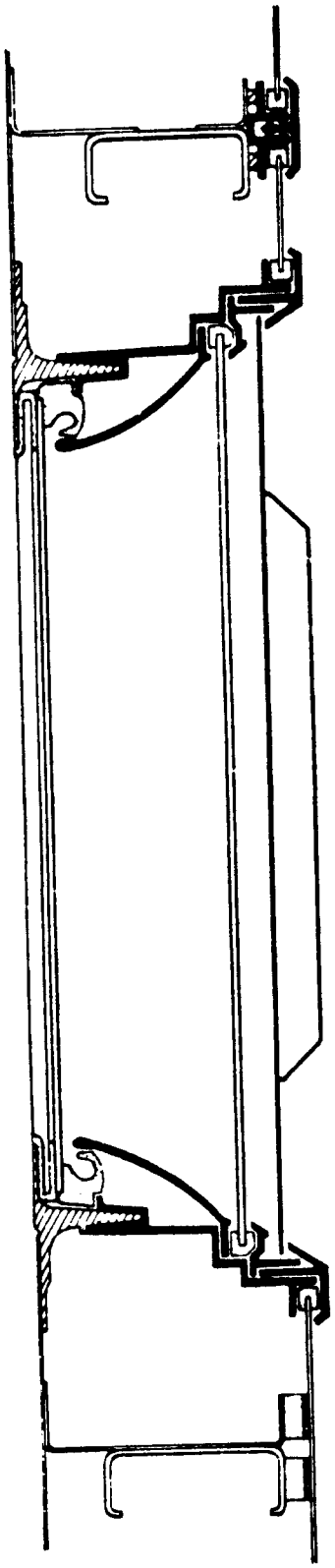

Figure 3.79 Typical Window Cross Section: Fokker F28

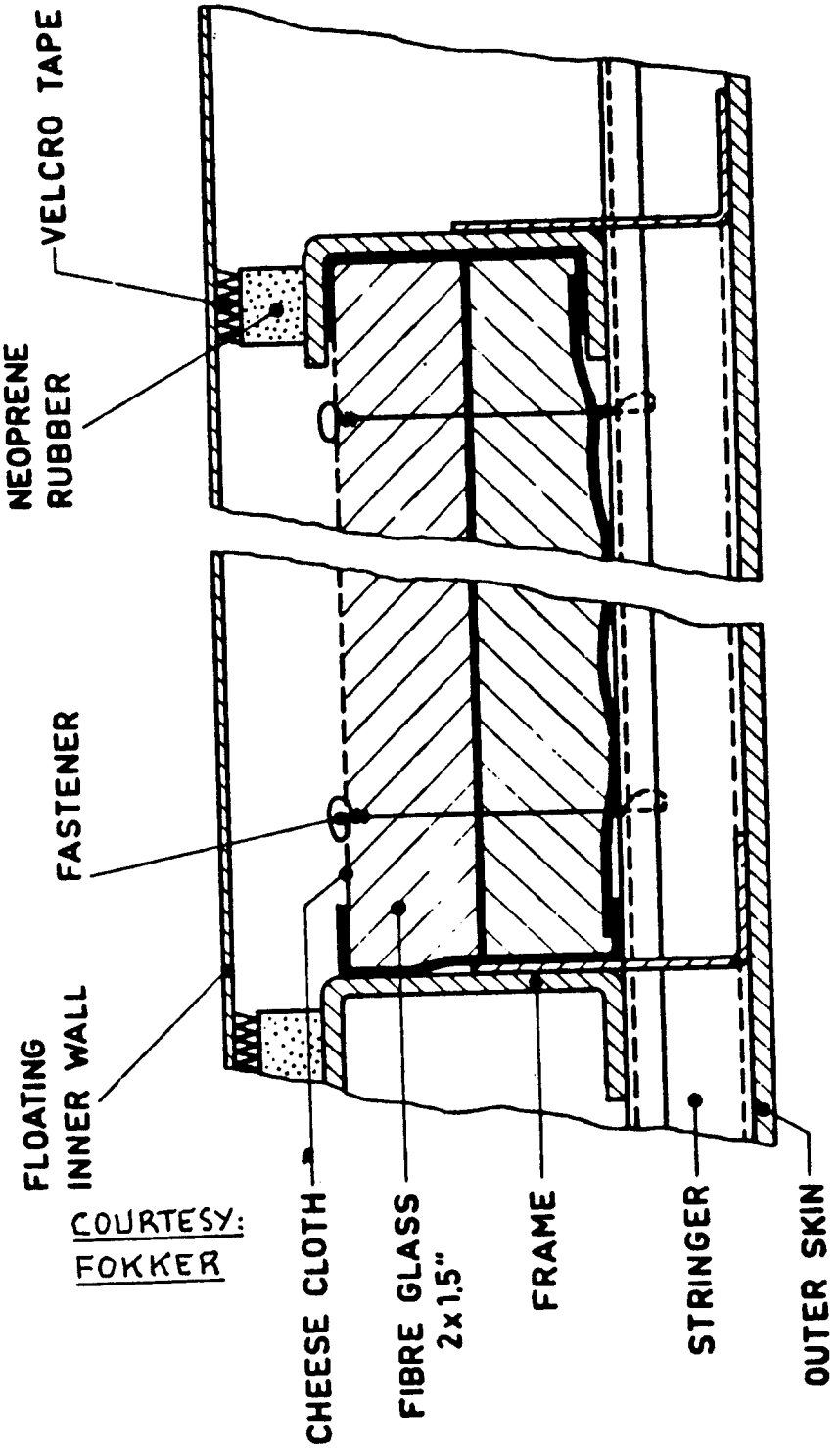

Figure 3.80 Typical Wall Cross Section: Fokker F28

3.5.6 Examples of Floor Design

For new general aviation airplanes the author recommends a review of Ref.24 before committing to a specific floor design. Floors and the attached seat rails for crew and passenger seats can now be designed for maximum protection in the case of a crash.

For cargo carrying airplanes, floors need to be equipped with cargo restraint systems. Examples of tied down cargoes with appropriate restraints are depicted in Figures 3.81a-b.

In large cargo airplanes it is essential that the cargo can be easily moved to its proper position. This can be done with the help of self-driving roller systems. Figure 3.82 shows an example of a floor equipped in this manner.

The possibility of liquid spillage exists in passenger and in cargo airplanes alike. Floors need to be equipped with a drainage system. To be effective, the surrounding floor areas need to be sealed to prevent liquids running into areas where they could cause corrosion or malfunctioning of equipment. Figures 3.83 and 3.84 show typical drainage provisions.

Floors are ideal components for application of composite materials. Figure 3.85 show the extent to which composite floors are used in the Boeing 757.

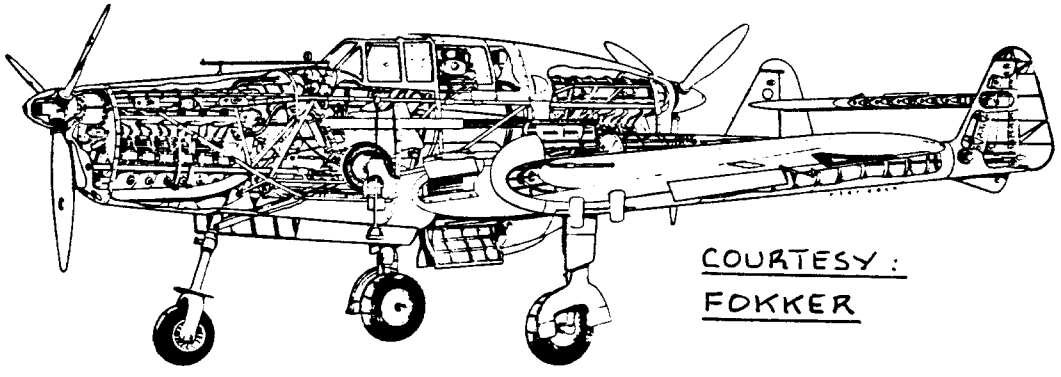

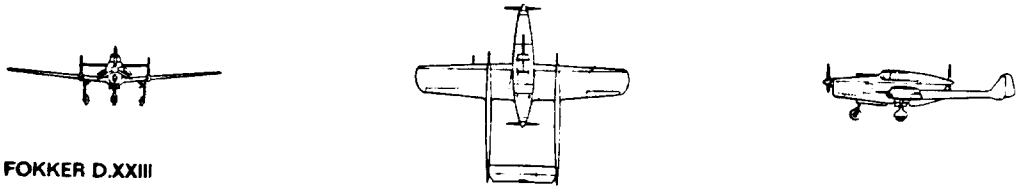

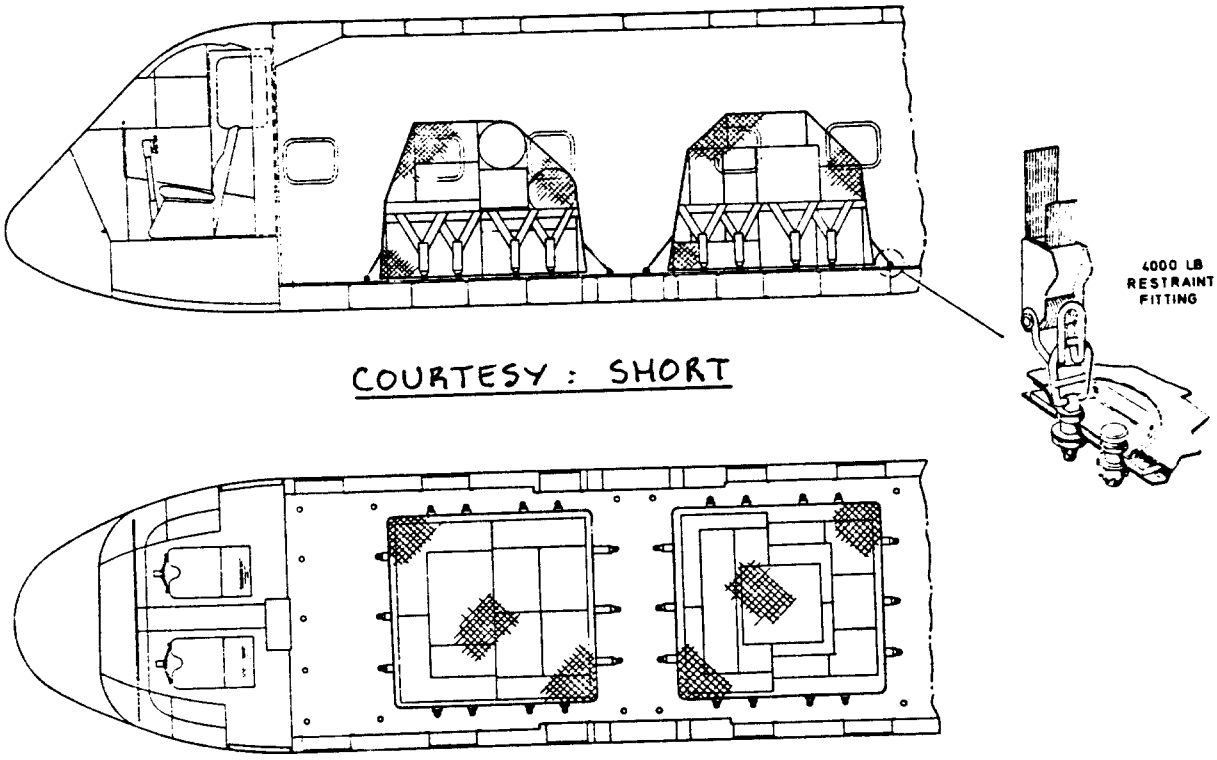

Figure 3.81a Palletized Cargo with Restraints in the Short Skyvan Series 3

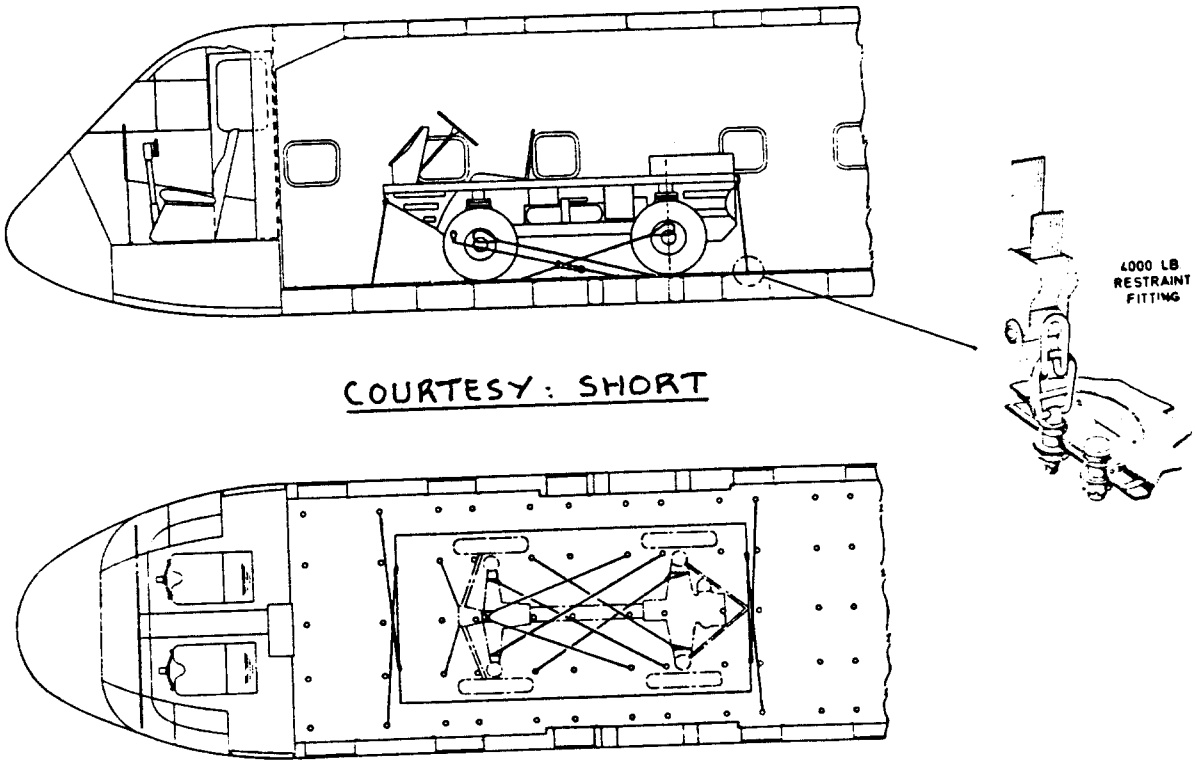

Figure 3.81b Vehicle with Restraints in the Short Skyvan Series 3

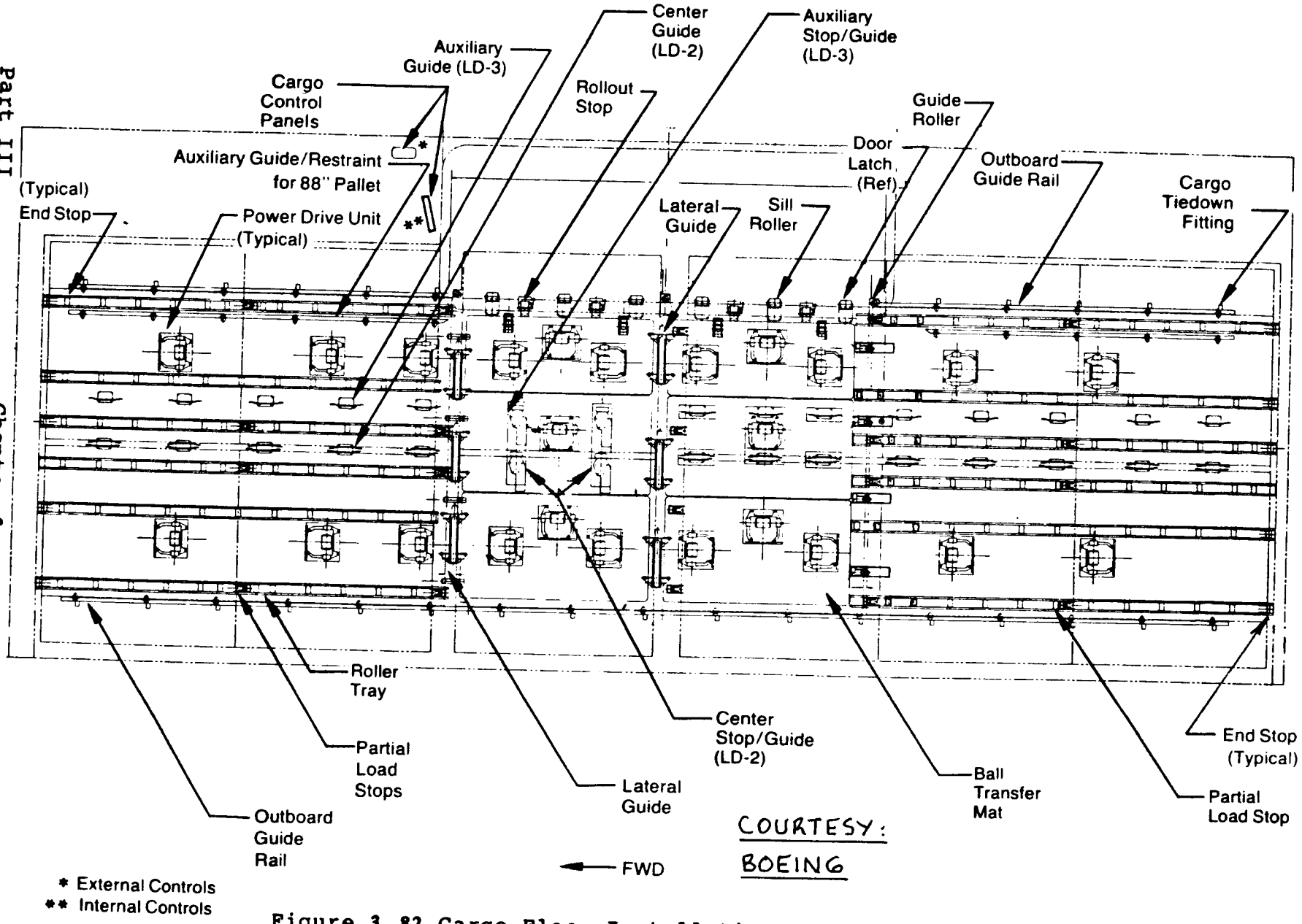

COURTESY: BOEING

Figure 3.82 Cargo Floor Installation: Boeing 767-200

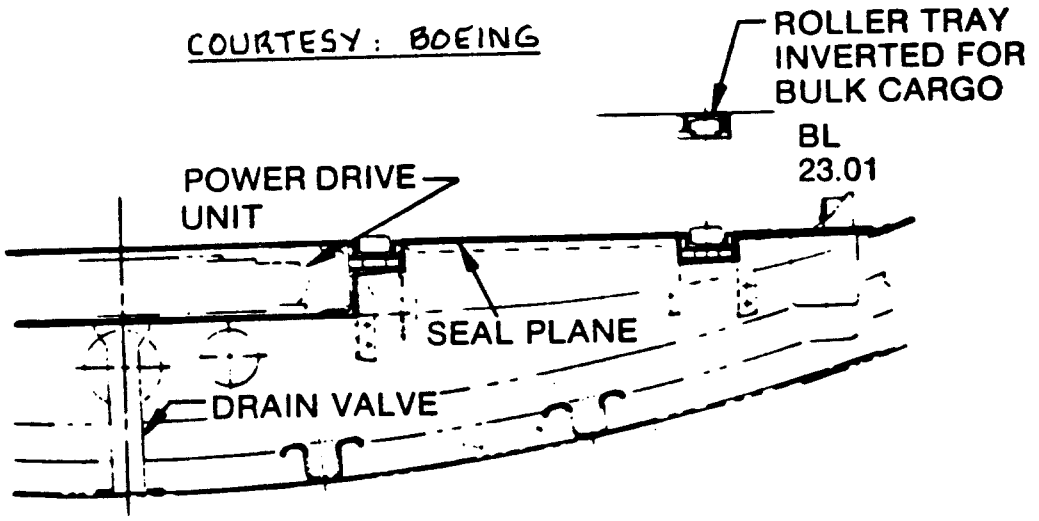

Figure 3.83 Cargo Floor with Drainage Provision: Boeing 757

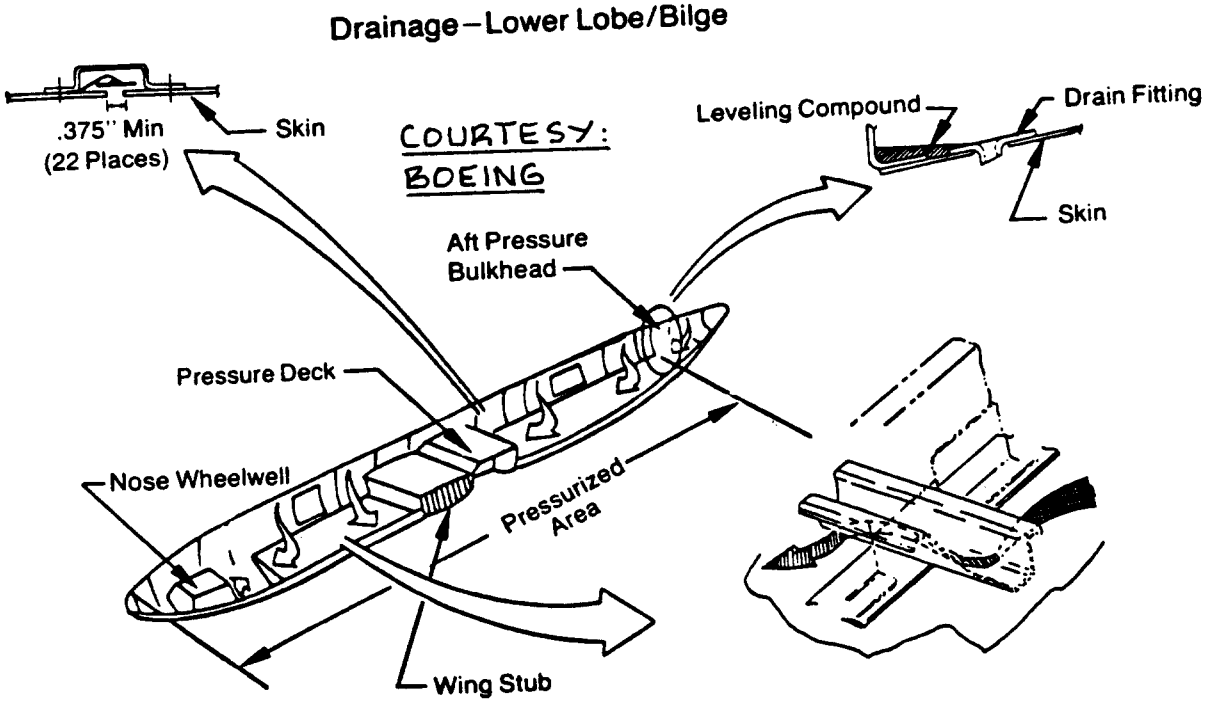

Figure 3.84 Drainage Provisions for the Boeing 767-200

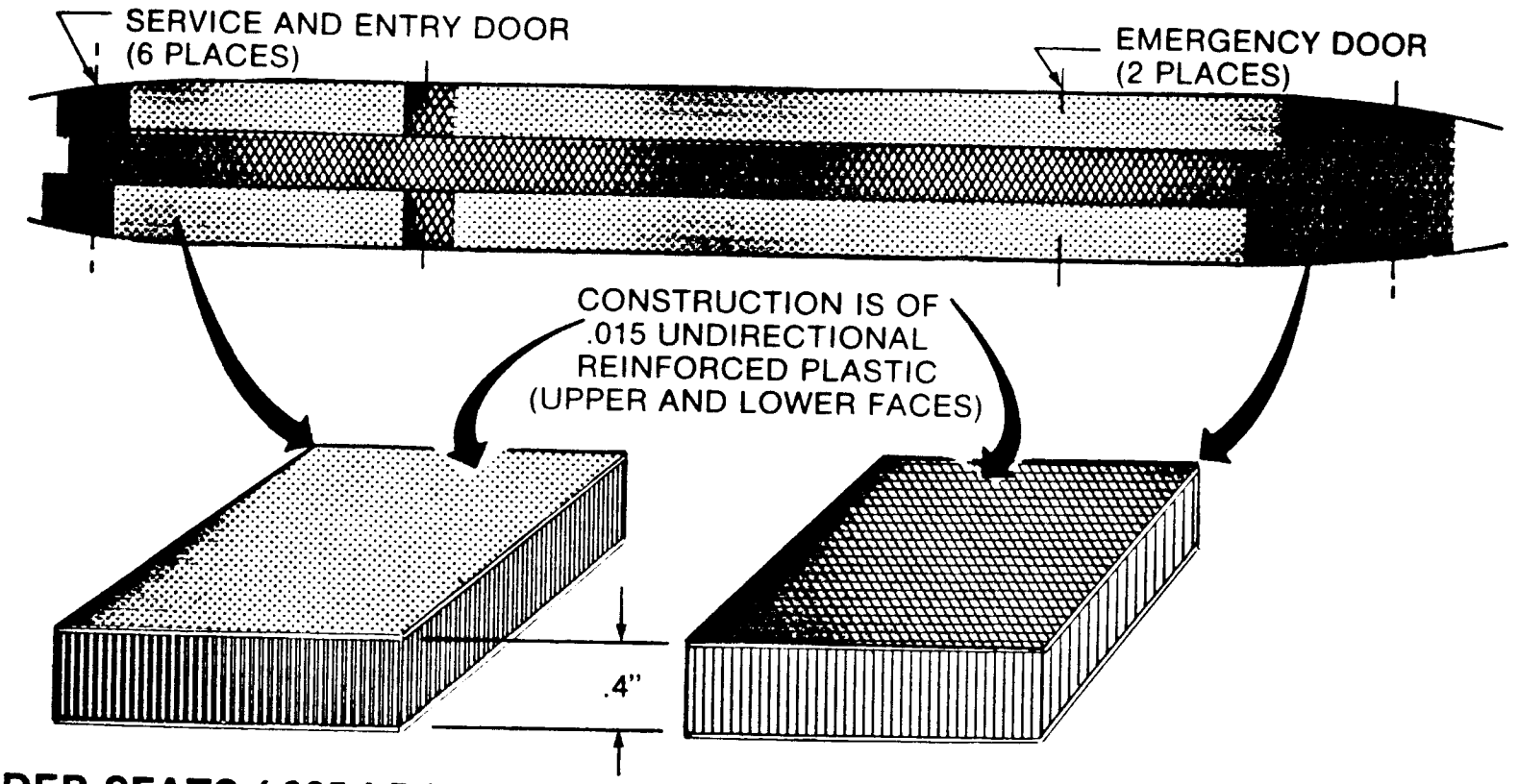

Design considerations:

- Service proven floor panels — 727/737/747
- Corrosion protected and sealed floors in entry ways, galleys and lavatories
- Positive entryway and galley floor drainage
- Floor panels replaceable without removing major components (galleys, lavatories, etc.)
- Full threaded screws to attach floor panels

COURTESY: BOEING

Figure 3.85 Composite Floor Application: Boeing 757

3.6 EXAMPLES OF INBOARD PROFILES

When the basic design decisions reflected by Sections 3.1 through 3.5 have been made it is useful to prepare a composite drawing showing the relative arrangement of important items. Such a composite drawing is called an 'inboard profile'. It is useful to include in the inboard profile all systems which are essential to the operation of the airplane. The latter implies that Step 4.7 of p.d. sequence I and Step 17 of p.d. sequence II have been completed.

The inboard profile serves primarily as an 'organizer' for the designer: it allows him to determine major conflicts. It also allows the designer to play the 'what-if' game, so essential to the ultimate flight safety of the proposed design. The 'what-if' game and its role in airplane design is discussed in Part IV.

Figures 3.86 through 3.94 provide examples of inboard profiles. The completeness of an inboard profile depends on the amount of detailed information available.

The inboard profiles are presented in the following sequence:

Figure 3.86 for a piston/propeller driven homebuilt: the Piel CP-80

Figure 3.87 for a jet powered homebuilt: the BD-5J

Figure 3.88 for a turbo/propeller driven twin: the Mitsubishi MU-2G

Figure 3.89 for a Jet Transport: the Boeing 767-200

Figure 3.90 for a military trainer/attack airplane: the SIAI-Marchetti S-211

Figure 3.91 for a military trainer: the Fairchild-Republic T-46A

Figure 3.92 for a fighter: the Macchi MB.339

Figure 3.93 for an experimental fighter: the Grumman X-29

Figure 3.94 for a turbo/propeller driven flying boat: the Shinmeiwa US-1

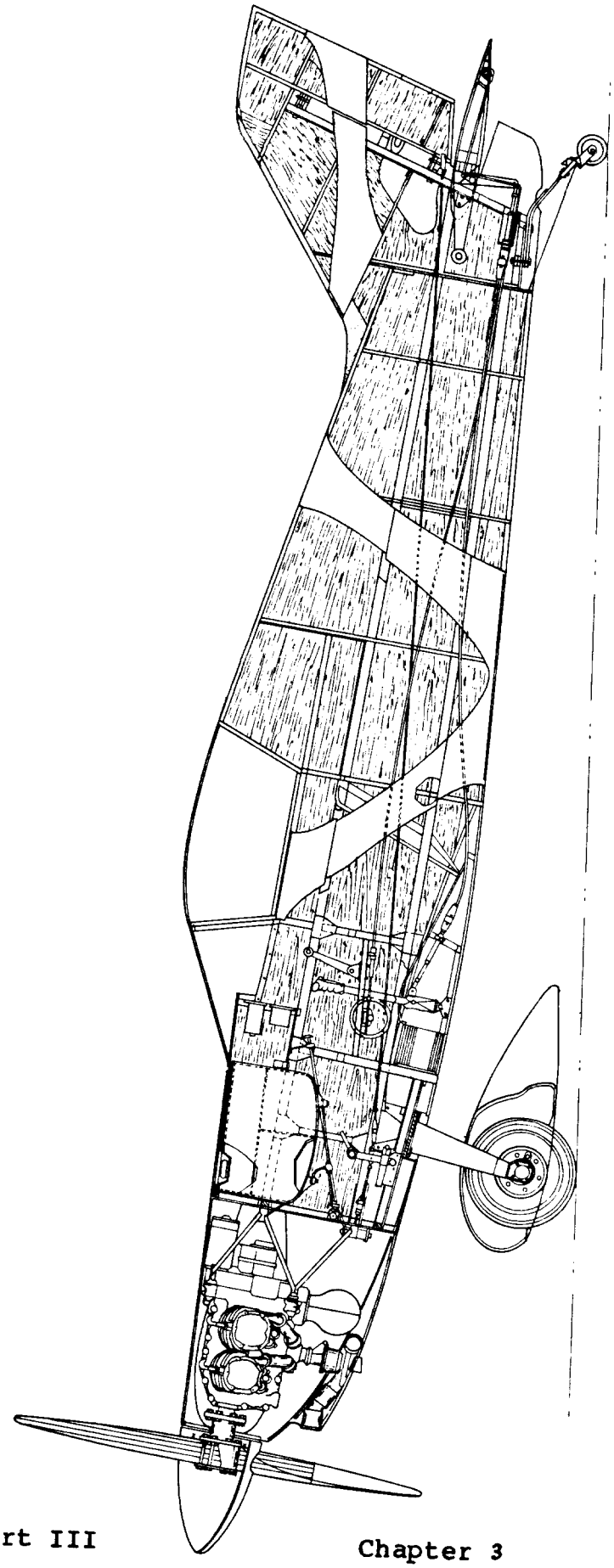

Figure 3.86 Inboard Profile: Piel CP-80

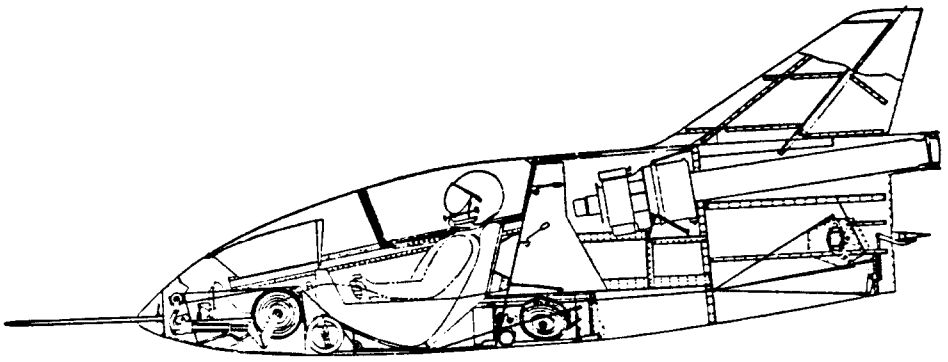

Figure 3.87 Inboard Profile: BD-5J

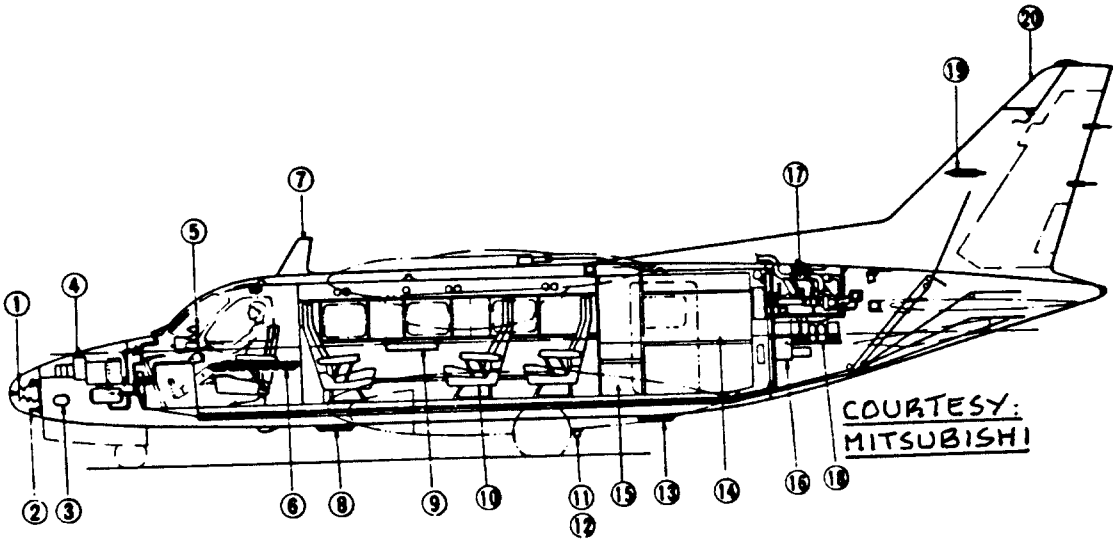

① Weather radar antenna
② Glide slope antenna
③ Landing and taxi light
④ Nose avionics compartment
⑤ Instrument panel
⑥ Circuit breaker panel
⑦ #1 VHF antenna
⑧ Marker beacon antenna
⑨ Table
⑩ Passenger seat
⑪ DME antenna (L.H)
⑫ ATC transponder antenna (R.H)
⑬ #1 ADF loop antenna
⑭ Baggage compartment
⑮ Toilet
⑯ Batteries
⑰ Air-conditioning system
⑱ Rear avionics compartment
⑲ VOR antenna
⑳ #2 VHF antenna

Figure 3.88 Inboard profile: Mitsubishi MU-2G

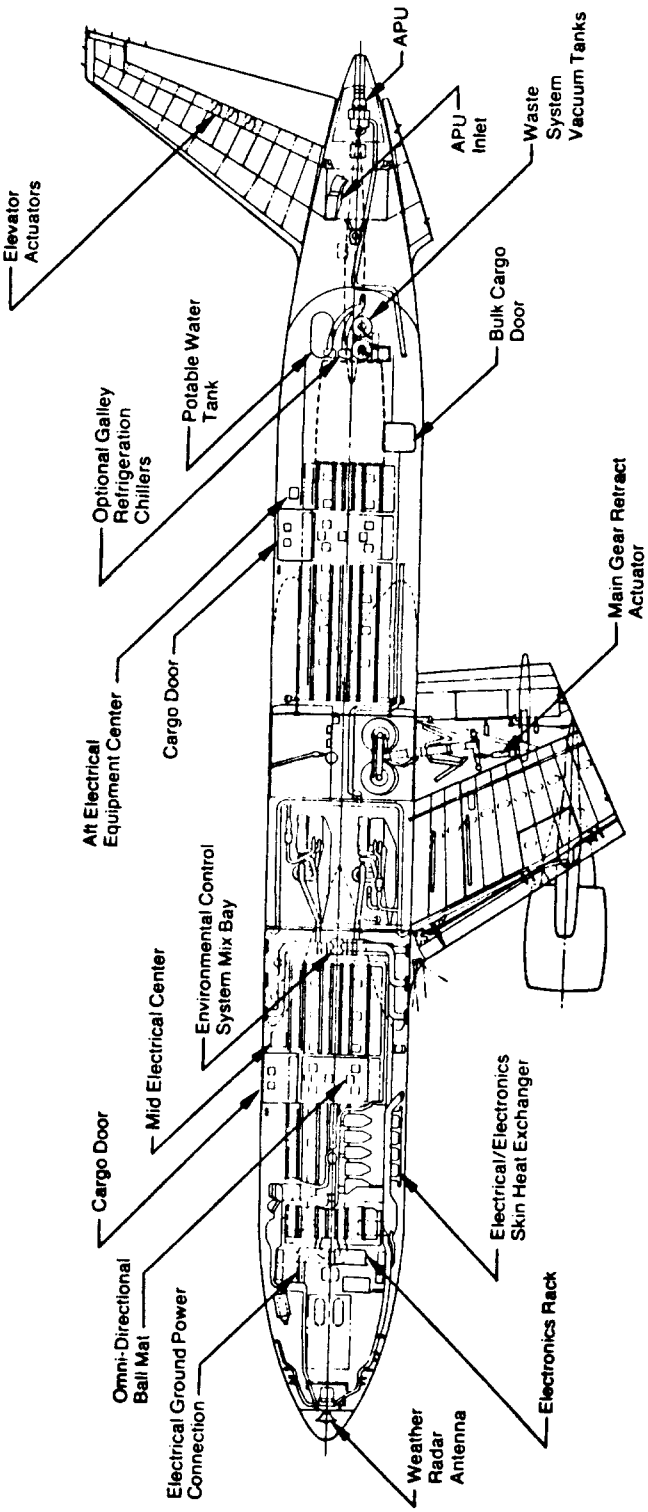

COURTESY: BOEING

Figure 3.89a Inboard Profile Below Floor: Boeing 767-200

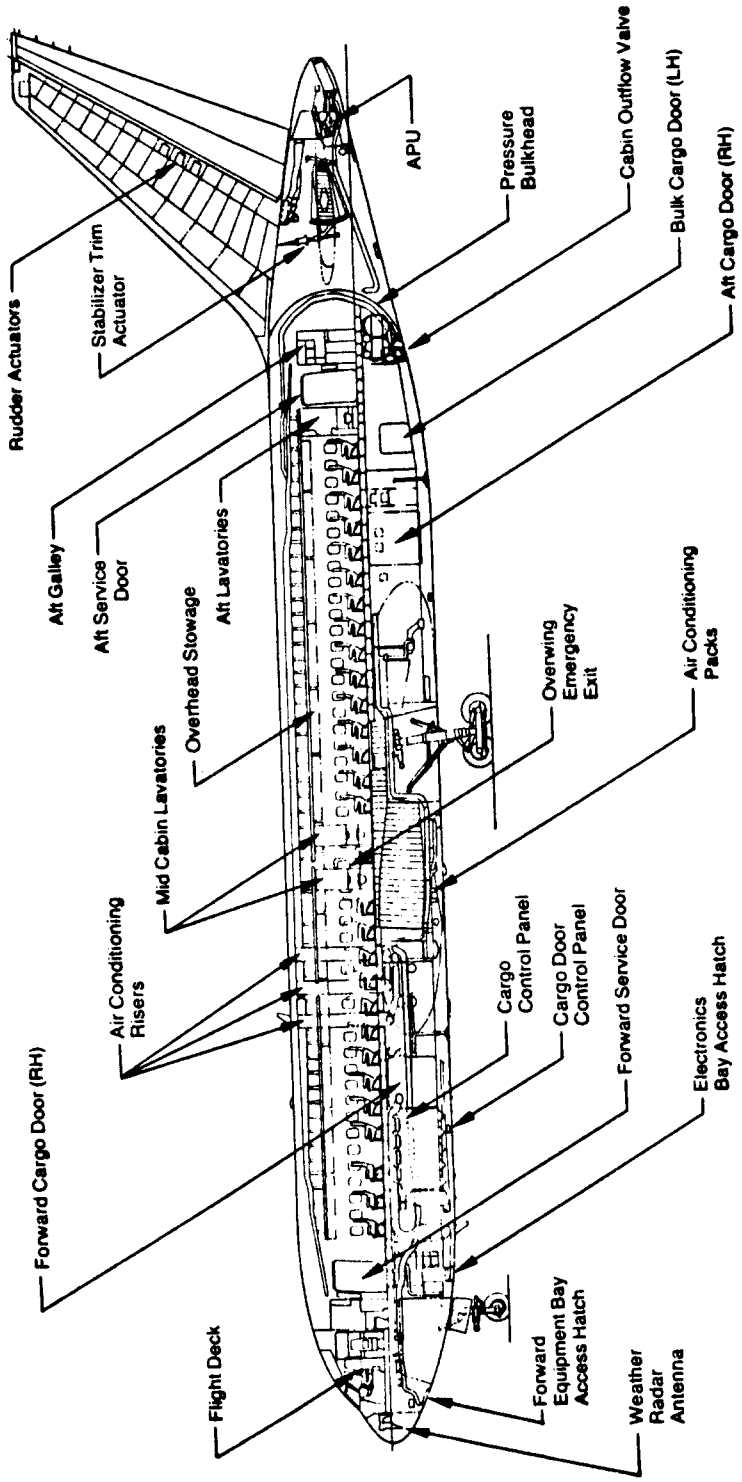

COURTESY: BOEING

Figure 3.89b Inboard Profile: Boeing 767-200

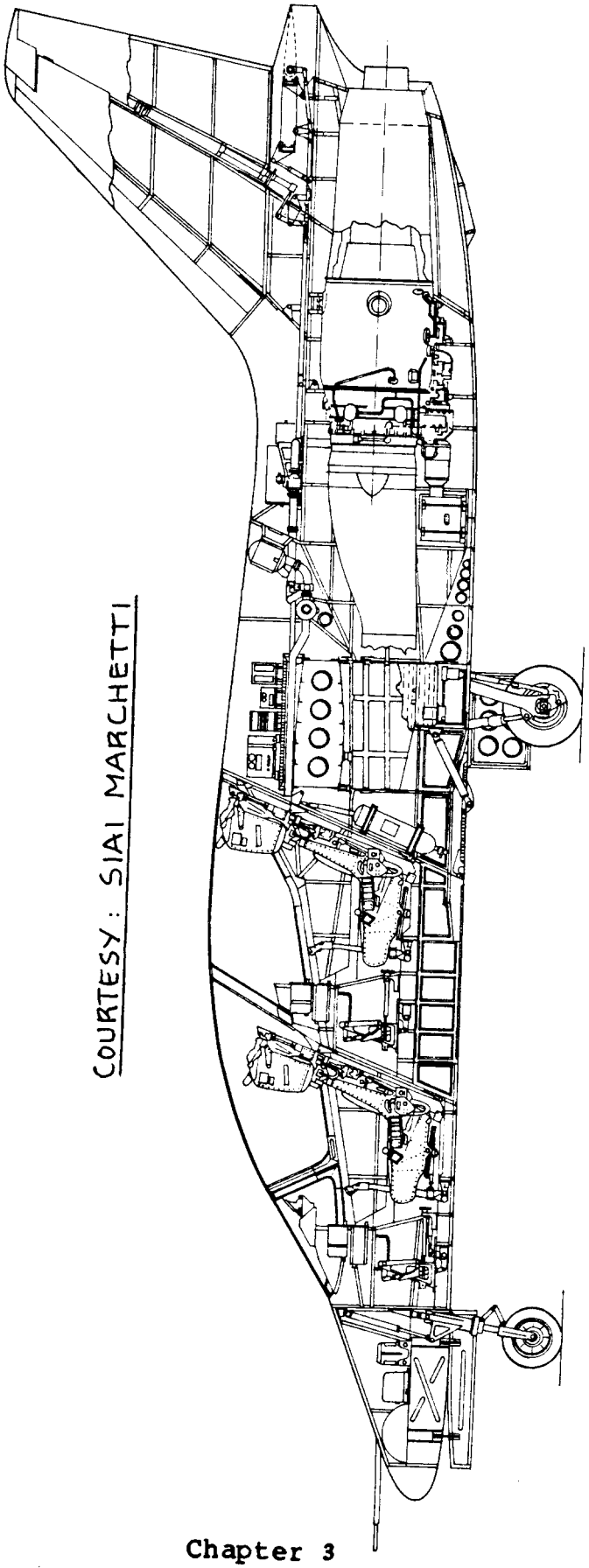

COURTESY: SIAI MARCHETTI

Figure 3.90 Inboard Profile: SIAI Marchetti S-211

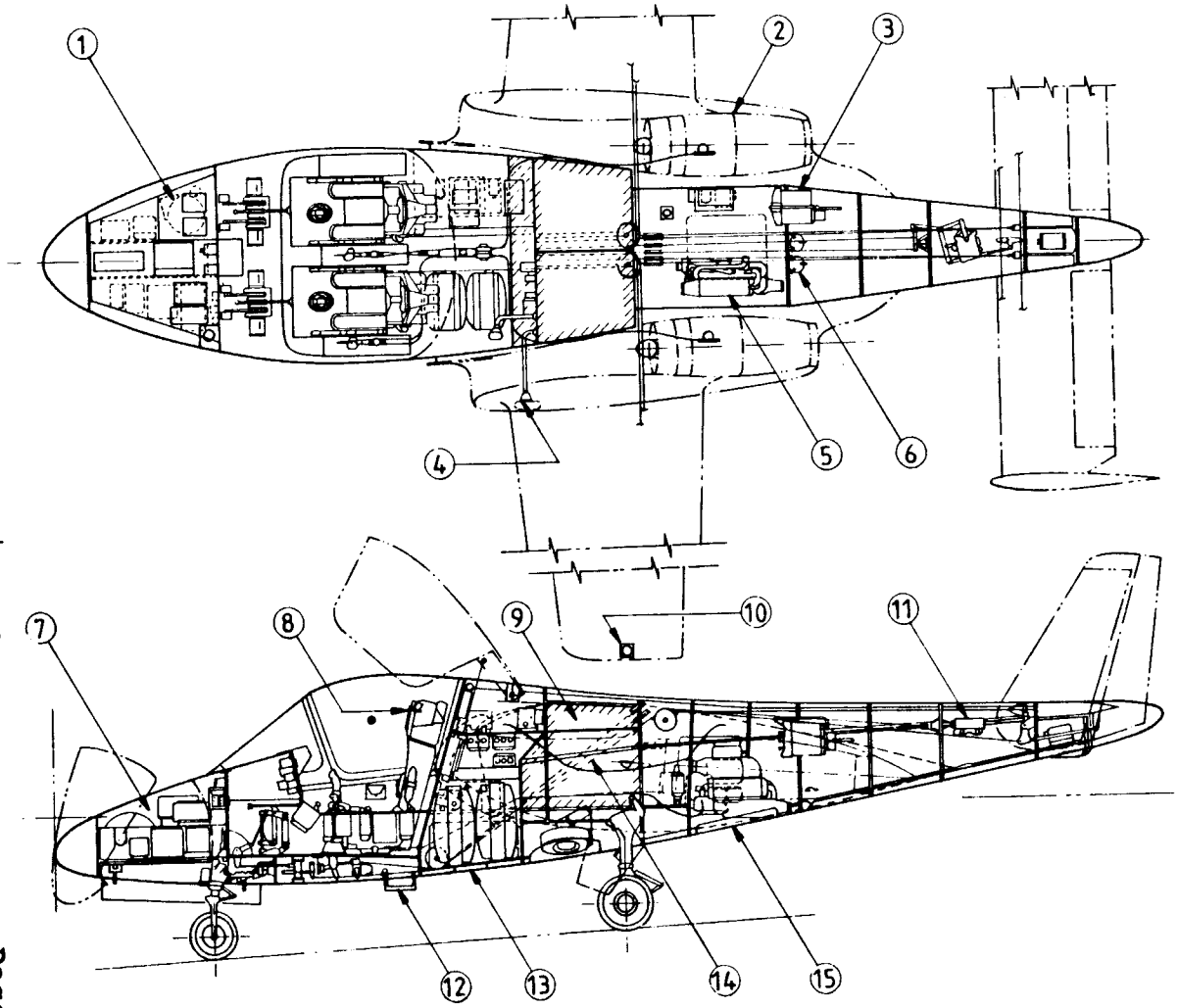

1. OXYGEN SYSTEM
2. GARRETT F109-GA-100
3. HYDRAULIC RESERVOIR
4. SINGLE POINT REFUELING
5. ENVIRONMENTAL CONTROL SYSTEM UNIT
6. FIRE EXTINGUISHER SYSTEM
7. NOSE AVIONICS COMPARTMENT
8. ACES II SEATS
9. FUEL CELLS
10. REMOTE COMPASS
11. RUDDER ACTUATOR
12. BOARDING STAIR (EXTENDED)
13. BAGGAGE & AVIONICS COMPARTMENT
14. CONTROL CABLES
15. AFT COMPARTMENT DOOR

COURTESY:
FAIRCHILD REPUBLIC

Figure 3.91 Inboard Profile: Fairchild-Republic T-46A

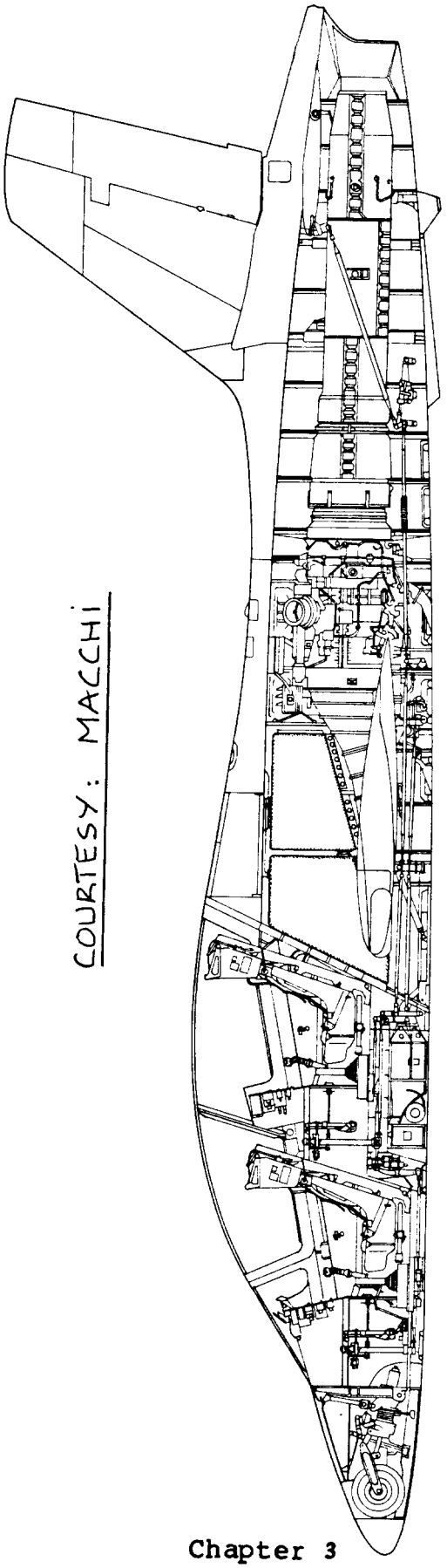

COURTESY: MACCHI

Figure 3.92 Inboard Profile: Macchi MB.339

1. F-5A FORWARD FUSELAGE ASSEMBLY
2. ENVIRONMENTAL CONTROL UNIT
3. CANARD ACTUATOR (2)
4. STRAKE FUEL TANKS
5. PITOT STATIC PROBE (2)
6. ANGLE OF ATTACK VANE (2)
7. GENERATOR 5 KVA
8. OUTBOARD FLAPERON ACTUATOR (2)
9. INBOARD FLAPERON ACTUATOR (2)
10. JET FUEL STARTER
11. STRAKE ACTUATOR
12. FLIGHT TEST INSTRUMENTATION
13. TOTAL TEMPERATURE PROBES (2)
14. MARTIN BAKER EJECTION SEAT
15. FUEL TANKS
16. ACCESSORY DRIVE GEARBOX GENERATOR 40/50 KVA
17. BLEED AIR HEAT EXCHANGER
18. RUDDER ACTUATOR

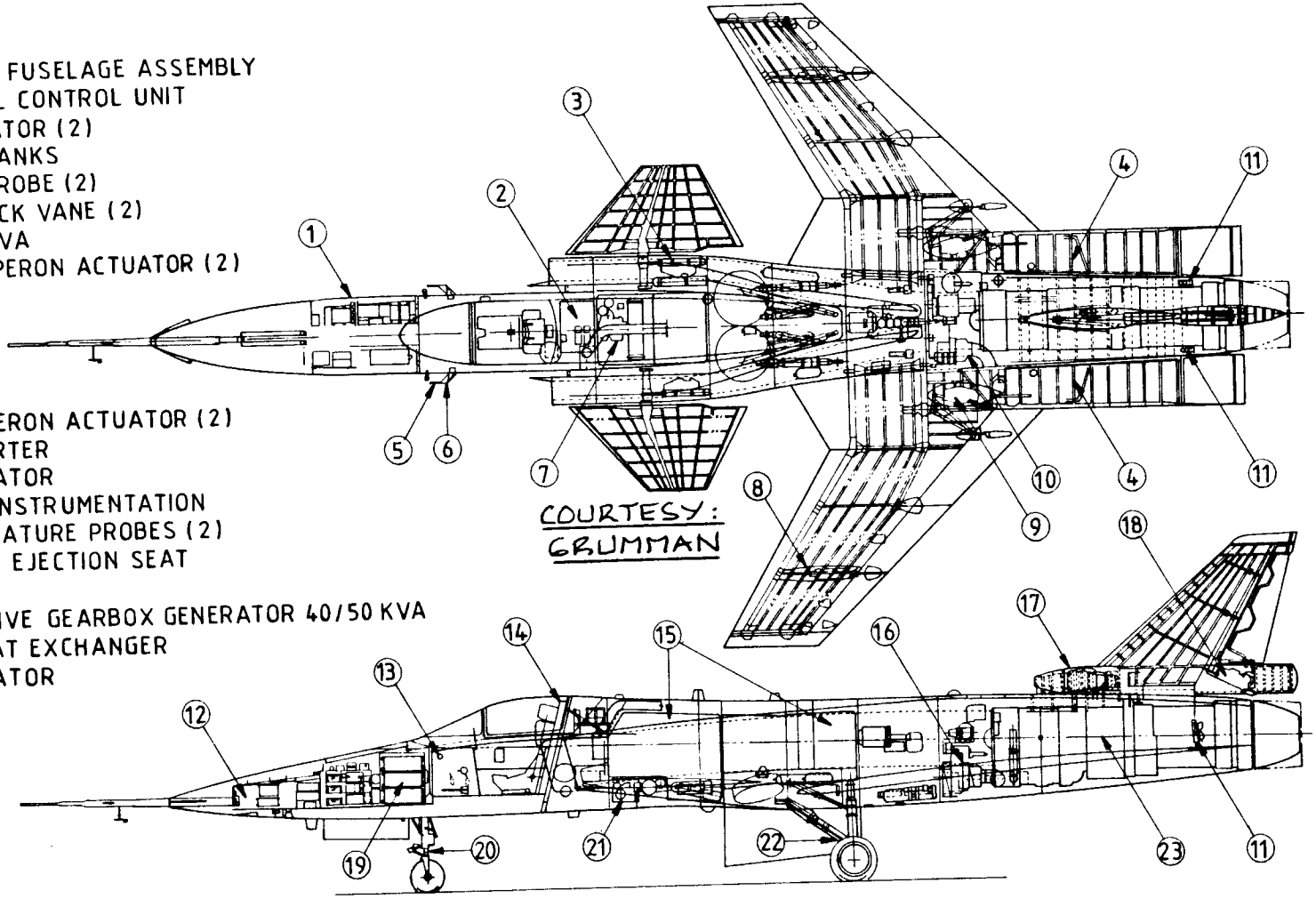

19. FLIGHT CONTROL COMPUTER
20. F-5A NOSE LANDING GEAR
21. EMERGENCY POWER UNIT
22. F-16 MAIN LANDING GEAR
23. GENERAL ELECTRIC TURBOFAN F 404-GE-400

Figure 3.93 Inboard Profile: Grumman X-29

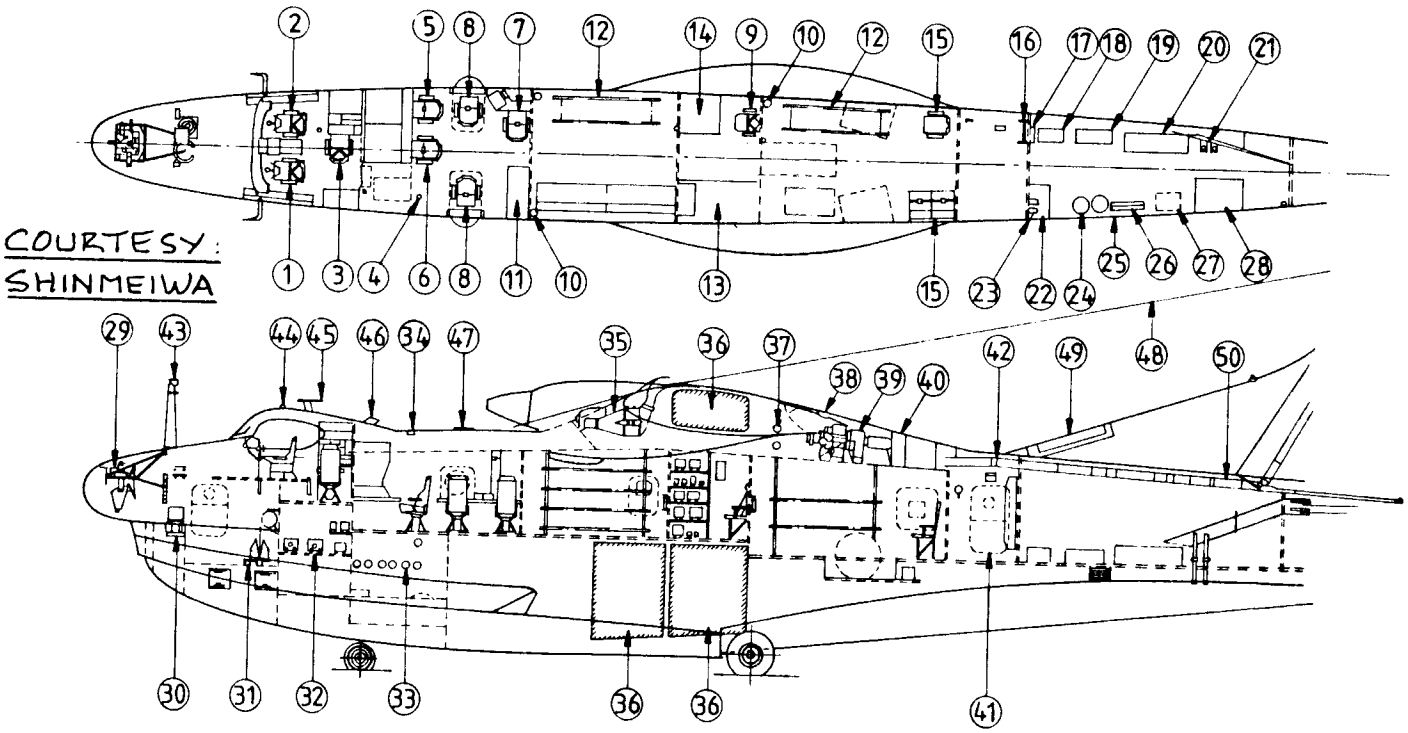

1. PILOT
2. CO-PILOT
3. FLIGHT ENGINEER
4. DRIFT METER
5. RADAR OPERATOR
6. NAVIGATOR
7. RADIO OPERATOR
8. OBSERVER
9. RESCUE MAN
10. PORTABLE OXYGEN
11. MAIN ELECTRICAL PANEL
12. STRETCHER X 12 (OR CANVAS SHEET FOR 3-MAN X 4 OR 2-MAN X 2)
13. SHELVES
14. ELECTRONICS RACK
15. RESERVE SEAT
16. RESCUE KIT THROWER
17. PORTABLE LADDER
18. CAMERA STOWAGE
19. LINE-THROWING APPLIANCES BOX
20. OUTBOARD-MOTOR BOAT
21. PYROTECHNICS-DROPPING DEVICES
22. GALLEY
23. DRINKING WATER
24. RESCUE KIT X 2
25. GUIDE LINE
26. RESCUE RAMP
27. LIVE RAFT, WITH TRANSCEIVER
28. PYROTECHNICS STORAGE
29. SEARCH RADAR
30. RADAR TRANSCEIVER
31. ANCHOR AND ROPE
32. ELECTRONICS
33. OXYGEN BOTTLES
34. SEXTANT MOUNT
35. AIR CONDITIONER
36. FUEL TANKS
37. FIRE EXTINGUISHER
38. BLC ENGINE AND COMPRESSOR
39. APU
40. LIVE RAFT (EMERGENCY)
41. MAIN HATCH
42. RESCUE HOIST
43. LB SENSOR
44. TACAN/IFF ANTENNA
45. VHF ANTENNA
46. UHF ANTENNA
47. ADF LOOP ANTENNA
48. HF ANTENNA
49. ADF SENSE ANTENNA
50. BLC DUCTING

Figure 3.94 Inboard Profile: Shinmeiwa US-1

4. WING LAYOUT DESIGN

The purpose of this chapter is to provide design considerations, design data and design examples for the layout design of wings.

A step-by-step procedure for arriving at a satisfactory Class I preliminary wing layout was presented in Chapter 6 of Part II. That procedure is meant to be used in conjunction with p.d. sequence I of Chapter 2 in Part II. During the next phase of wing design (Class II in p.d. sequence II as outlined in Chapter 2 of Part II) it is recommended that the reader use the same procedure, but now augmented with the broad range of wing design considerations presented in this chapter.

The reader should also review the large number of wing/airplane configurations presented in Chapter 3 of Part II. It is always useful to determine what has been done by various manufacturers.

Section 4.1 presents a general discussion of wing configuration design aspects: aerodynamic as well as operational.

Section 4.2 contains a discussion of wing design integration considerations. Guidelines for the structural design of wings are presented. In addition, the structural integration of the wing into the fuselage is discussed with examples. Mechanizations of flaps and wing mounted lateral controls are also given.

Section 4.3 provides a discussion of several military/operational design considerations such as: stores, pivoting stores , wing folding, and wing pivot construction.

Section 4.4 contains examples of the overall structural arrangement of wings for a number of airplanes.

4.1 WING CONFIGURATION: AERODYNAMIC AND OPERATIONAL DESIGN CONSIDERATIONS

An overview of airplane configurations including discussions of wing configurations is presented in Chapter 3 of Part II. A step-by-step procedure for arriving at a satisfactory preliminary wing layout is contained in Chapter 6 of Part II.

The purpose of this section is to present additional design information relative to the choice of the wing configuration.

References 12, 13 , 14 and 29 should be consulted for additional information on wing design.

The following wing configuration aspects will be discussed:

4.1.1 Wing size: large or small? Or,
Wing loading: low or high?
4.1.2 High, mid or low wing?
4.1.3 Forward sweep, no sweep or aft sweep?
4.1.4 Variable sweep: one pivot or two?
4.1.5 Bi-plane, braced wing or joined wing?
4.1.6 Wing aspect ratio: high, low and/or winglets?
4.1.7 Wing thickness ratio: large or small?
4.1.8 Wing taper ratio: high or low?
4.1.9 Straight taper or variable taper?
4.1.10 Wing twist: how much?
4.1.11 Wing dihedral angle: how much?
4.1.12 Wing incidence on the fuselage: how much?
4.1.13 Variable camber (MAW = Mission Adaptive Wing)?
4.1.14 Wing leading edge strakes (Lexes)
4.1.15 Planform tailoring: why and when?
4.1.16 Area ruling: when is it required?
4.1.17 Wing span: when is it too high?
4.1.18 Aerodynamic coupling?
4.1.19 Flaps: what size and which type(s)?
4.1.20 Lateral controls: what size and which type(s)?

Finally, a review of wing drag contributions is presented:

4.1.21 Review of wing drag contributions.

The reader is referred to Tables 6.1 through 6.12 and 8.1 through 8.12 in Part II for detailed wing airfoil and wing planform design information.

4.1.1 Wing Size: Large or Small? Or, Wing Loading: Low or High?

The question of wing size (or wing loading) depends mostly on performance oriented objectives. Chapter 3 of Part I has addressed the general question of wing and thrust sizing to a wide range of performance objectives.

Wing size or wing loading primarily affects the following characteristics:

1. Take-off/landing field length
2. Cruise performance (L/D)
3. Ride through turbulence
4. Weight

Two examples will be discussed of trade studies showing the effect of wing loading on fieldlength performance and on cruise efficiency. The reader can develop similar relations for other performance objectives such as: climb performance, maximum speed performance and maneuvering performance. During Class II wing design it is essential to carry out these individual trade studies to ensure the proper sizing of the wing.

1. Take-off/landing field length: To achieve short field lengths, large wings (low wing loading) are better than small wings (high wing loading). The wing can be kept small by using flaps. Flaps provide the possibility to obtain high values of $C_{L_{max}}$

Figure 4.1 illustrates the trends based on the following equations which are valid for sealevel only:

For landing field length at sealevel standard:

$$s_L = 429(W/S)_L / C_{L_{max_L}} \qquad (4.1)$$

For take-off field length at sealevel standard:

$$s_{TOFL} = 37.5(W/S)_{TO} / (T/W)_{TO} C_{L_{max_{TO}}} \qquad (4.2)$$

These equations are approximations of FAR 23 and 25 fieldlength Eqns. (3.8), (3.14) and (3.16) of Part I.

The strong influence of maximum lift coefficient in the landing configuration and of wing loading on required landing field length is apparent.

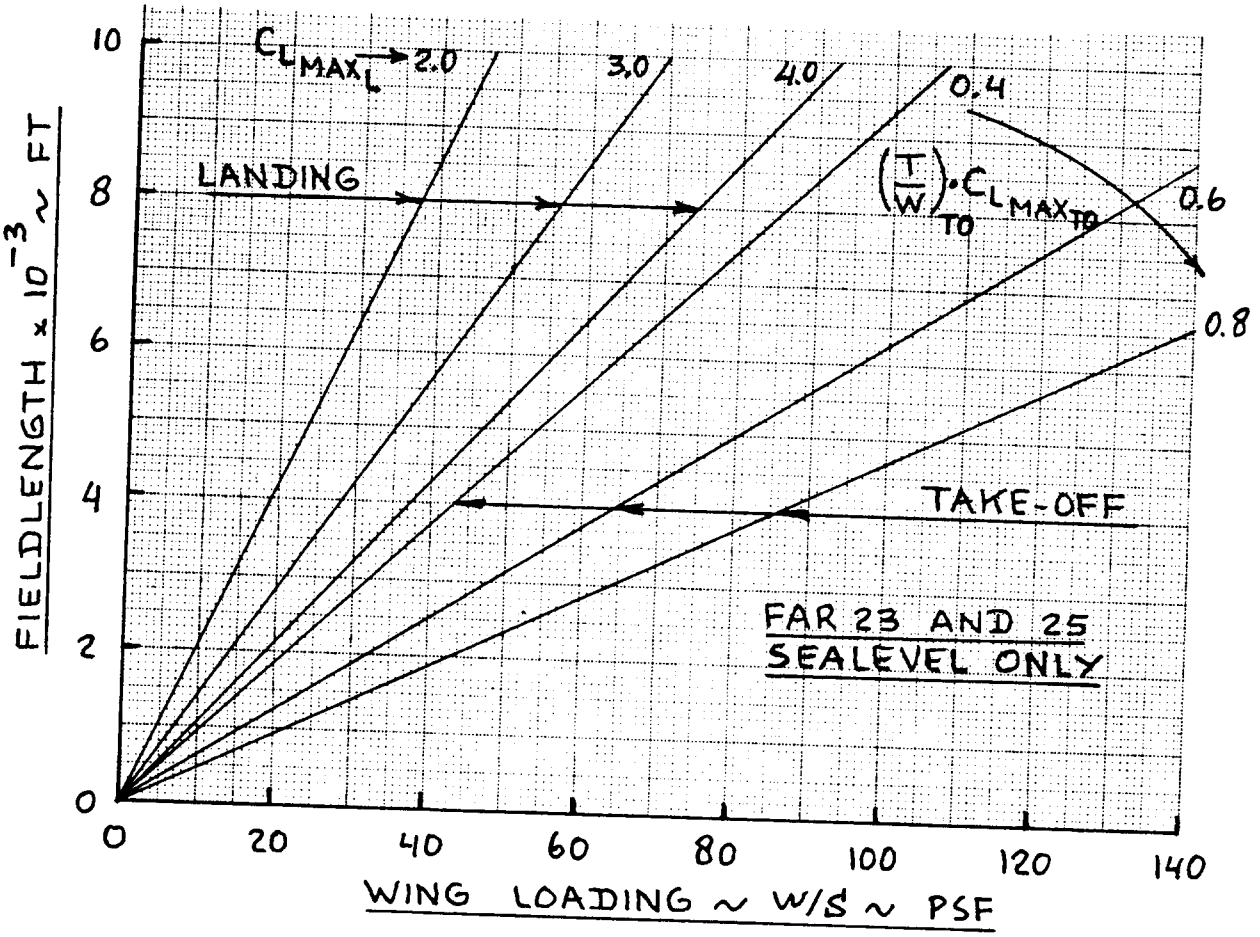

Figure 4.1 Effect of Wing Loading on Field Performance

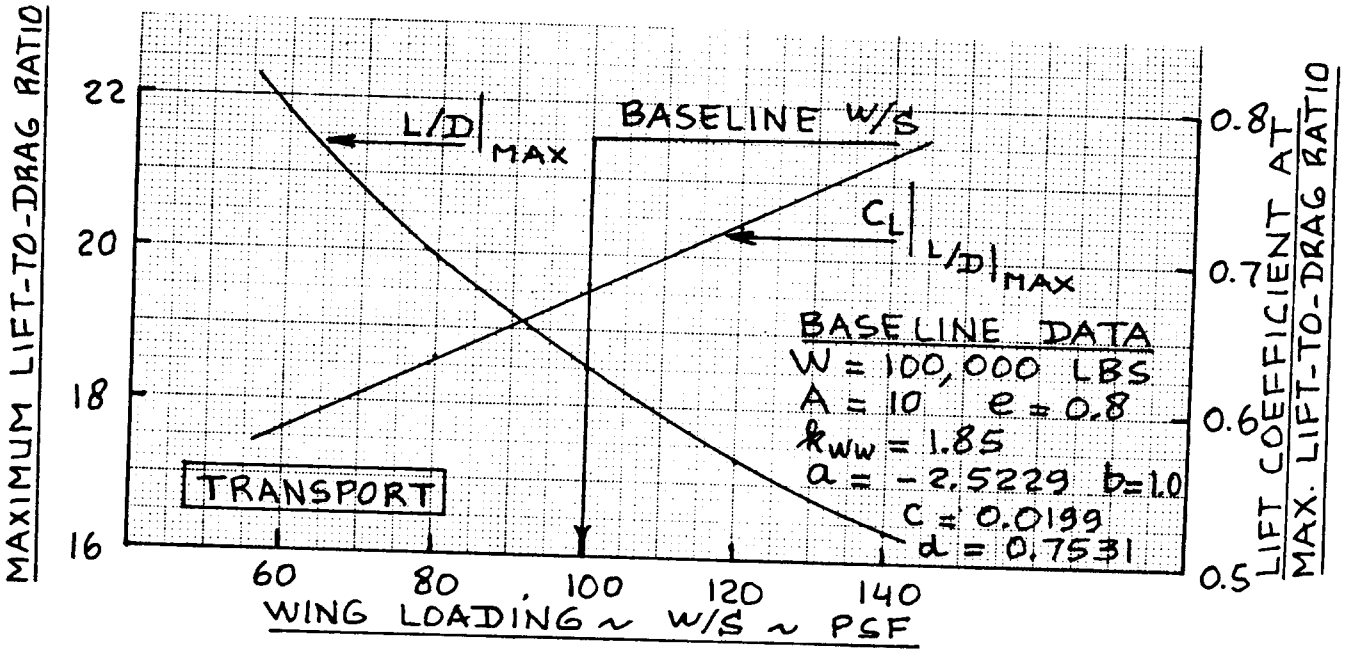

Figure 4.2 Effect of Wing Loading on Cruise Parameters

2: Cruise performance (L/D): To achieve cruise flight close to $(L/D)_{max}$ a high wing loading is needed, so that the cruise lift coeffcient can be close to that at $(L/D)_{max}$. On the other hand, if flight at extremely high altitudes and moderate speeds is required, a large wing area may be essential (U-2 and Canberra).

An appreciation for the effect of wing loading on $(L/D)_{max}$ can be obtained as follows:

$$(L/D)_{max} = (\pi Ae/4C_{D_o})^{1/2} \qquad (4.3)$$

with:

$$C_{D_o} = (1/S)\text{invlog}_{10}[a + b\log_{10}\{(\text{invlog}_{10}(c + d\log_{10}W_{TO})) + k_{ww}(S - S_{baseline})\}] \qquad (4.4)$$

Equations (4.3) and (4.4) can be used to study the effect of varying wing area (wing loading) on $(L/D)_{max}$ for a given type airplane. To perform such a study the following input information is required:

*Aspect ratio, A

*Oswald's Efficiency Factor, e

*Regression constants a, b, c and d: (See Tables 3.4 and 3.5 in Part I)

*Take-off weight, W_{TO}

*Baseline wing loading, $(W/S)_{baseline}$

*k_{ww} = 1.85 (approximately)

The constant k_{ww} accounts for that part of the wing which is 'buried' in the fuselage and which therefore does not contribute to wetted area.

The value for $S_{baseline}$ in Eqn.(4.4) follows from:

$$S_{baseline} = W_{TO}/(W/S)_{baseline} \qquad (4.5)$$

The lift coefficient at $(L/D)_{max}$ follows from:

$$C_{L_{(L/D)_{max}}} = (C_{D_o}\pi AE)^{1/2} \qquad (4.6)$$

Figure 4.2 illustrates the results of a trade study of the effect of wing loading on these cruise performance parameters for a transport type airplane. By varying the input data in the appropriate manner similar results can be generated for any type airplane. The reader is encouraged to do this for any new design.

WARNING: do not assume that an airplane will always be able to cruise at the lift coefficient for $(L/D)_{max}$ as given by Eqn.(4.6). Verify the actual cruise lift coefficient from:

$$C_{L_{cruise}} = W_{cruise}/\bar{q}S = W_{cruise}/14\,826M^2 \qquad (4.7)$$

It will be found that most airplanes cruise at significantly lower values of lift coefficient than the one indicated by Eqn.(4.6).

3. Ride through turbulence: Wing loading also has a significant effect on the ride quality of an airplane through turbulence. Ride response to turbulence is proportional to the parameter n_α:

$$n_\alpha = \bar{q}C_{L_\alpha}/(W/S) \qquad (4.8)$$

Eqn.(4.8) clearly shows that airplanes with low wing loading have high values of n_α which translates into 'poor' ride qualities.

4. Weight: The larger the wing area, the greater the weight of the wing and therefore the weight of the airplane. The wing weight equations in Part V allow for the calculation of wing weight as a function of wing size (area).

Table 4.1 summarizes the range of typical take-off wing loadings found in twelve types of airplanes. The reader is reminded of the fact that additional data on airplane wing loadings may be found in Ref.30.

Table 4.2 summarizes the effect of wing loading on a number of design characteristics.

Table 4.1 Typical Values For Take-off Wing Loadings

Note: Ranges for take-off wing loadings are in psf.

Airplane Type	$(W/S)_{TO}$	Airplane Type	$(W/S)_{TO}$
1. Homebuilts	5 - 15	9. Fighters	
2. Single Engine Prop. Driven	10 - 25	Jets	70 - 140
		Props	40 - 70
3. Twin Engine Prop. Driven	20 - 45	10. Mil. Patrol, Bomb and Transport Airplanes	70 - 120
4. Agricultural	15 - 30		
		11. Flying Boats, Amphibious and Float Airplanes	
5. Business Jets	40 - 80	Jets	50 - 90
6. Regional TBP	30 - 55	Props	30 - 60
		Floats	20 - 50
7. Transport Jets	80 - 120		
8. Mil.Trainers		12. Supersonic Cruise Airplanes	80 - 120
Jets	40 - 80		
Props	20 - 40		

Table 4.2 Summary of the Effect of Wing Loading

Item	Effect of Wing Loading on Item	
	High W/S	Low W/S
Stall speed	High	Low
Fieldlength (landing and take-off)	Long	Short
Max. lift-to-drag ratio	High	Low
Ride quality in turbulence	Good	Bad
Weight	Low	High

4.1.2. High, Mid or Low Wing?

The vertical location of the wing on a fuselage affects the following characteristics:

1. Drag 2. Dihedral effect

3. Operational considerations

To a large extent the choice of high, mid or low wing configuration depends on operational considerations associated with the mission of the airplane. Therefore, which type of airplane is being considered plays an important role in deciding the vertical location of the wing.

Cargo Transports: For cargo transports, the requirement for easy loading and unloading via self-contained ramps, virtually dictates a high wing configuration. Floor levels must be close to the ground. This would not be possible with the wing carry-through structure passing below the floor in a low wing configuration.

Figure 4.3 illustrates these points.

Passenger Transports: For passenger transports a high wing configuration offers good visibility for all passengers. The Fokker F27 and the BAe 146 (Figures 3.18a and 3.21d in Part II) are examples of such configurations. If baggage and cargo needs to be carried below the floor of the passenger cabin, this results in a very heavy landing gear if the gear is wing mounted (F27). If the gear is fuselage mounted (BAe 146), this results in draggy bulges and/or marginal lateral stability during ground operations.

In the case of small high wing passenger transports it is possible to allow passenger loading without the help of external loading ramps and without the penalty self-contained stairs impose.

A synergistic advantage of a swept, high wing layout is that it allows the use of negative dihedral (anhedral) to obtain better dutch roll damping. In a low wing transport this is difficult to do because it results in long landing gear legs. The BAe 146 and the SAAB 105XT (Fig.4.4) illustrate these points.

In the case of large passenger transports, efficient access to baggage and cargo space is possible only with

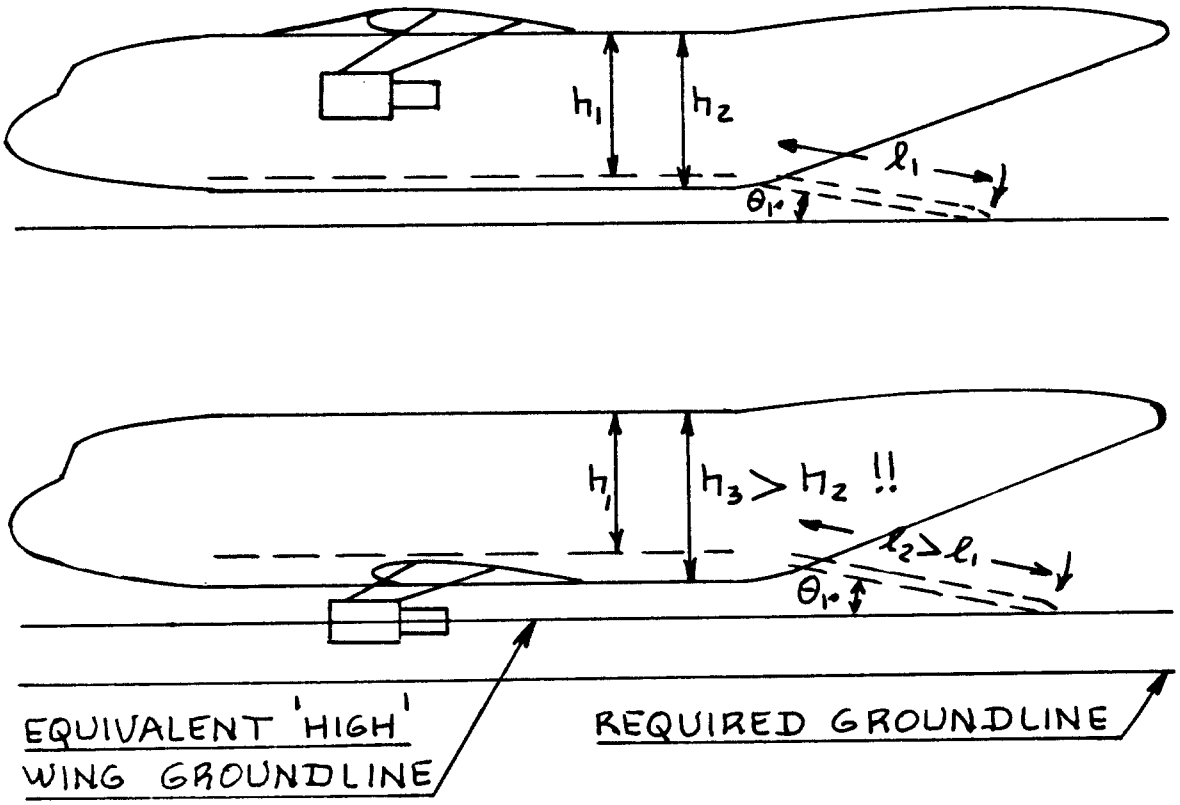

Figure 4.3 Effect of Wing Location on Ground Clearance

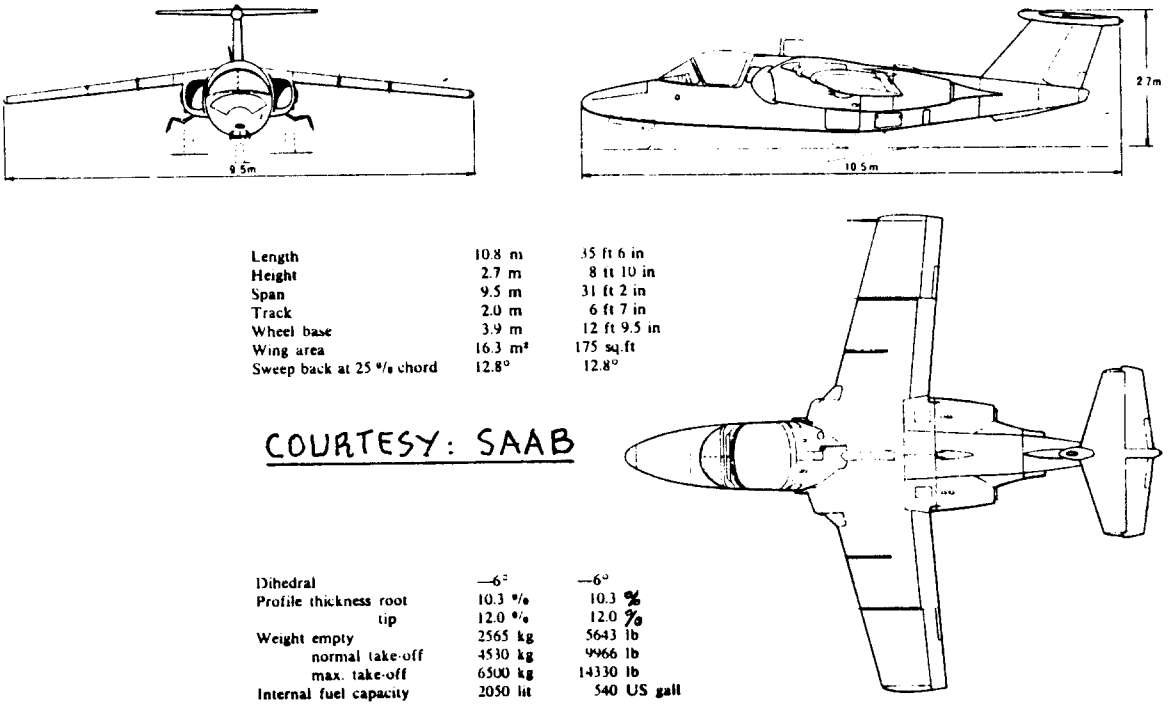

Length	10.8 m	35 ft 6 in
Height	2.7 m	8 ft 10 in
Span	9.5 m	31 ft 2 in
Track	2.0 m	6 ft 7 in
Wheel base	3.9 m	12 ft 9.5 in
Wing area	16.3 m²	175 sq.ft
Sweep back at 25 % chord	12.8°	12.8°

COURTESY: SAAB

Dihedral	−6°	−6°
Profile thickness root	10.3 %	10.3 %
tip	12.0 %	12.0 %
Weight empty	2565 kg	5643 lb
normal take-off	4530 kg	9966 lb
max. take-off	6500 kg	14330 lb
Internal fuel capacity	2050 lit	540 US gall

Figure 4.4 Use of Anhedral on the SAAB 105XT

the cargo holds close to the ground. This leads to the choice of a low wing configuration.

Both low and high wing configurations must carry fairings to smooth out the flow at the wing-fuselage intersection. If this is not done the interference drag becomes too high. Such fairings can be very large and cause an increase in weight and in manufacturing cost. Figures 3.30a and 3.15b in Part II illustrate these points.

Light Airplanes: For light airplanes, the choice of wing location seems to be more a matter of company tradition than anything else. A solid case pro or con either location is difficult to make.

A considerable aerodynamic (drag) advantage is associated with the mid wing configuration. Such a wing arrangement tends to minimize interference drag. A structural problem is the requirement for a carry-through structure passing through the middle of the fuselage. This makes it necessary to keep the passenger cabin either forward or behind the wing carry-through. Examples of this wing configuration are shown in Fig.4.5 and in Fig.3.47 of Part II.

Placing the passenger cabin forward of the wing usually results in large c.g. excursions which require special attention in empennage design. By utilizing canard and/or three-surface layouts it is possible to overcome these trim problems caused by large c.g. excursions. Figures 3.42 and 3.47 of Part II are examples of such layouts.

Fighters and Trainers: In fighter and trainer airplanes the mid wing configuration is often selected because of the favorable drag effect. No passengers need to be carried so the c.g. excursion argument does not apply in these cases.

Mid to high wing layouts in fighter airplanes also lead to easier loading and unloading of underwing stores.

Flying Boats, Amphibians and Float Airplanes: In this airplane category the high wing layout is often dictated by water clearance requirements. In float equipped airplanes the low wing layout has also been used.

Table 4.3 summarizes the effect of wing location on the fuselage.

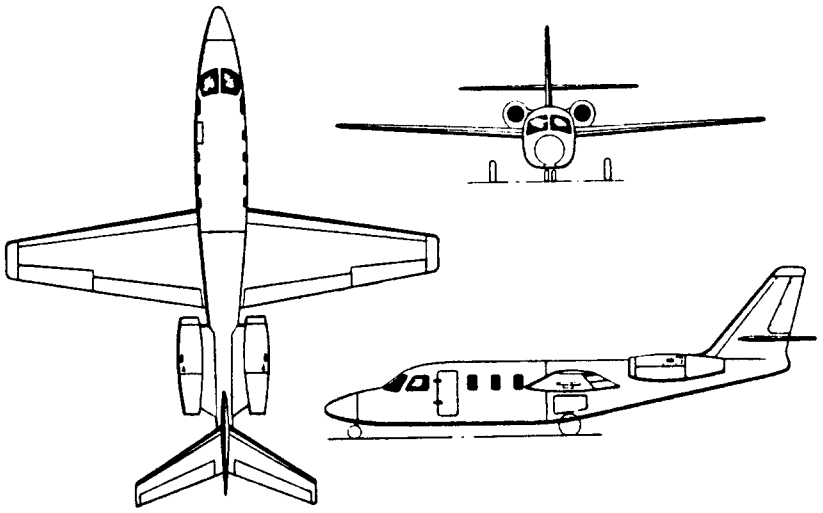

Figure 4.5 Use of Mid Wing Location on the Jet Commander

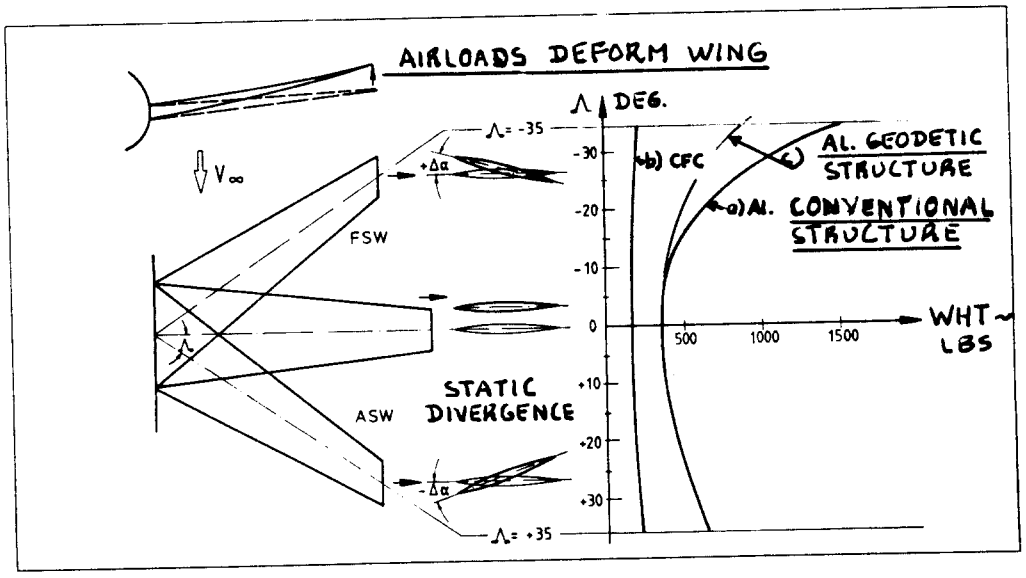

Figure 4.6 Effect of Sweep on Wing Weight

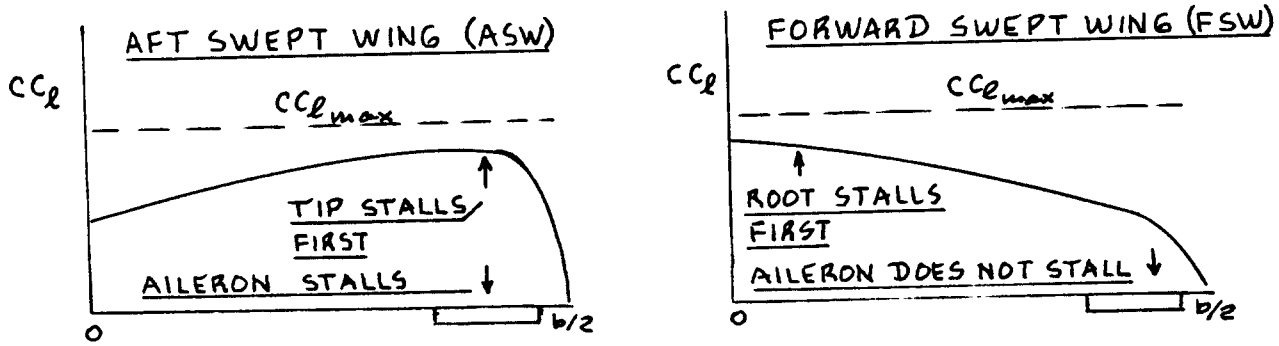

Figure 4.7 Effect of Sweep on Stall Behavior

Table 4.3 Summary of the Effect of Wing Location on the Fuselage

Item	Effect of Wing Location on Item		
	High	Mid	Low
Interference Drag	Poor	Good	Poor
Dihedral Effect	Negative	Neutral	Positive
Passenger Visibility	Good	Good	Poor for some
Landing Gear:			
Wing mounted	Long/heavy		Short/light
Fuselage mounted	Possibly draggy		
Loading and unloading	easy	easy	need stairs

Table 4.4 Summary of the Effect of Wing Sweep

Item	Effect of Increased Wing Sweep on item		
	Forward	None	Aft
Lift-curve Slope	Low	High	Low
Pitch attitude in low speed, level flight	High	Low	High
Ride through turbulence	Good	Poor	Good
Asymmetric stall	Best	Good	Poor
Lateral control at stall	Best	Good	Poor
Compressibility drag	Low	High	Low
Wing weight	Highest	Low	High

Tables 6.1 through 6.12 in Part II provide data on overall wing type and wing location for a wide range of airplanes.

4.1.3 Forward Sweep, No Sweep or Aft Sweep?

Adding sweep to a wing has important consequences to the following characteristics:

1. Compressibility drag 2. Weight 3. Stall behavior

4. Balance 5. Pitch attitude and ride 6. Good looks

There is a substantial weight penalty associated with the addition of sweep to a wing. Figure 4.6 illustrates this point for aft and for forward sweep.

1. Compressibility drag: It is clear from Fig. 6.1 in Part II that sweep has a very favorable effect on compressibility drag. Note that the sign of the sweep angle is not influenced by this: aft sweep and forward sweep yield similar reductions in compressibility drag.

2. Weight: Adding sweep to a wing increases wing weight substantially. The wing weight equations of Part V demonstrate this quantitatively for aft swept wings. Figure 4.6 illustrates this point for both aft swept and forward swept wings.

Figure 4.6 shows that aft sweep does translate into a weight advantage compared with forward sweep. The reason is the structural divergence phenomenon associated with forward sweep. By tailoring the ratio of bending to torsion stifness it is possible to make the weight penalty associated with forward swept wings quite acceptable. Such tailoring is inherently possible with composite structures. However, by using tailored machined skins (geodetic structure) and ribs it is possible to achieve similar results with metal wings. References 31 and 32 discuss these concepts in some detail.

3. Stall behavior: A significant advantage of forward sweep over aft sweep is the superior stall characteristics. Figure 4.7 illustrates the potential advantage of forward sweep. An important consequence of the superior stall behavior is the fact that outboard mounted lateral controls maintain their effectiveness well into the stall. Aft swept wings need to be twisted to protect against roll-off in the stall.

4. Balance: If a new design of an airplane with an unswept wing runs into minor trouble with its weight and balance (for example the c.g. is a bit too far aft) then it may be possible to 'fix' the problem by a slight amount of aft sweep. This has the effect of moving the airplane a.c. aft faster than the c.g. thereby bringing the airplane back into balance. This is in fact the reason for the fairly pronounced sweep of the Douglas DC2! The wing sweep feature of the DC2 was inherited by the DC3 and became one of its recognition features.

Adding aft sweep to a flying wing has a beneficial effect on the inherent longitudinal damping characteristics of such a configuration.

Adding aft sweep to a wing will also create the necessary moment arm for the addition of directionally stabilizing surfaces. The Beech Starship I of Fig. 3.42 (Part II) is a case in point.

5. Pitch attitude and ride: Sweep angle also has a significant effect on the lift-curve slope, C_{L_α} and therefore on:

1. Pitch attitude at low speed and therefore on runway visibility
2. Ride characteristics: high sweep improves ride and low sweep worsens the ride through turbulence

Figures 4.8 and 4.9 illustrate point 1. Point 2 can be visualized with Equation (4.8) which allows the calculation of the 'change in load factor with angle of attack derivative. This equation shows that lowering C_{L_α} by increasing sweep angle lowers the load factor reaction to turbulence induced angles of attack. Note that Eqn.(4.8) also shows that increased wing loading improves the ride!

6. Good looks: The 'good looks' aspects of sweep selection should not be dismissed as entirely frivolous. There is plenty of evidence that 'good looks' helps sell airplanes!

Table 4.4 summarizes the effect of wing sweep angle on a number of important characteristics.

The reader should refer to Tables 6.1 through 6.12 in Part II for data on wing sweep angles used on a wide range of airplanes.

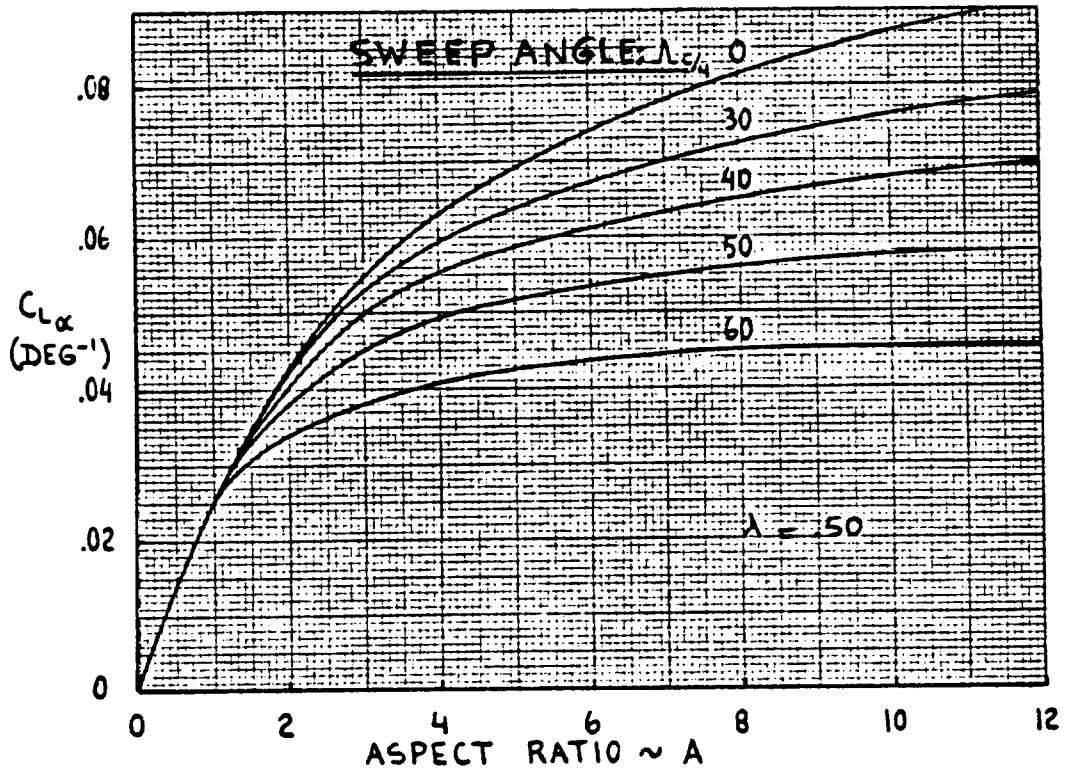

Figure 4.8 Effect of Sweep on Lift Curve Slope

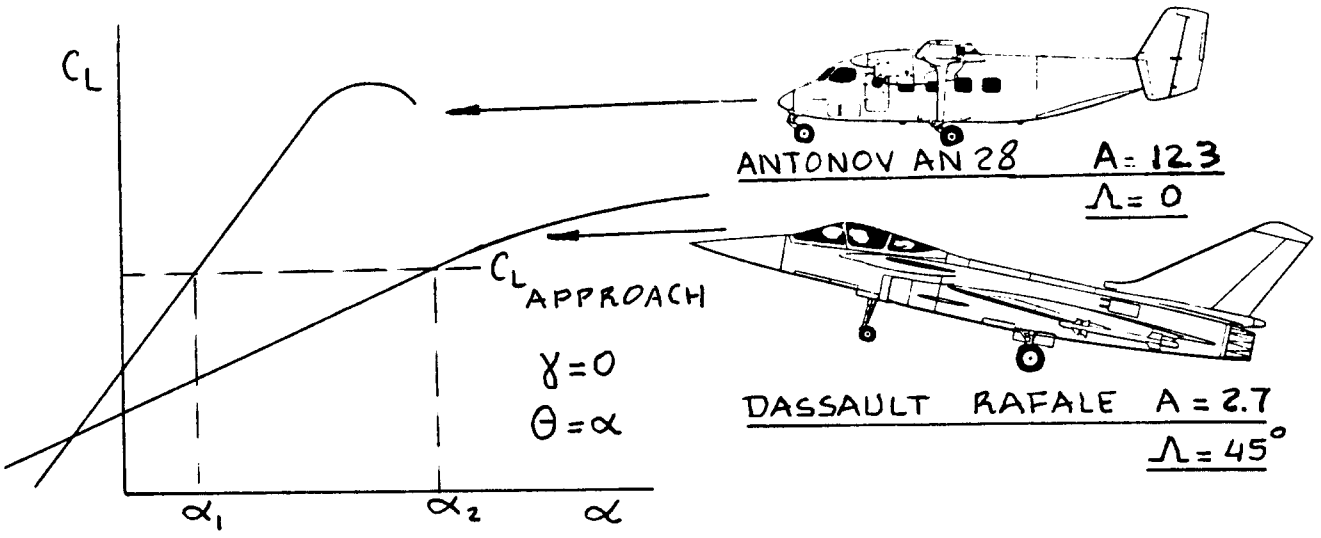

Figure 4.9 Effect of Sweep on Approach Attitude

4.1.4 Variable Sweep: One Pivot or Two?

The primary reasons for using variable sweep are:

1. for good take-off and landing performance as well as good handling characteristics very low sweep angles are best.
2. for low drag and good ride characteristics at high speed, high sweep angles are best.
3. to obtain optimum values of L/D throughout a wide performance envelope, variable sweep is best.

1. Take-off/landing and handling: Sub-section 4.11 shows that a high value of maximum lift coefficient is required to achieve good fieldlength performance. Sub-section 4.1.3 shows that at high sweep angles asymmetric stall problems may arise which compromise good handling qualities.

High sweep angles cause a drop in maximum lift coefficient according to the so-called cosine rule:

$$C_{L_{max_\Lambda}} = C_{L_{max_{\Lambda=0}}} \cos\Lambda \qquad (4.9)$$

This cosine rule applies below 35 degrees of sweep.

2. Low drag and good ride: The dragrise data of Fig.6.1, Part II and Eqn.(4.8) demonstrate the correctness of statement 2.

3. Lift-to-drag ratio: Figure 4.10 illustrates the possibilities with regard to L/D thereby showing the correctness of statement 3.

Evidently, with variable sweep all these things are possible. However, at a price: the variable sweep wing results in a significant weight penalty due to the need for a pivot structure and a system to change wing sweep angle in flight. A major design question with a variable sweep wing is: where to place the pivot(s)?

The chordwise pivot location is fairly obvious: close to the mid-chord position of the wing torque box. The spanwise pivot(s) position depends on whether one or two pivots are used.

If two pivots are used (symmetrical variable sweep) the weight penalty can be lessened by using outboard pivot locations. Outboard pivot locations also result in a reduction of a.c. travel due to sweep which in turn

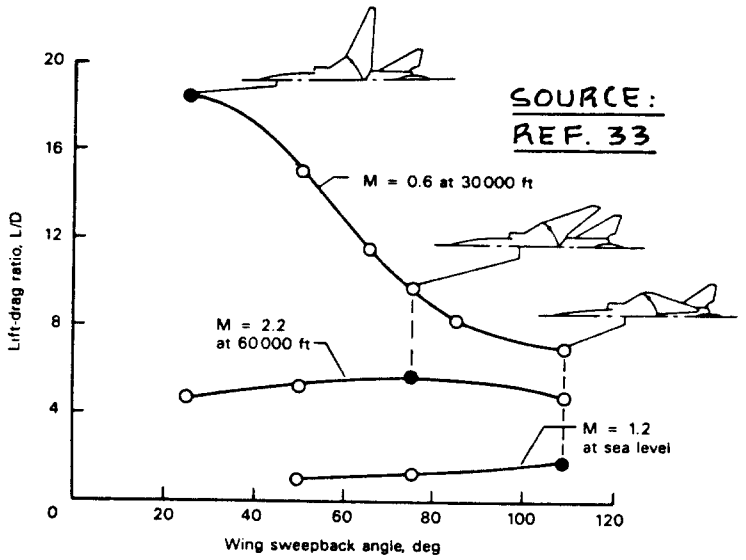

Figure 4.10 Effect of Sweep on Lift-to-Drag Ratio

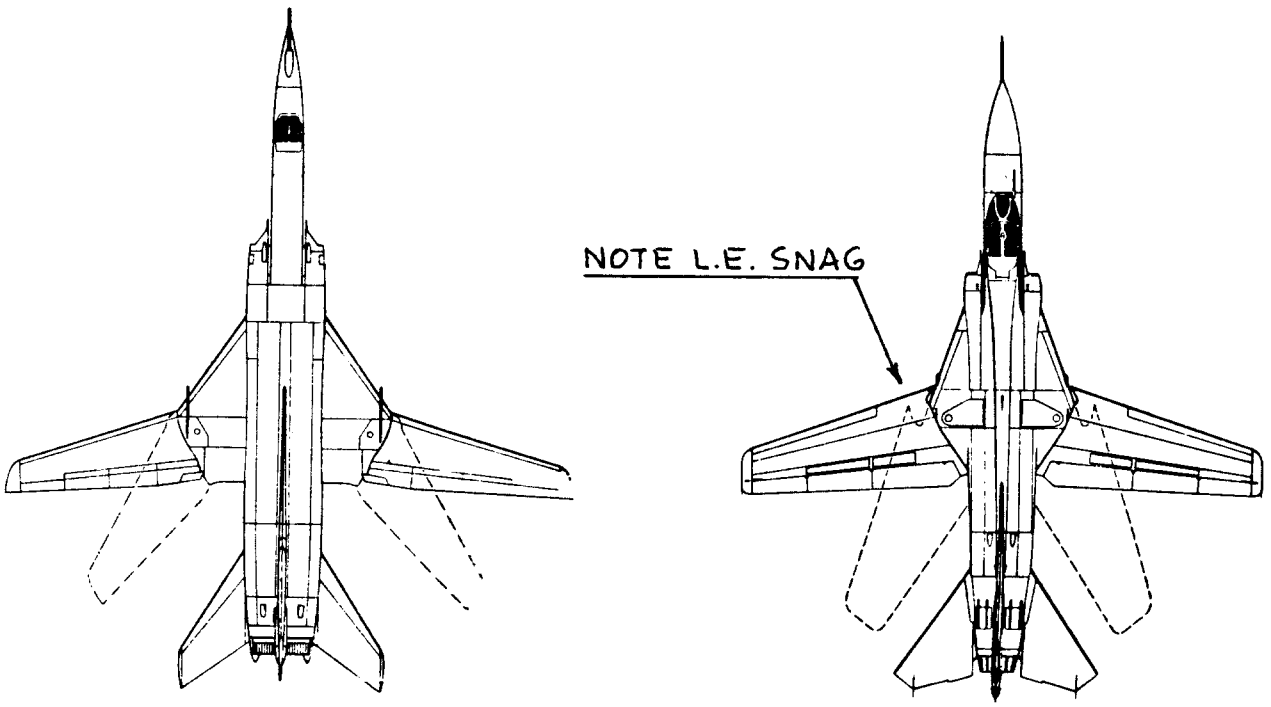

TU-22M BACKFIRE
32% PIVOT LOCATION

MIG-23 FLOGGER-G
21% PIVOT LOCATION

Figure 4.11 Example of Inboard and Outboard Wing Pivot Locations

results in less trim drag penalties. Outboard pivot locations result in large highly swept strakes which in turn result in formidable 'pitch-up' behavior at high angles of attack.

With inboard pivot locations the 'pitch-up' problem is less dominant. Weight is larger and aeroelastic effects become more important.

Figure 4.11 illustrates both inboard and outboard pivot locations.

Variable aft sweep has been used on airplanes such as: XF10F, F14, F111, Tornado, B-1, Backfire, Flogger and other Soviet airplanes.

Variable forward sweep has not yet been used operationally despite its obvious advantages.

Asymmetrical variable sweep (oblique wing) has been demonstrated in theory and in the windtunnel to result in considerable drag reductions, particularly in the transonic speed range. Because of the presence of only one pivot, a weight reduction relative to conventional VSW airplanes may be possible. The divergence behavior of the forward panel will require some increase in weight and partially off-set the pivot weight advantage.

Figure 4.12 shows why the oblique wing is (in principle) lighter than a conventional variable sweep wing. A flight test program on the NASA AD-1 (Fig. 4.13) has shown that the handling characteristics of the oblique wing are quite acceptable even without stability augmentation systems. With the advent of multiple surface, digital control systems the handling qualities issue against the oblique wing has become a non-issue.

Figure 4.14 shows a high speed application of an oblique wing to an F-8 fighter airplane.

A more radical approach to the problem of variable sweep is the so-called 'slewed wing' concept advanced by Handley Page. Figure 4.15 shows a potential application to a transport airplane. With the use of multiple trailing edge mounted flight control surfaces and modern control system design the controllability of this type of configuration is beyond question.

Table 4.5 summarizes the pros and cons of fixed versus variable sweep wing configurations, including the location of the pivot.

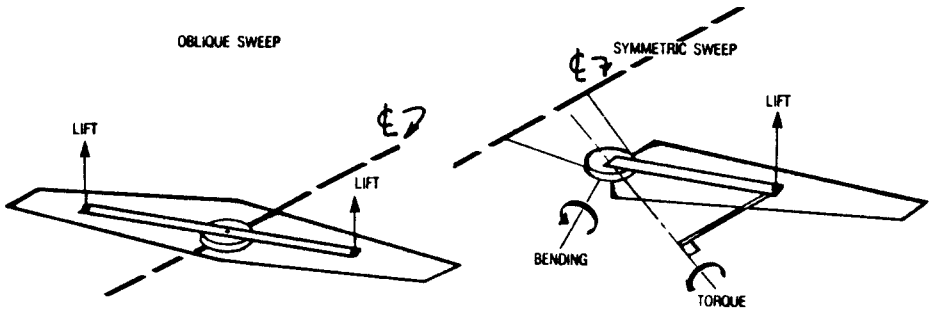

Figure 4.12 Load Comparison of Oblique and Symmetrically Variable Sweep Wings

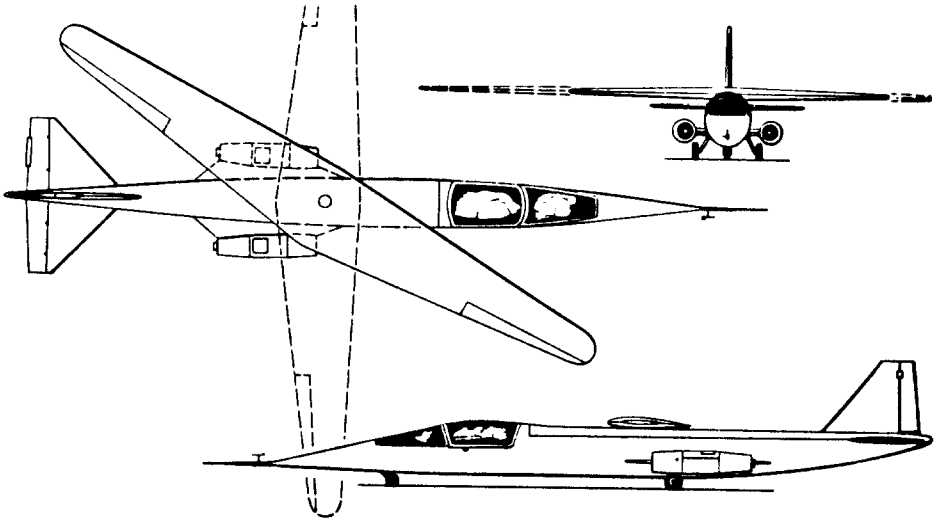

Figure 4.13 Experimental Oblique Wing Airplane: NASA AD-1

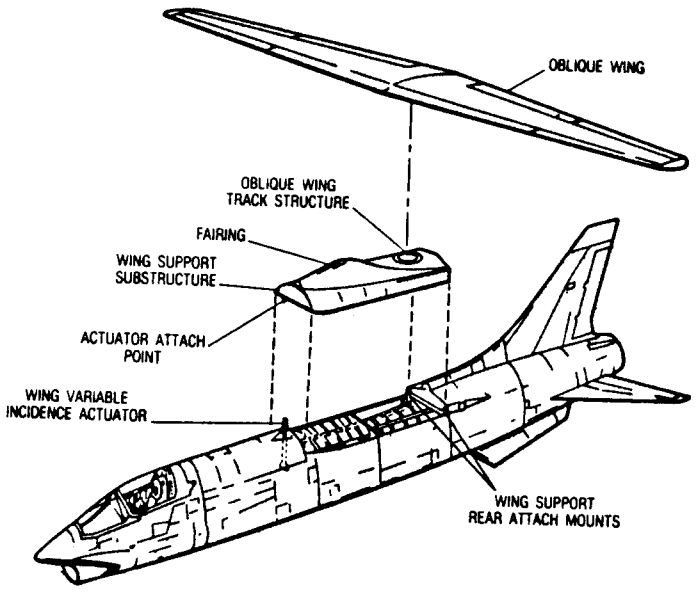

Figure 4.14 Experimental Oblique Wing Airplane: NASA F-8

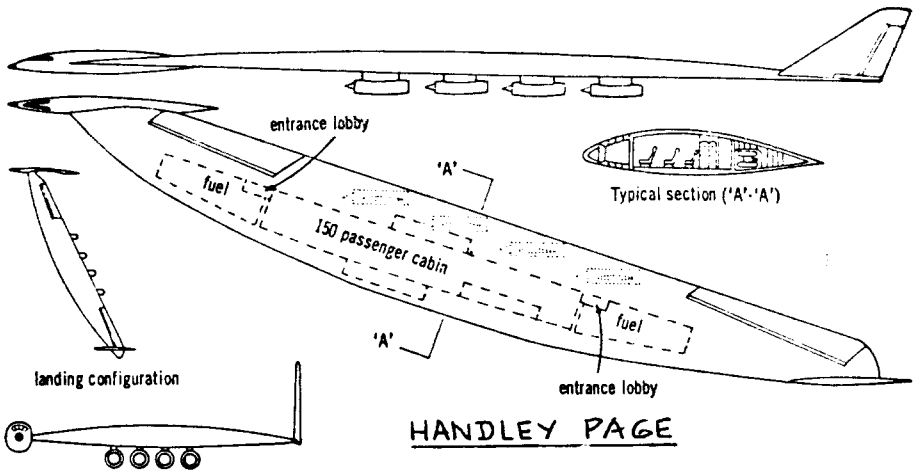

Figure 4.15 Proposed Slewed Wing Configuration

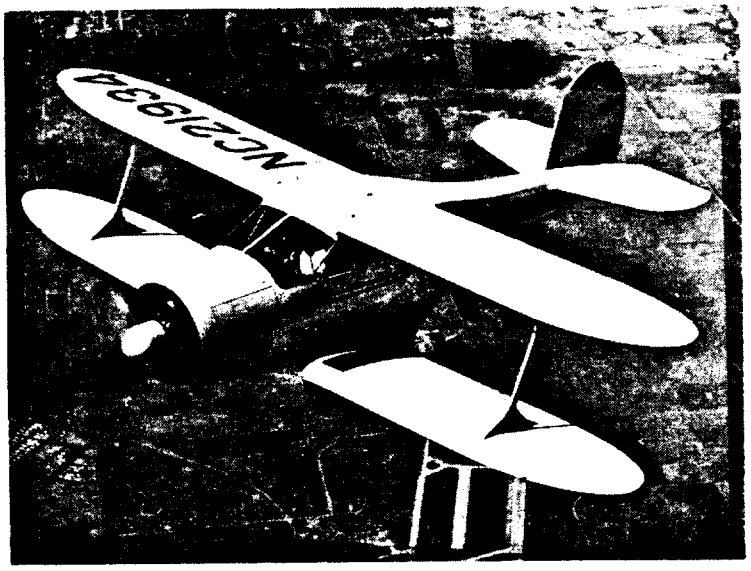

COURTESY: BEECH

Figure 4.16 Bi-plane Example: Beech Model 17 Staggerwing

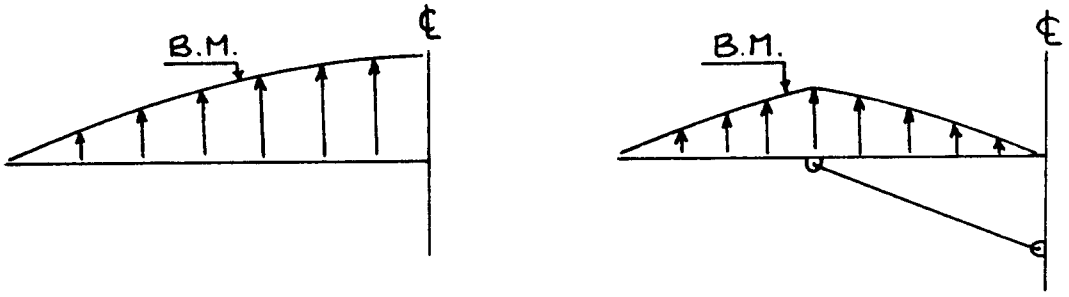

Figure 4.17 Comparison of Bending Moment Distributions of Braced and Cantilever Wings

Table 4.5 Summary of the Effect of Wing Pivot Location

Item	Effect of Wing Pivot Location		
	Two Pivots		One Pivot
	Inboard	Outboard	Oblique
Wing weight	Highest	High	Low
Aeroelastic effects	Severe	Moderate	Moderate
Aerodynamic center shift	Large	Small	Little
Pitch-up at high alpha	Moderate	Severe	Moderate

Table 4.6 Summary of Effect of Monoplane/Bi-plane/Joined

Item	Effect of Wing Configuration			
	Monoplane		Bi-plane	Joined
	Cantilever	Braced		
Wing weight	High	Low	Very Low	Low
Profile Drag	Low	High	Higher	Moderate
Interf. drag	Low	High	Higher	High

Table 4.7 Summary of the Effect of Aspect Ratio

Item	Effect of Aspect Ratio on Item	
	High	Low
Induced Drag	Low	High
Lift-curve slope	High	Low
Pitch attitude (approach)	Low	High
Ride in turbulence	Poor	Good
Wing weight	High	Low
Wing span	Large	Small

4.1.5 Bi-plane, Braced Wing or Joined Wing?

Bi-planes, compared to cantilever monoplanes have the following advantages, according to Reference 14:

1. Compactness: for the same required area they can have smaller spans which results in easier storage

2. For a given size airplane a bi-plane can carry more wing area which results in shorter field length requirements

3. Particularly the wire or strut-braced bi-planes are cheaper to build than comparable monoplanes, all else remaining equal.

For the low subsonic speed range it is not at all clear that a properly designed bi-plane should have poor L/D ratios. The 'old' Beech 17 Staggerwing of Fig. 4.16 sported a cruise speed of 202 mph and an $(L/D)_{max}$ of 11.7 (despite its suspension wires) according to Reference 33.

For fundamental aerodynamic data and theories on bi-planes the reader is referred to References 14 and 34.

Braced wings, compared with strutted wings have the advantage of lower structural weight. Figure 4.17 shows the reason: much less root-bending moment resulting in lower weight. Part V, p.70 suggests a factor of 30 percent wing weight advantage for the strutted wing over the cantilevered wing!

Whether or not this difference in weight offsets the difference in drag (the strut can cause a significant increase in profile and interference drag) depends on detail design and on the required speed range. Detailed trade studies must provide the answer to this question.

It is possible to combine the weight advantage of the braced wing with the drag advantage of the cantilever wing by adapting the so-called joined wing. Figures 3.44 and 3.45 in Part II show examples of such an arrangement. Ref.35 claims significant weight and drag advantages for such a wing arrangement. A problem is that no such airplane has yet been built and certified. Therefore, many designers are weary of this possibility.

Table 4.6 summarizes the pros and cons of cantilever versus braced wing configurations.

4.1.6 Wing Aspect Ratio: High, Low and/or Winglets?

Wing aspect ratio, $A = b^2/S$ affects the following characteristics:

1. Induced drag 2. Lift-curve-slope 3. Weight 4. Span

1. Induced drag: High aspect ratio wings tend to have lower induced drag and therefore larger values of $(L/D)_{max}$. However, to utilize this advantage the associated larger value of lift coefficient requires flight at higher altitudes or at lower speeds. Equations (4.3), (4.6) and (4.7) demonstrate these points.

2. Lift-curve-slope: High aspect ratio wings tend to have high lift-curve slopes. Figure 4.8 illustrates this. High lift curve slopes have two consequences:

a) At low speed the approach attitude is conducive to good runway visibility from the cockpit. See Figure 4.9.

b) The ride through turbulence is rougher: Eqn.(4.8) shows this.

3. Weight: High aspect ratio wings tend to weigh more than low aspect ratio wings. The wing weight equations in Chapter 5 of Part V demonstrate this.

4. Span: High aspect ratio wings tend to have large spans. The definition of aspect ratio, $A = b^2/S$ shows this. Sub-section 4.1.17 presents a discussion of factors which can constrain wingspan.

Table 4.7 summarizes the effect of aspect ratio.

In some instances it is possible to increase the 'effective' aspect ratio of a wing by the use of winglets. Figure 4.18 shows an example application. The following question has been raised by designers: is it better to design a new wing with or without winglets? There still are no definitive answers to this question. Here are some opinions of the author:

a) New airplane design: A lower overall wing weight can be achieved by going to a higher aspect ratio instead of using a lower aspect ratio with winglets. However, if 'good looks' dictate the use of winglets, use them!

If, because of the configuration (aft located wing such as the Starship I) winglets are needed also for directional stability and control, it is advantageous to use winglets.

b) Retrofit or growth of an existing airplane: To improve cruise L/D of an existing airplane it is often lighter to add winglets than to extend the wingspan. In some cases a combination of the two works out best. An example of the latter case is the 747-400: See Fig.4.18.

There are situations where the choice of high aspect ratio leads to wing spans which are too high for reasons of operational constraints. Sub-section 4.1.17 addresses some of those constraints.

Table 4.7 summarizes the effect of wing aspect ratio on several important characteristics.

Refer to Tables 6.1 through 6.12 in Part II for values of aspect ratio used in a wide range of airplanes.

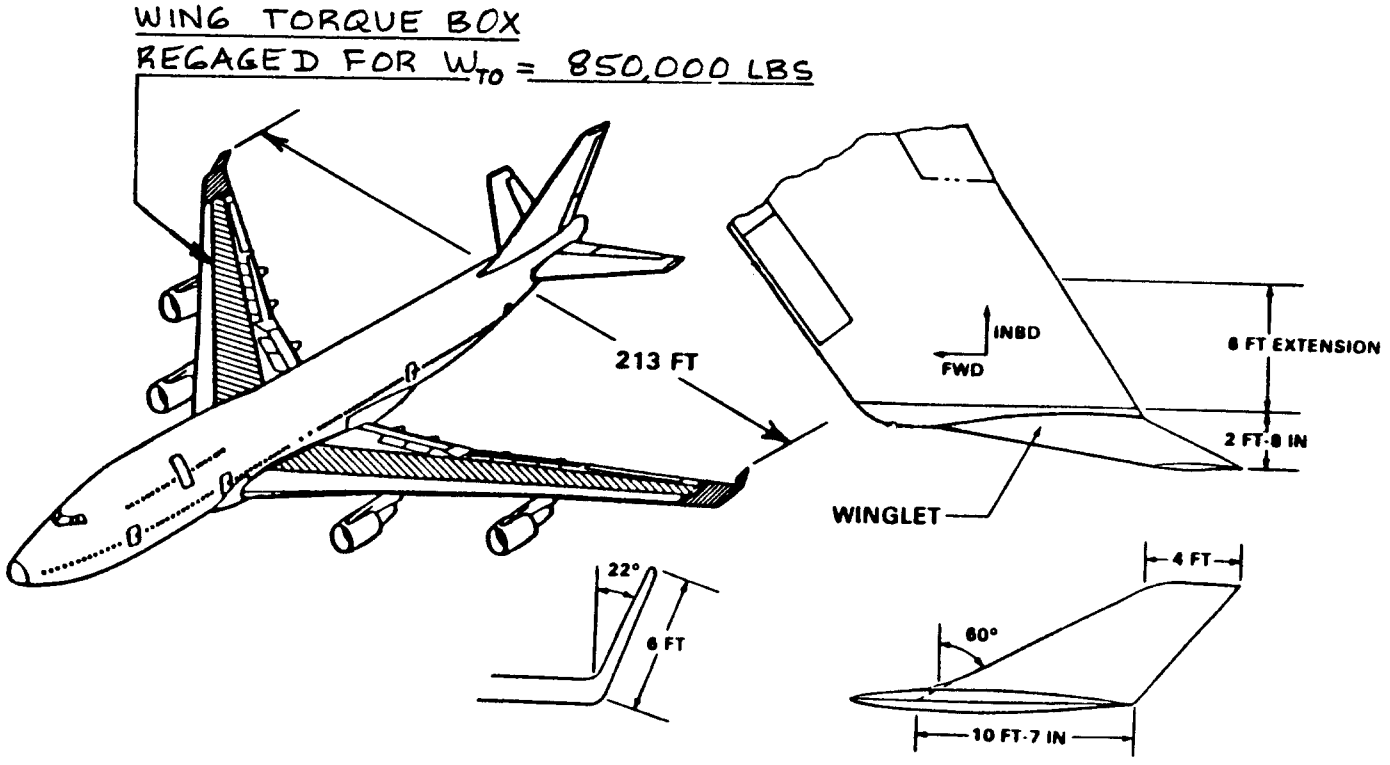

Figure 4.18 Winglet Example on the Boeing 747-400

4.1.7 Wing Thickness Ratio: Large or Small?

Wing (airfoil) thickness primarily affects the following characteristics:

1. Drag 2. Weight 3. Maximum Lift 4. Fuel Volume

1. Drag: Increased thickness means higher profile drag in the subsonic flight regime. It also means higher wave drag in the transonic and supersonic flight regime. In the transonic flight regime, Fig. 6.1 of Part II shows the large effect of thickness on compressibility drag. Use of super-critical airfoils allows designers to use larger thickness ratios and maintain fairly high subsonic Mach Numbers. Fig. 6.2 (Part II) shows this effect.

Reference 36 shows that wave drag is proportional to the parameter $(t/c)^2$ in the supersonic flight regime. Because of the very rapid increase of wave drag with t/c, the thickness of wing and empennage surfaces of supersonic airplanes must be very carefully selected.

2. Weight: Increased wing thickness means decreased wing weight since both bending and torsional stiffness increase with increasing thickness. The wing weight formulas in Chapter 5 of Part V indicate this trend.

3. Maximum Lift: Figure 7.1 in Part II shows that up to 12-14 percent thickness, maximum lift coefficients of airfoils tend to increase with increasing thickness.

4. Fuel Volume: Increased thickness translates into greater fuel volume. The effect of thickness ratio on fuel volume is given by Eqn.(6.3) in Part II. If possible fuel should be carried in the wing: this helps reduce wing weight (inertial relief) and tends to make the fuel system simpler as well.

Designers should always try to use as high a thickness ratio as possible, consistent with performance constraints. The weight decrease which results from this improves the operating economics of all airplanes.

Figure 4.19 illustrates the drag and weight trends.

Table 4.8 summarizes the primary effects of thickness ratio.

Tables 8.1 through 8.12 in Part II provide data on taper ratios used in a wide range of airplanes.

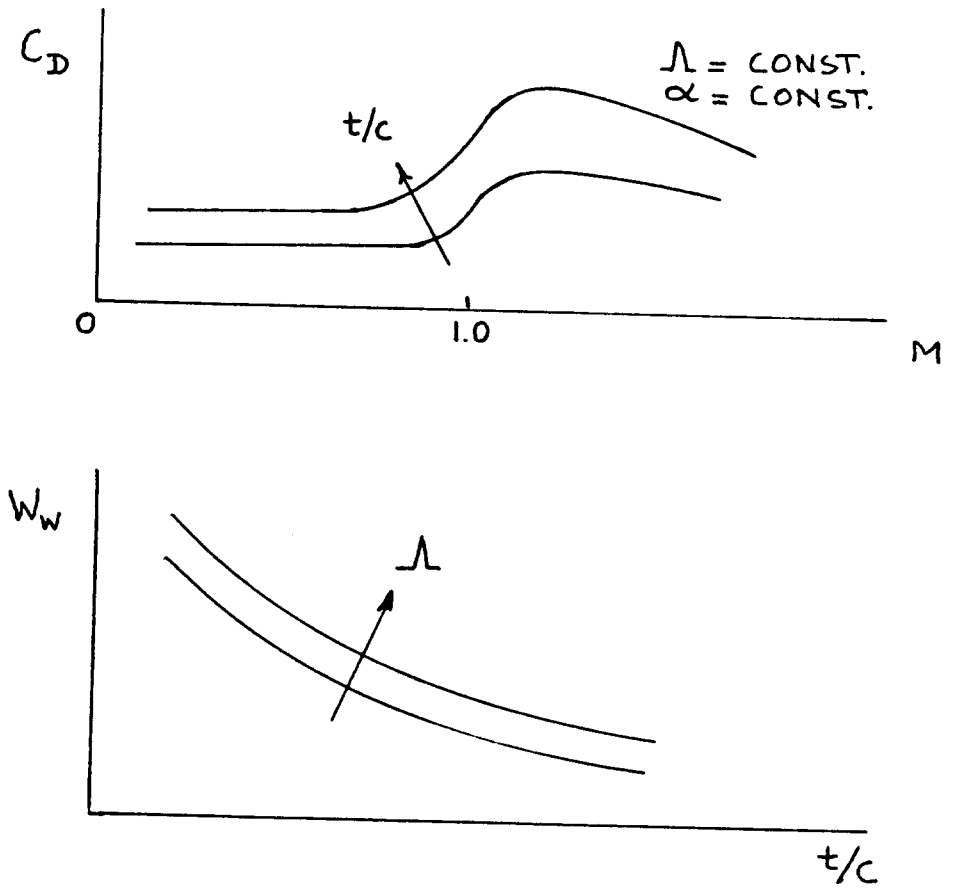

Figure 4.19 Effect of Thickness Ratio on Compressibility Drag and on Wing Weight

Table 4.8 Summary of the Effect of Thickness

Item	Effect of Thickness	
	Low t/c	High t/c
Wing weight	High	Low
Wing drag: subsonic	Low	High
supersonic	Acceptable	Very high
Wing fuel volume	Poor	Good
Maximum lift	Poor	Good
		Up to 12-14 percent depends on airfoil

4.1.8 Wing Taper Ratio: Large or Small?

Wing taper ratio: $\lambda = c_t/c_r$, tends to affect primarily the following items:

1. Weight 2. Tip stall 3. Fuel volume 4. Cost

1. Weight: Because wing lift distributions tend to zero at the wing tip the area near the tip of a wing is not very effective. A wing with $\lambda = 1$ will therefore 'waste' area and because of that weigh more than a wing with a smaller taper ratio.

2. Tip stall: Wings with small taper ratios tend to have small tip chords. This implies lower tip Reynold's numbers and therefore lower maximum lift coefficients. This is conducive to tip stall. An extreme example is a delta wing. Decreasing taper ratio also shifts the spanload distribution outboard : see Figure 4.20. This further aggravates tip stall.

3. Fuel volume: Large taper ratios mean more fuel volume. Eqn.(6.3) of Part II shows this effect.

4. Cost: Straight, untapered wings (no sweep, constant thickness ratio and $\lambda = 1.0$) allow for common wing ribs. This tends to lower manufacturing cost. Several light airplanes employ such wings as seen in Figures 3.4d and 3.6b,c in Part II.

Note: any value of taper ratio different from 1.0 will eliminate this advantage.

The reader may wonder if anyone has ever tried to build a wing with inverse taper? The answer is yes! An extreme example of such a wing is found in the Republic XF-91 Thunderceptor of Figure 4.21.

Reasons for using inverse taper (despite the wing weight penalty) were:

1. Improved tip stall. This was a real problem in early jet fighters. Stall protection by control-law algorithms did not exist at the time of the XF-91.

2. Improved cross sectional area distribution allowed the fuselage to be kept smaller, regaining some weight and drag.

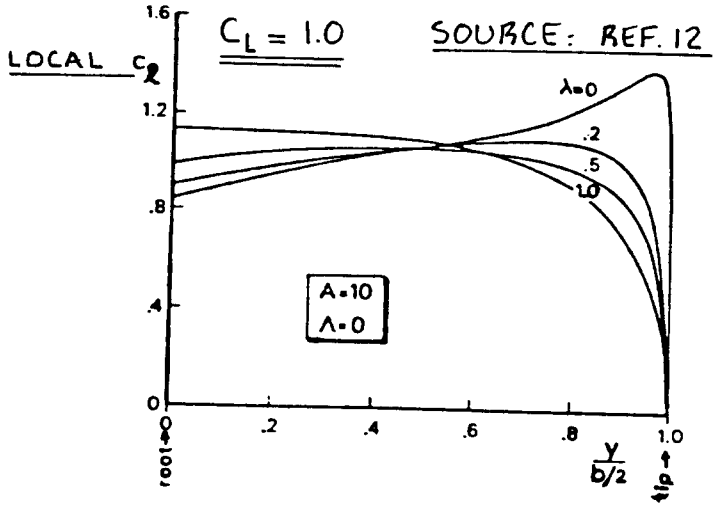

Figure 4.20 Effect of Taper Ratio on Span loading

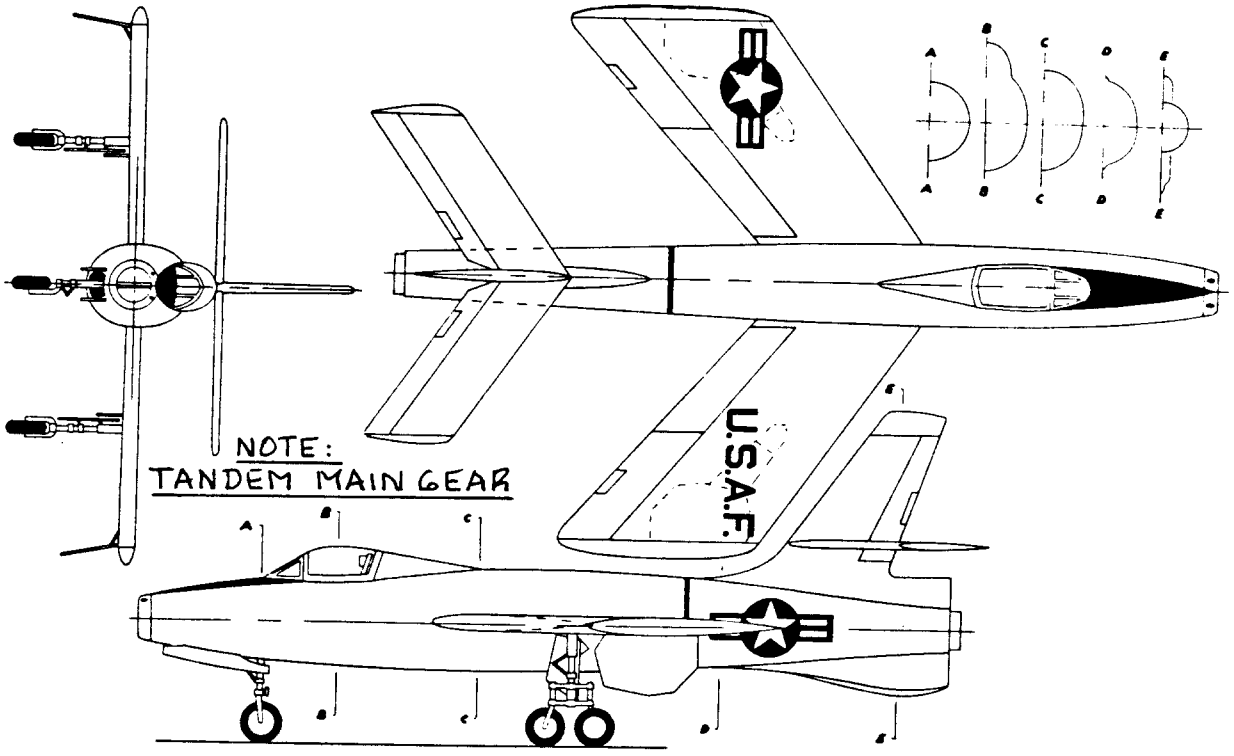

Figure 4.21 Republic XF-91 Thunderceptor: Example of an Inversely Tapered Wing

An interesting consequence of the inverse tapered wing was that the landing gear would no longer fit into the wing. To solve that problem the gear was configured as a tandem gear and retracted into the outboard wing. Note the large gear doors almost at the wingtips in Figure 4.21.

Other interesting features of the XF-91 were its variable incidence wing and its wing slats which gave it very good low speed characteristics. The XF-91 was the first USAF fighter to exceed Mach 1 on its first flight!

Table 4.9 summarizes the effect of wing taper ratio.

Tables 6.1 through 6.12 in Part II list values for wing taper ratio used in a wide range of airplanes.

4.1.9 Straight Taper or Variable Taper?

Wings with constant taper ratio are also called straight-tapered wings.

As the configuration drawings in Chapter 3 of Part II indicate, straight tapered wings are used in many airplanes. The taper ratio is then selected as a compromise between weight and good handling in the stall.

In many instance the use of 'broken' or 'curved' leading and trailing edge wings is advantageous. The following examples are offered:

1.) Cessna has been using planforms without taper inboard and straight taper outboard. Such wings have proved very effective in the low speed regime. Figures 3.5a and 3.5b in Part II are examples.

2.) In many transports, yehudis and or gloves are used in the inboard wing section. The reasons for this are:

a) to increase the root thickness which allows for a lighter wing.

b) to decrease the root thickness ratio which allows for higher drag divergence Mach number.

c) to increase the leading edge sweep angle at the root which allows for higher drag divergence Mach number (glove).

d) to create room behind the wing spar for the moun-

Table 4.9 Summary of the Effect of Taper Ratio

Item	Effect of Taper Ratio	
	High	Low
Wing weight	High	Low
Tipstall	Good	Poor
Wing fuel volume	Good	Poor

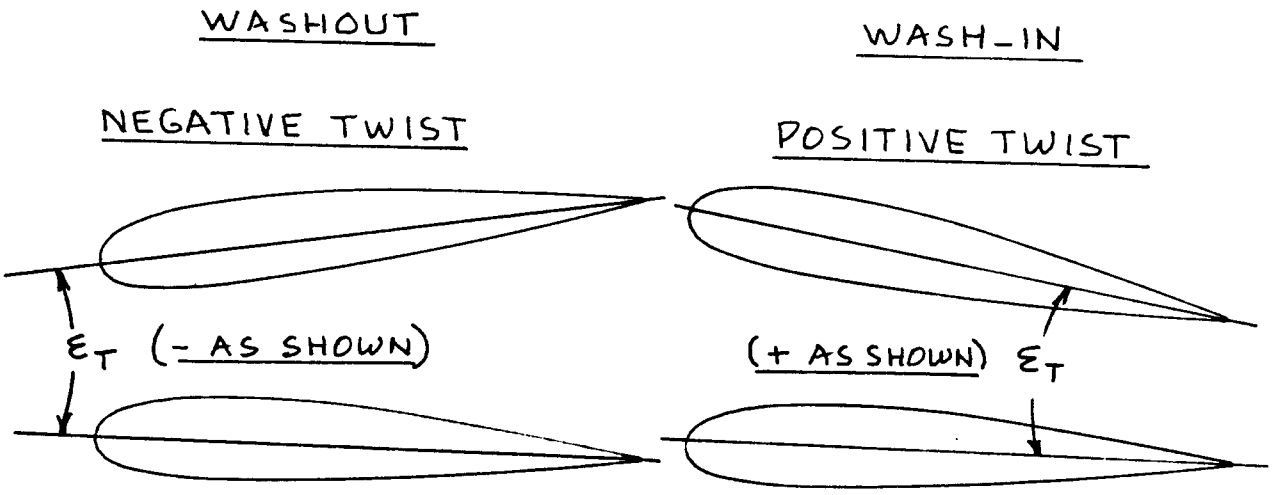

Figure 4.22 Definition of Wing Twist

Table 4.10 Summary of the Effect of Twist

Item	Effect of Twist Angle (Washout)	
	Large	Small
Induced drag	High	Small
Tipstall	good	poor
Wing weight	mildly lower	mildly higher

ting and retraction of the main landing gear. Gear retraction can thus be done without interfering with the flaps (yehudi).

Particularly Boeing has used the glove/yehudi combination with success: Figures 3.19 in Part II show examples.

4.1.10 Twist: How Much?

The wing twist angle affects primarily:

1. Wing tip stall 2. Induced drag 3. Wing weight

Figure 4.22 defines the wing twist angle ε_t: it is referred to as wing washout as drawn.

1. Wing tip stall: Many wings are designed with built-in twist so that the wing incidence angle actually decreases in the outboard direction. The reason for this is to delay tip stall. Tip stall is generally felt to be undesirable because it inevitably occurs in an asymmetrical manner causing serious roll control problems when approaching stall or when in a stall. Particularly aft swept wings must be twisted to prevent tip stall from happening.

2. Induced drag: A penalty which is caused by twist is an increase in induced drag. Forward swept wings (see 4.1.3) have an advantage in this regard since they can be built without twist.

In supersonic applications the use of conical camber was introduced on the F106 and B58 airplanes. The reason for this form of twist was a reduction in drag at high speed.

3. Weight: Washout as defined by Figure 4.22 tends to decrease the aerodynamic loading at the tip. This shifts the center of pressure inboard and results in a decrease in wing root bending moment. In turn this results in lower weight.

Table 4.10 summarizes the effect of twist.

Tables 6.1 through 6.12 in Part II contain typical values of wing incidence angles at the root and at the tip from which the twist angle (in case of linear twist distribution) may be deduced as:

$$\varepsilon_t = i_{w_{tip}} - i_{w_{root}} \qquad (4.10)$$

4.1.11 Wing Dihedral: How Much?

The choice of wing geometric dihedral affects the following characteristics:

1. Spiral stability
2. Dutch roll stability
3. Ground and water clearance

Figure 4.23 defines positive and negative dihedral.

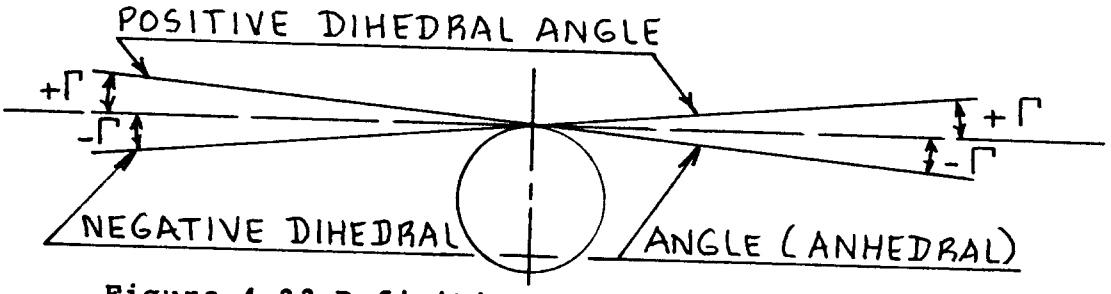

Figure 4.23 Definition of Wing Dihedral Angle

1. Spiral stability and 2. Dutch Roll Stability:

Positive wing geometric dihedral causes the rolling moment due to sideslip derivative, C_{l_β} to be negative.

This derivative in turn affects both spiral and dutch roll stability:

More negative C_{l_β} means more spiral stability but also less dutch roll stability! Reference 37 contains detailed discussions of these effects.

Airplanes must have a certain minimum amount of negative rolling moment due to sideslip: dihedral effect. This is needed to prevent excessive spiral instability. Too much dihedral effect tends to lower dutch roll damping.

High wing airplanes have inherent dihedral effect due to wing position while low wing airplanes tend to be deficient in inherent dihedral effect. For this reason low wing airplanes tend to have considerably greater geometric dihedral than high wing airplanes.

Swept wing airplanes tend to have too much dihedral effect due to sweep. This can be offset in high wing airplanes by giving the wing negative dihedral (anhedral). The BAe 146 of Figure 3.21d (Part II) is an example.

3. Ground and water clearance: Airplane wings, nacelles and/or propellers must have a minimum amount of ground and water clearance.

Chapter 9 in Part II presents the minimum ground clearance criteria for land based airplanes. For water based airplanes Reference 14 gives some indications of waterspray directions. Propellers and inlets should not be located in such areas.

In some airplanes positive or negative wing dihedral at the root is used for entirely different reasons. On the F4U Corsair fighter of WWII (See Figure 4.24) the reasons were: 1. low interference drag and 2. Propeller clearance with a reasonably short landing gear.

On the Piaggio 122-DL3 (See Figure 4.25) the reasons are: 1) low interference drag and 2) retain the wing of an earlier Piaggio amphibian which needed the large positive root dihedral to keep the propellers away from water spray during take-off.

In airplanes with highly elastic wings (B52, B747) the elastic deformation of the wing in flight creates extra geometric dihedral. This must be accounted for in the design of such airplanes.

Table 4.11 summarizes the effect of wing dihedral.

Tables 6.1 through 6.12 in Part II provide numerical data on wing dihedral angles used in a wide range of airplanes.

4.1.12 Wing Incidence on the Fuselage: How Much?

The following factors affect the decision of wing incidence angle relative to the fuselage:

1. Cruise drag
2. Floor attitude in cruise
3. Landing gear configuration

Figure 4.26 gives a definition of wing incidence angle, i_w.

1. Cruise drag: If i_w is made too large, the fuselage will 'cruise' nose down thereby probably increasing drag. The opposite is true as well.

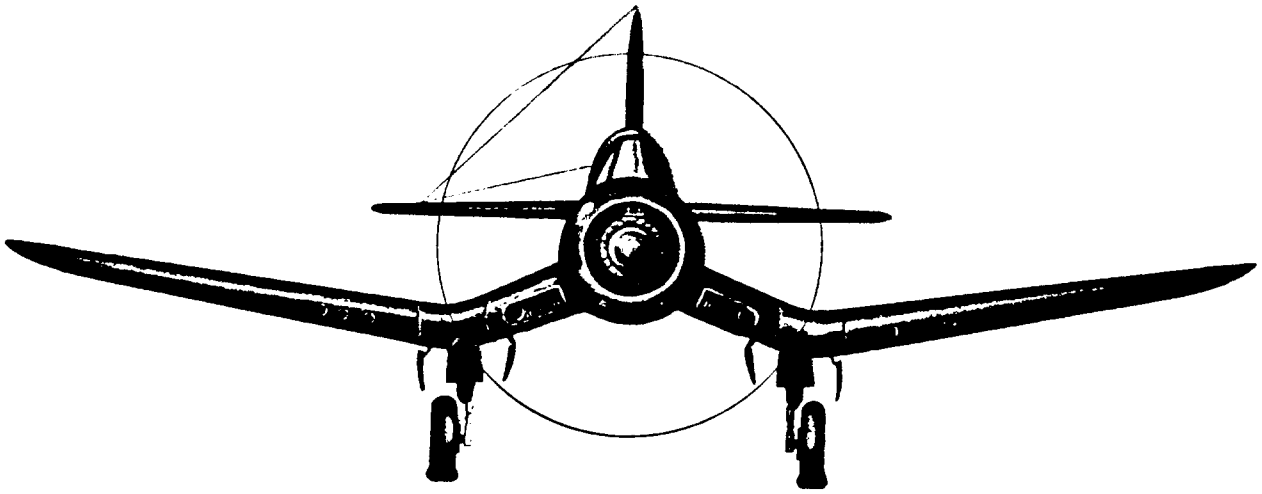

Figure 4.24 Vought F4U Corsair: Example of a Wing with Root Anhedral and Tip Dihedral

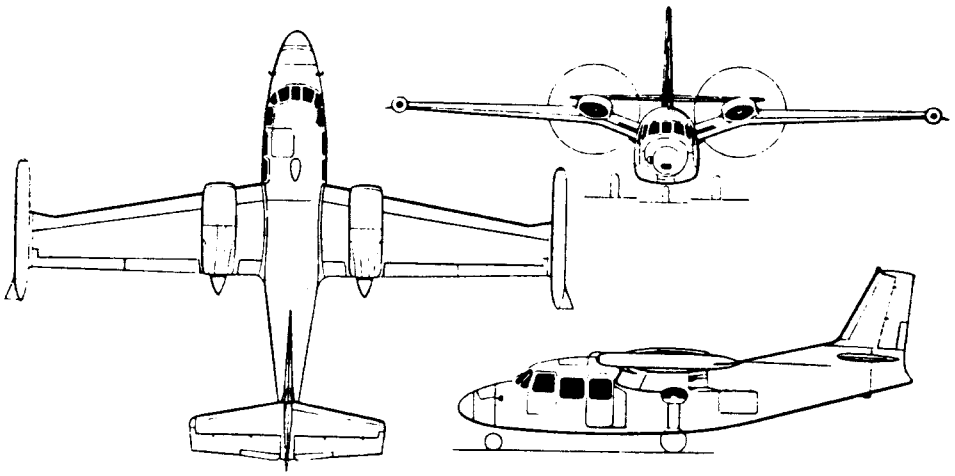

Figure 4.25 Piaggio P166-BL2: Example of a Wing with Root Dihedral and Tip Anhedral

Table 4.11 Summary of the Effect of Wing Dihedral Angle

Item	Effect of Dihedral Angle	
	Positive	Negative
Spiral stability	Increased	Decreased
Dutch roll stability	Decreased	Increased
Ground clearance of wing, nacelle, propeller or landing gear	Increased	Decreased

2. Floor attitude in cruise: It is also evident from Figure 4.26 that the 'floor attitude' in cruise is influenced by the choice of i_w.

If the floor attitude in cruise differs too much from horizontal it will be difficult for people to walk. Pushing beverage service carts through the aisles may also become a problem. In cruise, floor levels should not be greater than +/- 2 degrees.

The following equation may be used to determine a preliminary value for i_w:

$$i_w = (C_{L_{cr}})/C_{L_\alpha} + (d\alpha_{o_L}/d\varepsilon_t)\varepsilon_t + \alpha_{o_L} \qquad (4.11)$$

The cruise lift coefficient, $C_{L_{cr}}$ is assumed to be the lift coefficient for which the floor is supposed to be level.

The derivative $d\alpha_{o_L}/d\varepsilon_t$ may be taken as 0.4 for straight tapered wings with linear twist distribution.

Wing incidence angle can be made variable if both low cruise drag and good forward visibility in the approach mandate it. Examples are the Vought F-8 and the Republic XF-91.

In canard airplanes the relative selection of canard and wing incidence (after airfoils have been decided upon) is of great importance to the stall characteristics of the wing. Wing bending moment distribution due to canard vortex interference is another important consideration in selecting wing incidence.

3. Landing gear configuration: If a tandem landing gear is required (for example: because of a requirement for an uninterrupted bomb bay) the wing must have enough incidence so that the airplane can lift off without rotation. The Boeing B52 of Figure 4.27 is an example of this.

Table 4.12 summarizes the effect of wing incidence angle.

Tables 6.1 through 6.12 contain numerical data in wing incidence angles used on a wide range of airplanes.

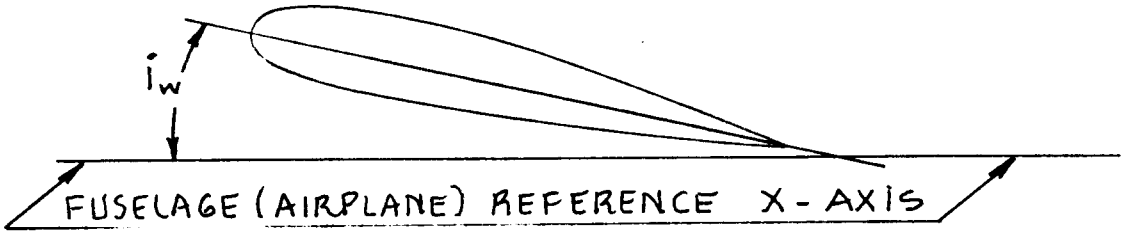

Figure 4.26 Definition of Wing Incidence Angle

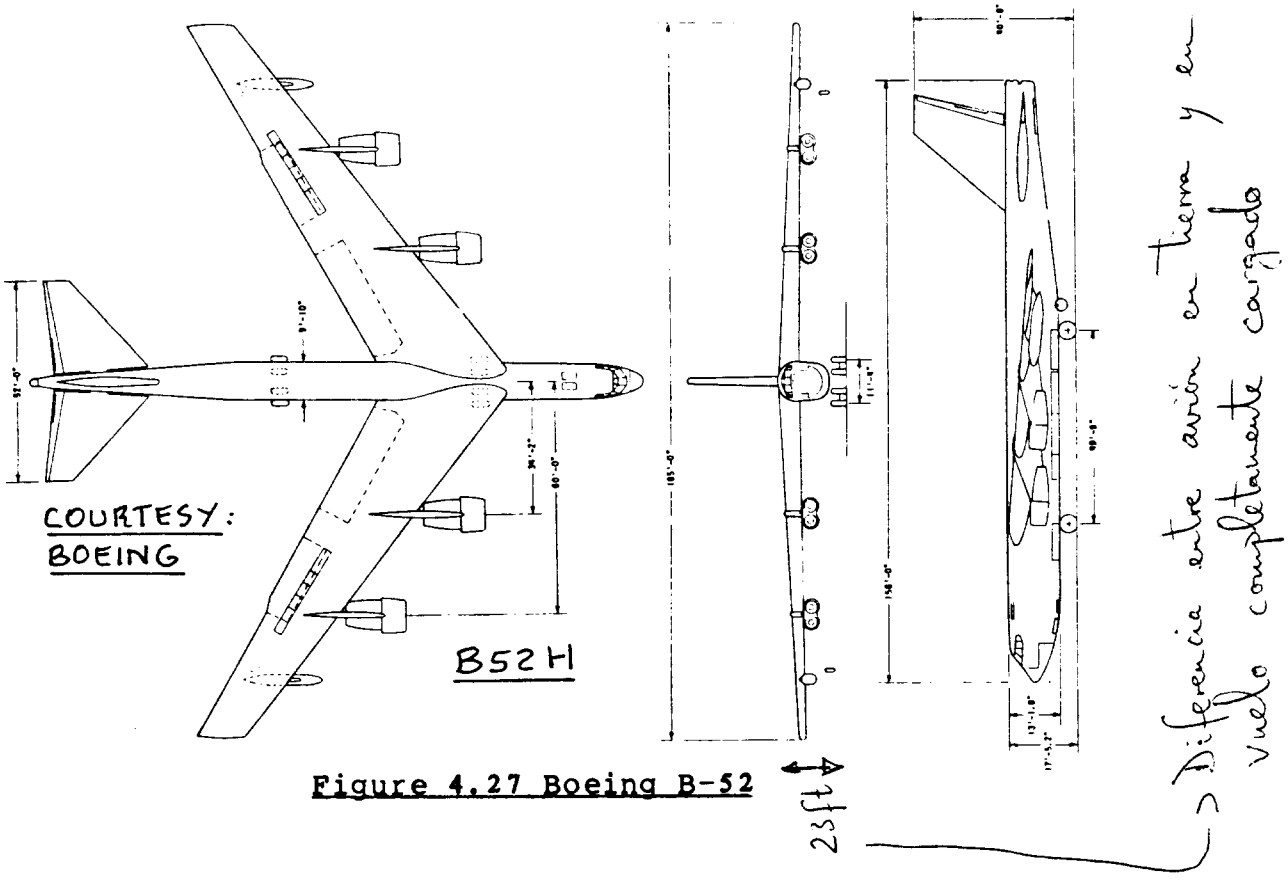

Figure 4.27 Boeing B-52

Table 4.12 Summary of the Effect of Wing Incidence Angle

Item	Large i_w	Small i_w
Cruise drag	High	Low
Cockpit visibility	Good	Watch out
Landing attitude in terms of nose gear hitting runway first	Watch out	No problem

4.1.13 Variable Camber (MAW = Mission Adaptive Wing)?

Birds have the ability to vary wing camber in flight in a more or less continuous manner. The advantage of this is the ability to adjust maximum lift and drag almost at will.

Wings with leading and trailing edge devices come close to this albeit for low speed flight only: the flap-placard speed inhibits operation at higher speed. Recent flight tests on an F111 with a Boeing designed variable camber wing (MAW) indicate that fighter maneuvering ability can be significantly enhanced by such a feature. The price is: weight and complexity (cost).

Figure 4.28 illustrates the MAW concept for the wing trailing edge as used in the F111 test program. The leading edge employs a similar system.

Another example of in-flight variable camber is found in the maneuvering flaps used in the Grumman X-29 (Figure 3.46, Part II).

4.1.14 Leading Edge Strakes (Lexes)

By using highly swept relatively sharp leading edge strakes (also called lexes) significant increases in lift at moderate to high angles of attack can be obtained.

The F18 and SR71 are examples of such strakes: see Figures 4.29 and 4.30. Figure 4.31 shows the additional vortex lift which can be obtained from very highly swept lifting surfaces. Lexes in fact are very highly swept lifting surfaces. Reference 36 provides data and theoretical discussions of vortex lift and vortex bursting.

A major design problem is to determine what happens to the strake/body generated vortices as they proceed downstream. If they envelop the vertical tail while still intact, they can enhance directional stability, a synergistic effect. If however, they burst before getting to the vertical tail, they can induce significant structural oscillations and lead to early fatigue problems.

The separation and bursting behavior of vortices shed from slender fuselages and/or strakes can also lead to the so-called wing-rock phenomenon. A modern theory for predicting this phenomenon is given in Reference 38.

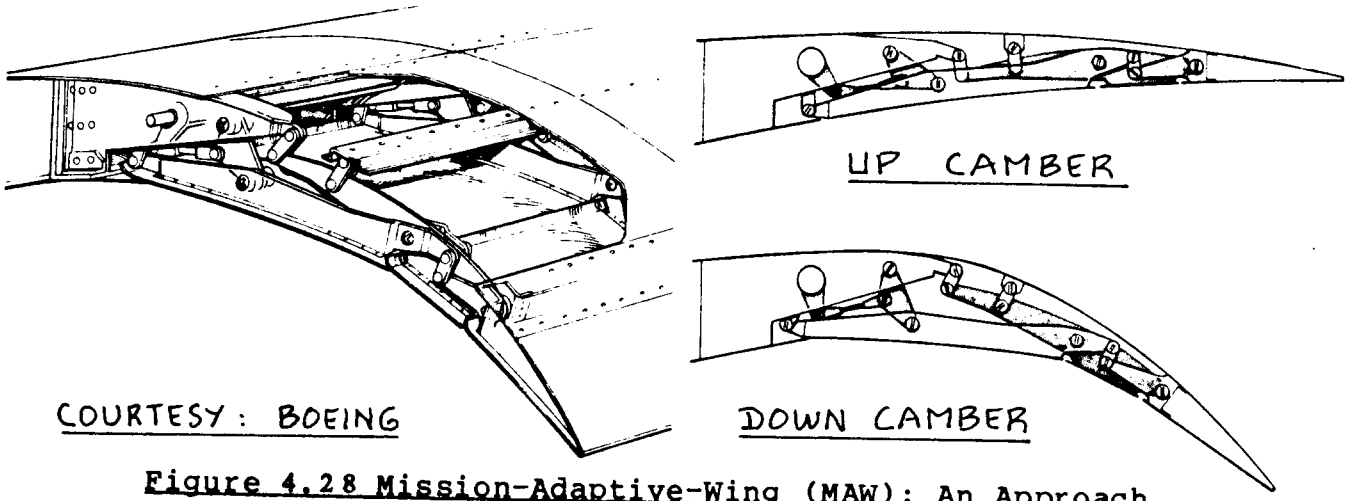

Figure 4.28 Mission-Adaptive-Wing (MAW): An Approach to Continuous Variable Camber

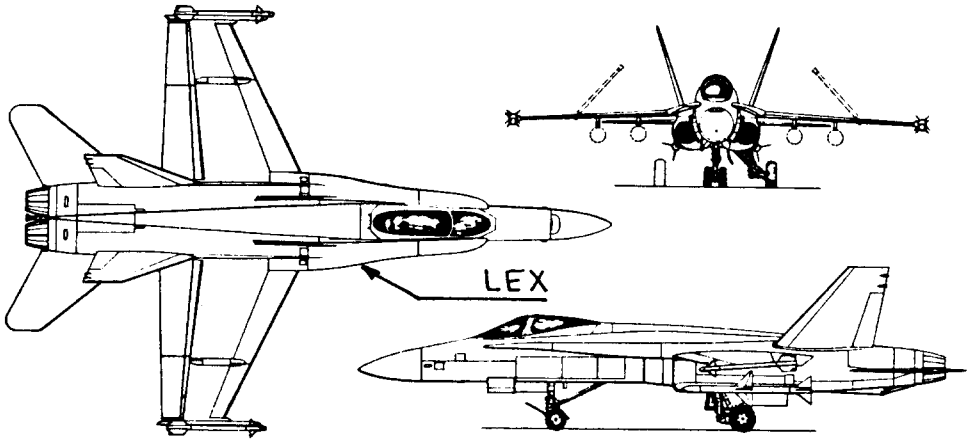

Figure 4.29 F-18: Example of Leading Edge Strakes

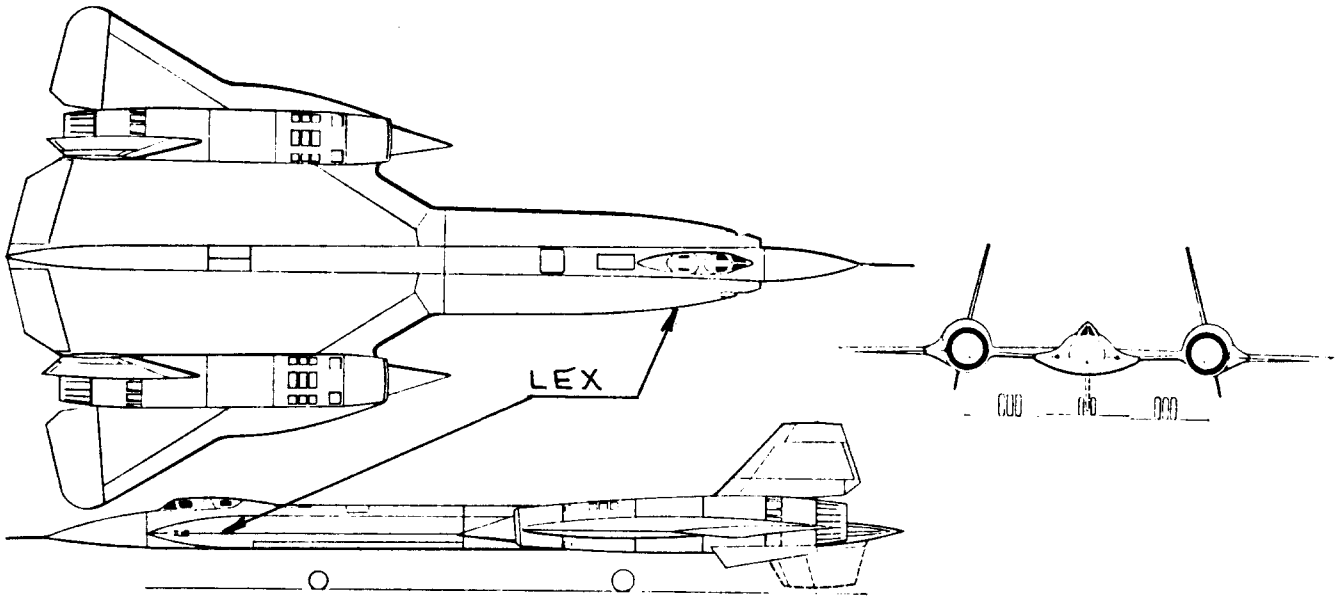

Figure 4.30 YF12A: Example of Leading Edge Strakes

4.1.15 Planform Tailoring: Why and How?

Many airplanes end up with significant planform irregularities: broken and/or curved leading edges, large fences, snags and leading edge droop and/or extensions. Examples of such planform tailoring are shown in Figures 4.32 through 4.35.

Some reasons for using planform tailoring are:

1. Stall behavior 2. Spin and/or stall entry/recovery behavior 3. Pitching moment behavior at high Mach 4. Aileron buzz 5. Aeroelastic behavior

The reasons for inboard leading edge and for trailing edge extensions were already discussed in Sub-section 4.1.9.

To improve the stall behavior of a wing (i.e. delay stall to a higher angle of attack and/or make the ensuiing recovery more gentle) leading edge extensions and/or droop may be used. See Figure 4.32.

Leading edge snags and stall fences have been used in many airplanes as 'aerodynamic afterthoughts' or 'fixes' of problems ranging from high Mach pitching moment to low speed stall behavior. Figures 4.33 and Figure 4.23 (Part II) show examples.

Aileron buzz can occur if the wing sections at the aileron stations develop shocks close to the aileron hingeline. If the aileron is cable controlled (eleastic element) the aileron can develop a severe vibration which is known as aileron buzz. Such problems can be relieved by leading edge extensions (lower t/c and thus delayed shock formation) and sometimes by a row of vortex generators (Learjet 25).

At high subsonic speeds transport and bomber wings tend to develop significant aeroelastic behavior: aft swept wings 'unload' themselves outboard and forward swept wings do just the opposite. These effects can be lessened by assuring that the loci of aerodynamic centers and the elastic axis coincide. If that is achieved, aeroelastic deformations are minimized. The Handley Page Victor (Fig.4.34) uses such a (aero-isoclinic) wing. A remarkable aspect of this wing is that it was developed without the help of digital computers!!

Observe the so-called Küchemann bodies mounted midspan at the trailing edge of the wing. These bodies

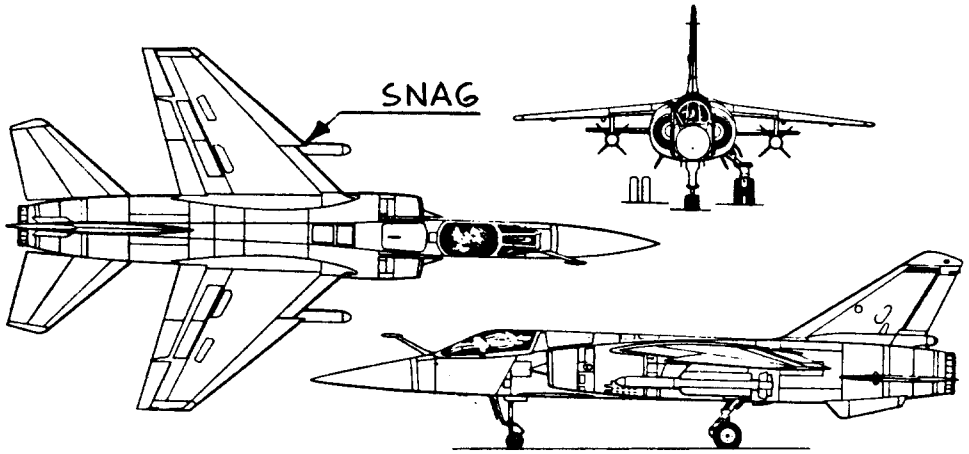

Figure 4.33 Example of Leading Edge Snags: Mirage F1-C

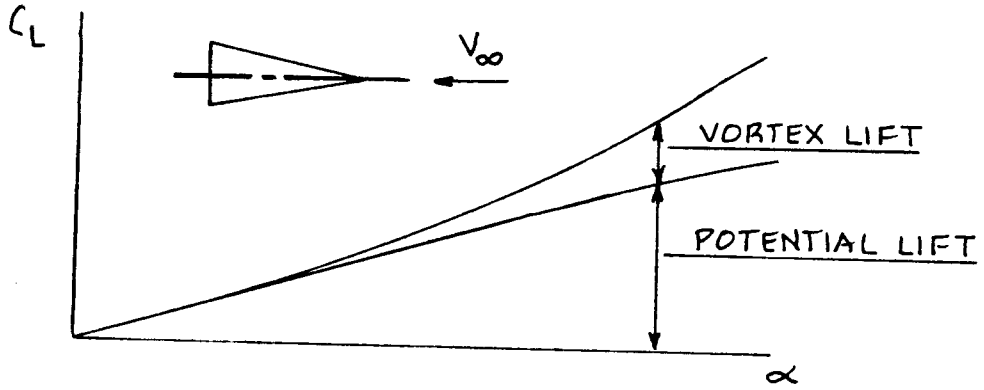

Figure 4.31 Vortex Lift Compared with Potential Lift

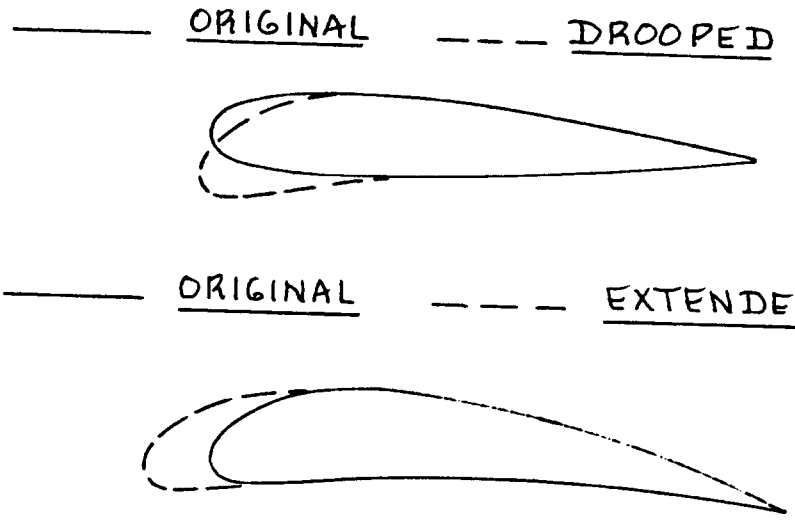

Figure 4.32 Leading Edge Droop and Leading Edge Extension

delay critical Mach number through local area ruling. Several Soviet airplanes also employ these Küchemann bodies to retract the main landing gear.

Figure 4.35 shows another example of significant leading edge tailoring in a high subsonic jet bomber, the AVRoe Vulcan.

Several supersonic airplanes employ leading edge tailoring to achieve the proper balance between acceptable subsonic and supersonic performance. The Concorde of Figure 3.35d (Part II) is an interesting example.

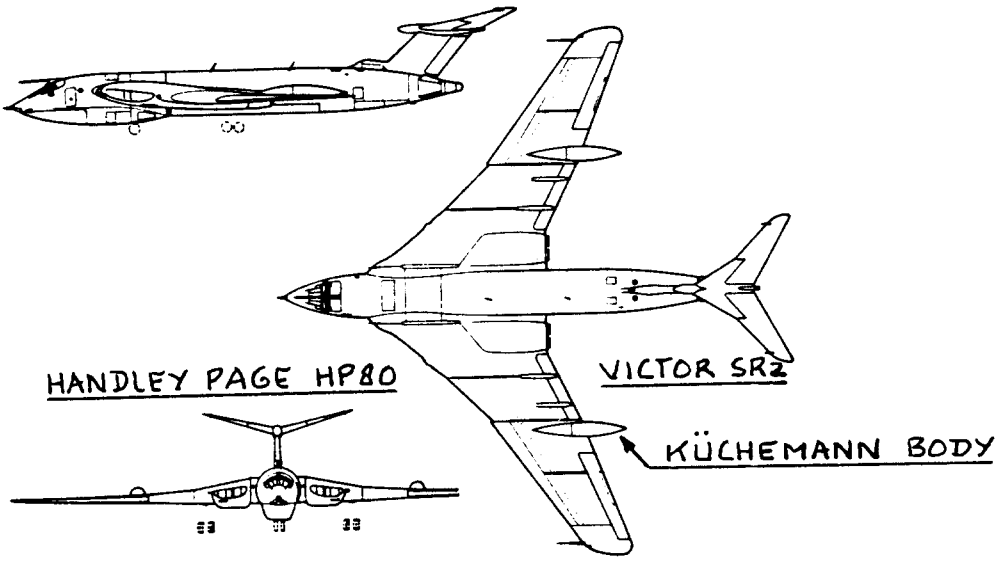

Figure 4.34 Example of Planform Tailoring: HP-Victor

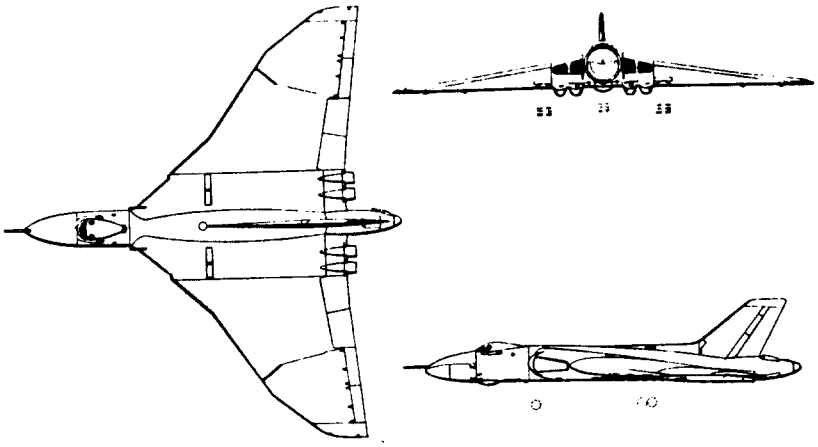

Figure 4.35 Example of Planform Tailoring: AVRoe Vulcan

4.1.16 Area Ruling: When is it Required?

Area ruling is required in those Mach ranges where the drag due to compressibility becomes unacceptably high. Figure 4.36 shows some early experimental results obtained by Whitcomb (Ref.39): with area ruling a large reduction in wave drag can be obtained.

Area ruling has also been succesfully applied in the local sense as follows:

1. Tiptank area ruling (F5)
2. Wing/nacelle arear ruling (737 and GP180)

For further discussions of the area rule concept the reader should consult Part VI and Refs 13, 29 and 36.

An interesting observation is that a swept forward wing 'integrates' much smoother into a wing/fuselage combination than a swept aft wing. Figure 4.37 illustrates this point.

4.1.17 Wing Span: When is it Too Large?

For a given wing area, increasing span means increased aspect ratio. The effect of aspect ratio was discussed in Sub-sections 4.1.1 and 4.1.6. Non-aerodynamic constraints may prevent the use of wing spans beyond some specific value. Examples of such constraints are:

1. Aircraft carrier space limitations: This may result in the need to 'fold' wings or to limit the span.

2. Hangar width limitations: If building larger hangars is not justified by aerodynamic efficiencies from increased span, this may be an important constraint.

3. Gate space limitations: If the investment in a change in the terminal/gate infra-structure is too high, this may lead to span limitations. In such a case winglets may be used instead of physical span increases of a wing. The Boeing 747-400 is an example case! The possibility of wing-tip folding may also have to be considered at some point in the future.

4. Cartwheeling: Very large spans can lead to 'cartwheeling' accidents while making S-turns close to the ground. An example of an airplane with a very large wing span was the Hurel-Dubois 321 shown in Figure 4.38. The wing span of this airplane was 148.5 ft with an aspect ratio of 20.2!

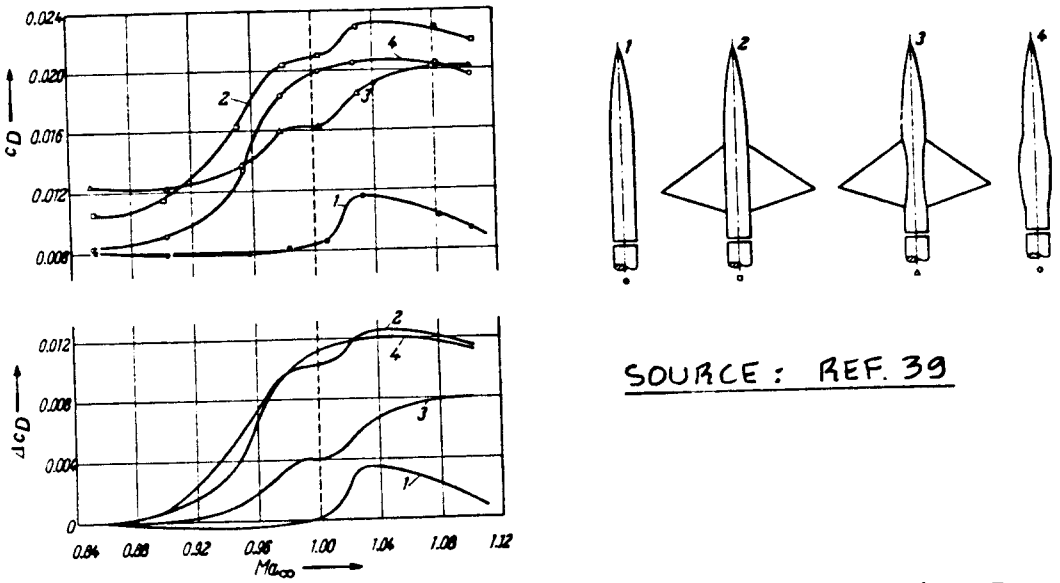

SOURCE: REF. 39

Figure 4.36 Effect of Area Ruling on Compressibility Drag

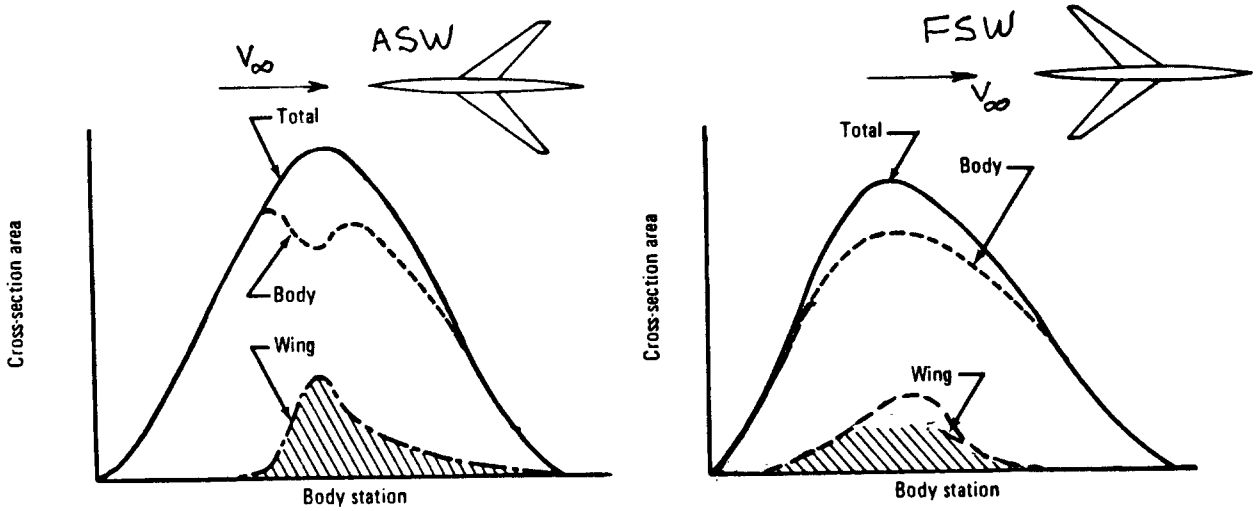

Figure 4.37 Comparison of Fuselage Area Ruling for Aft and Forward Swept Wings

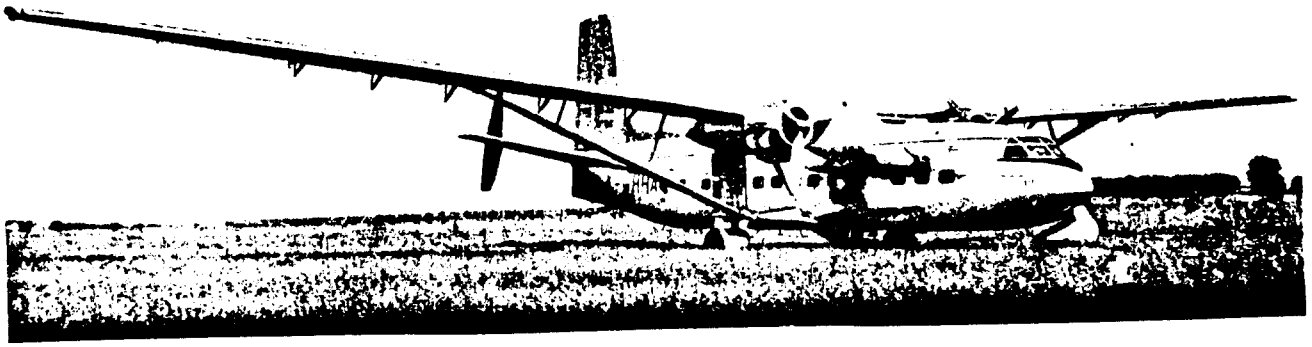

Figure 4.38 Example of a Very Large Span Wing: HD-321

4.1.18 Aerodynamic Coupling

Aerodynamic coupling is the intentionally adding of a closely coupled lifting surface forward of the wing. Figure 4.39 illustrates the vortex coupling which can occur between a wing and a closely coupled canard. This principle was used first on the SAAB 37 Viggen fighter airplane. Figure 4.40 shows the potential effect of this type of coupling on airplane lift-curve characteristics.

4.1.19 Flaps: What Size and Which Type?

The following factors affect the decision of wing flap size and type:

1. High lift requirements
2. Trim considerations
3. Drag considerations
4. Cost, complexity and maintenance.

1. High lift requirements: Figure 4.41 reviews typical values of wing maximum lift coefficients achievable with different types of flaps for an unswept wing with A=6.

Figure 4.42 shows values of maximum lift coefficients achievable with swept wings.

The reader is reminded that required values of overall airplane (trimmed) maximum lift coefficients were obtained from the performance sizing calculations described in Part I. Class I methods for sizing the required flaps were presented in Chapter 7 of Part II. Part VI contains methods for 'fine-tuning' the required flaps.

2. Trim considerations: Flaps cause significant changes in pitching moment. There are two sources for these pitching moments:

1. The pitching moments induced by flap camber.

2. Pitching moments induced by downwash changes on a horizontal tail and/or by upwash on a canard.

To 'trim' out these flap induced pitching moments considerable down loads may be required on a horizontal tail. Similarly, considerable uploads may be required on a canard. The resulting 'trimmed' maximum lift coefficient is usually less than the maximum lift coefficient generated by the flapped wing in a

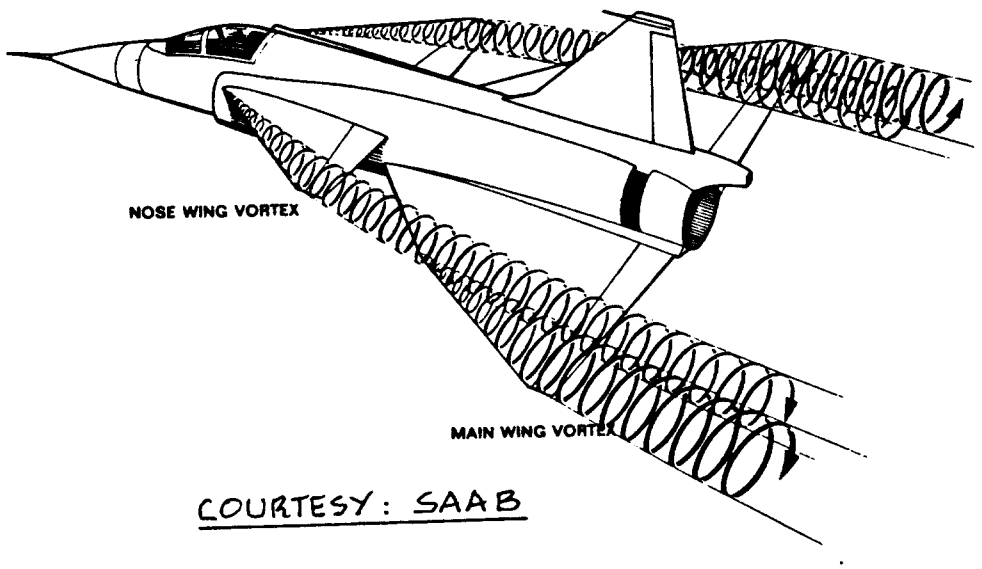

Figure 4.39 Aerodynamic Coupling Between a Wing and a Canard on the SAAB 37 Viggen

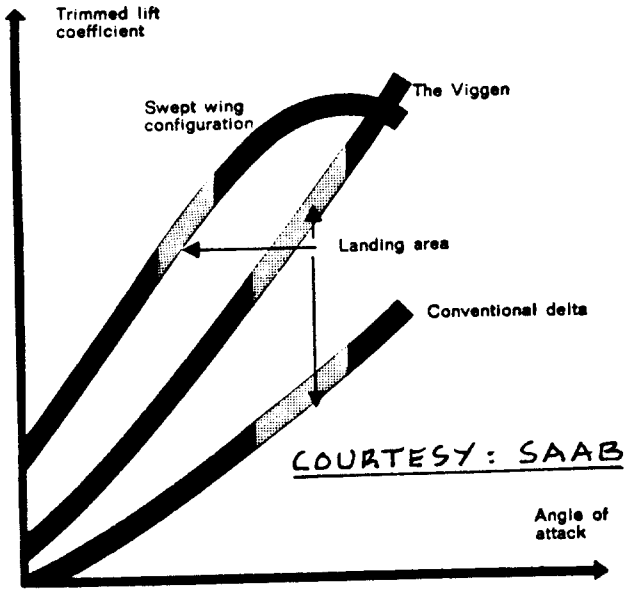

Figure 4.40 Effect of Canard/Wing Coupling on Lift

conventional configuration. In a canard configuration the potential exists for an increase in 'trimmed' maximumt lift coefficient. Interference of the canard tip vortex system with the wing may alter this conclusion!

The reader should be aware that from a performance viewpoint, the only maximum lift coefficient which is of practical interest is the 'trimmed' maximum lift coefficient. Conventional configurations are normally critical at forward c.g. while canard configurations tend to be critical at aft c.g.

For detailed information on lift, drag and pitching moments associated with flaps, see Refs 15, 40 and 41.

Reference 37 contains detailed discussions of airplane trim diagrams. Part VI contains methods for constructing trim diagrams for new designs.

3. Drag considerations: Flap deployment always results in an increase in drag. An important design consideration in the selection of a flap system is the flaps-down lift-to-drag ratio in an engine out climb. Part I addressed this problem by presenting a rapid method for determining thrust/power to weight ratios needed to satisfy engine out climb requirements. The drag estimates used in those sizing methods were very preliminary in nature (Class I). More accurate methods for estimation of drag due to flaps are given in Part VI.

4. Cost, complexity and maintenance: As a general rule of thumb, the higher the trimmed value of maximum lift coefficient with the flaps down, the greater the complexity, the maintenance requirements and therefore the cost. By careful attention to the detail mechanical design of the flaps and the associated systems, cost can be kept within acceptable limits. The Boeing 727 still is an outstanding example of a highly complex yet reliable and maintainable flap system.

Section 4.2 presents examples of a number of flap mechanizations.

4.1.20 Lateral Controls: Type, Size and Location?

The following types of wing mounted lateral control device are prevalent today:

1. Ailerons
2. Spoilers

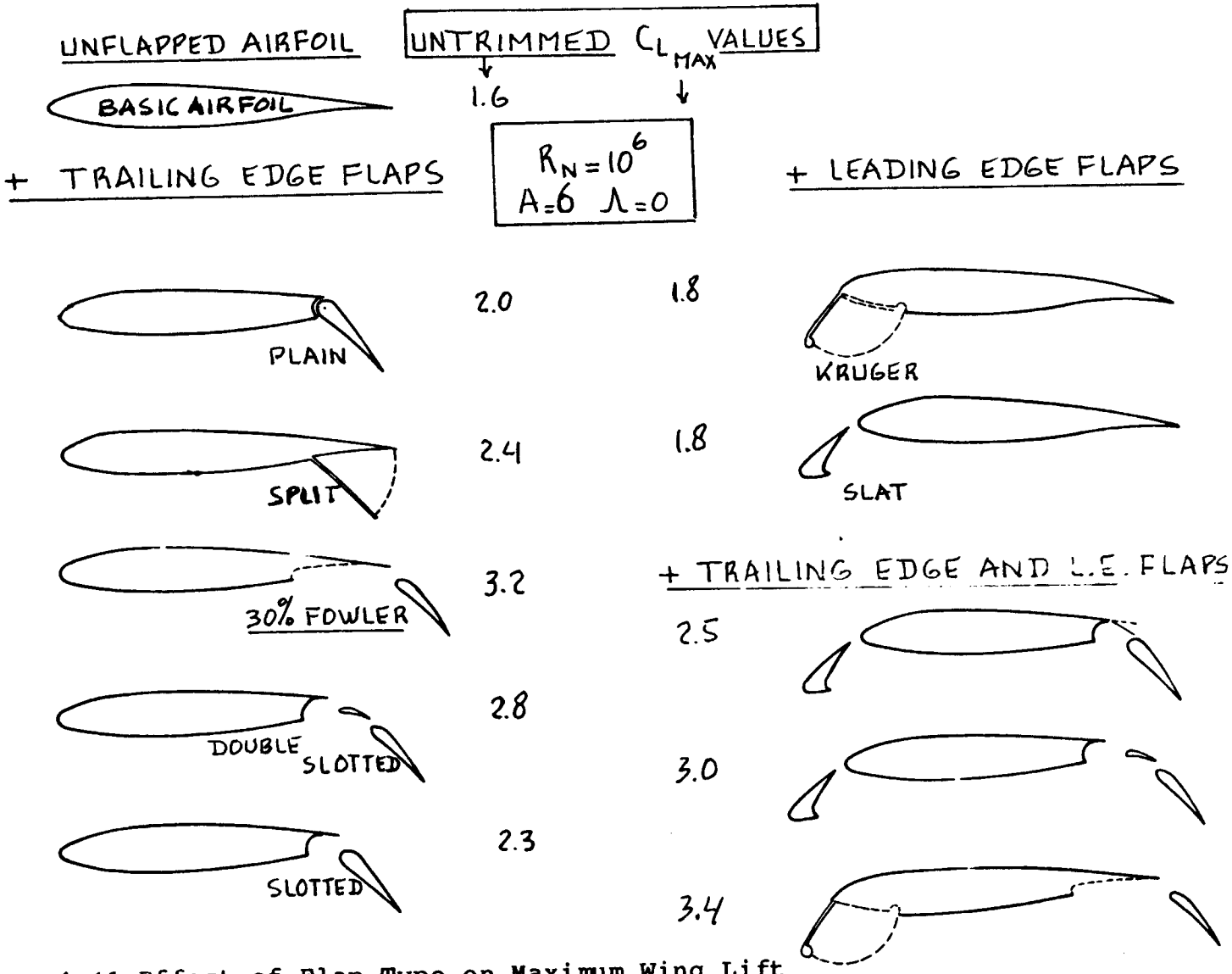

Figure 4.41 Effect of Flap Type on Maximum Wing Lift Coefficient for an Unswept, A=6 Wing

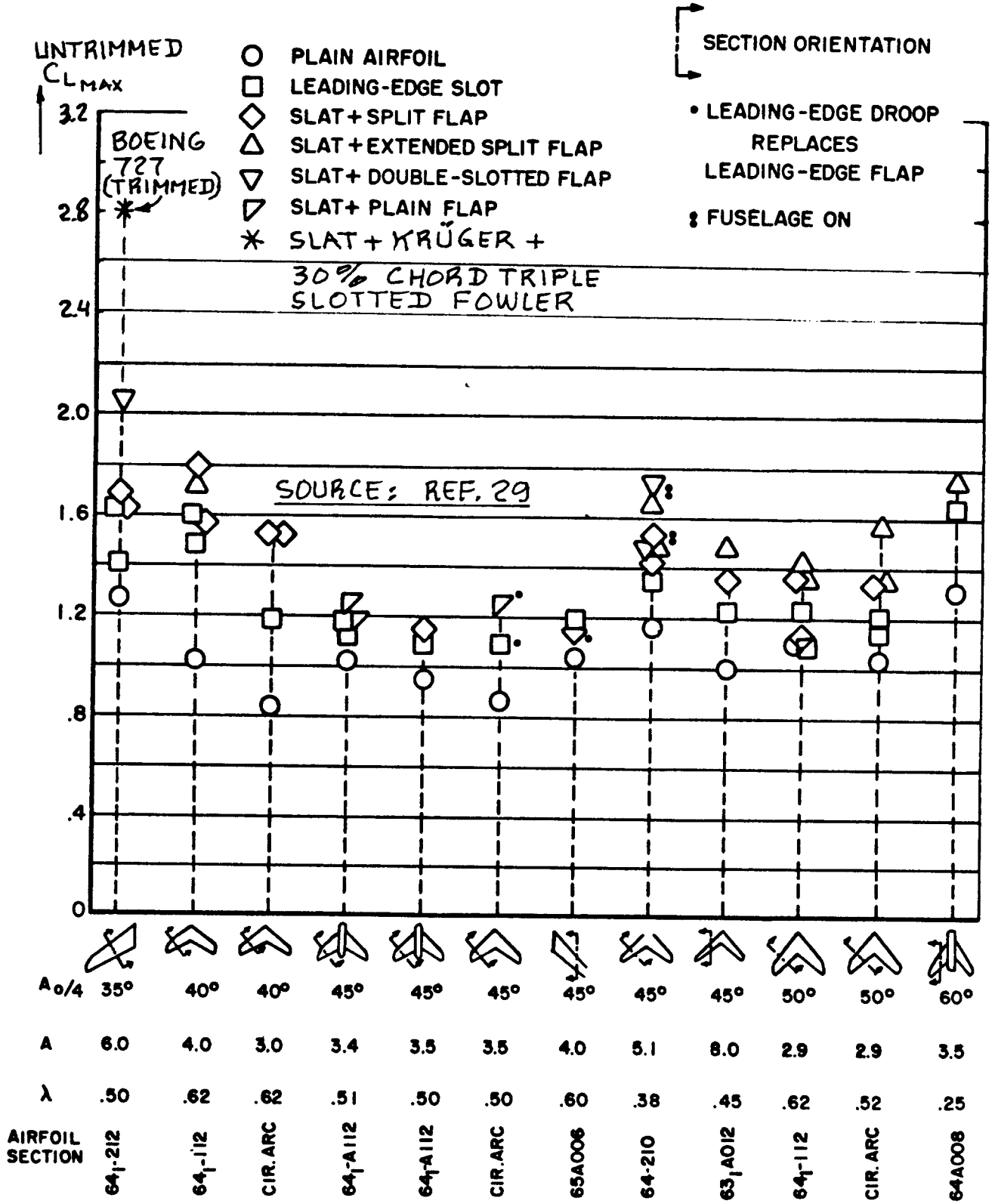

Figure 4.42 Effect of Aspect Ratio, Sweep Angle and Flap Type on Wing Maximum Lift Coefficient

Most airplanes use wing mounted ailerons and/or spoilers for lateral control. The reason is to take advantage of the largest possible moment arm. Fighter airplanes and some military trainers use differential stabilizers to enhance their lateral control effectiveness.

Tables 8.1 through 8.12 in Part II contain data for aileron and spoiler sizes and locations employed on a wide range of airplanes. More detailed methods for sizing of lateral controls may be found in Part VI and Part VII.

1. Ailerons: Ailerons are 'plain' flaps mounted close to the wing tips for lateral control. They loose effectiveness at high angles of attack. They create a negative yawing moment, called adverse yaw. The magnitude of adverse yaw may be decreased by the application of 'differential' aileron controls (See Figure 4.43) or by the use of so-called Frise ailerons (See Figure 4.44).

When ailerons are used on swept aft wing airplanes they loose effectiveness at high dynamic pressures because of a phenomenon called 'aileron reversal. This aeroelastic phenomenon can be so severe that outboard ailerons must be 'locked-in-place' in some airplanes : Boeing 707, 727, 747.

At very high sweep angles ailerons loose effectiveness also because of the fact that the outboard flow over the top of the wing tends to become parallel to the aileron hinge line.

The English Electric Lightning fighter employed an interesting tip mounted aileron which neatly overcame the aerodynamic and aeroelastic degradations in effectiveness. Figure 4.45 shows the Lightning configuration.

2. Spoilers: Spoilers literally 'spoil' the lift over the part of the surface immediately behind the spoiler. Figure 4.46 illustrates the effect. Spoilers are extremely effective with flaps down. Most high speed airplanes use spoilers for roll control at high speed and a combination of ailerons and spoilers at low speed.

Spoilers generate a positive yawing moment: proverse yaw. Proverse yaw is to be preferred over adverse yaw. However, too much proverse yaw is also disliked by pilots.

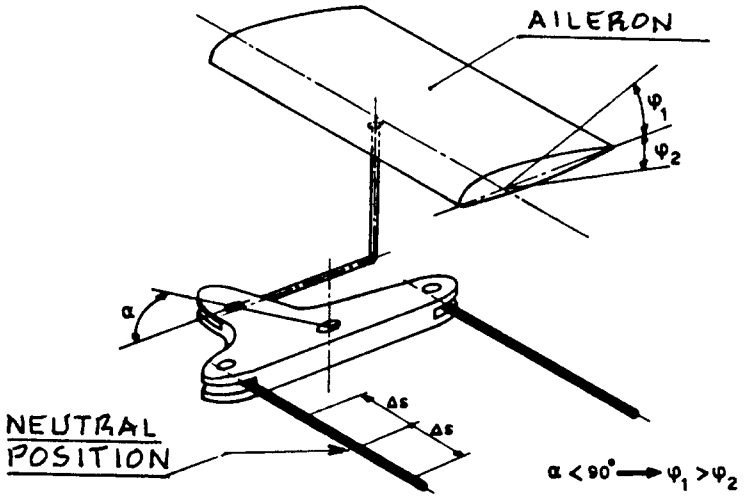

Figure 4.43 Example of Differential Aileron Control

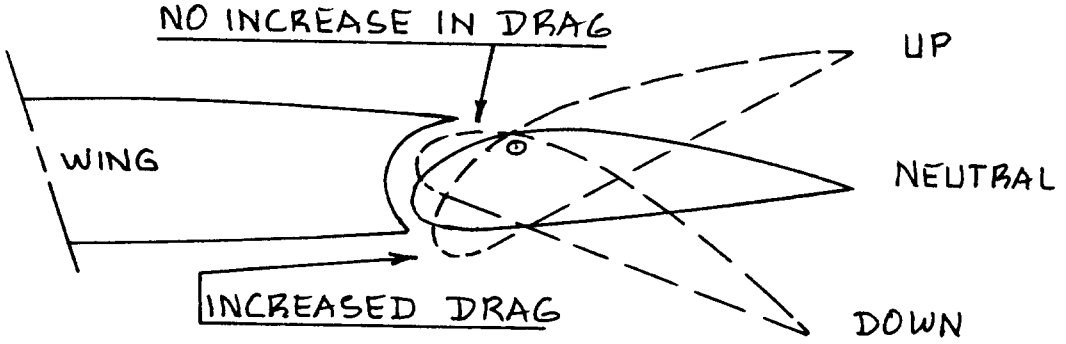

Figure 4.44 Example of Frise Ailerons

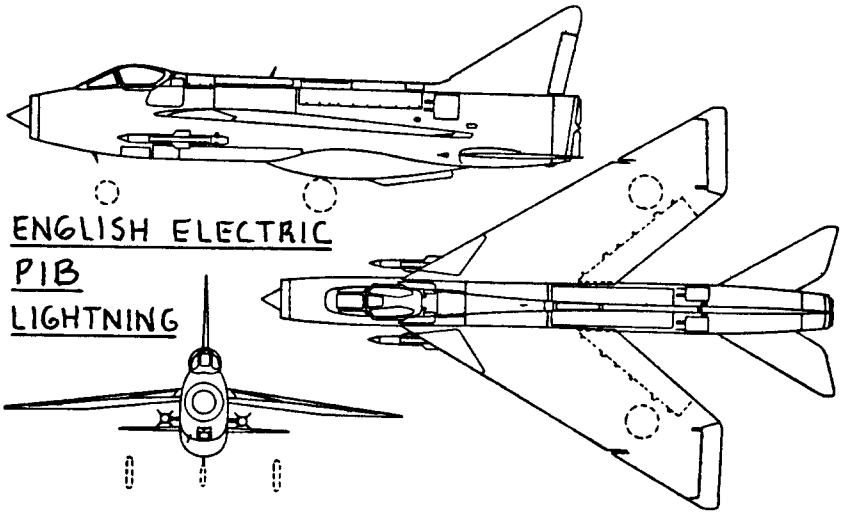

Figure 4.45 Example of Tip Mounted Ailerons

Because spoilers separate the airflow they also cause drag. For this reason it is not a good idea to use spoilers alone when flying on autopilot through turbulent air: drag is continually being 'integrated'. A better solution is to use a small inboard aileron (inboard to avoid aeroelastic effects) for moderate autopilot inputs. For large autopilot inputs a spoiler can be 'picked-up' after using say 15 degrees of the inboard aileron. This type of 'nonlinear' gearing of lateral controls is widely used on transports. Nearly all Boeing transports use this type of lateral control system.

Section 4.2 presents examples of wing mounted lateral control mechanizations.

Part VI contains methods for estimating lateral control effectiveness.

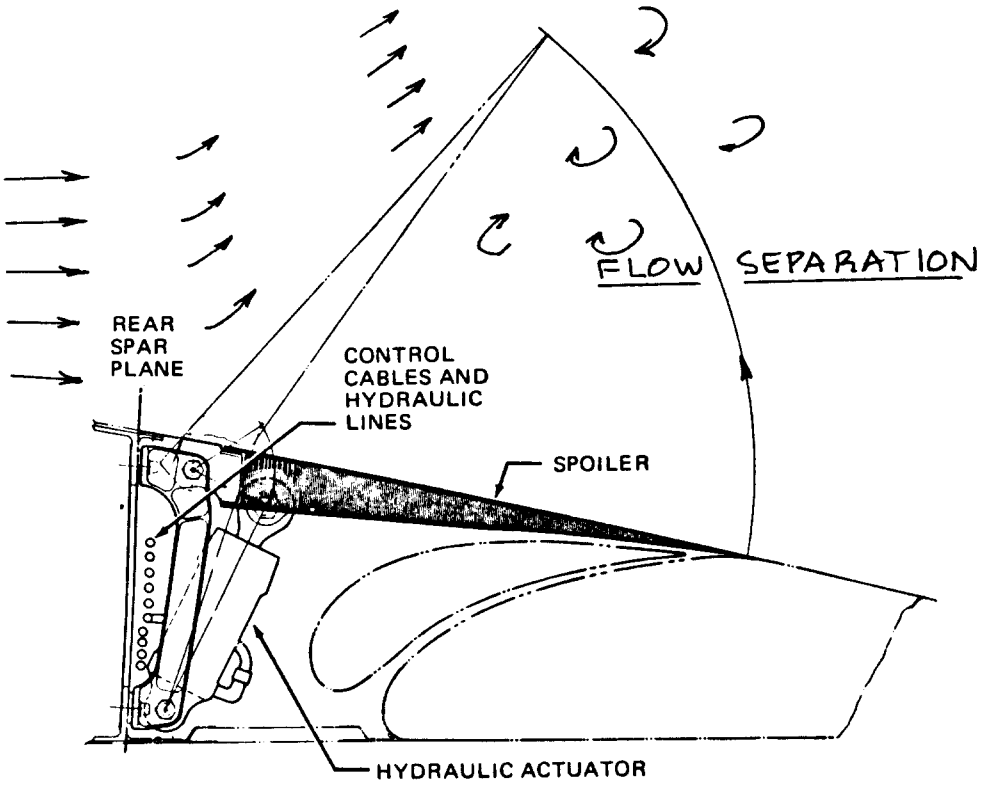

COURTESY: MCDONNELL DOUGLAS

Figure 4.46 Example of Spoiler Operation

4.1.21 Review of Wing Drag Contributions

The wing is responsible for generating most of the lift on an airplane: 90 to 95 percent. The wing is also responsible for generating a large amount of drag: 20 - 40 percent of the total drag of an airplane. It is obviously desirable to design the wing so that it provides the highest possible value of lift-to-drag ratio in those flight conditions where aerodynamic efficiency is important. Such flight conditions are:

*cruise *loiter *climb *engine-out climb

The reader is referred to references 12, 13 and 29 for excellent discussions on the aerodynamic design of wings. A summary of important design considerations is given in the following.

Wings, in addition to generating lift, are responsible for generating the following types of drag:

1. Friction drag
2. Induced drag
3. Compressibility drag
4. Interference drag
5. Profile drag

Detailed procedures for predicting wing drag are presented in Part VI.

1. Friction drag: Friction drag is directly related to wetted area and to the type of boundary layer which is present in a given flight condition.

Wing wetted area is itself related to wing planform area (wing reference area), and to airfoil thickness: Equation (12.1) in Part II shows this.

For a given wetted area the friction drag depends on how much of the boundary layer is laminar and how much is turbulent.

Figure 4.47 shows the major drag reduction which can be obtained with laminar flow as compared to turbulent flow.

Until fairly recently it was generally believed that except for gliders and certain smoothly finished homebuilts, most airplanes were 'turbulent' airplanes. In predicting drag of most airplanes the boundary layer was assumed to be fully turbulent.

References 42 and 43 show that very significant

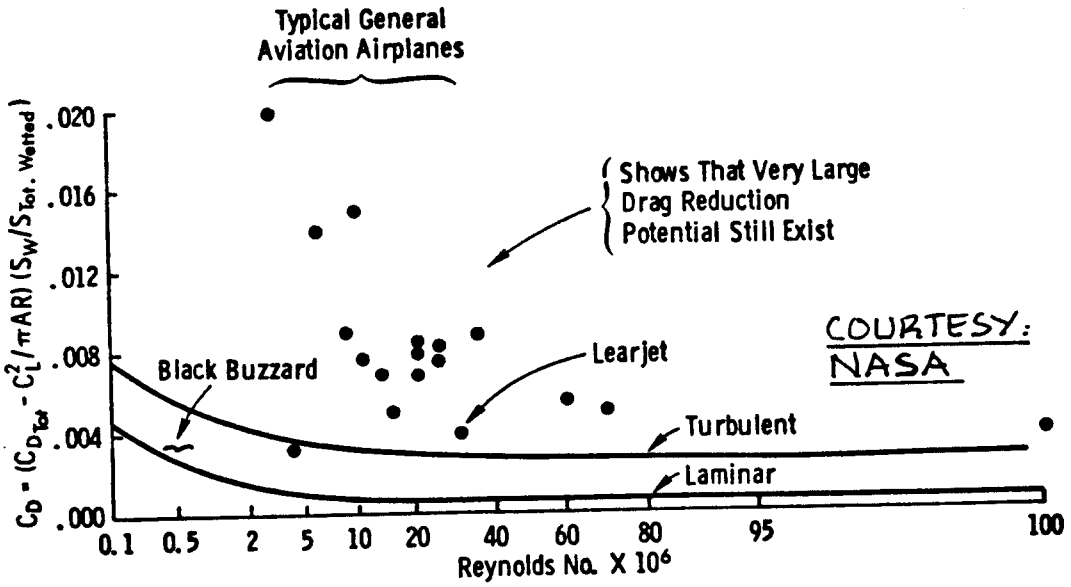

Figure 4.47 Example of Drag Reduction Potential With Laminar Flow

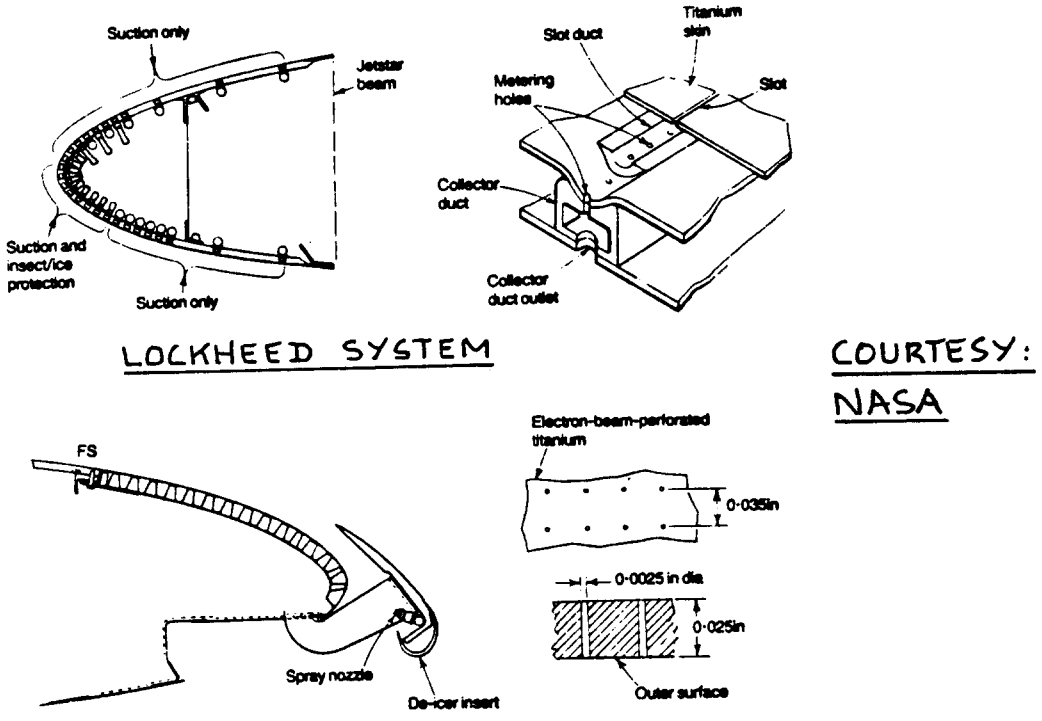

Figure 4.48 Examples of Hybrid Laminar Flow Control

laminar flow runs are indeed feasible at typical operational combinations of Mach Number and Reynold's Number for airplanes ranging from general aviation airplanes to large jet transports.

Reference 44 shows the significant performance advantages which can accrue due to natural laminar flow.

Typical questions which arise in wing design with regard to the possibility of achieving natural laminar flow are:

1. What roughness and waviness criteria need to be used in the wing manufacturing process?

2. What combinations of sweep angle, Mach number and Reynold's Number lead to stable laminar flow?

3. What about insect contamination?

References 45 and 46 provide some answers to these questions.

If natural laminar flow cannot be achieved in a stable, reliable manner, the next approach is that of 'hybrid' laminar flow. Here, the leading edge is artificially kept laminar by boundary layer suction. This then allows longer 'natural' laminar flow runs over the airfoil. Figure 4.48 shows two design approaches to 'hybrid' laminar flow. Reference 47 contains a discussion of these approaches.

Methods for estimating wing friction drag are provided in Part VI.

2. Induced drag: The amount of induced drag generated by the wing is dependent on the amount of lift being generated, on the aspect ratio of the wing and on the so-called Oswald efficiency factor.

Methods for estimating the induced drag of wings are presented in Part VI.

3. Compressibility drag: How much compressibility drag is generated by a wing depends on the Mach Number, the sweep angle, the thickness ratio and the blending of the wing into the fuselage. In chapter 6 of Part II a simple method was provided to select wing sweep and wing thickness so that the wing operates below the drag rise Mach Number in subsonic flow. The compressibility drag in supersonic flow (also referred to as wave drag)

depends also on sweep angle, on thickness ratio on lift coefficient and on Mach number.

Part VI contains methods for estimating the wing contribution to compressibility drag. Area ruling of the wing fuselage intersection is nearly always required to keep the compressibility drag within acceptable bounds.

4. Interference drag: Interference drag is a poorly understood component of drag. It is well known, that interference drag depends greatly on the 'fairing' of a wing into a fuselage. The same can be said for the interference drag created by other bodies installed under or on a wing. Examples of such bodies are: nacelles, tanks, radar pods and typical military stores. In some instances 'local' arear ruling is required to bring the interference drag down. The reader should consult Reference 15 for more information on interference drag.

5. Profile drag: Profile drag in wings comes about only after flow separation has occurred. Properly designed wings do not exhibit significant areas of flow separation in most flight regimes. An exception is formed by vehicles which spend a significant amount of time maneuvering close to the maximum lift coefficient. In those cases profile drag becomes important. Use of experimental data is recommended whenever drag due to flow separation needs to be estimated.

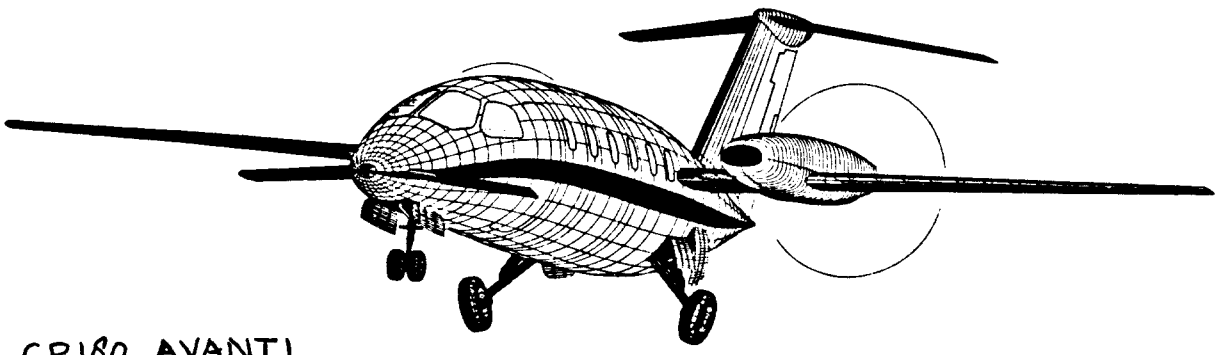

GP180 AVANTI
COURTESY:
GATES LEARJET / PIAG610

4.2 STRUCTURAL DESIGN CONSIDERATIONS AND EXAMPLES OF STRUCTURAL LAYOUT DESIGN OF WINGS

The purpose of this section is to provide some guidelines and examples of how the structural layout design and the integration of the wing structure into the airplane can be accomplished.

The material in this section is organized as follows:

4.2.1 Typical Spar, Rib and Stiffener Spacings

4.2.2 Examples of wing structural arrangements

4.2.3 Examples of wing/fuselage integration

4.2.4 Examples of wing cross section design

4.2.5 Examples of lateral control mechanizations

4.2.6 Examples of high lift device mechanizations

4.2.7 Examples of wing skin gages

4.2.8 Maintenance and Access Requirements

Chapter 7 contains a procedure for preparing the overall structural arrangement of an airplane. For additional insight into airplane structural arrangements the reader should consult Chapter 8.

4.2.1 Typical Spar, Rib and Stiffener Spacings

The actual structural arrangement of spars, ribs and skin stiffeners depends very much on the type of airplane being designed and the loads to which it will be subjected. The reader should refer to Refs. 11, 19 and 23 for detailed information on the types of loads to which airplane structures are subjected. Reference 20 contains detailed methods for the preliminary structural analysis of wing structures.

Figure 4.49 defines the locations of major structural components for wings.

Wing Spar Locations: Most airplane wings use a so-called torque-box (wing-box) as the main load carrying component. The torque box should be located to take maximum advantage of the structural height available within the airfoil contours. This will save weight. The

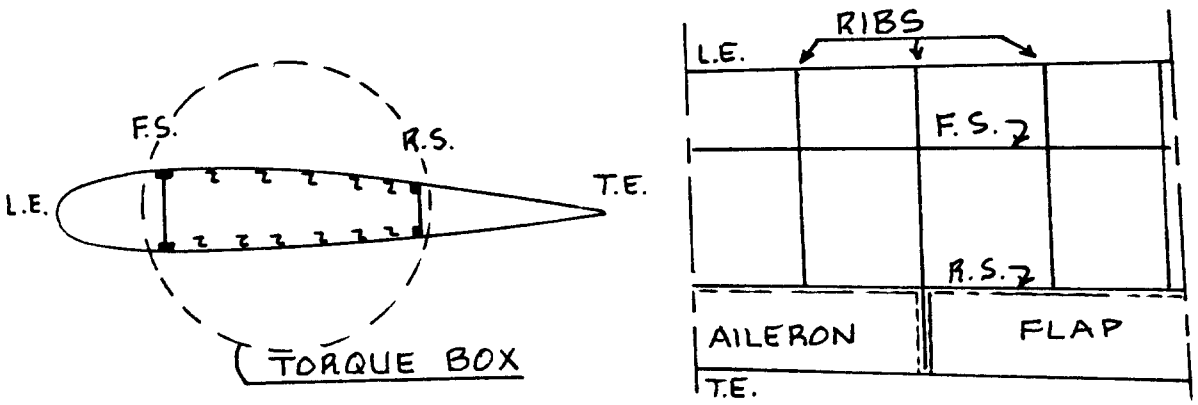

Figure 4.49 Definition of Major Structural Wing Components and Their Location

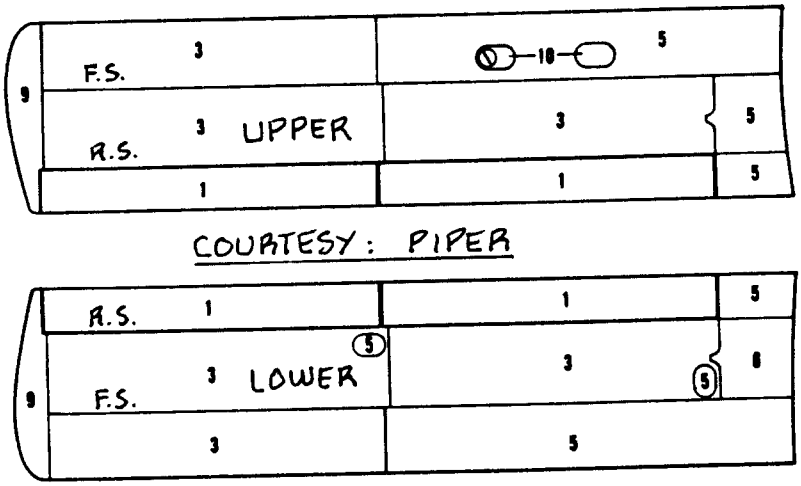

COURTESY: PIPER

SKIN NO.	MATERIAL	THICKNESS
1	2024-T3	.016
2	2024-0*	.032
3	2024-T3	.020
4	2024-T3	.025
5	2024-T3	.032
6	2024-T3	.040
7	2024-0*	.040
8	FIBERGLASS	
9	THERMOPLASTIC	
10	2024-T3	.080

Figure 4.50 Wing Structural Arrangement Piper PA-38-112 Tomahawk

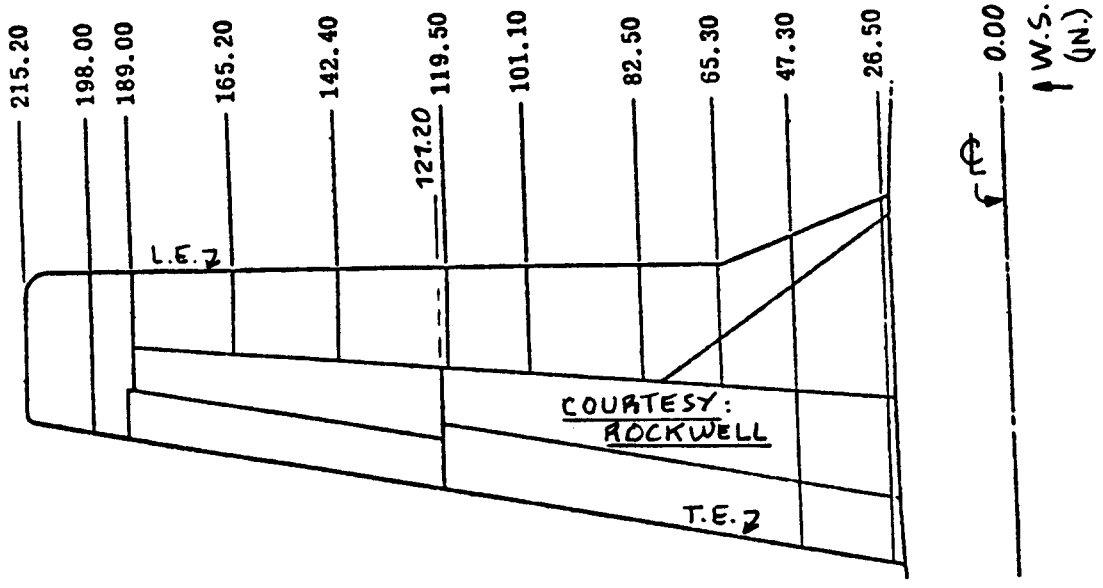

Figure 4.51 Wing Structural Arrangement Rockwell 112B

torque box is normally closed off by a front spar (F.S.), a rear spar (R.S.) and an upper and lower skin. The spar locations are often constrained by requirements for high lift devices.

Typical spar locations are:

Front spar: 15-30 percent chord

Rear spar: 65-75 percent chord

Multiple spar construction is often applied in the case of fighter wings. The F16 wing has 11 spars, 5 ribs and a machine-tapered skin without stiffeners.

Wing Rib Locations: To help stabilize torque box skins and to serve as attachment points for leading edge skins, trailing edge skins and/or flaps, ailerons and spoilers, wing ribs are used. Typical rib spacings are:

Light Airplanes: 36 inches

Transports: 24 inches

Fighters and Trainers: rib spacings vary widely.

Ribs are always required at those spanwise locations where stores are attached to a wing. Examples of such ribs are shown in Section 4.3.

Wing Stiffener Spacings: These vary widely and depend on the relative stiffness of the wing skin. For example spacings see sub-section 4.2.2.

4.2.2 Examples of Wing Structural Arrangements

A procedure for arriving at the overall structural arrangement for any new airplane is given in Chapter 7. Figures 4.50 through 4.59 present examples of wing structural arrangements for the following airplanes:

Fig. 4.50 Piper Tomahawk	Fig. 4.51 Rockwell 112B
Fig. 4.52 Short Skyvan	Fig. 4.53 McDD DC9-30
Fig. 4.54 McDD DC-10	Fig. 4.55 Boeing 767
Fig. 4.56 Aerospatiale Corvette	Fig. 4.57 Douglas A4
Fig. 4.58 Piaggio P166	Fig. 4.59 Canadair CL-215

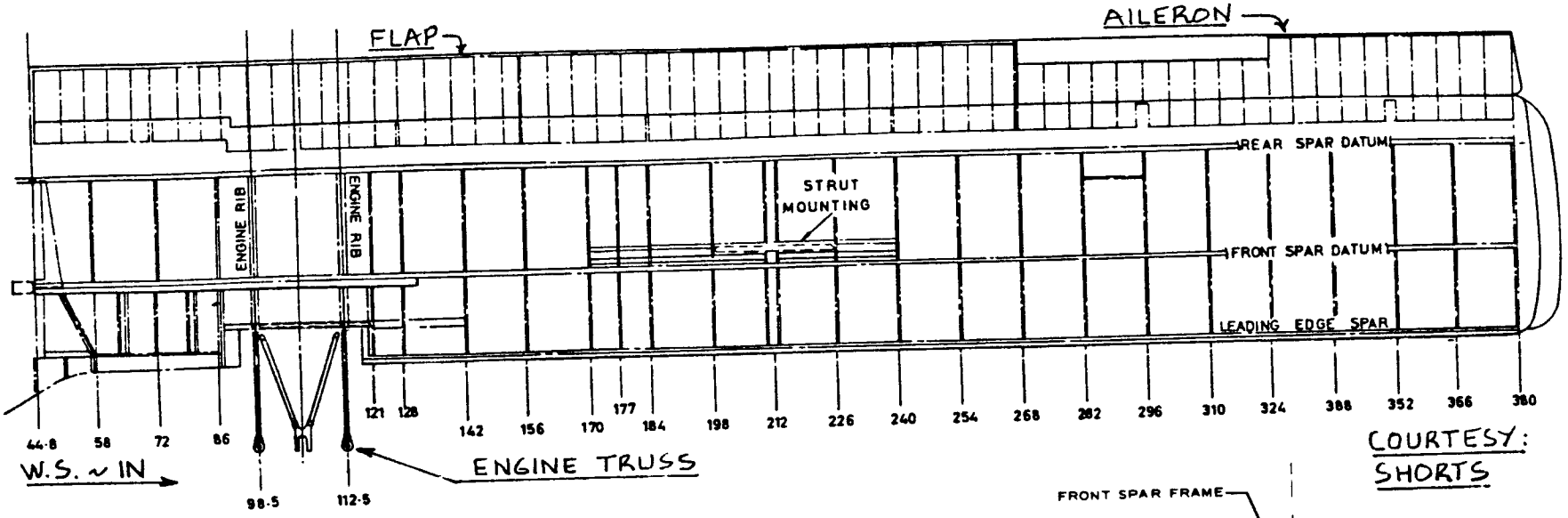

Figure 4.52 Wing Structural Arrangement Short Skyvan

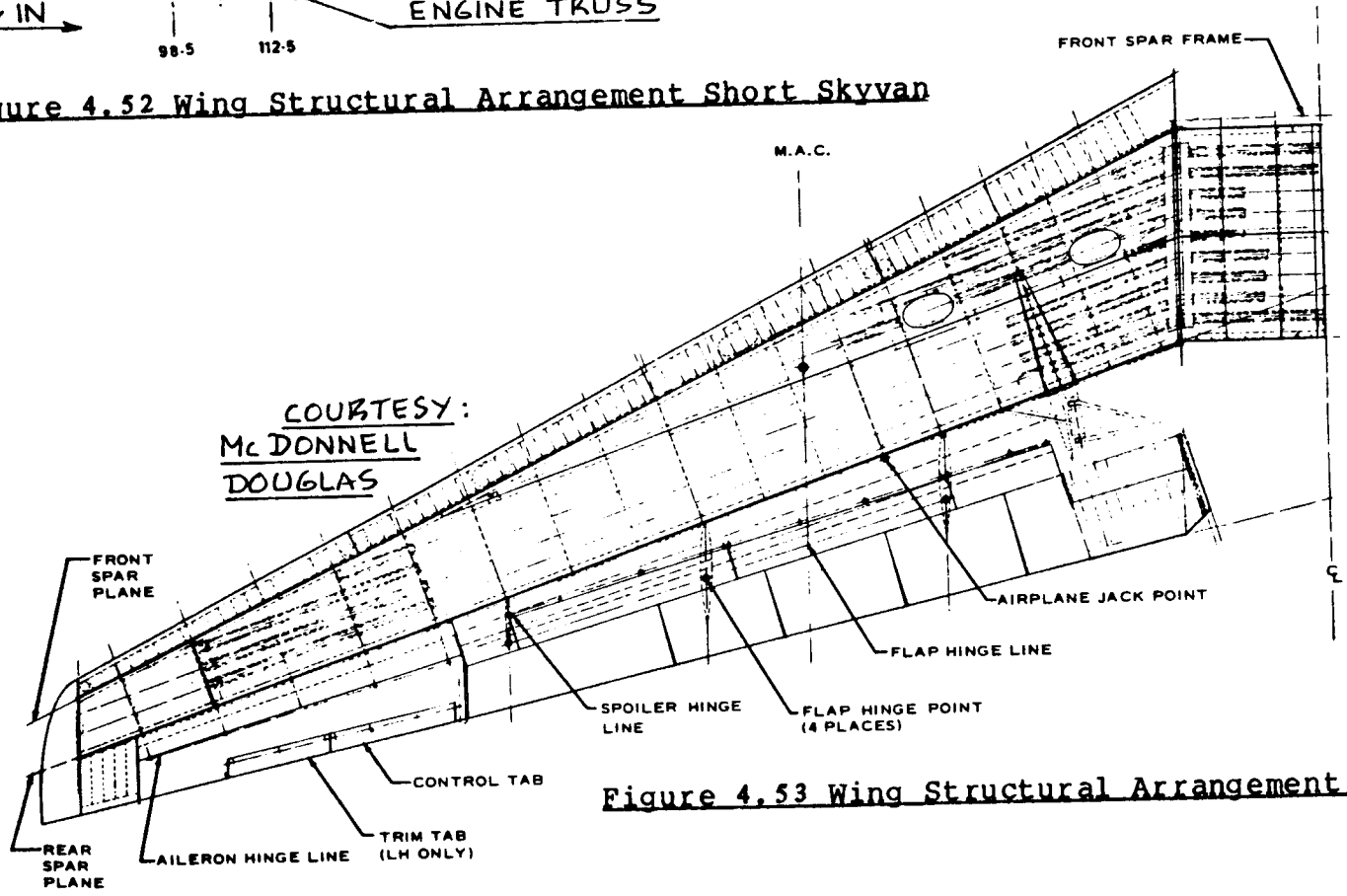

Figure 4.53 Wing Structural Arrangement McDD DC-9-30

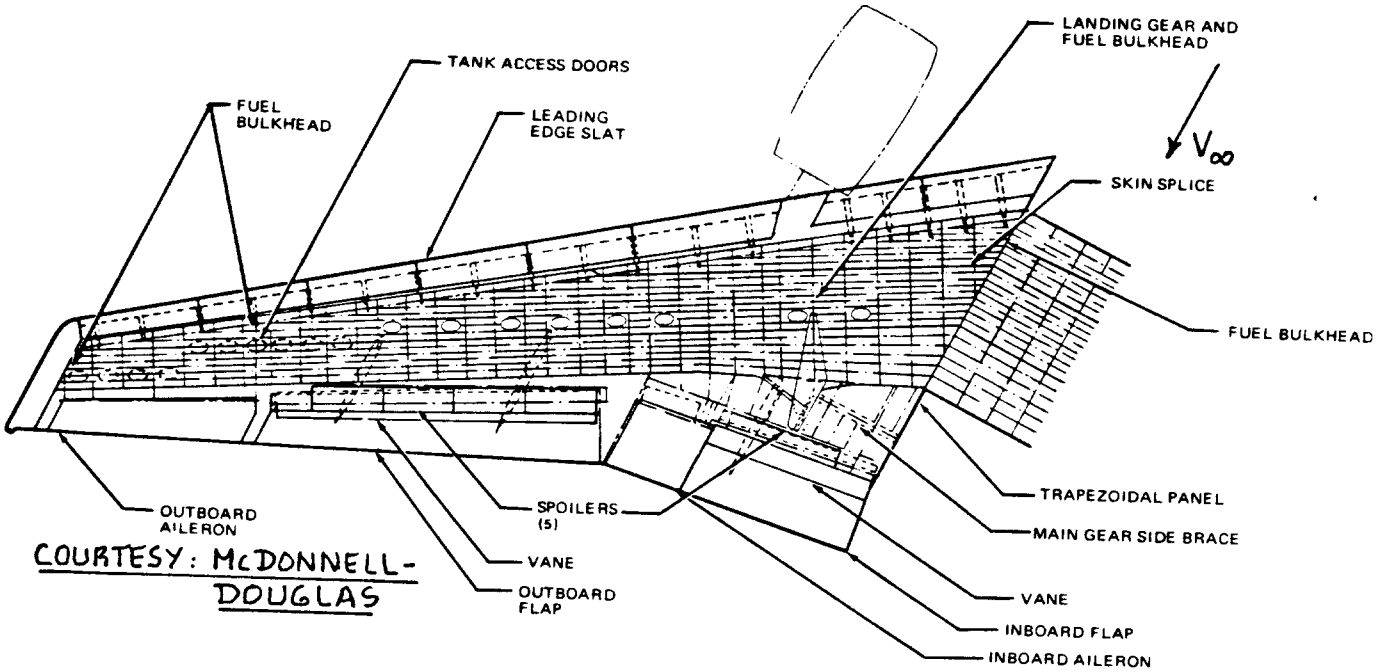

Figure 4.54 Wing Structural Arrangement McDD DC-10

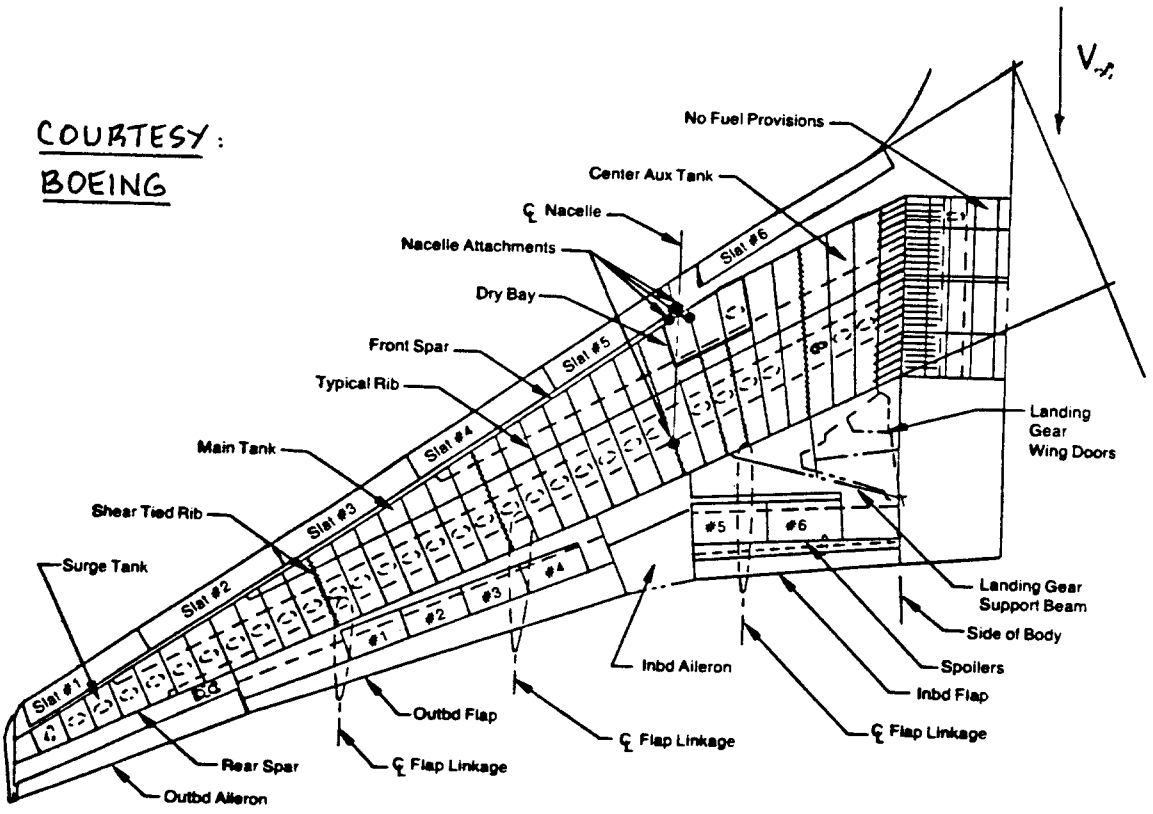

Figure 4.55 Wing Structural Arrangement Boeing 767

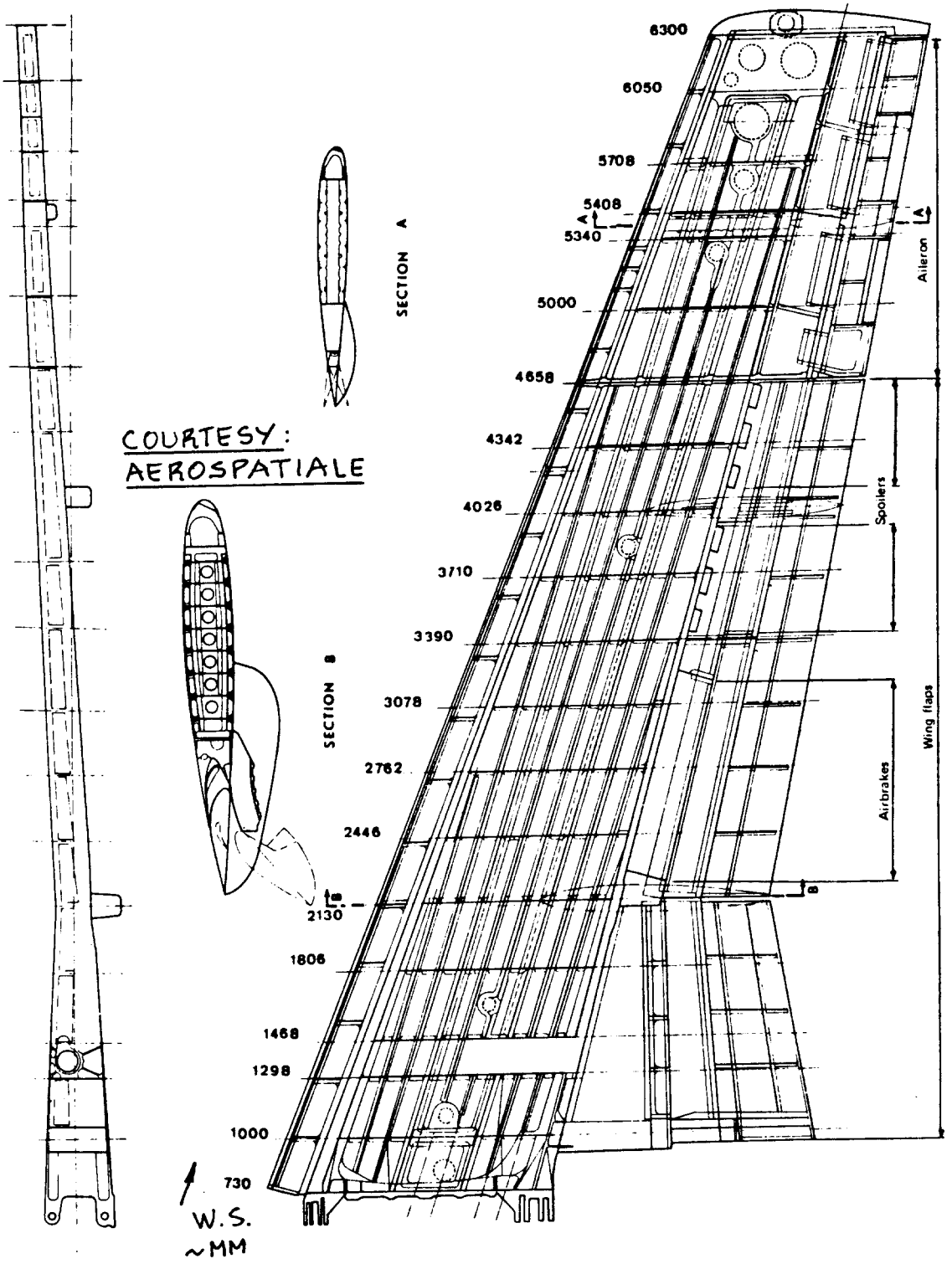

Figure 4.56 Wing Structural Arrangement Aerospatiale Corvette

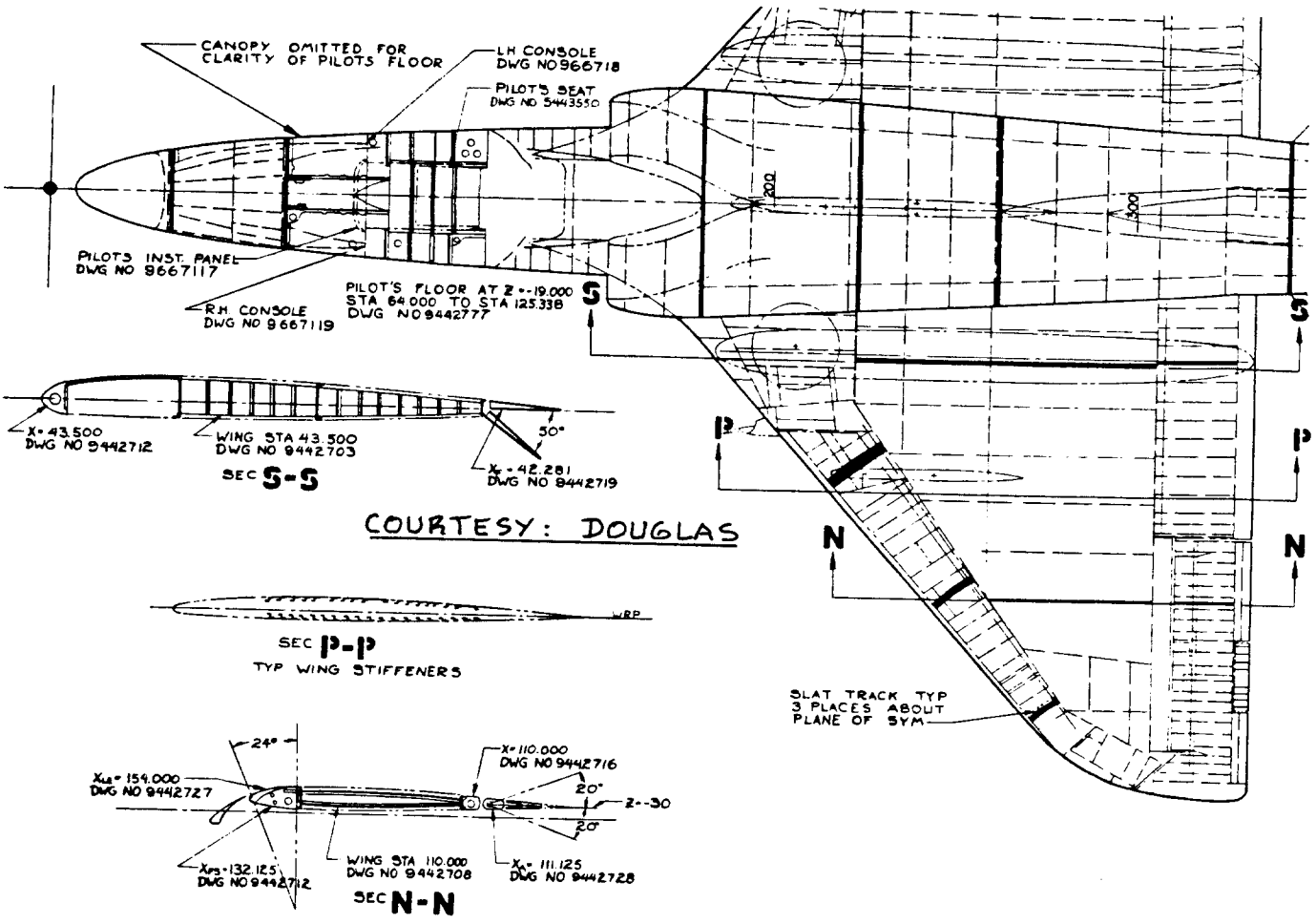

Figure 4.57 Wing Structural Arrangement Douglas A4D-2N

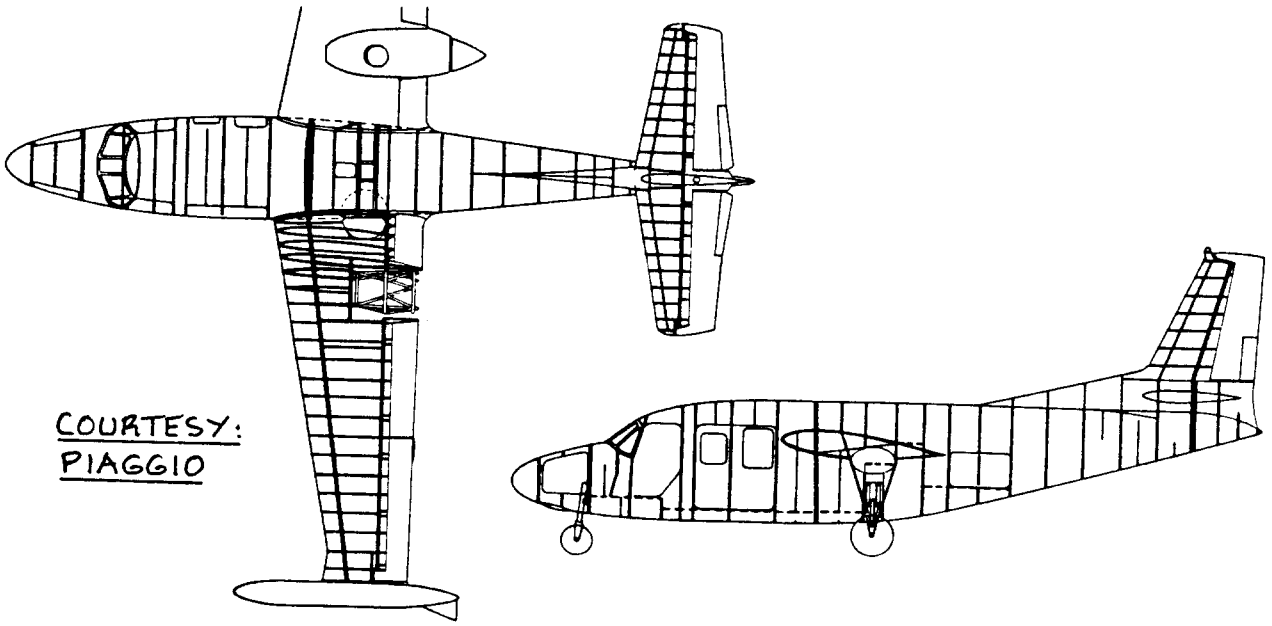

Figure 4.58 Overall Structural Arrangement Piaggio P166-DL3

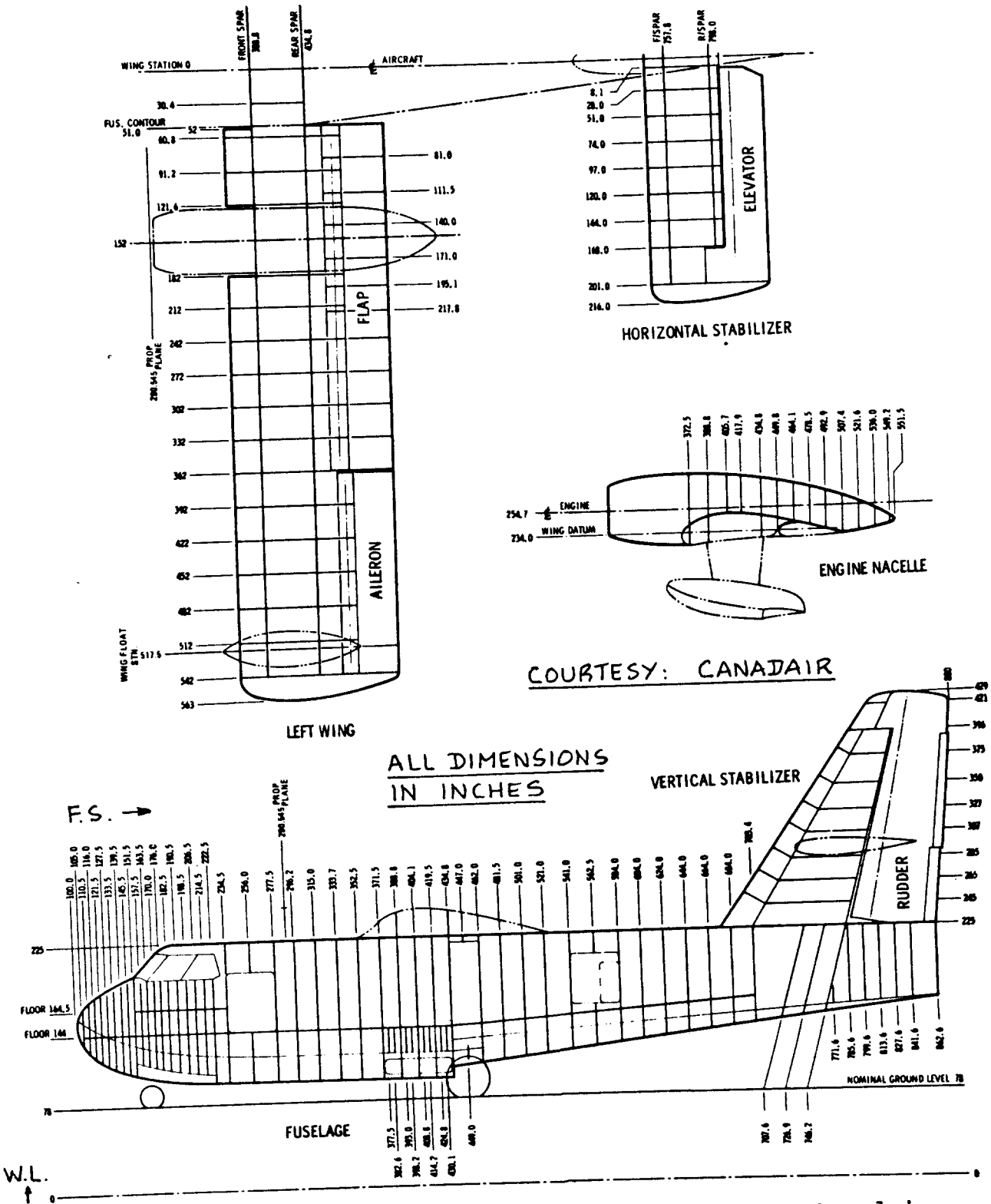

Figure 4.59 Overall Structural Arrangement Canadair CL-215

Note that in most of these structural arrangements the wing stations of major structural elements are defined. A complete structural arrangement must contain that information!

The structural arrangements for the P166 and the CL 215 are given in their entirety.

4.2.3 Examples of Wing/Fuselage Integration

Wings are normally joined to a fuselage in one of the following manners:

1. Wings are 'bolted' to a fuselage 'carry-through' section.

Figures 4.60 and 4.61 are examples of this type of wing/fuselage joint. Note that in Fig. 4.61 the attachments bolts are in tension/compression. In most other wing fuselage joints the attachment bolts are in shear.

Note that in the wing/fuselage attachment of Fig.4.60 the front spar attachment takes care of all bending loads while the rear spar attachment can only transmit a normal force (pin-joint!).

The Corvette wings (Fig. 4.56) are joined to the fuselage through a total of four large bolts in shear.

2. Wings, including the carry-through section are joined to the fuselage by a large number of 'small' bolts.

Figures 4.57 and 4.62 are examples of this type of arrangement

4.2.4 Examples of Wing Cross Section Design

Figures 4.63 and 4.64 provide examples of typical wing cross section designs for the DC9-30 and the DC-10 respectively. Figure 4.57 shows the wing cross sections in a typical fighter.

Figures 4.65 through 4.67 privide details of typical wing box construction methods. Conventional riveted, bonded honeycomb and composite constructions are shown respectively.

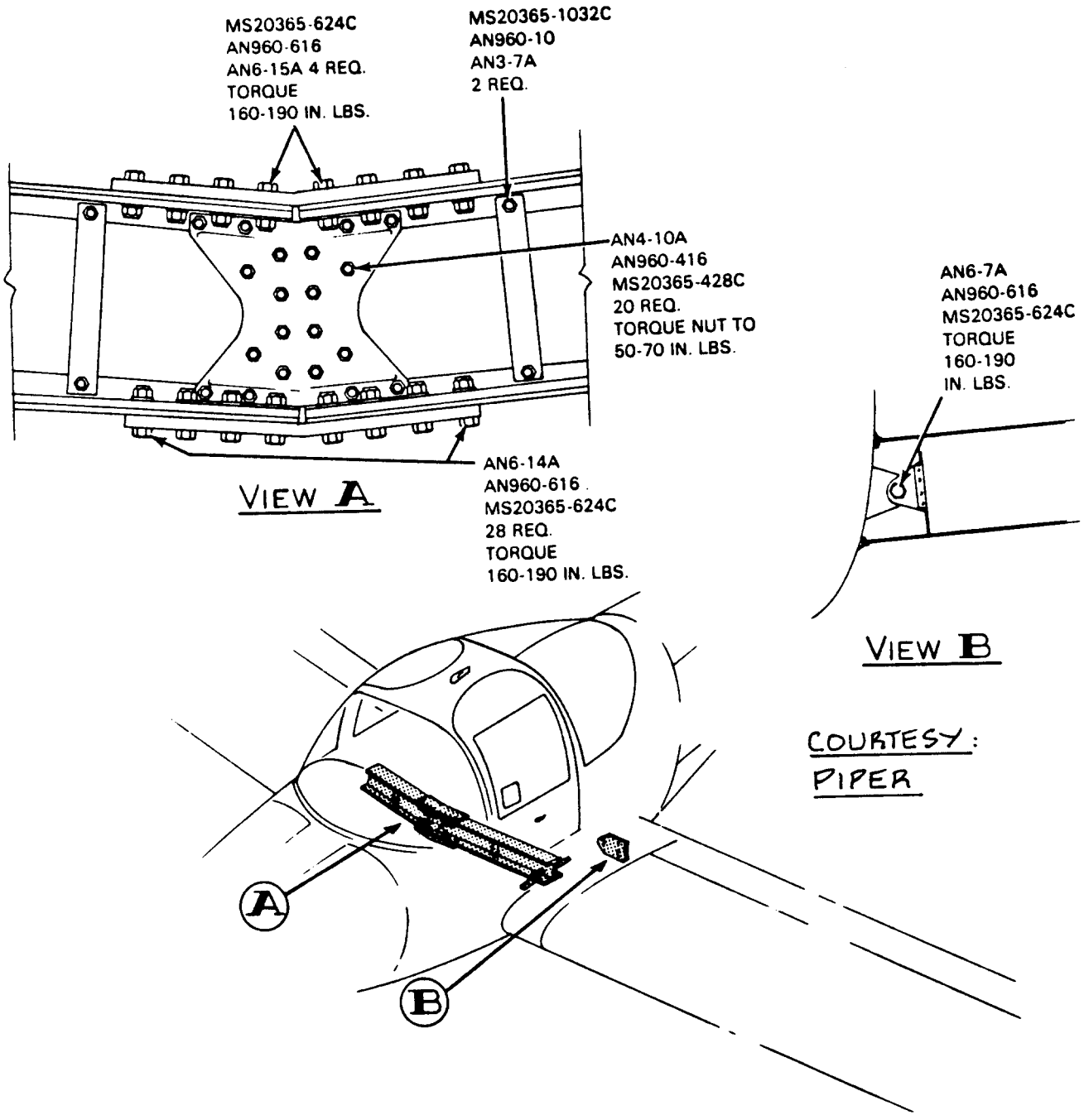

Figure 4.60 Wing/Fuselage Attachment Piper PA-38-112 Tomahawk

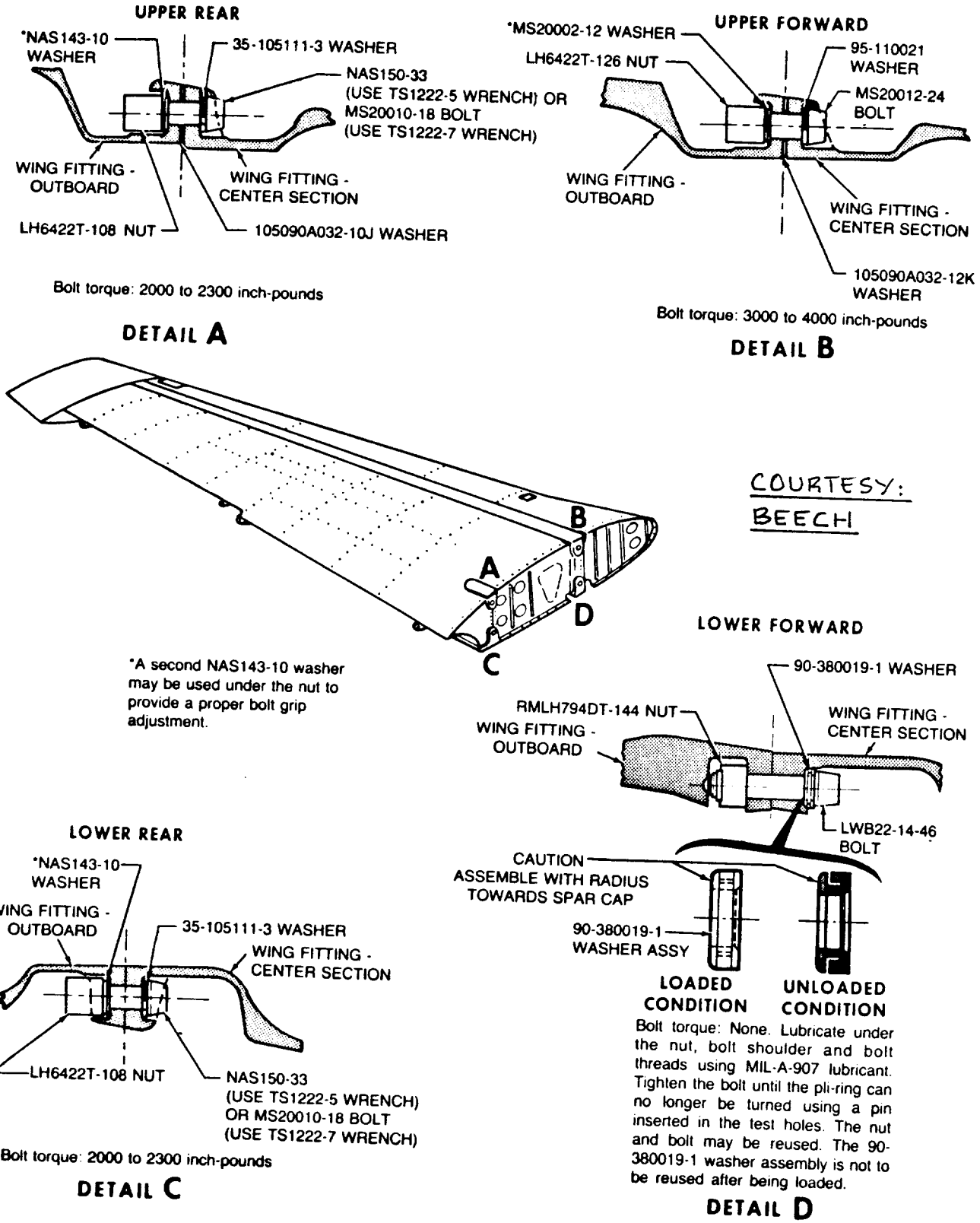

Figure 4.61 Wing/Center Section Attachment Beech King Air F90

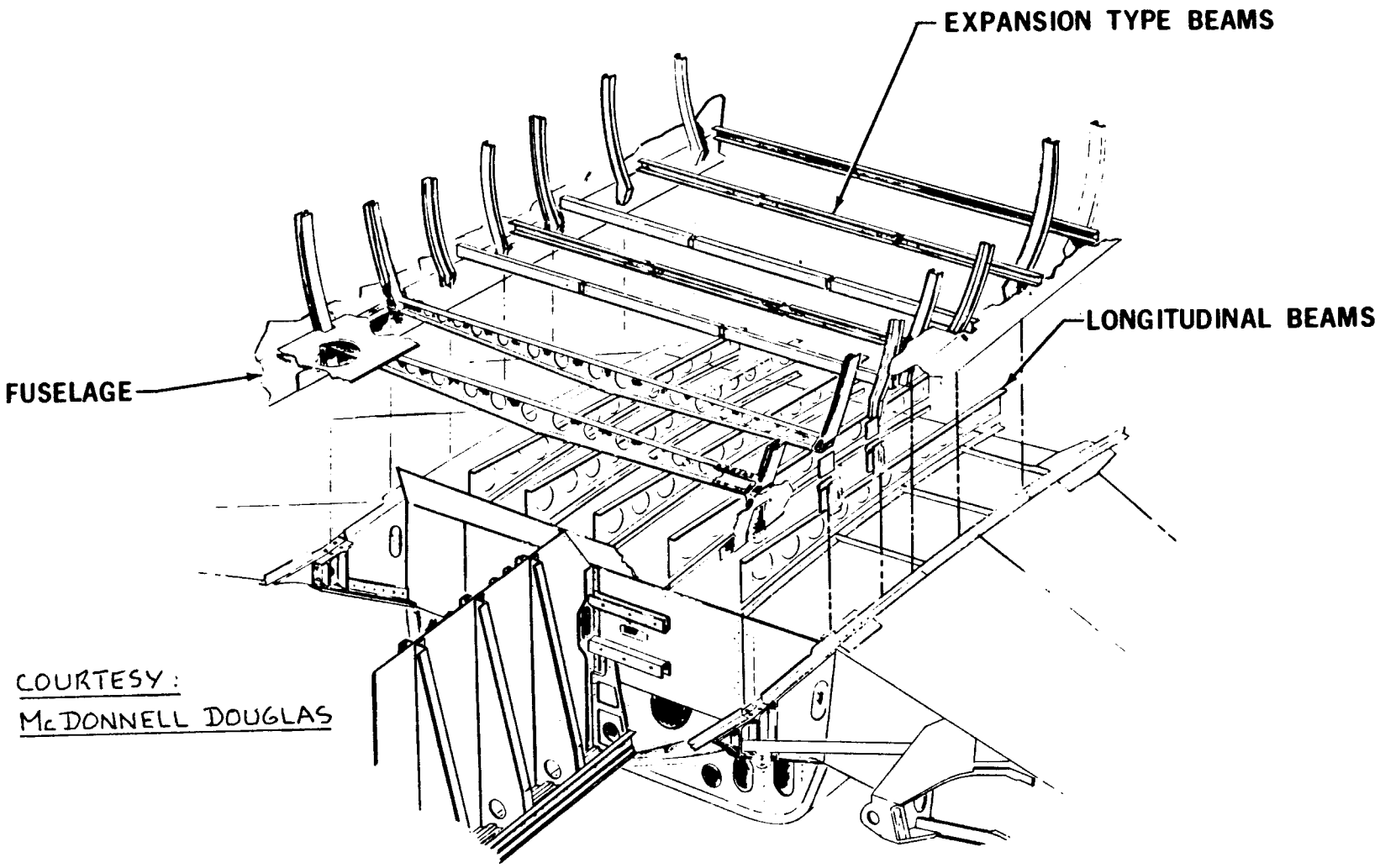

Figure 4.62 Wing/Fuselage Attachment McDD DC-10

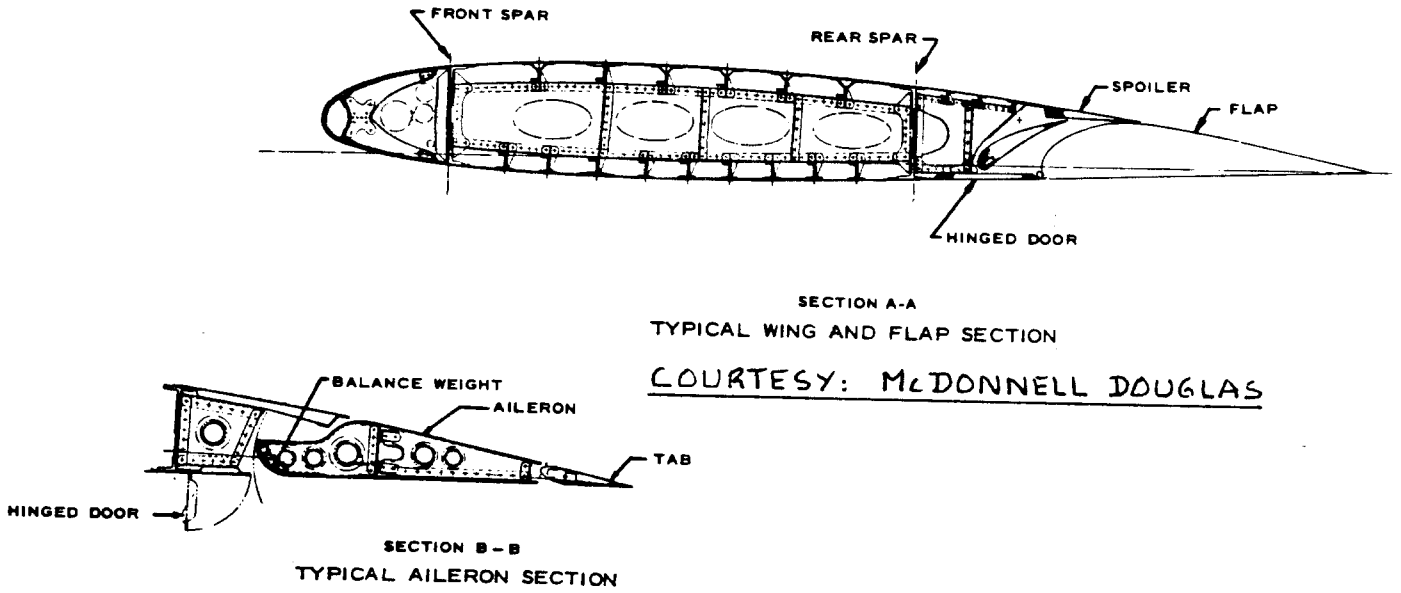

Figure 4.63 Wing Cross Section Design McDD DC-9-30

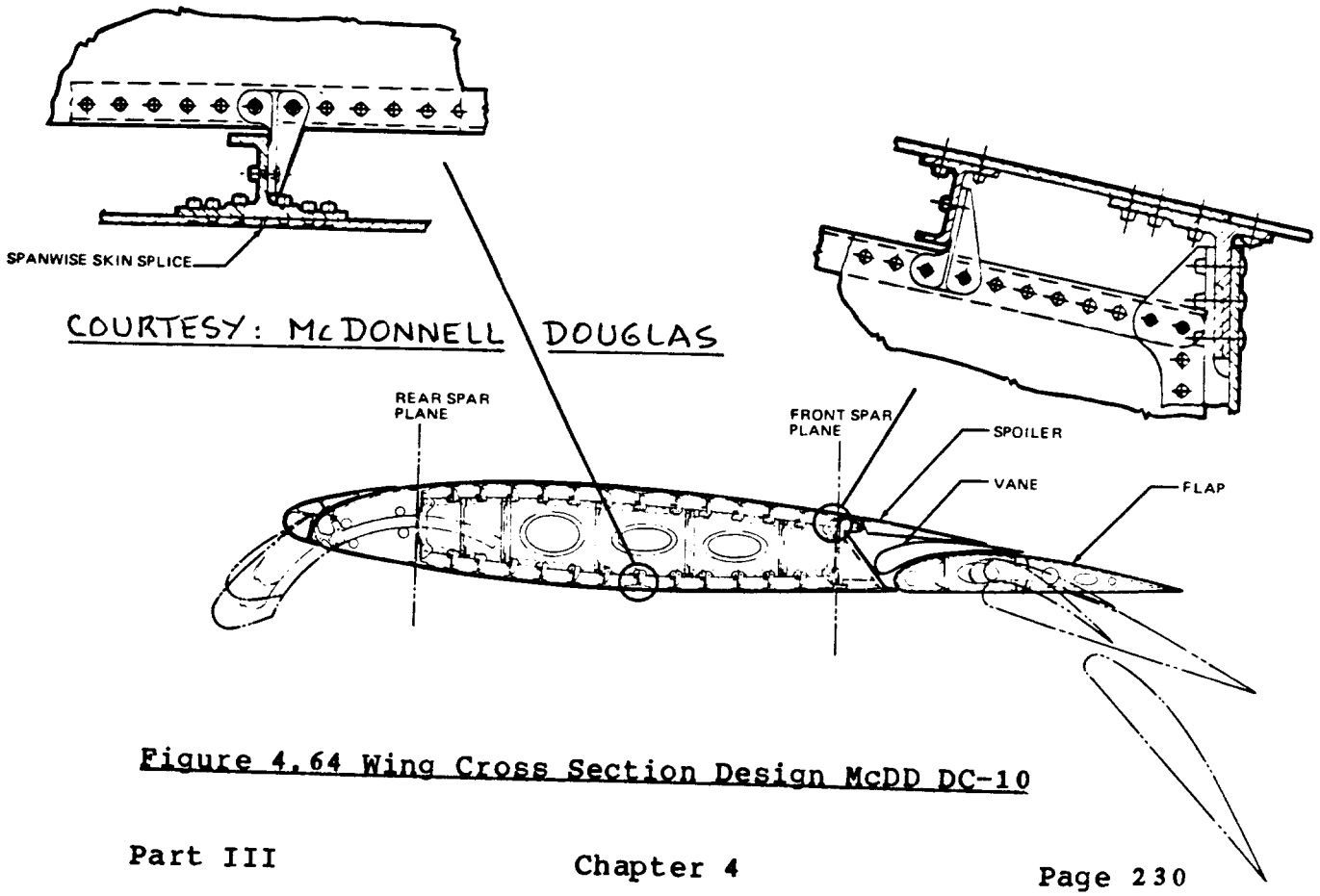

Figure 4.64 Wing Cross Section Design McDD DC-10

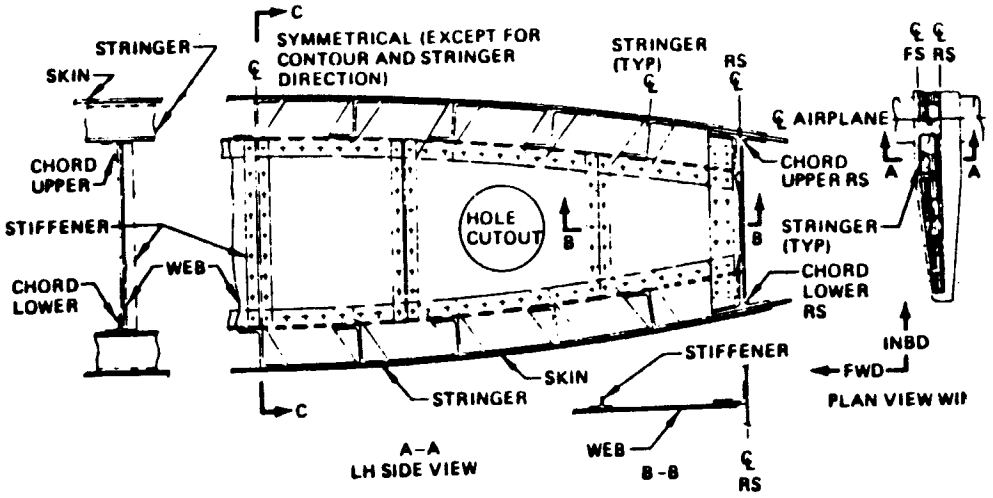

Figure 4.65 Conventional Wing Box Construction

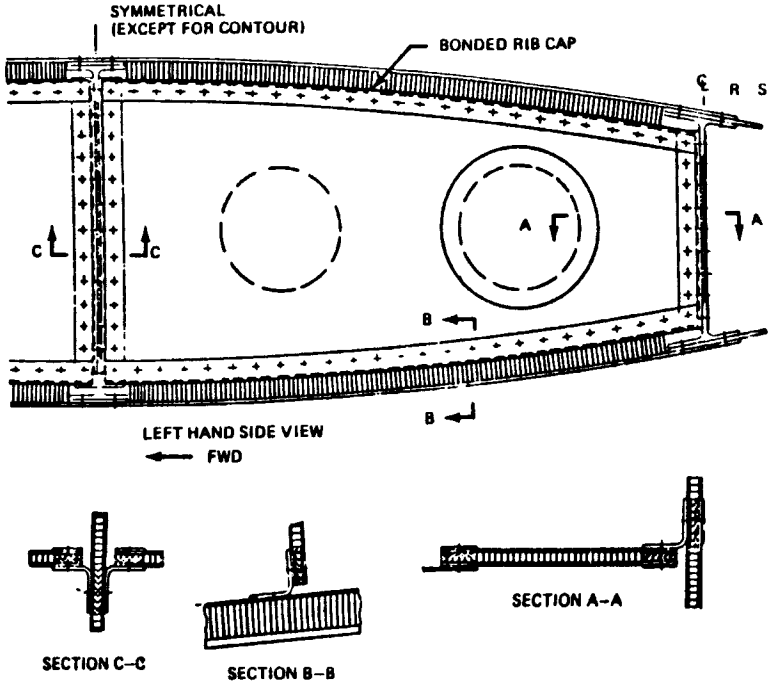

Figure 4.66 Bonded Honeycomb Wing Box Construction

SOURCE : REF. 28

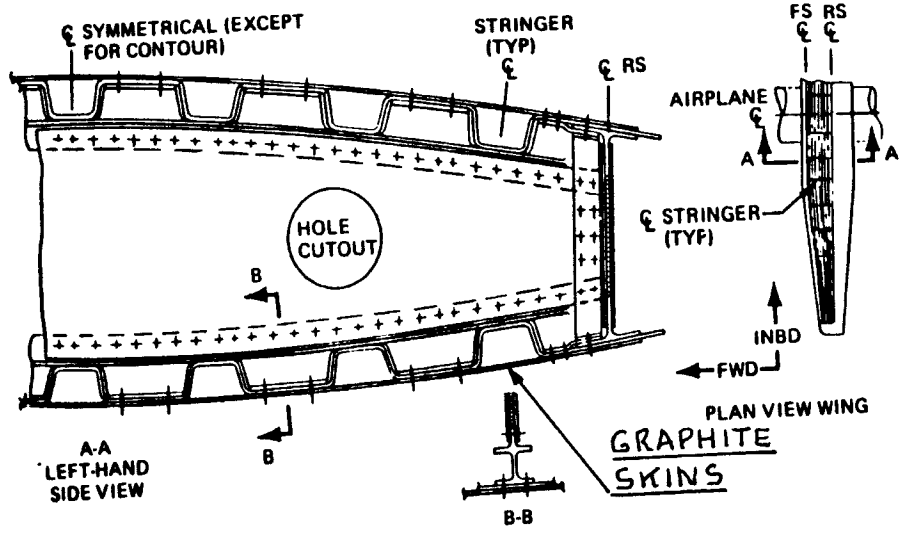

Figure 4.67 Composite Wing Box Construction

4.2.5 Examples of Lateral Control Mechanizations

Figures 4.68 and 4.69 show examples of outboard and inboard aileron mechanizations in a large transport airplane. Figure 4.70 shows a roll control spoiler mechanization also for a transport airplane.

Figure 4.56 and 4.57 show the aileron mechanizations used in a business jet and in a fighter airplane respectively.

4.2.6 Examples of High Lift Device Mechanizations

Figures 4.71 through 4.77 show examples of high lift device mechanizations in a large transport airplane.

Double slotted flap mechanizations are shown in Figures 4.71 through 4.74 while the corresponding leading edge slat mechanizations are shown in Figures 4.75 and 4.76.

A single slotted flap design is seen in Fig. 4.77.

A plain type flap for a fighter airplane is shown in Figure 4.57, cross section NN.

4.2.7 Examples of Wing Skin Gages

Figure 4.78 and 4.79 show examples of typical wing skin gages and materials used in light twin turboprop business airplanes. The actual skin gages used depend very much on the V-n diagram for which the airplane is designed. The reader is referred to Ref. 30 for descriptions of typical structural materials and construction methods used in a wide variety of airplanes.

4.2.8 Maintenance and Access Requirements

Wing structures must be inspectable. That implies inspection covers of a size sufficiently large that inspection and if necessary maintenance functions can be carried out. Figures 4.53 - 4.56, 4.78 and 4.79 give examples of different types of inspection holes. Note that large numbers of these are required.

In many airplanes the leading and trailing edges of the wing are used to house high lift devices, lateral controls and their associated systems. All of these require maintenance and therefore access. The comments made about accessibility in Sub-section 3.3.6 also apply to wing access.

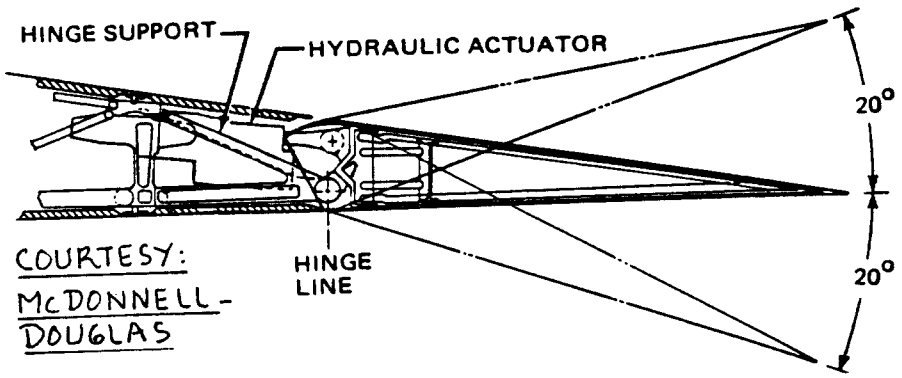

Figure 4.68 Inboard Aileron Installation McDD DC-10

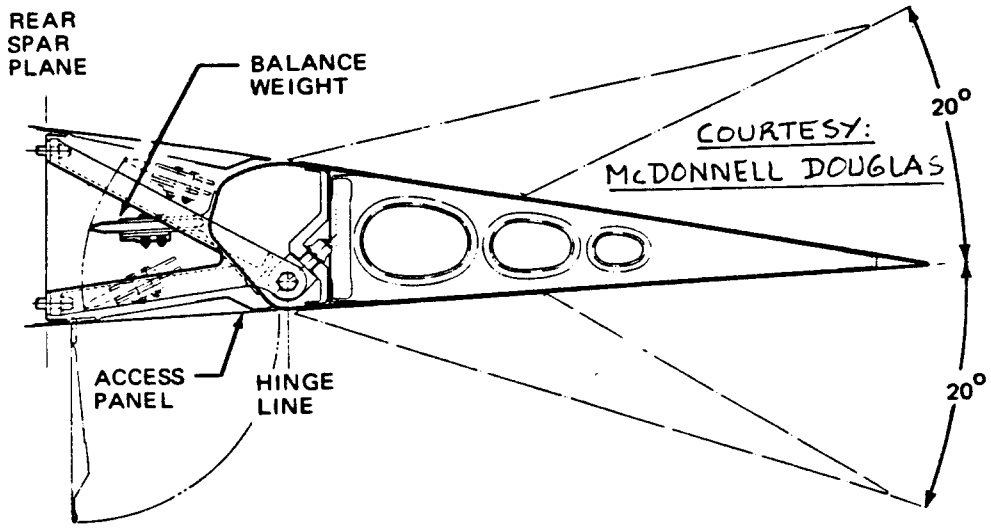

Figure 4.69 Outboard Aileron Installation McDD DC 10

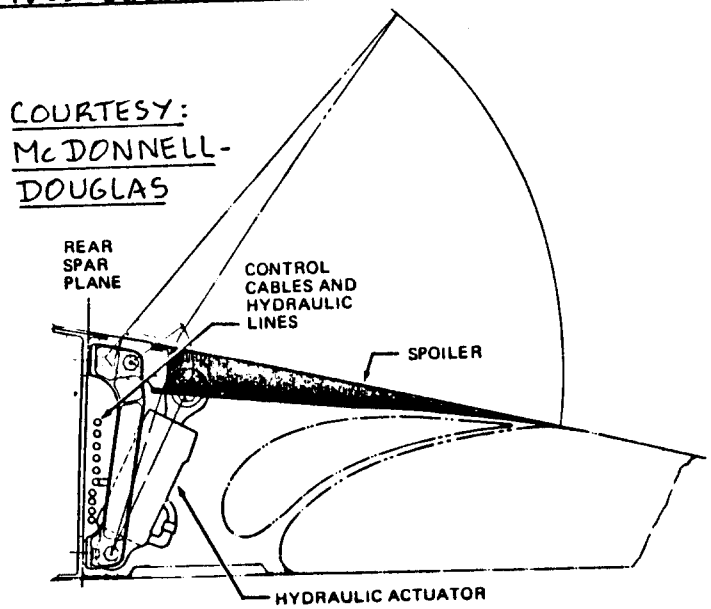

Figure 4.70 Outboard Spoiler Installation McDD DC-10

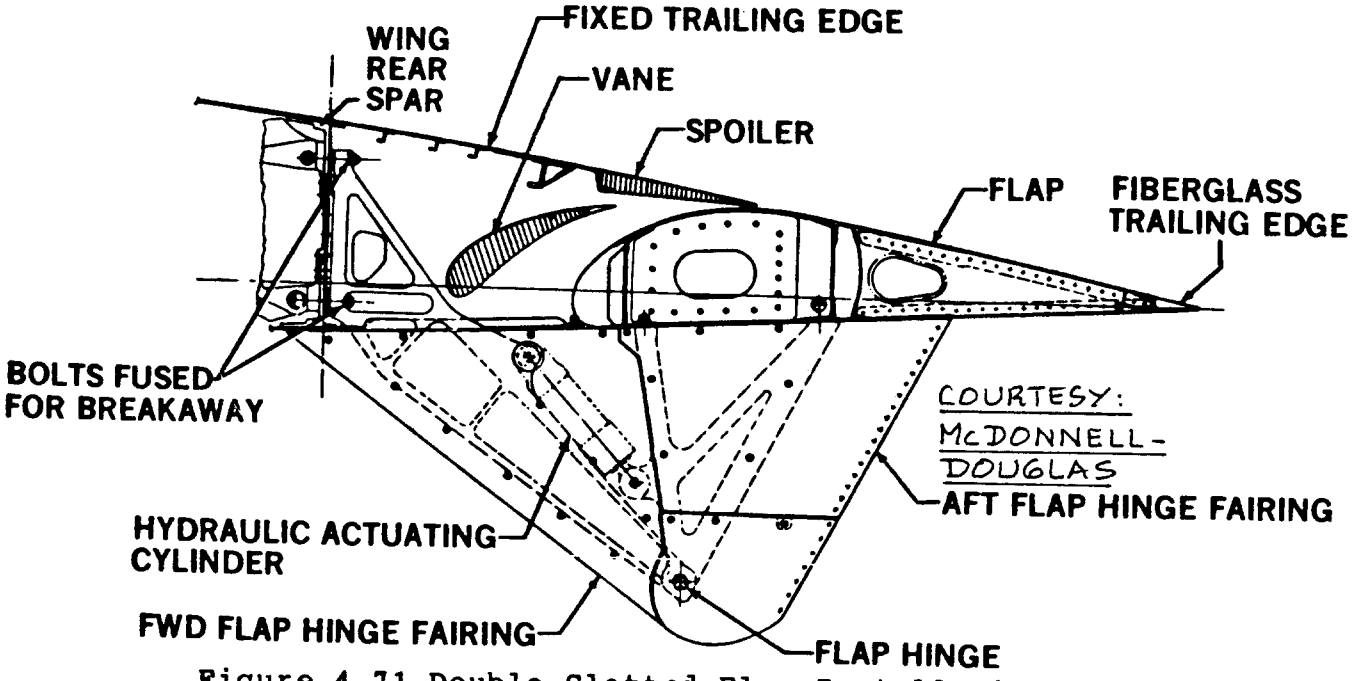

Figure 4.71 Double Slotted Flap Installation McDD DC-9-30

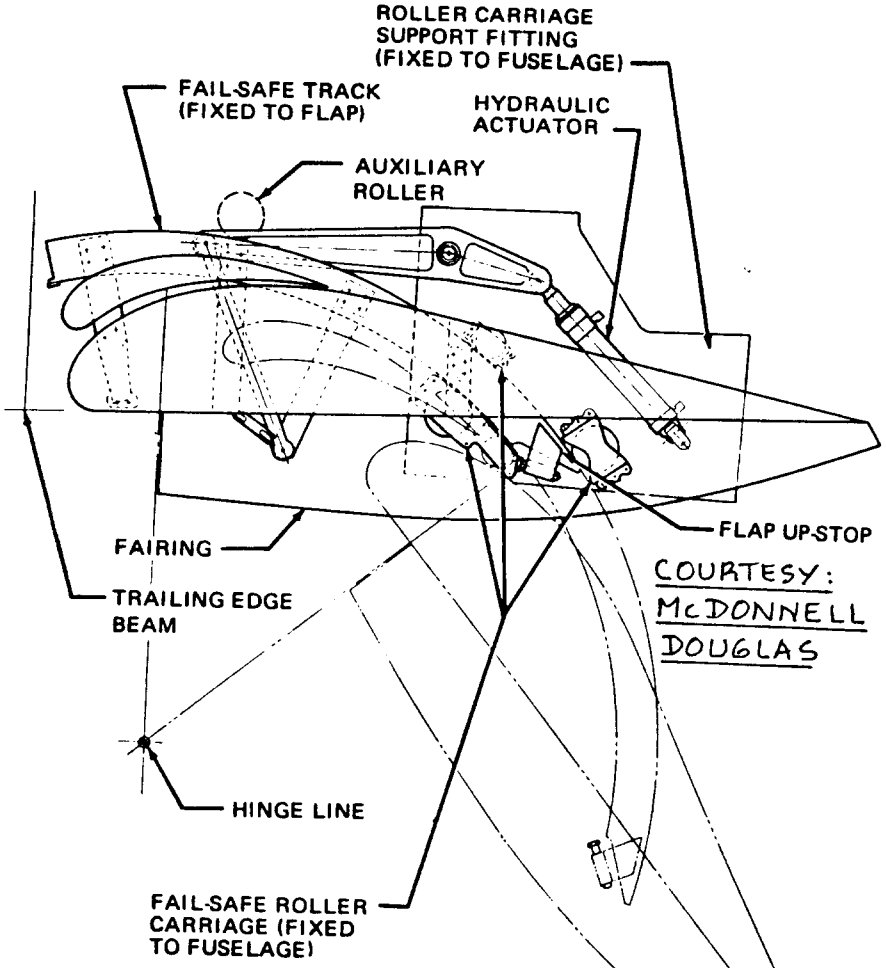

Figure 4.72 Double Slotted Flap Installation McDD DC-10: Inboard Flap, Inboard Support

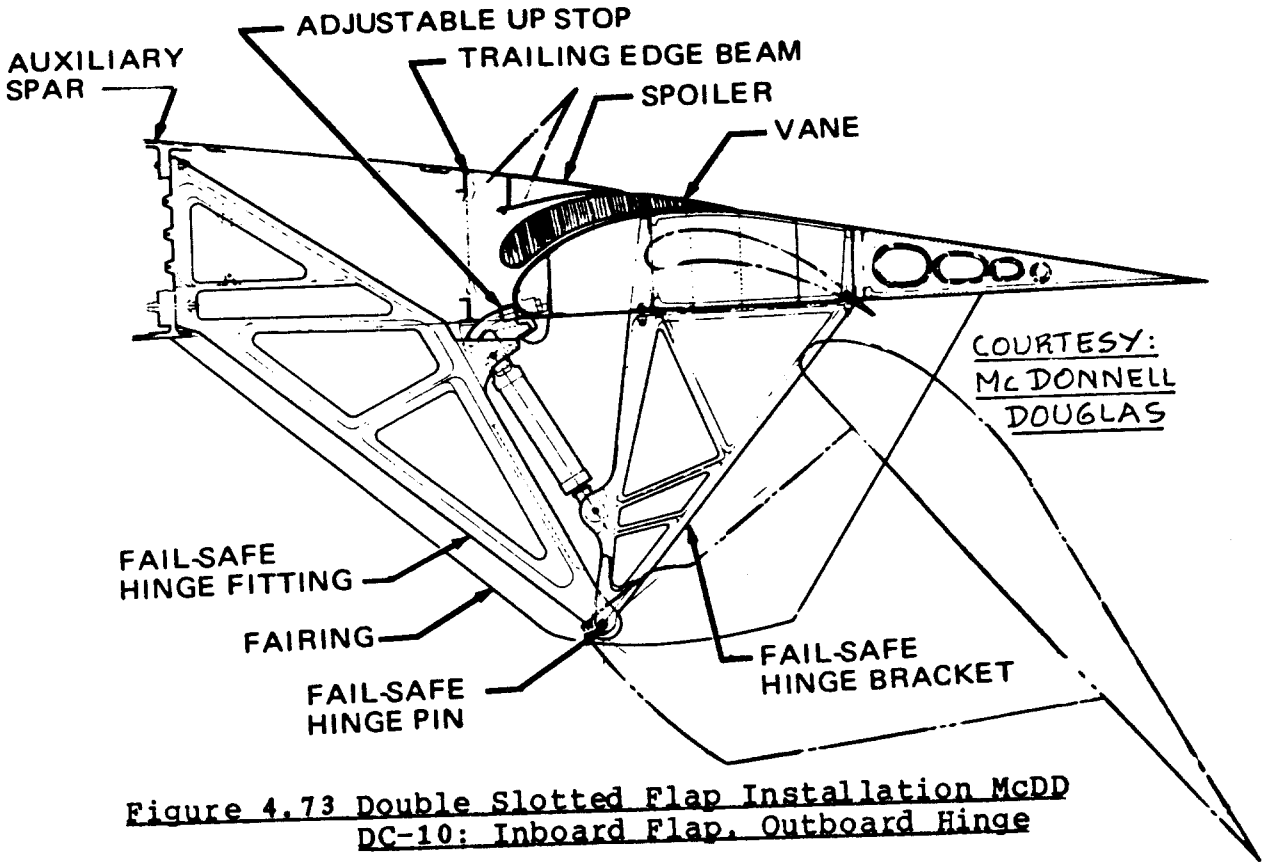

Figure 4.73 Double Slotted Flap Installation McDD DC-10: Inboard Flap, Outboard Hinge

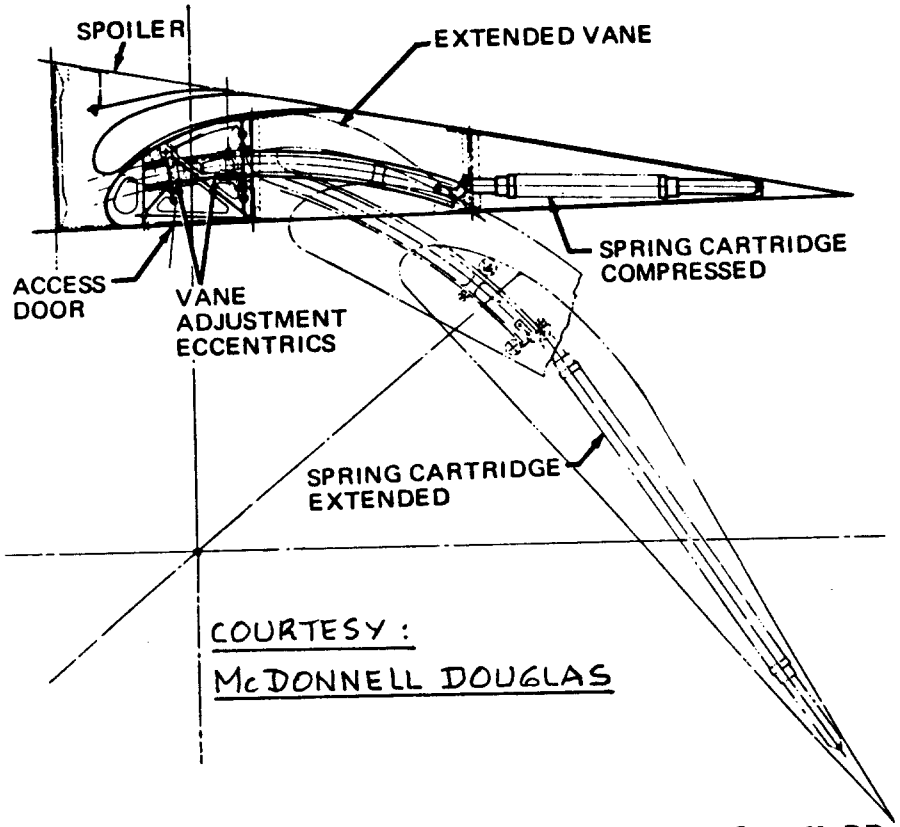

Figure 4.74 Flap Vane Support and Actuation for McDD DC-10: Double Slotted Flaps

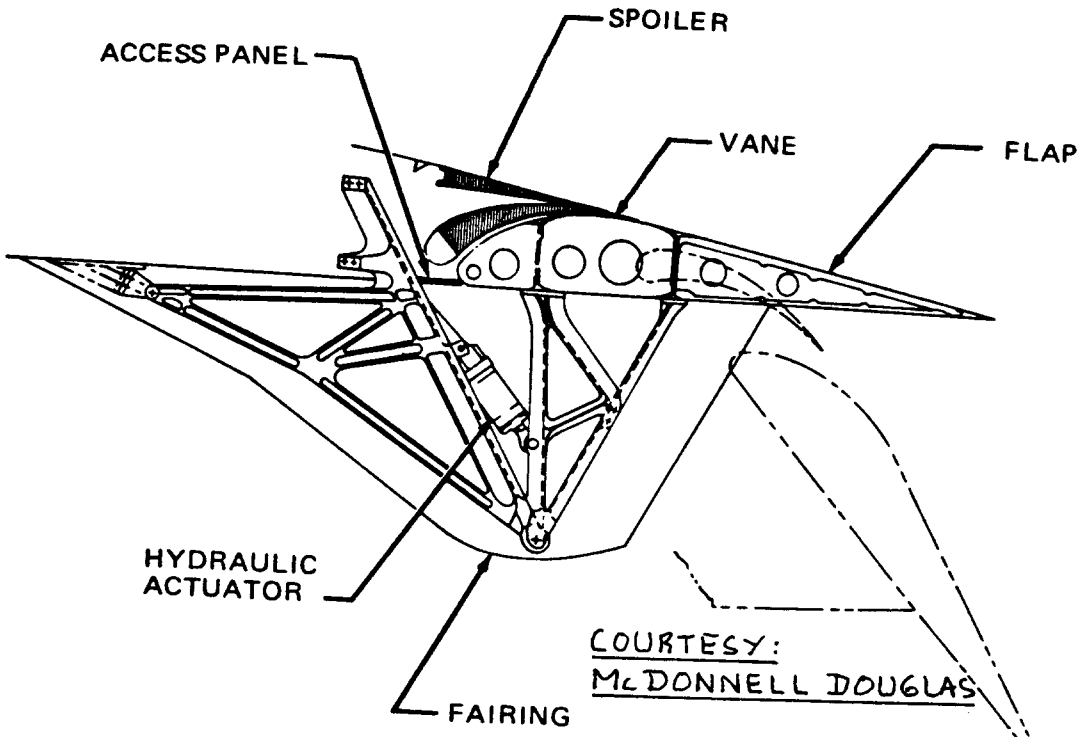

Figure 4.75 Double Slotted Flap Installation McDD DC-10: Outboard Flap Drive Hinge

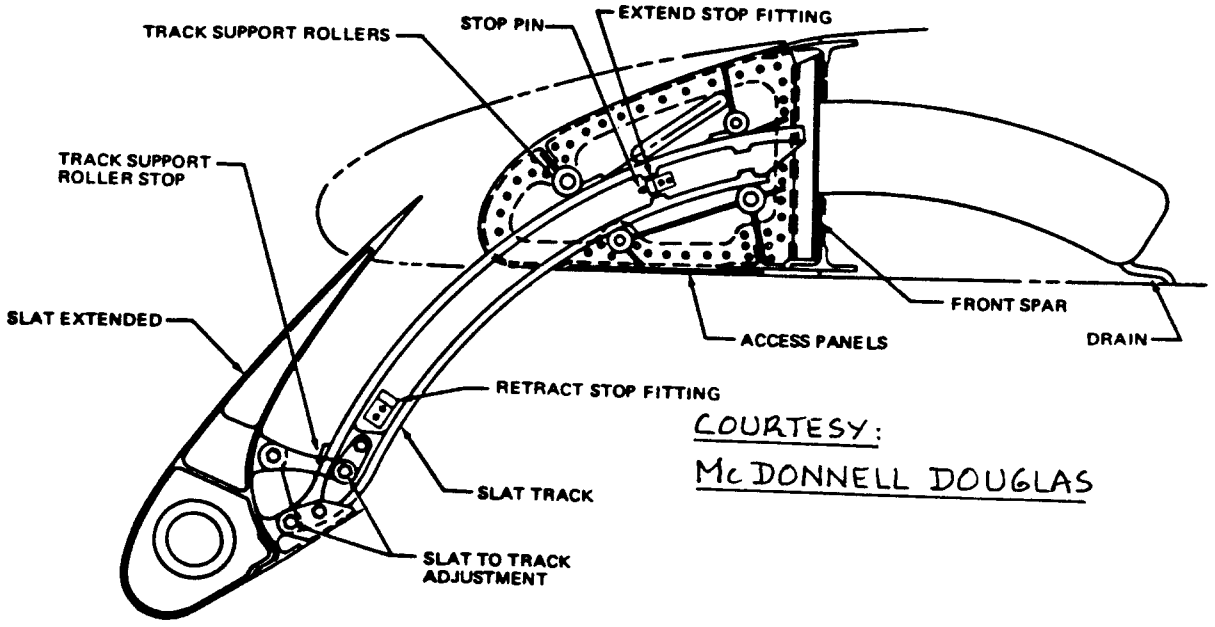

Figure 4.76 Leading Edge Slat Installation McDD DC-10

Figure 4.77 Single Slotted Flap Installation FR T-46

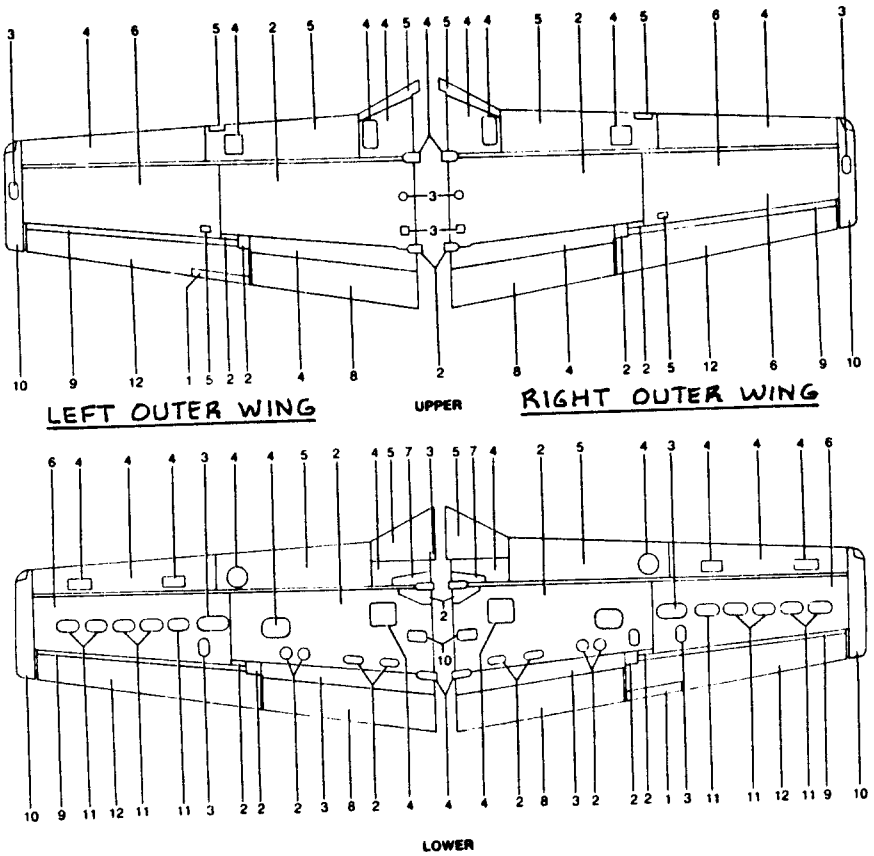

NUMBER	MATERIAL	THICKNESS IN INCHES
1.	2024-T3	.016
2.	2024-T3	.020
3.	2024-T3	.025
4.	2024-T3	.032
5.	2024-T3	.040
6.	2024-T3	.090
7.	2024-T42	.064
8.	6061-T6	.020
9.	6061-T6	.025
10.	6061-T6	.032
11.	6061-T6	.250
12.	AZ-31B-0 (Magnesium Alloy)	.020

COURTESY : BEECH

Figure 4.78 Typical Wing Skin Gages and Materials in a Beech King Air F90: Outer Wings

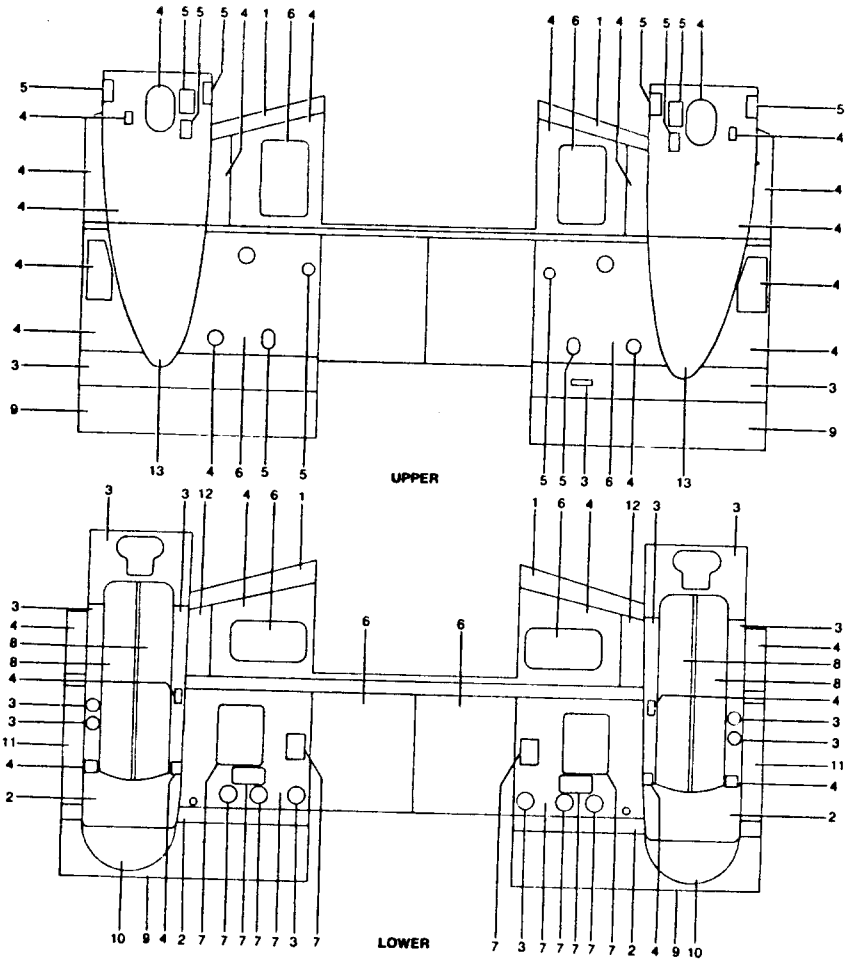

NUMBER	MATERIAL	THICKNESS IN INCHES
1.	2024-T3 (Four layers of .012 material are bonded together with Epibond 104 adhesive)	.012
2.	2024-T3	.020
3.	2024-T3	.025
4.	2024-T3	.032
5.	2024-T3	.040
6.	2024-T3	.050
7.	2024-T3	.063
8.	2024-T42 (Bonded Honeycomb)	.016
9.	2024-T42	.020
10.	2024-T42	.025
11.	2024-T42	.032
12.	2024-T42	.040
13.	6061-T62	.040

COURTESY: BEECH

Figure 4.79 Typical Wing Skin Gages and Materials in a Beech King Air F90: Center Section

4.3 MILITARY DESIGN CONSIDERATIONS

In many military airplanes there is a need for carrying external stores, for folding wings and for incorporating variable wing sweep.

Figure 4.80 shows an example of a typical wing 'hard point' and the method used to attach stores via a so-called weapons pylon. Note the major strengthening that is used at such a 'hard point'.

Particularly in the case of aircraft carrier based airplanes the need for wing folding (and sometimes vertical tail folding) often exists. Figures 4.81 through 4.84 show examples of folding applications.

A typical design problem associated with such folds is the way any controls are routed through such folding joints. Figure 4.85 shows an example of a wing fold joint. The controls are routed through this joint with a method shown in Figure 4.86.

Figure 4.87 shows a typical variable sweep wing pivot construction method. The reader is reminded of the fact that all wing loads must be passed through that one pivot. It is evident that this will incur a major structural weight penalty. In part V this penalty is assessed as 17.5 percent of the wing weight! Figure 4.87 also shows an application of a 'swiveling' wing store. In a variable sweep airplane this can become an additional complication.

4.4 DETAILED OVERALL STRUCTURAL ARRANGEMENTS

Because wing structural design cannot always be easily separated from the structural layout design of the entire airplane a number of overall structural layouts are presented to conclude this chapter on wing design. Figures 4.88 through 4.92 show structural cutaways for the following airplanes:

Figure 4.88 Cessna 441 Conquest
Figure 4.89 Cessna Citation II
Figure 4.90 Caproni Vizzola C22J
Figure 4.91 Fairchild Republic A-10
Figure 4.92 Douglas A4D-2N

For additional examples of wing structural arrangements the reader is referred to the airplane cutaway drawings in Chapter 9.

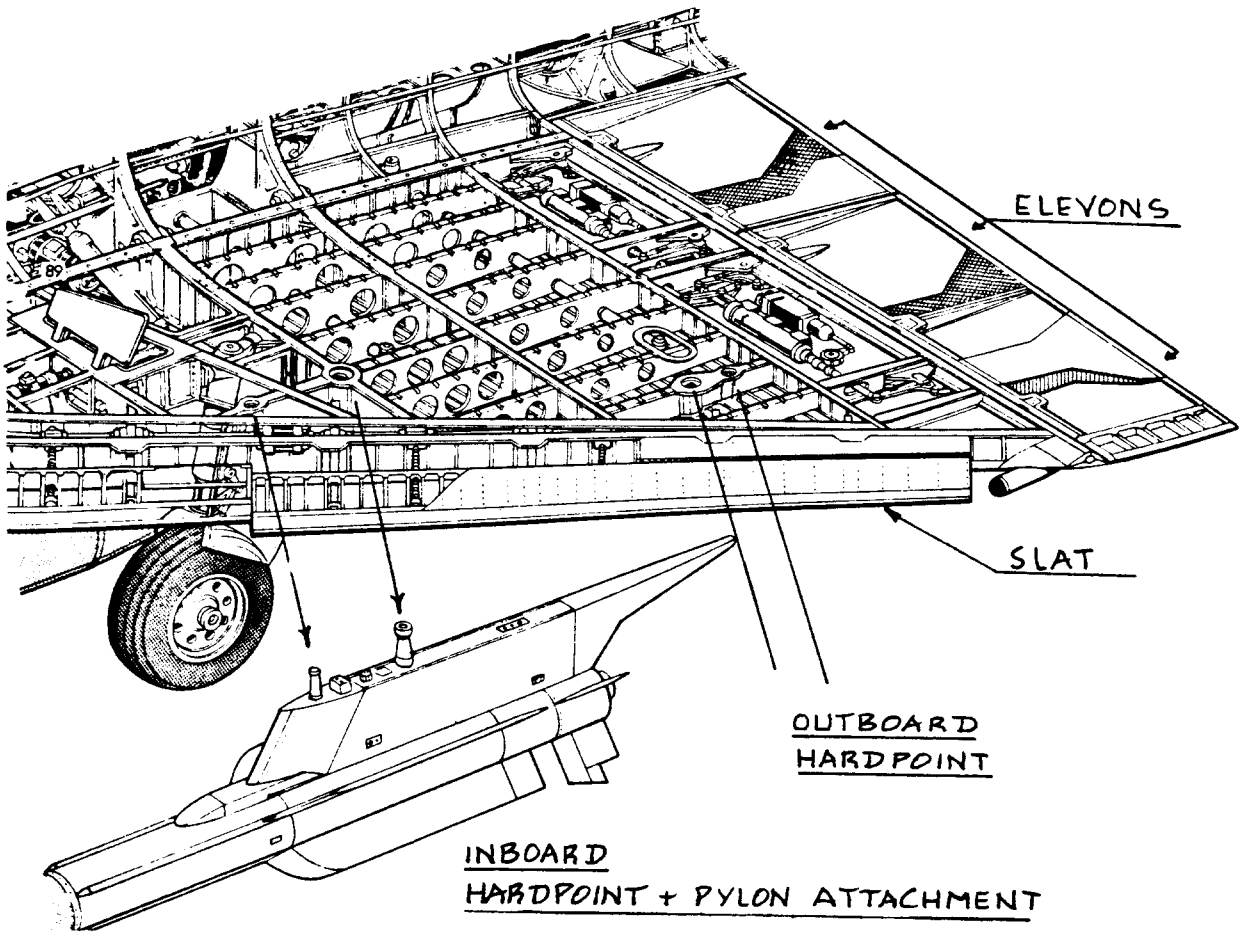

Figure 4.80 Example of a Wing Hard Point

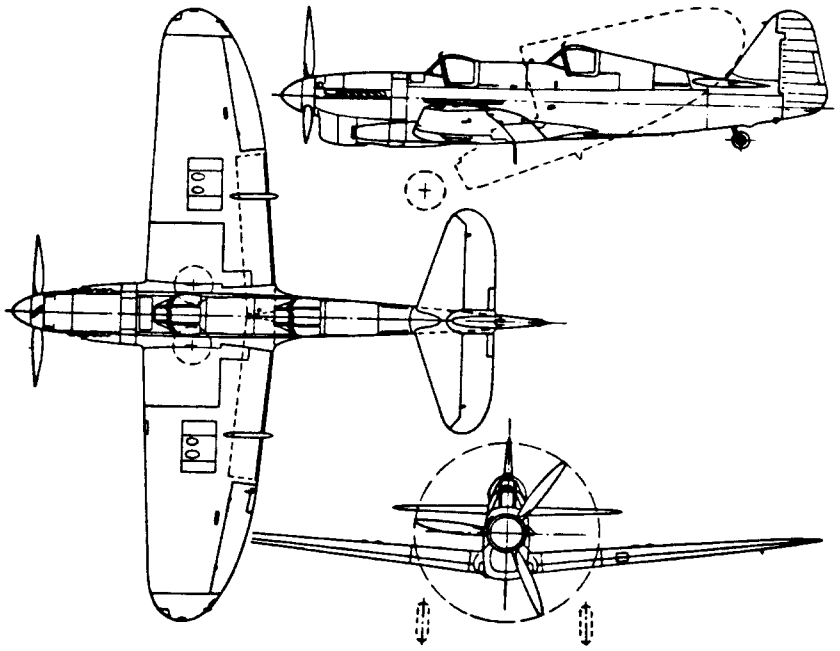

Figure 4.81 Wing Folding Fairey Firefly T1

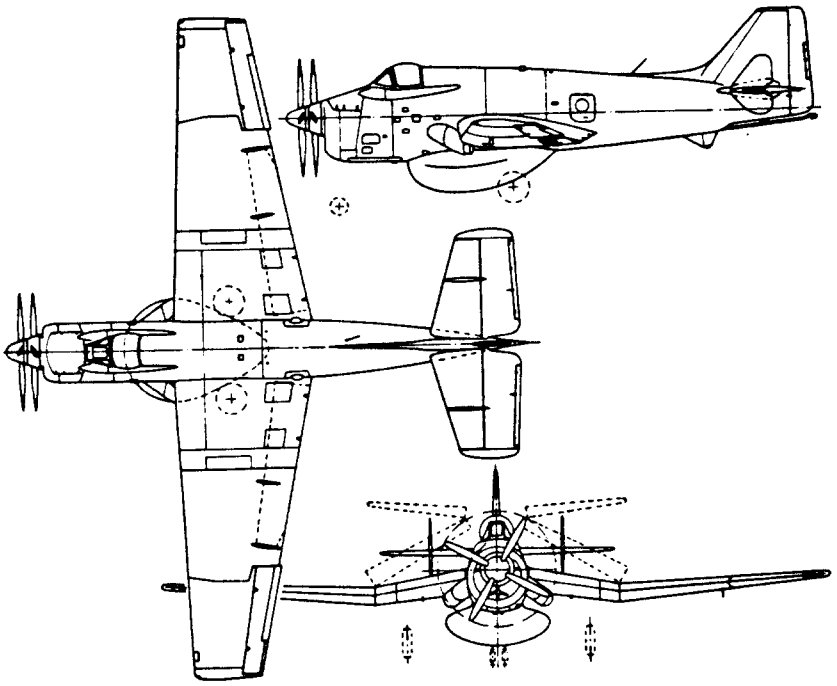

Figure 4.82 Wing Folding Fairey Gannett AEW3

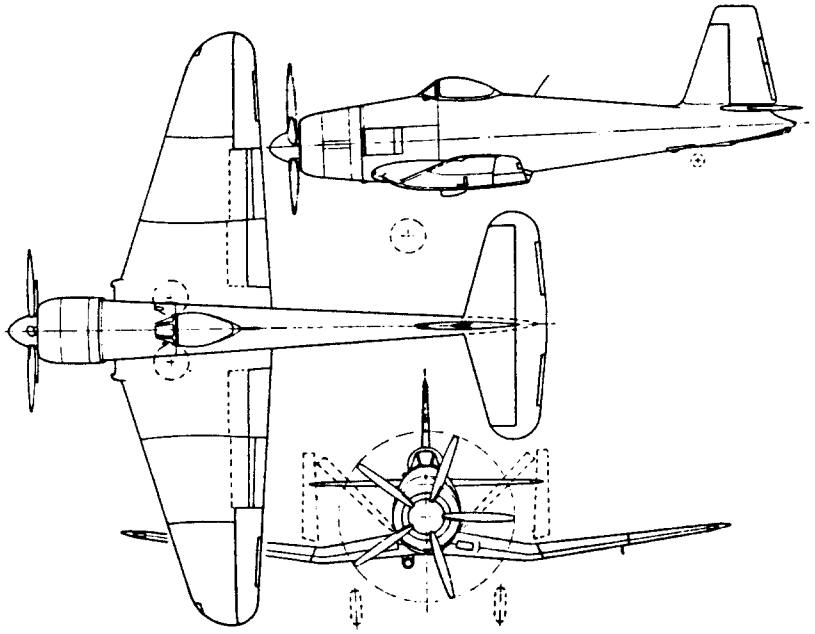

Figure 4.83 Wing Folding Blackburn B-48

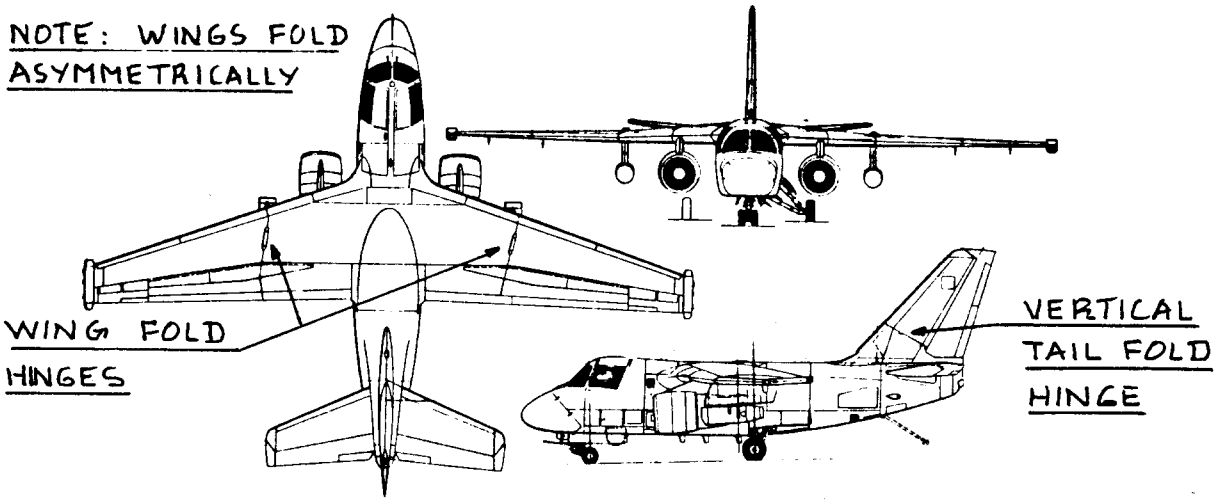

Figure 4.84 Wing and Vertical Tail Folding Lockheed S3-A

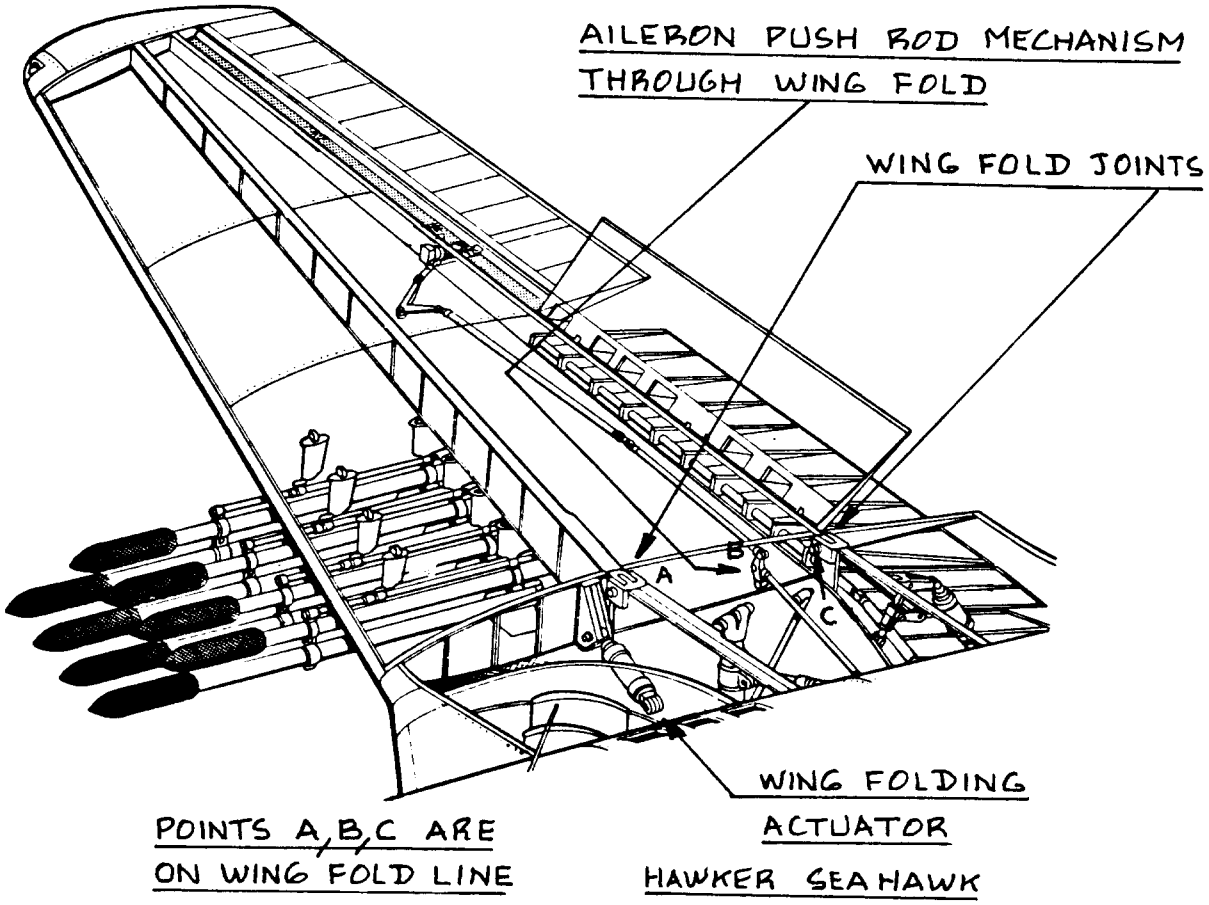

Figure 4.85 Example Wing Folding Mechanization

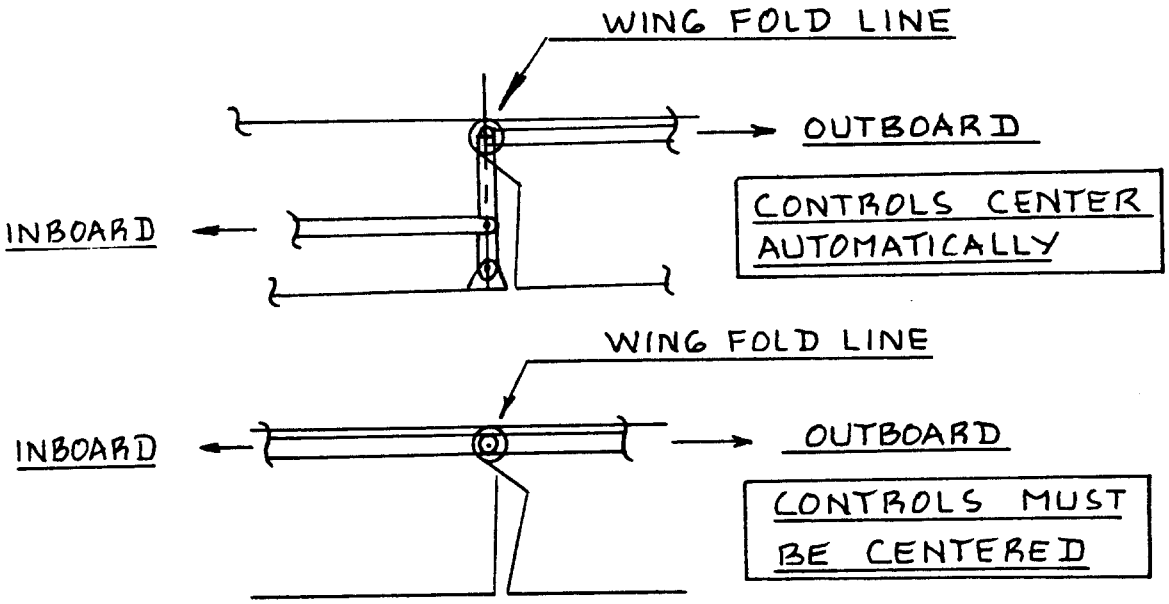

Figure 4.86 Controls Routing Through Wing Fold

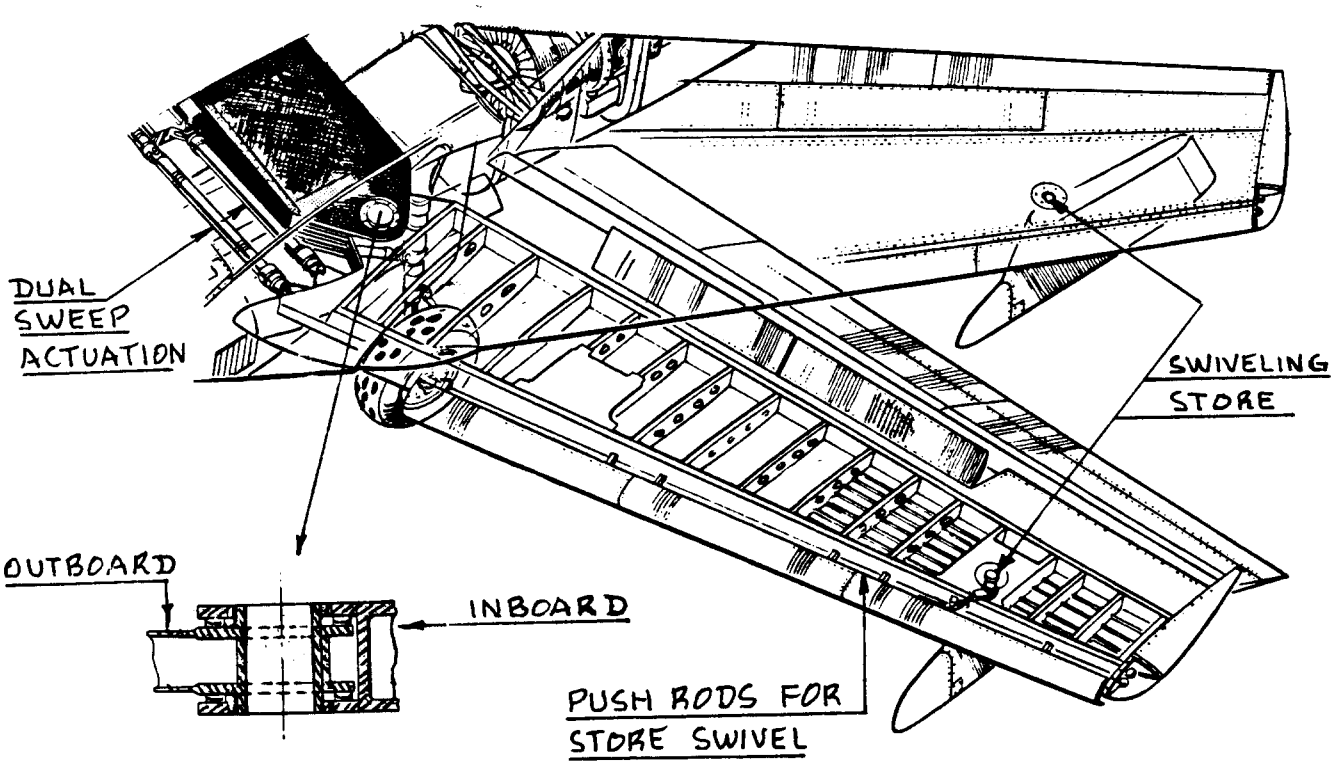

Figure 4.87 Example of Wing Pivot Construction and Swiveling Store Application

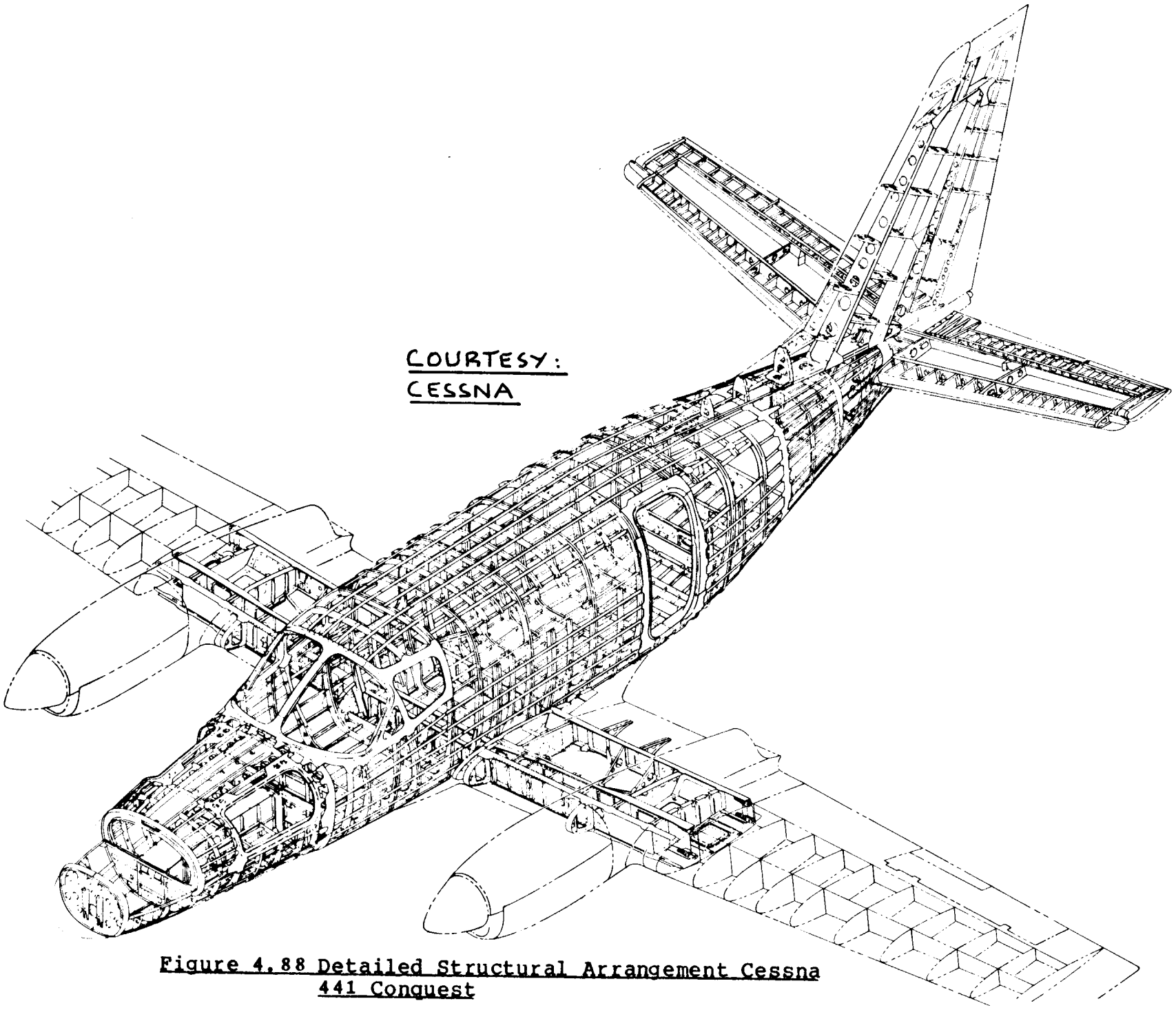

Figure 4.88 Detailed Structural Arrangement Cessna 441 Conquest

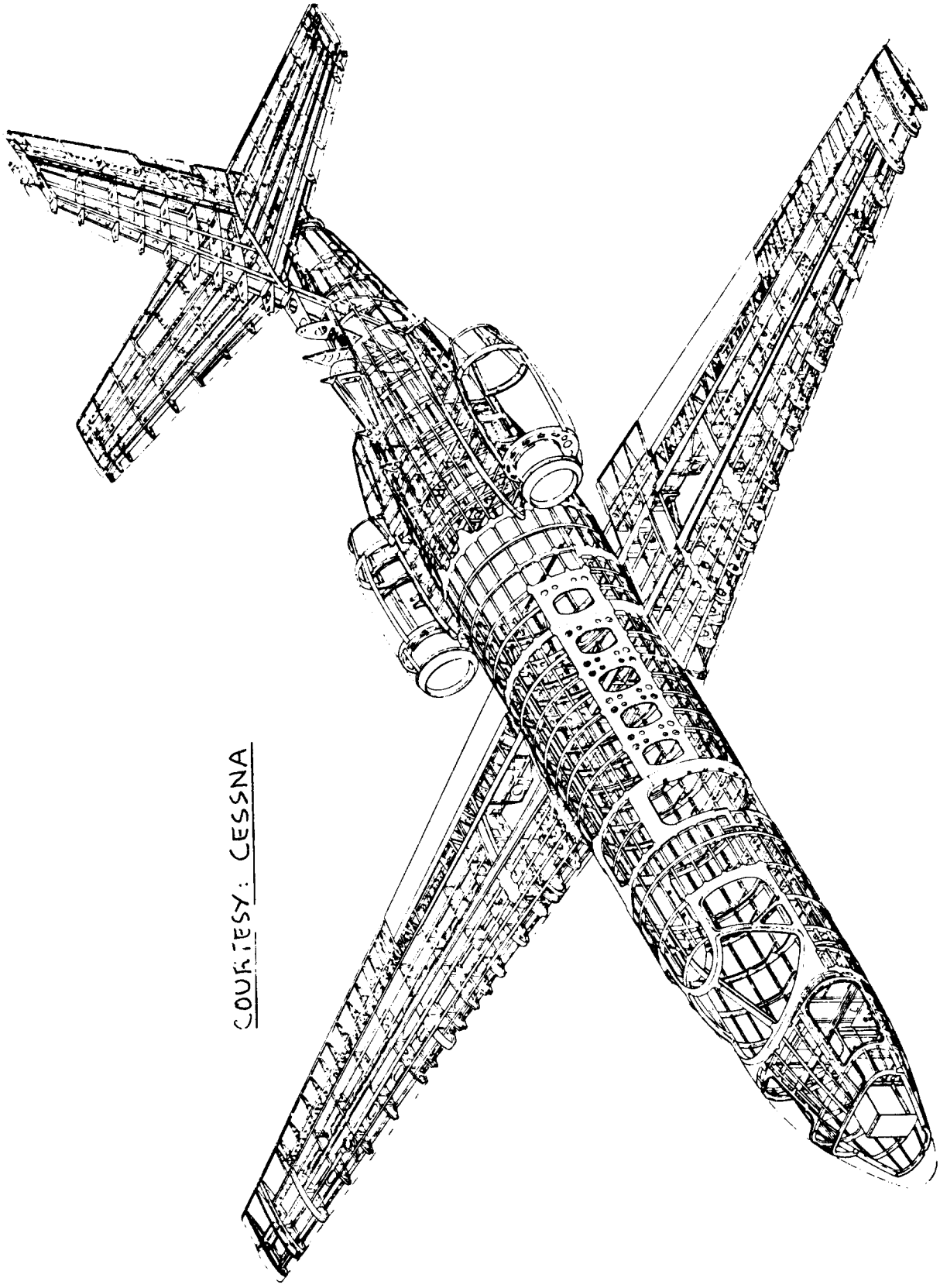

COURTESY: CESSNA

Figure 4.89 Detailed Structural Arrangement Cessna Citation II

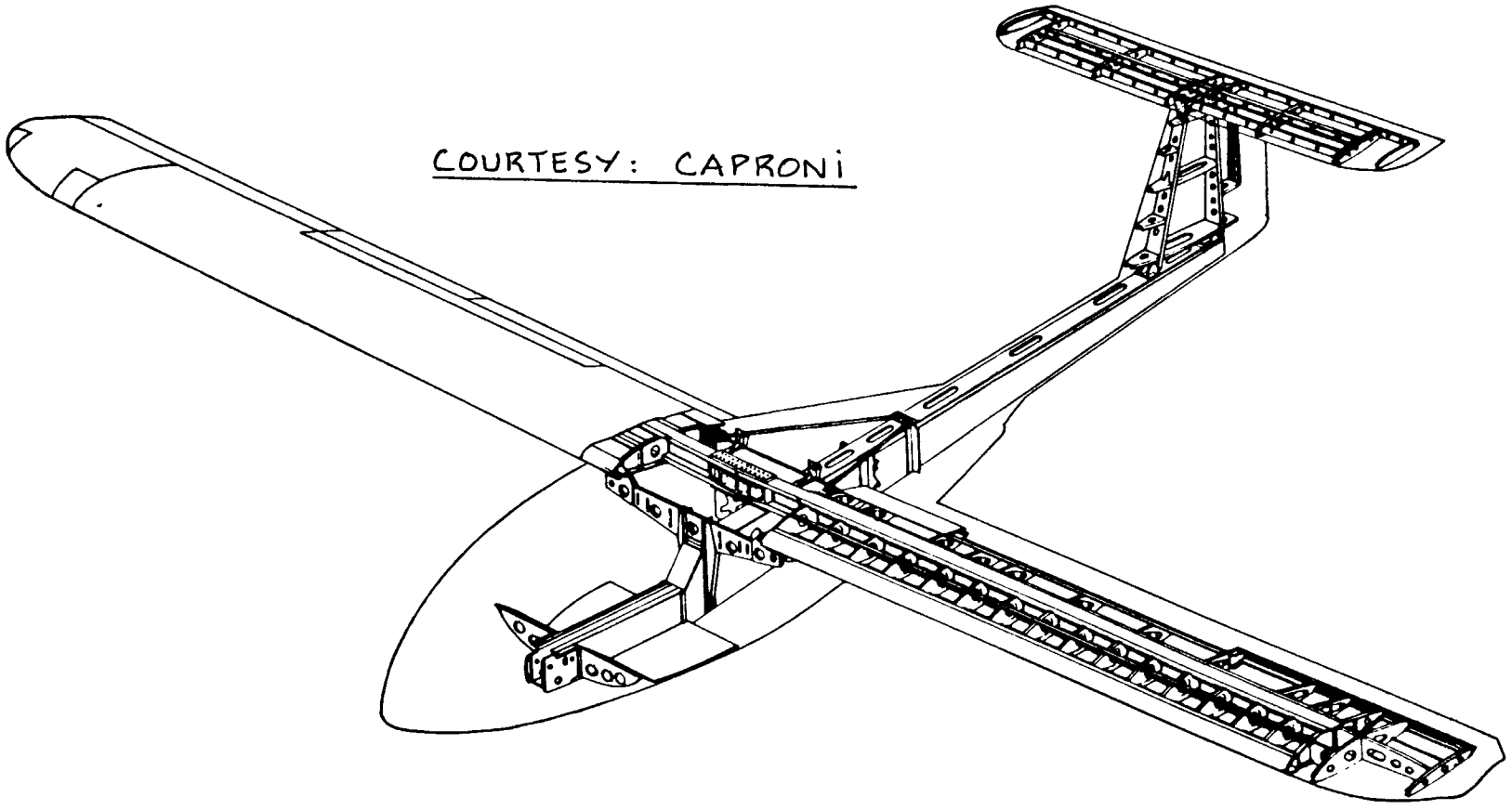

Figure 4.90 Detailed Structural Arrangement Caproni Vizzola C22J

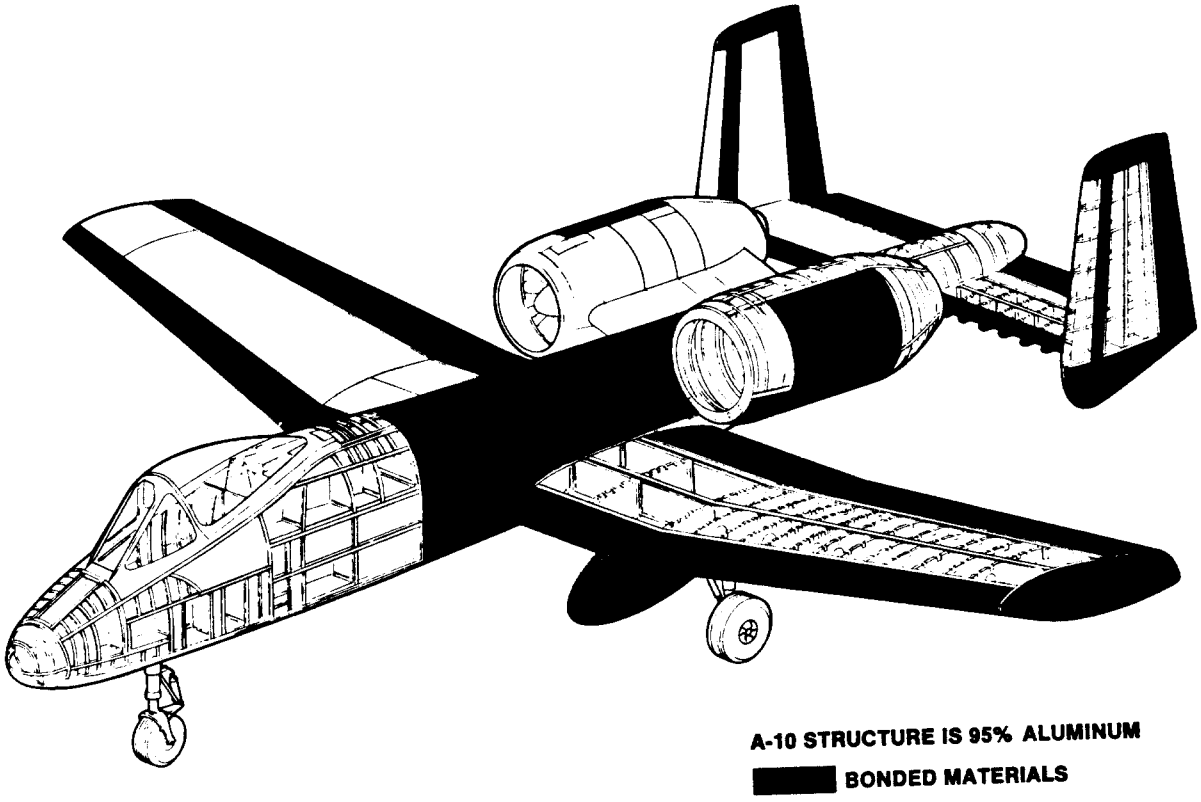

COURTESY: FAIRCHILD REPUBLIC

Figure 4.91 Detailed Structural Arrangement Fairchild Republic A-10

COURTESY: DOUGLAS

Figure 4.92 Detailed Structural Arrangement Douglas A4D-2N

5. EMPENNAGE LAYOUT DESIGN

The purpose of this chapter is to provide design considerations, design data and design examples for the layout design of the empennage.

A step-by-step procedure for arriving at a satisfactory Class I preliminary empennage layout is presented in Chapter 8 of Part II. That procedure is meant to be used together with p.d. sequence I of Chapter 2 in Part II. During the next phase of empennage design (Class II in p.d. sequence II as outlined in Chapter 2 of Part II) it is recommended to use the same procedure, but now augmented with the empennage design considerations presented in this chapter.

The reader should also review the large number of empennage/wing configurations presented in Chapter 3 of Part II. It is always useful to determine what has been done by various manufacturers.

Section 5.1 presents a general discussion of empennage design aspects: aerodynamic as well as operational.

Section 5.2 contains a discussion of empennage design integration considerations. Guidelines for structural design of the empennage are also given. Furthermore the structural integration of the empennage into the entire airplane configuration is discussed with examples.

5.1 EMPENNAGE CONFIGURATION: AERODYNAMIC AND OPERATIONAL DESIGN CONSIDERATIONS

An overview of airplane configurations including some discussions of empennage configurations is presented in Chapter 3 of Part II. A step-by-step procedure for arriving at a satisfactory preliminary empennage layout is contained in Chapter 8 of Part II.

The purpose of this section is to present additional design information relative to the choice of the empennage configuration.

References 12, 13, 14 and 37 should be consulted for further information on empennage design.

The following empennage configuration aspects will be discussed:

5.1.1 Conventional (Tails aft), canard or three-surface?
5.1.2 Additional empennage configuration choices.
5.1.3 Empennage and control surface size: stability, control and handling considerations.
5.1.4 Stall and spin considerations.
5.1.5 Empennage planform design.
5.1.6 Empennage airfoil design or selection.

Finally, a review of empennage drag contributions is presented:

5.1.7 Review of empennage drag contributions.

5.1.1 Conventional (Tails Aft), Canard or Three-surface?

The choice of conventional, canard and/or three-surface empennage configurations is strongly coupled with the overall airplane configuration design philosophy:

Important aspects to be considered are:

1. Achievable trimmed lift-to-drag ratio

2. Achievable trimmed maximum lift coefficient (flaps up)

3. Achievable trimmed maximum lift coefficient in landing and/or in take-off (flaps down)
   NOTE: This must be done AT THE CRITICAL C.G. LOCATION FOR THE CONFIGURATION BEING STUDIED

4. Distribution of major airplanes masses (examples are: engines, fuel, payload) and their relation to the weight and balance problem

5. Structural design synergism

6. Good looks

1. Achievable trimmed lift-to-drag ratio: Ref.48 shows that three-surface configurations can achieve higher trimmed cruise lift-to-drag ratios than either conventional or canard configurations. It is shown that three-surface configurations can achieve this at ANY location of the c.g.!

However, Ref.48 also observes, that these conclusions are based on the so-called Prandtl/Munk requirement of elliptical lift distributions and that

these conclusions may be invalid if actual spanload distributions are accounted for.

In Ref.49 it is shown that if actual spanload distributions are accounted for, the conventional configuration has higher trimmed L/D value. The Ref.48 data are valid for one c.g. location only and the method does not account for the effect of the propulsive installation on the lift distribution. Particularly for propeller driven airplanes this effect is known to be important.

Conclusion: no concensus exists with respect to the question which type of configuration yields the highest trimmed L/D in cruise.

2. Achievable trimmed maximum lift coefficient flaps up: No systematic studies have been carried out to determine which configuration can yield the maximum trimmed lift coefficient in a flaps up condition or with the use of maneuvering flaps. Unpublished work done by Grumman and by Rockwell seems to indicate the fact that in fighters the canard canard configuration has a definite edge in this regard.

3. Achievable trimmed maximum lift coefficient in landing and/or in take-off (flaps down): No systematic studies have been carried out to determine which configuration can yield the maximum trimmed lift coefficient in take-off and/or in landing (flaps down) conditions.

If canard/wing interference from canard tip vortices can be minimized the canard configuration and the three-surface configuration have (in principle) the higher trimmed maximum lift capability. The reason is quite simply the additive lift due to the canard when compared to the down lift from a conventional tail.

NOTE: This argument will be invalid for inherently unstable airplanes: in those cases the tail lifts up!

The reader should consult Part VII for detailed discussions of trim diagrams for stable and for unstable configurations.

4. Distribution of major airplane masses and their relation to the weight and balance problem: With the engines located forward (Cessna 172, Beech King Air, Boeing 737 and 747) the overall weight and balance of the airplane virtually dictates a conventional empennage

configuration. To minimize wetted area it is always desirable to have as little empennage area as possible.

To achieve the latter, the empennage surfaces must be placed in locations which maximize the product of the lift-curve-slope and the moment arm of each empennage surface! Figure 5.1 illustrates the principles involved here.

With the engines located aft (Rutan Varieze, Beech Starship I, Piaggio P 180, Boeing 727, Il-62) a conventional empennage arrangement becomes awkwardly large at some point. The Varieze wing/engine/fuselage combination has so much longitudinal stability that the only practical solution is a pure canard configuration. The 727 and the Il-62 use a very highly swept vertical tail to gain enough moment arm to still 'get away' with a conventional empennage arrangement.

5. Structural design synergism: In some cases it is possible by a unique combination of structural components to achieve a particularly favorable ratio of empty weight to take-off weight. The GP180 is an example: the wing torque box, the rear pressure bulkhead and the main landing gear are essentially attached to a common fuselage structure. Couple this with the favorable wing/fuselage intersection (mid wing) and a significant synergism has been achieved. What makes airplane configuration design decision making so difficult is that this type of 'synergism' needs to be weighed against other (sometimes negative) aspects of a particular layout. To make such decisions based on 'hard' data requires a lot of 'up-front' engineering effort. Time for such an effort is not always available.

Another example is the design case history of the Boeing 727. Ref.50 shows that in the early 727 design studies the landing gear was retracted into Küchemann bodies (See Fig.4.34 for an example), there was no acceptable spot for the APU and the rear cargo door was simply too small. By deciding to retract the gear into the fuselage (via a yehudi in the wing) which resulted in the need for a local enlargement of the fuselage cross section, sufficient room was created for the APU as well as for a cargo door of acceptable size.
These examples should indicate to the reader the importance of synergistic design thinking.

6. Good looks: This aspect of airplane design should not be considered as trivial. The 'good looks' question is obviously a very subjective one: de gustibus

non disputandum! An airplane designer should always consider the aesthetics of his creations. An example of this is the swept vertical tail on Cessna single engine airplanes. Those sweep angles are incorporated not for high Mach reasons but only for 'good looks'.

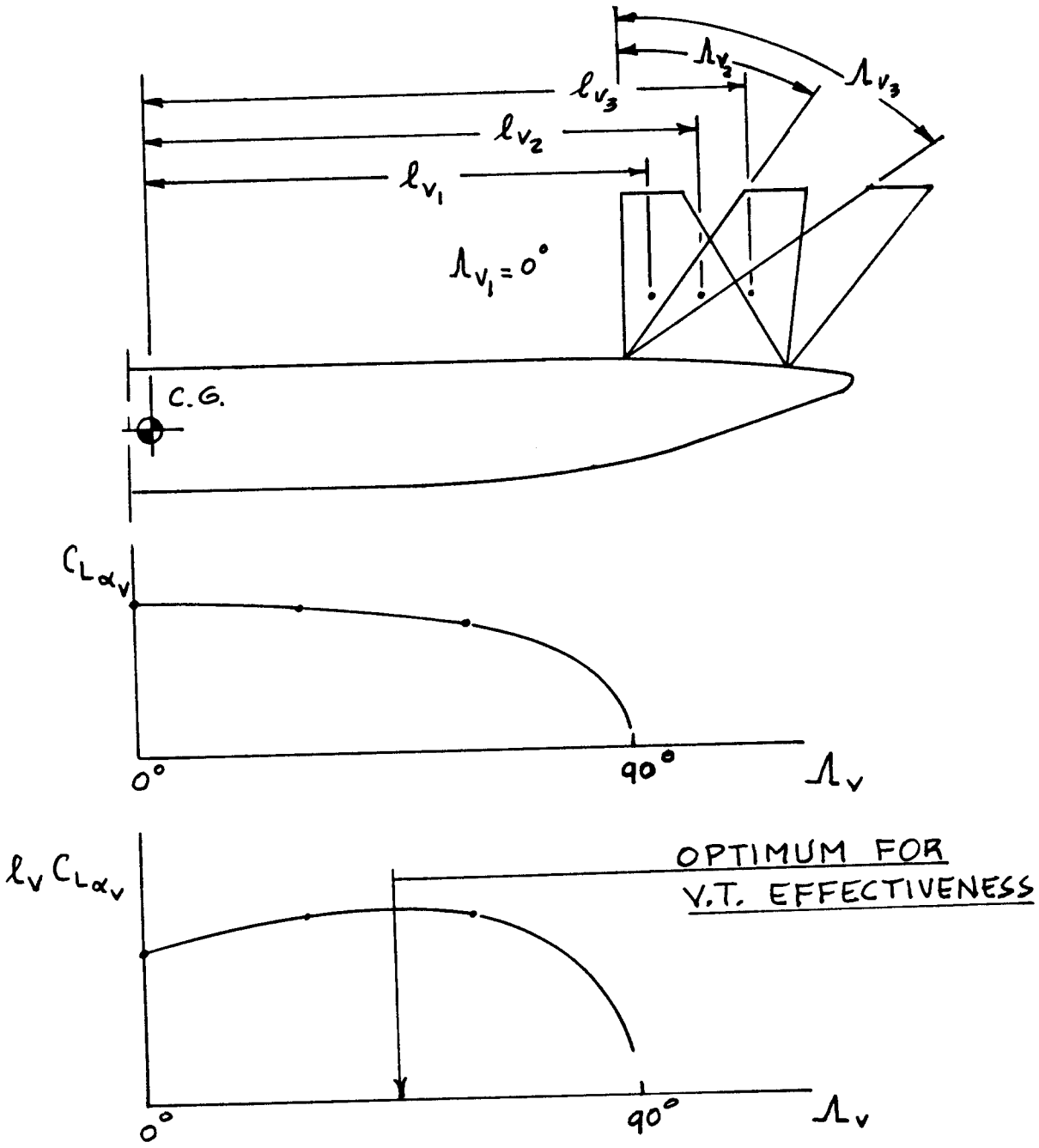

Figure 5.1 Illustration of Optimization of the Aerodynamic Effectiveness of an Empennage Surface

5.1.2 Additional Empennage Configuration Choices

Once the fundamental questions regarding the overall empennage configuration have been settled, a number of detailed configuration choices remain:

1. V-tail
2. T-tail
3. Single vertical tail
4. Multiple vertical tail
5. Twin boom tail
6. Vertical tail on wing

1. V-tail: Examples of V-tail (Butterfly tail) applications are found in the following airplanes:

1. Beech Twin Quad (Fig.5.2)
2. Beech Bonanza (Fig.5.3)
3. Fouga Magister (Fig.5.4)
4. Heinkel He211 (Fig.5.5)

Potential advantages of the V-tail configuration are small savings in wetted area and in weight when compared with a conventional empennage arrangement.

A so-called 'mixer' unit is needed to achieve uncoupled longitudinal and directional control. Figure 5.6 shows an example of such a 'mixer' in an airplane with a mechanical flight control system.

2. T-tail: Examples of T-tail applications are found in Figures 3.4, 3.8, 3.17, 3.21 and 3.32 in Part II.

From a viewpoint of vertical tail effectiveness per unit area, the 'best' locations for a horizontal tail in relation to the vertical tail is either the T-tail or the low tail configuration. The horizontal tail acts like an 'end-plate' which increases the lift-curve-slope of the vertical tail. Part VI contains a detailed procedure which accounts for this 'end-plate' effect.

From a structural weight viewpoint the low horizontal tail location is to be preferred over the T-tail location. This statement is not necessarily true in cases such as the 727, the DC9 and the BAC 111. In those airplanes (because of the aft engine mounts on the fuselage) it would be very difficult to find an acceptable 'low' position for the horizontal tail. Also, by sweeping the vertical tail aft, moment arm is gained for the T-tail mounted horizontal tail. This saves horizontal tail area.

Most T-tail mounted horizontal tails are given a slight amount of anhedral. Flutter calculations for the T-tail arrangement usually show that doing this saves weight.

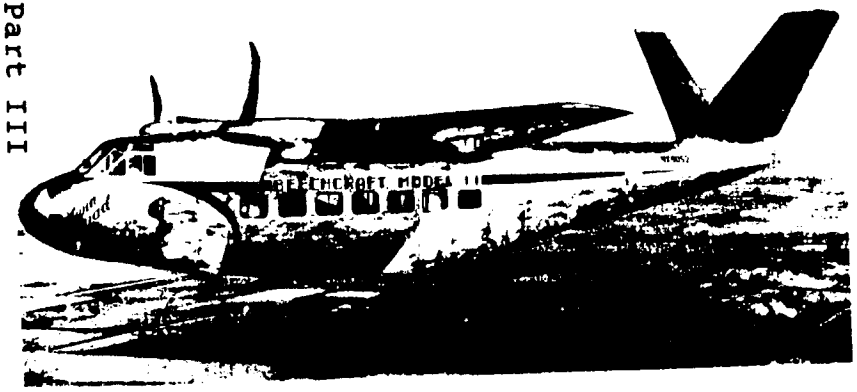

Figure 5.2 Beech Twin Quad

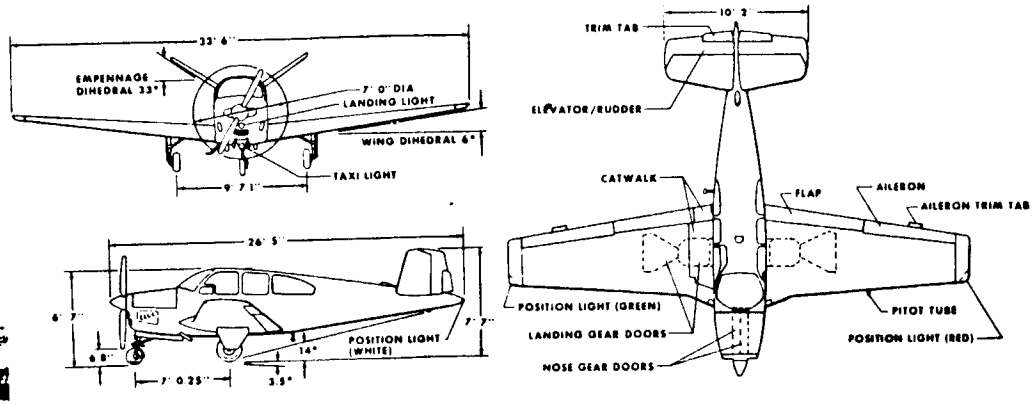

Figure 5.3 Beech Bonanza

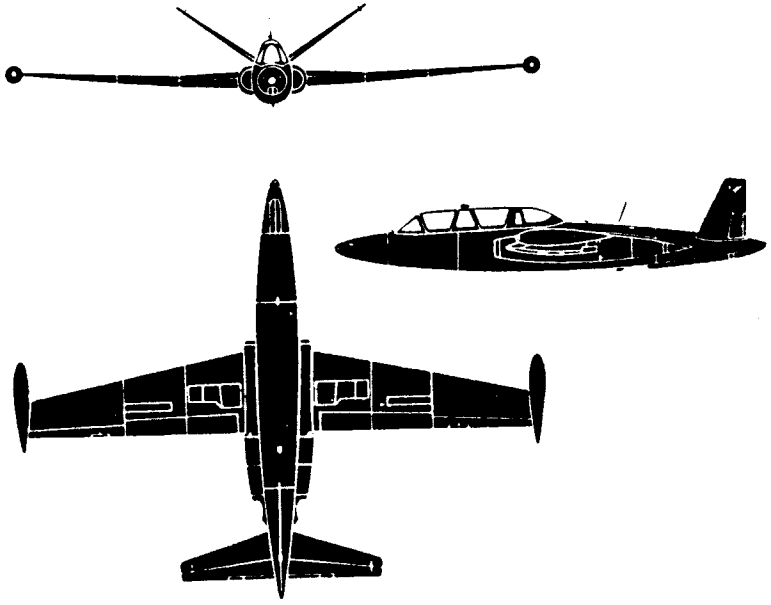

Figure 5.4 Fouga Magister

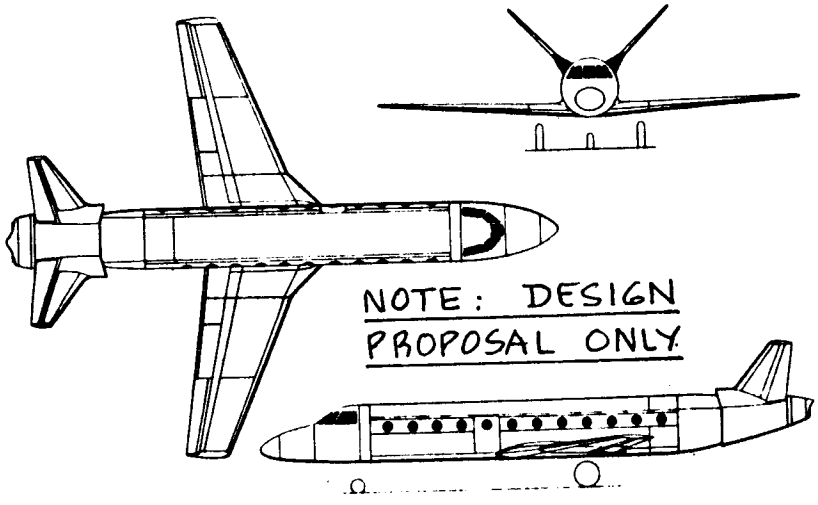

Figure 5.5 Heinkel He 211

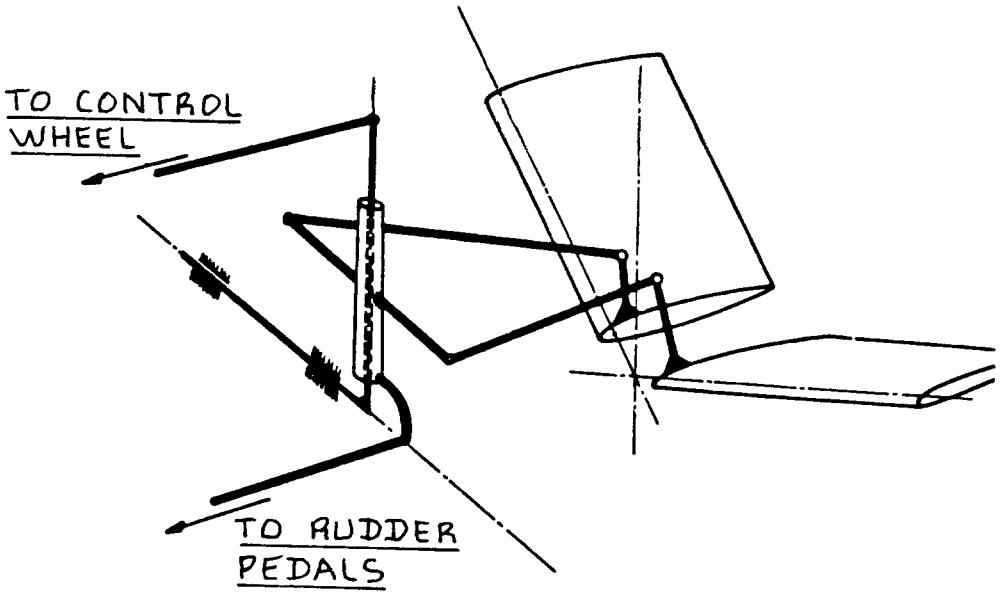

Figure 5.6 Control Mixer for a V-tail

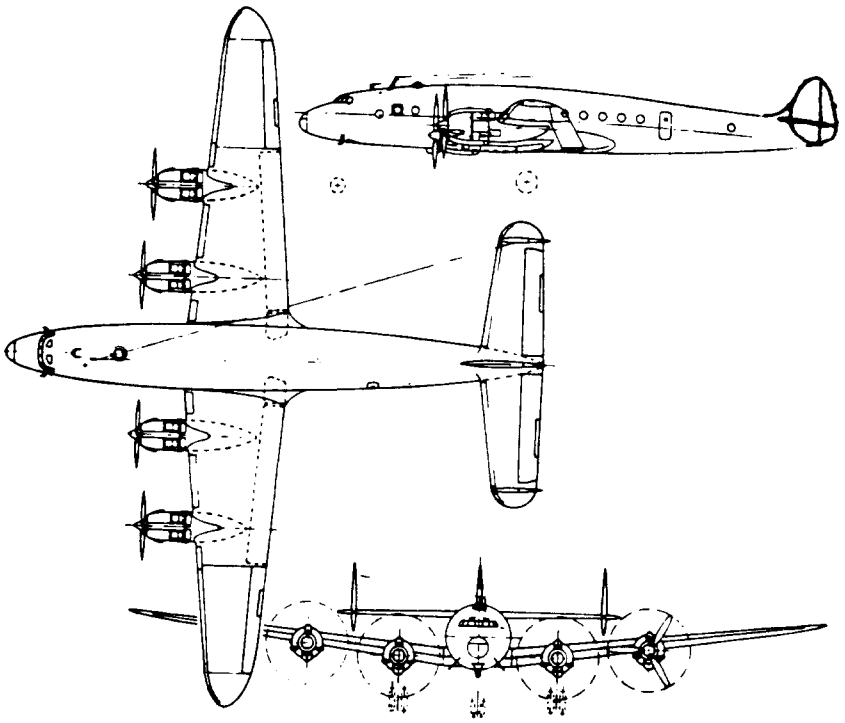

Figure 5.7 Lockheed Constellation

T-tail configurations often are prone to the so-called 'deep-stall trim-point problem'. This problem is discussed in more detail in sub-section 5.1.4.

3. Single vertical tail: Most airplanes have the single vertical tail configuration. Chapter 3 of Part II contains examples of single vertical tail applications.

From a weight viewpoint as well as from several aerodynamic viewpoints the single vertical tail is the most effective one for civil airplanes in the low s subsonic speed range. The reason is that a single vertical tail can be built with a higher aspect ratio and therefore be more effective per unit area.

Potential disadvantages of large single vertical tails are:

1. Large rolling moment due to rudder deflection: to 'fix' this requires an aileron/rudder interconnect system.

2. Problems with servicing and hangering because of excessive height.

For supersonic airplanes a single vertical tail is usually not a good design solution. The reason is the fact that the vertical tail normally is located in an expansion wave behind the wing. The dynamic pressure at the vertical tail tends to be less than the free stream dynamic pressure. For such airplanes a vertical tail located below the wing would be best above Mach 1.

Solutions to this problem are: folding vertical fins (Mig-27 Flogger), fixed ventral fins and/or multiple vertical tails. Many fighters in Chapter 3, Part II use some of these solutions.

The XB-70A of Fig.3.34b (Part II) employs folding wingtips to enhance directional stability in supersonic flight and at the same time reduce the aft shift of aerodynamic center which is a problem in nearly all supersonic airplanes.

If there are good reasons not to use either a low horizontal tail or a T-tail, a so-called 'cruciform' arrangement may be used. Examples of 'cruciform' arrangements are found in Part II as:

1. Dassault Falcon 50 (Fig.3.13d)
2. BAE HS 125 (Fig.3.15b)
3. Cessna Crusader (Fig.3.8c)
4. Lockheed Jetstar (Fig.3.13a)

A disadvantage of the cruciform arrangement is the lower vertical tail effectiveness due to lack of 'end-plate' effect. In some airplanes it is possible to use the cruciform arrangement to place the horizontal tail outside the slipstream to prevent tail buffeting (fatigue). This can be an important consideration in propeller driven airplanes with high power-to-weight ratios.

An interesting aspect of the Lockheed Jetstar is that the entire vertical pivots so that its leading edge sweep angle is altered. This is done to achieve longitudinal trim!

4. Multiple vertical tails: Examples of multiple vertical tail applications are:

1. Lockheed Constellation (Fig.5.7)
2. Grumman E2C Hawkeye (Fig.3.30c in Part II)
3. Antonov AN-22 Antheus (Fig.3.28d in Part II)
4. Fairchild Republic T-46A (Fig.3.23b in Part II)
5. Grumman F-14A Tomcat (Fig.3.25a in Part II)
6. F.R. A-10A Thunderbolt II (Fig.3.27c in Part II)
7. McDD F-15C Eagle (Fig.3.27b in Part II)

Potential advantages of multiple vertical tails are:

1. low rolling moment due to rudder deflection
2. redundancy to combat damage (A-10A!!)
3. in propeller driven airplanes: slipstream augmentation of one of the vertical tails in an engine out situation

5. Twin boom tails: Examples of twin boom tail applications are:

1. Cessna Skymaster (Fig.3.9c in Part II)
2. Fairchild Packet II (Fig.3.41 this part)
3. Armstrong Whitworth Argosy (Fig.3.2 this part)
4. WSK Mielec M-15 (Fig.3.11c in Part II)
5. Eris (Fig.13.3 in Part II)

Twin boom configurations are usually heavier that layouts with a conventional fuselage. One reason is that the fuselage of a twin boom airplane tends to have a low fineness ratio which increases drag which in turn results

in higher required installed power and thus weight.

In cargo transports the high wing twin boom layout can be advantageous from a loading and unloading viewpoint.

If the booms can also be used to carry fuel (this makes sense only for extremely long range airplanes) the twin boom design can in fact come out lighter. An example of such a case is the Rutan Voyager 'around-the-world' airplane.

6. Vertical tail on wing: The Beech Starship I and the XB-70A are examples of this approach (Figures 3.42 and 3.34b, Part II respectively).

There have not been many instances where the vertical tail was mounted on the fuselage, forward of the c.g. This approach would reduce directional stability! The AFTI F16 and an experimental German modified F4 both of which used their 'vertical canards' to reduce directional stability and to allow pure sideforce control, are notable exceptions.

5.1.3 Empennage Size: Stability, Control and Handling Considerations

A step-by-step Class I method for empennage and control surface sizing is presented in Chapter 8 of Part II. In Class II empennage sizing methods much more detailed analyses of the stability and control characteristics of an airplane are needed. A detailed review of airplane stability and control theory and applications may be found in Ref.37. Part VII contains Class II methods for determining the required stability, control and handling characteristics of airplanes. This sub-section will highlight some of the most important aspects of empennage design as it relates to stability, control and handling requirements.

WARNING: Whether or not an airplane is structurally rigid or elastic can make a great deal of difference to stability and control behavior. The reader should not automatically assume that all airplanes are reasonably rigid. Most jet transports and even fighters in high 'g' flight conditions should be considered as 'elastic' airplanes. Ref.37 contains methods for analyzing the effects of aeroelasticity on stability and control.

5.1.3.1 Longitudinal considerations

From a viewpoint of longitudinal stability, control and handling, the horizontal empennage surfaces must satisfy the following requirements:

1. Longitudinal stability requirements
2. Longitudinal control requirements
3. Longitudinal stick (or wheel) force requirements

1. Longitudinal stability requirements: Longitudinal stability at forward and at aft c.g. must be consistent with requirements for static, dynamic as well as maneuvering stability. Stability requirements (inherent or de-facto) determine primarily the size of the horizontal empennage surfaces, once the disposition (i.e. moment arms) has been decided.

The stability requirements of Ref.51 should be used in conjunction with the methods of Part VII to determine the adequacy of any proposed empennage configuration and size.

2. Longitudinal control requirements: The following longitudinal control requirements must be considered:

2a. Control power for trim at forward and aft c.g. must be consistent with the operational flight envelope and weight of the airplane.

2b. Control power for take-off rotation at forward c.g. (for tricycle gear airplanes) and at aft c.g. (for taildraggers) must be consistent with the operational flight envelope and weight of the airplane. If control power for take-off rotation is not sufficient a consequence is that the take-off fieldlength is much larger than predicted.

2c. Control power for maneuvering (in calm and in gusty air) must be consistent with the operational flight envelope, c.g. location and weight of the airplane. This requirement is particularly important in the case of inherently unstable (highly augmented) airplanes.

2d. Control power must be sufficient to allow for any requirements for artificial static and/or dynamic stability.

Control power requirements determine both the size and the maximum lift of the horizontal empennage surfaces. Ref.51 should be used in conjunction with the

methods of Part VII to assure that empennage and control surface sizes are sufficient.

3. Longitudinal stick (or wheel) force requirements: These requirements cover such concepts as: stick-force speed gradients, trim speed and return-to-trim-speed, stick-force per 'g' and maximum incremental stick force needed to cope with changes in airplane configuration such as: power or thrust changes, flap changes and/or failures.

References 11 and 51 should be consulted for details. Ref.37 and Part VII contain detailed methods for analyzing stick force requirements.

5.1.3.2 Lateral-Directional considerations

From a viewpoint of lateral-directional stability, control and handling the vertical empennage surfaces must satisfy the following requirements:

1. Lateral-directional stability requirements
2. Lateral-directional control requirements
3. Lateral-directional stick (or wheel) and rudder pedal force requirements.

1. Lateral-directional stability requirements: The following lateral-directional stability requirements must be considered:

1a. Lateral stability must be consistent with requirements for static and dynamic stability at all c.g. locations and the operational flight envelope of the airplane. This requirement is usually dominated by the inherent lateral stability designed into the wing. It is shown in Ref.37 that wing dihedral angle, wing sweep angle and wing location on the fuselage dominate the magnitude and the sign of the stability derivative C_{l_β}.

Since the wing is designed primarily by performance and operational considerations, the empennage is often used to 'fine-tune' the lateral stability of airplanes. Examples of this fine-tuning are: F-4 and AV8B.

1b. Directional stability must be consistent with requirements for static and dynamic stability at all c.g. locations and the operational flight envelope of the airplane. This requirement often dictates the size of the vertical tail.

2. Lateral-directional control requirements: The following lateral-directional control requirements must be considered:

2a. Lateral control power must be sufficient to meet the time-to-bank and response requirements of Refs 11 and 51.

2b. Directional control power must be sufficient to handle the most critical engine-out situation (V_{mc}).

2c. Directional control power must be sufficient to allow for cross-wind landing conditions

2d. Directional control power must be sufficient to allow for maneuvering.

2e. Directional control power must be sufficient to provide for any requirements for artificial static and/or dynamic stability.

These control power requirements determine the size, type and location of ailerons, spoilers, differential stabilizers and rudders. Requirement 2b) also may determine the maximum lift capability demanded of the vertical tail with full rudder deflection. References 11 and 51 should be used in conjunction with the methods of Part VII to assure the correct size of the lateral-directional control surfaces.

3. Lateral-directional stick (or wheel) and rudder pedal force requirements: It takes a definite physical effort by a pilot to move the primary cockpit controls. It is obvious that the cockpit control forces needed by the pilot to satisfy the control power requirements outlined under 2) must be within the capabilities of the pilot. References 11 and 51 specify the allowable control force limits for temporary and for prolonged situations. Ref.37 and Part VII contain methods for the analysis of pilot control force requirements.

5.1.4 Stall and Spin Characteristics

For satisfactory stall and spin characteristics it is necessary that sufficient control power and stability can be maintained up to levels of angle of attack and sideslip consistent with the operational requirements for the airplane.

The following characteristics will be discussed:

1. Stable and unstable pitch breaks
2. The stall scenario
3. The deep stall trim problem
4. Pitch-up in high speed airplanes
5. Spin departure
6. Spin Recovery

1. Stable and unstable pitch breaks: The C_m-C_L behavior of the airplane at forward and at aft c.g. is of major importance here as well as the associated behavior of the C_L-α curve.

Figure 5.8a illustrates the C_L-C_m behavior for airplanes with a stable pitch break. It is noted that stable pitch breaks are required for FAR23 airplanes.

Figure 5.8b shows the C_L-C_m character for airplanes with an unstable pitch break. Unstable pitch breaks are acceptable for FAR25 and for military airplanes. However, depending on the dynamic behavior of the airplane following pilot induced stall entry (or gust induced stall entry) the airplane may have to be outfitted with stick-shakers and/or stick-pushers. In the latter case, the value for $C_{L_{max}}$ which may be used in the certification of the airplane is not the 'aerodynamic' $C_{L_{max}}$ but instead is a value somewhere between 'stick-shaker C_L' and 'stick-pusher C_L' (See Fig.5.8b). This can lead to significant performance penalties, particularly in field length.

2. The stall scenario: Two types of configurations will be discussed: conventional (aft tail) configurations and canard configurations.

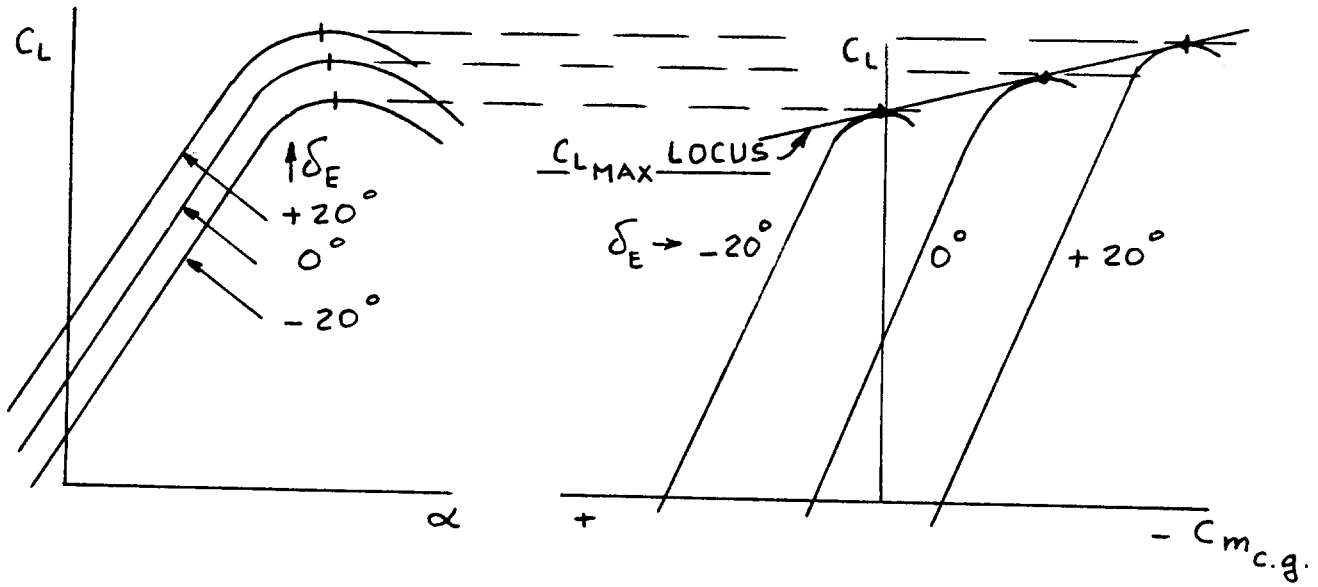

Figure 5.8a Stable Pitch Break Behavior

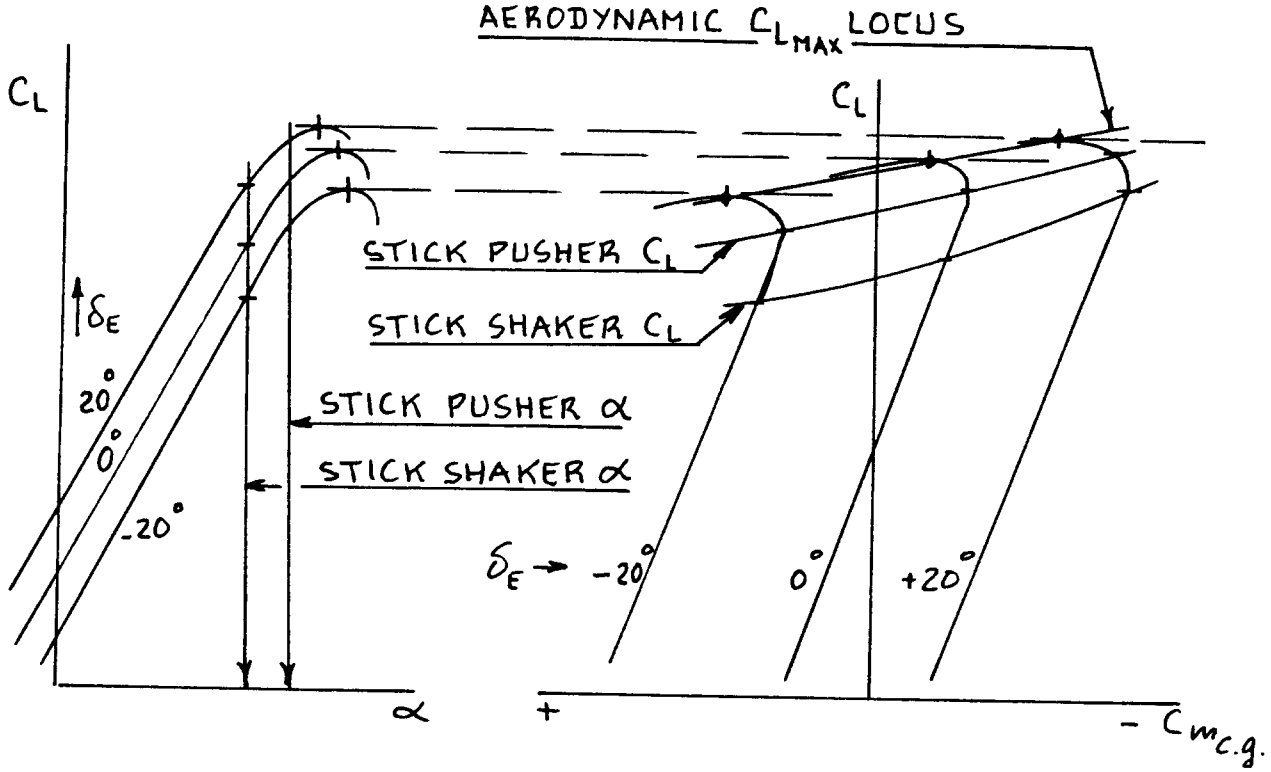

Figure 5.8b Unstable Pitch Break Behavior

2a) Conventional (aft tail) configurations: The high angle of attack pitching moment behavior of a conventional airplane depends on the behavior of the wing-body and on that of the horizontal tail.

The stall scenario for a conventional airplanes is as follows:

Once the wing stalls along the inboard trailing edge, the downwash from that part of the wing over the horizontal tail disappears. This is seen by the horizontal tail as a positive increase in angle of attack. This creates a nose down pitching moment which is perceived by the pilot as a 'stable' pitch break.

However: the breakdown of the flow over the inboard part of the wing can change the wing contribution to airplane pitching moment. If the wing contribution to pitching moment becomes 'larger positive' than the tail contribution is 'negative', an unstable pitchbreak results.

Figure 5.9 shows the classical pitch stability boundary for wings in terms of aspect ratio and sweep angle. Note that wings with very high aspect ratios will have unstable pitchbreaks even at low sweep angles. The tail must be designed to overcome this if a net stable break for the entire airplane is required.

Figure 5.10 identifies four regions for the location of the horizontal tail: A, B, C and D.

Figure 5.11 shows the net result of adding the horizontal tail in each of these regions:

in Region A: the wing wake does not affect the tail. This is normally the best place for a horizontal tail. With flaps down, the flap wake may alter this!

in Region B: same as A at low speeds. However, at high subsonic speeds, particularly when maneuvering, there could be a problem.

in Region C: the horizontal tail will enter the wing wake only when the latter is unstable.

in Region D: a reversal of the C_m-C_L curve will usually occur leading to the 'deep-stall' trim-point phenomenon which is discussed under 3.

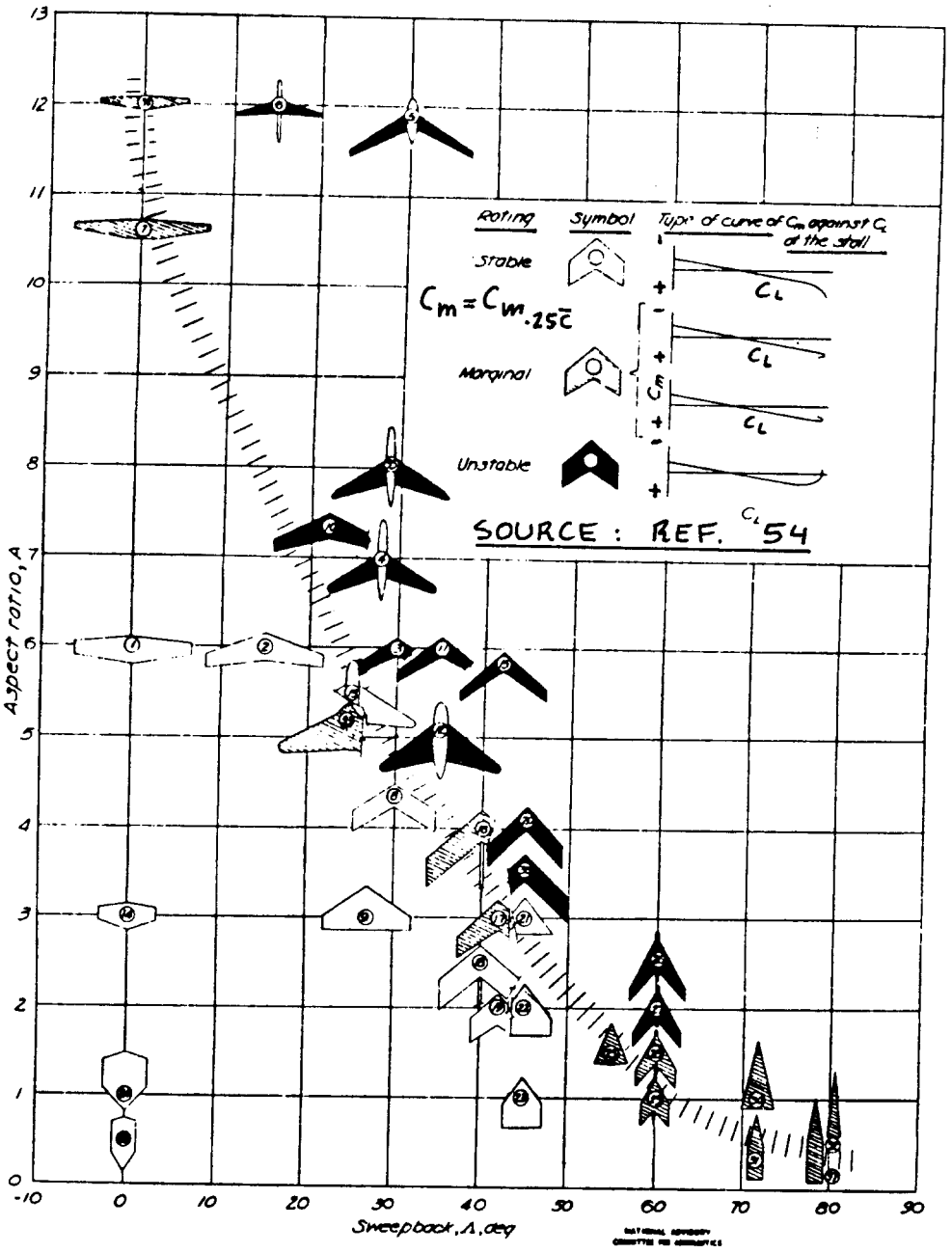

Figure 5.9 Wing Alone Pitch Break Stability Boundary

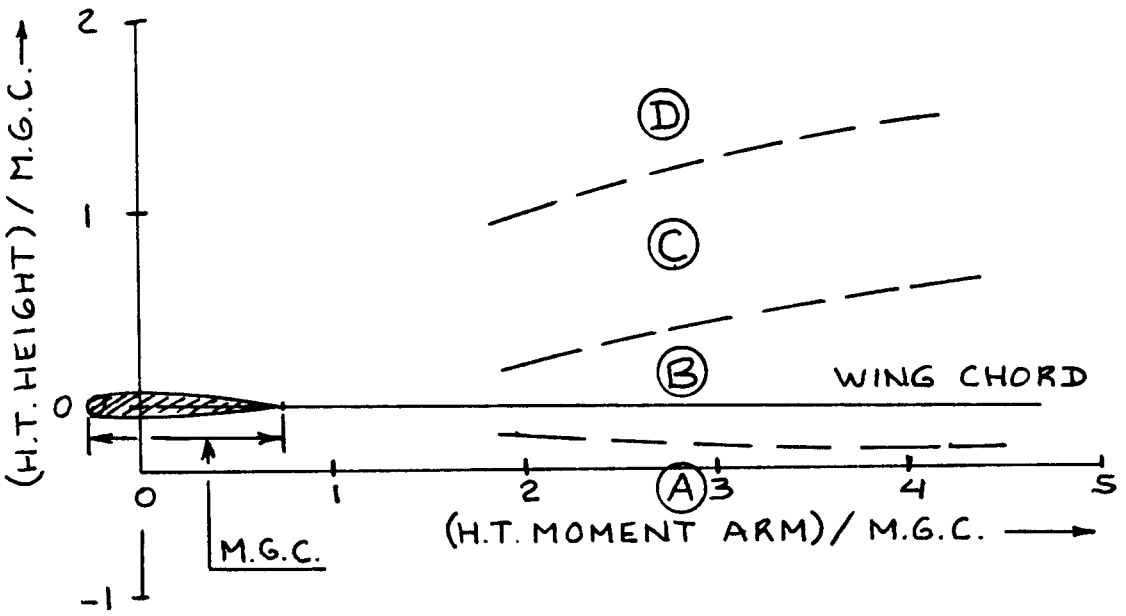

Figure 5.10 Four Regions for Horizontal Tail Location in Relation to Pitch Break Stability

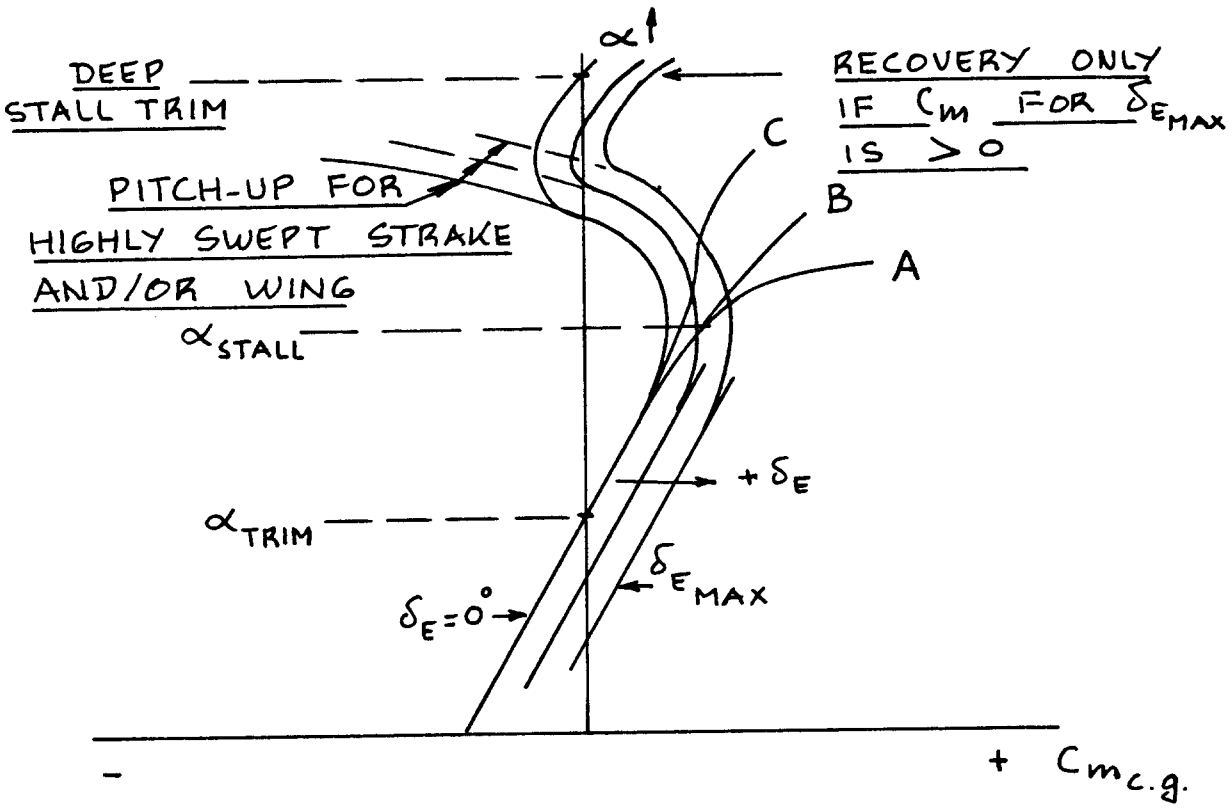

Figure 5.11 Pitch Break Behavior of Airplanes with the Horizontal Tail Located in the Regions of Figure 5.10

2b) Canard configurations: These must be designed so that the canard stalls before the wing.

The stall scenario for a canard airplane should be as follows:

When the canard stalls, a nose-down pitching moment is automatically generated: the canard lift drops and the canard downwash at the wing disappears which has the effect to slightly increase wing lift. Both factors contribute to the nose-down pitching moment.

The following design decisions must be made:

i) What type airfoil to use in the canard surface.
ii) What incidence angle should the canard have.

i) The selection of canard airfoil affects the value of $C_{L_{max}}$ which can be generated by the canard. If the canard airfoil is a laminar flow airfoil its sensitivity to transition to turbulent flow (for example due to flying into rain) must be carefully considered if major trim changes are to be avoided. Whether any such trim changes are acceptable depends on available control power as well as on the required stick (or wheel) force to compensate for these trim changes.

The reader should be aware of the fact that these considerations apply to ALL flap configurations which may be operationally encountered!

ii) The canard incidence angle determines when canard stall will occur relative to wing stall.

Sofar it has been assumed that the canard incidence angle is 'fixed'. If the canard incidence is variable it must be recognized that this makes canard stall a function of the trim state (i.e. c.g. location). This can be undesirable.

In canard equipped fighters, the canard incidence is used as the primary longitudinal control. In that case the flight control system must be able to detect situations of impending stall and prevent the pilot from entering flight conditions from which recovery may be questionable. This can be done by control signal limiting.

WARNINGS: 1.) The canard configuration shown in Figure 3.43 in Part II, has unacceptable stall recovery characteristics, despite the fact that it has a stable pitch break: Read page 83 in Part II!!

2. Figure 5.12 illustrates the potential interference effect of a canard on wing spanwise lift distribution. This effect can have an adverse effect on wing stall: in an extreme case it could induce wing tip stall. The reader should also be aware of the fact that this type of interference may result in induced drag penalties (deviation from elliptical spanloading) as well as in root-bending-moment penalties. This type of canard-wing interference can be reduced by adding camber to the wing as suggested in Figure 5.12. The Beech Starship I incorporates such camber in its wing.

3. The deep stall trim problem: Airplanes with T-tail empennage configurations and the wing relatively aft on the fuselage usually have the horizontal tail in the region marked D in Figure 5.10. Figure 5.11 shows the 'deep-stall' trim point which then may occur. When an airplane is 'parked' in that flight condition recovery is possible only with sufficient longitudinal control power and even then after considerable loss of altitude.

To obtain the required level of control power for deep stall recovery a large span horizontal tail is needed: this keeps the outboard part of the tail out of the wing/nacelle wake. (Probar en túnel: la única solución)

Most swept wing T-tail airplanes are equipped with stick-shakers and stick-pushers to prevent pilots from entering the deep stall trim point.

4. Pitch-up in high speed airplanes: In high speed airplanes the wing inboard section is usually given a very high sweep angle (or a highly swept strake). In such cases the center of pressure of the wing will move forward rapidly at high angles of attack: the trailing edge will begin to separate while the leading edge start to develop additional vortex lift! The resulting unstable pitchbreak is impossible to overcome by reasonably sized horizontal tails. Nearly all airplanes with variable swept wings have this problem. Figure 5.11 also illustrates this problem. In such airplanes the flight control system must be automated to prevent the pilot from inadvertently entering the strong, uncontrollable pitch-up region.

To maintain controllability in spins (not required

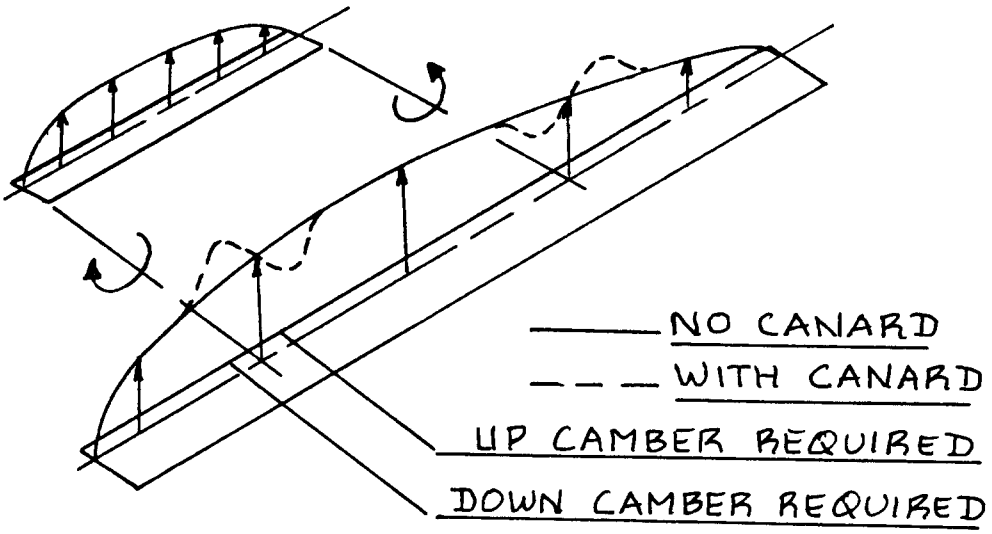

Figure 5.12 Effect of Canard Downwash on the Wing Span Lift Distribution

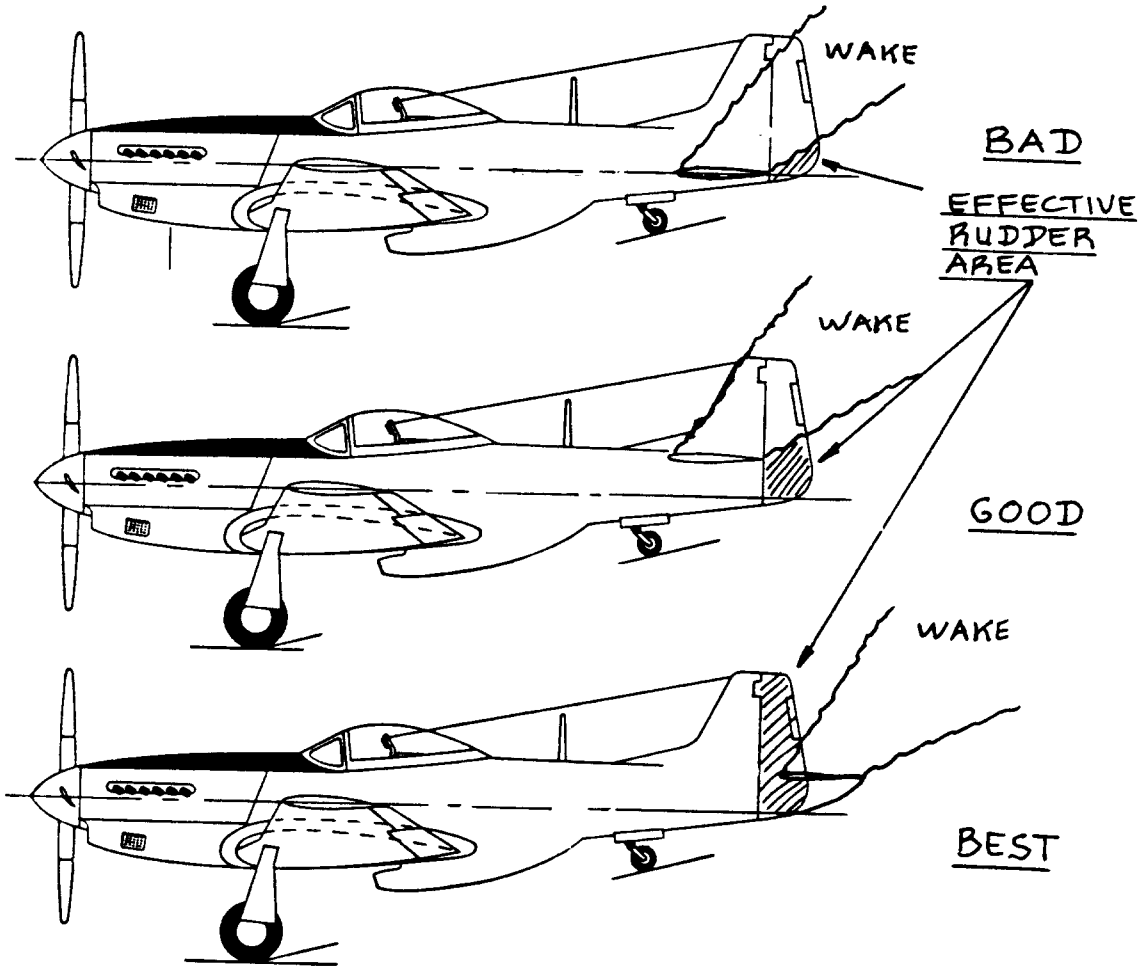

Figure 5.13 Empennage Configurations as Related to Stall/Spin Characteristics

for FAR25 airplanes and for comparable military airplanes) it is necessary to prevent separated wakes from interfering with control surfaces. Figure 5.13 illustrates desirable empennage configurations from a stall and spin viewpoint.

5. Spin Departures: Once an airplane is placed in an angle of attack where stall occurs, it is essential that the airplane be 'spin-resistant' to prevent a so-called spin departure. Ref.52 shows that to prevent inherent spin departures the following parameter must be positive:

$$C_{n_{\beta_{dyn}}} = \{C_{n_{\beta_B}} - (I_{zz_B}/I_{xx_B})C_{l_{\beta_B}} \tan\alpha\}\cos\alpha > 0 \qquad (5.1)$$

Note: the stability derivatives C_{n_β} and C_{l_β} in Eqn.(5.1) are in the body axis system!

It is normally necessary to run a windtunnel test to determine how this parameter varies with angle of attack.

6. Spin recovery: Once the airplane is in a spin it is required in FAR 23.221 (Ref.11) that recovery can be effected by control procedures which do not require exceptional pilot skills. The placement of the longitudinal and directional flight controls is of great importance in determining whether an airplane can meet this requirement.

Another way to make an airplane spin resistant is to design the wing so that auto-rotation is delayed to much higher angles of attack. Once a wing stalls the roll damping derivative normally reverses sign. It is this fact which drives the spinning motion in most airplanes. By careful planform and airfoil design it possible to achieve this. Ref.53 provides a useful overview of recent NASA research results in this area. Ref.14 contains an excellent discussion of airplane spin characteristics.

NOTE: there is no requirement that commercial transports be recoverable from a spin. These airplanes are not supposed to be operated near flight conditions where spin could be possible.

For fighter airplanes a requirement for recovery from extreme angles of attack (up to 90 degrees!) is that the planform centroid is behind the most aft c.g. This requirement can be readily verified from a threeview

drawing and a weight and balance calculation.

5.1.5 Empennage Planform Design

The discussions in Chapter 4 on the subject of wing planform design also apply to empennage planform design. Chapter 8 in Part II contains tabulated information on planform design parameters used in a large number of airplanes.

For reasons of structural weight it is usually not feasible to use high aspect ratios in empennage surfaces. The reader should not deviate too far from the aspect ratios of Tables 8.1-8.12 in Part II!

In high speed airplanes the empennage should be designed so that its critical Mach numbers are above that of the wing.

Historically the subjective judgement of 'good or bad looks' has had a significant influence on the planform design of empennage surfaces. In many airplanes the planform design of the vertical tail reflects almost a company 'trademark'!

5.1.6 Empennage Airfoil Design or Selection

Most horizontal and vertical tails use symmetrical airfoils. The reason is that these surfaces must be able to provide 'lift' in either direction.

If the horizontal tail is found to be critical in either 'download to trim at forward c.g., flaps down' or in take-off rotation an inversely cambered airfoil may be useful to keep down the size of the horizontal tail. In the take-off rotation case, the down lift capability must be determined in the presence of ground effect!

Tables 8.1-8.12 show which airfoil types are used in the empennage surfaces of twelve types of airplanes.

For canard surfaces the problem of airfoil selection and/or design is far less straightforward. The designer should make a list of the critical lift requirements placed on any canard design. The effect of Reynolds number, Mach number and surface condition in icing conditions and rain conditions must be carefully assessed before selecting a canard airfoil.

5.1.7 Review of Empennage Drag Contributions

The empennage generates the same types of drag as the wing:

1. Friction drag
2. Induced drag
3. Compressibility drag
4. Interference drag
5. Profile drag

The total drag generated by the empennage varies from 10 - 20 percent of the total drag of an airplane, depending on the size and disposition.

Detailed procedures for predicting empennage drag are contained in Part VI.

The discussion of friction drag, compressibility drag, interference drag and profile drag for the wing in Chapter 4 applies almost verbatum to the empennage. For that reason it will not be repeated.

The induced drag generated by the empennage depends on the amount of lift which the empennage must provide.

Keep in mind that the induced drag due to individual empennage surfaces is independent of the direction in which the lift is generated: induced drag is proportional to the square of the lift coefficient.

The conditions under which a conventional tail and/or a canard lift up or down to provide moment trim for an airplane are delineated in Part VII. The prevailing situation is as follows:

- *Conventional tails usually provide down lift to trim.
- *Canards usually provide up lift to trim.

Note: although a canard does normally lift 'up', this can interfere with the wing in an unfavorable manner. Figure 5.12 illustrates the potential downwash effect of a lifting canard on the wing. This effect needs to be accounted for in determining the actual aerodynamic performance of the wing. By providing down/up camber in the wing as indicated in Fig.5.12 this problem can be eliminated for one flight condition only! The cruise flight condition normally would be the one for which this is done.

Canards can have a favorable interference effect on a wing due to the interaction of canard vortices with

wing vortices. Figure 4.39 illustrates this for the Viggen fighter. Recent examples of this type of configuration are shown in Figures 5.14 and 5.15.

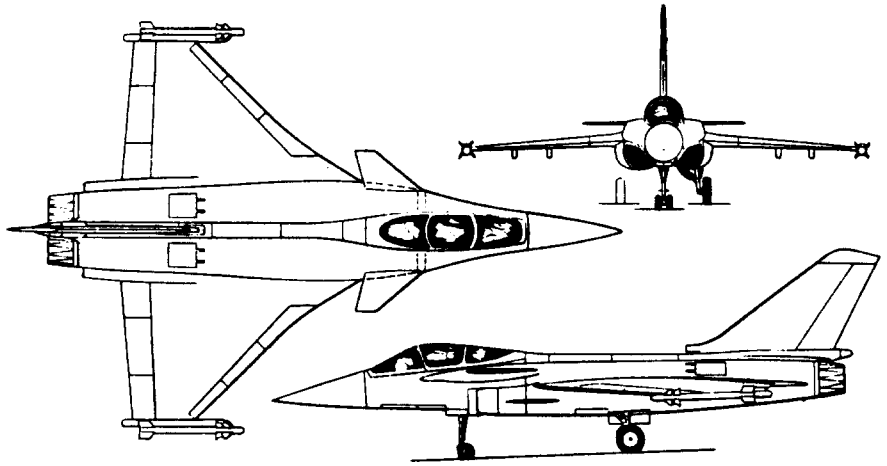

Figure 5.14 Dassault Breguet Rafale

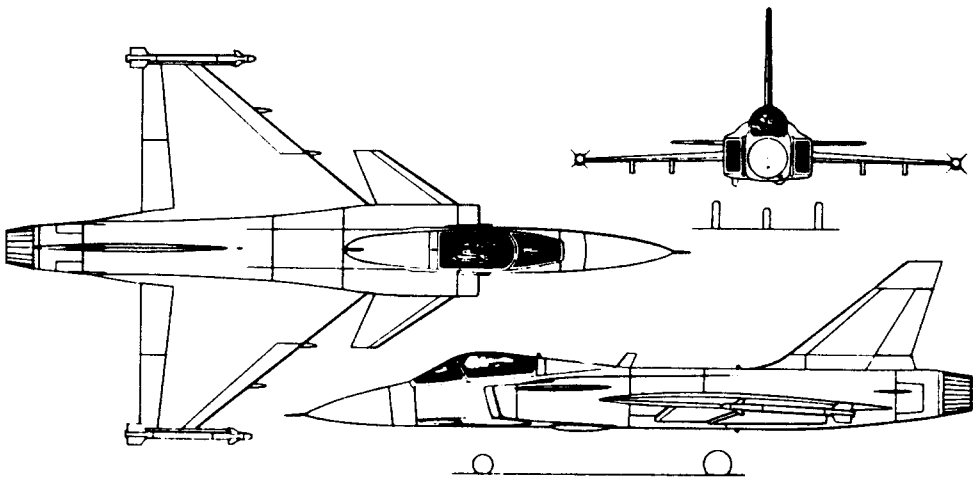

Figure 5.15 SAAB 2110 Gripen

5.2 STRUCTURAL AND INTEGRATION DESIGN CONSIDERATIONS FOR THE EMPENNAGE

The purpose of this section is to provide guidelines and examples of how the structural layout design and the integration of the empennage structure into the airplane can be accomplished.

The decision about empennage size and disposition (overall empennage configuration) has been made as a result of the work described in Section 5.1.

The material in this section is organized as:

5.2.1 Typical spar, rib and stiffener spacings.

5.2.2 Examples of empennage structural arrangements

5.2.3 Examples of fuselage/empennage integration and/or vertical/horizontal tail integration

5.2.4 Examples of empennage cross section design

5.2.5 Examples of longitudinal control mechanizations

5.2.6 Examples of directional control mechanizations

5.2.7 Examples of empennage skin gages

5.2.8 Maintenance and access requirements

A procedure for preparing the overall structural arrangement of an airplane is given in Chapter 7. For further insight into empennage structural arrangements the reader should consult Chapter 8.

5.2.1 Typical Spar, Rib and Stiffener Spacings

The actual arrangement of empennage spars, ribs and stiffeners depends ver much on the type of airplane being designed and the loads to which it will be subjected. The reader should refer to Refs. 11, 19 and 23 for detailed information on the types of loads to which empennange structures are subjected. Reference 20 contains detailed methods for the preliminary structural analysis of empennage structures.

Figure 5.16 defines the locations of major structural components for empennage surfaces. Tail booms

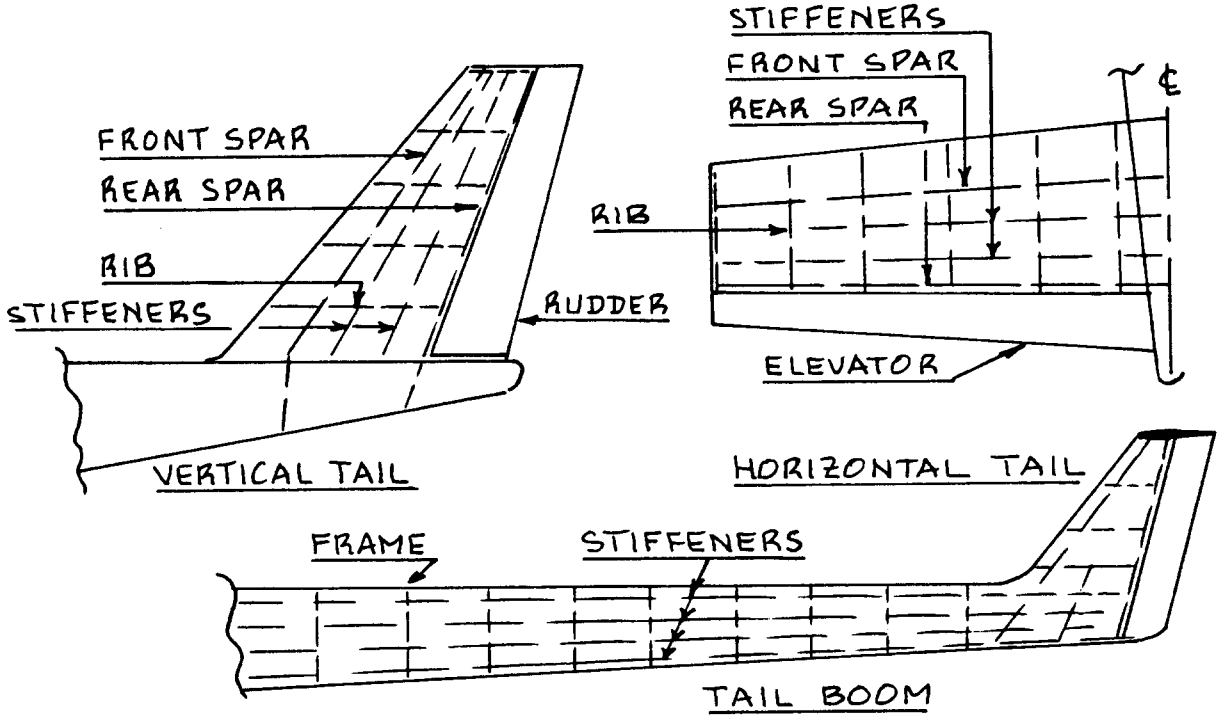

Figure 5.16 Definition of Empennage Spar, Rib and Stiffener Locations

SKIN NO.	MATERIAL	THICKNESS
1	2024-T3	.016
2	2024-0*	.032
3	2024-T3	.020
4	2024-T3	.025
5	2024-T3	.032
6	2024-T3	.040
7	2024-0*	.040
8	FIBERGLASS	
9	THERMOPLASTIC	
10	2024-T3	.080

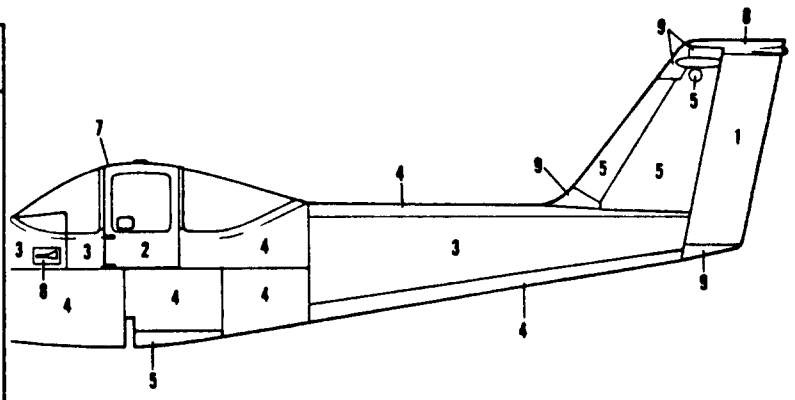

COURTESY : PIPER

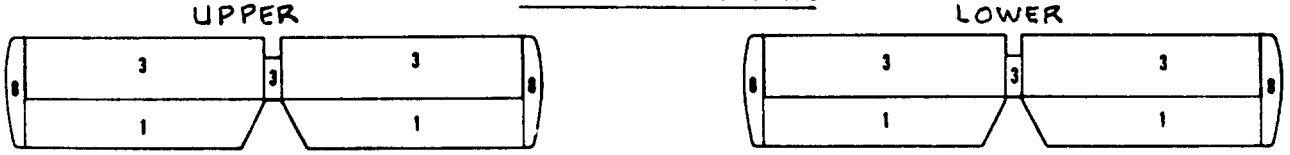

Figure 5.17 Empennage Structural Arrangement Piper PA-38-112 Tomahawk

in the case of twin boom configurations are included in this definition.

Empennage Spar Locations: Most airplanes use a so-called torque-box to carry the main loads on empennage surfaces. The torque-box should be located to take maximum advantage of the airfoil thickness distribution.: this will save weight. A torque-box is normally closed off by a front spar (F.S.), a rear spar (R.S.) and an upper and lower skin. The rear spar location is often constrained by control surface size requirements. The front spar location is not normally so constrained in the case of empennage surfaces.

Typical spar locations are:

Front spar: 15-25 percent chord

Rear spar: 70-75 percent chord

Multiple spar construction is often used in the case of fighter empennage surfaces.

Empennage Rib Locations: To help stabilize the torque-box of the empennage and to serve as anchors for control surface attachment brackets, ribs are used. Typical empennage rib spacings are:

Light airplanes: 15 - 30 inches

Transports: 24 inches

Fighters and Trainers: rib spacings vary widely.

Remember: wherever 'point loads' are expected a rib will be required. Examples of point loads are: control surface loads, taillet loads (Beech Model 1900, see Figure 3.16b), intersections with other surfaces.

Empennage Stiffener Spacings: These vary widely depending on the airplane type. The relative empennage skin stiffness determines the number and type of stiffeners needed: See Sub-section 5.2.2 for examples.

5.2.2 Examples of Empennage Structural Arrangements

A procedure for arriving at the overall structural arrangement for any new airplane is presented in Chapter 8.

Figures 5.17 through 5.24 present examples of

empennage structural arrangements for the following airplanes:

Fig. 5.17 Piper Tomahawk	Fig. 5.18 Rockwell 112B
Fig. 5.19 Short Skyvan	Fig. 5.20 McDD DC9-30
Fig. 5.21 McDD DC-10	Fig. 5.22 Boeing 767
Fig. 5.23 Aerospatiale Corvette	Fig. 5.24 Douglas A4

Note that in several of these structural arrangement drawings the fuselage stations, buttock line locations and waterline locations are indicated. A complete structural arrangement must contain that information!

Additional examples for the structural arrangement of the empennage may be found in Figures 4.58, 4.59 and in Section 4.4.

5.2.3 Examples of Fuselage/Empennage Integration and/or Vertical/Horizontal Tail Integration

The fuselage frames or bulkheads where empennage surfaces are attached must be able to carry the empennage loads into the fuselage, usually the fuselage skin. This requires proper location of empennage spars in relation to their fuselage attachment frames and vice versa. Figure 5.25 illustrates two types of vertical-tail/fuselage-frame attachment methods. Figures 4.88 and 4.89 provide more specific examples.

The fuselage structural depth at the location of empennage attachment should not be too shallow: bending and torsion moments exerted on the fuselage by the empennage can be very high! This is the reason for the upper fuselage bulges in most military cargo transports: the aft loading ramps cut so severely into the fuselage structure as to leave little depth for empennage attachment. This depth is then created by bulging the fuselage upward at the point of vertical tail attachment. Examples of this type of fuselage 'bulging' are seen in Figures 3.28c, 3.29b and 3.30a in Part II.

Figures 5.20 and 5.22 provide examples of the structural empennage integration for a transport and for a business jet.

Figures 5.26 and 5.27 show examples of horizontal/vertical tail integration in the case of small T-tail

airplanes. Figure 5.27 also gives a good idea about the component breakdown from a manufacturing viewpoint.

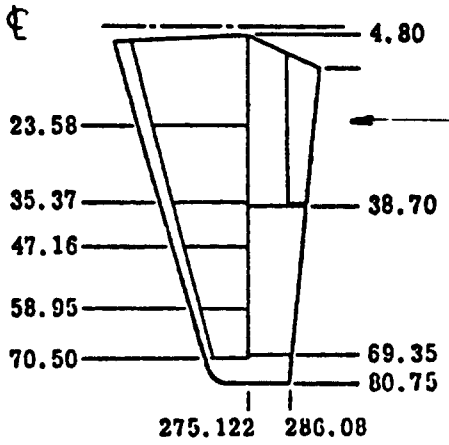

FOR VERTICAL TAIL
SEE FIG. 3.56

COURTESY: ROCKWELL

Figure 5.18 Empennage Structural Arrangement
Rockwell 112B

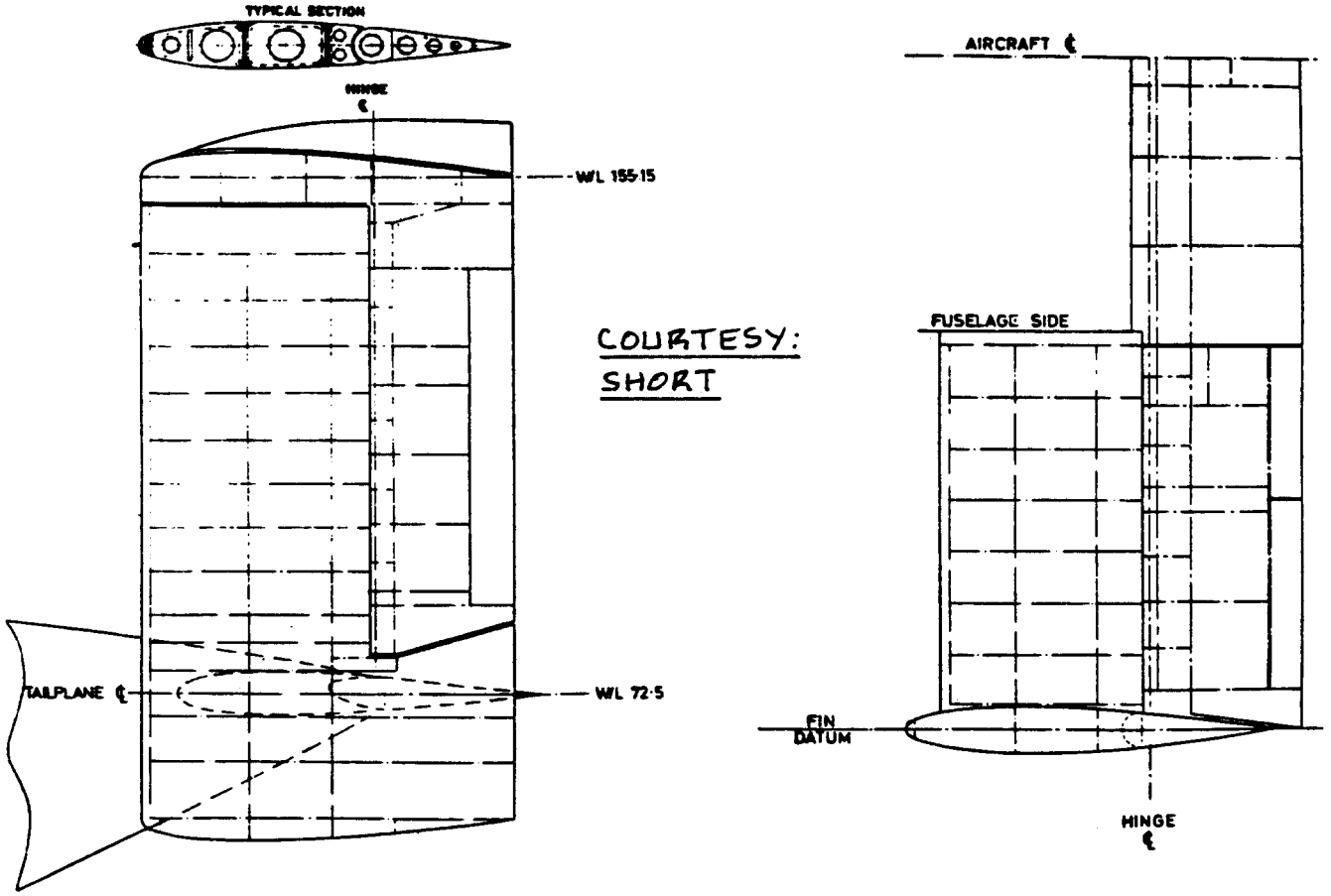

COURTESY: SHORT

Figure 5.19 Empennage Structural Arrangement Short Skyvan

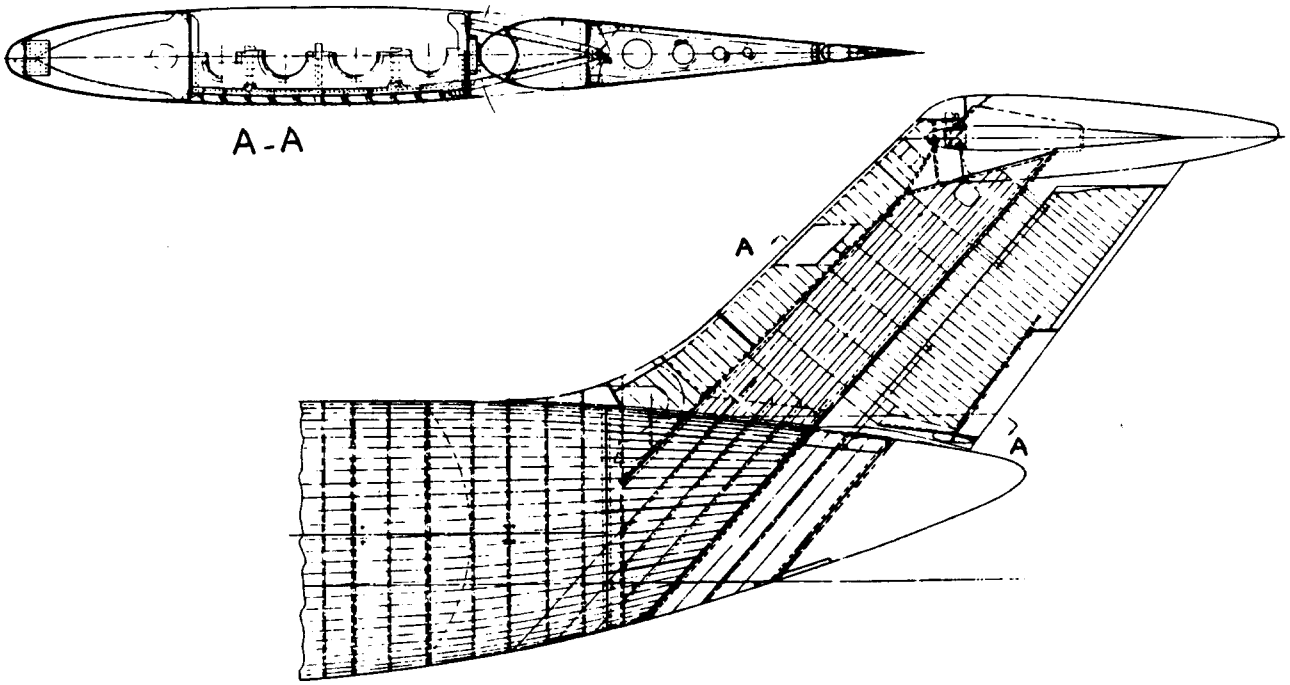

Figure 5.20a Vertical Tail Structural Arrangement
McDonnell Douglas DC9-30

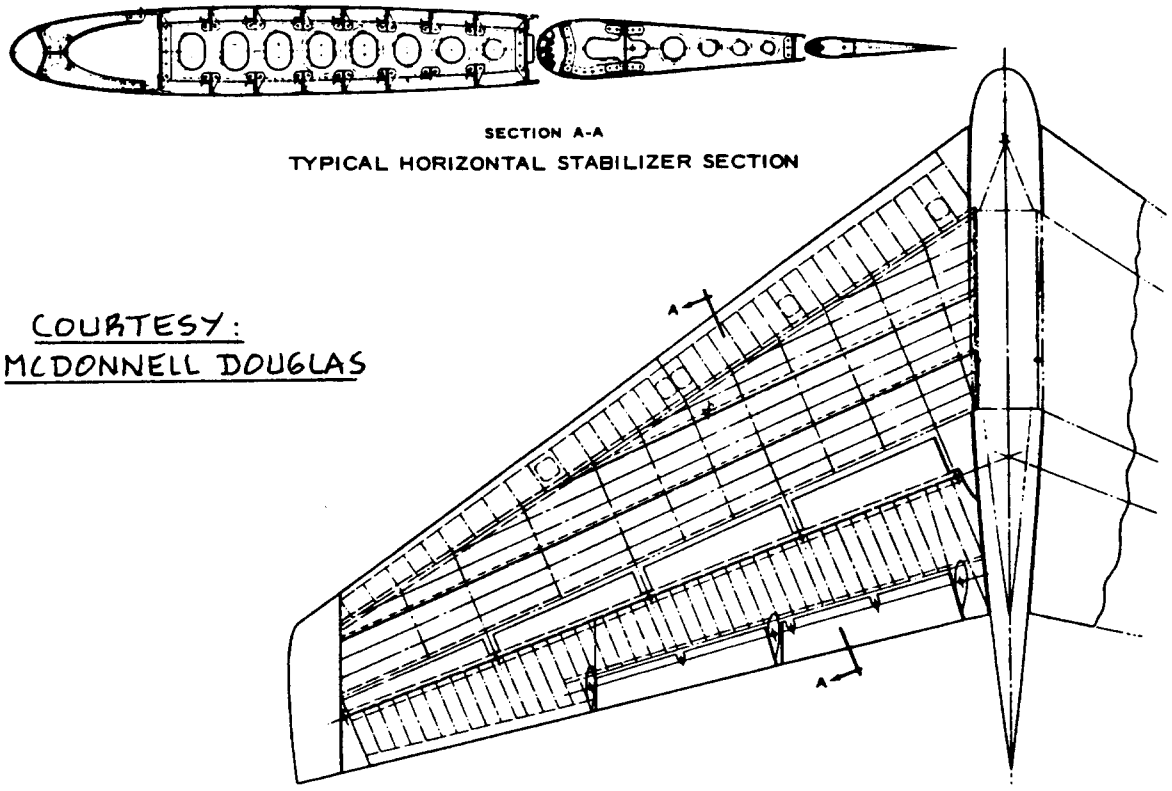

COURTESY:
MCDONNELL DOUGLAS

Figure 5.20b Horizontal Tail Structural Arrangement
McDonnell Douglas DC9-30

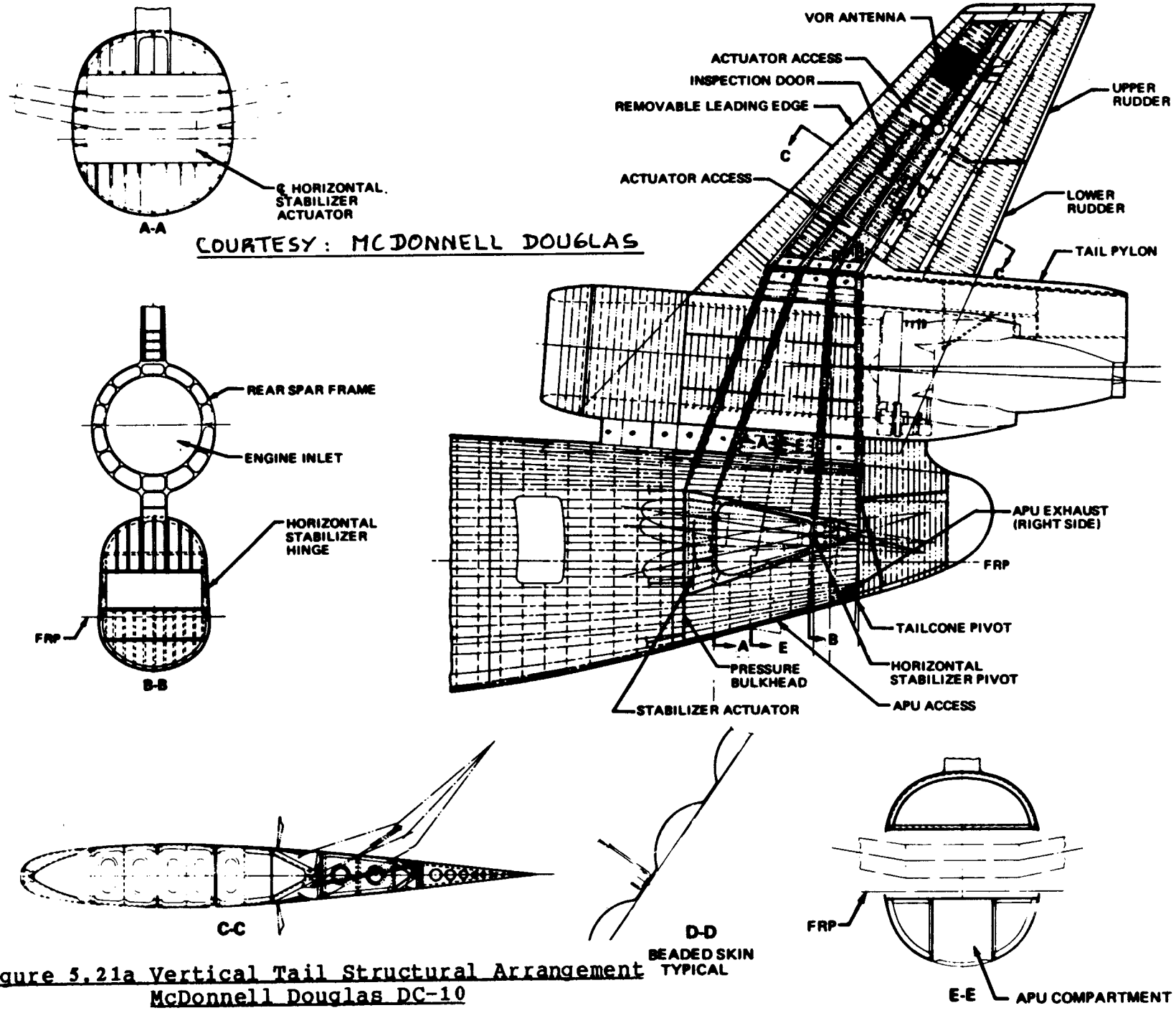

COURTESY: MCDONNELL DOUGLAS

Figure 5.21a Vertical Tail Structural Arrangement
McDonnell Douglas DC-10

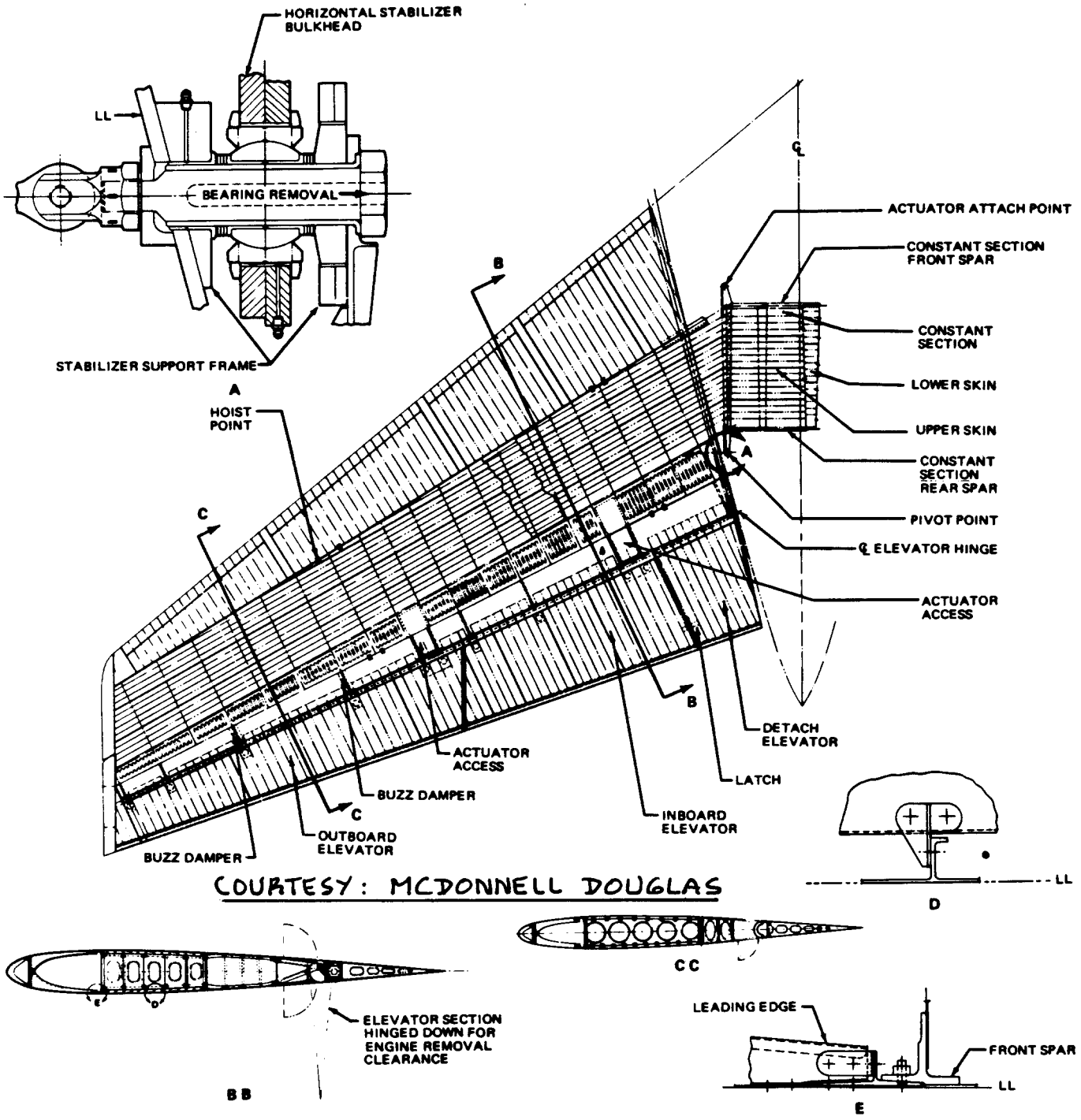

Figure 5.21b Horizontal Tail Structural Arrangement
McDonnell Douglas DC-10

Vertical Tail

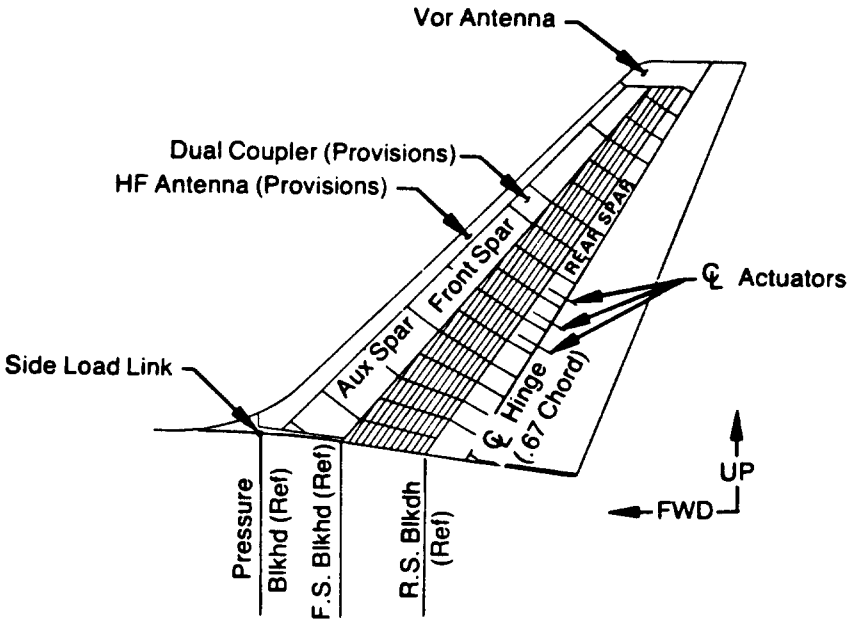

Horizontal Tail

COURTESY: BOEING

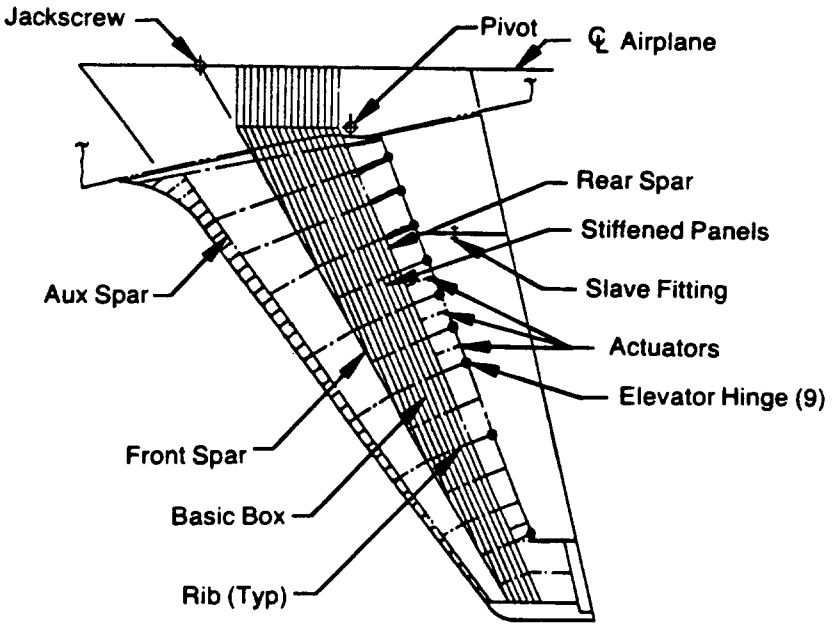

Figure 5.22 Empennage Structural Arrangement Boeing 767

COURTESY: AEROSPATIALE

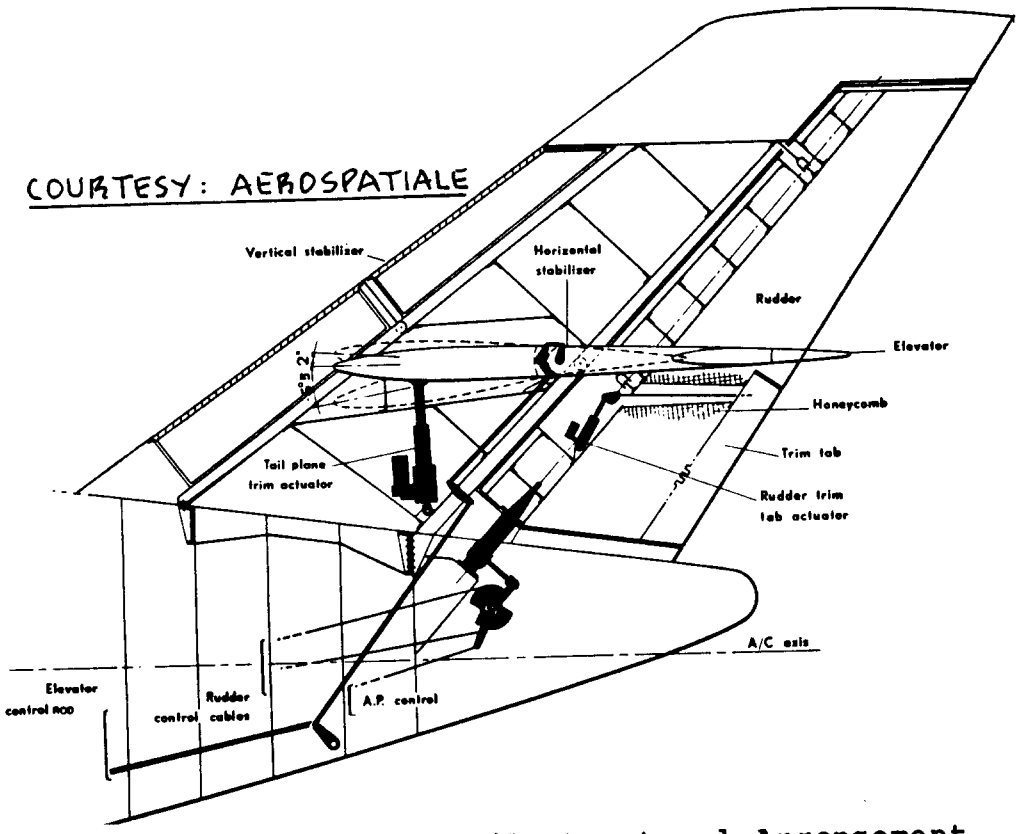

Figure 5.23a Vertical Tail Structural Arrangement
Aerospatiale Corvette

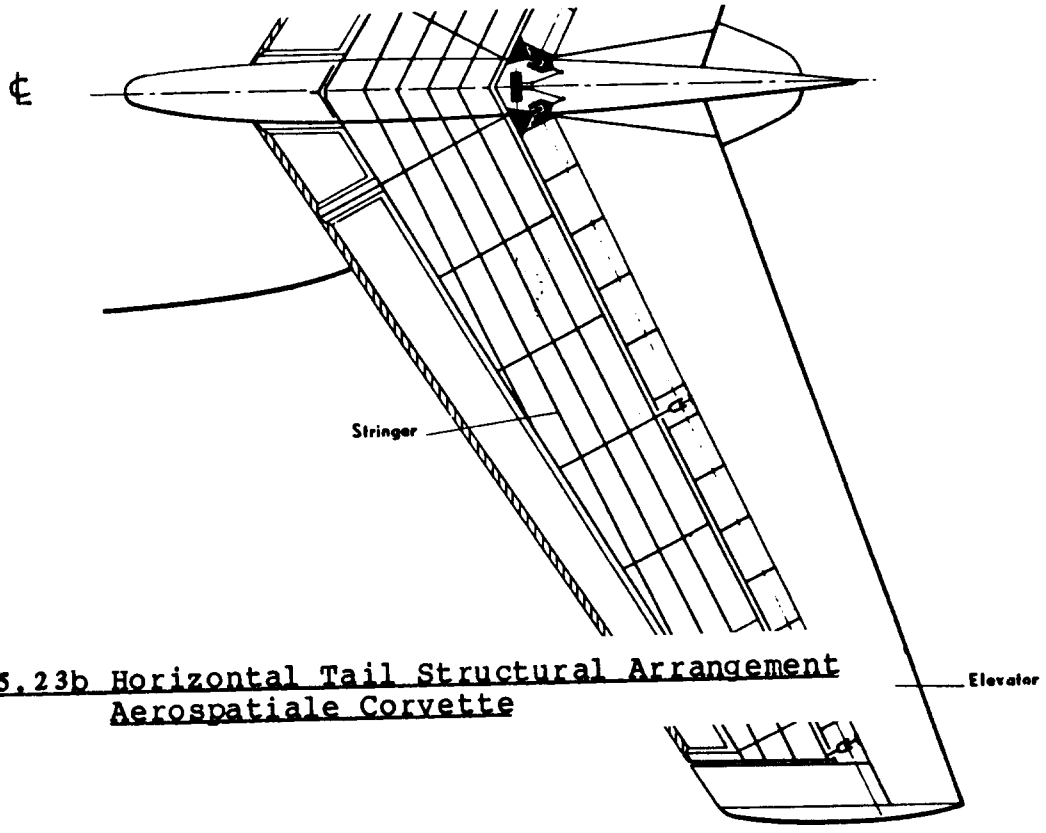

Figure 5.23b Horizontal Tail Structural Arrangement
Aerospatiale Corvette

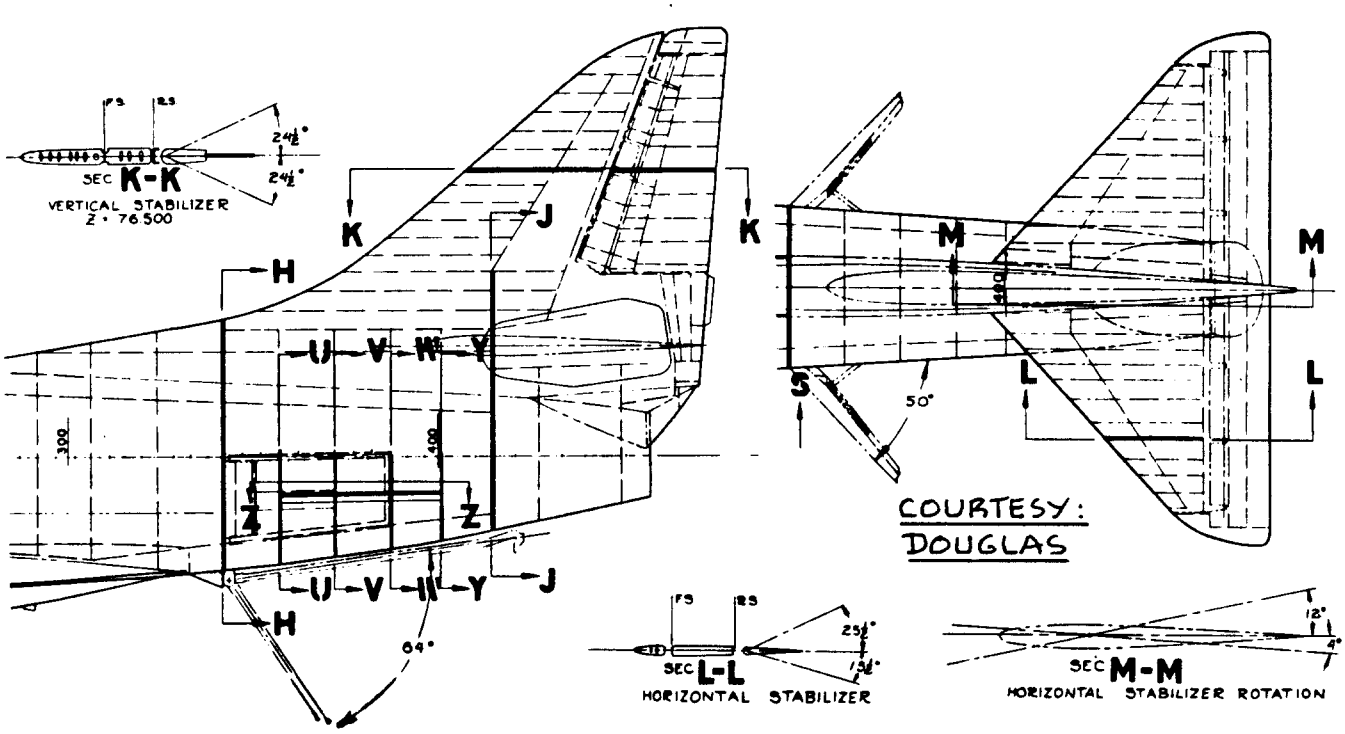

Figure 5.24 Empennage Structural Arrangement Douglas A4

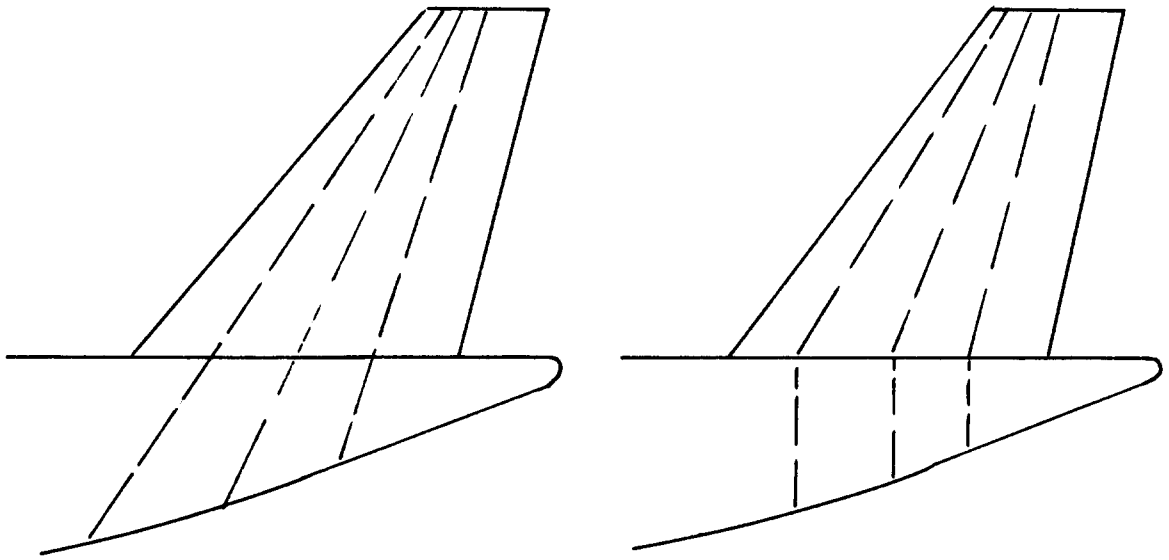

Figure 5.25 Example of Two Methods for Vertical Tail to Fuselage Attachment

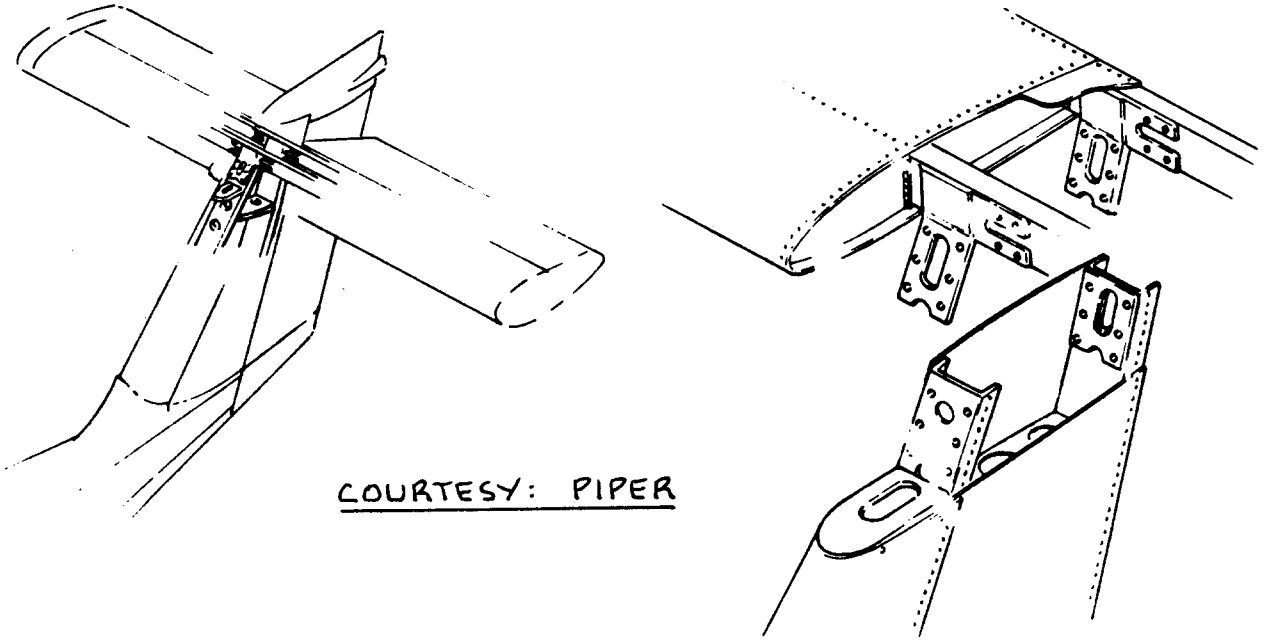

Figure 5.26 T-tail Structure Piper PA-38-112 Tomahawk

1. Dorsal Fin
2. Vertical Stabilizer
3. Fairing
4. Horizontal Stabilizer

5. Elevator
6. Rotating Beacon
7. Fairing
8. Tail Fairing and Tail Light

9. Elevator Control Horn
10. Elevator Tab
11. Rudder
12. Rudder Tab

13. Rudder Torque Tube
14. Rudder Control Horn
15. Rudder Bell Crank Hinge Bracket
16. Rudder Hinge Bracket

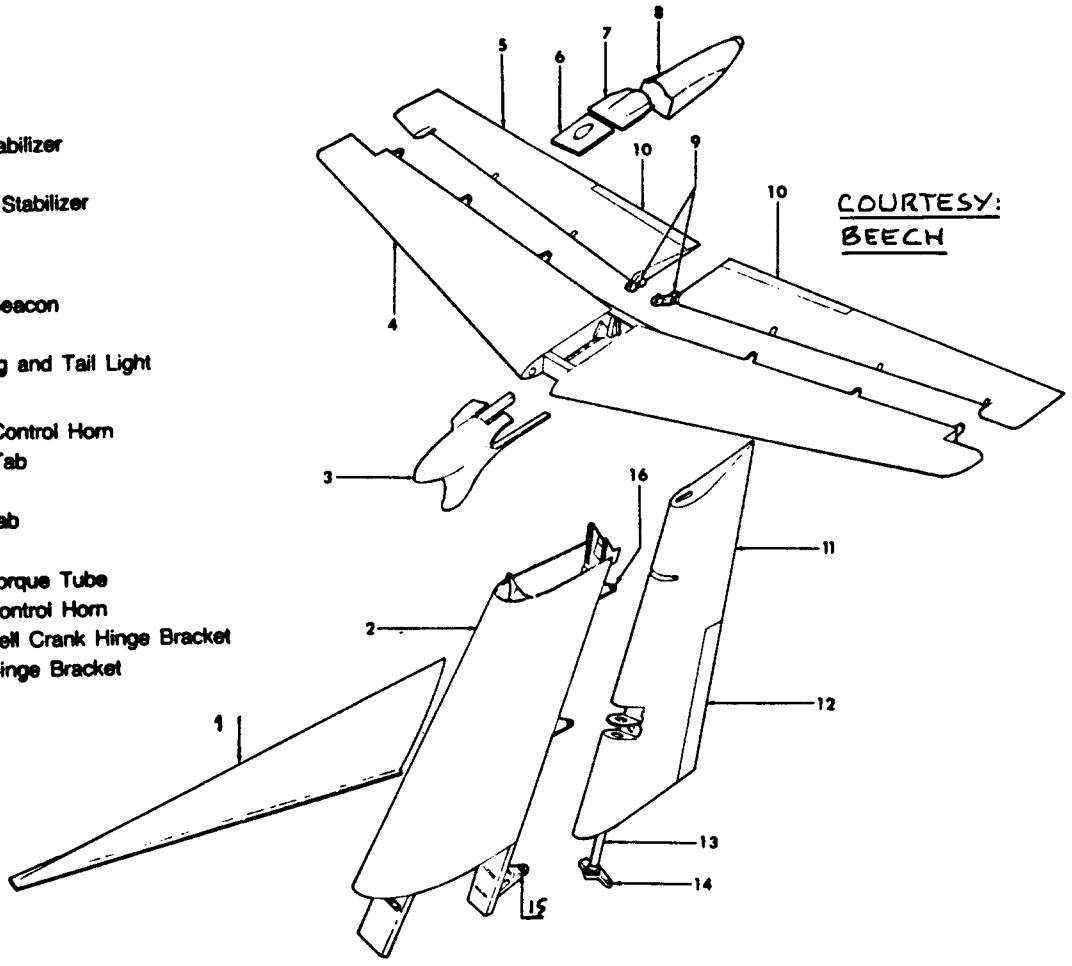

Figure 5.27 T-tail Structure Beech King Air F90

5.2.4 Examples of Empennage Cross Section Design

Figures 5.19, 5.20 and 5.21 present examples of typical cross section designs for vertical and horizontal tails. Observe the similarity with wing cross section designs shown in Chapter 4.

5.2.5 Examples of Longitudinal Control Mechanizations

Figure 5.28 shows the structural mechanization of the elevator control of the Piper Tomahawk, a typical light airplane.

Figures 5.20 and 5.21 provide examples of elevator mechanizations in the DC9 and DC10 respectively.

Examples of elevator control surface designs are seen in Figures 5.28, 5.29 and 5.30.

In most high performance airplanes the entire horizontal tail is used for trim and in most fighters also for primary longitudinal control. In such cases the stabilizer pivots about a fixed point and one or more actuators are used to control the stabilizer. Figures 5.21 and 5.22 show two examples.

A unique solution to obtaining variable incidence stabilizer angles was used by Lockheed on the XF-90 and on the Jetstar. Figure 5.31 shows the XF-90 and identifies the pivot location for the vertical tail: by in effect varying the leading edge sweep angle of the vertical tail, the horizontal stabilizer was given variable incidence!

5.2.6 Examples of Directional Control Mechanizations

This type of rudder design results in much improved rudder effectiveness when compared to a single hinge rudder.

Figure 5.20a shows a rudder plus tab arrangement as used in the DC-9.

Figure 5.27 shows the rudder of the Beech King Air. The rudder is actuated by cables which attach to the control horn labelled no.14 in Fig. 5.27.

5.2.7 Examples of Empennage Skin Gages

Figure 5.17 gives an example of the empennage skin

gages in a very light airplane: Tomahawk. Figure 5.32 shows the same for a Beech King Air.

For fighters and transports the skin gages vary widely depending on the size of the airplane, its performance envelope and on loads.

5.2.8 Maintenance and Access Requirements

The comments made in Chapters 3 and 4 in regard to maintenance and accessibility also apply here. Because of the smaller sizez associated with empennage surfaces there is always a strong temptation to make inspection and access covers too small. This saves weight but is not conducive to safety: any design feature which inhibits accessibility should be considered a detrement to flight safety!

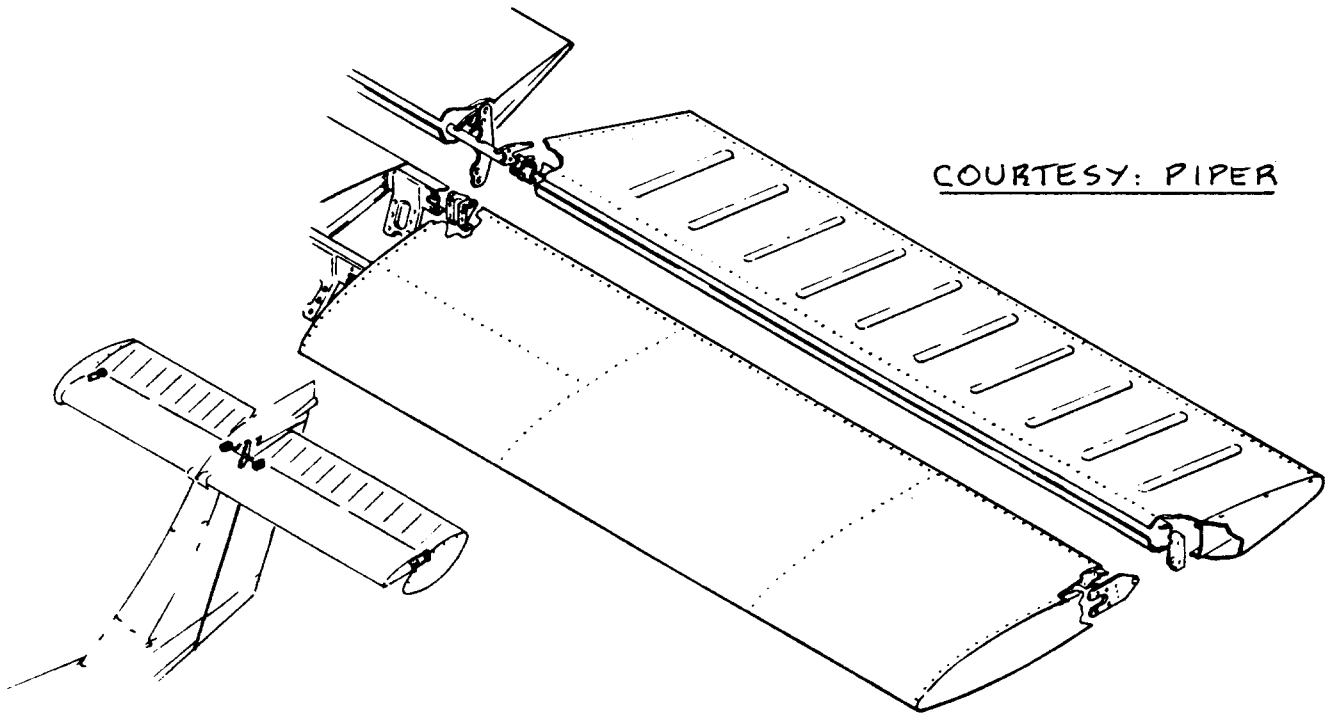

Figure 5.28 Elevator Arrangement Piper PA-38 112 Tomahawk

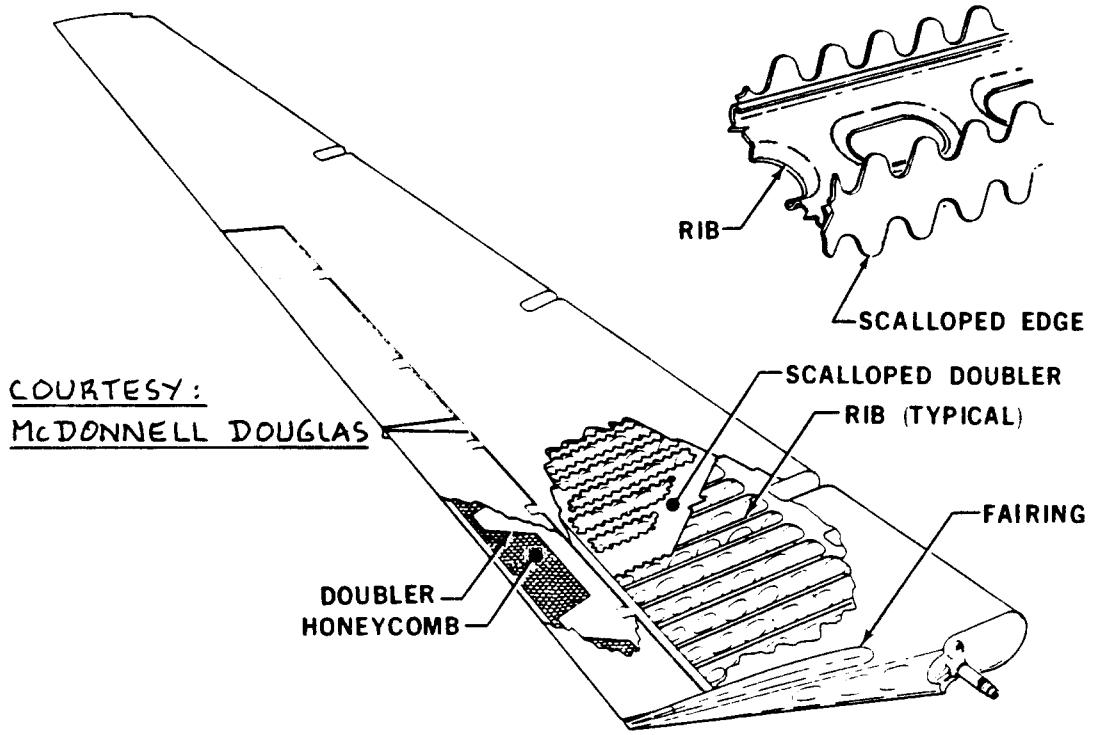

Figure 5.29 Elevator Construction McDD DC9-30

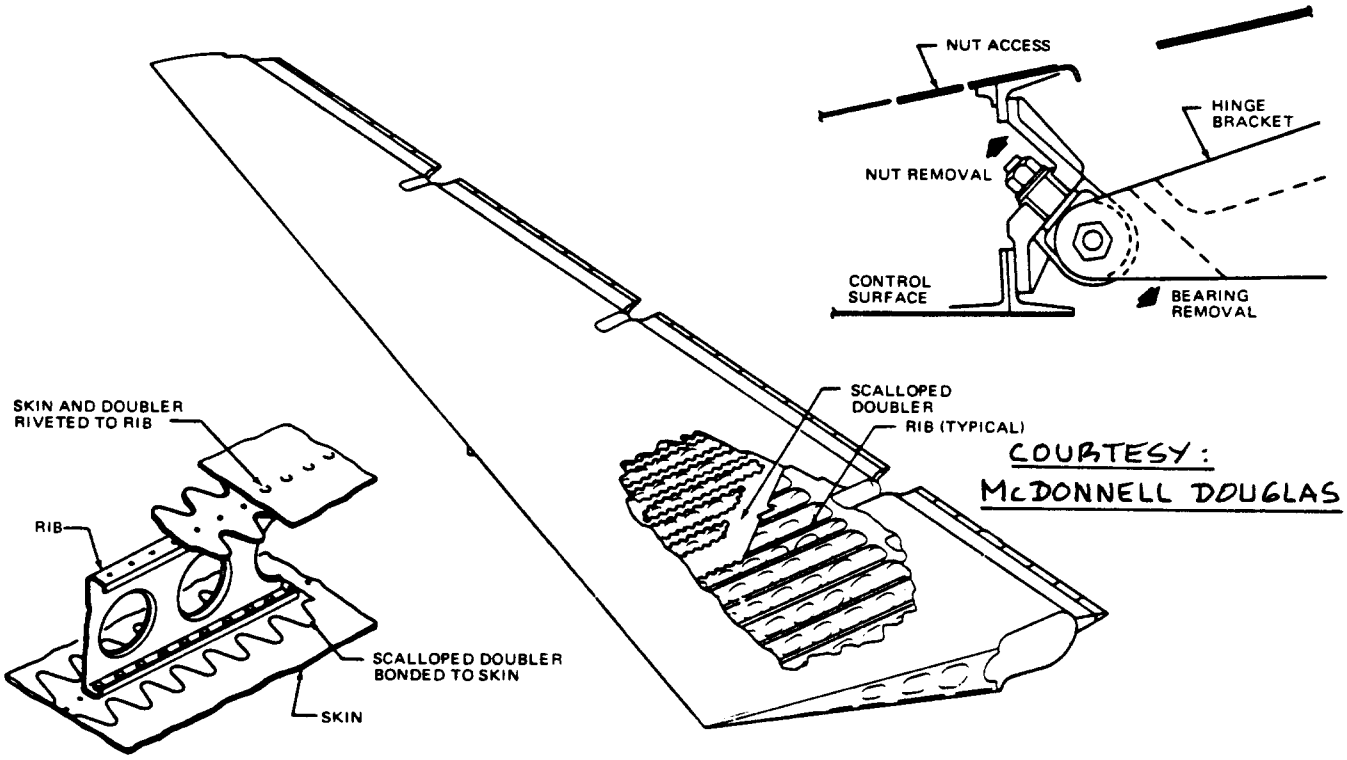

Figure 5.30 Elevator Construction McDD DC-10

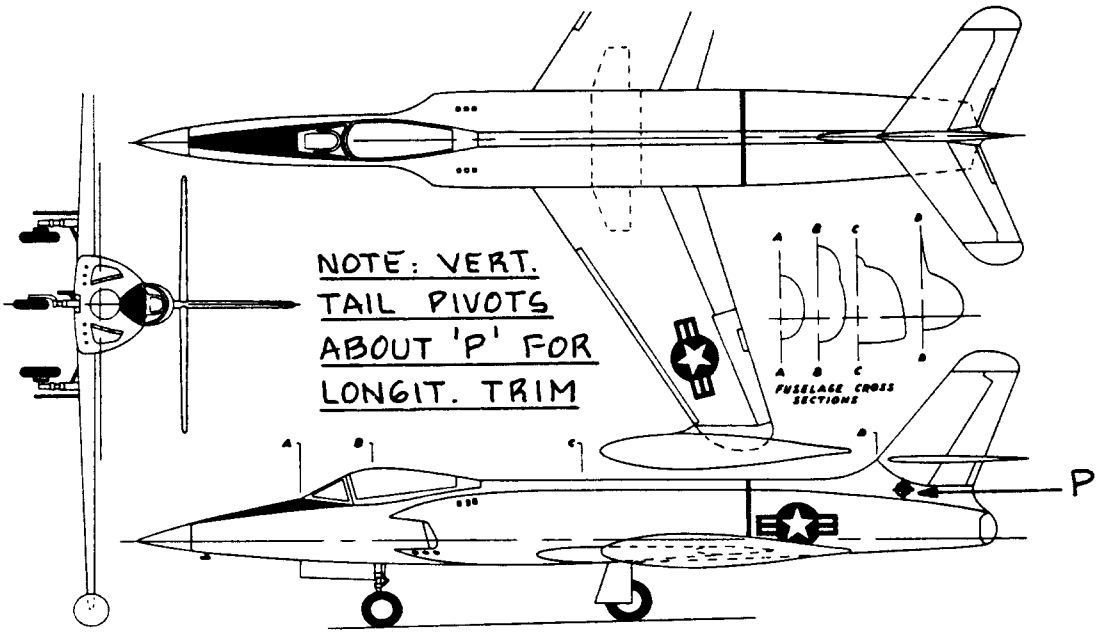

Figure 5.31 Lockheed XF-90

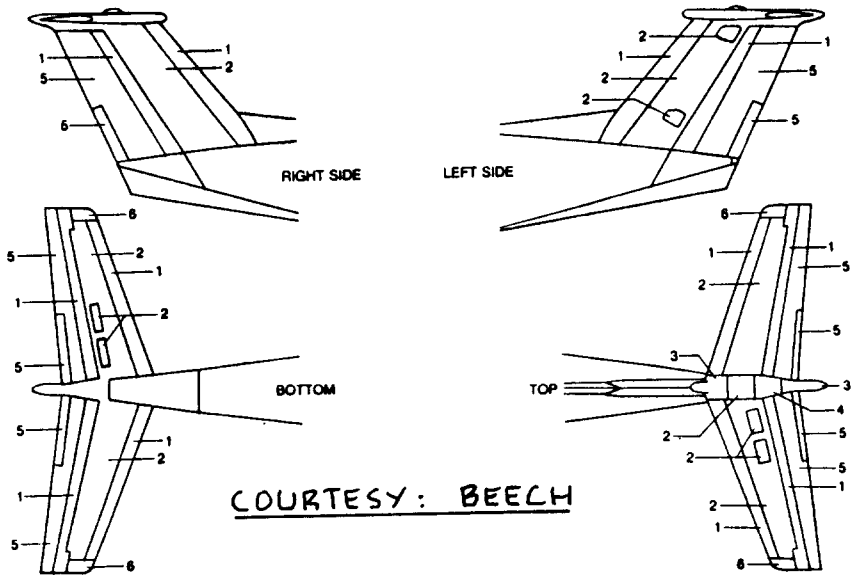

ITEM	MATERIAL	THICKNESS IN INCHES
1	2024T3	.032
2	2024T3	.040
3	Glass Cloth (MIL-C-9084, Type VIII, with MIL-R-7575 Resin)	3 Plies
4	6061T4	.032
5	6061T6	.020
6	Laminated of 2024-T3 and Glass Cloth (MIL-C-9084, Type VIII)	.020 3 Plies

Figure 5.32 Typical Empennage Skin Gages in a Beech King Air F90

6. INTEGRATION OF THE PROPULSION SYSTEM

A Class I procedure for selecting propulsion system type, how many engines to use and where to put these engines was presented as Step 5 of preliminary design sequence 1 as discussed in Chapter 2 of Part II.

The purpose of this chapter is to provide additional information to guide the reader in making these difficult design decisions. The material in this chapter is organized as follows:

6.1 Presentation of engine and propeller data

6.2 Relation between flight envelope and engine type

6.3 Installed thrust/power, inlet and efficiency considerations

6.4 Stability and control considerations (thrust line location and inclination)

6.5 Structural considerations (whirlmode flutter, extension shafts, propeller blade excitations)

6.6 Maintenance and accessibility considerations

6.7 Safety considerations

6.8 Noise considerations

6.9 Example engine and propeller installations

NOTE: Methods for calculating propeller thrust, installed engine thrust/power and other significant engine performance characteristics are presented in Part VI.

6.1 PRESENTATION OF ENGINE AND PROPELLER DATA

In this section tabulated and pictorial data are provided for those engine and propeller characteristics which are important to the preliminary layout designer. The material is organized as follows:

6.1.1 Propellers
6.1.2 Piston engines
6.1.3 Turbo/propeller driven engines
6.1.4 Turbojet and turbofan engines
6.1.5 Propfan engines

For more detailed discussions of the fundamental thermodynamic, performance and mechanical aspects of engines the reader should refer to the following references depending on propulsion system type:

For propellers: Refs.12, 14, 55, 56 and 57

For piston engines: Refs.12, 14, 58 and 59

For turbojets and turbofans: Refs.12, 60 and 61

For propfans Refs.62 and 63

6.1.1 Propellers

Methods for computing installed propeller thrust data are presented in Part VI. The following subjects will be addressed:

1. Propeller efficiency
2. Examples of propeller thrust data
3. Examples of existing propellers
4. Propeller weight data

1. Propeller efficiency: Figure 6.1 shows examples of the installed efficiencies which can be expected from propellers in the subsonic speed range.

The following equation defines what is meant by installed propeller efficiency, η_p:

$$THP = \eta_p SHP \qquad (6.1)$$

Installed propeller efficiency depends on such factors as:

- *Activity factor, AF
- *Airfoil(s)
- *Pitch distribution
- *Blockage
- *Number of blades, n_p
- *Tip Mach number
- *Single or Counter rotation
- *Disk loading/Power loading

Figure 6.1 also shows the improvement in efficiency which can be obtained from counter rotating propellers: the reason is the recovery of swirl losses caused by any individual propeller. The price paid for this improved efficiency is higher installed weight and increased complexity.

Note also in Figure 1, that 'advanced' turboprops do quite well in the high subsonic speed range. The word

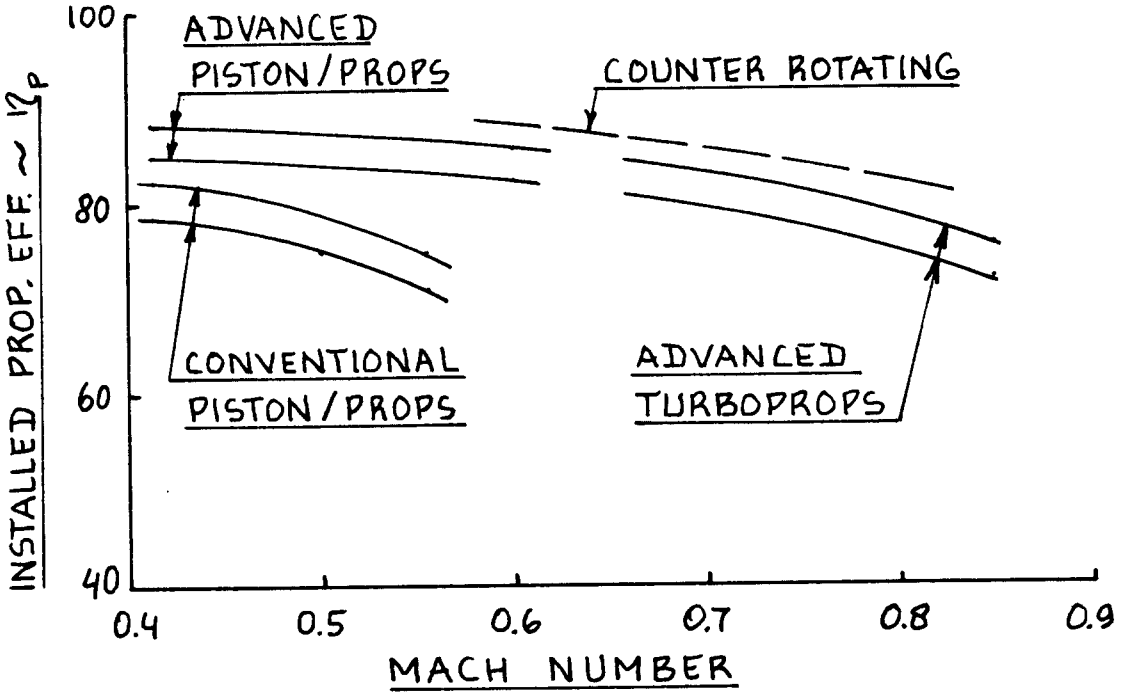

Figure 6.1 Potential Installed Propeller Efficiencies

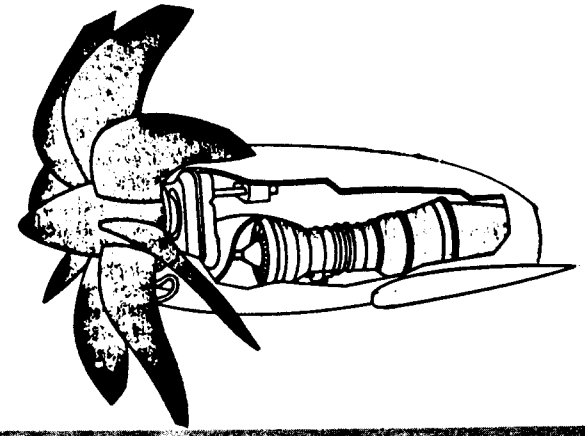

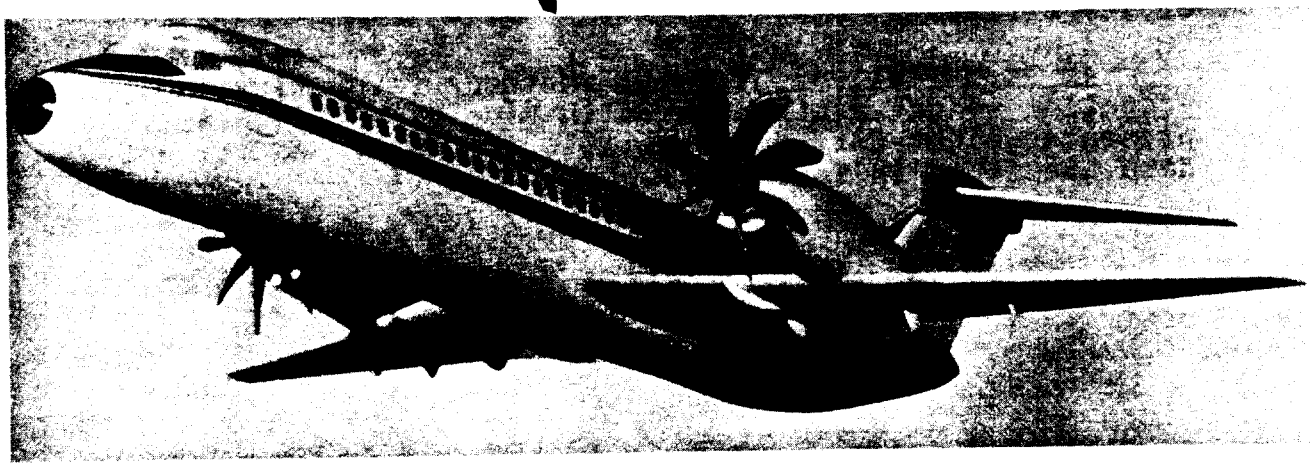

Figure 6.2 Example of a Propfan Arrangement

'advanced' means that thin, supercritical airfoils and swept blades are used. An extreme consequence of this is shown in Figure 6.2 which shows a possible 'propfan' arrangement in a transport type airplane.

Figure 6.3 shows how the number of blades and the diskloading affect ideal propeller efficiency. It is seen that multibladed propellers have a significant performance advantage. The price for this again is increased complexity and increased weight.

2. Examples of propeller thrust data: Figure 6.4 presents typical free propeller thrust data as a function of speed and propeller rpm and shaft horsepower. Methods for computing both free and installed propeller thrust data are outlined in Part VI.

3. Examples of existing propellers: Tables 6.1 and 6.2 present detailed design data for current technology as well as for advanced technology propellers.

Figure 6.5 shows an example of a fixed (but ground adjustable) pitch propeller. The pitch angle can be adjusted by inserting 'pitch blocks' with different angles.

Figure 6.6 illustrates the blade geometry used in a conventional variable pitch propeller. The mechanism used to achieve variable pitch capability varies from one manufacturer to another. An example mechanism is shown in Figure 6.7.

Figure 6.8 shows the blade construction of a modern four-bladed propeller. This propeller also is fully reversible, a feature essential in slowing down airplanes on icy surfaces.

4. Propeller weight data: Methods for estimating propeller weight are presented in Part V. Table 6.3 presents weight data for several propellers. Additional data are found in Tables 6.1 and 6.2.

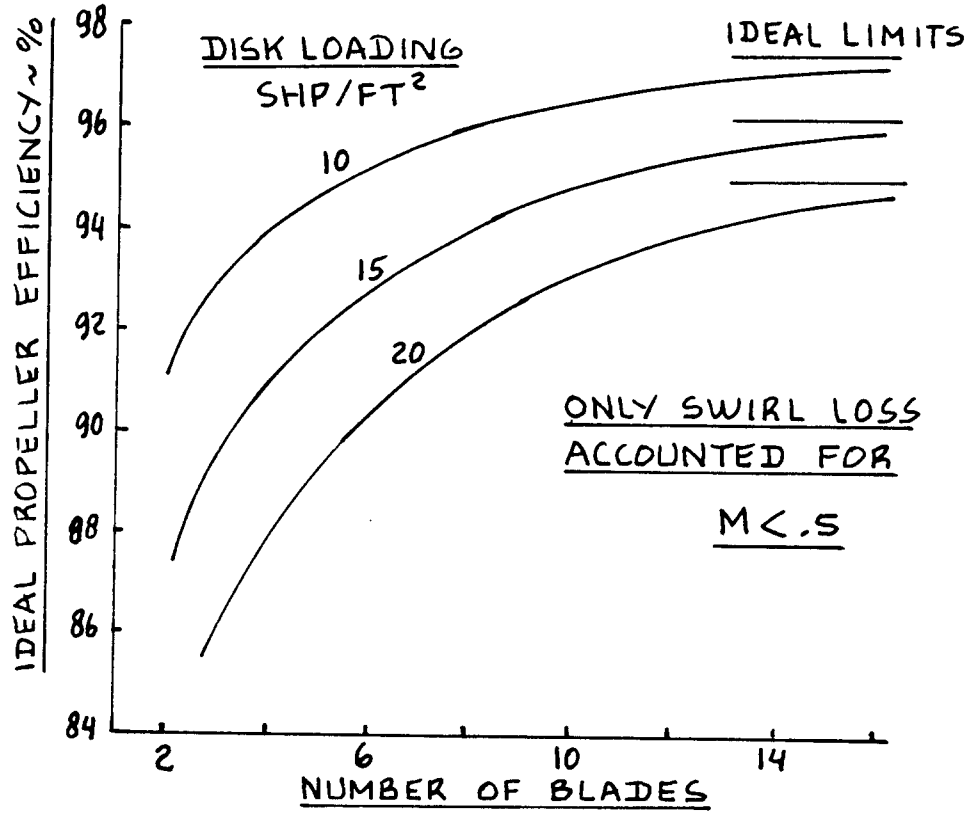

Figure 6.3 Effect of Number of Blades and of Disk Loading on Propeller Efficiency

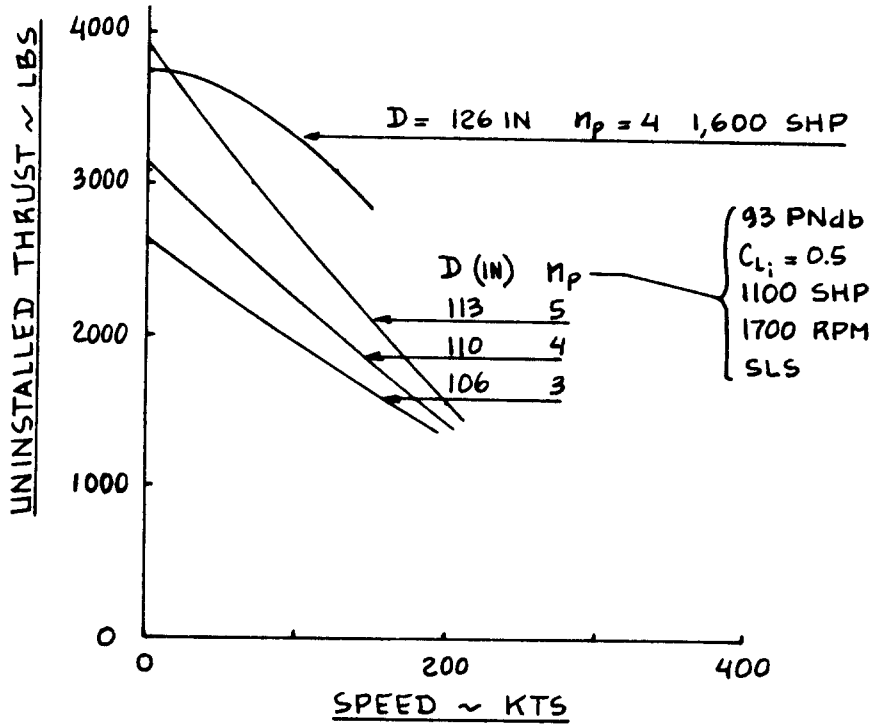

Figure 6.4 Example of the Variation of Propeller Thrust with Flight Speed at Sealevel

Table 6.1 Current Technology Propeller Data (From Ref.64)

Airplane	Cessna 172N	Cessna 210M	Cessna 414A	Cessna 441	Cessna A188B	STAT
Engine	Lycoming O-320-H2AD	Continental IO-520-L	Continentel TSIO-520-NB	Garrett TPE-331-8	Continental IO-520D	PW PT65
Power, hp	160	285	310	635	285	1,270
Prop. RPM	2,700	2,700	2,700	2,000	2,700	1,700
Diameter, in	75	80	76.5	90	80	110
No. of blades	2	3	3	3	3	3
Tipspeed, fps	885	942	901	785	942	816
Cr.speed, kts	120	170	215	295	105	290
Activ. Factor	170	243	267	390	240	360
t/c at .75R	0.085	0.081	0.083	0.065	0.080	0.063
Airfoil	RAF-6	Clark-Y	RAF-6	NACA 16-64	RAF-6	NACA 16-64
Tip sweep deg	0 deg	0 deg	0 deg	1 deg	0 deg	0.5
Proplets	none	none	none	none	none	none
Weight, lbs	36	68	70	117	65	166
Material	Al.	Al.	Al.	Al.	Al.	Al.

Table 6.2 Advanced Technology Propeller Data (From Ref.64)

Airplane	Cessna 172N	Cessna 210M	Cessna 414A	Cessna 441	Cessna A188B	STAT
Engine	Lycoming O-320-H2AD	Continental IO-520-L	Continentel TSIO-520-NB	Garrett TPE-331-8	Continental IO-520D	PW PT65
Power, hp*	145/147	270/272	260/263	515/525	275/278	1075/1080
Prop. RPM*	2665/2388	2653/2399	2699/2429	2051/1822	2653/2399	1818/1627
Diameter, in	83	90	85	100	90	120
No. of blades	2	4	4	4	4	5
Tipspeed, fps*	965/865	1042/942	1001/901	895/795	1042/942	952/852
Cr.speed, kts	120	170	215	295	105	290
Activ. Factor	170	243	267	390	240	360
t/c at .75R	0.060	0.060	0.063	0.040	0.060	0.040
Airfoil	all have advanced NASA propeller airfoils					
Tip sweep	all have 25 degrees tip sweep					
Proplets	all have proplets with height to radius ratio of 0.05					
Weight, lbs	32	55	60	99	48	127
Material	E-glass	Kevlar	Kevlar	Kevlar	Kevlar	Kevlar

* first number meets FAR 36/second number meets FAR 36 minus 5 db

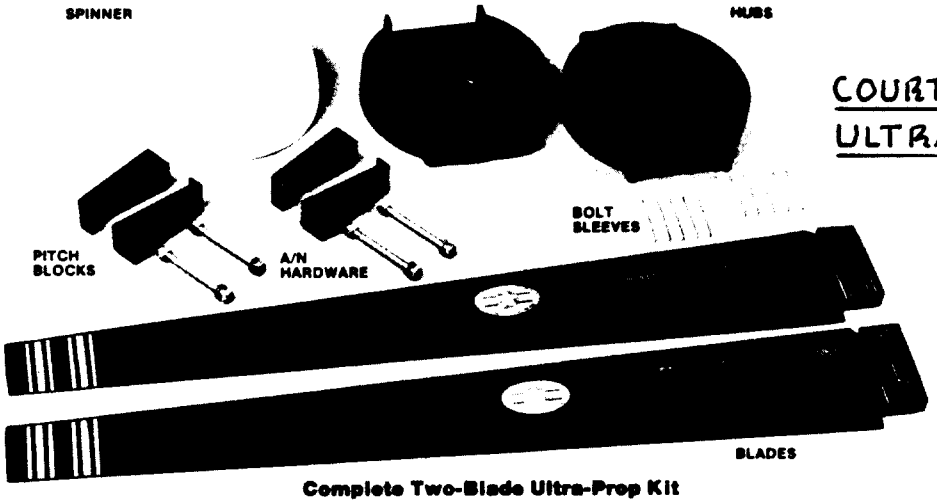

COURTESY: ULTRA PROP

Figure 6.5 Example of a Fixed Pitch Propeller

Station Inches from Centerline	Width-In.		Thickness-In.		*Angle - Degrees				Edge Alignment-In.		Face Alignment-In.	
					New Blade		Reworked Blade					
	Min	Max	Min	Max	Min	Max	Min	Max	Min	Max	Min	Max
9	5.157	5.344	1.761	1.885	6.6	7.6	6.6	7.6	2.355	2.511	0.844	0.934
12	5.966	6.090	1.182	1.232	4.6	5.6	4.6	5.6	2.699	2.761	0.518	0.580
15	6.293	6.417	0.817	0.867	2.2	3.2	2.2	3.2	2.803	2.865	0.319	0.381
18	6.478	6.602	0.675	0.725	0.0	0.0	0.0	0.0	2.886	2.948	0.260	0.322
24	6.598	6.722	0.525	0.575	5.8	6.2	5.9	6.1	2.939	3.001	0.198	0.260
30	6.144	6.206	0.407	0.457	9.9	10.3	10.0	10.2	2.723	2.785	0.149	0.211
36	5.054	5.116	0.298	0.348	12.4	12.8	12.5	12.7	2.237	2.299	0.103	0.165
39	4.349	4.411	0.245	0.295	13.4	13.8	13.5	13.7	1.922	1.984	0.081	0.143
42	3.574	3.636	0.193	0.243	14.2	14.6	14.3	14.5	1.577	1.639	0.060	0.122
45	2.741	2.803	0.100	0.150	14.9	15.3	15.0	15.2	1.205	1.267	0.021	0.083

* For the purpose of measuring blade angles, a plane passing through the thrust face at the 18-inch station is the reference plane. For stations either side of the 18-inch station, the angles are measured on opposite sides of the reference plane.

COURTESY: McCAULEY

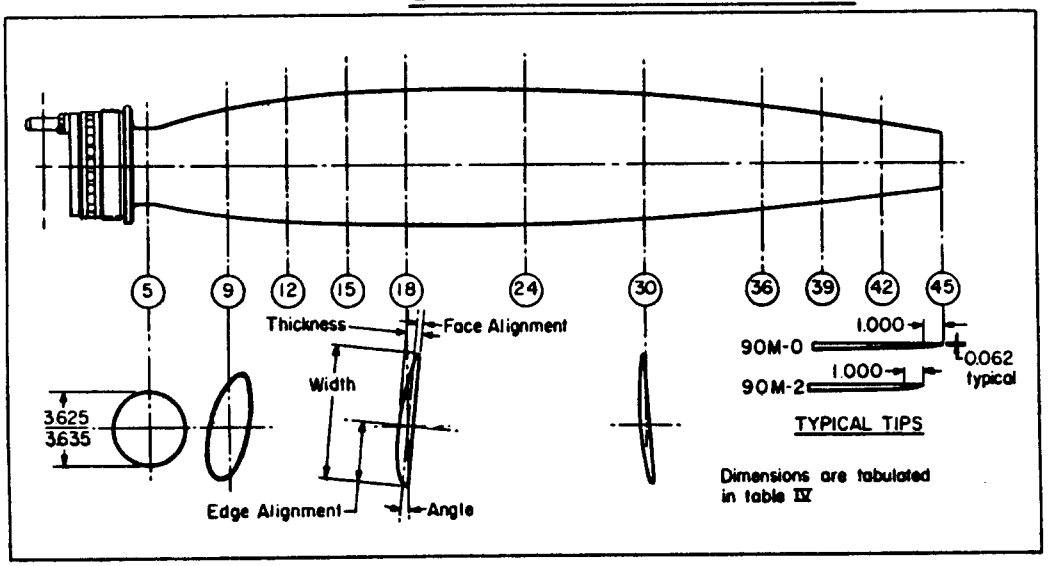

Figure 6.6 Example of Propeller Blade Geometry and Airfoils for a Low Speed Variable Pitch Propeller

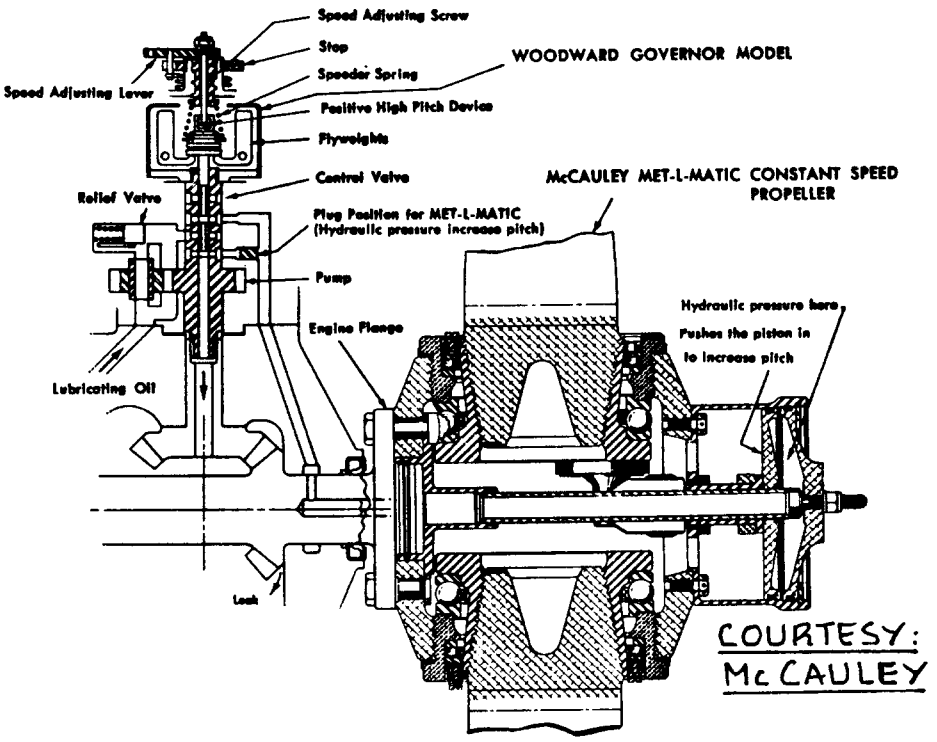

Figure 6.7 Example of a Variable Pitch Mechanism

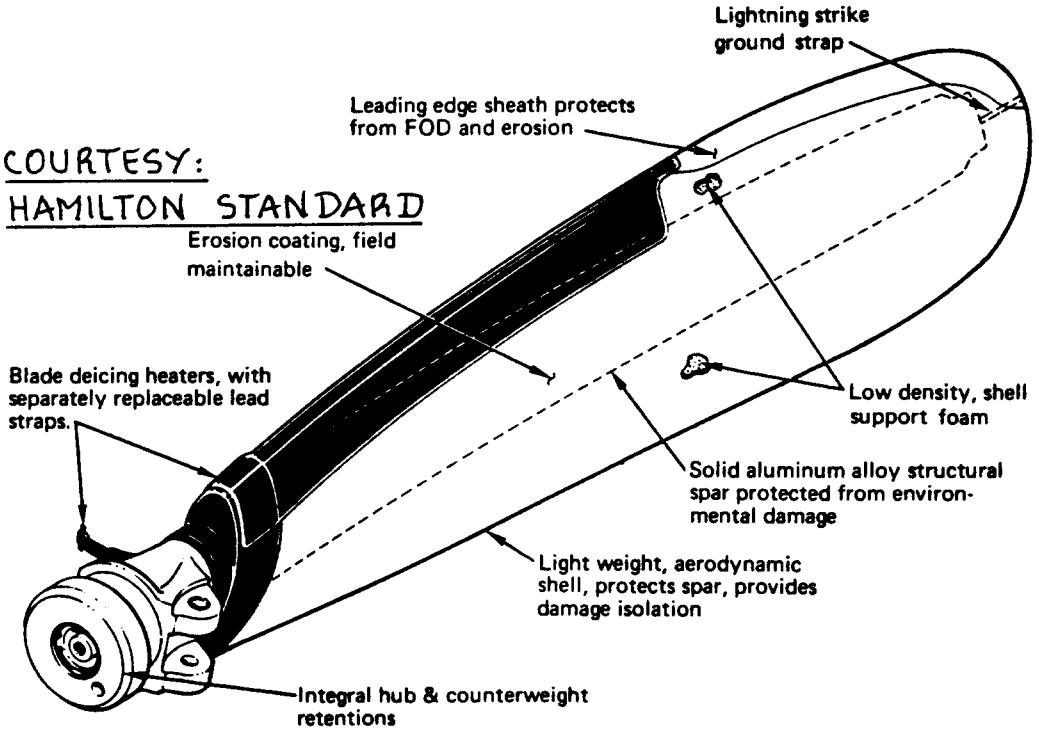

Figure 6.8 Blade Construction of a Modern Four Bladed, Reversible Pitch Propeller

Table 6.3 Propeller Weight Data

Airplane	TOHP	TO RPM	Prop. Diam.	No. of Blades	Weight*	Propeller Control F/V/R**
	hp	rpm	in		lbs	
Cessna 180	225	2,660	84	2	62	F
Cessna 310	240	2,600	80	2	68	V
Beech Baron 95-55	290	2,625	76	2	97	V
Aero Comm. 560	320	2,060	90	2	103	V
DHC-6 Twin Otter	620	2,110	102	3	134	V/R
Beech 99	850	2,000	97	3	131	V/R
Shorts Skyvan	715	2,000	99	4	143	V/R
Beech A-100	680	2,200	90	4	154	V/R
Shorts SD3-30	1,120	1,700	111	5	218	V/R
Hamilton Standard Propfan for 150 Pax Airliner	3,000	1,000	120	8	430	V/R

* Weights exclude spinners. Typical spinner weights 5-12 lbs

** F = Fixed pitch V = Variable pitch R = Reversible

6.1.2 Piston Engines

Airplane piston engines are available in three configurations:

1. Horizontally opposed cylinders
2. Radially arranged cylinders (radials)
3. In-line and/or V- arranged cylinders.

The great majority of modern piston engines are of the horizontally opposed type. Figures 6.9 and 6.10 show an example of a horizontally opposed, aircooled piston engine.

Figure 6.11 shows a 14-cylinder, double row radial piston engine. This engine is no longer in production but hundreds are still available. It is installed in the Canadair CL-215 (Figure 3.31b in Part II) which is still in production.

Smaller radials are still in production in Poland. They are used primarily in agricultural airplanes.

The in-line and/or V- arranged engine configurations were very popular in WWII but have lost favor with most airframers. Small in-lines are still in production in Czechoslovakia. They are used primarily in aerobatic and trainer airplanes.

Reference 30 contains basic design data on piston engines.

Piston engines rapidly loose power with altitude. Too counteract this a co-called 'super-charger' is used. Superchargers use the exhaust gasses from the cylinders to drive a turbine which in turn drives a compressor. The latter compresses the air which is then fed into the cylinders. Super-chargers were in widespread use in WWII in fighter and bomber airplanes. A modern super-charger installation is shown in Figure 6.12.

During preliminary design of airplanes basic data on engine geometry, weight, power output and specific fuel consumption must be available. Ref. 30 provides this information. Tables 6.4 and 6.5 list such preliminary design information for a number of piston engines. The gemetric data used in these tables are defined in Fig.6.13.

Figures 6.14 and 6.15 provide examples of manufacturers engine data for two typical piston engines.

6.1.3 Turbopropeller Engines

A turbopropeller engine is a turboshaft engine which drives a gearbox which in turn drives a propeller. Examples of modern turbopropeller engines are presented in Figures 6.16 and 6.17.

Tables 6.6 and 6.7 present basic design data for a number of turbopropeller engines. Note that propeller weights are not included in these data, but the gearboxes are. More design data on turboshaft engines (no gearbox) and turbopropeller engines (with gearbox but without propeller) are found in Ref.30.

Figures 6.18 and 619a present typical manufacturers performance information for turbopropeller engines. Figure 19b also provides the installation information needed to integrate this powerplant into an airframe.

6.1.4 Turbojet and Turbofan Engines

The difference between a turbojet and a turbofan engine is primarily in the management of air: in a turbojet all the inlet air passes through the combustion process (BPR = 0), while in a turbofan part of the air is 'by-passed' through a fan which accelerates the bypassed air aft (BPR > 0).

At subsonic speeds turbofans have essentially replaced turbojets in most applications. The reason is the much lower specific fuel consumption associated with the turbofan.

For supersonic operations there is a trend toward replacement of pure turbojets with low by-pass ratio turbofans. What complicates the installation of engines in a supersonic airplane is the requirement for special inlets and frequently the requirement for afterburning (=augmentation).

Figure 6.20 through 6.22 show cutaways of modern turbofan engines for subsonic applications. Performance and geometry data for two of these engines are presented in Figures 6.23 and 6.24. Figure 6.25 presents data for the GE TF39 engine (similar to the PW JT9D engine).

Figures 6.26 through 6.29a show examples of afterburning turbojet and turbofan engines, all for use in supersonic airplanes. Thrust and sfc data for the F100 engine of Fig.6.29a are given in Figure 6.29b.

Tables 6.8 through 6.11 contain basic design data on selected turbojet and turbofan engines. Ref.30 contains information on a large number of turbojets and turbofans.

6.1.5 Propfan Engines

Figures 6.30 and 6.31 show examples of two types of propfan engines. The associated performance predictions for these powerplants are reflected in Figures 6.32 and 6.33 respectively. These engines and their derivatives are expected to become operational in the early 90's. At the time of publication of this text none had been certificated for civil nor for military operation.

NOTE: This note applies to all types of engines which have a gasgenerator as the primary source of power:

Engine weight data for these engines DO NOT include the weight of any associated nacelles, inlets and exhaust pipes and/or nozzles. Manufacturers thrust and sfc data are normally given for 'ideal' inlets (bellmouths) and for 'ideal' exhaust systems. The reason is that engine manufacturers cannot anticipate the different types of engine installations an airframe manufacturer may wish to use. Section 6.9 contains examples of nacelle, inlet and exhaust system configurations.

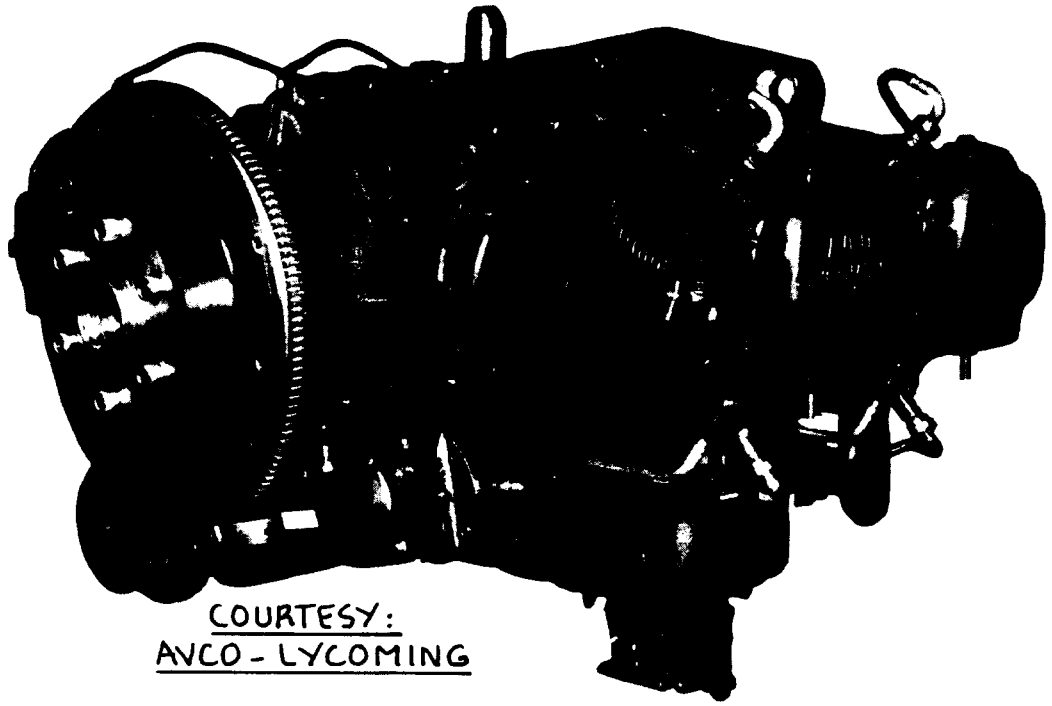

Figure 6.9 AVCO-Lycoming O-320 Series Horizontally Opposed 4-Cylinder Piston Engine

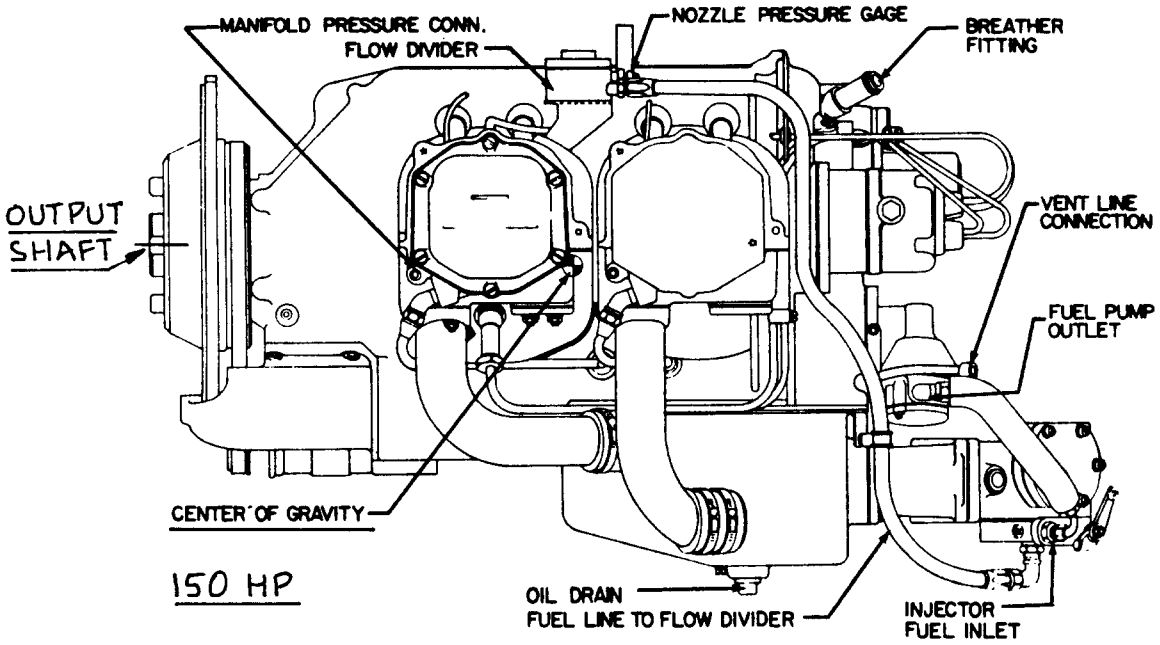

COURTESY: AVCO-LYCOMING

P: ENGINE MOUNTING POINTS

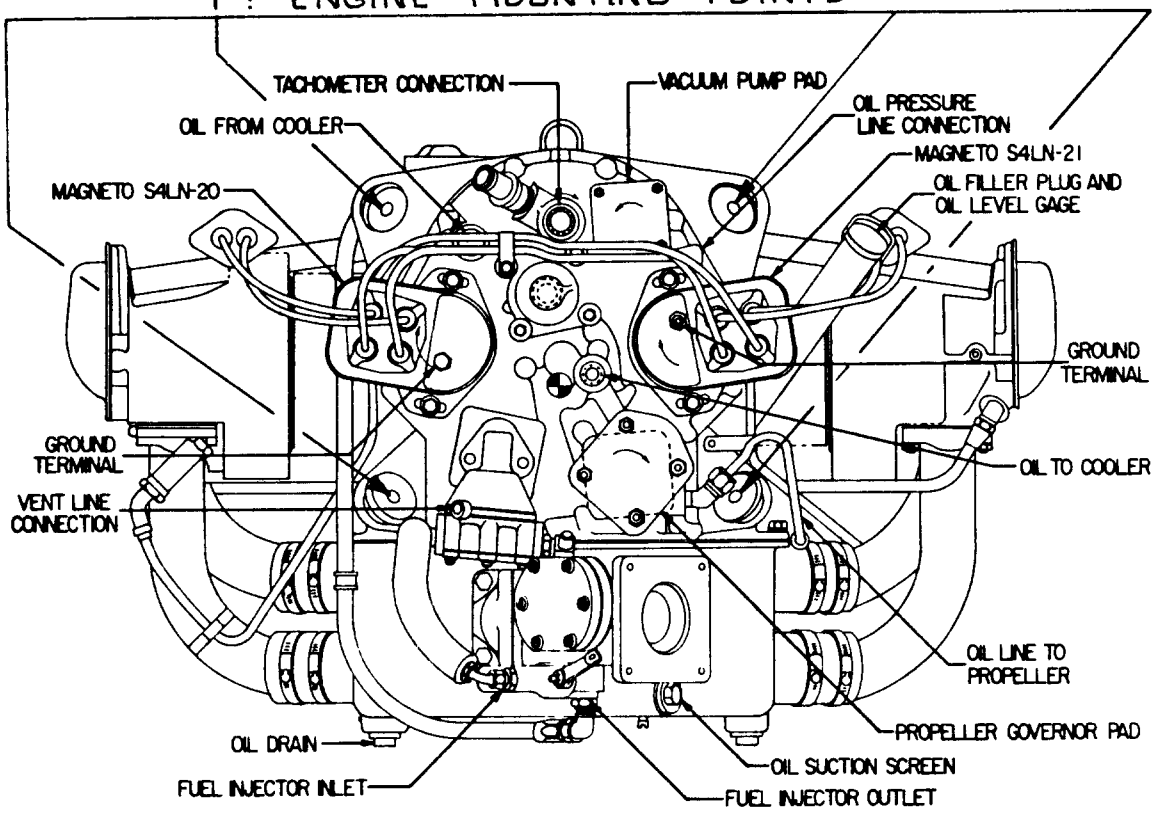

Figure 6.10 Side View and Rear View of AVCO-Lycoming O-320 Series 4-Cylinder Piston Engine

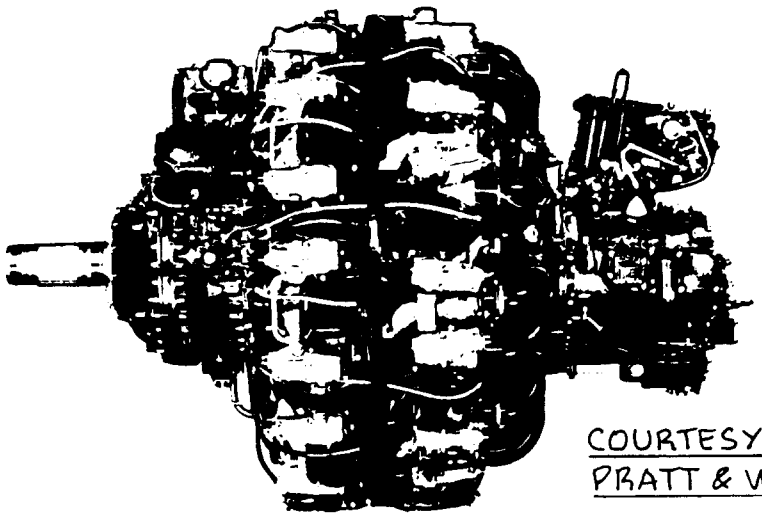

Figure 6.11 Pratt and Whitney R2800 Double Row Radial 14-cylinder Piston Engine

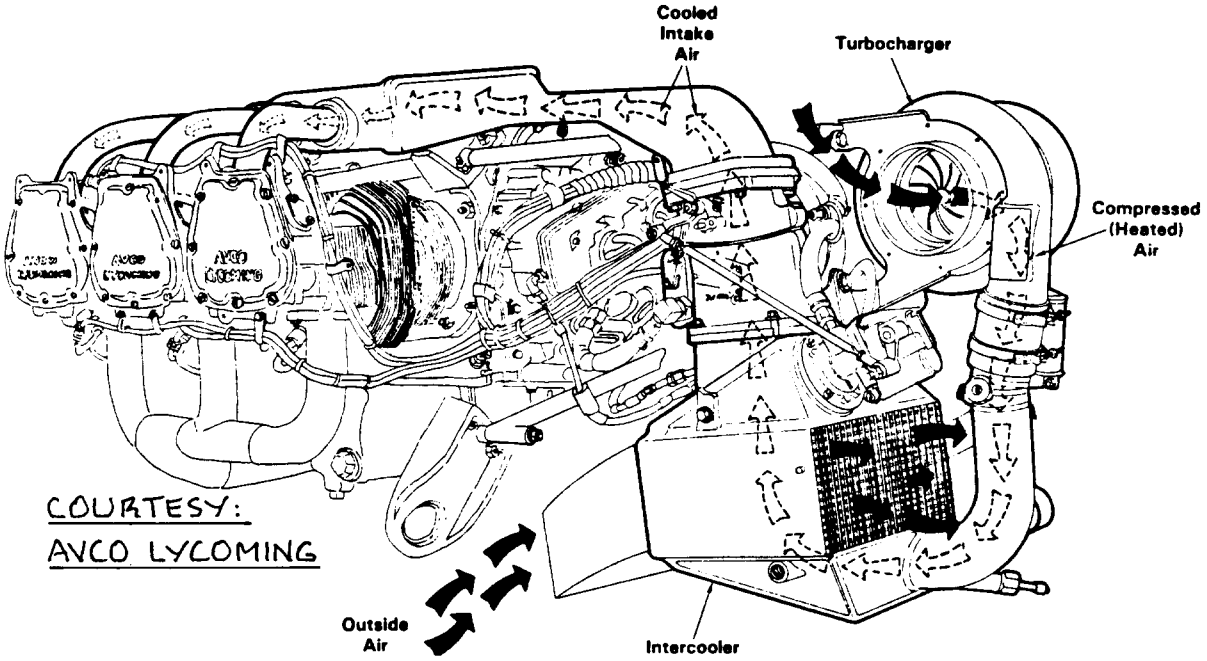

Figure 6.12 Typical Supercharger Installation

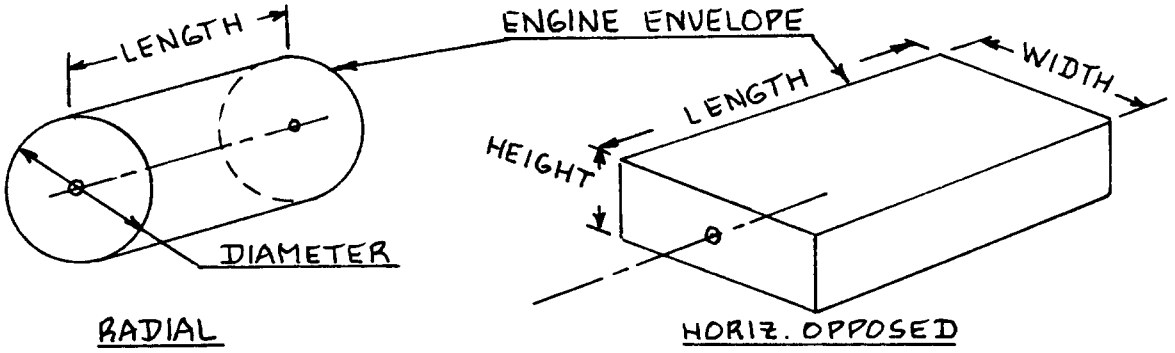

Figure 6.13 Definition of Piston Engine Geometric Data

Table 6.4 Manufacturer Performance Data for Piston Engines

Type	Avco Lycoming 10-320-B1A	IO-360-A1B6D	TIO-540-A1A	TIGO-541-E1A	PZL-3S
Supercharged	no	no	yes	yes	no
Direct drive	yes	yes	yes	geared 0.8	yes
Max. T.O. Power (hp) at Prop. RPM/to alt.	160 2,700/SL	200 2,700	310 2,575/15K	425 2,133/15K	600 2,200/SL
SFC (lbs/hp/hr)	0.51	0.50	0.565	0.753	0.610
Cruise Power* (hp) at RPM	120 2,350	150 2,450	233 2,575	319 1,833	415 2,000
SFC (lbs/hp/hr)	0.489	0.481	0.516	0.502	0.510
No. of cylinders	4	4	6	6	7(radial)
Dry weight** (lbs)	287	330	540	700	906
Length (in)	33.6	31.3	51.3	57.6	43.7
Width (in)	32.2	34.3	34.3	34.9	49.9
Height (in)	19.2	19.4	22.7	22.7	diam.
Octane	91/96	100/130	100/130	100/130	91+

*normally at 75 percent rated power, static sealevel.

**includes accessories needed for operation

Table 6.5 Manufacturer Performance Data for Piston Engines

Type	Franklin/PZL*** 2A-120	4A-235-B2	6A-350-C1	Teledyne-Continental O-200A	TSIO-	IO-520-A
Supercharged	no	no	no	no	no	no
Direct drive	yes	yes	yes	yes	yes	yes
Max. T.O. Power (hp) at Prop. RPM, SLS	60 3,200	125 2,800	220 2,800	100 2,750	225 2,800	285 2,700
SFC (lbs/hp/hr)	0.53	0.52	0.460	0.60	0.62	0.50
Cruise Power* (hp) at RPM	45 2,200	94 2,080	165 2,100	75 2,450	169 2,550	214 2,500
SFC (lbs/hp/hr)	0.620	0.440	0.480	0.585	0.52	0.452
No. of cylinders	2	4	6	4	6	6
Dry weight** (lbs)	137	224	333	218	300	471
Length (in)	29.7	30.5	32.1	28.5	35.3	41.4
Width (in)	30.7	31.5	31.6	31.6	33.1	33.6
Height (in)	22.7	25.1	27.5	23.2	23.7	19.8
Octane	100/130	100/130	100/130	80/87	100/130	100/130

*normally at 75 percent rated power **includes accessories needed for operation

***Franklin engines are manufactured in Poland by PZL

PERFORMANCE

Rated Power (Sea Level) . . . 100
Take-Off Power (Sea Level). . 100
Cruise Power (Sea Level) . . . 75
Power corrected to 29.92 in. Hg.
60° F. Inlet Air Temp.

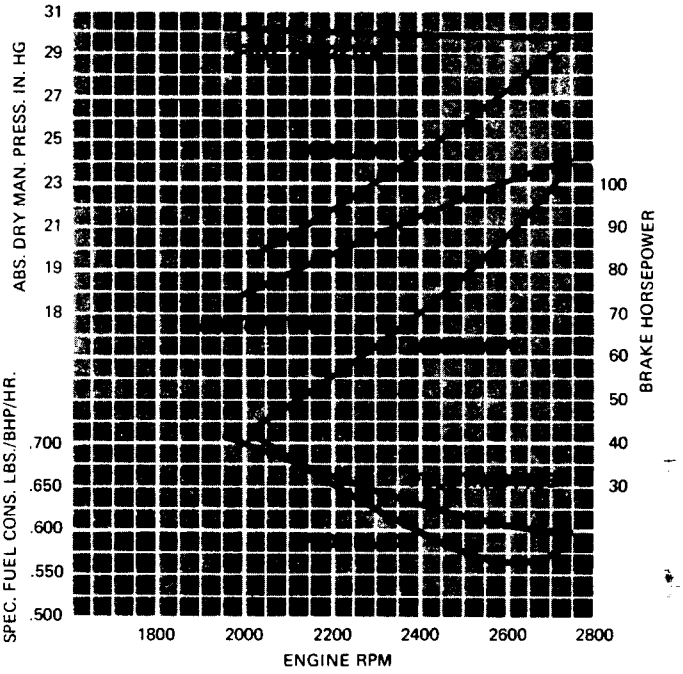

OPERATING DATA

Oil Required . . . Below 40°F: SAE-20
Above 40°F: SAE-40
Oil Temperature . . . . . 75°F.–170°F.
Oil Pressure, Idling . . . . .10 p.s.i. Min.
Oil Pressure, Cruising . . . . .30-60 p.s.i.
Oil Sump Capacity . . . . . 6 quarts
Allowable Temperatures:
Cylinder Head . . . . . .525°F. Max.
Cylinder Barrel . . . . .290°F. Max.
Oil Temperature . . . . . .225°F. Max.

SPECIFICATIONS

Type Certificate Number 252
Number of Cylinders 4
Bore (Inches) 4.06
Stroke (Inches) 3.88
Displacement (cubic inches) 201
Type of Propeller Drive, Flanged . . . . . Direct
Compression Ratio 7.0:1

RPM at Rated Power 2750
RPM at Take-Off 2750
Cruising RPM 2500
Recommended Fuel Grade Min. 80/87
Dry Weight (With Accessories Below Included) . . . 217.87
Crankshaft Rotation . . . . . Clockwise
Ignition . . . . . Dual

COURTESY:
TELEDYNE CONTINENTAL

STANDARD EQUIPMENT

ITEM	MAKE	WEIGHT
Spark Plugs	A.C.	1.75
Magnetos	Slick	12.12
Ignition Harness (Shielded)	Continental	3.81
Starter	Delco-Remy	15.50
Generator	Delco-Remy	10.12
Oil Cooler	Harrison	4.25
Tachometer Drive	Continental	0.12

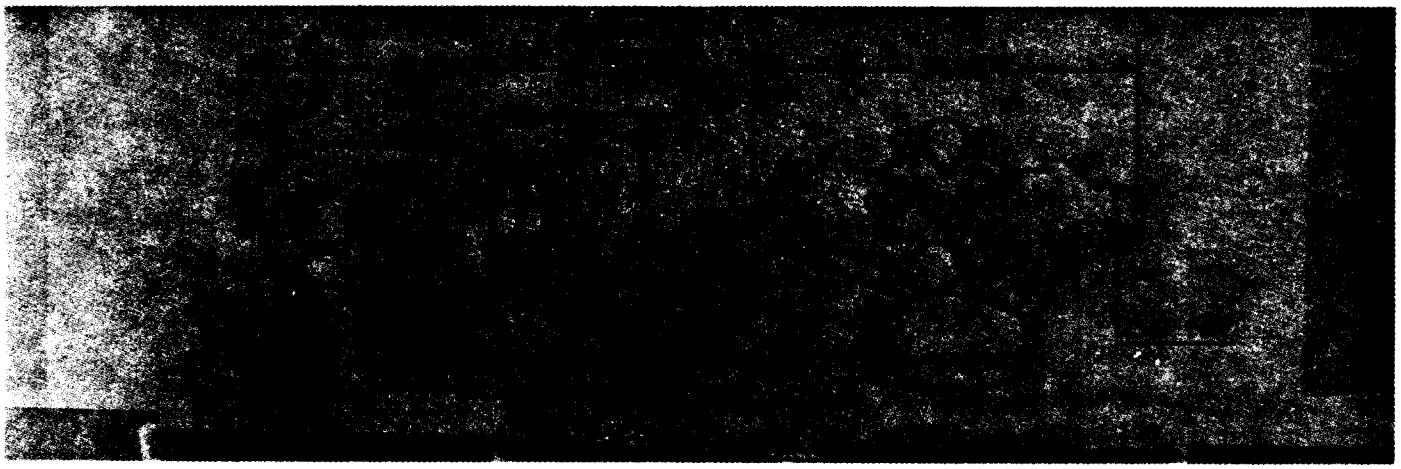

Figure 6.14 Tel.-Continental O-200-A Manufacturer Data

PERFORMANCE

Rated Power (Sea Level)	225
Take-Off Power (Sea Level)	225
Recommended Cruise Power (Sea Level)	172
Critical Altitude	
Rated Manifold Pressure	20,000
Cruise Power	25,000
Power Corrected to 29.92 In. Hg 60°F. Inlet Air Temperature	

OPERATING DATA

Oil Required	Below 40°F: SAE No. 30 10W-30 Optional Above 40°F: SAE No. 50
Oil Temperature	75°F–240°F
Oil Pressure, Idling	10 p.s.i. Min.
Oil Pressure, Cruising	30-60 p.s.i.
Oil Sump Capacity	10 quarts
Allowable Temperatures:	
Cylinder Head	460°F Max.
Cylinder Barrel	310°F Max.

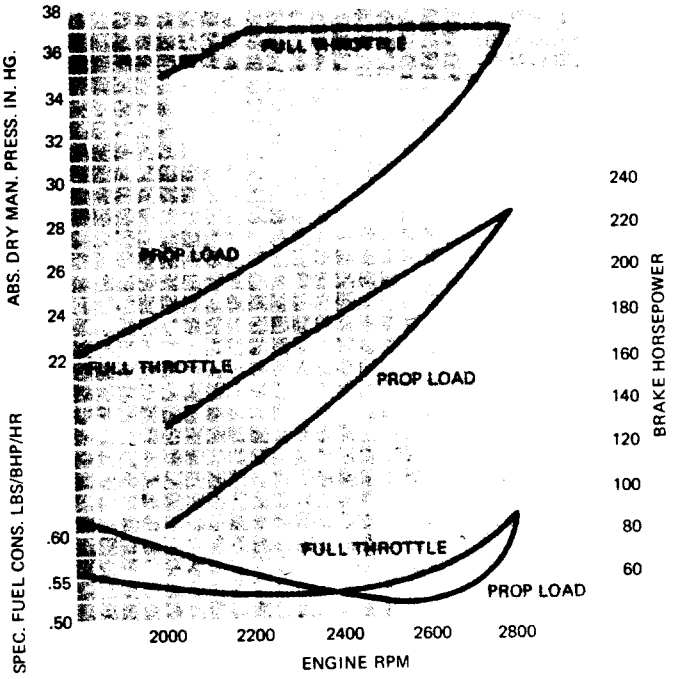

COURTESY:
TELEDYNE CONTINENTAL

SPECIFICATIONS

Type Certificate Number	E9CE
Number of Cylinders	6
Bore (inches)	4.438
Stroke (inches)	3.875
Displacement (cubic inches)	.360
Type of Propeller Drive, Flanged	Direct
Compression Ratio	7.5:1
Max. Continuous M.P., to 20,000 Ft. Critical Altitude, In. Hg	37
RPM @ Cruise Power	.2600
RPM @ Rated Power	.2800
Max. Cruise M.P., to 25,500 Ft. Critical Altitude, In. Hg	30
Recommended Fuel, Grade Min.	100/130
Dry Weight (With Accessories Below Included)	300.25
Crankshaft Rotation	Clockwise
Ignition	Dual
Dimensions With Standard Equipment Installed	
Length	35.34
Width	33.11
Height	23.74

STANDARD EQUIPMENT

ITEM	MAKE	WEIGHT
Spark Plugs	A.C.	3.03
Fuel Injector System	Continental	8.75
Magnetos	Scintilla	11.00
Ignition Harness (Shielded)	Continental	2.41
Starter	Delco-Remy	16.38
Alternator	Autolite	10.81
Oil Cooler	Harrison	4.25

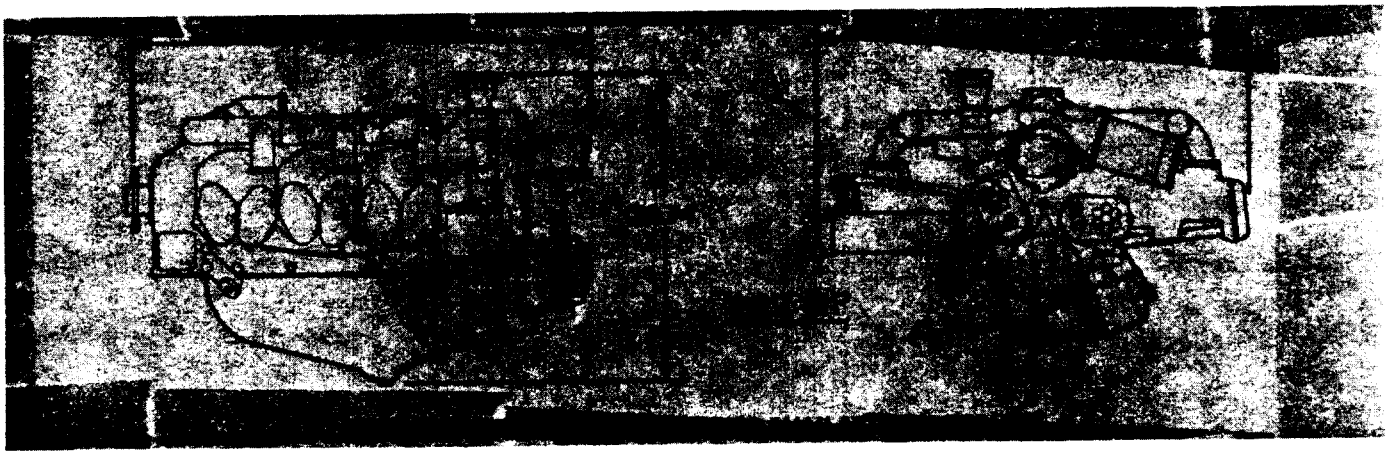

Figure 6.15 Tel.-Continental TSIO-360-C Manufacturer Data

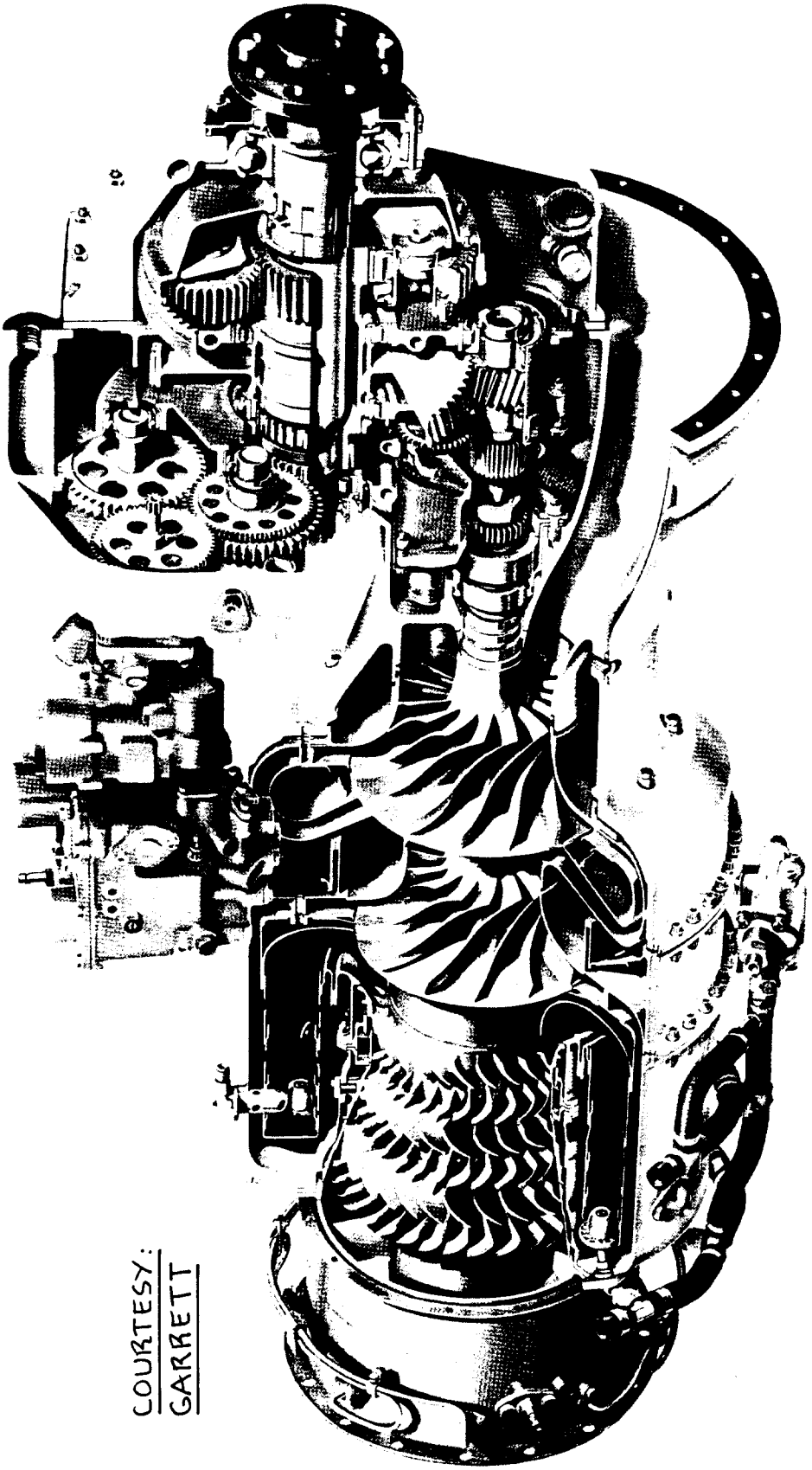

Figure 6.16 Garrett TPE331 Turboprop Engine Cutaway

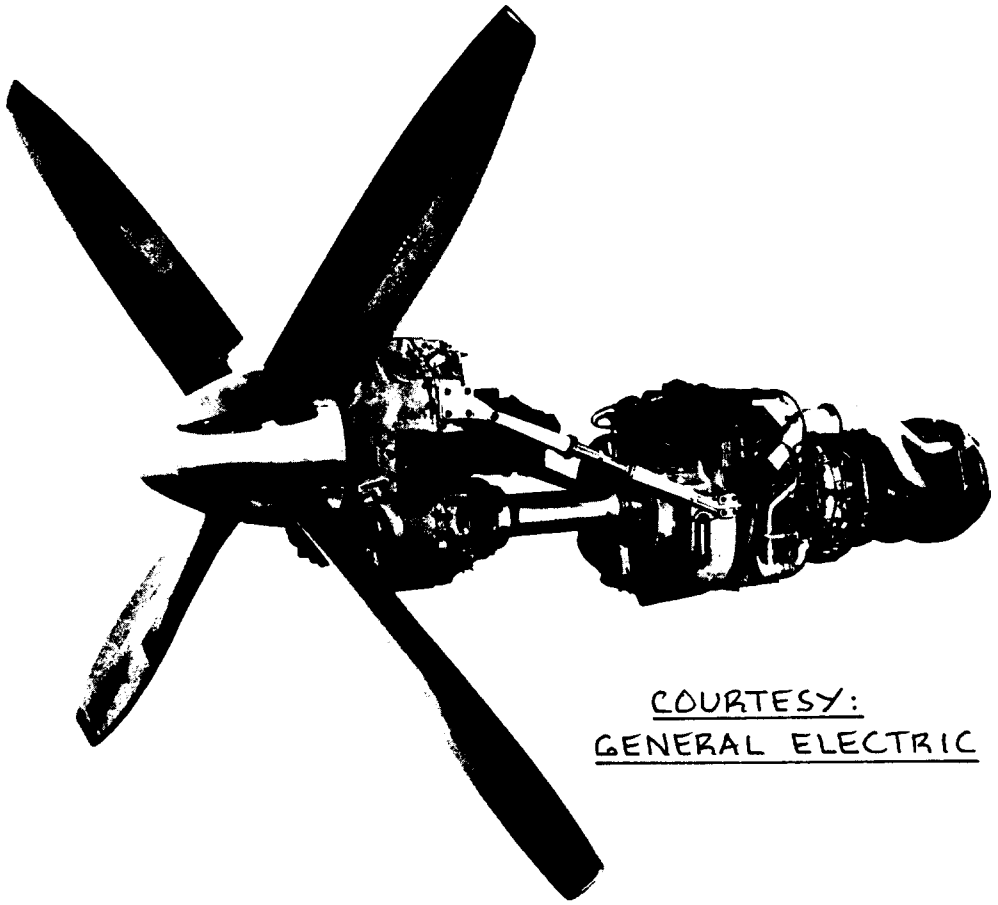

COURTESY:
GENERAL ELECTRIC

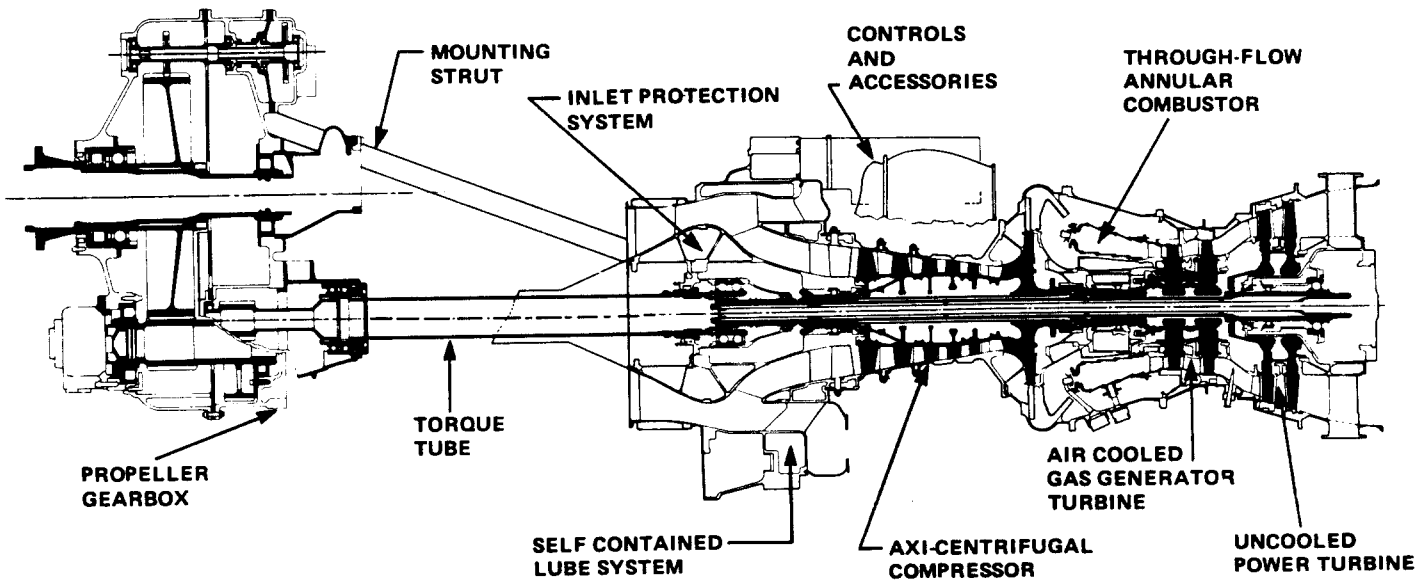

Figure 6.17 General Electric CT7-5 Turboprop Engine Layout and Perspective

Table 6.6 Manufacturer Performance Data for Turboprop Engines

Type	Pratt and Whitney of Canada Ltd. PT6A-21	PT6A-41	PT6A-65R	PW115	PW120	PW124
For SLS (static shaft horsepower, hp):						
Max. T.O.	550	850	1,173	1,500	1,800	2,150
Max. Cont.	550	850	1,173	1,500	1,700	NA
Max. Cruise	550	850	956	1,500	1,619	2,030
Max. Massflow (lbs/sec)	6.1	8.0	9.4	14.3	14.8	NA
For SLS (specific fuel consumption, lbs/ESHP/hr):						
Max. T.O.	0.630	0.591	0.549	0.529	0.499	0.473
Max. Cont.	0.630	0.591	0.564	0.529	0.506	NA
Max.Cruise	0.649	0.591	0.581	0.529	0.514	NA
SHP/Altitude/speed	316/20K/ 245kts	488/20K/ 245kts	549/20K/ 245kts	861/20K/ 245kts	929/20K/ 245kts	1,165/20K/ 245kts
Rated Propeller RPM	2,200	2,000	1,700	1,300	1,200	1,200
Weight (lbs)	303	380	464	841	921	1,060
Length (in), cold	62	67	74	81	84	84
Max. diam. (in)	19	19	19	25	25	25
Application	Beech C90	Piper Cheyenne III	Shorts 360	EMB-120	DHC-8	BAe-ATP

Table 6.7 Manufacturer Performance Data for Turboprop Engines

Type	General Electric CT7-5A	CT64-820	Rolls R. Dart RDa7 TS1637	Rolls R. Turbomeca AZ-14	Garrett TPE 331-3	T.Lyc. LTP101
For SLS (static shaft horsepower, hp):						
Max. T.O.	1,699	3,133	1,835	800	840	592
Max. Cont.	1,476	2,745	1,835	800	840	592
Max. Cruise	1,417	2,745	1,650	720	770	NA
Max. Massflow (lbs/sec)	10	26.2	23.5	5.5	7.8	4.8
For SLS (specific fuel consumption, lbs/ESHP/hr):						
Max. T.O.	0.456	0.486	0.676	0.521	0.548	0.550
Max. Cont.	0.465	0.505	0.676	0.521	NA	NA
Max.Cruise	0.471	0.505	0.676	0.532	NA	NA
SHP/Altitude/speed	1,655/ 15+K/NA	NA	1,220/ 15K/0kts	NA	NA	NA
Rated Propeller RPM	1,200 (estim.)	1,160	1,400	1,783	1,600	1,924
Weight (lbs)	676	1,145	1,369	454	355	241
Length (in), cold	80.4	110.1	97.6	80.6*	43.5	30.9
Height (in)	31	20.1	37.9	22.9	26.0	18.6
Width (in)	26	diam.	diam.	22.9	21.0	diam.
Application	SF340	G222	F-50	BAe Jetstream	BAe Jetstream	P166-D1-3

*includes propeller!

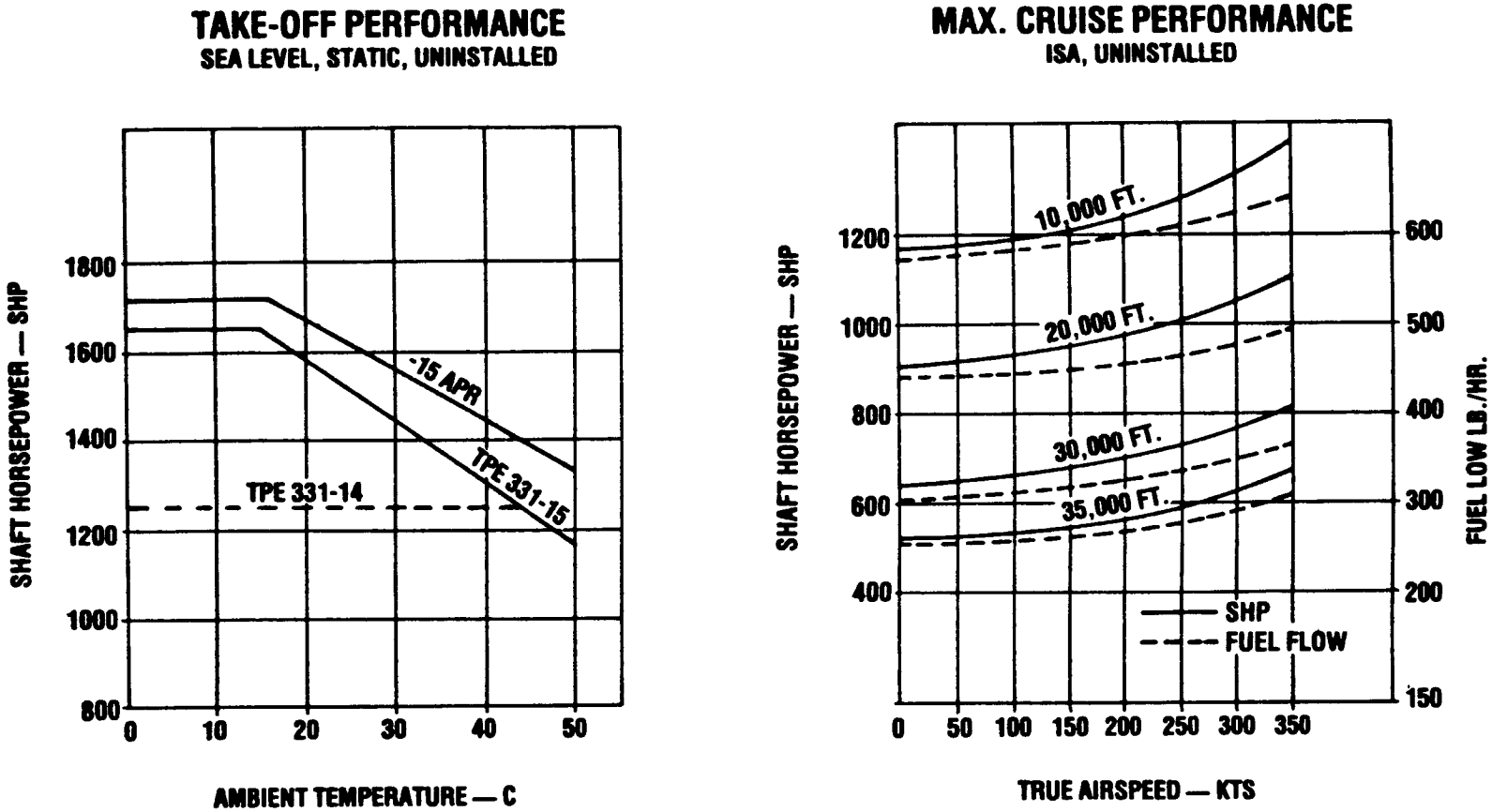

Figure 6.18 Uninstalled Performance Data for Garrett TPE331-14 Turboprop Engine

PT6A-41

PERFORMANCE

Guaranteed calibration stand performance at 2000 RPM propeller speed, sea level static output.

Ratings:	ESHP	SHP	Specific Fuel Consumption lb/eshp/hr
Take-off Max. Continuous	903	850(1)	.591
Max. Climb Max. Cruise	903	850(2)	.591

(1) Available to 106°F
(2) Available to 84°F

COURTESY: PRATT & WHITNEY

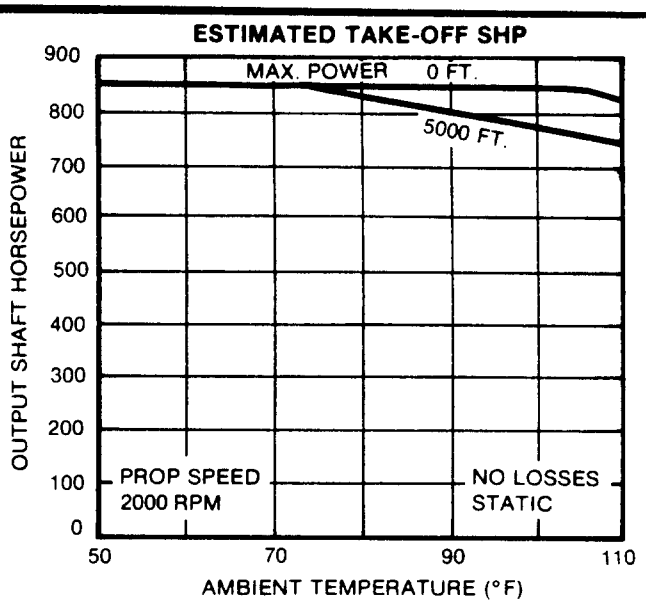

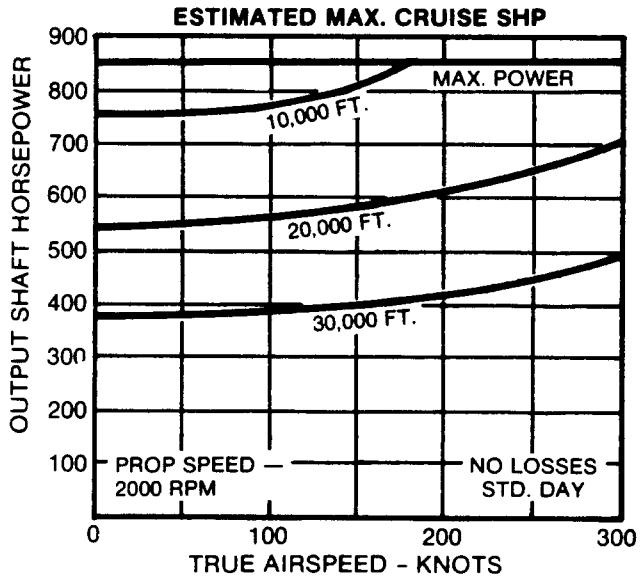

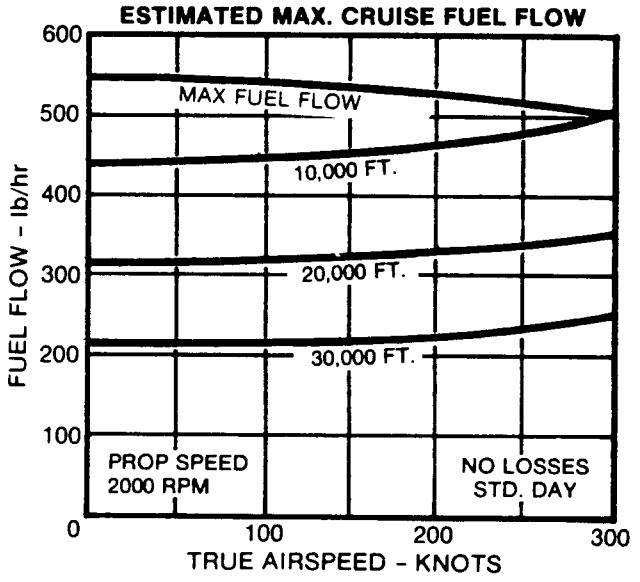

STANDARD EQUIPMENT

- Fuel System — including fuel pump and altitude compensated fuel control unit
- Engine Ignition System — without power source
- Gas Temperature Thermocouples
- Integral Oil Tank
- Torquemeter
- Marinization
- Inlet Screen
- Accessory Drives
  - — power section: propeller control unit and tachometer generator
  - — gas generator section: starter generator and tachometer generator

ADDITIONAL EQUIPMENT

- Fireseal mounting rings
- Fuel heater with hoses

OPTIONAL EQUIPMENT

- Propeller Control System including propeller control unit
- Accessory Drives
  - — gas generator section: three (3) aircraft accessories
  - — power section: propeller overspeed governor
- Torque limiter
- Compressor wash ring
- Provision for fuel flowmeter
- Provision for fuel temperature

Figure 6.19a Uninstalled Performance Data for Pratt and Whitney PT6A-41 Turboprop Engine

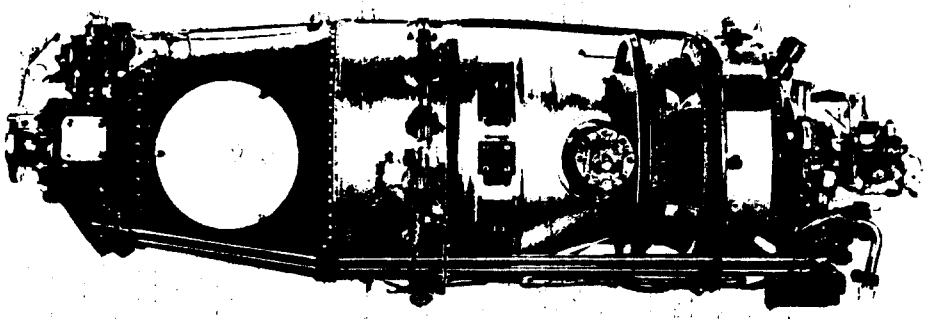

The PT6A-41 is a free turbine propulsion engine incorporating a multi-stage compressor, single-stage compressor turbine, and independent two-stage power turbine driving the output shaft through integral planetary gearing. A single annular combustion chamber, 14 simplex fuel nozzles and two spark igniter plugs comprise the combustion system. Engine accessories are conveniently grouped on the rear of the engine. The free turbine design permits selection of propeller speed from a wide RPM band to suit aircraft operation.

Engine dry weight (with standard equipment); 380 lbs.

Output shaft speed (max.): 2000 RPM.

COURTESY: PRATT & WHITNEY

Sold under current edition of Production Specification No.723.

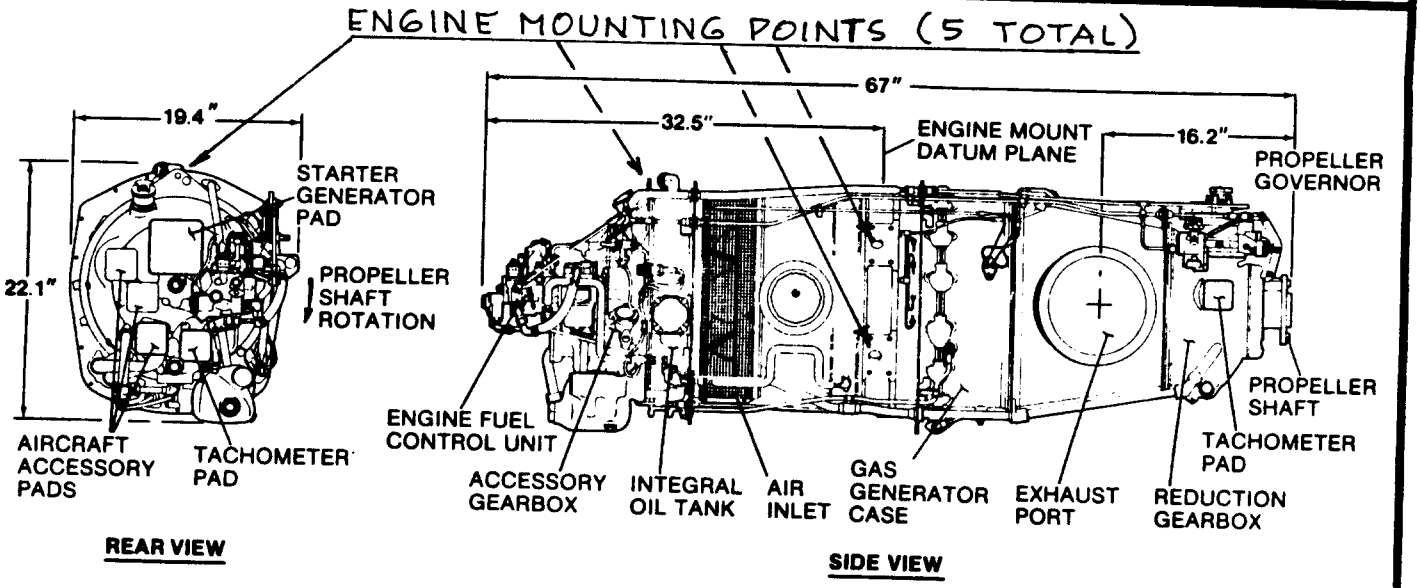

Figure 6.19b Installation Geometry for Pratt and Whitney PT6A-41 Turboprop Engine

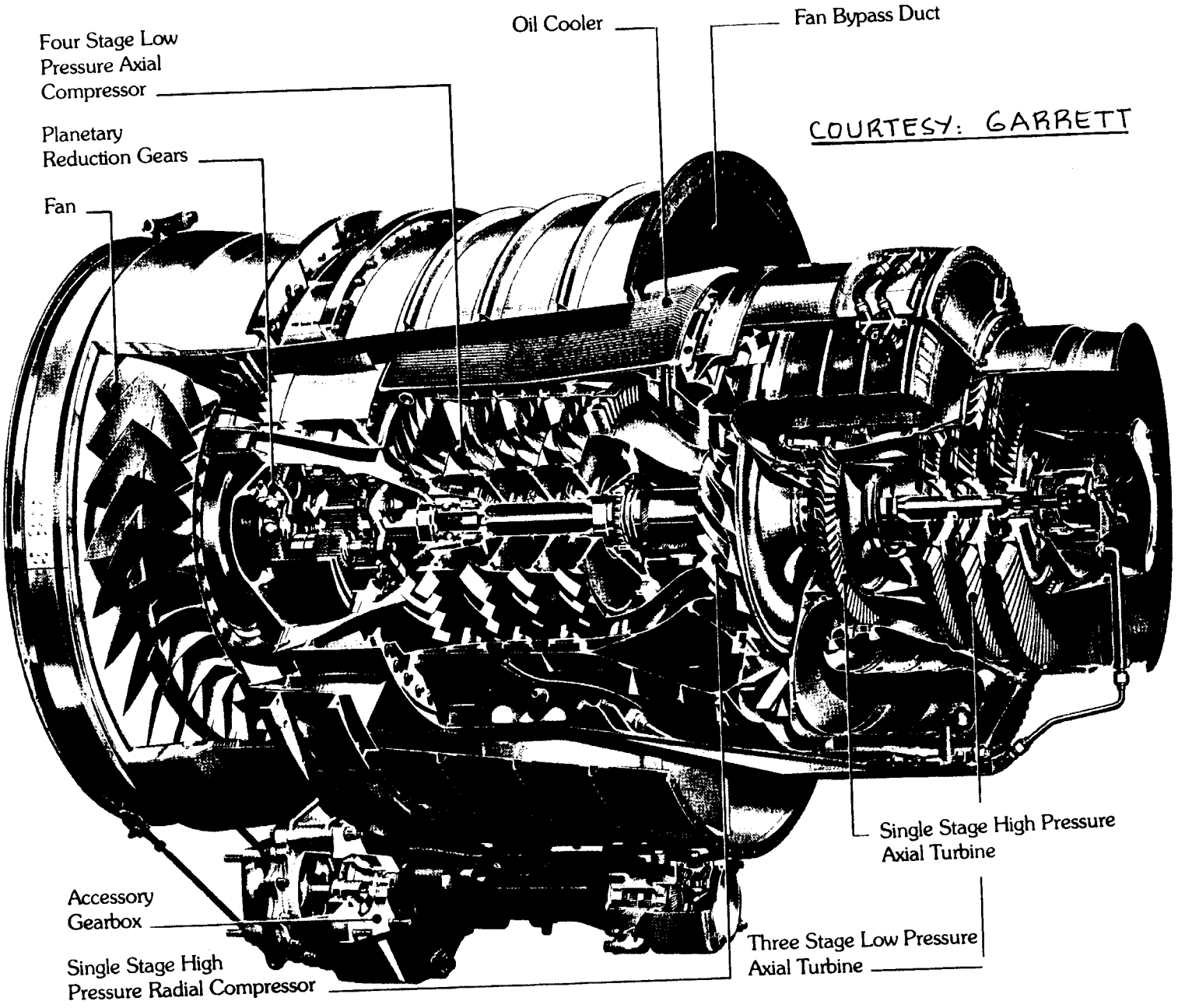

Figure 6.20 Cutaway of Garrett TFE731 Turbofan

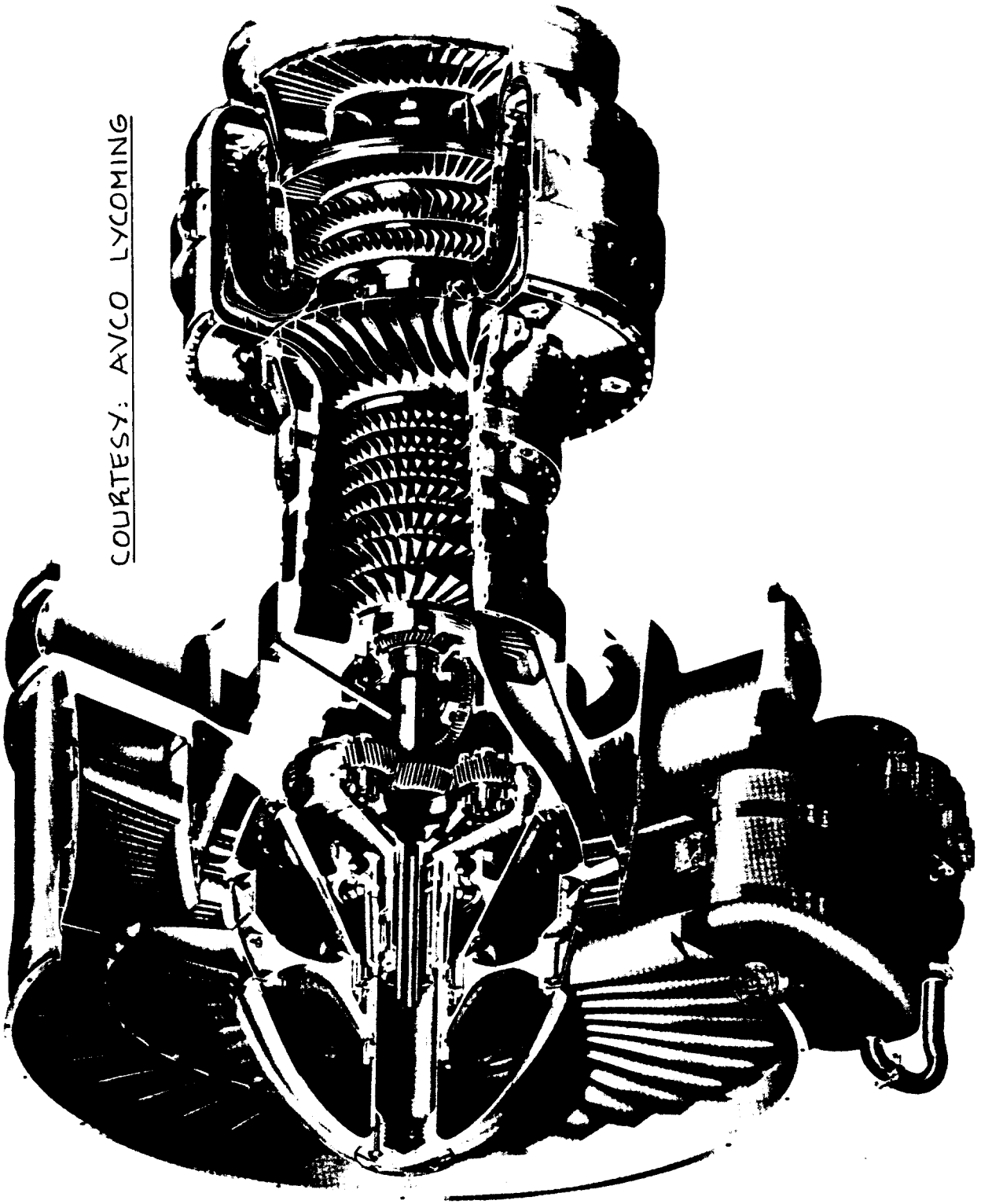

COURTESY: AVCO LYCOMING

Figure 6.21 Cutaway of AVCO Lycoming ALF-502R-5 Turbofan

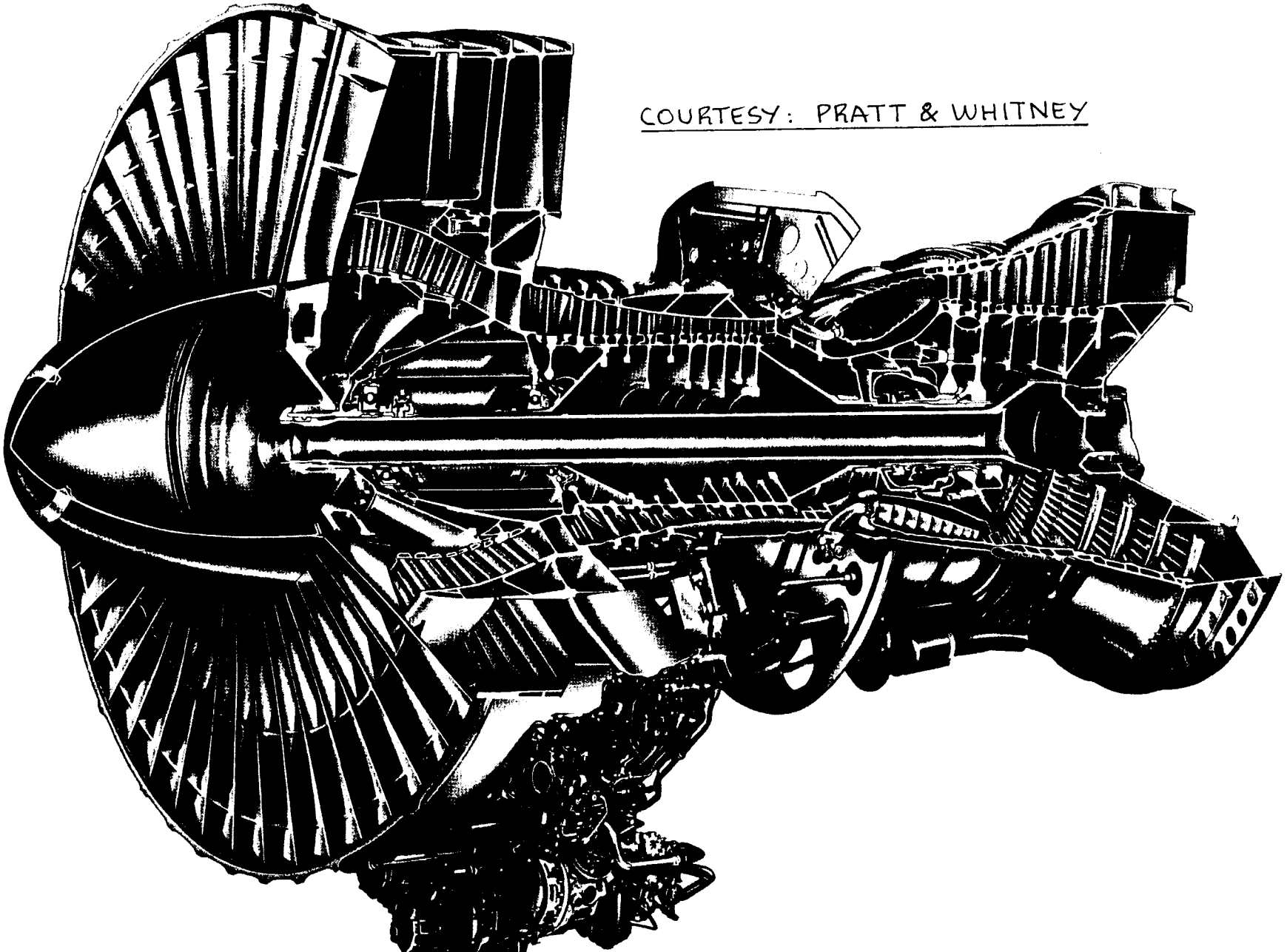

Figure 6.22 Cutaway of Pratt and Whitney JT9D Turbofan

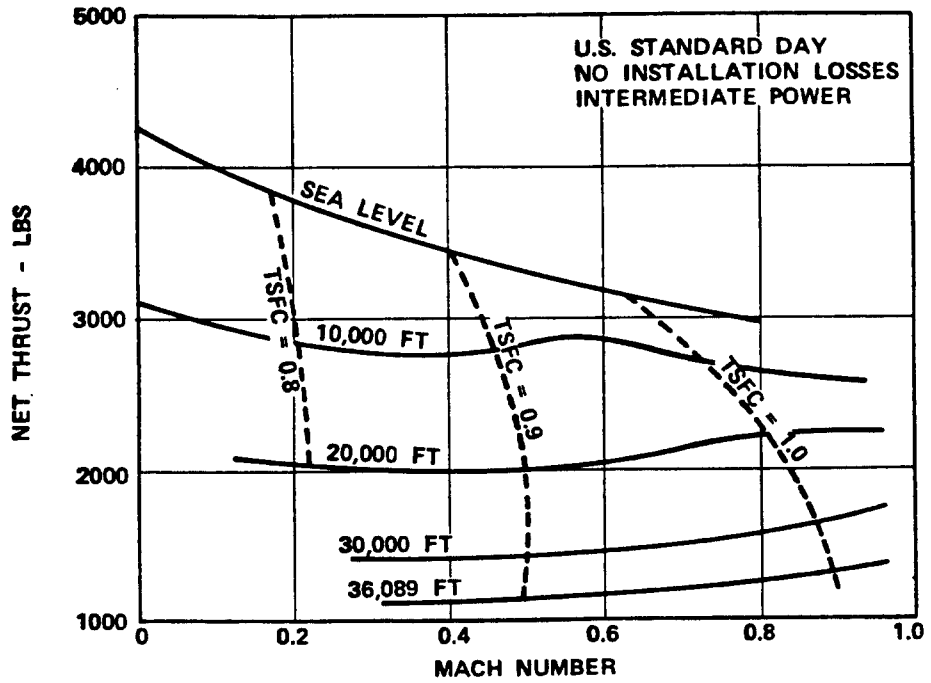

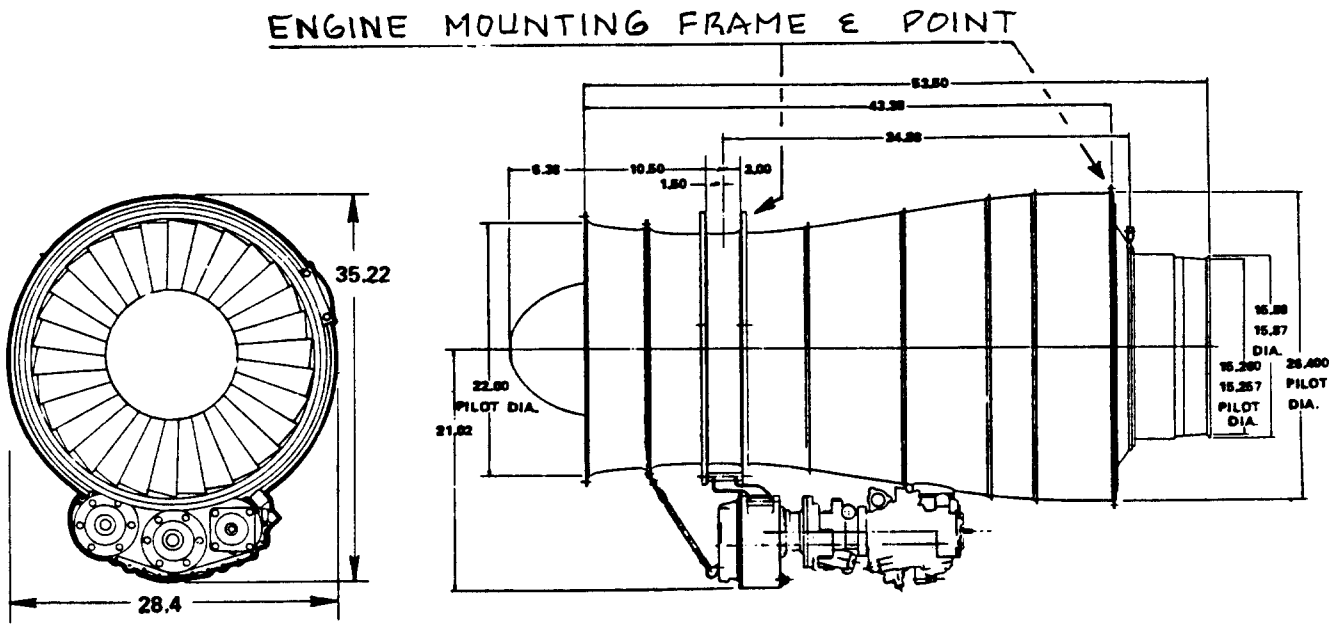

COURTESY: GARRETT

Figure 6.23 Uninstalled Performance and Geometry Data for Garrett TFE731-1042 Engine

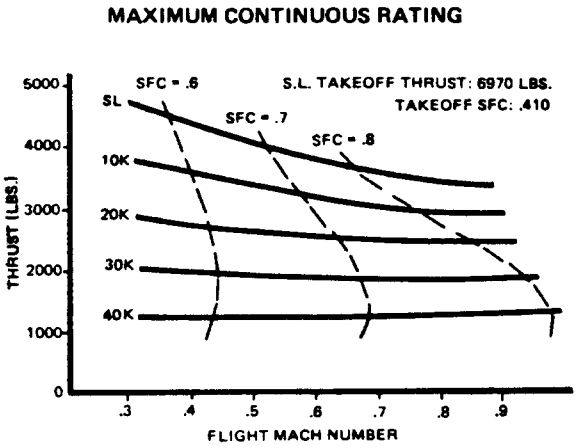

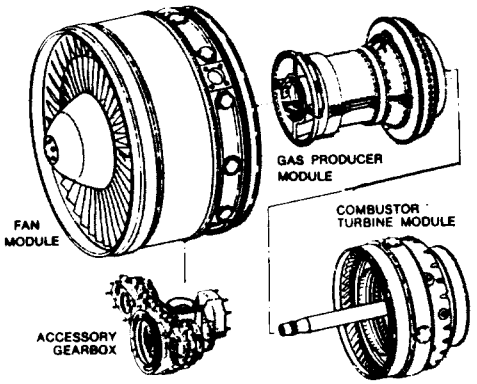

FULL MODULAR DESIGN AND CONSTRUCTION

COURTESY: AVCO LYCOMING

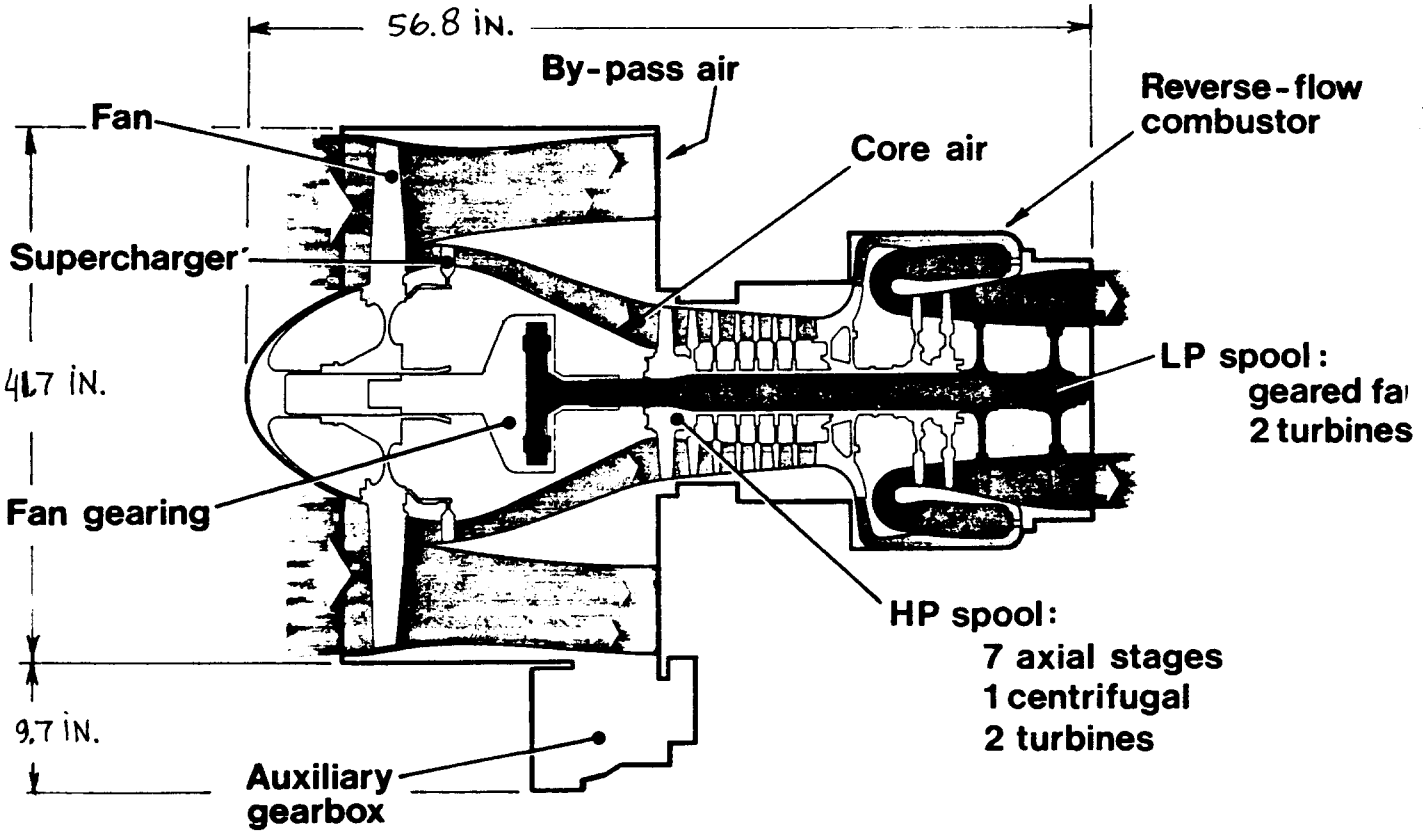

Figure 6.24 Uninstalled Performance and Geometry Data for AVCO Lycoming ALF-502R-5 Turbofan

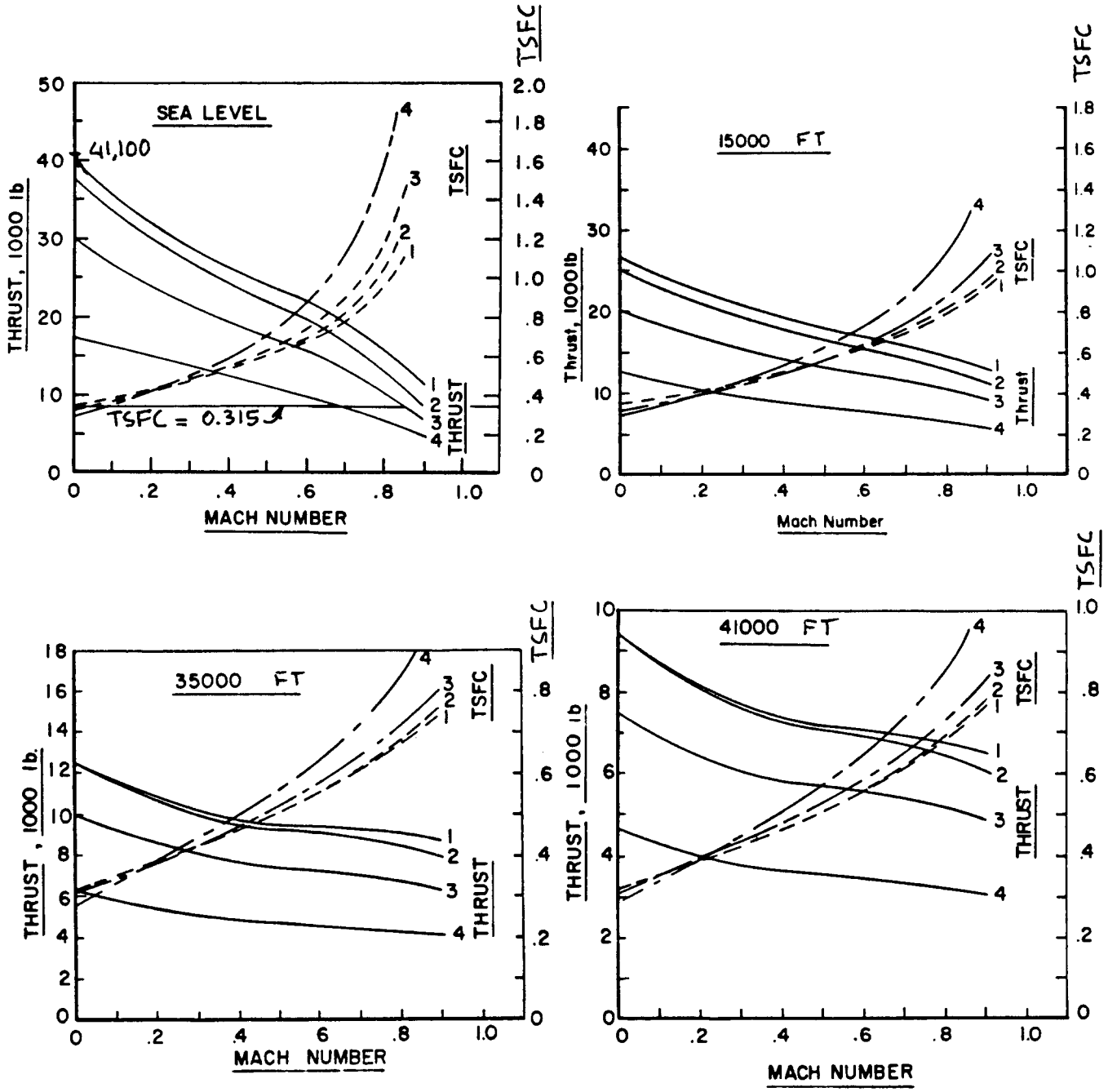

LEGEND:

1. MILITARY THRUST
2. NORMAL (CONT.) THRUST
3. 80% NORMAL
4. 50% NORMAL

S.L.S.T.O. MASSFLOW 1,541 LBS/SEC
LENGTH : 271 IN.
MAX. DIAMETER : 100 IN.
BPR : 8

COURTESY: L. NICOLAI
REF. 29

Figure 6.25 Estimated C5-A Installed Performance Data for General Electric TF-39-GE-1 Turbofan

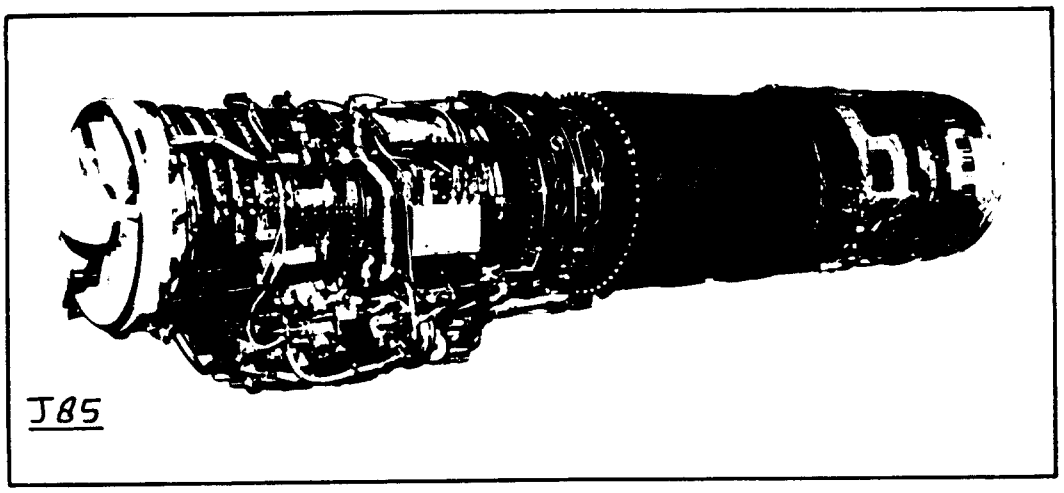

Figure 6.26 General Electric J-85 Augmented Turbojet

SPECIFICATIONS

	J85-13	J85-21A
Weight (lb)	597	684
Length (in.) (cold)	105.6	112.5
Max Dia (in.)(cold)	17.7	21
Max Radius (in.) (cold)	17.6	17.6
Comp/Turbine Stages	8/2	9/2
Thrust/Weight	6.8	7.3
Pressure Ratio	6.9	8.3
Air Flow (lb/sec)	44.0	53.0
RPM	16,500	16,600
T_4 (T O/^{o}F)	1745	1800
EGT Limit (^{o}F)	1325	1345
Max Thrust/HP (SLS)	4080	5000
SFC	2.22	2.13
MIL Thrust/HP (SLS)	2720	3500
SFC	1.03	1.00
Max Mach No/Alt	2.35/65K	2.35/65K
Cruise Mach No/Alt	.9/36K	.9/36K
Thrust	770	1200
SFC	1.29	1.23

SPECIFICATIONS

	J79-17	J79-17X*
Weight (lb)	3873	3847
Length (in) (cold)	208.69	208.69
Max. Dia. (in) (cold)	39.06	39.06
Max Radius	19.5	19.5
Comp/Turbine Stages	17/3	17/3
Thrust/Weight	4.60	4.9**
Pressure Ratio (MIL)	13.4	13.4
Air Flow (lb/sec)	170.0	170.0
RPM	7685	7839
T4 (T.O./Cruise) ^{o}F	1810	1837
EGT Limit (^{o}F)	1240	1300
Max Thrust (SLS)	17,820	18,730**
SFC	1.98	1.98
MIL Thrust (SLS)	11,810	11,810
SFC	0.85	0.85
Max Mach No./Alt.	2.4/45K	2.0/50K
Thrust (M2.0/35K)	18,600	20,840**
SFC (M2.0/35K)	2.07	2.05
Cruise Mach No./Alt	.9/35K	.9/35K
Thrust	2600	2600
SFC	0.98	0.98

*Various of these engine parameters are specifications and have not been verified by testing.
**Combat plus mode

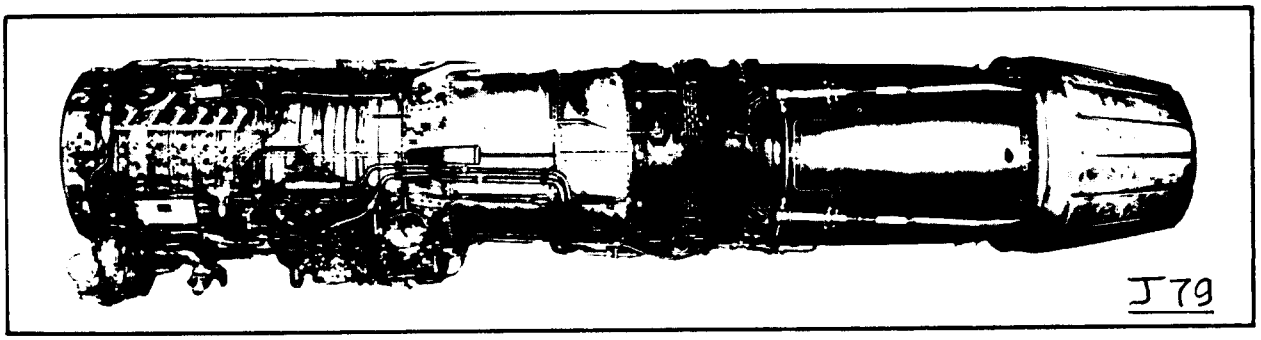

Figure 6.27 General Electric J-79 Augmented Turbojet

COURTESY : GENERAL ELECTRIC

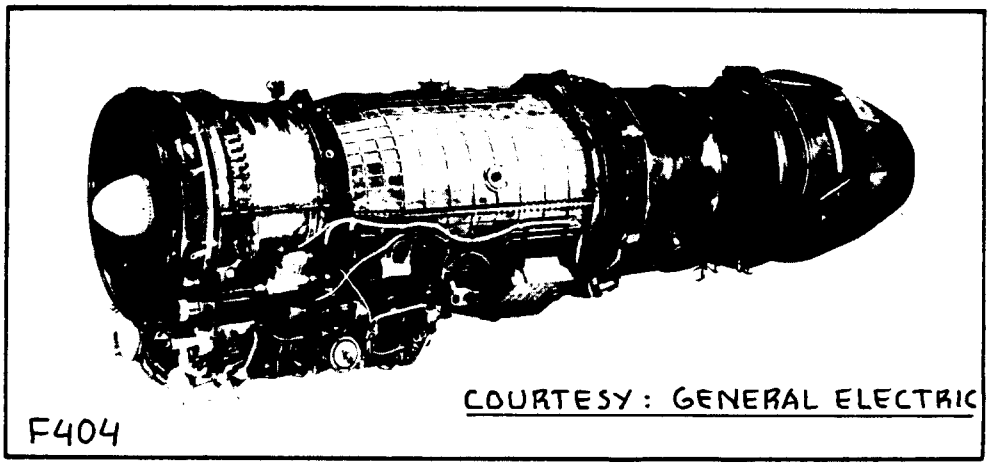

Figure 6.28 General Electric F404 Augmented Turbofan

SPECIFICATIONS

	F404
Thrust	16,000-lb Class
Length (in.)	158.8
Maximum Diameter (in.)	34.8
Fan Stages	3
Compressor Stages	7
Compressor Pressure Ratio	Over 25:1 Class
Combustor	One Piece Annular
Turbine Stages	
High Pressure	1
Low Pressure	1
Control	Electrical-Hydromechanical
Variable Exhaust Nozzle	Hydraulically Actuated Converging-Diverging Type

F100-PW-100

MAXIMUM THRUST (FULL AUGMENTATION)	25,000-POUND (111.2 kN) CLASS
INTERMEDIATE THRUST (NON-AUGMENTED)	15,000-POUND (66.7 kN) CLASS
WEIGHT	3020 POUNDS (1371 kg)
LENGTH	191 INCHES (4.85 m)
INLET DIAMETER	36 INCHES (0.91 m)
MAXIMUM DIAMETER	46.5 INCHES (1.18 m)
BYPASS RATIO	0.6
OVERALL PRESSURE RATIO	24 to 1

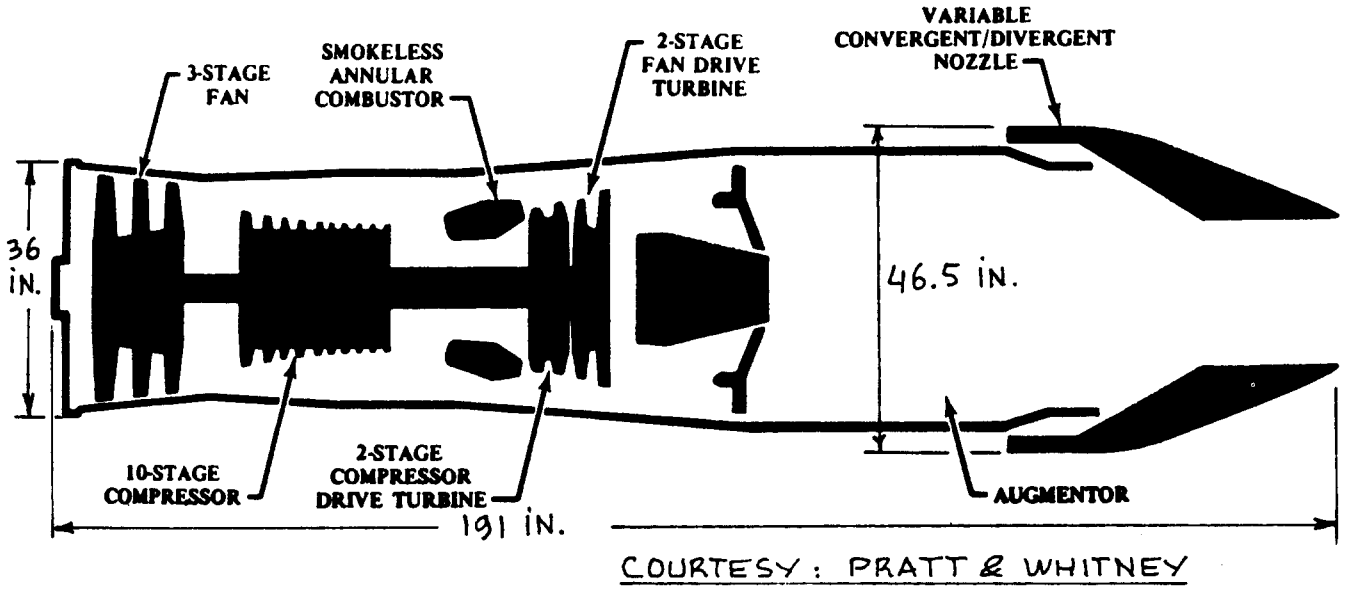

Figure 6.29a Pratt and Whitney F100-PW-100 Augmented Turbofan

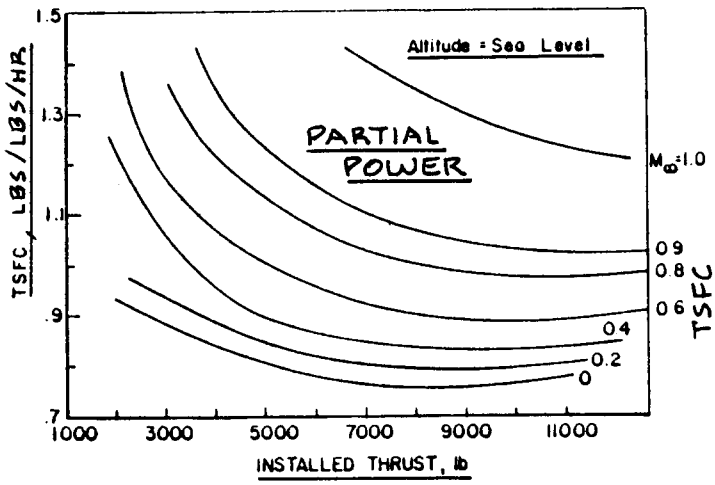

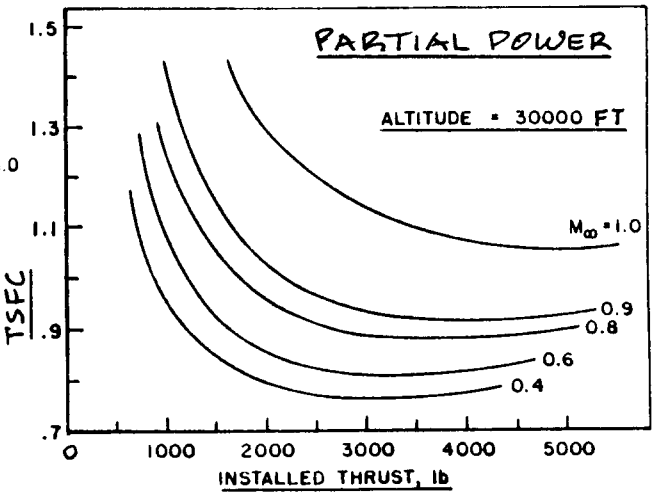

* 70 HP FOR AUXILIARY EQPMT AT ALL POWER SETTINGS

* 0.4 LBS/SEC BLEEDAIR AT ALL POWER SETTINGS

S.L.S.T.O. MASSFLOW 217 LBS/SEC

COURTESY: L. NICOLAI, REF. 29

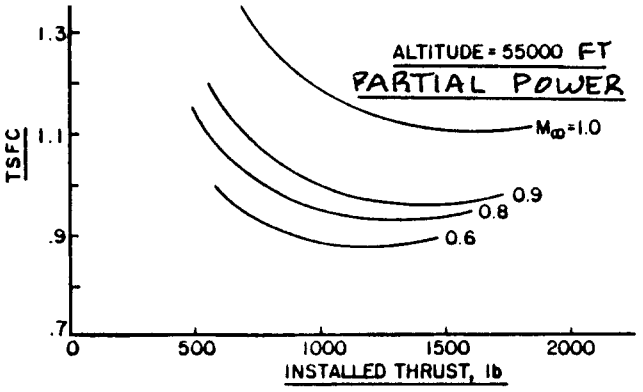

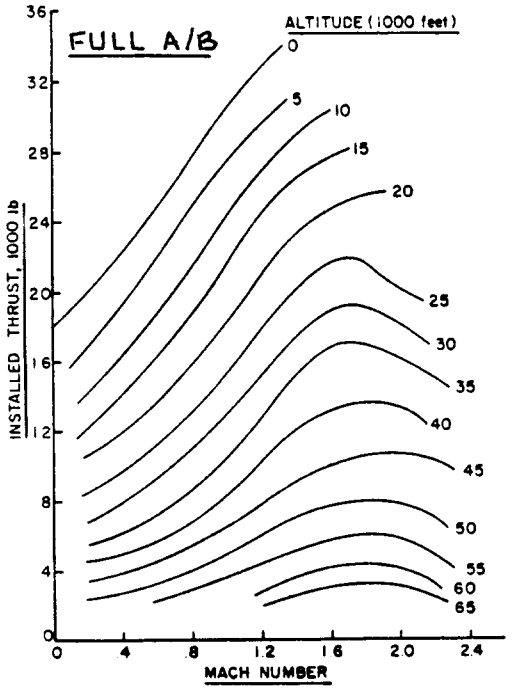

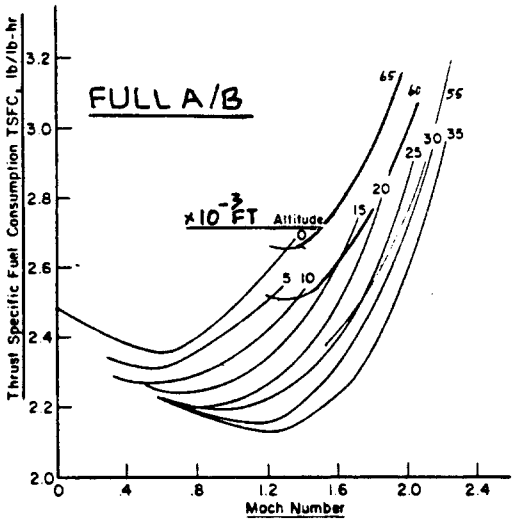

Figure 6.29b Estimated Installed Performance Data for Pratt and Whitney F100-PW-100 Augmented Turbofan

Table 6.8 Manufacturer Performance Data for Turbofan Engines

Type	Pratt and Whitney JT15D-1	JT15D-4C *	Garrett TFE731	ATF3-6 -2c	Teled. CAE 490-4**	Avco Lycoming ALF-502L-3
Max.T.O. Thrust (lbs)	2,200	2,500	3,500	5,440	2,965	7,500
T.O. Condition (static)	SLS	SLS	SLS	SLS	SLS	SLS
T.O. SFC (lbs/lbs/hr)	0.540	0.562	0.493	0.506	0.703	0.411
T.O. Massflow (lbs/sec)	69.4	77.7	112	162	61	256
T.O. BPR	3.3	2.6	2.82	2.55	1.13	5.0
Cruise Thrust (lbs) at 80 percent max.	2,065	2,125	755	1,047	1,400 max. contin.	2,100
Cruise Condition	SLS	SLS	0.8/40K	0.8/40K	0.8/20K	0.8/30K
Cruise SFC (lbs/lbs/hr)	0.537	0.556	0.815	0.816	1.00	0.750
Weight*(lbs)	514	575	725	1,125	640	1,270
Length (in), cold	56.6	63.3	49.7	33.6	51.2	56.8
Max. diam. (in)	27	27.3	39.1	102	h=28.3 w=23.2	41.7
Application	Cessna Citation	SIAI-M S211	Learjet M36	Falcon 200	Alphajet	BAe 146

* Military version ** Same as SNECMA/Turbomeca Larzac

Table 6.9 Manufacturer Performance Data for Turbojet and Turbofan Engines

Type	General Electric J79***	J85-21A ***	CF700	CJ610-5 (J85-4B)	F404***	F101***
Max.T.O. Thrust (lbs)	17,820	5,000	4,200	2,950	16,000	28,000
T.O. Condition (static)	SLS	SLS	SLS	SLS	SLS	SLS
T.O. SFC (lbs/lbs/hr)	1.98	2.13	0.66	0.980	NA	NA
T.O. Massflow (lbs/sec)	170	53	43/85**	44	NA	270
T.O. BPR	0	0	NA	0	NA	0.85
Cruise Thrust (lbs) at 80 percent max.	2,600 (dry)	1,200	1,060	870	NA	NA
Cruise Condition	0.9/35K	0.9/36K	0.8/36K	0.8/36K	NA	NA
Cruise SFC (lbs/lbs/hr)	0.98	1.23	0.98	1.15	NA	NA
Weight*(lbs)	3,873	684	725	402	2,000 (dry)	4,400 (dry)
Length (in), cold	209	113	53.6	51.1	159	181
Max. diam. (in)	39.1	21	33.1	17.7	34.8	55
Application	F4/F16	F-5E/F	Falcon	Learjet	F18	B1B

* No tailpipe, no thrust-reverser **generator/fan ***incl. afterburner

Table 6.10 Manufacturer Performance Data for Turbofan and Turbojet Engines

Type	Pratt and Whitney JT8D-217	2037= JT10D	JT9D-7	Rolls Royce RB211-22B	RB163 Spey	Ames TRS-18
Max.T.O. Thrust (lbs)	20,000	37,600	45,600	42,000	10,410	200
T.O. Condition (static)	SLS	SLS	SLS	SLS	SLS	SLS
T.O. SFC (lbs/lbs/hr)	0.562	NA	NA	NA	0.563	1.12
T.O. Massflow (lbs/sec)	483	1,340	1,509	1,380	203	N.A.
T.O. BPR	1.7	5.8	5.15	4.8	1.0	0
Cruise Thrust (lbs) max.continuous	5,350	NA	10,200	9,700	3,070	150
Cruise Condition	0.8/35K	0.8/35K	0.85/35K	0.8/35K	0.77/32K	0.3/5K
Cruise SFC (lbs/lbs/hr)	0.753	0.563	0.620	0.618	0.760	1.45
Weight*(lbs)	4,430	6,906	8,850	9,195	2,257	68
Length (in), cold	154	141.4	128.2	119.4	110	36.5
Max. diam. (in)	49.2	85.0	95.6	85.9	37	13
Application	MD-80	757	747-200	L-1011	BAC111	BD5J

Table 6.11 Manufacturer Performance Data for Turbofan Engines

Type	General Electric CF6-50C	CF6-50C1	CF6-6D	CF6-6K	CF6-32C1	CFM56-2	CF34
Max.T.O. Thrust (lbs)	51,000	52,500	40,000	41,500	36,500	24,000	8,650
T.O. Condition (static)	SLS	SLS	SLS	SLS	SLS	SLS	SL/59F
T.O. SFC (lbs/lbs/hr)	0.390	0.394	0.346	0.350	0.357		0.359
T.O. Massflow (lbs/sec)	1,450	1,470	1,303	1,328	1,104	830	307
T.O. BPR	4.26	4.24	5.72	5.67	4.9	6.0	6.3
Cruise Thrust (lbs) at 80 percent max.	8,720	9,080	7,160	7,270	6,630	N.A.	1,420
Cruise Condition	0.8/35K	0.8/35K	0.8/35K	0.8/35K	0.8/35K	0.8/30K	0.8/40K
Cruise SFC (lbs/lbs/hr)	0.628	0.626	0.616	0.616	0.609	0.650	0.690
Weight*(lbs)	8,731	8,731	7,896	7,896	7,140	4,610	1,580
Length (in), cold	173	173	177	177	140	95.7	100
Fan tip diam. (in)	86.4	86.4	86.4	86.4	76.3	68.3	49
Application	KC-10A	747 E4A	DC-10	DC-10	757	DC-8 Challenger (mod)	

* No tailpipe, no thrust-reverser

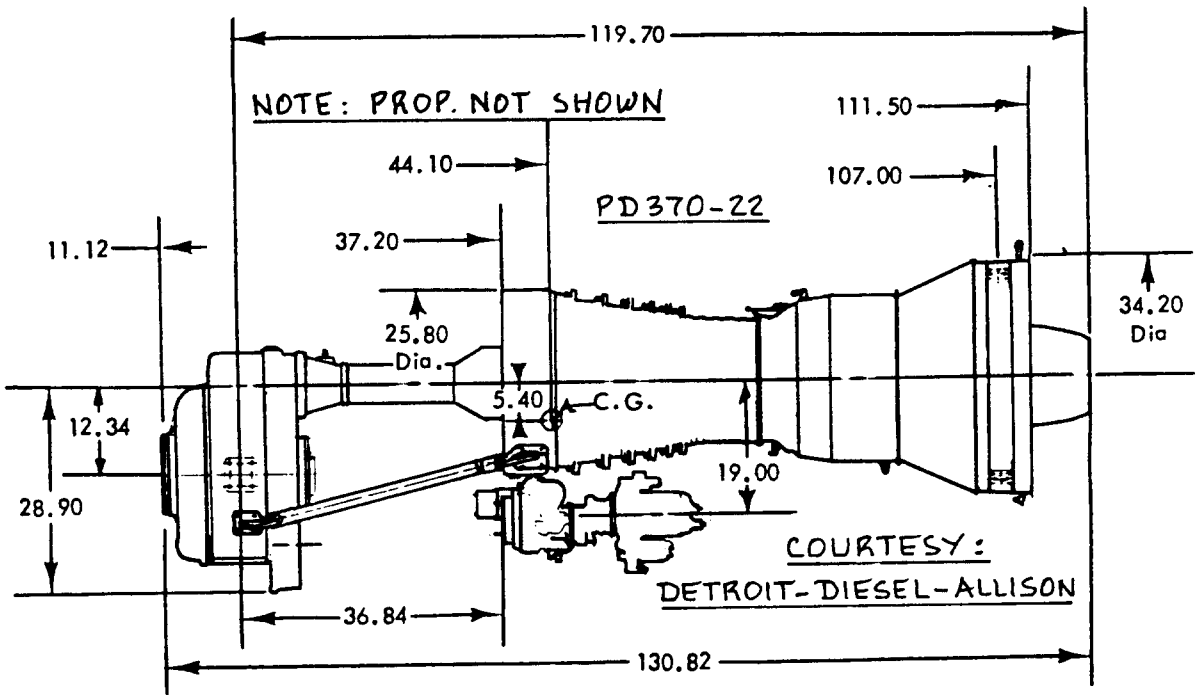

Figure 6.30 Detroit Diesel Allison PD370-22 Propfan

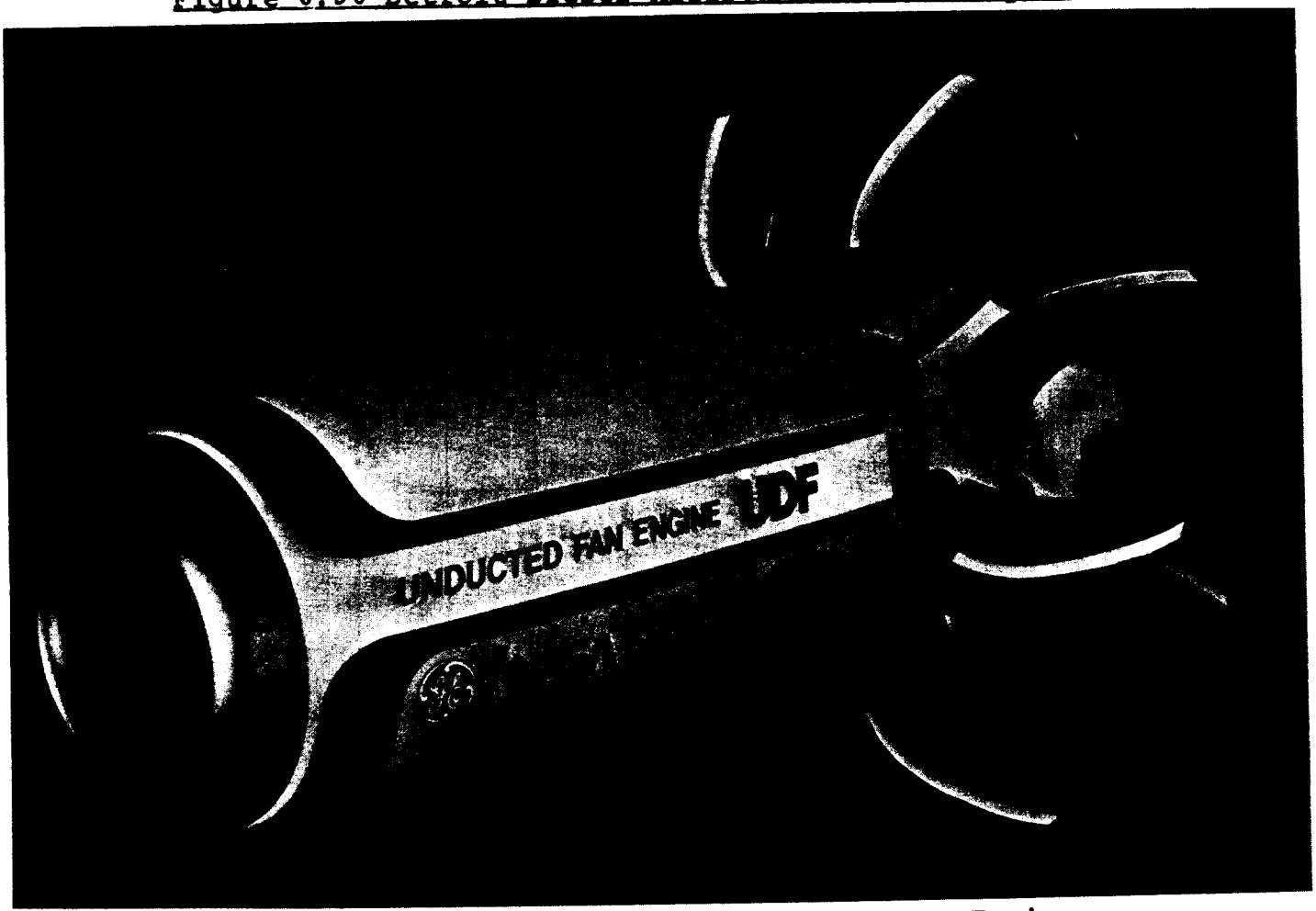

Figure 6.31 General Electric Ultra Bypass Engine

NOTE : THIS GASGENERATOR IS DESIGNED FOR DRIVING 8-BLADE OR 10-BLADE PROPELLERS (PROPFAN)

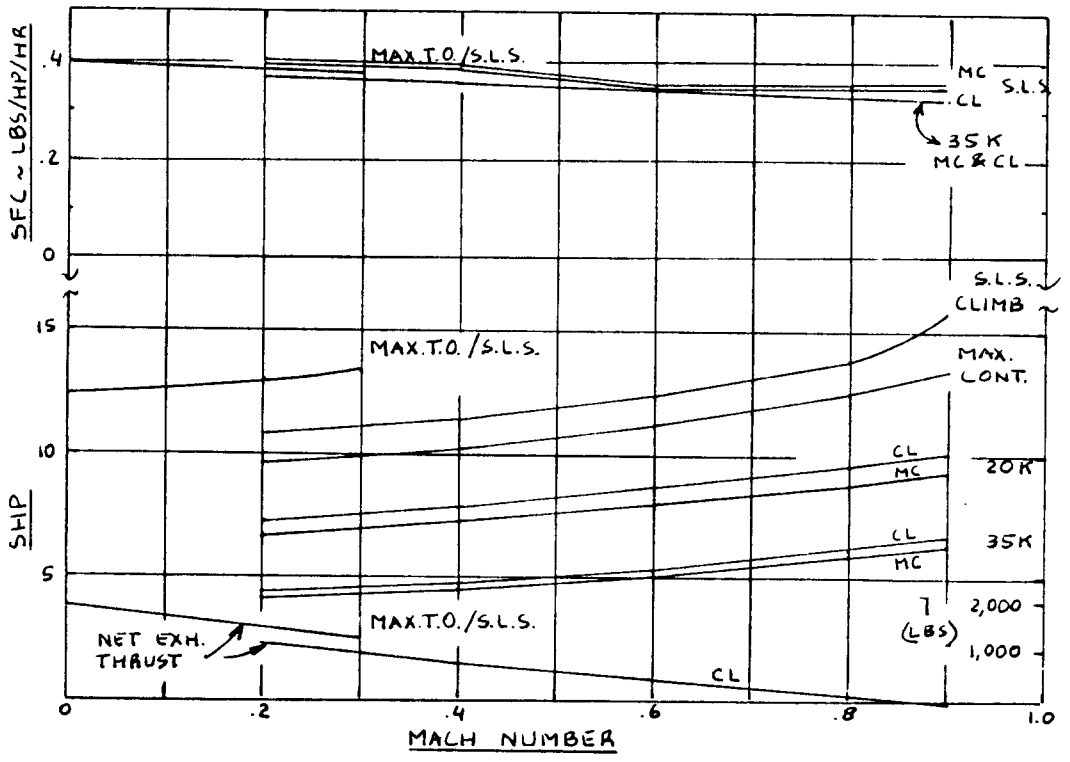

Figure 6.32 Uninstalled Performance Data for Detroit Diesel Allison PD370-22 Propfan

NO DATA AVAILABLE AT PRESS TIME. MAXIMUM S.L.S. T.O. THRUST ESTIMATED AT 30,000 LBS WITH T.S.F.C. OF 0.250

Figure 6.33 Guestimated Uninstalled Performance Data for General Electric Ultra Bypass Engine

6.2 RELATION BETWEEN FLIGHT ENVELOPE AND ENGINE TYPE

Matching engine type to the flight envelope of airplanes is of key importance to the ultimate succes (or lack thereof) of any airplane.

Figure 6.34 shows some fundamental relations between flight speed, mass flow rate, thrust and various efficiency parameters for piston engines, for turbojets and for turboprops.

Figure 6.35 shows the typical sfc values associated with different powerplants across the Mach range. For cruise range dominated airplanes it is usually the amount of fuel burned during the cruise phase of the mission which is decisive in selecting the type of powerplant. In such airplanes the achievable payload-range performance and the associated return-on-investment (ROI) play a dominant role in powerplant selection. Part VII shows how the payload range performance of an airplane can be predicted. Part VIII shows how the ROI characteristics of an airplane can be predicted.

There are however other considerations which may influence the powerplant decision. In military airplanes the acceleration potential, the radar cross section, the infrared signature and the physical size of the powerplant may be important considerations.

In commercial airplanes, the installed weight of the total powerplant package plus its fuel requirements, the cost of ownership and the reliability potential all may be deciding factors over and beyond pure efficiency considerations.

Figures 6.34 and 6.35 indicate that many areas of overlap exist. In these overlap areas it is not usually straightforward to select the 'proper' engine type. Customer preference, considerations of growth potential also play an important role in ultimately deciding the proper engine type.

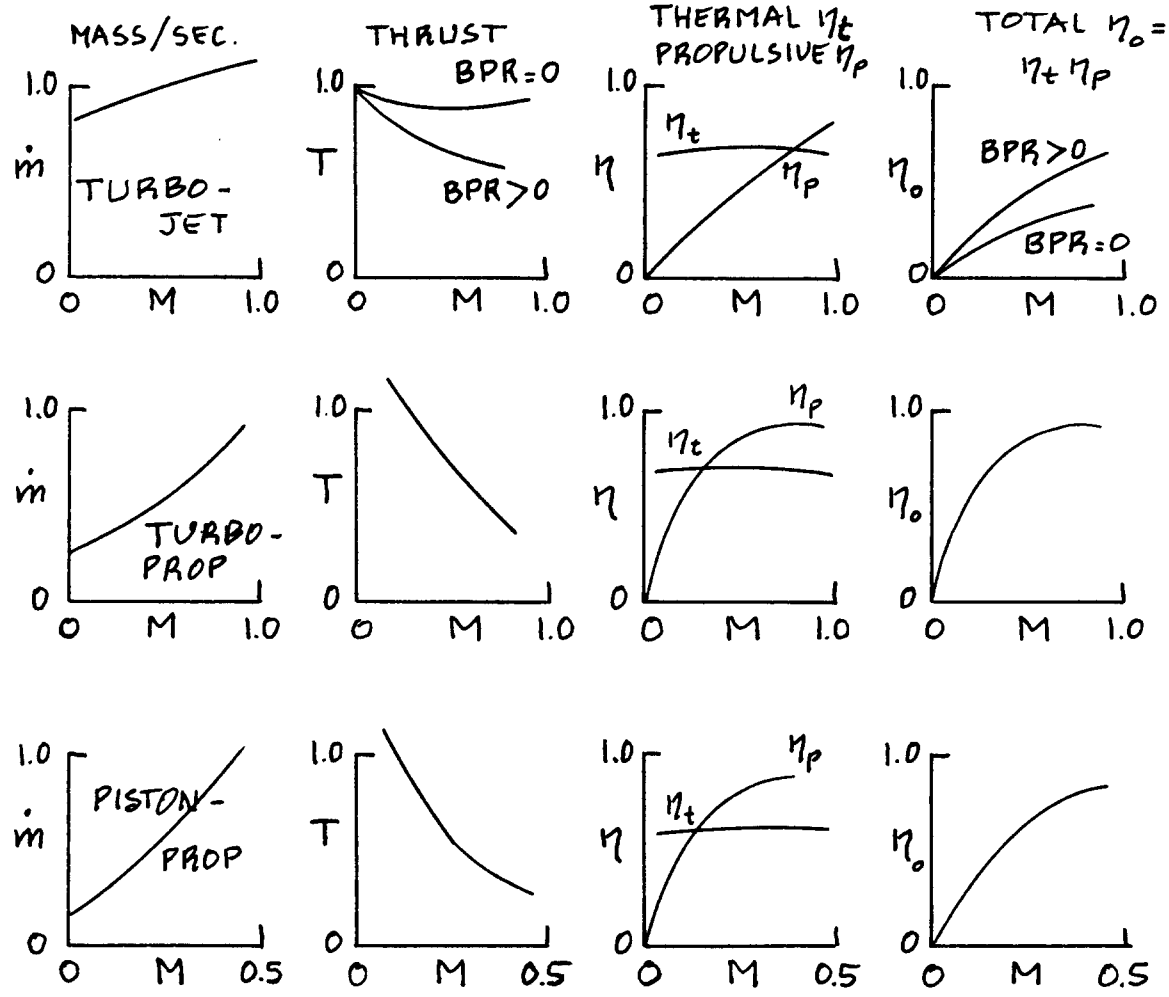

Figure 6.34 Variation of Fundamental Powerplant Parameters with Flight Speed

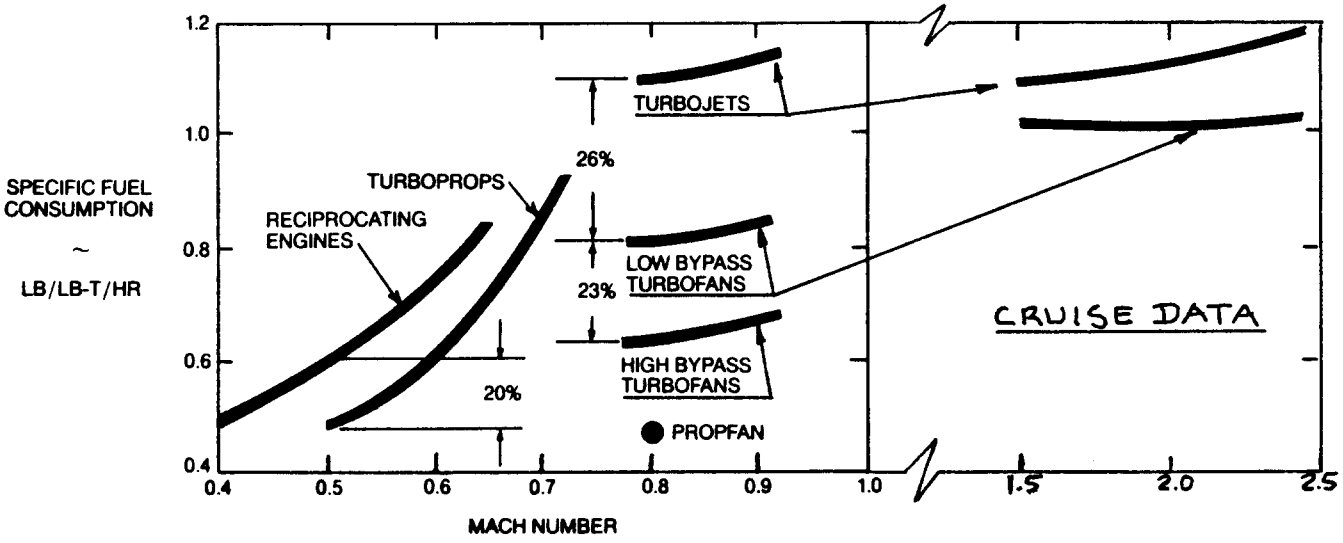

Figure 6.35 Effect of Mach Number on SFC for a Range of Powerplant Types

6.3 INSTALLED THRUST, POWER AND EFFICIENCY CONSIDERATIONS

To achieve the best combination of installed thrust and efficiency from any given powerplant installation requires a lot of attention to details. Requirements for power generation, airconditioning and other operationally required services all cause reductions in propulsive thrust and/or efficiency.

This section is organized as follows:

6.3.1 Power extraction
6.3.2 Propeller installations
6.3.3 Piston-engine installations
6.3.4 Subsonic and supersonic turbojet and turbofan installations

6.3.1 Power Extraction

To determine the amount of power extraction required from the engines it is necessary to make a list of all systems and services which take energy from the engines. Part IV contains a discussion of most system types found in civil and military airplanes. Once the system requirements for a given airplane have been defined (Step 17 in p.d. sequence II, p.18, Part II) such a list of power extraction requirements can be made.

The power extraction list should be subdivided into requirements for:

1. electrical power, in hp
2. bleedair mass flow, in lbs/sec

With this list it is possible to estimate the effect of power extraction on installed engine performance.

For typical cruise operations in passenger transports a total power loss of 2-5 percent should be used in preliminary design calculations.

In military operations the requirements for power extraction depend on the airplane mission: radar/search missions require large amounts of electrical power.

In fighters, typically 70 hp is needed to drive essential generators and auxiliary equipment while bleedair flow rates typically amount to 0.5 lbs/sec.

It is often desirable (notably in transports) to install auxiliary power units (APU) for power generation

on the ground. This makes an airplane independent of ground based power. Whether or not the APU is designed to be used in flight depends on in-flight power requirements and on the question of system reliability for those systems which derive power from the propulsive installation.

6.3.2 Propeller Installations

For any given propeller design and for a given combination of rpm and delivered shaft horsepower, the thrust output of a propeller depends on the shape and the size of airplane components behind or ahead of it.

In tractor installations, the effect of the nacelle and/or wing directly behind the propeller is referred to as the 'blockage' effect. Figure 6.36 shows an example of a good and a poorly shaped installation.

In pusher installations, the effect of the nacelle and/or the wing directly in front of the propeller affects the propeller 'inflow field' and can affect propeller performance. Figure 6.37 shows an example of a good and a poorly shaped installation.

6.3.3 Piston-Engine Installations

The management of cooling air and of exhaust gasses plays a significant role in the ultimate propulsive efficiency of a given installation. Sub-section 6.9.1 contains further discussions of this subject.

6.3.4 Subsonic and Supersonic Turbojet and Turbofan Installations

Inlet design: The design of the inlet plays a very important role in determining overall installed engine performance. For a discussion of inlet types and their performance effects the reader should consult Refs 12, 14, 29, 60 and 65.

Part VI contains rapid methods for accounting for inlet effects on drag and thrust.

Nozzle design: The design of the nozzle (exhaust configuration) also plays a significant role in determining installed drag and thrust. References 12 and 65 should be consulted for details on exhaust (tailpipe) configurations. Reference 60 contains useful information on the design of exhaust nozzles. Examples of inlet and exhaust configurations are presented in Section 6.9.

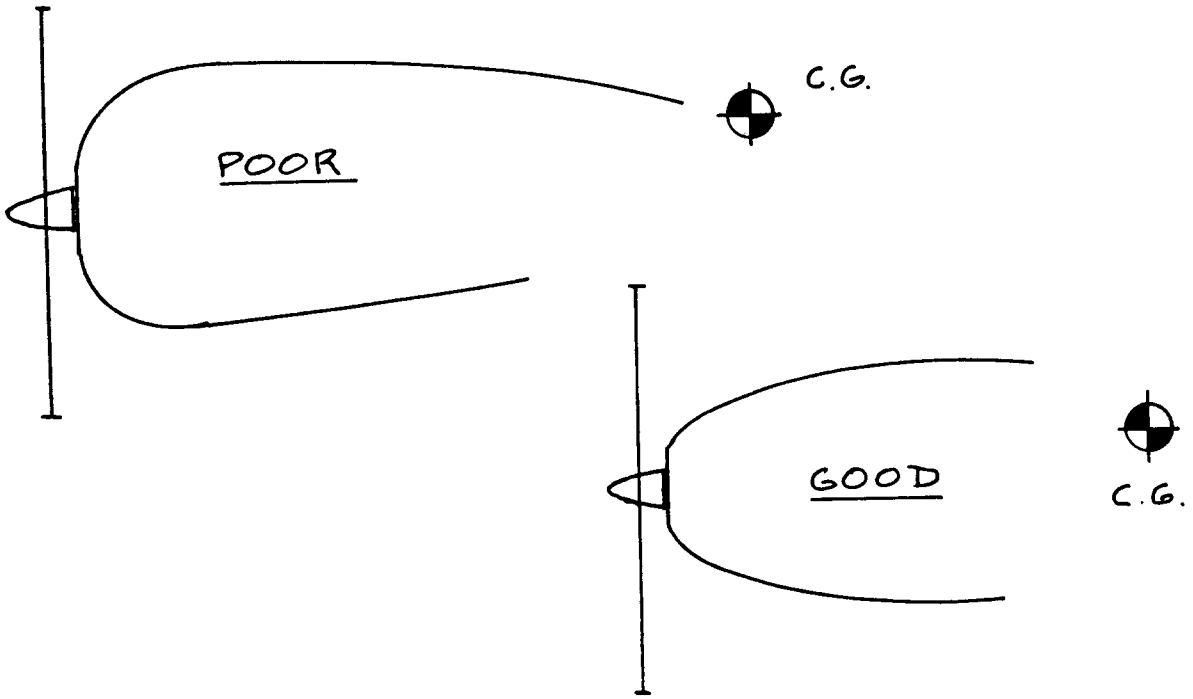

Figure 6.36 Example of 'Good' and 'Poor' Nacelle Shaping in a Tractor Installation

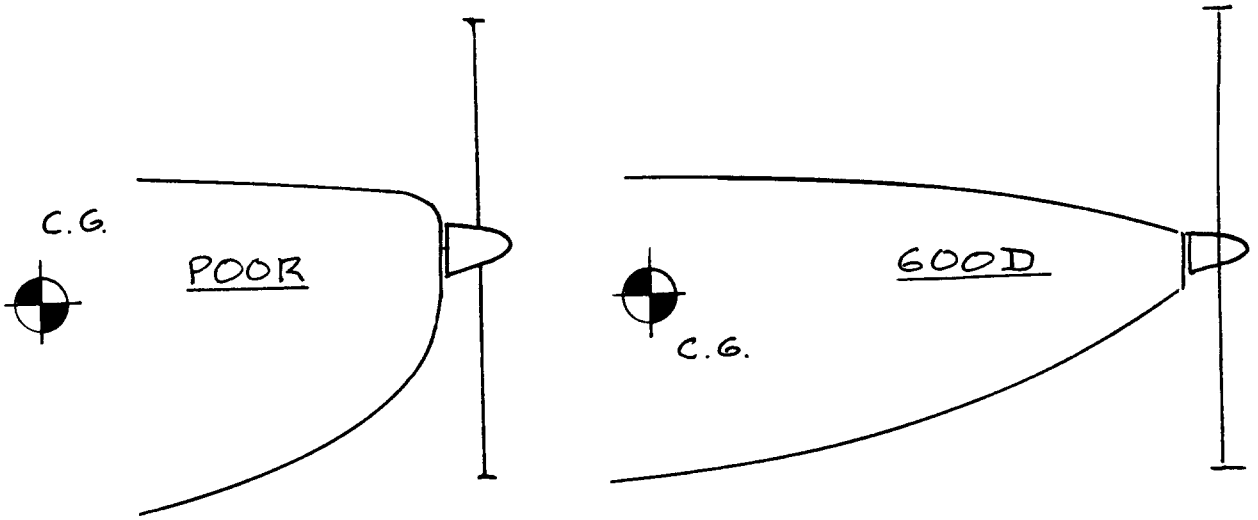

Figure 6.37 Example of 'Good' and 'Poor' Nacelle Shaping in a Pusher Installation

6.4 STABILITY AND CONTROL CONSIDERATIONS

The following stability and control effects should be considered:

6.4.1 Effect of one or more engines inoperative and effects of power transients

6.4.2 Tractor versus pusher

6.4.3 Effect of engine/propeller thrust line location and inclination

In preliminary design a good rule of thumb is: if the engine disposition differs significantly from that of existing, certified airplanes, considerable power effects on stability and control characteristics can be expected. In such cases the safest thing to do is to perform the necessary stability and control calculations before freezing the design. Part VII contains methods for doing this.

6.4.1 Effect of One or More Engines Inoperative and Effects of Power Transients

If the engines are disposed so that large yawing moment arms and/or large pitching moment arms prevail the effect of one or more engines becoming suddenly inoperative must be considered. Ref.37 and Part VII contain methods for computing engine-out effects on handling and on controllability.

6.4.2 Tractor Versus Pusher

Figures 6.36 and 6.37 define what is meant by a tractor and a pusher propeller installation. Part VI shows that tractor installations act to decrease longitudinal stability while pushers act to increase it.

The reader should not infer from this that pushers are good nor that tractors are bad. How much stabilizing effect or destabilizing effect is desirable depends entirely on the type of airplane and on its mission requirements.

Sub-section 6.4.3 presents a simple approximate equation from which the incremental stability of tractors and pushers may be estimated for preliminary layout purposes.

6.4.3 Effect of Engine/Propeller Thrust Line Location and Inclination

Figure 6.38 shows the geometry of propeller thrust line location with respect to the c.g. of the airplane. It is shown in Part VI that the static longitudinal stability of a propeller driven airplane varies roughly with z_T and with x_T in the following manner:

for vertical thrust line location:

$$(dC_m/dC_L)_T = 0.25(z_T/\bar{c})N_p \qquad (6.2)$$

for horizontal thrust line location:

$$(dC_m/dC_L)_T = 0.02(x_T/\bar{c})N_p \qquad (6.3)$$

These equations are valid for airplanes with power-to-weight ratios of about 0.1.

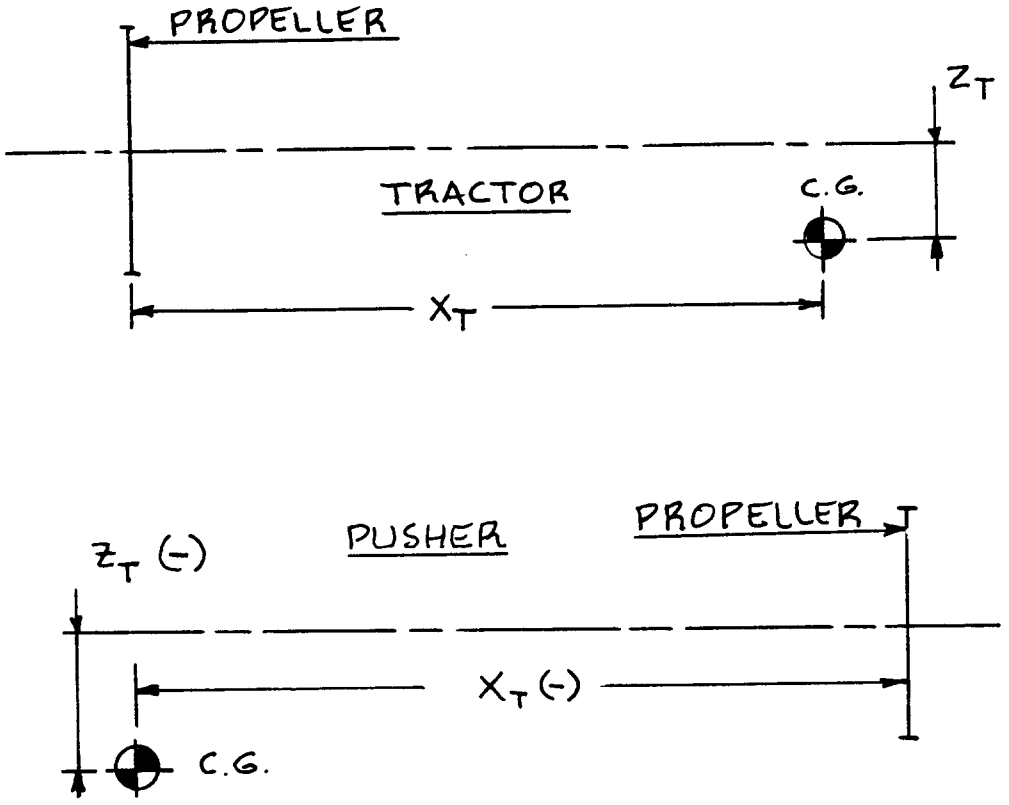

Figure 6.38 Geometry for Propeller Thrust Line Location

6.5 STRUCTURAL CONSIDERATIONS

The following structural considerations play an important role in the integration of the propulsion system into the airframe:

6.5.1 Transmission of thrust into the airframe
6.5.2 Lateral location of engines on the wing
6.5.3 Extension shafts and propeller blade excitation
6.5.4 Flutter

6.5.1 Transmission of Thrust into the Airframe

To transmit thrust forces into the airframe it is necessary to have a number of 'hard points' where the engine is physically attached to the airframe. The number of these hardpoints depends on the type of engine used.

Figure 6.39a shows an example of the principal method used to mount piston engines in airframes. Note that this is accomplished with a truss (usually made of welded steel tubes) or with a support cradle. Note that where the truss or cradle is attached to the airframe thrust and engine weight determine the attachment point loads.

The reader must realize that the attachment (mounting) points on the engine itself cannot be changed easily. Their location depends on the internal design of the engine and is normally determined by the engine manufacturer. Changing these attachment points is very expensive!

Since most piston engines transmit significant vibrations into the airframe it is essential to use some type of shock mount(s) to reduce these vibrations. Section 6.9 shows an example of such a shock mount in Figure 6.69.

Figure 6.39b shows the principal mounting arrangement used for jet engines. Note that there are usually two or three attachment points which are designed to transmit thrust as well as most of the engine weight. The rear attachment point is usually designed to allow for the considerable thermal expansion which a jet engine undergoes. This rear attachment point normally carries only part of the engine weight.

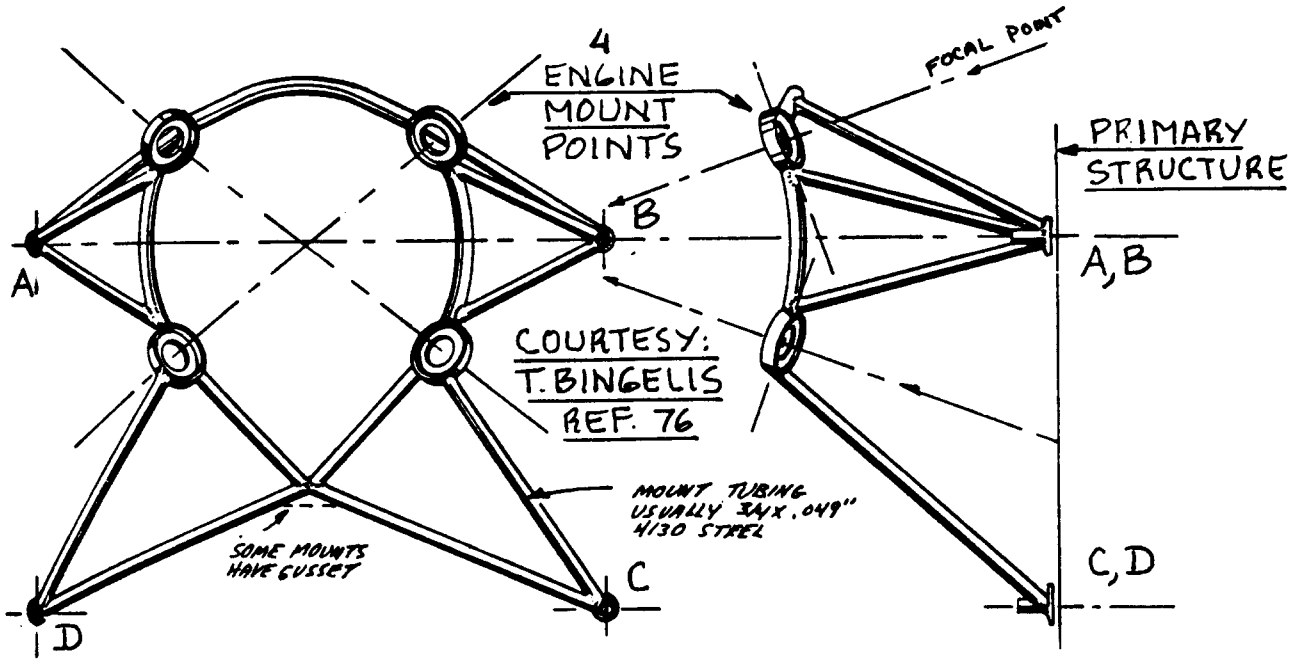

Figure 6.39a Method for Mounting Piston Engines in Airframes

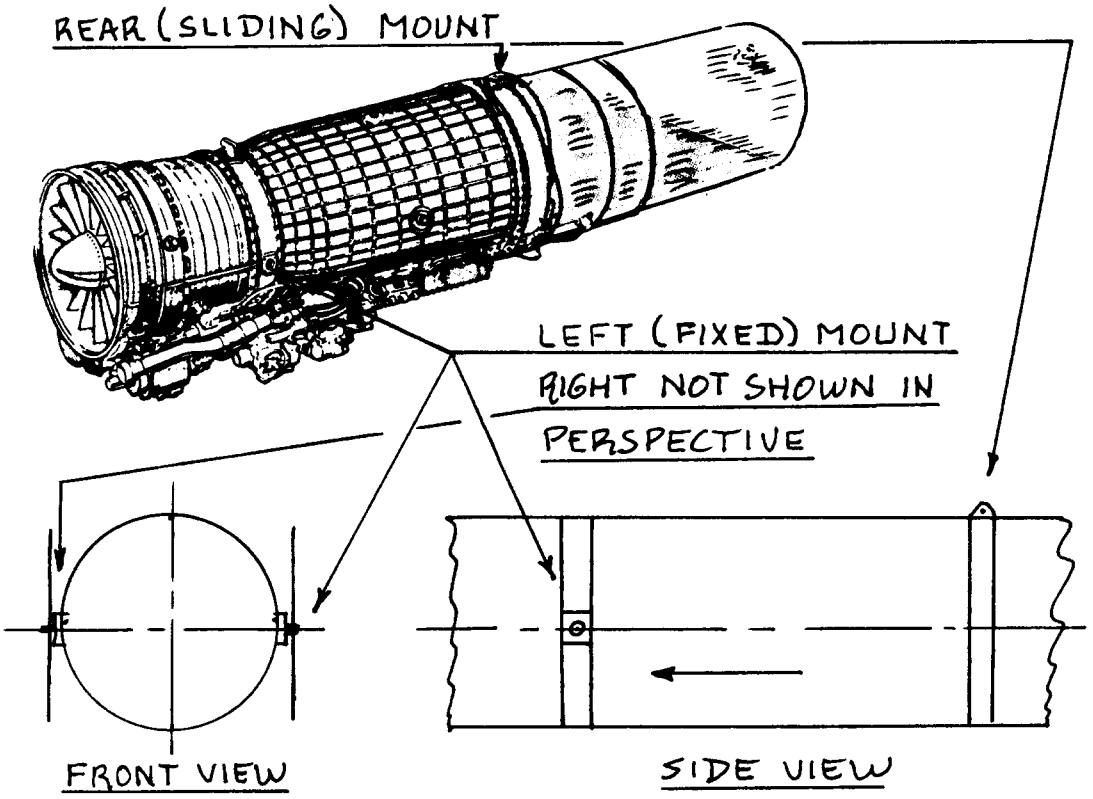

Figure 6.39b Method for Mounting Jet Engines in Airframes

Figure 6.39c shows a typical turboprop attachment. Note that the gasgenerator part of the engine is mounted in basically the same manner as a jet engine. However, in many turboprop engines the propeller and the gearbox must be separately supported. The transmission of thrust is normally done via the forward mounting points.

In jet engines as well as in turboprops, the engine attachment points cannot easily be changed. The engine manufacturer normally determines their location.

The reader should refer to Section 6.9 for more examples of engine installations.

6.5.2 Lateral Disposition of Engines over the Wing

Figure 6.40 shows head-on views of two types of four-engined jet transports. It is clear that a difference in design philosophy exists between these two designs.

Design 1 (compared to Design 2) will have a lower wing root bending moment due to the relieving bending moments induces by the engines. Design 1 (again compared to Design 2) will require a larger vertical tail and rudder to compensate for the larger asymmetric yawing moment which results from operation with one engine inoperative. Which design approach is best depends on how these trades affect the overall empty weight of the airplane.

6.5.3 Extension Shafts and Propeller Blade Excitation

Figure 6.41 shows examples of two airplanes with extension shafts between the engines and the propeller(s). This design approach has the advantage of giving excellent control over the c.g. location of an airplane: putting engines and propellers all the way back in an airplane can lead to stability problems which may be impossible to solve.

A serious problem associated with extension shaft installations is the vibration problems introduced by relatively flexible shafts. Bending vibrations can be eliminated by the use of more closely spaced bearings. Torsion vibrations can be reduced by a stiffer shaft. Both solutions cost extra weight: this must be considered before committing to such an installation. The airplanes of Figure 6.41 did suffer from serious vibration problems.

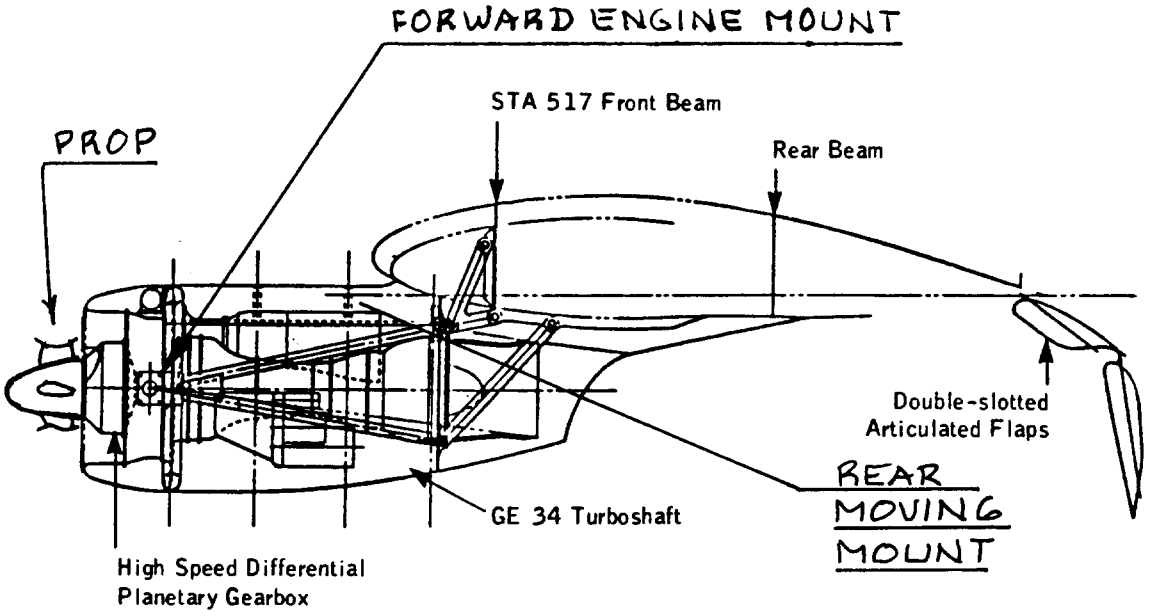

Figure 6.39c Method for Mounting Turboprop Engines in Airframes

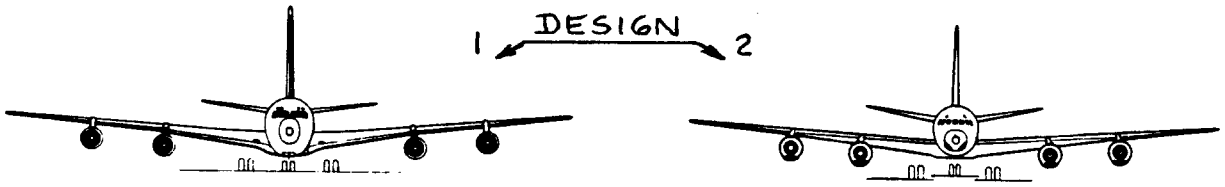

Figure 6.40 Examples of Lateral Disposition of Engines

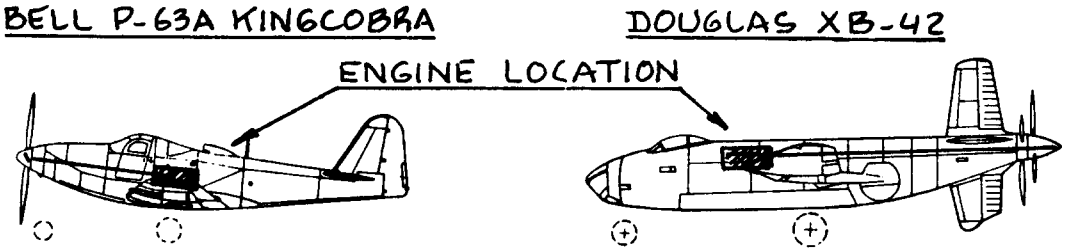

Figure 6.41 Examples of Application of Extension Shafts

Another structural problem may be caused by separated flow exciting the propeller blades whenever the propeller is mounted behind a wing, nacelle or a fuselage where flow separation can occur. Careful streamlining of the 'body' ahead of the propeller is essential. Fig.6.42 shows 'good' and 'poor' propeller locations behind a wing.

6.5.4 Flutter

The lateral and the longitudinal placement of engines relative to a slender wing is important from a wing flutter viewpoint. Detailed flutter analyses are required to ultimately decide on the best engine disposition.

In turbopropeller installations a so-called whirlmode flutter may occur. Such a flutter mode usually consists of a combination of propeller-plus-gearbox coning motion excited by a wing and/or nacelle osscilation. It is of great importance to assure that the landing gear is installed such that structural damage due to hard landings cannot weaken key structural components in the whirlmode scenario. Again, only detailed flutter analyses with and without assumed damage can identify the lightest ultimate installation.

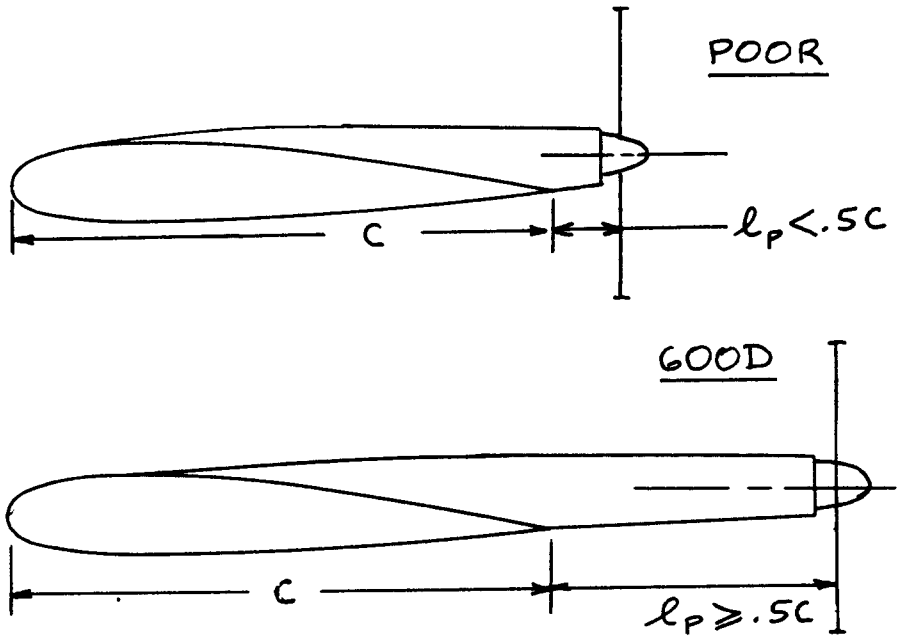

Figure 6.42 Example of 'Good' and 'Poor' Propeller Location From a Viewpoint of Blade Excitation

6.6 MAINTENANCE AND ACCESSIBILITY CONSIDERATIONS

Because engines need frequent servicing, inspection and component replacement, accessibility of the powerplant installation is a requirement in nearly all airplanes.

Figures 6.43 through 6.45 show how accessibility is provided in the case of a propeller driven single, a jet trainer and a small jet transport. Note the use of large clamshell doors. These doors must be designed so that they are supported in the 'open' position under prevailing wind conditions!

It must be possible to replace engines with relative ease. Figures 6.46 through 6.49 show how this requirement is addressed in a jet trainer, a jet fighter and in two jet transports respectively.

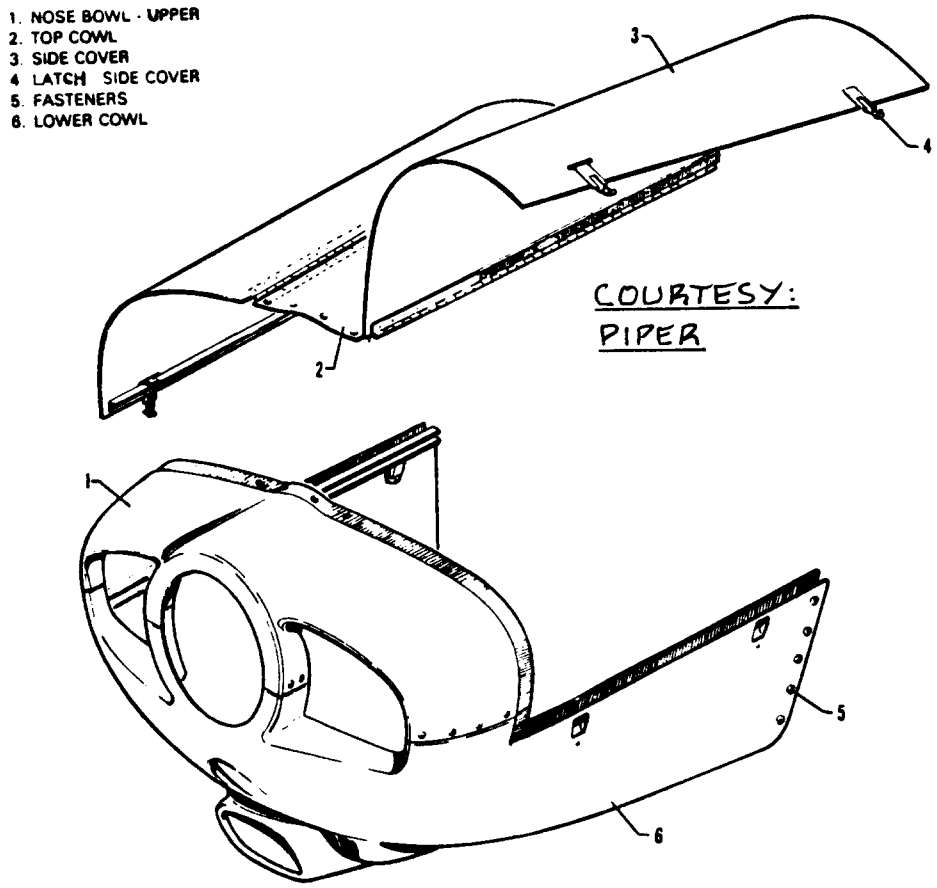

Figure 6.43 Accessibility of Engine Installation of the Piper PA-38-112 Tomahawk

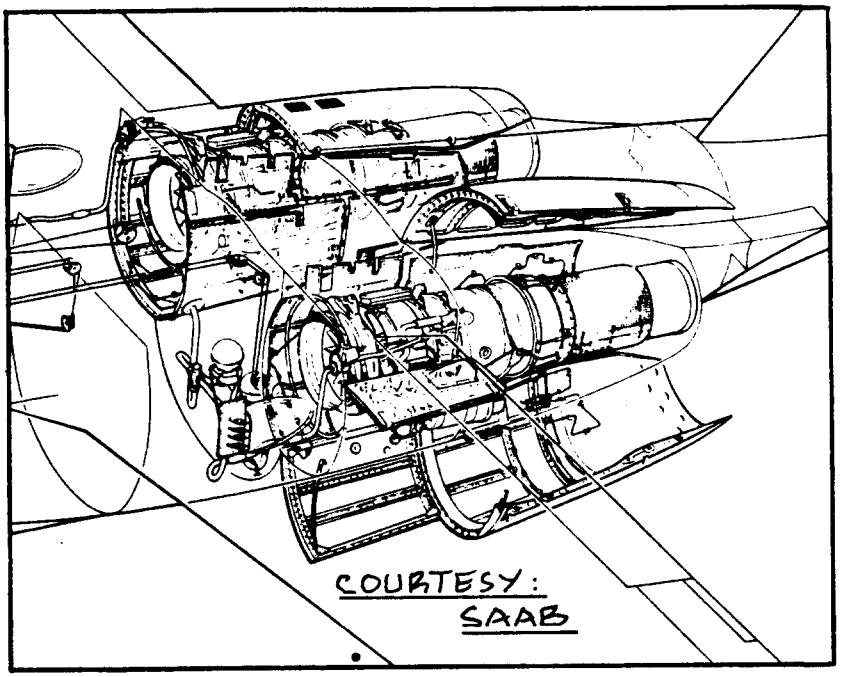

Figure 6.44 Accessibility of Engine Installation of the SAAB 105-XT

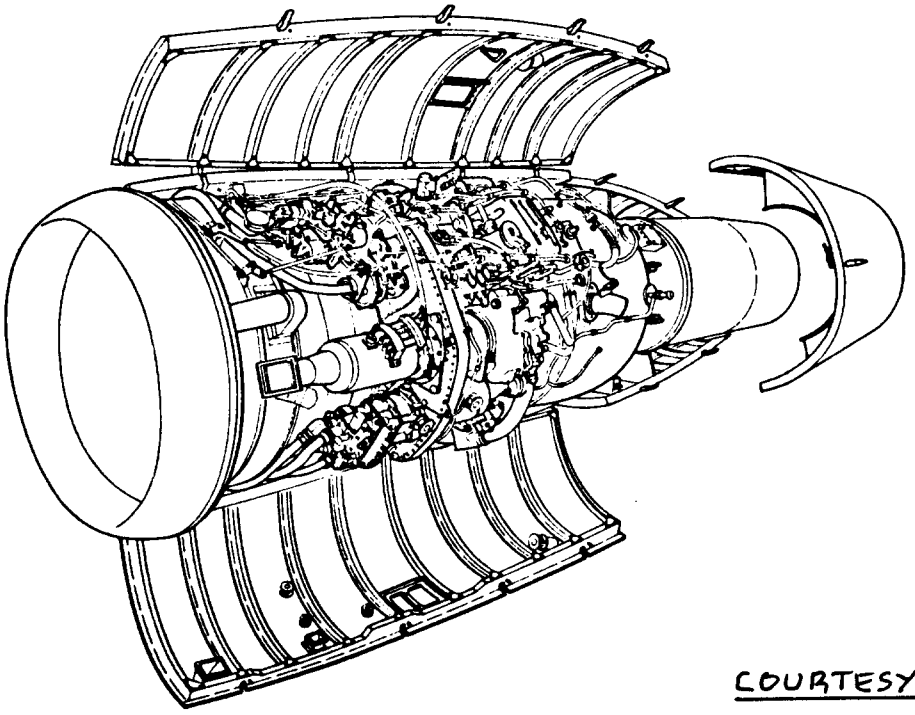

Figure 6.45 Accessibility of Engine Installation of the Fokker F28

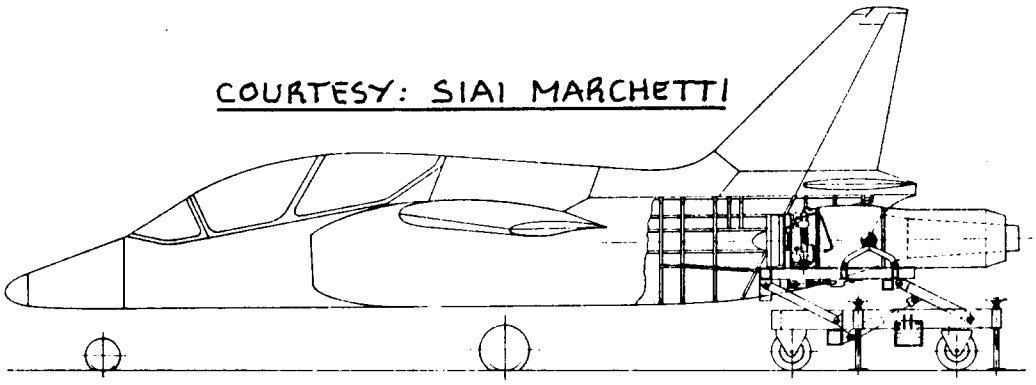

Figure 6.46 Engine Removal for the SIAI Marchetti S211

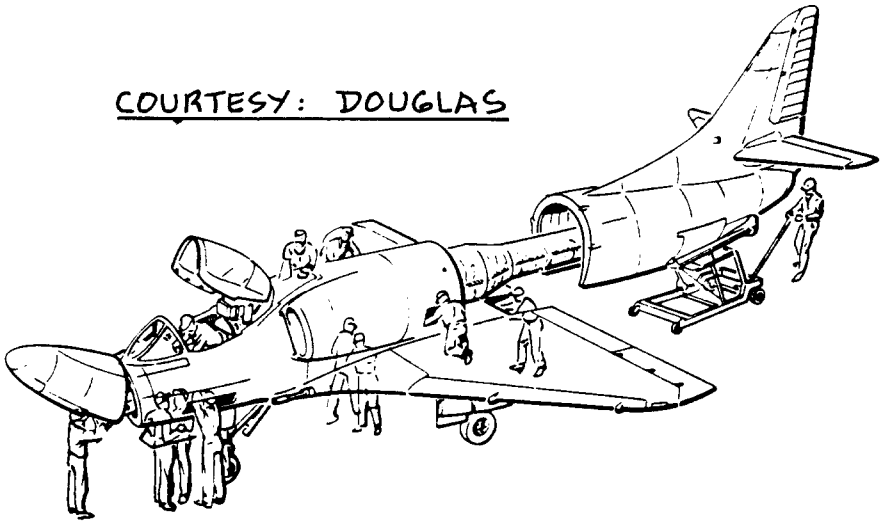

Figure 6.47 Engine Removal for the Douglas A4 Skyhawk

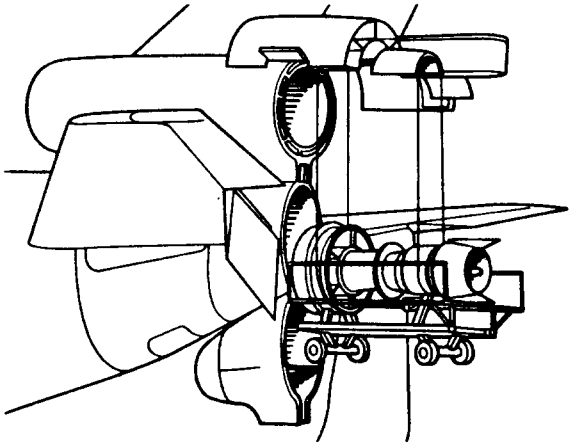

Figure 6.48 Engine Removal for the McDD DC10

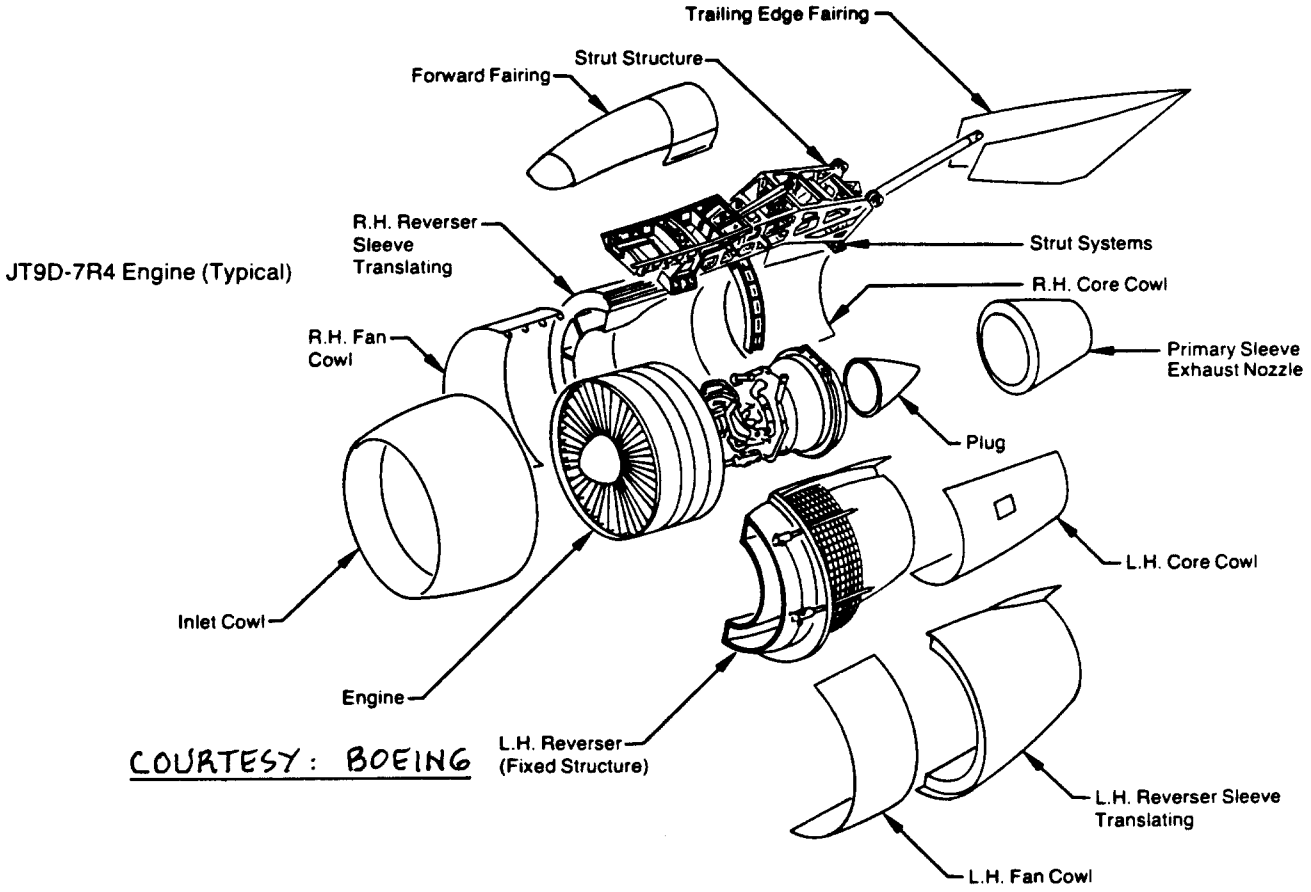

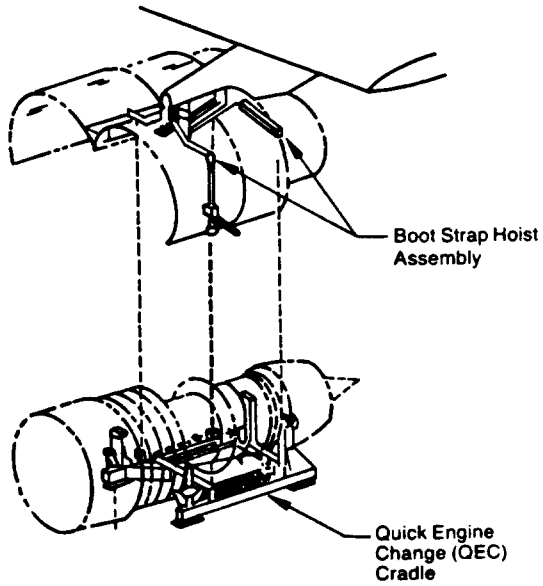

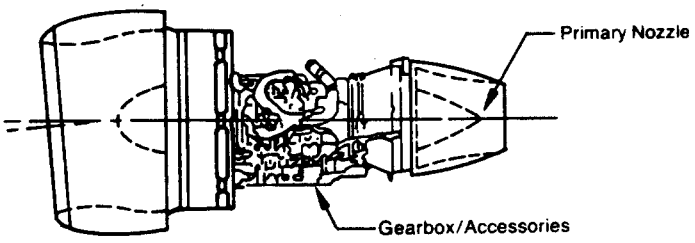

Engine Removed

Figure 6.49 Engine Removal for the Boeing 767

6.7 SAFETY CONSIDERATIONS

The following safety aspects will be discussed:

6.7.1 Installation safety
6.7.2 Safety during ground operation
6.7.3 Foreign object damage (FOD)
6.7.4 Engine reliability and shutdown rates

6.7.1 Installation Safety

All engines and other heat generating equipment must be isolated from the rest of the airplane by means of firewalls and/or other suitable shrouds. This requirement is of great importance in isolating engines from fuel tanks. Rules to be followed in laying out fuel tanks and fuel systems are discussed in Part IV.

FAR 23.1191 and 25.1191 deal with this requirement for commercial airplanes. A similar requirement exists for military airplanes.

Figure 6.50 shows where insulating blankets can be applied in a jet engine nacelle. The material properties are also listed.

Figure 6.51 shows a typical firewall installation in a light airplane. Fire walls should be made out of stainless steel and/or titanium. DO NOT USE ASBESTOS!!!

The structural integrity of engines and propellers is historically less than that of airplane primary structure: the frequency of occurrence of disintegration type failures (although low) is one to two orders of magnitude greater than the likelihood of the primary structure failing. In deciding on any powerplant installation the following failures must be accounted for:

*Propeller blade failure
*Compressor and turbine wheel disintegration

Because of the very high kinetic energies associated with these items it is not acceptable to locate the crew, the passengers, flight crucial systems or primary structure in the path of such items. Figure 2.14 illustrates the so-called 5 degree cone criterion which is frequently used in layout design to satisfy this requirement with regard to humans. The designer should use the same criterion with regard to flight crucial systems and with regard to primary structure.

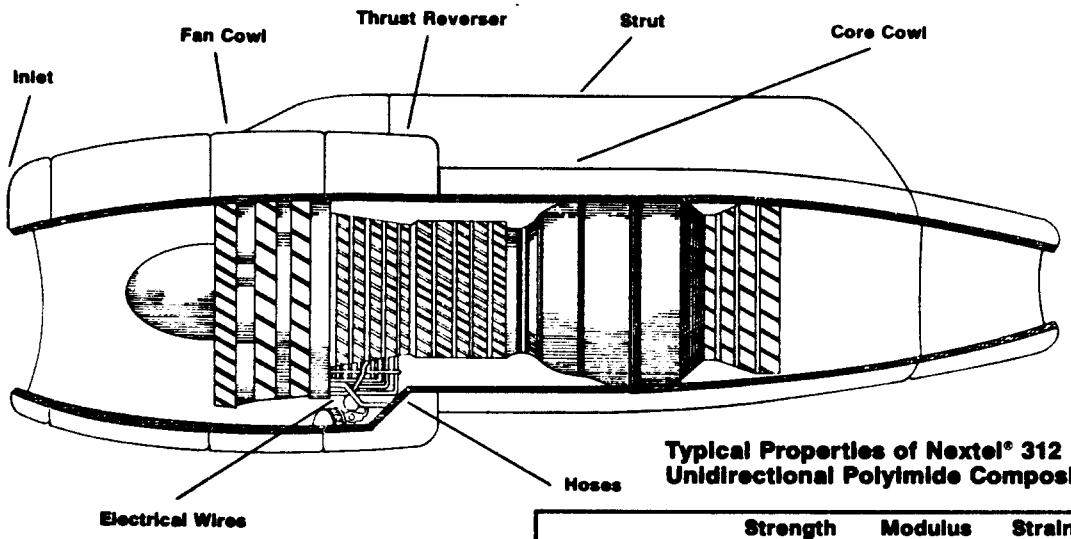

Typical Properties of Nextel® 312 Unidirectional Polyimide Composites

	Strength (PSI)	Modulus (PSI × 10^6)	Strain @ Break (in./in. × 10^{-3})
Tensile	75,000	10.300	7.04
Compressive	88,100	9.150	9.63
Shear	3,840	.358	10.73

WEIGHT: 50% OF STAINLESS STEEL

CONTAINS FIRES ≤ 2,200°F

COURTESY: 3M CORP.

Figure 6.50 Application of Fire Insulating Blankets

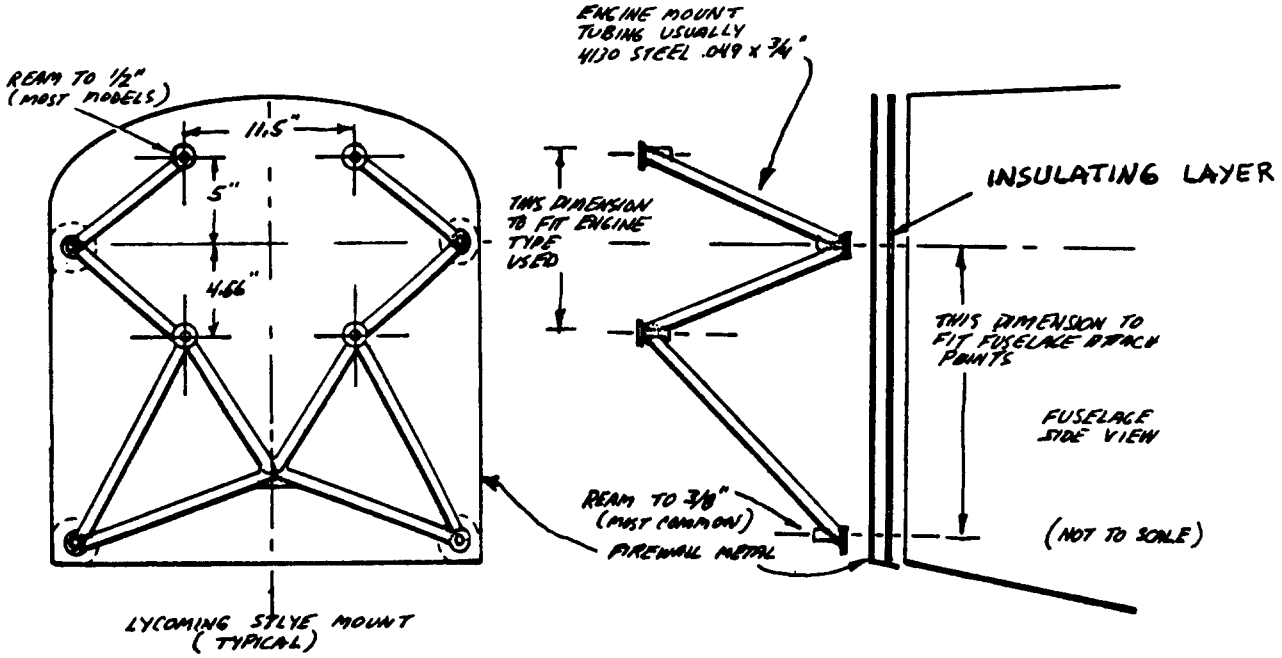

COURTESY: T. BINGELIS
REF. 76

Figure 6.51 Fire Wall Installation in a Light Airplane

It should be obvious that powerplants must not be located in such a manner, that a disintegration type failure would result in serious damage to an adjacent powerplant. The reader should observe that all transport jets have the engines located to prevent this from happening!

6.7.2 Safety During Ground Operation

Propellers and jet engines create potential hazards for people who need to work in close proximity to airplanes while on the ground. It is not feasible to arrange for protection from running propellers and/or jet engines under most operating circumstances. Awareness of the potential danger and constant reminders must serve to deter serious accidents. Figure 6.52 illustrates the potential danger areas in the case of a large turbofan engine.

6.7.3 Foreign Object Damage (FOD)

Jet engines are sensitive to ingestion of many types of debris. Apart from the so-called bird strike requirement, it is necessary to assure that debris (gravel, slush, mud, snow add ice) thrown up by the landing gear cannot enter into inlets or cannot damage propellers or other critical components of the propulsive installation. To provide reasonable assurance in preliminary design that a proposed installation is not prone to landing gear FOD the reader should check the relative location of engine inlets and landing gears on existing airplanes and verify that critical angular relationships are not violated. Figure 6.53 illustrates a number of such relationships. By using special deflectors on the nose gear it is possible to prevent FOD despite a marginal angular relationship. To certify the 737 for operation from gravel runways, Boeing added such deflector shields to special versions of the 737.

Turbopropeller installations (with their relatively small air inlets) can be sensitive to ingestion of ice, dust particles, small birds and other particles. In such installations frequent use is made of so-called 'particle separators'. Figure 6.54 illustrates such a separator system. Note that even if the particle screen ices up a path must be provided for air to enter the engine even though some pressure loss may be associated with that.

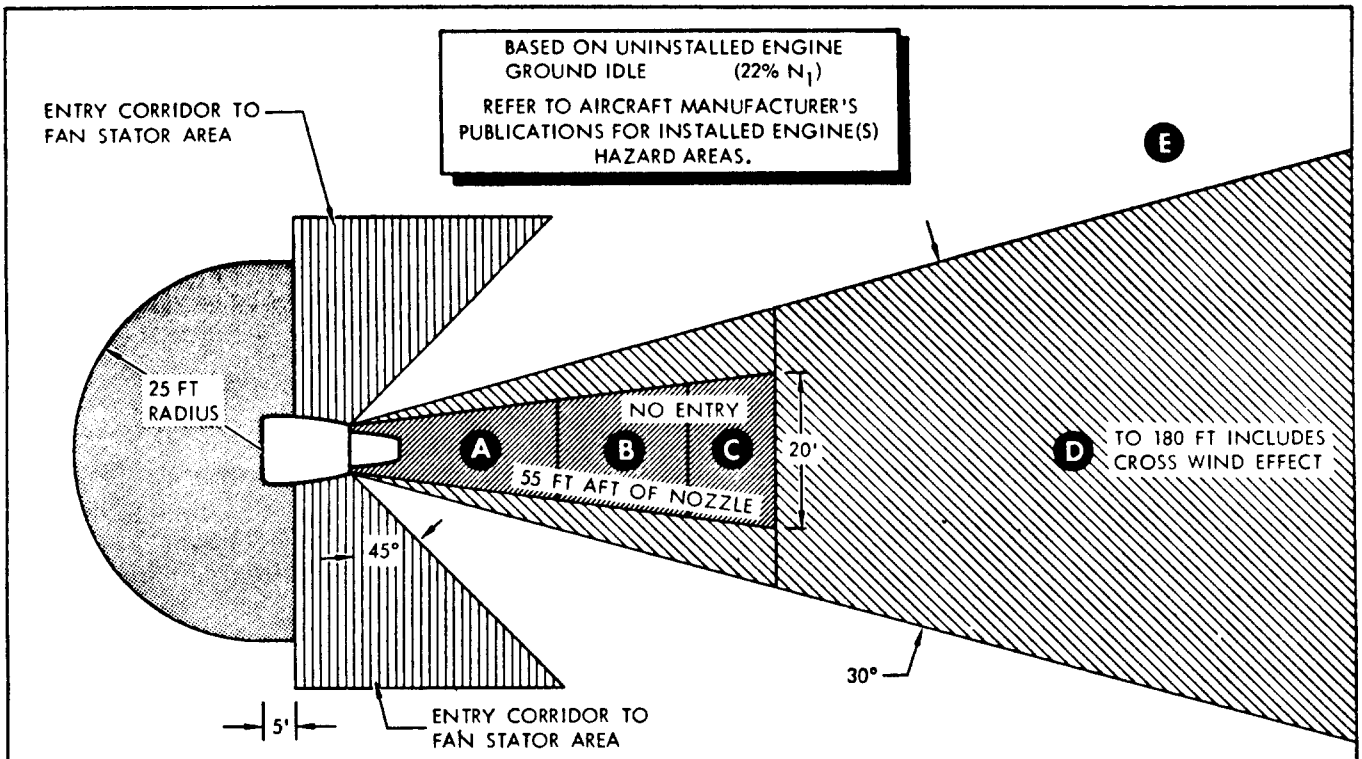

EXHAUST WAKE DANGER AREA 65 MPH OR GREATER

INLET SUCTION DANGER AREA

EXHAUST WAKE DANGER AREA 65 MPH OR LESS

ENTRY CORRIDOR

CF6-6D Engine Hazard Areas (Uninstalled)

NOTE: REFER TO AIRCRAFT MANUFACTURER'S PUBLICATIONS FOR INSTALLED ENGINE HAZARD AREAS.

COURTESY: GENERAL ELECTRIC

AREA	APPROX. WIND VELOCITY (MPH)	POSSIBLE EFFECTS WITHIN DANGER ZONE BASED ON "RADIOLOGICAL DEFENSE" VOL II ARMED FORCES SPECIAL WEAPONS PROJECT, NOV. 1951
A	210 TO 145	A MAN STANDING WILL BE PICKED UP AND THROWN; AIRCRAFT WILL BE COMPLETELY DESTROYED OR DAMAGED BEYOND ECONOMICAL REPAIR; COMPLETE DESTRUCTION OF FRAME OR BRICK HOMES.
B	145 TO 105	A MAN STANDING FACE-ON WILL BE PICKED UP AND THROWN; DAMAGE NEARING TOTAL DESTRUCTION TO LIGHT INDUSTRIAL BUILDINGS OR RIGID STEEL FRAMING; CORRUGATED STEEL STRUCTURES LESS SEVERELY
C	105 TO 65	MODERATE DAMAGE TO LIGHT INDUSTRIAL BUILDINGS AND TRANSPORT TYPE AIRCRAFT.
D	65 TO 20	LIGHT TO MODERATE DAMAGE TO TRANSPORT-TYPE AIRCRAFT.
E	< 20	BEYOND DANGER AREA.

CF6-6155-2-A2A

Figure 6.52 Danger Zone Behind a Turbofan

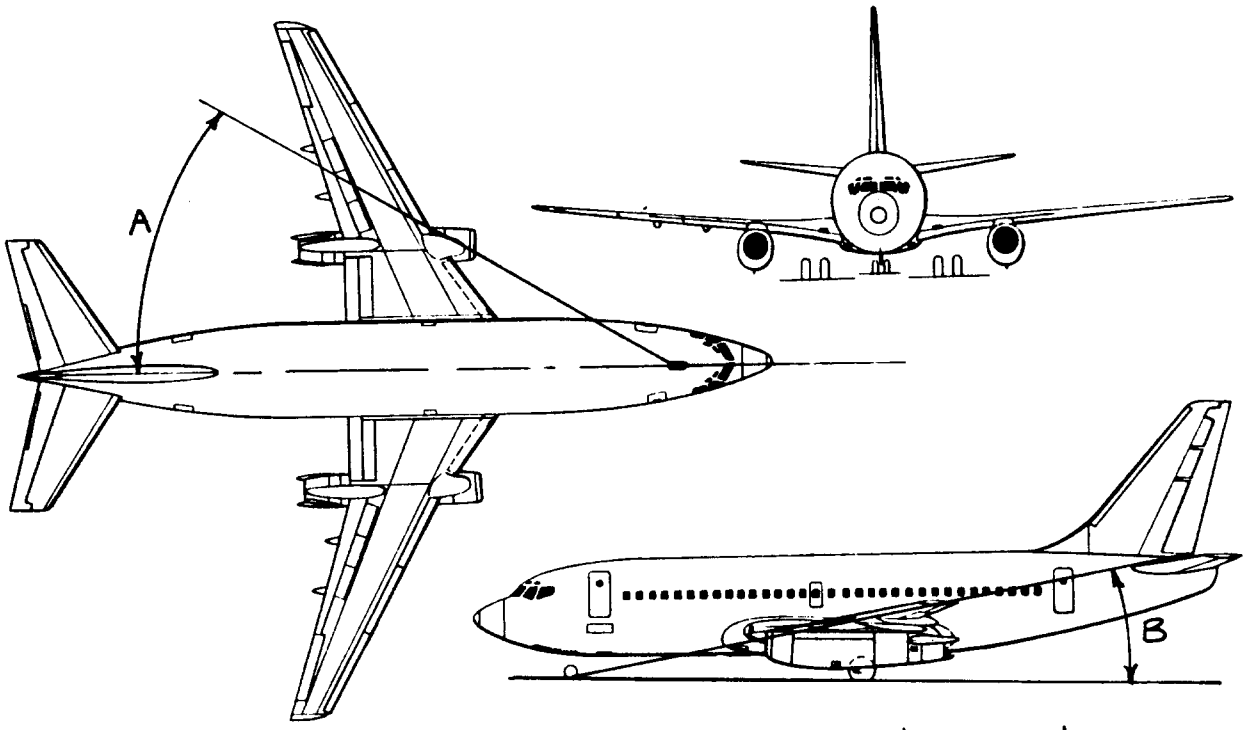

TYPE:	737-200	-300	757-200	L-1011	DC10-30	BAe-146-200
A	31°	32°	30°	43°	39°	33°
B	12°	10°	11°	11°	12°	21°

Figure 6.53 Critical Angles for FOD in Jet Engines

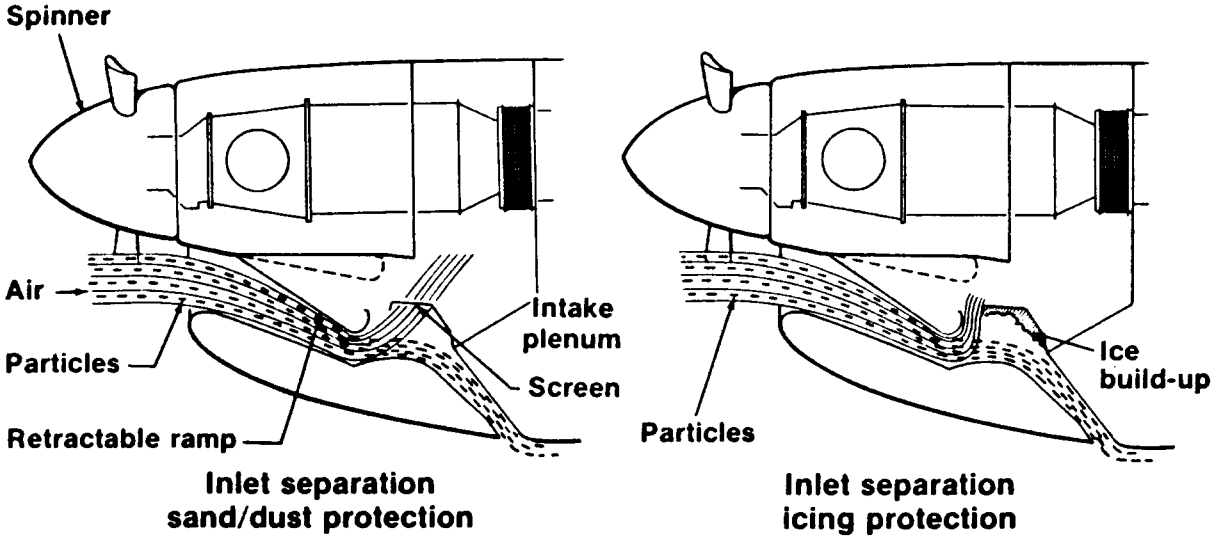

Figure 6.54 Particle Separator System for a Turboprop

6.7.4 Engine Reliability and Shutdown Rates

The following engine related scenarios need to be considered:

1. engine failure during take-off and/or go-around
2. engine failure during overwater flight

Case 1 is adequately addressed by the required one engine inoperative climb requirements which are imposed on all multi-engine airplanes. Part I, Chapter 3 has addressed these requirements in terms of basic airplane design parameters. Case 1 also can have stability and control consequences. These were addressed in Part II, Chapter 11. Part VII deals with this problem in detail.

Case 2 is of concern primarily in the case of twin engined passenger airplanes operating over long stretches of water. Figure 6.55 shows a recent study which indicates how long it takes to achieve certain mean diversion times at different engine cruise failure rates. The reader should monitor the flight safety articles published in 'Flight International' (British, weekly) at regular interval for recent information on actual engine shutdown rates. These shutdown rates depend not only on engine type but also on the type of airplane operations.

The concern over engine-out operation during extended overwater flights centers not merely on the engine itself but in particular on the effect on flight crucial systems. Part IV deals with this question in detail.

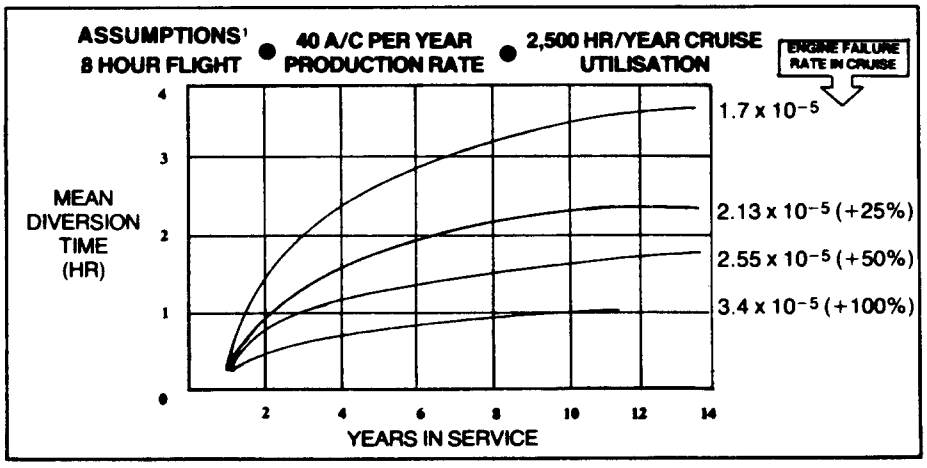

SOURCE: AEROSPACE - DEC. 1985, P.11, R.A.E.S.

Figure 6.55 Relation Between Mean Diversion Time and Calendar Time as a Function of Engine Shutdown Rate in Oceanic Twins

6.8 NOISE CONSIDERATIONS

Airplanes and their engines create a substantial amount of both interior and exterior noise. The interior noise levels should not be so high as to cause discomfort to the passengers or to make safe operation by the crew impossible.

The exterior noise levels should meet the requirements of FAR 36 (Ref.11). These requirements impose severe restrictions on the type of engine and/or propeller technology which can be utilized.

Figure 6.56 shows those noise sources which are of major importance to airplane designers.

The material in this section is organized as follows:

6.8.1 Interior noise design considerations
6.8.2 Exterior noise design considerations

6.8.1 Interior Noise Design Considerations

Reference 66 contains information about noise levels which are acceptable from a speech interference level and a hearing damage level viewpoint. Table 6.11 shows the noise levels permissible by OSHA standards. Table 6.12 relates noise levels to various activities.

Interior noise levels are of primary concern in propeller driven airplanes. Reference 67 reviews procedures for the prediction of cabin interior noise levels. Figure 6.57 shows typical interior noise levels measured inside the cabin of a light, propeller driven airplane.

Reductions of cabin noise levels can normally be achieved only by:

1. relocation of the propellers and/or powerplants
2. redesign of the propeller(s)
3. addition of sound damping materials

Examples of 1) are the Beech Starship I and the Piaggio 180 (Part II, Figures 3.42 and 3.47 respectively).

Item 2) normally amounts to lowering the tip Mach number of the propeller. This can be done by lowering propeller rpm and by lowering the propeller diameter.

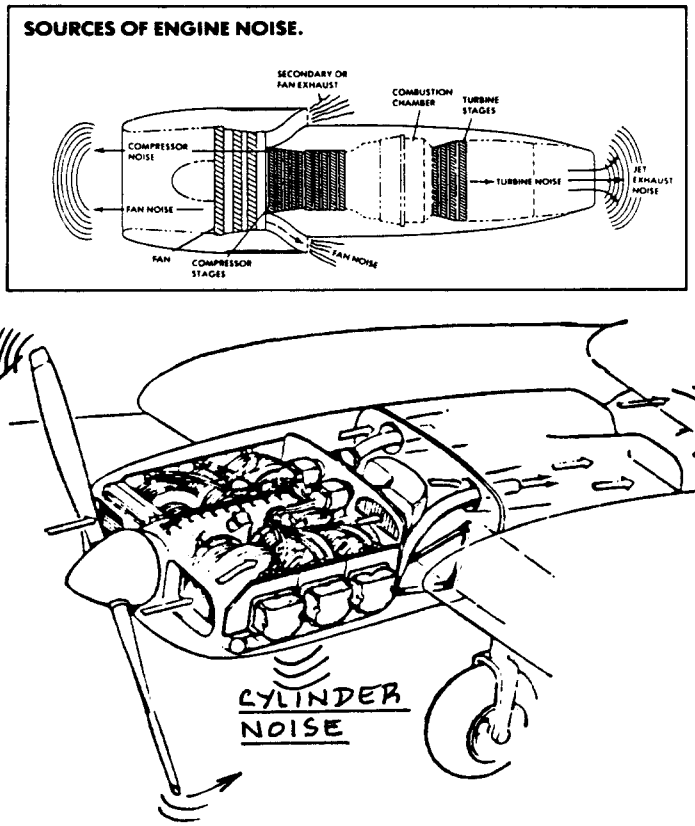

Figure 6.56 Sources of Engine Noise

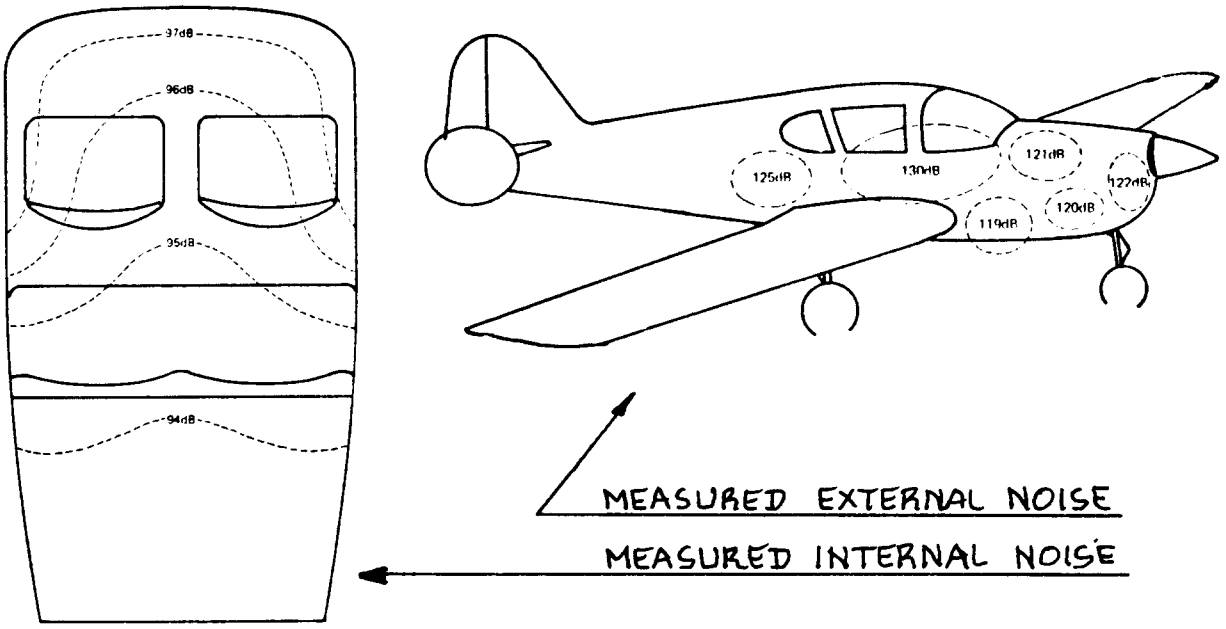

Figure 6.57 Typical Noise Contours in a Light Airplane

Table 6.11 Permissible Noise Exposure by OSHA Standard

Duration per day in hours:	Permissible Level in db:	Duration per day in hours:	Permissible Level in db:
8	90	1.5	102
6	92	1	105
4	95	0.5	110
3	97	0.25 or less	115
2	100		

Table 6.12 Noise Levels Associated with Activities

Overall Effect	Level in db	Activity
Extreme danger	155	Rifle blast, siren, jet engine (close to)
	140	Shotgun blast, drag strip (close to)
	120	Some rock music, rock drill (close to)
Probable permanent hearing damage	115-125	Drop hammers
	110-115	Routers, planers
	90-100	Subway, weaving mill
	90-95	Riveter, punch press
Possible hearing damage, depending on duration	80-95	Spinners, looms, lathes
	80	Heavy traffic
No hearing damage	65-75	Noisy typewriter
	70	Busy street
	60	Normal speech
	50	Average office
	20-30	Sleeping limit
	15	Leaf rustling

Changes in propeller airfoil to delay drag rise phenomena are also beneficial. Reference 68 contains a discussion of the penalties and the potential associated with propeller noise reduction.

Examples of item 3) are shown in Figure 6.58. Addition of sound damping materials adds to airplane empty weight and usually reduces airplane payload (or fuel) weight. In the F27 example discussed in Ref.69, the following weight penalties were identified:

For a 2 dbA reduction, 55 lbs for using 'tuned dampers' (Fig.6.58).

For a 5 dbA reduction, 66 lbs for using blankets (Fig.6.58)

6.8.2 Exterior Noise Design Considerations

The following specific exterior noise considerations are important to the design of airplanes:

1. Take-off noise
2. Approach noise
3. Sideline noise
4. Sonic boom generated noise

Regulations containing allowable noise levels and methods for demonstrating compliance are contained in Ref.11 (FAR 36). Figures 6.59a through 6.59d show the FAR 36 noise standards in relationship to airplane type and take-off weight. These figures also show the degree of compliance of several existing airplanes.

Refs 70 and 71 contain procedures for the prediction of fly-over noise from propeller driven airplanes.

Ref.72 presents a discussion on the noise from turbomachinery. Ref.73 presents two design conclusions:

1) If an airplane is designed to meet the take-off and approach performance requirements of Ref.11 by minimizing required thrust, it tends to also be optimum for minimizing noise within plus or minus 1 EPNdb.

2) The powerplant installation should be designed to allow for adequate sound attenuation treatment. About 10 to 12 EPNdb cen be expected from this source.

With regard to sonic boom overpressure, Reference 74 contains a simple procedure for its prediction.

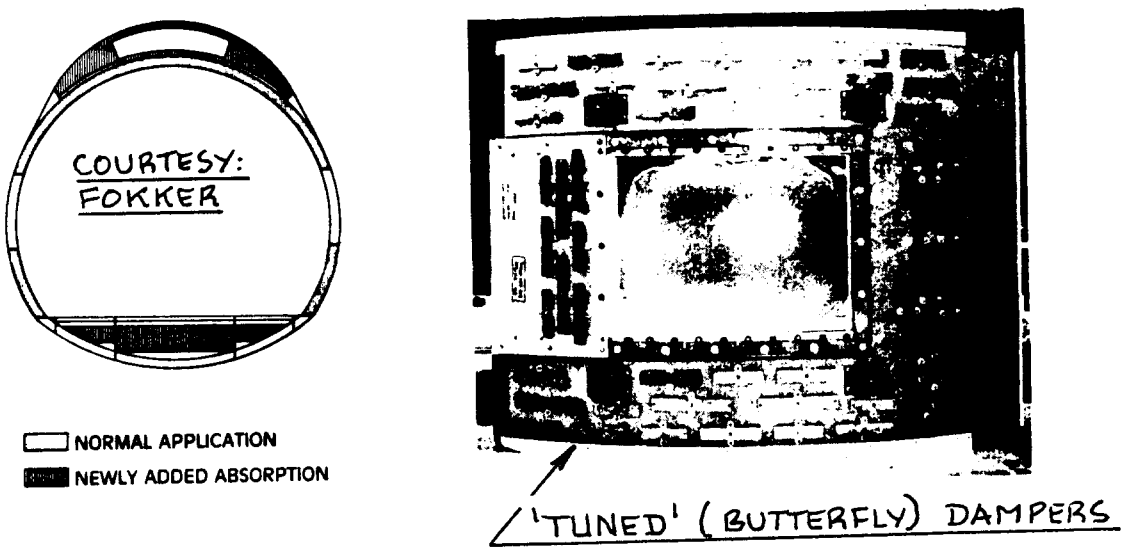

Figure 6.58 Examples of Sound Damping Treatment in the Fokker F27

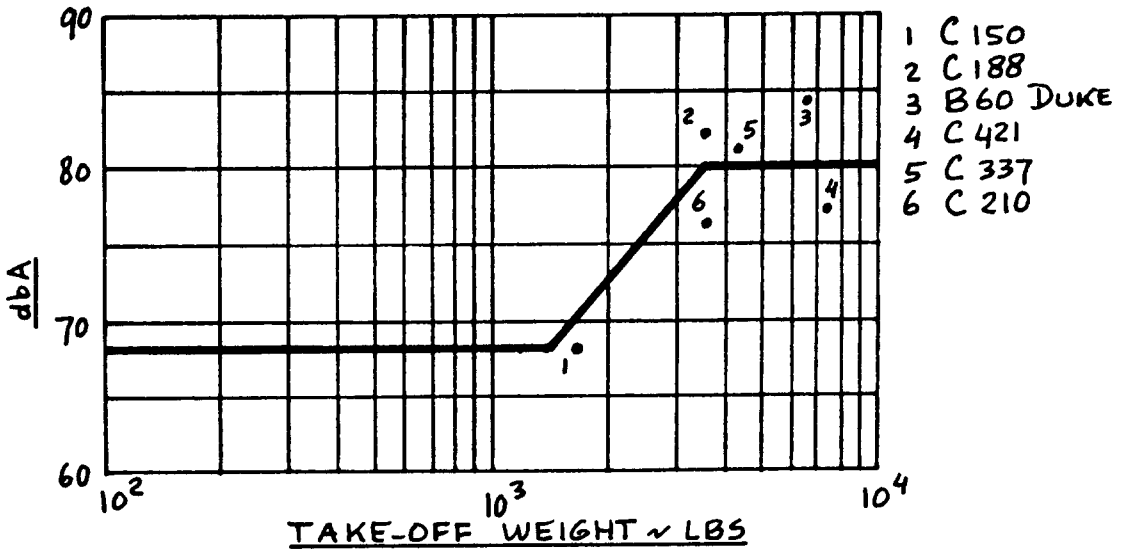

Figure 6.59a FAR 36 Noise Criteria For Light Airplanes

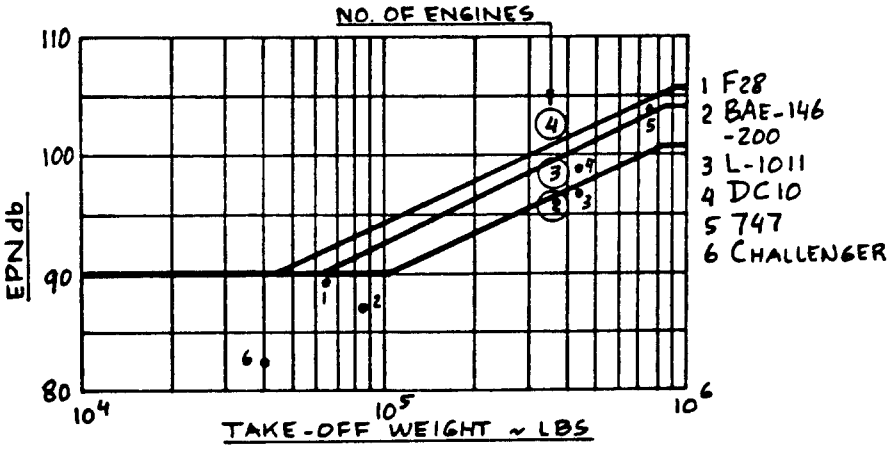

Figure 6.59b FAR 36 Take-off Noise Criteria for Jets

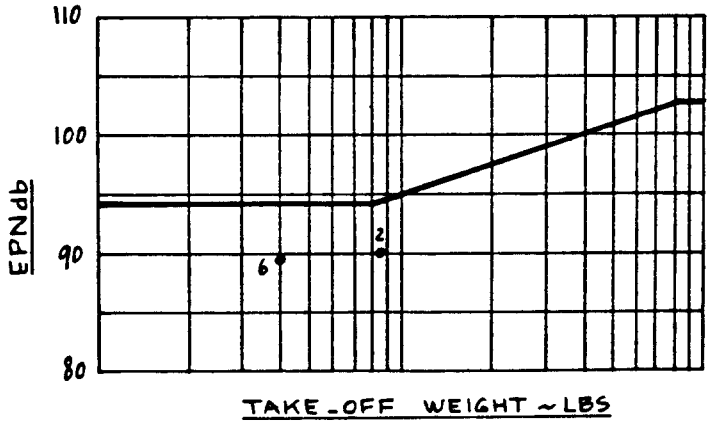

Figure 6.59c FAR 36 Sideline Noise Criteria for Jets

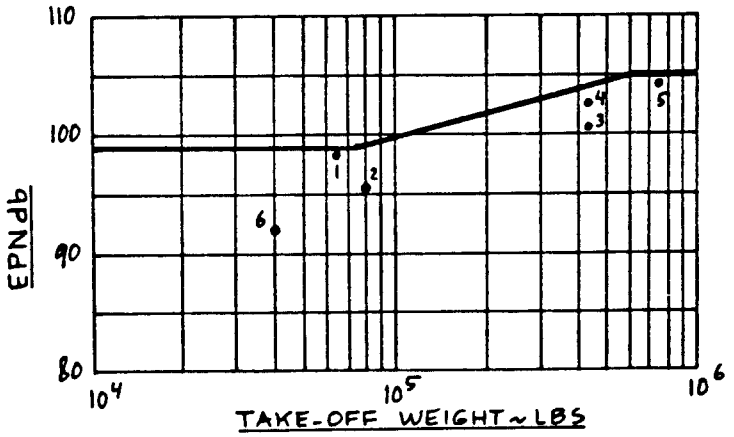

Figure 6.59d FAR 36 Approach Noise Criteria for Jets

6.9 EXAMPLE EGINE INSTALLATIONS

Examples will be presented for the following types of engine installations:

6.9.1 Piston-propeller ínstallations
6.9.2 Turbopropeller installations
6.9.3 Turbojet and turbofan installations
6.9.4 Propfan and ultra-bypass installations
6.9.5 Nozzles and thrust reversers

The reader should recognize that it is not clear at which point a propeller becomes a fan nor at which point a ducted fan becomes a ducted propeller.

6.9.1 Piston-Propeller Installations

Figure 6.60 shows a conventional piston-propeller installation, tractor fashion in a fuselage. Figs 3.1 through 3.6 in Part II contain many examples of this type of installation.

Significant design problems associated with piston/propeller installations are:

1. management of exhaust gasses
2. management of cooling air
3. reduction of airframe vibration
4. reduction of noise

1. Management of exhaust gasses: Note in Fig.6.60 that the exhaust stack is mounted perpendicular to the free stream. From a drag viewpoint this is very bad. Figure 6.61 shows how this can be improved somewhat. Reference 75 shows that poorly designed exhaust configurations can increase the zero lift drag coefficient of an airplane by 16 percent.

By directing the exhaust rearward, drag can be reduced and some thrust can be recovered as well: Ref.75 estimates that for highly powered general aviation twins the thrust recovery possible in a typical cruise flight condition amounts to some 15 percent of zero lift drag!

2. Management of cooling air: Figures 6.62 and 6.63 show the conventional ram-air cooling system as used in a tractor and a pusher arrangement respectively.

Warning: most piston engines are designed with the assumption that the cooling air will flow from top to bottom: downdraft. Figure 6.64 shows an updraft cooling

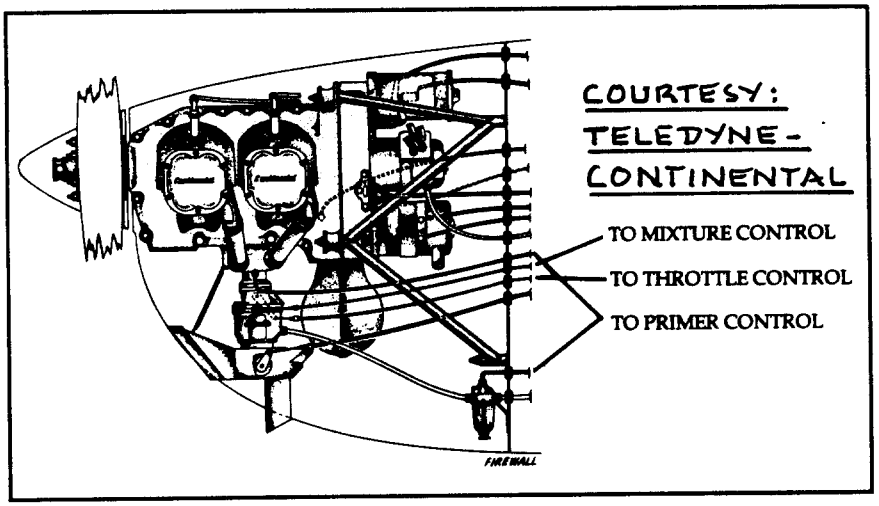

Figure 6.60 Light Airplane Piston Engine Installation

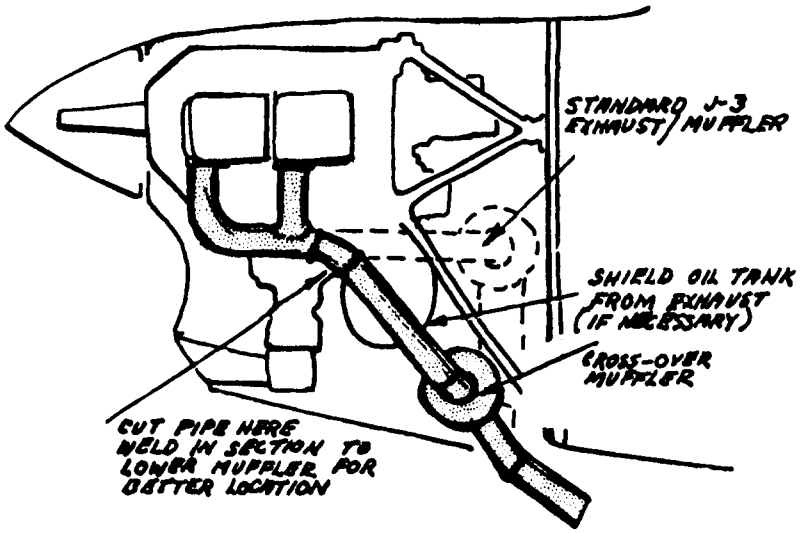

COURTESY: T. BINGELIS, REF. 76

Figure 6.61 Improved Exhaust System Installation

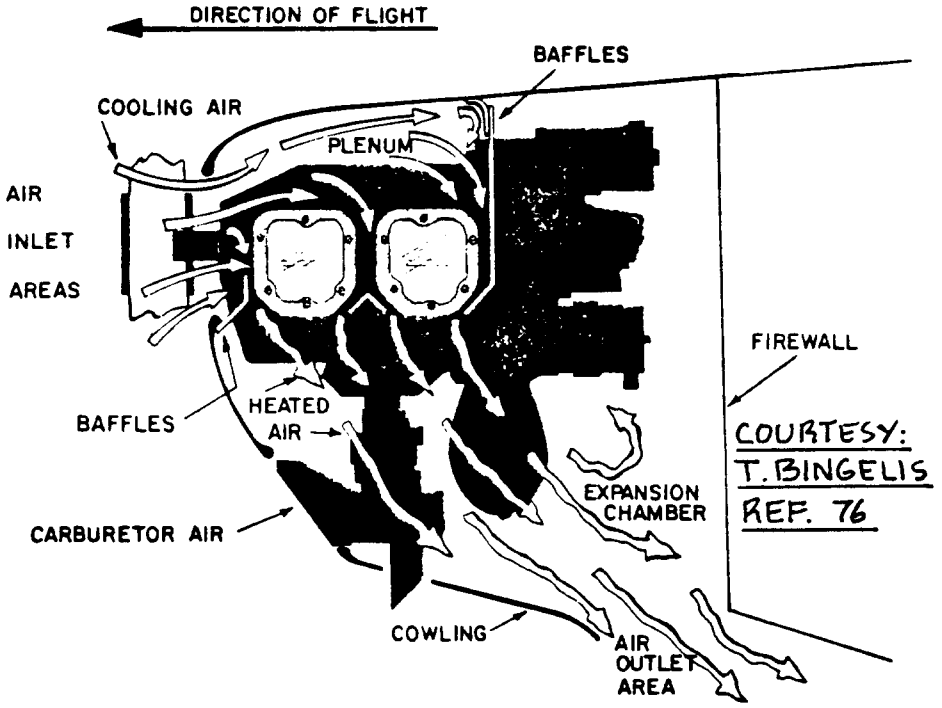

Figure 6.62 Conventional Ram Air Cooling for a Tractor Piston Engine Installation

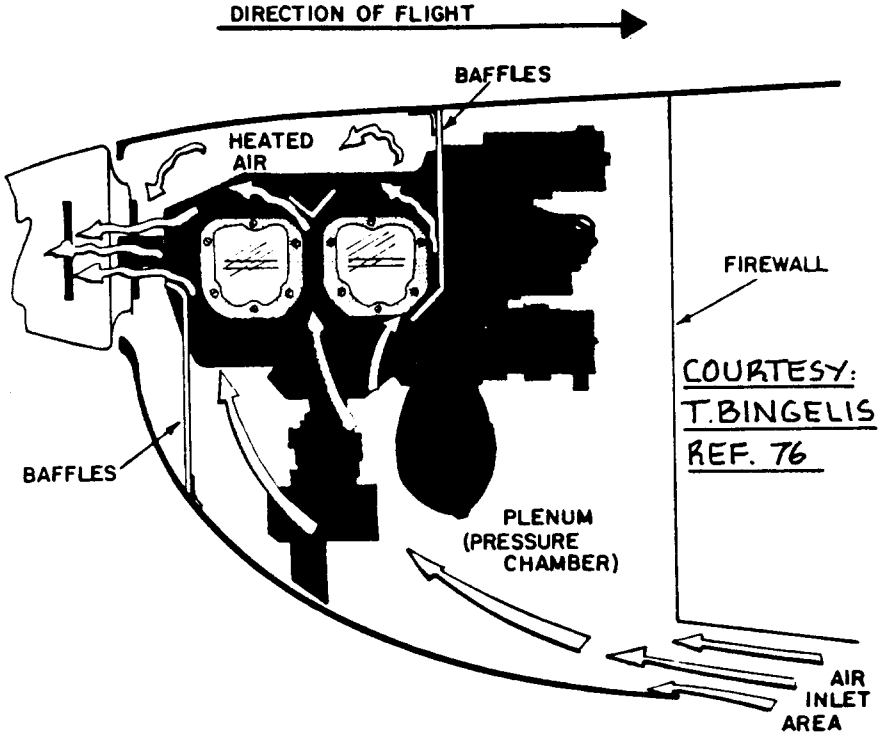

Figure 6.63 Conventional Ram Air Cooling for a Pusher Piston Engine Installation

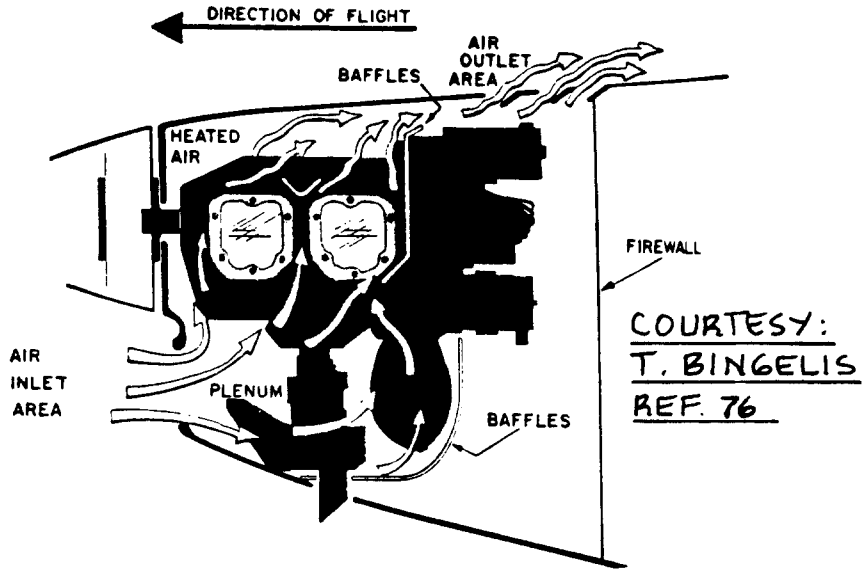

Figure 6.64 Updraft Cooling for a Tractor Piston Engine Installation

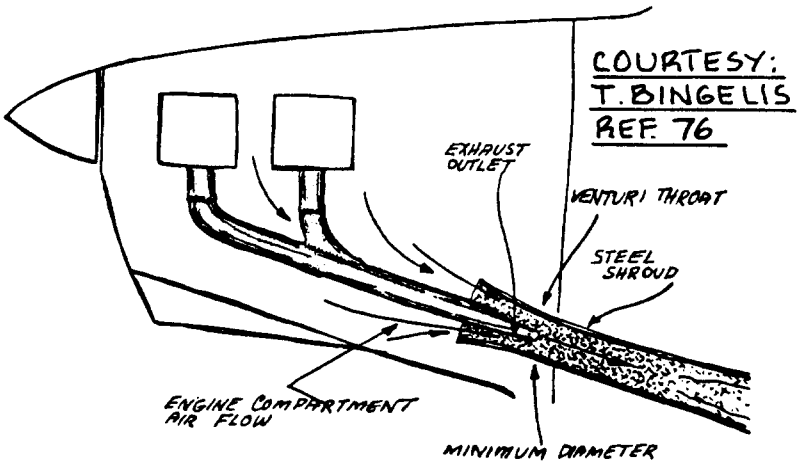

Figure 6.65 Example Ejector Installation in a Single

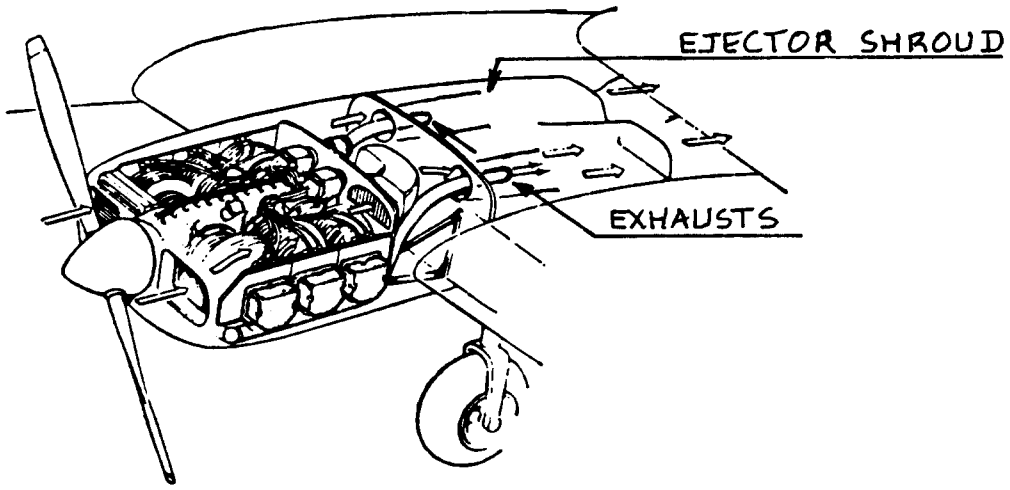

Figure 6.66 Example Ejector Installation in a Twin

arrangement. This may look good, but can result in the cooling air being heated by the exhaust stack thereby reducing cooling effectiveness! In pusher installations such as that of Fig.6.63 this can be a problem. Special engine driven cooling fan(s) may have to be installed to solve this problem.

Mismanagement of cooling air can cause drag increases up to 9 percent of zero lift drag according to Ref.75. Significant reductions in cooling air drag and exhaust configuration drag can be obtained by using so-called ejector systems. Figures 6.65 and 6.66 show examples of ejector installations. However: ejectors will increase weight and initial cost: this must be evaluated against the potential benefits.

Most of todays piston engines are of the horizontally opposed type. For installed power requirements above roughly 750 hp it has been found that the in-line or radial piston engines offer lighter and less 'draggy' installations. Examples of in-line engine installations are found in WWII fighters. Fig.6.67 shows an example of a modern radial engine installation. Note the 'tight' cowling system used in this arrangement. Figure 6.67 also shows the extra cowl flaps used to improve engine cooling during take-off.

Piston engines tend to loose power rapidly at altitude. Most high performance piston/propeller driven airplanes use supercharging to increase power available at altitude. Figures 6.12 and 6.68 show typical arrangements used in supercharger installations.

3. Reduction of airframe vibration: Most piston engines transmit significant vibrations into the airframe to which they are attached. To reduce such vibrations, piston engines are normally mounted on shock absorbing engine mounts. Figure 6.69 shows an example. References 76 and 77 contain many more examples of shock mount installations.

Section 6.8 presents a discussion of airplane noise. Piston-propeller combinations tend to be very noisy unless special steps are taken to reduce noise. It is possible to achieve major reductions in powerplant noise by using ducted fans. Figure 6.70 shows a potential application of a ducted fan driven by a piston engine. Whether the additional weight and wetted area is worth the reduction in noise remains to be seen.

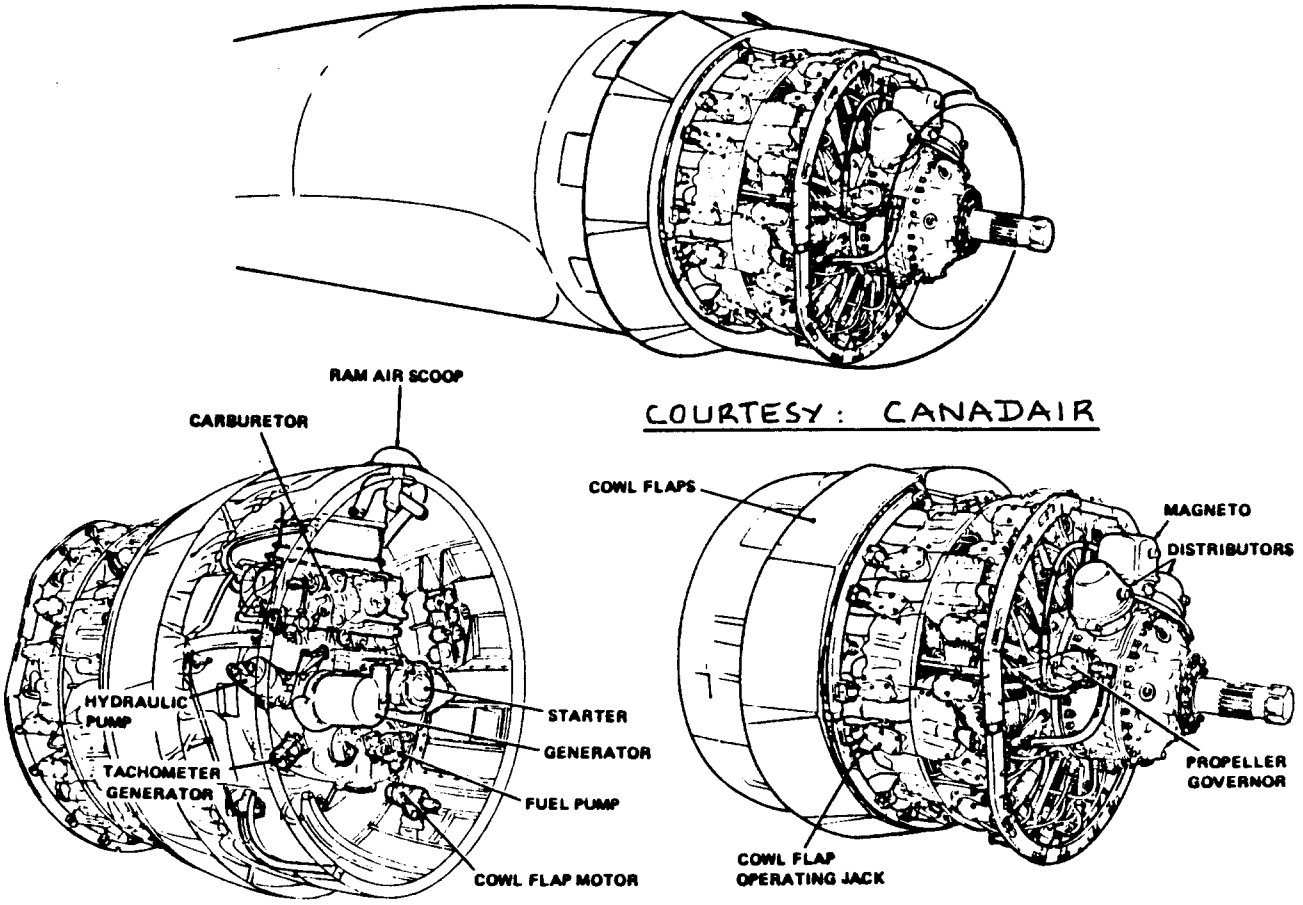

Figure 6.67 Radial Piston Engine Installation

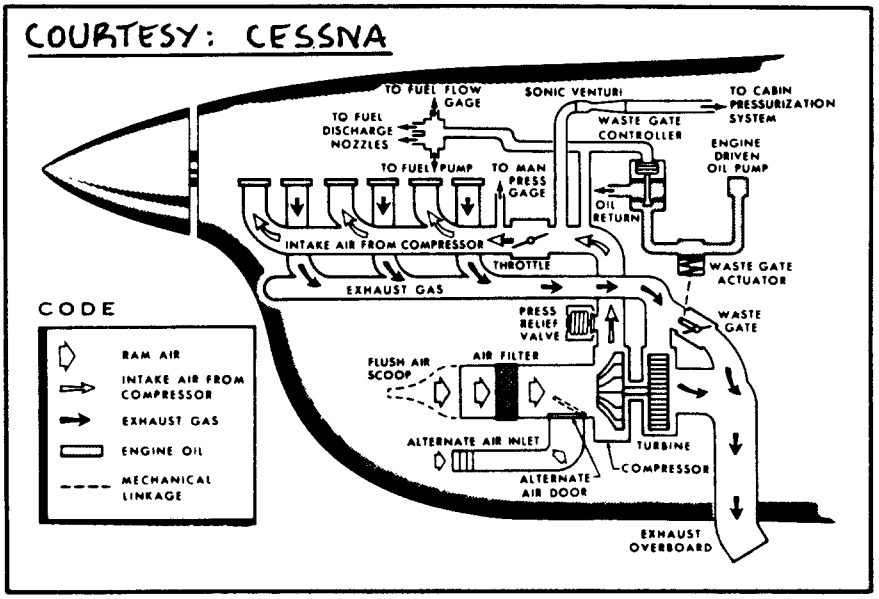

Figure 6.68 Schematic of a Supercharger Installation

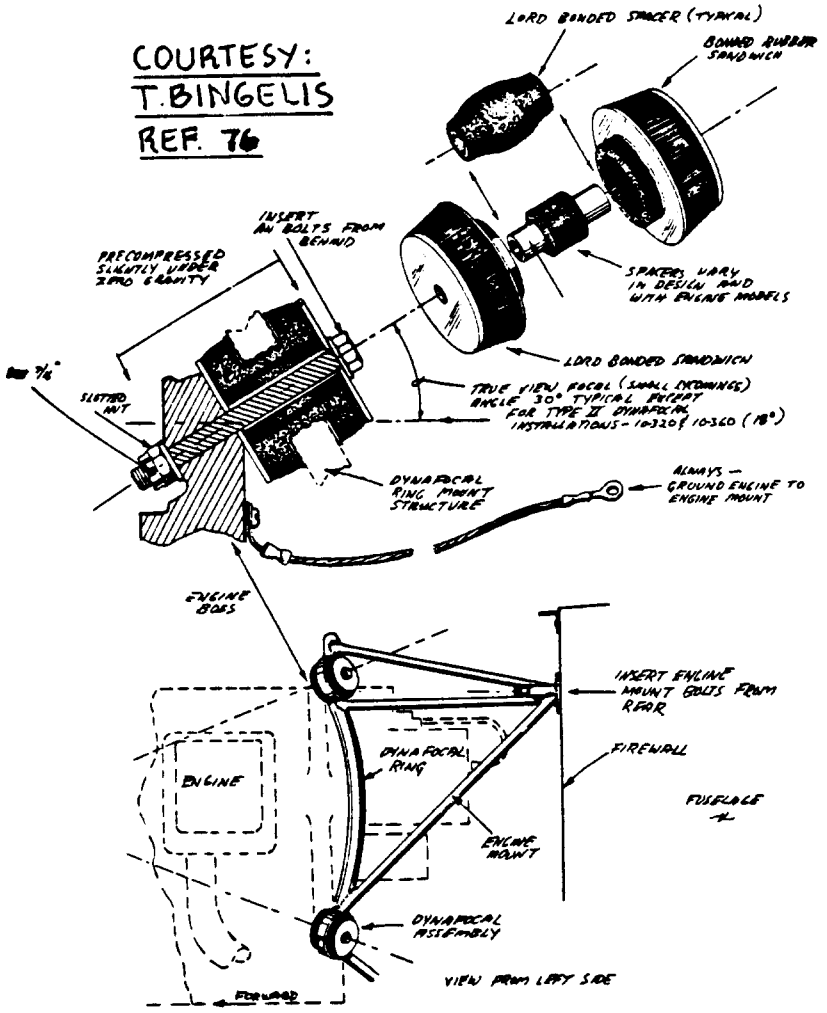

Figure 6.69 Shock Mount Installation

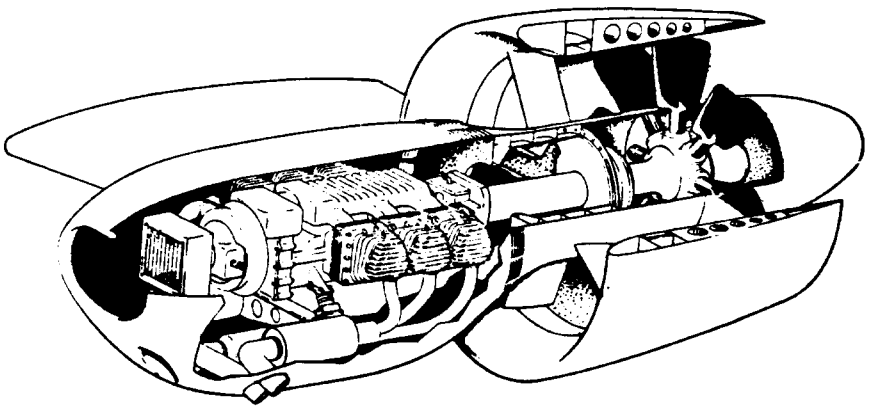

SOURCE:
NASA CR
114665

Figure 6.70 Piston Engine Driving a Ducted Fan

4. Reduction of noise: The problem of exterior and interior noise was discussed in Section 6.8. Major noise reductions due to the powerplant installation can be obtained by using a ducted propeller. An example of such an arrangement is shown in Figure 6.70. The reader should carefully evaluate the weight and drag penalties associated with this type of installation before deciding on its use. Figure 3.22d in Part II shows an airplane which uses a similar ducted propeller installation.

6.9.2 Turbo-Propeller Installations

Figure 6.71 shows a typical single engine turboprop tractor installation. Note the engine truss mount connecting to the firewall bulkhead.

Examples of 'over-the-wing' and 'under-the-wing' turboprop installations are shown in Fig.6.72. A counter-rotating turboprop installation is shown in Fig.6.73.

A cutaway drawing of a complete turboprop/nacelle/landing-gear installation is provided in Figure 6.74.

Figure 6.75 shows a pusher propeller installation driven by two gas generators. This installation was flown on the Learfan, also shown in Figure 6.75. An advantage of this installation is the absence of any yawing moment following an engine failure.

Many turboprop engines are sensitive to bird and/or (sand) particle ingestion. For that reason particle separators and/or screens are included in many turboprop installations. Figure 6.54 shows an example of such a particle separator.

6.9.3 Turbojet and Turbofan Installations

In transports and bombers the so-called 'buried' engine installation has been used in airplanes such as the DeHavilland Comet, the Vulcan and the Valiant: see Figure 6.76.

A major advantage of buried installations is the low installed drag. Disadvantages include: interruption of spars, relatively poor accessibility and long tailpipes.

In most of todays transports the engines are installed in external pods: wing or fuselage mounted. Fig.6.77 is a typical example of a wing mounted installation. Observe the forward and aft engine mounting points: recall the material in Section 6.5 on engine mounting.

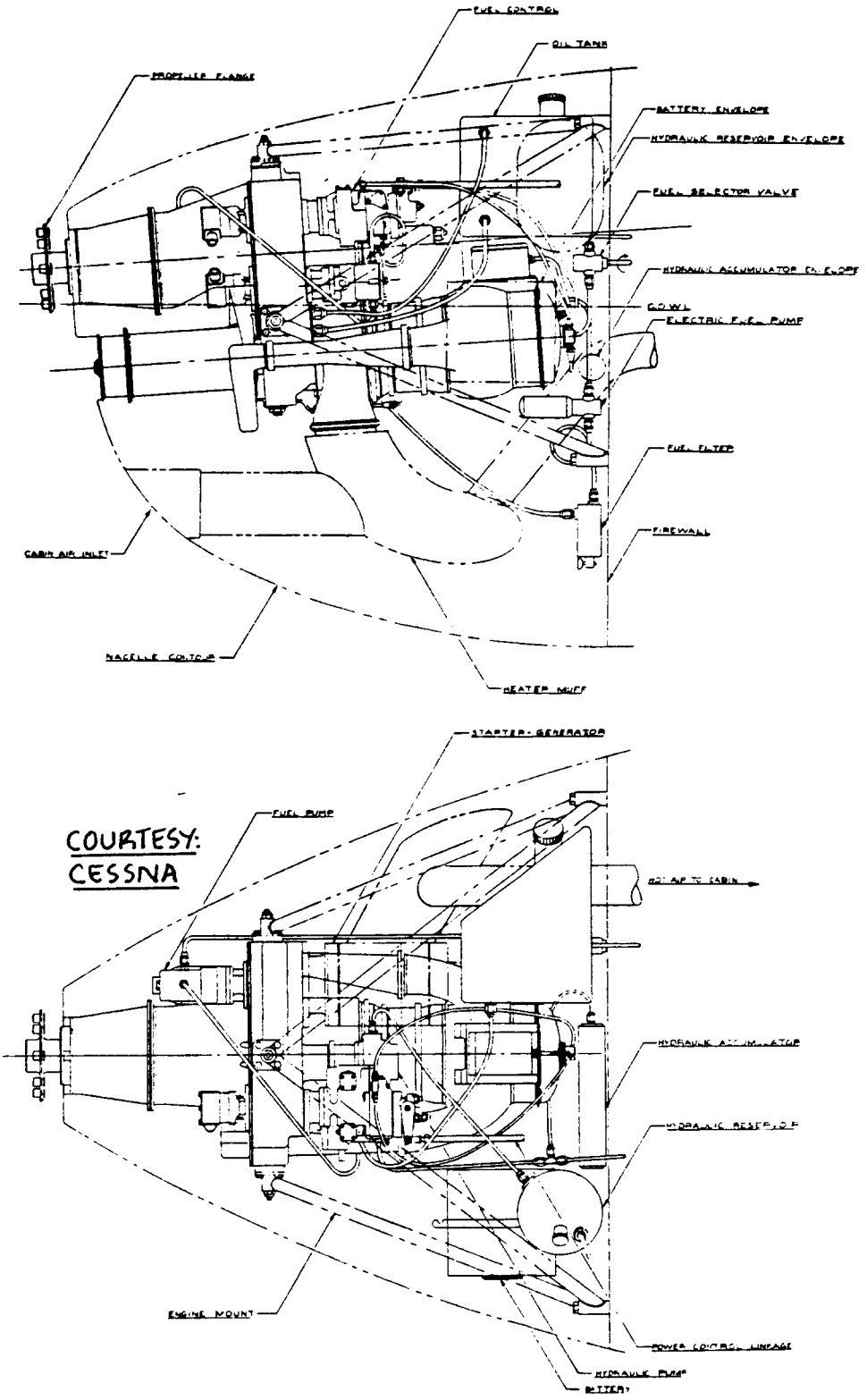

Figure 6.71 Turboprop Installation in a Cessna 406

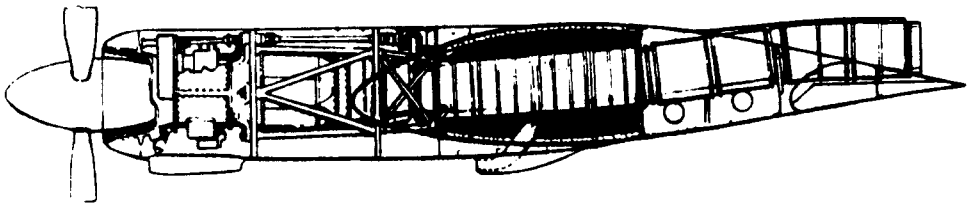

Detail of jet pipe, showing roller and link mounting for thermal expansion.

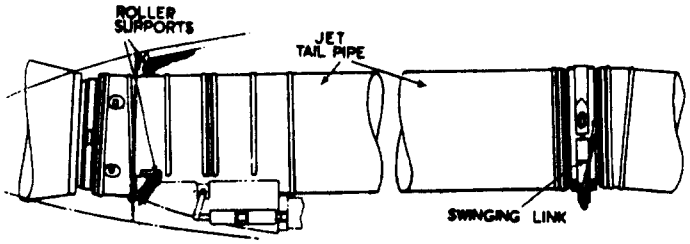

COURTESY: VICKERS - ARMSTRONG

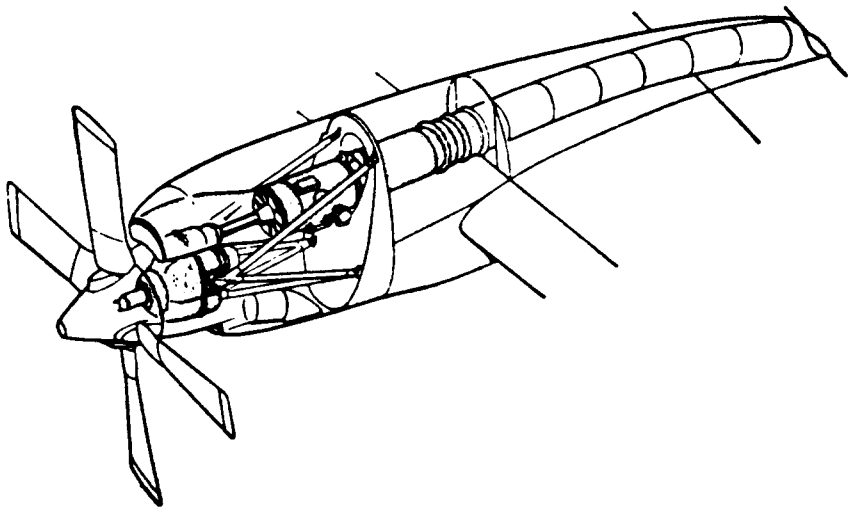

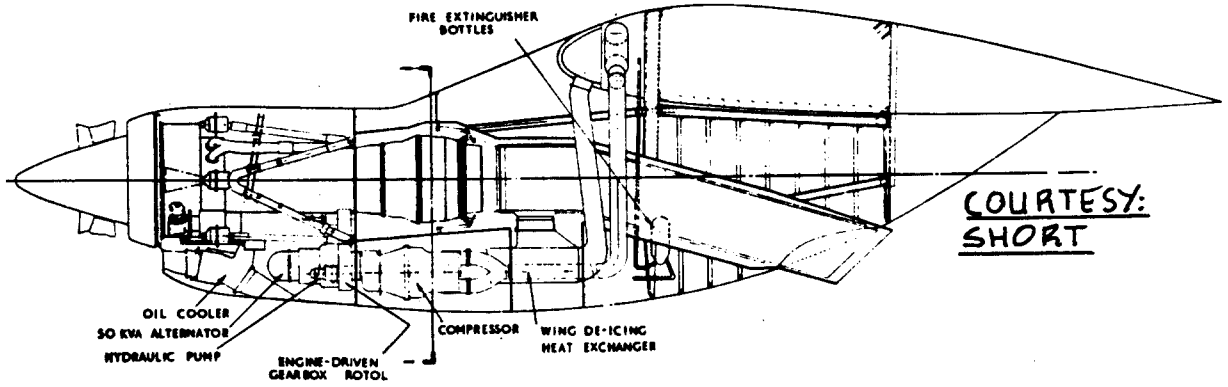

COURTESY: SHORT

Figure 6.72 Examples of Over-Wing and Under-Wing Turbo-Prop Installations

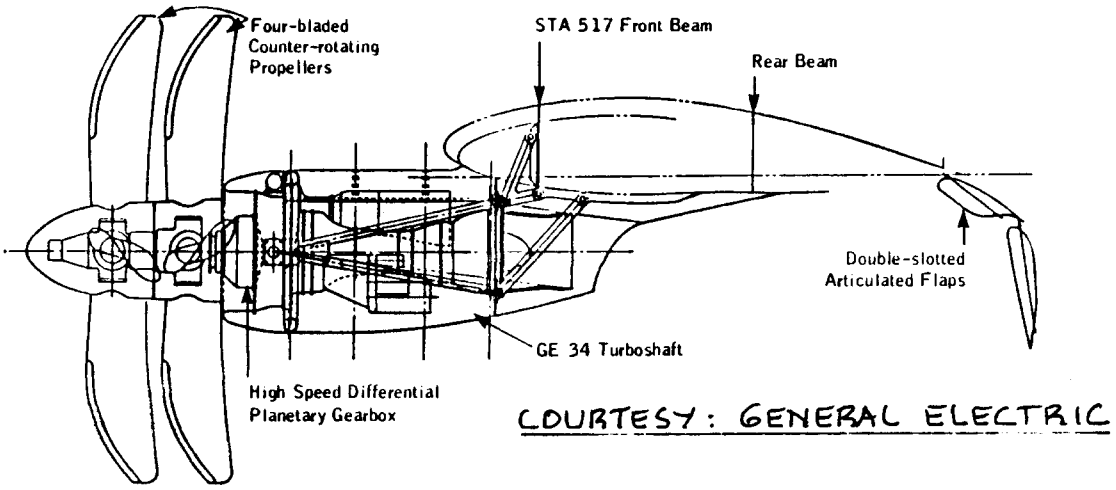

Figure 6.73 Counter Rotating Turboprop Installation

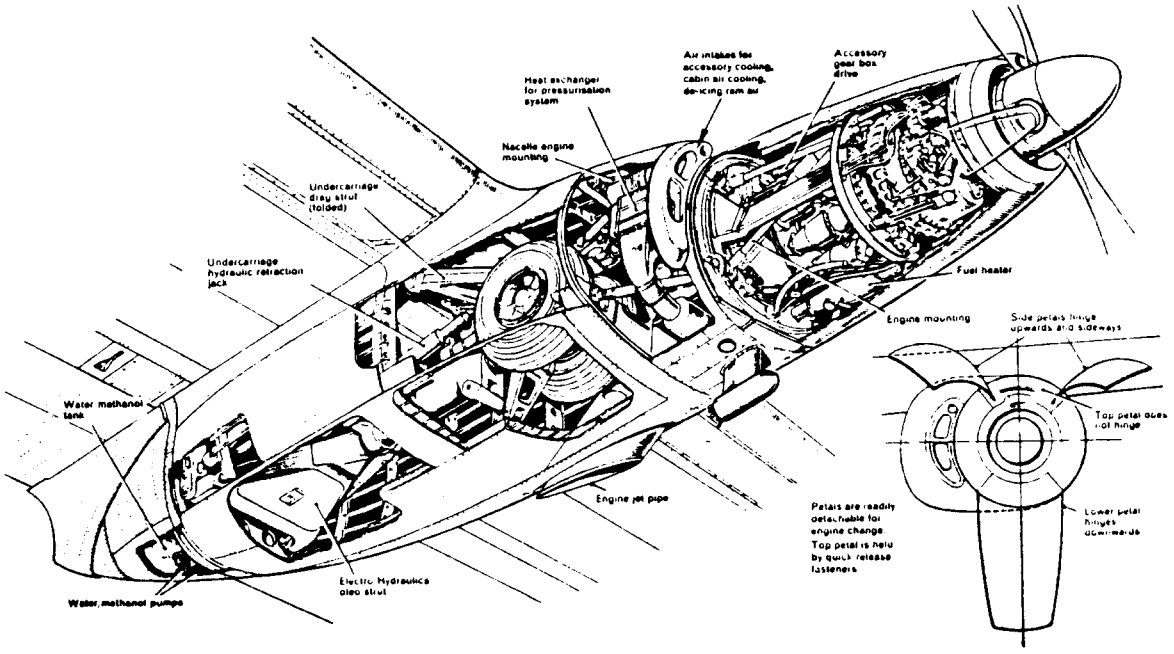

Figure 6.74 Cutaway of Turboprop Installation in the Handley Page Dart Herald

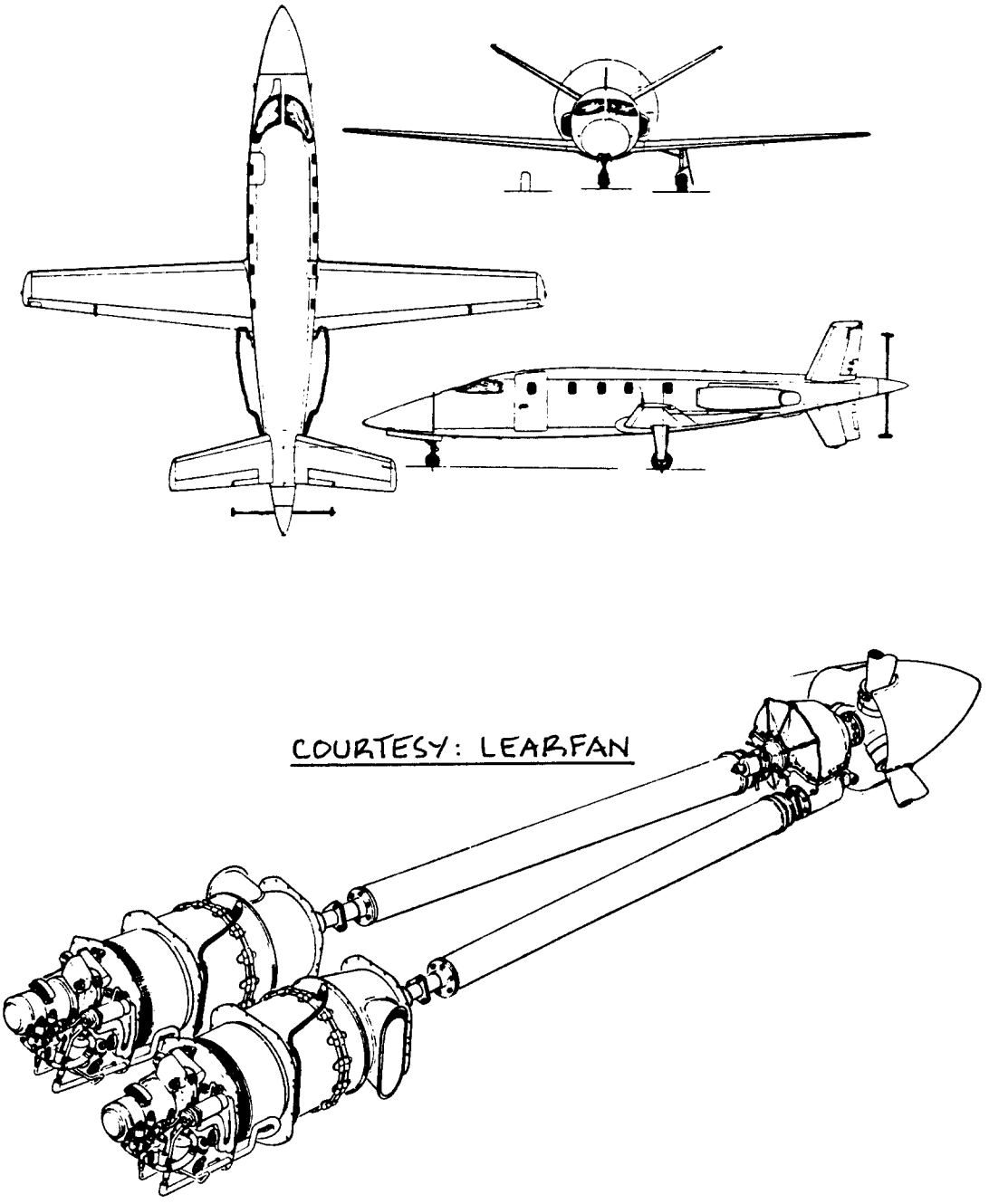

Figure 6.75 Turboprop and Drive Shaft Installation in the Learfan

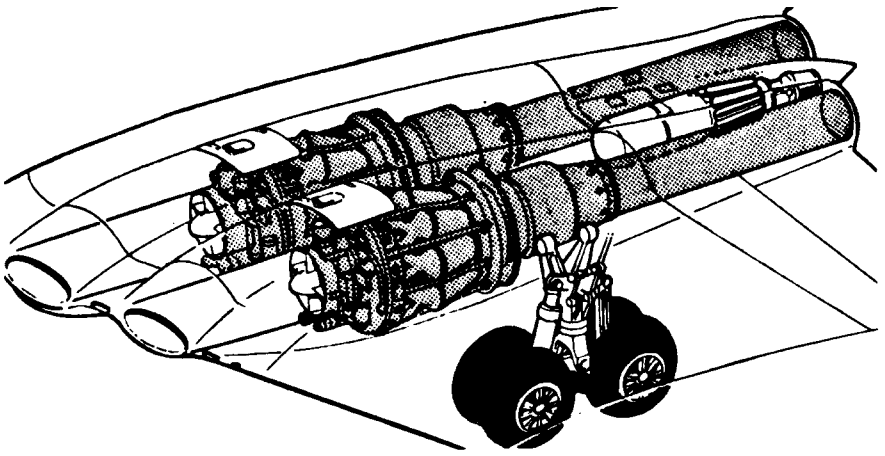

Figure 6.76 Example of Buried Turbojet Installation

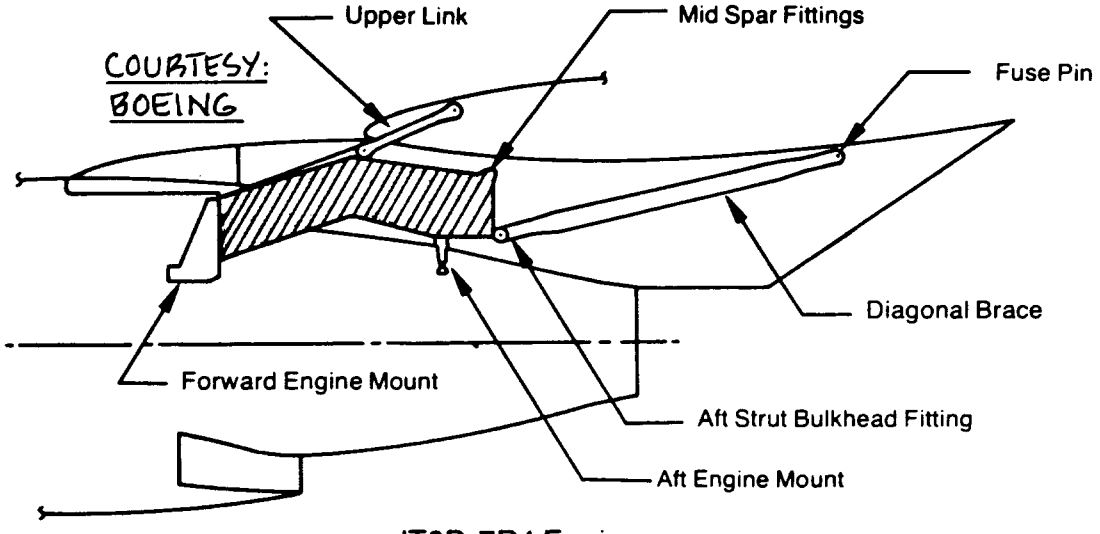

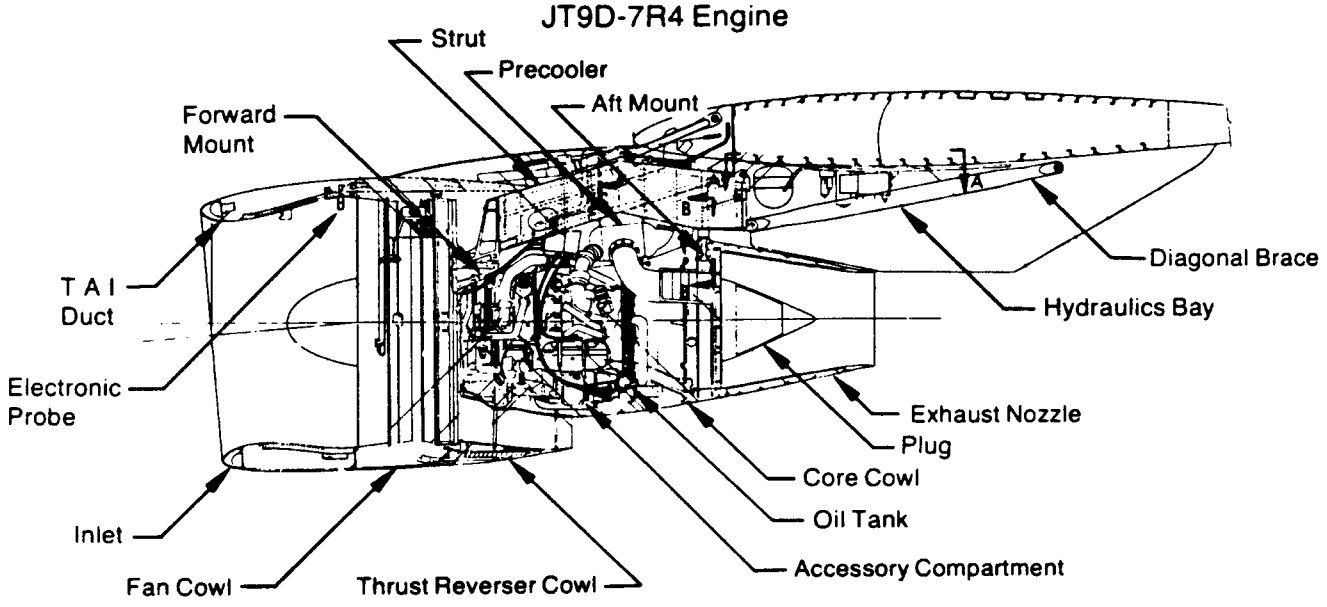

Figure 6.77 Nacelle/Engine Installation in the Boeing 767

Examples of fuselage mounted nacelles are found in the B727 and the McDD DC9. Figure 6.78 shows the 727 installation. Note the buried center engine: this requires a long duct which causes some loss in pressure recovery as well as a weight increase. Even high bypass ratio fans can be installed in this manner. The L1011 installation of Figure 6.79 is an example. An interesting contrast to this arrangement is that of the center engine of the McDD DC10 shown in Figure 6.80.

The DC10 center engine installation eliminates the need for a long inlet duct but complicates the design of the vertical tail.

In fighter airplanes the engines are normally buried in the fuselage. The A10 of Figure 3.27c in Part II is an exception.

Figures 6.81 and 6.82 are examples of subsonic fighter engine installations.

In supersonic fighters the installation is complicated because of the requirement of inlet shock management. Figures 6.83 through 6.85 show examples of supersonic installations. For best efficiencies at Mach numbers of 2.0 and above variable geometry inlets are required. The F15 inlet of Figure 6.84 has a variable ramp inlet.

Supersonic transports above Mach 2.0 also require vaiable geometry inlets. The Concorde inlet of Figure 6.86 illustrates such a system.

References 65 and 78 contain discussions of the characteristics of various types of inlets. Part VI also addresses this question.

6.9.4 Propfan and Ultra-bypass Installations

These installations are currently in the preliminary design and development stage. It appears likely that 'range-payload' driven airplanes will be strong candidates for these engines.

Figures 6.87 show several proposed propfan installations arranged as tractors. Counter rotating arrangements are also possible: Figure 6.88 shows a tractor and a pusher installation.

Figure 6.89 puts the large propfan diameter in

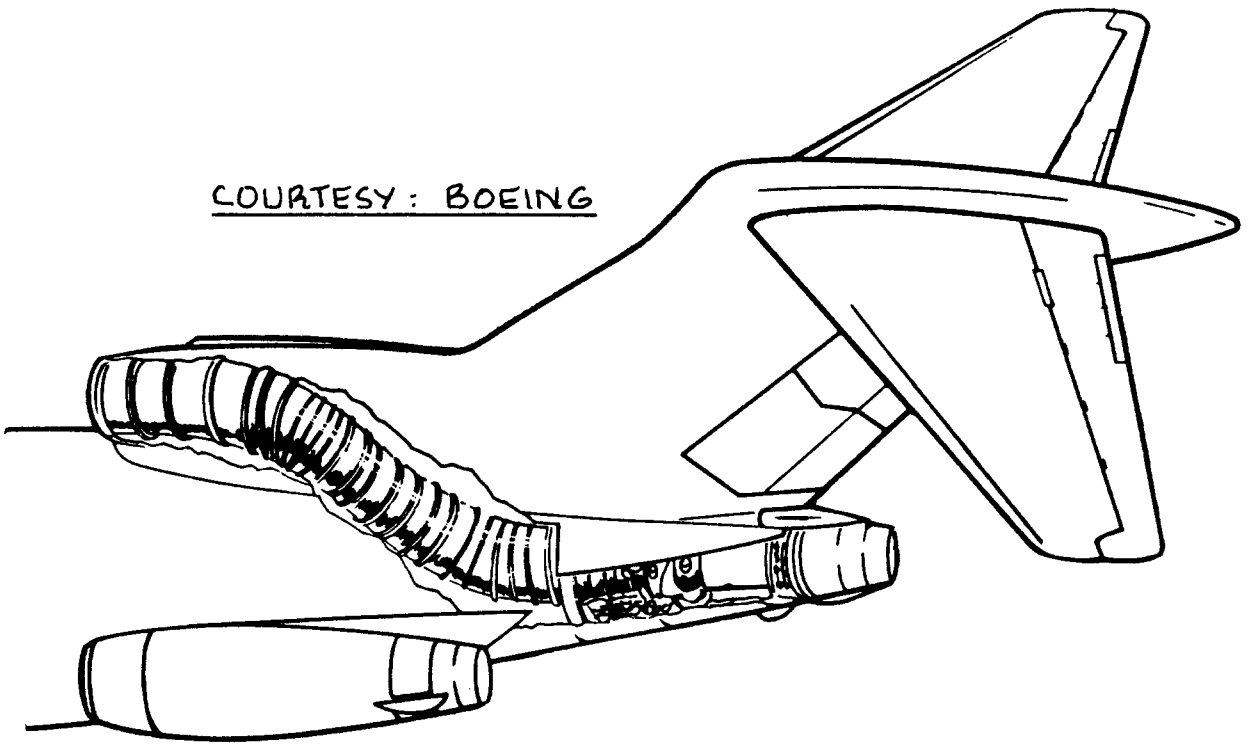

Figure 6.78 Center Engine Installation in the Boeing 727

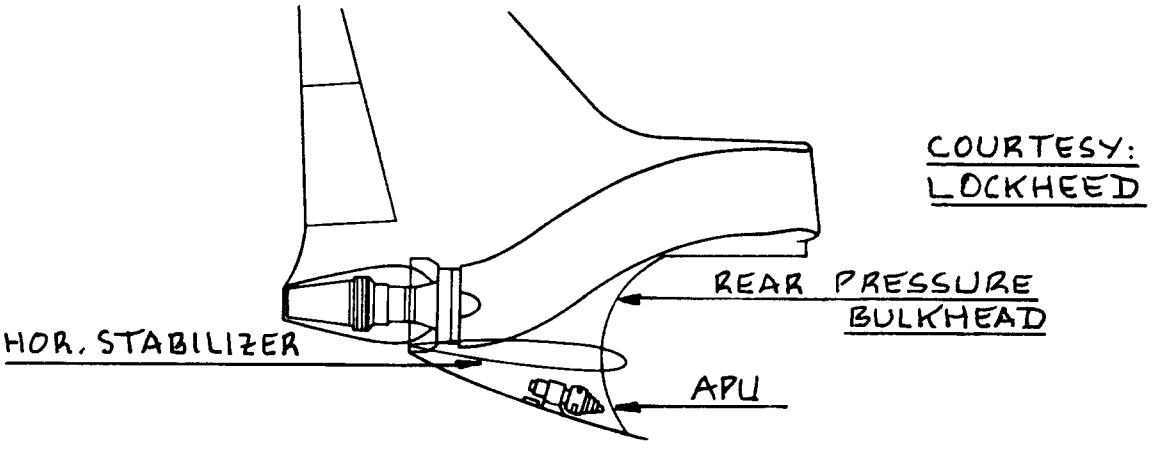

Figure 6.79 Center Engine Installation in the Lockheed L-1011

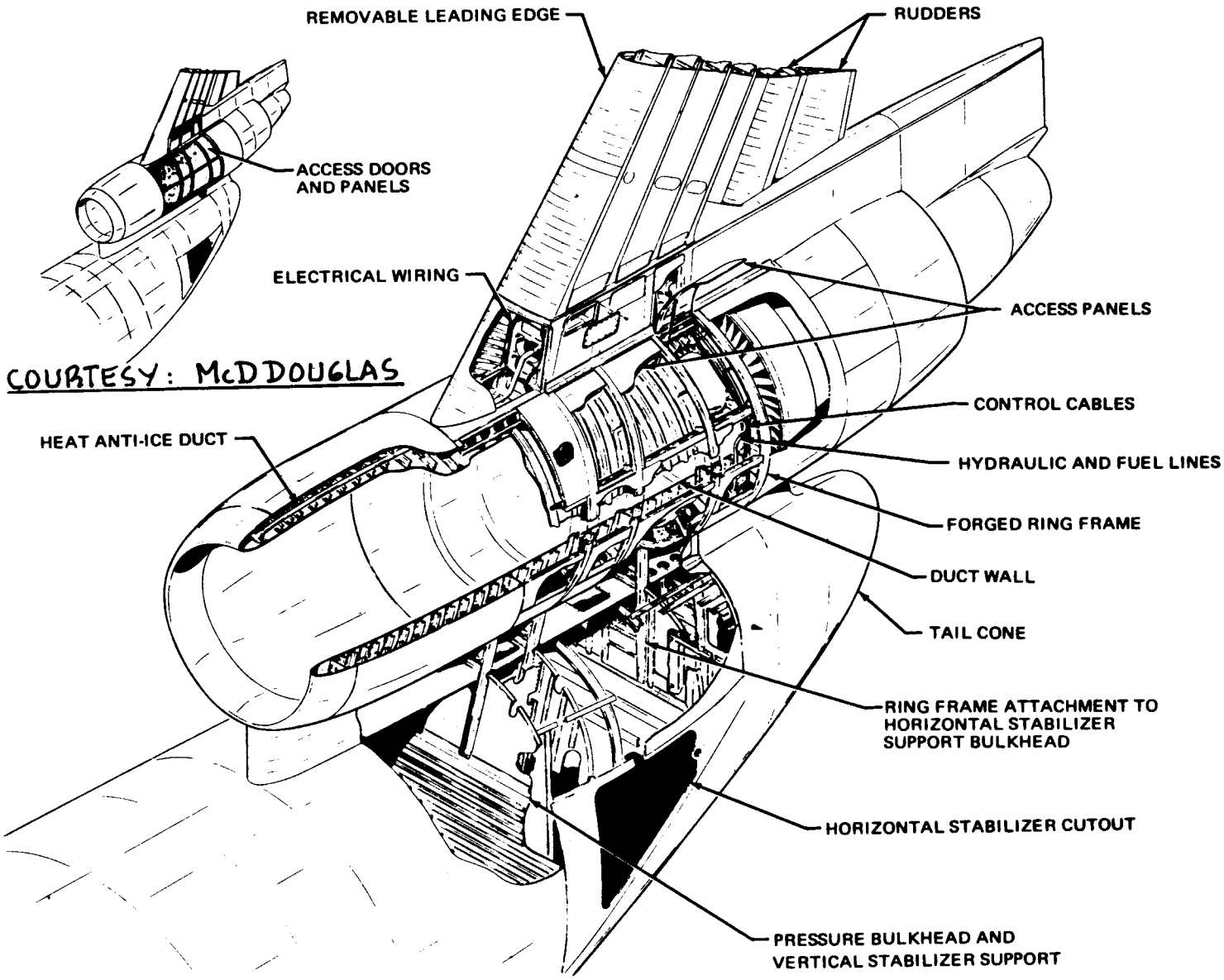

Figure 6.80 Center Engine Installation McDD DC10

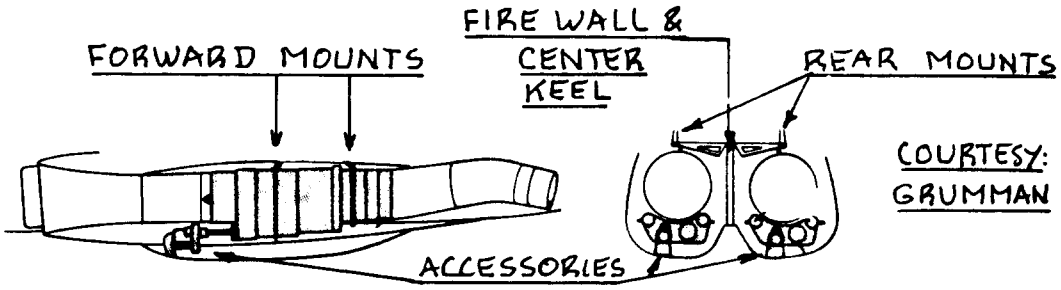

Figure 6.81 Subsonic Engine Installation: Grumman A6

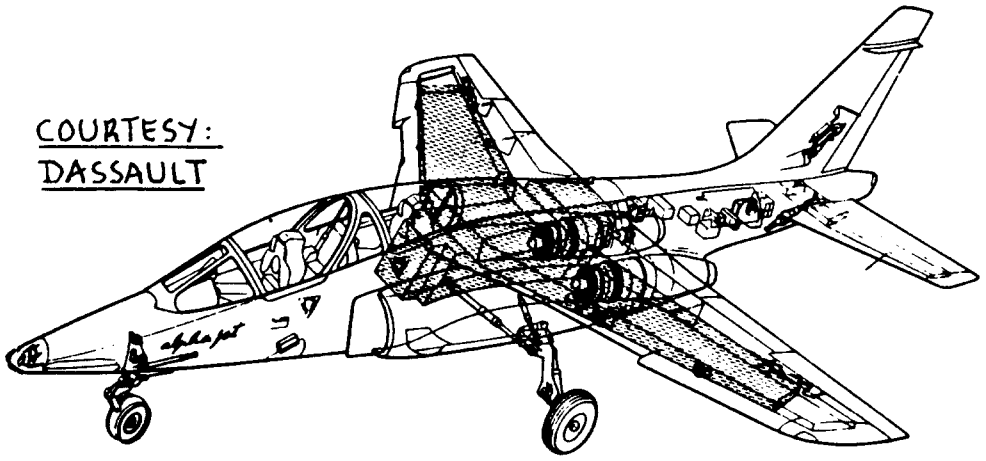

Figure 6.82 Subsonic Engine Installation: DBD Alphajet

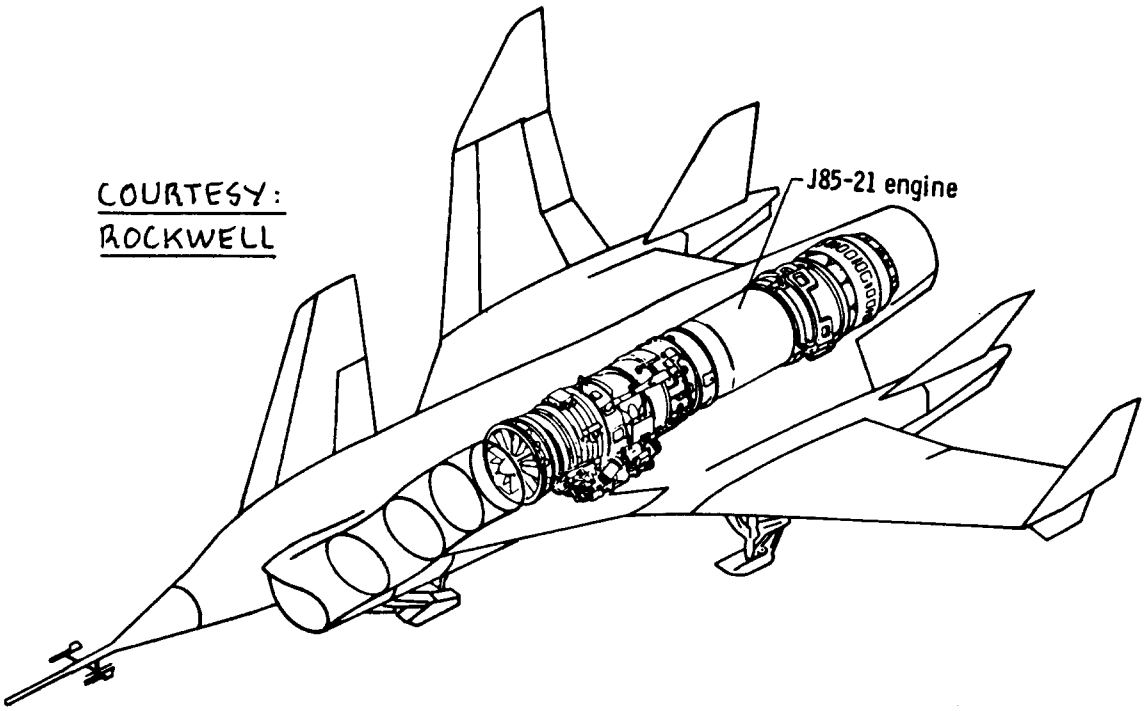

Figure 6.83 Subsonic Engine Installation: Rockwell HiMat

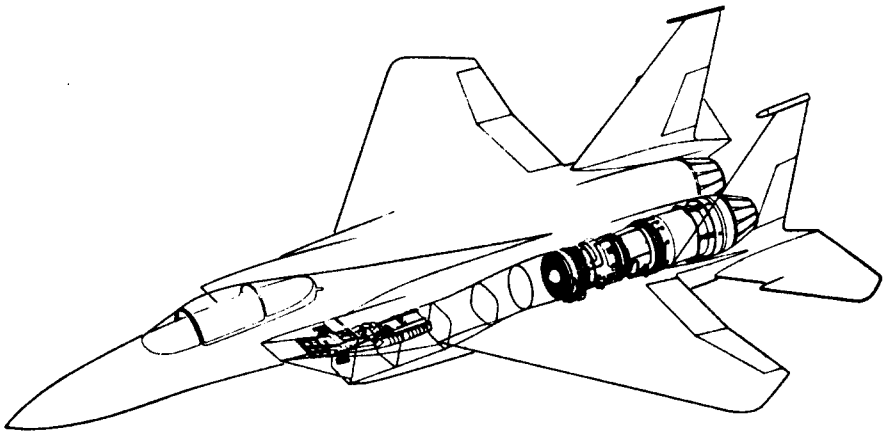

COURTESY:
McDONNELL DOUGLAS

Figure 6.84 Supersonic Engine Installation: McDD F15

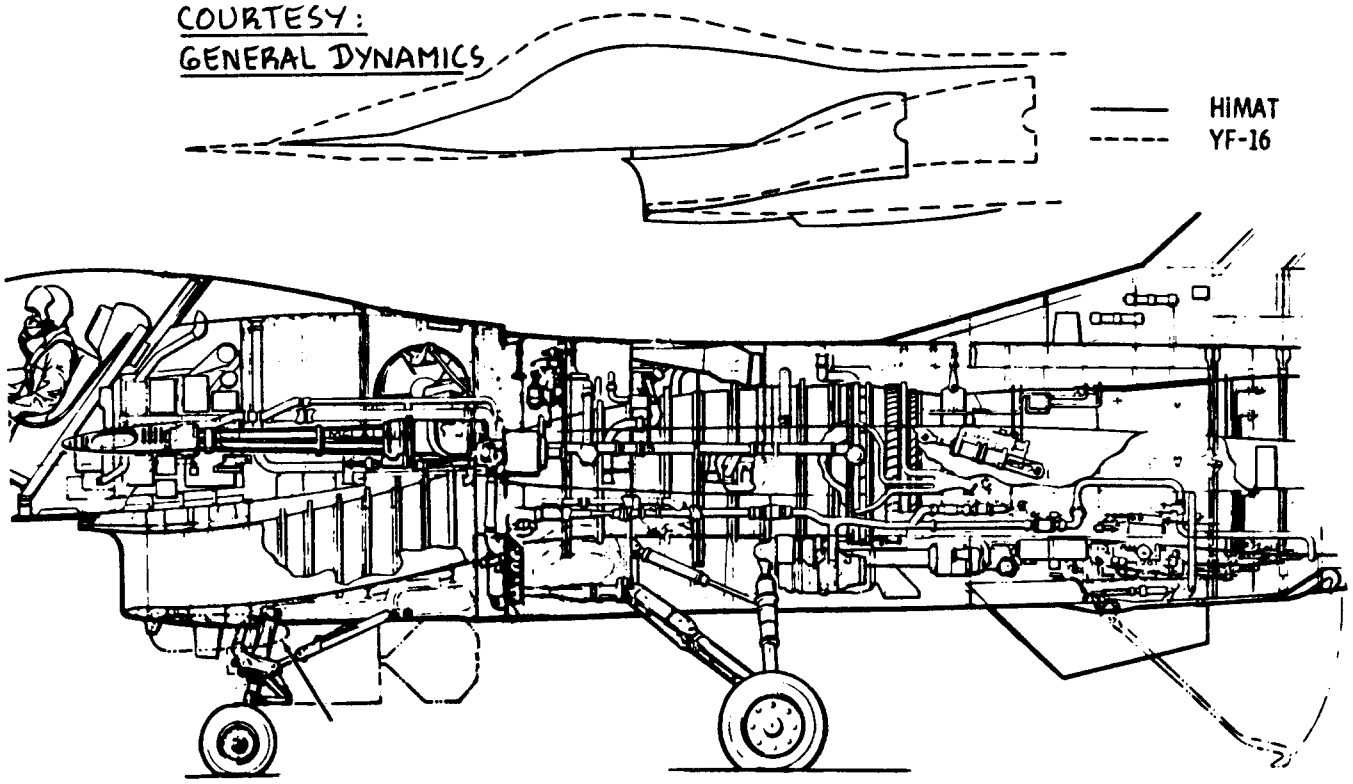

Figure 6.85 Supersonic Engine Installation: GD F16

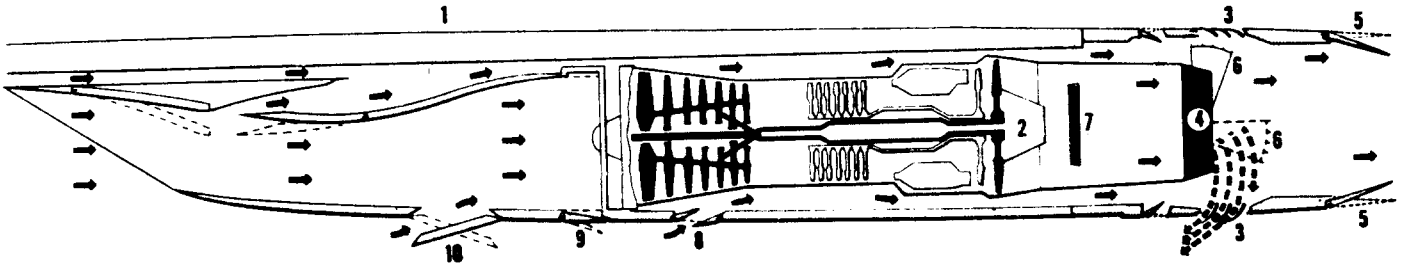

LEGEND:

1. WING
2. TURBINES
3. THRUST REVERSERS
4. PRIMARY NOZZLE
5. SECONDARY NOZZLE
6. THRUST REV. BUCKET
7. AFTERBURNER
8. COOLING AIR FLAP
9. BYPASS FOR EXCESS AIR
10. INLET FOR EXTRA AIR

Figure 6.86 Supersonic Engine Installation: Concorde

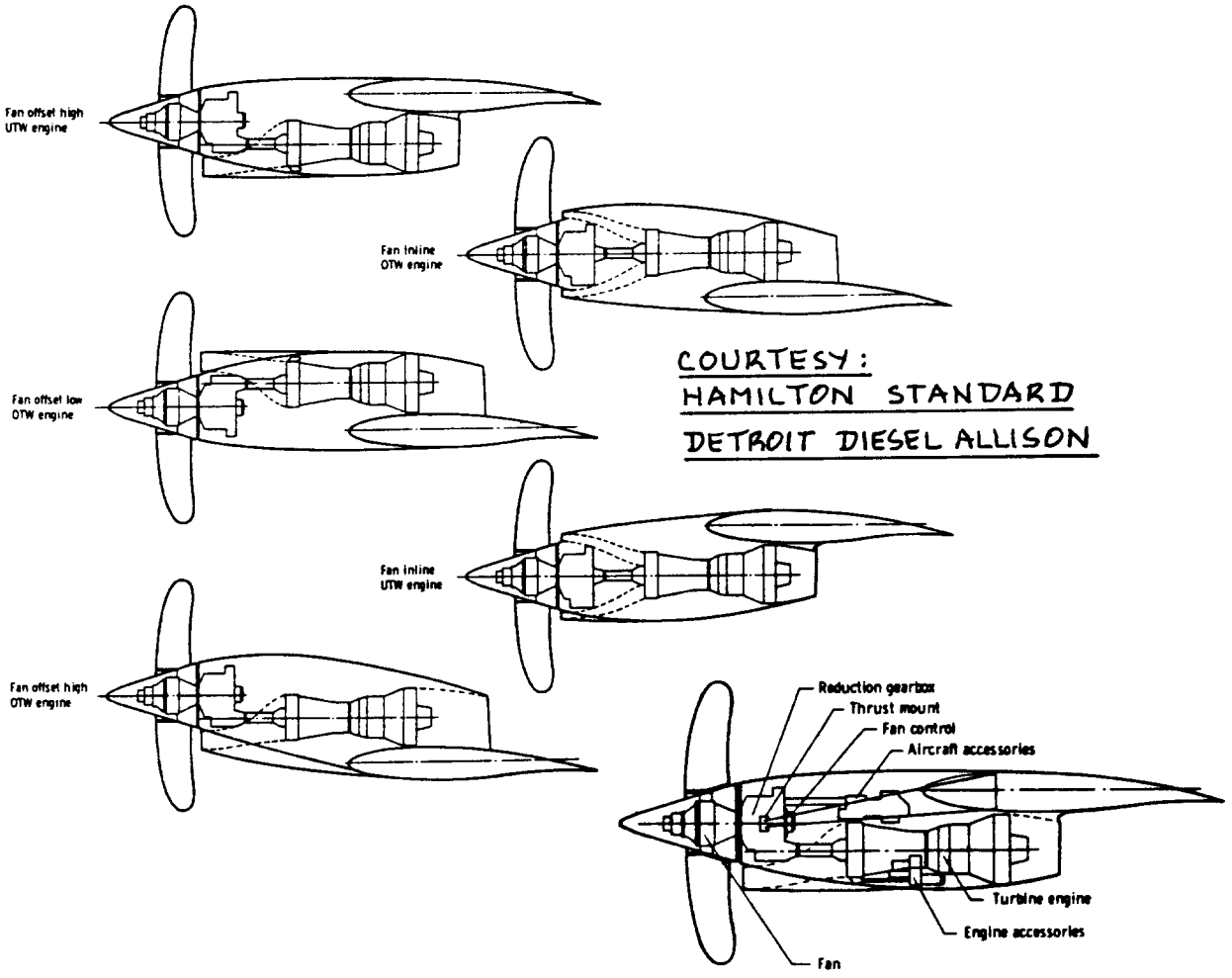

Figure 6.87 Single Rotating Propfan Installations

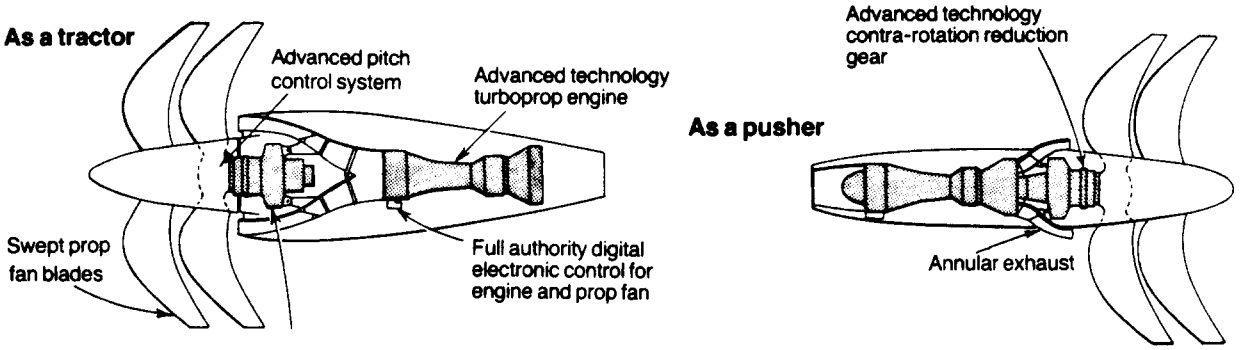

COURTESY: PRATT & WHITNEY

Figure 6.88 Counter Rotating Propfan Installations

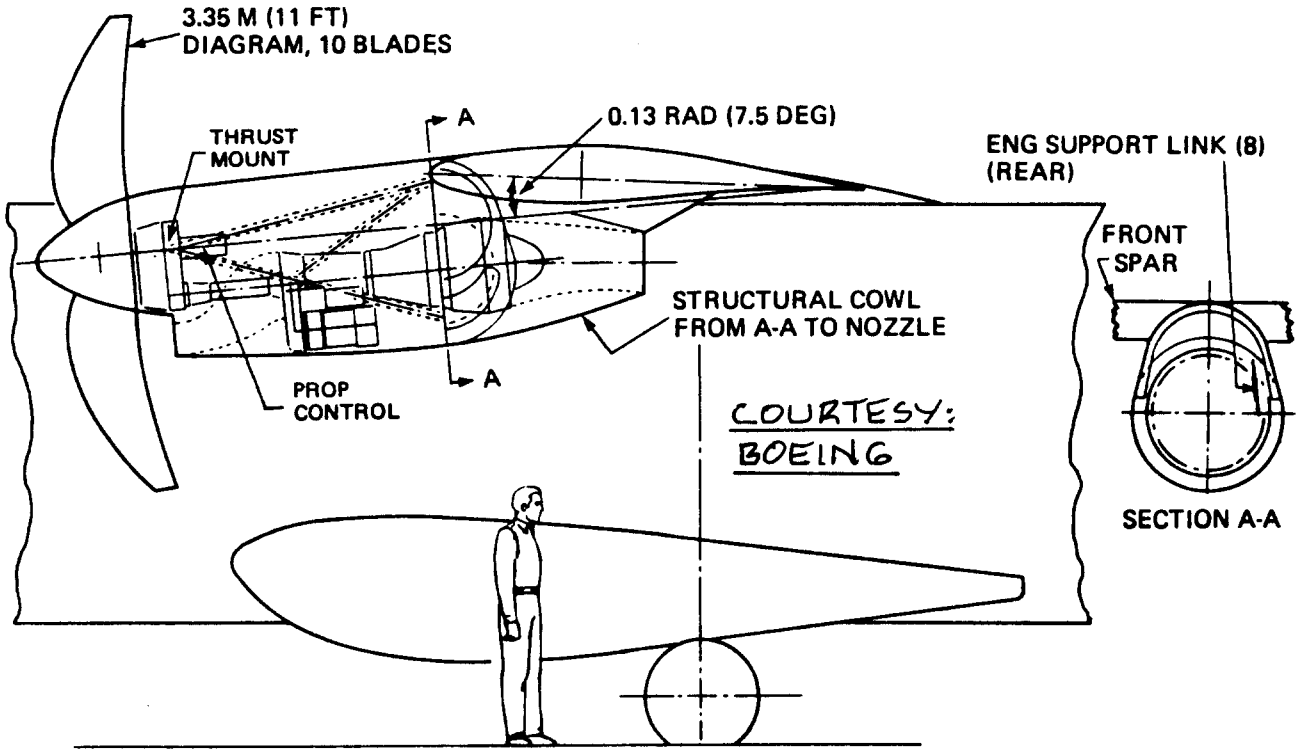

Figure 6.89 Propfan Installation in a High Wing Commuter

perspective in a small commuter transport proposal.

A variant of the propfan is the General Electric ultra-bypass-engine (UBE), shown in the proposed Boeing 7J7 in Figure 6.90. Figure 6.91 shows a tractor and a pusher arrangement for the UBE powerplant.

6.9.5 Nozzles and Thrust Reversers

All jet engines must have exhaust nozzles to generate thrust. Figures 6.77 through 6.86 all show such nozzles. A close-up view of a typical nozzle installation is given in Figure 6.92.

A desirable feature of most exhaust systems is that they be reversible for landing operations. Although this adds complexity to the nozzle installation such reversers are incorporated in most transports to provide improved slowdown capability. The latter is essential when operating on slick surfaces such as icy runways. Figures 6.93 through 6.95 show example installations on transports.

Even some fighters use thrust reversers: the SAAB 37 Viggen is an example. Figure 6.96 shows its thrust reverser installation.

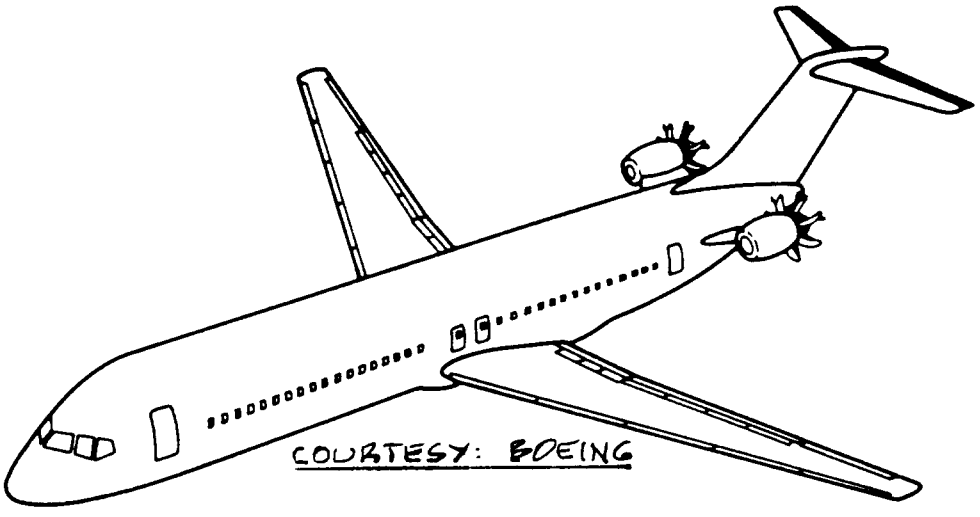

Figure 6.90 Ultra Bypass Engine Installation: Boeing 7J7

COURTESY : GENERAL ELECTRIC

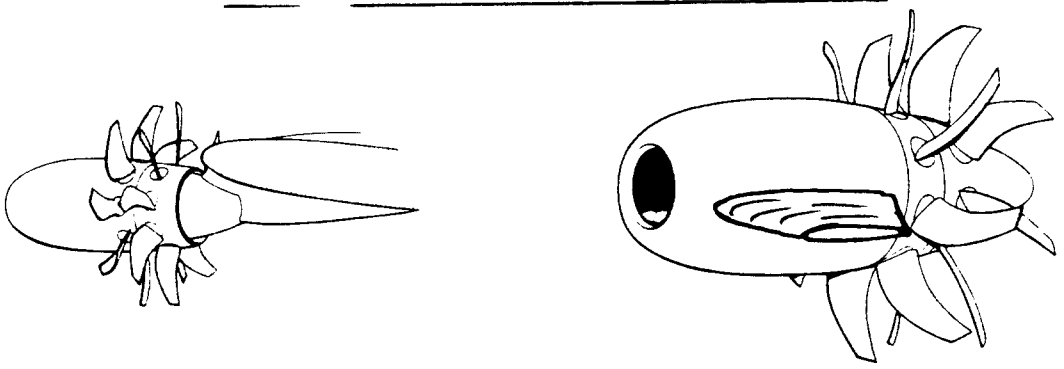

TRACTOR
STING MOUNT

PUSHER
PYLON MOUNT
(SEE FIG. 6.90)

Figure 6.91 Ultra Bypass Engine Arranged as Pusher or as Tractor

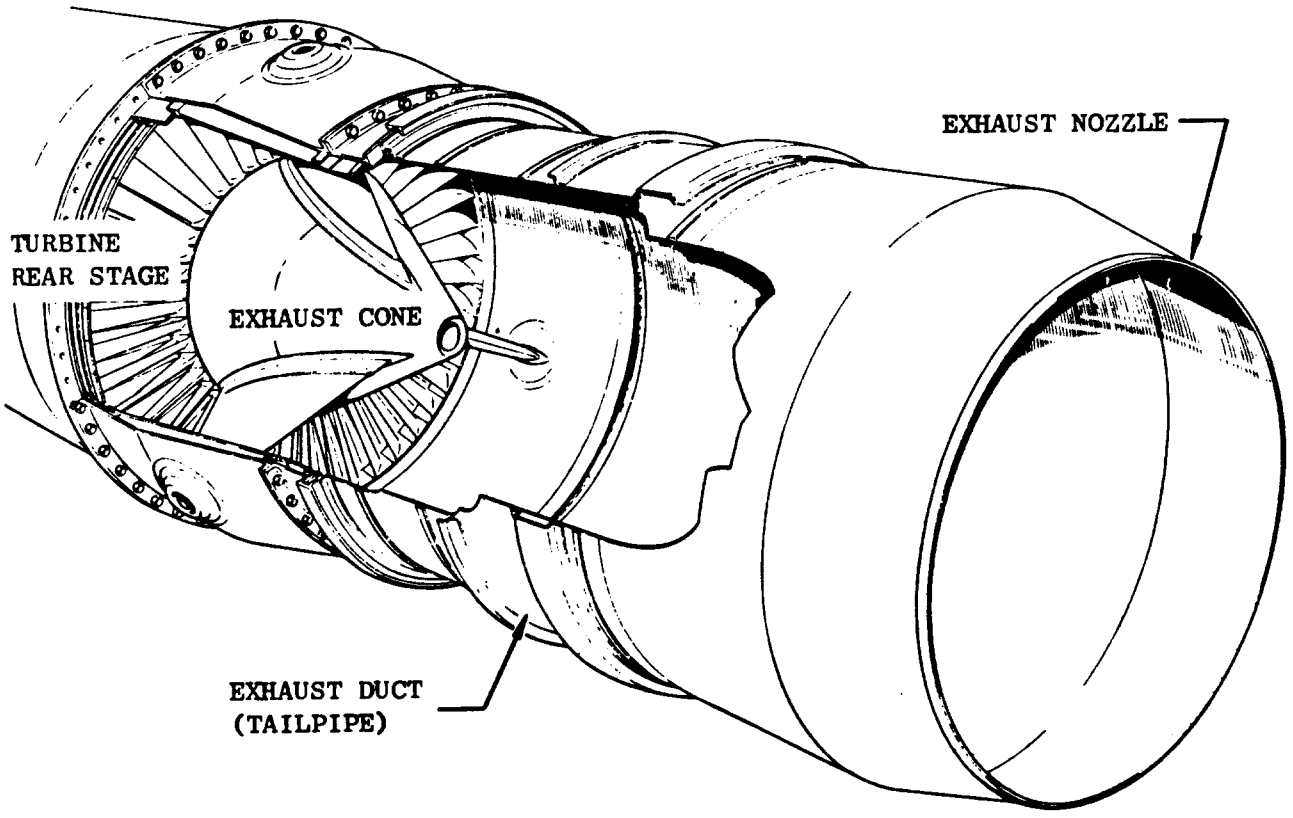

Figure 6.92 Typical Turbojet Exhaust Nozzle Arrangement

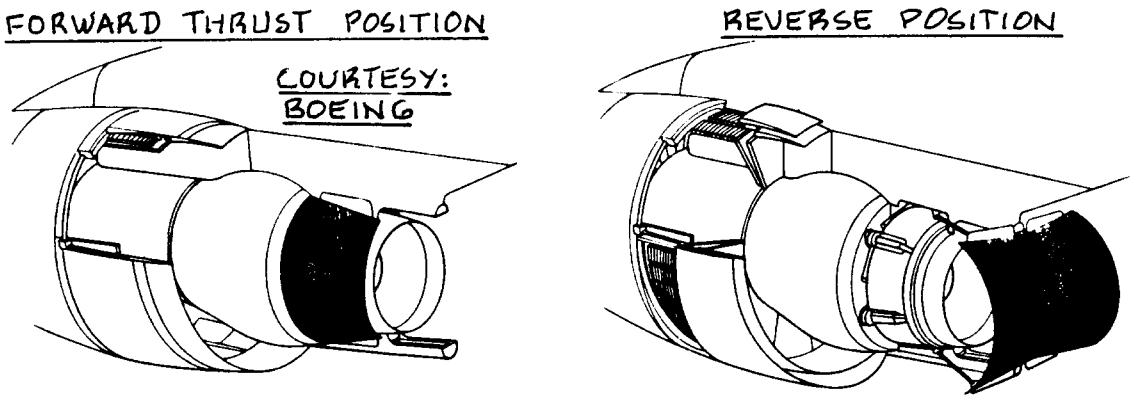

Figure 6.93 Thrust Reverser Installation: Boeing 747

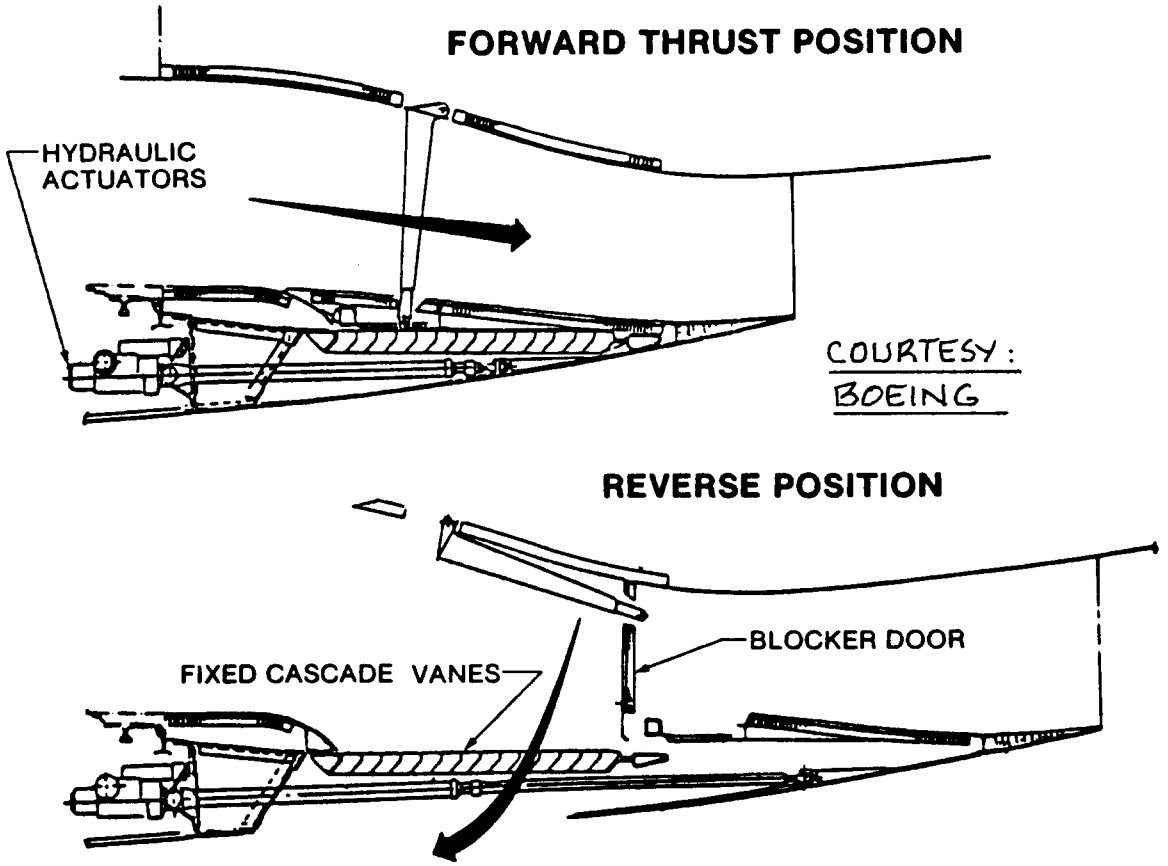

Figure 6.94 Thrust Reverser Schematic: Boeing 757

Figure 6.95 Thrust Reversers: Lockheed Jetstar

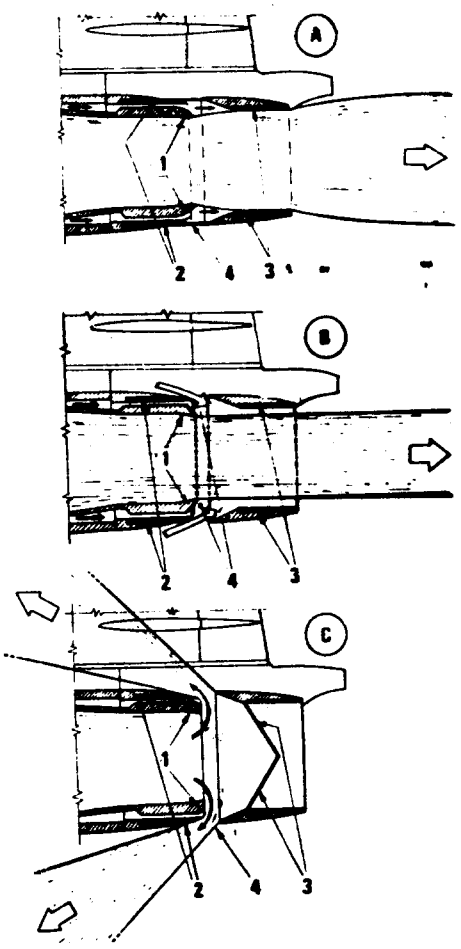

A MAXIMUM THRUST

B CRUISE THRUST

C REVERSE THRUST

1. VARIABLE PRIMARY NOZZLE
2. THRUST REVERSER SLIDE
3. THRUST REVERSER CLAMSHELL DOORS
4. THRUST REVERSER NOZZLES

Figure 6.96 Thrust Reverser: SAAB 37 Viggen

7. PRELIMINARY STRUCTURAL ARRANGEMENT, MATERIAL SELECTION AND MANUFACTURING BREAKDOWN

The purpose of this chapter is threefold:

1. to provide a logical method for arriving at a reasonable structural arrangement: Step 19 in Chapter 2 of Part II.

2. to provide a preliminary basis for the selection of structural materials.

3. to provide data for deciding on a manufacturing breakdown.

Sections 7.1 through 7.3 present discussions of these subjects.

7.1 PREPARING A PRELIMINARY STRUCTURAL ARRANGEMENT*

Before a structural arrangement can be decided upon, it is required that the following is available:

1. A dimensioned threeview, including an indication where all moving surfaces are.

From Step 15 in p.d. sequence I (p.17, Part II) a dimensioned threeview of the proposed design is available. For examples, see Chapter 13 of Part II.

2. A weight and balance calculation and the resulting c.g. excursion diagram.

From Steps 10-13 in p.d. sequence I (p.15-16, Part II) a weight and balance analysis is available.

With the threeview and the weight and balance analysis at hand, it is suggested that the following steps be taken:

Step 1: On all lifting surfaces, identify the moving control surfaces and/or the flaps. Locate the rear and the front spar of each lifting surface so that a sufficient amount

---

* This section is based on suggestions made to the author by Dr.H.W.Smith of the Department of Aerospace Engineering of The University of Kansas.

of room is available for hinges and/or for tracks. Draw in these spar locations.

Note: the information needed to do this, is available after carrying out Steps 6,7 and 8 of p.d. sequence I (p.12-14, Part II). Preliminary design procedures for the wing, for the layout of high lift devices, for the empennage and for control surface layouts are presented in Chapters 6,7 and 8 in Part II.

Step 2: Carry the spars, which form the so-called torque boxes of the structure of the lifting surfaces through to where they intersect with the fuselage. At the point of intersection of these spars with the fuselage, draw in the required fuselage frames or bulkheads.

Note: in most airplanes the torque box actually passes through the fuselage (at the top or at the bottom). Several wing design examples which illustrate this are given in Chapter 4.

Step 3: Determine the location of major structural cutouts for such items as doors and emergency exits. Draw in the necessary frames. If these cutouts are in the wing or in another lifting surface then ribs need to be drawn in at those locations.

Note: in fuselages there are specific requirements for doors and for exits. These requirements MUST be adhered to! However, they strongly impact the location and spacing of fuselage frames and longerons.

Examples of door and exit requirements and specific layouts which satisfy these requirements are given in Chapter 3.

Step 4: Determine the location of the landing gears.

Note: this information is available after carrying out Step 9 of p.d. sequence I (p.14-15, Part II). A preliminary design procedure for landing gear design is presented in Chapter 9 of Part II.

a) If the gears are attached to the fuselage, then it will be necessary to support the attachment points with frames or bulkheads. Draw these in.

b) If the gears are attached to the wings, then it

will be necessary to draw in local ribs to support the attachment points. Draw these in.

Part IV contains more details on the subject of landing gear design as well as specific examples of landing gear arrangements and layouts.

Step 5: Determine the location of the powerplants. From engine manufacturer's data, locate where on the engine the attachment pads are. It is at these points that the engines will be attached to surrounding structure.

Note: this information is available after carrying out Step 5 of p.d. sequence I (p.12 of Part II). A procedure for the preliminary integration of the propulsion system into the airframe is contained in Chapter 5 of Part II.

a) If the powerplants are attached to the wing then locally, ribs for attachment are required. Draw these in.

b) If the powerplants are attached to the fuselage, for example with the help of pylons, then locally frames or bulkheads are required. Draw these in.

Chapter 6 contains examples of many types of engine installations.

Step 6: Determine where major masses (other than powerplants) are located.

Examples of major masses are:

a) Guns, pods and bombracks: these normally require extra ribs and/or frames. Typical wing 'hard point' requirements are discussed in Chapter 4.

b) Radar antennas: depending on their size, these may require extra frames or bulkheads for attachment.

c) special fuel tanks and/or hoppers: these may require extra ribs, spars, frames and/or bulkheads.

d) passenger seats: these require tracks to move on and to attach to. These tracks in turn are mounted on stiffened floors. See Ch.3 for floor design examples.

f) concentrated payloads such as large vehicles and/or machine equipment: these require special floor

strengthening and special tie-down provisions to prevent accidental 'sliding' of the payload. All this usually results in the need for special structural provisions in the form of longerons, frames, ribs and/or spars. See Chapter 3 for cargo floor design examples.

g) auxiliary power units (APU): these require special installation provisions and firewalls. Part IV deals with APU installations.

Draw in the required ribs, frames, bulkheads and floor beams to account for ALL major masses.

For data on typical spacings, see the following chapters:

Chapter 3 for fuselage framedepths, frame spacings and longeron spacings.

Chapter 4 for typical wing rib spacings.

Chapter 5 for typical empennage rib spacings.

Step 7: Locate the pressure bulkheads and draw those in.

Note: pressure bulkheads are required in most transports and fighters. See Chapter 3 for examples of pressure bulkhead arrangements.

Step 8: Draw in the major fuselage cross sections.

Note: major cross sections, from a structural arrangement viewpoint are those where intersections with other major structural components occur. Major cross sections are also those, where major cutouts, such as doors and windows, occur.

In each of these cross sections, locate where longerons need to be placed and draw them in.

Examples of fuselage cross section design are found in Chapter 3.

Step 9: Take a good look at the resulting 'skeleton structure' and see if any items can be relocated such that structural synergism can be achieved.

The following examples illustrate what is meant by 'structural synergism'.

Synergism Example 1: Where the vertical tail and horizontal tail spars intersect the fuselage, four frames could be required. It would save a lot of weight if they could both attach to the same two frames. It is not always possible to achieve this, but it certainly is a desirable target to shoot for. If the front spars of both tails can be made to intersect the fuselage at the rear pressure bulkhead, additional weight savings will accrue.

Synergism Example 2: Placement of the landing gear was dictated by a number of nonstructural considerations, as seen in Chapter 7. It would save weight, if the landing gear locations could me made to coincide with already existing major structural components.

Step 10: In the spaces between the frames, bulkheads, spars, ribs and longerons, it is normally necessary to install minor similar items. The spacings for these items differ from one airplane type to another.

The following general rules can be used in a preliminary layout:

For fuselage frames typical frame spacings are: 18 inches for transports and 24 inches for general aviation airplanes.

For wing ribs typical rib spacings are: 24 inches for transports and 36 inches for general aviation airplanes.

For fighter and military trainer airplanes the spacings vary considerably, depending on the mission and on the design flight envelope.

Draw in these additional structural items.

This completes the initial structural arrangement.

For additional guidance in preparing a structural arrangement, the reader is encouraged to consult the inboard profile drawings in Chapter 3 (p.154-162), the structural arrangement drawings in Chapter 4 (p.244-248) and the cut-away drawings in Chapter 8.

Next, attention needs to be focussed on material selection and on manufacturing breakdown. These topics are covered in Sections 7.2 and 7.3 respectively.

7.2 PRELIMINARY SELECTION OF STRUCTURAL MATERIALS

The following considerations determine which materials are selected in the structural design of an airplane:

1. Design strength to weight ratio
2. Fatigue characteristics
3. Crack propagation behavior
4. Dominant failure mode(s)
5. Damage and corrosion tolerance and/or resistance
6. Familiarity and experience with a given matarial
7. Existing manufacturing facilities
8. Cost of material
9. Manufacturing cost
10. Customer requirements

These considerations are not listed in an intended order of importance.

Table 7.1 presents a list of typical airplane structural materials which are in use. The reader should consult the following materials for information on the use of structural materials:

For light airplanes: pages 132, 133, 219, 238, 276 and 286.

For fighter airplanes: Figures 7.1 and 7.2a-b.

For transport airplanes: Figures 7.3a-d.

References 12,20,31,79,80 and 81 contain data which provide further insight into the problem of airplane material selection.

Table 7.1 Examples of Use of Airplane Materials (Data Source: Ref. 82)

Material	Aluminum	Steel	Titanium	Composites
Shapes and Forms	Sheet Extrusions Plate Forgings Tubes	Sheet Extrusions Plate Forgings Tubes	Sheet Extrusions Plate Forgings Tubes	Sheet Extrusions Plate Forgings Tubes
Typical Airplane usage	Skins Spar webs and Spar caps Stiffeners Control surfaces and flaps Fittings	Engine and/or fuselage trusses Landing gear, system and engine parts	Skins Stringers and spars Stiffeners Fittings	Skins Spar webs and spar caps Stiffeners Control surfaces and flaps Fairings
Major design consideration	Light weight Corrosion resistant	High strength Suited for high temp.	High strength Suited for high temp. Expensive and difficult to manufacture	Light weight Can be layed up in any shape Low temp. Needs anti-lightning
Commonly used Alloys	2024-T3, T8, T81 T861, 2124-T3, T8 6061-T6 7075-T73, T76 7175-T73, 76 7050-T736, T76 T73, T736	Stainless Steels 5Cr-Mo-V AlSi4340 300M	Ti-140A, Ti-155A Ti-4Al-3Mo-V Ti-8Al-Mo-V Ti-6Al-25N-4Zr-2Mo	Graphite epoxy Kevlar Fiberglass Boron Aluminum

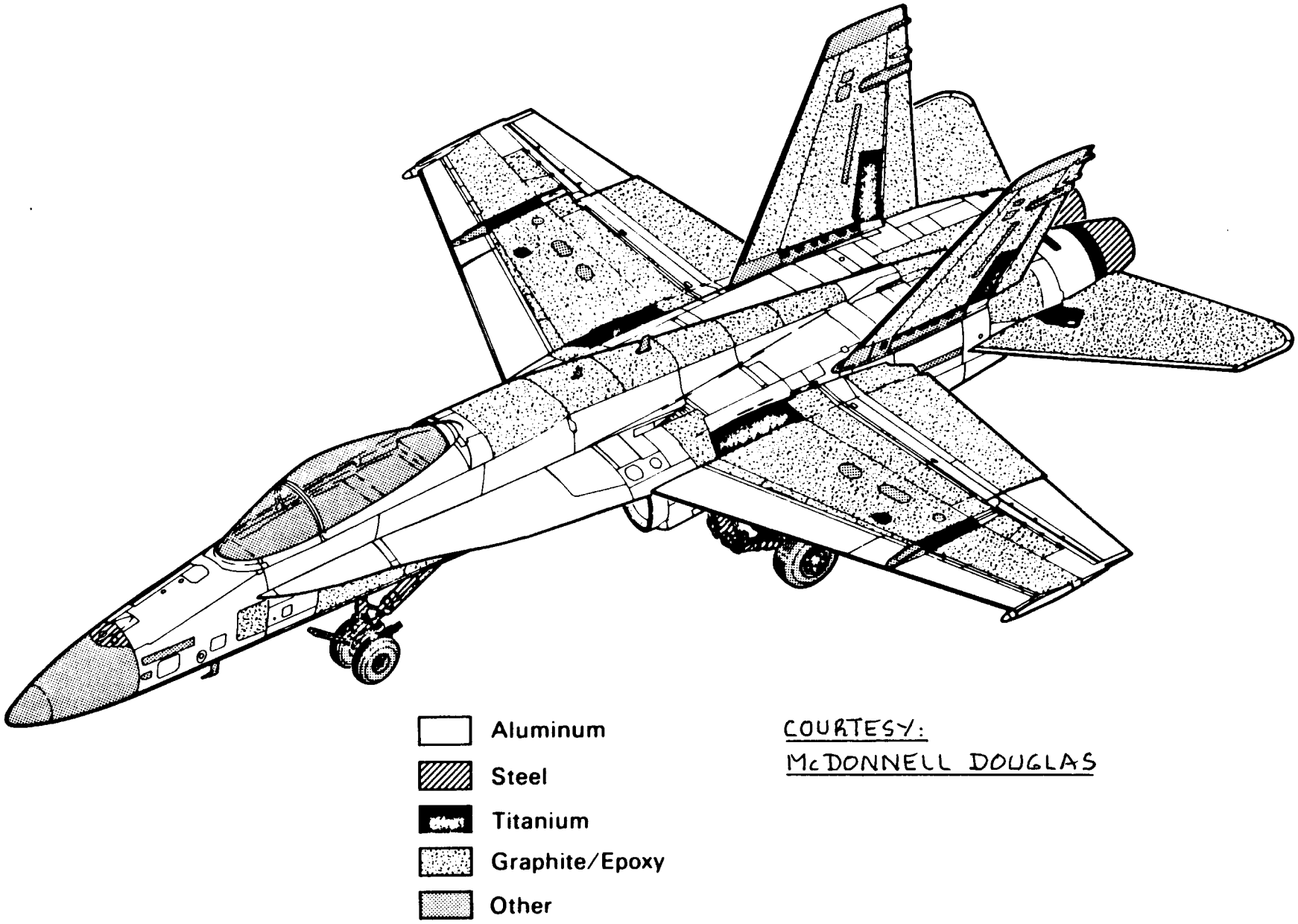

Figure 7.1 Material Distribution: McDonnell Douglas F-18

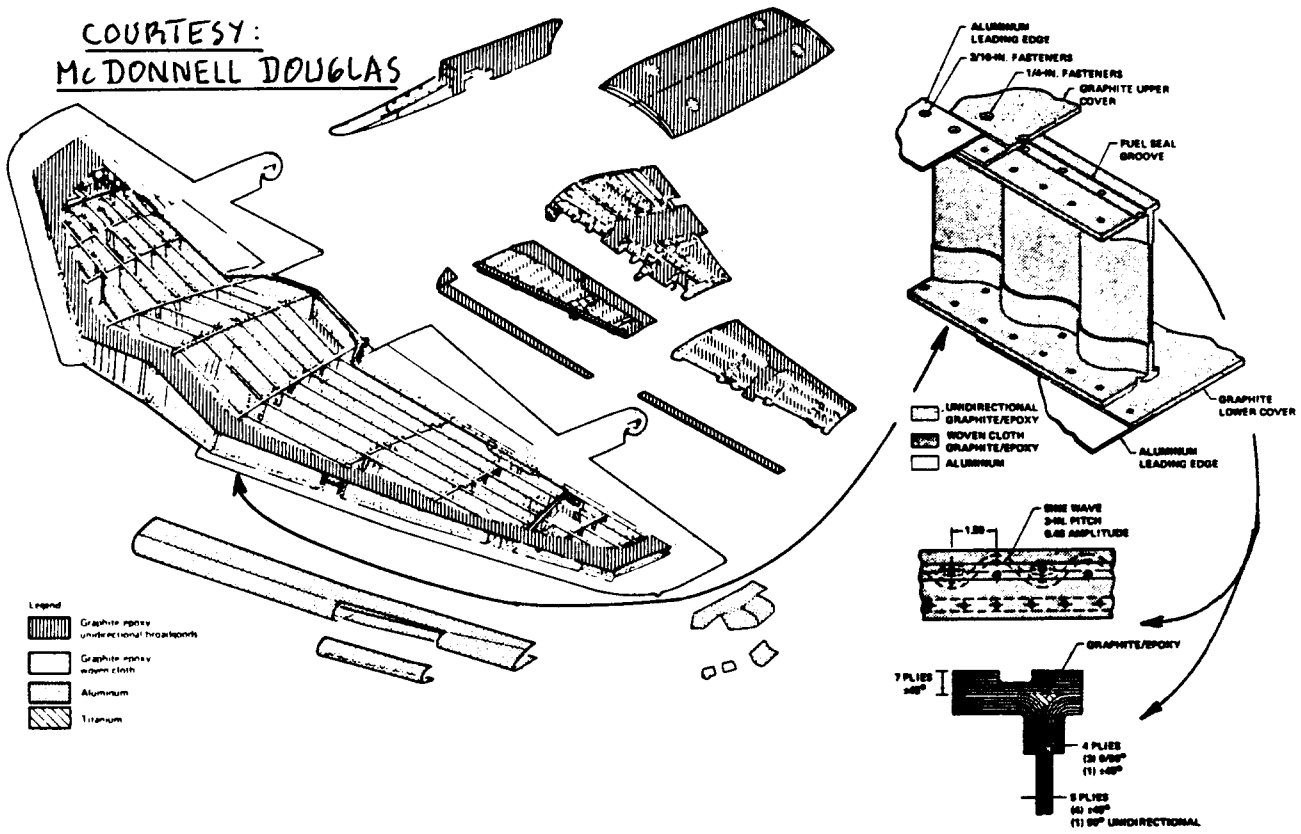

Figure 7.2a Material Distribution, Wing: McDD AV-8B

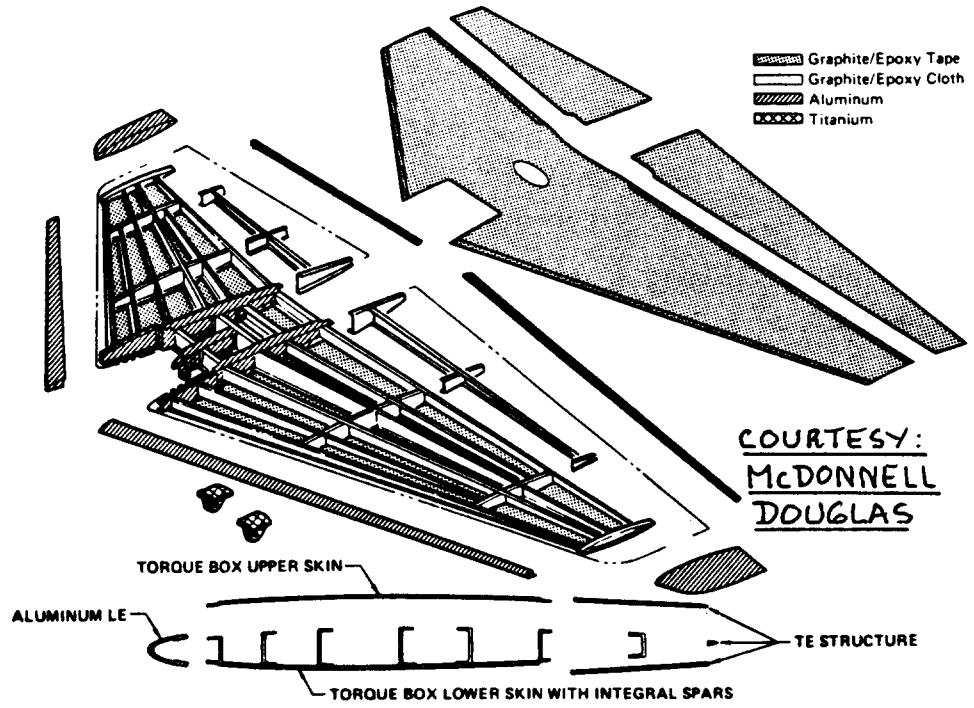

Figure 7.2b Material Distribution, Hor. Tail: McDD AV-8B

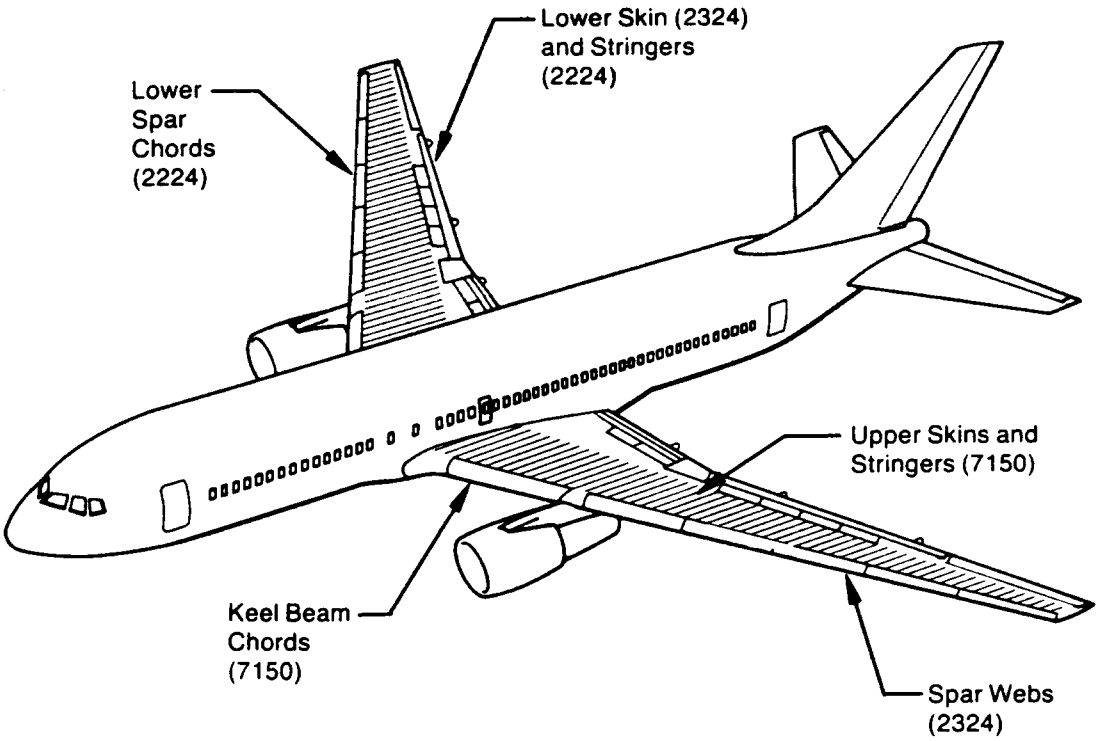

COURTESY: BOEING

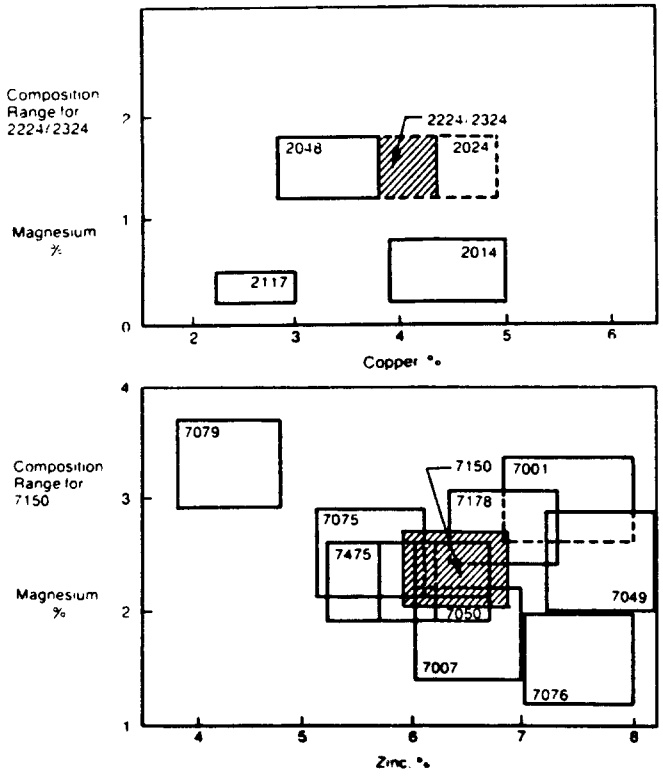

- Alloy designations 2224/2324 and 7150
- Similarity to conventional alloys (2024 and 7075)
  - Narrower composition ranges
  - Modified milling procedures
- Improved strength
  - 2224/2324 ..... 5 to 8%
  - 7150 ..... 11 to 13%
- Equivalent fatigue, toughness, and corrosion resistance

Figure 7.3a Aluminum Usage: Boeing 767-200

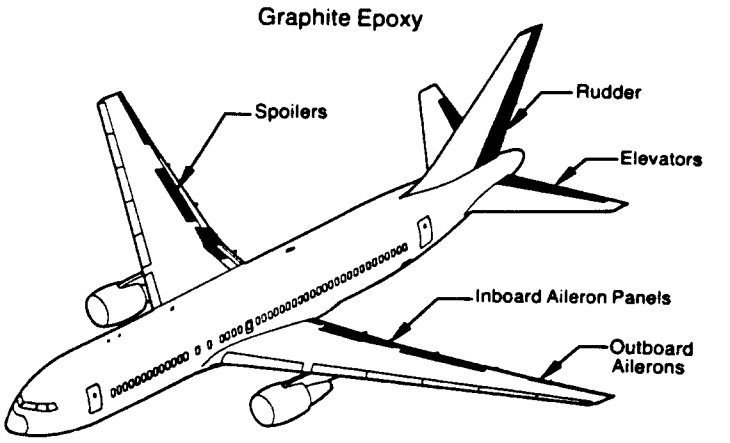

COURTESY: BOEING

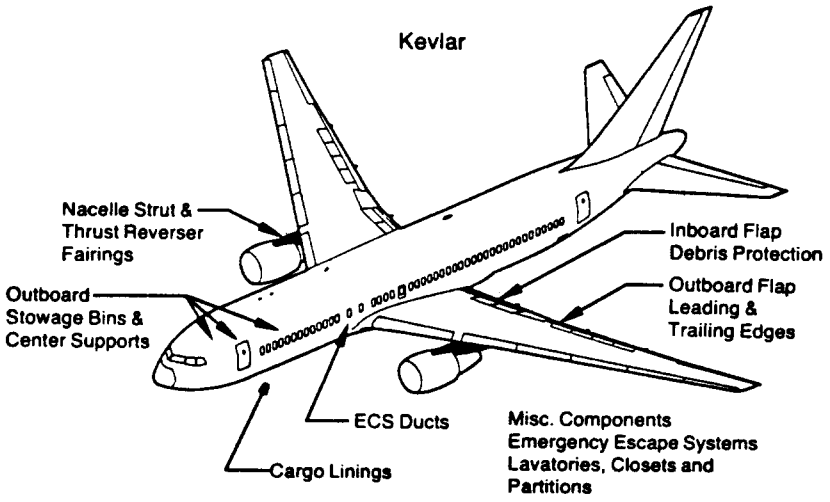

Hybrid Composite (Kevlar/Graphite)

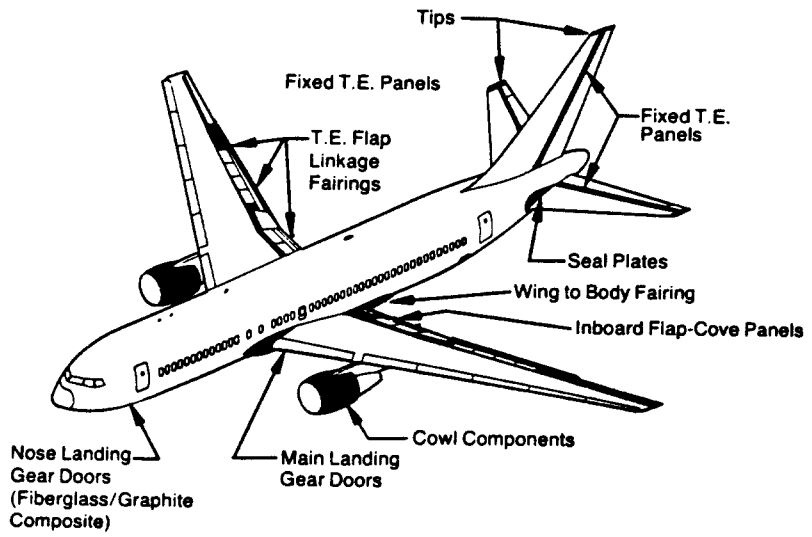

Figure 7.3b Advanced Composites Usage: Boeing 767-200

Material	Application
Graphite/Epoxy	Inboard Aileron Outboard Aileron Inboard and Outboard Spoilers Rudder Elevator
Hybrid (Kevlar/Graphite) Hybrid (Fiber-Glass/Graphite	Fixed Panels-Wing T.E. Cowls-Thrust Reverser, Inlet and Fan Fairing-T.E. Flap Linkage Cove Panels-Inbd T.E. Flap Wing/Body Fairing Landing Gear Doors-Body Fixed T.E. Panels, Tip-Empennage Seal Plates-Stabilizer Nose Landing Gear Doors (Graphite Weight Only)
Kevlar	ECS Ducts Cargo Liner Outboard Stowage Bins & Center Stowage Supports Emergency Escape System Lavs, Closets, & Partitions Fairings-Engine Pylon Outboard Flap-L.E. and T.E. Inboard Flap-Debris Protection Fairing-Thrust Reverser

Composite Applications Example
Main Landing Gear Door
(Kevlar/Graphite Composite)

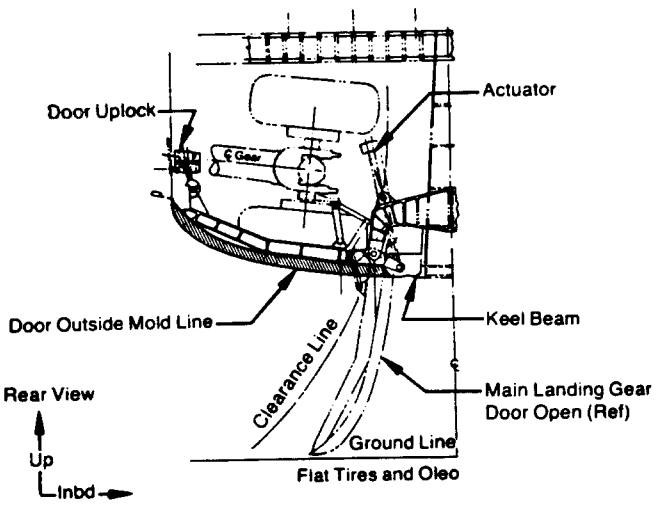

COURTESY: BOEING

Figure 7.3c Composites Applications: Boeing 767-200

COURTESY: BOEING

Fiberglass Usage

- Durable
- Lightweight
- Sonic and buffet resistant
- Easily repairable
- Corrosion resistant

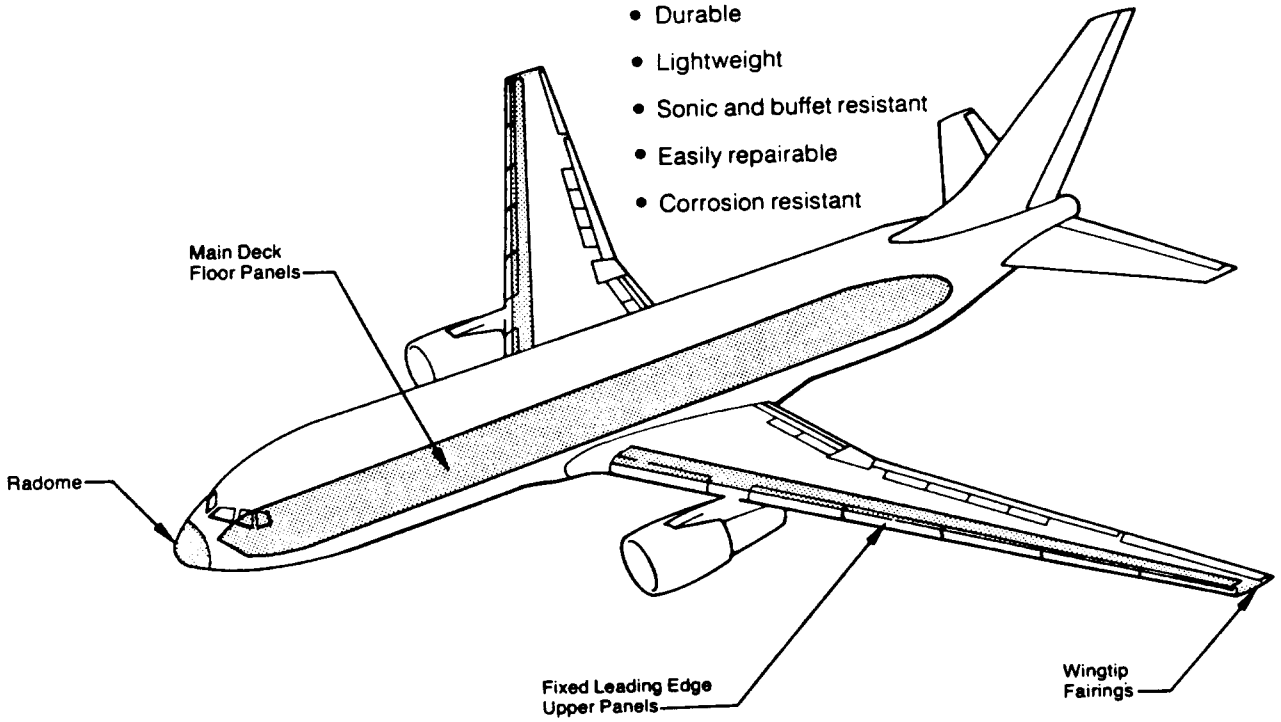

Figure 7.3d Fiberglass Usage: Boeing 767-200

7.3 PRELIMINARY SELECTION OF MANUFACTURING BREAKDOWN

The following considerations play a role in deciding on the manufacturing breakdown for an airplane:

1. Number of units to be produced
2. Available sub-assembly and final assembly facilities
3. Agreements for sub-assemblies to be performed in other areas or in other countries (international programs)
4. Future growth potential
5. Questions of production optimization: how many workers can perform their jobs without interfering with one another

The material presented in this chapter does not address these considerations. Part VIII contains methods for predicting manufacturing cost which depends to a large extent on the manufacturing materials and the manufacturing breakdown selected. Figures 7.4 through 7.9 present examples of manufacturing breakdowns used in a range of airplanes:

For a light airplane: Figure 7.4 Beech Musketeer

For a military trainer: Figure 7.5 SIAI Marchetti S-211

For a jet transport: Figure 7.6 Boeing 767-200

For fighters: Figure 7.7 Fairchild Republic A-10

Figure 7.8 McDonnell Douglas F-15

Figure 7.9 McDonnell Douglas F-18

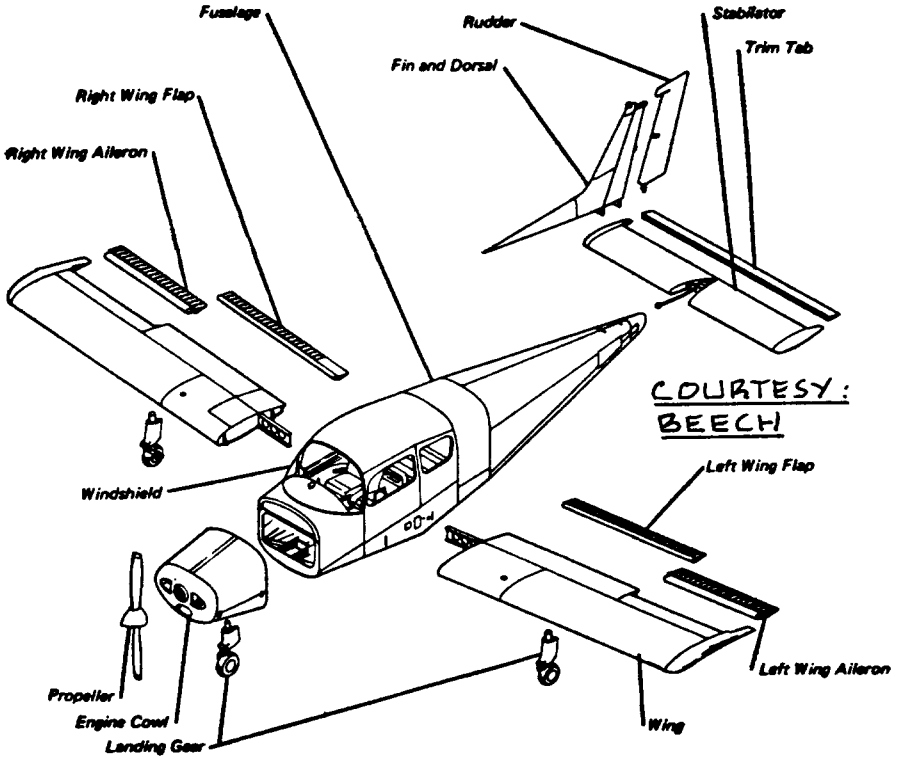

Figure 7.4 Manufacturing Breakdown: Beech Sport

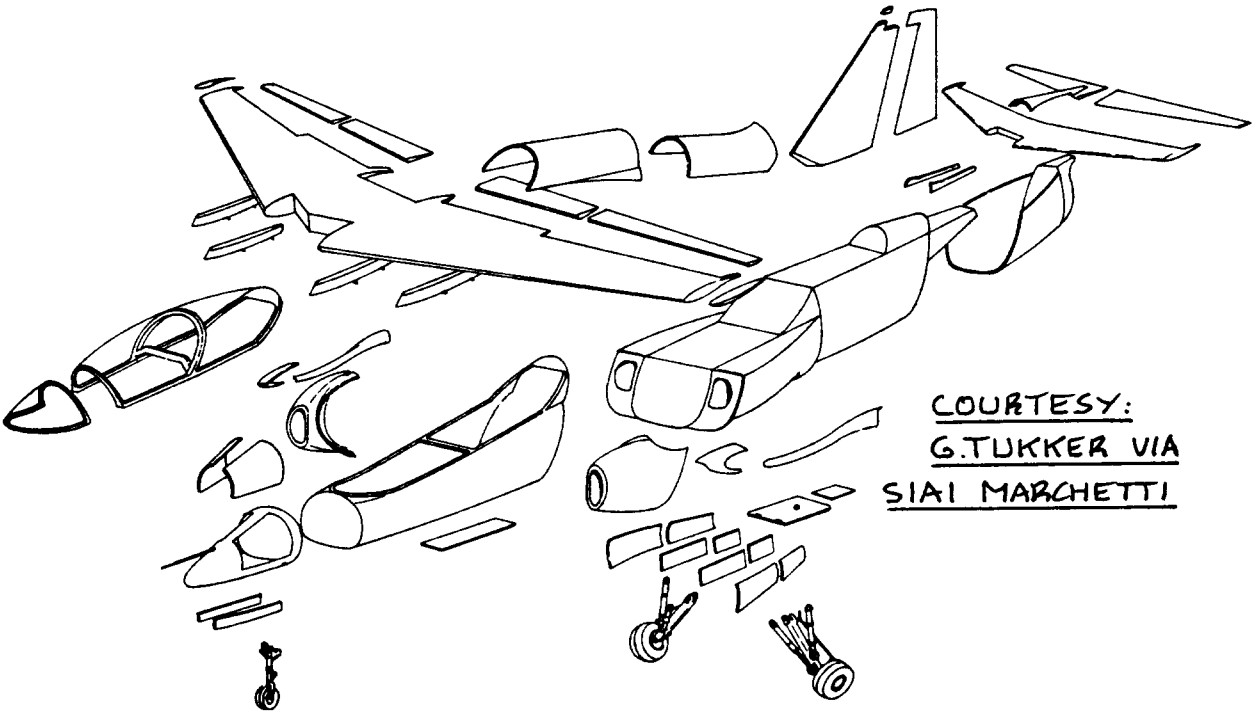

Figure 7.5 Manufacturing Breakdown: SIAI Marchetti S-211

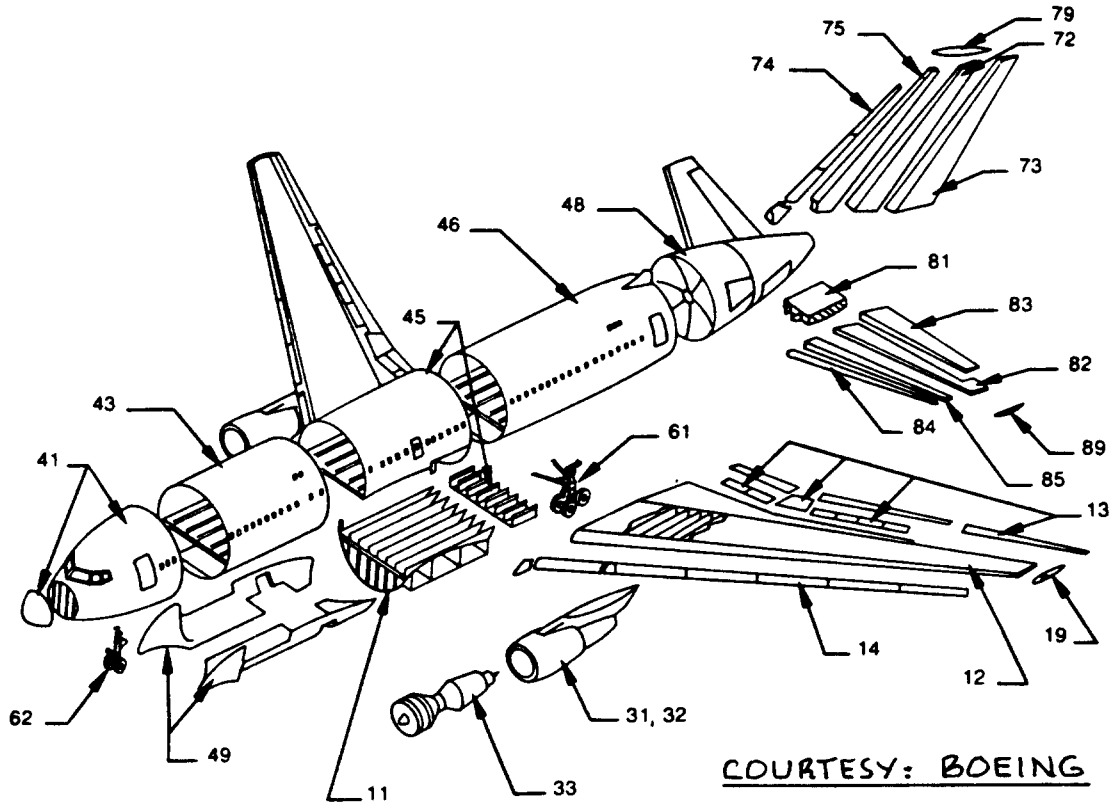

Section Number	Description	Section Number	Description
11	Wing Center Section	49	Multi-Section (Wing/Body Fairings)
12	Wing Outboard Structural Box	61	Main Landing Gear
13	Wing Trailing Edge (Includes Ailerons, Flaps, and Spoilers)	62	Nose Landing Gear
14	Wing Leading Edge (Fixed and Movable)	72	Vertical Tail – Aft Torque Box
19	Wingtip	73	Vertical Tail – Trailing Edge (Fixed and Movable)
31	Propulsion – Wing Installation (Strut and Cowling)	74	Vertical Tail – Leading Edge
32	Propulsion – Center Installation (Mount, Inlet, Ducting & Thrust Reverser	75	Vertical Tail – Forward Torque Box
33	Propulsion – Built-Up Engine	79	Vertical Tail – Tip
41	Fuselage Nose Section (Includes Radome)	81	Horizontal Tail – Center Section
43	Forward Fuselage Section	82	Horizontal Tail – Aft Torque Box
45	Fuselage Section, Wing Join	83	Horizontal Tail – Trailing Edge (Fixed and Movable)
46	Aft Fuselage Section	84	Horizontal Tail – Leading Edge
48	Fuselage Tail Section	85	Horizontal Tail – Forward Torque Box
		89	Horizontal Tail – Tip

Figure 7.6 Manufacturing Breakdown: Boeing 767-200

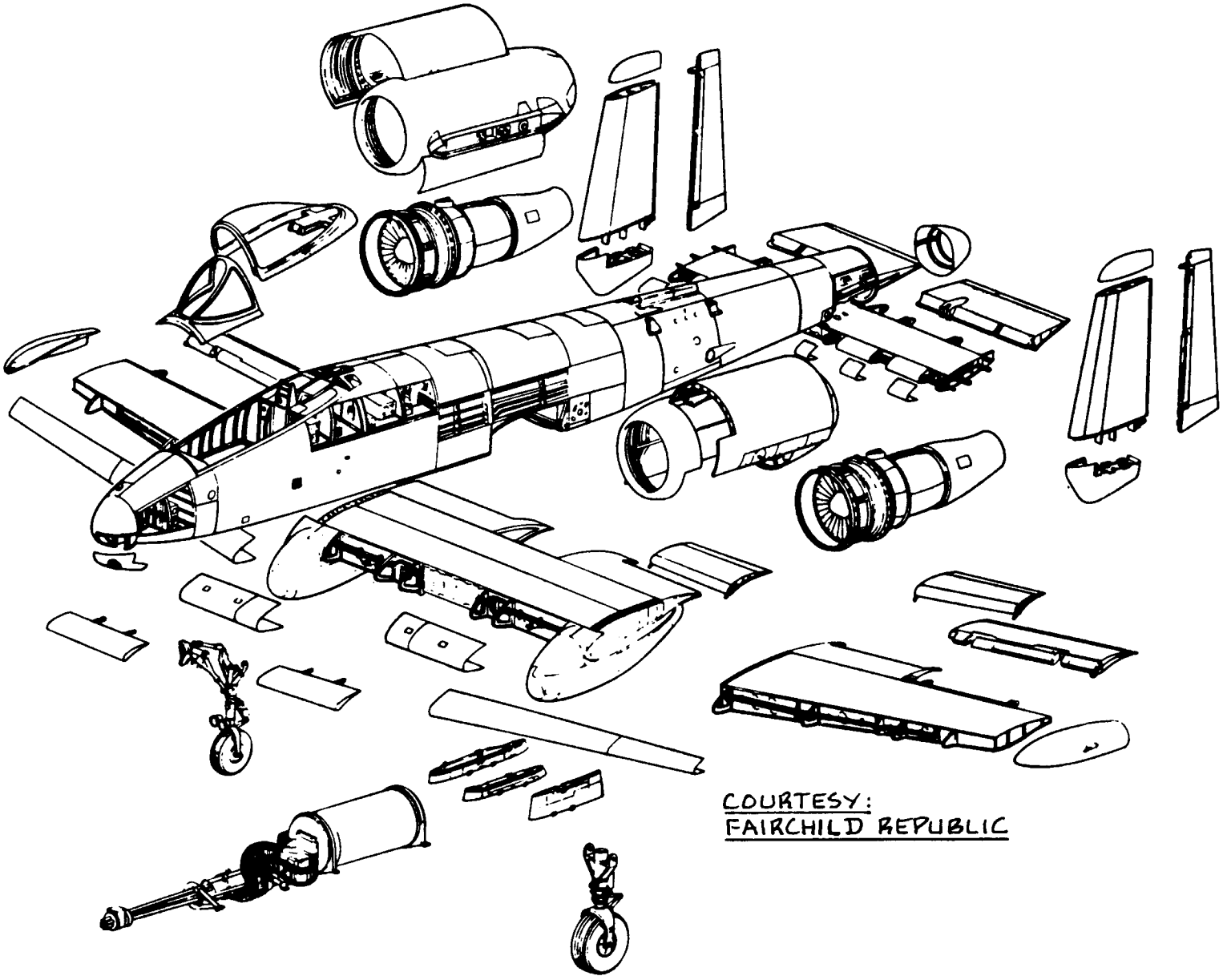

Figure 7.7 Manufacturing Breakdown: Fairchild Republic A-10

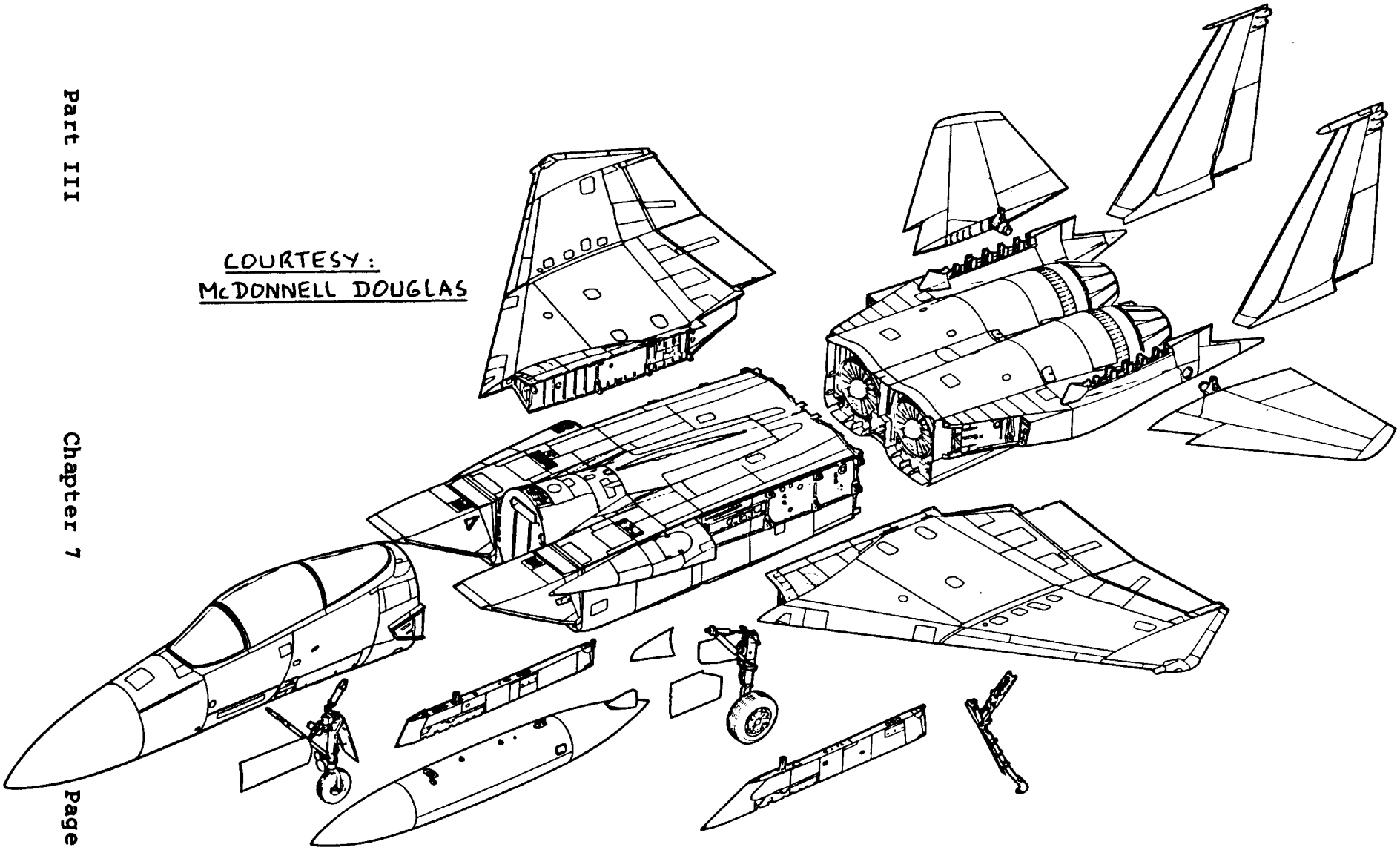

Figure 7.8 Manufacturing Breakdown: McDonnell Douglas F-15

COURTESY : McDONNELL DOUGLAS

Figure 7.9 Manufacturing Breakdown: McDonnell Douglas F-18

8. COLLECTION OF CUTAWAY DRAWINGS

The purpose of this chapter is to provide a number of airplane cutaway drawings. Such cutaway drawings show the overall internal structural, systems and propulsion layout of an airplane. They also serve to provide the aeronautical engineering student with the opportunity to 'look' at airplanes from a 3-dimensional viewpoint.

Cutaways are presented for modern airplanes and for some older airplanes. The reason for the latter is to provide some historical perspective. The indicated years are approximate. The following cutaways are included:

1. Homebuilt Airplanes:

   Piston-Propeller Driven:

   Figure 8.1 Scaled Down Focke-Wulf 190 (1943)

2. Single Engine Propeller Driven Airplanes:

   Piston-Propeller driven:

   Figure 8.2 Percival Prentice (1938)
   Figure 8.3 Fokker Promotor (1948)
   Figure 8.4 Cessna 150 (1962)
   Figure 8.5 Cessna 172 (1964)
   Figure 8.6 Beech 77 Skipper (1978)

   Turbo-Propeller driven:

   Figure 8.7 Pilatus Turbo-porter (1980)

3. Twin Engine Propeller Driven Airplanes:

   Piston-Propeller driven:

   Figure 8.8 Italair F.20 Pegaso (1970)
   Figure 8.9 Beech 76 Duchess (1978)

   Turbo-Propeller Driven:

   Figure 8.10 Beech Super King Air 200 (1980)

4. Agricultural Airplanes:

   Piston-Propeller Driven:

   Figure 8.11 Hollandair HA-001 Libel (1960)

5. Business Jets:

Figure 8.12 Gulfstream Peregrine (1980 proposal)
Figure 8.13 Gates Learjet 25 (1972)
Figure 8.14 Aerospatiale Corvette (1976)
Figure 8.15 Gates Learjet 28 (1980)
Figure 8.16 Gulfstream GIII (1984)

6. Regional Propeller Driven Airplanes:

Piston-Propeller Driven:

Figure 8.17 Scottish Av. Twin Pioneer (1950)
Figure 8.18 Britten Norman Trislander (1970)

Turbo-Propeller Driven:

Figure 8.19 Armstrong Whitworth Apollo (1952)
Figure 8.20 Handley Page Dart Herald (1956)
Figure 8.21 Short Skyvan (1958)
Figure 8.22 Fokker F-27 Friendship (1958)
Figure 8.23 Piper T-1040 (1982)

7. Transports and Transport Jets

Piston-Propeller Driven:

Figure 8.24 Fokker F22 (1938)

Jet Driven:

Figure 8.25 McDonnell Douglas DC9 (1962)
Figure 8.26 Fokker F28 (1964)
Figure 8.27 McDonnell Douglas DC10 (1972)

8. Military Trainers

Piston-Propeller Driven:

Figure 8.28 Fokker S12 (1948)

Turbo-Propeller Driven:

Figure 8.29 Beech T-34C-1 (1978)

Jet Driven:

Figure 8.30 Fokker S14 (1952)
Figure 8.31 SAAB XT-105 (1958)
Figure 8.32 British Aerospace Hawk (1980)

Figure 8.33 Microturbo Microjet 200 (1984)

9. Fighters

Piston-Propeller Driven:

Figure 8.34 Fokker G.1 (1938)

Turbo-Propeller Driven:

Figure 8.35 Piper PA-48 Enforcer (1980)

Jet Driven:

Figure 8.36 Gloster Meteor (1945)
Figure 8.37 Douglas A4 Skyhawk (1960)
Figure 8.38 General Dynamics F-16 (1980)
Figure 8.39 McDonnell Douglas F-4E (1970)
Figure 8.40 McDonnell Douglas F-15 (1978)
Figure 8.41 McDonnell Douglas F-18 (1982)
Figure 8.42 McDonnell Douglas AV-8B (1984)

10. Military Patrol, Bomb and Transport Airplanes:

Piston-Propeller Driven:

Figure 8.43 Fokker T.IX (1939)

Turbo-Propeller Driven:

Figure 8.44 CASA C212A (1978)

11. Flying Boats, Amphibious and Float Airplanes

Piston-Propeller Driven:

Figure 8.45 Fokker T.VIII-W (1940)
Figure 8.46 Riviera Amphibian (1965)

12. Supersonic Cruise Airplanes

No cutaways available

13. NACA/NASA Experimental Airplanes:

Figure 8.47 Bell X2 (1952)
Figure 8.48 Ryan X13 (1956)
Figure 8.49 North American X15 (1959)

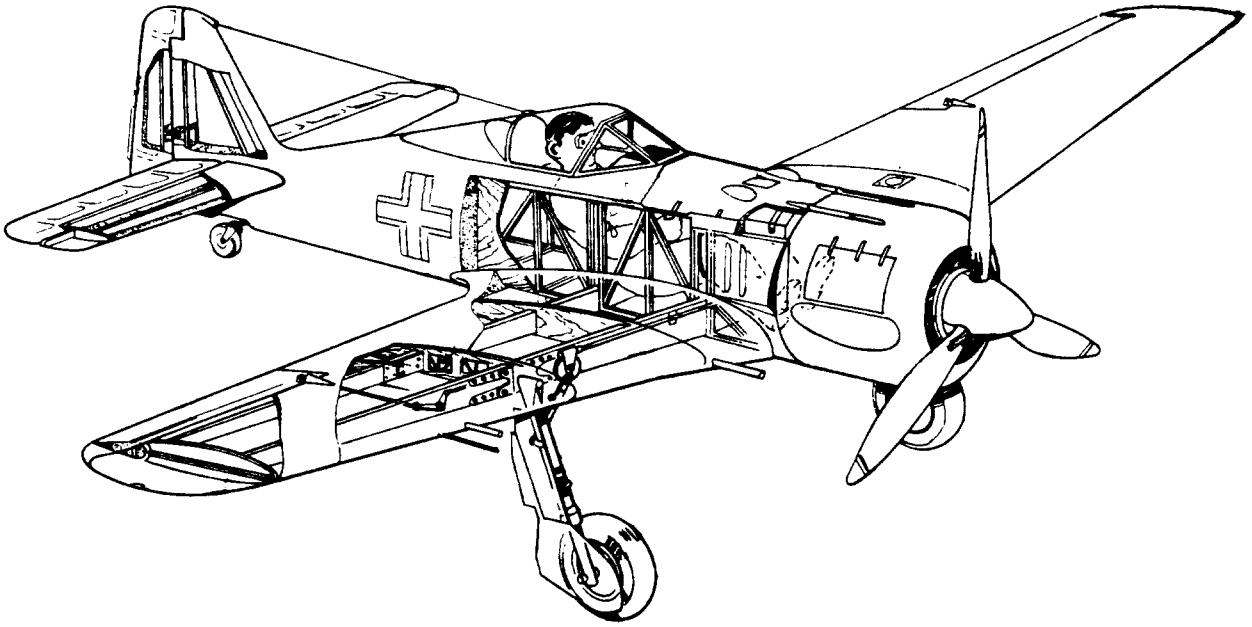

Figure 8.1 Scaled Down Focke-Wulf 190

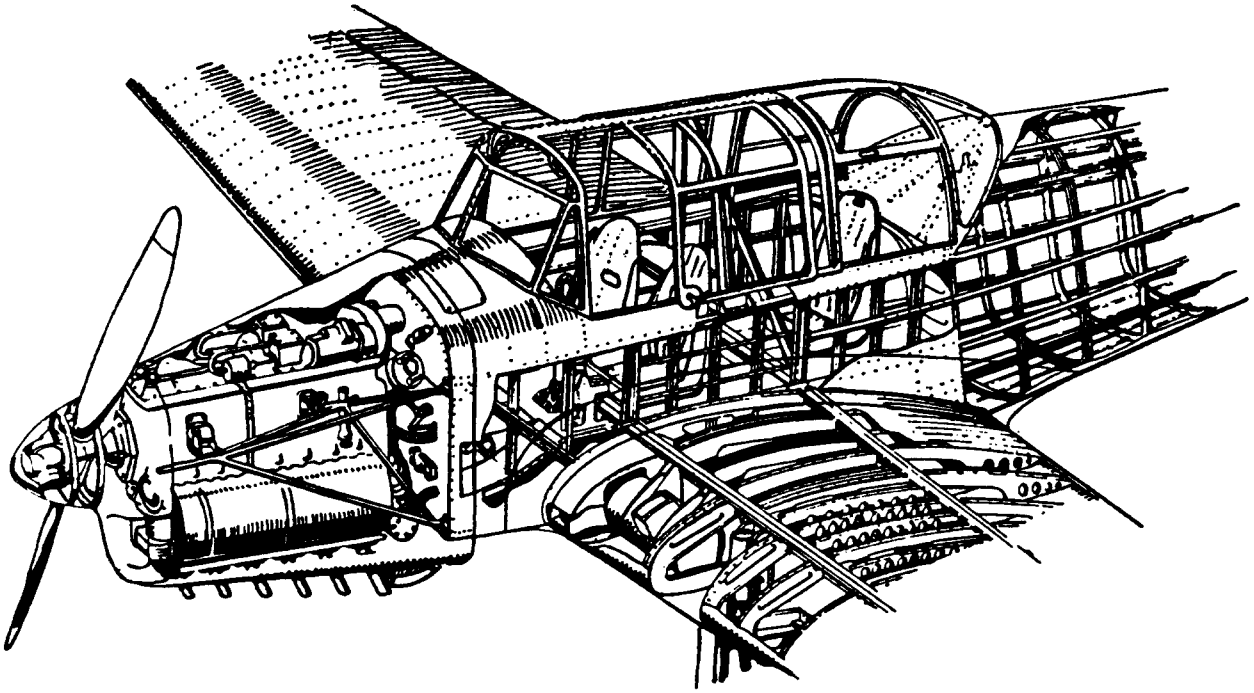

Figure 8.2 Percival Prentice

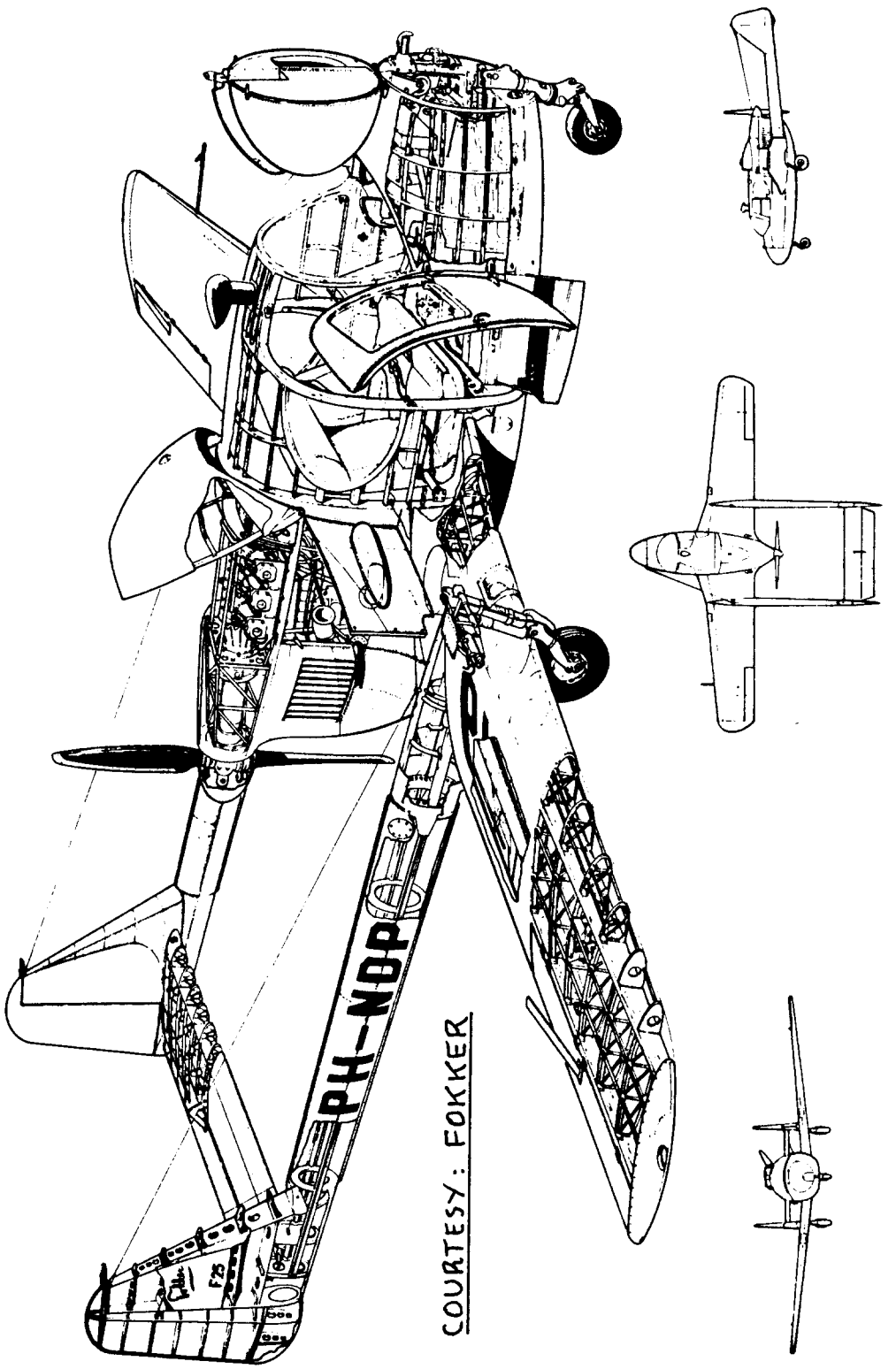

Figure 8.3 Fokker Promotor

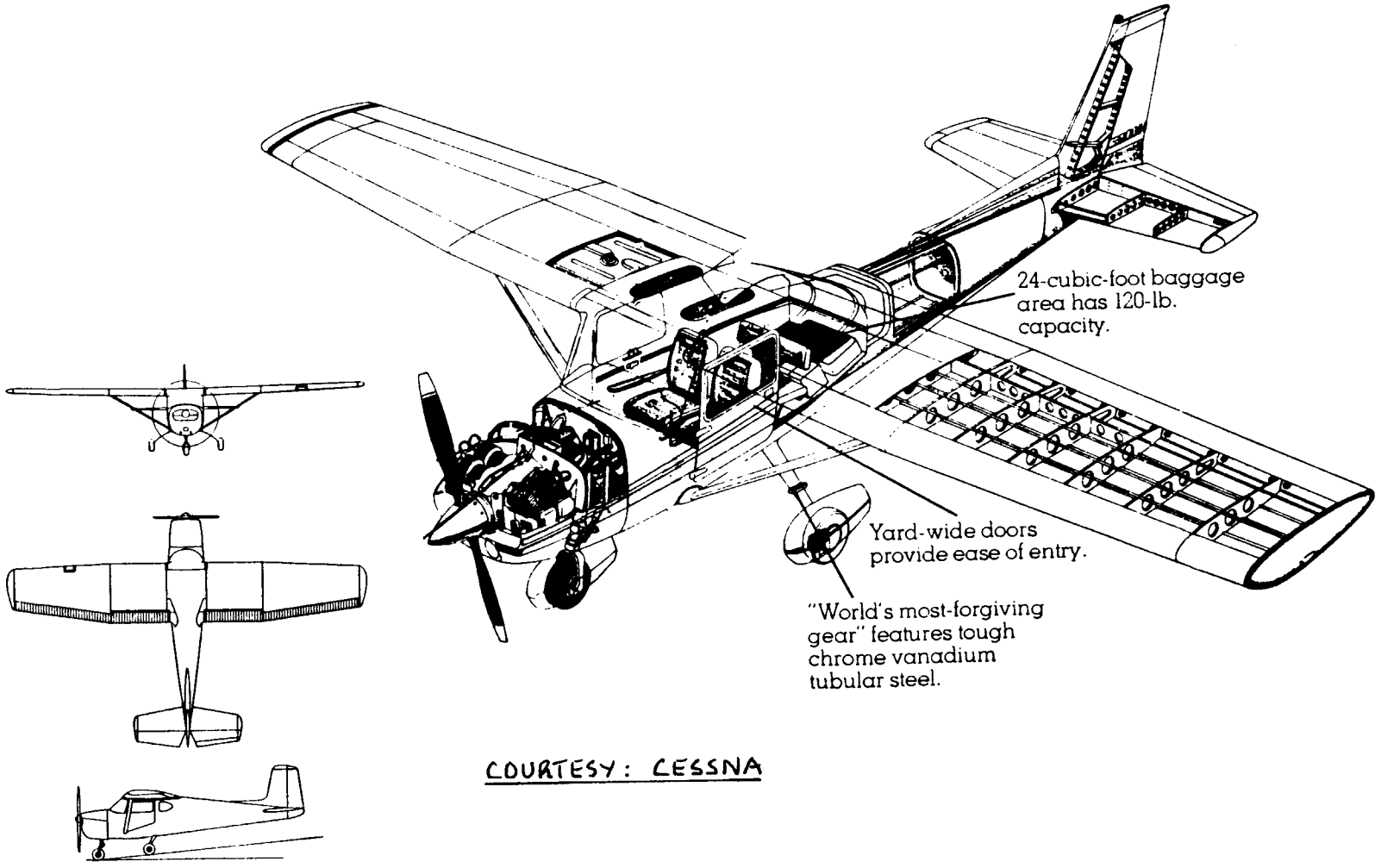

COURTESY: CESSNA

Figure 8.4 Cessna 150

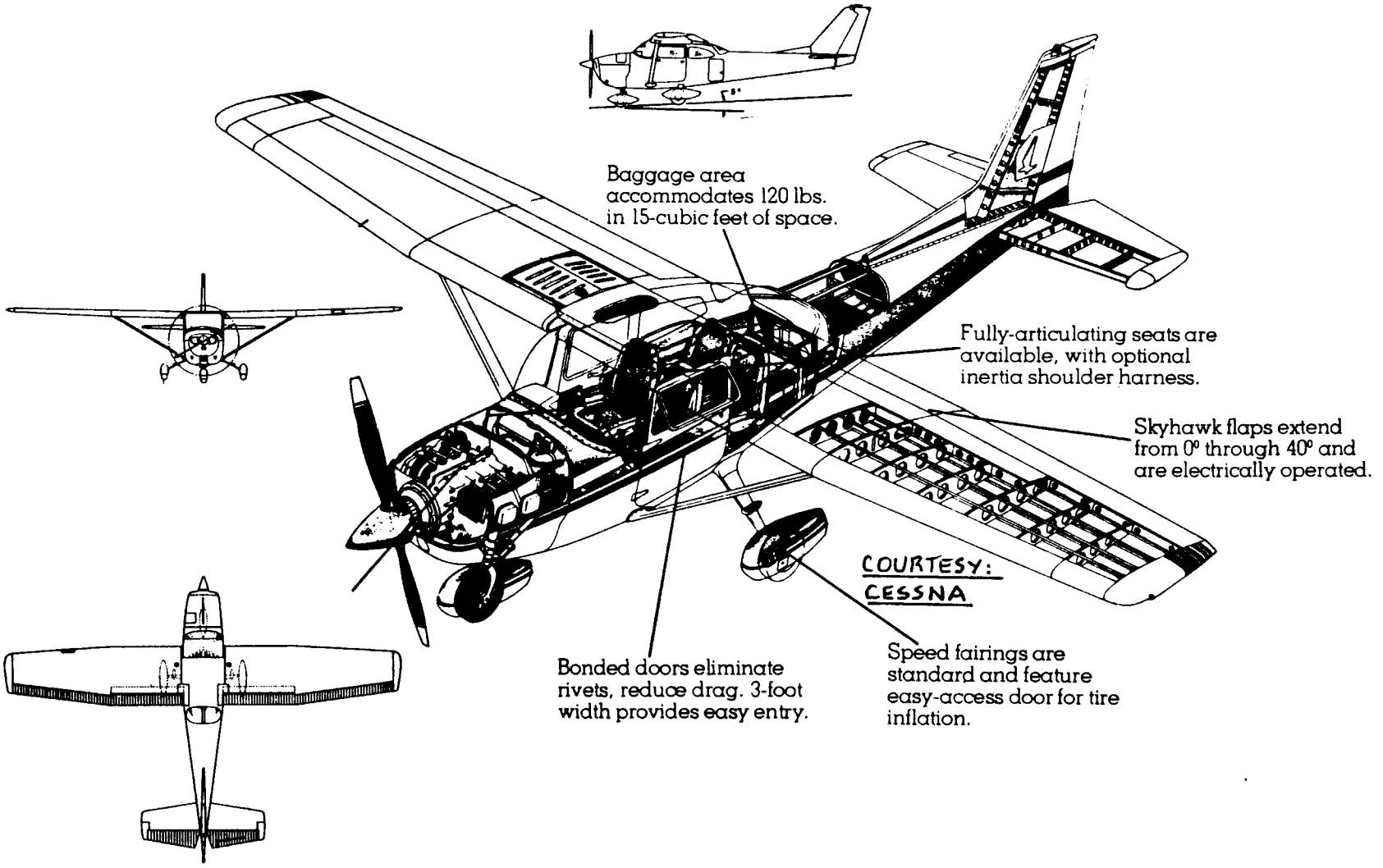

Figure 8.5 Cessna 172

Figure 8.6 Beech 77 Skipper

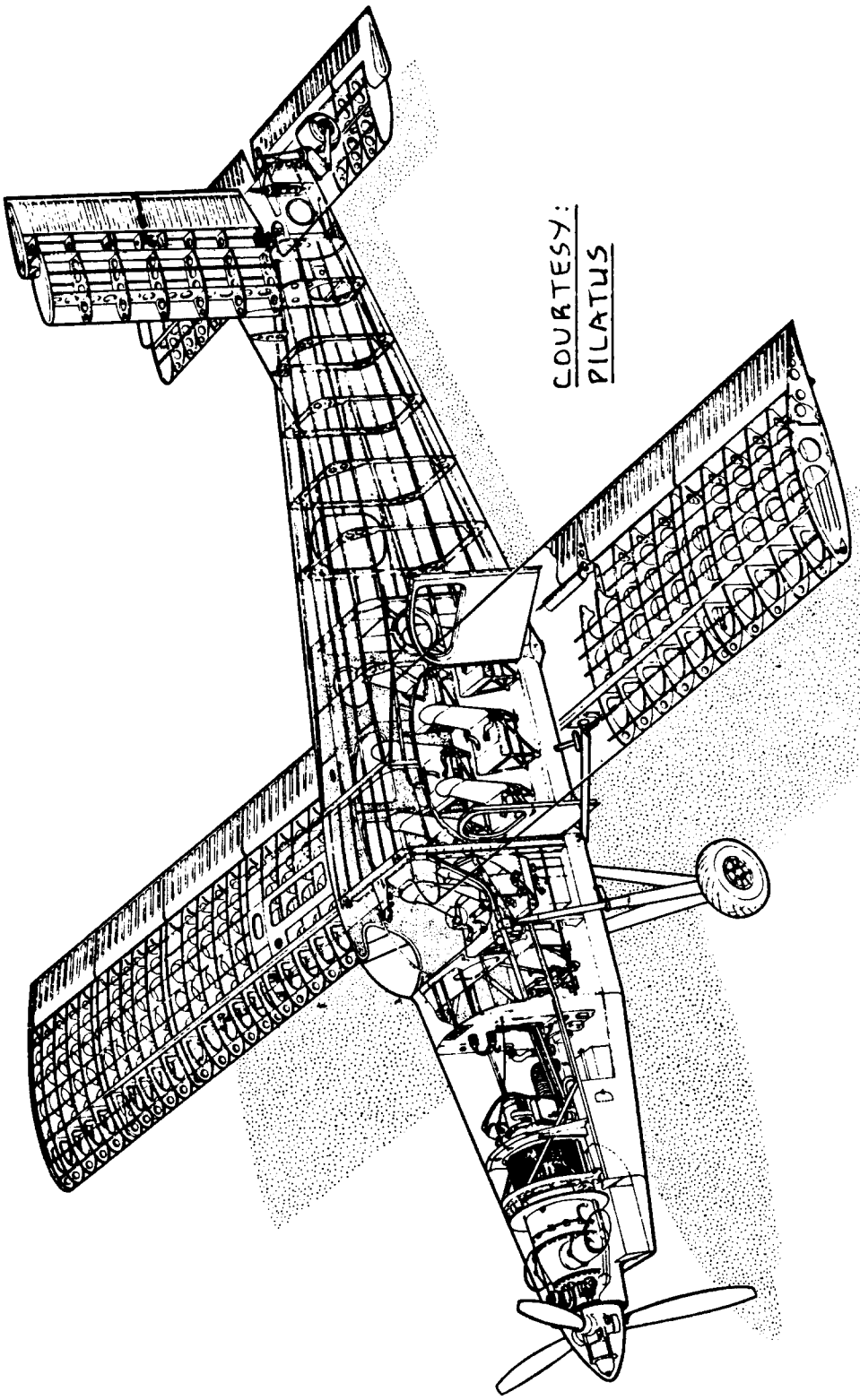

Figure 8.7 Pilatus Turbo-porter

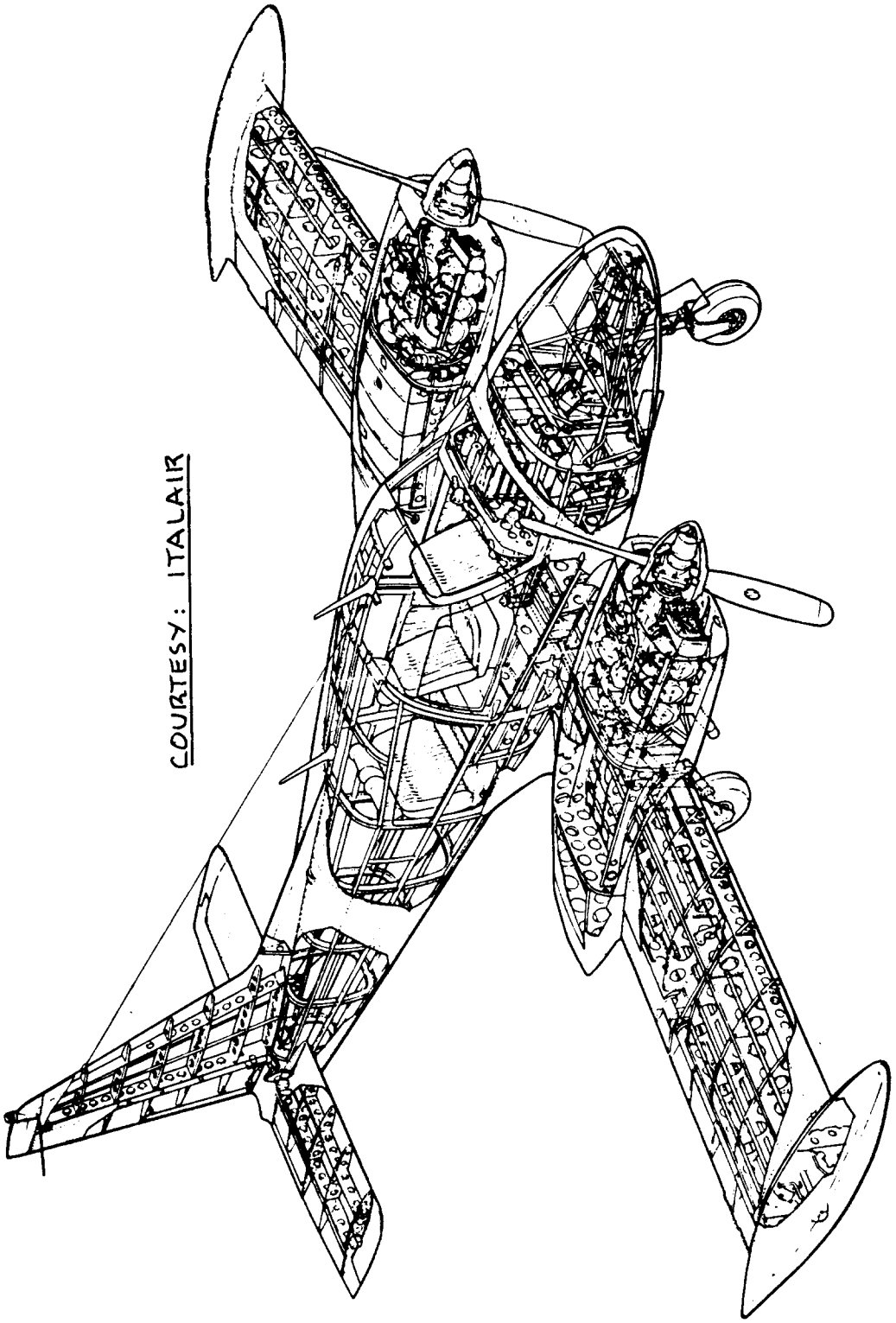

COURTESY: ITALAIR

Figure 8.8 Italair F.20 Pegaso

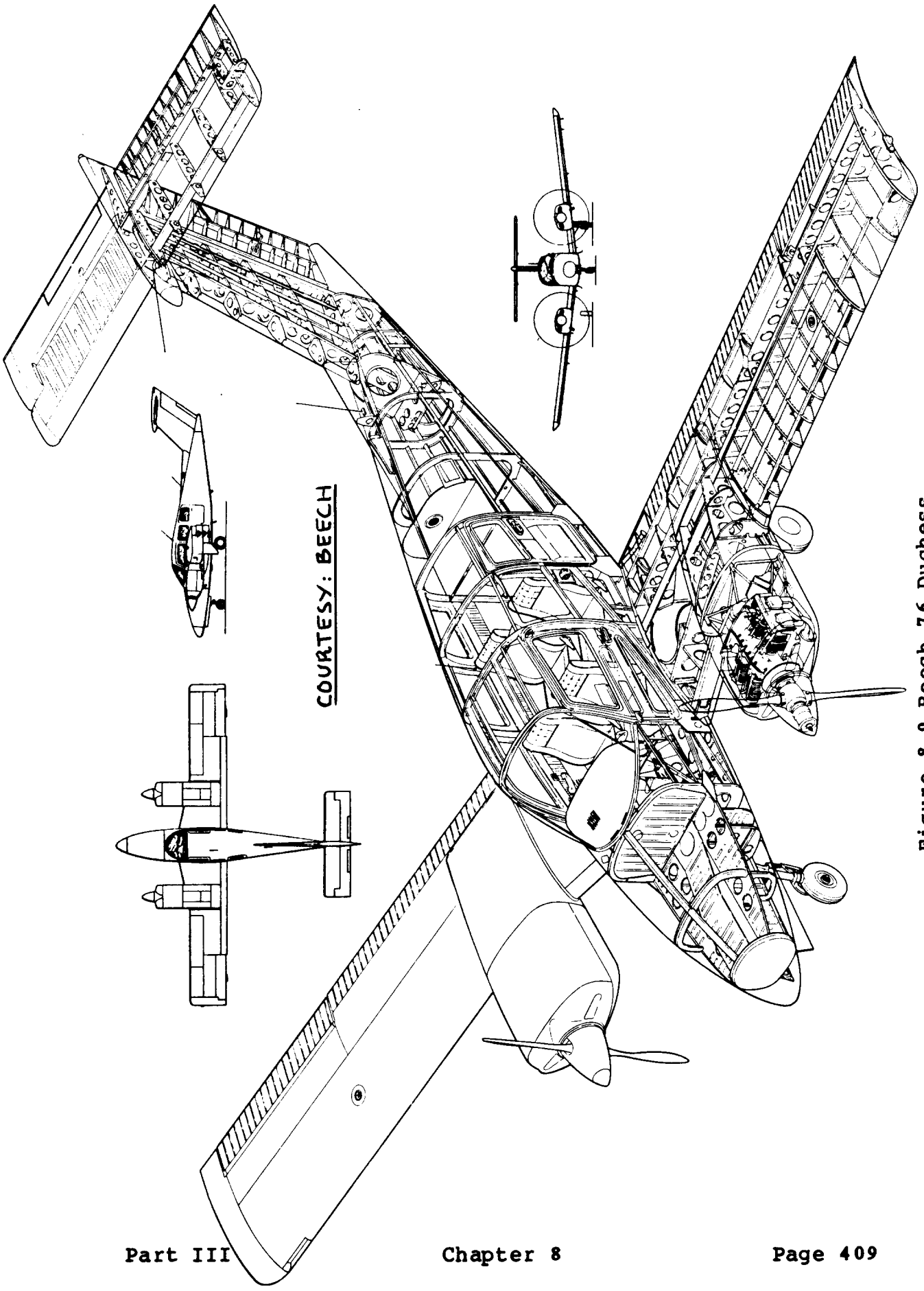

Figure 8.9 Beech 76 Duchess

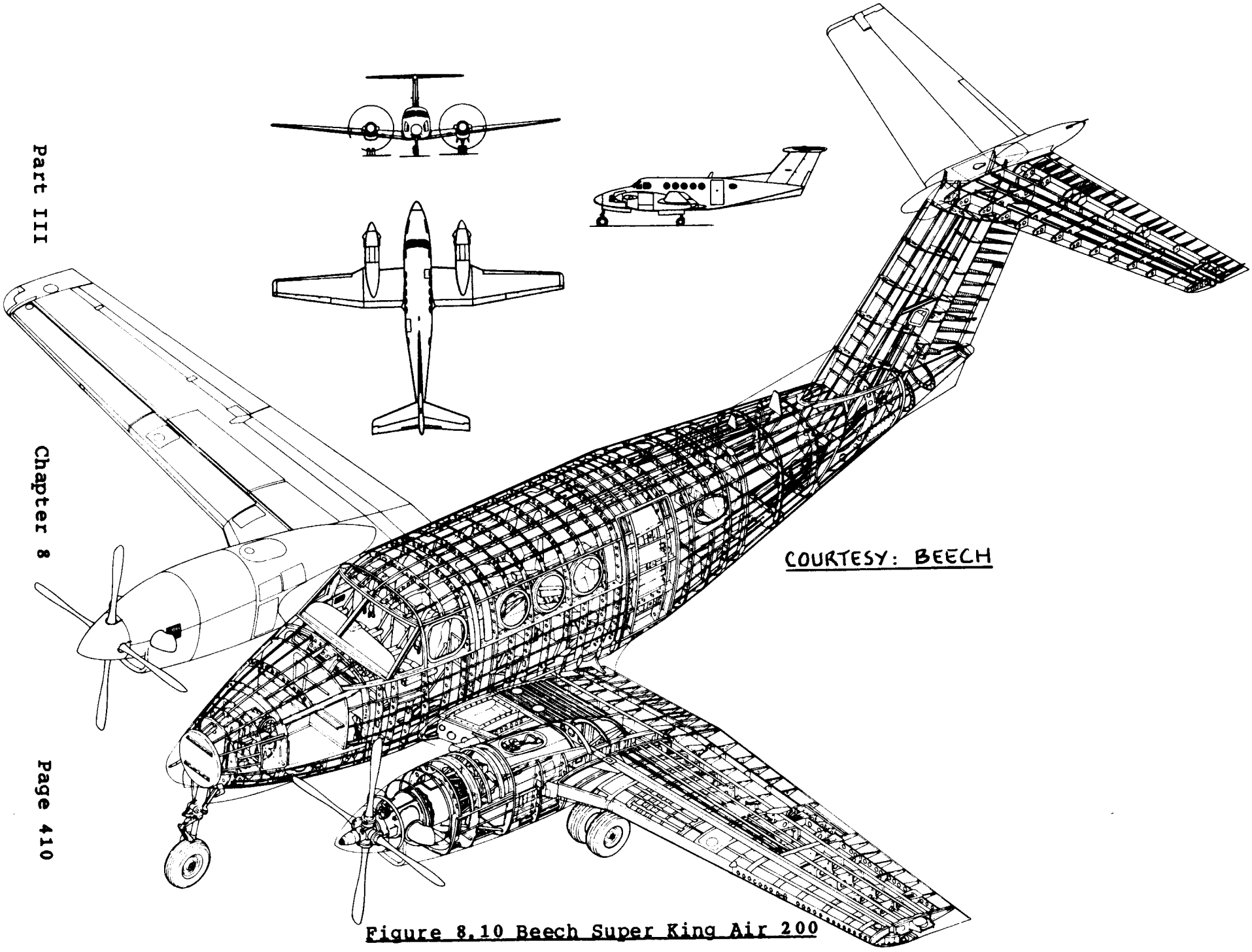

Figure 8.10 Beech Super King Air 200

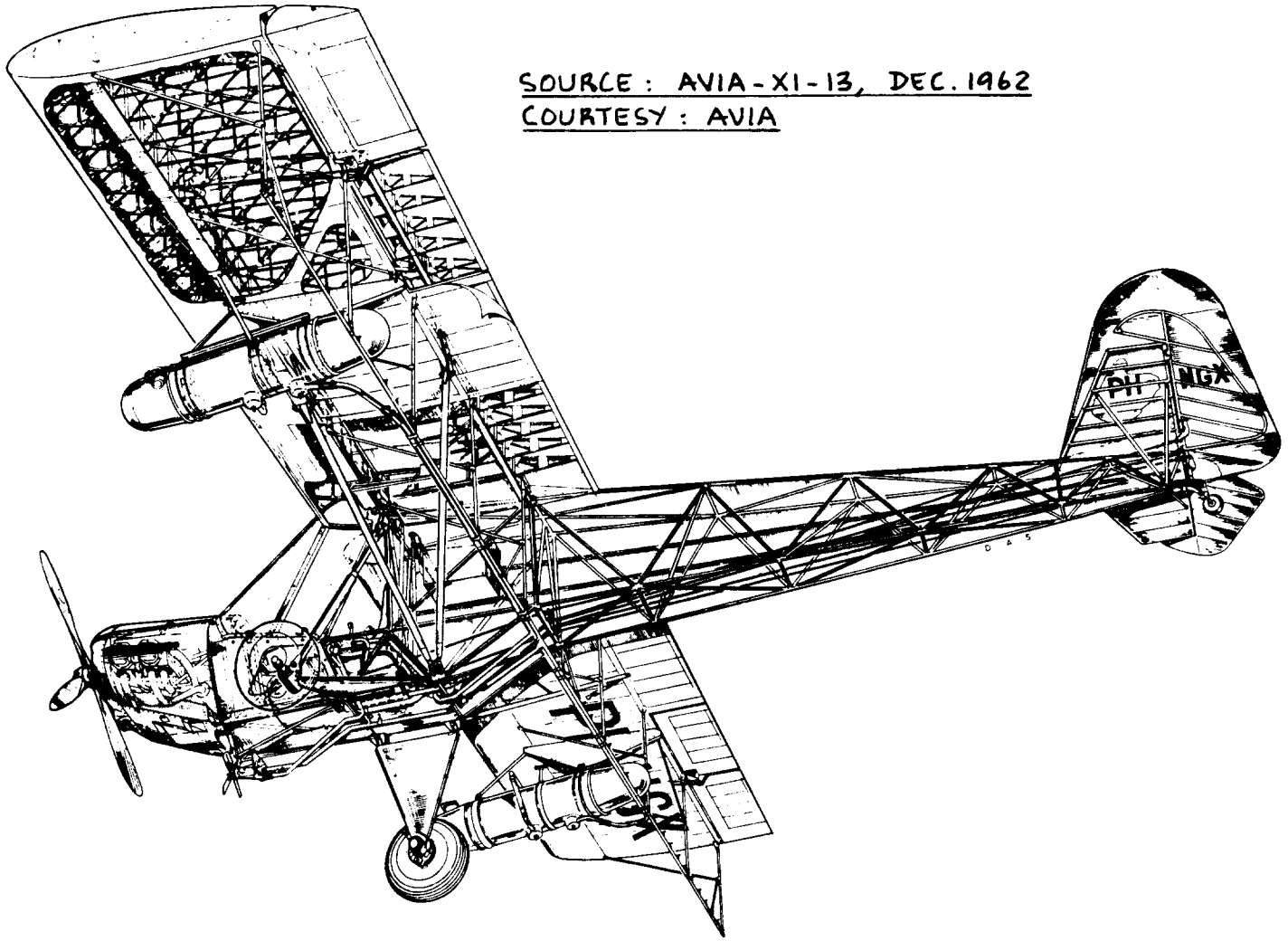

SOURCE : AVIA-XI-13, DEC. 1962
COURTESY : AVIA

Figure 8.11 Hollandair HA-001 Libel

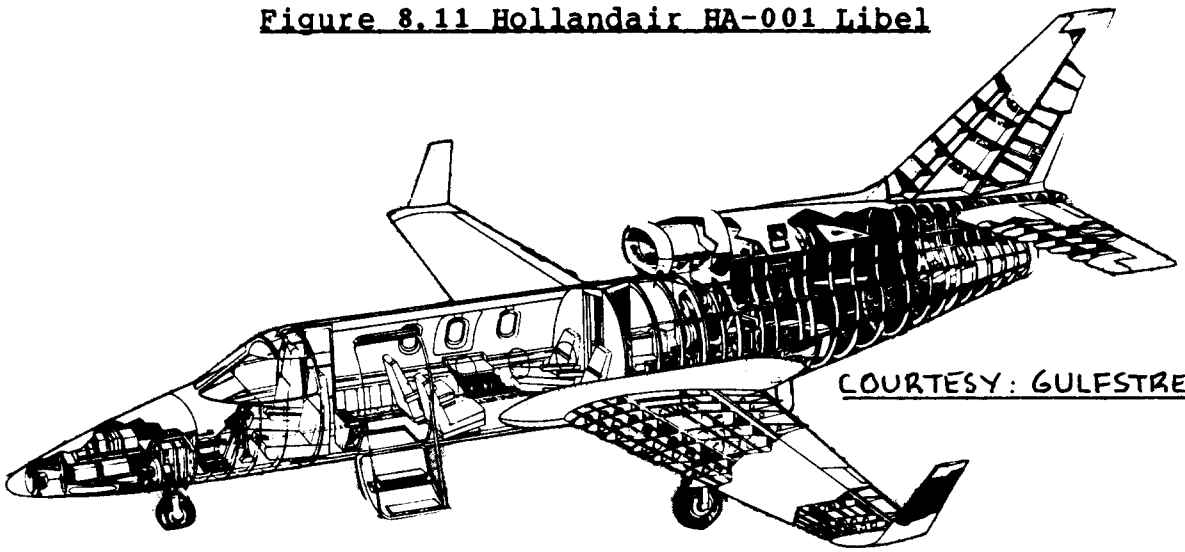

COURTESY: GULFSTREAM

Figure 8.12 Gulfstream Peregrine

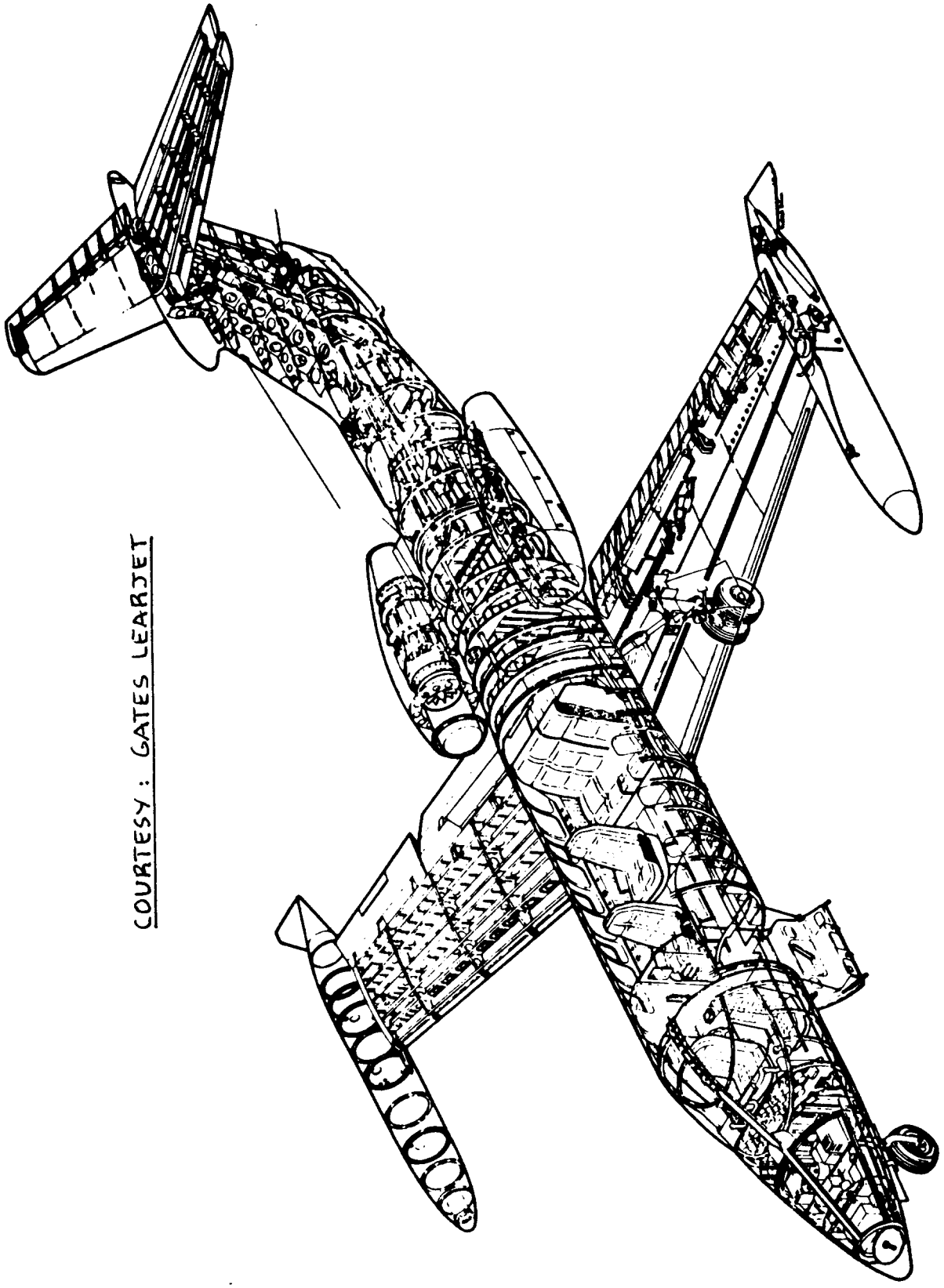

COURTESY: GATES LEARJET

Figure 8.13 Gates Learjet 25

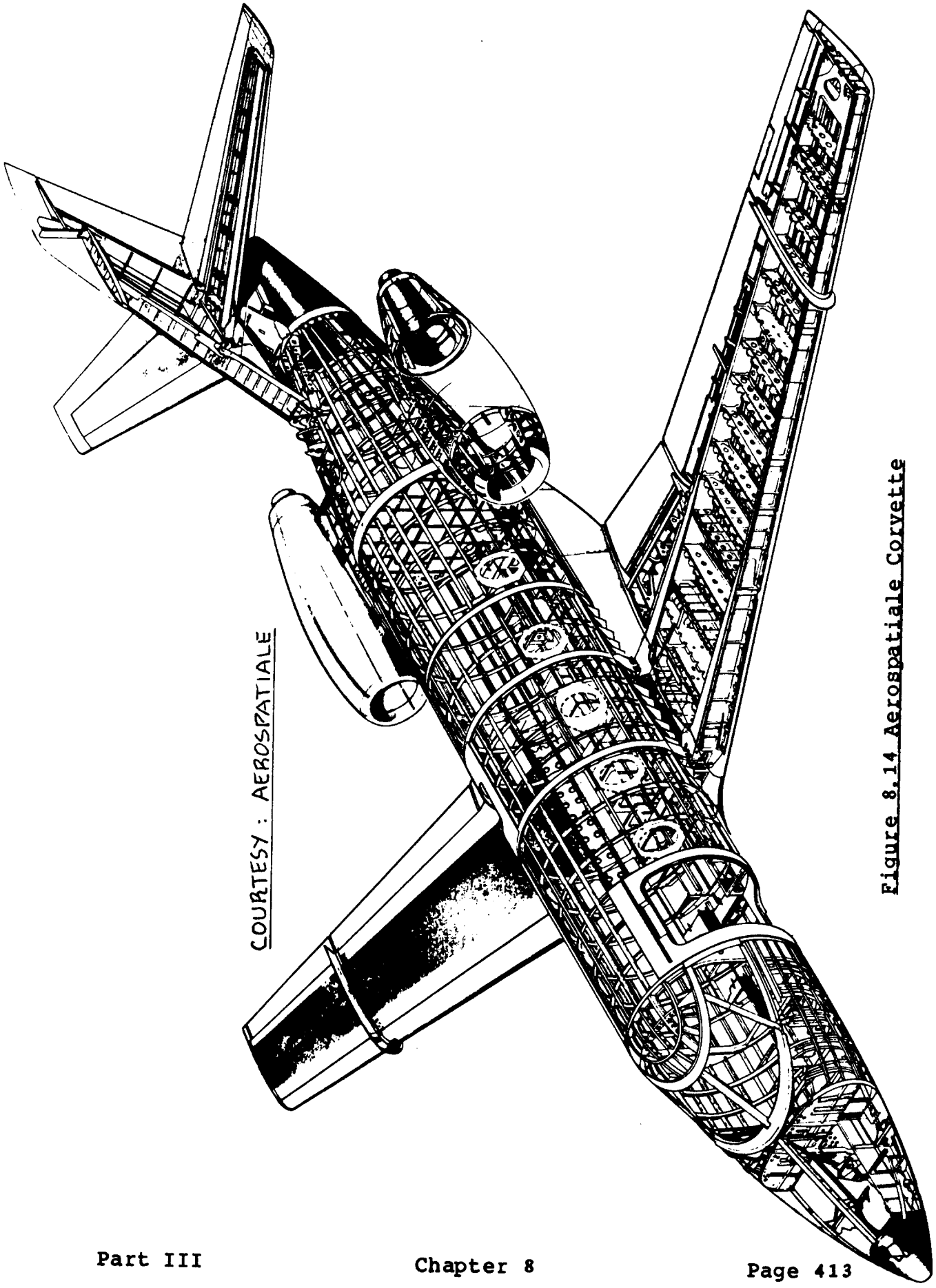

COURTESY : AEROSPATIALE

Figure 8.14 Aerospatiale Corvette

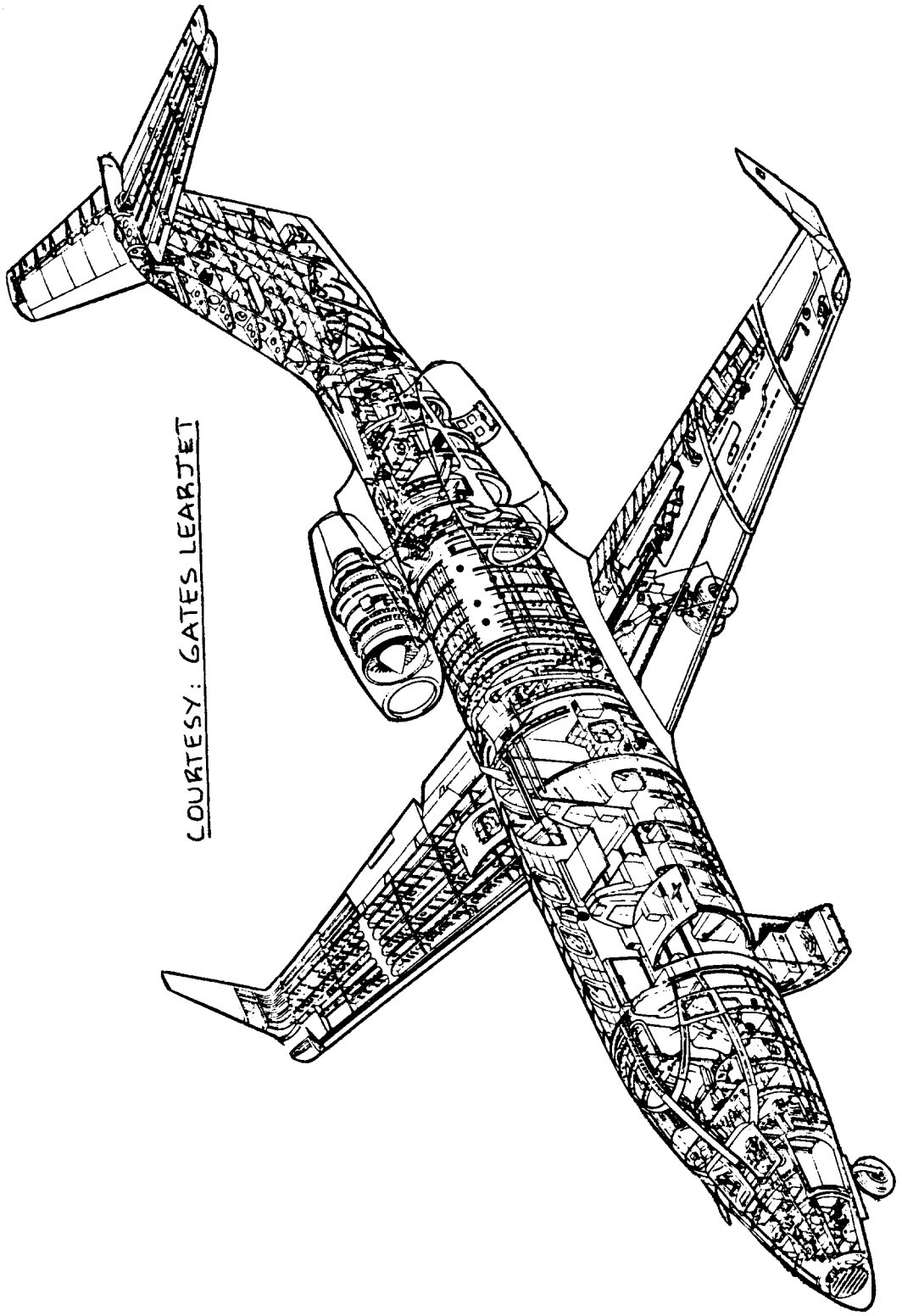

COURTESY: GATES LEARJET

Figure 8.15 Gates Learjet 28

Figure 8.16 Gulfstream GIII

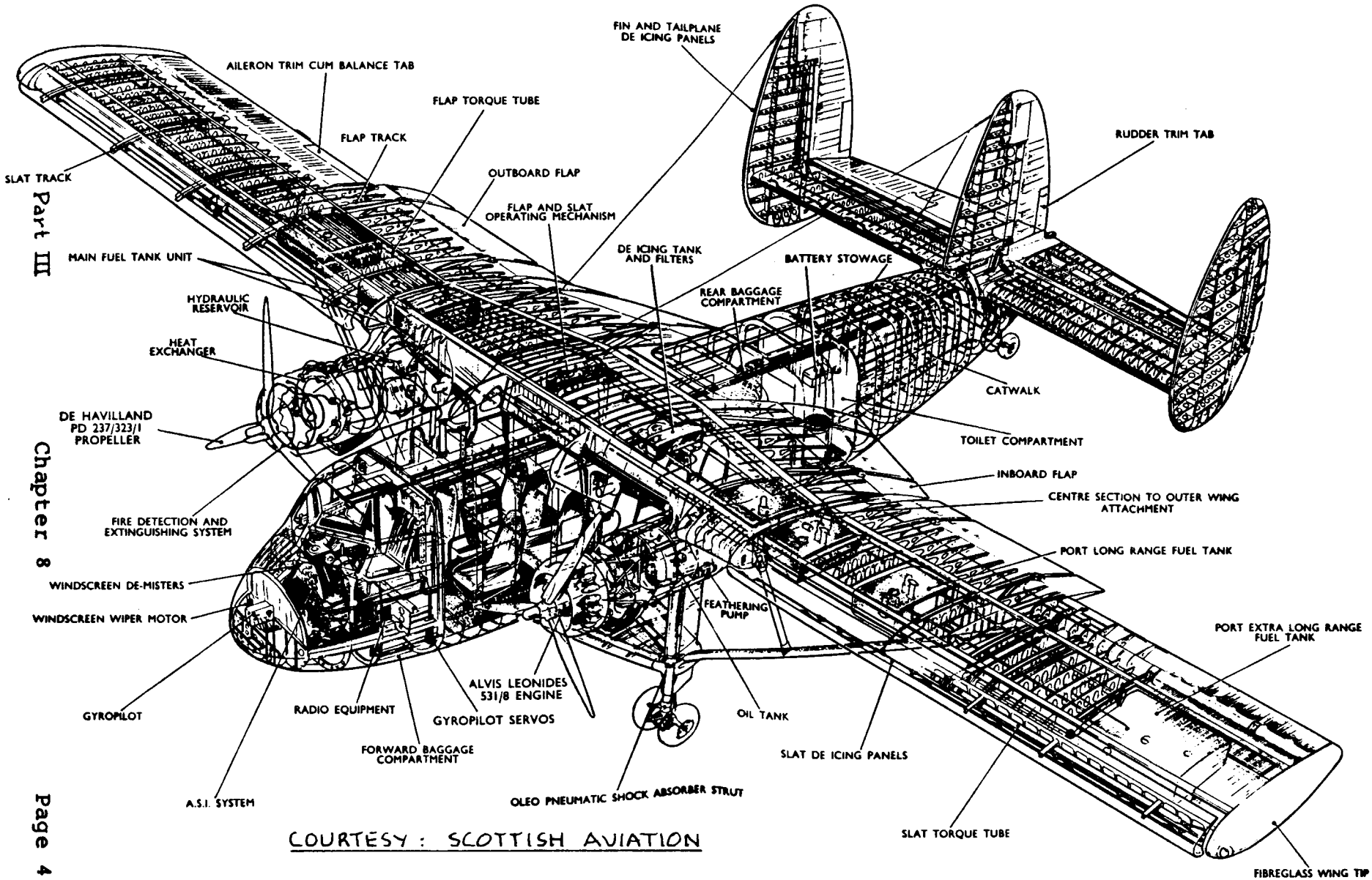

COURTESY : SCOTTISH AVIATION

Figure 8.17 Scottish Aviation Twin Pioneer

Figure 8.18 Britten Norman Trislander

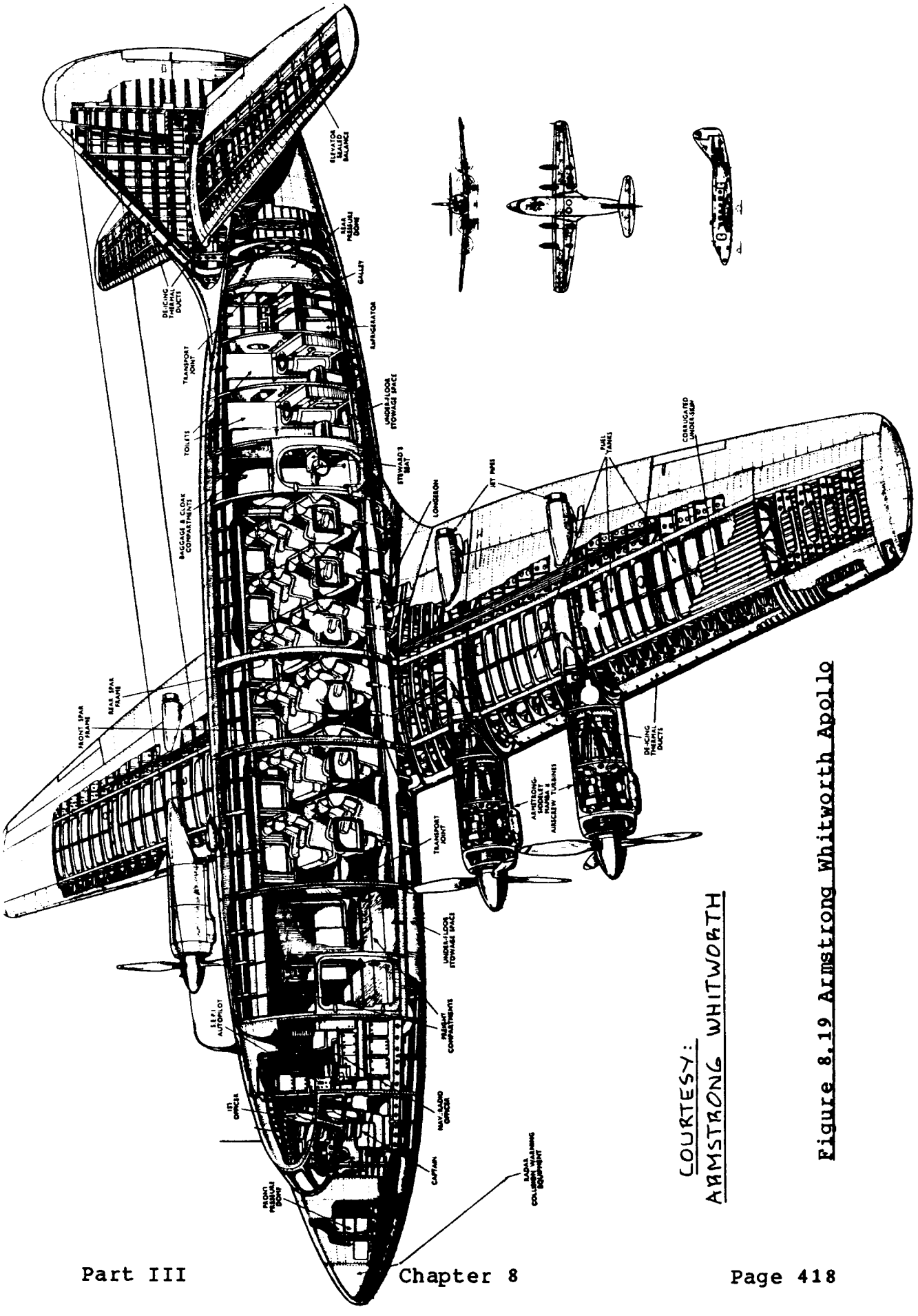

COURTESY:
ARMSTRONG WHITWORTH

Figure 8.19 Armstrong Whitworth Apollo

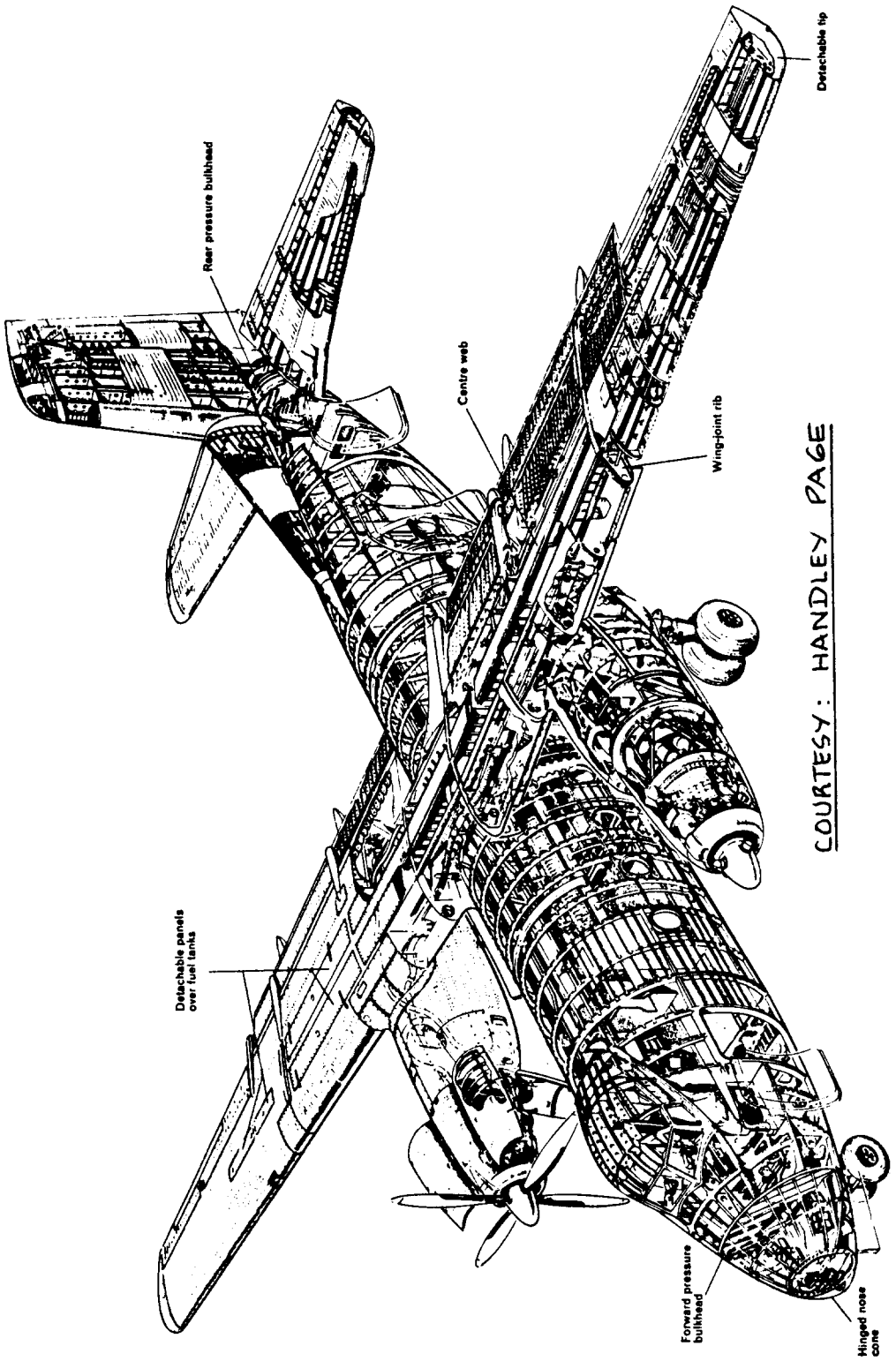

COURTESY: HANDLEY PAGE

Figure 8.20 Handley Page Dart Herald

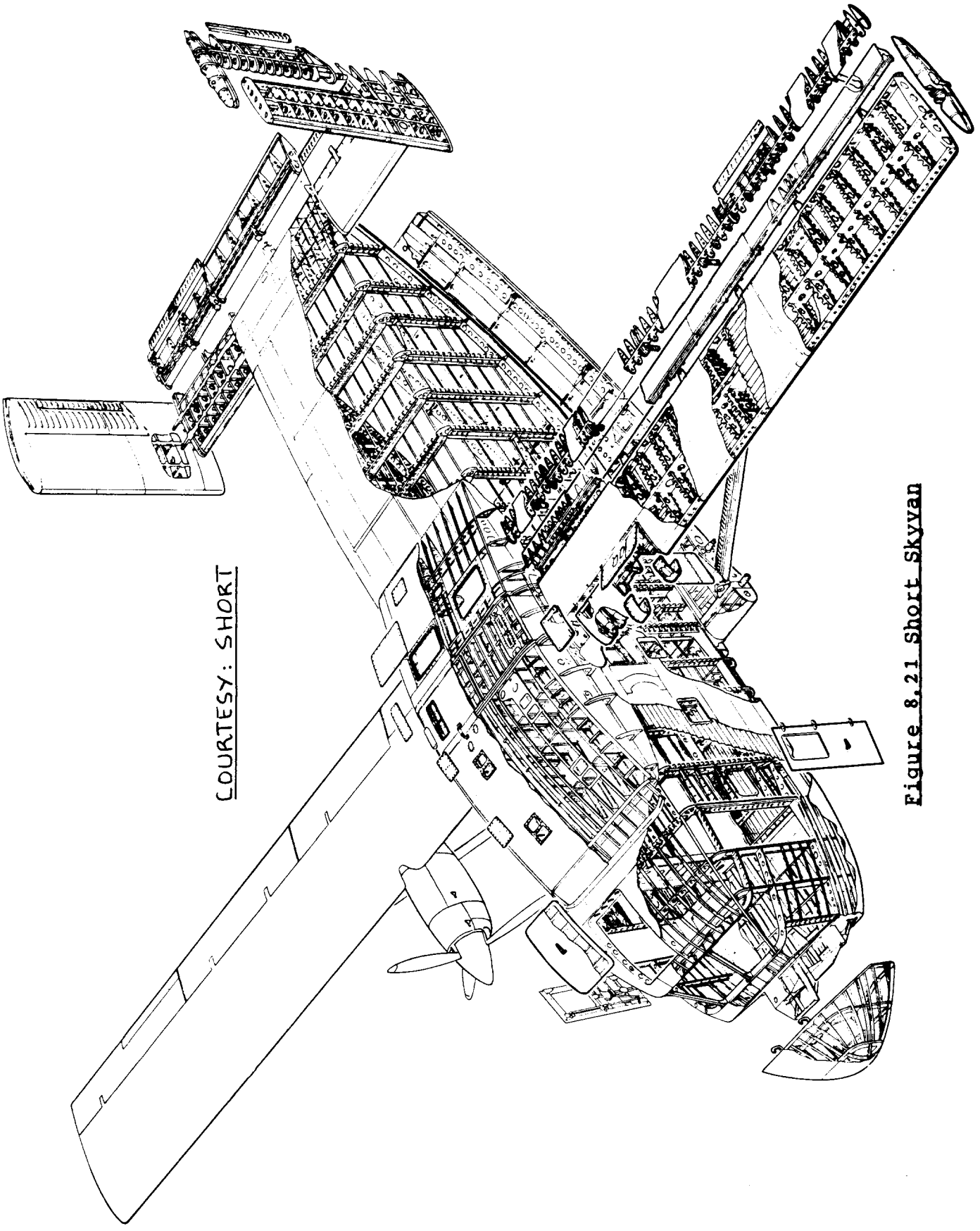

COURTESY: SHORT

Figure 8.21 Short Skyvan

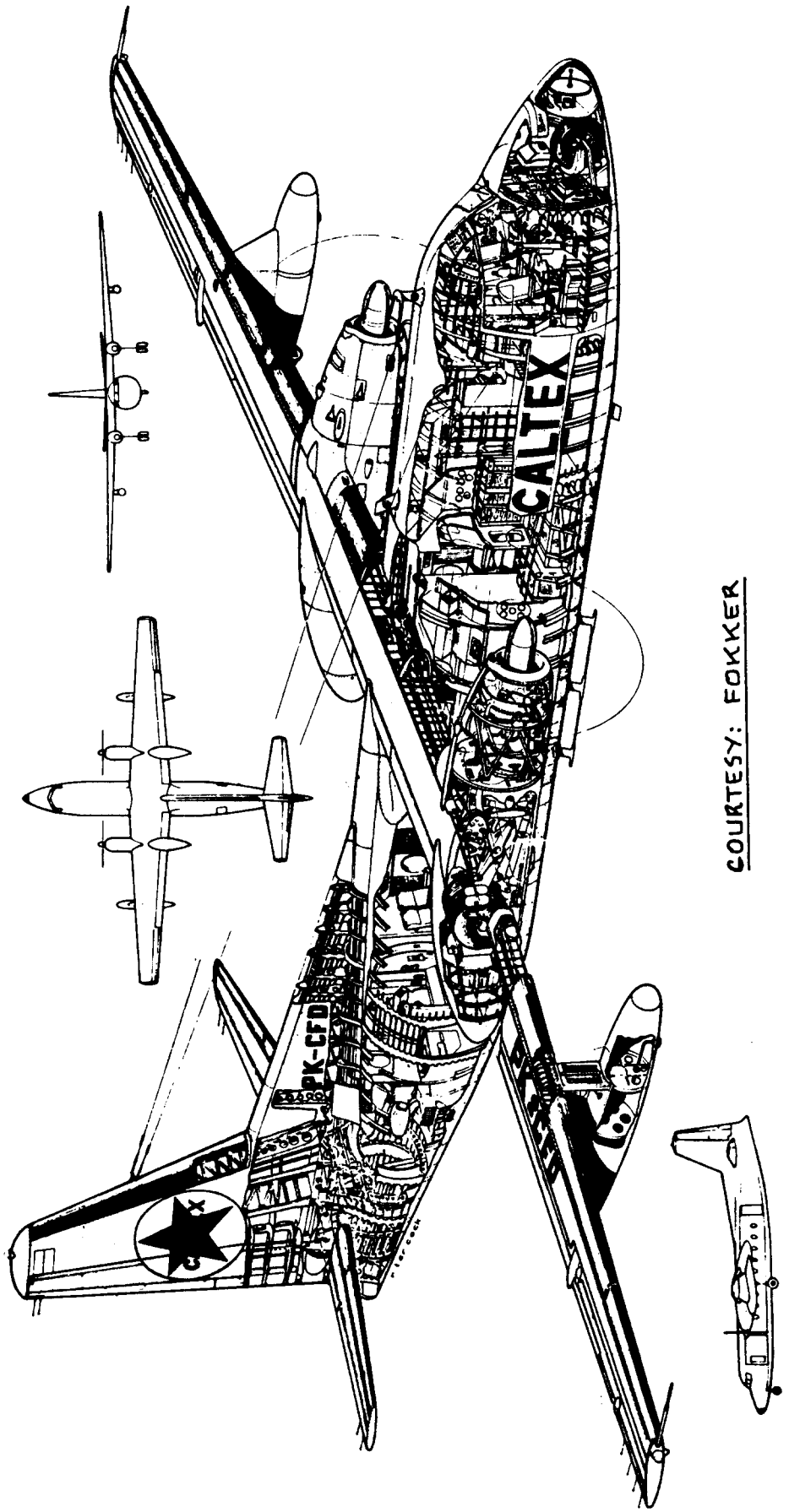

COURTESY: FOKKER

Figure 8.22 Fokker F-27 Friendship

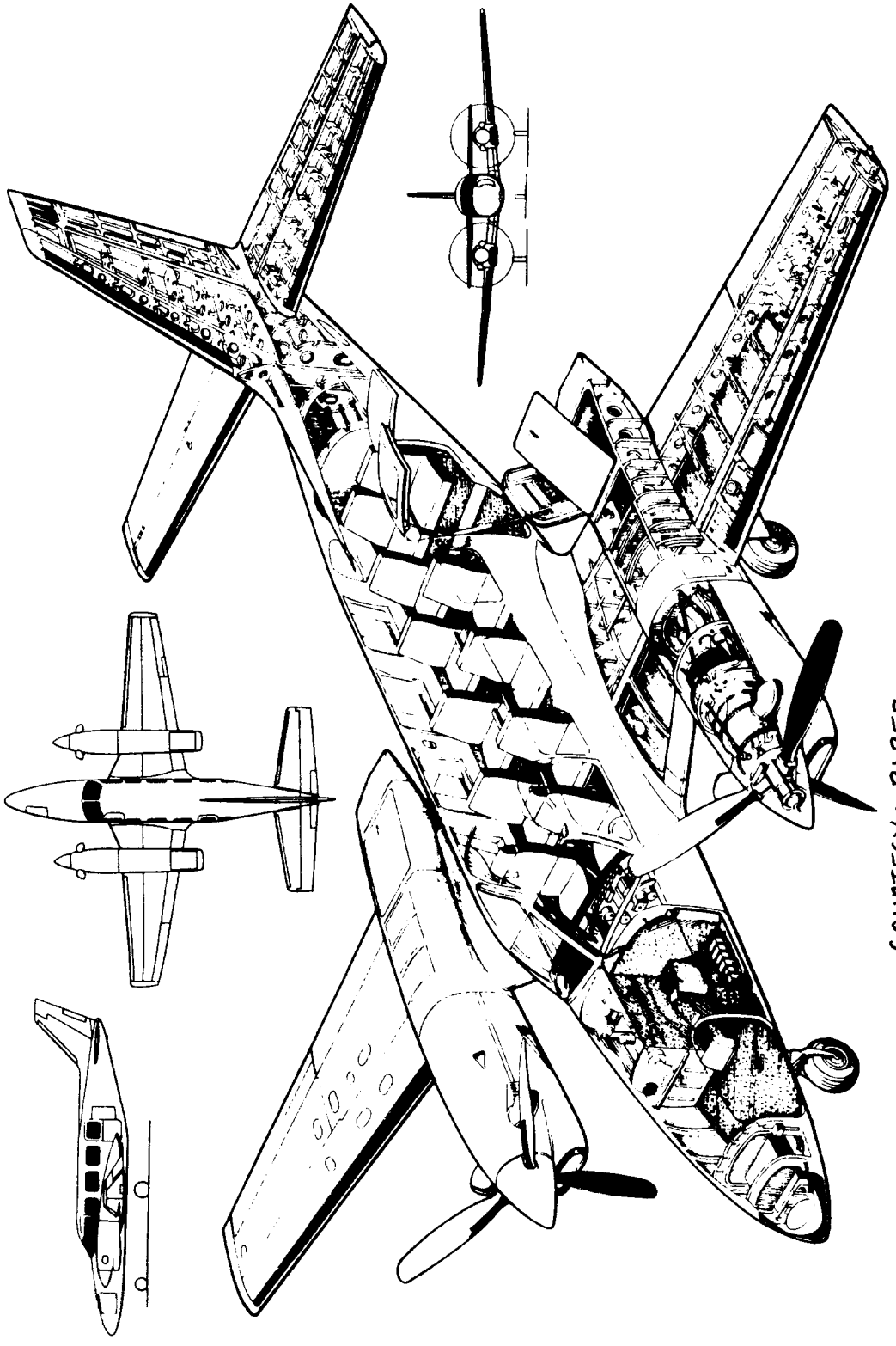

COURTESY: PIPER

Figure 8.23 Piper T-1040

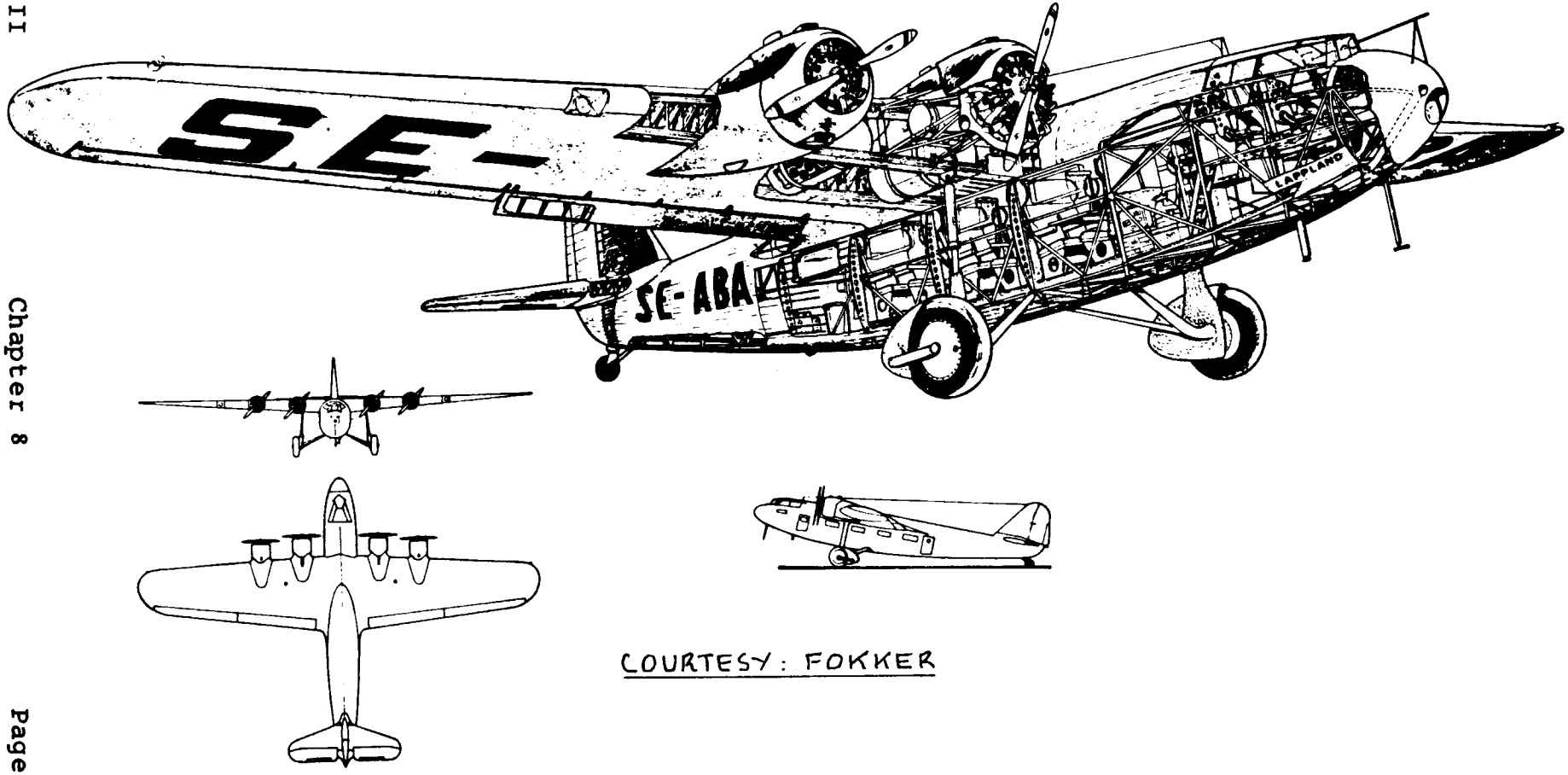

COURTESY: FOKKER

Figure 8.24 Fokker F22

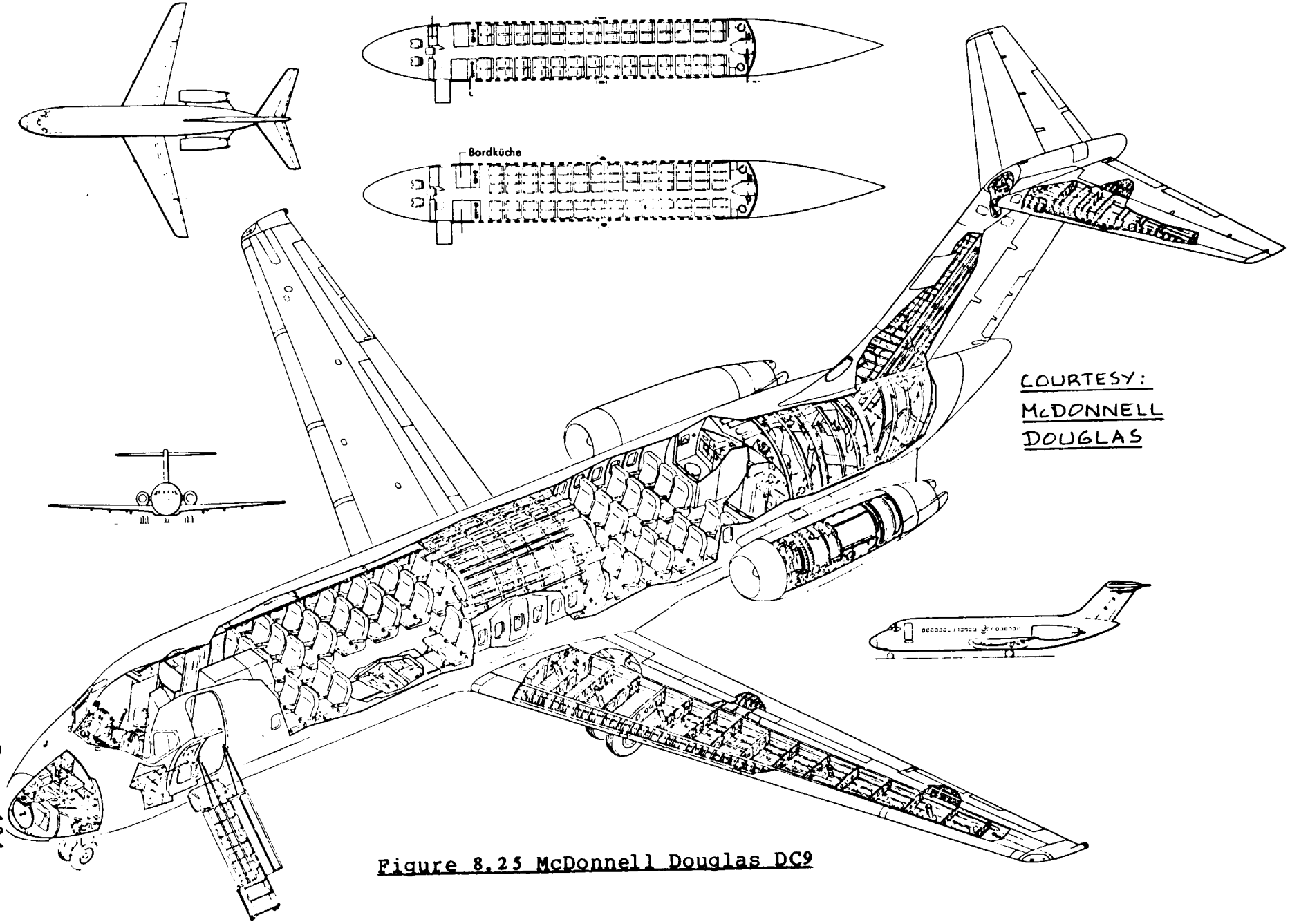

Figure 8.25 McDonnell Douglas DC9

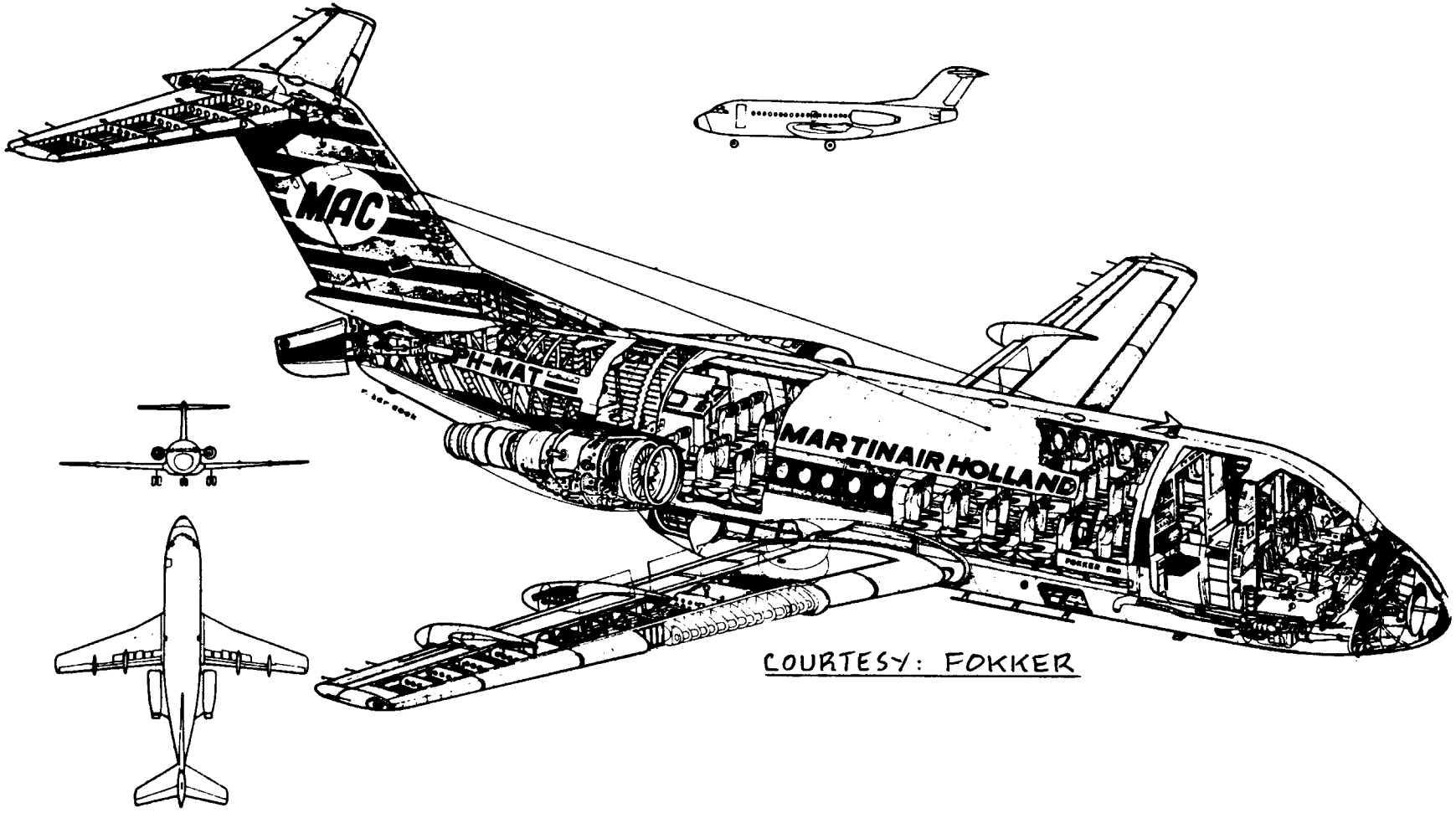

Figure 8.26 Fokker F28

Figure 8.27 McDonnell Douglas DC10

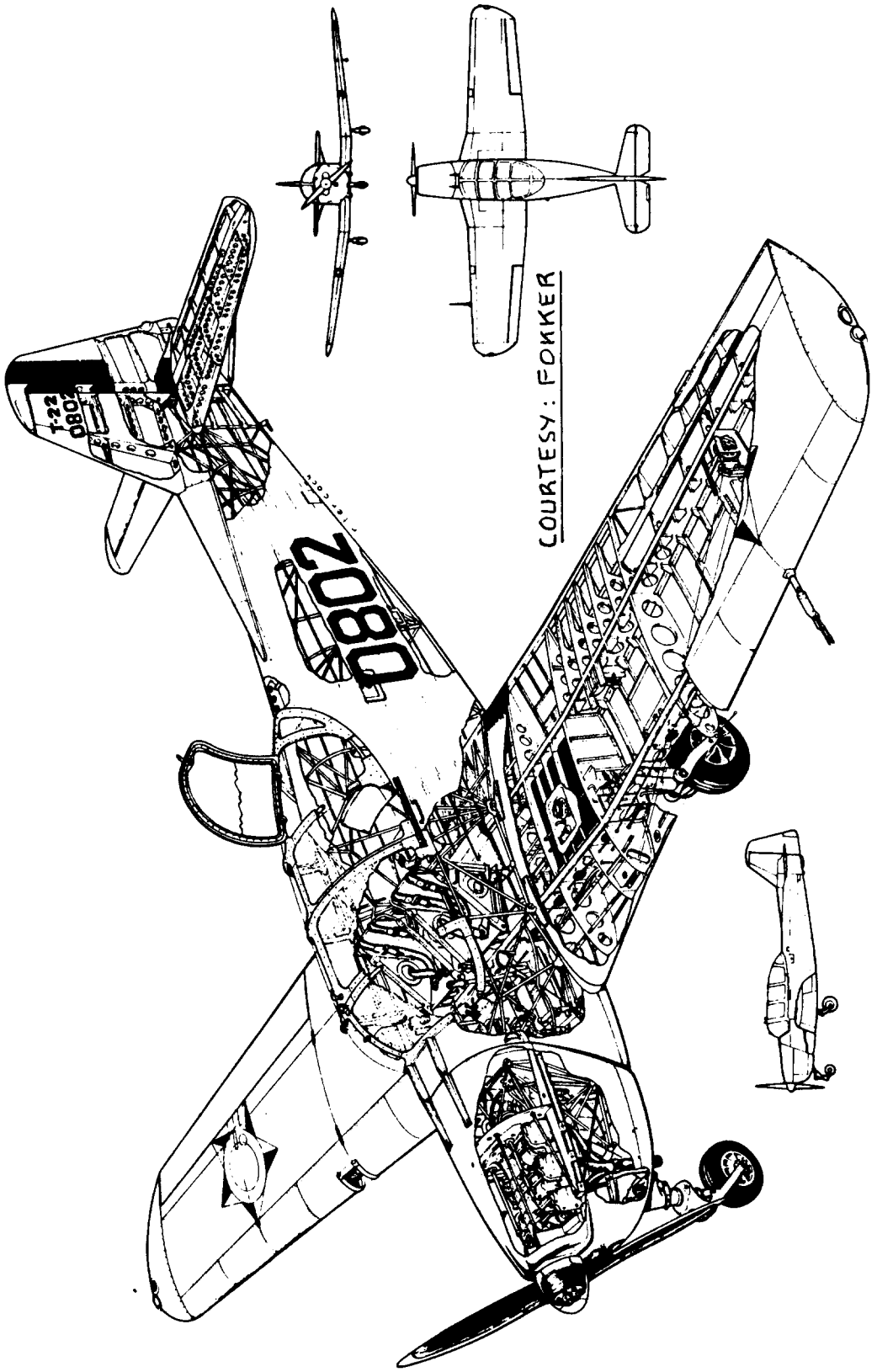

Figure 8.28 Fokker S12

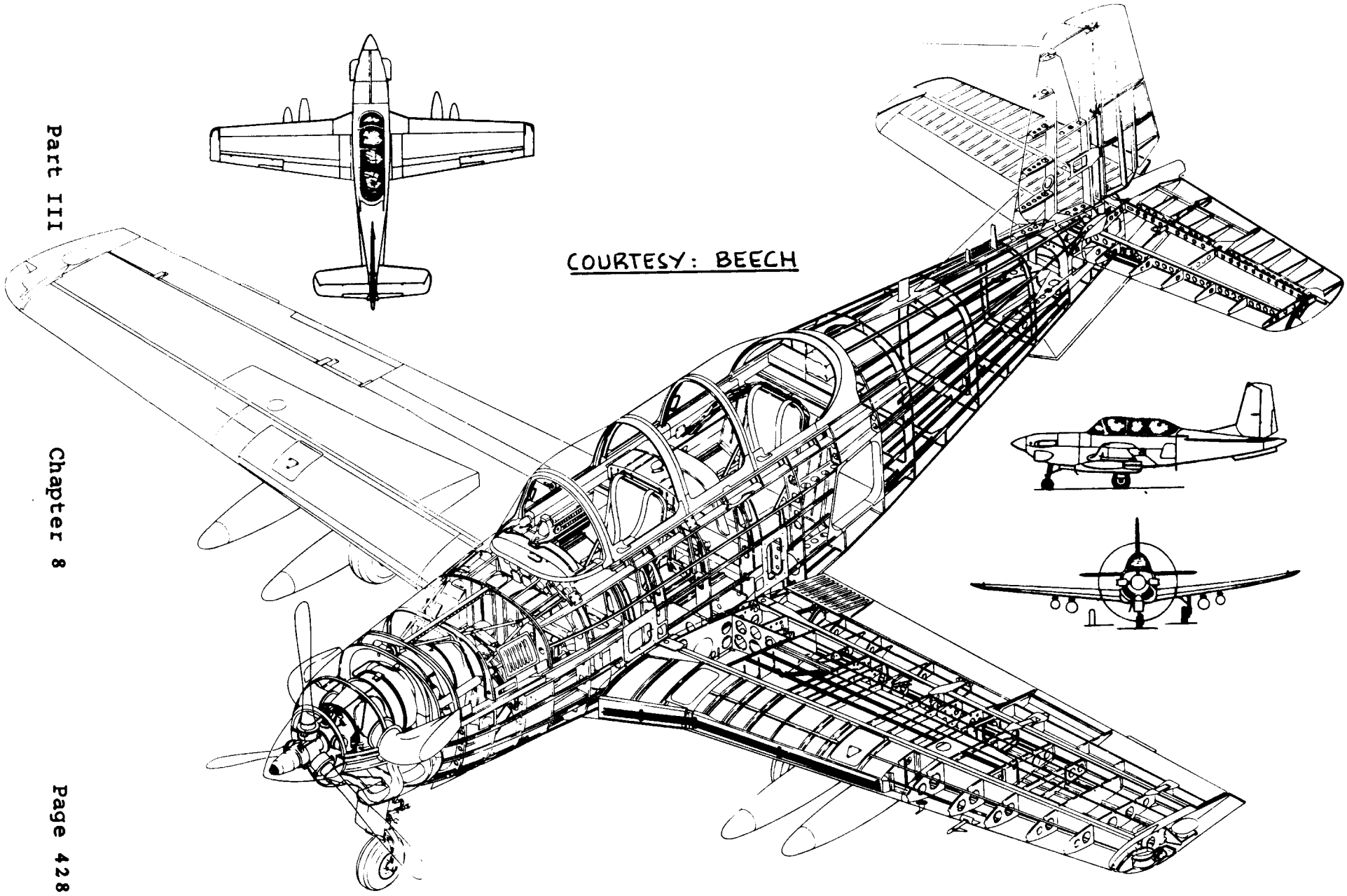

Figure 8.29 Beech T-34C-1

Figure 8.30 Fokker S14

COURTESY: SAAB

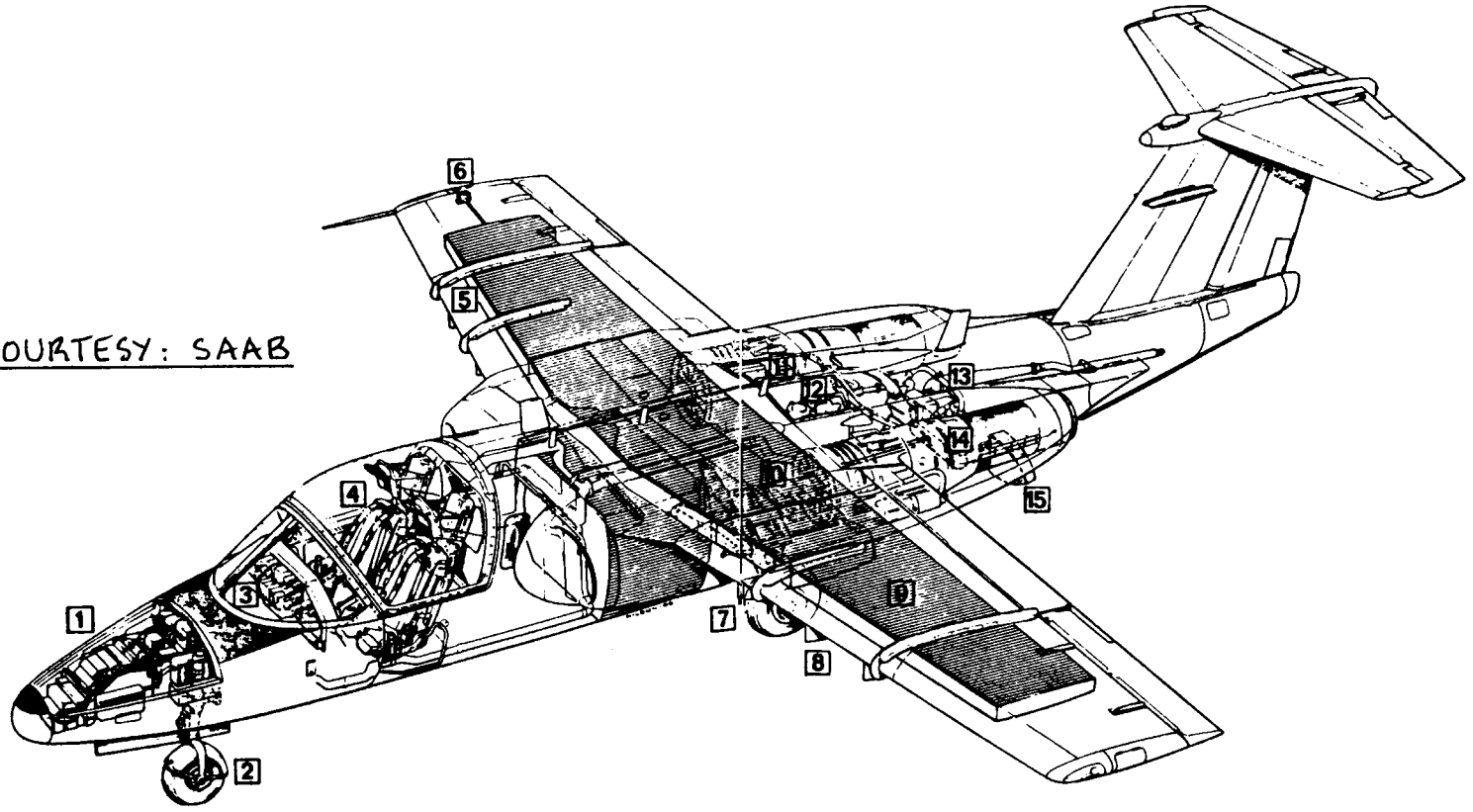

1 Forward equipment compartment housing nav/com equipment.
2 Nose landing gear, steerable, with shimmy damper retracts forward.
3 Instrument panel, with duplicated instruments and controls, under bird-proof windshields and acrylic hood.
4 Pressurized cabin seating two in ejection seats or four in standard seats. Light cargo and other cabin arrangements are also possible.
5 Wing, thin, moderately swept and with negative dihedral. Two-spar, one piece design.
6 Pressure refuelling point. Gravity refuelling also possible.
7 Main landing gear, retracting into fuselage, hydraulically operated, in emergency gravity lowered. Hydraulic anti-skid disk brakes.
8 Six weapon pylons for up to 2000 kg (4400 lb) stores.
9 2050 litres (540 US gallons) fuel tanks. 920 litres (243 US gallons) in fuselage and 1130 litres (297 US gallons) in wing.
10 Lower equipment compartment.
11 Rear equipment and electronics compartment. 28 V DC and 115/200 V 400 c/s AC electric systems. Engine start on internal or external power.
12 Hydraulic compartment. Hydraulic system driven by both engines, operational on one idling engine.
13 Cabin pressure and air-conditioning system.
14 Two General Electric J85-17B jet engines giving 1293 kg (2850 lb) thrust each.
15 Air brakes, hydraulically operated, continuously variable with position indicated in cockpit. Air brakes permit controlled vertical dive.

Figure 8.31 SAAB XT-105

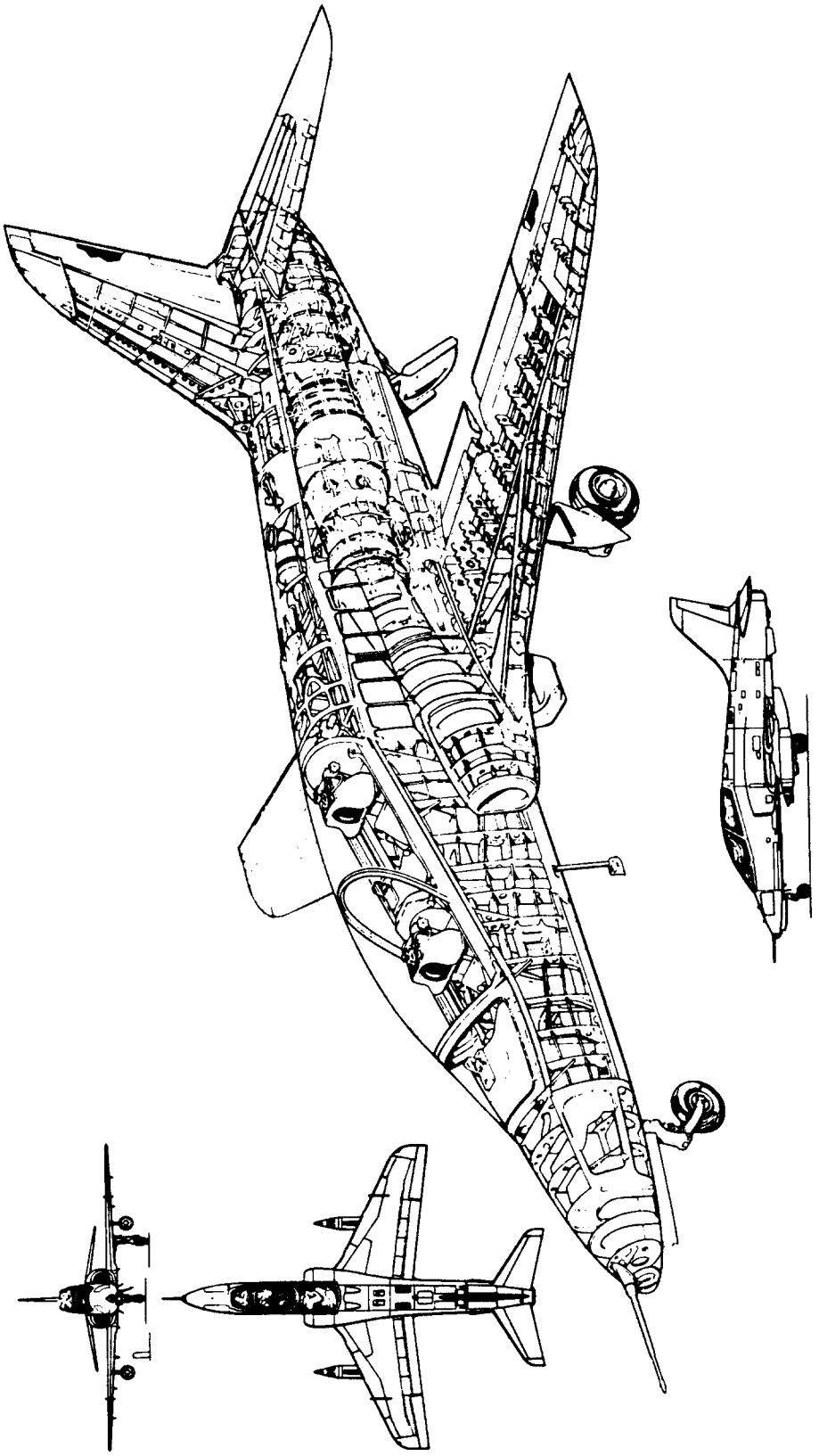

Figure 8.32 British Aerospace Hawk

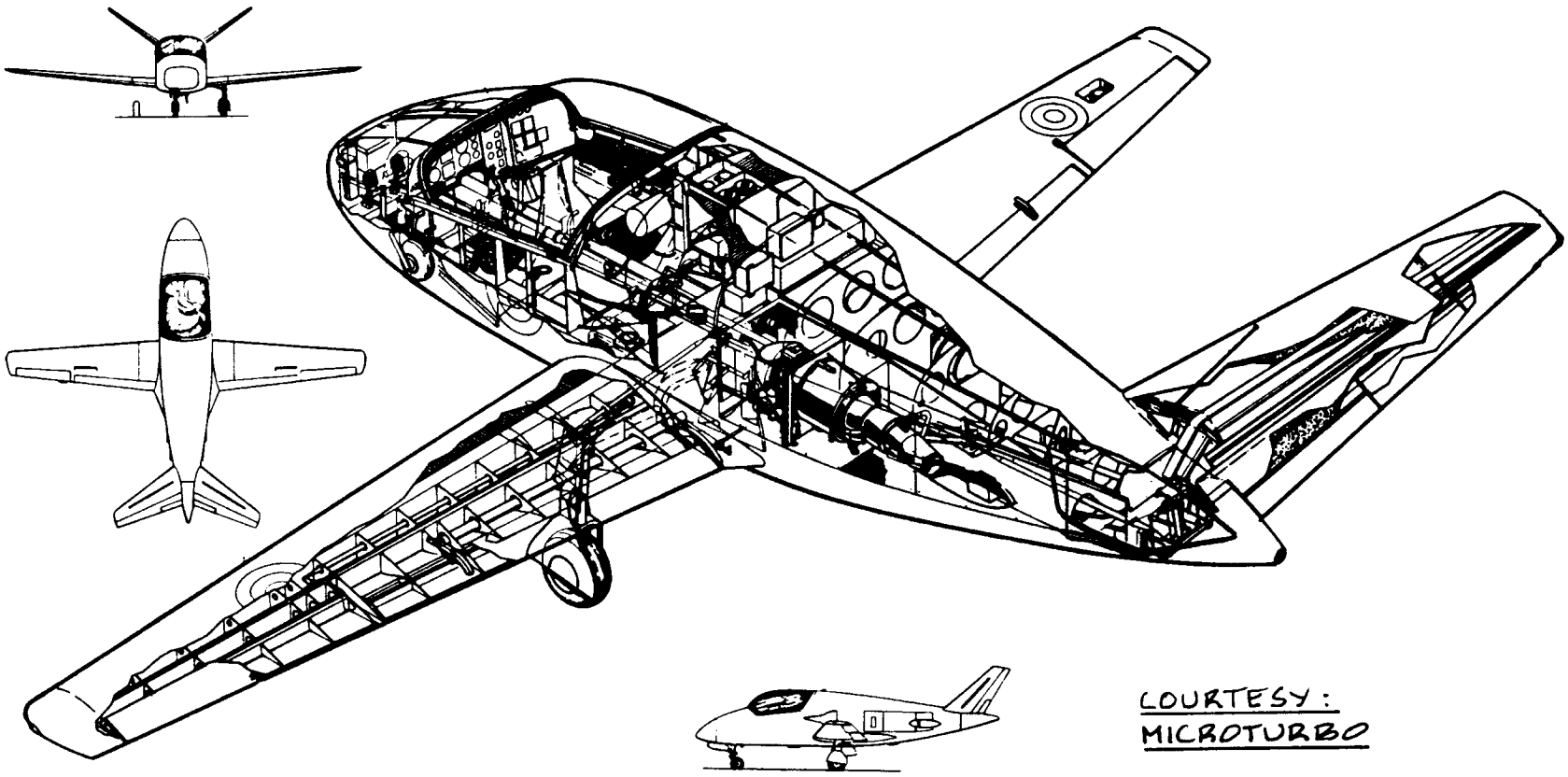

Figure 8.33 Microturbo Microjet 200

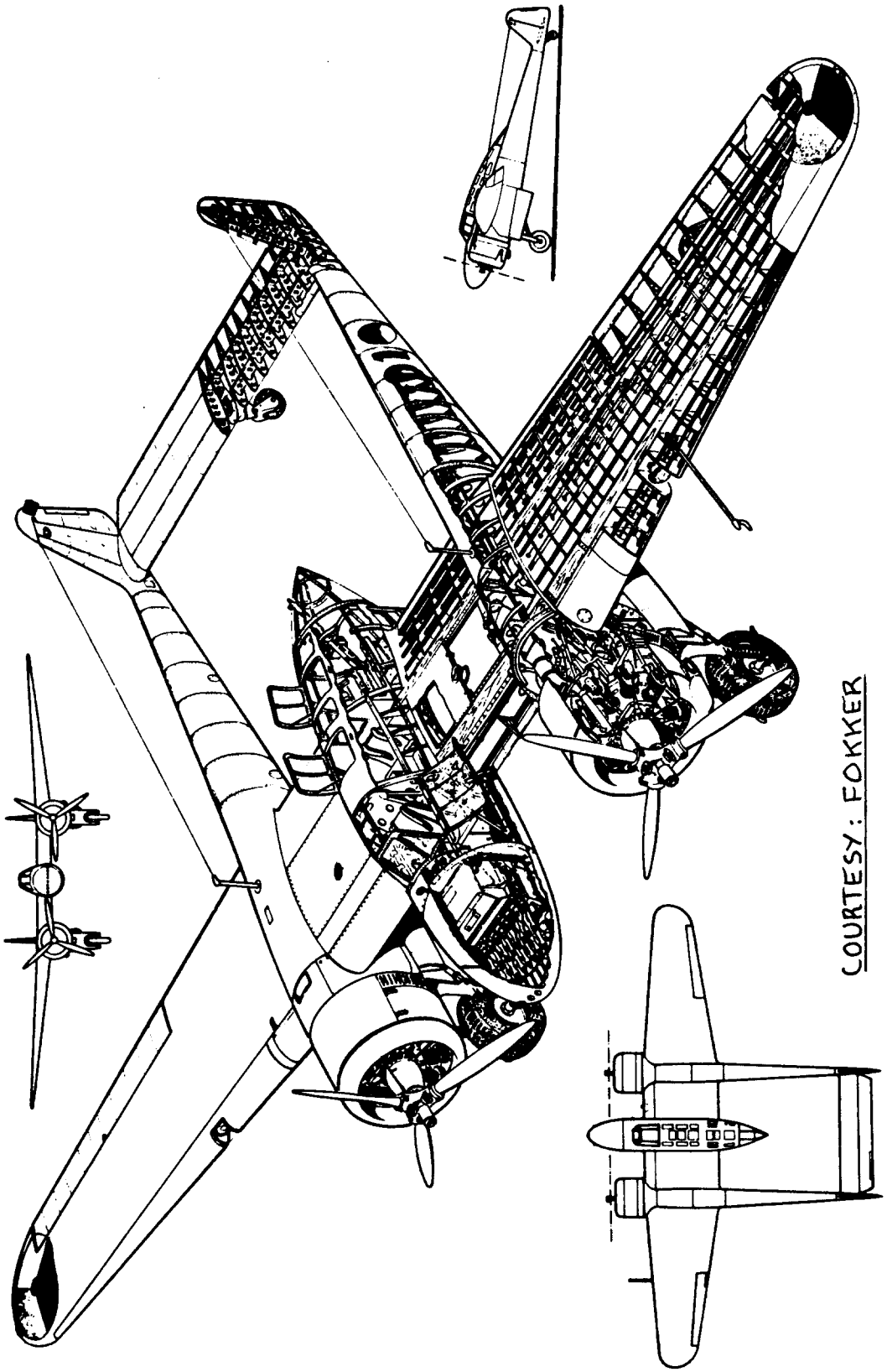

COURTESY: FOKKER

Figure 8.34 Fokker G.1

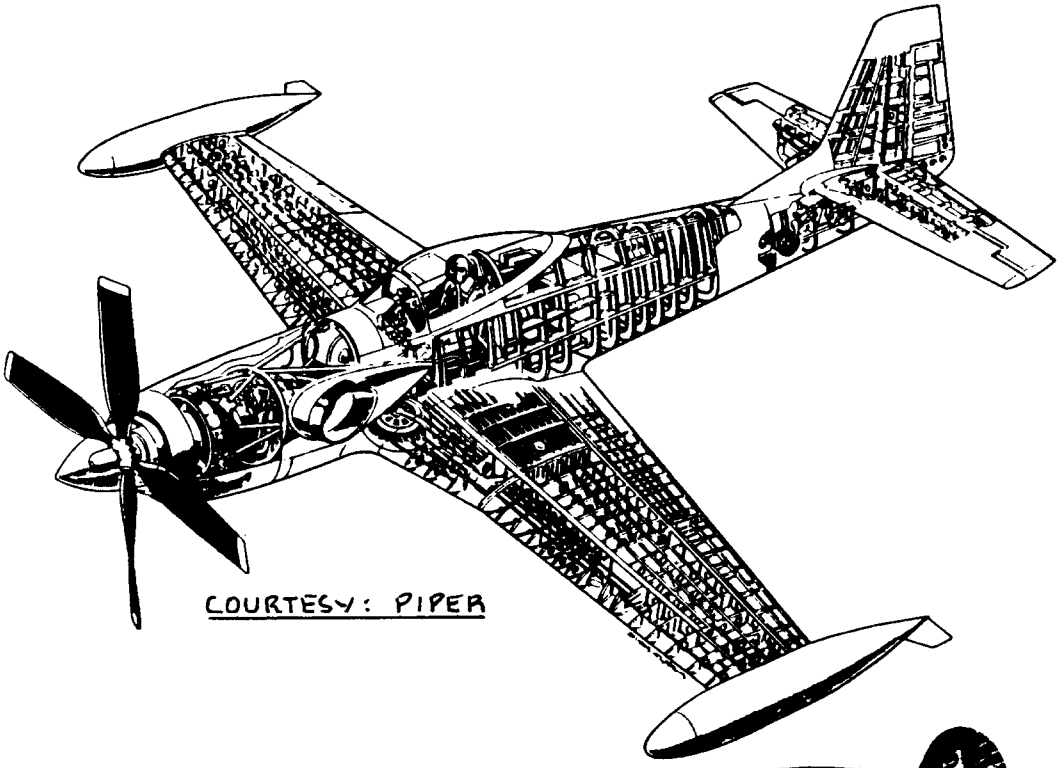

Figure 8.35 Piper PA-48 Enforcer

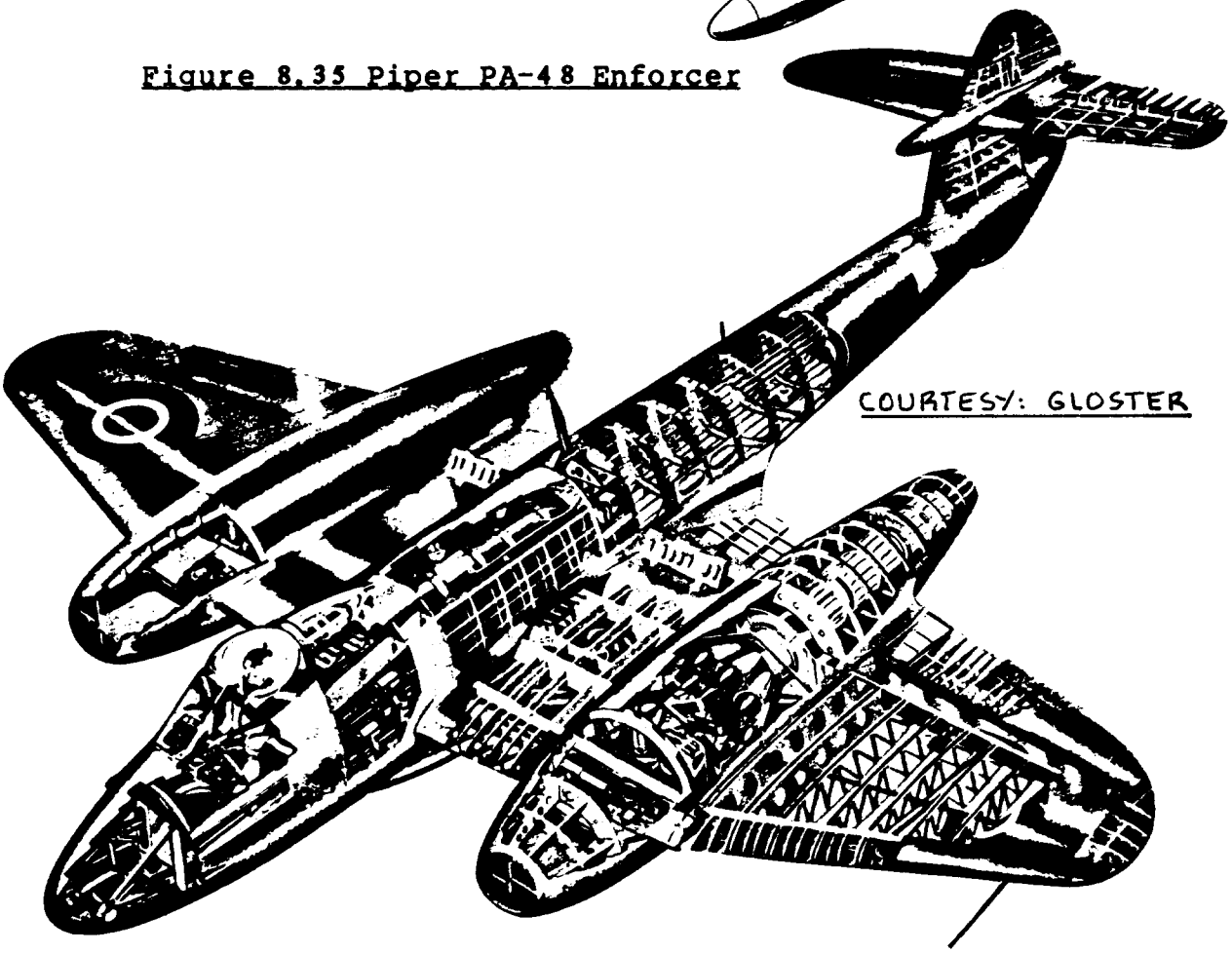

Figure 8.36 Gloster Meteor

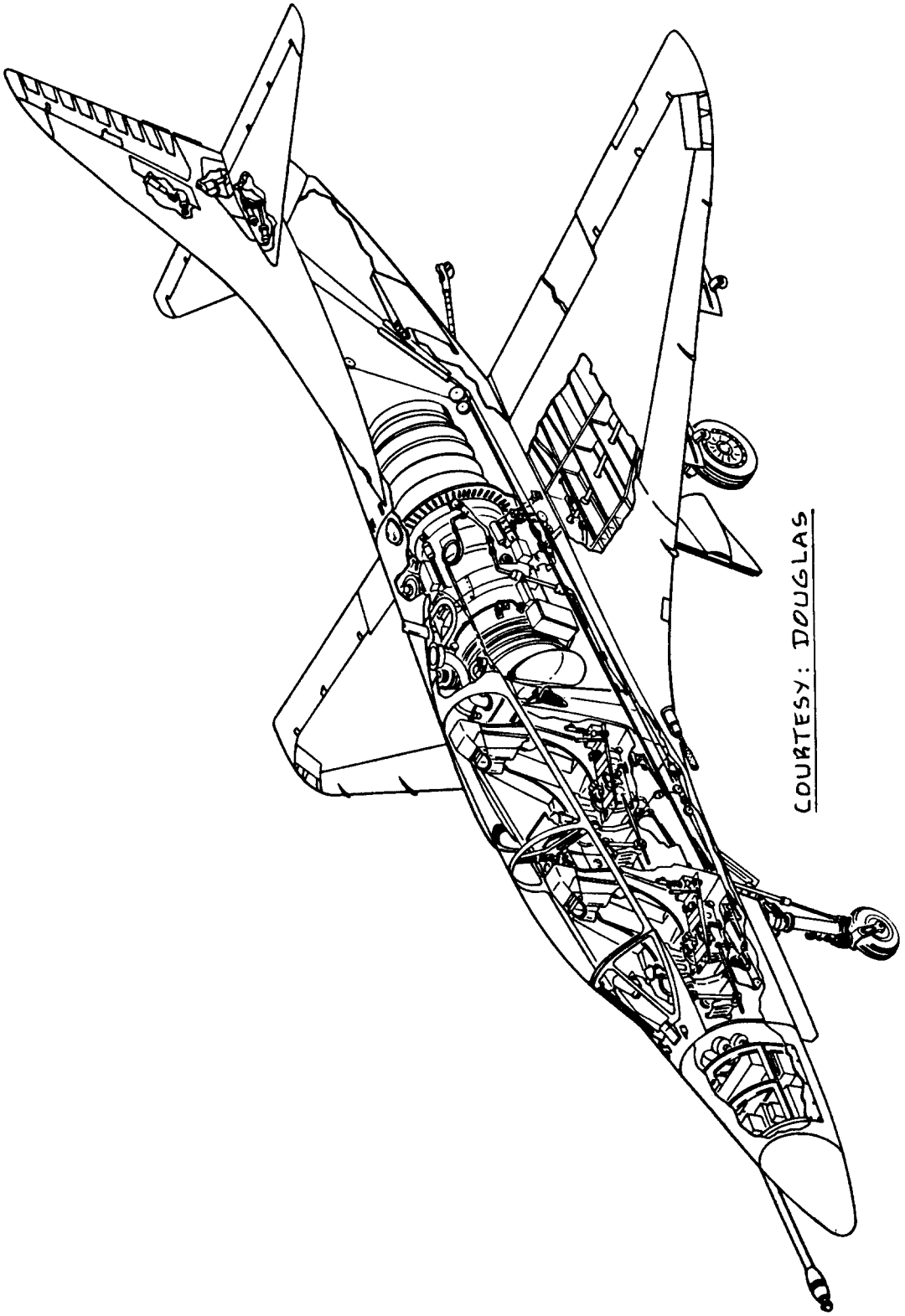

COURTESY: DOUGLAS

Figure 8.37 Douglas A4 Skyhawk

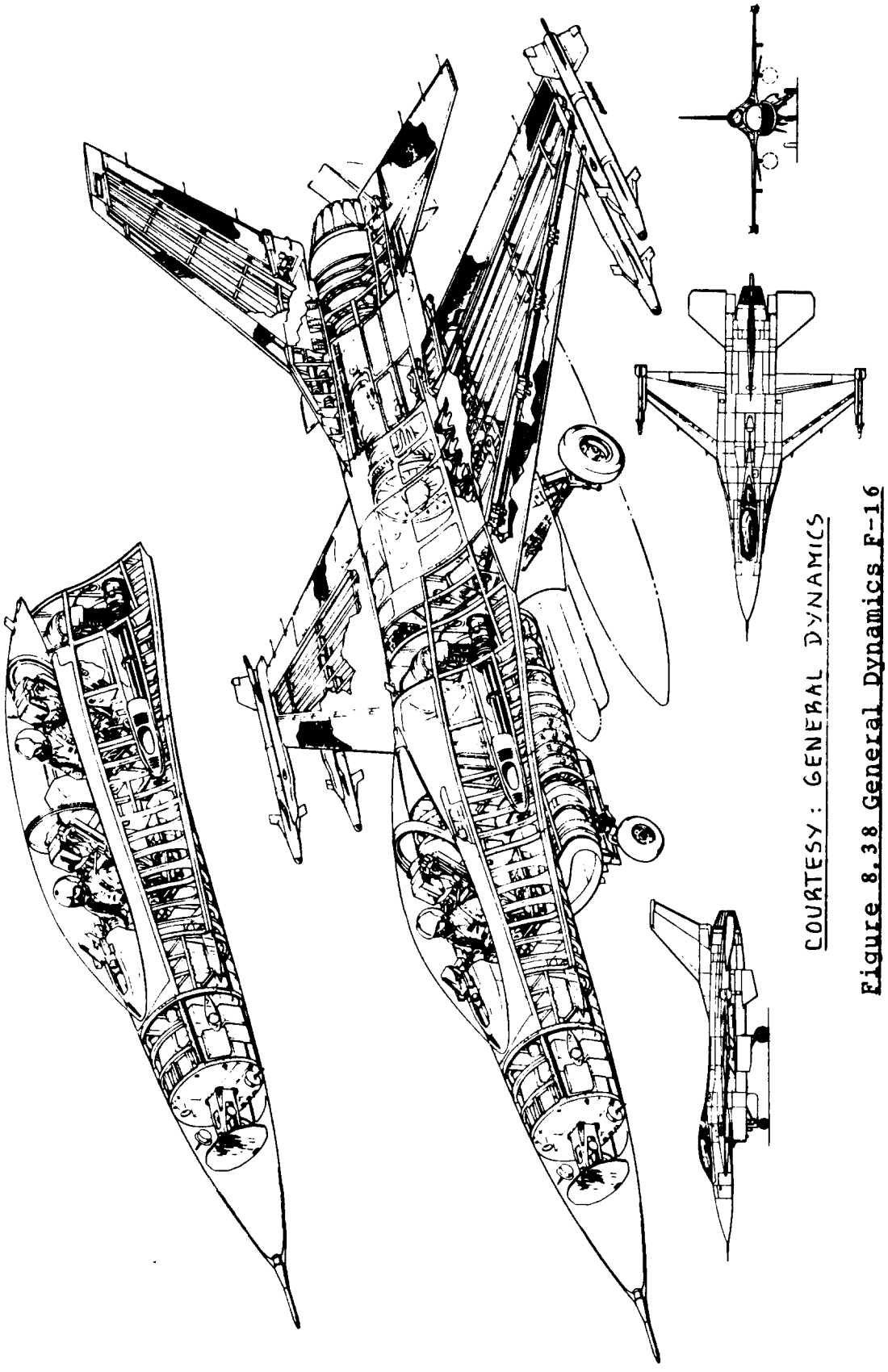

COURTESY: GENERAL DYNAMICS

Figure 8.38 General Dynamics F-16

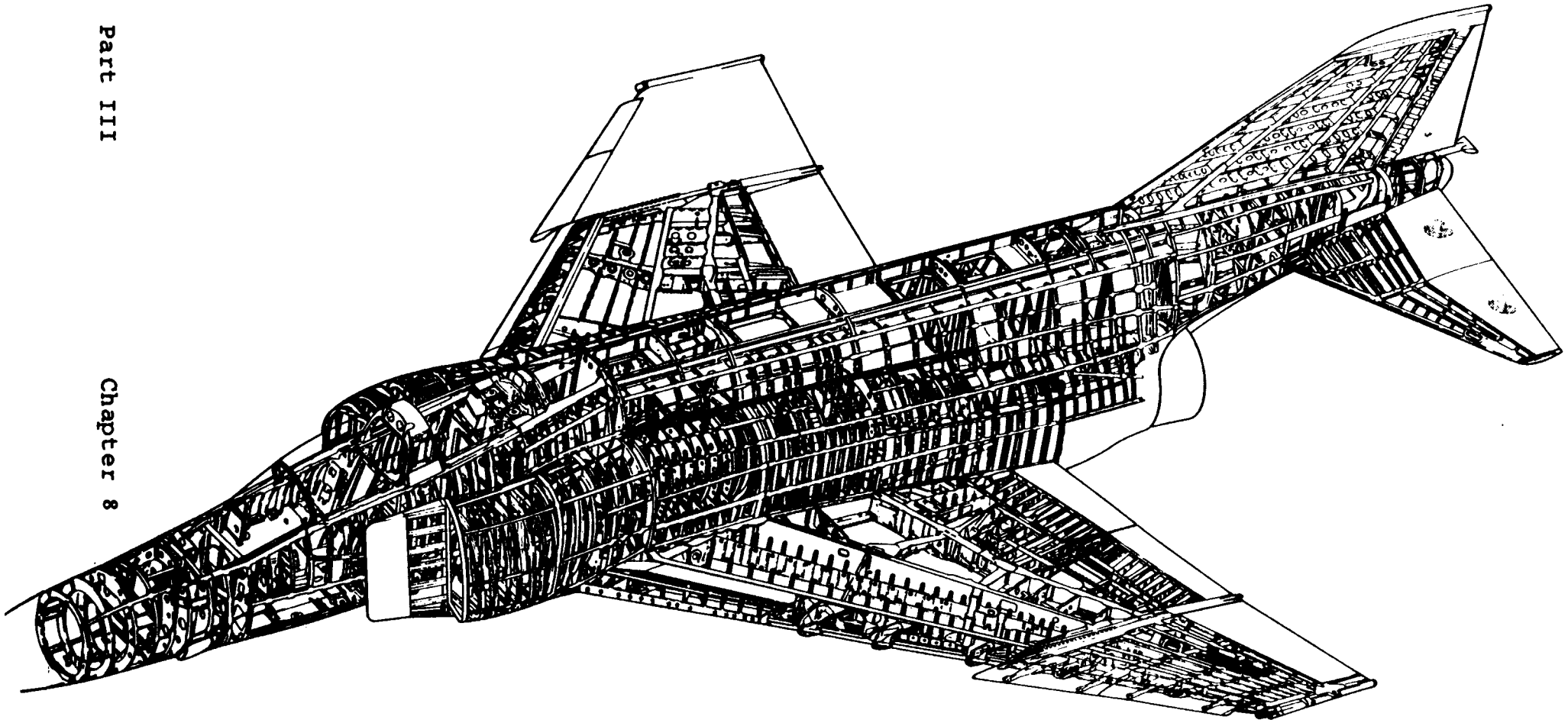

COURTESY: McDONNELL DOUGLAS

Figure 8.39 McDonnell Douglas F-4E

Figure 8.40 McDonnell Douglas F-15

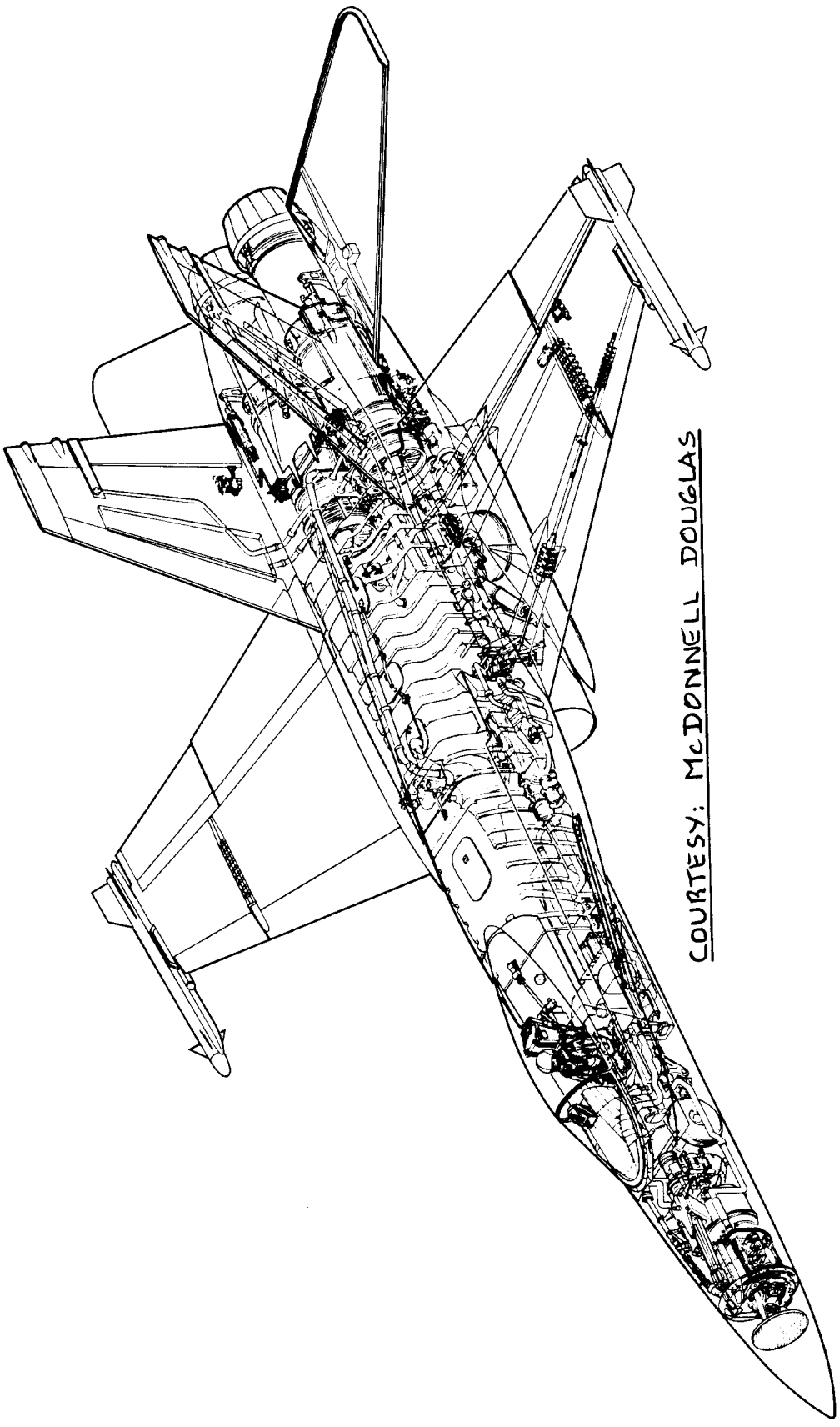

COURTESY: McDONNELL DOUGLAS

Figure 8.41 McDonnell Douglas F-18

COURTESY: McDONNELL DOUGLAS

Figure 8.42 McDonnell Douglas AV-8B

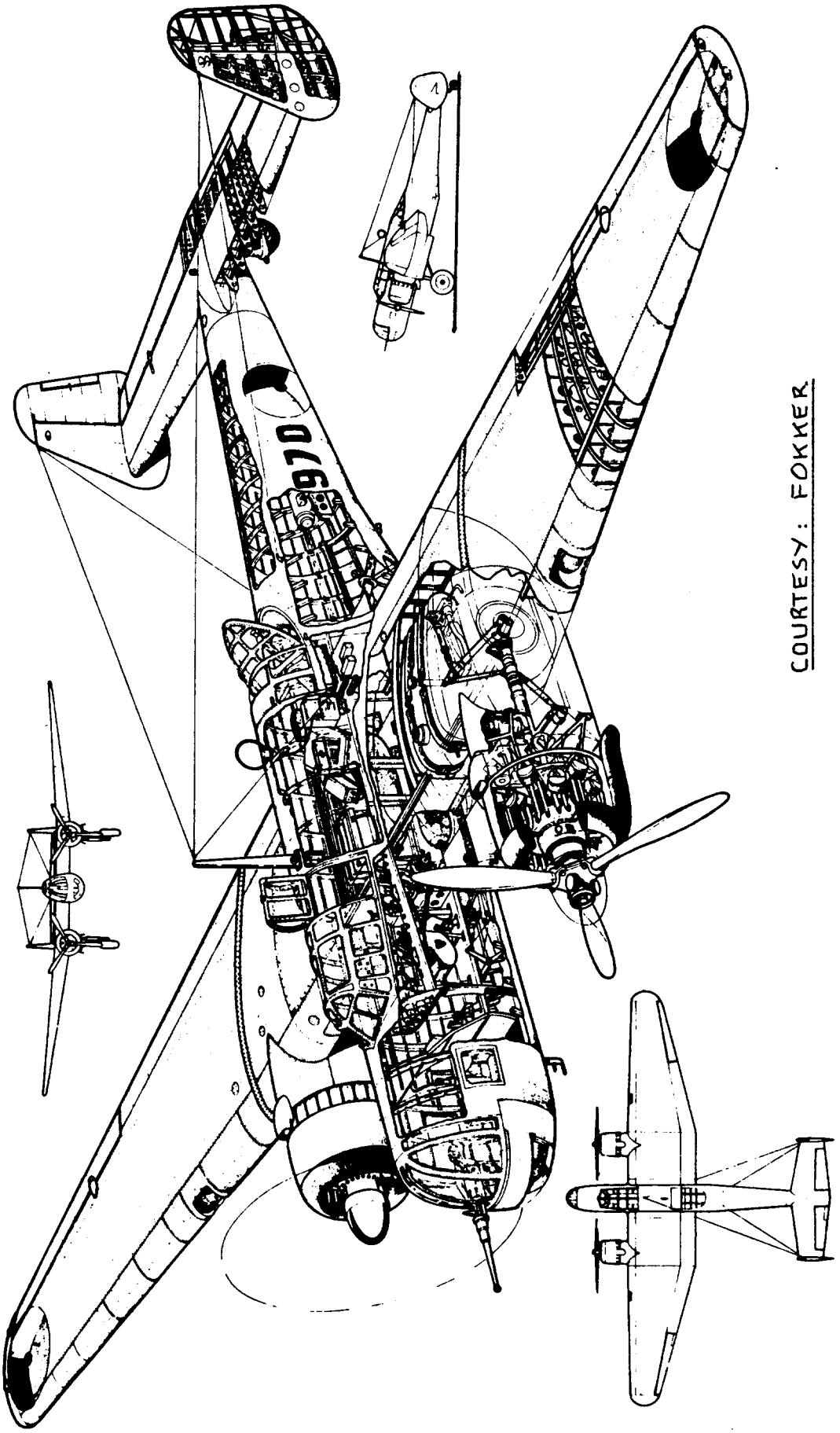

COURTESY: FOKKER

Figure 8.43 Fokker T.IX

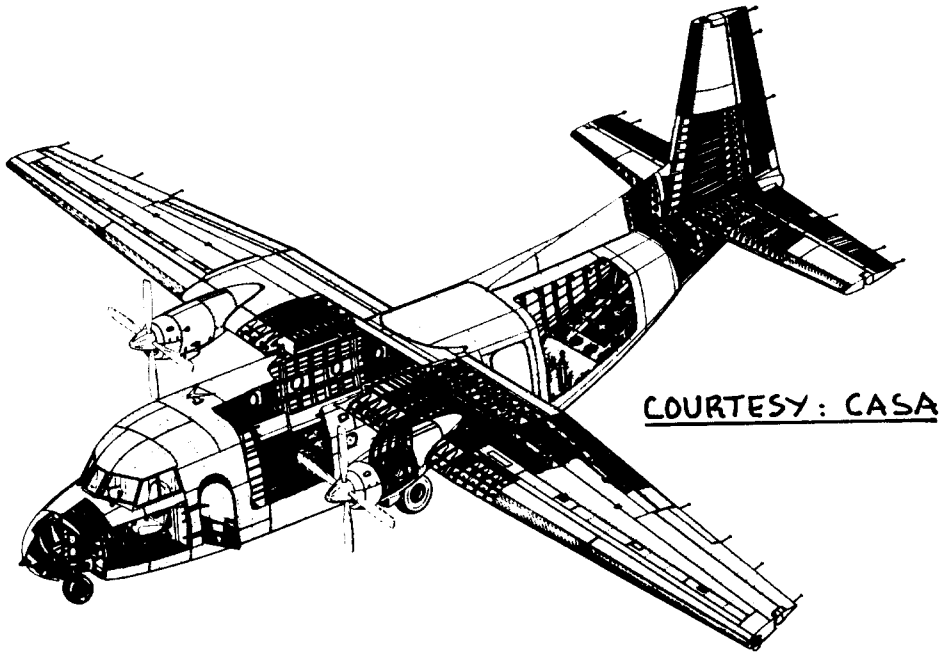

Figure 8.44 CASA C212A

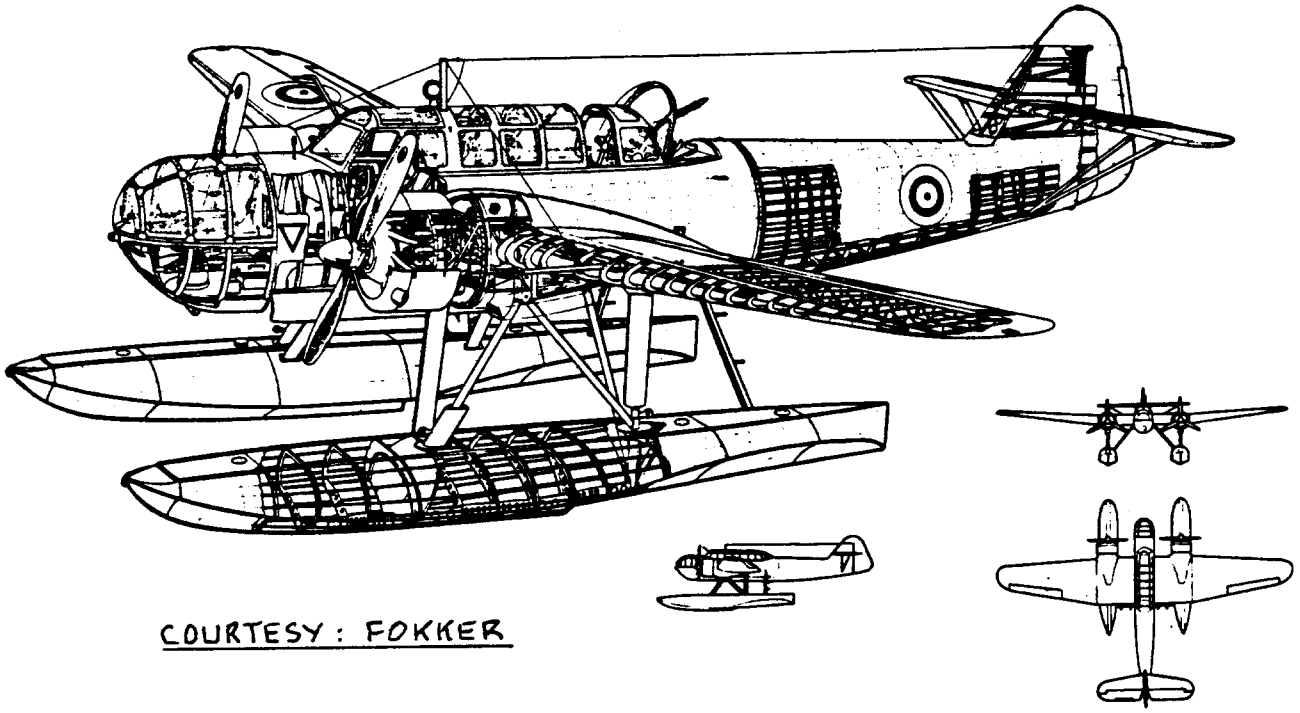

Figure 8.45 Fokker T.VIII-W

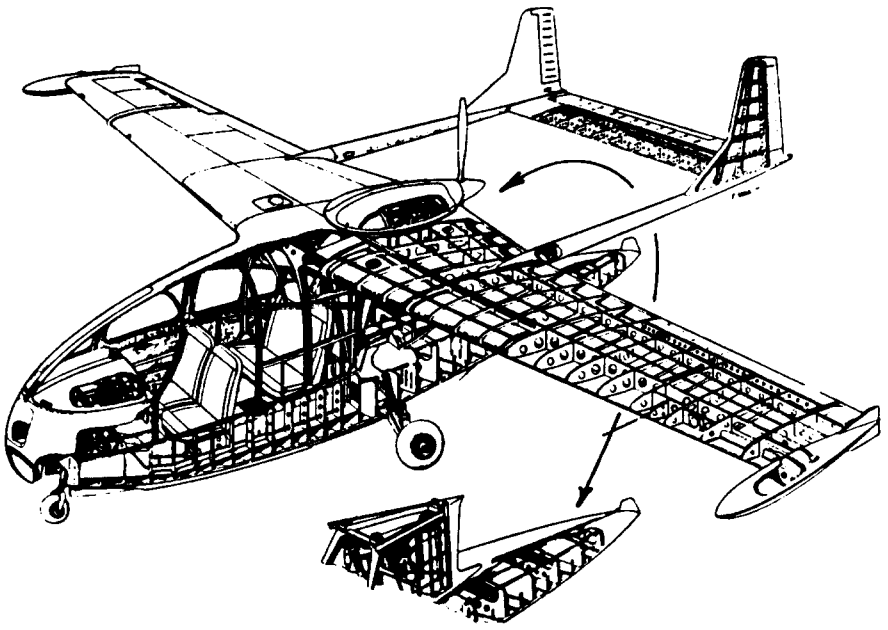

Figure 8.46 Riviera Amphibian

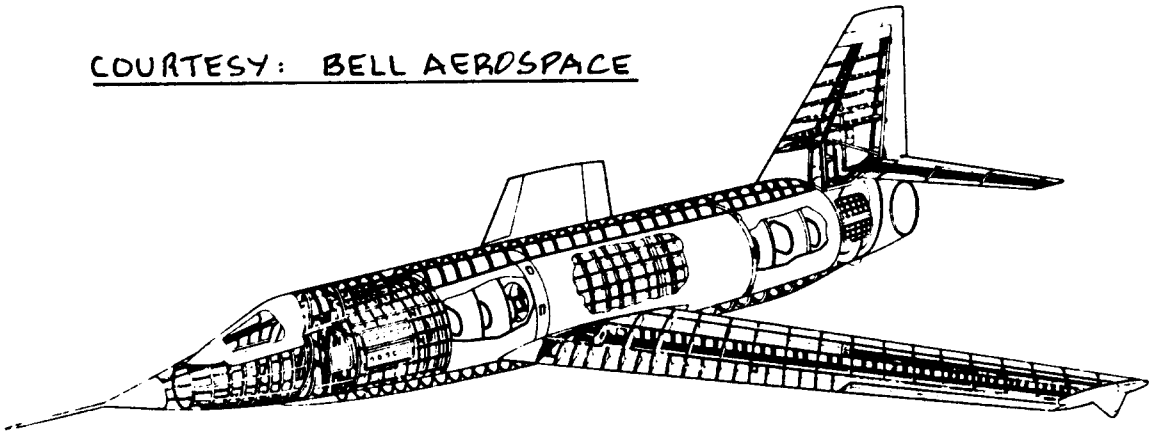

Figure 8.47 Bell X2

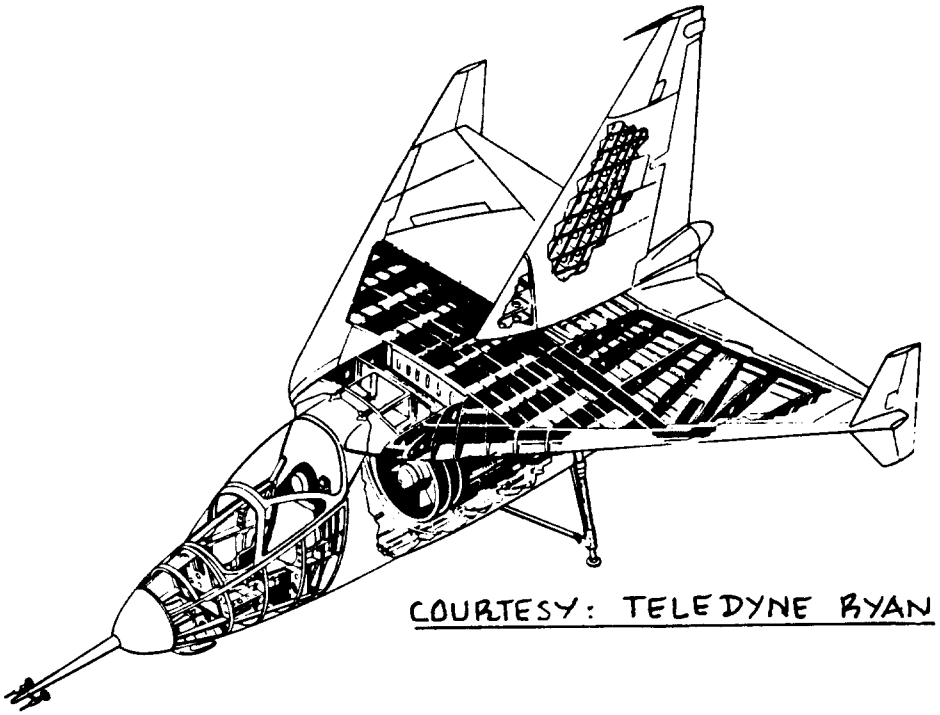

Figure 8.48 Ryan X13

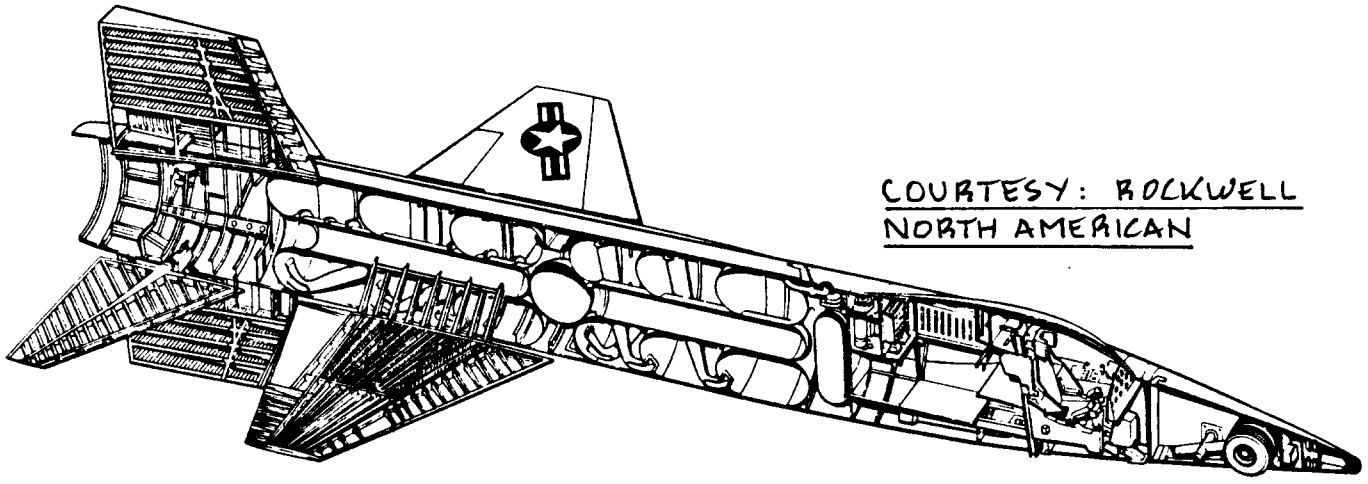

Figure 8.49 North American X15

9. REFERENCES

1. Roskam, J., Airplane Design: Part I, Preliminary Sizing of Airplanes.

2. Roskam, J., Airplane Design: Part II, Preliminary Configuration Design and Integration of the Propulsion System.

3. Roskam, J., Airplane Design: Part IV, Layout Design of Landing Gear and Systems.

4. Roskam, J., Airplane Design: Part V, Component Weight Estimation.

5. Roskam, J., Airplane Design: Part VI, Preliminary Calculation of Aerodynamic, Thrust and Power Characteristics.

6. Roskam, J., Airplane Design: Part VII, Determination of Stability, Control and Performance Characteristics: FAR and Military Requirements.

7. Roskam, J., Airplane Design: Part VIII, Airplane Cost Estimation and Optimization: Design, Development Manufacturing and Operating.

Note: These books are all published by: Roskam Aviation and Engineering Corporation, Rt4, Box 274, Ottawa, Kansas, 66067, Tel. 913-2421624.

8. Human Factors, Flight Safety Foundation, 468 Park Ave. South, New York, N.Y., 10016.

9. Damon, A., Stoudt, H.W. and McFarland, R.A., The Human Body in Equipment Design, Harvard University Press, Cambridge, Mass., 1966.

10. Anon., AFSC Design Handbook, Series DH2-2, Crew Station and Passenger Accomodations, AFWAL, WPAFB, Ohio, 45433.

11. Anon., Federal Aviation Regulations, Part 23 and Part 25, Department of Transportation, Federal Aviation Administration, Distribution Requirements Section, M-482.2, Washington, D.C., 20590.

12. Torenbeek, E., Synthesis of Subsonic Airplane Design, Kluwer Boston Inc., Hingham, Maine, 1982.

13. Küchemann, D., The Aerodynamic Design of Aircraft, Pergamon Press Ltd, Oxford, England, 1978.

14. Stinton, D., The Design of the Aeroplane, Granada, London, England, 1983.

15. Hoerner, S.F., Fluid Dynamic Drag, Hoerner Fluid Dynamics, P.O. Box 342, Brick Town, N.J., 08723, 1965.

16. Roskam, J., Proceedings of the NASA/Industry/University General Aviation Drag Reduction Workshop, Space Technology Center, University of Kansas, Lawrence, Kansas, 66045, 1975.

17. Thurston, D.B., Design for Flying, McGraw Hill Book Co., N.Y., 1978.

18. Olson, R.E. and Land, N.S., Effect of Afterbody Length and Keel Angle on Minimum Depth of Step for Landing Stability and on Take-off Stability of a Flying Boat, NACA TR 923, 1949.

19. Anon., MIL-A-8861(ASG), Military Specification, Airplane Strength and Rigidity, Flight Loads, May, 1960.

20. Bruhn, E.F., Analysis and Design of Flight Vehicle Structures, Tri-State Offset Co., Cincinnati, Ohio, 45202, 1965.

21. Anon., Fatigue Design Handbook, Society of Automotive Engineers, 400 Commonwealth Drive, Warrendale, Pennsylvania, 15096, 1968.

22. Smith, H.W., Airplane Designer's Checklist for Occupant Injury Prevention, AIAA Paper 84-2520, 1984.

23. Anon., British Civil Airworthiness Regulations, Civil Aviation Authority, United Kingdom.

24. Anon., Energy Absorbing Structure Improves Aircraft Safety, Automotive Engineering, Volume 89, Number 12, 1981, Society of Automotive Engineers.

25. Carden, H.D., Impulse Analysis of Airplane Crash Data with Consideration Given to Human Tolerance, SAE Paper 830748, 1983.

26. Snyder, R.G., Impact Protection in Air Transport Passenger Seat Design, SAE Paper 821391, 1982.

27. Saczalski, K., Singley, G.T., Pilkey, W.D. and Huston, R.L., Aircraft Crashworthiness, University Press of Virginia, Charlottesville, 1975.

28. Andrews, D.G. et al, Application of Advanced Technologies to Small Short Haul Aircraft, NASA CR 152089, March 1, 1978.

29. Nicolai, L.M., Fundamentals of Aircraft Design, METS, Inc., 6520 Kingsland Court, San Jose, CA, 95120.

30. Taylor, J.W.R., Jane's All The World Aircraft, Published annually by: Jane's Publishing Company, 238 City Road, London, EC1V 2PU, England.

31. Weisshaar, T., Aeroelastic Stability and Performance Characteristics of Aircraft with Advanced Composite Swept Forward Wing Structures, AFFDL-TR-78-116, 1978.

32. Cook, E., On the Feasibility of Aluminum Forward Swept Wings, Bristol Forward Swept Wing Conference, Bristol, England, 1985.

33. Loftin, L.K., Jr., Quest for Performance, NASA SP-468, 1985.

34. Von Mises, R., Theory of Flight, Dover Publishing Co, N.Y., N.Y., 1960.

35. Wolkovitch, J., Principles of the Joined Wing, Engel Engineering Report No. 80-1, 28603 Trailriders Drive, Rancho Pales Verdes, CA, 90274.

36. Schlichting, H. and Truckenbrodt, E., Aerodynamics of the Airplane, McGraw-Hill International Book Company, N.Y., N.Y., 1979.

37. Roskam, J., Airplane Flight Dynamics and Automatic Flight Controls, Part I, Roskam Aviation and Engineering Corp., Rt 4, Box 274, Ottawa, Ks, 66067, 1984

38. Hsu, C.H. and Lan, C.E., Theory of Wing Rock, Journal of Aircaft, Vol.22, No.10, pp 920-924, October 1985.

39. Whitcomb, R.T., A Study of the Zero-Lift Drag-Rise Characteristics of Wing-Body Combinations Near the Speed of Sound, NACA TR 1273, 1956.

40. Abbott, I.H. and Von Doenhoff, A.E., Theory of Wing Sections, Dover Publications, N.Y., N.Y., 1959.

41. Hoerner, S. and Borst, H.V., Fluid Dynamic Lift, Hoerner Fluid Dynamics, P.O. Box 342, Brick Town, N.J., 08723

42. Holmes, B.J., Obara, C.J. and Yip, L.P., Natural Laminar Flow Experiments on Modern Airplanes, NASA TP 2256, 1984.

43. Gratzer, B., Results of Natural Laminar Flow Flight Tests on a Boeing 757, Oral Presentation at the AIAA Aircraft Design and Operations Meeting, Oct., 1985.

44. Williams, K.L., Vijgen, P. and Roskam, J., Natural Laminar Flow and Regional Aircraft, SAE Paper 850864, General Aviation Aircraft Meeting and Exposition, April 16-19, 1985, Wichita, Ks.

45. Holmes, B.J. et al, Manufacturing Tolerances for Natural Laminar Flow Airframe Surfaces, SAE Paper 850863, as ref. 44.

46. Croom, C.C. and Holmes, B.J., Flight Evaluation of an Insect Contamination Protection System for Laminar Flow Wings, SAE Paper 850860, as ref. 44.

47. Warwick, G., Jetstar Smooths the Way, Flight International, September 1985, pp 32-34.

48. Kendall, E.R., The Minimum Induced Drag, Longitudinal Trim and Static Longitudinal Stability of Two-Surface and Three-Surface Airplanes, AIAA Paper 84-2164, 2nd Applied Aerodynamics Conference, August, 1984.

49. Rokhsaz, K. and Selberg, B.P., Analytical Study of Three-Surface Lifting Systems, SAE Paper 850866, as ref. 44.

50. Steiner, J.E. et al, Case Study in Aircraft Design, The Boeing 727, Professional Study Series, AIAA, September 14, 1978.

51. Anon., Military Specification for Flying Qualities of Piloted Airplanes, MIL-F-8785, B and C, 1984.

52. Pelikan, R.J., Evaluation of Aircraft Departure Divergence Critaria with a Six-Degree-of-Freedom Digital Simulation Program, AIAA Paper 74-68, 1974.

53. Chambers, J.R., Overview of Stall/Spin Technology, AIAA Paper 80-1580, 1980.

54. Shortal, J.A. and Maggin, B., Effect of Sweepback and Aspect Ratio on Longitudinal Stability Characteristics of Wings at Low Speeds, NACA TN 1093, '46.

55. Larrabee, E.E., Five Years Experience with Minimum Loss Propellers-Part I: Theory, SAE Paper 840026, International Congress and Exposition, 1984.

56. Larrabee, E.E., Five Years Experience with Minimum Loss Propellers-Part II: Applications, SAE Paper 840027, as Ref.55.

57. Lan, C.E. and Roskam, J., Airplane Aerodynamics and Performance, Roskam Av. and Engrg Corp. as ref.7.

58. McKinley, J.L. and Bent, R.D., Powerplants for Aerospace Vehicles, McGraw Hill Book Co., NY, NY, 1965.

59. Taylor, C.F., The Internal Combustion Engine in Theory and Practice, Volumes 1 and 2, MIT Press, 1966.

60. Kerrebrock, J.L., Aircraft Engines and Gas Turbines, MIT Press, 1977.

61. Treager, I.E., Aircraft Gas Turbine Engine Technology, Mc Graw Hill Book Co., NY, NY, 1970.

62. Godston, J. and Reynolds, C.N., Prop-fan Powered Aircraft, Journal of Aircraft, December, 1985.

63. Whitlow, J.B. and Sievers, G.K., Fuel Savings Potential of the NASA Advanced Turboprop Program, NASA TM 83736, September, 1984.

64. Keiter, I.D., Impact of Advanced Technology on Aircraft/Mission Characteristics of Several General Aviation Aircraft, SAE Paper 810584, 1981.

65. Covert, E.E. et al, Thrust and Drag: Its Prediction and Verification, Volume 98, Progress in Aeronautics and Astronautics, AIAA, NY, NY, 1985.

66. Anon., MIL-STD-1474(MI), Military Standard, Noise Limits for Army Materiel, March 1973.

67. Wilby, J.F., The Prediction of Interior Noise of Propeller Driven Aircraft: A Review, SAE Paper 830737, 1983.

68. Klatte, R.J., General Aviation Propeller Noise Reduction: Penalties and Potential, SAE Ppr 810585, 1981.

69. Waterman, E.H., Kaptein, D. and Sarin, S.L., Fokker's Activities in Cabin Noise Control for Propeller Aircraft, SAE Paper 830736, 1983.

70. Smith, M.H., A Prediction Procedure for Propeller Aircraft Flyover Noise Based on Empirical Data, SAE Paper 810604, 1981.

71. Anon., Prediction Procedure for Near-Field and Far-Field Propeller Noise, AIR 1407, SAE Aerospace Information Report, May 1977.

72. Feiler, C.E. and Conrad, W., Noise from Turbomachinery, AIAA Paper 73-815, AIAA 5th Aircraft Design and Operations Meeting, August 1973.

73. Drell, H., Impact of Noise on Subsonic Transport Design, SAE Paper 700806.

74. Carlson, H.W., Simplified Sonic Boom Prediction, NASA TP-1122, 1978.

75. Roskam, J. et al, Proceedings of the NASA/Industry/University General Aviation Drag Reduction Workshop, Space Technology Center, The University of Kansas, Lawrence, Kansas, 1975.

76. Bingelis, T., Firewall Forward, Engine Installation Methods, Tony Bingelis, 8509 Greenflint Lane, Austin, Texas, 78759, 1983.

77. Anon., Lord Kinematics Catalog, Technical Reference LB-571, Lord Kinematics, 1635 West 12th Street, Erie, Pennsylvania, 16512, 1974.

78. Stinton, D., The Anatomy of the Aeroplane, Granada Publishing, England, 1980.

79. Warwick, G., Aluminum Fights Back, Flight International, March 2, 1985.

80. Brahney, J., Polyamide-imide Resins Examined, Aerospace Engineering, December, 1985.

81. Langston, P.R., Design and use of Kevlar in Aircraft Structures, SAE Paper 850893, General Aviation Aircraft Meeting and Exposition, Wichita, April, 1985.

82. Heinemann, E., Rausa, R. and Van Every, K., Aircraft Design, The Nautical and Aviation Publ. Co., 1985.

10. INDEX

CONSTRUCCIONES AERONAUTICAS, S. A.
- D. PROYECTOS Y SISTEMAS -
2351
BIBLIOTECA TECNICA
- INFORMACION Y DOCUMENTACION -
GETAFE (Madrid)

AIRPLANE DESIGN

PART IV: LAYOUT DESIGN OF LANDING GEAR AND SYSTEMS

by

Dr. Jan Roskam
Ackers Distinguished Professor
of Aerospace Engineering
The University of Kansas
Lawrence, Kansas

NO PART OF THIS BOOK MAY BE REPRODUCED WITHOUT
PERMISSION FROM THE AUTHOR

Copyright: Roskam Aviation and Engineering Corporation
Rt4, Box 274, Ottawa, Kansas, 66067
Tel. 913-2421624

First Printing: 1986 (softbound)
Second Printing: 1989 (hardbound)

TABLE OF CONTENTS

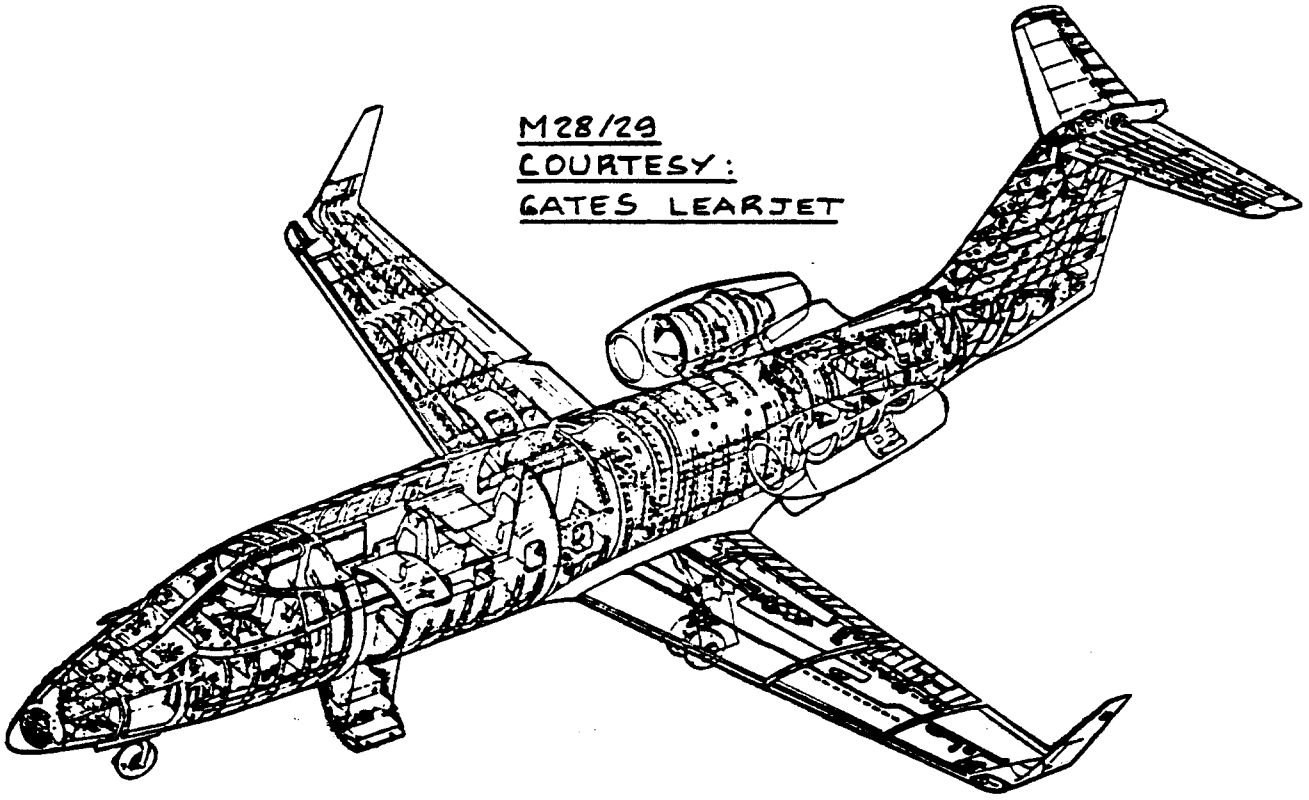

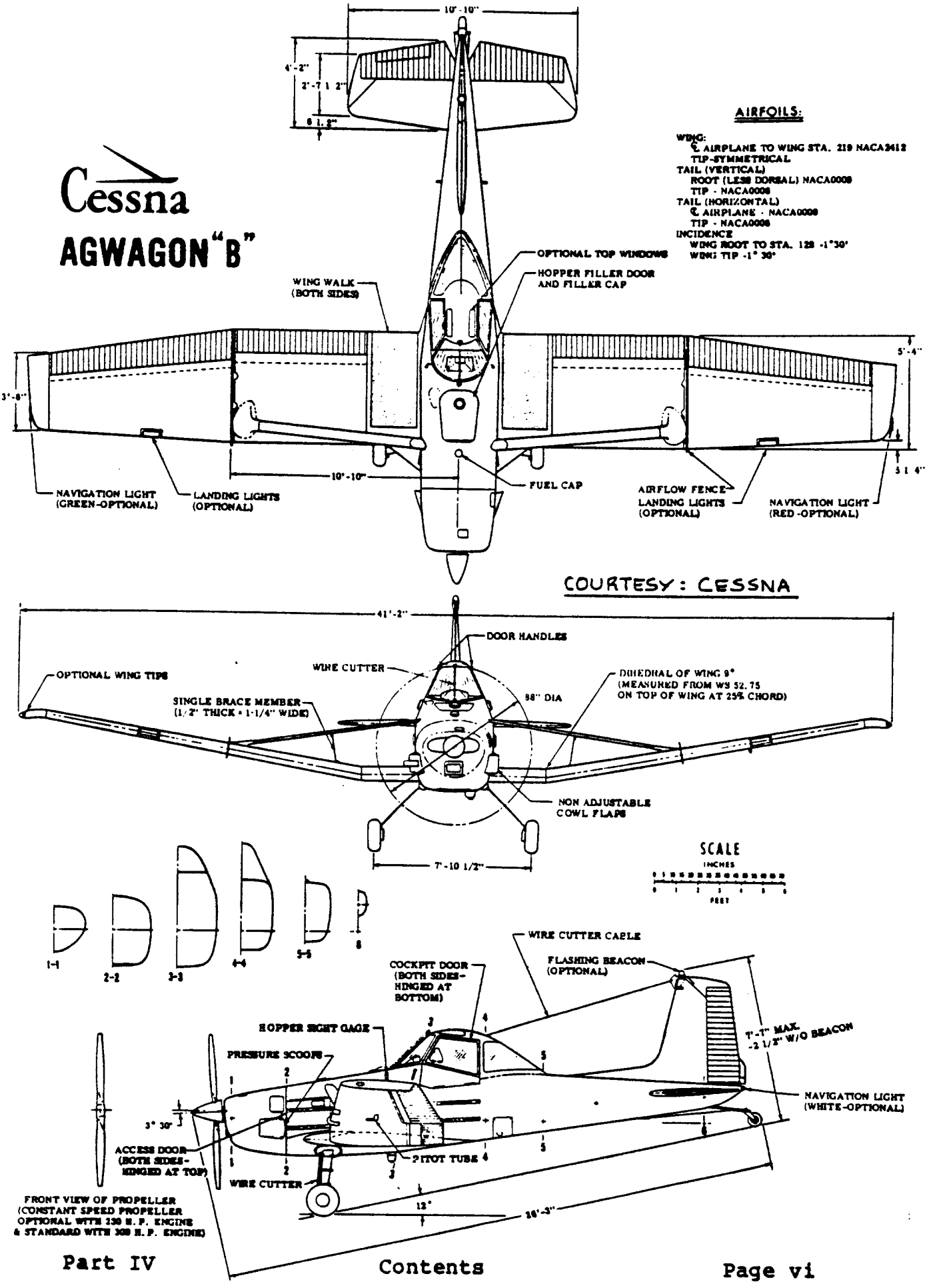
Cessna
AGWAGON "B"
AIRFOILS:
WING:
℄ AIRPLANE TO WING STA. 219 NACA2412
TIP-SYMMETRICAL
TAIL (VERTICAL)
ROOT (LESS DORSAL) NACA0008
TIP - NACA0008
TAIL (HORIZONTAL)
℄ AIRPLANE - NACA0008
TIP - NACA0008
INCIDENCE
WING ROOT TO STA. 128 +1°30'
WING TIP +1° 30'
10'-10"
4'-2"
2'-7 1 2"
6 1 2"
OPTIONAL TOP WINDOWS
HOPPER FILLER DOOR AND FILLER CAP
WING WALK (BOTH SIDES)
5'-4"
3'-8"
10'-10"
FUEL CAP
NAVIGATION LIGHT (GREEN-OPTIONAL)
LANDING LIGHTS (OPTIONAL)
AIRFLOW FENCE
LANDING LIGHTS (OPTIONAL)
NAVIGATION LIGHT (RED-OPTIONAL)
3 1 4"
COURTESY: CESSNA
41'-2"
DOOR HANDLES
OPTIONAL WING TIPS
WIRE CUTTER
DIHEDRAL OF WING 9° (MEASURED FROM WS 52.75 ON TOP OF WING AT 25% CHORD)
SINGLE BRACE MEMBER (1/2" THICK x 1-1/4" WIDE)
98" DIA
NON ADJUSTABLE COWL FLAPS
7'-10 1/2"
SCALE
INCHES
FEET
1-1
2-2
3-3
4-4
5-5
6
WIRE CUTTER CABLE
FLASHING BEACON (OPTIONAL)
COCKPIT DOOR (BOTH SIDES-HINGED AT BOTTOM)
HOPPER SIGHT GAGE
PRESSURE SCOOPS
7'-7" MAX. -2 1/2" W/O BEACON
NAVIGATION LIGHT (WHITE-OPTIONAL)
3° 30'
ACCESS DOOR (BOTH SIDES-HINGED AT TOP)
PITOT TUBE
WIRE CUTTER
12"
26'-3"
FRONT VIEW OF PROPELLER (CONSTANT SPEED PROPELLER OPTIONAL WITH 230 H. P. ENGINE & STANDARD WITH 300 H. P. ENGINE)

TABLE OF SYMBOLS

Symbol	Definition	Dimension
a_x	forward deceleration	ft/sec^2
b	wing span	ft
b_t	maximum tire width	
c	wing mean geometric chord	ft
c_j	specific fuel cons.(jet)	lbs/lbs/hr
c_p	specific fuel cons.(pist)	lbs/hp/hr
C.F.	Centrifugal force	lbs
C_h	Hingemoment coefficient	----
C_{m_r}	Recoil pitching mom. coeff.	----
C_{n_r}	Recoil yawing mom. coeff.	----
C_R	Top tire clearance	in
d_s	shock absorber diameter	ft
D	Tire bead seat diameter	in
D_i	Drag in Fig.2.66a	lbs
D_o	Outside tire diameter	in
D_F	Tire flange diameter	in
D_G	Grown tire diameter	in
D_s	Tire shoulder diameter	in
D_t	Outside tire diameter	in
E_t	Kinetic energy	ftlbs
f_{dyn}	factor which multiplies tire static load to get dynamic load	-----
F	Force on landing gear	lbs
F_c	cable or push-rod control force	lbs
F_p	Pilot control force	lbs
F_r	Retraction force, also gun recoil force	lbs

g	acceleration of gravity	ft/sec^2
G	Gearing ratio	rad/ft
h_{cg}	distance from the center of gravity to the runway	ft
H	Tire section height	in
HM	Hingemoment	ftlbs
i_H	Stabilizer incidence	deg or rad
l_i	See Fig.2.66a	ft
l_m	Distance from main gear to the center of gravity	ft
l_n	Distance from the nose gear to the center of gravity	ft
m	airplane mass	slugs
n	load factor	-----
n_s	number of struts in main gear	-----
n_t	number of tires (nosegear)	-----
N_g	Landing gear load factor	-----
P	Force on landing gear	lbs
P_n	Static load on nosegear as defined in Fig.2.14	lbs
P_m	Static load on main gear strut defined in Fig.2.14	lbs
P_{TO}	Take-off power	hp
$\bar{q}$	dynamic pressure	psf
R	See Fig.2.66b	ft
s_p	cockpit control travel	in or ft
s_s	allowable shock absorber deflection	ft
s_t	allowable tire deflection	ft
s_x	tire shoulder clearance	in
S	Wing area	ft^2
S_p	Effective piston area	in^2
t	Tire deflection	in/ft
T_{TO}	Take-off thrust	lbs
V	Airplane speed	fps/kts
V_{s_l}	Stall speed, landing	mph

$V_{s_{TO}}$	Stall speed, take-off	mph
$V_{tire/max}$	Maximum allowable tire speed	mph
w_t	Touchdown rate	fps
W	Airplane weight	lbs
W (note!)	Maximum tire width, also called Tire section width	in
W_g	Landing gear weight	lbs
W_G	Grown tire width	in
W_s	Tire shoulder width	in
x_i	See Fig.2.66a	ft
x_p	See Fig.2.66b	ft
y_r	See Fig.3.7	ft
z_i	See Fig.2.66a	ft
z_p	See Fig.2.66b	ft
z_r	See Fig.3.7	ft

Greek Symbols
==========

γ	Flight path angle	deg
η_s	Shock abs. efficiency	-----
η_t	Tire abs. efficiency	-----
δ	Control deflection angle	deg or rad
μ	friction coefficient	-----
phi	gear retraction angle	deg

Subscripts
==========

ave	average
dyn	dynamic
g	ground
h	horizontal
L	Landing
m	main gear

max	maximum
n	nose gear
r	recoil
R	Rudder
TO	Take-off
v	vertical

Acronyms
========

ac	alternating current
ACLS	Air cushion landing system
AGM	Air-to-ground missile
AIM	Air intercept missile
ARM	Anti radiation missile
ASM	Air-to-surface missile
BBL	Body Buttock Line
CCW	Counterclock wise
CW	Clock wise
dc	direct current
ESWL	Equivalent Single Wheel Load
FAA	Federal Aviation Administration
FAR	Federal Aviation Regulation
FOD	Foreign Object Damage
HUD	Heads up display
ICAO	International Cicil Aviation Organization
KVA	Kilovolt-amperes
LCN	Load Classification Number
N.A.	Not available
NTSB	National Transportation and Safety Board
RCS	Radar cross section
SMTD	STOL and maneuver demonstrator
STOL	Short take-off and landing
VDC	Volts direct current
V/STOL	Vertical/Short Take-off and Landing

ACKNOWLEDGEMENT

Writing a book on airplane design is impossible without the supply of a large amount of data. The author is grateful to the following companies for supplying the raw data, manuals, sketches and drawings which made the book what it is:

Aerospatiale
Beech Aircraft Corp.
The Boeing Company
British Aerospace Corp.
Cessna Aircraft Company
Fairchild Republic Co.
Gates Learjet Corporation
Piper Aircraft Corporation
General Dynamics Corporation
Grumman Aerospace Corp.
Gulfstream Aerospace Corp.
Lockheed Aircraft Corp.
McDonnell Douglas Corp.
Short Brothers and Harland Ltd.

The author wishes to specifically acknowledge the cooperation received from Boeing and from McDonnell Douglas Corporation in providing large numbers of layout drawings with permission to publish.

A significant amount of airplane design information has been accumulated by the author over many years from the following magazines:

Interavia (Swiss, monthly)
Flight International (British, weekly)
Business and Commercial Aviation (USA, monthly)
Aviation Week and Space Technology (USA, weekly)
Journal of Aircraft (USA, AIAA, monthly)

The author wishes to acknowledge the important role played by these magazines in his own development as an aeronautical engineer. Aeronautical engineering students and graduates should read these magazines regularly.

Nearly all weapons and military payload drawings in this book were drawn by Mr. Govert Tukker of Molenaarsgraaf, The Netherlands. The author is grateful to Mr. Tukker for his skill and patience in carrying out this most difficult assignment.

CHANCELLOR

Cessna

1981 MODEL 414A

AIRFOILS

WING
- ℄ AIRCRAFT-NACA 23018 MODIFIED
- ℄ NACELLE-NACA 23015 MODIFIED
- TIP-NACA 23009 MODIFIED

TAIL (VERTICAL)
- ROOT (LESS DORSAL)-NACA 0012 MODIFIED
- TIP-NACA 0009 MODIFIED

TAIL (HORIZONTAL)
- ROOT-NACA 0009 MODIFIED
- TIP-NACA 0006 MODIFIED

INCIDENCE
- WING ROOT - +2° 30'
- WING TIP - — 0° 30'
- STABILIZER - 0° 0'

DIHEDRAL
- WING - 5°
- HORIZONTAL STABILIZER - 0°

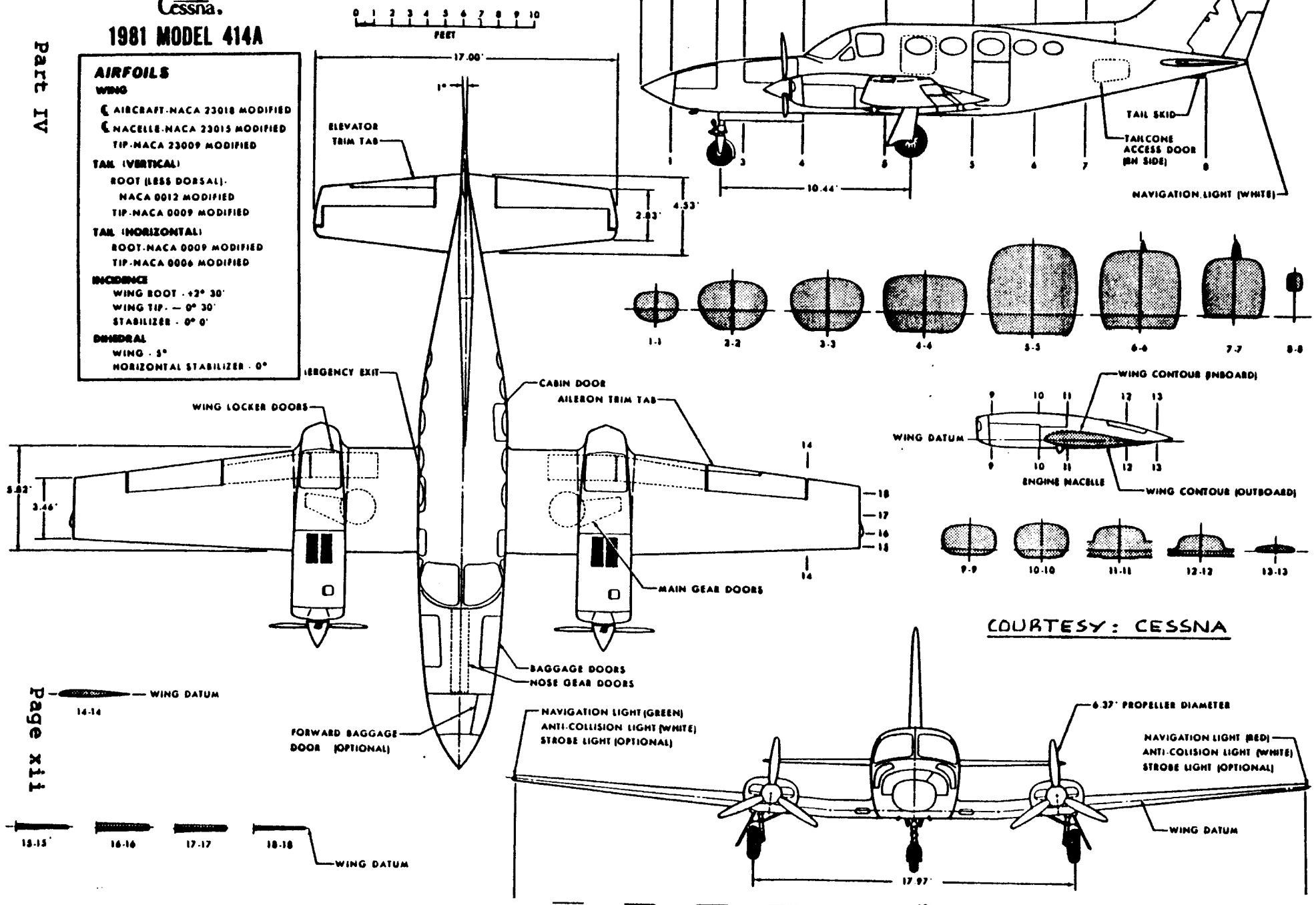

COURTESY: CESSNA

1. INTRODUCTION

The purpose of this series of books on Airplane Design is to familiarize aerospace engineering students with the design methodology and design decision making involved in the process of designing airplanes.
The series of books is organized as follows:

PART I:	PRELIMINARY SIZING OF AIRPLANES
PART II:	PRELIMINARY CONFIGURATION DESIGN AND INTEGRATION OF THE PROPULSION SYSTEM
PART III:	LAYOUT DESIGN OF COCKPIT, FUSELAGE, WING AND EMPENNAGE: CUTAWAYS AND INBOARD PROFILES
PART IV:	LAYOUT DESIGN OF LANDING GEAR AND SYSTEMS
PART V:	COMPONENT WEIGHT ESTIMATION
PART VI:	PRELIMINARY CALCULATION OF AERODYNAMIC, THRUST AND POWER CHARACTERISTICS
PART VII:	DETERMINATION OF STABILITY, CONTROL AND PERFORMANCE CHARACTERISTICS: FAR AND MILITARY REQUIREMENTS
PART VIII:	AIRPLANE COST ESTIMATION: DESIGN, DEVELOPMENT, MANUFACTURING AND OPERATING

The purpose of PART IV is to present a systematic approach to the problem of airplane landing gear design and airplane systems design during the preliminary design phase.

Chapter 2 presents a discussion of methods employed to yield realistic layouts of landing gears. Specific problems addressed are:

a) tire selection and sizing
b) strut sizing
c) landing gear disposition in view of turnover criteria, rotation and ground handling requirements
d) retraction kinematics

Chapter 3 contains data on weapons integration problems encountered during the preliminary design of military airplanes. In laying out military airplane designs, geometric and weights data on weapons and other military payloads are needed. Such data are given in Chapter 3.

Chapter 4 contains a discussion of design considerations for primary and secondary flight control systems. Both reversible and irreversible flight control systems are addressed and many example layouts included.

The layout design of airplane systems is an important subject during the preliminary design phase. The main reason for this is the fact that many systems have a large impact on flight safety. Another reason is that early design decisions tend 'lock in' most of the life cycle cost of an airplane. It is therefore essential, that attention be given to the layout design of all systems which are important to the operation of an airplane. The following systems are covered:

Chapter 5 addresses the problem of preliminary fuel system design. A number of guidelines for 'design for safety' are included.

Chapter 6: provides an introduction to hydraulic system layout design.

Chapter 7: Gives a brief overview of design decisions involved in laying out airplane electrical systems.

Chapter 8: Environmental systems are important components of many airplanes. This chapter deals with the layout design of the pressurization system, the airconditioning systen and the oxygen system.

Chapter 9: This chapter deals with layout design problems associated with cockpit instrumentation, flight management and other avionics systems.

De-icing, anti-icing, rain removal and defog systems are covered in Chapter 10.

Chapter 11 presents examples of the layout design problems encountered in the preliminary design of emergency escape and ejection systems.

Particularly in passenger transports the design of the potable water and waste system is an important aspect of layout design. Chapter 12 covers these systems.

Chapter 13 addresses the role of safety and survivability in preliminary design thinking and in preliminary design decision making. A review of aviation safety and how it is measured is also given.

2. LANDING GEAR LAYOUT DESIGN

The purpose of this chapter is to provide methods and data to assist in preparing satisfactory landing gear layouts. The material presented here is meant to be used in conjunction with Steps 18 and 29 in p.d. sequence II of Part II. Methods consistent with p.d. sequence II are referred to as Class II methods. The Class I landing gear layout design procedure was presented in Chapter 9 of Part II.

The material is organized as follows:

2.1 Function of landing gear components
2.2 Discussion of landing gear types
2.3 Compatibility of landing gear and runway surface: determination of allowable wheel loads
2.4 Tires: types, performance, sizing and data
2.5 Strut-wheel interface, struts and shock absorbers
2.6 Brakes and braking capability
2.7 Design considerations for landing gears of carrier based airplanes
2.8 Review of landing gear layout geometry
2.9 Steering, turnradii and ground operation
2.10 Retraction kinematics
2.11 Examples of landing gear layouts
2.12 Unconventional landing gear configurations

References 1 through 5 are excellent sources for additional information on landing gear design.

2.1 FUNCTION OF LANDING GEAR COMPONENTS

There are five reasons for incorporating landing gears in airplanes:

1. To absorb landing shocks and taxiing shocks.

2. To provide ability for ground maneuvering: taxi, take-off roll, landing roll and steering.

3. To provide for braking capability.

4. To allow for airplane towing.

5. To protect the ground surface.

Landing gears must be capable of absorbing landing

and taxi loads as well as transmit part of these loads to the airframe. The magnitude of these loads depends on the type of airplane as well as on its mission. Ref.2 contains detailed discussions of landing gear loads. Three types of loads must be considered in the layout design of landing gears:

1. Vertical loads, primarily caused by non-zero touchdown rates and taxiing over rough surfaces.

2. Longitudinal loads primarily caused by 'spin-up' loads, braking loads and rolling friction loads.

3. Lateral loads primarily caused by 'crabbed landings', cross-wind taxiing and ground turning.

1. Vertical Landing Gear Loads

The magnitude of vertical landing gear loads depends on the touchdown rate. Design touchdown rates (also called sink speeds) are as follows:

FAR 23: $w_t = 4.4(W/S)_L^{1/4}$, but no less than 7 and no more than 10 fps (Derived from FAR 23.725)

FAR 25: w_t = 12 fps (FAR 25.723)

USAF: w_t = 10 fps (13 fps for trainers)

USN: w_t = 10 fps for transports

w_t = 17 fps for other non-carrier based airplanes

w_t = 22 fps for carrier based airplanes: these must contend with heaving decks.

Except for trainers and carrier based airplanes these sink speeds are hardly ever experienced: they are very conservative. A 4 fps sink rate is considered a 'hard' landing. Figure 2.1 illustrates the probabilities associated with encountering specific sink speeds.

To properly absorb the shock associated with any sink speed most landing gears contain two elements: tires and shock absorbers. Figure 2.2 shows both components in a typical landing gear layout.

The role of tires is discussed in Section 2.4.

Shock absorbers can be designed as separate elements

or they can be integrated into the gear strut. Section 2.5 presents a discussion on struts and on shock absorbers.

Figure 2.3 shows what happens to the ground reaction force during a typical landing. Note that longitudinal and lateral tire-ground forces are not considered here.

Figure 2.4 shows the interplay between spring and damping forces acting on the shock absorber. Figure 2.5 shows the same for the tire. More detailed design considerations for tires and shock absorbers (shock struts) are presented in Sections 2.4 and 2.5 respectively.

2. Longitudinal and Lateral Loads

In addition to the 'vertical' landing gear loads just mentioned, there are the longitudinal and lateral loads. Figure 2.6 illustrates these loads. The landing gear elements which resist these loads are called the drag-brace and the side-brace respectively. Figure 2.7 shows a landing gear with all elements mentioned sofar. In simple landing gears such as shown in Figure 2.8 the drag-brace and side-brace capability are all included in the main strut design. In the case of Figure 2.8 the strut is normally referred to as the 'spring-leaf' or the 'spring-tube'.

For details regarding the structural design of landing gear elements the reader should consult Ref. 2.

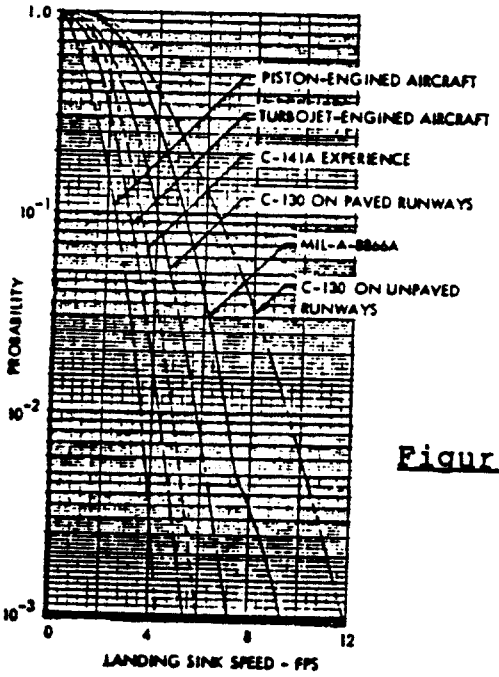

Figure 2.1 Probability of Encountering Certain Sink Speeds

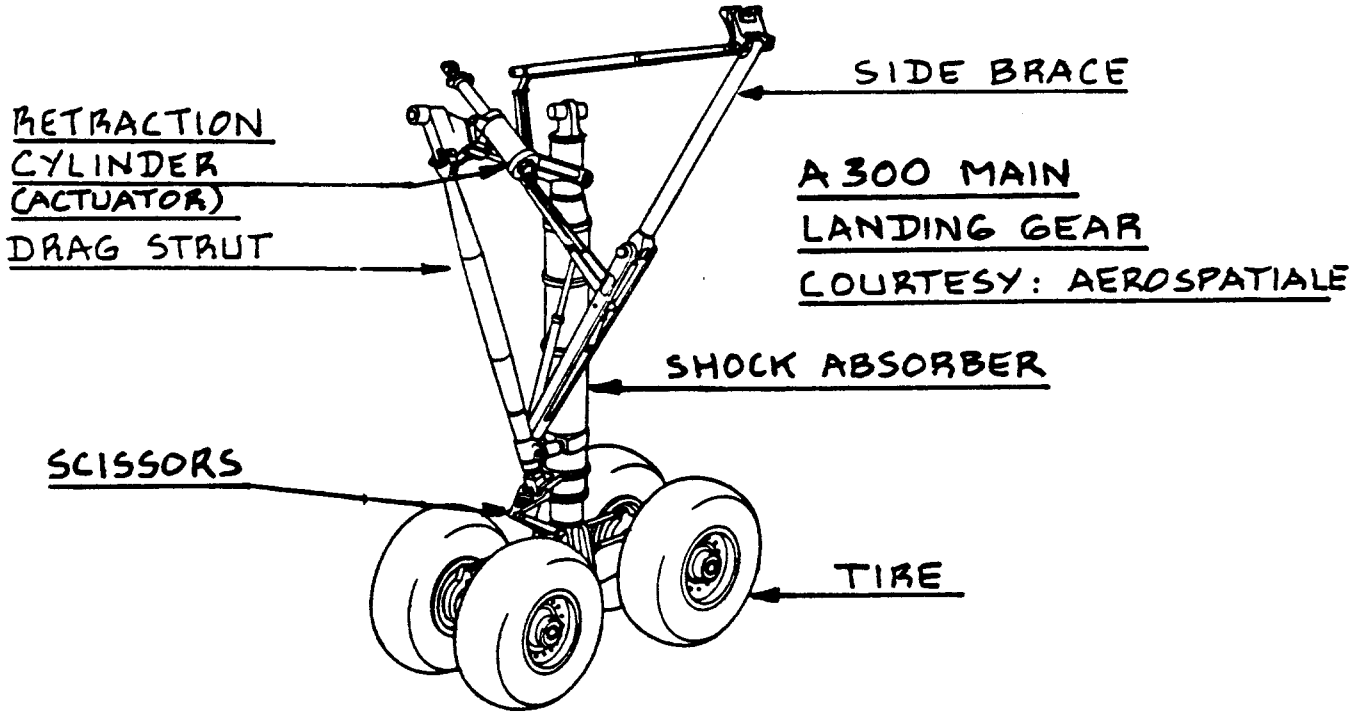

Figure 2.2 Example of Shock Absorber and Tires

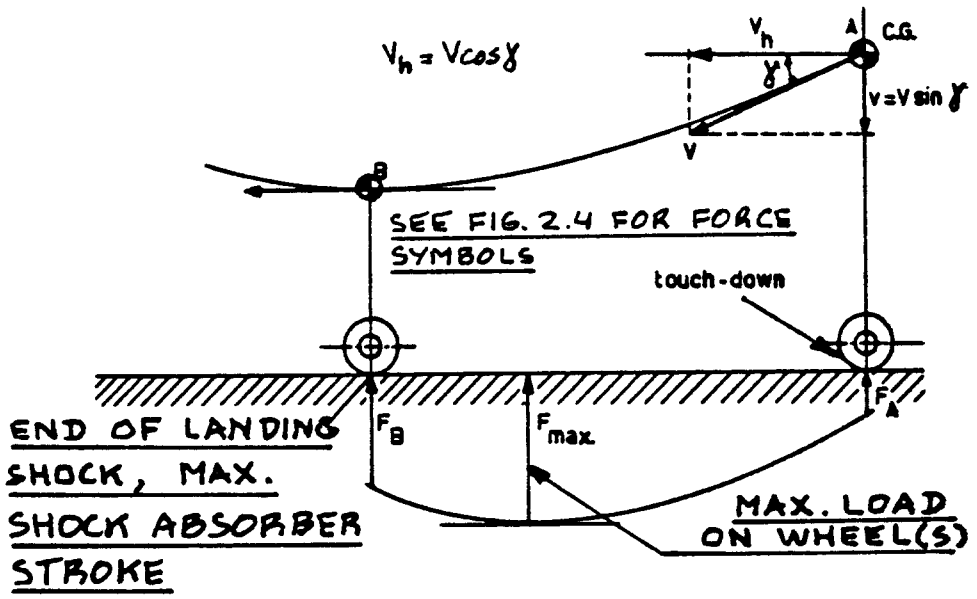

Figure 2.3 Change of Ground Reaction Force During Landing

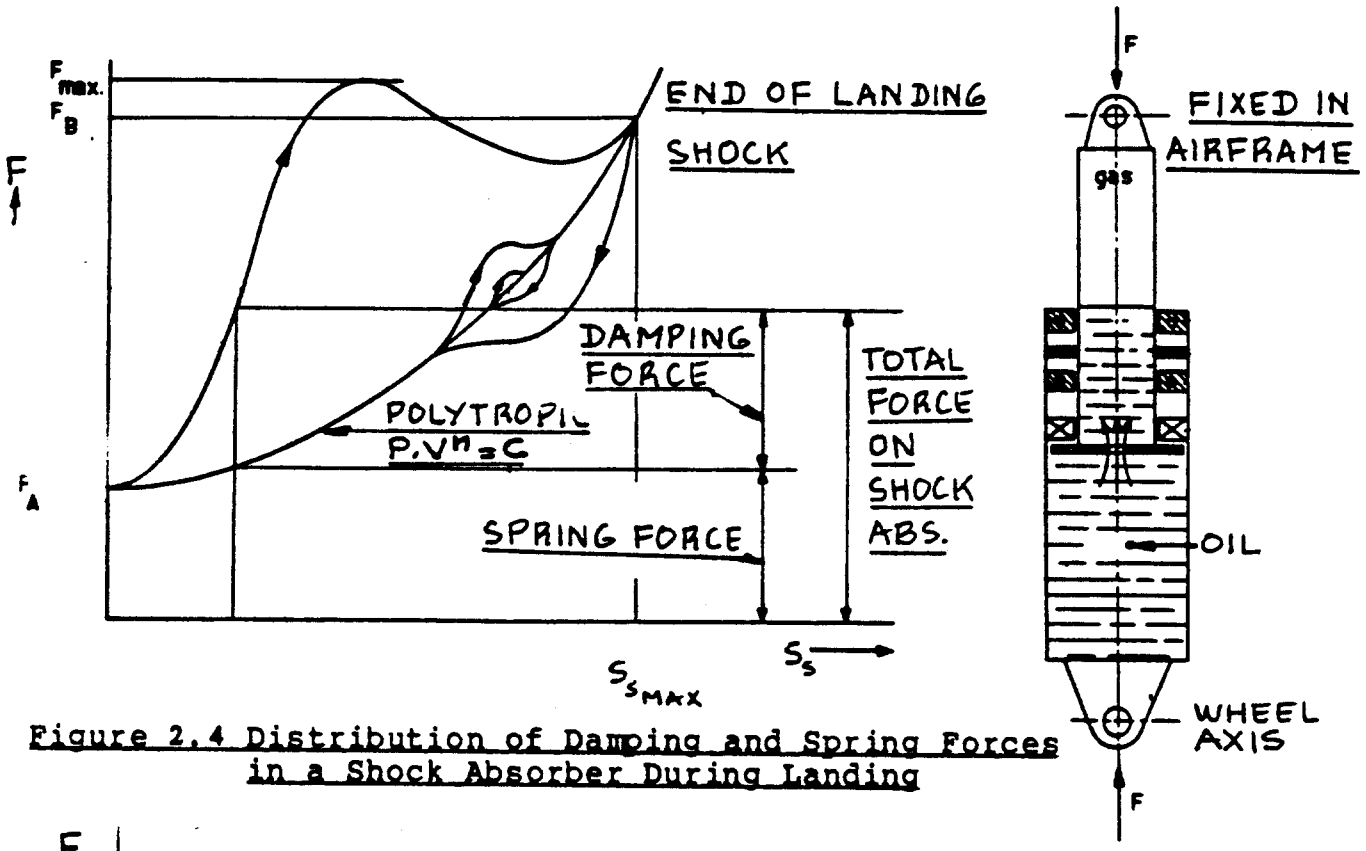

Figure 2.4 Distribution of Damping and Spring Forces in a Shock Absorber During Landing

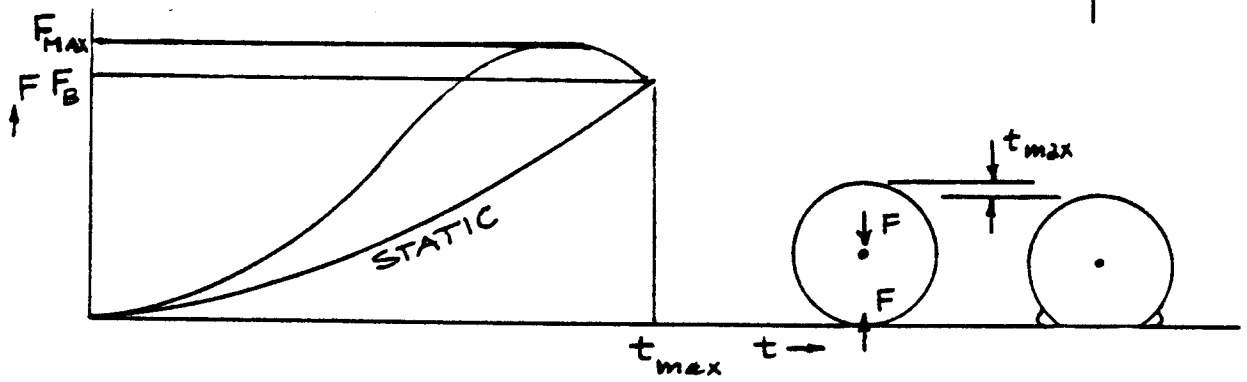

Figure 2.5 Distribution of Damping and Spring Forces in a Tire During landing

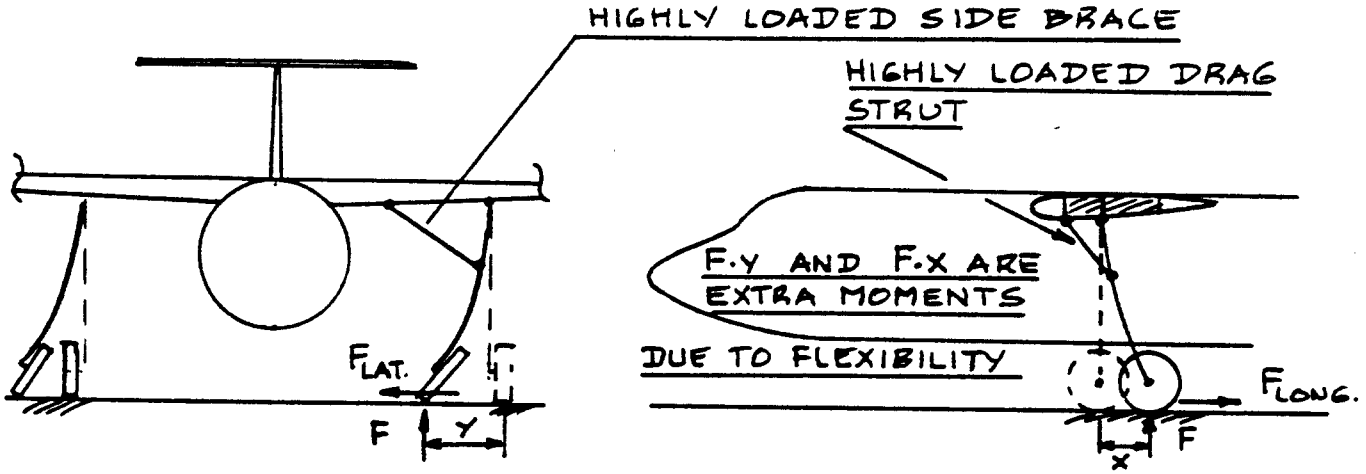

Figure 2.6 Lateral and Longitudinal Loads Acting on a Landing Gear

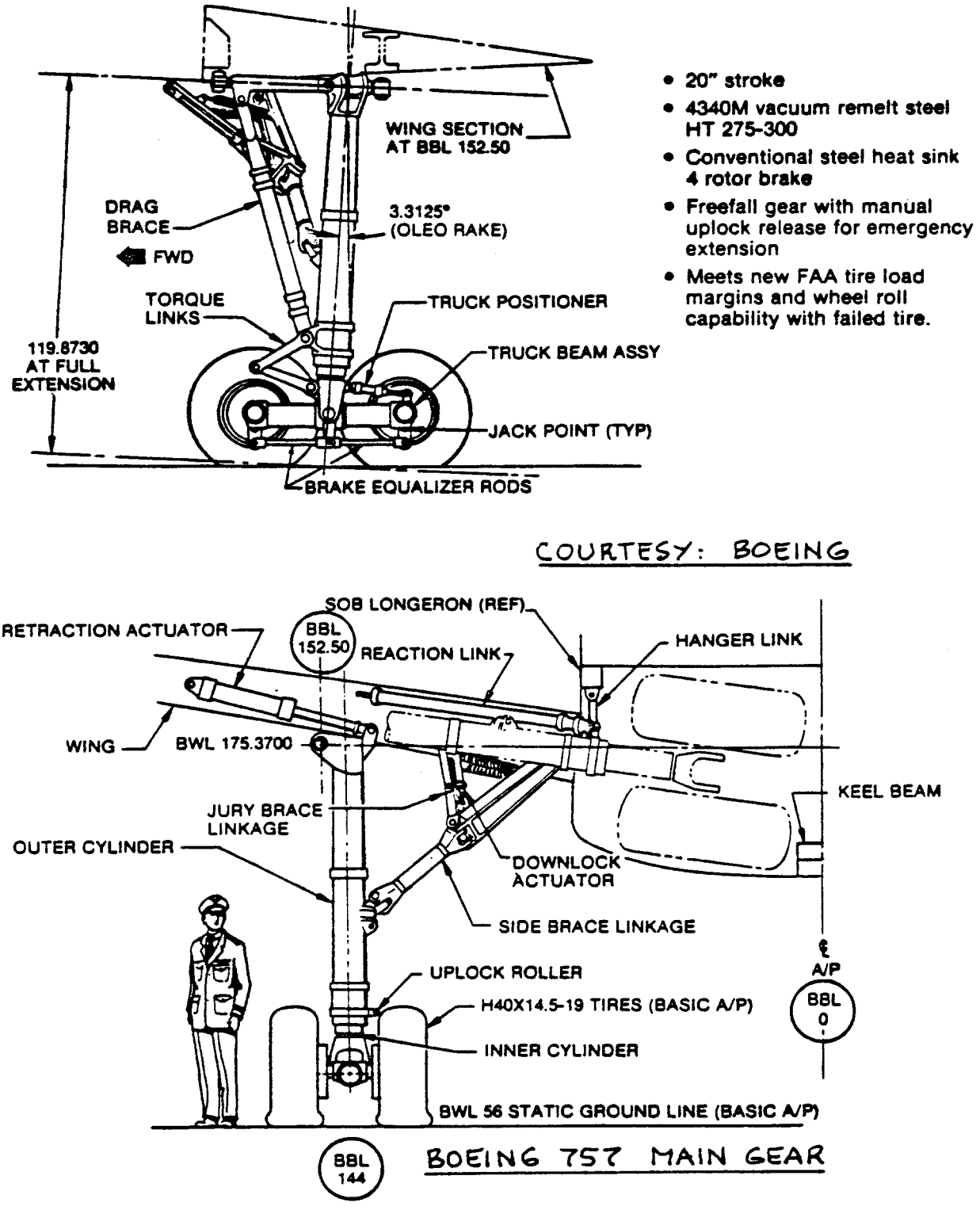

Figure 2.7 Example of a Jet Transport Landing Gear

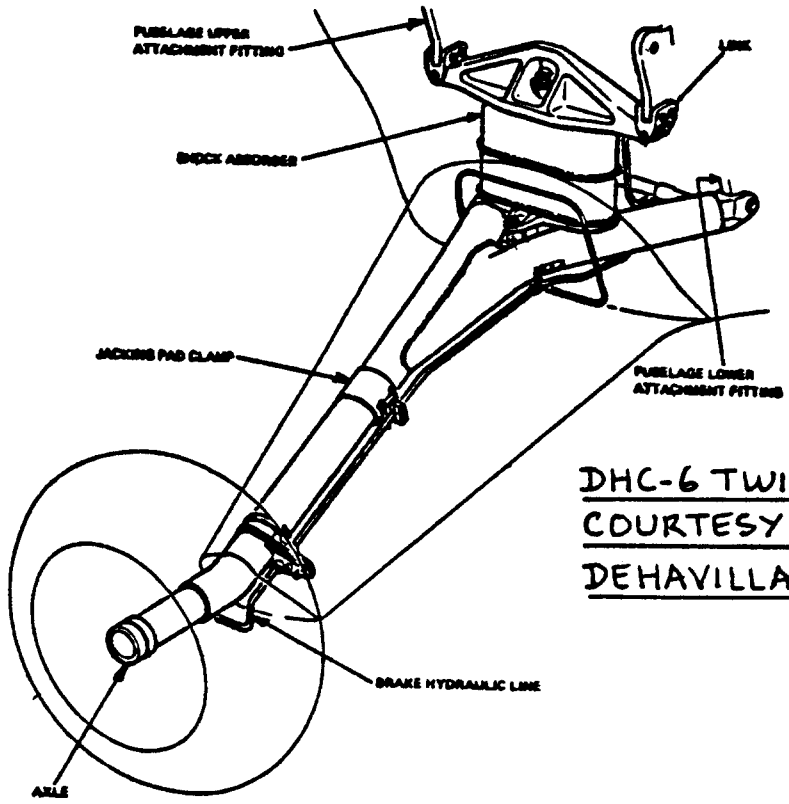

DHC-6 TWIN OTTER
COURTESY:
DEHAVILLAND CANADA

Figure 2.8 Example of a Commuter Landing Gear

EMB-121B XINGU

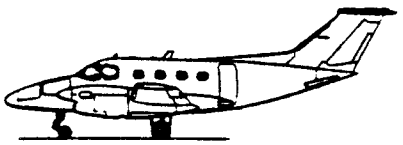

A) TRICYCLE

BAC HARRIER GR.MK3

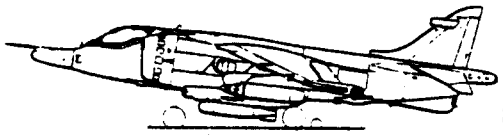

B) BICYCLE
NOTE OUTRIGGERS

LET XZ-37T

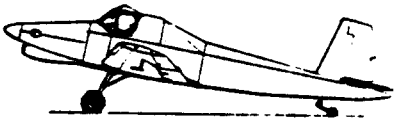

C) TAILGEAR

Figure 2.9 Example of Tricycle, Bicycle and Tailwheel Landing Gears

2.2 DISCUSSION OF LANDING GEAR TYPES

In this section some fundamental aspects of the overall landing gear configuration are discussed. For further discussions of landing gear configurations the reader should consult Refs 1-5.

Two major decisions which must be made before the landing gear layout process can be started are:

1. Decide on a fixed (non-retractable) or a retractable gear.

2. Decide on the use of a tricycle, bicycle, tailwheel or unconventional gear. In some cases outrigger gears may be needed.

The pros and cons of these decisions will now be discussed.

Decision 1 is a trade-off between gear induced aerodynamic drag, weight and complexity (cost!). Ref.6 contains information on the type of gear used in a wide range of airplanes. The reader should study Ref.6 to get some insight into which types of gears are used by various manufacturers for different types of airplanes. Experience indicates that airplanes with cruise speeds above 150 kts tend to use retractable landing gears because of the gear drag penalty.

Table 2.1 summarizes the pros and cons of fixed versus retractable landings gears.

Decision 2 depends strongly on the airplane mission. Figure 2.9 presents an example of each type of gear. There are pros and cons associated with each type. These will now be discussed.

The tricycle gear configuration (see Fig.2.9a) has become the most frequently used gear layout. Important reasons for this are:

1. Good visibility over the nose during ground operation.

2. Stability against groundloops: see Fig.2.10.

3. Good steering characteristics.

4. Level floor while on the ground. This is important in cargo and passenger transports.

Table 2.1 SUMMARY OF PROS AND CONS OF FIXED VERSUS RETRACTABLE LANDING GEARS

Gear Type:	Fixed	Retractable
Characteristics:		
Aerodynamic drag	High	Minimal
Weight	Low	High
Complexity and cost	Low	High
Maintenance cost	Insignificant	Significant

Table 2.2 SUMMARY OF PROS AND CONS FOR THREE GEAR TYPES

Gear Type:	Tricycle	Bicycle	Tailwheel
Characteristic:			
Groudloop behavior:	Stable	Stability depends on c.g. location	Unstable
Visibility over the nose:	Good	Good	Poor
Floor attitude on the ground:	Level	Can be level	Not level
Weight:	Medium	High	Low
Steering after touchdown:	Good	Marginal to good	Poor
Steering while taxiing:	Good	Good	Poor
Take-off rotation:	Good	Marginal to impossible	Good
Take-off procedure	Easy	Easy	Needs skill

The bi-cycle gear configuration (see Fig.2.9b) is used in cases where placement of essential components prohibits the use of either the tricycle or the tailwheel configuration. Examples are: the B52 bomber (Fig.3.28a, Part II) and the AV8B Harrier V/STOL fighter (Bottom of p.221, Part II).

In the case of the B52 bomber, a large uninterrupted bombbay was desired. This made retraction of the main gear into the middle of the fuselage impossible. The high wing layout ruled against gear retraction into the wing. The remaining option of a bicycle gear was used.

In the case of the Harrier, the entire center area of the fuselage is occupied by the Pegasus 'four-poster' engine with swiveling nozzles. This made main gear retraction into the fuselage impossible. Because of the thin wing, retraction of the main gear into the wing was also ruled out. That left the bicycle gear layout.

The reader will note that in the case of bicycle gear layouts so-called 'outrigger' gears are needed to provide lateral stability during ground operation. These ourigger gears are normally retracted into the wings (B52) or into wingtip fairings (Harrier).

An important consequence of the bicycle gear arrangement is that take-off rotation is made difficult if not impossible. The wing must therefore be set at an incidence angle governed by take-off considerations instead of by cruise drag considerations. The B52 is an example of this!

The tailwheel configuration (See Fig.2.9c) is used primarily in homebuilt airplanes and in airplanes which must operate from rather rough surfaces. Nose-gear configurations tend to become very heavy if the nosegear is designed to withstand the severe stresses which are the consequence of operating from rough fields.

Tailwheel gears are nearly always lighter than other types of gears. The following disadvantages are the reason for the demise of the tailwheel configuration in most airplanes:

1. Strong tendency to groundloop: see Fig.2.10.

2. Visibility over the nose is poor during ground operation. This results in the need to zig-zag during taxiing.

3. Steering while taxiing is compromised.

Table 2.2 summarizes the pros and cons of the tricycle, bicycle and tailwheel type landing gears. If none of these landing gear configurations are suitable an unconventional layout may be called for. Section 2.12 presents some thoughts on unconventional landing gear configurations.

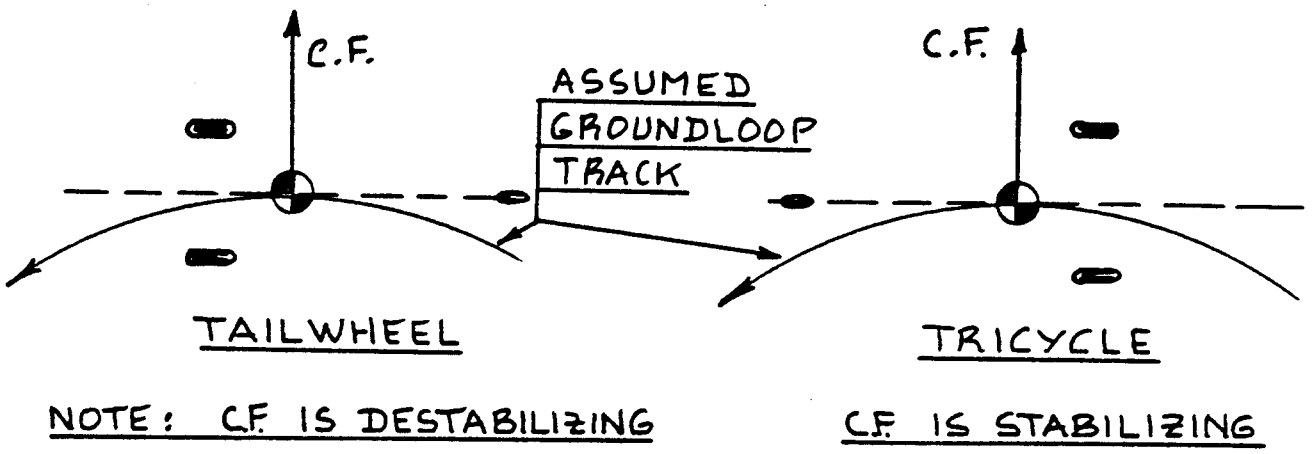

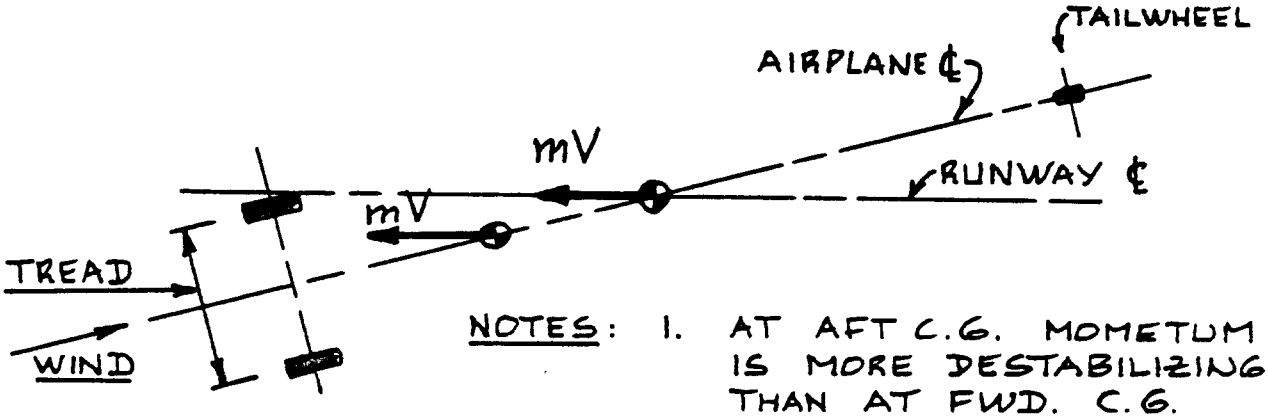

NOTES:
1. AT AFT C.G. MOMETUM IS MORE DESTABILIZING THAN AT FWD. C.G.
2. LARGE TREAD IS BETTER THAN SMALL TREAD
3. IF TAILWHEEL SWIVELS FREELY IT RIDES WITH THE DEVELOPING LOOP

Figure 2.10 Groundloop Characteristics of the Tricycle and the Tailwheel Landing Gear Configurations

2.3 COMPATIBILITY OF LANDING GEAR AND RUNWAY SURFACE: DETERMINATION OF ALLOWABLE WHEEL LOADS

The load on each landing gear strut (also called landing gear leg) as well as the load on each tire may not exceed values which:

1. cause structural damage to the gear or to the airplane
2. cause tire damage
3. cause runway damage or excessive surface deformations

This text does not consider structural design details. For aspects of landing gear structural design the reader is referred to References 2 and 7.

This section deals with permissible landing gear and wheel loads from a runway surface viewpoint.

The subject of permissible tire loads is discussed in Section 2.4.

2.3.1 Nosegear Steering Loads

To allow for adequate nosewheel steering, a minimum normal force must act on the nose gear so that the appropriate levels of friction forces needed for steering can be generated.

IMPORTANT NOTE: The normal force on the nosegear should not be less than $0.08W_{TO}$ for adequate steering.

2.3.2 Gear Loads From A Surface Viewpoint

Three types of runway surface will be considered:

Type 1 Surfaces: Runways with unprepared or simply prepared surfaces: grassy surfaces and gravel surfaces are examples of these. Surface failure occurs normally due to severe local indentation (ruts) caused by excessive tire loads.

Type 2 Surfaces: Runways with flexible pavement: asphalt or tarmacadam. These are normally very thick surfaces. Surface failure normally occurs due to local indentation caused by excessive tire loads. Severe surface waviness may result from this.

Type 3 Surfaces: Runways with rigid pavement: concrete. These surfaces normally have about one half the thickness of flexible pavements. Failure often occurs due to corner fracture of a slab caused by excessive tire loads.

Figure 2.11 illustrates the very heavy pavement requirements imposed by modern jet transport airplanes.

2.3.2.1 Allowable gear loads for Type 1 surfaces:

To avoid gear induced surface damage for Type 1 surfaces the tire pressures should not exceed the values given in Table 2.3. Note that this table does NOT apply whenever the load per strut exceeds 10,000 lbs. If the load per strut is greater than 10,000 lbs the gear design practices associated with surface types 2 and 3 must be used.

2.3.2.2 Allowable gear loads for Types 2 and 3 surfaces:

To avoid gear induced surface damage for Type 2 and for Type 3 surfaces the so-called LCN method (LCN = Load Classification Number) is suggested. This method has been established by the ICAO (International Civil Aviation Organization). All major runways in the world have been assigned an LCN. Landing gears must be designed so that their LCN number does not exceed the lowest runway LCN from which the airplane is intended to operate.

Table 2.4 presents typical LCN design values associated with transport airplanes.

For landing gears with a SINGLE WHEEL PER STRUT the relationship between its LCN, its load per wheel and its tire pressure is illustrated in Figure 2.12. When operating from runways with a given LCN value, Fig.2.12 can be used to find the allowable combinations of load per wheel and tire pressure.

For landing gears with MULTIPLE WHEELS PER STRUT the so-called ESWL (Equivalent Single Wheel Load) must be determined first, before Figure 2.12 can be used. The definition of ESWL is as follows:

Definition: The ESWL of a group of two or more wheels equals the load of a single wheel with the same pressure and causing the same pavement stresses.

Precise methods for computing the ESWL for arbitrary

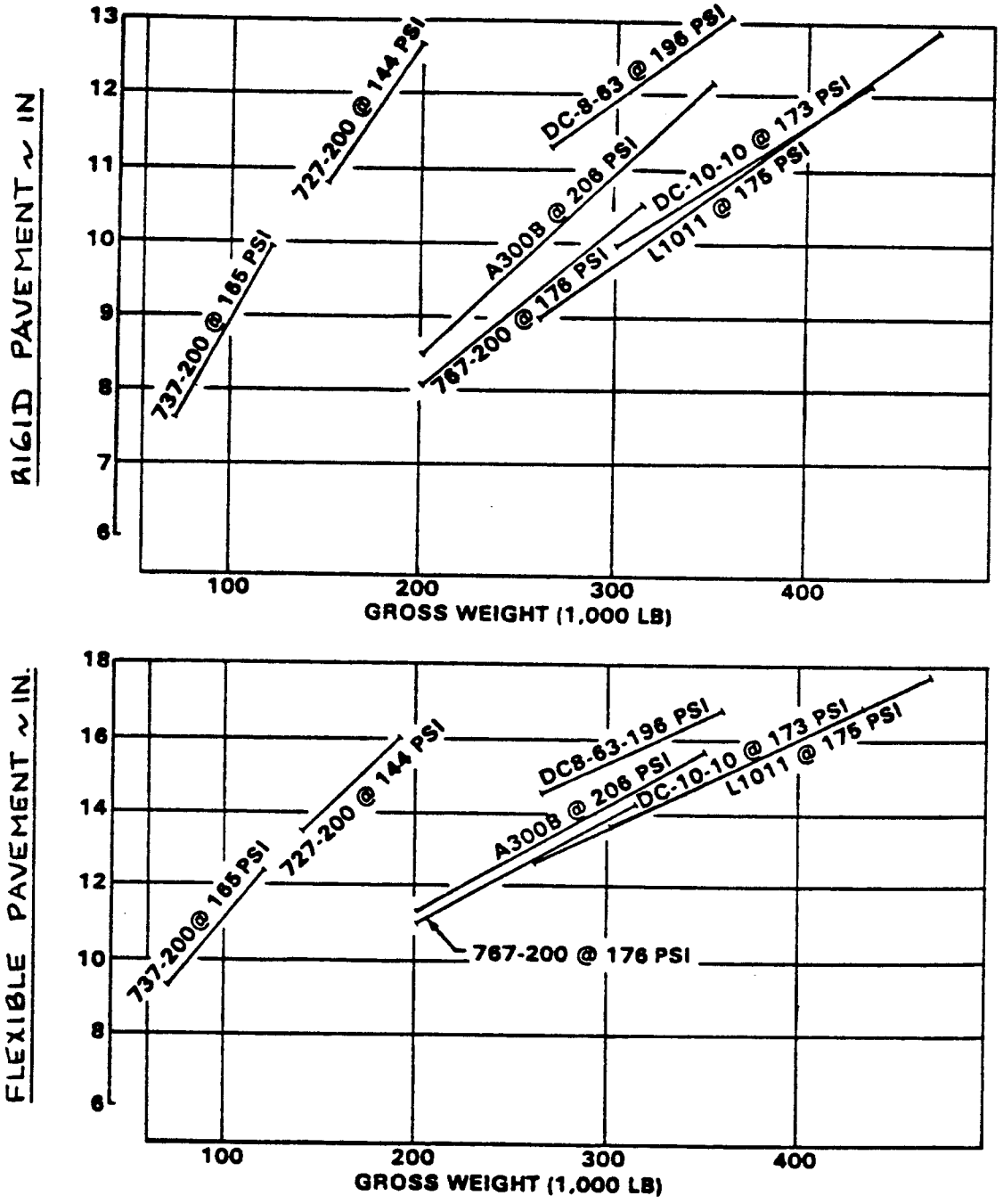

Figure 2.11 Pavement Thickness Needed for Jet Transports

Table 2.3 Recommended Tire Pressures for Various Surfaces

Description of Surface	Maximum Allowable Tire Pressure	
	kg/cm^2	psi
Soft, loose desert sand	1.8 - 2.5	25 - 35
Wet, boggy grass	2.1 - 3.2	30 - 45
Hard desert sand	2.8 - 4.2	40 - 60
Hard grass depending on the type of subsoil	3.2 - 4.2	45 - 60
Small tarmac runway with poor foundation	3.5 - 5.0	50 - 70
Small tarmac runway with good foundation	5.0 - 6.3	70 - 90
Large, well maintained concrete runways	8.5 - 14	120 - 200

Table 2.4 Tire Pressure and LCN Data for Transports

Airplane Type	W_{TO}	Tire Pressure	LCN
	lbs	psi	
Fokker F-27 Mk 500	45,000	80	19
Fokker F-28 Mk 2000	65,000	100	27
McDD DC-9/10	90,700	129	39
Boeing 737-200	110,110	162	49
Boeing 727-200	190,000	160	80
Boeing 757-200	210,000	157	50
Boeing 707-320C	300,000	180	80
McDD DC-10/10	410,000	175	88

gear configurations may be found in References 2 and 3. For preliminary design purposes the following equations give reasonable results:

For DUAL WHEEL layouts (See Fig.2.13 for examples):

$$ESWL = P_n/1.33 \text{ or } P_m/1.33 \qquad (2.1)$$

For TANDEM TWIN layouts (See Fig.2.13 for examples):

$$ESWL = P_n/2 \text{ or } P_m/2 \qquad (2.2)$$

Definitions for P_n and P_m are given in Figure 2.14.

For landing gears with more than four wheels per strut the ESWL should be determined with the methods given in References 2 and 3.

For military airplanes operating from soft fields or steelmatted fields the design procedures of Reference 2 should be used.

Tables 9.1 and 9.2 in Part II provide information on the number of struts and the number of wheels per strut used by a range of airplane types. Reference 6 contains considerably more data on this subject.

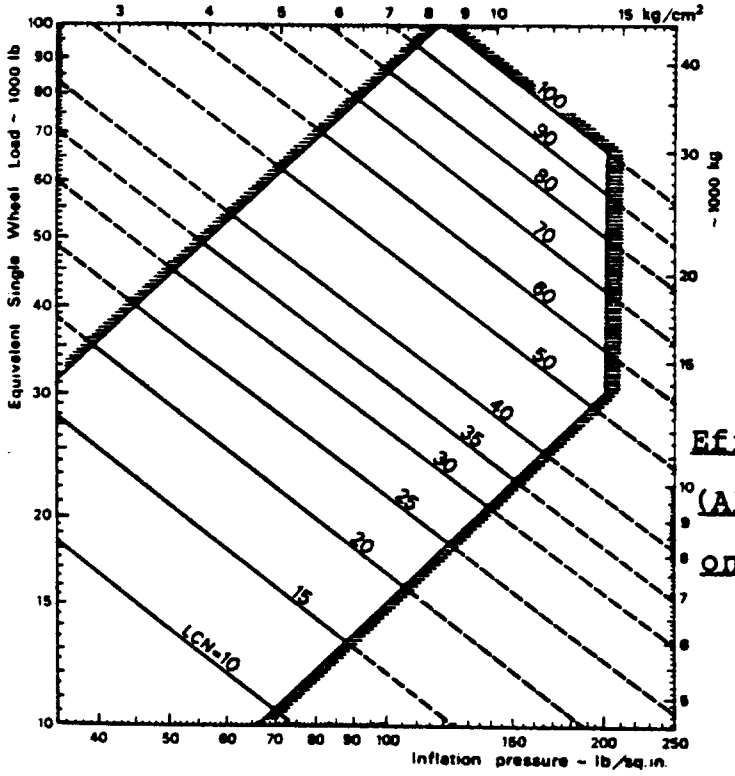

COPIED FROM REF.3
COURTESY: E.TORENBEEK

Figure 2.12

Effect of Tire Pressure and Tire Load (Also: Equivalent Single Wheel Load) on LCN (Load Classification Number)

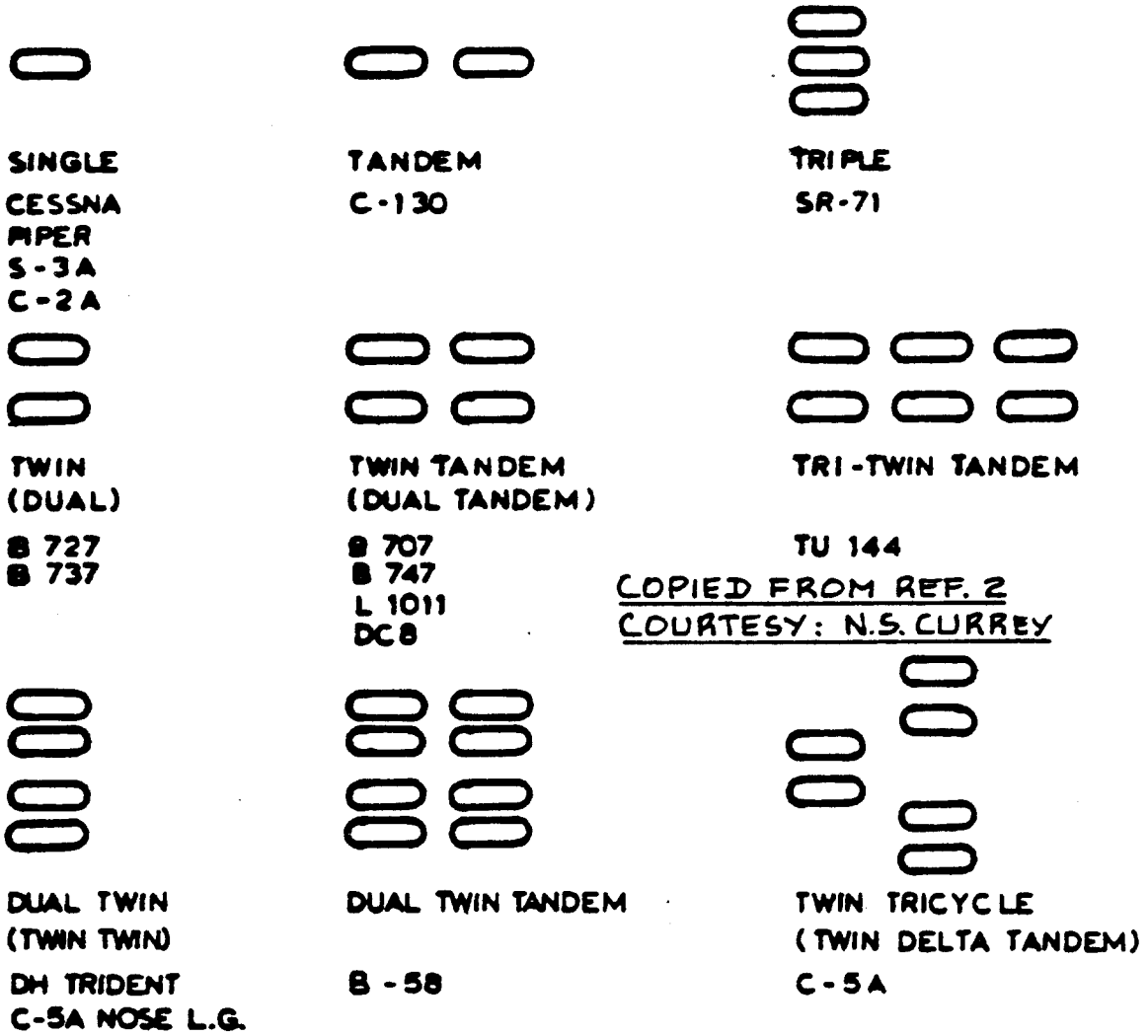

COPIED FROM REF. 2
COURTESY: N.S. CURREY

Figure 2.13 Examples of Landing Gear Wheel Layouts

NOTE : $P_n + n_s P_m = W$

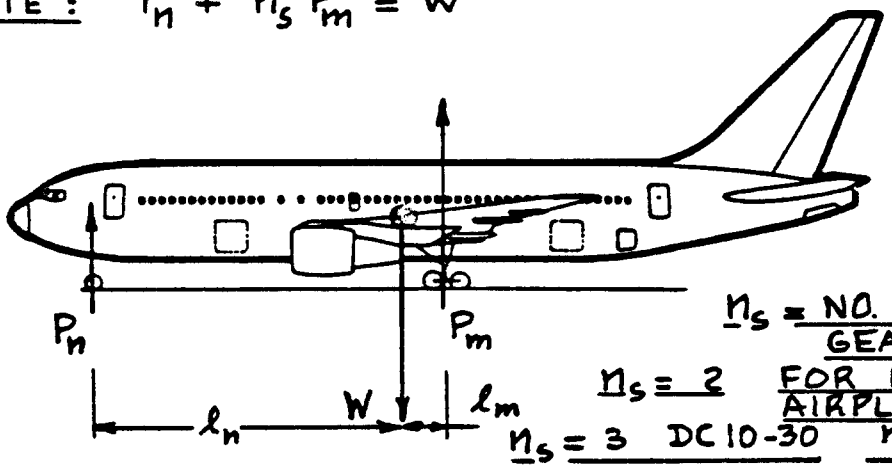

n_s = NO. OF MAIN GEAR STRUTS

$n_s = 2$ FOR MOST AIRPLANES

$n_s = 3$ DC10-30 $n_s = 4$ B747

Figure 2.14 Definition of P_m and P_n

2.4 TIRES: TYPES, PERFORMANCE, SIZING AND DATA

The following information is presented in this section:

1. A discussion of tire types, tire construction and tire descriptions: see sub-section 2.4.1.
2. A discussion of tire performance: load, deflection and shock absorption capability: see sub-section 2.4.2.
3. A discussion of tire clearance requirements: see sub-section 2.4.3.
4. A method for determining the correct tire size for airplane applications: see sub-section 2.4.4.
5. Tabulated data on tire geometry, tire load carrying capability and tire applications: see sub-section 2.4.5.

2.4.1 Tire Types, Tire Construction, and Tire Descriptions

Figure 2.15 shows seven tire types which are frequently used in airplanes. A description of each type is given next to each tire.

Figure 2.16 shows how typical airplane tires are constructed.

Tire manufacturers rate tires in terms of:

1. Ply rating 2. Maximum allowable static loading

3. Recommended (unloaded) inflation pressure

4. Maximum allowable runway speed

The ply rating of a tire identifies the tire with its maximum recommended static load and corresponding inflation pressure when used in a specific type of operation. The ply rating is an index of tire strength and DOES NOT indicate the actual number of fabric core plies.

For any given tire application the maximum allowable static loading and the associated unloaded inflation pressure must be compatible with the allowable values determined from a runway surface viewpoint. The latter are discussed in Section 2.3. Sub-section 2.4.4 contains a tire sizing procedure which accounts for the tire/surface interface. Specific tire data are found in sub-section 2.4.5.

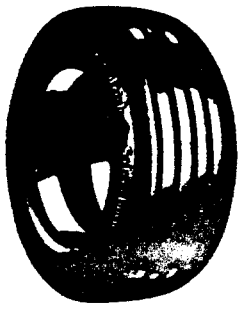

NEW DESIGN

New Design: This is a recent design. The outside tire dimensions are reflected in the type designation: D xW. All new tires will be designated with this system.

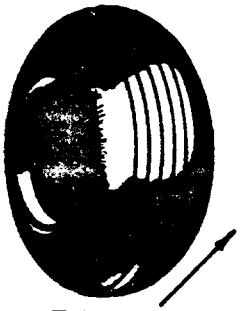

TYPE I

Type I: Smooth Contour. This type was designed for airplanes with non-retractable landing gears. Although this type is still available, its use in newly designed airplanes is discouraged because this tire type is considered obsolete.

Type II: High Pressure. This type, although still available is also considered obsolete. It was designed for airplanes with retractable gears. It has been replaced by Type VII which has considerably greater load carrying capacity.

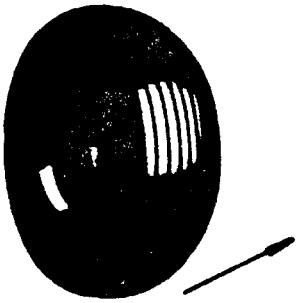

TYPE III

Type III: Low Pressure. This type is comparable to Type I but has beads of smaller diameter. It also has larger volume and lower pressure. Any new sizes in this type will be listed under the 'New Design' designation.

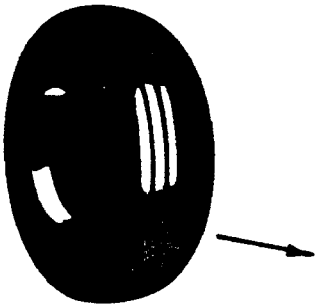

TYPE VII

Type VI: Low Profile (Inactive). This Type was designed for nosewheel applications only. It was designed to reduce wheel drop following complete deflation of the tire.

Type VII: Extra High Pressure. This Type is almost universal on military and civil jets and turboprops. It has high load capacity and narrow width. Any new sizes in this type will be listed under the 'New Design' designation.

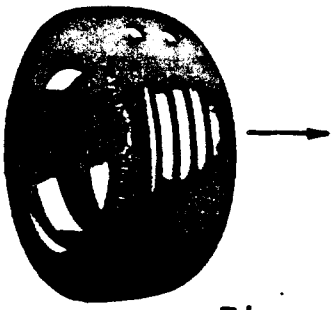

TYPE VIII

Type VIII: Low Profile High Pressure. This is a new design for very high take-off speeds. Any new sizes in this type will be listed under the 'New Design' designation.

Figure 2.15 Types of Airplane Tires

Aircraft Tire Construction

Aircraft tires, tubeless or tube type, provide a cushion of air that helps absorb the shocks and roughness of landings and takeoffs. They support the weight of the aircraft while on the ground and provide the necessary traction for braking and stopping aircraft on landing. Thus, aircraft tires must be carefully maintained to meet the rigorous demands of their basic job...to accept a variety of static and dynamic stresses in a wide range of operating conditions.

THE TREAD is a layer of rubber on the outer circumference of the tire, which serves as the wearing surface. With the sidewall, it helps protect the cord body from cuts, snags, bruises and moisture.

FABRIC TREAD REINFORCEMENT consists of plies added to reduce tire squirm and increase stability for high speed operation.

THE UNDERTREAD is a layer of special rubber which provides adhesion of the tread to the cord body, and enables the tire to be retreaded.

THE CORD BODY consists of layers (PLIES) of rubber-coated nylon cord. Since a layer of these cords (a ply) has all of its strength in only one direction, the cords of every succeeding ply run diagonally to each other to give balanced strength. The plies are folded around the wire beads, creating the PLY TURNUPS.

BEADS are layers of steel wire imbedde in rubber and then wrapped with fabri They give a base around which the plies are anchored and provide a firm fit on the wheel.

THE SIDEWALL is a cover over the side o the cord body to protect the cords from injury and exposure.

CHAFER STRIPS protect the plies from damage when mounting or demounting the tire, and minimize the effects of chafing contact with the wheel.

THE LINER in tubeless tires is a layer of rubber specially compounded to resist diffusion of air. It is vulcanized to the inside of the tire, extending from bead to bead. In tube-type tires, a thin liner is provided to prevent tube chafing.

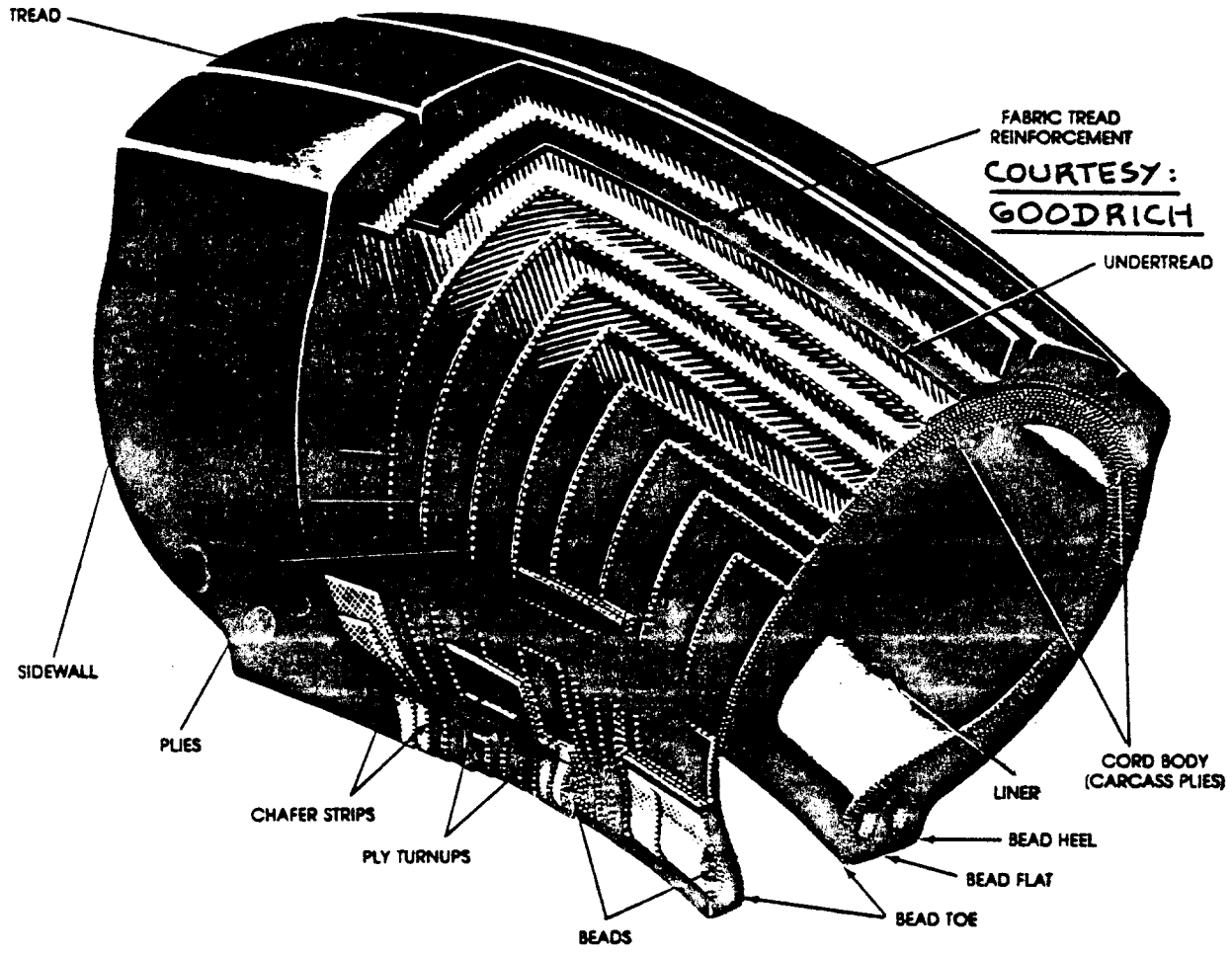

Figure 2.16 Conventional Airplane Tire Construction

Tires are described in terms of certain geometric parameters:

D_o or D_t, the tire outside diameter

W or b_t, the tire maximum width

D, the tire rim diameter

Figure 2.17 shows how these parameters are defined

With these geometric parameters, the following tire descriptions are being used:

Type I: D_o Type II: D_oxW Type III: W-D

Type VI: D_oxW-D Type VII or New Design: D_oxW

Type VIII or NS: D_oxW-D

There is a recent trend toward radial tires. See Figure 2.18 for how a radial tire is constructed. The advantages of radial tires over conventional tires are: up to 25 percent less weight and longer life. No systematic data on radial airplane tires were available when this text went to the printer.

2.4.2 Tire Performance: Load, Deflection and Shock Absorption Capability

Tires are subjected to rather severe static and dynamic loads during taxiing, during the take-off roll and during the landing roll. Figure 2.19 illustrates qualitatively what is typically demanded of an airplane tire.

Tires also participate significantly in the process of shock absorption following a touchdown. How much the tires participate, depends on the design of the shock absorbers. The amount of energy absorbed by the tires can be computed with the method discussed in Section 2.5.

Each tire is designed to operate at a so-called maximum allowable static load. The tire data tables in sub-section 2.4.4 indicate the maximum allowable static load for each tire. These loads must not be exceeded for the most critical weight/c.g. combination.

In selecting airplane tires, it is usually a good idea to keep future airplane growth capabilities in mind.

Once a given tire size is selected it is not always possible to accomodate larger tires within the geometric constraints of wheel wells. It is recommended to allow for 25 percent growth in tire load in selecting tires for a new airplane.

Nosewheel tires are designed for maximum allowable dynamic loads. These dynamic loads are obtained as follows:

$$\text{Dynamic load} = f_{dyn}(\text{static load}) \qquad (2.3)$$

The factor f_{dyn} is defined as follows:

For tires of Types I and III: $f_{dyn} = 1.45$

For tires of Type II: $f_{dyn} = 1.25$

For tires of Types VI, VII, VIII and for New Design: $f_{dyn} = 1.50$

Allowable tire deflections are determined by the tire manufacturer. The allowable tire deflection, s_t may be computed from:

$$s_t = D_o - 2(\text{loaded radius}) \qquad (2.4)$$

Values for D_o and for the 'loaded radius' are given in tire tables such as presented in sub-section 2.4.5

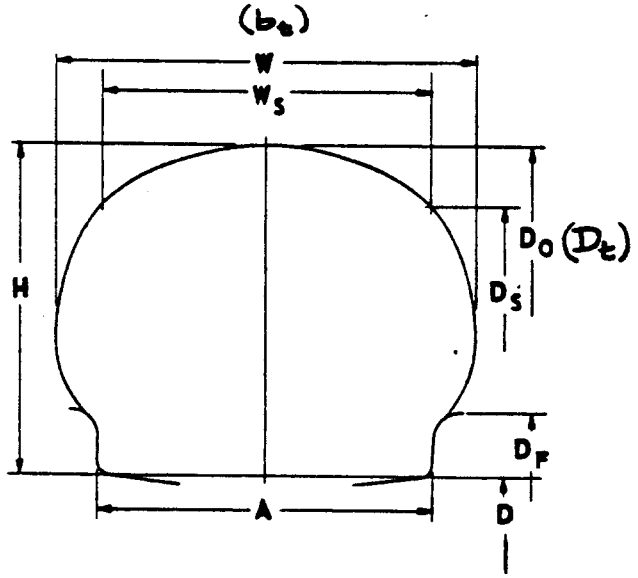

D	=	Bead Seat Diameter
D_F	=	Flange Diameter
D_o	=	Outside Diameter — Tire
D_s	=	Shoulder Diameter — Tire
W	=	Section Width — Tire
W_s	=	Shoulder Width — Tire
H	=	Section Height — Tire
W_s (max)	=	.85 W (max) for Type III Tires
W_s (max)	=	.88 W (max) for all other Types
D_s (max)	=	1.64 H + D
H	=	$\frac{D_o - D}{2}$

Figure 2.17 Definition of Tire Geometry Parameters

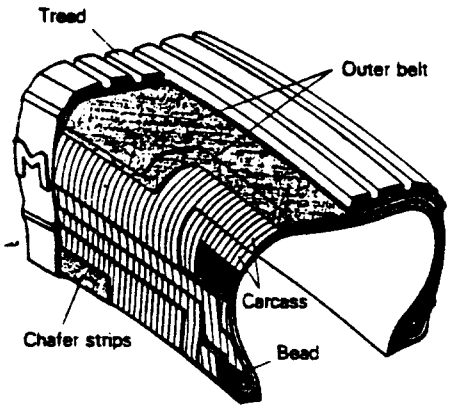

Figure 2.18 Radial Airplane Tire Construction

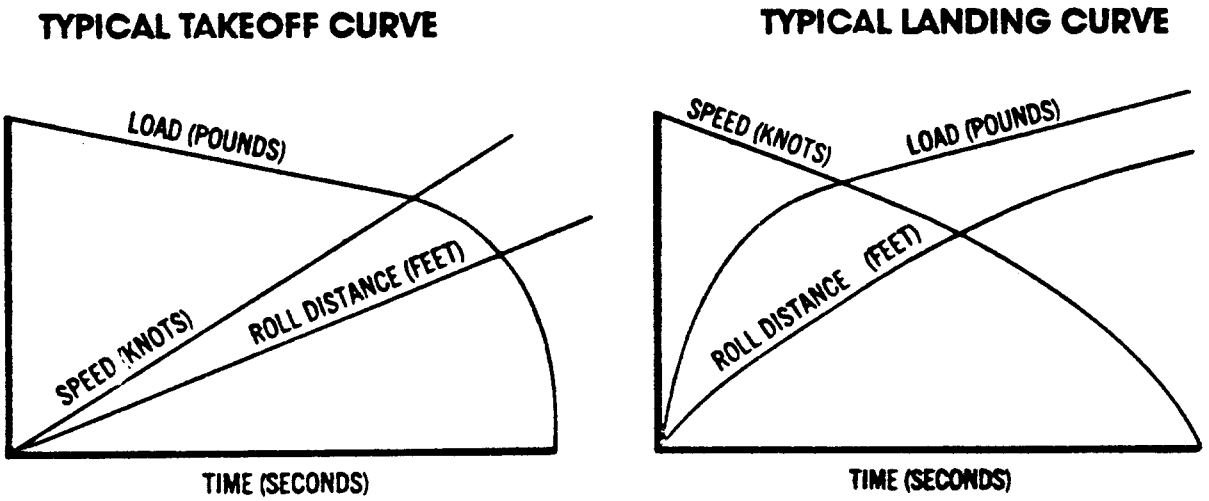

Figure 2.19 Typical Tire Performance Requirements During Take-off and Landing Rolls

2.4.3 Tire Clearance Requirements

The following tire clearance requirements must be observed:

1. Wheel well clearance (after retraction)
2. Tire-to-fork and/or tire-to-strut clearance
3. Tire-to-tire clearance in multiple wheel arrangements

Figure 2.20 defines what is meant by these clearance requirements. The physical reasons for these tire clearance requirements are:

a) Tires grow in size during their service life: 4 percent in width and 10 percent in diameter

b) Tires grow in size under the influence of centrifugal forces. This type of growth depends on the maximum tire operating speed on the ground

Figure 2.21 shows the required lateral (width) and radial clearances due to centrifugal forces as a function of the 'grown tire width'. The 'grown tire width' in Figure 2.21 may be taken as: 1.04W.

For preliminary design purposes it is acceptable to account for the following tire clearances:

In width: 0.04W + lateral clearance due to centrifugal forces + 1 inch

In radius: $0.1D_o$ + radial clearance due to centrifugal forces + 1 inch

For more precise methods to compute clearance requirements, see Ref.2.

2.4.4 Tire Sizing Procedure

The following procedure is recommended for airplane tire sizing:

1. Main gear tire(s): Determine the maximum static load on each main gear. This can be done with the help of Figure 2.14. Make sure that this load is computed for that weight/c.g. location which results in the maximum load per tire.

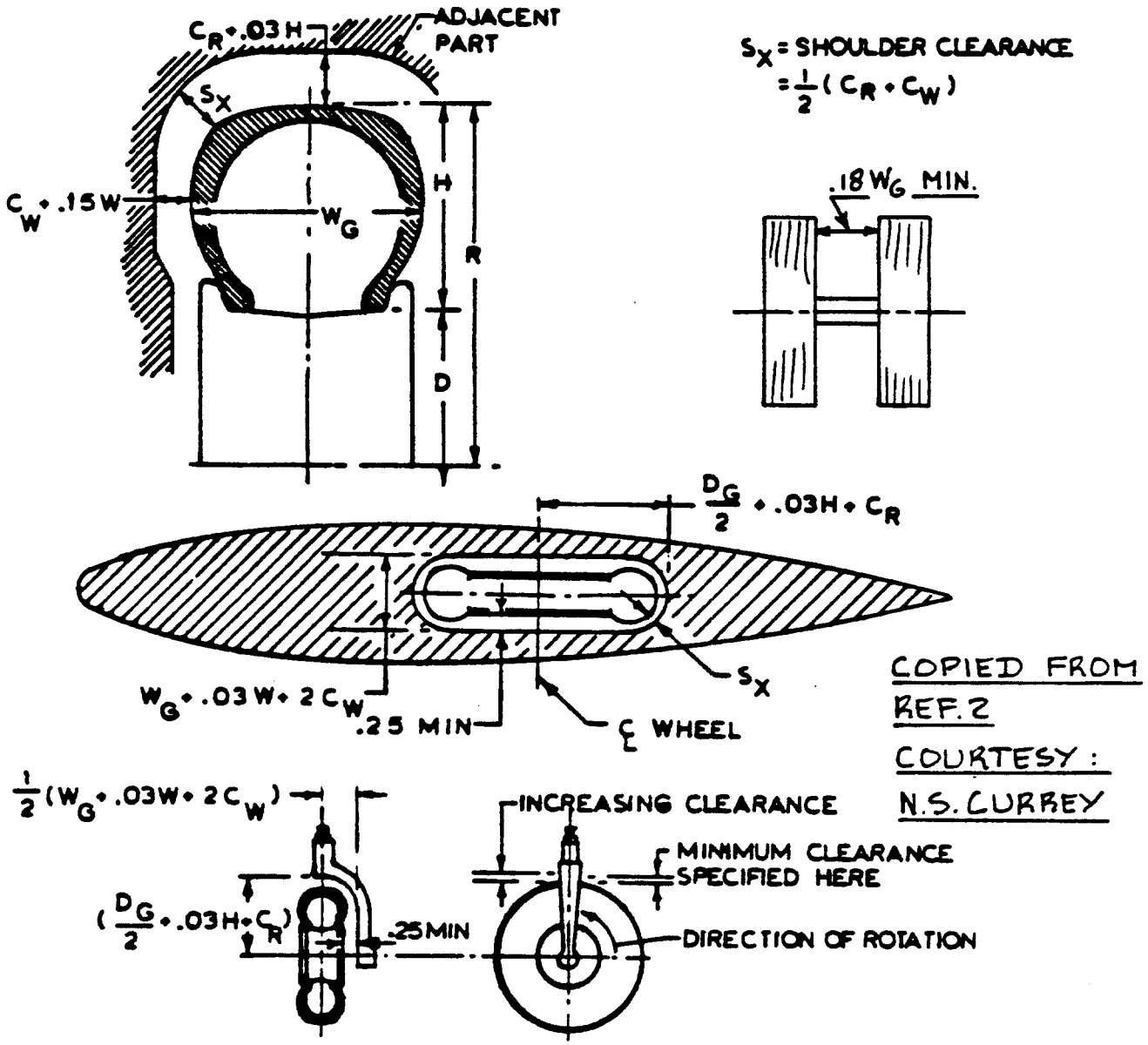

COPIED FROM REF. 2
COURTESY: N.S. CURREY

Figure 2.20 Geometry of Lateral and Radial Tire Clearance Requirements

W_G GROWN TIRE WIDTH

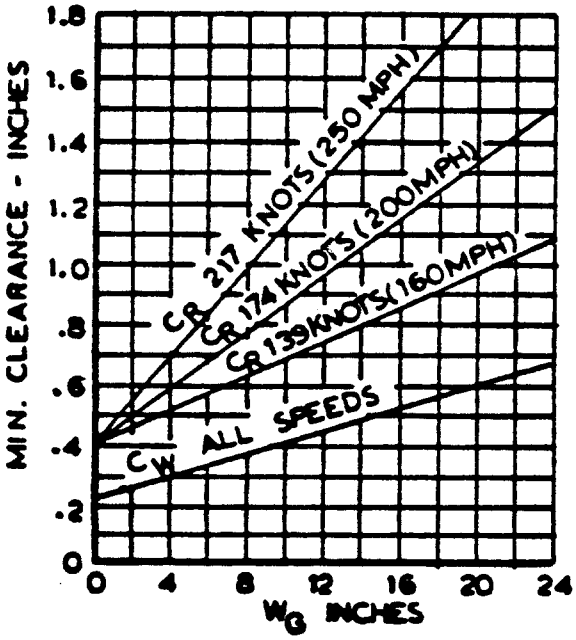

Figure 2.21 Minimum Tire Clearance Requirements

Note 1: If the airplane is to be FAR 25 certified, multiply this load by 1.07.

Note 2: If the airplane c.g. locations are not yet known, assume that the total main gear load is 90 percent of the maximum ramp weight. Maximum ramp weight may be taken as 1.005 to 1.01 times W_{TO}.

Note 3: To allow for growth in airplane weight, multiply the design load by 1.25.

Divide the maximum static load on each main gear by the number of tires per main gear. The result is the design maximum static load per main gear tire.

2. Nose gear tire(s): Determine the maximum static and dynamic loads on each tire. This can be done with the help of Figure 2.14. Make sure that these loads are computed for that weight/c.g. location which results in the maximum load per nose gear tire.

Note 1: If the airplane is to be FAR 25 certified, multiply these loads by 1.07.

Note 2: If the airplane c.g. locations are not yet known, assume that the nose gear load is 10 percent of the maximum ramp weight. Maximum ramp weight may be taken as 1.005 to 1.01 times W_{TO}.

Note 3: To allow for growth in airplane weight, multiply the design load by 1.25.

Divide the maximum static load on the nose gear by the number of tires on the nose gear. The result is the design maximum static load per nose gear tire.

3. Determine the maximum dynamic load per nose gear tire from:

$$P_{n_{dyn_t}} = W_{TO}\{l_m + a_x/g(h_{cg})\}/n_t(l_m + l_n) \qquad (2.5)$$

The definitions for l_m and for l_n are given in Figure 2.14. Values for a_x may be taken as:

$a_x/g = 0.35$ for dry concrete with simple brakes

$a_x/g = 0.45$ for dry concrete with anti-skid brakes

The design maximum static load may be obtained from the maximum dynamic load obtained with Eqn.(2.5) by dividing by the following factor:

For Type I and III tires: 1.45

For Type II tires: 1.25

For Type VI, VII and VIII tires: 1.50

For New Design tires: 1.50

This value for design maximum static load needs to be compared with the load computed under 2. The highest load value should be used.

4. Determine the maximum tire operating speed. This speed is the highest of the design take-off or landing speed of the airplane:

$$\text{For landing: } V_{tire/max} = 1.2V_{s_L} \qquad (2.6)$$

$$\text{For take-off: } V_{tire/max} = 1.1V_{s_{TO}} \qquad (2.7)$$

5. Using Tables 2.5 through 2.12 (Sub-section 2.4.5) list all tires which meet the load/speed conditions of the airplane.

6. Based on the ESWL calculation of Eqns (2.1) or (2.2) select the tires which meet the load/pressure criteria for surface compatibility.

7. For airplanes which operate from rough surfaces or from carriers the so-called 'crush-load' may be critical. This crush-load arises when the tire runs over a relatively sharp object such as sharp bump or a deck cable. A method for estimating the crush-load is given in Ref.2, p.6-14.

8. From the remaining candidate tires select a tire. This final selection can be made on the basis of the following criteria:

1. weight
2. minimum size
3. customer preference
4. wear and tear

Tire size and weight data are also listed in Tables 2.5-2.12 in sub-section 2.4.5.

Figures 2.22 present an example application of this tire sizing procedure.

2.4.5 Tire Data

For the most recent tire data the reader should consult tire catalogs published by tire manufacturers. In the USA airplane tires are most frequently selected from the following manufacturers:

Goodrich
Goodyear
Dunlop (United Kingdom)
Michelin (France)

In this text only a limited amount of tire data can be included. Tables 2.5 through 2.12 present tire data for Goodrich tires.

The reader should check his tire selection by comparison with the data in Tables 2.13 through 2.16. The latter tables contain information on which tire types were selected by a different manufacturers for their airplanes. For more information of this type Ref.6 should be consulted.

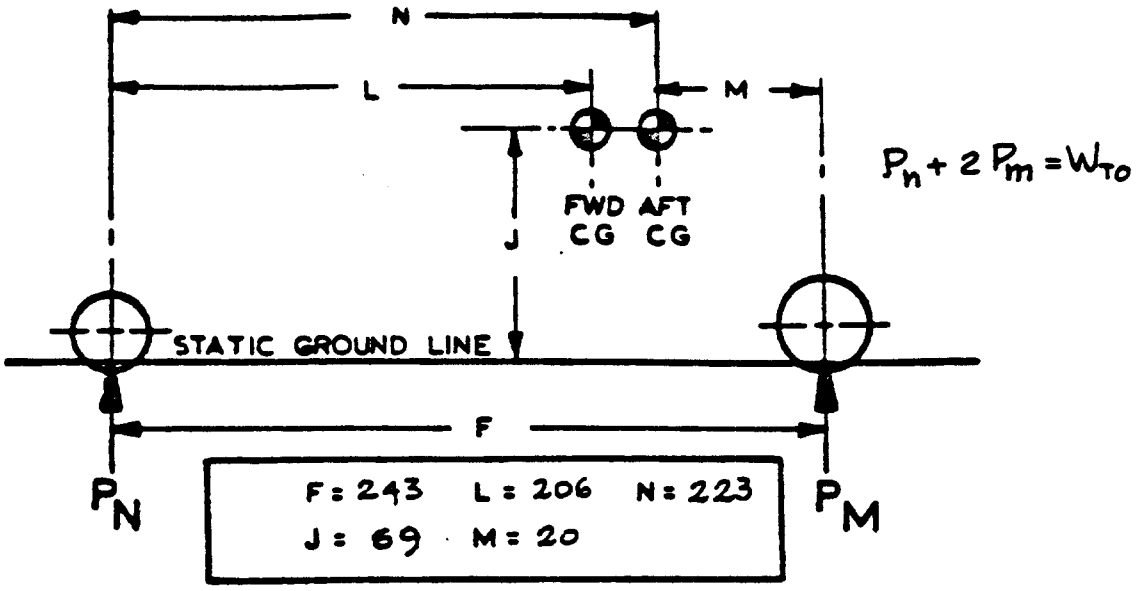

MAXIMUM STATIC MAIN GEAR LOAD (PER STRUT) (ASSUMING 2 STRUTS/a/c) ($n_s = 2$)

$$= \frac{\text{GROSS WEIGHT}(F - M)}{2F}$$

$$= \frac{40{,}000\ (223)}{486}$$

$$P_M = \underline{18{,}330}$$

MAXIMUM STATIC NOSE GEAR LOAD

$$= \frac{\text{GROSS WEIGHT}(F - L)}{F}$$

$$= \frac{40{,}000\ (37)}{243}$$

$$P_{NS_{MAX}} = \underline{6{,}100}$$

MINIMUM STATIC NOSE GEAR LOAD

$$= \frac{\text{GROSS WEIGHT}(F - N)}{F}$$

$$= \frac{40{,}000\ (20)}{243}$$

$$P_{NS_{MIN}} = \underline{3{,}950}$$

DYNAMIC NOSE GEAR LOAD (10 FT/SEC/SEC DECELERATION) ($a_x = 10$ FT/SEC^2)

$$= P_{NS_{MAX}} + \frac{10J \times \text{GROSS WEIGHT}}{32.2\ F} \quad \text{(EQN. 2.3)}$$

$$= 6{,}100 + \frac{690\ (40{,}000)}{7820}$$

$$P_{ND} = \underline{9{,}630}$$

Figure 2.22 Tire Sizing Example

WITH (2) TIRES ON EACH MAIN GEAR, MAX STATIC TIRE LOAD = 9165 LB.
WITH (2) TIRES ON NOSE GEAR, MAX STATIC TIRE LOAD = 3050 LB.
MAX. DYN. NOSE TIRE LOAD = 4815 LB.

ALLOWING FOR 25% AIRPLANE GROWTH, USE THE FOLLOWING VALUES FOR BASIC SIZE SELECTION, & USE ABOVE VALUES FOR PLIES SELECTION:

MAIN GEAR TIRE STATIC LOAD = 11,450 LB.
NOSE GEAR TIRE STATIC LOAD = 3,810 LB.
NOSE GEAR TIRE DYNAMIC LOAD = 6,200 LB.

ASSUME MAX GROUND SPEED IS 180 MPH (156 KTS)

CANDIDATE TIRES MAIN GEAR

NO.	SIZE	PR	LOAD RATING STATIC LB.	LOAD RATING DYNAM. LB.	INFL PRESS PSI	SPEED RATING MPH (KTS)	TIRE O.D. INS	BEAD LEDGE DIA. INS	WIDTH INS	BUMP CAPAB INS	QUALIFIC^N STATUS
1	24 x 5.5	16	11,500	N.A.	355	200	24.15	14.0	5.70	1.6	MIL
2	25 x 6.0	16	12,000	N.A.	330	160	SPEED RATING			INADEQUATE.	
3	22 x 6.6-10	20	12,000	N.A.	290	225	22.20	10.0	6.80	2.2	MIL
4	26 x 6.6	16	12,000	N.A.	270	200	25.75	14.0	6.65	1.9	MIL
5	30 x 6.6	14	12,950	N.A.	320	225	30.12	20.0	6.50	1.1	MIL
6	25 x 6.75	18	13,000	N.A.	300	275	25.50	14.00	6.85	1.6	MIL
7	29 x 7.7	16	13,800	N.A.	230	200	28.40	15.00	7.85	2.1	COMML.
8	26 x 8.0-14	16	12,700	N.A.	235	275	26.00	14.00	8.00	1.6	MIL.
9	32 x 11.50-15	12	11,200	N.A.	120	200	32.00	15.00	11.50	3.2	COMML.

SELECTION FACTORS

INFLATION PRESSURE ELIMINATES: 1, 2, 3, 4, 5, 6
WHEEL DIAMETER ELIMINATES: 5, 9 (D TOO LARGE)
DIMENSIONS ELIMINATES:
OTHER: (MINOR FACTOR: NOT QUAL. FOR MIL. USE) 7

SELECTED TIRES MAIN No. 8 26 x 8.0-14 16PR, OPER. AT 170 PSI
NOSE NOT DONE IN THIS EXAMPLE

COPIED FROM REF. 2
COURTESY: N.S. CURREY

Figure 2.22 (Cont'd) Tire Sizing Example

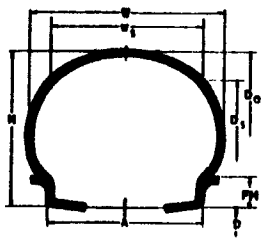

Table 2.5 Tire Data, Courtesy: B.F.Goodrich

Tire Description			Ply Rating	Tube Type Tubeless	Tire Dimensions (Inches)						Type	Max. Loading (Lbs.)	Unloaded Inflation Pressure (PSI)	Tread Patterns	Max. Speed (MPH)	Aspect Ratio	Loaded Radius		Rim Dimensions (Inches)			Qualification		WEIGHT
					D_o		W		D_o Max.	W_o Max.							Static	Flat Tire	A	B	FH	MIL	TSO	lbs
D_o	W	D			Max.	Min.	Max.	Min.																
	5.00	- 4	4	TT	13.25	12.70	5.05	4.75	11.60	4.30	III	700	35	Rib	120		5.2	3.5	3.50	4.00	.750	MIL	TSO	
	5.00	- 4	6	TT	13.25	12.70	5.05	4.75	11.60	4.30	III	1,200	56	Rib	120		5.7	3.9	3.50	4.00	.750	MIL	TSO	
	5.00	- 5	4	TL	14.20	13.65	4.95	4.65	12.55	4.20	III	800	31	Rib	120	.93	5.7	4.0	3.50	5.00	.750	MIL	TSO	5.5
	5.00	- 5	4	TT	14.20	13.65	4.95	4.65	12.55	4.20	III	800	31	Rib	120	.93	5.7	4.0	3.50	5.00	.750	MIL	TSO	5.0
	5.00	- 5	6	TL	14.20	13.65	4.95	4.65	12.55	4.20	III	1,260	49	Rib	120	.93	5.7	4.0	3.50	5.00	.750		TSO	6.0
	5.00	- 5	6	TT	14.20	13.65	4.95	4.65	12.55	4.20	III	1,260	49	Rib	120	.93	5.7	4.0	3.50	5.00	.750	MIL	TSO	5.5
	5.00	- 5	10	TT	14.20	13.65	4.95	4.65	12.55	4.20	III	2,150	88	Rib	120	.93	5.7	4.0	3.50	5.00	.750	MIL		6.0
	5.50	- 4	8	TT	13.47	12.99	5.54	5.28	13.47	4.27	III	1,225	50	Channel	120	.88	5.4	4.8	3.50	4.00	.750	MIL		
	6.00	- 6	4	TL	17.50	16.80	6.30	5.90	15.45	5.35	III	1,150	28	Rib	120	.91	6.9	4.6	5.00	6.00	.750		TSO	6.0
	6.00	- 6	6	TT	17.50	16.80	6.30	5.90	15.45	5.35	III	1,750	42	Rib	120	.91	6.9	4.6	5.00	6.00	.750	MIL	TSO	6.0
	6.00	- 6	6	TL	17.50	16.80	6.30	5.90	15.45	5.35	III	1,750	42	Rib	120	.91	6.9	4.6	5.00	6.00	.750	MIL	TSO	6.0
	6.00	- 6	8	TL	17.50	16.80	6.30	5.90	15.45	5.35	III	2,350	56	Rib	120	.91	6.9	4.6	5.00	6.00	.750	MIL	TSO	6.0
	6.00	- 6	8	TT	17.50	16.80	6.30	5.90	15.45	5.35	III	2,350	56	Rib	120	.91	6.9	4.6	5.00	6.00	.750	MIL	TSO	6.0
	6.50	- 8	4	TL	19.85	19.15	6.90	6.50	17.70	5.85	III	1,500	30	Rib	120	.88	8.0	5.6	5.25	8.00	.812	MIL	TSO	9.5
	6.50	- 8	6	TT	19.85	19.15	6.90	6.50	17.70	5.85	III	2,300	51	Rib	120	.88	8.0	5.6	5.25	8.00	.812		TSO	
	6.50	- 8	6	TL	19.85	19.15	6.90	6.50	17.70	5.85	III	2,300	51	Rib	120	.88	8.0	5.6	5.25	8.00	.812	MIL	TSO	
	6.50	- 8	8	TL	19.85	19.15	6.90	6.50	17.70	5.85	III	3,150	70	Rib	120	.88	8.0	5.6	5.25	8.00	.812	MIL	TSO	
	6.50	- 8	8	TT	19.85	19.15	6.90	6.50	17.70	5.85	III	3,150	70	Rib	120	.88	8.0	5.6	5.25	8.00	.812	MIL	TSO	
	6.50	- 10	6	TL	22.10	21.35	6.65	6.25	19.90	5.65	III	2,770	69	Rib	120	.91	9.1	6.9	4.75	10.00	.812	MIL	TSO	
	6.50	- 10	6	TT	22.10	21.35	6.65	6.25	19.90	5.65	III	2,770	69	Rib	120	.91	9.1	6.9	4.75	10.00	.812	MIL	TSO	
	6.50	- 10	8	TL	22.10	21.35	6.65	6.25	19.90	5.65	III	3,750	80	Rib	120	.91	9.1	6.9	4.75	10.00	.812	MIL	TSO	
	6.50	- 10	8	TT	22.10	21.35	6.65	6.25	19.90	5.65	III	3,750	80	Rib	120	.91	9.1	6.9	4.75	10.00	.812	MIL	TSO	
	6.50	- 10	10	TL	22.10	21.35	6.65	6.25	19.90	5.65	III	4,750	100	Rib	120	.91	9.1	6.9	4.75	10.00	.812	MIL	TSO	
	6.50	- 10	10	TT	22.10	21.35	6.65	6.25	19.90	5.65	III	4,750	100	Rib	120	.91	9.1	6.9	4.75	10.00	.812	MIL	TSO	
	6.50	- 10	12	TL	22.10	21.35	6.65	6.25	19.90	5.65	III	5,750	125	Rib	120	.91	9.1	6.9	4.75	10.00	.812	MIL	TSO	
	7.00	- 6	4	TL	18.75	18.00	7.00	6.60	16.45	5.95	III	1,250	23	Rib	120	.91	7.3	4.6	5.00	6.00	.750		TSO	10.0
	7.00	- 6	4	TT	18.75	18.00	7.00	6.60	16.45	5.95	III	1,250	23	Rib	120	.91	7.3	4.6	5.00	6.00	.750		TSO	9.0
	7.00	- 6	6	TL	18.75	18.00	7.00	6.60	16.45	5.95	III	1,900	38	Rib	120	.91	7.3	4.6	5.00	6.00	.750		TSO	9.0
	7.00	- 6	6	TT	18.75	18.00	7.00	6.60	16.45	5.95	III	3,180	66	Rib	120	.91	7.3	4.6	5.00	6.00	.750	MIL		
	7.00	- 6	6	TT	18.75	18.00	7.00	6.60	16.45	5.95	III	1,900	38	Rib	120	.91	7.3	4.6	5.00	6.00	.750	MIL	TSO	
	7.00	- 6	8	TT	18.75	18.00	7.00	6.60	16.45	5.95	III	2,550	54	Rib	120	.91	7.3	4.6	5.00	6.00	.750	MIL	TSO	
	7.00	- 8	4	TT	20.65	20.10	7.30	6.85	18.55	6.25	III	1,600	30	Rib	120	.88	8.4	5.9	5.50	8.00	.812		TSO	
	7.00	- 8	6	TT	20.65	20.10	7.30	6.85	18.55	6.25	III	2,400	46	Rib	120	.88	8.4	5.9	5.50	8.00	.812		TSO	
	7.00	- 8	12	TL	20.65	20.10	7.30	6.85	18.55	6.25	III	5,300	95	Rib	120	.88	8.4	5.9	5.50	8.00	.812	MIL		
	7.00	- 8	16	TL	20.65	20.10	7.30	6.85	18.55	6.25	III	6,650	125	Rib	150	.88	8.4	5.9	5.50	8.00	.812	MIL		
	7.50	- 10	6	TL	24.15	23.30	6.75	7.20	21.60	6.50	III	3,000	40	Rib	120	.92	9.7	6.9	5.50	10.00	.812	MIL	TSO	17.0
	7.50	- 10	6	TT	24.15	23.30	6.75	7.20	21.60	6.50	III	3,000	40	Rib	120	.92	9.7	6.9	5.50	10.00	.812	MIL	TSO	14.5
	7.50	- 10	8	TT	24.15	23.30	6.75	7.20	21.60	6.50	III	4,070	67	Rib	120	.92	9.7	6.9	5.50	10.00	.812	MIL		
	7.50	- 10	12	TL	24.15	23.30	6.75	7.20	21.60	6.50	III	1,800	80	Rib	120	.92	9.7	6.9	5.50	10.00	.812	MIL		
	7.50	- 10	12	TT	24.15	23.30	6.75	7.20	21.60	6.50	III	1,800	80	Channel	120	.92	9.7	6.9	5.50	10.00	.812	MIL		
	7.50	- 14	8	TL	27.75	27.00	7.65	7.20	25.30	6.50	III	5,700	67	Rib	160	.90	11.6	9.2	5.50	14.00	.812		TSO	
	7.50	- 14	8	TT	27.75	27.00	7.65	7.20	25.30	6.50	III	5,700	67	Rib	160	.90	11.6	9.2	5.50	14.00	.812	MIL	TSO	
	7.50	- 14	10	TL	27.75	27.00	7.65	7.20	25.30	6.50	III	7,200	110	Rib	160	.90	11.6	9.2	5.50	14.00	.812		TSO	

Table 2.6 Tire Data, Courtesy: B.F.Goodrich

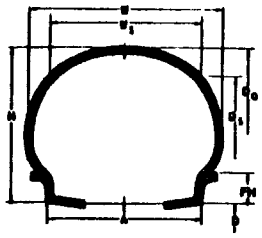

Tire Description			Ply Rating	Tube Type Tube-less	Tire Dimensions (Inches)						Type	Max. Loading (Lbs.)	Unloaded Inflation Pressure (PSI)
					D_o		W		D_o Max.	W_o Max.			
D_o	W	D			Max.	Min.	Max.	Min.					
	7.00	- 14	12	TL	27.75	27.00	7.65	7.20	25.30	6.50	III	8,700	120
8.00"			6	TT	8.10	7.86	3.08	2.94	7.32	1.86	I	450	55
	8.00	- 4	6	TT	18.00	17.15	8.30	7.80	15.50	7.05	III	1,700	35
	8.00	- 6	4	TL	19.50	18.75	7.95	7.50	17.05	6.75	III	1,350	23
	8.00	- 6	4	TT	19.50	18.75	7.95	7.50	17.05	6.75	III	1,350	23
	8.00	- 6	6	TT	19.80	18.75	7.95	7.50	17.05	6.75	III	2,080	35
	8.50	- 4	4	TL	22.10	21.15	8.65	8.30	19.20	7.50	III	1,600	20
	8.50	- 6	4	TT	22.10	21.15	8.65	8.30	19.20	7.50	III	1,600	20
	8.50	- 6	6	TT	22.10	21.15	8.65	8.30	19.20	7.50	III	2,275	30
	8.50	- 10	6	TL	25.65	24.70	8.70	8.20	22.80	7.40	III	3,250	41
	8.50	- 10	6	TT	25.65	24.70	8.70	8.20	22.80	7.40	III	3,250	41
	8.50	- 10	8	TL	25.65	24.70	8.70	8.20	22.80	7.40	III	4,400	55
	8.50	- 10	8	TT	25.65	24.70	8.70	8.20	22.80	7.40	III	4,400	55
	8.50	- 10	10	TL	25.65	24.70	8.70	8.20	22.80	7.40	III	5,500	70
	8.50	- 10	10	TT	25.65	24.70	8.70	8.20	22.80	7.40	III	5,500	70
	8.50	- 10	12	TL	25.65	24.70	8.70	8.20	22.80	7.40	III	8,000	100
	8.50	- 12.50	8	(See 27.50 x 8.90-12.50)									
	9.00	- 8	8	TT	22.40	21.40	9.25	8.70	19.45	7.85	III	4,000	50
	9.00	- 8	10	TT	22.40	21.40	9.25	8.70	19.45	7.85	III	4,500	55
	9.50	- 16	10	TT	33.35	32.50	9.70	9.10	30.25	8.25	III	9,250	80
	9.50	- 16	12	TL	33.35	32.50	9.70	9.10	30.25	8.25	III	11,200	110
10.00"			6	TT	10.08	9.76	4.15	4.00	9.00	2.52	I	650	45
	10.00	- 7	12	TT	25.45	24.30	10.25	9.85	22.15	8.70	III	7,100	80
	11.00	- 12	8	TL	32.20	31.00	11.20	10.50	28.55	9.50	III	8,300	45
	11.00	- 12	8	TT	32.20	31.00	11.20	10.50	28.55	9.50	III	8,300	45
12.50"			6	TT	12.50	12.10	5.40	4.98	11.16	3.44	I	1,800	80
12½	x 4½		10	TT	12.86	12.10	4.85	4.45	12.40	4.20	VII	1,800	75
	12.50	- 16	12	TL	28.45	27.50	12.75	12.00	34.40	10.85	III	12,800	75
	12.50	- 16	12	TT	28.45	27.50	12.75	12.00	34.40	10.85	III	12,800	75
	13.50	- 16	24	TL	39.80	38.85	14.00	13.25	35.10	12.00	III	27,500	145
14.50"			8	TT	14.70	14.28	6.24	5.98	13.14	3.70	I	2,000	80
14.5	x 5.5	- 6	14	TL	14.50	14.00	5.50	5.15	13.00	4.85	NS	3,550	155
15	x 6.00	- 6	4	TT	15.20	14.58	6.30	5.90	13.55	5.55	III	1,250	45
15	x 6.00	- 6	6	TL	15.20	14.55	6.30	5.90	13.55	5.55	III	1,950	68
15	x 6.00	- 6	6	TT	15.20	14.55	6.30	5.90	13.55	5.55	III	1,950	68
15	x 6.00	- 6	6	TT	15.20	14.55	6.30	5.90	13.55	5.55	III	3,525	110
	15.00	- 10	10	TL	34.80	34.20	15.00	14.60	30.35	13.20	III	8,850	38
	15.00	- 16	10	TL	42.40	41.40	15.30	14.40	37.65	13.00	III	12,200	53
	15.00	- 16	14	TL	42.40	41.40	15.30	14.40	37.65	13.00	III	17,100	70
	15.00	- 16	16	TL	42.40	41.40	15.30	14.40	37.65	13.00	III	20,300	90
	15.50	- 20	14	TT	45.25	44.30	16.00	15.05	40.70	13.60	III	20,800	90
	15.50	- 20	16	TL	45.25	44.30	16.00	15.05	40.70	13.60	III	24,000	105
	15.50	- 20	16	TT	45.25	44.30	16.00	15.05	40.70	13.60	III	24,000	105
	15.50	- 20	20	TL	45.25	44.30	16.00	15.05	40.70	13.60	III	29,900	135
	15.50	- 20	20	TL	45.25	44.30	16.00	15.05	40.70	13.60	III	29,900	135

Tread Patterns	Max. Speed (MPH)	Aspect Ratio	Loaded Radius		Rim Dimensions (Inches)			Qualification		WEIGHT
			Static	Flat Tire	A	D	FH	MIL	TSO	lbs
Rib	160	.90	11.8	9.2	5.50	14.00	.812		TSO	
Smooth	120	.85	3.2	2.5	2.66	2.66	.491	MIL	TSO	1.5
Rib	120	.84	6.7	3.5	5.50	4.00	.880	MIL	TSO	
Rib	120	.85	7.5	4.7	5.00	6.00	.750		TSO	12.0
Rib	120	.85	7.5	4.7	5.00	6.00	.750		TSO	11.0
Rib	120	.85	7.5	4.7	5.00	6.00	.750		TSO	11.0
Rib	120	.91	8.4	4.8	6.00	6.00	.875		TSO	
Rib	120	.91	8.4	4.8	6.00	6.00	.875		TSO	
Rib	120	.91	8.4	4.8	6.00	6.00	.875		TSO	14.0
Rib	120	.90	10.2	7.3	6.25	10.00	.812		TSO	22.0
Rib	120	.90	10.2	7.3	6.25	10.00	.812		TSO	20.0
Rib	120	.90	10.2	7.0	6.25	10.00	.812	MIL	TSO	
Rib	120	.90	10.2	7.0	6.25	10.00	.812	MIL	TSO	22.0
Rib	120	.90	10.2	6.8	6.25	10.00	.812	MIL	TSO	25.0
Rib	120	.90	10.2	6.8	6.25	10.00	.812		TSO	23.0
Rib	120	.90	10.2	6.9	6.25	10.00	.812	MIL		
	(See 27.50 x 8.90-12.50)									
Rib	120	.89	8.5	5.7	6.75	6.00	.875		TSO	
Rib	120	.89	8.5	5.7	6.75	6.00	.875	MIL	TSO	
Rib	160	.90	13.8	10.5	7.00	16.00	1.000	MIL		
Rib	160	.90	13.9	10.5	7.00	16.00	1.000		TSO	
Smooth	120	.82	3.9	2.7	3.624	3.19	.514	MIL	TSO	8.0
Rib	120	–	8.9	6.5	8.0	7.00	1.25	MIL	TSO	
Rib	120	.90	12.6	8.4	8.25	12.00	1.000	MIL	TSO	
Rib	120	.90	12.8	8.4	8.25	12.00	1.000		TSO	
Smooth	120	–	10.3	6.5	4.75	3.94	.881	MIL	TSO	
Channel	120	.86	6.4	4.2	3.625	4.50	.625	MIL	TSO	
Rib	160	.89	15.7	11.2	10.00	16.00	1.250	MIL	TSO	
Rib	160	.89	15.7	11.2	10.00	16.00	1.250		TSO	
Rib	160	.86	16.3	11.8	11.00	16.00	1.625		TSO	
Smooth	120	.80	5.8	3.9	5.624	4.66	.845	MIL	TSO	
Rib CH	200	.78	6.1	4.6	4.25	6.00	.875		TSO	
Rib	120	.73	6.2	4.6	5.00	6.00	.750	MIL	TSO	
Rib	120	.73	6.2	4.6	5.00	6.00	.750		TSO	
Rib	69	.73	6.2	4.6	5.00	6.00	.750	MIL		
Rib	120	.73	6.2	4.6	5.00	6.00	.750		TSO	
Univ.	160	.83	13.3	7.3	11.00	10.00	1.000		TSO	58.0
Rib	160	.87	16.8	11.1	11.25	16.00	1.375	MIL	TSO	
Dimple	160	.87	16.9	11.1	11.25	16.00	1.375		TSO	93.0
Dimple	160	.87	16.9	11.1	11.25	16.00	1.375		TSO	
Dimple	160	.80	18.6	13.4	13.25	20.00	1.625	MIL	TSO	130.0
Dimple	160	.80	18.6	13.4	13.25	20.00	1.625		TSO	
Dimple	160	.80	18.6	13.4	13.25	20.00	1.625		TSO	
Rib	160	.80	18.6	13.4	13.25	20.00	1.625	MIL		
Rib	160	.80	18.6	13.4	13.25	20.00	1.625	MIL		156.0

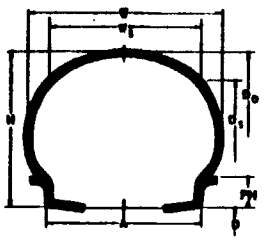

Table 2.7 Tire Data, Courtesy: B.F.Goodrich

Tire Description			Ply Rating	Tube Type Tubeless	Tire Dimensions (inches)						Type	Max. Loading (Lbs.)	Unloaded Inflation Pressure (PSI)
					Do		W		Do Max.	Wo Max.			
Do	W	D			Max.	Min.	Max.	Min.					
	15.50	- 20	20	TT	45.25	44.30	16.00	15.05	40.70	13.60	III	29,900	135
	15.50	- 20	20	TT	45.25	44.30	16.00	15.05	40.70	13.60	III	29,900	135
16 x 4.4			4	TL	16.00	15.50	4.45	4.15	14.55	3.90	VII	1,100	55
16 x 4.4			6	TL	16.00	15.50	4.45	4.15	14.55	3.90	VII	1,700	85
16 x 4.4			8	TT	16.00	15.50	4.45	4.15	14.55	3.90	VII	1,700	85
16 x 4.4			8	TL	16.00	15.50	4.45	4.15	14.55	3.90	VII	2,300	120
17.00"			10	TT	17.00	16.56	7.20	6.92	15.28	4.52	I	2,300	55
	17.00	- 16	10	TT	45.05	43.70	17.40	16.35	39.80	14.80	III	13,500	40
	17.00	- 16	12	TT	45.05	43.70	17.40	16.35	39.80	14.80	III	16,000	60
	17.00	- 20	22	TL	46.75	47.70	17.25	16.40	43.60	14.65	III	34,500	130
	17.00	- 20	22	TT	46.75	47.70	17.25	16.40	43.60	14.65	III	34,500	130
17.5 x 5.75		- 6	12	TL	17.5	16.85	5.75	5.40	15.80	5.10	NS	5,000	100
17.5 x 6.25		- 8	10	TL	17.5	16.85	6.25	5.90	15.45	5.90	NS	3,750	80
18 x 4.25		- 10	6	TL	18.25	17.75	4.70	4.46	16.75	4.15	NS	2,300	100
18 x 4.4			6	TL	17.90	17.40	4.45	4.15	14.55	3.79	VII	2,100	100
18 x 4.4			6	TL	17.90	17.40	4.45	4.15	14.55	3.79	VII	2,100	100
18 x 4.4			8	TL	17.90	17.40	4.45	4.15	14.55	3.79	VII	2,660	150
18 x 4.4			10	TL	17.90	17.40	4.45	4.15	14.55	3.79	VII	3,550	185
18 x 4.4			10	TL	17.90	17.40	4.45	4.15	14.55	3.79	VII	3,550	165
18 x 4.4			12	TL	17.90	17.40	4.45	4.15	14.55	3.79	VII	4,360	225
18 x 4.4			12	TL	17.90	17.40	4.45	4.15	14.55	3.79	VII	4,360	225
18 x 4.4			12	TT	17.90	17.40	4.45	4.15	14.55	3.79	VII	4,360	225
18 x 5.5			8	TL	17.90	17.30	5.70	5.36	16.20	5.00	VII	3,060	105
18 x 5.5			8	TL	17.90	17.30	5.70	5.36	16.20	5.00	VII	3,060	105
18 x 5.5			8	TT	17.90	17.30	5.70	5.36	16.20	5.00	VII	3,060	110
18 x 5.5			10	TL	17.90	17.30	5.70	5.36	16.20	5.00	VII	4,000	140
18 x 5.5			12	TL	17.90	17.30	5.70	5.36	16.20	5.00	VII	5,050	170
18 x 5.5			12	TT	17.90	17.30	5.70	5.36	16.20	5.00	VII	5,050	170
18 x 5.5			14	TL	17.90	17.30	5.70	5.36	16.20	5.00	VII	6,200	215
18 x 5.5			14	TL	17.90	17.30	5.70	5.36	16.20	5.00	VII	6,200	200
18 x 5.7		- 8	14	TL	17.8	17.25	5.80	5.25	16.20	5.00	NS	6,200	215
	19.00	- 23	16	TT	56.10	53.15	19.38	18.25	49.30	16.50	III	29,000	85
19.5 x 6.75		- 8	10	TL	19.50	18.90	6.75	6.35	17.45	5.95	NS	4,270	110
19.5 x 6.75		- 8	10	TT	19.50	18.90	6.75	6.35	17.45	5.95	NS	4,270	110
20 x 4.4			10	TL	20.00	19.50	4.45	4.15	19.45	3.95	VII	4,250	190
20 x 4.4			10	TT	20.00	19.50	4.45	4.15	19.45	3.95	VII	4,250	190
20 x 4.4			12	TL	20.00	19.50	4.45	4.15	19.45	3.95	VII	5,150	225
20 x 4.4			14	TL	20.00	19.50	4.45	4.15	19.45	3.95	VII	6,000	265
20 x 5.5			12	TL	20.15	19.55	5.70	5.36	19.30	4.75	VII	6,150	190
20 x 5.5			14	TL	20.15	19.55	5.70	5.36	19.30	4.75	VII	7,200	230
20 x 5.5			16	TL	20.15	19.55	5.70	5.36	19.30	4.75	VII	8,750	270
	20.00	- 20	20	TL	56.00	54.30	20.10	19.20	49.50	17.10	III	46,500	125
	20.00	- 20	22	TL	56.00	54.30	20.10	19.20	49.50	17.10	III	38,500	95
	20.00	- 20	26	TL	56.00	54.30	20.10	19.20	49.50	17.10	III	46,500	125
21 x 7.25		- 10	8	TL	21.25	20.60	7.20	6.80	19.25	6.35	NS	4,000	95

Tread Patterns	Max. Speed (MPH)	Aspect Ratio	Loaded Radius		Rim Dimensions (Inches)			Qualification		WEIGHT
			Static	Flat Tire	A	B	Rh	MIL	TSO	lbs
Rib	160	.80	16.6	13.4	13.25	20.00	1.625	MIL		158.0
Dimple	160	.80	16.6	13.4	13.25	20.00	1.625		TSO	
Rib	200	.80	6.9	5.7	3.50	8.00	.812	MIL	TSO	7.5
	160	.80	6.9	5.7	3.50	8.00	.812		TSO	5.5
Rib	160	.80	6.9	5.7	3.50	8.00	.812	MIL	TSO	
Rib	160	.80	6.9	5.7	3.50	8.00	.812	MIL		8.0
Smooth	120	.81	6.1	4.4	5.662	5.44	.733	MIL	TSO	
Rib	160	.84	17.7	11.2	13.25	16.00	1.875	MIL	TSO	
Rib	160	.84	17.7	11.2	13.25	16.00	1.875	MIL	TSO	185.0
Rib	160	.84	16.7	13.6	13.25	20.00	1.750	MIL	TSO	
Rib	160	.84	16.7	13.6	13.25	20.00	1.750	MIL	TSO	178.0
Rib	210	.83	7.4	4.3	4.25	8.00	.875		TSO	
Rib	120	.82	6.9	5.3	5.00	6.00	.750		TSO	
Rib CH	210	.87	8.0	6.6	3.625	10.00	.900		TSO	
Rib	200	.88	7.9	6.6	3.50	10.00	.812	MIL	TSO	8.0
Rib Du CH	200	.88	7.9	6.6	3.50	10.00	.812		TSO	
Rib CH	210	.88	7.9	6.6	3.50	10.00	.812		TSO	
Rib CH	200	.88	7.9	6.6	3.50	10.00	.812		TSO	11.5
Rib Du CH	200	.88	7.9	6.6	3.50	10.00	.812		TSO	
Rib CH	300	.88	7.9	6.6	3.50	10.00	.812	MIL		11.5
Rib CH	200	.88	7.9	6.6	3.50	10.00	.812		TSO	
Rib	220	.88	7.9	6.6	3.50	10.00	.812	MIL		10.4
Rib	160	.87	7.5	6.2	4.25	8.00	.875	MIL		11.0
Rib	160	.87	7.5	6.2	4.25	8.00	.875	MIL	TSO	13.5
Rib	160	.87	7.5	6.2	4.25	8.00	.875	MIL		
Rib	210	.87	7.5	6.2	4.25	8.00	.875		TSO	
Rib	160	.87	7.5	6.2	4.25	8.00	.875	MIL		14.0
Rib	160	.87	7.5	6.2	4.25	8.00	.875	MIL		13.0
Rib	275	.87	7.5	6.2	4.25	8.00	.875	MIL		
Rib	160	.87	7.5	6.2	4.25	8.00	.875	MIL		15.0
Rib	250	.87	7.46	6.1	4.25	8.00	.875	MIL		
Rib	160	.83	22.6	15.6	14.75	23.00	2.000		TSO	174.0
Rib	160	.85	6.1	5.5	5.25	8.00	.812		TSO	
Rib	160	.85	6.1	5.5	5.25	8.00	.812		TSO	
Rib	160	.90	8.9	8.0	3.50	12.00	.812	MIL		
Rib	160	.90	8.9	8.0	3.50	12.00	.812	MIL		13.5
Rib	225	.90	8.9	8.0	3.50	12.00	.812	MIL		
Rib	235	.90	8.9	8.0	3.50	12.00	.812	MIL		
Rib	160	.88	8.6	7.1	4.25	10.00	.875	MIL		17.0
Rib	200	.88	8.6	7.1	4.25	10.00	.875	MIL		
Rib	185	.88	8.6	7.1	4.25	10.00	.875	MIL		20.5
Rib	200	.88	22.0	13.9	15.50	23.00	2.000	MIL		
Rib	200	.88	22.0	13.9	15.50	23.00	2.000	MIL		202.0
Rib	200	.88	22.0	13.9	15.50	23.00	2.000	MIL		260.0
Rib CH	200	.78	9.1	7.1	5.50	10.00	1.000		TSO	

Table 2.8 Tire Data, Courtesy: B.F.Goodrich

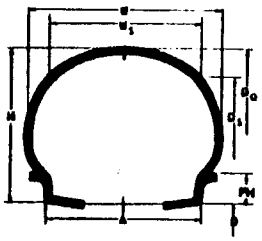

Tire Description				Ply Rating	Tube Type Tube-less	Tire Dimensions (inches)						Type	Max. Loading (Lbs.)	Unloaded Inflation Pressure (PSI)
						D_o		W		D_s Max.	W_s Max.			
D_o	W		D			Max.	Min.	Max.	Min.					
21	x 7.25	-	10	20	TL	21.25	20.60	7.20	6.80	19.25	6.35	NS	12,000	320
21	x 7.25	-	10	20	TL	21.25	20.60	7.20	6.80	19.25	6.35	NS	12,000	320
22	x 5.5			10	TL	22.15	21.55	5.70	5.35	21.30	4.95	VII	5,700	185
22	x 5.5			12	TL	22.15	21.55	5.70	5.35	21.30	4.95	VII	7,100	235
22	x 5.75	-	12	8	TL	22.00	21.40	5.75	5.40	20.20	5.05	NS	4,350	135
22	x 5.75	-	12	10	TL	22.00	21.40	5.75	5.40	20.20	5.05	NS	5,700	180
22	x 6.5	-	10	16	TL	22.00	21.60	6.80	6.40	20.00	6.00	NS	7,900	180
22	x 6.5	-	10	16	TL	22.00	21.60	6.80	6.40	20.00	6.00	NS	9,150	180
22	x 6.5	-	10	18	TL	22.00	21.60	6.80	6.40	20.00	6.00	NS	10,700	280
22	x 6.5	-	10	20	TL	22.00	21.60	6.80	6.40	20.00	6.00	NS	12,000	280
22	x 6.5	-	10	20	TL	22.00	21.60	6.80	6.40	20.00	6.00	NS	12,000	270
22	x 6.75	-	10	8	TL	22.00	21.30	6.75	6.35	19.85	5.95	NS	4,450	95
22	x 7.75	-	11.50	8	TT	22.34	21.75	7.43	7.00	22.18	7.37	NS	4,600	80
22	x 7.7	-	12	16	TL	22.35	21.75	7.70	7.25	20.25	6.80	NS	10,500	280
22	x 7.75	-	10	8	TL	22.00	21.30	7.75	7.30	19.85	6.80	NS	4,700	90
22	x 8.00	-	10	10	TL	22.00	21.35	8.00	7.55	19.84	7.04	NS	6,500	110
22	x 8.5	-	11	16	TL	22.00	21.40	8.50	8.10	19.65	7.50	NS	10,000	210
23	x 7.00	-	12	10	TL	23.20	22.60	7.20	6.80	21.15	6.30	NS	6,500	110
24	x 5.5			12	TL	24.15	23.55	5.70	5.45	23.30	4.95	VII	8,070	230
24	x 5.5			12	TT	24.15	23.55	5.70	5.45	23.30	4.95	VII	7,500	250
24	x 5.5			14	TT	24.15	23.55	5.70	5.45	23.30	4.95	VII	9,700	275
24	x 5.5			16	TT	24.15	23.55	5.70	5.45	23.30	4.95	VII	11,500	355
24	x 7.25	-	12	10	TL	24.50	23.80	7.50	7.00	22.75	6.50	NS	6,600	120
24	x 7.7			10	TL	24.15	23.50	7.65	7.20	21.50	6.75	VII	5,400	90
24	x 7.7			10	TT	24.15	23.50	7.65	7.20	21.50	6.75	VII	5,400	85
24	x 7.7			10	TT	24.15	23.50	7.65	7.20	21.50	6.75	VII	5,100	85
24	x 7.7			12	TL	24.15	23.50	7.65	7.20	21.50	6.75	VII	6,800	110
24	x 7.7			14	TL	24.15	23.50	7.65	7.20	21.50	6.75	VII	8,200	135
24	x 7.7			14	TL	24.15	23.50	7.65	7.20	21.50	6.75	VII	8,200	135
24	x 7.7			14	TL	24.15	23.50	7.65	7.20	21.50	6.75	VII	8,200	135
24	x 7.7			16	TL	24.15	23.50	7.65	7.20	21.50	6.75	VII	9,725	165
24	x 7.7			16	TL	24.15	23.50	7.65	7.20	21.50	6.75	VII	9,700	165
24	x 7.7			18	TL	24.15	23.50	7.65	7.20	21.50	6.75	VII	11,900	180
24	x 8.0	-	13	18	TL	24.00	23.40	8.00	7.55	22.00	7.05	NS	12,500	285
25	x 8.0			16	TT	25.00	24.35	8.15	7.80	23.70	5.00	VII	12,000	330
25	x 6.75			16	TL	25.50	24.80	6.85	6.45	23.44	6.03	VII	11,000	240
25	x 6.75			18	TL	22.50	24.80	6.85	6.45	23.44	6.03	VII	13,000	300
		25.00	- 28	30	TT	71.15	69.30	25.70	24.70	63.40	21.85	III	55,000	85
25.5	x 8.0	-	14	18	TL	25.50	24.80	8.00	7.55	23.14	6.89	NS	15,300	275
25.00*				12	TL	25.00	24.96	11.00	10.56	23.24	7.16	I	6,300	70
26	x 6			10	TT	25.75	25.10	6.65	6.25	–	–	II	5,150	130
26	x 6.6			8	TL	25.75	25.05	6.65	6.25	23.55	5.85	VII	5,300	120
26	x 6.6			8	TL	25.75	25.06	6.65	6.25	23.55	5.85	VII	5,300	120
26	x 6.6			10	TL	25.75	25.06	6.65	6.25	23.55	5.85	VII	6,900	158
26	x 6.6			10	TL	25.75	25.06	6.65	6.25	23.55	5.85	VII	6,900	158

Tread Patterns	Max. Speed (MPH)	Aspect Ratio	Loaded Radius		Rim Dimensions (Inches)			Qualification		WEIGHT
			Static	Flat Tire	A	D	FH	MIL	TSO	lbs
Rib CH	225	.78	9.1	7.1	5.50	10.00	1.000			
Rib	225	.78	9.1	7.1	5.50	10.00	1.000	MIL		
Rib	160	.89	9.6	8.0	4.25	12.00	.875	MIL		
Rib	160	.89	9.6	8.0	4.25	12.00	.875	MIL		21.0
Rib	160	.89	9.6	8.0	4.25	12.00	.875		TSO	
Rib	160	.89	9.6	8.0	4.25	12.00	.875		TSO	
Rib	200	.80	9.4	7.2	5.50	10.00	1.000	MIL		
Ribh CH	230	.80	9.4	7.2	5.50	10.00	1.000	MIL		
Rib	230	.80	9.4	7.2	5.50	10.00	1.000	MIL		
Rib	225	.80	9.4	7.2	5.50	10.00	1.000	MIL		
Rib CH	160	.80	9.4	7.2	5.50	10.00	1.000	MIL		
Rib	160	.89	9.1	6.9	4.75	10.00	.812		TSO	
Smooth	160	.73	9.2	7.8	4.63	11.50	*1.222	MIL		
Rib	275	.67	9.7	8.2	6.00	12.00	1.000	MIL		
Rib	160	.77	9.1	6.8	4.75	10.00	.812		TSO	
Rib	190	.75	9.0	6.9	5.00	10.00	.500		TSO	
	250	.84	9.4	7.8	7.25	11.00	.875	MIL		
Rib	210	.78	9.9	7.8	6.25	12.00	.650		TSO	
Rib	200	.89	10.6	9.0	4.25	14.00	.875	MIL		
Rib	160	.89	10.6	9.0	4.25	14.00	.875	MIL		
Rib	160	.89	10.6	9.0	4.25	14.00	.875	MIL		23.5
Rib	200	.89	10.6	9.0	4.25	14.00	.875	MIL		27.5
Hib CH	180	.84	10.4	8.0	6.25	12.00	.700		TSO	
Rib	180	.82	10.0	7.5	5.50	10.00	.906		TSO	
Rib	160	.82	10.0	7.5	5.50	10.00	.906	MIL		
Rib	180	.82	10.0	7.5	5.50	10.00	.906	MIL		
Rib	200	.82	10.0	7.5	5.50	10.00	.906		TSO	
Rib	250	.82	10.0	7.5	5.50	10.00	.906	MIL		
Rib	200	.82	10.0	7.5	5.50	10.00	.906	MIL	TSO	
Rib	225	.82	10.0	7.5	5.50	10.00	.906		TSO	
Rib	210	.82	10.0	7.5	5.50	10.00	.906		TSO	
Rib	225	.82	10.0	7.5	5.50	10.00	.906		TSO	
Rib	190	.82	10.0	7.5	5.50	10.00	.906		TSO	
Rib	265	.84	10.4	7.7	5.75	13.00	1.00	MIL		
Rib	160	.89	11.0	9.2	4.27	14.00	.875	MIL		
Rib	275	.84	11.2	9.6	4.00	14.00	1.00	MIL		
Rib	275	.84	11.2	9.6	4.00	14.00	1.00	MIL		
Rib	160	.84	28.6	18.5	19.50	28.00	2.625	MIL		488
Rib	200	.72	11.0	9.2	5.75	14.00	1.000	MIL		
Rib	120	.80	10.3	8.5	10.0	8.25	1.125	MIL	TSO	25.0
Rib	160	.89	11.5	8.4	5.00	14.00	.725	MIL		21.0
Rib CH	200	.88	11.2	8.9	5.0	14.00	1.00		TSO	27.0
Rib CH	225	.88	11.2	8.9	5.0	14.00	1.00		TSO	25.5
Rib CH	200	.88	11.3	9.2	5.0	14.00	1.00		TSO	28.5
Rib CH	225	.88	11.3	9.2	5.0	14.00	1.00		TSO	27.0

*Size 22x7.25-11.50: Deflection is calculated from tire height of .812 not from flange height of 1.222.

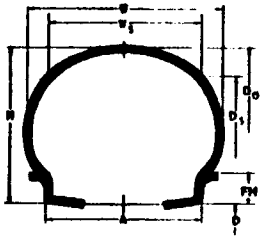

Table 2.9 Tire Data, Courtesy: B.F.Goodrich

Tire Description			Ply Rating	Tube Type Tubeless	Tire Dimensions (Inches)						Type	Max. Loading (Lbs.)	Unloaded Inflation Pressure (PSI)
					D_o		W		D_o	W_o			
D_o	W	D			Max.	Min.	Max.	Min.	Max.	Max.			
26 x 6.6			10	TL	25.75	25.05	6.65	6.25	23.55	5.85	VII	6,900	155
26 x 6.6			10	TL	25.75	25.05	6.65	6.25	23.55	5.85	VII	6,900	155
26 x 6.6			12	TL	25.75	25.05	6.65	6.25	23.55	5.85	VII	8,600	195
26 x 6.6			12	TL	25.75	25.05	6.65	6.25	23.55	5.85	VII	8,600	195
26 x 6.6			14	TL	25.75	25.05	6.65	6.25	23.55	5.85	VII	10,000	225
26 x 6.6			14	TL	25.75	25.05	6.65	6.25	23.55	5.85	VII	10,000	210
26 x 6.6			14	TL	25.75	25.05	6.65	6.25	23.55	5.85	VII	10,000	225
26 x 6.6			14	TT	25.75	25.05	6.65	6.25	23.55	5.85	VII	10,000	225
26 x 6.6			16	TL	25.75	25.05	6.65	6.25	23.55	5.85	VII	12,000	270
26 x 6.75	- 14		14	TL	26.00	25.30	6.75	6.30	23.85	5.95	NS	10,300	230
26 x 6.75	- 14		16	TL	26.00	25.30	6.75	6.30	23.85	5.95	NS	11,900	270
26 x 7.75	- 13		10	TT	26.20	25.50	7.90	7.45	23.80	6.95	NS	7,050	130
26 x 8.0	- 14		16	TL	26.00	25.30	8.00	7.50	23.35	6.00	NS	12,700	235
26 x 10	- 11		10	TL	26.00	25.20	10.00	9.45	23.30	8.80	NS	9,700	110
27			10	TT	26.16	27.22	9.86	9.14	26.30	5.70	I	5,500	70
27.5 x 7.5	- 16		22	TL	27.50	26.80	7.50	7.00	24.45	6.60	NS	20,500	400
27.50 x 8.80	- 12.50		8	TL	27.70	27.30	9.00	8.67	24.95	7.85	NS	4,300	50
28 x 7.7			10	TL	27.40	26.60	7.85	7.40	24.90	6.95	VII	7,400	125
28 x 7.7			14	TL	27.40	26.60	7.85	7.40	24.90	6.95	VII	11,000	195
28 x 9.0	- 12		22	TL	27.60	26.80	8.85	8.35	24.80	7.80	VII	16,650	235
28 x 9.0	- 14		22	TL	27.70	27.00	9.10	8.60	25.25	8.00	NS	18,100	260
29 x 7.7			12	TL	28.40	27.60	7.85	7.40	25.90	6.95	VII	9,800	160
29 x 7.7			16	TL	28.40	27.60	7.85	7.40	25.90	6.95	VII	13,800	230
29 x 7.7			16	TL	28.40	27.60	7.85	7.40	25.90	6.95	VII	13,800	230
29 x 7.7			16	TT	28.40	27.60	7.85	7.40	25.90	6.95	VII	13,800	220
29 x 11.00	- 10		8	TT	29.06	28.10	11.00	10.40	25.60	9.35	NS	5,000	45
29 x 11.00	- 10		10	TL	29.00	28.10	11.00	10.40	25.60	9.35	NS	7,070	60
30 x 8.8			14	TT	30.12	29.40	8.50	5.95	26.20	5.50	VII	12,950	320
30 x 7.7			12	TT	29.40	28.60	7.85	7.40	26.90	6.95	VII	10,000	165
30 x 7.7			16	TL	29.40	28.60	7.85	7.40	26.90	6.95	VII	16,500	270
30 x 7.7			22	TL	29.40	28.60	7.85	7.40	26.90	6.95	VII	21,300	360
30 x 7.7			26	TL	29.40	28.60	7.85	7.40	26.90	6.95	VII	24,100	395
30 x 8.8			26	TL	29.80	29.40	7.98	7.76	26.90	6.95	VII	24,100	360
30 x 8.8			22	TL	30.44	29.50	8.90	8.35	27.40	7.90	VII	21,000	235
30 x 11.0	- 14		4	TT	30.00	29.20	11.00	10.40	27.10	9.70	NS	3,500	35
30 x 11.50	- 14.50		24	TL	29.75	28.75	11.50	11.00	27.00	10.10	NS	25,000	243
30 x 11.50	- 14.50		24	TL	29.75	28.75	11.50	11.00	27.00	10.10	NS	25,000	245
30 x 11.50	- 14.50		28	TL	29.75	28.75	11.50	11.00	27.00	10.10	NS	25,000	245
31 x 11.50	- 16		22	TL	31.00	30.20	11.50	10.80	28.30	10.10	NS	23,300	275
H31 x 13	- 12		20	TL	31.00	30.10	13.00	12.30	27.60	11.45	NS	17,200	135
32 x 8.8			12	TL	31.00	30.05	8.90	8.35	28.05	7.90	VII	11,000	140
32 x 8.8			12	TT	31.00	30.05	8.90	8.35	28.05	7.90	VII	11,000	135
32 x 8.8			16	TT	31.00	30.05	8.90	8.35	28.05	7.90	VII	15,100	200
32 x 8.8			16	TT	31.00	30.05	8.90	8.35	28.05	7.90	VII	15,600	200
32 x 8.8			20	TL	31.00	30.05	8.90	8.35	28.05	7.90	VII	15,000	300

Tread Patterns	Max. Speed (MPH)	Aspect Ratio	Loaded Radius		Rim Dimensions (Inches)			Qualification		WEIGHT
			Static	Flat Tire	A	D	FH	MIL	TSO	lbs
Rib	200	.86	11.3	9.2	5.0	14.00	1.00		TSO	28.5
Rib	225	.86	11.3	9.2	5.0	14.00	1.00		TSO	27.0
Rib	200	.89	11.3	9.4	5.0	14.00	1.00	MIL		30.0
Rib	210	.88	11.3	9.4	5.0	14.00	1.00		TSO	
Rib	200	.88	11.3	9.4	5.0	14.00	1.00	MIL		
Rib	180	.86	11.3	9.4	5.0	14.00	1.00	MIL		36.0
Rib	210	.88	11.3	9.4	5.0	14.00	1.00	MIL	TSO	
Rib	200	.88	11.3	9.4	5.0	14.00	1.00	MIL		
Rib	200	.88	11.2	9.5	5.0	14.00	1.00	MIL		36.0
Rib	190	.89	11.3	9.2	5.00	14.00	1.000		TSO	
Rib	180	.89	11.3	9.2	5.00	14.00	1.000		TSO	
Rib CH	200	.84	11.1	8.6	6.00	13.00	.700		TSO	
Rib	275	.75	11.2	9.6	6.375	14.00	1.125	MIL		
Rib	88	.75	10.25	7.25	6.00	11.00	1.000	MIL		
Rib	160	.73	11.6	8.6	8.94	14.00	.688	MIL	TSO	
Dimple	275	.84	12.3	11.0	8.0	16.00	1.125	MIL		
Rib	180	.84	12.0	8.1	6.75	12.80	.875		TSO	
Rib	180	.85	11.7	9.2	6.00	14.00	1.00		TSO	
Rib	200	.85	11.7	9.2	6.00	14.00	1.00	MIL		
Rib	173	.89	11.7	9.1	7.00	12.00	1.250	MIL		
Rib	200	.75	11.9	8.9	6.00	16.00	1.000	MIL		
Rib	200	.85	12.2	10.1	6.00	15.00	1.000		TSO	38.0
Rib	200	.85	12.2	10.1	6.00	15.00	1.000		TSO	47.0
Rib	225	.85	12.2	10.1	6.00	15.00	1.000		TSO	
Rib	200	.85	12.2	10.1	6.00	15.00	1.000	MIL		44.0
Rib	180	.87	11.4	7.2	8.50	10.00	1.000	MIL	TSO	
Rib	120	.87	11.4	7.2	8.50	10.00	1.000	MIL	TSO	
Rib	225	.78	13.8	12.5	5.00	20.00	1.000	MIL		
Rib	200	.85	12.7	10.8	6.00	16.00	1.00	MIL		
Rib	180	.85	12.7	10.7	6.00	16.00	1.00	MIL		
Rib	180	.85	12.7	10.7	6.00	16.00	1.00	MIL		
Rib	224	.85	12.7	10.8	6.00	16.00	1.00	MIL		
Rib	248	.86	12.8	10.8	6.00	16.00	1.00	MIL		58.0
Rib	250	.87	12.9	10.4	7.00	15.00	1.125	MIL		57.0
Univ.	120	.73	12.8	8.2	9.00	14.00	.750		TSO	
Rib	240	.86	12.5	10.4	9.75	14.50	1.250	MIL		
Rib	247	.86	12.5	10.4	9.75	14.50	1.250	MIL		
Rib	247	.86	12.5	10.4	9.75	14.50	1.250	MIL		
Rib	275	.86	13.2	11.0	9.00	18.00	1.250	MIL		
Rib	210	.73	12.4		8.00	12.00	1.200		TSO	
Rib	180	.84	13.3	10.9	7.00	16.00	1.125		TSO	
Rib	180	.84	13.3	10.9	7.00	16.00	1.125	MIL		41.0
Rib	180	.84	13.3	10.9	7.00	16.00	1.125	MIL		49.5
Rib	180	.84	13.3	10.9	7.00	16.00	1.125	MIL		59.0
Rib	260	.84	13.3	10.9	7.00	16.00	1.125	MIL		

Table 2.10 Tire Data, Courtesy: B.F.Goodrich

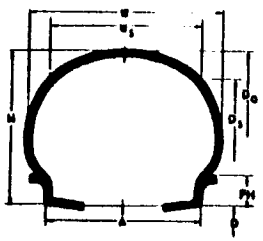

Tire Description			Ply Rating	Tube Type Tube-less	Tire Dimensions (inches)						Type	Max. Loading (Lbs.)	Unloaded Inflation Pressure (PSI)	Tread Patterns	Max. Speed (MPH)	Aspect Ratio	Loaded Radius		Rim Dimensions (inches)			Qualification		WEIGHT
					D_o		W		D_o Max.	W_o Max.							Static	Flat Tire	A	D	FH	MIL	TSO	lbs
D_o	W	D			Max.	Min.	Max.	Min.																
32 x 8.8			24	TL	31.00	30.05	8.90	8.35	28.05	7.90	VII	23,300	336	Rib	275	.84	13.3	10.8	7.00	16.00	1.125	MIL		
32 x 11.50		- 15	12	TL	32.00	31.10	11.50	10.80	29.00	10.50	NS	11,200	120	Rib CH	210	.74	13.5	10.3	9.00	15.00	1.250		TSO	67.0
32 x 11.50		- 15	12	TL	32.00	31.10	11.50	10.80	29.00	10.50	NS	11,200	120	Rib CH	225	.74	13.5	10.3	9.00	15.00	1.250		TSO	82.0
33			10	TT	33.06	32.06	11.30	10.84	31.30	6.60	I	8,000	70	Rib	160	.73	13.8	10.3	10.78	16.50	.813	MIL	TSO	
34 x 9.25		- 16	16	TL	34.00	33.15	9.25	8.75	30.75	8.15	NS	18,500	156	Rib	200	.88	14.3	10.4	7.00	16.00	1.125		TSO	55.5
34 x 8.9			12	TL	33.40	32.45	10.20	9.55	30.10	8.80	VII	11,200	115	Rib	200	.86	14.2	10.7	8.00	16.00	1.250		TSO	53.0
34 x 8.9			14	TL	33.40	32.45	10.20	9.55	30.10	8.80	VII	14,000	150	Rib	160	.86	14.2	10.7	8.00	16.00	1.250	MIL		55.0
34 x 8.9			14	TT	33.40	32.45	10.20	9.55	30.10	8.80	VII	14,000	150	Rib	160	.86	14.2	10.7	8.00	16.00	1.250	MIL		
34 x 11			16	TL	33.40	32.60	11.30	10.60	29.90	9.95	VII	16,100	145	Rib	200	.87	13.9	10.0	9.00	14.00	1.500		TSO	78.0
34 x 11			20	TL	33.40	32.60	11.30	10.60	29.90	9.95	VII	18,300	185	Rib	200	.87	13.9	10.0	9.00	14.00	1.500		TSO	77.0
34 x 11			22	TL	33.40	32.60	11.30	10.60	29.90	9.95	VII	20,500	186	Rib	200	.87	13.9	10.0	9.00	14.00	1.500		TSO	73.5
34 x 11			22	TL	33.40	32.60	11.30	10.60	29.90	9.95	VII	20,500	186	Rib	225	.87	13.9	10.0	9.00	14.00	1.500		TSO	76.0
34 x 12		- 12	12	TL	34.00	33.10	12.00	11.35	30.00	10.55	NS	10,400	70	Rib	160	.92	13.4	8.3	9.00	12.00	1.125		TSO	58.0
34 x 12		- 12	14	TL	34.00	33.10	12.00	11.35	30.00	10.55	NS	11,300	86	Rib	160	.92	13.4	8.3	9.00	12.00	1.125		TSO	64.5
34.5 x 8.75		- 18	22	TL	34.50	33.76	9.75	9.15	31.55	8.60	NS	23,400	260	Rib	260	.85	14.9	11.6	7.50	18.00	1.125	MIL		
34.5 x 8.75		- 18	26	TL	34.50	33.76	9.75	9.15	31.55	8.60	NS	30,100	340	Rib	250	.85	14.9	11.6	7.50	18.00	1.125	MIL		
35 x 9.00		- 17	16	TL	34.80	33.95	9.40	8.90	31.60	8.25	NS	16,300	170	Rib	200	.95	14.8	11.6	7.25	17.00	1.100		TSO	
36 x 11.50		- 16	22	TL	36.00	31.80	11.50	10.80	31.80	10.10	NS	23,000	210	Rib	225	.83	14.8	9.7	9.00	16.00	1.375	MIL		
36			12	TT	36.86	35.40	13.08	12.56	34.84	7.02	I	10,500	70	Rib	160	.72	16.3	11.1	12.46	17.75	.875	MIL	TSO	
36 x 11			20	TL	35.10	34.00	11.50	10.80	31.65	10.10	VII	21,000	185	Rib	225	.83	14.7	11.3	9.00	16.00	1.375		TSO	78.0
36 x 11			22	TL	35.10	34.00	11.50	10.80	31.65	10.10	VII	23,300	200	Rib	200	.83	14.7	11.3	9.00	16.00	1.375	MIL		84.5
36 x 11			22	TL	35.10	34.00	11.50	10.80	31.65	10.10	VII	23,300	200	Rib	225	.83	14.7	11.3	9.00	16.00	1.375		TSO	
36 x 11			24	TL	35.10	34.00	11.50	10.80	31.65	10.10	VII	26,000	235	Rib	180	.83	14.7	11.3	9.00	16.00	1.375	MIL		90.5
36 x 11			24	TL	35.10	34.00	11.50	10.80	31.65	10.10	VII	26,000	235	Rib	250	.83	14.7	11.3	9.00	16.00	1.375	MIL		85.0
36 x 11			28	TL	35.10	34.00	11.50	10.80	31.65	10.10	VII	31,500	280	Rib	200	.83	14.7	11.3	9.00	16.00	1.375	MIL		87.0
37 x 11.50		- 16	28	TL	37.00	36.10	11.50	10.90	33.20	10.10	NS	31,200	246	Rib	180	.91	16.1	10.4	8.00	16.00	1.375	MIL		90.0
37 x 13		- 16	20	TL	37.00	36.10	13.00	12.30	33.20	11.45	NS	22,200	185	Rib	210	.81	15.4	10.8	9.00	16.00	1.375		TSO	
37 x 13		- 16	26	TL	37.00	36.10	13.00	12.30	33.20	11.45	NS	29,300	220	Rib	225	.81	15.4	10.8	9.00	16.00	1.375		TSO	
37 x 14		- 14	24	TL	37.00	36.05	14.00	13.30	32.85	12.30	NS	25,000	180	Rib	225	.83	16.1	10.4	11.00	14.00	1.500		TSO	90.0
H37 x 14.0		- 15	22	TL	37.00	36.10	14.00	13.30	33.05	12.30	NS	24,100	165	Rib	225	.79	15.0		9.00	15.00	1.300		TSO	
38 x 11			14	TL	37.10	36.00	11.50	10.80	33.65	10.10	VII	15,400	130	Rib	225	.83	15.7	12.3	9.00	16.00	1.375	MIL		80.5
38 x 13			14	TL	38.25	37.30	13.00	12.25	34.25	11.45	VII	15,000	100	Rib	180	.86	15.8	11.0	10.00	16.00	*1.375		TSO	
38 x 13			14	TL	38.25	37.30	13.00	12.25	34.25	11.45	VII	15,000	100	Rib	200	.86	15.8	11.0	10.00	16.00	*1.375		TSO	87.0
38 x 13			14	TT	38.25	37.30	13.00	12.25	34.25	11.45	VII	15,000	100	Rib	180	.86	15.8	11.0	10.00	16.00	*1.375		TSO	
38 x 13			16	TL	38.25	37.30	13.00	12.25	34.25	11.45	VII	17,200	115	Rib	210	.86	15.8	11.0	10.00	16.00	*1.375		TSO	
38 x 13			16	TL	38.25	37.30	13.00	12.25	34.25	11.45	VII	17,200	115	Rib	225	.86	15.8	11.0	10.00	16.00	*1.375	MIL	TSO	94.0
38 x 13			20	TL	38.25	37.30	13.00	12.25	34.25	11.45	VII	22,300	150	Rib	200	.86	15.8	11.0	10.00	16.00	1.375		TSO	107.0
38 x 13			22	TL	38.25	37.30	13.00	12.25	34.25	11.45	VII	24,600	165	Rib	200	.86	15.8	11.0	10.00	16.00	1.375		TSO	114.0
38 x 13			22	TL	38.25	37.30	13.00	12.25	34.25	11.45	VII	24,600	165	Rib	225	.86	15.8	11.0	10.00	16.00	1.375		TSO	104.0
40 x 12			14	TT	39.40	38.04	12.35	11.70	35.50	10.90	VII	14,500	95	Rib	180	.87	16.6	12.3	10.00	18.00	1.500	MIL		78.0
40 x 12			16	TL	39.40	38.40	12.35	11.70	35.50	10.90	VII	18,500	130	Rib	180	.87	16.6	12.3	10.00	18.00	1.500		TSO	95.0
40 x 12			18	TL	39.40	38.40	12.35	11.70	35.50	10.90	VII	21,000	150	Rib	180	.87	16.6	12.3	10.00	18.00	1.500		TSO	102.0
40 x 12			18	TL	39.40	38.40	12.35	11.70	35.50	10.90	VII	21,000	150	Rib	200	.87	16.6	12.3	10.00	18.00	1.500		TSO	
40 x 12			22	TL	39.40	38.40	12.35	11.70	35.50	10.90	VII	26,700	190	Rib	180	.87	16.6	12.3	10.00	18.00	1.500		TSO	107.0
40 x 14			20	TL	39.80	38.95	14.00	13.25	35.10	12.00	VII	22,300	200	Rib	200	.86	16.5	11.6	11.00	16.00	1.625		TSO	

*Rim with FH of 1.25 is optional for 38x13, 14 and 16 PR tires

Table 2.11 Tire Data, Courtesy: B.F.Goodrich

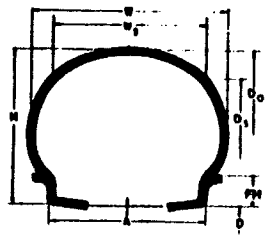

Tire Description Do	W	D	Ply Rating	Tube Type Tube-less	Tire Dimensions (Inches) Do Max.	Do Min.	W Max.	W Min.	Do Max.	Wo Max.	Type	Max. Loading (Lbs.)	Unloaded Inflation Pressure (PSI)	Tread Patterns	Max. Speed (MPH)	Aspect Ratio	Loaded Radius Static	Loaded Radius Flat Tire	Rim Dimensions (Inches) A	Rim Dimensions (Inches) D	Rim Dimensions (Inches) FH	Qualification MRL	Qualification TSO	WEIGHT lbs
46 x 14			20	TL	39.80	38.85	14.00	13.25	35.10	12.00	VII	22,300	135	Rib	225	.86	16.5	11.6	11.00	16.00	1.625		TSO	114.0
46 x 14			22	TL	39.80	38.85	14.00	13.25	35.10	12.00	VII	25,000	156	Rib	200	.86	16.5	11.6	11.00	16.00	1.625		TSO	124.0
46 x 14			22	TL	39.80	38.85	14.00	13.25	35.10	12.00	VII	25,000	156	Rib	225	.86	16.5	11.6	11.00	16.00	1.625		TSO	112.0
46 x 14			24	TL	39.80	38.85	14.00	13.25	35.10	12.00	VII	27,700	170	Rib	200	.86	16.5	11.6	11.00	16.00	1.625		TSO	129.0
46 x 14			24	TL	39.80	38.85	14.00	13.25	35.10	12.00	VII	27,700	170	Rib	225	.86	16.5	11.6	11.00	16.00	1.625		TSO	130.0
46 x 14			26	TL	39.80	38.85	14.00	13.25	35.10	12.00	VII	30,500	175	Rib	200	.86	16.5	11.6	11.00	16.00	1.625	MIL		118.0
46 x 14			26	TL	39.80	38.85	14.00	13.25	35.10	12.00	VII	30,500	185	Rib	210	.86	16.5	11.6	11.00	16.00	1.625		TSO	
46 x 14			26	TL	39.80	38.85	14.00	13.25	35.10	12.00	VII	33,500	200	Rib	200	.86	16.5	11.6	11.00	16.00	1.625	MIL		127.0
46 x 14			26	TL	39.80	38.85	14.00	13.25	35.10	12.00	VII	33,100	200	Rib	210	.86	16.5	11.6	11.00	16.00	1.625		TSO	
C46 x 14		- 21	22	TL	40.0	38.90	14.00	13.25	37.75	11.10	NS	25,400	155	Rib	225	.68	16.9	13.4	6.75	21.00	.800		TSO	132.0
C46 x 14		- 21	24	TL	40.0	38.90	14.00	13.25	37.75	11.10	NS	25,400	155	Rib	210	.68	16.9	13.4	6.75	21.00	.800		TSO	
H46 x 14.5		- 19	22	TL	40.0	38.90	14.00	13.25	37.75	11.10	NS	25,400	155	Rib	210	.73	16.7	13.3	9.50	19.00	1.400		TSO	
H46 x 14.5		- 19	24	TL	40.0	39.10	14.50	13.75	38.25	12.80	NS	33,200	200	Rib	210	.73	16.7	13.3	9.50	19.00	1.400		TSO	
46 x 15.5		- 19	26	TL	40.00	39.05	15.50	14.75	35.70	13.85	NS	36,300	180	Rib	235	.78	16.1	11.6	10.00	16.00	1.250		TSO	
946 x 18.0		- 19	20	TL	40.00	39.00	18.00	17.15	35.70	15.85	NS	27,800	130	Rib	190	.67	18.08	11.4	11.00	16.00	1.625	MIL		
41 x 15.0		- 19	22	TL	41.00	40.05	15.00	14.25	36.90	13.20	NS	28,600	170	Rib	225	.77	17.2	12.3	12.75	19.00	1.625		TSO	134.0
41 x 15.0		- 19	24	TL	41.00	40.05	15.00	14.25	36.90	13.20	NS	31,400	190	Rib	225	.77	17.2	12.3	12.75	19.00	1.625		TSO	128.0
42 x 13.0		- 19	26	TL	41.25	40.38	13.50	12.80	37.15	11.80	NS	35,900	205	Rib CH	230	.67	17.2	12.9	10.50	19.00	1.625	MIL		
H43 x 15.5		- 20	26	TL	43.00	42.10	15.50	14.75	38.65	13.65	NS	38,500		Rib	225	.74	18.1		11.00	20.00	1.900		TSO	
44*			12	TT	44.94	43.64	15.78	14.12	45.20	8.52	I	15,000	70	Rib	180	.72	18.7	13.4	14.87	22.00	1.063	MIL		
44*			12	TT	44.94	43.64	15.78	15.12	42.50	8.52	I	15,000	70	Dimple	180	.72	18.7	13.4	14.87	22.00	1.063		TSO	
44*			14	TT	44.94	43.64	15.78	15.12	42.50	8.53	I	18,200	86	Dimple	180	.72	18.7	13.4	14.87	22.00	1.063		TSO	
44 x 13			26	TL	43.55	42.30	13.50	12.80	39.45	12.80	VII	35,000	200	Rib	200	.87	18.4	13.7	11.00	20.00	1.875	MIL		126.0
44 x 16			26	TL	43.25	42.30	16.00	15.05	38.20	13.70	VII	38,400	185	Rib	200	.80	17.9	12.5	13.25	18.00	1.625	MIL		160.0
44 x 16			28	TL	43.25	42.30	16.00	15.05	38.20	13.70	VII	38,400	200	Rib	200	.80	17.9	12.5	13.25	18.00	1.625		TSO	167.0
44 x 16			28	TL	43.25	42.30	16.00	15.05	38.20	13.70	VII	38,400	200	Rib	225	.80	17.9	12.5	13.25	18.00	1.625		TSO	169.0
44 x 16			30	TL	43.25	42.30	16.00	15.05	38.20	13.70	VII	41,700	210	Rib	210	.80	17.9	12.5	13.25	18.00	1.625		TSO	172.0
44 x 16			30	TL	43.25	42.30	16.00	15.05	38.20	13.70	VII	41,700	210	Rib	225	.80	17.9	12.5	13.25	18.00	1.625		TSO	168.0
44 x 16			32	TL	43.25	42.30	16.00	15.05	38.20	13.70	VII	45,000	225	Rib	225	.80	17.9	12.5	13.25	18.00	1.625		TSO	180.0
44.5 x 16.0		- 21	24	TL	44.50	43.50	16.00	15.20	40.70	14.10	NS	40,500	195	Rib	225	.74	18.4	13.4	10.50	21.00	1.250	MIL		
44.5 x 16.0		- 21	28	TL	44.50	43.50	16.00	15.20	40.70	14.10	NS	45,400	240	Rib	280	.74	18.4	13.4	10.50	21.00	1.250	MIL		
44.5 x 16.0		- 21	34	TL	44.50	43.50	16.00	15.20	40.70	14.10	NS	60,900	315	Rib	283	.74	18.4	13.4	10.50	21.00	1.250	MIL		
44.5 x 16.5		- 19	30	TL	44.50	43.50	16.50	15.70	39.70	14.50	NS	42,500	195	Rib	225	.81	18.4	13.0	13.25	18.00	1.625		TSO	
44.5 x 16.5		- 19	30	TL	44.50	43.50	16.50	15.70	39.70	14.50	NS	42,500	195	Rib	200	.81	18.4	13.0	13.25	18.00	1.625		TSO	
H44.5 x 16.5		- 20	24	TL.	44.50	43.50	16.50	15.70	40.10	14.50	NS	38,200	165	Rib	225	.75	18.3		10.50	20.00	1.500		TSO	
H46 x 17.0		- 20	28	TL	45.00	44.00	17.80	16.20	40.50	14.95	NS	39,800	195	Rib	225	.74	18.8		11.00	20.00	1.600		TSO	
46 x 16			20	TL	45.25	44.03	16.00	15.50	40.70	14.10	VII	28,900	145	Rib	200	.80	19.0	13.6	13.25	20.00	*1.875		TSO	
46 x 16			24	TL	45.25	44.30	16.00	15.05	40.70	14.10	VII	35,700	170	Rib	210	.80	19.0	13.6	13.25	20.00	1.75		TSO	161.0
46 x 16			26	TL	45.25	44.30	16.00	15.05	40.70	14.10	VII	38,300	185	Rib	200	.80	19.0	13.6	13.25	20.00	1.75		TSO	168.0
46 x 16			26	TL	45.25	44.30	16.00	15.05	40.70	14.10	VII	38,300	185	Rib	225	.80	19.0	13.6	13.25	20.00	1.75		TSO	166.0
46 x 16			26	TL	45.25	44.30	16.00	15.05	40.70	14.10	VII	41,800	210	Rib	225	.80	19.0	13.6	13.25	20.00	1.75		TSO	185.0
46 x 16			26	TL	45.25	44.30	16.00	15.05	40.70	14.10	VII	41,800	210	Rib	210	.80	19.0	13.6	13.25	20.00	1.75		TSO	
46 x 16			28	TL	45.25	44.30	16.00	15.05	40.70	14.10	VII	41,800	225	Rib	225	.80	19.0	13.6	13.25	20.00	1.75	MIL	TSO	
46 x 16			30	TL	45.25	44.30	16.00	15.05	40.70	14.10	VII	44,800	225	Rib	225	.80	19.0	13.6	13.25	20.00	1.75		TSO	186.0
46 x 16			30	TL	45.25	44.30	16.00	15.05	40.70	14.10	VII	44,800	225	Rib	210	.80	19.0	13.6	13.25	20.00	1.75		TSO	191.0

*Rim with FH of 1.625 is optional for 46x16 20 PR tire.

Table 2.12 Tire Data, Courtesy: B.F.Goodrich

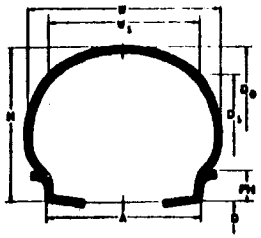

Tire Description			Ply Rating	Tube Type Tube-less	Tire Dimensions (inches)						Type	Max. Loading (Lbs.)	Unloaded Inflation Pressure (PSI)
					D_o		W		D_s	W_s			
D_o	W	D			Max.	Min.	Max.	Min.	Max.	Max.			
46 x 16			30	TL	45.25	44.30	16.00	15.05	40.70	14.10	VII	44,800	225
846 x 16.0		- 23.5	28	TL	46.00	45.10	16.00	15.20	41.95	14.10	NS	45,400	220
H46 x 16.0		- 20	26	TL	46.00	45.00	16.00	17.15	41.30	15.85	NS	40,700	185
47*			14	TT	44.88	47.02	17.00	16.32	44.24	10.66	I	17,500	70
47 x 16		- 16	26	TL	46.90	46.00	18.00	17.25	41.60	16.34	NS	38,100	150
47 x 16		- 16	30	TL	46.90	46.00	18.00	17.25	41.60	16.34	NS	43,700	175
47 x 16		- 16	36	TL	46.90	46.00	18.00	17.25	41.60	16.34	NS	54,000	215
48 x 17			26	TL	48.75	47.70	17.25	16.40	43.00	14.50	VII	39,600	170
48 x 17			28	TL	48.75	47.70	17.25	16.40	43.00	14.50	VII	39,600	170
48 x 17			28	TL	48.75	47.70	17.25	16.40	43.00	14.50	VII	43,200	180
48 x 17			28	TL	48.75	47.70	17.25	16.40	43.00	14.50	VII	43,200	180
48 x 17			30	TL	48.75	47.70	17.25	16.40	43.00	14.50	VII	50,400	195
48 x 17			30	TL	48.75	47.70	17.25	16.40	43.00	14.50	VII	50,400	210
48 x 17			30	TL	48.75	47.70	17.25	16.40	43.00	14.50	VII	46,700	195
48 x 17			30	TL	48.75	47.70	17.25	16.40	43.00	14.50	VII	46,700	195
48 x 17			32	TL	48.75	47.70	17.25	16.40	43.00	14.50	VII	50,400	210
48 x 18		- 20	32	TL	48.00	48.00	19.00	18.15	43.80	16.70	NS	51,900	195
50 x 20		- 20	24	TL	50.00	49.00	20.00	19.10	44.60	17.60	NS	38,200	135
50 x 20		- 20	26	TL	50.00	49.00	20.00	19.10	44.60	17.60	NS	41,800	150
50 x 20		- 20	30	TL	50.00	49.00	20.00	19.10	44.60	17.60	NS	49,400	175
50 x 20		- 20	32	TL	50.00	49.00	20.00	19.10	44.60	17.60	NS	53,800	190
50 x 20		- 20	34	TL	50.00	49.00	20.00	19.10	44.60	17.60	NS	57,000	205
50 x 21		- 20	30	TL	50.00	49.00	21.00	20.10	44.60	18.50	NS	49,000	180
50 x 21		- 20	30	TL	50.00	49.00	21.00	20.10	44.60	18.50	NS	49,000	180
52 x 20.5		- 20	34	TL	52.00	51.00	20.50	19.60	46.25	18.05	NS	57,800	185
52 x 20.5		- 20	36	TL	52.00	51.00	20.50	19.60	46.25	18.05	NS	62,500	200
52 x 20.5		- 23	26	TL	52.00	51.00	20.50	19.60	46.80	18.05	NS	55,000	165
52 x 20.5		- 23	28	TL	52.00	51.00	20.50	19.60	46.80	18.05	NS	59,400	180
56*			20	TT	56.62	55.44	19.92	19.12	53.44	11.44	I	35,000	100
56*			20	TT	56.62	55.44	19.92	19.12	53.44	11.44	I	35,000	100
56*			22	TL	56.62	55.44	19.92	19.12	53.44	11.44	I	37,500	110
56*			22	TT	56.62	55.44	19.92	19.12	53.44	11.44	I	37,500	110
56 x 16			24	TL	55.90	54.80	16.20	15.50	50.85	14.30	VII	45,000	175
56 x 16			32	TL	55.90	54.80	16.20	15.50	50.85	14.30	VII	60,000	250
56 x 16			36	TL	55.90	54.80	16.20	15.50	50.85	14.30	VII	76,000	315
56 x 20		- 20 -	24	TL	56.00	54.80	20.00	19.10	49.50	17.60	NS	38,500	110

Tread Patterns	Max. Speed (MPH)	Aspect Ratio	Loaded Radius		Rim Dimensions (inches)			Qualification		WEIGHT
			Static	Flat Tire	A	D	FH	MIL	TSO	lbs
Rib	225	.80	19.0	13.6	13.25	20.00	1.750		TSO	186.0
Rib	225	.71	19.4	14.75	10.50	23.50	1.250	MIL		
Rib	225	.73	19.1		11.00	20.00	1.600		TSO	
Rib	160	.72	20.1	14.2	16.25	23.50	1.125	MIL		108.0
Rib	230	.81	19.2	12.8	14.75	18.00	1.625	MIL		150.0
Rib	225	.81	19.2	12.5	14.75	18.00	1.625	MIL		179.0
Rib	250	.81	19.2	12.5	14.75	18.00	1.625	MIL		
Rib	200	.84	20.2	14.0	13.25	20.00	1.750	MIL		
Rib	225	.84	20.2	14.0	13.25	20.00	1.750	MIL		204.0
Rib	210	.84	20.2	14.0	13.25	20.00	1.750		TSO	212.0
Rib	225	.84	20.2	14.0	13.25	20.00	1.750		TSO	204.0
Rib	225	.84	20.2	14.0	13.25	20.00	1.750		TSO	
Rib	225	.84	20.2	14.0	13.25	20.00	1.750		TSO	
Rib	210	.84	20.2	14.0	14.00	20.00	1.750		TSO	
Rib	210	.84	20.2	14.0	14.00	20.00	1.750		TSO	
Rib	225	.84	20.2	14.0	13.25	20.00	1.750		TSO	
Rib	225	.84	20.2	14.0	14.00	20.00	1.750		TSO	
Rib	235	.77	20.3	13.9	13.25	20.00	1.875		TSO	
Rib	200	.75	20.6	13.6	16.25	20.00	1.875		TSO	220.0
Rib	200	.75	20.6	13.6	16.25	20.00	1.875		TSO	238.0
Rib	210	.75	20.6	13.6	16.25	20.00	1.875		TSO	245.0
Rib	225	.75	20.6	13.6	16.25	20.00	1.875		TSO	244.0
Rib	225	.75	20.6	13.6	16.25	20.00	1.875		TSO	
Rib	210	.72	20.2	14.6	13.25	20.00	1.750		TSO	
Rib	225	.72	20.2	14.6	13.25	20.00	1.750		TSO	
Rib	235	.79	21.3	14.3	16.25	20.00	1.875		TSO	
Rib	225	.79	21.3	14.3	16.25	20.00	1.875		TSO	
Rib	235	.71	21.3	15.9	13.00	23.00	1.500		TSO	
Rib	235	.71	21.3	15.9	13.00	23.00	1.500		TSO	
Rib	160	.74	23.6	16.9	16.94	27.00	1.375	MIL		203.0
Rib	160	.74	23.6	16.9	16.94	27.00	1.375	MIL		187.0
Dimple	160	.74	23.6	16.9	16.94	27.00	1.375		TSO	238.0
Dimple	160	.74	23.6	16.9	16.94	27.00	1.375		TSO	226.0
Rib	200	.88	24.1	18.7	12.75	28.00	2.25	MIL		
Rib	250	.88	24.1	18.7	12.75	28.00	2.25	MIL		
Rib	250	.88	24.1	18.7	12.75	28.00	2.25	MIL		
Rib	200	.90	22.7	15.2	15.50	20.00	2.000		TSO	

Table 2.13 Tire Applications, Courtesy: B.F.Goodrich

Business, Personal, Utility

Aircraft	Model	Popular Name	MAIN GEAR		AUXILIARY GEAR	
			Tire Size	Ply Rating	Tire Size	Ply Rating
Air Products Co.	F-1A	Aircoupe	6.00-6	4 TT	6.00-6	4 TT
Bede Aircraft Corp.	XBD-2		15x6.00-6	4 TT	5.00-5	4 TT
	BD-3, BD-5, BD-5J, BD-4		7.00-6	6 TT	5.00-5	6 TT
Beech Aircraft Corp.	18	Twin Beech	8.50-10	8 TL	8.50-10	8 TL
	19	Musketeer Sport	6.00-6	4 TT	6.00-6	4 TT
	23	Musketeer	6.00-6	4 TT	6.00-6	4 TT
	23-C	Sundowner	6.00-6	4 TT	6.00-6	4 TT
	24	Musketeer	6.00-6	4 TT	15x6.00-6	4 TT
	24-R, 25-R	Super Musketeer	6.00-6	4 TT	5.00-5	4 TT
	33, 33A	Debonair	6.00-6	6 TT	5.00-5	4 TT
	35, 35B, 36	Bonanza	7.00-6	6 TT	5.00-5	4 TT
	50	Twin Bonanza	8.50-10	6 TT	8.50-10	8 TT
	B55, C55, E55	Baron	6.50-8	8 TT	5.00-5	6 TT
	56TC, 56TO, 58	Baron	6.50-8	6 TT	5.00-5	6 TT
	58TC, 58P	Baron	6.50-8	8 TT	5.00-5	6 TT
	60	Duke	19.5x6.75-8	10 TT	6.00-6	4 TT
	D18S, D18C, E18S, R18S, 9700, G18S	Twin Beech	11.00-12	8	14.50 (Tail)	6 TT
	H18	Twin Beech	8.50-10	10	14.50 (Tail)	6 TT
	H18 (opt. equip.)	Twin Beech	8.50-10	8/10	8.50-10 (NW)	8/10
	65, A65, 70, 80, A80, B80, 88	Queen Air	8.50-10	8 TL	8.50-10	6 TL
	80, A90, B90, C90	King Air	8.50-10	8 TL	8.50-10	6 TL
	E90	King Air	8.50-10	10 TL	8.50-10	6 TL
	99, 99A, A99, A99A, B99	Airliner	18x5.5	8 TL	8.50-10	8 TL
	99, 99A, A99, A99A, B99 (opt. equip.)	Airliner	8.50-10	6 TL	8.50-10	6 TL
	95	Travelair	7.00x6	6 TT	5.00-5	6 TT
	100, A100, B100	King Air	18x5.5	8 TL	6.50x10	6 TL
	100, A110, B100 (opt.)	King Air	6.50-10	8 TL	6.50x10	6 TL
	200	Super King Air	18x5.5	8 TL	22x6.75-10	8 TL
	200 (opt.)	Super King Air	22x6.75-10	8 TL	22x6.75-10	8 TL
Bellanca Inter Air	260A	Bellanca	6.00-6	6 TL	6.00-6	4 TT
		Viking	6.00-6	6 TL	6.00-6	4 TT
	17-30A	Viking	6.00-6	6/8	15x6.00-6	6/8 TT
	17-31A	Super Viking	6.00-6	6/8	15x6.00-6	6/8 TT
	17-31ATC	Turbo Viking	6.00-6	6/8	15x6.00-6	6/8 TT
	7ECA, 7GCAA	Citabria	6.00-6	4/6		
	7BCBC	Citabria	7.00-6	4/6 TT		
	7KCAB	Citabria	8.00-6	4 TT		
	8GC5BC	Scout	8.50-6	4/6		
Cessna	150, 152, A152		6.00-6	4 TT	5.00-5	4 TT
	172	Skyhawk	6.00-6	4 TT	5.00-5	4 TT
	R172	Hawk XP	6.00-6	6 TL	5.00-5	6 TT
	F172		6.00-6	4 TT	5.00-5	4 TT
	175	Sky Lark	6.00-6	4 TT	5.00-5	4 TT
	177	Cardinal	6.00-6	6 TT	5.00-5	4 TT
	177RG	Cardinal RG	15x6.00-6	6 TT	5.00-5	4 TT
	180	Skywagon	6.00-6	8 TL	8" SC	6 TT
	182, 182-N	Skylane	6.00-6	8 TL	5.00-5	6 TT
	R182	Skylane RG	15x6.00-6	6 TT	5.00-5	6 TT
	185	Skywagon	6.00-6	6 TT, TL	10" SC	8 TT
	A185	Skywagon	6.00-6	6 TT	8.00-3	4 TT
	A185 (opt.)	Skywagon	8.00-6	6 TT	8.00-3	4 TT
	188	AG Wagon	8.00-6	6 TT	8.00" SC	8 TT
	188 (opt.)	AG Wagon	6.50-10	6 TT	10.00"	8 TT
	A188	AG Wagon & AG Truck	8.00-6	6 TT	10.00-3.5	4 TT
	A188 (opt.)	AG Wagon & AG Truck	8.5-10	6 TT	10.00-3.5	4 TT
	206, P206	Super Skylane	6.00-6	6 TT	5.00-5	6 TT
	TP206	Super Skylane Turbo	6.00-6	6 TT	5.00-5	6 TT
	U206/	Super Skywagon	6.00-6/	6 TT	6.00-6	6 TT
	Opt.		8.00-6	6 TT	6.00-6	4 TT
	TU206/	Super Skywagon Turbo	6.00-6/	6 TT	6.00-6	6 TT
	Opt.		8.00-6	6 TT	6.00-6	4 TT
	U206E	Station Air	6.00-6	6 TT	5.00-5	6 TT
	TV206E	Station Air Turbo	6.00-6	6 TT	5.00-5	6 TT
	207	Skywagon	6.00-6	6 TT	5.00-5	6 TT
	207 (opt.)	Skywagon	8.00-6	6 TT	6.00-6	4 TT

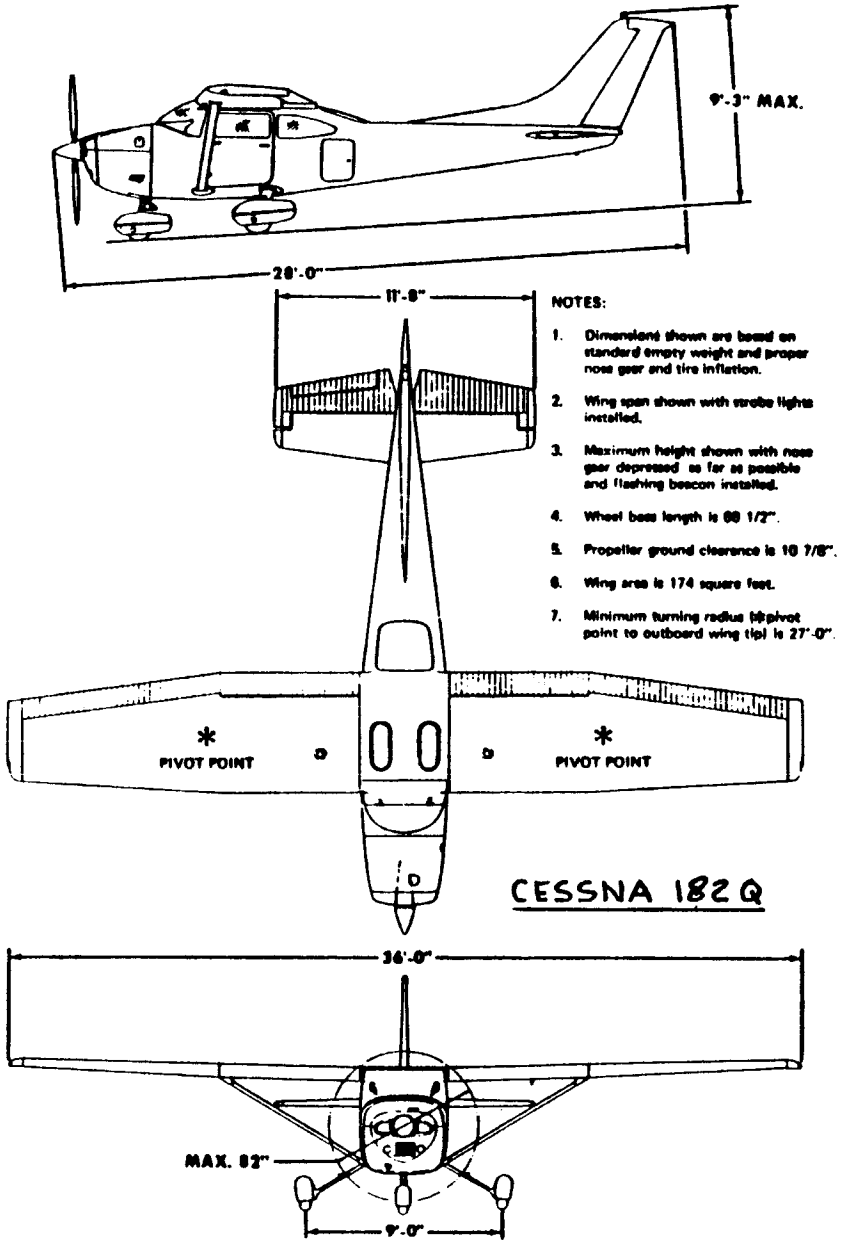

Table 2.14 Tire Applications, Courtesy: B.F.Goodrich

Business, Personal, Utility (Continued)

Aircraft	Model	Popular Name	MAIN GEAR Tire Size	MAIN GEAR Ply Rating	AUXILIARY GEAR Tire Size	AUXILIARY GEAR Ply Rating
Cessna (Cont.)	T207/	Turbo Skywagon	6.00-6	8 TT	5.00-5	6 TT
	Opt		6.00-6	6 TT	6.00-6	4 TT
	210, 210-2	Centurion	6.00-6	6 TT	5.00-5	6 TT
	T210, T210-2	Turbo Centurion	6.00-6	8 TT	5.00-5	8 TT
	P210	Pressurized Centurion	6.00-6	8 TL, TT	5.00-5	10 TL
	310, 310-2, 310 (Turbo)		6.50-10	6 TL, TT	6.00-6	6 TT
	320	Skyknight	6.50-10	6 TL	6.00-6	6 TL
	336		6.00-6	8 TL, TT	15x6.00-6	4 TT
	337	Super Skymaster	6.00-6	6 TL, TT	6.00-6	6 TL
	337 (opt), T337, P337	Super Skymaster	18x5.5	8 TT	15x6.00-6	4 TT
	340, 340-A		6.50-10	8 TT	6.00-6	8 TT
	401, 402, 402-B		6.50-10	8 TT	6.00-6	8 TT
	404, 441		22x7.75-10	8 TL	6.00-6	6 TT
	411, 414, 421		6.50-10	8 TT	6.00-6	6 TT
	500	Citation I	22x8.0-10	10 TL	18x4.4 CH-DU	10 TL
	550	Citation II	22x8.0-10	10 TL	18x4.4 CH-DU-LG	10 TL
Champion Aircraft	75RS	Citabria	6.00-6	4 TT	5.00-5	4 TT
	7EC	Traveler	6.00-6	4 TT	5.00-5	4 TT
	7FC	Tri-Traveler	6.00-6	4 TT	5.00-5	4 TT
	7GCB	Challenger	7.00-6	4 TT	5.00-5	4 TT
	402	Lancer	7.00-6	4 TT	5.00-5	4 TT
	7GCB-A	Challenger	8.00-6	4 TT	5.00-5	4 TT
Custer Channel Wing	CCW5		6.50-10	8 TL	6.00-6	4 TL, TT
Grumman Aircraft	AA1B, AA5	Trainer	6.00-6	4 TT	5.00-5	4 TT
	AA1B	TR-2	6.00-6	4 TT	5.00-5	4 TT
	158A	AG-CAT	8.50-10	6 TT	10.00"	8 TT
	159	Gulfstream I	7.50-14	12 TL	6.50-8	6 TL
	164	Gulfstream II	34x9.25-16	16 TL	21x7.25-10 CH	8 TL
	164	AG-CAT	8.50-6	6 TT	10"	8 TT
Hawker-Siddeley	HS125 Up to Series 700		23x7.00-12	10 TL	18x4.25-10 CH	6 TL
Helio Aircraft Corp.	250	Courier	6.50-8	6 TL	6.00-6	6 TL, TT
	295	Super Courier	8.00-6	6 TT	6.00-6	8 TT
	550-A	Stallion	7.50-10	6 TT	5.00-5	4 TT
	634	Twin Stallion	7.50-10	6 TT	5.00-5	4 TT
Howard Aero Mfg.		500	15.00-16	14/16 TT/TL	17" SC	10 TT
		Super Ventura	16.00-16	14 TT	17" SC	10 TT
Lake Aircraft Corp.	4	Buccaneer	6.00-6	4 TT	5.00-4	4 TT
	4, 4-200	(Amphibian)	6.00-6	4 TT	5.00-4	4 TT
Lear	23	Learjet	18x5.5	8 TL	18x4.4 CH-DU	10 TL
	24, 25	Learjet	18x5.5	10 TL	18x4.4 CH-DU	10 TL
	35, 36	Learjet	17.5x5.75-8	12 TL	18x4.4 CH-DU	10 TL
		Learstar	15.00-16	10 TT	17" SC	10 TT
Lockheed Aircraft Co.		Lodestar	15.00-16	10 TT	17" SC	10 TT
		Jetstar-6	26x6.6	14 TL	18x4.4 CH	10 TL
		Jetstar-8/11	26x6.6	14 TL	18x4.4 CH	12 TL
	SA80	Azacarte-80	6.50-8	4 TT	6.00-6	4 TT
Maule	4-220C	Lunar Rocket	8.50-6	6 TT	–	–
	5-210-C		8.00-6	4 TT	–	–
			6.00-6	4 TT	–	–
Meyers	200B		6.50-8	6 TT	6.00-6	4 TT
Mitsubishi	MU-2		8.50-10	8 TL	5.00-5	6 TT
	MU-2		8.50-10	10 TL	5.00-5	8 TT
Mooney	Mark 20	Ranger	6.00-6	6 TT	5.00-5	4 TT
	Mark 21C	Super	6.00-6	6 TT	5.00-5	4 TT
	Mark 22	Mustang	6.00-6	6 TT	15x6.00-6	4 TT
	20E	Chaparral	6.00-6	6 TT	5.00-5	4 TT
	20F	Executive	6.00-6	6 TT	5.00-5	6 TT
	20J	201	6.00-6	6 TT	5.00-5	6 TT
Mystere (Dassault)	Fanjet Falcon 10		22x5.75-12	8/10 TL	18x5.75-8 CH	8 TL
	Fanjet Falcon 20 (thru F Models)		26x6.6	10 TL	14.5x5.5-6 CH	14 TL
	Fanjet Falcon 20G and 50		26x6.6	14 TL	14.5x5.5-6 CH	14 TL
Navion	Navion G.H.T.	Rangemaster	6.50-8	4 TT	6.00-6	4 TT
Piper	18-135	Cub	6.00-4	4 TT	6x2.00	Solid
	18A-150	Super Cub	6.00-4	4 TT	6x2.00	Solid
	22	Caribbean	6.00-6	4 TT	6.00-6	4 TT

Aircraft	Model	Popular Name	MAIN GEAR Tire Size	MAIN GEAR Ply Rating	AUXILIARY GEAR Tire Size	AUXILIARY GEAR Ply Rating
Piper (Cont.)	22-108	Colt	6.00-6	4 TT	6.00-6	4 TT
	22-150	Tri-Pacer	6.00-6	4 TT	6.00-6	4 TT
	23, 23-235, 23-180	Apache	7.00-6	6 TT	6.00-6	4 TT
	23-250	Aztec	7.00-6	8 TT	6.00-6	4 TT
	24-180	Comanche	6.00-6	4 TT	6.00-6	4 TT
	24-250, 24-260	Comanche	6.00-6	6 TT	6.00-6	4 TT
	24-400, 25-400	Comanche	6.00-6	6 TT	6.00-6	6 TT
	25-150	Pawnee	7.00-6	4 TT	8.00x3-4	4 TT
	25-135, 25-235, 25-260	Pawnee	8.00-6	4 TT	8.00x3-4	4 TT
	28, 28-180R, 28-200R	Arrow	6.00-6	4 TT	5.00-5	4 TT
	28-140, 28-235, 28-180,					
	28-180, 28-150	Cherokee	6.00-6	4 TT	6.00-6	4 TT
	28-151	Warrior	6.00-6	4 TT	5.00-5	4 TT
	30	Twin Comanche	6.00-6	6 TT	6.00-6	4 TT
	31, 31-350, 31-300, 31-310	Navajo	8.50-10	8 TT	6.00-6	6 TT
	31P-425	Navajo	8.50-10	8 TT	6.00-6	8 TT
	31T	Navajo	8.50-10	10 TT, TL	18x4.4	8 TT, TL
	34, 34-200	Seneca	6.00-6	8 TT	6.00-6	6 TT
	32, 32-300	Cherokee (6 ply)	6.00-6	6 TT	6.00-6	6 TT
(See Ted Smith Aircraft)	32-260	Cherokee	6.00-6	8 TT	6.00-6	6 TT
	36-285, 300, 375	Brave	8.50-10	6 TT	6x2.00	solid
	42	Cheyenne	8.50-10	12 TL	17.5x6.25-6	10 TT
Rockwell Int. (Aero Commander)	112, 112A	Commander	6.00-6	4/6 TT	5.00-5	4 TT
	200	Commander	7.00-6	6 TT	6.00-6	4 TT
	500A	Commander	8.50-10	6 TL	6.00-6	6 TL, TT
	680FP	Commander	8.50-10	6 TT	6.00-6	6 TL, TT
	(Turbo 11) 681	Commander	8.50-10	10 TT, TL	6.00-6	6 TL, TT
	500B	Commander	8.50-10	8 TL	6.00-6	6 TL, TT
	500S	Shrike Commander	8.50-10	8 TL, TT	6.00-6	6 TL, TT
	720, 560E, 560F, 680F	Aero Commander	8.50-10	8 TL	6.00-6	6 TL, TT
	680FL, 680FLP	Grand Commander	8.50-10	8 TL	6.00-6	6 TL, TT
	680T	Turbo Commander	8.50-10	8 TL	6.00-6	6 TL, TT
	685, 690, 690A, 690B	Commander	8.50-10	10 TL	6.00-6	8 TL, TT
	1121	Jet Commander	24x7.7	14 TL	18x4.4	4 TL
	5ZR	Thrvs H Commander	8.50-10	10 TL	12.5-4.6	4 TT
Rockwell Int. (North American)	40	Sabreliner (Low Pressure)	26x6.75-14	14 TL	18x4.4 CH	10 TL
		(Standard)	26x8.6	14 TL	18x4.4 CH	10 TL
	60	Sabreliner (Low Pressure)	26x6.75-14	14 TL	18x4.4 CH	10 TL
		(Standard)	26x8.6	14 TL	18x4.4 CH	10 TL
	70	Sabreliner	22x5.75-12	10 TL	18x4.4 CH	10 TL
	75-A	Sabreliner	22x5.75-12	10 TL	18x4.4 CH	10 TL
	265	Sabreliner	26x8.6	14 TL	18x4.4	6 TL
					18x4.4 CH	10 TL
Smith (L.B.) Aircraft	C465 Conver		17.00-20	20 TT	10.00-7	12 TT
	B26 Conver	Tempo II	17.00-20	16 TT		
Swearingen Aircraft		Metro	18x5.5	8/10 TL	16x4.4	8 TT
		Merlin	8.50-10	8 TL	8.50-10	8 TT
	226-R-TC, AT		18.5x6.75-8	10 TT, TL	16x4.4	8 TT
	3, 4		22x8.75-10	8 TL	16x4.4	8 TT
Taylorcraft, Inc.	F19		6.00-6	4 TT	6.00-2	
	20	Topper	7.00-6	4 TT	Tail Skid	
Ted Smith Aircraft (Piper)	600, 601	Aerostar	7.00-6	8 TT	6.00-6	6 TL, TT
	600, 601, 601P		6.50-8	8 TT	6.00-6	6 TT
	600, 601, 601P		19.5x6.75-8	8 TT	6.00-6	6 TT
Thurston		Teal	6.00-6	4 TT	6x3.00-4	
Ranoland Aircraft	T-17		5.00-5	6 TT	5.00-5	4 TT
Trecker Aircraft	166		8.50-10	8 TT	6.00-6	6, 8 TT
	L-2, L-2	Gull Amphibian	8.50-10	6 TT		
Velairaft	10	1900	6.00-6	4 TT	6.00-6	4 TT
			8.00-6	4 TT	6.00-6	4 TT
			15x6.00-6	4 TT		
Velper		Tri Gear	8.50-10	10 TL	8.50-10	10 TL
		Turboliner	8.50-10	10 TL	8.50-10	10 TL
Wees Aircraft	250	Vega	6.00-6	6 TT	5.00-5	6 TT
	260	Meteor	6.00-6	6 TT	5.00-5	6 TT

Table 2.15 Tire Applications, Courtesy: B.F.Goodrich

Commercial Transport

Manufacturer	Model	MLG Size	MLG PR	NLG Size	NLG PR
Airbus	A300B	46x16	24 TL	40x14	20 TL
	A300B1-B2-B4	46x16	24/28 TL	40x14	20 TL
	A300B1-B2-B4 (Optional)	49x17	28 TL	40x14	22 TL
Boeing	707-120	46x16	24 TL	39x13	14 TL
	707-320B	46x16	28 TL	39x13	16 TL
	707-320C	46x16	28 TL	39x13	16 TL
	720	40x14	24 TL	34x9.9	12 TL
	720B	40x14	24 TL	39x13	14 TL
	727-100	49x17	28 TL	32x11.50-15 CH	12 TL
	727/200	49x17	28 TL	32x11.50-15 CH	12 TL
		50x20-20	30 TL	32x11.50-15 CH	12 TL
	727 ADV	50x21-20	28/30 TL	32x11.50-15 CH	12 TL
	737-100	40x14	22 TL	24x7.7	14 TL
	737-200	40x14	24 TL	24x7.7	14 TL
	737-200	C40x14-21	22, 24 TL	24x7.7	14 TL
		C40x18-17	20 TL	C24.5x8.5-12	12 TL
	747-100	46x16	28 TL	46x16	28 TL
	747-200	49x17	30 TL	49x17	30 TL
	747-200F	49x19-20	32 TL	49x19-20	32 TL
	747SP	46x16	28 TL	46x16	28 TL
	757	H40x14.5-19	22 TL	H31x13-12	20 PR TL
	767	H45x17.20	28 TL	H37x14-15	22 TL
	767	H46x18-20	28 TL	H37x14-15	22 TL
British Aircraft	BAC-111-200	40x12	16 TL	24x7.25-12 CH	10 TL
	BAC-111-400	40x12	18 TL	24x7.25-12 CH	10 TL
	500/510	40x12	20 TL	24x7.25-12 CH	10 TL
	475	40x12	16/18 TL	24x7.75-12	12 TL
Bristol Freighter		46x18.0-18	14		
Britannia	300	15.50-20			
		40x12	22 TL	32x8.8	12
Canadair	CL440D-2	40x12	22 TL	32x8.8	12 TL
	CL600	26x6.6	12 TL	18x4.4	8 TL
Caravelle	48C, 50C	35x9.00-17	14 TL	26x7.75-13 CH	10 TL
	52C, 56C	35x9.00-17	16 TL	26x7.75-13 CH	10 TL
	58C	35x9.00-17	16 TL	26x7.75-13 CH	10 TL
Convair	240	34x9.9	14 TT	26x6.6	12 TL
	340	12.50-16	12 TT	7.50-14	8 TT
	440	12.50-16	12 TT	7.50-14	8 TT
	540	12.50-16	12 TT	7.50-14	8 TT
	580/600/640	12.50-16	14 TT	7.50-14	8 TT
		39x13	14 TT	7.50-14	8 TT
	880	39x13	20 TL	29x7.7	12 TL
	880M	39x13	22 TL	29x7.7	12 TL
	990	41x15.0-19	22 TL	29x7.7	16 TL
	990HV	41x15.0-19	24 TL	29x7.7	16 TL
Comet		35x9.00-17	16	30x9.10-15	10
Curtis	C46	19.00-23	16 TT	10.00-7	12 TT
De Havilland	DHC-6 Twin Otter	11.00-12	8 TT	8.90-12.50	6 TT
	Flotation	15.00-12	10 TL	15.00-12	10 TL
	DHC-7	30x9.00-15	12 TL	8.90-12.50	8 TL
Fairchild Hiller	F-27/227	9.50-16	10-12 TL	8.50-10	10 TL
	F-28	39x13	14 TL	24x7.7	10 TL
Fokker	F-27	34x10.75-16	10 TL	8.50-10	10 TL
	F-28	39x13	14 TL	24x7.7	10 TL
	F-28 (Flotation)	40x14	14 TL	24.5x8.5-10 CH	10 TL
	F-227	9.50-16	12 TL	8.50-10	10 TL
Hawker-Siddeley	HS 748, HFB-330	32x8.8	12 TL	25.65x8.5-10	
	HS 748	32x10.75-14	12 TL	8.50-10	6 TT/TL

Manufacturer	Model	MLG Size	MLG PR	NLG Size	NLG PR
Lockheed	049	17.00-20	20 TT	33"	10 TT
	747	17.00-20	20 TT	33"	10 TT
	1049	17.00-20	22 TT	34x9.9	10 TT
	188	13.50-18	24 TL	7.50-14	10 TL
	188 (AR.)	40x14	24 TL	29x7.7	10-14 TL
	L-1001-1	56x20.0-20	24 TL	39x13	14 TL
	L-1011-1	50x20.0-20	32 TL	36x11	20-22 TL
	L-1011-14/15	52x20.5-20	34/36 TL	37x13-18	20 TL
	L-1011-500	52x20.5-20	36 TL	37x13-18	26 TL
Martin	202/404	12.50-18	12 TL	9.50-16	10 TT
McDonnell-Douglas Co. (Douglas Div.)	DC-3 (Super)	17.00-16	12 TT	9.00-6	10 TT
	DC-4	15.50-20	14-16 TT	44" SC	12 TT
	DC-6, DC-6A	15.50-20	16 TT	44" SC	12 TT
	DC-6B	15.50-20	20 TL	44" SC	12 TT
	DC-7, DC-7B	17.00-20	20 TL	44" SC	14 TL
	DC-7C, DC-7C/F	17.00-20	22 TL	18.00-18	14 TL
	DC-8	44x16	26 TL	34x11	18 TL
	DC-8 (HV)	44x16	28 TL	34x11	20 TL
	DC-8 (50F)	44x16	28 TL	34x11	20-22 TL
	DC-8 (61, 62)	44x16	30 TL	34x11	22 TL
	DC-8 (62F, 62H)	44.5x16.5-18	30 TL	34x11	22 TL
	DC-8 (63)	44x16	32 TL	34x11	22 TL
	DC-8 (63, 63F)	44.5x16.5-18	30 TL	34x11	22 TL
	DC-8F	44x16	28 TL	34x11	22 TL
	DC-9 (10, 11, 12, 14, 15)	40x14	20 TL	26x6.6 (CH)	8 TL
	DC-9 (20)	40x14	22 TL	26x6.6 (CH)	10 TL
	DC-9 (30, 31)	40x14	24 TL	26x6.6 (CH)	10 TL
	DC-9 (30, 32)	42x15.0-16	20 TL	26x6.6 (CH)	10 TL
	DC-9 (30, 33, 41, 80)	41x15.0-19	22, 24 TL	26x6.6 (CH)	10 TL
	DC-10 (10)	50x20.0-20	32 TL	37x14-14	24 TL
	DC-10 (20, 30, 40)	52x20.5-23	26/26 TL	40x15.5-16	26 TL
Mercure	02	46x16	20	30x8.8	12
Nihon	YS-11	12.50-16	12 TL	24x7.7	10 TL
Nord	262	12.50-16	10 TT	6.00-6	8 TT
Potez	840	26x7.75-13	10 TL		
Swiss	Caravelle 46, 50	35x9.00-17	14 TL	26x7.75-13 CH	10 TL
	52, 56	35x9.00-17	16 TL	26x7.75-13 CH	10 TL
	58	35x9.00-17	18 TL	26x7.75-13 CH	10 TL
	Concorde Preprod	47x15.75-22	26	31x10.75-14	20
	Prod	1195x400-22		785x275-14	
Shorts	SD3-30	34x10.75-16	10 TL	9.00-6	10 TL
Trident	1	34x9.50-16	12 TL	26x8.0-15	12 TL
	1E, 2E, 3E	36x10.0-16	16 TL	26x8.0-15	12 TL
Vickers	742/745	36x10.75-16.50	12 TT	24x7.25-12 (CH)	8 TT
	VC-10	50x16	26 TL	39x13	16 TL
	Vanguard	46x17	24 TL	33x9.75-16	10 TL

Table 2.16 Tire Applications, Courtesy: B.F.Goodrich

MILITARY AIRPLANES

Manufacturer	DOD Designation	Popular Name	Old Designation	MAIN GEAR Tire Size	MAIN GEAR Ply Rating	AUXILIARY GEAR Tire Size	AUXILIARY GEAR Ply Rating
Beech	T34B	Mentor	T34B	6.50-8	6 TT	5.00-5	6 TT
	U8F	Seminole	L23F	8.50-10	8 TT	6.50-10	8 TT
	T42A			6.50-8	6 TL	5.00-5	6 TL
	VC8A	King Air		8.50-10	8 TL	6.50-10	6 TL, TT
Boeing	B47E	Stratojet	B47E	56x16	36 TL	26x6.6	14 TT
	B52F, G, H	Stratofortress	B52, F, G, H	56x16	38 TL	32x8.8	12 TT
	C97D	Stratofreighter	C97D	56x16	32 TT	36" SC	12 TT
	C135B	Stratolifter	C135B	49x17	28 TL	38x11	14 TL
	VC137C		VC137C	46x16	26 TL	39x13	16 TL
	E3A	707		46x16	36 TL	39x16	16 TL
	E4A	747		49x17	30 TL	49x17	30 TL
	T43A	737		40x14	24 TL	24x7.7	14 TL
	YC14	STOL		B40x16.0-16	20 TL	B40x16.0-16	20 TL
Cessna	O-1E	Bird Dog	L19A	6.00-6	6 TL	8x3.0-4	4 TT
	T37B		T37B	20x4.4	10 TL	16x4.4	8 TT
	A37		T-37A	7.00-8	12 TL	6.00-6	6 TT
	T41A	Skyhawk	172	6.00-6	4 TL	5.00-5	4 TL
	U3B		U3B	6.50-10	8 TT	6.00-6	6 TT
	U17A	Skywagon		6.00-6	8 TT	10" SC	8 TT
	O2A, B			6.00-6	8 TT	15x6.00-6	4 TT
De Havilland	CV-2B	Caribou	AC-1A	11.00-12	8 TL	7.50-10	8 TL
	CV-7A	Buffalo	AC-2	15.00-10			
				15.00-12	10 TL	8.90-12.50	8 TL
	U-1A	Otter		11.00-12	6 TT	6.00-6	6 TT
	U-6A	Beaver	L-20	8.50-10	6 TT	5.50-4	6 TT
Fairchild-Hiller	C-119J	Flying Boxcar	C-119J	15.50-20	14 TT	9.50-16	10 TT
	C-123B	Provider	C-123B	17.00-20	22 TT, TL	11.00-12	8 TT
	C-123J	Provider	C-123J	17.00-20	22 TT, TL	9.50-16	10 TT
(Republic Division)	F-84F	Thunder Streak	F-84F	30x6.6	14 TT	20x4.4	12 TL, TT
	F-105	Thunder Chief	F-105	36x11	24 TL	24x7.7	14 TL
	A-10A	–	–	36x11	22 TL	24x7.7	10 TL
General Dynamics	B-58A	Hustler	B-58A	22x7.7-12	16 TL	22x7.7-12	16 TL
	F102A	Delta Dagger	F102A	30x8.8	22 TT	24x5.5	12 TT
	F106A	Delta Dart	F106A	30x8.8	22 TL	18x4.4	12 TT
	C131A	Samaritan	C131A	34x9.9	14 TL	26x6.6	14 TL
	C131B, C, D, E, F	Samaritan	C131B, C, D, E, F	12.50-16	12 TT	7.50-14	8 TT
	RB-57F			44x13	26 TT	24x5.5	12 TT
	T29D		T29D	34x9.9	14 TT	26x6.6	14 TL
	F-16			25.5x8.0-14	18 TL	18x5.5	14 TL
	F111A			47x18-18	30 TL	22x6.6-10	16 TL
	FB111A			47x18-18	36 TL	22x6.6-10	20 TL
	F8-111B			47x18-18	36 TL	21x7.25-10	20 CH, TL
Grumman	A6A	Intruder	A2F-1	36x11	24 TL	20x5.5	12 TL
	E16B	Intruder		36x11	24 TL	20x5.5	16 TL
	F11A	Tiger	F11F-1	26x6.6	16 TL	18x5.5	8 TL
	OV-1C	Mohawk	AO-1C	8.50-10	12 TL	8.50-8	6 TL
	S-2D	Tracker	S2F-3	34x9.9	14 TT	18x5.5	12 TT
	F-14A	Tomcat		37x11.50-16	28 TL	22x8.6-10	20 TL
	E-1B	Tracer	WF-2	34x9.9	14 TT	18x5.5	12 TT
	E-2A	Hawkeye	W2F-1	36x11	24 TL	20x5.5	12 TL
	C-1A	Trader	TF-1	34x9.9	14 TT	18x5.5	12 TT
	C-2A		C-2A	36x11	24 TL	20x5.5	12 TL
	HU-16E	Albatross	UF-2G	40x12	14 TT	26x6	10 TT

Manufacturer	DOD Designation	Popular Name	Old Designation	MAIN GEAR Tire Size	MAIN GEAR Ply Rating	AUXILIARY GEAR Tire Size	AUXILIARY GEAR Ply Rating
Helio	U10A	Courier	L28A	6.50-8	6 TT	10" SC	8 TT
Ling-Temco-Vought (Vought Aeronautics Div.)	A7A, B, E	Corsair II		28x9.0-12	22 TL	22x5.5	12 TL
	A7D	Corsair II		28x9.0-14	22 TL	22x5.5	16 TL
	F8H, J	Crusader	F8E	26x6.6	16 TL	20x5.5	14 TL
	XC142A		XC-142A	11.00-12	8 TL	8.50-10	10 TL
Lockheed	F104A, B	Starfighter		25x6.75	18 TL	18x5.5	14 TT
	F104C, D, J, DJ	Starfighter		25x6.75	18 TL	18x5.5	14 TT
(Early Version)	F104G	Starfighter		25x6.75	18 TL	18x5.5	14 TT
	F104G	Starfighter	F104FG	26x8.0-14	18 TL	18x5.5	14 TL
	YF12A			27.5x7.5-16	22 TL	26x6.75	16 TL
	SR71			27.5x7.5-16	22 TL	25x8.75	16 TL
	P2H	Neptune	P2V-7	56" SC	30 TL	34x9.9	14 TL
	P3A	Orion	P3V	40x14	26 TL	26x7.7	14 TL
	P3B, C	Orion	P3V-1	40x14	26 TL	26x7.7	14 TL
	C121G	Super Constellation	C121G	17.00-20	22 TL	33" SC	10 TT
	C130A, B, D, E	Hercules	–	20.00-20	22 TT	12.50-16	12 TT
	S3A	Viking	–	30x11.5-14.5	24 TL	22x6.75-10	18 TL
	HC130H	Hercules	C130	20.00-20	26 TL	12.50-16	12 TT
	C140A	Jetstar	C140A	26x6.6	14 TL	16x4.4 CH	10 TL
	C141	Starlifter	C141	44x16	26 TL	36x11	22 TL
	T33	Shooting Star	T33	26x6.6	14 TL	22x7.25-11.50	8 TL
	C5A	Galaxy		49x17	26 TL	49x17	26 TL
	AH56A	Cheyenne		29x11.00-10	10 TL	6.00-4	8 TL
Martin McDonnell-Douglas Co. (Douglas Division)	P5B	Martin	P5M-2	15.50-20	14 TT	10.00-7	12 TT
	A1	Skyraider	AD-7	32x8.8	16 TT	12½x4½	14 TT
	A3	Skywarrior	A3D-2	44x13	26 TL	32x8.8	16 TT
	A4	Skyhawk	A4D-5	24x5.5	16 TT	18x5.5	12 TL
	A-26A	Counter Invader		15.50-20	14 TT	36" SC	12 TT
	B66	Destroyer	B66D	49x17	26 TL	38x11	22 TT
	F6A	Skyray	F4D-1	26x6.6	16 TL	22x5.5	12 TT
	C47	Skytrain	C47E	17.00-16	12 TT	8.00-6	10 TT
	C54	Skymaster	C54	15.50-20	14 TT	44" SC	12 TL
	C9A	Nightingale		40x14	24 TL	26 4-6-CH	10 TL
	C117		R4D8	17.00-16	12 TT	8.00-6	10 TT
	VC118	Liftmaster	C118A	15.50-20	20 TL	44" SC	12 TL
	C124	Globemaster	C124C	25.00-28	30 TT	15.50-20	14 TL
	C133	Cargomaster	C133B	20.00-20	22 TT	15.00-16	10 TL
McDonnell-Douglas Co. (McDonnell)	F-101A, C	Voodoo	F-101A, C	32.x8.8	24 TL	18x5.5	14 TL
	F-101B	Voodoo	F-101B	31x11.50-16	22 TL	18x5.5	14 TL
	F4B	Phantom II	F4H	30x8.0	26 TL	18x5.7	14 TL
	F4C	Phantom II		30x11.50-14.5	24 TL	18x5.5	14 TL
	F4J	Phantom II		30x11.50-14.5	24 TL	18x5.7	14 TL
	F-15	Eagle	101	34.5x9.75-16	22 TL	22x6.6-10	16 TL
	F-15		103	34.5x9.75-16	26 TL	22x6.6-10	20 TL
	F-18A			30x11.5-14.5	26 TL	22x6.6-10	20 TL
Rockwell Int.	F86	Sabre	F86A	26x6.6	14 TL	22x7.25-11.50	8 TL
	F100	Super Sabre	F100	30x8.8	22 TL	18x4.4	12 TL
	RA5C	Vigilante	A3J-3	36x11	28 TL	26x6.6	16 TL
	OV10A	Bronco	Coin	29x11.00-10	10 TL	7.50-10	12 TL
	U4A	Aero Commander	U4B	8.50-10	6 TT	6.00-16	6 TT
	T-2B	Buckeye	T2J	24x5.5	12 TL	20x4.4	10 TL
	T-28D	Trojan		24x7.7	10 TT	24x7.7	10 TT
	T-39	Sabreliner	T39A	26x6.6	14 TL	18x4.4	8 TL
	X-15			Skids		18x4.4	12 TL
	XB70A	Valkyrie		40x17.50-18	40 TL	14x4.5-6	8 TL
	Shuttle			44.5x16.0-21	28 TL	32x8.0	28 TL
Northrop	F5A, B	Freedom Fighter		22x8.5-11	16 TL	18x6.5-8	12 TL
	F5E			24x8.0-13	16 TL	18x6.5-8	12 TL
	T38	Talon	T38A	20x4.4	12 TL	18x4.4	8 TL
	F19L			28x9.5-15	20 TL	18x6.5-8	16 TL
Piper	U7A		L-21	6.00-4	4 TT	TAILSKID	
	U11A	Aztec	UO-1	7.00-6	8 TT	6.00-6	4 TT

2.5 STRUT-WHEEL INTERFACE, STRUTS AND SHOCK ABSORBERS

The landing gear must absorb the shocks of landing as well as taxiing. Two elements for shock absorption are incorporated in most landing gears: the tire(s) and the shock absorber(s). This section will discuss various ways in which shocks can be absorbed through the struts and through the tires. A rapid method for shock absorber sizing is also presented. A method for tire sizing was presented in Section 2.4. This section is organized as follows:

2.5.1 Strut-wheel interface
2.5.2 Devices used for shock absorption
2.5.3 Shock absorption capability of tires and shock absorbers: sizing of struts

2.5.1 Strut-Wheel Interface

Landing gear wheels are attached to some type of strut. Figure 2.23 illustrates two important strut-wheel interface parameters: the 'rake' and the 'trail'. These parameters are important to the static and dynamic stability behavior of the wheel relative to the strut.

The 'rake' is defined as the angle between the wheel swivel axis and a line vertical to the runway surface. Figure 2.23a defines positive and negative rake. The wheel swivel axis is identified as X-X.

The 'trail' is defined as the distance between the runway-wheel contact point and the point where the wheel swivel axis intersects the ground. Positive and negative trail are defined in Figures 2.23c and 2.23d.

The wheel rotation axis is the line perpendicular to the paper through point P.

In Figure 2.23a the wheel swivel axis, X-X passes below the wheel rotation axis P. This arrangement is statically stable because any wheel swivel about X-X would tend to 'lift' the airplane.

In Figure 2.23b the wheel swivel axis passes above the wheel rotation axis P. This arrangement is statically unstable because any wheel swivel about X-X would tend to 'lower' the airplane: the wheel therefore has a tendency to 'flop over'!

The arrangement shown in Figure 2.23c (positive trail) is called dynamically stable: when the wheel has

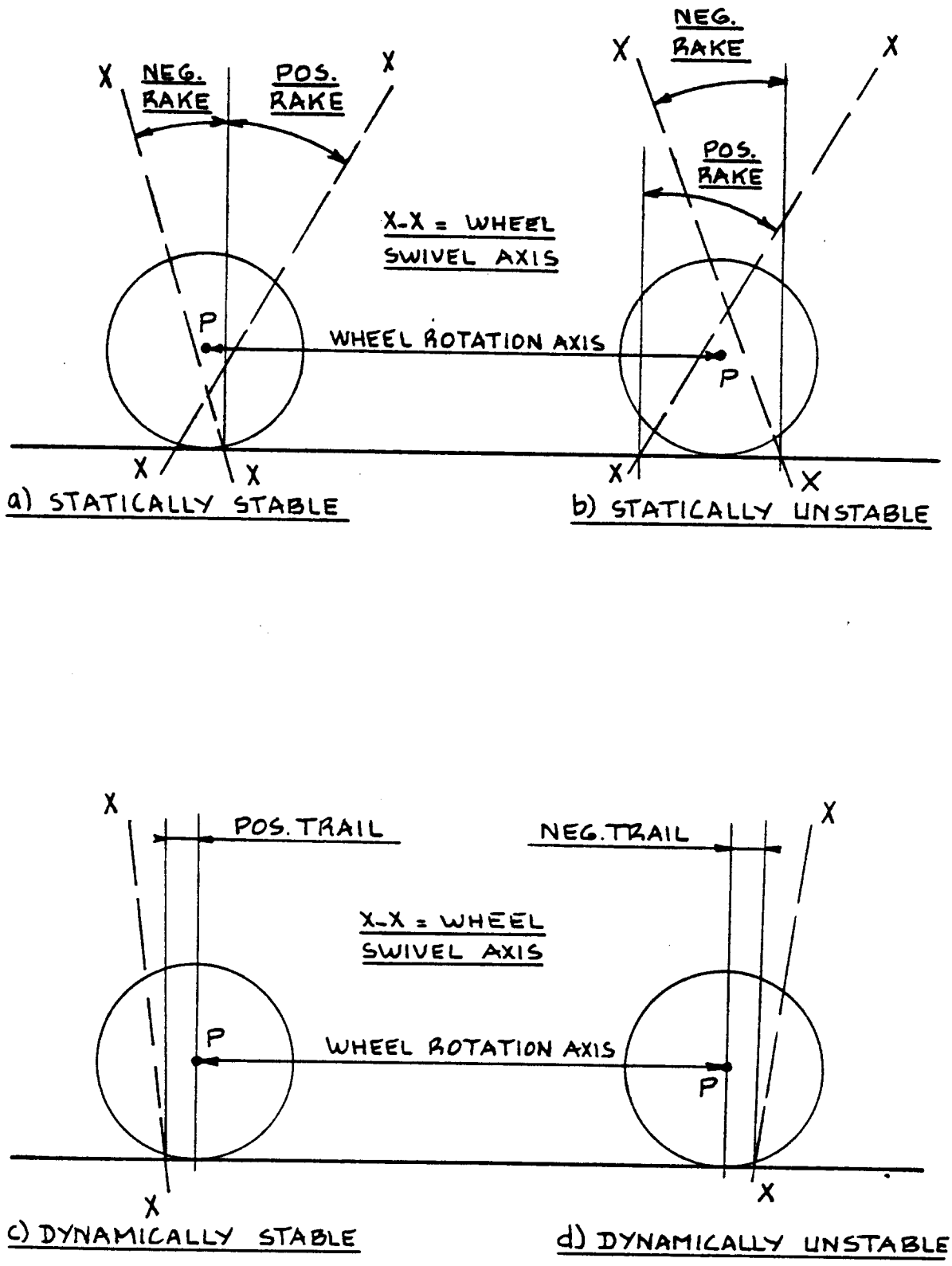

Figure 2.23 Definition of Rake and Trail

swiveled about X-X, the runway-to-tire friction would tend to rotate the wheel back to its original position.

Figure 2.23d (negative trail) depicts a dynamically unstable situation: when the wheel has swiveled about X-X, the runway-to-tire friction force would tend to rotate the wheel away from its original position.

In most airplane applications either stable or neutrally stable strut-wheel arrangements are favored. Unstable combinations do occur, but rarely so.

Figure 2.24 shows a number of strut-wheel combinations used in nose gear, tail gear and main gear designs.

Another form of dynamic instability is 'shimmy'. When a wheel shimmies, it oscillates about the wheel swivel axis. This is not only annoying, but can result in structural failure(s).

The physical causes for shimmy can be any combination of the following factors:

1. Overall torsional stiffness of the gear is insufficient. Torsional stiffness is defined about the swivel axis. Torsional movement is restricted by the 'scissors' and by the combined 'stiffness of the gear attachment to the structure, including any side- and(or) drag-bracing. Fig.2.7 shows a scissor (=torque-link) application.

2. Inadequate trail. Positive trail reduces shimmy.

3. Improper wheel mass balancing about the wheel rotation axis P.

To reduce and/or to damp shimmy, a so-called shimmy damper is often installed. A shimmy damper 'acts' like a shock absorber, but in a 'rotary' fashion.

2.5.2 Devices Used For Shock Absorption

The following devices are available for absorbing energy associated with landing and taxi loads:

- *Tires
- *Air springs
- *Oleo-pneumatic struts
- *Shock chords and/or rubbers
- *Cantilever springs
- *Liquid springs

Figure 2.25 shows examples of each device for shock absorption as well as typical load-deflection relation-

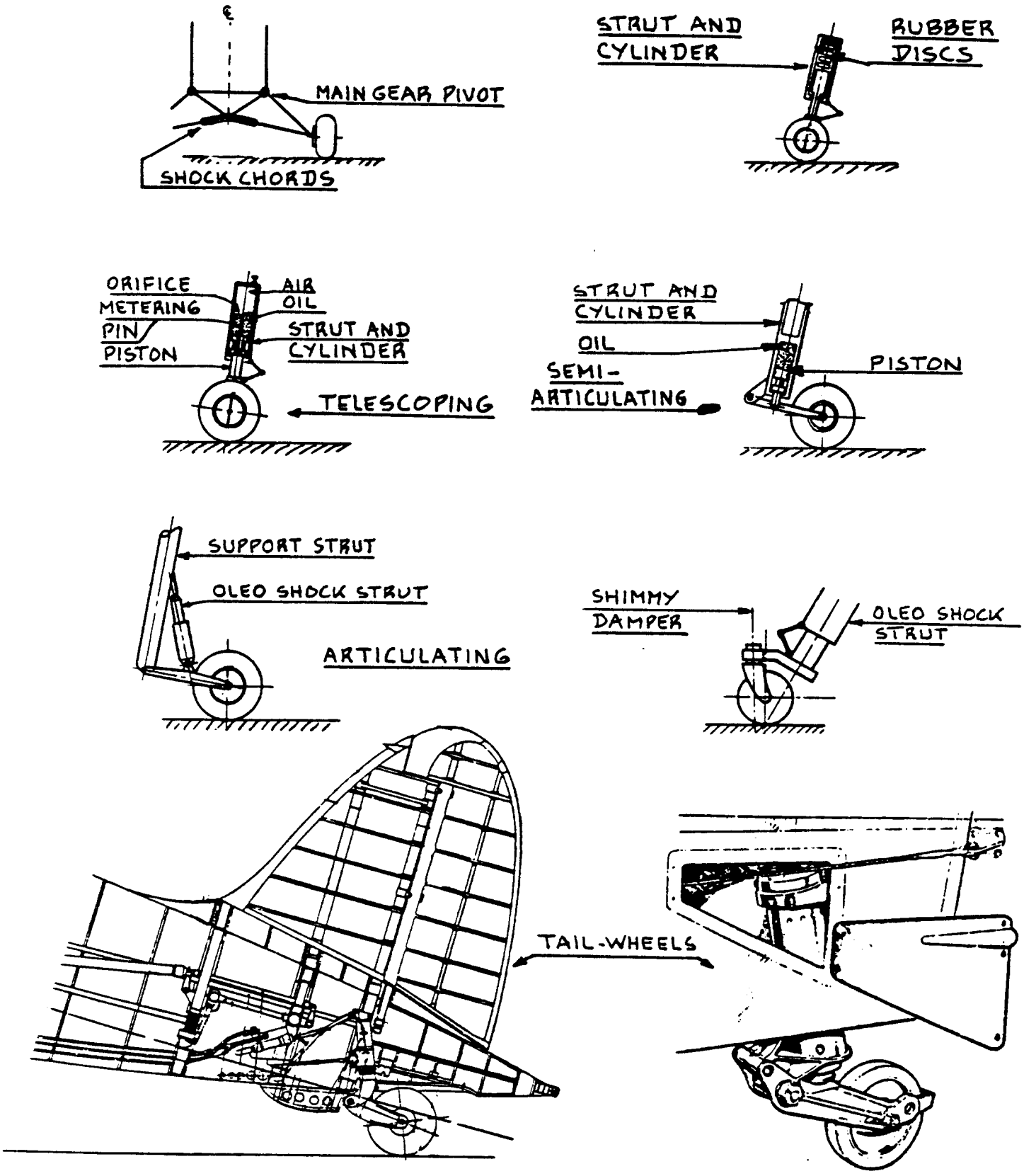

Figure 2.24 Examples of Strut-Wheel Combinations

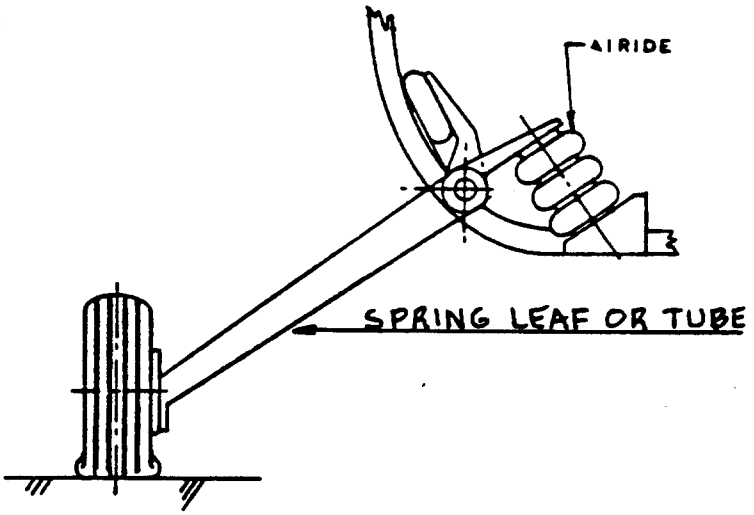

Possible Airide Spring Application

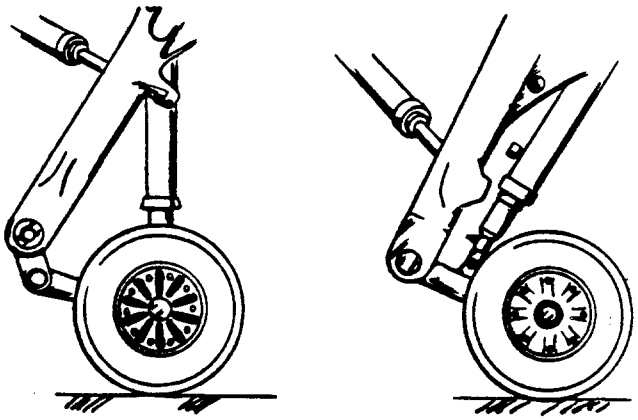

Trailing Link Main Gears

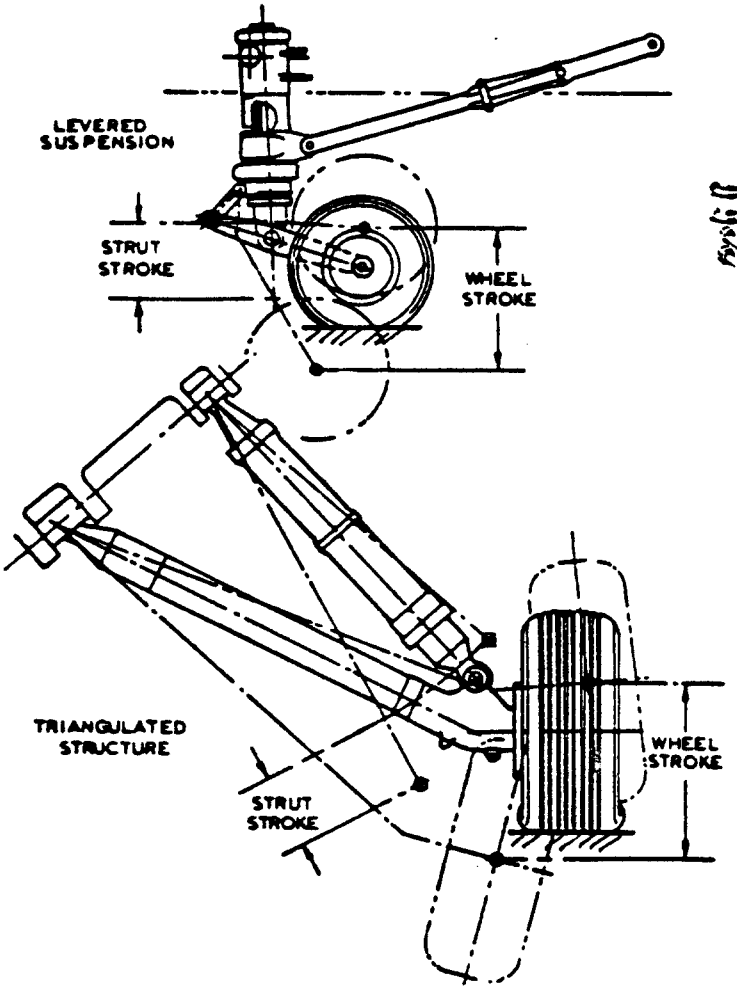

Levered Suspension and Triangulated Structure

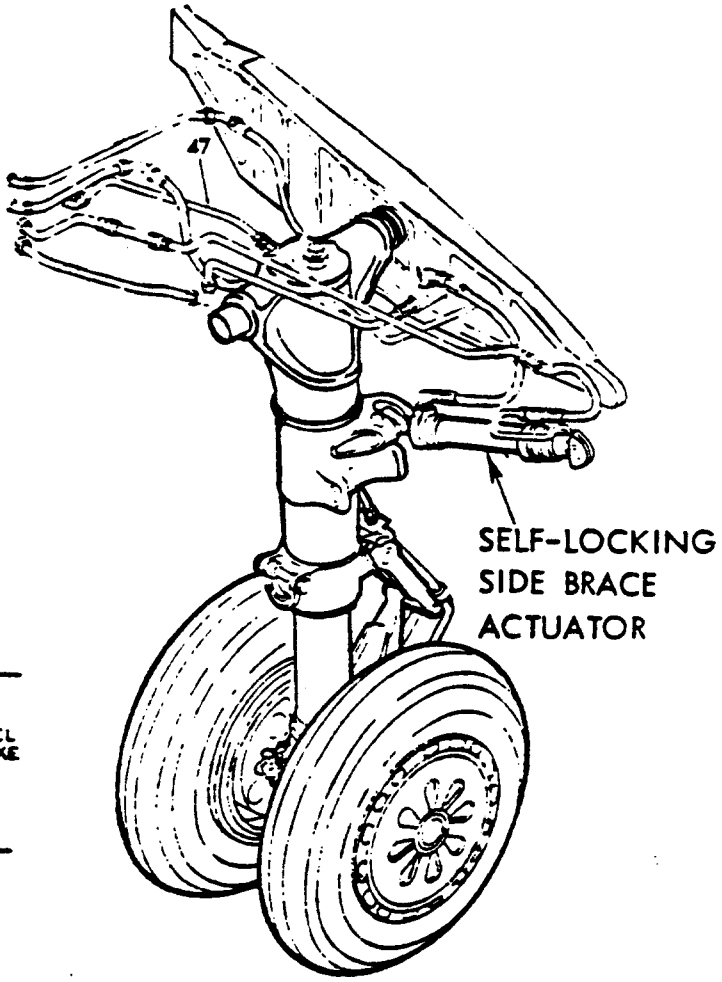

Figure 2.24 (Cont'd) Examples of Strut-Wheel Combinations

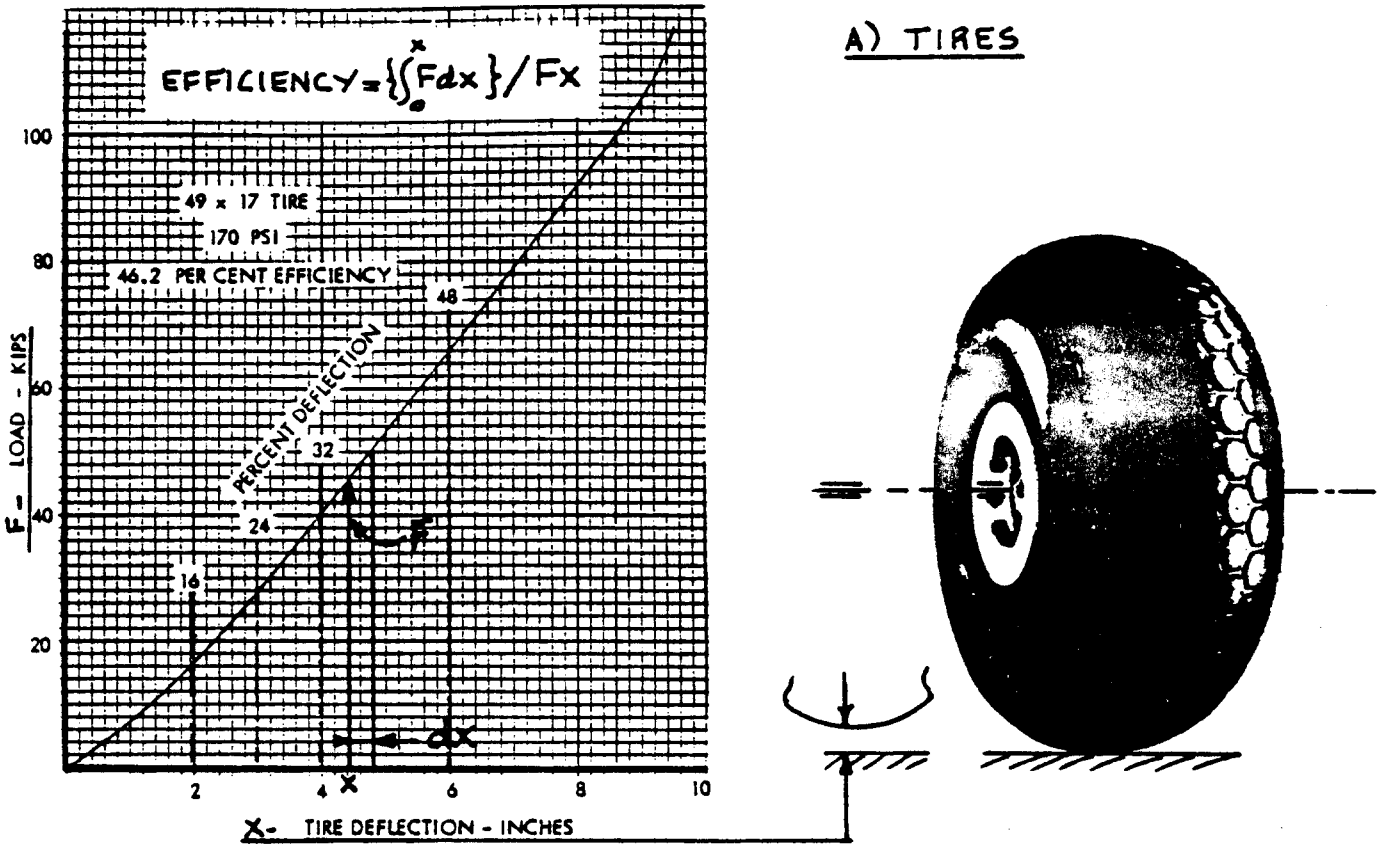

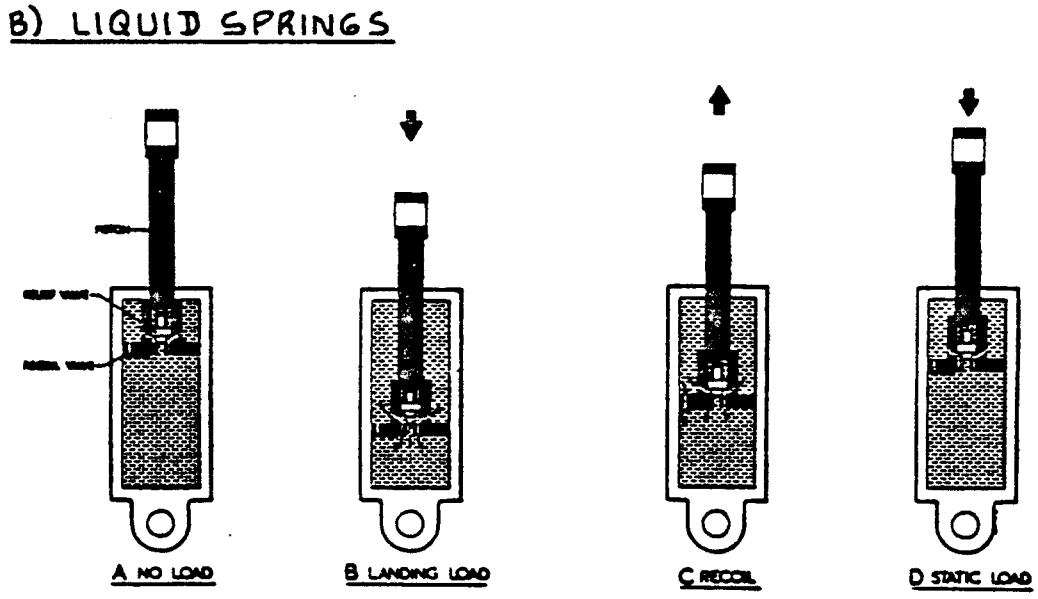

Figure 2.25 Examples of Shock Absorbing Devices

c) OLEO-PNEUMATIC STRUTS

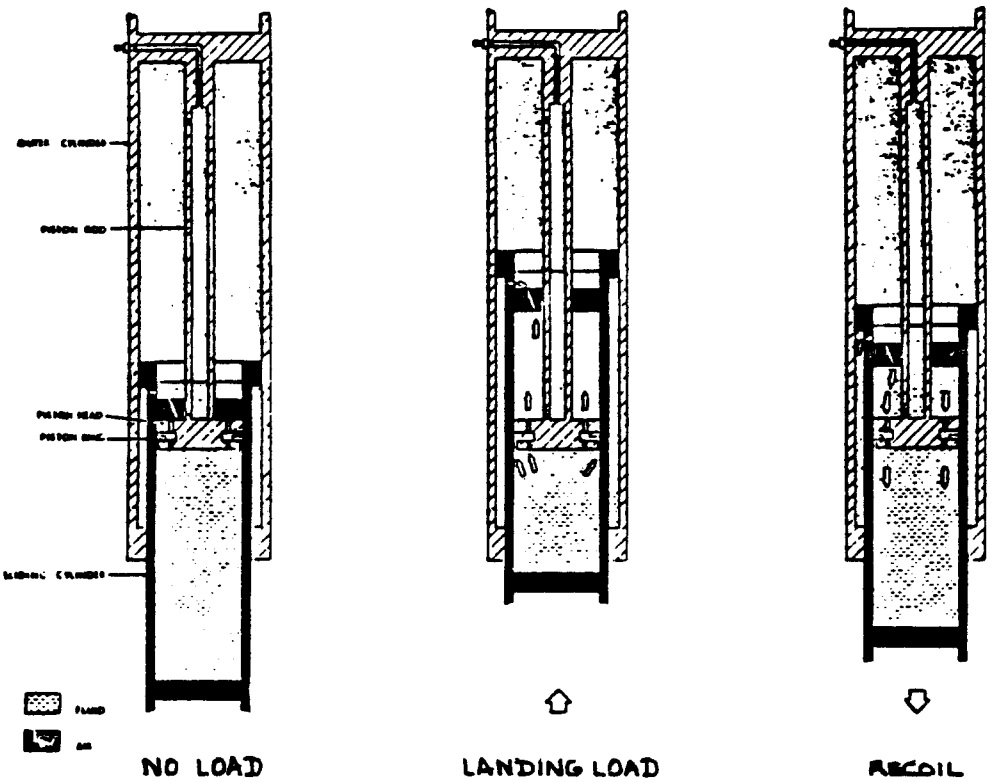

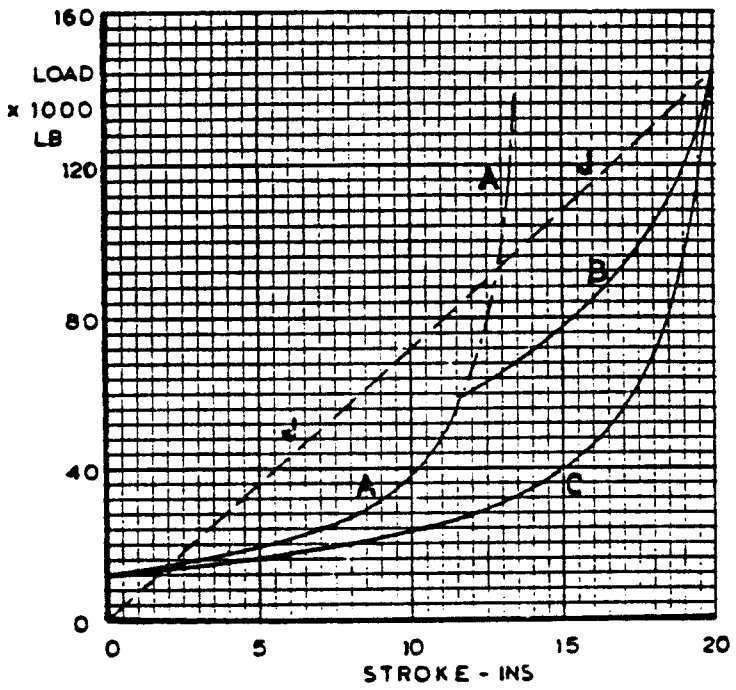

Comparison of Double and Single-Acting Struts

AB DOUBLE ACTING
C SINGLE ACTING
JJ LIQUID SPRING

NOTE: ALL FIGURES FROM REF. 2
COURTESY: N.S. CURREY

Figure 2.25 (Cont'd) Examples of Shock Absorbing Devices

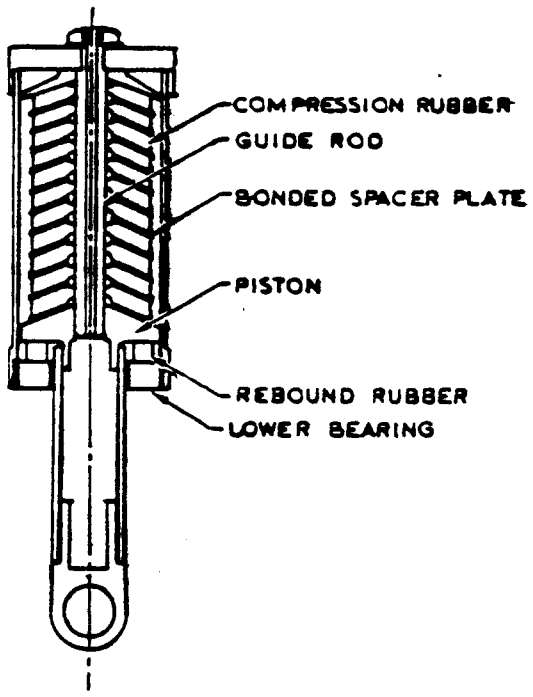

D) RUBBER SHOCK STRUT

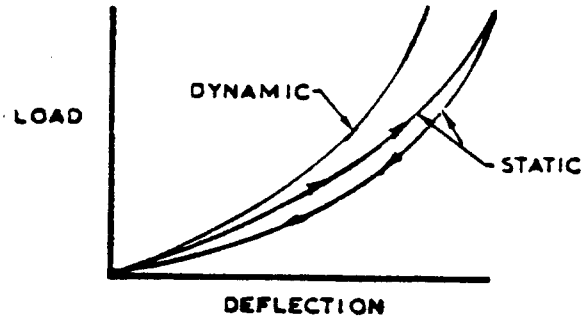

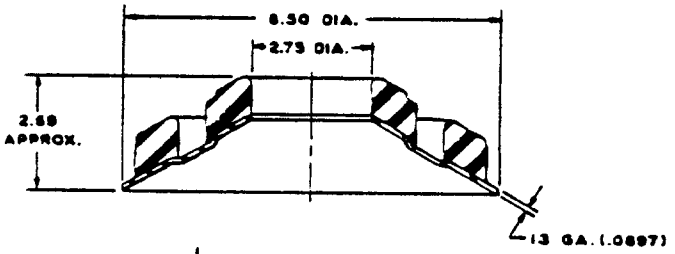

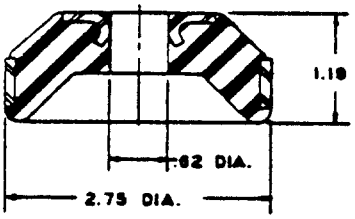

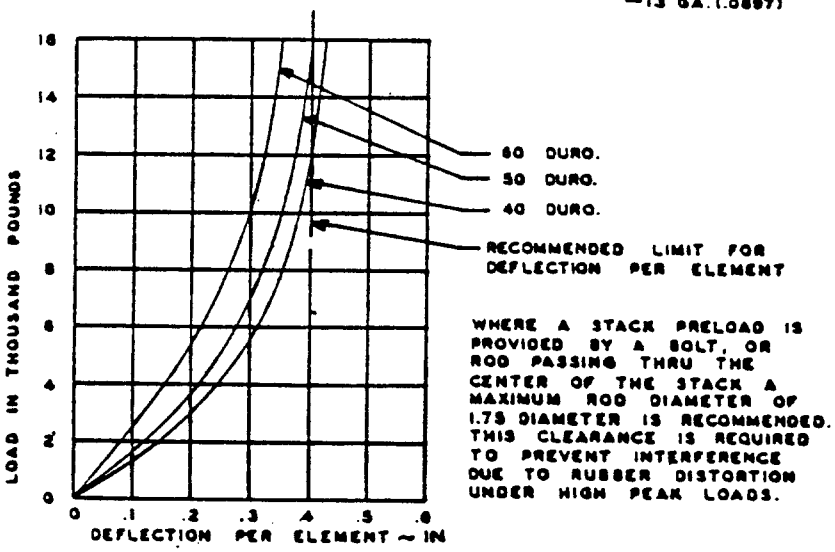

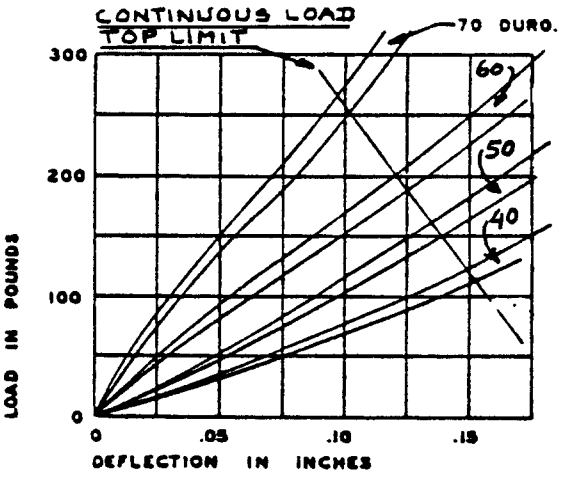

THESE DISCS MAY BE STACKED ONE ON THE OTHER IN ORDER TO OBTAIN THE LENGTH OF SPRING AND THE DEFLECTION WHICH IS DESIRED. WHEN USED IN THIS MANNER, THE VERTICAL HEIGHT OF EACH DISC IS APPROXIMATELY 1-1/2" WHEN UNLOADED A CENTER ROD MAY BE USED FOR STABILITY IF NEEDED.

Figure 2.25 (Cont'd) Examples of Shock Absorbing Devices

ships for each. The energy absorbed by each type follows from the area under its load-deflection curve. The ratio of that area to the rectangular area around the load-deflection curve is called the shock absorption efficiency. Table 2.17 presents typical values for tire and shock absorber efficiencies.

Figure 2.24 showed a number of ways in which these shock absorbing elements can be integrated into a landing gear/strut arrangement.

2.5.3 Shock Absorption Capability of Tires and Shock Absorbers: Sizing of Struts

When an airplane touches down, the maximum kinetic energy which needs to be absorbed is:

$$E_t = 0.5(W_L)(w_t)^2/g \qquad (2.8)$$

The landing weight, W_L follows from Table 3.3 in Part I. The design vertical touchdown rate, w_t follows from Section 2.1, page 4.

The energy of Eqn.(2.8) needs to be aborbed by the landing gear. How this energy is distributed over the landing gear components is discussed in the following.

For the main landing gear it is assumed that the entire touch-down kinetic energy is absorbed by the main landing gear. This is a conservative assumption. The participants in this shock absorption process are: the tires and the shock absorbers.

The following equation is used:

$$E_t = n_s P_m N_g (\eta_t s_t + \eta_s s_s) \qquad (2.9)$$

In Eqn.(2.9) it is assumed that:

$$W_L = n_s P_m \qquad (2.10)$$

The various quantities in Eqns(2.9) are defined as:

n_s is the number of main gear stuts (or legs), assumed to be equal to the number of shock absorbers. Note: $n_s = 2$ for most main gears.

P_m is the maximum static load per main gear strut.

N_g is the landing gear load factor: ratio of maximum

Table 2.17 Energy Absorption Efficiency of Tires and Shock Absorbers

Element:	Energy Absorption Efficiency:
Tires:	η_t = 0.47
Shock absorbers:	
air springs	η_s = 0.60 t0 0.65
metal springs with oil damping	= 0.70
liquid springs	= 0.75 to 0.85
oleo-pneumatic	= 0.80
cantilever spring	= 0.50

Table 2.18 Suggested Landing Gear Load Factors

Certification Base:	Landing Gear Load Factor, N_g:
FAR 23	N_g = 3.0
FAR 25	N_g = 1.5 to 2.0
Fighters and Trainers	N_g = 3.0 - 8.0: See Fig.2.25 for more details
Military transports	N_g = 1.5 - 2.0

load per leg to the maximum static load per leg.

η_t is the tire energy absorption efficiency.

η_s is the energy absorption efficiency of the shock absorber.

s_t is the maximum allowable tire deflection as determined from Eqn.(2.4).

s_s is the stroke of the shock absorber.

Eqn.(2.9) may be used to compute the required shock absorber length:

$$s_s = [\{0.5(W_L/g)(w_t)^2/(n_s P_m N_g)\} - \eta_t s_t]/\eta_s \qquad (2.11)$$

It is suggested to add one inch to this length:

$$s_{s_{design}} = s_s + 1/12 \qquad (2.12)$$

Table 2.18 shows the values for landing gear load factors which may be used in preliminary design. How these landing gear load factors are related to design touchdown rate and to shock absorber stroke is shown in Figure 2.26 for some example airplanes.

The diameter of the shock absorber (strut) may be estimated from:

$$d_s = 0.041 + 0.0025(P_m)^{1/2} \qquad (2.13)$$

Note that Eqn.(2.9) tacitly assumes that the main gear reaction load is transferred directly into the shock absorber. This condition is not satisfied for gears where the reaction load is not 'in line' with the shock absorber. A landing gear where the reaction load is aligned with the shock absorber is given in Fig.(2.7). Examples of landing gears where this alignment is absent, are given in Fig.(2.24). For the latter type gears, the required value for shock absorber stroke (and thus strut length) must be determined for the particular landing gear geometry at hand. No general rules can be given.

For main gears where the design calls for a simple cantilever (leaf or tube) spring, Ref.8 contains an example sizing calculation. Figure 2.27 shows an example application, seen mostly in light airplanes.

For the nose gear, the shock absorber length may be computed from Eqn.(2.11), BUT WITH ALTERATIONS:

1. Replace W_L with P_n (See Figure 2.14).
2. The load P_m must be replaced by the maximum dynamic nose wheel load which is equal to the maximum dynamic nose wheel tire load from Eqn.(2.5) multiplied by the number of tires. For the nose gear: $n_s = 1.0$
3. The tire deflection, s_t in this case is the nose gear tire deflection.

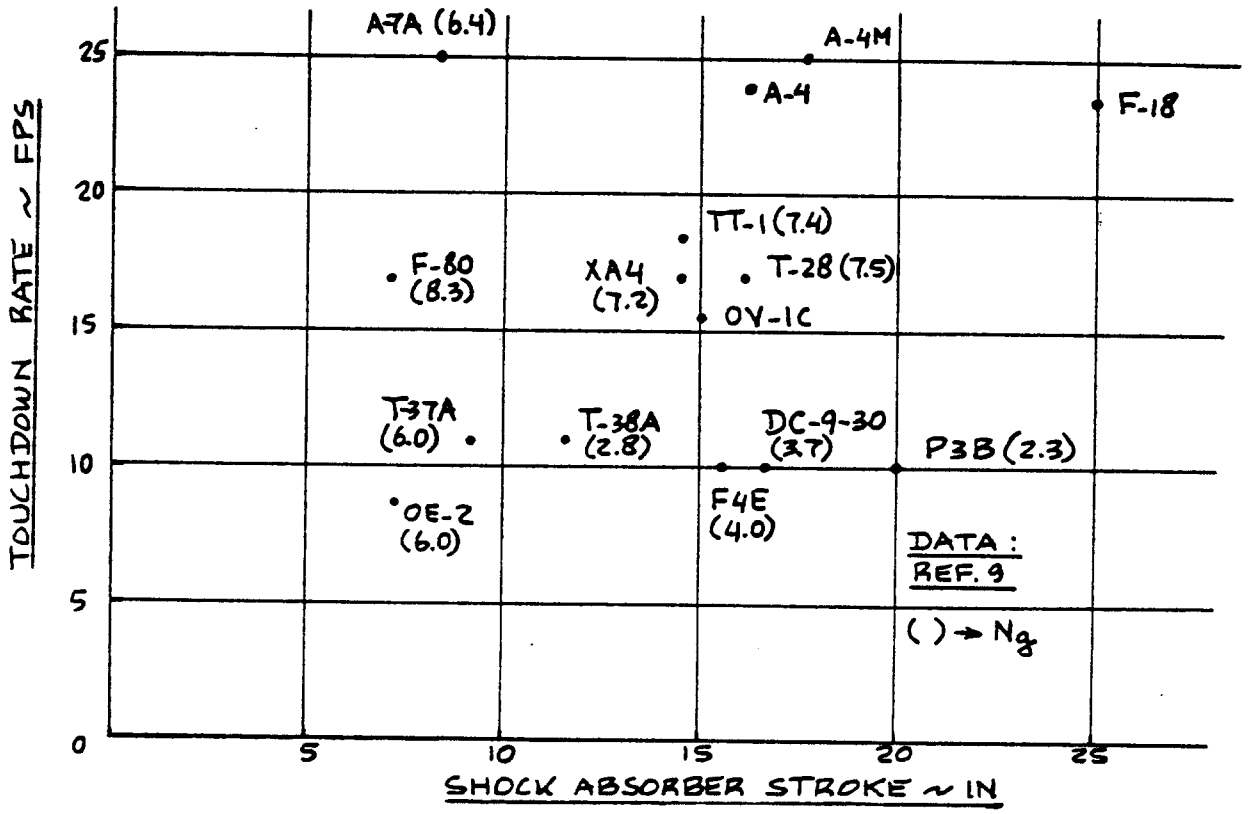

Figure 2.26 Landing Gear Load Factor as Related to Shock Stroke and Sink Speed

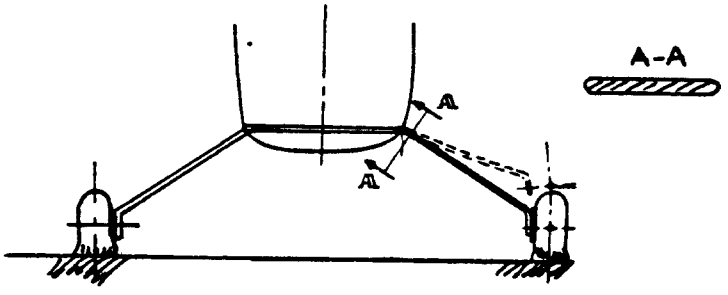

Figure 2.27 Example of Cantilever Spring Leaf Main Gear

2.6 BRAKES AND BRAKING CAPABILITY

2.6.1 Braking and Brakes

The purpose of brakes is to:

1. help stop an airplane
2. help steer an airplane by differential braking action
3. hold the airplane when parked
4. hold the airplane while running up the engines
5. control speed while taxiing.

Since virtually all modern airplanes use disc type brakes, only these will be discussed.

Figure 2.28 shows a cross section through a tire/wheel/brake assembly: wheels are made of two halves.

Figure 2.29 shows the wheel construction for a B767. Note the heat shields used to prevent overheating of the tire from the inside. A cross section of the B767 brakes which fit into the wheel cavity is shown in Figure 2.30.

Brakes turn kinetic energy (due to forward motion of the airplane) into heat energy through friction. This friction generated heat is dissipated to the immediate environment of the brake: wheel, tire and surrounding air. Figure 2.31 indicates how the braking heat flows into the wheel and into the tire: these elements act as heat sinks. The capacity of wheel and tire to absorb heat is limited. This must be accounted for in the design of wheel and tire. The methods used in heat sink sizing for brakes and wheels are beyond the scope of this text: Ref.2 deals with such methods.

Ultimately, it is the rolling friction (while applying braking action) between the tire(s) and the runway surface which slows the airplane. Fig.2.32 shows how the rolling friction coefficient is related to the so-called slip ratio. The slip ratio of a wheel is defined as:

$$\text{Slip ratio} = \{1 - (\text{Wheel RPM})_{\text{brakes on}} / (\text{Wheel RPM})_{\text{brakes off}}\} \qquad (2.14)$$

As shown in Figure 2.32, at zero slip ratio (free rolling wheel without braking) the friction coefficient is 0.02 to 0.05 depending on the surface characteristics. At a slip ratio of 1.0, the brakes have 'locked' the wheel and the friction coefficient is about 0.4, corresponding to a skidding condition (This will wear out a

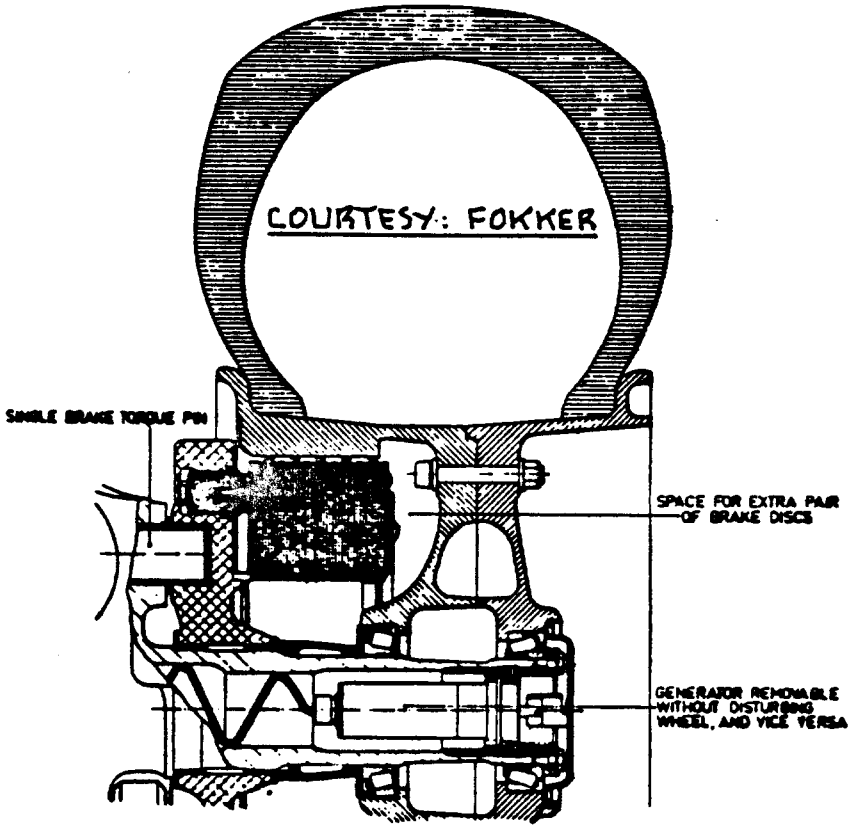

Figure 2.28 Cross Section Through a Typical Tire/Wheel/Brake Installation

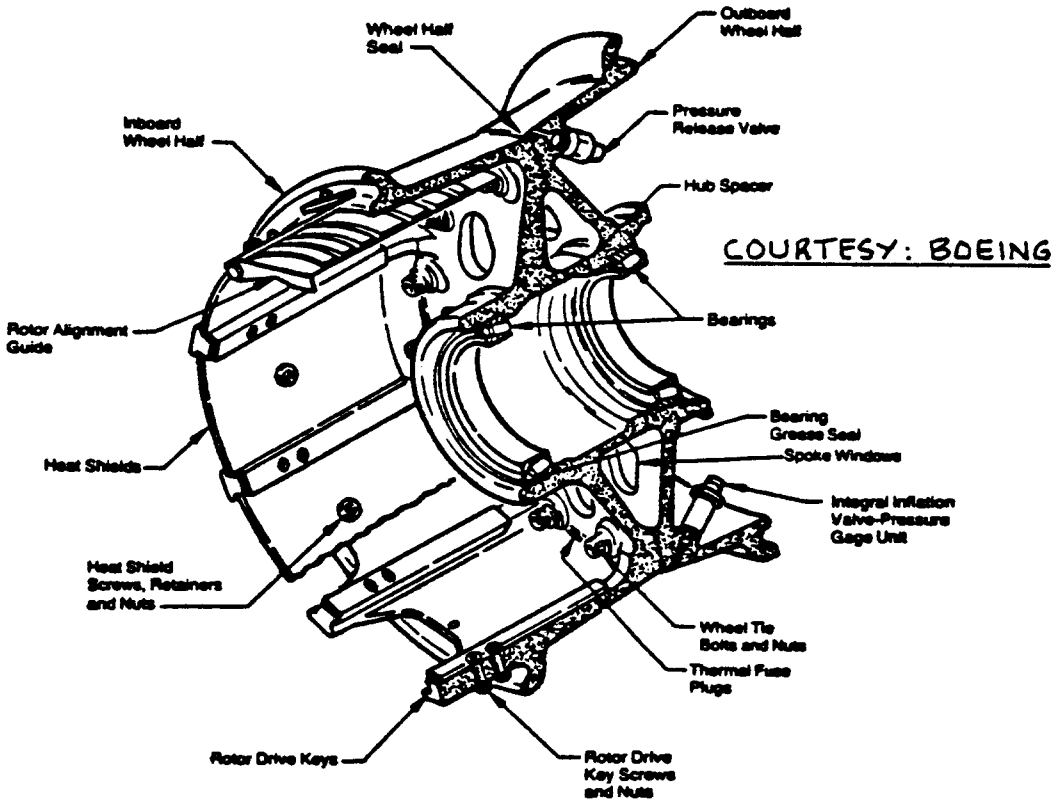

Figure 2.29 Wheel Construction for a Boeing 767

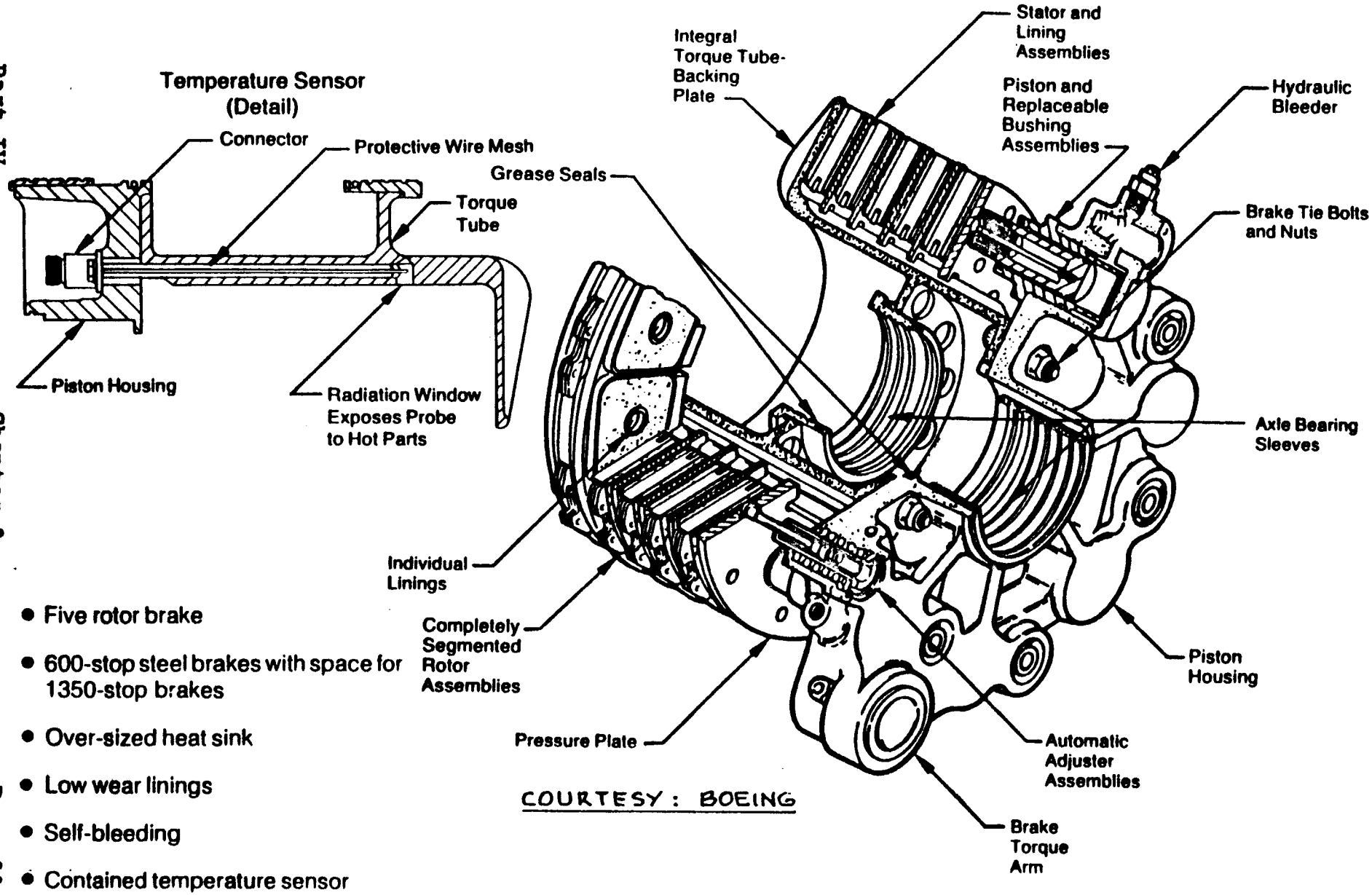

- Five rotor brake
- 600-stop steel brakes with space for 1350-stop brakes
- Over-sized heat sink
- Low wear linings
- Self-bleeding
- Contained temperature sensor

Figure 2.30 Brake Design for a Boeing 767

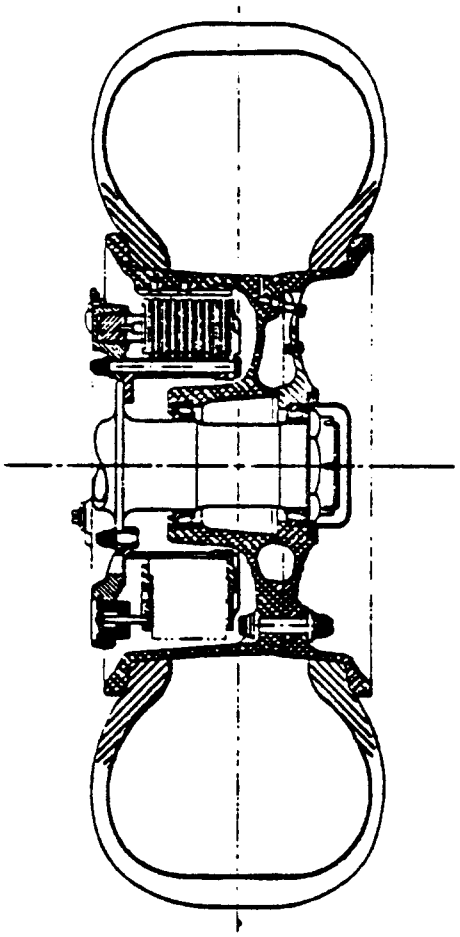

COURTESY:
N. CURREY
REF. 2

Figure 2.31 Example of Heat Flow into Wheel and Tire

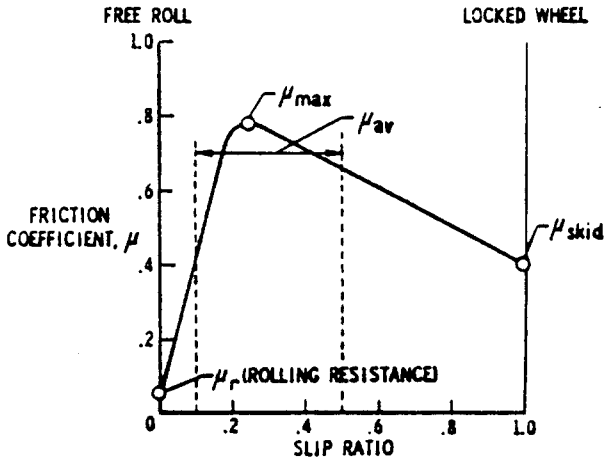

COPIED FROM:
REF. 10

Figure 2.32 Effect of Slip Ratio on Ground Friction Coefficient

tire and cause tire blow-out in less than 100 ft!). If an anti-skid system is used to control wheel RPM during braking, the average value of friction coefficient which can be attained is about 0.70.

In practical situations, accounting for the fact that tires will be a bit worn and that brakes do not operate at their best efficiency, the following deceleration values can be obtained during roll-out:

Conventional brakes:	0.35g on a dry surface
Carbon brakes:	0.40g on a dry surface
Anti-skid brakes:	0.45g on a dry surface
Anti-skid carbon brakes:	0.50g on a dry surface

Note that carbon brakes offer a significant improvement. Carbon brakes are also about 40 percent lighter than conventional brakes. Their cost is about twice the cost of conventional brakes.

On other than dry surfaces the friction coefficient while braking deteriorates significantly. Fig.2.33 shows the effect of surface condition on available braked friction coefficient values. Note that the braked friction coefficient also depends on the ground speed!

For jet transports, the average friction coefficients depicted in Figure 2.34 should be used in preliminary stop distance calculations. How to perform such calculations is shown in Part VII.

When a sufficient amount of water is present on a runway surface, a condition known as hydroplaning can arise. Fig.2.35 shows that the tire is actually 'lifted' off the runway and rides on a cushion of water: the friction coefficient values now are extremely low: approximately 0.05. When hydroplaning conditions prevail, the only way to slow down the airplane is with reverse thrust.

For a detailed discussion of available braked friction coefficients under a wide variety of conditions, Ref.10 should be consulted.

2.6.2 Brake Actuation

Brakes are normally actuated with the help of a hydraulic system. Figure 2.36 shows the main gear brake actuation system used in a Piper PA-38 Tomahawk. Figure 2.27 depicts the main gear brake actuation system used in a B767.

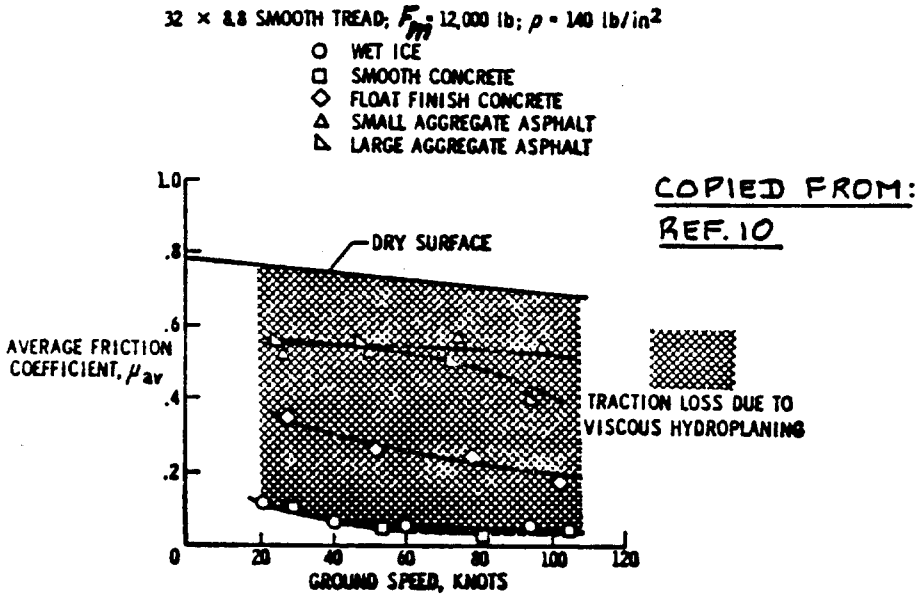

Figure 2.33 Effect of Surface Condition on Ground Friction Coefficient

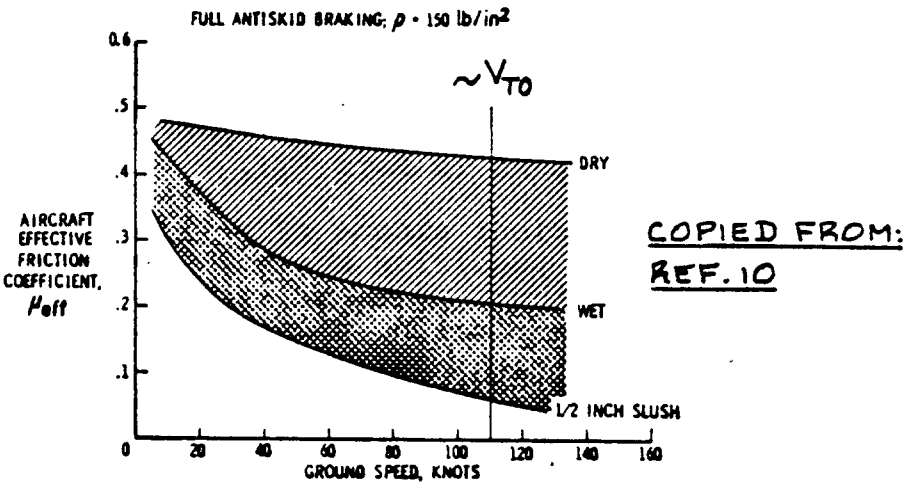

Figure 2.34 Typical Ground Friction Coefficients Encountered by Jet Transports

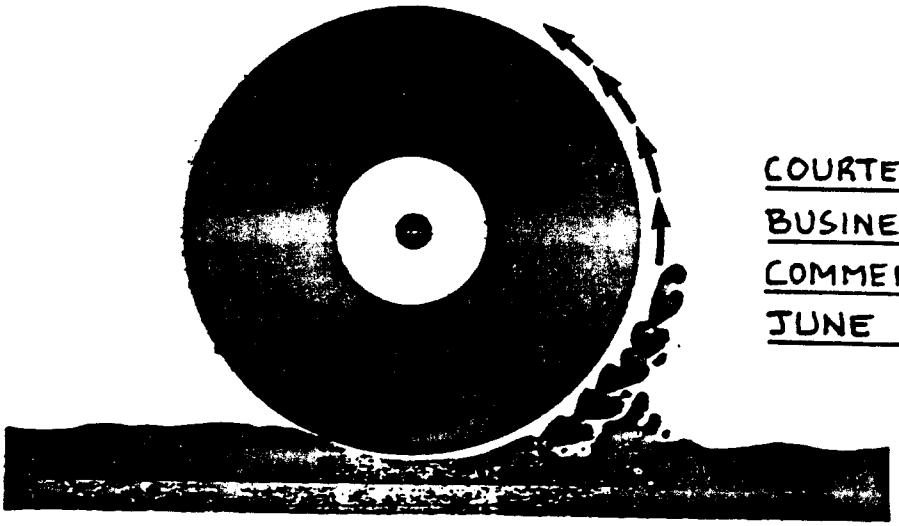

COURTESY:
BUSINESS AND
COMMERCIAL AVIATION
JUNE 1974

In standing water a wedge will build at the forward rolling point on the tire, lift it from the runway and impart vectors that cause the wheel to begin rotating backwards. NASA has demonstrated this phenomenon on aircraft as large as a DC-8.

Figure 2.35 Hydroplaning Tire

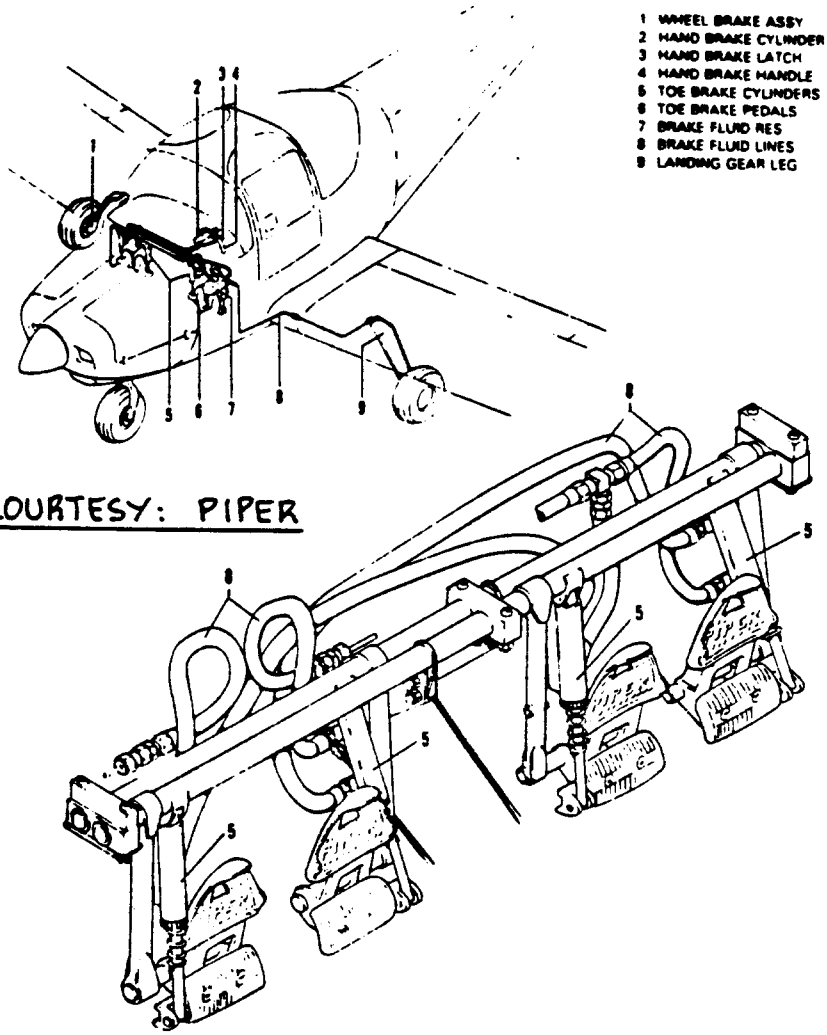

COURTESY: PIPER

Figure 2.36 Brake Installation Piper PA-38-112

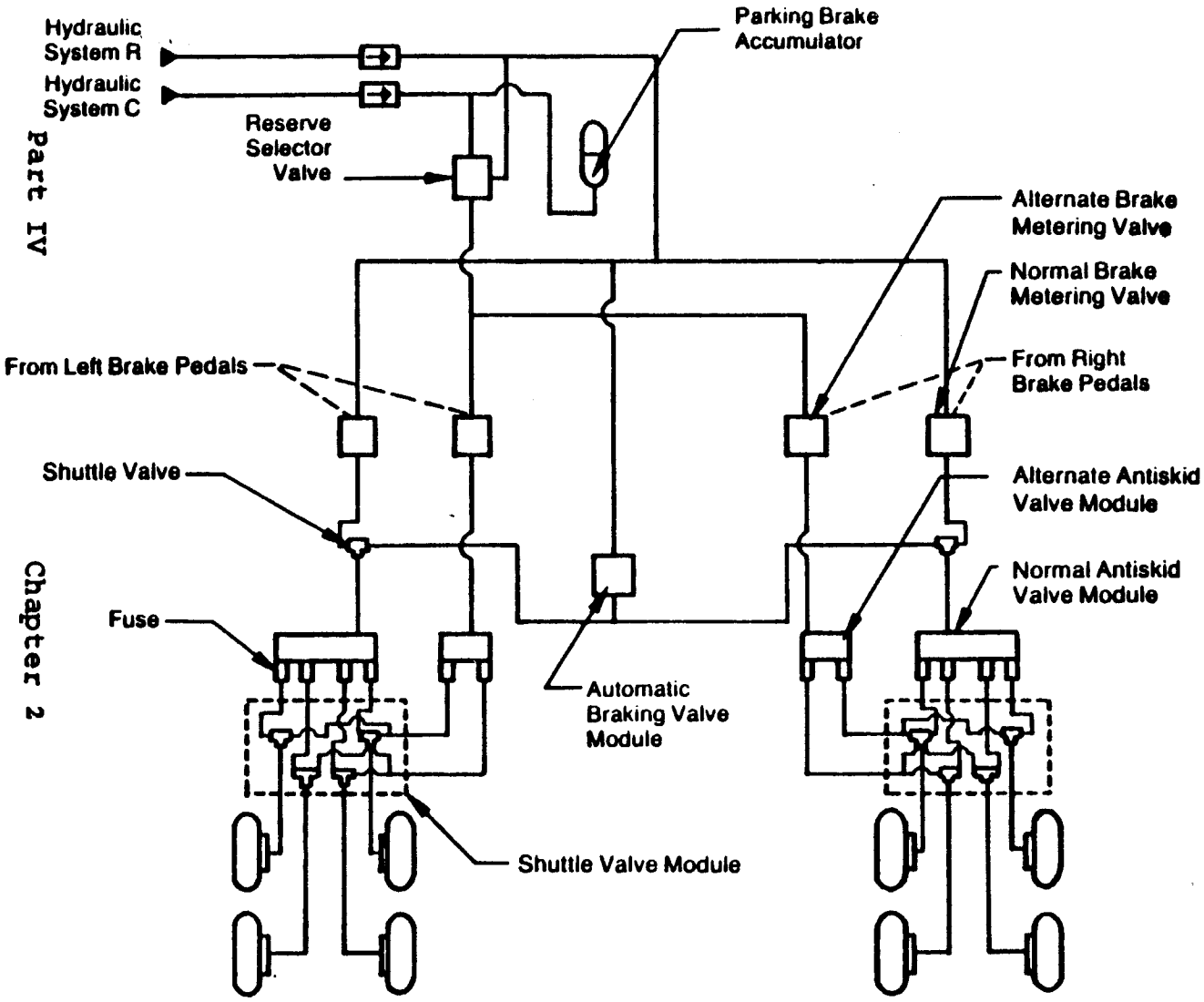

COURTESY: BOEING

Normal and alternate, 3000 psi brake system with automatic switching

Two systems independent with respect to:

- Hydraulic sources
- Plumbing down to the shuttle valves
- Metering valves
- Antiskid control valves

Normal brakes with individual wheel antiskid, automatic braking with selectable deceleration rates

- Alternate brakes, paired wheel antiskid and parking brake
- Reserve brake pressure from isolated electric motor-driven pump, crew selectable
- Parking brake effective for 8 hours minimum
- Braking capability during towing

Figure 2.37 Main Gear Brake System Boeing 767

2.7 DESIGN CONSIDERATIONS FOR LANDING GEARS OF CARRIER BASED AIRPLANES

Because of the requirements to catapult and arrest carrier based airplanes, special provisions must be made in their landing gear design. The purpose of this section is to discuss the most important aspects of landing gear design for carrier based airplanes. The material is organized as follows:

2.7.1 Description of flight deck features
2.7.2 Description of a catapult system
2.7.3 Catapulting procedures and required landing gear provisions
2.7.4 Description of arresting gear system
2.7.5 Arresting procedures and required landing gear provisions

2.7.1 Description of Flight Deck Features

Figure 2.38 shows the flight deck layout of the aircraft carrier Enterprise (CVN 65). Note the four catapults and the four deck pendants of the arresting gear. Also note the four elevators. All naval aircraft must fit within the geometry of the elevators: it must be possible to move aircraft from the flight deck to the hangar deck for repairs and for special outfittings.

It is essential to fit as many airplanes as possible on the flight deck and on the hangar deck below. A carrier airplane must also fit on an elevator to transport it from the flight deck to the hangar deck. This requires naval airplanes to be sufficiently small and/or to have folding surfaces. Examples of wing folding are given in Chapter 4 of Part III.

To determine how many airplanes fit on the flight deck during launching and recovery operations, so-called 'deck-spotting' studies are performed. Figure 2.39 shows a typical spotting study result for a small escort carrier (CVE 2/53: never built).

2.7.2 Description of a Catapult System

For detailed in formation on catapulting systems Ref.11 should be consulted. Figure 2.40 shows an example of how a catapult system works.

The airplane is attached to the shuttle and to a so-called holdback unit. The launching force is applied to the airplane via the shuttle. The shuttle is attached

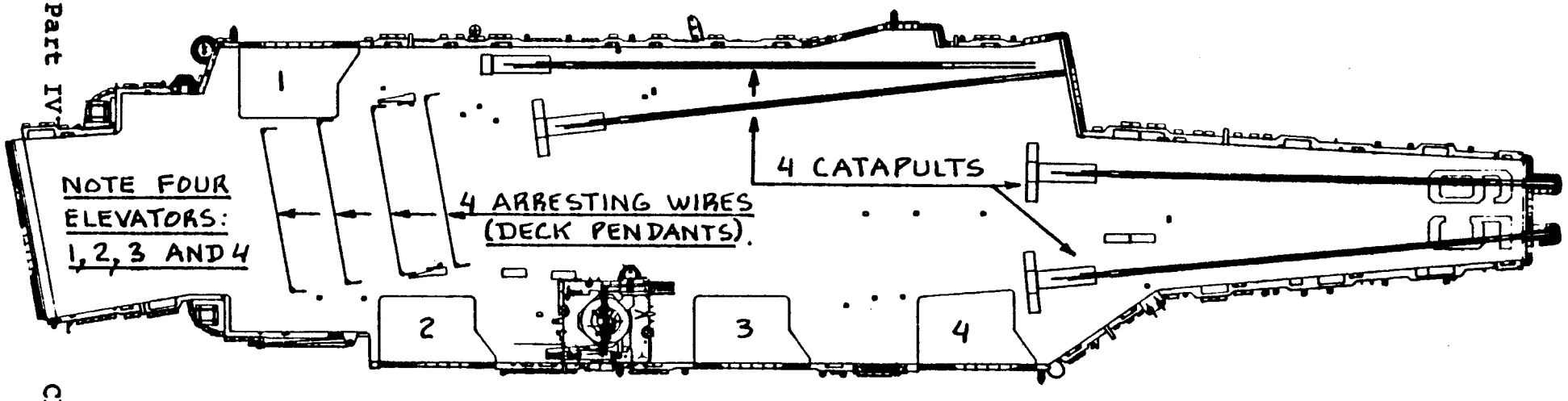

Figure 2.38 Flight Deck Layout: Enterprise (CVN 65)

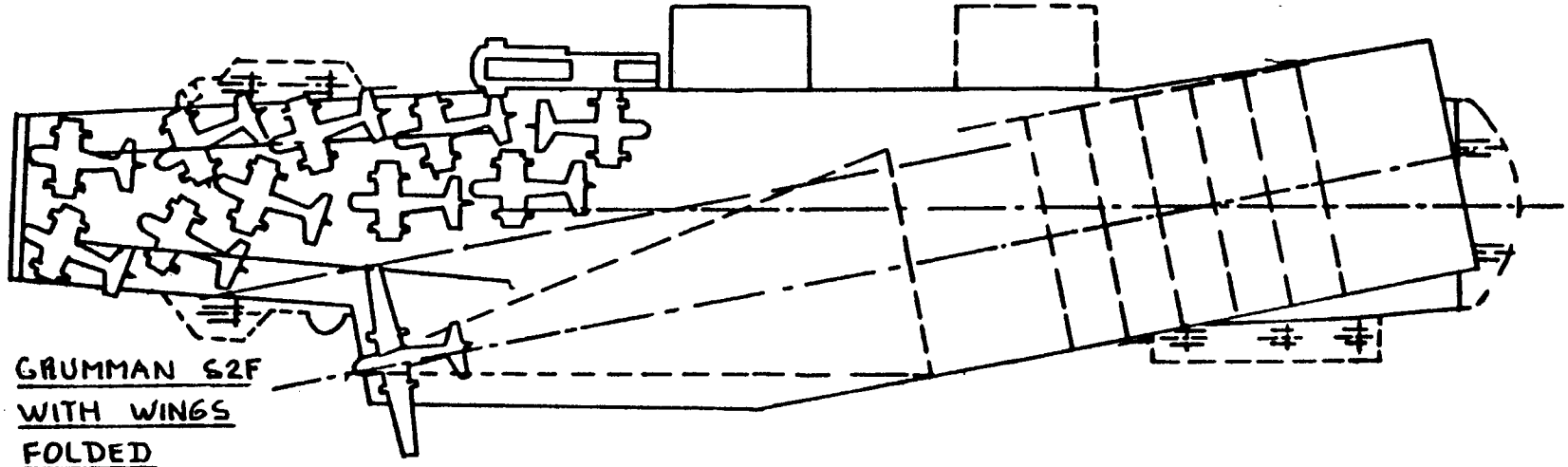

Figure 2.39 Example of a Flight Deck Spotting Study

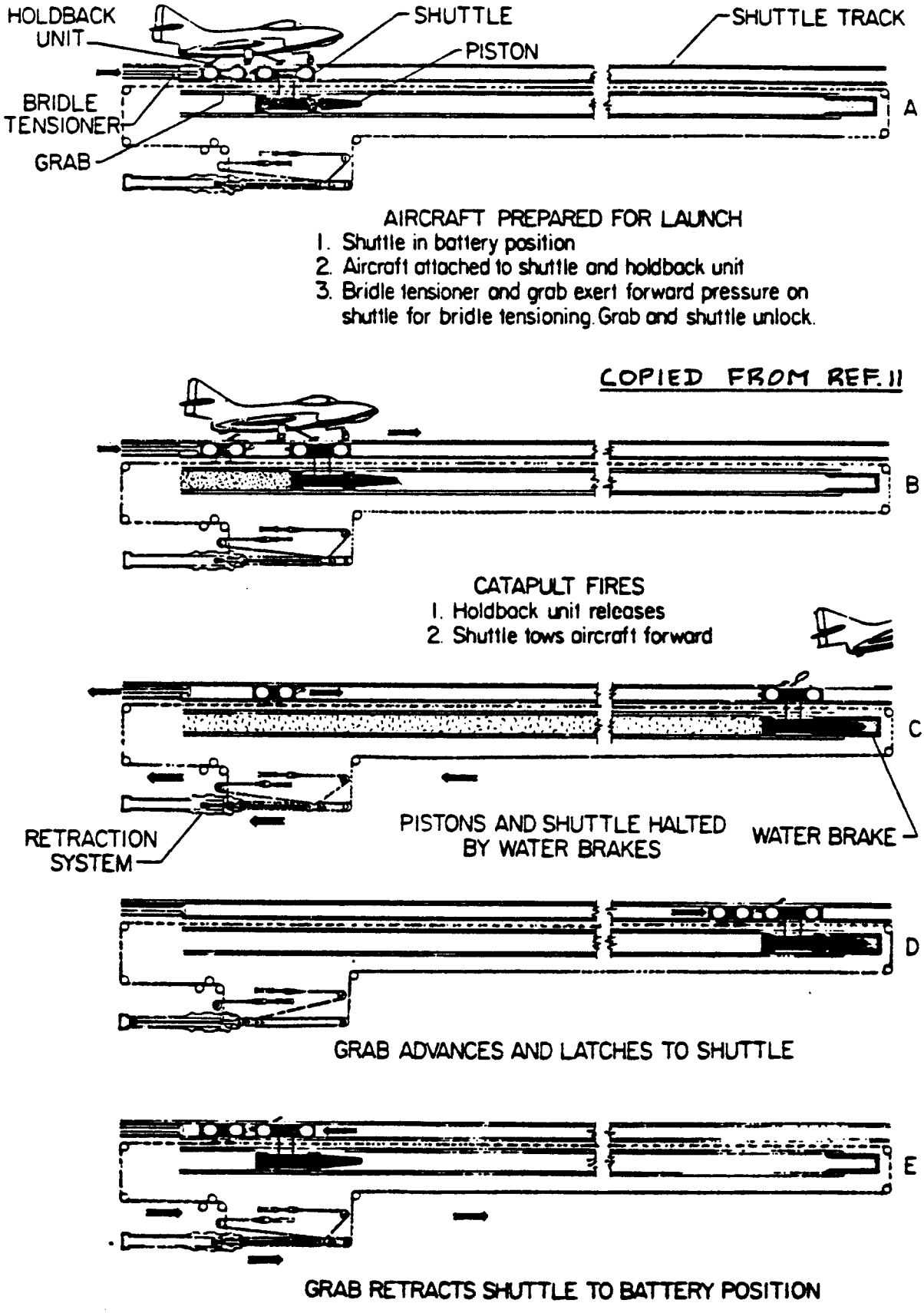

Figure 2.40 Typical Catapult Operation

either to the nosegear or to one or more points with a pendant or a bridle.

A catapult can be thought of as a device which accelerates a given mass (the airplane) from zero speed relative to the carrier deck to the catapult end-speed. The aerodynamic characteristics of the airplane are not important in this process. Figure 2.41 shows a typical catapult performance relationship. Any point within the limits represents a possible mass/end-speed combination. The steam pressure used during catapulting determines the actual performance obtained.

The airplane 'sizing' implications of catapult performance limitations are discussed in Chapter 3 of Pt I.

Note: To account for full thrust during the catapult stroke 3 kts may be added to the catapult end speed.

2.7.3 Catapulting Procedures and Required Landing Gear Provisions

Figure 2.42 shows the general arrangement of an airplane on the catapult. The airplane is positioned on the catapult and attached to the catapult tow fitting. The element which attaches an airplane to the tow fitting is:

1. a bridle (See Fig.2.42a)
2. a pendant
3. a launch bar (See Fig.2.42b)

Figures 2.43 and 2.44 show an example of a bridle and a nosegear launch bar arrangement respectively.

A holdback device (Fig.2.42) connects the airplane holdback fitting to the deck holdback attachment point. This holdback is needed for the following reasons:

1. to prevent the airplane from moving forward due to pitching of the carrier deck.

2. to prevent the airplane from moving under full thrust or power.

3. to prevent the airplane from moving when the bridle (or pendant) is tensioned prior to launch.

When the catapult is fired the shuttle attempts to move the tow fitting forward. The holdback device continues to restrain the airplane until a pre-set force level is reached whereupon the holdback releases the airplane.

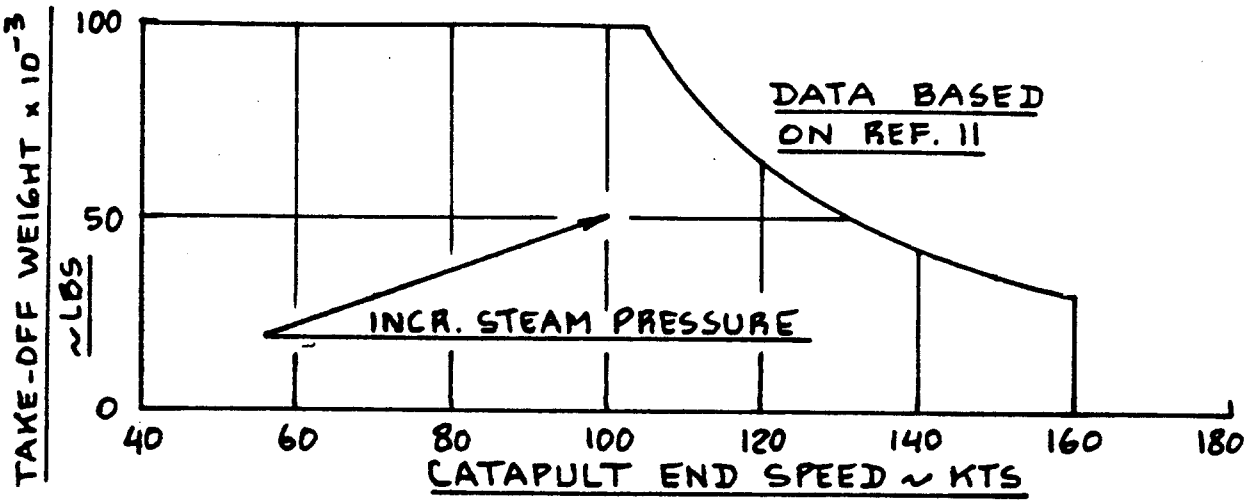

Figure 2.41 Performance Limitations C7 Catapult System

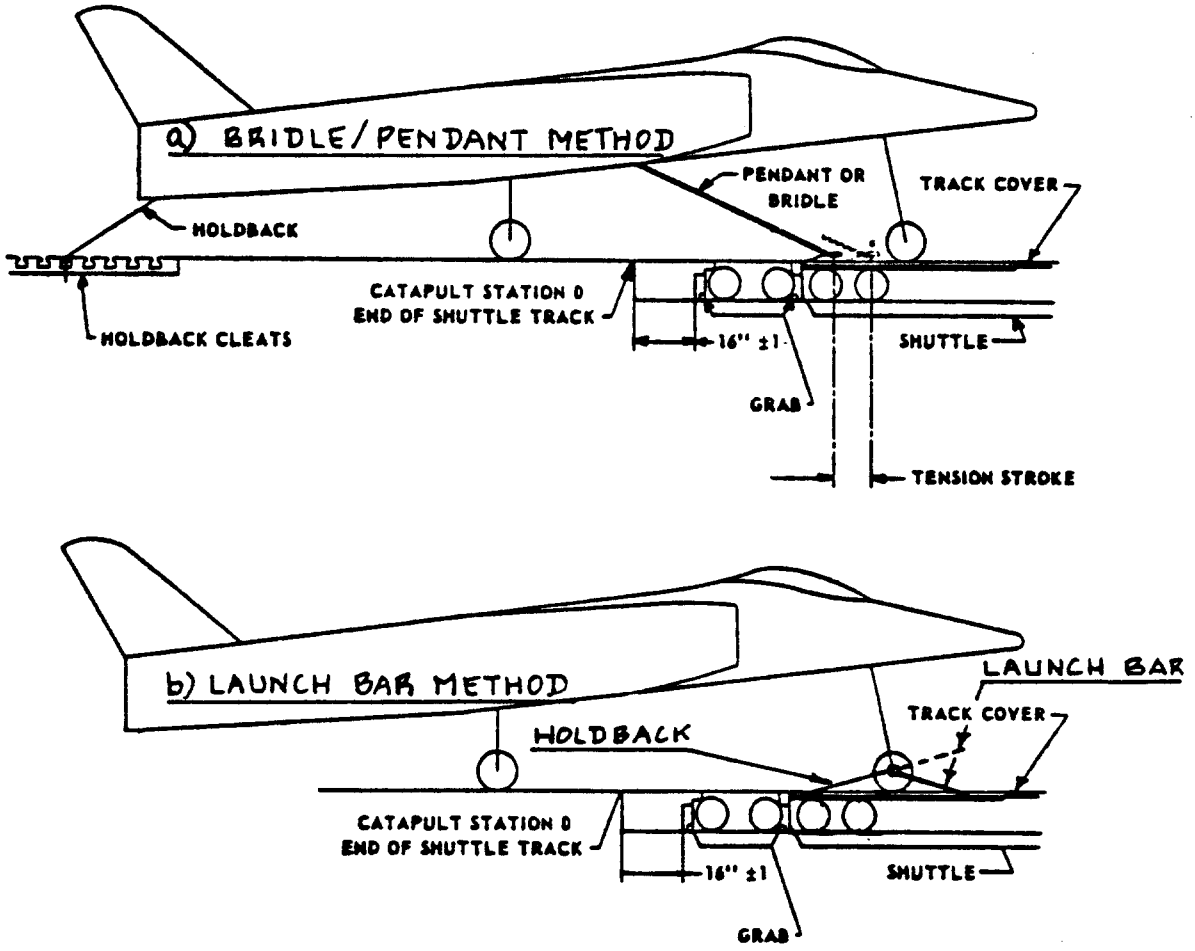

Figure 2.42 Airplane/Catapult Arrangements

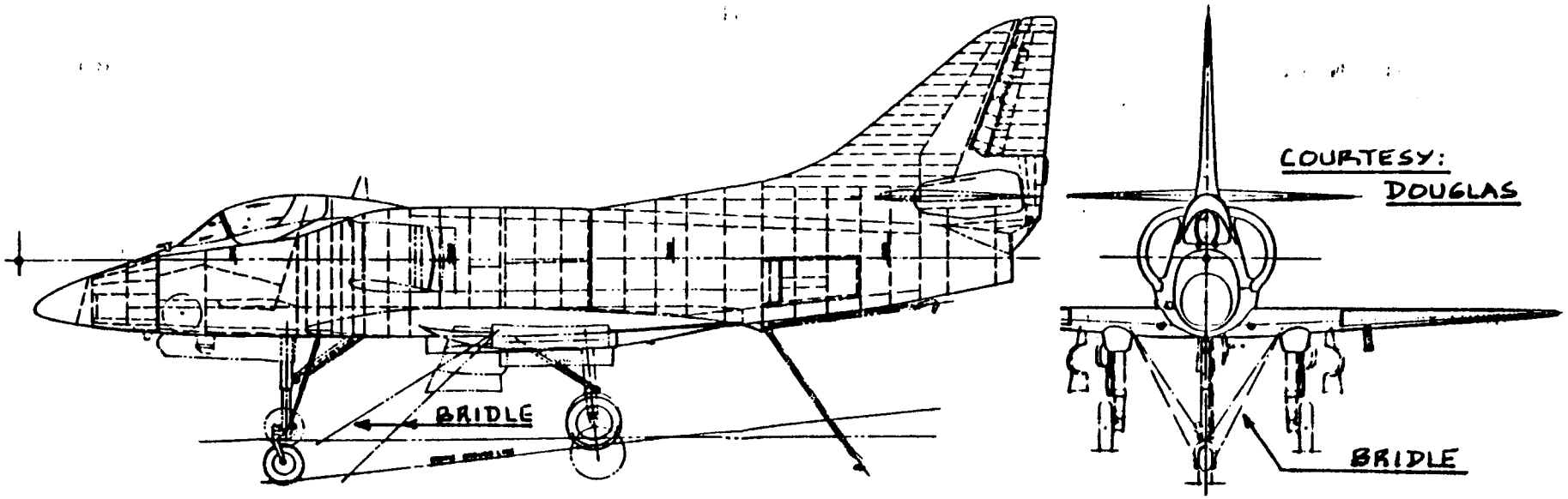

Figure 2.43 Bridle Installation: Douglas A4D-2N

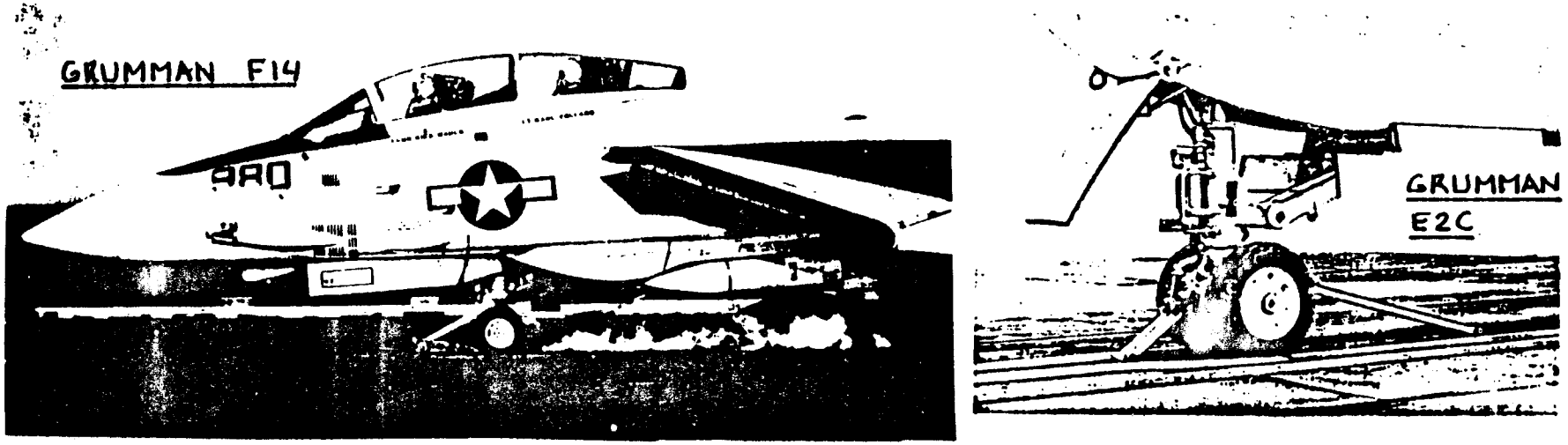

Figure 2.44 Nosegear Launch Bar Installations

At the end of the catapult stroke the airplane automatically disengages from the catapult tow fitting. The airplane then continues under its own thrust or power.

When using the bridle/pendant method, the airplane is attached to the catapult tow fitting with a V-shaped bridle (requires two attachment points on the airplane) or with a pendant (requires one attachment point on the airplane). This method requires the deck crew to manually attach the airplane to the catapult tow fitting and to the holdback cleats: See Figure 2.42a.

When using the nose-gear launch-bar method, the airplane is coupled to the catapult tow fitting with a nose-gear mounted launch-bar. This launch-bar retracts with the nose gear into the airplane after launch. The holdback device is also attached to the nose gear.

Note: All new carrier based airplanes must be designed for the nosegear launch method.

The forces which act on an airplane on the catapult are large: structural provisions must be made to transmit these forces into the airframe. In the case of the F14, the design load imposed by the shuttle on the nosegear is 120,000 lbs! Couple this with the touchdown rates of p.4 and it is clear why naval airplanes have much higher landing gear weight fractions than other types of airplanes.

2.7.4 Description of Arresting Gear System

The arresting gear consists of an arresting engine, reeved with a purchase cable coupled to a deck pendant which is the arresting cable on the flight deck. A typical arresting gear arrangement is shown in Figure 2.45.

An arresting hook, located in the rear of the airplane (See Figs 2.43 and 2.46) engages the deck pendant to stop the airplane. On modern carriers there are four arresting cables. Older carriers have six such cables.

The kinetic energy of the airplane is absorbed in the arresting engine which (like the catapult) is located below the flight deck. Figure 2.47 shows typical performance capabilities for various types of arresting gear: the allowable engaging speed of the arresting hook is a function of the airplane weight.

The airplane 'sizing' implications of arresting gear performance limitations are discussed in Ch.3 of Part I.

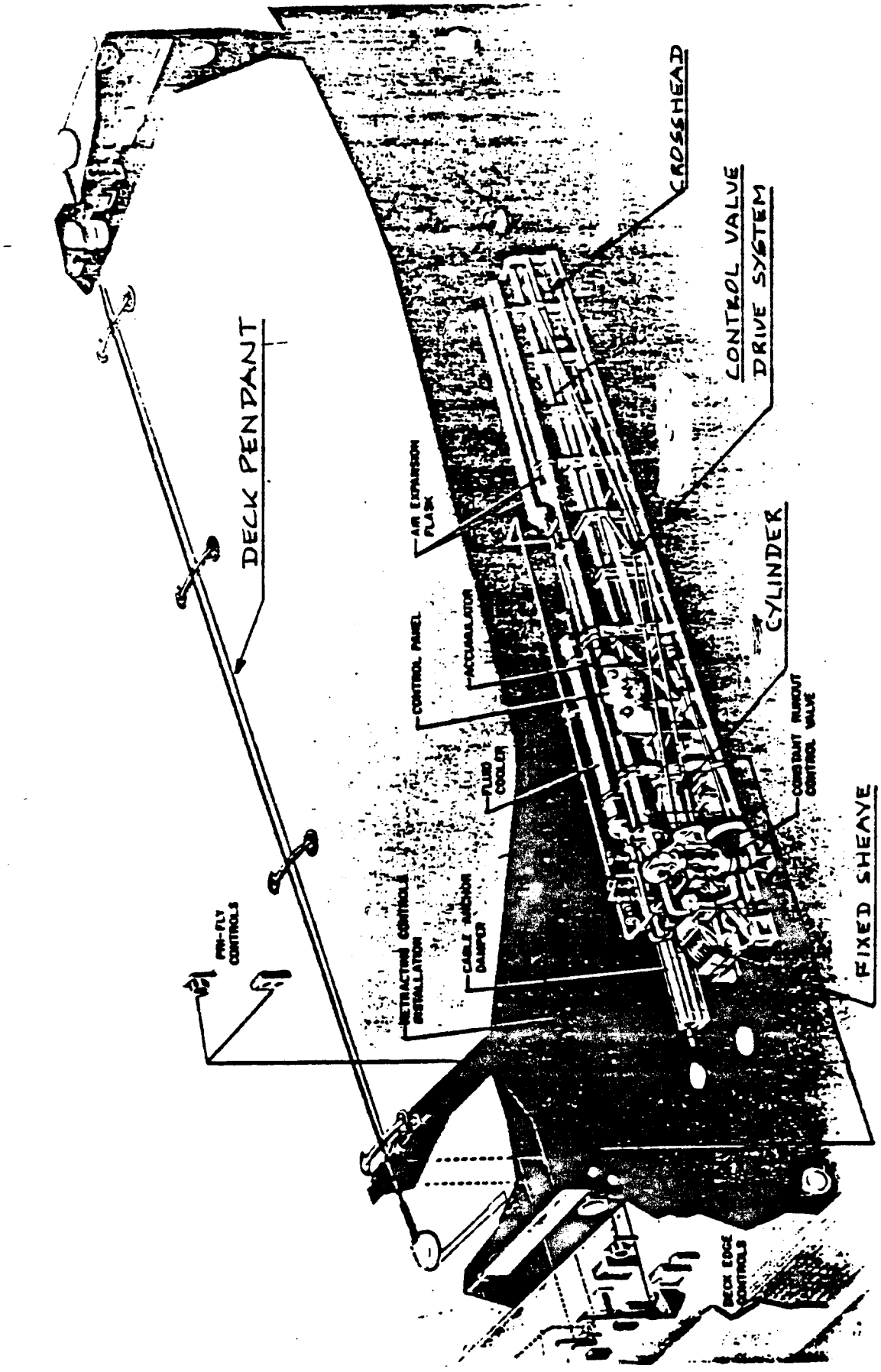

Figure 2.45 Example Arresting Gear Installation

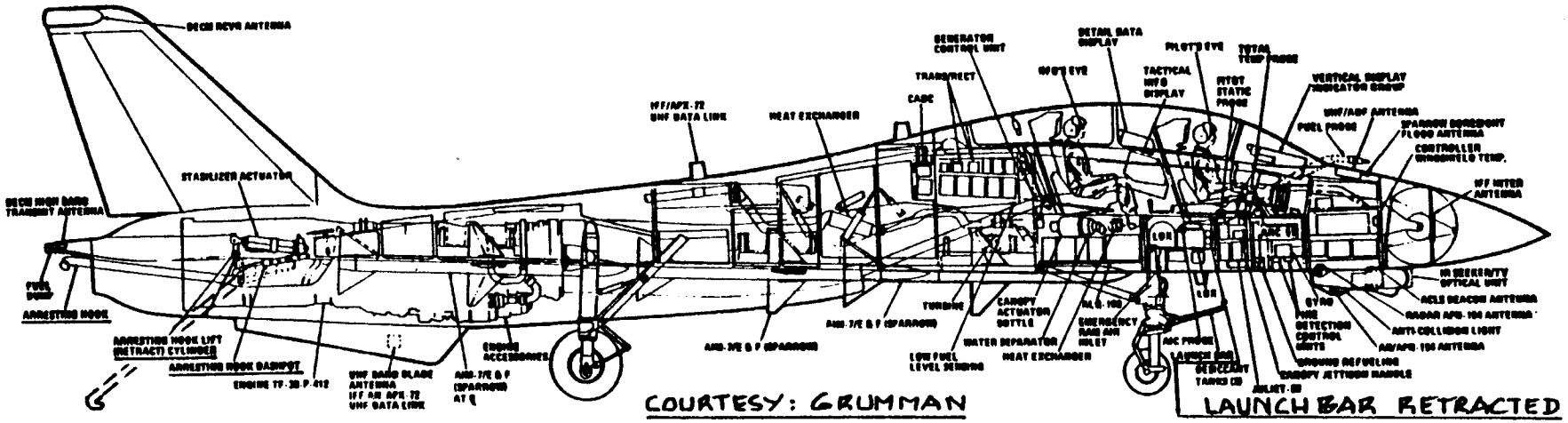

Figure 2.46 Arresting Hook Installation: Grumman F14

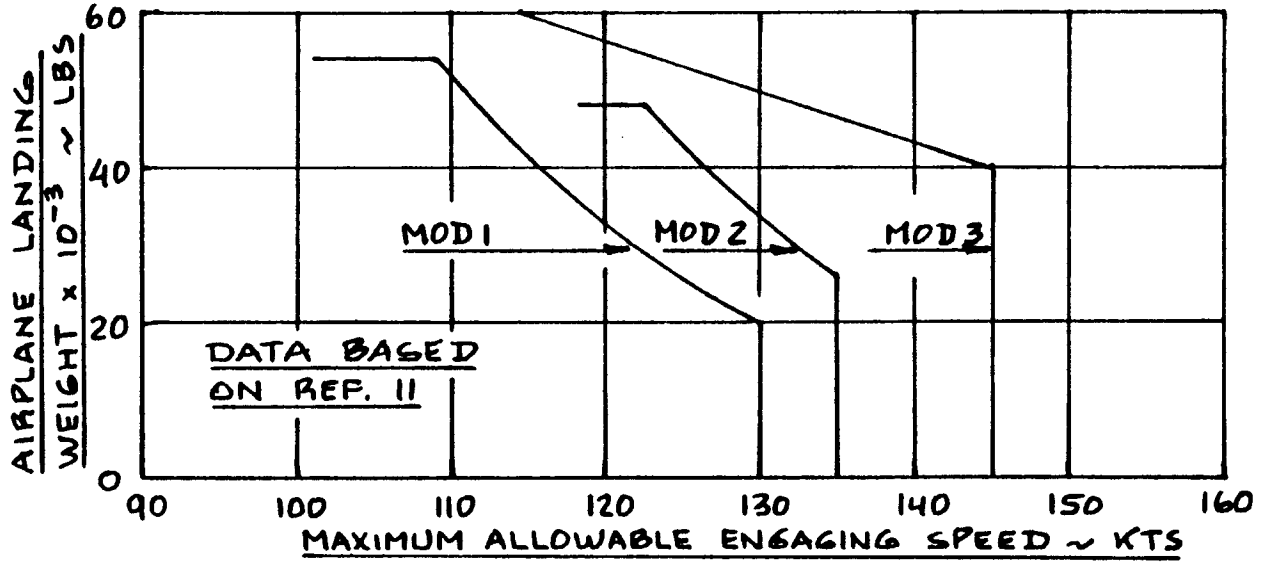

Figure 2.47 Performance Limitations Mk7 Arresting Gear

2.7.5 Arresting Procedures and Required Landing Gear and Arresting Hook Provisions

Carrier based airplanes fly a 3-4 degree flight path toward the deck. The arresting hook engages a deck pendant resting on wire supports on the deck: See Figures 2.38 and 2.45.

The forward motion of the airplane is transferred to the purchase cable system which consists of two lengths of cable reeved on a set of movable and on a set of fixed sheaves on the arresting engine. One end of each purchase cable is attached to one end of the deck pendant cable. The other ends of the purchase cables are coupled to a cable anchor damper or to a fixed anchor at the arresting engine. The fixed sheaves are attached to a cylinder filled with fluid. The movable sheaves are attached to the crosshead of a ram which extends from the cylinder. As the purchase cables are pulled out, the crosshead moves toward the fixed sheaves and the fluid is forced by the ram from the cylinder. The flow of the moving fluid is metered through a constant runout control valve to an accumulator. The control valve is set prior to engagement to determine the required degree of metering consistent with the kinetic energy level of the incoming airplane.

When the forward motion of the airplane has stopped, strain energy in the deck pendant and purchase cable will normally pull the airplane back enough to cause the arresting hook to automatically disengage.

The arresting hook of the airplane needs to be mounted such that:

1. the deceleration loads corresponding to 2.0g to 3.5g are transferred into the structure without significant deformations.

2. no large moments are imposed on the airplane.

Figures 2.43 and 2.46 show typical arresting hook installations.

2.8 REVIEW OF LANDING GEAR LAYOUT GEOMETRY

The purpose of this section is to review the overall landing gear layout geometry. The material is organized as follows:

2.8.1 Overall landing gear disposition

2.8.2 Critical landing gear dimensions: tires, struts, drag links and side braces

2.8.3 Landing gear layout checklist

2.8.1 Review of Overall Landing Gear Disposition

Figures 2.48 and 2.49 summarize the pertinent ground clearance and tip-over requirements (criteria) already mentioned in Chapter 9 of Part II. If these criteria are not met, the proposed landing gear disposition MUST be changed!

Figure 2.50 shows typical FOD (=foreign object damage) angles which should be observed. It may be possible in some cases to 'relocate' spray patterns by the use of deflector devices. Figure 2.51 shows two possibilities: a chine tire and a nosegear splash guard (sometimes called deflector shield). If an airplane must operate from 'gravel' covered runways it is essential that tests be carried out to demonstrate that any nosegear deflector shields really work!

Tests under actual slush conditions must be conducted to verify their proper operation. Figure 2.52 shows a typical spray pattern thrown up by the nose gear when travelling through water on the runway. Note that the sprays do not enter into the engine inlets.

2.8.2 Critical Landing Gear Dimensions: Tires, Struts, Drag Links and Side Braces

Figure 2.53 and 2.54 summarize the dimensions associated with the tire/wheel/shock-absorber system. Sections 2.3 through 2.5 address the sizing procedures for these landing gear components.

With the help of these dimensions and the landing gear disposition geometry of sub-section 2.8.1 it is now possible to identify the required attachment points to the airframe. The structural integration of the landing gear into the airframe is of major importance: if major additional structure is needed for the landing gear

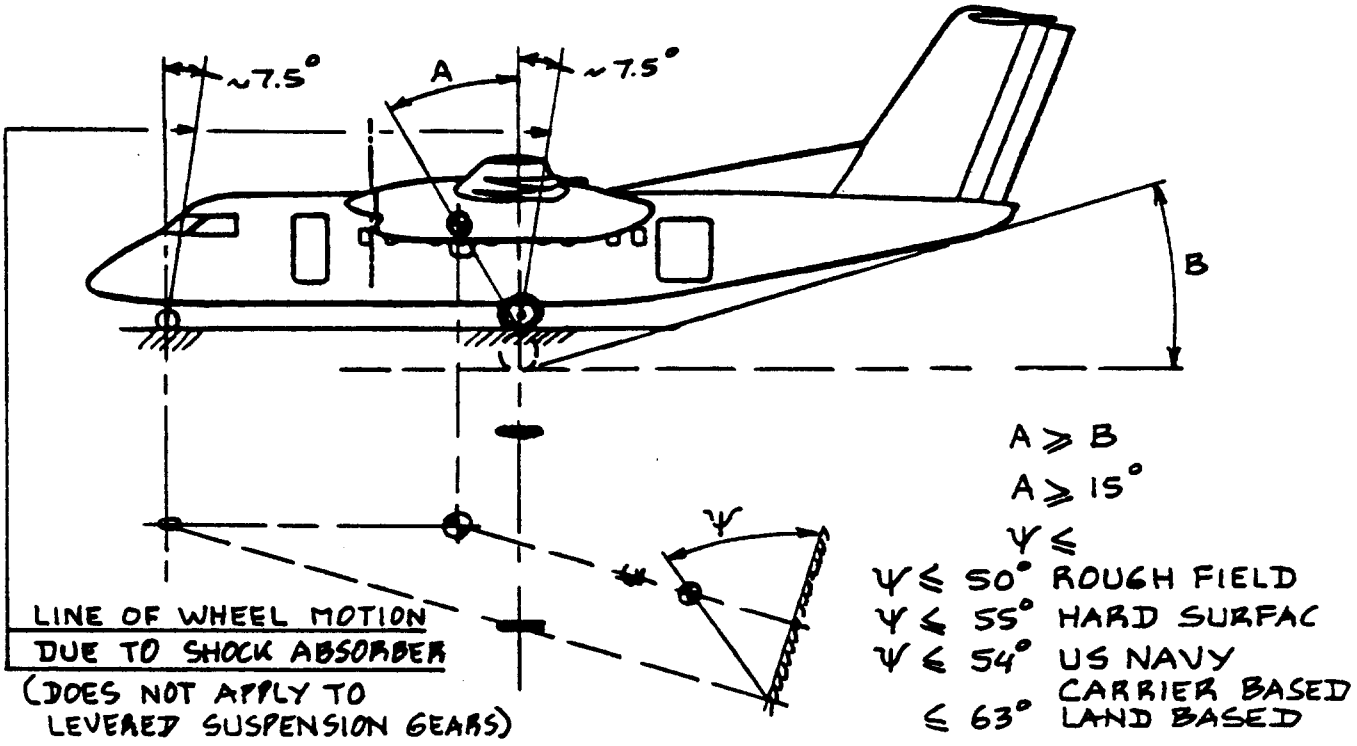

Figure 2.48a Tricycle Landing Gear Layout Requirements

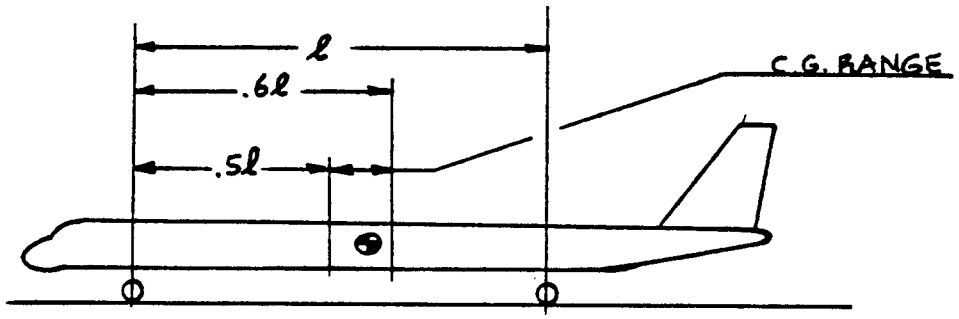

Figure 2.48b Tandem Landing Gear Layout Requirements

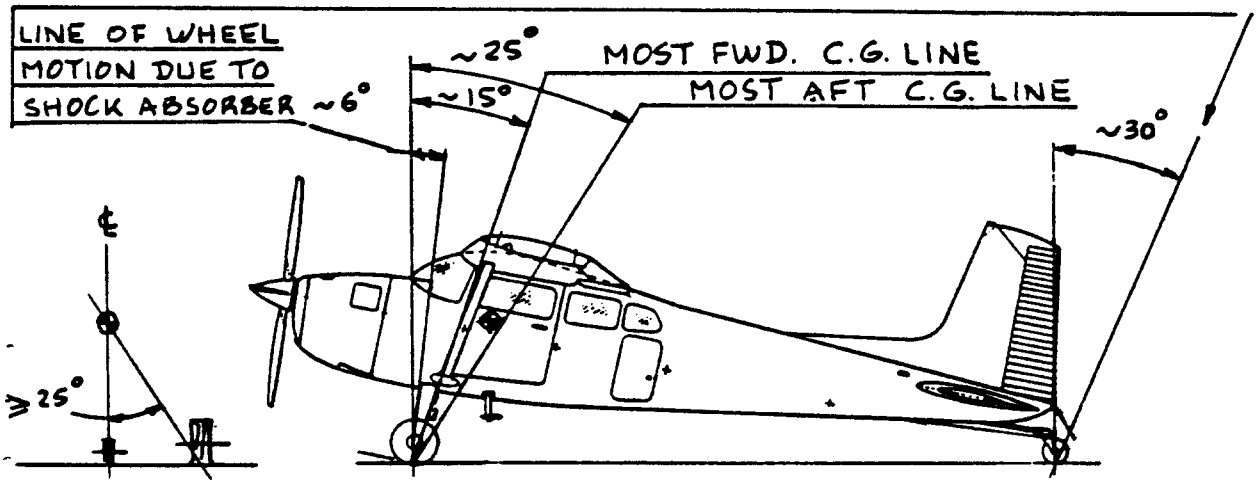

Figure 2.48c Tail Landing Gear Layout Requirements

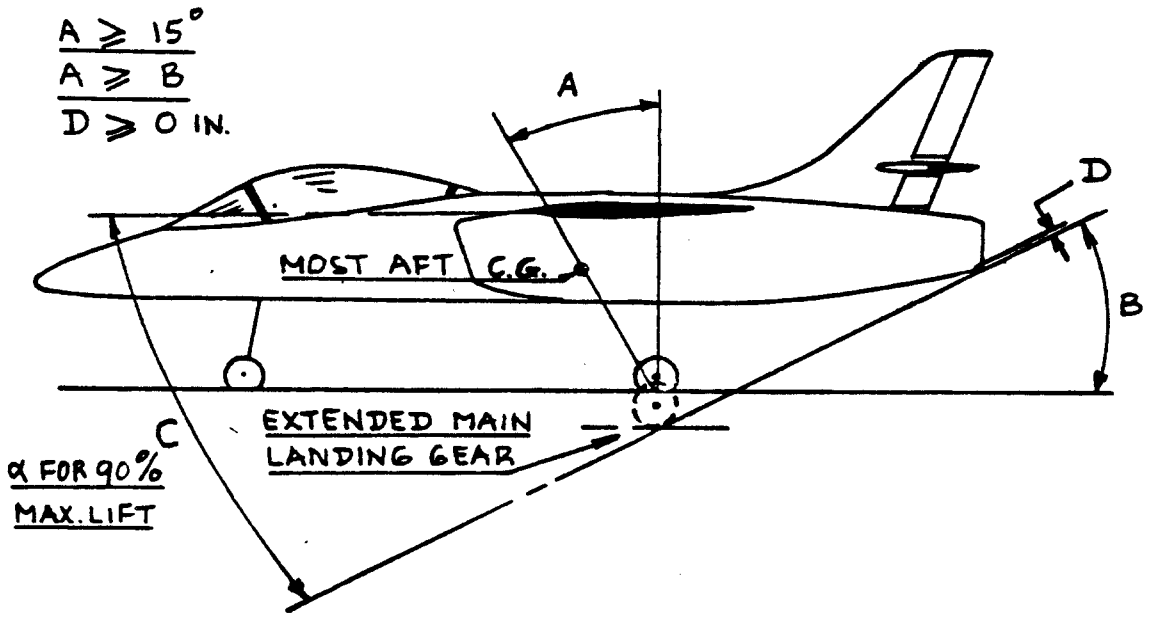

Figure 2.49 US Navy Landing Gear Layout Requirements

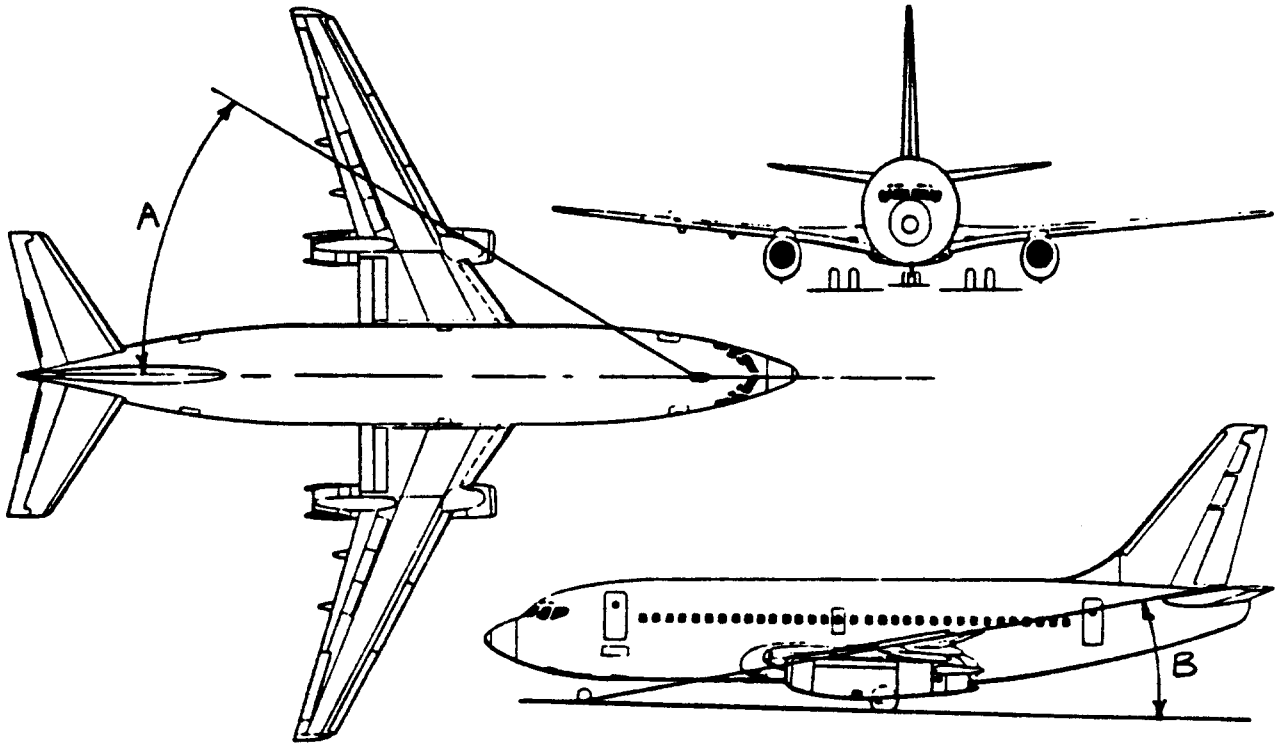

TYPE:	737-200	-300	757-200	L-1011	DC10-30	BAe-146-200
A	31°	32°	30°	43°	39°	33°
B	12°	10°	11°	11°	12°	21°

Figure 2.50 Critical Angles for FOD in Jet Engines

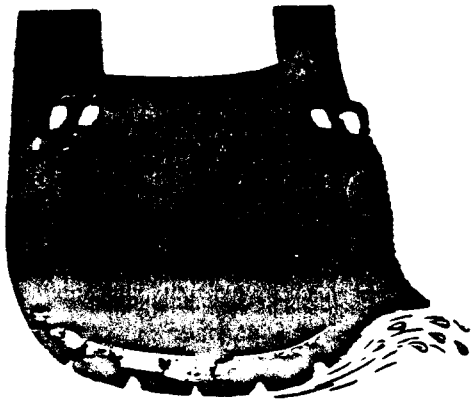

Figure 2.51a Example of a Chine Tire Application

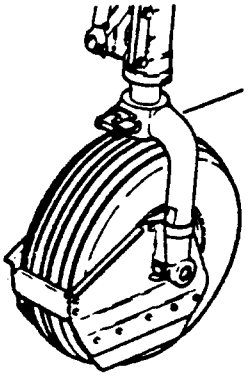

Figure 2.51b Example of a Splash Guard Application

Figure 2.52 Nose Gear Spray Pattern for the Boeing 767

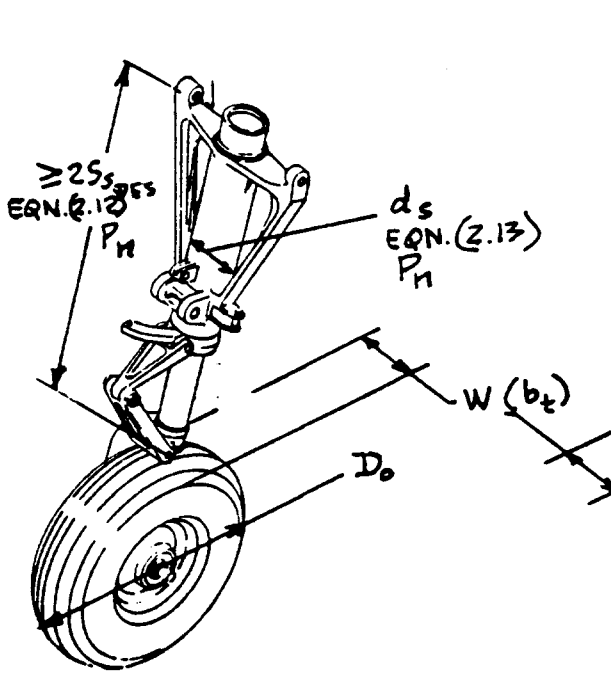

Figure 2.53 Summary of Important Dimensions of a Nose Gear

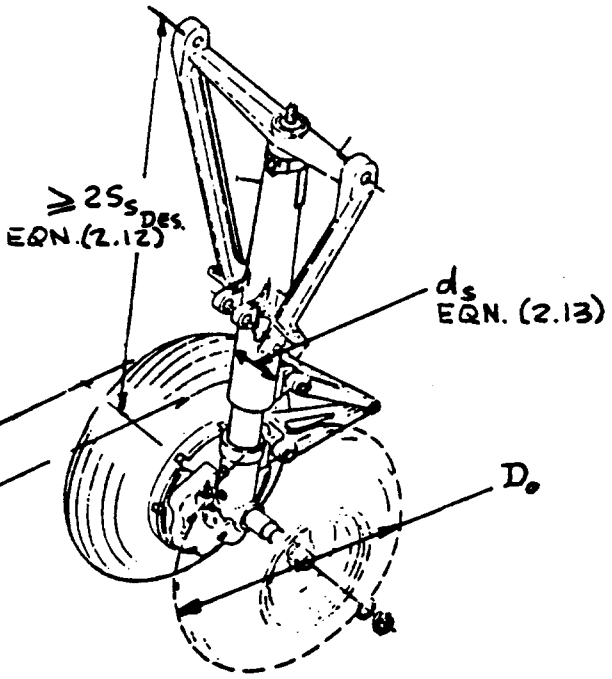

Figure 2.54 Summary of Important Dimensions of a Main Gear

attachments, the entire gear design should be reviewed.

Note: The reader should use the checklist of sub-section 2.8.3 to determine whether or not the proposed gear layout is satisfactory.

2.8.3 Landing Gear Layout Checklist

The reader is reminded again that a valid solution to a landing gear design problem cannot be claimed until ALL items in the following checklist have been addressed:

1. ALL geometric clearance and tip-over criteria are satisfied: See Chapter 9 in Part II and sub-section 2.8.1 in this part.

2. The proper tire size, shock absorber stroke and strut diameter have been determined: See Sections 2.3, 2.4 and 2.5 respectively.

3. The need for drag braces and side braces have been satisfied: See Section 2.1.

4. The structural attachment points for the gear should NOT require the introduction of significant additional structure.

5. Any 'spray' caused by the tires (particularly the nose gear) on wet or slushy runways must not enter the engine inlets. The spray (=FOD) angle criteria of Figure 2.50 must be met.

6. The gear can retract without interfering with other components of the airplane: the tire clearance requirements discussed in Section 2.4 must be met.

7. The retraction kinematics (to be discussed in Section 2.10) is feasible and does not require excessive actuator forces to retract or to lower.

Important Comment:

In Part II, Chapter 2, Step 9, the point is made that whether or not a 'valid' solution to the landing gear problem is obtained may well determine the viability of the entire airplane design.

2.9 STEERING, TURNRADII AND GROUND OPERATION

The purpose of this section is to show how steering during ground operations is accomplished. The material is organized as follows:

2.9.1 Steering systems

2.9.2 Turnradii and ground operation

2.9.1 Steering Systems

To operate airplanes on the ground it must be possible to 'steer' them. The steering feature used on most airplanes is a steerable nosegear or a steerable tailwheel. The steering capability in most airplanes is augmented by the use of differential braking on the main gear and in some cases by the use of differential thrust.

In very light airplanes, steering can be accomplished by a direct mechanical link from the rudder pedals. However, many light airplanes are equipped with a hydraulic type steering system. Section 2.11 contains a number of examples of light airplane nose gear installations with the steering system identified.

In the case of transport airplanes, nosegear steering requires a considerable force. This force is normally generated with the help of a hydraulic system. The hydraulic system itself receives its 'signal' to move from the rudder pedals and/or from a cockpit mounted 'steering tiller wheel'. Figure 2.55 shows an example of a nosegear steering system.

2.9.2 Turnradii and Ground Operation

It is essential that the airplane can be maneuvered on the ground without requiring excessive real estate. This is of particular importance to transport airplanes which need to maneuver in crowded terminal areas. The ground maneuvering capability of an airplane is normally expressed in terms of its minimum turn radius. This minimum turn radius is dependent on the location of the landing gears and on the nosewheel steering ability incorporated in the nose gear. Whther or not an airplane can turn about one main gear also influences its turnradius. Figures 2.56 and 2.57 illustrate the maneuvering capability of two typical jet transports.

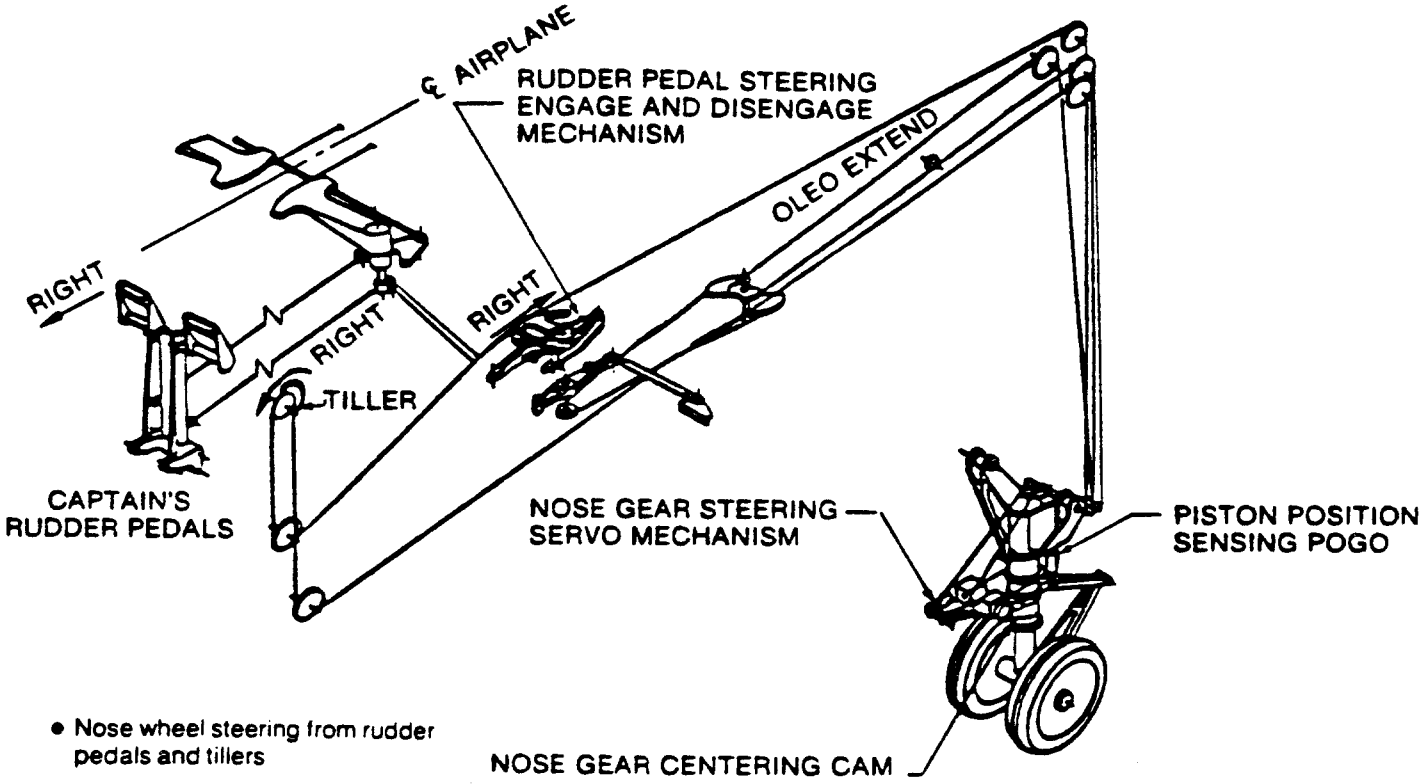

- Nose wheel steering from rudder pedals and tillers
- Steering authority – tiller, ± 65° rudder pedals, ± 16°
- Ground towing to ± 68° nose wheel angle without torque link disconnect

COURTESY: BOEING

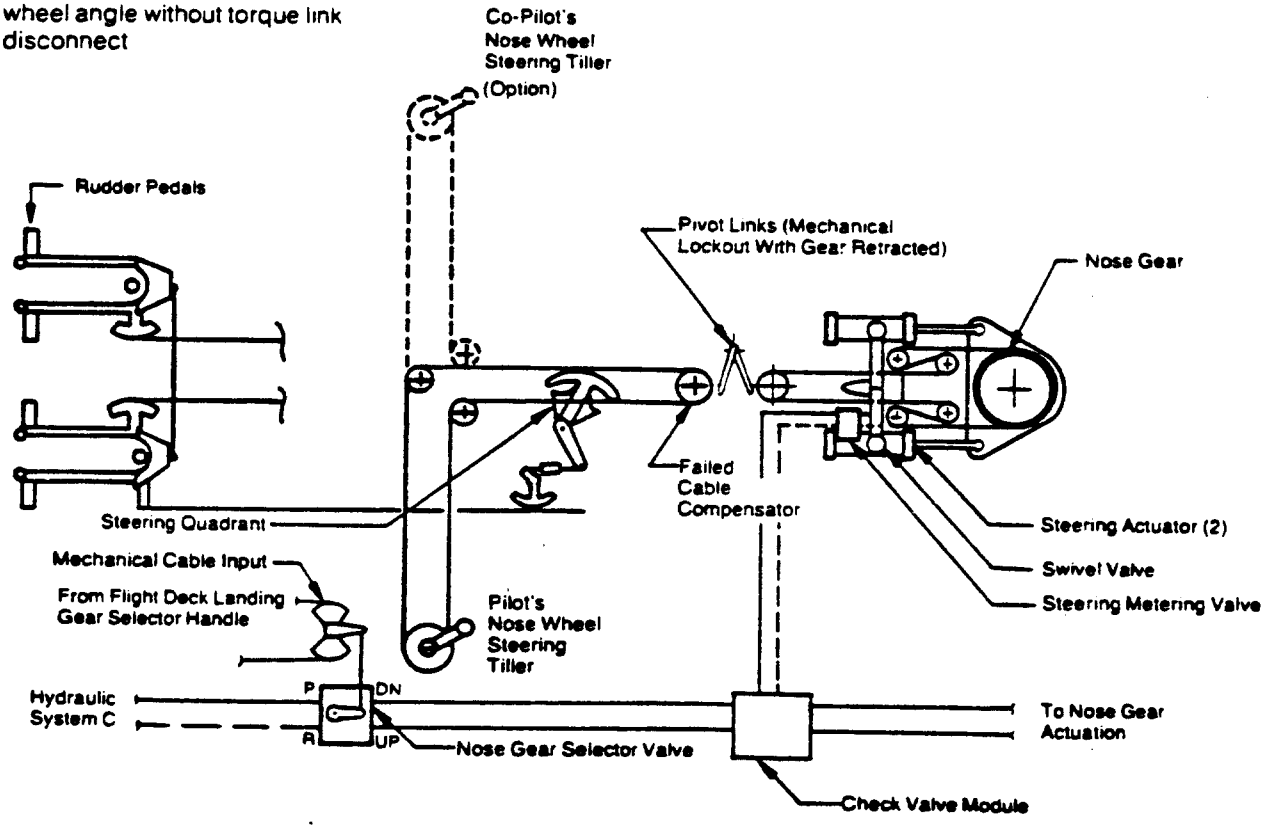

Figure 2.55 Boeing 767 Nose Gear Steering System

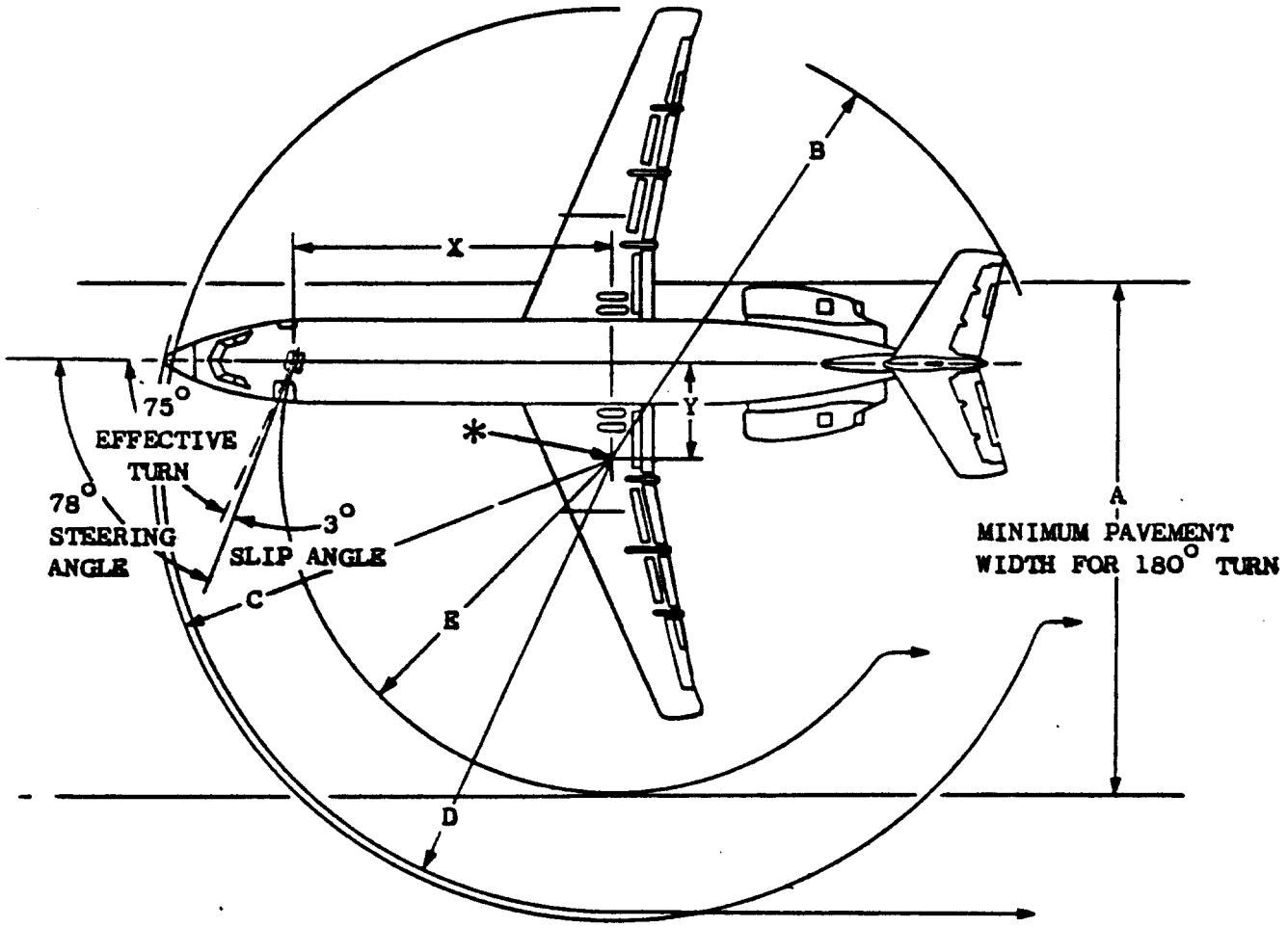

NOTE: 78° IS MAXIMUM POWERED STEERING ANGLE.
3° SLIPPAGE HAS BEEN ASSUMED TO OCCUR GIVING AN EFFECTIVE ANGLE OF 75°.

COURTESY:
BRITISH AEROSPACE

NOTE: * THEORETICAL CENTRE OF TURN AT MINIMUM TURNING RADIUS SLOW CONTINUOUS TURNING APPROXIMATELY IDLE THRUST ON ALL ENGINES. NO DIFFERENTIAL BRAKING.

DIMENSIONS IN FT / METRES

MODEL	EFFECTIVE TURN ANGLE	X	Y	A	B	C	D	E
400	75°	33 / 10.06	8 / 2.44	53 / 16.15	50 / 15.24	50 / 15.24	54 / 16.46	34 / 10.36
475	75°	33 / 10.06	8 / 2.44	53 / 16.15	50 / 15.24	50 / 15.24	56 / 17.07	34 / 10.36
500	75°	41 / 12.50	8 / 2.44	64 / 19.50	56 / 17.07	59 / 17.98	59 / 17.98	43 / 13.11

Figure 2.56 Ground Turning Capability of a BAC 111

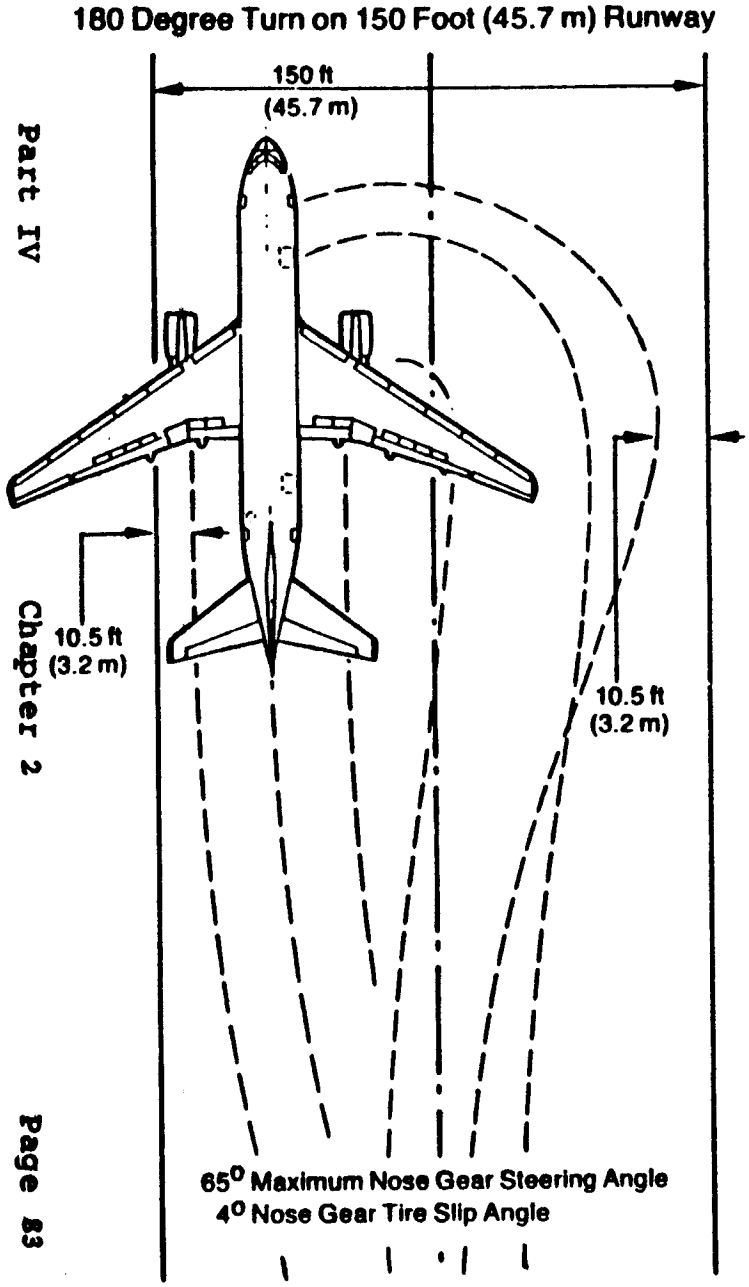

		767-200	727-200	707-320B	DC-8-63	DC-10-10
Wingtip Clearance - A	ft	109.8	71.0	112.0	99.5	112.4
	(m)	(33.5)	(21.6)	(34.1)	(30.3)	(34.3)
Nose Clearance - B	ft	84.7	79.5	84.0	96.0	104.6
	(m)	(25.8)	(24.2)	(25.6)	(29.3)	(31.9)
Wing Gear Clearance - C	ft	46.5	25.3	47.1	33.8	49.7
	(m)	(14.2)	(7.7)	(14.4)	(10.3)	(15.1)
Wing Clearance - D	ft	97.4	80.0	96.0	104.3	101.0
	(m)	(29.7)	(24.4)	(29.3)	(31.8)	(30.8)
Nose Gear Clearance - E	ft	72.3	66.5	69.4	81.5	79.5
	(m)	(22.0)	(20.3)	(21.2)	(24.8)	(24.2)
Minimum Turn Center - X	ft	28.8	13.5	34.0	21.5	29.6
	(m)	(8.8)	(4.1)	(10.4)	(6.6)	(9.0)
Min Width for 180° Turn - Y	ft	118.8	91.8	116.5	115.3	129.2
	(m)	(36.2)	(28.0)	(35.5)	(35.1)	(39.4)
Max Nose Gear Steering Angle	Deg	65	78	50	74.5	68

COURTESY : BOEING

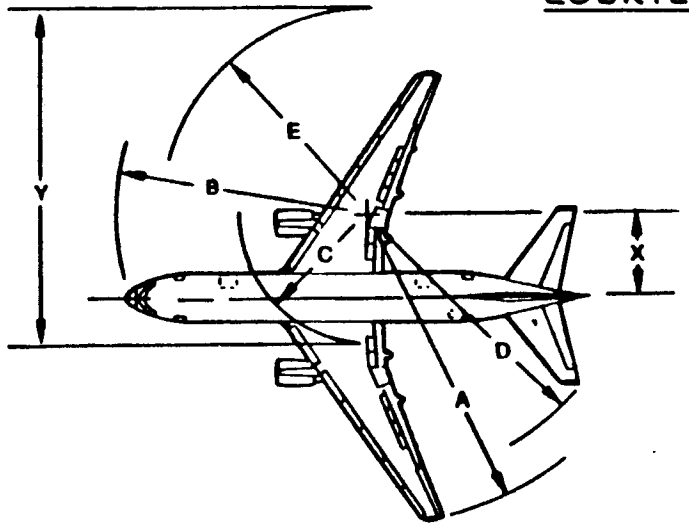

Figure 2.57 Ground Turning Capability of a Boeing 767 Compared to Other Jet Transports

2.10 RETRACTION KINEMATICS

In this section some fundamental principles of the operation of retraction mechanisms are discussed. Actual examples of landing gear retraction methods are provided. The material is presented as follows:

2.10.1 Fundamentals of retraction kinematics
2.10.2 Location of the retraction actuator
2.10.3 Special problems in landing gear retraction
2.10.4 Examples of landing gear retraction methods

2.10.1 Fundamentals of Retraction Kinematics

References 1 and 2 contain detailed discussions of a large number of kinematic possibilities for landing gear retraction. A number of these will be discussed.

Most landing gear retraction schemes are based on a version of so-called multiple bar linkages. For a detailed theoretical treatment on the subject of multiple bar mechanisms, References 12 and 13 are suggested.

To determine the feasibility of a proposed landing gear retraction scheme, so-called 'stick diagrams' are drawn. In the following, a number of retraction schemes are discussed using the stick diagram method.

Figures 2.58 through 2.60 show landing gear retraction schemes with a so-called floating link.

In Figure 2.58 the main gear strut (AC) rotates about point A. The drag strut BE has a pin joint at point D so that BD forms the floating link and link DE rotates about point E. Note that points A and E are fixed points in the airframe. The retraction cylinder (not shown in Figure 2.58) could be attached anywhere between points D and E. In the design of this type of linkage care must be taken, that landing loads do not collapse the drag strut BE at point D. Since the main direction of landing loads are in the CA direction, this does not represent a major problem.

In Figures 2.59 and 2.60 the main gear strut BD itself is the floating link. The drag strut CE is one piece. Points A and E are fixed points in the airframe. The retraction cylinder (not shown) can be attached anywhere between points A and B. Note that the gear can be made to go up almost vertically with a system as shown in Fig.2.59.

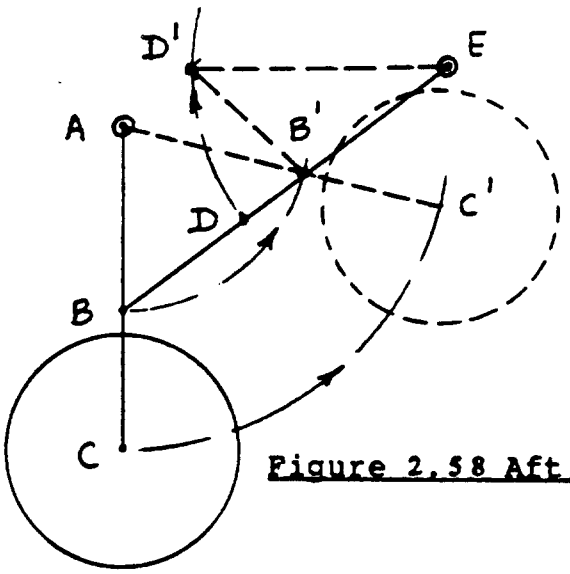

A AND E ARE FIXED POINTS IN AIRFRAME

Figure 2.58 Aft Retracting Gear with Floating Link

A AND E ARE FIXED POINTS IN AIRFRAME

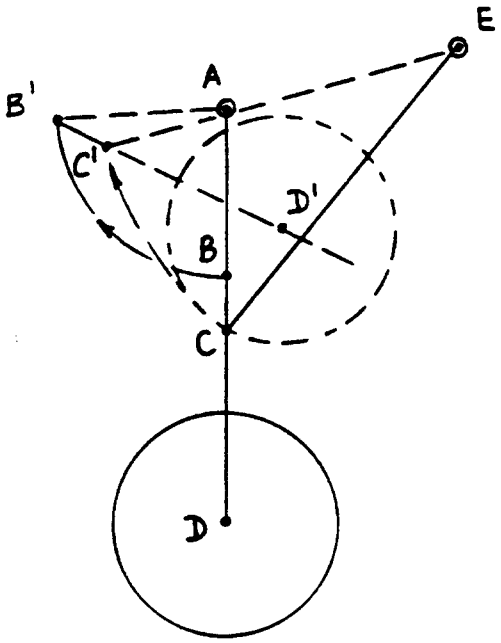

Figure 2.59 Upward Retracting Gear with Floating Link

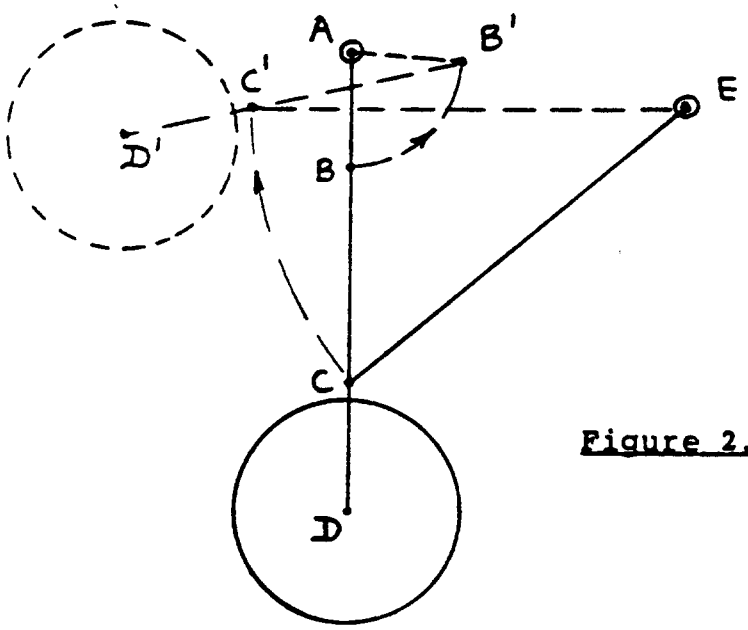

A AND E ARE FIXED POINTS IN AIRFRAME

Figure 2.60 Forward Retracting Gear with Floating Link

In the design of this type of linkage care must be taken that landing loads do not collapse struts AB and BD at point B. Since the main landing load is in the direction of DB this can be a major design problem. The system of Figure 2.58 is therefore preferred.

Observe that the system of Fig.2.60 allows the gear to 'free drop': aerodynamic drag helps to lower the gear.

Figures 2.61 through 2.63 represent solutions with a so-called 'slot'. From a kinematic viewpoint, a slot can be interpreted as a system for which the link AB is infinitely long. The slot as well as one other point are fixed in the airframe. A major disadvantage of slots is that mud, snow and ice can accumulate and cause the system to be prone to wear and tear or to be unreliable.

For more kinematic options in landing gear retraction, References 1 and 2 should be consulted.

2.10.2 Location of the Retraction Actuator

To retract a landing gear, so-called retraction actuators are used. Retraction actuators are normally of the hydraulic or electro-mechanical type. The retraction actuator can be thought of as a link of variable length. Figures 2.64 and 2.65 show examples of retraction actuators in the 'up' and 'down' position.

In deciding where to locate the retraction actuator, the following location criteria must be kept in mind:

Location Criterion 1: The retracted actuator length can't be less than one half the extended actuator length.

Location Criterion 2: The force-stroke diagram of the retraction actuator should not be 'peaky'.

To determine a satisfactory location for the retraction cylinder the following steps are suggested:

Step 1: Draw a 'stick diagram' of the proposed retraction scheme. This stick diagram should contain as a minimum the information depicted in Figs 2.58 - 2.63.

Step 2: Make certain that the 'fixed points' in the proposed stick diagram correspond to points of feasible structure on the airplane.

Step 3: Construct a number of intermediate landing gear positions in the stick diagram. See Figure 2.66a.

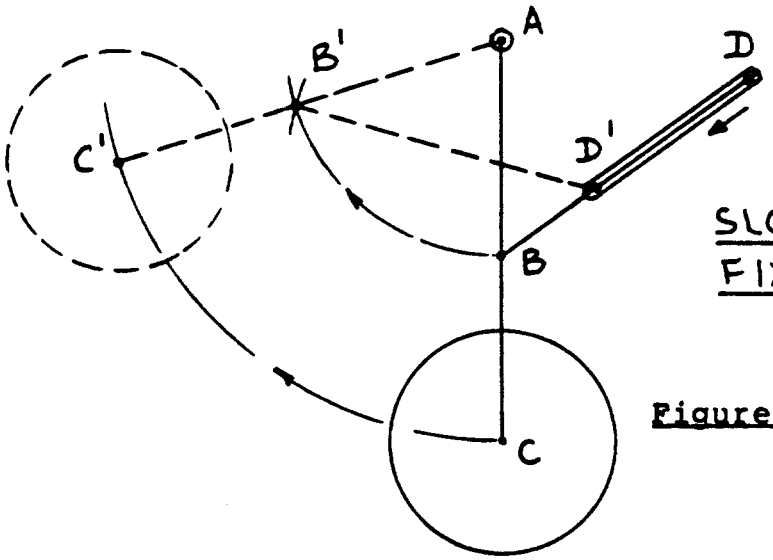

SLOT DD' AND A ARE FIXED IN AIRFRAME

Figure 2.61 Forward Retracting Gear with Angled Slot

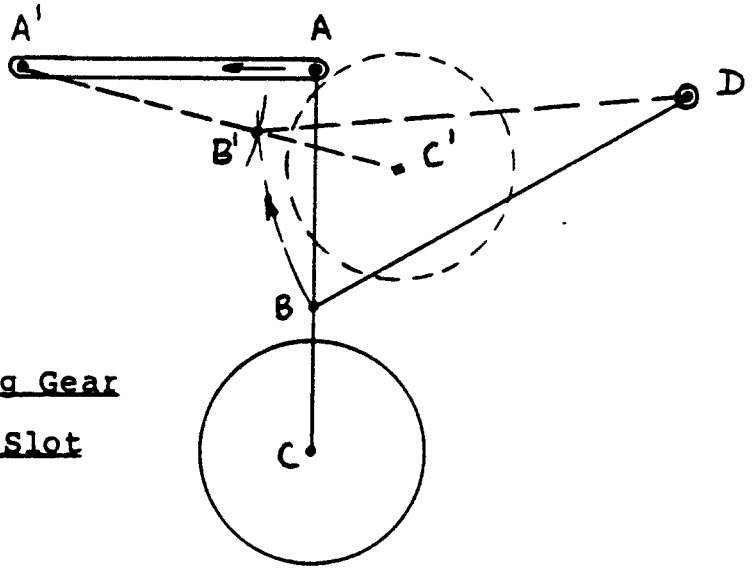

SLOT AA' AND D ARE FIXED IN AIRFRAME

Figure 2.62 Upward Retracting Gear with Horizontal Slot

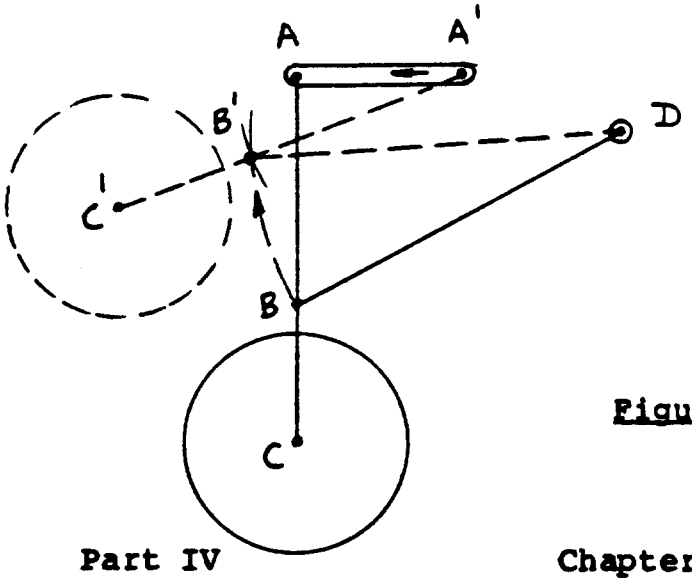

SLOT AA' AND D ARE FIXED IN AIRFRAME

Figure 2.63 Forward Retracting Gear with Horizontal Slot

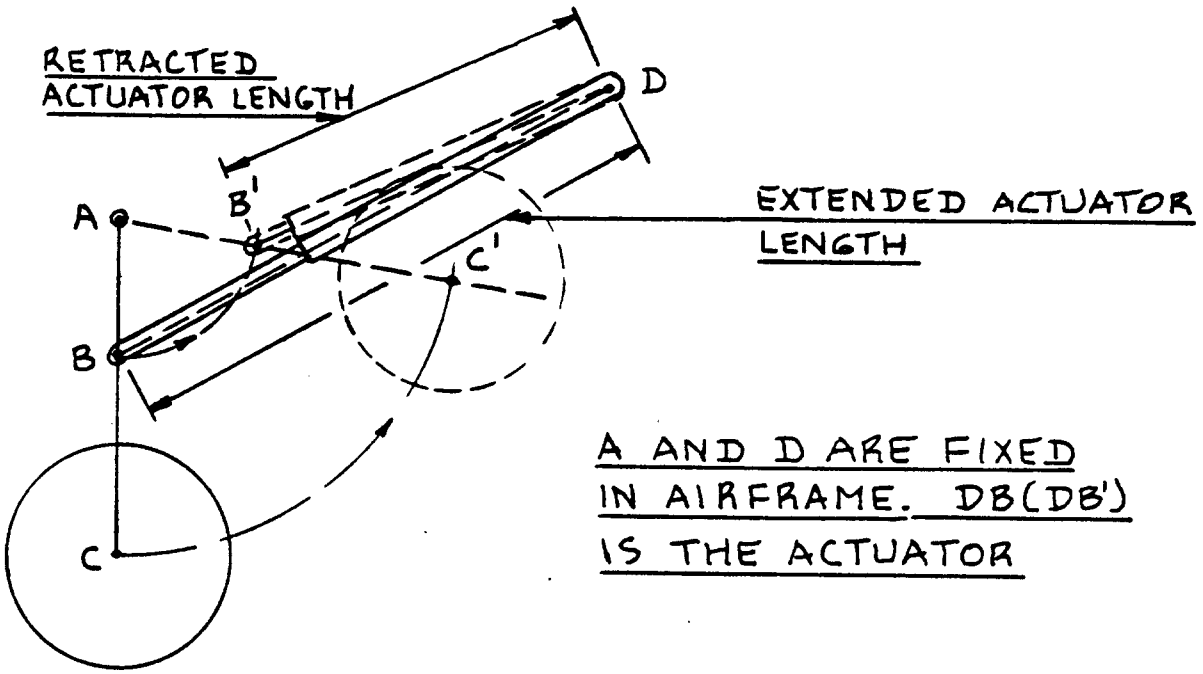

Figure 2.64 Retraction Actuator as Part of the Drag Brace

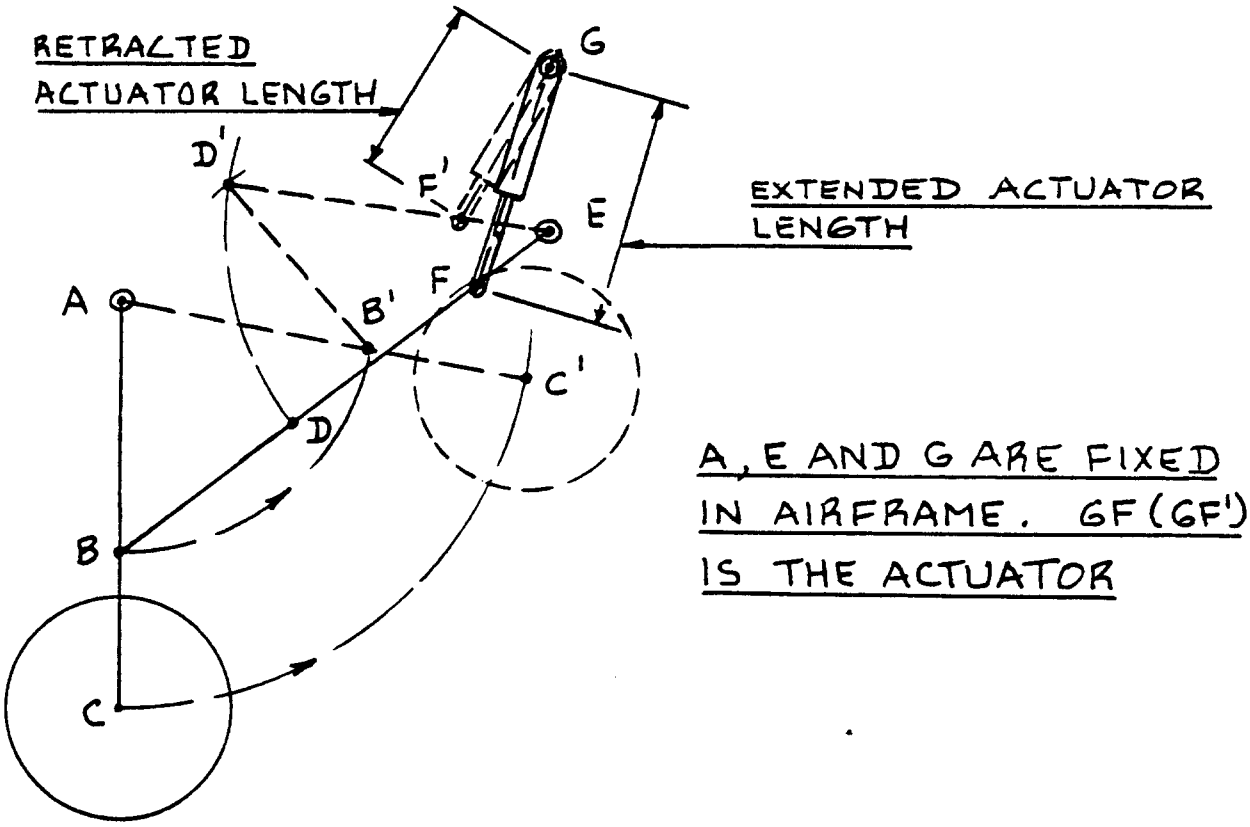

Figure 2.65 Retraction Actuator with Folding Main Strut

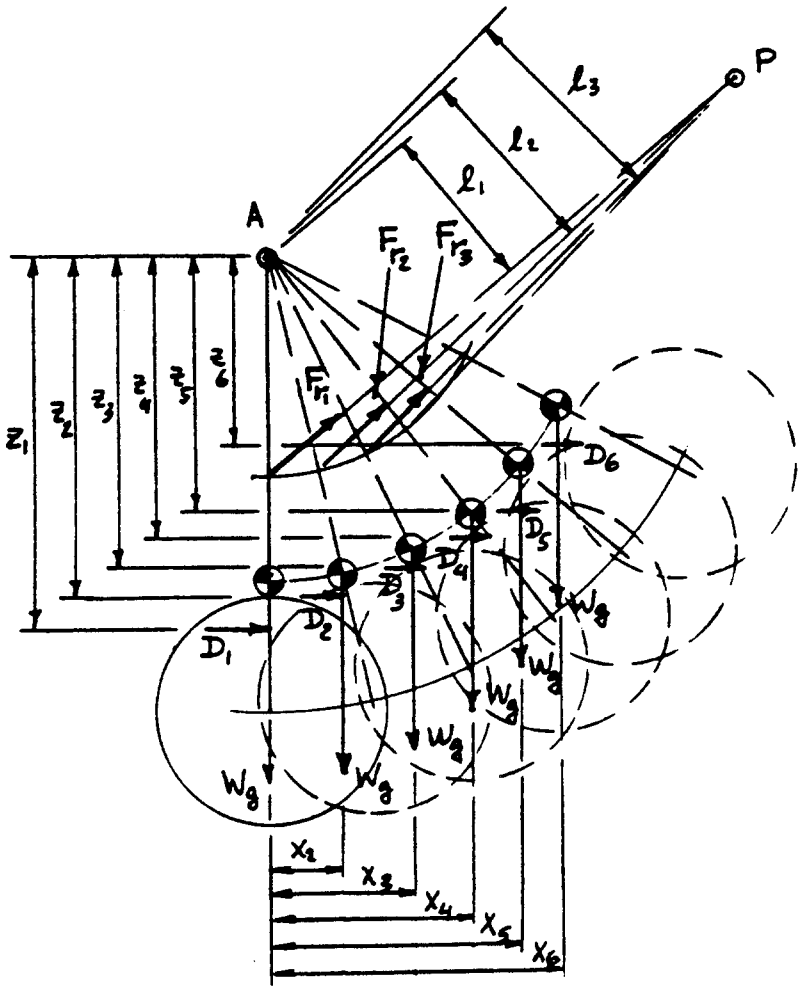

Figure 2.66a Landing Gear in Retraction Process

P AND A ARE FIXED POINTS IN AIRFRAME

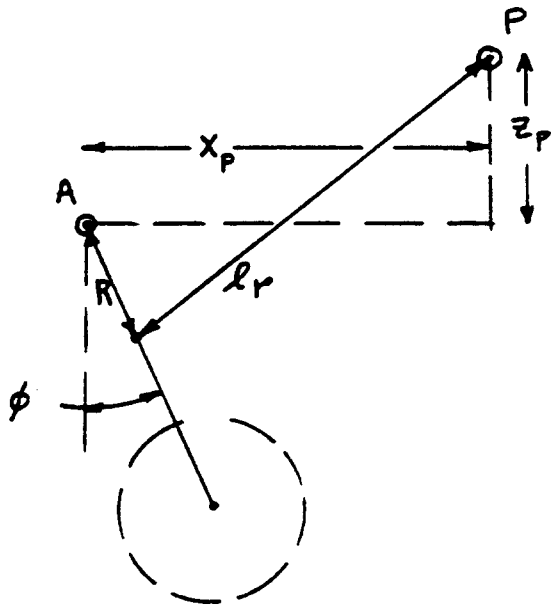

Figure 2.66b Definition of Retraction Actuator Length

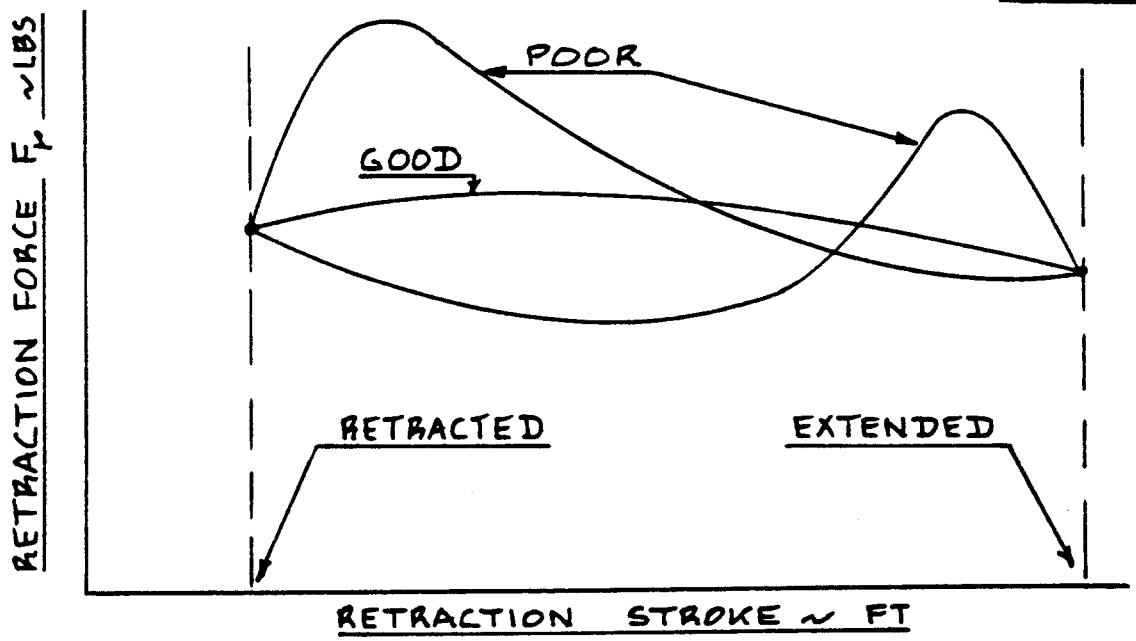

Figure 2.67 Good and Poor Force-Stroke Diagrams

Step 4: Select a location for the retraction actuator and make certain that location criterion 1 is satisfied before moving on to Step 5.

Step 5: Indicate in the stick diagram the forces which act on the landing gear during retraction. These forces are normally the weight of the gear and the aerodynamic drag force. Figure 2.66a shows these forces: W_g for the gear weight and D_i for the gear drag.

Notes: 1. The gear weight, W_g may be determined from the Class II weight estimating methods of Part V.

2. The gear drag, D_i may be determined from the gear drag estimating methods of Part VI.

Figure 2.66a shows these forces properly drawn in.

Step 5: Compute the retraction force, F_{r_i} from:

$$F_{r_i} = (W_g x_i - D_i z_i)/l_i \qquad (2.15)$$

Moment arms x_i, z_i and l_i are defined in Fig.2.66a.

The retraction force F_{r_i} must be plottes versus the retraction stroke (change in length of the retraction cylinder). The retraction cylinder length, l_r may be computed from:

$$l_r = \{(z_p + R\cos\phi)^2 + (x_p - R\sin\phi)^2\}^{1/2} \qquad (2.16)$$

Figure 2.66b defines the quatities R, z_p and x_p. The reader must realize that the form taken by Eqns(2.15) and (2.16) will be different for each gear layout.

Step 6: To satisfy location criterion 2, the plot of retraction force, F_r versus retraction length, l_r must not contain any major fluctuations in force (must not be 'peaky'). Figure 2.67 shows an example of a good and a poor force-stroke diagram.

Note: The retraction force/stroke diagram does not contain any information about the time needed to retract or to extend the gear. Table 2.19 summarizes the allowable 'retract' and 'extend' times for landing gears.

Table 2.19 Landing Gear Operating Times

Type of retraction and extension	Temperature	Max. time to extend and lock gear	Max. time to retract and lock gear
Power operated	above -20°F	15 sec.	10 sec.
	from -65°F to -20°F	30 sec.	10 sec.
	Note: The gear must be retracted BEFORE the airplane reaches 75 percent of the gear placard speed at maximum forward acceleration		
Manually operated	above -20°F	15 sec.	30 sec.
	from -65°F to -20°F	30 sec.	60 sec.
	Note: The power required to operate the system must NOT exceed 3000 ftlbs/min. and the force required on the operating handle shall NOT exceed 50 lbs.		

Note: For multi-engine airplanes these requirements must be met with the critical engine inoperative.

These requirements apply to military and civilian airplanes

Examples of extension and retraction times are:

Airplane	Extend	Retract	Airplane	Extend	Retract
A-10	6-9	6-9	F-5	6	6
			F-100	6-8	6-8
B-52	10-12	8-10	F-105	5-9	4-8
B-66	8	10	F-111	26	18
C-5	20	20	T-37	8	10
C-123	6	9	T-38	6	6
C-130	19	19			
C-135	10	10			

These times together with the force/stroke diagram determine the power required for gear retraction.

2.10.3 Special Problems in Gear Retraction

The examples of retraction kinematics illustrated sofar were extremely simple. It is not always possible to use such simple methods. In many landing gear applications it is necessary to use additional kinematic features to make retraction possible. Examples are:

1. Wheel rotates relative to the strut while retracting.

2. Main strut must shorten while retracting.

3. Bogie rotates relative to the strut while retracting.

4. Tandem gears sometimes must retract synchronously.

Figure 2.68 shows examples of a retraction scheme where the wheel rotates 90 degrees while retracting. This scheme is useful when the 'vertical' volume for receiving the tire is limited. Note that an additional link is required to accomplish this.

Figure 2.69 shows an example of a main strut which must 'shorten' while retracting. This scheme is used when the 'horizontal' volume for receiving the gear is limited. Additional links are needed to accomplish this.

Figure 2.70 shows examples of a 'folding' bogie in the case of a four-wheel landing gear. In jet transports this is often used to prevent having to reroute major structural components. Note that an additional actuator is needed in cases a) and b) but not in case c).

Figure 2.71 is an illustration of a main landing gear consisting of two units in tandem. These units retract in a synchronous manner.

2.10.4 Examples of Landing Gear Retraction Methods

Figures 2.72 through 2.84 are presented to illustrate a variety of solutions to retraction problems which are in use. Note the so-called 'tilted' pivot used in retracting landing gears into fuselages: Figures 2.72b, 2.80 and 2.81 are typical examples. This method is most often used in fighters.

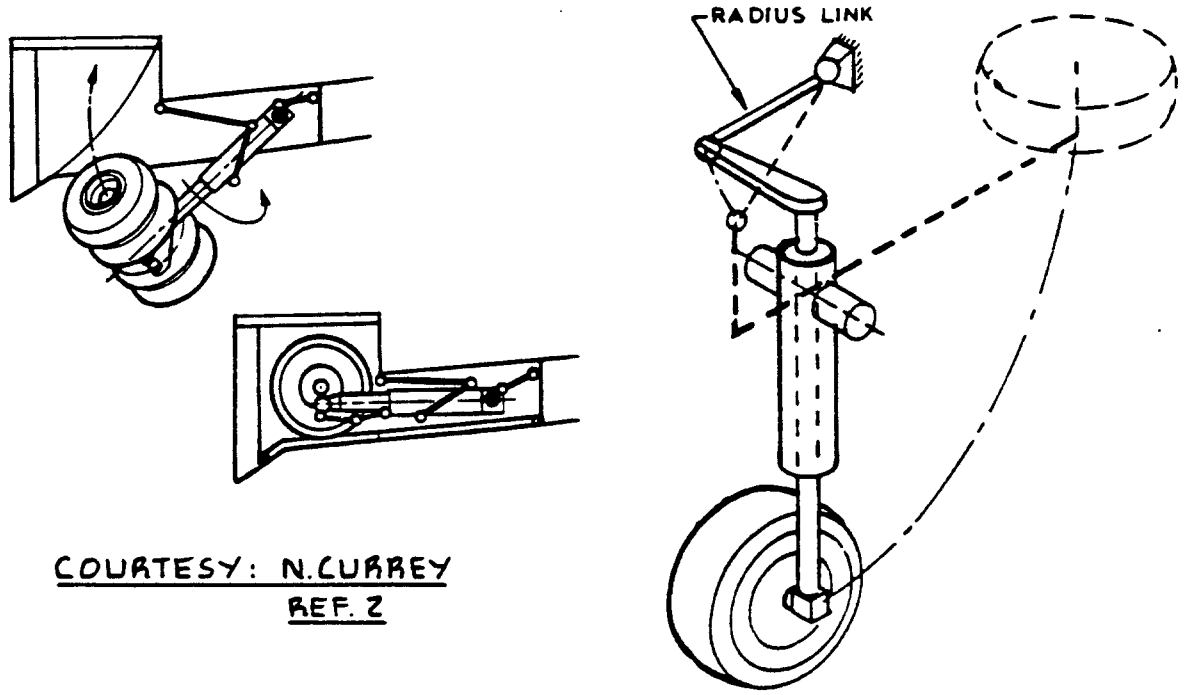

COURTESY: N.CURREY
REF. 2

Figure 2.68 Examples of Wheels Rotating Relative to Strut During Retraction

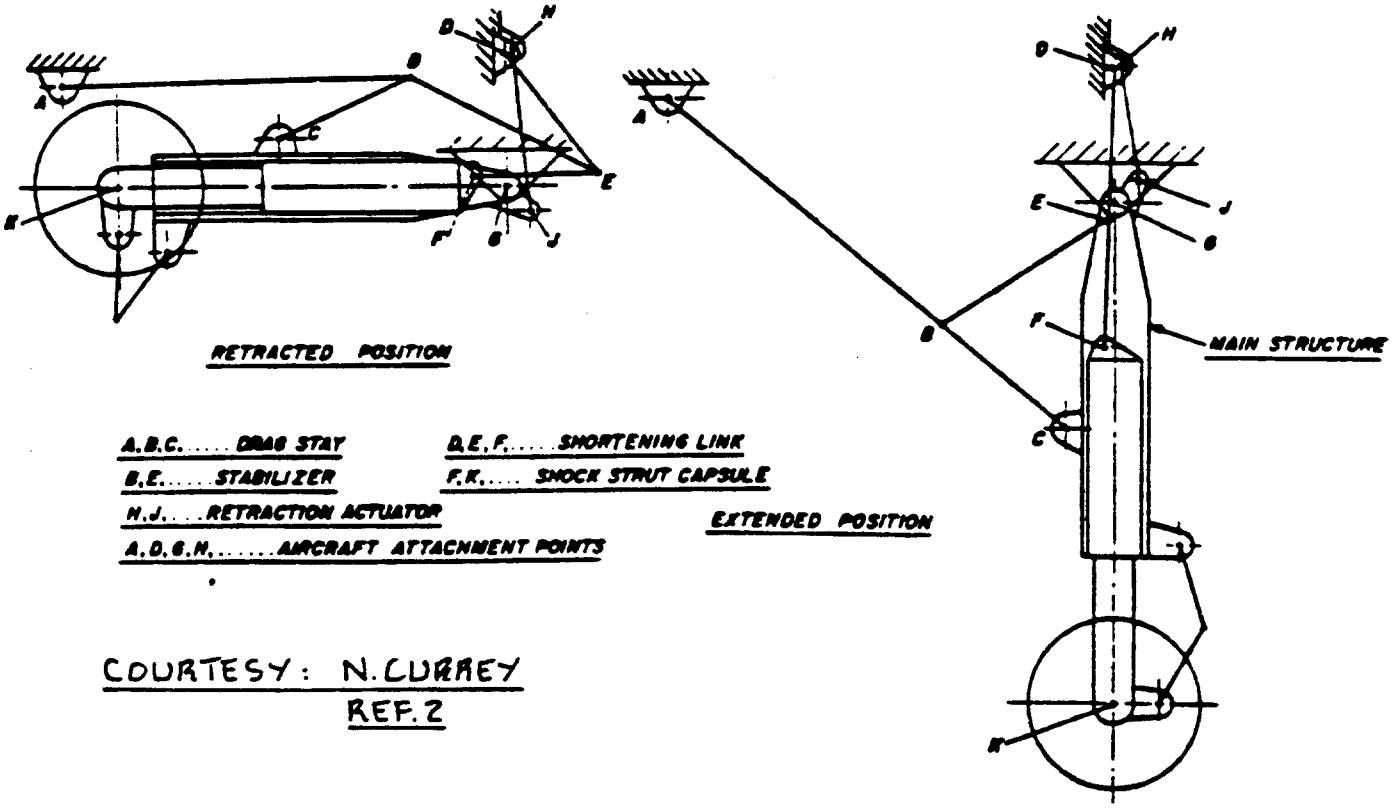

COURTESY: N.CURREY
REF. 2

Figure 2.69 Example of Strut Shortening During Retraction

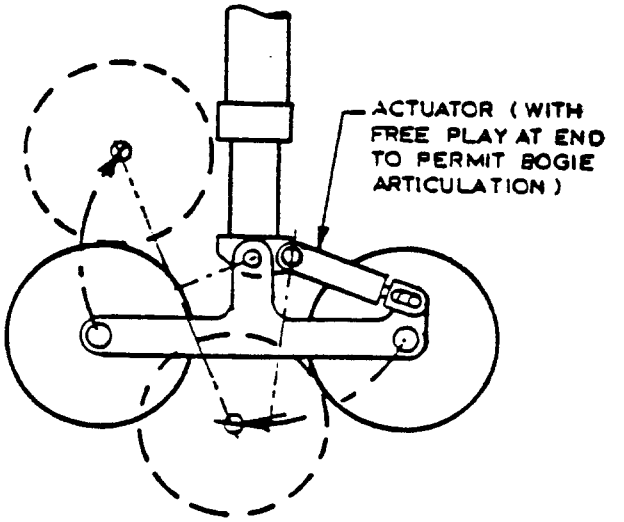

COURTESY:
N. CURREY
REF. 2

Figure 2.70a Partial Bogie Folding During retraction

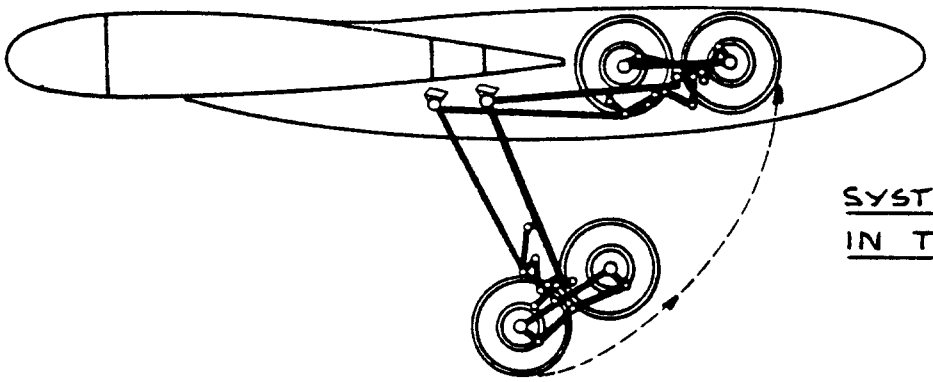

SYSTEM USED
IN Tu 134

Figure 2.70b Bogie Reversal During Retraction

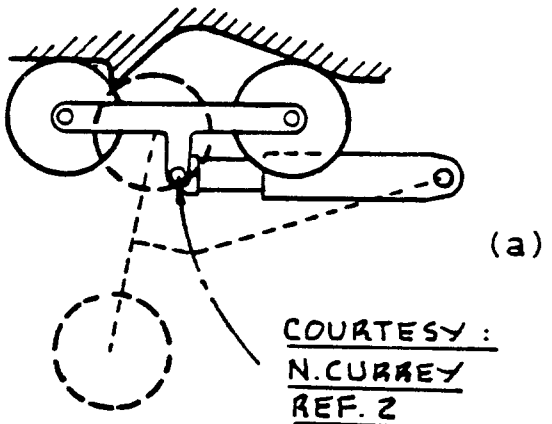

(a)

COURTESY:
N. CURREY
REF. 2

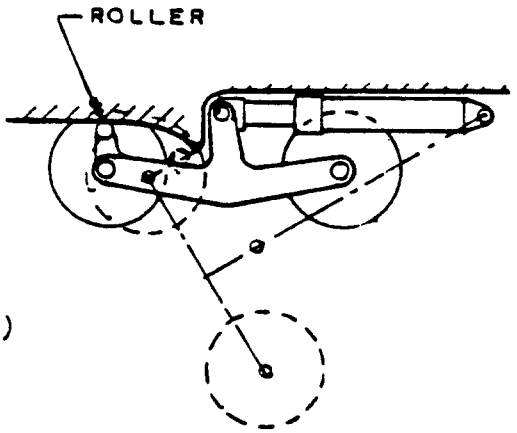

(b)

Figure 2.70c Bogie Folding Using Ramps

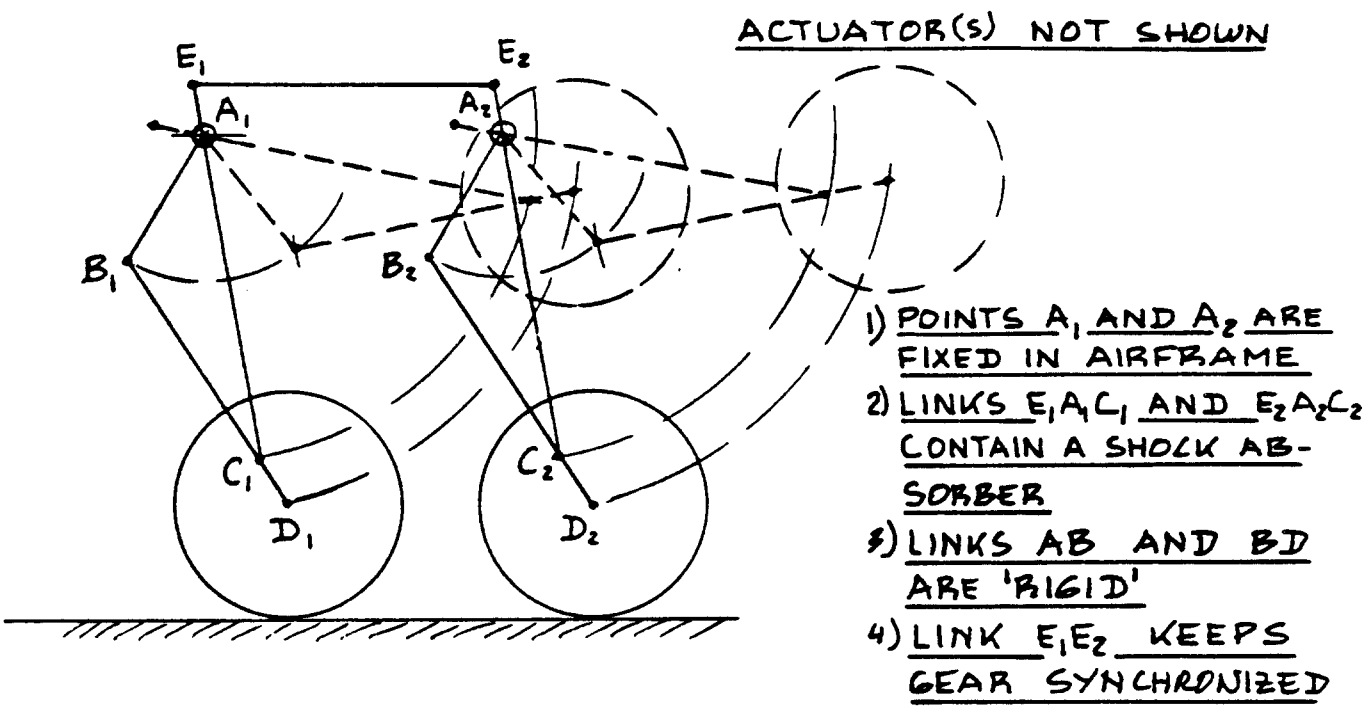

Figure 2.71 Tandem Gear Retraction Example

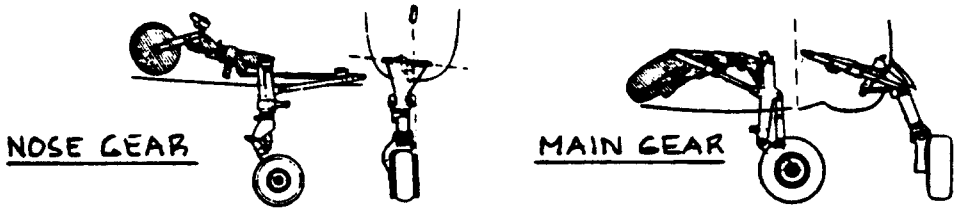

Figure 2.72 Gear Retraction: DBD Alphajet Trainer

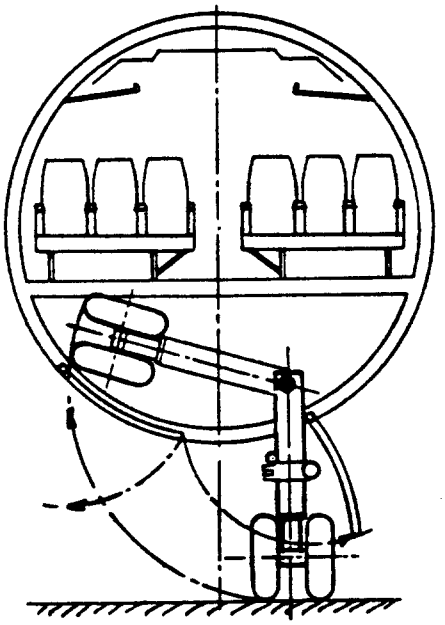

Figure 2.73 Sidewise Nosegear Retraction: DH 121 Trident

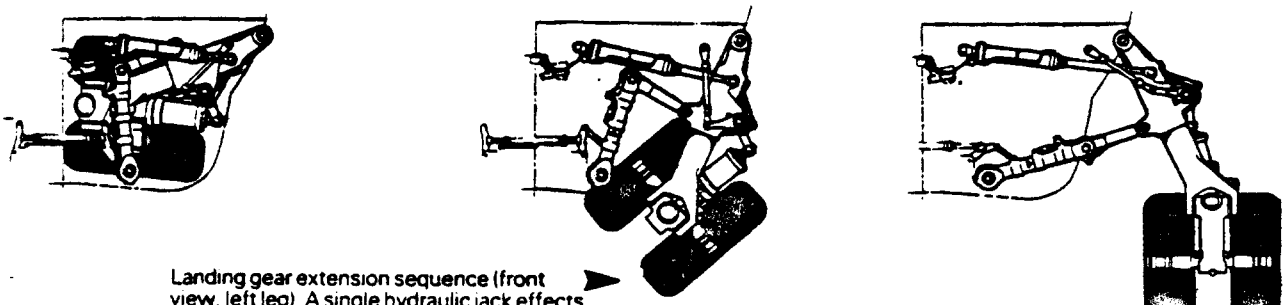

Landing gear extension sequence (front view, left leg). A single hydraulic jack effects extension/retraction of each leg; there is thus no jack sequencing. When viewed from rear, locking/bracing geometry and ease of oleo removal are clear.

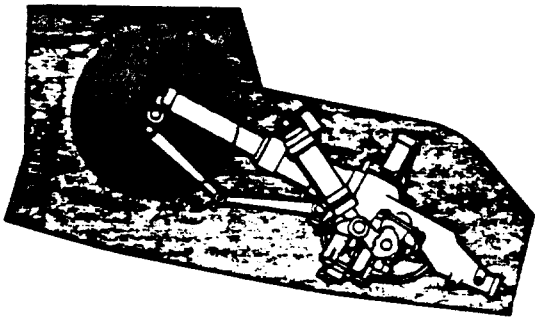

As with main gear, nose gear actuation is by a single jack with mechanically linked doors. Photo shows how closed doors keep nosewheel bay clean.

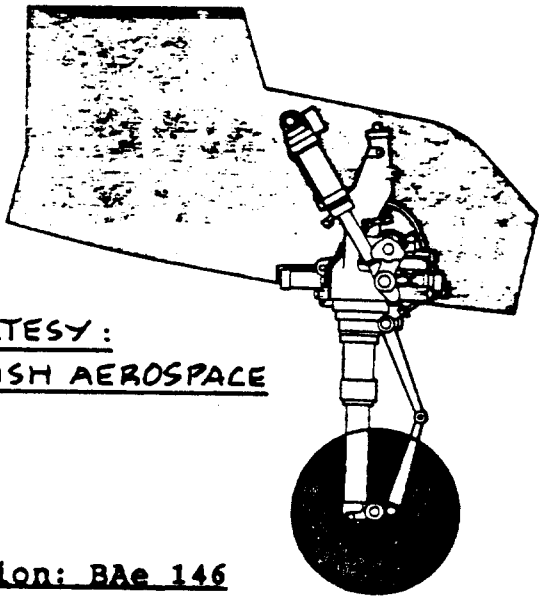

COURTESY:
BRITISH AEROSPACE

Figure 2.74 Gear Retraction: BAe 146

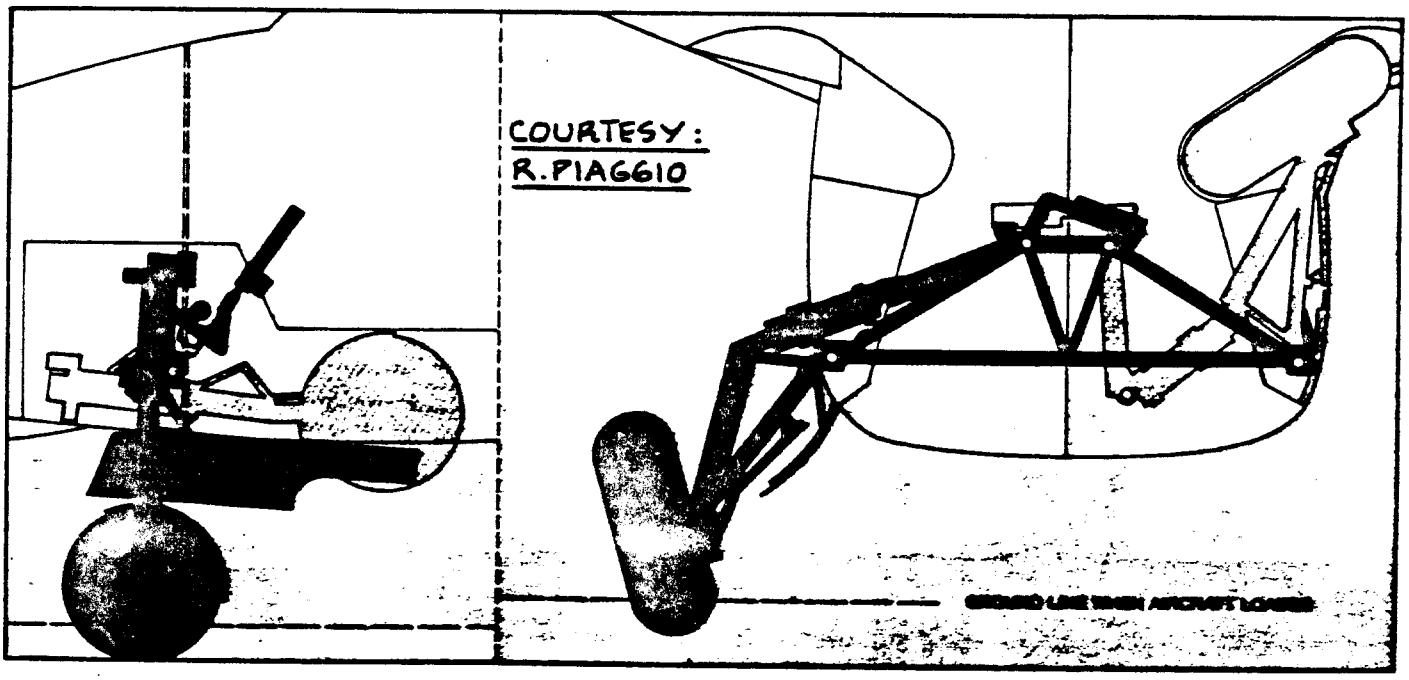

COURTESY:
R.PIAGGIO

Figure 2.75 Gear Retraction: Piaggio P.166-DL3

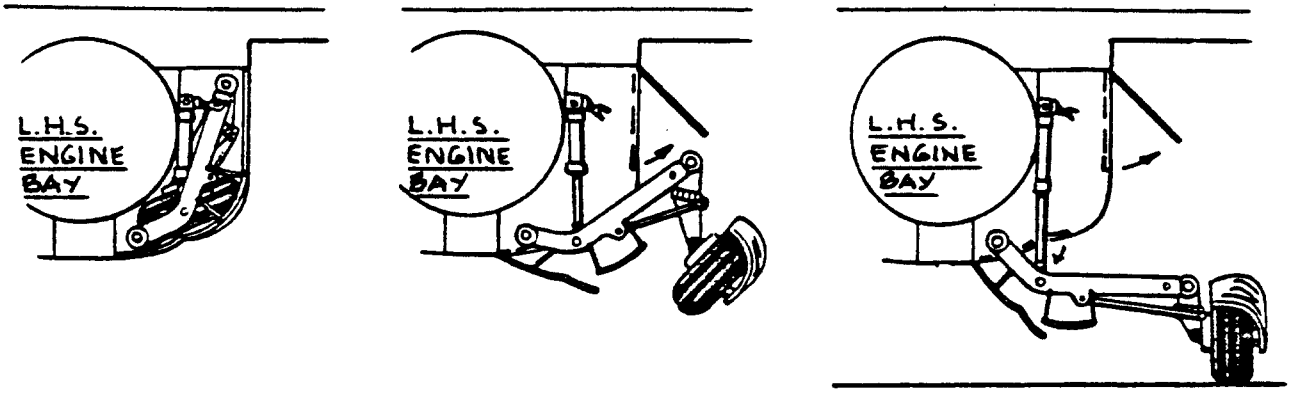

Figure 2.76 Gear Retraction: Mig-23 Flogger

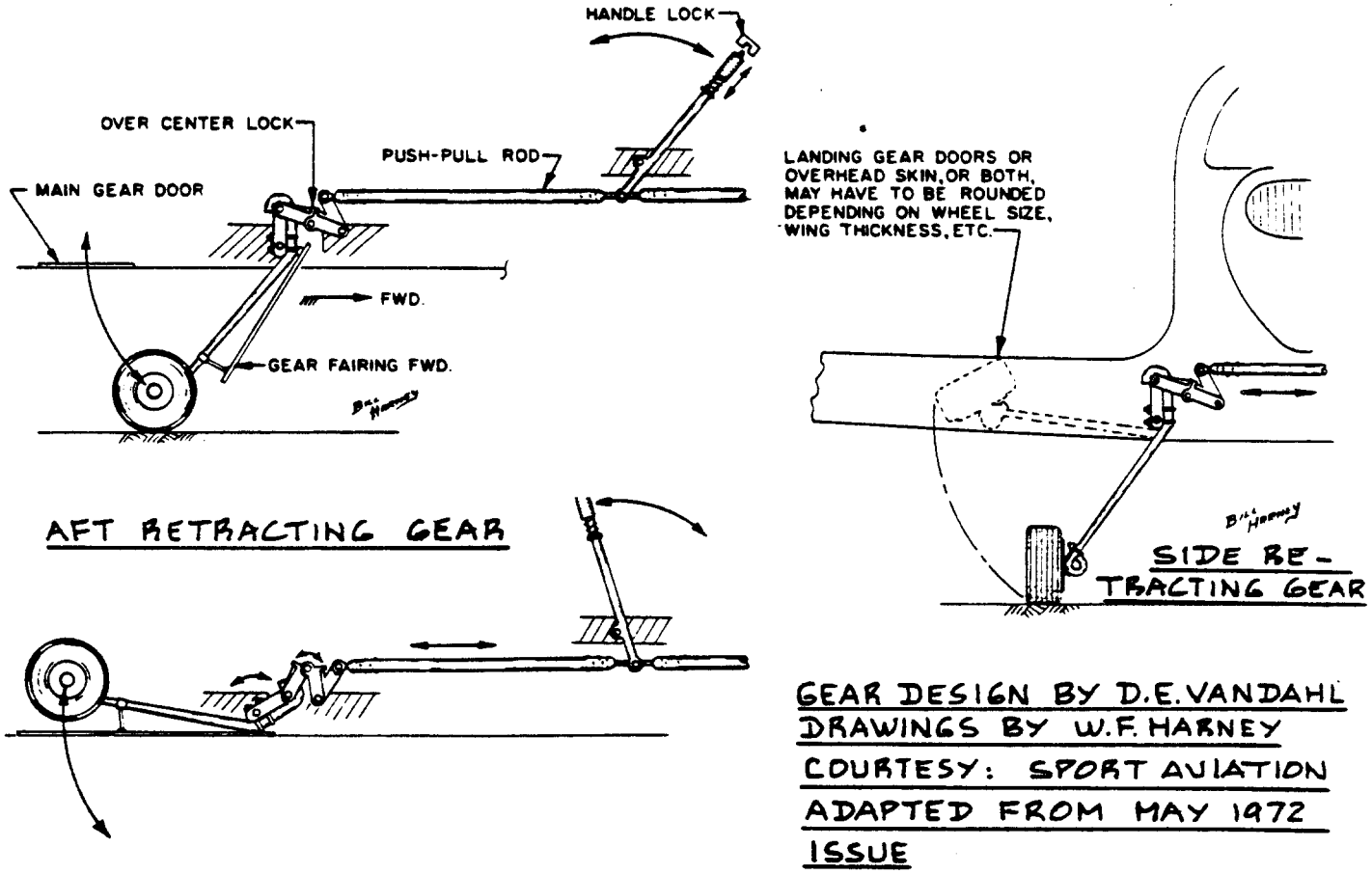

Figure 2.77 Example of Manual Gear Retraction

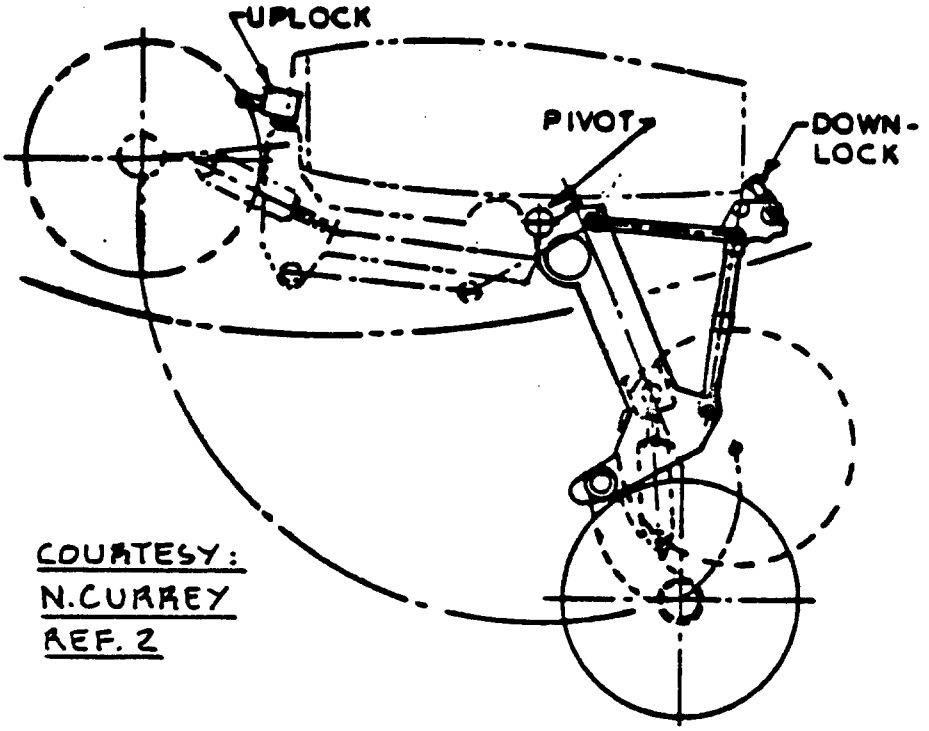

Figure 2.78 Forward Retracting Gear Clearing Wing Box

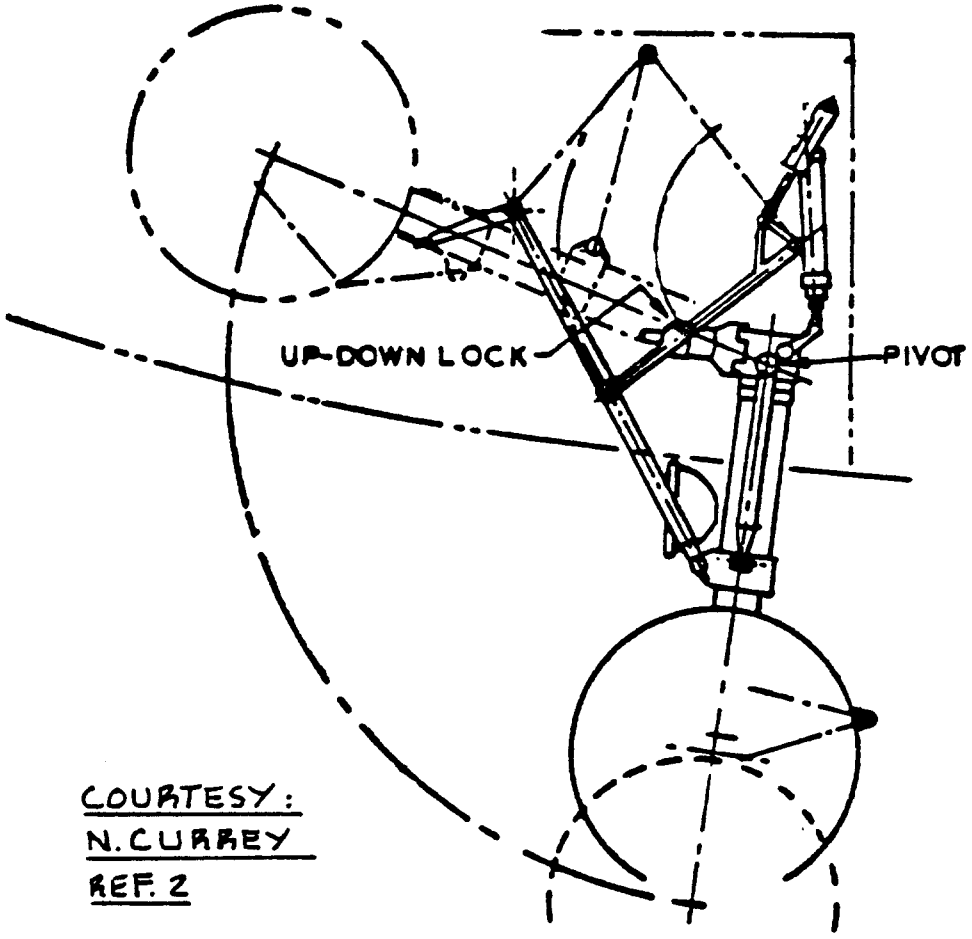

Figure 2.79 Forward Retracting Nose Gear

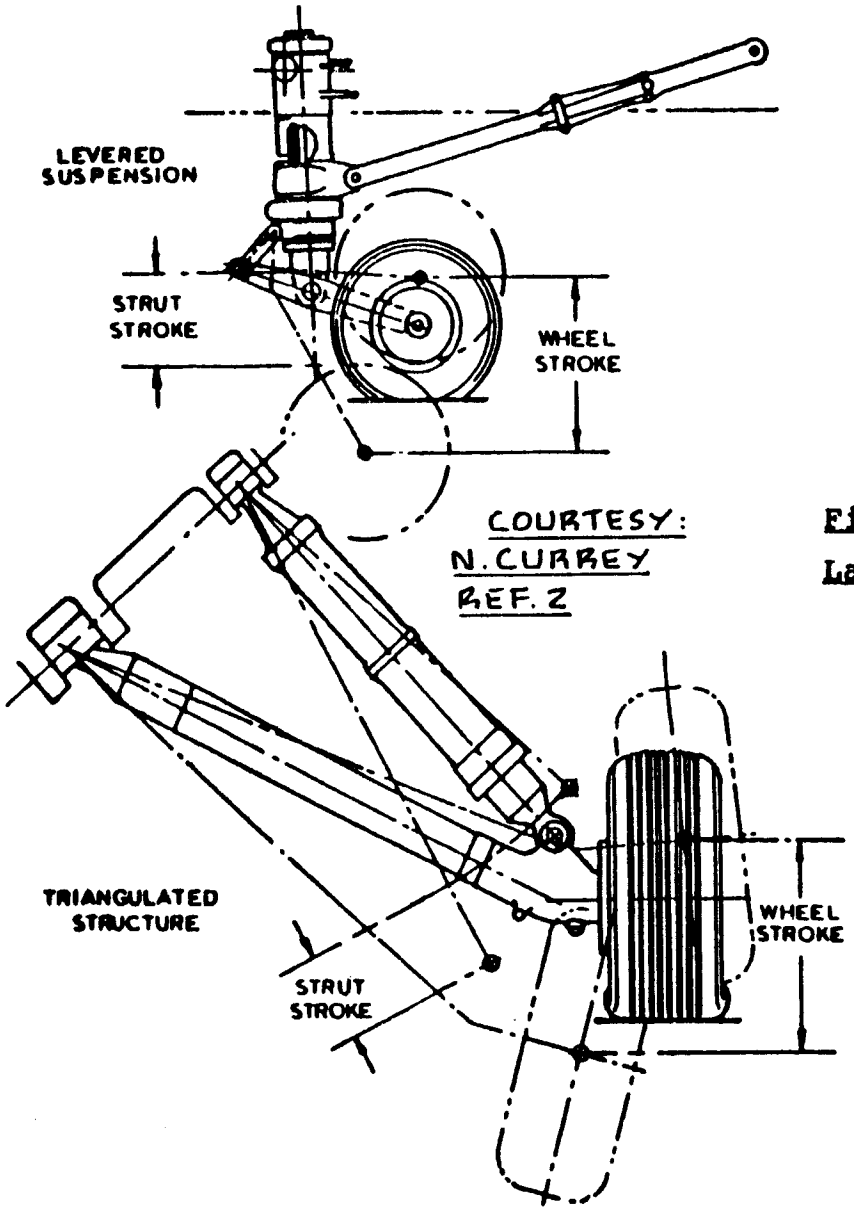

COURTESY: N.CURREY REF. 2

Figure 2.80 Main Gear with Tilted Pivot

COURTESY: N.CURREY REF. 2

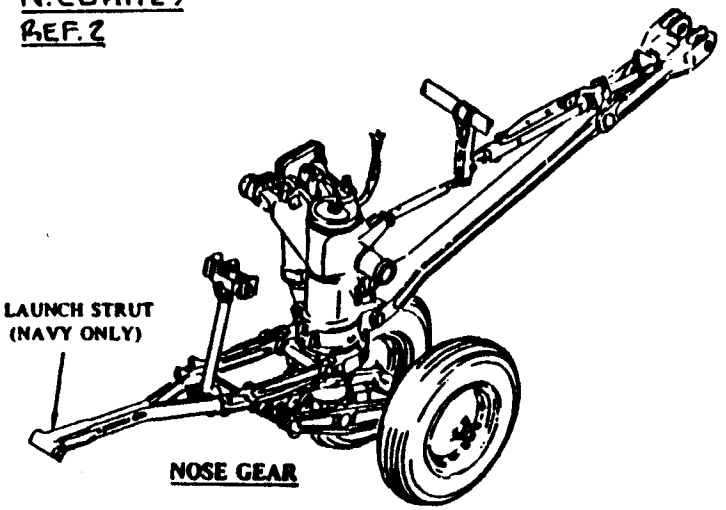

Figure 2.81a Nosegear with Launch Bar: Vought A-7E

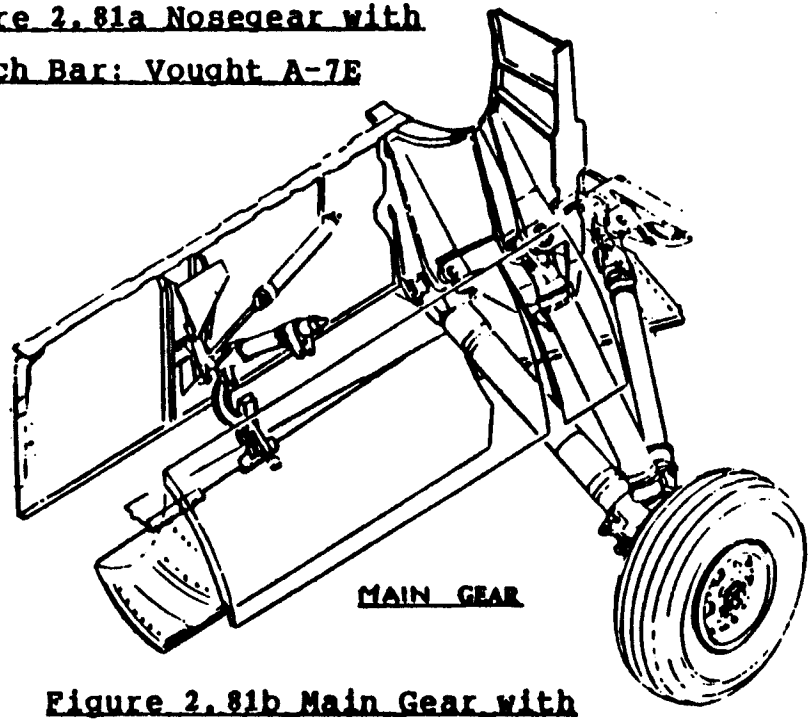

Figure 2.81b Main Gear with Tilted Pivot: Vought A-7E

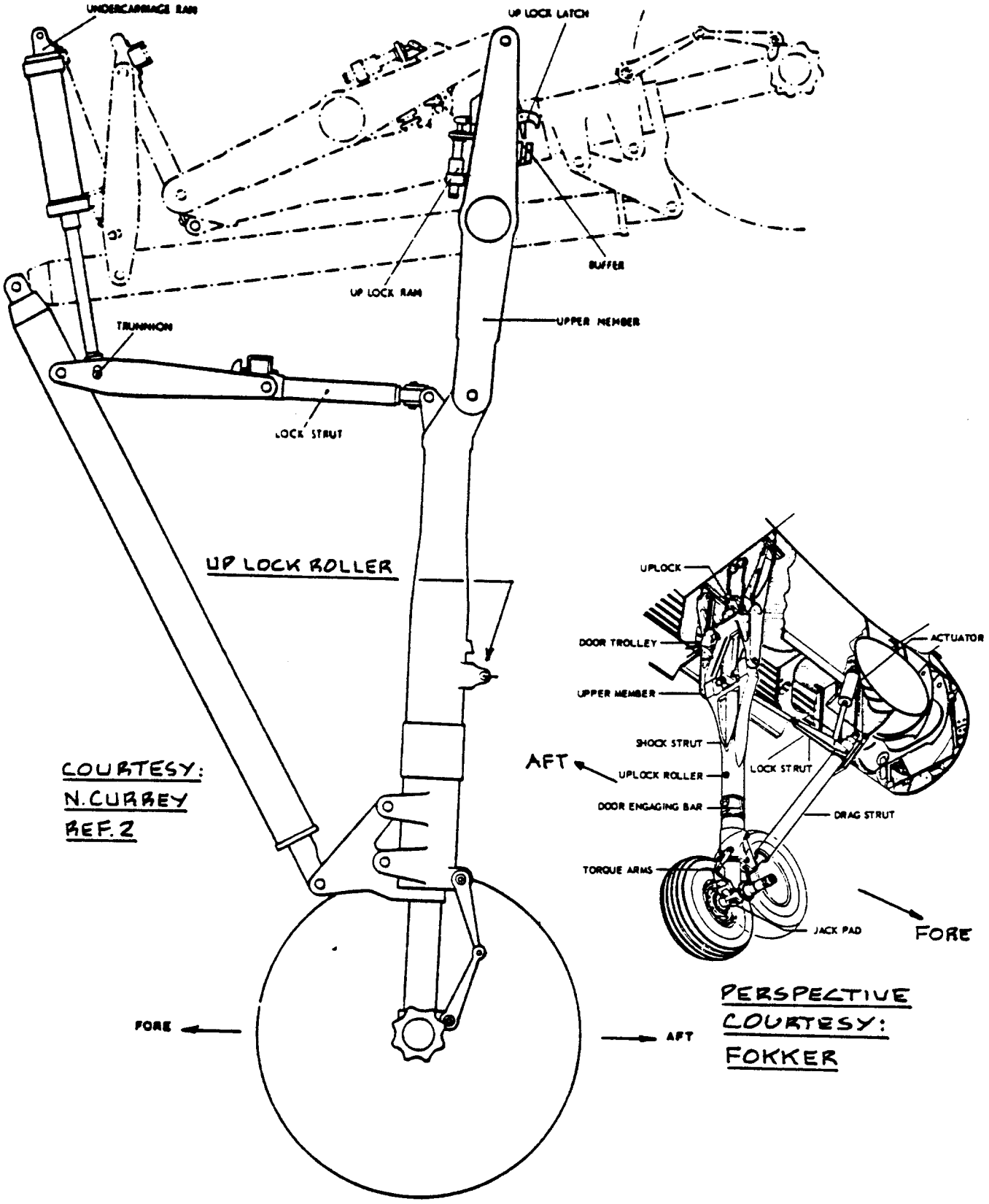

Figure 2.82 Main Gear Retraction: Fokker F-27

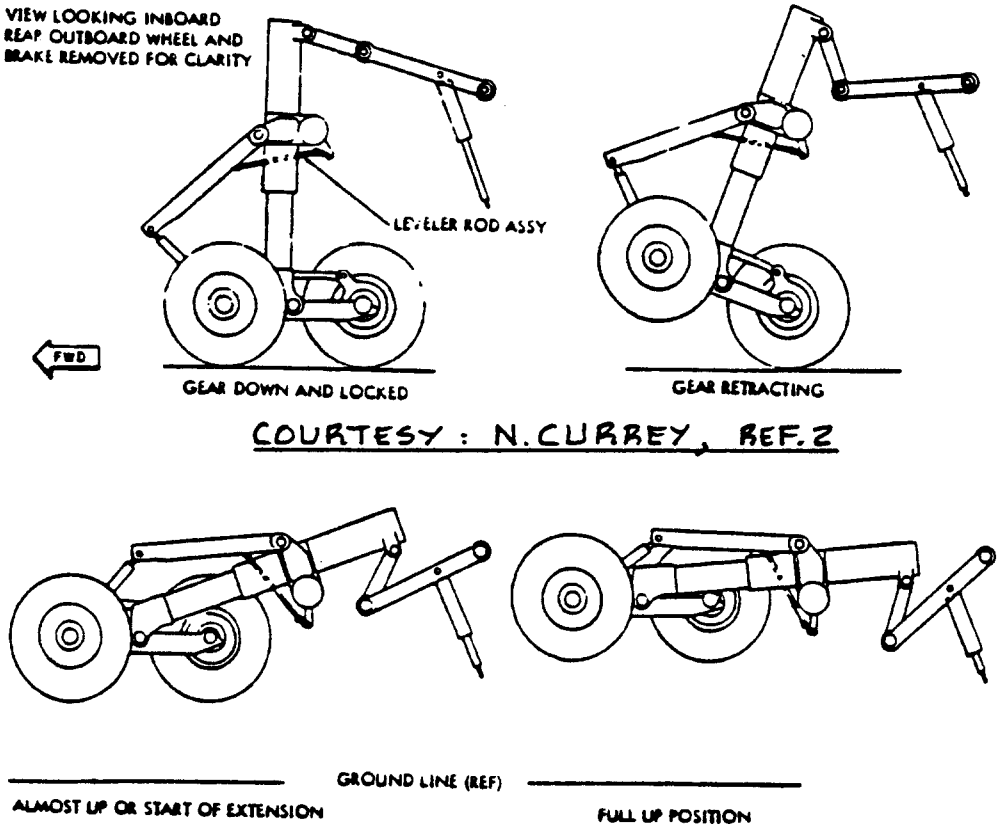

Figure 2.83 Main Gear Retraction: Lockheed C-141

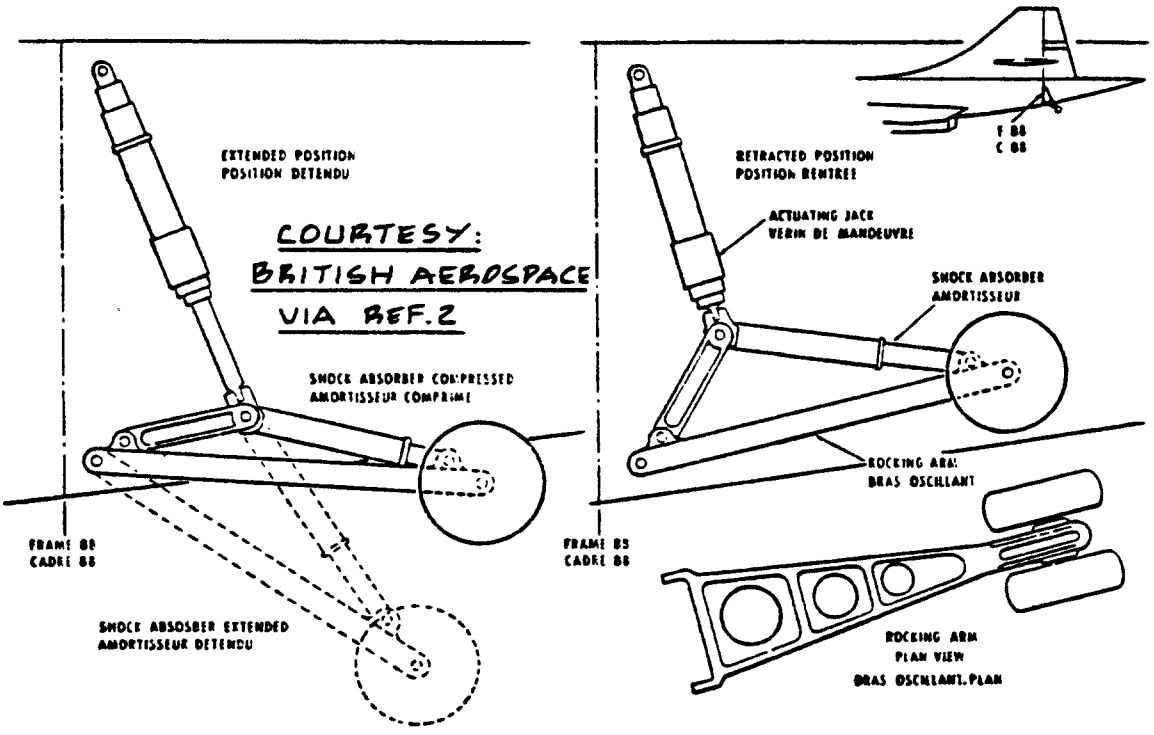

Figure 2.84 Tail Bumper Retraction: Concorde

2.11 EXAMPLE LANDING GEAR LAYOUTS

In this section a number of example layouts of landing gears will be presented. The material is presented as follows:

2.11.1 Fixed Gear Layouts
2.11.2 Retractable Gear Layouts

2.11.1 Fixed Gear Layouts

Figure 2.85 is an example of a simple fixed gear installation in a two-place, single engine light airplane: the Piper PA-38-112 Tomahawk. The main gear strut is of the spring-leaf type. All shocks are absorbed by the tire and by strut deflection. The nose gear which is steerable consists of a simple oleo strut attached to the engine truss and to the firewall.

Figure 2.86 shows the fixed gear installation for a typical four-place, single engine light airplane: the Cessna 172. Note that the tubular strut (spring-tube instead of spring-leaf) is one unit extending through the fuselage and attached at four points. The nose gear strut is attached to the firewall at two points.

Figure 2.87 also shows a fixed gear installation, but for a much larger airplane, the DHC Twin Otter. Note the rubber disk shock absorber installation.

2.11.2 Retractable Gear Layouts

Any retractable landing gear requires positive 'up' and 'down' indications in the cockpit. Figure 2.88 shows a simple method to provide 'up' and 'down' indications with the help of simple micro-switches.

Figure 2.89 shows the landing gear installation of a twin engine turboprop commuter airplane: the SF-340. This type of gear installation if frequently found in twin engined business airplanes as well.

Figure 2.90 presents the landing gear installation for the amphibious Canadair CL215. Note that the main gear retraction actuator doubles as the drag strut!

Figure 2.91 illustrates the landing gear of a small jet transport: the Fokker F28. The main gear retracts into the wing-fuselage area behind the rear wing spar.

Figure 2.92 shows the gear installation for the McDD

DC10, a heavy jet transport. The main gear retracts into the wing-fuselage junction behind the rear wing spar.

For very large transports, more than two main gears may be needed. Figure 2.93 shows the 'four-poster' main gear design for the B747.

Figures 2.94 show a detailed layout for the Boeing 767 landing gear including the retraction system.

Fighters present many landing gear design problems due to severe space limitations. Figures 2.76, 2.80, 2.81 and 2.95 illustrate several fighter landing gear arrangements.

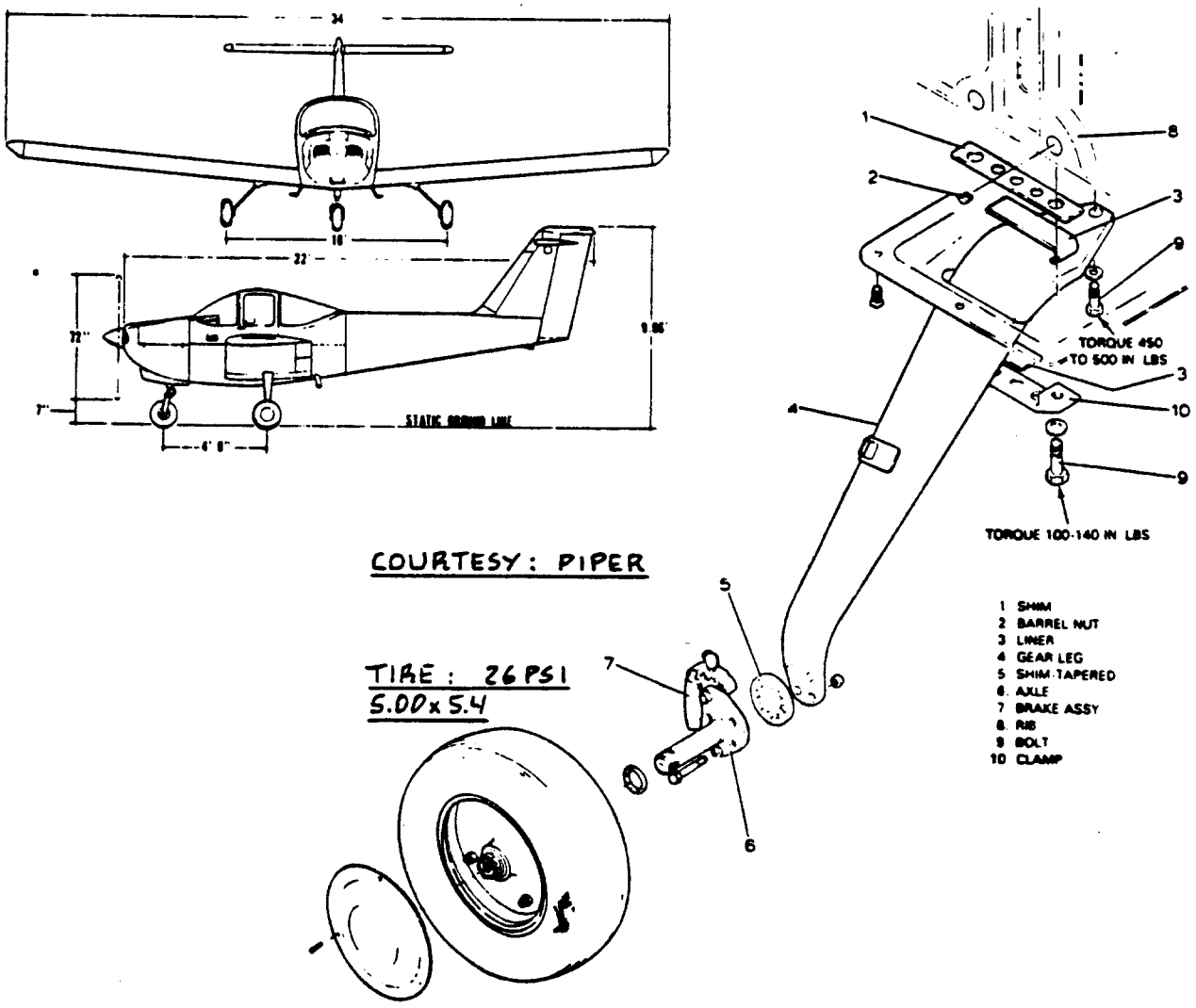

Figure 2.85a Fixed Main Gear Layout: Piper PA-38-112

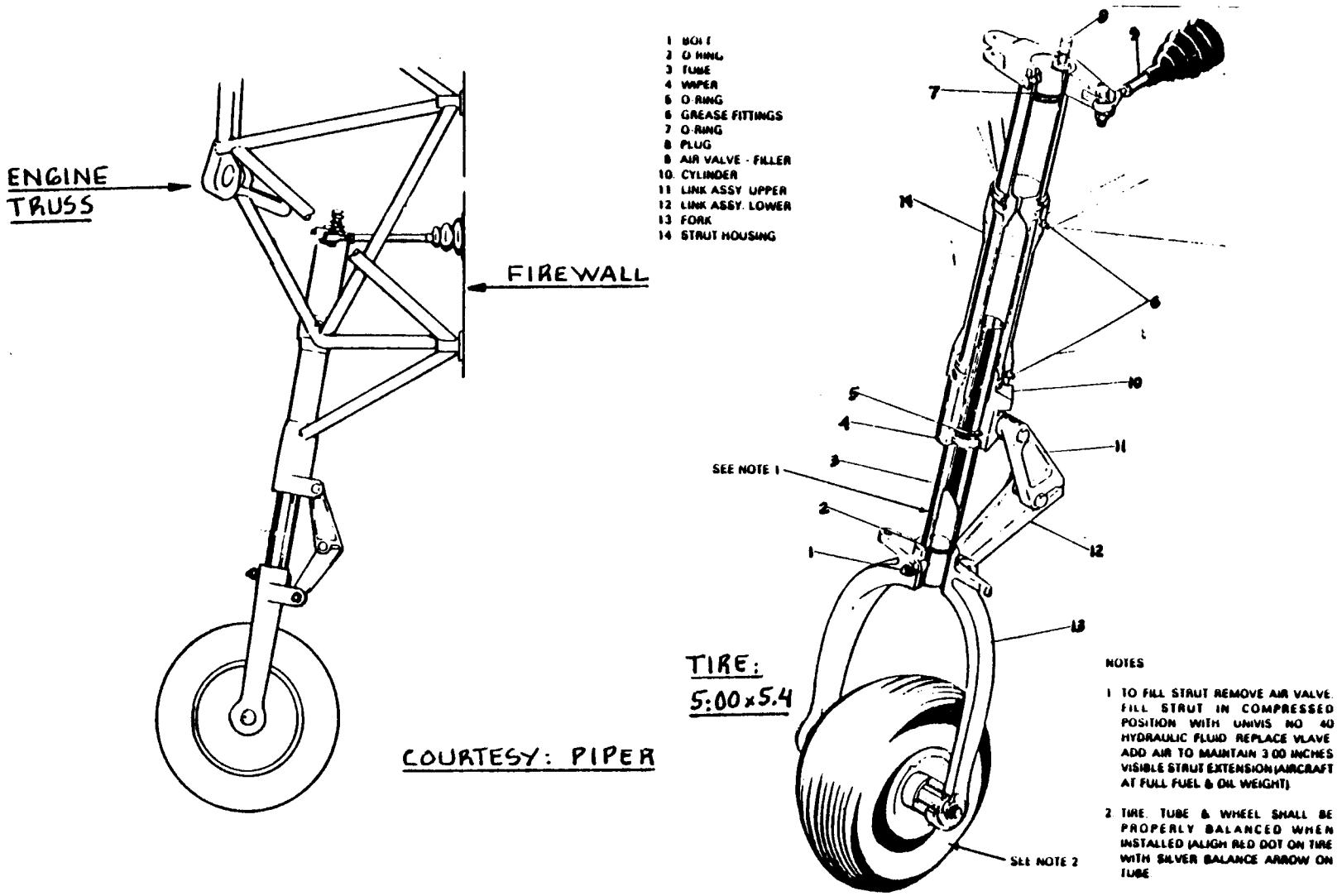

Figure 2.85b Fixed Nosegear Layout: Piper PA-38-112

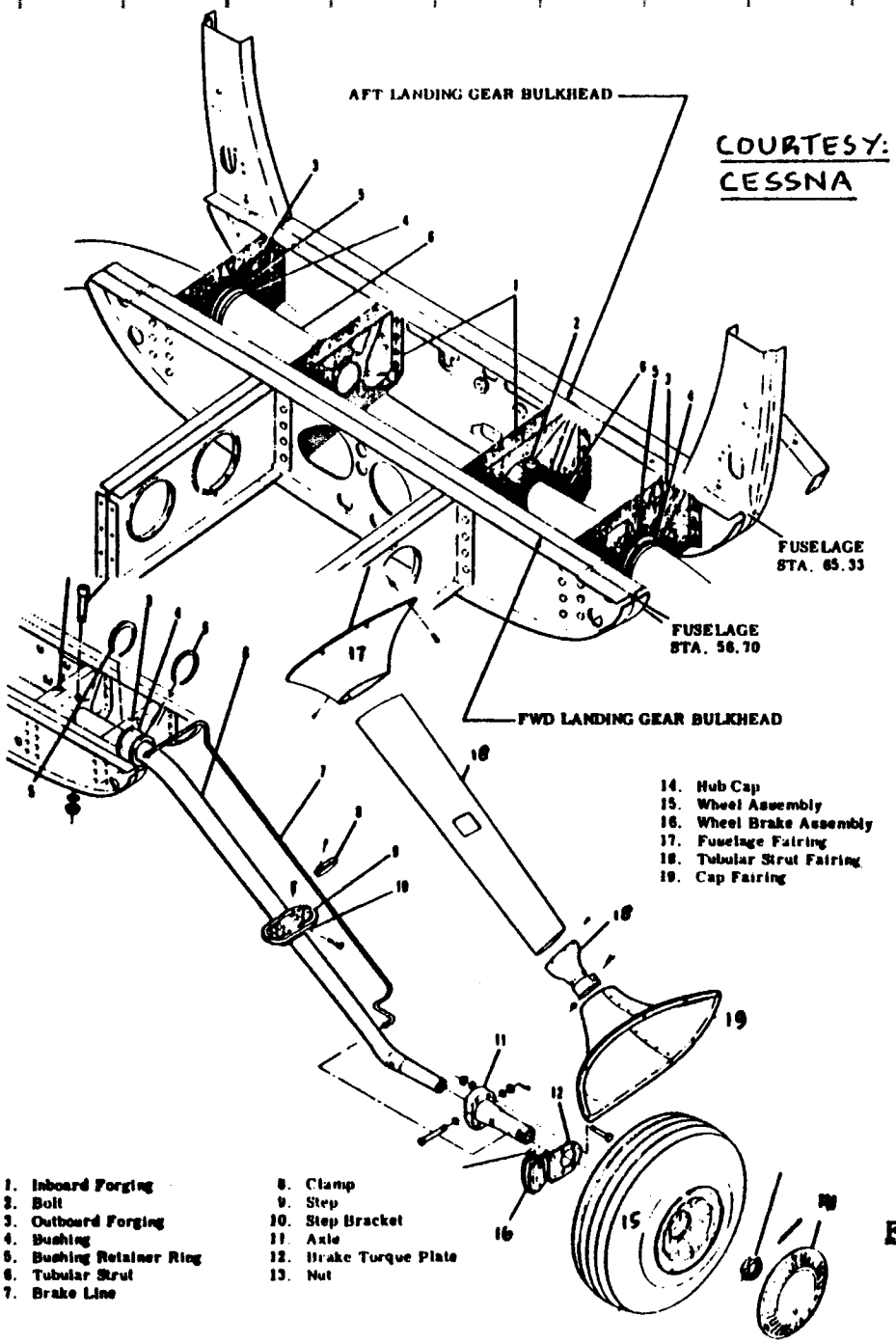

Figure 2.86a Fixed Main Gear Layout: Cessna 172

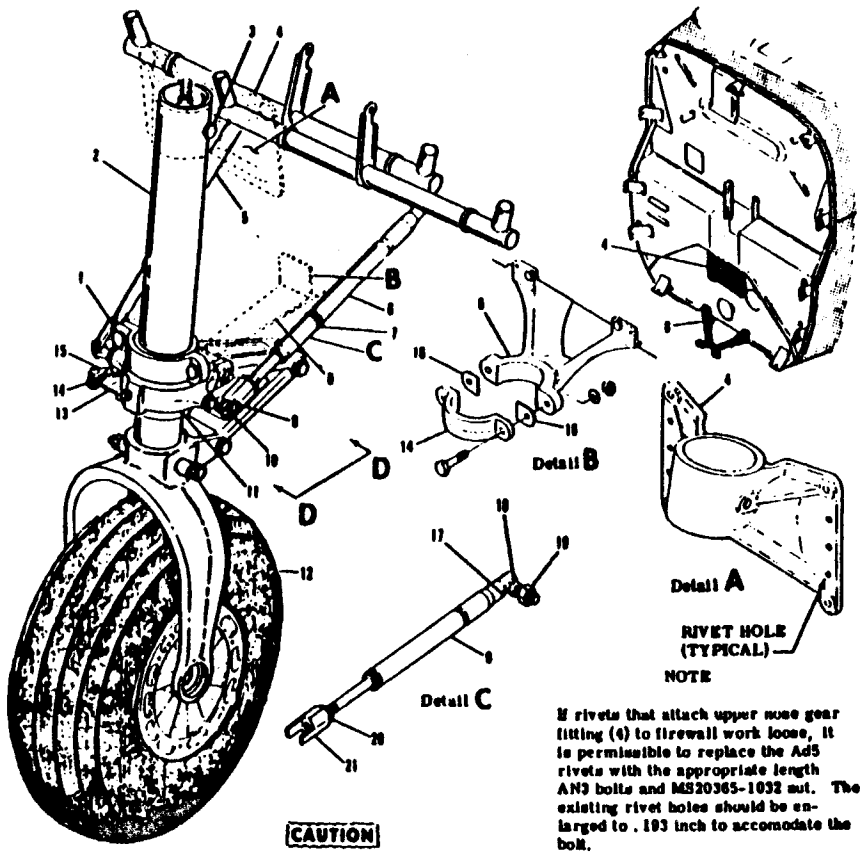

Figure 2.86b Fixed Nosegear Layout: Cessna 172

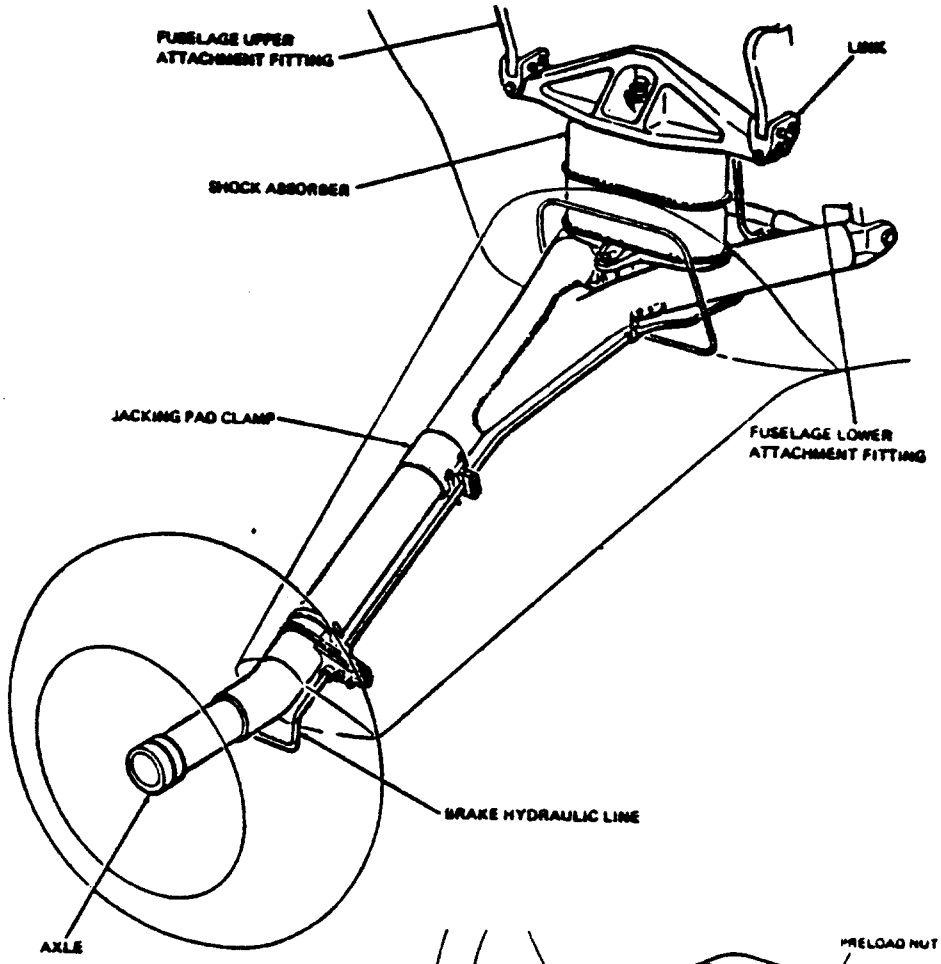

COURTESY: DH CANADA
VIA N.CURREY, REF.2

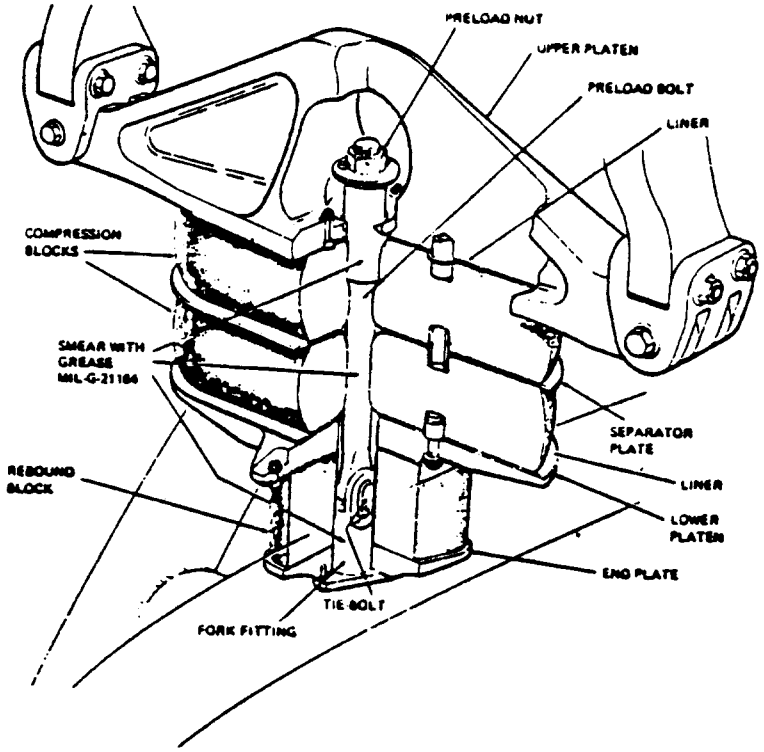

SHOCK ABSORBER DETAIL

Figure 2.87 Fixed Main Gear Layout: DHC-Twin Otter

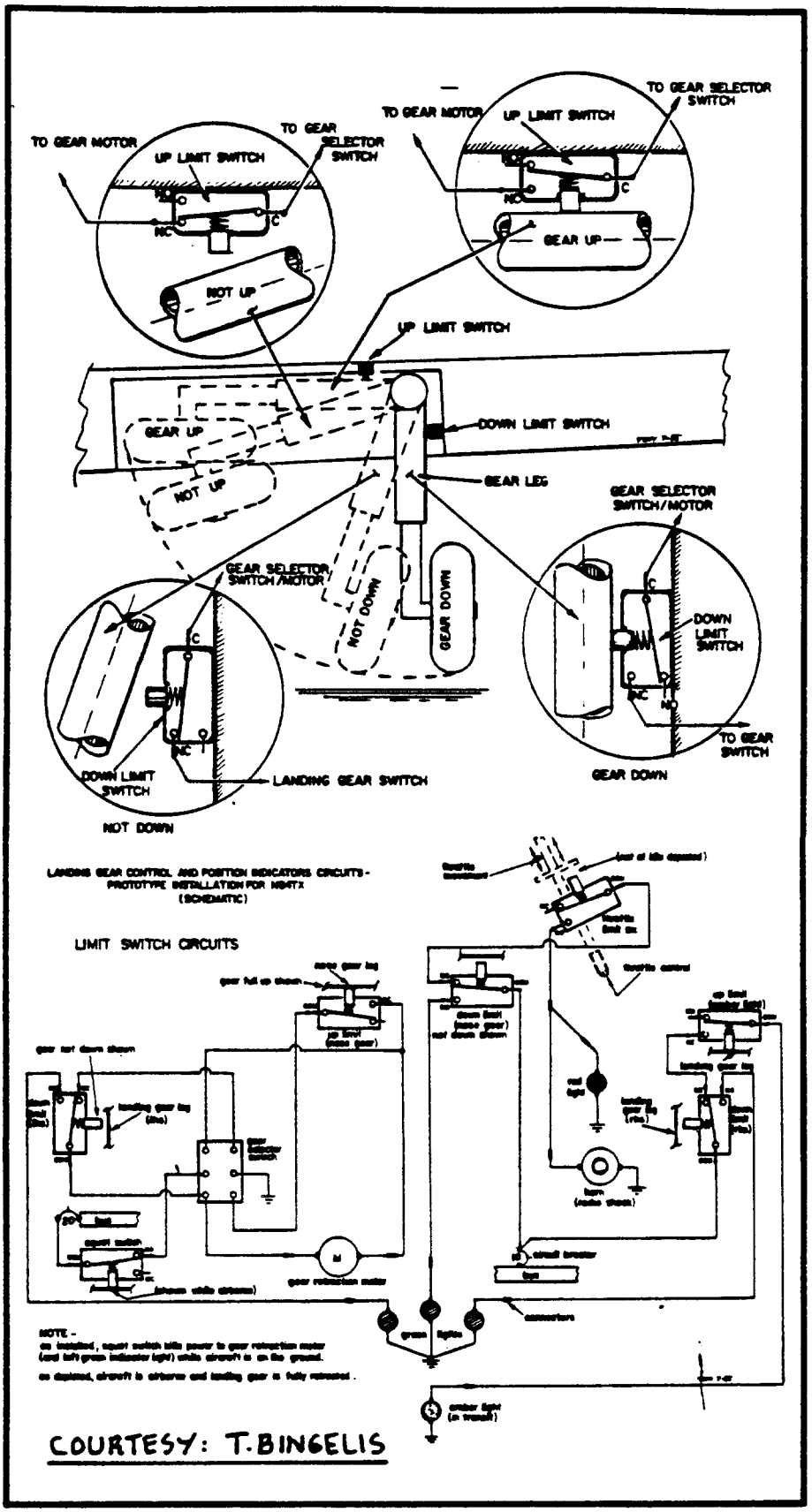

Figure 2.88 Up and Down Limit Switch Installation

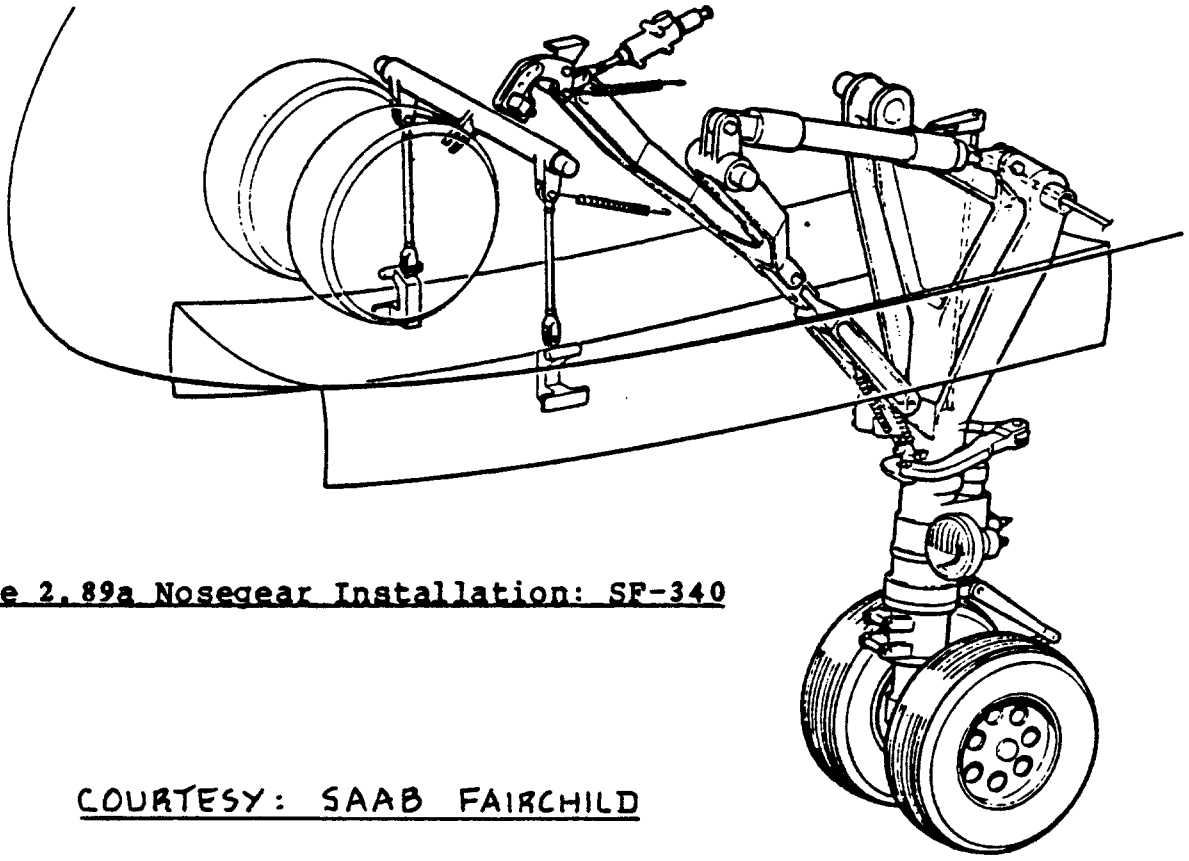

Figure 2.89a Nosegear Installation: SF-340

COURTESY: SAAB FAIRCHILD

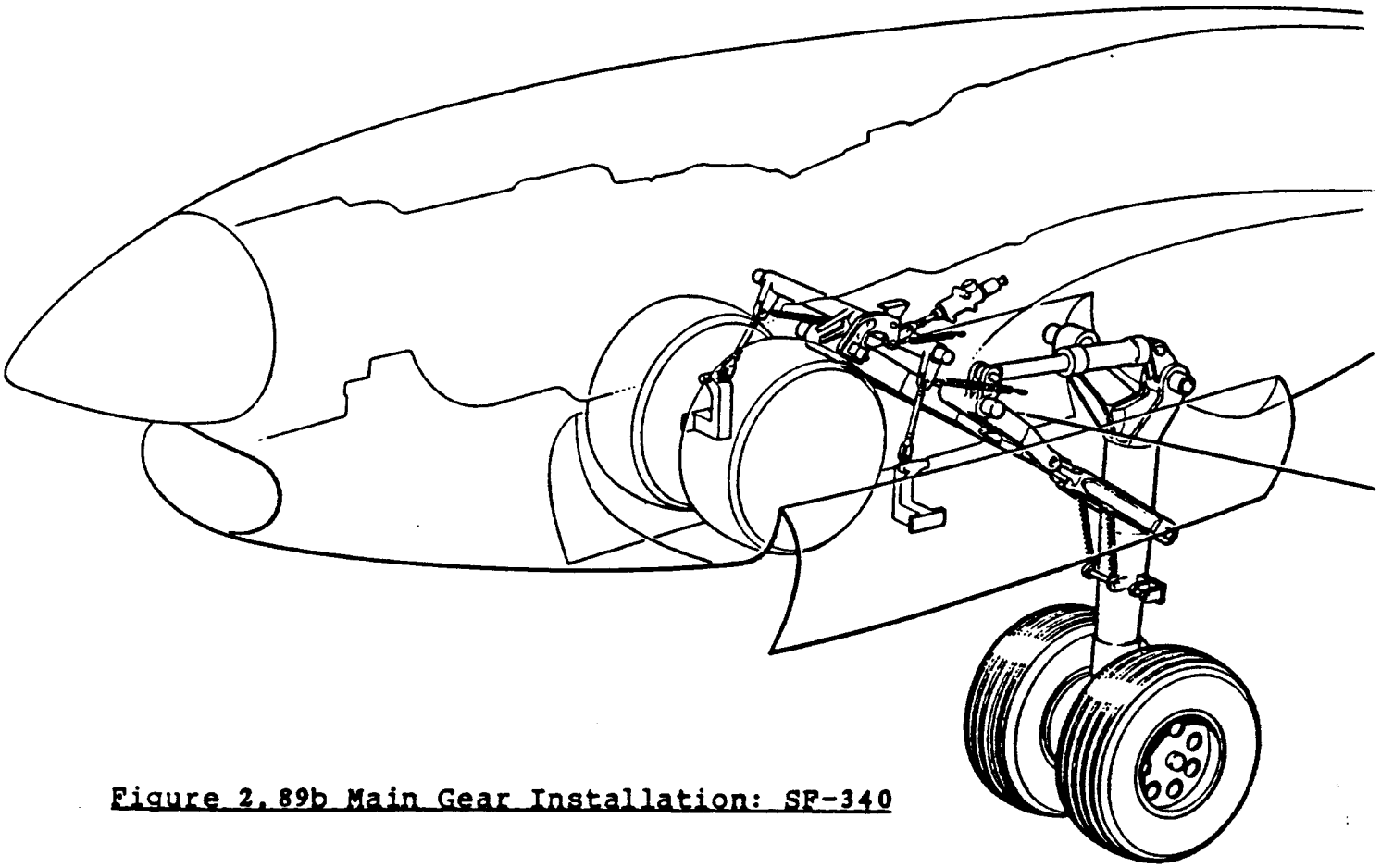

Figure 2.89b Main Gear Installation: SF-340

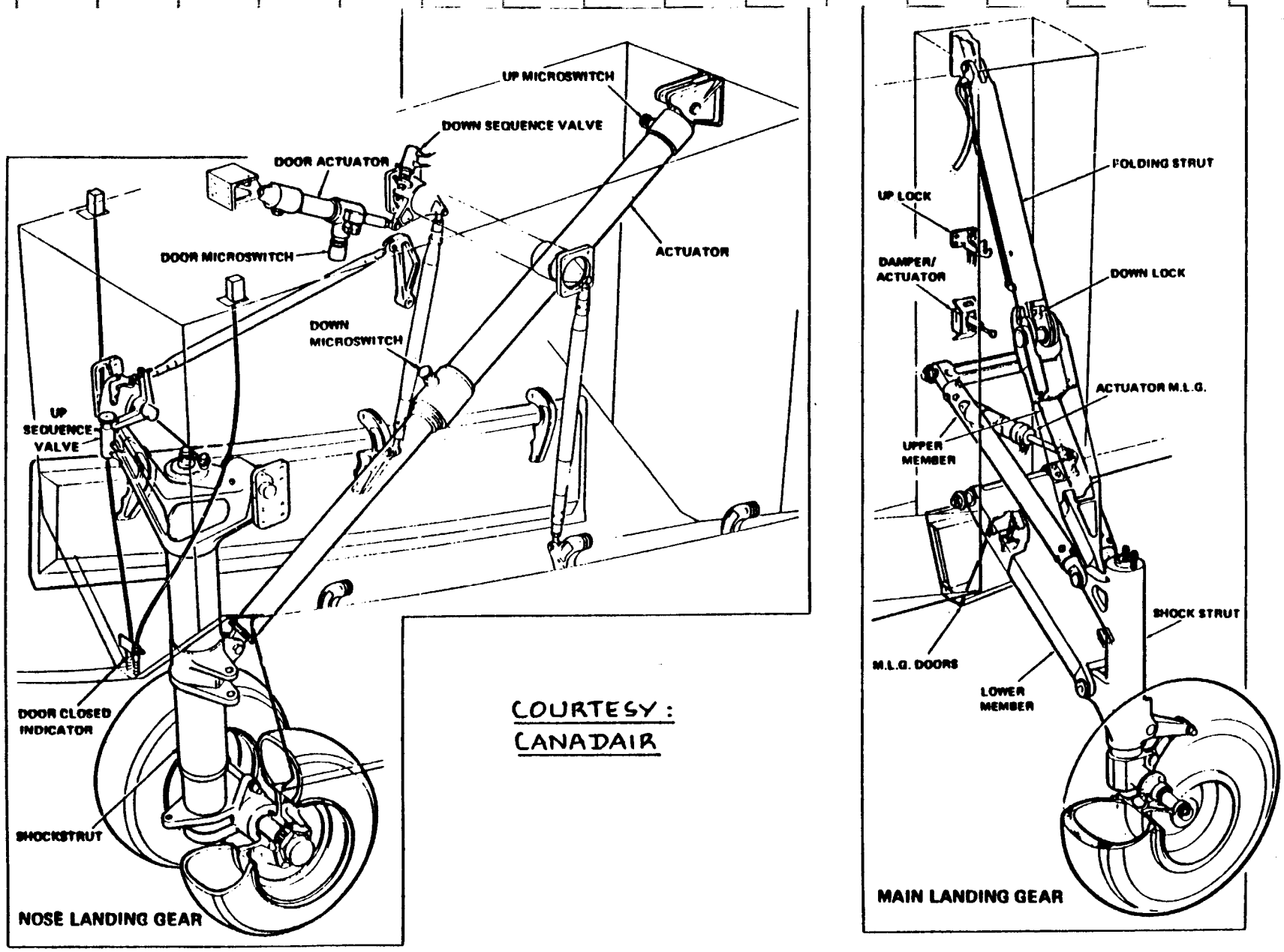

Figure 2.90 Landing Gear Installation: Canadair CL-215

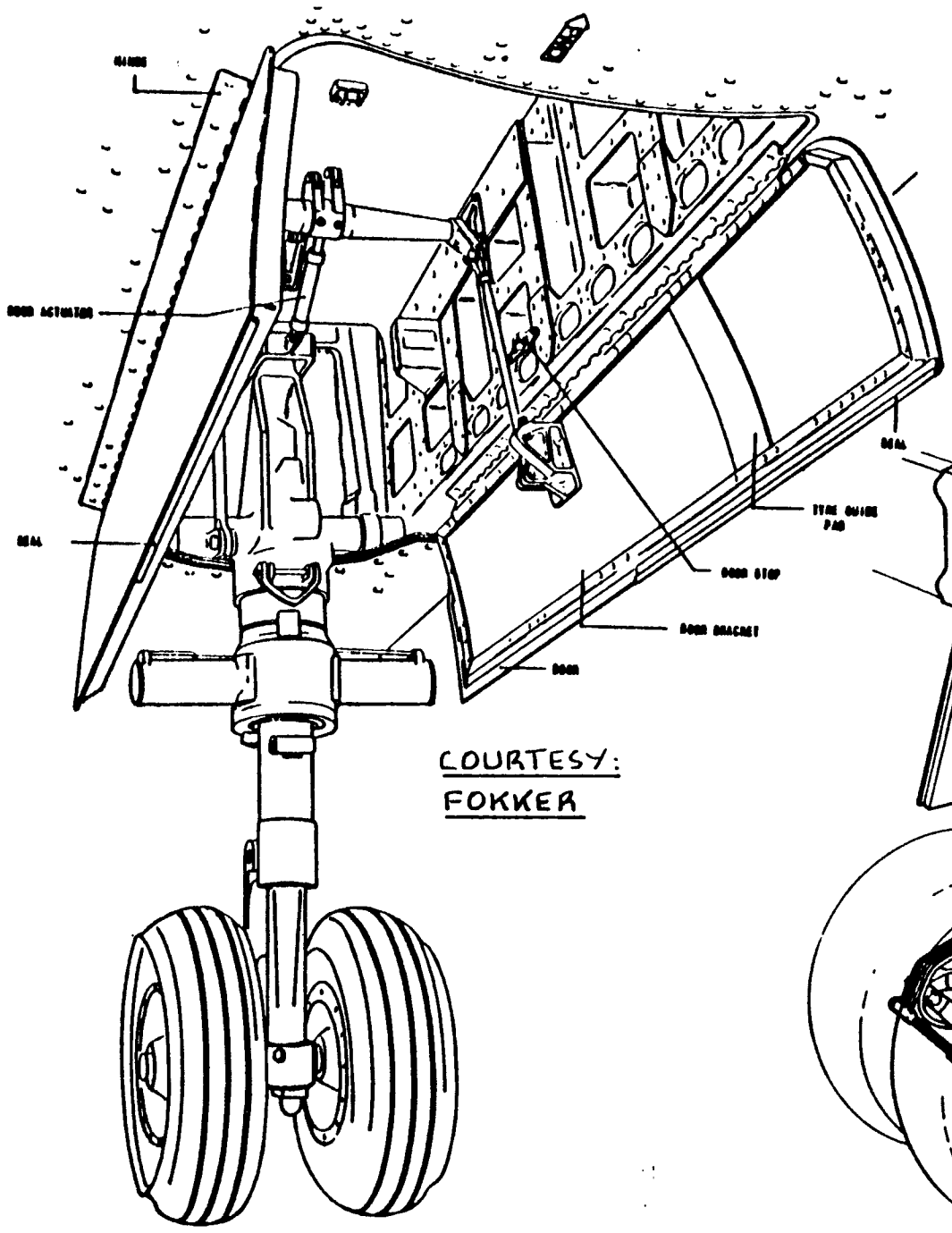

Figure 2.91a Nosegear Installation: Fokker F-28

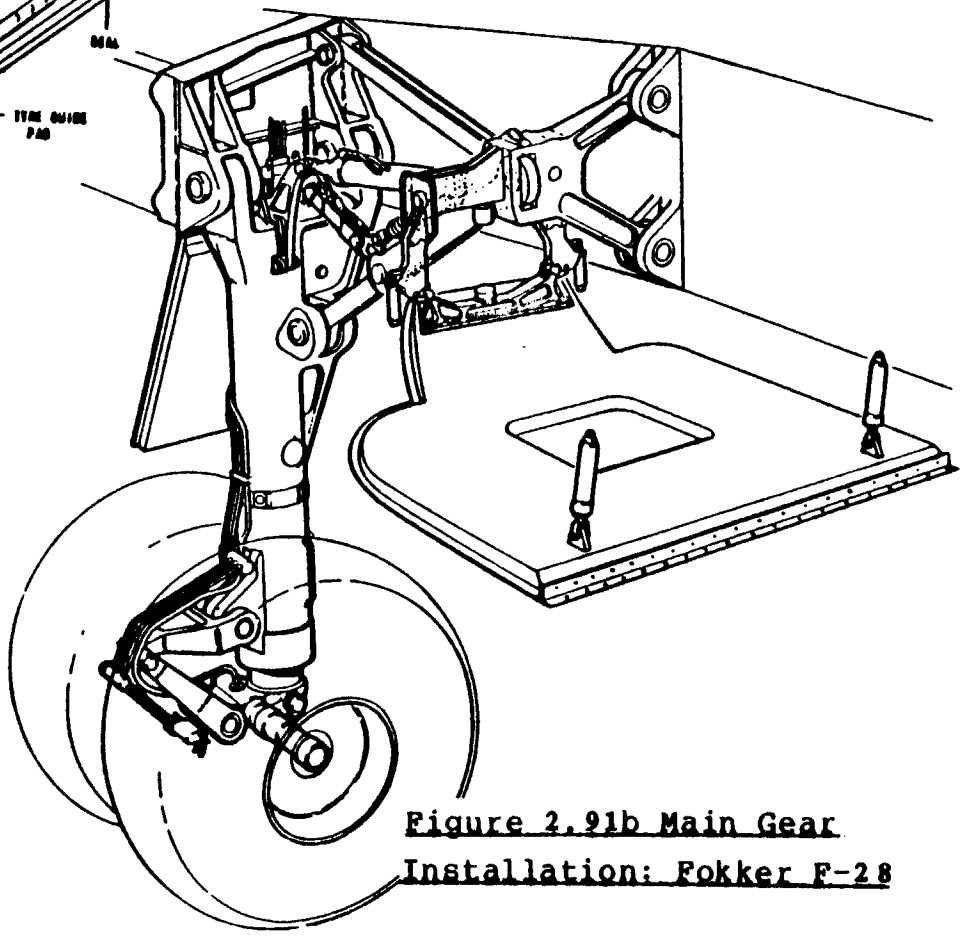

Figure 2.91b Main Gear Installation: Fokker F-28

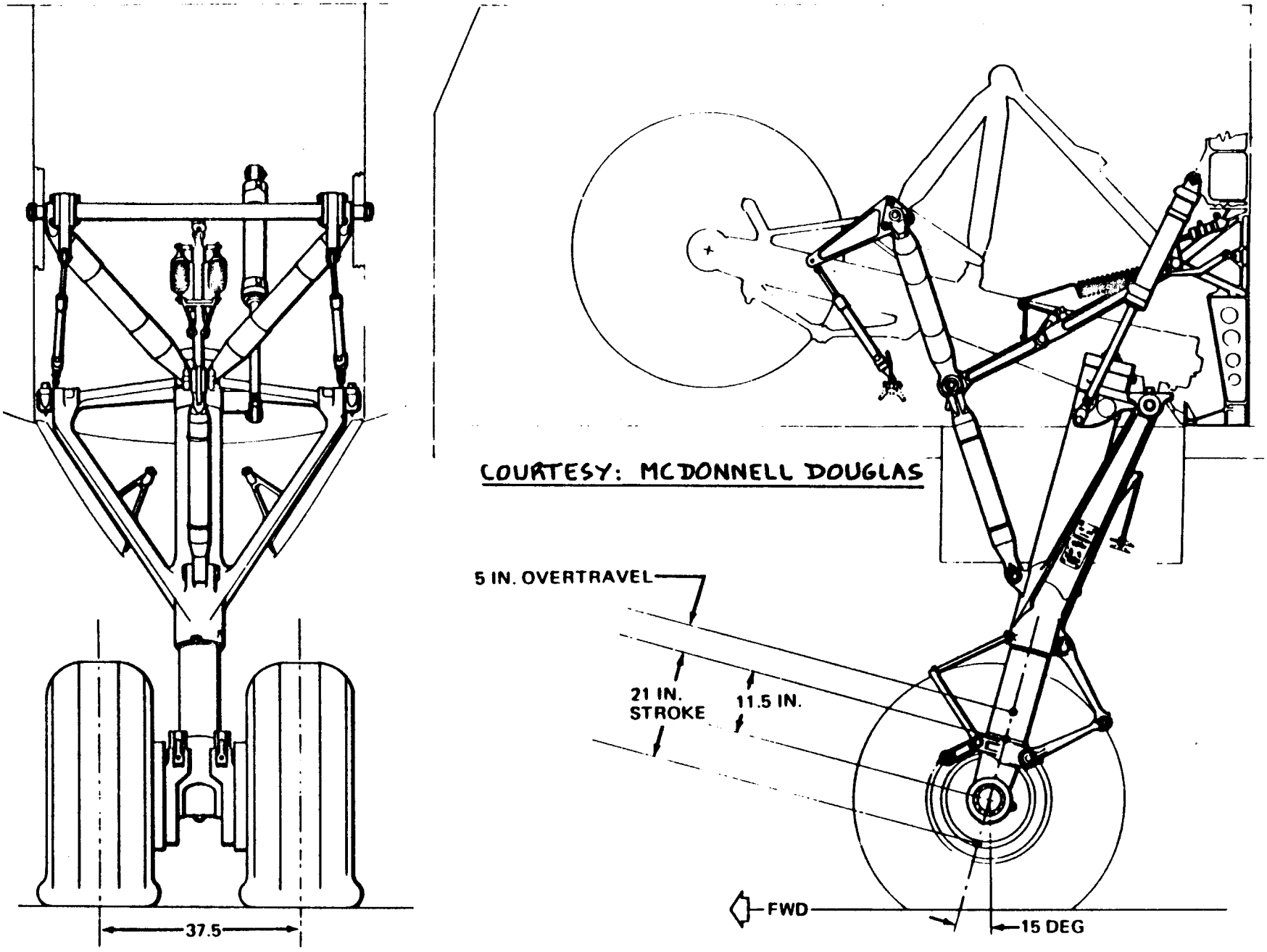

Figure 2.92a Nosegear Installation: McD-Douglas DC-10

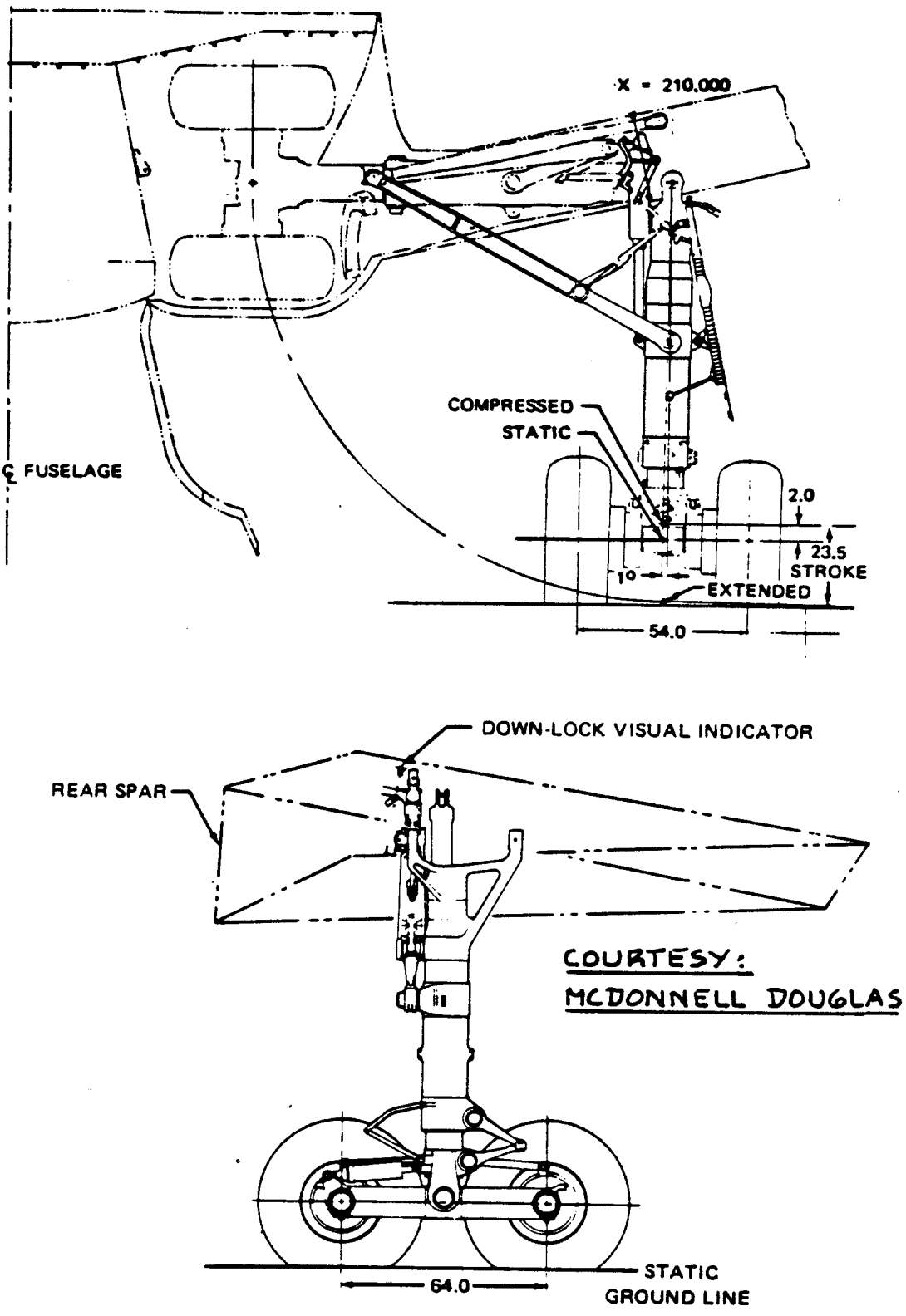

Figure 2.92b Main Gear Installation: McD-Douglas DC-10

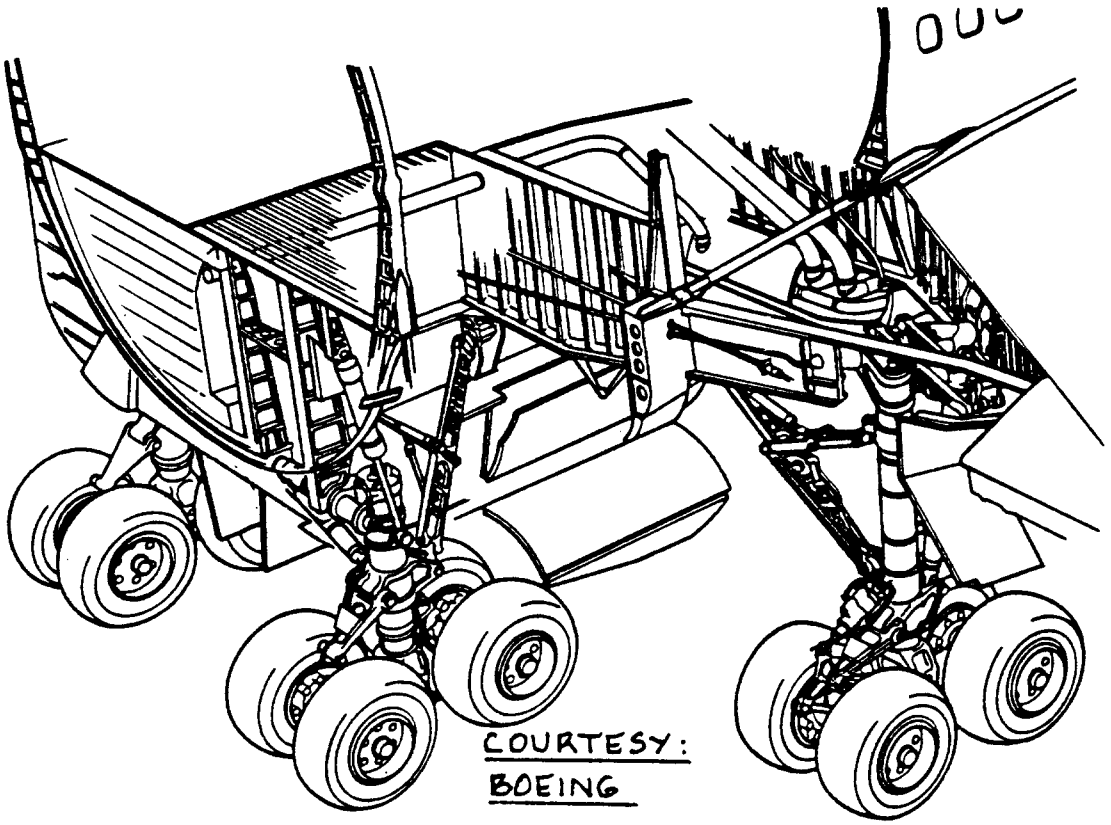

Figure 2.93 Main Gear Installation: Boeing 747

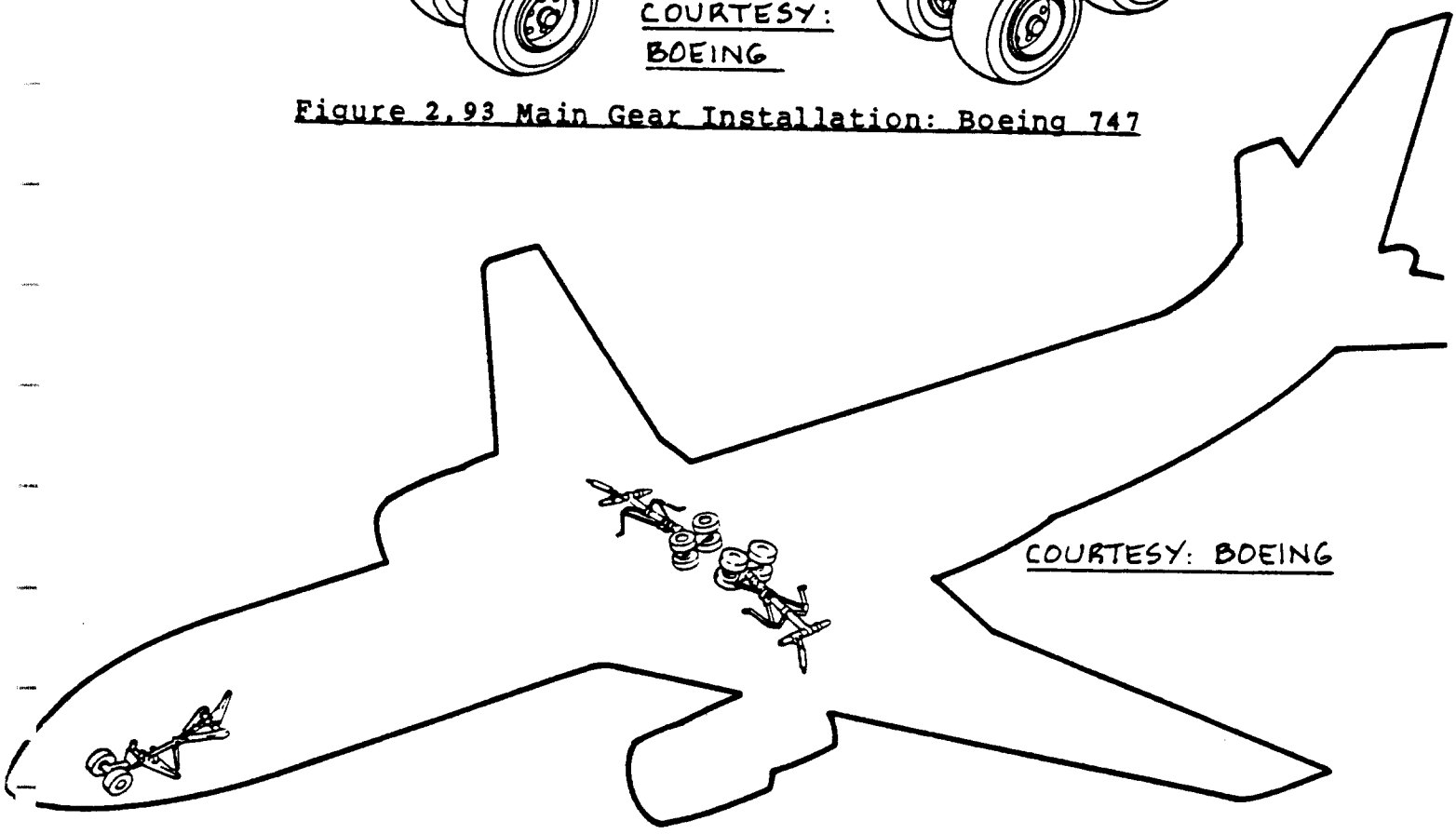

Figure 2.94a Landing Gear Overview: Boeing 767

- ±65° steering
- Replaceable tow lugs
- No mechanical disconnect of torque links for towing (Disconnect feature optional)
- All doors slaved to gear

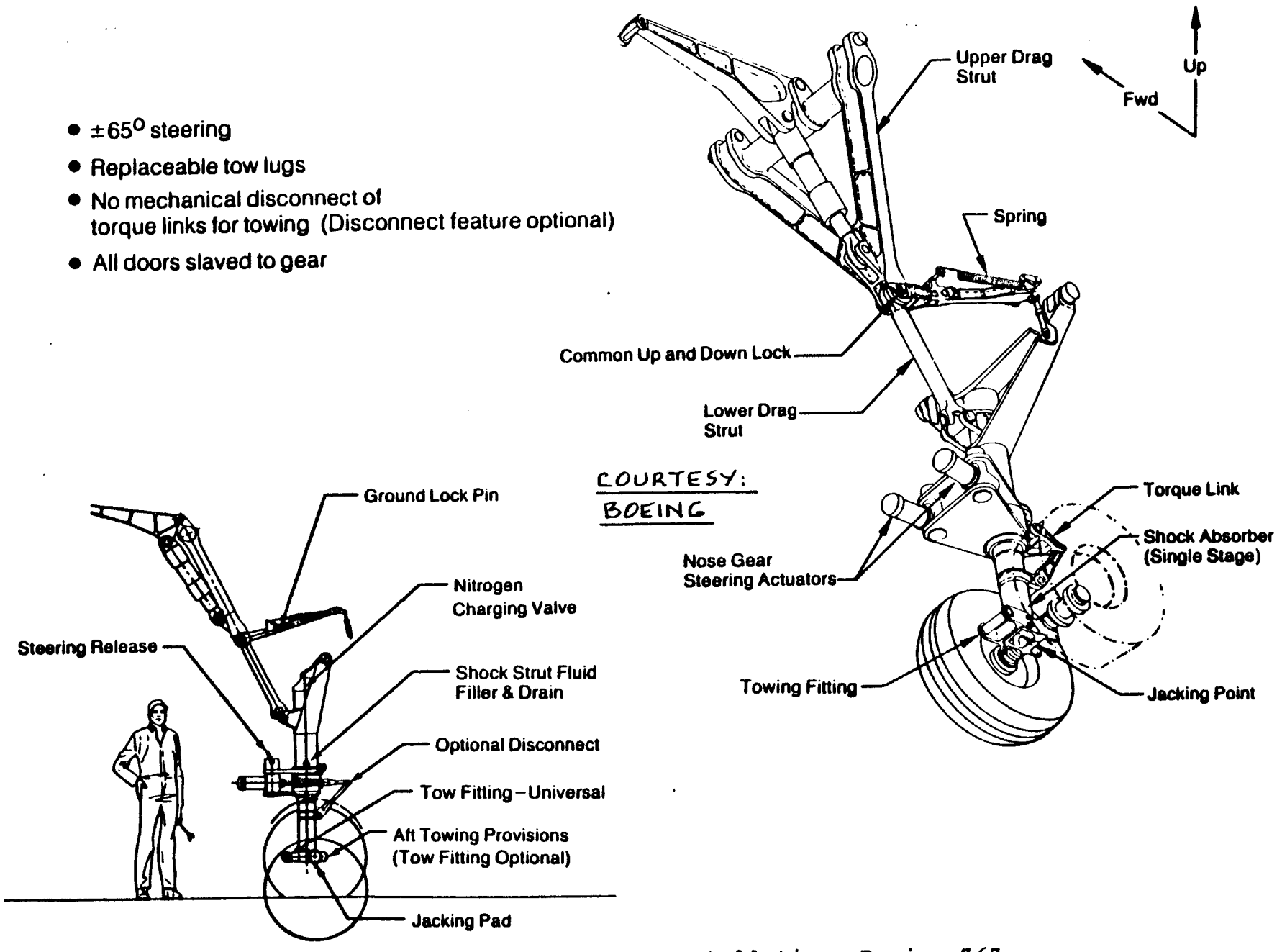

Figure 2.94b Nosegear Installation: Boeing 767

- Double braced for stiffness and clean break-away
- Low profile tires
- Five rotor brake
- Carbon brake provisions
- Long stroke shock strut

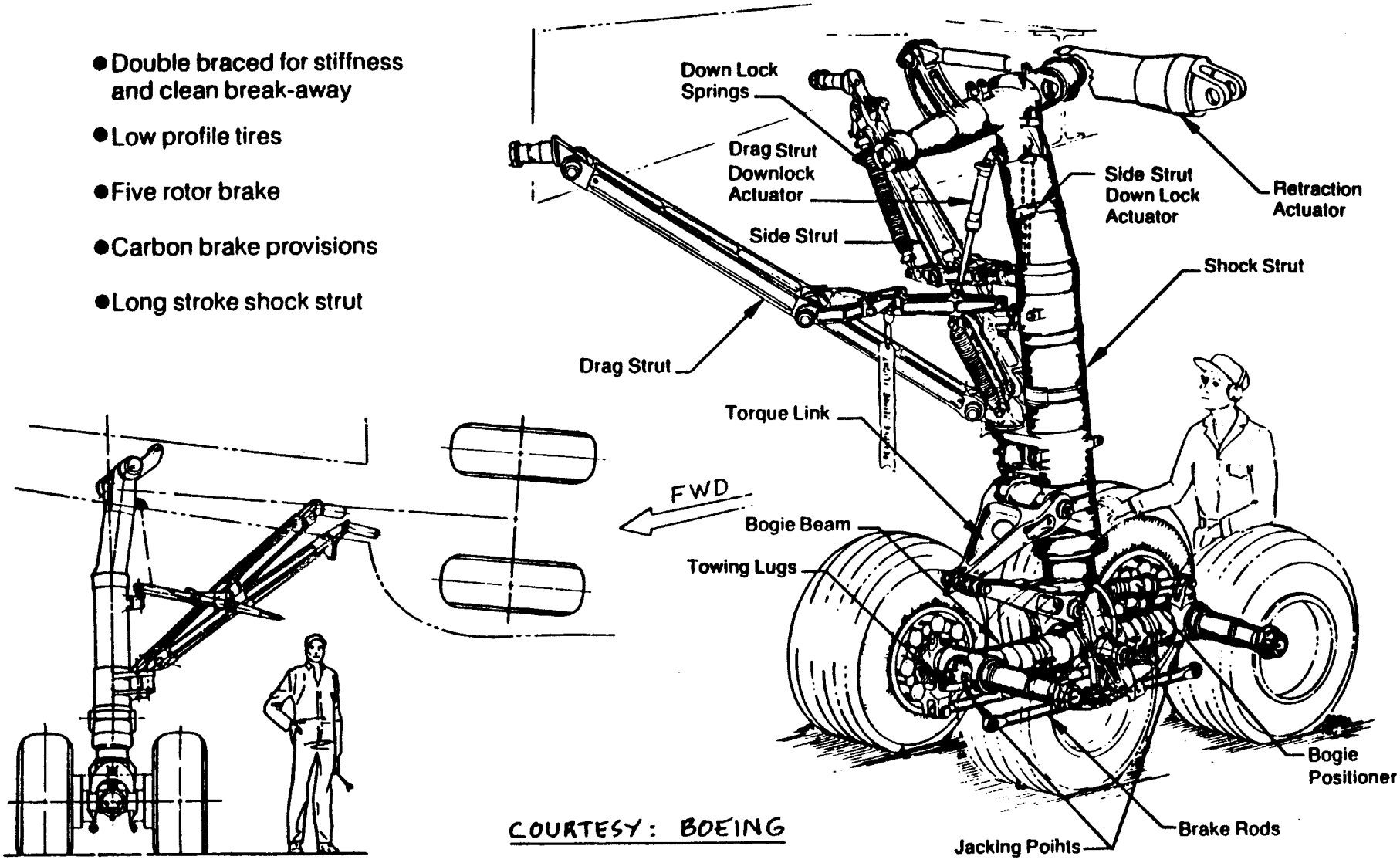

Figure 2.94c Main Gear Installation: Boeing 767

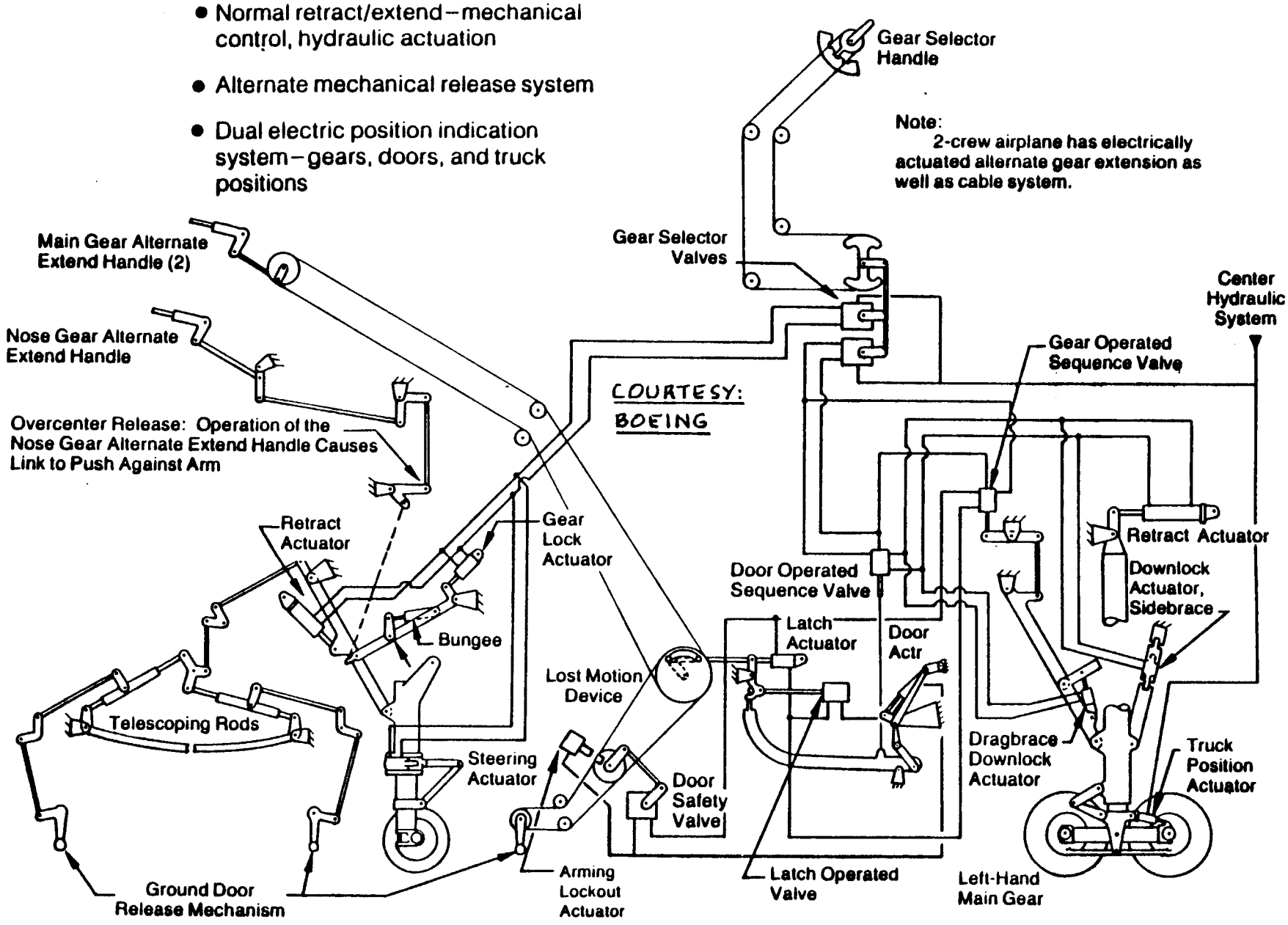

Figure 2.94d Landing Gear Retraction System: Boeing 767

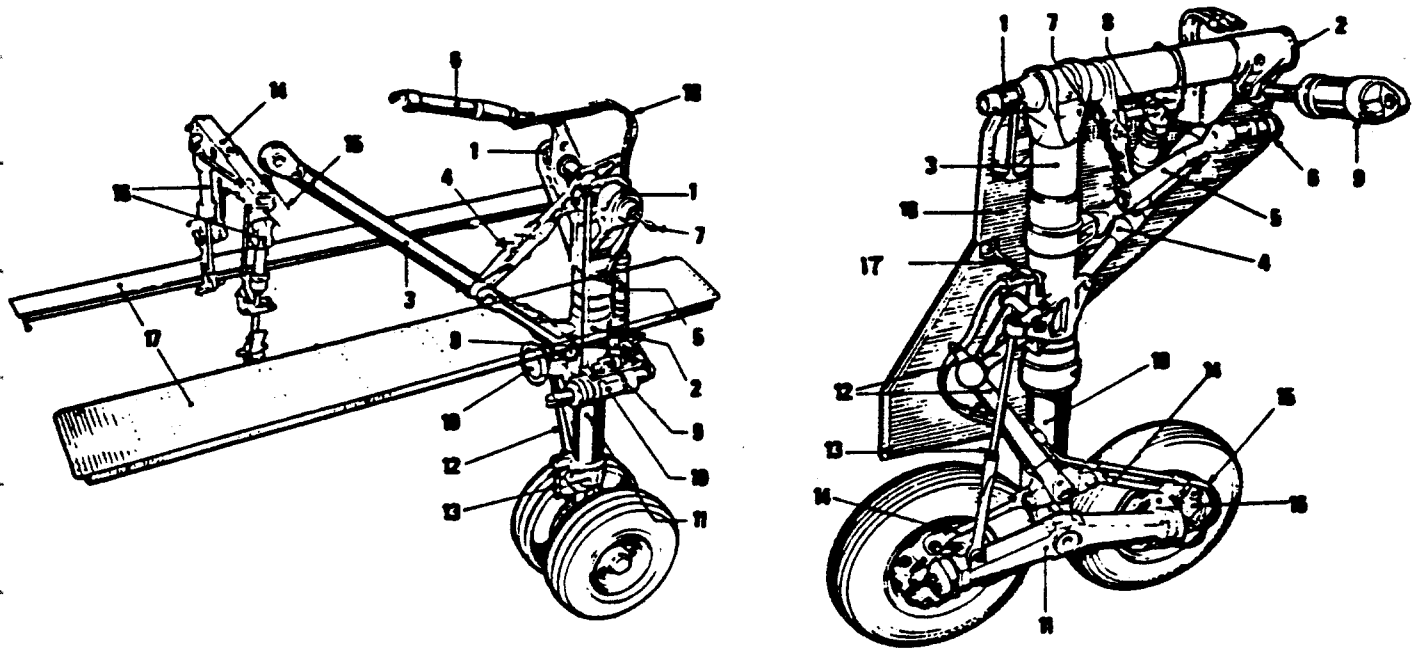

COURTESY: SAAB

NOSE GEAR

1. Attachment Points
2. Strut
3. Drag Link
4. Down Lock Support Link
5. Up/Down Lock Actuator
6. Retraction Actuator
7. Steering Command Rod
8. Steering Control Links
9. Steering Control Valve
10. Steering Actuator
11. Shock Absorber
12. Torque Link
13. Up Lock Reference (Gear)
14. Up Lock Reference (Nose)
15. Door Command Link
16. Door retraction actuators
17. Doors
18. Steering hydraulic lines
19. Landing light

MAIN GEAR

1. Fwd Attachment Point
2. Rear Attachment Point
3. Strut
4. Drag Link
5. Side Brace
6. Side Brace Support
7. Down Lock Support Link
8. Up/Down Lock Actuator
9. Retraction Actuator
10. Shock Absorber
11. Bogie
12. Torque Link
13. Bogie Pitch Stabilizer
14. Brake actuators
15. Brake Hydraulic Lines
16. Hydraulic Brakes
17. Door Retraction Link
18. Main Door

Figure 2.95 Landing Gear: SAAB Viggen

2.12 UNCONVENTIONAL LANDING GEAR CONFIGURATIONS

The purpose of this section is to review a number of alternative solutions to landing gear design. These are:

2.12.1 Cross wind landing gears
2.12.2 Gears with driven wheels
2.12.3 Jump-struts and ski-jumps
2.12.4 Droppable gears
2.12.5 Beaching Gears
2.12.6 Skis
2.12.7 Floats
2.12.8 Air cushion landing gears

2.12.1 Cross Wind Landing Gears

Figure 2.96a illustrates the potential consequence of too much directional stability during a cross wind landing. The control of the airplane on the runway can be particularly 'tricky' if the runway surface is slick and if the landing gear is of the tailwheel type.

One solution to this problem is to build into the gear the ability to be positioned in a manner to allow crabbed, wings level landings. Figure 2.96b shows an example of such a gear arrangement. The Boeing B52 has such a landing gear, called a cross wind landing gear. Airplanes with cross wind gears must have a cockpit control and display panel such as that of Fig.2.96c.

A penalty associated with cross wind landing gears is larger weight, cost and maintenance. Also, the possibility of the pilot turning the wheels in the wrong direction exists: if it can be done, it will be done!

2.12.2 Gears With Driven Wheels

Airplanes move along the ground under their own power or by being towed. Moving under power costs fuel and engine wear and tear. The alternate solution of towing costs additional manpower and requires special equipment.

One obvious solution to these problems is to build into the landing gear the ability to be self-driven. For a detailed discussion of such systems Ref.2 should be consulted. Figure 2.97 shows an example of such a system. One reason why this system has not been adopted as yet is its weight and its cost.

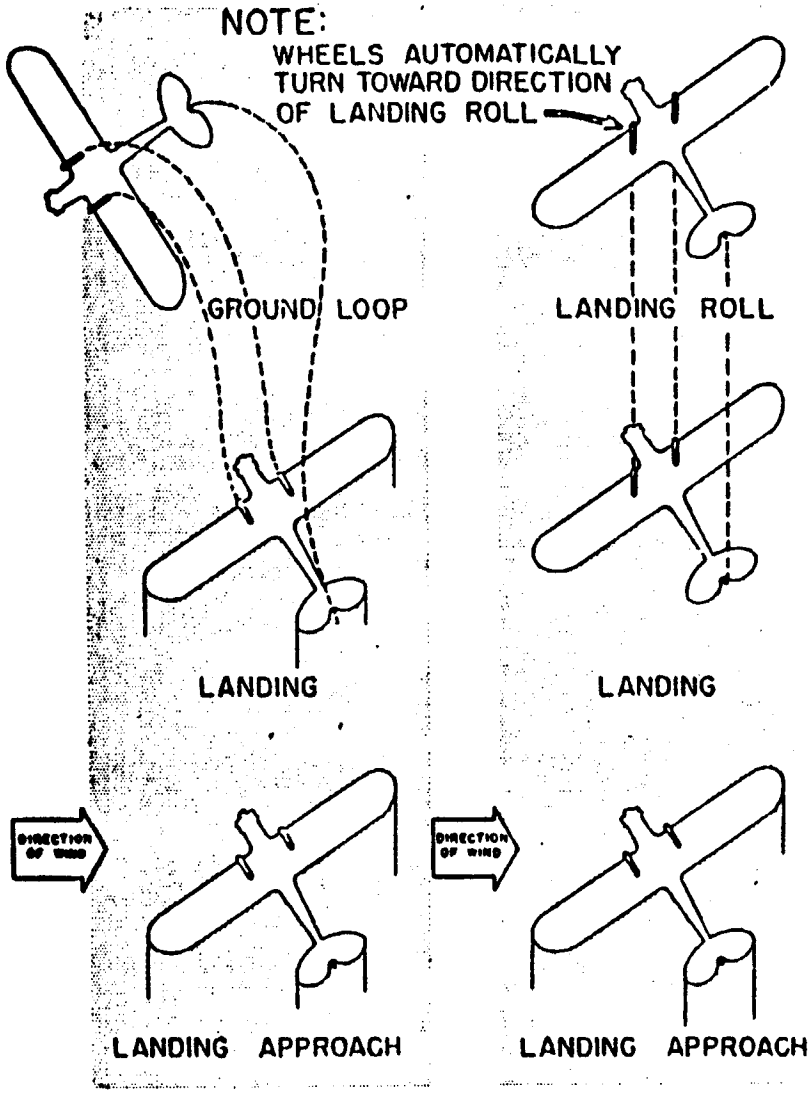

Figure 2.96a
Cross Wind Landing Without Cross Wind Landing Gear

Figure 2.96b
Cross Wind Landing With Cross Wind Landing Gear

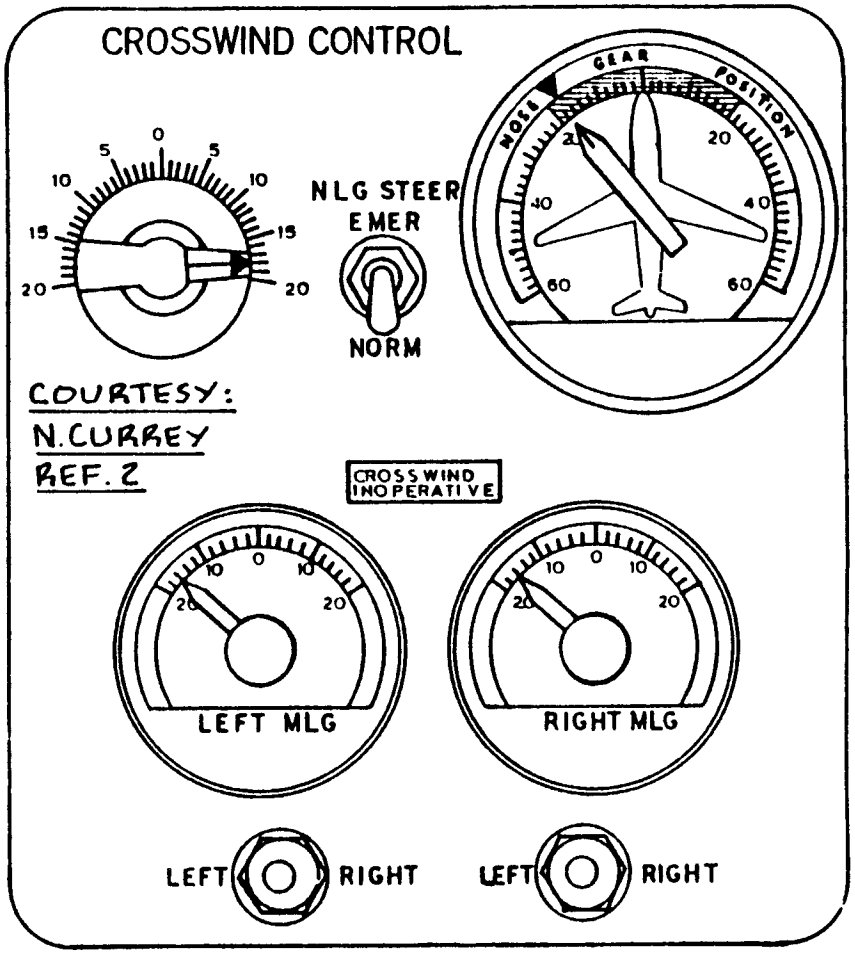

Figure 2.96c Control and Display Panel for a Cross Wind Landing Gear

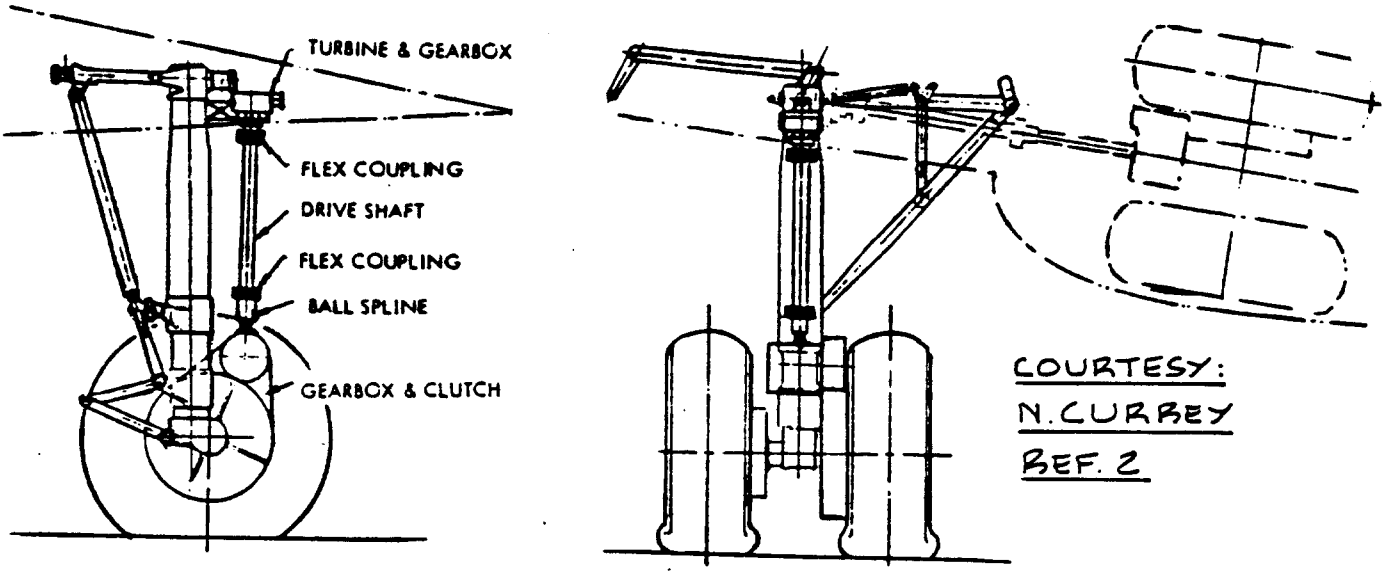

Figure 2.97 Self Driven Main Landing Gear

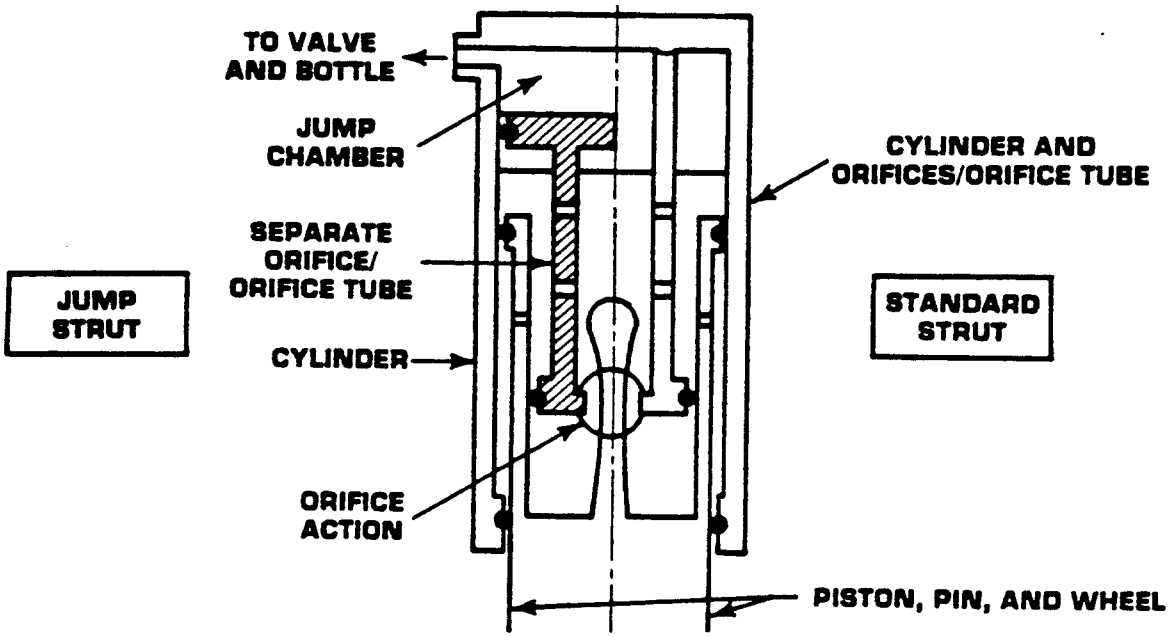

Figure 2.98 Jump Strut/Conventional Strut Comparison

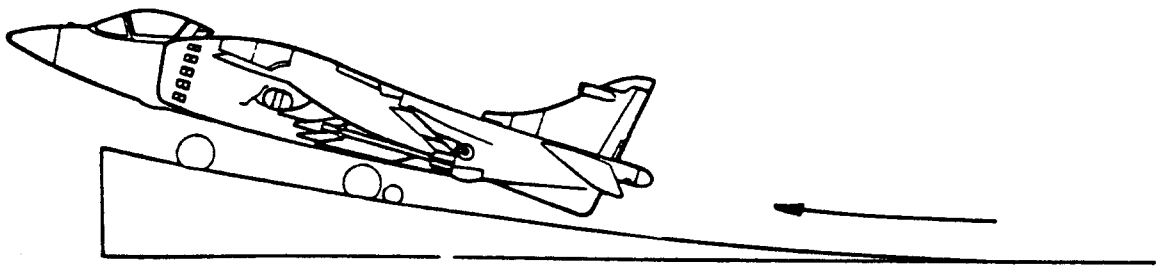

Figure 2.99 Example Ski-Jump Installation

2.12.3 Jump-Struts and Ski-Jumps

Many airplanes are critical in take-off rotation. This means that the longitudinal control system is sized by the need to rotate the airplane to the required take-off attitude toward the end of the take-off roll. The consequence of this is that the airplane is encumbered with too large a tail for its entire life.

Also, conventional fighters will have a tough time getting airborne in an environment where the enemy has 'cratered' the runways.

One method which has been proposed to eliminate this problem is to equip the airplane with 'jump-struts'. Figure 2.98 shows a jump-strut which has been tried experimentally on a Northrop T-38. With a jump-strut an airplane can be made to 'jump' upward at a speed significantly below the normal lift-off speed. The airplane will then trade potential energy for kinetic energy (like some carrier airplanes do after leaving the catapult) but stay airborne. This technique allows conventional fighters to get airborne in much shorter distances.

Another method to shorten the landing run of fighters is to use the so-called 'ski-jump'. This method was pioneered for use with the Harrier V/STOL fighter. Figure 2.99 illustrates such a ski-jump. The regular landing gear must be able to take the additional centrifugal forces imposed on the airplane on the ski-jump.

2.12.4 Droppable Gears

The landing gear weighs approximately 4 to 7 percent of the airplane take-off weight. This represents a sizeable amount of 'dead-weight' which is carried in the airplane only to allow relatively independent landing and take-off operations.

It is possible to equip an airplane with a landing gear which resembles a cart or series of carts on which the airplane rests. These carts allow normal ground maneuvering during take-off and are dropped immediately following lift-off.

The WWII Messerschmitt 263 of Figure 2.100 used such a gear. It landed on skis.

The British Hotol aerospace plane will also use such

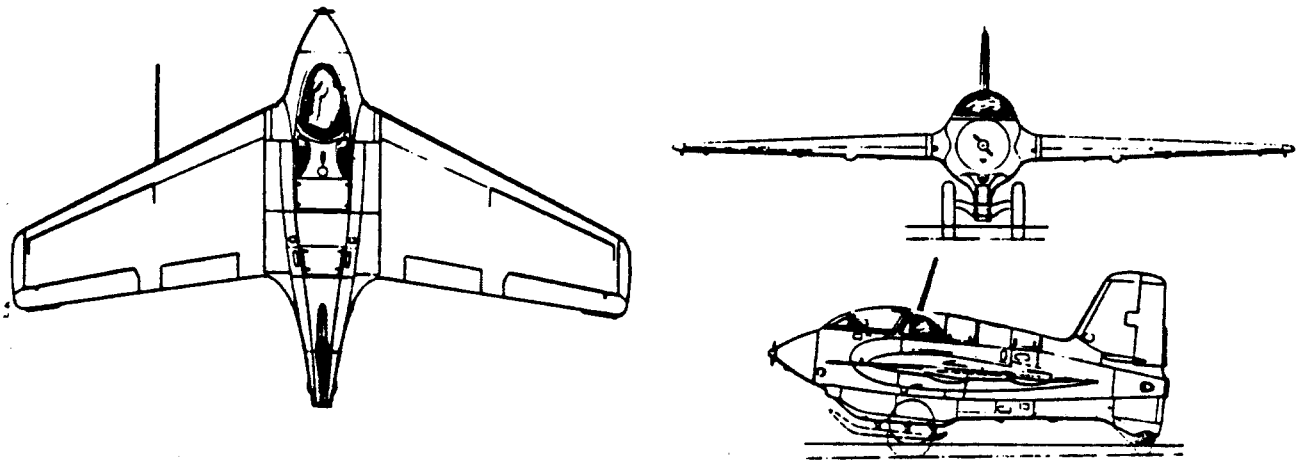

Figure 2.100 Example of a Droppable Landing Gear

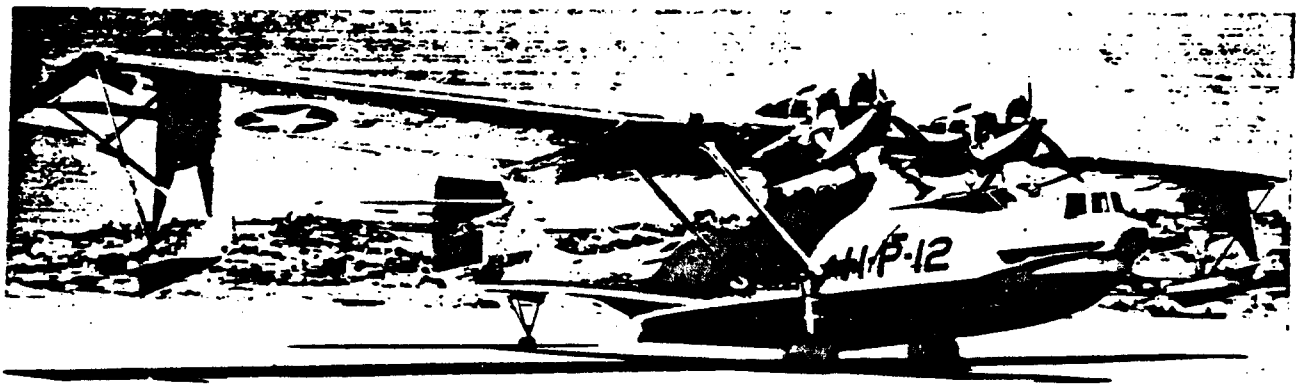

Figure 2.101 Example of a Beaching Gear

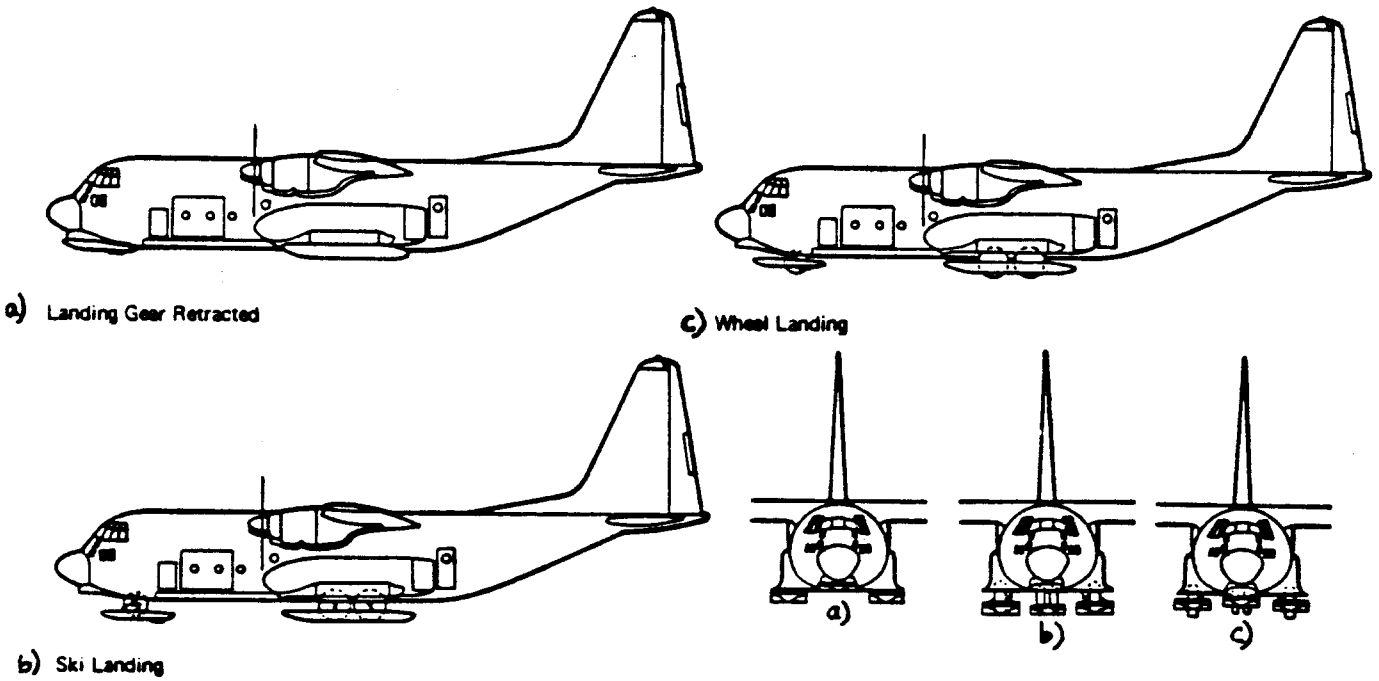

Figure 2.102 Example Ski Installation for Land Use

a gear. The Hotol will however still have a conventional retractable gear which is designed for the landing weight only.

An interesting possibility with a droppable gear is that the method for ground and take-off propulsion can also be built into the droppable gear system, allowing lift-off without any fuel having been used.

2.12.5 Beaching Gears

Flying boats are often equipped with beaching gears. These gears are attached to the flying boat after landing on the water. After the beaching gears have been attached, the flying boat can taxi up a ramp onto terra firma and then maneuver like any other land-plane. Figure 2.101 shows an example of such a beaching gear.

2.12.6 Skis

Skis are used to allow airplanes to land on snow, ice and water. Examples of skis are shown in Figs. 2.102 and 2.103.

2.12.7 Floats

Floats are added to some airplanes to enhance their operational capability in areas with large bodies of water. Canada and Alaska are examples of such areas. Figure 2.104 shows an example of an airplane on floats. A structural detail of a typical float attachment is given in Figure 2.105.

The hydrodynamic performance of floats depends strongly on their cross sectional shape. Figure 2.106 summarizes typical float geometries.

2.12.8 Air Cushion Landing System (ACLS)

The air cushion landing system was developed to make an airplane independent of prepared surfaces. Figures 2.107 and 2.108 show examples of such a system. References 2, 14 and 15 should be consulted for data on the design of air cushion landing systems.

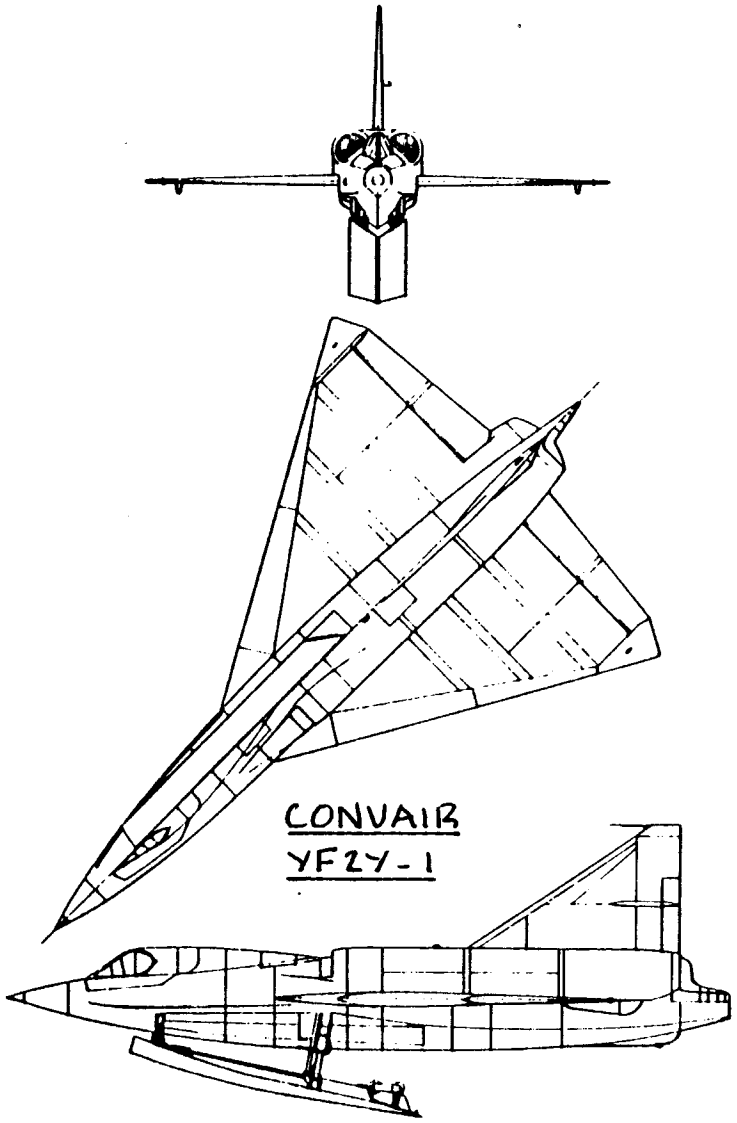

Figure 2.103 Example Ski Installation for Water Use

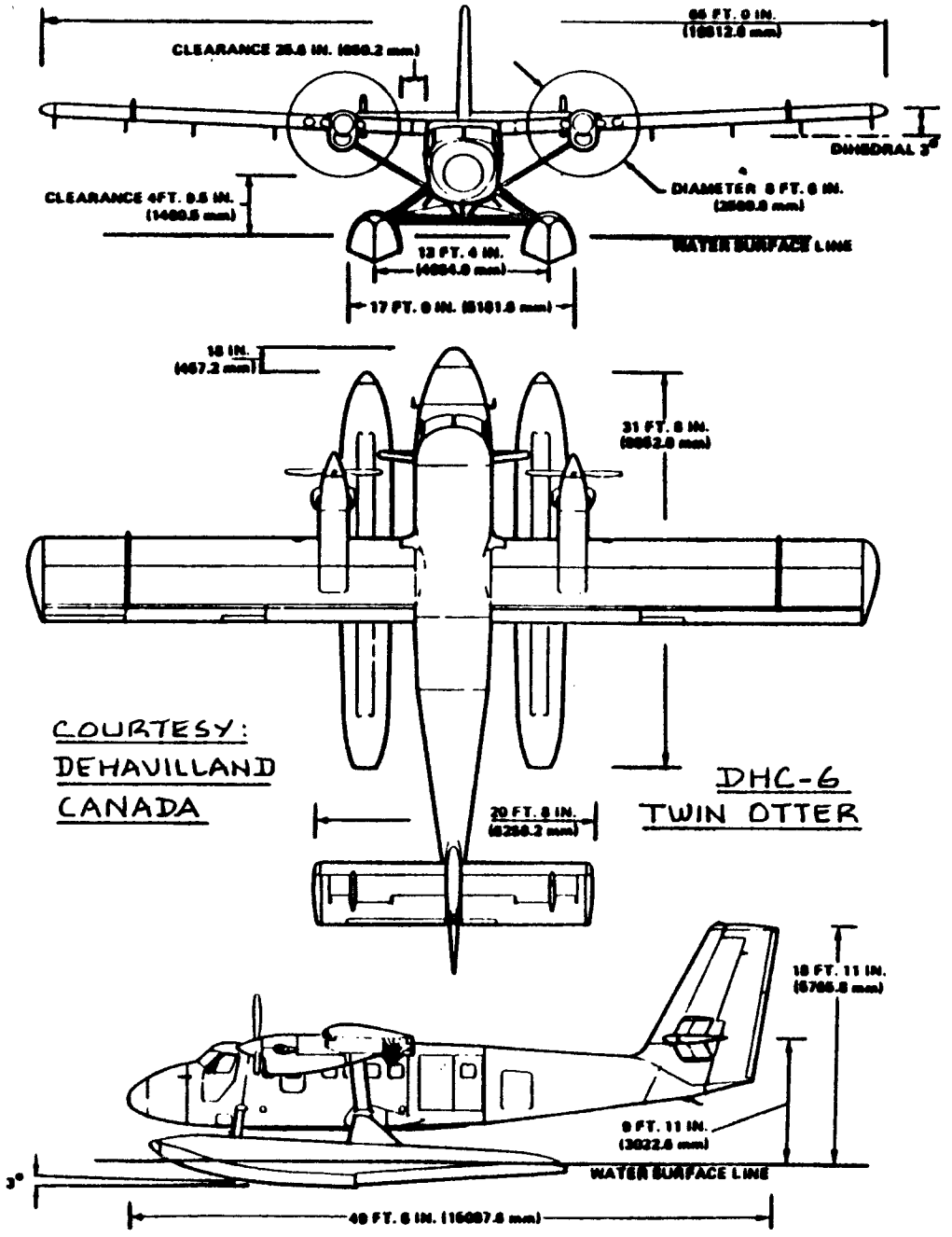

Figure 2.104 Example of a Float Installation

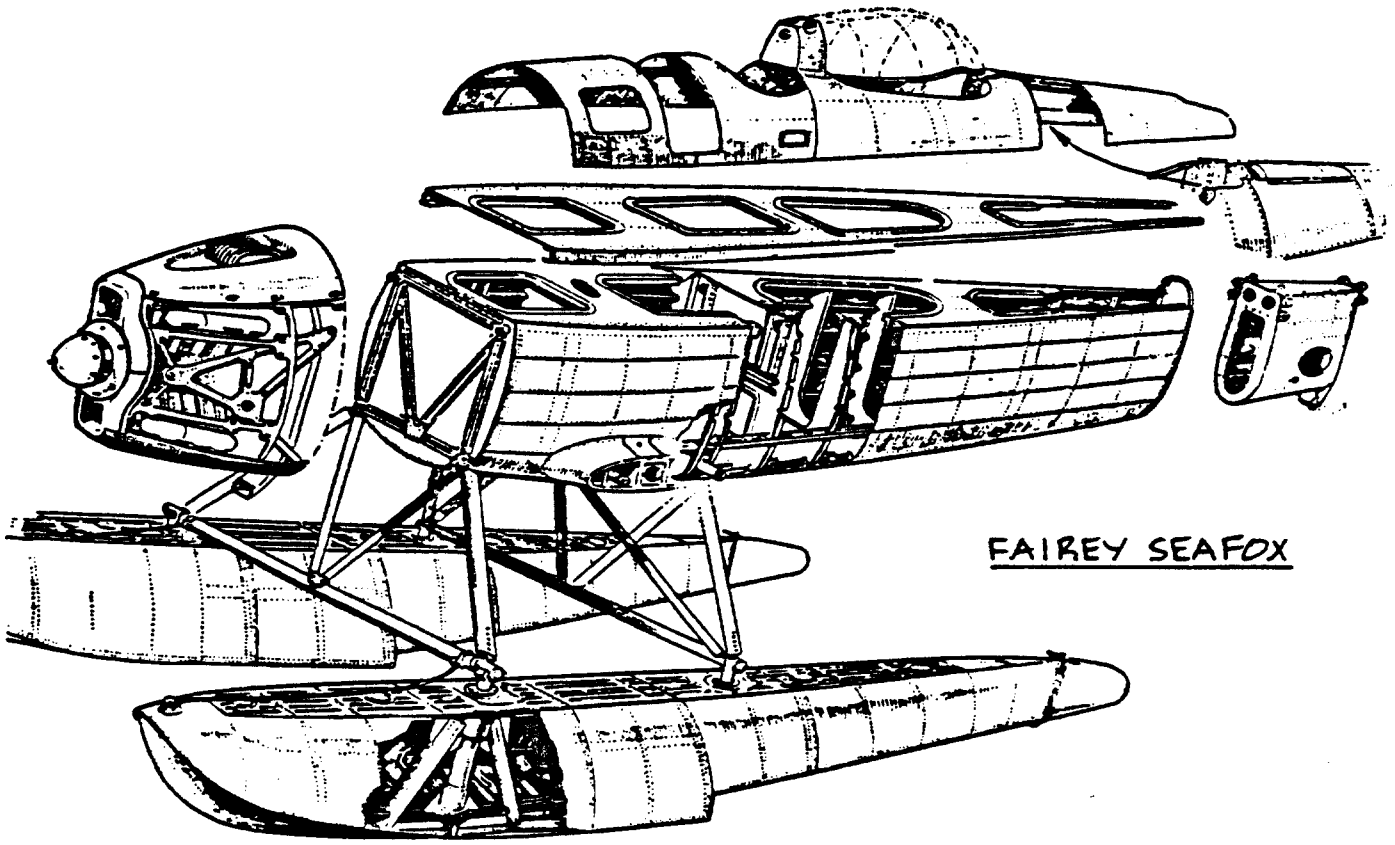

Figure 2.105 Example of a Float Structural Attachment

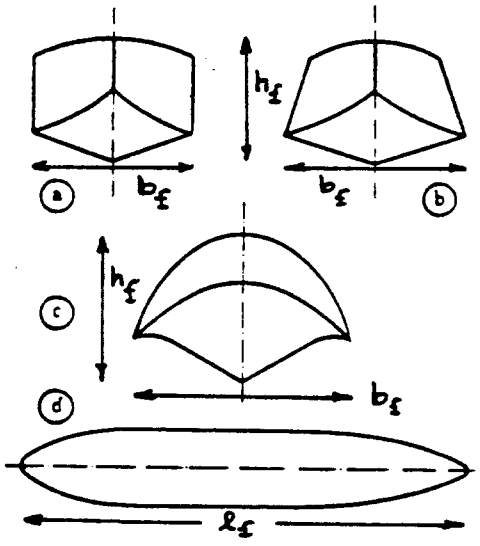

- TOTAL RECOMMENDED FLOAT VOLUME : 1.8 W_{TO} FOR LAKES
  2.0 W_{TO} FOR SEA
- FLOAT VOLUME PER FLOAT: V_f FT^3
- $b_f \cong 0.645\sqrt[3]{V}$
- $\ell_f \cong 0.775\, b_f$
- $h \cong 0.9\, b_f$
- SEE NACA TR488
- SEE SECTION 3.2 PART III
- © IS LESS 'DRAGGY' THAN @ AND ⓑ

Figure 2.106 Summary of Float Geometries

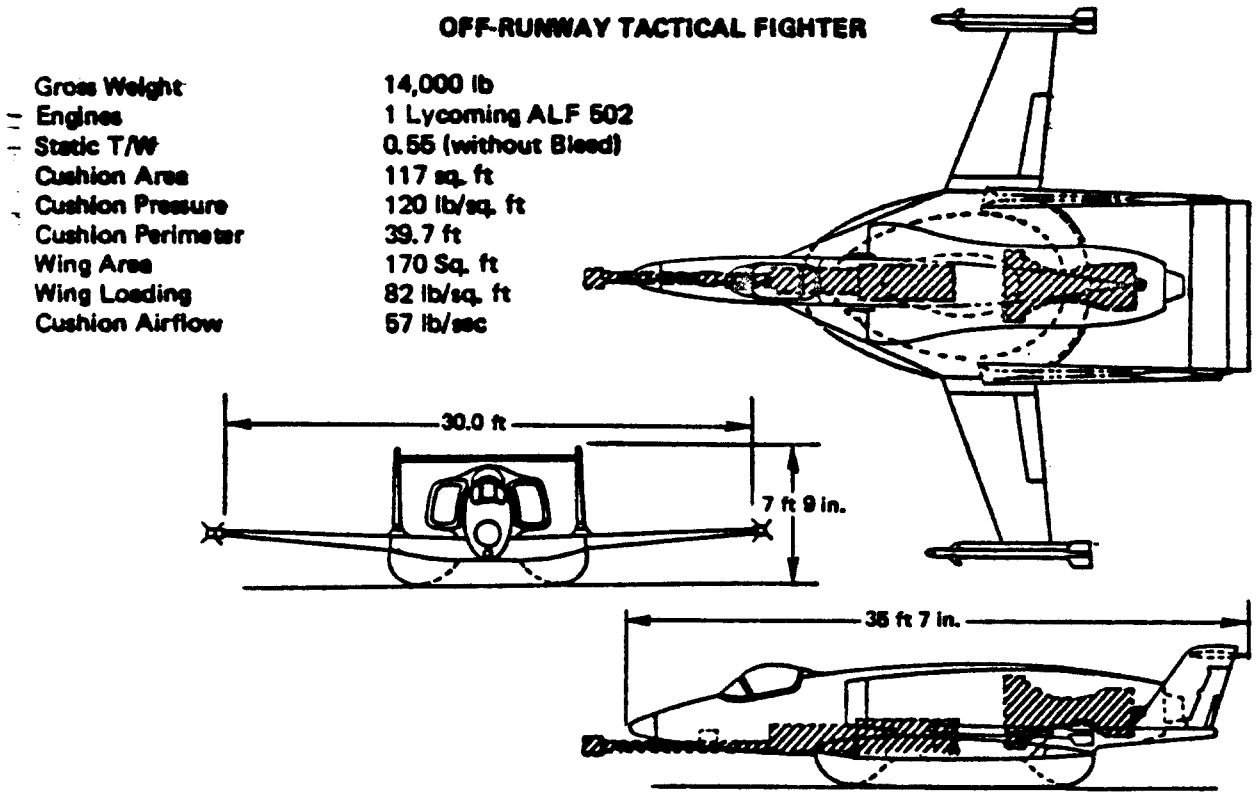

Figure 2.107 ACLS Installation in a Proposed Fighter

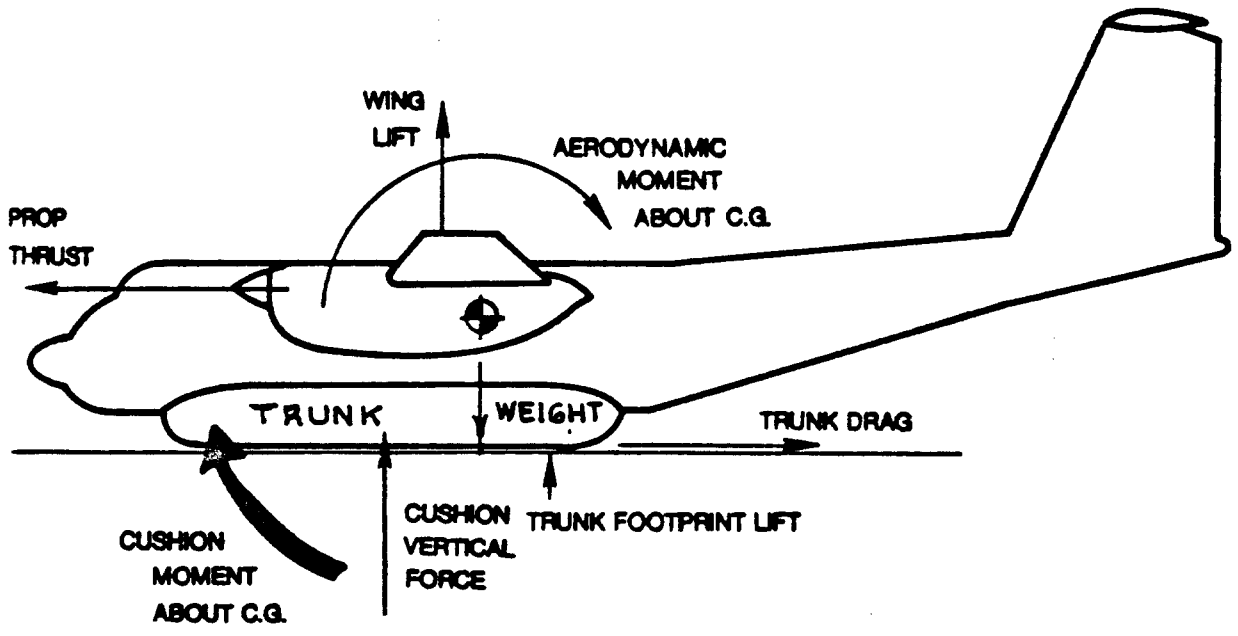

Figure 2.108 ACLS Installation in the XC-8A Transport

3. WEAPONS INTEGRATION AND WEAPONS DATA

The purpose of this chapter is to discuss a number of special design considerations which arise when integrating weapons and stores into military airplanes. In addition, data on typical weapons, stores and military cargo are presented.

The material is organized as follows:

3.1 Aerodynamic design considerations

3.2 Structural design considerations

3.3 Design for low radar and infrared detectability

3.4 Examples of weapon installations

3.5 Weapon and military payload data

3.1 AERODYNAMIC DESIGN CONSIDERATIONS

The following problem areas need to be considered when integrating weapons and/or stores into an airplane:

1. Drag 2. Stability and control 3. Separation

4. Gun exhaust gasses entering into engine inlets

3.1.1 Drag Considerations

When mounting stores under a wing or fuselage additional friction, profile and interference drag will be generated. Figures 3.1 and 3.2 show several 'rack' or 'pylon' mounted stores. For typical 'rack' geometries, the reader is referred to sub-section 3.5.2.

The incremental drag caused by the stores shown in Figures 3.1 and 3.2 can be estimated with the drag estimating methods of Part VI. The following general rules must be observed if drag increases due to stores are to be kept to a minimum:

1. For rack or pylon mounted stores which are roughly bodies of revolution, the distance from the store exterior to the wing or fuselage exterior should be larger than one half of the store diameter. This recommendation is illustrated in Figure 3.3.

COURTESY:
L.T.V.

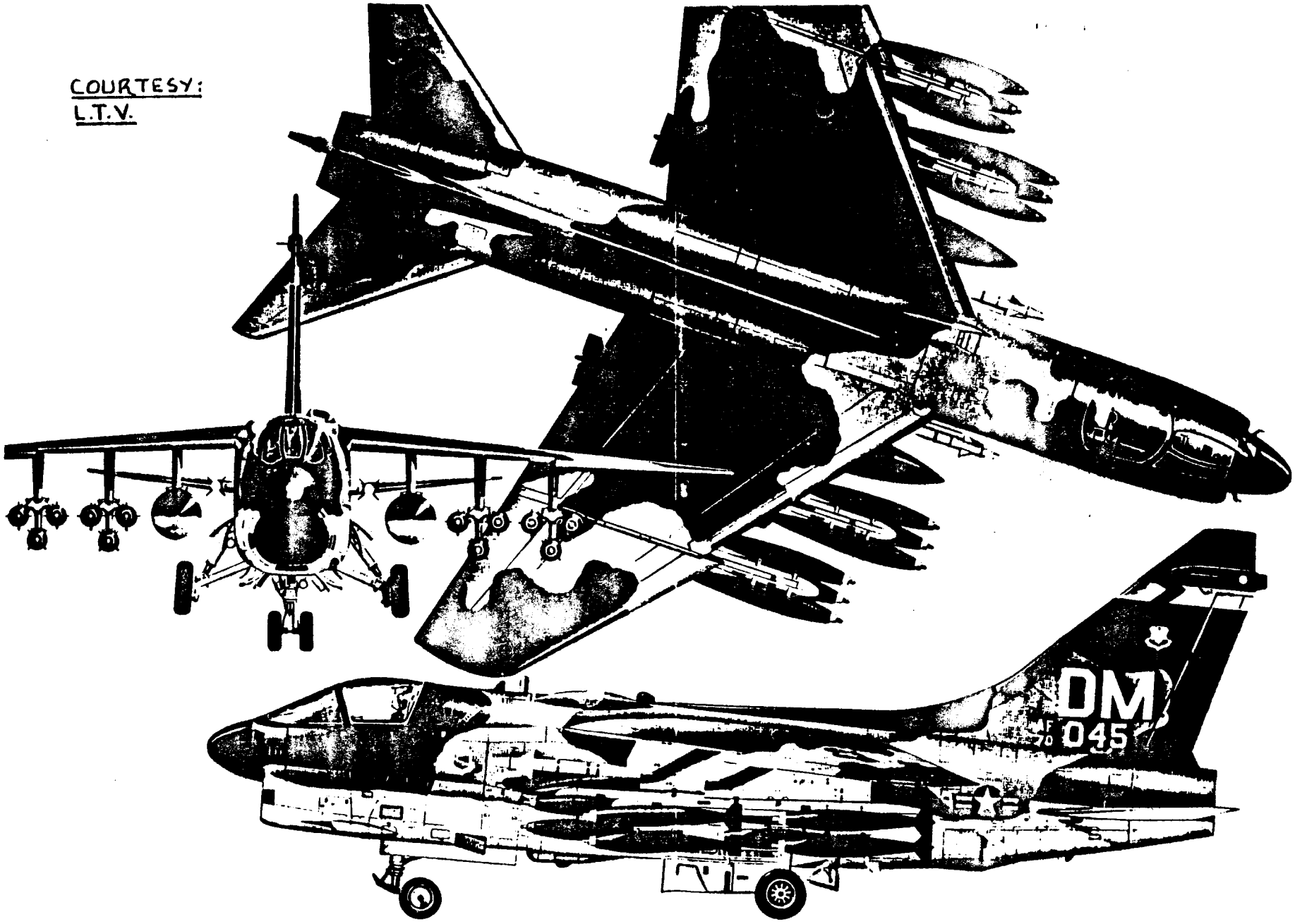

Figure 3.1 Example of Rack and Pylon Mounted Stores

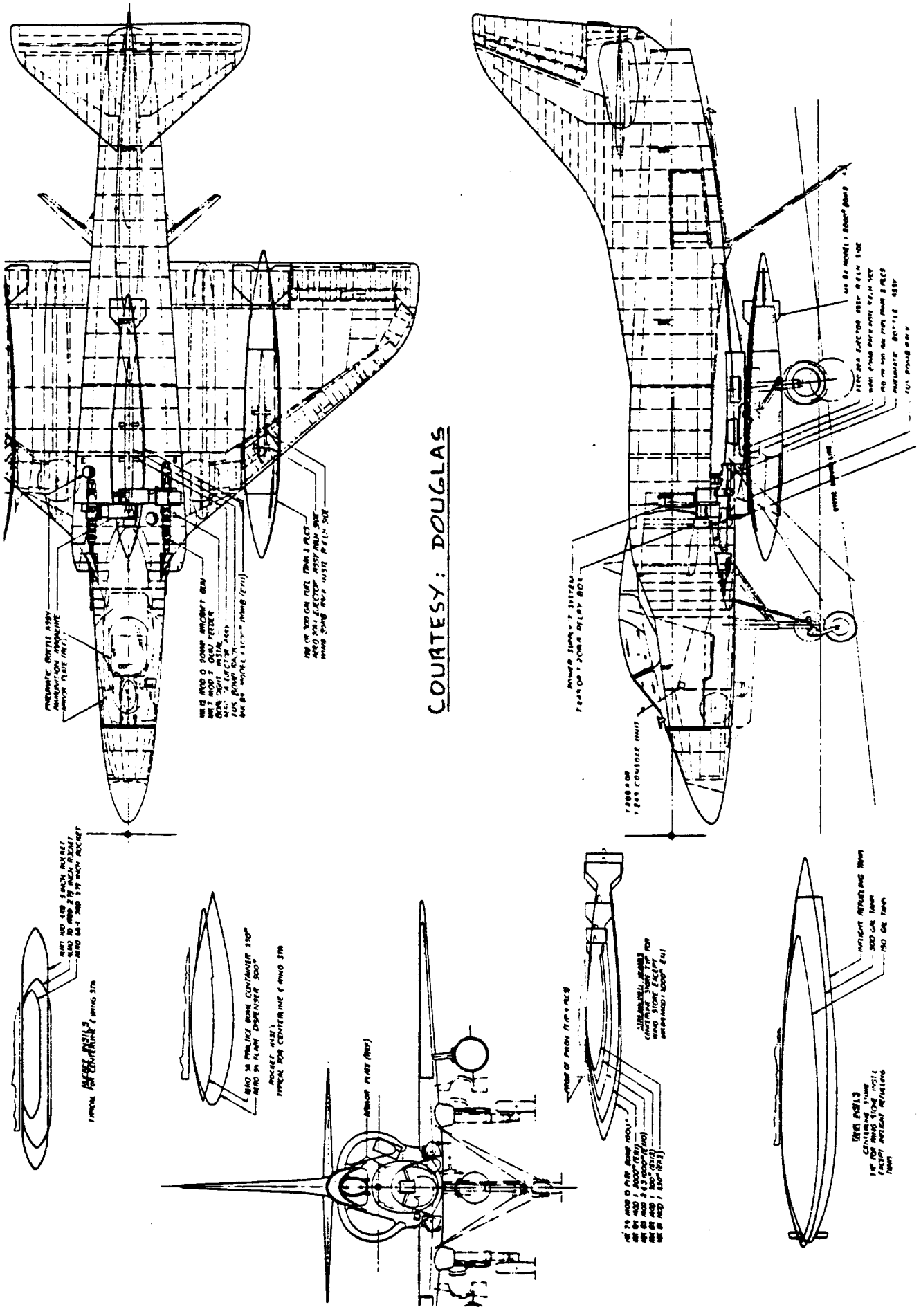

Figure 3.2 Example of Rack and Pylon Mounted Stores

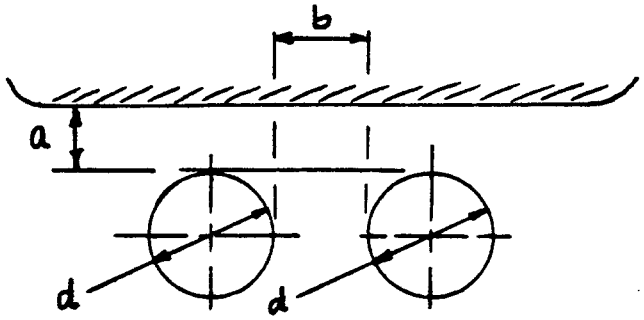

HEAD-ON VIEW

$a \geq d/2$

$b \geq d/2$

Figure 3.3 Recommended Mounting for Pylon and Rack Mounted Stores

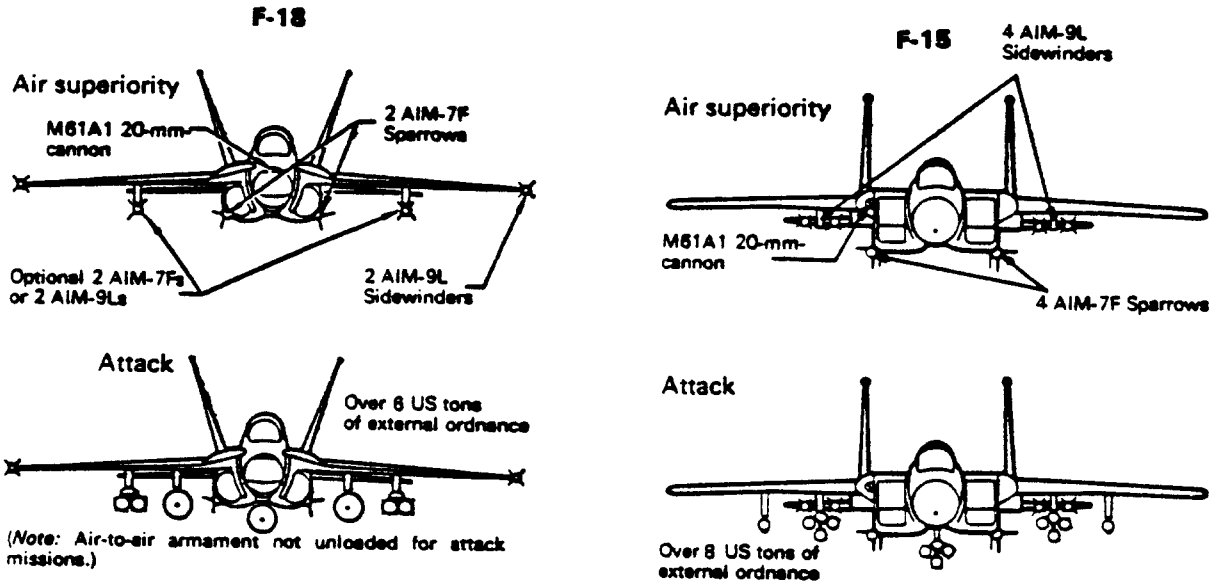

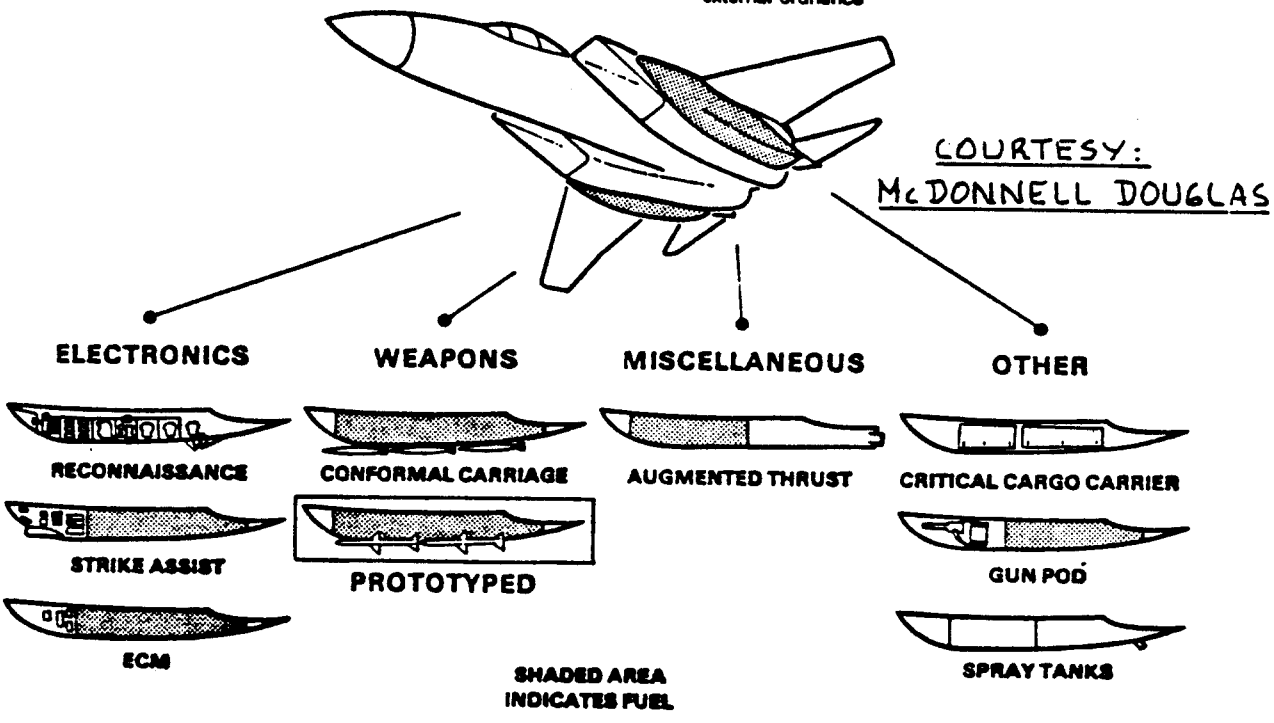

COURTESY: McDONNELL DOUGLAS

Figure 3.4 Examples of Conformal Store Mounting

Significant reductions in store drag increments can be achieved by mounting the stores 'conformally'. Examples of conformal and pylon mounted store arrangements are shown in Figure 3.4.

2. Figure 3.5 illustrates the drag reductions which can be achieved with a 'conformal' arrangement.

3.1.2 Stability and Control Considerations

Stores can alter the static longitudinal and static directional stability of an airplane. Figure 3.6 shows examples of store arrangements with such effects. The methods of Part VI and Part VII may be used to estimate the effects of stores on stability.

Stores and guns can add large moments about the center of gravity. These moments must be controllable without significant increase in pilot workload.

Store induced moments are primarily caused by drag. These drag induced moments need to be 'trimmed' in steady state flight. Upon release of the store a moment transient will occur. This moment transient should be minor.

Gun induced moments are caused by gun recoil forces. The data in Section 3.5 show that these recoil forces can be considerable.

In both cases the problem centers around the estimation of the moments imposed on the airplane by these recoil forces or/and by these drag forces.

Figure 3.7 shows a typical fuselage gun installation. If the recoil force imposed on the airframe is called: F_r and the moment arms are as shown in Figure 3.7,

then it is possible to estimate the resulting recoil moments from:

$$\Delta C_{m_r} = F_r z_r / \bar{q} S \bar{c} \qquad (3.1)$$

$$\Delta C_{n_r} = F_r y_r / \bar{q} S b \qquad (3.2)$$

The required control deflections to compensate for these moments follow from:

$$\Delta i_{H_r} = \Delta C_{m_r} / C_{m_{i_H}} \qquad (3.3)$$

$$\Delta \delta_{R_r} = \Delta C_{n_r} / C_{n_{\delta_R}} \qquad (3.4)$$

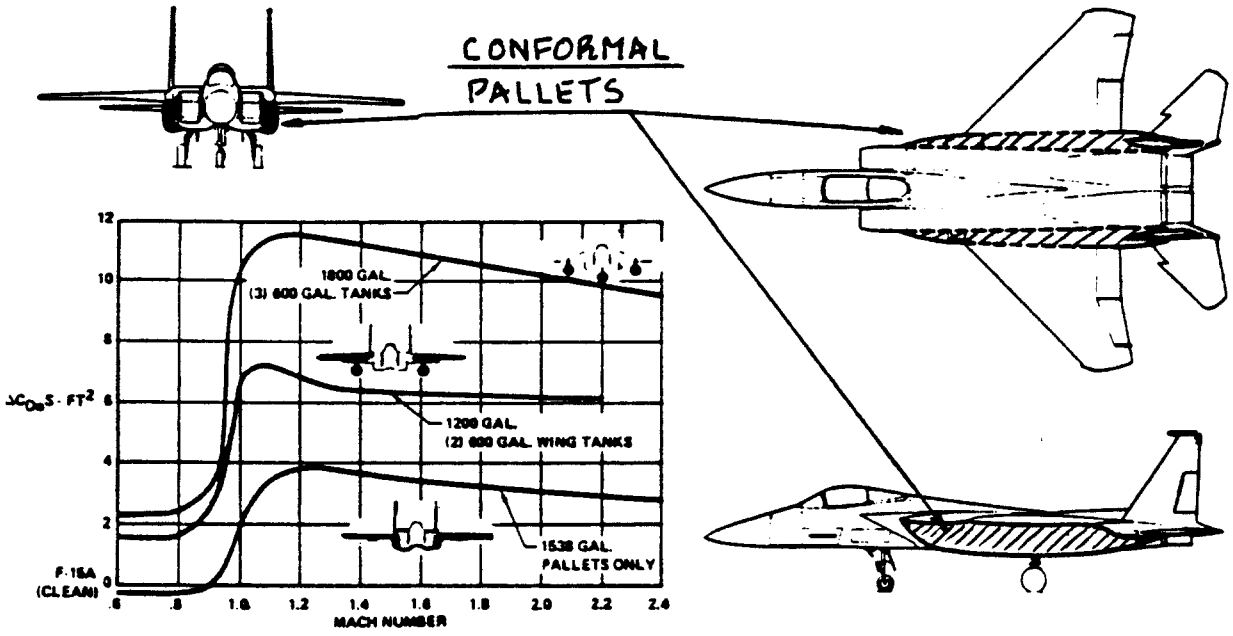

COURTESY: McDONNELL DOUGLAS

Figure 3.5 Typical Drag Reductions Due to Conformal Store Mounting

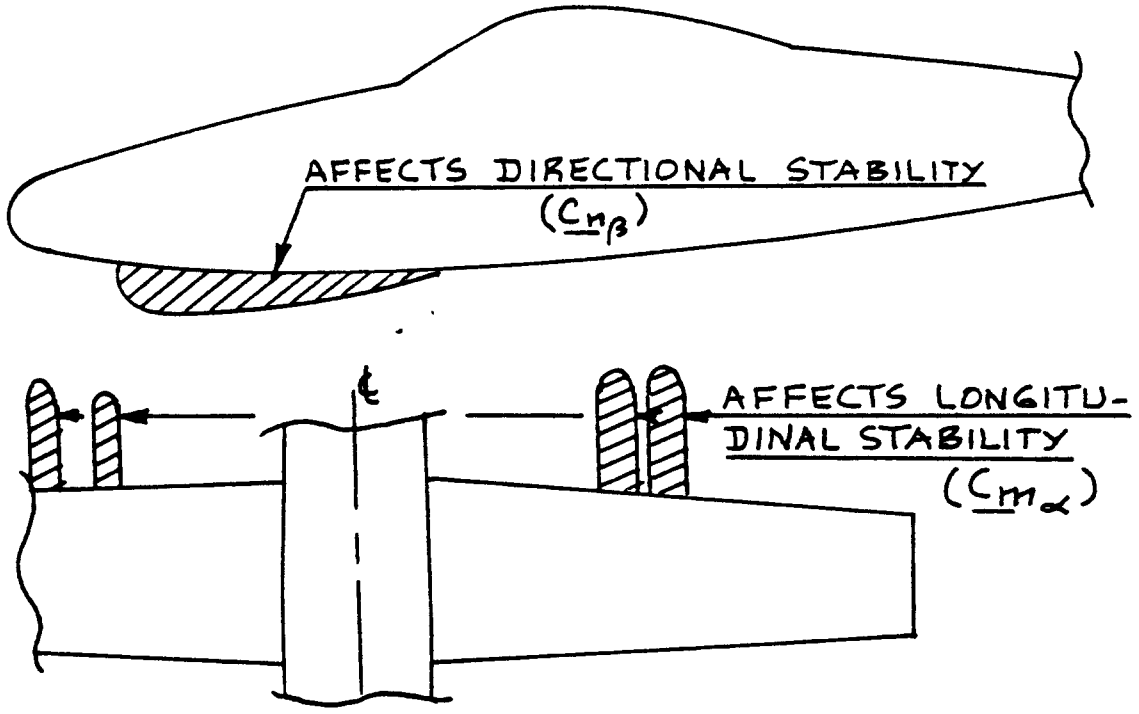

Figure 3.6 Example of Store Mountings Which Affect Longitudinal and Directional Stability

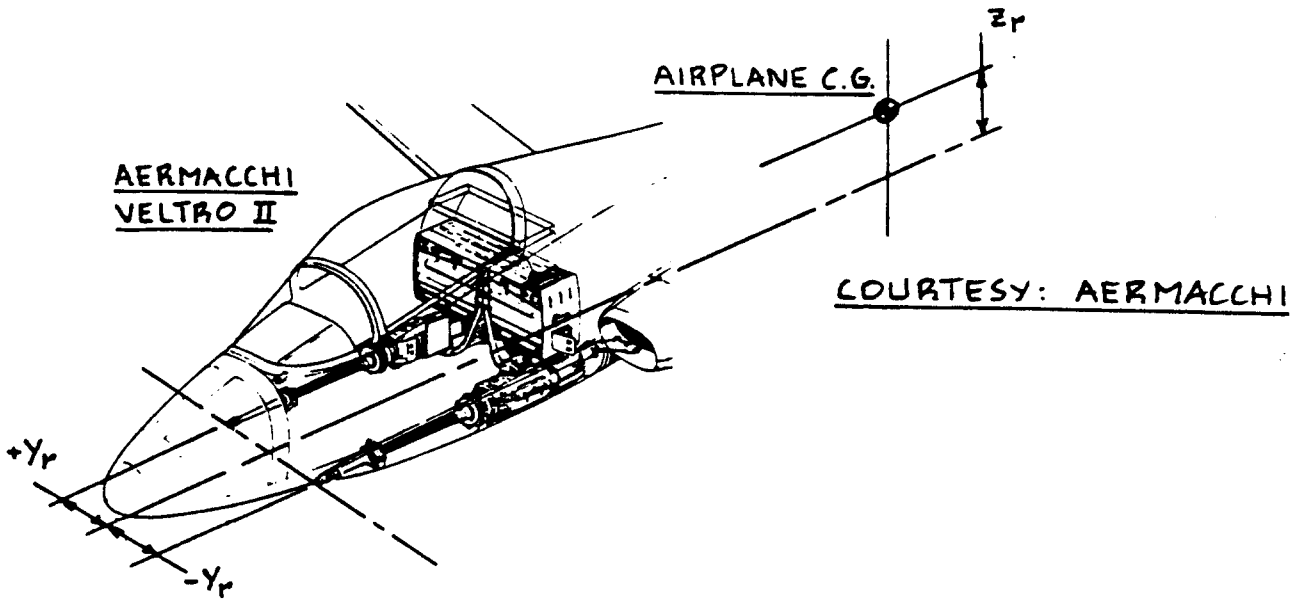

Figure 3.7 Example of a Fuselage Mounted Gun Installation

CANON RECOIL EFFECT ON CONTROL SYSTEM DESIGN

- THE SHOULDER MOUNTED GUN WAS THE OPTIMUM F-15 LOCATION:
  - PERMITTED ELEVATED BORE LINE FOR TRACKING STABILITY
  - ELIMINATED GAS INGESTION IN INLETS
  - MINIMIZED CROSSECTION AREA AND PERMITTED READY ACCESS
- THE LOCATION CAUSES A RECOIL MOMENT ON THE AIRCRAFT, WHICH IS NEGLIGIBLE WITH THE PRESENT 20MM GUN
- THE F-15 WAS DESIGNED TO ACCOMMODATE THE GAU-7A, 25MM GUN WHICH HAS NOT BEEN DEVELOPED, SIMULATION SHOWED COMPENSATION TO BE NEEDED TO ACCOMMODATE THE FACTOR OF 3 INCREASE IN RECOIL
- THE FOLLOWING SYSTEM WAS DESIGNED VIA SIMULATION AND WOULD BE ADDED WITH THE GAU-7A GUN

COURTESY: McDONNELL DOUGLAS

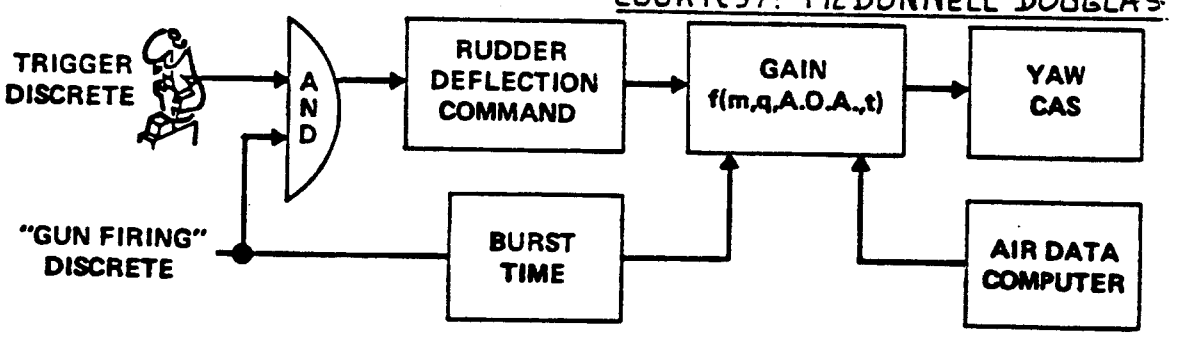

Figure 3.8 Automatic Compensation of Recoil Effects

The control power derivatives in Eqns.(3.3) and (3.4) may be estimated with the methods of Part VI. The incremental control deflections as determined in Eqns.(3.3) and (3.4) should not be 'too large'. What 'too large' means depends on the type of airplane and on its flight control system. Acceptable control deflections are in the 0.5 to 2 degree range.

For airplanes with reversible flight control systems the control deflections due to gun recoil must be obtained through a pilot induced force on the cockpit controls. These pilot control forces should not be excessive. Methods for computing pilot control forces are presented in Part VII.

For airplanes with irreversible flight control systems it is relatively easy to arrange for automatic compensation of the recoil moments. This can be done via the flight control computer system signalled by the pilot's triggering of a fire control switch. An example of such a system is shown in Figure 3.8.

3.1.3 Separation Considerations

Any store or missile which needs to be dropped or fired from an airplane must have 'clean' separation characteristics relative to the airplane as well as relative to other ordnance released at the same time.

To assure positive separation an analysis or test must be conducted which shows conclusively that upon release the now 'free' store or missile will not hit the airplane. This is a very difficult problem to analyze because the store or missile, upon release is not at first in a uniform flowfield but is instead in the complicated flowfield surrounding the airplane.

Separation trajectories are normally calculated with the help of finite element aerodynamic programs. The results of these calculations are then verified by windtunnel tests arranged so that the forces and moments on both airplane and store (or missile) can be measured. The US Navy David Taylor facility in Corduroc, Maryland is probably the best equipped facility for this type of testing.

After these windtunnel tests in-flight verification of positive separation is normally carried out at weapons test ranges, before the store or missile is released for

operational deployment.

Figure 3.9 shows an example of a positive separation system as used frequently in separating fuel tanks from airplanes.

3.1.4 Gun Exhaust Gas Considerations

When installing a gun or cannon in an airplane, make sure that the gun exhaust gasses cannot enter the inlet of a jet engine or gas generator. Most gun exhaust gasses are highly corrosive to jet engine compressor and/or turbine blades.

Figure 3.10 shows examples of 'good' and 'poor' installations from this viewpoint.

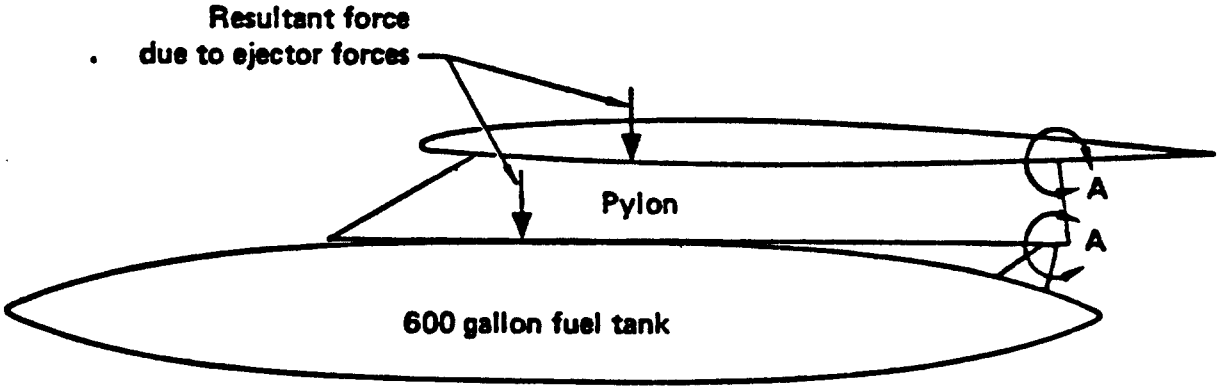

COURTESY: McDONNELL DOUGLAS

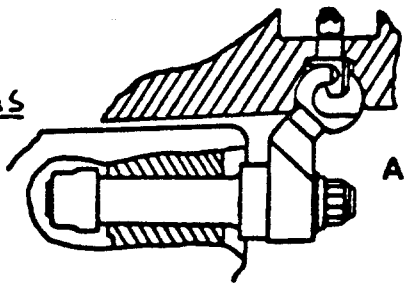

Figure 3.9 System for Positive Store Separation

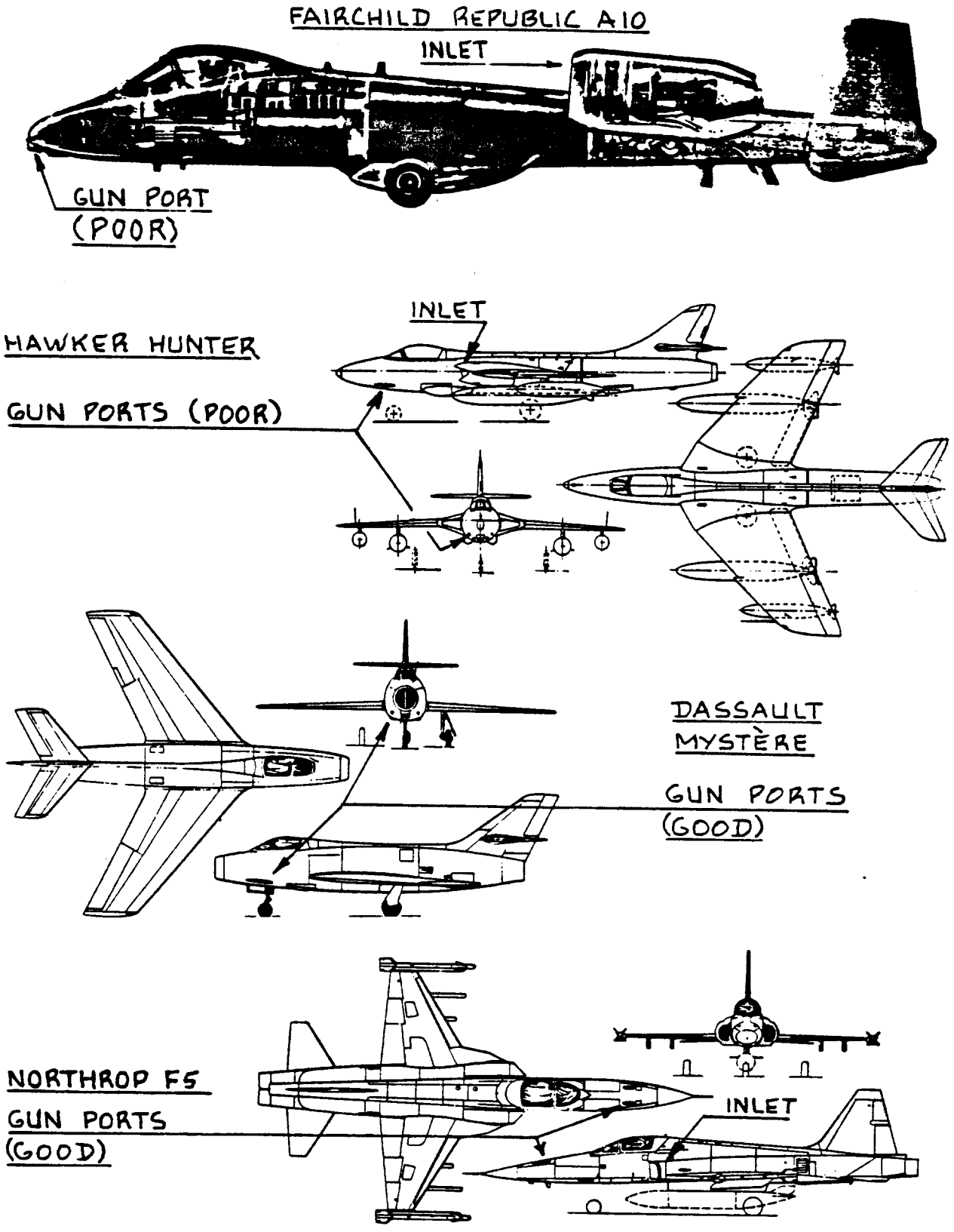

Figure 3.10 Example of Good and Poor Gun Locations From a Viewpoint of Gun Exhaust Versus Engine Inlet Locations

3.2 STRUCTURAL DESIGN CONSIDERATIONS

The following structural design considerations can be important in weapon and store integration:

1. Effect of gun recoil forces on the structure.

These recoil forces can be considerable (12,000 lbs in the case of some multi-barrel cannons!). These forces must be transitioned in to the airframe structure without causing undue deformations or fatigue problems.

2. Effect of gun induced vibrations on the structure and on sensors located close by.

Gun induced vibrations can cause ride quality problems at the pilot station. The gun attachment structure needs to be sufficiently stiff to prevent this.

Gun induced vibrations can cause local accelerations at places where flight crucial sensors are located. This can have two effects:

a) damage to the sensors

b) the sensors will interpret these accelerations as 'rigid' body signals thereby causing improper operation of the flight control system. Particularly this latter effect has been happening frequently during early weapons testing on several fighter programs. Relocating of sensors or the addition of notch filters can solve these problems.

3. Inertial load of stores and aerodynamic loads on stores need to be transmitted to the structural 'hard points' to which the stores are attached.

These hard points need to be designed so they do not deform excessively during maneuvering flight and so they do not induce unduly large stresses in the surrounding structure. Figure 3.11 shows an example of typical hard point installations. Another example was shown in Figure 4.80 in Part III.

4. Stores may cause flutter.

During flight testing in many fighters it is found that excessive vibration and/or flutter problems arise with certain store configurations. To prevent this from occurring it is necessary to conduct realistic flutter calculations (and sometimes flutter model tests)

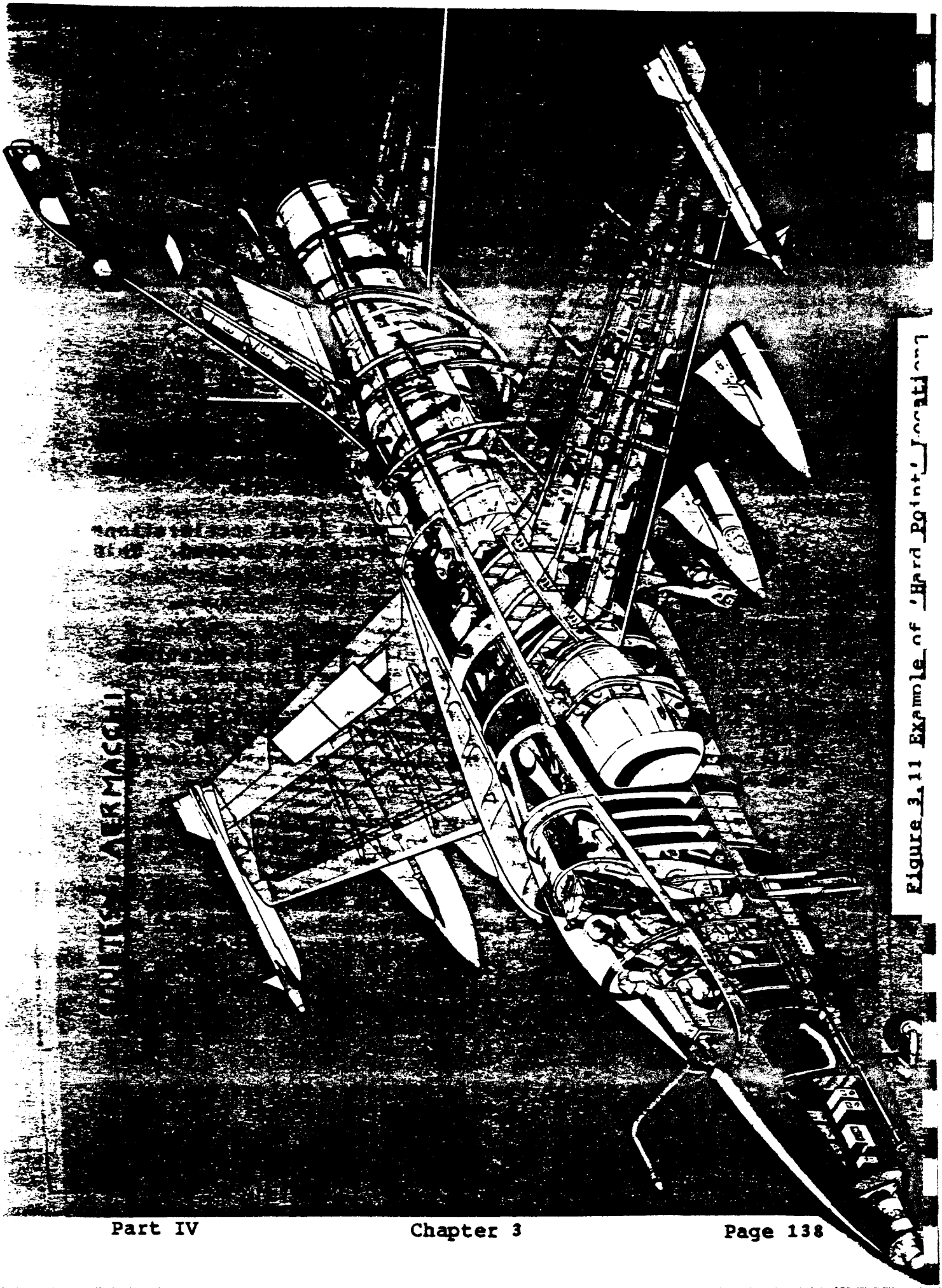

Figure 3.11 Example of 'Hard Point' Location

before committing to flight test and certainly before committing to production. Required 'fixes' late in a production program tend to be very expensive.

Figure 3.12 recalls an incident of store flutter (in this case a relatively benign 'limit cycle' oscillation) and indicates the 'fix'.

STORES EFFECT ON MECHANICAL CONTROL SYSTEM DESIGN

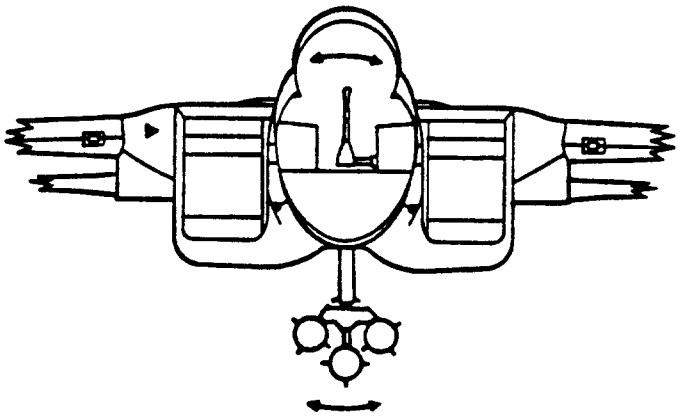

PROBLEM

- A 5.9hz DIVERGENT OSCILLATION WAS DISCOVERED AT 0.9M, 5000 FT DURING FLIGHT FLUTTER TESTING WITH MK-82 BOMBS. REACHED ±1g LATERAL.
- PILOT HAD TO JETTISON STORES

CAUSE

- COUPLED AEROELASTIC MODE INVOLVING: PYLON YAW, RACK BENDING, FUSELAGE SIDE BENDING AND LATERAL MECHANICAL CONTROL SYSTEM.
- REQUIRED HIGH EXCITATION LEVEL TO INDUCE.

SOLUTION

- ADDED EDDY-CURRENT DAMPER TO LATERAL CONTROL SYSTEM

Figure 3.12 Example of a Store Flutter Incident

3.3 DESIGN FOR LOW RADAR AND INFRARED DETECTABILITY

When an airplane is difficult to detect with radar and/or with infrared sensors its combat survivability is improved. Combat survivability is also determined by the vulnerability of critical airplane systems to hostile action. Reference 16 contains a thorough treatise on analysis and design for combat survivability.

3.3.1 Design Considerations for Low Radar Detectability

The following design considerations for low radar detectability (low radar cross section or low RCS) were obtained from Dr. Alan E. Fuhs of the US Naval Postgraduate School in Monterey, California. Ref.17 presents the corresponding theories and methods for determining the radar cross section of an airplane. This sub-section summarizes those recommendations for low RCS which are important to the preliminary layout designer.

What makes an airplane visible to radar is a phenomenon called radar wave reflection or radar wave scattering. To understand scattering, it is useful to think of an airplane as a 'porcupine' with quills pointing outward as normal vectors to the surface. If the airplane is to be 'stealthy' it should not point any quills in the direction of a radar antenna.

To shape an airplane for low RCS a decision must be made regarding the primary radar threat: it makes a difference whether the radar sees an airplane from below, from the side up, from the side down or from above.

In shaping an airplane for low RCS some unfavorable trades will have to be accepted in regard to aerodynamic drag, inlet efficiency and cockpit visibility.

The following factors tend to promote radar wave scattering and therefore increase the RCS of an airplane:

1. Fuselages with square cross sections: round the fuselage cross section as gently as possible. Cant the fuselage sides away from radar looking at it from the side: a fuselage with a rounded triangular cross section tends to have a low RCS.

Figure 3.13 illustrates the good and the bad.

2. Inlets with sharp flat surfaces: locate the inlets above the airplane when the primary radar threat is from below. If propulsion considerations allow it,

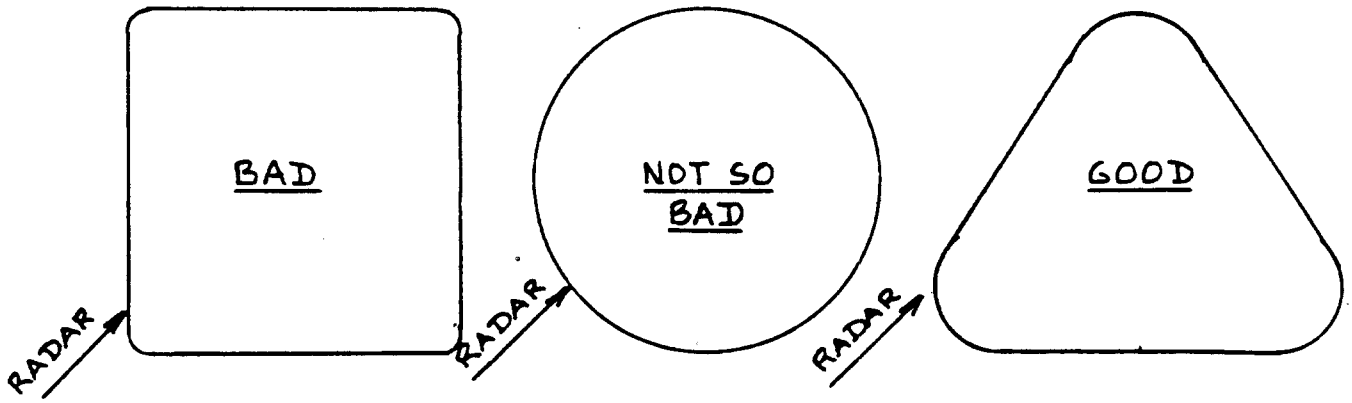

Figure 3.13 RCS: Good and Bad Fuselage Cross Section

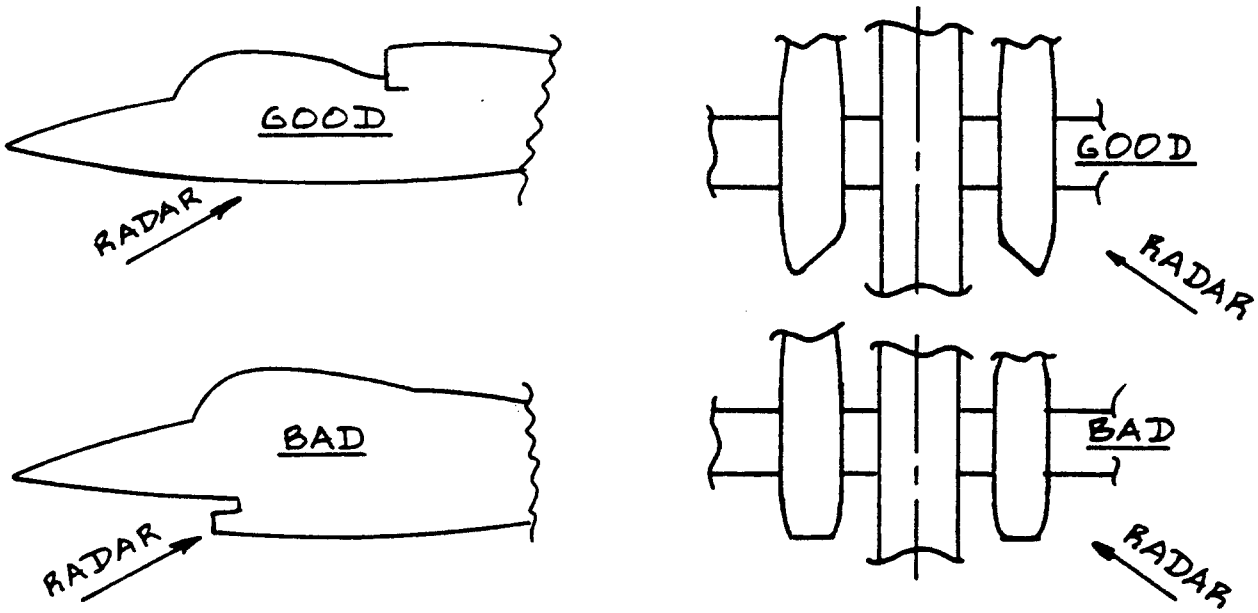

Figure 3.14 RCS: Good and Bad Inlet Design

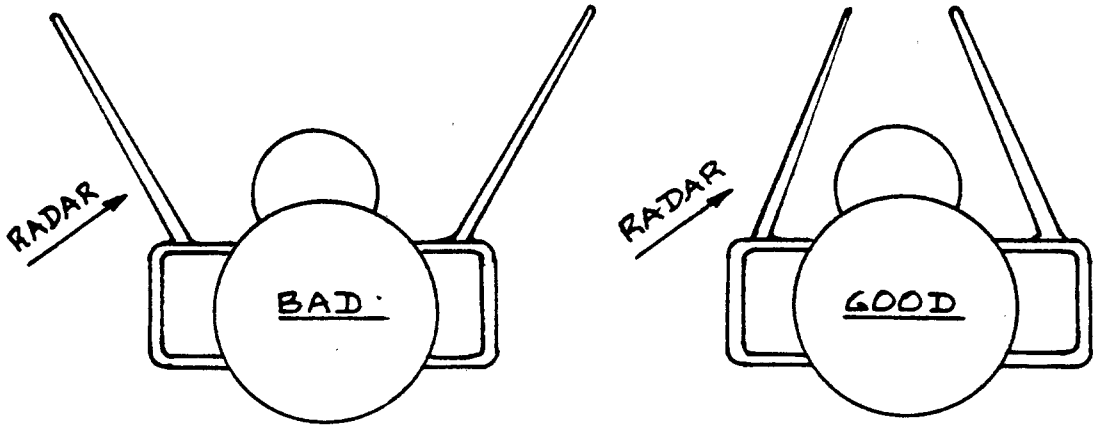

Figure 3.15 RCS: Good and Bad Vertical Tail Design

placing a wire mesh over the inlet helps reduce the RCS. The mesh spacing should be as small a fraction of the radar wavelength as possible.

In multi-engine installations the inlets may have to be angled inward to shield them from detection by side-looking radar.

Figure 3.14 illustrates the good and the bad.

3. Vertical tails which are tilted outward: cant the vertical tails inward for low RCS. The way most vertical tails are put on fighters today (with outward cant) is good from an aerodynamic viewpoint but it is bad from an RCS viewpoint.

Figure 3.15 illustrates the good and the bad.

4. Exhaust Nozzles: should be shielded from radar.

Figure 3.16 illustrates the good and the bad.

5. Wings with straight leading edges and tips: against head-on radar, the more sweep a wing has, the lower its detectability. For up-looking radar, a leading edge and wingtip which have a continuously varying curvature (rounding) are less detectable than straight leading edges and straight wing tips.

Figure 3.17 illustrates the good and the bad.

6. Large canopies: the use of low profile canopies tends to lower the RCS. The designer must make a compromise between the 'see and be seen' features.

Any thin layer of metal (preferably gold) which covers the canopy without hurting visibility from within helps reduce the RCS enormously.

Figure 3.18 illustrates the good and the bad.

7. Ordnance carried outside the airplane: to lower the RCS carry ordnance inside the airplane as much as possible.

Conformal stores are better than pylon mounted stores.

Figure 3.19 illustrates the good and the bad.

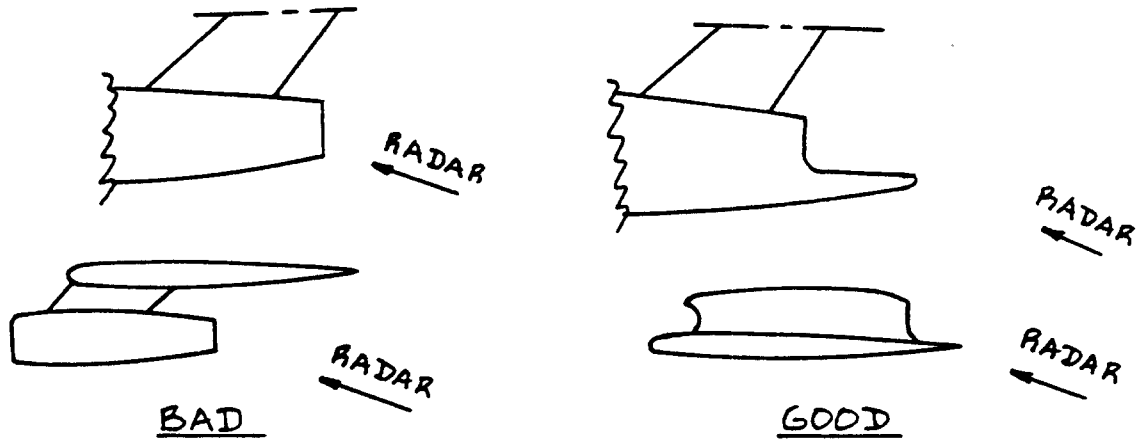

Figure 3.16 RCS: Good and Bad Exhaust Nozzle Design

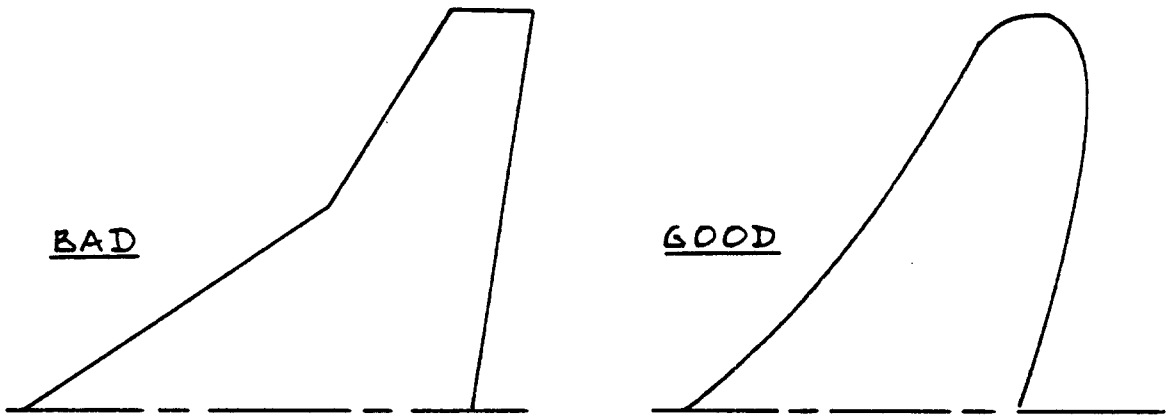

Figure 3.17 RCS: Good and Bad Wing Planform Design

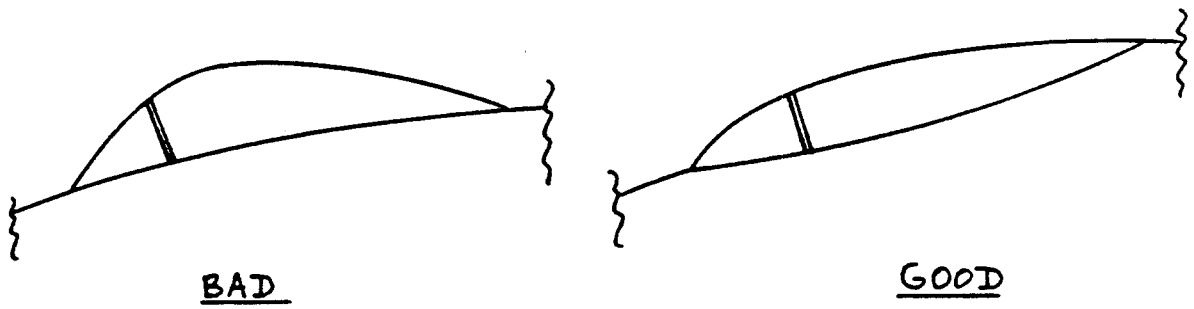

Figure 3.18 RCS: Good and Bad Canopy Design

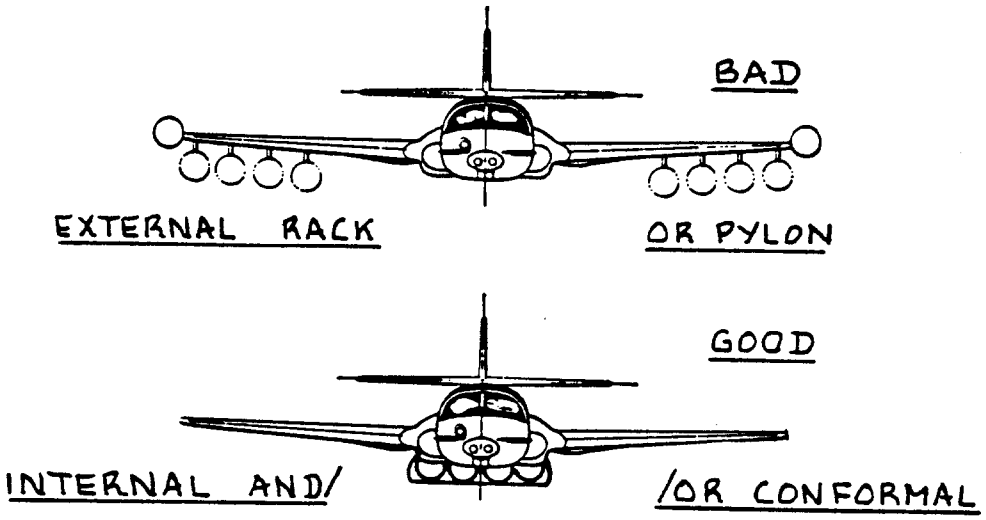

Figure 3.19 RCS: Good and Bad Ordnance Installations

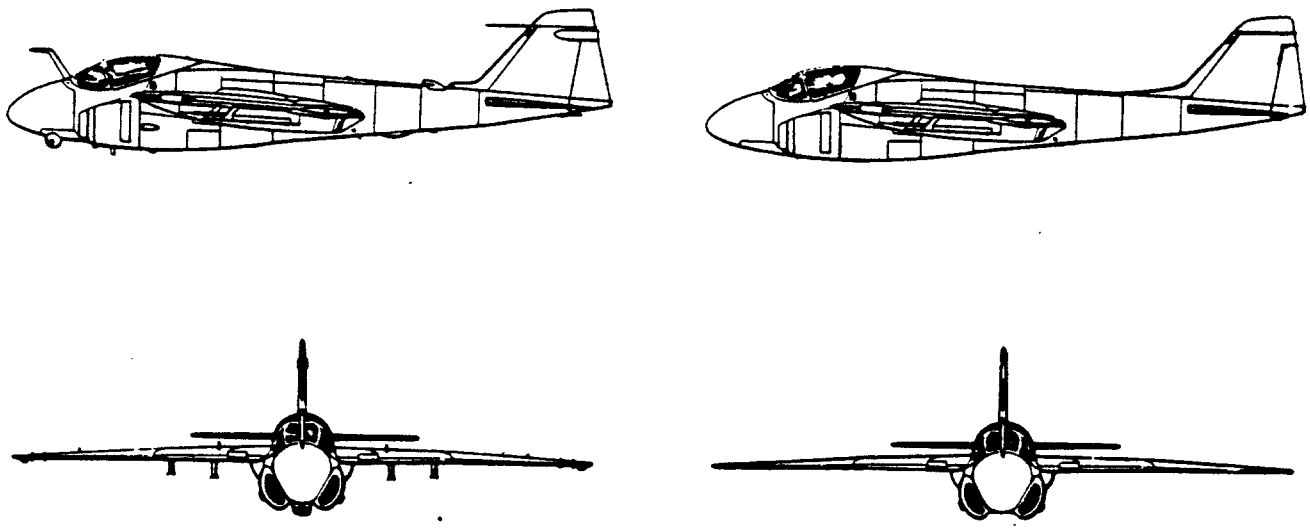

Figure 3.20 RCS: Good and Bad Bumps and Protrusions

8. Bumps and protrusions: eliminate these as much as possible to achieve a low RCS.

Figure 3.20 illustrates the good and the bad.

9. Radar antennas: A radar antenna when 'looked at' by enemy radar looks like the reflection of light from a cat's eyes at night. Making the radar dome (radome) opaque at the search radar wavelength cuts down on RCS.

Finally: anything that can be done to smoothly blend surfaces and bodies helps lower the RCS of an airplane.

10. Radar absorbing materials: Not much can be said about this subject other than that this can be rather effective.

Reference 18 contains some interesting discussions of the characteristics of 'stealthy' aircraft.

3.3.2 Design Considerations for Low Infrared Detectability

All bodies emit infrared radiation. The 'warmer' a body is relative to its surroundings, the easier it can be detected by infrared sensors. Contrary to popular opinion, infrared seeking missiles do not home in on exhaust plumes but on the surrounding metal which, although cooler than the exhaust plume, emits 95 percent of the infrared energy.

To suppress infrared detectability the following guidelines are offered:

1. Shield all exhaust nozzles from any direction from which a threat can be expected.

2. High by-pass ratio engines are much more difficult to detect by infrared sensors than straight turbojet engines. Carrying the by-pass air duct all the way aft also serves to reduce the infrared signature.

3. Carry heat generating flares and release these whenever the threat of infrared seeking weapons exists. Heat generating flares can confuse infrared seeking weapons and thus lead them to the wrong target.

Figure 3.21 illustrates a method for infrared shielding. It is clear that a significant increase in

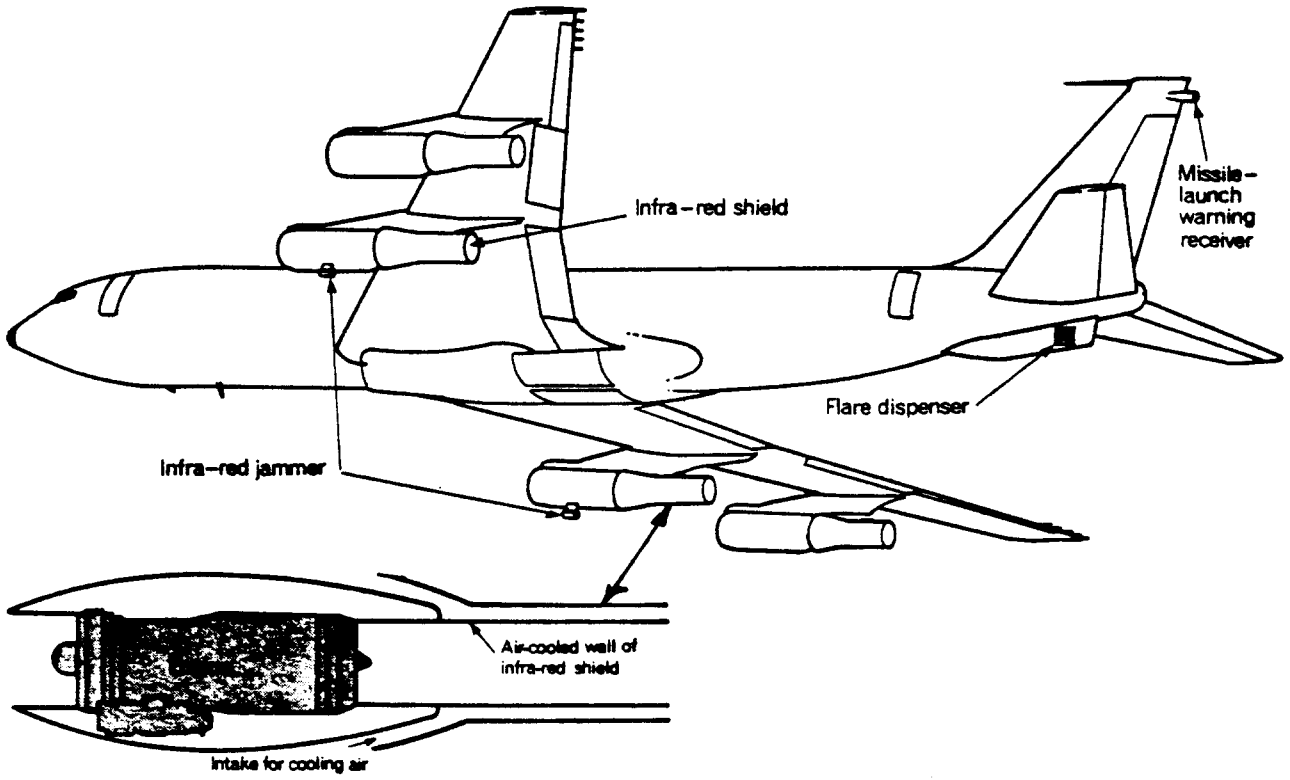

Figure 3.21 Example of Infrared Engine Shielding

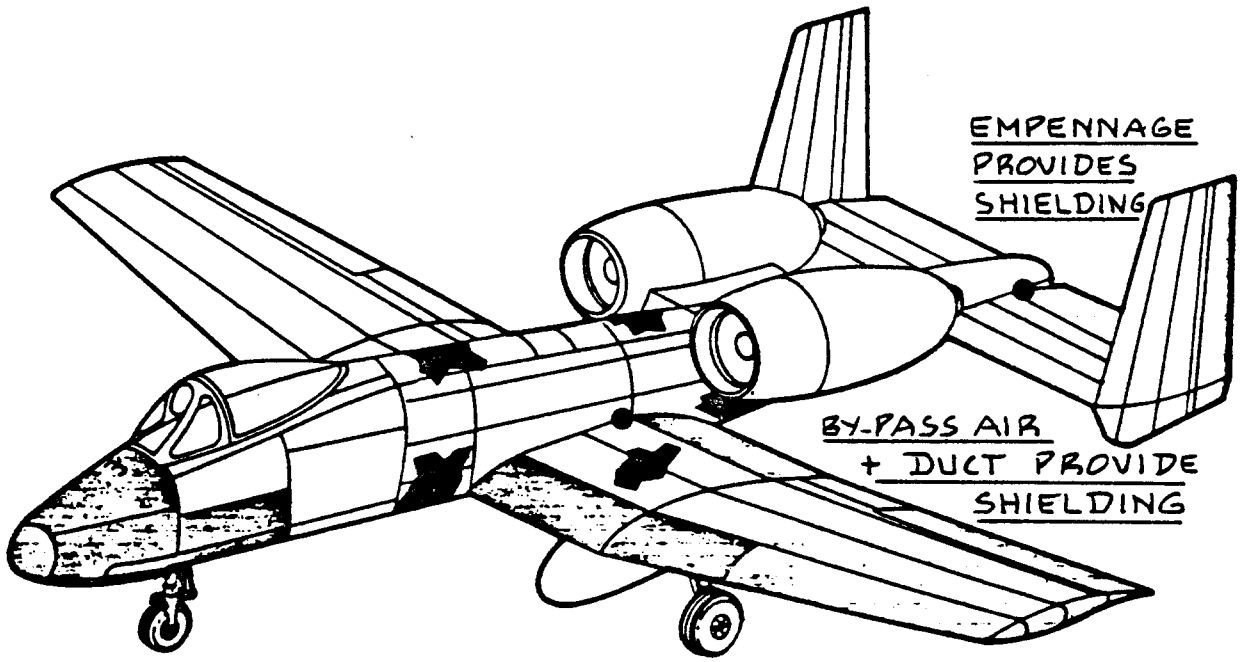

Figure 3.22 Example of an Engine Installation with Low Infrared Signature

empty weight will be incurred.

Figure 3.22 shows the Fairchild Republic A-10 with its engines very well placed to avoid a large infrared signature from its area of greatest vulnerability: missile attack from below and behind.

Figure 3.21 also shows infrared jammers. A typical infrared jammer is the Xerox ALQ-123 system. This is a 378 lbs externally mounted pod, powered by a ram-air turbine with a modulated caesium lamp as its infrared source. Since infrared seekers produce an error signal for any infrared source which is not on its optical axis, a modulated, high intensity signal in its field of vision will produce errors in its steering commands causing the missile to stray off course.

Finally, Figure 3.23 shows a Pratt and Whitney concept of a fighter designed with low RCS and low infrared signature.

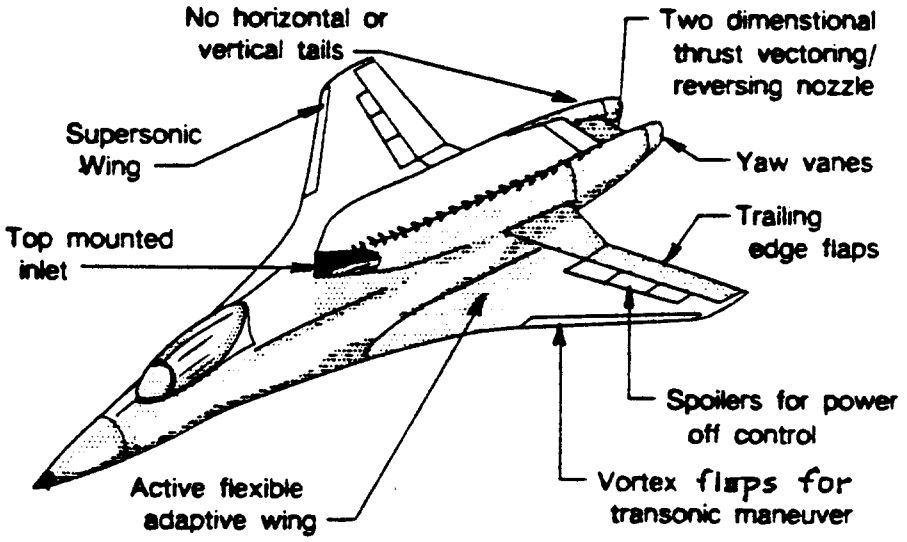

Figure 3.23 Fighter Concept for Low RCS and Low Infrared Detectability

3.4 EXAMPLES OF WEAPON INSTALLATIONS

In this section several examples are presented of airplane weapon installations.

3.4.1 Examples of Gun Installations

Typical gun/cannon installations are shown in the following figures:

Figure 3.7: Aermacchi Veltro II
Figure 3.24: Douglas A4D-2N Skyhawk (Also Fig.3.2)
Figure 3.25: Grumman F-14
Figure 3.26: General Dynamics F-16
Figure 3.27: Fairchild Republic A-10

3.4.2 Examples of External Store Arrangements

Examples of regular and conformal external store arrangements are shown in the following Figures:

Figure 3.28 Cessna YAT-37D
Figure 3.29 Grumman F-14
Figure 3.30 General Dynamics F-16
Figure 3.31 Sidewinder Installation on a Wing Tip
Figure 3.32 Panavia Tornado

3.4.3 Example of an Internal Store Installation

Figure 3.33 shows the internal weapons bay configuration of the B-1B bomber.

3.4.4 Example of Avionics Installations

Figure 3.34 shows a variety of military avionics installations used in the British Aerospace Hawk 200.

3.4.5 Example of Armor Plating

In a number of military airplanes it is deemed necessary to provide the pilot some degree of protection against enemy fire. Armor plating is the method normally used. Figure 3.24 shows the armor plating used in the Skyhawk. Armor plating is heavy (the armor is made of special steels) and provides only limited protection.

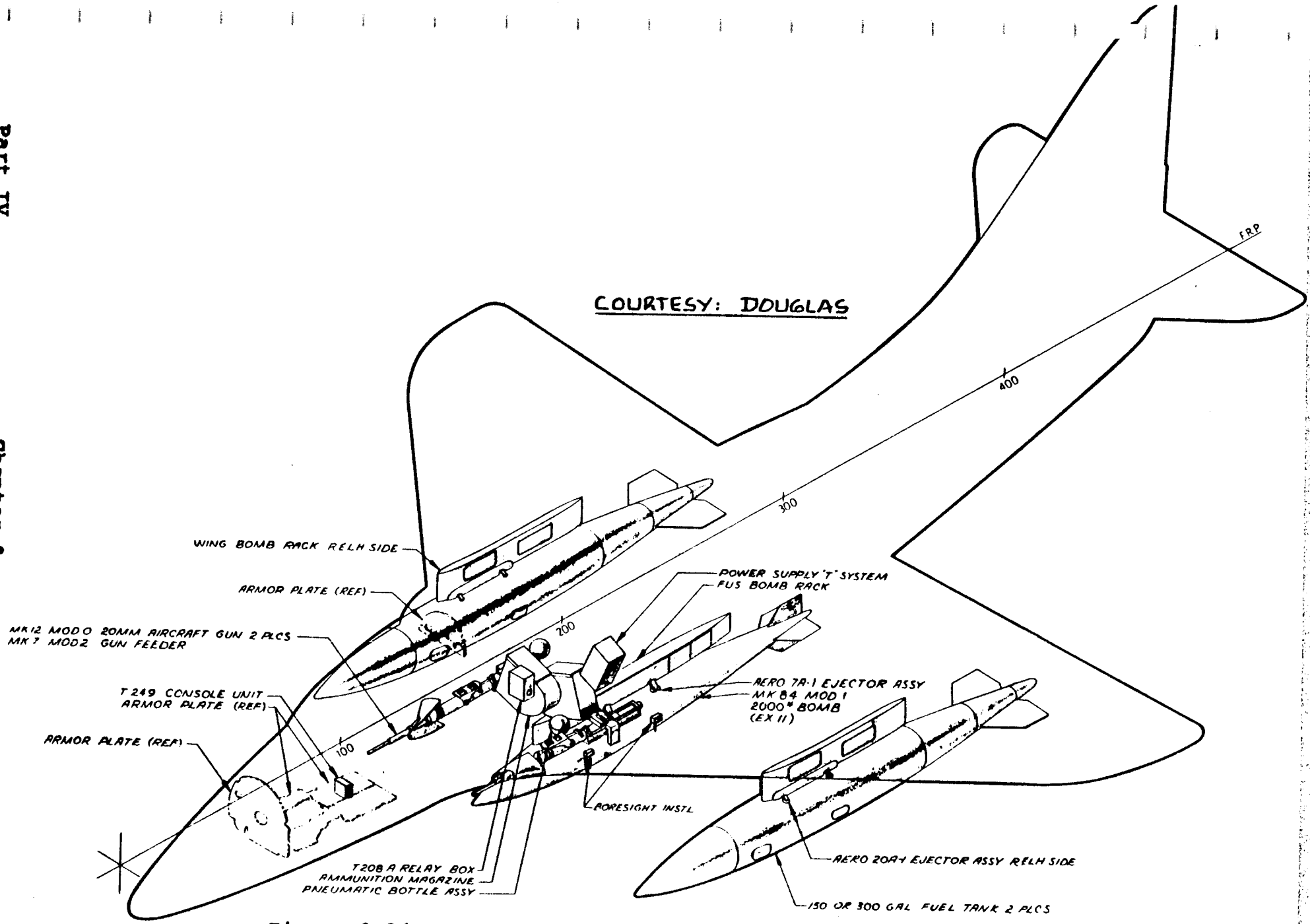

Figure 3.24 Gun Installation Douglas A4D-2N Skyhawk

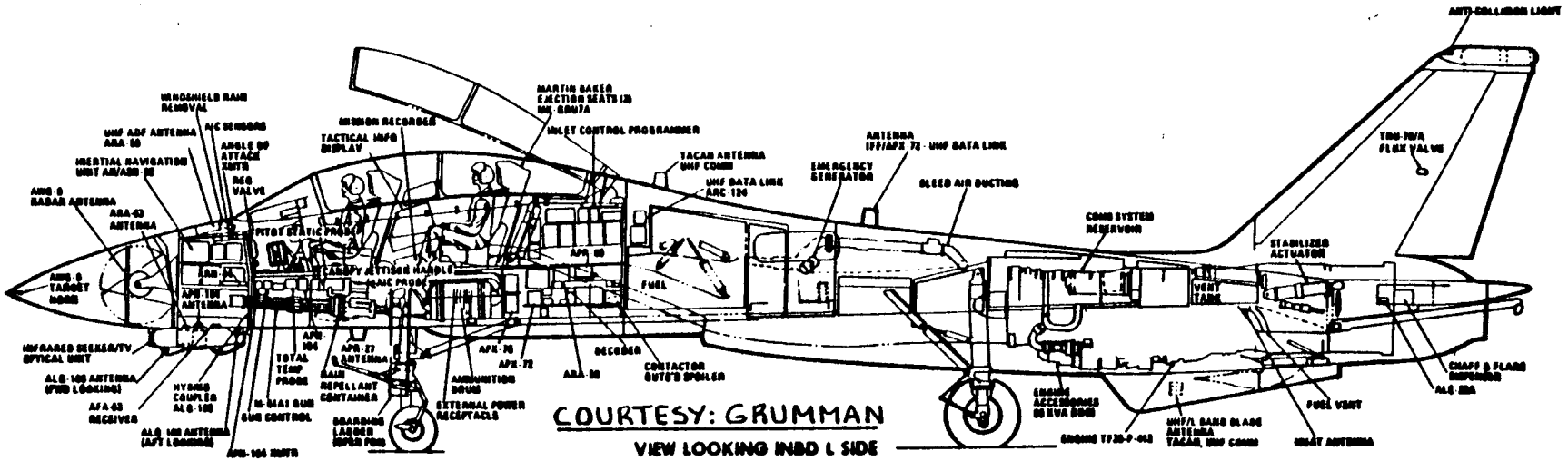

Figure 3.25 Gun Installation Grumman F-14

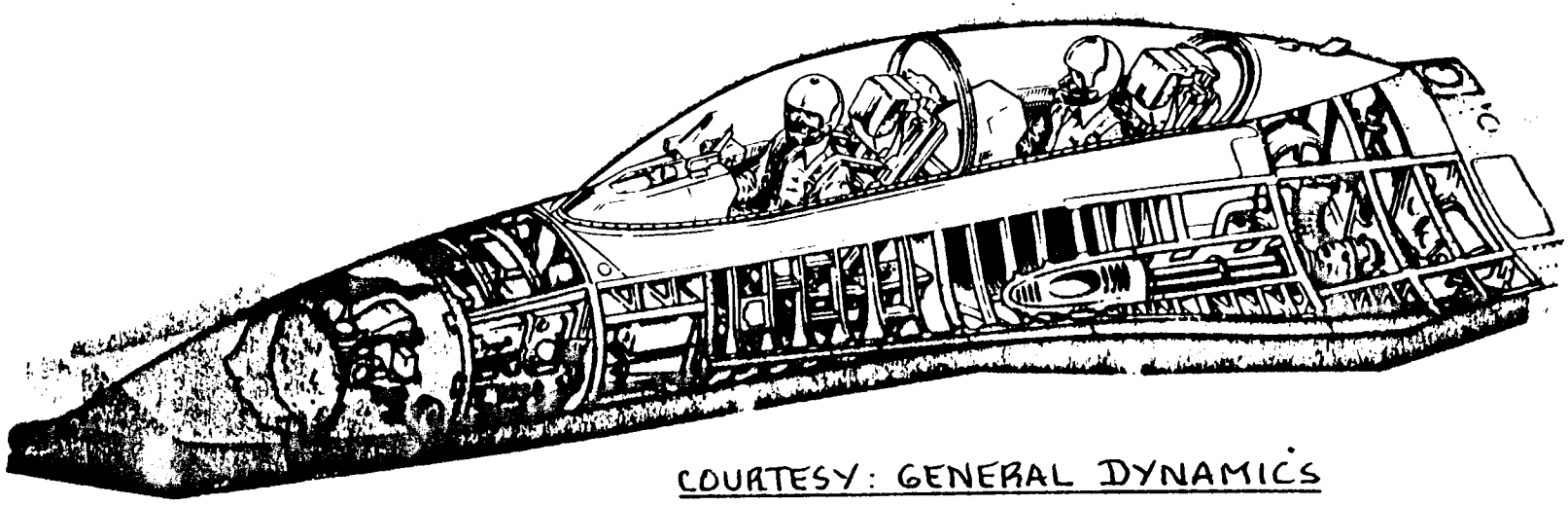

Figure 3.26 Gun Installation General Dynamics F-16

COURTESY:
FAIRCHILD-
REPUBLIC

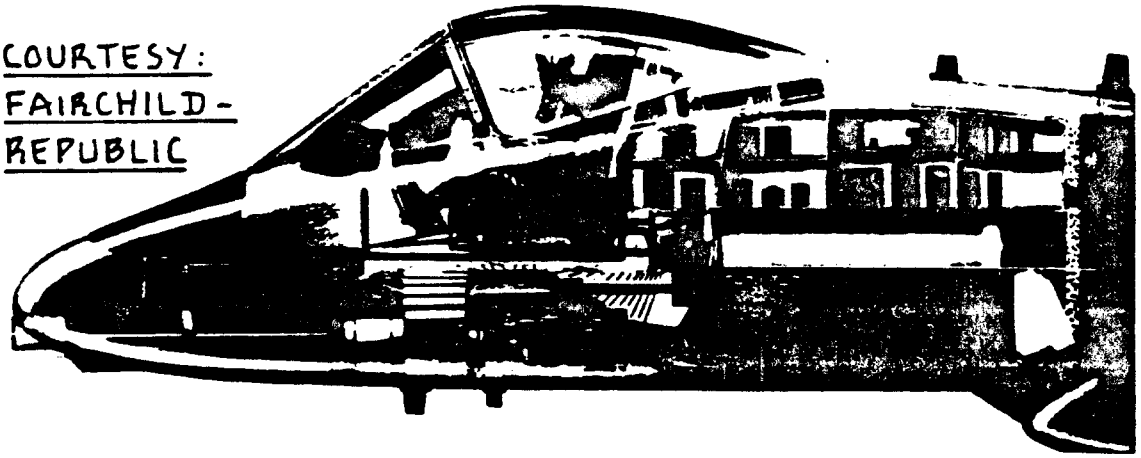

Figure 3.27 Gun Installation Fairchild Republic A-10

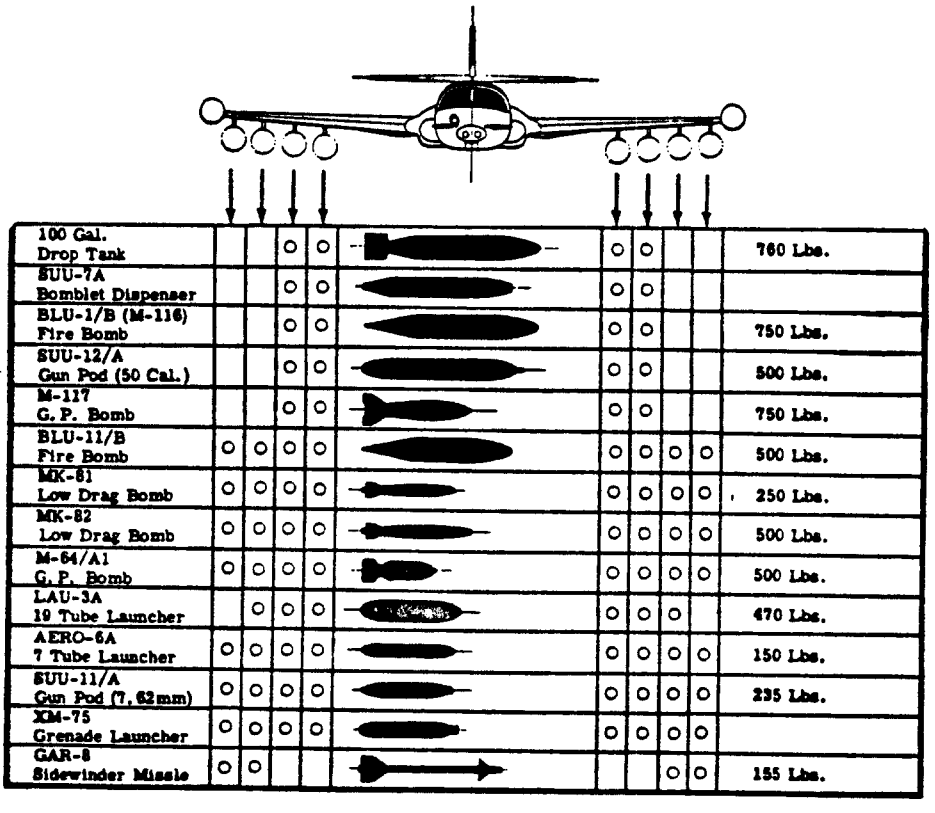

100 Gal. Drop Tank			o	o		o	o			760 Lbs.
SUU-7A Bomblet Dispenser			o	o		o	o			
BLU-1/B (M-116) Fire Bomb			o	o		o	o			750 Lbs.
SUU-12/A Gun Pod (50 Cal.)			o	o		o	o			500 Lbs.
M-117 G. P. Bomb			o	o		o	o			750 Lbs.
BLU-11/B Fire Bomb	o	o	o	o		o	o	o	o	500 Lbs.
MK-81 Low Drag Bomb	o	o	o	o		o	o	o	o	250 Lbs.
MK-82 Low Drag Bomb	o	o	o	o		o	o	o	o	500 Lbs.
M-64/A1 G. P. Bomb	o	o	o	o		o	o	o	o	500 Lbs.
LAU-3A 19 Tube Launcher		o	o	o		o	o	o		470 Lbs.
AERO-6A 7 Tube Launcher	o	o	o	o		o	o	o	o	150 Lbs.
SUU-11/A Gun Pod (7.62mm)	o	o	o	o		o	o	o	o	235 Lbs.
XM-75 Grenade Launcher	o	o	o	o		o	o	o	o	
GAR-8 Sidewinder Missle	o	o						o	o	155 Lbs.

COURTESY: CESSNA

Figure 3.28 External Store Arrangement Cessna YAT-37D

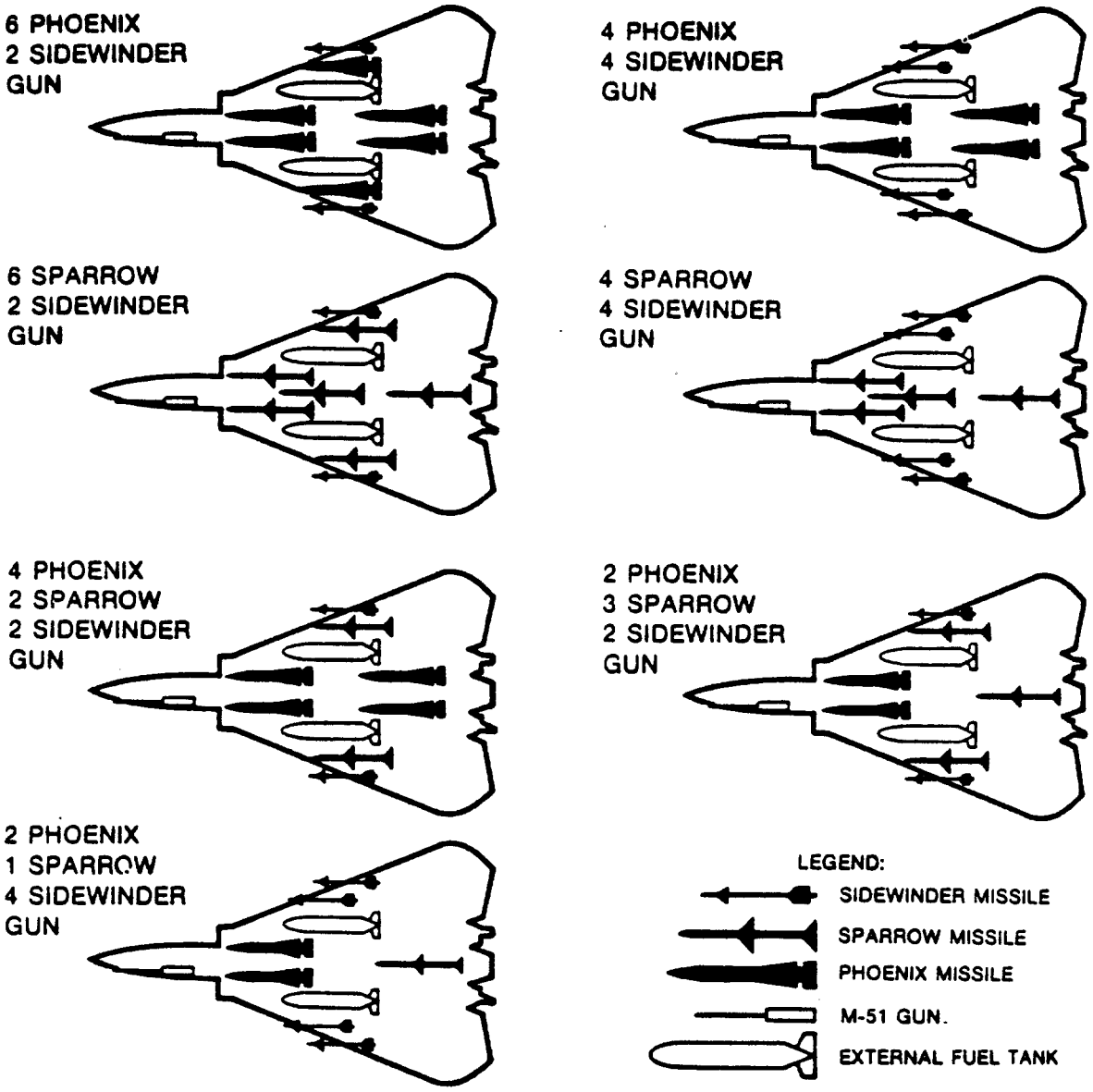

COURTESY: GRUMMAN

Figure 3.29 External Store Arrangement Grumman F-14

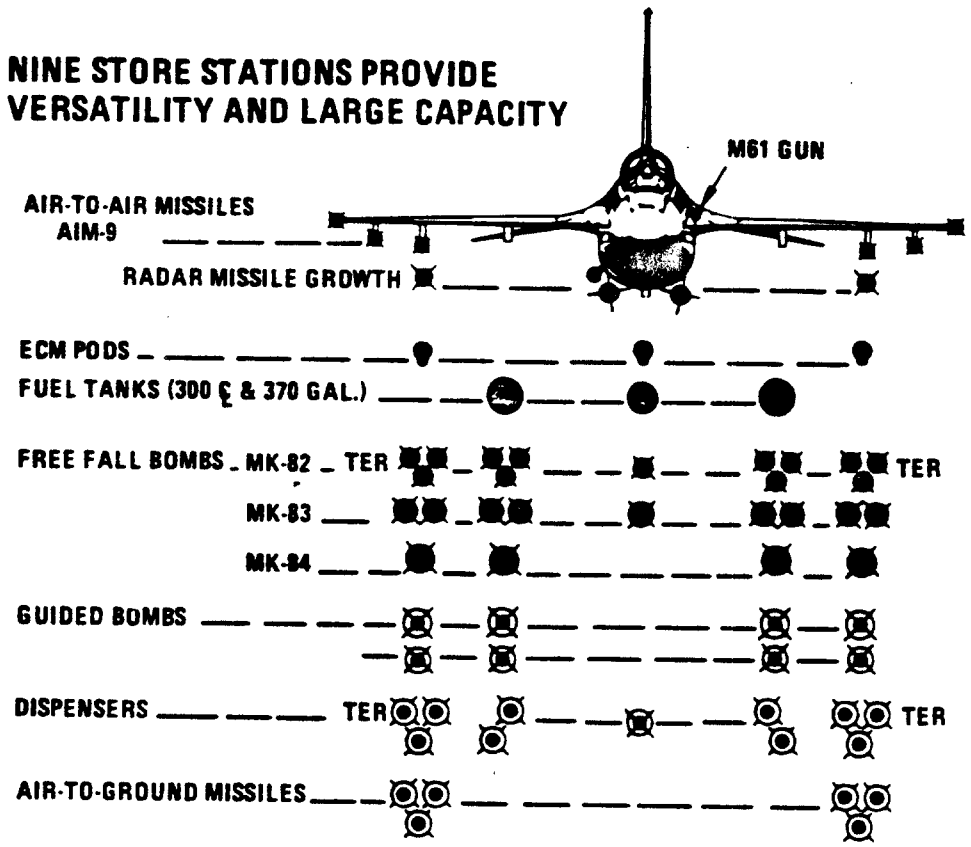

CAPACITY (LB)	250	250	2500	3500	2200	3500	2500	250 250
LOAD FACTOR ('g')	9.0	9.0	5.5	5.5	5.5	5.5	5.5	9.0 9.0

HARD POINT CAPACITY = 15,200 LBS

COURTESY: GENERAL DYNAMICS

Figure 3.30 External Store Arrangement Gen. Dynamics F-16

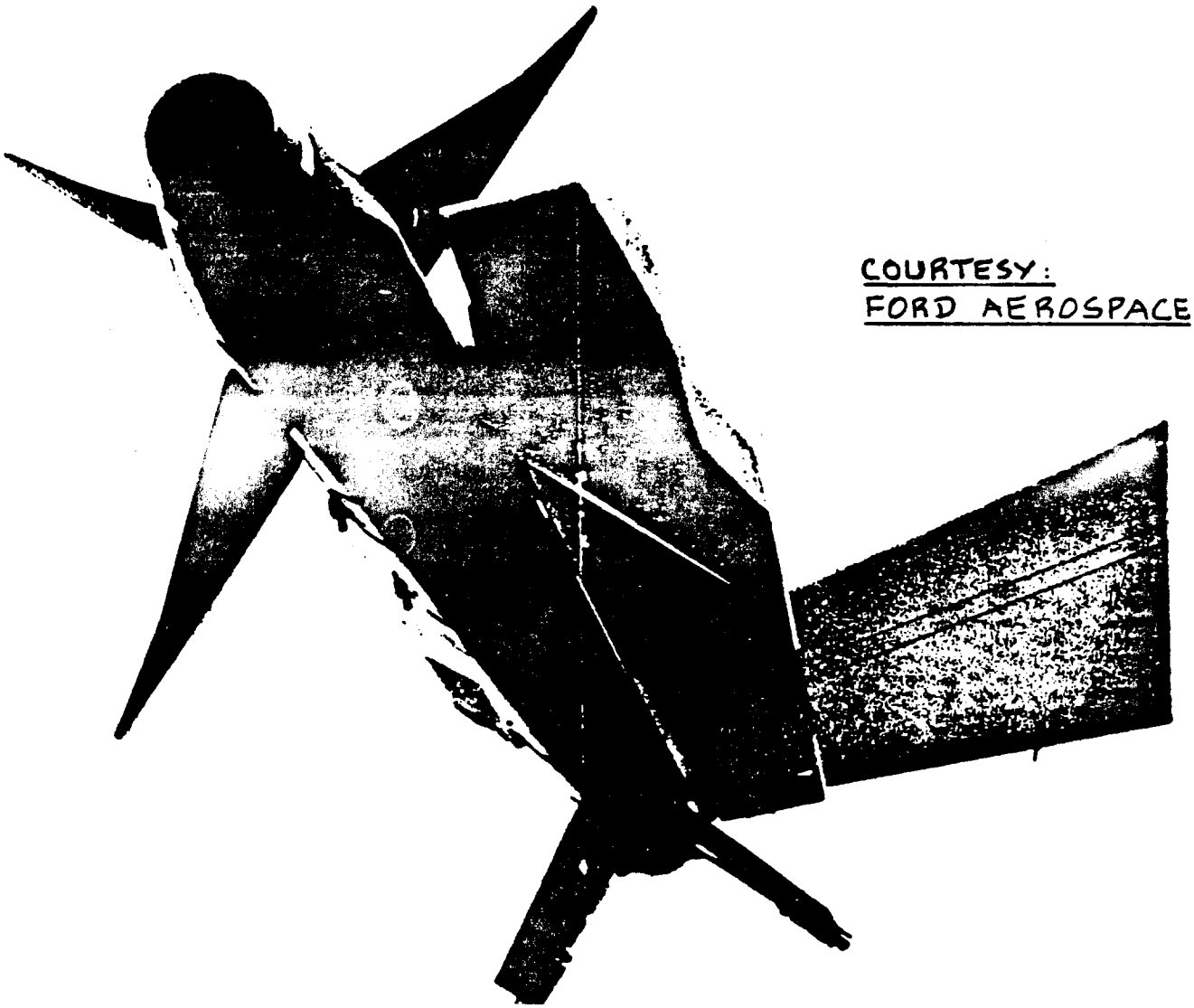

Figure 3.31 Sidewinder Installation on a Wing Tip

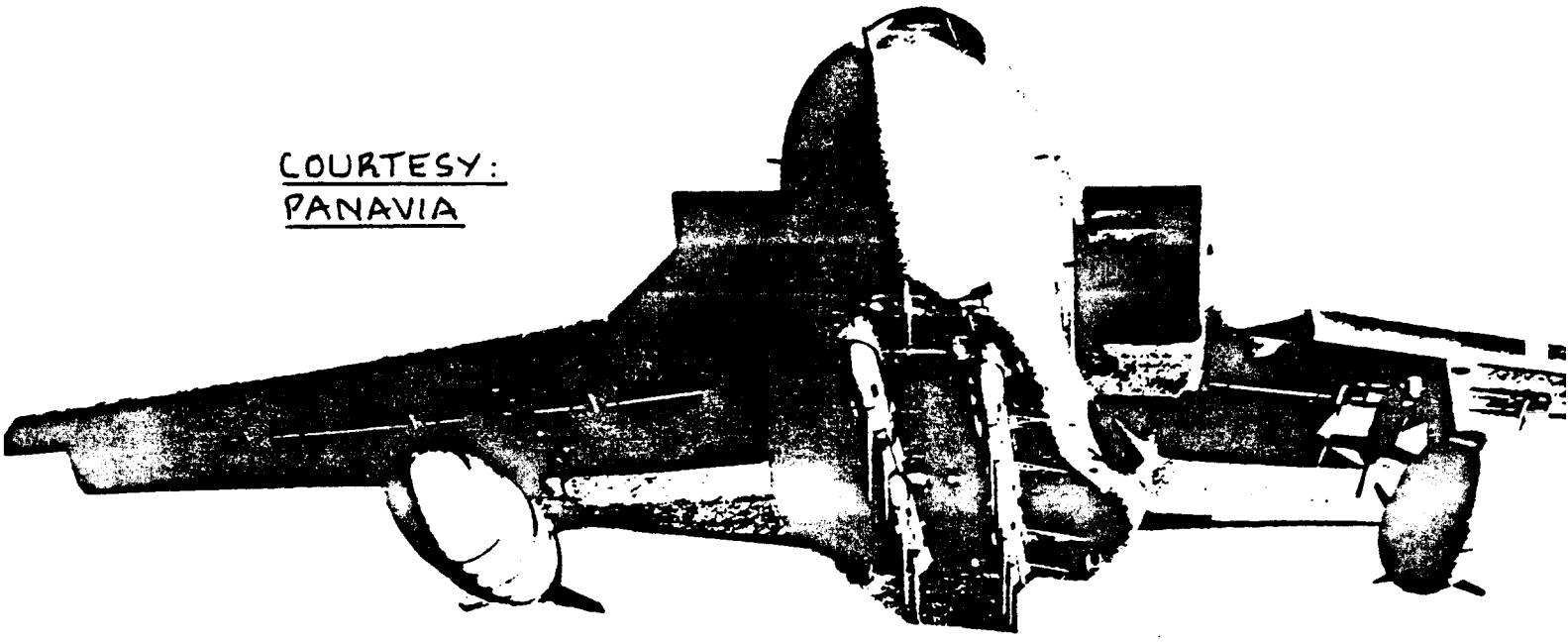

Figure 3.32 Conformal and Regular External Store Arrangement Panavia Tornado

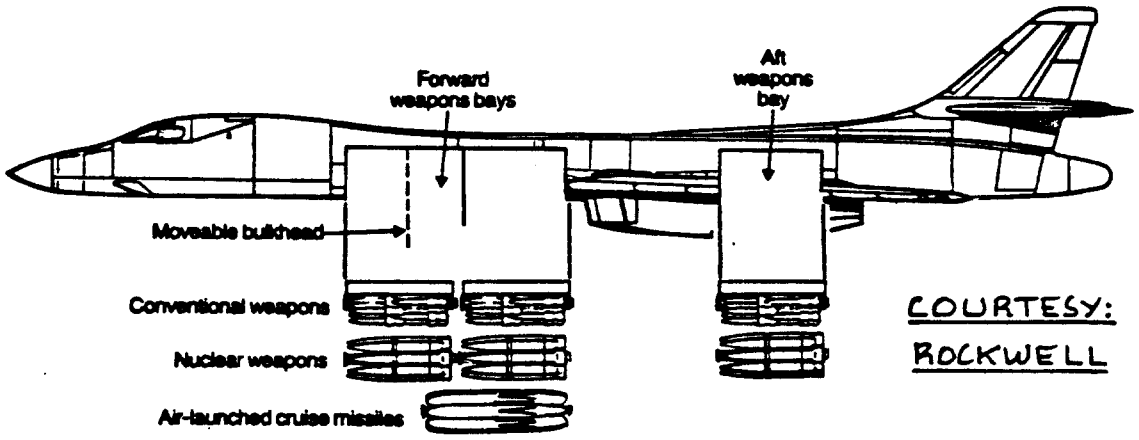

Figure 3.33 Internal Weapons Bay Rockwell B-1B

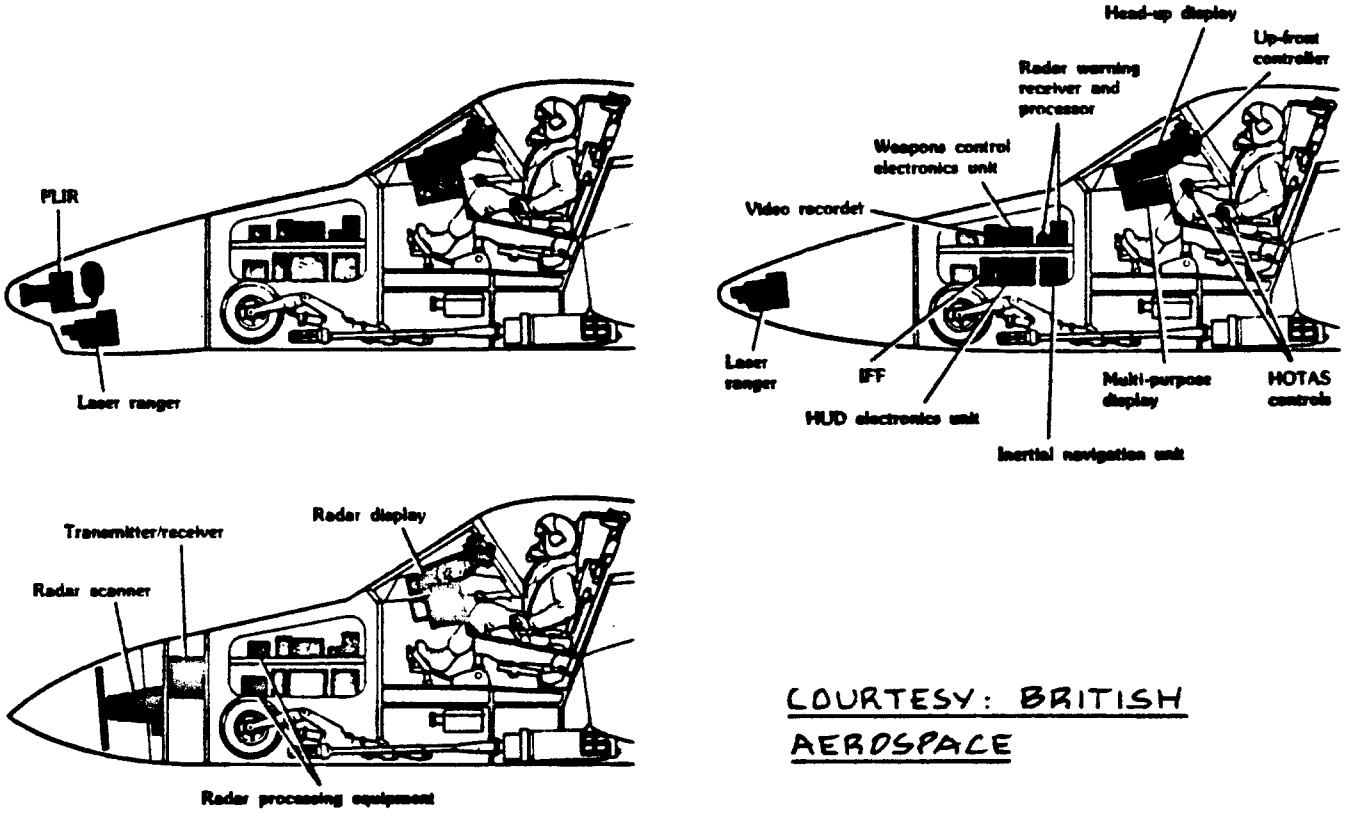

Figure 3.34 Avionics Options British Aerospace Hawk 200

3.5 WEAPON AND MILITARY PAYLOAD DATA

The purpose of this section is to provide a data base for a variety of weapons and other payloads carried by military airplanes.

The material is organized as follows:

3.5.1 Guns, gun pods, and rocket launchers

3.5.2 Free-fall munitions (bombs) and ejector racks

3.5.3 Missiles

3.5.4 External fuel stores

3.5.5 Special purpose stores

3.5.6 Military vehicles

3.5.1 Guns, Gun Pods, and Rocket Launchers

Figures 3.35 and 3.36 show dimensional data for rotating barrel guns used in military airplanes. A summary of the corresponding weight and ammunition data for these guns is given below:

GAU-2B/A 7.62mm Minigun (Fig.3.35a)

The General Electric GAU-2B/A is a six-barrel weapon which operates on the rotating barrel (Gatling) principle. It is intended for use primarily against personnel, trucks and other relatively light vehicles ('soft' targets). This gun is used on Cessna OA-37 light attack airplanes as well as on helicopters.

Weight: 67 lbs uninstalled.
Rate of fire: 4000-6000 RPM (rounds per minute), selectable.
Ammunition: NATO 7.62 mm standard.
Unit ammo weight: 0.053 lbs.
Average recoil force: 300 lbs at 6000 RPM firing rate.

GAU-4/A and M61A1 Vulcan 20mm Cannon (Fig.3.35b)

The General Electric Vulcan cannon operates on the same principle as the previously described Minigun. Ammunition is fed into the weapon chamber via a machanism that pulls the rounds from a drum. The rounds may be fed into the chamber by electrical or by hydraulic power.

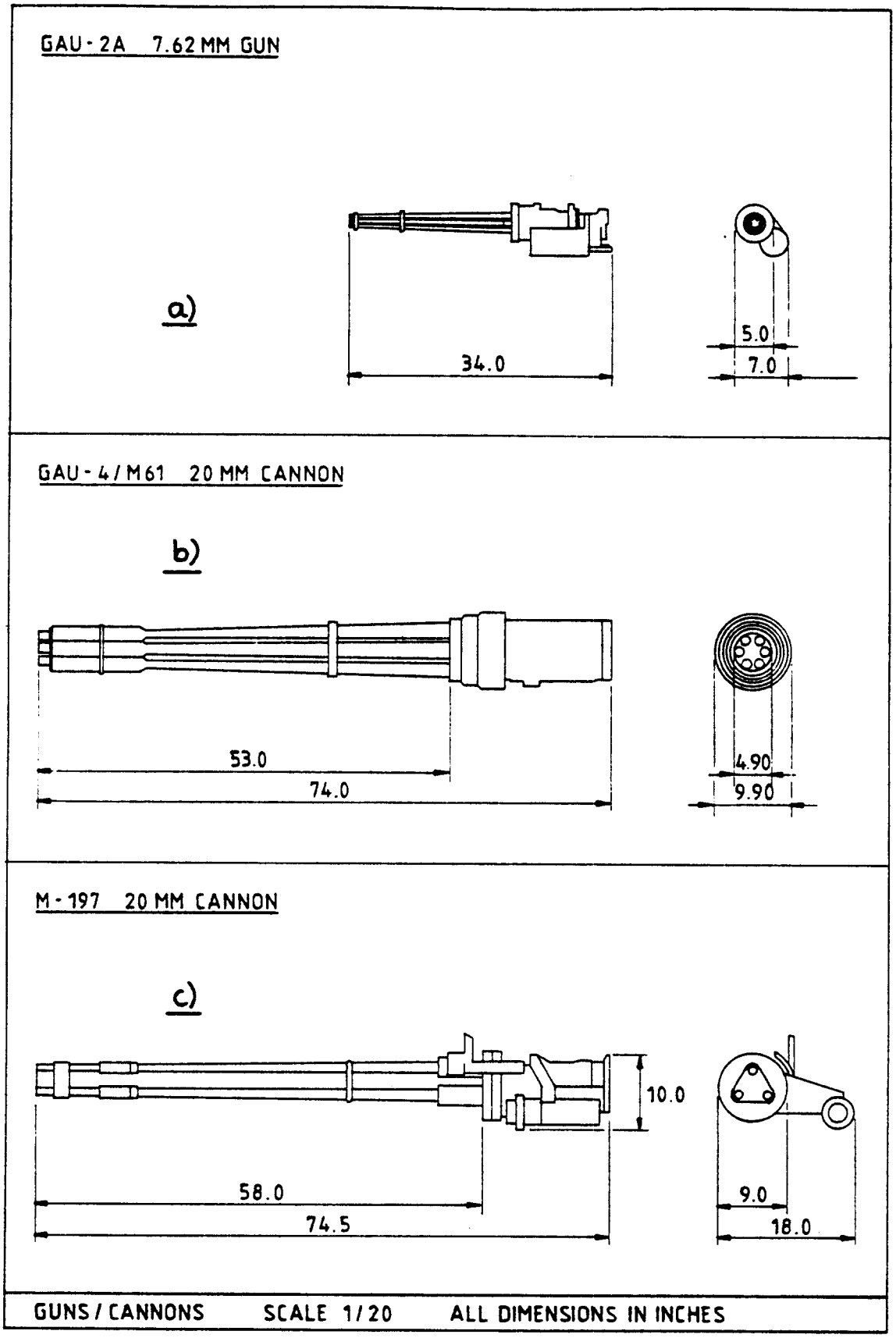

Figure 3.35 Dimensions of Typical Multi-Barrel Guns

Spent cases can be jettisoned or retained.

The Vulcan is standard armament in nearly all US fighter airplanes.

	GAU-4/A	M61A1
Weight: uninstalled	275 lbs	264 lbs

Rate of fire: maximum 6000 RPM
Ammunition: M50 series 20 mm
Unit ammo weight: 0.55 lbs
Average recoil force: 3,980 lbs at 6000 RPM.

A typical ammunition feed system weight with 1020 round capacity is 418 lbs for the LTV A-7 airplane.

M-197 20mm Cannon (Fig.3.35c)

The General Electric M-197 lightweight cannon was developed for use on light attack airplanes and for helicopters. It also operates on the Gatling principle but uses only three barrels. The weapon requires 3 hp to operate and can accept linkless or belted ammunition.

Weight: uninstalled 145 lbs
Rate of fire: 400-6000 RPM, selectable
Ammunition: M50 series 20 mm
Unit ammo weight: 0.55 lbs
Average recoil force: 1,500 lbs at 1500 RPM

GAU-8/A 30mm Cannon (Fig.3.36)

The General Electric GAU-8/A seven barrel cannon is designed for use against armoured vehicles with medium thickness armour. The cannon is hydraulically powered from the airplane hydraulic system. This Gatling type cannon is currently in use on the Fairchild A-10 attack airplane.

Weight: empty 2014 lbs
loaded 3799 lbs
Rate of fire: 6000 RPM
Ammunition: 30 mm
Unit ammo weight: 1.521 lbs
Standard ammo capacity: 1174 rounds
Average recoil force: 12,000 lbs (estimated)

Figure 3.37 presents geometric data for typical gun-pods. These are used in airplanes which do not have a separate gun installation. They may also be used on airplanes which already have built-in guns, to increase the firepower.

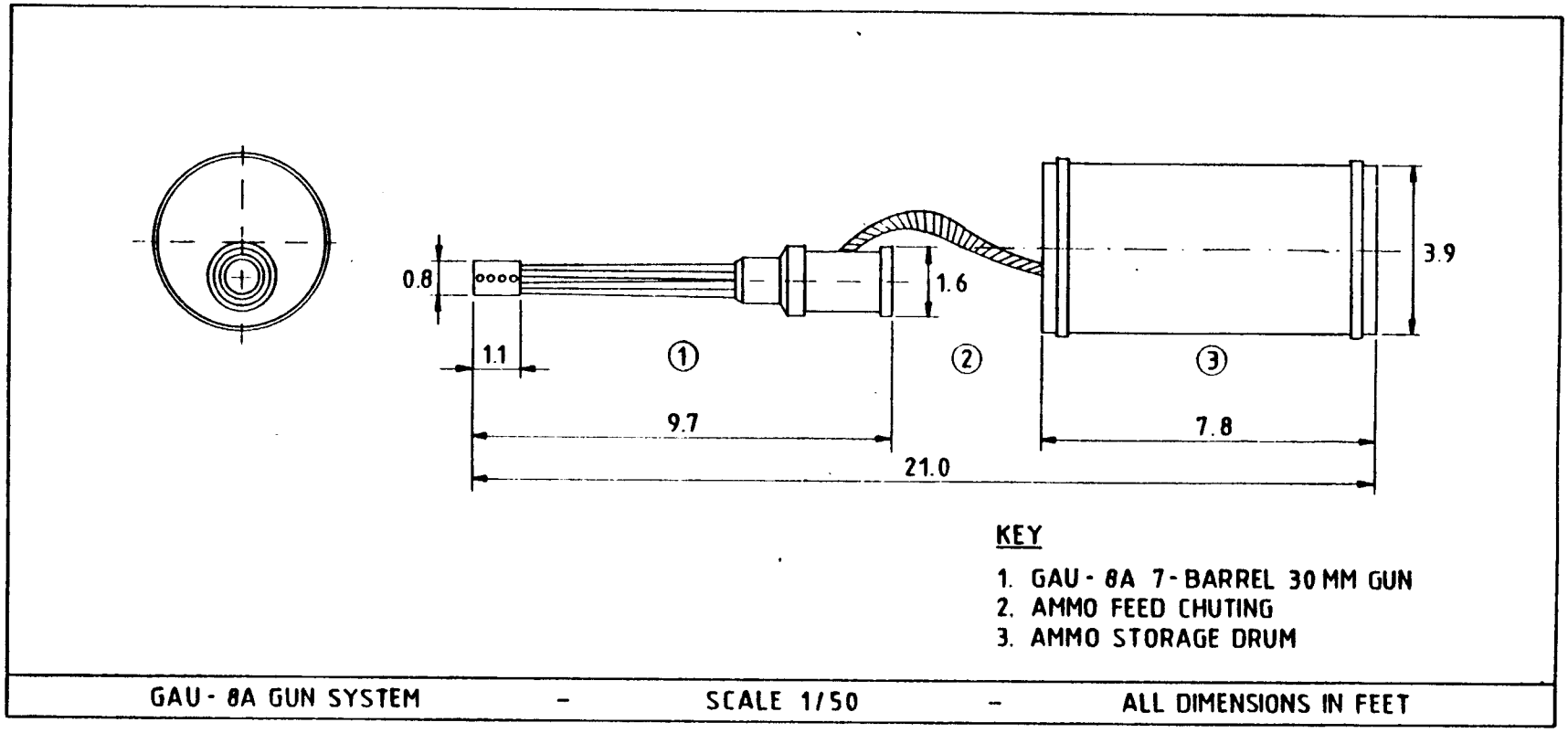

Figure 3.36 Dimensions of GAU-8A Gun System

SUU-11B/A 7.62mm Minigun Pod (Fig.3.37a)

This pod contains the GAU-2 minigun. An external power source is required. The pod is mounted on standard hard-points or on a pylon.

Weight: empty 245 lbs
loaded 324 lbs
Ammo: 7.62 mm NATO standard
Standard ammo capacity: 1,500 rounds

SUU-16/A and SUU-23/A 20mm Gun Pods (Fig.3.37b)

These pods are geometrically similar. The aft end of these pods contains a cylindrical ammo drum. The difference between these pods is that they carry different types of guns.

The SUU-16/A uses the externally powered M61A1 gun. The external power source can be in the form of a ram-air turbine which generates the required electrical power. An airspeed of 350 kts is needed for achieving full firing performance.

The SUU-23/A uses the self-powered GAU-4 gun.

	SUU-16/A	SUU-23/A
Weight: empty	1,067 lbs	1,078 lbs
loaded	1,720 lbs	1,731 lbs

Ammo: 20 mm
Ammo unit weight: 0.55 lbs
Standard ammo capacity: 1,500 rounds

Mark-4 Mod 0 20mm Gun Pod (Fig.3.37c)

This gun pod is in use with the US Navy on F-4, A-4 and A-7 airplanes. The Mk.4 employs a twin barrel (fixed) Mk.5 gun which has a selectable rate of fire from 750 to 4,200 RPM. Ammo is belt-fed into the weapon. The pod is powered by the gun exhaust gas.

Weight: empty 797 lbs
loaded 1,390 lbs
Ammo: 20 mm
Ammo unit weight: 0.55 lbs
Ammo capacity: 750 rounds
Ammo weight including links: 593 lbs

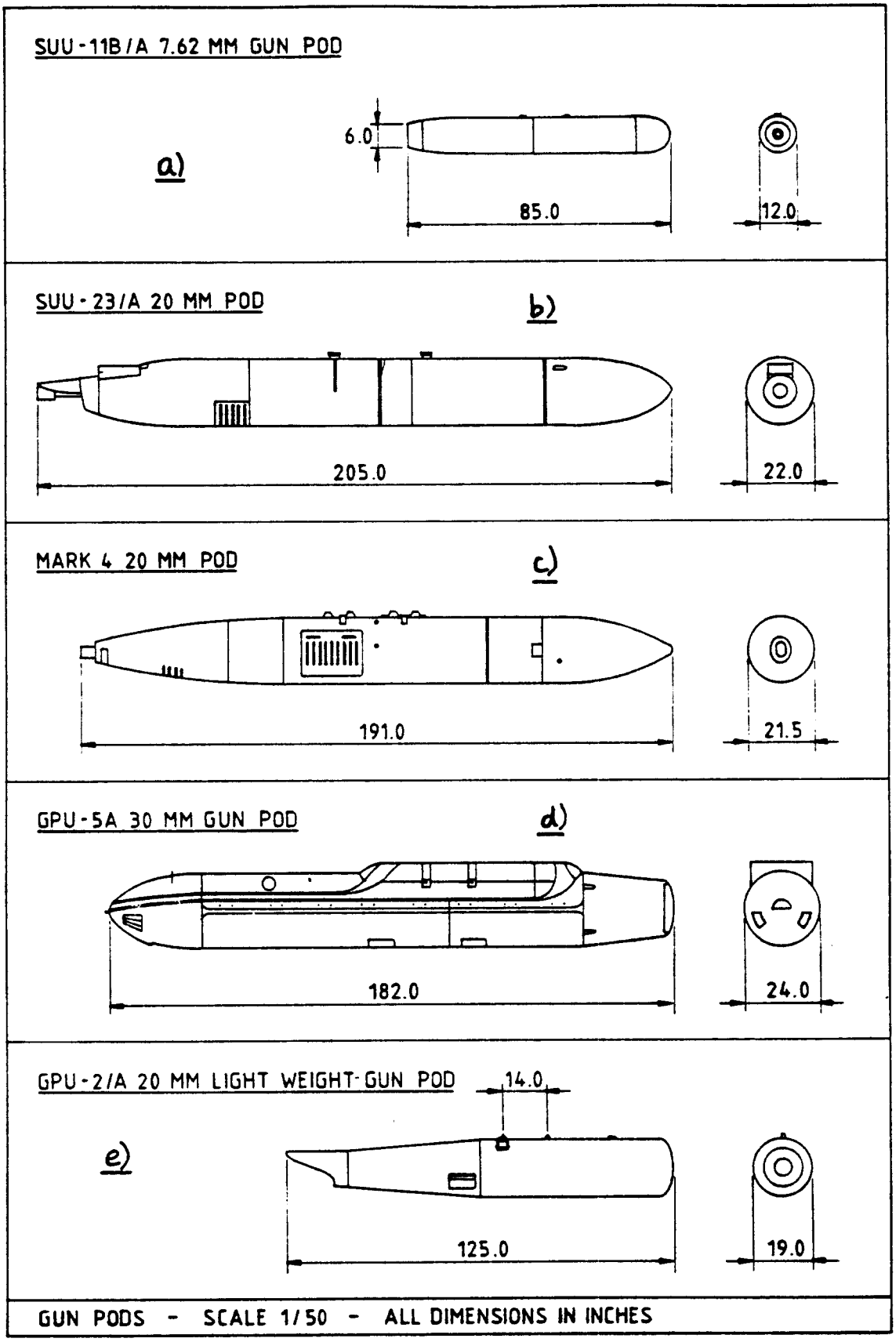

Figure 3.37 Dimensions of Gun Pods

GPU-5/A 30mm-Gun Pod (Fig.3.37d)

This pod is based on the GAU-13/A 5-barrel gun. The GAU-13 gun is a derivative of the GAU-8/A weapon. Anti-armor capability is similar to that of the GAU-8/A. This pod has been designed to be compatible with nearly all US attack airplanes.

Weight: empty 1,369 lbs
loaded 1,900 lbs
Ammo: 30 mm
Ammo unit weight: 1.79 lbs per round
Ammo capacity: 300 rounds
Firing rate: 2,400 RPM

GPU-2/A 20mm Lightweight Gun Pod (Fig.3.37e)

This pod is powered by a NiCad battery which provides power sufficient for three reloads (900 rounds of total ammo) before needing a recharge. The pod contains the M-197 gun which can be set to fire 750 or 1,500 RPM.

Weight: empty 433 lbs
loaded 595 lbs
Ammo: 20 mm
Ammo unit weight: 0.54 lbs
Ammo capacity: 300 rounds

Rockets fired from airplanes can be very effective in concentrating a large amount of fire power onto ground targets. In recent years most of these rockets are of the 'folding fin' type. The rocket fins are spring loaded and deployed immediately following their launch. The folding fin feature permits denser storage and lower installed drag. The rockets are normally installed in rocket launchers which can be dropped or retained.

Figure 3.38 shows two rocket launchers used on USAF airplanes.

LAU-68 7 Round 2.75 in. Rocket Launcher

The LAU-68 is the standard 7 round rocket launcher in the USAF. Figure 3.38a shows the geometry of this launcher.

Weight: empty 67 lbs
loaded 218 lbs

LAU-3 19 Round 2.75 in. Rocket Launcher

The LAU-3 is the standard 19 round rocket launcher for the USAF. Fighter airplanes may carry several of these rocket launchers. The 19 rounds can be fired within 2 seconds. Figure 3.38b shows the geometry of this rocket launcher.

Weight: empty 78 lbs
loaded 415 lbs

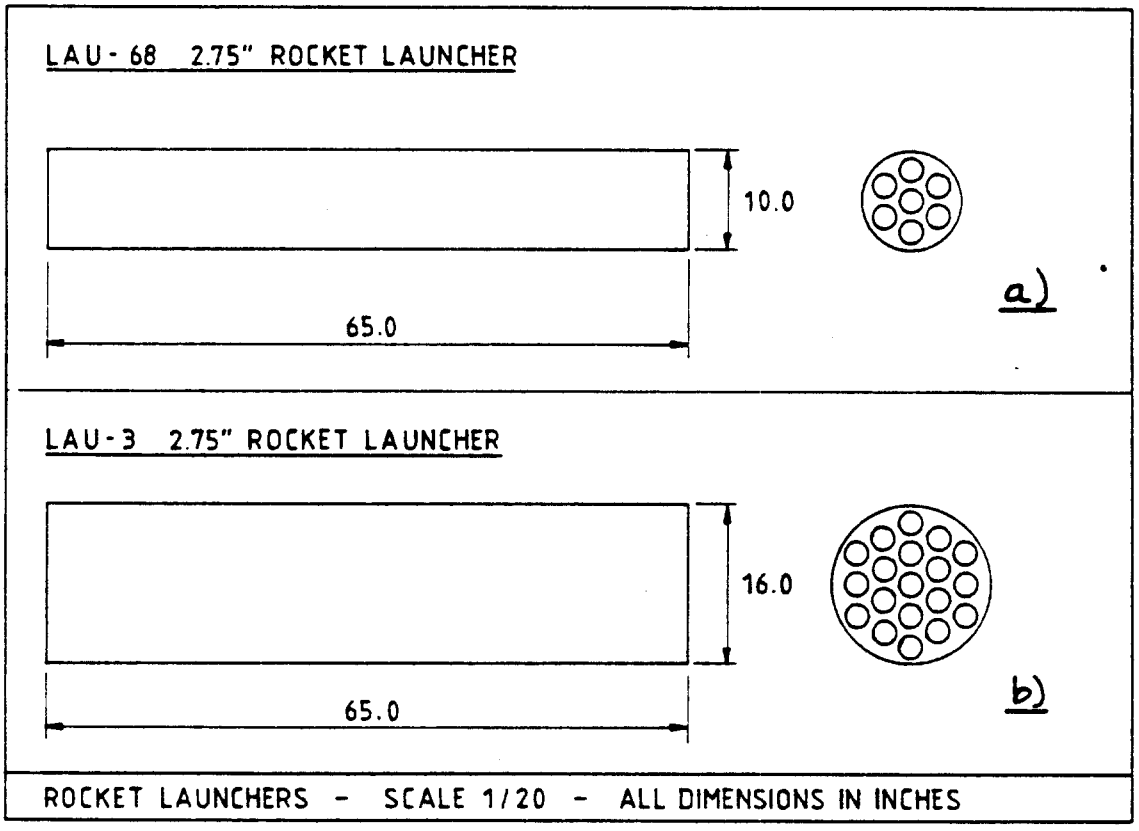

Figure 3.38 Dimensions of Rocket Launchers

3.5.2 Free-Fall Munitions (Bombs) and Ejector Racks

This class of munitions is subdivided into unguided and guided free-fall types. Both types are normally released from ejector racks. These racks can be mounted externally or internally.

Unguided Free-Fall Munitions

Free-fall munitions (also called bombs) are steel cased explosives designed for blast and fragmentation effects. A more recent version is the so-called cluster bomb, designed to disperse a large amount of 'bomblets'.

Figure 3.39 shows the geometries for these weapons. Table 3.1 lists the corresponding weights.

Table 3.1 Weights for Free-fall Munitions

Type	Nominal Weight lbs	Actual Weight lbs	Explosives Weight lbs	Comment
Mk81	250	270	96	No longer in production
Mk82	500	531	192	
Mk82-Snakeye	500	560	192	This high drag bomb uses the Mk15 retardation device to allow low altitude delivery.
Mk83	1,000	985	N.A.	Used by US Navy
Note: Mk80 series are compatible with 14 in. racks only.				
Mk84	2,000	1,970	N.A.	Compatible with 30 in. racks only
SUU-30	500	500*	N.A.	*varies with type of sub-munition carried
Mk20 Rockeye	500	476	N.A.	carries Mk118 sub-munition which can penetrate light to medium armor

Bombs, when carried internally or externally are mounted below racks from which they may be released by the pilot following an electrical command.

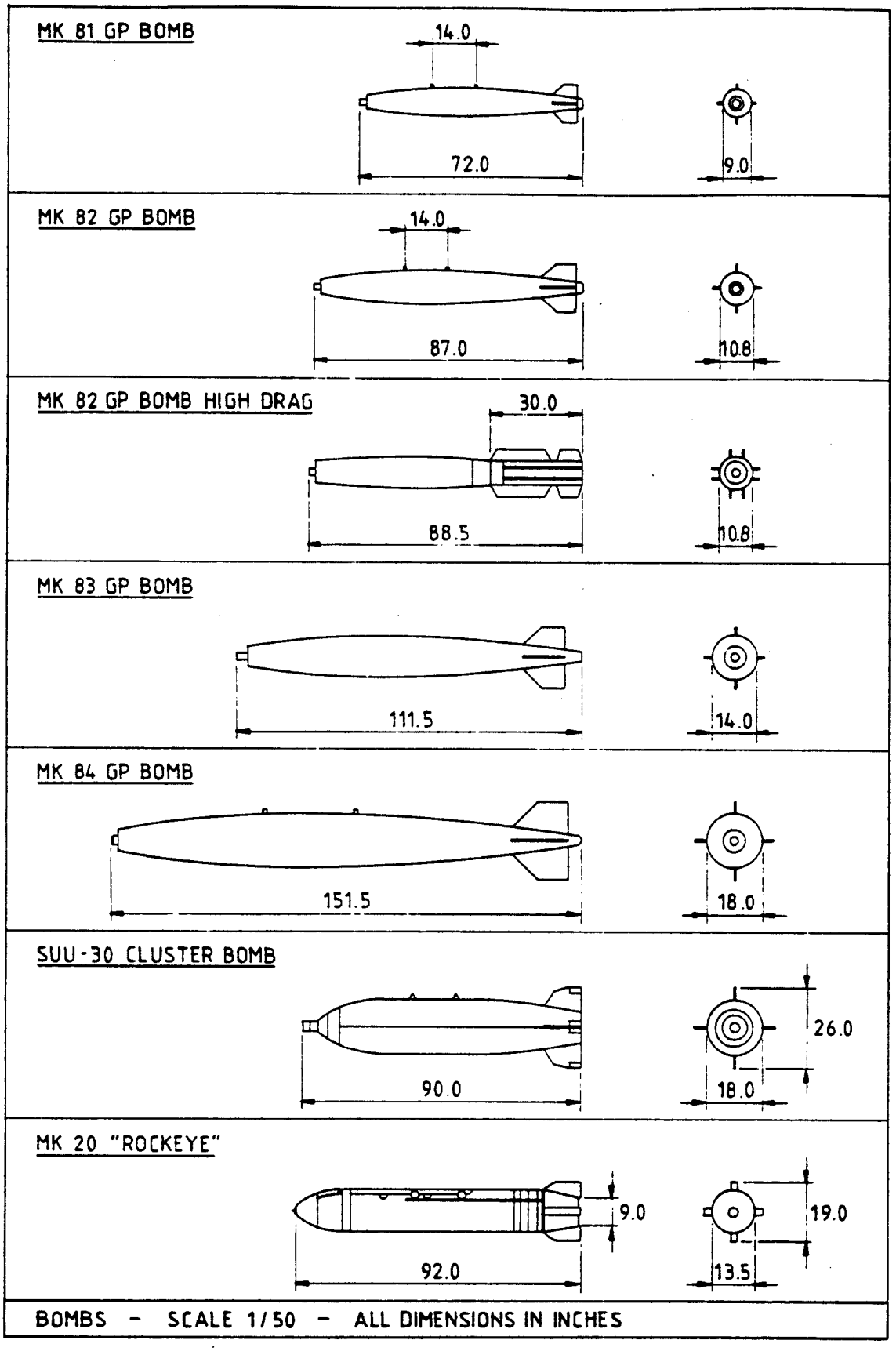

Figure 3.39 Dimensions of Free Fall Munitions (Bombs)

Bomb racks tend to be very 'draggy' as well as to present a large radar cross section (RCS). Conformal and internal installations tend to reduce these problems. Figures 3.4 and 3.34 show examples of such installations.

The most frequently used racks are the MER (Multiple Ejector Rack) and the TER (Triple Ejector Rack), both shown in Figure 3.40. The weights of these racks are:

MER weight: 220 lbs TER weight: 93 lbs

Fig.3.41 shows EDO built 14 in. and 14/30 in. racks.

Guided Free-Fall Munitions

Two types of guided free-fall weapons will be presented: electro-optical and laser guided weapons.

Electro-optical guided weapons use one or more television cameras and data links to visually lock-on and home-to the target.

Laser guided weapons use the target reflection of a laser beam to lock-on and home-to the target. A device which 'illuminates' the target is required.

Figure 3.42 shows the geometries of several of these weapons. Most are based on Mk80 series bombs.

Table 3.2 provides the weight and range data for these weapons.

Table 3.2 Weights and Range Data for Guided Free-Fall Munitions

Type	Based on	Weight lbs	Range miles	Comment
GBU-15	Mk84 or SUU-54 Cluster	2,515	N.A.	Rockwell
AGM-62-Walleye I		1,100	10	Martin
AGM-62-Walleye II		2,340	10	Martin
GBU-10/B Paveway-II	Mk84 series	2,052	N.A.	Texas Instr.
GBU-12/B	Mk82	627	N.A.	Texas Instr.

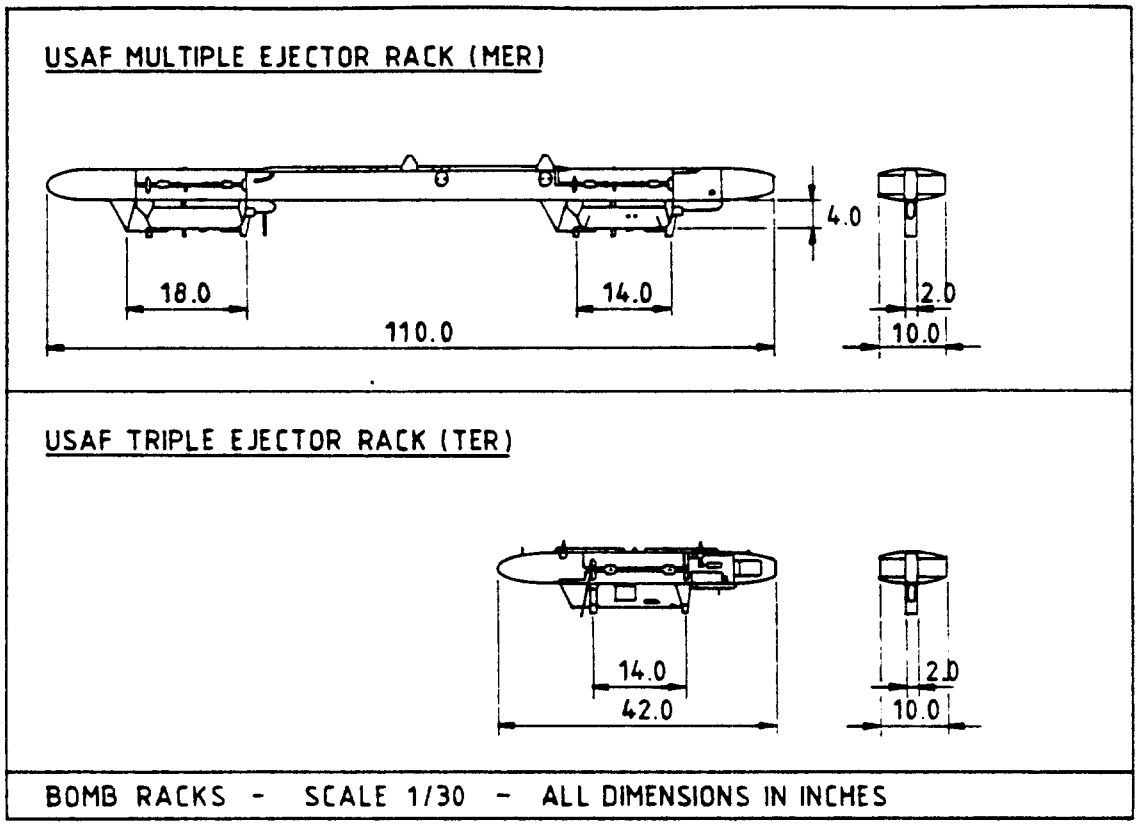

Figure 3.40 Dimensions of Ejector Racks

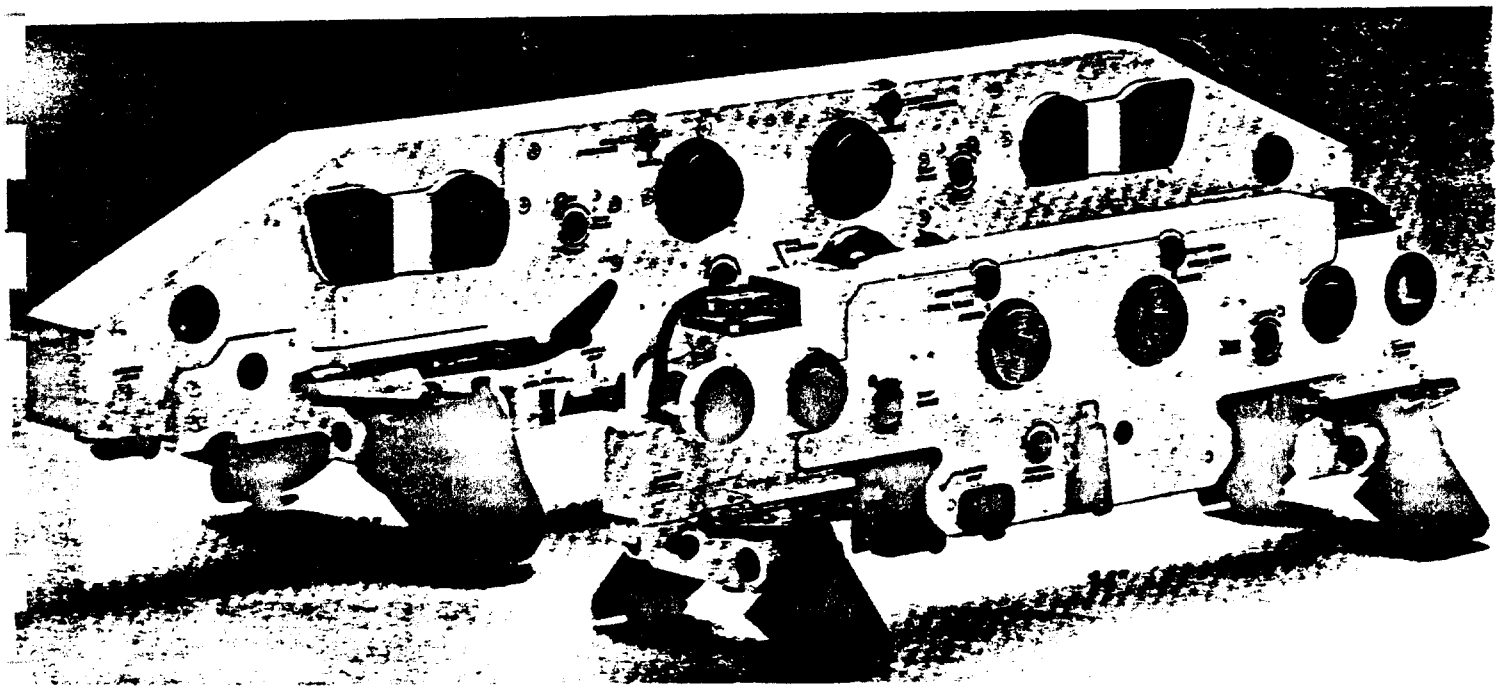

Figure 3.41 Perspective View of EDO Ejector Racks

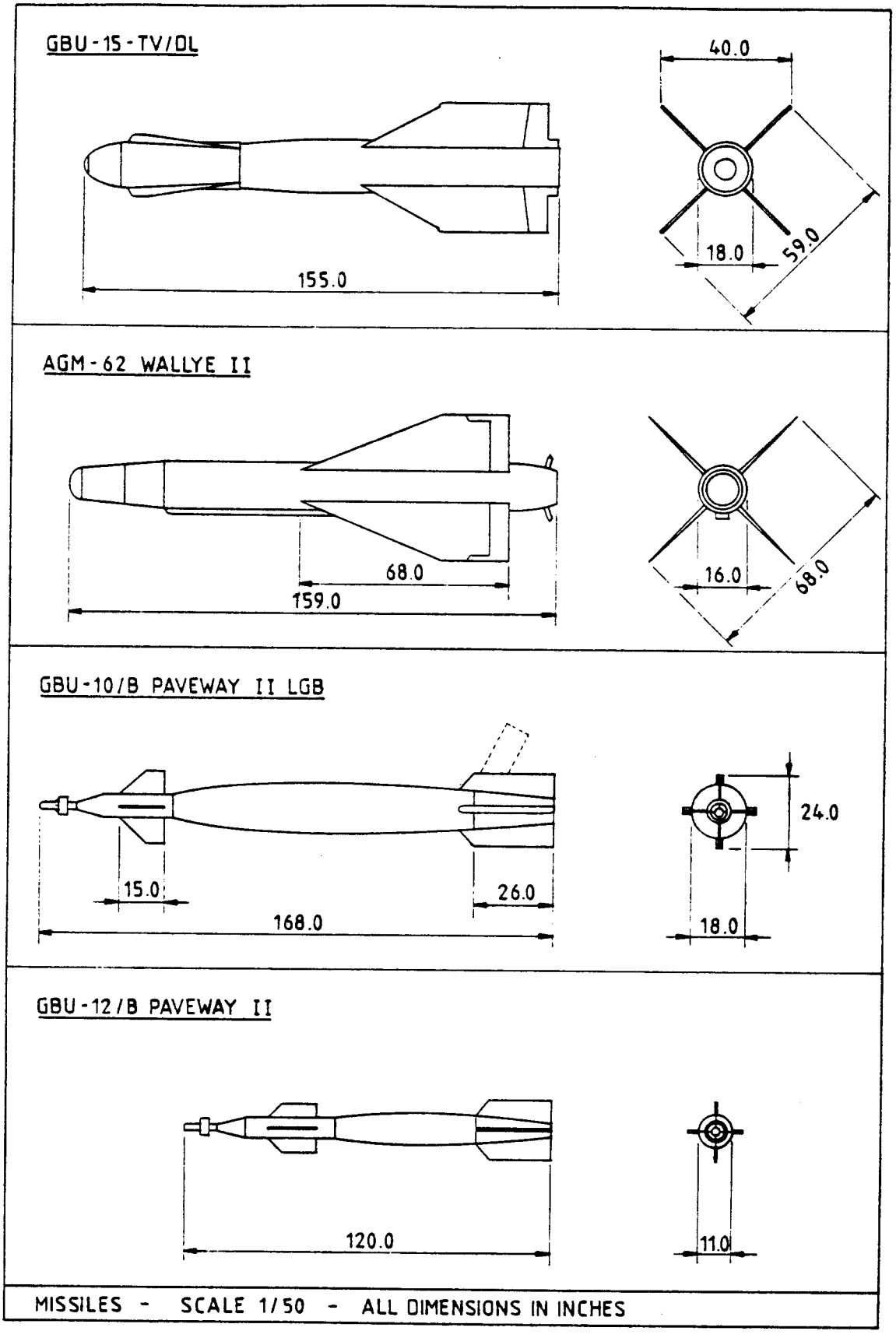

Figure 3.42 Dimensions of Guided Free Fall Munitions

3.5.3 Missiles

The data presented in this sub-section cover two types of missiles: Air-to-air missiles and Air-to-surface missiles.

Air-to-air Missiles

Air-to-air missiles are normally used in an air intercept role against enemy fighters, bombers and reconnaissance airplanes. For that reason they are also referred to as Air-Intercept-Missiles (AIM).

Air-to-air missiles are classified in terms of range and in terms of the guidance systems used:

Short range: less than 10 miles. These are mostly infrared seekers: passive guidance.

Medium range: 10-30 miles. These are mostly guided via radar illumination of the target: semi-active guidance.

Long Range: 30 miles or more. These are also mostly guided via radar illumination of the target: semi-active guidance.

Figure 3.43 contains geometric information for five air-to-air missiles. Table 3.3 provides weight and range data for these missiles.

Table 3.3 Weight and Range Data: Air-to-air Missiles

Type	Weight (lbs)	Range (miles)	Warhead (lbs)	Launch Method
Infrared Guided AIM's				
AIM-9J Sidewinder	170	6	N.A.	Rail
AIM-9L Sidewinder	191	10	25	Rail
Radar Guided AIM's				
AIM-7F Sparrow	514	24	66	Rail or eject.
AIM-54C Phoenix	1,000	120	132	eject.
AIM-120 AMRAAM	327	>100	N.A.	eject.

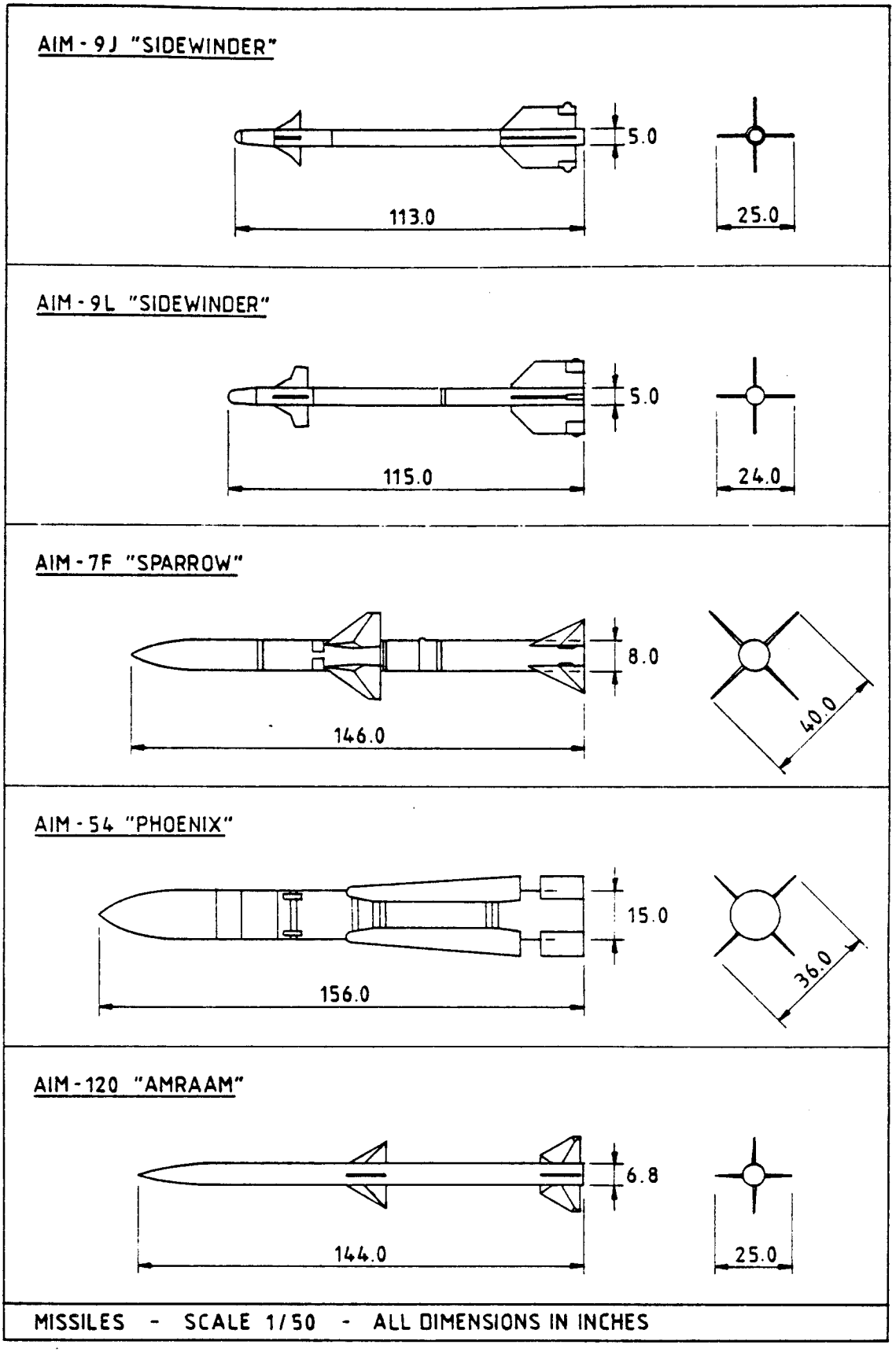

Figure 3.43 Dimensions of Air-to-air Missiles

Air-to-surface Missiles

Air-to-surface missiles are also referred to as Air-to-ground (AGM) missiles.

AGM's or air-to-ground missiles use a wide variety of guidance systems depending on range and purpose. Figure 3.44 presents the geometries of five such missiles. Table 3.4 contains weight and range data for these missiles.

Table 3.4 Weight and Range Data: Air-to-surface Missiles

Type	Guidance	Purpose	Weight	Warhead	Range
Maverick AGM-65A/B	TV	Anti-tank+ Anti-ship	463	125	N.A.
Maverick AGM-65C	Laser	same	463	not produced	
E			634	299	N.A.
Maverick AGM-65D	IFR	same	463	N.A.	N.A.
F			634	N.A.	N.A.
Standard ARM AGM-78D	Radar	Anti-radar	1,397	N.A.	>15.5
Shrike AGM-45	Radar	Anti-radar	400	145	10
HARM AGM-88A	Radar	Anti-radar	807	145	13
Hellfire AGM-114A	Laser	Anti-tank	95	N.A.	N.A.

For further information on missile systems the reader should consult Reference 19.

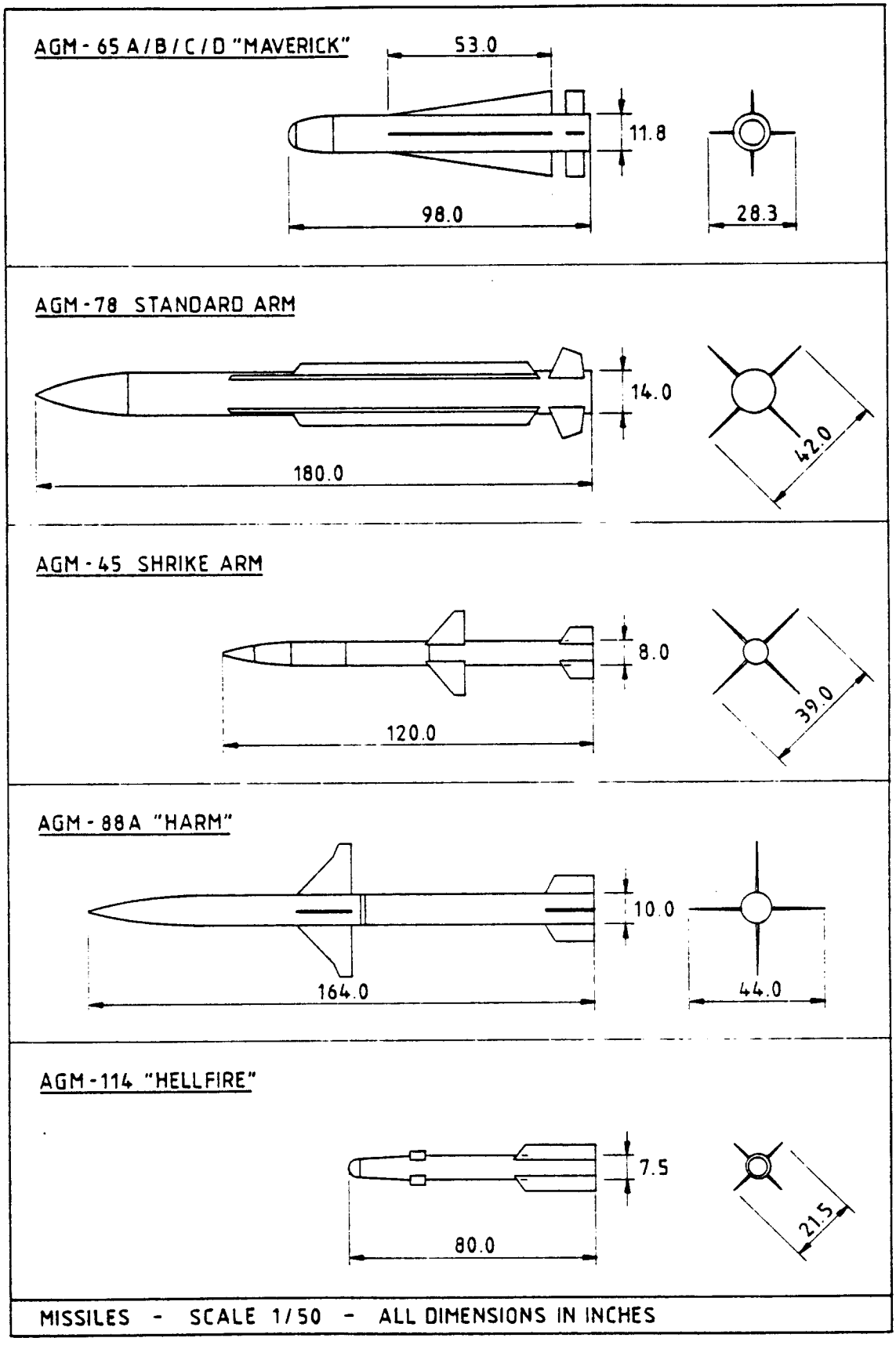

Figure 3.44 Dimensions of Air-to-surface Missiles

3.5.4 External Fuel Stores

For aerodynamic, structures and mission oriented reasons there is not much interchangeability between external fuel stores. As a general rule these external fuel stores are developed uniquely for each airplane.

In preliminary design it is useful to have data relating tank weights (empty) to usable tank volume. This information is given in Fig.3.45. Figures 3.46 and 3.47 define dimensions for five external fuel stores (tanks).

3.5.5 Special Purpose Stores

Most combat airplanes can be equipped with external stores to enhance their effectiveness in combat zones. These external stores can have several functions:

electronic warfare, navigation, offensive avionics and reconnaissance.

Figures 3.48-3.50 contain information on the geometries of special purpose stores. Table 3.5 provides weight and function data for these stores.

Table 3.5 Special Purpose Stores

Type	Purpose	Figure	Weight gross	empty
AN/ALQ-101 V-6	ECM	3.48a	400	
V-10	ECM	3.48b	540	
AN/ALQ-119 V-15	ECM	3.48c	580	
AN/ALQ-131 V	ECM	3.48d	675	
Pave Penny Sensor	Targetting (via HUD)	3.49a	32	
LANTIRN Pod 1	Targeting	3.49b	431	
Pod 2	Navigation	3.50a	544	
AN/ASQ-153 Pave Spike	Targeting (Laser)	3.49c	425	
AN/ALE 43	Chaff Pod	7.49d	534	184
Lundy Conformal	Chaff Pod+ IR decoys	7.50b	31.3	12

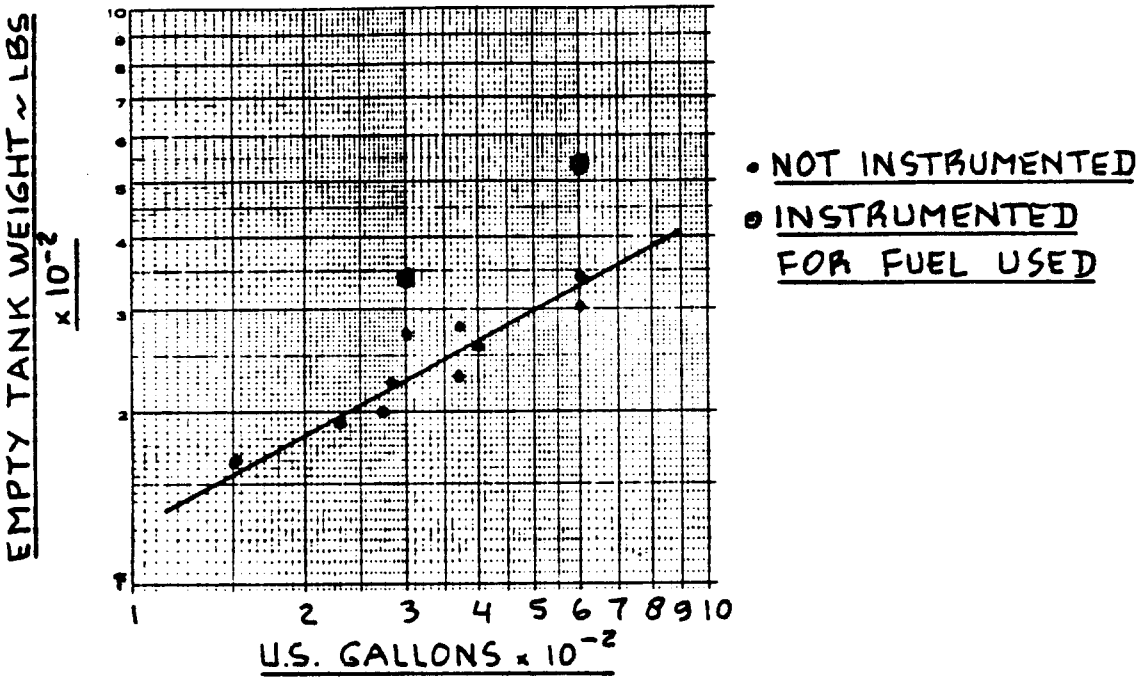

Figure 3.45 Tank Volume and Tank Empty Weight for a Range of External Fuel Tanks

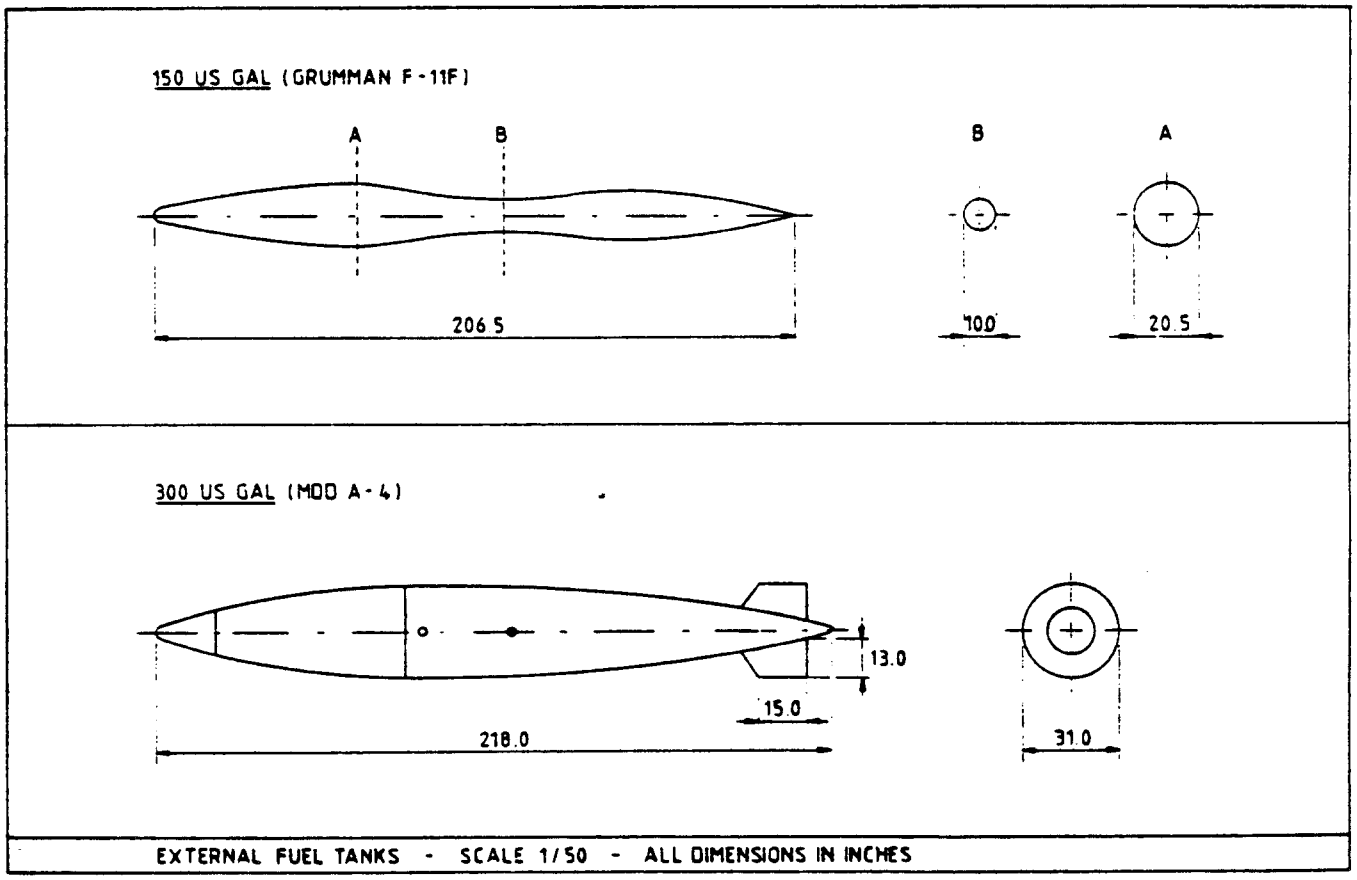

Figure 3.46 Dimensions of External Fuel Tanks

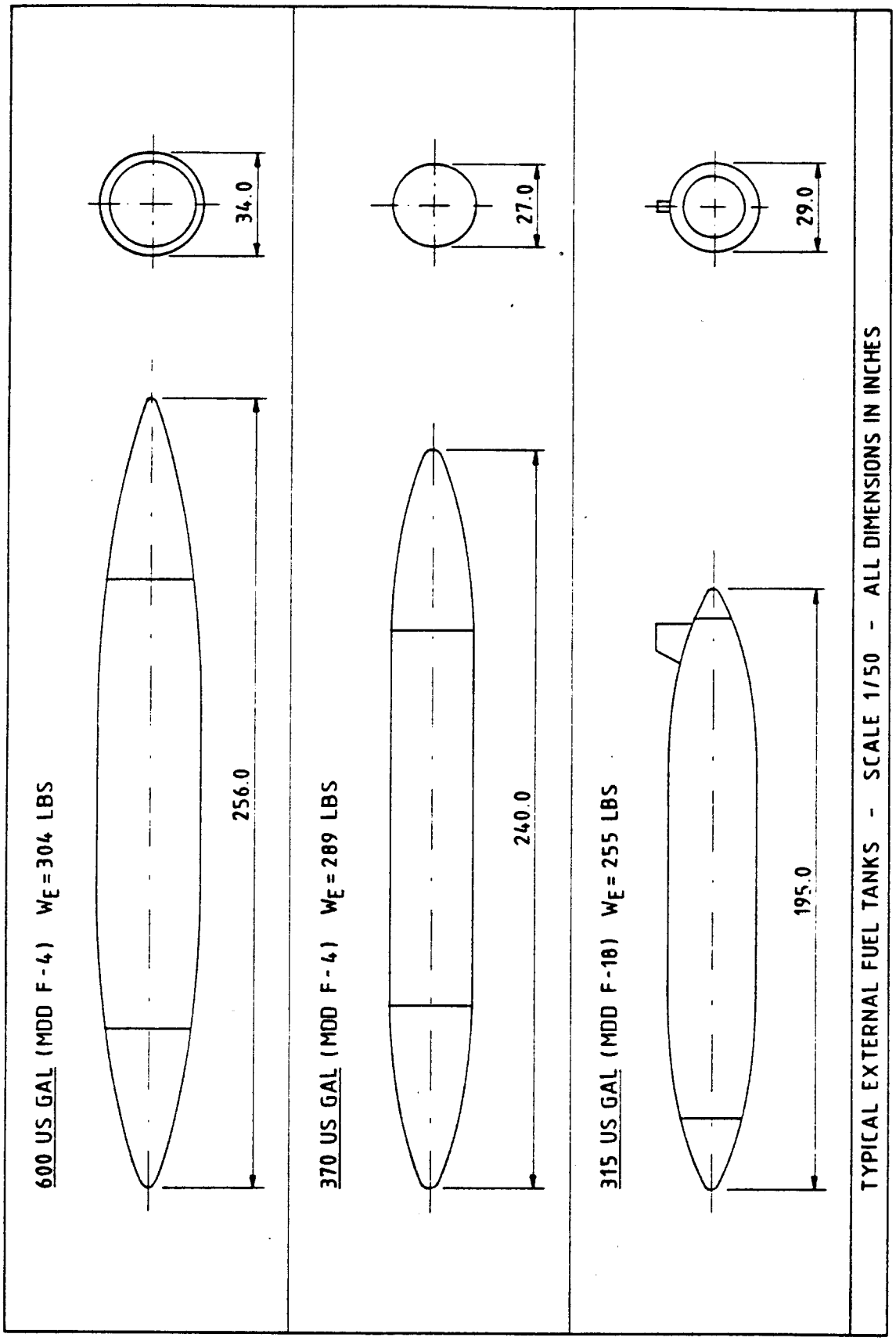

Figure 3.47 Dimensions of External Fuel Tanks

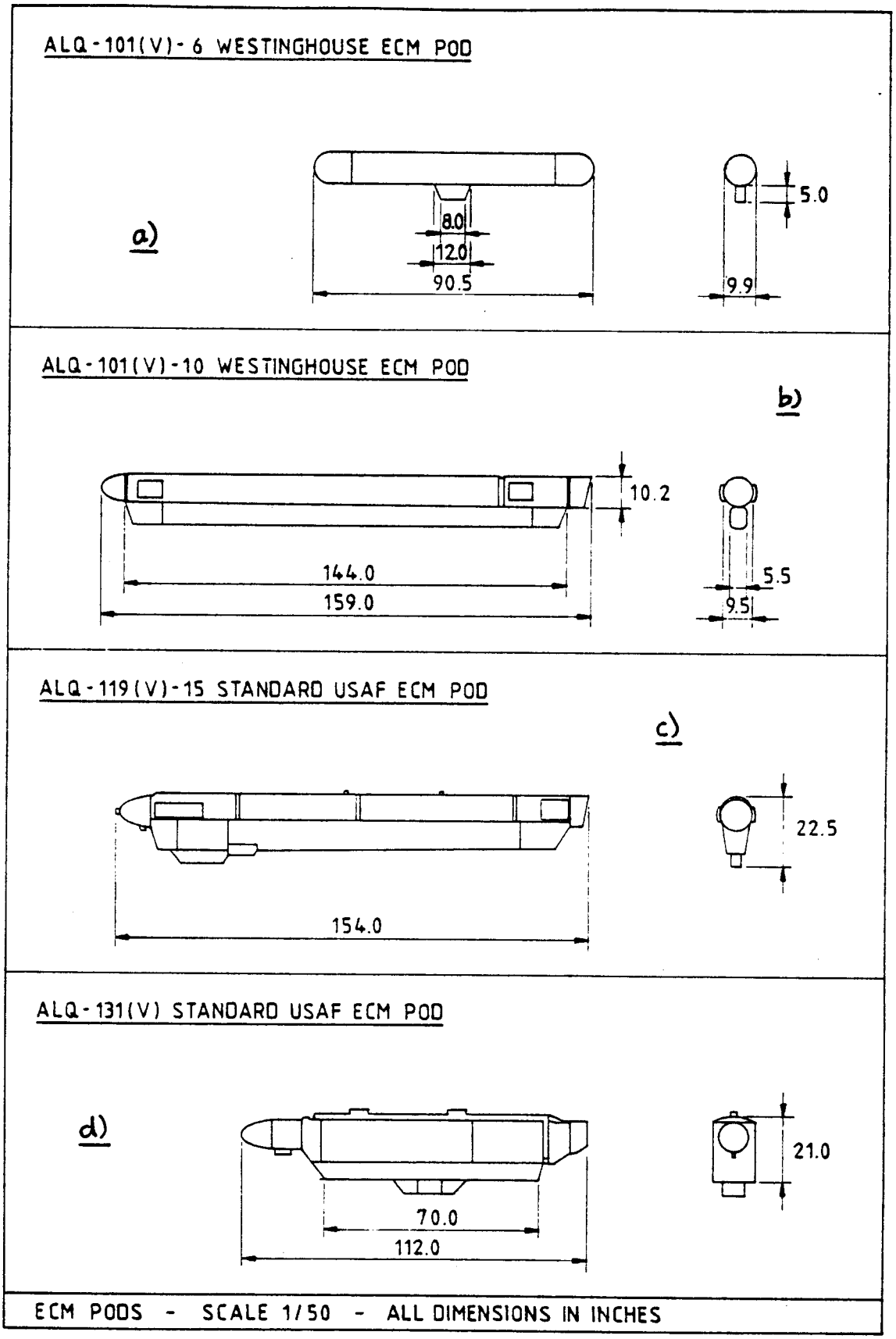

Figure 3.48 Dimensions of Special Purpose Pods

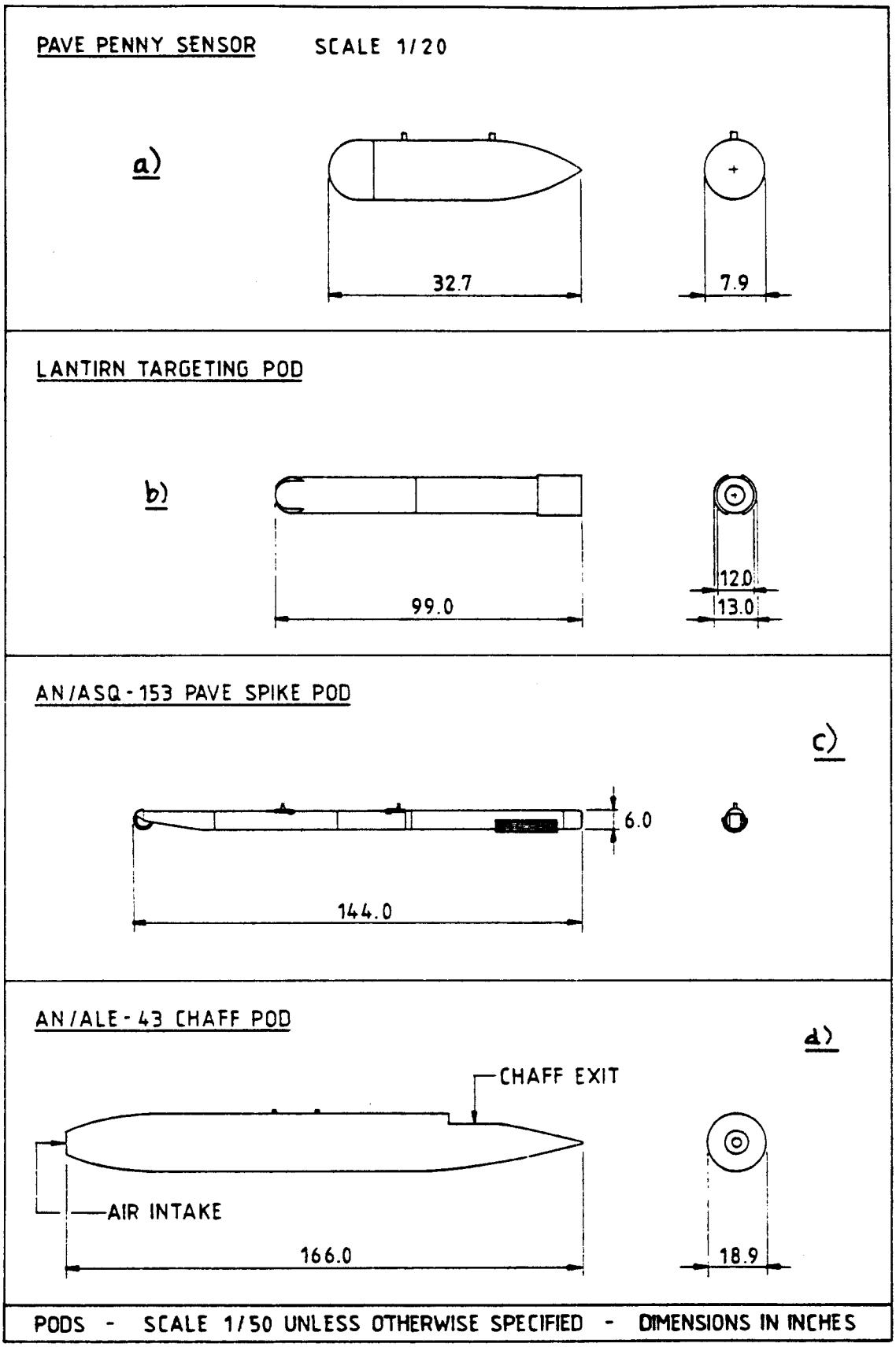

Figure 3.49 Dimensions of Special Purpose Pods

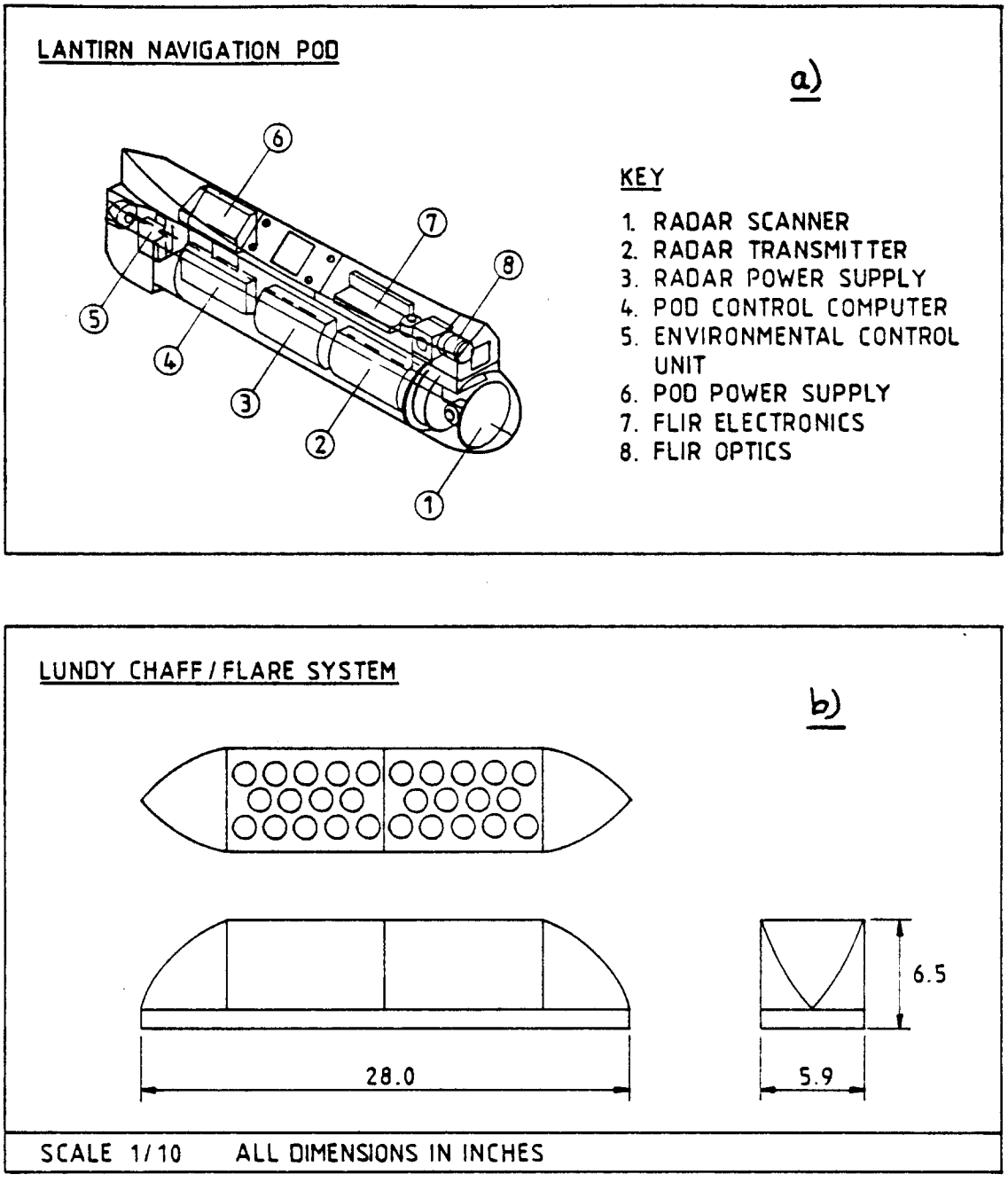

Figure 3.50 Dimensions of Special Purpose Pods

3.5.6 Military Vehicles

Military transport airplanes must be designed so that they can load, carry and unload a wide range of military vehicles. The number and type of vehicles to be carried are normally given in the mission specification of the airplane. The purpose of this sub-section is to present weight and geometric data on a range of large military vehicles. Reference 19 should be consulted for further data on military vehicles.

Table 3.6 lists the type, purpose and weight of each vehicle. Figures 3.51 through 3.58 provide geometric information for these vehicles.

Table 3.6 Typical Military Vehicles

Type	Purpose	Weight Loaded	Figure
M1 Abrams	Main battle tank	117,600*	3.51
M60	Battle tank	108,000	3.52
M2 Bradley	Fighting vehicle	50,000	3.53
M113	Personnel Carrier	22,520	3.54
M107(175mm)	Self-propelled Gun	62,027	3.55
M108(105mm)	Self-propelled Gun	49,458	3.56
M109(155mm)	Self-propelled Gun	52,428	3.57
M110(203mm)	Self-propelled Gun	62,370	3.58

*Empty weight: 100,000 lbs

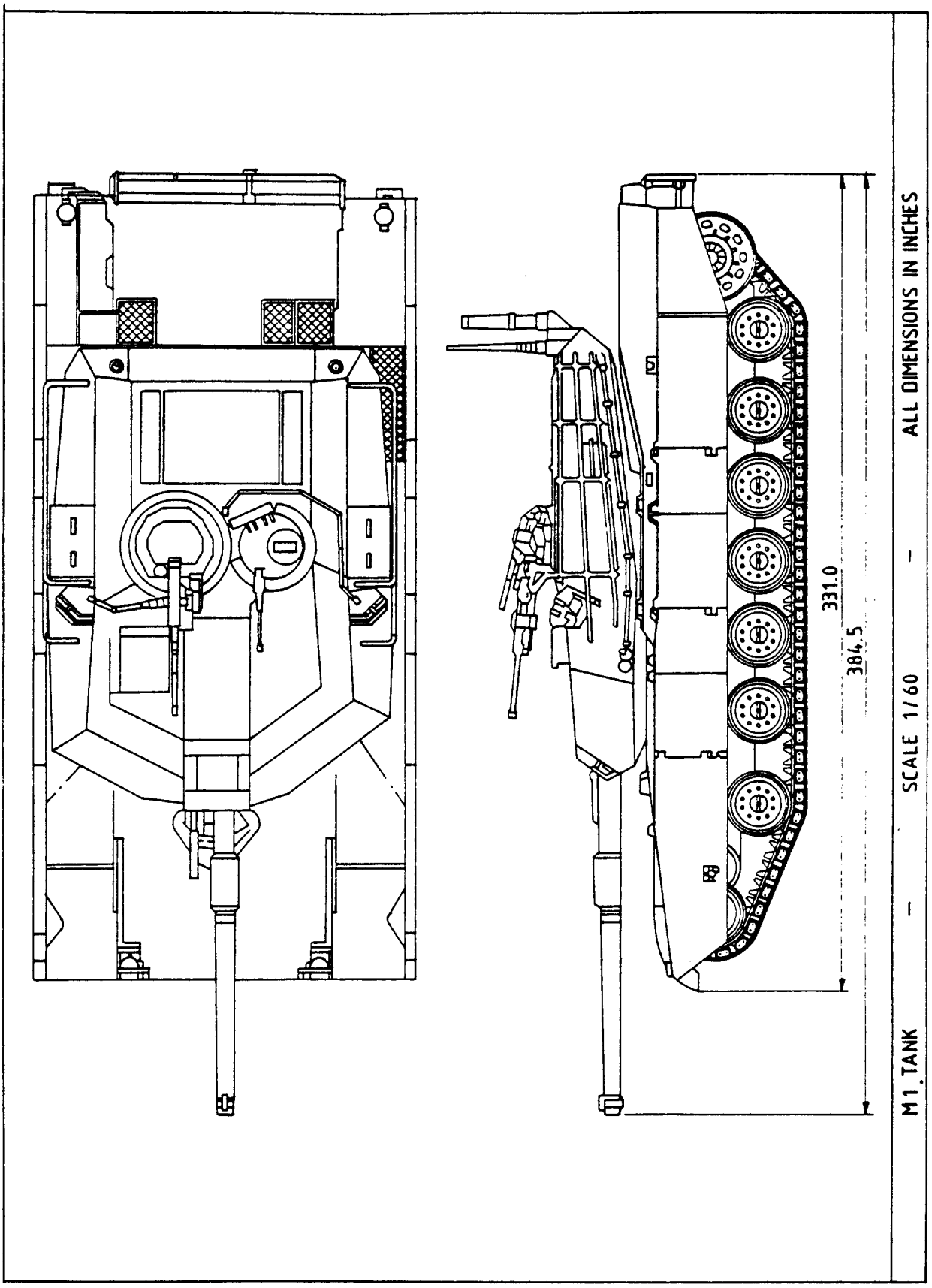

Figure 3.51 Dimensions of M1 Tank

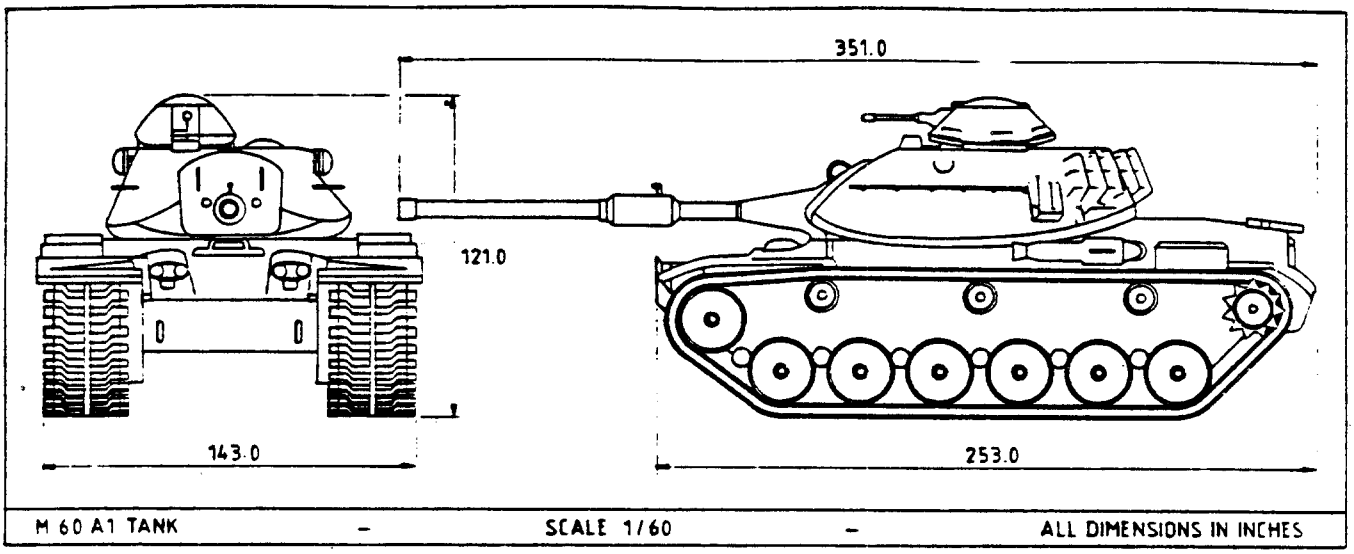

Figure 3.52 Dimensions of M60-A1 Tank

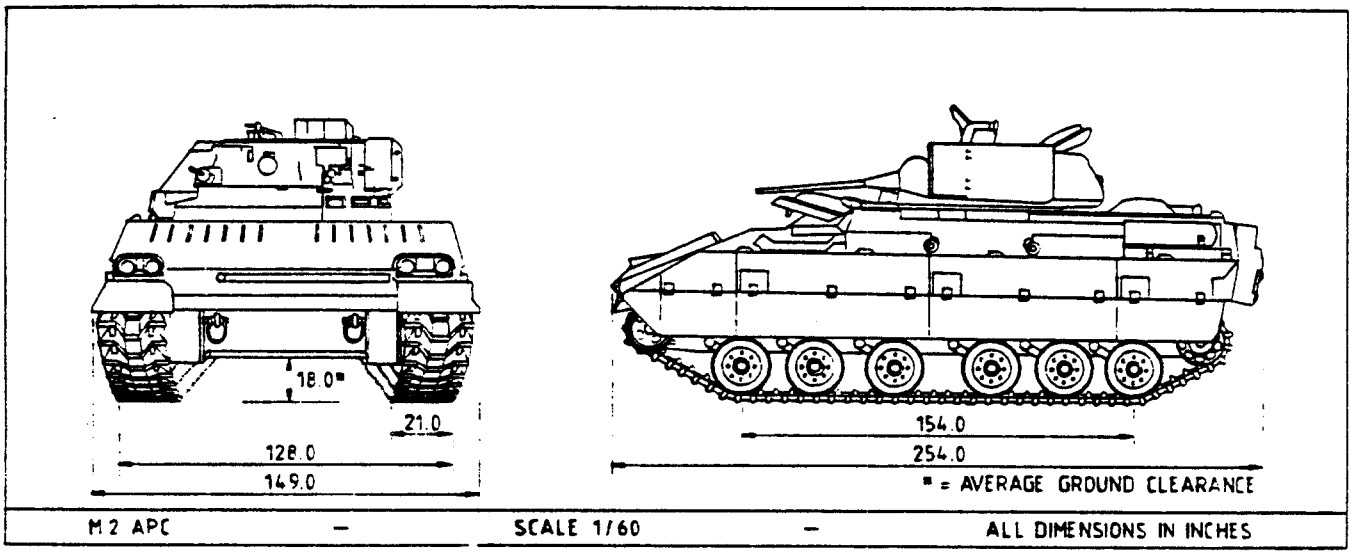

Figure 3.53 Dimensions of M2 Bradley Fighting Vehicle

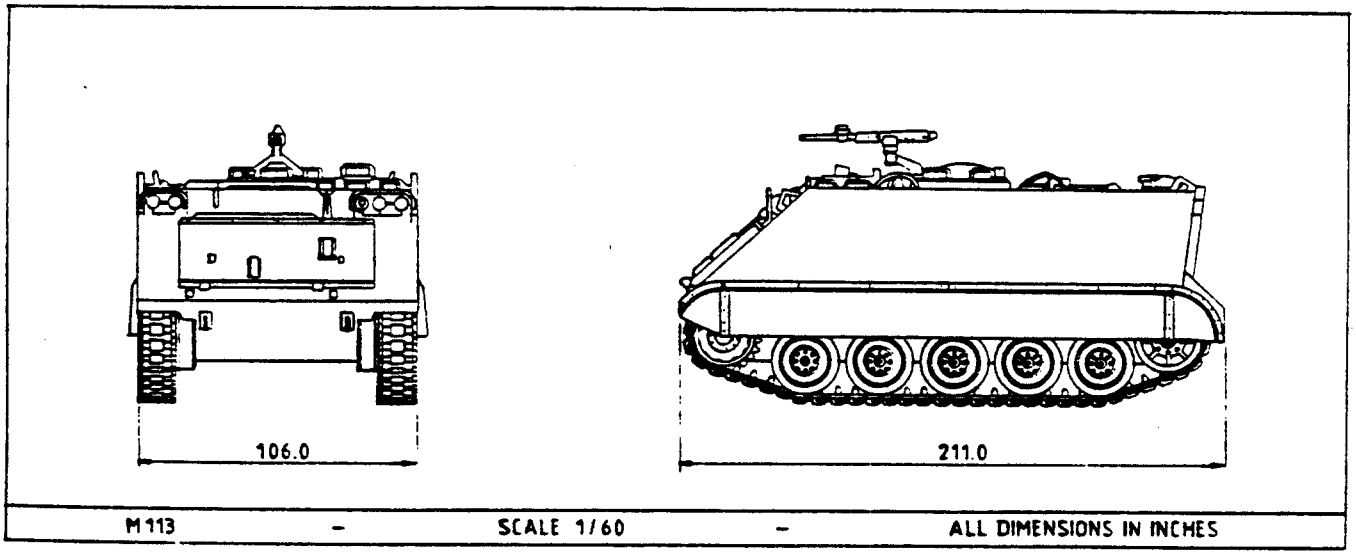

Figure 3.54 Dimensions of M113 Personnel Carrier

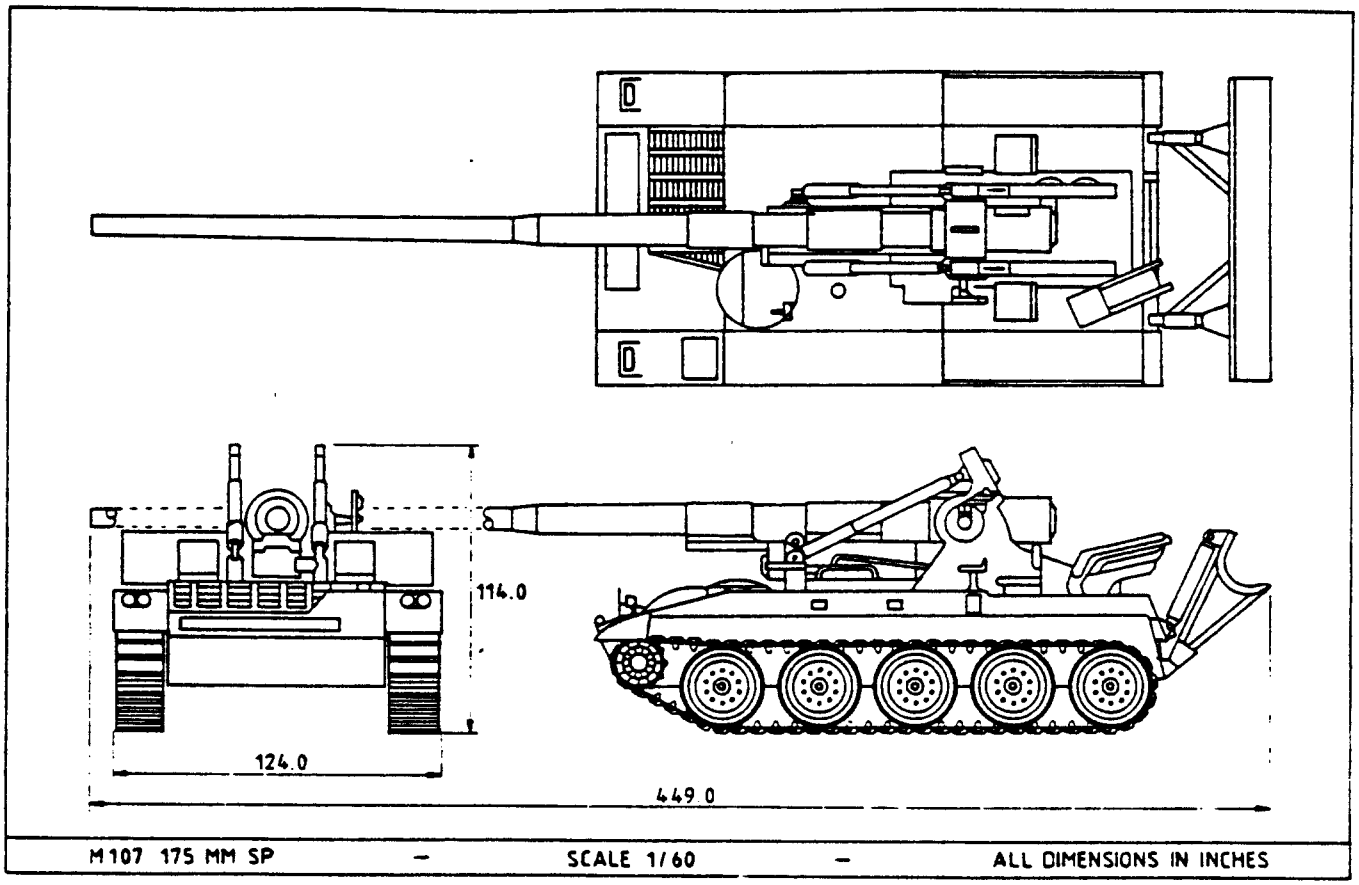

Figure 3.55 Dimensions of M107 Self-propelled Gun

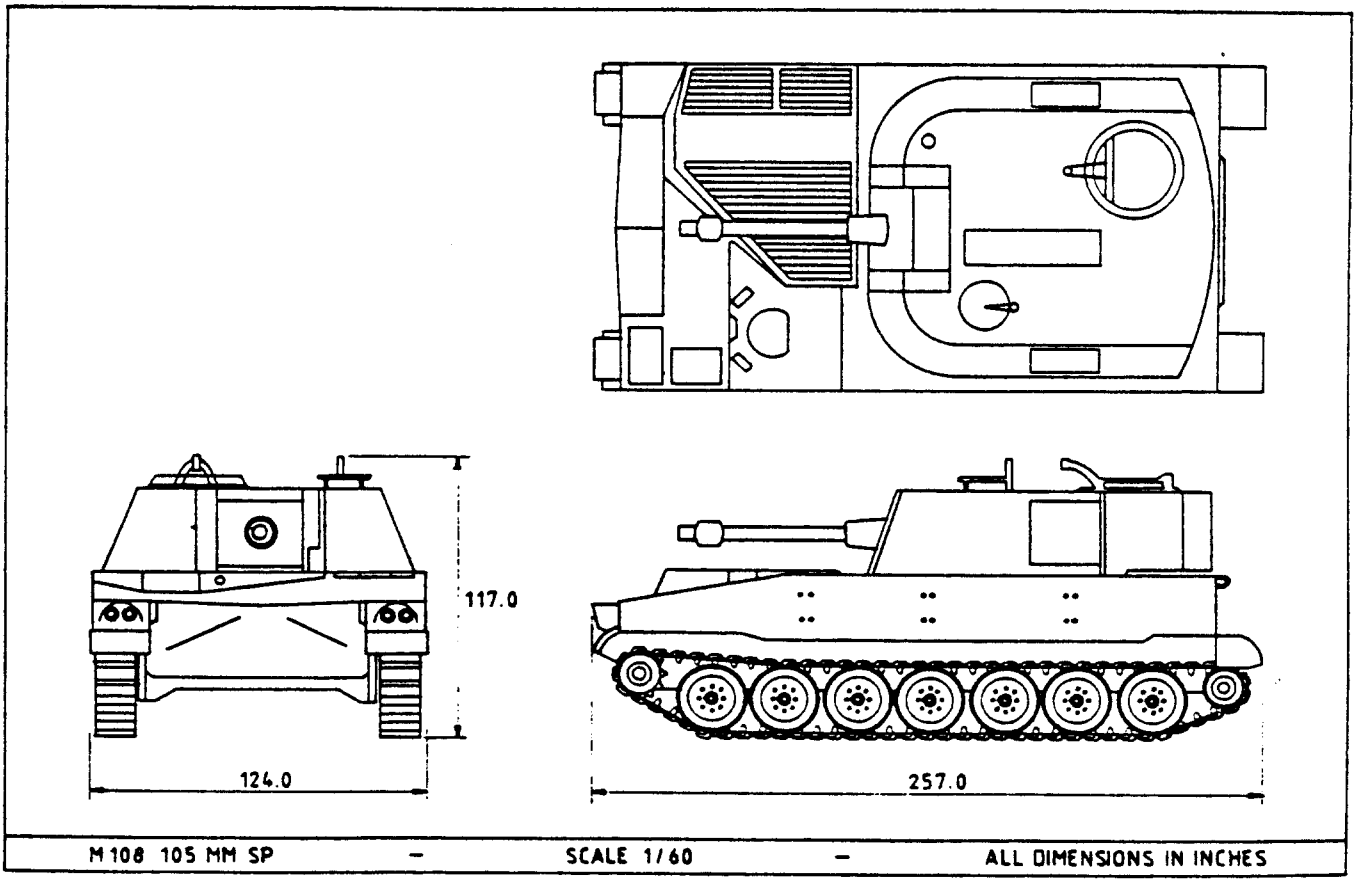

Figure 3.56 Dimensions of M108 Self-propelled Gun

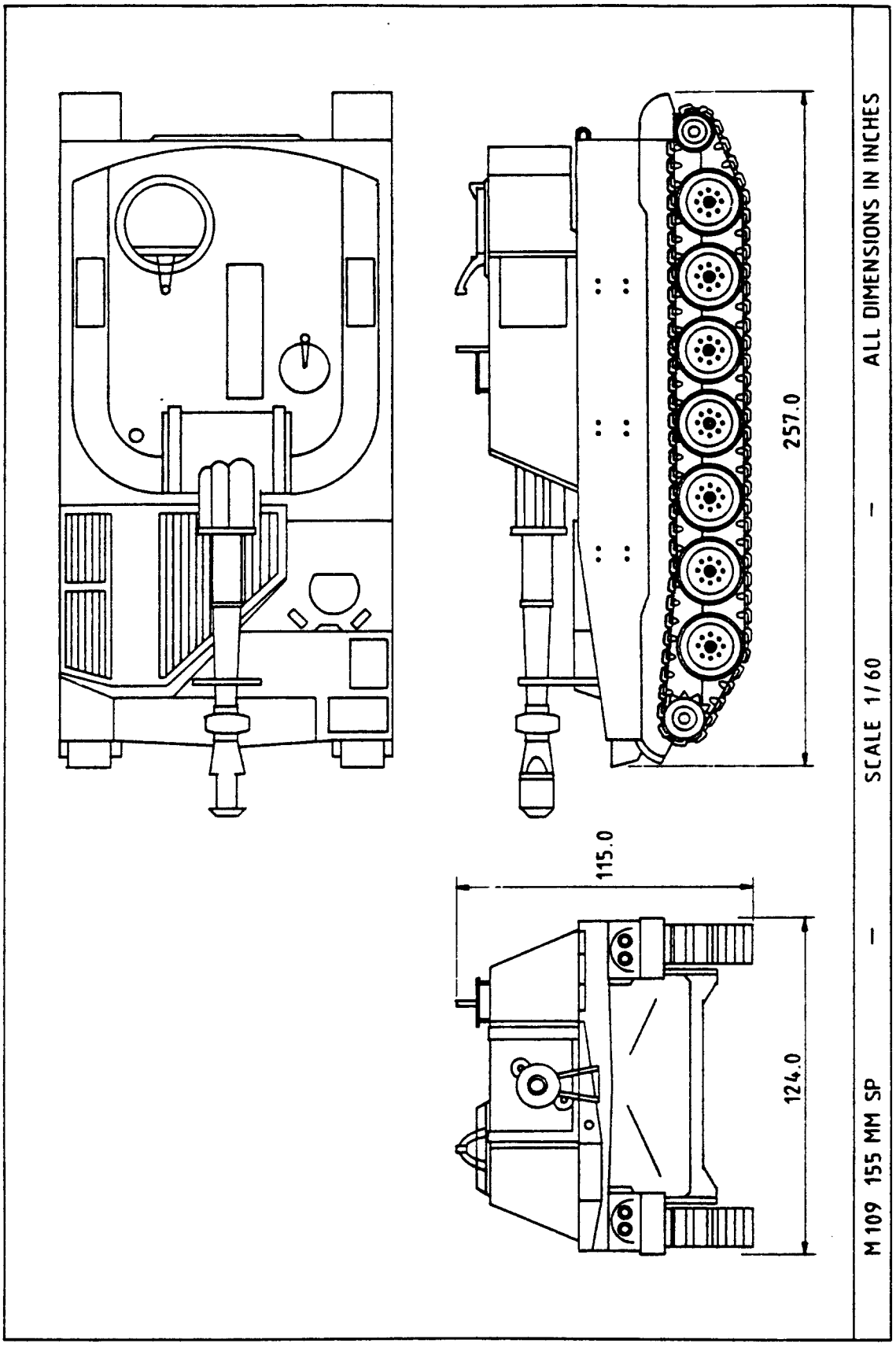

Figure 3.57 Dimensions of M109 Self-propelled Gun

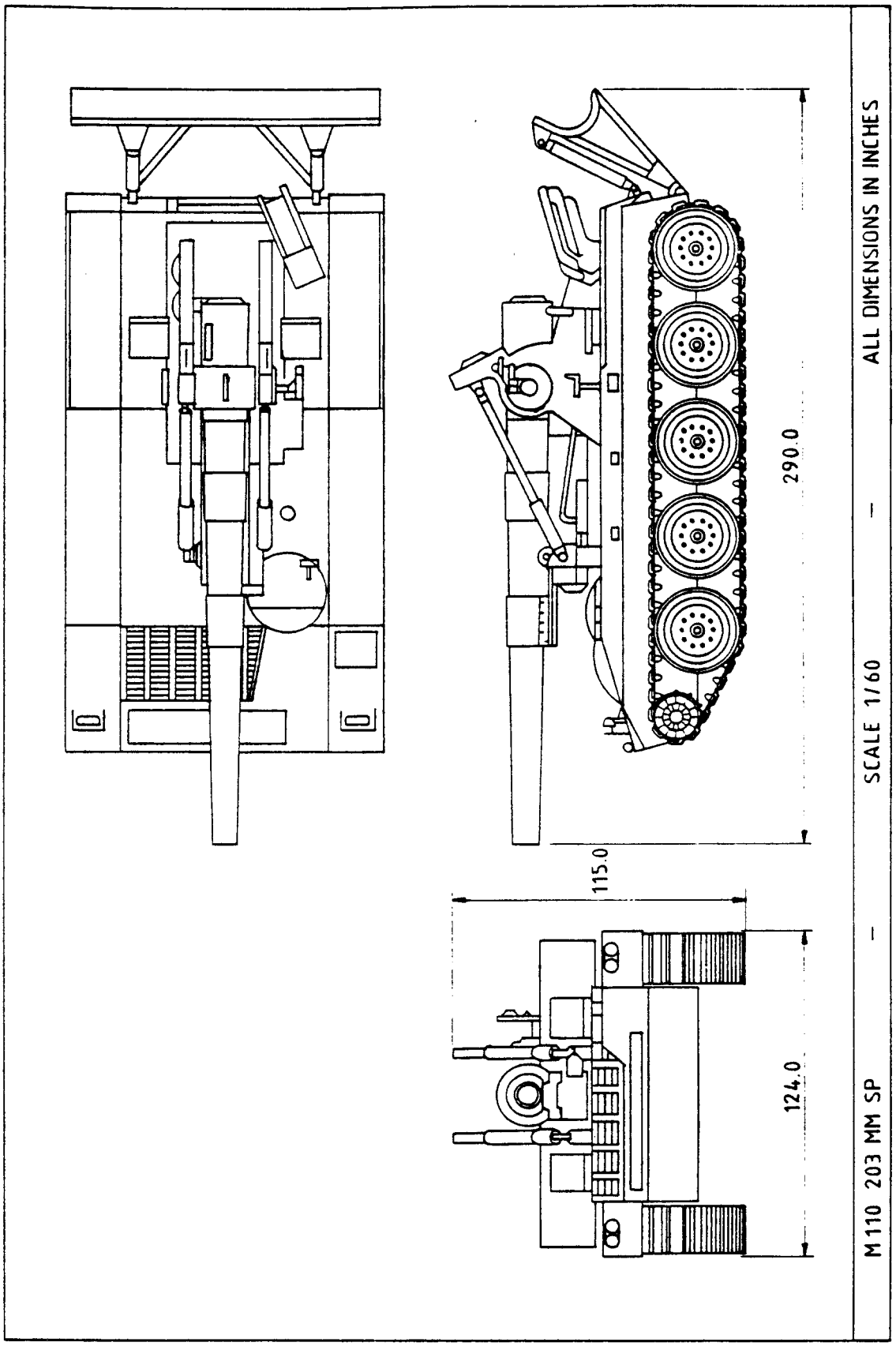

Figure 3.58 Dimensions of M110 Self-propelled Gun

4. FLIGHT CONTROL SYSTEM LAYOUT DESIGN

The purpose of this chapter is to discuss the preliminary layout design of flight control systems.

Flight control systems can be divided into: Primary and Secondary flight control systems.

Examples of primary flight control systems are:

Lateral Controls to:	Longitudinal Controls to:	Directional Controls to:
Ailerons, Spoilers Differential Stabilizer	Elevator Stabilizer Canard	Rudder

Examples of secondary flight control systems are:

Trim controls Controls to:	High lift Controls to:	Thrust (or Power) Controls to:
Lateral, Longitudinal and Directional primary flight controls	Trailing and/or leading edge flaps	Engine fuel controls (Throttles), Manifold gates, Propeller blade incidence

In the case of automated and powered flight control systems the split between primary and secondary flight controls is not clear. In several fighter airplanes the thrust controls and the flight controls are in fact already integrated or combined with the primary (aerodynamic) flight controls. Examples are : the Harrier AV8B (reaction controls use bleed air from the compressor) and the F15 SMTD demonstrator have integrated aerodynamic and propulsion controls. Such integration of primary and secondary controls into one flight control system will probably be commonplace in most high performance airplanes.

Preliminary sizing of the aerodynamic flight controls is discussed in Chapters 6 and 8 of Part II. Preliminary sizing of high lift devices is discussed in Chapter 7 of Part II.

The preliminary layout design of flight control systems is presented in the following manner:

4.1 Layout of reversible flight control systems

4.2 Examples of reversible flight control systems

4.3 Layout of irreversible flight control systems

4.4 Examples of irreversible flight control systems

4.5 Trim systems

4.6 High lift control systems

4.7 Power control systems

4.1 LAYOUT OF REVERSIBLE FLIGHT CONTROL SYSTEMS

Definition: In a reversible flight control system, when the cockpit controls are moved, the aerodynamic surface controls move and vice versa.

Reversible flight control systems are typically mechanized with cables, push-rods or a combination thereof.

Major design problems associated with this type of flight controls are:

1. Friction 2. Cable stretch 3. Weight

4. Handling qualities 5. Flutter

Major advantages associated with this type of flight controls are:

1. Simplicity (= reliability) 2. Low cost

3. Relatively maintenance free

4.1.1 Reversible Lateral Flight Control Systems

Figure 4.1 shows several possible layouts for reversible lateral flight control systems.

Note: the lateral cockpit control movement must be consistent with the ranges specified for commercial and for military airplanes in Section 2.2 of Part III.

Credit: Most figures in this section were adapted from: Bok, F.P. and Beulink, D.G., Aircraft Mechanisms (in Dutch), Report: VTH-D22, June 1974, Delft Technological University, The Netherlands.

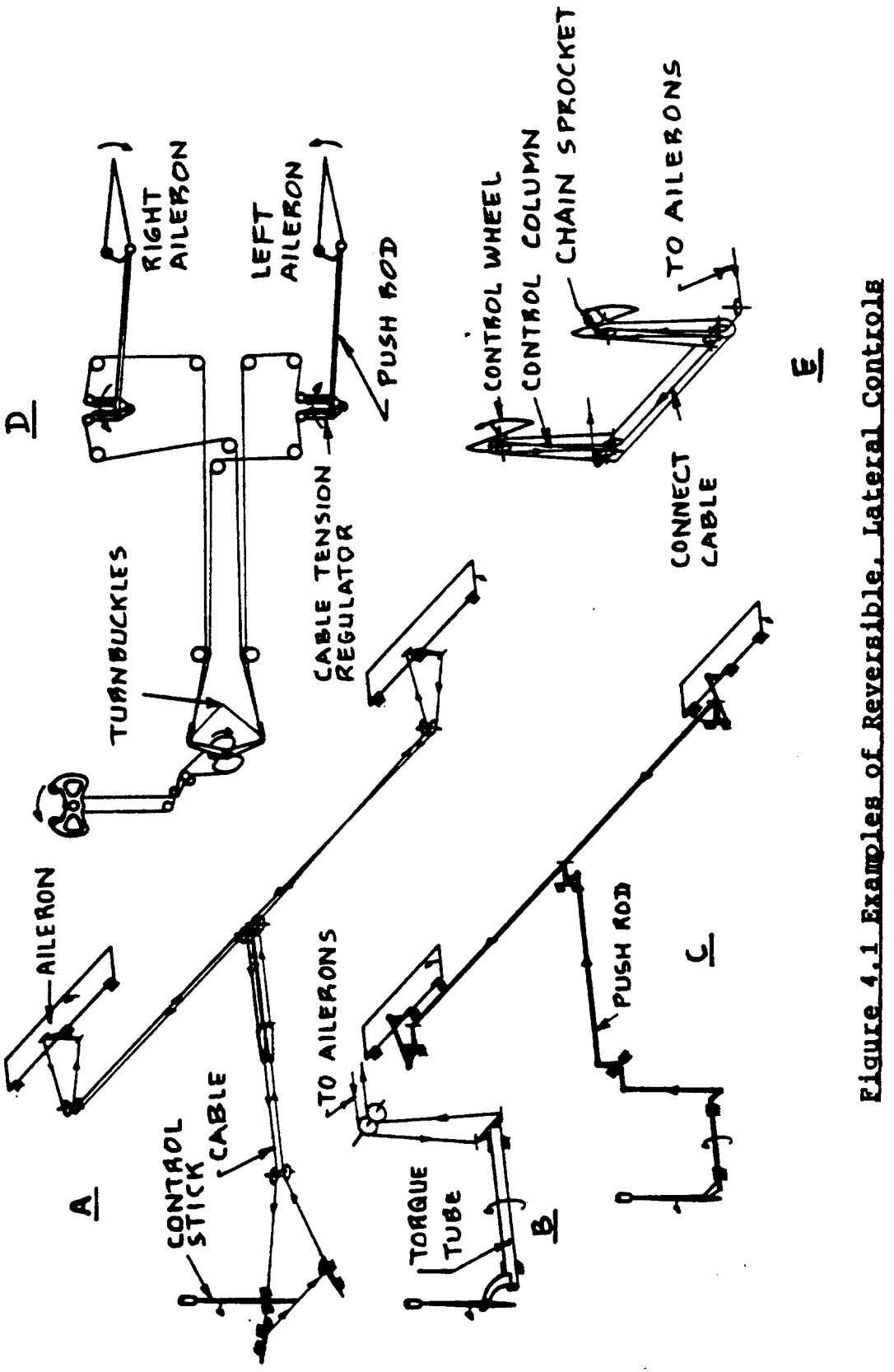

Figure 4.1 Examples of Reversible, Lateral Controls

System type A in Figure 4.1 is commonly used in light airplanes. The lateral stick motion is translated directly into cable motion. Figure 4.2 shows the stick-to-cable arrangement in more detail. Experience shows that this direct attachment method works satisfactorily only as long as: (l/s) > 6. If this criterion is violated, excessive cable stretch problems result.

In airplanes with tandem cockpit arrangements the lateral cockpit controls are often combined with the longitudinal cockpit controls through a concentric cable/tube arrangement. Figure 4.1B shows such an arrangement with more detail presented in Figure 4.3. The (l/s) > 6 criterion applies here also.

Figure 4.1C shows an example of a push-rod driven lateral control system.

In many airplanes a wheel mounted on a control column is used to actuate the lateral flight controls. Figure 4.1D is an example of a single control wheel installation. Figure 4.1E shows a dual control wheel installation. The latter are frequently used in airplanes with a side-by-side cockpit.

Most ailerons when deflected asymmetrically over the same angle, induce an adverse yawing moment onto the airplane. Ref.20 (Ch.4) contains a physical explanation of this effect. To counteract this adverse yawing moment the ailerons may be deflected 'differentially': Fig.4.4 shows a simple method for achieving this.

Note that the systems of Figures 4.1B through 4.1E avoid the cable stretch problem associated with the system of Figure 4.1A.

4.1.2 Reversible Longitudinal Flight Control Systems

Figure 4.5 presents a number of layouts used in reversible longitudinal flight controls systems.

Note: The longitudinal cockpit control movement must be consistent with the ranges specified for commercial and for military airplanes defined in Ch.2 of Part III.

The cable-crossing feature shown in Fig.4.5A is acceptable only as long as the cables do not rub together.

The system of Figure 4.5B employs a mixture of cables and push-rods. The system of Figure 4.5C uses only push-rods. Push-rod systems tend to have less

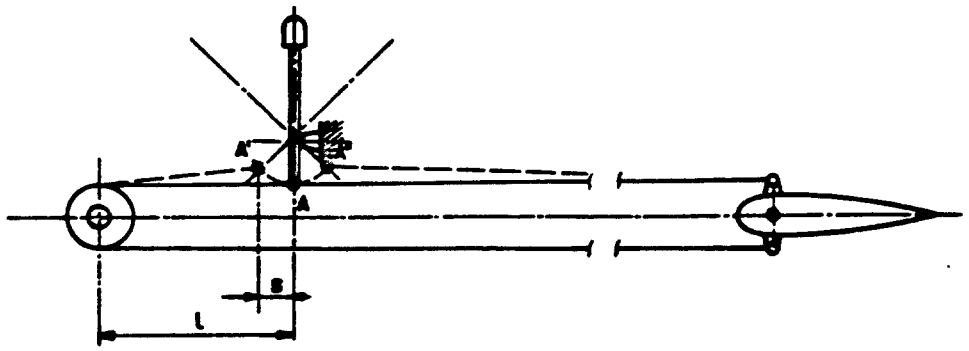

Figure 4.2 Occurrence of Cable Stretch in a System with Direct Stick-to-Cable Attachment

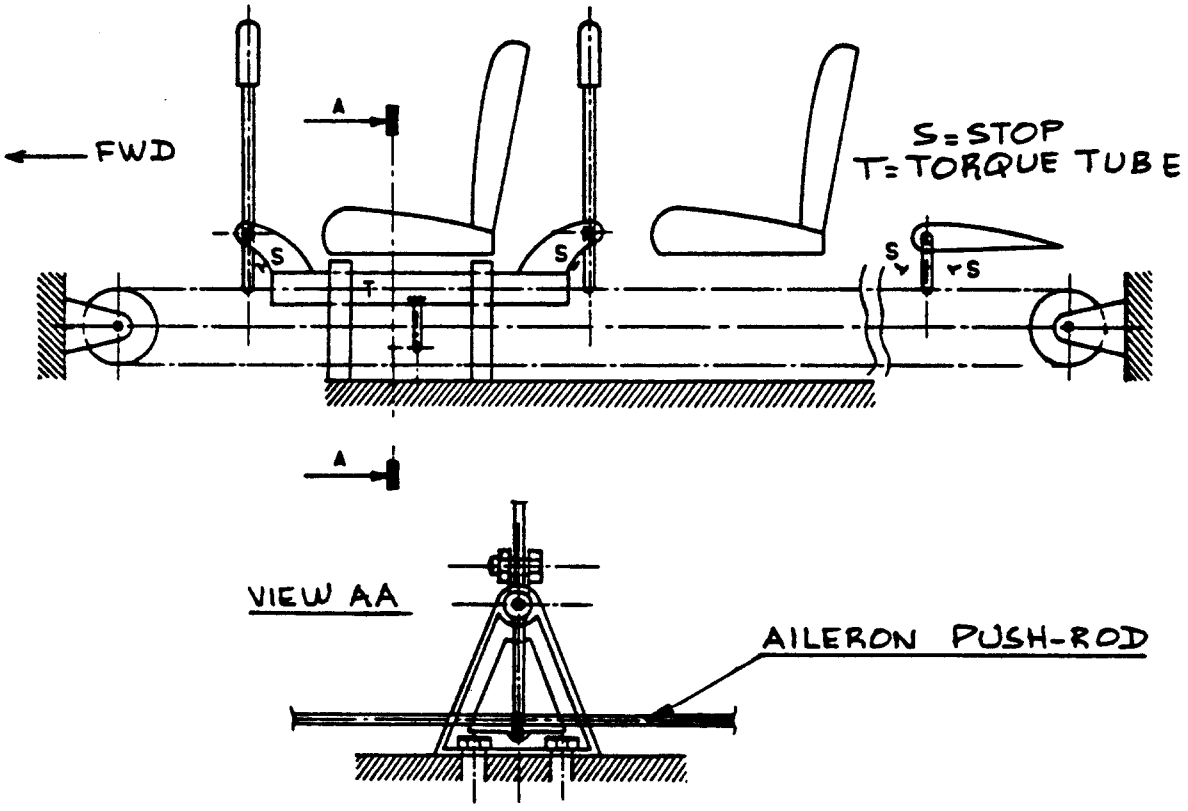

Figure 4.3 Example Layout for Combined Lateral and Longitudinal Cockpit Controls

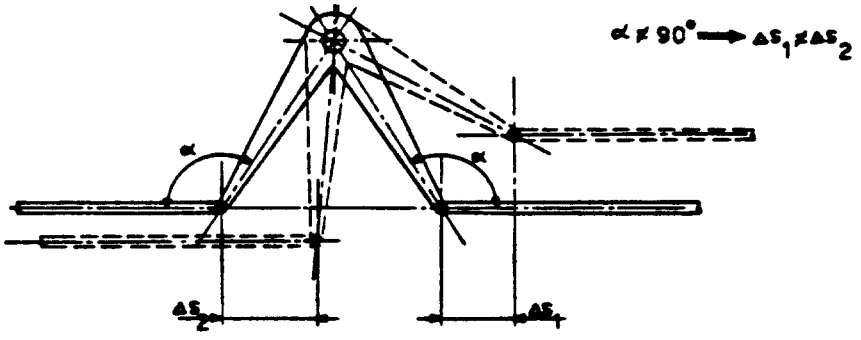

Figure 4.4 Mechanism for Differential Control Action

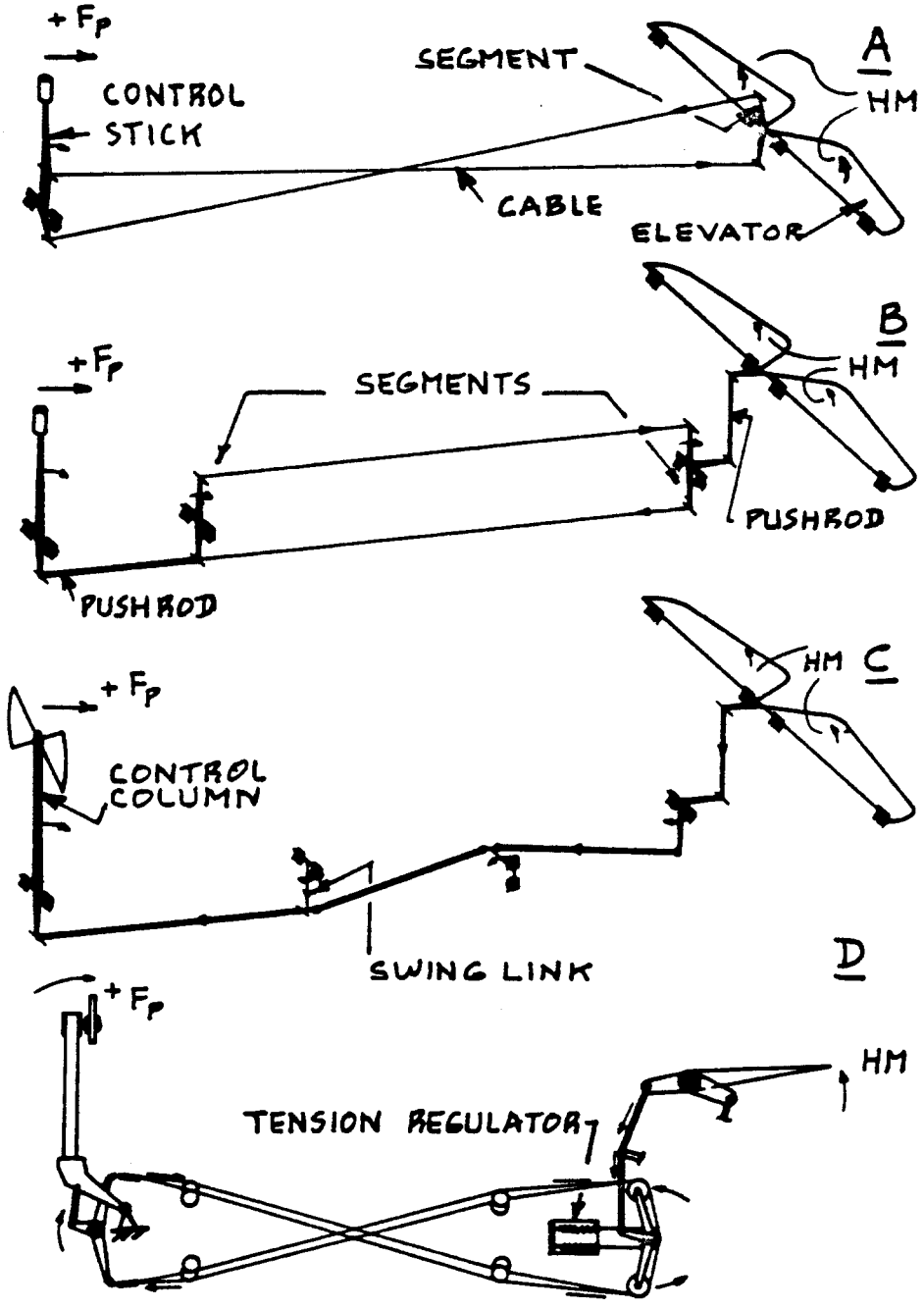

Figure 4.5 Examples of Reversible, Longitudinal Controls

friction than cable systems. They also tend to be a bit heavier.

Note the redundant cable system shown in Fig.4.5D: this type of cable redundancy is required in FAR25 certified airplanes only. In FAR23 airplanes single cable routings are acceptable.

4.1.3 Reversible Directional Flight Control Systems

Figure 4.6 shows examples of reversible directional flight control systems. The system of Figure 4.6A is found in many light airplanes.

Note: The directional cockpit control movement must be consistent with the ranges specified for commercial and for military airplanes defined in Section 2.2 of Part III.

Whenever dual cockpit controls are needed, the layouts shown in Figures 4.6B or C are employed. When redundancy is required, a cable layout such as shown in Figure 4.6D may be used.

In airplanes with V-tails (butterfly tails) the tail-mounted control surfaces normally serve both longitudinal and directional control functions. The separation of these functions is accomplished with a so-called mechanical mixer unit. Figure 4.7 shows example schematics of such mixer units.

4.1.4 Important Design Aspects of Reversible Flight Control Systems

In laying out a reversible flight control system, the following important design aspects need to be kept in mind:

- *Mechanical design requirements for cable and for push-rod systems
- *Efficiency considerations
- *Cable and push-rod control force levels
- *Control surface types and hinge moments
- *Aerodynamic balance requirements
- *Mass balance requirements

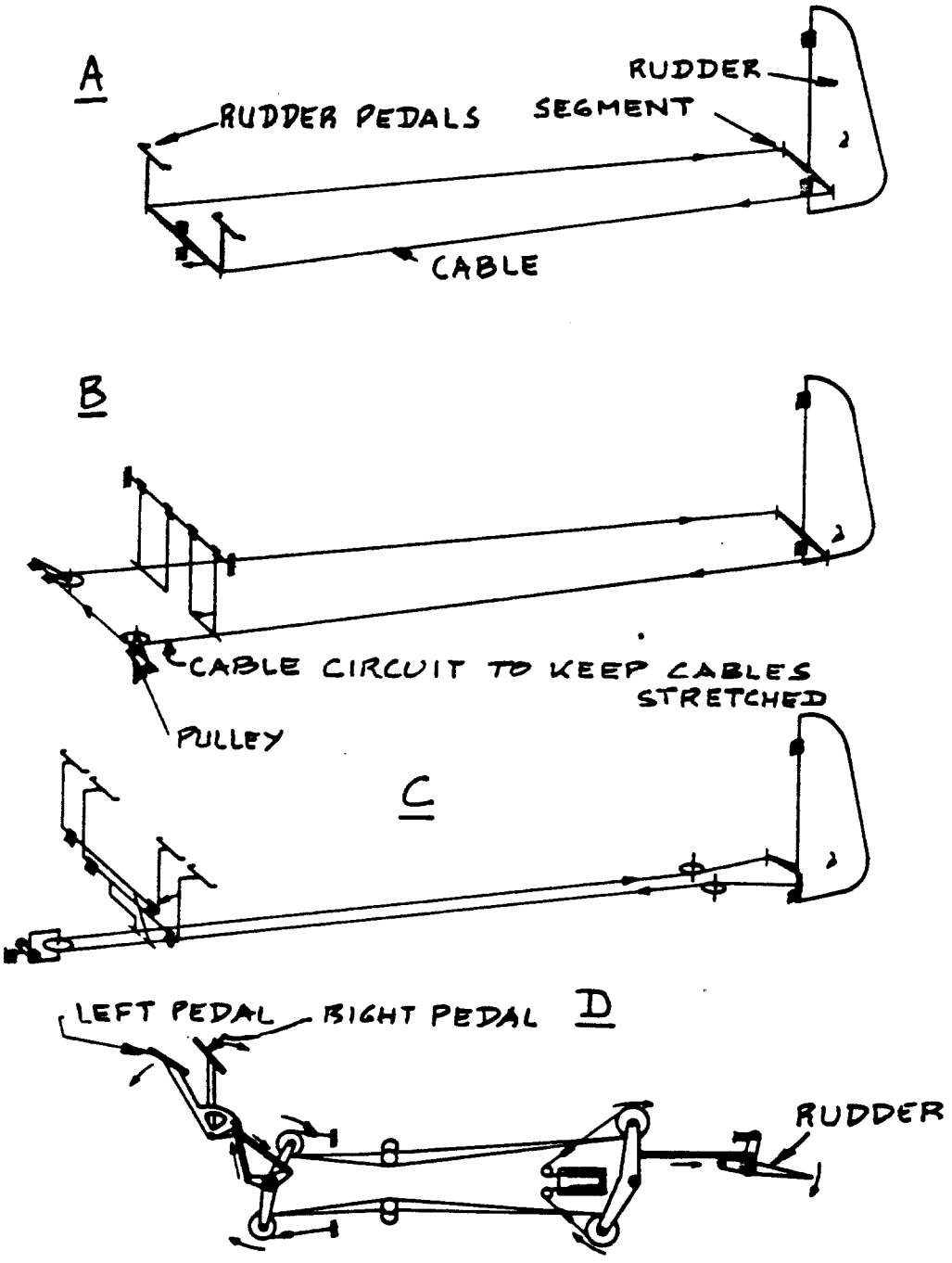

Figure 4.6 Examples of Reversible, Directional Controls

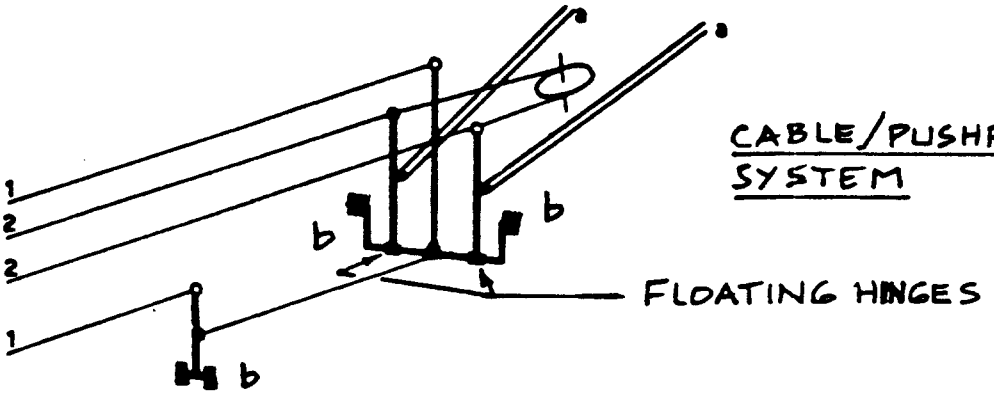

a TO RUDDERVATORS b FIXED HINGE

1 CABLES FOR LONGITUDINAL CONTROL

2 CABLES FOR DIRECTIONAL CONTROL

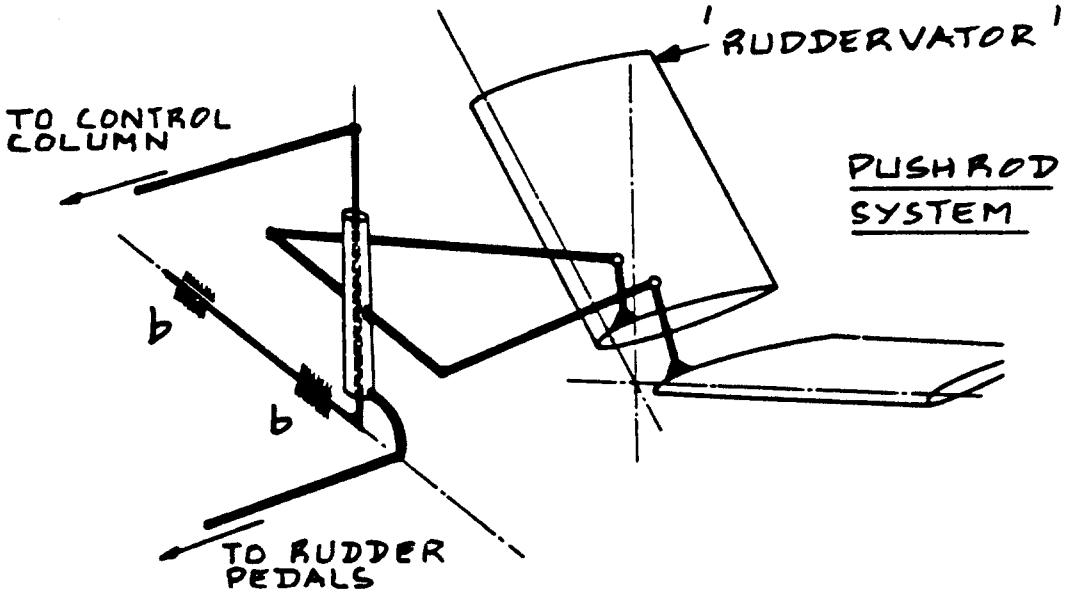

Figure 4.7 Examples of Longitudinal/Directional Control Mixers

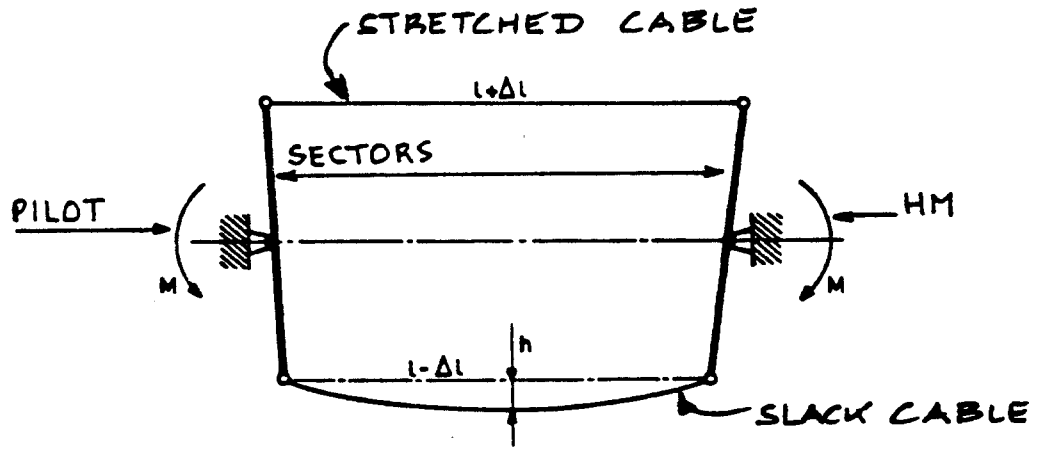

Figure 4.8 Occurrence of Cable Stretch and Cable Slack

4.1.4.1 Mechanical design requirements associated with cable systems

The designer of cable driven flight control systems is confronted with a range of mechanical design problems:

1. Cable stretch and cable slack
2. System friction
3. System elastic deformation
4. Kinematic feasibility

These problems are discussed in the following.

1. Cable stretch and cable slack

Figure 4.8 shows how cable stretch occurs in a simple cable system. The pilot's control force (moment) is opposed by an aerodynamically induced hinge moment. The consequence is that one cable will be stretched while the other cable will develop slack.

To prevent a 'slack' cable from leaving its pulley(s) or to prevent the cable from getting tangled into some other system a number of precautions must be taken:

1. Each pulley must have cables guards as shown in Figure 4.9.

2. For long cable runs, additional pulleys and/or cable guides must be installed. Figure 4.10 shows an example of a cable guide.

3. Turnbuckles and/or cable stretchers may have to be used to pre-stretch the cable system so that slack cables do not occur. Figures 4.11 and 4.12 show examples of these.

Cable slack can also occur for thermal reasons:

When an airplane cruises at high altitude for long periods of time the airplane becomes 'cold-soaked'. If the cruise was preceeded by take-off from a 'hot' field, the airplane may have been 'warm-soaked' before take-off.

An aluminum airplane with steel cables will experience cable slackening in cruise due to the differences in thermal coefficient of expansion between aluminum and steel. Such cable slackening can have serious consequences to controllability. In some cases cable slackening can contribute to control surface flutter.

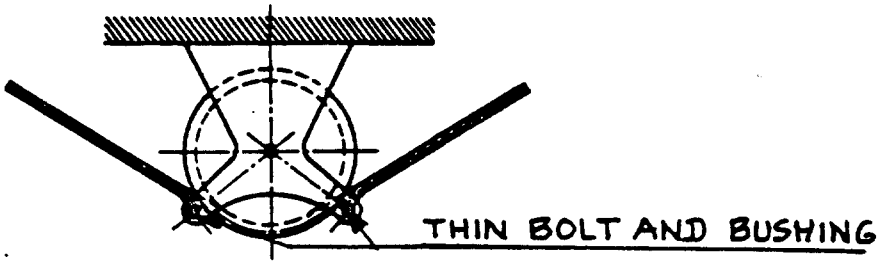

Figure 4.9 Example of a Cable Guard Installation

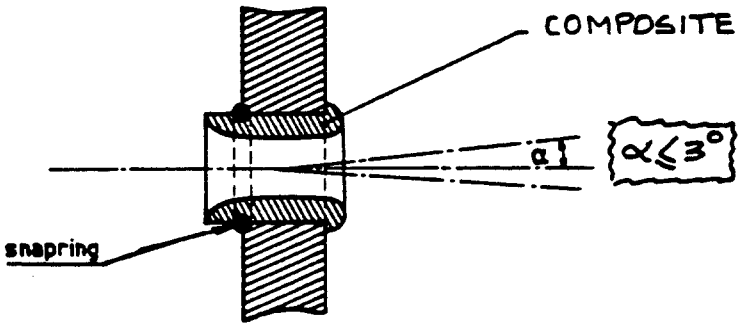

Figure 4.10 Example of a Cable Guide Installation

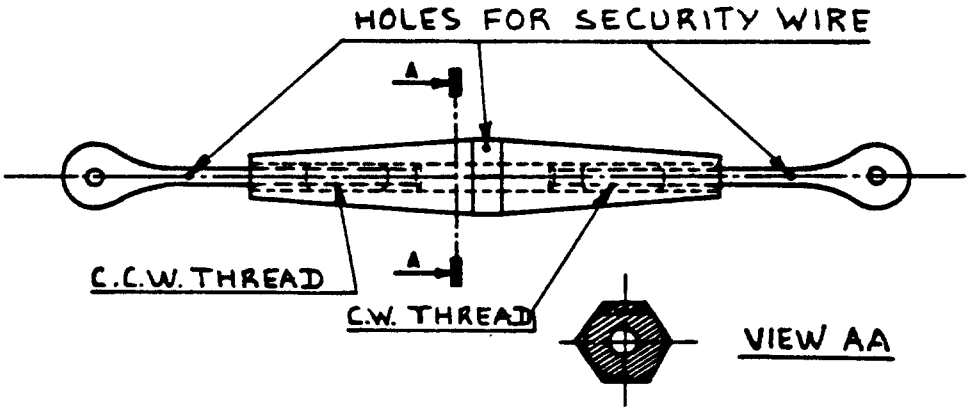

Figure 4.11 Example of a Turnbuckle

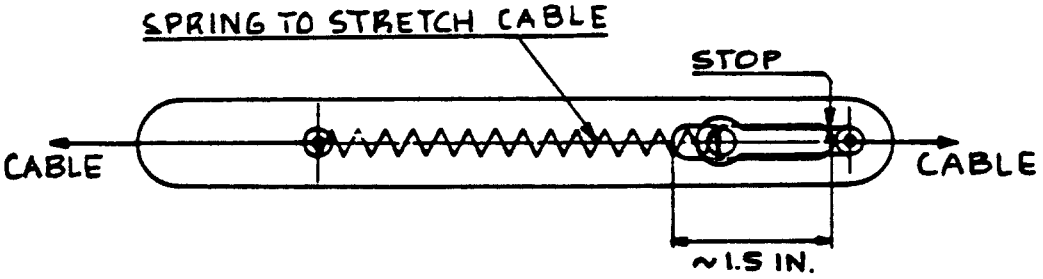

Figure 4.12 Example of a Cable Stretcher

A composite airplane with steel cables will experience exactly the opposite scenario.

This type of cable slack can be prevented by the installation of cable tension regulators: see Fig.4.13.

2. System friction

A major cause of handling quality problems with airplanes is control system friction. The effect of control system friction on the so-called 'return-to-trim-speed' behavior of an airplane is discussed in Ref.20, Ch.5.

To prevent too much friction, the following ground rules must be observed:

1. Keep cable runs as straight as possible.

2. Keep the number of pulleys and guides as small as possible.

Remember that at every cable turn an additional pulley is needed which introduces extra friction and extra weight.

3. System elastic deformations

Another major problem in the design of cable systems is the occurrence of elastic deformations. Sources for these deformation are the cables themselves and the pulley attachment structure. Excessive elastic deformation in a cable system means that full control surface travel will not be attained.

To prevent elastic control system deformation the following groundrules should be observed:

1. Use oversized cables (This will 'cost' weight)

2. Make sure pulleys are attached to 'stiff' structural components. Note: do NOT attach pulleys to flat plates: they deform too easily.

4. Kinematic feasibility

For a cable system to be acceptable it must be kinematically sound. Figure 4.14 shows a number of possible arrangements for cable systems. Mechanisms A and B are kinematically sound: the quadrangles ABFE and CDFE remain parallelograms when the system is used. System A is better than system B because of its higher

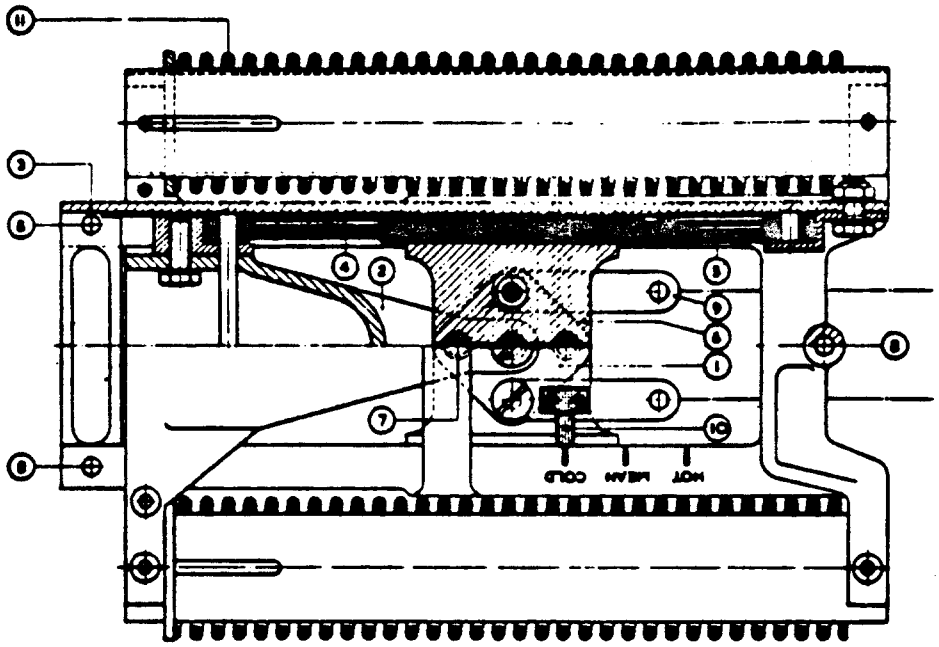

1 Rotating plate

2 Beam, attached to tension reg.

3 Beam, attached to airplane

4 Brake plate attached to 2

5 Brake plate attached to 3

6 Brake lining

7 Pins

8 Attachment points to airplane structure

9 Clevis for control cable attachment

10 Pointer

11 Springs

Airplane Temperature		Distance from HOT to pointer	
deg.C.	deg.F.	mm.	in.
52	125	0	0
38	100	4.6	0.18
24	75	9.1	0.36
10	50	13.7	0.54
-4	25	18.2	0.72
-18	0	22.5	0.89
-32	-25	27.2	1.07
-46	-50	31.8	1.25

Figure 4.13 Example of a Cable Tension Regulator

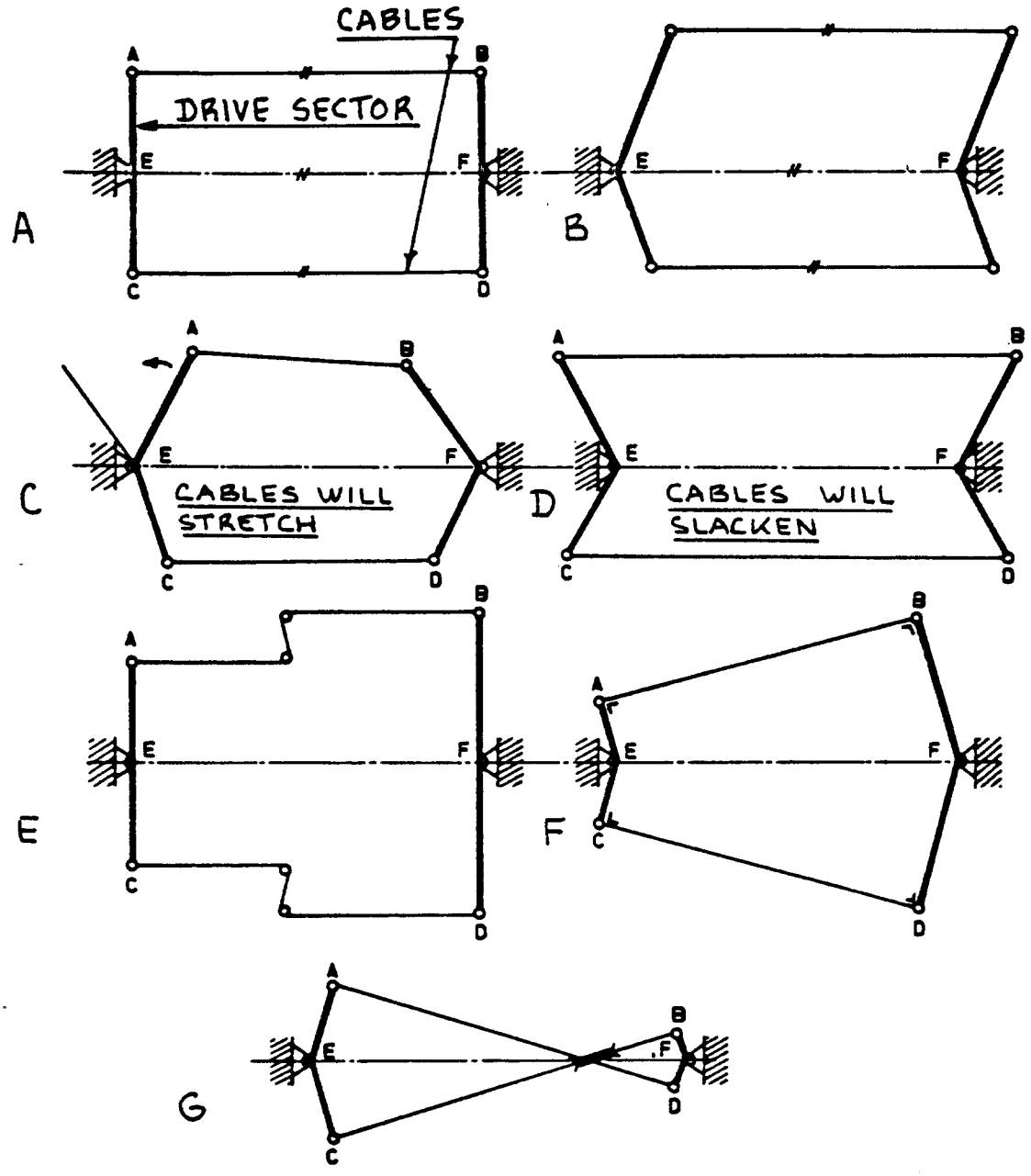

Figure 4.14 Examples of Cable Mechanisms

rotation efficiency. Rotation efficiency is highest if the angle between the cable and the driving sector is 90 degrees with the system in its neutral position.

Mechanisms C and D in Figure 4.14 are unworkable because the cable lengths AB and CD do not remain constant after some rotation: this is undesirable. The reader will recall that the system of Figure 4.2 also violates the 'constant-cable-length' requirement. Despite this shortcoming the system is used in several light airplanes. It is important that the $l/s > 6$ criterion be met to prevent excessive cable stresses!

Mechanism E is kinematically sound but it requires more pulleys: increased weight, complexity, friction and maintenance.

Mechanism F is kinematically sound (it meets the previously stated 90 degree requirement).

Note that the output rotation in both systems E and F is not the same as the input rotation. This effect is sometimes desirable.

Mechanism G employs 'crossing' cables but is kinematically sound. In detail design it is essential that the 'crossing' cables do not in fact touch each other: that would cause extra friction and chafing.

One way to always maintain the 90 degree angle between a cable and its sector is to use a cable-quadrant. Figure 4.15 shows an example of a cable-quadrant.

Cables have 'built-in' redundancy because of the multiple strands from which they are made. This built-in redundancy is only as good as the reliability of the devices used to connect cables to sectors, to quadrants, to turnbuckles and to cable tension regulators. These connections often take the form of 'swaged ends'. Fig.4.16 shows an example of a swaged end in the form of a clevis. The quality control used in manufacturing such swaged ends must be very good.

For detailed requirements which flight control systems must meet the reader should read Ref.21, Subpart D.

Primary flight control system cables should have a diameter of greater than 0.15 in.

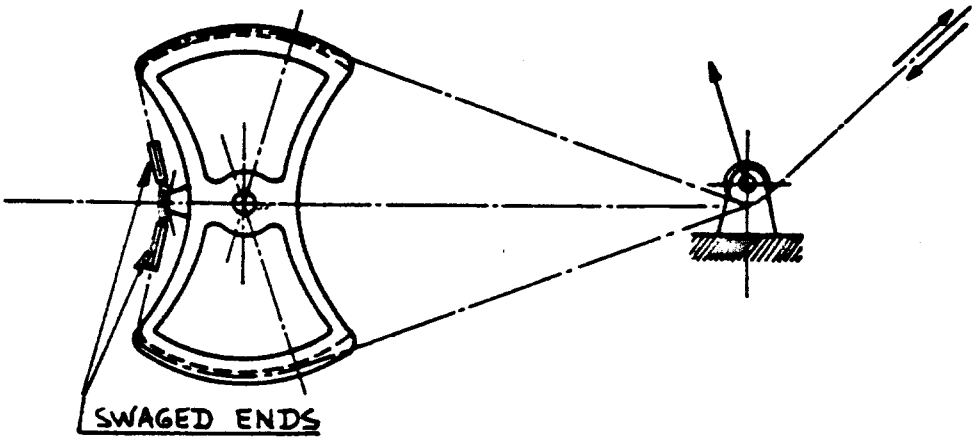

Figure 4.15 Example of a Cable Quadrant

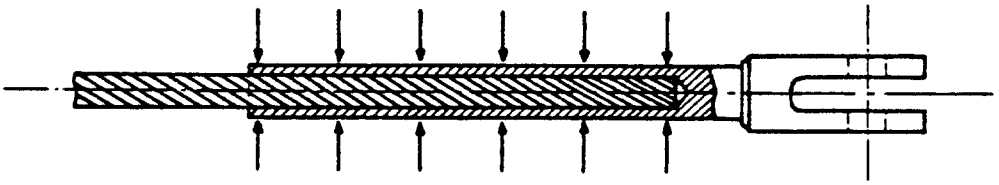

Figure 4.16 Example of a Swaged Fork End

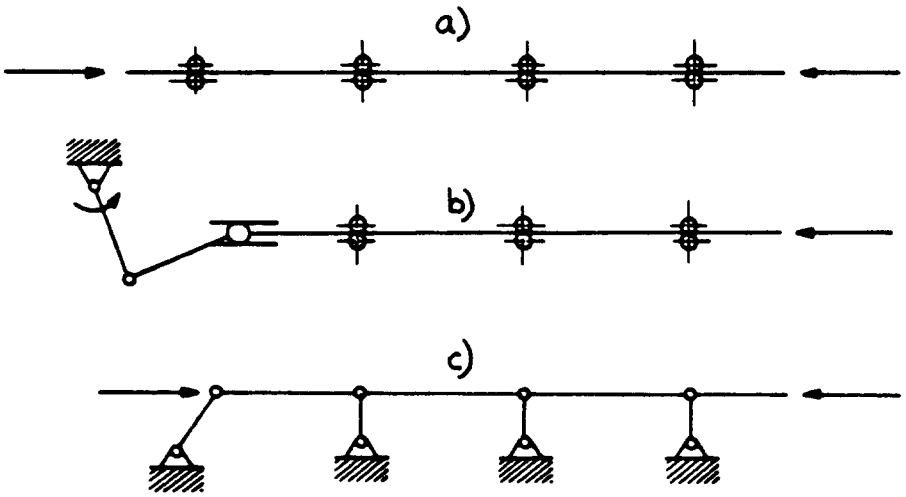

Figure 4.17 Prevention of Buckling in Push-rod Systems

4.1.4.2 Mechanical design requirements associated with push-pull (push-rod) systems

Figures 4.1C and 4.5C show examples of applications of push-rod flight control systems. A major problem associated with push-rod systems is buckling of the push-rods. Clearly, such buckling is unacceptable.

Figure 4.17 shows what can be done to guard against the buckling of push-rods. The unsupported length of each push-rod must be selected so that under a push load of 1.5 times the maximum expected control force application in each rod, no buckling will occur.

Typical push-rod dimensions which normally will prevent buckling are:

Push-rod diameter: > 0.5 in.

Push-rod wall thickness: > 0.08 in.

Push-rod length: < 45 in.

For accurate dimensioning of pushrods, Ref.7 should be consulted.

Whether or not a push-rod system is lighter or heavier than a cable system depends on the controls layout of an airplane.

The comments made under 4.1.4.1 about friction, kinematic feasibility and elastic deformations also apply to push-rod systems.

4.1.4.3 Efficiency considerations

The efficiency of a mechanical flight control system is defined as:

$$\eta_{cs} = W_e/W_i \qquad (4.1)$$

where: W_e = work done by the control surface against the aerodynamic hinge moments

W_i = work done by the pilot on the cockpit control(s)

The work done by the pilot consists of three contributions:

$$W_i = W_e + W_v + W_w \qquad (4.2)$$

where: W_v = the work done to overcome elastic deformation in the control system

W_w = the work done to overcome system friction

A well designed mechanical flight control system has efficiency values in the range of 0.85 to 0.90.

The work done by the pilot can be expressed as:

$$W_i = \int F_p ds_p \qquad (4.3)$$

The pilot control force, F_p and the cockpit control travel, s_p are defined in Figure 4.5.

Using considerations of virtual work it can be shown that:

$$F_p = G(HM), \qquad (4.4)$$

where: HM is the control surface hingemoment defined in Eqn.(4.7) and

G is the control system gearing ratio defined as:

$$G = \delta/ds_p \qquad (4.5)$$

where: δ is the control surface deflection.

The gearing ratio is normally expressed in rad/ft. Table 4.1 contains typical values for G.

4.1.4.4 Calculation of cable and/or push-rod forces from control surface hingemoments

To determine the minimum required sizes of control cables and/or control push-rods, the maximum operating forces must be determined. These operating forces follow from equilibrium considerations between control surface hinge moments and the control force needed to oppose it. Figure 4.18 depicts a typical layout.

It is assumed that the control surface hingemoment, HM (in ftlbs) is known. The cable control force, F_c required to oppose this hingemoment follows from:

$$F_c = (HM/a)(b/c) \qquad (4.6)$$

Table 4.1 Control Deflections and Gearing Ratios

Airplane Type	Elevator			Aileron			Rudder		
	Surface Travel degrees	Wheel Travel	Gearing Ratio rad/ft	Surface Travel degrees	Wheel Travel	Gearing Ratio rad/ft	Surface Travel degrees	Pedal Travel	Gearing Ratio rad/ft
Cessna 172	28 up 23 dwn	6.6 in. total	1.62	20 up 15 dwn	+/-90 deg	0.50	+/-16 deg	4.0 in. total	1.68
Cessna 210	23 up 17 dwn	7.5 in. total	1.12	25 up 15 dwn	+/-90 deg	0.50	+/-24	2.8 in. total	3.59
Cessna 303	28 up 15 dwn	6.0 in. total	1.50	20 up 15 dwn	+/-85 deg	0.50	+/-30 deg	4 in. total	3.14
SIAI-M S211		stick	0.70		stick	0.67			1.42
GL M36			0.86			0.39			2.29
Transp. Jets			0.72			0.35			1.30

Note: The gearing ratios are all defined so that:

$$F_p = (G) * (HM)$$

(lbs) (rad/ft) (ftlbs)

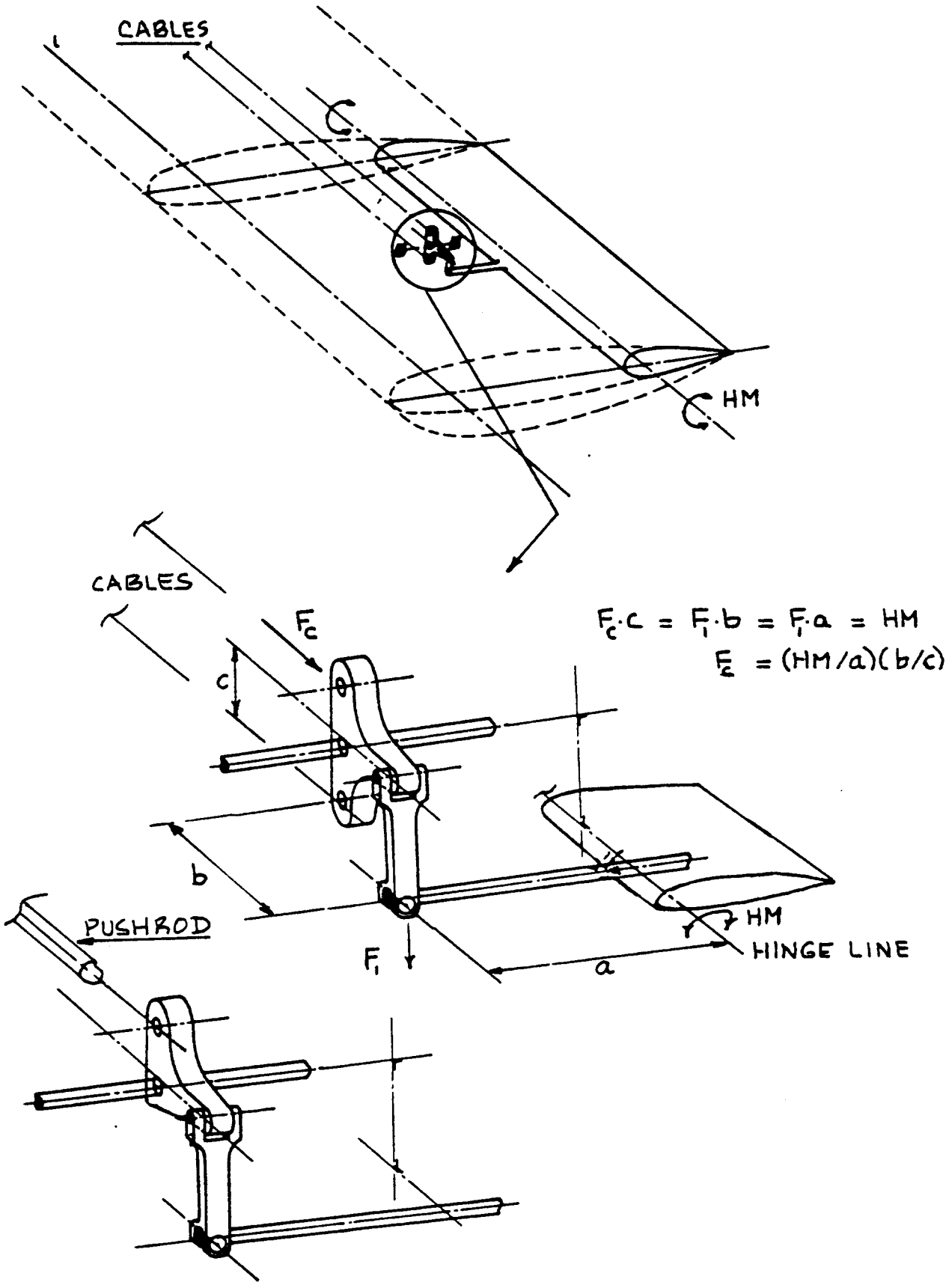

Figure 4.18 Layout for Translating Cable Motion or Push-rod Motion into Control Surface Deflection

Note from Figure 4.18 that for the control force in a push-rod system the same equation (4.6) applies.

The value of the control surface hinge moment, HM depends on the control surface deflection, on the flight condition and on the control surface geometry and design. Reference 21 defines the conditions for determining control system limit and ultimate loads. A brief discussion on the dependence of control surface hinge moments on parameters such as control surface geometry and design is provided next.

4.1.4.5 Control surface hinge moments and control surface tabs and types

Figure 4.19 shows a typical control surface cross section. The hingemoment acting about the control surface hinge line can be computed from:

$$HM = C_h \bar{q} (S\bar{c})_{\text{control surface}} \qquad (4.7)$$

The hinge moment coefficient, C_h depends on such factors as:

1. hinge line location
2. gap size
3. nose shape
4. trailing edge angle
5. overhang
6. horn size and shape
7. tab configuration
8. surface deflection
9. Reynold's Number
10. Mach Number

Figure 4.19 also shows a sealed gap and two control surface horn configurations.

It is shown in Reference 20 (Ch.5) and in Part VI that the hinge moment coefficient, C_h can be expressed as:

$$C_h = C_{h_o} + C_{h_\alpha}\alpha + C_{h_\delta}\delta + C_{h_{\delta_t}}\delta_t \qquad (4.8)$$

Part VI contains methods for estimating the control surface hinge moment derivatives used in Eqn.(4.8).

Figure 4.20 shows a number of control surface tab configurations. An indication of their potential applications is given below. For a discussion of tab

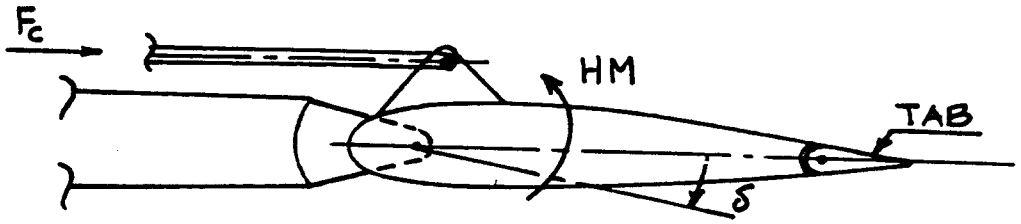

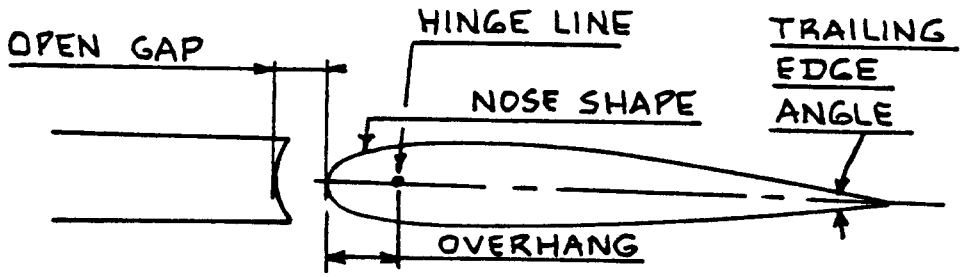

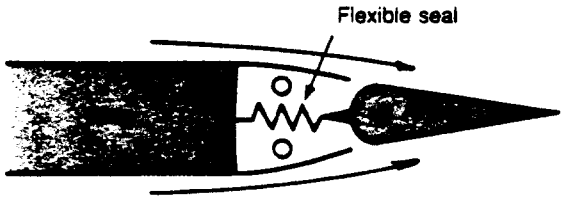

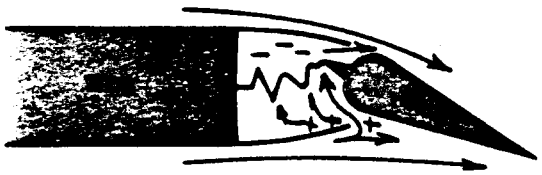

SEALED GAP WITH INTERNAL BALANCE

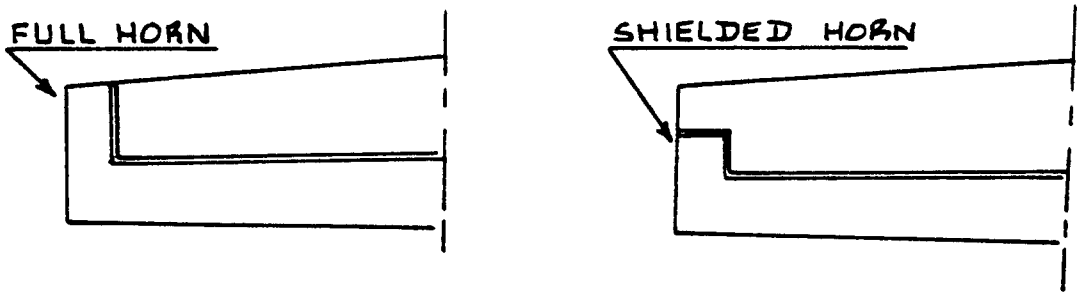

Figure 4.19 Typical Control Surface Cross Section and Control Surface Horn Arrangements

effects on pilot control forces (and thus on handling qualities) the reader should refer to Ref.20 and/or to Part VI.

Ground Adjustable Tabs: Figures 4.20A and 4.20B show potential applications.

These tabs allow the pilot control forces to be 'trimmed' in one flight condition only. These tabs are light, cheap and simple.

Flight Controllable Trim Tabs: Figure 4.20C shows an application.

These tabs allow the pilot control forces to be 'trimmed' in any flight condition. An additional control system connecting the trim tab with the cockpit must be provided. This increases weight, cost and complexity.

Geared Tabs (also called Balance Tabs): Figure 4.20D shows an application.

These tabs allow the hinge moment derivative C_{h_δ} to be increased or decreased depending on the sign and magnitude of gearing used. In some instances the gearing ratio may be varied in flight. These tabs also increase weight, cost and complexity.

Blow Down Tabs: Figure 4.20E shows an application.

These tabs can be used to alter the apparent stability level in airplanes. Ref.20 contains a detailed discussion of such tabs.

Servo Tabs and Spring Tabs: Figures 4.20F and 4.20G show applications.

These tabs are used to allow reversible flight control systems to be used in airplanes of such size and performance that direct control over the flight control surfaces would yield pilot control forces which are too high.

Control surface types: Figure 4.21 shows a range of control surface types.

When the elevator and the rudder are mounted in close proximity (Figure 4.21A) it is necessary to arrange for a 'cutout' in one of these surfaces to prevent mechanical interference.

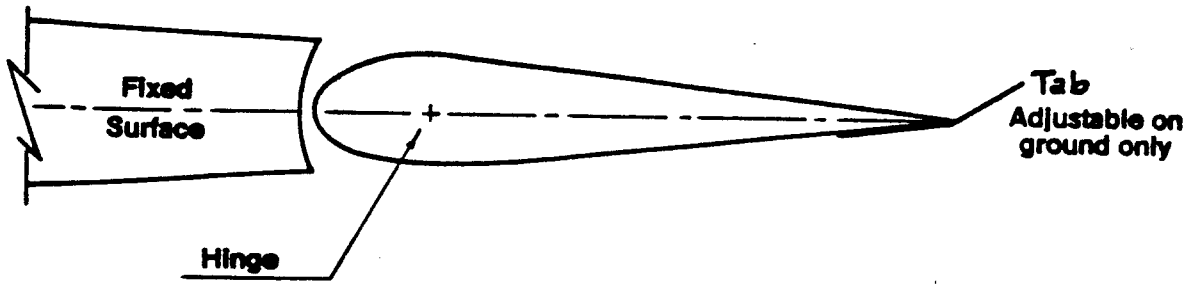

A SIMPLE GROUND ADJUSTABLE TRIM TAB

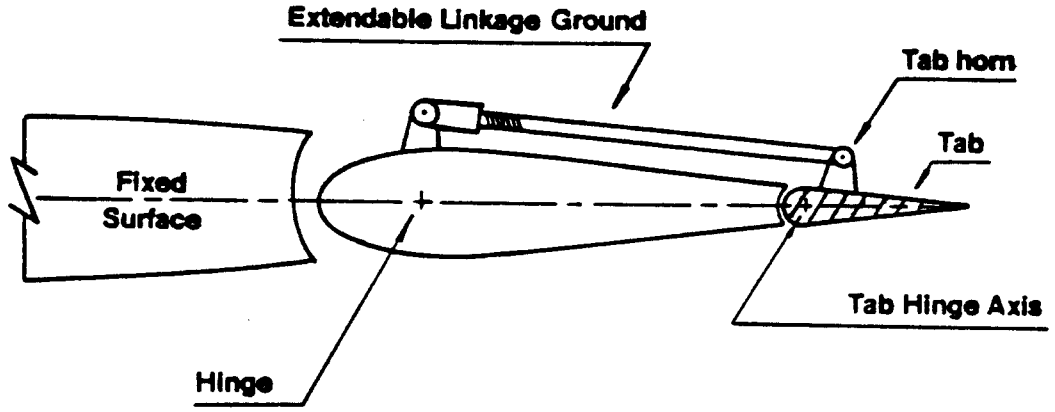

B GROUND AJUSTABLE TRIM TAB

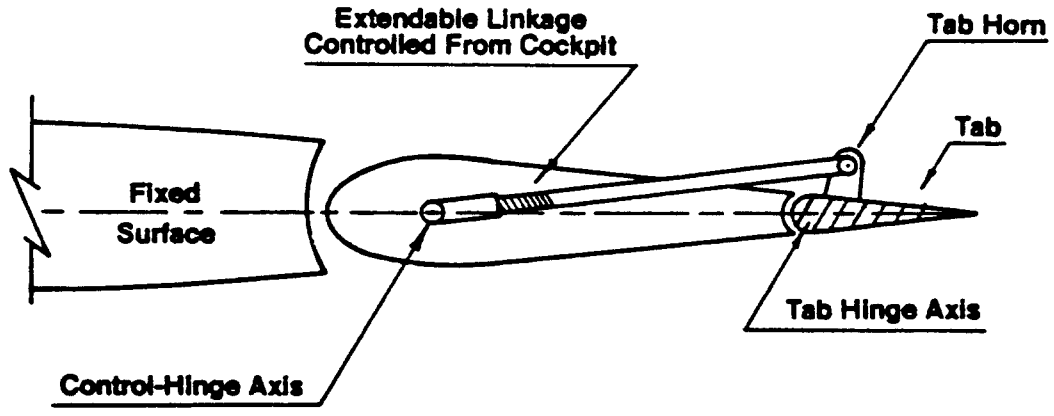

C FLIGHT CONTROLLABLE TRIM TAB

Figure 4.20 Example Tab Configurations

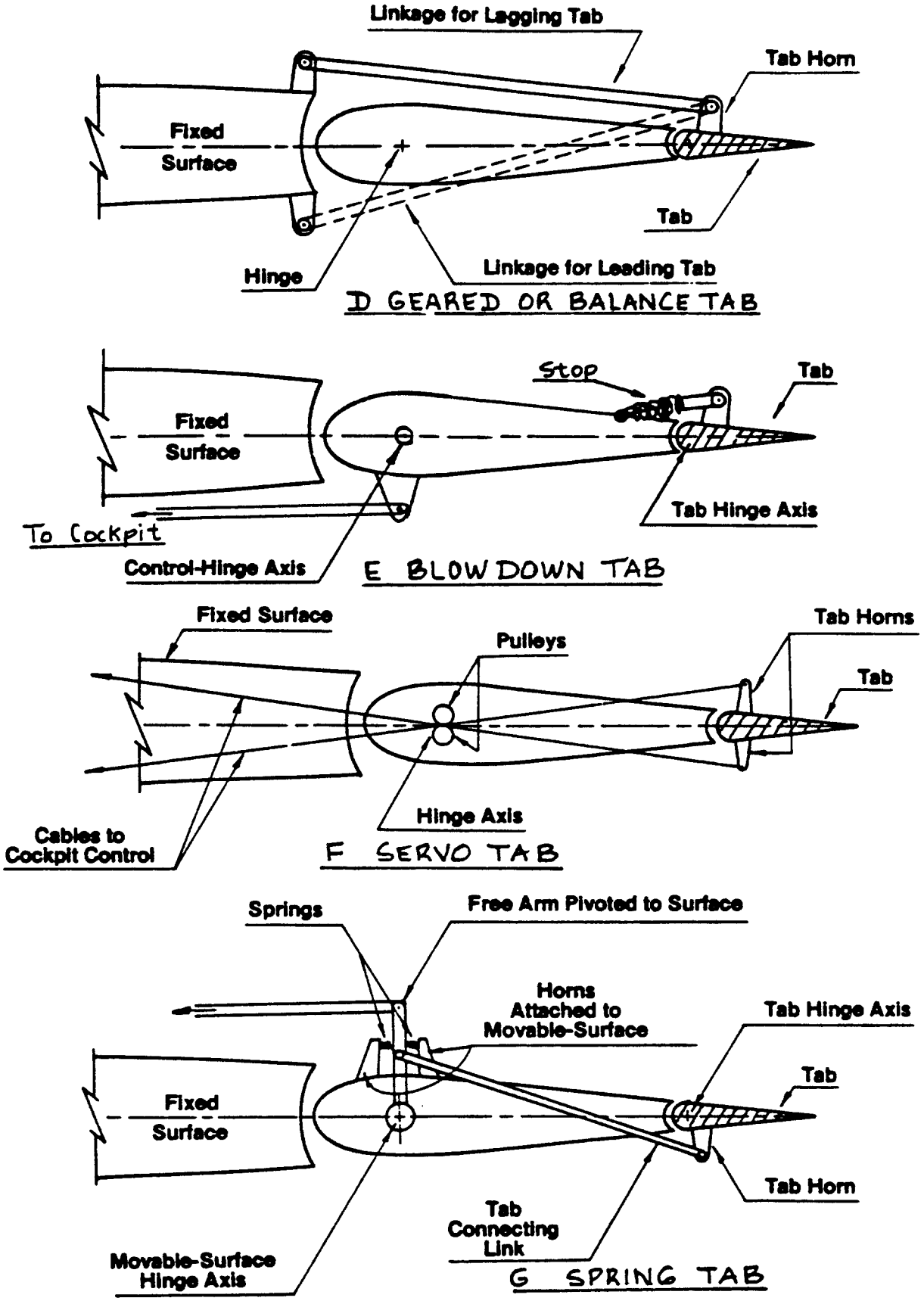

Figure 4.20 (Cont'd) Example Tab Configurations

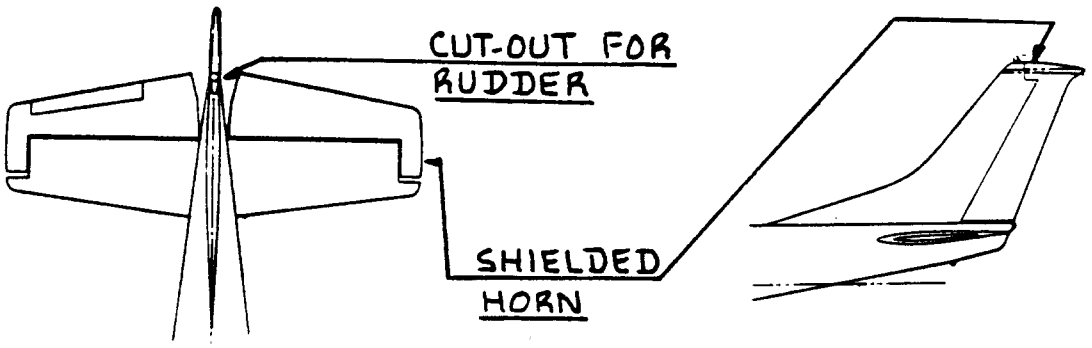

CESSNA SUPER SKYLANE

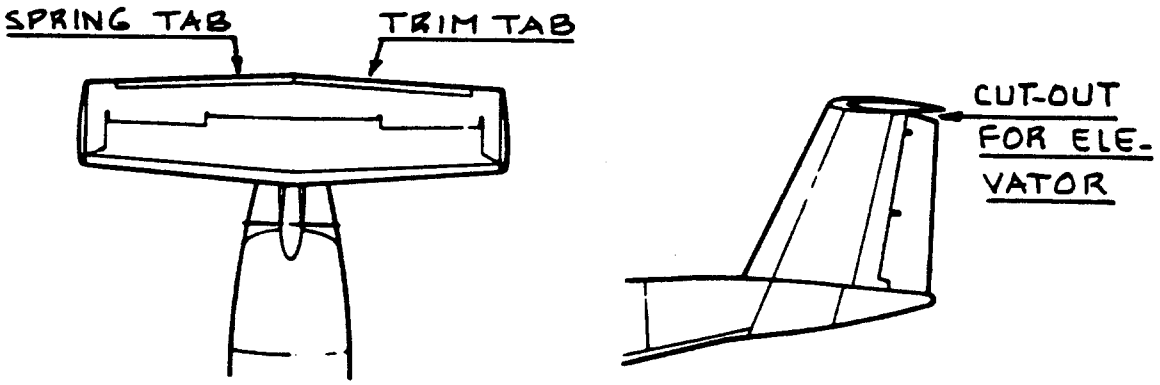

DHC 5D BUFFALO

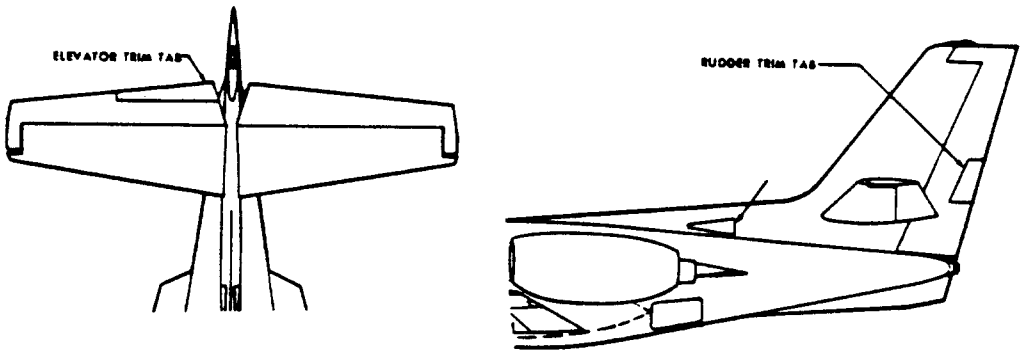

CESSNA CITATION

NOTE: WITH ANY TYPE HORN BALANCE WATCH OUT FOR ICING

Figure 4.21 Examples of Control Surface Configurations

Most control surfaces in airplanes with reversible flight control systems need special design provisions for aerodynamic and for mass balancing. Sub-sub-sections 4.1.4.6 and 4.1.4.7 contain more information on these balancing requirements.

4.1.4.6 Aerodynamic balance requirements and control system gadgets

To keep the pilot control force, F_p and the pilot control force gradients with respect to speed and load factor, $\partial F_p/\partial V$ and $\partial F_p/\partial n$ within acceptable limits, the hinge moment derivatives in Eqn.(4.8) must be kept within certain bounds. These bounds are dictated by handling quality requirements laid down in Refs 21 and 22.

Part VI addresses the relationship between the hingemoment derivatives and the handling quality requirements of Refs 21 and 22 from a design viewpoint.

The process used to 'tailor' the aerodynamic hinge moments to achieve certain handling quality objectives is referred to as aerodynamic balancing of the flight controls.

Aerodynamic balancing can be achieved by careful selection of items 1 through 7 mentioned in sub-sub-section 4.1.4.5.

Control surface tabs (Figure 4.20) and control surface horns (Figure 4.21) are important tools used to achieve satisfactory aerodynamic balance.

CAUTION: The tab configurations of Figures 4.20B through 4.20G are prone to flutter if special precautions to the design and maintenance of their attachments are not taken. Failure of a tab attachment rod and/or a tab spring can have serious consequences. References 23-25 contain methods for analyzing the flutter characteristics of various control surface/tab arrangements.

In many instances it turns out that desirable handling qualities cannot be attained without the use of so-called control system gadgets. Typical of such gadgets are:

Downspring: Figure 4.22 shows an example of a downspring. The downspring adds a force to the pilot control force,

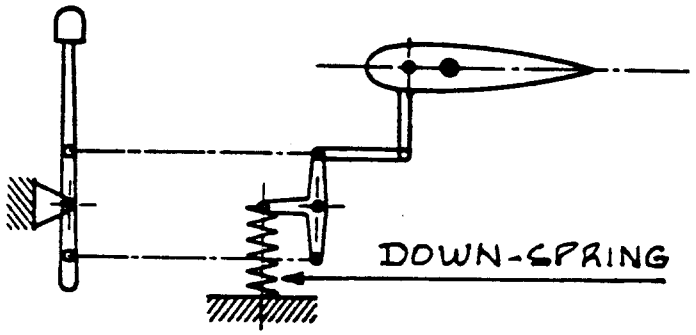

Figure 4.22 Example of a Down-spring

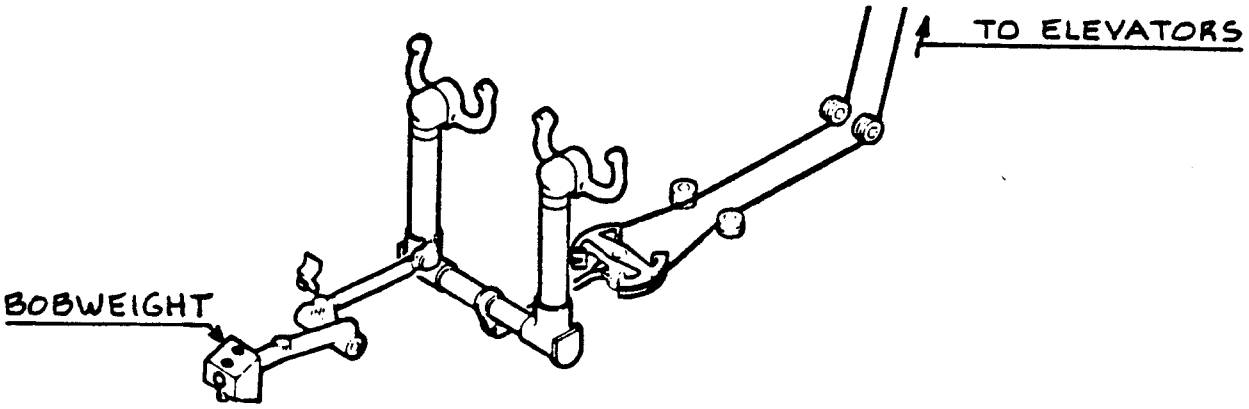

Figure 4.23 Example of a Bob-weight

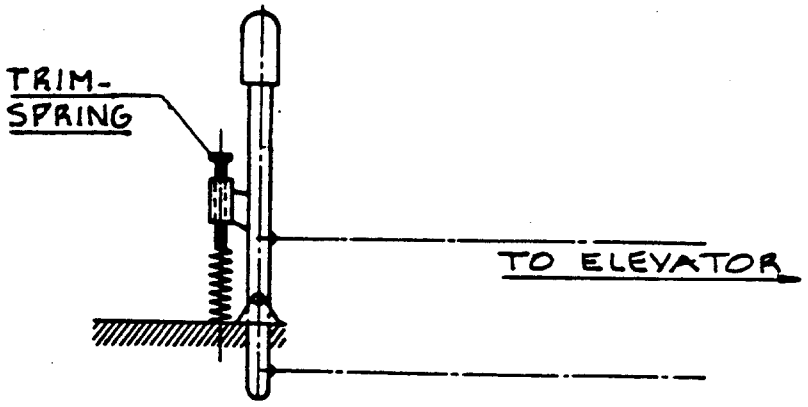

Figure 4.24 Example of a Trim-spring

F_p. This added force is proportional to control stick or to control surface deflection.

Bob-weight: Figure 4.23 shows an example of a bob-weight. Such bob-weights are used to alter the stick-force-per-g gradients of an airplane.

Reference 20 (Chapter 5) contains detailed analyses of the influence of downsprings and bob-weights on airplane handling qualities.

Trim-spring: Figure 4.24 shows an example of a trim-spring. The trim-spring is a simple method for obtaining stick force trim. The trim spring does cause the stick to move and care must be taken that the stick motion does not fall outside the recommended ranges of Section 2.2 in Part III.

4.1.4.7 Mass balancing requirements

All mechanical flight controls and all reversible flight control surfaces must be mass balanced.

Figure 4.25 shows what is meant by the mass balancing of a mechanical flight control system. It is clear from Figure 4.25 what would happen to the flight control surface if the mechanical system itself is not balanced: the control surface may be forced to move when the airplane is perturbed by vertical accelerations. This could lead to undesirable oscillations and in some cases could also lead to flutter.

Figure 4.26 illustrates several potential methods for balancing of a mechanical control system.

Figure 4.27 shows what is meant by the mass balancing of a flight control surface. Under-balancing of a flight control surface can lead to flutter.

The attachment structure of mass balances as well as the torsional stiffnes of the control surfaces itself are extremely important detail design considerations.

Figure 4.28 illustrates several methods of mass balancing of a flight control surface.

CAUTION 1: Painting of flight control surfaces must be done BEFORE mass balancing. The distribution of paint over a flight control surface can seriously change its mass balance.

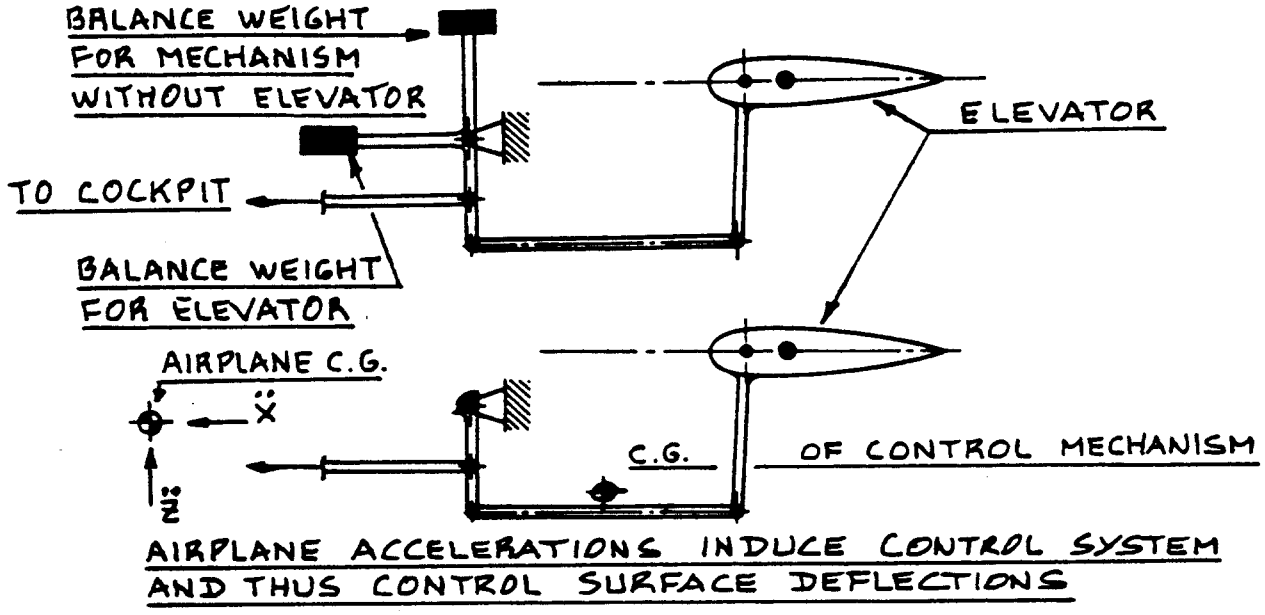

Figure 4.25 Effect of Underbalancing of a Control System

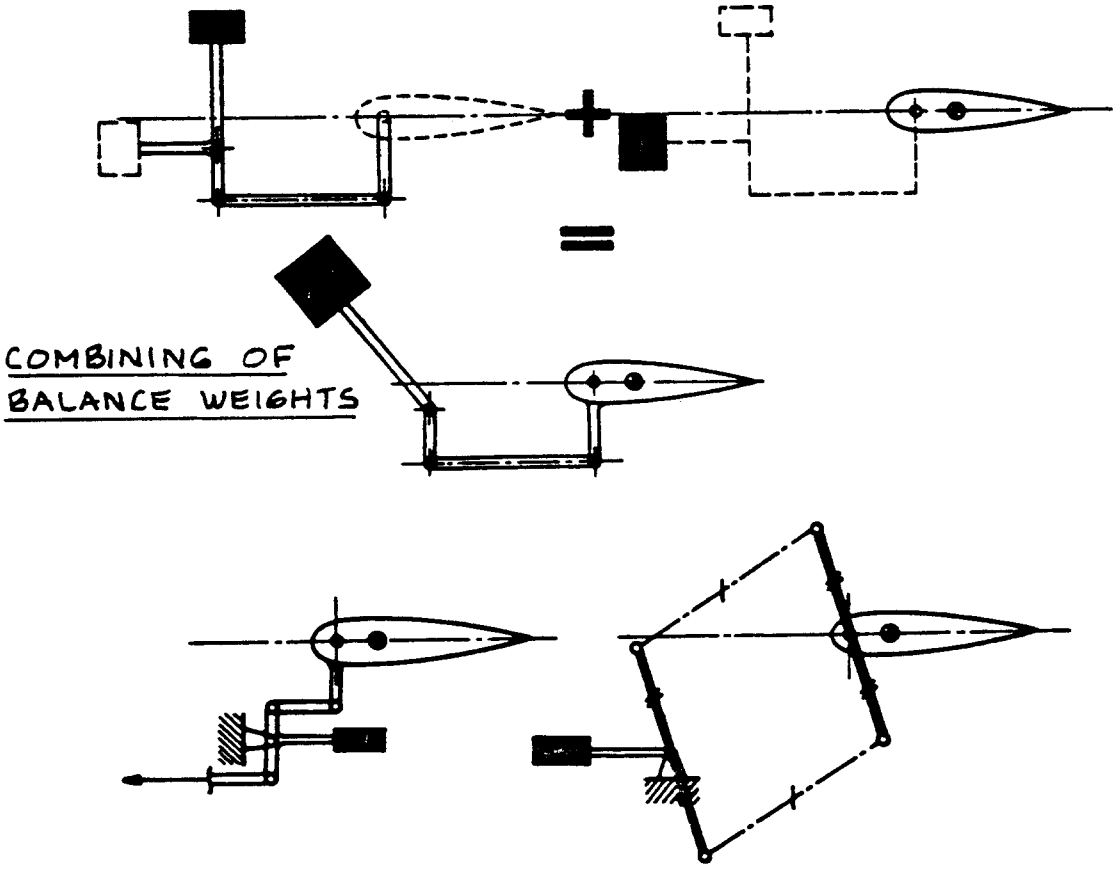

Figure 4.26 Examples of Balancing of a Control System

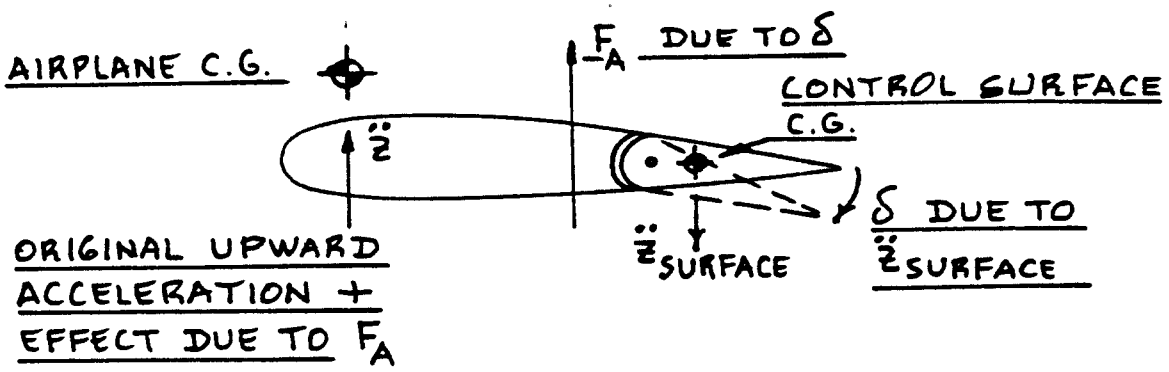

Figure 4.27 Effect of Underbalancing of a Control Surface

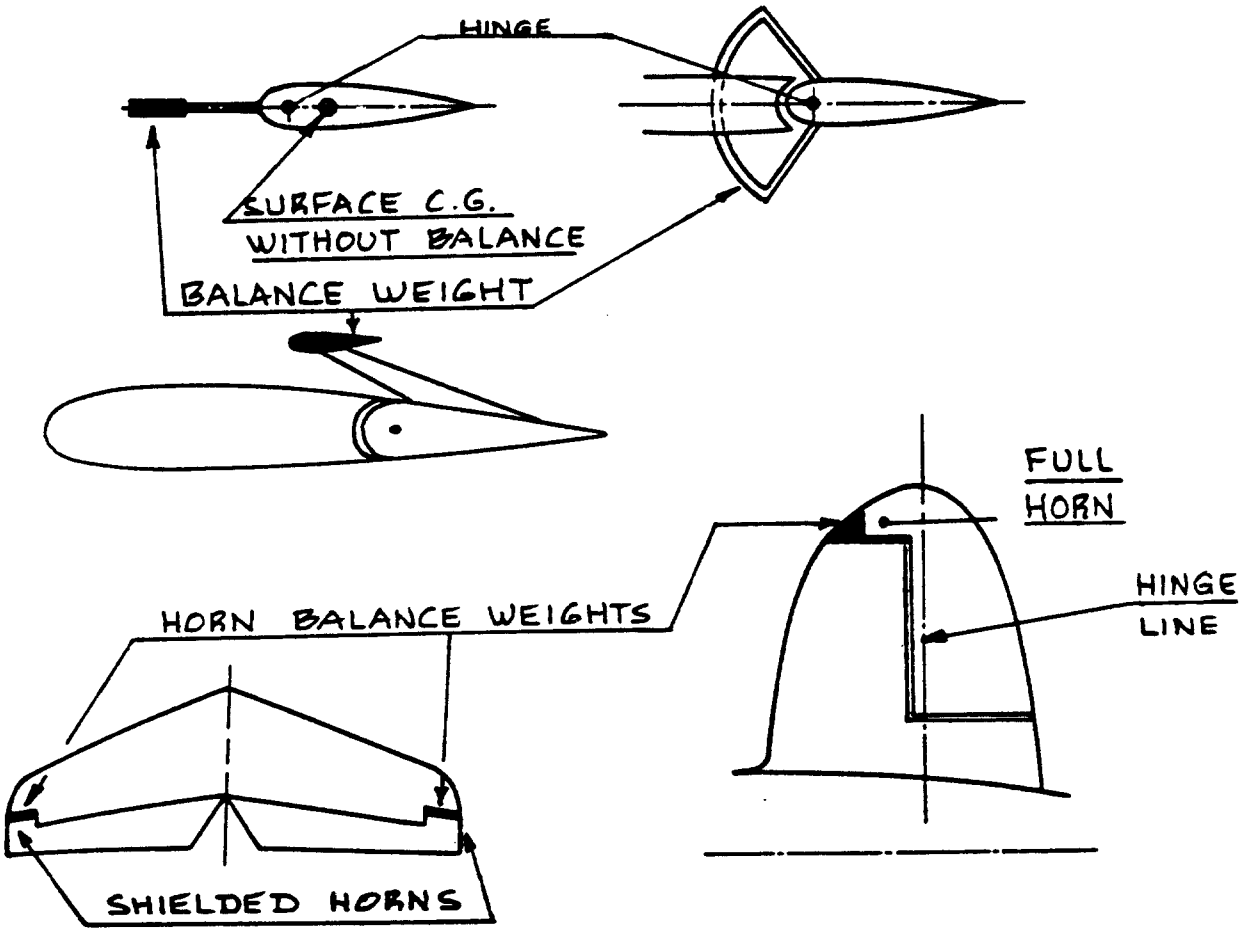

Figure 4.28 Examples of Balancing of a Control Surface

CAUTION 2: The stiffness of a flight control surface and the distribution of the mass balance weights are extremely important design considerations. Figure 4.29 illustrates what can happen if this point is ignored.

References 23-25 contain methods for analyzing the effect of mass balance and stiffness on the flutter characteristics of airplane plus its control system(s).

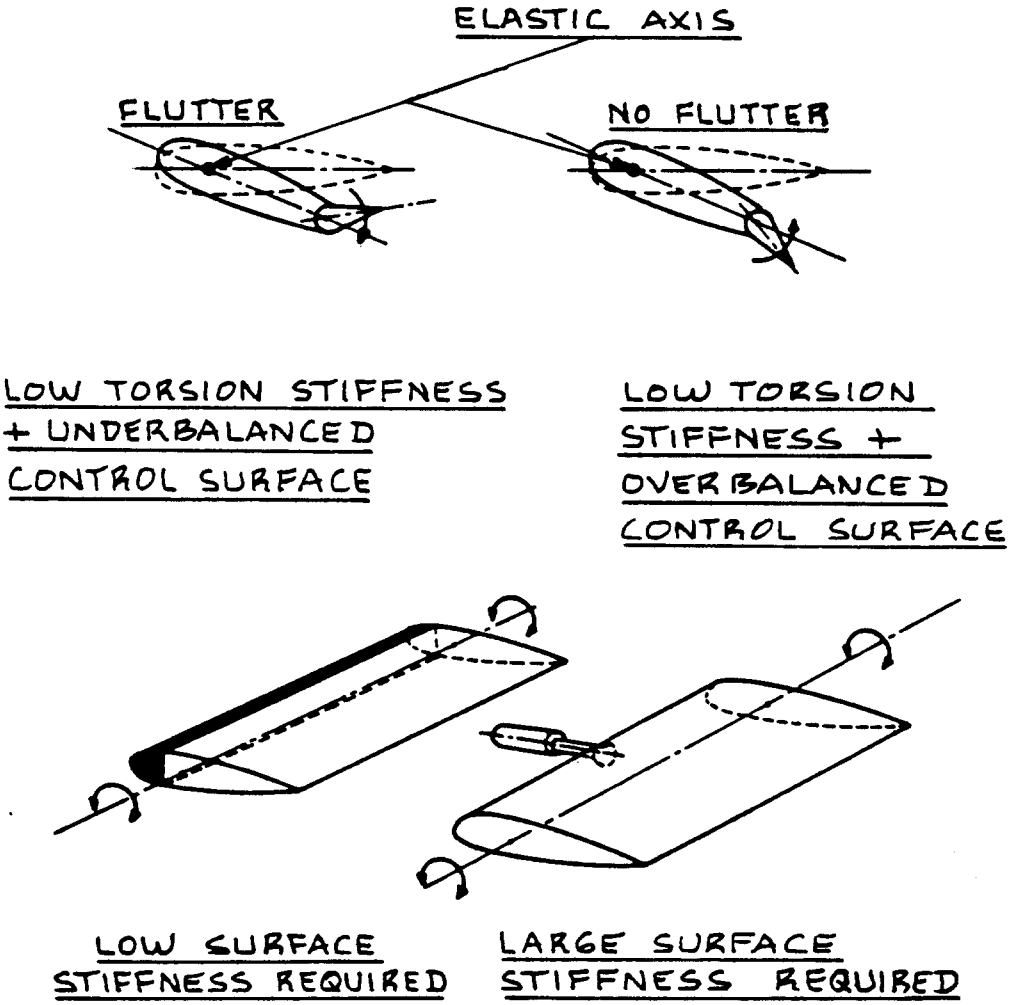

Figure 4.29 Effect of Control Surface Stiffness on the Distribution of Mass Balance Weights

4.2 EXAMPLES OF REVERSIBLE FLIGHT CONTROL SYSTEMS

In this section a number of example layouts of reversible flight control systems are presented in the form of '3-D' layout drawings. Such drawings are also referred to as 'ghost' layout drawings. The ghost layouts are presented in Figures 4.30 through 4.42. Commentary on these drawings is given below.

==========

Figure 4.30: Lateral Controls Piper PA-38-112

This is a dual control installation. Note that lateral control motion is translated into the cable system via two sets of torque tubes. These torque tubes must have sufficient torsional stiffness to prevent significant loss of control authority!

Note also the chain-sprocket arrangement used to drive the aileron torque tube.

To reduce aileron induced adverse yaw the ailerons are deflected differentially. The bellcrank installation which provides this differential motion is shown in an insert in Fugure 4.30.

Figure 4.31: Control Column Assembly Piper PA-38-112

Observe that the control column is arranged in the form of a large T-bar. For longitudinal control the T-bar pivots about point 9. For lateral control the chain-sprocket drive rotates the aileron torque tube 7.

Figure 4.32: Longitudinal Controls Piper PA-38-112

Note that the bottom of the T-bar assembly is directly attached to one of the longitudinal control cables. This is similar to the arrangement discussed in Figure 4.2!

The longitudinal cables are routed via pulleys which use mountings common to the directional control pulleys. The longitudinal cables finally attach to a sector mounted on the elevator torque tube.

Figure 4.33: Directional Controls Piper PA-38-112

Rudder pedal motion in the cockpit is translated into rudder deflection via cables which use pulleys for guidance. Note that these pulleys use mountings common also to the longitudinal control pulleys.

The rudder cables attach to a sector mounted at the bottom of the rudder. This arrangement makes it necessary for the rudder to be fairly stiff to assure that rudder torsion does not reduce directional control effectiveness.

==========

Figure 4.34 Lateral Controls Cessna 441

Aileron motion is generated through wing mounted cables which are actuated by a differential sector (See detail B) which itself is rigidly attached to a 'wheel' mounted in the wing. This 'wheel' in turn is controlled by cables operated by a chain/sprocket system mounted in the cockpit control column.

Observe the autopilot servo tie-in to the wing mounted 'wheel'.

Figure 4.35: Longitudinal Controls Cessna 441

Longitudinal cockpit control motion is translated into motion of cables which in turn move a sector mounted in the fuselage tail cone. This sector moves a push-rod which drives the elevator torque-tube. Note again the autopilot servo tie-in.

Figure 4.36 Directional Controls Cessna 441

Pedal motion is translated into cable motion which eventually drives a sector mounted at the bottom of the rudder torque-tube. The autopilot servo drives the rudder sector via separate cables.

Note the tie-in between the rudder and aileron system through springs in Detail A. This tie-in is to overcome a mild deficiency in rolling moment due to sideslip.

==========

Figure 4.37 Flight Controls Canadair CL215

Note the extensive use of redundant cabling in this ghost view.

Because of the amphibious role of this airplane all control cables are routed up behind the cockpit and then routed aft.

Figure 4.38 Lateral Controls Canadair CL215

The lateral cockpit control system does not use the chain/sprocket method but instead a cable-drum system.

Note that the control yokes in the cockpit are not interconnected as they were in the previous examples.

Figure 4.39 Longitudinal Controls Canadair CL215

The cockpit yokes are directly attached to the elevator control cables. Note that the elevator is controlled directly with assist from a spring tab. Also note that the elevator halves are connected with a torque-tube.

Figure 4.40 Directional Controls Canadair CL215

Observe that the rudder pedals again control a sector at the bottom of the rudde torque-tube. This sector itself is controlled by a cable system. There is an interconnect between the lateral and the directional controls via an aileron tab.

Figure 4.41 Flight Controls Short Skyvan

Note that this system is a total push-rod system. The controls are routed up behind the cockpit. The high wing layout makes this a logical choice.

Note from detail A the extensive anti-buckling measures taken in this system.

Figure 4.42 Flight Controls Learjet M23

Despite the high performance capabilities of this airplane its flight control system is completely reversible. Cables are used throughout except for the final control run to the elevators. Here a redundant push-rod system is used.

Note the autopilot tie-ins in all three systems.

1. CONTROL WHEELS
2. CONTROL WHEEL TORQUE TUBE
3. FLEXIBLE JOINT
4. ROLLER CHAIN
5. CONTROL WHEEL SPROCKET
6. TENSIONER SPROCKET
7. WASHER
8. TEE BAR ASSY.
9. CHAIN TENSIONER ASSY.
10. LOWER SPROCKET
11. AILERON TORQUE TUBE
12. BALANCE CABLE - LEFT
13. TURNBUCKLE PRIMARY CABLE - LEFT
14. INTERCONNECT BALANCE CABLE PULLEY
15. TURNBUCKLE - BALANCE CABLE
16. TURNBUCKLE PRIMARY CABLE - RIGHT
17. PULLEY - PRIMARY CABLE - RIGHT
18. PRIMARY CABLE - RIGHT
19. BELLCRANK-AILERON - RIGHT
20. ROD-AILERON CONTROL - RIGHT
21. AILERON CENTERING SPRING

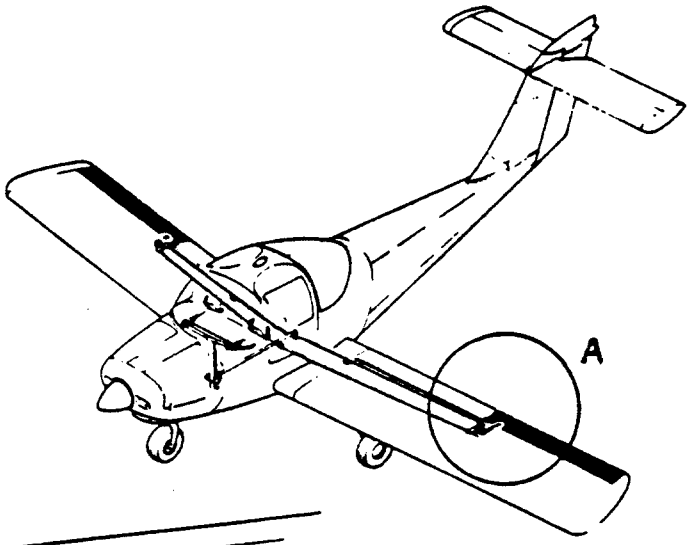

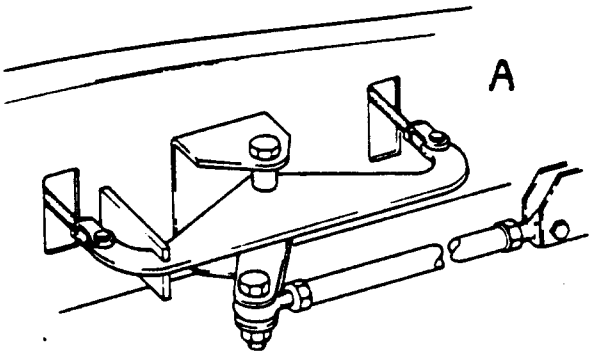

COURTESY: PIPER

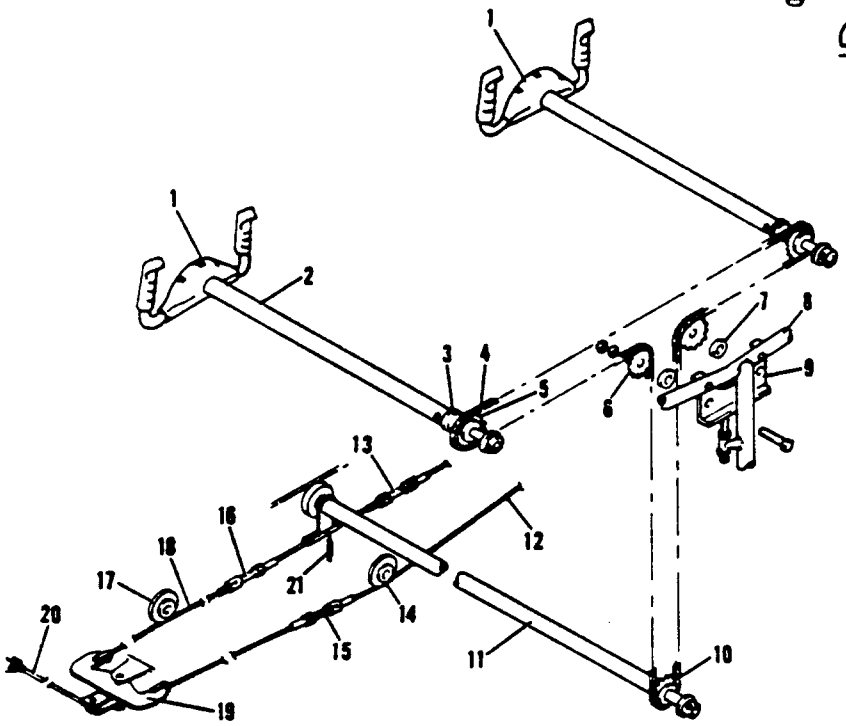

Figure 4.30 Lateral Controls Piper PA-38-112

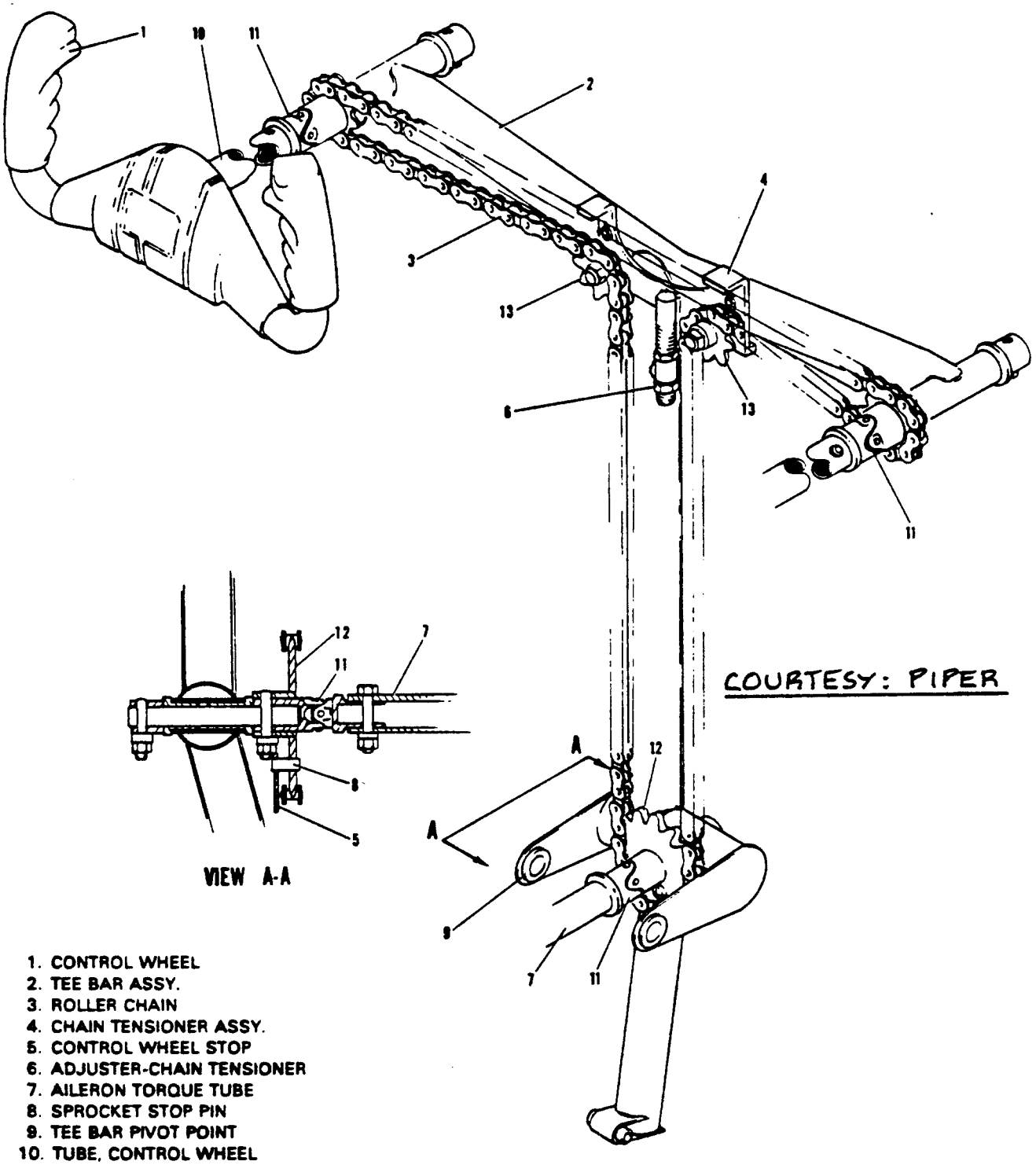

1. CONTROL WHEEL
2. TEE BAR ASSY.
3. ROLLER CHAIN
4. CHAIN TENSIONER ASSY.
5. CONTROL WHEEL STOP
6. ADJUSTER-CHAIN TENSIONER
7. AILERON TORQUE TUBE
8. SPROCKET STOP PIN
9. TEE BAR PIVOT POINT
10. TUBE, CONTROL WHEEL
11. FLEXIBLE JOINT
12. SPROCKET
13. IDLER SPROCKETS

Figure 4.31 Control Column Assembly Piper PA-38-112

1. ELEVATOR BELLCRANK
2. ELEVATOR PULLEY - UPPER
3. ELEVATOR PULLEY - LOWER
4. ELEVATOR CABLE - UPPER - AFT
5. ELEVATOR CABLE - LOWER - AFT
6. PULLEY CLUSTER - BASE OF FIN
7. ELEVATOR TURNBUCKLE
8. ELEVATOR TURNBUCKLE
9. PULLEY CLUSTER - AFT - BAGGAGE AREA
10. PULLEY CLUSTER - MAIN SPAR
11. CABLE ATTACHMENT - TEE BAR
12. PULLEY CLUSTER - FORWARD
13. ELEVATOR CABLE - FORWARD
14. TEE BAR ASSEMBLY

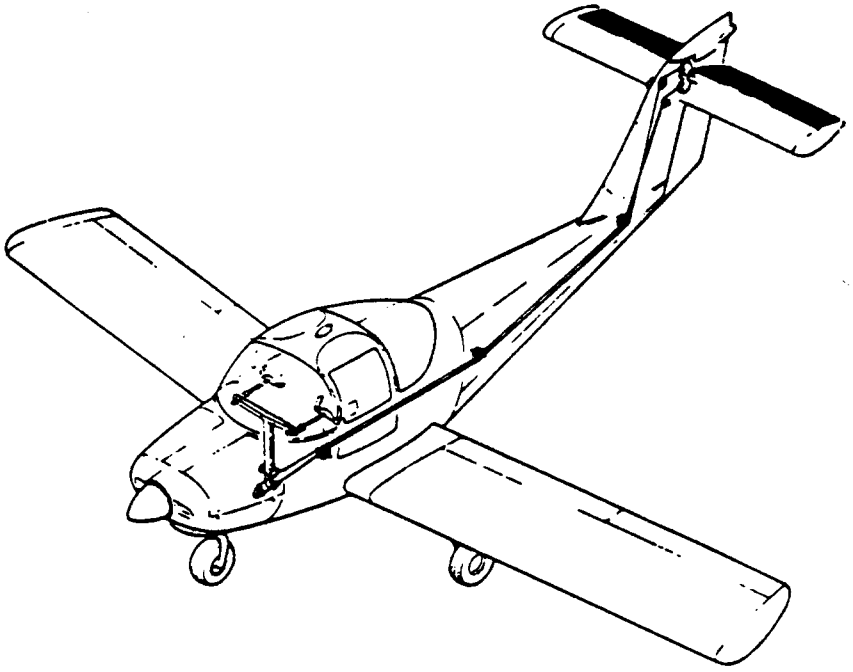

COURTESY: PIPER

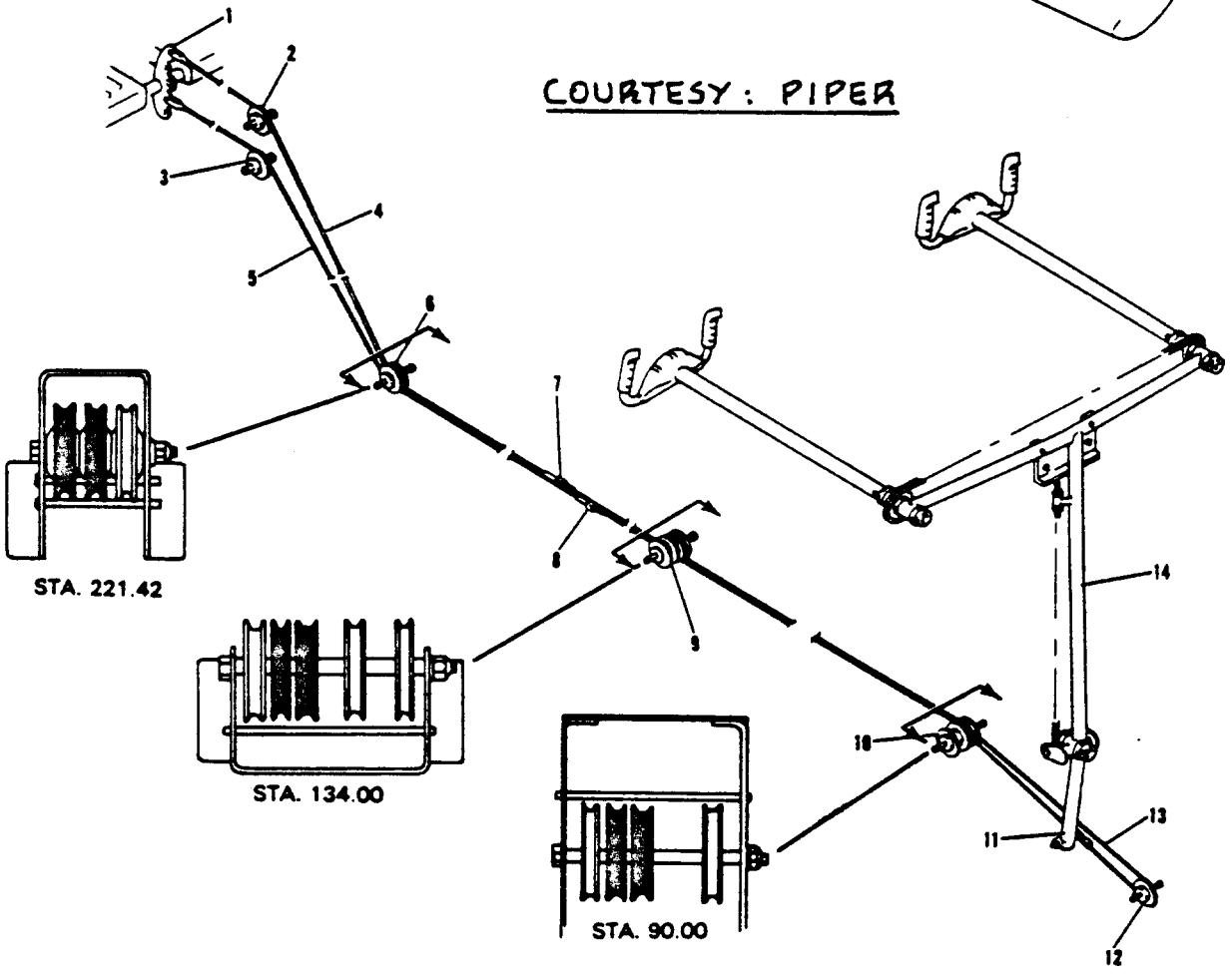

Figure 4.32 Longitudinal Controls Piper PA-38-112

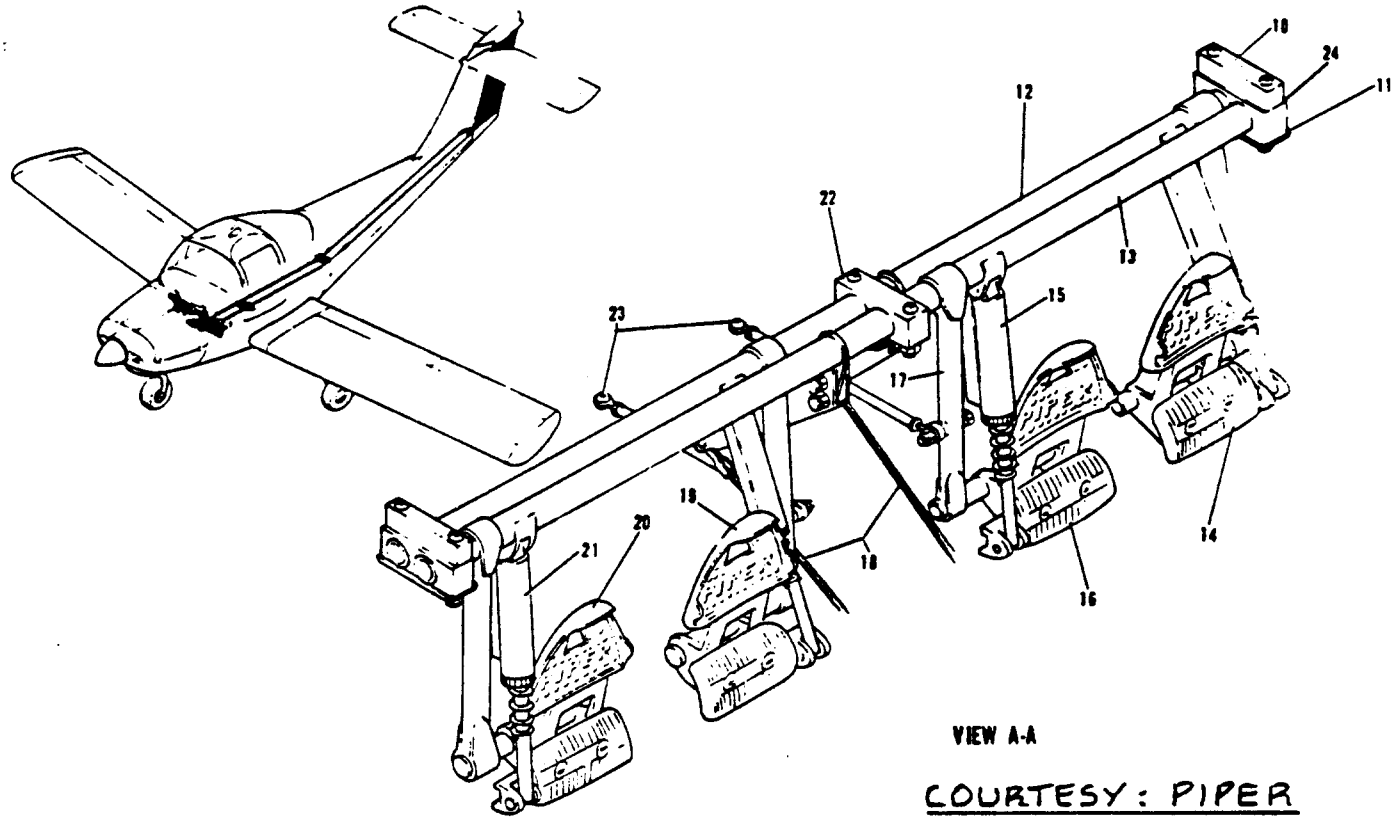

COURTESY: PIPER

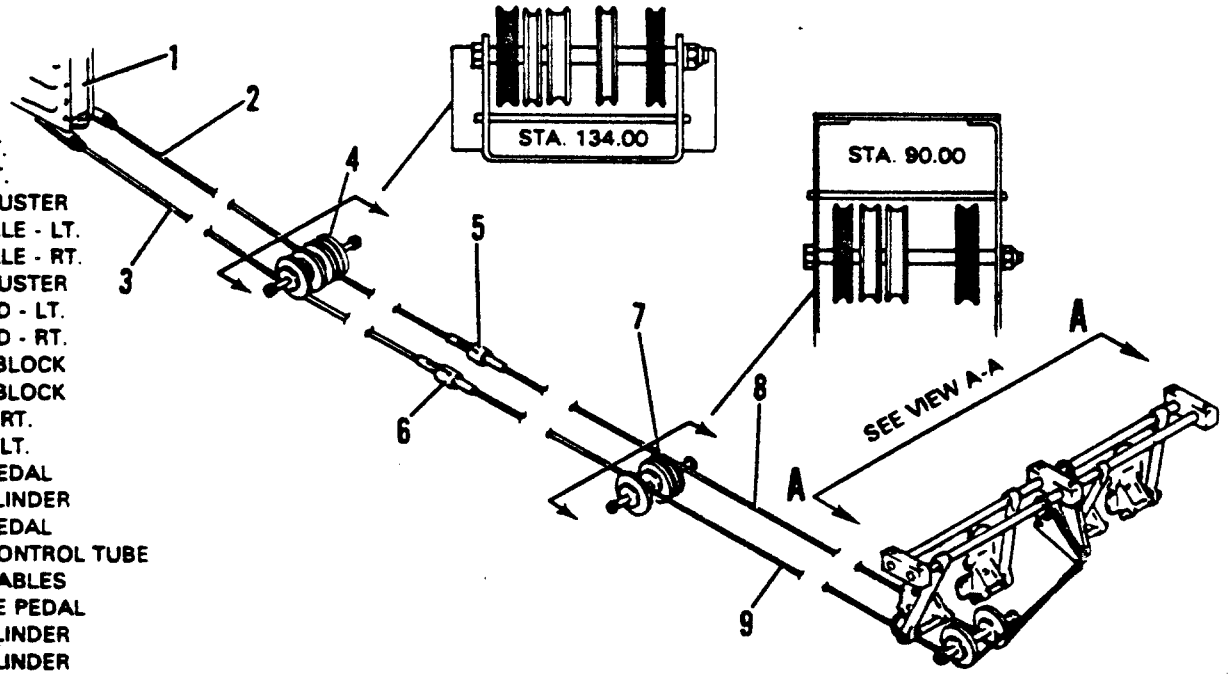

1. RUDDER
2. CABLE - LT.
3. CABLE - RT.
4. PULLEY CLUSTER
5. TURNBUCKLE - LT.
6. TURNBUCKLE - RT.
7. PULLEY CLUSTER
8. CABLE-FWD - LT.
9. CABLE-FWD - RT.
10. SUPPORT BLOCK
11. SUPPORT BLOCK
12. HANGER - RT.
13. HANGER - LT.
14. RUDDER PEDAL
15. BRAKE CYLINDER
16. RUDDER PEDAL
17. RUDDER CONTROL TUBE
18. RUDDER CABLES
19. TOE BRAKE PEDAL
20. BRAKE CYLINDER
21. BRAKE CYLINDER
22. CENTER SUPPORT BLOCK AND SPACER
23. NOSE GEAR STEERING RODS
24. SPACER

Figure 4.33 Directional Controls Piper PA-38-112

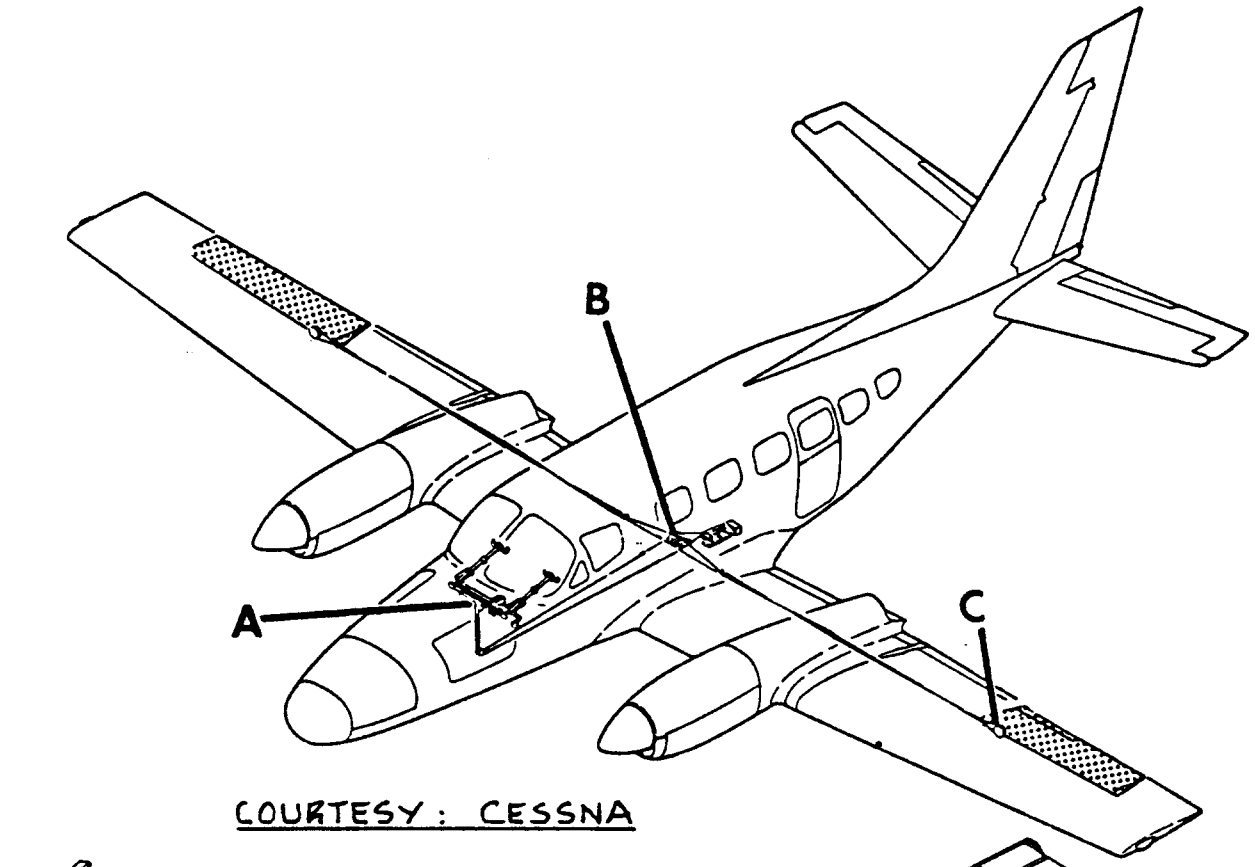

COURTESY : CESSNA

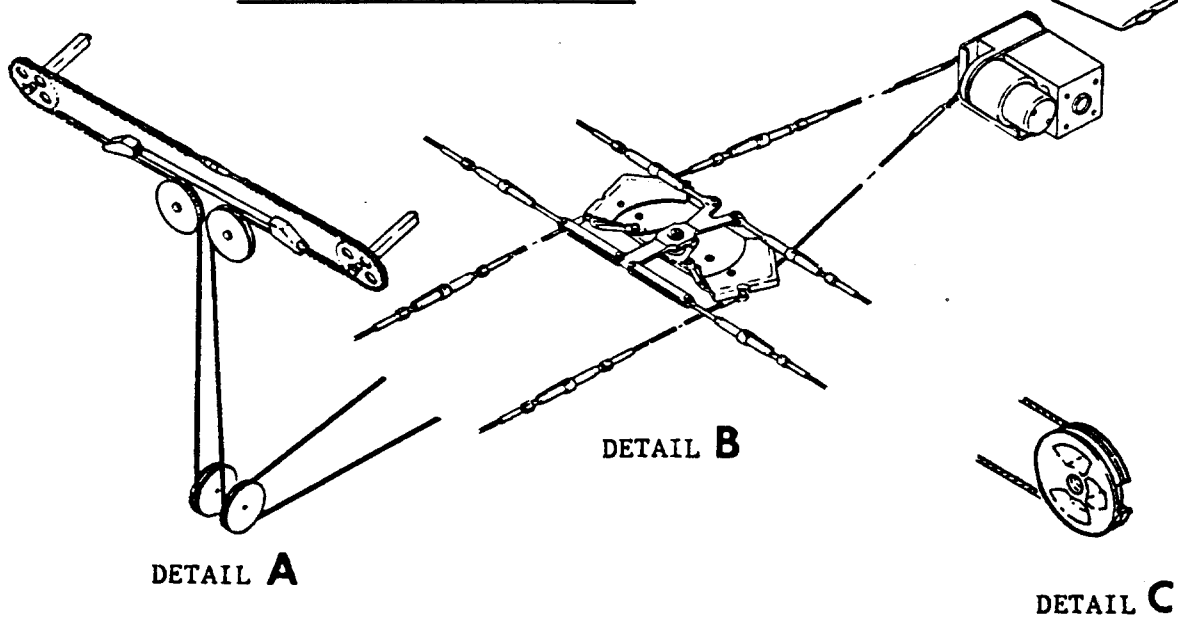

Figure 4.34 Lateral Controls Cessna 441

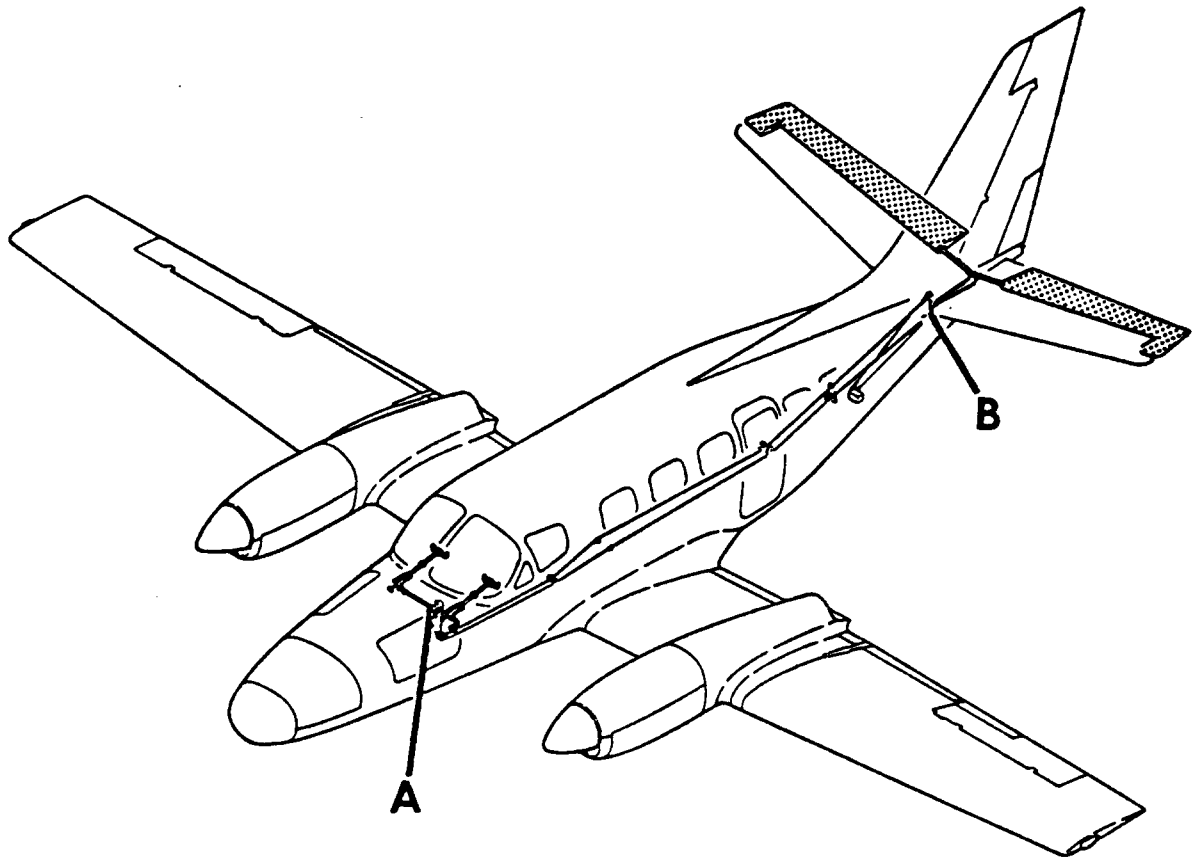

COURTESY : CESSNA

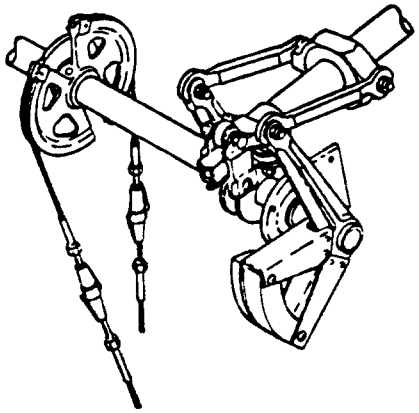

DETAIL A

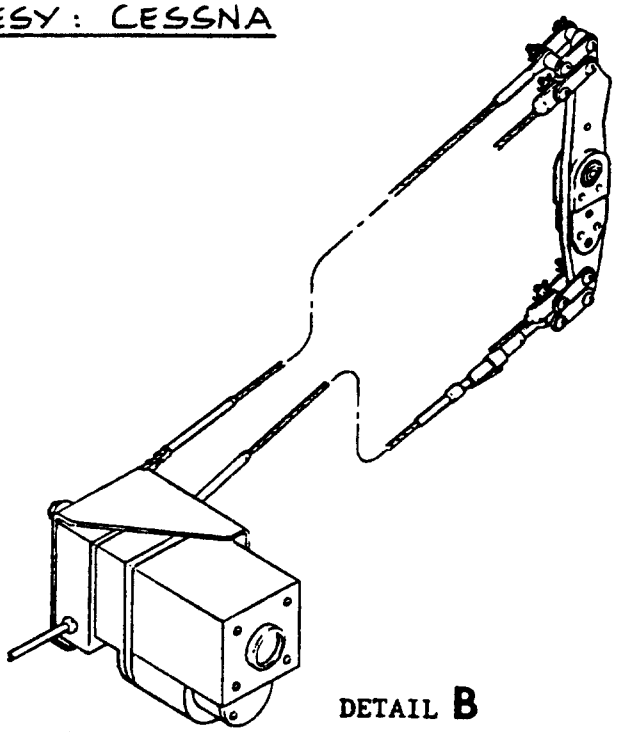

DETAIL B

Figure 4.35 Longitudinal Controls Cessna 441

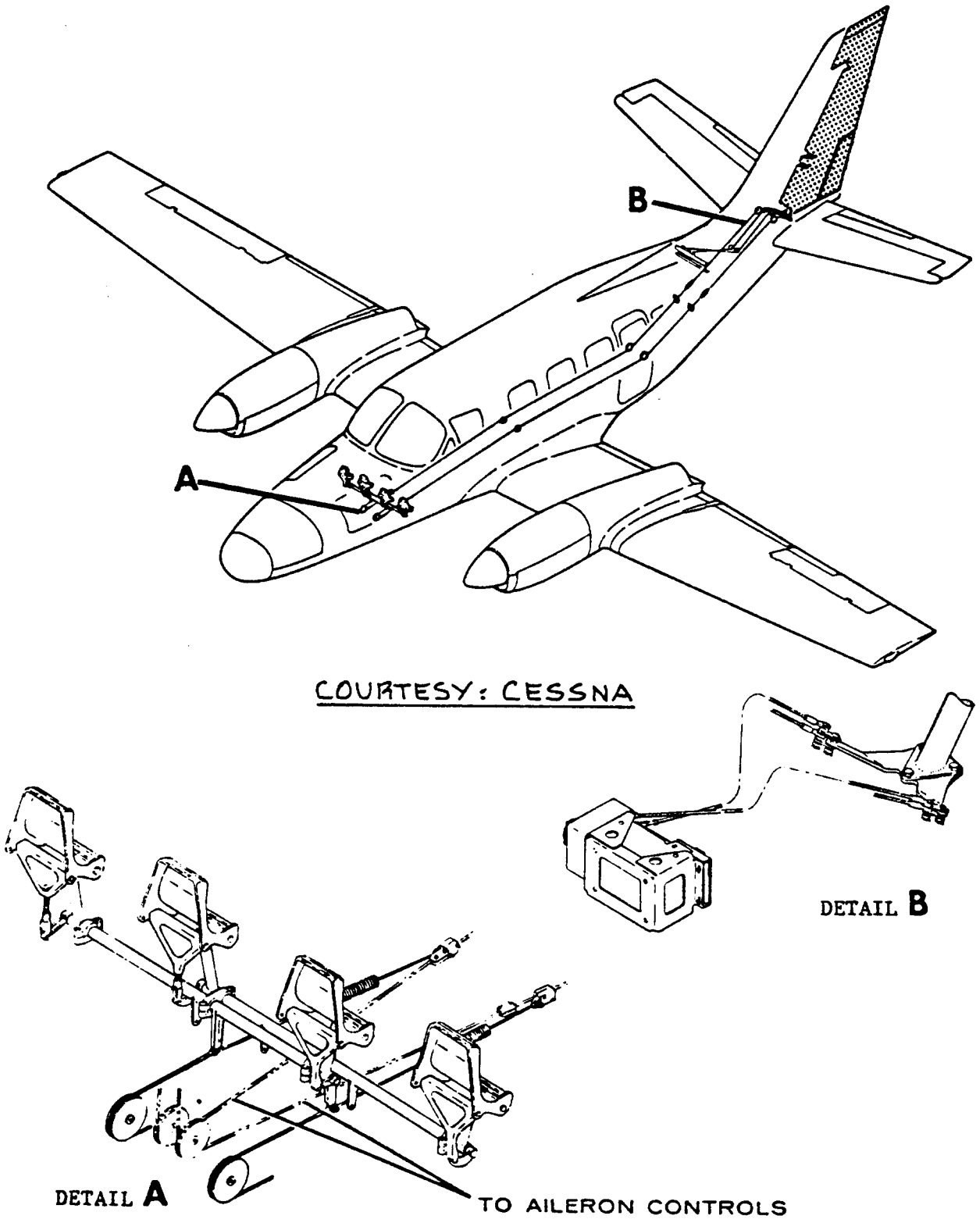

Figure 4.36 Directional Controls Cessna 441

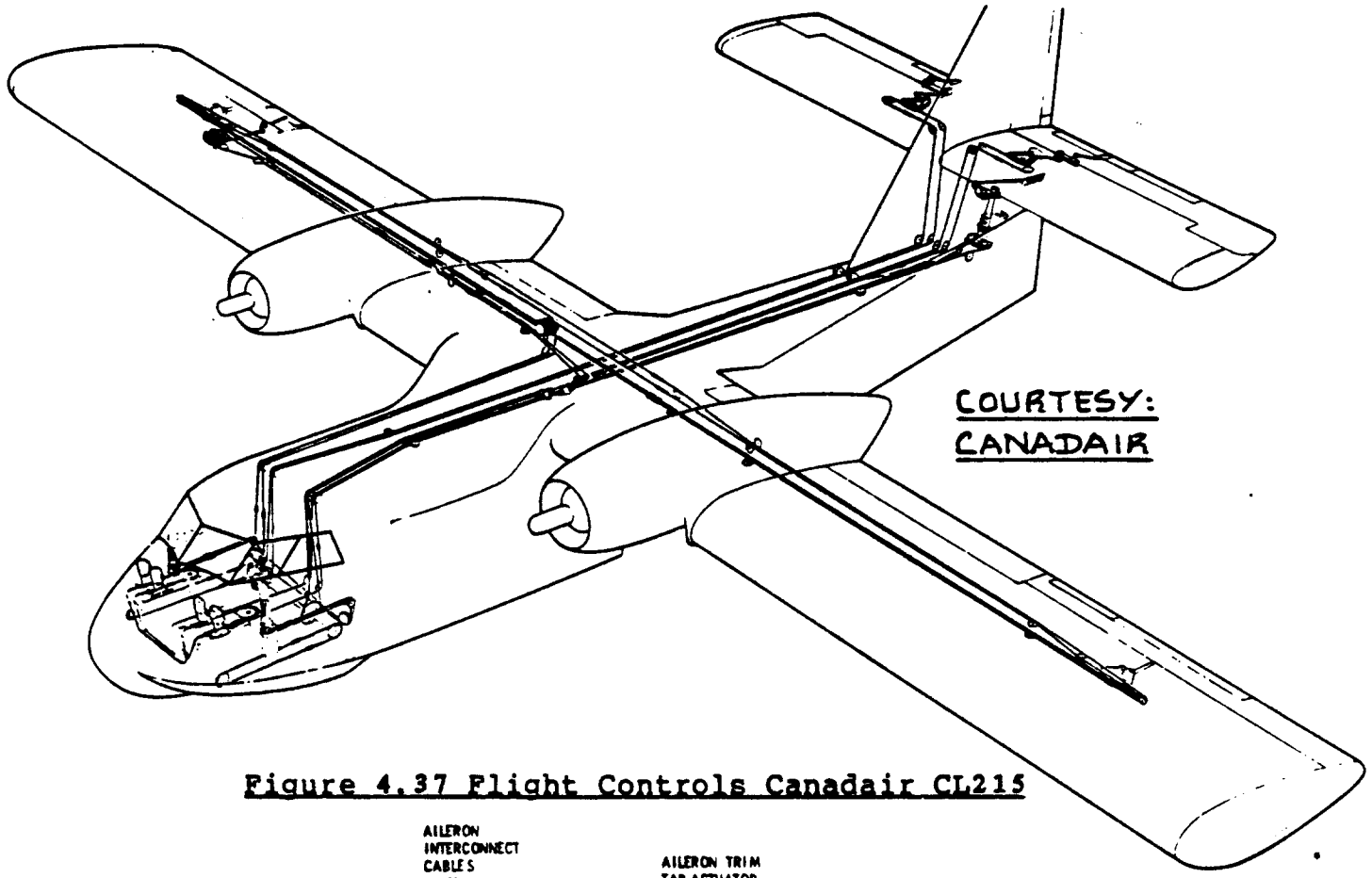

Figure 4.37 Flight Controls Canadair CL215

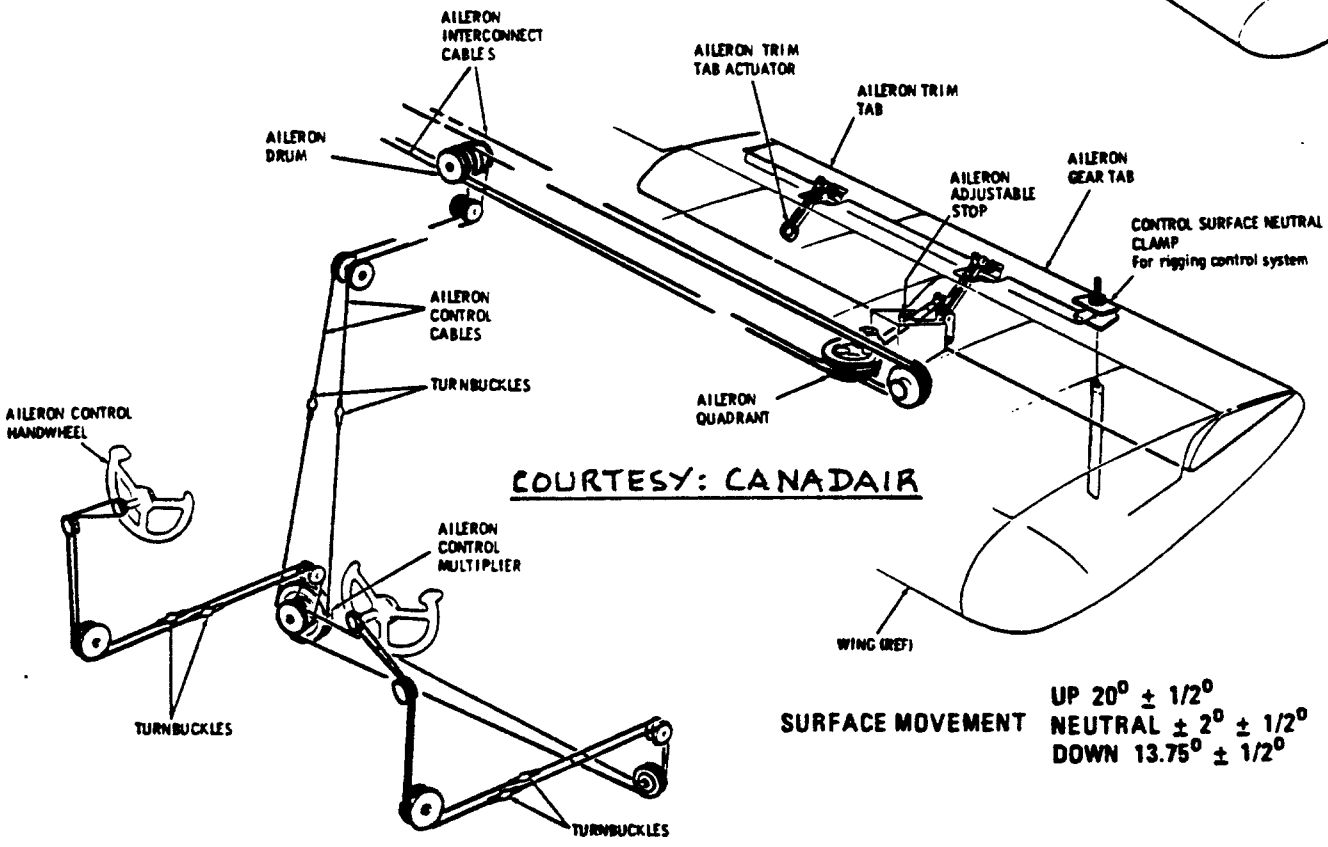

Figure 4.38 Lateral Controls Canadair CL215

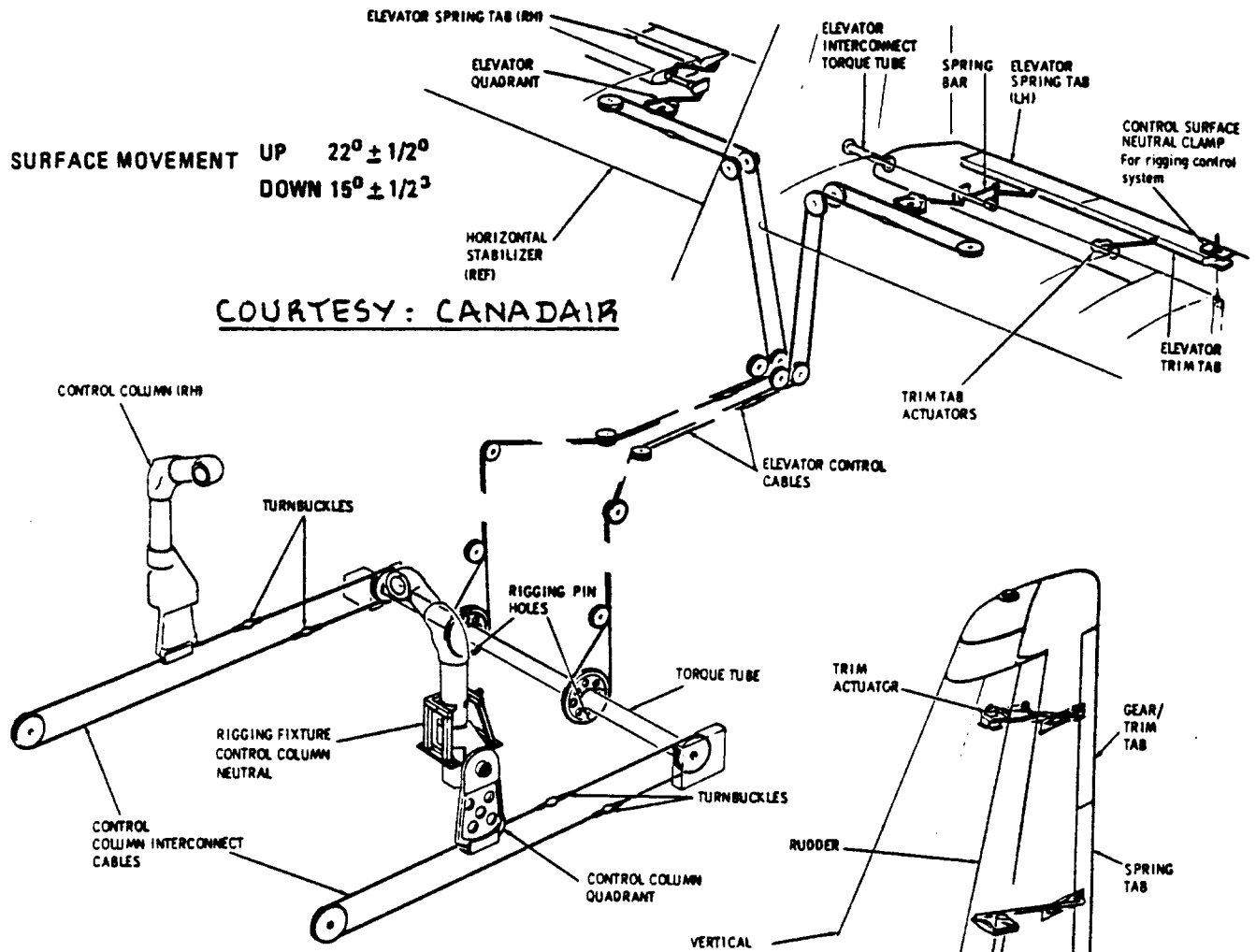

Figure 4.39 Longitudinal Controls Canadair CL215

Figure 4.40 Directional Controls Canadair CL215

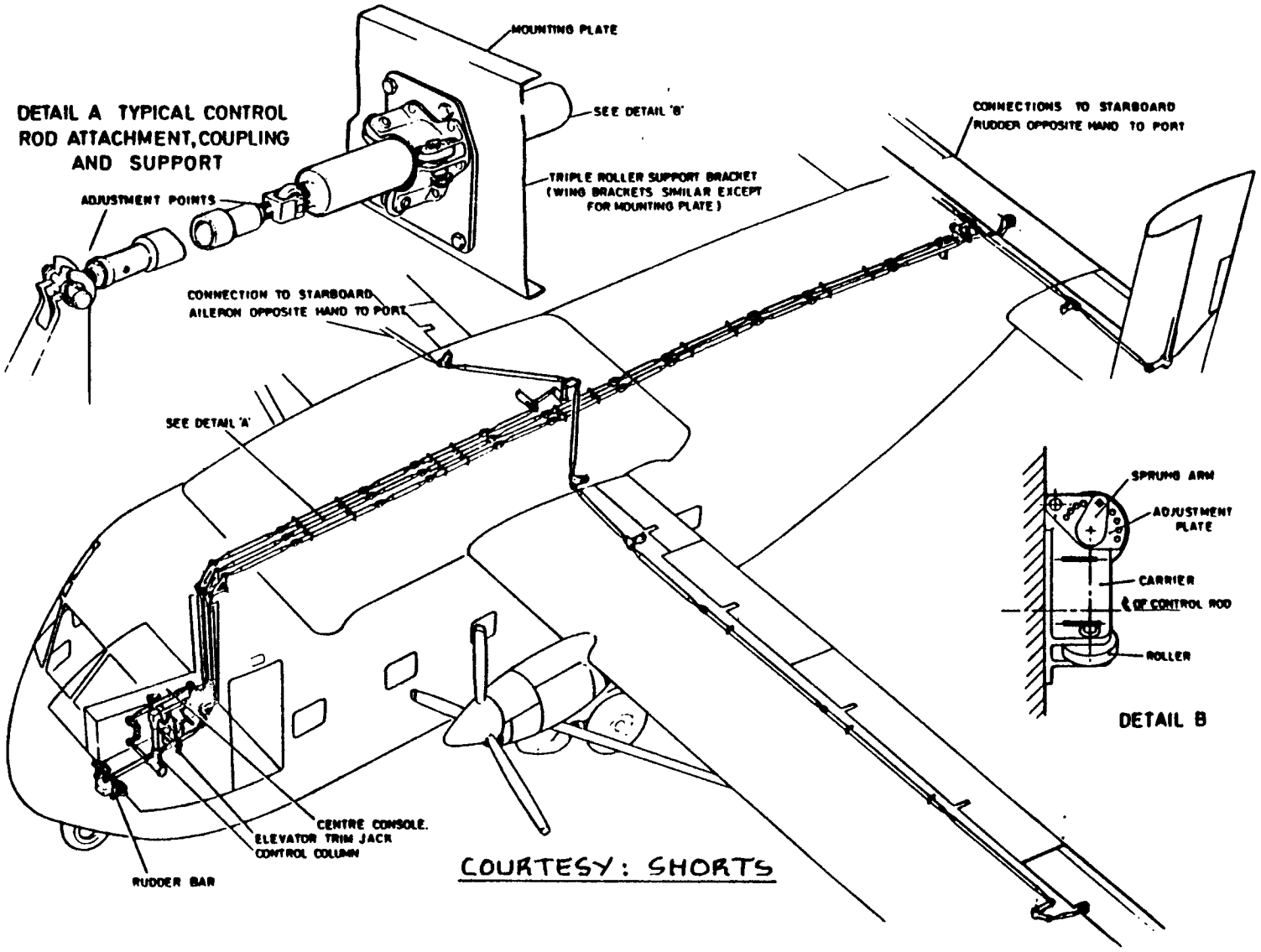

Figure 4.41 Flight Controls Short Skyvan

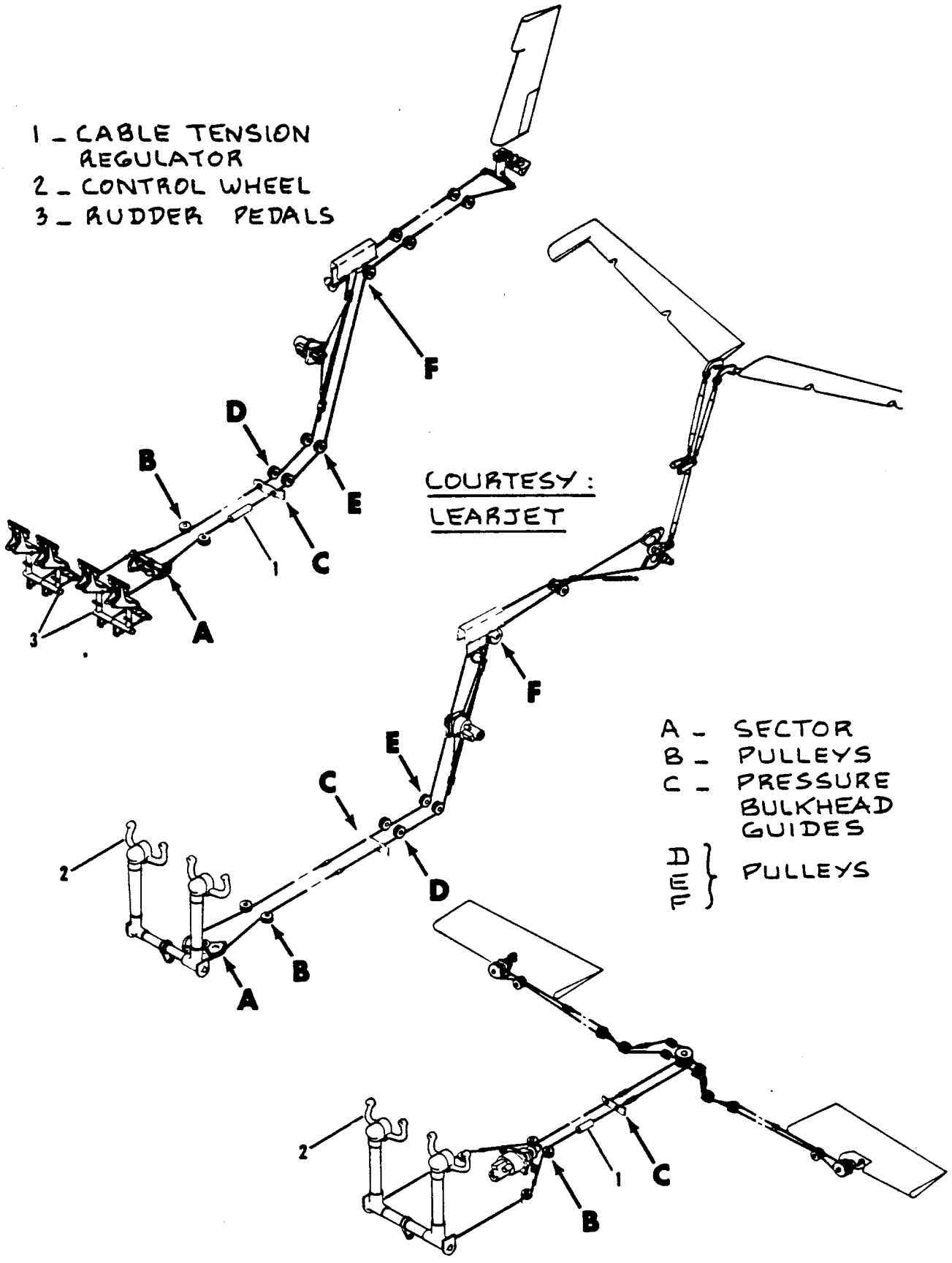

Figure 4.42 Flight Controls Learjet M23

4.3 LAYOUT OF IRREVERSIBLE FLIGHT CONTROL SYSTEMS

Definition: In an irreversible flight control system (hydraulic and/or electrical), when the cockpit controls are moved, the aerodynamic surface controls move and NOT vice versa.

Another way of stating this is to say that in an irreversible flight control system an actuator moves the aerodynamic surface controls. The pilot merely 'signals' the actuator to move. This signalling process is usually an irreversible process.

The material in this chapter is organized as:

4.3.1 Actuators (Servos)

In irreversible flight control systems the flight controls are moved by means of actuators (also called servos). Figure 4.43 shows a typical actuator-to-control-surface arrangement.

Actuators have two ends: a fixed and a moving end. The fixed end is attached to airplane structure. The moving end (also called the control rod) is attached to an aerodynamic surface control.

Two types of actuators are used most frequently: hydraulic and electromechanical. Figs 4.44 and 4.45 show examples of hydraulic and electromechanical actuators respectively. Sofar, in primary flight control systems the hydraulic actuator is the most frequently used type.

Actuators can be designed for linear or for rotary outputs. Figure 4.46 shows example installations.

Note: The structure at the fixed actuator end must be stiff. If this condition is not satisfied, the control surface will not deflect as much as the installation geometry would predict. This is called servo-elasticity.

For the actuator rod to move, the actuator must

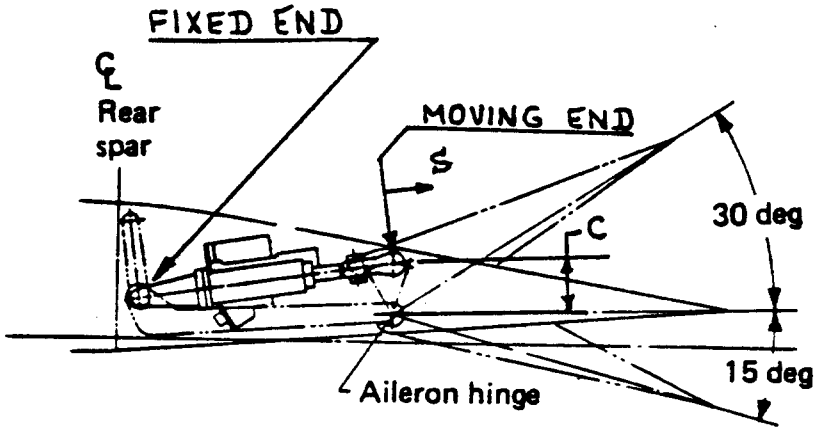

Figure 4.43 Typical Actuator-to-Surface Installation

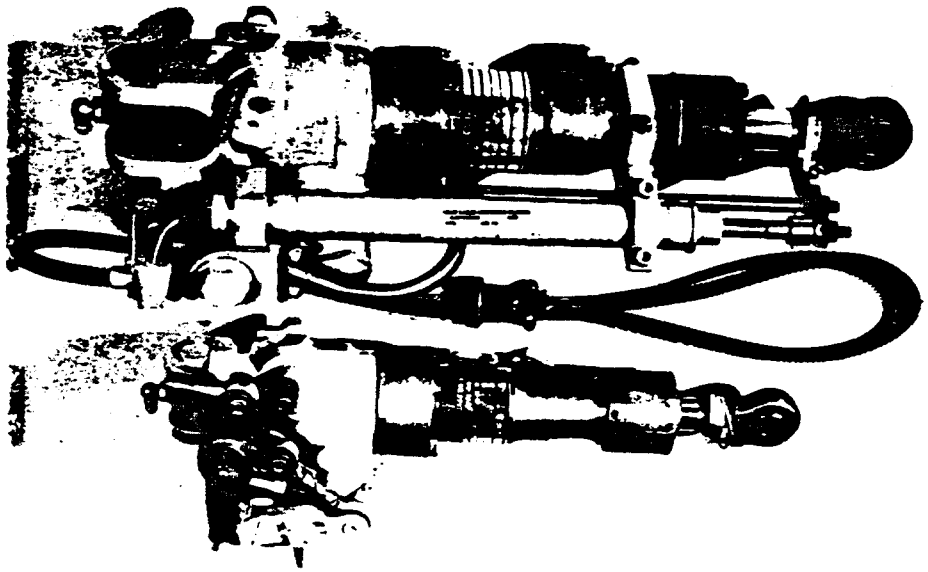

Figure 4.44 Hydraulic Actuator Examples

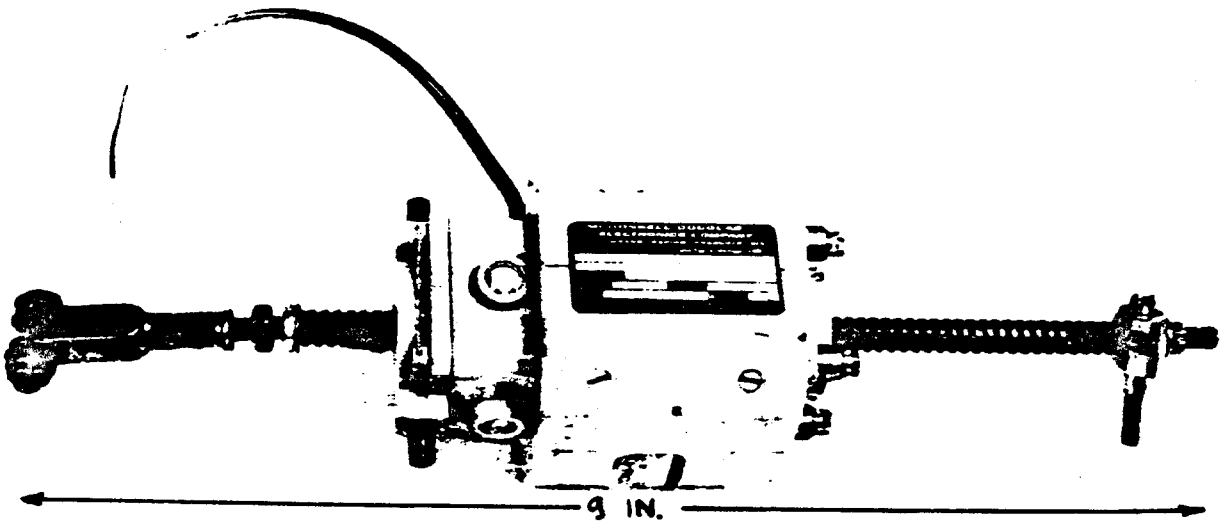

Figure 4.45 Electromechanical Actuator Example

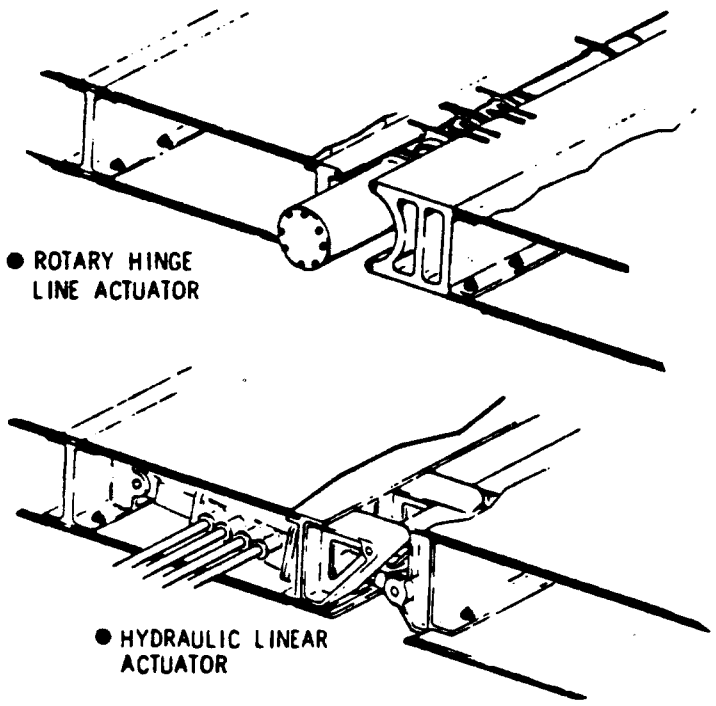

Figure 4.46 Rotary and Linear Actuator Installations

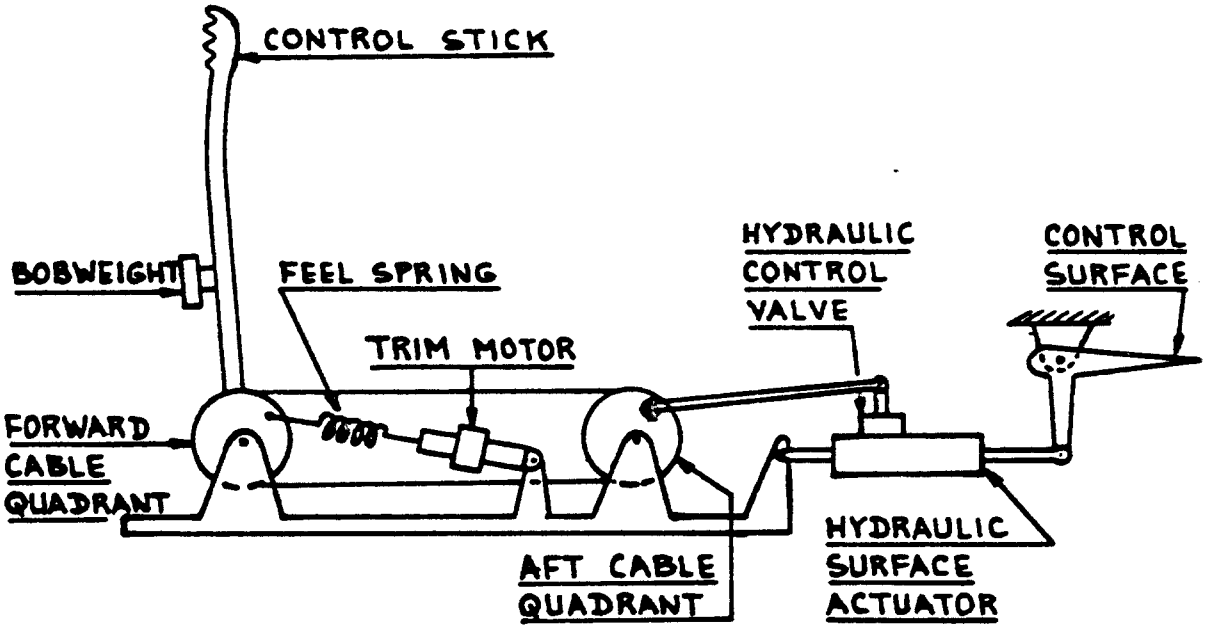

Figure 4.47a Mechanical Signalling of the Actuator

receive two inputs:

1) a command input signal, and 2) power

The general characteristics of these inputs will now be discussed.

1) Command input signal

The command input signal to an actuator can be sent by one or more of three methods:

a) mechanical signalling: this is done with cables and/or with push-rods

b) electrical signalling (Analog and/or digital): this is called fly-by-wire.

c) optical signalling: this is called fly-by-light

Figures 4.47a, b and c illustrate how actuator command signals may be transmitted from cockpit to actuator.

2) Power

Power to drive actuators (also called servos) is normally derived from a hydraulic system and/or from an electrical system*. The layout design of hydraulic and electrical systems is discussed in Chapters 6 and 7.

The basic operating characteristics of hydraulic and electromechanical actuators will now be discussed.

4.3.1.1 Operation of hydraulic actuators

Figure 4.48 shows a schematic of a hydraulic actuator as installed in an irreversible longitudinal flight control system. Note that the input command opens a control valve which admits high pressure hydraulic fluid to one side of the actuating cylinder. This high pressure hydraulic fluid then moves the piston (moving end or actuator rod) which in turns moves the control surface.

As drawn in Figure 4.48 the actuator would in fact move all the way to its mechanical stop. This is not usually desired: the output displacement is normally desired to be proportional to the input displacement.

---

* In some older installations pneumatic actuators are still used. These are not discussed in this text.

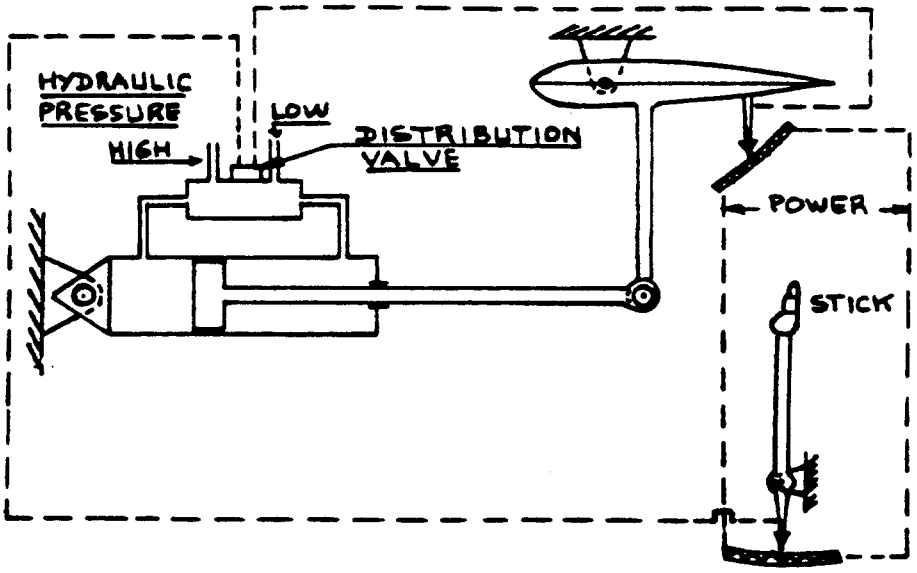

Figure 4.47b Electrical Signalling of the Actuator

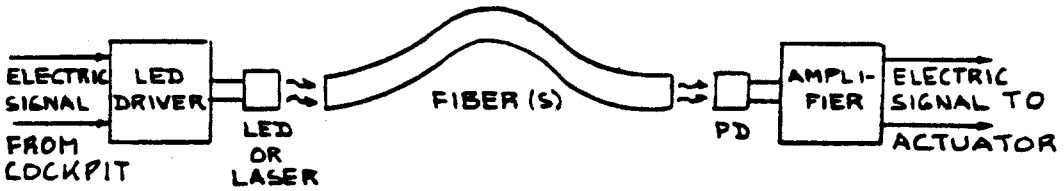

LED = LIGHT EMITTING DIODE
PD = PHOTODIODE

Figure 4.47c Optical Signalling of the Actuator

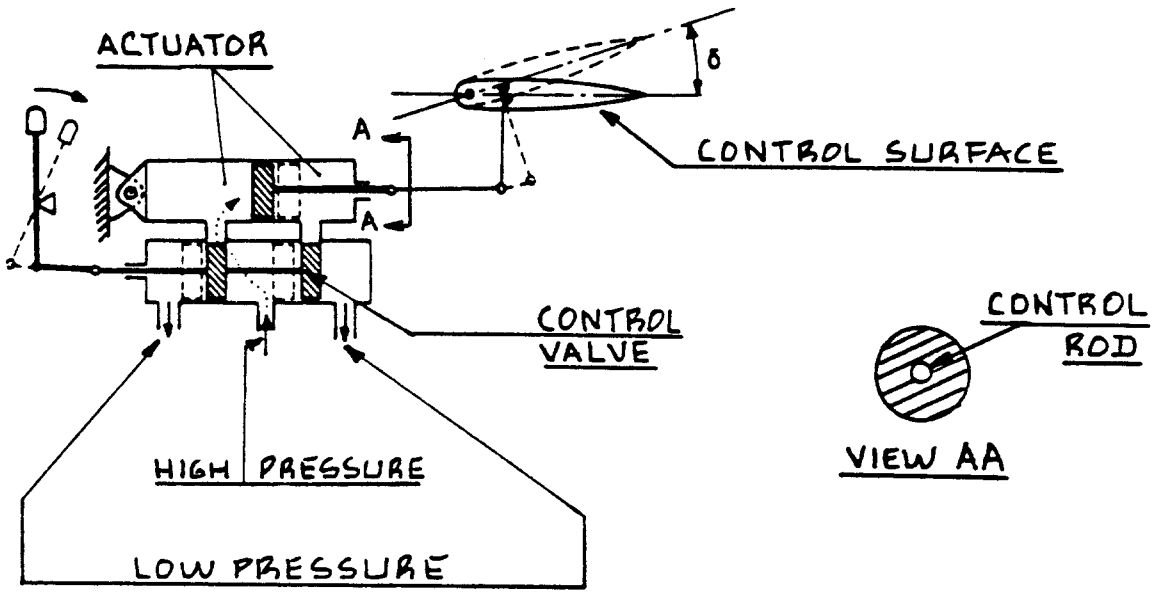

Figure 4.48 Mechanically Signalled Hydraulic Actuator Without Feedback

Such proportionality can be achieved with the help of feedback. Fig.4.49 shows how position feedback works in a hydraulic actuator with mechanical signalling.

In the design and/or selection of all actuators the following characteristics are critical to the operation of the flight control system:

1. Maximum output force capability
2. Maximum output stroke capability
3. Maximum output velocity (rate) versus load capability
4. Stall load magnitude
5. Actuator weight and volume
6. Actuator power requirements

The maximum required actuator rate depends on its application. Typical ranges for maximum actuator rates must be consistent with the following ranges of maximum control surface rates:

Transport flight controls:	100-200 deg/sec
Fighter flight controls:	
inherently stable fighters:	100-300 deg/sec
de-facto stable fighters:	200-800 deg/sec
Gust alleviation and structural mode control systems:	500-800 deg/sec

If cost, weight and complexity were not limiting factors, actuator rates would always be selected to be as high as technically feasible.

4.3.1.2 Operation of electrohydrostatic actuators

A recent development of the electrically signalled hydraulic actuator is the so-called electrohydrostatic actuator. This actuator does not require an airplane hydraulic system. EHS actuators have their own miniature hydraulic system, including a pump and an electric motor (rare earth) which drives the pump. EHS actuators are driven by electric power and signalled by fly-by-wire or by fly-by-light systems. Figure 4.50 shows an example.

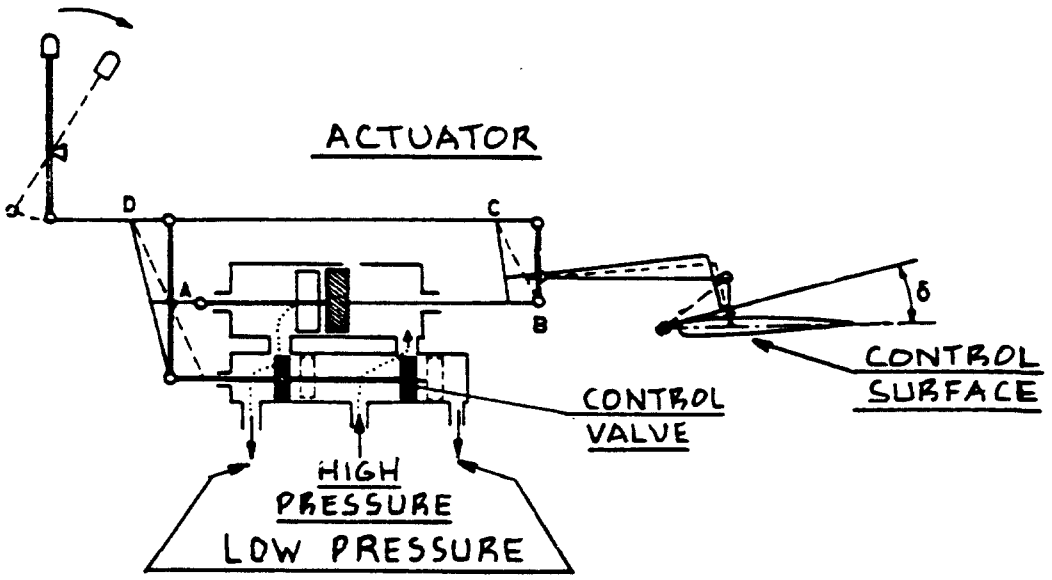

Figure 4.49 Mechanically Signalled Hydraulic Actuator With Position Feedback

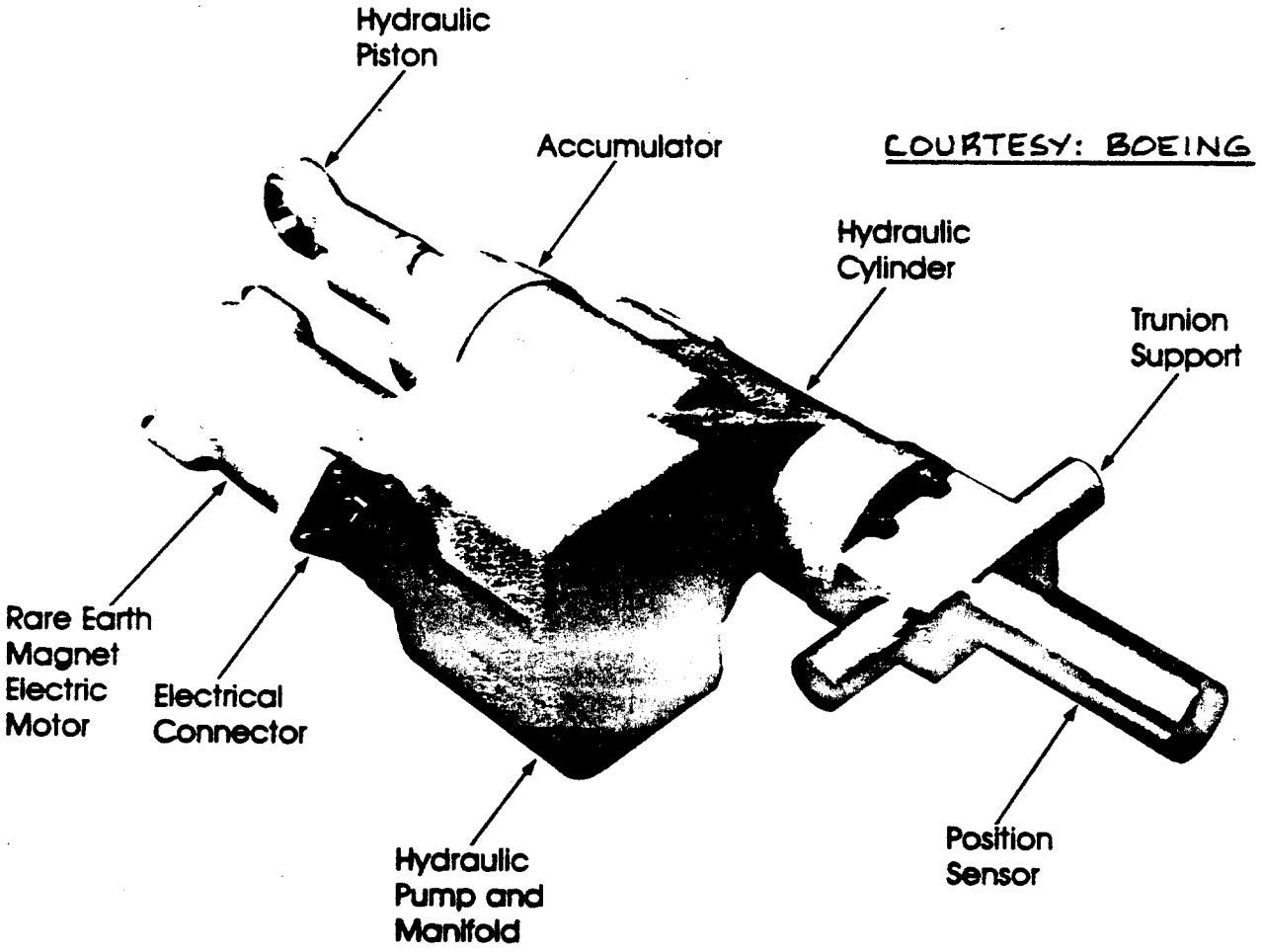

Figure 4.50 Example Electrohydrostatic Actuator

4.3.1.3 Operation of electromechanical actuators

Electromechanical actuators consist of an electric motor which drives an output shaft via a gear box or via a ball-screw jack. In flight control systems with hinge-line installations the first type is used. For linear installations the second type is used. Figures 4.51 and 4.52 show schematics for both types.

The weight, volume and performance characteristics of electric motors depends strongly on the magnetic field strength capability of the magnets used. Figure 4.53 shows a comparison of the fieldstrength associated with conventional ALNICO magnets and with the more recent Nd-Fe-B magnets. These latter magnets (also called rare earth magnets) have considerably greater performance. This enhanced field strength capability makes it possible to use electromechanical actuators: with the new magnet materials these actuators are quite competitive in weight, in volume and in performance.

Reference 26 contains a design study of electromechanical systems, indicating their competitiveness with hydraulic systems.

4.3.2 Sizing of Actuators

References 21 and 27 should be consulted for specific maximum design requirements associated with actuators used in flight control systems. In this section only the sizing to normal operating conditions will be discussed.

The control force, F_c required to overcome the control surface hingemoment may be computed from Eqn.(4.6) on page 202. If the actuator stroke is called 's' and the control surface deflection is called 'δ' the following relationship follows from an 'equal work' condition:

$$F_c = \{C_{h_\delta} \bar{q} (Sc)_{\text{control surface}}\}/c \qquad (4.9)$$

The moment arm c is defined in Figure 4.43 and is normally given in inches.

If the desired control surface deflection rate is $d\delta/dt$ (normally given in deg/sec), the required control rod velocity ds/dt (normally given in in/sec), follows from:

$$ds/dt = (57.3)(c)d\delta/dt \qquad (4.10)$$

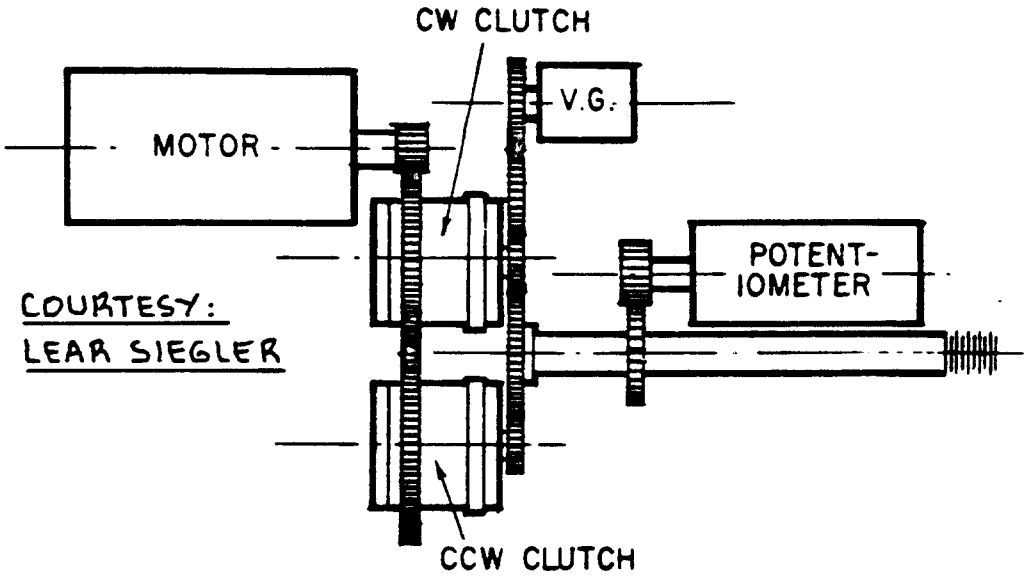

Figure 4.51 Schematic: Rotary Electromechanical Actuator

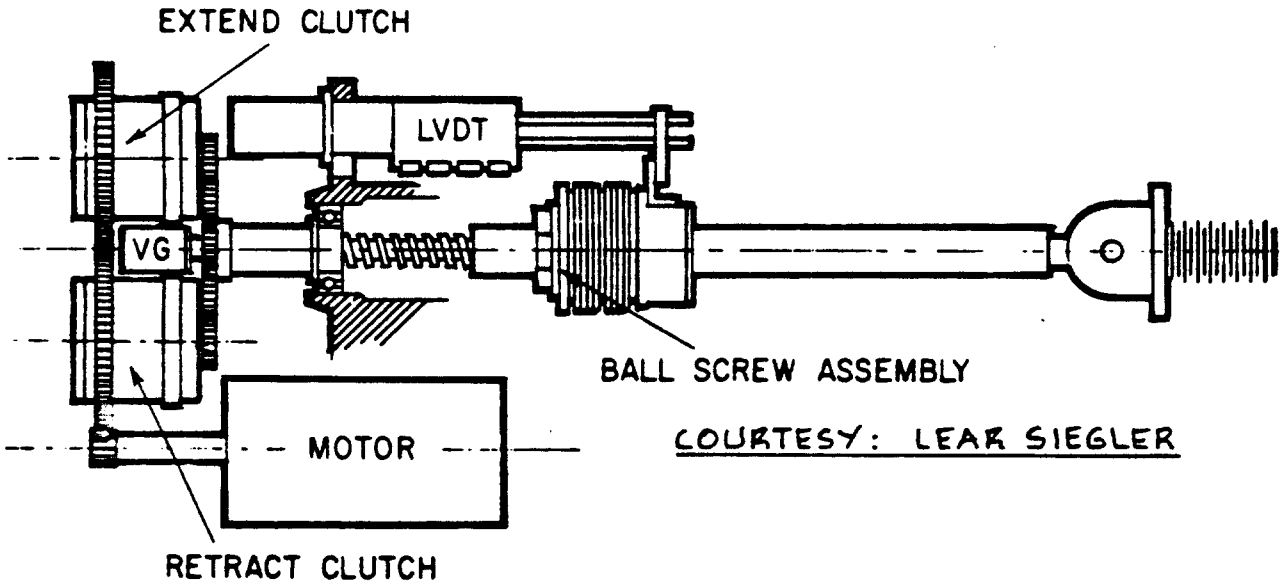

Figure 4.52 Schematic: Linear Electromechanical Actuator

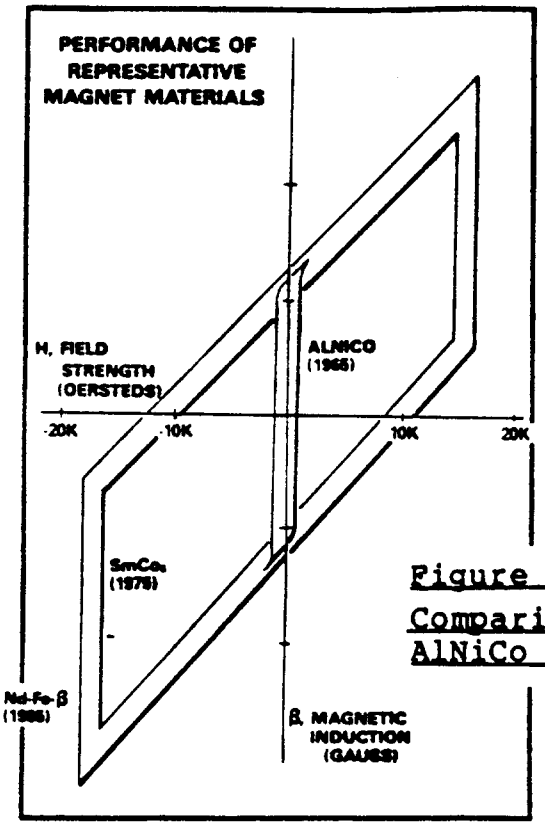

Figure 4.53

Comparison of Fieldstrength Capability of AlNiCo with Neodymium/Iron/Boron Magnets

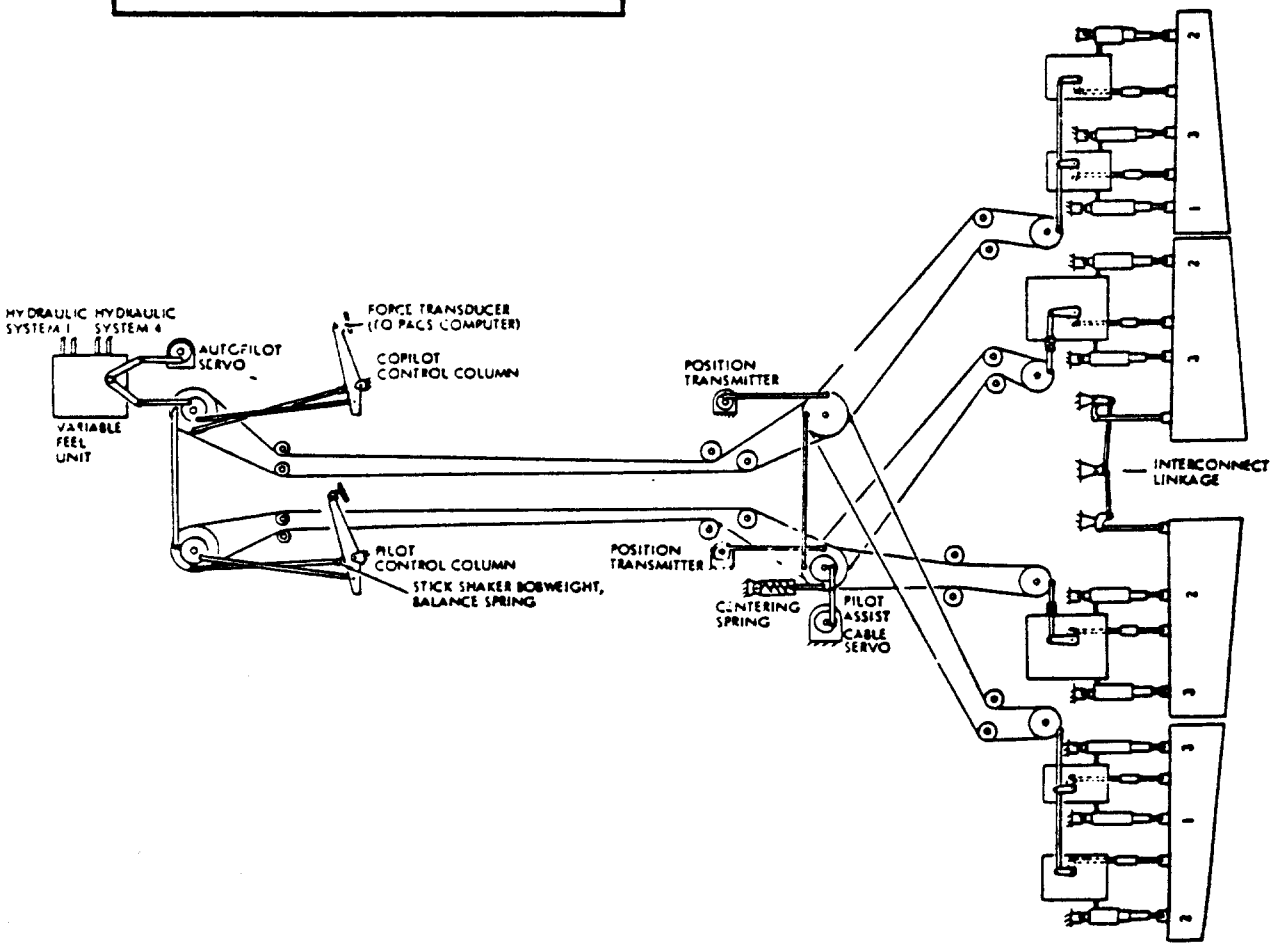

Figure 4.54 Lockheed C5-A Elevator Control Schematic

Hydraulic Actuators

If the hydraulic system operating pressure is p_h (normally given in psi), while the effective piston area is S_p (normally given in $in.^2$), the following relation may be used to compute the required actuator size:

$$S_p = F_c/(p_h - 200) \qquad (4.11)$$

Figure 4.48 defines the effective piston area, S_p.

The hydraulic system backport pressure is assumed to be typically 200 psi. The required hydraulic fluid flow follows from:

$$\text{Hydraulic fluid flow} = S_p(ds/dt) \ in^3/sec \qquad (4.12)$$

Typical operating pressures in current hydraulic systems are 3000-3500 psi for commercial applications and 5000 psi for military applications. Ref.28 states that systems with 8000 psi pressure may become feasible. Chapter 6 discusses the layout of hydraulic systems.

Electromechanical Actuators

These actuators are rated in terms of their normal operating load as given in Eqn.(4.9), their stroke velocity as given by Eqn.(4.10) and their stall load. By using an actuator efficiency of 80 percent the required electrical operating power follows once the basic operating voltage of the system is known. Typical operating voltages are 12-28 VDC and 60-90 KVA. Chapter 7 presents a discussion of electrical systems.

4.3.3 Basic Arrangements of Irreversible Flight Control Systems

Table 4.2 lists example applications of different types of irreversible flight control systems.

4.3.3.1 Hydraulic system with mechanical signalling

Figure 4.54 shows a schematic for the elevator control system of the Lockheed C5-A. It is a hydraulically powered, irreversible system with mechanical signalling.

This type of system is typical of that used in most commercial jet transports as well.

Table 4.2 Examples of Control System Applications

Airplane Type	Type of Signalling	Actuators	Redundancy	Reversibility	Trim System
Boeing 737					
Lateral	Mechanical	Hydraulic	2 systems	Full reversion	Through feel system
Longitudinal	Mechanical	Hydraulic	2 systems	Full reversion	El.Mech./Stabilizer
Directional	Mechanical	Hydraulic	3 systems	No reversion	Through feel system
Boeing 747					
Lateral	Mechanical	Hydraulic	4 systems	No reversion	Through feel system
Longitudinal	Mechanical	Hydraulic	4 systems	No reversion	Through feel system
Directional	Mechanical	Hydraulic	4 systems	No reversion	Through feel system
Rockwell B-1B					
Lateral	Mechanical Fly-by-wire	Hydraulic	4 systems	No reversion	Through feel system using diff. stabil.
Longitudinal	Mechanical	Hydraulic	4 systems	Fly-by-wire	Through feel system using stabilizers
Directional	Mechanical	Hydraulic	4 systems	Fly-by-wire	Through feel system
McDonnell-Douglas F/A-18A					
Lateral	Fly-by-wire	Hydraulic	2 systems	No back-up	Through feel system
Longitudinal	Quadriplex	Hydraulic	2 systems	Mechanical	Through feel system
Directional	Digital	Hydraulic	2 systems	No back-up	Through feel system
Aeritalia/Aermacchi/EMBRAER AM-X					
Lateral					
Spoilers	Fly-by-wire	Hydraulic	2 systems	None	Through feel system
Ailerons	Mechanical	Hydraulic	2 systems	Full reversion	Through feel system
Longitudinal	Mechanical	Hydraulic	2 systems	Full reversion	Through feel system
Directional	Fly-by-wire	Hydraulic	2 systems	No back-up	Through feel system

Figure 4.55 shows a schematic for the longitudinal control system of the YF-17 fighter. The hydraulic actuators control the left and right stabilizer.

Mechanical signalling is done with cable and/or with push-rod systems. Such systems are mechanically similar to those used in reversible control systems. Section 4.1 deals with the layout design of reversible flight control systems and section 4.2 gives example applications.

A problem with powered controls is: redundancy. If no mechanical reversion is provided it is necessary to design redundancy into the hydraulics, the electrics and the actuators so that complete system failure is an 'extremely' remote event. (Ch.13 defines event probability)

In powered flight controls designing for redundancy means the following:

In hydraulically driven systems: a large number of hydraulic pumps, at least three independent power sources for the hydraulic pumps and redundant actuators.

In electrically driven systems: a large number of electric generators, two independent standby sources for electric power and redundant actuators.

A fundamental advantage of mechanical signalling is that provisions for mechanical reversion can be incorporated for only a minor weight penalty.

Figures 4.56 through 4.58 show schematics for the Boeing 737 flight control system. Note that the rudder axis incorporates complete hydraulic system redundancy. The lateral and longitudinal axes incorporate complete mechanical reversion and thus do not need hydraulic redundancy. Observe that both aerodynamic balance and mass balance were added to make this certifiable.

Mechanical signalling involves a large weight penalty. Electrical and/or optical signalling avoid this.

4.3.3.2 Hydraulic system with electrical or optical signalling

Figure 4.59 shows a schematic for this system type. Note the triplicated signal paths and the use of three actuators per elevator.

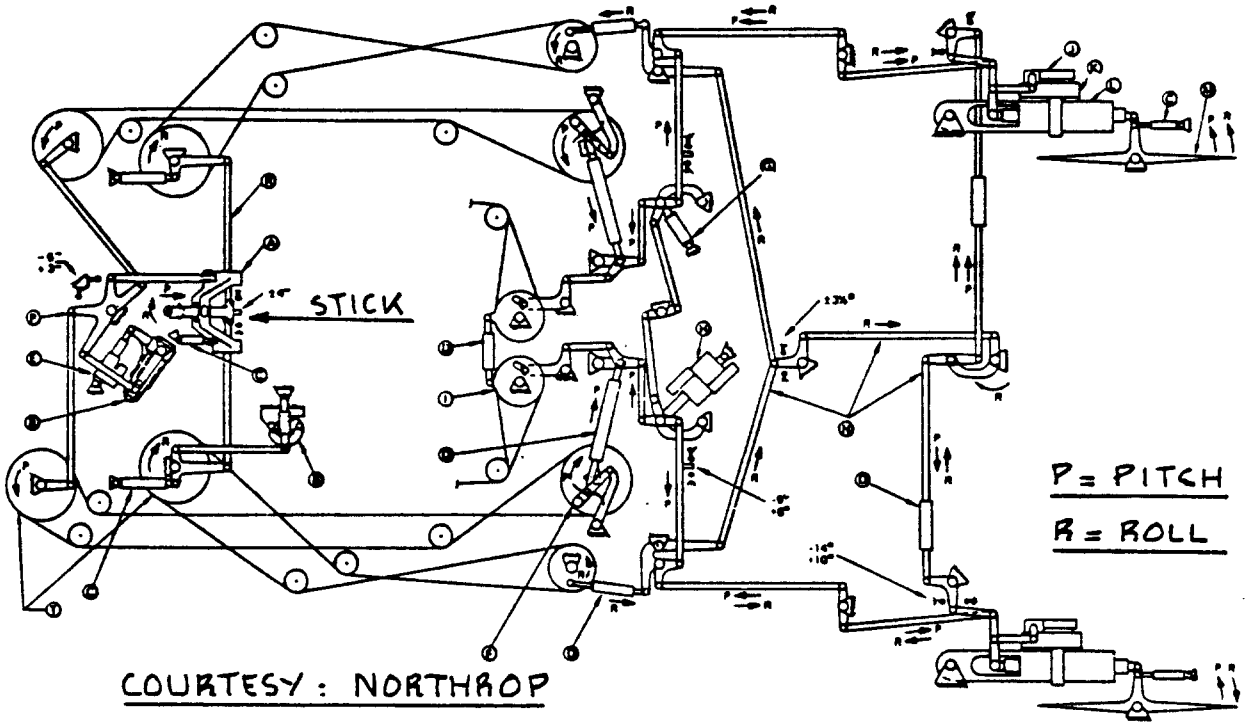

Figure 4.55 Northrop YF-17 Stabilizer Control Schematic

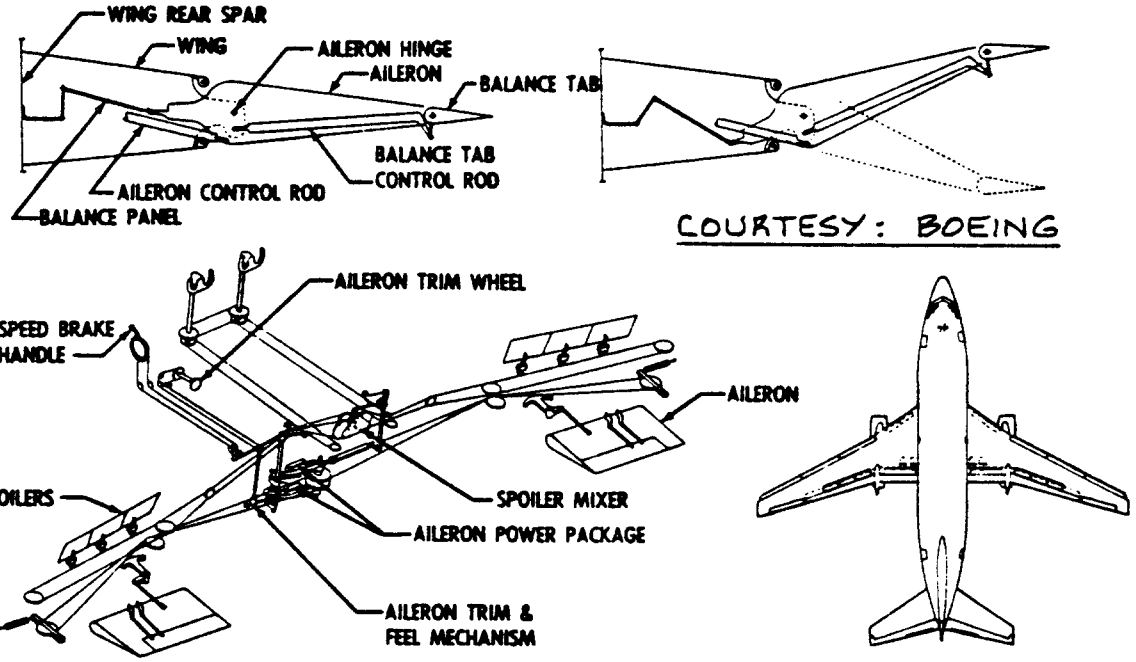

Figure 4.56 Lateral Control Schematic: Boeing 737

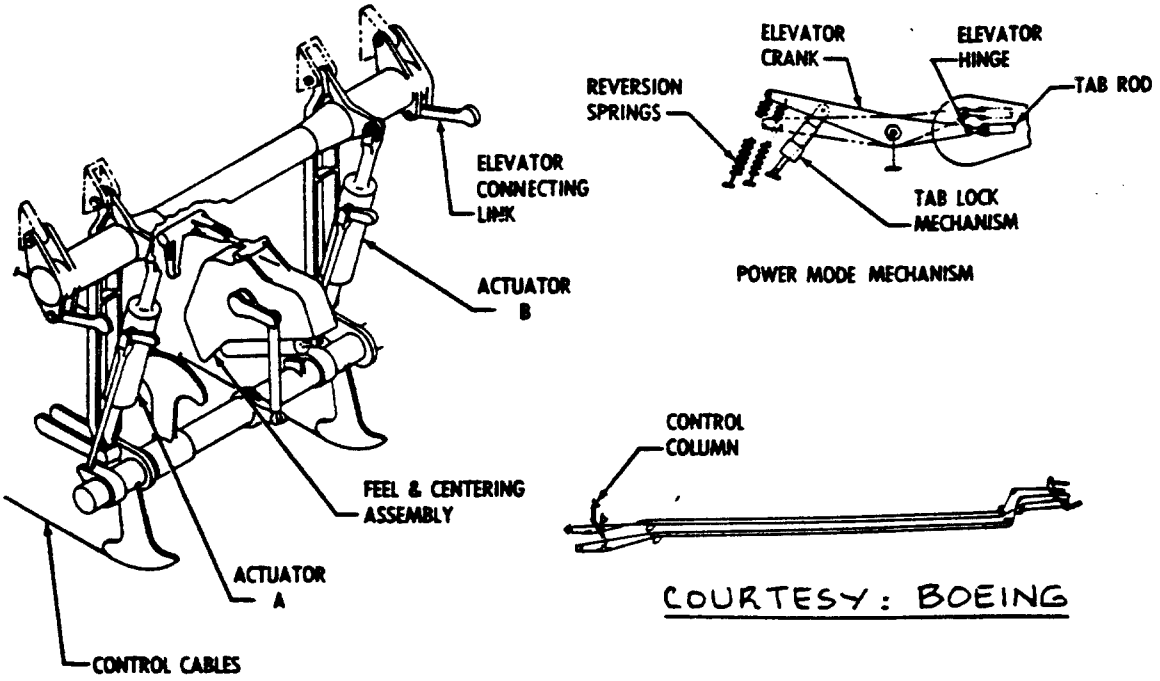

Figure 4.57 Elevator Control Schematic: Boeing 737

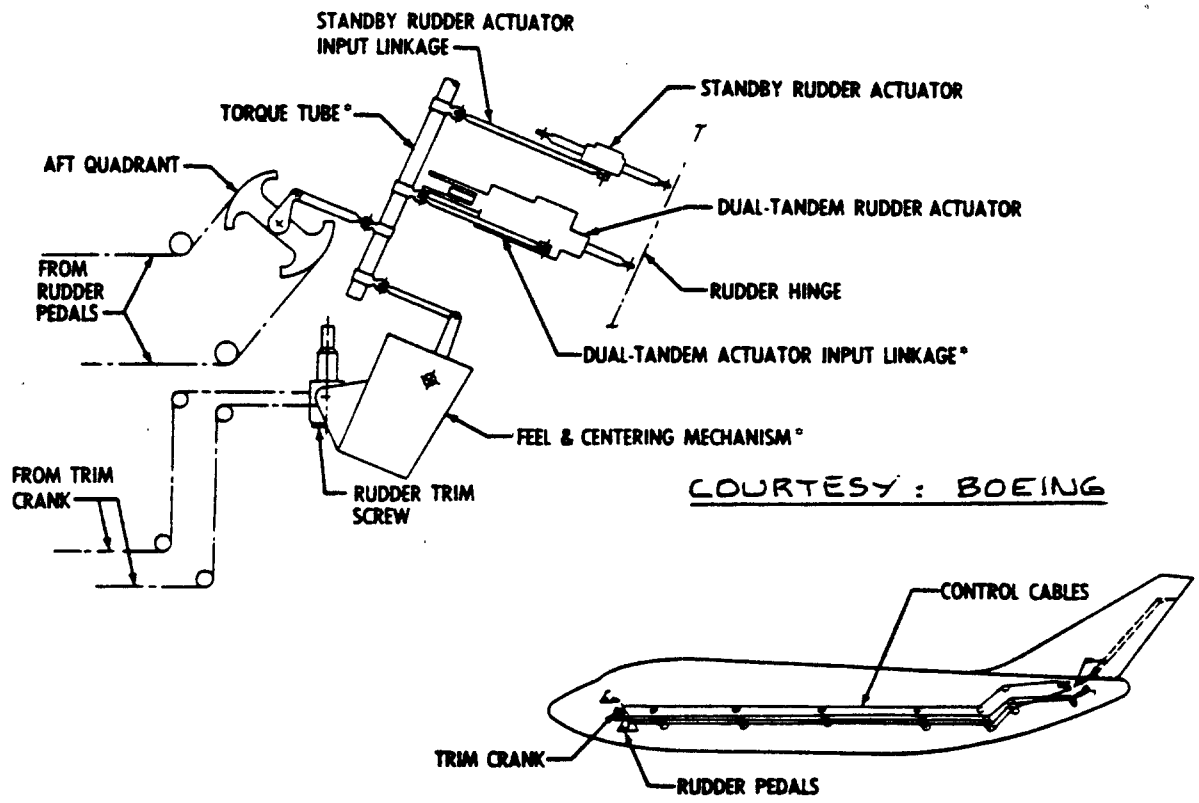

* DUAL PATH TO ACTUATOR VALVE

Figure 4.58 Rudder Control Schematic: Boeing 737

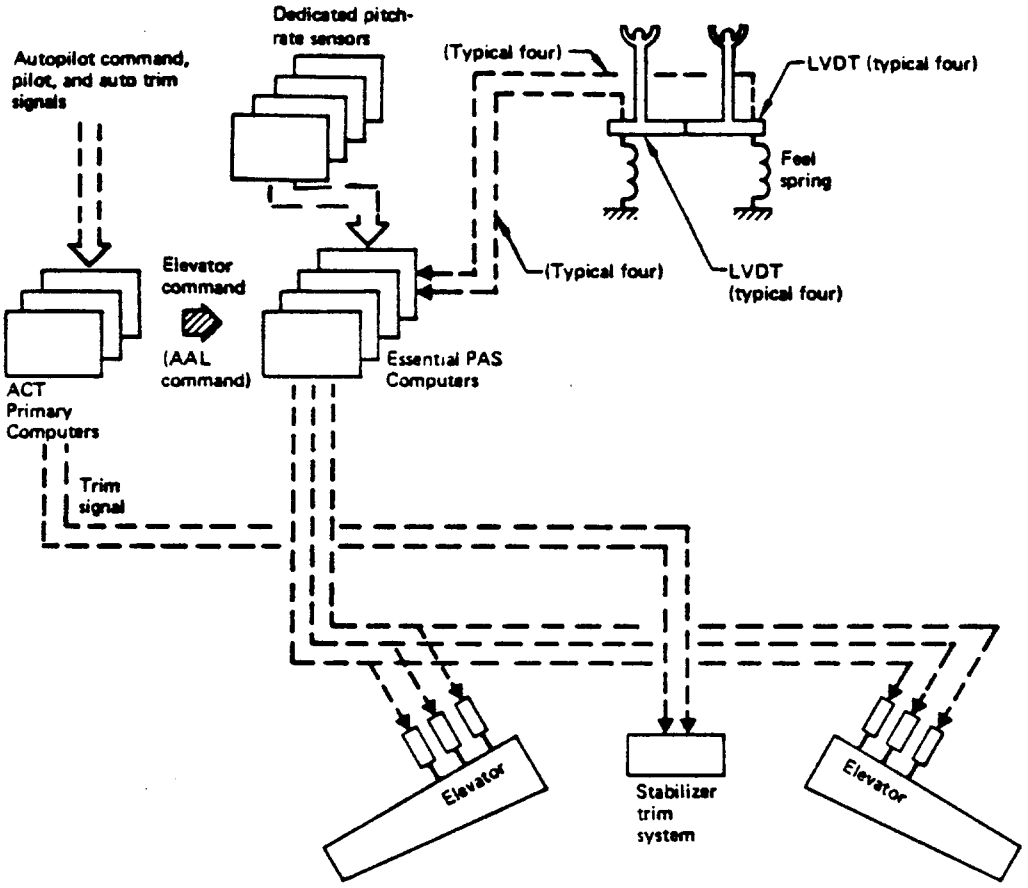

Figure 4.59 Schematic of Fly-by-wire, Hydraulically Powered Elevator Control System

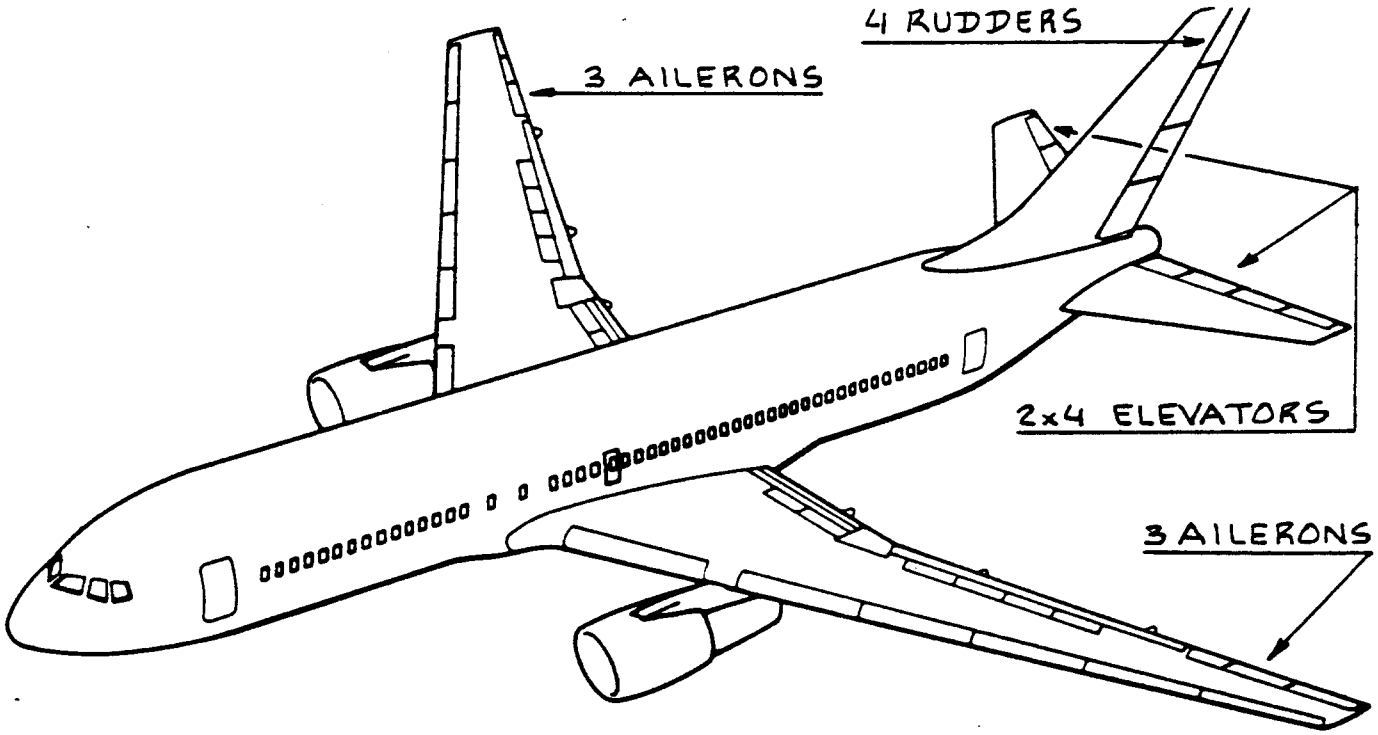

Figure 4.60 Proposed Separate Surface Flight Control Layout for and Advanced Transport Airplane

4.3.3.3 Separate surface control systems with electrical or optical signalling

Because of requirements for redundancy and because primary flight control system actuators are normally sized to each control surface individually, these actuators tend to be large, complex and very expensive. In fighter airplanes these actuators contribute significantly to maintenance, cost and inventory problems.

An attractive way around these problems is a system where all flight control surfaces are split into smaller separate surfaces. These surfaces can be sized so that they all require the same type of actuator. This way, large numbers of these actuators can be produced which reduces unit cost. Also, because of the large number of actuators per airplane it won't be necessary to design redundancy into each actuator, again lowering its cost.

Figure 4.60 illustrates a possible separate surface control system configuration.

4.3.3.4 Electromechanical flight control systems

Application of these systems has sofar been restricted to secondary flight controls. Flaps and trim systems frequently employ electromechanical actuators. Examples are shown in Section 4.5.

Figure 4.61 shows a potential system layout for an electromechanical flight control system.

4.3.4 Design Problems With Irreversible Flight Control Systems

Major problems associated with reversible flight controls are:

1. Complexity
2. Reliability
3. Redundancy
4. Cost
5. Accessibility for repairs
6. Susceptibility to lightning strikes in the case of electrically signalled systems

Major advantages associated with reversible flight control systems are:

1. Flexibility in combining pilot control commands with automatic control commands

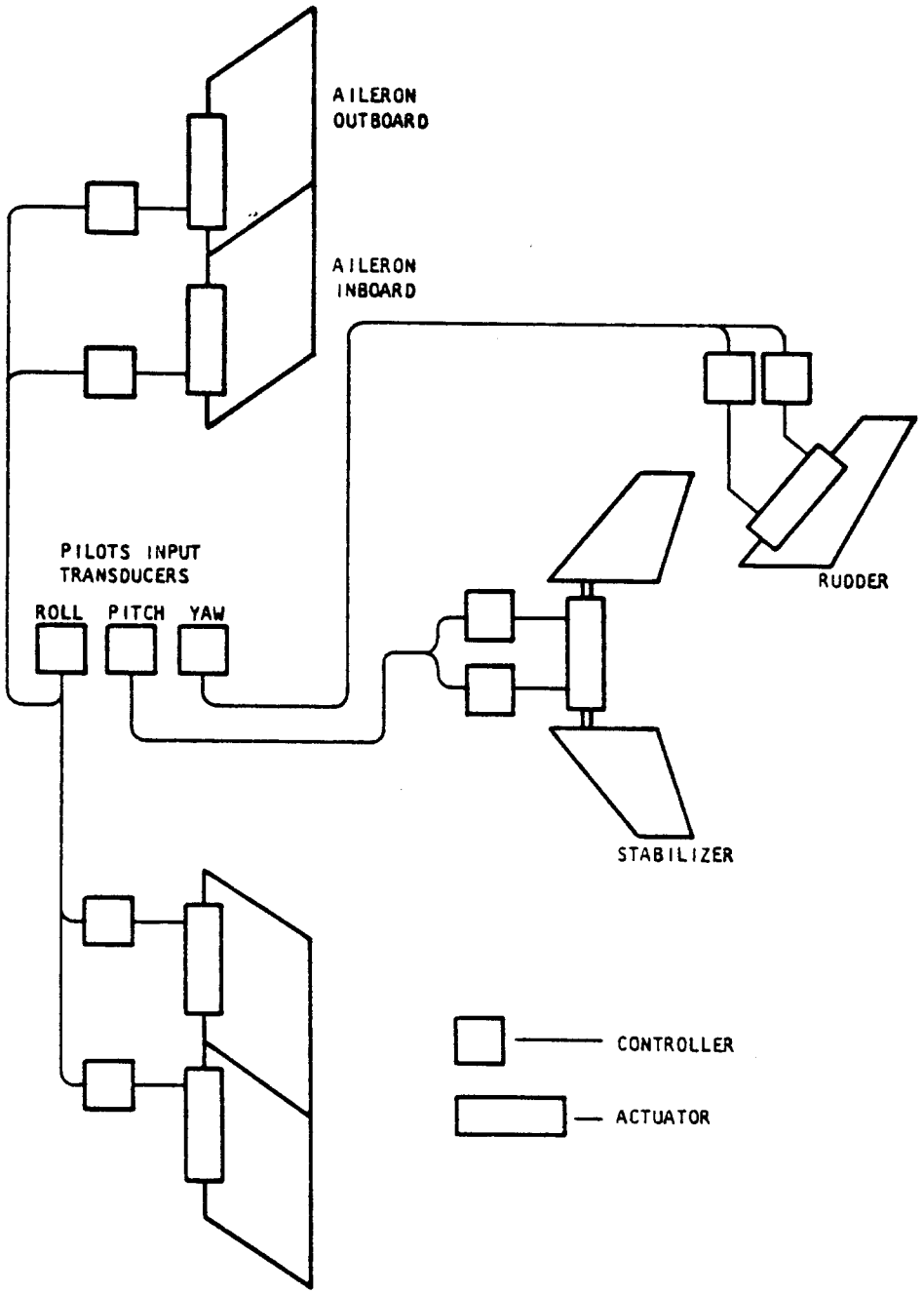

Figure 4.61 Proposed Schematic for an Electromechanical Flight Control System for a Fighter

2. Ability to tailor handling qualities

3. Potential of lower weight, particularly if electrical and/or optical signalling is used.

In the design and development of irreversible systems key roles are played by the following design considerations:

A. Reliability of all system components and the resulting need for redundancy.

B. Relative location of system components to assure that failures or damage induced by outside causes cannot cause total failure of the system.

C. Maintenance and accessibility.

It is useful to list a number of DO'S and DON'TS with regard to the layout design of irreversible flight controls:

DO'S:

Actuators: should be located at the aerodynamic surface controls such that maximum system stiffness is attained.

should be located such that inspection, maintenance and removal can be easily carried out.

DON'TS:

Actuator signal paths:

do not locate redundant signal paths close together. Closeness invites disaster due to such causes as: engine component disintegration, propeller blade separation, local structural failure due failure of another system, terrorist action or combat damage.

do not locate the signal paths so that lightning strikes can cause the system to fail.

4.3.5 Control Routing Through Folding Joints

Carrier based airplanes and some cargo airplanes require folding joints in wing, empennage or fuselage. Control routing through wing joints is discussed in Part III, Section 4.3. Figure 4.62 shows a typical folding

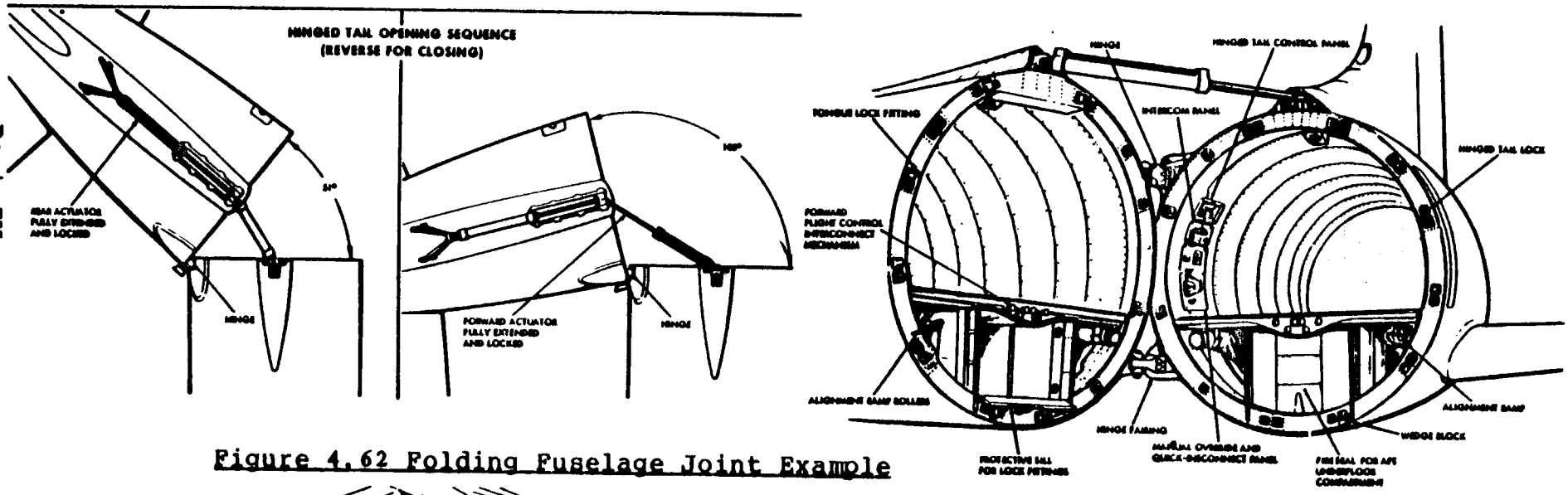

Figure 4.62 Folding Fuselage Joint Example

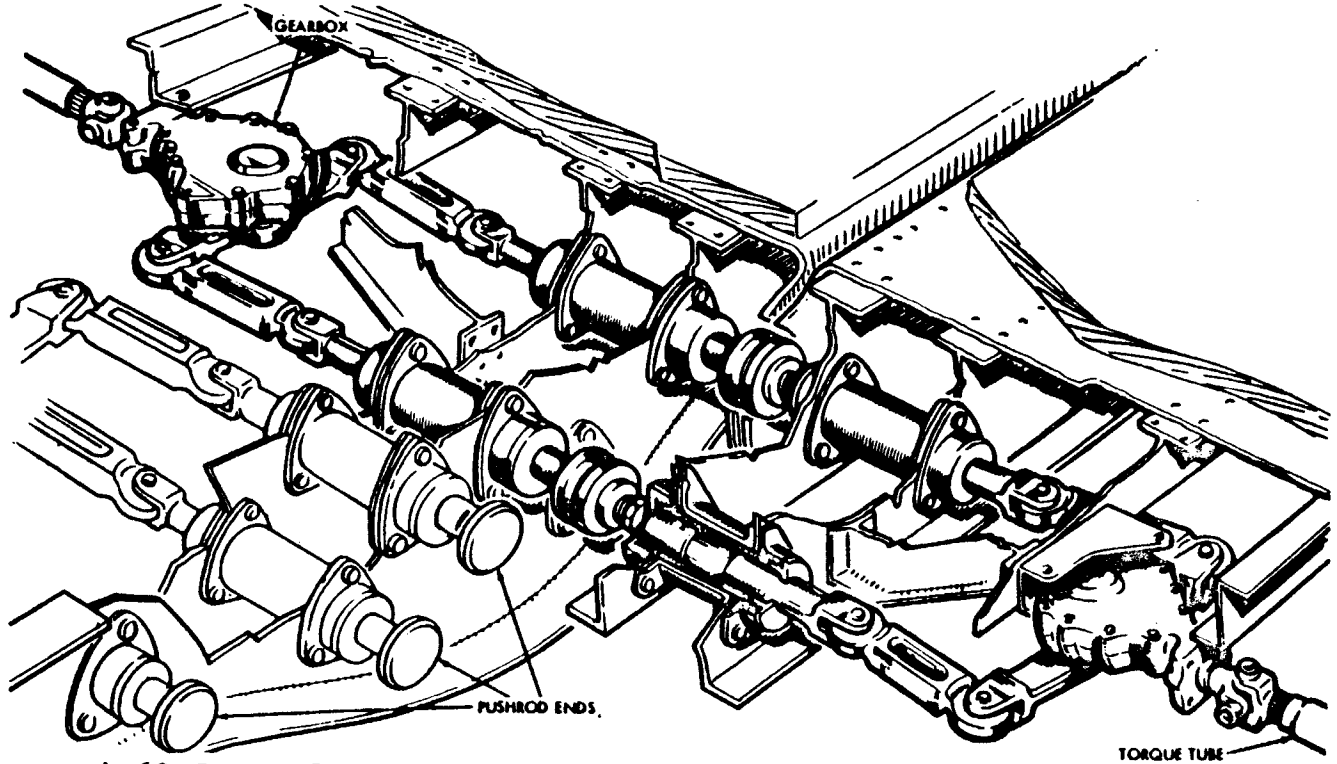

Figure 4.63 Control Routing Through the Folding Fuselage Joint of Figure 4.62

fuselage joint. The control routing through this joint is shown in Figure 4.63.

4.3.6 Iron Birds

To ensure the proper operation of complex flight control systems it is highly desirable to construct a so-called Iron Bird. Such an iron bird represents a full scale working model of the entire flight control system. Actual components used in the airplane are also installed in this iron bird. Figure 4.64 shows an example of an iron bird. Any defects in the design of the flight control system can be relatively easily 'ironed' out in this manner.

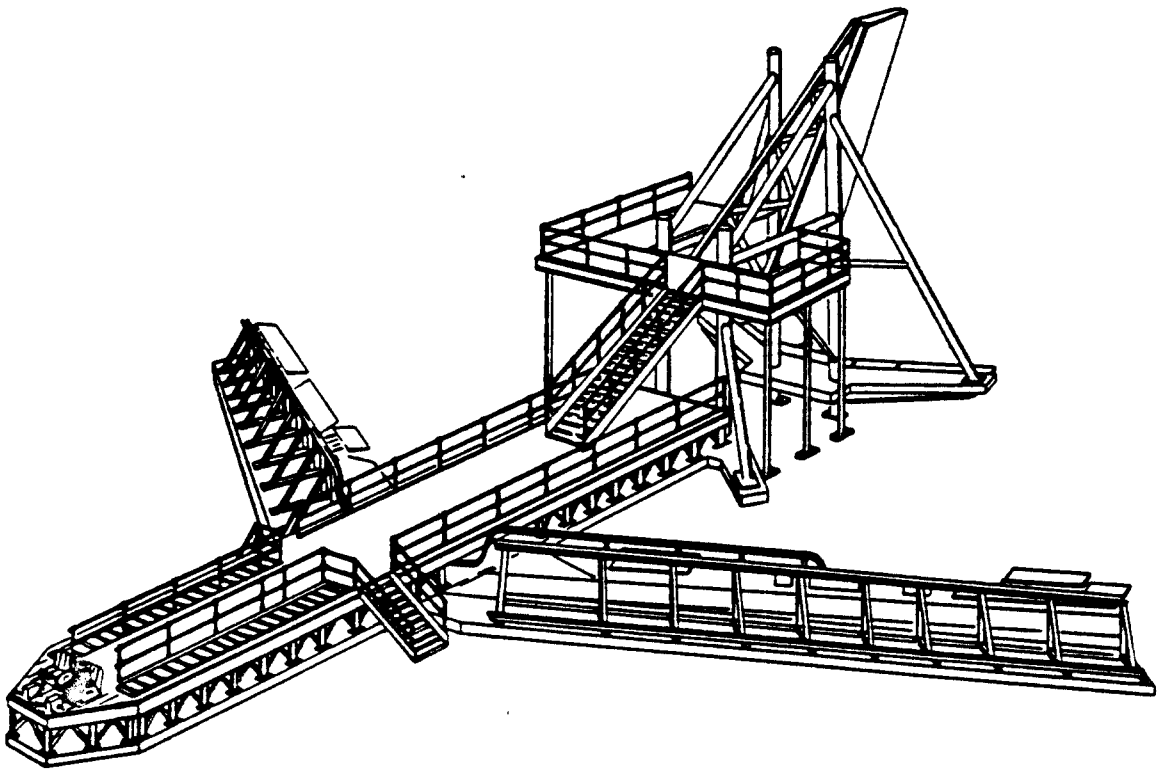

Figure 4.64 Iron Bird for Boeing 737

4.4 EXAMPLES OF IRREVERSIBLE FLIGHT CONTROL SYSTEMS

In this section a number of example layouts of irreversible flight control systems are presented as Figures 4.65 through 4.79. Commentary on these figures is given below.

==========

Figure 4.65 Flight Control Features: Boeing 767

The Boeing 767 has a hydraulically powered, mechanically signalled flight control system for all aerodynamic controls except the spoilers. The spoilers are hydraulically powered but signalled by a fly-by-wire system.

Hydraulic power is provided by three independent systems. Two are powered by engine driven pumps, one by engine bleed-air. An emergency hydraulic power source is provided by a ram-air driven turbine (RAT). A description of the 767 hydraulic system is given in Chapter 6.

Figure 4.66 Control Surface Actuation: Boeing 767

Observe the redundancy in the actuator layout.

Figure 4.67 Aileron Control System: Boeing 767

The pilot lateral control inputs are translated into valve displacements in the central control actuators. If this system were to fail, an override is available: there is a direct mechanical link from the right control wheel to the aileron control actuators.

Each aileron is powered by two independent actuators. The distribution of hydraulic power to these actuators is indicated. Observe the lockout system for the outboard ailerons: this is necessary to prevent aileron/wing reversal at high speed. The lockout system is commanded by flap position.

The autopilot inputs to the aileron controls are routed to the central control actuators. These in turn signal the aileron actuators.

Figure 4.68 Spoiler Control System: Boeing 767

The spoilers are signalled by a fly-by-wire system using control wheel steering transducers. Logic circuits decide whether the spoilers are operated as lateral controls, as in-flight speedbrakes or as ground spoilers.

Note the emergency evacuation system spoiler over-

ride. This system lowers the spoilers when the emergency evacuation system is activated. This prevents the evacuation slides from being damaged by extended spoilers.

Figure 4.69 Elevator Control System: Boeing 767

Note that the primary elevator control circuit uses mechanical signalling. The autopilot flight control computer signals 3 autopilot actuators which in turn drive the mechanical system to signal the elevator actuators. Three autopilot actuators are required for Category 3A automatic landing operation.

Figure 4.70 Directional Control System: Boeing 767

The 767 uses a one-piece rudder driven by three independent actuators. The rudder pedals are mechanically connected to the actuator valves. The yaw dampers use two independent servos to signal the rudder servos.

Figure 4.71 Primary Flight Control System: McDD DC-10

The McDonnell-Douglas DC-10 employs a hydraulically powered, mechanically signalled flight control system. Note the split elevators and the split rudder. In the roll control axis, low speed and high speed ailerons are used (as in the 767) in addition to spoilers.

Hydraulic power is provided by three independent systems. Each system is powered by two engine driven pumps. One system also receives power from an electrically driven pump. This system allows control of the airplane if all engines were to fail.

Figure 4.72 Distribution of Hydraulic System Power to the Flight Controls

The distribution of hydraulic power to the flight controls was arranged to be able to cope with complete failure of two hydraulic systems.

Figure 4.73 Cockpit Flight Controls: McDD DC-10

Note the cable runs extending aft and below the cabin floor. Access to the control cables is from below.

Figure 4.74 Lateral Control System: McDD DC-10

Note that ALL lateral controls are mechanically signalled in this airplane. There is an electrical interconnect between the landing gear and the spoiler controls

to provide for ground speedbrake operation.

The spoilers are used in a direct lift control mode with the flaps down. A mixing unit tells the spoilers which mode of operation is desired. This mixer unit is illustrated in Figure 4.75.

Figure 4.75 Aileron-Spoiler Mixer Unit: McDD DC-10

This unit decides the mode of operation of the aileron/spoiler combination. The unit is totally mechanical.

Figure 4.76 Elevator Control System: McDD DC-10

Note the direct link between the elevator cockpit control and the elevator control cables.

Pilot inputs to the elevator actuators are mechanical. Autopilot inputs to these actuators are electrical!

In an irreversible flight control system it is necessary to arrange for control force 'feel' artificially. This is done with the help of a control feel unit.

Figure 4.77 Control Feel Unit: McDD DC-10

This figure indicates schematically the types of input signals required to provide the pilot with the proper control-force/speed and control-force/'g' gradients.

Figure 4.78 Directional Control System: McDD DC-10

Note that the rudder is split into two parts, each driven by different hydraulic systems.

Figure 4.79 Control Surface Damper: McDD DC-10

In irreversible flight controls mass balancing of aerodynamic surface controls is not required as long as mechanical failure of the actuator is an extremely remote event. Whether or not it is depends on the design choices made in the actuator installation. If actuator failure were to occur, either mass balancing has to be included (to prevent flutter) or a control surface damper unit must be installed. The DC-10 uses control surface dampers. The Boeing 767 uses mass balancing as shown in Figure 4.69.

- Service-proven system and hardware concepts
- Fly-by-wire spoilers for system simplification
- Control wheel steering through autopilot for pilot workload reduction
- Maintenance improvements – less complex line replaceable units
- Control surfaces and actuators replaceable without rerigging control cable
- Faired position of control surfaces defined by permanent indices (except ailerons) – rigging pin positions are readily accessible
- Only one hydraulic system is disturbed when a flight control actuator is replaced on the airplane
- All spoiler control valves replaceable without actuator removed
- All autopilot and yaw damper servos replaceable with control surface actuators installed

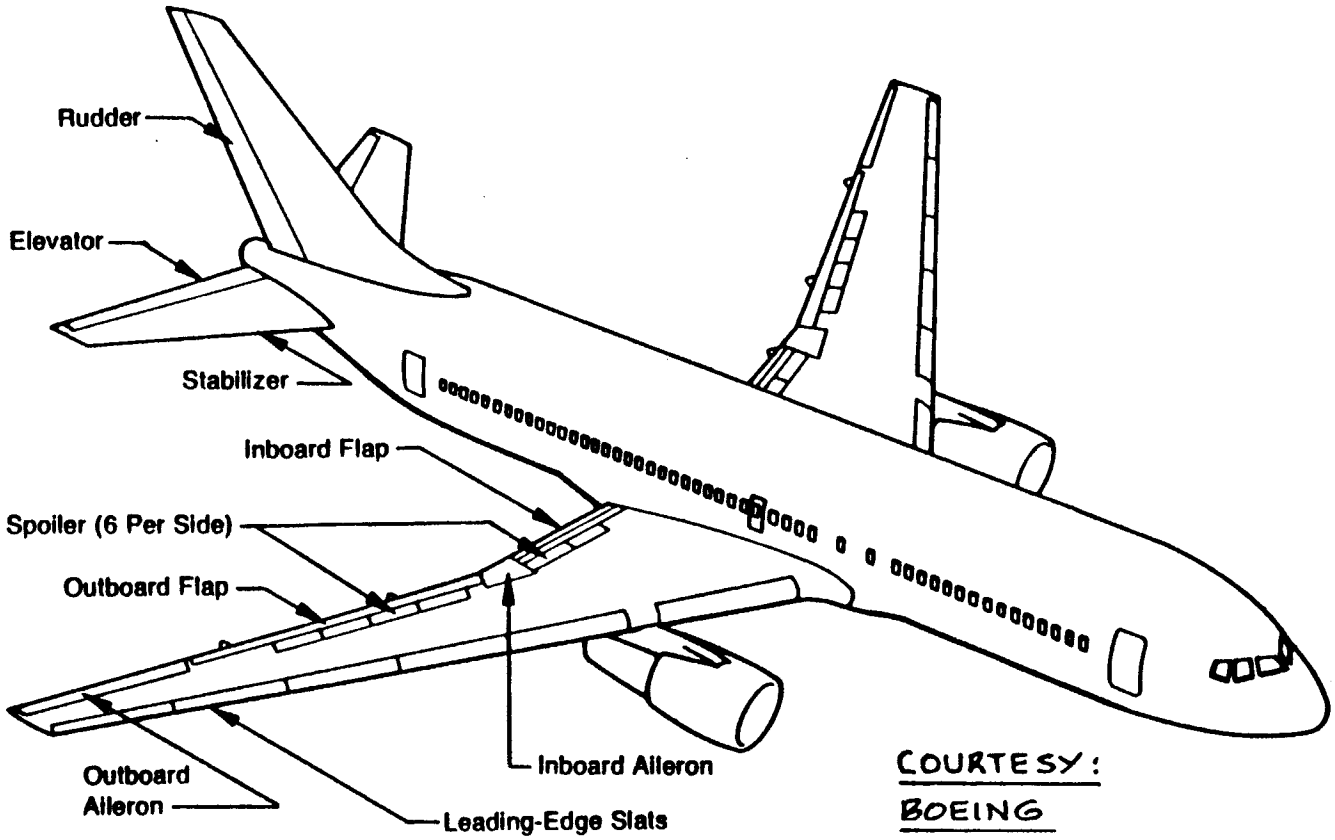

Figure 4.65 Flight Control Features: Boeing 767

COURTESY: BOEING

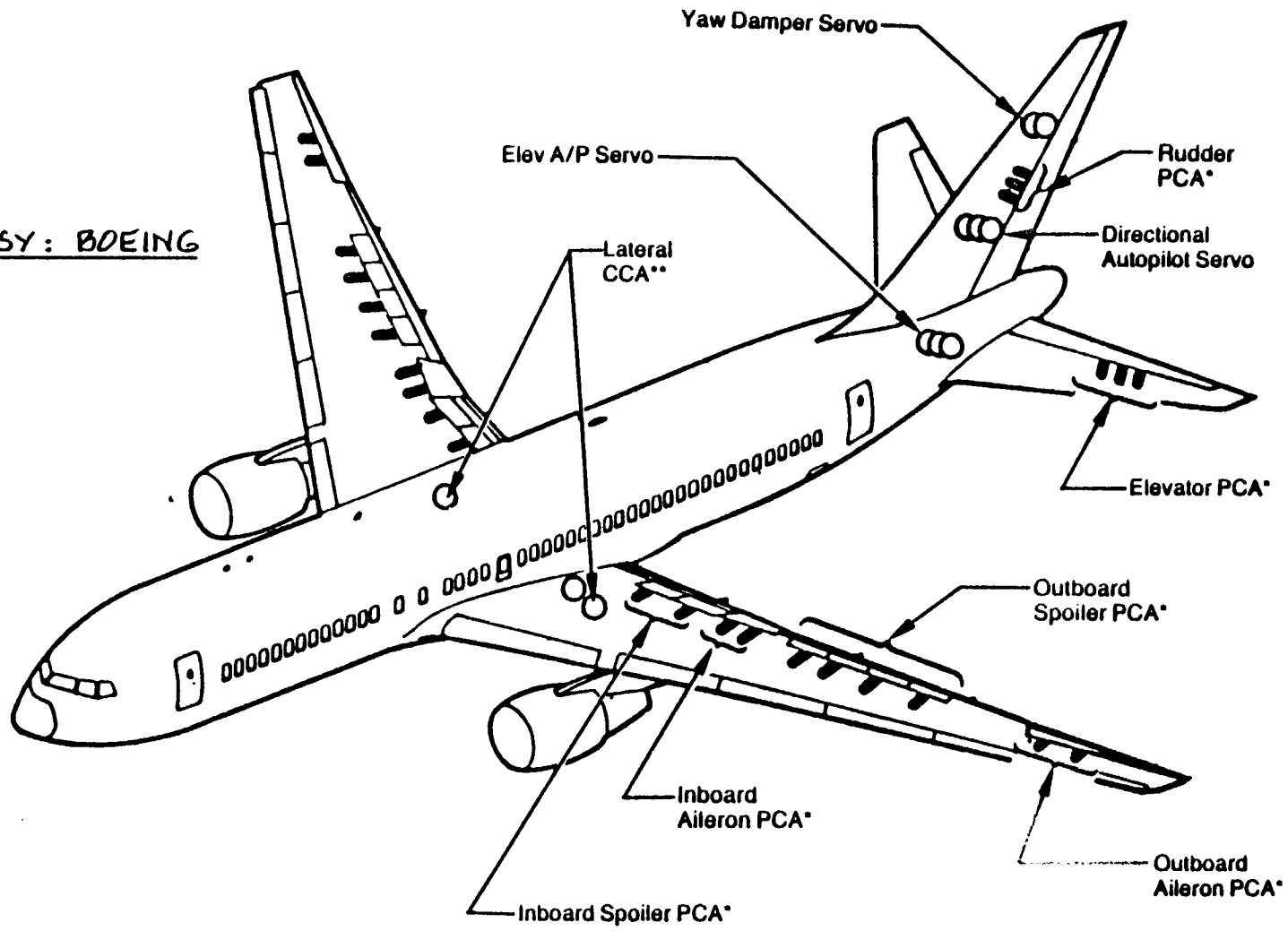

*PCA – Power Control Actuator
**CCA – Central Control Actuator

Figure 4.66 Control Surface Actuation: Boeing 767

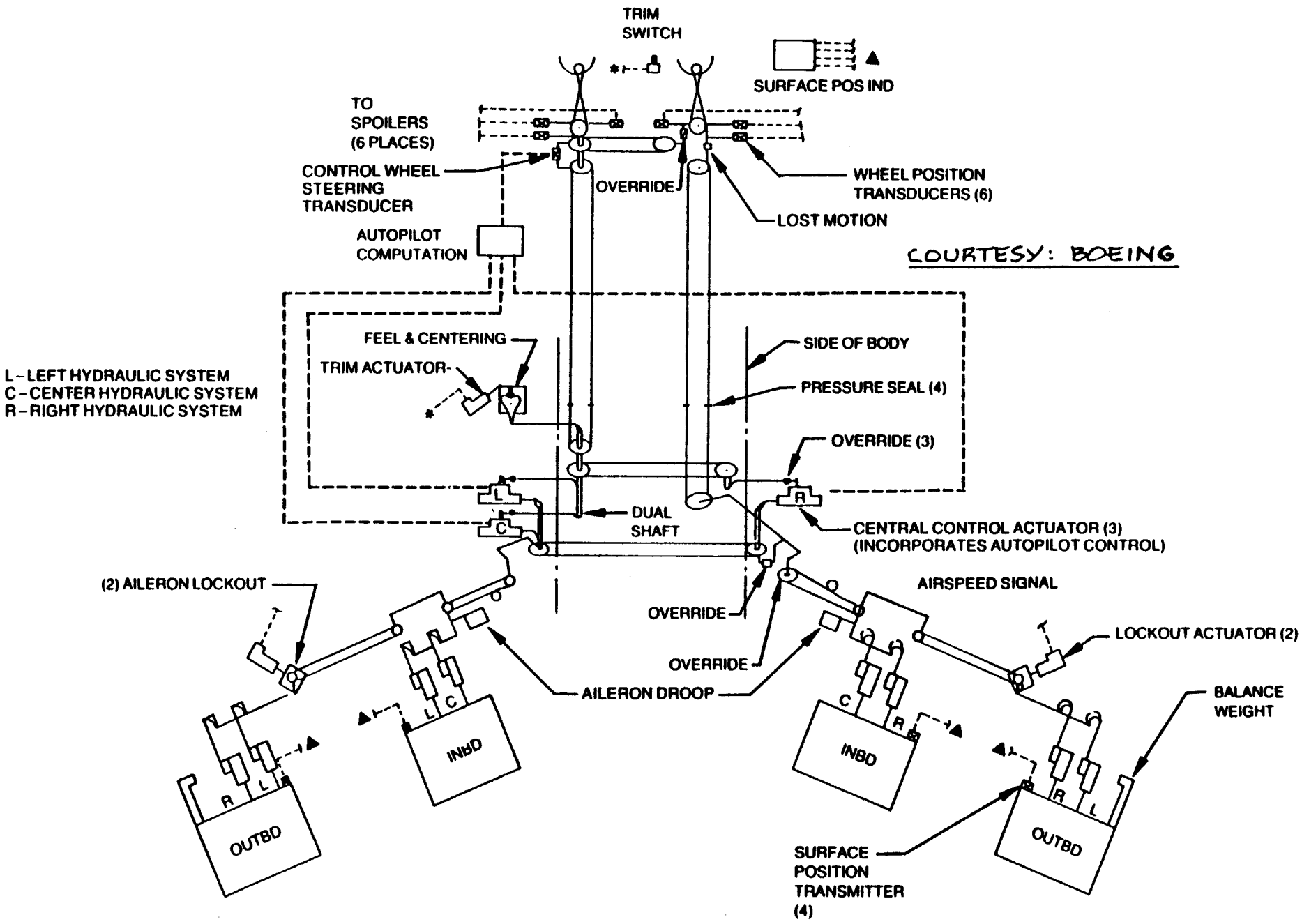

Figure 4.67 Aileron Control System: Boeing 767

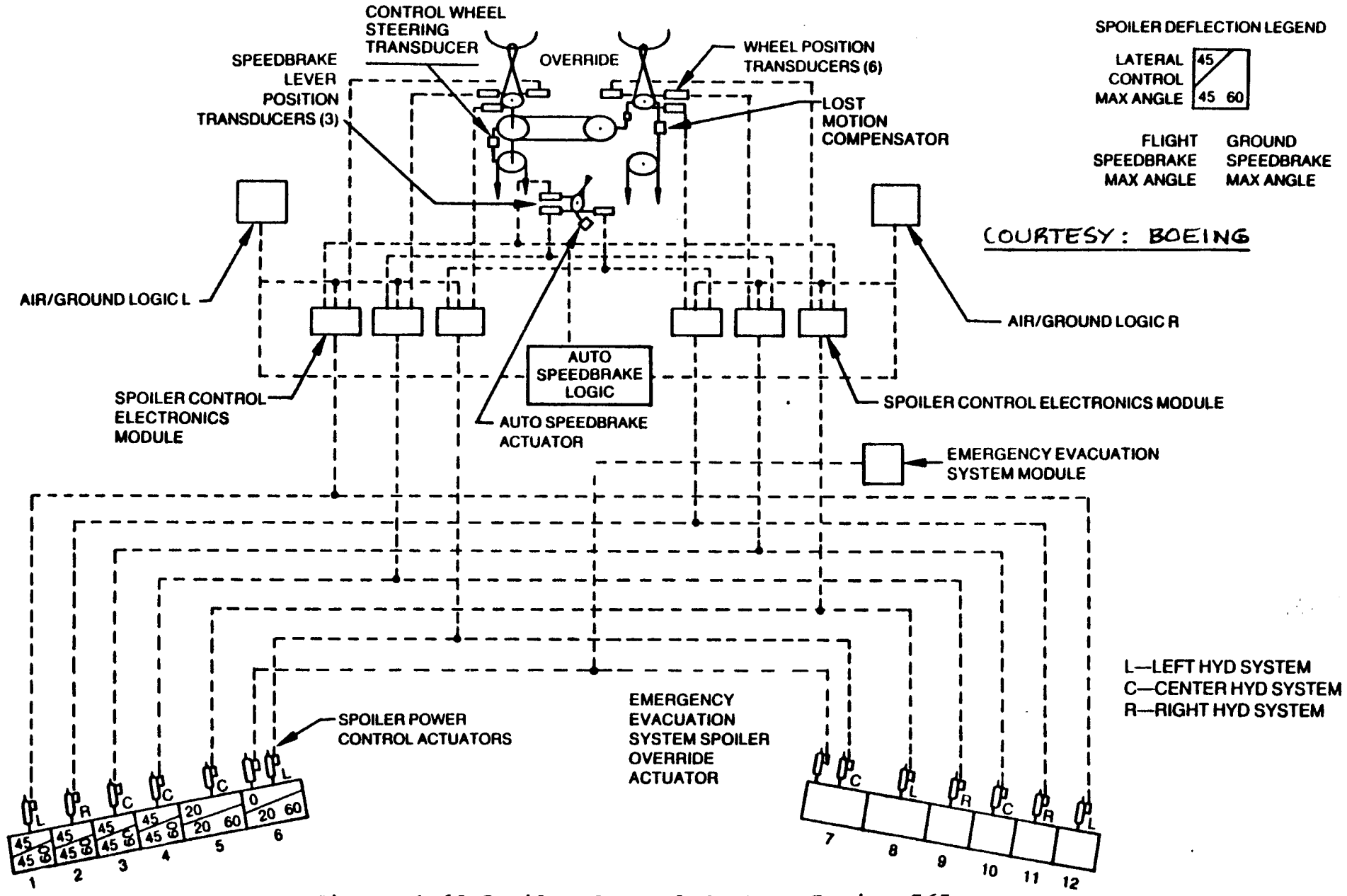

Figure 4.68 Spoiler Control System: Boeing 767

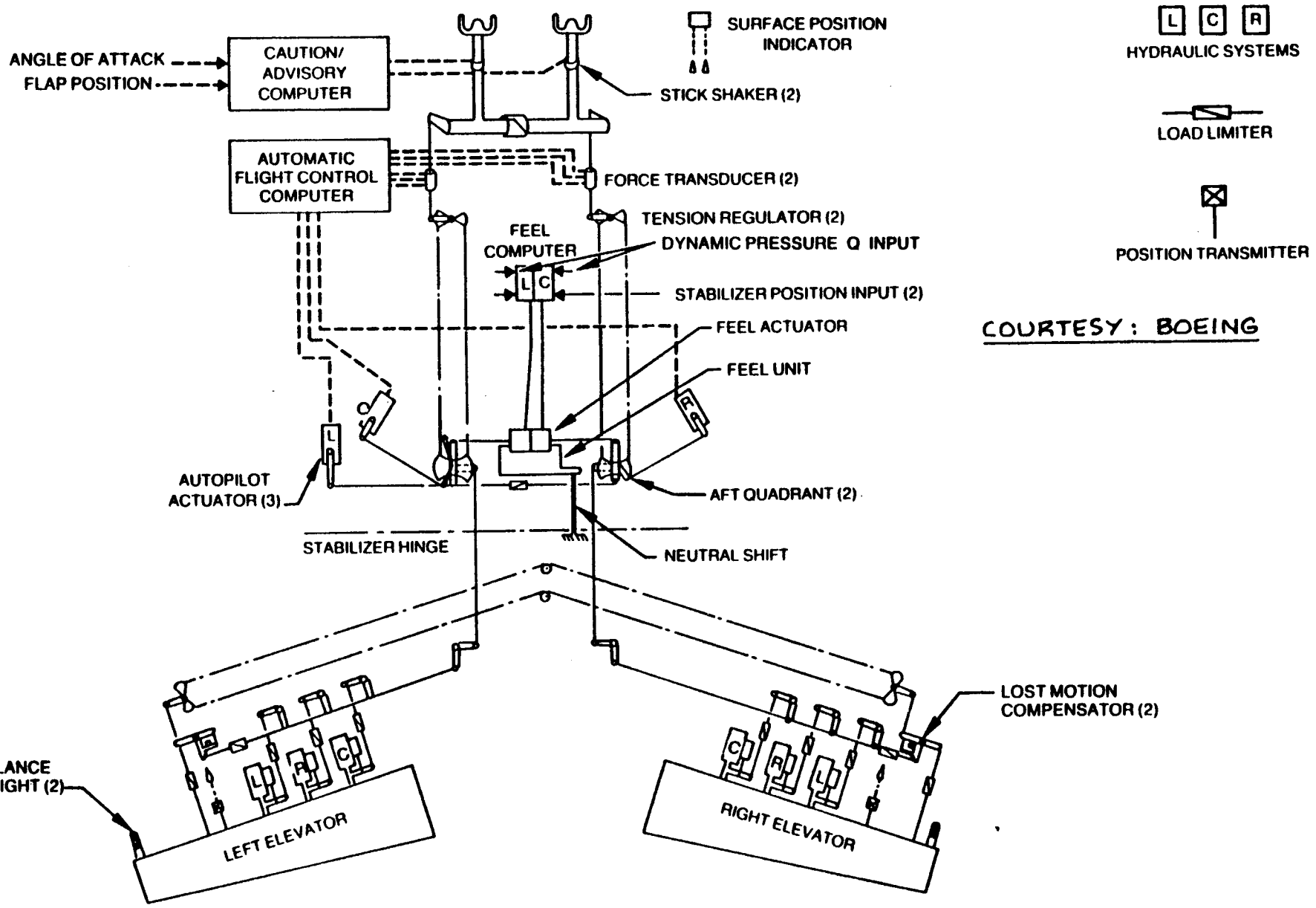

Figure 4.69 Elevator Control System: Boeing 767

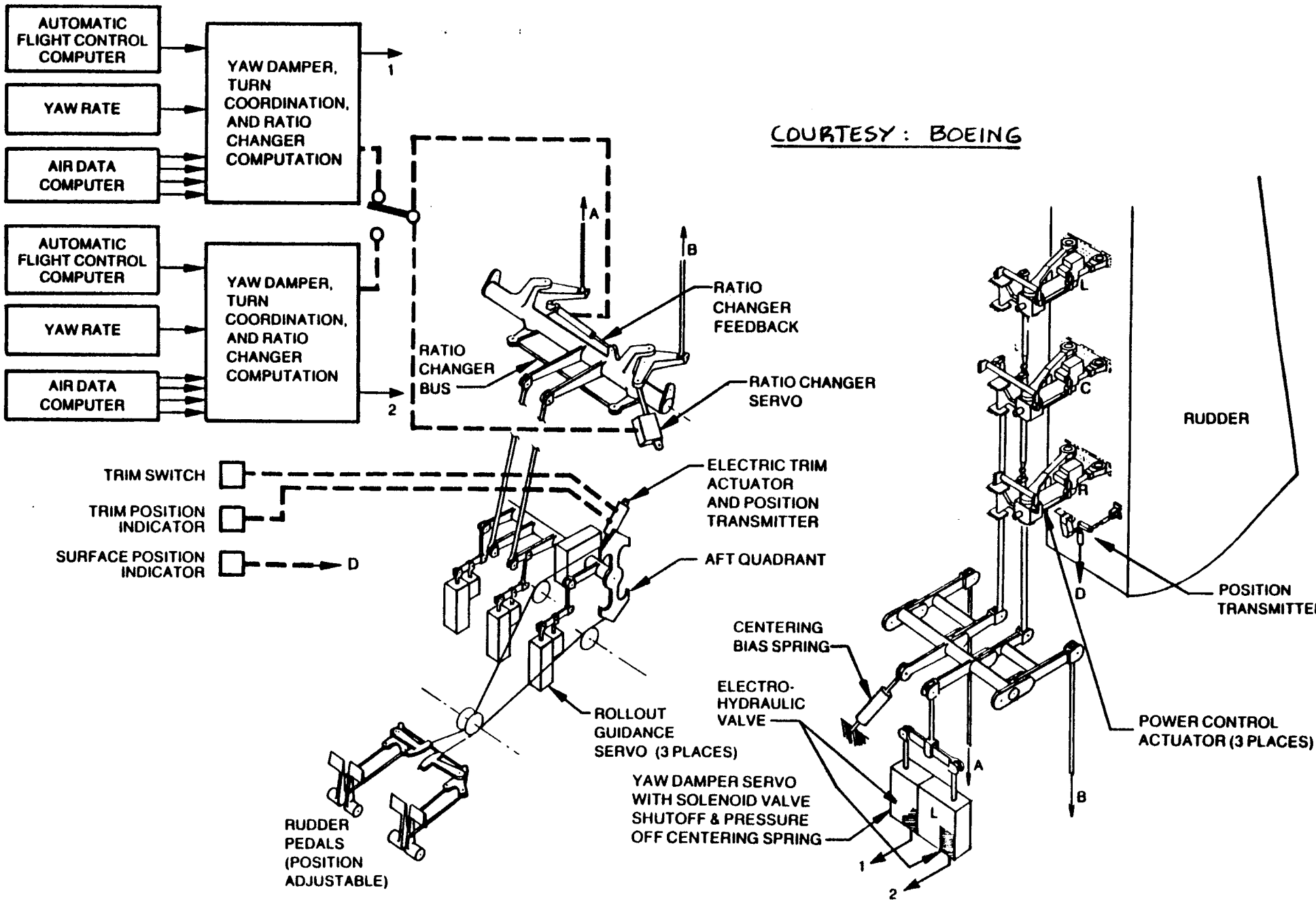

Figure 4.70 Directional Control System: Boeing 767

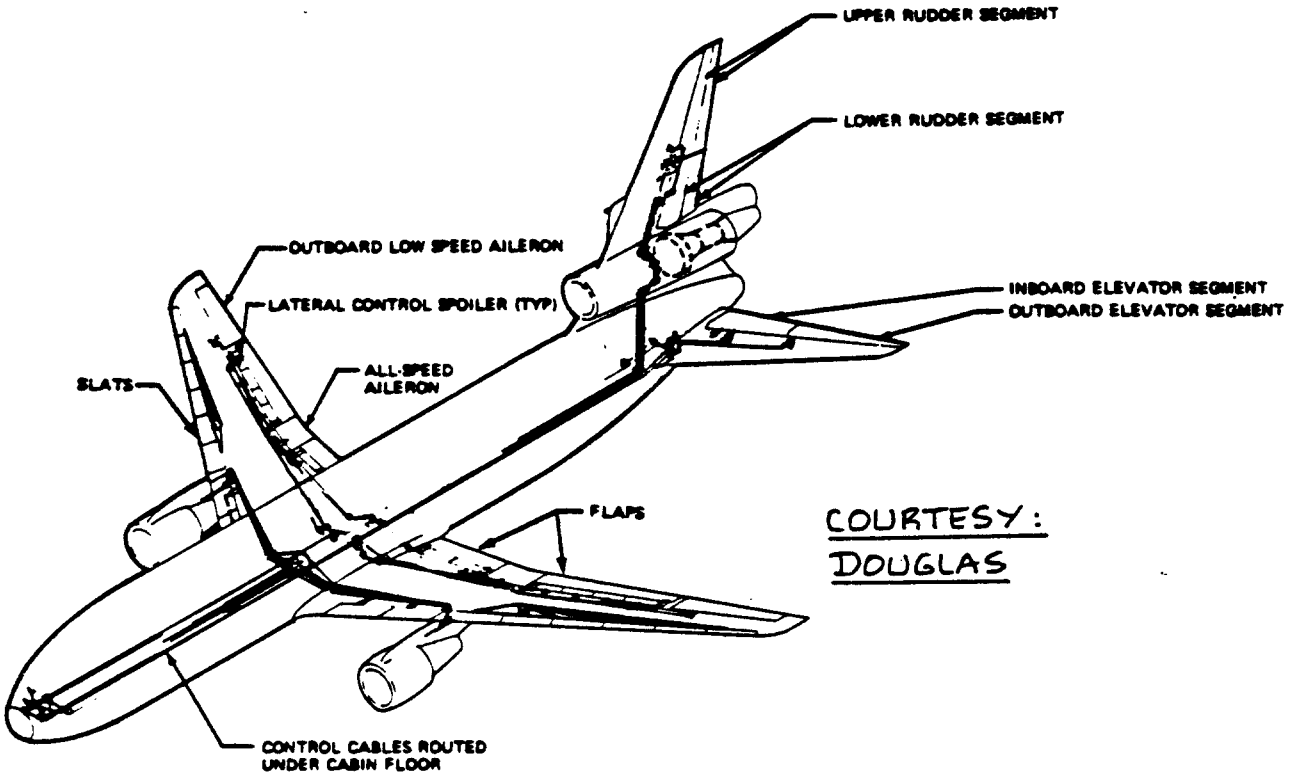

Figure 4.71 Primary Flight Control System: McDD DC-10

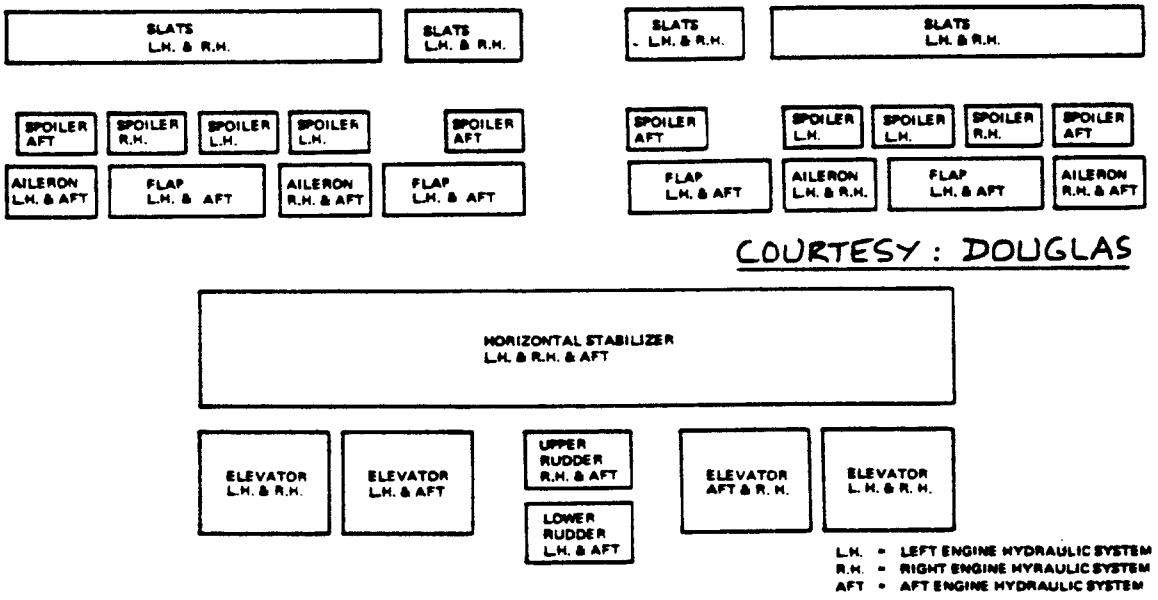

Figure 4.72 Distribution of Hydraulic System Power to the Flight Controls: McDD DC-10

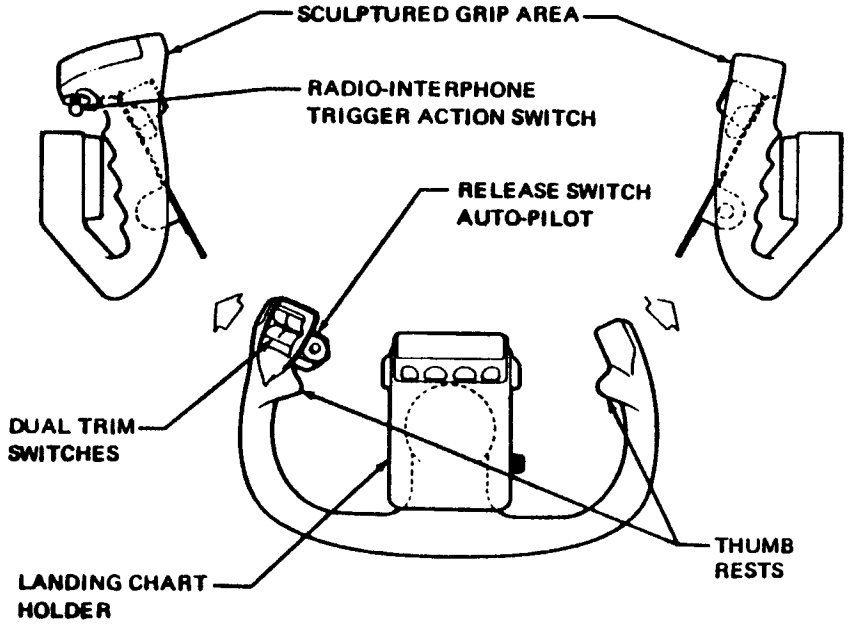

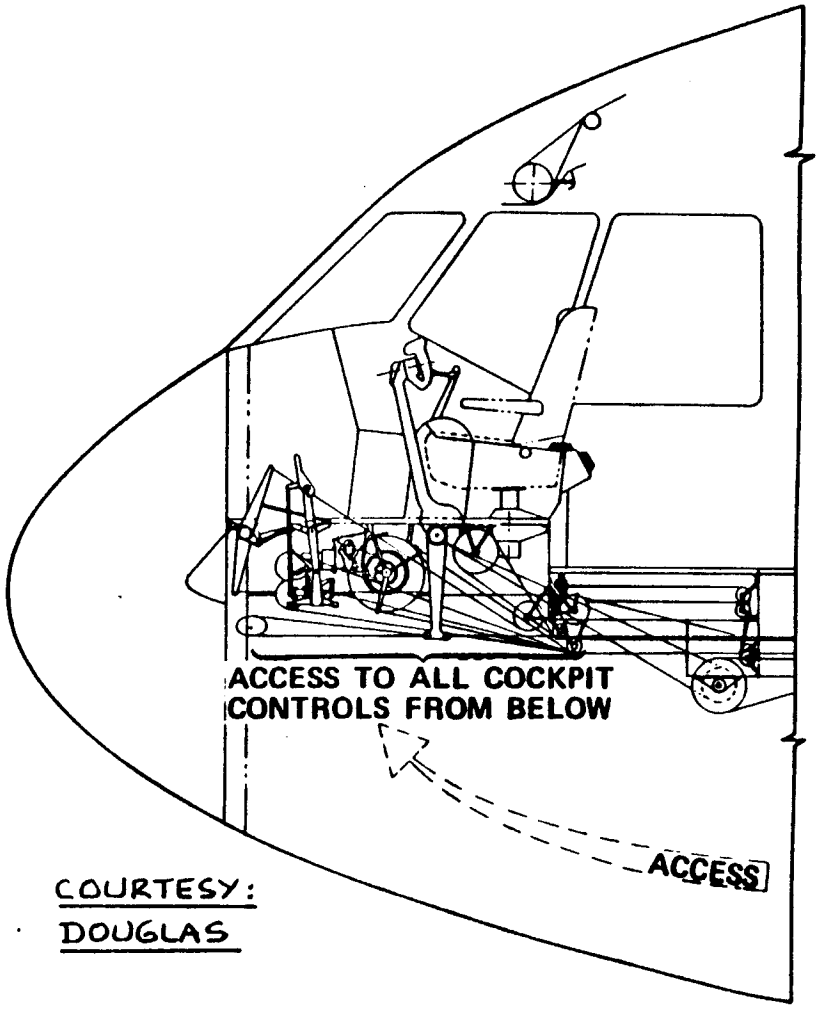

COURTESY: DOUGLAS

- Maximum utilization of properly designed and rigged closed-loop cable systems to provide long life, low friction, and adequate rigidity. Special cable tension regulators are not required.
- Use of carefully designed guards to prevent mechanical jamming
- Ample structural clearances on rotating or swinging parts of the control system
- Elevator, rudder, and lateral control systems provide instinctive override capability to protect against a jammed or runaway control.

Figure 4.73 Cockpit Flight Controls: McDD DC-10

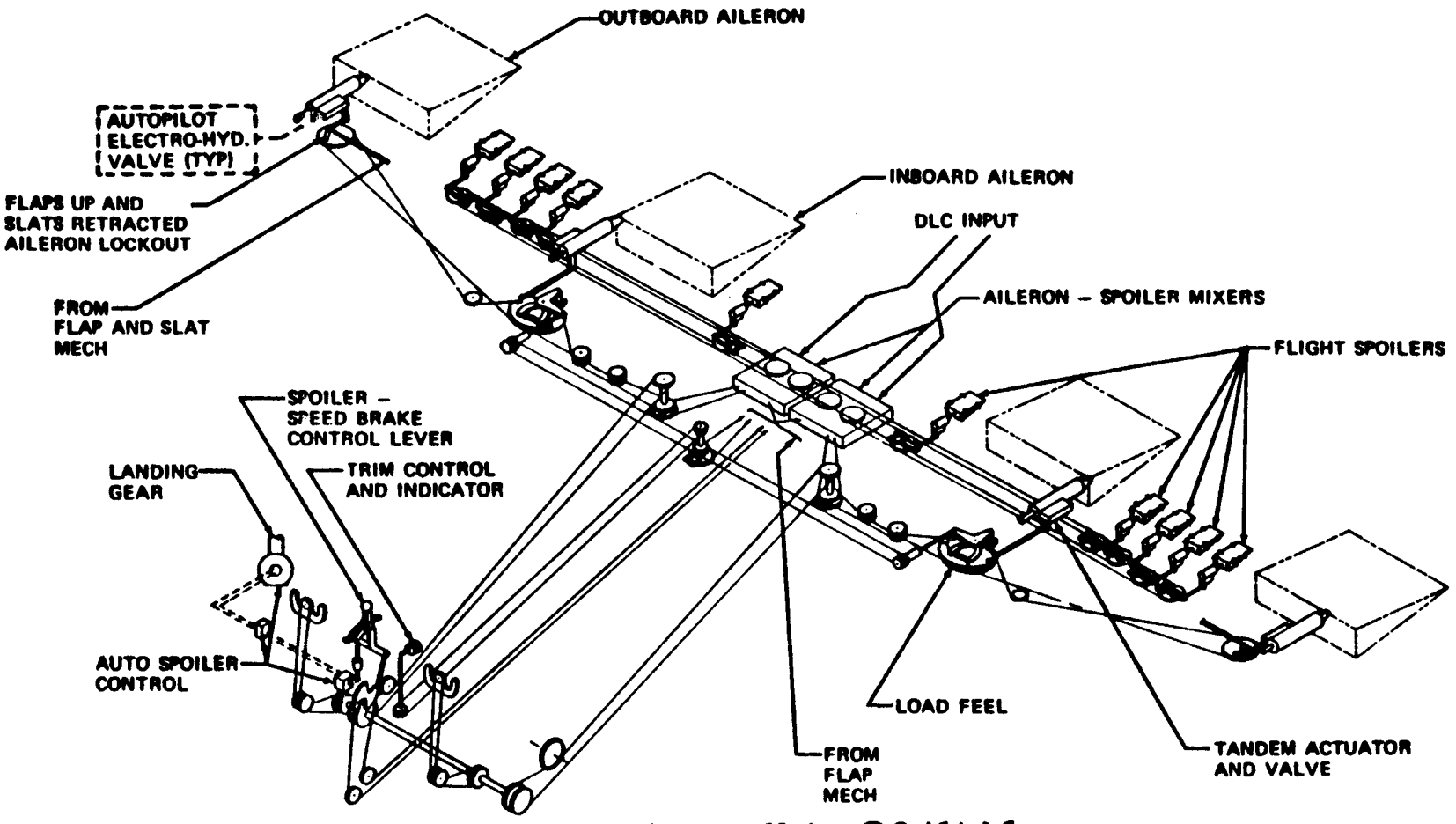

COURTESY : DOUGLAS

Figure 4.74 Lateral Control System: McDD DC-10

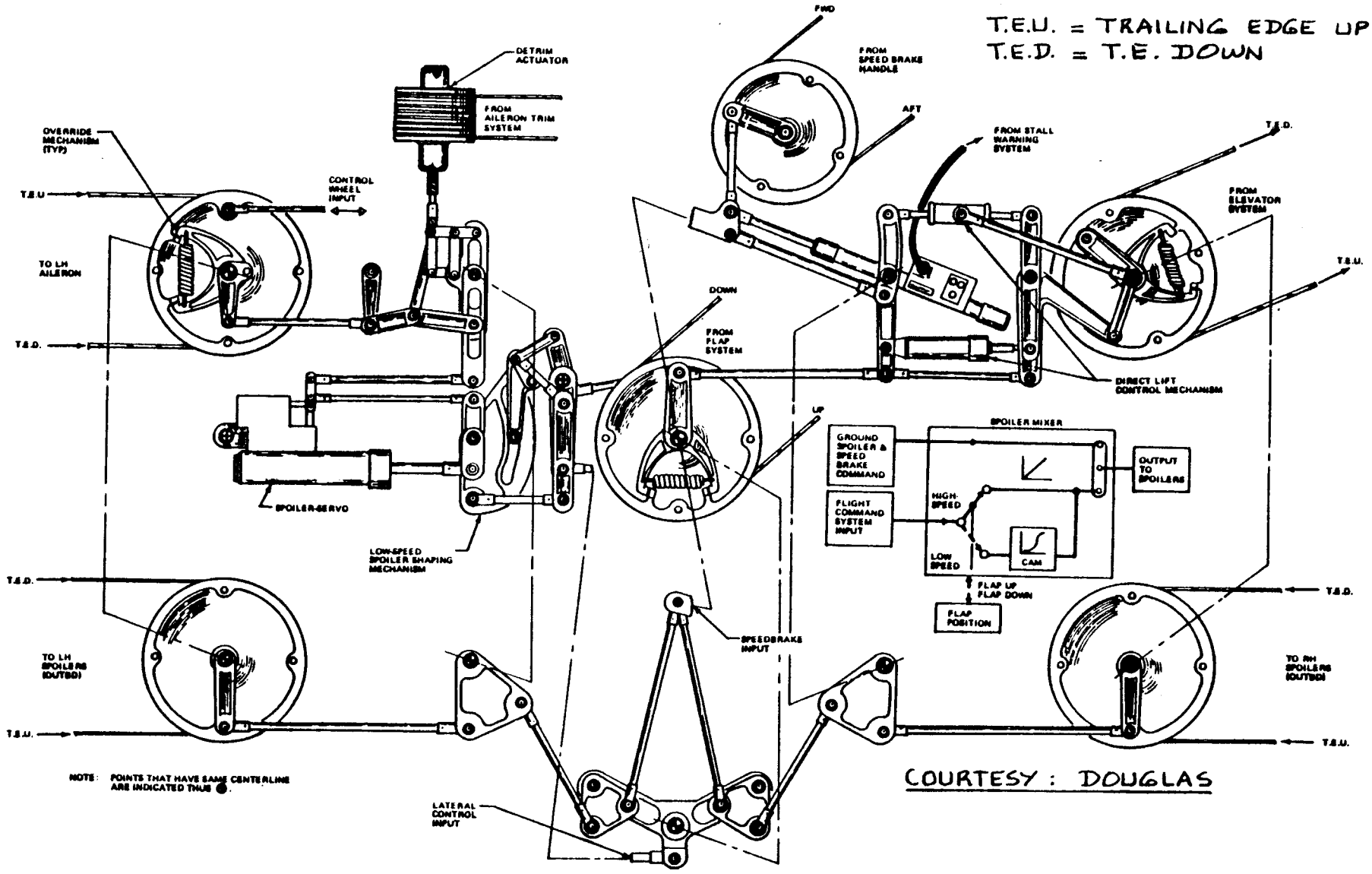

Figure 4.75 Aileron-Spoiler Mixer Unit: McDD DC-10

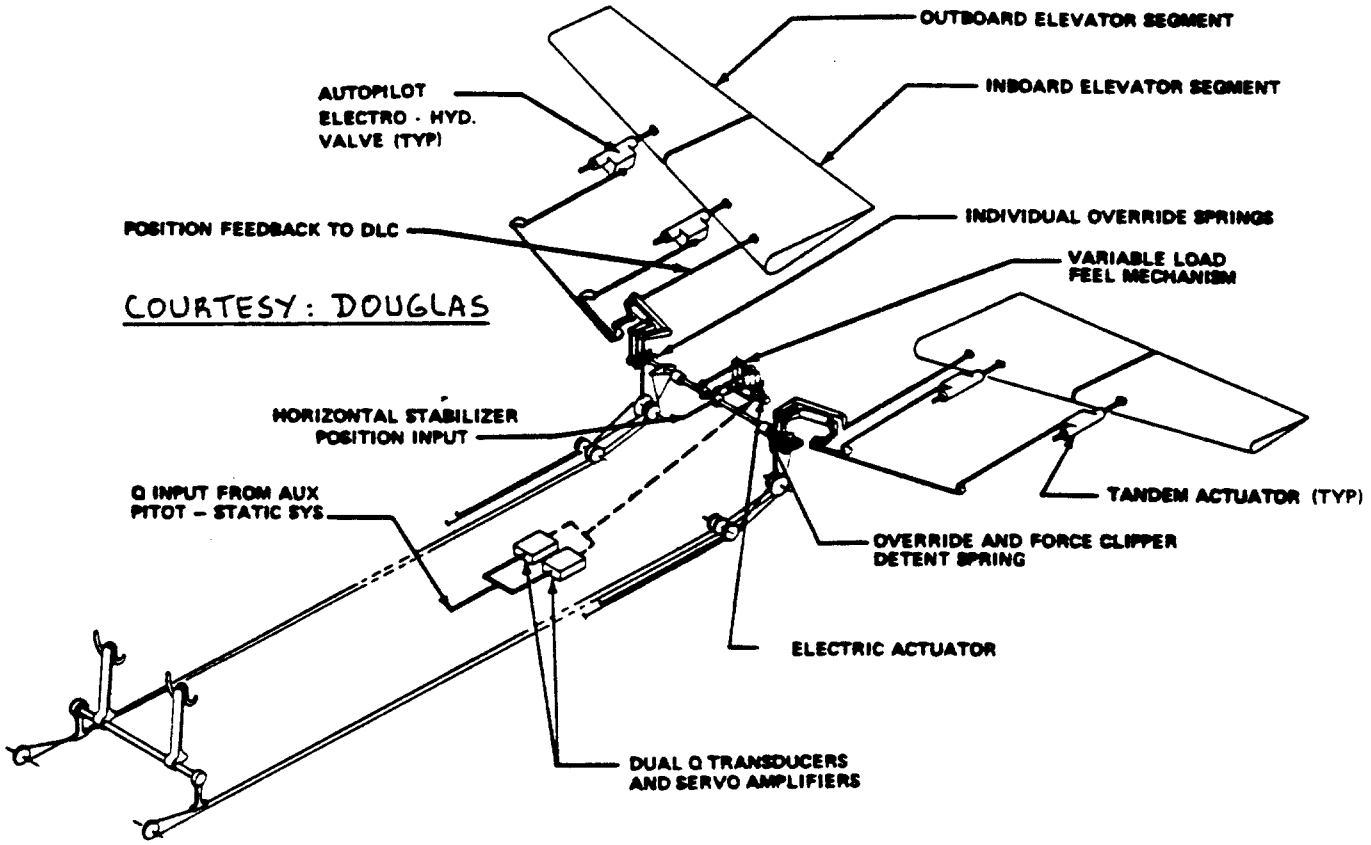

Figure 4.76 Elevator Control System: McDD DC-10

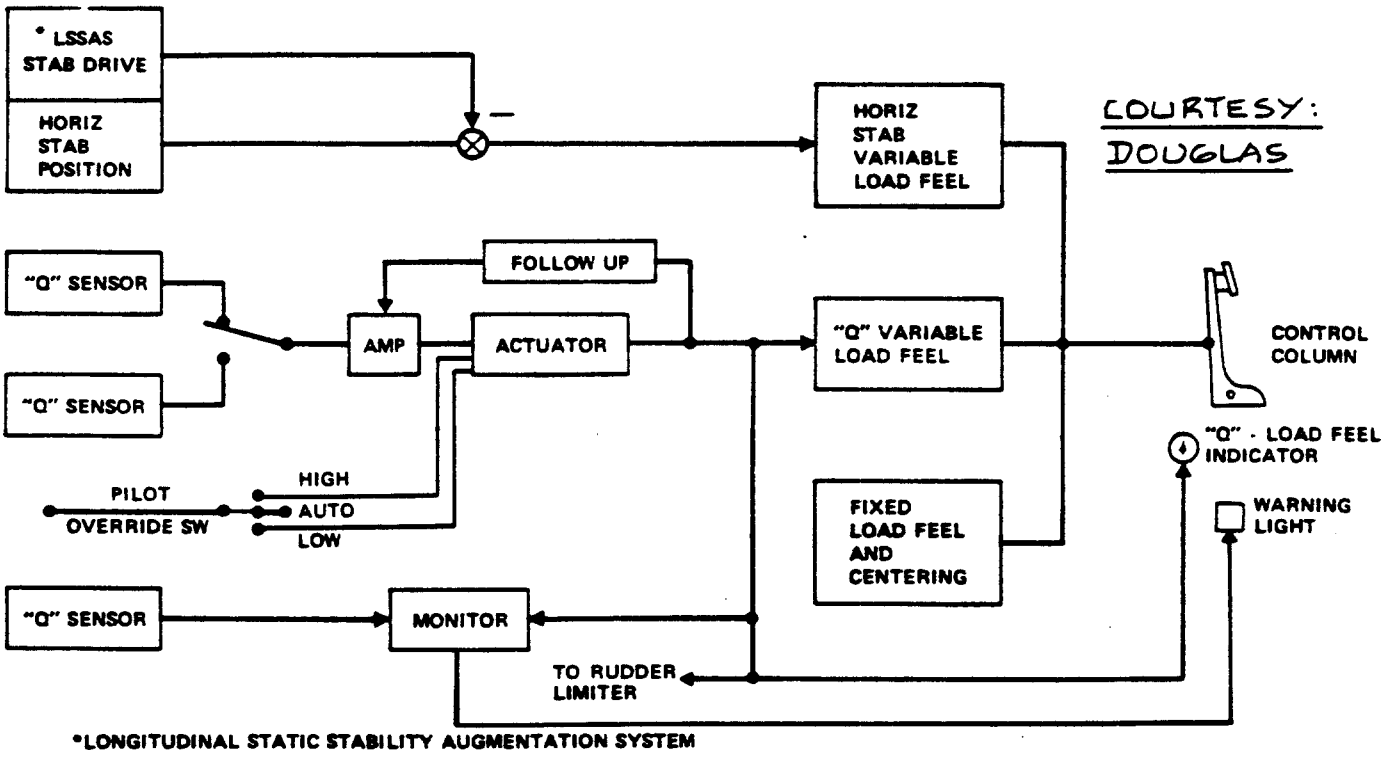

Figure 4.77 Control Feel Unit: McDD DC-10

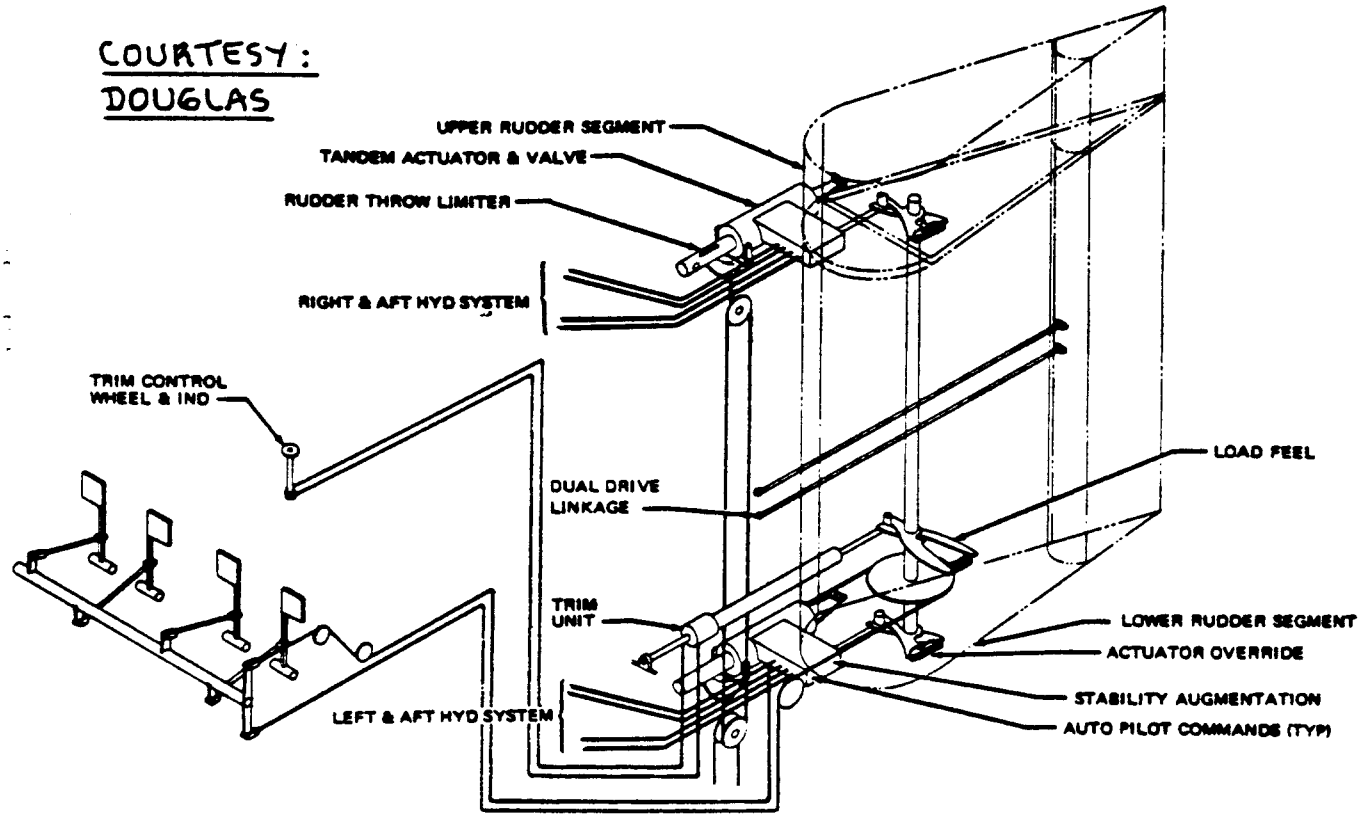

Figure 4.78 Directional Control System: McDD DC-10

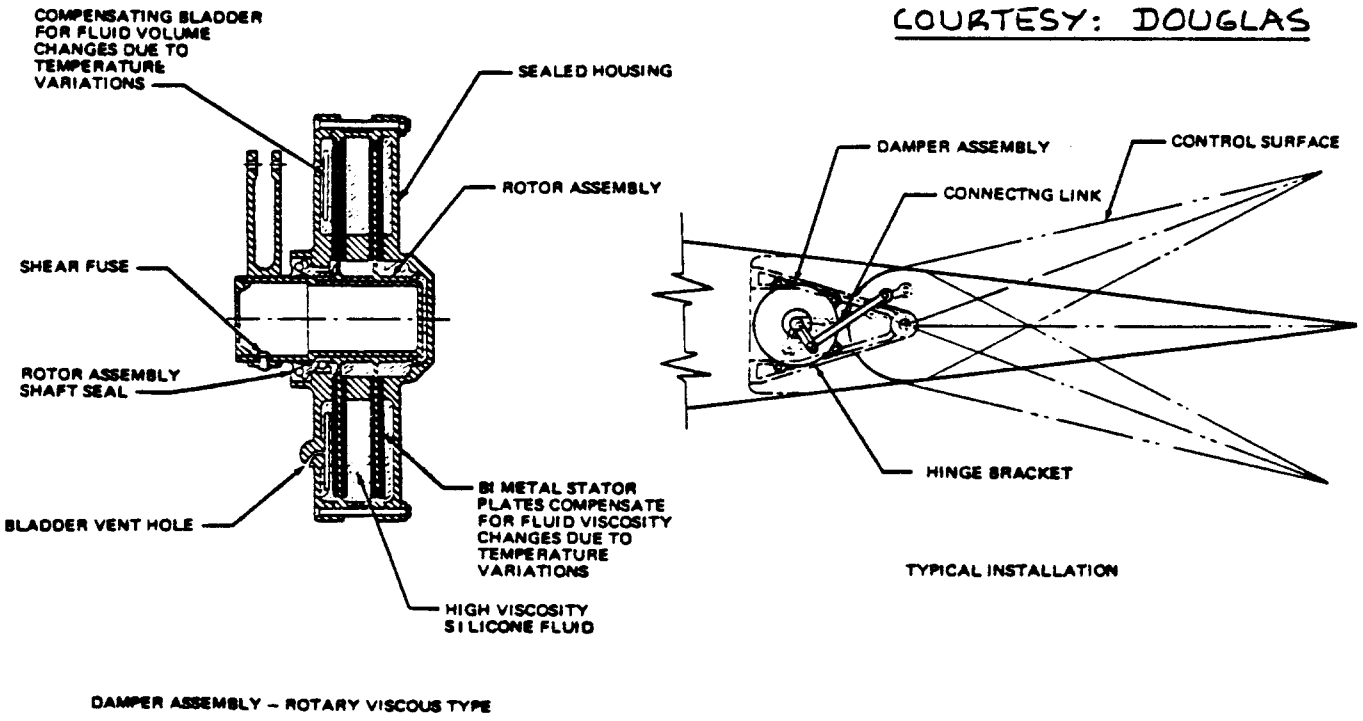

Figure 4.79 Control Surface Damper: McDD DC-10

4.5 TRIM SYSTEMS

A trim system helps the pilot maintain zero cockpit control forces in a given flight condition. In most airplanes it is desirable that cockpit control force trim can be maintained in nearly all flight conditions.

For a detailed discussion of the longitudinal and lateral-directional trim state of airplanes the reader should consult Chapter 5 of Ref.20.

Pilot force trim can be obtained as follows:

A) In reversible control systems by:

1. adding trim-tabs to the primary flight control surfaces. Figures 4.80 through 4.83 provide examples of trim tab systems.

2. the use of a variable incidence stabilizer. Figure 4.84 shows an example of a stabilizer trim system.

3. a trim-spring system as shown in Fig.4.24.

B) In an irreversible system the cockpit control forces are simulated by means of a so-called force-feel system. By nulling out the output of the force-feel system a trimmed condition can be obtained.

Figures 4.69 and 4.77 show examples of such control force feel systems.

CAUTION: In nearly all trim systems care must be taken that the airplane will not fly with the control surfaces in a so-called 'jack-knifed' condition. Figure 4.85 illustrates a stabilizer/elevator combination in a 'jack-knifed' position. Such jack-knifing of the controls leads to extra drag. Trading of elevator angle for stabilizer angle eliminates this problem.

In most jet transports the trim system is arranged to drive the stabilizer angle to prevent jack-knifing. Figures 4.86 and 4.87 show example trim systems used in typical jet transports.

Notes: 1. Trim systems are nearly always mechanized as irreversible systems. They are either powered or unpowered.

2. If trim systems are powered (electrical or hydraulic) redundancy must be provided: run-away trim deflections can cause loss of control.

3. Figs 4.80 - 4.83 show examples of unpowered trim systems: redundancy is not needed.

4. Figs 4.84, 4.86 and 4.87 show examples of powered trim systems. Redundancy is required by Refs 21 and 22. In addition, 'trim-in-motion' indicators are required in the cockpit.

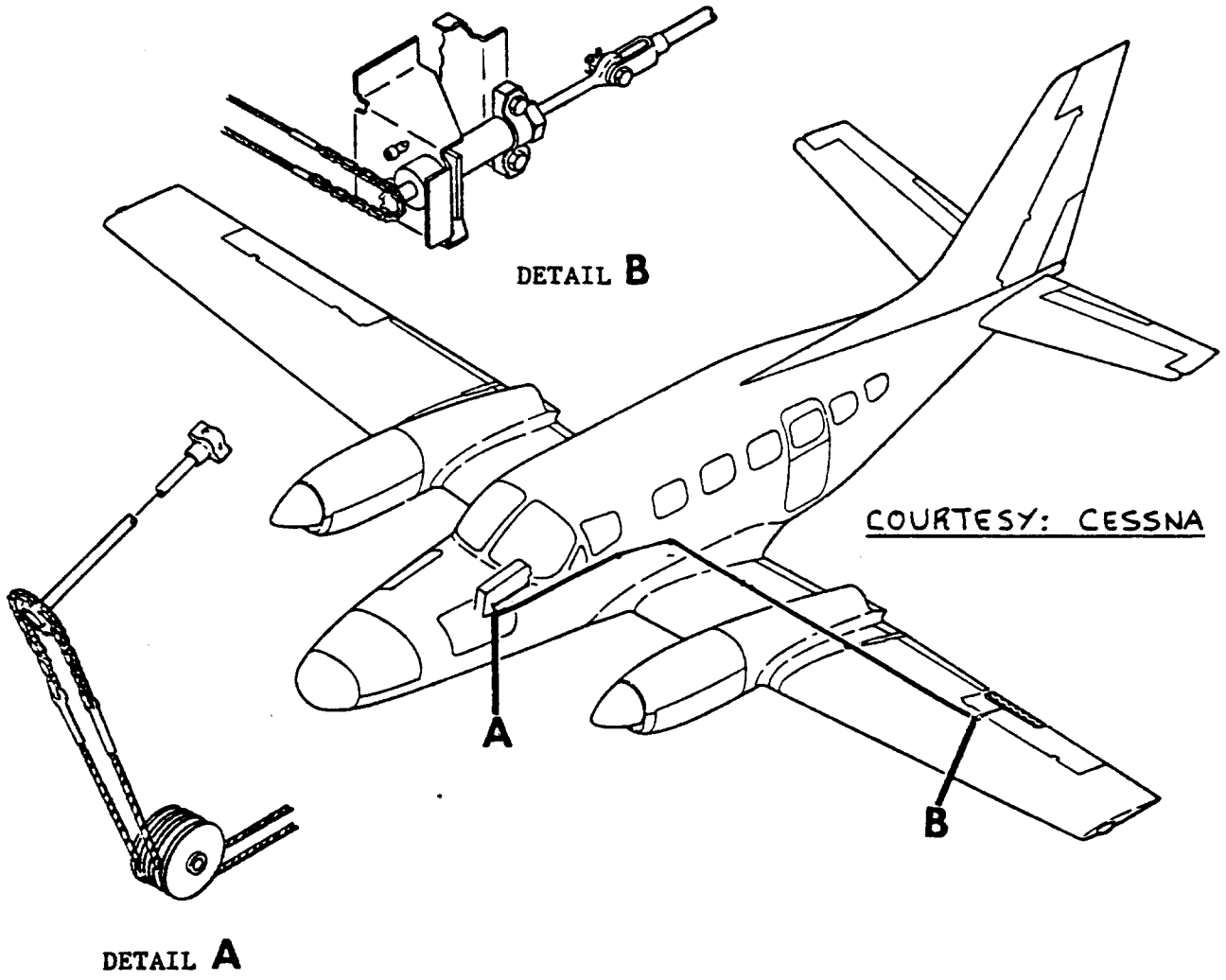

Figure 4.80 Aileron Trim System: Cessna 441

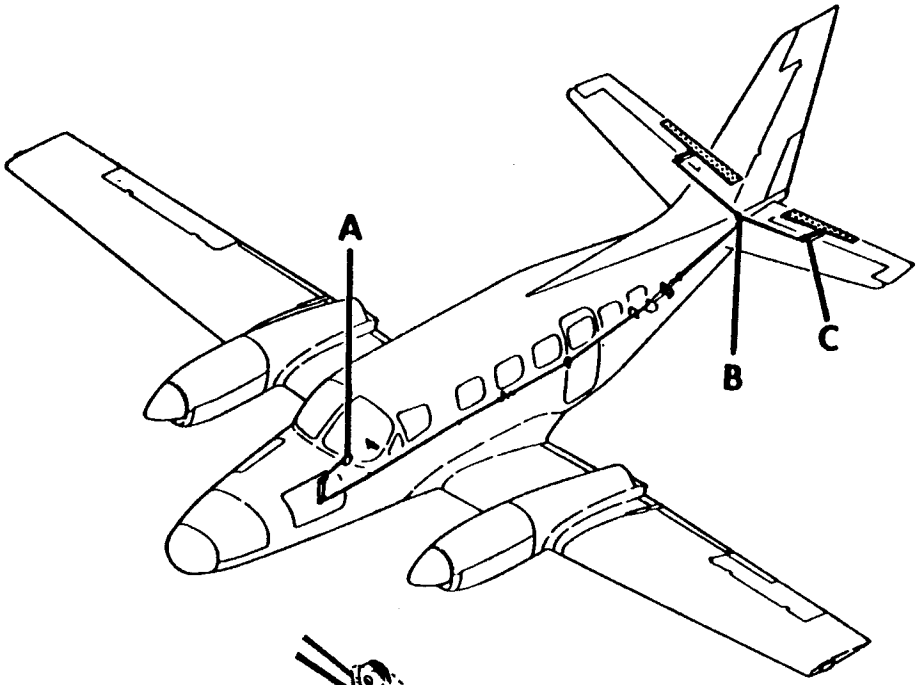

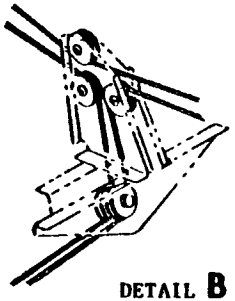

COURTESY: CESSNA

DETAIL B

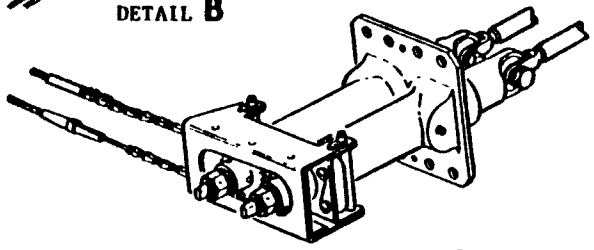

DETAIL C

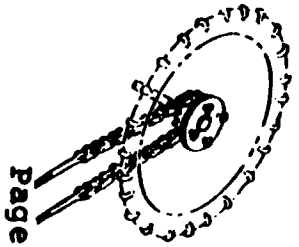

DETAIL A

Figure 4.81 Elevator Trim System: Cessna 441

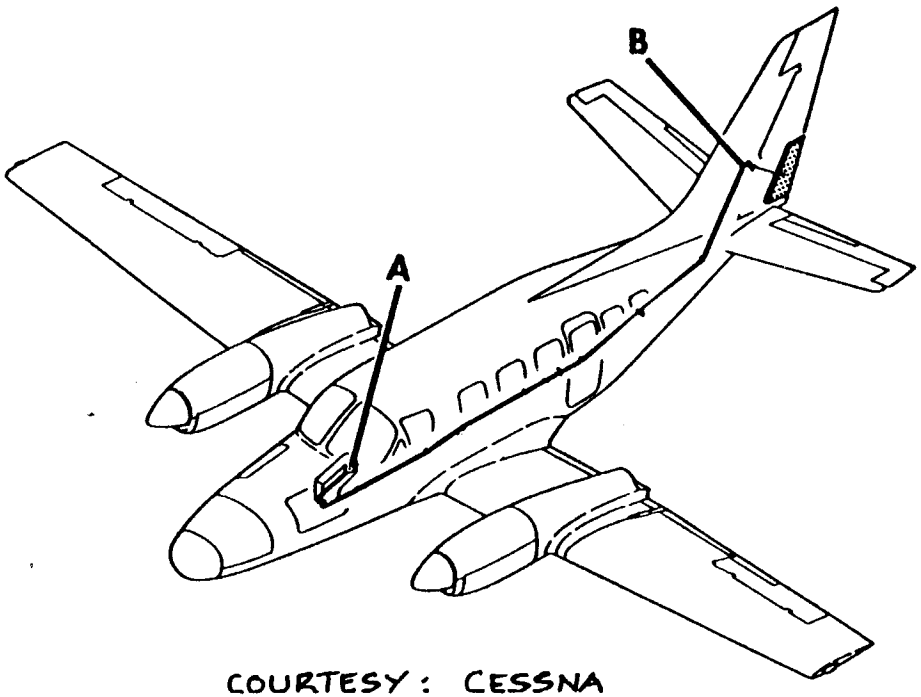

COURTESY: CESSNA

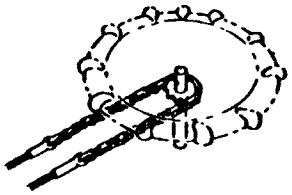

DETAIL A

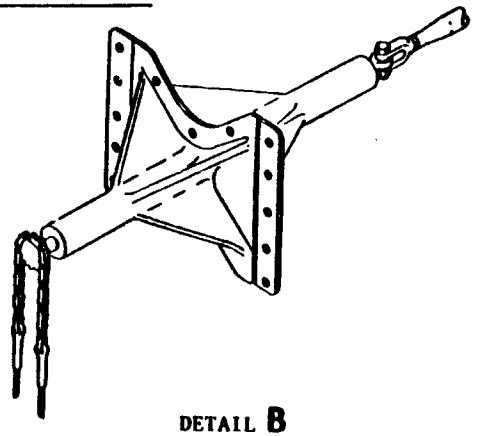

DETAIL B

Figure 4.82 Rudder Trim System: Cessna 441

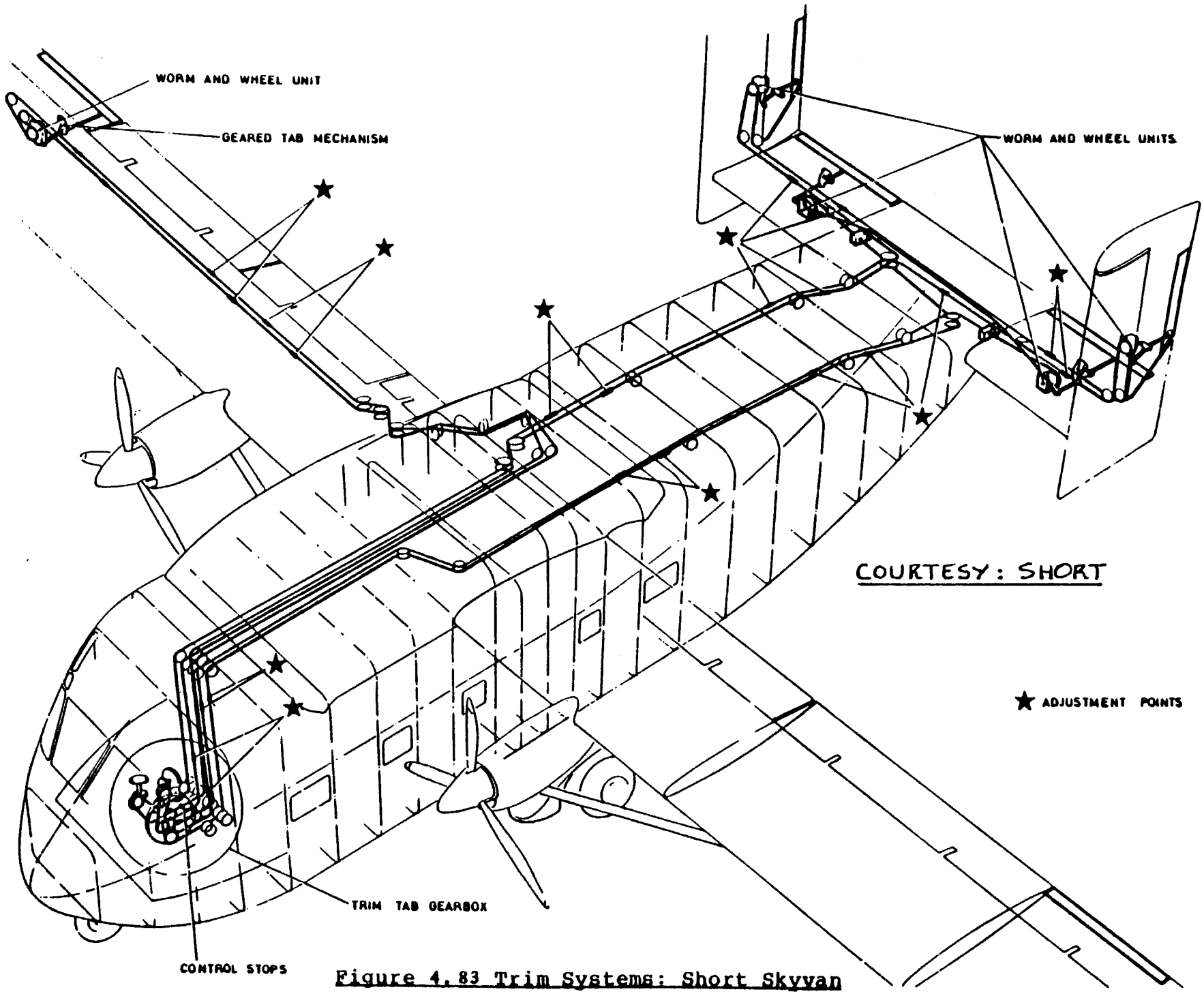

Figure 4.83 Trim Systems: Short Skyvan

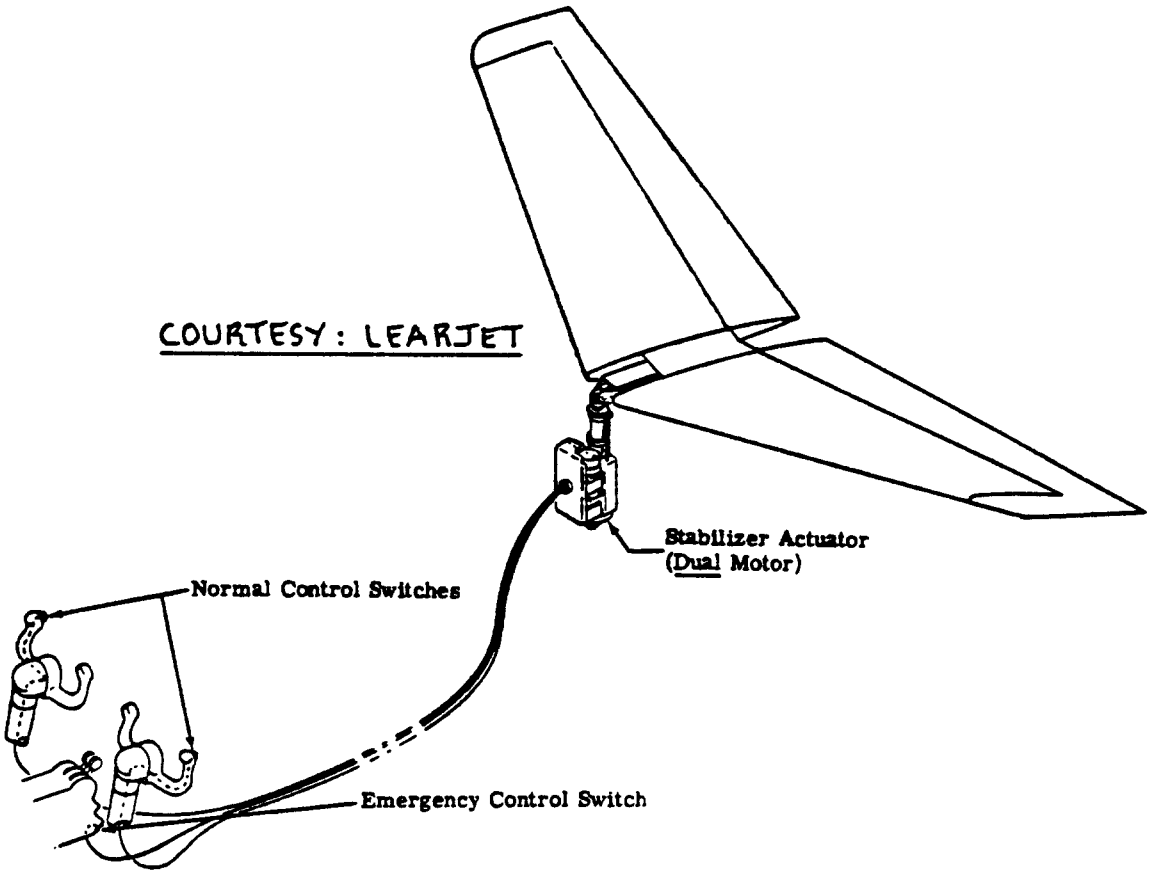

Figure 4.84 Stabilizer Trim System: Learjet M23

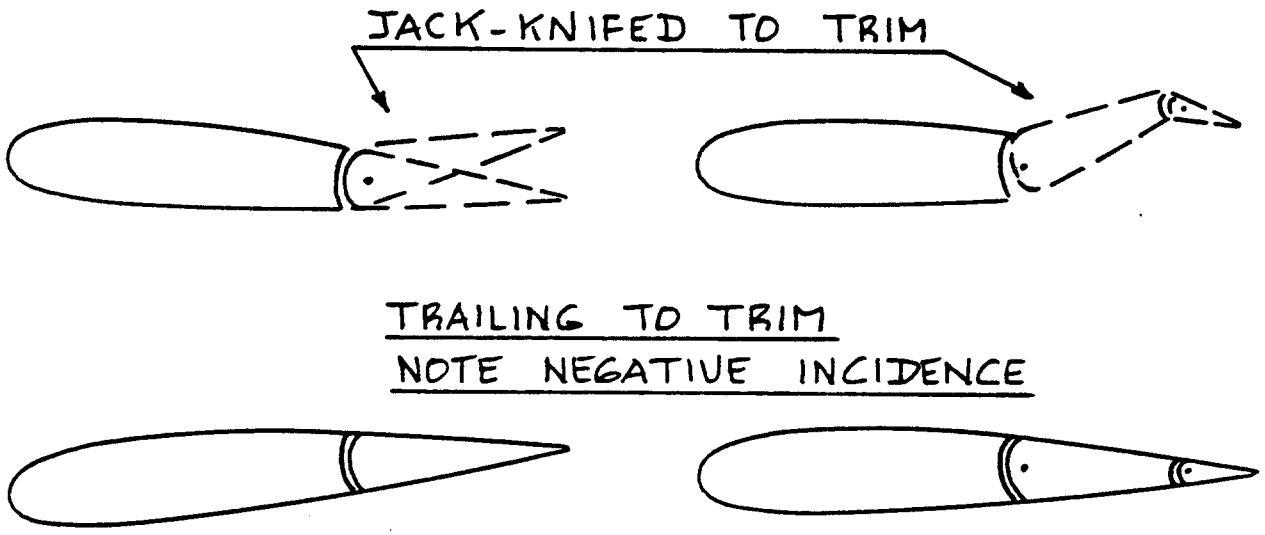

Figure 4.85 Examples of Jack-knifing of Controls

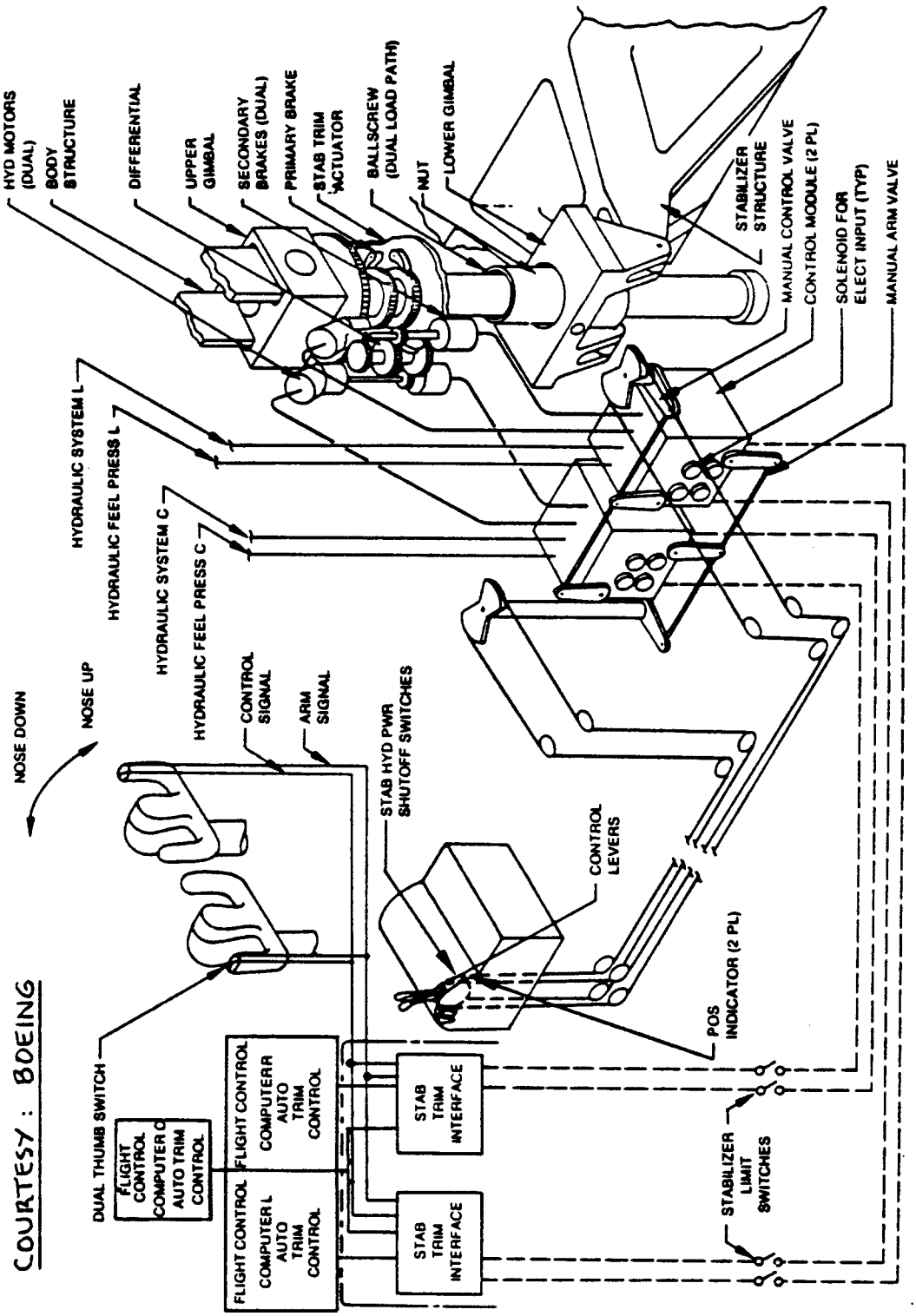

Figure 4.86 Stabilizer Trim Schematic: Boeing 767

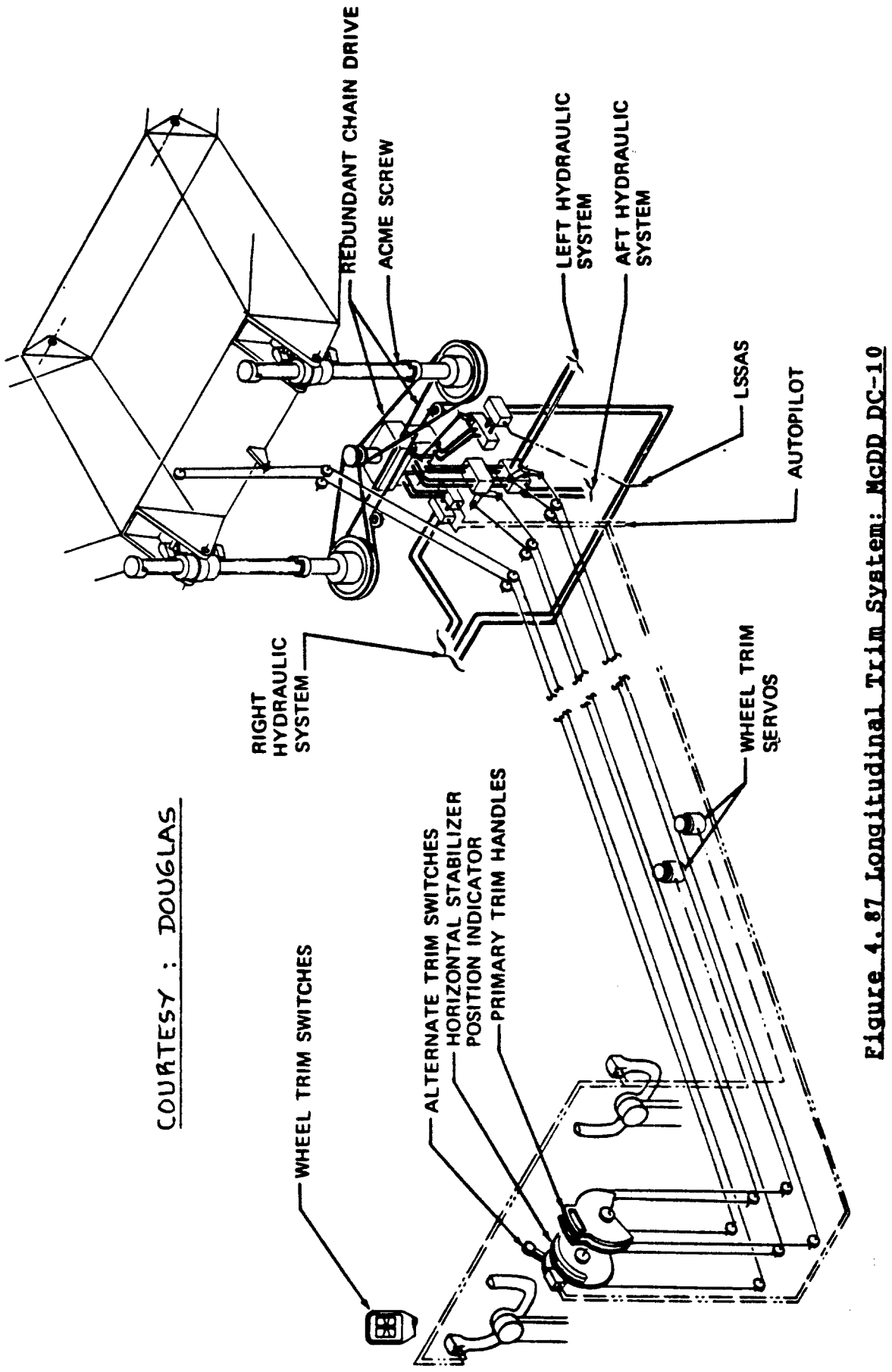

Figure 4.87 Longitudinal Trim System: McDD DC-10

4.6 HIGH LIFT CONTROL SYSTEMS

Most airplanes need flaps to achieve the lift coefficients required for take-off and landing. It was shown in Parts I and II that the following lift coefficients are important in airplane preliminary design:

Clean: $C_{L_{max}}$ Take-off: $C_{L_{max_{TO}}}$

Landing: $C_{L_{max_L}}$

Methods for determining the magnitudes required for these lift coefficients were discussed in Chapter 3 of Part I. How to design the wing planform and what size and type of flaps are required to attain these maximum lift coefficient values was discussed in Chapter 7 of Part II.

In this section examples will be given of how the flaps of typical airplanes are mechanized.

In basic airplanes the flaps are normally mechanized for manual control. Figure 4.88 shows an example.

Many single engine airplanes use electromechanically driven flaps. Figure 4.89 presents an example.

In larger airplanes the flaps are usually mechanized for hydraulic control. Figures 4.90 through 4.95 show examples of flap systems in such airplanes.

Figures 4.92 - 4.95 show the flap system used in the Boeing 767. Note that such systems become very complex and require a lot of attention to detail design, operation and maintenance.

The reader is reminded that Figures 4.71 through 4.76 in Part III provided details of the flap installation of the McDD DC-10.

A critical problem encountered in the design of most high lift systems is that of asymmetric deployment. If flap asymmetry would lead to loss of control, it is mandatory to prevent asymmetric flap deployment. One way to do this is to install flap travel sensors which in turn drive asymmetry logic circuits. These logic circuits can then halt flap deployment beyond some tolerable level of asymmetry.

1. FLAP
2. CONTROL ROD
3. ARM - TORQUE TUBE
4. BEARING - OUTBOARD
5. TORQUE TUBE - OUTBOARD
6. TORQUE TUBE - INBOARD
7. BEARING - INBOARD
8. ARM - ACTUATOR
9. TORQUE TUBE - CENTER
10. INTERCONNECT ROD
11. FLAP HANDLE
12. LOCK BUTTON
13. MOUNTING BRACKET HANDLE
14. TUBE - SPACER

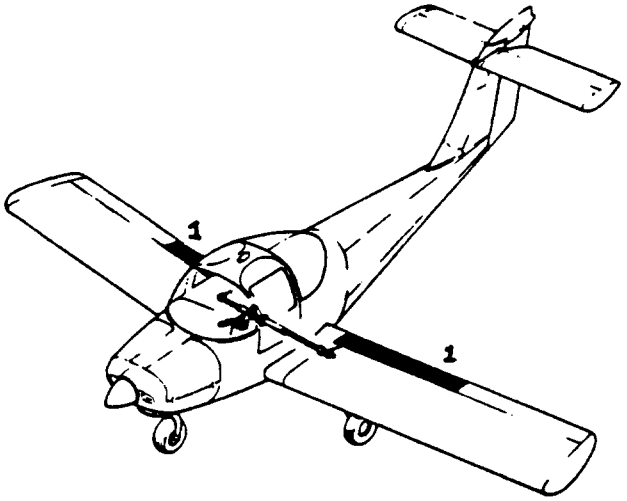

COURTESY: PIPER

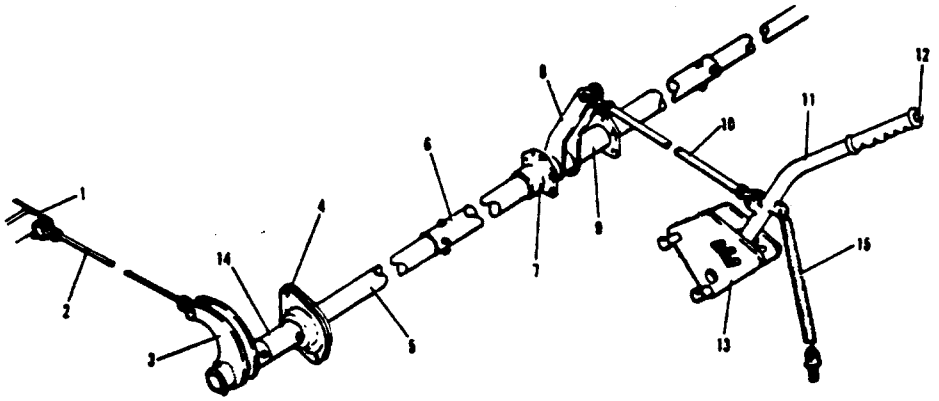

Figure 4.88 Flap Control System: Piper PA-38-112

COURTESY : CESSNA

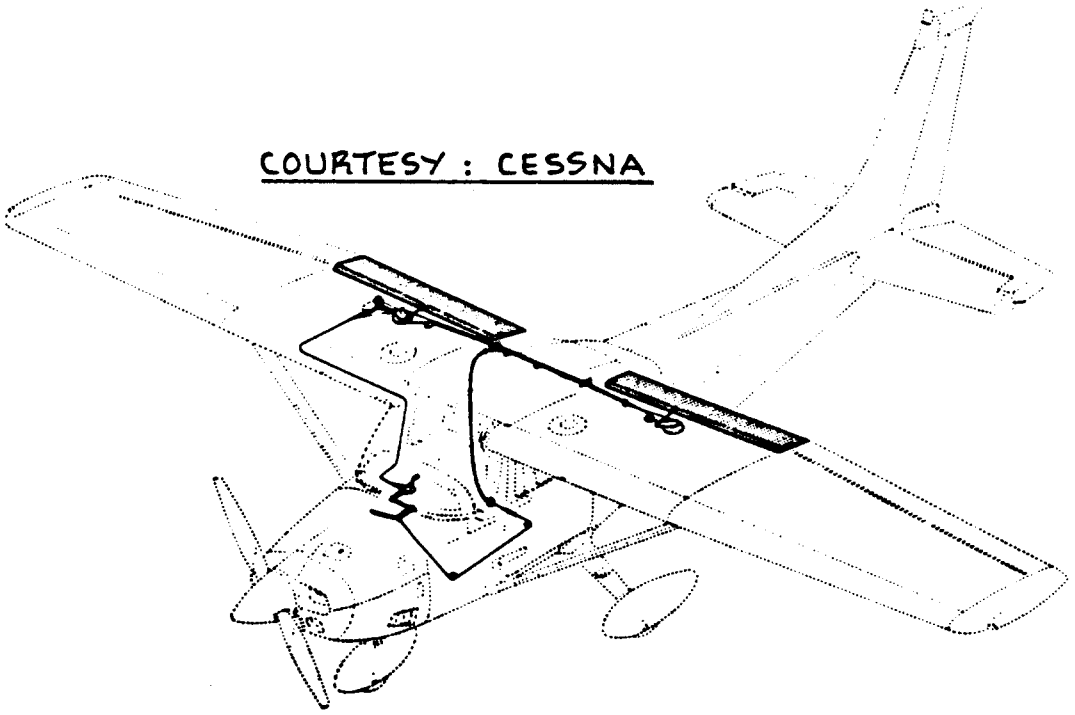

Figure 4.89 Flap Control System: Cessna 182Q Skylane

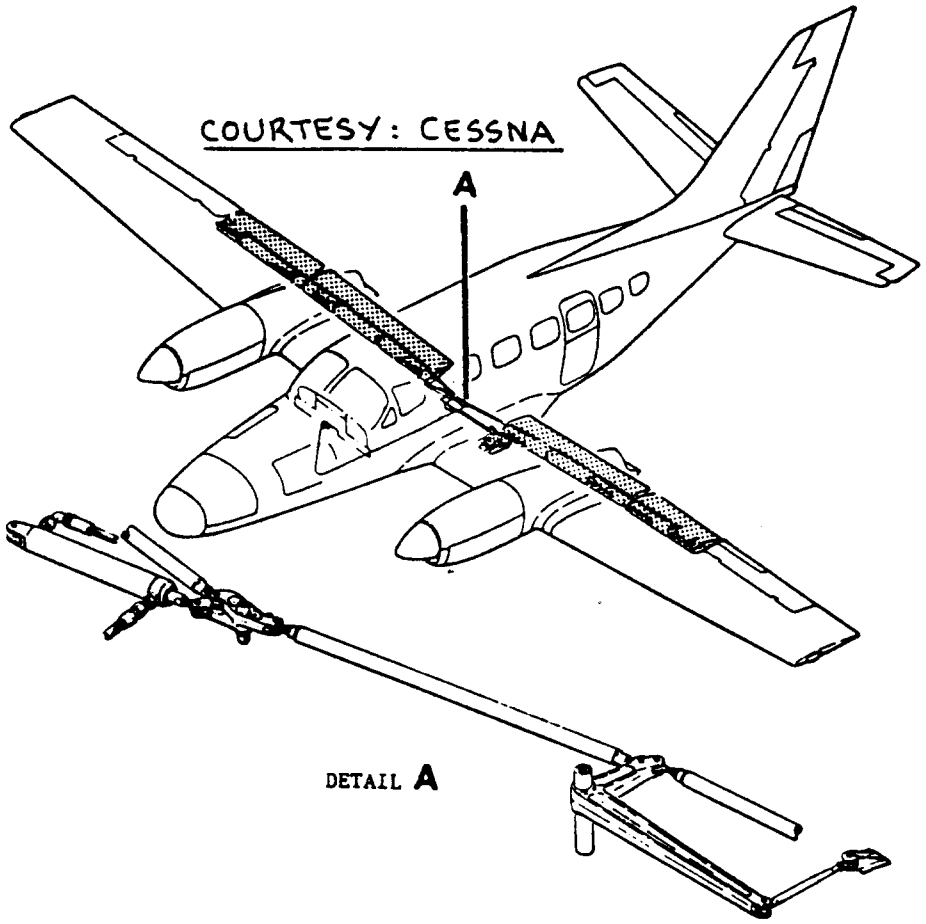

Figure 4.90 Flap Control System: Cessna 441

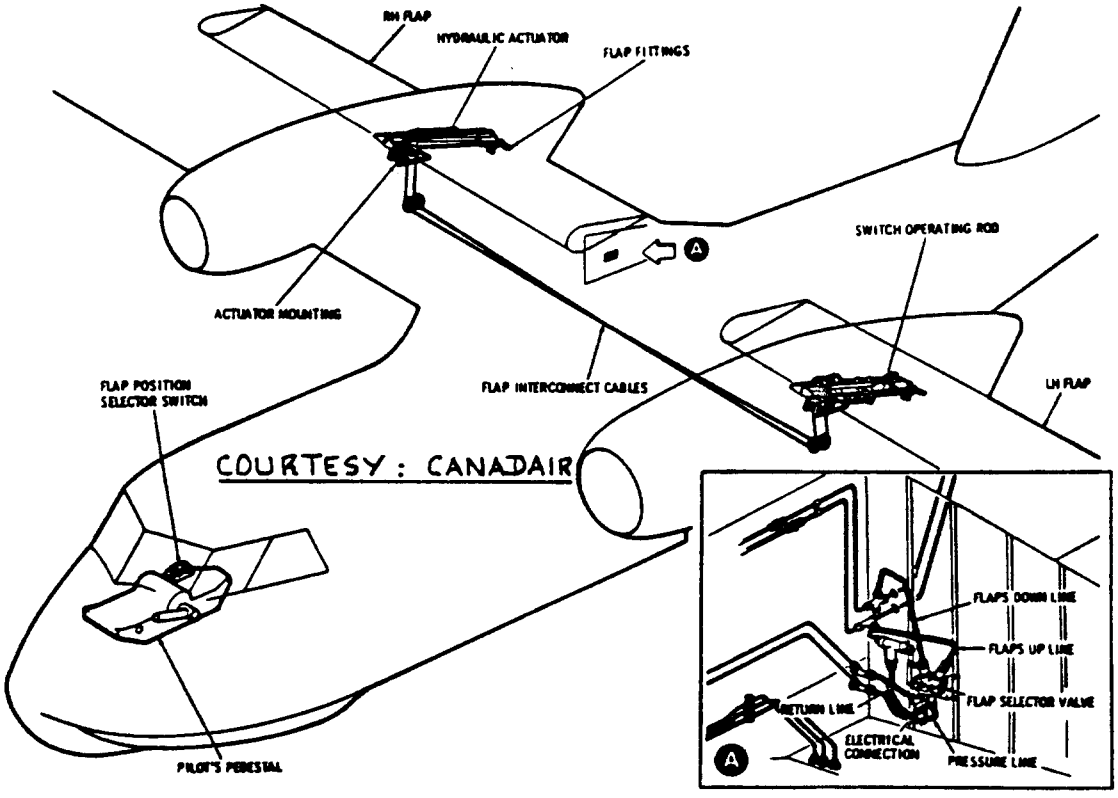

Figure 4.91 Flap Control System: Canadair CL215

COURTESY: BOEING

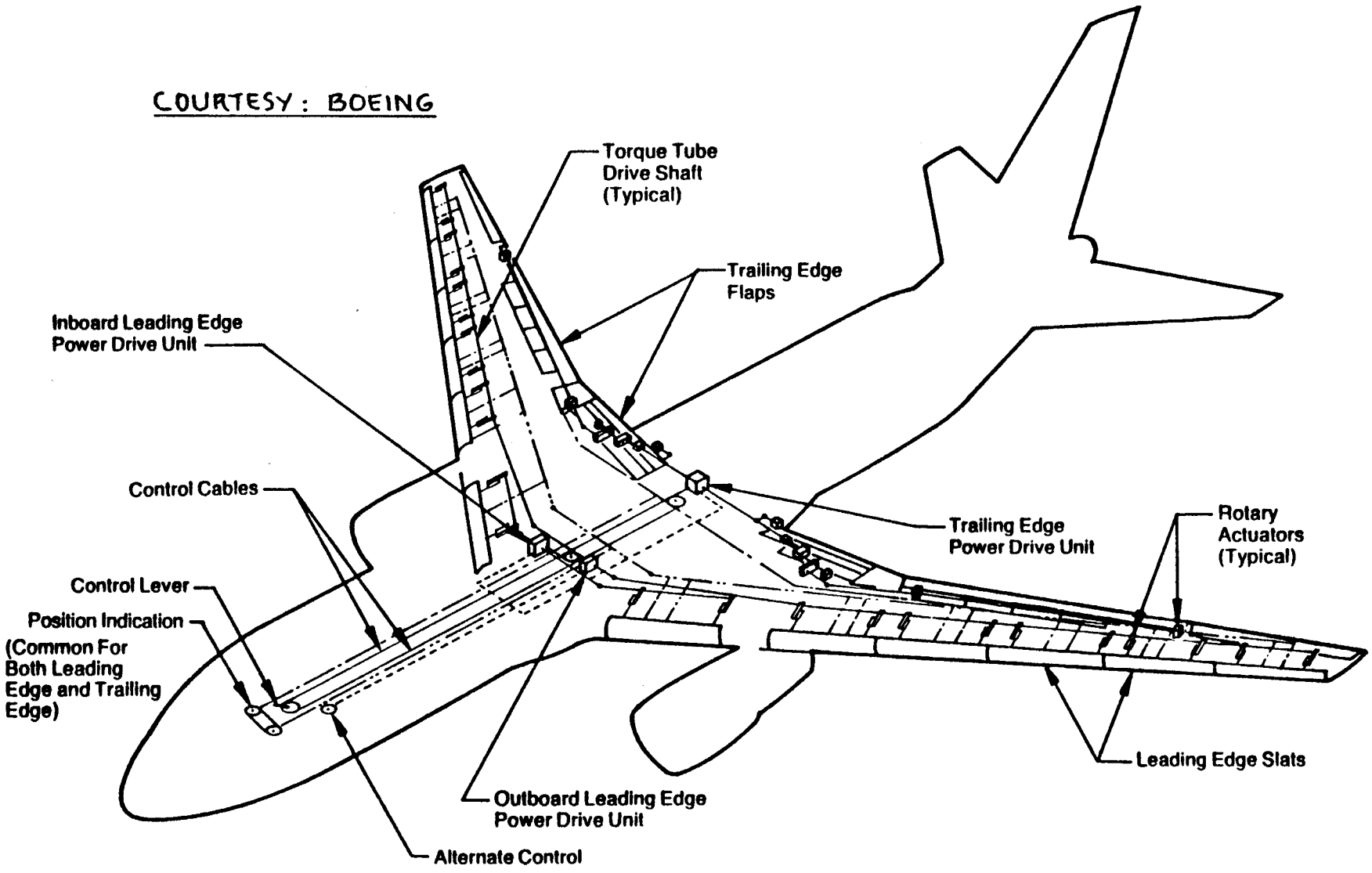

Figure 4.92 High Lift Device Schematic: Boeing 767

Leading edge slats are translating track supported (1) are programmed by fixed cams (2) and are moved by slat actuators (3)

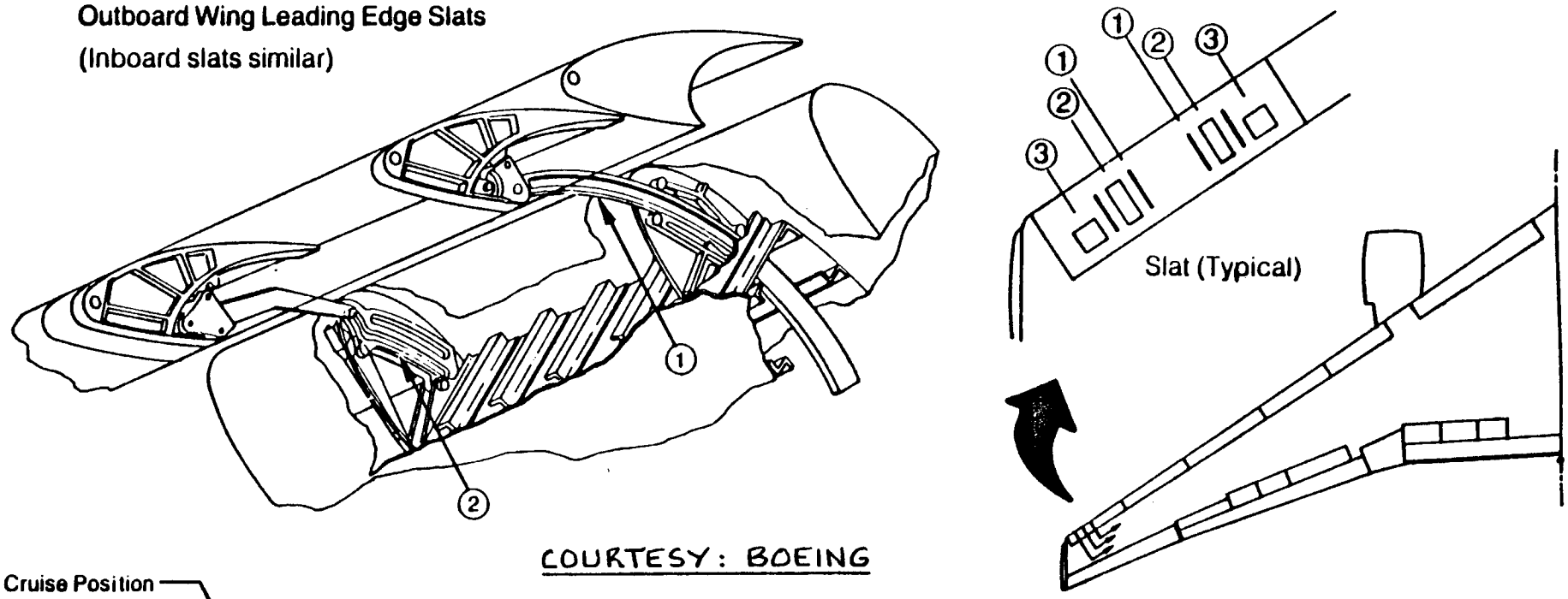

COURTESY: BOEING

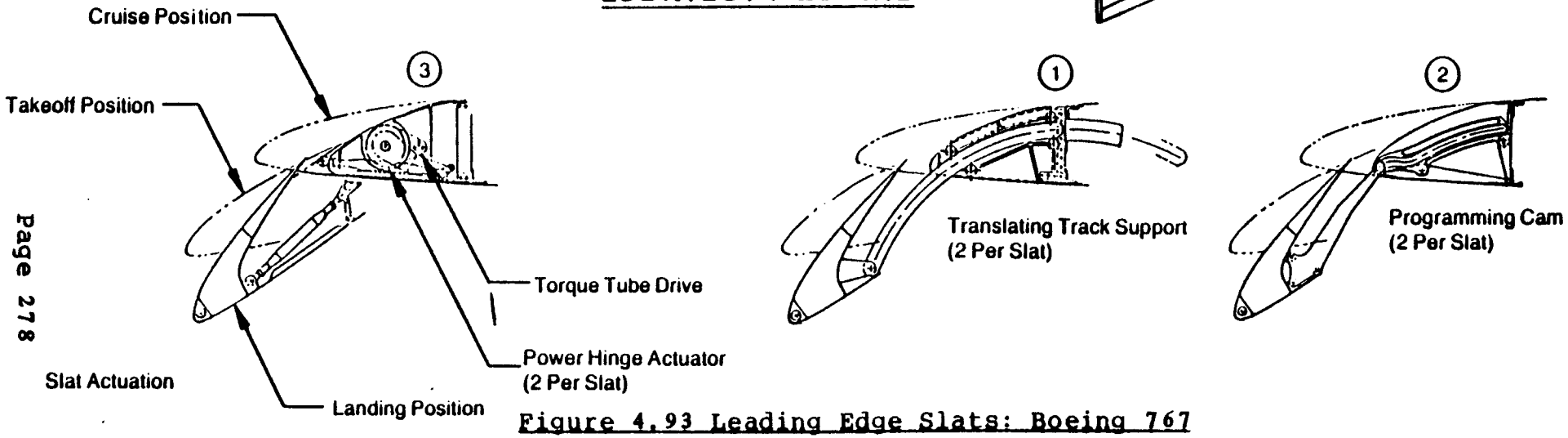

Figure 4.93 Leading Edge Slats: Boeing 767

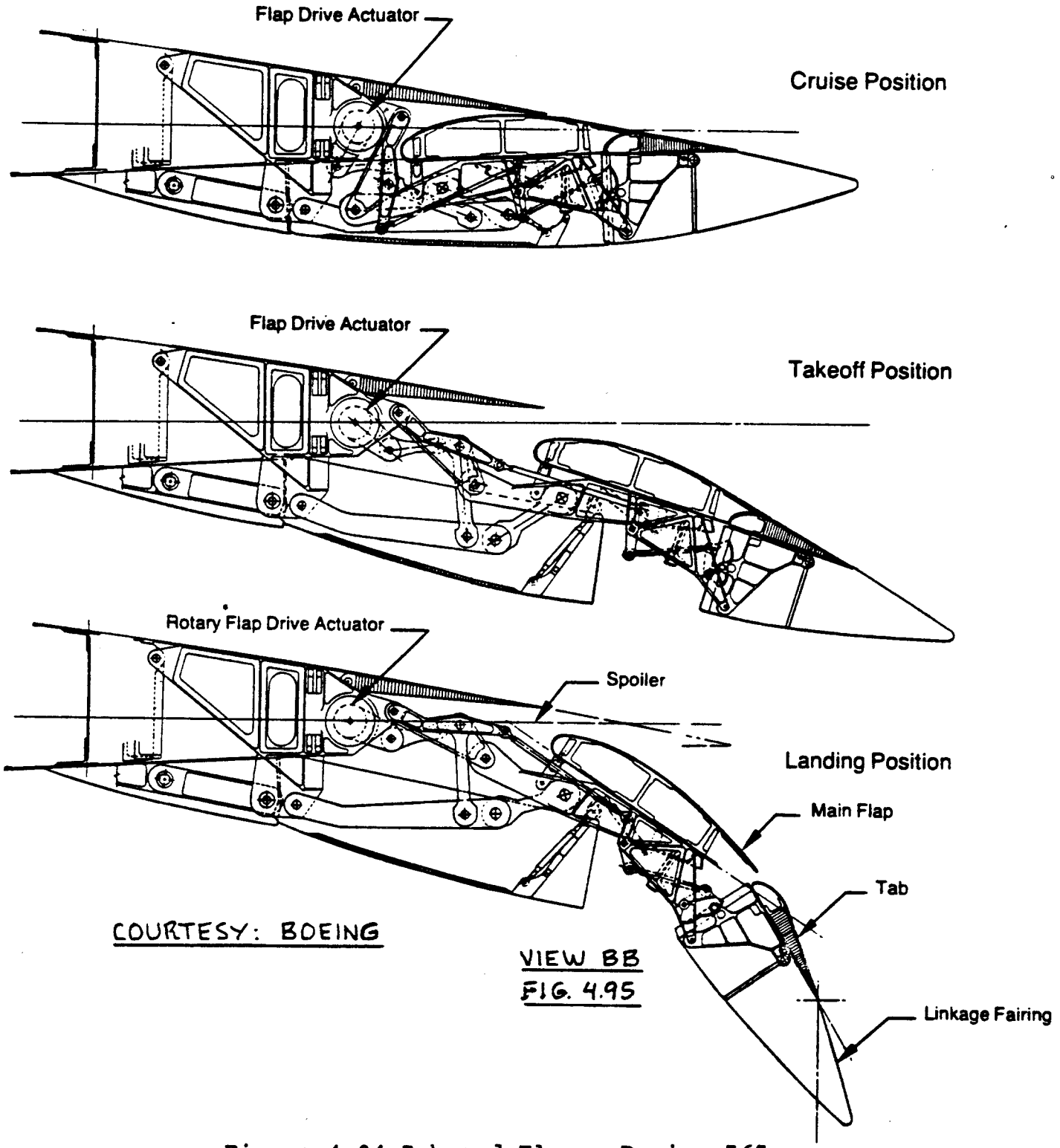

Figure 4.94 Inboard Flaps: Boeing 767

- Simple flaps
- Link supported
- Mechanically linked trailing edge tab on inboard flap– extends for landing, faired for takeoff

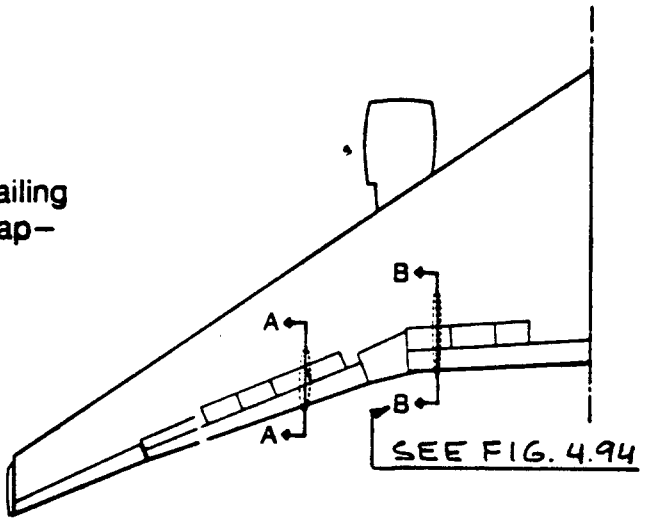

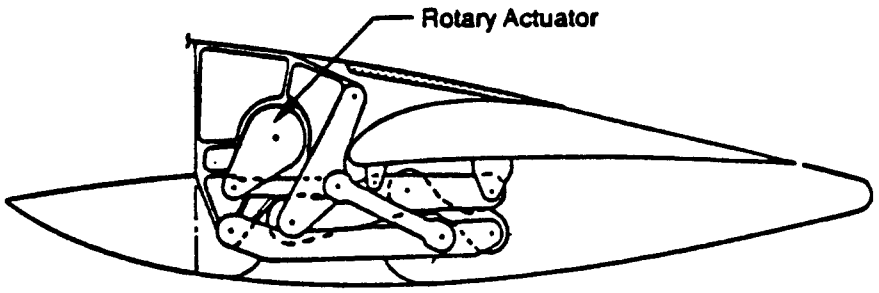

A-A

COURTESY: BOEING

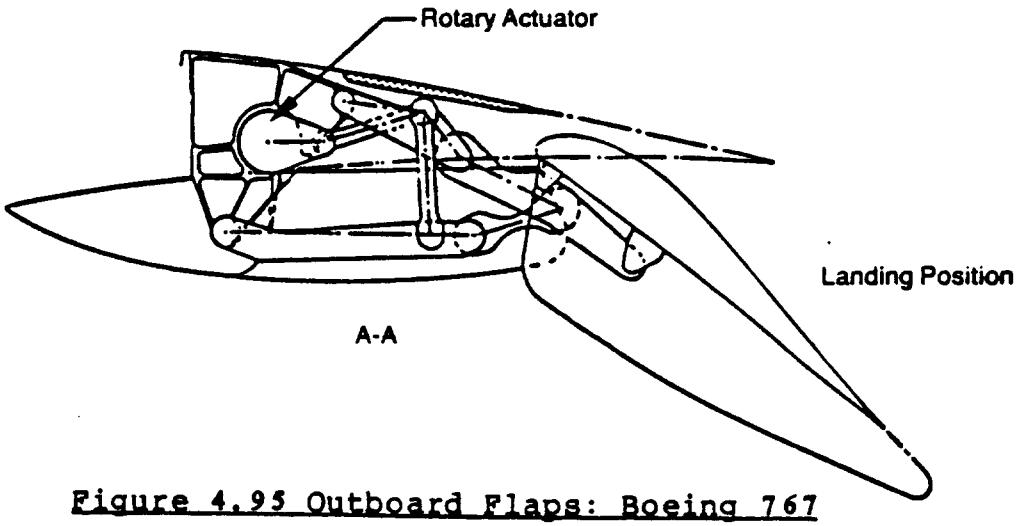

Figure 4.95 Outboard Flaps: Boeing 767

4.7 PROPULSION CONTROL SYSTEMS

Except for gliders, all other airplanes use some form of propulsion to control their flight paths. The propulsion system in turn needs to be controlled by the pilot. This is done with the help of a propulsion control system.

The reader is referred to Chapter 6 in Part III for a discussion of the integration of the propulsion system into airplanes.

Most propeller driven airplanes require six types of propulsion control systems:

1. Ignition control
2. Starter system
3. Fuel flow (=throttle) control
4. Manifold (= mixture) control
5. Propeller control
6. Cooling flap control

In most jet powered airplanes four types of propulsion control systems are needed:

1. Ignition control
2. Starter system
3. Fuel flow (= throttle) control
4. Thrust reverser control

A brief discussion of each propulsion control system follows.

Ignition Controls

Ignition controls are normally a part of the electrical system. Chapter 7 deals with the layout of electrical systems.

Starter System

In most airplanes the starter system consists of an electric starter motor which is geared to the engine. In

some military jet engine installations so-called cartridge starters are used. Cartridge starters generate a burst of high velocity, hot gas which drives a small turbine geared to the engine shaft.

Fuel Flow (= Throttle) Control

The pilot controls the power or thrust output of engines with the help of throttles. In most airplanes these throttles in turn operate a cable and/or a push-rod system which is linked to the engine fuel controls.

A separate fuel system with its own controls supplies the fuel to the engines. The layout design of fuel systems is discussed in Chapter 5.

Manifold (= Mixture) Control

This type of control is found only in piston-propeller combinations. These controls are also mechanized with cable and/or push-rod systems.

Propeller Control

All propeller driven airplanes require two forms of propeller controls: propeller speed (rpm) and propeller pitch. In many airplanes the propeller pitch controls incorporate a so-called 'beta-range': in this pitch range the propeller generates reverse thrust. This is normally used only for ground (landing) operations. Propeller controls can be mechanical, electrical or hydraulic.

Cooling Flap Control

Particularly piston engines require special cooling provisions. To admit extra cooling air during take-off operations, cooling flaps are used. These cooling flaps are operated from the cockpit with a cable and/or push-rod system. In large airplanes the cooling flaps are driven by hydraulic actuators

Thrust Reverser Control

Most jet powered airplanes are equipped with thrust reversers. These are used to help slow the airplane after touchdown. Thrust reversers are normally operated with hydraulic controls.

Figure 4.96 shows the complex nature of the propulsion controls in a large piston/propeller powered airplane.

Figures 4.97 illustrates a typical thrust control system layout for a jet transport. A thrust reverser installation is shown in Figure 4.98.

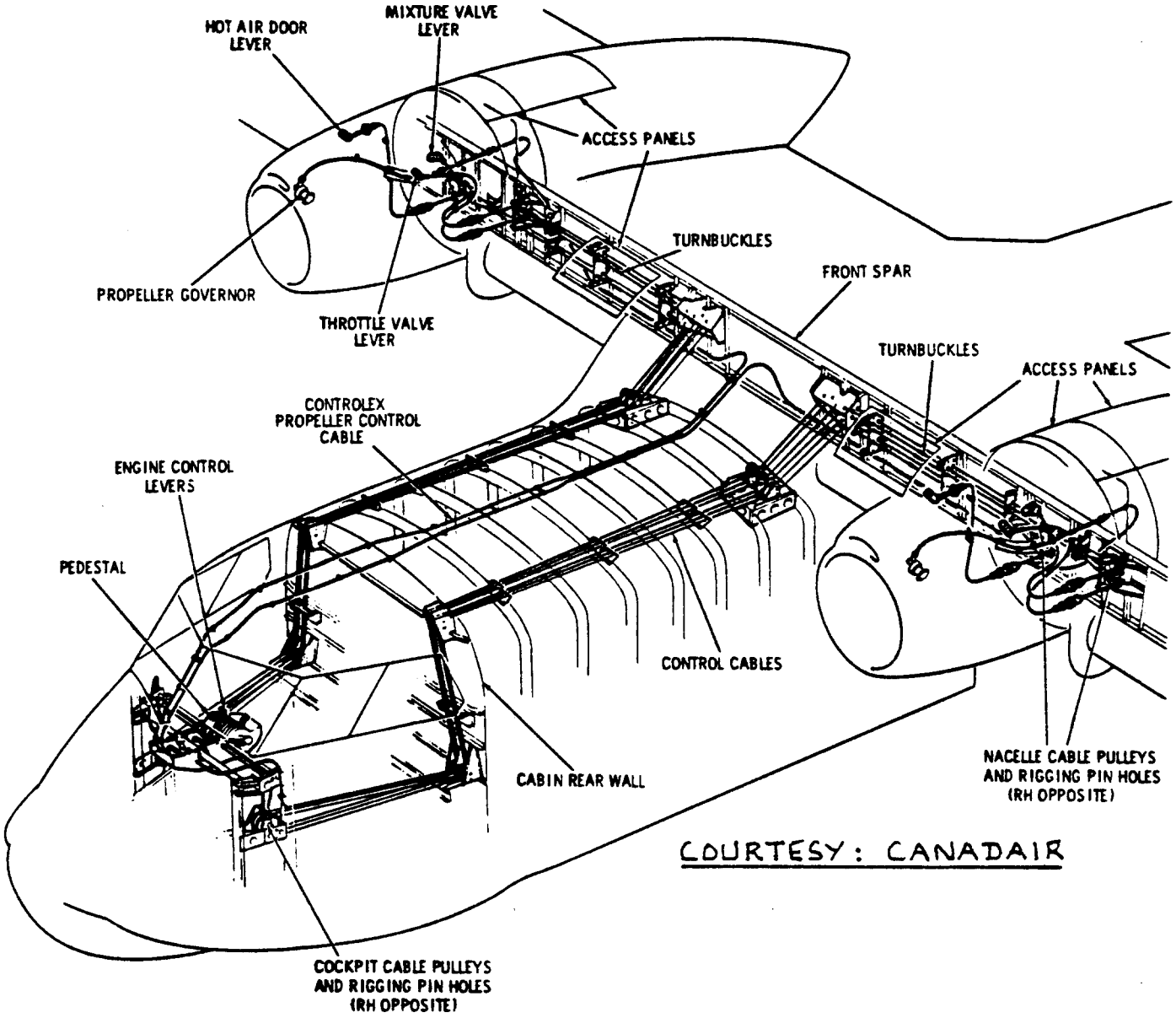

Figure 4.96 Propulsion System Controls: Canadair CL215

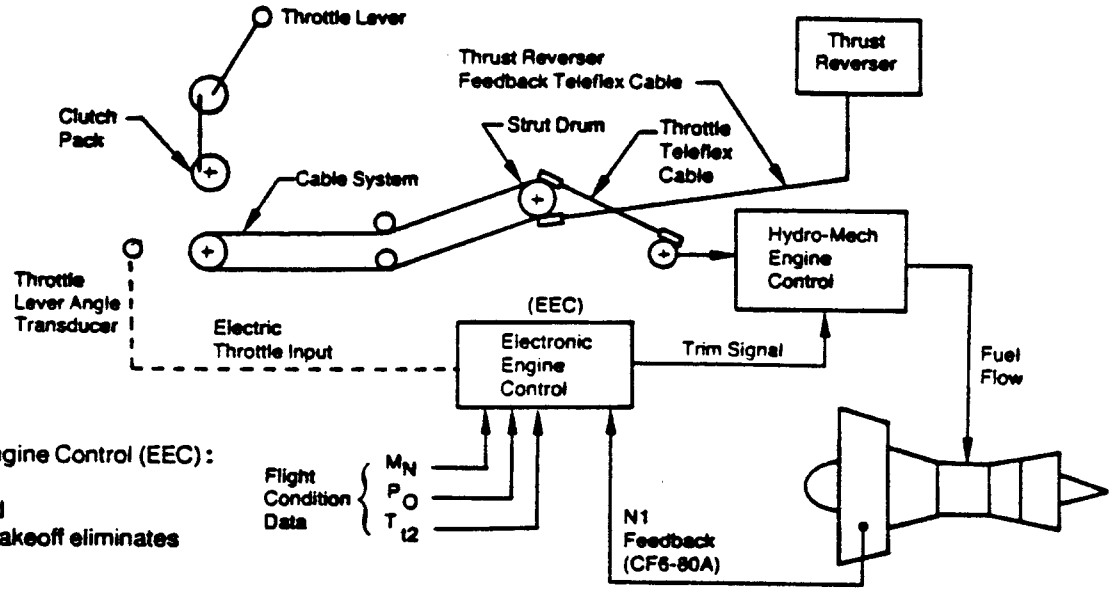

COURTESY : BOEING

Advantages of Electronic Engine Control (EEC):

- Lowers flight crew work load
  - One throttle setting for takeoff eliminates EPR/N1 overshoot
  - Constant climb setting
  - One throttle position for max reverse
  - Use full throttle travel at all ambient temperatures
- Reduces chance of inadvertent overboost
  - Extends engine life
  - Reduces hot parts consumption
  - Prevents overtemperature

Figure 4.97 Thrust Control System: Boeing 767

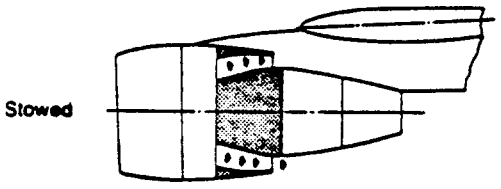

- Fan reversers only
- Hydraulic Actuators
- Mechanically actuated hydraulically driven fan reverser cowl
- Remains on strut during engine change

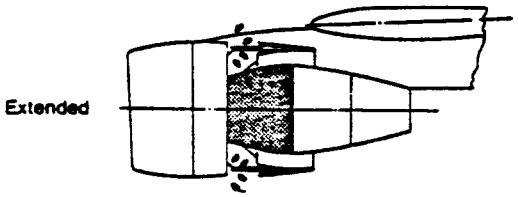

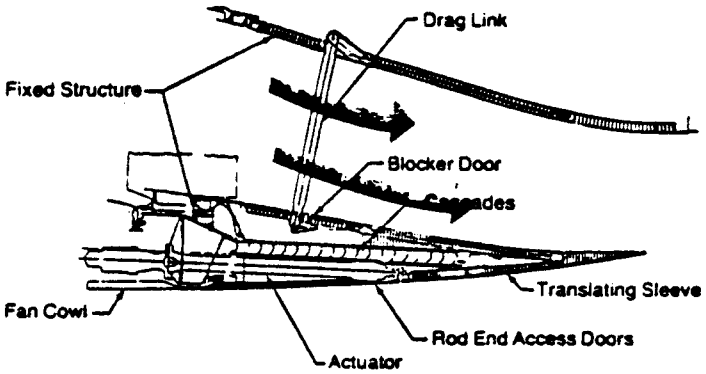

COURTESY: BOEING

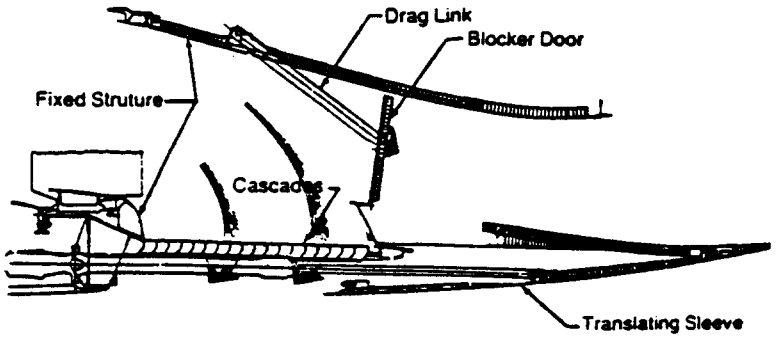

Figure 4.98 Thrust Reverser Control: Boeing 767

5. FUEL SYSTEM LAYOUT DESIGN

The purpose of this chapter is to discuss the most fundamental principles of fuel system layout design for airplanes.

For a detailed discussion on airplane fuels, the operation and the layout of airplane fuel systems references 29 and 30 should be consulted.

Since airplane fuels are very combustible liquids, the design, location, operation, accessibility and maintenance aspects of the fuel system are of great importance to airplane safety as well as to airplane economy.

To operate properly, most fuel systems need the following components:

1. Fuel tanks or fuel bays with a total volume sufficient to cover the design range of the airplane plus reserves.

2. Fuel pump(s) and fuel lines to carry the fuel from the fuel tanks to the propulsion units (engines).

   The fuel pumps and fuel lines must be dimensioned so they can supply 1.5 times the maximum required fuel flow by the engines.

   In aerobatic and in fighter airplanes this fuel supply system must also be able to supply fuel under high 'g' maneuvers and/or under inverted flight conditions.

3. A fuel venting system to prevent excessive pressures from building up in the tanks (this could happen when parked in the hot sun). The fuel venting system also must provide positive pressure in the tanks during flight.

4. A fuel quantity indicating system so the crew can tell how much fuel has been used and how much fuel is left. In some systems fuel flow indicators are also needed.

5. A fuel management system (= tank selection system), to allow the crew to regulate the flow from various tanks to different engines. This includes a shut-off system so that fuel supply to inoperative engines (or egines on fire) can be stopped.

6. In airplanes where the center of gravity travel is large, automatic fuel management systems may be required.

7. An easy method for refuelling must be provided. In transport and in military airplanes single point refuelling is operationally desirable. In many military airplanes in-flight refuelling is also required.

8. If the airplane ramp weight exceeds the maximum design landing weight by more than 5 percent a fuel dumping system must be provided.

The material in this chapter is organized as follows:

5.1 Sizing of the fuel system

5.2 Guidelines for fuel system layout design

5.3 Fire extinguishing systems

5.4 In-flight refuelling systems

5.5 Examples of fuel system layouts

5.1 SIZING OF THE FUEL SYSTEM

Fuel system sizing encompasses the following design decisions:

1. Total fuel volume required

2. Size, location and number of fuel tanks needed

3. Number of fuel pumps, location of fuel pumps and required capacity of fuel pumps and fuel lines

The total amount of fuel required by an airplane depends on its mission. It was shown in Part I, Chapter 2 how a first estimate of the mission fuel required, W_F can be obtained. This estimate was later refined with the help of preliminary design Steps 14 and 28 in Chapter 2 of Part II. In any case, the mission fuel weight, W_F is assumed to be known.

In most airplanes fuel is stored in tanks located in the wing or in the empennage. Estimates of available fuel volume in lifting surfaces can be obtained with Eqn.(6.3) of page 153, Part II.

Reference 3 contains methods for determining the volume of 'irregularly' shaped fuel containers.

Fuel pumps need to be sized so that they can deliver 1.5 times the maximum required amount of fuel flow to the engines. Maximum fuel flow normally occurs during take-off. In military airplanes, maximum fuel flow normally occurs during afterburning operations.

In either case the required engine fuel flow is obtained from the engine manufacturer or, in early preliminary design by multiplying the maximum required thrust by the associated fuel consumption:

$$\text{Max. Fuel Flow} = T_{TO}(c_j) \qquad (5.1)$$

or from:

$$\text{Max. Fuel Flow} = P_{TO}(c_p) \qquad (5.2)$$

The number of fuel tanks should be kept to a minimum from a weight and cost viewpoint.

For the sizing of fuel lines and the determination of necessary fuel pump pressures the method of Ref.31 (Section 3, Flow of Liquids Through Pipes) can be used.

5.2 GUIDELINES FOR FUEL SYSTEM LAYOUT DESIGN

Figure 5.1 shows a so-called gravity fuel system in a high wing light airplane. In such a system only one fuel pump may be required.

Figure 5.2 shows a typical fuel system layout in a low wing light airplane. In this type of system at least two fuel pumps are required.

Figure 5.3 shows an example of a fuselage mounted fuel tank in a fighter airplane. This fuel tank is designed for 'inverted' operation: the inner tank is equipped with flapper valves which trap fuel around the pump during inverted flight.

Each fuel system must be equipped with a fuel vent and a fuel sump system.

The fuel vent system prevents excessive pressure from building up in the fuel tanks. It also serves to maintain ram-air pressure in the tanks while in flight. In some fighter airplanes the tanks are pressurized by

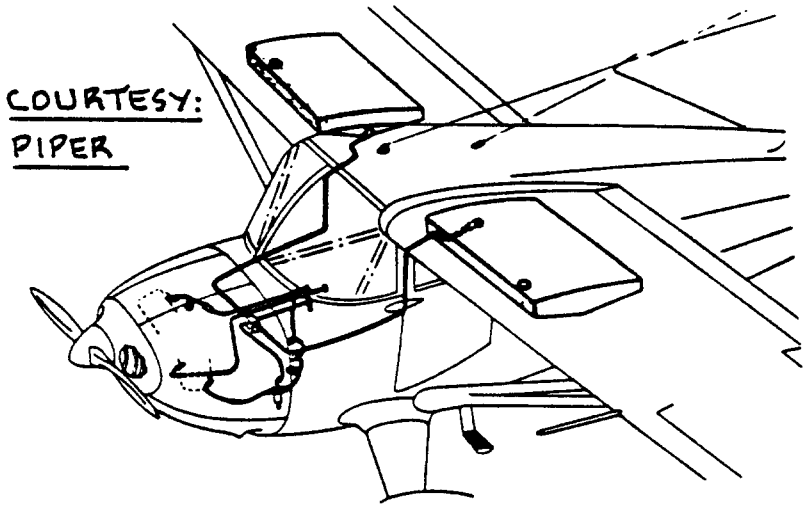

Figure 5.1 Fuel System Layout for a High Wing Airplane

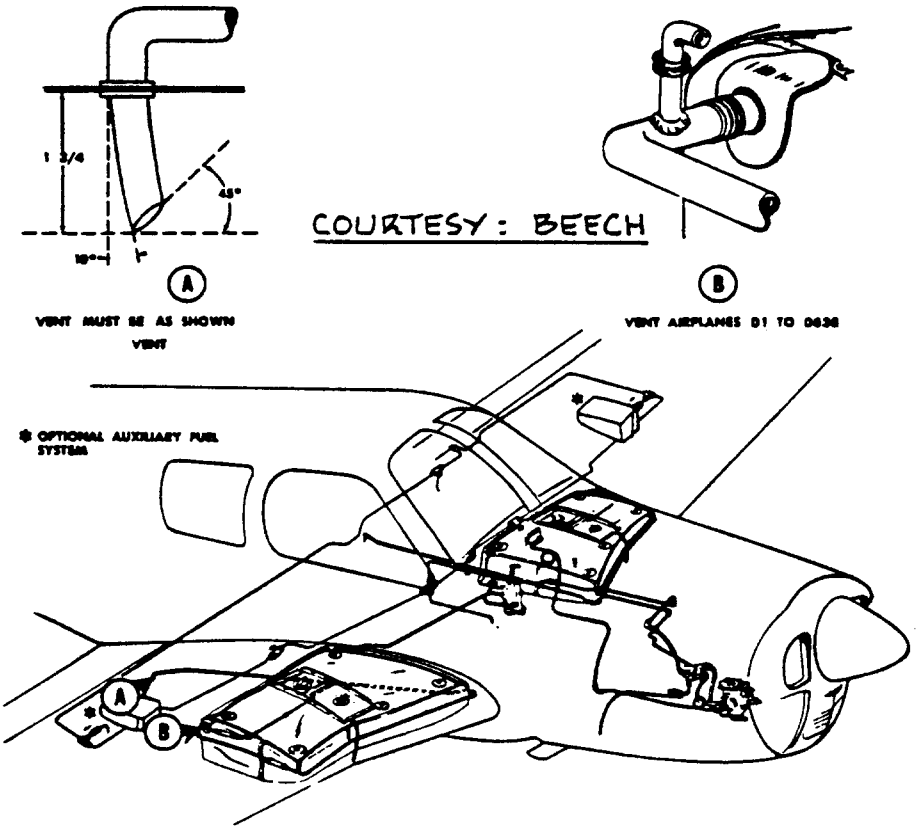

Figure 5.2 Fuel System Layout for a Low Wing Airplane

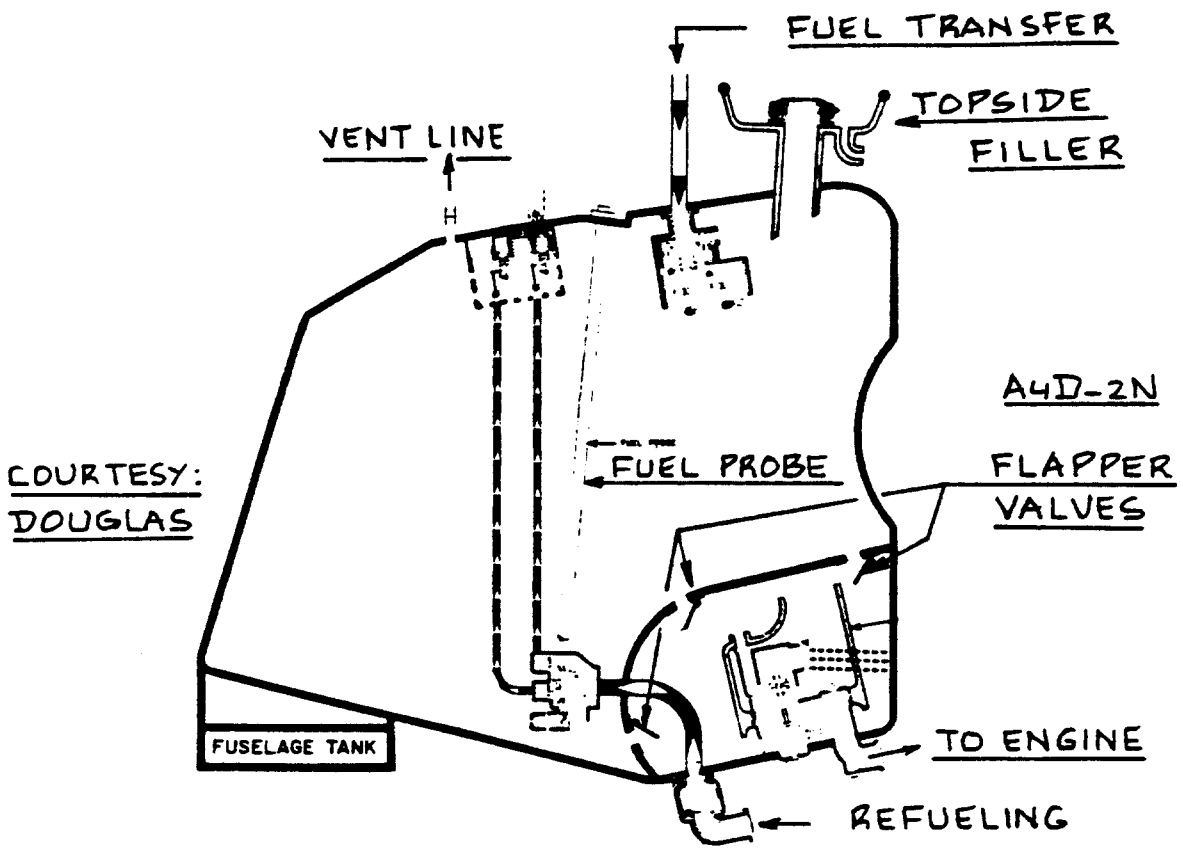

Figure 5.3 Fighter Fuselage Tank for Inverted Flight

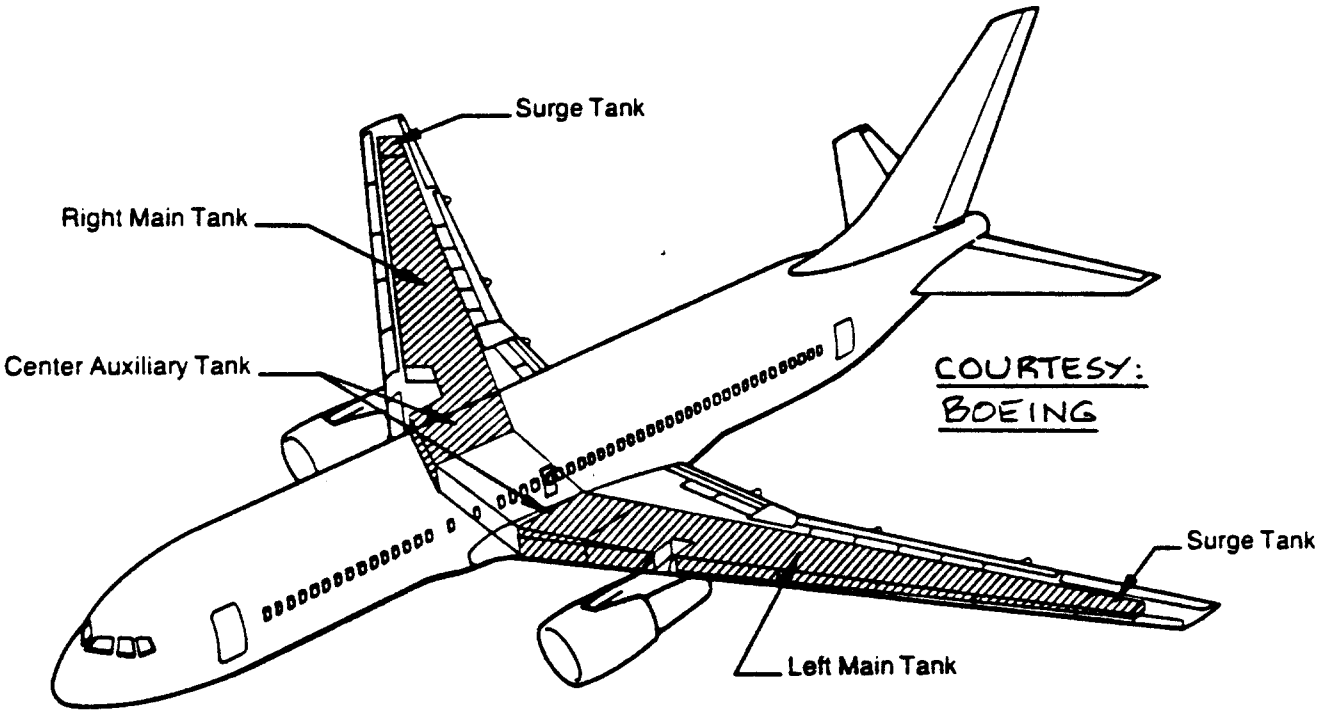

Figure 5.4 Example of Surge Tank Location: Boeing 767

engine bleed-air.

In transports so-called surge tanks are installed to collect and condense any excess fuel vapor before it exits through the overboard fuel vents.

At the lowest point(s) in each fuel system drainage capability must be provided to eliminate condensed water from the tanks. In transports condensed liquids are sometimes automatically removed through the use of a sumping system.

Figure 5.2 shows the location of fuel vent and drain lines (sump). Figure 5.4 provides an example of a surge tank installation.

Following are some important guidelines for safe fuel system design during the preliminary design phase of airplanes.

1. Make sure that the fuel tanks cannot easily rupture in otherwise survivable crashes. Reference 21 contains regulations for fuel tank integrity.

Example: design the landing gear attachments so that rupture of gear struts and braces during a crash is not likely to damage any fuel tanks.

2. Locate fuel lines safely away from easily damaged structure in case of a survivable crash.

Example: do not place fuel lines in the vicinity of landing gear attachment points which are easily damaged or even separated from the airframe in the case of hard landings or aborted take-offs. Fuel lines are easily ruptured in such cases.

3. Do not place fuel lines in the vicinity of equipment which can generate sparks such as many electrical components.

Example: do not locate fuel lines and/or fuel line connectors close to electric genrators.

4. Do not locate fuel lines in or near landing gear wells.

Example: overheated tires can explode inside the wheel well. If fuel lines are present, catastrophic fire may result.

5. Do not locate the fuel tanks close to engines if at all possible. Use dry bays to separate engines from fuel tanks. Fire walls (stainless steel) must separate all engines and all passenger and crew compartments from fuel tanks.

Example: Figure 5.4 shows small dry bays directly behind the engines.

6. Locate the fuel vent lines and the fuel dump lines so that positive separation of fuel and fuel vapor from the airframe is assured.

Example: determine the local pressures which surround fuel vents. It has occurred that due to adverse pressure gradients vented fuel was drawn into a cabin heating system leading to a fatal accident.

7. Locate ram-air inlets for vent systems so that large asymmetric pressures are unlikely to occur.

Example: when asymmetric ram pressures occur in the vent system it is possible that fuel will be transferred from one wing into the other. This can lead to serious lateral control problems.

8. Locate fuel quantity sensors in fuel tanks such that in extreme airplane attitudes (climb, dive or glide) the correct level of fuel remaining is indicated to the crew.

Example: in wing tip mounted fuel tanks, placing the fuel quantity sensors at one end of the tank may cause it to indicate wrongly during prolonged climbs or glides.

9. Locate fuel pumps in fuel systems so that in extreme airplane attitudes fuel is still delivered to the engine(s).

Example: locating fuel pumps at one end of a long fuel container may cause it to run dry (which can cause pump failure and/or engine flame-out) during prolonged climbs or glides.

10. Avoid the use of tiptanks.

Example: tiptanks may cause large changes in the airplane rolling moment of inertia between their full and empty condition. This in turn may cause detrimental effects on the lateral control of the airplane.

11. Most fuel tanks require access panels and fuel caps. If improperly designed, these can cause explosions due to arcing inside the fuel tank when struck by lightning. Figure 5.5 shows airplane regions where lightning strikes occur most frequently.

Example: Figure 5.6 shows a properly and improperly designed fuel cap. Reference 32 presents design procedures which minimize adverse effects of lightning strikes on airplanes.

5.3 FIRE EXTINGUISHING SYSTEM

Reference 21 contains regulations regarding the need for and installation of fire extinguishing systems. All FAR 25 certified airplanes must have such systems aboard.

Figures 5.7 and 5.8 show example installations for fire extinguishing systems.

5.4 IN-FLIGHT REFUELING SYSTEMS

In-flight refueling is required in many military airplanes. Two types of systems are in use:

1. Refueling Boom System

2. Probe and Drogue System

An example of a refueling boom installation is shown in Figure 5.9. This system requires a boom operator stationed in the tanker airplane.

An example of a probe and drogue system is shown in Figure 5.10.

Figure 5.11 presents an example of an airplane modification proposal which includes both refueling systems.

The receiving airplane must be equipped with a refueling probe. Figure 5.12 shows an example.

5.5 EXAMPLES OF FUEL SYSTEM LAYOUTS

Figures 5.13 through 5.20 contain examples of fuel system schematics and/or layouts. Commentary on these drawings is given next.

Figure 5.13 Fuel System Installation: Piper PA-38-112

This is a low wing airplane: two pumps are required to operate this system. Note the location of the fuel vents below each wing. Also note that the fuel tanks are well away from the engine compartment.

==========

Figure 5.14 Fuel System Schematic: Canadair CL215

Only the right side of the system is shown. The left side is mirror symmetric. Note the ram air scoop associated with the vent system. In this system fuel is pumped from the main fuel tanks (numbers 1-8) to an engine collector tank, one for each engine. The engines are fed only from the collector tanks.

==========

Figure 5.15 Fuel System Schematic: Short Skyvan

Note again the presence of the collector tanks. The fuel vent lines in this case protrude into the airstream adjacent to the fuselage.

==========

Figure 5.16 Fuel System Schematic: Boeing 767

Observe the dry bays behind the engines. Note also the surge tanks near the wing tips. These surge tanks are not normally filled with fuel. The system can be filled from over the wing if the airplane is landed at an airport where pressure refueling is not available.

Figure 5.17 Fueling/Defueling System: Boeing 767

Note the single point refueling in the left wing only. The overfill sensor installed in the surge tanks prevents overfilling and overpressuring of the fuel tanks. Defueling is done close to the center of the airplane: low point in the fuel system.

Figure 5.18 Engine Fuel Feed System: Boeing 767

Observe the tie-ins with the airplane APU system located in the fuselage tailcone.

Figure 5.19 Fuel Tank Vent System: Boeing 767

Note that the vent lines are equipped with flame arrestors. The center wing drainmast allows fuel dumping if required.

Figure 5.20 Automatic Sumping System: Boeing 767

In airline operation it is desirable not to have to inspect the fuel system all the time for condensates which may collect at the bottom of the tanks. The automatic sumping system clears condensates automatically.

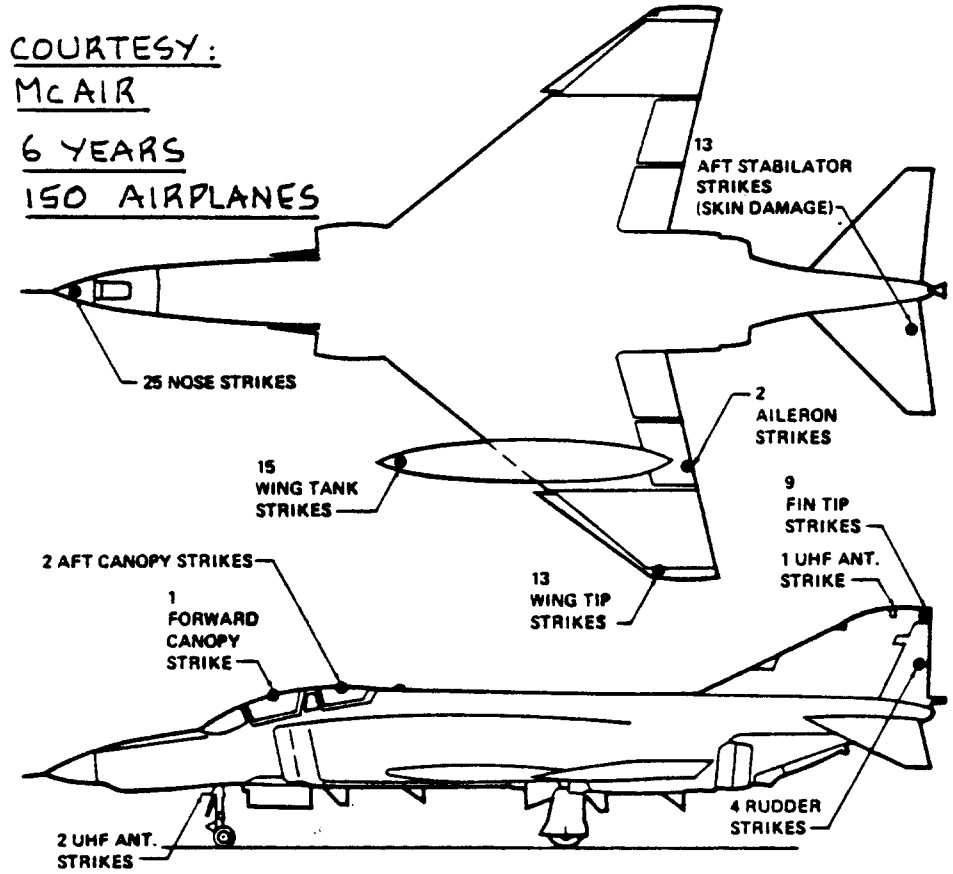

Figure 5.5 Likely Locations for Lightning Strikes

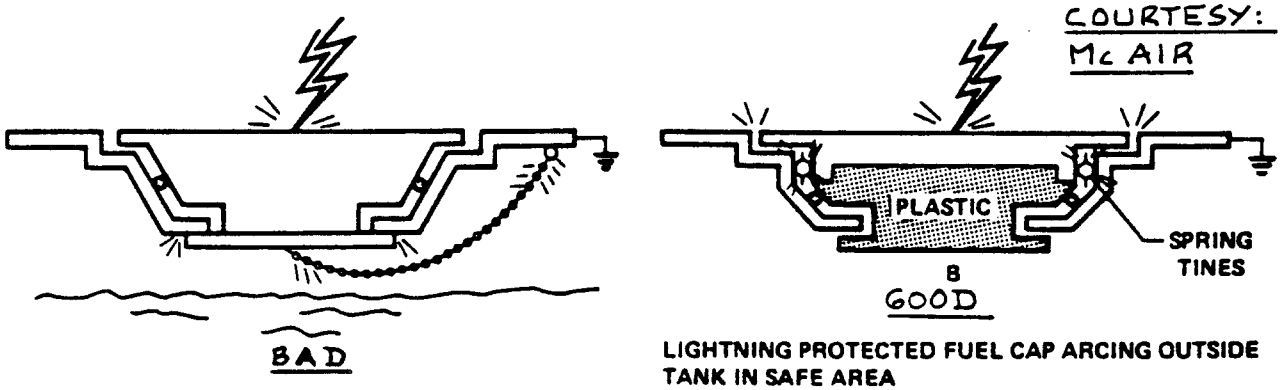

LIGHTNING PROTECTED FUEL CAP ARCING OUTSIDE TANK IN SAFE AREA

USUALLY SEMI-INSULATED FUEL CAP ARCING INSIDE TANK DUE TO DIRECT STROKE

Figure 5.6 Good and Bad Design Of Fuel Caps

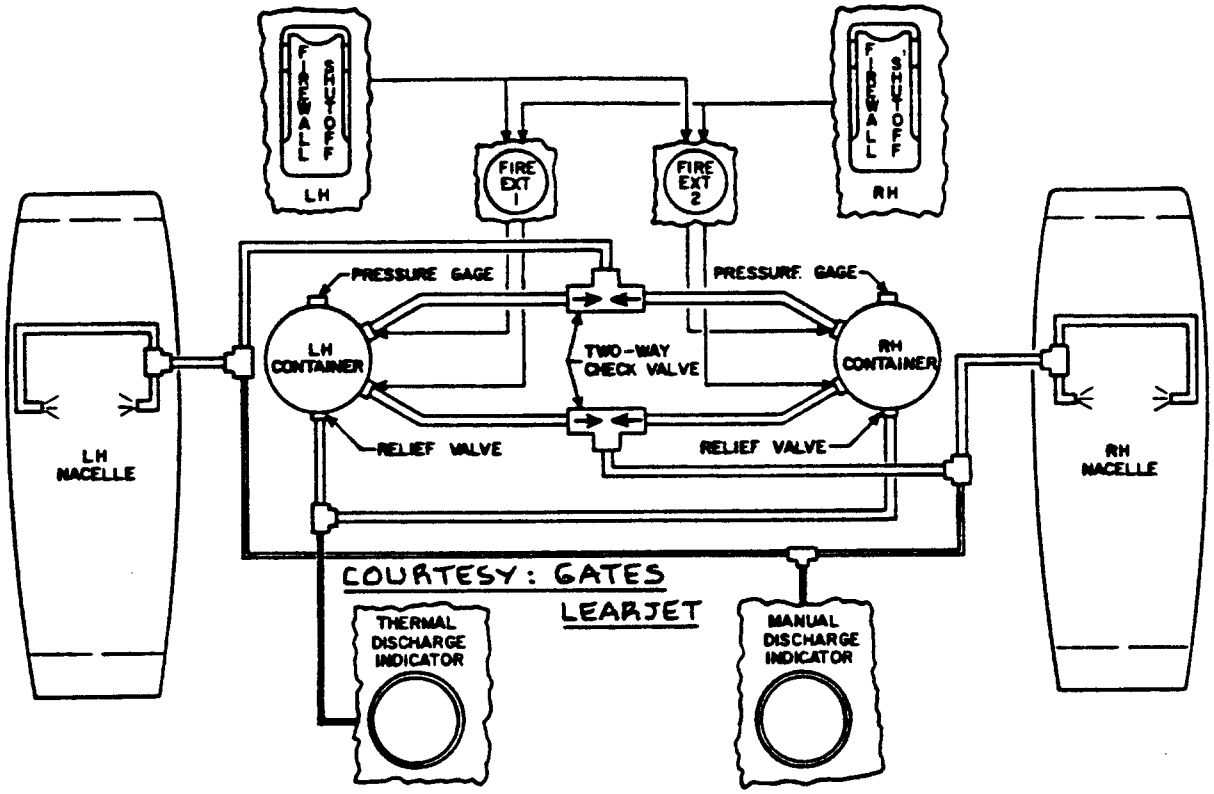

Figure 5.7 Fire Extinguishing System Schematic: Gates Learjet Model 25

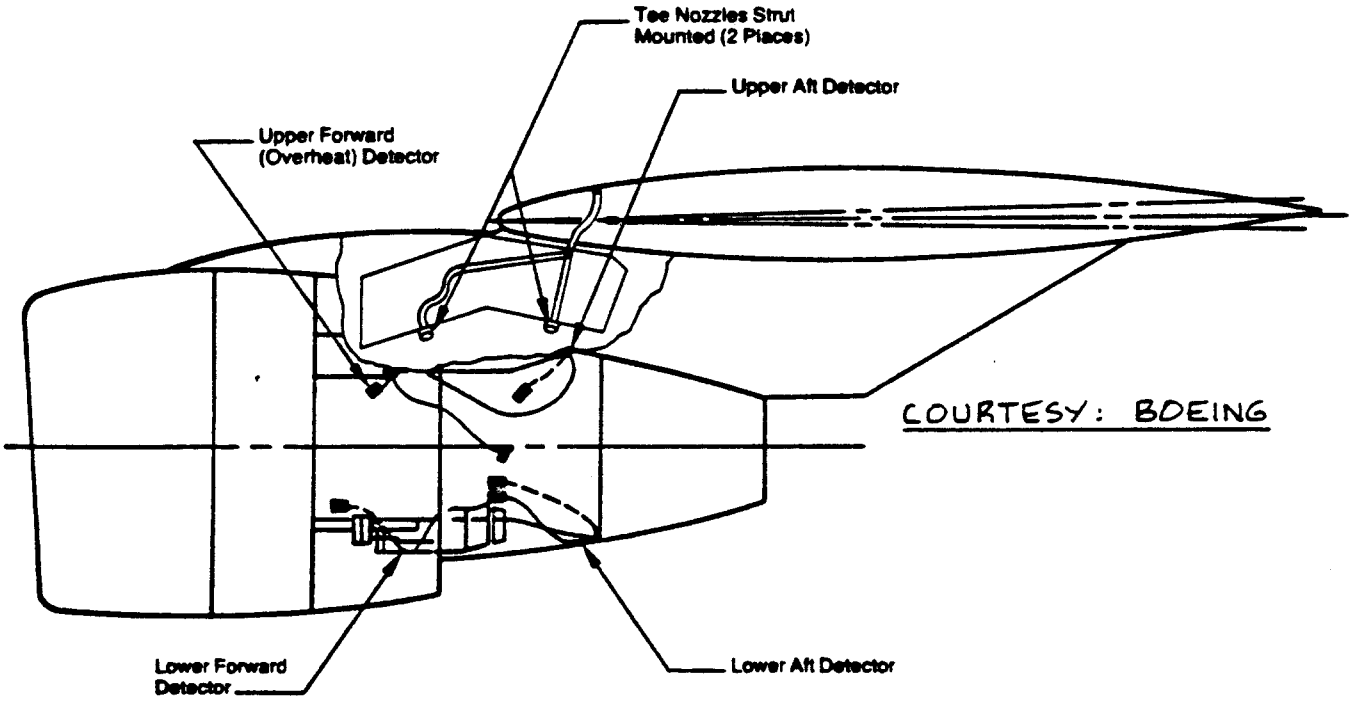

Figure 5.8 Location of Fire Detectors and Fire Extinguishing Nozzles: Boeing 767

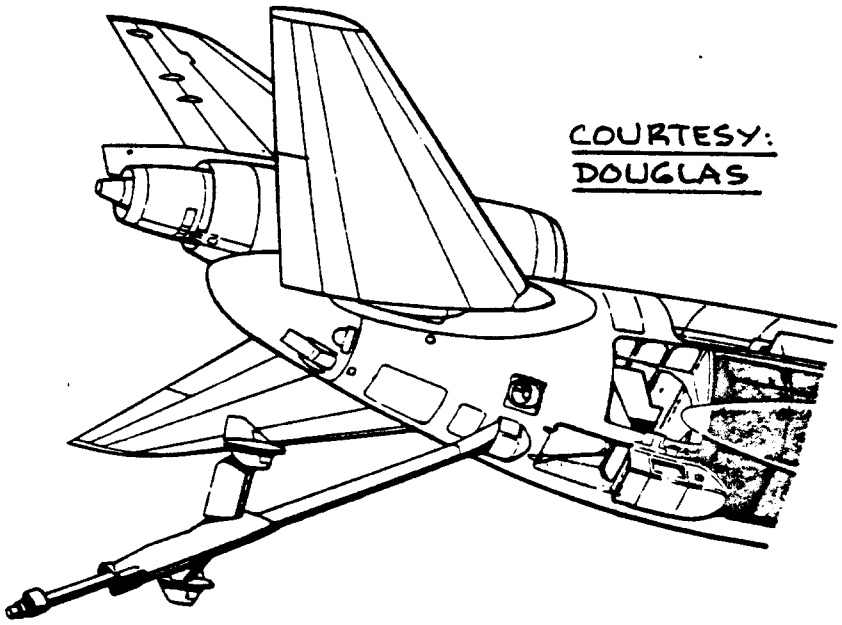

Figure 5.9 Refueling Boom Installation McDD KC-10A

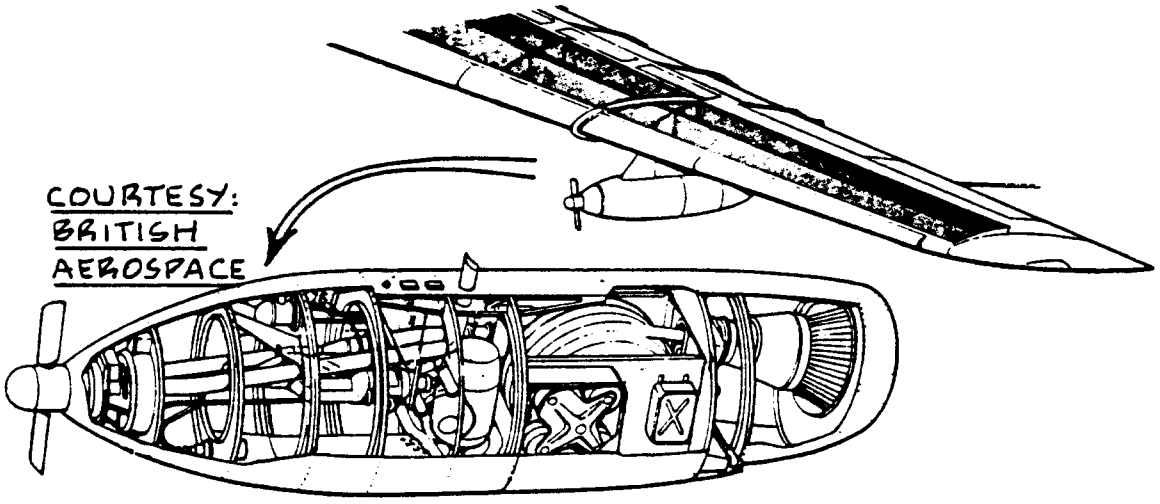

Figure 5.10 Probe and Drogue Refueling Installation: Vickers VC10 K.2

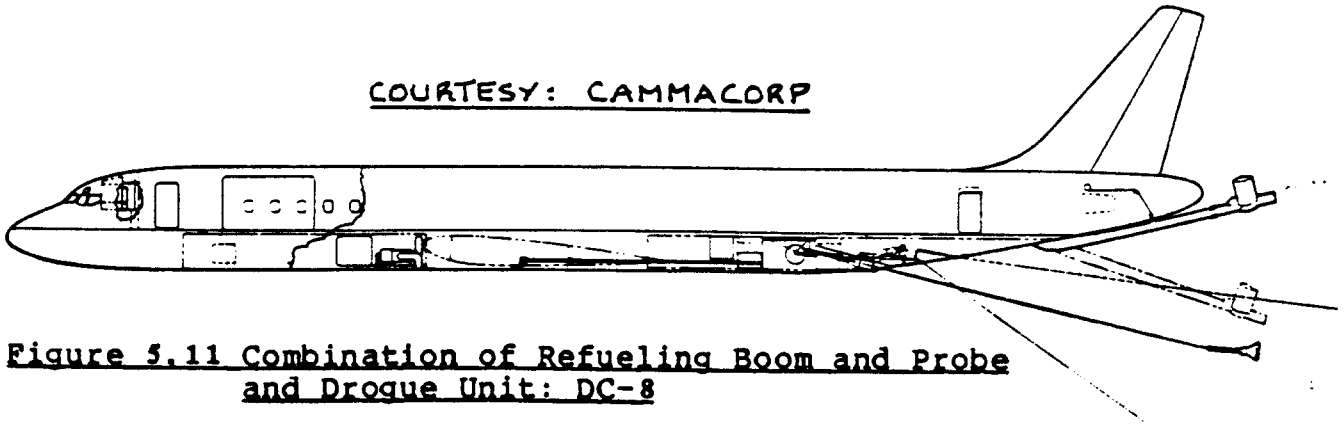

Figure 5.11 Combination of Refueling Boom and Probe and Drogue Unit: DC-8

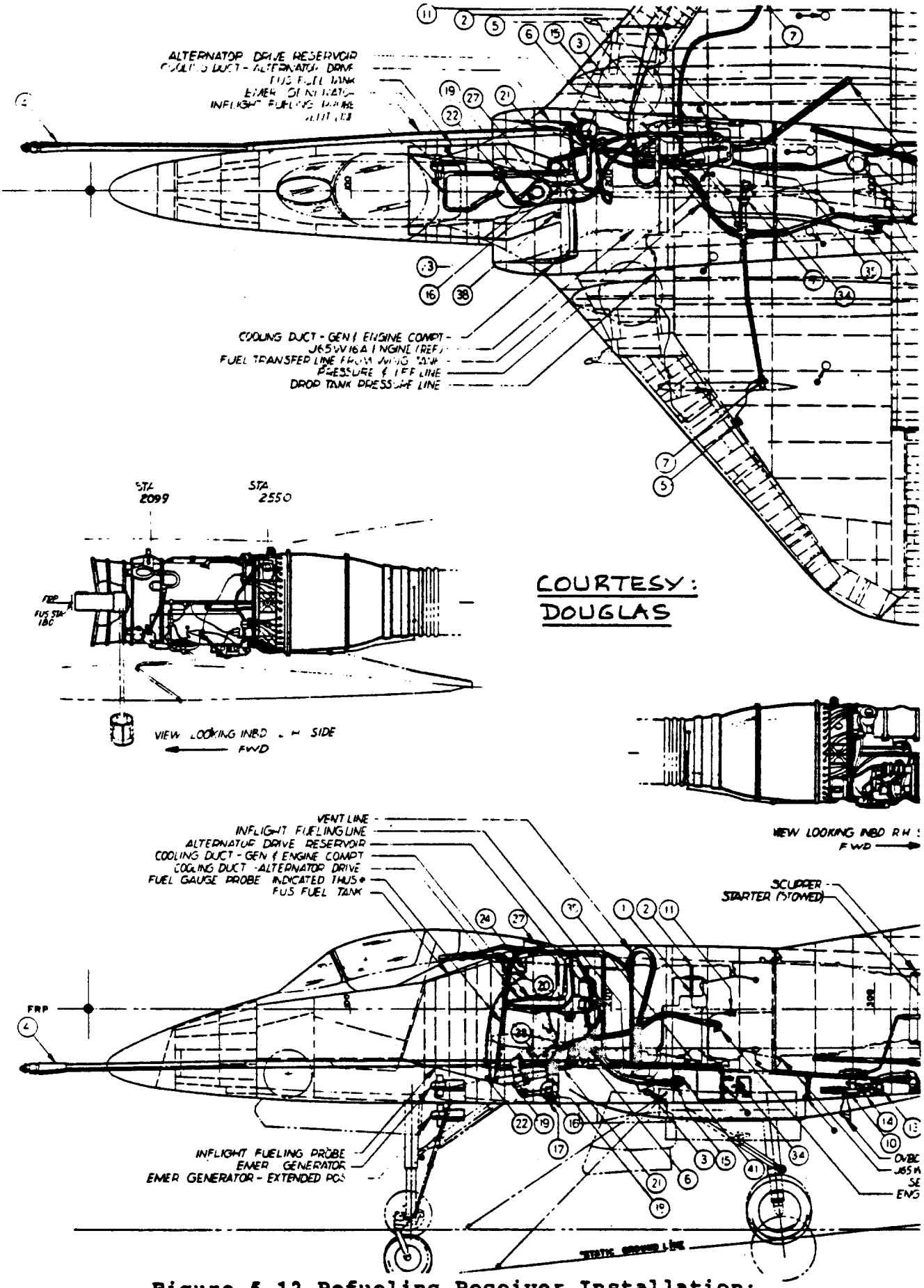

Figure 5.12 Refueling Receiver Installation: Douglas A4D-2N

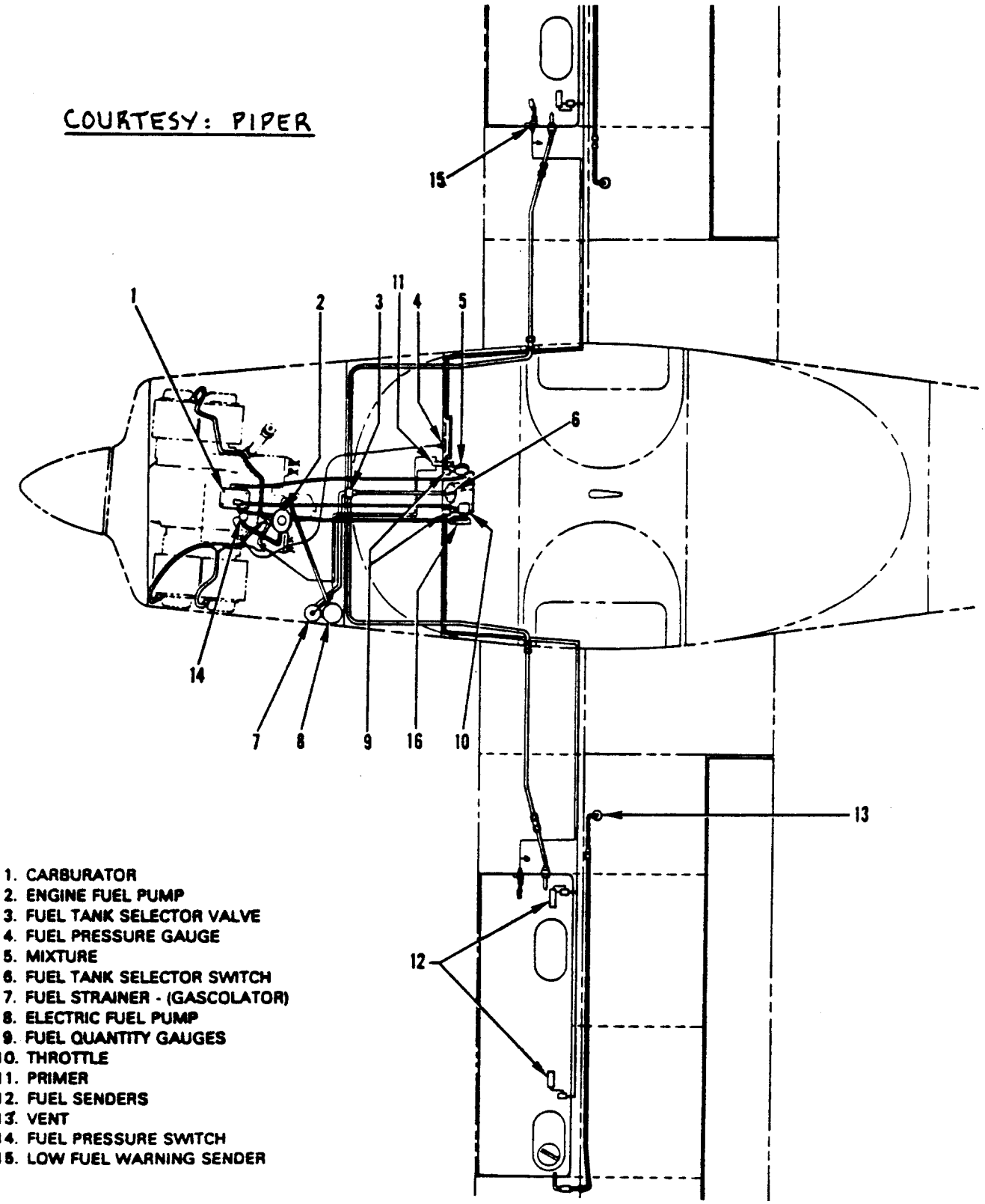

Figure 5.13 Fuel System Installation: Piper PA-38-112

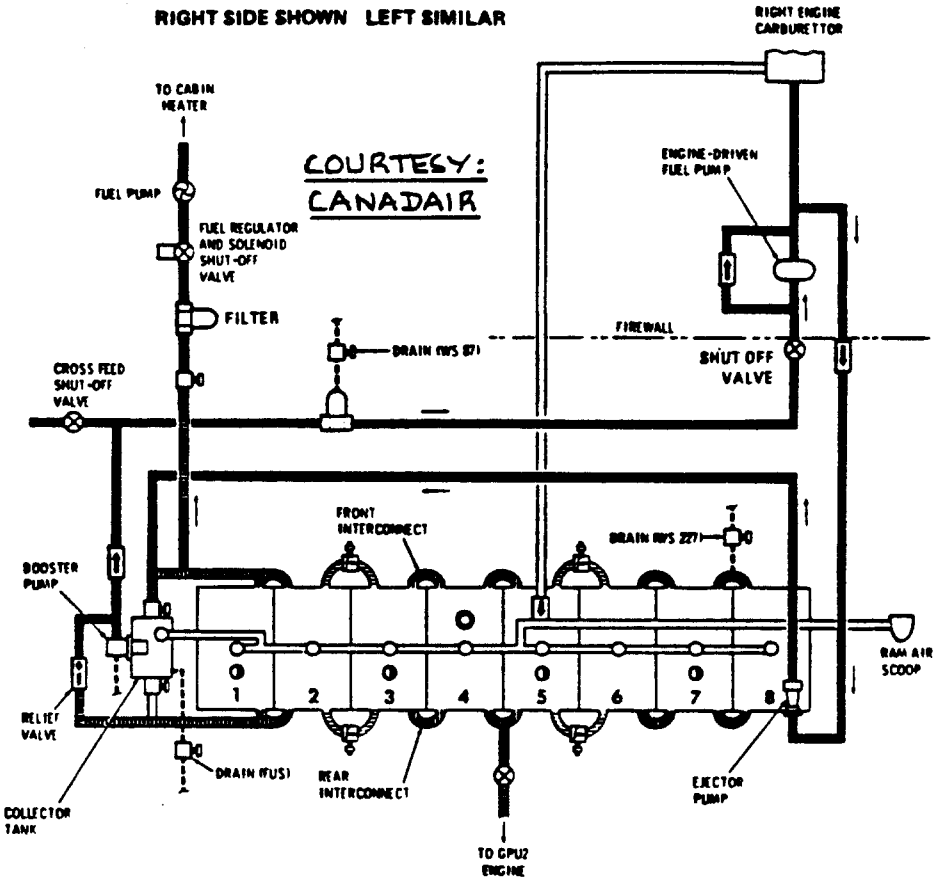

Figure 5.14 Fuel System Schematic: Canadair CL215

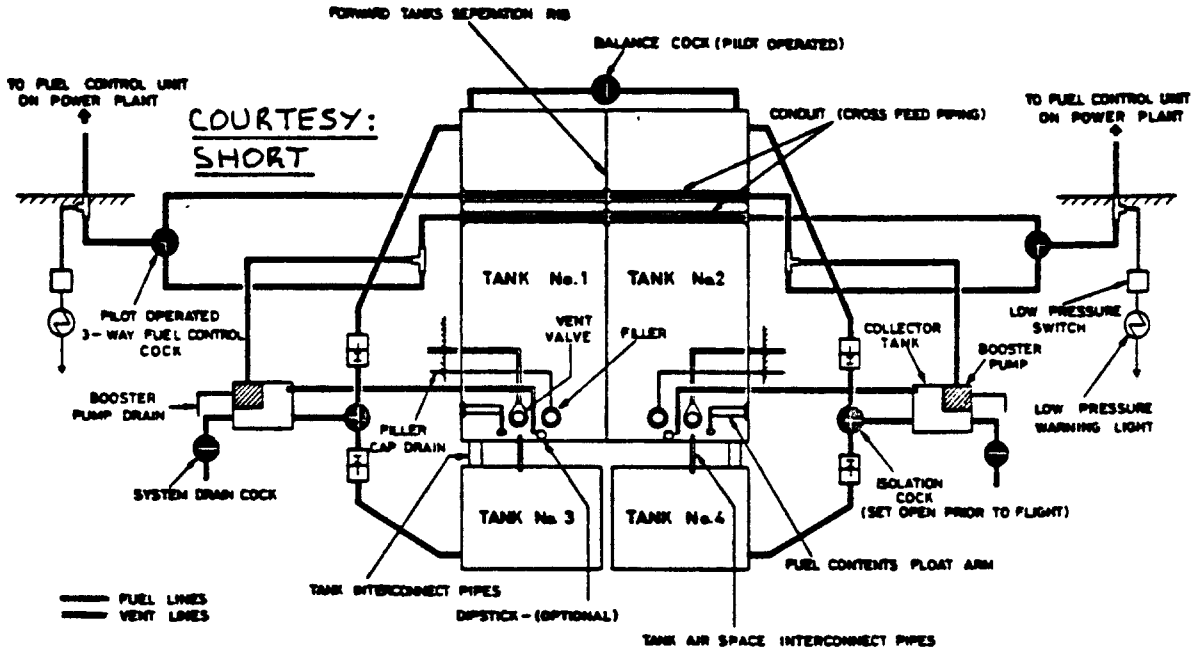

Figure 5.15 Fuel System Schematic: Short Skyvan

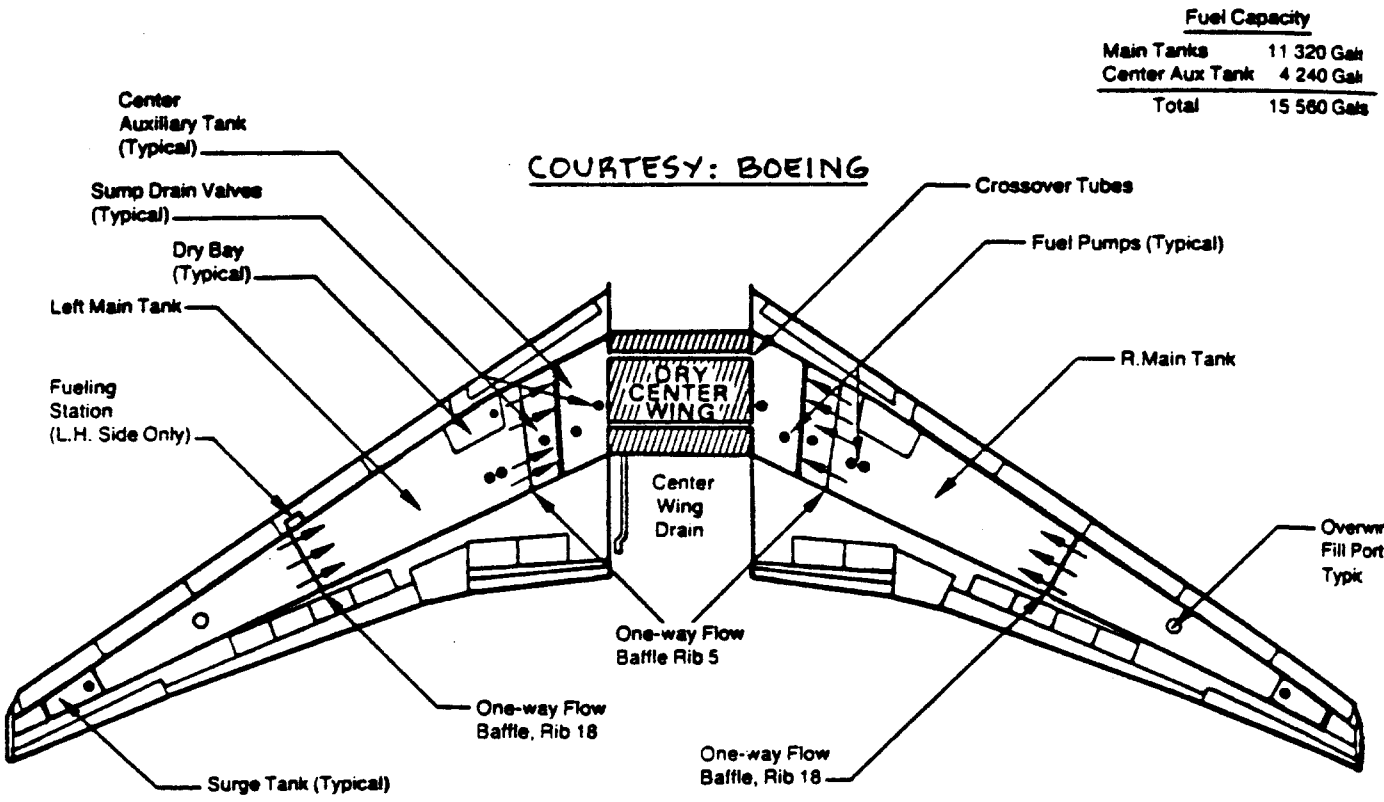

Figure 5.16 Fuel System Schematic: Boeing 767

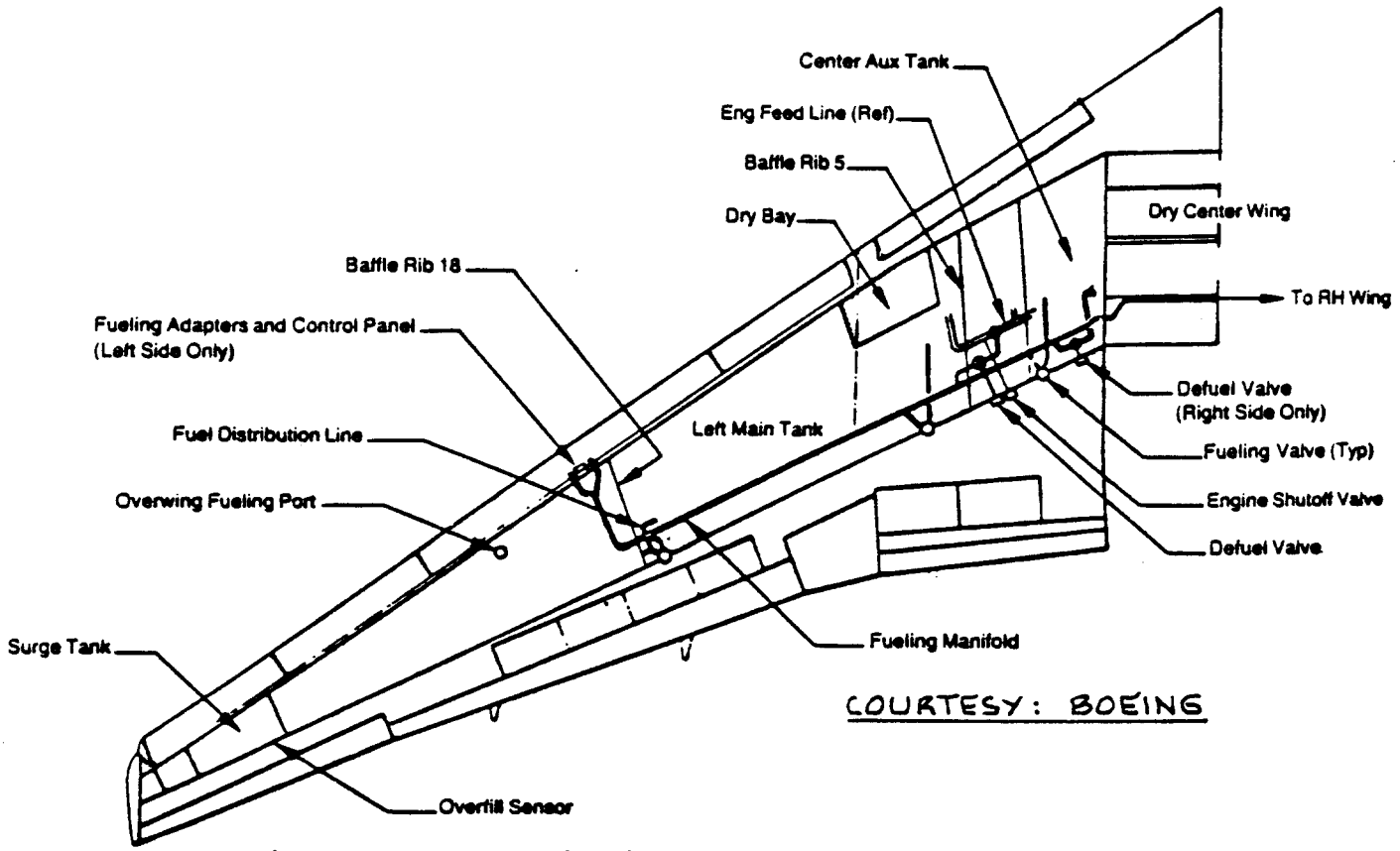

Figure 5.17 Fueling/Defueling System: Boeing 767

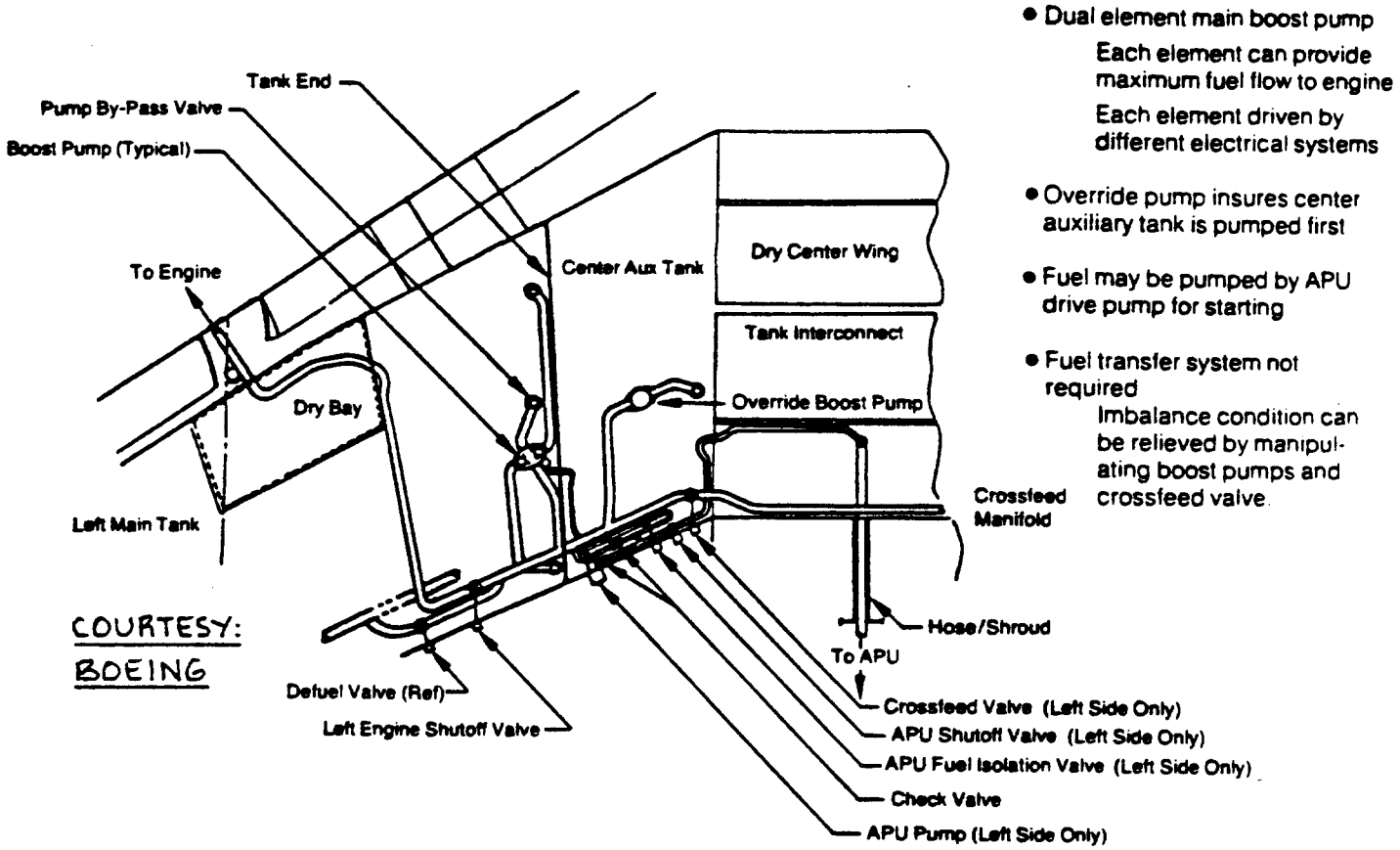

Figure 5.18 Engine Fuel Feed System: Boeing 767

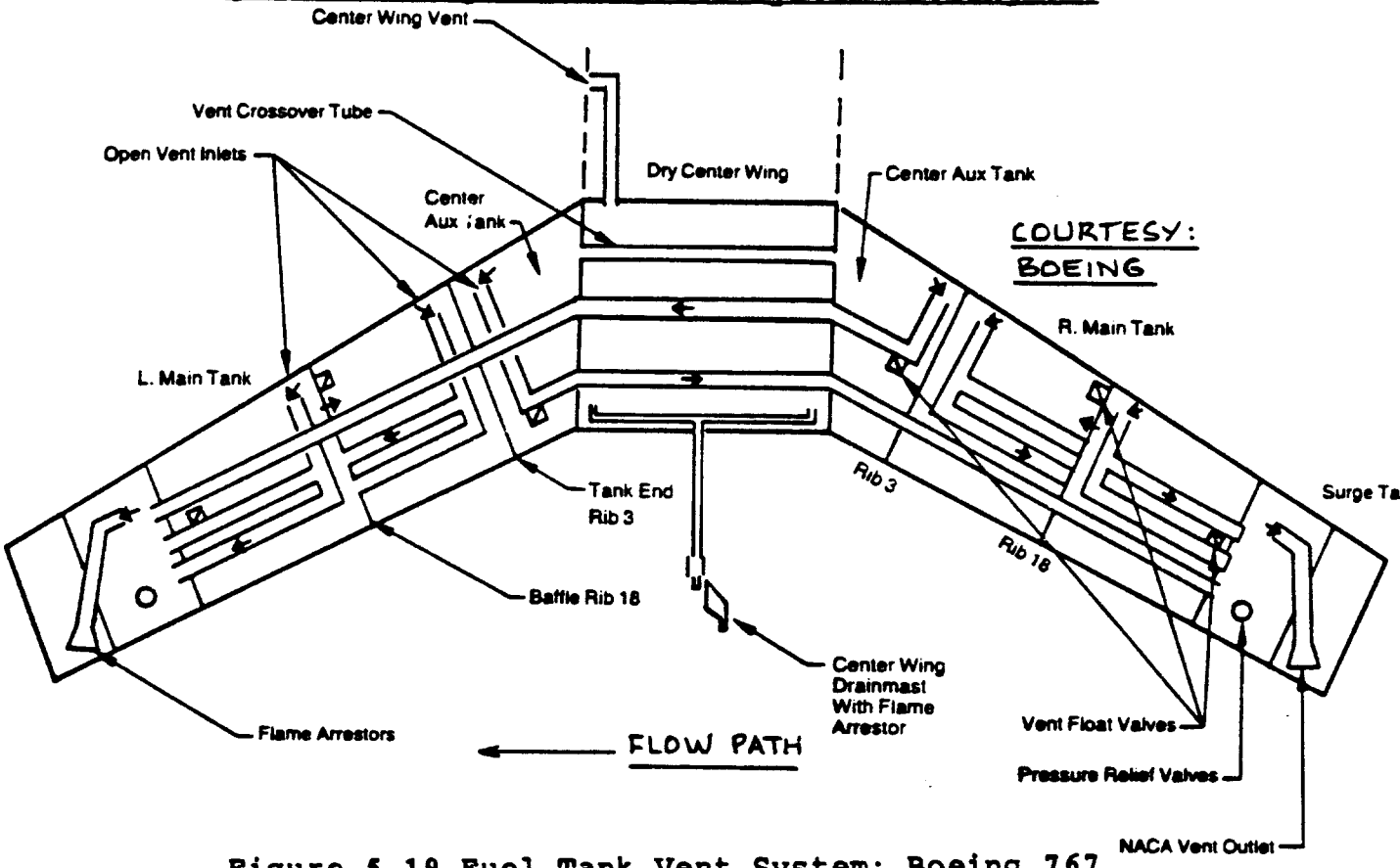

Figure 5.19 Fuel Tank Vent System: Boeing 767

- Inlets to ejector pumps located between ribs of lower wing skin
- Ejector pumps draw out any condensate in bottom of tanks before large amounts collect
- Outputs of ejector pumps removed through boost pumps

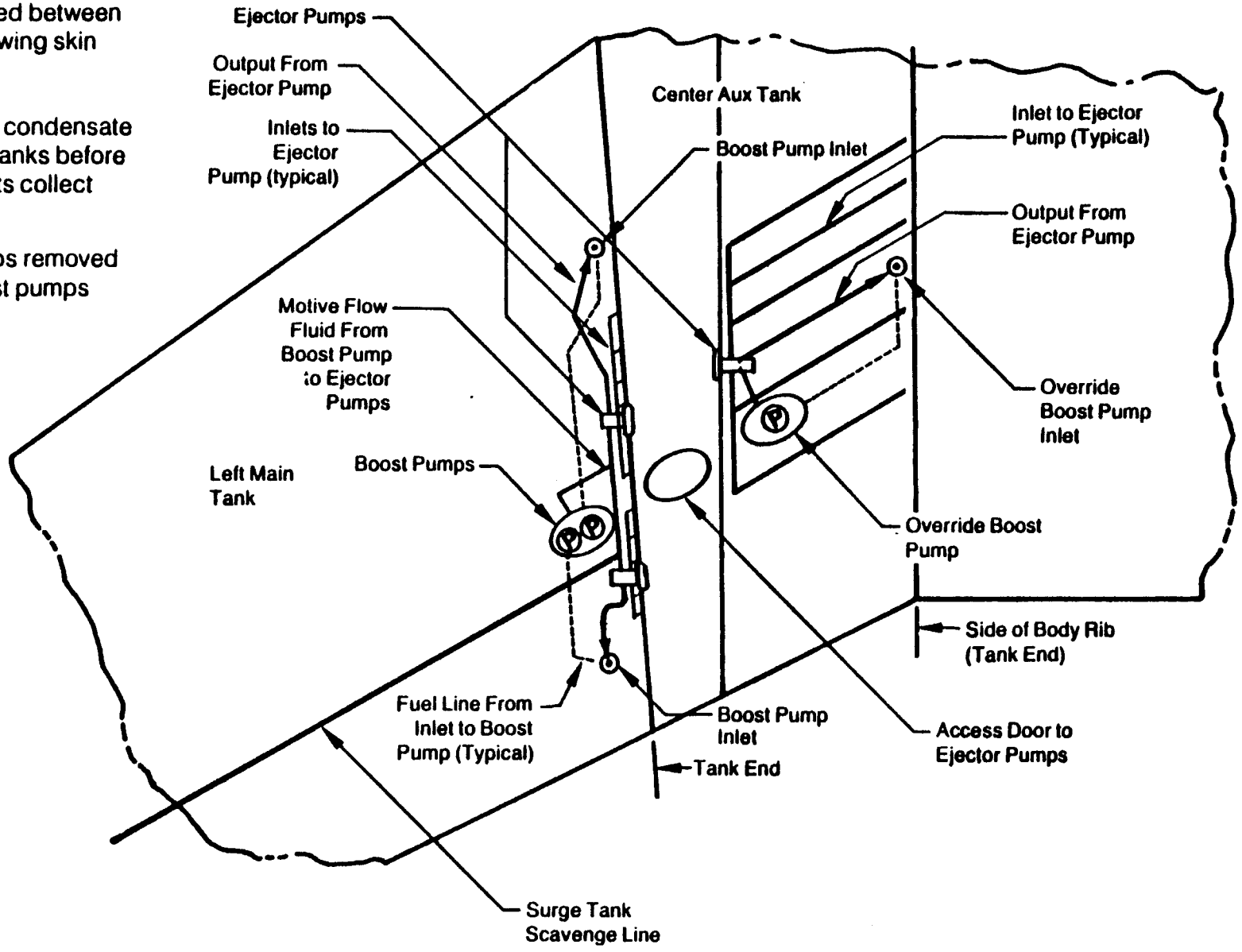

Figure 5.20 Automatic Sumping System: Boeing 767

6. HYDRAULIC SYSTEM LAYOUT DESIGN

In this chapter some fundamental design layout requirements for hydraulic systems will be discussed. The material is organized as follows:

6.1 Functions of the hydraulic system

6.2 Sizing of the hydraulic system

6.3 Guidelines for hydraulic system design

6.4 Hydraulic system layout examples

6.1 FUNCTIONS OF HYDRAULIC SYSTEMS

The functions of hydraulic systems vary from one airplane to the other. Typical functions are to provide hydraulic power to actuators with the following tasks:

1. Moving primary flight controls: ailerons, elevator, stabilizer, rudder and spoilers.

2. Moving secondary flight controls:

   a) high lift devices (flaps)
   b) trim controls
   c) speed brakes

3. Extending and retracting of the landing gear

4. Controlling wheel brakes

5. Landing gear steering

6. Operating thrust reversers

Hydraulic systems usually consist of the following components:

1. Hydraulic fluid reservoir: Figure 6.1 shows an example.

2. Hydraulic pumps (engine driven, air-driven, electric driven or RAT driven): Figure 6.2 shows an example. RAT = Ram Air Turbine.

   Note: in some light airplanes a hand driven pump is provided for emergencies.

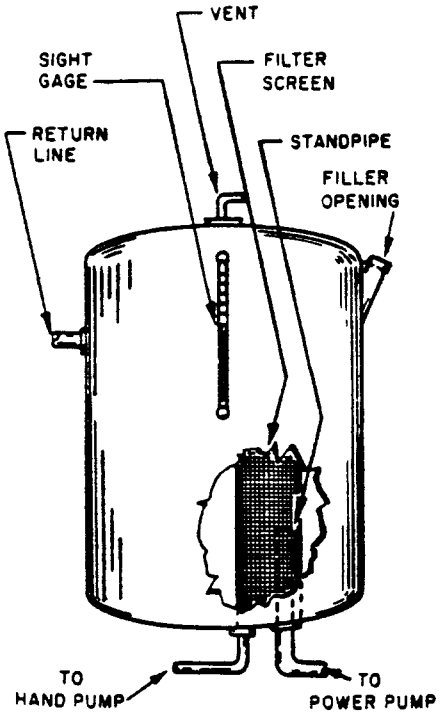

Figure 6.1 Example of a Hydraulic Reservoir

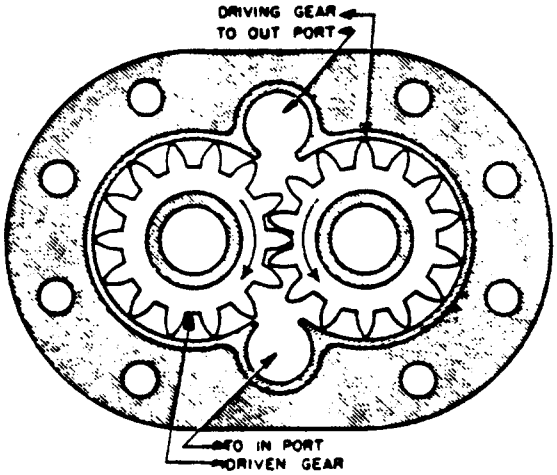

Figure 6.2 Example of a Hydraulic Pump

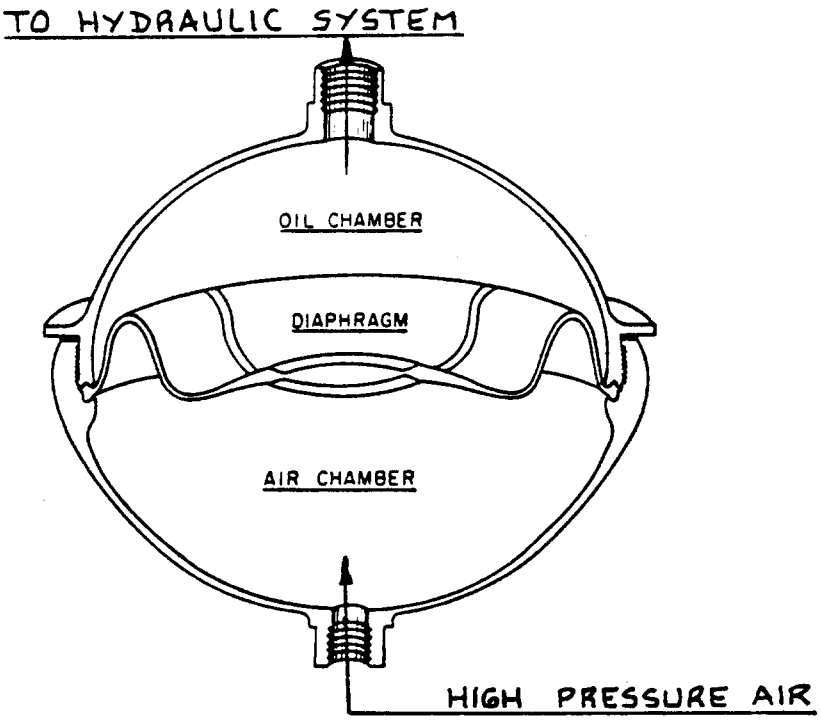

Figure 6.3 Example of a Hydraulic Accumulator

3. Accumulators (mostly used for emergencies): Figure 6.3 shows an example.

4. a) Lines and valves for fluid distribution to all operating points.

   b) Cockpit controls to operate the functions served by the hydraulic system.

   Figure 6.4 shows an example schematic of a hydraulic system used in a light twin. Note the hand driven pump.

The number of hydraulic pumps required depends on the criticality of the hydraulic system to safe flight operations. If the hydraulic system is essential for safe flight operations a large number of pumps and 3-4 independent hydraulic systems may be required. If the hydraulic system is not critical for safe flight operations, a hydraulic accumulator is often used to provide temporary hydraulic pressure if the pumps have failed.

Most hydraulic systems today operate at a pressure level of 3,000 psi and use some version of Skydrol 500 as the operating fluid.

Reference 28 contains a discussion of the design requirements for future 8,000 psi systems. The major advantages of such high pressures are much reduced weight and installed volume.

References 29 and 33 contain excellent detailed discussions of the functions of hydraulic system components.

In Chapter 4 the possible use of electrohydrostatic actuators was mentioned. With such actuators it is in principle possible to eliminate the hydraulic system entirely from future airplane.

6.2 SIZING OF THE HYDRAULIC SYSTEM

6.2.1 Normal Operation

The maximum amount of hydraulic fluid flow required for the operation of an airplane normally occurs in the landing phase: the primary and secondary flight controls, the landing gear and speed brakes may all have to be operated simultaneously.

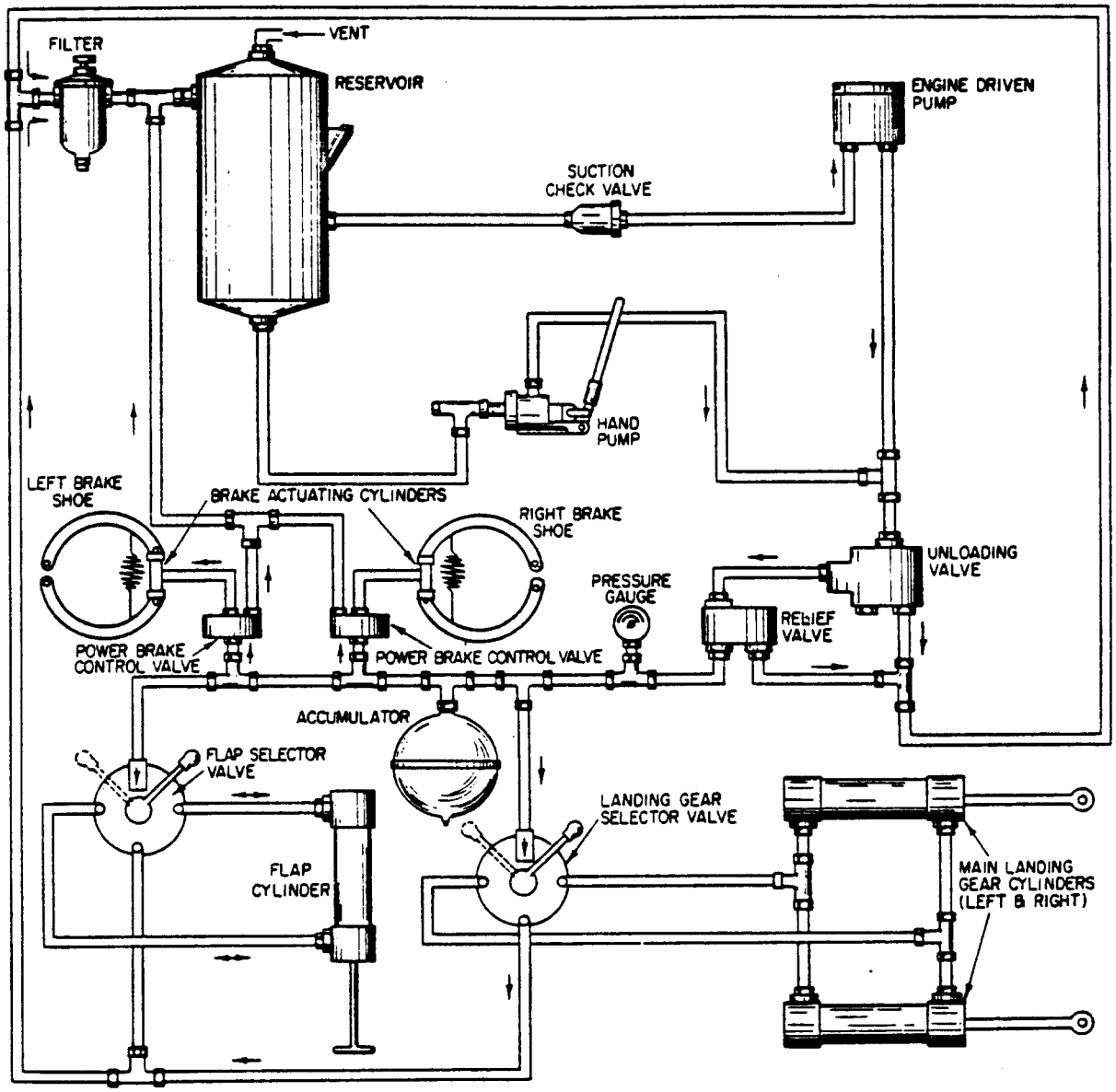

COURTESY : NORTHROP UNIVERSITY

Figure 6.4 Hydraulic System Schematic for a Light Twin

A convenient way to analyze the total fluid flow requirements is to make a list of the actuator rate and force requirements from which the 'gallons-per-minute' flow requirement is obtainded by summation. Such a hydraulic system load analysis will be different for each type of airplane.

Table 6.1 provides some data on hydraulic system capabilities of several airplanes.

Power requirements for hydraulic systems range from 1-5 hp in light airplanes to 200-300 hp in transports and up to 700 hp in large tactical fighters.

6.2.2 Emergency Operation

Hydraulic pumps or their power source (such as the engines or electric power sources) can fail. It depends on the type of airplane and the criticality of functions served by the hydraulic system whether or not back-up systems need to be provided.

Typical back-up systems used in many airplanes include:

1. Accumulators to provide short duration hydraulic pressure for lowering the landing gear. Figure 6.4 gives an example.

2. APU and/or RAT to provide long duration emergency stand-by popwer to operate the flight controls. APU installations are discussed in Chapter 7. Fig.6.5 gives an example of a RAT installation. APU = Auxiliary Power Unit, RAT = Ram Air Turbine.

6.3 GUIDELINES FOR HYDRAULIC SYSTEM DESIGN

1. It is essential to make a list of functions to be served by the hydraulic system under normal and under emergency operating conditions. Table 6.2 shows such a list for the Boeing 737-200.

2. Many hydraulic system components require service and maintenance. Make sure that these components can be accessed.

3. Do not route the hydraulic supply lines to flight critical controls such that they all fail together in case of:

a) engine component disintegration

Table 6.1 Airplane Hydraulic System Capabilities

Airplane Type	Hydraulic Pressure	Systems Serviced	System Flow Capacity	System Pumps
Canadair CL215	3,000 psi	Flaps, landing gear, wheel brakes, water doors	4 gpm 1.1 gpm	2 engine driven 1 auxiliary
Short Skyvan	2,500 psi	Flaps, nosewheel steering, wheel brakes		1 electric 1 accumulator
Gates Learjet M25	1,500 psi	Flaps, spoilers, landing gear, wheel brakes	4 gpm 0.3 gpm	2 engine driven 1 auxiliary
Boeing 757	3,000 psi	Flight controls, landing gear, wheel brakes, nose-wheel steering, thrust reversers	74 gpm 27 gpm 11 gpm	2 engine driven 3 electric RAT*
Boeing 767	3,000 psi	Flight controls, landing gear, nose-wheel steering wheel brakes, thrust reversers	74 gpm 37 gpm 16 gpm 9.6 gpm	2 engine driven 1 air driven by APU* 2 electric 1 RAT*

* RAT = Ram Air Turbine APU = Auxiliary Power Unit

Ram Air Turbine (RAT) Features

- Automatic or manual deployment
  - Manual deployment by pushbutton on pilot's overhead panel
  - Automatic deployment if both engines fail when airborne
- Fully deployed in 2 seconds
- Drives a hydraulic pump to operate flight controls on center hydraulic system
- Proper operation shown in flight deck display
- Deployment/retraction by DC motor, powered by separate battery
- Retraction by manual switch in wheelwell

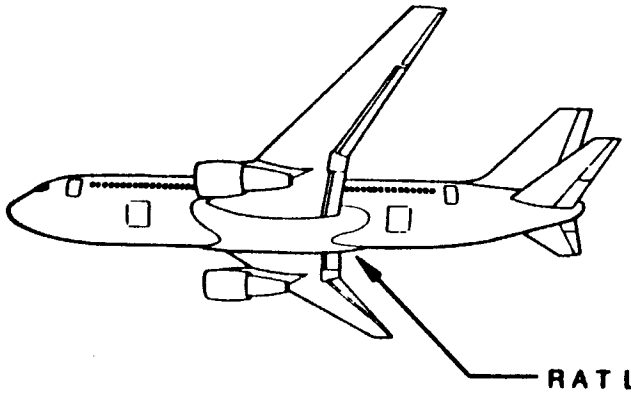

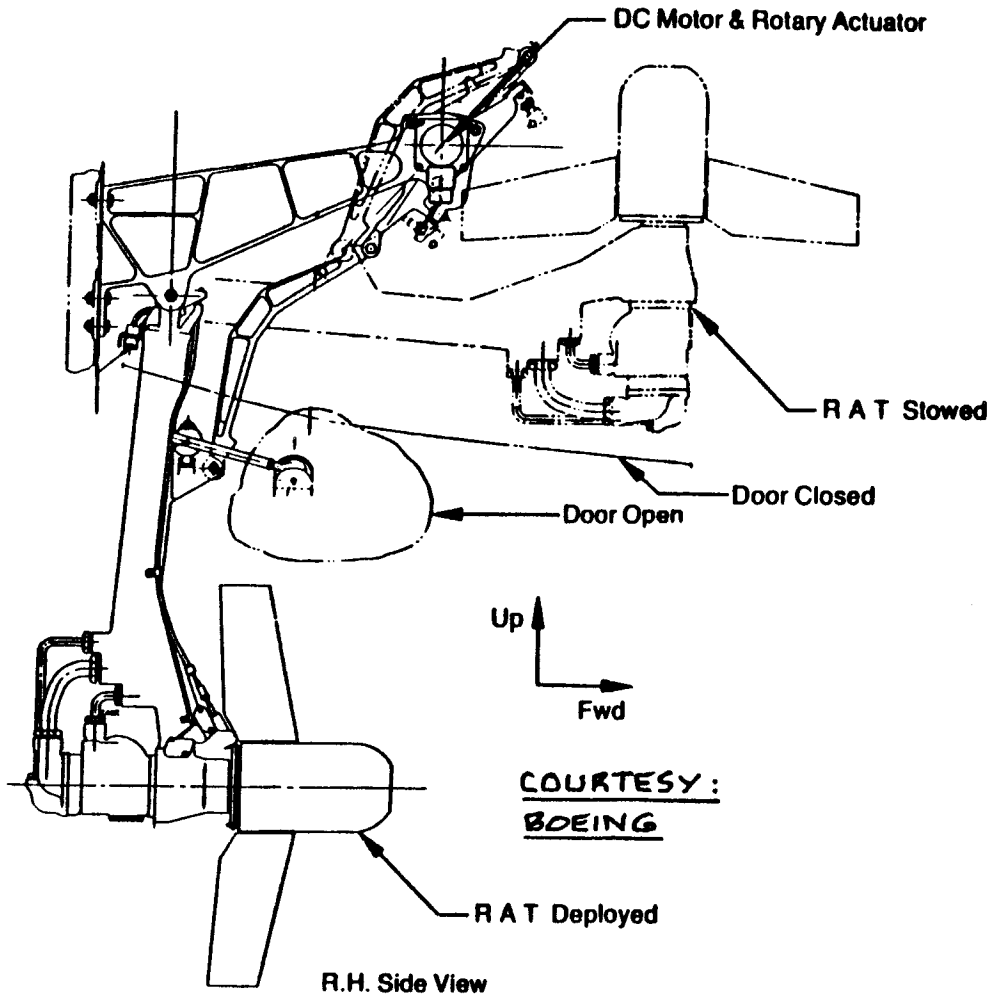

Figure 6.5 Ram Air Turbine Installation: Boeing 767

Table 6.2 Hydraulic System Function Distributions for the Boeing 737-200

Powered units	Normal hydraulic system power	Alternate operation
Flight controls		
• Ailerons	A and B	Manual reversion
• Elevators	A and B	Manual reversion
• Rudder	A and B	Standby hydraulic system
• Flight spoilers		
• Inboard	A	Outboard spoilers available
• Outboard	B	Inboard spoilers available
• Ground spoilers	A	-
• Trailing-edge flaps	A	Electrical
• Leading-edge flaps and slats	A	Standby hydraulic (extension only)
Landing gear		
• Main and nose gear	A	Manual release and "free fall" extension
• Nose gear steering	A	Differential braking
• Brakes		
• Inboard wheels	A	Outboard brakes available, brake accumulator
• Outboard wheels	B	Inboard brakes available, brake accumulator
Thrust reverser	A	

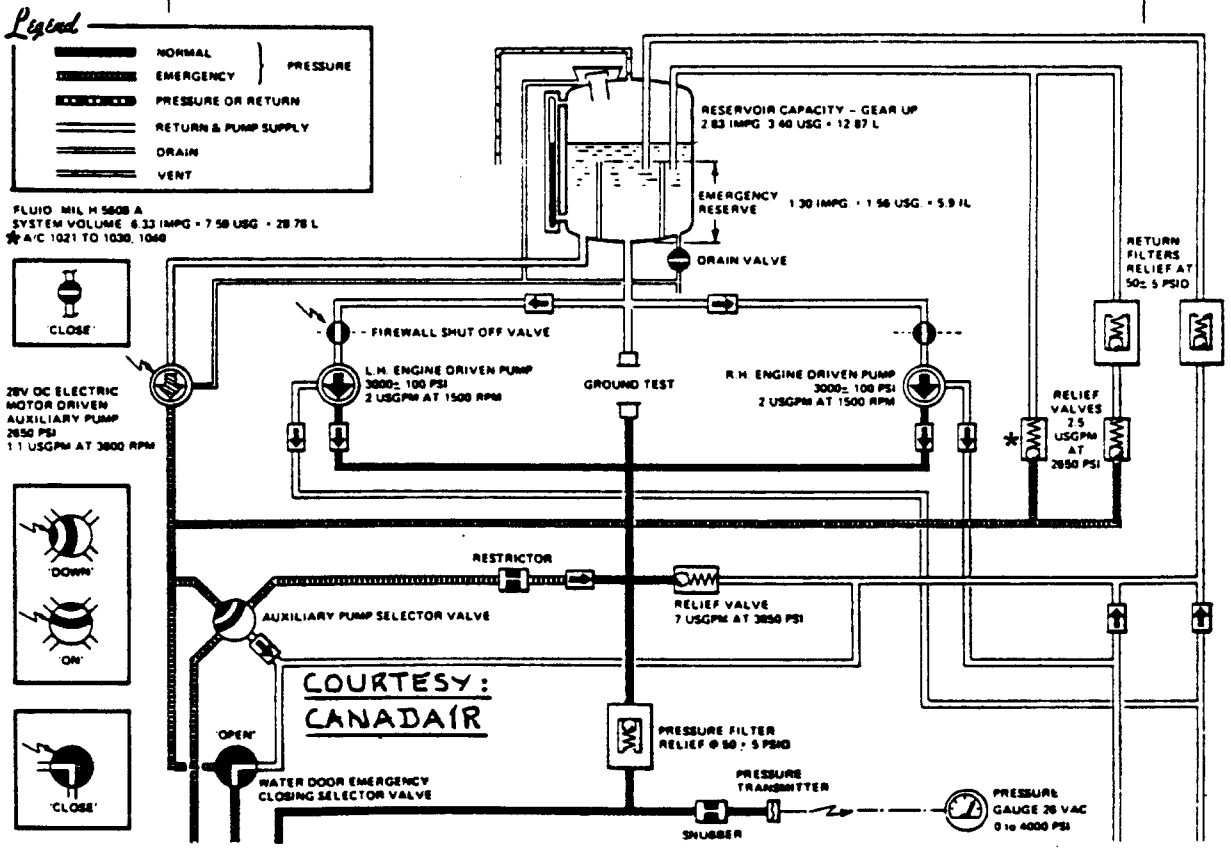

Figure 6.6 Hydraulic System Schematic: Canadair CL215

b) terrorist action
c) failure of adjacent structure

In other words: do not route critical hydraulic lines close together.

4. Make sure that 'independent' systems are truly independent.

6.4 HYDRAULIC SYSTEM LAYOUT EXAMPLES

Figures 6.6 through 6.13 provide examples of hydraulic system layouts. Comments on these figures are given next.

Figure 6.6 Hydraulic System Schematic: Canadair CL215

Note that this system has two engine driven pumps and one electric auxiliary pump.

Figure 6.7 Hydraulic System Schematic: Short Skyvan

The hydraulic power pack employs one electric pump and a nitrogen charged accumulator for emergency use.

Figure 6.8 Hydraulic System Schematic: Gates Learjet M25

This system has two engine driven pumps and an accumulator for emergency services.

Figure 6.9 Hydraulic System Functions: Boeing 767

Because of the flight criticality of this hydraulic system it uses three independent systems each with their own power supply. Note that there are three different types of hydraulic pump: engine driven, electric driven and air driven. On top of these there is a RAT driven pump, if all else fails.

Figure 6.10 Hydraulic System Schematic: McDD DC-10

Because of the flight criticality of this hydraulic system it uses three independent systems. Each system is driven by two engine driven pumps. One system may also be driven by an electric pump.

Note that the landing gear has a mechanical free-fall capability.

Figures 6.11 - 6.13 illustrate the redundant aspects of critical flight control hydraulics in more detail.

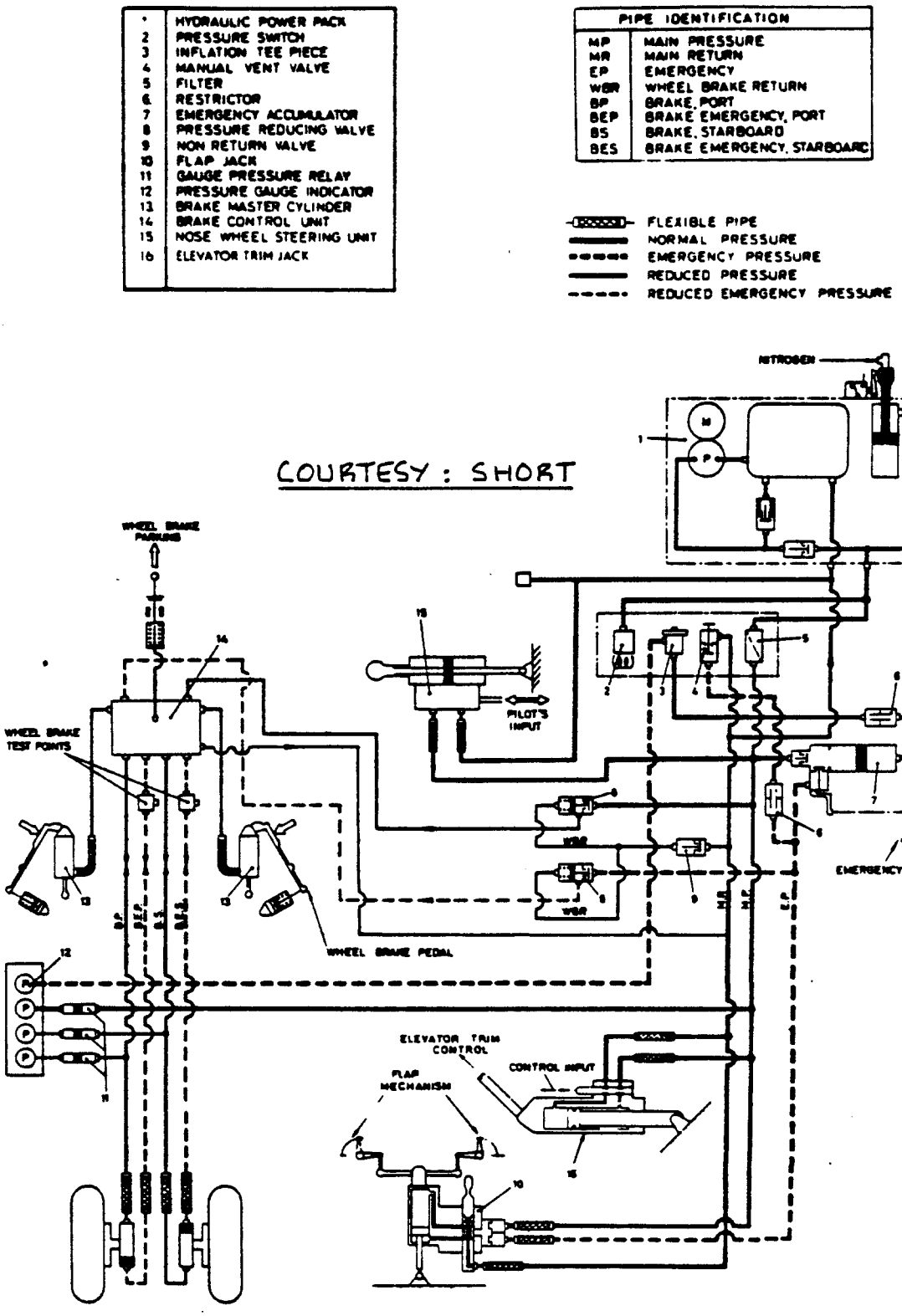

Figure 6.7 Hydraulic System Schematic: Short Skyvan

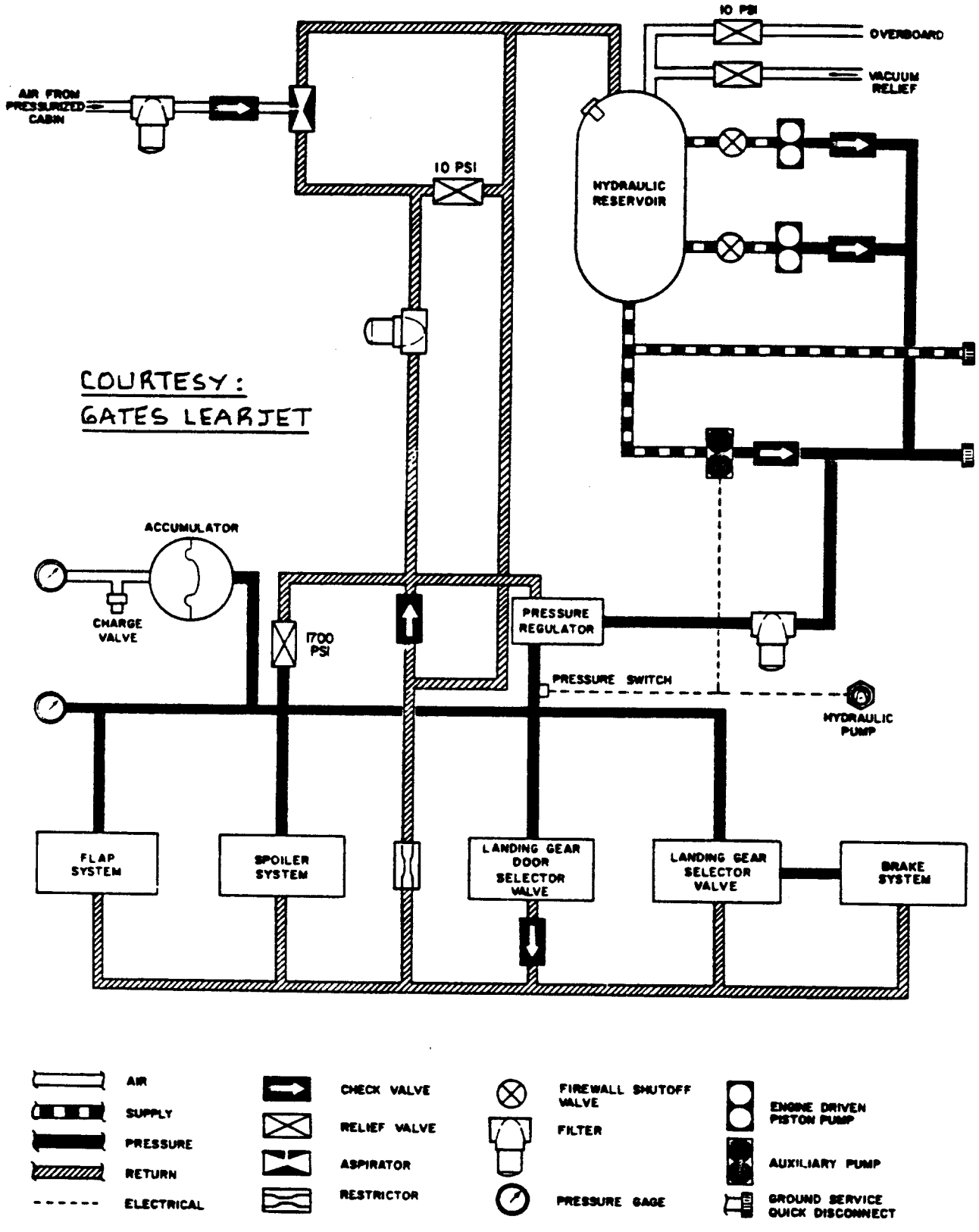

Figure 6.8 Hydraulic System Schematic: Gates Learjet M25

- Three independent 3000 psi systems
- 747 type engine-driven pumps
- Electric motor pumps on all systems available for ground operations
- All power components located to facilitate servicing
- Erosion reduction through use of type IV fluid and improved valve design
- Titanium pressure tubing (3Al-2.5V)
- Ram air turbine for emergency flight control hydraulic power source—retractable, located aft of landing gear wells

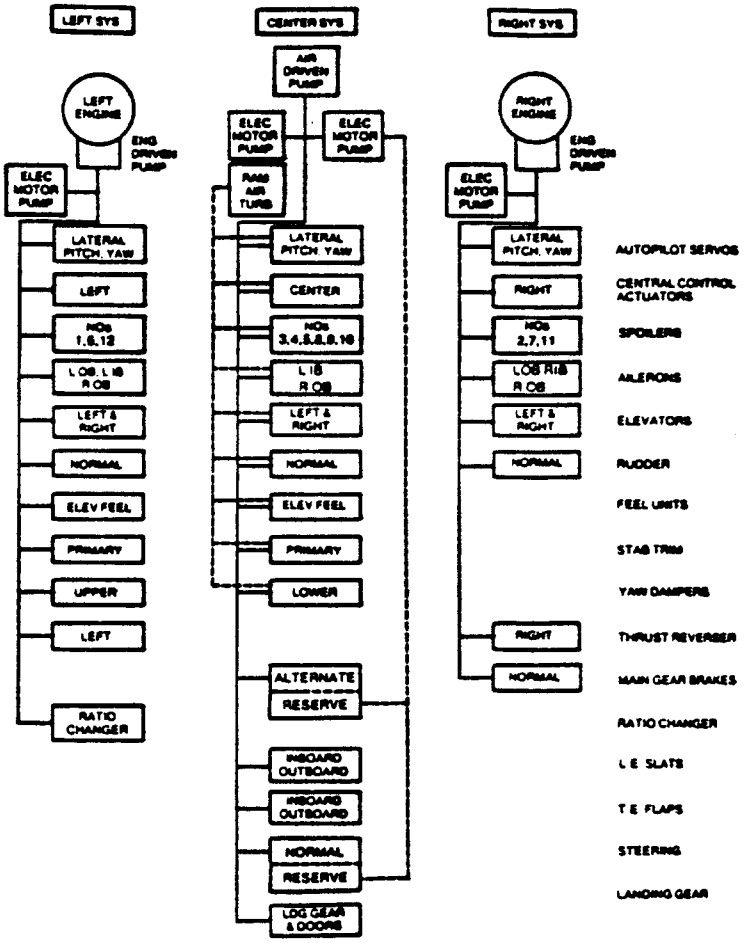

COURTESY: BOEING

Figure 6.9 Hydraulic System Functions: Boeing 767

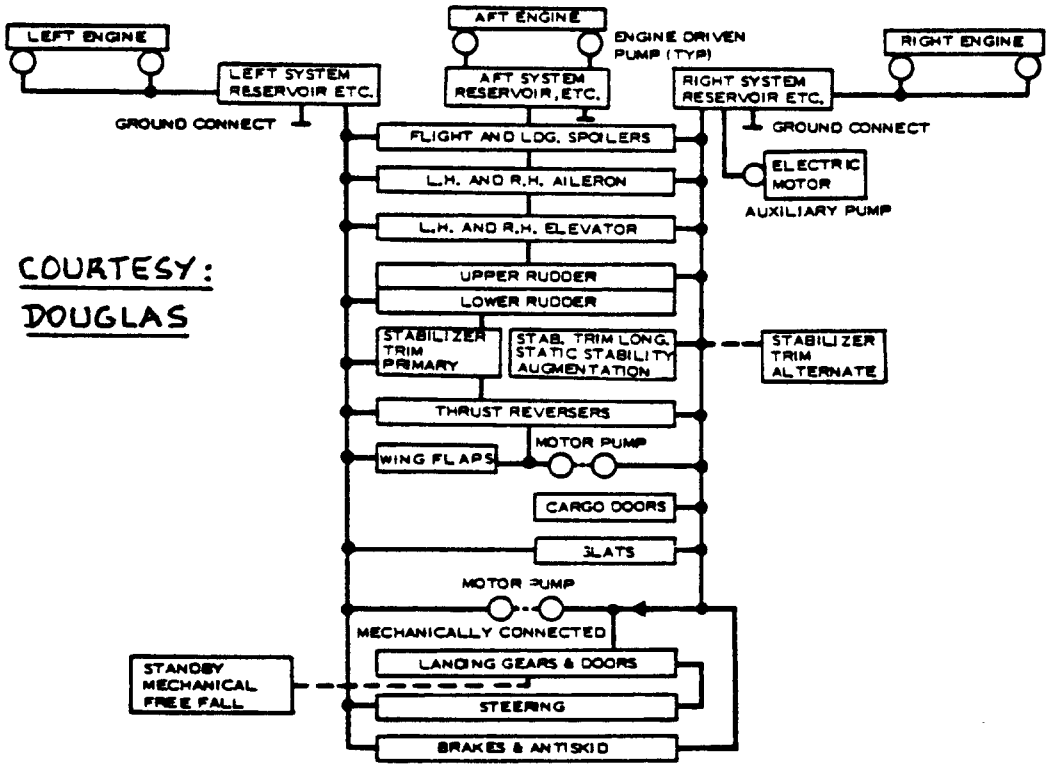

COURTESY: DOUGLAS

Figure 6.10 Hydraulic System Schematic: McDD DC-10

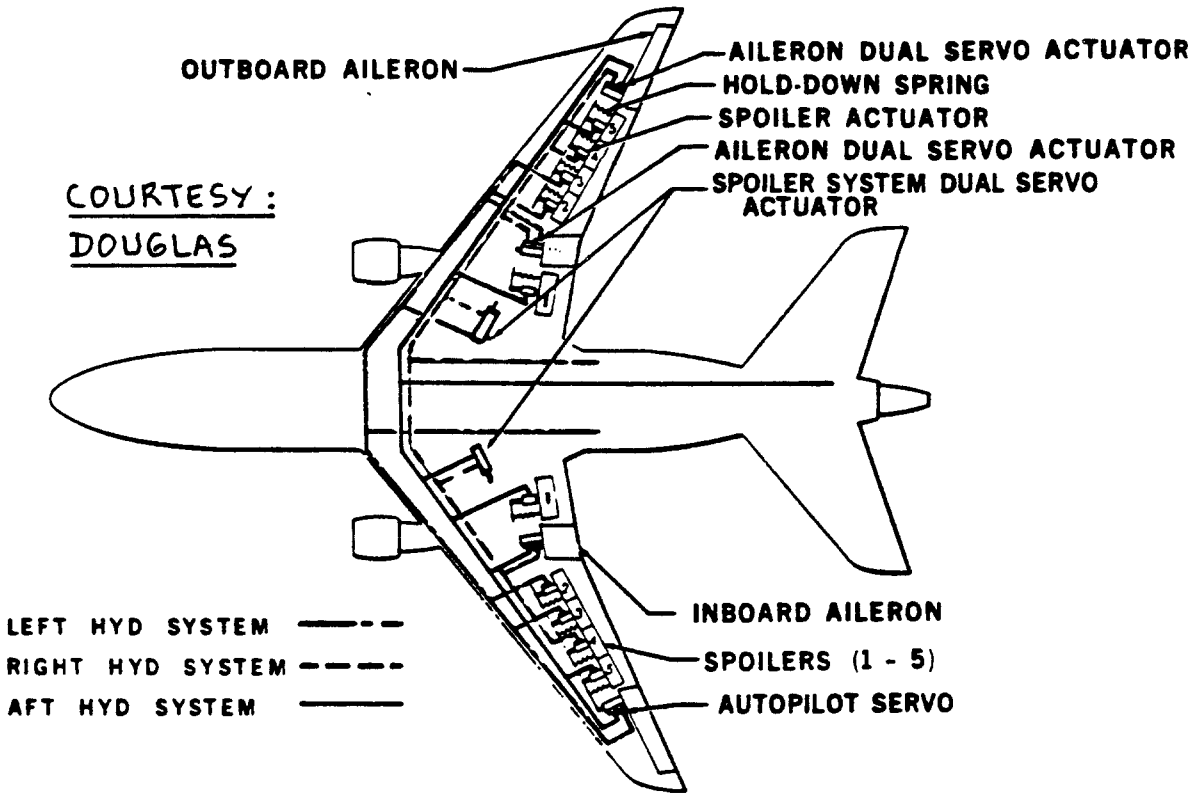

Figure 6.11 Lateral Control and Ground Spoiler Hydraulic System: McDD DC-10

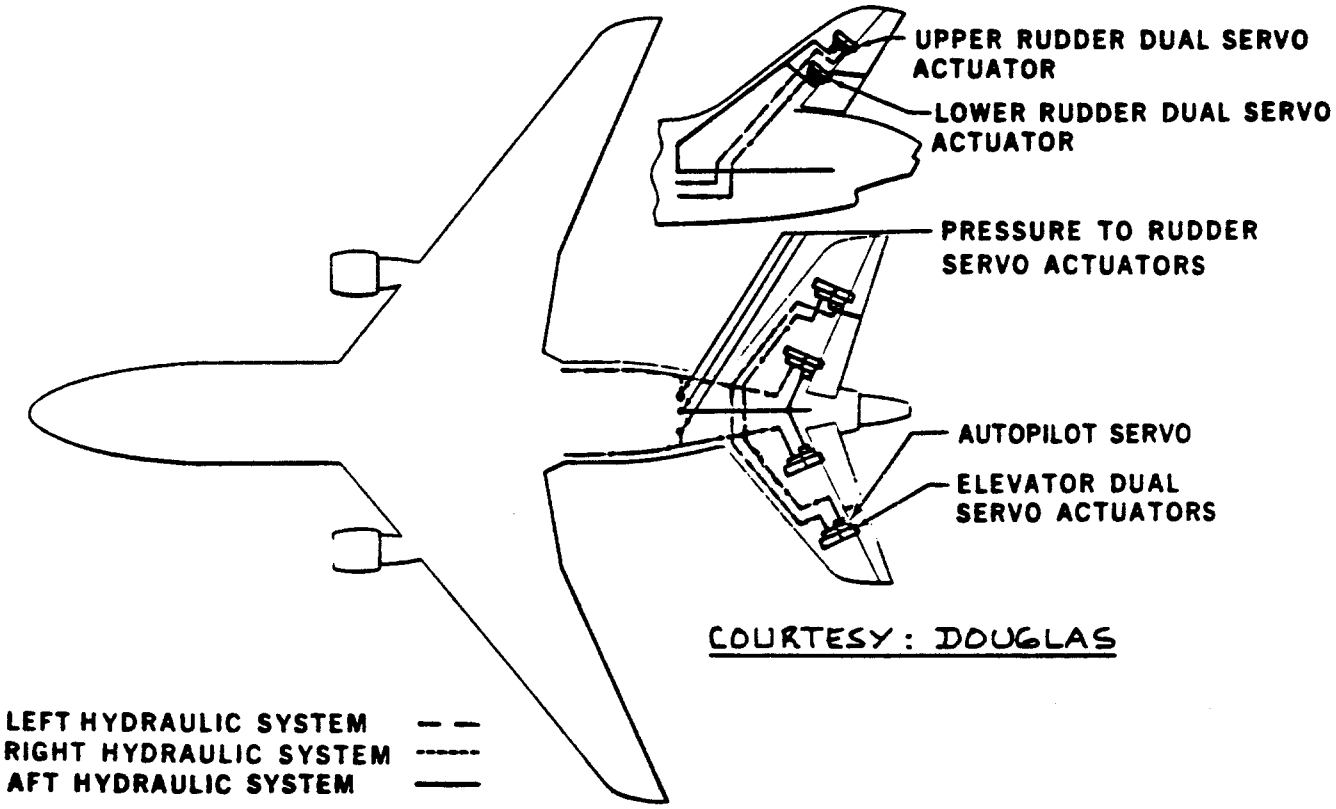

Figure 6.12 Longitudinal and Directional Control Hydraulic System: McDD DC-10

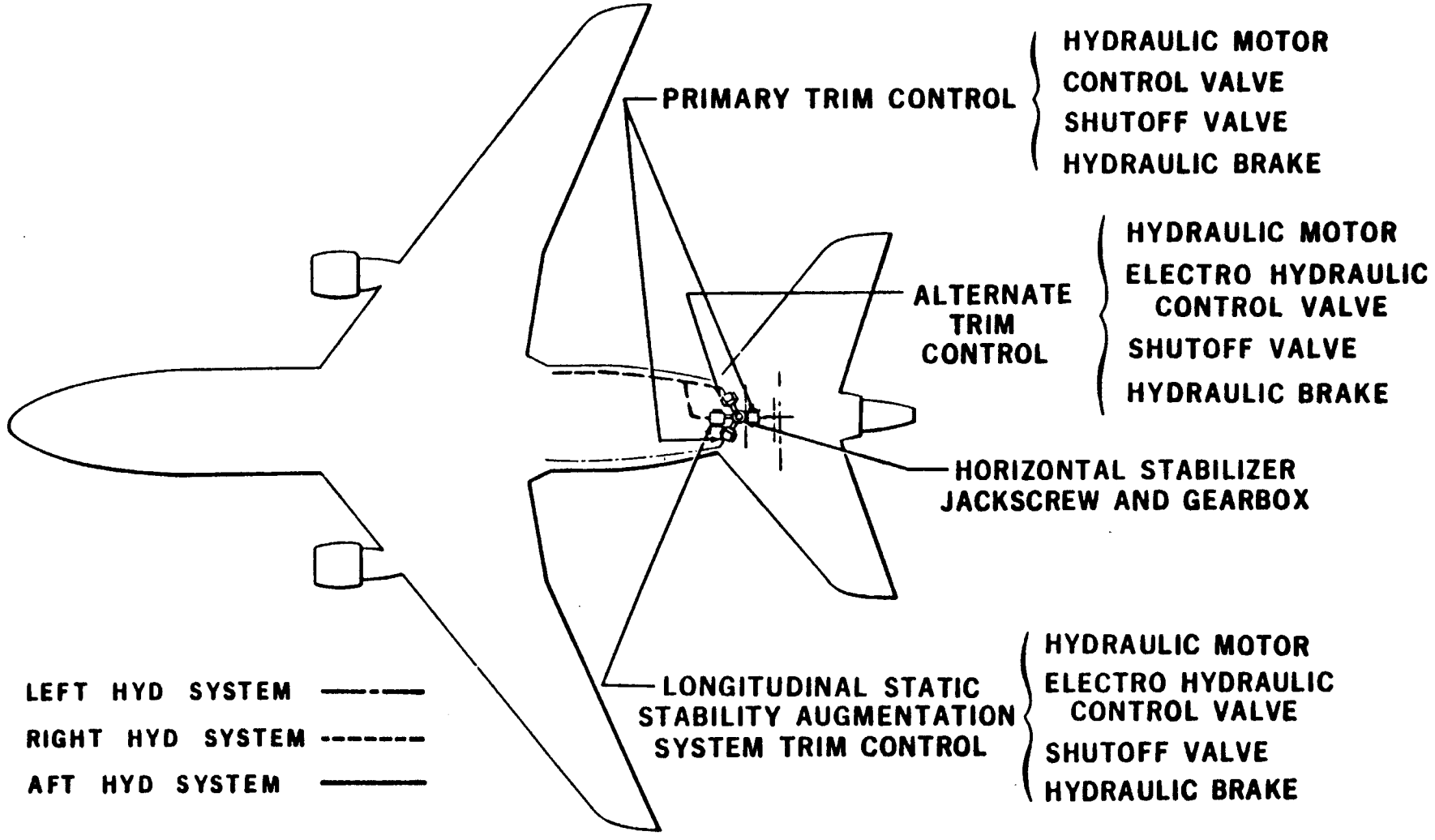

Figure 6.13 Horizontal Stabilizer Hydraulic System: McDD DC-10

7. ELECTRICAL SYSTEM LAYOUT DESIGN

Virtually all airplanes require electrical power for the operation of a large number of systems. Examples of systems requiring electrical power are:

1. Internal and external lighting

   Figure 7.1 shows an example of the external light installation in a jet transport. The angles from which landing lights and navigation lights must be visible are important. Figure 7.2 illustrates typical visibility angles for exterior lights.

2. Flight instruments and avionics systems

   Chapter 9 addresses the layout of these systems.

3. Food and beverages heating systems

   These systems are not addressed in this text: the reader should consult manufacturers brochures which cover passenger amenities.

4. Engine starting systems

   These systems are not addressed in this text.

5. Flight control systems (primary and secondary)

   Chapter 4 contains detailed descriptions of flight control systems.

Electric power is normally provided by two systems:

1.) Primary power generating system

   Primary power is usually delivered by engine driven generators.

2.) Secondary (stand-by) power generating system(s)

   Secondary power systems supply electrical power in case of failure of the primary system. These secondary power systems may consist of:

   a) Battery system
   b) Auxiliary power unit (APU)
   c) Ram-air turbine (RAT)

- Emergency lights battery powered
  - Illuminated automatically with electric power loss
  - May be illuminated upon command from flight deck panel or forward attendant panel
- Landing lights in each wing root (1) and on nose gear (2)
  - Each wing root light and nose gear light may be illuminated separately
  - Nose gear lights aimed along glide path
  - Wing root lights aimed horizontally
- Anticollision strobe lights on fuselage (red) and wingtips (white)
- Two forward-facing position lights and two aft-facing position lights on each wingtip
- Taxi light, logo lights, and external cargo handling lights optional

COURTESY : BOEING

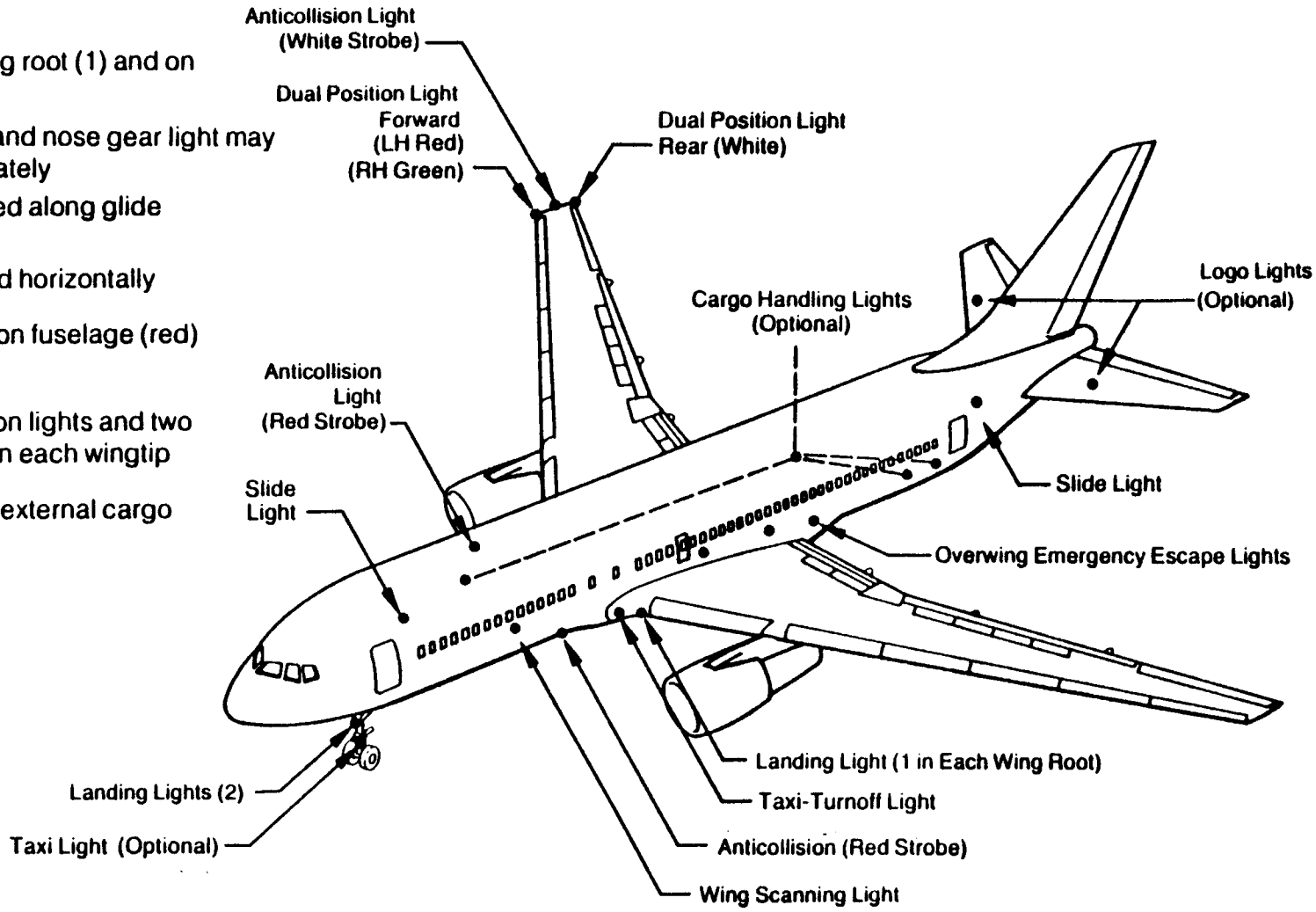

Figure 7.1 Exterior Light Installations: Boeing 767

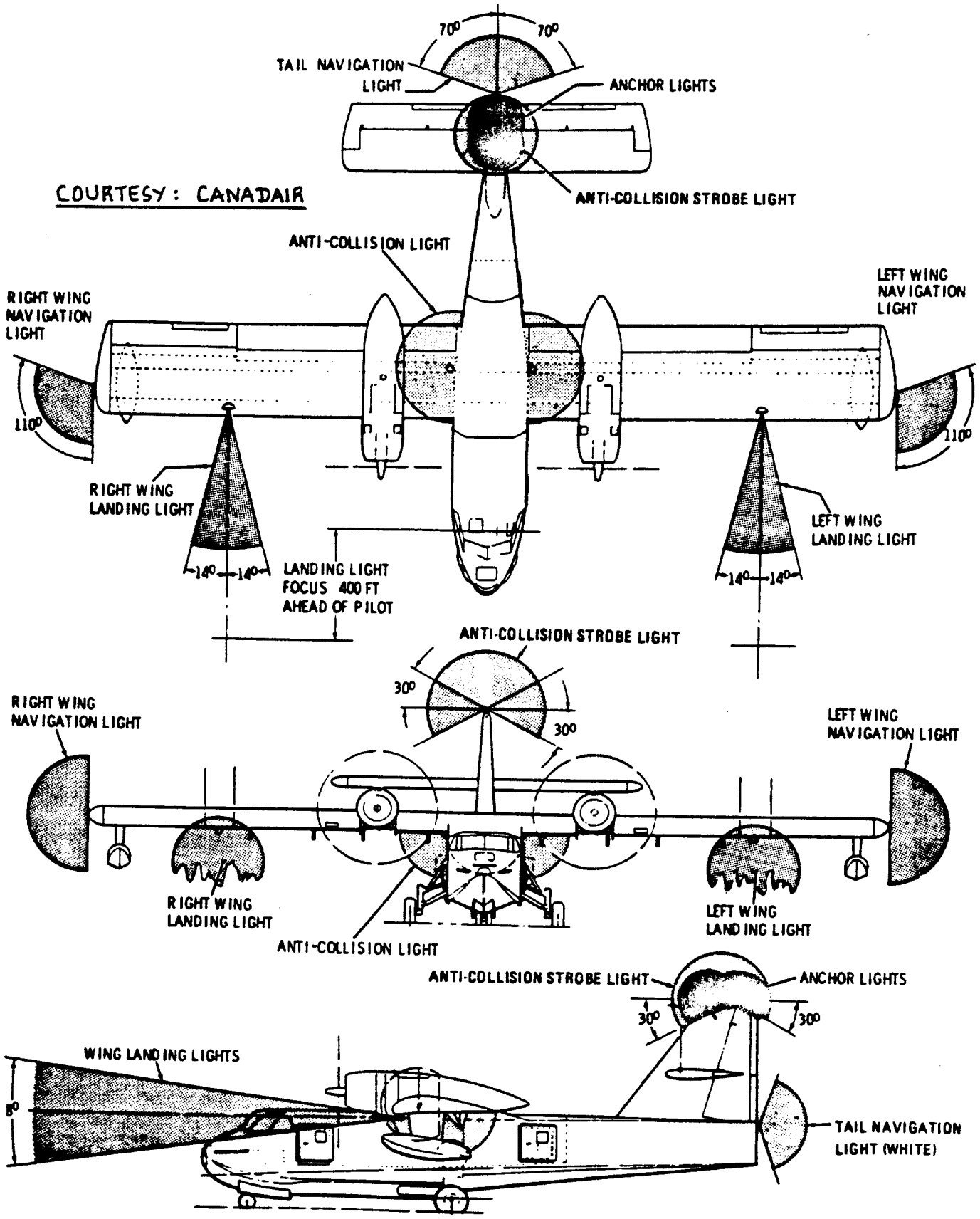

Figure 7.2 Exterior Lighting Visibility Angles: Canadair CL215

Reference 34 contains excellent descriptions of airplane electrical system operation, sizing and design.

Many experts in the airplane field believe that in the near future electrical systems will also replace existing pneumatic and hydraulic systems. An excellent article which foreshadows this change is Reference 35.

The material in this chapter is organized as:

7.1 Major components of electrical systems

7.2 Sizing of electrical systems

7.3 Example layouts of electrical systems

7.1 MAJOR COMPONENTS OF ELECTRICAL SYSTEMS

Under normal operating conditions electrical power is generated by engine driven generators and/or alternators. These devices may be designed for generation of DC or AC power. In some airplanes DC generators can be reversed and also used as starter motors. Figure 7.3 shows a cross section through a modern 90 KVA generator such as used in the Boeing 767.

In the case of DC generators their primary power is fed to the DC bus(es) of the airplane and/or to inverters to derive AC power.

In the case of AC generators, their primary power is fed to the AC bus(es) of the airplane and to transformer/rectifier systems to derive DC power.

Reference 34 contains methods for sizing of electrical wiring and buses. Descriptions of other essential components of electrical systems are also included.

7.2 SIZING OF ELECTRICAL SYSTEMS

To determine the maximum amount of electric power needed in an airplane it is necessary to construct so-called electric power load profiles for the airplane.

Figure 7.4 shows an example of such a profile. Tables 7.1 - 7.3 summarize the electric power requirements needed during ground loading, take-off and climb and during cruise. Similar tables must be constructed for all mission phases of the airplane.

Electrical systems are designed for two types of

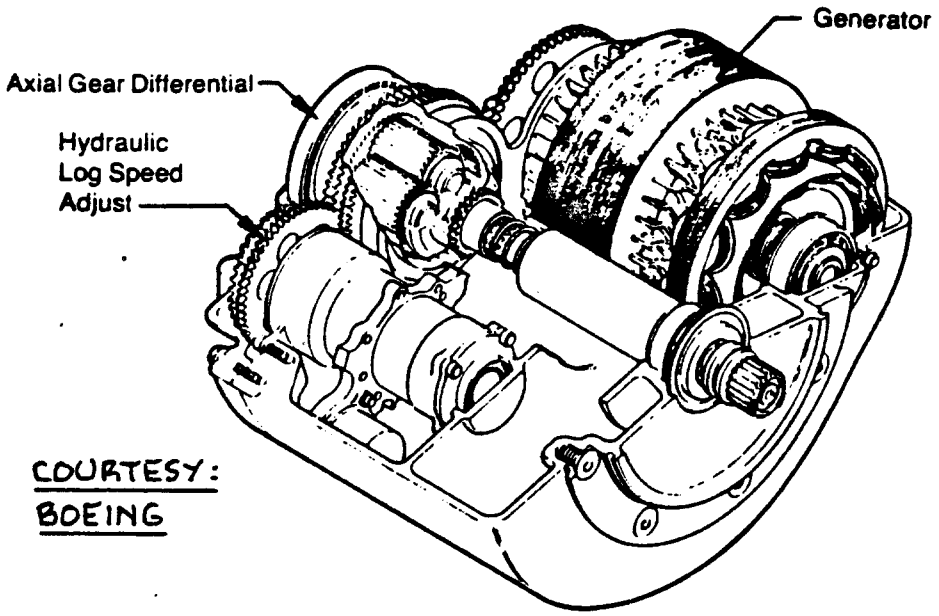

Figure 7.3 Integrated Drive/Generator: Boeing 767

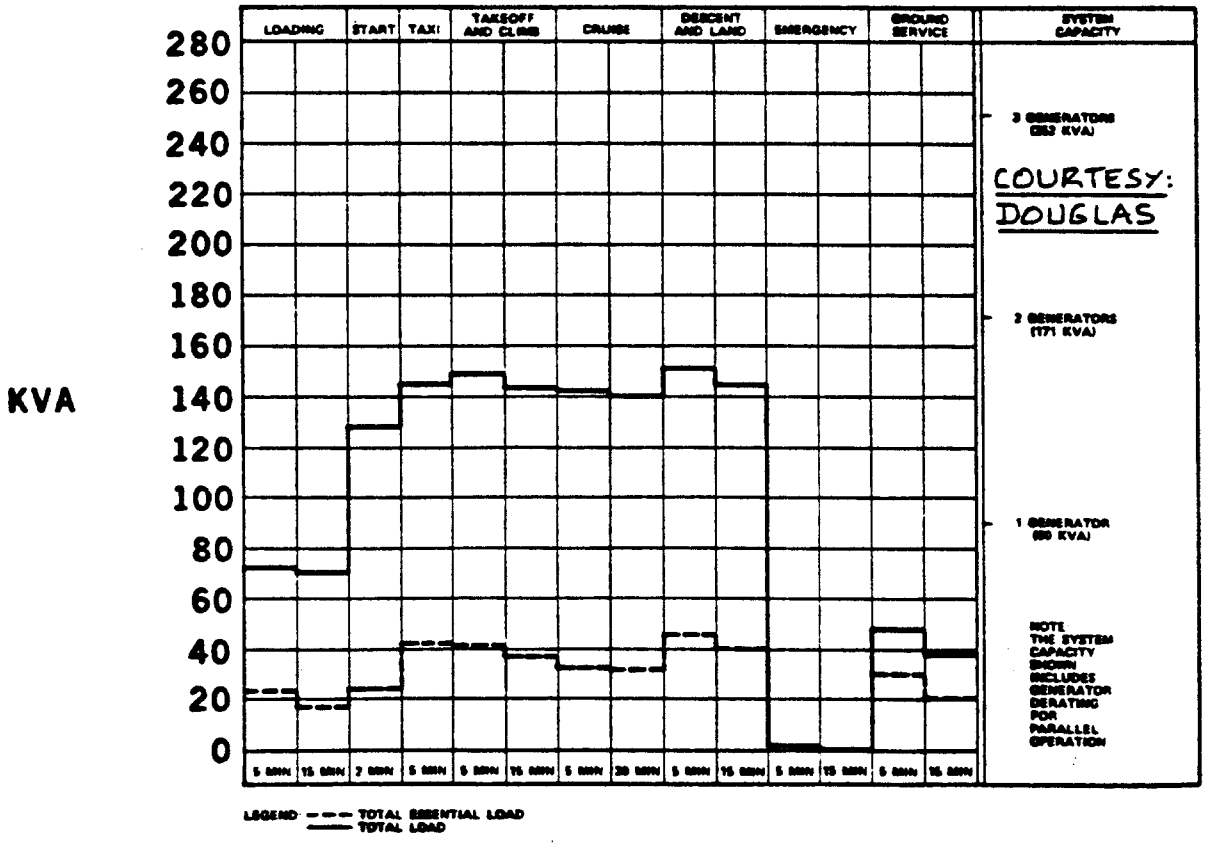

Figure 7.4 Electrical Load Profile: McDD DC-10

COURTESY : DOUGLAS

Table 7.1 Electrical Load Summary:

Ground Loading

(15 Min.) for the McDD DC-10

EXTERIOR LIGHTING	2,600
FLIGHT COMPARTMENT LIGHTING	650
PASSENGER CABIN LIGHTING	13,400
GALLEY	30,000
TOILETS	3,100
ENTERTAINMENT	50
WINDSHIELD HEATING	1,000
AVIONICS	5,300
AIR CONDITIONING	1,600
FUEL	0
HYDRAULIC	0
FLIGHT CONTROL	1,250
ELECTRICAL POWER (CONVERTED DC)	7,900
CARGO HANDLING	2,750
MISCELLANEOUS	200
TOTAL	69,800 VA

Table 7.2 Electrical Load Summary:

Take-off and Climb

(15 Min.) for the McDD DC-10

EXTERIOR LIGHTING	3,850
FLIGHT COMPARTMENT LIGHTING	1,200
PASSENGER CABIN LIGHTING	14,200
GALLEY	84,000
TOILETS	0
ENTERTAINMENT	0
WINDSHIELD HEATING	6,000
AVIONICS	7,400
AIR CONDITIONING	1,600
FUEL	6,500
HYDRAULICS	8,800
FLIGHT CONTROL	2,000
ELECTRICAL POWER (CONVERTED TO DC)	7,900
MISCELLANEOUS	250
TOTAL	143,700 VA

Table 7.3 Electrical Load Summary:

Cruise (30 min) for

the McDD DC-10

EXTERIOR LIGHTING	200
FLIGHT COMPARTMENT LIGHTING	1,200
PASSENGER CABIN LIGHTING	14,700
GALLEY	84,000
TOILETS	6,100
ENTERTAINMENT	3,000
WINDSHIELD HEATING	7,200
AVIONICS	7,250
AIR CONDITIONING	1,600
FUEL	6,500
HYDRAULICS	0
FLIGHT CONTROL	2,000
ELECTRICAL POWER (CONVERTED TO DC)	6,000
MISCELLANEOUS	250
TOTAL	140,000 VA

load requirements:

1. Essential load requirements

Essential load requirements are determined by the sum of all electric loads required by systems which are essential to the safe operation of the airplane.

2. Normal operating load requirements

Normal operating load requirements are determined by the maximum sum of all electric power requirements during certain mission phases.

The probability that the essential electric power requirements cannot be met during any flight must be extremely remote. This is why in passenger transports usually a minimum of three main electrical systems is employed with one or more back-up systems just in case.

In the case of the DC-10 in Figure 7.4 it is seen that two generators can supply the maximum electric power load needed during a typical mission. One generator can handle the essential load. That is why three generators were selected for the electrical system. Each generator is driven from an engine mounted accessory pad. A fourth generator of the same capacity is driven by the APU. Figure 7.5 shows the APU system integration with its 90 KVA generator attached.

Figure 7.6 shows an example of one possible DC-10 APU installation. Figure 7.7 shows a similar installation in the Boeing 767.

7.3 GUIDELINES FOR LAYOUT OF ELECTRICAL SYSTEMS

Following are some basic guidelines which must be followed when laying out electrical systems:

1. Electrical systems must be carefully shielded from the effects of lightning strike.

2. Electrical systems must be designed so that they are shielded from each other. Electromagnetic interference is one of the major development headaches during the certification of airplanes.

3. Electrical systems must be designed so that airplane dispatch is possible with certain system components failed. For example: in most passenger transports it is highly desirable to be able to dispatch

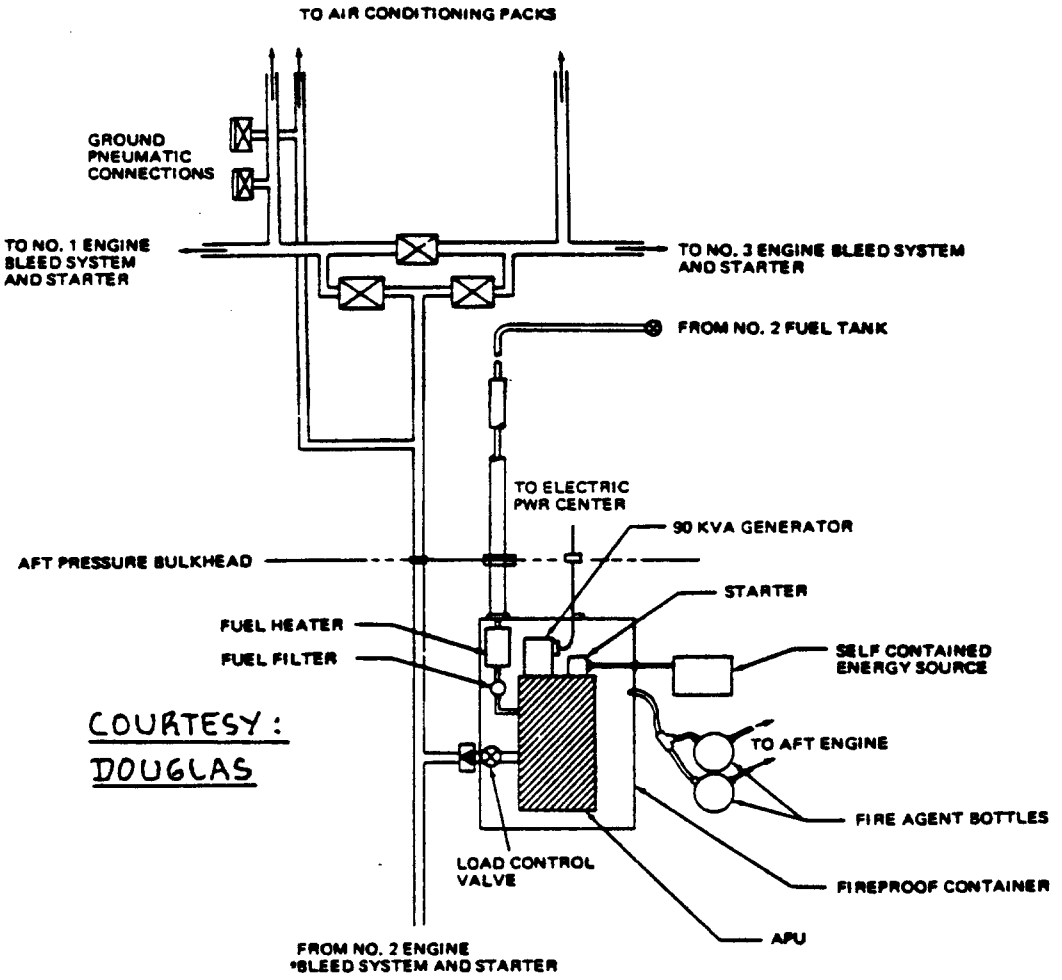

Figure 7.5 APU System Integration: McDD DC-10

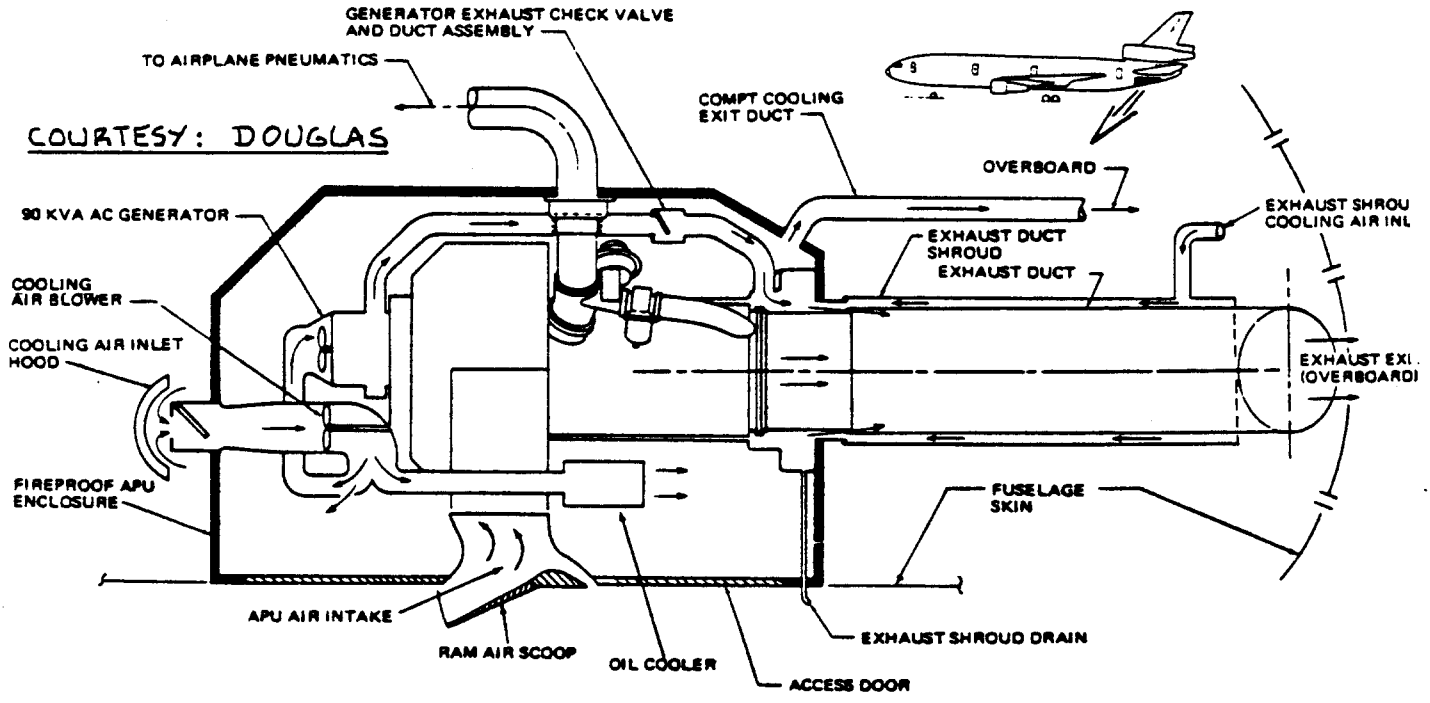

Figure 7.6 APU Installation Schematic: McDD DC-10

- Provides ground power (90 kVA) bleed air for air conditioning pack operation and engine start capability
- Inflight power capability to 35 000 feet, air start to 25 000 feet
- Supplies air-driven pump for hydraulic system (if one engine air source unavailable)
- Electronic APU control unit installed in aft cargo compartment
- Low noise level at ramp work-stations
  - APU installed in aft fuselage
  - Inlet high above ramp
  - Inlet muffler
  - APU engine acoustic treatment incorporated

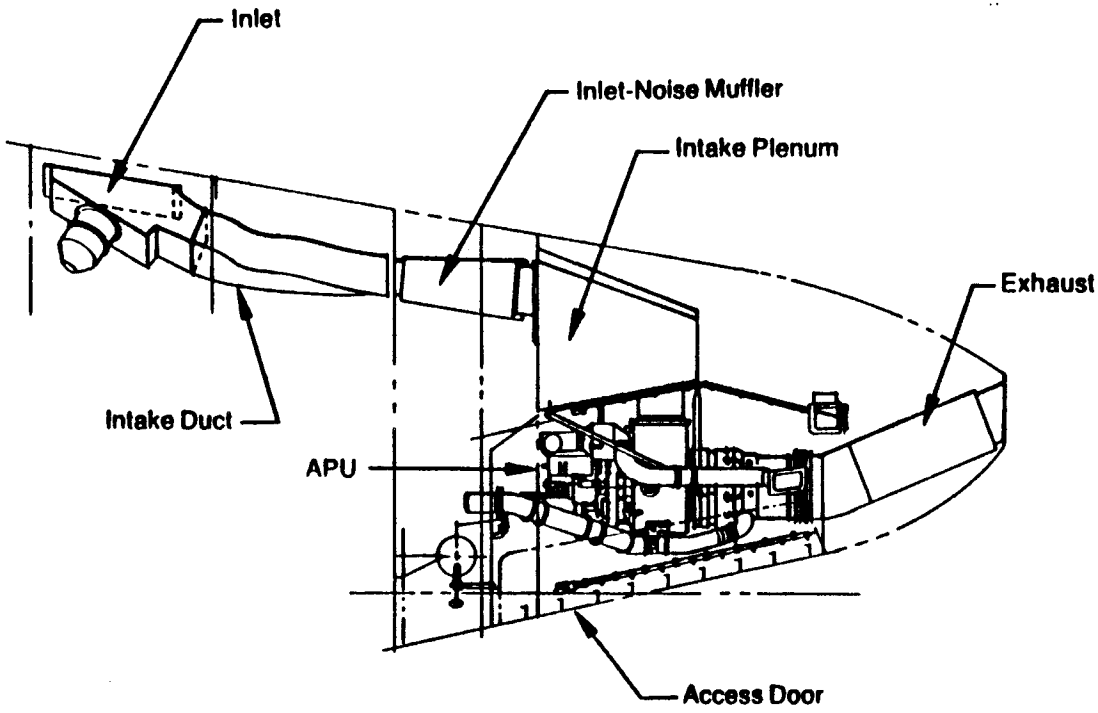

COURTESY: BOEING

Aft Equipment Center
- APU Controller
- TRU APU (Std Option)
- APU Battery Charger
- APU Battery
- Airplane/APU Interface Module

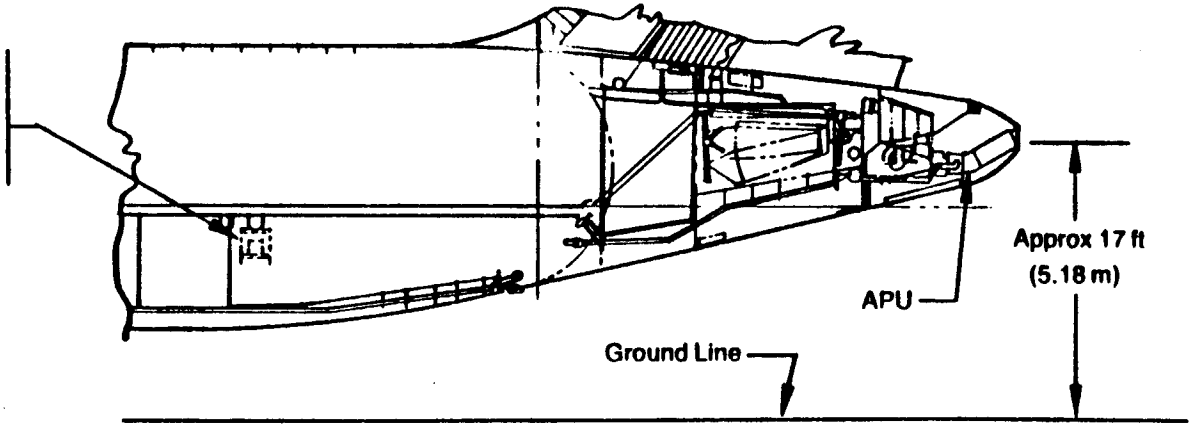

Figure 7.7 APU Installation Schematic: Boeing 767

with one failed system. That means a minimum of four independent systems are needed.

4. Servicing and accessibility of electrical system components must be easy and safe.

5. Flight crucial buses and/or wiring bundles should be widely separated to avoid catastrophic results under the following scenarios:

a) uncontained failure of engine components
b) terrorist action
c) failure of adjacent structure
d) localized in-flight fires

6. In most passenger transports and in military airplanes provisions for hooking up to ground power are required.

7. Most airplanes require batteries for various standby functions. Airplane batteries must be physically shielded from primary structure and from essential airplane services: batteries can leak highly corrosive fluids. Batteries can als pose a fire hazard following certain failure scenarios. They must therefore also be shielded from flammable materials.

For these reasons many batteries are installed in fire-proof and corrosion proof containers. These containers may have to be vented to the atmosphere to prevent excessive pressures from building up.

7.4 EXAMPLE LAYOUTS OF ELECTRICAL SYSTEMS

Figures 7.8 - 7.11 show examples of electrical system layouts. Comments on these figures are given next.

Figure 7.8 Electrical System Schematic: Canadair CL215

This airplane is equipped with two engine driven 28-volt, 200 amp., DC generators. AC power is provided by monophase, 400 cycle, 115 AC static inverters.

A 36 ampere-hour lead-acid battery is capable of carrying essential electric power loads.

Figure 7.9 Electrical System Schematic: Short Skyvan

This airplane uses two engine driven, 28-volt, 200 amp., DC starter generators. For some systems the DC power is inverted to 115 and 26 volt, 400 cycle, AC power.

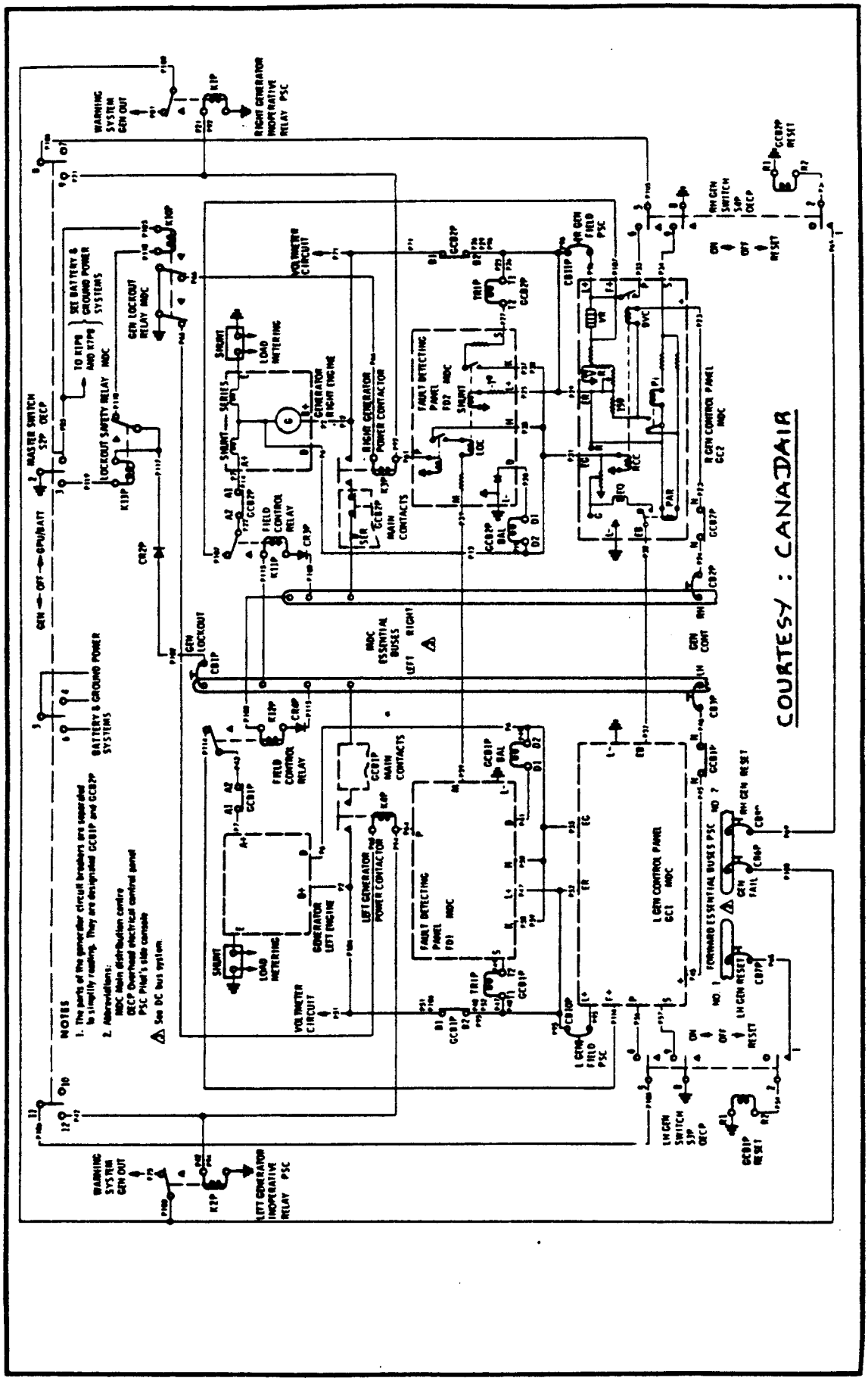

Figure 7.8 Electrical System Schematic: Canadair CL 215

Figure 7.10 AC And DC Power Distribution Schematics: Gates Learjet M25

This airplane uses two engine driven, 28-volt, 400 amp., DC starter generators. The schematics show which types of power are required for the various functions. Note that the DC power is inverted to 115 and 26 volt, 400 cycle, AC power. The inverters are rated at 400 volt-amperes.

Figure 7.11 Electrical Power System McDD DC-10

Note the four generators used in this system. Section 7.3 gave the reasons for this selection.

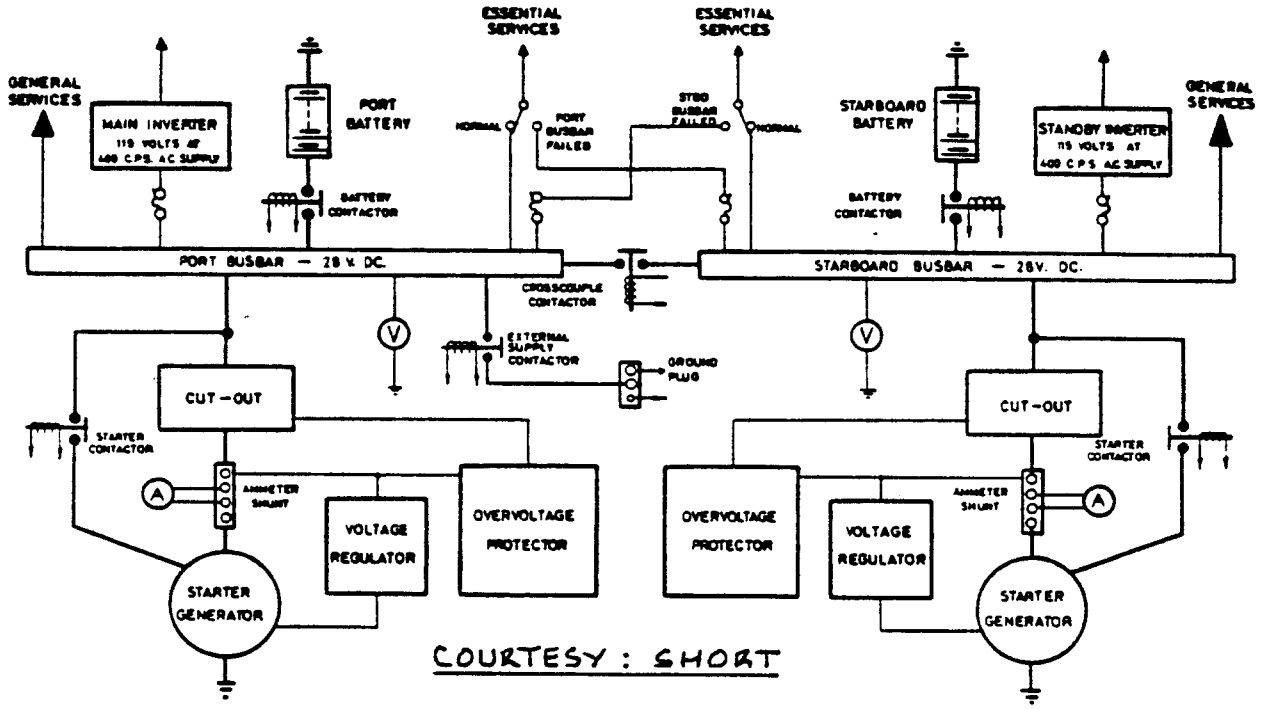

Figure 7.9 Electrical System Schematic: Short Skyvan

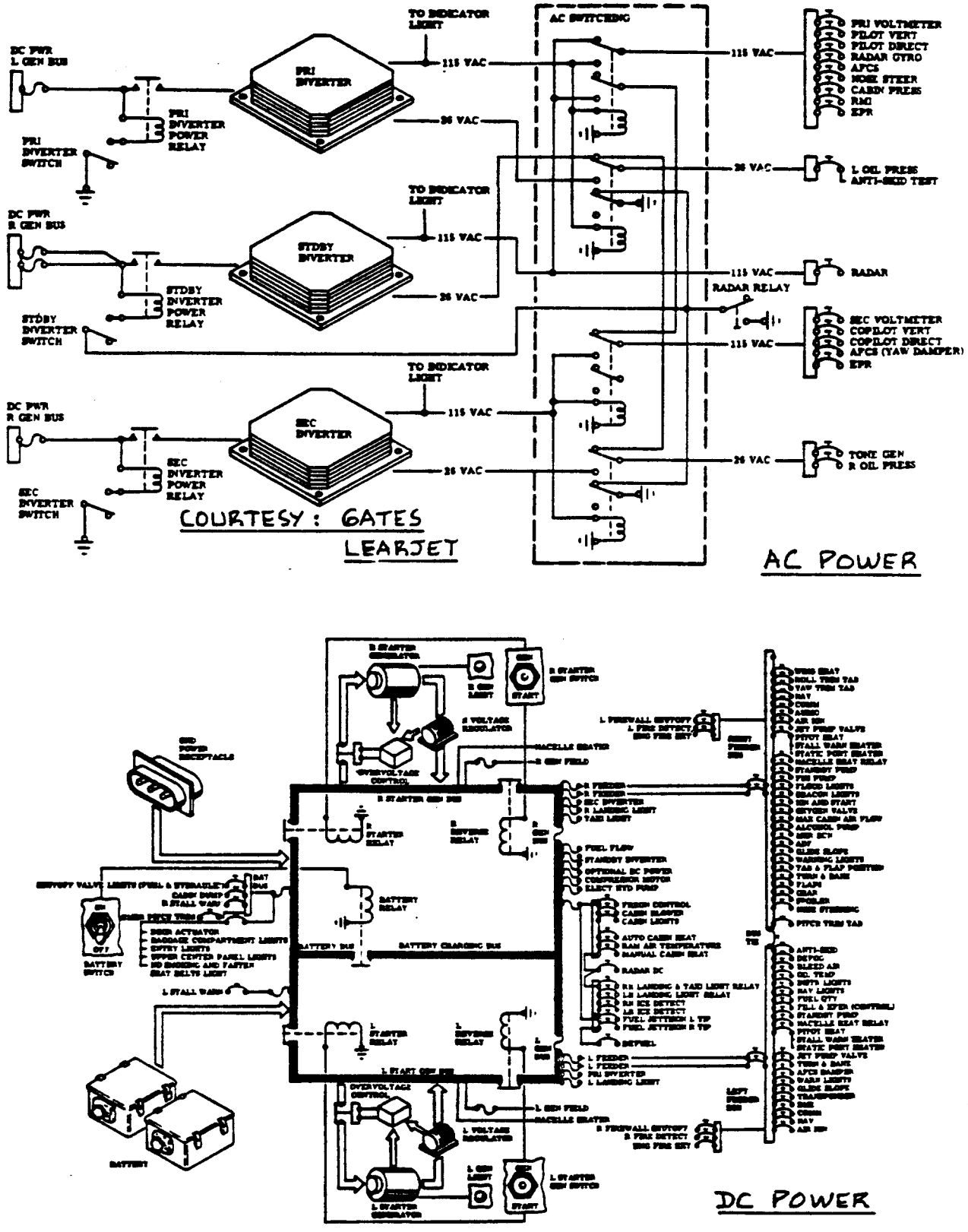

Figure 7.10 AC and DC Power Distribution Schematics: Gates Learjet M25

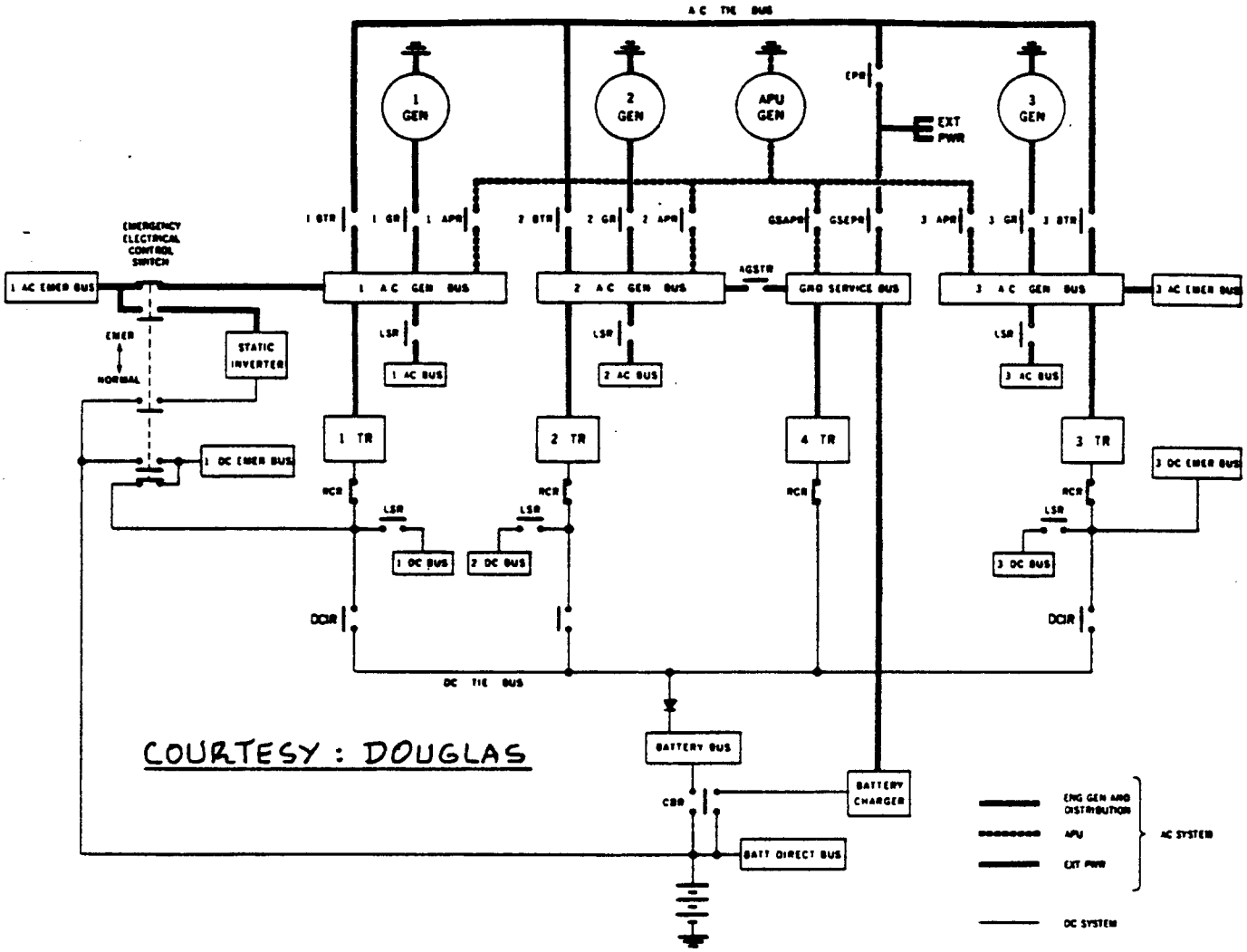

Figure 7.11 Electrical Power System: McDD DC-10

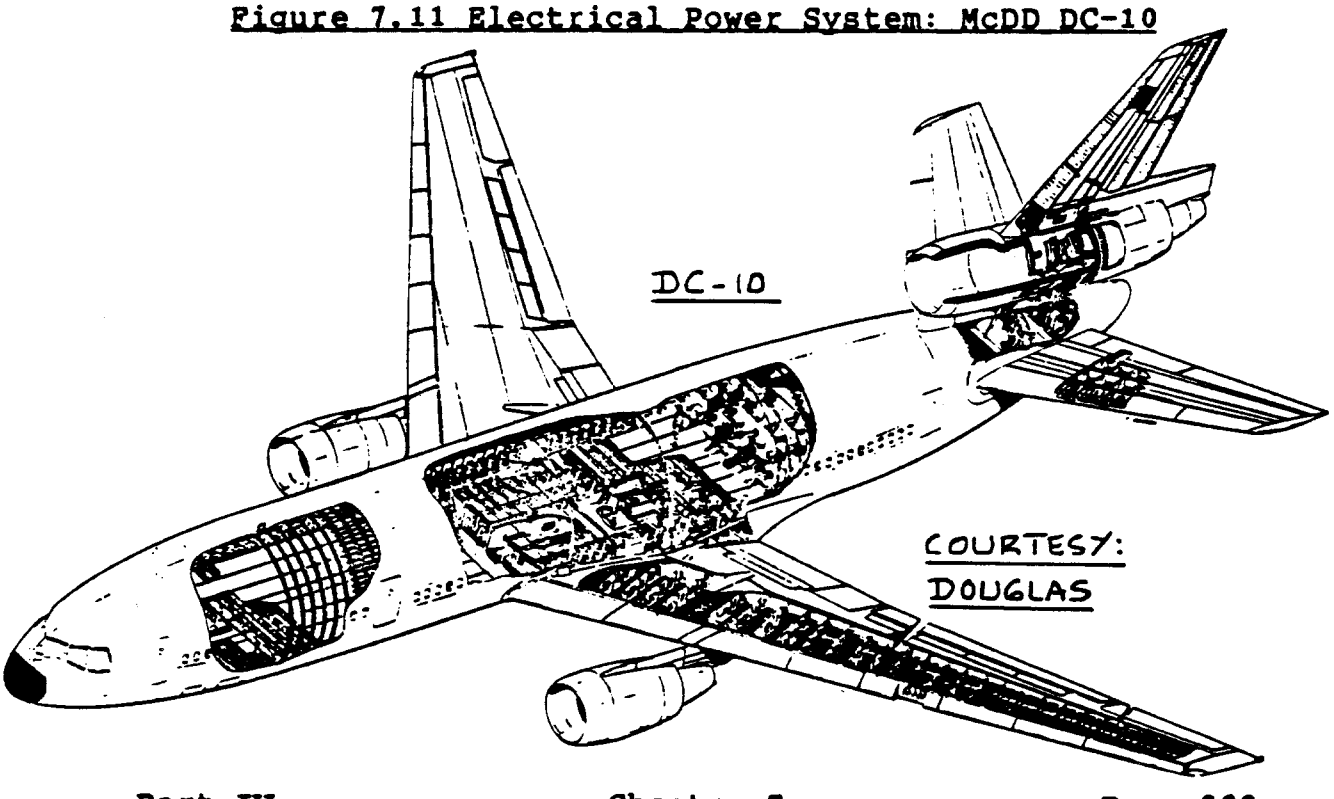

8. ENVIRONMENTAL CONTROL SYSTEMS LAYOUT DESIGN

In this chapter some fundamental design layout requirements for environmental control systems will be discussed. The material is organized as follows:

8.1 Pressurization system

8.2 Pneumatic system

8.3 Airconditioning system

8.4 Oxygen system

8.1 PRESSURIZATION SYSTEM

The purpose of this system is to maintain sufficient cabin air pressure during flight at high altitudes so that passengers remain comfortable. Typical differential pressure capabilities in jet transports are designed to maintain a cabin altitude from 1000 ft below sealevel to 10,000 ft above sealevel.

Figure 8.1 shows a typical pressurization schedule used in a transport. To reduce crew workload the pressurization schedule with altitude should be automatic.

Cabin pressurization systems need the following components:

1. A source of high pressure air (high relative to the outside air pressure). The air source is normally the airplane pneumatic system. The pneumatic system is discussed in Section 8.2.

2. A control and metering system to:

   a) provide positive pressure relief to protect the structure. This pressure relief is typically set for a pressure differential larger than 9-10 psi.

   b) provide negative pressure relief. This lets air into the cabin when outside air pressure exceeds the inside pressure. This system is normally set for a pressure differential corresponding to about 10 inches of water.

The reliability of the cabin pressurization system is of great importance to the safety of the passengers.

CONSTRUCCIONES AERONAUTICAS PROYECTOS Y SISTEMAS
BIBLIOTECA TECNICA
INFORMACION Y DOCUMENTACION
GETAFE (Madrid)

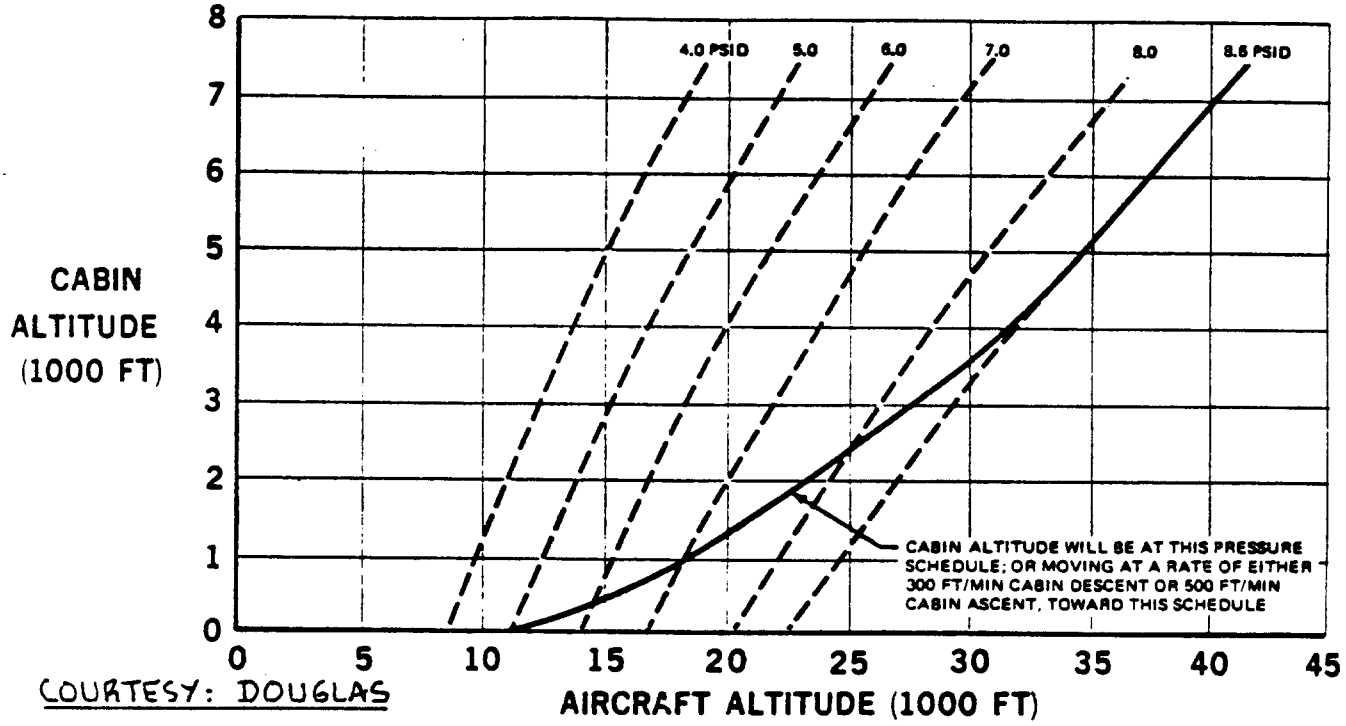

COURTESY: DOUGLAS

Figure 8.1 Cabin Pressurization Schedule: McDD DC-10

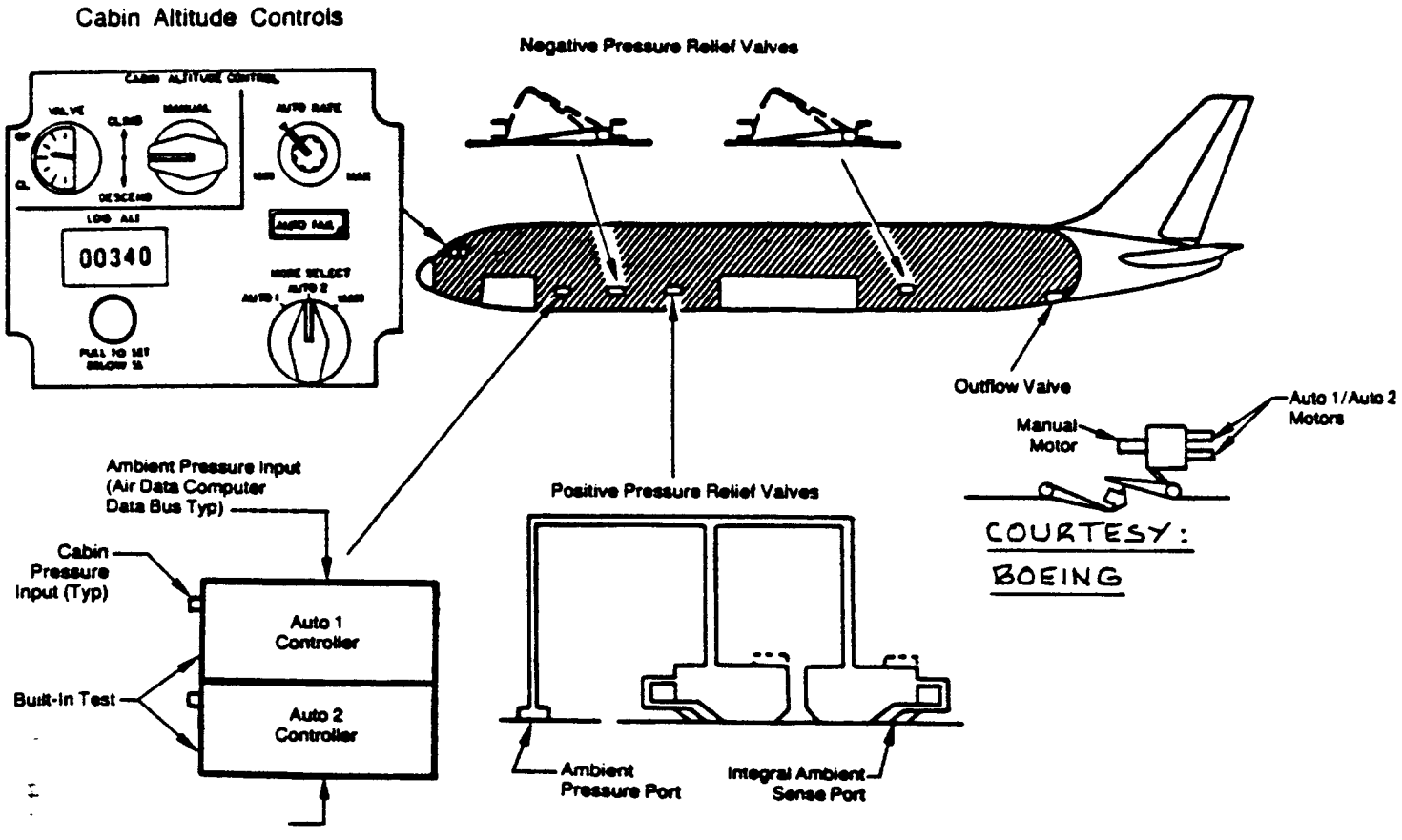

COURTESY: BOEING

Figure 8.2 Pressurization System Arrangement: Boeing 767

If this system fails at altitude, serious breathing problems would arise. That is the reason why an emergency oxygen system must be installed in all jet transports. Section 8.4 covers oxygen system layout design.

If the pressurization system fails at landing it would be impossible to open the cabin doors. For that reason a cabin depressurization system is also included.

A major problem can arise if cargo doors located below the cabin floor accidentally blow out. In that case the pressure in the cargo hold bleeds off very rapidly. The pressure differential which then exists between the passenger cabin and the cargo hold may cause the cabin floor to fail. If flight crucial systems (such as flight control cables or wire bundles) are located in that area, loss of control can occur. These problems can be avoided only by a combination of:

a) proper location of essential controls
b) providing pressure relief for the cabin if a cargo door fails
c) fail-safe design of the cargo door latch mechanism

Figure 8.2 shows a typical arrangement for a cabin pressurization system. For detailed discussions of the associated control systems the reader should consult Ref.33 and manufacturers brochures describing such systems for a particular airplane.

8.2 PNEUMATIC SYSTEM

The purpose of the pneumatic system is to supply air for the following functions:

1. Cabin pressurization and airconditioning
2. Ice protection system (See Chapter 10)
3. Cross engine starting (not in all airplanes)

Figure 8.3 shows a typical schematic for a pneumatic system used in jet transports. Note that the primary source of air is engine compressor bleed air. A secondary source is air from the APU.

8.3 AIRCONDITIONING SYSTEM

The purpose of the airconditioning system is to 'condition' cabin air in terms of temperature (cooling or heating) and humidity.

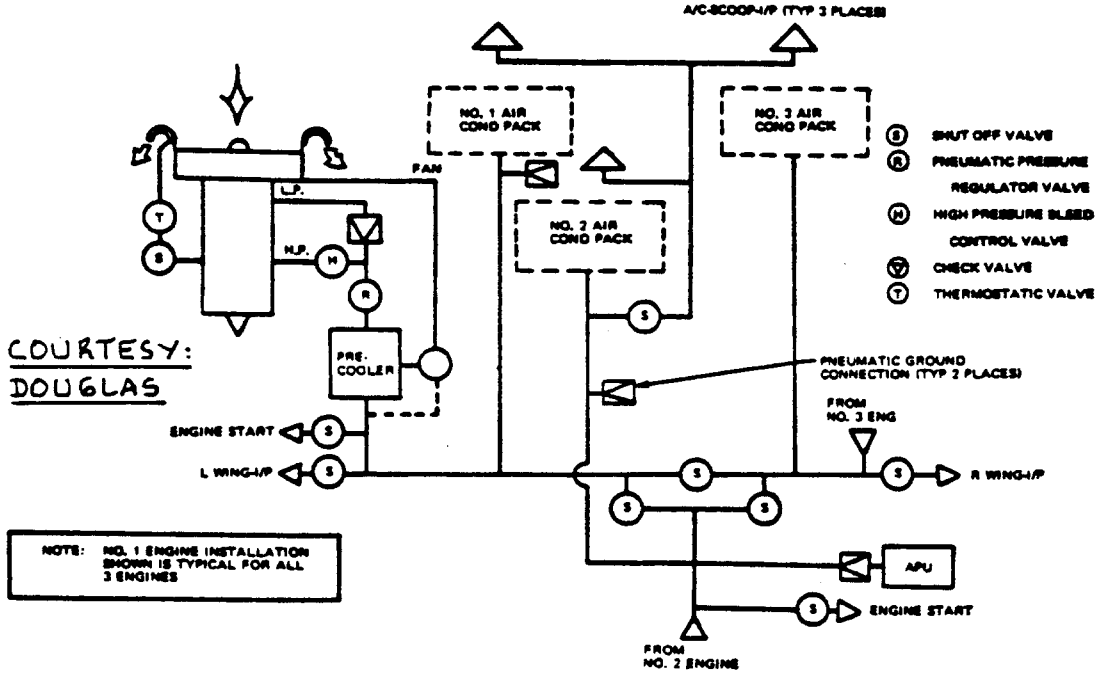

Figure 8.3 Pneumatic System Schematic: McDD DC-10

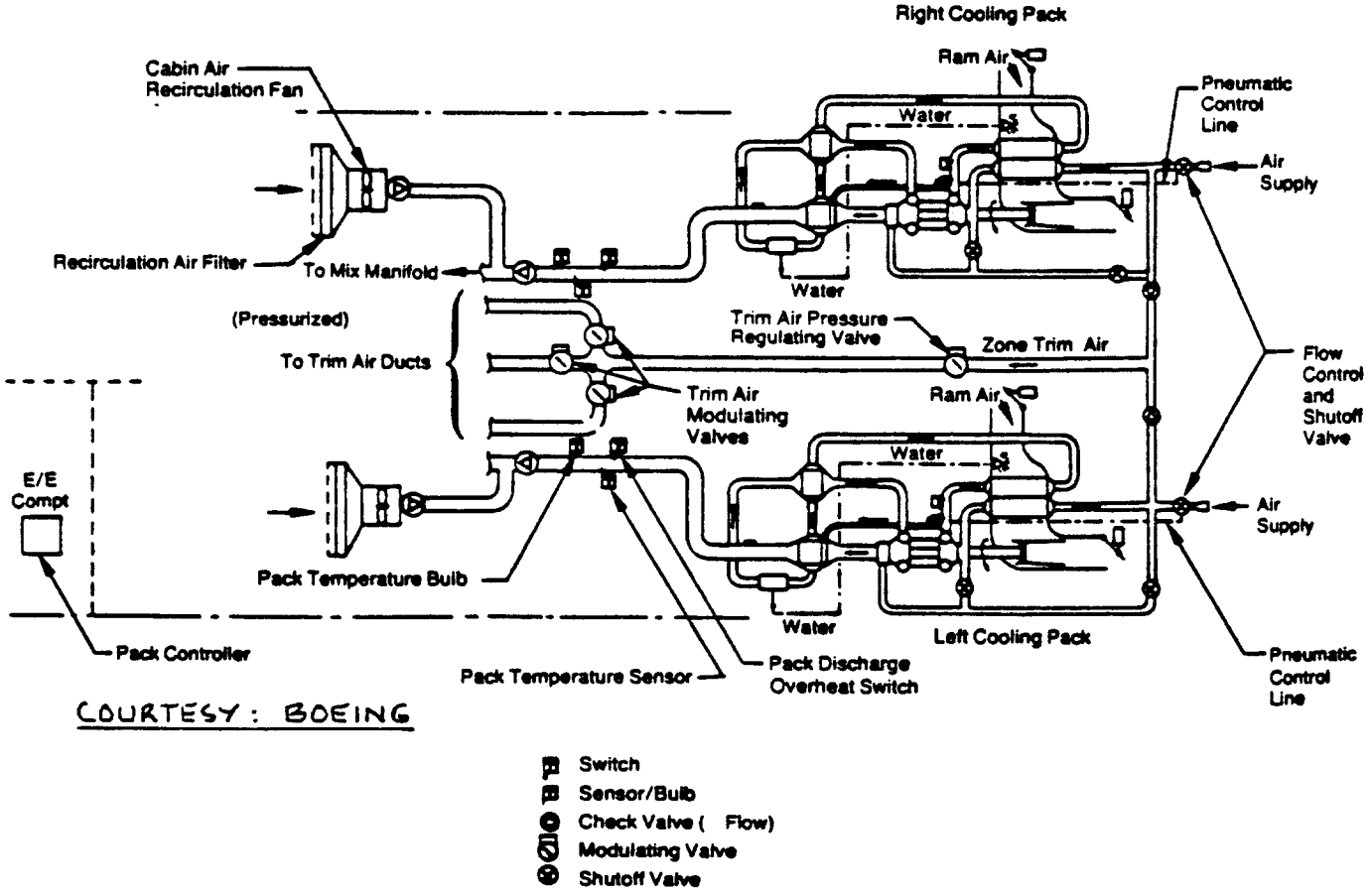

Figure 8.4 Airconditioning System: Boeing 767

Figure 8.4 provides a schematic of a typical airconditioning system used in jet transports. Since the engine bleedair is always hot, cabin heating requires less air cooling than cabin cooling. In the design of these systems a critical condition is normally a descent at flight idle power. This flight condition leads to minimal bleedair availability.

The overall efficiency of the cabin airconditioning system depends a great deal on the thermal insulation of the cabin wall. Figure 8.5 shows a cross section through a cabin wall with the associated temperature gradients.

The air coming from the airconditioning system must be distributed into the cabin. In passenger transports this requires a complex network of airducts. In large transports the cabin temperature is controlled in individual cabin zones. This temperature control is achieved by a system which mixes hot air with cooled air in the desired proportion.

The amount of cabin air required in jet transports is typically 20 cubic feet per minute per passenger.

Figure 8.6 shows the location of airconditioning units in a jet transport with the primary air ducts indicated. Note the separate line leading to the electrical/avionics bay: these systems require a significant amount of cooling or they will malfunction.

Figure 8.7 shows an air distribution network in more detail. A cross section through the passenger cabin with the various air distribution ducts indicated is given in Figure 8.8.

In the detail design of the air distribution system careful attention must be paid to duct acoustics: improperly designed air distribution systems can be extremely noisy.

In many unpressurized airplanes cabin heating systems are used. Figures 8.9 and 8.10 show schematics of such systems. Note that these systems use fuel and a combustor (heat exchanger) as a source of heat. Great care must be taken in the design and location of these systems: they are a potential source of hazards: carbon-monoxide poisoning and fires are two of these.

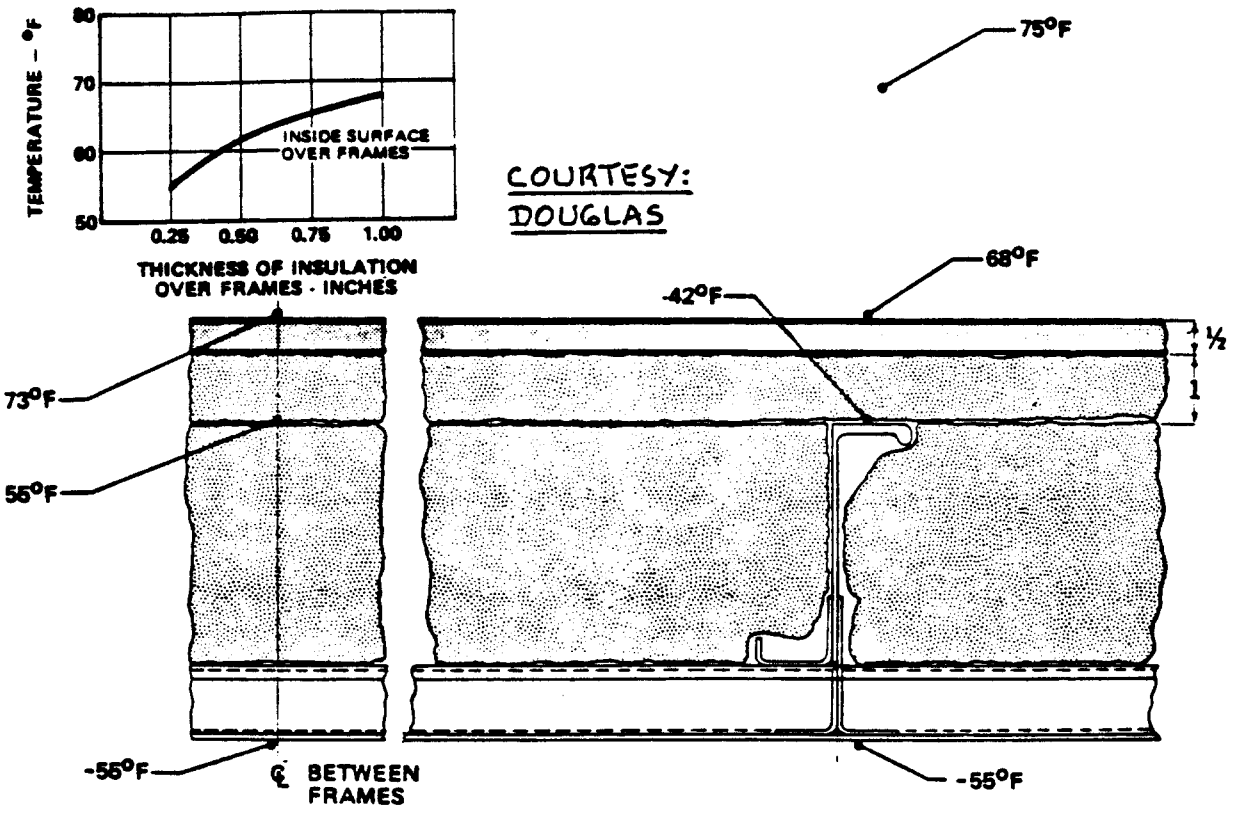

Figure 8.5 Sidewall Temperature Gradients: McDD DC-10

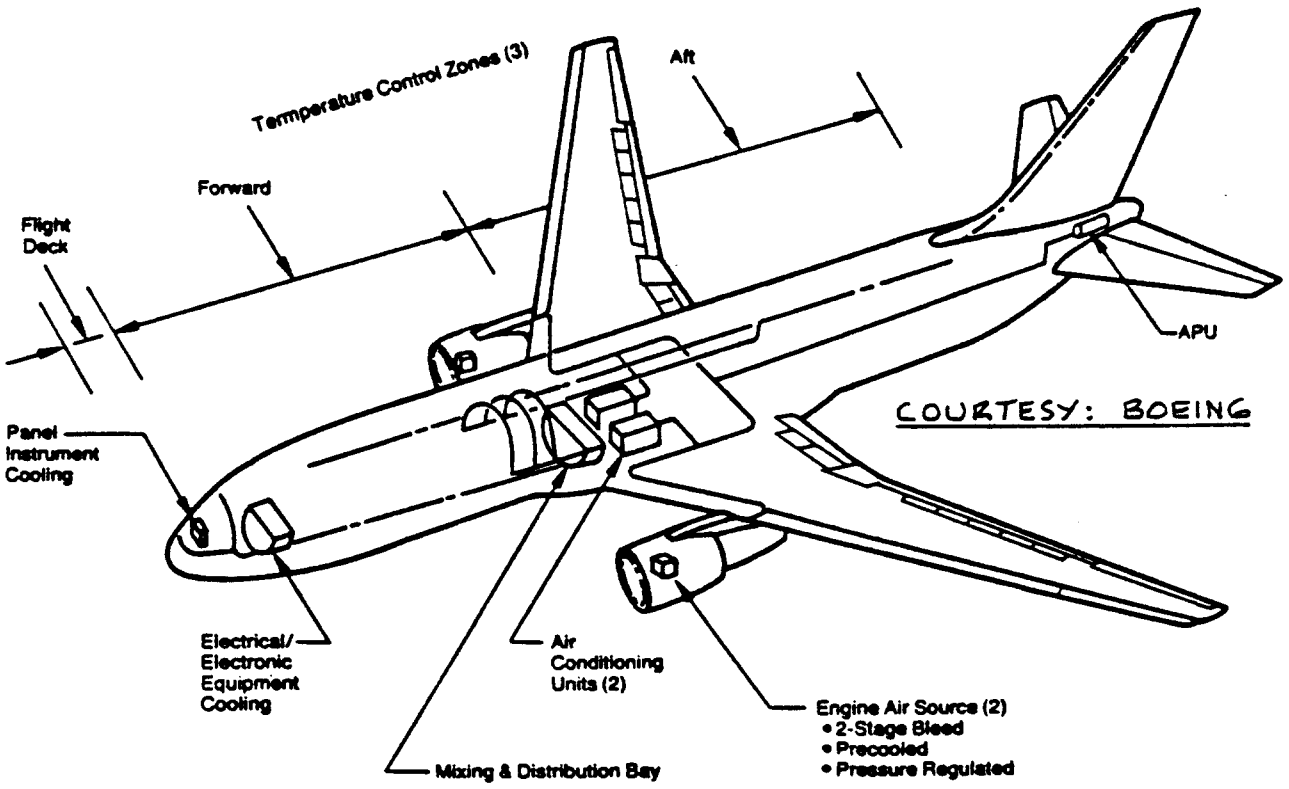

Figure 8.6 Airconditioning Component Location: Boeing 767

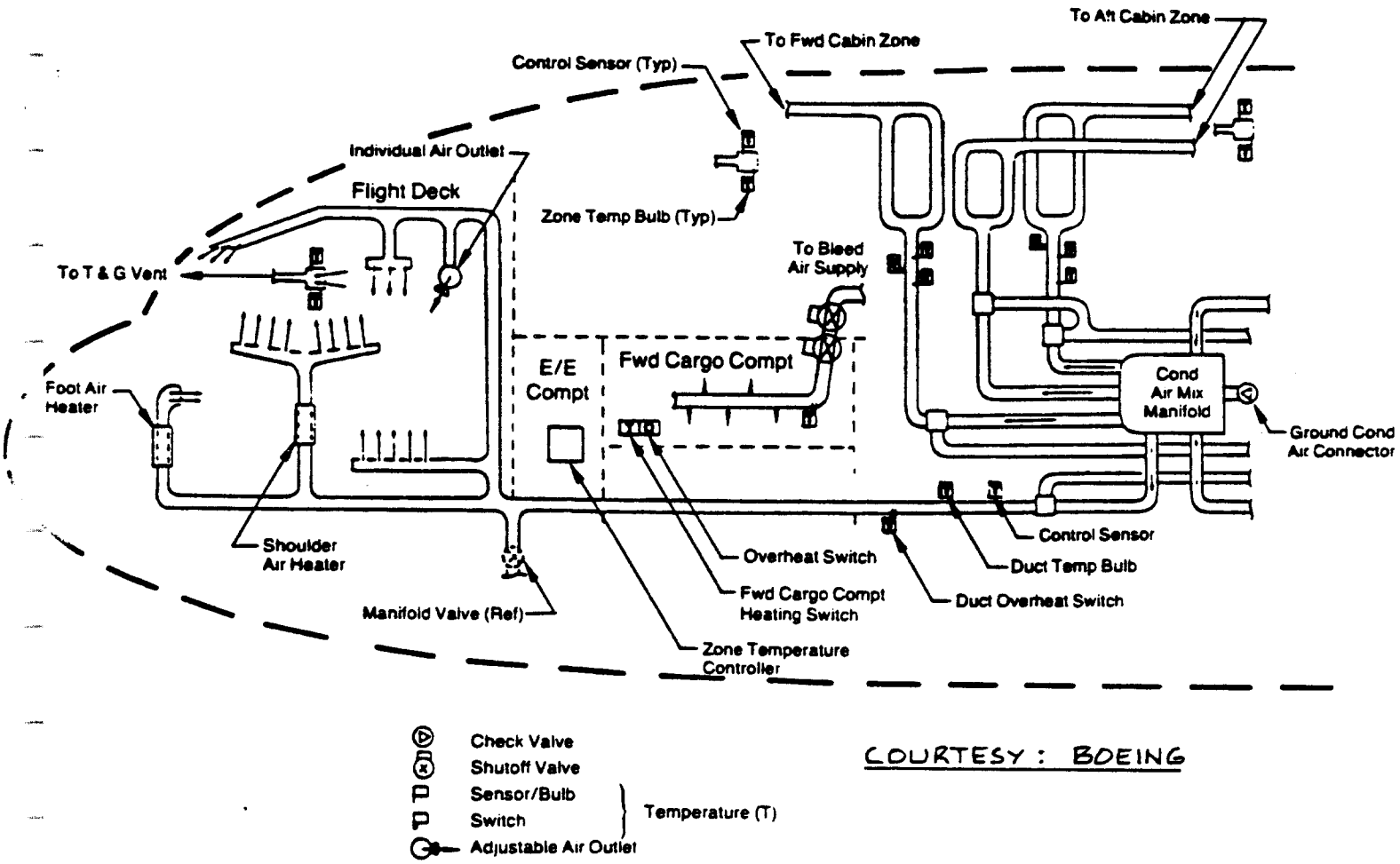

COURTESY : BOEING

Figure 8.7 Air Distribution System: Boeing 767

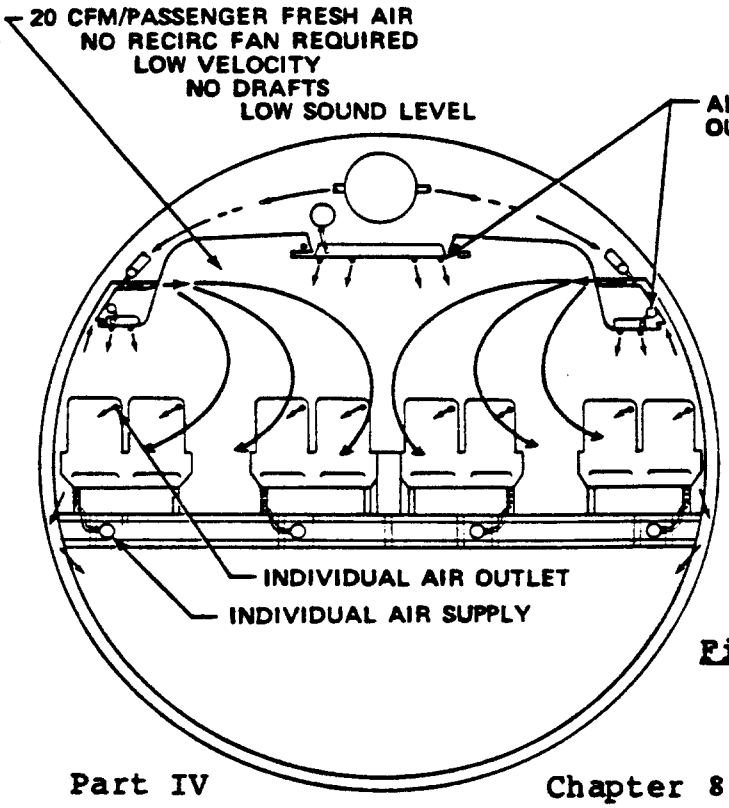

COURTESY: DOUGLAS

Figure 8.8 Cabin Air Circulation: McDD DC-10

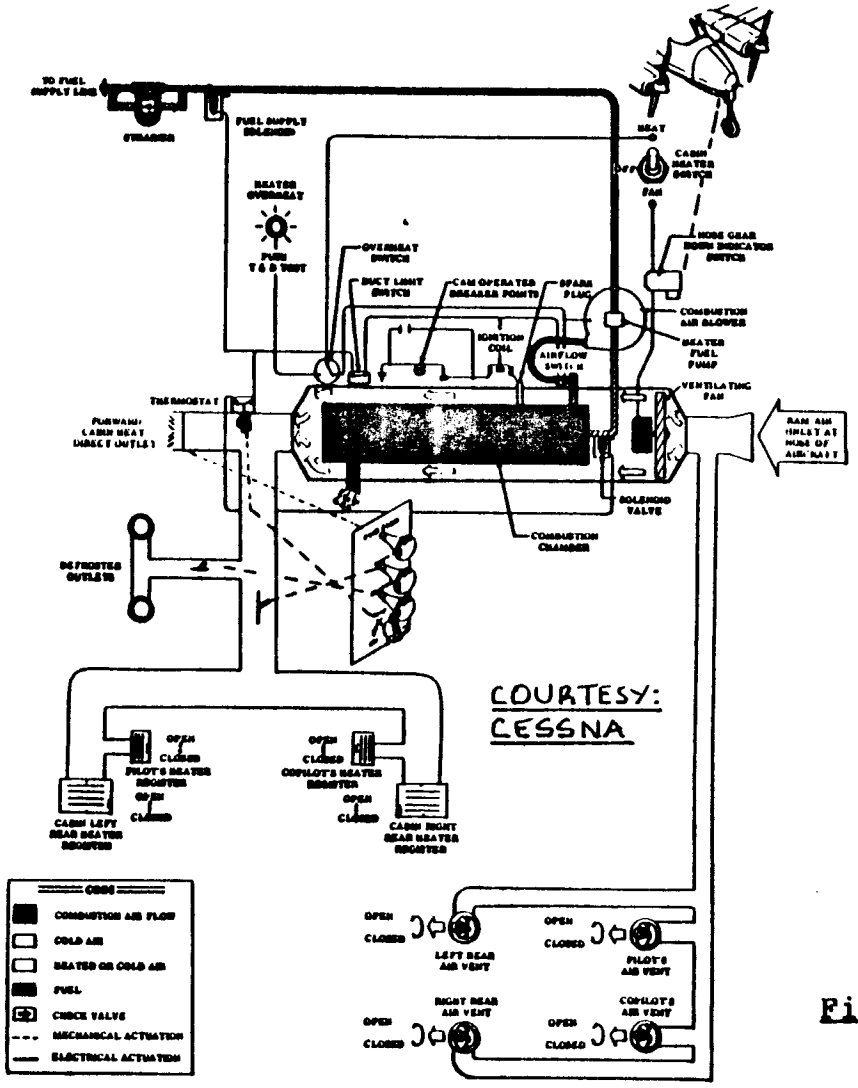

Figure 8.9 Cabin Heating System: Cessna 310

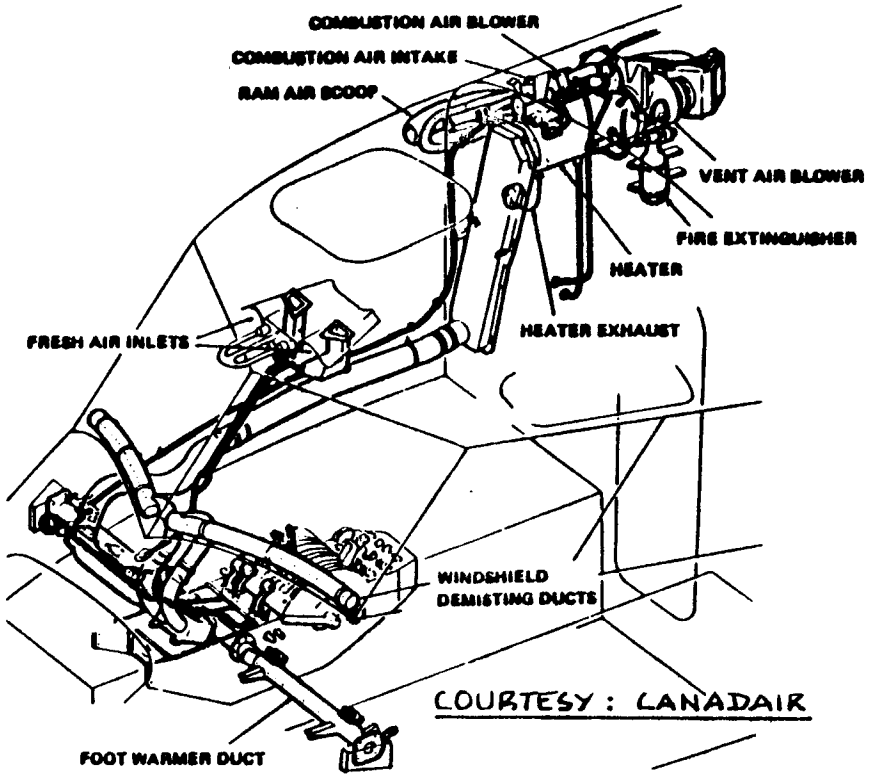

Figure 8.10 Cabin Heating System: Canadair CL215

8.4 OXYGEN SYSTEM

For flight at high altitudes oxygen is required after failure of the cabin pressurization system.

Oxygen systems use either gaseous oxygen or chemically obtained oxygen. Crew oxygen systems are normally supplied from a gaseous source. Passenger oxygen is usually supplied from a chemical source.

The main disadvantage associated with gaseous oxygen is that it presents a fire hazard during servicing and during cylinder replacement. The main disadvantage of chemical oxygen systems is their larger weight.

Figure 8.11 shows a crew oxygen delivery system in detail. Figure 8.12 shows a schematic of the entire oxygen system in a typical jet transport.

Reference 33 is an excellent source for more information on oxygen systems.

In military airplane liquid oxygen systems are often used. Although more hazardous, these systems save weight and volume. Figure 8.13 shows a typical oxygen system layout used in a fighter airplane.

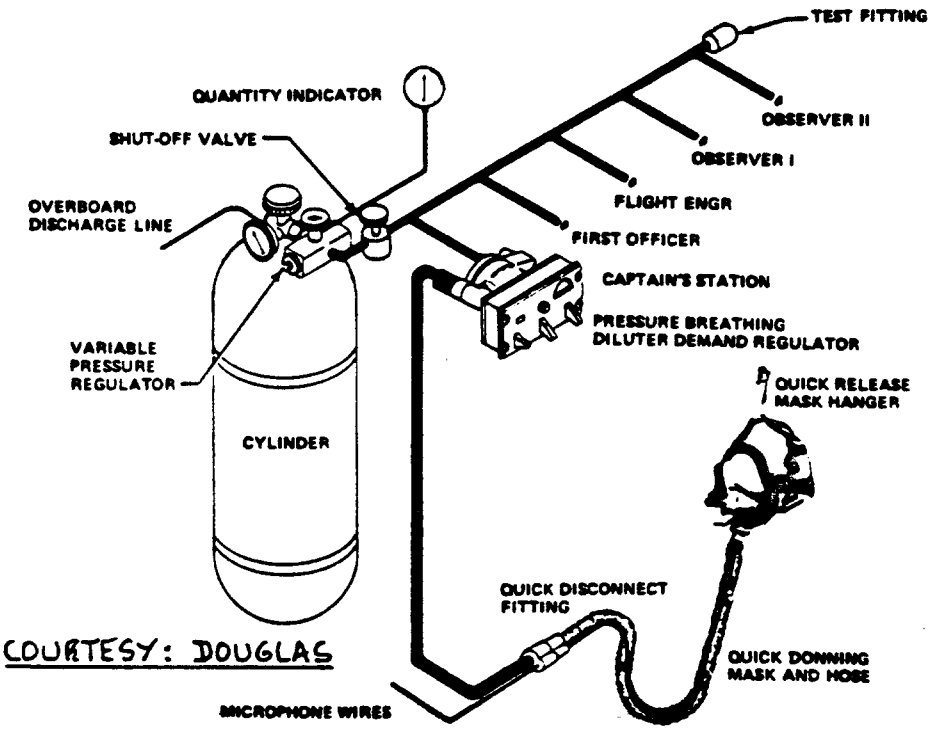

COURTESY: DOUGLAS

Figure 8.11 Crew Oxygen System: McDD DC-10

- Gaseous oxygen system for crew
- Overhead chemical oxygen for passengers
- Use of one mask starts generator for seat unit
- Reduces high pressure passenger oxygen bottles and associated risk in servicing and replacing bottles
- Reduced maintenance in passenger system
  - No bottle regulators or valves to leak
  - Eliminate dispatch inspection of oxygen supply

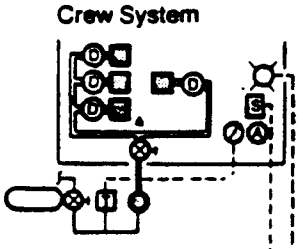

COURTESY : BOEING

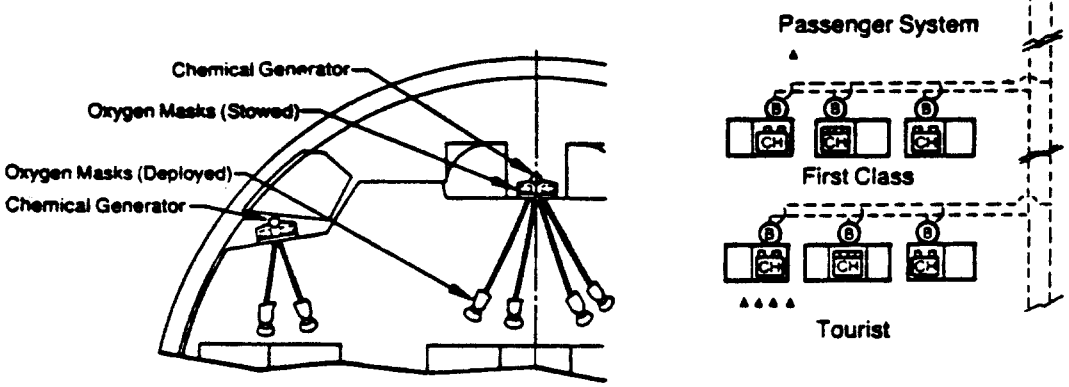

- Portable Oxygen Cylinder 4.25 ft Capacity
- Crew Mask Coupling
- Passenger Outlet With Mask
- Electric Switch
- Pressure Reducing Regulator
- Pressure Transducer
- Automatic Switch Barometrically Operated
- Electrical Actuated Door Latch
- Shutoff Valve, Manual
- Pressure Indicator
- Indicating Light
- Electrical Connection
- Low-Pressure Tubing
- Overboard Discharge
- High-Pressure Tubing
- Chemical Oxygen Supply
- Oxygen Cylinder Assembly 76 cu ft Capacity
- Diluter Demand Regulator

Figure 8.12 Oxygen System Schematic: Boeing 767

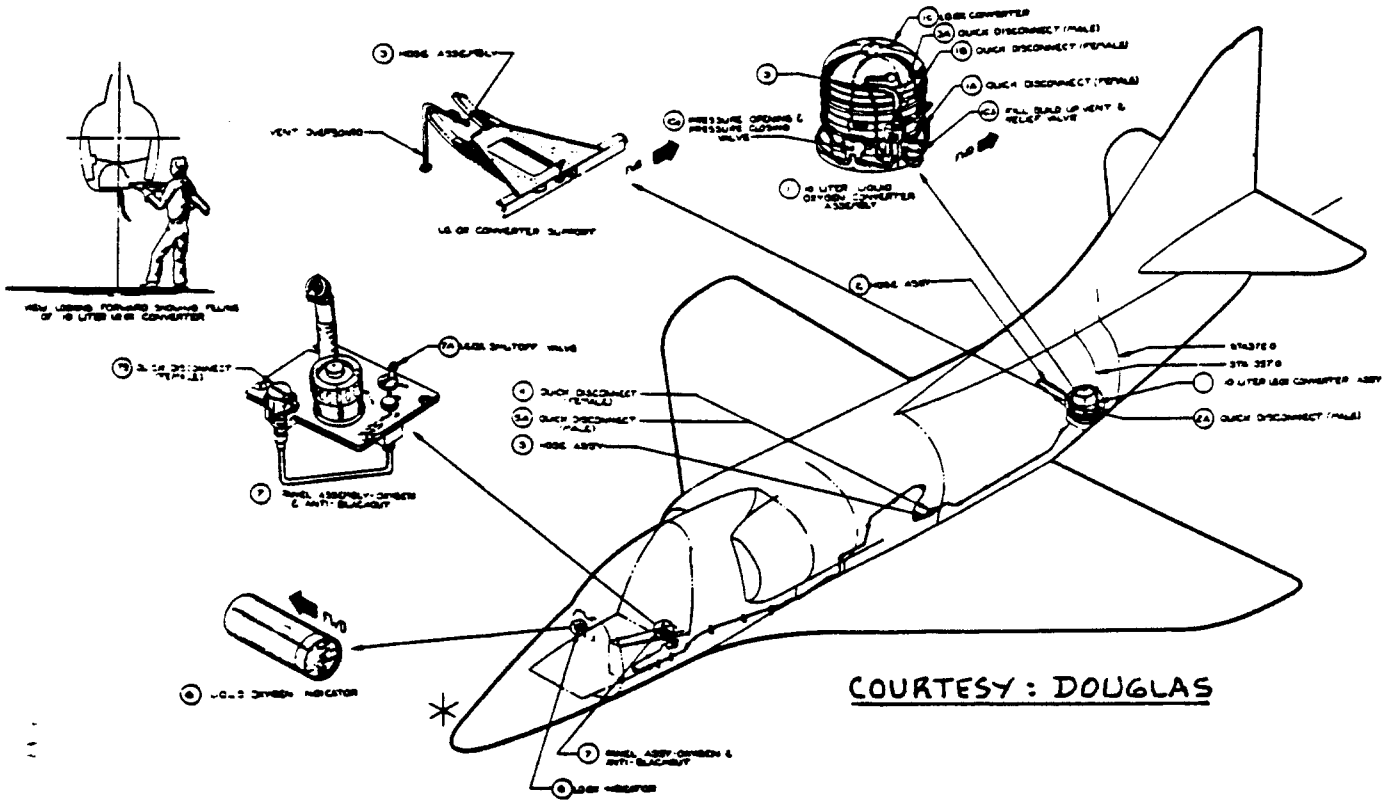

COURTESY : DOUGLAS

Figure 8.13 Oxygen System Schematic: Douglas A4D-2N

9. COCKPIT INSTRUMENTATION, FLIGHT MANAGEMENT AND AVIONICS SYSTEM LAYOUT DESIGN

In this chapter some fundamental design layout requirements for cockpit instrumentation, flight management systems and avionics systems will be discussed.

The material is organized as follows:

9.1 Cockpit instrumentation system

9.2 Flight management and avionics system layout

9.3 Antenna system layout

9.4 Installation, maintenance and servicing considerations

9.1 COCKPIT INSTRUMENTATION LAYOUT

The cockpit instrumentation layout should be uncluttered and functional. The crew must be able to see all flight crucial instruments, controls and warning devices.

Figure 9.1 shows a typical cockpit instrumentation layout used in light airplanes.

In larger airplanes the cockpit instrumentation is organized into panels. Figure 9.2 shows an example of a panel organization in a small turboprop twin.

Figure 9.3 gives a general flight compartment view for a piston/prop twin engine amphibian.

A cockpit impression of an older technology twin jet transport is given in Figure 9.4. This is contrasted with the more recent CRT (Cathode Ray Tube) type of instrumentation in Figure 9.5.

Since cockpit instrumentation and airplane avionics are evolving rapidly, changes occur almost each year. Figure 9.6 speculates on a near future cockpit arrangement consisting almost exclusively of advanced flat panel displays.

Because of classification problems no cockpit arrangements of recent operational fighters are included in this text.

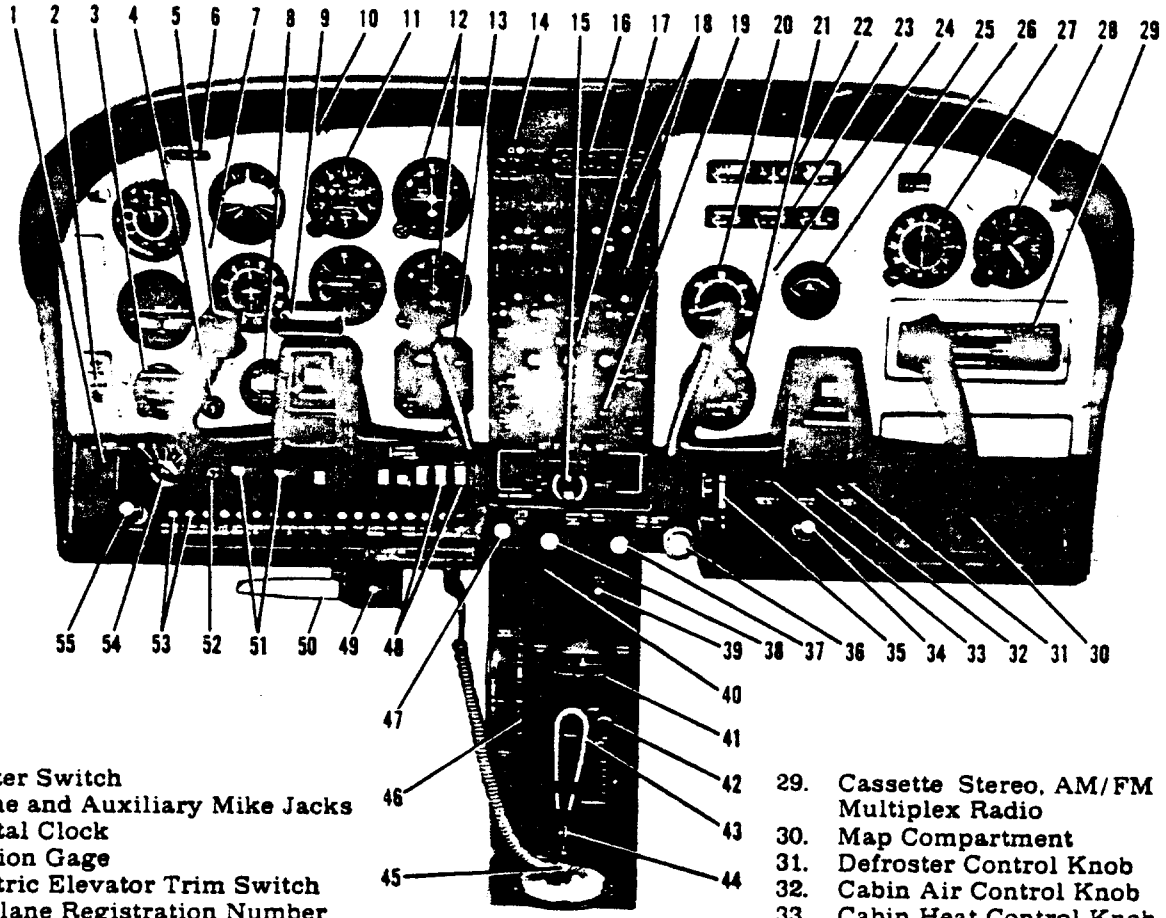

1. Master Switch
2. Phone and Auxiliary Mike Jacks
3. Digital Clock
4. Suction Gage
5. Electric Elevator Trim Switch
6. Airplane Registration Number
7. Flight Instrument Group
8. Carburetor Air Temperature Gage
9. Approach Plate Holder
10. Approach Plate Light and Switch
11. Encoding Altimeter
12. Course Deviation and ILS Glide Slope Indicators
13. DME
14. Marker Beacon Indicator Lights and Switches
15. Autopilot Control Unit
16. Audio Control Panel
17. ADF Radio
18. Nav/Com Radios
19. Transponder
20. Manifold Pressure Gage
21. Tachometer
22. Fuel Quantity Indicators and Ammeter
23. Cylinder Head Temperature, Oil Temperature, and Oil Pressure Gages
24. Low-Voltage Warning Light
25. Economy Mixture Indicator
26. Flight Hour Recorder
27. ADF Bearing Indicator
28. Secondary Altimeter
29. Cassette Stereo, AM/FM Multiplex Radio
30. Map Compartment
31. Defroster Control Knob
32. Cabin Air Control Knob
33. Cabin Heat Control Knob
34. Cigar Lighter
35. Wing Flap Switch and Position Indicator
36. Mixture Control Knob
37. Propeller Control Knob
38. Throttle (With Friction Lock)
39. Electric Elevator Trim Circuit Breaker
40. Control Pedestal Light
41. Rudder Trim Control Wheel and Position Indicator
42. Cowl Flap Control Lever
43. Microphone
44. Fuel Selector Light
45. Fuel Selector Valve Handle
46. Elevator Trim Control Wheel and Position Indicator
47. Carburetor Heat Control Knob
48. Electrical Switches
49. Static Pressure Alternate Source Valve
50. Parking Brake Handle
51. Instrument and Radio Dial Light Dimming Rheostats
52. Avionics Power Switch
53. Circuit Breakers
54. Ignition Switch
55. Primer

Figure 9.1 Cockpit Instrumentation: Cessna 182Q

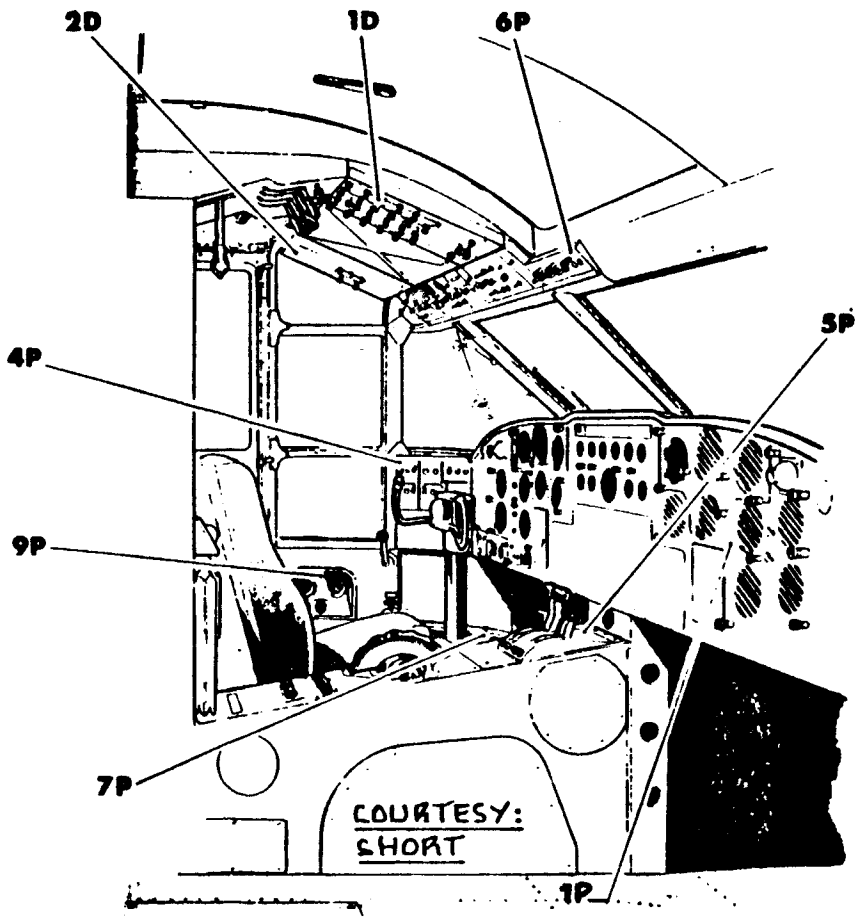

INSTALLATION OF PANELS

PANEL 1P	PILOT'S FLIGHT INSTRUMENT PANEL.	PANEL 7P	HYDRAULICS PANEL.
PANEL 4P	DE-ICING PANEL.	PANEL 9P	AIR CONDITIONING PANEL.
PANEL 5P	PILOT'S CONSOLE.	PANEL 1D	DISTRIBUTION PANEL.
PANEL 6P	STARTING & ELECTRICAL PANEL.	PANEL 2D	A.C. POWER SUPPLY PANEL.
			ROOF CONSOLE

Figure 9.2 Flight Deck Panel Organization: Short Skyvan

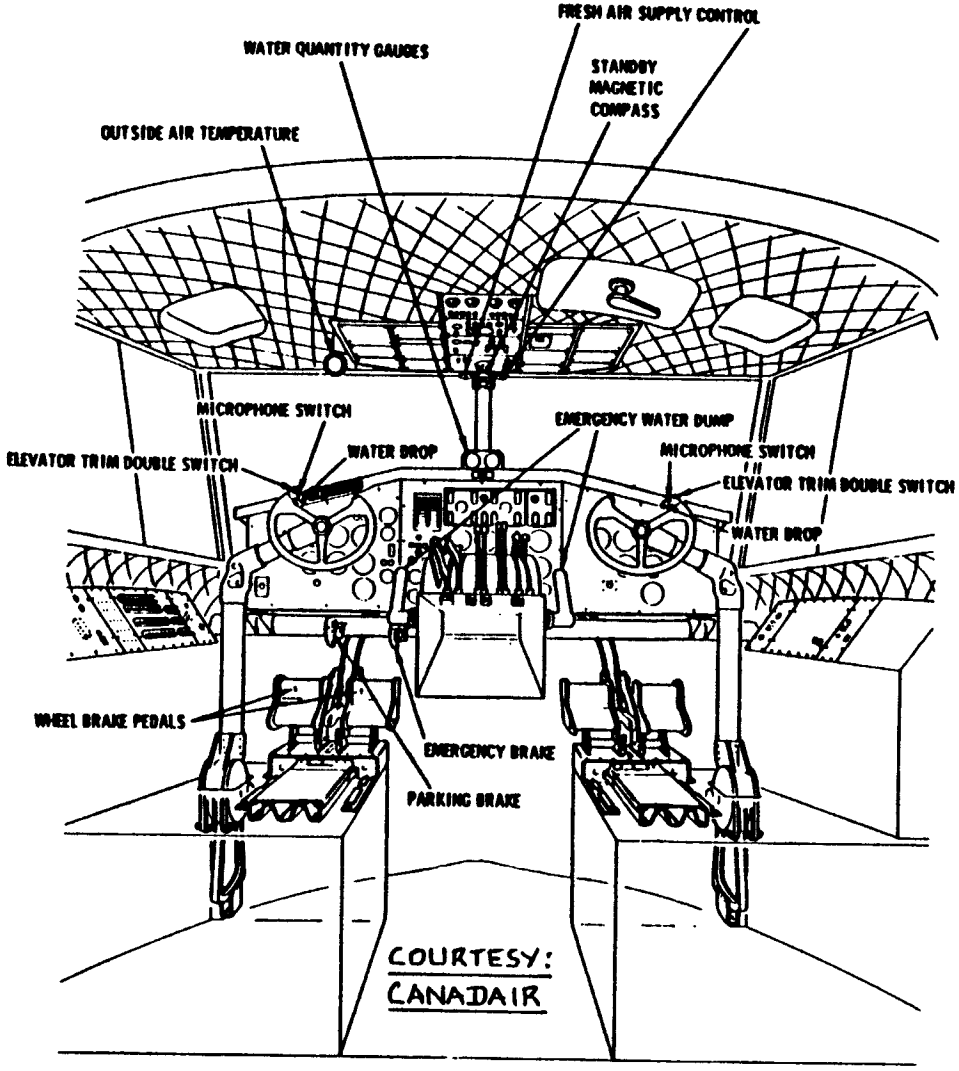

Figure 9.3 Flight Compartment View: Canadair CL215

Figure 9.4 Cockpit Impression: Fokker F-28

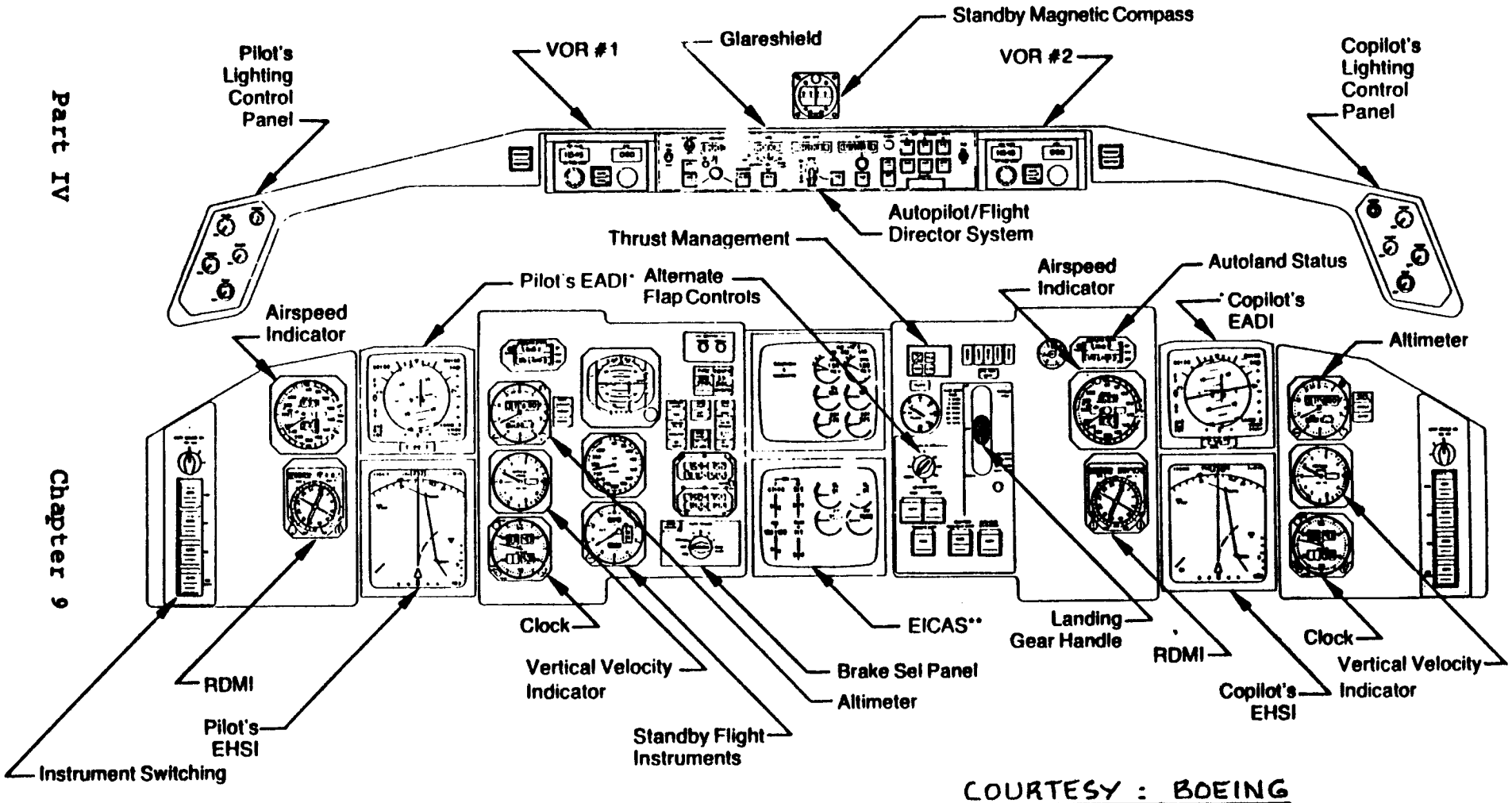

COURTESY : BOEING

*Cathode Ray Tube (CRT)
**Engine Indication and Crew Alerting System CRTs

Figure 9.5 Cockpit Instrumentation: Boeing 767

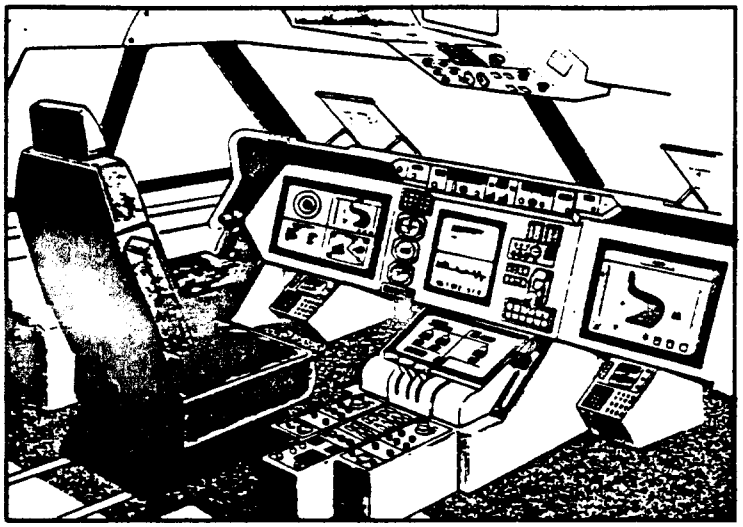

COURTESY:
LOCKHEED

Figure 9.6 Proposed Flat Panel Cockpit Display

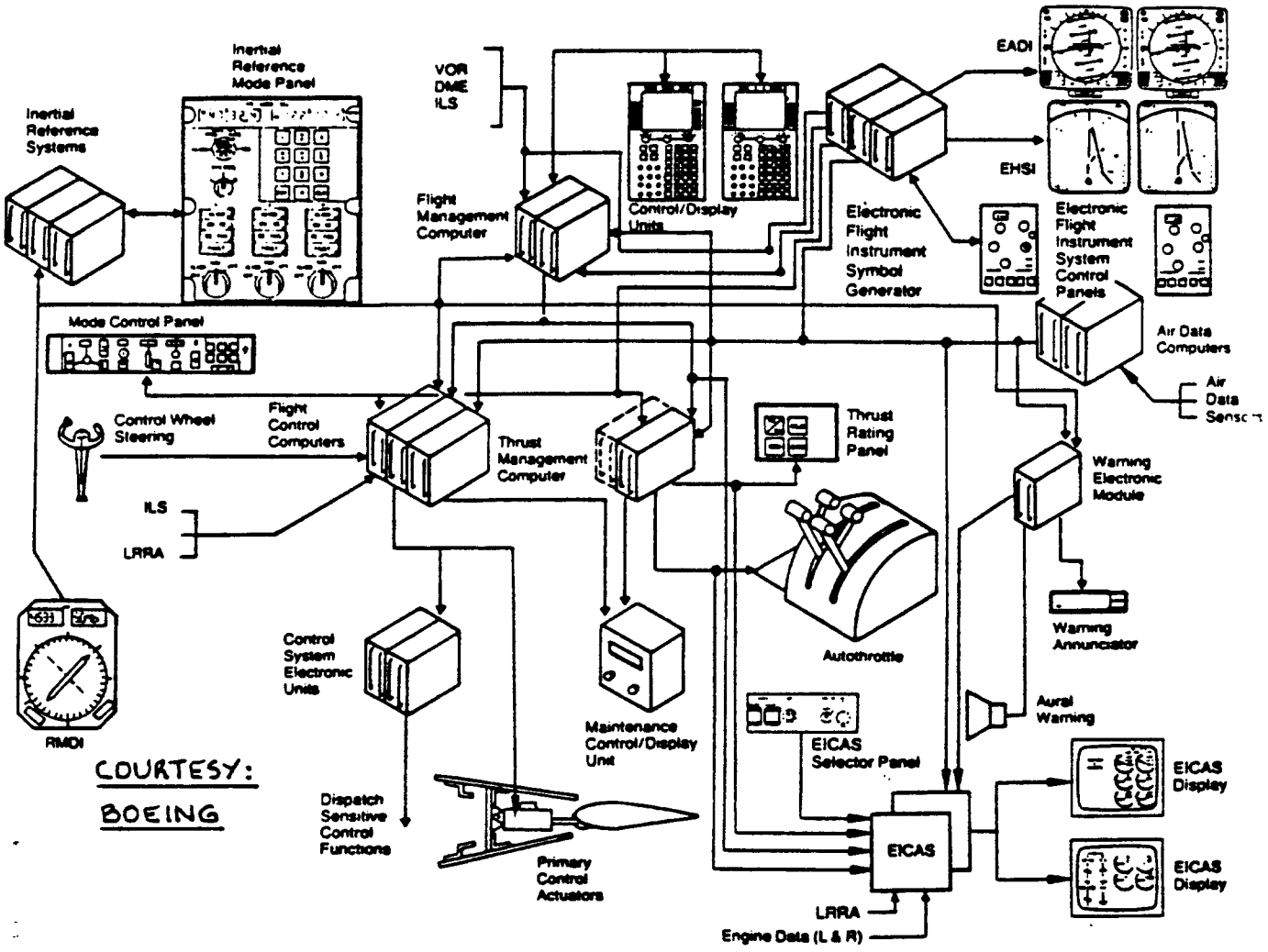

COURTESY:
BOEING

Figure 9.7 Flight Management System Schematic Boeing 767

9.2 FLIGHT MANAGEMENT AND AVIONICS SYSTEM LAYOUT

Flight management and avionics systems are undergoing very rapid development. Also, the number of different systems available to the user is so large that a concise summary in a textbook on airplane design cannot be given in a few pages. For older avionics and flight management systems the reader should refer to Ref.34. For an annual summary of available avionics systems the reader should consult the magazine: 'Business and Commercial Aviation' which each year publishes an up-to-date list of available equipment including data on weight, power requirements and pricing. Reference 36 contains a 1986 state of the art description of what advanced avionics can do for an airplane.

In nearly all recently built transports the pilot interfaces with the airplane controls through the so-called flight management system. These systems have now progressed to the point of integrating propulsion controls, flight controls and autopilot functions. Figure 9.7 shows a flight management system schematic as used in a modern jet transport.

A flight management system requires a number of sub-systems. In the following the sub-system breakdown employed in the Boeing 767 will be illustrated.

1. Flight control computer

   Figure 9.8 shows a diagram indicating the flight control computer functions.

2. Autopilot/autothrottle controls

   Figure 9.9 shows the autopilot/autothrottle control panel with its various function selectors indicated.

3. Thrust management computer

   Figure 9.10 presents a schematic of the thrust management computer functions.

Figure 9.11 summarizes the flight control avionics functions of the 767 flight mangement system.

4. Inertial reference system

In long range airplanes in particular, inertial re-

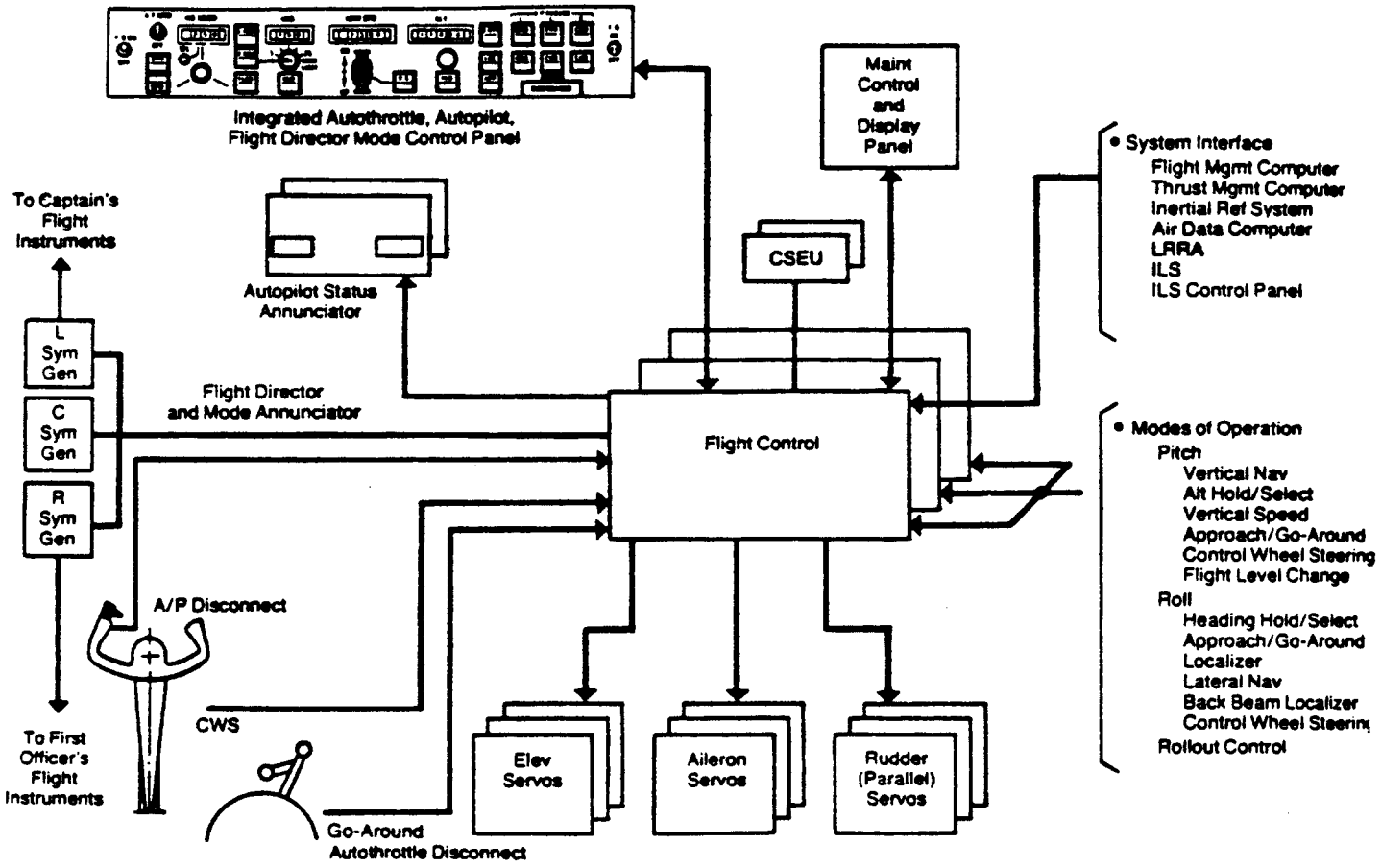

Figure 9.8 Flight Control Computer Functions: Boeing 767

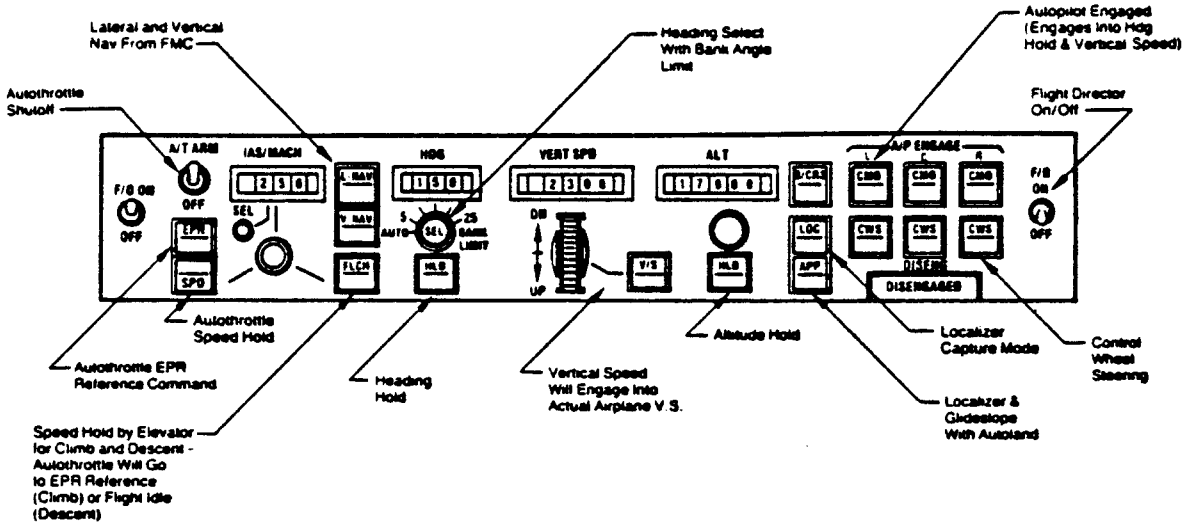

Figure 9.9 Autopilot/Autothrottle Control Panel: Boeing 767

- Thrust rating
  - Thrust limit computation
  - Thrust derate
- Autothrottle control
  - Controls to thrust limit
  - IAS/Mach select
  - Autoland flare retard
  - Overspeed protection
  - Overboost protection

COURTESY: BOEING

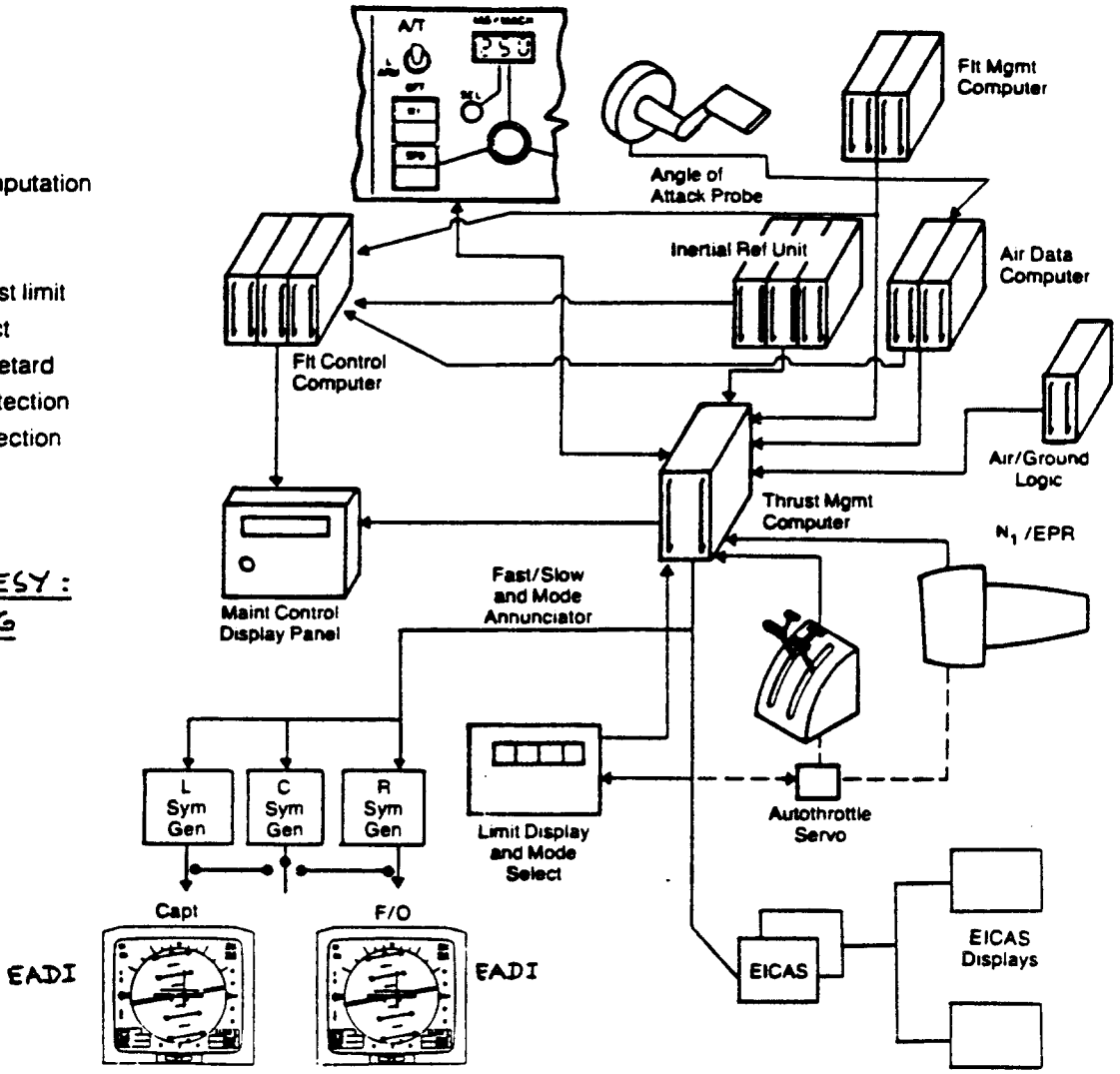

Figure 9.10 Thrust Management Computer Functions: Boeing 767

COURTESY: BOEING

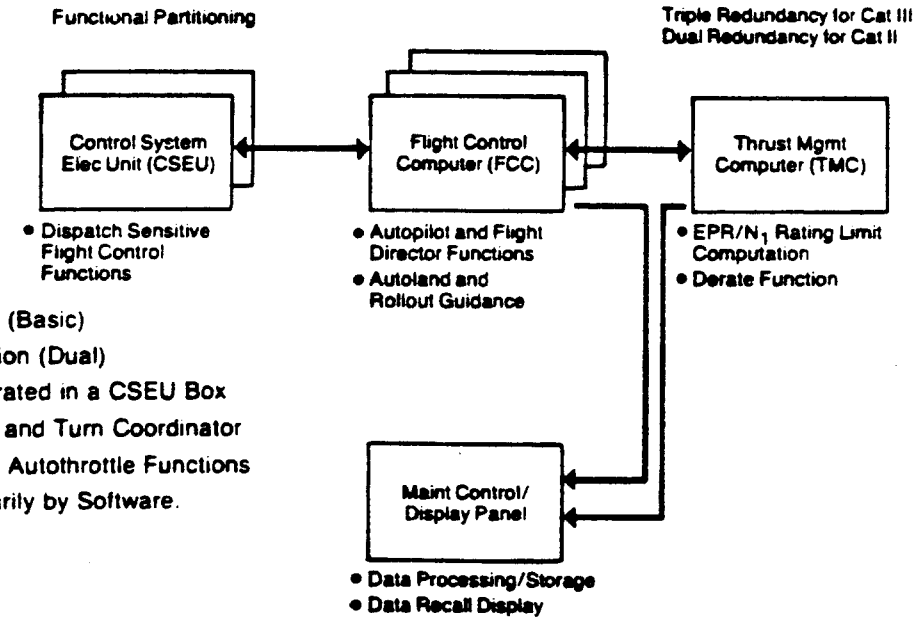

- Category IIIb and Rollout Guidance (Basic)
- Category II Achieved by LRU Deletion (Dual)
- Dispatch Sensitive Functions Separated in a CSEU Box
- Integrated Autopilot, Flight Director and Turn Coordinator
- Integrated Thrust Management and Autothrottle Functions
- Growth/Operational Changes Primarily by Software.
- Advanced Maintenance Capability

Figure 9.11 Flight Control Avionics Functions: Boeing 767

ference systems are required. Figure 9.12 indicates the functions of the inertial reference system.

5. Flight data acquisition system

Flight data are an essential input to all flight management systems. Figure 9.13 shows the flight data inputs needed by the 767 system.

6. Communication and advisory system

During any flight a large number of communications take place between the cockpit and air traffic control stations. In addition the crew advises the passengers of the flight status. Figure 9.14 provides a functional flow diagram of the communication and advisory system.

9.3 ANTENNA SYSTEM LAYOUT

For communication between the ground and the airplane a large number of antenna systems are required. Figure 9.15 shows an example of the antennae installed in a Boeing 767.

9.4 INSTALLATION, MAINTENANCE AND SERVICING CONSIDERATIONS

Much of the avionics equipment in airplanes consumes a considerable amount of electrical power. Most of that power is eventually transformed into heat. In turn this would lead to major malfunctions in avionics equipment. Therefore cooling is a necessity. Figure 9.16a shows a schematic of the instrument and equipment cooling needed in a Boeing 767. Figure 9.16b shows how some of the flight deck instruments are cooled.

A reasonable assumption is that most electrical and electronic equipment will fail rather frequently. Therefore, easy access to this equipment is an essential feature of good layout design.

Figure 9.17 shows an example of accessibility to a cockpit instrument panel. Other avionics equipment is located in five equipment centers. Figure 9.18 shows where these equipment centers are located in the airplane.

Figure 9.19 indicates where the maintenance control and display panel is located and what its functions are. This type of maintenance control is also being used in

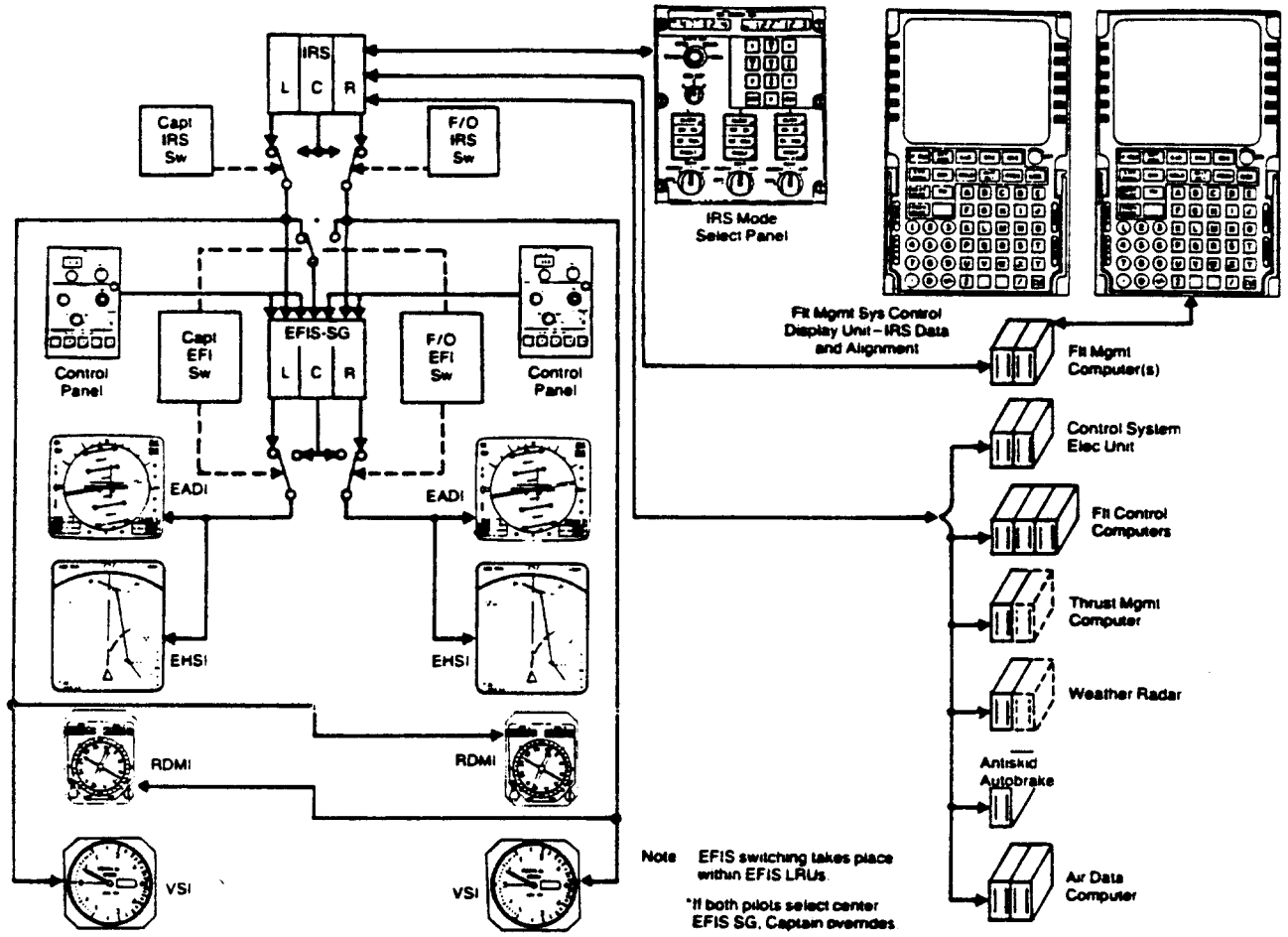

Figure 9.12 Inertial Reference System Functions: Boeing 767

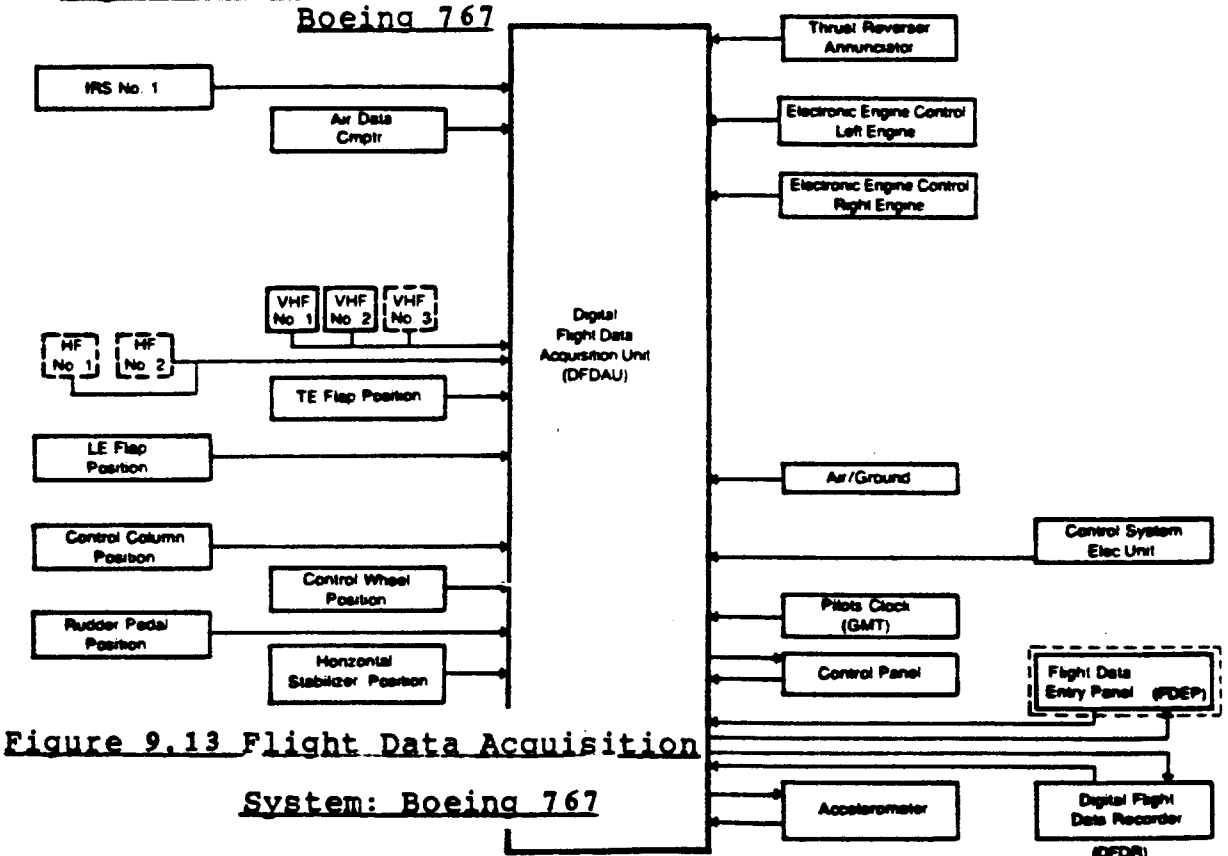

Figure 9.13 Flight Data Acquisition System: Boeing 767

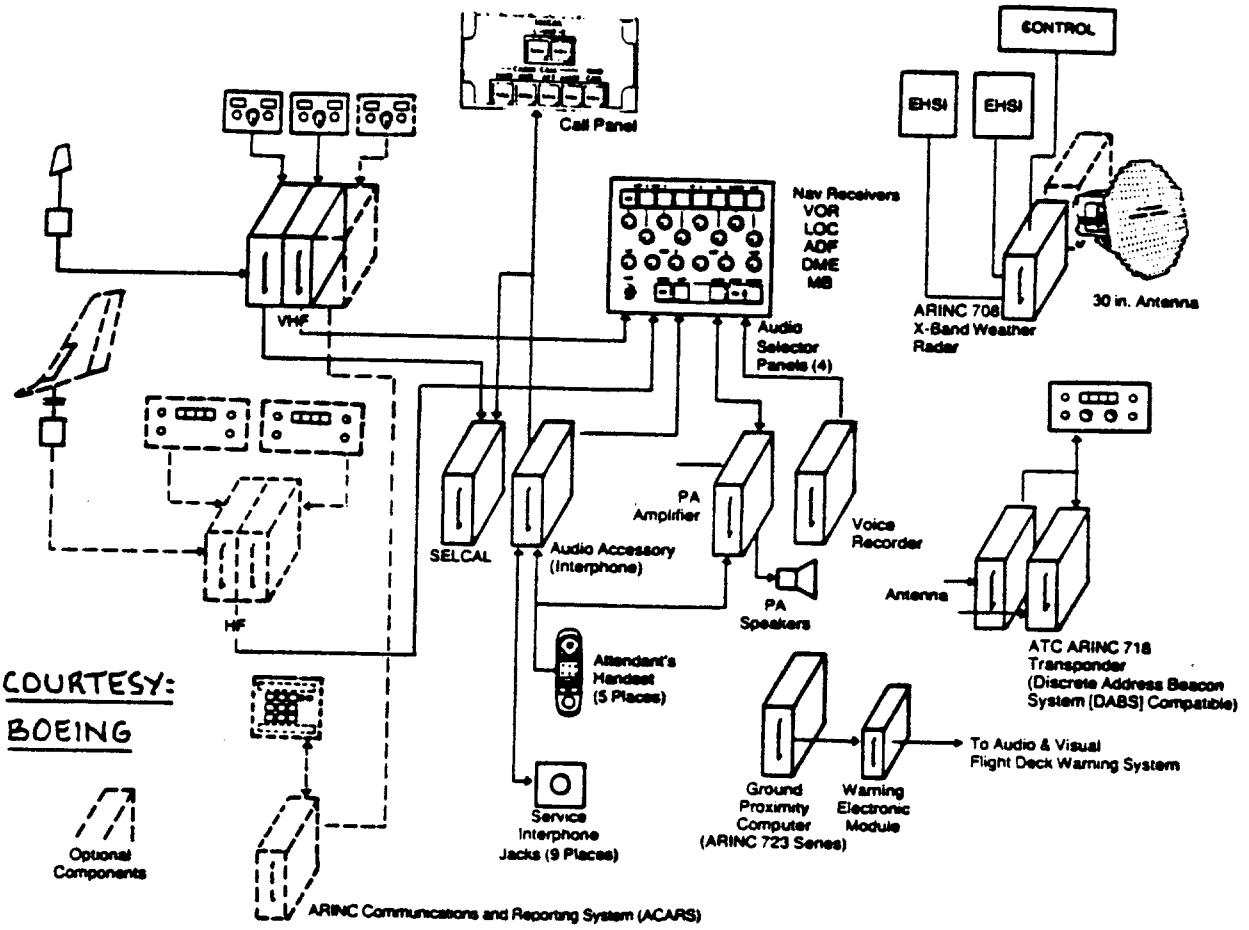

Figure 9.14 Communications and Advisory Systems Functional Flow: Boeing 767

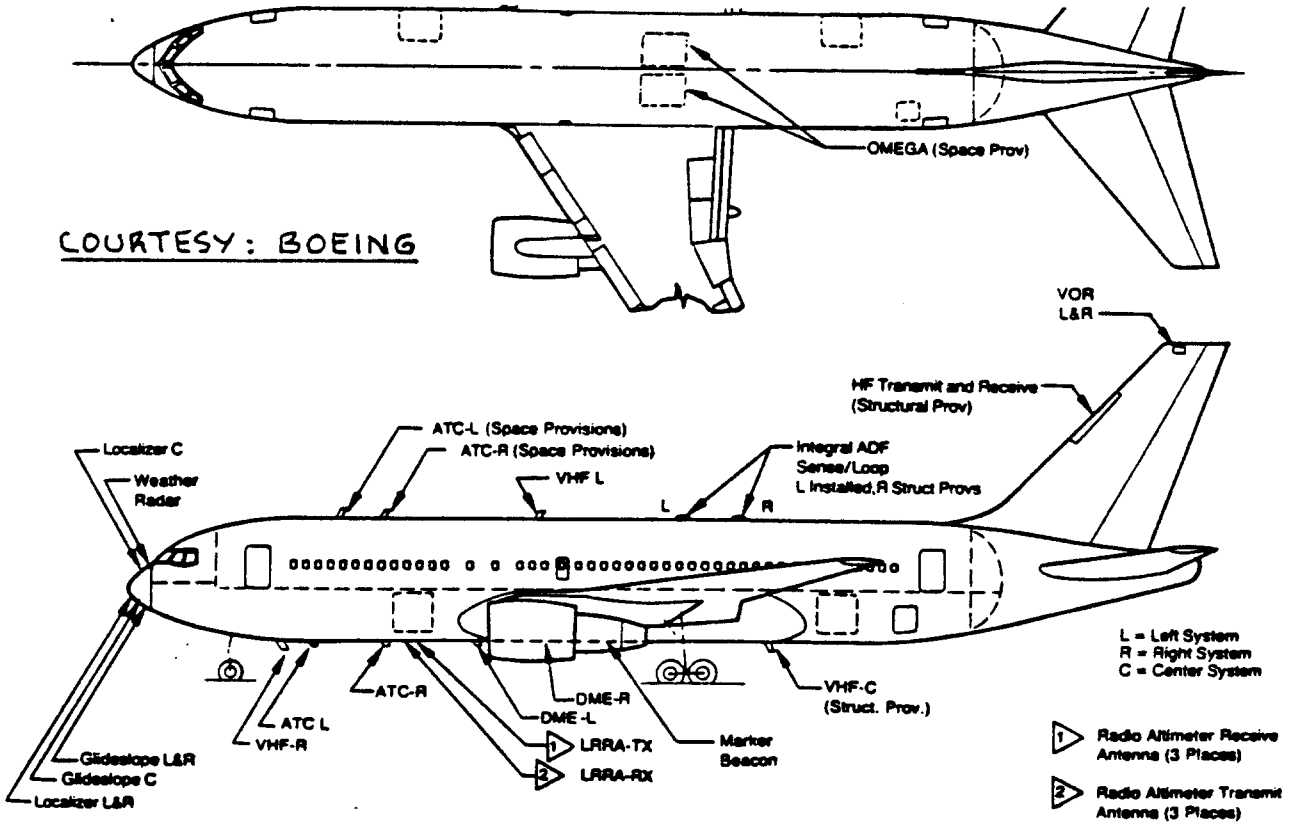

Figure 9.15 Antenna Installations: Boeing 767

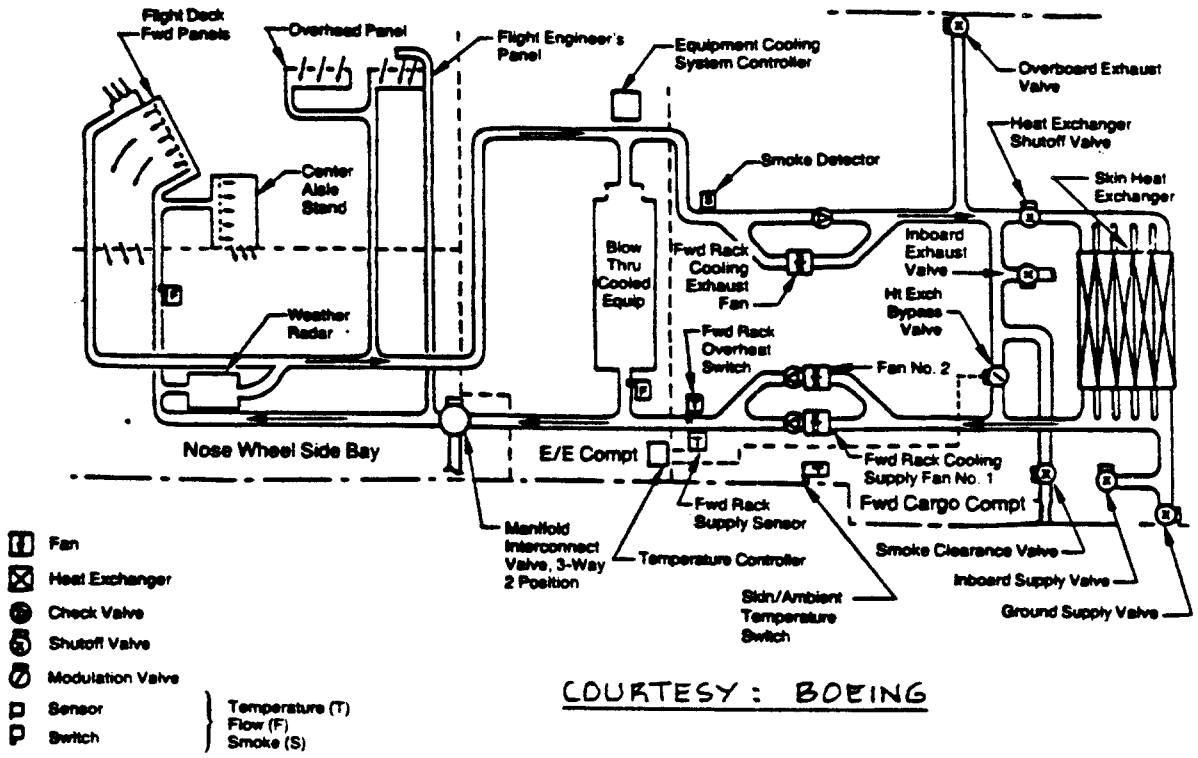

COURTESY: BOEING

Figure 9.16a Instrument and Equipment Cooling System: Boeing 767

Instrument Cooling

- Positive cooling for flight deck instruments
- Improved ground cooling
- Closed loop in-flight cooling
  - Reduced equipment contamination without using filters
  - Reduces system impact on main cabin air distribution
  - Permits control of cooling air temperature
  - Skin heat exchanger

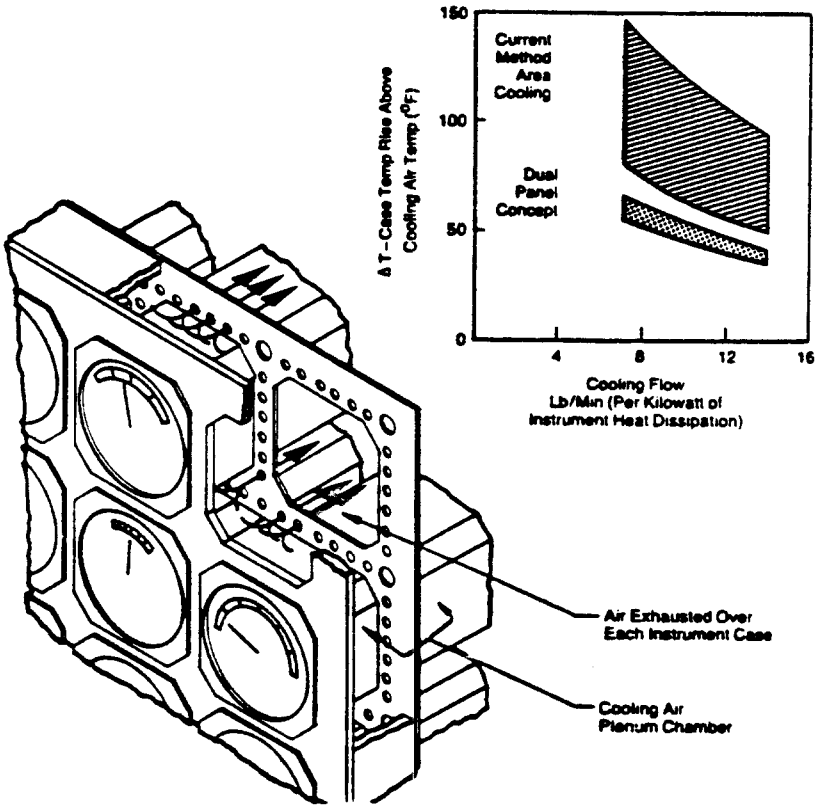

COURTESY: BOEING

Figure 9.16b Cooling of Flight Deck Instruments: Boeing 767

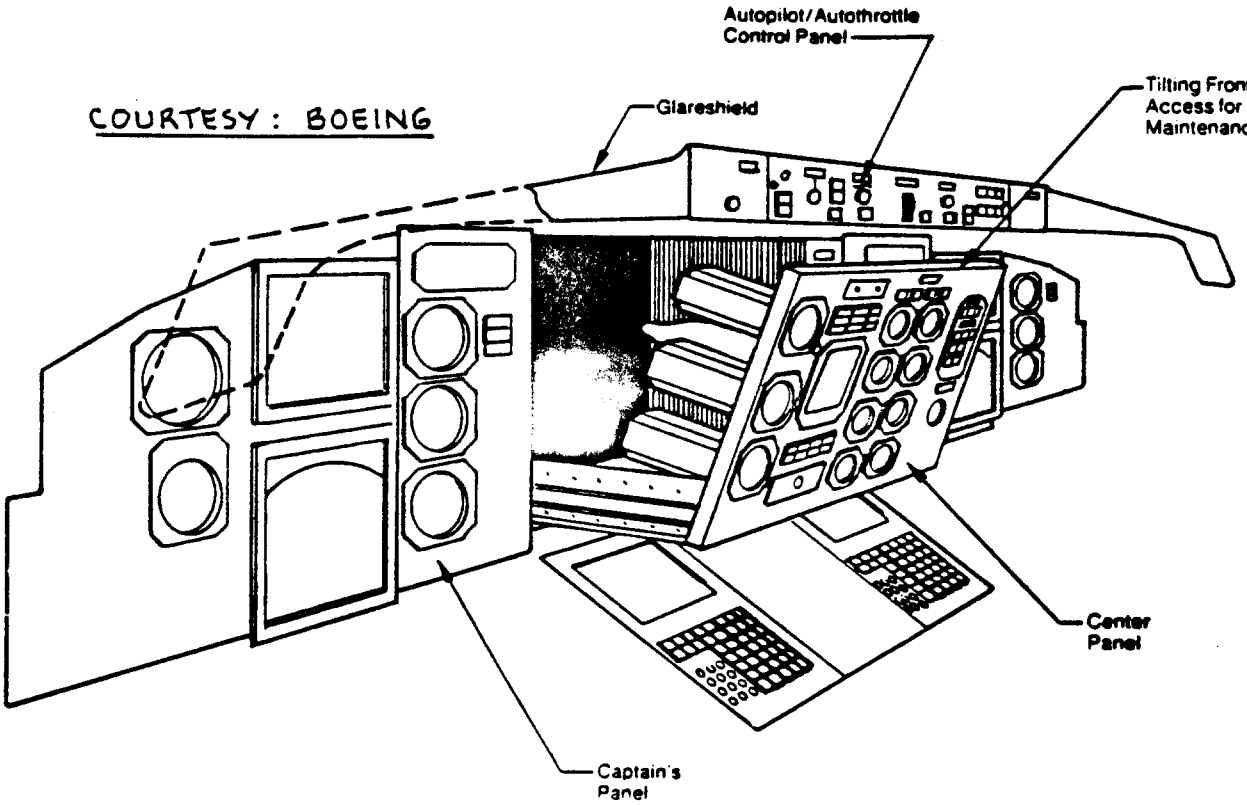

Figure 9.17 Cockpit Instrument Accessibility: Boeing 767

Main Equipment Center

- Flight Management System
- Flight Control System Electronics
- Inertial Reference System
- Thrust Management System
- Air Data Computers
- Maintenance Control & Display
- Caution Advisory Computer
- VHF Communications & Selcal
- ILS, VOR, DME and ATC Avionics
- Passenger Service & Entertainment System
- Environmental Control System Electronics
- Flight Data Acquisition Unit
- Ground Proximity System
- Electrical Power System Controls
- Anti-Skid/Auto Brake System
- Engine Vibration Monitor Electronics

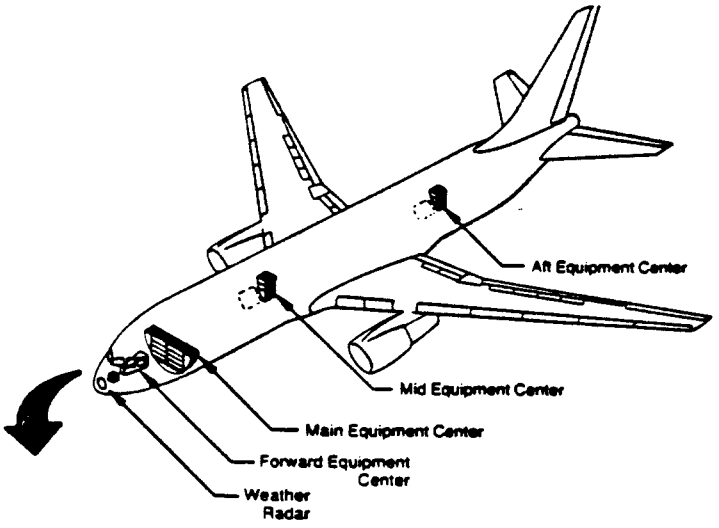

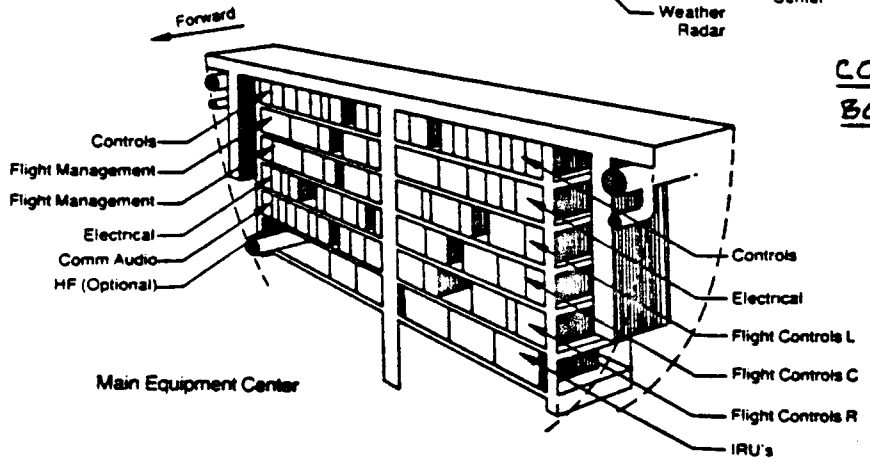

COURTESY: BOEING

Figure 9.18 Location of Avionics Equipment Centers: Boeing 767

many fighter airplanes.

Figure 9.20 shows how the mid and aft equipment centers can be accessed.

The radar system and flight control antennae are accessed through removal of the radome. Figure 9.21 shows how the forward equipment center can be accessed.

(Ground Use Only)

- Provides means to store and readout identification of LRU's which have failed in flight
  - •Flight squawk oriented system
  - •Designed for quick turnaround operation
- Provides means to readout faulted LRU interfaces following maintenace action for the following:
  - •Flight control computers
  - •Thrust management computer
  - •Flight management computers
- Provides means to display test and maintenance instructions to fault isolate to the LRU level
  - •Instructions are function oriented
  - •Designed for overnight maintenance activity

COURTESY: BOEING

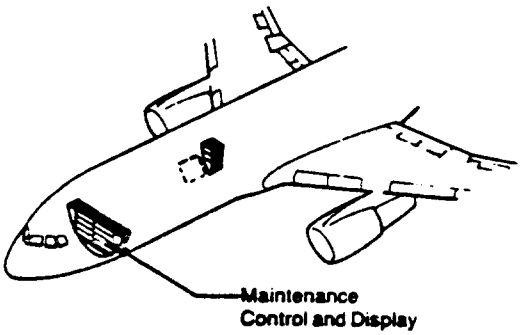

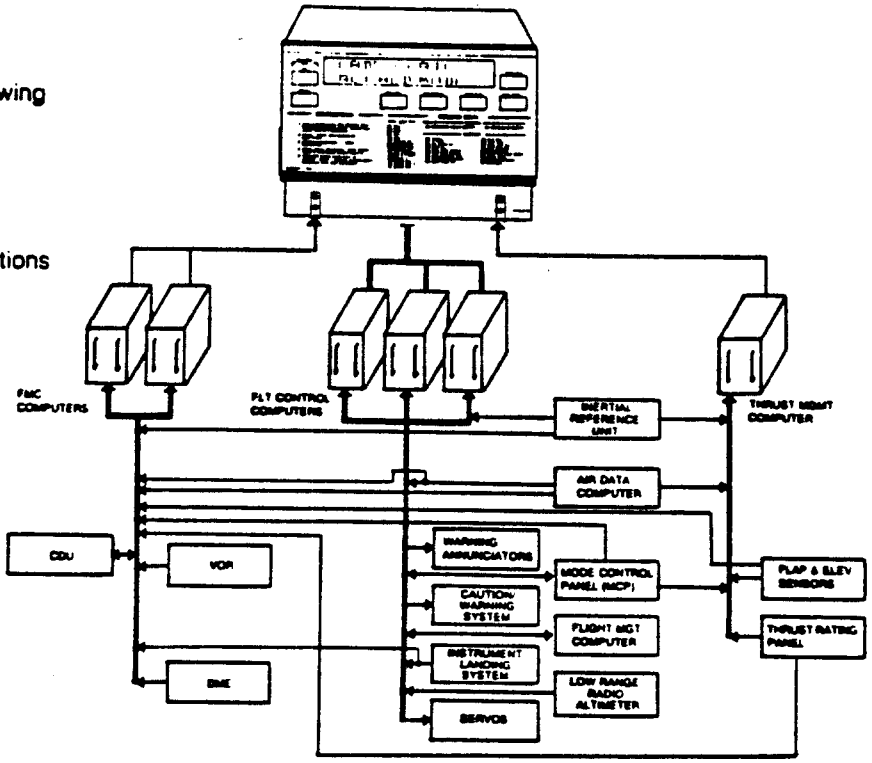

Figure 9.19 Maintenance Control and Display Panel: Boeing 767

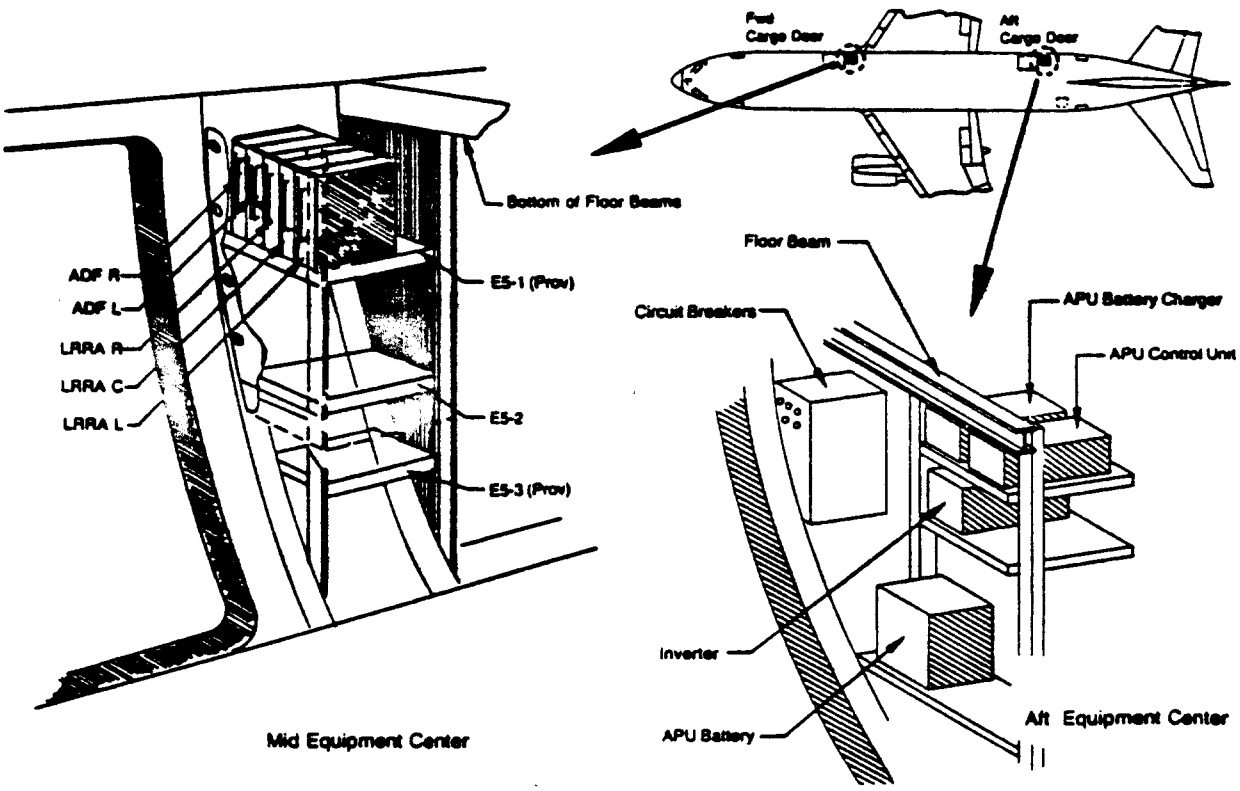

Figure 9.21 Forward Equipment Center, Radar and Flight Control Antennae Access: Boeing 767

Features of Weather Radar

- Visual indication of storm conditions and areas of turbulence at ranges up to 320 miles
- Color-coded displays for levels of turbulence/precipitation
- Built-in test (BIT) capability to check system performance
- Meets requirements of ARINC 708 and FAA T50 C63b

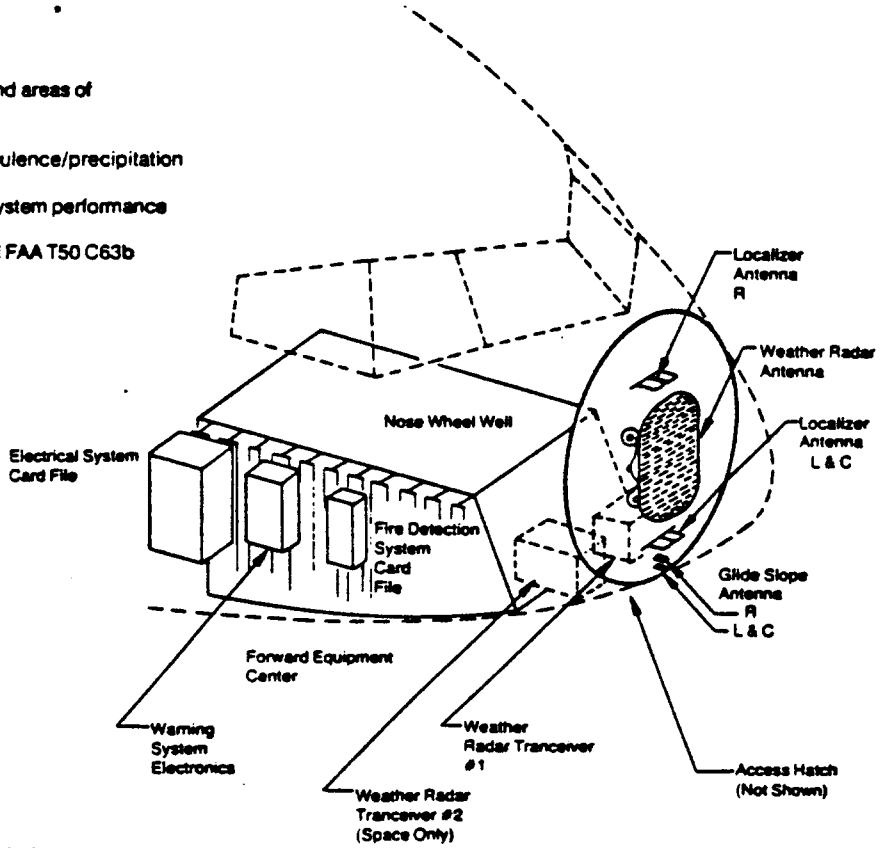

Figure 9.20 Mid and Aft Equipment Center Access: Boeing 767

10. DE-ICING, ANTI-ICING, RAIN REMOVAL AND DEFOG SYSTEMS

Whenever an airplane can be expected to be operated into known icing conditions, special systems must be installed to prevent the accumulation of ice and/or to remove ice which has formed.

In addition, when flying through severe rain it is possible that water accumulates on the windshields such that visibility is seriously degraded. A rain removal system must then be available.

Under certain combinations of humidity and temperature fog forms on the windshields, again restricting visibility. A defog system helps to combat this.

Reference 33 contains detailed descriptions of de-icing, anti-icing and rain removal systems.

The material in this chapter is organized as:

10.1 De-icing and anti-icing systems

10.2 Rain removal and defog systems

10.1 DE-ICING AND ANTI-ICING SYSTEMS

Ice formation can have the following consequences:

1. Ice formed on wings and tails can distort the aerodynamic contours such that:

a) the drag increases markedly which may cause the airplane to slow down or to loose climb capability.

b) the lift decreases. Particularly a sharp drop in maximum lift coefficient may lead to earlier than normal stalls when the pilot maneuvers the airplane.

c) the pitching moment changes. This can lead to unexpected trim changes as well as to changes in the stick-force-speed and/or stick-force-per-'g' gradients.

Figure 10.1 illustrates typical ice accumulation shapes which can occur on airplane lifting surfaces.

2. Ice formed in engine inlets can result in serious degradation of engine performance. In addition, when ice breaks loose from the inlet it can cause serious damage to the engine.

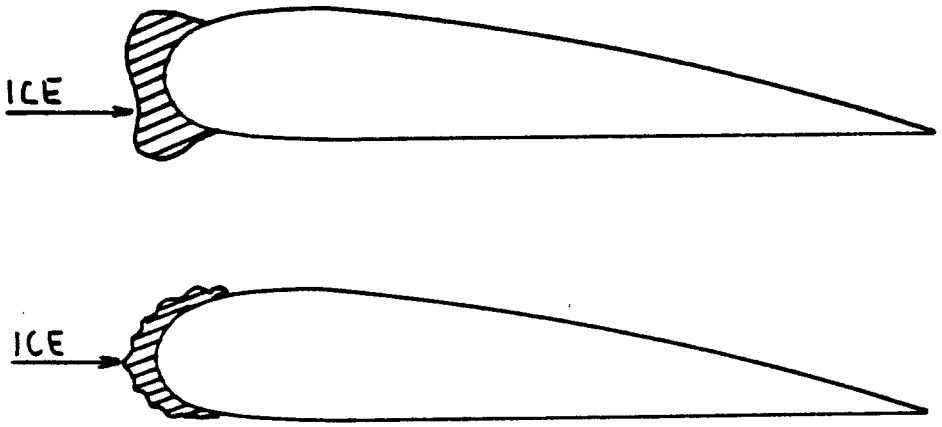

Figure 10.1 Ice Accumulation Shapes

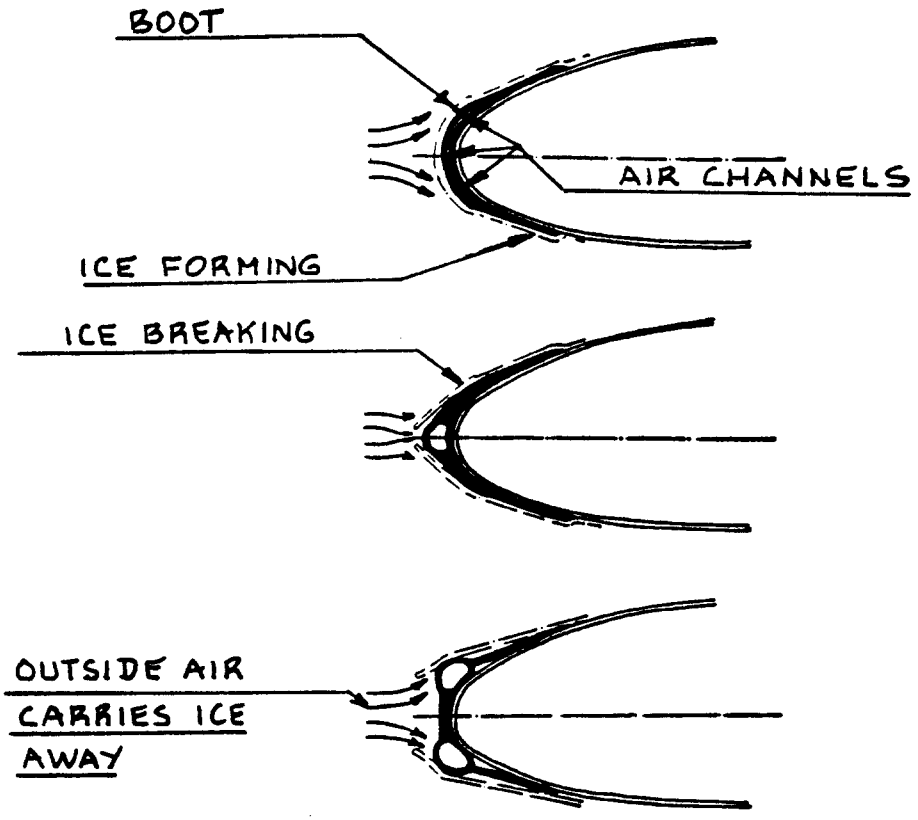

Figure 10.2 Operation of a De-icing Boot

3. Ice formed on pitot inlets, stall vanes or other sensors crucial to the safe operation of an airplane can result in accidents.

The purpose of this section is to discuss the following systems:

10.1.1 De-icing Systems: these are systems which are designed to remove ice which has already formed.

10.1.2 Anti-icing Systems: these are systems designed to prevent the formation of ice.

10.1.1 De-Icing Systems

The following de-icing systems will be discussed:

1. De-icing boots

2. Electro-impulse systems

1. De-icing Boots

De-icing boots consist of a thin rubber bag attached to the leading edge of a lifting surface. Figure 10.2 shows a cross section of a boot installation. Note that three separate air channels are pressurized in an alternating manner. This cracks and breaks the ice away.

Figure 10.3 shows an example of a de-icing boot system installed in a Beech King Air. The system uses engine bleed-air to pressurize the boots.

2. Electro-Impulse Systems

These systems operate by delivering mechanical impulses to the surfaces on which ice has formed. These impulses are delivered by electromagnetic coils installed on these surfaces. Figure 10.4 shows a cross section through a leading edge with an electro-impulse system installed. Ref.37 should be consulted for further details.

NOTE: Airplane configurations must be laid out so that ice which breaks away does not enter jet engines.

10.1.2 Anti-Icing Systems

The idea behind anti-icing systems is to prevent the formation of ice. These systems are to be turned on as soon as the crew suspects that their flight will

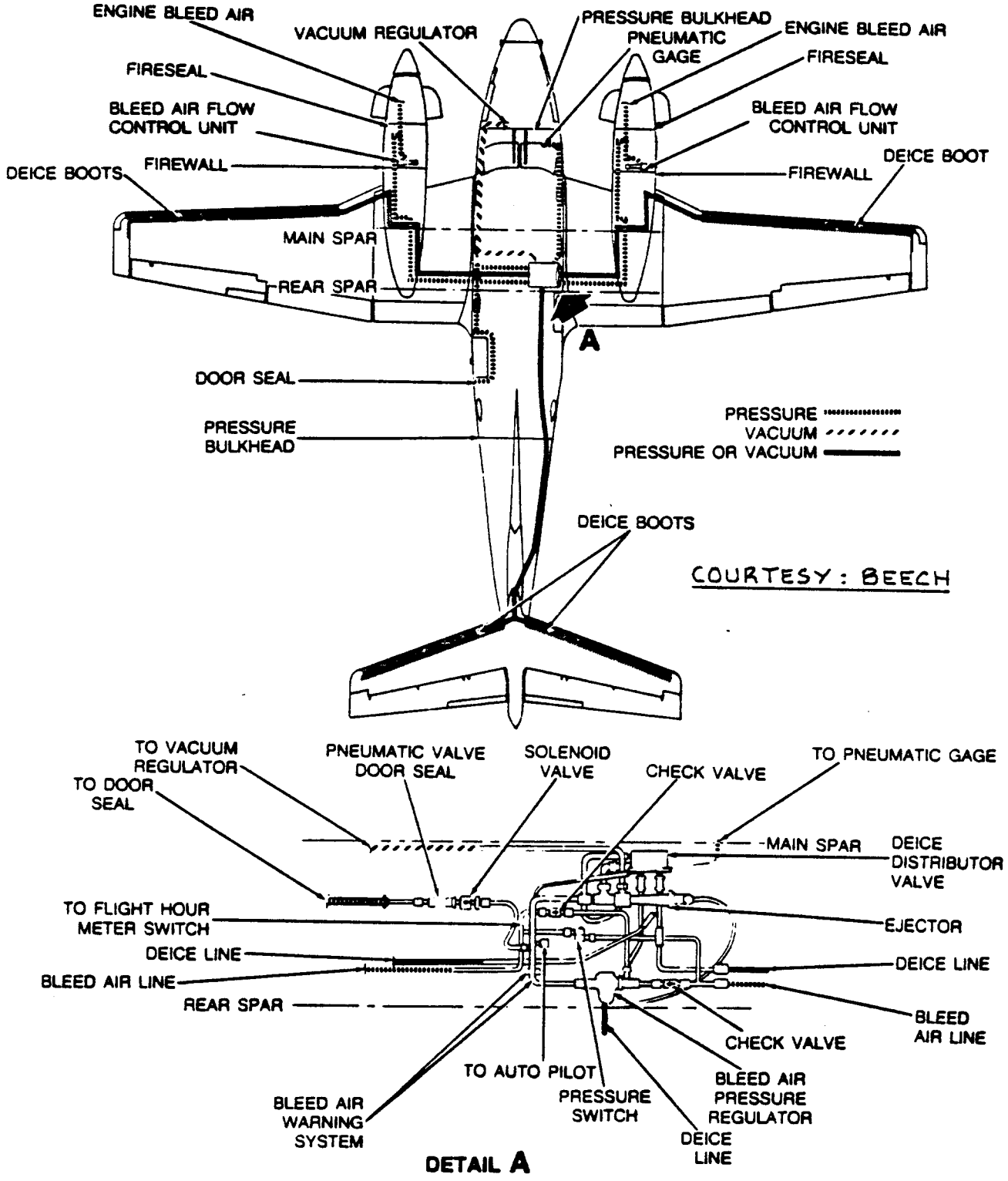

Figure 10.3 De-icing Boot System: Beech King Air F90

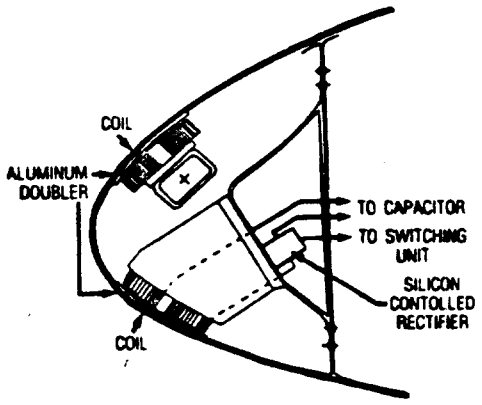

COURTESY:
DR. G.W. ZUMWALT

Figure 10.4 Electro-Impulse De-icing System

Thermal Anti-Ice (TAI)

Engine bleed air is used to prevent ice buildup on the engine inlet cowl and the three outboard slats on each wing leading edge.

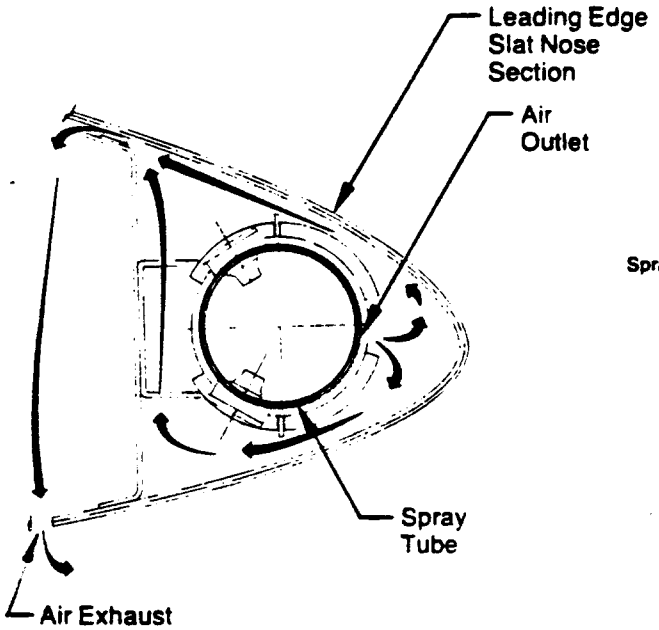

Spray Tube Cross Section (Typical)

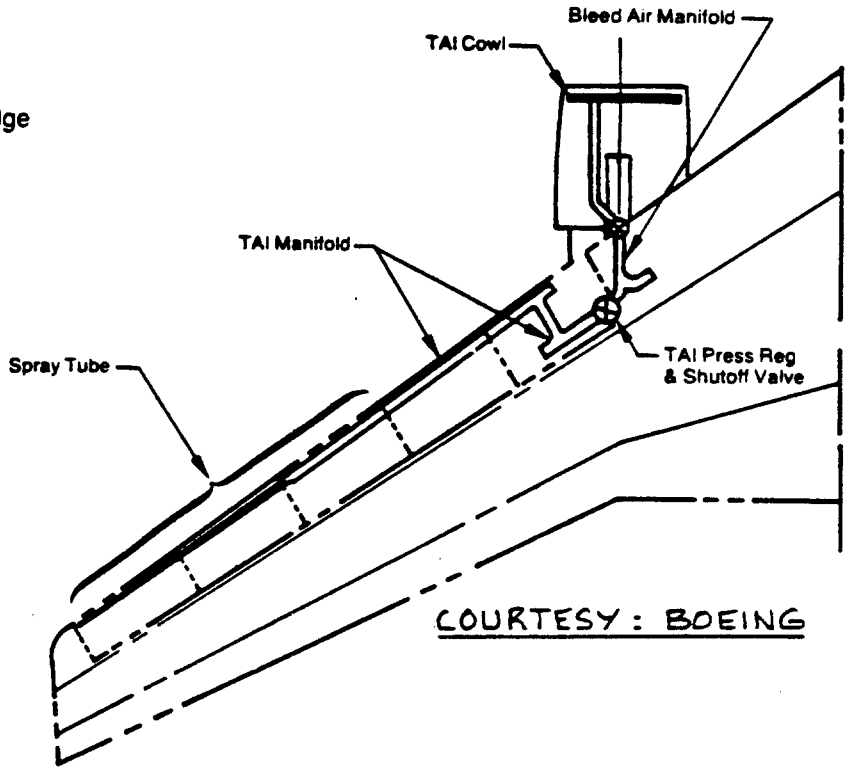

COURTESY: BOEING

Figure 10.5 Air Heated Anti-Icing System: Boeing 767

encounter conditions favorable to the formation of ice.

The following anti-icing systems will be discussed:

1. Thermal anti-icing system

2. Chemical system

   NOTE: thermal and chemical anti-icing systems can be used in a de-icing mode. If this is done, ice which breaks away must not enter jet engines.

3. Carburetor heating system

4. Inertial anti-icer system

1. Thermal Anti-icing Systems

Two types of thermal anti-ice systems are in use: air heated systems and electrically heated systems.

Air heated anti-icing systems employ hot air to heat surfaces where ice would otherwise form. Thermal anti-icing systems are sometimes used also to de-ice a surface. However, it is far better to prevent ice formation than to get rid of it after it has formed.

Figure 10.5 shows how an air heated system operates. Detailed schematics of air heated anti-icing systems are shown in Figures 10.6 and 10.7.

Air heated systems are also used to protect leading edge slats as well as engine nose cowls (inlet lips). Figure 10.8 shows such a system on the DC-10.

In electrically heated systems electrical resistances are used to heat those surfaces where ice otherwise would form. Electrical heating is used to prevent ice formation on pitot tubes, stall vanes, total air temperature probes, drain masts and engine inlet lips.

Figure 10.9 shows an electric anti-ice system schematic used on the Boeing 767.

2. Chemical Anti-icing System

In this type of system an anti-freeze liquid (for example a glycol base) is 'oozed' through a system of very small holes located in the leading edge. The leading edge is therefore covered with a liquid which does not freeze and thus prevents the formation of ice.

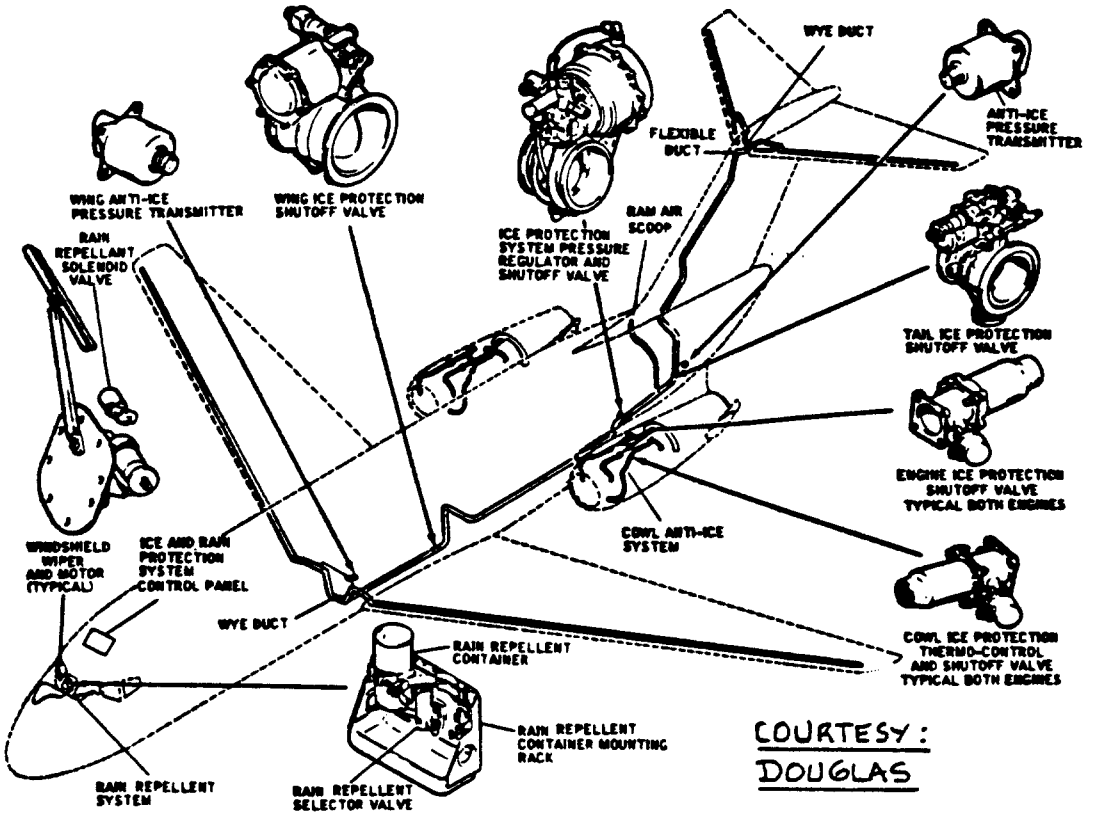

Figure 10.6 Anti-Icing System Layout: McDD DC-9

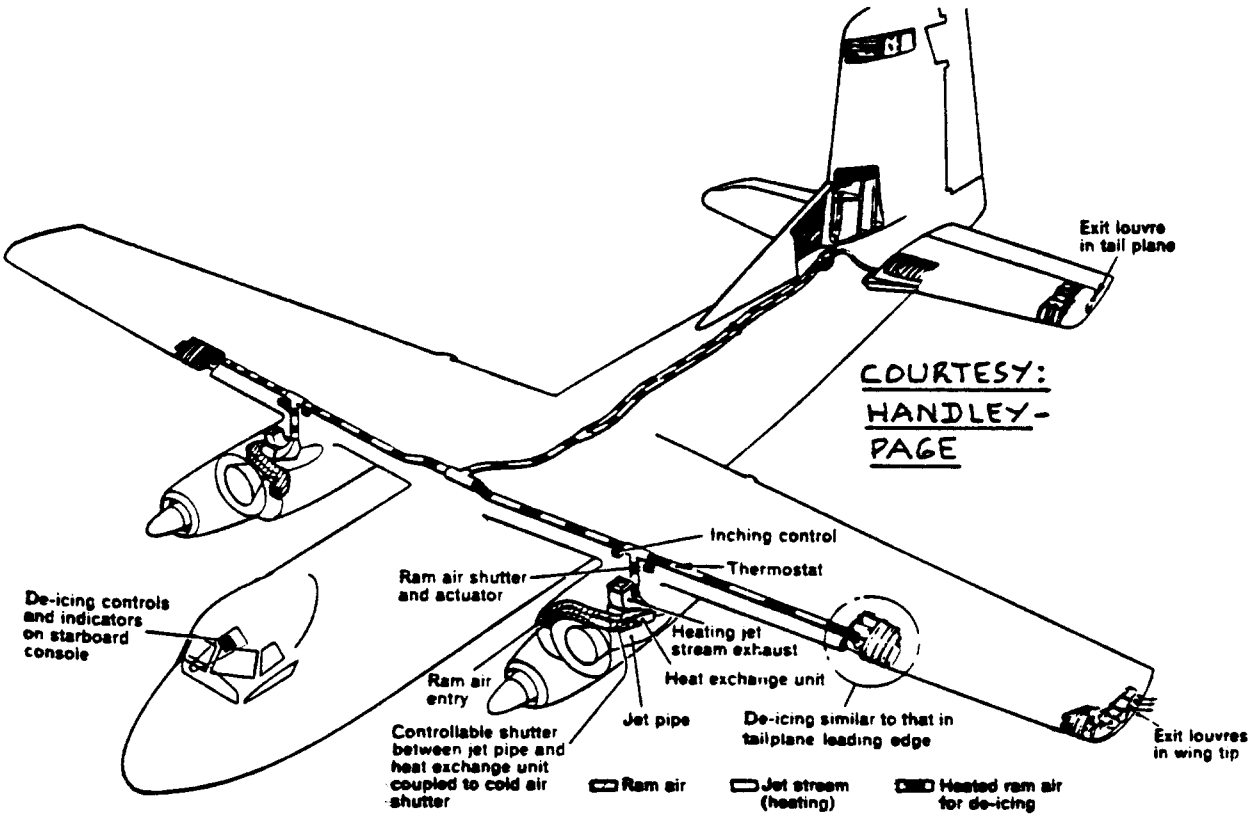

Figure 10.7 Anti-Icing System Layout: Handley Page Dart Herald

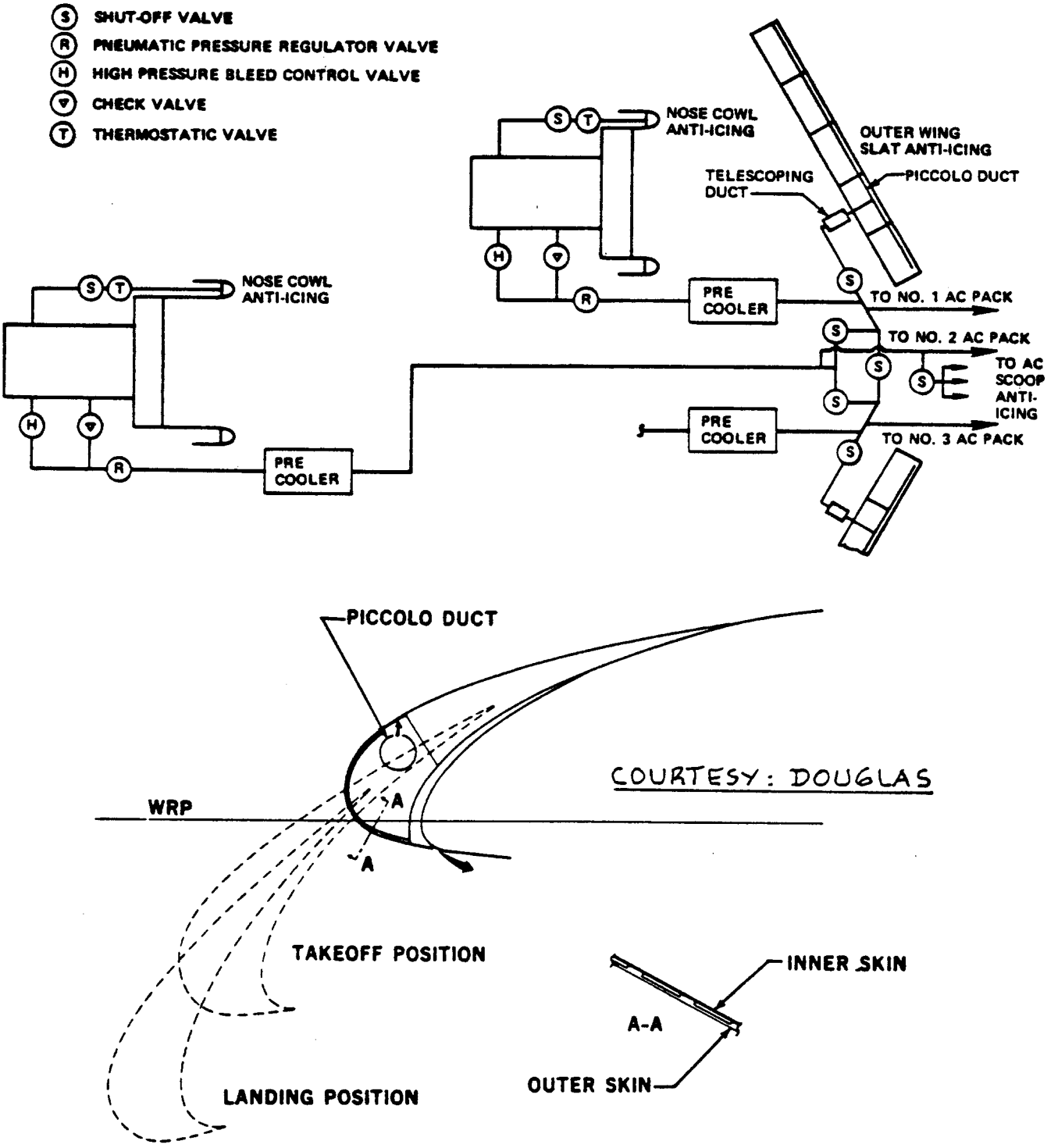

Figure 10.8 Anti-Icing System for Slats and Engine Nose Cowls: McDD DC-10

Electric Heat Anti-Ice

Electric heater icing protection is provided for the angle of attack sensors, the total air temperature sensors, the pitot-static probes, and the drain masts. The two forward flight compartment windshields are electrically heated to antifog those surfaces.

Rain Removal

Dual speed electrically operated windshield wipers are provided for the two forward windshields. A rain repellent solution is available to independently apply fluid to each of the two forward windshields.

COURTESY: BOEING

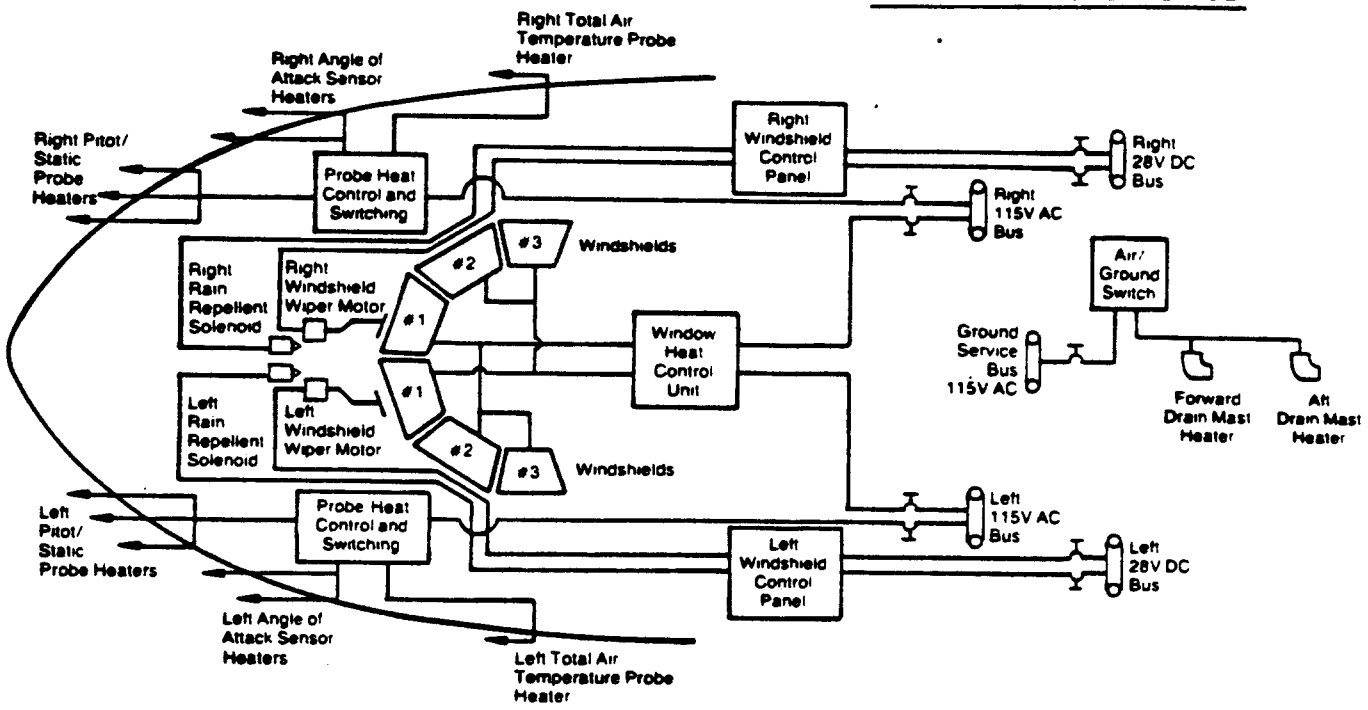

Figure 10.9 Electric Heat Anti Ice and Rain Repellant System: Boeing 767

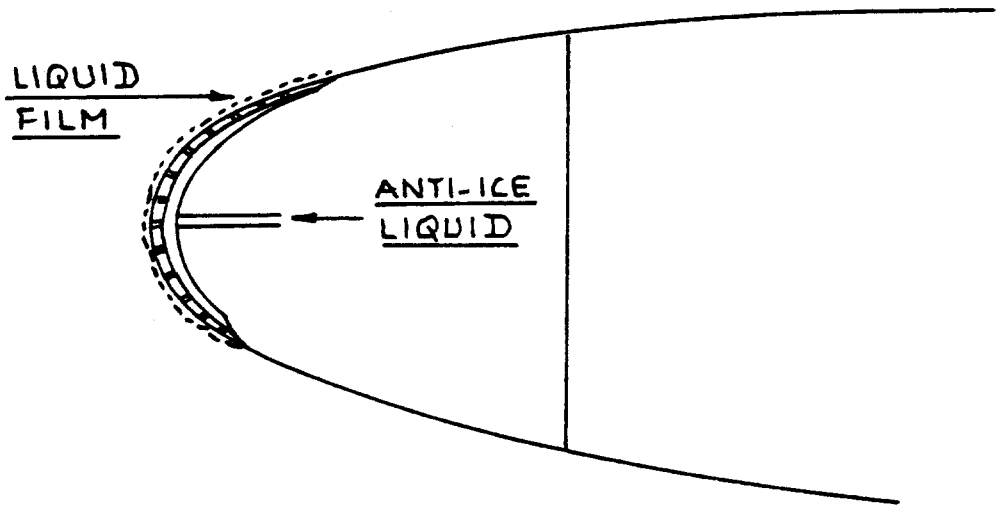

Figure 10.10 Operation of Chemical Anti-Icing System

Figure 10.10 shows how this system works. A disadvantage of this system is that it operates from a finite supply of anti-freeze. A major design question is: how much liquid should be carried? An advantage of this system is that it can be used to keep the wing leading edge clean from bugs and thus helps to maintain laminar flow.

Figure 10.11 shows an example of a liquid anti-icing system installation in a Short Skyvan.

3. Carburetor Heating Systems

In piston engines with carburetors it is mandatory to install a carburetor heating system to prevent ice formation. Because a carburetor operates on the principle of evaporation, it tends to cool the mixture below the prevailing temperature. Ice formation in a carburetor is therefore possible at fairly high outside air temperatures. For details on carburetor heating see Ref.38.

4. Inertial Anti-icer Systems

Figure 10.12 shows an example. When icing conditions are encountered, the vane in Figure 10.12 is extended into the inlet airflow. This vane increases the velocity of the incoming air by Bernoulli's Law. Any ice and snow particles are rushed past the entrance to the inlet plenum because of their inertia. The lighter air turns the corner to enter the plenum. The penalty is a decrease in pressure recovery and a decrease in engine performance.

10.2 RAIN REMOVAL AND DEFOG SYSTEMS

Rain removal is normally accomplished with windshield wipers similar to those in cars. Figure 10.13 shows an example installation. In most instances it is necessary to add a rain repellant into the wiper paths. Fig.10.14 shows a system for dispersing a rain repellant.

To prevent windshields from fogging up on the inside and/or on the outside a defog system can be installed. Figure 10.15 shows such a system.

Defogging can also be achieved with the help of electrical wiring buried inside the windshield material.

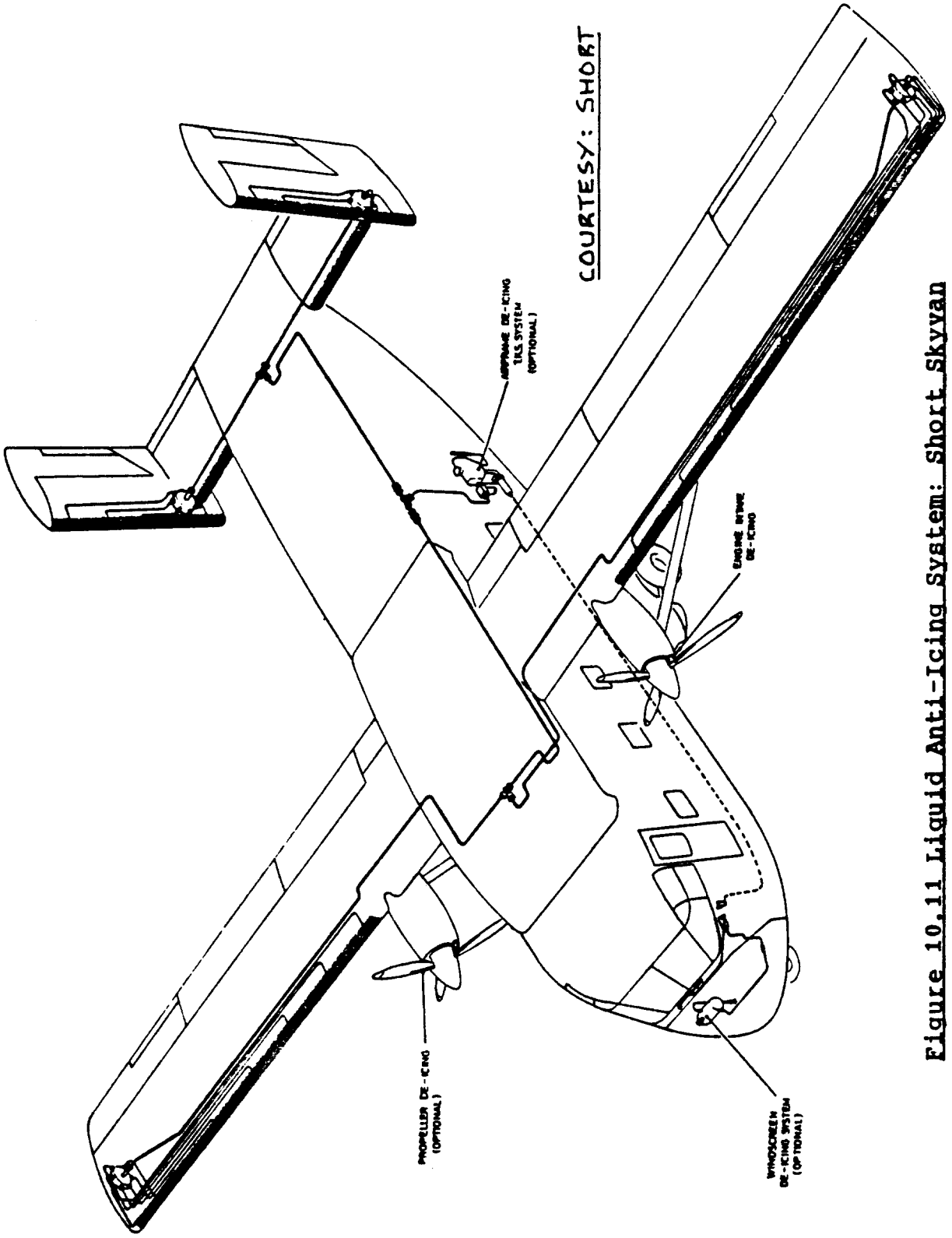

Figure 10.11 Liquid Anti-Icing System: Short Skyvan

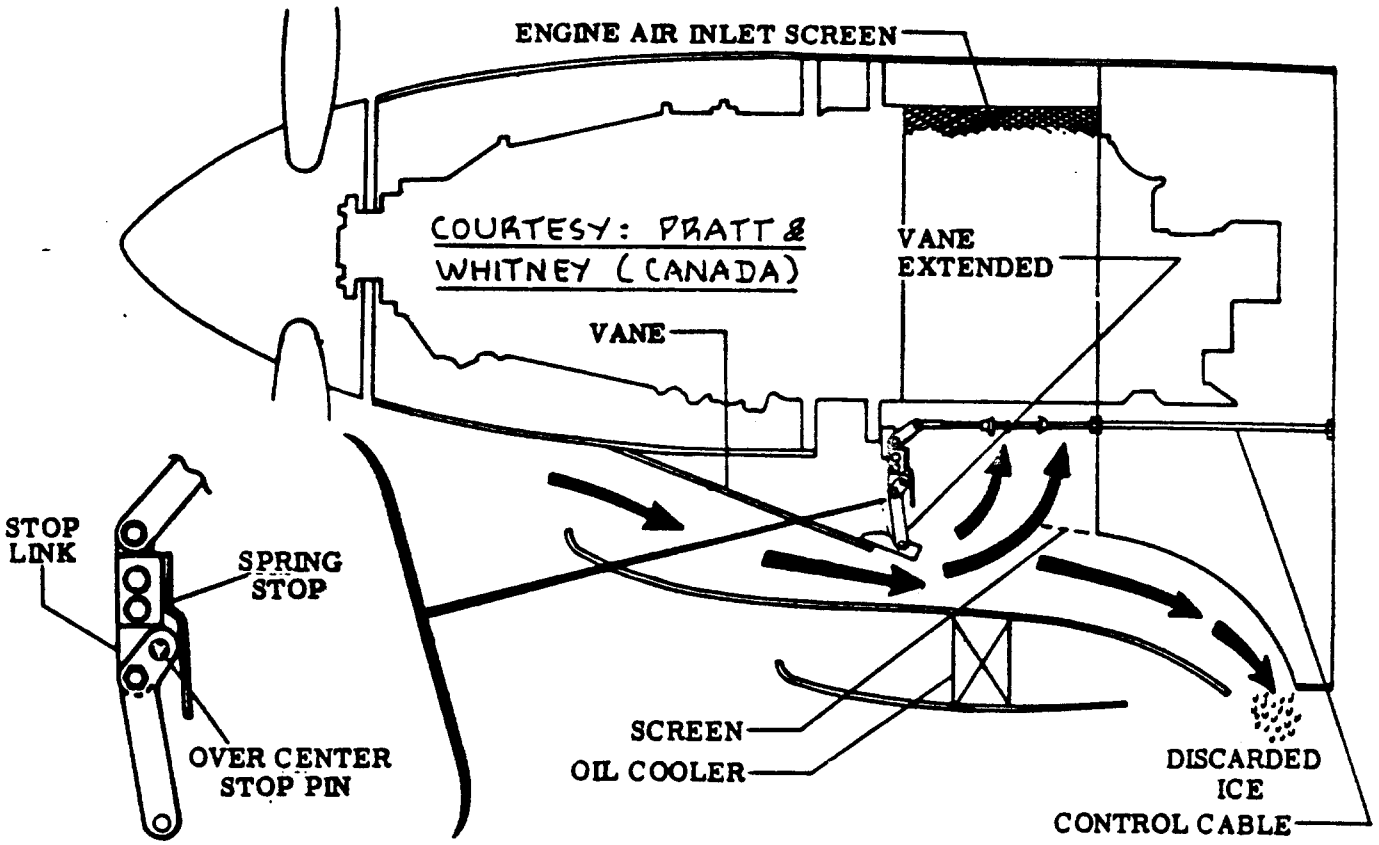

Figure 10.12 Inertial Anti-Icer System

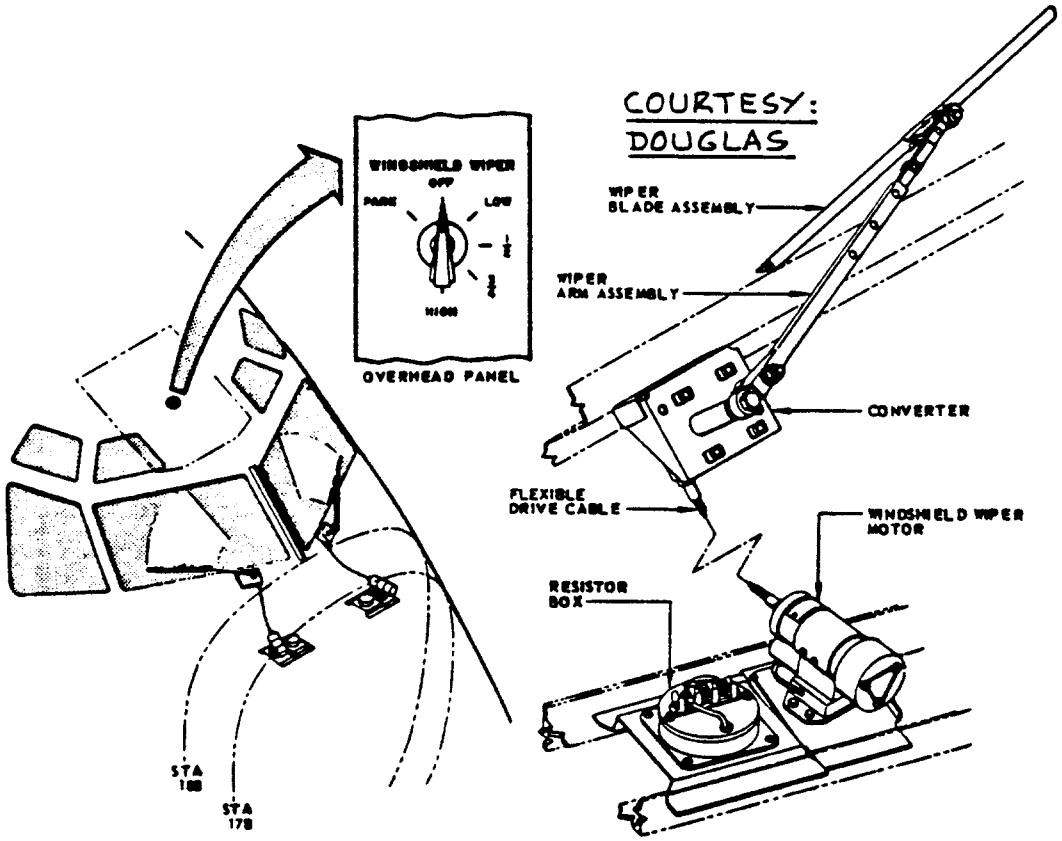

Figure 10.13 Windshield Wiper System: McDD DC-9

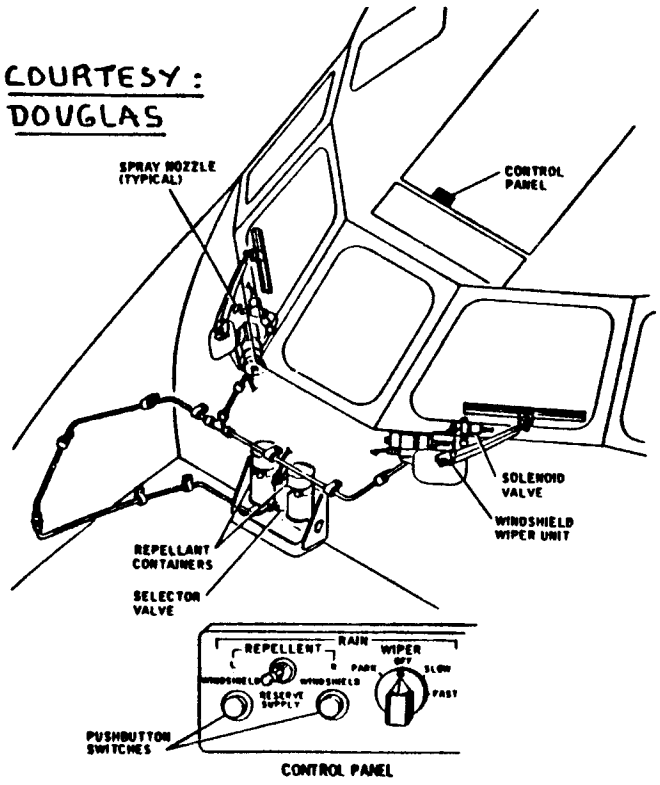

Figure 10.14 Rain Repellant System: McDD DC-9

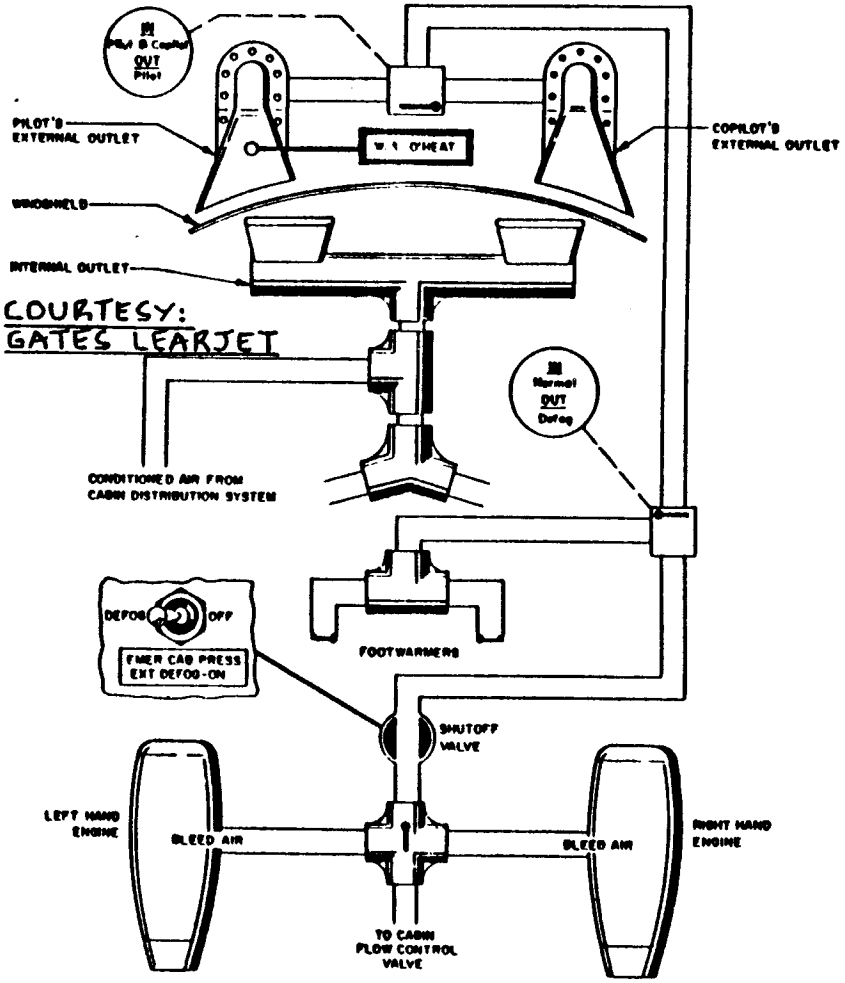

Figure 10.15 Defog System: Gates Learjet M25

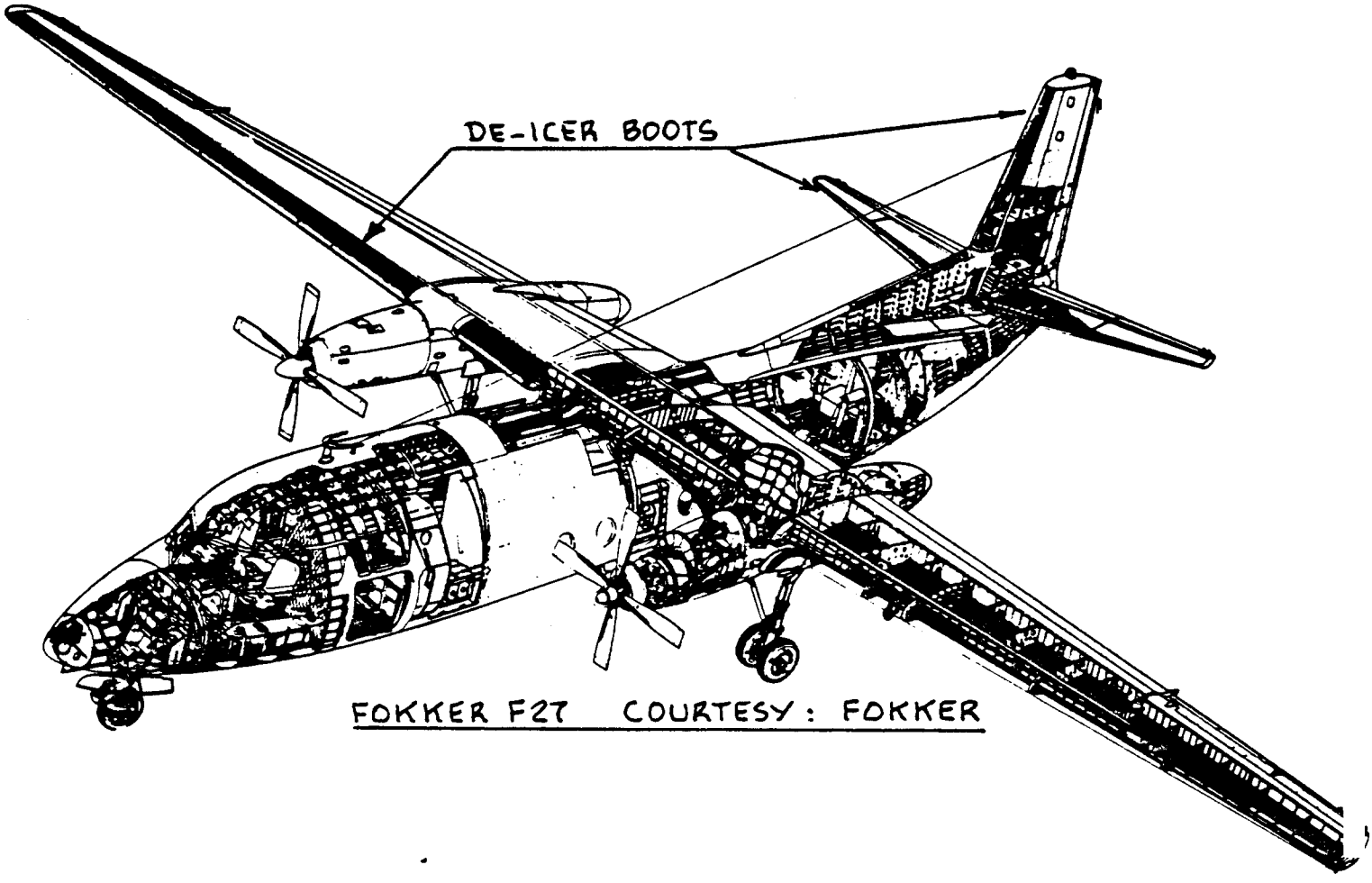

FOKKER F27 COURTESY: FOKKER

11. ESCAPE SYSTEM LAYOUT DESIGN

The purpose of this chapter is to discuss the layout design of emergency exits and escape systems for commercial and for military airplanes.

The material is organized as:

11.1 Emergency exits and escape systems for commercial airplanes.

11.2 Emergency exits and escape systems for military airplanes.

11.1 EMERGENCY EXITS AND ESCAPE SYSTEMS FOR COMMERCIAL AIRPLANES

All passenger airplanes must have reasonable means for passenger egress in emergency situations. Ref.21 contains the pertinent regulations for the determination of size and number of exits required. Ch.3 in Part III (pages 68-72) provides design guidelines for the number, size and type of emergency exits required for FAR 25 certified airplanes.

All exits must be properly marked. They must also be equipped with self illuminating signs. The operation of each emergency exit must be prominently displayed on the exit. Figure 11.1 shows an example escape hatch.

All passenger transports must be equipped with life jackets. These life jackets must be within easy reach of each passenger. For that reason these jackets are normally installed under the seat.

Figure 11.2 shows the emergency system layout of the BAC 111. Note the break-in areas which are marked on the airplane. This is a requirement on military airplanes, not on commercial airplanes.

Large, low-wing commercial transports which sit high on the landing gear must be equipped with escape hatches and escape slides. To prevent passengers from slipping on a smooth wing surface, that part of the wing which can be expected to be used as an escape route must be covered with an anti-skid material. Note that this makes laminar flow over this part of the wing impossible! Figure 11.3 shows an example situation.

Figure 11.4 illustrates the overall deployment of

emergency slides in a Boeing 767.

For overwater flights (in excess of 30 minutes) passenger transports must carry emergency rafts. Fig.11.5 shows an example of a design where the fore and aft emergency slides are in fact configured as rafts. There must be sufficient space in the rafts to carry all passengers and crew members. Figure 11.5 also shows the additional equipment which rafts must include.

11.2 EMERGENCY EXITS AND ESCAPE SYSTEMS FOR MILITARY AIRPLANES

In military transports the requirements for emergency exits are similar to those for commercial transports. In addition, break-in areas must me prominently marked on the outside of the airplane.

Many military airplanes must be equipped with ejection systems. All modern fighters must be equipped with so-called zero-zero ejection seats. Such seats allow the pilot to eject from an airplane which is at standstill on the ground and survive the process.

An ejection seat would be useless if the canopy were not automatically ejected or if the seat could not be propelled straight through the canopy. Many fighters are equipped with systems which have both capabilities.

Figure 11.6 shows two examples of ejection seats. For ejection seat dimensions and ejection seat clearance requirements the reader should see pgs 20-22 of Chapter 2 of Part III.

An example of a detailed ejection seat plus canopy installation is given in Figures 11.7 and 11.8. Note in Figure 11.7 the underwater jettison relief valve. This system allows the pilot to open the canopy under water after allowing the cockpit to flood.

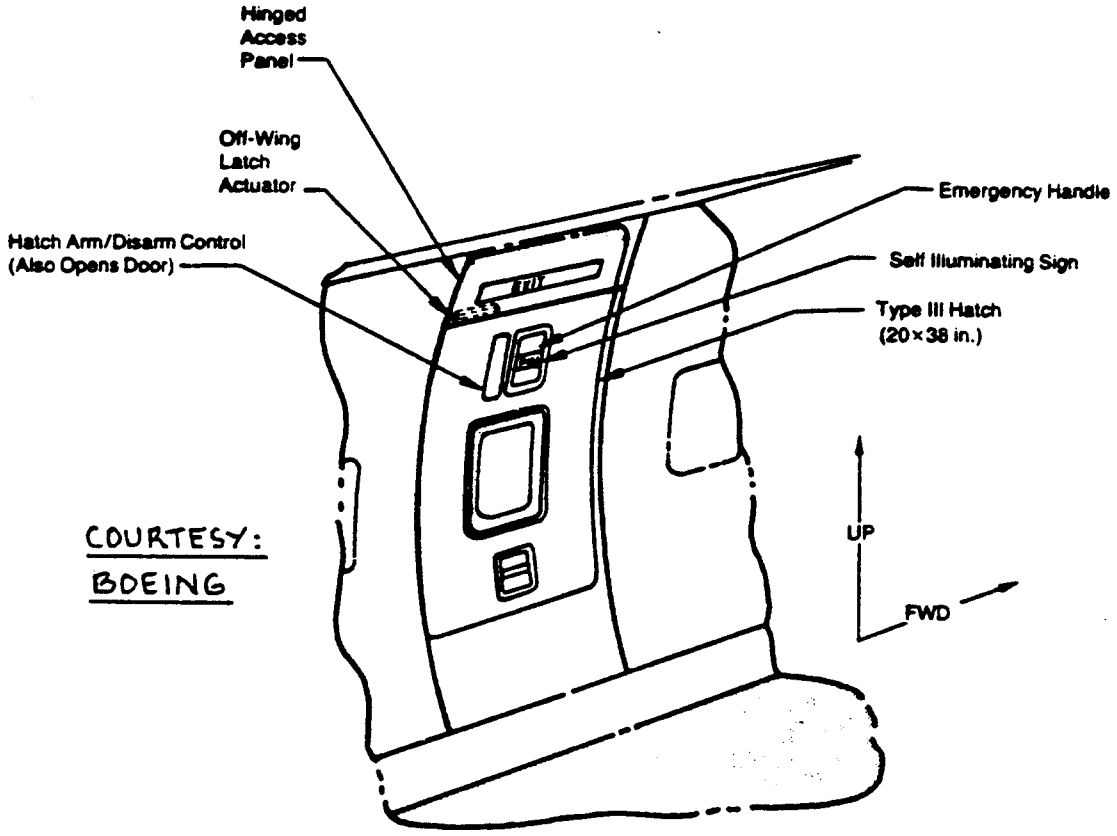

Figure 11.1 Example of an Overwing Escape Hatch

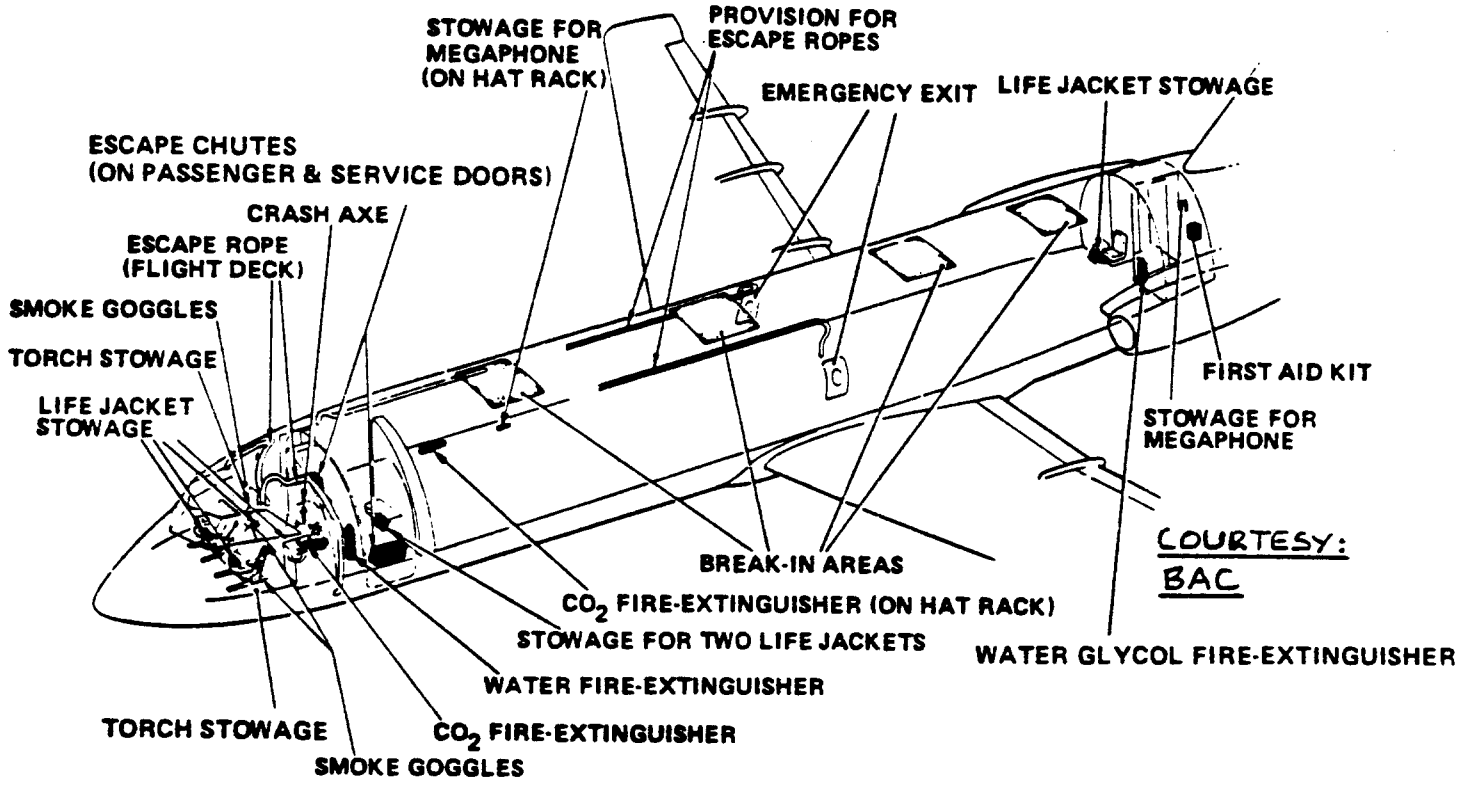

Figure 11.2 Emergency System Layout: BAC 111

- Stowage compartment in body
- Automatic deployment with escape exit door removal
- Automatic spoiler retraction

COURTESY : BOEING

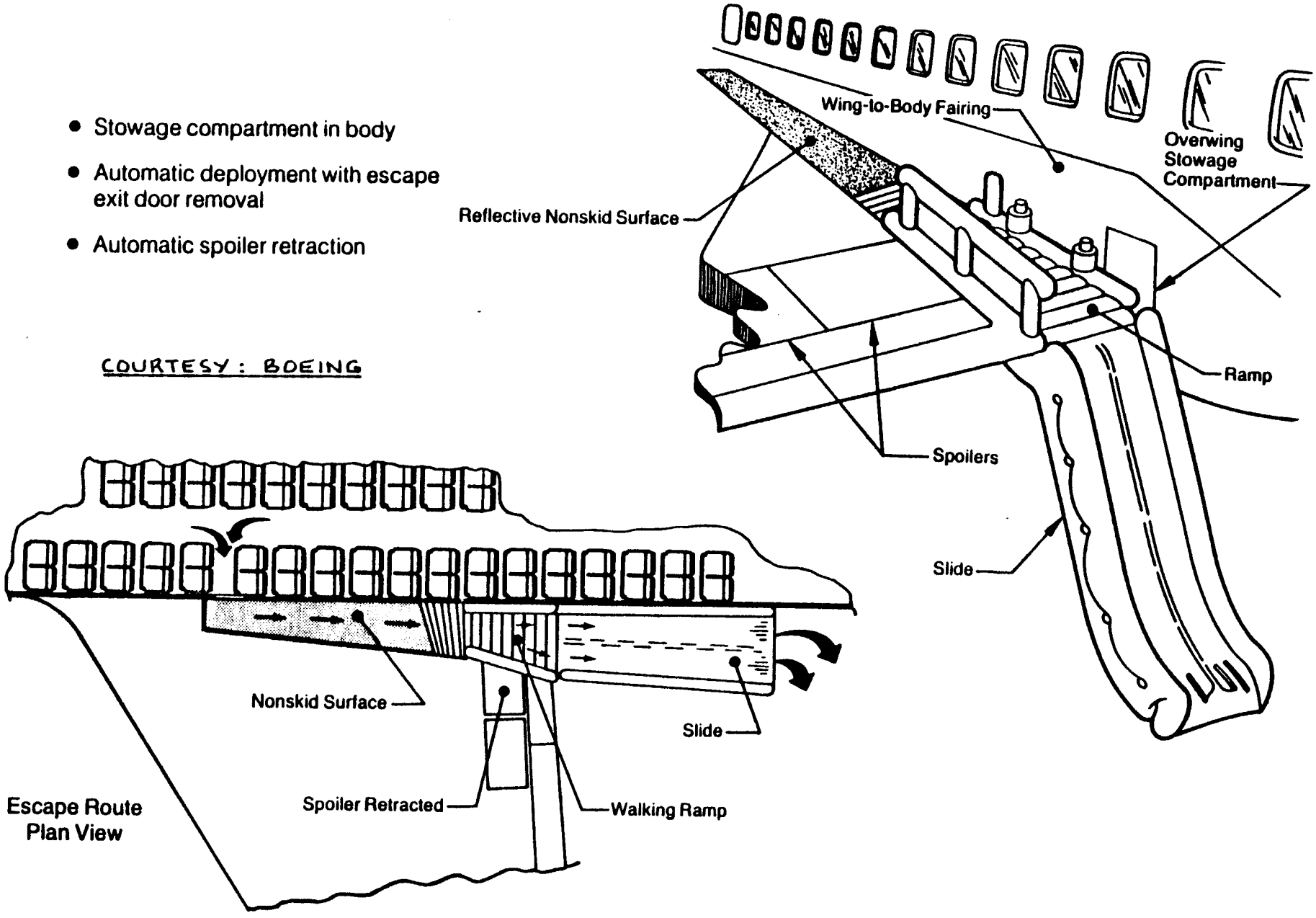

Figure 11.3 Overwing Escape Slide: Boeing 767

- Inflatable slides automatically deploy upon opening each exit
- Inflation by stored gas
- Escape system disarmed when door opened from outside airplane
- Slides usable in all landing gear conditions
- Optional slide/rafts available at type "A" doors.*

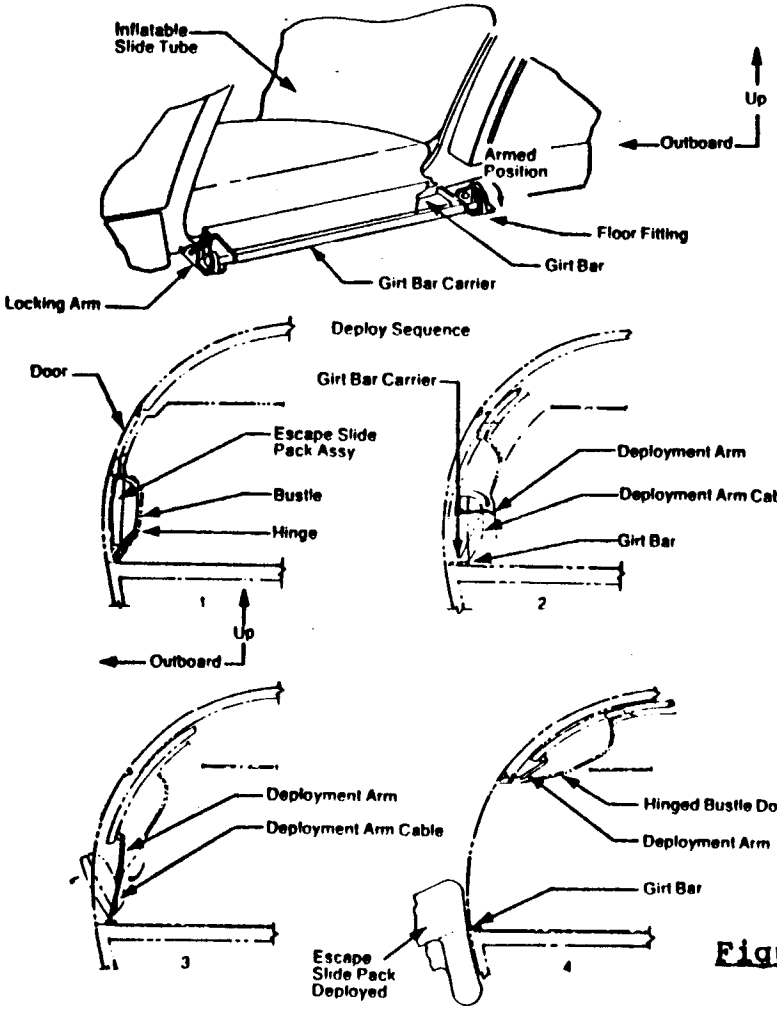

COURTESY: BOEING

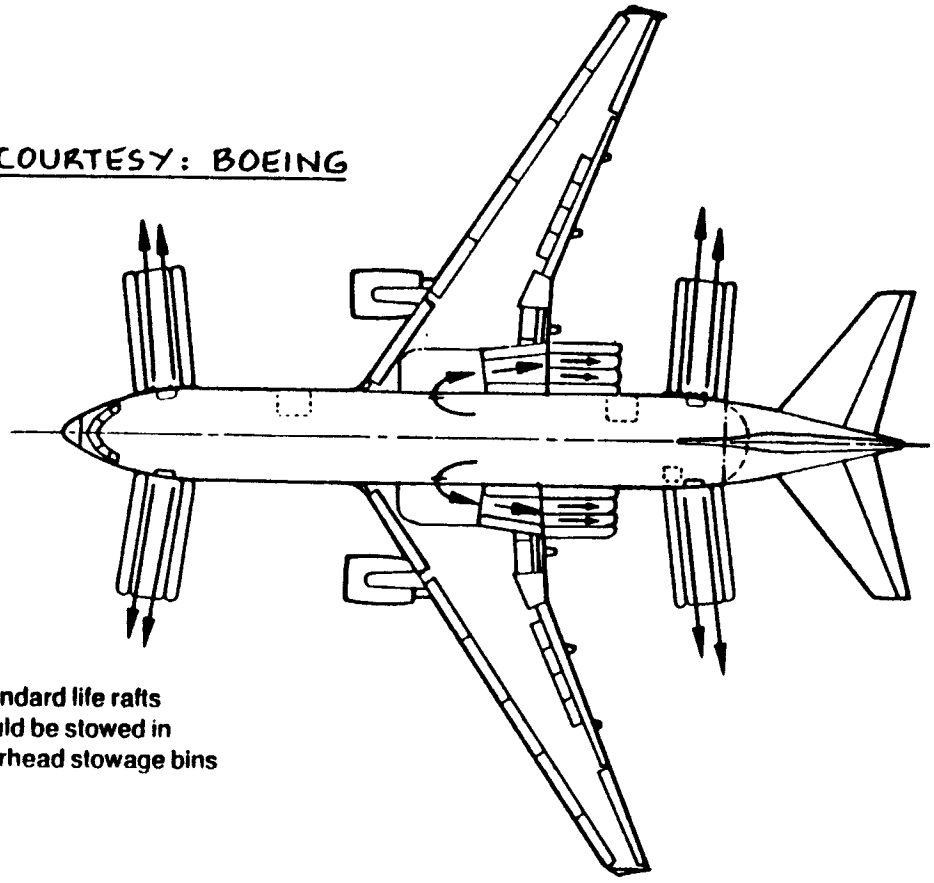

*Standard life rafts would be stowed in overhead stowage bins

Slides Deployed

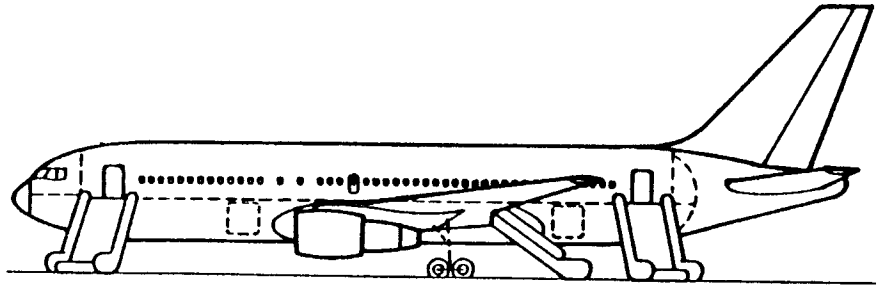

Figure 11.4 Emergency Evacuation Slide Deployment: Boeing 767

Emergency Slide/Raft Assembly (Optional)

- Capacity for 58 evacuees*
- One at each Type A door
- Includes
  - Survival kit
  - Provision for radio transmitter
  - Canopies
  - Sea Anchor
- Attached and stored very similar to emergency evacuation slides (pg 2-22)

*Auxiliary life rafts required for interior configurations over 232 (including crew)

COURTESY : BOEING

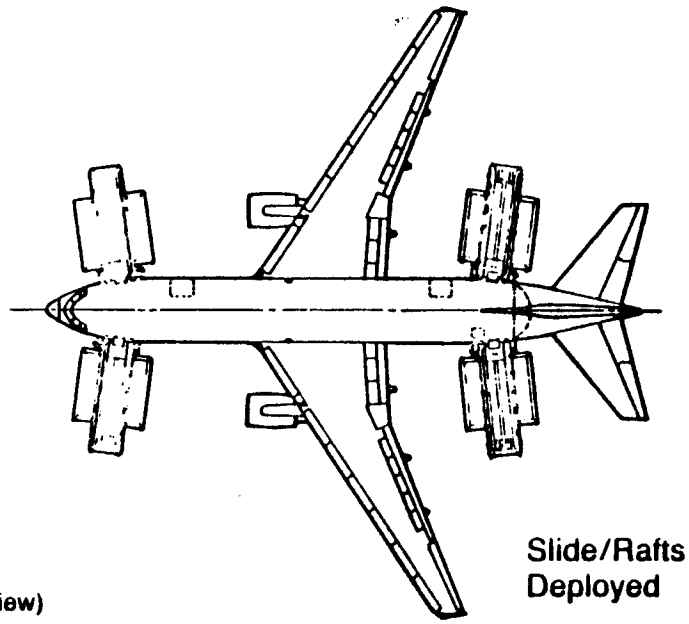

Slide/Rafts Deployed

(Plan View)

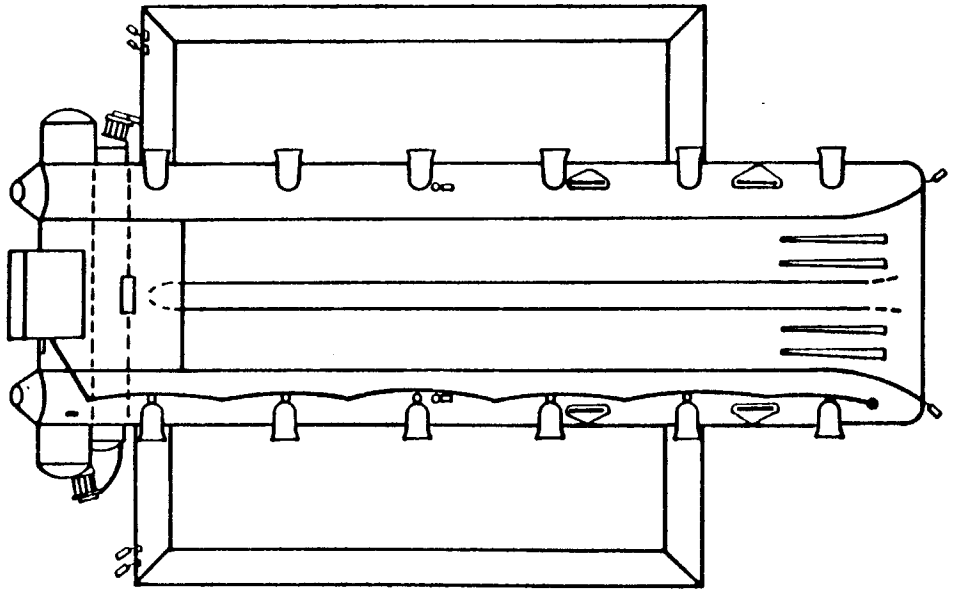

Figure 11.5 Combination Emergency Slide/Raft Assembly: Boeing 767

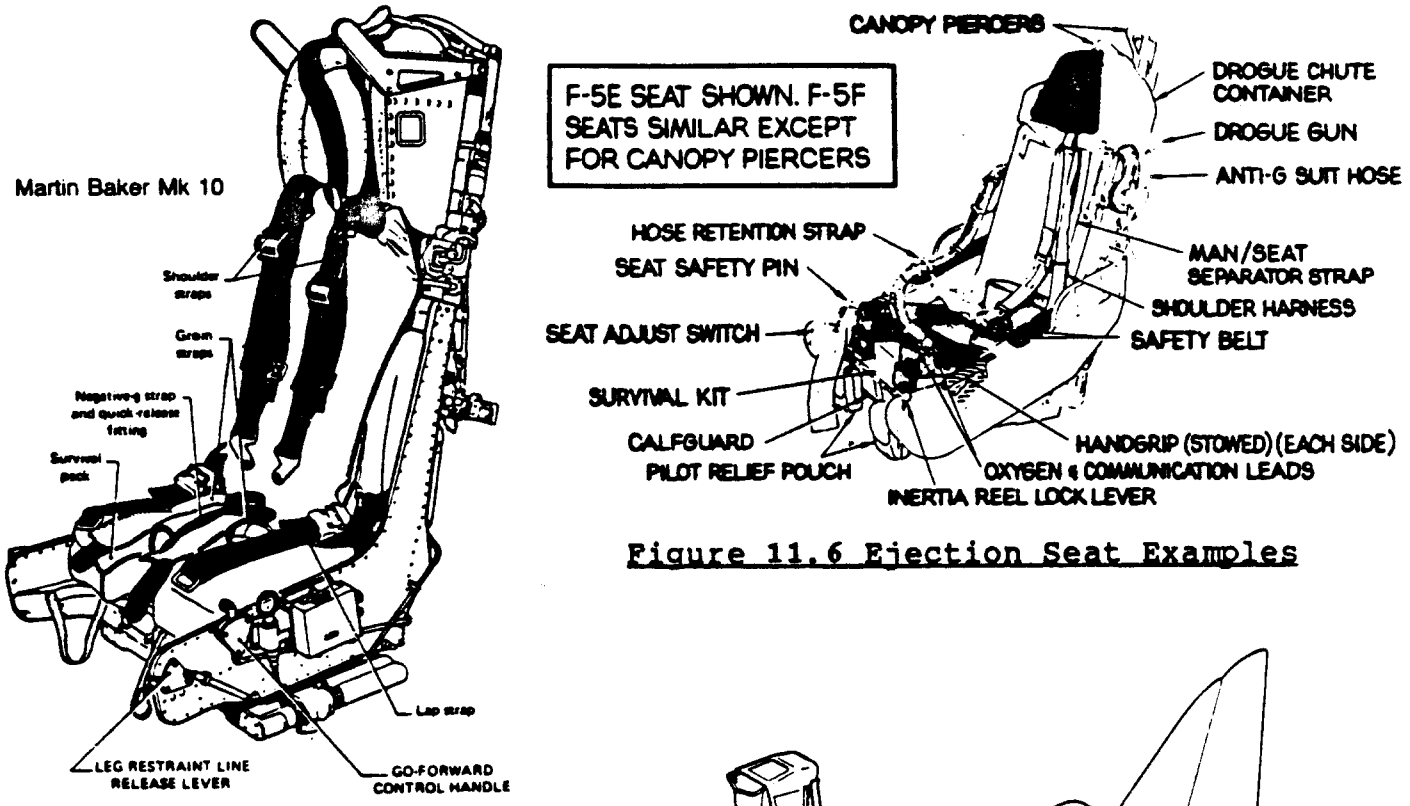

Figure 11.6 Ejection Seat Examples

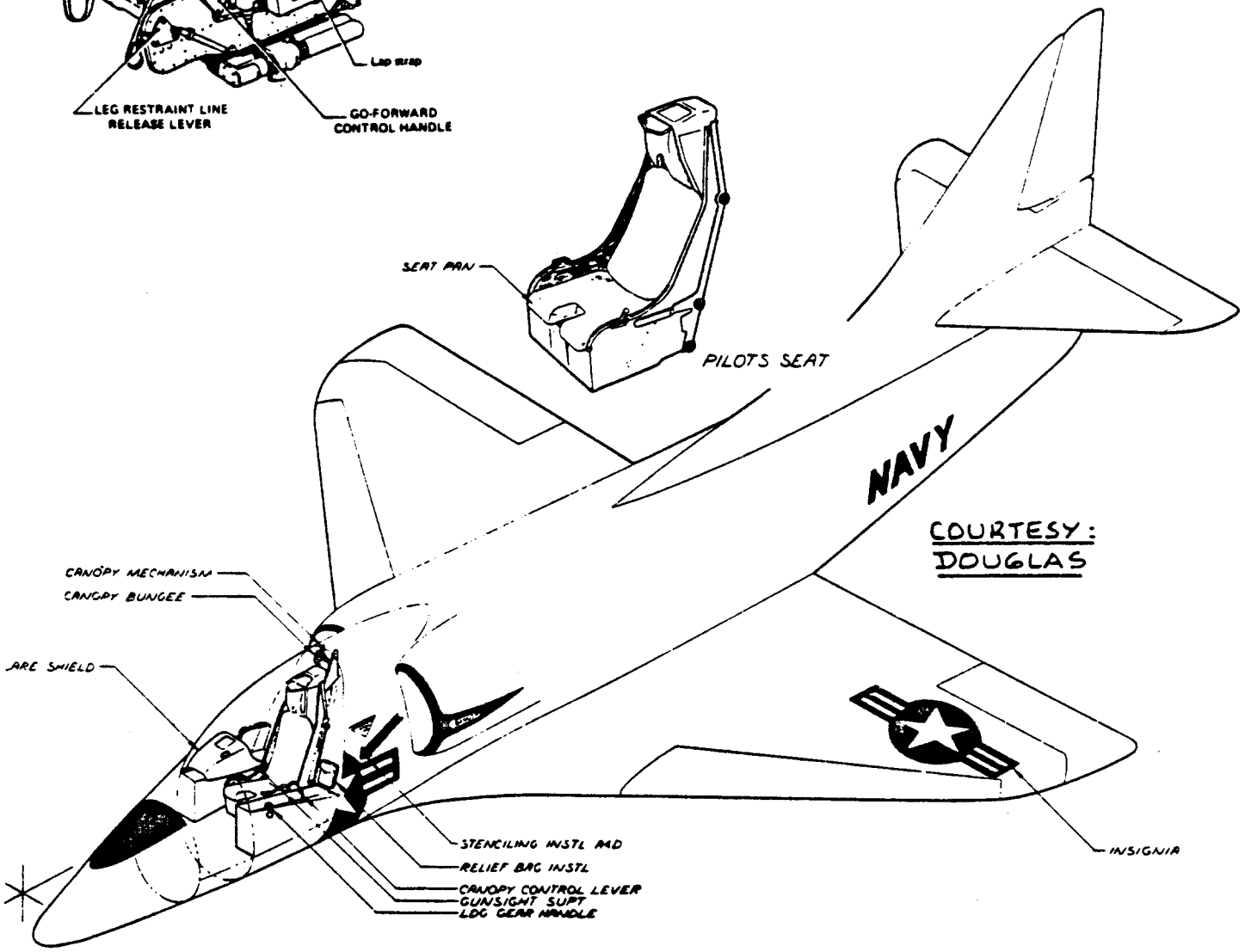

Figure 11.7 Ejection Seat Arrangement: Douglas A4D-2N

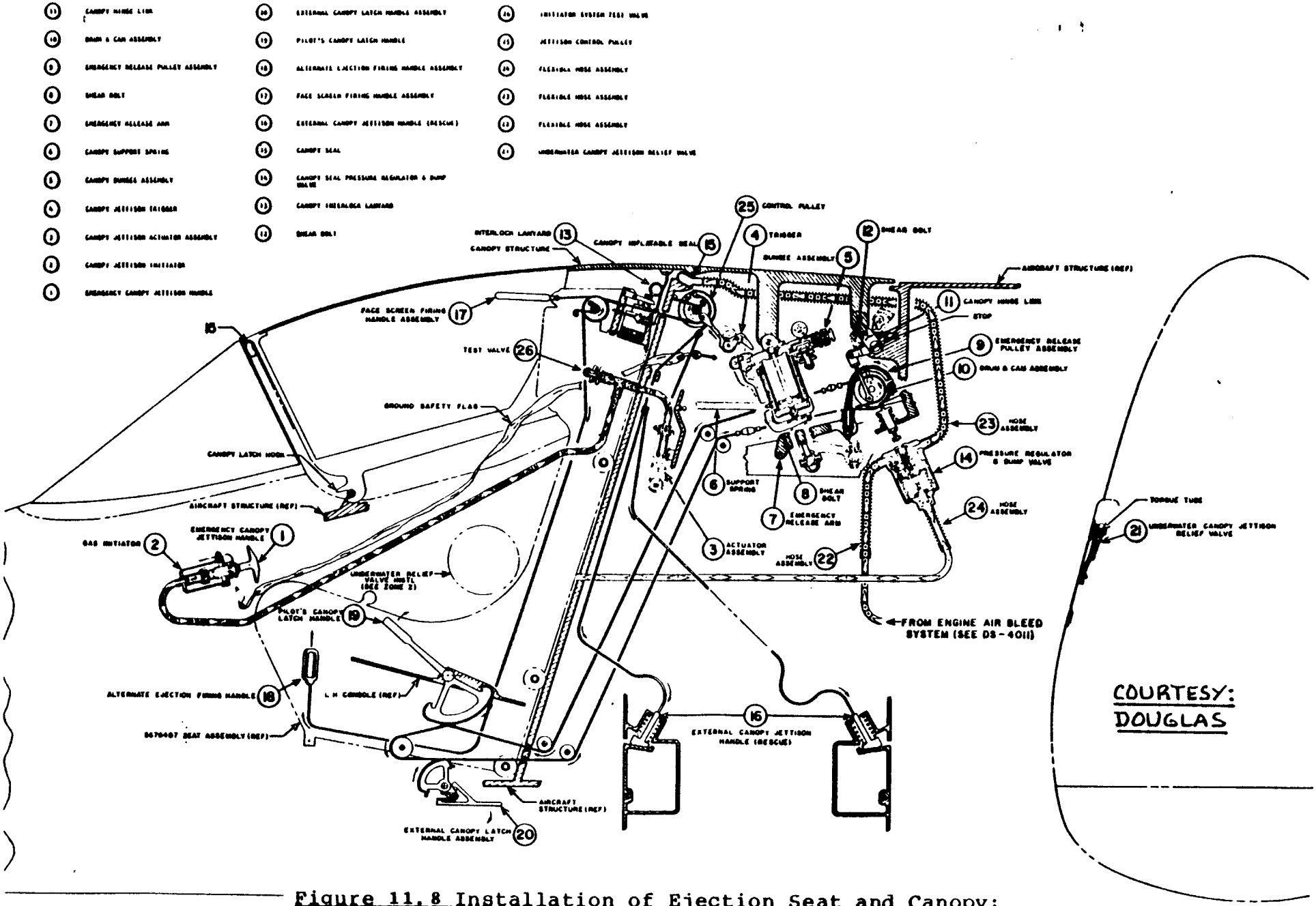

COURTESY: DOUGLAS

Figure 11.8 Installation of Ejection Seat and Canopy: Douglas A4D 2N

12. LAYOUT DESIGN OF WATER AND WASTE SYSTEMS

Nearly all passenger transports are equipped with water and waste systems. These systems represent a large investment in weight and volume. It is important to include these systems in preliminary design considerations. Section 12.1 presents the fundamental layout design considerations for such systems.

For use in fighting large fires (such as forest fires) airplanes are frequently used. The flying boat and/or the amphibious airplane is ideally suited for this purpose. Section 11.2 addresses the problem of laying out systems to rapidly take on water as well as to disperse the water over a fire.

12.1 WATER AND WASTE SYSTEMS

Reference 33 contains detailed descriptions of water and waste systems.

Water systems in passenger transports are typically sized for 0.3 US gallon per passenger. The system is usually pressurized with air from the airplane pneumatic system (discussed in Chapter 8). Figures 12.1 and 12.2 show potable water systems as used in jet transports.

Note the drain masts in these systems. These drain masts must be heated to prevent freezing. An item of concern in the location of these drain masts is what happens if the drain mast heating system fails. Large blobs of ice can then form. When these ice blobs break away from the airplane they should not be ingested by engines!

In most transports both warm and cold water is available. Warm water is supplied by running cold water through an electrically heated heat exchanger.

Waste systems in passenger transports are self-contained: these systems have waste tanks (collector tanks) and flushing units which mix the waste with chemicals contained in the flushing liquid.

The number of lavatories per passenger varies with the use of the airplane. On the average, 1 lavatory per 30 passengers is deemed sufficient.

Figures 12.3 and 12.4 show examples of waste systems in passenger transports.

Both water and waste systems need to be serviced after each flight. Access to the service panels for these systems should not interfere with access to other services required during loading and unloading of the airplane.

The service drain locations of both water and waste systems is of concern to preliminary designers: if failures occur in the drain valves so that fluids leak out, ice can form. When this ice breaks away from the airplane it should not be ingested by the engines!

12.2 WATER BOMBING SYSTEMS

The system selected for inclusion in this section is that of the Canadair CL215, an airplane specifically designed for the water bombing role.

Figure 12.5 shows the interior arrangement of this airplane. Note the two water tanks in the center of the fuselage.

Figure 12.6a illustrates how water is taken onboard: a bucket is rotated into the water while the airplane is skimming a lake (or another large body of water). When the tanks are filled, the bucket is retracted.

Figure 12.6b shows the water door mechanism. The water doors are opened over the fire as indicated by the door operating sequence in Figure 12.6c. The water system controls in the cockpit are shown in Figure 12.7.

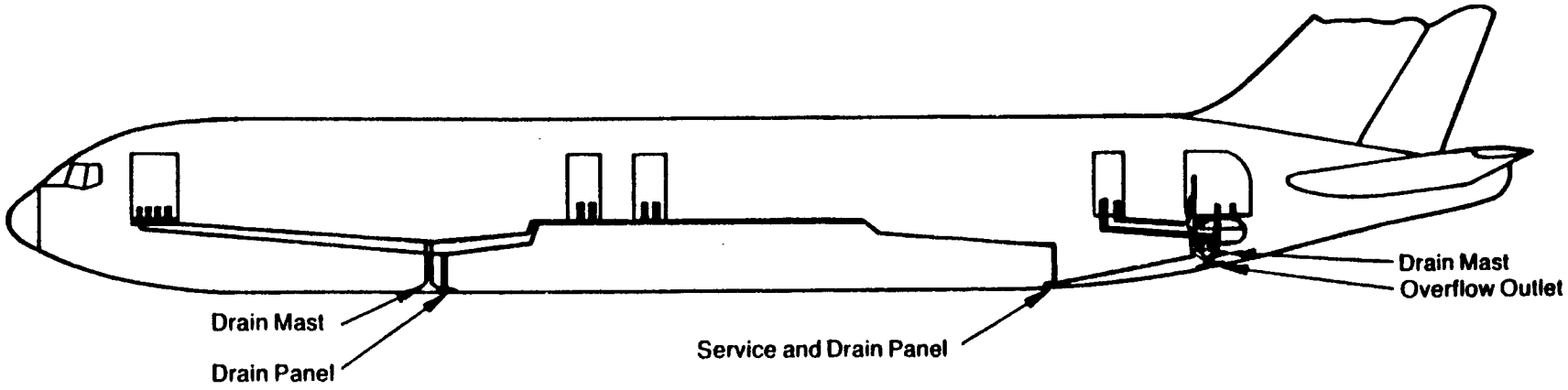

COURTESY : BOEING

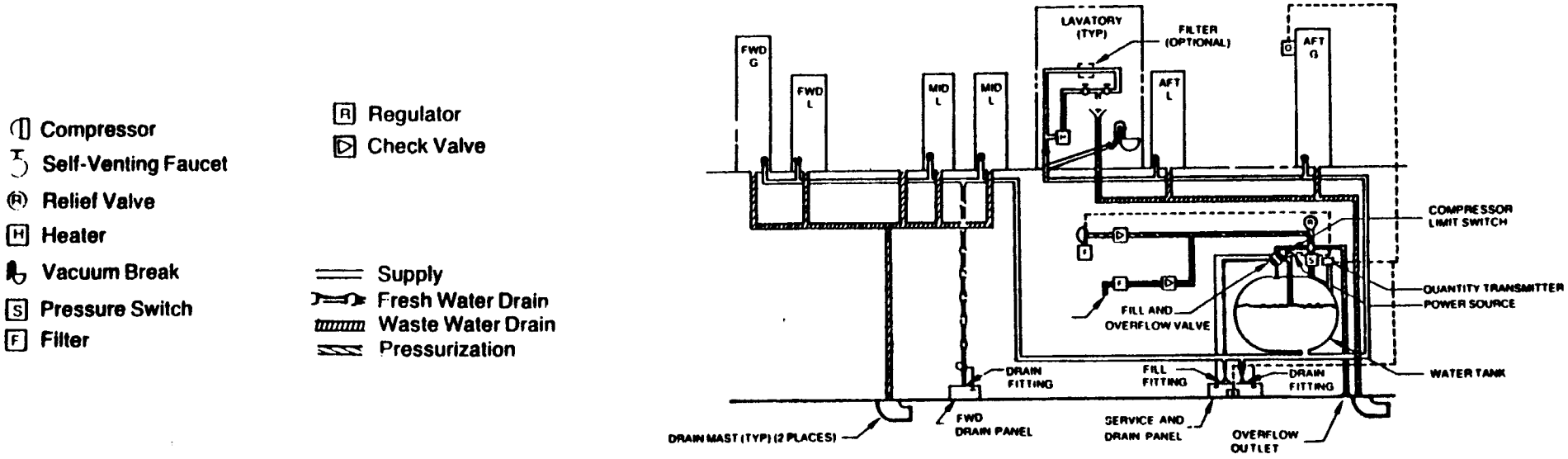

Figure 12.1 Potable Water System: Boeing 767

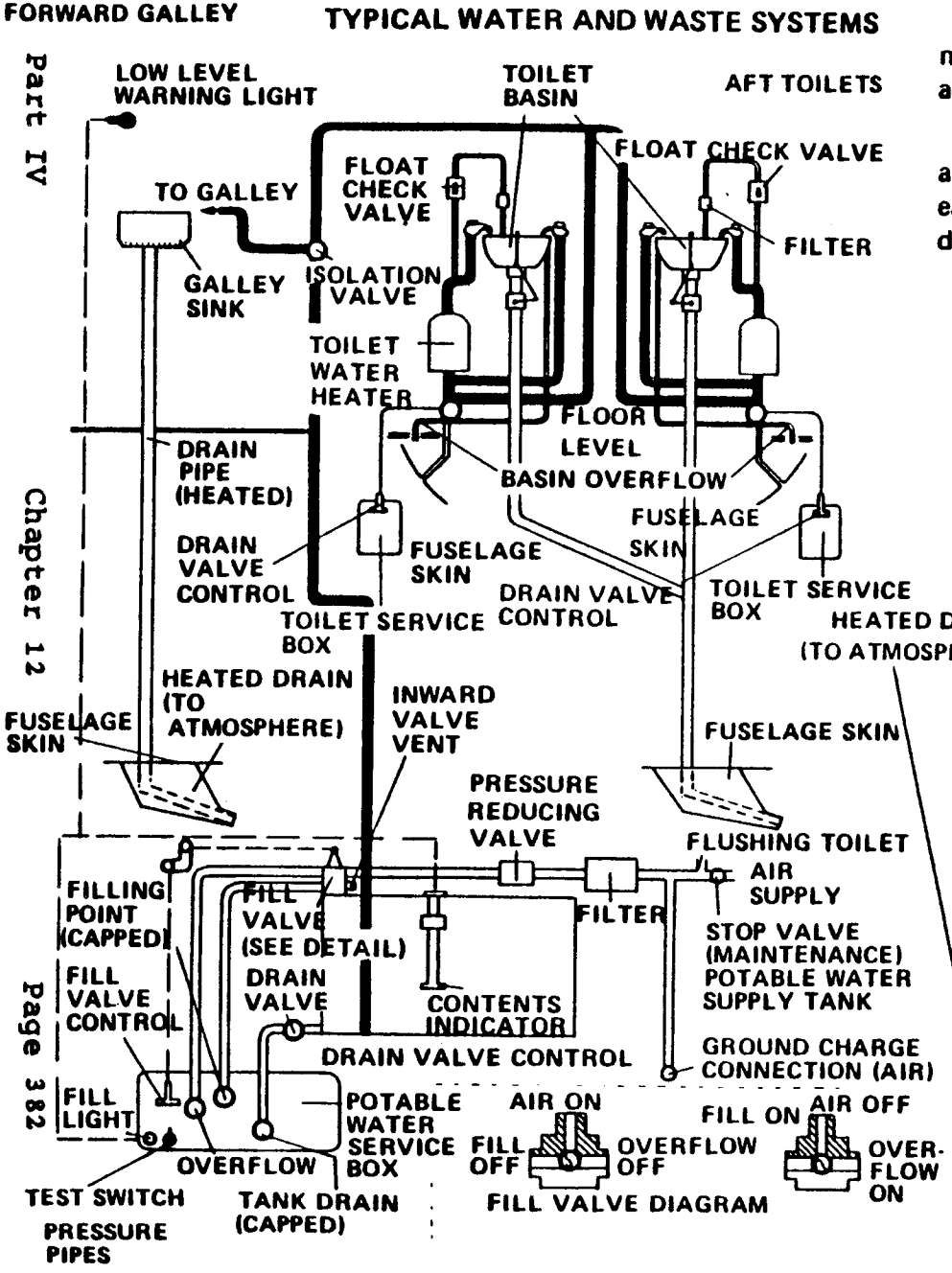

Fresh water is contained in a 20 Imperial gallon stainless steel tank mounted below the floor line on the right hand side of the fuselage adjacent to the nosewheel bay.

The system is pressurized by filtered bleed air from the integrated air system. An electric heater provides warm water to the washbasin in each toilet. Waste water from the two toilets and the galley is discharged directly overboard through electrically heated drains.

COURTESY : BAC

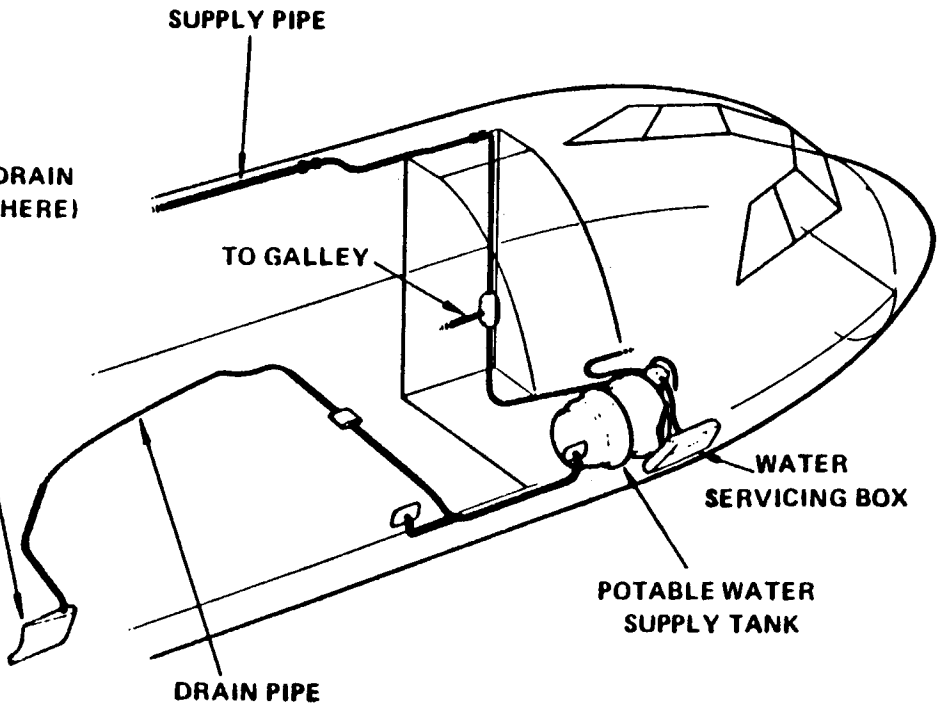

Figure 12.2 Potable Water System: BAC 111

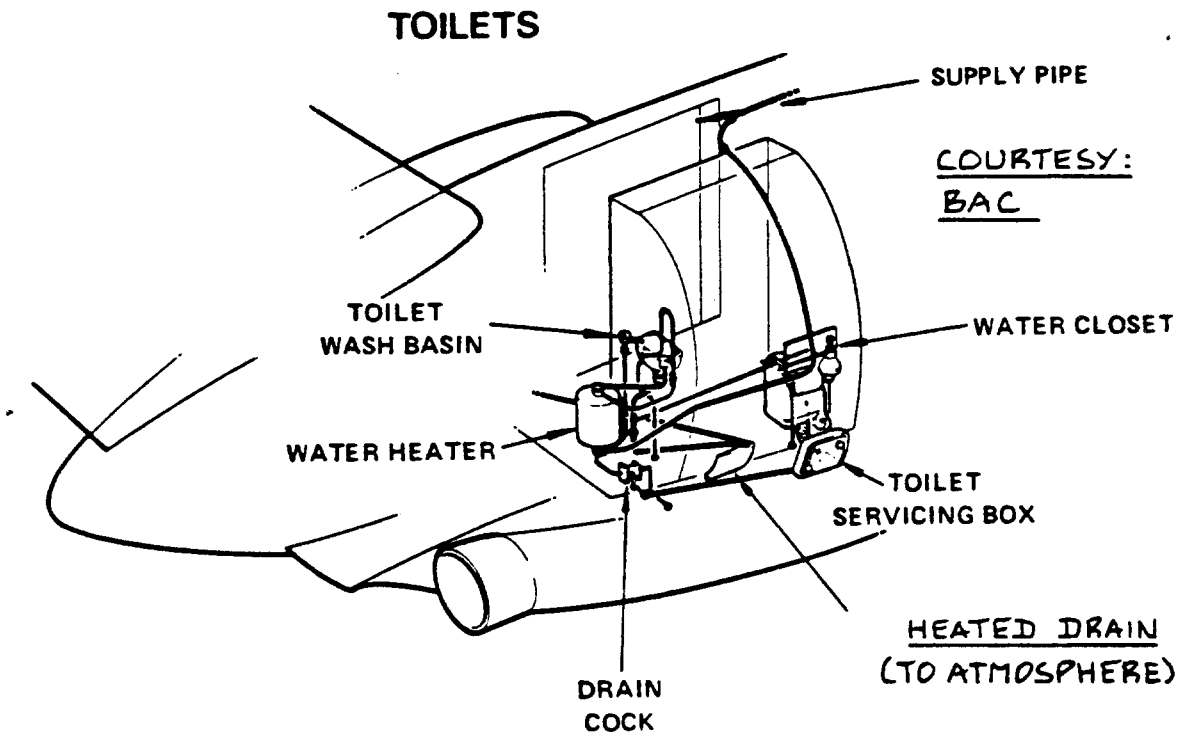

Figure 12.3 Waste System: BAC 111

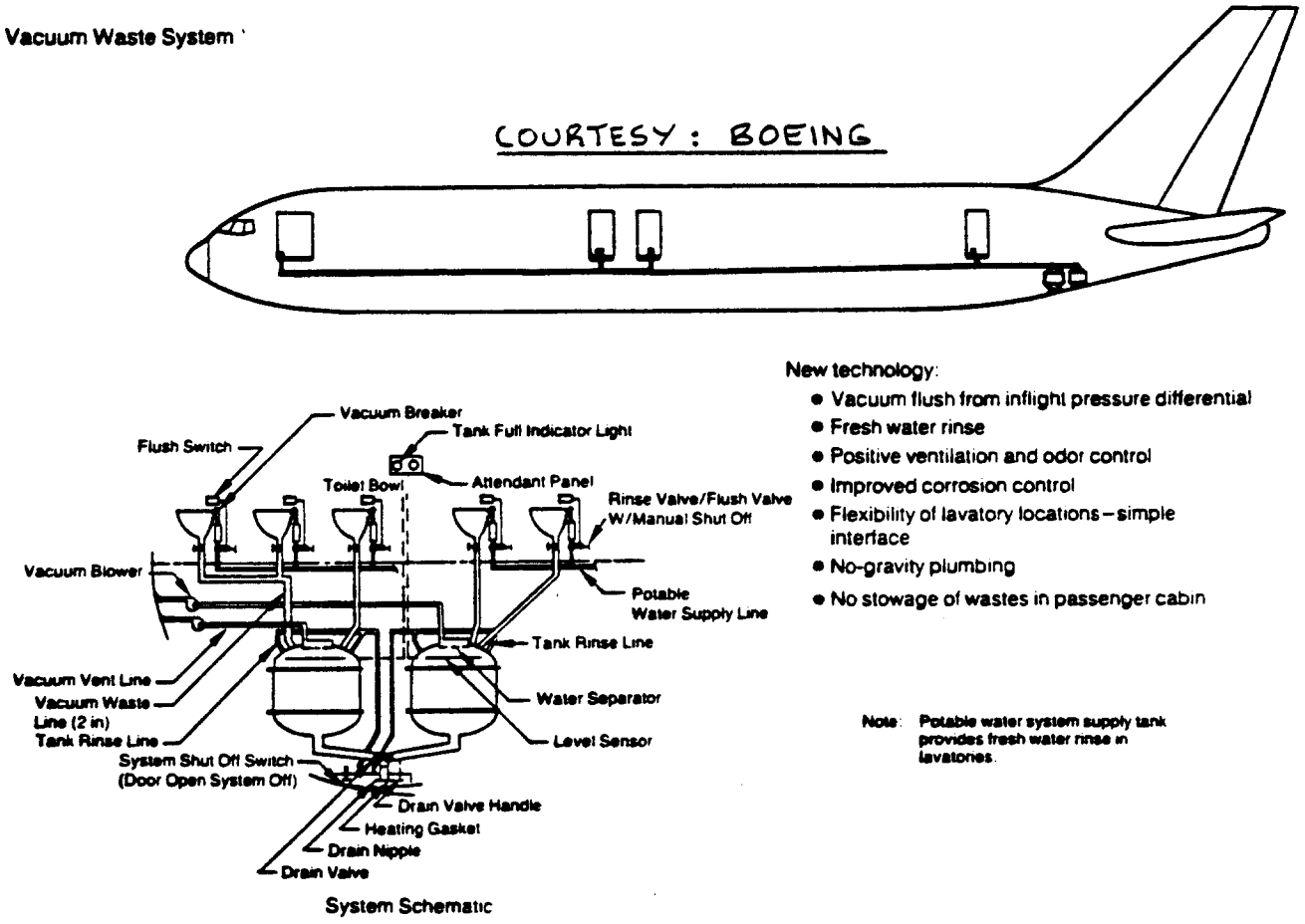

Figure 12.4 Waste System: Boeing 767

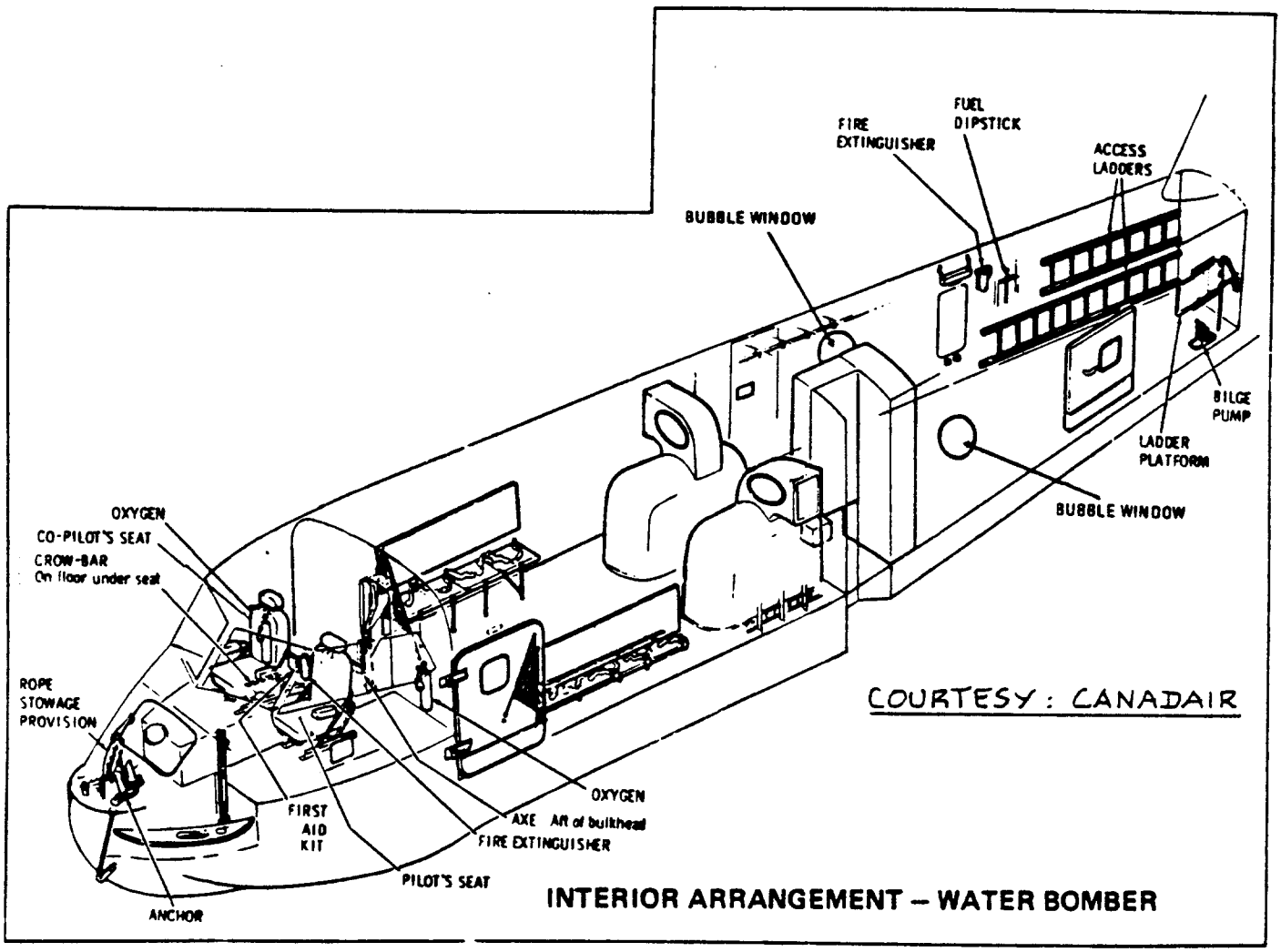

Figure 12.5 Interior Arrangement: Canadair CL215

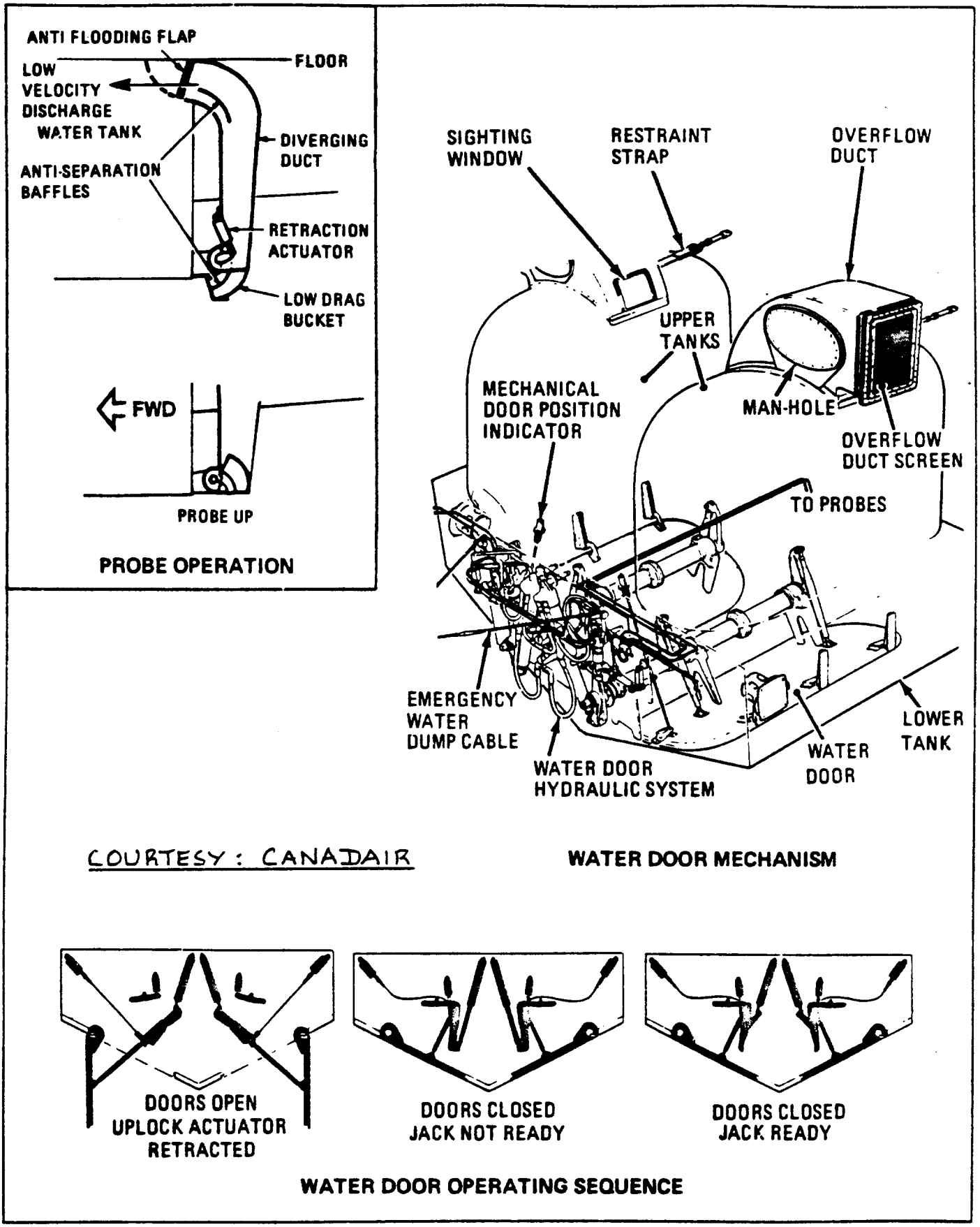

Figure 12.6 Water Bombing System: Canadair CL215

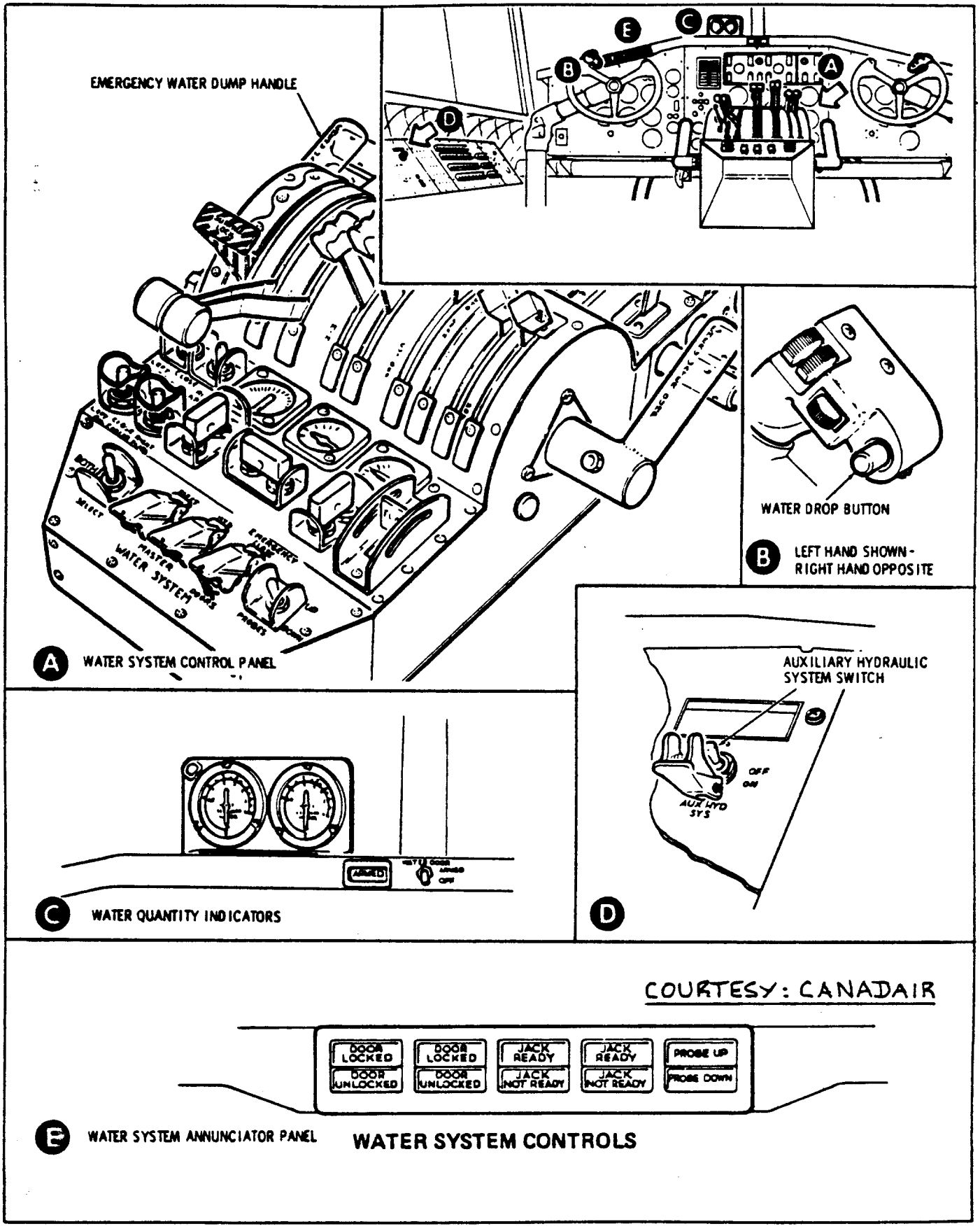

Figure 12.7 Water System Controls: Canadair CL215

13. SAFETY AND SURVIVABILITY

The purpose of this chapter is to provide some insight into design problems associated with safety and survivability considerations. These considerations are important both to commercial and to military airplanes.

The problems of safety and survivability are addressed as follows:

13.1 How safe is safe enough?

13.2 Safety and survivability in commercial airplanes

13.3 Safety and survivability in military airplanes

13.4 The role of the preliminary design engineer and management in creating safe airplanes

13.1 HOW SAFE IS SAFE ENOUGH?

Definitions: 1. An accident is defined as an occurrence which causes the death of at least one passenger or crew member.

2. An incident is defined as an occurrence which falls outside the normal operating events but which causes no fatalities. Non-fatal injuries may be incurred during incidents.

Lemma: It is IMPOSSIBLE to design airplanes such that the probability of fatal accidents is zero.

Accepting this lemma (which is presented here without proof), the question is: how many fatalities are acceptable?

This is a cruel question. The answer to this question will be different, depending on such matters as religion, morality and personal experiences. Neither of these matters are addressed in this text. Instead, the position will be taken that acceptable levels of safety arise as a result of societal trade-offs made between the number of fatalities and the cost incurred to lower them.

Figure 13.1 illustrates how safety (expressed as a relative accident rate) and costs are related. Aviation tends to operate to the left of the minimum cost level.

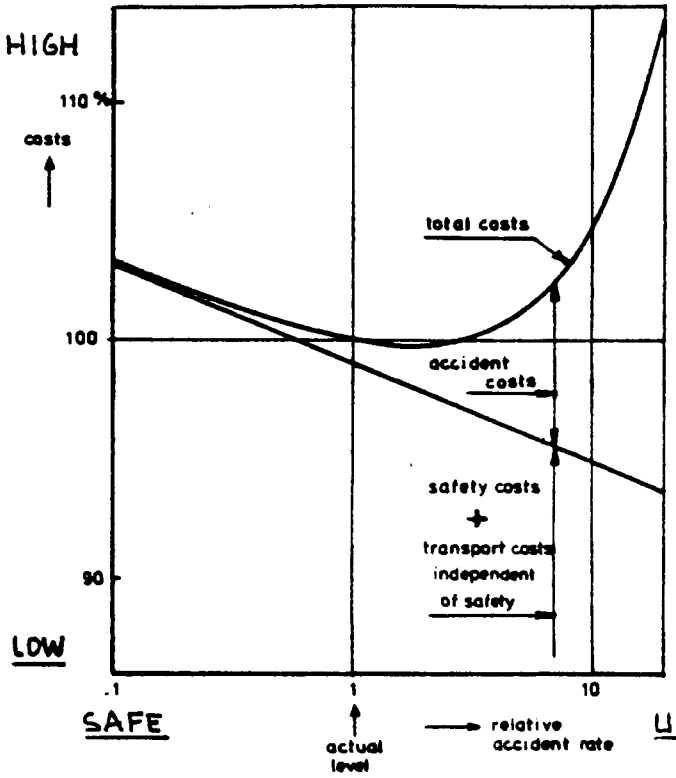

FROM: REF. 39

Figure 13.1 The Relationship Between Cost and Safety

Table 13.1 Safety Comparisons for Several Modes of Transportation

Transport mode		Average speed (km/h)	Number of fatalities *) per 10^9 pass.km	Number of fatalities *) per 10^7 pass.hrs
public transport	European Railways, 1968-1975 (Union Int. des Chemin de Fer)	80	.4	.32
	ICAO-world-scheduled air services (excl. USSR, China), 1975-1977	590	.9	5.3
private transport	Road traffic, the Netherlands, 1976			
	- private car	70	10	7
	- autocycle	20	92	18
	- motorcycle/scooter	60	150	90
	USA general aviation, 1975-1977 .	280	68	190

*) For private transport: driver/pilot included

FROM: REF. 39

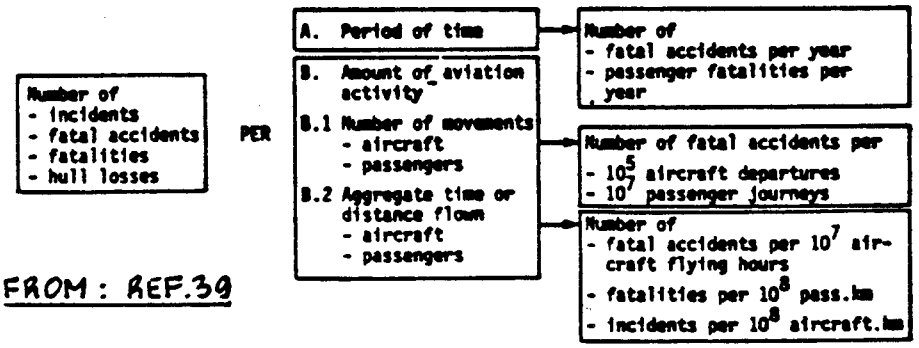

FROM: REF.39

Figure 13.2 Fourteen Yardsticks for Measuring Safety

It is of interest to compare the safety levels associated with various modes of transportation. Table 13.1 presents this comparison. Observe that there are two ways of presenting relative safety:

1. fatalities per passenger mile (or km)

2. fatalities per passenger hour

Note that different conclusions are arrived at depending on which method of comparison is used:

I. on the basis of distance travelled, the safety record of aviation equals that of railway transportation. Note the poor safety record of cars and motorcycles.

II. on the basis of time spent, the safety record of aviation is only slightly better than that of the car. The safety record of railway transportation is an order of magnitude better than that of aviation.

At this point it is useful to point out how the safety yardsticks just mentioned are derived from statistical data on aviation accidents. The derivation has been taken from Reference 39.

The follwowing definitions are required:

P = the number of passenger miles (or km) flown
U = the number of airplane flight hours produced
S = the number of airplane miles (or km) flown
K = the number of passenger fatalities
R = the number of fatal accidents

The fatality rate per passenger mile (or km) is: K/P

The fatal accident rate per flight hour is: R/U

It is possible to write:

$$K/P = (R/U)(K/R)(U/P) =$$

$$= (R/U)\{(K/R)/(P/R)\}(U/S) \qquad (13.1)$$

Introduce the following quantities:

k = K/R = the average number of fatalities per fatal accident

p = P/S = the average number of passengers per airplane

V_B = the average block speed in mph (or km/hr)

Eqn.(13.1) can now be written as:

$$K/P = \{(R/U)(k/p)\}/V_B \qquad (13.2)$$

or in words:

$$\frac{\text{passenger fatalities}}{\text{passenger mile}} = \left(\frac{\text{fatal accidents}}{\text{flight hours}}\right) * \frac{\text{fatalities per accident}}{\text{passengers per airplane}} * \frac{1}{\text{block speed}} \qquad (13.3)$$

Which yardstick should be used in safety comparisons depends on the objective.

Figure 13.2 presents fourteen yardsticks for measuring safety levels. From an engineering viewpoint, yardsticks B are to be preferred over yardsticks A. Relations between 'the amount of aviation' and 'accidents per amount of aviation' are usable in rational design procedures. However: engineers should not forget that the total numbers of people killed (yardsticks A) are important not only in human terms BUT ALSO in terms of public perception of safety. Never forget that the public ultimately decides on aviation activity levels: it does so in the market place and in the polling place!!!!

Table 13.2 presents aviation accident data using the quantities of Eqn.(13.2). Note that in the time period considered, the fatality rate per passenger mile (or km) has decreased much more than the fatal airplane accident rate per hour. The reason for this is twofold: the block speed has increased due to the introduction of jets and the average number of passengers per airplane has increased due to the introduction of larger airplanes.

One significant point needs to be made: the general public appears to 'accept' these safety levels!

An important question is: what should future aviation safety targets be? Table 13.3 compares aviation fatalities with death rates due to all causes. It is interesting to note that aviation fatality rates (per flight

Table 13.2 Safety Statistics for World Air Travel

year	1945	1950	1955	1960	1965	1970	1975
transport in 10^8 pass.km(P)	80	280	610	1090	1980	3820	5750
total distance flown in 10^8 aircr.km (S)	6	14.5	23	31	41	71	74
total flight time in 10^6 aircr.hrs (U)	2.5	5.0	7.3	8.6	8.8	12.2	12.5
no of fatal accidents (R)	20.	27	26	34	25	28	20
no of passenger fatalities(K)	240	551	407	873	684	687	445
no of fatalities per accident (k = K/R)	12	20.4	15.7	25.8	27.4	24.5	22.3
no of pass. per aircraft (p = P/S)	13.3	19.3	26.5	35.2	48.3	53.8	77.7
average block speed in km/h (V_B = S/U)	240	290	315	360	446	582	592
no of aircraft acc. per 10^6 aircr.hrs (R/U)	8.0	5.4	3.6	4.0	2.8	2.3	1.6
no of pass. fatalities per 10^8 pass.km (K/P)	3.00	1.97	.67	.80	.35	.19	.08

PERIOD 73-84 AVE.

15.6
518

FROM: REF. 39

Table 13.3 The Safety Target for the Year 2000

Passenger fatality rates in aviation	Fatalities per 10^9 pass.km	Fatalities per 10^7 pass.hrs
Scheduled air services, 1975-1977 (ICAO-world, Fig. 9)	.9	5.3
Future target for the year 2000	.2	1.2
Average population death rate by all causes (The Netherlands, 1976): - age group 15-44 years: 1.05 deaths per 10^7 person.hrs - whole population : 9.5 " " " " "		

FROM: REF. 39

hour) appear to be similar to overall death rates (per person hour).

If the demand for public air transportation keeps growing at current rates (about 7 percent per year) a factor 3 increase in fatalities can be expected by the year 2000. The assumption is made here that such an increase in absolute number of fatalities will not be accepted by the public. Instead, the assumption is made that the total fatality level should not increase. However, this implies an increase in relative safety. That target safety level is also shown in Table 13.3.

Such improvements in relative safety level are not going to happen automatically. Remember:

SAFETY IS NO ACCIDENT.

It will take a major effort on the part of airplane designers, airplane design management, airplane air and ground crews and the air traffic control system to make this happen.

Sections 13.2 and 13.3 discuss the safety and survivability aspects of commercial and military airplanes in some detail. The role of the preliminary design engineer and design management in assuring safe and survivable designs is discussed in Section 13.4.

13.2 DESIGN FOR SAFETY AND SURVIVABILITY IN COMMERCIAL AIRPLANES

The FAA (Federal Aviation Administration) is responsible for setting up airworthiness regulations, air carrier operating rules as well as enforcing these rules and regulations. The FAA is also responsible for the operation of the air traffic control system.

Commercial airplane accidents in the USA are investigated by the NTSB (National Transportation and Safety Board). The results of all NTSB investigations are made public, including the recommendations made to the FAA for changes in airworthiness regulations or directives, or for changes in air traffic control procedures.

The author believes that a major reason for the relatively high safety of US commercial aviation is the openness with which the overall business of aviation is conducted AND the fact that rule-making/rule enforcement is separated from investigative efforts.

It is useful to quote from FAR 25, par.1309(b):

'The airplane system and associated components, considered separately and in relation to other systems, must be designed so that the occurrence of any failure condition which would prevent the continued safe flight and landing of the airplane is 'extremely improbable'.'

From a design engineering viewpoint the words 'extremely improbable' are interpreted to mean a probability level of less than $1x10^{-9}$ per 1-hour flight.

Table 13.4 defines the relationship between frequency of occurrence of a failure and its allowable effect on flight safety. Fig.13.3 illustrates this relationship.

Overall, the factors which contribute to safety in aviation are listed in Table 13.5. Accidents are usually classified by causes as defined in Table 13.6. In accident analyses, two types of accidents are considered:

1. Predominantly airworthiness and

2. Predominantly operational.

Table 13.7 shows accident breakdowns according to this classification.

A summary of the statistics in Table 13.7 is given in Table 13.8: note that operational accidents dominate.

A study of the human factor in aviation accidents reveals the data in Table 13.9: over half of all accidents are caused by human factors. A breakdown of the human factor into identifiable deficiencies is given in Table 13.10. Clearly, the contribution of the flight crew to accidents is greater than that of ground crews.

Table 13.11 shows a comparison of commercial accident statistics by region: the USA and Canada have a better safety record than other areas of the world.

An alarming trend is clear from Table 13.11 and from Table 13.12: the airplane hull loss rate per million flight hours is very high: more than two hull losses per million flight hours are registered worldwide. This is approaching two hull losses per month on a world wide basis! If the hull loss rate is not curbed significantly, airplane hull insurance rates will increase out of sight.

Table 13.4 The Airworthiness Code for Airplanes

Frequency of Occurrence			Allowable Effect on Flight Safety		Probability	
Code FROM: REF.39		Description	Effect	Description	Probability P per hour of flight	Safety Class S
Frequent	Re-current	Occurring from time to time for each individual aircraft	Minor	At most small increase of crew work load and slight degradation of flight characteristics	10^{-0} - 10^{-3}	0-3
Reasonably Probable	Re-current	Occurring from time to time for each individual aircraft	Minor	At most small increase of crew work load and slight degradation of flight characteristics	10^{-3} - 10^{-5}	3-5
Remote		Not likely to occur for an individual aircraft, but may happen a few times during the total operational life of all aircraft of one type	Major	Significant increase of crew work load and considerable change in flight characteristics. Emergency procedures may be applied, but safe flight and landing still possible	10^{-5} - 10^{-7}	5-7
Extremely Remote		Unlikely to occur during total operational life of all aircraft from one type, but nevertheless possible	Hazardous	Dangerous increase of crew work load and serious degradation of aircraft performance, handling qualities or aircraft structure. Immediate landing necessary; marginal conditions for occupants/injuries	10^{-7} - 10^{-9}	7-9
Extremely Improbable		So extremely remote that it can be considered not to occur	Catastrophic	Loss of aircraft and/or human lives	$<10^{-9}$	>9

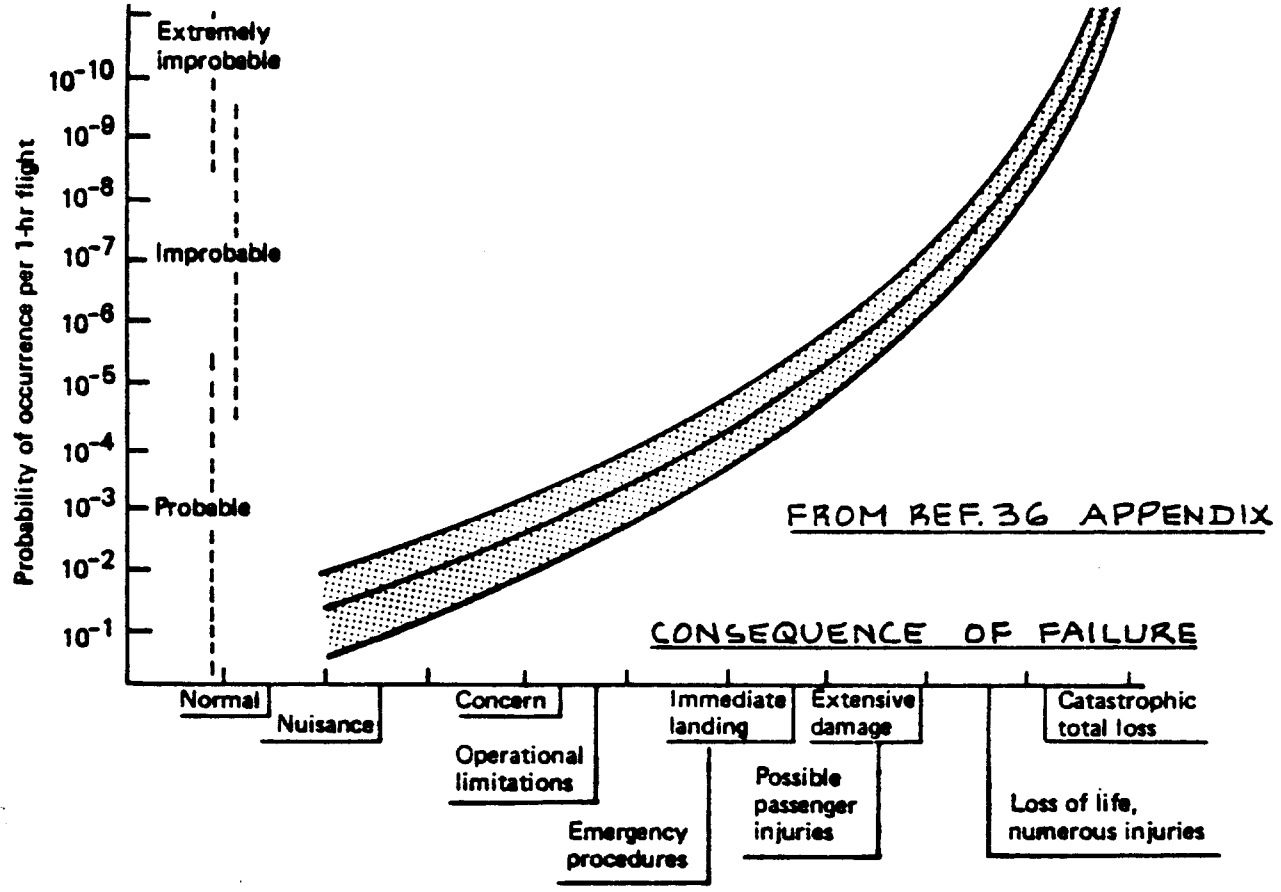

Figure 13.3 Failure Consequence and Failure Probability

Table 13.5 Factors Which Contribute to Aviation Safety

Topic	Contributing Factors
Aircraft design and manufacturing	Airworthiness requirements: - performance and flying qualities - aircraft structure and loads - powerplants - aircraft systems - crashworthiness Aircraft production control
Aircraft flight operations	Flightplanning Air Traffic Control and Air Navigation Airport lay-out and facilities Aircraft maintenance
Personnel	Selection, training and licensing of - operational staff - technical staff
Abnormal events	Occurrence reporting and accident investigation

FROM: REF. 39

Table 13.6 Classification of Airplane Accidents by Cause

Aircraft condition prior to accident	Basic accident cause	Occurrences, leading to accident
Normal (aircraft under full control, engines running)	Collision with ground, obstacle, birds or other aircraft	Navigational error by flight crew
		Failure nav. equipment of aircraft
		Failure ATC-services
Abnormal flight condition	Loss of control	Mechanical or electrical failures in aircraft systems
		Piloting error with loss of lift, stability and control (stall, dive)
	Loss of engine power	Engine failure
		Mismanagement of engines or fuel system
		Fuel shortage
	Loss of structural integrity	Structural fractures e.g. by fatigue, corrosion
		Outbreak of fire
		Structural failure by excessive loads due to - wrong manoeuvres - extreme bad weather - hard landing - flutter

FROM: REF. 39

Table 13.7 Analysis of Airplane Accident Types

Accident type (1969 - 1975)		Number of accidents		
		Total	Fatal	Fatal / Total
Predominantly Airworthiness	Fire (cabin, toilet)	7	2	29%
	Structural failure	21	1	5
	Landing gear mechanism (G)	13	0	0
	Landing gear failure/fire (G)	20	1	5
	Engine failure/fire	58	5	9
	System failure	14	7	50
	Sub-total	133	16	12%
Predominantly Operational	Bird strike	19	0	0
	Weather	18	6	33
	Struck high ground	14	14	100
	Under-shoot	45	23	51
	Overshoot/over-run (G)	28	4	14
	Running off runway (G)	23	0	0
	Heavy landing (G)	16	0	0
	Miscellaneous	42	8	19
	Sub-total	205	55	27%
	Grand-total	338	71	21%

(G) = low-speed accidents at or near ground, few fatal accidents.

FROM: REF. 39

Table 13.8 Airworthiness and Operational Accident Causes

Accident cause predominantly	Number of accidents	
	Total	Fatal
Airworthiness	39%	23%
Operational	61%	77%
Total	100%	100%
Flying hours: 7.8×10^7 hrs; number of flights: 5×10^7		

FROM: REF. 39

Table 13.9 Airplane Accidents Classified by Causes

Fatal accident causes for commercial aircraft (139 accidents; 47 with jets, 29 with turbo-props, 63 with piston-engined aircraft)	
Human factor, HF	51%
Technical factor, T	14%
Both HF and T	14%
Weather, W	7%
Both HF and W	8%
Sabotage and others	6%
Total	100%

FROM: REF. 39

Table 13.10 The Human Factor in Airplane Accidents

Flight crew	Failed to follow approved procedures (improper IFR-operation included)	34%
	Misjudged speed/altitude/distance (improper level-off included)	19%
	Spatial disorientation	8%
	Failed to see and avoid other aircraft	4%
	Inadequate supervision of flight	5%
	Inadequate preflight preparation/planning	7.5%
	Other crew failures	10%
Ground personnel	Improper maintenance and others	12.5%
Total		100%

FROM: REF. 39

Table 13.11 Fatal Airplane Accidents by Region

Region	Scheduled air services (ICAO, 1970-1976, excl. USSR and China)	Civil jet Aircraft registered per region (1959-Sept.1978)
	Fatal accidents per 10^6 aircr.flight hrs	Hull loss rate per 10^6 aircr. flight hrs.
U.S.A.	.55	1.31
Canada		2.13
Europe	1.9	2.43
Africa	-	4.61
Central and South America	7.4	8.62
Asia	3.6	4.26
World average (jets only)	2.3 (.85)	2.17

FROM: REF. 39

Table 13.12 Summary of World Jet Hull Loss Rate

WORLD JET HULL LOSS RATE
by generation of aircraft
(Cumulative 1975 – Sept 1980)

Area	1st	2nd	3rd	Total
World	1/385,000	1/767,000	1/1,112,000	1/640,000
Australasia	—	—	1/399,000	1/1,427,000
USA	1/818,000	1/1,468,000	1/941,000	1/1,180,000
Europe	1/426,000	1/599,000	1/1,643,000	1/599,000
Canada	—	1/759,000	—	1/1,297,000
Africa	1/222,000	1/736,000	—	1/413,000
Asia	1/258,000	1/227,000	1/976,000	1/313,000
C&S America	1/182,000	1/544,000	—	1/321,000
World excl. USA	1/301,000	1/497,000	1/1,282,000	1/458,000

FROM: REF. 40 OCT. '80

In designing for safety and survivability the following factors are offered for consideration:

I. Preventive factors:

1. Benign flying qualities.

   This means plenty control power with moderate cockpit control forces, certainly in engine-out emergencies. Changes in flap setting and power setting should be easily controlled. Good damping characteristics are needed.

2. Easy inspectability of the structure for fatigue crack detection and monitoring.

3. Production and materials quality control: know what goes into the airplane.

4. Design systems for ease of operation and prevention of design induced mistakes.

5. Remember: as a general rule, inherent component reliability is better than redundancy.

II. Post crash factors

Crashes will occur despite the best of care in preventive design. For survivabilty: make the cabin environment survivable in a survivable crash.

1. The structure and the seats should not fail in a hazardous manner under g loadings which are survivable by the human body.

2. Prevent fires by safe fuel system design, see Chapter 5.

3. Prevent the use of materials which generate toxic fumes when ignited by fires.

4. Arrange emergency exits so that people really have a chance of getting out.

Review the system design guidelines and design considerations given in Chapters 2 through 12.

13.3 DESIGN FOR SAFETY AND SURVIVABILITY IN MILITARY AIRPLANES

Military accidents are investigated only by military authorities as long as no loss of civilian life has occurred. Since military organizations are not compelled to publish the findings of their accident investigations openly, not much statistical information is available.

Reference 40 publishes listings of military airplane accidents on a regular basis. Aeronautical engineers should study these lists carefully because they often reveal design problems with certain types of airplanes. Selected data from Ref.40 are given in Table 13.13.

Table 13.13, excerpted from Reference 40, is presented here without comment.

Military airplanes are subject to combat damage of a variety of types. Reference 41 provides detailed methods of analysis for combat survivability.

Table 13.14 shows the loss rates sustained in several military conflicts.

Table 13.15 shows the causes of combat inflicted losses in five wars.

Table 13.16 shows the probability of military crews completing a combat tour under different values of assumed loss rate.

It is clear that safety in military aviation is a difficult subject. Even in peace time, by the nature of the military business (need for training in extreme circumstances is one example) it will be virtually impossible to achieve safety levels comparable to those achieved in commercial aviation.

From a design viewpoint, all factors mentioned in Section 13.2 also apply to the design of military airplanes.

13.4 THE ROLE OF THE PRELIMINARY DESIGN ENGINEER AND DESIGN MANAGEMENT IN CREATING SAFE AIRPLANES

The process of airplane sizing (Part I) and preliminary airplane configuration design (Part II) was seen to be dominated by airworthiness requirements (civil or military). Minimum performance requirements as well as stability and control requirements were seen to exert

Table 13.13 Summary of Military Airplane Accidents for 1985, from Reference 40.

Date	Type	Service	Location	F*	I*	S*	Remarks
17.1	F-14A Tomcat	USN	USS Constellation	0	10	2	Clipped nose of A-6 on landing
22.1	C-130 Hercules	USAF	1/2 n.m. off Trujillo, N.Honduras	21			
23.1	VA-3B Skywarrior	USN	Between Atsugi, Japan and Guam	9			Missing at sea
29.1	A-4M Skyhawk	USMC	San Clemente, CA			1	Pilot ejected during post maint. check-flight
?.1	A-10A Th'bolt II	USAF	New York	no data			
7.2	A-7E Corsair	USN	NAS Fallon, Nv			1	departed in IMC climb at low level
7.2	F-16A Ftg'Falcon	USAF	Townsend Range			1	
8.2	F-16A Ftg'Falcon	USAF	La Cesa			1	pilot ejected
9.2	A-10A Th'bolt II	USAF	30 n.m. of Flagstaff, Az.	1			Weapons sortie
10.2	F-16A Ftg'Falcon	USAF	Near Luke AFB, Az	no data			
13.2	TA-4J Skyhawk	USN	NAS Pensacola		1	2	Thrust loss in circuit, crew ejected

* F = fatality I = injured S = survived, no injury

Table 13.14 Airplane Loss Rates in High Intensity Sorties

Data taken from Reference 43.

Operation	Loss Rate in Percent
RAF Bomber Command, Night attacks, January,1942 - June, 1944	> 4
RAF Bomber Command, Battle of Berlin November, 1943 - March, 1944	6.4
U.S. 8th Air Force, January, 1943 - September, 1943 (Airplanes penetrating enemy defenses over Germany only)	8.2
U.S. 20th Bomber Command over Japan, June, 1944 - December, 1944	4
Israeli Air Force, 1973, Golan, days 1-4	4

Table 13.15 Causes of Combat Losses in Several Wars

Data taken from Reference 43.

War	Losses due to: AAA	SAM	Fighters
U.S., WWII	10,287	---	8,743
U.S., Korea	1,109	---	144
U.S., Vietnam	1,605	196	82
Israel, 1973	31	46	15
Arab Forces, 1973	72	25	334

Table 13.16 Probability of Completion of Combat Tour

Data taken from Reference 43.

Attrition Rate per sortie	Probability of completing sorties 25	50	100
0.1	98	95	90
0.5	88	78	61
1.0	78	61	37
2.0	60	36	13
4.0	36	13	2
8.0	12	2	-

much influence on the sizing and the configuration design process of commercial as well as military airplanes.

The preliminary design engineer must therefore be thoroughly familiar with civil and military airworthiness regulations.

The role of the preliminary design engineer in designing airplane systems for safety and for reliability was first hinted at in Part II. In Step 17 of p.d. sequence II (p.18 of Part I) the designer was asked to do the following:

> Step 17: List the major systems needed in the airplane. Also: prepare 'ghost' views indicating the general system arrangements and their location in the airframe.

As a follow-up to Step 17, in Step 32 (p.22, p.d. sequence II in Part II) the designer was also asked to:

> Step 32: Prepare a preliminary layout drawing for all essential airplane systems, in particular the primary and secondary flight control systems.

Chapters 2 through 12 in this part dealt with the layout design of the most important systems which are normally required by airplanes. What is meant by system layout design in Step 32 is the completion of the following 'what-if' safety and maintenance checklist:

'WHAT-IF' SAFETY AND MAINTENANCE CHECKLIST

1. Check whether all performance requirements which are critical to the airworthiness of the airplane are satisfied. Determine how close the airplane is to NOT satisfying one or more of these requirements and identify the reason. Start thinking about possible design fixes.

2. Check whether all stability and control requirements which are critical to the airworthiness of the airplane have been met. Determine how close the airplane is to NOT satisfying one or more of these requirements and identify the reason. Start thinking about possible design fixes.

3. Prepare the following drawings:

   3a) a system schematic drawing

3b) a system inboard profile
3c) a system 'ghost' view

Table 13.17 provides a key to where in this text examples of schematic drawings, inboard profiles and ghost views of systems can be found.

4. Prepare a functional description of the system.

   This should include a description of all system components with their function.

5. Identify all component attachments to surrounding structure and identify the implications for structural design and analysis.

6. Prepare a list of required redundancies in the system with preliminary reasons explaining the need for the redundancy.

7. Prepare a list of servicing and/or maintenance requirements. This must include an analysis of requirements for accessibility.

8. Play the 'WHAT-IF' game. How to do this is explained below.

One idea behind completing the items in the checklist is to be able to identify possible conflict situations. Conflict situations exist if:

A. two systems or system components apparently occupy the same space.

B. two systems or system components are so close together that in case of system failure or local structural failure other serious failures would result.

With the help of Computer Aided Design (CAD) systems it is relatively easy to spot such conflict situations: various 'ghost' layouts can be overlaid on the computer display. Conflicts are immediately obvious.

At this point it is essential that the designer play the so-called 'WHAT-IF' game. The 'what-if' game consists of asking the question:

<u>What happens if: component X in system Y fails?</u>

The answer to this question must be spelled out in

Table 13.17 Examples of System Schematics, System Inboard Profiles and System Ghost Views

System	Chptr	Schematic		Inboard Profile		Ghost View	
		Fig.	Pg.	Fig.	Pg.	Fig.	Pg.
Landing Gear	2	2.94d	116	2.46	73	2.89b	108
Weapons	3	3.8,	133	3.2	129	3.7	133
Flight Controls	4	4.68	258	4.94	279	4.96	283
Fuel	5	5.15	299	5.13	298	5.2	288
Hydraulic	6	6.4	306	6.11	315	6.5	309
Electrical	7	7.8	327	7.7	325	7.1	318
Environmental	8	8.4	334	8.7	337	8.6	336
Cockpit Instr. and Flight Management	9	9.7	346	9.15	352	9.20	356
De-icing etc.	10	10.3	360	10.12	368	10.11	367
Escape	11	11.8	378	11.3	374	11.7	377
Water and Waste	12	12.2	382	12.1	381	12.3	383

terms of detailed failure and consequence scenarios. Depending on the seriousness of the consequences, modifications of the proposed design layout may be required.

The 'what-if' game is the follow-up to Step 32 in p.d. sequence II as described on p.22 in Part II.

What follows now is a list of rules for designing safe airplanes. Each aeronautical engineering student and each practicing design engineer should always keep this list in mind!

RULES FOR DESIGNING SAFE AIRPLANES:
==========

1. Know the airworthiness regulations!

2. Never be complacent about the safety of any aspect of your design.

3. Pay attention to details: often the 'little' things cause serious accidents

4. Do not become a specialist in any design area. Design engineers should be as broad as possible in their knowledge of the airplane and all its systems.

5. LEARN TO FLY! The author considers it essential that airplane design engineers be licensed pilots. This teaches additional respect and understanding for the products being designed and appreciation for the problems encountered by those who professionally fly and maintain airplanes.

6. READ, READ, READ. The design engineer should spend at least 20 percent of his time reading airplane accident reports and the airplane literature. The author recommends regular reading of the following periodicals:

   1. Aviation Week and Space Technology (USA)
   2. Interavia (Switzerland)
   3. Flight International (England)
   4. AOPA Pilot (USA)
   5. Flying (USA)
   6. Journal of Aircraft (USA)
   7. US Naval and Air Force Safety Reviews
   8. NTSB accident reports and recommendations

   The designer must learn from mistakes made by

others and not repeat these mistakes. There is only one way to prevent making the same mistakes over and over again: READ, READ, READ.

7. An ethical point: whenever the question of the airworthiness of a design arises, the first question the designer should ask is:

   Is it safe enough for myself and/or my family to ride on? Only when the answer to this question is YES, should reference be made to airworthiness specifications. Remember that all airworthiness specifications represent MINIMUM safety requirements. If at all possible the designer should do better than the minimum which is demanded of him.

8. If management fails to alter a design which is judged to be unsafe by the design engineer he should insist on a review of the design by a peer group in the organization. Normally the decision of this group should prevail.

   If management ignores the peer group decision and wants to proceed with the unsafe design, the engineer has only two options:

   A. write a memo outlining the problem, its solution and its status. Address this memo to the appropriate level of management. In extreme cases this may mean the bypassing of immediate supervision!

   B. if design changes are not made, send a copy of the memo to the certifying authority.

In this regard it is sad to observe that certifying agencies not always react with due speed to problems with air safety. Ref.42 contains many examples of cases where certifying agencies as well as corporations failed to react on time in the face of known design deficiencies.

The role of management in the process of creating safe designs is that of monitoring engineering decision making, insisting on meeting at least the minimum requirements AND insisting on ethical conduct of the design, development and certification process.

14. REFERENCES

1. Conway, H.G., Landing Gear Design, Chapman Hall, London, England, 1958.

2. Currey, N.S., Landing Gear Design Handbook, Lockheed Georgia Company, Marietta, Georgia, 30063, 1982.

3. Torenbeek, E., Synthesis of Subsonic Airplane Design, Kluwer Boston Inc., Hingham, Maine, 1982.

4. Stinton, D., The Design of the Aeroplane, Granada Publishing, London, England, 1983.

5. Bingelis, T., The Sportplane Builder, T.Bingelis, 8509 Greenflint Lane, Austin, Texas, 78759, 1979.

6. Taylor, J.W.R., Jane's All The World Aircraft, Published annually by: Jane's Publishing Company, 238 City Road, London EC1V 2PU, England.

7. Bruhn, E.F., Analysis and Design of Flight Vehicle Structures, Tri-State Offset Co., Cincinnati, Ohio, 45202, 1965.

8. Thurston, D.B., Design for Flying, McGraw-Hill Book Co., New York, 1978.

9. Heinemann, H., Rausa, R. and Van Every, K., Aircraft Design, The Nautical Publishing Company of America, Inc, Baltimore, Md, 21201, 1985.

10. Horne, W.B., Yager, T.J. and Taylor, G.R., Recent Research on Ways to Improve Tire Traction on Water, Slush or Ice, De Ingenieur, September, 1966. (Journal of the Royal Netherlands Inst. for Engineers).

11. Anon., Aircraft Carrier Reference Data Manual, NAEC MISC 06900, Naval Air Engineering Center, 1974.

12. Erdman, A.G. and Sandor, G.N., Mechanical Design: Analysis and Synthesis, Volume 1, Prentice Hall, N.J., 1984.

13. Erdman, A.G. and Sandor, G.N., Advanced Mechanical Design: Analysis and Synthesis, Volume 2, Prentice Hall, N.J., 1984.

14. Buzzard, W.C. et al, Tests of the Air Cushion Landing System on the XC-8A, AFFDL-TR-78-61, 1978.

15. Anon., Air Cushion Landing Gear Application Studies, Report D7605-927001, NASA Contract NAS1-15202, Bell Aerospace, Buffalo, N.Y., 1978.

16. Ball, R.E., The Fundamentals of Aircraft Combat Survivability Analysis and Design, AIAA Education Series, AIAA, N.Y., 1985.

17. Fuhs, A.E., Radar Cross Section Lectures, US Naval Postgraduate School, Monterey, CA, 93940, 1984.

18. Sweetman, B., Stealth Aircraft, Motorbooks International, Osceola, Wisconsin, 54028, 1986.

19. Pretty, R.T., Jane's Weapon Systems, 1984-1985. See Reference 6.

20. Roskam, J., Airplane Flight Dynamics and Automatic Flight Controls, 1981, Roskam Aviation and Engineering Corp., Rt 4, Box 274, Ottawa, Kansas, 66067.

21. Anon., Federal Aviation Regulations, Part 23 and Part 25, Department of Transportation, Distribution Requirements Section, M-482.2, Wash., D.C., 20590.

22. Anon., MIL-F-8785-B/C, Military Specification-Flying Qualities of Piloted Airplanes, 1969 and 1982.

23. Scanlan, R.H. and Rosenbaum, R., Aircraft Vibration and Flutter, Dover Publications, N.Y., 1968.

24. Fung, Y.C., An Introduction to the Theory of Aeroelasticity, J.Wiley and Sons, 1955.

25. Bisplinghoff, R.L., Ashley, H. and Halfman, R., Aeroelasticity, Addison-Wesley, 1955.

26. Wood, N.E. et al, Electromechanical Actuation Feasibility Study, AFFDL-TR-76-42, WPAFB, OH, 45433.

27. Anon., MIL-F-9490D, Military Specification-Flight Control Systems-Design, Installation and Test of, Piloted Aircraft, June 1975.

28. Brahney, J.H., Pumps for 8000 psi Hydraulic Systems Examined, Aerospace Engineering, July 1986.

29. McKinley, J.L. and Bent, R.D., Basic Science for Aerospace Vehicles, Northrop University, McGraw Hill Book Co., N.Y., 1965.

30. Casamassa, J.V. and Bent, R.D., Jet Aircraft Power Systems, Northrop University, McGraw Hill Book Co., N.Y., 1965.

31. Marks, L.S., Mechanical Engineer's Handbook, McGraw Hill Book Co., N.Y., 1951.

32. Weinstock, G.L., Lightning Protection on Advanced Fighter Aircraft, SAE/AFAL Lightning and Static Electricity Conference, McDonnell Douglas Paper, MDC 70-035, 1970.

33. McKinley, J.C. and Bent, R.D., Maintenance and Repair of Aerospace Vehicles, Northrop University, McGraw Hill Book Co., N.Y., 1967.

34. McKinley, J.C. and Bent, R.D., Electricity and Electronics for Aerospace Vehicles, Northrop University, McGraw Hill Book Co., N.Y., 1971.

35. Beauchamp, E.D., Opportunities and Challenges for Electric-Drive Systems on Aircraft, SAE Paper 841627, Aerospace Congress and Exposition, 1984.

36. Anon., Integrated Application of Active Controls (IAAC) Technology to an Advanced Subsonic Transport Project, NASA Contractor Report 3880, 1986.

37. Zumwalt, G.W. and Mueller, A.A., Flight and Wind Tunnel Tests of an Electro-Impulse De-icing System, AIAA/NASA General Aviation Technology Conference, AIAA Paper No. 84-2236, Hampton, VA, 1984.

38. Bingelis, T., Firewall Forward, Published by T.Bingelis, 8509 Greenflint Lane, Austin, Texas, 78759.

39. Wittenberg, H., Safety in Aviation, Achievements and Targets, Memorandum M-353, Delft University of Technology, Department of Aerospace Engineering, Delft, The Netherlands, 1979.

40. Flight International, British Aerospace Weekly Magazine, Business Press International USA, 205 East 42nd Street, New York, N.Y., 10017.

41. Ball, R.E., The Fundamentals of Aircraft Combat Survivability Analysis and Design, AIAA Education Series, AIAA, 1633 Broadway, New York, N.Y., 10019.

42. Tench, Bill, Safety is no accident, Collins, 8 Grafton Street, London, W1X 3LA, England.

43. Greene, T.E., Surviving Modern Air Defenses, Aerospace America, August 1986.

15. INDEX

AIRPLANE DESIGN

PART V: COMPONENT WEIGHT ESTIMATION

by

Dr. Jan Roskam
Ackers Distinguished Professor
of Aerospace Engineering
The University of Kansas
Lawrence, Kansas

NO PART OF THIS BOOK MAY BE REPRODUCED WITHOUT
PERMISSION FROM THE AUTHOR

Copyright: Roskam Aviation and Engineering Corporation
Rt4, Box 274, Ottawa, Kansas, 66067
Tel. 913-2421624
First Printing: 1985

TABLE OF CONTENTS

TABLE OF SYMBOLS

Symbol	Definition	Dimension
A	wing aspect ratio	-----
$A_{h,v,c}$	Hor. tail, Vert. tail or Canard aspect ratio	-----
A_{inl}	Inlet capture area per inlet	ft^2
A_g	constant in Eqn.(5.42) and Table 5.1	
b	wing span	ft
$b_{h,v,c}$	Hor. tail, Vert. tail or Canard span	ft
B_g	constant in Eqn.(5.42) and Table 5.1	
$\bar{c}$	wing mean geometric chord	ft
$\bar{c}_{h,v,c}$	mean geometric chord of hor. tail, vert. tail or canard	ft
C_g	constant in Eqn.(5.42) and Table 5.1	
C_D	Drag coefficient	-----
C_L	Lift coefficient	-----
C_{L_α}	Airplane lift-curve slope	rad^{-1}
C_N	Normal force coefficient	-----
D_g	constant in Eqn.(5.42) and Table 5.1	
D_p	Propeller diameter	ft
$e = (b + L)/2$	Used in inertia calcs.	ft
FAR	Federal Air Regulation	-----
g	acceleration of gravity	ft/sec^2
GW	Flight design gross wht	lbs
h	altitude	ft
h_f	maximum fuselage height	ft
int	fraction of fuel tanks which are integral	-----
I	Moment of inertia	$slugs/ft^3$

K = constant as defined in equations below:

K_{api} (7.32)	K_b (6.34)	K_{bc} (7.48)	K_{buf} (7.44)
K_c (4.6)	K_d (6.9) and (6.10) but note that values differ		K_{ec} (6.23)
K_f (5.27)	K_{fcf} (7.9)	K_{gr} (5.42)	K_h (5.19)
K_{inl} (5.26) and (5.28)		K_{lav} (7.44)	K_m (6.9)
K_n (5.29)	K_{osc} (6.38)	K_p (6.2)	K_{pg} (6.4)
$K_{prop1 \text{ or } 2}$ (6.13) or (6.14)			K_r (6.11)
K_s (6.12)	K_{thr} (6.6)	K_v (5.20)	K_w (5.9), (5.10)
K_{st} (7.46)			

K_{fsp}	specific weight of fuel	lbs/gal
K_g	Gust alleviation factor, see Eqn. (4.16)	
l_f	length of fuselage	ft
l_{f-n}	length of fuselage minus nacelle	ft
$l_{h,v,c}$	Distance from wing 1/4c to $1/4c_{h,v,c}$	ft
l_{inl}	inlet length from lip to compressor face	ft
l_{pax}	length of passenger cabin	ft
$l_{s_{m \text{ or } n}}$	shock strut length for main gear or for nose gear	ft
L	Overall airplane length	ft
L_d	inlet duct length	ft
L_r	ramp length	ft
M	Mach number	
M_{ff}	Mission fuel fraction (M_{ff}= End weight/Begin weight)	none
n	Load factor	-----
N	Number of (see subscript)	-----

p_{max}	maximum fusel. perimeter	ft
P_c	design ult. cabin press.	psi
P_{TO}	required take-off power	hp
P_2	maximum static pressure at engine compressor face	psi
$\bar{q}$	dynamic pressure	psf
R	Range	nm or m
$R_{x,y,z}$	Radius of inertia about x,y,z axis respectively	ft
$\bar{R}_{x,y,z}$	Non-dimensional radius of inertia about x,y,z axiz resp.	-----
S	Wing area	ft^2
S_{cs}	Total control surface area	ft^2
S_{ff}	freight floor area	ft^2
S_{fgs}	Fuselage gross shell area	ft^2
$S_{h,v,c}$	Hor., Vert. or Can. area	ft^2
S_r	Rudder area	ft^2
SHP	Shaft horsepower	hp
t/c	thickness ratio	-----
t_r	maximum root thickness	ft
U_{de}	Derived gust velocity	fps
V	True airspeed	mph, fps, kts
V_A	Design maneuvering speed	KEAS
V_B	Design speed for maximum gust intensity	KEAS
V_C	Design cruise speed	KEAS
V_D	Design dive speed	KEAS
V_H	Maximum level speed at at sealevel	KEAS

V_{pax}	Volume of passenger cabin	ft^3
$V_{pax+cargo}$	Vol. of pass. and cargo	ft^3
V_S, V_{S_1}	+1g stall speed	KEAS
w_f	maximum fuselage width	ft
W	Weight	lbs
W_i	Weight of component i	lbs
x	distance from some ref.	ft
x_i	distance from some ref. of component i	ft
z_h	Distance from vert.tail root to where h.t. is mounted on the v.t.	ft

Greek Symbols
==========

α	angle of attack of airplane	rad.
ε	downwash angle at h.t.	rad.
ρ	air density	$slugs/ft^3$
λ	wing taper ratio	-----
$\lambda_{h,v,c}$	taper ratio for hor. tail, vert. tail or canard	-----
μ_g	airplane mass ratio, see Eqn.(4.17)	
Λ_n	sweep angle at n^{th} chord station	

Subscripts
==========

ai	air induction
api	airconditioning, pressurization, de-icing and anti-icing system
apsi	accessory drives, powerplant controls, starting and ignition system
apu	auxiliary power unit
arm	armament
aux	auxiliary
bal	ballast
bc	baggage and cargo handling equipment
bl	blades
c	canard
cc	cabin crew
cg	center of gravity
cr	crew
crew	crew
C	Cruise

D	Dive
e	engines (all!)
ec	engine controls
els	electrical system
emp	empennage
eng	engine (one only)
ess	engine starting system
etc	etcetera (please pronounce as eTcetera and not as eKcetera)
E	Empty
f	fuselage
fc	flight control system
fd	fuel dumping system
fdc	flight deck crew
feq	fixed equipment
fl.boat	flying boat
fs	fuel system
fti	flight test instrumentation
fur	furnishings
F	Mission fuel
g	landing gear
glw	guns, launchers and weapons provisions
h	horizontal tail
hps	hydraulic and pneumatic system
H	maximum level flight at sealevel
i	instrumentation
iae	instrumentation, avionics and electronics
inflref	in-flight refuelling system
inl	inlet(s)
lim	limit
L	Landing (subscript to W)
L	maximum dive (subscript to V)
LE	Leading Edge
m	maximum
max	maximum
MZF	Maximum zero fuel
n	nacelle
neg	negative
ops	operational items
osc	oil system and oil cooler
ox	oxygen system
pax	passengers
p	propellers (subscript to N)
p	propulsion system (subscript to W)
pc	propeller controls
pos	positive
prop	propeller
pt	paint
pwr	powerplant
PL	Payload

ramp	ramp
sprchr	supercharger
struct	structure
supp	bladder support structure
t	fuel tanks
tfo	trapped fuel and oil
tr	thrust reverser system
troop	troop(s)
TO	Take-off
ult	ultimate
ult.l.	ultimate landing
v	vertical tail
w	wing
wb	wing + body
wi	water injection system
xx, yy, zz	about x-, y-, z-axis respectively

Acronyms
========

APU	Auxiliary power unit
C.G., c.g.	Center of gravity
OWE	Operating weight empty
TBP	Turboprop

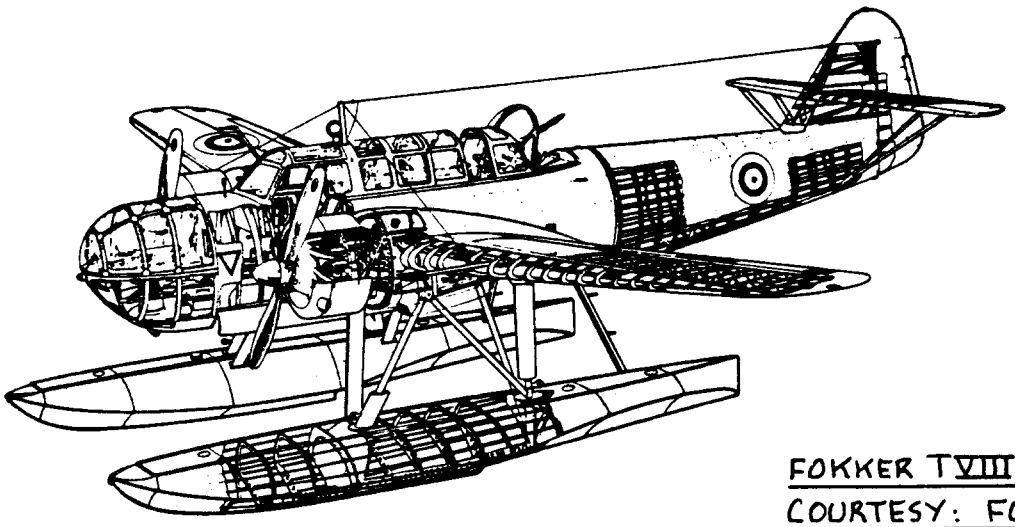

FOKKER TVIII-W
COURTESY: FOKKER

ACKNOWLEDGEMENT

Writing a book on airplane weight estimation is impossible without the supply of a large amount of data. The author is grateful to the following companies for supplying the weight data, the weight manuals and the weight estimating procedures which made the book what it is:

Beech Aircraft Corporation
Boeing Commercial Airplane Company
Canadair
Cessna Aircraft Company
DeHavilland Aircraft Company of Canada
Gates Learjet Corporation
Gulfstream Aerospace Corporation
Lockheed Aircraft Corporation
McDonnell Douglas Corporation
NASA, Ames Research Center
Rinaldo Piaggio S.p.A.
Rockwell International
Royal Netherlands Aircraft Factory, Fokker
SIAI Marchetti S.p.A.

A significant amount of airplane design information has been accumulated by the author over many years from the following magazines:

Interavia (Swiss, monthly)
Flight International (British, weekly)
Business and Commercial Aviation (USA, monthly)
Aviation Week and Space Technology (USA, weekly)
Journal of Aircraft (USA, AIAA, monthly)

The author wishes to acknowledge the important role played by these magazines in his own development as an aeronautical engineer. Aeronautical engineering students and graduates should read these magazines regularly.

FOKKER F.27 FRIENDSHIP

COURTESY: FOKKER

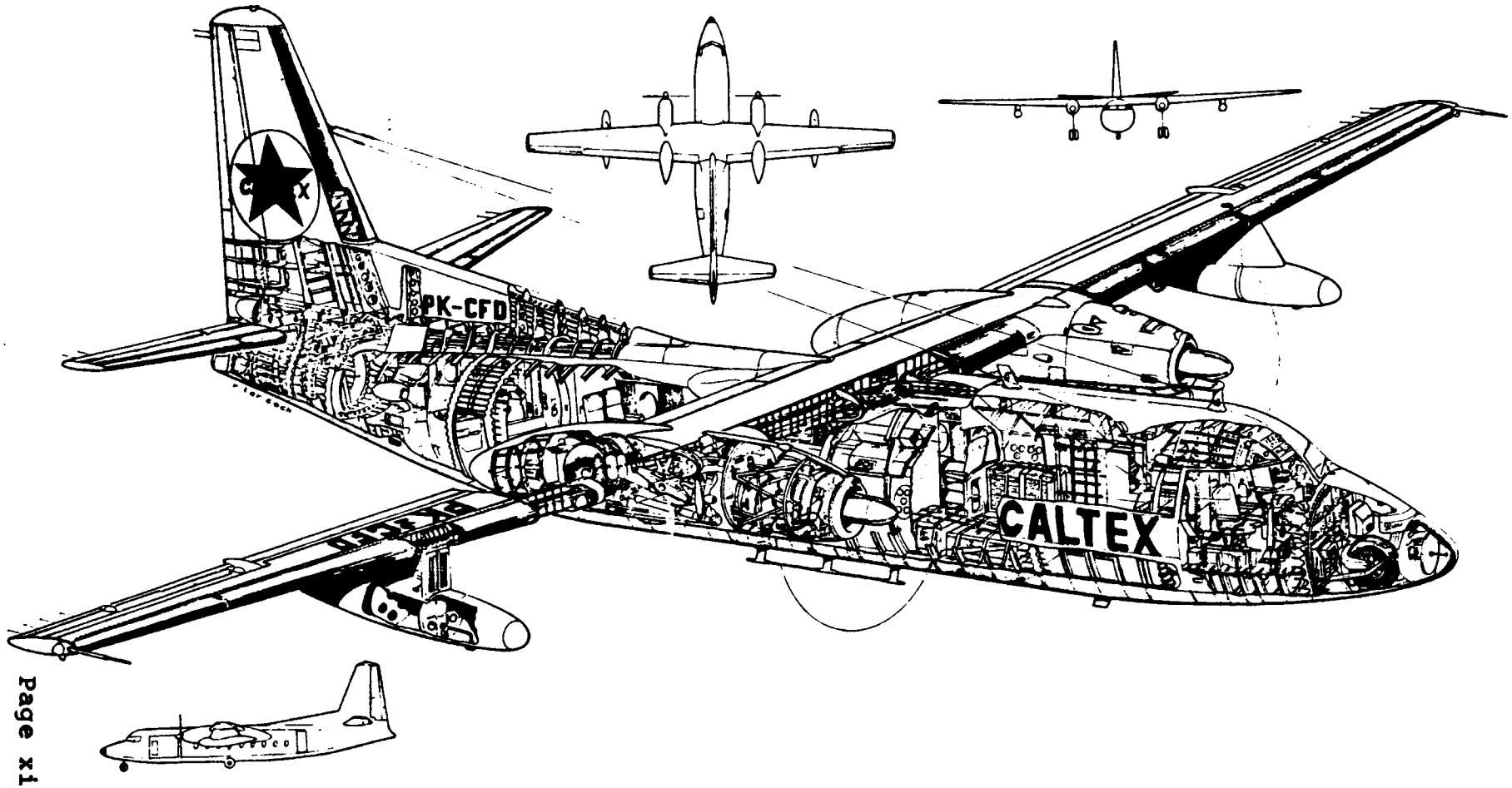

1. INTRODUCTION

The purpose of this series of books on Airplane Design is to familiarize aerospace engineering students with the design methodology and design decision making involved in the process of designing airplanes.

The series of books is organized as follows:

PART I:	PRELIMINARY SIZING OF AIRPLANES
PART II:	PRELIMINARY CONFIGURATION DESIGN AND INTEGRATION OF THE PROPULSION SYSTEM
PART III:	LAYOUT DESIGN OF COCKPIT, FUSELAGE, WING AND EMPENNAGE: CUTAWAYS AND INBOARD PROFILES
PART IV:	LAYOUT DESIGN OF LANDING GEAR AND SYSTEMS
PART V:	COMPONENT WEIGHT ESTIMATION
PART VI:	PRELIMINARY CALCULATION OF AERODYNAMIC, THRUST AND POWER CHARACTERISTICS
PART VII:	DETERMINATION OF STABILITY, CONTROL AND PERFORMANCE CHARACTERISTICS: FAR AND MILITARY REQUIREMENTS
PART VIII:	AIRPLANE COST ESTIMATION: DESIGN, DEVELOPMENT, MANUFACTURING AND OPERATING

The purpose of PART V is to present methods for estimating airplane component weights and airplane inertias during airplane preliminary design.

Two methods are presented: they are called the Class I and the Class II method respectively.

The Class I method relies on the estimation of a percentage of the flight design gross weight (= take-off weight for most airplanes) of major airplane components. These percentages are obtained from actual weight data for existing airplanes. The usual procedure is to average these percentages for a number of airplanes similar to the one being designed. These averaged percentages are multiplied by the take-off weight to obtain a first estimate of the weight of each major component.

The method can be used with minimal knowledge about the airplane being designed and requires very little engineering work. However, the accuracy of this method is limited. It should be used only in association with preliminary design sequence I as outlined in Part II (See Step 10, p.15).

Chapter 2 presents the Class I method for estimating

airplane component weights in the form of a step-by-step precedure. Three example applications are also given.

Chapter 3 presents a Class I method for estimating airplane moments of inertia. Example applications are also given.

Class II methods are based on weight equations for more detailed airplane components and groupings. These equations have a statistical basis. They do allow the designer to account for fairly detailed configuration design parameters. To use this method it is necessary to have a V-n diagram, a preliminary structural arrangement and to have decided on all systems which are needed for the operation of the airplane under study.

The Class II method should be used in conjunction with preliminary design sequence II as outlined in Part II (See Step 21, p.19).

Chapter 4 presents the Class II method for estimating airplane component weights in the form of a step-by-step procedure. A method for construction of a V-n diagram is included. Example applications are given.

As part of the Class II weight estimation procedure the airplane empty weight is split into three major groupings:

1. Structure weight
2. Powerplant weight
3. Fixed equipment weight

Chapters 5, 6 and 7 present the detailed methodologies used in determining the component weights within each of these three groupings.

Chapter 8 contains data and methods for rapidly determining the c.g. location of individual components.

A Class II method for performing a weight and balance analysis is discussed in Chapter 9.

Chapter 10 presents a Class II method for computing airplane moments and products of inertia.

Appendix A contains a data base for airplane component weights and weight fractions.

Appendix B contains a data base for non-dimensional radii of gyration for airplanes.

2. CLASS I METHOD FOR ESTIMATING AIRPLANE COMPONENT WEIGHTS

The purpose of this chapter is to provide a methodology for rapidly estimating airplane component weights. The emphasis is on rapid and on spending as few engineering manhours as possible. Methods which fit meet these objectives are referred to as Class I methods. They are used in conjunction with the first stage in the preliminary design process, the one referred to as 'p.d. sequence I' in Part II (See Step 10, p.15).

The Class I weight estimating method relies on the assumption, that within each airplane category it is possible to express the weight of major airplane components (or groups) as a simple fraction of one of the following weights:

1. Gross take-off weight, W_{TO}
2. Flight design gross weight, GW
3. Empty weight, W_E

The reader is already familiar with the definition of W_{TO} and W_E. The flight design gross weight, GW is that weight at which the airplane can sustain its design ultimate load factor, n_{ult}. For civil airplanes GW and W_{TO} are often the same, although there are exceptions. For military airplanes GW and W_{TO} are frequently quite different.

In this book, all component weight fractions are given relative to the flight design gross weight, GW. In the component weight and weight fraction data presented in Appendix A, both GW and W_{TO} are listed for all airplanes for which data are presented.

Since W_{TO} is known from the preliminary sizing work described in Part I, the value of GW can be established.

The weight of any major airplane component or group can now be found rapidly through multiplication of GW by

an appropriate weight fraction. For this reason, the Class I weight method is also referred to as the 'weight fraction' method.

Section 2.1 presents a step-by-step procedure for using weight fractions to estimate the component weight breakdown of airplanes.

Section 2.2 presents example applications to three airplanes.

2.1 A METHOD FOR ESTIMATING AIRPLANE COMPONENT WEIGHTS WITH WEIGHT FRACTIONS

In this section the Class I method for estimating airplane component weights is presented in the form of a step-by-step procedure.

Step 1: List the following overall weight values for the airplane:

1. Gross take-off weight, W_{TO}
2. Empty weight, W_E
3. Mission Fuel Weight, W_F
4. Payload weight, W_{PL}
5. Crew weight, W_{crew}
6. Trapped fuel and oil weight, W_{tfo}
7. Flight design gross weight, GW

Weight items 1-6 are already known from the preliminary sizing process described in Part I (See Chapter 2).

For most airplanes, W_{TO} and GW are the same. In the case of many military airplanes there is a difference. Appendix A contains tables with airplane weight data on basis of which a decision can be made about the ratio between W_{TO} and GW. Sometimes the mission specification will include this information.

Step 2: Proceed to Appendix A and determine which airplane category best fits the airplane which is being designed. Identify those

airplanes which will be used in estimating the weight fractions for the airplane which is being designed.

Step 3: Make a list of the significant airplane components for which weights need to be estimated. This list will vary some from one airplane type to the other. In many cases certain weight items are already specified in the mission specification.

A typical Class I component weight list contains the following items:

I. Structure Weight, W_{struct}

1. Wing
2. Empennage
   2.1 Horizontal tail and/or canard
   2.2 Vertical tail and/or canard
3. Fuselage (and/or tailbooms)
4. Nacelles
5. Landing gear
   5.1 Nose gear
   5.2 Main gear
   5.3 Tail gear
   5.4 Outrigger gear
   5.5 Floats

II. Powerplant Weight, W_{pwr}

1. Engine(s), this may include afterburners or thrust reversers
2. Air induction system
3. Propeller(s)
4. Fuel system
5. Propulsion system

III. Fixed Equipment Weight, W_{feq}

1. Flight control system
2. Hydraulic and pneumatic system
3. Electrical system
4. Instrumentation, avionics and electronics
5. Air conditioning, pressurization, anti-icing and de-icing system
6. Oxygen system
7. Auxiliary power unit
8. Furnishings
9. Baggage and cargo handling equipment
10. Operational items

11. Armament
12. Guns, launchers and weapons provisions
13. Flight test instrumentation
14. Auxiliary gear
15. Ballast
16. Paint
17. Other weight items not listed above

Consult the mission specification as well as the appropriate tables in Appendix A for any weight items not listed above.

The airplane empty weight, W_E is expressed as:

$$W_E = W_{struct} + W_{pwr} + W_{feq} \qquad (2.1)$$

Whether or not it is necessary to split weight groupings II and III in as many components as listed above depends on the expected effect of these components on the accuracy of the airplane c.g. location.

Use as much detail as necessary for realism in the Class I weight and balance analysis of Chapter 10, Part II.

Step 4: From the appropriate Table(s) in Appendix A decide on the weight fractions to be used.

Frequently it will be sufficient to use average fraction values obtained from a number of airplanes with missions not too much different from the mission of the airplane being designed. The reader should familiarize himself with what the airplanes for which weight fraction data are available, look like and what their missions were. This can be done by referring to Jane's All the World Aircraft (Ref.8). Jane's contains an index identifying which issue of Jane's contains descriptions of certain types of airplanes.

It is of great importance to observe whether or not:

1. an airplane has a strutted (braced) wing
2. an airplane is pressurized
3. the landing gear is mounted on the fuselage or on the wing
4. the engines are mounted on the wing or fuselage

The reader should note, that most weight and weight fraction data in Appendix A are for airplanes with largely aluminum primary structures. If the airplane being designed will have to contain a significant amount

of primary structure made from composites, from lithium-aluminum or from other materials, it will be necessary to modify the weight fractions. Table 2.16, p.48, Part I may be useful in this regard.

After thus 'massaging' the weight fraction data, list the weight fractions to be used. Make careful notes of reasons why specific fractions were selected.

Step 5: Multiply the selected weight fractions by the GW value of Step 1 and list all significant airplane component weights.

The Class I component weight data thus obtained are used in the Class I weight and balance analysis described in Chapter 10 of Part II.

To illustrate the use of this procedure, three examples are presented in Section 2.2.

Step 6: Document the decisions made under Steps 1 through 5 in a brief, descriptive report.

2.2 EXAMPLE APPLICATIONS

In this section, three example applications of the Class I component weight estimating method will be discussed:

2.2.1 Twin Engine Propeller Driven Airplane: Selene
2.2.2 Jet Transport: Ourania
2.2.3 Fighter: Eris

2.2.1 Twin Engine Propeller Driven Airplane

Step 1: Overall weight values for this airplane were determined as a result of the preliminary sizing performed in Part I. These weight values are summarized in sub-sub-section 3.7.2.6, Part I, p.178:

W_{TO} = 7,900 lbs W_E = 4,900 lbs

W_F = 1,706 lbs W_{PL} = 1,250 lbs (Part I, p.49)

W_{tfo} = 44 lbs makes up the balance.

The crew weight is included in the payload of this airplane. It will be assumed that GW = W_{TO}. This is consistent with the data in Tables A3.1 and A3.2.

For easy reference the airplane will be referred to as the Selene, the name of the Greek Moon Goddess.

Step 2: Tables A3.1 and A3.2 contain component weight data for airplanes in the same category as the Selene. Specifically, the following airplanes have comparable sizes and missions: Cessna 310C, Beech 65 Queen Air, Cessna 404-3 and Cessna 414A.

Step 3: For reasons of brevity, only the following component weights are considered:

Wing	Empennage	Fuselage	Nacelles
Landing Gear	Power Plant	Fixed Eqpmt	

Step 4: The following table lists the pertinent weight fractions and their averaged values. Because the intent is to apply conventional metal construction methods to the Selene there is no reason to alter the averaged weight fractions.

	Beech 65 QA	Cessna 310C	Cessna 404-3	Cessna 414A	Selene Average
Pwr Plt/GW	0.219	0.259	0.194	0.206	0.220
Fix Eqp/GW	0.123	0.103	0.134	0.167	0.132
Empty Wht/GW	0.638	0.628	0.596	0.665	0.631
Wing Grp/GW	0.091	0.094	0.102	0.094	0.095
Emp. Grp/GW	0.021	0.024	0.022	0.024	0.023
Fus. Grp/GW	0.082	0.066	0.073	0.100	0.080
Nac. Grp/GW	0.039	0.027	0.034	0.029	0.032
Gear Grp/GW	0.060	0.054	0.038	0.045	0.049

Note that the ratio of W_E/GW which follows from the preliminary sizing, is 4,900/7,900 = 0.62. This is close to the average value of 0.631 in the above tabulation.

Step 5: Using the averaged weight fractions from Step 4, the following preliminary component weight summary can be determined:

Component	First weight estimate	Adjustment	Selene Class I weight (alum.)	Selene Class I weight (compos.)
	lbs	lbs	lbs	lbs
Wing	751	-13	738	627
Empennage	182	- 3	179	152
Fuselage	632	-11	621	528
Nacelles	253	- 4	249	212
Landing Gear	387	- 7	380	380
Power Plant	1,738	-30	1,708	1,708
Fixed Eqp.	1,043	-18	1,025	1,025
Empty Wht	4,986	-86	4,900	4,632
Payload			1,250	1,250
Fuel			1,706	1,706
Trapped fuel and oil			44	44
Take-off Gross Weight			7,900	7,632

When the numbers in the first column are added, they yield an empty weight of 4,986 lbs instead of the desired 4,900 lbs. The difference is due to round-off errors in the weight fractions used. It is best to 'distribute' this difference over all items in proportion to their component weight value listed in the first column.

For example, the wing adjustment number is arrived at by multiplying 86 lbs by 751/4986.

It is quite possible that in other airplanes the adjustment will turn out to be positive instead of negative.

If the judgement is made to manufacture the Selene with composites as the primary structural materials significant weight savings can be obtained. A conservative assumption is to apply a 15 percent weight reduction to wing, empennage, fuselage and nacelles. The resulting weights are also shown in the Class I weight tabulation. Note the reduction in empty weight of 268 lbs. Using the weight sensitivity $\partial W_{TO}/\partial W_E = 1.66$ as computed in sub-sub-section 2.7.3.1 in Part I, an overall reduction in W_{TO} of 1.66x268 = 545 lbs can be achieved.

The designer has the obvious choice to fly the same mission with (545 - 268) = 277 lbs less fuel or to simply add the 545 lbs to the useful load of the Selene.

The component weight values in the column labelled: 'Class I weight (alum.)' are those to be used in the Class I weight and balance analysis of the Selene. This corresponds to Step 10 as outlined in Chapter 2, Part II. The Class I weight and balance analysis for the Selene is carried out in Chapter 10 of Part II (See pp. 246-250).

Step 6: To save space, this step has been omitted.

2.2.2 Jet Transport

Step 1: Overall weight values for this airplane were determined as a result of the preliminary sizing performed in Part I. These weight values are summarized in sub-sub-section 3.7.3.6, Part I, p.183:

W_{TO} = 127,000 lbs W_E = 68,450 lbs

W_F = 25,850 lbs W_{PL} = 30,750 lbs (Part I, p.54)

W_{tfo} = 925 lbs W_{crew} = 1,025 lbs (Part I, p.58)

It will be assumed that GW = W_{TO} for this airplane. This is consistent with the data in Tables A7.1 through A7.5.

For easy reference the airplane will be referred to as the Ourania, the name of the Greek Muse of Astronomy.

Step 2: Tables A7.1 through A7.5 contain component weight data for airplanes in the same category as the Ourania. Specifically the following airplanes have comparable sizes and missions: McDonnell-Douglas DC-9-30 and MD-80, Boeing 737-200 and 727-100.

Step 3: For reasons of brevity, only the following component weights are considered:

Wing	Empennage	Fuselage	Nacelles
Landing Gear	Power Plant	Fixed Eqpmt	

Step 4: The following table lists the pertinent weight fractions and their averaged values. Because the intent is to apply conventional metal construction methods to the Ourania, there is no reason to alter the averaged weight fractions.

	McDonnell-Douglas DC-9-30	MD-80	Boeing 737-200	727-100	Ourania Average
Pwr Plt/GW	0.076	0.079	0.071	0.078	0.076
Fix Eqp/GW	0.175	0.182	0.129	0.133	0.155
Empty Wht/GW	0.538	0.564	0.521	0.552	0.544
Wing Grp/GW	0.106	0.111	0.092	0.111	0.105
Emp. Grp/GW	0.026	0.024	0.024	0.026	0.025
Fus. Grp/GW	0.103	0.115	0.105	0.111	0.109
Nac. Grp/GW	0.013	0.015	0.012	0.024	0.016
Gear Grp/GW	0.039	0.038	0.038	0.045	0.040

Note that the ratio of W_E/GW which follows from the preliminary sizing, is 68,450/127,000 = 0.539. This is close to the average value of 0.544 in the above tabulation.

Step 5: Using the averaged weight fractions just determined, the following preliminary component weight summary can be determined:

Component	First weight estimate lbs	Adjustment lbs	Ourania Class I weight (alum.) lbs	Ourania Class I weight (li/alum.) lbs
Wing	13,335	+329	13,664	12,298
Empennage	3,175	+ 78	3,253	2,928
Fuselage	13,843	+341	14,184	12,766
Nacelles	2,032	+ 50	2,082	1,874
Landing Gear	5,080	+125	5,205	5,205
Power Plant	9,652	+239	9,891	9,891
Fixed Eqp.	19,685	+486	20,171	20,171
Empty Wht	66,802	+1,648	68,450	65,133
Payload			30,750	30,750
Crew			1,025	1,025
Fuel			25,850	25,850
Trapped fuel and oil			925	925
Take-off Gross Weight			127,000	123,683

When the numbers in the first column are added, they yield an empty weight of 66,802 lbs instead of the desired 68,450 lbs. The difference is due to round-off errors in the weight fractions used. It is best to 'distribute' this difference over all items in proportion

to their component weight values listed in the first column.

For example, the wing adjustment number is arrived at by multiplying 1,648 lbs by 13,335/66,802. When so doing, the sum of the adjusted component weights is still 41 lbs shy of the desired goal. That new difference is then redistributed in the same manner.

It will be noted that the adjustments here are positive whereas for the light twin they were negative. It all depends on the weight fraction roundoffs, how this comes out.

If the judgement is made to manufacture the Ourania with lithium/aluminum as the primary structural material, sigificant weight savings can be obtained. A reasonable assumption is to apply a 10 percent weight reduction to wing, empennage, fuselage and nacelles. The resulting weights are also shown in the Class I weight tabulation. Note the reduction in empty weight of 3,317 lbs. Using the weight sensitivity $\partial W_{TO}/\partial W_E = 1.93$ as computed in sub-sub-section 2.7.3.2 in Part I, an overall reduction in W_{TO} of 1.93x3,317 = 6,402 lbs can be achieved.

The designer has the obvious choice to fly the same mission with (6,402 - 3,317) = 3,085 lbs less fuel or to add the 6,402 lbs to the useful load of the Ourania.

The component weight values in the column labelled: 'Class I weight (alum.)' are those to be used in the Class I weight and balance analysis of the Ourania. This corresponds to Step 10 as outlined in Chapter 2, Part II. The Class I weight and balance analysis of the Ourania is carried out in Chapter 10 of Part II (See pp. 250-254.

Step 6: To save space, this step is omitted.

2.2.3 Fighter

Step 1: Overall weight values for this airplane were determined as a result of the preliminary sizing performed in Part I. These weight values are summarized in sub-sub-section 3.7.4.5, Part I, p.191:

W_{TO} = 64,500 lbs W_E = 33,500 lbs

W_F = 18,500 lbs W_{PL} = 12,000 lbs (Part I, p.60)

W_{tfo} = 300 lbs W_{crew} = 200 lbs (Part I, p.66)

It will be assumed that GW = $0.95W_{TO}$ for this airplane. This is consistent with the data in Tables A9.1 through A9.6.

For easy reference the airplane will be referred to as the Eris, the name of the Greek Goddess of War.

When looking up the actual bomb weight for a nominal 500 lbs bomb, it will be discovered that this weight is 531 lbs and not 500 lbs. That is a difference of 20x31 = 620lbs. On the other hand, the normal ammunition for the standard GAU-8A gun drum weighs 1,785 and not 2,000 lbs. The difference is -215 lbs. The actual payload is therefore 405 lbs more than originally planned.

Step 2: Tables A9.1 through A9.6 contain component weight data for airplanes in the same category as the Eris. Specifically the following airplanes have comparable sizes and missions: Republic F105B, Vought F8U, and Grumman A2F.

Step 3: For reasons of brevity only the following component weights are considered:

Wing	Empennage	Fuselage	Eng. Sect.
Landing Gear	Power Plant	Fixed Eqpmt	

Step 4: The following table lists the pertinent weight fractions and their averaged values. Since Eris will be made from conventional aluminum materials, there is no reason to alter the averaged weight fractions.

	Republic F105B	Vought F8U	Grumman A2F(A6)	Eris Average
Pwr Plt/GW	0.246	0.257	0.162	0.222
Fix Eqp/GW	0.155	0.135	0.159	0.150
Empty Wht/GW	0.797	0.722	0.651	0.723
Wing Grp/GW	0.109	0.135	0.136	0.127
Emp. Grp/GW	0.031	0.034	0.024	0.030
Fus. Grp/GW	0.187	0.126	0.102	0.138
Eng.Sect./GW	0.003	0.003	0.002	0.003
Gear Grp/GW	0.059	0.031	0.067	0.052
Engine(s)/GW	0.197	0.197	0.115	0.170
$n_{ult.}$	13	9.6	N.A	Use: 12
GW/W_{TO}	0.92	0.79	1.0	Use: 0.95

Note: all fraction data were based on GW without external stores!

Note that the ratio of W_E/GW which follows from the preliminary sizing, is 33,500/54,500 = 0.615. This is lower than the average value of 0.723 in the above tabulation. The reason is that the data base is for older fighters, two of which are USN fighters. Also note the large value $n_{ult.}$ for the F105B.

Step 5: Using the averaged weight fractions just determined, the following preliminary component weight summary can be determined:

Component	First weight estimate	Adjustment	Eris Class I weight (alum.)
	lbs	lbs	lbs
Wing	6,922	-160	6,762
Empennage	1,635	- 38	1,597
Fuselage	7,521	-174	7,347
Eng.Sect.	164	- 4	160
Landing Gear	2,834	- 66	2,768
Power plant	12,099 predicted from fraction data		
Engines	9,265 predicted from fraction data		
Engines	6,000 actual for F404's with A/B		
Engines			6,000
Eng.Sect.		12,099-9,265 =	2,834
Fix.Eqpmt	8,175 predicted from fraction data		
Ammo	2,000 (original estim.)		
Fix.Eqpmt-Ammo	6,175	-143 = 6,032	
GAU-8A Gun (Actual weight)			2,014
Fix.Eqpmt-Gun			4,018
Empty Wht	39,350	-585	33,500
Pilot			200
Payload: ammo			1,785
: bombs			10,620
Trapped fuel and oil			300
Fuel			18,500
Take-off Gross Weight			64,905

When the numbers in the first column are added, they yield an empty weight of 39,350 lbs instead of the

desired 33,500 lbs., obtained from preliminary sizing. The difference is due to:

1. 2,000 lbs of ammo are included.
2. 3,265 lbs because of the much more favorable engine weight (9,265-6,000).
3. the remaining -585 lbs is due to round-off errors in the weight fractions.

The -585 lbs is distributed over all items which are computed with the weight fractions. This distribution is done in proportion to their component weight values in the first column.

For example, the wing adjustment number is arrived at by multiplying -585 lbs by 6,922/25,251*.

Note:

*25,251 = 6,922 + 1,635 + 7,521 + 164 + 2,834 + 6,175

The component weight values in the last column are those to be used in the Class I weight and balance analysis of the Eris. This corresponds to Step 10 as outlined in Chapter 2, Part II. The Class I weight and balance analysis of the Eris is carried out in Chapter 10 of Part II (See pp. 254-258).

Step 6: To save space, this step is omitted.

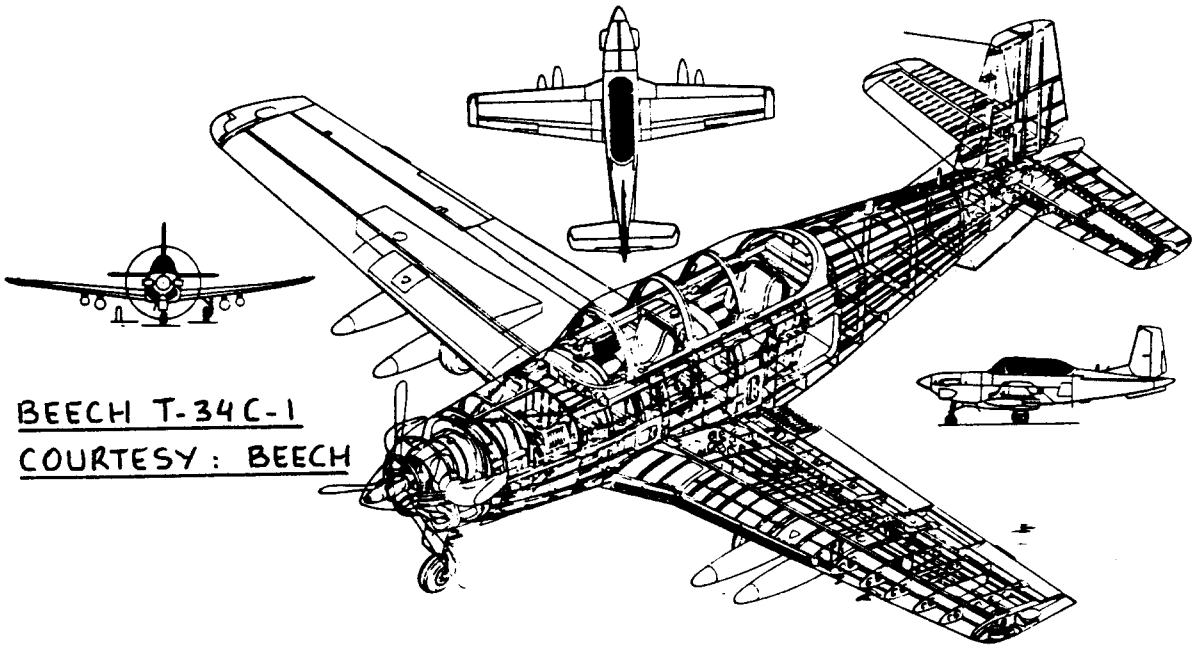

BEECH T-34C-1
COURTESY: BEECH

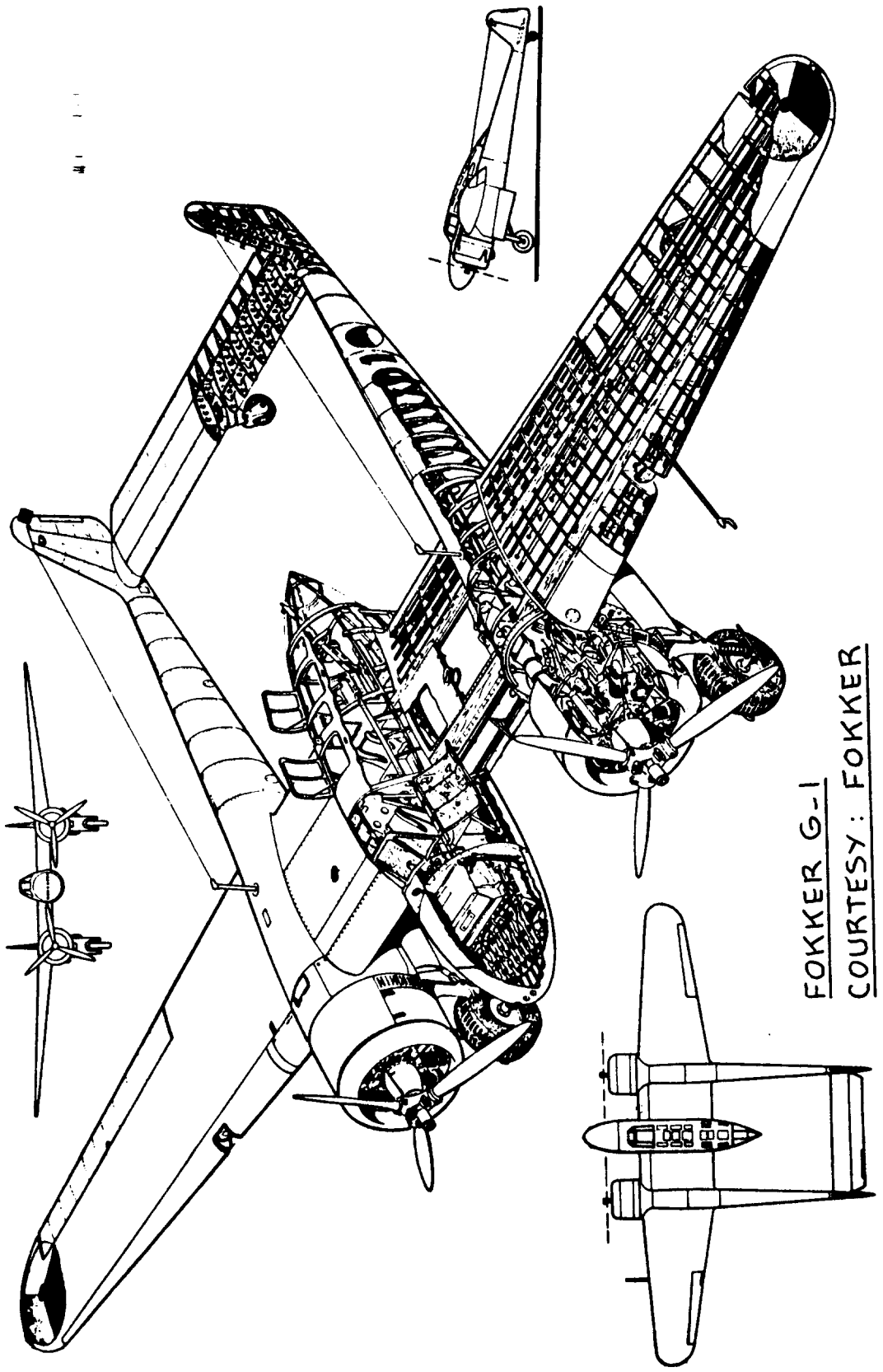

FOKKER G-1
COURTESY: FOKKER

3. CLASS I METHOD FOR ESTIMATING AIRPLANE INERTIAS

The purpose of this chapter is to provide a methodology for rapidly estimating airplane inertias. The emphasis is on rapid and on spending as few engineering manhours as possible. Methods which fit meet these objectives are referred to as Class I methods. They are used in conjunction with the first stage in the preliminary design process, the one referred to as 'p.d. sequence I' in Part II (Ref.2).

Section 3.1 presents a Class I method for estimating I_{xx}, I_{yy} and I_{zz}. These inertia moments are useful whenever it is necessary to evaluate undamped natural frequencies and/or motion time constants for airplanes during p.d. sequence I.

Example applications are discussed in Section 3.2.

3.1 ESTIMATING MOMENTS OF INERTIA WITH RADII OF GYRATION

The Class I method for airplane inertia estimation relies on the assumption, that within each airplane category it is possible to identify a radius of gyration, $R_{x,y,z}$ for the airplane. The moments of inertia of the airplane are then found from the following equations:

$$I_{xx} = (R_x)^2 W/g \qquad (3.1)$$

$$I_{yy} = (R_y)^2 W/g \qquad (3.2)$$

$$I_{zz} = (R_z)^2 W/g \qquad (3.3)$$

Research in References 9, 10 and 11 has shown that a non-dimensional radius of gyration can be associated with each R component in the following manner:

$$\bar{R}_x = 2R_x/b \qquad (3.4)$$

$$\bar{R}_y = 2R_y/L \qquad (3.5)$$

$$\bar{R}_z = 2R_z/e, \text{ with: } e = (b + L)/2 \qquad (3.6)$$

The quantities b and L in Eqns.(3.4) and (3.5) are the wing span and the overall airplane length respectively.

Airplanes of the same mission orientation tend to have similar values for the non-dimensional radius of gyration. Tables B.1 through B.12 (See Appendix B) present numerical values for these non-dimensional radii of gyration for different types of airplanes.

The procedure for estimating inertias therefore boils down to the following simple steps:

Step 1: List the values of W_{TO}, W_E, b, L and e for the airplane being designed.

Step 2: Identify which type of airplane in Tables B.1 through B.12 best 'fit' the airplane being designed.

Step 3: Select values for the non-dimensional radii of gyration corresponding to W_{TO} and W_E. It must be kept in mind that the distribution of the mass difference between W_{TO} and W_E is more important than the mass difference itself.

Acquiring the knowledge of what the airplanes in Tables B.1 through B.12 are like is therefore essential. As usual, Jane's (Ref.8) is the source for acquiring that knowledge.

Step 4: Compute the airplane moments of inertia from:

$$I_{xx} = b^2 W(\bar{R}_x)^2/4g \tag{3.7}$$

$$I_{yy} = L^2 W(\bar{R}_y)^2/4g \tag{3.8}$$

$$I_{zz} = e^2 W(\bar{R}_z)^2/4g \tag{3.9}$$

Values for b and for L follow from the airplane threeview. The value for e follows from Eqn.(3.6).

The reader will have noted that there is no rapid method for evaluating I_{xz}. This product of inertia can be realistically evaluated only from a Class II weight and balance analysis. Such an analysis is presented in Chapter 9. In the first stages of preliminary design I_{xz} is not usually important. Therefore, it is normally

ignored until later stages in the design process.

Step 5: Compare the estimated inertias of Step 4 with the data of Figures 3.1 through 3.3. If the comparison is poor, find an explanation and/or make adjustments.

Step 6: Document the results obtained in Steps 1 through 5 in a brief, descriptive report. Include illustrations where necessary.

3.2 EXAMPLE APPLICATIONS

Three example applications will now be discussed:

3.2.1 Twin Engine Propeller Driven Airplane: Selene
3.2.2 Jet Transport: Ourania
3.2.3 Fighter: Eris

3.2.1 Twin Engine Propeller Driven Airplane

Step 1: The following information is available for the Selene airplane:

W_{TO} = 7,900 lbs W_E = 4,900 lbs b = 37.1 ft

L = 43.0 ft e = 40.05 ft (Part II, p.247, p.297)

Step 2: From Table B3 (Appendix B) the following airplanes are judged to be comparable to the Selene in terms of mass distribution: Beech D18S, Cessna 404 and Cessna 441.

Step 3: From Table B3 (Appendix B) it is estimated that the following non-dimensional radii of gyration apply to the Selene:

$\bar{R}_x$ = 0.30 $\bar{R}_y$ = 0.34 $\bar{R}_z$ = 0.40

Step 4: With Eqns.(3.7) through (3.9) the following moments of inertia can now be calculated:

At W_{TO}:

$I_{xx} = 37.1^2 \times 7{,}900 \times 0.30^2 / 4 \times 32.2 = 7{,}598$ slugft^2

$I_{yy} = 43.0^2 \times 7{,}900 \times 0.34^2 / 4 \times 32.2 = 13{,}109$ slugft^2

$I_{zz} = 40.05^2 \times 7{,}900 \times 0.40^2 / 4 \times 32.2 = 15{,}741$ slugft^2

At W_E:

I_{xx} = (4,900/7,900)x7,598 = 4,713 slugft^2

I_{yy} = (4,900/7,900)x13,109 = 8,131 slugft^2

I_{zz} = (4,900/7,900)x15,741 = 9,763 slugft^2

Step 5: Figures 3.1 through 3.3 show that the inertia estimates of Step 4 are reasonable.

Step 6: This step has been omitted to save space.

3.2.2 Jet Transport

Step 1: The following information is available for the Ourania airplane:

W_{TO} = 127,000 lbs W_E = 68,450 lbs b = 113.8 ft

L = 127.0 ft e = 120.4 ft (Part II, p.251, p.299)

Step 2: From Table B7a (Appendix B) the following airplanes are judged to be comparable to the Ourania in terms of mass distribution: Convair 880, Convair 990, Boeing 737-200, McDonnell Douglas DC8.

Step 3: From Table B7a (Appendix B) it is estimated that the following non-dimensional radii of gyration apply to the Ourania:

At W_{TO}: $\bar{R}_x$ = 0.25 $\bar{R}_y$ = 0.38 $\bar{R}_z$ = 0.46

At W_E: $\bar{R}_x$ = 0.27 $\bar{R}_y$ = 0.46 $\bar{R}_z$ = 0.52

Step 4: With Eqns.(3.7) through (3.9) the following moments of inertia can now be calculated:

At W_{TO}:

I_{xx} = 113.8^{2}x127,000x0.25^2/4x32.2 = 798,090 slugft^2

I_{yy} = 127.0^{2}x127,000x0.38^2/4x32.2 = 2,296,479 slgft^2

I_{zz} = 120.4^{2}x127,000x0.46^2/4x32.2 = 3,024,520 slgft^2

At W_E:

$I_{xx} = 113.8^2 x 68,450 x 0.27^2 / 4 x 32.2 = 501,730$ slugft^2

$I_{yy} = 127.0^2 x 68,450 x 0.46^2 / 4 x 32.2 = 1,813,764$ slugft^2

$I_{zz} = 120.4^2 x 68,450 x 0.52^2 / 4 x 32.2 = 2,083,134$ slugft^2

Step 5: Comparison with Figures 3.1 through 3.3 indicates that the inertia estimates of Step 4 are reasonable.

Step 6: To save space, this step has been omitted.

3.2.3 Fighter

Step 1: The following information is available for the Eris airplane:

$W_{TO} = 64,905$ lbs $W_E = 33,500$ lbs $b = 68.7$ ft

$L = 50.7$ ft $e = 59.7$ ft (Part II, p.255, p.301)

Step 2: From Table B9a (Appendix B) the following airplanes are judged to be comparable to the Eris in terms of mass distribution: DH Vampire 20 and Gloster Meteor II. The reader should note that the Vampire is the only jet fighter in Table B9a with a twin boom configuration.

Step 3: From Table B9a (Appendix B) it is estimated that the following non-dimensional radii of gyration apply to the Eris:

$\bar{R}_x = 0.29$ $\bar{R}_y = 0.32$ $\bar{R}_z = 0.40$

Step 4: With Eqns.(3.7) through (3.9) the following moments of inertia can now be calculated:

At W_{TO}:

$I_{xx} = 68.7^2 x 64,905 x 0.29^2 / 4 x 32.2 = 200,019$ slugft^2

$I_{yy} = 50.7^2 x 64,905 x 0.32^2 / 4 x 32.2 = 132,641$ slugft^2

$I_{zz} = 59.7^2 x 64,905 x 0.40^2 / 4 x 32.2 = 287,363$ slugft^2

At W_E:

$I_{xx} = 68.7^2 \times 33,500 \times 0.29^2 / 4 \times 32.2 = 103,237 \text{ slugft}^2$

$I_{yy} = 50.7^2 \times 33,500 \times 0.32^2 / 4 \times 32.2 = 68,461 \text{ slugft}^2$

$I_{zz} = 59.7^2 \times 33,500 \times 0.40^2 / 4 \times 32.2 = 148,319 \text{ slugft}^2$

Step 5: Comparison of the results of Step 4 with Figures 3.1 through 3.3 indicate that the inertia estimates are reasonable.

Step 6: This step has been omitted to save space.

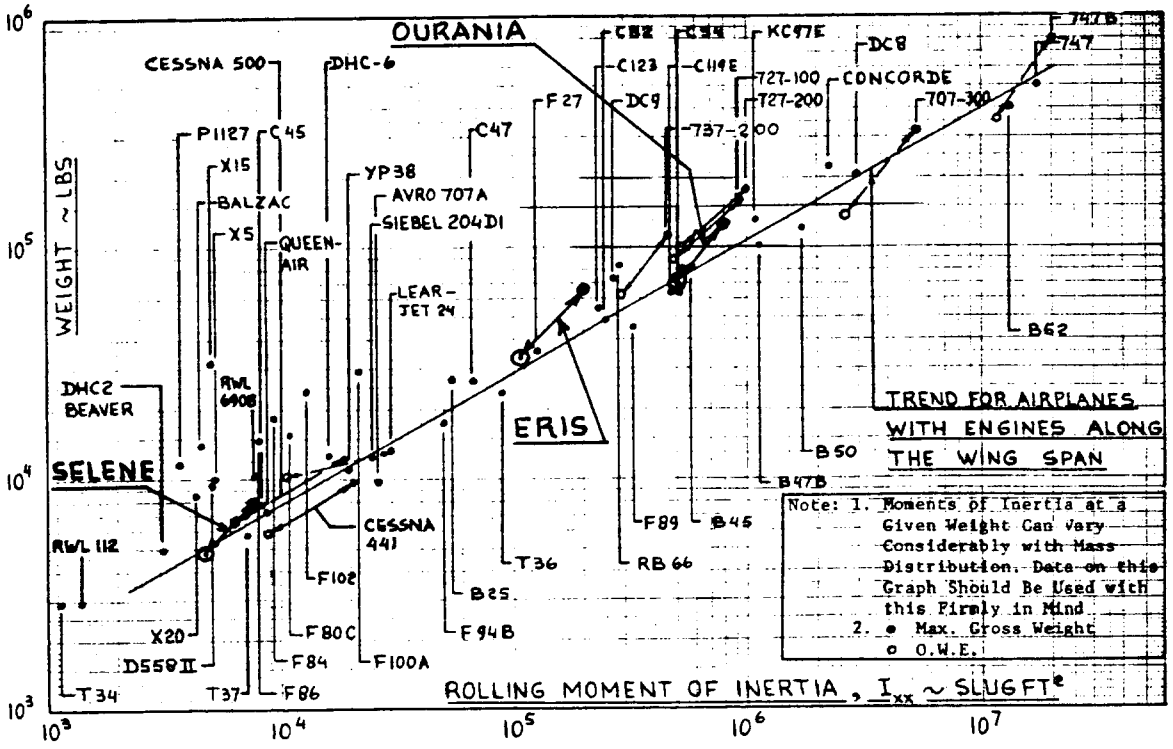

Figure 3.1 Correlation of Rolling Moments of Inertia with Weight

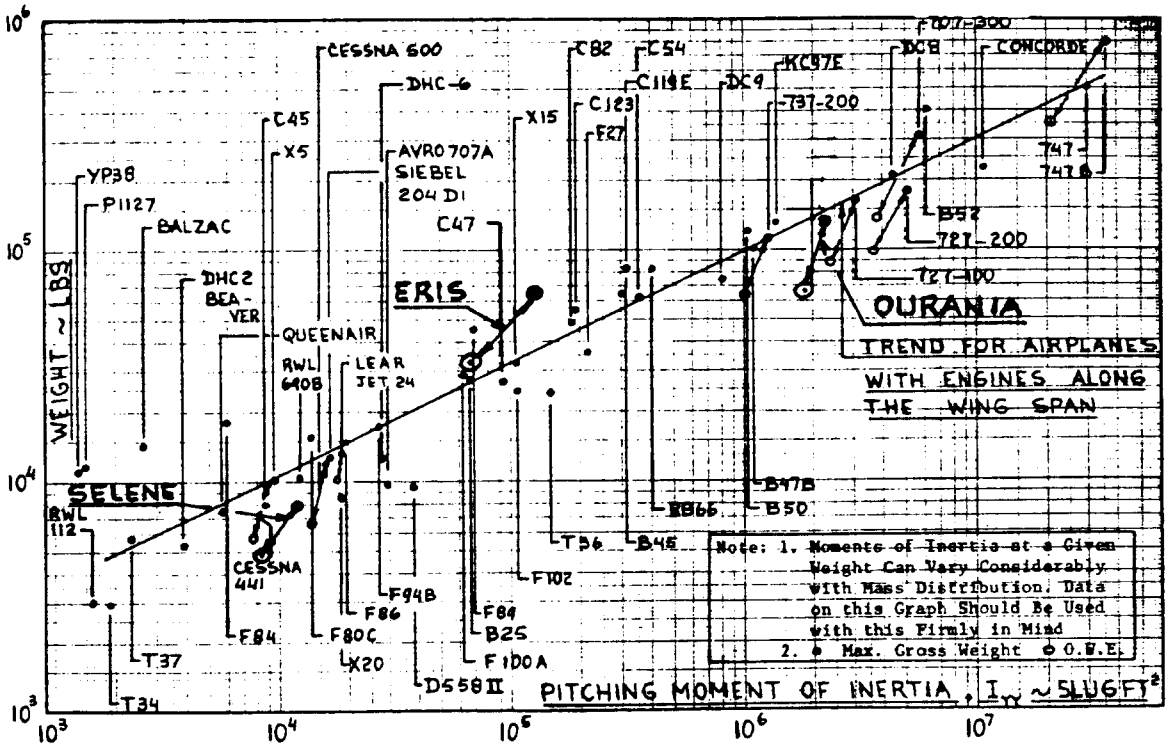

Figure 3.2 Correlation of Pitching Moments of Inertia with Weight

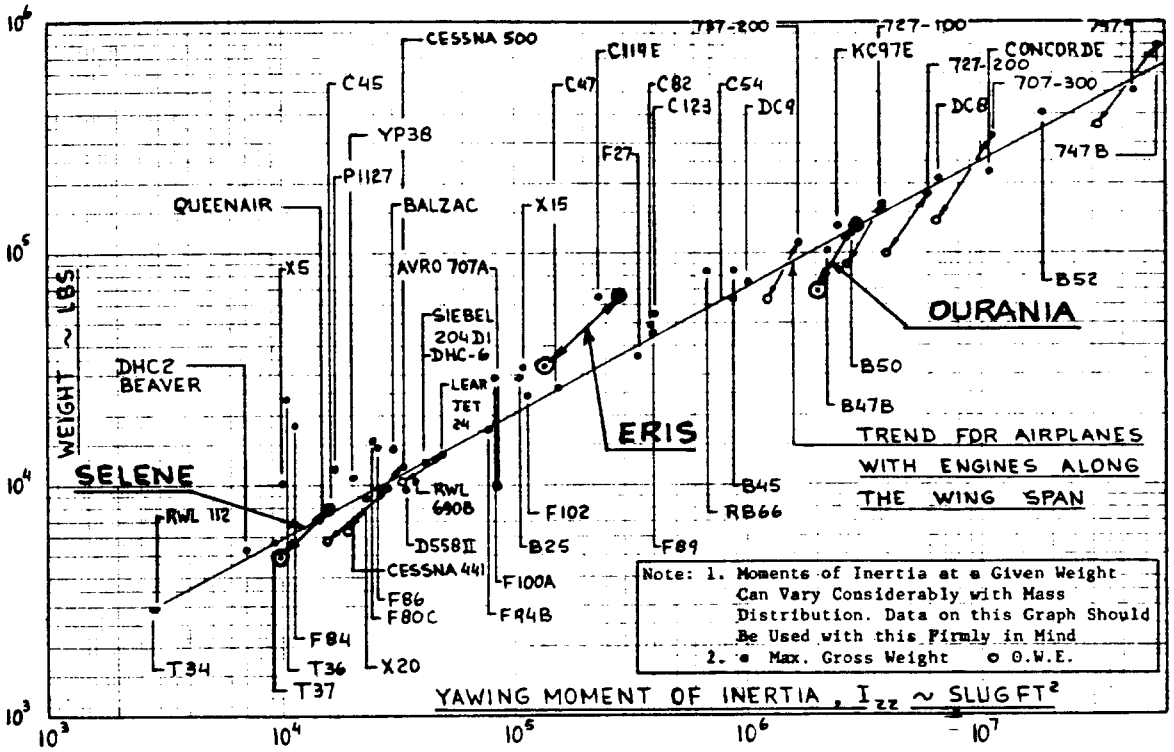

Figure 3.3 Correlation of Yawing Moments of Inertia with Weight

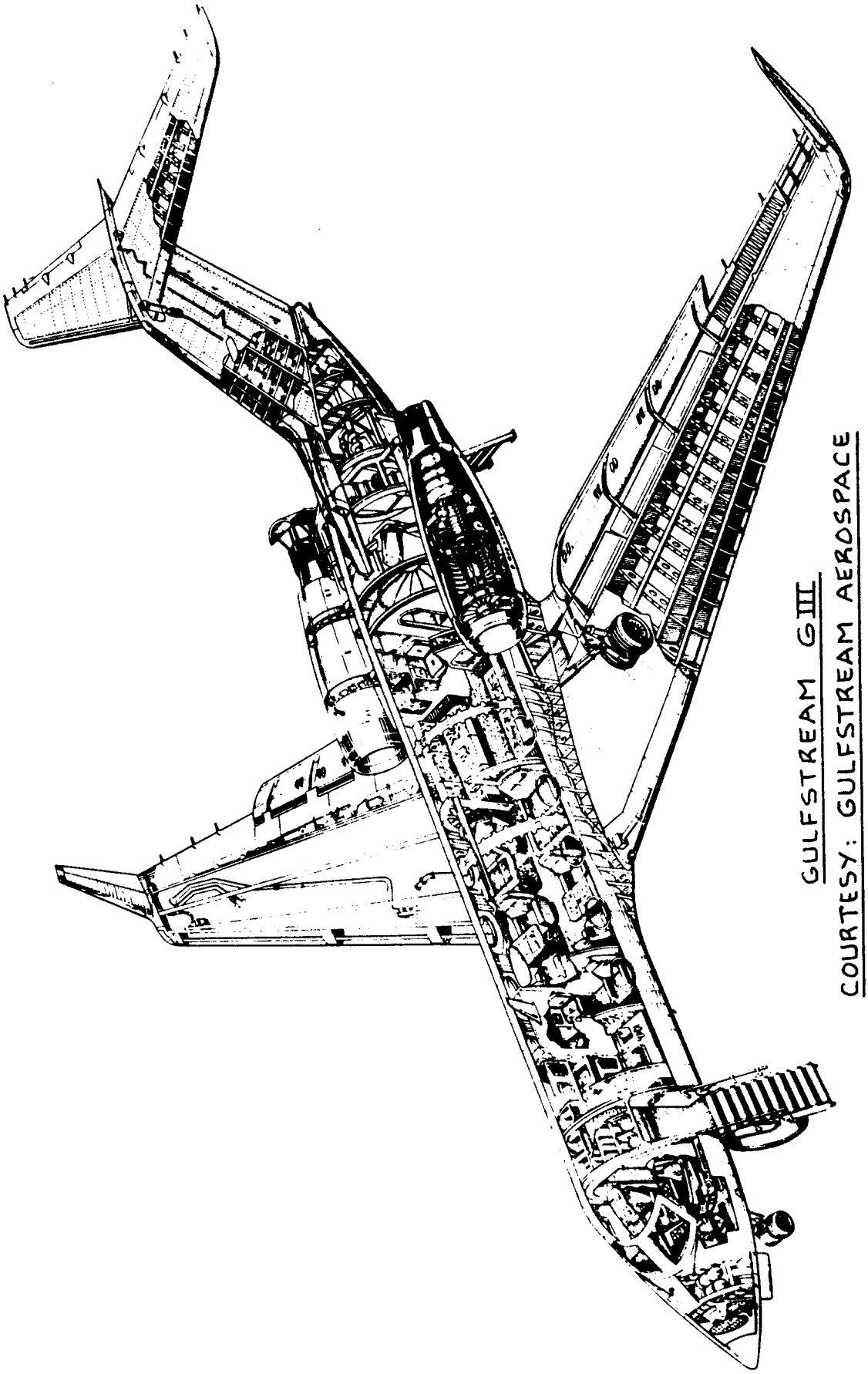

GULFSTREAM GIII

COURTESY: GULFSTREAM AEROSPACE

4. CLASS II METHOD FOR ESTIMATING AIRPLANE COMPONENT WEIGHTS

The purpose of this chapter is to present a Class II method for estimating airplane component weights. Class II methods are those used in conjunction with preliminary design sequence II as defined in Part II, pp 18-23. The Class II weight estimating method accounts for such details as:

1. Airplane take-off gross weight

2. Wing and empennage design parameters such as:

   a. area
   b. sweep angle,
   c. taper ratio, λ
   d. thickness ratio, t/c

3. Load factor, n_{lim} or n_{ult}

4. Design cruise and/or dive speed, V_C or V_D

   Note: items 3 and 4 follow from a V-n diagram.

5. Fuselage configuration and interior requirements

6. Powerplant installation

7. Landing gear design and disposition

8. Systems requirements

9. Preliminary structural arrangement

To apply the Class II method for estimating component weights requires a fairly comprehensive knowledge about the airplane being designed. This knowledge was developed as a result of p.d. sequence I, discussed in Part II, pp 11-18.

Almost all airframe manufacturers have developed their own Class II methods for estimating airplane component weights. Many of these methods are proprietary. The Class II methods used in this text are based on those of References 12, 13 and 14. These methods employ empirical equations which relate component weights to airplane design characteristics such as items 1-9 above.

The following basic weight definition from Part I (Eqn. 2.17) will be used:

$$W_{TO} = W_E + W_F + W_{PL} + W_{tfo} + W_{crew}, \qquad (4.1)$$

where: W_E = empty weight, defined by Eqn. (4.2).

W_F = mission fuel weight, defined by: Eqn. (2.15) in Part I.

W_{PL} = payload weight, defined by the mission specification and on page 8, Part I.

W_{tfo} = weight of trapped fuel and oil, found from p.7, Part I.

W_{crew} = crew weight, defined by the mission specification and on page 8, Part I.

The Class II weight estimating method to be developed here will focus on estimating the components of empty weight, W_E which are defined as:

$$W_E = W_{struct} + W_{pwr} + W_{feq}, \qquad (4.2)$$

where: W_{struct} = structure weight, discussed in Chapter 5.

W_{pwr} = powerplant weight, discussed in Chapter 6.

W_{feq} = fixed equipment weight, discussed in Chapter 7.

In Chapters 5-7 the specific Class II methods are identified as follows:

1. Cessna method: from Ref.12
2. USAF method from Ref.13
3. GD (General Dynamics) method from Ref.13
4. Torenbeek method from Ref.14

Section 4.1 presents a step-by-step procedure for using the Class II weight estimation method.

Section 4.2 presents a method for constructing the V-n diagram, needed in several of the weight equations employed in Chapters 5-7.

Example applications are presented in Section 4.3.

4.1 A METHOD FOR ESTIMATING AIRPLANE COMPONENT WEIGHTS WITH WEIGHT EQUATIONS

In this section a step-by-step procedure is presented for estimating airplane component weights and use these weights in estimating airplane empty weight, W_E.

As will be seen, this procedure is iterative. The reason is, that almost all airplane component weights themselves are a function of W_{TO}. A first estimate for W_{TO} was obtained during the preliminary sizing of the airplane. The reader will have noticed that during the Class I weight estimates (Chapter 2), the original estimate of W_{TO} remained unaltered. That will no longer be the case in the Class II method.

The method is presented as part of Step 21 in p.d. sequence II, as outlined on p.19 of Part II.

For the inexperienced reader, it is suggested that the following procedure be followed exactly as suggested.

Step 1: List all airplane components for which the weights are already known and tabulate their weights. This information can normally be obtained from the mission specification.

Typical items of known weight are:

1. Payload
2. Crew
3. Certain operational systems
4. Certain military loads
5. Engines (these are sometimes specified)

Step 2: List all airplane components for which the weights will have to be estimated. This list will contain at least the same items used in Class I. However, particularly in the systems area the list will contain much more detail at this point.

In preparing this list, use the groupings of components as indicated by Eqn.(4.2). Subdivision of these groupings should be done in accordance with Chapters 5-7, Eqns.(5.1), (6.1) and (7.1).

Step 3: Refer to the structural arrangement drawing prepared under Step 19, p.19, Part II.

The initial structural arrangement drawing is needed to identify those areas of the structure where special provisions were made or where, because of a clever structural arrangement a weight saving can be claimed.

Step 4: Determine from the tabulation below which weight estimation category best represents the airplane being designed.

Airplane Type		Weight Category for Component Weight Estimation Equations
1.	Homebuilts	General Aviation Airplanes
2.	Single Engine Props	General Aviation Airplanes
3.	Twin Engine Props	General Aviation Airplanes
4.	Agricultural	General Aviation Airplanes
5.	Business Jets	Commercial Transports
6.	Regional Turboprops	
	below 12,500 lbs	General Aviation Airplanes
	above 12,500 lbs	Commercial Transports
7.	Jet Transports	Commercial Transports
8.	Military Trainers	
	low speed	General Aviation Airplanes
	high speed	Fighter and Attack Airplanes
9.	Fighters	Fighter and Attack Airplanes
10.	Military Patrol, Bomb and Transport Airplanes	Military Patrol, Bomb and Transport Airplanes
11.	Flying boats, Amphibious and Float Airplanes	
	small and low speed	General Aviation Airplanes
	large and high speed	Commercial Transports and/or Mil.Patr., Bomb and Transp.
12.	Supersonic cruise	
	Commercial	Commercial Transports, but use Fighter inlet data
	Fighter and Attack	Fighter and Attack
	Patrol, Bomb, Transp.	Mil.Patr., Bomb and Transp.

The weight estimation equations in Chapters 5-7 are all given in terms of the categories on the right side of the above table.

Step 5: Determine which equations in Chapters 5-7 apply to the airplane for which the Class II weight estimate is to be made. List these equations for each weight component.

Step 6: Make a list of all required input data needed in the equations of Step 5.

Step 7: Compute the component weights with the applicable equations of Step 5.

Notes:

1. The reader will observe that Chapters 5-7 often contain more than one equation to estimate the weight of a particular component. In that case estimate the weights with all applicable equations and use an average.

2. Sometimes it is desirable to 'calibrate' a component weight equation with the help of known weight data from existing airplanes. The component weight data of Appendix A can be used for this purpose. Calibration is done by applying the weight equations to the appropriate components and comparing the answers with the actual weight data of Appendix A. The so-called 'fudge-constants' which appear in all Class II weight equations can then be altered to obtain a better estimate. The reader should be careful and only use this 'calibration' method in conjunction with airplanes which have similar missions.

3. In the systems area, there are not enough reliable equations available. In that case it is desirable to also estimate the average applicable weight fraction for each system component. This can be done with the data in Appendix A. The examples in Section 4.3 show how this is done.

Step 8: Add all component weights and obtain an estimate for W_E, from Eqn.(4.2).

Step 9: Compute a new value for W_{TO} with Eqn.(4.1),

but: 1. use for W_E the value obtained in Step 8.

2. use for W_F a value obtained from Eqn.(2.15) in Part I. This implies that the mission fuel needed must be adjusted for the new value of W_{TO}. The result is:

$$W_{TO} = \qquad (4.3)$$

$$= (W_E + W_{PL} + W_{crew})/\{M_{ff}(1 + M_{res}) - M_{res} - M_{tfo}\}$$

Values for M_{ff}, M_{res} and M_{tfo} were already obtained during the preliminary sizing work described in Chapter 2 of Part I. These fractions may have changed if, during the Class I drag polar analysis of Chapter 12, Part II a significant change in L/D was discovered. In that case it was recommended in Step 14, Part II (p.16-17) to redo the preliminary sizing. This in turn would result in new values for the fractions in Eqn.(4.3).

Step 10: Use this new estimate for W_{TO} to iterate back through Steps 7-9 until the W_{TO} values agree within 0.5 percent.

Notes:

1. If the new value of W_{TO} obtained in Step 9 differs from the original one by more than 5 percent it will be necessary to account for the effect on required engine thrust (or power) at take-off. This in turn will affect the engine weight.

2. Accounting for a change in required take-off thrust (or power) may be done by using the ratio $(T/W)_{TO}$ (or $(W/P)_{TO}$ obtained from the preliminary sizing process of Chapter 3, Part I.

Step 11: Document all calculations including all assumptions made, all decisions made and all interpretations made in a brief, descriptive report. Where needed, include clearly drawn sketches.

Include a final Class II weight statement, using the groupings suggested by Eqns.(4.2), (5.1), (6.1) and (7.1).

4.2 METHODS FOR CONSTRUCTING V-n DIAGRAMS

In this section a step-by-step procedure is presented for constructing V-n diagrams for the following types of airplanes:

4.2.1 FAR 23 Certified Airplanes
4.2.2 FAR 25 Certified Airplanes
4.2.3 Military Airplanes

Example applications for three airplanes are provided in sub-section 4.2.4.

The V-n diagrams are used to determine design limit and design ultimate load factors as well as the corresponding speeds to which airplane structures are designed. As will be seen in the Class II weight equations of Chapters 5-7, many require as input a design load factor and/or a design speed.

Important notes:

1. The V-n diagrams given here are simplified versions of those defined in Refs 15-17. They should be used only in conjunction with Class II weight estimation methods.

2. In the Class II method only flaps-up cases are considered.

4.2.1 V-n Diagram for FAR 23 Certified Airplanes

Reference 15, in Part 23.335 presents the V-n diagram shown in Figure 4.1. The following definitions apply to the various speeds given in the diagram:

Note: all speeds are normally given in KEAS.

V_S = +1g stall speed or the minimum speed at which the airplane is controllable

V_C = design cruising speed

V_D = design diving speed

V_A = design maneuvering speed

Determination of these speeds and determination of the critical points A, C, D, E, F and G in Figure 4.1 is discussed in sub-sub-sections 4.2.1.1 through 4.2.1.7.

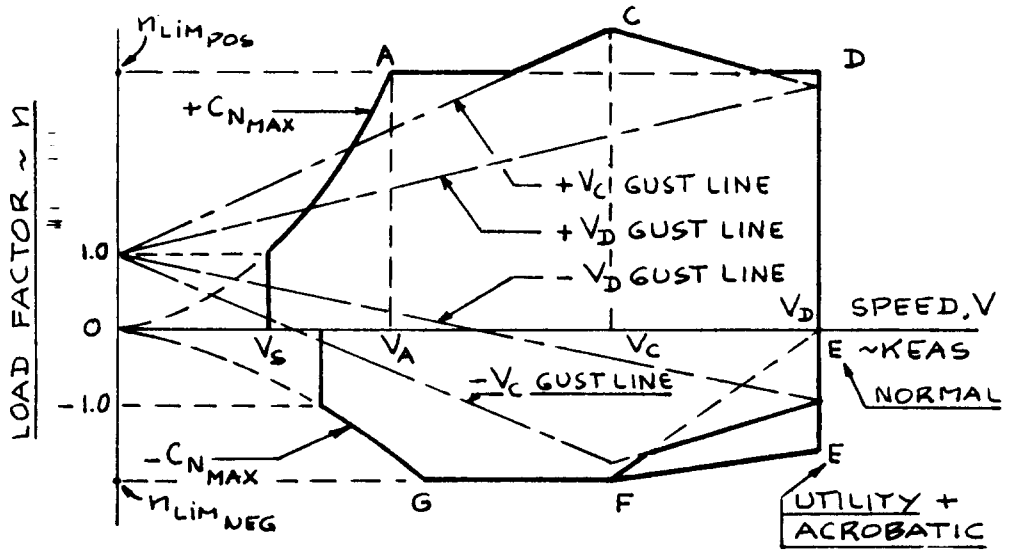

Figure 4.1 V-n Diagram According to FAR 23

4.2.1.1 Determination of +1g stall speed, V_S

$$V_S = \{2(GW/S)/\rho C_{N_{max}}\}^{1/2}, \qquad (4.4)$$

where: GW = flight design gross weight in lbs

S = wing area in ft^2

ρ = air density in $slugs/ft^3$

$C_{N_{max}}$ = maximum normal force coefficient.

The maximum normal force coefficient follows from:

$$C_{N_{max}} = \{(C_{L_{max}})^2 + (C_{D_{at\ C_{L_{max}}}})^2\}^{1/2} \qquad (4.5)$$

In preliminary design it is acceptable to set:

$$C_{N_{max}} = 1.1 C_{L_{max}} \qquad (4.6)$$

4.2.1.2 Determination of design cruising speed, V_C

$$V_C \geq k_c (GW/S)^{1/2}, \qquad (4.7)$$

where the constant k_c takes on the following values:

k_c = 33 for normal and utility category airplanes up to W/S = 20 psf.

k_c varies linearly from 33 to 28.6 as W/S varies from 20 to 100, for normal and utility category airplanes.

k_c = 36 for acrobatic category airplanes.

Note: V_C need not be more than $0.9V_H$, where V_H is the maximum level speed obtained with maximum power or with maximum thrust.

4.2.1.3 Determination of design diving speed, V_D

$$V_D \text{ (or } M_D) \geqslant 1.25V_C \text{ (or } 1.25M_C), \tag{4.8}$$

where: V_C follows from Eqn.(4.7).

4.2.1.4 Determination of design maneuvering speed, V_A

$$V_A \geqslant V_S n_{lim}^{1/2}, \tag{4.9}$$

where: n_{lim} is the limit maneuvering load factor given by Eqn.(4.13).

Note: V_A need not exceed V_C

4.2.1.5 Determination of negative stall speed line

$$V_{S_{neg}} = \{2(GW/S)/\rho C_{N_{max_{neg}}}\}^{1/2}, \tag{4.10}$$

where $C_{N_{max_{neg}}}$ is given by:

$$C_{N_{max_{neg}}} = \{(C_{L_{max_{neg}}})^2 + (C_{D_{atC_{L_{max_{neg}}}}})^2\}^{1/2} \tag{4.11}$$

In preliminary design it is acceptable to use:

$$C_{N_{max_{neg}}} = 1.1C_{L_{max_{neg}}} \tag{4.12}$$

where: $C_{L_{max_{neg}}}$ is the maximum negative lift coefficient.

4.2.1.6 Determination of design limit load factor, n_{lim}

The positive, design limit load factor is given by:

$$n_{lim_{pos}} \geq 2.1 + \{24,000/(GW + 10,000) \quad (4.13)$$

Exceptions:

n_{lim} need not be greater than 3.8

$n_{lim} = 4.4$ for utility category airplanes

$n_{lim} = 6.0$ for acrobatic airplanes

The negative, design limit load factor is given by:

$$n_{lim_{neg}} \geq 0.4n_{lim} \text{ for normal and for utility category airplanes} \quad (4.14)$$

$$\geq 0.5n_{lim} \text{ for acrobatic airplanes} \quad (4.15)$$

4.2.1.7 Construction of gust load factor lines in Fig.4.1

The gust load factor lines in Figure 4.1 are defined by the following equation:

$$n_{lim} = 1 + (K_g U_{de} V C_{L_\alpha})/498(GW/S), \quad (4.16)$$

where: K_g is the gust alleviation factor given by:

$$K_g = 0.88\mu_g/(5.3 + \mu_g), \quad (4.17)$$

where:

$$\mu_g = 2(GW/S)/\rho \bar{c} g C_{L_\alpha} \quad (4.18)$$

The derived gust velocity, U_{de} is defined as follows:

For the V_C gust lines:

$U_{de} = 50$ fps between sealevel and 20,000 ft

$U_{de} = 66.67 - 0.000833h$ between 20,000 and 50,000 ft

For the V_D gust lines:

$U_{de} = 25$ fps between sealevel and 20,000 ft

$U_{de} = 33.34 - 0.000417h$ between 20,000 and 50,000 ft

4.2.2 V-n Diagram for FAR 25 Certified Airplanes

Reference 16, in Part 25.335 presents the two V-n diagrams shown in Figures 4.2a and 4.2b. The following definitions apply to the various speeds given in the diagrams:

Note: all speeds are normally given in KEAS.

V_{S_1} = +1-g stall speed or the minimum steady flight speed which can be obtained

V_C = design cruising speed

V_D = design diving speed

V_A = design maneuvering speed

V_B = design speed for maximum gust intensity

Determination of these speeds and determination of the critical points A, D, E, F, H, B', C', D', E', F' and G' is discussed in sub-sub-sections 4.2.2.1 through 4.2.2.8.

4.2.2.1 Determination of +1g stall speed, V_{S_1}

$$V_{S_1} = \{2(GW/S)/\rho C_{N_{max}}\}^{1/2}, \qquad (4.19)$$

where: GW = flight design gross weight in lbs

S = wing area in ft^2

ρ = air density in slugs/ft^3

$C_{N_{max}}$ = maximum normal force coefficient, as computed from Eqn. (4.5) or (4.6).

4.2.2.2 Determination of design cruising speed, V_C

V_C must be sufficiently greater than V_B to provide for inadvertent speed increases likely to occur as a result of severe atmospheric turbulence. For V_B, see sub-sub-section 4.2.2.5.

$$V_C \geqslant V_B + 43 \text{ kts} \qquad (4.20)$$

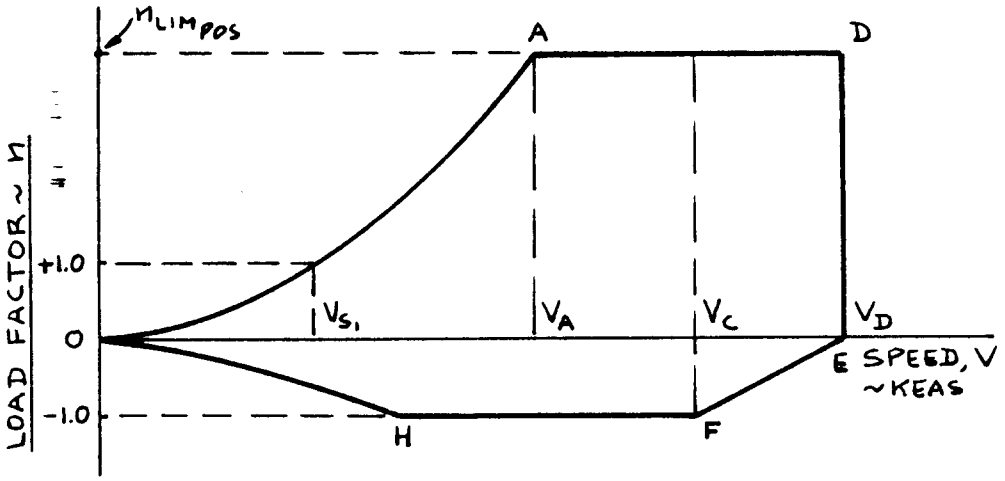

Figure 4.2a V-n Maneuver Diagram According to FAR 25

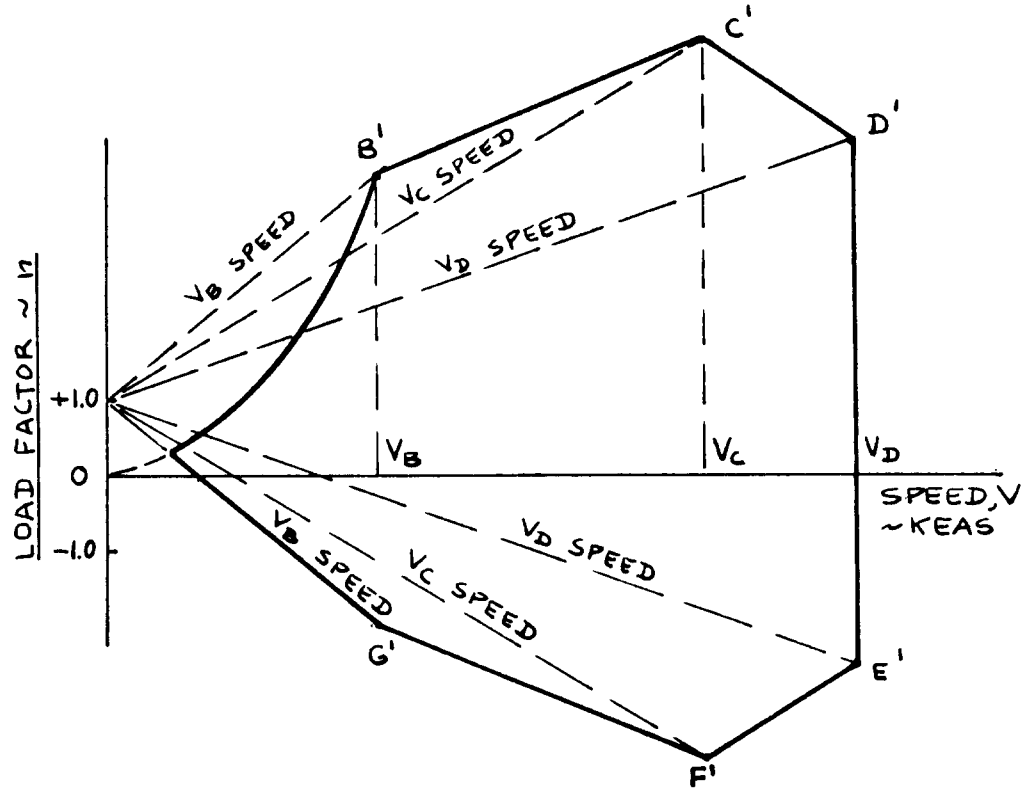

Figure 4.2b V-n Gust Diagram According to FAR25

4.2.2.3 Determination of design diving speed, V_D

$$V_D \text{ (or } M_D) \geqslant 1.25V_C \text{ (or } 1.25M_C) \qquad (4.21)$$

where: V_C follows from Eqn.(4.20).

4.2.2.4 Determination of design maneuvering speed, V_A

$$V_A \geqslant V_{S_1} n_{lim}^{1/2}, \qquad (4.22)$$

where: n_{lim} is the limit maneuvering load factor at V_C.

The limit maneuvering load factor in Eqn.(4.22) follows from 4.2.2.7 or from 4.2.2.8 depending on which is the more critical.

Note: V_A need not exceed V_C.

4.2.2.5 Determination of design speed for maximum gust intensity, V_B

V_B need not be greater than V_C.

V_B may not be less than the speed determined from the intersection of the $C_{N_{max}}$ line and the gustline marked V_B.

4.2.2.6 Determination of negative stall speed line

The negative stall speed line in Figure 4.2a is determined with the method of sub-sub-section 4.2.1.5.

4.2.2.7 Determination of design limit load factor, n_{lim}

The positive limit maneuvering load factor, $n_{lim_{pos}}$ is determined from:

$$n_{lim_{pos}} \geqslant 2.1 + \{24,000/(W + 10,000)\} \qquad (4.23)$$

Exceptions:

$n_{lim_{pos}} \geqslant 2.5$ at all times

$n_{lim_{pos}}$ need not be greater than 3.8 at W_{TO}

The negative, design limit load factor is determined from:

$n_{lim_{neg}} \geq -1.0$ up to V_C

$n_{lim_{neg}}$ varies linearly from the value at V_C to zero at V_D

4.2.2.8 Construction of gust load factor lines in Fig.4.2b

The gust load factor lines in Figure 4.2b are arrived at with the help of Eqns.(4.16) through (4.18). The derived gust velocities, U_{de} in FAR 25 are as follows:

For the gust line marked V_B:

U_{de} = 66 fps between sealevel and 20,000 ft

U_{de} = 47.33 - 0.000933h between 20,000 and 50,000 ft

For the gust line marked V_C:

U_{de} = 50 fps between sealevel and 20,000 ft

U_{de} = 66.67 - 0.000833h between 20,000 and 50,000 ft

For the gust line marked V_D:

U_{de} = 25 fps between sealevel and 20,000 ft

U_{de} = 16.67 - 0.000417h between 20,000 and 50,000 ft

4.2.3 V-n Diagram for Military Airplanes

Reference 17, provides the V-n diagram given in Figure 4.3. The indicated limit load factors must not be less than those defined in Table 4.1.

The speeds in Figure 4.3 are normally given in KEAS and are defined as follows:

V_H = maximum level speed which can be attained at the combination of weight and altitude under consideration

V_L = maximum dive speed, typically $1.25V_H$

Gust lines are as in FAR 25. Gust induced load factors are normally not critical for military airplanes with limit load factors above 3.00.

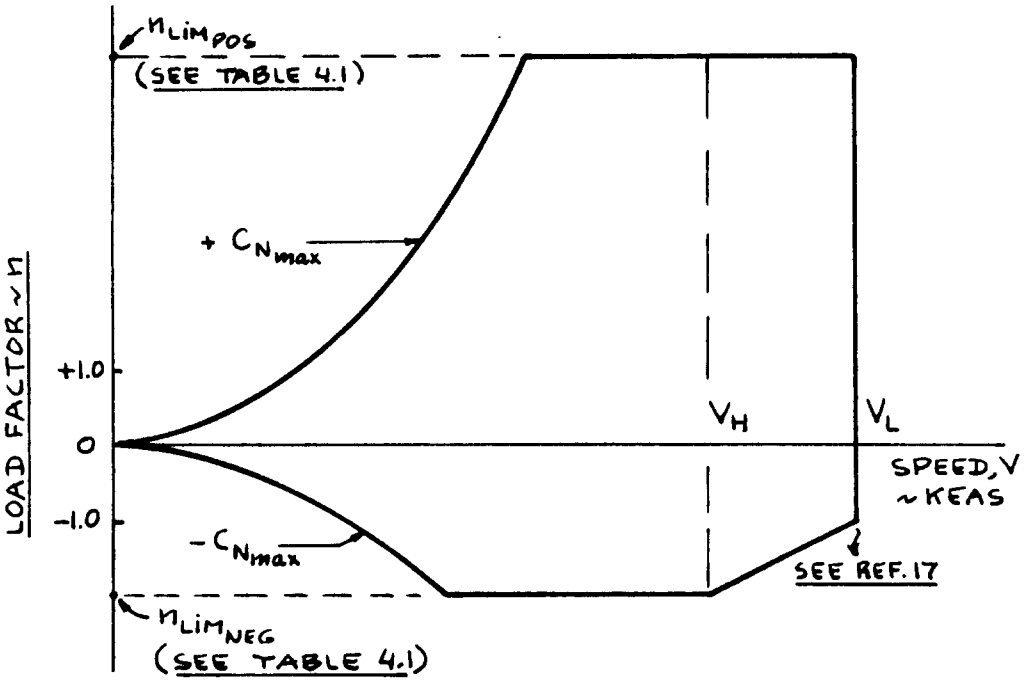

Figure 4.3 V-n Diagram According to MIL-A 8861(ASG)

Table 4.1 Limit Load Factors for Military Airplanes

Airplane Type		Limit Load Factor, n_{lim} at Flight Design Gross Weight, GW	
USAF	USN	Positive	Negative
Fighter		8.67	-3.00
Attack	Fighter, Attack, Trainer	7.33	-3.00
	Observation	6.00	-3.00
Trainer		5.67	-2.33
Utility	Utility	4.00	-2.00
Small Bomber		3.67	-1.67
Medium Bomber, Assault Transp.	Patrol, Weather, Anti-submarine, Reconnaissance	3.00	-1.00
Medium Transp.		2.50	-1.00
Heavy Bomber, Heavy Transp.		2.00	-1.00

4.2.4 Example Applications

The following example applications will be discussed:

4.2.4.1 Twin Engine Propeller Driven Airplane: Selene
4.2.4.2 Jet Transport: Ourania
4.2.4.3 Fighter:Eris

4.2.4.1 Twin Engine Propeller Driven Airplane

According to the mission specification (Table 2.17, Part I) this is a FAR 23 airplane. It will be assumed that under FAR 23 it will be certified under the normal category.

Determination of V_S:

Since $C_{L_{max}} = 1.7$ (Part I, p.178), it follows from Eqn.(4.6) that: $C_{N_{max}} = 1.1 \times 1.7 = 1.87$.

Since $(W/S)_{TO} = 46$ psf (Part I, p.178), the value for stall speed as found from Eqn.(4.4) is:

$$V_S = \{2 \times 46 / 0.002378 \times 1.87\}^{1/2} = 144 \text{ fps} = 85 \text{ kts.}$$

Determination of V_C

The design wing loading for the Selene is 46 psf. This yields $k_c = 31.6$. With Eqn.(4.7) this in turn gives $V_C \geqslant 214$ kts.

The Selene was to have a cruise speed of 250 kts at 75 percent power at 10,000 ft (Part I, Table 2.17). For 100 percent power this would yield a maximum cruise speed which is a factor $(100/75)^{1/3} = 1.1$ higher, or 275 kts. According to sub-sub-section 4.2.1.2, V_C need not be higher than $0.9 \times 275 = 248$ kts.

Thus: $V_C = 248$ kts.

Determination of V_D

According to sub-sub-section 4.2.1.3, the design dive speed is: $V_D = 1.25 \times 248 = 310$ kts.

Determination of n_{lim}

The positive limit load factor of the Selene as given by Eqn.(4.13) is:

$$n_{lim_{pos}} \geq 2.1 + \{24,000/(7,900 + 10,000)\} = 3.44$$

The negative limit load factor as given by Eqn.(4.14) is:

$$n_{lim_{neg}} = 0.4 \times 3.44 = 1.38$$

Determination of Gust Load Factor Lines, V_C and V_D

The overall airplane liftcurve slope, C_{L_α} can be shown to be 0.095 deg^{-1} = 5.44 rad^{-1}. With $\bar{c}$ = 4.92 ft (Table 13.1, Part II), the value of μ_g is: 44.8, according to Eqn.(4.18).

The gust alleviation factor follows from Eqn.(4.17) as:

$$K_g = 0.88 \times 44.8/(5.3 + 44.8) = 0.787$$

The gust load factor lines now follow from Eqn.(4.16) as:

$n_{lim_{gust}}$ = 1 + 0.0094V for the V_C line and:

$n_{lim_{gust}}$ = 1 + 0.0047V for the V_D line.

Determination of V_A

From Eqn.(4.9): V_A $85 \times (3.44)^{1/2}$ = 158 kts.

Determination of Negative Stall Line

It will be assumed that $C_{L_{max_{neg}}} = -1.18$. This yields $C_{N_{max_{neg}}} = -1.3$. Using Eqn.4.4 it is found that the negative 1g stall speed is 102 kts.

With these data it is now possible to draw the V-n diagram for the Selene. The result is shown in Fig.4.4.

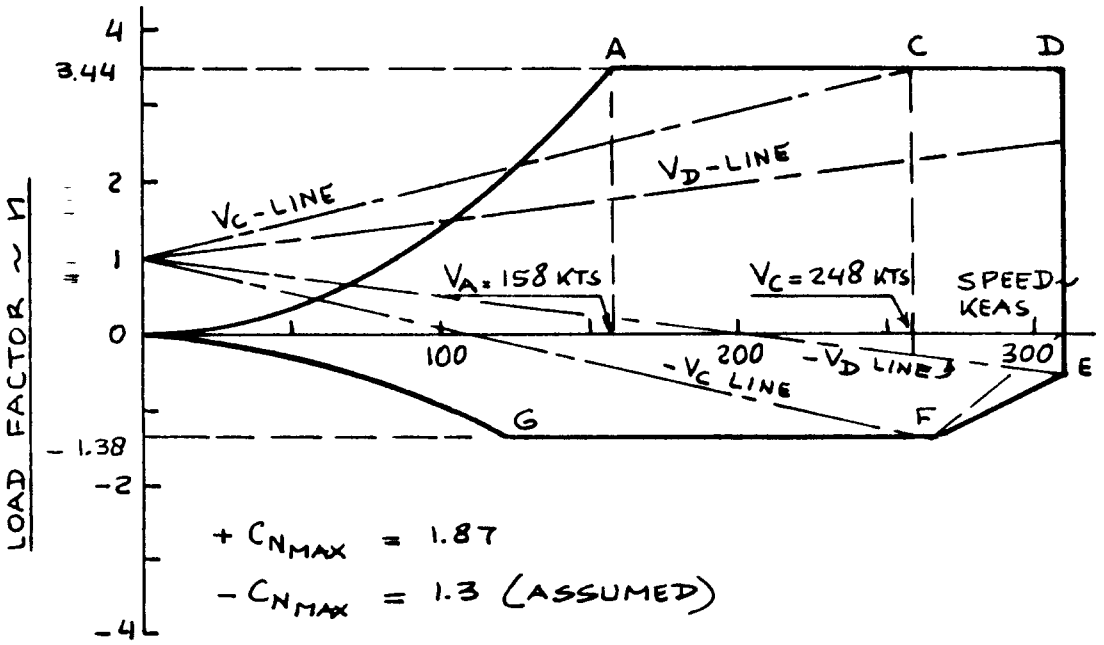

Figure 4.4 Example V-n Diagram for the Selene

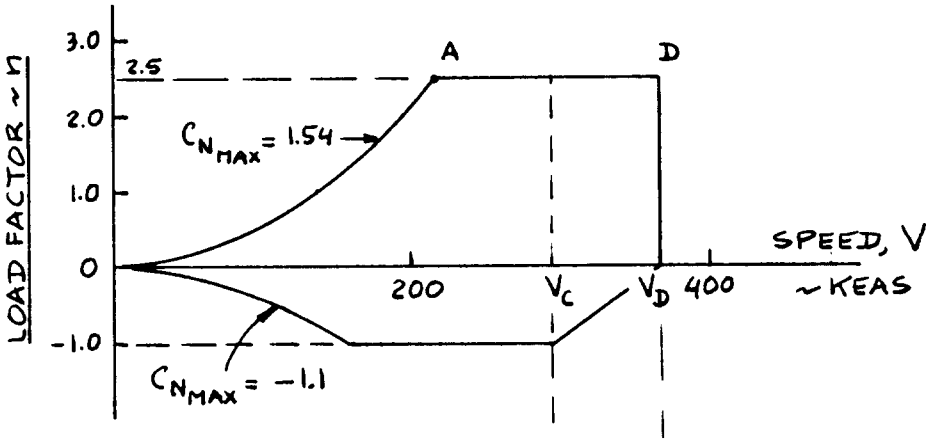

Figure 4.5a Example V-n Maneuver Diagram for the Ourania

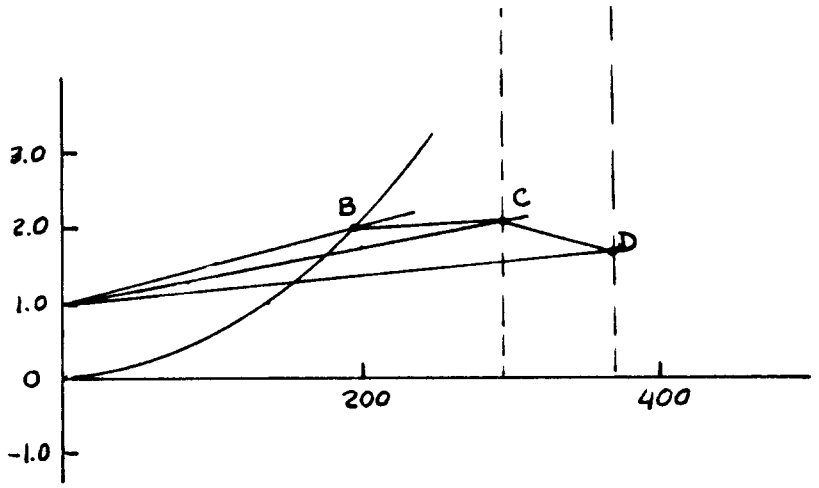

Figure 4.5b Example V-n Gust Diagram for the Ourania

4.2.4.2 Jet Transport

According to the mission specification (Table 2.18, Part I) this is a FAR 25 airplane.

Determination of V_{S_1}:

Since $C_{L_{max}}$ = 1.4 (Part I, p.184), it follows from Eqn.(4.6) that: $C_{N_{max}}$ = 1.1x1.4 = 1.54.

Since $(W/S)_{TO}$ = 98 psf (Part I, p.184), the value for stall speed as found from Eqn.(4.4) is:

$V_S = \{2x98/0.002378x1.54\}^{1/2}$ = 231 fps = 137 kts.

Determination of V_A

V_A follows from the intersection of the +1g stall line and the +2.50 load factor line: V_A = 195 kts.

Determination of V_B

V_B follows from the intersect of the +1g stall line and the V_B gust line. This intersect will be determined upon calculation of the V_B gust line.

Determination of V_C

According to Eqn.(4.20): V_C V_B + 43 kts.

Therefore: V_C 195 + 43 = 238 kts. However, the mission specification of Table 2.18 (Part I) calls for a cruise speed of M = 0.82 at 35,000 ft. This corresponds to 483 kts at 35,000 ft or a dynamic pressure of 296 psf. At sealevel, the corresponding value in KEAS is 295 kts. Since this is larger 238 kts, V_C = 295 kts.

Determination of V_D

According to sub-sub-section 4.2.2.3, the design dive speed is: $V_D = 1.25xV_C = 1.25x295$ = 369 kts.

Determination of n_{lim}

The positive limit load factor of the Ourania as

given by Eqn.(4.23) is:

$$n_{lim_{pos}} = 2.1 + \{24,000/(127,000 + 10,000)\} = 2.28$$

The exceptions in sub-sub-section 4.2.2.7 demand that this load factor never be less than 2.5. Therefore:

$$n_{lim_{pos}} = 2.5$$

The negative limit load factor is -1 up to V_C and varies linearly to zero at V_D.

Determination of Gust Load Factor Lines, V_B, V_C and V_D

The overall airplane liftcurve slope, C_{L_α} can be shown to be 0.085 deg^{-1} = 4.87 rad^{-1}. With $\bar{c}$ = 12.5 ft (Table 13.2, Part II), the value of μ_g is: 42.0, according to Eqn.(4.18).

The gust alleviation factor follows from Eqn.(4.17) as:

$$K_g = 0.88x42.0/(5.3 + 42.0) = 0.781$$

The gust load factor lines now follow from Eqn.(4.16) as:

$n_{lim_{gust}}$ = 1 + 0.0051V for the V_B line,

$n_{lim_{gust}}$ = 1 + 0.0039V for the V_C line and:

$n_{lim_{gust}}$ = 1 + 0.0019V for the V_D line.

Determination of V_B

From the intersection of the +1g stall line with the V_B gust line it follows that V_B = 195 kts.

Determination of Negative Stall Line

It will be assumed that $C_{L_{max_{neg}}} = -1.00$. This yields $C_{N_{max_{neg}}} = -1.1$. Using Eqn.4.4 it is found that the negative 1g stall speed is 162 kts.

With these data it is now possible to draw the V-n diagram for the Selene. The result is shown in Figures 4.5a and 4.5b.

4.2.4.3 Fighter

According to the mission specification (Table 2.19, Part I) the Selene is an attack fighter. From Table 4.1 it follows that $n_{lim_{pos}} = 7.33$ and $n_{lim_{neg}} = -3.0$.

The maximum level speed at sealevel is $V_H = 450$ kts.

The design dive speed, $V_L = 1.25 \times 450 = 563$ kts.

The gust lines are far within the maneuvering V-n diagram and are not computed for this airplane. Fig.4.6 presents the V-n diagram for the Eris.

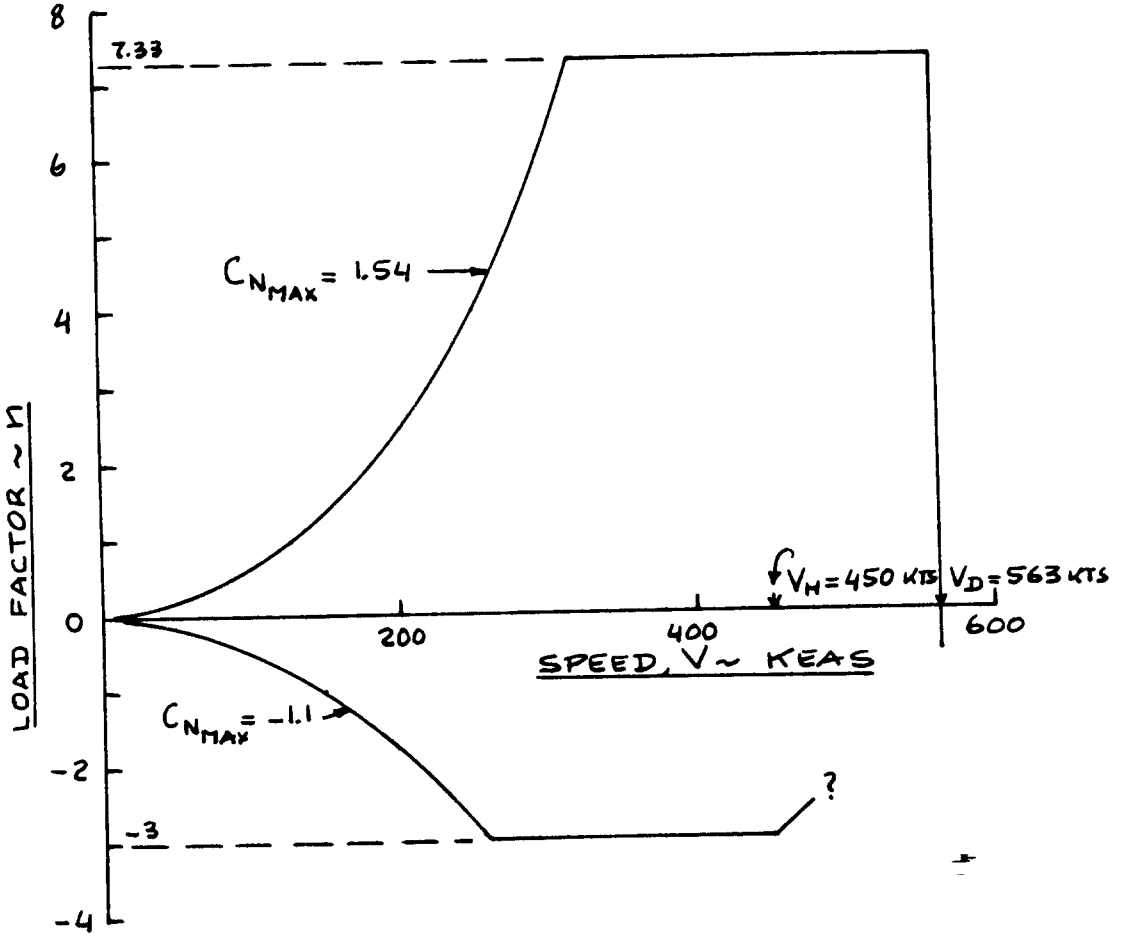

Figure 4.6 Example V-n Diagram for the Eris

4.3 EXAMPLE APPLICATIONS FOR CLASS II WEIGHT ESTIMATES

In this section, three example applications of the Class II weight estimation method described in Section 4.1 are discussed:

4.3.1 Twin Engine Propeller Driven Airplane: Selene
4.3.2 Jet Transport: Ourania
4.3.3 Fighter: Eris

4.3.1 Twin Engine Propeller Driven Airplane

Step 1: The following weight items are already known:

From Table 10.4, Part II:

Payload: W_{PL} = 1,250 lbs

Fuel: W_F = 1,706 lbs

TFO: W_{tfo} = 44 lbs

From Part II, p.135:

Engine dry weight: W_e = 1,400 lbs

Step 2: Weights need to be estimated for the following items:

Structural Weight, W_{struct}:

1) Wing 2) Adjustment for Fowler flaps 3) Empennage

4) Fuselage 5) Nacelles 6) Landing Gear

Powerplant Weight, W_{pwr}:

1) Engines 2) Air induction system 3) Propellers

4) Fuel System 5) Propulsion installation

Fixed Equipment Weight, W_{feq}:

1) Flight controls 2) Electrical system

3) Instrumentation, avionics and electronics

4) Air-conditioning and de-icing 5) Oxygen

6) Furnishings 7) Paint

Step 3: The structural arrangement drawing for the Selene is presented in Chapter 8 of Part III.

Step 4: From a weight estimating viewpoint this airplane falls in the General Aviation Airplane category.

Step 5: The following weight equations apply to the Selene:

W_{struct}: 1) Wing: Eqns (5.4) and (5.5)

2) Adjustment for Fowler flaps: an extra factor of 2 percent will be added in accordance with 5.2.2.2.

3) Empennage: Eqns (5.14) - (5.16)

4) Fuselage: Eqns (5.25) and (5.27)

5) Nacelles: Eqn. (5.33)

6) Landing Gear: Eqns (5.40) and (5.42)

W_{pwr}: 1) Engines: see Step 1.

2) Air induction system: Eqn.(6.8)

3) Propellers: Eqns (6.13) and (6.14)

4) Fuel System: Eqns (6.17) and (6.18)

5) Propulsion system: Eqns (6.3) and (6.4)

W_{feq}: 1) Flight control system: Eqns (7.1), (7.2) and (7.4).
Note: hydraulics and pneumatics are included in item 1).

2) Electrical system: Eqns (7.12) - (7.14)

3) Instrumentation, avionics and electronics: Eqn.(7.21)

4) Air-conditioning + de-icing: Eqn.(7.28)

5) Oxygen system: Eqn.(7.35)

6) Furnishings: Eqns (7.41) and (7.43)

7) Paint: Table A3.2a

Step 6: The following list itemizes all required input data for estimating the weight items listed in steps 2 and 5.

W_{TO} 7,900 lbs n_{lim} = 3.44 S = 172 ft^2

V_C = 248 kts V_D = 310 kts n_{ult} = 5.16

A = 8 λ = 0.4 $\Lambda_{1/4}$ = 0 deg.

$(t/c)_m$ = 0.17 b = 37.1 ft t_r = 1.13 ft

S_h = 58 ft^2 b_h = 14.9 ft t_{r_h} = 0.53 ft

l_h = 24.3 ft

S_v = 38 ft^2 b_v = 6.16 ft t_{r_v} = 0.66 ft

l_f = 39.3 ft w_f = 4.5 ft h_f = 5.5 ft

K_f = 1.08 P_{TO} = 850 hp l_{s_m} = 6.00 ft

W_L = 7,505 lbs $n_{ult.l.}$ = 4.0

K_{prop1} = 31.92 N_p = 2 N_{bl} = 3

D_p = 7.8 ft

Notes: 1) The value for n_{lim} follows from the V-n diagram of Figure 4.4.

2) Most data were obtained from Selene data listed in Part II. The reader is reminded that a detailed geometric definition may be found in Part II as Table 13.1, a Class I weight statement as Table 10.4. Detailed definitions of fuselage, wing, tails, landing gear and powerplant may be found in Chapters 4,5,6,7,8 and 9 respectively in Part II.

Step 7: Table 4.1 lists all weights computed as part of the Class II weight estimation process. Observe that the Class I weight estimates (computed from weight fractions) are averaged into the new weight calculations to form the Class II weight estimate.

Step 8: The Class II empty weight of the Selene is 5,122 lbs. This compares with 4,900 lbs for the Class I weight estimate. This represents a difference of 222 lbs which is 4.5 percent of the Class I empty weight.

Several comments are in order:

1. an iteration through the equations of Step 7 should be performed, to determine the 'convergence' empty weight.

2. several weight savings can be made in the Selene:

a) by manufacturing the propellers out of composites, their weight can probably be cut by 40 percent for a weight saving of 93 lbs.

b) the empennage can be manufactured from composites which would yield a weight saving of about 15 percent, or 24 lbs.

c) the nacelles can be manufactured partially from composites which would yield a weight saving of about 10 percent, or 26 lbs.

d) by manufacturing the low stress areas of the wing and fuselage from composites, a weight saving of about 5 percent should be feasible. This would save 72 lbs.

e) combining a) through d) yields a saving of 215 lbs. It therefore appears quite possible to bring the overall Selene take-off weight in at the original estimate of 7,900 lbs.

Steps 9 and 10: Not needed, see item e), Step 8.

Step 11: To save space, this step has been omitted.

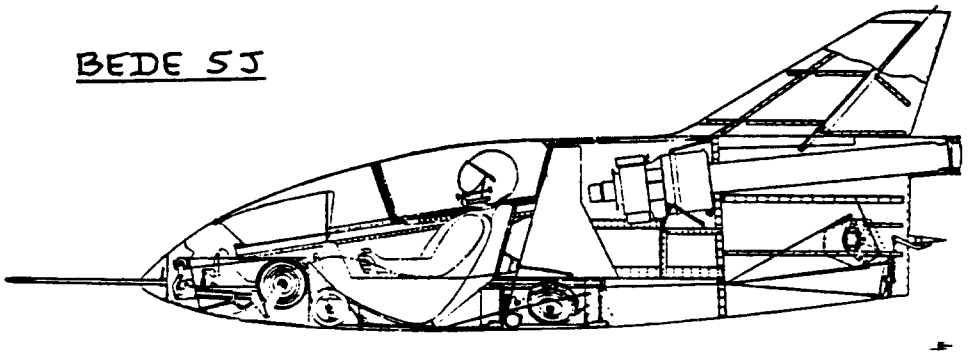

Table 4.1a Class II Weight Estimates for the Selene

Component	Methods: Class I Page 9	USAF	Torenbeek	Use as Class II Estimate
Structure weight, W_{struct}:				
Wing	738	580	410	576
Adjustment for Fowler flaps, 2 percent:				12
Empennage	179	149	155	161
Fuselage	621	830	1,130	860
Nacelles	249	N.A.	272	261
Landing gear	380	196	313	296
W_{struct}	2,167	1,755 excl.nac.	2,280	2,166
Powerplant weight, W_{pwr}:				
Engines	1,400	1,400	1,400	1,400
Air induction	in pwrplt		88	88
Propellers	200	250	250	233
Fuel system	in pwrplt	157	135	146
$W_{pwr}-W_{fs}$		2,162*	2,165**	
Powerplant inst.	108			108
W_{pwr}	1,708	2,319	2,300	1,975

* includes engine and propeller weight, Eqn.(6.3)

**includes engine and propeller weight, Eqn.(6.4)

Table 4.1b Class II Weight Estimates for the Selene

Component	Methods: Class I Page 9	Cessna	USAF	T'beek	Use as Class II Estimate
Fixed equipment weight, W_{feq}:					
W_{fc}		133	294	91	173
W_{hps}: this is included in W_{fc}					
W_{els}		212	210	209	210
W_{iae}				103	103
W_{api}				88	88
W_{ox}			GD: 25		25
W_{fur}		258		410	334
W_{pt}				Table A3.2a:	48
W_{feq}	1,025	not complete			981

Summary:

Class II empty weight, W_E follows from Eqn.(2.1):

$$W_E = 2,166 + 1,975 + 981 = 5,122 \text{ lbs}$$

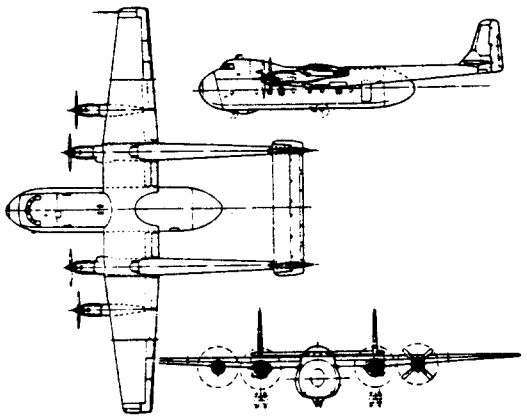

ARMSTRONG WHITWORTH
ARGOSY 222

4.3.2 Jet Transport

Step 1: The following weight items are already known:

From Table 10.5, Part II:

Payload weight: W_{PL} = 30,750 lbs

Crew weight: W_{crew} = 1,025 lbs

Fuel weight: W_F = 25,850 lbs

Trapped fuel and oil: W_{tfo} = 925 lbs

From Part II, p.138:

Engine dry wht: W_e = 9,224 lbs

Step 2: Weights need to be estimated for the following items:

Structural Weight, W_{struct}:

1) Wing 2) Adjustment for Fowler flaps 3) Empennage 4) Fuselage 5) Nacelles 6) Landing Gear

Powerplant Weight, W_{pwr}:

1) Engines 2) Fuel system 3) Propulsion system 4) Accessory drives, starting and ignition system 5) Thrust reversers

Fixed Equipment Weight, W_{feq}:

1) Flight controls 2) Electrical system 3) Instrumentation, avionics and electronics 4) Air-conditioning, pressurization and de-icing 5) Oxygen 6) APU 7) Furnishings 8) Baggage and cargo handling 9) Operational items 10) Paint

Step 3: The structural arrangement drawing for the Ourania is presented in Chapter 8 of Part III.

Step 4: From a weight estimating viewpoint this airplane falls in the Commercial Transport category.

Step 5: The following weight equations apply to the Ourania:

W_{struct}: 1) Wing: Eqns (5.6) and (5.7)

2) Adjustment for Fowler flaps: an extra factor of 2 percent will be added in accordance with 5.2.2.2.

3) Empennage: Eqns (5.17), (5.18), (5.20)

4) Fuselage: Eqns (5.26) and (5.27)

5) Nacelles: Eqns (5.35) and (5.37)

6) Landing Gear: Eqns (5.41) and (5.42)

W_{pwr}: 1) Engines: see Step 1.

2) Fuel system: Eqn. (6.24)

3) Propulsion system: Eqns (6.24), (6.29)

4) Accessory drives, starting and ignition system: Eqn. (6.34)

5) Thrust reversers: Eqn. (6.36)

W_{feq}: 1) Flight control system: Eqns (7.5), (7.6)

Note: hydraulics and pneumatics are included in item 1).

2) Electrical system: Eqns (7.15), (7.17)

3) Instrumentation, avionics and electronics: Eqns (7.23) and (7.25)

4) Air-conditioning, pressurization and de-icing: Eqns (7.29) and (7.30)

5) Oxygen system: Eqns (7.35) and (7.37)

6) APU: Eqn.(7.40)

7) Furnishings: Eqns (7.44) and (7.45)

8) Baggage and cargo handling: Eqn.(7.48)

9) Operational items: See Section 7.10.

10) Paint: See Section 7.15.

Step 6: The following list itemizes all required input data for estimating the weight items listed in steps 2 and 5.

W_{TO} 127,000 lbs n_{ult} = 2.5 S = 1,296 ft^2

V_C = 295 kts V_D = 369 kts n_{ult} = 3.75

A = 10 λ = 0.32 $\Lambda_{1/4}$ = 35 deg.

$\Lambda_{1/2}$ = 33.5 deg M_H = 0.85

$(t/c)_m$ = 0.13 b = 113.8 ft t_r = 2.26 ft

S_h = 254 ft^2 b_h = 35.6 ft t_{r_h} = 1.30 ft

$\bar{c}$ = 12.5 ft l_h = 32.5 ft

S_v = 200 ft^2 z_h/b_v = 0 l_v = 35.8 ft

S_r/S_v = 0.45 λ_v = 0.32 A_v = 1.8

$\Lambda_{1/4}$ = 45 deg.

l_f = 124.3 ft $w_f + h_f$ = 26.4 ft $\bar{q}_D$ = 461 psf

W_L = 7,505 lbs $n_{ult.l.}$ = 4.0 d_f = 13.2 ft

P_2 = 20 psi l_n = 11.7 ft A_{inl} = 28.3 ft^2

D_{inl} = 6.0 ft

Notes: 1) The value for n_{lim} follows from the V-n diagram of Figure 4.5.

2) Most data were obtained from Ourania data listed in Part II. The reader is reminded that a detailed geometric definition may be found in Part II as Table 13.2, a Class I weight statement as Table 10.5. Detailed definitions of layouts of fuselage, powerplant, wing, high lift system, empennage and landing gear may be found in Chapters 4,5,6,7,8 and 9 respectively.

Step 7: Tables 4.2a - 4.2c list all weights computed as part of the Class II weight estimation process.

Step 8: The Class II empty weight of the Ourania is 72,622 lbs. This compares with 68,450 lbs for the Class I weight estimate. This represents a difference of 4,172 lbs which is 6.1 percent of the Class I empty weight.

Several comments are in order:

1. an iteration through the equations of Step 7 should be performed, to determine the 'convergence' empty weight.

2. several weight savings can be made in the Ourania:

a) the empennage can be manufactured from composites which would yield a weight saving of about 15 percent, or 359 lbs.

b) the nacelles can be manufactured partially from composites which would yield a weight saving of about 10 percent, or 264 lbs.

c) by manufacturing the low stress areas of the wing and fuselage from composites, a weight saving of about 5 percent should be feasible. This would save 1,388 lbs.

d) by using a quadruplex digital flight control system and using fly-by-wire instead of mechanical flight controls, a weight saving of 15 percent over the estimated weight can be obtained. This would save 352 lbs.

e) by using lithium aluminum in the primary wing and fuselage structure, a weight saving of 6 percent is feasible. This saves 1,665 lbs.

By combining a) through e) a total weight saving of 4,028 lbs can be achieved. This is close to the discrepancy of 4,172 lbs. It is therefore judged possible to bring the Ourania in at the originally estimated empty weight of 68,450 lbs.

Steps 9-10: Not needed, see item e), Step 8.

Step 11: This step has been omitted to save space.

Table 4.2a Class II Weight Estimates for the Ourania

Component	Methods: Class I Page 11	GD	Torenbeek	Use as Class II Estimate
Structure weight, W_{struct}:				
Wing	13,664	11,753	15,973	13,797
Adjustment for Fowler flaps, 2 percent:				276
Horiz.Tail		949	1,218	1,319
Vert.Tail		920	829	1,071
Empennage	3,253	1,869	2,047	2,390
Fuselage	14,184	15,748	11,140	13,691
Nacelles	2,082	2,722	3,120	2,641
Nose Gear	573		783	716
Main Gear	4,632		4,208	3,904
Landing gear	5,205	3,663	4,991	4,620
W_{struct}	38,388			37,415
Powerplant weight, W_{pwr}:				
Engines	9,224	9,224	9,224	9,224
Fuel system	in pwrplt		1,009	1,009
Propulsion inst.	667	439		700
Acc.dr, Start, Ign			960	
Thrust reversers			1,660	1,660
W_{pwr}	9,891			12,593

Table 4.2b Class II Weight Estimates for the Ourania:
Average Weight Fractions for Fixed Equipment Breakdown

Note: these data were used in Table 4.2c.

Component	Similar Airplane Type: McDD DC-9-30	MD-80	Boeing 737-200	727-100	Use as Class II Estimate
Fixed equipment weight item:					
W_{fc}*	0.0220	0.0241	0.0279	0.0276	0.0254
W_{els}	0.0123	0.0123	0.0092	0.0134	0.0118
W_{iae}	0.0134	0.0152	0.0137	0.0147	0.0143
W_{api}	0.0148	0.0152	0.0123	0.0124	0.0137
W_{ox}	0.0014	0.0016			0.0015
W_{apu}	0.0076	0.0060	0.0072		0.0069
W_{fur}	0.0782	0.0814	0.0575	0.0641	0.0703
W_{ops}	0.0250	0.0261			0.0256
W_{pt} typical US airline paint scheme:					0.0035

* includes hydraulic and pneumatic system

Note: Specific airplane type data from Tables A7.1a and A7.2a in Appendix A.

Table 4.2c Class II Weight Estimates for the Ourania

Component	Methods: Table 4.2b x127,000	GD	Torenbeek	Use as Class II Estimate
Fixed equipment weight, W_{feq}:				
W_{fc}	3,226	2,200	1,617	2,348
W_{hps}: this is included in W_{fc}				
W_{els}	1,499	1,887	4,063	2,483
W_{iae}	1,810	1,593	1,775	1,726
W_{api}	1,737	4,251	2,166	2,718
W_{ox}	191	241	210	214
W_{apu}	881	1,016	1,016	982
W_{fur}	8,928	7,467	7,565	7,987
W_{bc}		466	466	466
W_{ops}	3,245		3,245	3,245
W_{pt}			Table 4.2b:	445
W_{feq}	21,517	19,121	22,123	22,614

Summary:

Class II empty weight, W_E follows from Eqn.(2.1):

$$W_E = 37,415 + 12,593 + 22,614 = 72,622 \text{ lbs}$$

4.3.3 Fighter

Step 1: The following weight items are already known:

From Table 10.6, Part II:

Payload weight: W_{PL} = 12,405 lbs

Crew weight: W_{crew} = 200 lbs

Fuel weight: W_F = 18,500 lbs

Trapped fuel and oil: W_{tfo} = 300 lbs

From Part II, p.140:

Engines, incl A/B: W_e = 6,000 lbs

Step 2: Weights need to be estimated for the following items:

Structural Weight, W_{struct}:

1) Wing 2) Adjustment for Fowler flaps 3) Empennage

4) Fuselage 5) Tailbooms 6) Engine section

7) Landing Gear

Powerplant Weight, W_{pwr}:

1) Engines 2) Afterburners 3) Air induction system

4) Fuel system 5) Propulsion system

Fixed Equipment Weight, W_{feq}:

1) Flight controls 2) Electrical system

3) Instrumentation, avionics and electronics

4) Air-conditioning, pressurization and de-icing

5) Armament 6) Furnishings 7) Oxygen system

8)Auxiliary gear 9) GAU-8A Gun

Step 3: The structural arrangement drawing for the Eris is presented in Chapter 8 of Part III.

Step 4: From a weight estimating viewpoint this airplane falls in the Fighter and Attack Airplane category.

Step 5: The following weight equations apply to the Eris:

W_{struct}: 1) Wing: Eqn. (5.9)

2) Adjustment for Fowler flaps: an extra factor of 2 percent will be added in accordance with 5.2.2.2.

3) Empennage: Eqns (5.17) and (5.18)

4) Fuselage: Eqn. (5.26)

5) Tailbooms: Eqn. (5.27)

6) Engine section: See Class I, p.14

7) Landing Gear: Eqns (5.41) and (5.42)

W_{pwr}: 1) Engines: see Step 1.

2) Air induction system: Eqn. (6.9)

3) Fuel system: Eqn. (6.20)

4) Propulsion system: Eqns (6.23), (6.27)

W_{feq}: The data of Table 4.3b are used, in addition to the following equations:

1) Flight control system: Eqn. (7.11)

Note: hydraulics and pneumatics are included in item 1).

2) Electrical system: Eqn. (7.19)

3) Instrumentation, avionics and electronics: Eqn. (7.25)

4) Air-conditioning, pressurization and de-icing: Eqn. (7.33)

5) Armament: Table 4.4b

6) Furnishings: Eqn. (7.47)

7) Oxygen system: Eqn. (7.39)

8) Auxiliary gear: Table 4.4b

9) GAU-8A Gun: See Part III under weapons

Step 6: The following list itemizes all required input data for estimating the weight items listed in steps 2 and 5.

$GW = 61,660$ lbs $\quad n_{ult} = 11.0 \quad S = 787$ ft^2

$V_D = 563$ kts $\quad \bar{q}_D = 1,072$ psf $\quad n_{ult} = 7.33$

$A = 6 \quad K_w = 1.0 \quad \lambda = 0.50 \quad \Lambda_{LE} = 3.5$ deg.

$(t/c)_m = 0.10 \quad M_H = 0.68 \quad \bar{c} = 11.9$ ft

$S_h = 93$ ft^2 $\quad b_h = 18.3$ ft $\quad t_{r_h} = 0.51$ ft

$l_h = 32.3$ ft

$S_v = 147^*$ ft^2 $\quad z_h/b_v = 1.0 \quad l_v = 26.0$ ft

$S_r/S_v = 0.22 \quad \lambda_v = 0.55 \quad A_v = 1.2$

$\Lambda_{1/4} = 41$ deg. $\quad$ *This is for both vertical tails

$K_{inl} = 1.25$

$l_f = 41.3$ ft $\quad h_f = 6.83$ ft for the fuselage

$l_f = 33.3$ ft $\quad w_f + h_f = 3.06$ ft for the booms

$S_{fgs} = 2x30.6 = 61.2$ ft^2 for the booms

	A_g	B_g	C_g	D_g
Nose gear:	12	0.06	0	0
Main gear:	33	0.04	0.021	0

$N_{inl} = 2 \quad L_d = 8$ ft $\quad A_{inl} = 6.31$ ft^2

$P_2 = 30$ psi $\quad K_d = 1.0 \quad K_m = 1.0$

Notes: 1) The value for n_{lim} follows from the V-n diagram of Figure 4.6.

2) Most data were obtained from Eris data listed in Part II. The reader is reminded that a

detailed geometric definition may be found in Part II as Table 13.3, a Class I weight statement as Table 10.6. Detailed definitions of layouts of fuselage, powerplant, wing, high lift system, empennage and landing gear may be found in Chapters 4,5,6,7,8 and 9 respectively.

Step 7: Tables 4.3a, 4.3b and 4.3c list all weights computed as part of the Class II weight estimation process.

Step 8: The Class II empty weight of the Eris is 35,755 lbs. This compares with 33,500 lbs for the Class I weight estimate. This represents a difference of 2,255 lbs which is 6.7 percent of the Class I empty weight.

Several comments are in order:

1. an iteration through the equations of Step 7 should be performed, to determine the 'convergence' empty weight.

2. several weight savings can be made in the Eris:

a) the entire primary structure can be made from composites. This could yield a potential savings of 10 percent or 2,246 lbs.

b) by using a quadruplex digital flight control system and using fly-by-wire instead of mechanical flight controls, a weight saving of 15 percent over the estimated weight can be obtained. This would save 254 lbs.

By combining a) and b) a total weight saving of 2,500 lbs can be achieved. It is therefore judged possible to bring the Eris in at a weight below the originally estimated empty weight.

Steps 9-10: Not needed, see item e), Step 8.

Step 11: This step has been omitted to save space.

Table 4.3a Class II Weight Estimates for the Eris

Component	Methods: Class II Page 14	GD	Torenbeek	Use as Class II Estimate
Structure weight, W_{struct}:				
Wing	6,762	9,490		8,126
Adjustment for Fowler flaps, 2 percent:				163
Horiz.Tail		720		707
Vert.Tail		938		921
Empennage	1,597	1,658		1,628
Fuselage	7,347 incl.booms	5,044		5,967*
Booms		458		458
Engine Section	160			160
Nose Gear	554		267	443
Main Gear	2,214		1,603	1,768
Landing gear	2,768	1,996	1,870	2,211
W_{struct}	18,634	20,304		18,713
Powerplant weight, W_{pwr}:				
Engines	4,000	4,000	4,000	4,000
Afterburners	2,000	2,000	2,000	2,000
Air ind. syst.	in propuls.	445		445
Fuel system	in propuls.	777		777
Propulsion inst.	2,834**	78		845***
W_{pwr}	8,834	7,632		8,067

*1/2(7,347 - 458 + 5,044) = 5967

**includes air induction and fuel system

***1/2(2,834 + 78 - 445 - 777) = 845

Table 4.3b Weight Fraction Estimates for the Eris:

Average Weight Fractions for Fixed Equipment Breakdown

Note: these data were used in Table 4.3c.

Component	Similar Airplane Type: Republic F105B	Chance Vought F8U	Grumman A2F(A6)	Use as Class II Estimate
Fixed equipment weight item:				
W_{fc}*	0.0561	0.0515	0.0317	0.0464
W_{els}	0.0223	0.0144	0.0200	0.0189
W_{iae}	0.0307	0.0337	0.0800	0.0481
W_{api}	0.0054	0.0108	0.0047	0.0070
W_{arm}	0.0229	0.0123	0.0093	0.0148
W_{fur}	0.0077	0.0069	0.0137	0.0094
W_{aux}	0.0029	0.0060		0.0045

* includes hydraulic and pneumatic system

Note: Specific airplane type data from Tables A9.2a, A9.3a and A9.4a in Appendix A.

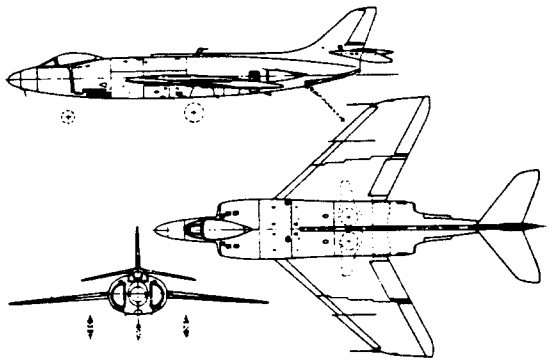

SUPERMARINE SCIMITAR F1

Table 4.3c Class II Weight Estimates for the Eris

Component	Methods: Table 4.3b x61,660	GD	Torenbeek	Use as Class II Estimate
Fixed equipment weight, W_{feq}:				
W_{fc}	3,459	1,513		2,486
$W_{fc_{cg}}$		102		102
W_{hps}: this is included in W_{fc}				
W_{els}	1,165	703		934
W_{iae}	1,893		1,033	1,463
W_{api}	431	347		389
W_{arm}	913			913
W_{fur}	580	214		397
W_{ox}	in W_{fur}	17		in W_{fur}
W_{aux}	277			277
GAU-8A Gun	2,014	Part II, Table 10.6:		2,014
W_{feq}	10,732*			8,975

* This disagrees significantly with W_{feq} in Table 10.6 of Part II.

Summary:

Class II empty weight, W_E follows from Eqn.(2.1):

$$W_E = 18,713 + 8,067 + 8,975 = 35,755 \text{ lbs}$$

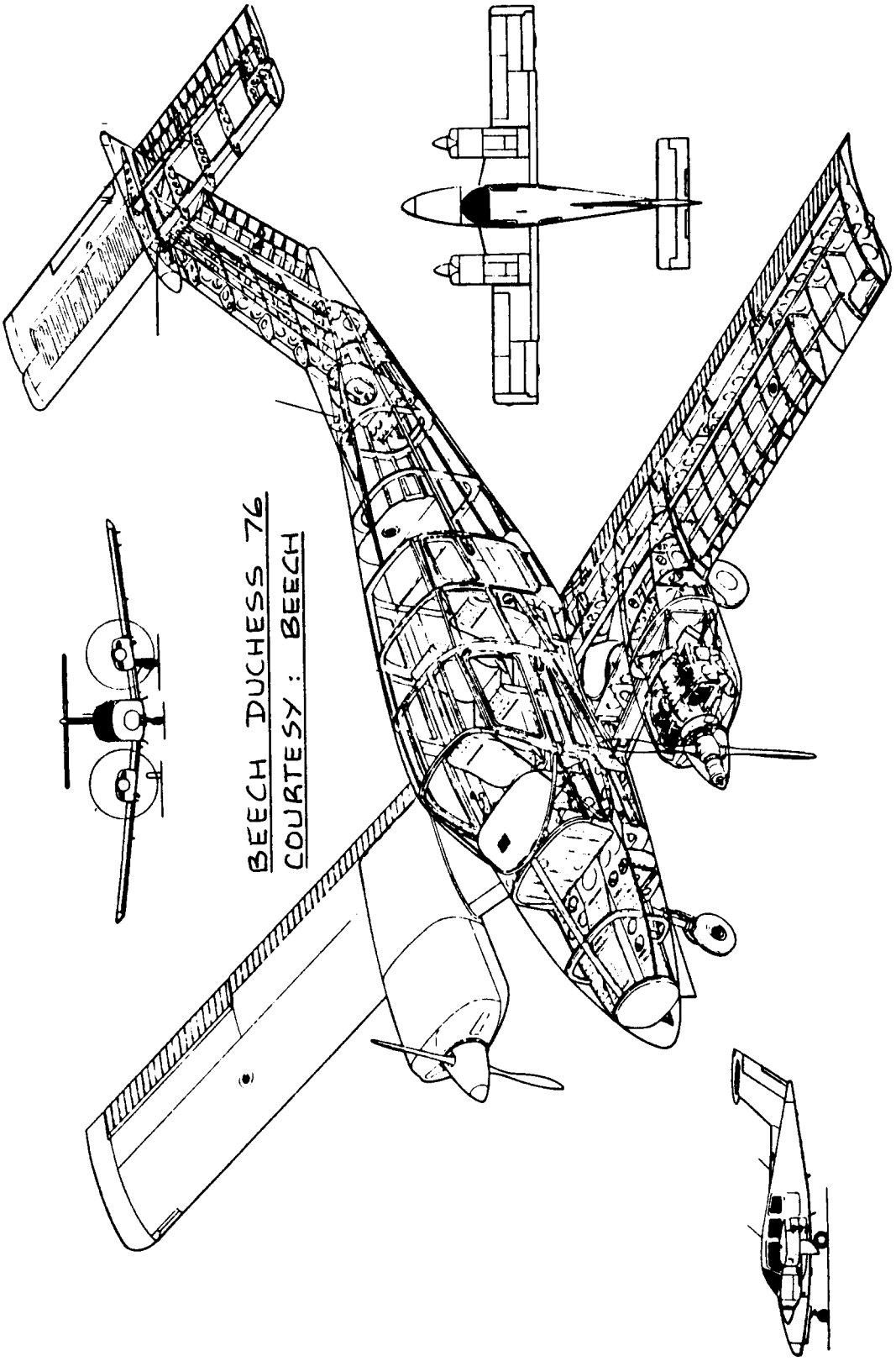

BEECH DUCHESS 76
COURTESY: BEECH

5. CLASS II METHOD FOR ESTIMATING STRUCTURE WEIGHT

The airplane structure weight, W_{struct} will be assumed to consist of the following components:

5.1 Wing, W_w — 5.2 Empennage, W_{emp}

5.3 Fuselage, W_f — 5.4 Nacelles, W_n

5.5 Landing gear, W_g — Therefore:

$$W_{struct} = W_w + W_{emp} + W_f + W_n + W_g \quad (5.1)$$

Equations for structure weight estimation are presented for the following types of airplanes:

1. General Aviation Airplanes
2. Commercial Transport Airplanes
3. Military Patrol, Bomb and Transport Airplanes
4. Fighter and Attack Airplanes

5.1 WING WEIGHT ESTIMATION

5.1.1 General Aviation Airplanes

5.1.1.1 Cessna method

The following equations should be applied only to small, relatively low performance type airplanes with maximum speeds below 200 kts. The equations apply to wings of two types:

Cantilever wings: Eqn.(5.2)
Strut braced wings: Eqn.(5.3)

Both equations include: weight of wing tip fairing
wing control surfaces

Both equations exclude: fuel tanks
wing/fuselage spar carry-through structure
effect of sweep angle

For cantilever wings:

$$W_w = 0.04674(W_{TO})^{0.397}(S)^{0.360}(n_{ult})^{0.397}(A)^{1.712} \quad (5.2)$$

For strut braced wings:

$$W_w = 0.002933(S)^{1.018}(A)^{2.473}(n_{ult})^{0.611} \quad (5.3)$$

Definition of terms:

W_{TO} = take-off weight in lbs,

S = wing area in ft^2,

n_{ult} = design ultimate load factor

A = wing aspect ratio

Note that Eqn.(5.3) does not account for W_{TO}. It should therefore be used with caution. The reader should also realize that wings in this category have maximum thickness ratios of around 18 percent.

5.1.1.2 USAF Method

The following equation applies to light and utility type airplanes with performance up to about 300 kts:

$$W_w = 96.948[(W_{TO}n_{ult}/10^5)^{0.65}(A/\cos\Lambda_{1/4})^{0.57}(S/100)^{0.61}x$$
$$x\{(1+\lambda)/2(t/c)_m\}^{0.36}(1 + V_H/500)^{0.5}]^{0.993} \qquad (5.4)$$

Definition of new terms:

$\Lambda_{1/4}$ = wing quarter chord sweep angle

λ = wing taper ratio

$(t/c)_m$ = maximum wing thickness ratio

V_H = maximum level speed at sealevel in kts

5.1.1.3 Torenbeek Method

The following equation applies to light transport airplanes with take-off weights below 12,500 lbs:

$$W_w =$$
$$= 0.00125W_{TO}(b/\cos\Lambda_{1/2})^{0.75}[1 + \{6.3\cos(\Lambda_{1/2})/b\}^{1/2}]x$$
$$x(n_{ult})^{0.55}(bS/t_rW_{TO}\cos\Lambda_{1/2})^{0.30} \qquad (5.5)$$

See special notes in Section 5.2.2.

Definition of new terms:

b = wing span in ft

$\Lambda_{1/2}$ = wing semi-chord sweep angle

t_r = maximum thickness of wing root chord in ft

5.1.2 Commercial Transport Airplanes

5.1.2.1 GD Method

$$W_w = \frac{\{0.00428(S^{0.48})(A)(M_H)^{0.43}(W_{TO}n_{ult})^{0.84}(\lambda)^{0.14}\}}{[\{100(t/c)_m\}^{0.76}(\cos\Lambda_{1/2})^{1.54}]} \quad (5.6)$$

Note: This equation is valid only in the following parameter ranges:

M_H from 0.4 to 0.8, $(t/c)_m$ from 0.08 to 0.15, and A from 4 to 12.

Definition of new term:

M_H = maximum Mach number at sealevel

5.1.2.2 Torenbeek Method

The following equation applies to transport airplanes with take-off weights above 12,500 lbs:

$$W_w = 0.0017W_{MZF}(b/\cos\Lambda_{1/2})^{0.75}[1 + \{6.3\cos(\Lambda_{1/2})/b\}^{1/2}]x$$
$$x(n_{ult})^{0.55}(bS/t_rW_{MZF}\cos\Lambda_{1/2})^{0.30} \quad (5.7)$$

Definition of new term:

W_{MZF} = maximum zero fuel weight = $W_{TO} - W_F$ (5.8)

Special notes:

1. Eqns.(5.6) and (5.7) include the weight of normal high lift devices as well as ailerons.
2. For spoilers and speed brakes 2 percent should be added.

3. If the airplane has 2 wing mounted engines reduce the wing weight by 5 percent.
4. If the airplane has 4 wing mounted engines reduce the wing weight by 10 percent.
5. If the landing gear is not mounted under the wing reduce the wing weight by 5 percent.
6. For braced wings reduce the wing weight by 30 percent. The resulting wing weight estimate does include the weight of the strut. The latter is roughly 10 percent of the wing weight.
7. For Fowler flaps add 2 percent to wing weight.

5.1.3 Military Patrol, Bomb and Transport Airplanes

For predicting wing weight it is suggested to use Eqns.(5.6) and (5.7) but with the appropriate value for n_{ult}. For this type of military airplane the usual value for n_{ult} is 4.5. Refer to Table 4.1 for a listing of military limit load factors.

Note: wing weight in military airplanes is often based on the flight design gross weight, GW, rather than W_{TO}. Check the mission specification and/or the applicable military specifications to determine which weight value to use in Eqns.(5.6) and (5.7).

5.1.4 Fighter and Attack Airplanes

5.1.4.1 GD Method

For USAF fighter and attack airplanes:

$$W_w = 3.08[\{(K_w n_{ult} W_{TO})/(t/c)_m\}\{(\tan\Lambda_{LE} - 2(1-\lambda)/A(1+\lambda))^2 + 1.0\}x10^{-6}]^{0.593}\{A(1+\lambda)\}^{0.89}(S)^{0.741} \quad (5.9)$$

For USN fighter and attack airplanes:

$$W_w = 19.29[\{(K_w n_{ult} W_{TO})/(t/c)_m\}\{(\tan\Lambda_{LE} - 2(1-\lambda)/A(1+\lambda))^2 + 1.0\}x10^{-6}]^{0.464}\{(1+\lambda)A\}^{0.70}(S)^{0.58} \quad (5.10)$$

Definition of new terms:

K_w = 1.00 for fixed wing airplanes and
= 1.175 for variable sweep wing airplanes

Λ_{LE} = leading edge sweep angle of the wing

Note: wing weight in military airplanes is often based on the flight design gross weight, GW, rather than W_{TO}. Check the mission specification and/or the applicable military specifications to determine which weight to use in Eqns. (5.9) and (5.10).

5.2 EMPENNAGE WEIGHT ESTIMATION

Empennage weight, W_{emp} will be expressed as follows:

$$W_{emp} = W_h + W_v + W_c, \qquad (5.11)$$

where: W_h = horizontal tail weight in lbs

W_v = vertical tail weight in lbs

W_c = canard weight in lbs

Equations for empennage weight components are presented in the remainder of this section.

5.2.1 General Aviation Airplanes

5.2.1.1 Cessna method

The following equations should be applied only to small, relatively low performance type airplanes with maximum speeds below 200 kts.

Horizontal tail:

$$W_h = \frac{3.184(W_{TO})^{0.887}(S_h)^{0.101}(A_h)^{0.138}}{57.5(t_{r_h})^{0.223}} \qquad (5.12)$$

Note that no factor for horizontal tail sweep is included.

Vertical tail:

$$W_v = \frac{1.68(W_{TO})^{0.567}(S_v)^{1.249}(A_v)^{0.482}}{15.6(t_{r_v})^{0.747}(\cos\Lambda_{1/4_v})^{0.882}} \qquad (5.13)$$

Canard: For a lightly loaded canard, Eqn.(5.12) may be used. For a significantly loaded canard (such as on the GP180 and the Starship I) it is suggested to use the appropriate wing weight equation.

Definition of terms:

W_{TO} = take-off weight ib lbs

S_h = horizontal tail area in ft^2

A_h = horizontal tail aspect ratio

t_{r_h} = horizontal tail maximum root thickness in ft

S_v = vertical tail area in ft^2

A_v = vertical tail aspect ratio

t_{r_v} = vertical tail maximum root thickness in ft

$1/4_v$ = vertical tail quarter chord sweep angle

5.2.1.2 USAF Method

The following equation applies to light and utility type airplanes with performance up to about 300 kts:

Horizontal tail:

$$W_h = 127\{(W_{TO}n_{ult}/10^5)^{0.87}(S_h/100)^{1.2}x$$
$$x0.289(l_h/10)^{0.483}(b_h/t_{r_h})^{0.5}\}^{0.458} \qquad (5.14)$$

Note that sweep angle is not a factor in this equation.

Vertical tail:

$$W_v = 98.5\{(W_{TO}n_{ult}/10^5)^{0.87}(S_v/100)^{1.2}x$$
$$x0.289(b_v/t_{r_v})^{0.5}\}^{0.458} \qquad (5.15)$$

Again, sweep angle is not a factor in this equation.

Canard:

The comments made under 5.2.1.2 also apply.

Definition of new terms:

l_h = distance from wing $\bar{c}/4$ to hor. tail $\bar{c}_h/4$ in ft

b_h = horizontal tail span in ft

b_v = vertical tail span in ft

5.2.1.3 Torenbeek Method

The following equation applies to light transport airplanes with design dive speeds up to 250 kts and with conventional tail configurations:

$$W_{emp} = 0.04\{n_{ult}(S_v + S_h)^2\}^{0.75}, \qquad (5.16)$$

If the airplane also has a canard, the comments made under 'canard' in 5.2.1.2 also apply here.

5.2.2 Commercial Transport Airplanes

5.2.2.1 GD Method

Horizontal tail:

$$W_h = 0.0034\{(W_{TO}n_{ult})^{0.813}(S_h)^{0.584}x$$
$$x(b_h/t_{r_h})^{0.033}(\bar{c}/l_h)^{0.28}\}^{0.915} \qquad (5.17)$$

Note: sweep angle is not a factor in this equation.

Vertical tail:

$$W_v =$$
$$0.19\{(1 + z_h/b_v)^{0.5}(W_{TO}n_{ult})^{0.363}(S_v)^{1.089}(M_H)^{0.601}x$$
$$x(l_v)^{-0.726}(1 + S_r/S_v)^{0.217}(A_v)^{0.337}(1+\lambda_v)^{0.363}x$$
$$x(\cos\Lambda_{1/4_v})^{-0.484}\}^{1.014} \qquad (5.18)$$

Canard: Comments made under 5.2.2.2 also apply here.

Definition of new terms:

z_h = distance from the vertical tail root to where the horizontal tail is mounted on the vertical tail, in ft. Warning: for fuselage mounted horizontal tails, set $z_h = 0$.

l_v = dist. from wing $\bar{c}/4$ to vert. tail $\bar{c}_v/4$ in ft

S_r = rudder area in ft^2

λ_v = vertical tail taper ratio

5.2.2.2 Torenbeek Method

The following equation applies to transport airplanes and to business jets with design dive speeds above 250 kts.

Horizontal tail:

W_h = (5.19)

$= K_h S_h [3.81\{(S_h)^{0.2} V_D\}/\{1,000(\cos \Lambda_{1/2_h})^{1/2}\} - 0.287]$

where K_h takes on the following values:

K_h = 1.0 for fixed incidence stabilizers

K_h = 1.1 for variable incidence stabilizers

Vertical tail:

W_v = (5.20)

$= K_v S_v [3.81\{(S_v)^{0.2} V_D/1,000(\cos \Lambda_{1/2_v})^{1/2}\} - 0.287]$

where K_v takes on the following values:

K_v = 1.0 for fuselage mounted horizontal tails

for fin mounted horizontal tails:

$K_v = \{1 + 0.15(S_h z_h/S_v b_v)\}$ (5.21)

Definition of new terms:

V_D = design dive speed in KEAS

$\Lambda_{1/2_h}$ horizontal tail semi-chord sweep angle

$\Lambda_{1/2_v}$ vertical tail semi-chord sweep angle

Canard: The comments made under 5.2.2.2 also apply here.

5.2.3 Military Patrol, Bomb and Transport Airplanes

See Sub-section 5.2.4.

5.2.4 Fighter and Attack airplanes

For estimation of empennage weight of airplanes in this category, use the methods of sub-section 5.2.2. Be sure to use the proper values for ultimate load factor. See Table 4.1.

Note: empennage weights of military airplanes are often based on the flight design gross weight, GW, rather than W_{TO}. Check the mission specification and/or the applicable military specifications to determine which weight to use.

5.3 FUSELAGE WEIGHT ESTIMATION

The equations presented for fuselage weight estimation are valid for land-based airplanes only. For flying boats and amphibious airplanes it is suggested to multiply the fuselage weight by 1.65:

$$W_{f_{fl.boat}} = 1.65 W_f \qquad (5.22)$$

For float equipped airplanes the weight due to the floats may be found with Eqn.(5.27), by substituting float wetted area for S_{fgs}.

For estimation of tailboom weight it is suggested to use Eqn.(5.27) applied to each tailboom individually, but with $K_f = 1$.

5.3.1 General Aviation airplanes

5.3.1.1 Cessna method

The following equations should be applied only to small, relatively low performance type airplanes with maximum speeds below 200 kts.

For low wing airplanes:

$$W_f = \qquad (5.23)$$

$$= 0.04682 (W_{TO})^{0.692} (N_{pax})^{0.374} (l_{f-n})^{0.590} \sqrt{/100}$$

For high wing airplanes:

$$W_f = 14.86(W_{TO})^{0.144}(l_{f-n}/p_{max})^{0.778}(l_{f-n})^{0.383}(N_{pax})^{0.455} \quad (5.24)$$

Definition of terms:

W_{TO} = take-off weight in lbs

N_{pax} = number of passengers

l_{f-n} = fuselage length, not including nose mounted nacelle length in ft

Notes:
1. These equations do not account for pressurized fuselages.
2. There is no explanation for why the fuselage weight of low wing airplanes does not depend on the number of passengers.
3. For this type airplane the crew is counted in the number of passengers.

5.3.1.2 USAF Method

The following equation applies to light and utility type airplanes with performance up to about 300 kts:

$$W_f = 200[(W_{TO}n_{ult}/10^5)^{0.286}(l_f/10)^{0.857}x \{(w_f + h_f)/10\}(V_C/100)^{0.338}]^{1.1} \quad (5.25)$$

Definition of new terms:

n_{ult} = ultimate load factor

l_f = fuselage length in ft

w_f = maximum fuselage width in ft

h_f = maximum fuselage height in ft

V_C = design cruise speed in KEAS

5.3.2 Commercial Transport Airplanes

5.3.2.1 GD Method

$$W_f = 2x10.43(K_{inl})^{1.42}(\bar{q}_D/100)^{0.283}(W_{TO}/1000)^{0.95}(l_f/h_f)^{0.71} \quad (5.26)$$

The factor K_{inl} takes on the following values:

K_{inl} = 1.25 for airplanes with inlets in or on the fuselage for a buried engine installation

K_{inl} = 1.0 for inlets located elsewhere

Definition of new term:

$\bar{q}_D$ = design dive dynamic pressure in psf

5.3.2.2 Torenbeek Method

The following equation applies to transport airplanes and to business jets with design dive speeds above 250 kts.

$$W_f = 0.021K_f\{(V_D l_h/(w_f + h_f)\}^{1/2}(S_{fgs})^{1.2} \qquad (5.27)$$

The constant K_f takes on the following values:

K_f = 1.08 for a pressurized fuselage

= 1.07 for a main gear attached to the fuselage.

= 1.10 for a cargo airplane with a cargo floor

These effects are multiplicative for airplanes equipped with all of the above.

Definition of new terms:

V_D = design dive speed in KEAS

l_h = distance from wing $\bar{c}/4$ to hor. tail $\bar{c}_h/4$ in ft

S_{fgs} = fuselage gross shell area in ft^2

5.3.3 Military Patrol, Bomb and Transport Airplanes

5.3.3.1 GD Method

For USAF airplanes, Eqn.(5.26) may be used.

For USN airplanes the following equation should be used:

W_f = (5.28)

$$= 11.03(K_{inl})^{1.23})(\bar{q}_L/100)^{0.245}(W_{TO}/1000)^{0.98}(l_f/h_f)^{0.61}$$

Values for K_{inl} are as given in 5.3.2.1.

Definition of new term:

$\bar{q}_L$ = design dive dynamic pressure in psf

5.3.4 Fighter and Attack Airplanes

For estimation of fuselage weights Equations (5.26) or (5.28) may be used.

Warning: In using Eqn. (5.26) for fighters, leave off the factor 2 at the beginning of the equation.

5.4 NACELLE WEIGHT ESTIMATION

The nacelle weight is assumed to consist of the following components:

1. For podded engines: the structural weight associated with the engine external ducts and or cowls. Any pylon weight is included.

2. For propeller driven airplanes: the structural weight associated with the engine external ducts and or cowls plus the weight due to the engine mounting trusses.

3. For buried engines: the structural weight associated with special cowling and or ducting provisions (other than the inlet duct which is included in the air induction system under powerplant weight, Section 6.2) and any special engine mounting provisions.

5.4.1 General Aviation Airplanes

5.4.1.1 Cessna Method

The following equations should be applied only to small, relatively low performance type airplanes with maximum speeds below 200 kts.

$$W_n = K_n W_{TO} \qquad (5.29)$$

The constant K_n takes on the following values:

K_n = 0.37 lbs/hp for radial engines

K_n = 0.24 lbs/hp for horizontally opposed engines

Definition of term:

W_{TO} = take-off weight in lbs

These data should not be applied to turbopropeller nacelles.

5.4.1.2 USAF Method

In this method, the nacelle weight is included in the powerplant weight: refer to Chapter 6.

5.4.1.3 Torenbeek Method

For single engine propeller driven airplanes with the nacelle in the fuselage nose:

$$W_n = 2.5(P_{TO})^{1/2} \quad (5.30)$$

This weight includes the entire engine section forward of the firewall.

For multi-engine airplane with piston engines:

$W_n = 0.32P_{TO}$ for horizontally opposed engines (5.31)

$W_n = 0.045(P_{TO})^{5/4}$ for radial engines (5.32)

$W_n = 0.14(P_{TO})$ for turboprop engines (5.33)

Notes: 1. Since P_{TO} is the total required take-off horsepower, these weight estimates include the weights of all nacelles.

2. If the main landing gear retracts into the nacelles, add 0.04 lbs/hp to the nacelle weight

3. If the engine exhausts over the wing, as in the Lockheed Electra, add 0.11 lbs/hp to the nacelle weight.

5.4.2 Commercial Transport Airplanes

5.4.2.1 GD Method

For turbojet engines:

$$W_n = 3.0(N_{inl})\{(A_{inl})^{0.5}(l_n)(P_2)\}^{0.731} \quad (5.34)$$

For turbofan engines:

$$W_n = 7.435(N_{inl})\{(A_{inl})^{0.5}(l_n)(P_2)\}^{0.731} \quad (5.35)$$

Definition of terms:

N_{inl} = number of inlets

A_{inl} = capture area per inlet inft^2

l_n = nacelle length from inlet lip to compressor face in ft

P_2 = maximum static pressure at engine compressor face in psi. Typical values range from 15 to 50 psi.

5.4.2.2 Torenbeek Method

For turbojet or low bypass ratio turbofan engines:

$$W_n = 0.055T_{TO} \quad (5.36)$$

For high bypass ratio turbofan engines:

$$W_n = 0.065T_{TO} \quad (5.37)$$

Since T_{TO} is the total required take-off thrust, these equations account for the weight of all nacelles.

5.4.3 Military Patrol Bomb and Transport Airplanes

For all airplanes in this category Eqns.(5.34) and (5.35) may be used.

5.4.4 Fighter and Attack Airplanes

For all airplanes in this category Eqns.(5.34) and (5.35) may be used.

5.5 LANDING GEAR WEIGHT ESTIMATION

5.5.1 General Aviation Airplanes

5.5.1.1 Cessna method

The following equations should be applied only to small, relatively low performance type airplanes with maximum speeds below 200 kts.

For non-retractable landing gears:

$$W_g = \quad (5.38)$$

$$0.013W_{TO} + 0.146(W_L)^{0.417}n_{ult.l})^{0.950}(l_{s_m})^{0.183} +$$

wheels + tires m.g. strut assembly m.g.

$$+ 6.2 + 0.0013W_{TO} + 0.000143(W_L)^{0.749}(n_{ult.l})(l_{s_n})^{0.788}$$

wheels + tires n.g. strut assembly n.g.

For retractable landing gears:

$$W_g = W_{g_{Eqn.(5.38)}} + 0.014W_{TO} \quad (5.39)$$

Definition of terms:

W_{TO} = take-off weight in lbs

W_L = design landing weight in lbs (See Table 3.3, Part I for data relating W_L to W_{TO})

$n_{ult.l}$ = ultimate load factor for landing, may be taken as 5.7

l_{s_m} = shock strut length for main gear in ft

l_{s_n} = shock strut length for nose gear in ft

5.5.1.2 USAF Method

The following equation applies to light and utility type airplanes with performance up to about 300 kts:

$$W_g = 0.054(l_{s_m})^{0.501}(W_L n_{ult.l})^{0.684} \quad (5.40)$$

Notes: 1) This equation includes nose gear weight.

2) $N_{ult.l}$ may be taken as 5.7.

5.5.2 Commercial Transport Airplanes

5.5.2.1 GD Method

$$W_g = 62.61(W_{TO}/1,000)^{0.84} \quad (5.41)$$

5.5.2.2 Torenbeek Method

The following equation applies to transport airplanes and to business jets with the main gear mounted

on the wing and the nose gear mounted on the fuselage:

$$W_g = \bar{K}_{g_r}\{A_g + B_g(W_{TO})^{3/4} + C_g W_{TO} + D_g(W_{TO})^{3/2}\} \qquad (5.42)$$

The factor K_{g_r} takes on the following values:

K_{g_r} = 1.0 for low wing airplanes

K_{g_r} = 1.08 for high wing airplanes

The constants A_g through D_g are defined in Table 5.1 which is taken from Reference 14.

Table 5.1 Constants in Landing Gear Weight Eqn.(5.42)

Airplane Type	Gear Type	Gear Comp.	A_g	B_g	C_g	D_g
Jet Trainers and Business Jets	Retr.	Main	33.0	0.04	0.021	0.0
		Nose	12.0	0.06	0.0	0.0
Other civil airplanes	Fixed	Main	20.0	0.10	0.019	0.0
		Nose	25.0	0.0	0.0024	0.0
		Tail	9	0.0	0.0024	0.0
	Retr.	Main	40.0	0.16	0.019	1.5×10^{-5}
		Nose	20.0	0.10	0.0	2.0×10^{-6}
		Tail	5.0	0.0	0.0031	0.0

5.5.3 Military Patrol, Bomb and Transport Airplanes

For USAF airplanes, Eqns.(5.41) and (5.42) may be used.

For USN airplanes the following equation should be used:

$$W_g = 129.1(W_{TO}/1{,}000)^{0.66} \qquad (5.43)$$

5.5.4 Fighter and Attack Airplanes

For USAF airplanes, Eqns.(5.41) and (5.42) may be used.

For USN airplanes, Eqn.(5.43) should be used.

6. CLASS II METHOD FOR ESTIMATING POWERPLANT WEIGHT

The airplane powerplant weight, W_{pwr} will be assumed to consist of the following components:

6.1 Engines, W_e: this includes engine, exhaust, cooling, supercharger and lubrication systems.

Note: afterburners and thrust reversers are not always included under engines. They are often treated as a separate powerplant component.

6.2 Air induction system, W_{ai}: this includes inlet ducts other than nacelles, ramps, spikes and associated controls.

6.3 Propellers, W_{prop}

6.4 Fuel System, W_{fs}

6.5 Propulsion System, W_p, this includes:

- *engine controls
- *starting systems
- *propeller controls
- *provisions for engine installation

Note: instead of the words 'propulsion system', the words 'propulsion installation' or even 'engine installation' are sometimes used.

Therefore:

$$W_{pwr} = W_e + W_{ai} + W_{prop} + W_{fs} + W_p \qquad (6.1)$$

General Note: for powerplant weight predictions it is highly recommended to obtain actual weight data from engine manufacturers.

Equations for powerplant weight prediction are presented for the following types of airplanes:

1. General Aviation Airplanes
2. Commercial Transport Airplanes
3. Military Patrol, Bomb and Transport Airplanes
4. Fighter and Attack Airplanes

6.1 ENGINE WEIGHT ESTIMATION

6.1.1 General Aviation Airplanes

6.1.1.1 Cessna method

The following equations should be applied only to small, relatively low performance type airplanes with maximum speeds below 200 kts.

$$W_e = K_p P_{TO} \tag{6.2}$$

The factor K_p takes on the following values:

For piston engines: K_p = 1.1 to 1.8, depending on whether or not supercharging is used.

For turbopropeller engines: K_p = 0.35 to 0.55.

These weights represent the so-called engine dry weight. Normal engine accessories are included in this weight but engine oil is not.

Definition of terms:

W_e = weight of all engines in lbs

P_{TO} = required take-off power in hp

6.1.1.2 USAF Method

$$W_e + W_{ai} + W_{prop} + W_p = 2.575(W_{eng})^{0.922} N_e \tag{6.3}$$

Use engine manufacturers data to obtain W_{eng} or use Eqn. (6.2).

Definition of new terms:

W_{eng} = weight per engine in lbs

N_e = number of engines

6.1.1.3 Torenbeek Method

For propeller driven airplanes:

$$W_{pwr} = K_{pg}(W_e + 0.24 P_{TO}) \tag{6.4}$$

The constant K_{pg} takes on the following values:

K_{pg} = 1.16 for single engine tractor installations

K_{pg} 1.35 for multi-engine installations

For superchargers the following additional weight is incurred:

$$W_{sprch} = 0.455(W_e)^{0.943} \quad (6.5)$$

For jet airplanes:

$$W_{pwr} = K_{pg}K_{thr}W_e \quad (6.6)$$

The constant K_{pg} takes on the following values:

K_{pg} = 1.40 for airplanes with buried engines

The constant K_{thr} takes on the following values:

K_{thr} = 1.00 for airplanes without thrust reversers

K_{thr} = 1.18 for airplanes with thrust reversers

6.1.2 Commercial Transport Airplanes

Use of actual engine manufactures data is highly recommended. Figure 6.1 provides a graphical summary of engine dry weights versus take-off thrust. Figure 6.2 gives a graphical summary of engine dry weights versus take-off shaft horsepower.

When using Figures (6.1) or (6.2), keep in mind that:

$$W_e = N_e W_{eng}, \quad (6.7)$$

where W_{eng} is the weight per engine.

Equations (6.5) and (6.6) may also be used to obtain an initial estimate.

6.1.3 Military Patrol, Bomb and Transport Airplanes

See Sub-Section 6.1.2.

6.1.4 Fighter and Attack Airplanes

See Sub-Section 6.1.2.

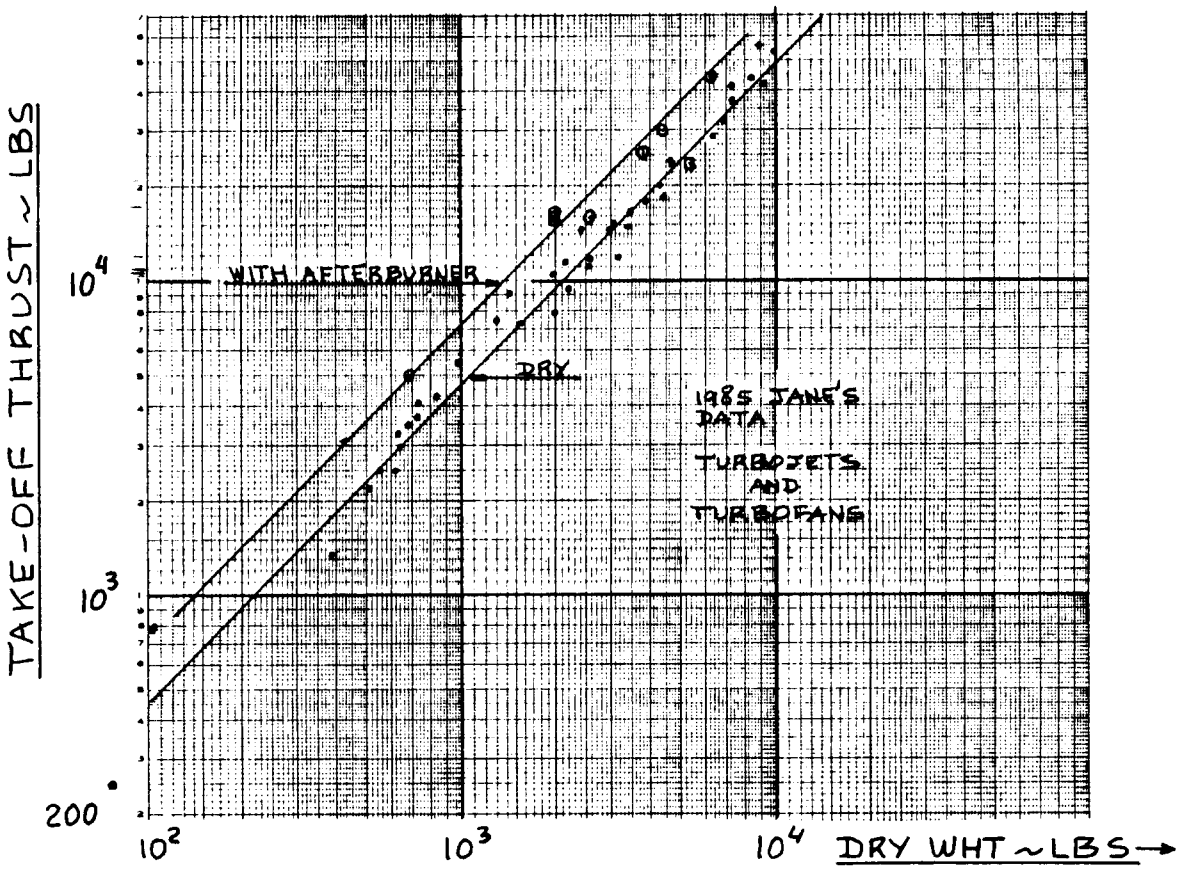

Figure 6.1 Turbojets and Turbofans: Take-off Thrust and Dry Weight Trends

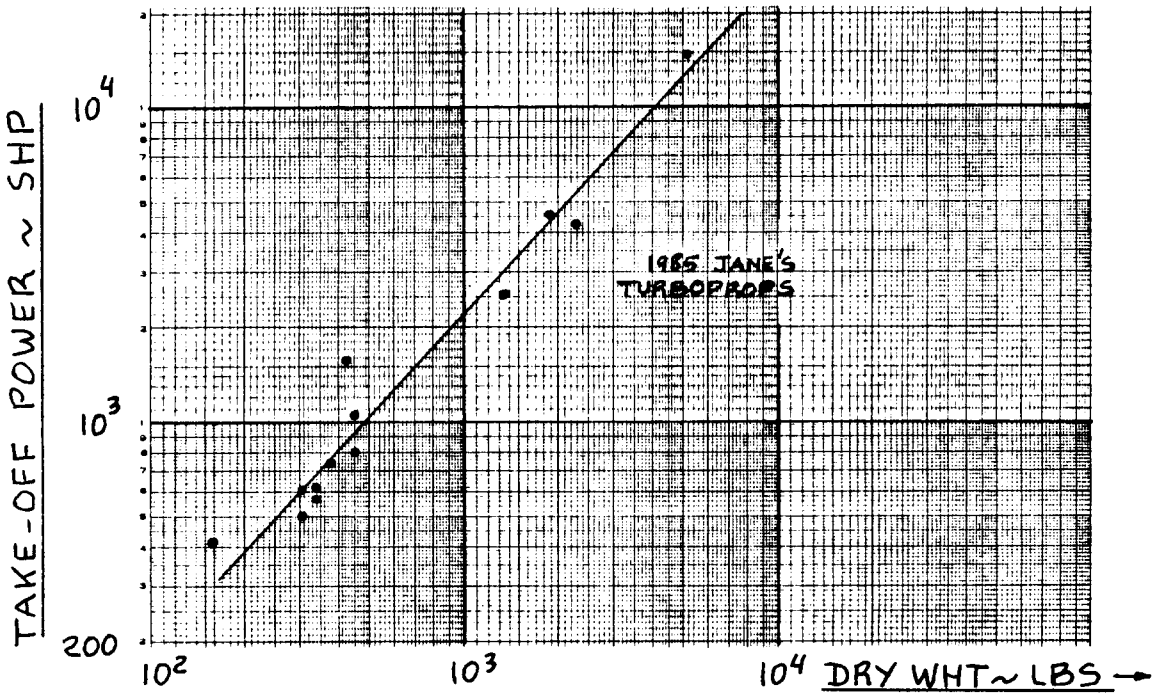

Figure 6.2 Turboprops: Take-off Shaft Horse Power and Dry Weight Trends

6.2 AIR INDUCTION SYSTEM WEIGHT ESTIMATION

6.2.1 General Aviation Airplanes

6.2.1.1 Cessna method

W_{ai} is included in the propulsion system weight, W_p.

6.2.1.2 USAF Method

See 6.2.1.1.

6.2.1.3 Torenbeek Method

$$W_{ai} + W_p = 1.03(N_e)^{0.3}(P_{TO}/N_e)^{0.7} \qquad (6.8)$$

6.2.2 Commercial Transport Airplanes

6.2.2.1 GD Method

For buried engine installations:

The air induction system weight is split into two items: the first one for duct support structure, the second one for the subsonic duct leading from the inlet lip to the engine compressor face.

$$W_{ai} = 0.32(N_{inl})(L_d)(A_{inl})^{0.65}(P_2)^{0.6} + \qquad (6.9)$$

(duct support structure)

$$1.735\{(L_d)(N_{inl})(A_{inl})^{0.5}(P_2)(K_d)(K_m)\}^{0.7331}$$

(subsonic part of duct)

The factors K_d and K_m are defined as follows:

K_d = 1.33 for ducts with flat cross sections

1.0 for ducts with curved cross sections

K_m = 1.0 for M_D below 1.4

= 1.5 for M_D above 1.4

Definition of terms:

L_d = duct length in ft

N_{inl} = number of inlets

A_{inl} = capture area per inlet in ft^2

P_2 = maximum static pressure at engine compressor face in psi. Typical values range from 15 to 50 psi.

For podded engine installations:

The air induction system weight is included in the nacelle weight, W_n.

6.2.2.2 Torenbeek Method

For buried engine installations:

$$W_{ai} = 11.45\{(L_d)(N_{inl})(A_{inl})^{0.5}(K_d)\}^{0.7331} \quad (6.10)$$

The constant K_d takes on the following values:

K_d = 1.0 for ducts with curved cross sections

1.33 for ducts with flat cross sections

For podded engine installations:

The air induction system weight is included in the nacelle weight, W_n.

Note: For supersonic installations additional weight items due to the special inlet requirements are needed. See Sub-section 6.2.4.

6.2.3. Military Patrol, Bomb and Transport Airplanes

See Section 6.2.2.

6.2.4 Fighter and Attack Airplanes

6.2.4.1 GD Method

For prediction of the duct support structure weight and the duct weight, Eqn.(6.9) may be used.

Particularly in supersonic applications the following additional weight items due to inlet provisions may be incurred:

For variable geometry ramps, actuators and controls:

$$W_{ramp} = 4.079\{(L_r)(N_{inl})(A_{inl})^{0.5}(K_r)\}^{1.201} \quad (6.11)$$

The factor K_r takes on the following values:

K_r = 1.0 for M_D below 3.0

= $(M_D + 2)/5$ for M_D above 3.0

Definition of new term:

L_r is the ramp length forward of the inlet throat in ft

For inlet spikes:

$$W_{sp} = K_s(N_{inl})(A_{inl}) \qquad (6.12)$$

The constant K_s takes on the following values:

K_s = 12.53 for half round fixed spikes
= 15.65 for full round translating spikes
= 51.80 for translating and expanding spikes

Note: these weights also apply to supersonic commercial installations.

6.3 PROPELLER WEIGHT ESTIMATION

6.3.1 General Aviation Airplanes

It is recommended to use propeller manufacturer data whereever possible. Lacking actual data the equation of Sub-Section 6.3.2 may be used.

Appendix A contains propeller installation data for a number of airplanes. Propeller installation weights usually include the propeller controls.

6.3.2 Commercial Transport Airplanes

6.3.2.1 GD Method

$$W_{prop} = \qquad (6.13)$$

$$K_{prop1}(N_p)(N_{bl})^{0.391}\{(D_p)(P_{TO}/N_e)/1,000\}^{0.782}$$

The constant K_{prop1} takes on the following values:

K_{prop1} = 24.0 for turboprops above 1,500 shp

= 31.92 for piston engines and for turboprops below 1,500 shp

Definition of terms:

N_p is the number of propellers

N_{bl} is the number of blades per propeller

D_p is the propeller diameter in ft

P_{TO} is the required take-off power in hp

N_e is the number of engines

6.3.2.2 Torenbeek Method

$$W_{prop} = K_{prop2}(N_p)^{0.218}\{D_p P_{TO}(N_{bl})^{1/2}\}^{0.782} \quad (6.14)$$

The factor K_{prop2} takes on the following values:

$K_{prop2} = 0.108$ for turboprops

$K_{prop2} = 0.144$ for piston engines

The reader is asked to show that equations (6.13) and (6.14) are in fact the same.

6.3.3 Military Patrol, Bomb and Transport Airplanes

See Sub-Section 6.3.2.

6.3.4 Fighter and Attack Airplanes

See Sub-Section 6.3.2.

6.4 FUEL SYSTEM WEIGHT ESTIMATION

Note: In some airplanes the fuel system is used to control the center of gravity location. Airplanes with relaxed static stability and/or supersonic cruise airplanes frequently require such a system. The weight increment incurred due to such a feature is included in the weight estimation of the flight control system, Section 7.1.

6.4.1 General Aviation Airplanes

6.4.1.1 Cessna method

For airplanes with internal fuel systems (no tiptanks):

$$W_{fs} = 0.40 W_F / K_{fsp} \quad (6.15)$$

For airplanes with external fuel systems (with tiptanks):

$$W_{fs} = 0.70W_F/K_{fsp} \quad (6.16)$$

The constant K_{fsp} takes on the following values:

K_{fsp} = 5.87 lbs/gal for aviation gasoline

= 6.55 for lbs/gal for JP-4

Definition of term:

W_F = mission fuel weight (includes reserves) in lbs

6.4.1.2 USAF Method

$$W_{fs} = \quad (6.17)$$

$$= 2.49[(W_F/K_{fsp})^{0.6}\{1/(1+int)\}^{0.3}(N_t)^{0.20}(N_e)^{0.13}]^{1.21}$$

The factor K_f is defined in 6.4.1.1.

Definition of new terms:

int = fraction of fuel tanks which are integral

N_t = number of separate fuel tanks

N_e = number of engines

6.4.1.3 Torenbeek Method

For turbine engines, see Sub-Section 6.4.2.

For single piston engine installations:

$$W_{fs} = 2(W_F/5.87)^{0.667} \quad (6.18)$$

For multi piston engine installations:

$$W_{fs} = 4.5(W_F/5.87)^{0.60} \quad (6.19)$$

6.4.2 Commercial Transport Airplanes

6.4.2.1 GD Method

For a fuel system with integral tanks see 6.4.2.2.

For a fuel system with self-sealing bladder cells:

$$W_{fs} = 41.6\{(W_F/K_{fsp})/100\}^{0.818} + W_{supp} \quad (6.20)$$

For a fuel system with non-self-sealing bladder cells:

$$W_{fs} = 23.1\{(W_F/K_{fsp})/100\}^{0.758} + W_{supp} \quad (6.21)$$

The factor K_{fsp} is defined in 6.4.1.1.

W_{supp} is the weight of the bladder support structure and is given by:

$$W_{supp} = 7.91\{(W_F/K_{fsp})/100\}^{0.854} \quad (6.22)$$

6.4.2.2 Torenbeek Method

For airplanes equipped with non-self-sealing bladder tanks:

$$W_{fs} = 3.2(W_F/K_{fsp})^{0.727} \quad (6.23)$$

For airplanes equipped with integral fuel tanks (wet wing):

$$W_{fs} = 80(N_e + N_t - 1) + 15(N_t)^{0.5}(W_F/K_{fsp})^{0.333} \quad (6.24)$$

6.4.3 Military Patrol, Bomb and Transport Airplanes

For basic fuel system weights, see Sub-Section 6.4.2.

Many military airplanes carry in flight refuelling systems. In addition, many are equipped with fuel dumping systems. The weights of these systems may be estimated from:

For in-flight refuelling:

$$W_{inflref} = 13.64\{(W_F/K_{fsp})/100\}^{0.392} \quad (6.25)$$

For fuel dumping:

$$W_{fd} = 7.38\{(W_F/K_{fsp})/100\}^{0.458} \quad (6.26)$$

6.4.4 Fighter and Attack Airplanes

See Sub-Sections 6.4.2 and 6.4.3.

6.5 PROPULSION SYSTEM WEIGHT ESTIMATION

Depending on airplane type, the propulsion system weight, W_p is either given as a function of total engine weight and/or mission fuel or by:

$W_p = W_{ec} + W_{ess} + W_{pc} + W_{osc}$, where: (6.22)

W_{ec} = weight of engine controls in lbs

W_{ess} = weight of engine starting system in lbs

W_{pc} = weight of propeller controls in lbs

W_{osc} = weight of oil system and oil cooler in lbs

6.5.1 General Aviation Airplanes

6.5.1.1 Cessna method

Use actual data.

6.5.1.2 USAF Method

W_p is included in Eqn.(6.3).

6.5.1.3 Torenbeek Method

W_p is included in Eqn.(6.3).

6.5.2 Commercial Transport Airplanes

6.5.2.1 GD Method

Engine controls:

For fuselage/wing-root mounted jet engines:

$$W_{ec} = K_{ec}(l_f N_e)^{0.792} \quad (6.23)$$

The factor K_{ec} takes on the following values:

K_{ec} = 0.686 for non-afterburning engines
= 1.080 for afterburning engines

For wing mounted jet engines:

$$W_{ec} = 88.46\{(l_f + b)N_e/100\}^{0.294} \quad (6.24)$$

For wing mounted turboprops:

$$W_{ec} = 56.84\{(l_f + b)N_e/100\}^{0.514} \quad (6.25)$$

For wing mounted piston engines:

$$W_{ec} = 60.27\{(l_f + b)N_e/100\}^{0.724} \quad (6.26)$$

Definition of terms:

N_e = number of engines

l_f = fuselage length in ft

b = wing span in ft

Engine starting systems:

For airplanes with one or two jet engines using cartridge or pneumatic starting systems:

$$W_{ess} = 9.33(W_e/1,000)^{1.078} \quad (6.27)$$

For airplanes with four or more jet engines using pneumatic starting systems:

$$W_{ess} = 49.19(W_e/1,000)^{0.541} \quad (6.28)$$

For airplanes with jet engines using electric starting systems:

$$W_{ess} = 38.93(W_e/1,000)^{0.918} \quad (6.29)$$

For airplanes with turboprop engines using pneumatic starting systems:

$$W_{ess} = 12.05(W_e/1,000)^{1.458} \quad (6.30)$$

For airplanes with piston engines using electric starting systems:

$$W_{ess} = 50.38(W_e/1,000)^{0.459} \quad (6.31)$$

Propeller controls:

For turboprop engines:

$$W_{pc} = 0.322(N_{bl})^{0.589}\{(N_p D_p P_{TO}/N_e)/1,000\}^{1.178} \quad (6.32)$$

For piston engines:

$$W_{pc} = 4.552(N_{bl})^{0.379}\{(N_p D_p P_{TO}/N_e)/1,000\}^{0.759} \quad (6.33)$$

Definition of term:

W_e = total weight of all engines in lbs

6.5.2.2 Torenbeek Method

For airplanes with turbojet or turbofan engines using cartridge or pneumatic starting systems, the weight for accessory drives, powerplant controls, starting and ignition systems is:

$$W_{apsi} = 36N_e(dW_F/dt)_{TO} \quad (6.34a)$$

The take-off fuel flow rate, $(dW_F/dt)_{TO}$ has the dimension of lbs/sec.

For airplanes with turboprop engines this weight is:

$$W_{apsi} = 0.4K_b(N_e)^{0.2}(P_{TO}/N_e)^{0.8} \quad (6.34b)$$

The factor K_b takes on the following values:

K_b = 1.0 without beta controls
= 1.3 with beta controls

It is usually acceptable to assume that:

$$W_{api} = W_p - W_{osc} \quad (6.35)$$

Definition of new terms:

$(dW_F/dt)_{TO}$ = fuel flow at take-off in lbs/sec

P_{TO} = required take-off power in hp

Thrust reversers for jet engines:

The weight of thrust reversers was already included in the engine weight estimate of Eq.(6.6). To obtain a better estimate of the c.g. effect due to thrust reversers a separate weight estimate is needed:

$$W_{tr} = 0.18W_e \quad (6.36)$$

Water injection system:

Water injection systems are used to increase take-off performance of all types of engines. The installation of such a system is optional.

$$W_{wi} = 8.586W_{wtr}/8.35 \qquad (6.37)$$

W_{wtr} = weight of water carried in lbs

Oil system and oil cooler:

$$W_{osc} = K_{osc}W_e \qquad (6.38)$$

The factor K_{osc} takes on the following values:

K_{osc} = 0.00 for jet engines (weight incl. in W_e)
= 0.07 for turboprop engines
= 0.08 for radial piston engines
= 0.03 for horizontally opposed piston engines

6.5.3 Military Patrol, Bomb and Transport Airplanes

See Section 6.5.2.

6.5.4 Fighter and Attack Airplanes

See Section 6.5.2.

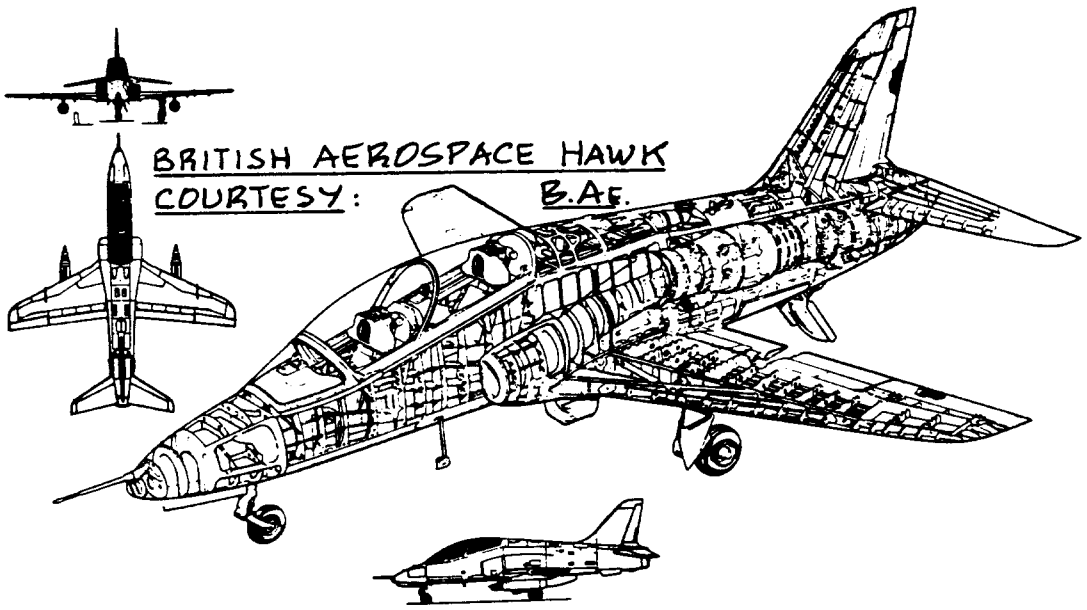

7. CLASS II METHOD FOR ESTIMATING FIXED EQUIPMENT WEIGHT

The list of fixed equipment carried on board airplanes varies significantly with airplane type and airplane mission. In this chapter it will be assumed that the following items are to be included in the fixed equipment category:

7.1. Flight control system, W_{fc}

7.2. Hydraulic and pneumatic System, W_{hps}

7.3. Electrical system, W_{els}

7.4. Instrumentation, avionics and electronics, W_{iae}

7.5. Air-conditioning, pressurization, anti- and de-icing system, W_{api}

7.6. Oxygen system, W_{ox}

7.7. Auxiliary power unit (APU), W_{apu}

7.8. Furnishings, W_{fur}

7.9. Baggage and cargo handling equipment, W_{bc}

7.10 Operational items, W_{ops}

7.11. Armament, W_{arm}

7.12. Guns, launchers and weapons provisions, W_{glw}

7.13. Flight test instrumentation, W_{fti}

7.14. Auxiliary gear, W_{aux}

7.15. Ballast, W_{bal}

7.16. Paint, W_{pt}

7.17. W_{etc}

Therefore:

$$W_{feq} = W_{fc} + W_{hps} + W_{els} + W_{iae} + W_{api} + W_{ox} + \\ + W_{apu} + W_{fur} + W_{bc} + W_{ops} + W_{arm} + W_{glw} + \\ + W_{fti} + W_{aux} + W_{bal} + W_{pt} + W_{etc} \qquad (7.1)$$

The exact definition of which item belongs in a particular fixed equipment category is hard to find. The category W_{etc} was added to cover any items not specifically listed.

Methods for predicting weights of typical fixed equipment items are presented for the following types of airplanes:

1. General Aviation Airplanes
2. Commercial Transport Airplanes
3. Military Patrol, Bomb and Transport Airplanes
4. Fighters and Attack Airplanes

The reader should always consult actual fixed equipment weight data for similar airplanes. Appendix A presents this information for a large number of airplanes.

7.1 FLIGHT CONTROL SYSTEM WEIGHT ESTIMATION

7.1.1 General Aviation Airplanes

7.1.1.1 Cessna Method

$$W_{fc} = 0.0168 W_{TO}, \qquad (7.1)$$

where: W_{TO} = take-off weight in lbs

This equation applies only to airplanes under 8,000 lbs take-off weight with mechanical flight controls. The equation includes all flight control system hardware: cables, pulleys, pushrods, cockpit controls plus any required back-up structure.

Airplanes in this category all tend to have two sets of flight controls in the cockpit.

7.1.1.2 USAF Method

For airplanes with un-powered flight controls:

$$W_{fc} = 1.066 (W_{TO})^{0.626} \qquad (7.2)$$

For airplanes with powered flight controls:

$$W_{fc} = 1.08 (W_{TO})^{0.7} \qquad (7.3)$$

7.1.1.3 Torenbeek Method

For airplanes with un-powered, unduplicated flight controls:

$$W_{fc} = 0.23(W_{TO})^{2/3} \qquad (7.4)$$

7.1.2 Commercial Transport Airplanes

7.1.2.1 GD Method

The following equation applies to business jets as well as to commercial transport airplanes:

$$W_{fc} = 56.01\ \{(W_{TO})(\bar{q}_D)/100,000\}^{0.576} \qquad (7.5)$$

where: $\bar{q}_D$ is the design dive dynamic pressure in psf

7.1.2.2 Torenbeek Method

$$W_{fc} = K_{fc}(W_{TO})^{2/3} \qquad (7.6)$$

The constant K_{fc} takes on the following values:

K_{fc} = 0.44 for airplanes with un-powered flight controls
= 0.64 for airplanes with powered flight controls

If leading edge devices are employed, these estimates should be multiplied by a factor 1.2. If lift dumpers are employed, a factor 1.15 should be used.

7.1.3 Military Patrol, Bomb and Transport Airplanes

7.1.3.1 GD Method

For transport airplanes:

$$W_{fc} = 15.96\{(W_{TO})(\bar{q}_L)/100,000\}^{0.815}, \qquad (7.7)$$

where: $\bar{q}_L$ is the design dive dynamic pressure in psf

For Bombers:

$$W_{fc} = 1.049\{(S_{cs})(\bar{q})/1,000\}^{1.21}, \qquad (7.8)$$

where: S_{sc} is the total control surface area in ft^2

Note: these estimates include the weight of all associated hydraulic and/or pneumatic systems!

7.1.4 Fighters and Attack Airplanes

7.1.4.1 GD Method

For USAF fighters:

$$W_{fc} = K_{fcf}(W_{TO}/1,000)^{0.581} \qquad (7.9)$$

The constant K_{fcf} takes on the following values:

K_{fcf} = 106 for airplanes with elevon control and no horizontal tail

= 138 for airplanes with a horizontal tail

= 168 for airplanes with a variable sweep wing

For USN fighters and attack airplanes:

$$W_{fc} = 23.77(W_{TO}/1,000)^{1.1} \qquad (7.10)$$

Note: these estimates include the weight of all associated hydraulic and/or pneumatic systems.

Certain airplanes require a center of gravity control system. This is normally implemented using a fuel transfer system. The extra weight due to a c.g. control system may be estimated from:

$$W_{fc_{cg}} = 23.38\{(W_F/K_{fsp})/100\}^{0.442} \qquad (7.11)$$

where: W_F is the mission fuel weight in lbs

K_{fsp} = 6.55 lbs /gal for JP-4

7.2 HYDRAULIC AND/OR PNEUMATIC SYSTEM WEIGHT ESTIMATION

As seen in Section 7.1 the weight of the hydraulic and/or pneumatic system needed for powered flight controls is usually included in the flight control system weight prediction.

The following weight ratios may be used to determine the hydraulic system weight separately:

For business jets: 0.0070 - 0.0150 of W_{TO}

For regional turboprops: 0.0060 - 0.0120 of W_{TO}

For commercial transports: 0.0060 - 0.0120 of W_{TO}

For military patrol, transport and bombers:

0.0060 - 0.0120 of W_{TO}

For fighters and attack airplanes:

0.0050 - 0.0180 of W_{TO}

The reader should consult the detailed weight data in Appendix A for more precise information.

7.3 ELECTRICAL SYSTEM WEIGHT ESTIMATION

The reader should consult the detailed weight data in Appendix A for electrical system weights of specific airplanes.

7.3.1 General Aviation Airplanes

7.3.1.1 Cessna Method

$$W_{els} = 0.0268 W_{TO} \tag{7.12}$$

7.3.1.2 USAF Method

$$W_{els} = 426\{(W_{fs} + W_{iae})/1,000\}^{0.51} \tag{7.13}$$

Note that the electrical system weight in this case is given as a function of the weight of the fuel system plus the weight of instrumentation, avionics and electronics.

7.3.1.3 Torenbeek Method

$$W_{hps} + W_{els} = 0.0078(W_E)^{1.2}, \quad (7.14)$$

where: W_E is the empty weight in lbs

7.3.2 Commercial Transport Airplanes

7.3.2.1 GD Method

$$W_{els} = 1{,}163\{(W_{fs} + W_{iae})/1{,}000\}^{0.506} \quad (7.15)$$

7.3.2.2 Torenbeek Method

For propeller driven transports:

$$W_{hps} + W_{els} = 0.325(W_E)^{0.8} \quad (7.16)$$

For jet transports:

$$W_{els} = 10.8(V_{pax})^{0.7}\{1 - 0.018(V_{pax})^{0.35}\}, \quad (7.17)$$

where: V_{pax} is the passenger cabin volume in ft^3

7.3.3 Military Patrol, Bomb and Transport Airplanes

7.3.3.1 GD Method

For transport airplanes:

Use Eqn.(7.15)

For Bombers:

$$W_{els} = 185\{(W_{fs} + W_{iae})/1{,}000\}^{1.268} \quad (7.18)$$

7.3.4 Fighters and Attack Airplanes

7.3.4.1 GD Method

For USAF fighters:

$$W_{els} = 426\{(W_{fs} + W_{iae})/1{,}000\}^{0.51} \quad (7.19)$$

For USN fighters and attack airplanes:

$$W_{els} = 347\{(W_{fs} + W_{iae})/1{,}000\}^{0.509} \quad (7.20)$$

7.4 WEIGHT ESTIMATION FOR INSTRUMENTATION, AVIONICS AND ELECTRONICS

The reader should consult the detailed weight data in Appendix A for weights of instrumentation, avionics and electronics for specific airplanes. Another important source of weight data on actual avionics and electronics systems for civil airplanes is Reference 18. For data on military avionics systems the reader should consult Reference 13, Tables 8-1 and 8-2.

Important comment: The weight equations given in this section are obsolete for modern EFIS type cockpit installations and for modern computer based flight management and navigation systems. The equations provided are probably conservative.

7.4.1 General Aviation Airplanes

7.4.1.1 Torenbeek Method

For single engine propeller driven airplanes:

$$W_{iae} = 33N_{pax}, \tag{7.21}$$

where: N_{pax} is the number of passengers, including the crew

For multi-engine propeller driven airplanes:

$$W_{iae} = 40 + 0.008W_{TO} \tag{7.22}$$

7.4.2 Commercial Transport Airplanes

7.4.2.1 GD Method (Modified)

For the weight of instruments:

$$W_i = \underbrace{N_{pil}\{15 + 0.032(W_{TO}/1{,}000)\}}_{\text{flight instruments}} + \underbrace{N_e\{5 + 0.006(W_{TO}/1{,}000)\}}_{\text{engine instruments}} + \underbrace{0.15(W_{TO}/1{,}000) + 0.012W_{TO}}_{\text{other instruments}} \tag{7.23}$$

where: N_{pil} is the number of pilots

N_e is the number of engines

7.4.2.2 Torenbeek Method

For regional transports:

$$W_{iae} = 120 + 20N_e + 0.006W_{TO} \quad (7.24)$$

For jet transports:

$$W_{iae} = 0.575(W_E)^{0.556}(R)^{0.25}, \quad (7.25)$$

where: W_E is the empty weight in lbs

R is the maximum range in nautical miles

7.4.3 Military Patrol, Bomb and Transport Airplanes

Use Sub-section 7.4.2.

7.4.4 Fighter and Attack Airplanes

Use Sub-section 7.4.2.

7.5 WEIGHT ESTIMATION FOR AIR-CONDITIONING, PRESSURIZATION, ANTI- AND-DEICING SYSTEMS

7.5.1 General Aviation Airplanes

7.5.1.1 USAF Method

$$W_{api} = 0.265(W_{TO})^{0.52}(N_{pax})^{0.68}x \\ x(W_{iae})^{0.17}(M_D)^{0.08}, \quad (7.26)$$

where: N_{pax} is the number of passengers, including the crew

M_D is the design dive Mach number

7.5.1.2 Torenbeek Method

For single engine, unpressurized airplanes:

$$W_{api} = 2.5N_{pax} \quad (7.27)$$

For multi-engine, unpressurized airplanes:

$$W_{api} = 0.018W_E \quad (7.28)$$

7.5.2 Commercial Transport Airplanes

7.5.2.1 GD Method

For pressurized airplanes:

$$W_{api} = 469\{V_{pax}(N_{cr} + N_{pax})/10,000\}^{0.419} \quad (7.29)$$

7.5.2.2 Torenbeek Method

For pressurized airplanes:

$$W_{api} = 6.75(l_{pax})^{1.28} \quad (7.30)$$

where l_{pax} = length of the passenger cabin in ft

7.5.3 Military Patrol, Bomb and Transport Airplanes

7.5.3.1 GD Method

$$W_{api} = K_{api}(V_{pr}/100)^{0.242} \quad (7.31)$$

The constant K_{api} takes on the following values:

K_{api} = 887 for subsonic airplanes with wing and tail anti-icing

= 610 for subsonic airplanes without anti-icing

= 748 for supersonic airplanes without anti-icing

7.5.4 Fighters and Attack airplanes

7.5.4.1 GD Method

For low subsonic airplanes:

$$W_{api} = K_{api}\{(W_{iae} + 200N_{cr})/1,000\}^{0.538} \quad (7.32)$$

The constant K_{api} takes on the following values:

K_{api} = 212 for airplanes with wing and tail anti-icing

= 109 for airplanes without anti-icing

For high subsonic and for supersonic airplanes:

$$W_{api} = 202\{(W_{iae} + 200N_{cr})/1,000\}^{0.735} \quad (7.33)$$

7.6 WEIGHT ESTIMATION FOR THE OXYGEN SYSTEM

7.6.1 General Aviation Airplanes

Use Sub-section 7.6.2.

Note: Equation number (7.34) has been intentionally deleted.

7.6.2 Commercial Transport Airplanes

7.6.2.1 GD Method

$$W_{ox} = 7(N_{cr} + N_{pax})^{0.702} \quad (7.35)$$

7.6.2.2 Torenbeek Method

For commercial transport airplanes and for business type airplanes:

For flights below 25,000 ft:

$$W_{ox} = 20 + 0.5N_{pax} \quad (7.36)$$

For short flights above 25,000 ft:

$$W_{ox} = 30 + 1.2N_{pax} \quad (7.37)$$

For extended overwater flights:

$$W_{ox} = 40 + 2.4N_{pax} \quad (7.38)$$

7.6.3 Military Patrol, Bomb and Transport airplanes

Use Sub-section 7.6.2.

7.6.4 Fighters and Attack airplanes

7.6.4.1 GD Method

$$W_{ox} = 16.9(N_{cr})^{1.494} \quad (7.39)$$

7.7 AUXILIARY POWER UNIT WEIGHT ESTIMATION

Auxiliary power units are often used in transport or patrol type airplanes, commercial as well as military.

Actual APU manufacturer data should be used, where possible. Reference 8 contains data on APU systems, under 'Engines'.

From the detailed weight statements in Appendix A it is possible to derive weight fractions for these systems as a function of the take-off weight, W_{TO}. The following ranges are typical of these weight fractions:

$$W_{apu} = (0.004 \text{ to } 0.013)W_{TO} \qquad (7.40)$$

7.8 FURNISHINGS WEIGHT ESTIMATION

The furnishings category normally includes the following items:

1. seats, insulation, trim panels, sound proofing, instrument panels, control stands, lighting and wiring
2. Galley (pantry) structure and provisions
3. Lavatory (toilet) and associated systems
4. Overhead luggage containers, hatracks, wardrobes
5. Escape provisions, fire fighting equipment

Note: the associated consumable items such as potable water, food, beverages and toilet chemicals and papers are normally included in a weight category referred to as: Operational Items: W_{ops}, see Section 7.10.

The reader is referred to the detail weight statements in Appendix A for actual furnishings weight data on specific airplanes.

7.8.1 General Aviation airplanes

7.8.1.1 Cessna Method

$$W_{fur} = 0.412(N_{pax})^{1.145}(W_{TO})^{0.489}, \qquad (7.41)$$

where: N_{pax} is the number of passengers including the crew

7.8.1.2 Torenbeek Method:

For single engine airplanes:

$$W_{fur} = 5 + 13N_{pax} + 25N_{row}, \quad (7.42)$$

where: N_{row} is the number of seat rows

For multi engine airplanes:

$$W_{fur} = 15N_{pax} + 1.0V_{pax+cargo}, \quad (7.43)$$

where: $V_{pax+cargo}$ is the volume of the passenger cabin plus the cargo volume in ft^3

7.8.2 Commercial Transport Airplanes

The weight of furnishings varies considerably with airplane type and with airplane mission. This weight item is a considerable fraction of the take-off weight of most airplanes, as the data in Appendix A illustrate.

Reference 14 contains a very detailed method for estimating the furnishings weight for commercial transport airplanes.

7.8.2.1 GD Method

$$W_{fur} = \quad (7.44)$$

$$55N_{fdc} + 32N_{pax} + 15N_{cc} + K_{lav}(N_{pax})^{1.33} + K_{buf}(N_{pax})^{1.12}$$

fdc sts pax sts cc sts lavs + water food prov.

$$+ 109\{(N_{pax}(1 + P_c)/100\}^{0.505} + 0.771(W_{TO}/1,000)$$

cabin windows miscellaneous

The factor K_{lav} takes on the following values:

K_{lav} = 3.90 for business airplanes
= 0.31 for short range airplanes
= 1.11 for long range airplanes

The factor K_{buf} takes on the following values:

K_{buf} = 1.02 for short ranges
= 5.68 for very long ranges

The term P_c is the design ultimate cabin pressure in psi. The value of P_c depends on the design altitude for the pressure cabin.

7.8.2.2 Torenbeek Method

$$W_{fur} = 0.211(W_{TO} - W_F)^{0.91} \quad (7.45)$$

In commercial transports it is usually desirable to make more detailed estimates than possible with Eqn.(7.45). Particularly if a more accurate location of the c.g. of items which contribute to the furnishings weight is needed, a more detailed method may be needed. Reference 14 contains the necessary detailed information.

7.8.3 Military Patrol, Bomb and Transport Airplanes

7.8.3.1 GD Method

W_{fur} = Sum ↓ in the tabulation below. (7.46)

Type	Patrol	Bomb	Transport
Crew Ej. Seats	$K_{st}(N_{cr})^{1.2}$	$K_{st}(N_{cr})^{1.2}$	
	K_{st} = 149 with survival kit = 100 without survival kit		
Crew Seats	$83(N_{cr})^{0.726}$	same	same
Passenger Seats			$32(N_{pax})$
Troop Seats			$11.2(N_{troop})$
Lav. and Water			$1.11(N_{pax})^{1.33}$
Misc.	$0.0019(W_{TO})^{0.839}$		$0.771(W_{TO}/1,000)$

7.8.4 Fighters and Attack Airplanes

$$W_{fur} = \quad (7.47)$$

$$= 22.9(N_{cr}\bar{q}_D/100)^{0.743} + 107(N_{cr}W_{TO}/100,000)^{0.585}$$

ejection seats — Misc. and emergency eqpmt

7.9 WEIGHT ESTIMATION OF BAGGAGE AND CARGO HANDLING EQUIPMENT

The GD method gives for military passenger transports:

$$W_{bc} = K_{bc}(N_{pax})^{1.456} \qquad (7.48)$$

The constant K_{bc} takes on the following values:

K_{bc} = 0.0646 without preload provisions
= 0.316 with preload provisions

The Torenbeek method gives for commercial cargo airplanes:

$$W_{bc} = 3S_{ff}, \qquad (7.49)$$

where: S_{ff} is the freight floor area in ft^2.

For baggage and for cargo containers, the following weight estimates may be used:

freight pallets:	88x108 in	225 lbs
(including nets)	88x125 in	262 lbs
	96x125 in	285 lbs

containers: 1.6 lbs/ft^3 (For container dimensions, see Part III.)

7.10 WEIGHT ESTIMATION OF OPERATIONAL ITEMS

Typical weights counted in operational items are:

*Food *Potable water *Drinks

*China *Lavatory supplies

Observe that Eqn. (7.44) includes these operational items. For more detailed information on operational items the reader should consult Reference 14, p.292.

7.11 ARMAMENT WEIGHT ESTIMATION

The category armament can contain a wide variety of weapons related items as well as protective shielding for the crew. Typical armament items are:

*Firing systems *Fire control systems

*Bomb bay or missile doors *Armor plating

*Weapons ejection systems

Note that the weapons themselves as well as any ammunition are not normally included in this item.

Appendix A contains data on 'armament' weight for several types of military airplanes.

7.12 WEIGHT ESTIMATION FOR GUNS, LAUNCHERS AND WEAPONS PROVISIONS

For detailed data on guns, lauchers and other military weapons provisions the reader is referred to Part III, Chapter 7.

Note: Ammunition, bombs, missiles, and most types of external stores are normally counted as part of the payload weight, W_{PL} in military airplanes.

7.13 WEIGHT ESTIMATION OF FLIGHT TEST INSTRUMENTATION

During the certification phase of most airplanes a significant amount of flight test instrumentation and associated hardware is carried on board. The magnitude of W_{fti} depends on the type of airplane and the types of flight tests to be performed. Appendix A contains weight data for flight test instrumentation carried on a number of NASA experimental airplanes (Tables A13.1-A13.4).

7.14 WEIGHT ESTIMATION FOR AUXILIARY GEAR

This item encompasses such equipment as:

*fire axes *sextants *unaccounted items

An item referred to as 'manufacturers variation' is sometimes included in this category as well. A safe assumption is to set:

$$W_{aux} = 0.01 W_E \qquad (7.50)$$

7.15 BALLAST WEIGHT ESTIMATION

When looking over the weight statements for various airplanes in Appendix A, the reader will make the startling discovery that some airplanes carry a

significant amount of ballast. This can have detrimental effects on speed, payload and range performance.

The following reasons can be given for the need to include ballast in an airplane:

1. The designer 'goofed' in the weight and balance calculations

2. To achieve certain aerodynamic advantages it was judged necessary to locate the wing or to size the empennage so that the static margin became insufficient. This problem can be solved with ballast. In this case, carrying ballast may in fact turn out to be advantageous.

3. To achieve flutter stability within the flight envelope ballast weights are sometimes attached to the wing and/or to the empennage.

Note: balance weights associated with flight control surfaces are not counted as ballast weight.

The amount of ballast weight required is determined with the help of the X-plot. Construction and use of the X-plot is discussed in Part II, Chapter 11. The Class II weight and balance method discussed in Chapter 9 of this part may also be helpful in determining the amount of ballast weight required to achieve a certain amount of static margin.

7.16 ESTIMATING WEIGHT OF PAINT

Transport jets and camouflaged military airplanes carry a considerable amount of paint. The amount of paint weight is obviously a function of the extent of surface coverage. For a well painted airplane a reasonable estimate for the weight of paint is:

$$W_{pt} = 0.003 - 0.006W_{TO} \qquad (7.51)$$

7.17 ESTIMATING WEIGHT OF W_{etc}

This weight item has been included to cover any items which do not normally fit in any of the previous weight categories.

8. LOCATING COMPONENT CENTERS OF GRAVITY

The purpose of this chapter is to provide guidelines for the determination of the location of centers of gravity for individual airplane components. Knowledge of component c.g. locations is essential in both Class I and Class II weight and balance analyses as discussed in Chapter 10 of Part II and Chapter 4 of this book.

In Part II, Chapter 10, Table 10.2 provides a summary of c.g. locations for the major structural components of the airplane only. In this chapter a slightly more extensive data base is provided. The presentation of component c.g. locations follows the weight breakdowns of Chapters 5-7:

8.1 C.G. Locations of Structural Components
8.2 C.G. Locations of Powerplant Components
8.3 C.G. Locations for Fixed Equipment

8.1 C.G. LOCATIONS OF STRUCTURAL COMPONENTS

Table 8.1 lists the most likely c.g. locations for major structural components. There is no substitute for common sense: if the preliminary structural arrangement of Part III (Step 19 of p.d. sequence 2, Part II) suggests that a given structural component has a different mass distribution than is commonly the case, an 'educated guess' must be made as to the effect on the c.g. of that component.

Example: Looking at the threeview of the GP-180 of Figure 3.47, p.86, Part II it is obvious that there is a concentration of primary structure at the aft end of the fuselage. The fuselage c.g. should therefore not be placed at 38-40 percent of the fuselage length, but probably at 55 to 60 percent.

8.2 C.G. LOCATIONS OF POWERPLANT COMPONENTS

Table 8.2 lists the most likely c.g. locations for powerplant components. Note that for engine c.g. locations manufacturers data should be used. 'Guessing' at engine c.g. locations is not recommended!

8.3 C.G. LOCATIONS OF FIXED EQUIPMENT

Table 8.3 lists guidelines for locating centers of gravity of fixed equipment components.

Table 8.1 Center of Gravity Location of Structural Components

Component:	Center of gravity location:
Wing (half):	Unswept wing: 38-42 percent chord from the L.E. at 40 percent of the semi-span. Swept wing: 70 percent of the distance between the front and rear spar behind the front spar at 35 percent of the semi-span
Horizontal Tail: (half)	Regardless of sweep angle: 42 percent chord from the L.E. at 38 percent of the semi-span.
Vertical Tail: (low tail)	Regardless of sweep angle: 42 percent chord from the L.E. at 38 percent vertical tail span from the root chord.
Vertical Tail: (T-tail) root	Regardless of sweep angle: 42 percent chord from the L.E. at 55 percent vertical tail span from the root chord.
Vertical Tail: (cruciform)	Regardless of sweep angle: 42 percent chord from the L.E. at between 38 and 55 percent vertical tail span from the root chord. Interpolate according to z_h/b_v.
Fuselage: Caution: Do not count the propeller spinner in fuselage or nacelle length!	Distances are given as a fraction of the fuselage length: Single engine tractors: 0.32-0.35 Single engine pusher: 0.45-0.48 Propeller driven twins: 0.38-0.40 (tractors on wing) Propeller driven twins: 0.50-0.53 (pushers on wing) Jet transports: 0.42-0.45 (wing mounted engines) Jet transports: 0.47-0.50 (rear fuselage mounted engines) Fighters: 0.45 (engines buried in the fuselage)
Tail booms:	0.40-0.45 of boom length starting from most forward structural attachment of the boom.
Nacelles:	0.40 of nacelle length from nacelle nose
Landing gear:	at 0.50 of strutlength for gears with mostly vertical struts

Table 8.2 Center of Gravity Location of Powerplant

Components

Component:	Center of Gravity Location:
Engine(s)	Use manufacturers data
Air induction system	Use the c.g. of the gross shell area of the inlets
Propellers	On the spin axis, in the propeller spin plane
Fuel system	Refer to the fuel system layout diagram required as part of Step 17 in p.d. sequence II, Part II, p.18.
Filled fuel tank 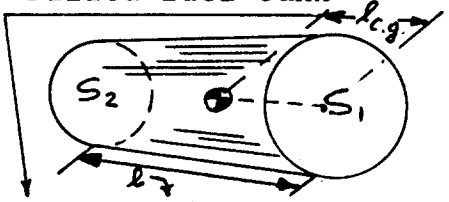	Assuming a prismoidal shape (See figure left), the c.g. is located relative to plane S_1 at: $l_{cg} = (1/4)\{S_1 + 3S_2 + 2(S_1S_2)^{1/2}\}/\{s_1 + S_2 + (S_1S_2)^{1/2}\}$ (8.1)
Trapped fuel and oil	Trapped fuel is normally located at the bottom of fuel tanks and fuel lines. Trapped oil is normally located close to the engine case.
Propulsion system	Make a list of which items contribute to the propulsion system weight and 'guestimate' their c.g. location by referring to the powerplant installation drawing required in Step 5.10, pages 133 and 134 in Part II.

Table 8.3 Center of Gravity Location of Fixed Equipment

Component:	Center of Gravity Location:
Flight Control System Hydraulic and Pneumatic System Electrical System Instrumentation, Avionics and Electronics Air-conditioning, Pressurization, Anti-icing and de-icing System Oxygen System	Note: for all systems, the c.g. location can be most closely 'guestimated' by referring to the system lay-out diagrams described in Part IV of this text. These system lay-outs were required as part of Step 17 in p.d. sequence 2, Part II, p.18.
Auxiliary Power Unit	See engine manufacturer data.
Furnishings Baggage and Cargo Handling Equipment	Refer to the fuselage internal arrangement drawing required by Steps 4.1 and 4.2 in Part II, pp 107 and 108.
Operational items	See furnishings
Armament	This item is normally close to the cockpit
Guns, launchers and weapons provisions	From manufacturer data.
Flight test instrumentation	A sketch depicting the locations of sensors, recorders operating systems should help in locating the overall c.g. of this item.
Auxiliary gear	Make a list of items in this category and 'guestimate' their c.g. locations.
Ballast	Ballast weights are normally made from lead. Ballast c.g. is thus easily located.
Paint	Centroid of painted areas.

9. CLASS II WEIGHT AND BALANCE ANALYSIS

The basic method used in performing a Class II weight and balance analysis is identical to that used for the Class I weight and balance analysis. The latter was discussed in detail in Part II, Chapter 10. The only difference is, that a more detailed weight statement is used: the Class II weight prediction method of Chapters 4-7 is used.

During this stage of the preliminary design frequent questions which are raised, are:

1. How much does the overall airplane c.g. move as a result of moving some component?

2. How much does the airplane static margin change as a result of moving the wing?

These questions are answered in Sections 9.1 and 9.2 respectively.

9.1 EFFECT OF MOVING COMPONENTS ON OVERALL AIRPLANE CENTER OF GRAVITY

Figure 9.1 illustrates an airplane, its c.g. location and the c.g. location of component i. The overall center of gravity of the airplane is found from:

$$x_{cg} = \left(\sum_{i=1}^{i=n} W_i x_i\right) / \left(\sum W_i\right) \qquad (9.1)$$

Evidently:

$$\sum_{i-1}^{i=n} W_i = W \qquad (9.2)$$

The rate at which overall airplane c.g. moves, when a component i is moved, can be found by differentiation of Eqn.(9.1):

$$\partial x_{cg}/\partial x_i = (W_i) / \left(\sum_{i=1}^{i=n} W_i\right) \qquad (9.3)$$

If component i is moved over a distance Δx_i, the

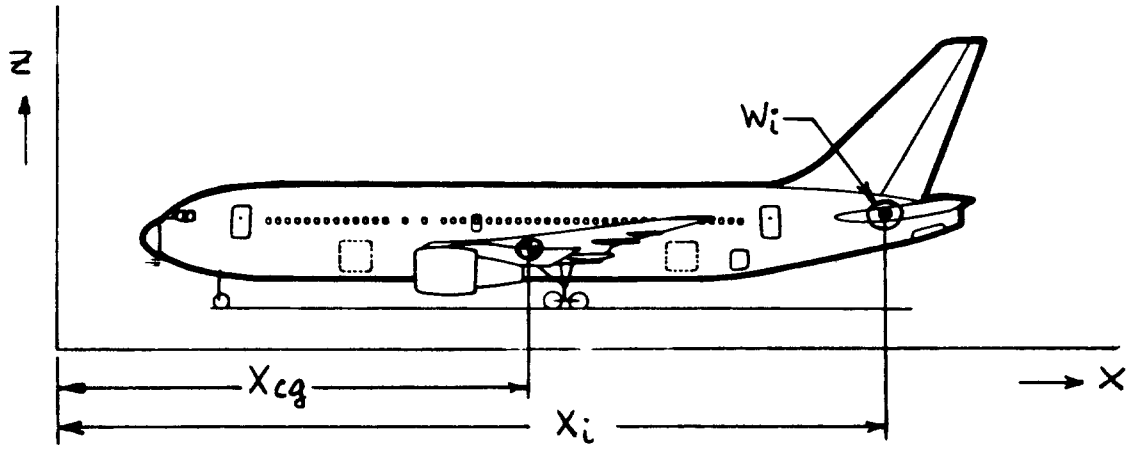

Figure 9.1 Definition of Overall C.G. Location and of Component C.G. Location

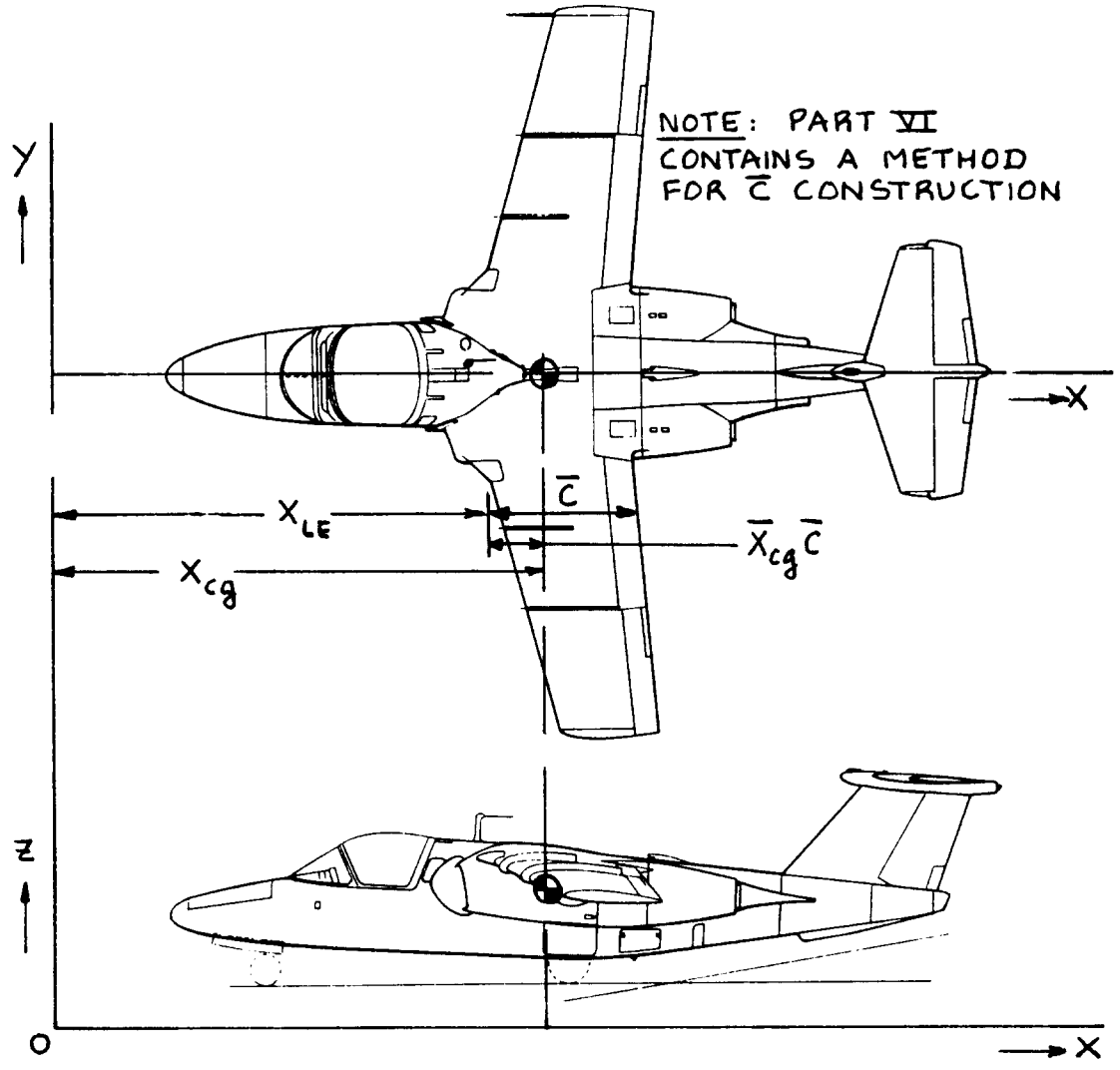

Figure 9.2 Definition of Mean Geometric Chord ($\bar{c}$) Location and Overall C.G. Location

overall airplane c.g. moves over a distance given by:

$$\Delta x_{cg} = (\Delta x_i)(W_i)/(\text{Sum}_{i=1}^{i=n} W_i) \qquad (9.4)$$

Equation (9.4) suggests that to move the overall c.g. of the airplane significantly, either a heavy weight component can be moved a small distance or a light weight component can be moved a large distance.

Items which are frequently moved about to achieve satisfactory weight and balance results are: batteries, air-conditioner units, certain 'black' boxes and sometimes just plain ballast. The reader will note from the detailed weight statements in Appendix A that several airplanes carry a relatively large amount of ballast.

9.2 EFFECT OF MOVING THE WING ON OVERALL AIRPLANE CENTER OF GRAVITY AND ON OVERALL AIRPLANE AERODYNAMIC CENTER

Figure 9.2 illustrates an airplane, its mean geometric chord location and its overall c.g. location.

If the leading edge of the mgc of the wing is at fuselage station (FS) x_{LE}, the airplane c.g. in terms of the wing mgc can be written as:

$$\bar{x}_{cg} = (x_{cg} - x_{LE})/\bar{c} \qquad (9.5)$$

When a component i is moved over a distance Δx_i, the overall airplane c.g. moves relative to the wing mgc as:

$$\Delta\bar{x}_{cg} = (\Delta x_i)(W_i)/\bar{c}(\text{Sum}_{i=1}^{i=n} W_i) \qquad (9.6)$$

For a conventional, tail-aft airplane, its aerodynamic center location can be written as:

$$\bar{x}_{ac} = \{C_1 + C_2(\bar{x}_{ac_h})\}/(1 + C_2) \qquad (9.7)$$

where: $C_1 = \bar{x}_{ac_w} + \Delta\bar{x}_{ac_{wb}}$ (9.8)

$$C_2 = (C_{L_{\alpha_h}}/C_{L_{\alpha_{wb}}})(1 - d\varepsilon/d\alpha)(S_h/S) \qquad (9.9)$$

A detailed derivation of Eqn. (9.7) may be found in Reference 19, p.133.

Part VI contains methods for computing the liftcurve slopes and aerodynamic centers which appear in C_1 and in C_2.

Warning: the wing-body aerodynamic center shift, $\Delta\bar{x}_{ac_{wb}}$ in Eqn.(9.8) is always a negative number: it shifts the a.c. forward!

If the wing is moved aft over a distance Δx_w, the overall airplane c.g. is:

$$\bar{x}_{cg_{new}} = \bar{x}_{cg_{old}} + (\Delta x_w W_w)/(\bar{c}(\text{Sum}_{i=1}^{i=n} W_i) \qquad (9.10)$$

The new a.c. location can now be written as:

$$\bar{x}_{ac_{new}} = \{C_1 + C_2(\bar{x}_{ac_h} - \Delta x_w/\bar{c})\}/(1 + C_2) \qquad (9.11)$$

Equations (9.10) and (9.11) can be used to 'redo' the X-plot of Part II, Chapter 11. This 'redone' X-plot in turn is used to:

1. determine how much the horizontal tail area must be changed as a result of moving the wing

or:

2. determine which other weight components need to be moved and by how much, to maintain some desired level of stability (or instability as the case may be).

For a canard airplane and/or for a three surface airplane similar equations are easily derived. The reader should consult Equations (11.1) and (11.2) in Part II for guidance.

10. CLASS II METHOD FOR ESTIMATING AIRPLANE INERTIAS

The purpose of this chapter is to provide an outline for a Class II method for estimating moments and products of inertia. It will be assumed that the Class II weight estimating method of Chapter 4 has been applied: a rather detailed weight and c.g. breakdown for the airplane is therefore presumed to be available.

The following equations are a slight modification of the general inertia equations 2.22a through 2.22c in Reference 19.

$$I_{xx} = \sum_{i=1}^{i=n} m_i\{(y_i - y_{cg})^2 + (z_i - z_{cg})^2\} \qquad (10.1)$$

$$I_{yy} = \sum_{i=1}^{i=n} m_i\{(z_i - z_{cg})^2 + (x_i - x_{cg})^2\} \qquad (10.2)$$

$$I_{zz} = \sum_{i=1}^{i=n} m_i\{(x_i - x_{cg})^2 + (y_i - y_{cg})^2\} \qquad (10.3)$$

$$I_{xy} = \sum_{i=1}^{i=n} m_i(x_i - x_{cg})(y_i - y_{cg}) \qquad (10.4)$$

$$I_{yz} = \sum_{i=1}^{i=n} m_i(y_i - y_{cg})(z_i - z_{cg}) \qquad (10.5)$$

$$I_{zx} = \sum_{i=1}^{i=n} m_i(z_i - z_{cg})(x_i - x_{cg}) \qquad (10.6)$$

Figure 10.1 defines the coordinates used in these equations.

The reader should recall that for a symmetrical airplane the inertia products I_{xy} and I_{yz} are zero.

Equations (10.1) through (10.6) are valid whenever the weight breakdown contains a 'sufficiently' large number of parts so that the inertia moment and/or product of each part about its own c.g. location is negligible.

Whenever the latter assumption is not satisfied,

equations (10.1) through (10.6) should be all modified as follows:

$$I_{xx} = \sum_{i=1}^{i=n} I_{xx_i} + \sum_{i=1}^{i=n} m_i\{(y_i - y_{cg})^2 + (z_i - z_{cg})^2\} \quad (10.7)$$

The first term in Eqn.(10.7) represents the moment (or product) of inertia of component i about its own center of gravity.

Moments (and products) of inertia of airplane components about their own center of gravity can be computed in a relatively straightforward manner by assuming uniform mass distributions for structural components and by using the 'lumped mass' assumption for distributed systems. An example of the latter would be the airplane fuel system. Major fuel system components such as pumps, bladders and the like can be considered to be concentrated masses distributed around the fuel system c.g.. Equations (10.1) through (10.2) are then used to compute the moments of inertia of the fuel system about its own c.g.

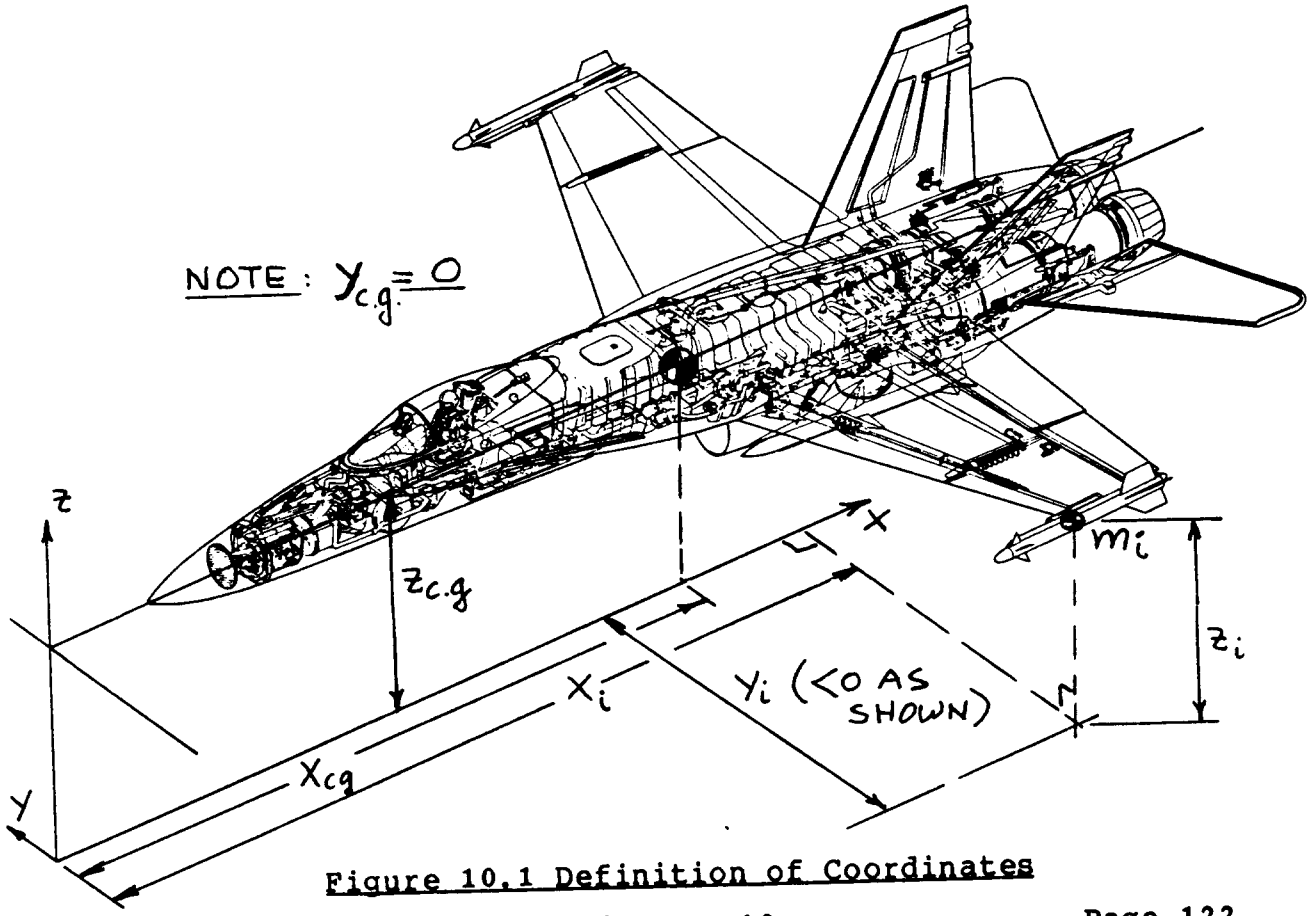

Figure 10.1 Definition of Coordinates

11. REFERENCES

1. Roskam, J., Airplane Design: Part I, Preliminary Sizing of Airplanes.

2. Roskam, J., Airplane Design: Part II, Preliminary Configuration Design and Integration of the Propulsion System.

3. Roskam, J., Airplane Design: Part III, Layout Design of Cockpit, Fuselage, Wing and Empennage: Cutaways and Inboard Profiles.

4. Roskam, J., Airplane Design: Part IV, Layout Design of Landing Gear and Systems.

5. Roskam, J., Airplane Design: Part VI, Preliminary Calculation of Aerodynamic, Thrust and Power Characteristics.

6. Roskam, J., Airplane Design: Part VII, Determination of Stability, Control and Performance Characteristics: FAR and Military Requirements.

7. Roskam, J., Airplane Design: Part VIII, Airplane Cost Estimation and Optimization: Design, Development Manufacturing and Operating.

Note: These books are all published by: Roskam Aviation and Engineering Corporation, Rt4, Box 274, Ottawa, Kansas, 66067, Tel. 913-2421624.

8. Taylor, J.W.R., Jane's All The World Aircraft, Published Annually by: Jane's Publishing Company, 238 City Road, London EC1V 2PU, England. (Issues used: 1945/46, 1968/84)

9. Chawla, J.P., Empirical Formulae for Radii of Gyration of Aircraft, SAWE Paper No.78, Hughes Aircraft Company, Culver City, California, 1952.

10. Anon., Empirical Formulae for Moments of Inertia of Aircraft, Royal Aircraft Establishment, Structures Report No. 28, Farnborough, England, 1948.

11. Garcia, D., Empirical Formulae for Radii of Gyration of Aircraft, Revision A, SAWE Paper No.78A, Republic Aviation Corporation, Farmingdale, Long Island, NY, 1962.

12. Schmitt, R.L., Foreman, K.C., Gertsen, W.M. and Johnson, P.H., Weight Estimation Handbook for Light Aircraft, Cessna Aircraft Company, 1959.

13. Nicolai, L.M., Fundamentals of Aircraft Design, METS, Inc., 6520 Kingsland Court, CA, 95120.

14. Torenbeek, E., Synthesis of Subsonic Airplane Design, Kluwer Boston inc., Hingham, Maine, 1982.

15. Anon., Federal Aviation Regulation, Part 23, Department of Transportation, Federal Aviation Administration, Distribution Requirements Section, M-482.2, Washington D.C., 20590.

16. Anon., Federal Aviation Regulation, Part 25, see Ref. 15.

17. MIL-A-8861(ASG), Military Specification, Airplane Strength and Rigidity, Flight Loads, May 1960.

18. Business and Commercial Aviation (Monthly magazine), 1985 Planning and Purchasing Handbook, April 1985.

19. Roskam, J., Airplane Flight Dynamics and Automatic Flight Controls, Part I, Roskam Aviation and Engineering Corporation, Rt 4, Box 274, Ottawa, Kansas, 66067.

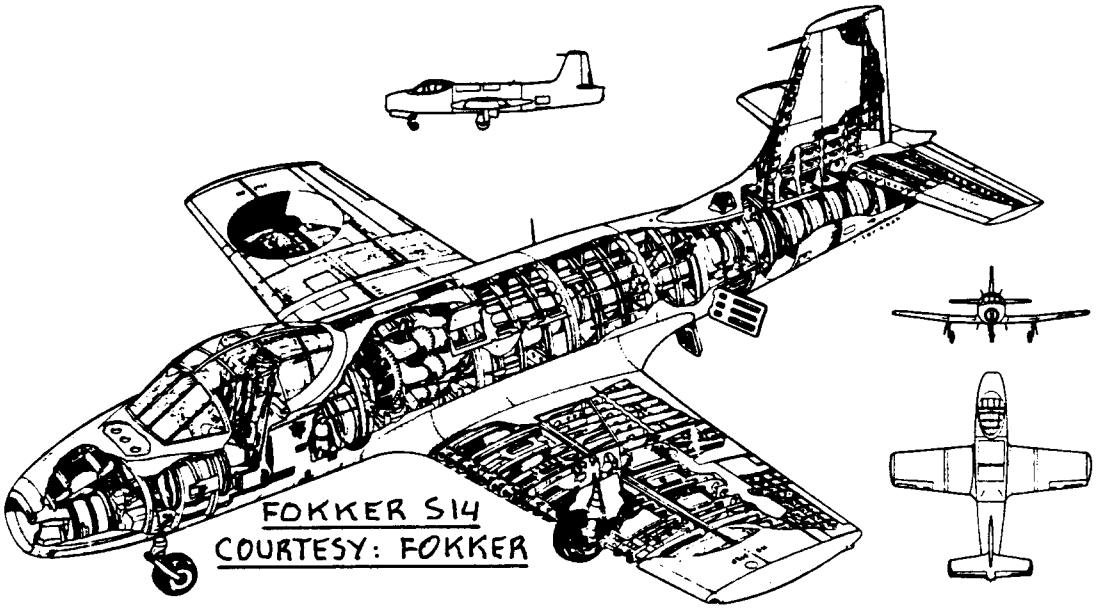

APPENDIX A: DATA SOURCE FOR AIRPLANE COMPONENT WEIGHTS AND FOR WEIGHT FRACTIONS

Tables A1 through A13 present component weight data for the following types of airplanes:

1. Homebuilt propeller driven airplanes: Tables A1.1.

2. Single engine propeller driven airplanes: Tables A2.1 and A2.2.

3. Twin engine propeller driven airplanes: Tables A3.1 and A3.2.

4. Agricultural airplanes: Tables A4.1. At the time of printing no data were available. The reader should use Tables A2 and add spray equipment weights.

5. Business Jets: Tables A5.1 and A5.2.

6. Regional turbopropeller airplanes: Tables A6.1 through A6.3.
   Regional piston/propeller airplanes: Tables A6.4.

7. Jet transports: Tables A7.1 through A7.5.
   Turbopropeller driven transports: Tables A7.6.

8. Military trainers: Tables A8.1.

9. Fighters: Tables A9.1 through A9.5.

10. Military jet transports: Tables A.10.1.
    Military turbopropeller driven transports: Tables A10.2.
    Military piston/propeller driven transports: Table A10.3 and A10.4.
    Military patrol airplanes: Tables A10.5.

11. Flying boats, amphibious and float airplanes: Tables A11.1. At the time of printing no data were available. The reader should use suitable tables in categories 1-10 and account for hull weight with the method of Chapter 4.

12. Supersonic cruise airplanes: Tables A12.1.

13. NACA and NASA X (experimental) airplanes: Tables A13.1 through A13.4.
    CAUTION: most of the X airplanes were built for experimental purposes only. They should not be regarded as 'optimized' for a given mission.

Table A1.1a Group Weight Data for Homebuilt Propeller Driven Airplanes

Type	Bede BD5B	At the time of printing no other data were available
Weight Item, lbs		
Wing Group	87	
Empennage Group	17	
Fuselage Group	89	
Nacelle Group	0	
Landing Gear Group	32	
Nose Gear	10	
Main Gear	22	
Structure Total	225	
Engine	146	
Air Induct. System	0	
Fuel System	25	
Propeller Install.	5	
Thrust Attenuator	3	
Engine Install.	10	
Power Plant Total	189	
Avionics + Instrum.	15	
Surface Controls	0	
Electrical System	10	
Electronics	0	
Ballast	30	
Parachute	20	
Furnishings + paint	50	
Auxiliary Gear	0	
Fixed Equipm't Total	125	
$W_{oil} + W_{tof}$	2	
Fuel	340	
Payload(pilot)	170	

Table A1.1b Group Weight Data for Homebuilt Propeller Driven Airplanes

Type	Bede BD5B	At the time of printing no other data were available
Flight Design Gross Weight, GW, lbs	1,051	
Structure/GW	0.214	
Power Plant/GW	0.180	
Fixed Equipm't/GW	0.119	
Empty Weight/GW	0.513	
Wing Group/GW	0.083	
Empenn. Group/GW	0.016	
Fuselage Group/GW	0.085	
Nacelle Group/GW	0.000	
Land. Gear Group/GW	0.030	
Take-off Gross Wht, W_{TO}, lbs	1,051	
Empty Weight, W_E, lbs	539	
Wing Group/S, psf	1.8	
Emp. Grp/S_{emp}, psf	1.1	
Ultimate Load Factor, g's	5.7	assumed
Surface Areas, ft^2		
Wing, S	47.4	
Horiz. Tail, S_h	10.5	
Vert. Tail, S_v	5.0	
Empenn. Area, S_{emp}	15.5	

Table A2.1a Group Weight Data for Single Engine Propeller Driven Airplanes

Type →	Cessna 150	172	175	180 **	182	L-19A* **
Weight Item, lbs						
Wing Group	216	226	227	235	235	238
Empennage Group	36	57	57	62	62	64
Fuselage Group	231	353	351	404	400	216
Nacelle Group	22	27	30	32	34	33
Landing Gear Group	104	111	111	112	132	135
Nose Gear						
Main Gear						
Structure Total	609	774	776	845	863	686
Engine	197	254	318	417	417	399
Air Induct. System	2	1	3	1	1	4
Fuel System	17	21	26	26	26	39
Propeller Install.	22	33	33	64	64	46
Engine Install.	28	36	36	37	37	62
Power Plant Total	267	345	416	545	545	550
Avionics + Instrum.	3	4	4	6	6	36
Surface Controls	31	31	31	36	36	47
Electrical System	34	38	38	43	43	86
Electronics	0	0	0	0	0	39
Air Cond. System	1	1	1	1	1	9
Anti-icing System	33	85	85	87	87	65
Furnishings	0	0	0	0	0	3
Auxiliary Gear						
Fixed Equipm't Total	102	159	159	173	173	285
W_{oil} + W_{tof}	11	15	19	22	22	19
Fuel	156	252	312	390	390	252
Payload	398	702	719	734	715	321

*Military observation airplane
**Taildragger

Table A2.1b Group Weight Data for Single Engine Propeller Driven Airplanes

Type	Cessna 150	172	175	180 **	182	L-19A* **
Flight Design Gross Weight, GW, lbs	1,500	2,200	2,350	2,650	2,650	2,100
Structure/GW	0.406	0.352	0.330	0.319	0.326	0.327
Power Plant/GW	0.178	0.157	0.177	0.206	0.206	0.262
Fixed Equipm't/GW	0.068	0.072	0.068	0.065	0.065	0.136
Empty Weight/GW	0.631	0.565	0.561	0.576	0.583	0.727
Wing Group/GW	0.144	0.103	0.097	0.089	0.089	0.113
Empenn. Group/GW	0.024	0.026	0.024	0.023	0.023	0.030
Fuselage Group/GW	0.154	0.160	0.149	0.152	0.151	0.103
Nacelle Group/GW	0.015	0.012	0.013	0.012	0.013	0.016
Land. Gear Group/GW	0.069	0.050	0.047	0.042	0.050	0.064
Take-off Gross Wht, W_{TO}, lbs	1,500	2,200	2,350	2,650	2,650	2,100
Empty Weight, W_E, lbs	946	1,243	1,319	1,526	1,545	1,527
Wing Group/S, psf	1.4	1.4	1.3	1.3	1.3	1.4
Emp. Grp/S_{emp}, psf	0.85	1.1	1.1	1.2	1.2	1.2
Ultimate Load Factor, g's	5.7	5.7	5.7	5.7	5.7	5.7
Surface Areas, ft^2						
Wing, S	160	175	175	175	175	174
Horiz. Tail, S_h	28.5	34.6	34.6	34.6	34.1	35.2
Vert. Tail, S_v	14.1	18.4	18.4	18.4	18.4	18.4
Empenn. Area, S_{emp}	42.6	53.0	53.0	53.0	52.5	53.6

*Military observation airplane
**Taildragger

Table A2.2a Group Weight Data for Single Engine Propeller Driven Airplanes

Type →	Cessna 210A	Beech J-35	Saab Safir	Rockwell 112TCA	Cessna 210J
Weight Item, lbs.					
Wing Group	261	379	276	334	335
Empennage Group	71	58	60	98	86
Fuselage Group	316*	200	386	358	408*
Nacelle Group	31	62	in fus.	61	28
Landing Gear Group	207	205	119	161	191
Nose Gear				35	50
Main Gear				126	141
Structure Total	886	904	841	1,082	1,048
Engine	390	432		475	450
Air Induct. System		3			7
Fuel System		30		17	24
Propeller Install.		73		in eng.	64
Engine Install.		45		65	36
Power Plant Total	577	583		557	581
Avionics + Instrum.	16	16		64	18
Surface Controls	44	56	in fus.	44	48
Hydraulic System	4			10	51
Electrical System	60	72		81	57
Air Cond. System	12	12		in misc.	10
Anti-icing System					
Furnishings	116	174		179	130
Oxygen System	0	0	0	20	0
Ballast	0	0	0	21	0
Auxiliary Gear	0	4	0	2	0
Misc. Equipment	20	0	0	24	0
Paint					21
Fixed Equipm't Total	272	334		445	335
W_{oil} + W_{tof}		11		31	24
Fuel (max. payload)		234		230	464**
Payload		845		740	693

*Includes wing-fuselage carry-through spars
**Maximum fuel

Table A2.2b Group Weight Data for Single Engine Propeller Driven Airplanes

Type	Cessna 210A	Beech J-35	Saab Safir	Rockwell 112TCA	Cessna 210J
Flight Design Gross Weight, GW, lbs	2,900	2,900	2,660	2,954	3,400
Structure/GW	0.306	0.312	0.316	0.366	0.308
Power Plant/GW	0.199	0.201		0.189	0.171
Fixed Equipm't/GW	0.094	0.115		0.151	0.099
Empty Weight/GW	0.598	0.628	0.620	0.705	0.578
Wing Group/GW	0.090	0.131	0.104	0.113	0.099
Empenn. Group/GW	0.024	0.020	0.023	0.033	0.025
Fuselage Group/GW	0.109	0.069	0.145	0.121	0.120
Nacelle Group/GW	0.011	0.021		0.021	0.008
Land. Gear Group/GW	0.071	0.071	0.045	0.055	0.056
Take-off Gross Wht, W_{TO}, lbs	2,900	2,900	2,660	2,954	3,400
Empty Weight, W_E, lbs	1,735	1,821	1,650	2,084	1,964
Wing Group/S, psf	1.5	2.1	1.9	2.2	1.9
Emp. Grp/S_{emp}, psf	1.3	1.6	1.4	2.0	1.5
Ultimate Load Factor, g's	5.7				5.7
Surface Areas, ft^2					
Wing, S	176	178	146	152	176
Horiz. Tail, S_h	38.6	*	27.6**	32.0	38.6
Vert. Tail, S_v	17.2	*	14.3**	17.0	17.2
Empenn. Area, S_{emp}	55.8	35.8	41.9	49.0	55.8

*V-tail
**Estimated

Table A3.1a Group Weight Data for Twin Engine Propeller Driven Airplanes

Type	Beech 65 QA*	E-18S	G-50 TB*	95 TA*	Cessna 310C
Number of engines:	2	2	2	2	2
Weight Item, lbs					
Wing Group	670	874	656	458	453
Empennage Group	153	180	156	79	118
Fuselage Group	601	768	495	276	319
Nacelle Group	285	331	261	180	129
Landing Gear Group	444	585**	447	218	263
Nose Gear					
Main Gear					
Structure Total	2,153	2,738	2,015	1,211	1,282
Engines	1,008	1,352	1,008	519	852
Air Induct. System	27	149	27	8	7
Fuel System	137	274	137	83	76
Propeller Install.	258	334	258	162	162
Engine Install.	180	172	172	101	153
Power Plant Total	1,610	2,281	1,610	873	1,250
Avionics + Instrum.	70	100	80	49	46
Surface Controls	132	115	120	73	66
Electrical System	166	295	184	96	121
Electronics	2	63	9	26	0
Air Cond. System	90	144	81	48	46
Anti-icing System					
Furnishings	438	524	333	194	154
Auxiliary Gear	5	0	7	0	65
Fixed Equipm't Total	903	1,241	814	486	498
W_{oil} + W_{tfo}	60	128	60	30	45
Fuel	1,380	1,908	1,380	672	612
Payload	1,287	1,474	1,311	733	1,186

*QA = Queen Air, TB = Twin Bonanza, TA = Travel Air
**Taildragger

Table A3.1b Group Weight Data for Twin Engine Propeller Driven Airplanes

Type	Beech 65 QA*	E-18S**	G-50 TB*	95 TA*	Cessna 310C
Flight Design Gross Weight, GW, lbs	7,368	9,700	7,150	4,000	4,830
Structure/GW	0.292	0.282	0.282	0.303	0.265
Power Plant/GW	0.219	0.235	0.225	0.218	0.259
Fixed Equipm't/GW	0.123	0.128	0.114	0.122	0.103
Empty Weight/GW	0.638	0.651	0.624	0.649	0.628
Wing Group/GW	0.091	0.090	0.092	0.115	0.094
Empenn. Group/GW	0.021	0.019	0.022	0.020	0.024
Fuselage Group/GW	0.082	0.079	0.069	0.069	0.066
Nacelle Group/GW	0.039	0.034	0.037	0.045	0.027
Land. Gear Group/GW	0.060	0.060	0.063	0.055	0.054
Take-off Gross Wht, W_{TO}, lbs	7,368	9,700	7,150	4,000	4,830
Empty Weight, W_E, lbs	4,701	6,318	4,459	2,595	3,032
Wing Group/S, psf	2.4	2.4	2.4	2.4	2.6
Emp. Grp/S_{emp}, psf	1.4	1.7	1.4	1.2	1.5
Ultimate Load Factor, g's	6.6		7.1		5.7
Surface Areas, ft^2					
Wing, S	277	361	277	194	175
Horiz. Tail, S_h	79.3	71.6	79.3	42.4	54.3
Vert. Tail, S_v	30.8	33.6	30.8	23.3	25.9
Empenn. Area, S_{emp}	110	105	110	65.7	80.2

*QA = Queen Air, TB = Twin Bonanza, TA = Travel Air
**Taildragger

Table A3.2a Group Weight Data for Twin Engine Propeller Driven Airplanes

Type	Cessna 404-3	414A	TP-441	Rockwell 690B
Number of engines:	2	2	2	2
Weight Item, lbs	(PP)	(PP)	(PP)	(TBP)
Wing Group	860	638	873	1,001
Empennage Group	181	160	233	207
Fuselage Group	610	678	873	1,377
Nacelle Group	284	200	258	in prop/eng
Land. Gear Group	316	303	346	437
Nose Gear	67	75	69	53
Main Gear	249	228	277	384
Structure Total	2,251	1,979	2,583	3,022
Engines	1,000	862	745	720
Air Induct. System	23	36	0	17
Fuel System	107	96	93	180
Propeller Install.	215	165	302	758
Engine Install.	281	240	130	
Power Plant Total	1,626	1,399	1,270	1,675
Avionics + Instrum.	311	334	250	344
Hydraulic System	52	14	49	99
Surface Controls	113	107	223	81
Electrical System	169	157	403	379
Electronics	1	1	150	0
Oxygen System	0	0	0	23
Air Cond. System	49	130*	182*	205*
Anti-icing System	11	3	78	84
Furnishings	370	342	538	612
Auxiliary Gear	5	3	7	41**
Paint	48	42	48	40
Fixed Equipm't Total	1,129	1,133	1,928	1,908
W_{oil} + W_{tfo}	116	113	98	65
Fuel	1,379	961	2,446	1,575
Payload***	1,900	1,200	1,600	1,960

*Includes pressurization system
**This is all ballast in this model
***Includes a crew of two

Table A3.2b Group Weight Data for Twin Engine Propeller Driven Airplanes

Type	Cessna 404-3 (PP)	414A (PP)	TP-441 (TBP)	Rockwell 690B (TBP)
Flight Design Gross Weight, GW, lbs	8,400	6,785	9,925	10,205
Structure/GW	0.268	0.292	0.260	0.296
Power Plant/GW	0.194	0.206	0.128	0.164
Fixed Equipm't/GW	0.134	0.167	0.194	0.187
Empty Weight/GW	0.596	0.665	0.582	0.647
Wing Group/GW	0.102	0.094	0.088	0.098
Empenn. Group/GW	0.022	0.024	0.023	0.020
Fuselage Group/GW	0.073	0.100	0.088	0.135
Nacelle Group/GW	0.034	0.029	0.026	
Land. Gear Group/GW	0.038	0.045	0.035	0.043
Take-off Gross Wht, W_{TO}, lbs	8,400	6,785	9,925	10,205
Empty Weight, W_E, lbs	5,006	4,511	5,781	6,605
Wing Group/S, psf	3.6	2.8	3.4	3.8
Emp. Grp/S_{emp}, psf	1.7	1.6	2.2	2.0
Ultimate Load Factor, g's	3.75*	3.75*	3.75*	3.75*
Surface Areas, ft^2				
Wing, S	242	226	254	266
Horiz. Tail, S_h	63.4	60.7	63.4	58.4
Vert. Tail, S_v	43.5	41.2	43.5	44.8
Empenn. Area, S_{emp}	107	102	107	103

*Assumed

Table A4.1a Group Weight Data for Agricultural Airplanes

Type	At the time of printing no data were available
Number of engines:	
Weight Item, lbs	
Wing Group	
Empennage Group	
Fuselage Group	
Nacelle Group	
Landing Gear Group	
Nose Gear	
Main Gear	
Structure Total	
Engines	
Air Induct. System	
Fuel System	
Propulsion System.	
Power Plant Total	
Spray equipment	
Avionics + Instrum.	
Surface Controls	
Hydraulic System	
Pneumatic System	
Electrical System	
Electronics	
Oxygen System	
Air Cond. System**	
Furnishings	
Auxiliary Gear	
Miscellaneous	
Fixed Equipm't Total	
$W_{oil} + W_{tfo}$	
Max. Fuel Capacity	
Max. Payload	

Table A4.1b Group Weight Data for Agricultural Airplanes

Type	At the time of printing no data were available
Flight Design Gross Weight, GW, lbs	
Structure/GW	
Power Plant/GW	
Fixed Equipm't/GW	
Empty Weight/GW	
Wing Group/GW	
Empenn. Group/GW	
Fuselage Group/GW	
Nacelle Group/GW	
Land. Gear Group/GW	
Take-off Gross Wht, W_{TO}, lbs	
Empty Weight, W_E, lbs	
Wing Group/S, psf	
Emp. Grp/S_{emp}, psf	
Ultimate Load Factor, g's	
Surface Areas, ft^2	
Wing, S	
Horiz. Tail, S_h	
Vert. Tail, S_v	
Empenn. Area, S_{emp}	

Table A5.1a Group Weight Data for Business Jets

Type	MS-760 Paris	Lockheed Jetstar	Gates-Learjet 25D	Gates-Learjet 28
Number of engines:	2	2	2	2
Weight Item, lbs				
Wing Group	897	2,827	1,467	1,939
Empennage Group	176	879	361	361
Fuselage Group	912	3,491	1,575	1,624
Nacelle Group	49*	792	241	214
Landing Gear Group	307	1,061	584	584
Nose Gear			102	102
Main Gear			482	482
Structure Total	2,341	9,050	4,228	4,722
Engines	609	1,750	792	792
Air Induct. System	31	135	0	0
Fuel System	240	360	179	237
Propulsion System.	136	230	255	255
Power Plant Total	1,016	2,475	1,226	1,284
Avionics + Instrum.	70	153	383	383
Surface Controls	188	768	291	275
Hydraulic System		262	119	114
Pneumatic System				
Electrical System	284	973	620	603
Electronics	158	868	0	0
Oxygen System			28	26
Air Cond. System**	48	510	293	285
Anti-icing System			82	162
Furnishings	169	1,521	720	768
Auxiliary Gear	0	10	0	0
Miscellaneous	0	0	-40	-11
Fixed Equipm't Total	917	5,065	2,496	2,605
$W_{oil} + W_{tfo}$	28	204	177	
Max. Fuel Capacity	2,460	11,229	6,098	4,684
Max. Payload	884	2,100	2,980	1,962

*Engines buried inside the fuselage
**Includes pressurization system

Table A5.1b Group Weight Data for Business Jets

Type	MS-760 Paris	Lockheed Jetstar	Gates-Learjet 25D	Gates-Learjet 28
Flight Design Gross Weight, GW, lbs	7,650	30,680	15,000	15,000
Structure/GW	0.306	0.295	0.282	0.315
Power Plant/GW	0.133	0.081	0.082	0.086
Fixed Equipm't/GW	0.120	0.165	0.166	0.174
Empty Weight/GW*	0.563	0.541	0.530	0.574
Wing Group/GW	0.117	0.092	0.098	0.129
Empenn. Group/GW	0.023	0.029	0.024	0.024
Fuselage Group/GW	0.119	0.114	0.105	0.108
Nacelle Group/GW	0.006*	0.026	0.016	0.014
Land. Gear Group/GW	0.040	0.035	0.039	0.039
Take-off Gross Wht, W_{TO}, lbs	7,650	30,680	15,000	15,000
Empty Weight, W_E, lbs	4,306	16,590	7,950	8,611
Wing Group/S, psf	4.6	5.4	6.3	7.3
Emp. Grp/S_{emp}, psf	3.5	3.4	3.9	3.9
Ultimate Load Factor, g's	3.75**	5.25	3.75**	3.75**
Surface Areas, ft^2				
Wing, S	194	521	232	265
Horiz. Tail, S_h	31.8	149	54.0	54.0
Vert. Tail, S_v	18.4	110	37.4	37.4
Empenn. Area, S_{emp}	50.2	259	91.4	91.4

*Engines buried inside the fuselage
**Assumed

Table A5.2a Group Weight Data for Business Jets

Type	Cessna Citation II	Rockwell JC-1121	Hawker-Siddeley 125	Gulfstr. American GII
Number of engines:	2	2	2	2
Weight Item, lbs				
Wing Group	1,288	1,322	1,968	6,372
Empenn. Group	295	425	608	1,965
Fuselage Group	1,069	1,622	1,628	5,944
Nacelle Group	220	350	in fusel.	1,239
Land. Gear Group	465	443	659	2,011
Nose Gear	87			321
Main Gear	378			1,690
Structure Total	3,337	4,162	4,863	17,531
Engine(s)	1,100			6,570
Air Induct. System	26			
Exhaust System	15			
Fuel System	189			316
Propulsion System	105			
Power Plant Total	1,435			6,886
Avionics + Instrum.	87			1,715
Surface Controls	203	223	217	1,021
Hydraulic System	96			959
Electrical System	340			1,682
Electronics	313			
Oxygen System				140
Air Cond. System*	264			927
Anti-icing System	98			
Furnishings	800			4,501
Auxiliary Gear	3			
Auxiliary power unit				258
Paint	47			
Fixed Equipm't Total	2,251			11,203
$W_{oil} + W_{tfo}$	143			
Max. Fuel Capacity	5,009	8,964	9,193	23,300
Max. Payload			1,905	5,380

*Includes pressurization system

Table A5.2b Group Weight Data for Business Jets

Type	Cessna Citation II	Rockwell JC-1121	Hawker Siddeley 125	Gulfstr. American GII
Flight Design Gross Weight, GW, lbs	13,500	20,500	23,300	64,800
Structure/GW	0.247	0.203	0.209	0.271
Power Plant/GW	0.106			0.106
Fixed Equipm't/GW	0.167			0.173
Empty Weight/GW	0.520	0.540	0.526	0.550*
Wing Group/GW	0.095	0.064	0.084	0.098
Empenn. Group/GW	0.022	0.021	0.026	0.030
Fuselage Group/GW	0.079	0.079	0.070	0.092
Nacelle Group/GW	0.016	0.017	in fusel.	0.019
Land. Gear Group/GW	0.034	0.022	0.028	0.031
Take-off Gross Wht, W_{TO}, lbs	13,500	20,500	23,300	64,800
Empty Weight, W_E, lbs	7,023	11,070	12,260	35,620
Wing Group/S, psf	4.6	4.4		8.0
Emp. Grp/S_{emp}, psf	2.4	3.3		5.8
Ultimate Load Factor, g's	3.75**			
Surface Areas, ft^2				
Wing, S	279	303	353	794
Horiz. Tail, S_h	70.6	70	100	182
Vert. Tail, S_v	50.9	59.3	51.6	155
Empenn. Area, S_{emp}	122	129	152	337

*Typical. Individual airplanes will vary. **Assumed

Table A6.1a Group Weight Data for Regional Turbopropeller Driven Airplanes

Type →	Grumman G-I	Fokker F-27-100	Nord 262	Embraer 110-P2
Number of engines:	2	2	2	2
Weight Item, lbs				
Wing Group	3,735	4,408	2,698	1,502
Empennage Group	874	977	805	454
Fuselage Group	3,718	4,122	3,675	1,354
Nacelle Group	1,136	628	236	198
Land. Gear Group	1,207	1,940	1,085	538
Nose Gear	219			
Main Gear	988			
Structure Total	10,670	12,075	8,499	4,046
Engines	2,688	2,427		622
Air Induct. System				
Fuel System	133	390		86
Propeller Install.	1,002	918		1,140
Propulsion System	698	612		in prop.
Power Plant Total	4,521	4,347		1,848
Avionics + Instrum.	97	81	133	364
Surface Controls	461	613	408	342
Hydraulic System	235	242	(incl.in electr.)	176
Pneumatic System				
Electrical System	966	835	765	452
Electronics	99	386	238	in avion.
APU	355	0	0	0
Air Cond. System	755*	1,225*	527*	192
Anti-icing System				73
Furnishings	415	2,291	1,324	882
Auxiliary Gear	6		33	
Fixed Equipm't Total	3,389	5,673	3,428	2,481
W_{oil} + W_{tfo}	329			
Max. Fuel Capacity	10,447	9,198	3,559	3,062
Maximum Payload	4,270	12,500	6,175	3,706

*Includes pressurization system

Table A6.1b Group Weight Data for Regional Turbopropeller Driven Airplanes

Type	Grumman G-I	Fokker F-27-100	Nord 262	Embraer 110-P2
Flight Design Gross Weight, GW, lbs	35,100	37,500	22,930	12,500
Structure/GW	0.304	0.322	0.371	0.324
Power Plant/GW	0.129	0.116		0.148
Fixed Equipm't/GW	0.097	0.151	0.149	0.198
Empty Weight/GW	0.624	0.615	0.663	0.670
Wing Group/GW	0.106	0.118	0.118	0.120
Empenn. Group/GW	0.025	0.026	0.035	0.036
Fuselage Group/GW	0.106	0.110	0.160	0.108
Nacelle Group/GW	0.032	0.017	0.010	0.016
Land. Gear Group/GW	0.034	0.052	0.047	0.043
Take-off Gross Wht, W_{TO}, lbs	35,100	37,500	22,930	12,500
Empty Weight, W_E, lbs	21,900	23,054	15,200	8,375
Wing Group/S, psf	6.1	5.8	4.6	4.8
Emp. Grp/S_{emp}, psf	3.6	3.0	2.9	2.8
Ultimate Load Factor, g's	3.75*	3.75*	3.75*	3.75*
Surface Areas, ft^2				
Wing, S	610	754	592	313
Horiz. Tail, S_h	127	172	169	105
Vert. Tail, S_v	117	153	109	59
Empenn. Area, S_{emp}	244	325	278	164

*Assumed

Table A6.2a Group Weight Data for Regional Turbopropeller Driven Airplanes

Type	Fokker F-27-200	F-27-500	Short* Skyvan
Number of engines:	2	2	2
Weight Item, lbs			
Wing Group	4,505	4,510	1,220
Empennage Group	1,053	1,060	374
Fuselage Group	4,303	5,142	2,154
Nacelle Group	667	668	254
Land. Gear Group	1,825	1,865	466
Nose Gear			
Main Gear			
Structure Total	12,353	13,245	4,468
Engines			714
Air Induct. System			
Fuel System			373
Propeller Install.			368
Propulsion System			87
Power Plant Total			1,542
Avionics + Instrum.		126	74
Surface Controls	620	626	265
Hydraulic System		256	64
Pneumatic System			
Electrical System		840	320
Electronics		329	12
APU		0	
Air Cond. System		1,257**	85
Anti-icing System			
Furnishings		3,035	135***
Auxiliary Gear		0	43
Paint			75
Fixed Equipm't Total		6,469	1,073
$W_{oil} + W_{tfo}$			44
Max. Fuel Capacity	9,146	9,146	4,924
Payload (Max.)	12,615	12,383	

*Strutbraced wing **Includes pressurization
***Cockpit furnishings only

Table A6.2b Group Weight Data for Regional Turbopropeller Driven Airplanes

Type	Fokker F-27-200	F-27-500	Short* Skyvan
Flight Design Gross Weight, GW, lbs	43,500	45,000	12,500
Structure/GW	0.284	0.294	0.357
Power Plant/GW			0.123
Fixed Equipm't/GW		0.144	0.086
Empty Weight/GW	0.537	0.548	0.570
Wing Group/GW	0.104	0.100	0.098
Empenn. Group/GW	0.024	0.024	0.030
Fuselage Group/GW	0.099	0.114	0.172
Nacelle Group/GW	0.015	0.015	0.020
Land. Gear Group/GW	0.042	0.041	0.037
Take-off Gross Wht, W_{TO}, lbs	43,500	45,000	12,500
Empty Weight, W_E, lbs	23,350	24,650	7,125
Wing Group/S, psf	6.0	6.0	3.3
Emp. Grp/S_{emp}, psf	3.2	3.3	2.2
Ultimate Load Factor, g's	3.75**	3.75**	3.75**
Surface Areas, ft^2			
Wing, S	754	754	373
Horiz. Tail, S_h	172	172	85
Vert. Tail, S_v	153	153	83
Empenn. Area, S_{emp}	325	325	168

*Strutbraced wing
**Assumed

Table A6.3a Group Weight Data for Regional Turbopropeller Driven Airplanes

Type →	De Havilland Canada DHC7-102	DHC6-300
Number of engines:	2	2
Weight Item, lbs		
Wing Group	4,888	1,263*
Empennage Group	1,318	303
Fuselage Group	4,680	1,705
Nacelle Group	1,841	221
Land. Gear Group	1,732	613
Nose Gear		
Main Gear		
Structure Total	14,459	4,105
Engines		
Air Induct. System		
Fuel System		
Propeller Install.		
Propulsion System		
Power Plant Total	4,701	1,248
Avionics + Instrum.	850	371
Surface Controls	710	145
Hydraulic System	493	43
Pneumatic System		
Electrical System	1,651	356
Electronics		
Air Cond. System	550	103**
Pressurization System		
Anti-icing System	176	
Furnishings	2,862	732
Paint	150	64
Fixed Equipm't Total	7,442	1,814
$W_{oil} + W_{tfo}$	150	35
Full oil	130	54
Max. Fuel Capacity	6,968	1,114
Water and supplies	130	
Payload (Max.)	9,500	3,610

*Strutbraced wing **Heating system only

Table A6.3b Group Weight Data for Regional Turbopropeller Driven Airplanes

Type	De Havilland Canada DHC7-102	DHC6-300
Flight Design Gross Weight, GW, lbs	44,000	12,500
Structure/GW	0.329	0.328
Power Plant/GW	0.107	0.100
Fixed Equipm't/GW	0.169	0.145
Empty Weight/GW	0.605	0.573
Wing Group/GW	0.111	0.101*
Empenn. Group/GW	0.030	0.024
Fuselage Group/GW	0.106	0.136
Nacelle Group/GW	0.042	0.018
Land. Gear Group/GW	0.039	0.049**
Take-off Gross Wht, W_{TO}, lbs	44,000	12,500
Empty Weight, W_E, lbs	26,602	7,167
Wing Group/S, psf	5.7	3.0
Emp. Grp/S_{emp}, psf	3.4	2.1
Ultimate Load Factor, g's	3.75***	3.75***
Surface Areas, ft^2		
Wing, S	860	420
Horiz. Tail, S_h	217	100
Vert. Tail, S_v	170	48
Empenn. Area, S_{emp}	387	148

*Strutbraced wing **Fixed gear
***Assumed

Table A6.4a Group Weight Data for Regional Piston/
Propeller Driven Airplanes

Type	SAAB Scandia	Handley Page Herald	Scottish* Aviation Twin Pion.	Convair 240
Number of engines:	2	4	2	2
Weight Item, lbs				
Wing Group	4,195	4,365	2,121	3,943
Empennage Group	584	987	576	922
Fuselage Group	2,773	2,986	1,381	4,227
Nacelle Group	1,479	830	230	1,215
Land. Gear Group	1,841	1,625	703	1,530
Nose Gear				
Main Gear				
Structure Total	10,872	10,793	5,011	11,837
Engines				
Air Induct. System				
Fuel System				
Propeller Install.				
Propulsion System				
Power Plant Total				7,299
Avionics + Instrum.				
Surface Controls	369	364	300	
Hydraulic System				
Pneumatic System				
Electrical System				
Electronics				
APU				
Oxygen System				
Air Cond. System				
Anti-icing System				
Furnishings				
Auxiliary Gear				
Fixed Equipm't Total				4,444
$W_{oil} + W_{tfo}$	not known			
Max. Fuel Capacity	11,080		1,740	6,700
Payload (Max.)			2,950	16,000

*Strutbraced wing

Table A6.4b Group Weight Data for Regional Piston/
Propeller Driven Airplanes

Type	SAAB Scandia	Handley Page Herald	Scottish Aviation Twin Pion.	Convair 240
Flight Design Gross Weight, GW, lbs	30,860	37,500	14,600	43,500
Structure/GW	0.352	0.288	0.343	0.272
Power Plant/GW				0.168
Fixed Equipm't/GW				0.102
Empty Weight/GW	0.641	0.673	0.683	0.542
Wing Group/GW	0.136	0.116	0.145	0.091
Empenn. Group/GW	0.019	0.026	0.039	0.021
Fuselage Group/GW	0.090	0.080	0.095	0.097
Nacelle Group/GW	0.048	0.022	0.016	0.028
Land. Gear Group/GW	0.060	0.043	0.048	0.035
Take-off Gross Wht, W_{TO}, lbs	30,860	37,500	14,600	43,500
Empty Weight, W_E, lbs	19,780	25,240	9,969	23,580
Wing Group/S, psf	4.5	4.9	3.2	4.8
Emp. Grp/S_{emp}, psf	2.0	2.2	1.7	
Ultimate Load Factor, g's	3.75*	3.75*	3.75*	3.75*
Surface Areas, ft^2				
Wing, S	922	886	670	817
Horiz. Tail, S_h	215	252	167	
Vert. Tail, S_v	82	193	167	
Empenn. Area, S_{emp}	297	445	334	

*Assumed

Table A7.1a Group Weight Data for Jet Transports

Type	McDonnell Douglas DC-9-30	MD-80	DC-10-10	DC-10-30
Number of engines:	2	2	3	3
Weight Item, lbs				
Wing Group	11,400	15,560	48,990	58,859
Empennage Group	2,780	3,320	13,660	14,676
Fuselage Group	11,160	16,150	44,790	47,270
Nacelle Group	1,430	2,120	8,490	9,127
Land. Gear Group	4,170	5,340	19,820	25,761
Nose Gear	470	550	1,520	1,832
Main Gear	3,700	4,790	18,300	23,929*
Structure Total	30,940	42,490	135,750	155,693
Engine(s)	6,410	8,820	23,688	26,163
Exhaust and Thrust Reverser System	1,240	1,540	7,232	6,916
Air Induct. System	0	0	0	0
Fuel System	600	640	2,040	4,308
Propulsion Install.	0	0	0	0
Power Plant Total	8,250	11,000	32,960	37,387
Avionics + Instrum.	1,450	2,130	3,410	4,274
Surface Controls	1,620	2,540	5,880	6,010
Hydraulic System	480	540	2,330	2,587
Pneumatic System	280	290	1,790	1,920
Electrical System	1,330	1,720	5,370	5,912
Electronics	Included in Avionics and Instrum.			
APU	820	840	1,590	1,643
Oxygen System	150	220	210	256
Air Cond. System**	1,120	1,580	2,390	2,723
Anti-icing System	480	550	420	471
Furnishings	8,450	11,400	35,810	34,124
Operating Items	2,700	3,650	13,340	16,274
Fixed Equipm't Total	18,880	25,460	72,540	76,194
W_{tfo}	Not known			
Max. Fuel Capacity	28,746	39,362	146,683	247,034
Max. Payload	28,930	43,050	93,750	98,726

*Includes 3,590 lbs for centerline gear
**Includes pressurization system

Table A7.1b Group Weight Data for Jet Transports

Type	Mc Donnell Douglas DC-9-30	MD-80	DC-10-10	DC-10-30
Flight Design Gross Weight, GW, lbs	108,000	140,000	430,000	555,000
Structure/GW	0.286	0.304	0.316	0.281
Power Plant/GW	0.076	0.079	0.077	0.067
Fixed Equipm't/GW	0.175	0.182	0.169	0.137
Empty Weight/GW	0.538	0.564	0.561	0.485
Wing Group/GW	0.106	0.111	0.114	0.106
Empenn. Group/GW	0.026	0.024	0.032	0.026
Fuselage Group/GW	0.103	0.115	0.104	0.085
Nacelle Group/GW	0.013	0.015	0.020	0.016
Land. Gear Group/GW	0.039	0.038	0.046	0.046
Take-off Gross Wht, W_{TO}, lbs	108,000	140,000	430,000	555,000
Empty Weight, W_E, lbs	58,070	78,950	241,250	269,274
Wing Group/S, psf	11.4	12.3	12.7	14.9
Emp. Grp/S_{emp}, psf	6.4	5.7	7.0	7.6
Ultimate Load Factor, g's	3.75*	3.75*	3.75*	3.75*
Surface Areas, ft^2				
Wing, S	1,001	1,270	3,861	3,958
Horiz. Tail, S_h	276	314	1,338	1,338
Vert. Tail, S_v	161	168	605	605
Empenn. Area, S_{emp}	437	582	1,943	1,943

*Assumed

Table A7.2a Group Weight Data for Jet Transports

Type	Boeing 737-200	Boeing 727-100	Boeing 747-100	Airbus A-300 B2
Number of engines:	2	3	4	2
Weight Item, lbs				
Wing Group	10,613	17,764	86,402	44,131
Empennage Group	2,718	4,133	11,850	5,941
Fuselage Group	12,108	17,681	71,845	35,820
Nacelle Group	1,392	3,870	10,031	7,039
Land. Gear Group	4,354	7,211	31,427	13,611
Nose Gear				
Main Gear				
Structure Total	31,185	50,659	211,555	106,542
Engines	6,217	9,325	34,120	16,825
Exhaust and Thrust-Reverser System	1,007	1,744	6,452	4,001
Air Induct. System	0	0	0	0
Fuel System	575	1,143	2,322	1,257
Propulsion Install.	378	250	802	814
Power Plant Total	8,177	12,462	43,696	22,897
Avionics + Instrum.	625	756	1,909	377
Surface Controls	2,348	2,996	6,982	5,808
Hydraulic System	873	1,418	4,471	3,701
Pneumatic System				
Electrical System	1,066	2,142	3,348	4,923
Electronics	956	1,591	4,429	1,726
APU	836	60	1,130	983
Air Cond. System*	1,416	1,976	3,969	3,642
Anti-icing System				
Furnishings	6,643	10,257	37,245	13,161
Miscellanous	124	85	-421	732
Fixed Equipm't Total	14,887	21,281	63,062	35,053
W_{oil} + W_{tfo}	Not known			
Max. Fuel Capacity	34,718	48,353	331,675	76,512
Max. Payload	34,790	29,700	140,000	69,865

*Includes pressurization system

Table A7.2b Group Weight Data for Jet Transports

Type	Boeing 737-200	727-100	747-100	Airbus A300-B2
Flight Design Gross Weight, GW, lbs	115,500	160,000	710,000	302,000
Structure/GW	0.270	0.317	0.298	0.353
Power Plant/GW	0.071	0.078	0.062	0.076
Fixed Equipm't/GW	0.129	0.133	0.089	0.116
Empty Weight/GW	0.521	0.552	0.498	0.559
Wing Group/GW	0.092	0.111	0.122	0.146
Empenn. Group/GW	0.024	0.026	0.017	0.020
Fuselage Group/GW	0.105	0.111	0.101	0.119
Nacelle Group/GW	0.012	0.024	0.014	0.023
Land. Gear Group/GW	0.038	0.045	0.044	0.045
Take-off Gross Wht, W_{TO}, lbs	115,500	160,000	710,000	302,000
Empty Weight, W_E, lbs	60,210	88,300	353,398	168,805
Wing Group/S, psf	10.8	10.4	15.7	15.8
Emp. Grp/S_{emp}, psf	4.9	5.6	5.2	4.8
Ultimate Load Factor, g's	3.75*	3.75*	3.75*	3.75*
Surface Areas, ft^2				
Wing, S	980	1,700	5,500	2,799
Horiz. Tail, S_h	321	376	1,470	748
Vert. Tail, S_v	233	356	830	487
Empenn. Area, S_{emp}	554	732	2,300	1,235

*Assumed

Table A7.3a Group Weight Data for Jet Transports

Type	Boeing 707-121	707-320	707-320C	720-022
Number of engines:	4	4	4	4
Weight Item, lbs				
Wing Group	24,024	29,762	32,255	22,850
Empennage Group	5,151	5,511	6,165	5,230
Fuselage Group	20,061	21,650	26,937	19,035
Nacelle Group	4,639	4,497	4,183	4,510
Land. Gear Group	9,763	12,700	12,737	8,110
Nose Gear				
Main Gear				
Structure Total	63,638	74,120	82,277	59,735
Engines	16,458	20,200	17,368	13,770
Exhaust and Thrust-Reverser System			3,492	
Air Induct. System	0	0	0	0
Fuel System	1,808		2,418	1,240
Propulsion Install.	1,738		798	885
Power Plant Total	20,004		24,076	15,895
Avionics + Instrum.	505		515	555
Surface Controls	2,159	2,400	3,052	2,450
Hydraulic System	484		1,086	505
Pneumatic System				
Electrical System	3,772		4,179	4,070
Electronics	1,708		2,338	1,200
APU			151	
Air Cond. System*	3,110		3,608	2,890
Anti-icing System				
Furnishings	13,651		9,527	13,055
Auxiliary Gear	0	0	0	0
Miscellanous	0	0	-389	0
Fixed Equipm't Total	25,389		24,456	24,725
W_{tfo}	704			
Max. Fuel Capacity	90,842	160,783	160,783	99,954
Max. Payload	42,600	55,000	84,000	28,200

*Includes pressurization system

Table A7.3b Group Weight Data for Jet Transports

Type	Boeing 707-121	707-320	707-320C	720-022
Flight Design Gross Weight, GW, lbs	246,000	311,000	330,000	203,000
Structure/GW	0.259	0.238	0.249	0.294
Power Plant/GW	0.081		0.073	0.078
Fixed Equipm't/GW	0.103		0.074	0.122
Empty Weight/GW	0.444	0.434	0.396	0.494
Wing Group/GW	0.098	0.096	0.098	0.113
Empenn. Group/GW	0.021	0.018	0.019	0.026
Fuselage Group/GW	0.082	0.070	0.082	0.094
Nacelle Group/GW	0.019	0.014	0.013	0.022
Land. Gear Group/GW	0.040	0.041	0.039	0.040
Take-off Gross Wht, W_{TO}, lbs	246,000	311,000	330,000	203,000
Empty Weight, W_E, lbs	109,111	135,000	130,809	100,355
Wing Group/S, psf	9.9	10.3	10.6	9.4
Emp. Grp/S_{emp}, psf	6.2	5.8	6.5	6.3
Ultimate Load Factor, g's	3.75	3.75	3.75	3.75
Surface Areas, ft^2				
Wing, S	2,433	2,892	3,050	2,433
Horiz. Tail, S_h	500	625	625	500
Vert. Tail, S_v	328	328	328	328
Empenn. Area, S_{emp}	828	953	953	828

Table A7.4a Group Weight Data for Jet Transports

Type	Boeing 707-321	McDonnell Douglas DC-8	McDonnell Douglas DC-9-10	Hawker-Siddeley 121-IC
Number of engines:	4	4	2	3
Weight Item, lbs				
Wing Group	28,647	27,556	9,470	12,600
Empennage Group	6,004	4,840	2,630	3,225
Fuselage Group	22,129	19,910	11,206	12,469
Nacelle Group	5,119	3,534	1,417	in fusel.
Land. Gear Group	11,122	10,910	3,660	4,413
Nose Gear				
Main Gear				
Structure Total	73,021	66,750	28,383	32,707
Engine(s)	19,192		6,160	
Exhaust and Thrust Reverser System			658	
Air Induct. System				
Fuel System	1,956		510	
Propulsive Install.	1,113		409	
Power Plant Total	22,261	27,677	7,737	
Avionics + Instrum.	561		719	
Surface Controls	2,408		1,264	1,792
Hydraulic System	498		714	
Pneumatic System				
Electrical System	3,959		1,663	
Electronics	1,716		914	
APU			818	
Air Cond. System*	3,290		1,476	
Anti-icing System				
Furnishings	14,854		7,408	
Auxiliary Gear	0		24	
Fixed Equipm't Total	27,286	25,650	15,000	
W_{tfo}	1,089			
Max. Fuel Capacity		30,256	18,778	31,060
Max. Payload			18,050	22,000

*Includes pressurization system

Table A7.4b Group Weight Data for Jet Transports

Type	Boeing 707-321	McDonnell Douglas DC-8	McDonnell Douglas DC-9-10	Hawker Siddeley 121-IC
Flight Design Gross Weight, GW, lbs	302,000	215,000	91,500	115,000
Structure/GW	0.242	0.310	0.310	0.284
Power Plant/GW	0.074	0.129	0.085	
Fixed Equipm't/GW	0.090	0.119	0.164	
Empty Weight/GW	0.406	0.562	0.495	0.587
Wing Group/GW	0.095	0.128	0.103	0.110
Empenn. Group/GW	0.020	0.023	0.029	0.028
Fuselage Group/GW	0.073	0.093	0.122	0.108
Nacelle Group/GW	0.017	0.016	0.015	in fusel.
Land. Gear Group/GW	0.037	0.051	0.040	0.038
Take-off Gross Wht, W_{TO}, lbs	301,000	215,000	91,500	115,000
Empty Weight, W_E, lbs	122,509	120,877	45,300	67,500
Wing Group/S, psf	9.9	9.9	10.1	9.3
Emp. Grp/S_{emp}, psf	6.4	5.6	5.5	5.7
Ultimate Load Factor, g's	3.75	3.75*	3.75*	3.75*
Surface Areas, ft^2				
Wing, S	2,892	2,773	934	1,358
Horiz. Tail, S_h	625	607**	275	310
Vert. Tail, S_v	312	263**	200**	259
Empenn. Area, S_{emp}	937	870	475	569

*Assumed
**Estimated from threeview

Table A7.5a Group Weight Data for Jet Transports

Type	VFW-Fokker 614	Fokker F28-1000	BAC 1-11/300	Sud/Aerospatiale Caravelle
Number of engines:	2	2	2	2
Weight Item, lbs				
Wing Group	5,767	7,330	9,643	14,735
Empennage Group	1,121	1,632	2,369	1,957
Fuselage Group	5,233	7,043	9,713	11,570
Nacelle Group	971	834	in fusel.	1,581
Land. Gear Group	1,620	2,759	2,856	5,110
Nose Gear				
Main Gear				
Structure Total	14,712	19,598	24,581	34,953
Engines	3,413	4,495		7,055
Exhaust and Thrust-Reverser System	119	127		975
Air Induct. System				
Fuel System	162	545		518
Propulsive Install	690	215		179
Power Plant Total	4,384	5,382		8,727
Avionics + Instrum.	215	302	182	236
Surface Controls	745	1,387	1,481	2,063
Hydraulic System	403	364	997	1,376
Pneumatic System				
Electrical System	1,054	1,023	2,317	2,846
Electronics	436	869	1,005	1,187
APU	305	346	457	0
Air Cond. System*	719	1,074	1,579	1,752
Anti-icing System				
Furnishings	2,655	4,030	4,933	6,481
Auxiliary Gear	49	0	0	0
Operating Items				
Fixed Equipm't Total	6,581	9,395	12,951	15,941
W_{tfo}	not known			
Max. Fuel Capacity	10,142	17,331	24,954	33,808
Max. Payload	8,201	14,380	22,278	29,100

*Includes pressurization system

Table A7.5b Group Weight Data for Jet Transports

Type	VFW Fokker 614	Fokker F28-1000	BAC 1-11/300	Sud-Aero spatiale Caravelle
Flight Design Gross Weight, GW, lbs	40,981	65,000	87,000	110,230
Structure/GW	0.359	0.302	0.283	0.317
Power Plant/GW	0.107	0.083		0.079
Fixed Equipm't/GW	0.161	0.145	0.149	0.145
Empty Weight/GW*	0.586	0.480	0.560	0.590
Wing Group/GW	0.141	0.113	0.111	0.134
Empenn. Group/GW	0.027	0.025	0.027	0.018
Fuselage Group/GW	0.128	0.108	0.112	0.105
Nacelle Group/GW	0.024	0.013	in fusel.	0.014
Land. Gear Group/GW	0.040	0.042	0.033	0.046
Take-off Gross Wht, W_{TO}, lbs	40,981	65,000	87,000	110,230
Empty Weight, W_E, lbs	24,000	31,219	48,722	65,050
Wing Group/S, psf	8.4	8.9	9.6	9.3
Emp. Grp/S_{emp}, psf	3.8	4.8	6.3	4.2
Ultimate Load Factor, g's	3.75*	3.75*	3.75*	3.75*
Surface Areas, ft^2				
Wing, S	689	822	1,003	1,579
Horiz. Tail, S_h	193	210	257	301
Vert. Tail, S_v	102	132	117	167
Empenn. Area, S_{emp}	295	342	374	468

*Assumed

Table A7.6a Group Weight Data for Turboprop. Transports

Type→	Bristol Britannia 300	Canadair CL-44C	Vickers Viscount 810	Lockheed Electra
Number of engines:	4	4	4	4
Weight Item, lbs				
Wing Group	13,433	15,710	6,250	7,670
Empennage Group	3,202	3,749	1,245	1,924
Fuselage Group	11,100	20,524	6,900	9,954
Nacelle Group	4,930	6,834	1,810	4,417
Land. Gear Group	5,785	7,083	2,469	3,817
Nose Gear				
Main Gear				
Structure Total	38,450	53,900	18,674	27,782
Engines	11,192	12,800		
Air Induct. System				
Fuel System	1,329	1,755		
Propeller Inst.	3,557	5,006		
Propulsion System	3,820	3,134		
Power Plant Total	19,898	22,695		13,733
Avionics + Instrum.	505	858	213	
Surface Controls	1,221	2,146	824	
Hydraulic System	650	630	457	
Pneumatic System				
Electrical System	1,800	3,040	2,826	
Electronics	1,040	1,229	617	
APU	0	0	0	
Air Cond. System*	3,000	2,536	2,092	
Anti-icing System				
Furnishings	6,866	12,349	3,476	
Auxiliary Gear	0	0	0	
Fixed Equipm't Total	15,082	22,788	10,505	14,469
$W_{oil} + W_{tfo}$				
Max. Fuel Capacity	69,395	82,170	13,897	37,205
Payload (Max.)	30,000	37,630	15,054	18,907

*Includes pressurization system

Table A7.6b Group Weight Data for Turboprop. Transports

Type	Bristol Britannia 300	Canadair CL-44C	Vickers Viscount 810	Lockheed Electra
Flight Design Gross Weight, GW, lbs	155,000	205,000	72,500	116,000
Structure/GW	0.248	0.263	0.258	0.240
Power Plant/GW	0.128	0.111		0.118
Fixed Equipm't/GW	0.097	0.111	0.145	0.125
Empty Weight/GW	0.587	0.516	0.569	0.491
Wing Group/GW	0.087	0.077	0.086	0.066
Empenn. Group/GW	0.021	0.018	0.017	0.017
Fuselage Group/GW	0.072	0.100	0.095	0.086
Nacelle Group/GW	0.032	0.033	0.025	0.038
Land. Gear Group/GW	0.037	0.035	0.034	0.033
Take-off Gross Wht, W_{TO}, lbs	155,000	205,000	72,500	116,000
Empty Weight, W_E, lbs	91,000	105,785	41,276	57,000
Wing Group/S, psf	6.5	7.6	6.5	5.9
Emp. Grp/S_{emp}, psf	3.4	4.0	2.9	3.1
Ultimate Load Factor, g's	3.75*	3.75*	3.75*	3.75*
Surface Areas, ft^2				
Wing, S	2,075	2,075	963	1,300
Horiz. Tail, S_h	588	588	307	399
Vert. Tail, S_v	356	356	124	212
Empenn. Area, S_{emp}	944	944	431	611

*Assumed

Table A8.1a Group Weight Data for Military Trainers

Type	Northrop T-38A	Rockwell NAA T-39A	Cessna T-37A	Fouga Magis-ter	Cana-dair CL-41
Number of engines:	2	2	2	2	2
Weight Item, lbs					
Wing Group	765	1,753	531	1,089	892
Empennage Group	305	297	128	165	201
Fuselage Group	1,985	2,014	839	743	955
Engine Section	147	315*		in fuse.	40
Land. Gear Group	457	728	330	459	318
Nose Gear					
Main Gear					
Structure Total	3,659	5,107	1,828	2,456	2,406
Engine(s)	1,038	959	751		
Air Induct. System	136	12	14		
Fuel System	285	190	225		
Propulsion System	171	140	205		
Power Plant Total	1,630	1,301	1,195		
Avionics + Instrum.	211	122	132		
Surface Controls	425	344	154		172
Hydraulic System	154	116	56		
Pneumatic System					
Electrical System	296	720	194		
Electronics	246	407	86		
Air Cond. System**	142	333	69		
Anti-icing System					
Furnishings	460	857	256		
Auxiliary Gear	24		3		
Fixed Equipm't Total	1,958	2,899	950		
$W_{oil} + W_{tfo}$	62	89	104		
Max. Fuel Capacity	3,916	5,805	1,959	1,299	2,082
Payload (Max. Fuel)***	426	1,500	400	400	400

*Nacelle group for T-39A
**Includes pressurization system
***Includes crew

Table A8.1b Group Weight Data for Military Trainers

Type	Northrop T-38A	Rockwell NAA T-39A	Cessna T-37A	Fouga Magis-ter	Cana-dair CL-41
Flight Design Gross Weight, GW, lbs	11,651	16,316	6,228	6,280	11,288
Structure/GW	0.314	0.313	0.294	0.391	0.213
Power Plant/GW	0.140	0.080	0.192		
Fixed Equipm't/GW	0.168	0.178	0.152	N.A.	N.A.
Empty Wt/GW	0.622	0.570	0.638	0.755	0.576
Wing Group/GW	0.066	0.107	0.085	0.173	0.079
Emp. Group/GW	0.026	0.018	0.021	0.026	0.018
Fusel.Group/GW	0.170	0.123	0.135	0.118	0.085
Engine Section/GW	0.013	0.019*		in fus.	0.004
Land. Gear Group/GW	0.039	0.045	0.053	0.073	0.028
Take-off Gross Wht, W_{TO}, lbs	11,651	16,701	6,436	6,280	11,288
Empty Weight, W_E, lbs	7,247	9,307	3,973	4,740	5,296
Wing Group/S, psf	4.5	5.1	3.9	5.9	4.1
Emp. Grp/S_{emp}, psf	2.9	2.5	1.7	3.4	3.4
Ultimate Load Factor, g's	10.0**	6.0	10.0		
Surface Areas, ft^2					
Wing, S	170	342	135	186	220
Horiz. Tail, S_h	59	77	54	***	41.3
Vert. Tail, S_v	47.8	41.6	20.4	***	17.5
Empenn. Area, S_{emp}	107	119	74.4	48.8	58.8

*Nacelle group for T-39A
**Assumed
***V-tail

Table A9.1a Group Weight Data for Fighters (USAF)

Type	NAA	McDonnell		Gen.Dyn.
	F-100F	F-101B	RF-101C	F-102A*
Number of engines:	1	2	2	1
Weight Item, lbs				
Wing Group	3,896	3,507	3,680	3,000
Empennage Group	979	812	837	535
Fuselage Group	4,032	3,901	3,955	3,409
Engine Section	104	99	103	39
Land. Gear Group	1,509	1,592	1,596	1,056
Nose Gear				
Main Gear				
Structure Total	10,520	9,911	10,171	8,039
Engine(s)	5,121	10,800	9,676	4,993
Air Induct. System	504	729	638	693
Fuel System	761	1,226	1,412	394
Propulsion System	414	892	599	278
Power Plant Total	6,800	13,647	12,325	6,358
Avionics + Instrum.	303	318	204	141
Surface Controls	1,076	772	780	413
Hydraulic System	157	433	359	318
Pneumatic System				
Electrical System	568	825	819	594
Electronics	496	2,222	629	2,001
Armament	794	228	36	589
Air Cond. System**	435	270	362	259
Anti-icing System				
Furnishings	427	480	242	227
Auxiliary Gear	77	84	91	78
Fixed Equipm't Total	4,333	5,632	3,522	4,620
$W_{oil} + W_{tfo}$	166	223	223	216
Max. Fuel Capacity	7,729	8,892	9,782	7,053
Payload (Max. Fuel)	250	1,881	704	1,241

*This airplane is a delta wing configuration
**Includes pressurization system

Table A9.1b Group Weight Data for Fighters (USAF)

Type	NAA F-100F	McDonnell F-101B	McDonnell RF-101C	Gen.Dyn. F-102A*
Flight Design Gross Weight, GW, lbs	29,391	39,800	37,000	25,500
Structure/GW	0.358	0.249	0.275	0.315
Power Plant/GW	0.231	0.343	0.333	0.249
Fixed Equipm't/GW	0.147	0.142	0.095	0.181
Empty Weight/GW	0.737	0.733	0.724	0.750
Wing Group/GW	0.133	0.088	0.099	0.118
Empenn. Group/GW	0.033	0.020	0.023	0.021
Fuselage Group/GW	0.137	0.098	0.107	0.134
Engine Section/GW	0.004	0.002	0.003	0.002
Land. Gear Group/GW	0.051	0.040	0.043	0.041
Take-off Gross Wht, W_{TO}, lbs	30,638	41,288	37,723	28,137
Empty Weight, W_E, lbs	21,653	29,190	26,774	19,130
Wing Group/S, psf	9.7	9.5	10.0	4.3
Emp. Grp/S_{emp}, psf	6.3	5.1	5.2	5.6
Ultimate Load Factor, g's	7.33	10.2	11.0	10.5
Surface Areas, ft^2				
Wing, S	400	368	368	698
Horiz. Tail, S_h	98.9	75.1	75.1	0
Vert. Tail, S_v	55.6	84.9	84.9	95.1
Empenn. Area, S_{emp}	155	160	160	95.1

* This airplane is a delta wing configuration

Table A9.2a Group Weight Data for Fighters (USAF)

Type	Republic F-105B	Gen.Dyn. F-106A*	North American F-107A	F-86H
Number of engines:	1	1	1	1
Weight Item, lbs				
Wing Group	3,409	3,302	3,787	2,702
Empennage Group	965	693	1,130	329
Fuselage Group	5,870	4,401	4,792	2,035
Engine Section	106	39	260	42
Land. Gear Group	1,848	1,232	1,410	989
Nose Gear				
Main Gear				
Structure Total	12,198	9,667	11,379	6,097
Engine	6,187	5,816	6,100	3,646
Air Induct. System	524	975	833	167
Fuel System	608	777	983	845
Propulsion System	406	503	368	340
Power Plant Total	7,725	8,071	8,284	4,998
Avionics + Instrum.	227	190	288	111
Surface Controls	1,311	445	1,454	358
Hydraulic System	449	431	150	339
Pneumatic System				
Electrical System	700	606	447	476
Electronics	737	2,743	382	230
Armament	719	626	1,006	828
Air Cond. System**	168	407	390	205
Anti-icing System				
Furnishings	243	290	282	182
Auxiliary Gear	92	69	42	12
APU	224	0	0	0
Fixed Equipm't Total	4,870	5,807	4,441	2,741
$W_{oil} + W_{tfo}$	198	303	143	57
Max. Fuel Capacity	7,540	8,476	11,050	3,660
Payload (Max. Fuel)	757	1,374	2,560	420

*This airplane is a delta wing configuration
**Includes pressurization system

Table A9.2b Group Weight Data for Fighters (USAF)

Type	Republic F-105B	Gen.Dyn. F-106A*	North American F-107A	F-86H
Flight Design Gross Weight, GW, lbs	31,392	30,590	29,524	19,012
Structure/GW	0.389	0.316	0.385	0.321
Power Plant/GW	0.246	0.264	0.281	0.263
Fixed Equipm't/GW	0.155	0.190	0.150	0.144
Empty Weight/GW	0.797	0.766	0.816	0.728
Wing Group/GW	0.109	0.108	0.128	0.142
Empenn. Group/GW	0.031	0.023	0.038	0.017
Fuselage Group/GW	0.187	0.144	0.162	0.107
Engine Section/GW	0.003	0.001	0.009	0.002
Land. Gear Group/GW	0.059	0.040	0.048	0.052
Take-off Gross Wht, W_{TO}, lbs	34,081	33,888	39,405	18,908
Empty Weight, W_E, lbs	25,022	23,448	24,104	13,836
Wing Group/S, psf	8.9	4.7	9.6	8.6
Emp. Grp/S_{emp}, psf	5.2	6.6	6.4	4.1
Ultimate Load Factor, g's	13.0	10.5	13.0	11.0
Surface Areas, ft^2				
Wing, S	385	698	395	313
Horiz. Tail, S_h	96.5	0	93.3	47.2
Vert. Tail, S_v	88.1	105	83.8	32.2
Empenn. Area, S_{emp}	185	105	177	79.4

* This airplane is a delta wing configuration

Table A9.3a Group Weight Data for Fighters (USN)

Type	Vought F8U-3	McDonnell F4H	Grumman F11F	F9F-5
Number of engines:	1	2	1	1
Weight Item, lbs				
Wing Group	4,128	4,343	2,180	2,294
Empennage Group	1,045	853	669	404
Fuselage Group	3,850	4,042	3,269	1,779
Engine Section	92	125	47	0
Land. Gear Group	949	1,735	907	728
Nose Gear				
Main Gear				
Structure Total	10,064	11,098	7,072	5,205
Engine(s)	6,010	6,940	3,489	2,008
Air Induct. System	673	1,037	159	225
Fuel System	849	953	463	529
Propulsion System.	338	106	192	116
Power Plant Total	7,870	9,036	4,303	2,878
Avionics + Instrum.	191	166	118	82
Surface Controls	1,425	919	760	345
Hydraulic System	150	441	166	267
Pneumatic System				
Electrical System	439	502	459	458
Electronics	840	1,386	439	292
Armament	376	446	358	416
Air Cond. System*	329	341	76	85
Anti-icing System				
Furnishings	210	321	166	144
Auxiliary Gear	183	0	131	51
Fixed Equipm't Total	4,143	4,522	2,673	2,140
$W_{oil} + W_{tfo}$	196	131	72	
Max. Fuel Capacity	14,306	13,410	6,663	7,160
Payload (Max. Fuel)	1,197	1,500	340	

*Includes pressurization system

Table A9.3b Group Weight Data for Fighters (USN)

Type	Vought F8U-3	McDonnell F4H	Grumman F11F	F9F-5
Flight Design Gross Weight, GW, lbs	30,578	34,851	17,500	14,900
Structure/GW	0.329	0.318	0.404	0.349
Power Plant/GW	0.257	0.259	0.246	0.193
Fixed Equipm't/GW	0.135	0.130	0.153	0.144
Empty Weight/GW	0.722	0.707	0.771	0.686
Wing Group/GW	0.135	0.125	0.125	0.154
Empenn. Group/GW	0.034	0.024	0.038	0.027
Fuselage Group/GW	0.126	0.116	0.187	0.119
Engine Section/GW	0.003	0.004	0.003	0
Land. Gear Group/GW	0.031	0.050	0.052	0.049
Take-off Gross Wht, W_{TO}, lbs	38,528	40,217	21,233	17,500
Empty Weight, W_E, lbs	22,092	24,656	13,485	10,223
Wing Group/S, psf	8.9	8.2	8.5	9.2
Emp. Grp/S_{emp}, psf	7.2	5.2	5.8	3.5
Ultimate Load Factor, g's	9.6		9.8	11.3
Surface Areas, ft^2				
Wing, S	462	530	255	250
Horiz. Tail, S_h	67.2	96.2	65.5	48
Vert. Tail, S_v	78.6	67.5	50.3	66
Empenn. Area, S_{emp}	146	164	116	114

Table A9.4a Group Weight Data for Fighters (USN)

Type	Grumman A2F(A6)	McDonnell F3H-2	NAA A3J	Vought F7U-1
Number of engines:	2	2	2	1
Weight Item, lbs				
Wing Group	4,733	4,314	5,072	3,583
Empennage Group	819	576	1,358	726
Fuselage Group	3,538	3,551	6,851	937
Engine Section	64	93	80	
Land. Gear Group	2,343	1,458	2,173	1,181
Nose Gear				
Main Gear				
Structure Total	11,497	9,992	15,534	6,427
Engine(s)	4,010	4,960	7,260	2,790
Air Induct. System	61	614	767	690
Fuel System	936	1,262	979	1,080
Propulsion System.	632	70	353	937
Power Plant Total	5,639	6,906	9,359	5,497
Avionics + Instrum.	133	145	210	108
Surface Controls	932	1,067	1,845	482
Hydraulic System Pneumatic System	170	474	275	317
Electrical System	695	535	821	371
Electronics	2,652	984	2,239	328
Armament	323	662	45	367
Air Cond. System* Anti-icing System	164	101	424	79
Furnishings	476	218	676	279
Auxiliary Gear		253		128
Fixed Equipm't Total	5,545	4,439	6,535	2,459
$W_{oil} + W_{tfo}$	195	147	320	97
Max. Fuel Capacity	8,764	9,789	19,074	5,826
Payload (Max. Fuel)	2,000	216	1,885	502

*Includes pressurization system

Table A9.4b Group Weight Data for Fighters (USN)

Type	Grumman A2F(A6)	McDonnell F3H-2	NAA A3J	Vought F7U-1*
Flight Design Gross Weight, GW, lbs	34,815	26,000	46,028	19,310
Structure/GW	0.330	0.384	0.337	0.333
Power Plant/GW	0.162	0.266	0.203	0.285
Fixed Equipm't/GW	0.159	0.171	0.142	0.127
Empty Weight/GW	0.651	0.818	0.679	0.746
Wing Group/GW	0.136	0.166	0.110	0.186
Empenn. Group/GW	0.024	0.022	0.030	0.038
Fuselage Group/GW	0.102	0.137	0.149	0.048
Engine Section/GW	0.002	0.004	0.002	
Land. Gear Group/GW	0.067	0.056	0.047	0.061
Take-off Gross Wht, W_{TO}, lbs	34,815	32,037	53,658	21,638
Empty Weight, W_E, lbs	22,680	21,272	31,246	14,397
Wing Group/S, psf	9.1	8.4	7.2	7.1
Emp. Grp/S_{emp}, psf	4.4	4.5	3.4	8.3
Ultimate Load Factor, g's		11.25		
Surface Areas, ft^2				
Wing, S	520	516	700	507
Horiz. Tail, S_h	120	82.5	304	0*
Vert. Tail, S_v	68.4	45.4	101	88
Empenn. Area, S_{emp}	188	128	405	88

*This airplane is essentially a flying wing with two vertical tails

Table A9.5a Group Weight Data for Fighters (USAF and USN)

Type	McDonnell Douglas F-4E (USAF)	F-15C (USAF)	F/A-18A (USN)	AV-8B* (USN)
Number of engines:	2	2	2	1
Weight Item, lbs				
Wing Group	5,226	3,642	3,798	1,443
Empennage Group	969	1,104	945	372
Fuselage Group	5,050	6,245	4,685	2,060
Engine Section	166	102	143	141
Land. Gear Group	1,944	1,393	1,992	1,011
Nose Gear	377	264	626	334
Main Gear	1,567	1,129	1,366	400
Outrigger Gear				277
Structure Total	13,355	12,486	11,563	5,027
Engine(s)	7,697	6,091	4,294	3,815
Air Induct. System	1,318	1,464	423	236
Fuel System	1,932	1,128	1,002	542
Propulsion System.	312	522	558	444
Power Plant Total	11,259	9,205	6,277	5,037
Instrument group	270	151	94	80
Surface Controls	1,167	810	1,067	698
Hydraulic System	543	433	364	176
Pneumatic System				
Electrical System	542	607	547	424
Electronics	2,227	1,787	1,538	697
Armament	641	627	387	152
Air Cond. System	406	685	593	218
Pressurization Syst.			21	
Anti-icing System				
Furnishings	611	294	317	298
Auxiliary Gear	412	119	189	
Photographic System		24		
Ballast		318	36	
Manuf. Variation	57	-97	-19	-16
Fixed Equipm't Total	6,900	5,734	5,134	2,727
Max. Fuel Capacity	12,058	13,455	17,592**	7,759
Expendable Payload	2,193	2,571	5,453	4,271
Fixed Payload***	incl. in armament		2,231	832

*V/STOL fighter **Incl. 6,732 lbs ext. fuel ***Pylons, racks, launchers, FLIR and camera pods

Table A9.5b Group Weight Data for Fighters (USAF and USN)

Type	McDonnell Douglas F-4E	F-15C	F/A-18A	AV-8B*
Flight Design Gross Weight, GW, lbs	37,500	37,400	32,357	22,950
Structure/GW	0.356	0.334	0.357	0.219
Power Plant/GW	0.300	0.246	0.194	0.219
Fixed Equipm't/GW	0.182	0.147	0.158	0.120
Empty Weight/GW	0.840	0.733	0.710	0.557
Wing Group/GW	0.139	0.097	0.117	0.063
Empenn. Group/GW	0.026	0.030	0.029	0.016
Fuselage Group/GW	0.135	0.167	0.145	0.090
Engine Section/GW	0.004	0.003	0.004	0.006
Land. Gear Group/GW	0.052	0.037	0.062	0.044
Take-off Gross Wht, W_{TO}, lbs	58,000	68,000	51,900	29,750
Empty Weight, W_E, lbs	31,514	27,425	22,974	12,791
Wing Group/S, psf	9.5	6.1	9.5	6.3
Emp. Grp/S_{emp}, psf	5.8	4.7	4.9	5.0
Ultimate Load Factor, g's	9.75	11.0	11.25	10.5
Surface Areas, ft^2				
Wing, S	548	599	400	230
Horiz. Tail, S_h	100	111	88.1	48.5
Vert. Tail, S_v	67.5	125	104	26.6
Empenn. Area, S_{emp}	168	236	192	75.1

*V/STOL Fighter

Table A10.1a Group Weight Data for Military Jet Transports

Type	Boeing KC135*	Lockheed C-141B	C-5A
Number of engines:	4	4	4
Weight Item, lbs			
Wing Group	25,251	35,272	100,015
Empennage Group	5,074	5,907	12,461
Fuselage Group	18,867	36,857	118,193
Nacelle Group	2,575	5,168	9,528
Land. Gear Group	10,180	10,850	38,353
Nose Gear		1,234	4,455
Main Gear		9,616	33,898
Structure Total	61,947	94,054	278,550
Engine(s)	16,687	23,665	38,035
Air Induct. System	172		
Fuel System	4,052	1,802	2,540
Propulsion System	591		
Power Plant Total	21,502	25,467	40,575
Avionics + Instrum.	553	3,078	3,823
Surface Controls	2,044	3,701	7,404
Hydraulic System		1,604	4,086
Pneumatic System	858		
Electrical System	2,470	2,826	3,503
Electronics	2,096	1,163	992
APU	0	534	987
Oxygen System		479	308
Air Cond. System**	1,464	2,283	3,416
Anti-icing System		453	229
Furnishings	1,518	5,210	19,272
Auxiliary Gear	1,899	103	39
Fixed Equipm't Total	12,902	21,434	44,059
$W_{oil} + W_{tfo}$	1,407	1,327	826
Max. Fuel Capacity	158,997	153,352	332,500
Payload (Max.)		73,873	200,000

*This is a tanker airplane
**Includes pressurization system

Table A10.1b Group Weight Data for Military Jet Transports

Type	Boeing KC135*	Lockheed C-141B	C-5A
Flight Design Gross Weight, GW, lbs	297,000	314,200	769,000
Structure/GW	0.209	0.299	0.362
Power Plant/GW	0.072	0.081	0.053
Fixed Equipm't/GW	0.043	0.068	0.057
Empty Weight/GW	0.323	0.449	0.472
Wing Group/GW	0.085	0.112	0.130
Empenn. Group/GW	0.017	0.019	0.016
Fuselage Group/GW	0.064	0.117	0.154
Nacelle Group/GW	0.009	0.016	0.012
Land. Gear Group/GW	0.034	0.035	0.050
Take-off Gross Wht, W_{TO}, lbs	297,000	314,000	769,000
Empty Weight, W_E, lbs	95,938	140,955	363,184
Wing Group/S, psf	10.4	10.9	16.1
Emp. Grp/S_{emp}, psf	6.2	6.6	6.5
Ultimate Load Factor, g's	3.75	3.75	3.75**
Surface Areas, ft^2			
Wing, S	2,435	3,228	6,200
Horiz. Tail, S_h	500	483	966
Vert. Tail, S_v	312	416	961
Empenn. Area, S_{emp}	812	899	1,927

*This is a tanker airplane
**after 100,000 lbs of fuel has been used.

Table A10.2a Group Weight Data for Turbo/Propeller

Driven Military Transports

	A.W.(HS) Argosy	Douglas C-133A	Lockheed C-130H	Breguet 941*
Number of engines:	4	4	4	4
Weight Item, lbs				
Wing Group	10,800	27,403	13,950	4,096
Empennage Group	1,300	6,011	3,480	1,387
Fuselage Group	11,100**	30,940	14,695	6,481
Nacelle Group	1,200	3,512	2,756	in wing
Land. Gear Group	3,180	10,635	5,309	2,626
Nose Gear			730	
Main Gear			4,579	
Structure Total	27,580	78,501	40,190	14,590
Engines		10,470	13,746	
Air Induct. System				
Fuel System		1,338	3,105	
Propeller Inst.		5,403	in eng.	
Propulsion System		2,081	in eng.	
Power Plant Total		19,292	16,851	
Avionics + Instrum.		578	3,582	
Surface Controls	in struct.	1,804	1,673	1,056
Hydraulic System		2,678	664	
Pneumatic System				
Electrical System		2,004	2,459	
Electronics		2,047	in avionics	
APU		188	651	
Oxygen System			231	
Air Cond. System***		2,973	1,684	
Anti-icing System			797	
Furnishings		3,632	4,472	
Auxiliary Gear		117	6	
Operating items			532	
Fixed Equipm't Total		16,021	16,219	
$W_{oil} + W_{tfo}$		1,693	1,089	
Max. Fuel Capacity		60,000	45,240	
Payload (Max.)		97,162	33,461	

*This is a STOL airplane **Tailbooms at 2,360 lbs are included ***Includes pressurization system

Table A10.2b Group Weight Data for Turbo/Propeller Driven Military Transports

Type	A.W.(HS) Argosy	Douglas C-133A	Lockheed C-130H	Breguet 941
Flight Design Gross Weight, GW, lbs	82,000	275,000	155,000	58,421
Structure/GW	0.336	0.285	0.259	0.250
Power Plant/GW		0.070	0.109	
Fixed Equipm't/GW		0.058	0.105	
Empty Weight/GW	0.561	0.414	0.473	0.508
Wing Group/GW	0.132	0.100	0.090	0.070
Empenn. Group/GW	0.016	0.022	0.022	0.024
Fuselage Group/GW	0.135	0.113	0.095	0.111
Nacelle Group/GW	0.015	0.013	0.018	in wing
Land. Gear Group/GW	0.039	0.039	0.034	0.045
Take-off Gross Wht, W_{TO}, lbs	82,000	275,000	155,000	58,421
Empty Weight, W_E, lbs	46,000	113,814	73,260	29,675
Wing Group/S, psf	7.4	10.3	8.0	4.5
Emp. Grp/S_{emp}, psf	2.3	4.2	4.2	2.6
Ultimate Load Factor, g's	3.75*	2.50	3.75*	3.75*
Surface Areas, ft^2				
Wing, S	1,458	2,673	1,745	902
Horiz. Tail, S_h	327	801	536	320
Vert. Tail, S_v	250	641	300	223
Empenn. Area, S_{emp}	577	1,442	836	543

*Assumed

Table A10.3a Group Weight Data for Piston/Propeller Driven Military Transports

Type	Beech L-23F*	Chase C-123B	DeHavill. Caribou	Fairchild C-119B
Number of engines:	2	2	2	2
Weight Item, lbs				
Wing Group	692	6,153	2,925	7,226
Empennage Group	156	1,103	790	1,193
Fuselage Group	679	7,763	2,849	7,157
Nacelle Group	279	1,633	781	2,538**
Land. Gear Group	453	2,081	1,230	4,197
Nose Gear				
Main Gear				
Structure Total	2,259	18,733	8,575	22,311
Engines	1,015	4,810	3,170	6,500
Propellers	260	1,430	871	
Fuel System	127	671	221	
Propulsion System	215	1,103	453	
Power Plant Total	1,617	8,014	4,715	11,979
Avionics + Instrum.	91	161	121	
Surface Controls	129	490	326	
Hydraulic System	0	148	85	
Pneumatic System	0			
Electrical System	190	904	436	
Electronics	80	452	273	
APU	0	136	0	
Air Cond. System	104	642	82	
Anti-icing System				
Furnishings	459	428	271	
Auxiliary Gear	7	0	16	
Fixed Equipm't Total	1,060	3,361	1,610	6,834
$W_{oil} + W_{tfo}$	92	420	406	
Water	0	225	0	
Max. Fuel Capacity	1,080	5,452		15,540
Payload (Max.)	1,090	16,000	7,344	

*Military version of Twin Bonanza
**Tailbooms included

Table A10.3b Group Weight Data for Piston/Propeller Driven Military Transports

Type	Beech L-23F*	Chase C-123B	DeHavill. Caribou	Fairchild C-119B
Flight Design Gross Weight, GW, lbs	7,368	54,000	26,000	64,000
Structure/GW	0.307	0.347	0.330	0.349
Power Plant/GW	0.219	0.148	0.181	0.187
Fixed Equipm't/GW	0.144	0.062	0.062	0.107
Empty Weight/GW*	0.670	0.558	0.635	0.641
Wing Group/GW	0.094	0.114	0.113	0.113
Empenn. Group/GW	0.021	0.020	0.030	0.019
Fuselage Group/GW	0.092	0.144	0.110	0.112
Nacelle Group/GW	0.038	0.030	0.030	0.040**
Land. Gear Group/GW	0.061	0.039	0.047	0.066
Take-off Gross Wht, W_{TO}, lbs	7,368	52,802	26,000	64,000
Empty Weight, W_E, lbs	4,936	30,108	16,500	41,017
Wing Group/S, psf	2.5	5.0	3.2	5.0
Emp. Grp/S_{emp}, psf	1.7	2.1	1.9	2.7
Ultimate Load Factor, g's	6.6	4.5	5.1	
Surface Areas, ft^2				
Wing, S	277	1,223	912	1,447
Horiz. Tail, S_h	29.3		206	297
Vert. Tail, S_v	65.1		211	151
Empenn. Area, S_{emp}	94.4	520	417	448

*This is a military version of the Twin Bonanza
**Tailbooms included

Table A10.4a Group Weight Data for Piston/Propeller

Driven Military Transports

Type	Douglas C-124C	Boeing C-97C	Lockheed C-69	C-121A
Number of engines:	4	4	4	4
Weight Item, lbs				
Wing Group	18,135	15,389	9,466	11,184
Empennage Group	3,025	2,078	2,026	2,094
Fuselage Group	18,073	13,572	6,794	8,520
Nacelle Group	6,119	4,753	2,505	3,970
Land. Gear Group	11,701	7,112	4,481	4,771
Nose Gear		963	1,019	1,077
Main Gear		6,149	3,462	3,694
Structure Total	57,053	42,904	25,272	30,539
Engine(s)	15,551	13,844	10,568	11,536
Air Induct. System	4,046			
Fuel System	4,059			
Propeller Inst.	4,363			
Propulsion System	in prop.			
Power Plant Total	28,019	23,051	15,633	15,676
Avionics + Instrum.	769			
Surface Controls	1,493			
Hydraulic System	582			
Pneumatic System				
Electrical System	1,952			
Electronics	1,886			
APU	410			
Air Cond. System*	3,294			
Anti-icing System				
Furnishings	7,539			
Auxiliary Gear	104			
Fixed Equipm't Total	18,029	9,997	7,625	13,710
W_{oil} + W_{tfo}	3,389			
Water and Alcohol	522			
Max. Fuel Capacity	22,000	23,094	33,470	41,496
Payload (Max.)	55,262	46,500	12,330	12,550

*Includes pressurization system

Table A10.4b Group Weight Data for Piston/Propeller Driven Military Transports

Type	Douglas C-124C	Boeing C-97C	Lockheed C-69	C-121A
Flight Design Gross Weight, GW, lbs	185,000	150,000	82,000	132,800
Structure/GW	0.308	0.286	0.308	0.230
Power Plant/GW	0.151	0.154	0.191	0.118
Fixed Equipm't/GW	0.097	0.067	0.093	0.103
Empty Weight/GW	0.552	0.506	0.592	0.450
Wing Group/GW	0.098	0.103	0.115	0.084
Empenn. Group/GW	0.016	0.014	0.025	0.016
Fuselage Group/GW	0.098	0.090	0.083	0.064
Nacelle Group/GW	0.033	0.032	0.031	0.030
Land. Gear Group/GW	0.063	0.047	0.055	0.036
Take-off Gross Wht, W_{TO}, lbs	185,000	150,000	82,000	132,800
Empty Weight, W_E, lbs	102,181	75,974	48,530	59,715
Wing Group/S, psf	7.2	8.7	5.7	6.8
Emp. Grp/S_{emp}, psf	2.6	3.3	2.9	3.0
Ultimate Load Factor, g's	3.75	3.75	3.75	3.75
Surface Areas, ft^2				
Wing, S	2,506	1,769	1,650	1,650
Horiz. Tail, S_h	681	333	464	464
Vert. Tail, S_v	465	306	262	242
Empenn. Area, S_{emp}	1,146	639	706	706

Table A10.5a Group Weight Data for Military Patrol Airplanes

Type	Grumman S2F-1	Lockheed P2V-4	Lockheed U2
Number of engines:	2	2	1
Weight Item, lbs	Piston/Propeller		Jet
Wing Group	2,902	7,498	2,034
Empennage Group	681	1,589	320
Fuselage Group	1,701	5,155	1,410
Nacelle Group	965	2,303	0
Land. Gear Group	1,396	3,715	263
Nose Gear		tail gear	60
Main Gear			203
Structure Total	7,645	20,260	4,027
Engines	2,953	5,726	4,076
Propellers	866	1,137	
Fuel System	215	2,827	311
Propulsion System	390	1,633	479**
Power Plant Total	4,424	11,323	4,866
Avionics + Instrum.	147	194	57
Surface Controls	714	960	362
Hydraulic System	208	284	66
Pneumatic System			
Electrical System	988	1,503	290
Electronics	2,310	2,903	166
Armament	256	1,705	
Air Cond. System*	356	496	135
Anti-icing System			
Furnishings	657	1,327	82
Auxiliary Gear	281	0	193
Fixed Equipm't Total	5,917	9,372	1,351
W_{oil} + W_{tfo}	332	1,640	97
Engine oil			120
Armament Provisions	18	5,951	
Water	0	1,480	
Max. Fuel Capacity	3,126	14,006	5,810
Payload (Max.)	1,938		518
Crew	N.A.	N.A.	285

*Incl. press. system **Incl. air induction and exhausts

Table A10.5b Group Weight Data for Military Patrol Airplanes

Type	Grumman S2F-1 Piston/Propeller	Lockheed P2V-4 Piston/Propeller	Lockheed U2 Jet
Flight Design Gross Weight, GW, lbs	23,180	67,500	17,000
Structure/GW	0.330	0.300	0.237
Power Plant/GW	0.191	0.168	0.286
Fixed Equipm't/GW	0.255	0.139	0.079
Empty Weight/GW	0.775	0.607	0.603
Wing Group/GW	0.125	0.111	0.120
Empenn. Group/GW	0.029	0.024	0.019
Fuselage Group/GW	0.073	0.076	0.083
Nacelle Group/GW	0.042	0.034	
Land. Gear Group/GW	0.060	0.055	0.015
Take-off Gross Wht, W_{TO}, lbs	24,167	67,500	19,913
Empty Weight, W_E, lbs	17,953	40,955	10,244
Wing Group/S, psf	6.0	7.5	3.4
Emp. Grp/S_{emp}, psf	3.5	3.9	2.3
Ultimate Load Factor, g's	4.5	4.0	3.75
Surface Areas, ft^2			
Wing, S	485	1,000	600
Horiz. Tail, S_h	103	241	90
Vert. Tail, S_v	90.2	170	49
Empenn. Area, S_{emp}	193	411	139

Table A11.1a Group Weight Data for Flying Boats,

Amphibious and Float Airplanes

Type	At the time of printing no data were available
Number of engines:	
Weight Item, lbs	
Wing Group	
Empennage Group	
Fuselage Group	
Nacelle Group	
Land. Gear Group	
Nose Gear	
Main Gear	

Structure Total	

Engines	
Propellers	
Fuel System	
Propulsion System	

Power Plant Total	

Avionics + Instrum.	
Surface Controls	
Hydraulic System	
Pneumatic System	
Electrical System	
Electronics	
Armament	
Air Cond. System	
Anti-icing System	
Furnishings	
Auxiliary Gear	

Fixed Equipm't Total	

W_{oil} + W_{tfo}	
Armament Provisions	
Water	
Max. Fuel Capacity	
Payload (Max.)	

Table A11.1b Group Weight Data for Flying Boats,
Amphibious and Float Airplanes

Type	At the time of printing no data were available
Flight Design Gross Weight, GW, lbs	
Structure/GW	
Power Plant/GW	
Fixed Equipm't/GW	
Empty Weight/GW	
Wing Group/GW	
Empenn. Group/GW	
Fuselage Group/GW	
Nacelle Group/GW	
Land. Gear Group/GW	
Take-off Gross Wht, W_{TO}, lbs	
Empty Weight, W_E, lbs	
Wing Group/S, psf	
Emp. Grp/S_{emp}, psf	
Ultimate Load Factor, g's	
Surface Areas, ft^2	
Wing, S	
Horiz. Tail, S_h	
Vert. Tail, S_v	
Empenn. Area, S_{emp}	

Table A12.1a Group Weight Data for Supersonic Cruise Airplanes

Type →	AST-100 *	SSXJET **	Super-cruiser ***
Number of engines:	4	2	2
Weight Item, lbs			
Wing Group	85,914	3,599	3,962
Empennage Group	10,655	481	225
Fuselage Group	52,410	3,494	2,195
Nacelle Group	16,803	505	700
Land. Gear Group	27,293	1,391	1,300
Nose Gear			
Main Gear			
Structure Total	193,075	9,470	8,382
Engines	52,000	3,016	4,781
Air Induct. System	incl. in propulsion system		
Fuel System	5,781	626	560
Propulsion System	1,780	59	165
Power Plant Total	59,561	3,701	6,756
Avionics + Instrum.	6,090	660	1,484
Surface Controls	9,405	564	1,207
Hydraulic System	5,600	266	302
Pneumatic System			
Electrical System	5,050	445	357
Electronics	incl. in avionics + instrum.		
Armament	0	0	600
Air Cond. System****	8,200	352	250
Anti-icing System	210	95	
Furnishings	25,111	417	242
Auxiliary Gear	0	0	40
Fixed Equipm't Total	59,666	2,799	4,482
W_{oil} + W_{tfo}	3,050	133	
Mission Fuel Reqd.	327,493	18,674	12,523
Payload	61,028	725	5,000

*NASA TM X-73936, M=2.2 large passenger transport
**NASA TM 74055, M=2.2 executive (business) jet
***NASA TM 78811, M=2.6 military missile carrying super cruiser
****Includes pressurization system

Table A12.1b Group Weight Data for Supersonic Cruise Airplanes

Type	AST-100 *	SSXJET **	Super-cruiser ***
Flight Design Gross Weight, GW, lbs	718,000	35,720	37,144
Structure/GW	0.269	0.265	0.226
Power Plant/GW	0.083	0.104	0.182
Fixed Equipm't/GW	0.083	0.078	0.121
Empty Weight/GW	0.435	0.447	0.528
Wing Group/GW	0.120	0.101	0.107
Empenn. Group/GW	0.015	0.013	0.006
Fuselage Group/GW	0.073	0.098	0.059
Nacelle Group/GW	0.023	0.014	0.019
Land. Gear Group/GW	0.038	0.039	0.035
Take-off Gross Wht, W_{TO}, lbs	718,000	35,720	47,900
Empty Weight, W_E, lbs	312,302	15,970	19,620
Wing Group/S, psf	8.6	3.7	10.7
Emp. Grp/S_{emp}, psf	11.0	3.9	3.1
Ultimate Load Factor, g's	3.75	3.75	6.0
Surface Areas, ft^2			
Wing, S	9,969	965	371
Horiz. Tail, S_h	579	62	0
Vert. Tail, S_v	386	62	73
Empenn. Area, S_{emp}	965	124	73

*NASA TM X-73936, M=2.2 large passenger transport
**NASA TM 74055, M=2.2 executive (business) jet
***NASA TM 78811, M=2.6 military missile carrying super cruiser

Table A13.1a Group Weight Data for NASA X Airplanes

Type	Ryan X-13*	North American X-15**	Hiller X-18***	Bell XV-15
Number of engines:	1	1	2	2
Weight Item, lbs	Jet	Rocket	TBP	TBP Tiltrotor
Wing Group	515	1,144	3,483	946
Empennage Group	146	1,267	928	259
Fuselage Group	415	3,806	4,694	1,589
Engine Section	69	187	728	nac. 369
Land. Gear Group	300	389	1,289	524
Nose Gear				
Main Gear				
Structure Total	1,445	6,793	11,122	3,687
Engine(s)	2,766	680	5,460	1,052
Fuel System	100	1,354	623	226
Propeller Inst.	0	0	3,679	863
Propulsion System	227	148	548	222
Drive system				1,340
Propeller Controls	0	0	2,023	****629
Power Plant Total	3,093	2,182	12,333	4,332
Avionics + Instrum.	41	172	141	231
Surface Controls	416	1,182	896	****777
Hydraulic System	214	240	863	util. 86
Electrical System	311	142	931	418
Electronics	29	175	63	
Test Instrumentation	139	1,328		1,160
Ballast				106
Air Cond. System	10	192		119
Furnishings	199	446	813	434
Auxiliary Gear	0	11	0	10
Fixed Equipm't Total	1,359	3,888	3,707	3,341
W_{oil} + W_{tfo}	43	0	353	32
Liquid Nitrogen		150	engine oil:	53
Max. Fuel Capacity	1,400	314	823	1,401
Payload	crew and test equipment only			

*Delta configuration, took off from vertical position
**Air launched by B-52
***Turbo/propeller driven, wing incidence variable over more than 90 degrees
****hydraulic system incl. in rotor and surface ctrls

Table A13.1b Group Weight Data for NASA X Airplanes

Type	Ryan X-13*	North American X-15**	Hiller X-18***	Bell **** XV-15
Flight Design Gross Weight, GW, lbs	7,000	13,592	33,000	13,226
Structure/GW	0.206	0.500	0.337	0.279
Power Plant/GW	0.442	0.161	0.374	0.328
Fixed Equipm't/GW	0.194	0.286	0.112	0.253
Empty Weight/GW	0.822	0.949	0.826	0.859
Wing Group/GW	0.074	0.084	0.106	0.072
Empenn. Group/GW	0.021	0.093	0.028	0.020
Fuselage Group/GW	0.059	0.280	0.142	0.120
Engine Section/GW	0.010	0.014	0.022	0.028
Land. Gear Group/GW	0.043	0.029	0.039	0.040
Take-off Gross Wht, W_{TO}, lbs	7,149	13,592	33,000	13,226
Empty Weight, W_E, lbs	5,755	12,901	27,272	11,360
Wing Group/S, psf	2.7	10.9	6.6	5.6
Emp. Grp/S_{emp}, psf	2.3	10.0	2.8	2.6
Ultimate Load Factor, g's	6.0	11.0		
Surface Areas, ft^2				
Wing, S	191	105	528	169
Horiz. Tail, S_h	0	52	201	50.3
Vert. Tail, S_v	62.8	74.9	133	50.5
Empenn. Area, S_{emp}	62.8	127	334	101

*Delta configuration, took off from vertical position
**Air launched by B-52
***Turbo/propeller driven, wing incidence variable over more than 90 degrees
****Tiltrotor research airplane

Table A13.2a Group Weight Data for NASA X Airplanes

Type	Bell X-2*	Bell X-5**	Northrop YP-61***	Bell XP-77****
Number of engines:	1	1	2	1
Weight Item, lbs	Rocket	Jet	Piston/ Prop.	Piston/ Prop.
Wing Group	2,856	1,683	3,969	463
Empennage Group	445	198	629	59
Fuselage Group	4,108	1,064	1,557	218
Engine Section	30	274	1,817 incl.booms	123
Land. Gear Group	421	532	1,803	344
Nose Gear	108	464	303	123
Main Gear (skids)	313	68	1,500	221
Structure Total	8,281	3,751	9,775	1,207
Engine(s)	607	2,223	4,974	738
Air Induction System		31		
Fuel System	898	108	914	91
Propulsion System	13	77	1,081	101
Propellers			1,111	206
Power Plant Total	1,518	2,439	8,080	1,136
Avionics + Instrum.	65	35	119	37
Surface Controls	364	195	400	42
Hydraulic System	442	139	240	0
Electrical System	604	127	668	92
Electronics	63	86	721	99
Anti-icing System			100	
Test Instrumentation	708	155		
Armament(incl. guns and ammo)			3,364	391
Ballast		98		
Air Cond. System	102	69		
Furnishings	158	84	252	56
Auxiliary Gear	0	90	352	15
Fixed Equipm't Total	2,506	1,078	6,216	732
W_{oil} + W_{tfo}	484		152	30
Liquid Oxygen	7,180			
Liquid Nitrogen	26	oil: 23	oil: 270	28
Max. Fuel Capacity	5,716	1,200	3,168	312
Payload	crew and test equipment only			

*Air launched by B50 **Variable sweep wing
***Twin boom fighter ****Wood built lightweight fighter

Table A13.2b Group Weight Data for NASA X Airplanes

Type	Bell X-2*	Bell X-5**	Northrop YP-61***	Bell XP-77****
Flight Design Gross Weight, GW, lbs	25,627	8,737	27,813	3,632
Structure/GW	0.323	0.429	0.351	0.332
Power Plant/GW	0.059	0.279	0.291	0.313
Fixed Equipm't/GW	0.098	0.123	0.223	0.202
Empty Weight/GW	0.480	0.832	0.865	0.847
Wing Group/GW	0.111	0.193	0.143	0.127
Empenn. Group/GW	0.017	0.023	0.023	0.016
Fuselage Group/GW	0.160	0.122	0.056	0.060
Engine Section/GW	0.001	0.031	0.065 incl.booms	0.034
Land. Gear Group/GW	0.016	0.061	0.065	0.095
Take-off Gross Wht, W_{TO}, lbs	25,627	8,737	27,813	3,632
Empty Weight, W_E, lbs	12,305	7,268	24,071	3,075
Wing Group/S, psf	11.0	9.6	6.0	4.6
Emp. Grp/S_{emp}, psf	4.1	3.4	3.0	2.1
Ultimate Load Factor, g's	not available			
Surface Areas, ft^2				
Wing, S	260	175	664	100
Horiz. Tail, S_h	49.5	31.8	120	18.7
Vert. Tail, S_v	58	25.8	92	9.0
Empenn. Area, S_{emp}	108	57.6	212	27.7

*Air launched by B50 **Variable sweep wing
***Twin boom fighter ****Wood built lightweight fighter

Table A13.3a Group Weight Data for NASA X Airplanes

Type	Mc Donnell XF-88A	Convair XF-92A**	NAA YF-93A***	Convair XFY-1
Number of engines:	2	1	1	1
Weight Item, lbs	Jet	Jet	Jet	TBP****
Wing Group	2,048	1,694	2,640	1,877
Empennage Group	472	590	444	623
Fuselage Group	3,267	2,149	2,850	1,084
Engine Section	29	0	44	157
Land. Gear Group	986	764	1,382	466
Nose Gear	193	155	254	gears on
Main Gear	793	609	1,128	four fins
Structure Total	6,802	5,197	7,360	4,207
Engine(s)	2,942*	2,254	2,787	2,935
Fuel System	920	362	1,520	185
Propeller Inst.	0	0		1,937
Propulsion System	261	198	396	470
Power Plant Total	4,123	2,814	4,703	5,527
Avionics + Instrum.	54	29	155	64
Surface Controls	509	672	686	364
Hydraulic System	307	406	210	214
Electrical System	662	408	488	377
Electronics	218	75	286	120
Test instrumentation				428
Ballast	337			230
Armament	479		1,008	
Guns or cannons	750		639	97
Air Cond. System	87	65	170	76
Furnishings	184	108	207	196
Miscellanous		30(paint)		121
Fixed Equipm't Total	3,587	1,793	3,849	2,287
$W_{oil} + W_{tfo}$	44	N.A.	50	102
Engine oil	75	23	18	94
Max. Fuel Capacity	4,404	4,440	10,593	1,839
Payload	829(ammo)	N.A.	863(ammo)	0
Crew	230	230	230	200

*Includes afterburners **Delta wing configuration
***F-86 modified with NACA flush side inlets
****Counter-rotating propeller driven tailsitter (VTOL)

Table A13.3b Group Weight Data for NASA X Airplanes

Type	Mc Donnell XF-88A	Convair XF-92A	NAA YF-93A	Convair XFY-1
Flight Design Gross Weight, GW, lbs	20,098	11,600	21,846	14,250
Structure/GW	0.338	0.448	0.337	0.295
Power Plant/GW	0.205	0.243	0.215	0.388
Fixed Equipm't/GW	0.178	0.155	0.176	0.160
Empty Weight/GW	0.722	0.845	0.728	0.844
Wing Group/GW	0.102	0.146	0.121	0.132
Empenn. Group/GW	0.023	0.051	0.020	0.044
Fuselage Group/GW	0.163	0.185	0.130	0.076
Engine Section/GW	0.001	0.000	0.002	0.011
Land. Gear Group/GW	0.049	0.066	0.064	0.033
Take-off Gross Wht, W_{TO}, lbs	20,098	11,600	27,788	15,185
Empty Weight, W_E, lbs	14,512	9,804	15,912	12,021
Wing Group/S, psf	5.9	4.0	8.6	5.3
Emp. Grp/S_{emp}, psf	4.3	7.8	5.6	3.5
Ultimate Load Factor, g's	11.0	11.0	11.0	11.3
Surface Areas, ft^2				
Wing, S	350	425	306	355
Horiz. Tail, S_h	N.A.	0	N.A.	N.A.
Vert. Tail, S_v	N.A.	76.0	N.A.	N.A.
Empenn. Area, S_{emp}	109	76.0	79.6	176

Table A13.4a Group Weight Data for NASA X Airplanes

Type	Lockheed XV-4A*	Lockheed XV-4B**	Ryan XV-5A***	Bell X-22A****
Number of engines:	2	6	4	4
Weight Item, lbs	Jet	Jet	Jet + liftfan	Turbo-shaft
Wing Group	350	395	1,059	789
Empennage Group	170	167	267	131
Fuselage Group	1,207	1,274	1,341	1,324
Engine Section	245	333	45	610
Land. Gear Group	291	389	482	432
Nose Gear	57	77	82	94
Main Gear	234	312	400	338
Structure Total	2,263	2,558	3,194	3,286
Engine(s) (main)	872	758	913	1,191
Engine(s) (lift)	0	1,500	1,855	
Exhaust system	520	608	304	8
Fuel System	155	142	124	175
Propeller Inst. including drives:				2,147
Ducts and supports: fwd 695, aft 686, total:				1,381
Propulsion System	101	88	80	246
Power Plant Total	1,648	3,096	3,276	5,148
Avionics + Instrum.	73	133	73	121
Surface Controls	486	655	440	1,256
Hydraulic System	62	116	115	162
Electrical System	376	394	196	376
Electronics	29	35	40	237
Test instrumentation	583	200	515	1,520
Auxiliary gear	52	27	158	10
Air Cond. System	32	58	34	45
Furnishings	209	391	235	376
Fixed Equipm't Total	1,902	2,009	1,806	4,103
$W_{oil} + W_{tfo}$	40	30	29	72
Engine oil	20	62	12	22
Max. Fuel Capacity	1,147	3,815	2,430	2,031
Crew	180	430	180	360
Payload				1,200

*Ejector type VTOL **Lift engine type VTOL Liftfan research airplane ****Tiltrotor research airplane

Table A13.4b Group Weight Data for NASA X Airplanes

Type	Lockheed XV-4A	Lockheed XV-4B	Ryan XV-5A	Bell X-22A
Flight Design Gross Weight, GW, lbs	7,200	12,000	9,200	14,700
Structure/GW	0.314	0.213	0.347	0.224
Power Plant/GW	0.229	0.258	0.356	0.350
Fixed Equipm't/GW	0.264	0.167	0.196	0.279
Empty Weight/GW	0.807	0.639	0.900	0.853
Wing Group/GW	0.049	0.033	0.115	0.054
Empenn. Group/GW	0.024	0.014	0.029	0.009
Fuselage Group/GW	0.168	0.106	0.146	0.090
Engine Section/GW	0.034	0.028	0.005	0.041
Land. Gear Group/GW	0.040	0.032	0.052	0.029
Take-off Gross Wht, W_{TO}, lbs	7,200	12,000	9,972	14,700
Empty Weight, W_E, lbs	5,813	7,663	8,276	12,537
Wing Group/S, psf	3.4	3.8	4.1	4.9
Emp. Grp/S_{emp}, psf	3.2	3.1	2.6	1.5
Ultimate Load Factor, g's	7.5	4.5	6.0	4.5
Surface Areas, ft^2				
Wing, S	104	104	260	160
Horiz. Tail, S_h	26.4	26.4	52.9	20
Vert. Tail, S_v	27.5	27.5	51.0	68.5
Empenn. Area, S_{emp}	53.9	53.9	104	88.5

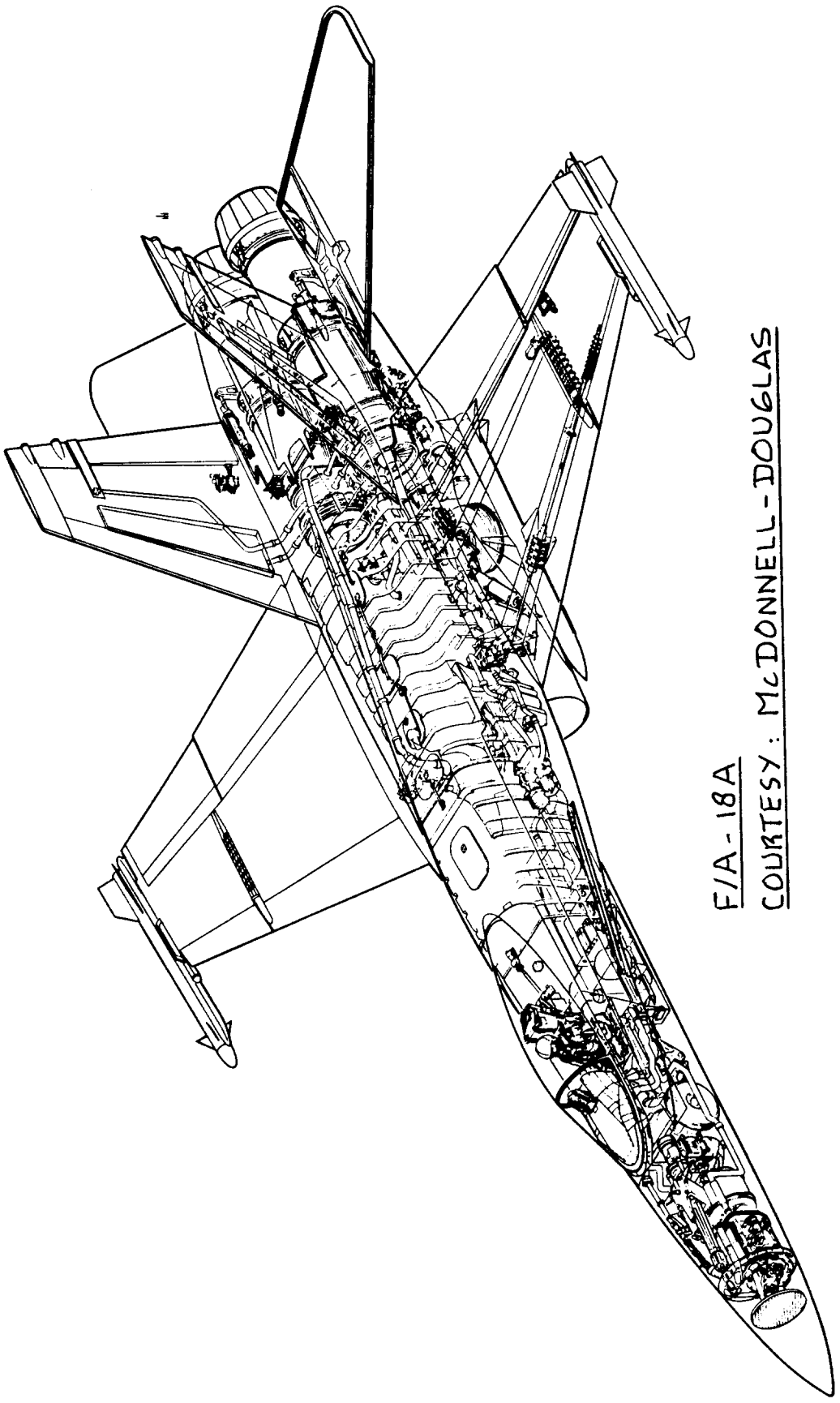

F/A-18A
COURTESY: McDONNELL-DOUGLAS

APPENDIX B: DATA SOURCE FOR NON-DIMENSIONAL RADII OF GYRATION FOR AIRPLANES

The purpose of this appendix is to present tabulated data for non-dimensional radii of gyration of airplanes. Actual moments of inertia can be estimated from these non-dimensional radii of gyration with the help of Equations 3.7 through 3.8.

The tables are organized as follows:

Table B1: Homebuilt propeller driven airplanes
Table B2: Single engine propeller driven airplanes
Table B3: Twin engine propeller driven airplanes
Table B4: Agricultural airplanes
Table B5: Business jets
Table B6: Regional turbopropeller driven airplanes
Table B7a: Jet transports
Table B7b: Piston-propeller driven transports
Table B7c: Turbopropeller driven transports
Table B8: Military trainers
Table B9a: Fighters (Jet)
Table B9b: Fighters (Propeller)
Table B10a: Bombers (Piston-Propeller)
Table B10b: Bombers (Jet)
Table B10c: Military patrol airplanes (Propeller)
Table B10d: Military transports (Propeller)
Table B11: Flying boats
Table B12: Supersonic cruise airplanes

The data in all these table were derived from manufacturers data and/or from Ref.11.

Table B1 Non-dimensional Radii of Gyration for Homebuilt Propeller

Driven Airplanes

Airplane Type	GW lbs	Wing Span, b, ft	Total Length, L, ft	e = (b+L)/2, ft	$\bar{R}_x$	$\bar{R}_y$	$\bar{R}_z$	Number of engines and disposition

At the time of printing, no data were available for this type airplane

Table B2 Non-dimensional Radii of Gyration for Single Engine

Propeller Driven Airplanes

Airplane Type	GW lbs	Wing Span, b, ft	Total Length, L, ft	e = (b+L)/2, ft	$\bar{R}_x$	$\bar{R}_y$	$\bar{R}_z$	Number of engines and disposition
Beech N-35*	3,125	32.8	25.1	29.0	0.248	0.338	0.393	1 in fusel.
Cessna 150M**	1,127	33.5	21.5	27.5	0.254	0.405	0.418	1 in fusel.
Cessna 172M**	1,477	36.2	26.5	31.4	0.242	0.386	0.403	1 in fusel.
Cessna 177A**	1,761	35.6	27.0	31.3	0.212	0.362	0.394	1 in fusel.
Cessna R182**	1,885	36.2	28.0	32.1	0.342	0.397	0.393	1 in fusel.
Cessna 210K***	2,700	36.8	28.3	32.6	0.222	0.356	0.379	1 in fusel.

*at W_{TO} **at W_{OE} ***atW_{OE} plus 25 percent fuel

Note: one pilot included in all data

Table B3 Non-dimensional Radii of Gyration for Twin Engine

Propeller Driven Airplanes

Airplane Type	GW lbs	Wing Span, b, ft	Total Length, L, ft	e = (b+L)/2, ft	$\bar{R}_x$	$\bar{R}_y$	$\bar{R}_z$	Number of engines and disposition
Beech 55	4,880	37.8	25.7	31.8	0.260	0.329	0.399	2 on wing
Beech 95	4,000	37.8	25.3	31.6	0.251	0.327	0.391	2 on wing
Beech D-50	6,500	45.9	31.5	38.7	0.240	0.313	0.384	2 on wing
Beech D18S	9,000	47.7	34.2	41.0	0.232	0.360	0.396	2 on wing
Cessna 402*	5,000	39.9	36.3	38.1	0.414	0.278	0.502	2 on wing
Cessna 402	6,200	39.9	36.3	38.1	0.373	0.269	0.461	2 on wing
Cessna 404*	4,851	46.7	39.5	43.1	0.324	0.318	0.446	2 on wing
Cessna 404	8,400	46.7	39.5	43.1	0.340	0.284	0.445	2 on wing
Cessna 441*	5,642	49.3	39.0	44.2	0.285	0.345	0.429	2 on wing
Cessna 441	9,925	49.3	39.0	44.2	0.256	0.212	0.336	2 on wing

*at W_E

Table B4 Non-dimensional Radii of Gyration for Agricultural Airplanes

Airplane Type	GW lbs	Wing Span, b, ft	Total Length, L, ft	e = (b+L)/2, ft	$\bar{R}_x$	$\bar{R}_y$	$\bar{R}_z$	Number of engines and disposition

At the time of printing, no data were available for this type of airplane

Table B5 Non-dimensional Radii of Gyration for Business Jets

Airplane Type	GW lbs	Wing Span, b, ft	Total Length, L, ft	e = (b+L)/2, ft	$\bar{R}_x$	$\bar{R}_y$	$\bar{R}_z$	Number of engines and disposition
Morane/S 760	7,066	33.3	32.9	33.1	0.374	0.328	0.486	2 in W/F
Lockh. Jetstar	39,288	53.7	58.8	56.3	0.370	0.356	0.503	4 on fusel.
Cessna 500*	6,505	47.1	43.5	45.3	0.236	0.384	0.430	2 on fusel.
Cessna 500**	12,000	47.1	43.5	45.3	0.306	0.303	0.423	2 on fusel.
Cessna 550*	7,036	51.7	47.2	49.5	0.243	0.400	0.447	2 on fusel.
Cessna 550**	13,500	51.7	47.2	49.5	0.293	0.312	0.420	2 on fusel.

*at W_e **at W_{TO}

Table B6 Non-dimensional Radii of Gyration for Regional Turbopropeller Driven Airplanes

Airplane Type	GW lbs	Wing Span, b, ft	Total Length, L, ft	e = (b+L)/2, ft	$\bar{R}_x$	$\bar{R}_y$	$\bar{R}_z$	Number of engines and disposition
Fokker F-27A	38,500	95.2	77.2	86.2	0.235	0.363	0.416	2 on wing
DHC6 Twin Otter	12,500	65.0	51.8	58.4	0.203	0.326	0.350	2 on wing

Table B7a Non-dimensional Radii of Gyration for Jet Transports

Airplane Type	GW lbs	Wing Span, b, ft	Total Length, L, ft	e = (b+L)/2, ft	$\bar{R}_x$	$\bar{R}_y$	$\bar{R}_z$	Number of engines and disposition
Convair 880	185,000	120.0	124.2	122.1	0.320	0.342	0.465	4 on wing
Convair 880	191,500	120.0	124.2	122.1	0.322	0.339	0.464	4 on wing
Convair 990	240,000	120.0	134.8	127.4	0.335	0.338	0.473	4 on wing
Convair 990	245,000	120.0	134.8	127.4	0.305	0.334	0.472	4 on wing
Boeing 727-100	165,000	108.0	133.2	120.6	0.249	0.375	0.452	3 on fusel.
Boeing 727-100*	89,000	108.0	133.2	120.6	0.247	0.442	0.518	3 on fusel.
Boeing 727-200	180,000	108.0	153.2	130.6	0.248	0.394	0.502	3 on fusel.
Boeing 727-200*	100,000	108.0	153.2	130.6	0.240	0.451	0.550	3 on fusel.
Boeing 737-200	113,000	93.0	100.0	96.5	0.246	0.382	0.456	2 on wing
Boeing 737-200*	62,000	93.0	100.0	96.5	0.264	0.456	0.517	2 on wing
Boeing 747-100B	800,000	195.7	231.3	213.5	0.290	0.329	0.445	4 on wing
Boeing 747-100B*	350,000	195.7	231.3	213.5	0.332	0.380	0.508	4 on wing
McDD DC9-10	74,000	89.4	104.3	96.9	0.242	0.360	0.435	2 on fusel.
McDD DC8	210,000	142.4	150.5	146.5	0.301	0.349	0.434	4 on wing

*at W_{OE}

Table B7b Non-dimensional Radii of Gyration for Piston-Propeller Driven Transports

Airplane Type	GW lbs	Wing Span, b, ft	Total Length, L, ft	e = (b+L)/2, ft	$\bar{R}_x$	$\bar{R}_y$	$\bar{R}_z$	Number of engines and disposition
Lockheed L-749A	107,000	123.0	95.2	109.1	0.300	0.298	0.426	4 on wing
Lockheed L-1049	120,000	123.0	113.6	118.3	0.316	0.336	0.448	4 on wing
Lockheed L-1649	146,500	150.0	116.2	133.1	0.371	0.278	0.473	4 on wing
Douglas DC-4	60,360	138.3	97.6	118.0	0.250	0.320	0.388	4 on wing
Douglas DC-6	97,200	117.5	100.5	109.0	0.322	0.324	0.456	4 on wing
Airspeed Ambass.	49,500	115.0	80.4	97.7	0.278	0.314	0.400	2 on wing
Martin 404	45,000	93.3	74.6	84.2	0.272	0.378	0.444	2 on wing
Convair T-240	41,800	91.7	74.7	83.2	0.286	0.351	0.443	2 on wing
Convair T-340	44,500	105.7	79.2	92.4	0.308	0.345	0.457	2 on wing
Beech Twin Quad	20,000	70.0	52.7	61.4	0.225	0.303	0.346	4 in wing

Table B7c Non-dimensional Radii of Gyration for Turbo-Propeller Driven Transports

Airplane Type	GW lbs	Wing Span, b, ft	Total Length, L, ft	e = (b+L)/2, ft	$\bar{R}_x$	$\bar{R}_y$	$\bar{R}_z$	Number of engines and disposition
Bristol 175(k)*	103,000	130.0	110.0	120.0	0.317	0.356	0.455	4 on wing
Bristol 167(1)**	187,000	230.0	177.0	203.5	0.330	0.356	0.478	4 on wing
Lockh. Electra	116,000	99.0	104.7	101.9	0.394	0.341	0.497	4 on wing

*Britannia **Brabazon

Table B8 Non-dimensional Radii of Gyration for Military Trainers

Airplane Type	GW lbs	Wing Span, b, ft	Total Length, L, ft	e = (b+L)/2 ft	$\bar{R}_x$	$\bar{R}_y$	$\bar{R}_z$	Number of engines and disposition
Cessna T-37A	6,300	38.4	30.0	34.2	0.220	0.142	0.245	2 in fusel.

Table B9a Non-dimensional Radii of Gyration for Fighters (Jet)

Airplane Type	GW lbs	Wing Span, b, ft	Total Length, L, ft	e = (b+L)/2, ft	$\bar{R}_x$	$\bar{R}_y$	$\bar{R}_z$	Number of engines and disposition
McD F2H-1	14,413	41.6	40.2	40.9	0.230	0.359	0.465	2 in W/F
McD F3H-2N	26,878	35.3	58.8	47.1	0.252	0.107	0.449	1 in fusel.
McD F-101A	36,969	39.7	67.4	53.6	0.209	0.329	0.428	2 in fusel.
VS Attacker	10,450	36.9	37.3	37.1	0.244	0.328	0.400	1 in fusel.
DH Vampire 20	10,891	40.0	30.1	35.1	0.286	0.318	0.409	1 in fusel.
Gl. Meteor II	11,100	43.0	41.4	42.2	0.286	0.330	0.404	2 in wing
Lockheed F-80A	11,940	38.9	34.3	36.6	0.286	0.356	0.444	1 in fusel.
Lockheed F-94B	13,650	37.5	40.1	38.8	0.284	0.396	0.488	1 in fusel.
Lockheed F-104G	20,900	21.9	54.8	38.4	0.224	0.392	0.563	1 in fusel.
NAA F-86A	13,900	37.1	37.5	37.3	0.266	0.346	0.400	1 in fusel.
NAA FJ-3	16,883	37.0	37.6	37.3	0.281	0.352	0.438	1 in fusel.
NAA F-100D	29,800	38.0	47.0	42.5	0.252	0.376	0.462	1 in fusel.
Vought XF8U-1	21,300	35.7	54.4	45.1	0.225	0.404	0.507	1 in fusel.
Vought F8U-3	30,600	40.0	58.9	49.5	0.225	0.375	0.467	1 in fusel.
GD XF-91	18,600	31.3	43.3	37.3	0.323	0.424	0.548	1 in fusel.
GD TF-102A	32,859	38.1	63.2	50.7	0.295	0.386	0.520	1 in fusel.
GD F-106B	36,834	38.3	70.7	54.5	0.247	0.379	0.516	1 in fusel.
Northrop F-89D	38,000	58.0	54.0	56.0	0.440	0.304	0.532	2 in fusel.
Republic RF-84F	19,000	33.6	47.5	40.6	0.310	0.308	0.432	1 in fusel.
Republic F-105D	34,058	35.0	64.4	49.7	0.231	0.425	0.567	1 in fusel.
Grumman F9F-8	16,744	34.5	41.9	38.2	0.248	0.374	0.454	1 in fusel.
Grumman XF10F-1	26,160	36.8	57.8	46.9	0.251	0.323	0.414	1 in fusel.
Grumman F11F-1	16,500	31.6	40.8	36.2	0.221	0.404	0.484	1 in fusel.

Table B9b Non-dimensional Radii of Gyration for Fighters (Propeller)

Airplane Type	GW lbs	Wing Span, b, ft	Total Length, L, ft	e = (b+L)/2, ft	$\bar{R}_x$	$\bar{R}_y$	$\bar{R}_z$	Number of engines and disposition
Brewster Buffalo	5,066	35.0	26.0	30.5	0.208	0.358	0.374	1 in fusel.
Seversky P35	5,788	36.0	26.8	31.4	0.198	0.367	0.360	1 in fusel.
VS Spitfire-I	6,250	36.8	29.9	33.4	0.240	0.334	0.384	1 in fusel.
BP Defiant	6,410	39.4	35.0	37.2	0.234	0.360	0.404	1 in fusel.
Curtiss P36	6,825	37.3	31.7	34.5	0.172	0.356	0.370	1 in fusel.
Bell P39	7,533	34.0	30.0	32.0	0.276	0.340	0.425	1 in fusel.
Grumman F6F	10,560	42.8	33.5	38.2	0.242	0.346	0.404	1 in fusel.
Hawker Typhoon	11,017	41.5	31.7	36.6	0.277	0.300	0.394	1 in fusel.
Republic P47	12,500	40.7	36.0	38.4	0.296	0.322	0.428	1 in fusel.
Vought F4U	12,850	41.0	34.5	37.8	0.268	0.360	0.420	1 in fusel.
Bl.Firebr'd-III	13,660	49.8	38.2	44.0	0.250	0.300	0.397	1 in fusel.
Westland Welkin	18,340	70.0	42.0	56.0	0.270	0.304	0.408	2 in wing
Bristol Beauftr	22,635	57.8	42.5	50.2	0.330	0.299	0.447	2 in wing
Bristol Brigand	39,000	71.7	46.4	59.1	0.299	0.338	0.438	2 in wing

Table B10a Non-dimensional Radii of Gyration for Bombers (Piston-Propeller)

Airplane Type	GW lbs	Wing Span, b, ft	Total Length, L, ft	e = (b+L)/2, ft	$\bar{R}_x$	$\bar{R}_y$	$\bar{R}_z$	Number of engines and disposition
Martin B-26	26,600	65.0	57.6	61.3	0.270	0.320	0.410	2 on wing
HP Halifax	55,000	99.0	71.6	85.3	0.346	0.306	0.395	4 on wing
Shorts Stirling	64,000	99.0	87.3	93.2	0.360	0.330	0.488	4 on wing
Boeing B-29	105,000	141.0	99.0	120.0	0.316	0.320	0.376	4 on wing
Boeing B-50	120,000	141.0	99.0	120.0	0.304	0.332	0.450	4 on wing
GD B-36	357,500	230.0	162.0	196.0	0.316	0.262	0.428	6 in wing

Table B10b Non-dimensional Radii of Gyration for Bombers (Jet)

Airplane Type	GW lbs	Wing Span, b, ft	Total Length, L, ft	e = (b+L)/2, ft	$\bar{R}_x$	$\bar{R}_y$	$\bar{R}_z$	Number of engines and disposition
Martin XB-51	53,785	53.0	81.0	67.0	0.194	0.404	0.498	3 in/on fus.
Martin B57A	48,554	64.0	66.0	65.0	0.312	0.278	0.412	2 in wing
Boeing XB-47	125,000	116.0	107.0	111.5	0.346	0.320	0.474	4 in wing
Boeing B-52A	390,000	185.0	156.5	170.8	0.346	0.306	0.466	8 on wing
Northrop RB-49A	213,500	172.0	53.0*	112.5	0.316	0.316	0.510	6 in wing
NAA B-45A	82,600	89.0	75.3	82.2	0.325	0.290	0.438	4 on wing
NAA B-45C	82,600	89.0	75.3	82.2	0.340	0.299	0.456	4 on wing

*Flying wing

Table B10c Non-dimensional Radii of Gyration for Military Patrol Airplanes

(Propeller Driven)

Airplane Type	GW lbs	Wing Span, b, ft	Total Length, L, ft	e = (b+L)/2, ft	$\bar{R}_x$	$\bar{R}_y$	$\bar{R}_z$	Number of engines and disposition
Piston-Propeller Driven								
Lockheed P2V-4	67,500	100.0	81.6	90.8	0.368	0.300	0.484	2 on wing
Lockheed P2V-7*	67,500	100.0	91.7	95.9	0.372	0.266	0.462	4 on wing
Grumman S2F-3	26,147	69.7	43.5	56.6	0.240	0.347	0.387	2 on wing
Grumman W2F-1	41,549	80.6	56.3	68.4	0.235	0.366	0.387	2 on wing
Turbo-propeller Driven								
Lockheed P3V-1	127,200	99.7	116.8	108.3	0.357	0.249	0.421	4 on wing

Table B10d Non-dimensional Radii of Gyration for Military Transports

(Propeller Driven)

Airplane Type	GW lbs	Wing Span, b, ft	Total Length, L, ft	e = (b+L)/2, ft	$\bar{R}_x$	$\bar{R}_y$	$\bar{R}_z$	Number of engines and disposition
Piston-Propeller Driven								
Douglas C-54	61,840	117.5	94.0	105.8	0.286	0.294	0.406	4 on wing
Fairchild C-119B	64,000	109.3	88.5	98.9	0.287	0.282	0.390	2 0n wing
in wing								
Boeing C-97	128,340	141.2	110.3	125.8	0.276	0.325	0.424	4 on wing
GD XC-99	265,000	230.0	182.5	206.3	0.276	0.346	0.432	6 on wing
Turbo-propeller Driven								
Lockheed C-130B	135,000	132.6	97.8	115.2	0.363	0.319	0.489	4 on wing
Lockheed C-130E	155,000	132.6	97.8	115.2	0.375	o.290	0.486	4 on wing

*Has two jet engines outboard of the piston engines

Table B11 Non-dimensional Radii of Gyration for Flying Boats

Airplane Type	GW lbs	Wing Span, b, ft	Total Length, L, ft	e = (b+L)/2, ft	$\bar{R}_x$	$\bar{R}_y$	$\bar{R}_z$	Number of engines and disposition
XBTM-1	20,009	50.0	41.2	45.6	0.230	0.340	0.380	1 in fusel.
XP4M-1	80,000	114.0	84.0	99.0	0.248	0.320	0.414	2 on wing
VS Seagull	14,230	52.5	44.0	48.3	0.297	0.364	0.402	1 in WF

Table B12 Non-dimensional Radii of Gyration for Supersonic Cruise Airplanes

Airplane Type	GW lbs	Wing Span, b, ft	Total Length, L, ft	e = (b+L)/2, ft	R_x	R_y	R_z	Number of engines and disposition
NAA A3J-1	44,305	53.0	72.5	62.8	0.240	0.372	0.472	2 in fusel.

12. INDEX

AIRPLANE DESIGN

PART VI: PRELIMINARY CALCULATION OF AERODYNAMIC, THRUST AND POWER CHARACTERISTICS

by

Dr. Jan Roskam
Ackers Distinguished Professor
of Aerospace Engineering
The University of Kansas
Lawrence, Kansas

NO PART OF THIS BOOK MAY BE REPRODUCED WITHOUT
PERMISSION FROM THE AUTHOR

Copyright: Roskam Aviation and Engineering Corporation
Rt4, Box 274, Ottawa, Kansas, 66067
Tel. 913-2421624
First Printing: 1987

TABLE OF CONTENTS

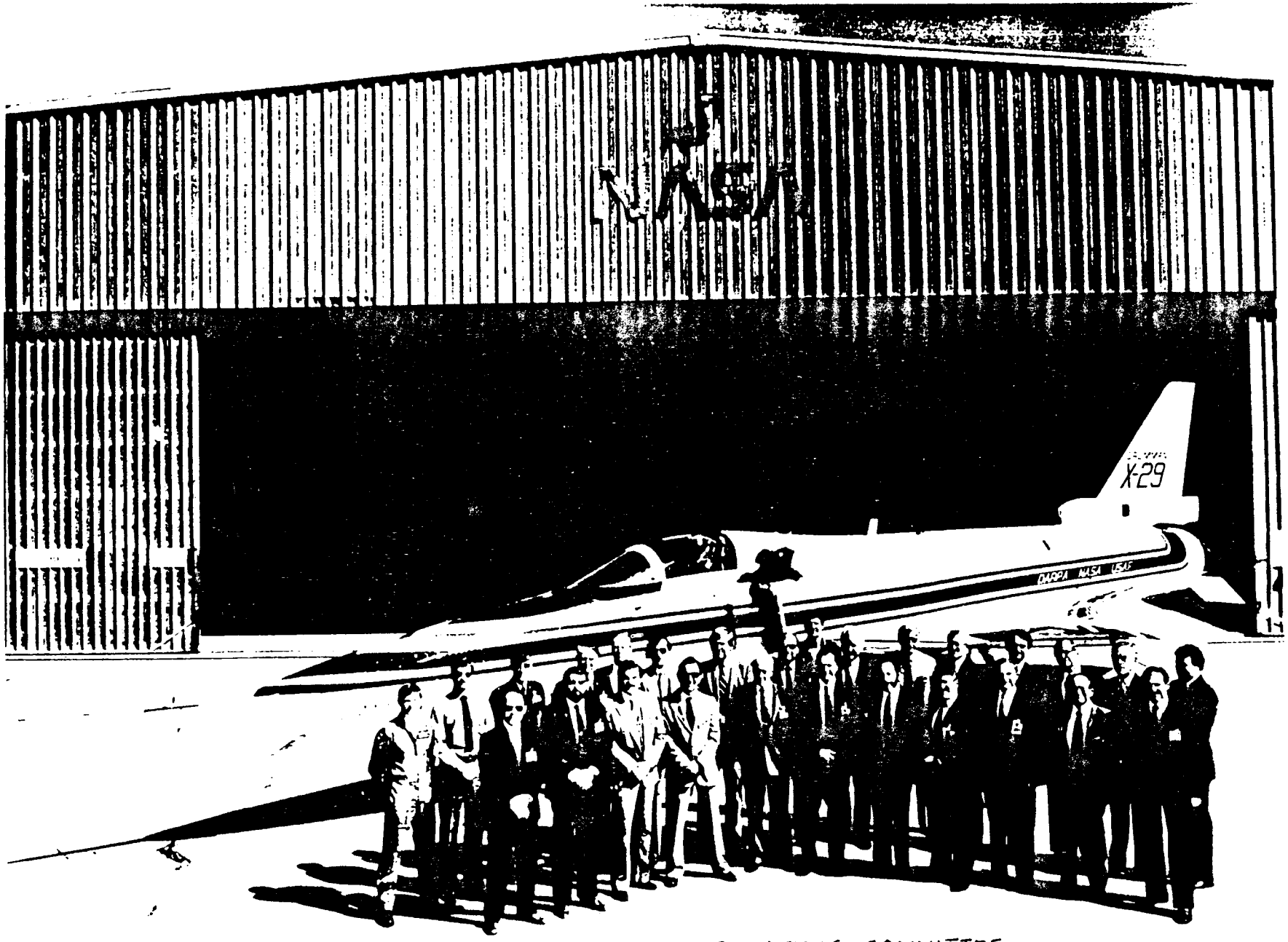

DARPA-NASA-USAF FUTURE APPLICATIONS COMMITTEE

TABLE OF SYMBOLS

The Table of Symbols is organized as follows:

1. GENERAL SYMBOLS

Symbol	Definition	Dimension
a	speed of sound	fps
a.c.	aerodynamic center	-----
$A = b^2/S$	Wing aspect ratio	-----
$A_c = b_c^2/S_c$	Canard aspect ratio	-----
$A_v = b_h^2/S_h$	Vert.tail aspect ratio	-----
A_∞	Inlet capture area	ft^2
A_c	Inlet area	ft^2
$\bar{A_c}$	Cowl cross section area at $\bar{d}_c$	ft^2
A_e	Nozzle (exit) area	ft^2
A_f	Internal area	ft^2
A_m	Cowl cross section area at d_m	ft^2
A_t	Nozzle throat area	ft^2
b	wing span	ft
b_c	canard span	ft
b_{f_i}	inboard flap span, p.89	ft

b_{f_o}	outboard flap span, p.89	ft
b_t	tire width	ft
b_v	vertical tail span, see p.387	ft
B	Compressible sweep correction factor, see Eqn.(10.64)	-----
c	chord	ft
c'	chord with flap extended	ft
$\bar{c}$	mean geometric chord	ft
c_b	control surface overhang, see p.471	ft
c_{d_c}	crossflow drag coeff	-----
c_e	elevator chord	ft
c_{δ_c}	canardvator chord	ft
c_f	flap chord	ft
c_h	two-dim. hingemoment coeff. about control surf. h.l.	-----
c^t_h	two-dim. hingemoment coeff. about tab h.l.	-----
c^*_l	airfoil lift coefficient at α^*	-----
$c_{m_{ac}}$	airfoil pitching moment coefficient about a.c.	-----
c_{m_o}	airfoil zero-lift pitching moment coeff.	-----
c_p	wing chord at wing pivot also: engine sfs	ft lbs/shp/hr
c_t, c_T	tip chord	ft
	c_t in Ch.10 also stands for tab chord, see p.473	ft
c_r, c_R	root chord	ft
$\bar{c}_{w_e}$	mean geometric chord of exposed wing	ft
C_D	Airplane drag coeff.	-----
C_{D_A}, $C_{D_{N_2}}$	wave drag coefficients see p.49 and 52	-----

$C_{D_{A(NC)}}$	interference drag coeff. see p.52	-----
C_{D_b}	base drag coefficient	-----
$C_{D_{L_i}}$	Drag due to lift coeff	-----
$C_{D_{L_v}}$	Viscous drag due to lift coefficient	-----
$C_{D_{min}}$	Drag coefficient at $C_{L_{min}}$	-----
$C_{D_{min_w}}$	Wing minimum drag coeff.	-----
$C_{D_{i_w}}$	Wing induced drag coeff.	-----
C_{D_o}	Zero-lift drag coeff.	-----
C_{D_p}	Profile drag coefficient	-----
C_f	turbulent flat plate friction coefficient	-----
C_{f_w}	turbulent flat plate friction coefficient of the wing	-----
C_h	Three-dim. hingemoment coeff. about contr. surf. h.l.	-----
C^t_h	Three-dim. hingemoment coeff. about tab h.l.	-----
c_l	airfoil lift coefficient	-----
c_{l_α}	airfoil lift curve slope	-----
$(c_{l_\alpha})_\delta$	section lift curve slope with the flaps down	1/deg, 1/rad
c_{l_δ}	derivative of airfoil lift coeff. with flap deflect.	-----
C_l	aerodynamic rolling moment coefficient	-----
$C_L = W/\bar{q}S$	Airplane lift coefficient	-----
C_{L_B}	Lift coefficient where drag rise due to separation begins	-----
C_{L_c}	Canard lift coefficient	-----
C_{L_h}	Hor. tail lift coeff.	-----

C_{L_o}	Lift coefficient for zero angle of attack	-----
$C_{L_{min}}$	Lift coefficient at minimum viscous drag due to lift	-----
C_{L_w}	Wing lift coefficient	-----
C_{L_α}	Airplane lift curve slope	1/deg, 1/rad
$C_{L_{\alpha_w}}$	Wing lift-curve slope	1/deg, 1/rad
C_m	Aerodynamic pitching moment coefficient	-----
c_{m_o}	Airfoil pitching moment coefficient at zero lift coefficient	-----
C_n	Aerodynamic yawing moment coefficient	-----
C_{p_b}	base pressure coeff., p.52	-----
C_R	Ram recovery factor	-----
C_y	Aerodynamic side force coefficient	-----
d_b	equivalent base diameter	-----
$\bar{d}_c$	cowl diameter at inlet area	ft
d_{exhnoz}	diam. of exhaust nozzle	in
d_{exhst}	exhaust stack diameter	in
d_f	equivalent fuselage diameter	--
d_{inl}	max. inlet diameter	ft
d_m	max. cowl diameter	ft
d_n	maximum nacelle (equivalent) diameter	ft
d_T	distance of thrustline to center of gravity, see Figure 8.126	ft
D	Drag	lbs
D_p	Propeller diameter	ft
D_t	Max. tire diameter	ft
e	span efficiency factor	-----

	(Also called Oswald's eff. factor)	
f	equivalent parasite area	ft^2
F_t	Factor in Eqn.(6.51)	-----
Δf	incremental eq. par. area	ft^2
F_{A_y}	Aerodynamic side force	lbs
i	incidence angle	deg
I_{xx}	Rolling moment of inertia in body axes	$slugft^2$
I_{xz}	XZ Product of inertia in body axes	$slugft^2$
I_{yy}	Piching moment of inertia in body axes	$slugft^2$
I_{zz}	Yawing moment of inertia in body axes	$slugft^2$
k	ratio of airfoil lift-curve slope to 2π, also:	-----
	equivalent sand roughness	-----
k'	correction factor for non-linear effects	-----
k_{cw}, k_{wc} and k_{wh}	interference factors, see pages 277, 278	-----
K	empirical constant, see p.86	--
K'	factor in Eqn.(3.6)	-----
K''	factor in Eqn.(3.6)	-----
K_B	factor in Eqn.(3.8)	-----
K_Λ	flap span factor for swept wings, p.313	-----
K_p	flap span factor, p.313	-----
K_t	constant in Eqn.(6.50)	-----
K_{wf}	wing-fuselage interference factor: see Eqn.(8.44)	
l	reference length	ft
l_f	fuselage length	ft
l_p	distance in Fig.10.34	ft
l_v	distance in Fig.10.27	ft
L	Lift	lbs
L'	Airfoil thickness location parameter	-----
L/D	Lift-to-drag ratio	-----

L_A	Aerodynamic rolling mom.	lbs
$\dot{m}_a$	engine massflow	slugs/sec
$\dot{m}_{bleed}$	bleed air massflow	slugs/sec
$\dot{m}_{comb}$	combustion massflow	slugs/sec
$\dot{m}_{cool}$	cooling air massflow	slugs/sec
M	Free stream Mach number	-----
M_A	Aerodynamic pitching moment	ftlbs
M_c	Crossflow Mach number	-----
M_{CR}, M_{crit}	Critical Mach number	-----
M_{DD}	Drag divergence Mach number	---
$n=W/\bar{q}S$	airplane load factor	-----
n_p	no. of blades per prop.	-----
N_A	Aerodynamic yawing moment	ftlbs
p	local static pressure	psf
	also: planform shape parameter, p.40	-----
P_{tot}	total pressure	psf
P_t	Factor in Eqn.(6.51)	-----
P_{av}	Power available	hp
P_{el}	Extracted electr. power	hp
P_{extr}	Extracted power	
P_{fp}	Extr. fuel pump power	hp
P_{hydr}	Extr. hydr. pump power	hp
P_{mech}	Extr. mechanical power	hp
P_{other}	Extr. other power	hp
P_{pneum}	Extr. pneumatic power	hp
P_{reqd}	Power required	hp

$\bar{q}$	free stream dyn. pressure	psf
R_N, R_l	Reynold's number	-----
R_{LS}	Lifting surface correction factor	-----
R_{wf}	Wing/fuselage interference factor	-----
S	Wing planform (ref) area	ft^2
$S_{b_{fus}}$	Fuselage base area	ft^2
S_c	Canard area	ft^2
S_{can}	Max. frontal area of canopy	ft^2
S_{cf}	Flapped canard area	ft^2
S_{ef}	Flapped hor.tail area	ft^2
S_{f_s}	Fuselage side area as defined in Fig.10.28	ft^2
S_{wf}	Flapped wing area	ft^2
S_h	Horiz.tail area	ft^2
S_n	Max. frontal area of nacelle	ft^2
S_v	Vertical tail area, see p.387	ft^2
S_{noz}	Nozzle cross section area	ft^2
S_{wet}	Total wetted area	ft^2
$S_{wet_{fus}}$	Wetted area of fuselage	ft^2
$S_{wet_{lam}}$	Wetted area with laminar flow	ft^2
$S_{wet_{turb}}$	Wetted area with turbulent flow	ft^2
S_{wet_w}	Wetted area of wing	ft^2

t/c	thickness ratio (at $\bar{c}$)	-----
T	Temperature of air	deg F
T_{av}	Thrust available	lbs
T_r	Remnant thrust	lbs
T_{reqd}	Thrust required	lbs
U_1 or U	Steady state airspeed	ft/sec
v	induced drag factor due to twist	-----
V_∞	Velocity at sta. A_∞	fps
V_c	Velocity at sta. A_c	fps
$\bar{V}_c$	Canard volume coefficient, see Eqn. (10.74)	-----
$\bar{V}_h$	Hor. tail volume coefficient, see Eqn. (10.23)	-----
VA_{plp}	Required electrical power	hp
$\dot{V}_{hydr}$	Hydr. fluid flow rate	gpm
V_{noz}	Average nozzle flow velocity	fps
w	zero-lift drag factor due to twist	-----
w_f	max. fuselage width	ft
W	Airplane weight	lbs
x_{ac}	position of a.c. on wing mgc,	ft
$\bar{x}_{ac}=x_{ac}/\bar{c}$	position of aerodynamic center on wing mgc, fr.$\bar{c}$	-----
x_{ac_h}	position of hor. tail a.c. on wing mgc	ft
$\bar{x}_{ac_h}=x_{ac}/\bar{c}$	position of hor. tail a.c. on wing mgc, fr.$\bar{c}$	-----
x_{cp}	position of wing center of pressure on wing mgc	ft
x_{ref}	position of reference point on wing mgc	ft

$\bar{x}_{ref}=x_{ref}/\bar{c}$	position of reference point on wing mgc, fr.$\bar{c}$	-----
NOTE: see Figure 8.114 for illustration!		
x_w	distance of wing quarter chord mgc to c.g., see Fig.10.39	----
y	spanwise coordinate	ft
z_f	vertical height of fuselage at wing root chord	ft
z_p	distance in Fig.10.34	ft
z_v	distance in Fig.10.27	ft
z_w	wing distance to fuselage centerline, see Fig.(10.9)	ft

2. STABILITY, CONTROL AND HINGEMOMENT DERIVATIVES

NOTE: All derivatives are presented in the airplane stability axes system. See pages 371 and 372 for a definition of axes.

STABILITY DERIVATIVES

Symbol	Definition	Dimension
C_{D_u}	$\partial C_D/\partial(u/U_1)$	-----
C_{L_u}	$\partial C_L/\partial(u/U_1)$	-----
C_{m_u}	$\partial C_m/\partial(u/U_1)$	-----
$C_{T_{x_u}}$	$\partial C_{T_x}/\partial(u/U_1)$	-----
$C_{m_{T_u}}$	$\partial C_{m_T}/\partial(u/U_1)$	-----
C_{D_α}	$\partial C_D/\partial\alpha$	rad^{-1}
C_{L_α}	$\partial C_L/\partial\alpha$	rad^{-1}
C_{m_α}	$\partial C_m/\partial\alpha$	rad^{-1}
$C_{m_{T_\alpha}}$	$\partial C_{m_T}/\partial\alpha$	rad^{-1}
$C_{D_{\dot\alpha}}$	$\partial C_D/\partial(\dot\alpha\bar{c}/2U_1)$	rad^{-1}
$C_{L_{\dot\alpha}}$	$\partial C_L/\partial(\dot\alpha\bar{c}/2U_1)$	rad^{-1}
$C_{m_{\dot\alpha}}$	$\partial C_m/\partial(\dot\alpha\bar{c}/2U_1)$	rad^{-1}

C_{y_β}	$\partial C_y / \partial \beta$	rad^{-1}
C_{l_β}	$\partial C_l / \partial \beta$	rad^{-1}
C_{n_β}	$\partial C_n / \partial \beta$	rad^{-1}
$C_{n_{T_\beta}}$	$\partial C_{n_T} / \partial \beta$	rad^{-1}
$C_{y_{\dot\beta}}$	$\partial C_y / \partial (\dot\beta b/2U_1)$	rad^{-1}
$C_{l_{\dot\beta}}$	$\partial C_l / \partial (\dot\beta b/2U_1)$	rad^{-1}
$C_{n_{\dot\beta}}$	$\partial C_n / \partial (\dot\beta b/2U_1)$	rad^{-1}
C_{y_p}	$\partial C_y / \partial (pb/2U_1)$	rad^{-1}
C_{l_p}	$\partial C_l / \partial (pb/2U_1)$	rad^{-1}
C_{n_p}	$\partial C_n / \partial (pb/2U_1)$	rad^{-1}
C_{D_q}	$\partial C_D / \partial (q\bar{c}/2U_1)$	rad^{-1}
C_{L_q}	$\partial C_L / \partial (q\bar{c}/2U_1)$	rad^{-1}
C_{m_q}	$\partial C_m / \partial (q\bar{c}/2U_1)$	rad^{-1}
C_{y_r}	$\partial C_y / \partial (rb/2U_1)$	rad^{-1}
C_{l_r}	$\partial C_l / \partial (rb/2U_1)$	rad^{-1}
C_{n_r}	$\partial C_n / \partial (rb/2U_1)$	rad^{-1}

CONTROL DERIVATIVES

$C_{D_{i_h}}$	$\partial C_D / \partial i_h$	rad^{-1}
$C_{L_{i_h}}$	$\partial C_l / \partial i_h$	rad^{-1}
$C_{m_{i_h}}$	$\partial C_m / \partial i_h$	rad^{-1}
$C_{D_{\delta_e}}$	$\partial C_D / \partial \delta_e$	rad^{-1}

$C_{L_{\delta_e}}$	$\partial C_L / \partial \delta_e$	rad^{-1}
$C_{m_{\delta_e}}$	$\partial C_m / \partial \delta_e$	rad^{-1}
$C_{D_{i_c}}$	$\partial C_D / \partial i_c$	rad^{-1}
$C_{L_{i_c}}$	$\partial C_L / \partial i_c$	rad^{-1}
$C_{m_{i_c}}$	$\partial C_m / \partial i_c$	rad^{-1}
$C_{D_{\delta_c}}$	$\partial C_D / \partial \delta_c$	rad^{-1}
$C_{L_{\delta_c}}$	$\partial C_L / \partial \delta_c$	rad^{-1}
$C_{m_{\delta_c}}$	$\partial C_m / \partial \delta_c$	rad^{-1}
$C_{y_{\delta_a}}$	$\partial C_y / \partial \delta_a$	rad^{-1}
$C_{l_{\delta_a}}$	$\partial C_l / \partial \delta_a$	rad^{-1}
$C_{n_{\delta_a}}$	$\partial C_n / \partial \delta_a$	rad^{-1}
$C_{y_{\delta_s}}$	$\partial C_y / \partial \delta_s$	rad^{-1}
$C_{l_{\delta_s}}$	$\partial C_l / \partial \delta_s$	rad^{-1}
$C_{n_{\delta_s}}$	$\partial C_n / \partial \delta_s$	rad^{-1}
$C_{y_{i_h}}$	$\partial C_y / \partial i_h$	rad^{-1}
$C_{l_{i_h}}$	$\partial C_l / \partial i_h$	rad^{-1}

$C_{n_{i_h}}$	$\partial C_n / \partial i_h$	rad^{-1}
$C_{y_{\delta_r}}$	$\partial C_y / \partial \delta_r$	rad^{-1}
$C_{l_{\delta_r}}$	$\partial C_l / \partial \delta_r$	rad^{-1}
$C_{n_{\delta_r}}$	$\partial C_n / \partial \delta_r$	rad^{-1}

HINGEMOMENT DERIVATIVES

Two-Dimensional Hingemoment Derivatives

Symbol	Definition	Dimension
c_{h_o}	zero-angle-of-attack, zero-control-surface-deflection, zero-tab-angle-deflection hingemoment coefficient	-----
c_{h_α}	$\partial c_h / \partial \alpha$	rad^{-1}
$c_{h_\delta} = c_{h_{\alpha_{bal}}}$	$\partial c_h / \partial \delta$	rad^{-1}
$c_{h_{\delta_t}}$	$\partial c_{h_t} / \partial \delta_t$	rad^{-1}

Three-Dimensional Hingemoment Derivatives

Symbol	Definition	Dimension
C_{h_o}	zero-angle-of-attack, zero-control-surface-deflection, zero-tab-angle-deflection hingemoment coefficient	-----
C_{h_α}	$\partial C_h / \partial \alpha$	rad^{-1}
C_{h_δ}	$\partial C_h / \partial \delta$	rad^{-1}
$C_{h_{\delta_t}}$	$\partial C_h / \partial \delta_t$	rad^{-1}

NOTE: Control surface hingemoment derivatives defined sofar, are taken about the control surface hingeline. Tab hingemoment derivatives taken about the tab hingeline are defined in a similar manner but carry the superscript 't' as in $c^t_{h_x}$ and $C^t_{h_x}$

3. GREEK SYMBOLS

Symbol	Definition	Dimension
α	airfoil angle of attack	deg, rad
α	airplane angle of attack with subscript w, h or c, the symbol indicates the angle of attack of that component	deg, rad
α^*	linear range of α	deg, rad
α_{o_l}	airfoil zero-lift angle of attack	deg, rad
α_{o_L}	airplane zero-lift angle of attack	deg, rad
α_δ	derivative of angle of attack w.r.t. surface deflection angle	-----
β	$(1 - M^2)^{1/2}$	-----
	also: sideslip angle	deg, rad
γ	flight path angle	deg, rad
Γ	dihedral angle	deg, rad
δ	pressure ratio,	-----
	also: flap or control surface deflection	deg, rad
δ_f	flap defl. angle	deg, rad
Δ	increment	depends
$\Delta\alpha_g$	change in angle of attack due to ground effect	deg, rad
$\Delta\alpha_{w/c}$	difference in stall angle of attack between wing and canard, see p.280	deg, rad
Δc_l	incremental airfoil lift coefficient due to flaps	-----
ΔC_L	incremental airplane lift coefficient due to flaps	-----
ΔC_{L_c}	incremental canard lift coefficient to trim, based on wing area, S	-----
ΔC_{L_h}	incremental tail lift coefficient to trim, based on wing area, S	-----
Δc_m	incremental airfoil pitching moment coefficient due to flaps	-----
ΔC_m	incremental airplane piching moment coefficient due to flaps	-----
$\Delta\varepsilon_f$	change in tail downwash angle due to flaps	deg, rad
Δp_{hydr}	hydraulic pressure differential	psi

$\Delta\bar{x}_{ac_f}$	shift in aerodynamic center due to the fuselage, fr.$\bar{c}$	-----
Δy	leading edge shape parameter	-----
ε	downwash angle at the horizontal tail	deg, rad
ε_c	upwash angle at the canard	deg, rad
ε_t	wing twist angle	deg, rad
η	span fraction, or see p.46	-----
η_c	ratio of canard to wing dynamic pressure	-----
η_{diff}	pressure recovery through diffuser	-----
η_{fp}	fuel pump efficiency	-----
η_{gear}	gearbox efficiency	-----
η_{gen}	generator efficiency	-----
η_h	ratio of hor.tail to wing dynamic pressure	-----
η_{hp}	hydr. pump efficiency	-----
η_{inl}	inlet pressure recovery	-----
$\eta_{inl/com}$	inlet pressure recovery, compressible	-----
$\eta_{inl/inc}$	inlet pressure recovery, incompressible	-----
η_p	propeller efficiency	-----
η_{shock}	pressure recovery through shock	-----
$\Lambda_{c/2}$	semi-chord sweep angle	deg, rad
$\Lambda_{c/4}$	quarter chord sweep angle	deg, rad
Λ_{LE}	leading edge sweep angle	deg, rad
λ	taper ratio	-----
μ	coefficient of viscosity for air	-----
μ_{inl}	area ratio A_c/A_∞	-----
π	3.14	-----
ρ	air density	slug/ft^3

σ	sidewash angle	deg, rad
$\bar{\Phi}$	effective turning angle	deg, rad
Φ_{te}	trailing edge angle	deg, rad

4. SUBSCRIPTS

1	steady state
a	aileron
av	available
A	Airplane
b	base
bal	balance
bw	basic wing
c	canard
can	canopy
cg	center of gravity
co	cut-off
cool	cooling
cw	canopy/windshield
e	elevator
eff	effective
emp	empennage
f	friction, sometimes: flap
flap	flap
fus	fuselage
g	ground effect
gear	landing gear
h	horizontal tail
int	interference
kf	krueger flap
lam	laminar
lef	leading edge flap
L	landing
LE, le	leading edge
max	maximum
misc	miscellaneous
M	(at a given) Mach Number
n	nacelle
np	nacelle/pylon
p	pylon
plf	planform
prof	profile
r	rudder
rated	rated, usually SHP
ref	reference, usually the wing, or a point on the wing
reqd	required
s	slat(ted)
sf	split flap
sp	spoiler (speedbrake)

std	standard
store	store(s)
T	thrust or power effect
TE, te	trailing edge
TL	thrustline offset effect
TS	propeller slipstream effect
turb	turbulent
TO	take-off
trim	trim
w	wing
wave	wave (drag)
wb	wing-body (same as wing-fuselage)
wet	wetted
wf	wing-fuselage (same as wing-body)
wing	wing
wmprop	windmilling propeller
ws	windshield

5. ACRONYMS

AEO	All engines operating
APU	Auxiliary power unit
AWACS	Airborne warning and control system
b.l.	boundary layer
BPR	Bypass ratio
CBR	California Bearing Ratio
c.g.	center of gravity
FRP	Fuselage Reference Plane
hl or h.l.	hingeline
i.e.	id est (that is)
l.e.	leading edge
mgc or m.g.c.	mean geometric chord
OEI	one engine inoperative
RAT	Ram air turbine
SHP	Shaft Horsepower
t.e.	trailing edge
W.R.P.	Wing Reference Plane
w.r.t	with respect to

ACKNOWLEDGEMENT

Writing a book on airplane design is impossible without the supply of a large amount of data. The author is grateful to the following companies for supplying data on airplane drag and on airplane stability and control characteristics:

Cessna Aircraft Company	Beech Aircraft Corporation
The Boeing Company	McDonnell Douglas Corp.
Lockheed Aircraft Corp.	Gates Learjet Corporation
Northrop Corporation	SIAI Marchetti

A significant amount of airplane design information has been accumulated by the author over many years from the following magazines:

Interavia (Swiss, monthly)
Flight International (British, weekly)
Business and Commercial Aviation (USA, monthly)
Aviation Week and Space Technology (USA, weekly)
Journal of Aircraft (USA, AIAA, monthly)

The author wishes to acknowledge the important role played by these magazines in his own development as an aeronautical engineer. Aeronautical engineering students and graduates should read these magazines regularly.

This part of the Airplane Design series presents rapid methods for estimating drag, lift, pitching moment, installed thrust and power data as well as stability, control and hingemoment derivatives. In preparing this part much use has been made of the USAF DATCOM, a most impressive and useful document which should be available in all aeronautical engineering design offices and libraries.

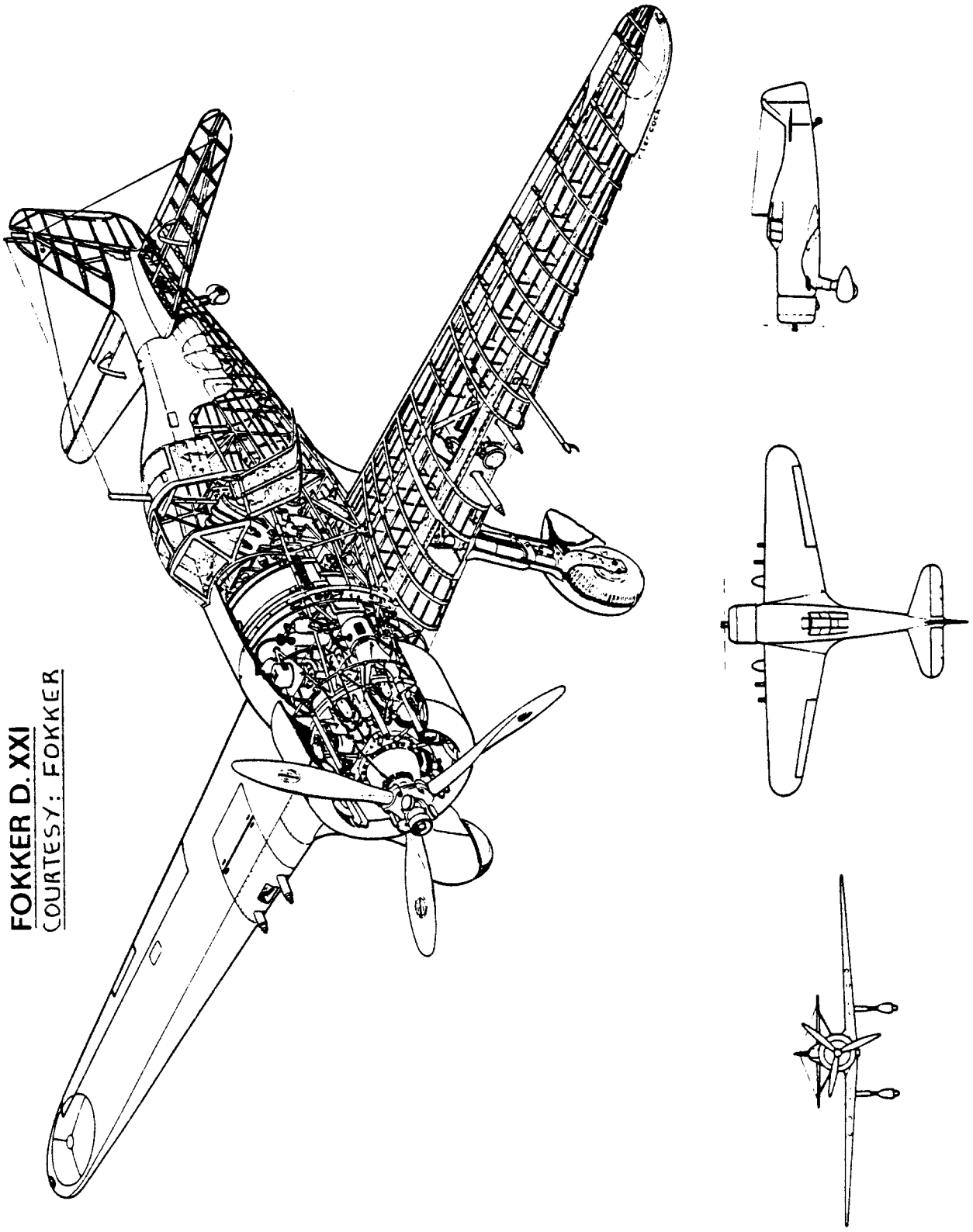

FOKKER D.XXI
COURTESY: FOKKER

1. INTRODUCTION

The purpose of this series of books on Airplane Design is to familiarize aerospace engineering students with the design methodology and design decision making involved in the process of designing airplanes.

The series of books is organized as follows:

PART I:	PRELIMINARY SIZING OF AIRPLANES
PART II:	PRELIMINARY CONFIGURATION DESIGN AND INTEGRATION OF THE PROPULSION SYSTEM
PART III:	LAYOUT DESIGN OF COCKPIT, FUSELAGE, WING AND EMPENNAGE: CUTAWAYS AND INBOARD PROFILES
PART IV:	LAYOUT DESIGN OF LANDING GEAR AND SYSTEMS
PART V:	COMPONENT WEIGHT ESTIMATION
PART VI:	PRELIMINARY CALCULATION OF AERODYNAMIC, THRUST AND POWER CHARACTERISTICS
PART VII:	DETERMINATION OF STABILITY, CONTROL AND PERFORMANCE CHARACTERISTICS: FAR AND MILITARY REQUIREMENTS
PART VIII:	AIRPLANE COST ESTIMATION: DESIGN, DEVELOPMENT, MANUFACTURING AND OPERATING

The purpose of PART VI is to present a systematic approach to the prediction of drag, installed power and thrust, lift, pitching moment and other important stability and control data needed in preliminary design.

The methods presented in this volume are meant to be used in conjunction with Preliminary Design Sequence II as outlined in Chapter 2 of Part II of this series. For that reason these methods are sometimes referred to as Class II methods. The preceeding Class I methods are covered in Part I and Part II of this series and are meant to be used with Preliminary Design Sequence I as outlined also in Chapter 2 of Part II.

In Chapter 2 some important definitions relating to flight regime and reference geometries are discussed.

Chapter 3 presents different ways by which airplane drag polars can be represented by simple mathematical models. Several examples are given.

Chapter 4 presents a method to predict the component drag breakdown and the total drag of airplanes. Example drag data are given in Chapter 5.

Methods for predicting installed thrust and power characteristics are presented in Chapter 6. Example thrust and power data are given in Chapter 7.

Chapter 8 contains methods for predicting lift and pitching moment characteristics of airplanes with and without (mechanical) flaps. Example data are given in Chapter 9.

Prediction methods for stability, control and hinge moment derivatives are presented in Chapter 10 with example data provided in Chapter 11.

To make the use of this book easy on students, a USER's GUIDE is presented in Chapter 12. Aeronautical engineering students should use this guide to prevent wasting a lot of time chasing non-existing problems.

Appendix A contains data on the atmosphere.

Appendix B contains data needed in the estimation of areas and volumes.

2. IMPORTANT DEFINITIONS

In this text frequent use is made of:

2.1 Flow regimes defined in terms of Mach number
2.2 Reference geometries defined in terms of areas and lengths

The purpose of this chapter is to define the physical and the mathematical meaning of these terms.

2.1 FLOW REGIME DEFINITIONS

In this text the following flow regimes are used:

2.1.1 Subsonic Flow Regime
2.1.2 Transonic Flow Regime
2.1.3 Supersonic Flow Regime

2.1.1 Subsonic Flow Regime

In terms of Mach number the subsonic flow regime is defined as:

SUBSONIC: $0 < M < 0.60$

It is assumed that in this flow regime all compressibility effects are negligible. The reader should keep in mind that whether or not compressibility effects are negligible depends not just on the free stream Mach number but also on thickness and on angle of attack.

Where the subsonic flow regime ends depends on the values of critical and drag divergence Mach numbers:

The critical Mach number is that free stream Mach number for which a condition of M=1 is first reached somewhere on the airplane.

Figure 2.1 shows how the critical Mach number varies with airfoil shape and with airfoil lift coefficient (or angle of attack).

The drag divergence Mach number is that free stream Mach number for which:

> Boeing definition: the drag coefficient first reaches a value of 0.0020 above that in the subsonic flow regime.

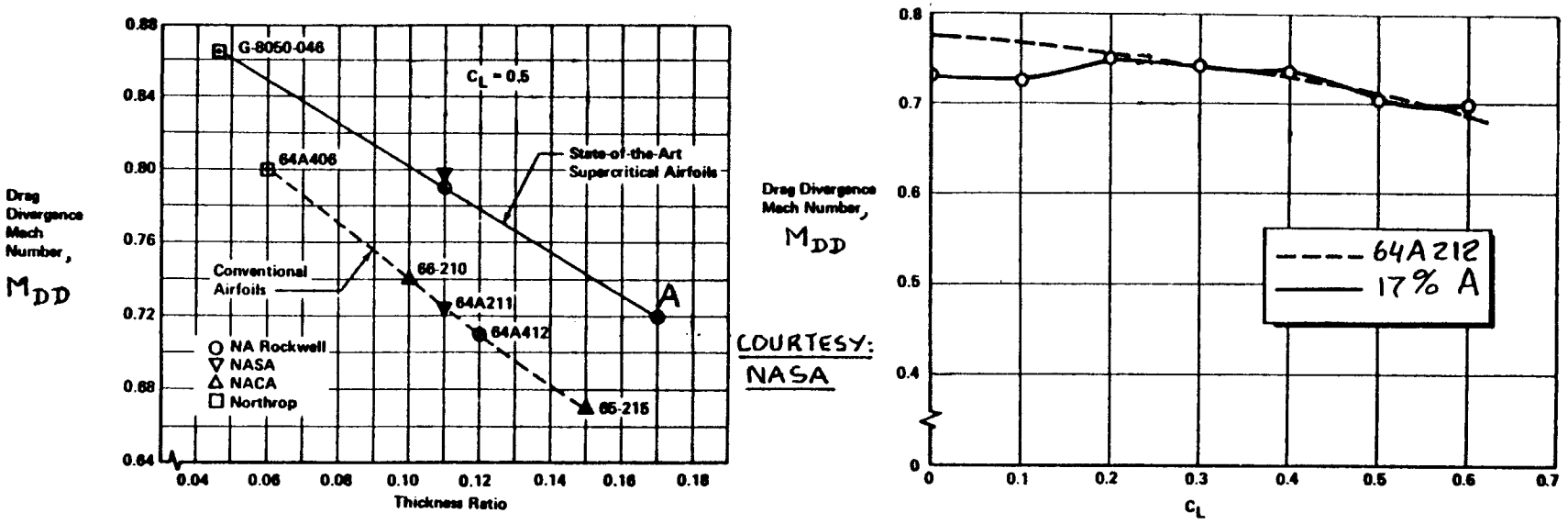

Figure 2.1 Effect of Airfoil Shape and Lift Coefficient on Drag Divergence Mach Number

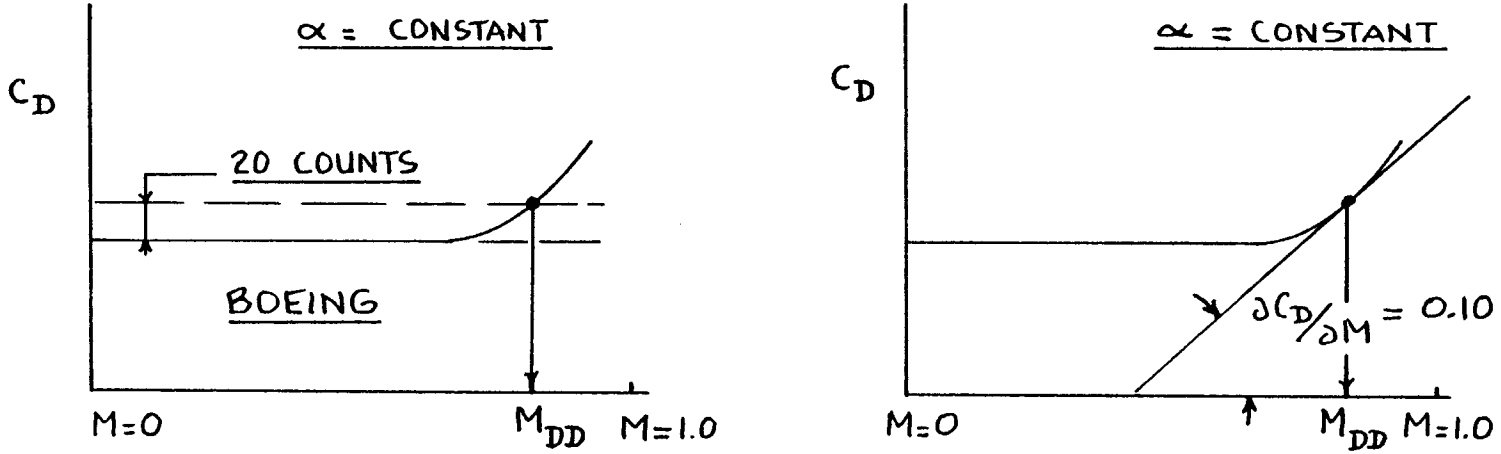

Figure 2.2 Boeing and Douglas Definitions for Drag Divergence Mach Number

Douglas definition: the slope of the drag coefficient versus Mach number first reaches the value of 0.10.

Figure 2.2 depicts these definitions graphically. Experience shows that there is no significant difference between these definitions.

The following equations may be used to estimate the drag divergence Mach number for airfoils:

For modern (aft-loaded) airfoils:

$$M_{DD} = 0.95 - (t/c)_{max} - c_l/10 \qquad (2.1)$$

For NACA airfoils:

$$M_{DD} = 0.90 - (t/c)_{max} - c_l/10 \qquad (2.2)$$

Figures 2.3 may be used to estimate the drag divergence Mach number of uncambered wings. For wings with camber, determine the lift coefficient for zero angle of attack, C_{L_o}. Then use Figures 2.3 with:

$$C_L = C_{L_{actual}} + C_{L_o} \qquad (2.3)$$

Reference 8 contains a wealth of information on the effect of the geometry of fuselages and wings on critical and on drag divergence Mach number.

2.1.2 Transonic Flow Regime

In terms of Mach number the transonic flow regime is defined as:

TRANSONIC: $0.60 < M < 1.2$

Mathematically speaking, the transonic flow regime starts at the critical Mach number.

Physically speaking, the transonic flow regime starts at the drag divergence Mach number.

In the transonic flow regime compressibility effects cannot be neglected. The reader should keep in mind that compressibility effects in this flow regime are a strong function of thickness ratio (for lifting surfaces such as wings, pylons and tails) and of cross sectional area distributions. The sweep angle of lifting surfaces is also an important parameter.

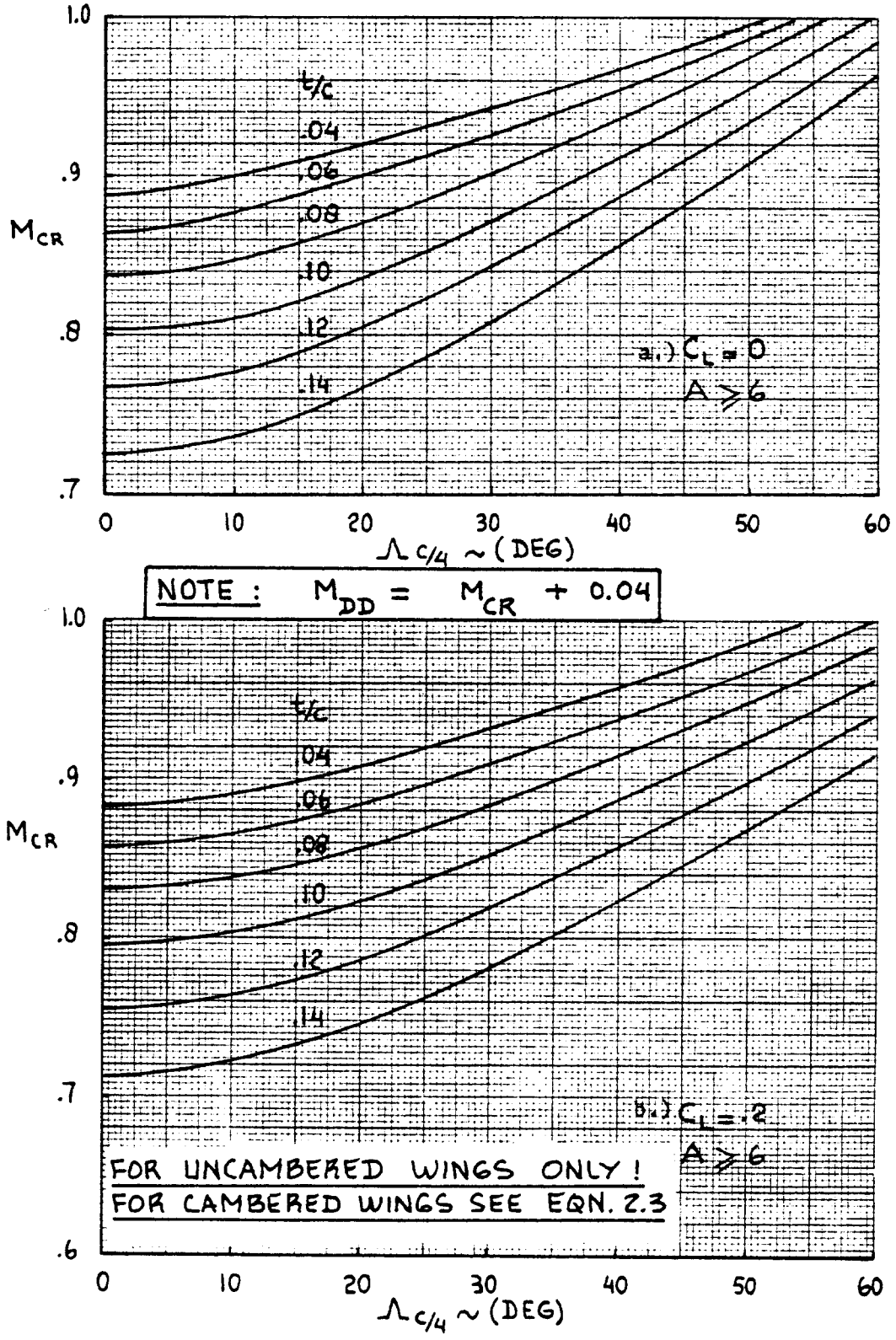

Figure 2.3 Effect of Thickness Ratio, Sweep Angle, Aspect Ratio and Lift Coefficient on the Drag Divergence Mach Number of Wings

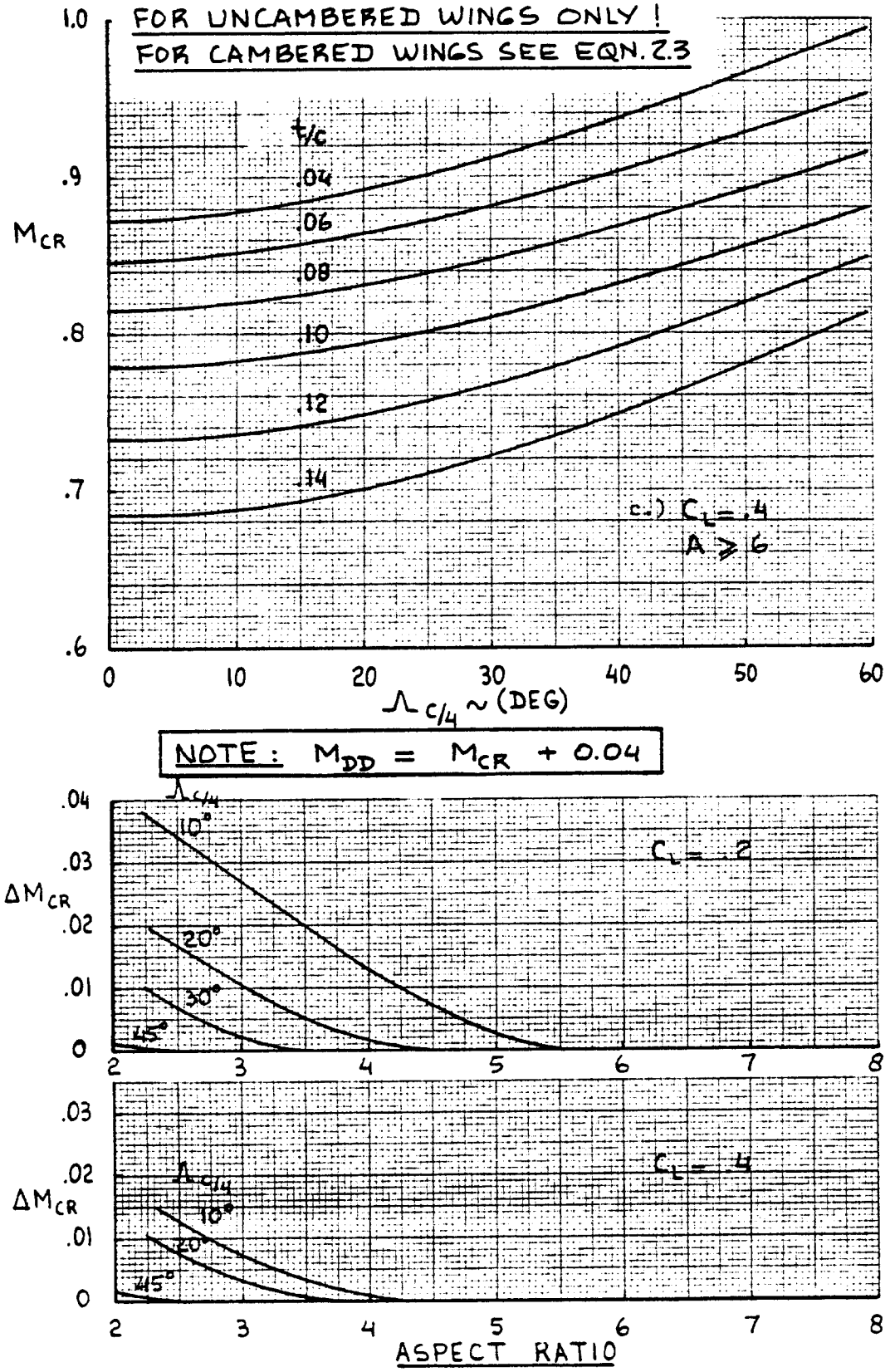

Figure 2.3 (Cont'd) Effect of Thickness Ratio, Sweep Angle, Aspect Ratio and Lift Coefficient on the Drag Divergence Mach Number of Wings

To reduce drag in the transonic flow regime the concept of area ruling plays an important role.

Reference 8 contains information on the variation of drag with Mach number in the transonic speed regime below M=1. Reference 9 should be used for the estimation of drag in the transonic flow regime above M=1.

For applications of the area rule concept, ref.10 should be consulted.

2.1.3 Supersonic Flow Regime

In terms of Mach number the supersonic flow regime is defined as:

SUPERSONIC: $1.2 < M < 3.0$

The aerodynamic behavior of airplanes in this flow regime depends strongly on the location of Mach lines relative to the airplane geometry. In particular whether or not the wing has a subsonic, supersonic or mixed flow leading edge has important consequences.

Figure 2.4 illustrates what is meant by subsonic/supersonic leading edges.

Reference 9 contains methods for estimating drag in this flow regime.

Note: Reference 11 is strongly recommended as a general text on the effect of Mach number and of angle of attack on the drag and lift characteristics of airplanes.

2.2 IMPORTANT GEOMETRIC DEFINITIONS

2.2.1 Wing Planform Geometries

In this text, all aerodynamic characteristics of airplanes are referred to so-called reference geometries. This is accomplished through the introduction of dimensionless coefficients for drag, lift, pitching moment, side force, rolling moment and yawing moment in the following manner:

For drag: $D = C_D \bar{q} S$ (2.4)

For lift: $L = C_L \bar{q} S$ (2.5)

For pitching moment: $M_A = C_m \bar{q} S \bar{c}$ (2.6)

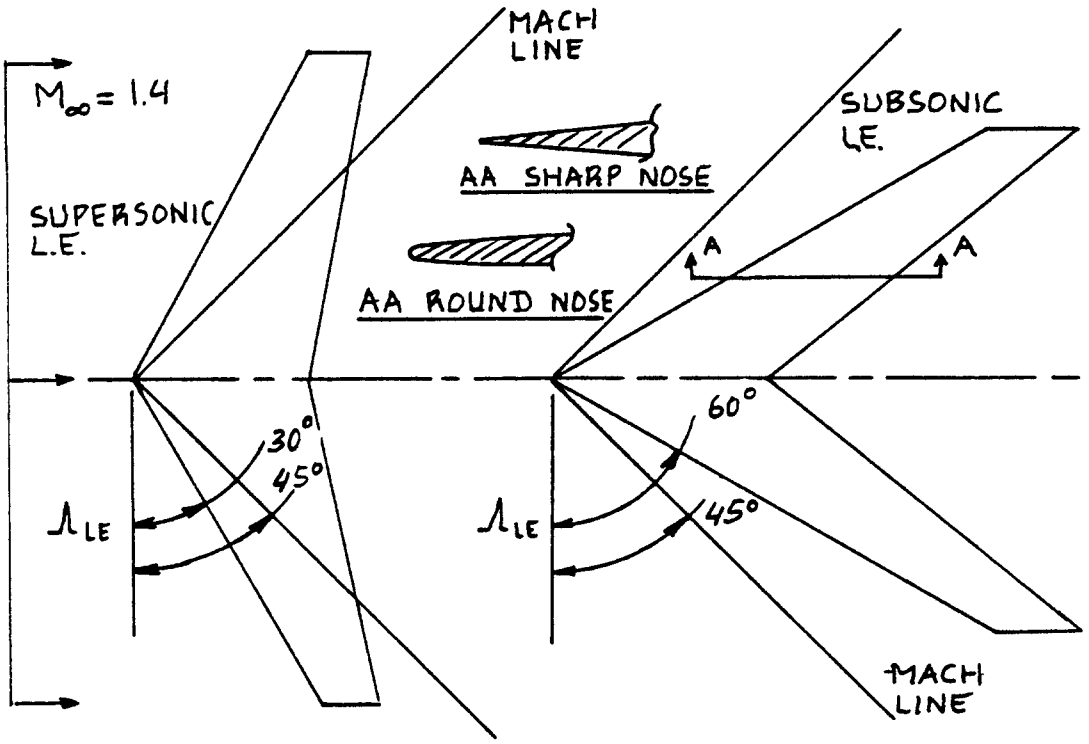

Figure 2.4 Subsonic and Supersonic Leading Edges

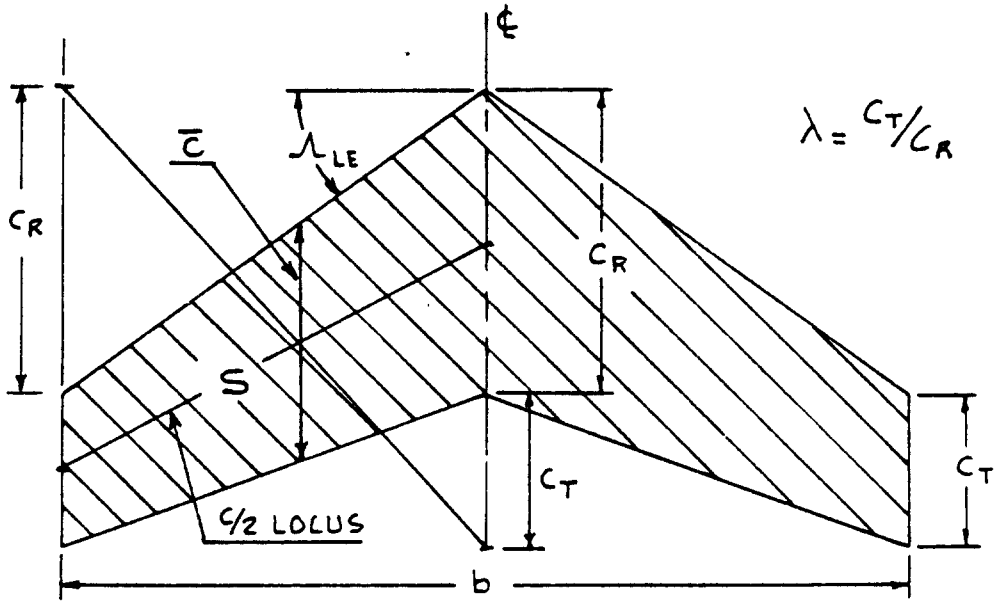

Figure 2.5 Reference Geometry for Straight, Tapered Wings

For side force: $F_{A_y} = C_y \bar{q} S$ (2.7)

For rolling moment: $L_A = C_l \bar{q} S b$ (2.8)

For yawing moment: $N_A = C_n \bar{q} S b$ (2.9)

The reference geometries in Equations (2.4) through (2.9) are S, $\bar{c}$ and b respectively. These reference geometries are normally based on the wing planform. For a straight, tapered wing these parameters are defined in Figure 2.5.

Most wings cannot be classified as straight, tapered wings. Leading edges and trailing edges are often broken or curved to achieve certain aerodynamic, structural or configurational objectives. Figure 2.6 shows how the parameters S, $\bar{c}$ and b are defined for non straight, tapered wings. Note that a so-called equivalent wing is defined for these planforms. This equivalent wing definition is found by 'averaging' areas.

In some airplanes the wings have very rapid changes in leading edge shape and/or trailing edge shape. Examples are shown in Figure 2.7. The definitions of S, $\bar{c}$ and b for such wings are also given in Figure 2.7.

Although the definition of airplane reference geometries is in principle arbitrary, the reader should not deviate too far from the definitions used here. The reason is that in the aerodynamic literature cited in this text the reference geometries are those defined here.

In addition to the parameters S, $\bar{c}$ and b, quantities such as taper ratio and sweep angle play an important role. Figures 2.5 and 2.6 also define these quantities.

2.2.2 Empennage Planform Geometries

To determine the contributions of empennage surfaces (horizontal tail, canard and/or vertical tail) to the aerodynamic characteristics of airplanes it is necessary to define their planform geometries. Figure 2.8 does this for horizontal tails and for canards. Figure 2.9 does this for vertical tails.

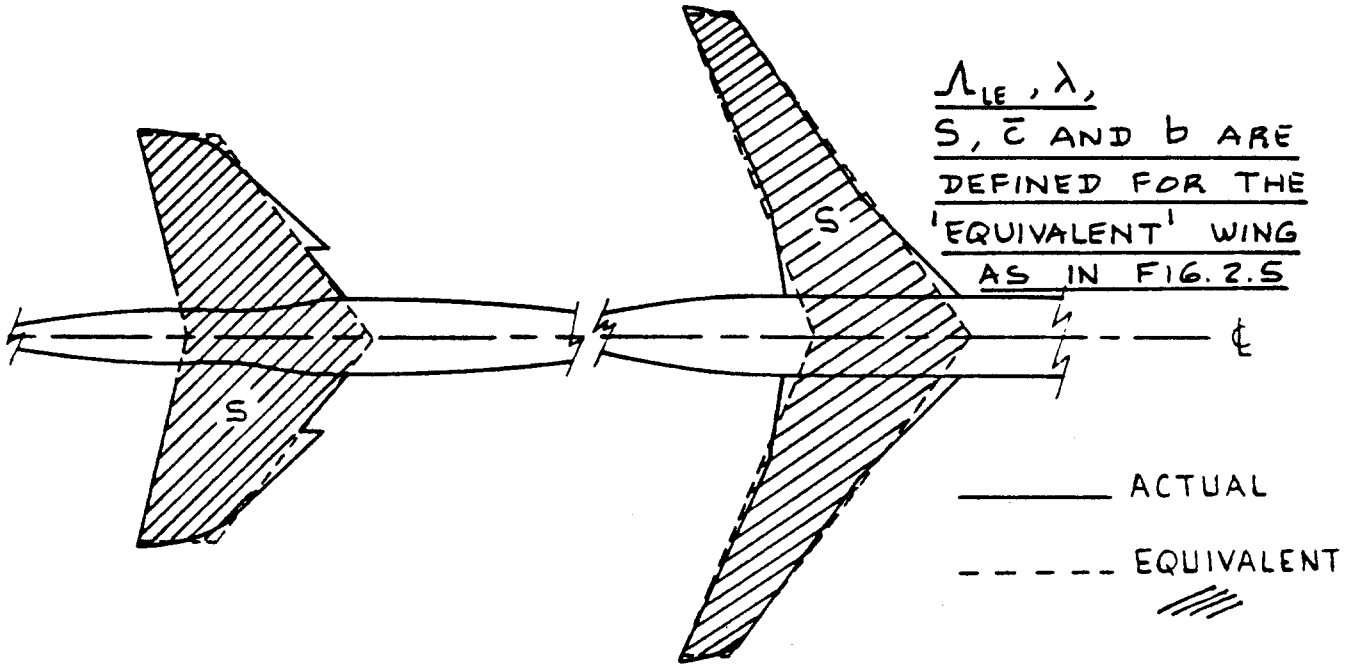

Figure 2.6 Reference Geometry and Equivalent Planform for Non Straight, Tapered Wings

$$y_{\bar{c}} = \frac{2}{S}\int_0^{b/2} y\,c(y)\,dy \qquad x_{LE_{\bar{c}}} = \frac{1}{S}\int_{-b/2}^{+b/2} x_{LE}(y)\,c(y)\,dy$$

$$S = \int_{-b/2}^{b/2} c(y)\,dy \qquad \bar{c} = \frac{1}{S}\int_{-b/2}^{+b/2} c^2(y)\,dy$$

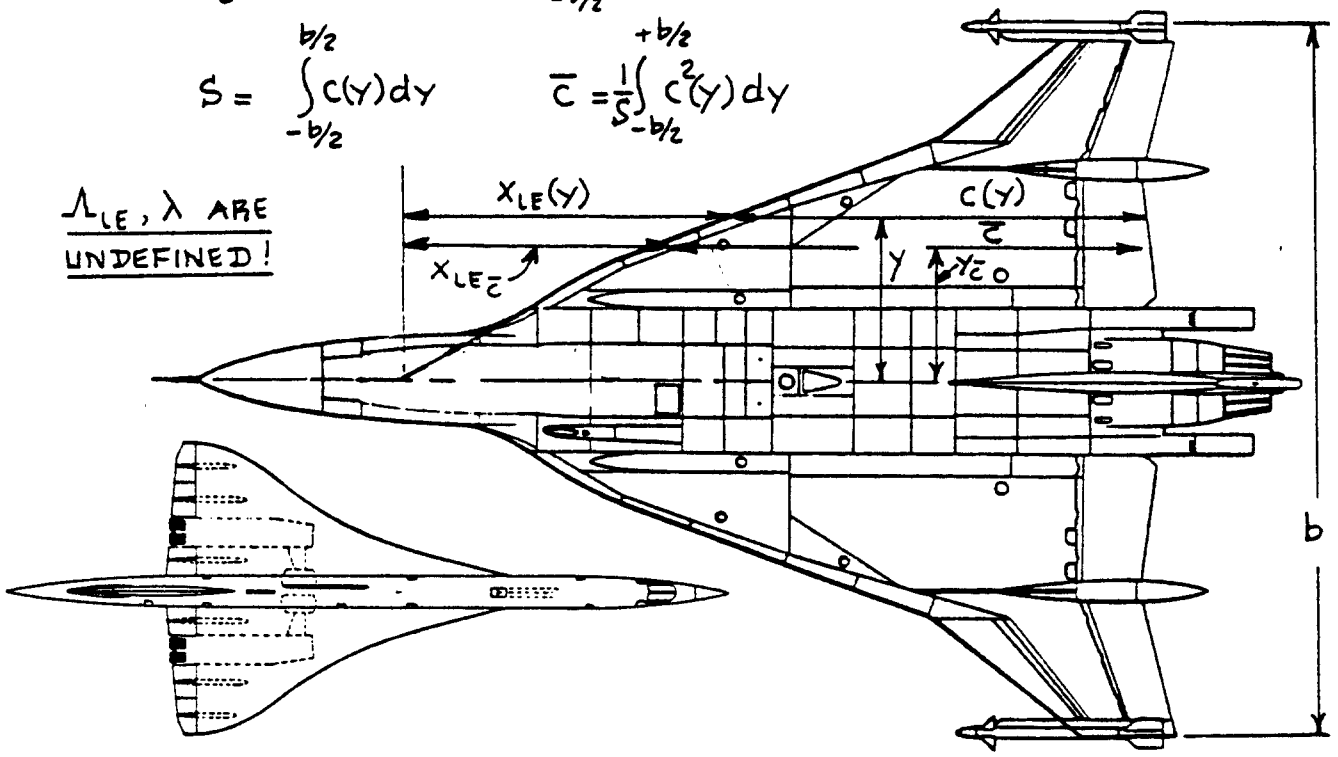

Figure 2.7 Reference Geometry for Arbitrary Wings

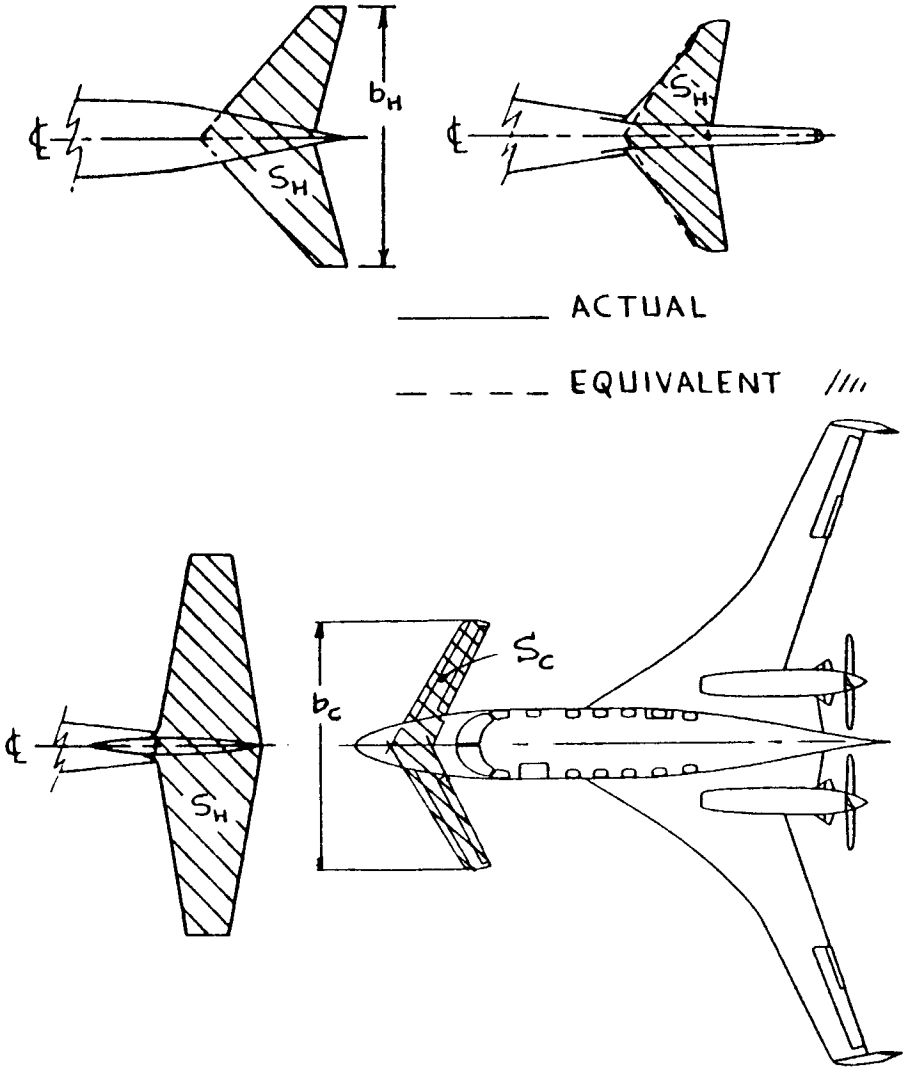

Figure 2.8 Reference Geometries for Horizontal Tails and for Canards

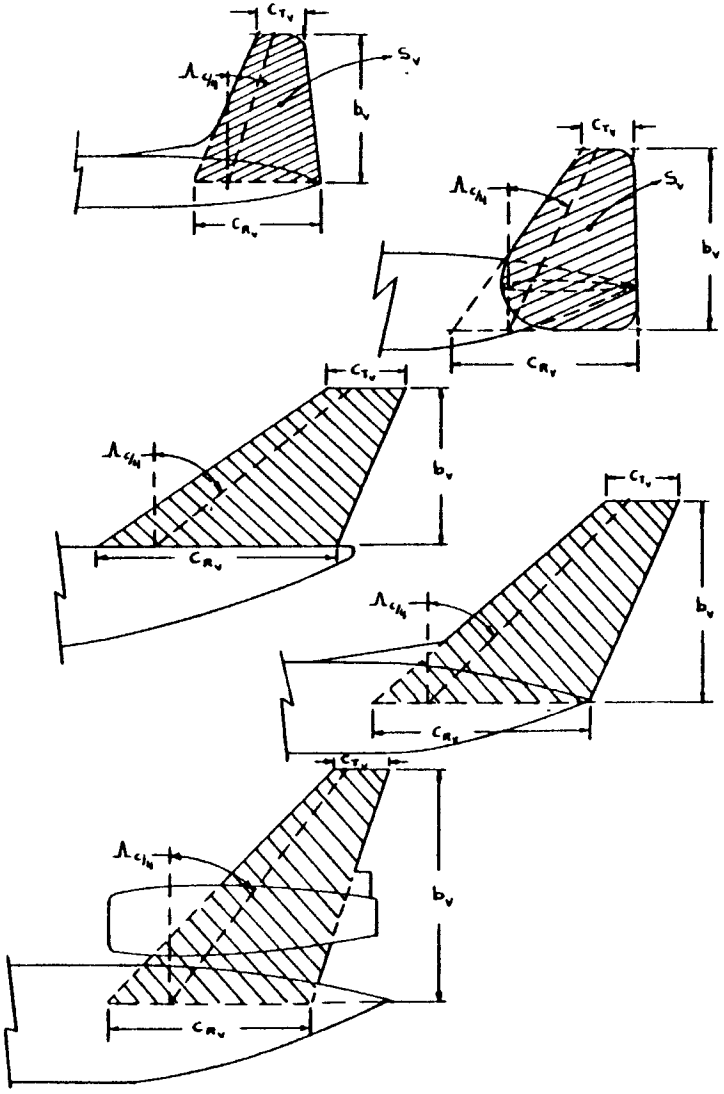

Figure 2.9 Reference Geometries for Vertical Tails

3. SUMMARY OF DRAG CAUSES AND DRAG MODELLING

The purpose of this chapter is to summarize the physical causes of drag, to present ways of breaking down drag and to discuss frequently used methods of modelling drag for use in airplane performance calculations.

For a more detailed study of drag, drag causes and drag computation methods the reader should consult references 8-15.

3.1 PHYSICAL CAUSES OF DRAG

Total drag is defined as the sum of zero-lift drag and induced drag (or drag due to lift):

$$\text{Total Drag} = \text{Zero-lift Drag} + \text{Drag-due-to-lift} \qquad (3.1)$$

This basic breakdown for will be used in all three speed ranges used in this text:

1. Subsonic speed range: $0 < M < 0.6$
2. Transonic speed range: $0.6 < M < 1.2$
3. Supersonic speed range: $1.2 < M < 3.0$

The zero-lift drag of an airplane is considered to be the sum of skin friction drag and pressure drag:

$$\text{Zero-lift Drag} = \text{Skin-friction Drag} + \text{Pressure Drag} \qquad (3.2)$$

Skin-friction drag is caused by the shearing stresses within the thin layer of air adjacent to the skin. This layer of air is called the boundary layer. It arises as a result of the viscosity of the air which resists a body passing through it.

The magnitude of this viscous resistance depends on whether the flow in the boundary layer is laminar or turbulent. Whether the boundary layer is laminar or turbulent depends on the Reynolds Number, on the pressure distribution and on the roughness of the skin (surface).

Pressure drag is caused by the displacement thickness of the boundary layer, which prevents full pressure recovery at the trailing edge. As long as the boundary layer remains attached, pressure drag tends to be small in subsonic flight. However, in transonic and in supersonic flight pressure drag is identified with wave drag and then becomes very significant.

When the boundary layer becomes separated and/or when bluntness is significant, pressure drag can be large in any speed regime.

Drag-due-to-lift is considered to be the sum of induced drag and viscous drag-due-to-lift:

$$\text{Drag-due-to-lift} = \text{Induced Drag} + \text{Viscous Drag-due-to-lift} \qquad (3.3)$$

The induced drag, also called trailing edge vortex drag (or simply vortex drag) depends on the spanwise distribution of lift. It is proportional to the square of the lift coefficient.

The viscous drag due to lift results from the change in the boundary layer development as a result of lift. The upper surface boundary layer thickness increases with increasing angle of attack. This in turn results in an increase in the so-called profile drag which itself is the sum of skin-friction drag and pressure drag.

Figure 3.1 illustrates a drag breakdown according to these physical causes. Intermediate drag types such as induced drag, form drag and profile drag are indicated also in Figure 3.1.

A major problem is that the basic drag causes in Equations (3.1)-(3.3) are interdependent. The flow regime in which the airplane is operating: Mach number, Reynold's number and angle of attack all influence the basic drag causes.

In predicting total airplane drag some 'book-keeping' procedures must be adopted. One 'book-keeping' decision which needs to be made is that which splits drag from thrust. In this text the position is taken that flow phenomena outside the airplane are associated with the generation of drag. Flow phenomena inside the airplane which are not associated with the production of thrust, are also considered to produce drag. An example of this is cooling air flow around a piston engine.

On the other hand, flow phenomena inside engine(s) (and/or nacelles) are associated with the production of thrust (or power).

Chapters 4 and 5 deal with airplane drag. Chapters 6 and 7 deal with airplane thrust (or power).

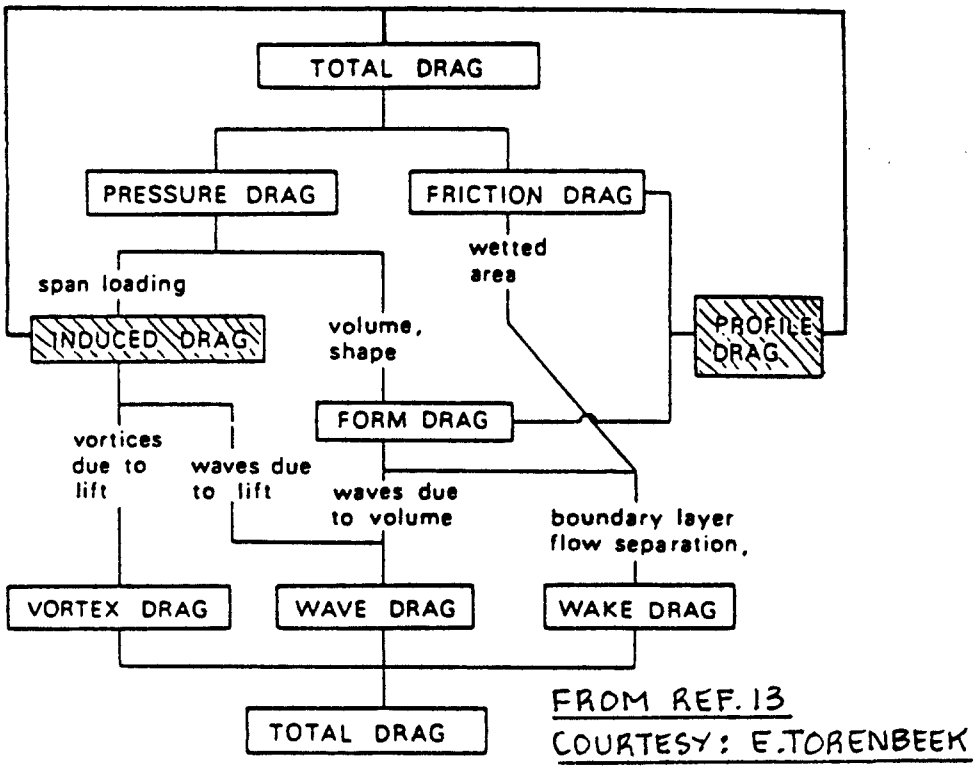

Figure 3.1 Drag Breakdown According to Physical Causes

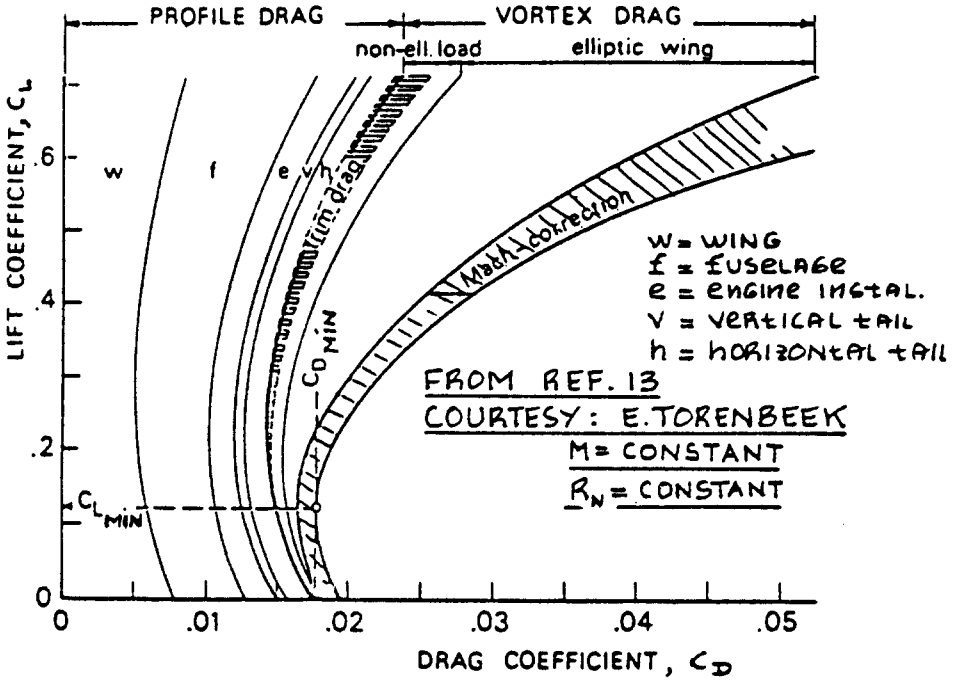

Figure 3.2 Typical Drag Breakdown for a Transport Jet

3.2 DRAG BREAKDOWN METHOD

It is useful to break down the drag of an airplane into that caused by its components. Figure 3.2 shows a typical drag breakdown for a transport operating at a high subsonic Mach number.

The drag breakdown method used in this text considers total airplane drag to be the sum of component drag contributions according to:

Airplane Drag = Component drag of (Wing + Fuselage + + Empennage + Nacelle/Pylon + Flap + + Landing Gear + Canopy/Windshield + + Store + Trim + Interference + + Miscellaneous) (3.4)

Chapter 4 presents a method for computing component drag for subsonic, transonic and supersonic flight.

3.3 DRAG MODELLING FOR PERFORMANCE CALCULATIONS

To enable the rapid calculation of airplane performance (discussed in Part VII), it is useful to represent airplane drag polars by simple mathematical models.

In addition, it is necessary to assume that the airplane can be held in a 'trimmed' state: no moments are acting on the airplane and the pilot does not have to exert a force on the cockpit controls. Requirements for trim are discussed in detail in Ref.16. Part VII contains methods for predicting trimmability.

To trim an airplane usually causes extra drag: trim drag. Eqn.(3.4) includes a term which accounts for trim drag. All drag polars used in performance calculations are assumed to be 'trimmed' drag polars.

For essentially uncambered airplanes in subsonic flight, the drag polar may be modelled as:

$$C_D = C_{D_o} + (C_L)^2/\pi Ae \qquad (3.5)$$

Note that the minimum drag occurs at $C_L = 0$.

The F4C fighter airplane is an example of an essentially uncambered airplane. Figure 3.3 shows its drag polar. It is very well represented by Eqn.(3.5).

For cambered airplanes, the minimum value of drag

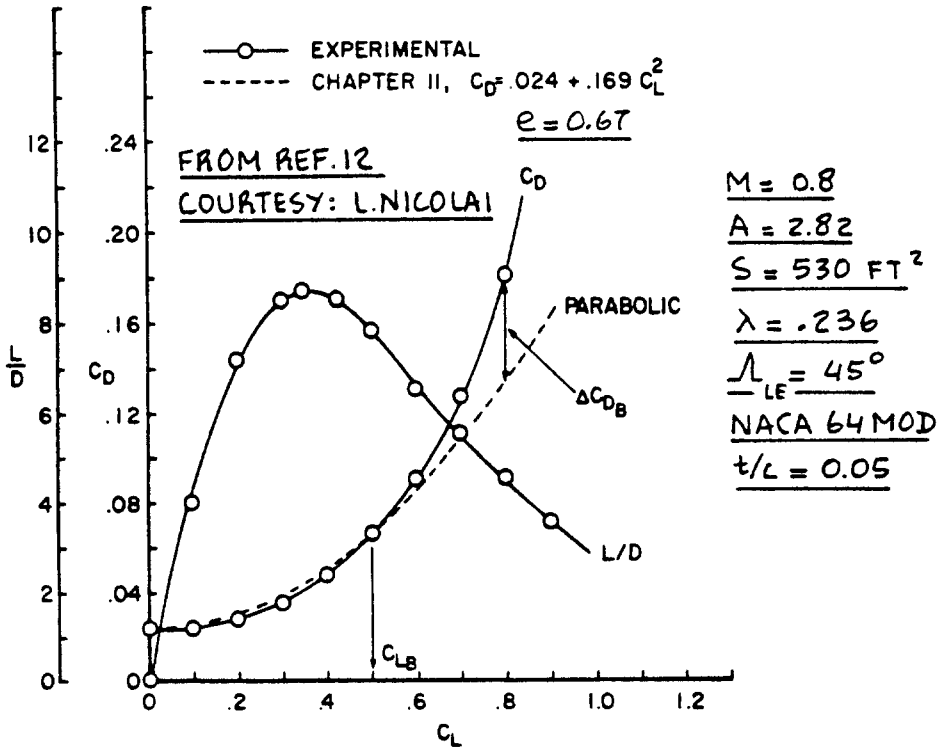

Figure 3.3 Drag Polar for the McDonnell-Douglas F4C

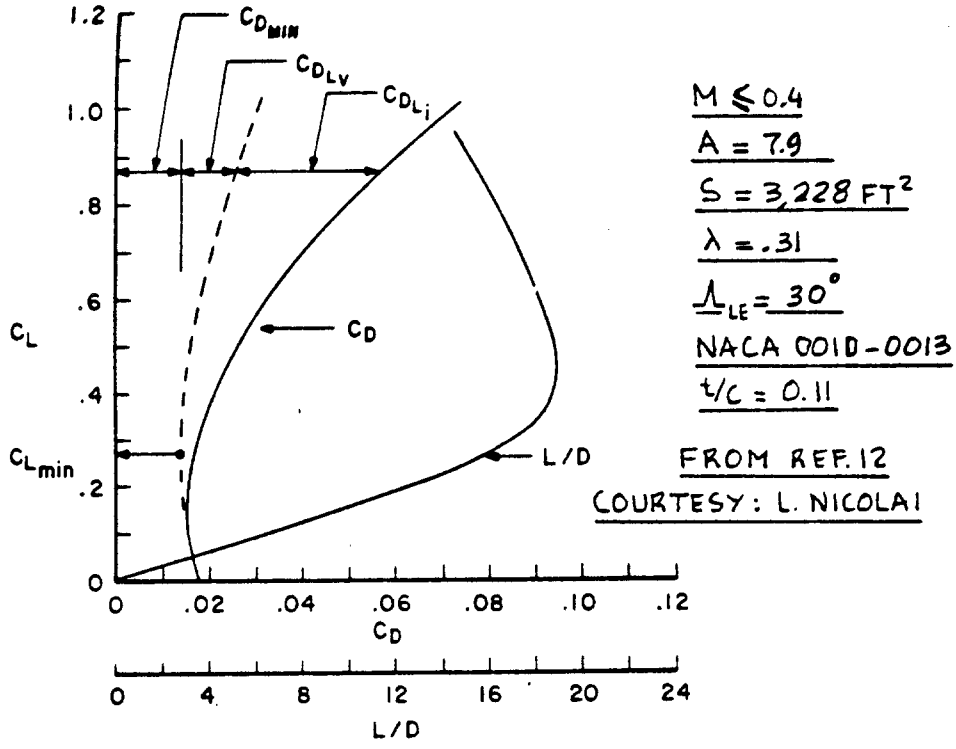

Figure 3.4 Drag Polar for the Lockheed C-141

does not occur at $C_L = 0$ and it becomes necessary to represent the drag polar as:

$$C_D = C_{D_{min}} + K''(C_L - C_{L_{min}})^2 + K'C_L^2 \qquad (3.6)$$

Note that minimum drag in this case occurs at a lift coefficient of $C_L = \{K''/(K''+K')\}C_{L_{min}}$.

The Lockheed C-141 Starlifter is a cambered airplane despite the fact that its wing uses symmetrical airfoil sections (average section is NACA 0011). Since the wing is installed at an incidence angle of 3.2 degrees the airplane acts like it is cambered. Figure 3.4 shows the C-141 low speed drag polar. Note that: $C_{D_{min}} = 0.0140$, which occurs at $C_{L_{min}} = 0.27$.

Note, that for an uncambered airplane Eqn.(3.6) reduces to Eqn.(3.5) since in that case: $C_{L_{min}} = 0$ and:

$$K'' + K' = 1/\pi Ae \text{ (no camber only!)} \qquad (3.7)$$

For airplanes flying at relatively high angles of attack, the drag polars deviate significantly from the parabolic shape. This is caused by flow separation resulting in a steep rise in pressure drag. In that case the polar is modelled as:

$$C_D = C_{D_{min}} + K''(C_L - C_{L_{min}})^2 + K'C_L^2 + K_B(C_L - C_{L_B})^2 \qquad (3.8)$$

Figure 3.5 illustrates a drag polar with this type of behavior.

C_{L_B} is the lift coefficient for which the steep drag rise due to separation begins. The factor K_B is called the break drag-due-to-lift factor and is defined as:

$$K_B = 0 \text{ for } C_L < C_{L_B} \qquad (3.9)$$
$$K_B > 0 \text{ for } C_L > C_{L_B}$$

Table 3.1 presents a summary of important lift-to-drag ratios based on the drag polar models of Eqns 3.5 and 3.6. These lift-to-drag ratios and the lift coefficients at which they occur are used in the performance calculations presented in Part VII.

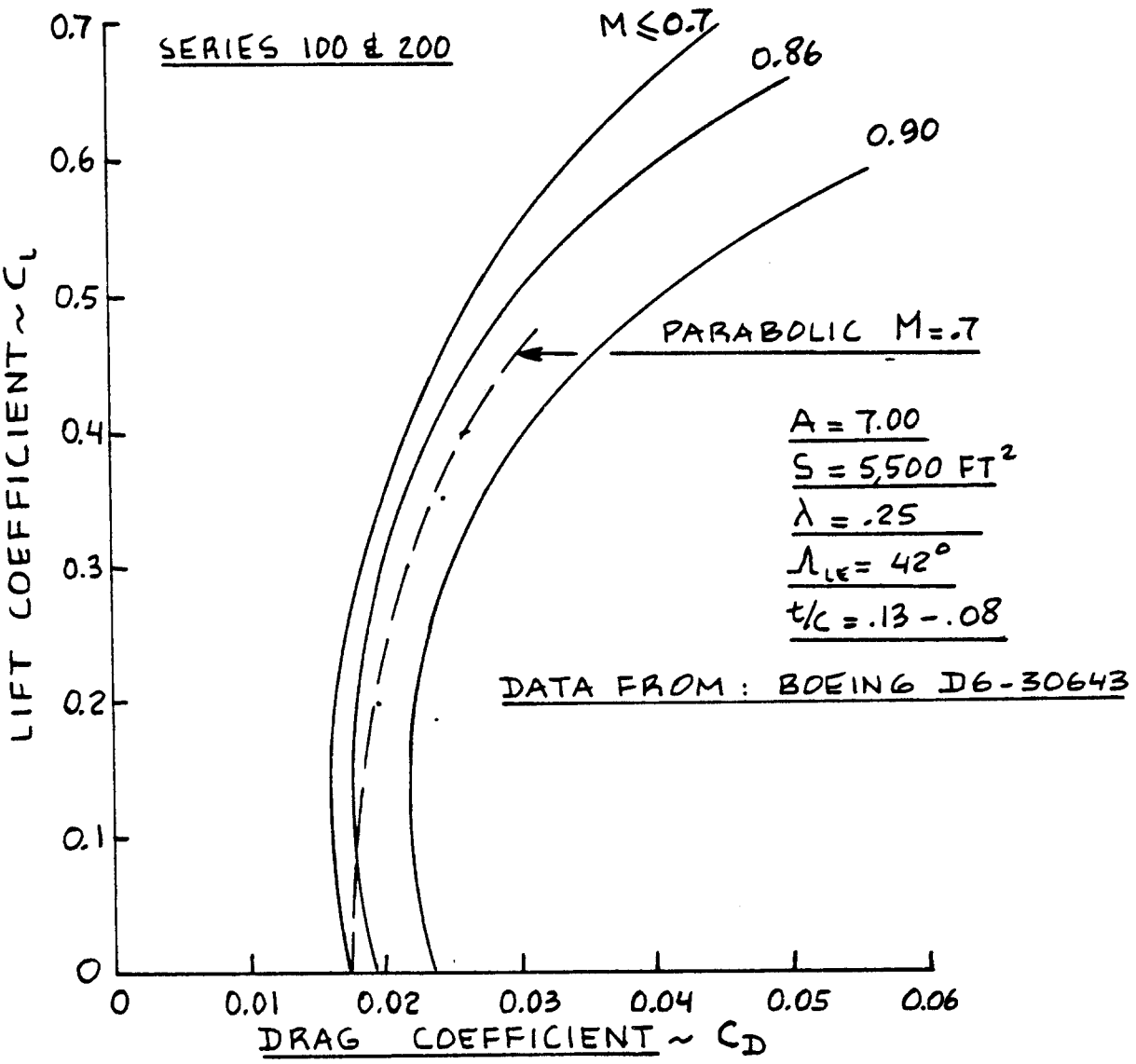

Figure 3.5 Drag Polars for the Boeing 747

Table 3.1 Maximum Lift-to-Drag Ratios and Corresponding Lift Coefficients

Drag Polar According to Eqn. (3.5)

$$(L/D)_{max} = 0.5/(KC_{D_o})^{1/2} \qquad (3.10)$$

$$C_{L_{(L/D)_{max}}} = (C_{D_o}/K)^{1/2} \qquad (3.11)$$

where: $K = 1/\pi Ae$ (3.12)

Drag Polar According to Eqn. (3.6)

$$(L/D)_{max} = (P^{1/2})/[C_{D_{min}} + K''\{(P^{1/2}) - C_{L_{min}}\}^2 + K'P] \qquad (3.13)$$

where: $P = \{C_{D_{min}} + K''(C_{L_{min}})^2\}/(K' + K'')$ (3.14)

$$C_{L_{(L/D)_{max}}} = (P)^{1/2} \qquad (3.15)$$

Note that equations (3.13) and (3.15) reduce to equations (3.10) and (3.11) for the case of $K''=0$ and $C_{D_{min}} = C_{D_o}$. In that case, $K' = K$.

4. DRAG POLAR PREDICTION METHODS

A Class I method for drag polar prediction was presented in Part I (Ch. 3). The purpose of this chapter is to present a Class II method for predicting drag polars of airplanes during the preliminary design phase. The method is based on Reference 9 and applies to airplanes with essentially straight, tapered wings. For other wing planforms, see Reference 9.

4.1 DRAG BREAKDOWN PROCEDURE

Total airplane drag in lbs is written as:

$$D = C_D \bar{q} S \tag{4.1}$$

where: C_D = the total airplane drag coefficient

$\bar{q}$ = $0.5\rho(U_1)^2 = 1482\delta M^2$, also called (4.2)

free stream dynamic pressure, with:

ρ = air density: see Appendix A.

U_1 = steady state airspeed

δ = pressure ratio: see Appendix A.

$M = U_1/a$ = Mach number (4.3)

a = speed of sound: see Appendix A.

S = the wing planform or reference area. Figures 2.5-2.7 define how this area is normally defined for a range of wing designs.

The total airplane drag coefficient is normally broken down into the following components:

$$C_D = C_{D_{wing}} + C_{D_{fus}} + C_{D_{emp}} + C_{D_{np}} + C_{D_{flap}} + C_{D_{gear}} + C_{D_{cw}} + C_{D_{store}} + C_{D_{trim}} + C_{D_{int}} + C_{D_{misc}} \tag{4.4}$$

where: $C_{D_{wing}}$ = wing drag coefficient: Section 4.2

$C_{D_{fus}}$ = fuselage drag coefficient: Section 4.3

$C_{D_{emp}}$ = empennage drag coefficient: Section 4.4

$C_{D_{np}}$ = nacelle/pylon drag coefficient, including cooling drag: Section 4.5

$C_{D_{flap}}$ = leading/trailing edge flap drag coefficient: Section 4.6

$C_{D_{gear}}$ = landing gear drag coefficient: Section 4.7

$C_{D_{cw}}$ = canopy/windshield drag coefficient: Section 4.8

$C_{D_{store}}$ = store(s) drag coefficient: Section 4.9

$C_{D_{trim}}$ = trim drag coefficient: Section 4.10

$C_{D_{int}}$ = interference drag coefficient: Section 4.11

$C_{D_{misc}}$ = miscellaneous drag coefficient, typically caused by such things as: speed brakes, struts, inlet drag, antennas, gaps and surface roughnesses: Section 4.12

Sections 4.2 through 4.12 present methods for predicting the drag coefficient components in Eqn.(4.2). Numerical examples of drag breakdowns and examples of airplane drag polars are presented in Chapter 5.

Important Notes: 1.) The drag prediction methods of Sections 4.2 through 4.5 apply only to flight cases where the boundary layer is mostly turbulent. If extensive laminar flow runs are present (for example because of use of natural laminar flow airfoils or because of use of 'forced' laminar flow by suction), Section 4.13 may be used to obtain the necessary drag corrections.

2.) The drag prediction methods of Sections 4.2 through 4.5 apply only to 'smooth' surfaces. If surface roughness is present, the procedure of Sub-section 4.12.2 should be used in conjunction with the methods of Sections 4.2 through 4.5.

4.2 WING DRAG COEFFICIENT PREDICTION

4.2.1 Subsonic Wing Drag Coefficient

The subsonic wing drag coefficient is found from:

$$C_{D_{wing}} = C_{D_{o_w}} + C_{D_{L_w}} \qquad (4.5)$$

where: $C_{D_{o_w}}$ = wing zero-lift drag coefficient, see 4.2.1.1.

$C_{D_{L_w}}$ = wing drag coefficient due to lift, see 4.2.1.2.

4.2.1.1 Wing zero-lift drag coefficient

The subsonic wing zero-lift drag coefficient may be computed from:

$$C_{D_{o_w}} = (R_{wf})(R_{LS})(C_{f_w})\{1 + L'(t/c) + 100(t/c)^4\}S_{wet_w}/S \qquad (4.6)$$

where: R_{wf} = wing/fuselage interference factor: see Figure 4.1. For a flying wing: $R_{wf} = 1.0$.

R_{LS} = lifting surface correction factor found from Figure 4.2.

C_{f_w} = turbulent flat plate friction coefficient of the wing.

The general turbulent, flat plate friction coefficient, C_f is shown in Figure 4.3 as a function of Mach number and of Reynolds number, R_N.

For the wing, use: $R_{N_w} = \rho U_1 \bar{c}_{w_e}/\mu \qquad (4.7)$

where: $\bar{c}_{w_e}$ = exposed wing m.g.c. (= wing m.g.c. for a flying wing)

μ = coefficient of viscosity of air: see Appendix A.

L' = airfoil thickness location parameter: see Figure 4.4.

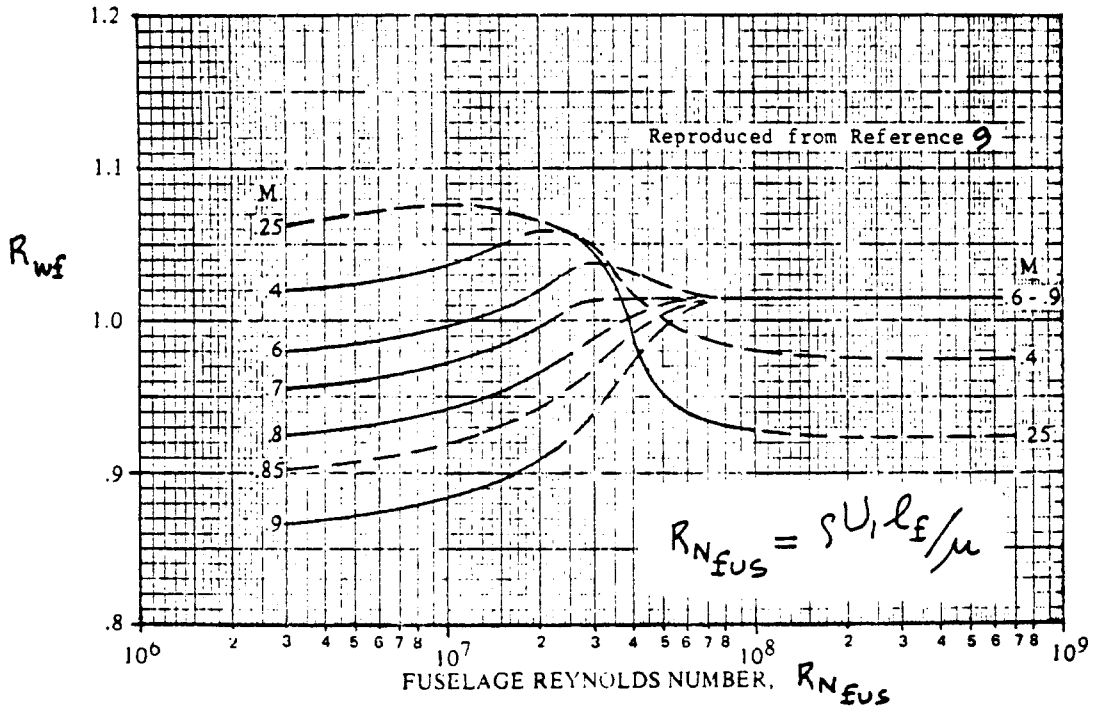

Figure 4.1 Wing Fuselage Interference Factor

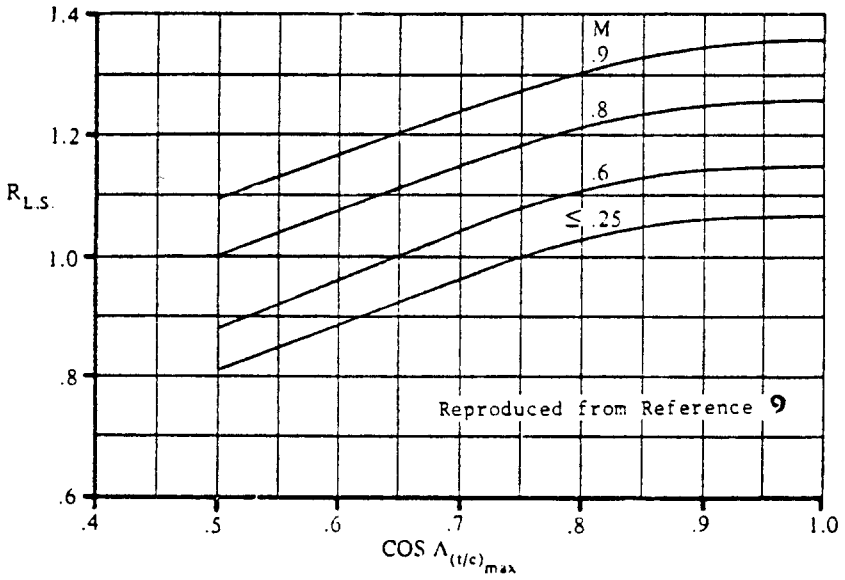

Figure 4.2 Lifting Surface Correction Factor

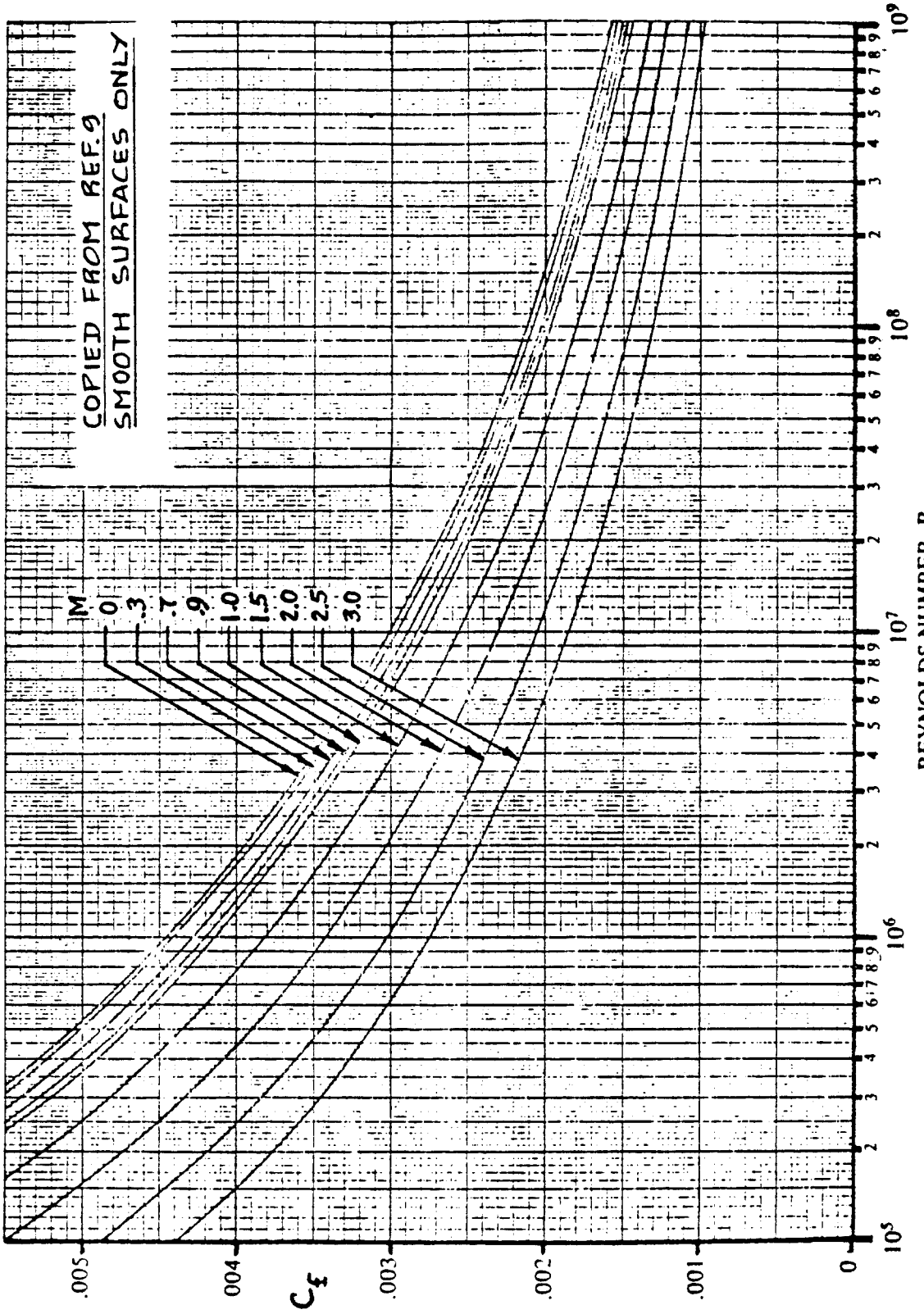

Figure 4.3 Turbulent Mean Skin-Friction Coefficient

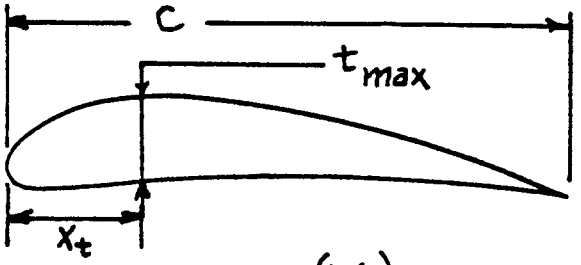

$L' = 1.2$ FOR $(t/c)_{max}$ AT $X_t \geq 0.30C$

$L' = 2.0$ FOR $(t/c)_{max}$ AT $X_t < 0.30C$

Figure 4.4 Airfoil Thickness Location Parameter

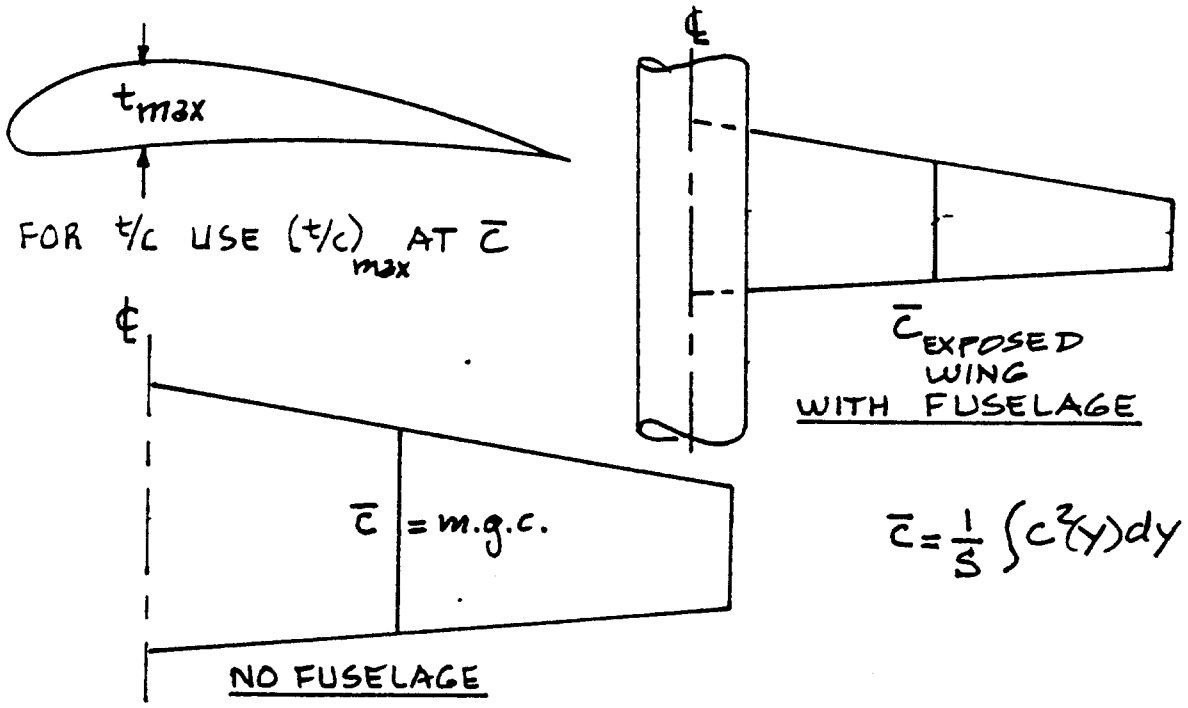

Figure 4.5 Definition of Thickness Ratio for a Wing

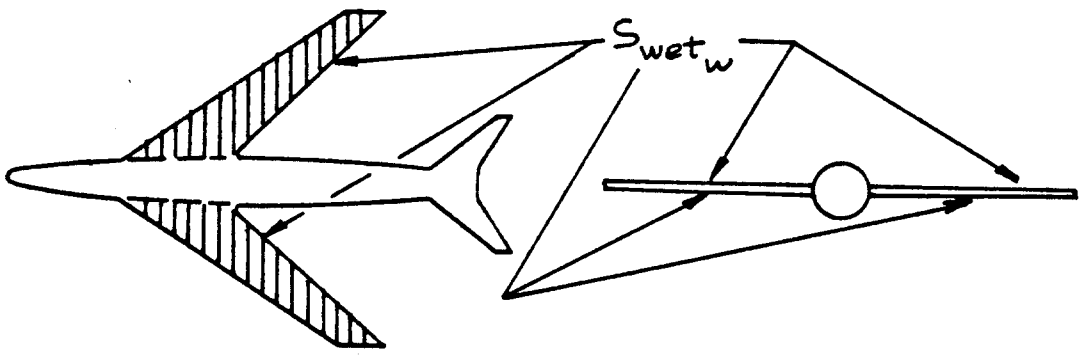

Figure 4.6 Definition of Wing Wetted Area

t/c = thickness ratio defined at the mean geometric chord of the wing: see Figure 4.5.

S_{wet_w} = wetted area of the wing: see Figure 4.6 and Appendix B.

S = wing or reference area. This is normally the wing planform area: see Figs 2.5-2.7.

4.2.1.2 Wing drag coefficient due to lift

The wing drag coefficient due to lift is found from:

$$C_{D_{L_w}} = (C_{L_w})^2/\pi Ae + 2\pi C_{L_w} \varepsilon_t v + 4\pi^2(\varepsilon_t)^2 w \qquad (4.8)$$

where: C_{L_w} = wing lift coefficient, defined as:

$$C_{L_w} = C_L - C_{L_c} S_c/S + C_{L_h} S_h/S \qquad (4.9)$$

where: $C_L = W/\bar{q}S$ (4.10)

The canard and horizontal tail lift coefficients, C_{L_c} and C_{L_h} respectively, are determined from trim considerations. Their values depend on the center of gravity location. To determine these empennage lift coefficients a trim calculation must be performed. This is done with the help of a trim diagram. Part VII contains a method for constructing a trim diagram.

In early preliminary design it is sufficiently accurate to set:

$$C_{L_w} = 1.05 C_L \qquad (4.11)$$

A = wing aspect ratio = b^2/S, where:
b = wing span: see Figures 2.5 - 2.7.

e = span efficiency factor, defined as:

$$e = 1.1(C_{L_{\alpha_w}}/A)/\{R(C_{L_{\alpha_w}}/A) + (1 - R)\pi\} \qquad (4.12)$$

where: $C_{L_{\alpha_w}}$ is the wing lift-curve slope which can be found with the help of Chapter 10.

R = leading edge suction parameter as defined in Figure 4.7.

ε_t = wing twist angle, positive for wash-in, negative for wash-out, see Figure 4.8.

v = induced drag factor due to linear twist, see Figures 4.9.

w = zero-lift drag factor due to linear twist, see Figures 4.10.

Note: this method for determining C_{L_w} applies only for $C_{L_w} < C_{L_B}$, the value of lift coefficient where the flow begins to separate.

4.2.2 Transonic Wing Drag Coefficient

The transonic wing drag coefficient is found from:

$$C_{D_{wing}} = C_{D_{o_w}} + C_{D_{L_w}} \qquad (4.13)$$

where: $C_{D_{o_w}}$ = wing zero-lift drag coefficient, see 4.2.2.1.

$C_{D_{L_w}}$ = wing drag coefficient due to lift, see 4.2.2.2.

4.2.2.1 Wing zero-lift drag coefficient

In the transonic speed range the wing zero-lift drag coefficient is found from:

$$C_{D_{o_w}} = C_{D_{o_w}\ \text{at } M=0.6} + C_{D_{w_{wave}}} \qquad (4.14)$$

where: $C_{D_{o_w}\ \text{at } M=0.6}$ = the drag coefficent due to friction. It is found from Eqn. (4.6) and is assumed to stay constant with Mach number in the entire transonic speed range.

$C_{D_{w_{wave}}}$ = the wing wave drag coefficient which depends on the wing sweep angle, $\Lambda_{c/4}$.

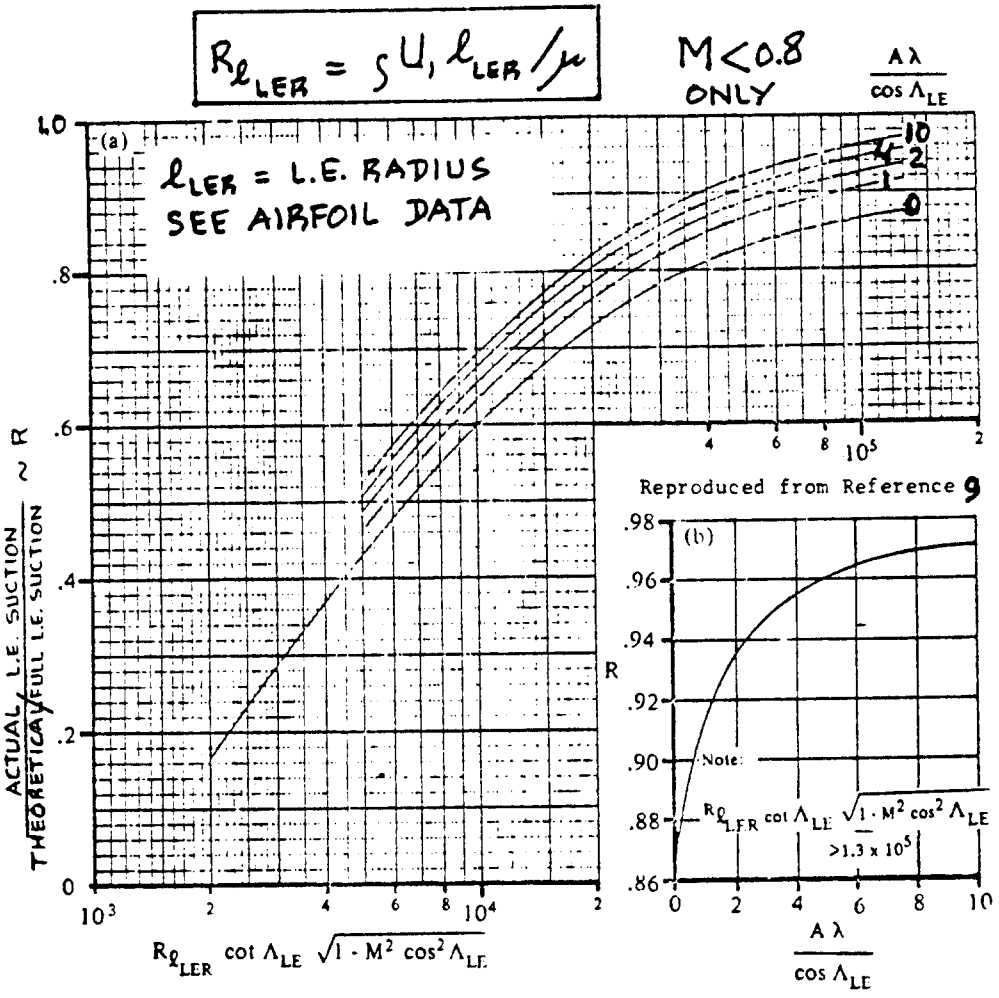

Figure 4.7 Leading Edge Suction Parameter

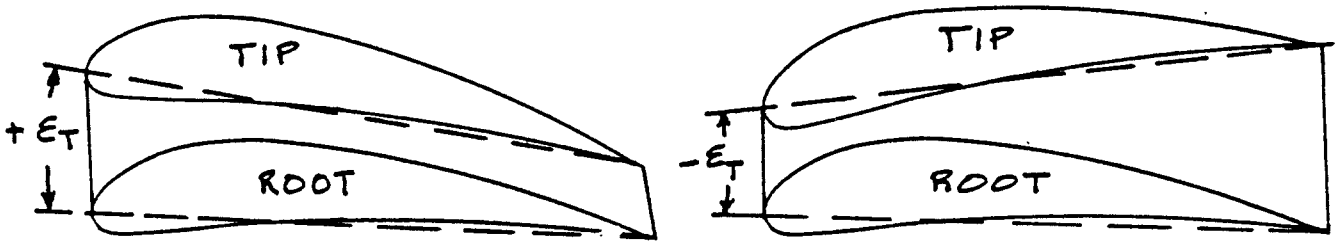

Figure 4.8 Definition of Wing Twist Angle

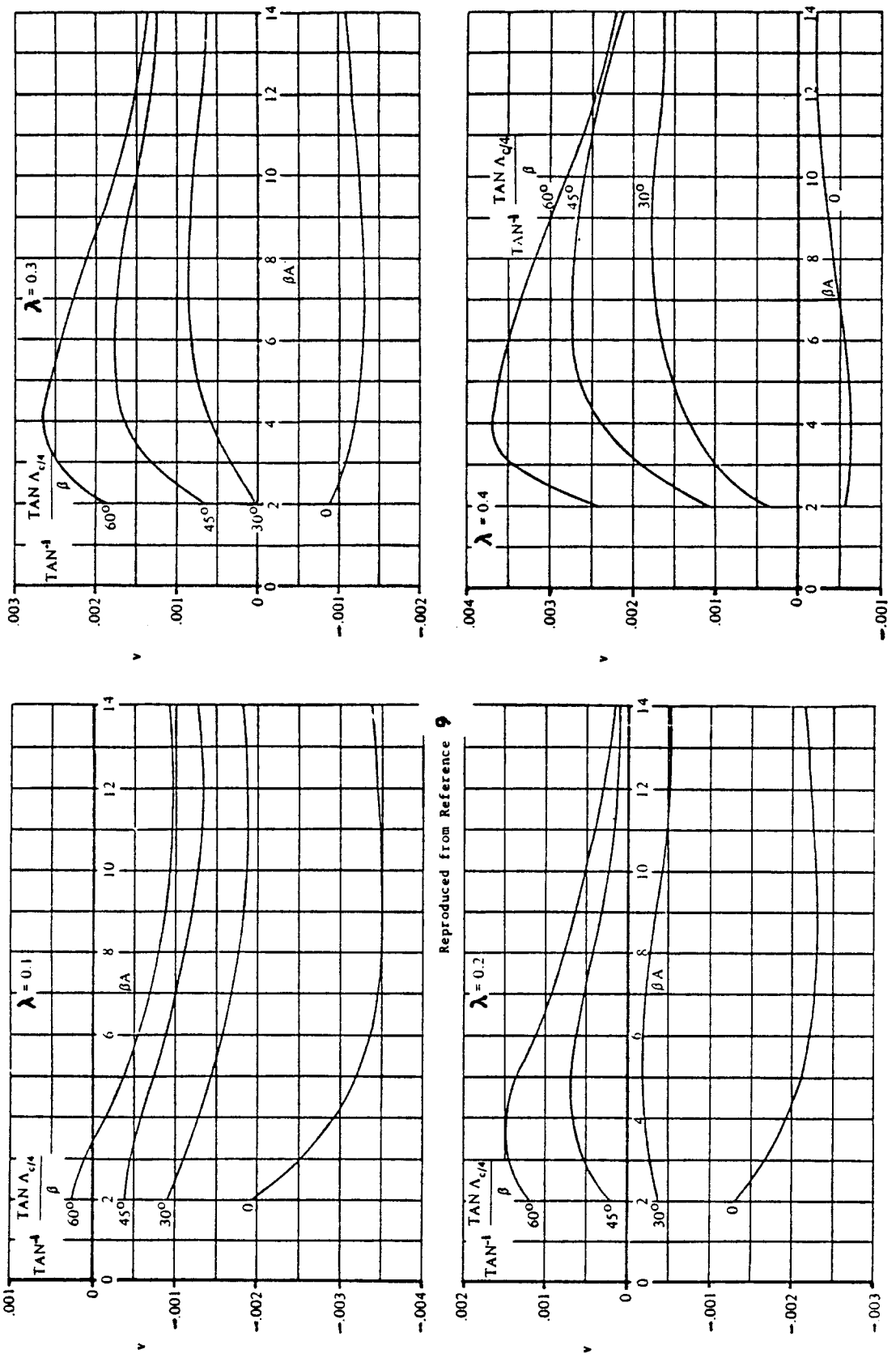

Figure 4.9a Induced Drag Factor due to Linear Twist

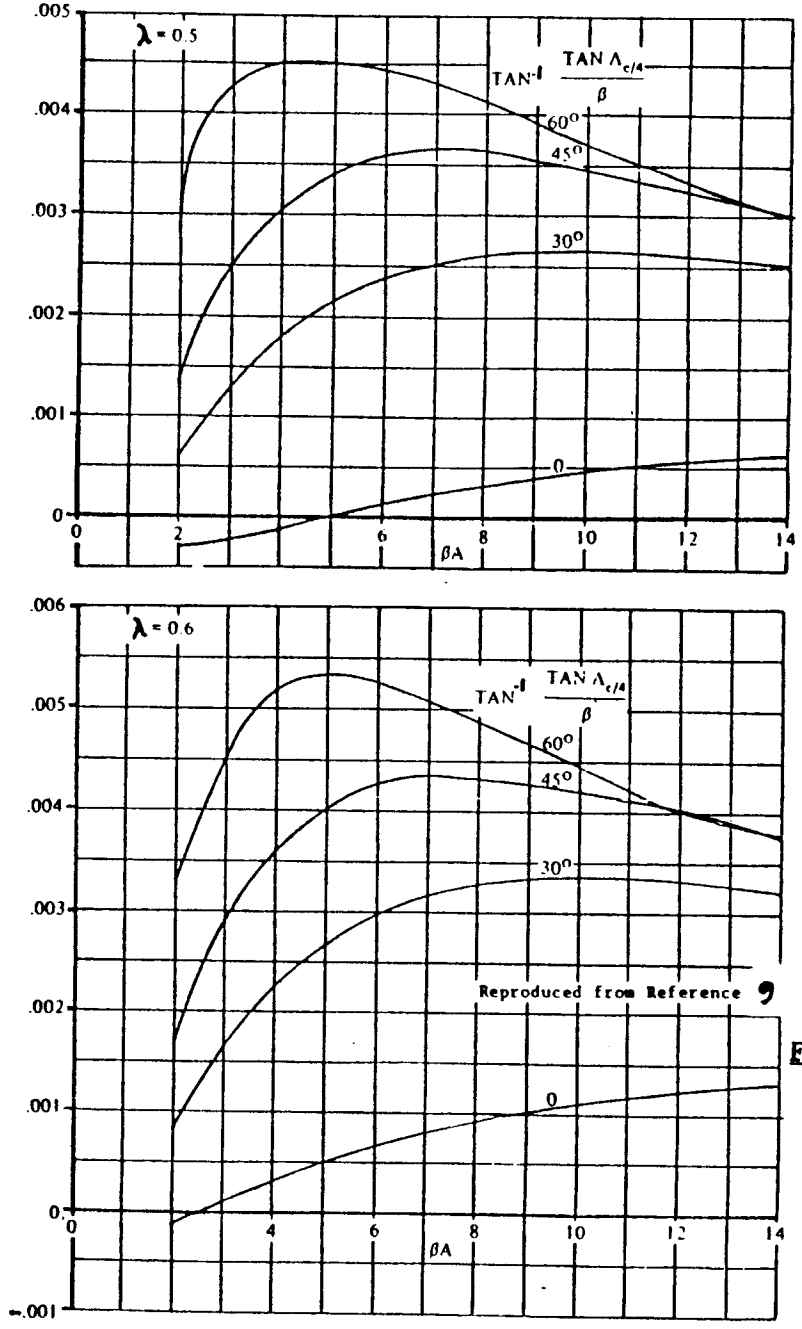

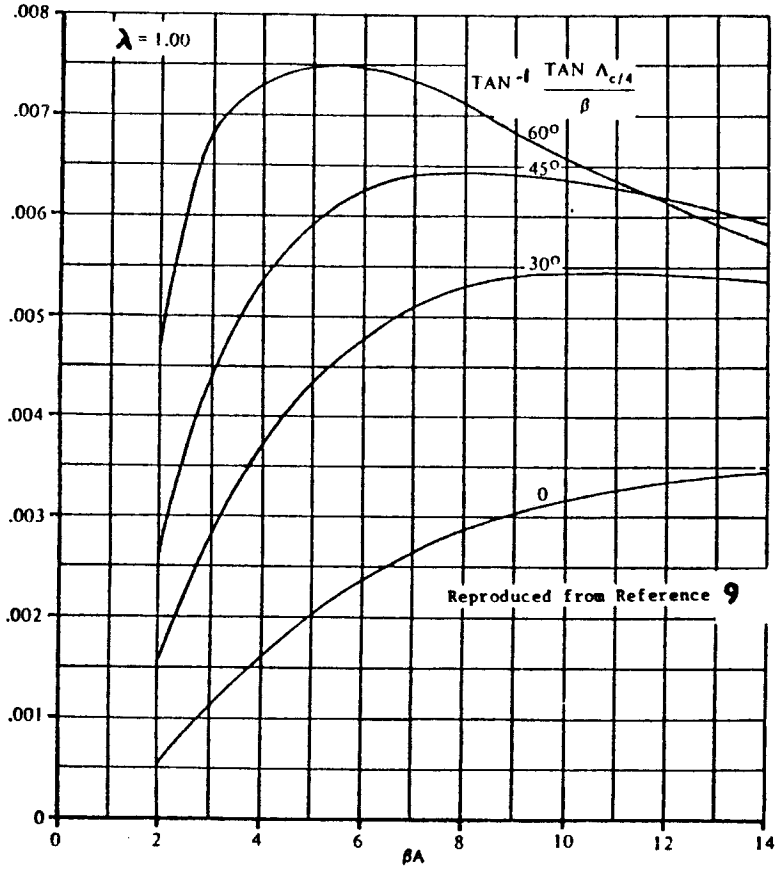

Figure 4.9b Induced Drag Factor due to Linear Twist

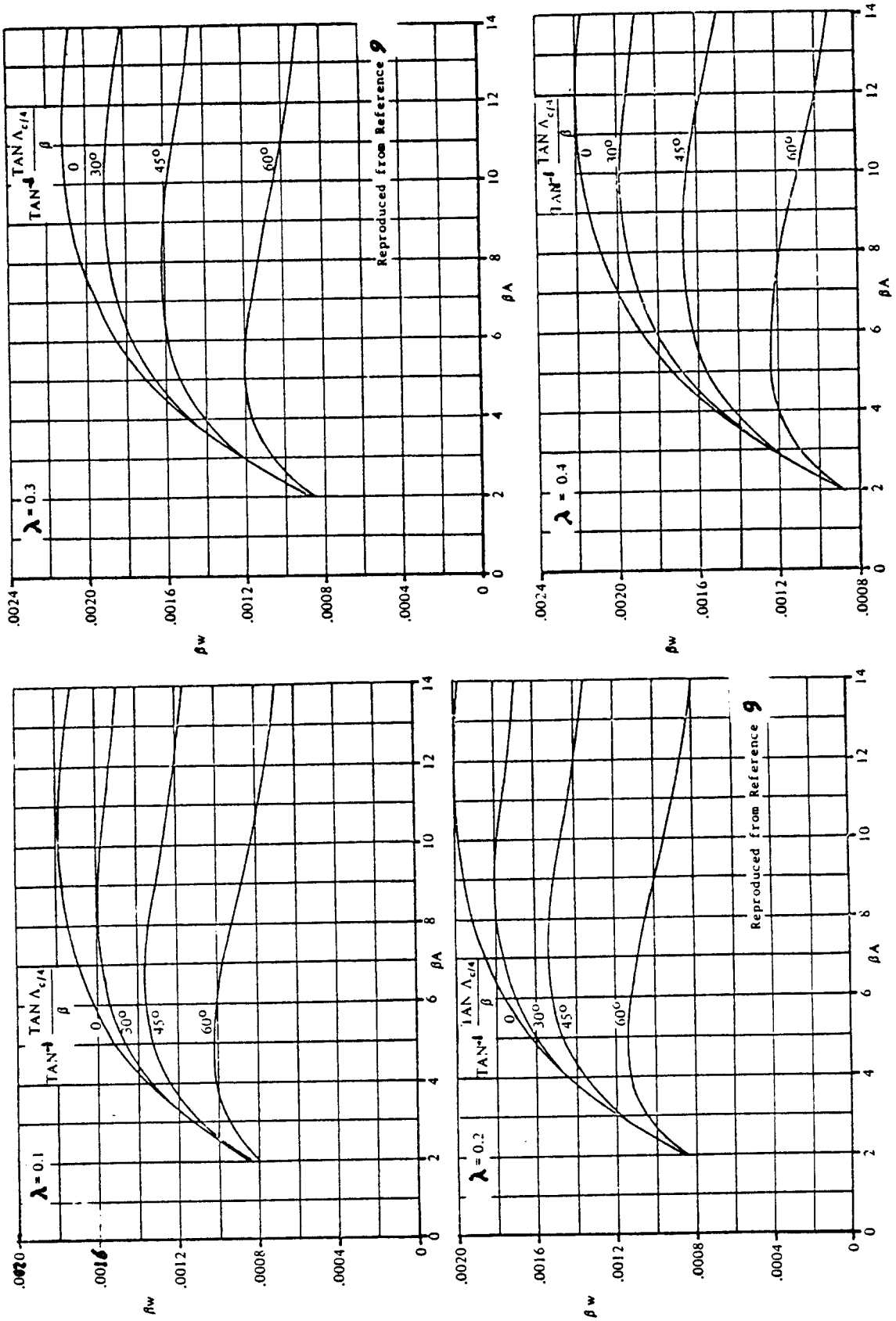

Figure 4.10a Zero-Lift Drag Factor due to Linear Twist

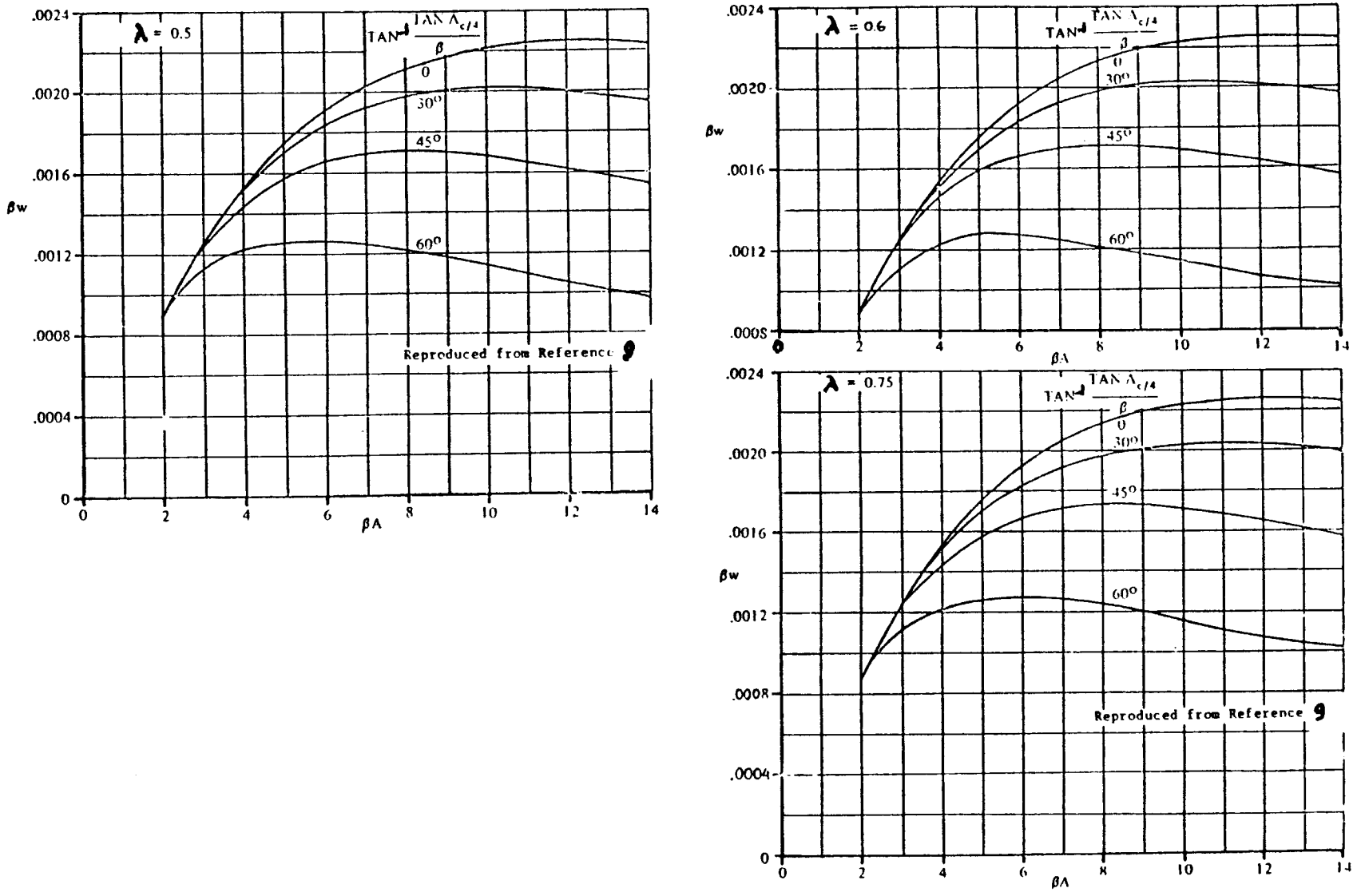

Figure 4.10b Zero-Lift Drag Factor due to Linear Twist

Unswept wings:

The wave drag coefficient, $C_{D_{w_{wave}}}$ for an unswept wing follows from Figure 4.11. This wave drag coefficient should be plotted against the Mach number in the transonic speed range.

Swept wings:

For a swept wing, proceed as follows:

From a plot of $C_{D_{w_{wave}}}$ versus M for the unswept wing of the same aspect ratio, and thickness ratio, read the following values:

M_{DD}, $C_{D_{w_{wave_{peak}}}}$ and $M_{at\ C_{D_{w_{wave_{peak}}}}}$.

Correct these values for sweep angle as follows:

$$M_{DD_{\Lambda_{c/4}}} = M_{DD}/(\cos\Lambda_{c/4})^{1/2} \quad (4.15)$$

$$C_{D_{wave_{peak_{\Lambda_{c/4}}}}} = C_{D_{wave_{peak}}} (\cos\Lambda_{c/4})^{2.5} \quad (4.16)$$

$$M_{at\ C_{D_{wave_{peak_{\Lambda_{c/4}}}}}} = \{M_{at\ C_{D_{wave_{peak}}}}\}/(\cos\Lambda_{c/4})^{1/2} \quad (4.17)$$

Draw in the line of $C_{D_{w_{wave_{\Lambda_{c/4}}}}}$ versus Mach number in the transonic speed range. A typical result is illustrated in Figure 4.12.

4.2.2.2 Wing drag coefficient due to lift

The transonic wing drag coefficient due to lift is written as:

$$C_{D_{L_w}} = (C_{D_L}/C_L^2)C_L^2 \quad (4.18)$$

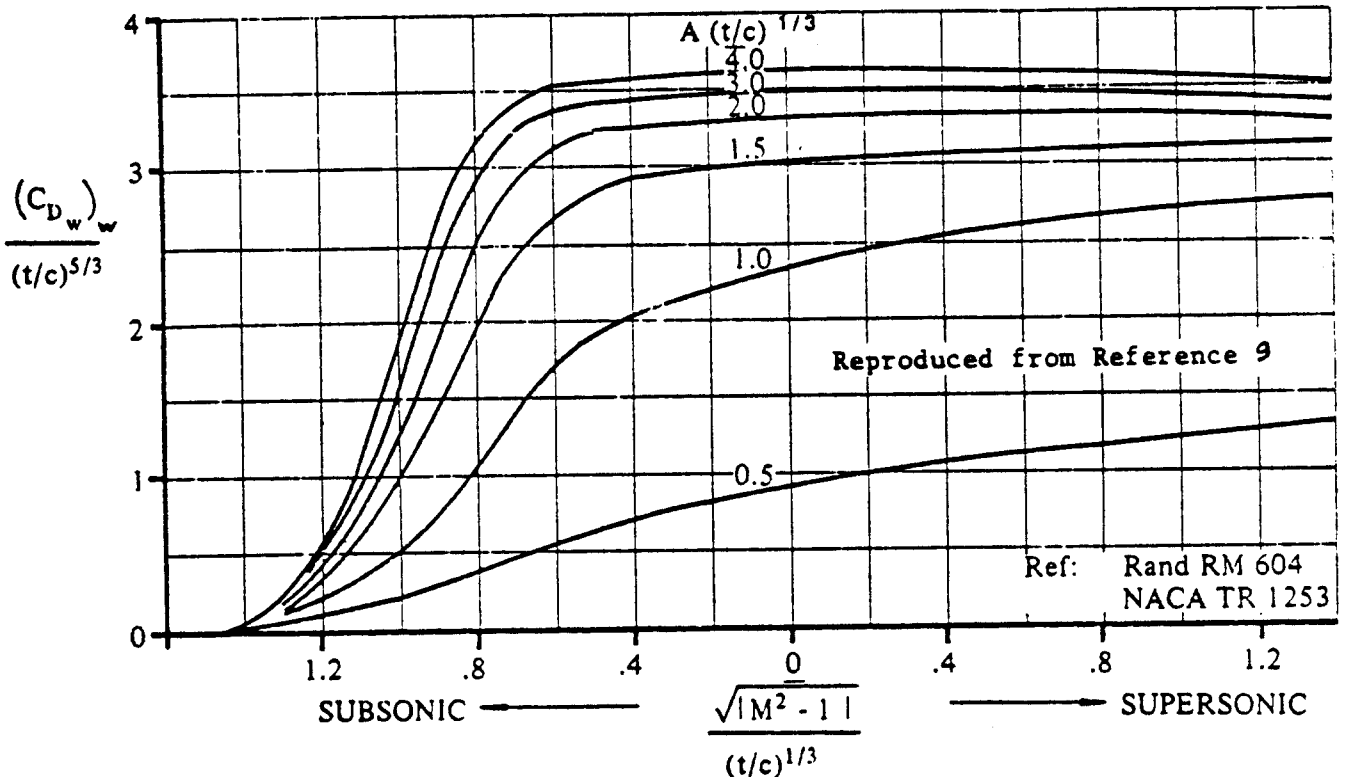

VALID ONLY AT TRANSONIC SPEEDS
VALID ONLY FOR UNSWEPT, ROUNDNOSE AIRFOILS

Figure 4.11 Zero-Lift Wave Drag Coefficient

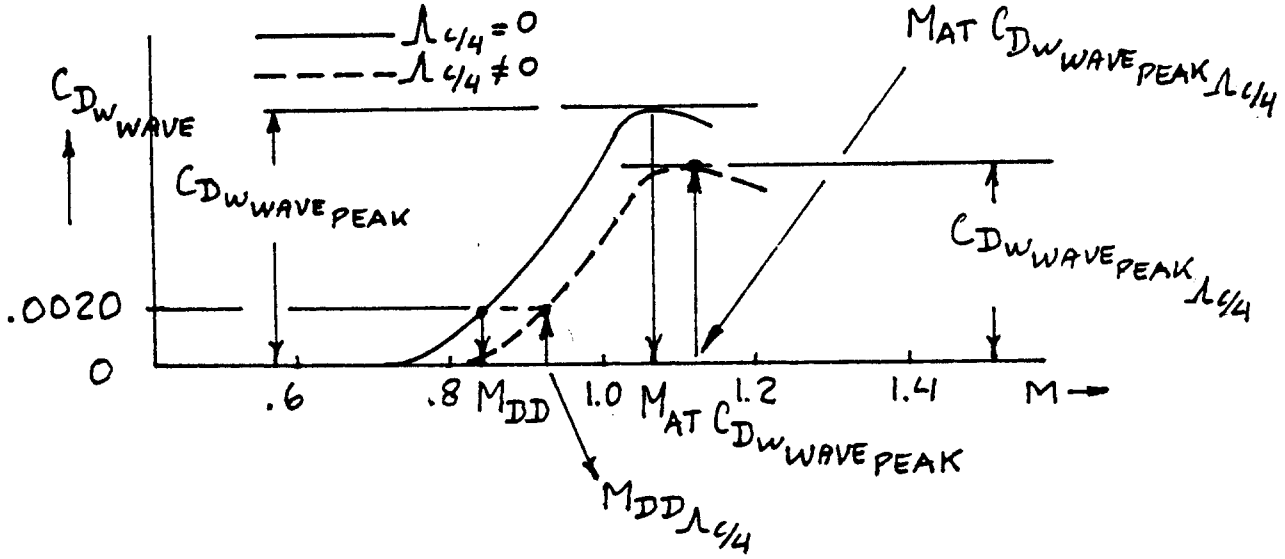

Figure 4.12 Transonic Fairing of Zero-Lift Wave Drag

The induced drag parameter (C_{D_L}/C_L^2) may be found as a function of transonic similarity parameters which are defined in Figures 4.13.

4.2.3 Supersonic Wing Drag Coefficient

The supersonic wing drag coefficient is found from:

$$C_{D_{wing}} = C_{D_{o_w}} + C_{D_{L_w}} \quad (4.19)$$

where: $C_{D_{o_w}}$ = wing zero-lift drag coefficient, see 4.2.3.1.

$C_{D_{L_w}}$ = wing drag coefficient due to lift, see 4.2.3.2.

4.2.3.1 Wing zero-lift drag coefficient

The supersonic wing zero-lift drag coefficient follows from:

$$C_{D_{o_w}} = C_{D_{w_f}} + C_{D_{w_{wave}}} \quad (4.20)$$

where: $C_{D_{w_f}}$ = the supersonic skin-friction drag coefficient, found from:

$$C_{D_{w_f}} = C_{f_w} S_{wet}/S \quad (4.21)$$

where: C_{f_w} may be found from Figure 4.3.

$C_{D_{w_{wave}}}$ = the wing wave drag coefficient which depends on the leading edge radius and on whether the wing has a subsonic or a supersonic leading edge: see Fig.2.4 for definitions. For wings with sharp nose airfoils, see Ref.9. For wings with round nose airfoils:

For wings with a supersonic leading edge:

$$C_{D_{w_{wave}}} = C_{D_{LE}} + (16/3\beta)\{(t/c)_{eff}\}^2 S_{bw}/S \quad (4.22)$$

For wings with a subsonic leading edge:

$$C_{D_{w_{wave}}} = C_{D_{LE}} + (16/3)\cot\Lambda_{LE_{bw}}\{(t/c)_{eff}\}^2 S_{bw}/S \quad (4.23)$$

COPIED FROM REF. 9

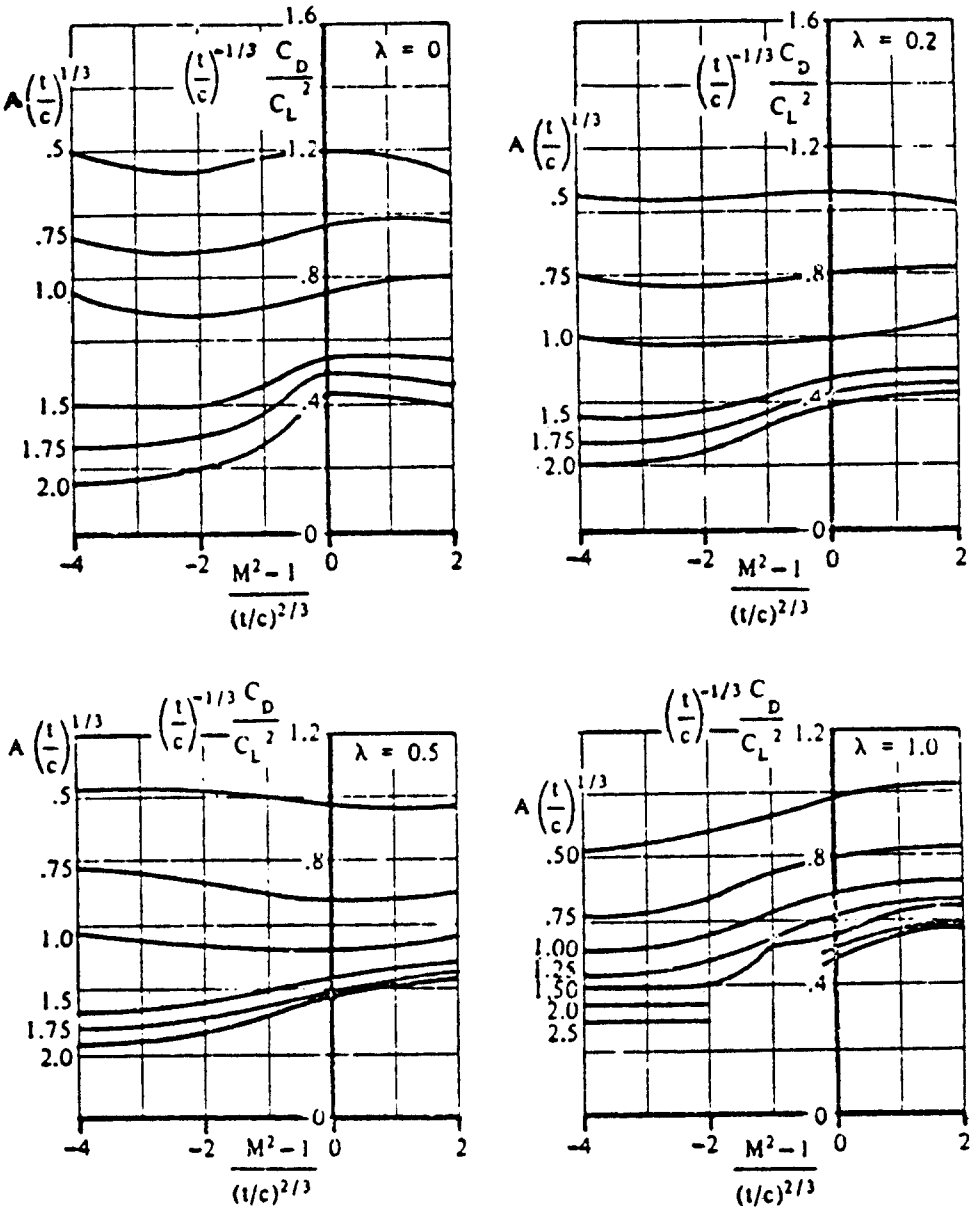

NOTE: $A \tan \Lambda_{LE} = 0$

Figure 4.13a Transonic Drag due to Lift

COPIED FROM REF.9

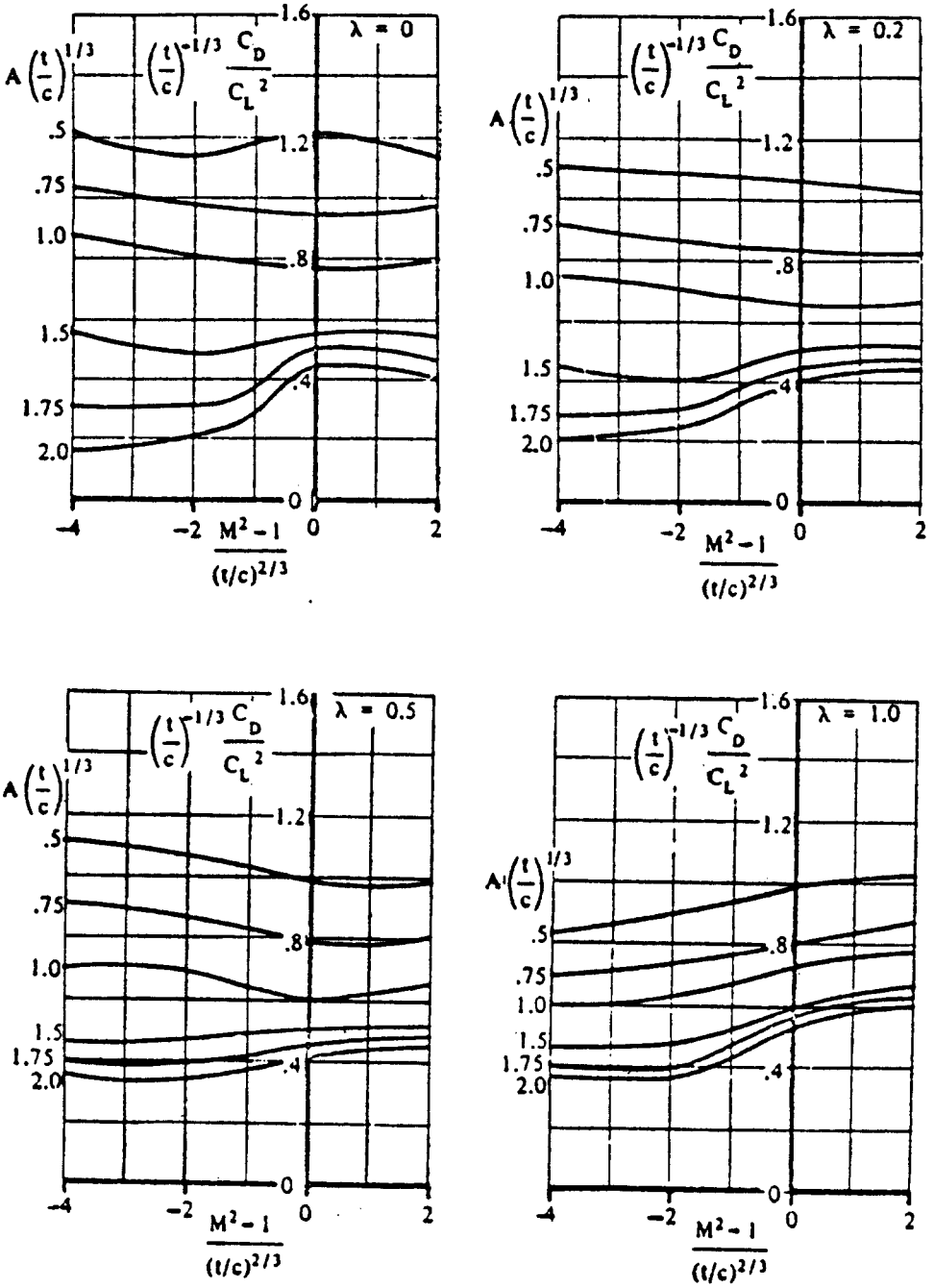

NOTE: $A\tan\Lambda_{LE} = 3$

Figure 4.13b Transonic Drag due to Lift

COPIED FROM REF. 9

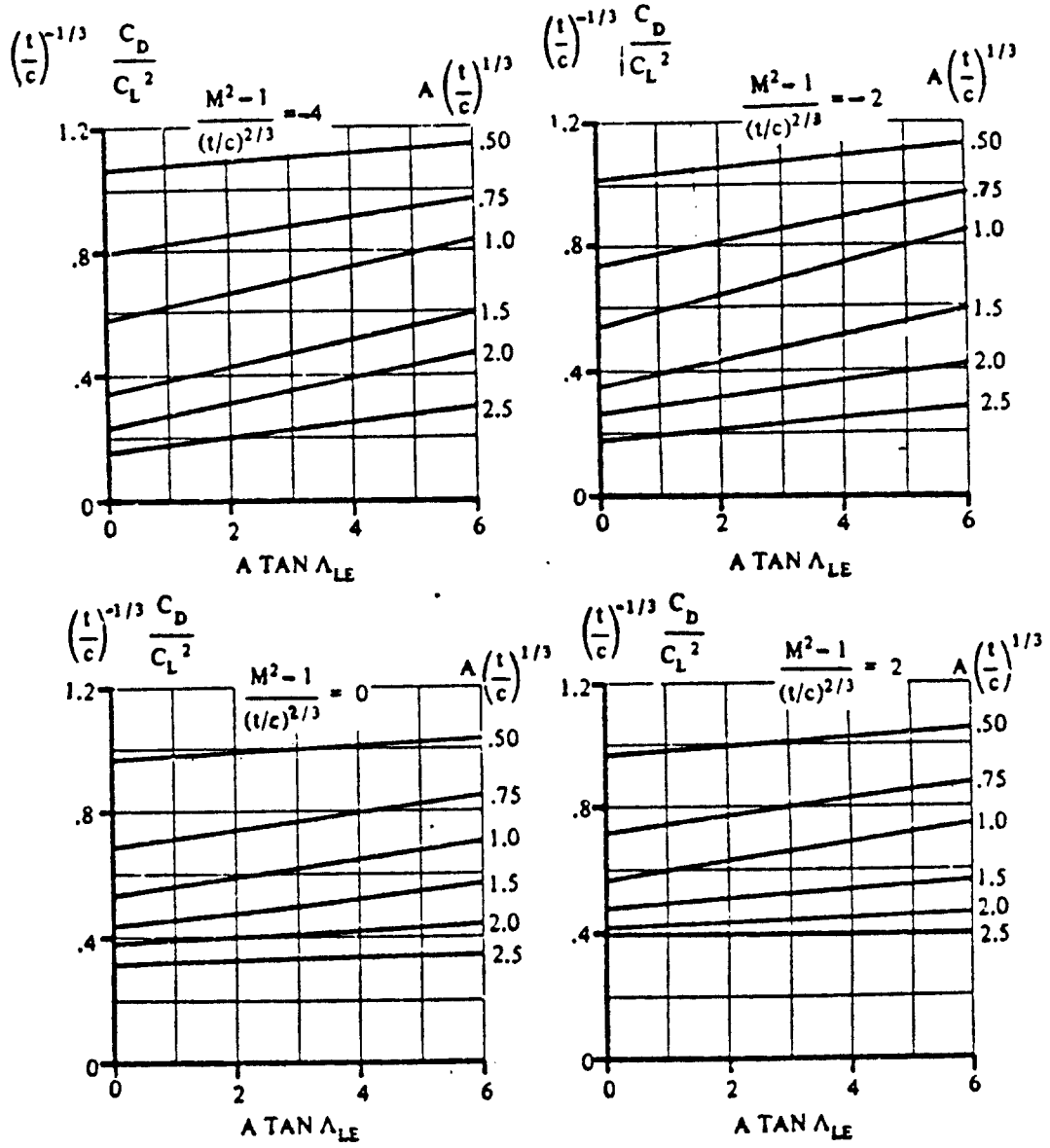

NOTE: $\lambda = 0.5$

Figure 4.13c Transonic Drag due to Lift

The value of the pressure drag coefficient, $C_{D_{LE}}$ follows from Figures 4.14.

Figure 4.15 defines the meaning of basic wing area, S_{bw} for several types of planform. The basic planform leading edge sweep angle, $\Lambda_{LE_{bw}}$ is also defined. Observe, that for a straight tapered wing: $S_{bw} = S$.

The term $(t/c)_{eff}$ in Eqns (4.22) and (4.23) is defined as follows:

$$(t/c)_{eff} = \{\int_0^{b/2} (t/c)^2 c_{bw} dy\}^{1/2} / (S_{bw}/2)^{1/2} \qquad (4.24)$$

4.2.3.2 Wing drag coefficient due to lift

The wing drag coefficient due to lift is found from:

$$C_{D_{L_w}} = (C_{D_L}/C_L^2) C_L^2 \qquad (4.25)$$

To compute the slope (C_{D_L}/C_L^2), proceed as follows:

1.) calculate two wing planform parameters:

planform shape parameter, $p = S/bc_r$

planform slenderness parameter, $b/2c_r$ (4.26)

Figure 4.15 illustrates the meaning of the quantities in Eqns (4.26) for some wing planforms.

2.) at the appropriate value of $\beta b/2c_r$, obtain the value of $\{(\pi A)(C_{D_L}/C_L^2)p/(p+1)\}$ from Fig.4.16. The symbol β is defined as:

$$\beta = (1 - M^2)^{1/2} \qquad (4.27)$$

3.) calculate the value of (C_{D_L}/C_L^2) from:

$$(C_{D_L}/C_L^2) = \{(\pi A)(C_{D_L}/C_L^2)p/(p+1)\}(1/\pi A)(1+p)/p \qquad (4.28)$$

COPIED FROM REF. 9

$$C_{D_{LE}}\left[\frac{S_{ref}}{2r_{LE_{bw}}\left(\frac{b_{bw}}{\cos\Lambda_{LE_{bw}}}\right)}\right] = 1.28\,\frac{M^3\cos^6\Lambda_{LE_{bw}}}{1+M^3\cos^3\Lambda_{LE_{bw}}}$$

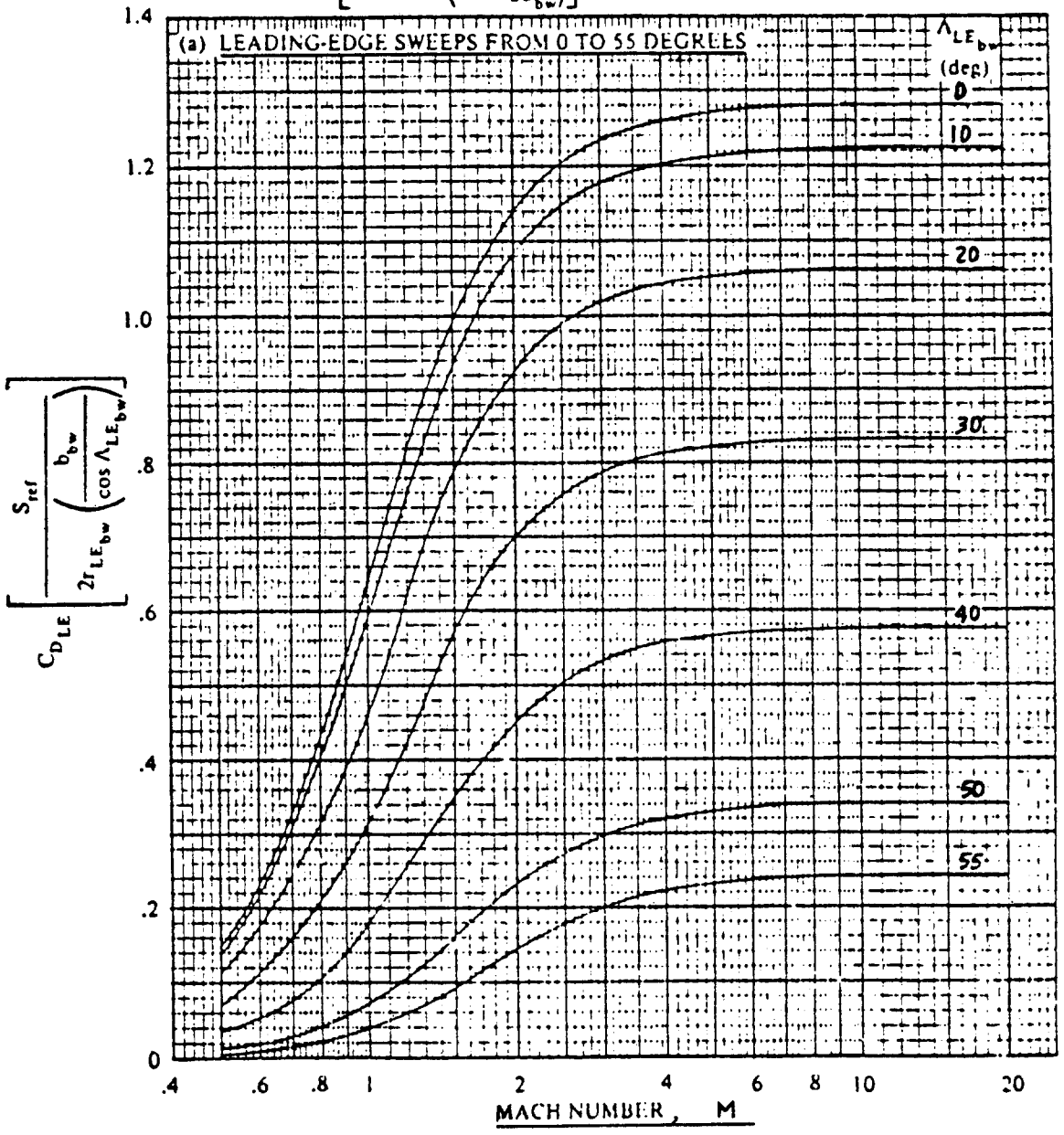

$r_{LE_{bw}}$ = BASIC WING L.E. RADIUS

Figure 4.14a Leading Edge Pressure Drag Coefficient

COPIED FROM REF. 9

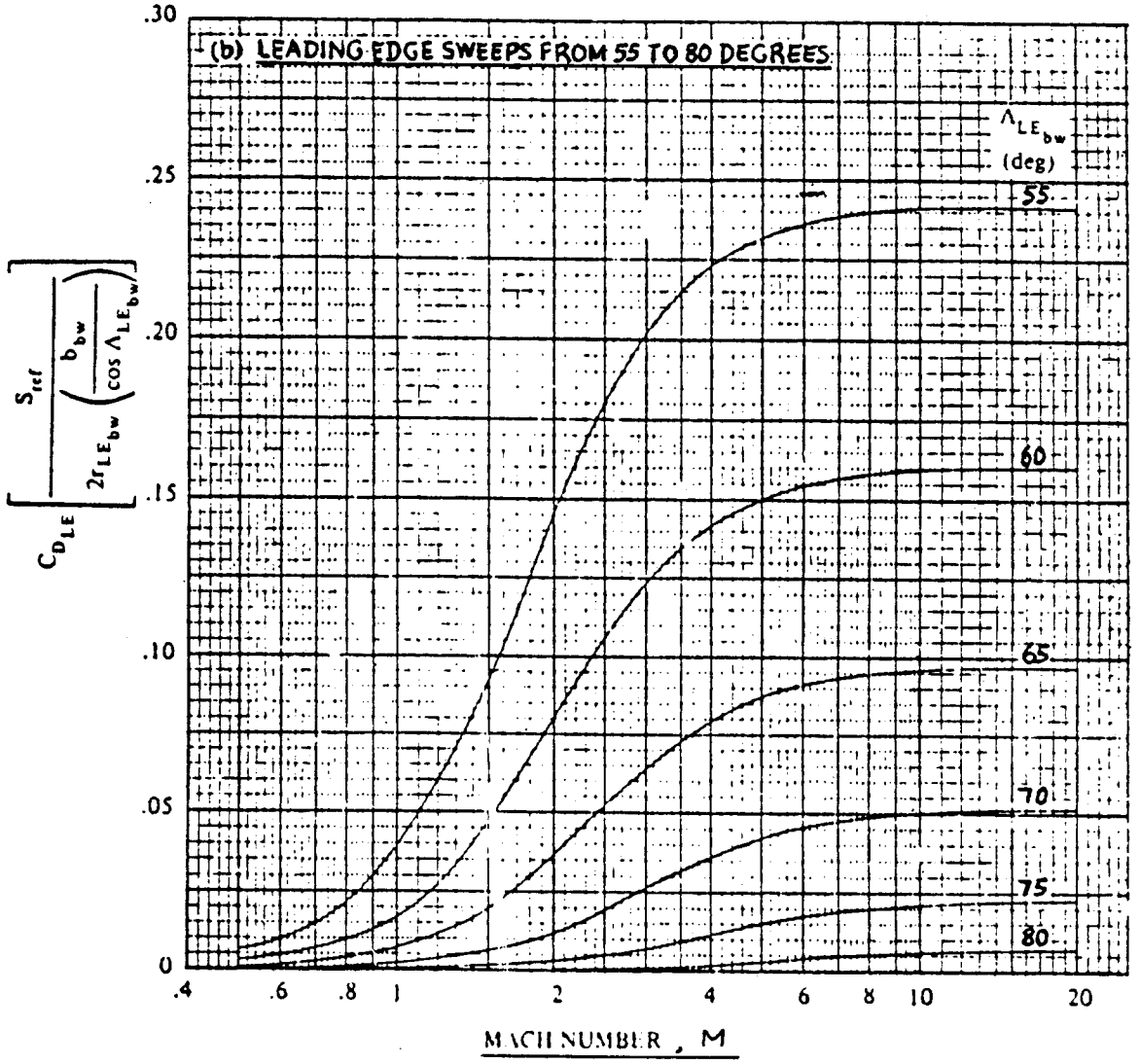

$r_{LE_{bw}}$ = BASIC WING L.E. RADIUS

Figure 4.14b Leading Edge Pressure Drag Coefficient

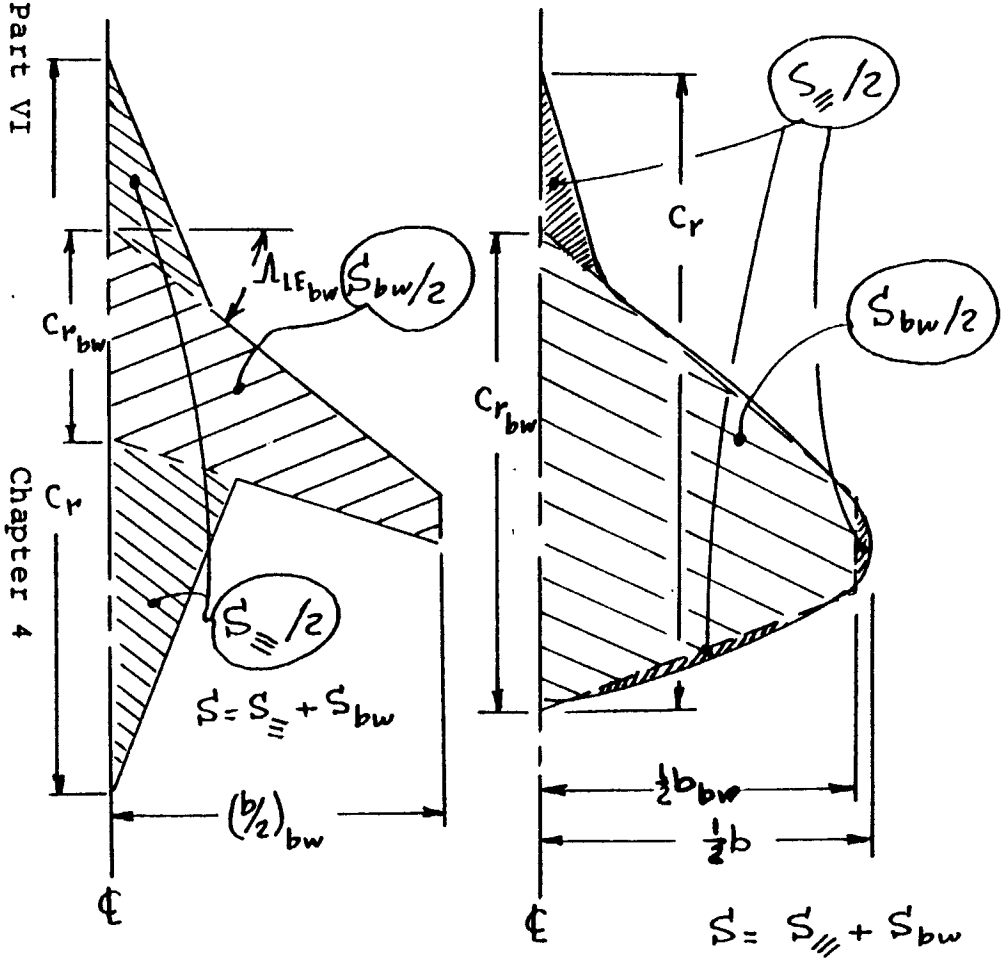

Figure 4.15 Basic Wing and Actual Wing Geometry

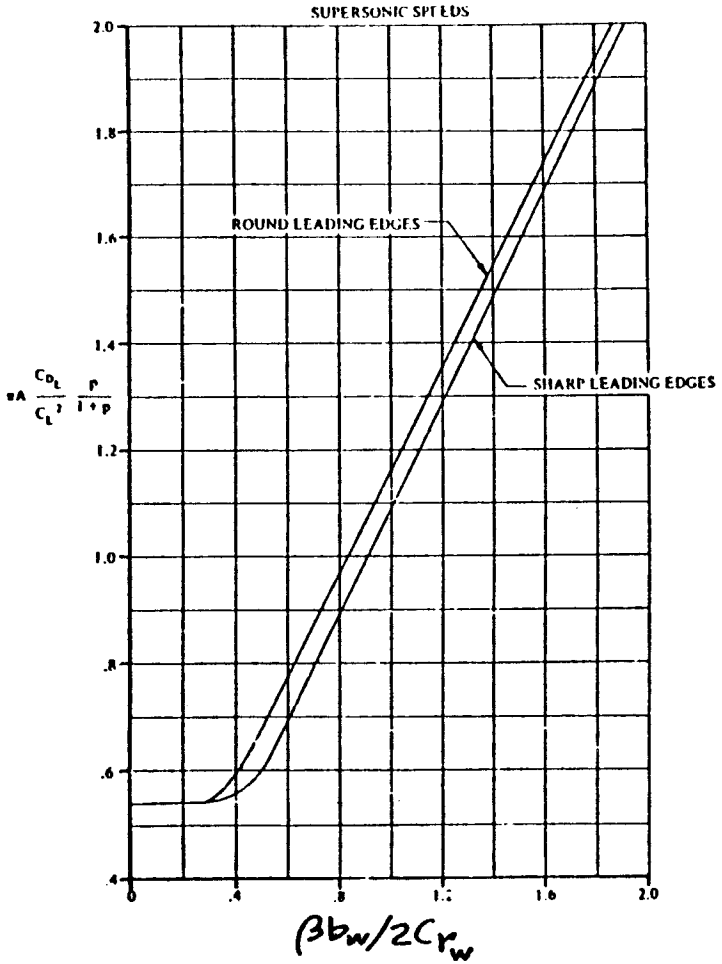

COPIED FROM REF. 9

Figure 4.16 Supersonic Drag due to Lift

4.3 FUSELAGE DRAG COEFFICIENT PREDICTION

4.3.1 Subsonic Fuselage Drag Coefficient

The subsonic fuselage drag coefficient is found from:

$$C_{D_{fus}} = C_{D_{o_{fus}}} + C_{D_{L_{fus}}} \qquad (4.29)$$

where: $C_{D_{o_{fus}}}$ = fuselage zero-lift drag coefficient, see 4.3.1.1.

$C_{D_{L_{fus}}}$ = fuselage drag coefficient due to lift, see 4.3.1.2.

4.3.1.1 Fuselage zero-lift drag coefficient

The subsonic fuselage zero-lift drag coefficient is found from:

$$C_{D_{o_{fus}}} = R_{wf} C_{f_{fus}} \{1 + 60/(l_f/d_f)^3 + 0.0025(l_f/d_f)\} S_{wet_{fus}}/S + C_{D_{b_{fus}}} \qquad (4.30)$$

where: R_{wf} = wing/fuselage interference factor, see Figure 4.1. Note: for a fuselage alone, use $R_{wf} = 1.0$.

$C_{f_{fus}}$ = turbulent flat plate skin-friction coefficient of the fuselage.

The general, turbulent, flat plate friction coefficient C_f is shown in Fig.4.3

as a function of Mach number and of Reynolds number, R_N.

For the fuselage, use:

$$R_{N_{fus}} = \rho U_1 l_f / \mu \qquad (4.31)$$

l_f = fuselage length as shown in Figure 4.17.

d_f = maximum fuselage diameter (equivalent diameter for fuselages with non-circular cross section, see Figure 4.17).

$S_{wet_{fus}}$ = wetted area of the fuselage. See Figure 4.17 and Appendix B.

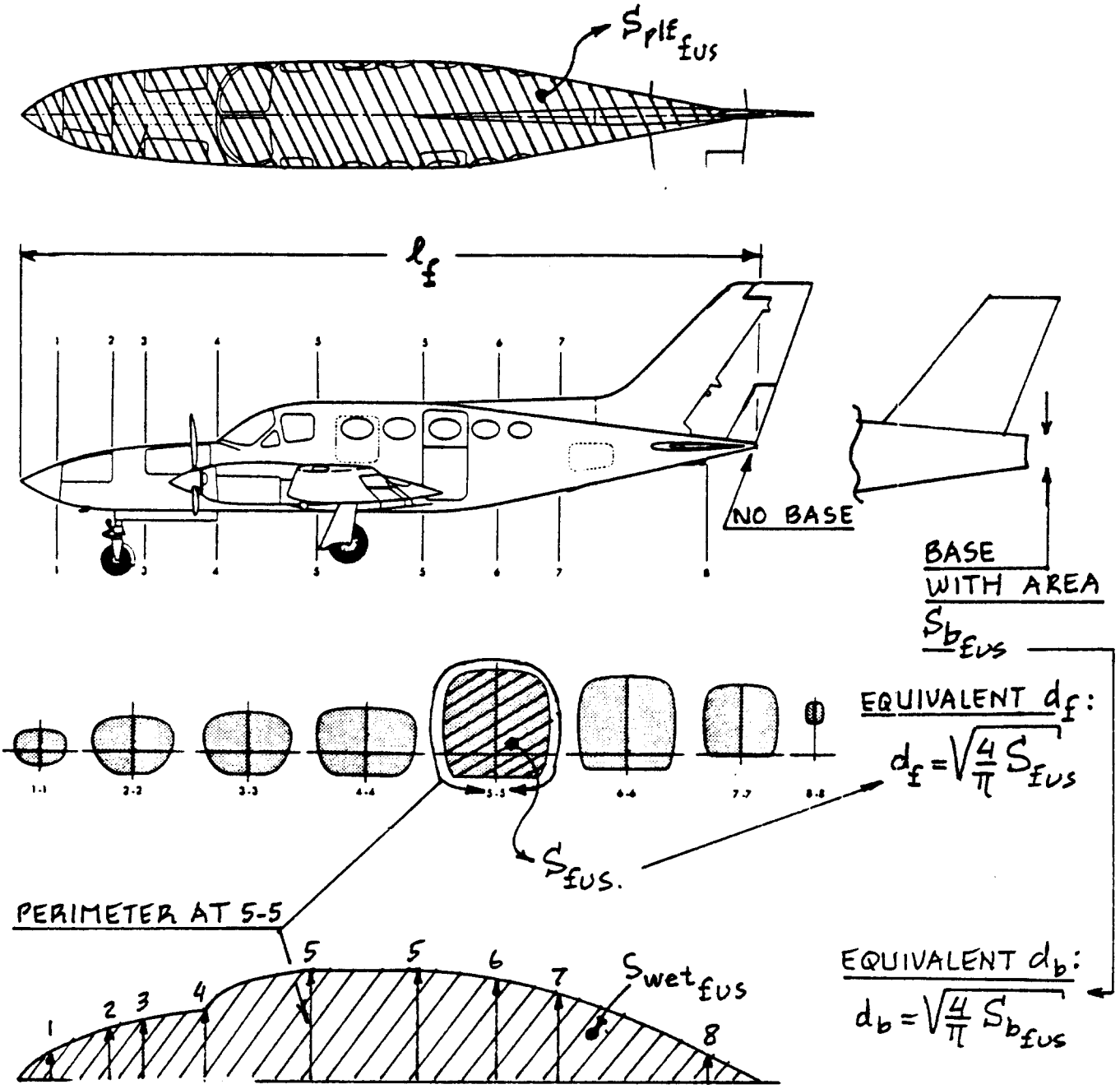

Figure 4.17 Definition of Fuselage Parameters

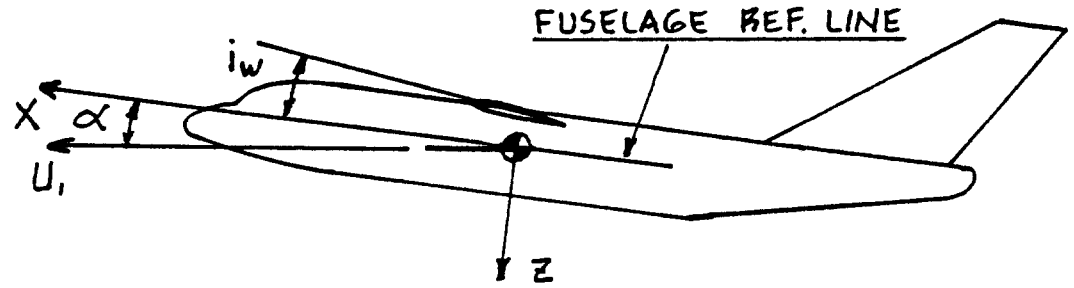

Figure 4.18 Defition of Fuselage Angle of Attack

$C_{D_{b_{fus}}}$ = fuselage base-drag coefficient, given by:

$$C_{D_{b_{fus}}} = [0.029(d_b/d_f)^3/\{C_{D_{o_{fus\text{-}base}}}(S/S_{fus})\}^{1/2}](S_{fus}/S) \quad (4.32)$$

where: d_b = fuselage base diameter, defined in Figure 4.17.

$C_{D_{o_{fus\text{-}base}}}$ = zero-lift drag coefficient of the fuselage exclusive of the base (see Figure 4.17) as determined from the first term on the right hand side in Eqn.(4.30).

S_{fus} = fuselage maximum frontal area as defined in Figure 4.17.

4.3.1.2 Fuselage drag coefficient due to lift

The fuselage drag coefficient due to lift is found from:

$$C_{D_{L_{fus}}} = 2\alpha^2 S_{b_{fus}}/S + \eta c_{d_c} \alpha^3 S_{plf_{fus}}/S \quad (4.33)$$

where: α is the fuselage angle of attack in radians, which is the same as the airplane angle of attack as seen in Figure 4.18.

The airplane angle of attack can be estimated as follows:

$$\alpha = \{(W/\bar{q}S) - C_{L_o}\}/C_{L_\alpha} \quad (4.34)$$

where: C_{L_o} = airplane zero-angle-of-attack lift coefficient, see Chapter 10.

C_{L_α} = airplane lift-curve slope, see Chapter 10.

$S_{b_{fus}}$ = fuselage base area defined in Fig.4.17.

η = ratio of the drag of a finite cylinder to the drag of an infinite cylinder, see Figure 4.19.

c_{d_c} = experimental steady state cross-flow drag coefficient of a circular cylinder, obtained from Figure 4.20.

$S_{plf_{fus}}$ = fuselage planform area, illustrated in Figure 4.17.

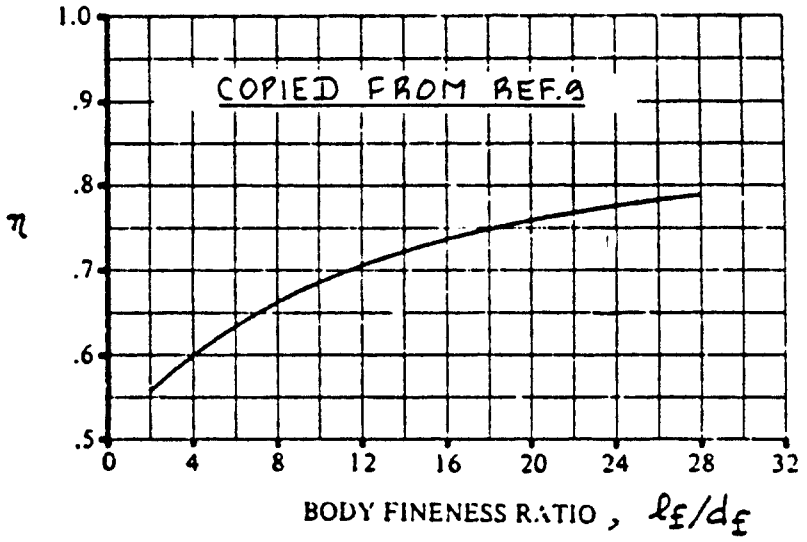

Figure 4.19 Ratio of the Drag Coefficient of a Circular Cylinder of Finite Length to that of a Cylinder of Infinite Length

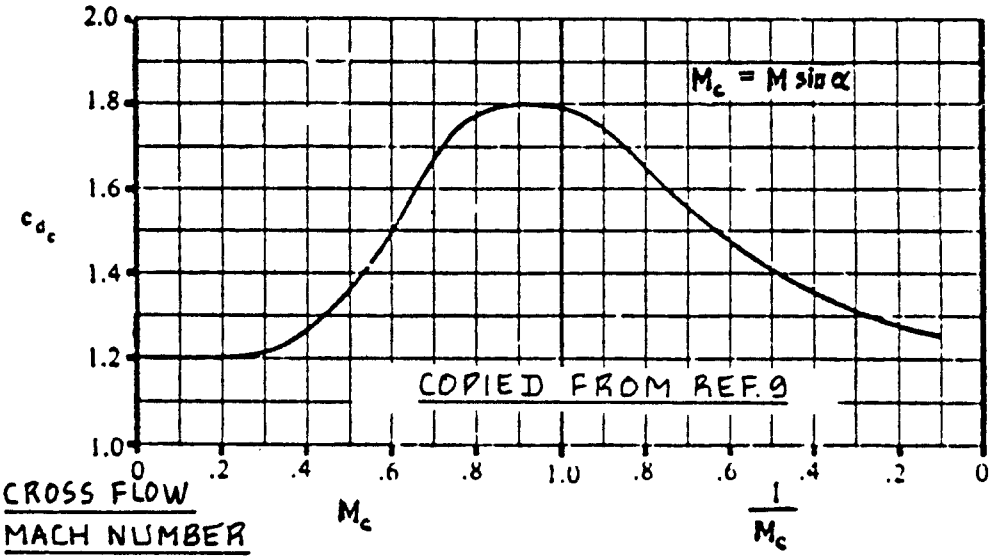

Figure 4.20 Steady State Cross-Flow Drag Coefficient for Two-Dimensional Circular Cylinders

4.3.2 Transonic Fuselage Drag Coefficient

The transonic fuselage drag coefficient is found from:

$$C_{D_{fus}} = C_{D_{o_{fus}}} + C_{D_{L_{fus}}} \quad (4.35)$$

where: $C_{D_{o_{fus}}}$ = fuselage zero-lift drag coefficient, see 4.3.2.1.

$C_{D_{L_{fus}}}$ = fuselage drag coefficient due to lift, see 4.3.2.2.

4.3.2.1 Fuselage zero-lift drag coefficient

The transonic fuselage zero-lift drag coefficient is found from:

$$C_{D_{o_{fus}}} = R_{wf}(C_{D_{f_{fus}}} + C_{D_{p_{fus}}}) + C_{D_{b_{fus}}} + (C_{D_{wave_{fus}}})S_{fus}/S \quad (4.36)$$

where: R_{wf} may be obtained from Figure 4.1 up to M=0.9.

For the remainder of the transonic speed range, R_{wf} = 1.0 should be used.

$C_{D_{f_{fus}}} = C_{f_{fus}}(S_{wet_{fus}})/S$, (4.37)
the fuselage skin-friction drag coefficient at M = 0.6 which is assumed to stay constant in the entire transonic range. The value of $C_{f_{fus}}$ follows from Fig.4.3.

$C_{D_{p_{fus}}} = (C_{f_{fus_{at\ M=0.6}}})\{60/(l_f/d_f)^3 + 0.0025(l_f/d_f)\}(S_{wet_{fus}})/S$, (4.38)
the fuselage pressure drag coefficient. This drag component is assumed to stay constant from M=0.6 to M=1.0 and then decrease linearly to zero at M=1.2.

$C_{D_{b_{fus}}}$ = the fuselage base drag coefficient as given by Eqn.(4.32) at M=0.6. From 0.6 > M < 1.2 this drag coefficient

may be determined by extrapolation, using the 'fairing lines' shown in Figure 4.21.

$C_{D_{wave_{fus}}}$ = the fuselage wave drag coefficient which follows from Figure 4.22.

Figure 4.23 illustrates how the transonic fuselage zero-lift drag coefficient is built up in this manner.

NOTE WELL: The wave drag component of zero lift drag can be much higher than predicted here if the cross sectional area distribution of the wing/fuselage combination is not 'smooth'. Sub-section 4.3.4 defines what is meant by 'smooth' cross sectional area distributions.

4.3.2.2 Fuselage drag coefficient due to lift

The transonic fuselage drag coefficient due to lift is found from:

$$C_{D_{b_{fus}}} = \alpha^2 (S_{base_{fus}})/S, \qquad (4.39)$$

with the angle of attack in radians.

4.3.3 Supersonic Fuselage Drag Coefficient

The supersonic fuselage drag coefficient is given as:

$$C_{D_{fus}} = C_{D_{o_{fus}}} + C_{D_{L_{fus}}} \qquad (4.40)$$

where: $C_{D_{o_{fus}}}$ = fuselage zero-lift drag coefficient, see 4.3.3.1.

$C_{D_{L_{fus}}}$ = fuselage drag coefficient due to lift, see 4.3.3.2.

4.3.3.1 Fuselage zero-lift drag coefficient

The supersonic fuselage zero-lift drag coefficient follows from:

$$C_{D_{o_{fus}}} = C_{f_{fus}} (S_{wet_{fus}})/S_{fus} + \{C_{D_{N_2}} + C_{D_A} + C_{D_{A(NC)}} + C_{D_{b_{fus}}}\}(S_{fus})/S \qquad (4.41)$$

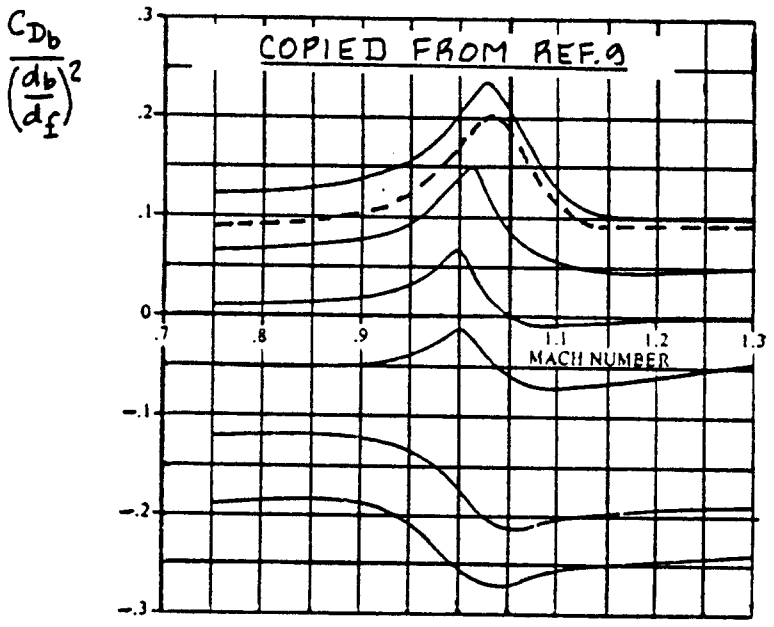

EXAMPLE:

ASSUME

$C_{D_b}/(d_b/d_f)^2 = .09$

THE PROPER FAIRING LINE TO BE USED IS ____

Figure 4.21 Transonic Fairing for Fuselage Base Drag Coefficient

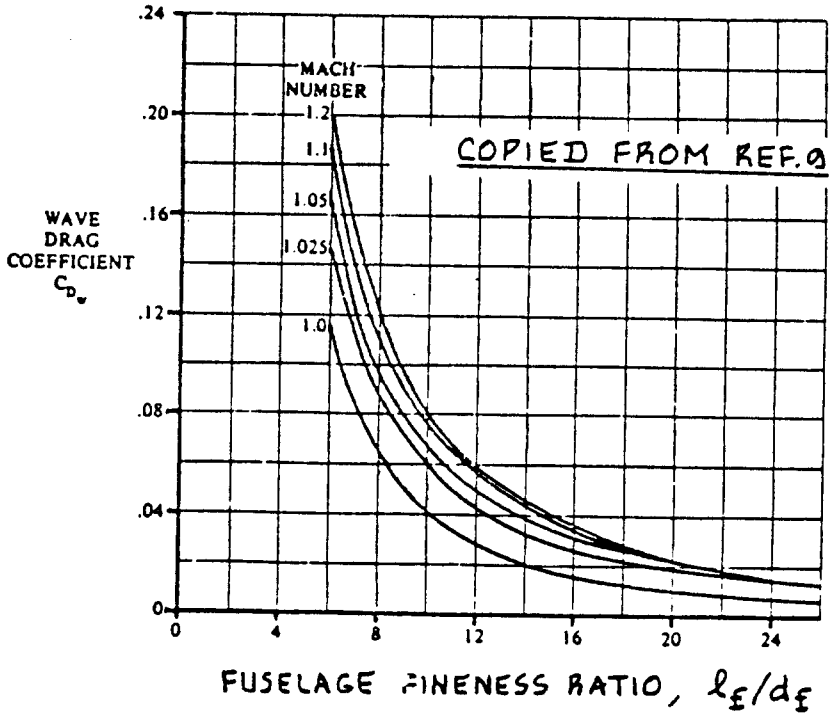

Figure 4.22 Wave Drag Coefficient for Parabolic Fuselages

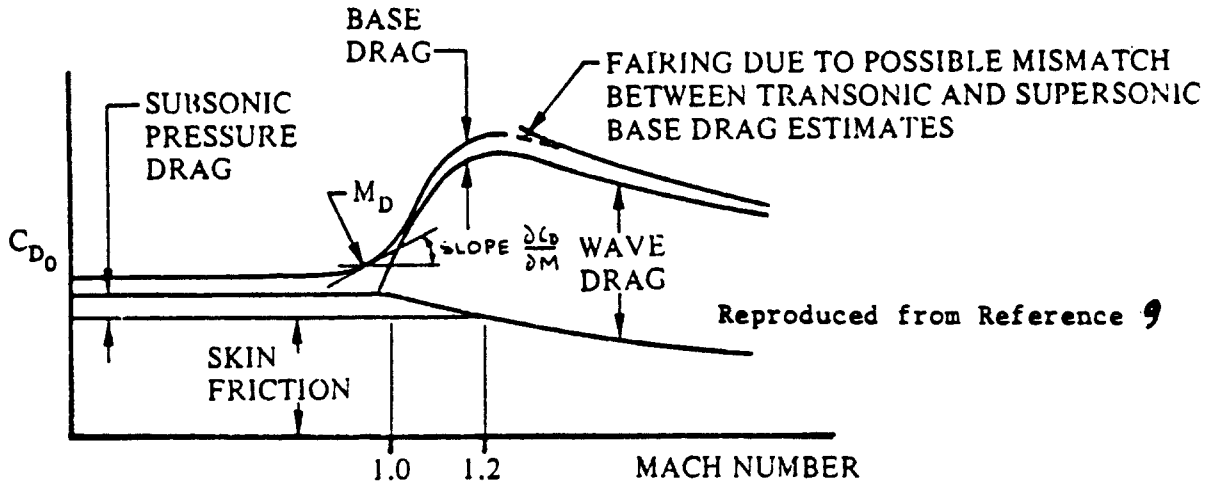

Figure 4.23 Build-up of Transonic Fuselage Drag

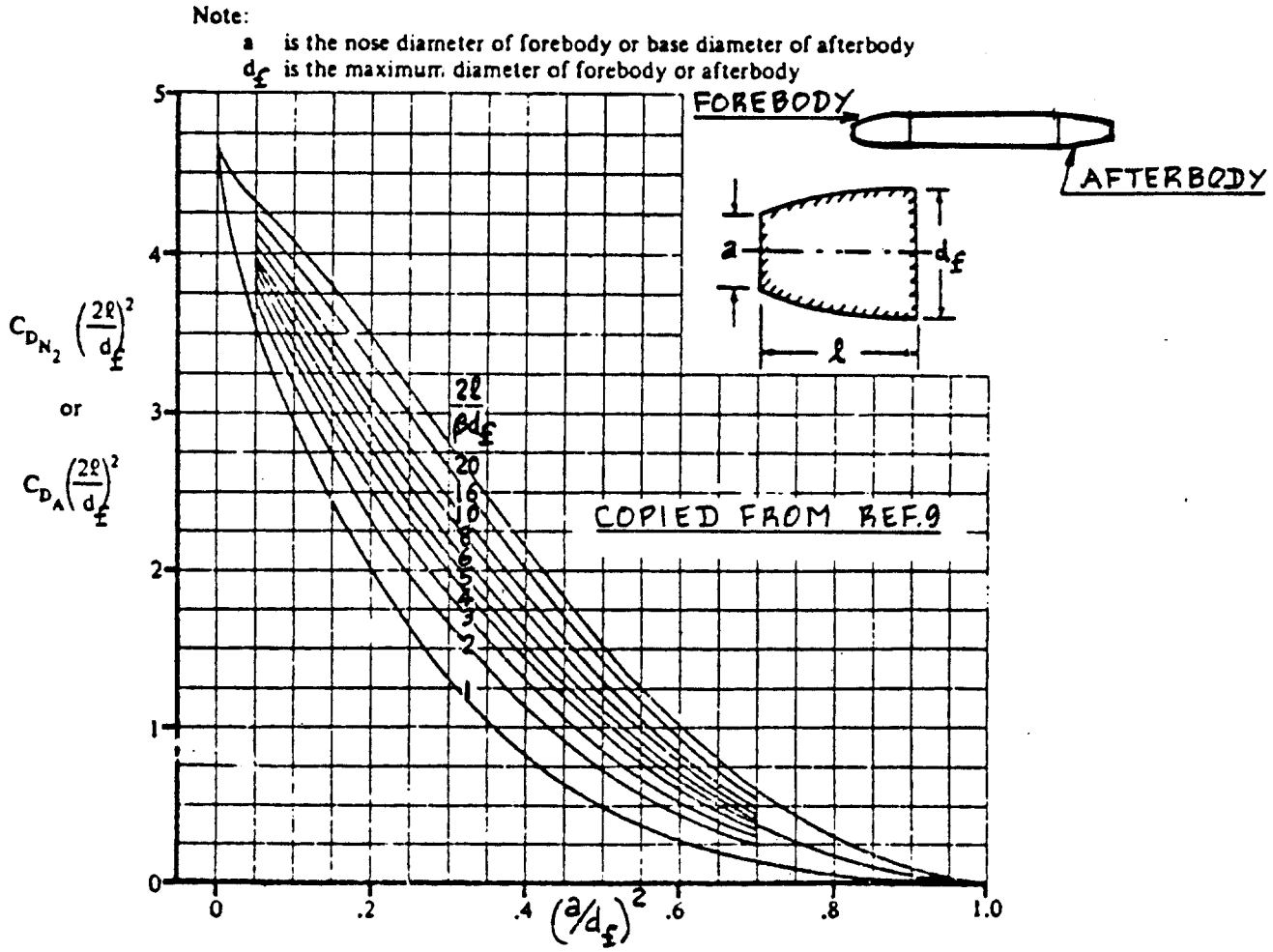

Figure 4.24 Drag of Slender Forebodies or Afterbodies of Parabolic Profile

where: $C_{f_{fus}}$ = turbulent flat plate skin-friction coefficient of the fuselage, determined as described under Eqn. (4.30).

$C_{D_{N_2}}$ and C_{D_A} are the wave drag coefficients of the fuselage nose and afterbody respectively.

These wave drag coefficients may be determined from Figures 4.24 and 4.25 respectively. If the fuselage does not have a circular cross section, the respective equivalent diameters should be used when using Figures 4.24 and 4.25.

NOTE WELL: The wave drag components of zero lift drag can be much higher than predicted here if the cross sectional area distribution of the wing/fuselage combination is not 'smooth'. Sub-section 4.3.4 defines what is meant by 'smooth' cross sectional area distributions.

$C_{D_{A(NC)}}$ = interference drag coefficient acting on the aft-fuselage due to the center-fuselage. This coefficient may be found in Figures 4.26 or 4.27.

$C_{D_{b_{fus}}}$ = fuselage base drag coefficient. For fuselages with an approximate circular cross section this coefficient may be read from Figure 4.28, provided the fuselage has no appreciable base area.

Note: if the fuselage has an appreciable base area (and this almost always is the case in fighter airplanes), the value for the fuselage base drag coefficient may be obtained from:

$$C_{D_b} = -C_{p_b}(d_b/d_f)^2 \qquad (4.42)$$

where the base pressure coefficient, C_{p_b} follows from Figures 4.29.

4.3.3.2 Fuselage drag coefficient due to lift

The supersonic fuselage drag coefficient due to lift depends strongly on the fuselage cross section:

$$C_{D_{L_{fus}}} = F\{(2\alpha^2)S_{b_{fus}}/S + c_{d_c}(S_{plf_{fus}}/S)\alpha^3\} \qquad (4.43)$$

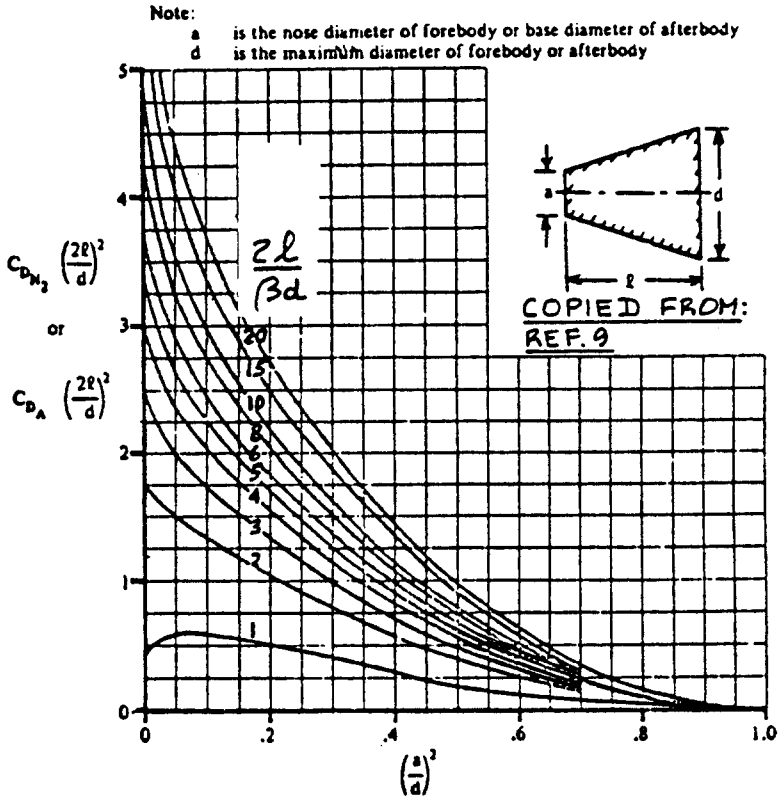

Figure 4.25 Drag of Slender, Conical Forebodies and Afterbodies

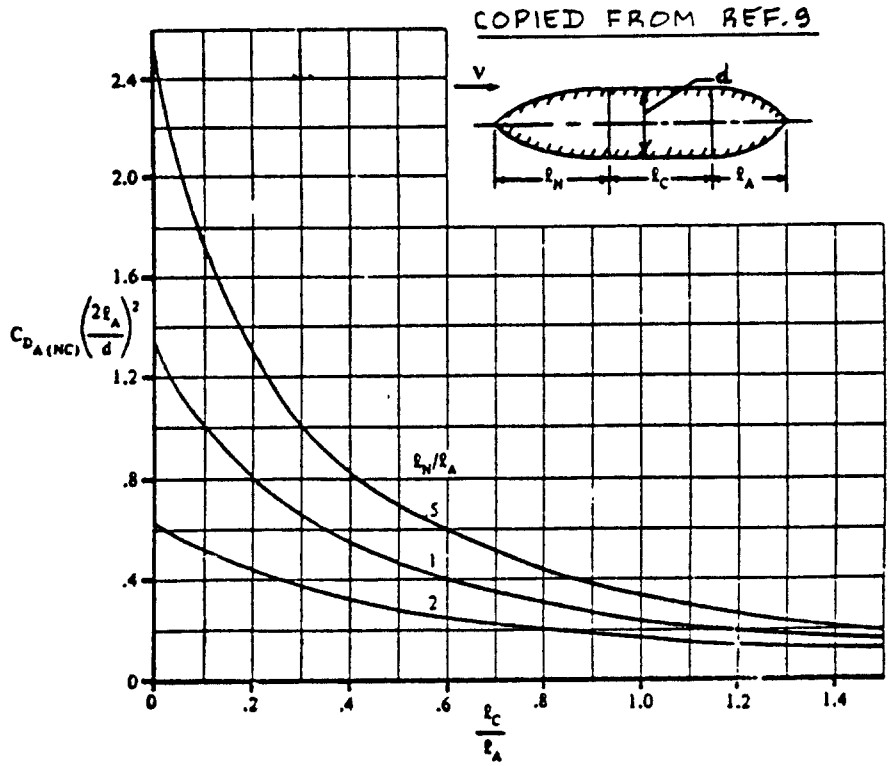

Figure 4.26 Interference Drag for Parabolic Bodies

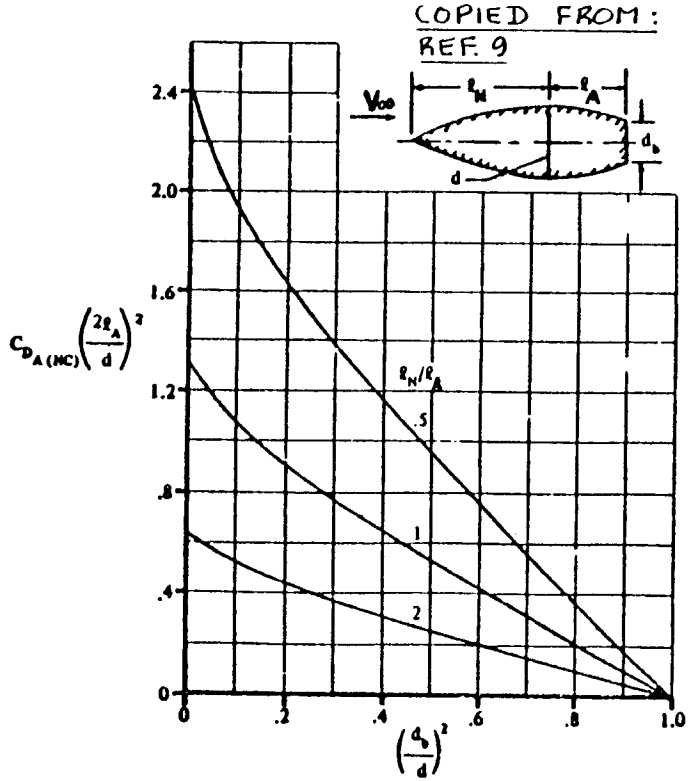

Figure 4.27 Interference Drag of Truncated Afterbodies Behind Parabolic Forebody with no Constant Centersection

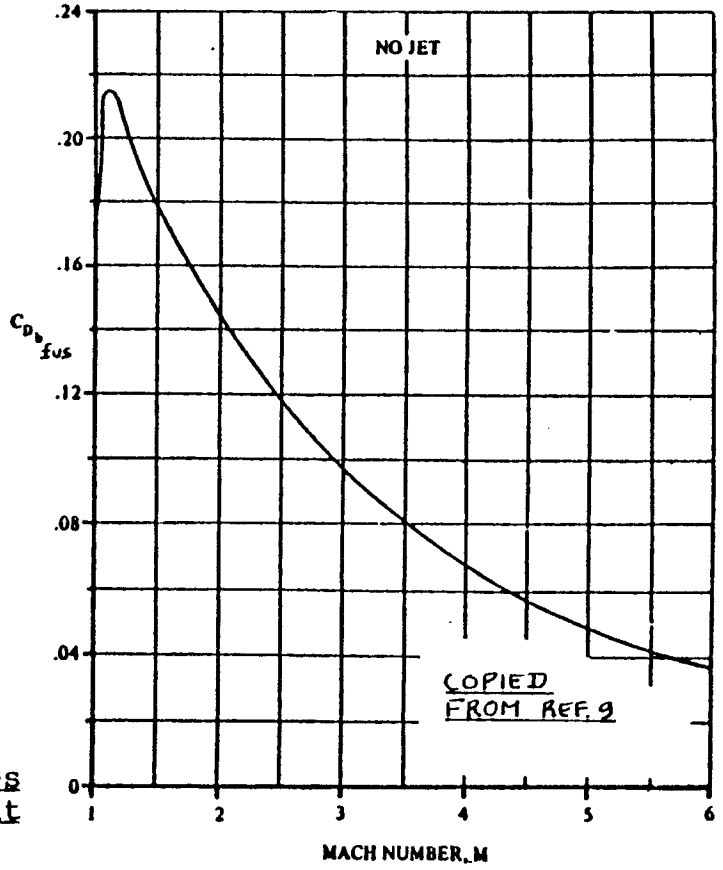

Figure 4.28 Base Drag Coefficient for Bodies of Revolution with no Boattail

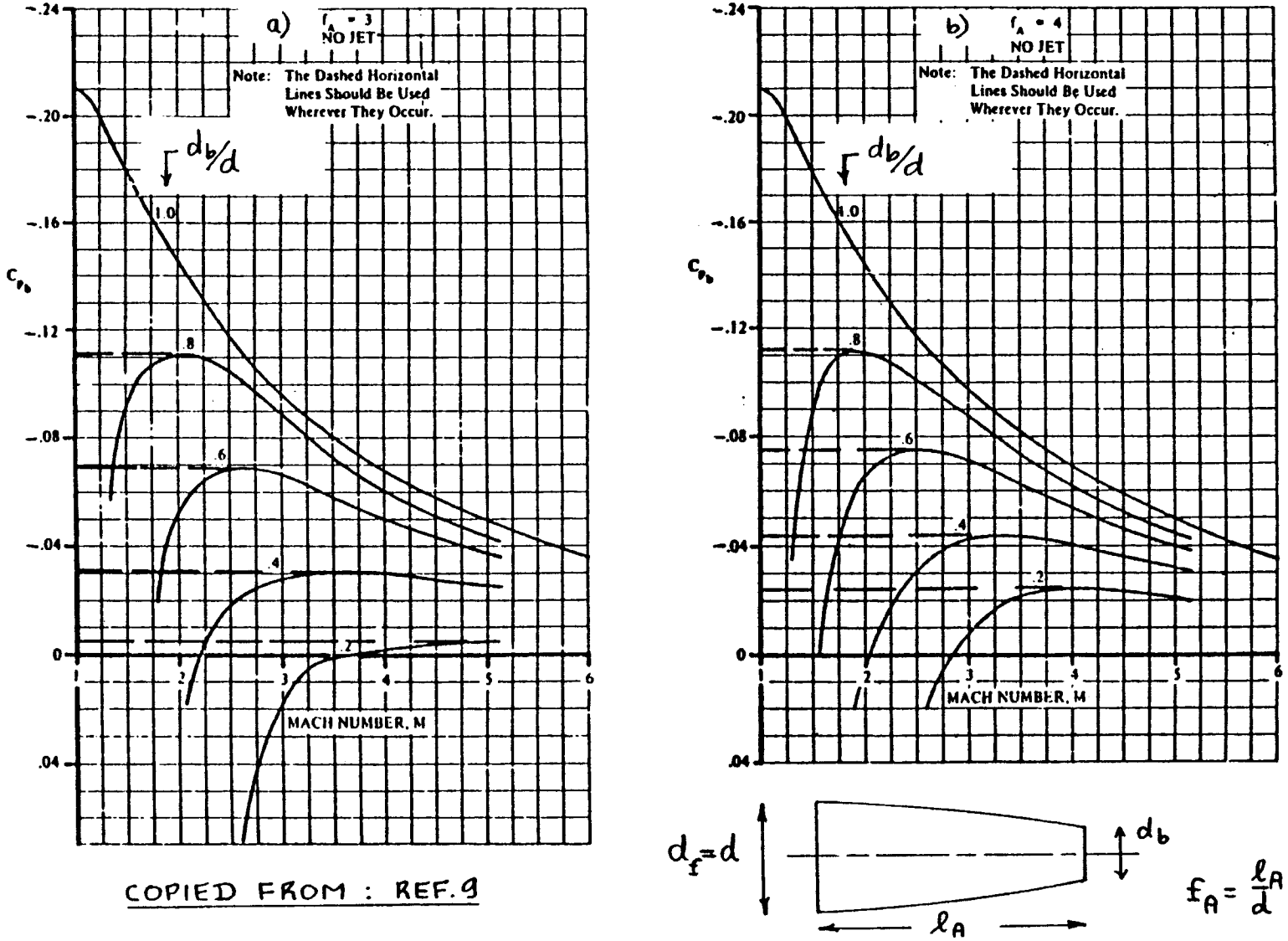

COPIED FROM : REF. 9

Figure 4.29 Base Pressure Coefficient for Boattails of Approximate Conical Shape

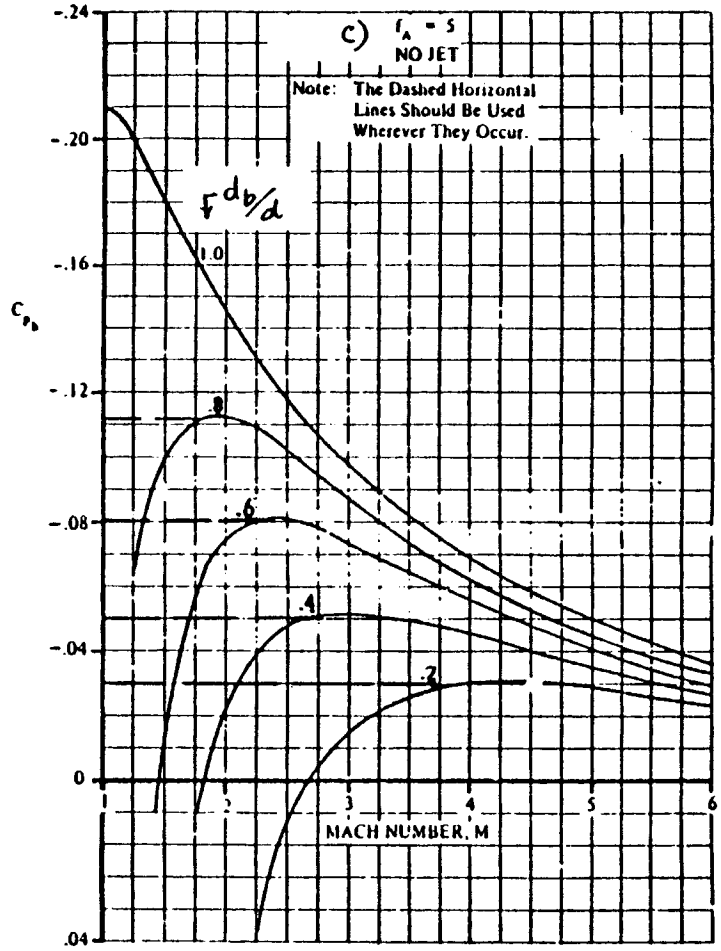

COPIED FROM: REF. 9

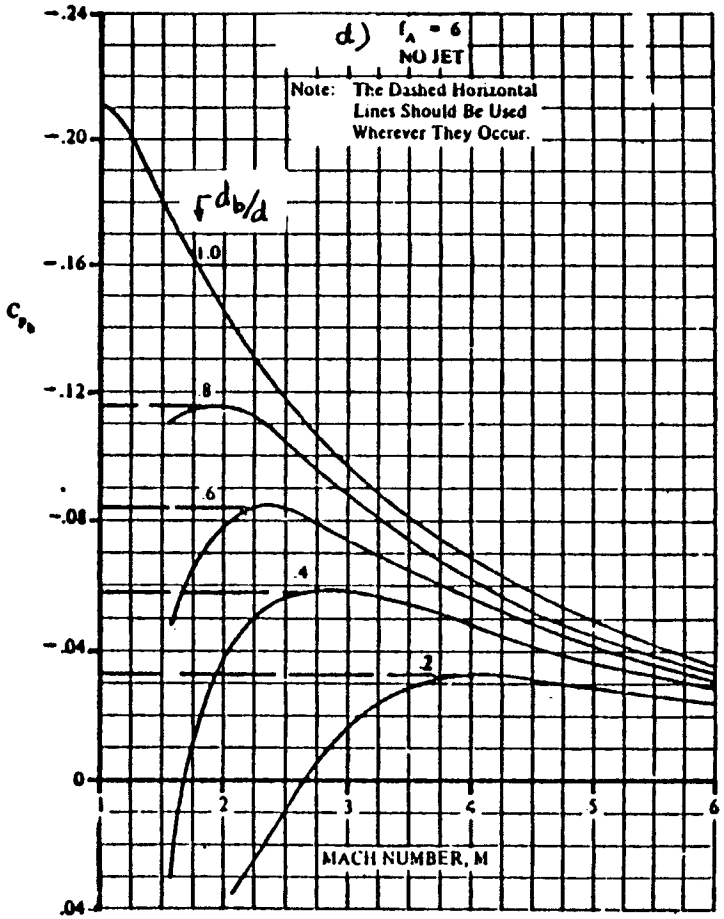

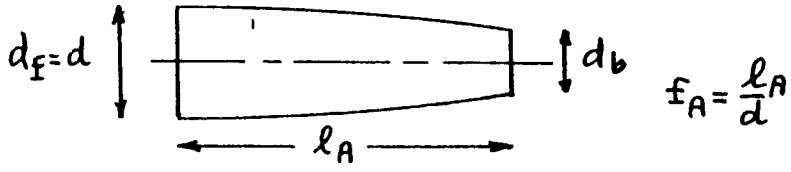

Figure 4.29 Base pressure Coefficient for Boattails of Approximate Conical Shape

For a fuselage with circular cross section: F = 1.0

For a fuselage with elliptical cross section:

$$F = \{(a/b)(\cos\omega)^2 + (b/a)(\sin\omega)^2\} \qquad (4.44)$$

where: a is the major axis of the elliptical cross section.

b is the minor axis of the elliptical cross section.

ω = 0 with the major axis horizontal.
ω = 90 deg. with the minor axis horizontal.

Values for c_{d_c} are found in Figure 4.20.

4.3.4 The Area Rule Concept

The methods for predicting wave drag in Sub-sections 4.3.2 and 4.3.3 are valid only if the wing/fuselage/empennage combination has a 'smooth' cross sectional area distribution. Figure 4.30 illustrates how a cross sectional area distribution of an airplane is obtained.

Whitcomb showed in Reference 17 that the wave drag of an airplane in the transonic speed range is roughly equal to the wave drag of its 'equivalent body of revolution. Figure 4.30 also shows the equivalent body of revolution for the same airplane. Note the irregularities in the equivalent body of revolution.

Minimum wave drag can be achieved by designing the wing/fuselage/empennage cross sectional area distribution in such a way that its equivalent body of revolution approximates the so-called Sears-Haack bodies. This design concept (due to Whitcomb) is referred to as area ruling.

Three types of Sears-Haack bodies are depicted in Figure 4.31:

Type I: used to minimize wave drag for a given length and volume.

Type II: used to minimize wave drag for a given length and diameter.

Type III: used to minimize wave drag for a given diameter and volume.

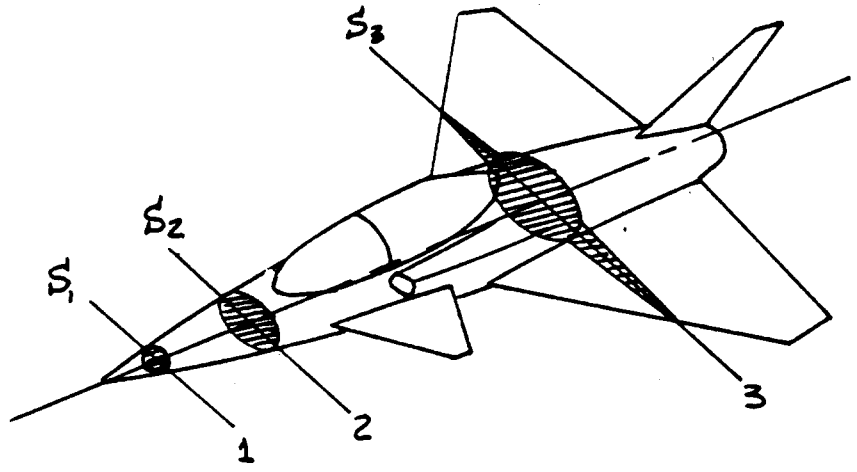

CONSTRUCT 'EQUIVALENT' BODY OF REVOLUTION SO THAT $S_{i\,AIRPLANE} = S_{i\,EQ.}$

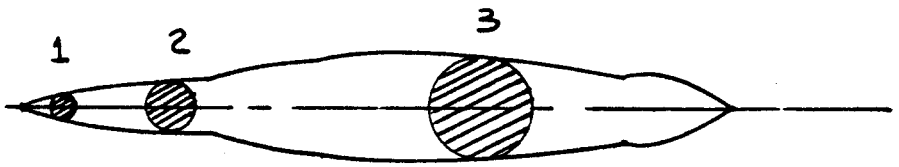

Figure 4.30 Development of a Cross Sectional Area Distribution and its Equivalent Body of Revolution

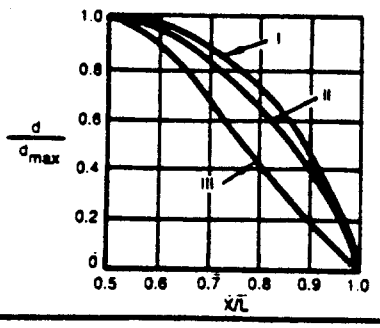

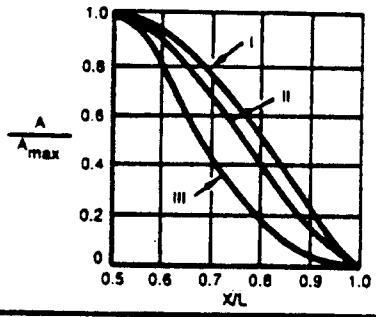

COPIED FROM: REF. 18. COURTESY: B. NELSON, NORTHROP

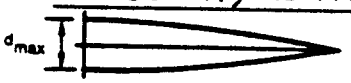

MINIMUM PRESSURE DRAG			VOL = $C_{p_n} \times A_{max} \times L$
TYPE I	$C_D = \frac{9}{8}\pi^2\left(\frac{d}{L}\right)^2$	GIVEN LENGTH & VOL	$C_{P_I} = 0.59$
TYPE II	$C_D = \pi^2\left(\frac{d}{L}\right)^2$	LENGTH & DIA	$C_{P_{II}} = 0.519$
TYPE III	$C_D = 3/2\,\pi^2\left(\frac{d}{L}\right)^2$	DIA & VOL	$C_{P_{III}} = 0.392$

Figure 4.31 Sears Haack Bodies and Drag Coefficients

The wave drag coefficients and volumes for the three Sears-Haack bodies are also given in Figure 4.31.

Note: these wave drag coefficients apply to supersonic Mach numbers only! To a first order of approximation these supersonic wave drag coefficients are independent of Mach number.

It is clear that to minimize wave drag it is essential to distribute any given volume over as much length as possible. However, in airplane layout design several constraints are encountered. Typical constraints are:

a) the airplane may not exceed a given length: this constraint is nearly always encountered in carrier based airplanes. Supersonic transports may encounter length limitations for reasons of ground maneuvering, gate space restrictions and hangar size limits.

b) the airplane must have a minimum total volume: this constraint comes about because of the need to carry fuel, payload, fixed equipment, landing gear and engines. Even airplane structures need a minimum amount of volume.

c) the airplane must have a minimum outside diameter: this constraint arises because of the need for cabin volume, engine size and/or payload size.

Because of these constraints on length, volume and diameter it may be necessary to strike a compromise in the layout design of transonic and supersonic airplanes.

From the previous discussion it is obvious that early knowledge of volume requirements inside the airplane is essential. The airplane layout design procedures of Chapters 4-9 in Part II must be augmented with the following step-by-step procedure:

Step 1: Tabulate preliminary volume requirements as indicated in Table 4.1.

Tables 4.2 give data for the volumetric requirements of the elements listed in Table 4.1. It is essential that the 'critical' (= minimum required) length for all elements is identified. The reader should use judgement in deciding where element critical lengths may overlap.

Step 2: Prepare a preliminary airplane layout which includes all elements listed in Step 1. Do not forget to cross-check with the design layout procedures of Chapters 4-9 of Pt.II.

Table 4.1 Critical Volume and Length Requirements

Airplane Element	Critical Volume (ft^3)	Critical Length (ft)
Forebody: radome, avionics, cockpit, nose gear		
Mid section: gun or weapons bay, main gear, avionics, control runs, body fuel, fixed equipment, wing sweep mechanism, inlets		
Aft body: engine bay(s), tail-pipes, nozzles, afterburners, body fuel, empennage carry-through		
Wing: total wing volume outside the body.		
Refuelling system: if required, this normally resides in the forward part of the fuselage.		
Empennage: total empennage volume outside the body.		
Streamtube: that volume taken up by the inlet, engines, tail-pipes, afterburners and nozzles.		
Inlet stream tube: that volume taken up by the inlet up to the engine compressor faces.		

Note: This table can be completed only after a preliminary layout of the airplane has been prepared. Chapters 4-9 in Part II provide step-by-step procedures for preparing such a layout. Tables 4.2a and 4.2b should be consulted for preliminary data on volumetric requirements of airplane elements.

Table 4.2a Critical Volume, Cross Section and Length Data

Notes: 1. Data given are minimum data for fighters. For transports the volume needs follow from layout design results of Chapters 4-9 in Part II.
2. All data refer to 'installed' volumes, not to actual volumes. Data based on Reference 18.

Element		Volume (ft^3)	Cross Section (ft^2)	Length (ft)
Radome:		$0.22(d_{rad} + 0.33)^4$	$(\pi/4)(d_{rad})^2$	
Cockpit:	today	70.0	14.0 upright	
	future	50.0	11.0 upright	
			7.0 semi-supine	
Nose gear:		15.0	3.0 (fighters only!)	
Weapons:	see Part IV, Chapter 3 for dimensioned data on weapons and stores. Some statistical data are:			
conformal carriage:		1.5 ft^3/1,000 lbs		3.0
internal bay:				
	tube launch:	20 ft^3/1,000 lbs		weapon
	ejector launch:	33 ft^3/1,000 lbs		weapon
Guns:	Mk61 20 mm	14.0		gun + 2
	Oerlikon 30 mm	4.8		gun + 2
Ammunition:	20 mm	0.013 ft^3/round		
	30 mm	0.052 ft^3/round		

Main Gear: $\{9 + 10^{-6}(2.56CBR - 4.86)W_{TO}(1.924CBR)^{-0.158}$

For CBR (California Bearing Ratio) definitions and its relation to airfield type, see Ref.19.

For fighters: CBR = 3.0 - 5.0 For transports: CBR = 12

Arresting gear: 4.0

Hydr./pneum. systems: $0.00046W_{TO}$

Electrical systems: 4.0 (for fighters only)

Armor: 1.0

Environmental system: 15.0 (for fighters only)

Table 4.2b Critical Volume, Cross Section and Length Data

Element	Volume (ft^3)	Cross Section (ft^2)	Length (ft)
Oxygen system:	6.0 per crew member for fighters		
Auxiliary gear:	$0.00005W_{TO}$		
Control runs:		1.0 ft^2 between the cockpit and empennage	
Fuselage structure:	$0.13(l_f/d_f)S_{wet_{fus}}$		

Wing: volume outside the body, computed from the wing layout drawing of Step 6.13 in Part II.

Wing sweep mechanism: $0.4(c_p)^2(t/c)_{max}w_f$, c_p= chord at pivot

Body fuel: use a volumetric efficiency of 85 percent for fuselage tanks.

Refuelling system: 2 ft^3, normally in the forebody

Empennage: volume outside the body, computed from the empennage layout drawing of Step 8.7, Part II.

Streamtube: that volume taken up by inlets, engines, tailpipes, afterburners and nozzles.

Wasted volume: it is not possible to package a fuselage without wasted volume. Many system components require accessibility: this adds volume. The following equation is suggested for computing wasted volume:

$$V_{waste} = 0.212\{3(Vol._{fus}/l_f) + 2.7(Vol_{fus}l_f)^{1/2}\}$$

where: Vol_{fus} = sum of all previous volume requirements.

l_f is the overall fuselage length

Total volume: = $Vol_{fus} + V_{waste}$.

Inlet stream tube: that volume taken up by the inlet up to the engine compressor faces. This volume is subtracted from the total volume in arriving at the net cross-sectional area distribution.

Step 3: Translate the preliminary airplane layout into a cross sectional area plot as shown in Figure 4.32. Make certain that all volumetric and critical length requirements of Step 1 are satisfied.

Step 4: Decide which of the Sears-Haack bodies of Figure 4.31 best fit the cross sectional area plot of Step 3. Overlay the selected Sears-Haack cross sectional area plots.

Step 5: Adjust the fuselage geometry until the airplane cross sectional area plot MINUS its inlet capture area conforms to the selected Sears-Haack shapes.

Figure 4.33 shows an example of a cross sectional area distribution of a fighter airplane. Figure 4.34 shows several critical cross sections.

Note that the 'bump' in the area distribution due to the canopy are eliminated by indenting the local fuselage cross section. The Dassault Rafale is an example of a fighter airplane where this has also been done.

Note that the 'bump' in the area distribution due to the wing has been eliminated also by indenting the local fuselage cross section. The result is a 'coke-bottle' shape. Further examples of this coke-bottling are shown in Figures 3.54 - 3.56 in Part II.

Airplanes which fly at high subsonic Mach numbers may require so-called 'local' area ruling. Examples of 'local' area ruling are found in the Boeing 737-300 wing/nacelle region, in the Northrop F-5 wing/tiptank region and in the DC-10 center-engine/vertical tail region.

In using 'local' area ruling, only local cross sectional area distributions are constructed. When these local cross sectional area distributions are 'smooth', no major problems in dragrise at high subsonic Mach numbers should be expected.

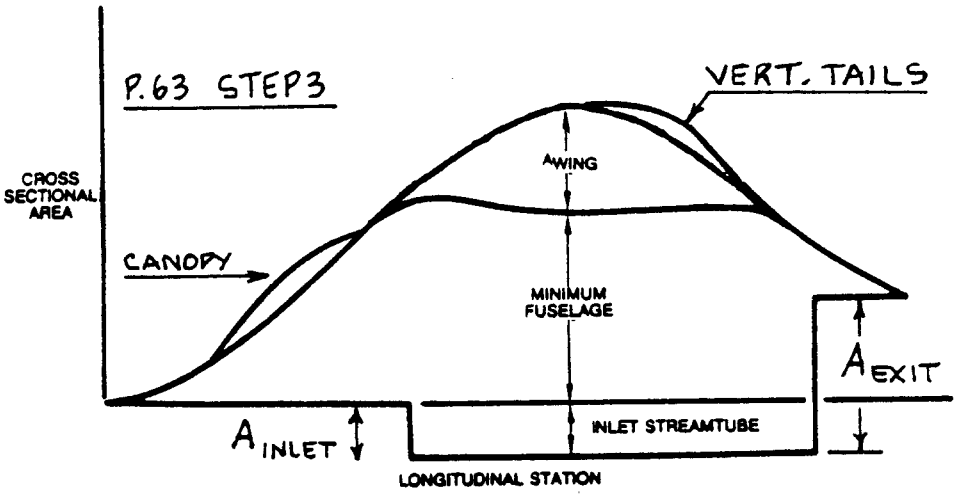

COPIED FROM REF. 18
COURTESY: B. NELSON
(NORTHROP)

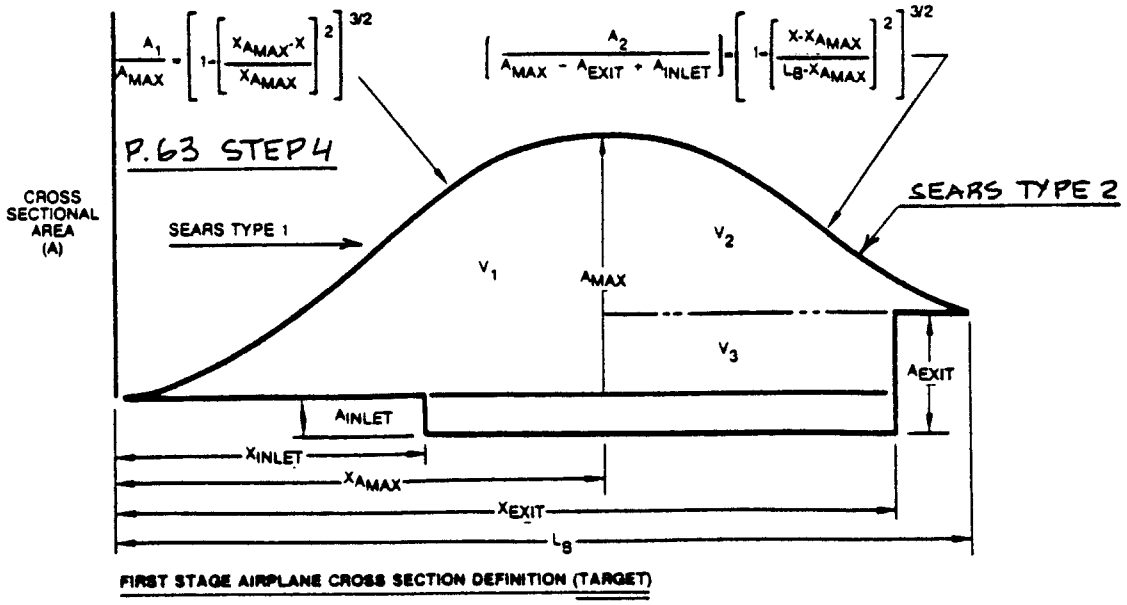

FIRST STAGE AIRPLANE CROSS SECTION DEFINITION (TARGET)

Figure 4.32 Development of a Cross Sectional Area Distribution from Volumetric Requirements

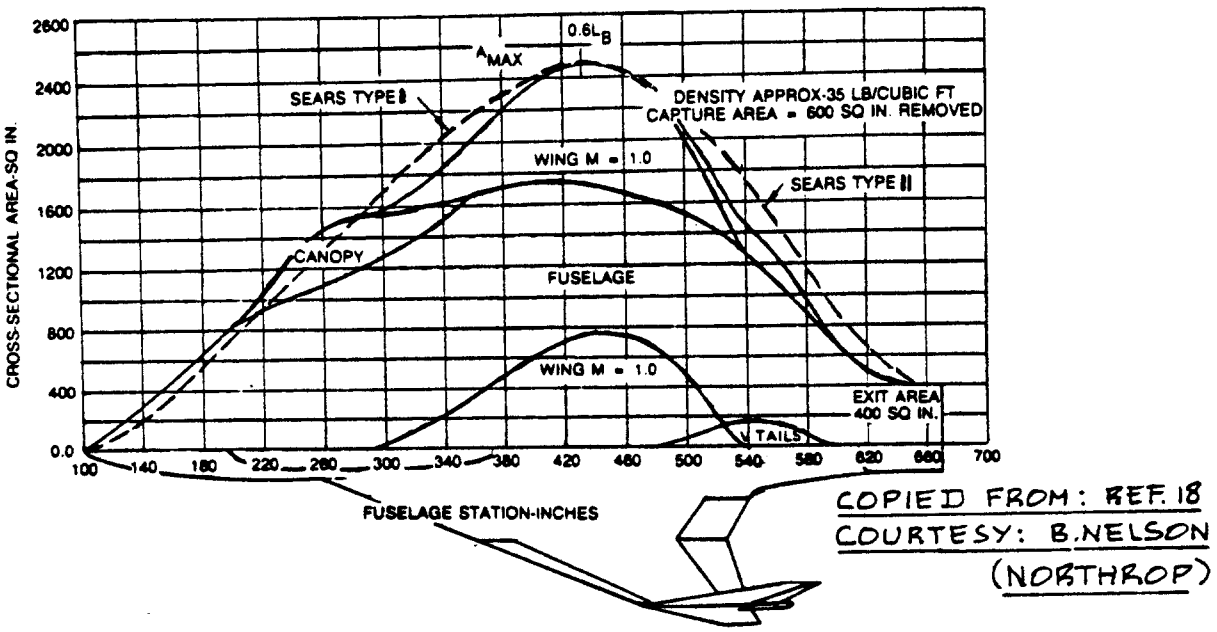

Figure 4.33 Example Cross Sectional Area Distribution

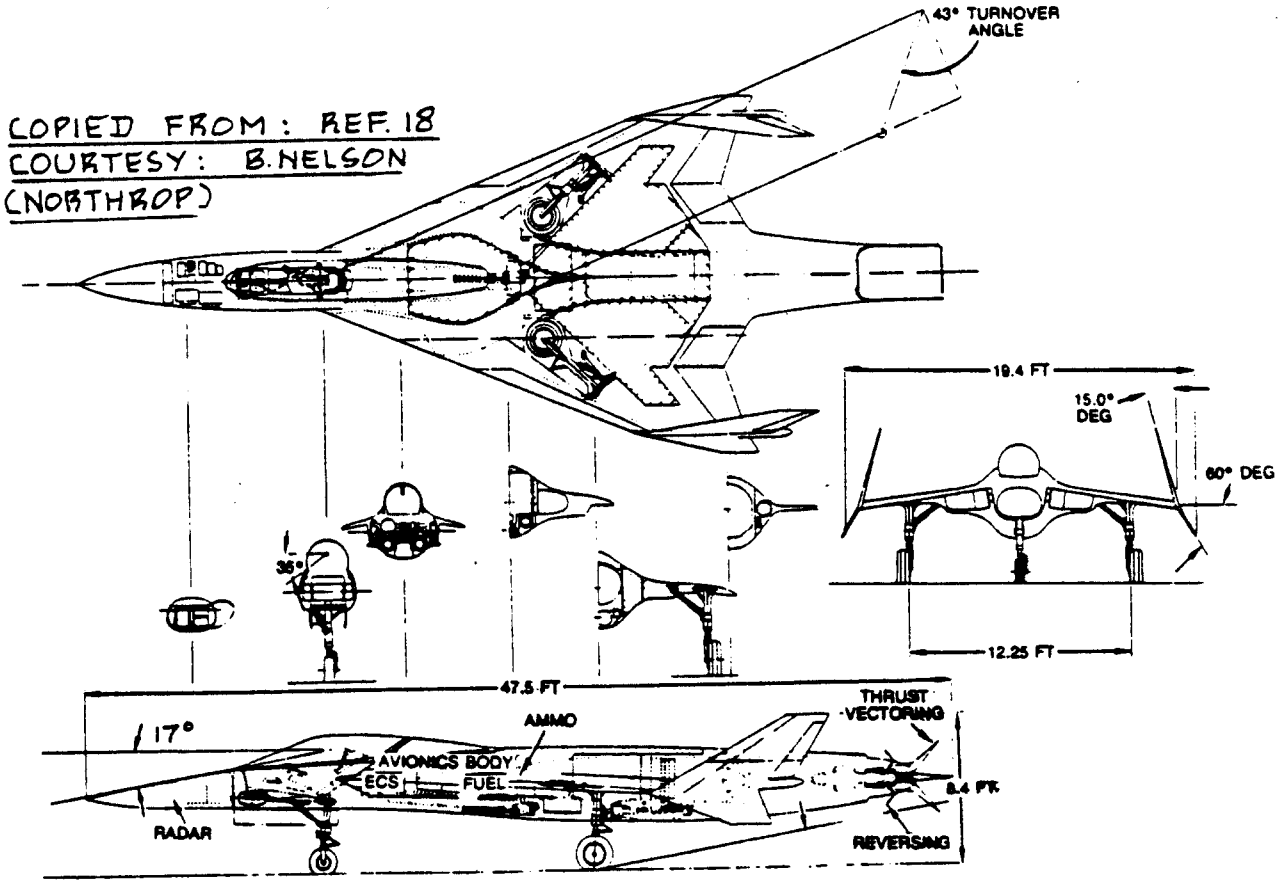

Figure 4.34 Critical Cross Sections for Figure 4.33

4.4 EMPENNAGE DRAG COEFFICIENT PREDICTION

4.4.1 Subsonic Empennage Drag Coefficient

The subsonic empennage drag coefficient is found from:

$$C_{D_{emp}} = SUM_i \{ (C_{D_{o_{emp}}})_i + (C_{D_{L_{emp}}})_i \} \qquad (4.45)$$

where: $(C_{D_{o_{emp}}})_i$ = empennage zero-lift drag coefficient of the number i empennage surface, see 4.4.1.1.

$(C_{D_{L_{emp}}})_i$ = empennage drag coefficient due to lift of the number i empennage surface, see 4.4.1.2.

4.4.1.1 Empennage zero-lift drag coefficient

The empennage zero-lift drag coefficient, $(C_{D_{o_{emp}}})_i$ may be computed with Equation (4.6) after replacing the appropriate wing parameters with those for the empennage.

It is assumed here that any airplane may have the following empennage surfaces:

* horizontal tail surface(s),
* canard surface(s) and
* vertical tail surface(s)

How many of these surfaces an airplane has and where they are located depends strongly on the configuration of the airplane. Chapter 3 of Part II presents more than 150 airplane configurations with different approaches to empennage layout design. Chapter 8 of Part II as well as Chapter V of Part III contain methods and examples for the sizing of empennage surfaces.

NOTE: For each of these empennage surfaces Eqn.(4.6) must be used with the following substitutions:

$$S_{wet_w} = (S_{wet_{emp}})_i$$

$$R_{wf} = 1.0$$

R_{LS} = as determined from Figure 4.2, but using the individual empennage surface sweep angle.

$C_{f_w} = C_{f_{emp}}$ which follows from Figure 4.3 at the appropriate empennage Reynolds number computed with as characteristic length, $\bar{c}_{emp_e}$, the exposed mean geometric chord for each empennage surface.

L' = as determined from Figure 4.4, using the maximum thickness location associated with each empennage airfoil.

(t/c) = maximum thickness ratio associated with each empennage airfoil, taken at its exposed mean geometric chord.

The empennage wetted area, $(S_{wet_{emp}})_i$ will normally be different for each empennage surface.

4.4.1.2 Empennage drag coefficient due to lift

The empennage drag coefficient due to lift, $(C_{D_{L_{emp}}})_i$ may be computed with the following method:

Horizontal Tail(s) and Canard(s)

Most canard and horizontal tail surfaces develop lift in a steady state flight condition. This lift causes induced drag.

In this text, the lift carried by empennage surfaces is split into two components:

1. Lift caused by the reference incidence setting of any empennage surface: the induced drag caused by this lift is accounted for in this paragraph.

2. Lift caused by the requirement to 'trim' the airplane at a particular center of gravity location: the induced drag caused by this lift is referred to as 'trim' drag: see Section 4.10.

If the empennage employs the so-called butterfly arrangement, the projection method of page 206 in Part II may be used to arrive at the 'equivalent horizontal' and the 'equivalent vertical' tail surface.

The amount of lift on a horizontal tail surface can

be computed from:

$$C_{L_h} = C_{L_{\alpha_h}} (\alpha_h - \alpha_{o_{L_h}}) \quad (4.46)$$

with: $\alpha_h = \alpha(1 - d\varepsilon/d\alpha) + i_h \quad (4.47)$

The amount of lift on a canard surface can be computed from:

$$C_{L_c} = C_{L_{\alpha_c}} (\alpha_c - \alpha_{o_{L_c}}) \quad (4.48)$$

with: $\alpha_c = \alpha(1 + d\varepsilon_c/d\alpha) + i_c \quad (4.49)$

Methods for predicting downwash ε, upwash ε_c and the zero lift angles of attack, $\alpha_{o_{L_h}}$ and $\alpha_{o_{L_c}}$, are presented in Chapter 10.

In airplanes with a fixed horizontal tailplane, i_h is usually zero. In airplanes with a fixed canard, i_c is normally set to assure that the canard stalls before the wing. In preliminary design it is acceptable to set:

$$i_c = \alpha_{stall_c} - \alpha_{stall_w} + i_w + 3 \quad (4.50)$$

where the values for α_{stall_c} and α_{stall_w} are taken as the airfoil stall angles of attack at the m.g.c. of their respective surfaces and where the wing incidence angle, i_w may be found from Tables 6.7 in Part II or from page 197 in Part III.

Since horizontal tails and canards are normally not twisted, their drag-due-to-lift may be computed from Eqn.(4.8) with ε_t=0, to yield:

$$C_{D_{L_{emp}}} = \{(C_{L_h})^2/\pi A_h e_h\} S_h/S + \{(C_{L_c})^2/\pi A_c e_c\} S_c/S \quad (4.51)$$

This equation applies to an airplane equipped with one horizontal tail and with one canard. If more empennage surfaces are present, they must be accounted for in a manner analogous to Eqn.(4.51).

Values for C_{L_h} and C_{L_c} follow from Eqns (4.46) and (4.48) respectively.

Values for A_h, A_c, S_h and S_c follow from airplane threeviews as developed in Chapter 13 of Part II.

For the Oswald efficiencies e_h and e_c the following values are suggested:

e_h = 0.5 for fuselage mounted tails

= 0.75 for T-tails

e_c = 0.5

Vertical Tail Surface(s)

Vertical tails are normally installed symmetrically so that the vertical tail drag contribution due to lift is usually zero. If the airplane is sideslipping over an angle β, this angle β should be considered as the angle of attack of the vertical tail. A modified version of Eqn.(4.51) may then be used to calculate the drag due to lift (in sideslip) of the vertical tail.

4.4.2 Transonic Empennage Drag Coefficient

The transonic empennage drag coefficient may be found from:

$$C_{D_{emp}} = SUM_i\{(C_{D_{o_{emp}}})_i + (C_{D_{L_{emp}}})_i\} \qquad (4.52)$$

where: $(C_{D_{o_{emp}}})_i$ = empennage zero-lift drag coefficient of the number i empennage surface, see 4.4.2.1.

$(C_{D_{L_{emp}}})_i$ = empennage drag coefficient due to lift of the number i empennage surface, see 4.4.2.2.

4.4.2.1 Empennage zero-lift drag coefficient

In the transonic speed range the empennage zero-lift drag coefficient is found from:

$$(C_{D_{o_{emp}}})_i = (C_{D_{o_{emp}}})_i + (C_{D_{emp_{wave}}})_i (S_{emp})_i / S \quad (4.53)$$

at M=0.6

where: $(C_{D_{o_{emp}}})_i$ at M=0.6 = empennage drag coefficient due to friction of the number i empennage surface at M=0.6. It is obtained from Eqn.(4.6) with the same substitutions as noted in 4.4.1.1.

$(C_{D_{emp_{wave}}})_i$ = empennage zero-lift wave drag coefficient obtained with the procedure of 4.2.2.2 but with the appropriate substitution of empennage (emp) parameters for wing (w) parameters.

To achieve acceptable wave drag characteristics, the entire configuration, including its empennage surfaces must be 'area-ruled'. A procedure for 'area-ruling' any configuration is given in Sub-section 4.3.4.

4.4.2.2 Empennage drag coefficient due to lift

The transonic empennage drag coefficient due to lift, $(C_{D_{L_{emp}}})_i$ may be computed from Eqn.(4.18), as long as the following substitutions are used:

To find $(C_{D_L}/C_L^2)_{emp_i}$ from Figures 4.13, use the appropriate transonic similarity parameters for the number i empennage surface.

For C_{L_i} use either C_{L_h} or C_{L_c} as in Equations (4.46) or (4.48).

4.4.3 Supersonic Empennage Drag Coefficient

The supersonic empennage drag coefficient is found from:

$$C_{D_{emp}} = SUM_i \{(C_{D_{o_{emp}}})_i + (C_{D_{L_{emp}}})_i\} \quad (4.54)$$

where: $(C_{D_{o_{emp}}})_i$ = zero lift drag coefficient of the number i empennage surface, see 4.4.3.1.

$(C_{D_{L_{emp}}})_i$ = drag coefficient due to lift of the number i empennage surface, see 4.4.3.2.

4.4.3.1 Empennage zero-lift drag coefficient

The supersonic empennage zero lift drag coefficient is found from:

$$(C_{D_{o_{emp}}})_i = (C_{D_{emp_f}})_i + (C_{D_{emp_{wave}}})_i \quad (4.55)$$

where: $$(C_{D_{emp_f}})_i = (C_{f_{emp}})_i (S_{wet_{emp}})_i / S \quad (4.56)$$

where: $(C_{f_{emp}})_i$ may be found from Fig.4.3 at the appropriate empennage Reynolds number computed with as characteristic length, $\bar{c}_{emp_e}$, the exposed mean geometric chord of each empennage surface.

$(C_{D_{emp_{wave}}})_i$ = wave drag coefficient of the number i empennage surface. This wave drag coefficient may be determined with the method of 4.2.3.1 as long as the appropriate empennage parameters are substituted for their wing counterparts.

4.4.3.2 Empennage drag coefficient due to lift

The supersonic empennage drag coefficient due to lift is found from:

$$(C_{D_{L_{emp}}})_i = (C_{D_L}/C_L^2)_{emp_i} (C_{L_{emp}}^2)_i \quad (4.57)$$

Values for $(C_{D_L}/C_L^2)_{emp_i}$ may be obtained from the method of 4.2.3.2, as long as the appropriate parameter substitutions are made.

Values for $(C_{L_{emp}})_i$ follow from either Eqn.(4.46) or from Eqn.(4.48).

4.5 NACELLE/PYLON DRAG COEFFICIENT PREDICTION

Methods for predicting nacelle/pylon drag are presented as follows:

4.5.1 Isolated Nacelle/Pylon Drag Coefficient

This method is applicable in all speed regimes considered in this text.

4.5.2 Installed Nacelle/Pylon Drag Coefficient Increment

This method applies only in the subsonic speed regime and provides the 'interference' drag increment due to nacelle/pylon installations.

It is assumed that this 'interference' drag increment is independent of Mach number as long as the appropriate area ruling is used in the transonic and supersonic speed ranges. See Sub-section 4.3.4 for details on area ruling.

4.5.3 Windmilling Drag and Propeller Drag Coefficients

This method provides the drag increase caused by engine and/or propeller stoppage.

These methods should be applied as follows:

Step 1: Determine the subsonic installed drag increment due to the nacelle or the nacelle/pylon combination from Sub-section 4.5.2. Again: this drag increment represents the interference drag of the installation.

Step 2: Determine the drag increments due to transonic and supersonic operations from Subsection 4.5.1 which assumes the nacelle/pylon to be isolated.

Step 3: Add the transonic and/or supersonic increments from Step 2 to the nacelle/pylon interference drag obtained in Step 1.

Step 4: For windmilling and/or propeller drag increments use Sub-section 4.5.3. Add this drag increment to the drag obtained in Step 3.

4.5.1 Isolated Nacelle/Pylon Drag Coefficient

The nacelle/pylon drag coefficient may be computed from:

$$C_{D_{np}} = C_{D_n} + C_{D_p} \qquad (4.58)$$

where: C_{D_n} = nacelle drag coefficient, see 4.5.1.1.

C_{D_p} = pylon drag coefficient, see 4.5.1.2.

4.5.1.1 Nacelle drag coefficient

Engine operating:

The nacelle drag coefficient is found from:

$$C_{D_n} = SUM_i (C_{D_n})_i \qquad (4.59)$$

The number i equals the number of nacelles on the airplane. Each nacelle drag coefficient, $(C_{D_n})_i$ is computed with the method of Section 4.3. This assumes that a nacelle can be treated as if it is a (small) fuselage.

Note: nacelles will generate lift when placed at an angle of attack. Local nacelle angle of attack should be expressed as:

$$\alpha_n = \alpha_w + i_n + \varepsilon_n \qquad (4.60)$$

where: α_w = wing angle of attack

i_n = nacelle incidence angle, see Figure 4.35.

ε_n = nacelle upwash or downwash angle. This depends on where the nacelle is installed on the airplane. Figure 4.36 illustrates two possibilities.

The nacelle up- or downwash angle follows from:

$$\varepsilon_n = (d\varepsilon_n/d\alpha)\alpha \qquad (4.61)$$

where: $d\varepsilon_n/d\alpha$ is computed with the methods described in Chapter 10.

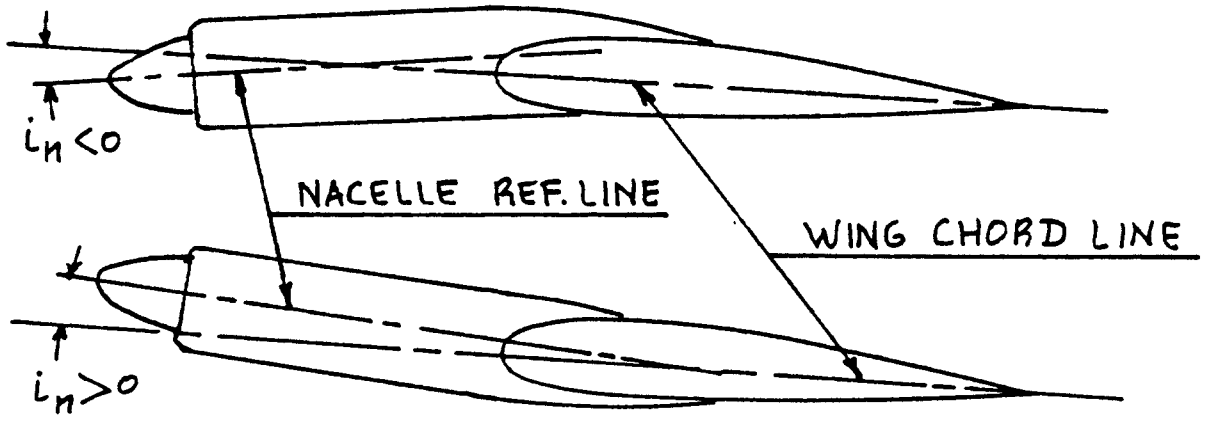

Figure 4.35 Definition of Nacelle Incidence Angle

a) NACELLE ON WING

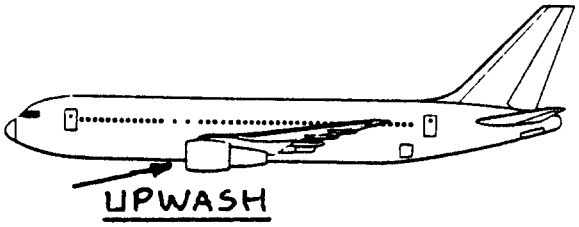

b) NACELLE ON FUSELAGE

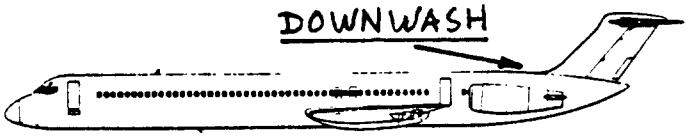

Figure 4.36 Examples for Nacelle Upwash and Downwash

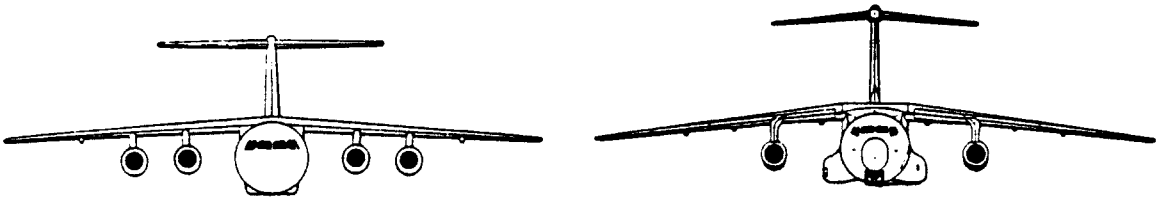

Figure 4.37 Examples of Vertically Installed Pylons

Engine Inoperative:

In addition to the drag given by Eqn.(4.59) there will be extra drag caused by engine or propeller windmilling. If a propeller is stopped, there will be extra drag due to that.

Sub-section 4.5.3 deals with such cases.

4.5.1.2 Pylon drag coefficient

The pylon drag coefficient may be found from:

$$C_{D_p} = SUM_i \ (C_{D_p})_i \qquad (4.62)$$

It will be assumed here that the drag behavior of a pylon can be modelled as that of an empennage. For this reason, values for $(C_{D_p})_i$ may be obtained by using the method of Section 4.4.

For vertically installed pylons (see Figure 4.37), the pylon should be treated as a vertical tail: the drag prediction method of Section 4.4 may be used.

For horizontally installed pylons (see Figure 4.38) the pylon should be treated as a horizontal tail or as a canard: use the drag prediction method of Section 4.4.

NOTA BENE 1: Nacelles installed in the proximity of wings (see Figure 4.37a) must be installed so that they are at zero local sideslip angle in the local flowfield. This results in the need for 'toe-in' for nacelles such as in the Boeing 747 series airplanes: see Figure 4.39.

NOTA BENE 2: The methods of 4.5.1.1 and 4.5.1.2 apply to all speed regimes. However, in the transonic and supersonic speed regimes the method is valid only as long as the nacelle/pylon combination is included in the area-ruling process described in Sub-section 4.3.3. Note: the nacelle stream tube should not be included in this area ruling process.

4.5.2 Installed Nacelle/Pylon Drag Coefficient Increment

Sub-section 4.5.1 provides a method for predicting the drag coefficient, $C_{D_{np}}$ due to isolated nacelle/pylon combinations.

In the following, a method for computing the interference drag increment caused by a nacelle/pylon

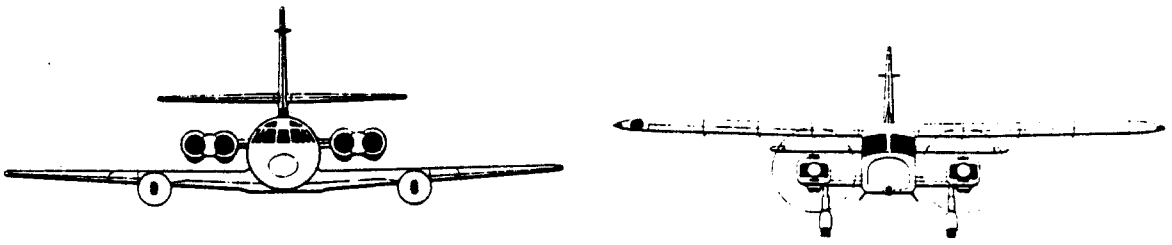

Figure 4.38 Examples of Horizontally Installed Pylons

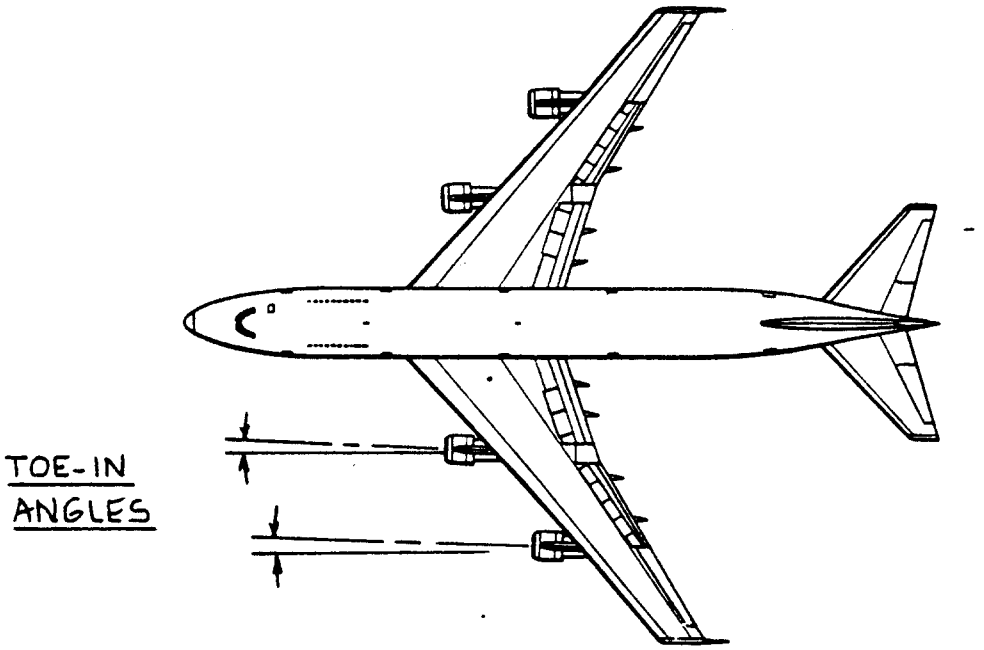

Figure 4.39 Example of Nacelles with Toe-in

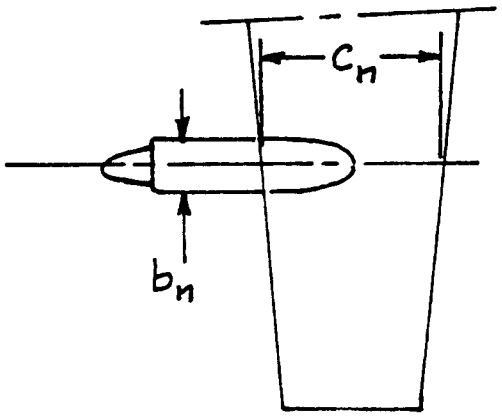

Figure 4.40 Definition of Nacelle Parameters

installation is presented. The method is broken down into three parts:

4.5.2.1 Wing/nacelle interference drag coefficient
4.5.2.2 Fuselage/nacelle interference drag coefficient
4.5.2.3 Cooling drag coefficient increment

Which drag increment should be accounted for depends on the airplane configuration.

4.5.2.1 Wing/nacelle interference drag coefficient

For turboprop and for piston-prop nacelle/wing installations the interference drag coefficient is found from:

$$C_{D_{n_{int}}} = 0.036\,(c_n b_n/S)(\Delta c_{l_1} + \Delta c_{l_2})^2 \qquad (4.63)$$

where: c_n and b_n are defined in Figure 4.40.

Δc_{l_1} = 0.2 for a nacelle on top of the wing

= -0.3 for a nacelle below the wing

$\Delta c_{l_2} = -0.056(i_n)$

i_n = nacelle incidence angle defined in Figure 4.35.

For jet-driven airplanes the wing/nacelle interference drag coefficient is found from:

$$C_{D_{n_{int}}} = F_{a_1}(\Delta C_{D_n}/C_{D_n})C_{D_n} \qquad (4.64)$$

where: $(\Delta C_{D_n}/C_{D_n})$ follows from Figure 4.41 at the Mach numbers indicated.

C_{D_n} = nacelle drag coefficient as determined in 4.5.1.1.

F_{a_1} = 1.0 for $M < 0.5$

1.0 for $M > 0.5$ and no local area ruling of the nacelle/pylon/wing intersection.

0.5 for $M > 0.5$ and a locally area ruled nacelle/pylon/wing intersection.

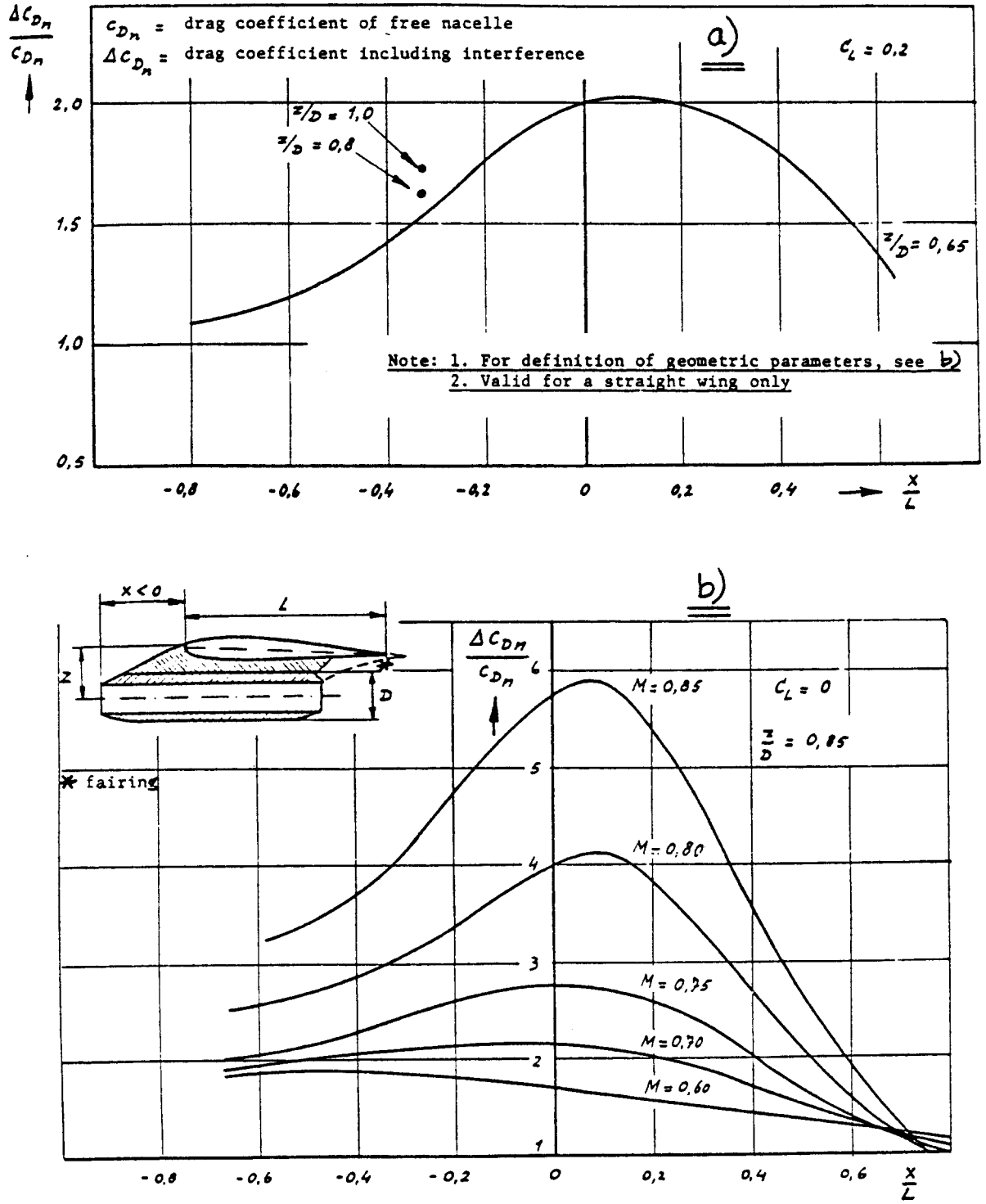

Note: Valid for swept wings only

COPIED FROM: REF. 21

Figure 4.41 Wing-Nacelle Drag Interference Factor

4.5.2.2 Fuselage/nacelle interference drag coefficient

The fuselage/nacelle interference drag coefficient may be found from:

$$C_{D_{n_{int}}} = F_{a_2}\{(C_{D_n})' - 0.05\}(S_n/S) \quad (4.65)$$

where: $(C_{D_n})'$ is found from Figure 4.42

S_n = maximum frontal area of the nacelle, excluding the pylon: see Figure 4.38.

F_{a_2} = 1.0 for fuselage/nacelle intersections without local area ruling

= 0.5 for fuselage/nacelle intersections with local area ruling.

4.5.2.3 Cooling drag coefficient increment

The cooling drag coefficient increment for radial air-cooled engine installations may be estimated from:

$$C_{D_{n_{cool}}} = (\Delta C_{D_{cool}})\{\pi(d_n)^2/4S\} \quad (4.66)$$

where: $\Delta C_{D_{cool}}$ follows from Figure 4.43.

d_n = the maximum nacelle diameter as shown in Figure 4.38.

4.5.3 Windmilling Drag and Propeller Drag Coefficients

The following cases should be considered:

1.) Windmilling drag coefficient due to jet engines: see 4.5.3.1.

2.) Windmilling drag coefficient due to propellers: see 4.5.3.2.

3.) Drag coefficient due to a stopped propeller: see 4.5.3.3.

4.5.3.1 Windmilling drag coefficient due to jet engines

The incremental drag coefficient due to a windmilling jet engine may be estimated from:

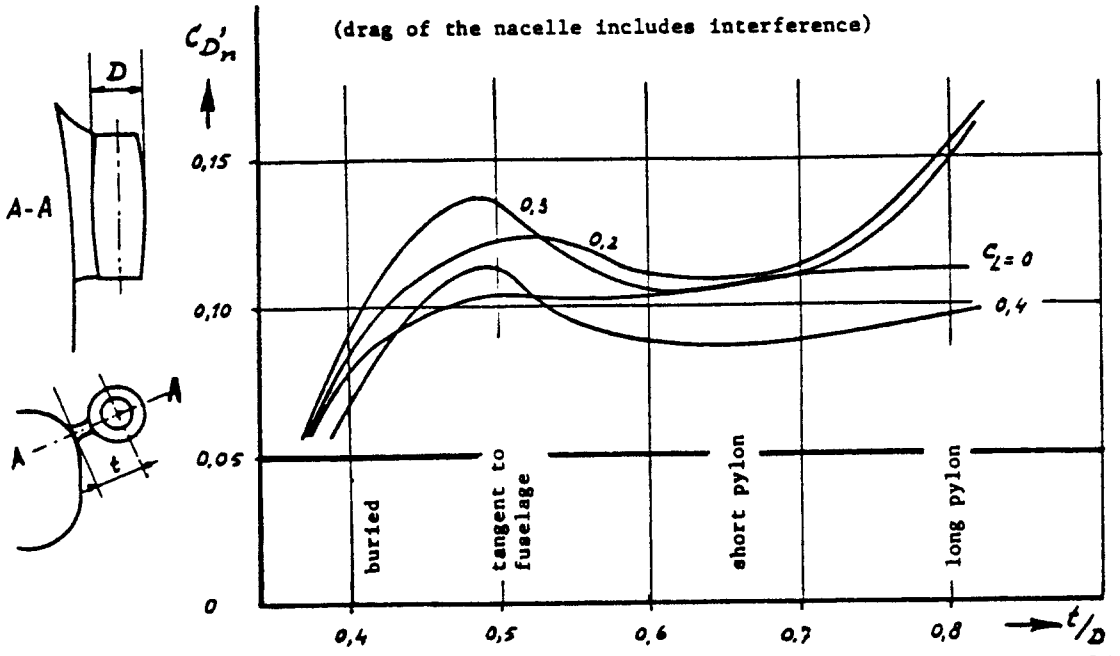

COPIED FROM: REF. 21

Note: 1. C_{D_n} is based on maximum nacelle frontal area

2. drag coefficient of the free nacelle is 0.05

Figure 4.42 Fuselage-Nacelle Drag Interference Factor

①	②	③	④	⑤	⑥	⑦	⑧
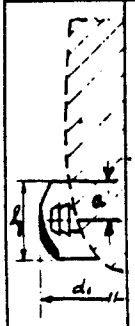							
$\frac{d_1}{\ell_1} = 1.78$	1,78	1,62	1,5	1,63	1,63	1,63	3,62
$\frac{a}{\ell_1} = 0.59$	0,59	0,59	0,63	0,66	0,66	0,66	0,16
$\Delta C_D^{*} = 0.16$	0,075	0,10	0,07	0,06	0,088	0,212	0,152

*) ΔC_D BASED ON: $\frac{\pi}{4} d_1^2$

COPIED FROM REF. 21

Figure 4.43 Cooling Drag Coefficient Increment

$$\Delta C_{D_{wmj}} = 0.0785(d_{inl}^2)/S +$$

$$+ \{2/(1 + 0.16M^2)\}(V_{noz}/U_1)(1 - V_{noz}/U_1)S_{noz}/S \quad (4.67)$$

where: d_{inl} = engine inlet diameter

S_{noz} = nozzle cross section area

V_{noz}/U_1 = ratio of average flow velocity in the nozzle to the steady state flight speed The following values are suggested for this ratio:

V_{noz}/U_1 = 0.25 for turbojets and turboprops

= 0.42 for low by-pass ratio jet engines

= 0.12 for the primary airflow of high by-pass jet engines

= 0.92 for the fan airflow of high bypass jet engines

4.5.3.2 Windmilling drag coefficient due to propellers

Reference 20 provides a method for estimating the windmilling drag due to a propeller. In absence of that reference it is suggested to use:

$$\Delta C_{D_{wmprop}} = 33(1/\bar{q}S)SHP_{rated}/U_1 \quad (4.68)$$

where: SHP_{rated} = maximum rated shaft horsepower of the engine in the flight condition being considered. Note: use hp!

U_1 = steady state flight speed, in fps.

4.5.3.3 Drag coefficient due to a stopped propeller

The incremental drag coefficient due to a stopped propeller may be estimated from:

$$\Delta C_{D_{prop}} = 0.0012\Im n_p(D_p)^2/S \quad (4.69)$$

where: n_p = number of blades per propeller

D_p = diameter of the propeller

4.6 FLAP DRAG PREDICTION

The assumption is made that flaps will be deployed only in the subsonic speed regime. For the effect of flap drag at high speed the reader should consult reference 9.

The drag coefficient due to flap deflection may be estimated from:

$$C_{D_{flap}} = \Delta C_{D_{prof_{flap}}} + \Delta C_{D_{i_{flap}}} + \Delta C_{D_{int_{flap}}} \quad (4.70)$$

where: $\Delta C_{D_{prof_{flap}}}$ = the flap profile drag increment, see 4.6.1.

$\Delta C_{D_{i_{flap}}}$ = the induced drag increment due to the flap, see 4.6.2.

$\Delta C_{D_{int_{flap}}}$ = the interference drag increment due to the flap, see 4.6.3.

4.6.1 Flap Profile Drag Increment

The following method applies to wings with sweep angles up to 40 degrees. For higher sweep angles the reader should consult Reference 9.

The flap profile drag increment may be found from:

$$\Delta C_{D_{prof_{flap}}} = (\Delta C_{d_{p_{\Lambda_{c/4}=0}}})(\cos\Lambda_{c/4})S_{wf}/S \quad (4.71)$$

where: $\Delta C_{d_{p_{\Lambda_{c/4}=0}}}$ = the two-dimensional profile drag increment due to flaps.

This increment depends on the type of flaps used:

For <u>plain</u> flaps: use Figure 4.44.

For <u>split</u> flaps, use Figure 4.45.

For <u>single slotted</u> flaps, use Figure 4.46.

For <u>double slotted</u> flaps: use Figure 4.47.

For <u>Fowler</u> flaps: use Figure 4.48.

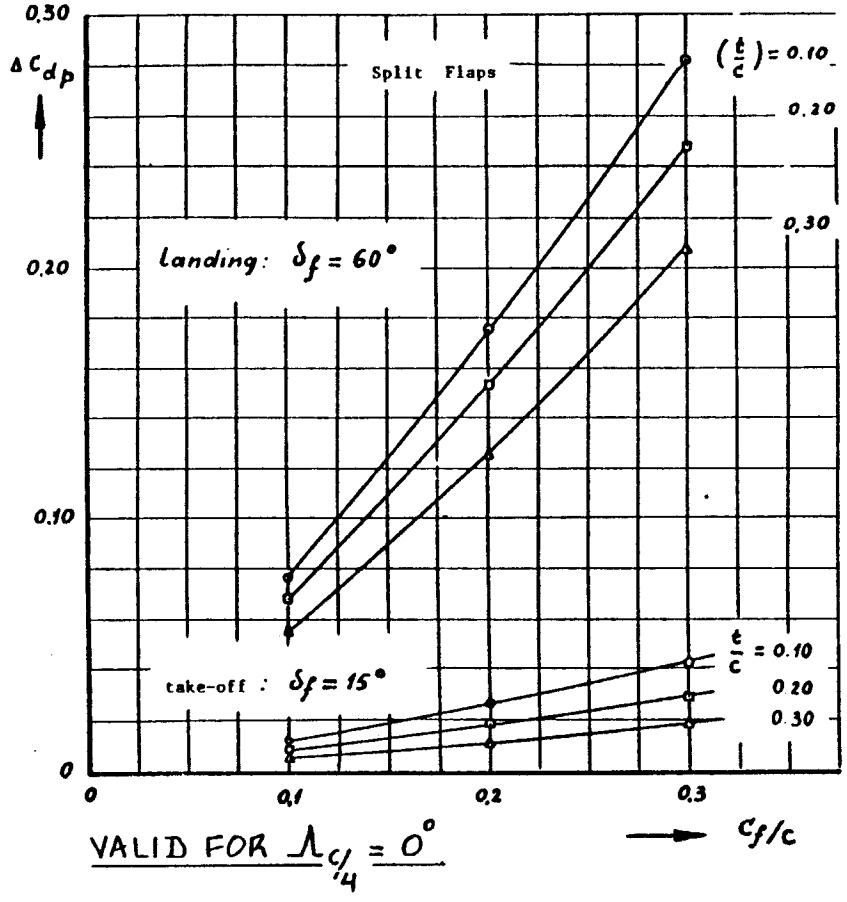

Figure 4.45 Profile Drag Increment: Split Flaps

COPIED FROM REF. 21

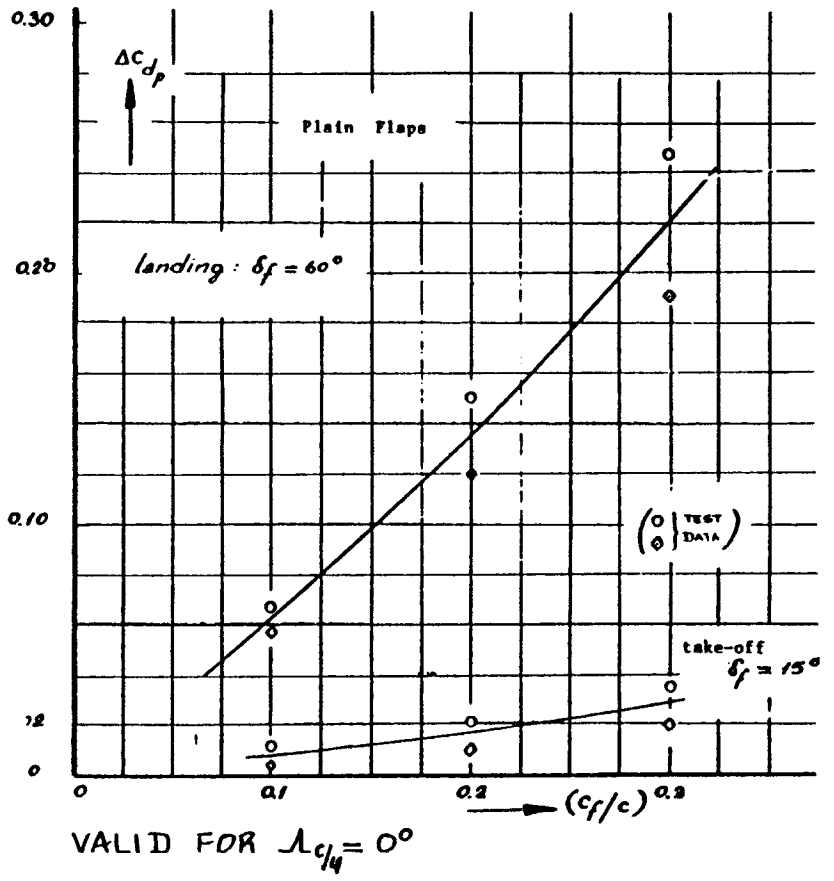

Figure 4.44 Profile Drag Increment: Plain Flaps

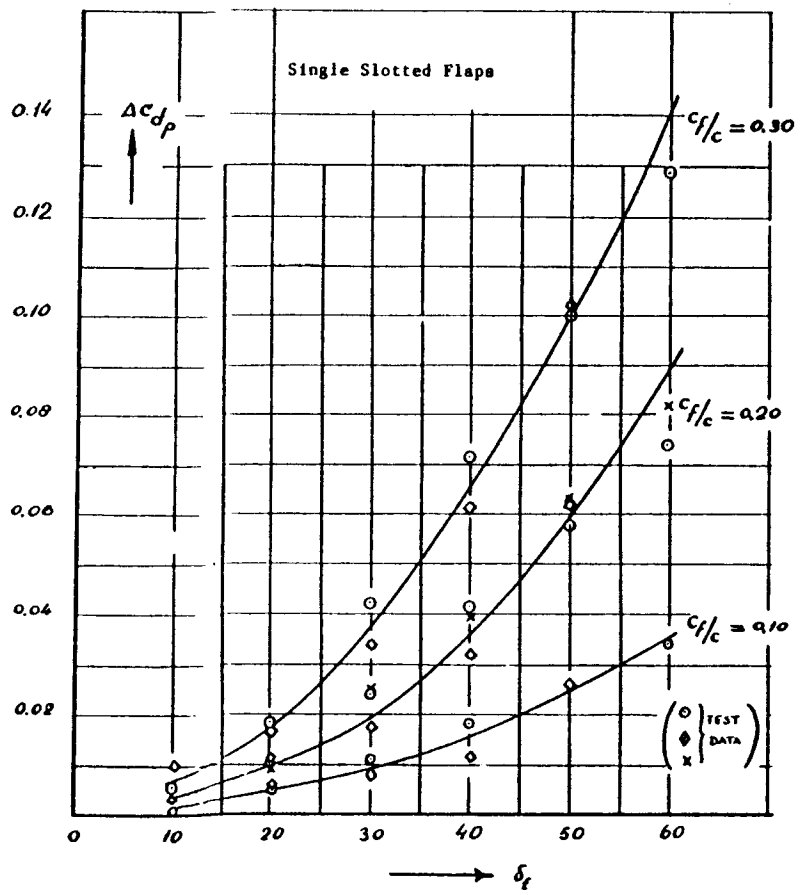

Figure 4.46 Profile Drag Increment:

Single Slotted Flaps

COPIED FROM REF. 21

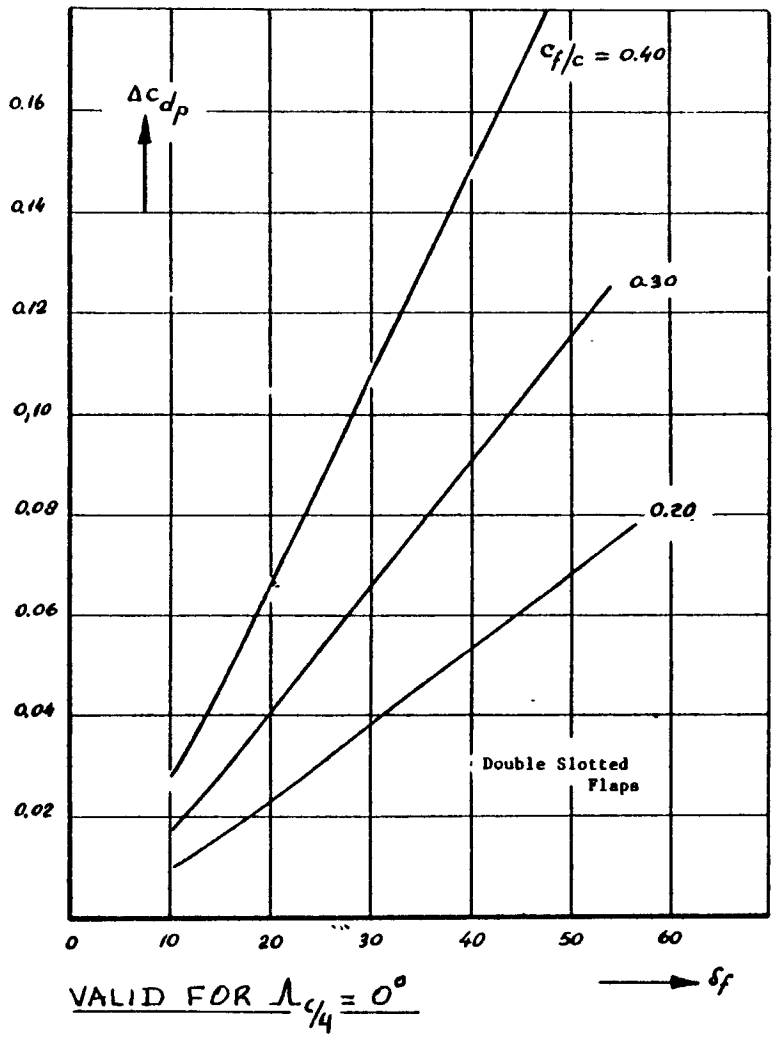

Figure 4.47 Profile Drag Increment:

Double Slotted Flaps

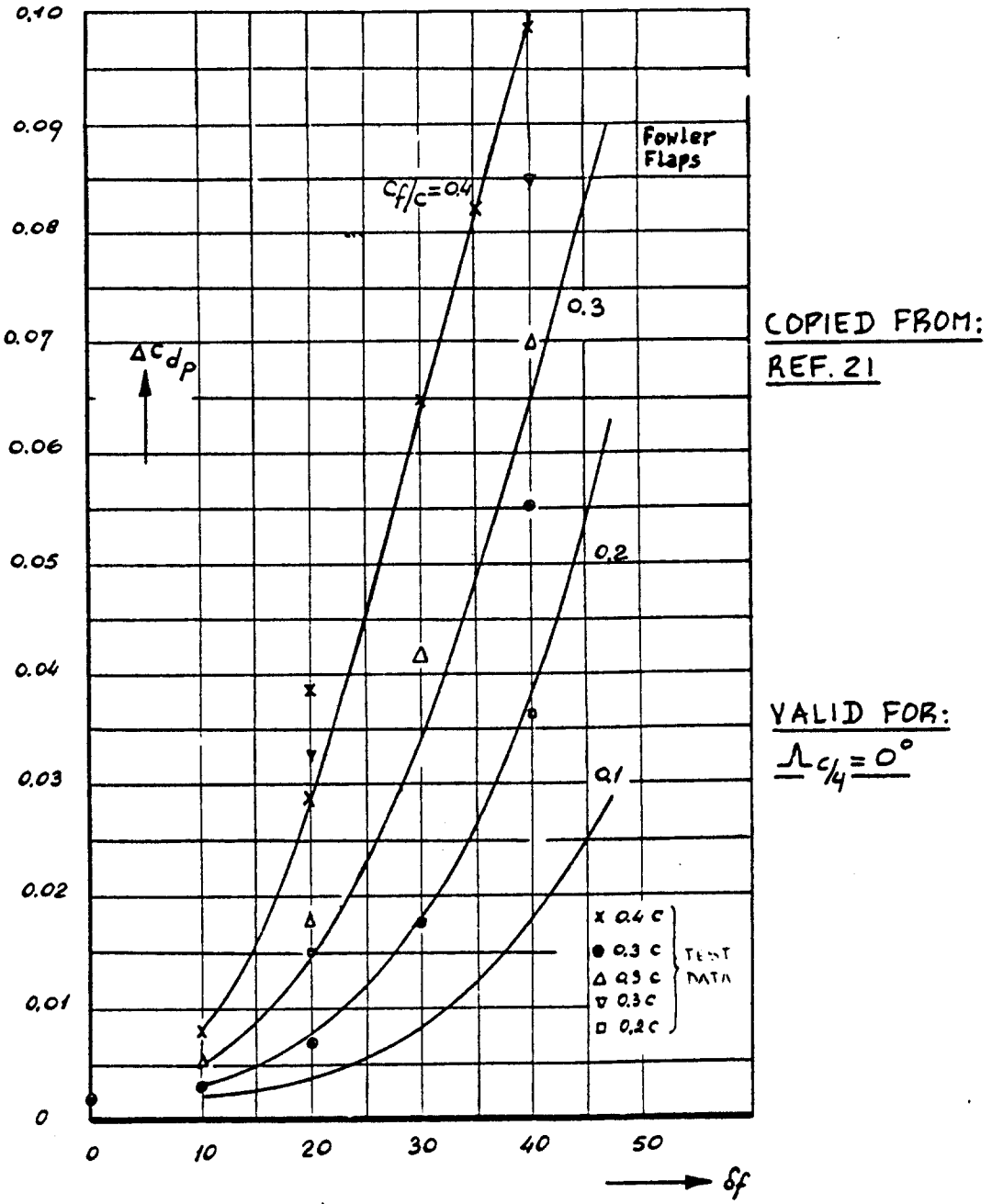

Figure 4.48 Profile Drag Increment: Fowler Flaps

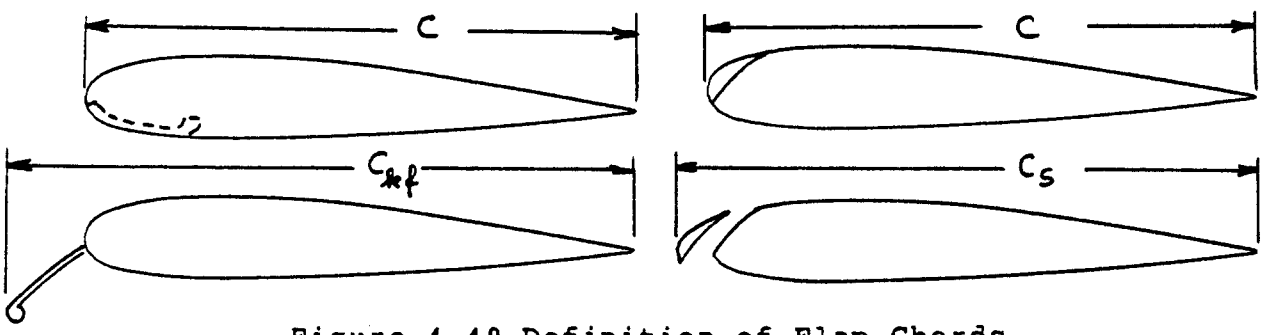

Figure 4.49 Definition of Flap Chords

For Krueger flaps, use:

$$\Delta C_{d_{p_{\Lambda_{c/4}=0}}} = C_{D_{o_w}} (c_{kf}/c) \qquad (4.72)$$

where: $C_{D_{o_w}}$ is obtained from Eqn.(4.1).

c_{kf}/c = ratio of wing chord with Krueger flap extended to that of the wing with the Krueger flap retracted: see Figure 4.49.

For slats, use:

$$\Delta C_{d_{p_{\Lambda c/4}=0}} = C_{D_{o_w}} (c_s/c) \qquad (4.73)$$

where: c_s/c = ratio of wing chord with slats extended to that of the wing with the slats retracted: See Figure 4.49.

Figure 4.50 illustrates these various flap types.

$\Lambda_{c/4}$ = wing quarter chord sweep angle.

S_{wf} = the flapped wing area: see Figure 4.50.

4.6.2 Induced Drag Increment due to Flaps

The induced drag increment due to flaps may be estimated from:

$$\Delta C_{D_{i_{flap}}} = K^2 (\Delta C_{L_{flap}})^2 \cos\Lambda_{c/4} \qquad (4.74)$$

where: $\Delta C_{L_{flap}}$ = the incremental lift coefficient due to the flap. This quantity follows from comparing a flaps-up with a flaps-down C_L-versus-α curve: see Figure 4.51.

Chapter 9 presents a method for constructing Fig.4.51.

K = an empirical constant which follows from Figures 4.52 and 4.53.

4.6.3 Interference Drag Increment due to Flaps

The interference drag increment due to flaps may be estimated from:

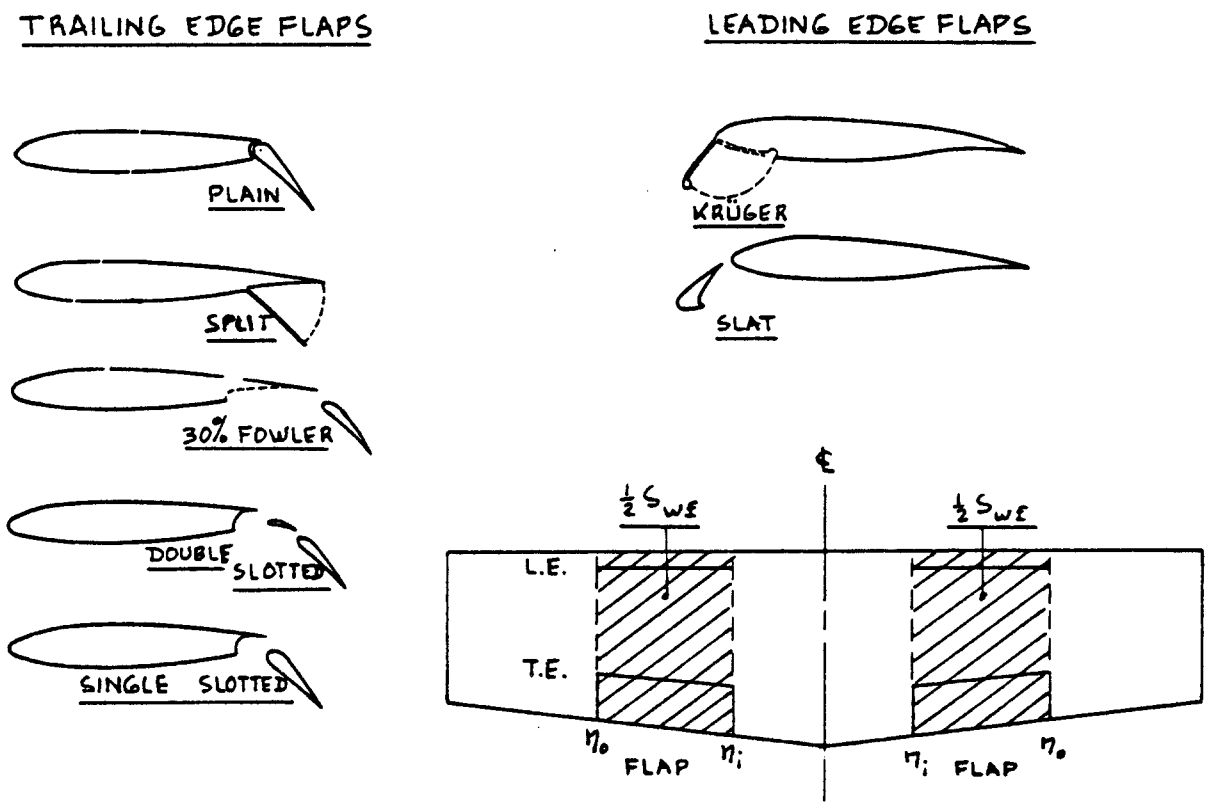

Figure 4.50 Typical Flap Types for Figures 4.44 - 4.48

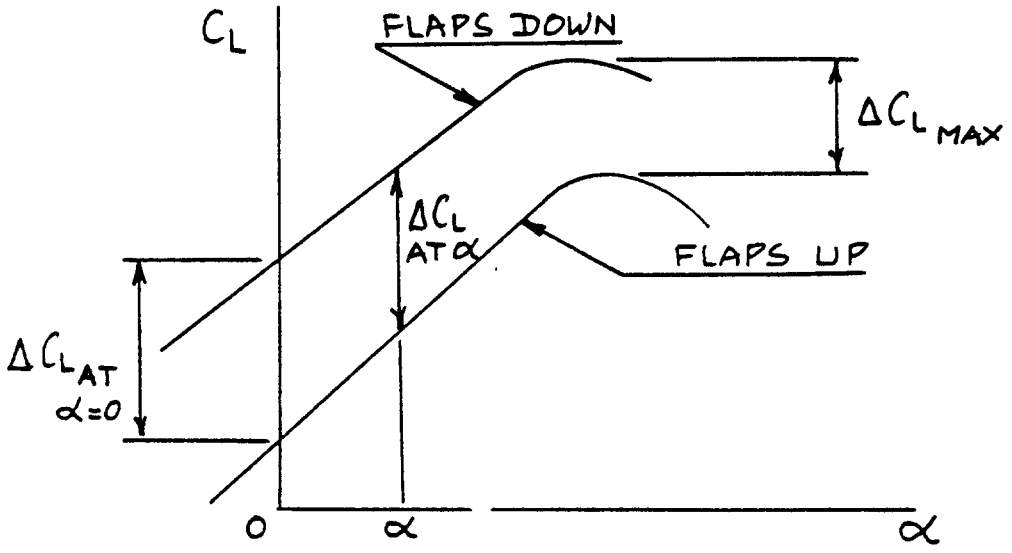

Figure 4.51 Example of Flaps-up and Flaps-down Lift Coefficient Versus Angle-of-Attack Behavior

$$\Delta C_{D_{int_{flap}}} = K_{int} \Delta C_{D_{prof_{flap}}} \quad (4.75)$$

where: $\Delta C_{D_{prof_{flap}}}$ follows Sub-section 4.6.1.

K_{int} = - 0.15 for split flaps

= 0 for plain flaps

= + 0.40 for slotted flaps

= + 0.25 for Fowler flaps

= + 0.10 for slats and for Kruegers

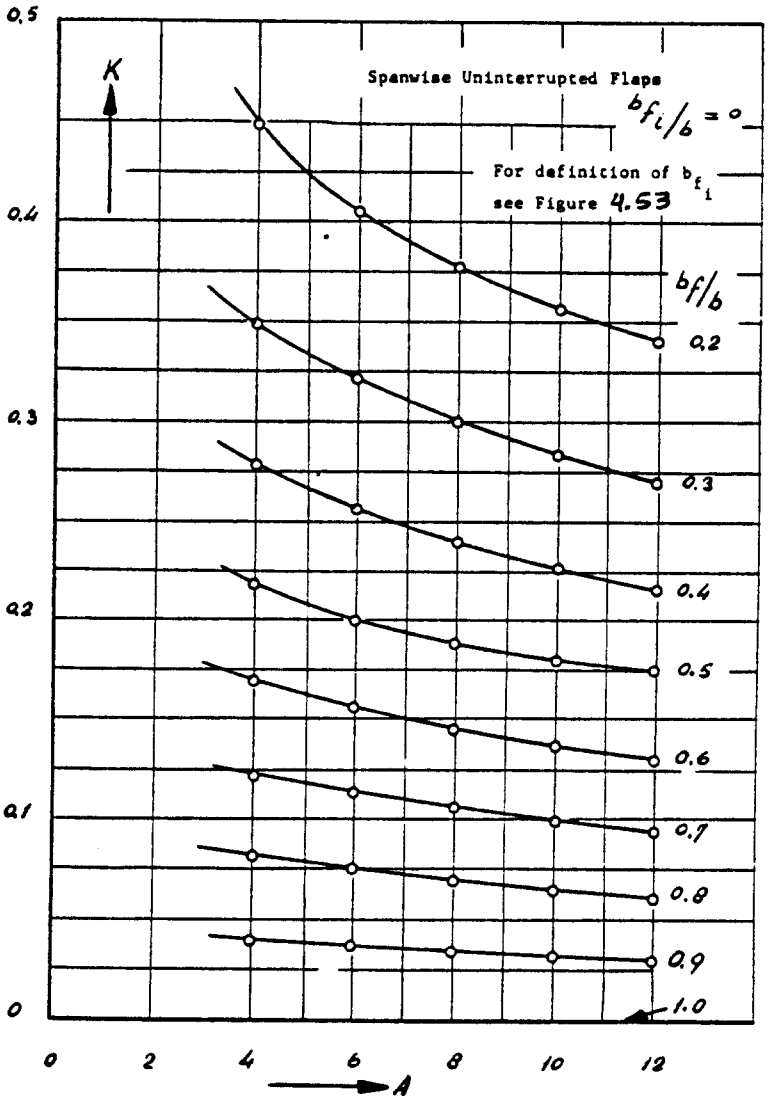

COPIED FROM: REF. 21

Figure 4.52 Induced Drag Factor for Uninterrupted Flaps

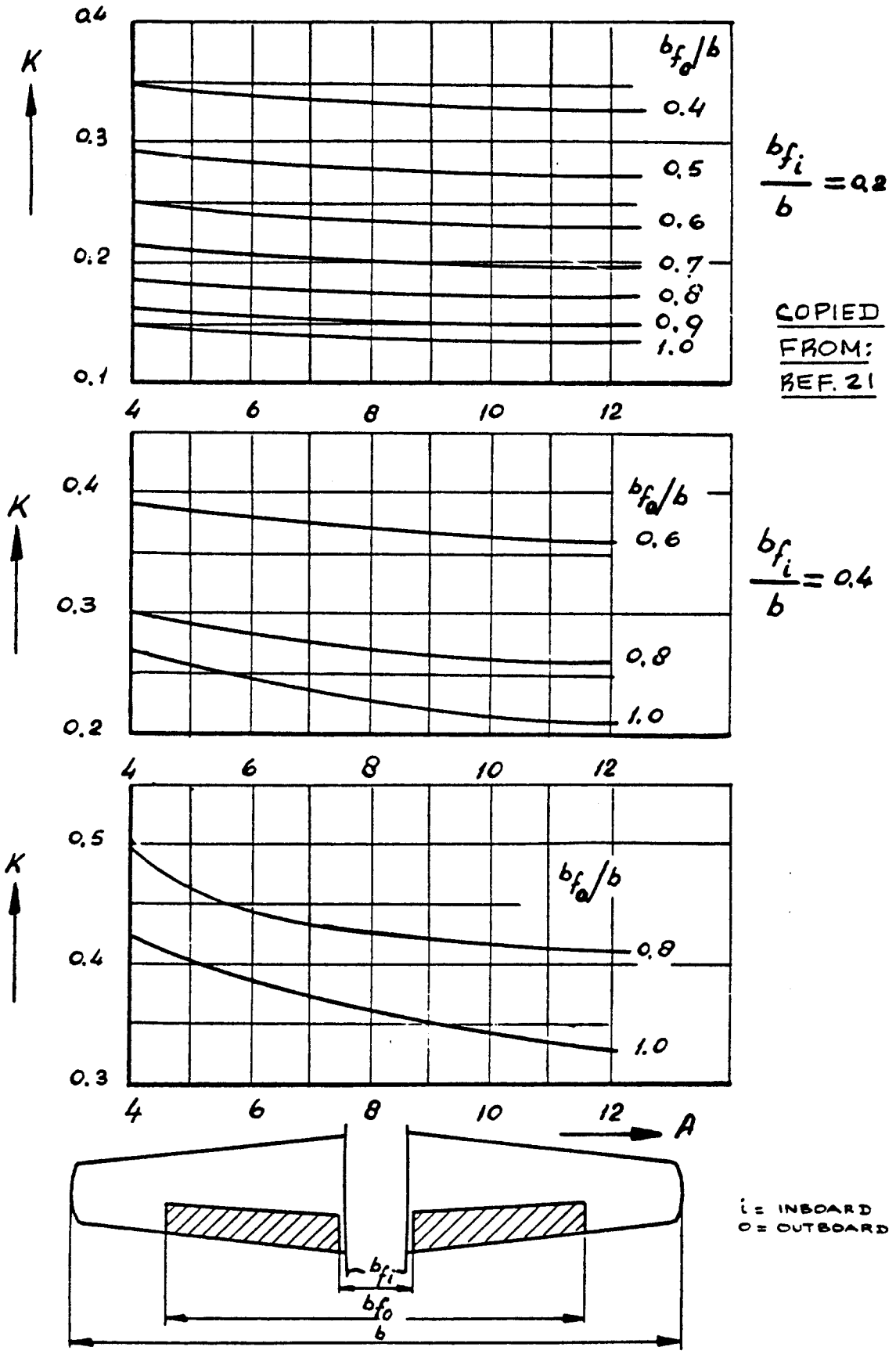

Figure 4.53 Induced Drag Factor for Interrupted Flaps

4.7 LANDING GEAR DRAG PREDICTION

The assumption is made that landing gear deployment will occur only in the subsonic speed regime. The method presented here applies only at low speed.

The landing gear drag coefficient for an airplane with i landing gears may be computed from:

$$C_{D_{gear}} = SUM_i [\{(C_{D_{gear_{C_L=0}}})_i + p_i C_L\}(S_{gear})_i / S] \qquad (4.76)$$

where: $C_{D_{gear_{C_L=0}}}$ = the zero-lift drag coefficient of the landing gear based on its own reference area, S_{gear}. Figures 4.54 through 4.60 provide data from which the zero-lift drag coefficient of the landing gear may be determined.

S_{gear} = reference area for the zero-lift gear drag coefficient. This reference area is defined in Figures 4.54-4.60. For most landing gear types: $S_{gear} = b_t x D_t$, where b_t is the tire width and D_t is the tire diameter.

p = a factor which accounts for the variation of gear drag with lift. Figure 4.61 gives a method for determining this factor p.

Airplanes can have a number of different types of landing gear. The summation over i landing gears in Eqn.(4.76) indicates this.

Figures 4.54 - 4.60 should be used as follows:

For fixed landing gears: Figures 4.54 and 4.55 apply to non-retractable (= fixed) landing gears attached to wing or fuselage. Note that these drag coefficients are based on: $S_{gear} = b_t x D_t$.

Figure 4.56 applies to non-retractable (= fixed) landing gears attached to nacelles. These drag coefficients are based on: $S_{gear} = b_t x D_t$.

Important note: The data in Figures 4.54 - 4.56 apply to the entire main gear which is assumed to consist of two of the legs shown in these figures.

Note: 1. All C_D values are referenced to $b_t x D_t$ and are valid for $C_L=0$

2. All landing gears shown in this figure are assumed to have streamlined tires such as shown in Figure 4.57

TYPE 1

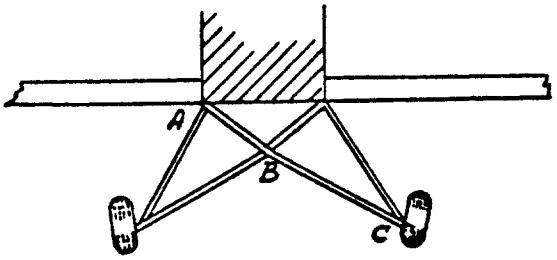

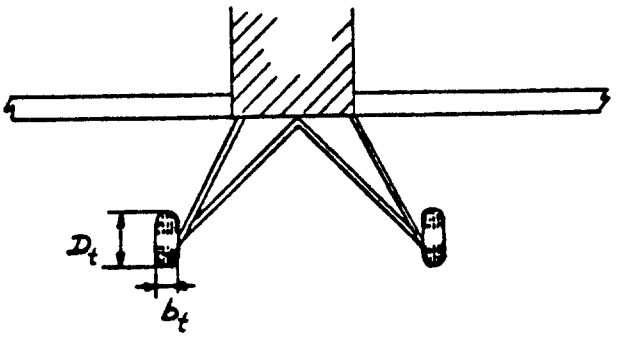

Effect of streamlining

Non streamlined struts	: $C_D=2.56$
Streamlined struts	: $C_D=1.11$
Struts also streamlined at intersections A and B	: $C_D=0.93$
Struts also streamlined at intersections A, B and C	: $C_D=0.85$

Effect of wheel fairings as shown in Figure 4.57

Fairing type A	: $C_D=1.15$
Fairing type B	: $C_D=1.05$
Fairing type C	: $C_D=0.71$

COPIED FROM REF. 21

TYPE 2

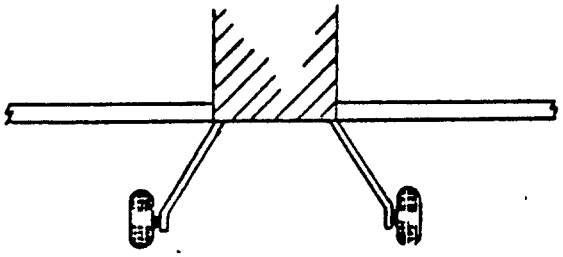

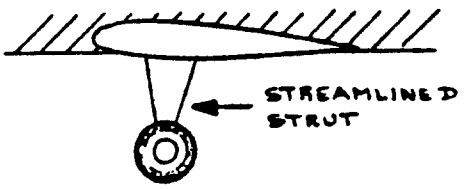

Without wheel fairing	: $C_D=0.565$
With fairing type B	: $C_D=0.54$
With fairing type C	: $C_D=0.49$

as shown in Figure 4.57

Figure 4.54 Gear Drag Increment: Non-retractable Gears Attached to Wing or Fuselage, Types 1-2

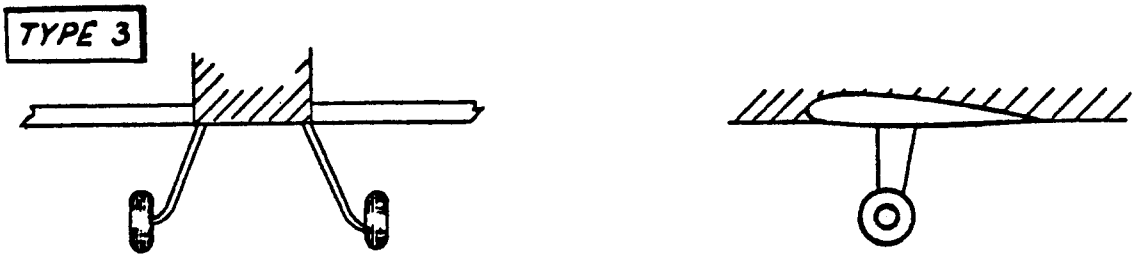

Without wheel fairing : C_D=0.62

With fairing type A : C_D=0.46
as shown in Figure 4.57

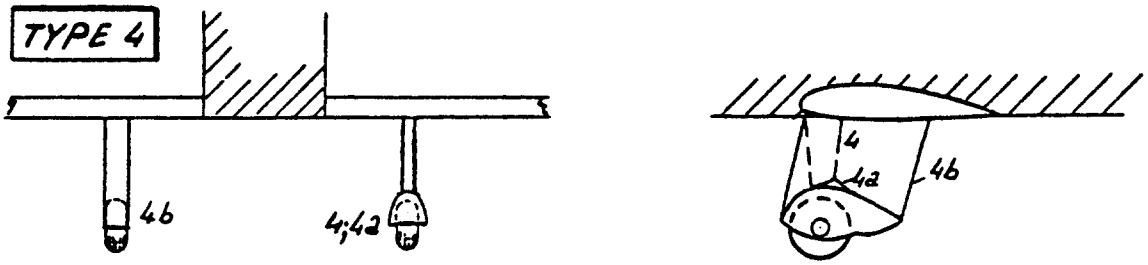

Type 4, narrow strut, no fairing : C_D=0.52

Type 4a, Narrow strut, small fairing : C_D=0.34

Type 4b, strut and wheel faired completely : C_D=0.34

COPIED FROM REF. 21

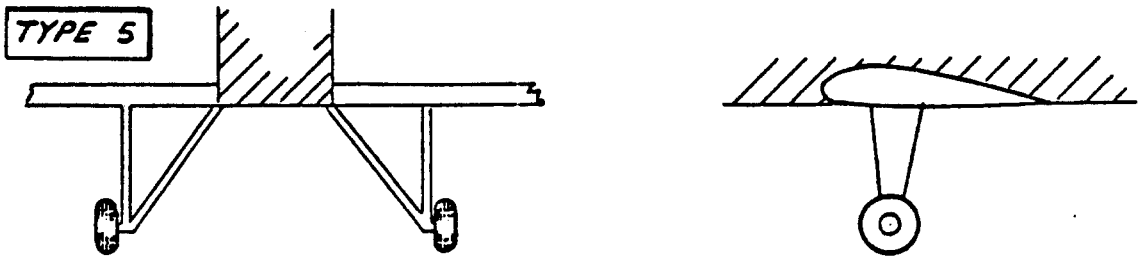

With wheel fairing type C, according to Figure 4.57 : C_D= .68

Without wheel fairing : C_D=1.05

Figure 4.55 Gear Drag Increment: Non-retractable Gears Attached to Wing or Fuselage, Types 3-5

Note: All C_D values are referenced to $b_t \times D_t$ of one wheel, but apply to the entire landing gear, including interference drag

COPIED FROM REF. 21

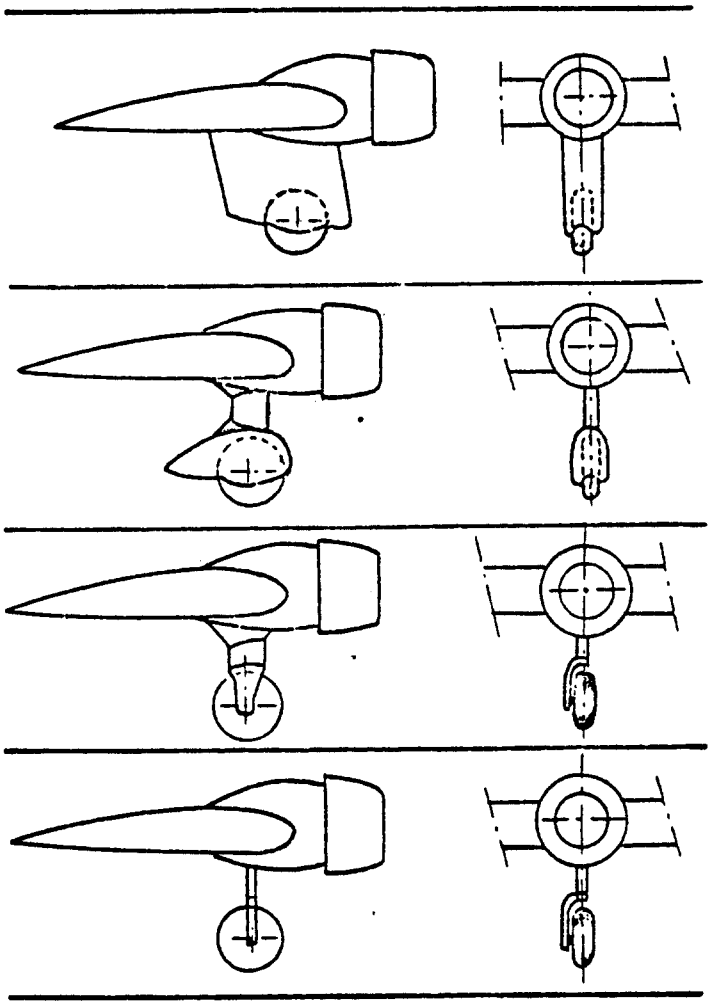

Valid for C_L=0 only

Figure 4.56 Gear Drag Increment: Non-retractable Gears Attached to Nacelles

For landing gear wheels alone: Figure 4.57 applies to wheels with and without streamline caps (fairings). Note that these drag coefficients are based on: $S_{gear} = b_t x D_t$.

For nose gears: Figure 4.58 applies to nose gears with closed nosewheel doors. Note that the reference area is again: $S_{gear} = b_t x D_t$.

For retractable landing gears: Figure 4.59 provides the data. Nota bene: these data are based on the reference area: (axb) as defined in Figure 4.59. The drag coefficients again apply to the entire gear which is assumed to consist of two legs.

For landing gears with more than one wheel per bogey: Figure 4.61 shows a relationship between Δf_{gear} and W_{TO} for different types of landing gear. From these data:

$$C_{D_{gear}} = \Delta f_{gear}/S \qquad (4.77)$$

Many airplane configurations employ 'landing-gear-bulge-fairings'. Many examples of this are depicted in Chapter 3 of Part II. The extra drag created by these bulge fairings should be accounted for in the the estimation of fuselage drag: see Section 4.3. Note that a bulge fairing will add to the cross sectional area of the fuselage and therefore will reduce the 'effective' fuselage slenderness ratio parameter l_f/d_f. This causes an increase in fuselage drag as given by Eqn.(4.30).

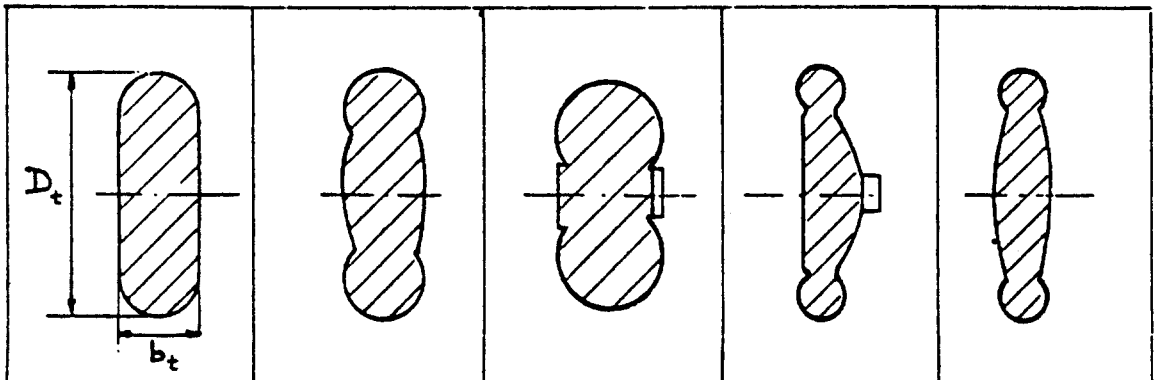

Streamlined Tire	Low Pressure Tire	Very Low Pressure Tire	High Pressure Tire	Standard Tire
$D_t.b_t$=27x9 1/4"	$D_t.b_t$=25x8½"	$D_t.b_t$=19,5x9"	$D_t.b_t$=26x5"	$D_t.b_t$=20x4"
C_D = 0,18	C_D = 0,25	C_D = 0,18	C_D = 0,30	C_D = 0,25

Drag Coefficients of Wheels

COPIED FROM REF. 21

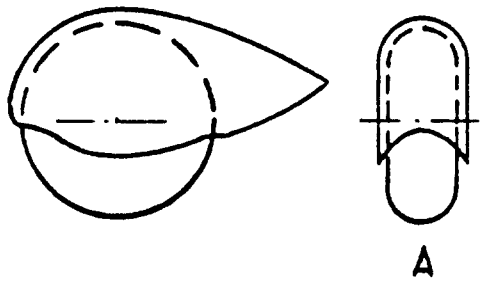

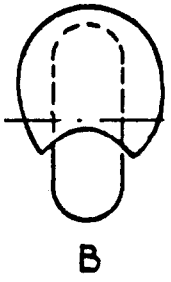

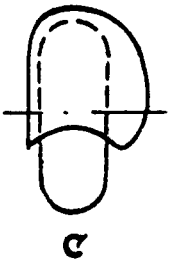

		A	B	C
Wheel without fairing	: C_D = 0,24		0,24	0,24
Wheel with fairing	: C_D= 0,12 - 0,14		0,22	0,19

Drag Coefficients of Wheels With Fairings

Figure 4.57 Wheel Drag Increments

COPIED FROM: REF.21

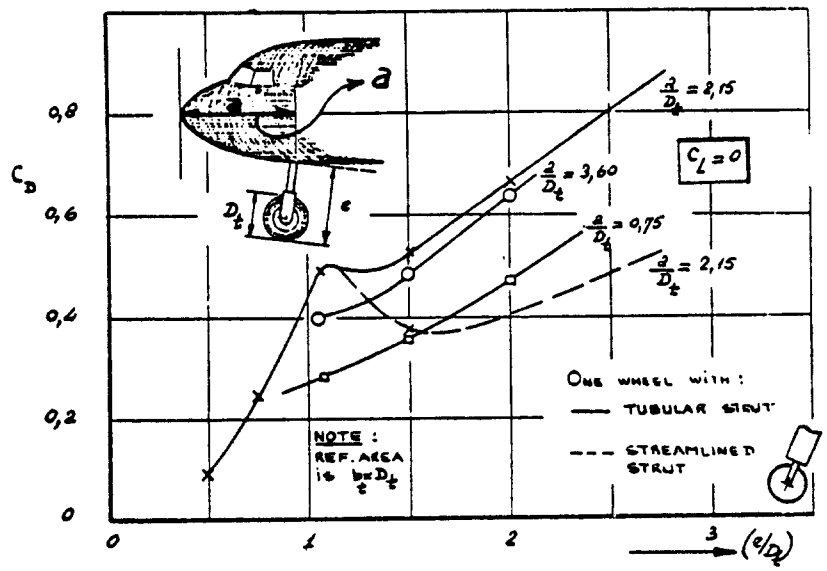

NOTE: GEAR CAVITY CLOSED!

Figure 4.58 Nosegear Drag Increments

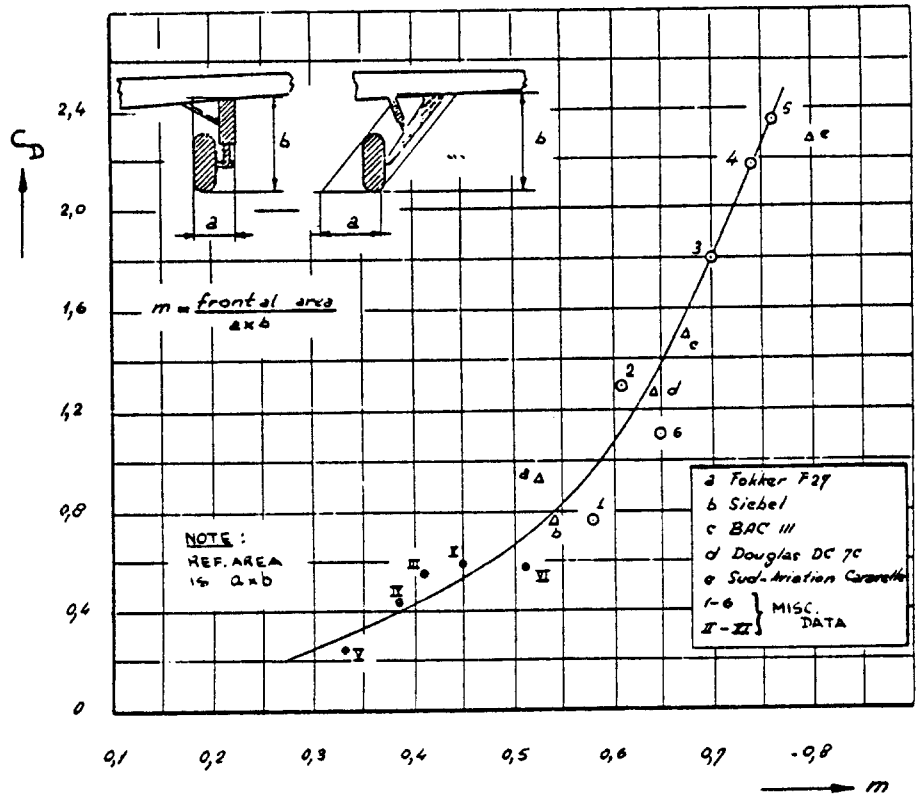

NOTE: GEAR CAVITY OPEN!

COPIED FROM: REF. 21

Note: All C_D values are referenced to axb of one gear, but apply to the entire landing gear, including interference drag

Figure 4.59 Gear Drag Increments: Retractable Gears

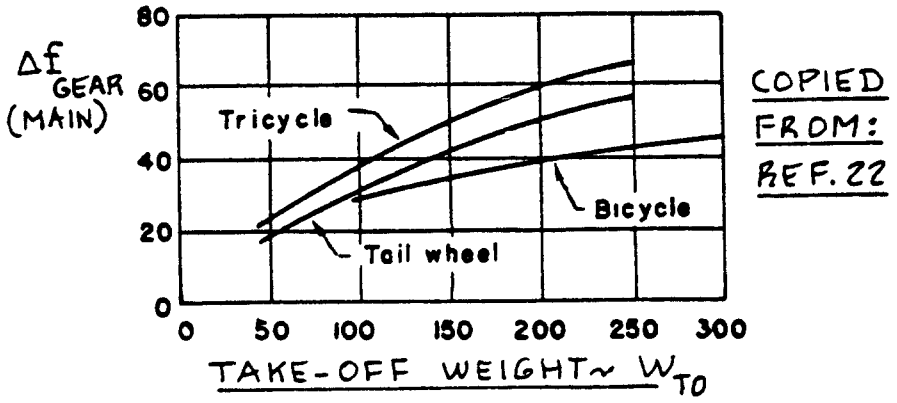

Figure 4.60 Equivalent Parasite Area Increment for Gears with Multiple Wheel Bogies

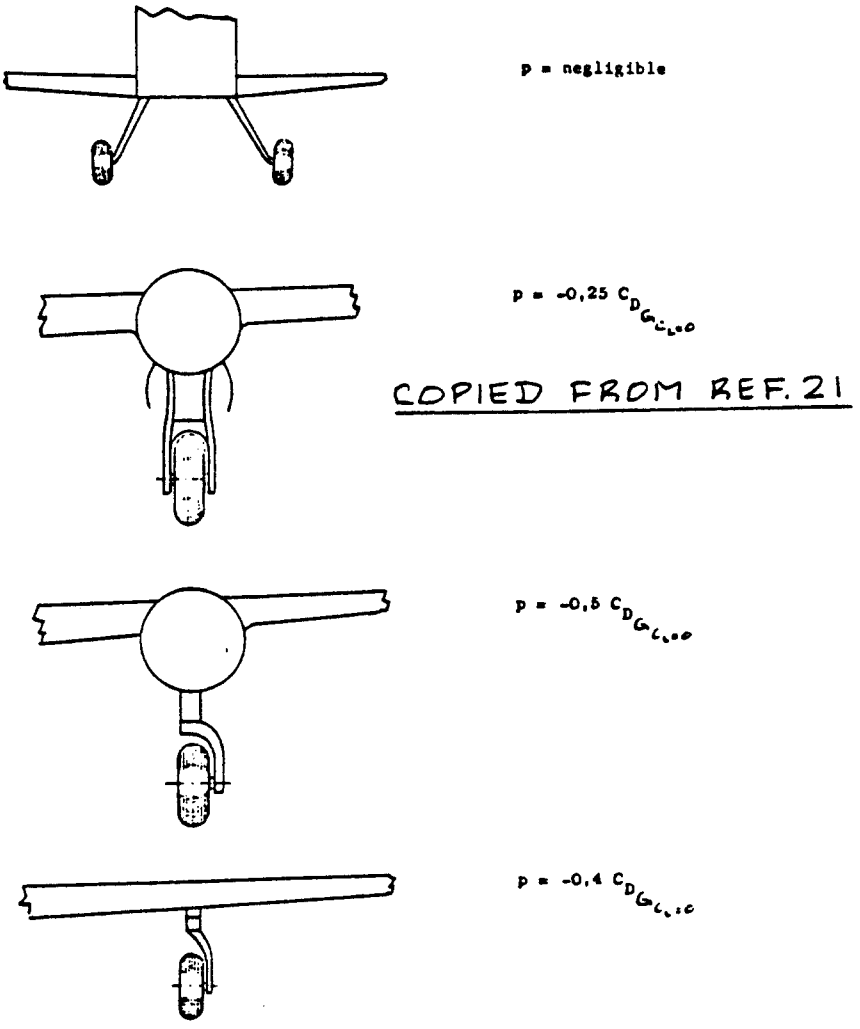

Figure 4.61 Landing Gear Induced Drag Factor

4.8 CANOPY/WINDSHIELD DRAG PREDICTION

The following method applies in the subsonic speed range. In the transonic and supersonic speed ranges the wave drag generated by canopies and windshields can be significant. In these speed ranges it will be necessary to employ area-ruling to cut wave drag to a minimum. Sub-section 4.3.4 presents a discussion on area-ruling.

The drag coefficient due to a canopy and/or a windshield may be found from:

$$C_{D_{cw}} = C_{D_{can}} + C_{D_{ws}} \qquad (4.78)$$

where: $C_{D_{can}}$ = drag coefficient due to a canopy, see 4.8.1.

$C_{D_{ws}}$ = drag coefficient due to a windshield, see 4.8.2.

4.8.1 Canopy Drag Prediction

The drag coefficient due to a canopy may be estimated from:

$$C_{D_{can}} = (\Delta C_{D_{can}})S_{can}/S \qquad (4.79)$$

where: $\Delta C_{D_{can}}$ = the incremental drag coefficient due to the canopy. Figures 4.62 through 4.67 provide data from which this increment may be found. Note from Figure 4.67, that this increment varies with Mach number in the subsonic speed range!

S_{can} = the maximum frontal area of the canopy as shown in Figure 4.62.

4.8.2 Windshield Drag Prediction

The drag coefficient due to a windshield may be determined from:

$$C_{D_{ws}} = (\Delta C_{D_{ws}})S_{fus}/S \qquad (4.80)$$

where: $\Delta C_{D_{ws}}$ = incremental drag coefficient due to a windshield: see Figure 4.68.

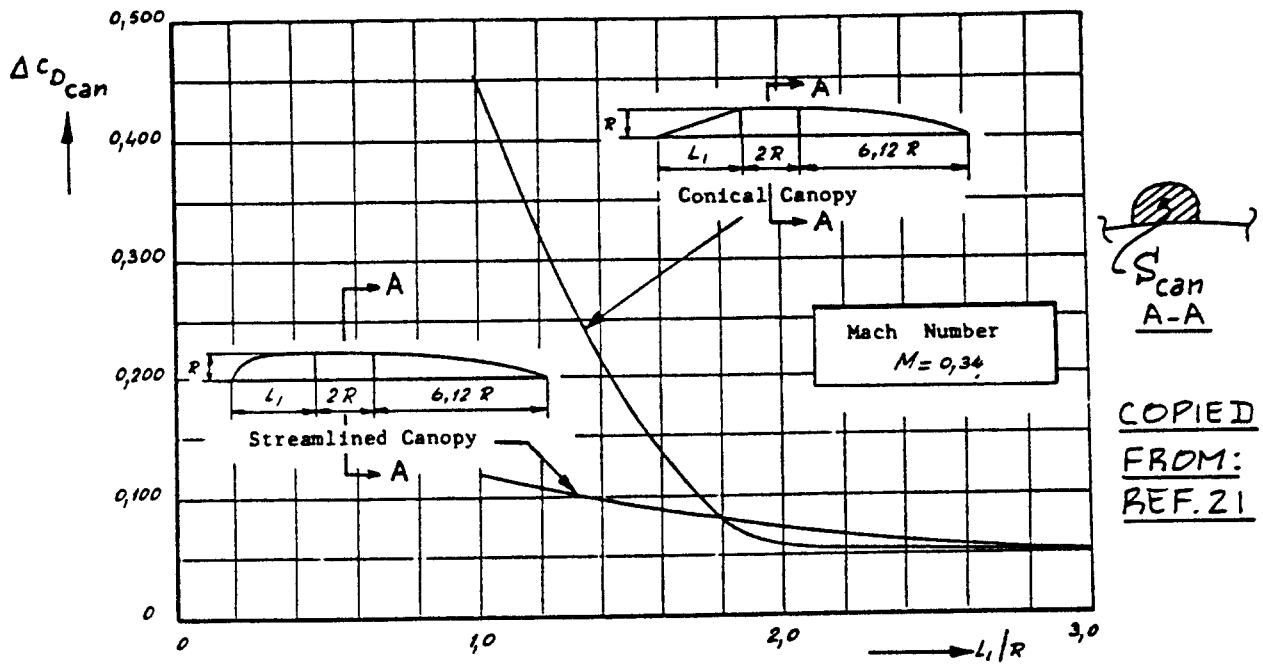

$\Delta C_{D_{can}}$ = Canopy Drag Coefficient Referenced to Frontal Area of Canopy, S_{can}

Figure 4.62 Effect of L_1 on Canopy Drag

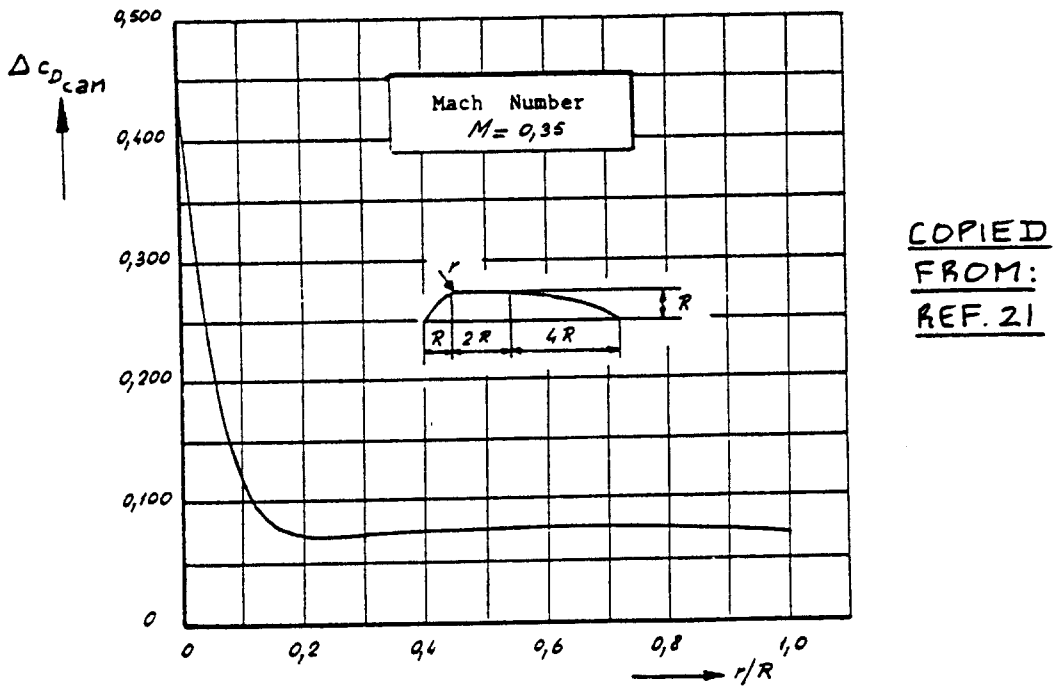

$\Delta C_{D_{can}}$ = Canopy Drag Coefficient Referenced to Frontal Area of Canopy, S_{can}

Figure 4.63 Effect of 'r' on Canopy Drag

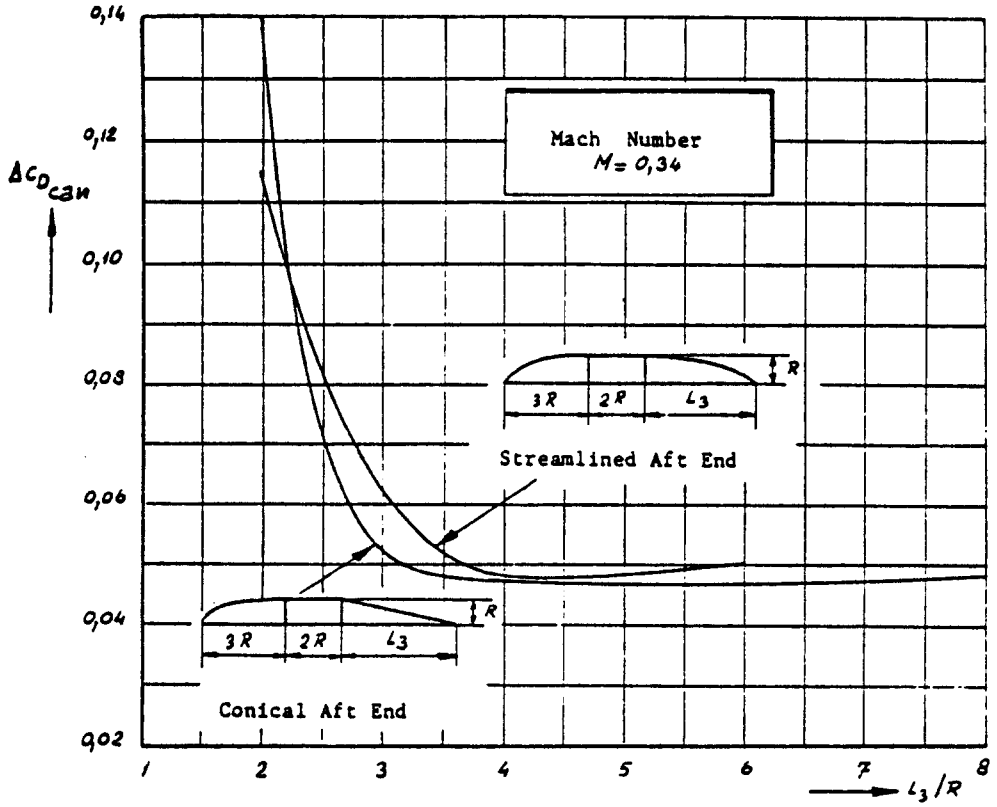

COPIED FROM: REF. 21

$\Delta C_{D_{can}}$ = Canopy Drag Coefficient Referenced to Frontal Area of Canopy, S_{can}

Figure 4.64 Effect of L_3 on Canopy Drag

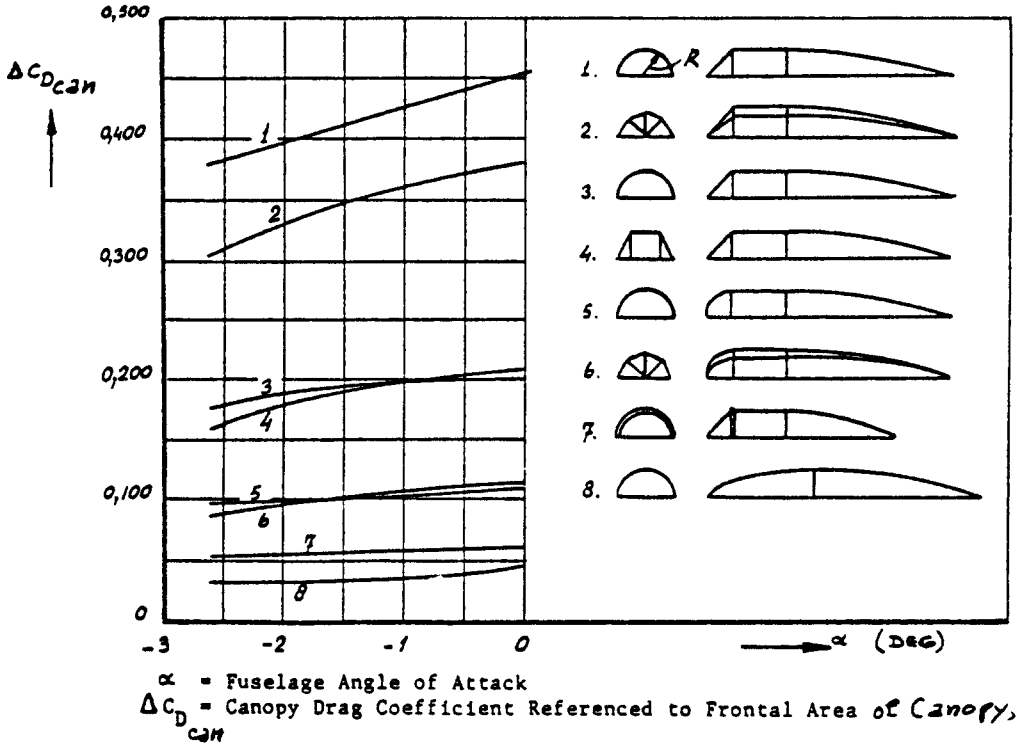

COPIED FROM: REF. 21

α = Fuselage Angle of Attack

$\Delta C_{D_{can}}$ = Canopy Drag Coefficient Referenced to Frontal Area of Canopy, S_{can}

Figure 4.65 Effect of Cross Section on Canopy Drag

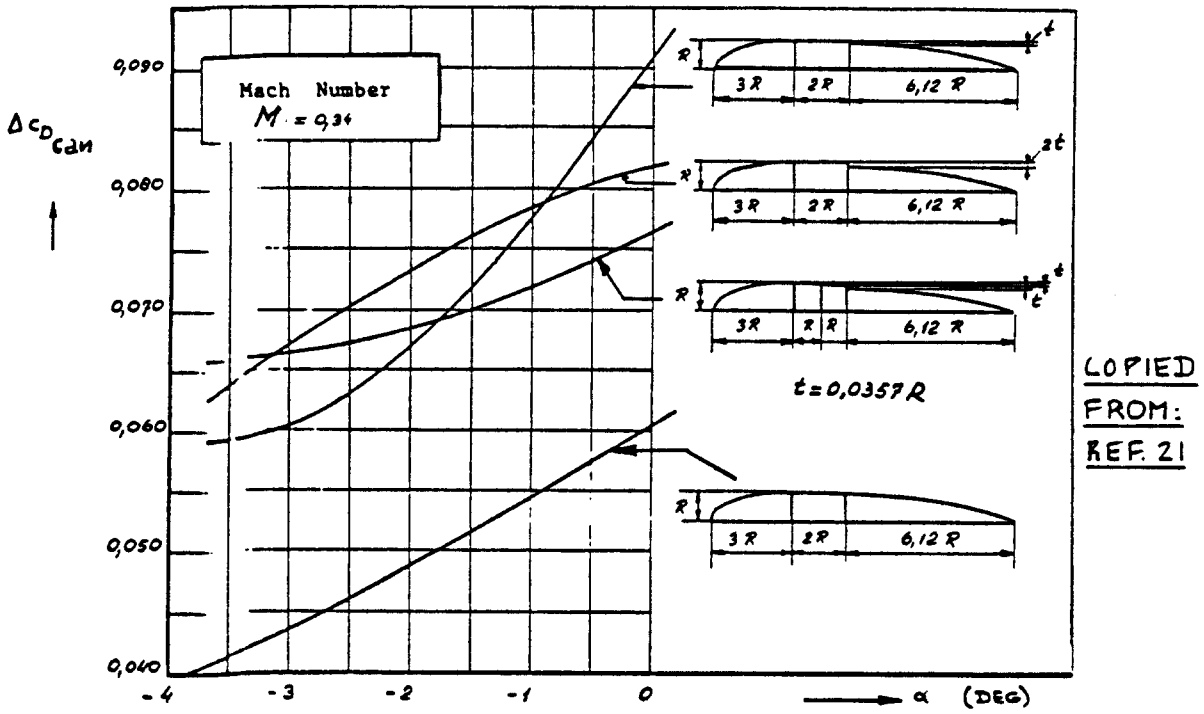

α = Fuselage Angle of Attack
$\Delta C_{D_{can}}$ = Canopy Drag Coefficient Referenced to Frontal Area of Canopy, S_{can}

Figure 4.66 Effect of Irregularities on Canopy Drag

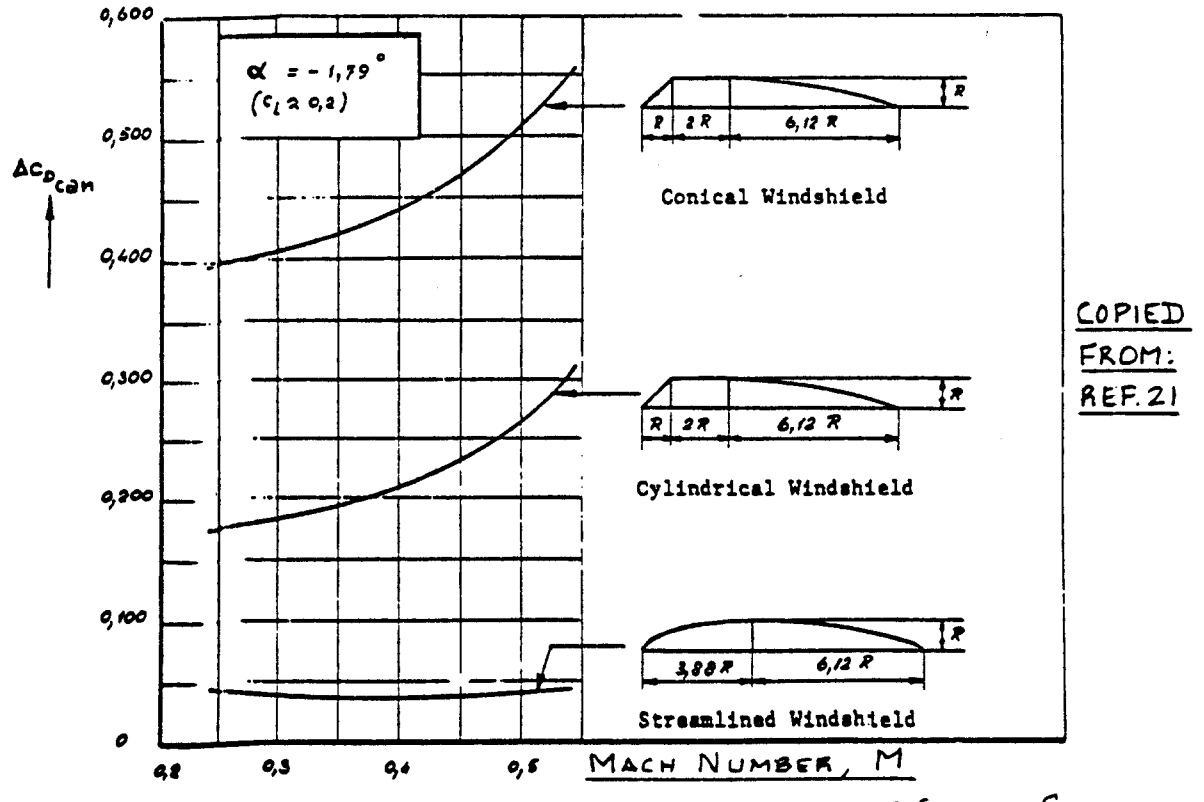

$\Delta C_{D_{can}}$ = Canopy Drag Coefficient Referenced to Frontal Area of Canopy, S_{can}

Figure 4.67 Effect of Mach Number on Canopy Drag

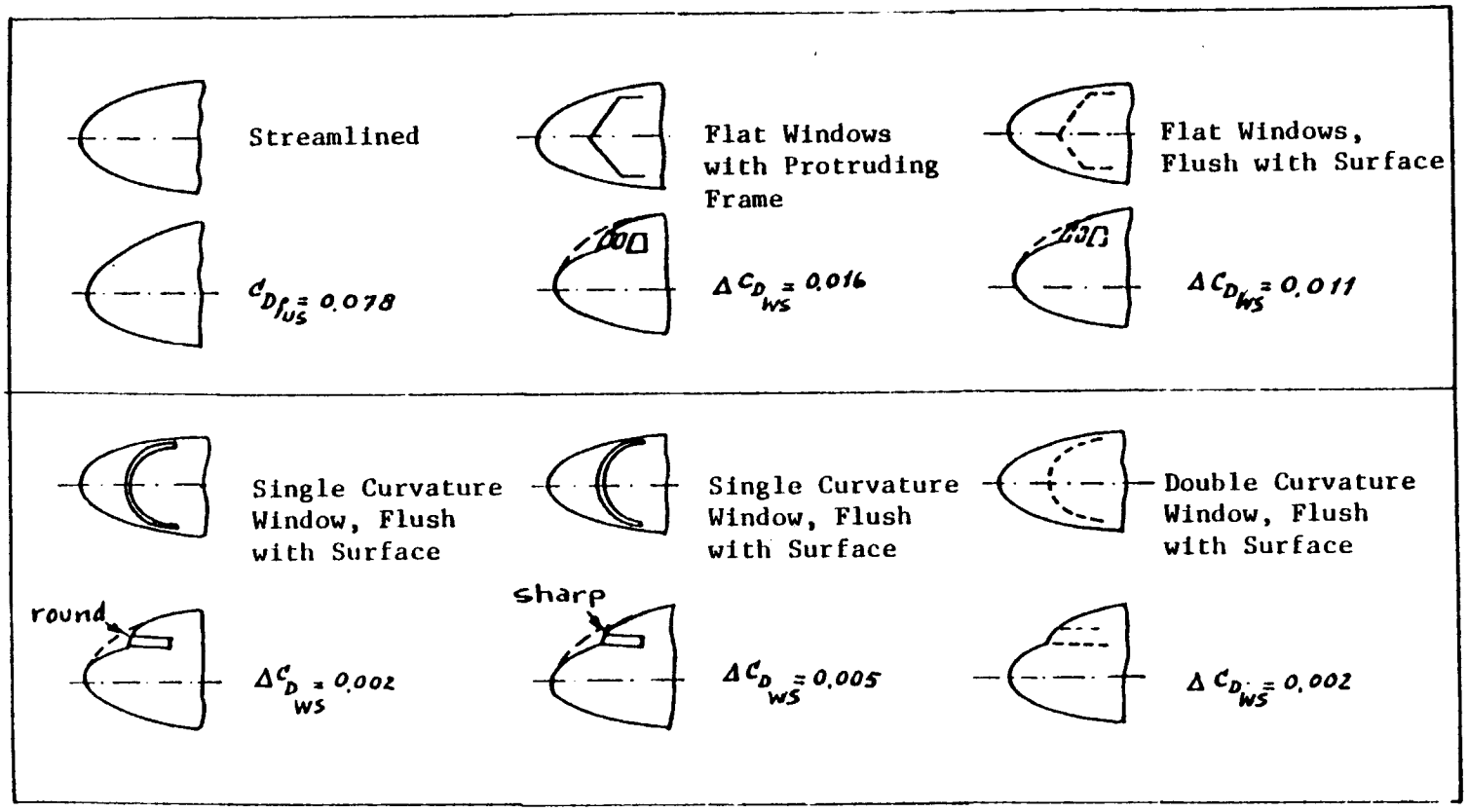

$C_{D_{fus}}$ = Fuselage Drag Coefficient Referenced to the Frontal Area of the Fuselage

$\Delta C_{D_{WS}}$ = Drag Coefficient of the Windshield Referenced to the Frontal Area of the Fuselage, S_{fus}

Figure 4.68 Effect of Windshield Configuration on Drag

4.9 STORE DRAG PREDICTION

Reference 9 provides detailed methods for estimating the drag due to many external store arrangements. Lacking that reference it is suggested to proceed as follows:

Step 1: Determine the isolated store drag coefficient, $(C_{D_{store}})_i$ for each store from the method of Section 4.3 by considering each isolated store to be like a fuselage.

Step 2: Compute the total store drag coefficient from:

$$C_{D_{store}} = SUM_i\{(K_{store})_i (C_{D_{store}})_i\} \qquad (4.81)$$

where: $(K_{store})_i$ = store interference factor:

For semi-submerged stores as shown in Figure 4.69: $K_{store} = 0.7$

For external stores as shown in Figure 4.70: $K_{store} = 1.3$

$(C_{D_{store}})_i$ = drag coefficient of the isolated store, see Step 1.

Additional data on the drag of various externally carried stores may be found in Reference 8.

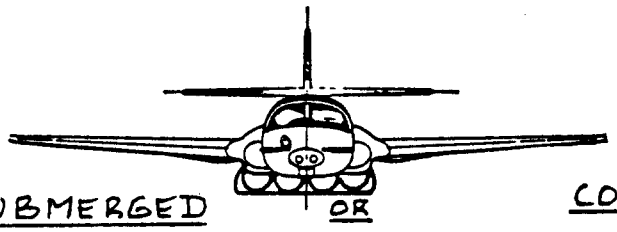

Figure 4.69 Example of Semi-submerged (Conformal) Stores

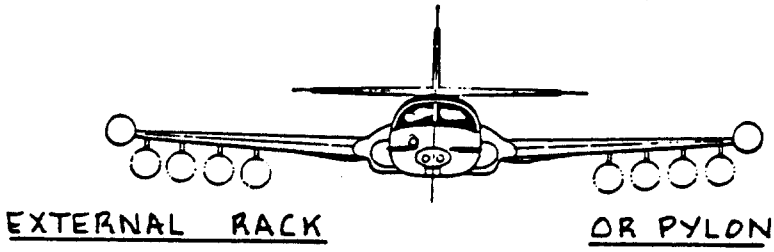

Figure 4.70 Example of External Stores

4.10 TRIM DRAG PREDICTION

Trim drag is caused by lift generated on a horizontal tail and/or a canard as a result of the requirement to 'moment trim' an airplane. Figure 4.71 illustrates two types of trim forces to be considered here. These trim force requirements result in two types of drag:

1. Trim drag due-to-lift generated on the trimming surface
2. Profile drag generated on the trimming surface as due to a control surface or a flap deflection.

The total trim drag coefficient may be found from:

$$C_{D_{trim}} = \Delta C_{D_{trim_{lift}}} + \Delta C_{D_{trim_{prof}}} \qquad (4.82)$$

where: $\Delta C_{D_{trim_{lift}}}$ = the induced drag coefficient increment due to the need for generating trim lift: see 4.10.1.

$\Delta C_{D_{trim_{prof}}}$ = the profile drag coefficient increment due to the need for generating trim lift: see 4.10.2.

4.10.1 Trim Drag Due to Lift

The trim drag due-to-lift increment, $\Delta C_{D_{trim_{lift}}}$ may be estimated from:

$$\Delta C_{D_{trim_{lift}}} = \{(\Delta C_{L_h})^2/\pi A_h e_h\} S/S_h + \{(\Delta C_{L_c})^2/\pi A_c e_c\} S/S_c \qquad (4.83)$$

where: ΔC_{L_h} = the horizontal tail incremental lift coefficient required for trim: see Section 8.3.

ΔC_{L_c} = the canard inremental lift coefficient required for trim: see Section 8.3.

A_h and A_c follow from the airplane threeview as developed in Chapter 13 of Part II.

e_h and e_c are defined on page 68.

4.10.2 Trim Drag Due to Profile Drag

The trim drag increment due to profile drag, is caused by the need to deflect an elevator, a canard-vator or a canard flap for purposes of trimming an airplane. The following equation assumes that trim is accomplished by a combination of elevator deflection and canard flap deflection:

$$\Delta C_{D_{trim_{prof}}} = \Delta C_{D_{p_{\Lambda_{c/4}=0}}} \cos\Lambda_{c/4} (S_{ef}/S_h)(S_h/S) + \Delta C_{D_{p_{\Lambda_{c/4}=0}}} \cos\Lambda_{c/4} (S_{cf}/S_c)(S_c/S) \quad (4.84)$$

where: $\Delta C_{D_{p_{\Lambda_{c/4}=0}}}$ = the profile drag coefficient due to an elevator and/or a canard control surface. It may be found with the method of Section 4.6, but with the following substitutions:

Elevator and/or canard-vator: these should be considered to be plain flaps. Elevator deflection, δ_e and/or canard-vator deflection, δ_{cv} are used instead of the flap deflection, δ_f.

Canard flap: if trimming is accomplished with a canard flap then it must be determined what type of flap the canard flap resembles most. The data of Sub-section 4.6.1 can be used to estimate the profile drag due to trim by a canard flap.

S_{ef} = flapped horizontal tail area, see Fig.4.72

S_{cf} = flapped canard area, see Fig.4.72

S_h and S_c are the canard and horizontal tail areas respectively.

Note: trim can be accomplished also with a variable incidence stabilizer or with an elevator trim tab. It is left up to the user to make the required modifications in Equations (4.83) and (4.84) to account for such cases.

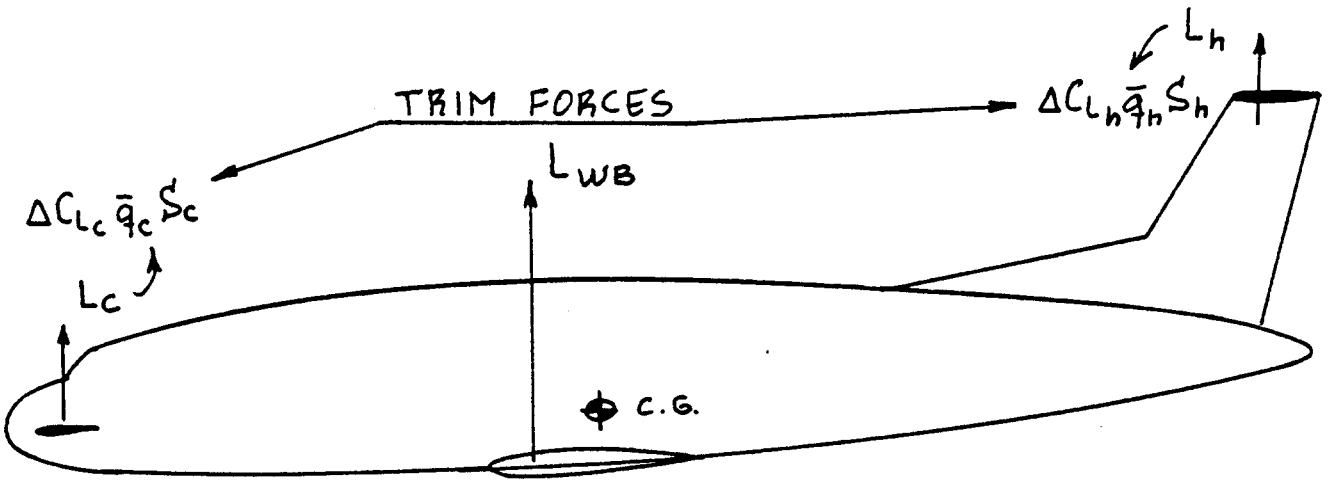

Figure 4.71 Example of Trim Force Requirements

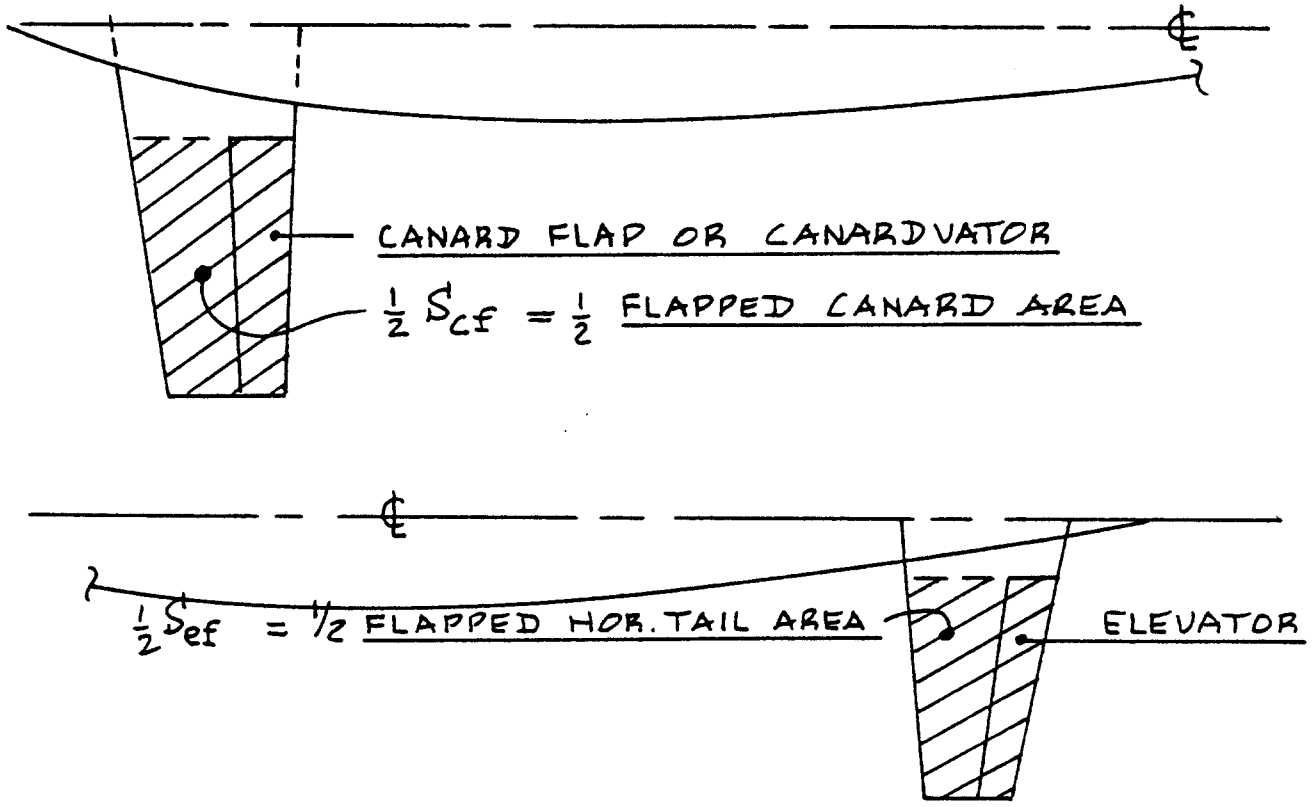

Figure 4.72 Definition of Flapped Areas

4.11 INTERFERENCE DRAG PREDICTION

Interference drag is a type of drag which is not yet fully understood. Its effect is that the total drag of two or more airplane components when integrated in a configuration is always larger than the sum of the individual component drags.

Several interference drag factors were already accounted for in Sections 4.2, 4.3, 4.5, 4.6 and 4.9. In addition to interference drag accounted for by these factors, extra interference drag may be caused by:

1. Wing struts meeting a wing and/or a fuselage at 'sharp' angles. Figure 4.73 shows such a case.

2. Empennage surfaces meeting each other or a fuselage at 'sharp' angles. Figure 4.74 illustrates several cases.

3. Low or high wing airplanes tend to have more interference drag than midwing airplanes: in the midwing configuration, the 'venturi' effect is absent. Figure 4.75 shows examples.

4. Wing/nacelle installations can have significantly greater interference drag than suggested by the the methods of 4.5.2.1 and 4.5.2.2.

In many instances it is possible to decrease interference drag by the use of so-called 'fairings'. Figures 4.73 - 4.75 show typical fairings.

The reader should carefully examine his configuration for additional causes of interference drag. To estimate their effect, the interference drag data base presented in Reference 8 should be used.

4.12 MISCELLANEOUS DRAG PREDICTION

The following drag items will be considered as miscellaneous drag contributions:

4.12.1 Drag due to spoilers (or speed brakes)
4.12.2 Drag due to surface roughness
4.12.3 Drag due to other causes

4.12.1 Drag Due to Spoilers (or Speed Brakes)

The incremental drag coefficient due to spoilers may be estimated from:

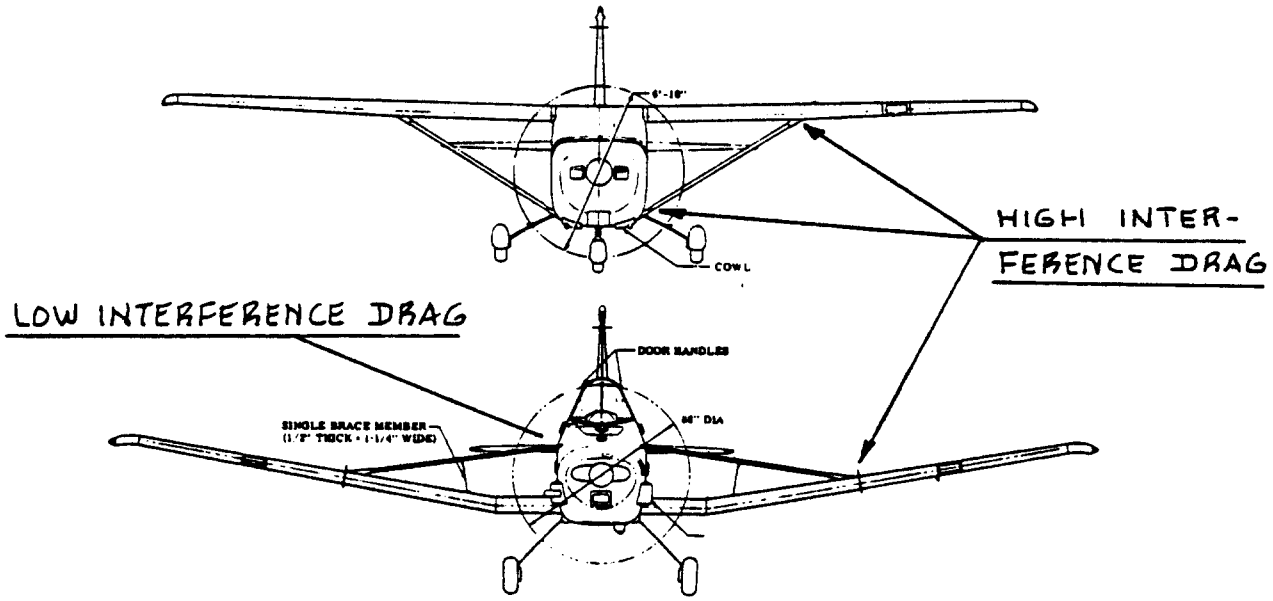

Figure 4.73 Wing Strut Arrangements With High and Low Interference Drag

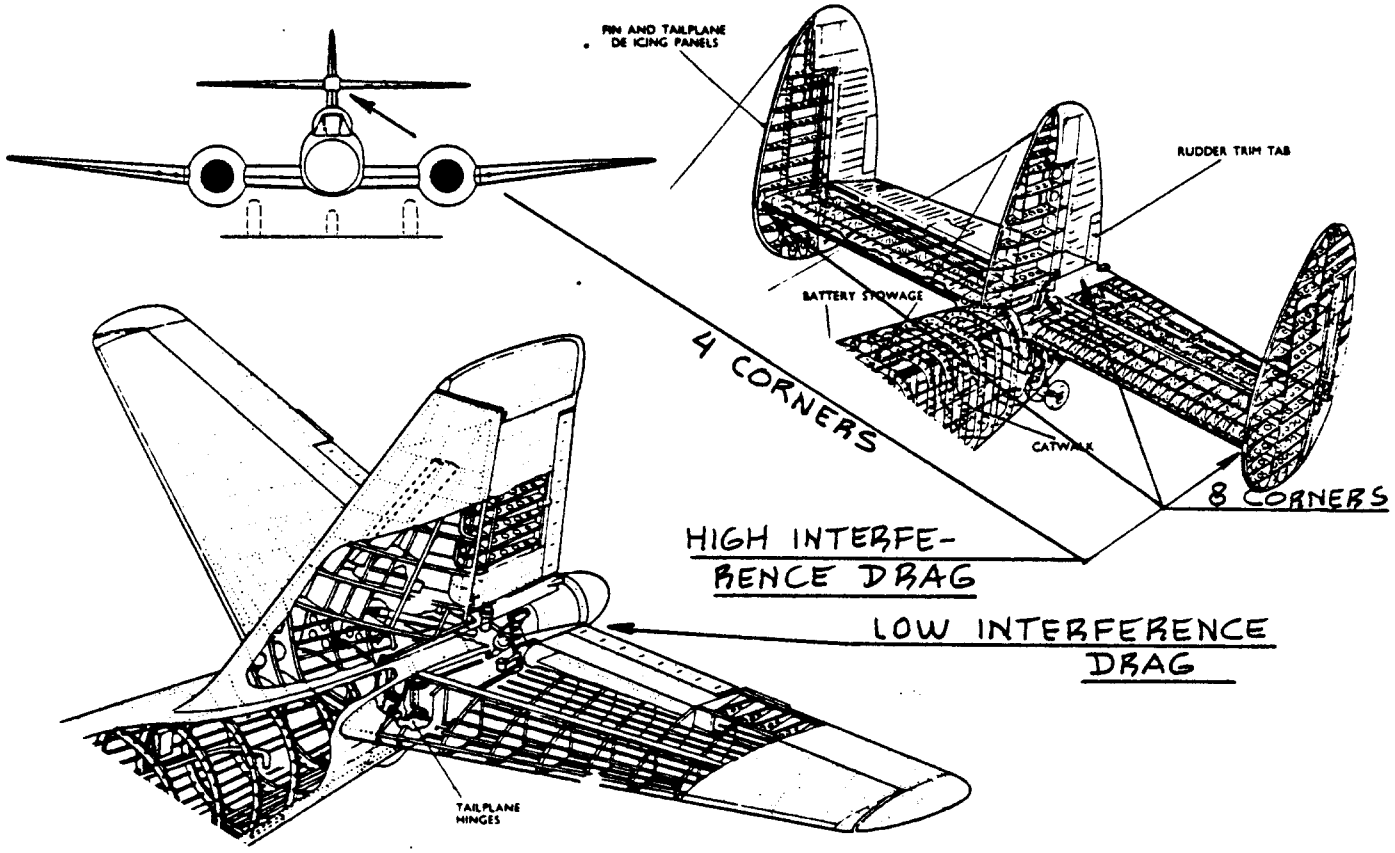

Figure 4.74 Empennage Arrangements with High and Low Interference Drag

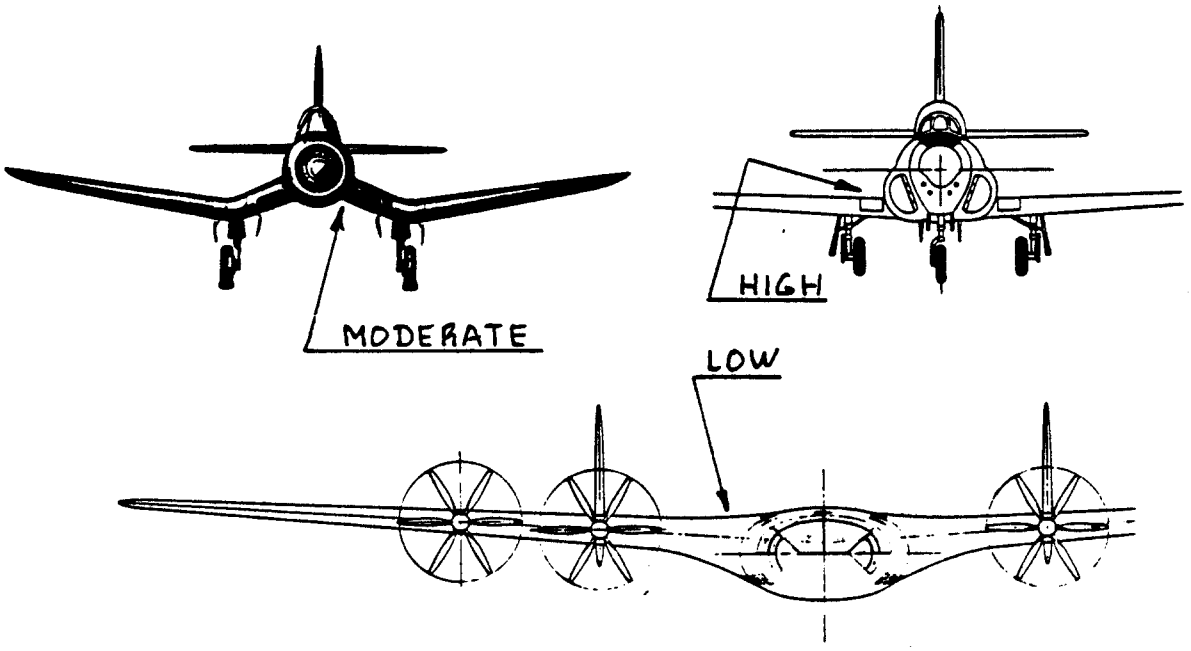

Figure 4.75 Wing/Fuselage Arrangements with High and Low Interference Drag

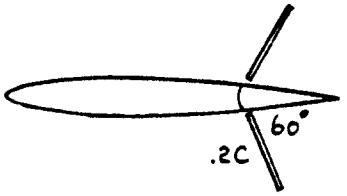

SOLID PLATES

$\Delta C_{D_{sp}} = 0.63$

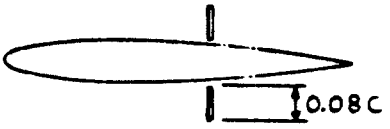

SHOWN AT .60 C

NACA 2412

$\Delta C_{D_{sp}} = 1.60$ AT .60 C

1.25 AT 1.00 C

FLAT PLATE DEFLECTED PERPENDICULAR TO FUSELAGE $\Delta C_D = 1.0$

Note: All coefficients are based on the area of the speed brake *or spoiler*

Figure 4.76 Drag Due to Spoilers and Speed Brakes

$$\Delta C_{D_{sp}} = \text{Sum}_i\{(\Delta C_{D_{sp_i}})(S_{sp_i}/S)\} \qquad (4.85)$$

where: $C_{D_{sp_i}}$ is found from Figure 4.76 for several spoiler locations.

S_{sp_i} is the flat plate area of each spoiler.

4.12.2 Drag Due to Surface Roughness

The methods for estimating friction and profile drag of wings and fuselages as discussed in Sections 4.2 and 4.3 apply only to 'smooth' surfaces. If a surface is 'rough', additional drag is created.

The actual level of turbulent boundary layer friction drag of 'rough' surfaces may be estimated with the following procedure:

Step 1: Determine the reference length l: this is $\bar{c}_{w_e}$ in the case of a wing and l_f in the case of a fuselage.

Step 2: Compute the parameter l/k, where k is determined from the following table:

Type of Surface	Equivalent Sand Roughness, k, in ft
Aerodynamically smooth	0.0
Polished metal or polished wood	0.00000167 to 0.00000667
Natural sheet metal	0.00001333
Smooth matte paint, carefully applied	0.00002083
Standard camouflage paint, average application	0.00003333
Camouflage paint, mass-production spray	0.0001
Dip-galvanized metal surface	0.0005
Natural surface of cast iron	0.00083

As a practical matter, use this information as follows:

For light airplanes with standard sheet metal manufacturing methods: use k = 0.00001333 ft.

For business jets and jet transports with sheet metal manufacturing methods but polished surfaces: use k = 0.000005 ft.

For airplanes made of composites and polished surfaces: use k = 0.00000167 ft.

For military airplanes with camouflage paint applied in the factory: use k = 0.00002083 ft.

For military airplanes with camouflage paint applied in the field: use k = 0.0001 ft.

Step 3: Determine the 'cut-off Reynolds number', $R_{N_{cut-off}}$ with the help of Figure 4.77.

Step 4: Determine the actual Reynolds number with Equation (4.7) or Equation (4.31).

Step 5: If $R_{N_{cut-off}} > R_N$ find C_f from Figure 4.3 at the actual Reynolds number.

If $R_{N_{cut-off}} < R_N$ find C_f from Figure 4.3 at the 'cut-off' Reynolds number.

Step 6: Substitute the appropriate value of C_f for C_{f_w} in Eqn.(4.6) or for $C_{f_{fus}}$ in Eqn.(4.30) and proceed with the determination of the desired zero-lift drag coefficients as indicated in Sections 4.2 and 4.3.

4.12.3 Drag Due to Other Causes

Other causes for drag may be items such as: struts, antennas, surface gaps, extra drag caused by inlet air spillage and by exhaust nozzle integration. Strut and antenna drag may be estimated by assuming these to be like small wings. For surface gap drag the reader should consult Ref. 8. For estimation of extra inlet drag the method of Sub-section 6.2.4 may be used. For estimation of drag due to exhaust nozzles, see Section 6.3.

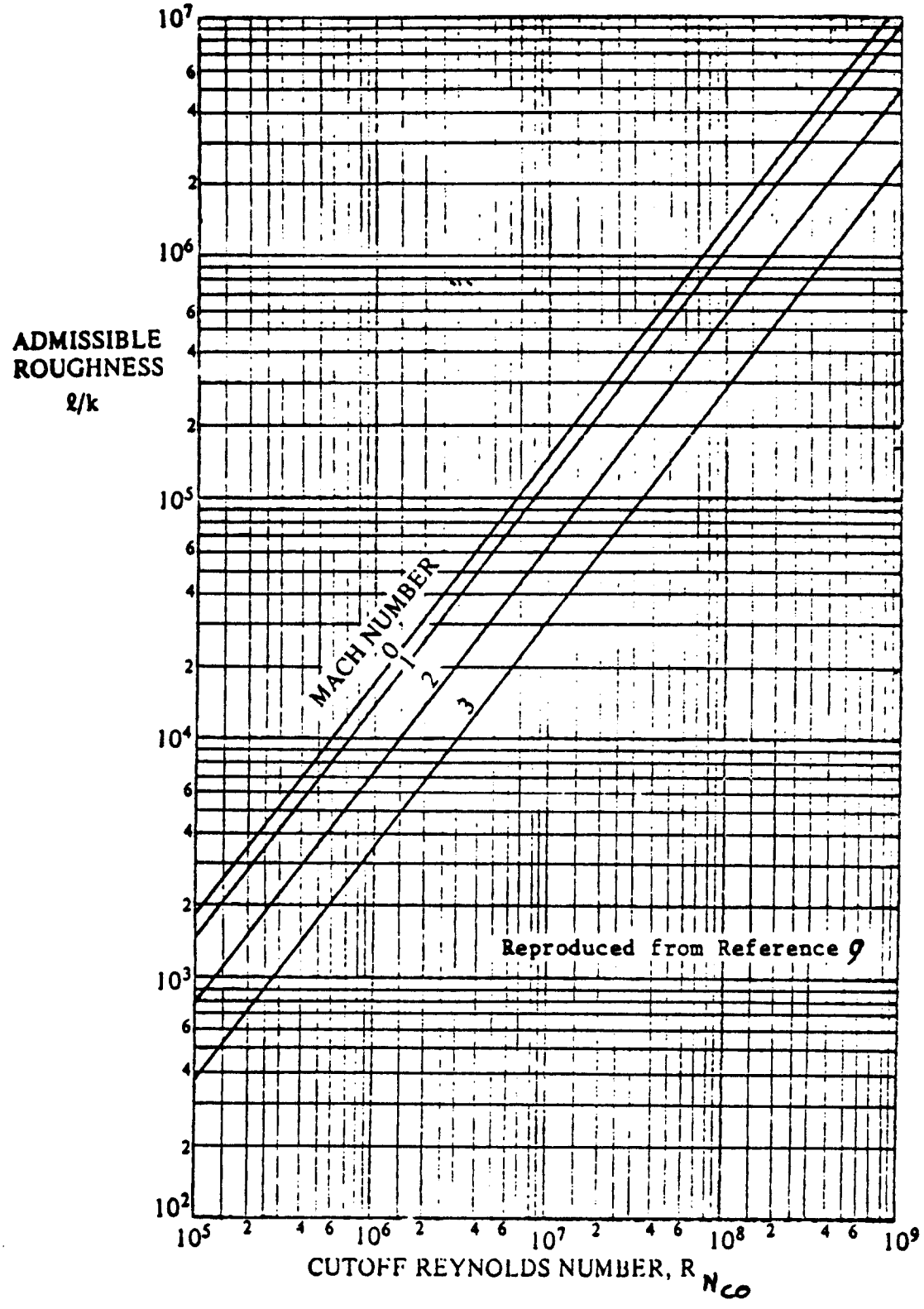

Figure 4.77 Effect of Mach Number on the Relation Between Cut-off Reynolds Number and Roughness

4.13 DRAG ADJUSTMENTS FOR LAMINAR FLOW

During the 70's and the 80's it has become increasingly evident that natural laminar boundary layer flow (instead of turbulent boundary layer flow) is practical in many instances. The resulting reduction in friction drag is very significant and should be accounted for in any realistic drag prediction procedure.

The methods presented in Sections 4.3 through 4.12 assume that the boundary layer is turbulent. To adjust the airplane zero-lift drag coefficient downward due to the existence of laminar flow, the following procedure is recommended:

If laminar flow is expected to occur naturally (natural laminar flow, also called NLF) start at Step 1.

If laminar flow is being forced, by suction or by blowing, start at Step 2.

Step 1: Determine which components of the airplane are likely to experience NLF.

In preliminary design the following criteria for the existence of NLF may be used:

$M < 0.65$ $\qquad$ $\Lambda_{LE} < 15$ degrees

$C_{L_{design}} < 0.65$ $\qquad$ $R_N < 10^7$

Note: by careful design it is possible to extend these criteria. Use of advanced airfoil design codes is recommended to verify that NLF is practical.

Step 2: Divide the surface area of all airplane components which according to Step 1 will have a certain amount of NLF in two parts: $S_{wet_{lam}}$ and $S_{wet_{turb}}$.

Figure 4.78 shows how these wetted areas are defined for a wing and for a fuselage respectively.

Step 3: For a wing or for an empennage surface, use Equation (4.6), but replace the term:

$\{(C_{f_w})S_{wet_w}/S\}$ by: (4.86)

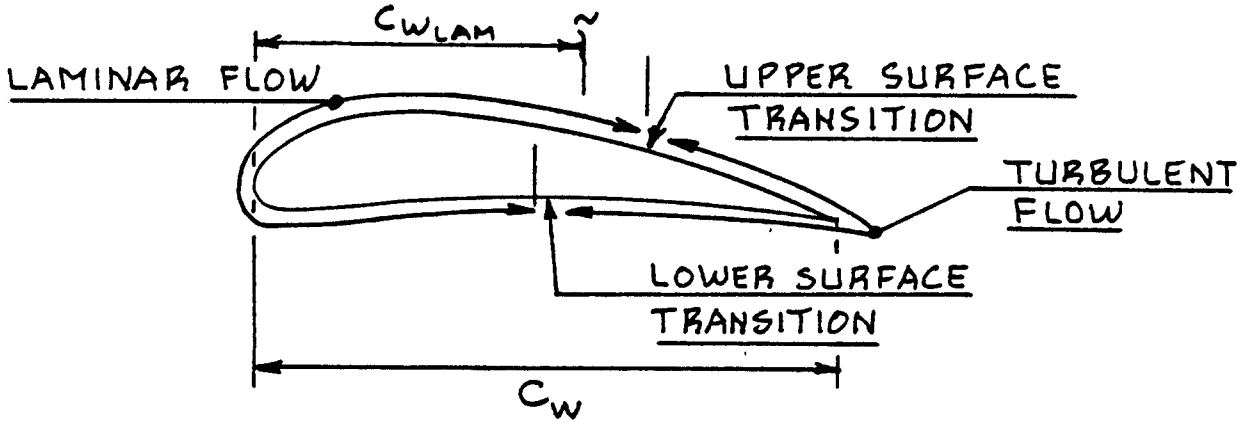

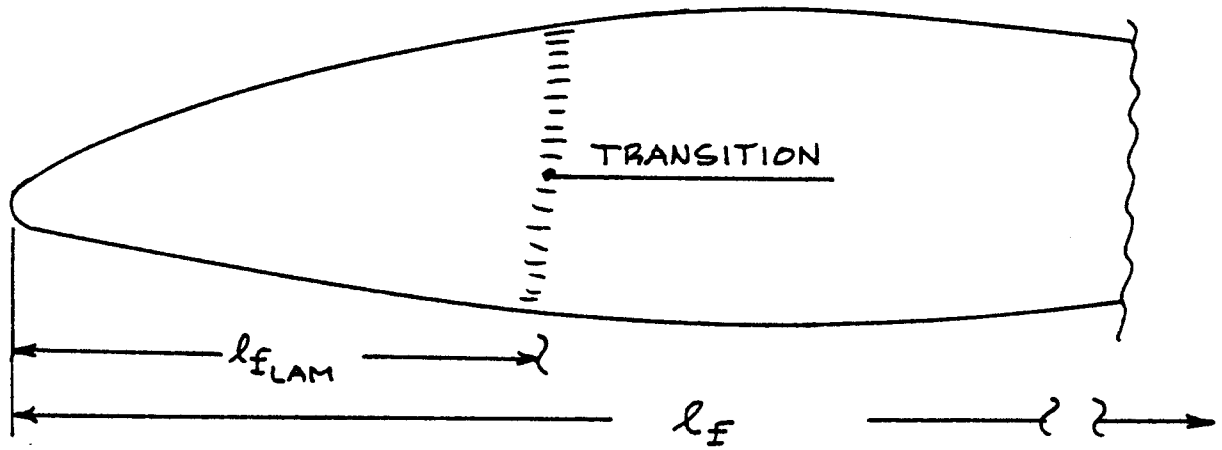

$S_{WET_{W_{LAM}}}$ = WETTED AREA OF THE WING IN THE LAMINAR FLOW REGION

$S_{WET_{FUS_{LAM}}}$ = WETTED AREA OF THE FUSELAGE IN THE LAMINAR FLOW REGION

Figure 4.78 Definition of Laminar and Turbulent Reference Lengths and Reference Areas

$$\{(C_{f_{w_{lam}}} - C_{f_{w_{tur}}})S_{wet_{w_{lam}}} + (C_{f_w})S_{wet_w}\}/S$$

For a fuselage or for a body similar to a fuselage, use Equation (4.30), but replace the term:

$$\{(C_{f_{fus}})S_{wet_{fus}}/S\} \text{ by:} \qquad (4.87)$$

$$\{(C_{f_{fus_{lam}}} - C_{f_{fus_{tur}}})S_{wet_{fus_{lam}}} + (C_{f_{fus}})S_{wet_{fus}}\}/S$$

where: C_{f_w} is the turbulent wing skin friction coefficient as found on p.23 of this text.

$$C_{f_{w_{lam}}} = 1.33/R_{N_{w_{lam}}}^{1/2}, \qquad (4.88)$$

with: $$R_{N_{w_{lam}}} = \rho U_1 c_{w_{lam}}/\mu \qquad (4.89)$$

$c_{w_{lam}}$ is the wing reference length of the laminar part of the wing: see Figure 4.78.

$S_{wet_{w_{lam}}}$ = the wing wetted area part exposed to laminar flow, see Figure 4.78.

$C_{f_{fus}}$ is the turbulent fuselage skin friction coefficient as found on p.44 of this text.

$$C_{f_{fus_{lam}}} = 1.33/(R_{N_{fus_{lam}}})^{1/2}, \qquad (4.90)$$

with: $$R_{N_{fus_{lam}}} = \rho U_1 l_{f_{lam}}/\mu \qquad (4.91)$$

$l_{f_{lam}}$ is the fuselage reference length of the laminar part of the fuselage: see Figure 4.78.

$S_{wet_{fus_{lam}}}$ = the fuselage wetted area part exposed to laminar flow, see Figure 4.78.

NOTES: 1. This procedure applies in the subsonic speed range only!

2. This procedure applies only as long as any surface irregularities (steps, waviness and roughness) are within the limits defined in Reference 23.

By using laminar flow control (sucking and/or blowing) it is possible to achieve laminar flow under conditions where natural laminar flow cannot be maintained. References 24 - 26 provide some data on the types of systems needed to achieve controlled laminar flow and on a number of operational considerations.

Once such systems are in place, the procedure given above for the adjustment of friction drag would apply except for the need to account for compressibility on the equations for skin friction coefficient. Reference 27 should be consulted for replacement of Eqns (4.88) and (4.90) by equations which account for compressibility effects in the transonic speed range below M=1.0

This text does not provide a method for accounting for laminar flow in the transonic speed range above M=1.0 nor for the supersonic flow regimes. This does not mean that laminar flow in these speed ranges is not feasible. Research in progress at NASA Langley indicates that in particular in the supersonic flow range extensive laminar flow may be possible. The conditions for which this can be achieved have not yet been firmly established.

References 28-30 provide some data on the design of fuselage shapes which are conducive to NLF. Design details such as inspection covers, doors and windshields must receive very careful attention, if laminar flow capability is to be retained after the airplane has been in service for some time!

5. AIRPLANE DRAG DATA

The purpose of this chapter is to present a range of actual airplane drag data. These data are given in the form of:

5.1 Drag polars
5.2 Equivalent parasite areas
5.3 Oswald's efficiency factors
5.4 Wetted area breakdown examples

Finally, once drag data for a new airplane have been computed, they should always be 'verified' by comparison against known drag data for similar airplanes. A method for verifying drag polar predictions is given in:

5.5 Verification of realism of computed drag polars

5.1 DRAG POLARS

Figures 5.1 through 5.19 present examples of actual airplane drag polars. The information is organized in the following manner:

Figure 5.1 Cessna 177: includes flap drag
Figure 5.2 Cessna 310: includes gear and flap drag
Figure 5.3 Gulfstream I: includes gear drag, flap drag and drag due to a feathered engine
Figure 5.4 SAAB 340
Figure 5.5 Fokker F-27: includes gear and flap drag
Figure 5.6 Lockheed C-130H: includes ground effect and compressibility data
Figure 5.7 SIAI-M S-211: includes gear and flap drag
Figure 5.8 NAA T2C: includes compressibility data
Figure 5.9 Convair F-106: includes supersonic drag
Figure 5.10 McDD AV8B: includes compressibility data
Figure 5.11 Learjet M25: includes compressibility data
Figure 5.12 Boeing 727-100: includes compressibility data
Figure 5.13 Boeing 707-320B: incl. compressibility data
Figure 5.14 Boeing 747-200: includes compressibility data
Figure 5.15 Boeing B-47B: includes compressibility data
Figure 5.16 Boeing B-52A: includes compressibility data
Figure 5.17 Lockheed C-141B: incl. compressibility data
Figure 5.18 Lockheed C-5A: includes compressibility data
Figure 5.19 Boeing SST Design: includes supersonic data

The reader should note that the wing (or reference) area, S, upon which the drag and lift coefficient data are based, is indicated on all Figures 5.1 through 5.19.

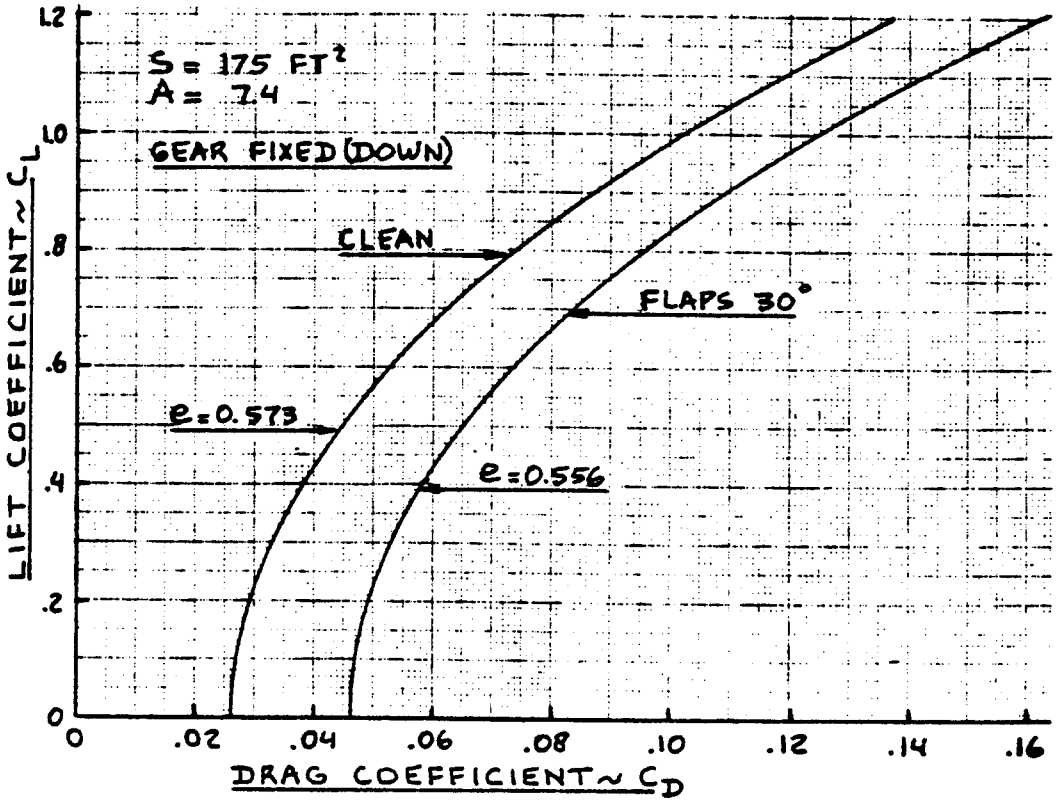

Figure 5.1 Drag Polars: Cessna 177

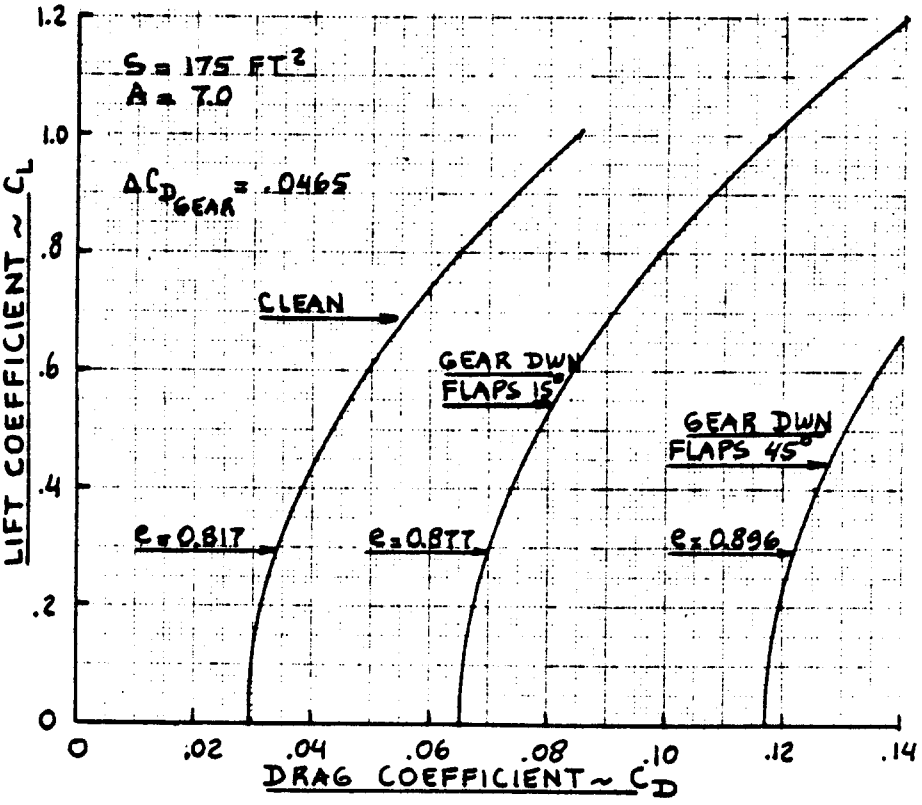

Figure 5.2 Drag Polars: Cessna 310

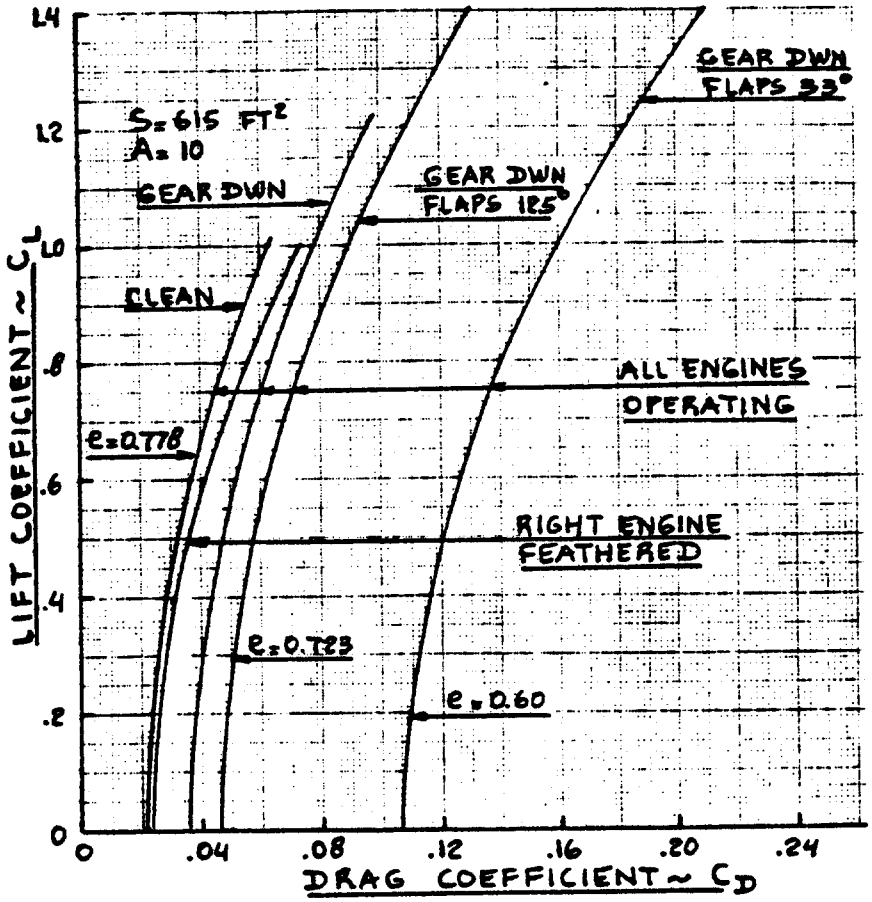

Figure 5.3 Drag Polars: Gulfstream I

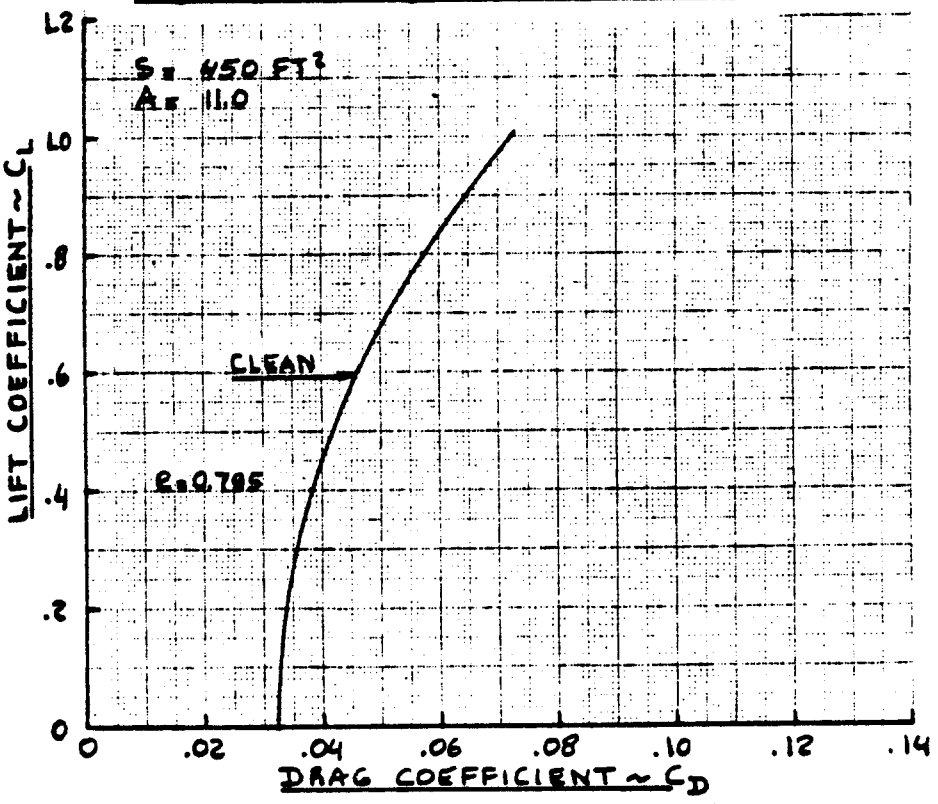

Figure 5.4 Drag Polar: SAAB 340

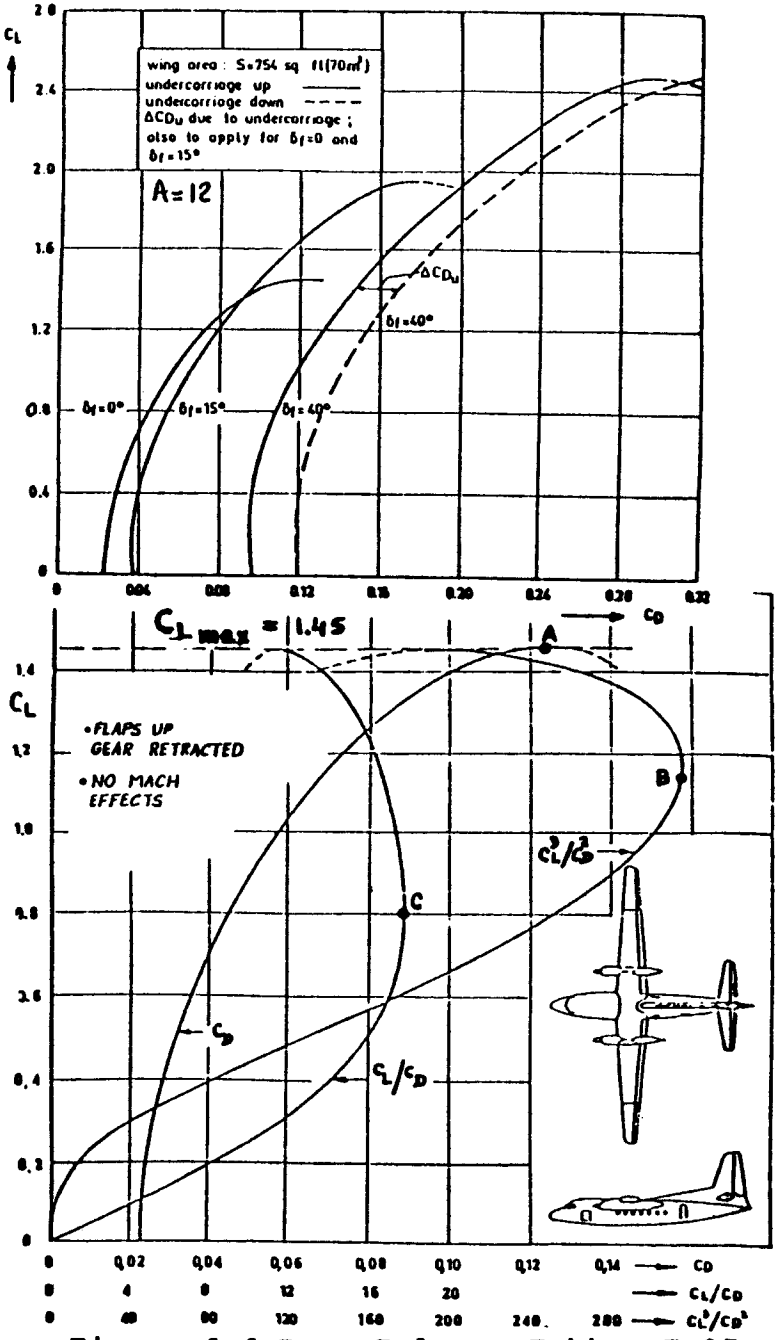

Figure 5.5 Drag Polars: Fokker F-27

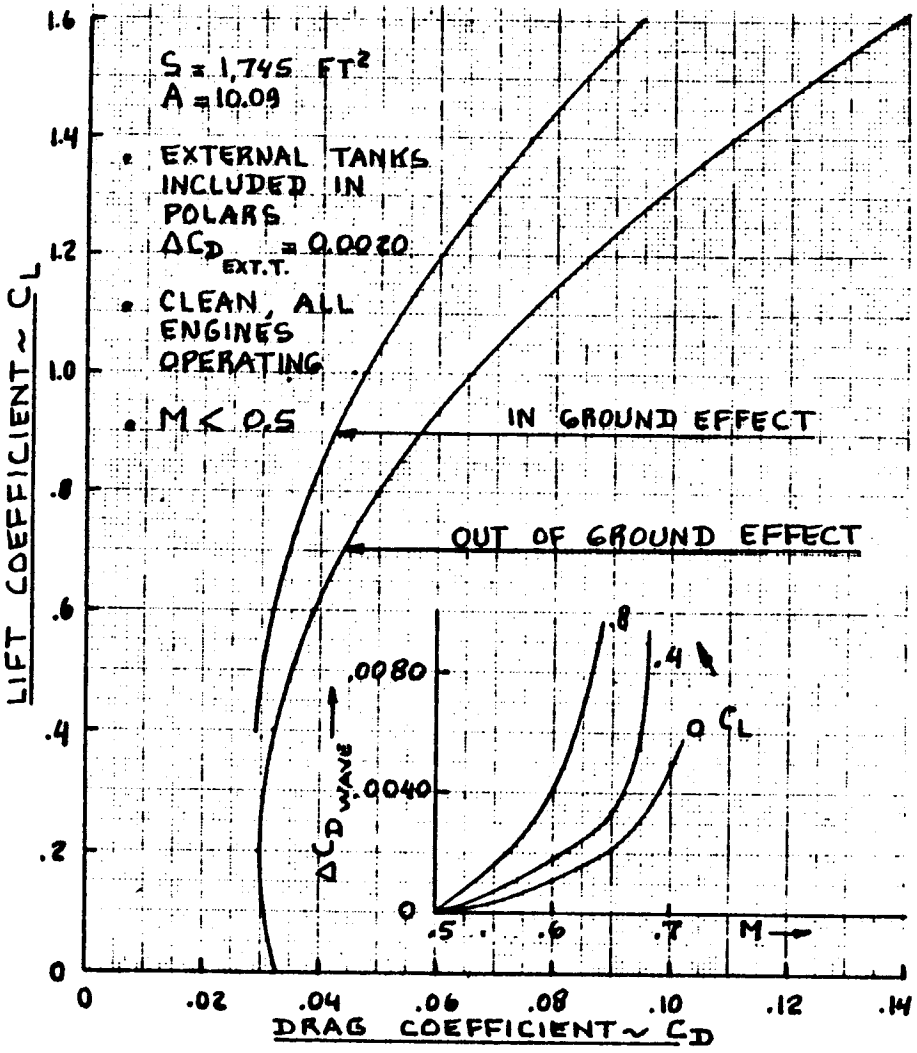

Figure 5.6 Drag Polars: Lockheed C-130B

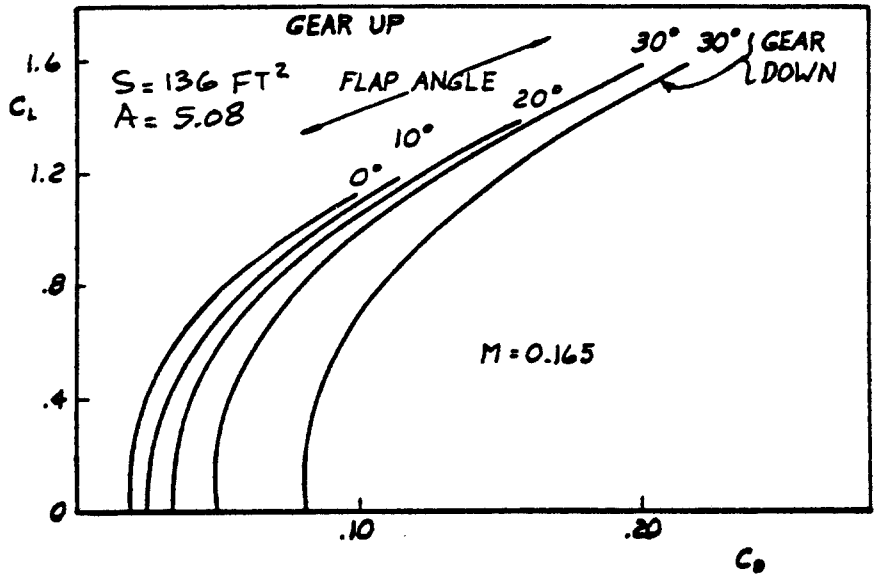

Figure 5.7 Drag Polars: SIAI-Marchetti S-211

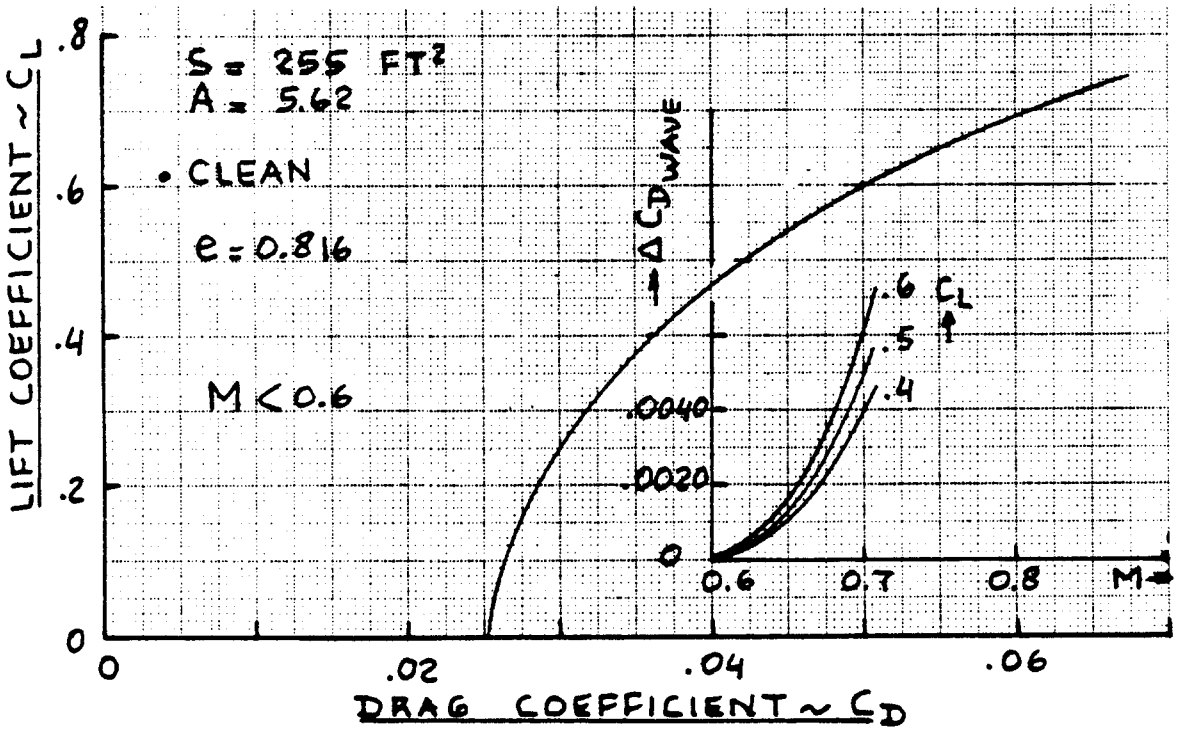

Figure 5.8 Drag Polars: NAA Rockwell T2C

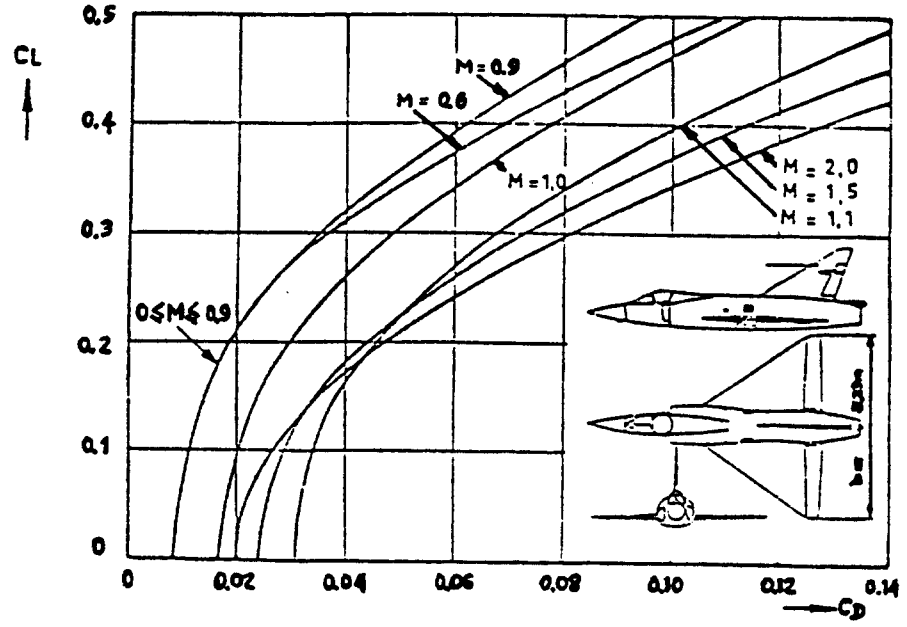

Figure 5.9 Drag Polars: Convair F-106

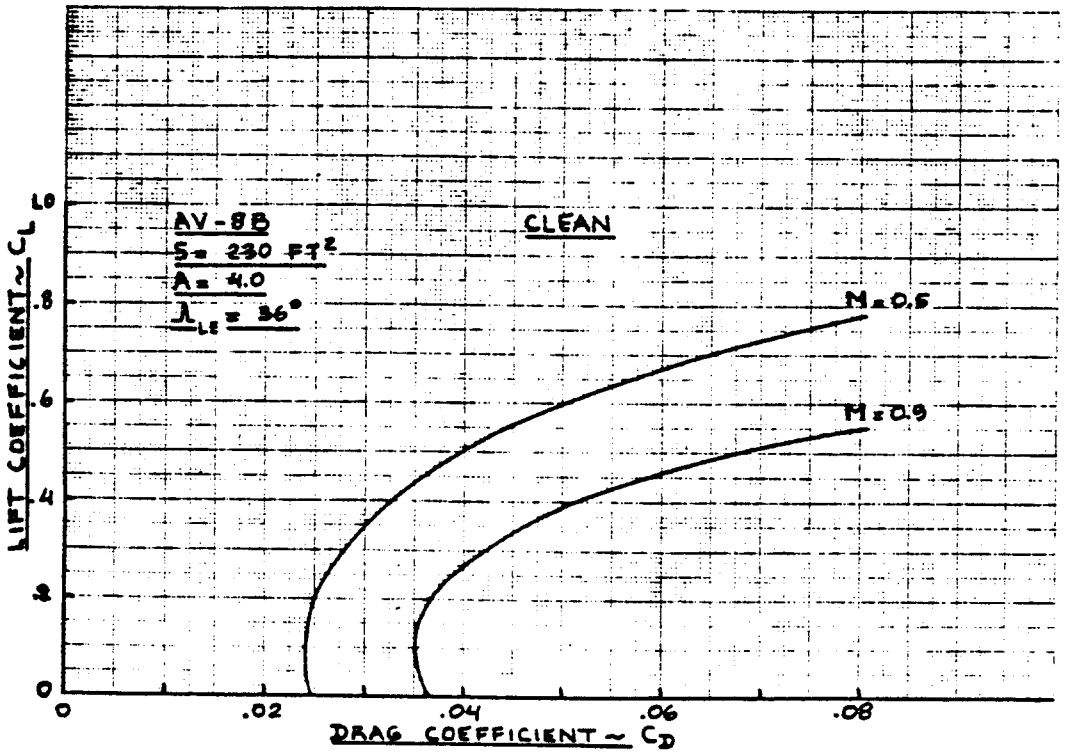

Figure 5.10 Drag Polars: McDonnell Douglas AV8B

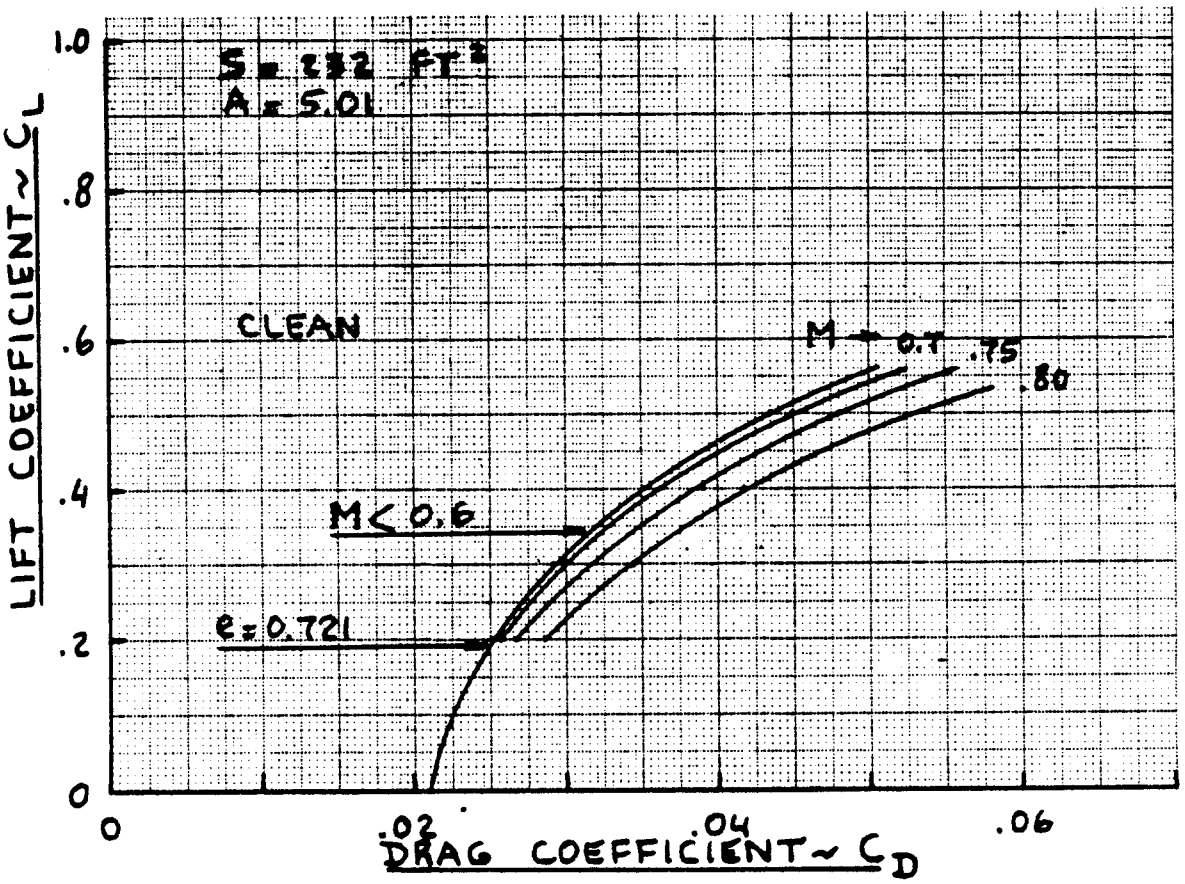

Figure 5.11 Drag Polars: Learjet M25

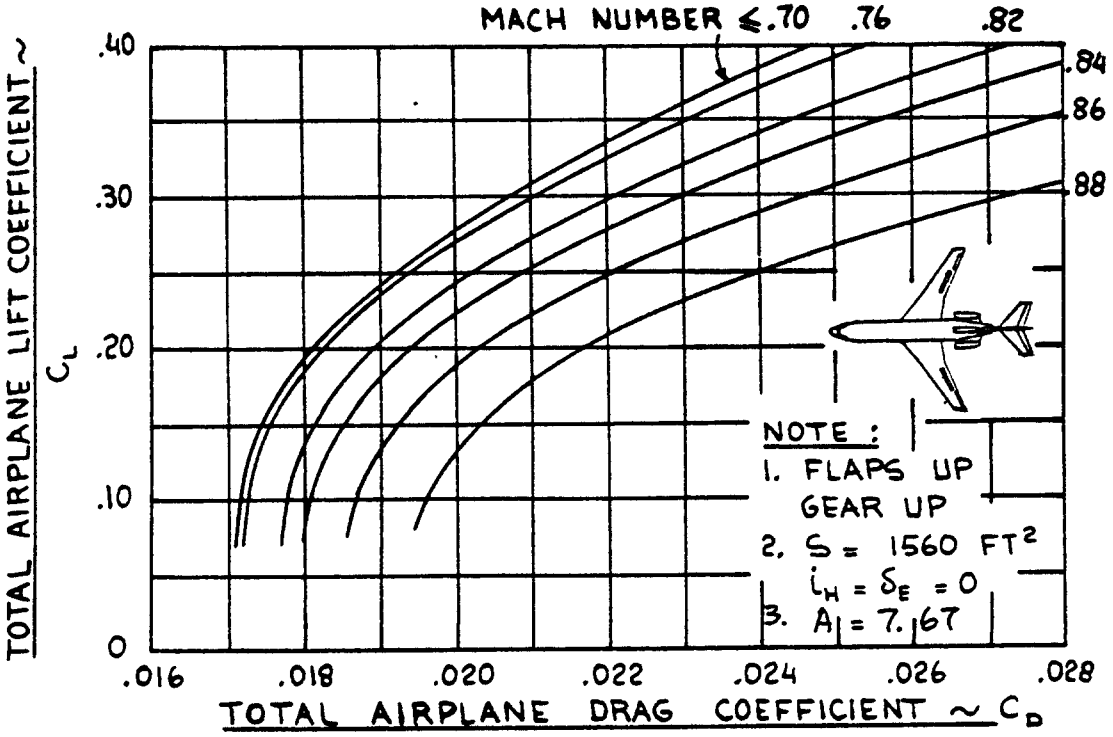

Figure 5.12 Drag Polars: Boeing 727-100

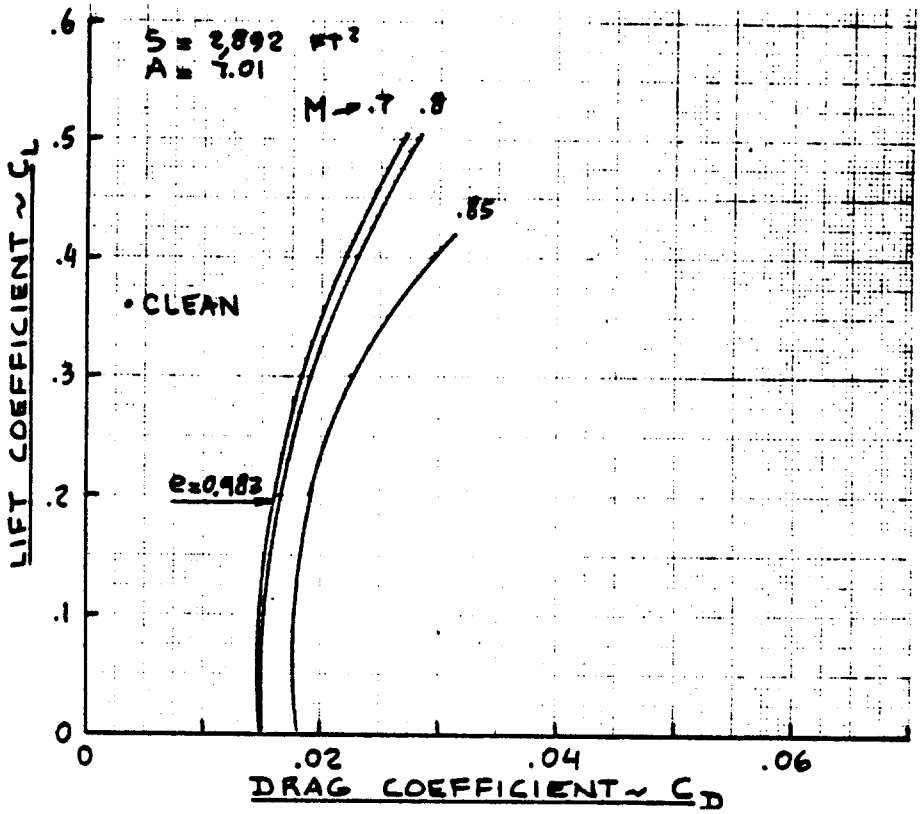

Figure 5.13 Drag Polars: Boeing 707-320B

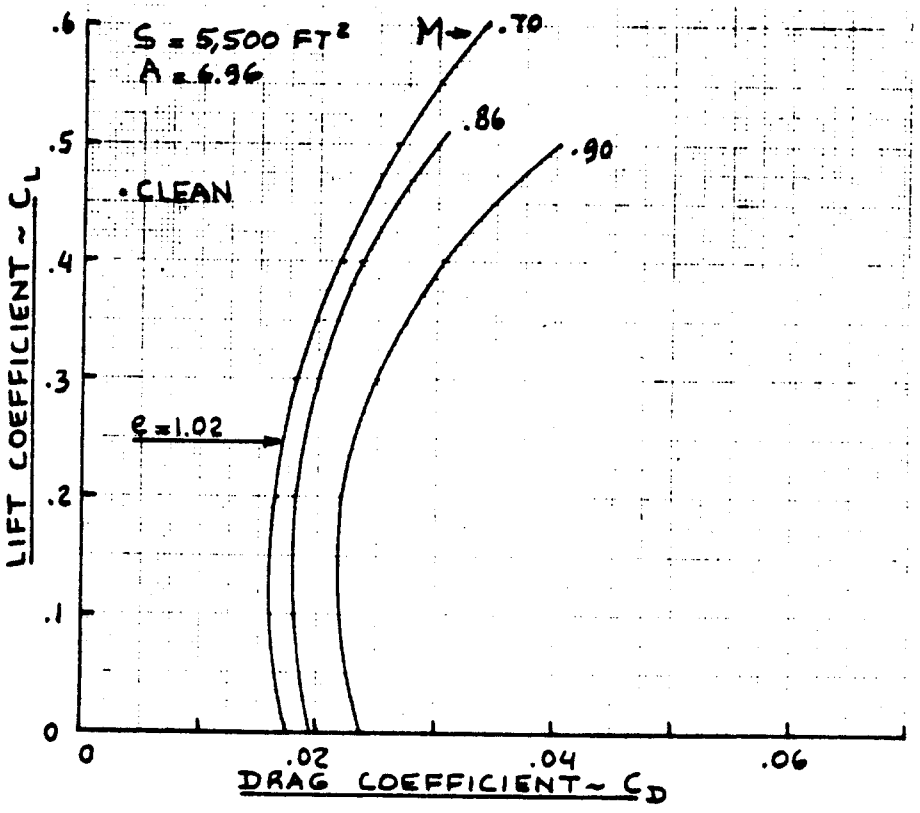

Figure 5.14 Drag Polars: Boeing 747-200

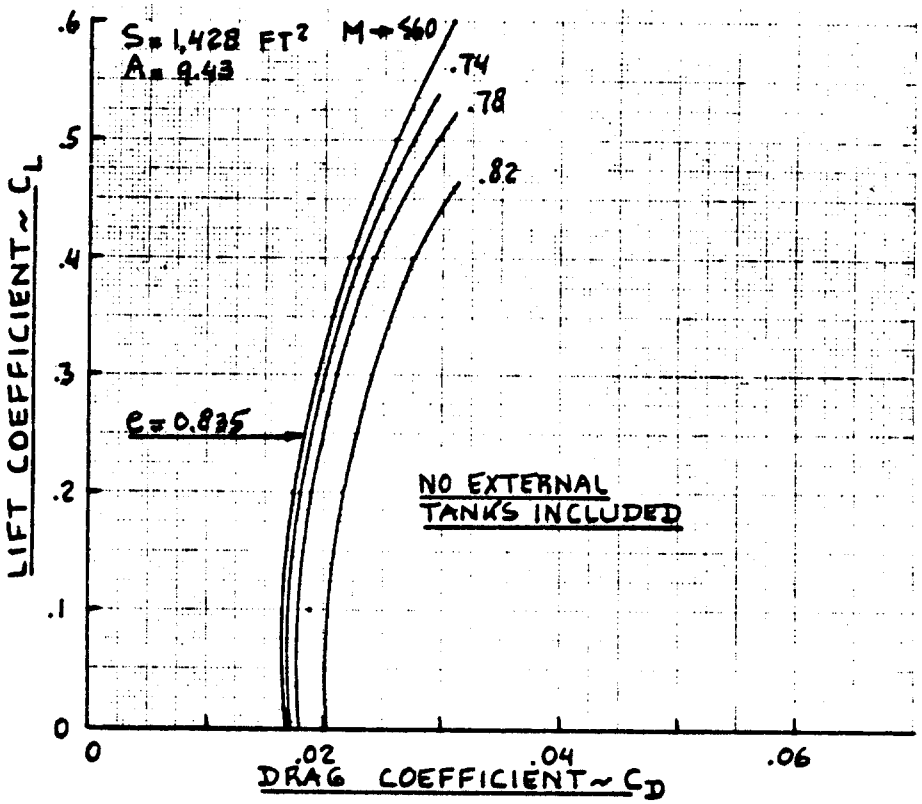

Figure 5.15 Drag Polars: Boeing B-47B

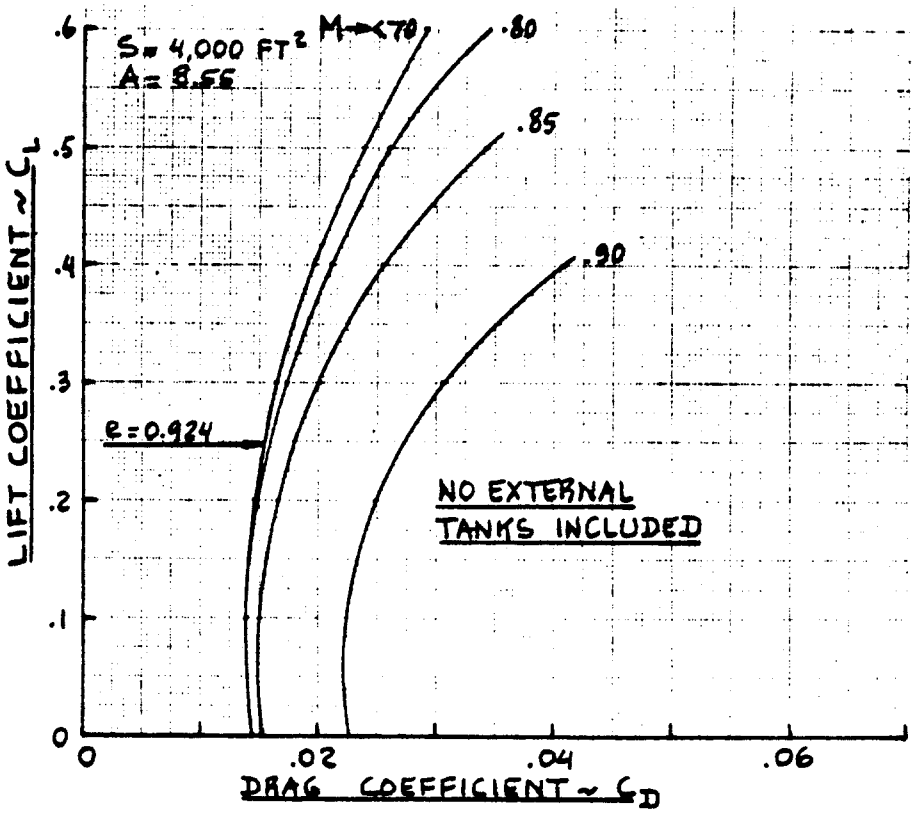

Figure 5.16 Drag Polars: Boeing B-52A

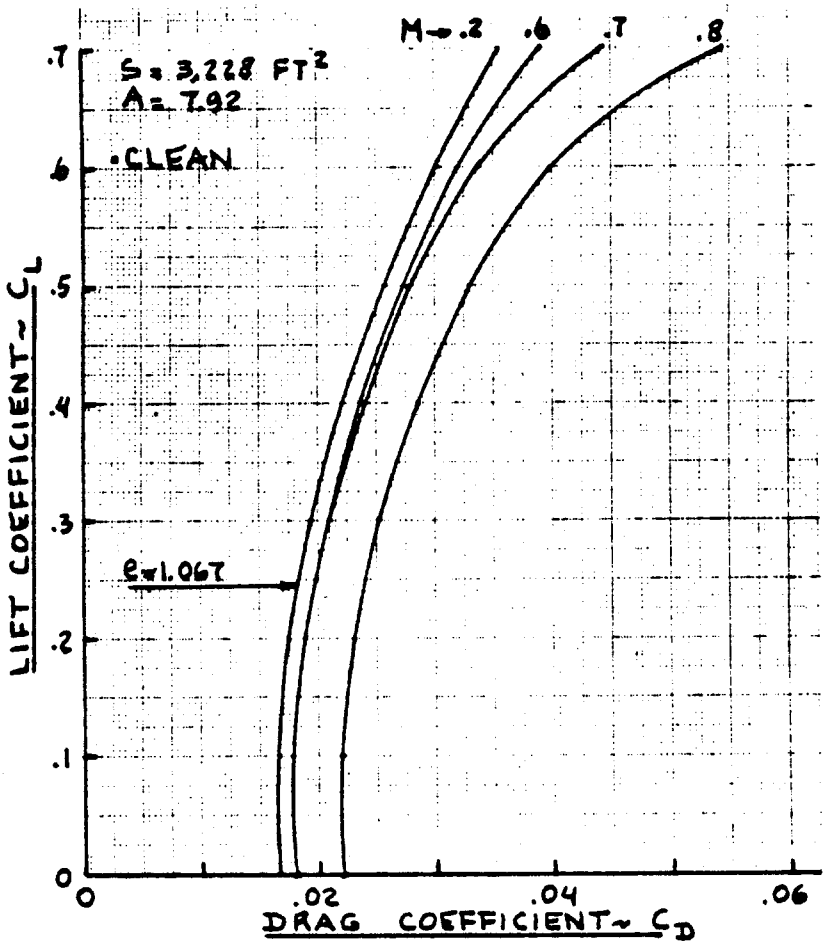

Figure 5.17 Drag Polars: Lockheed C-141B

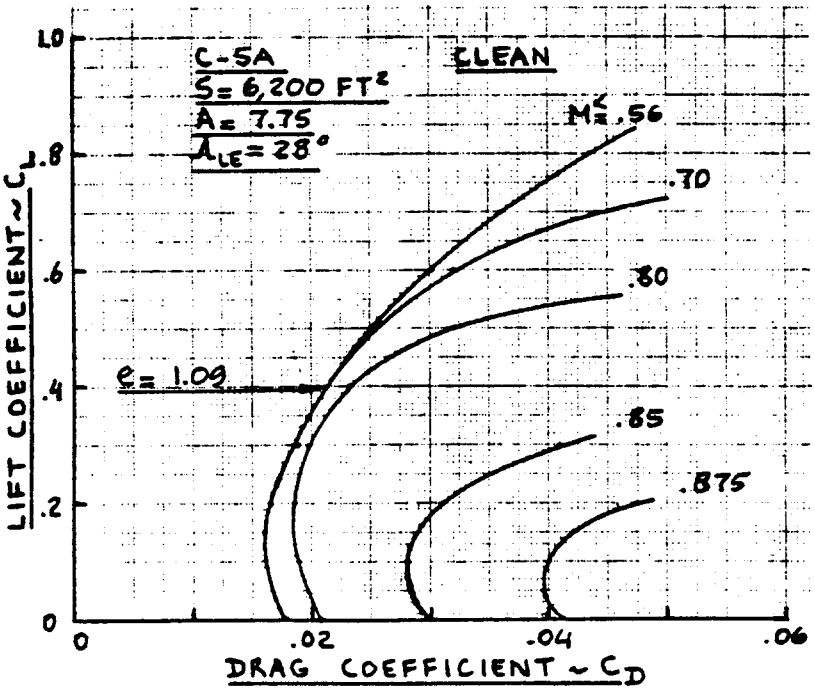

Figure 5.18 Drag Polars: Lockheed C-5A

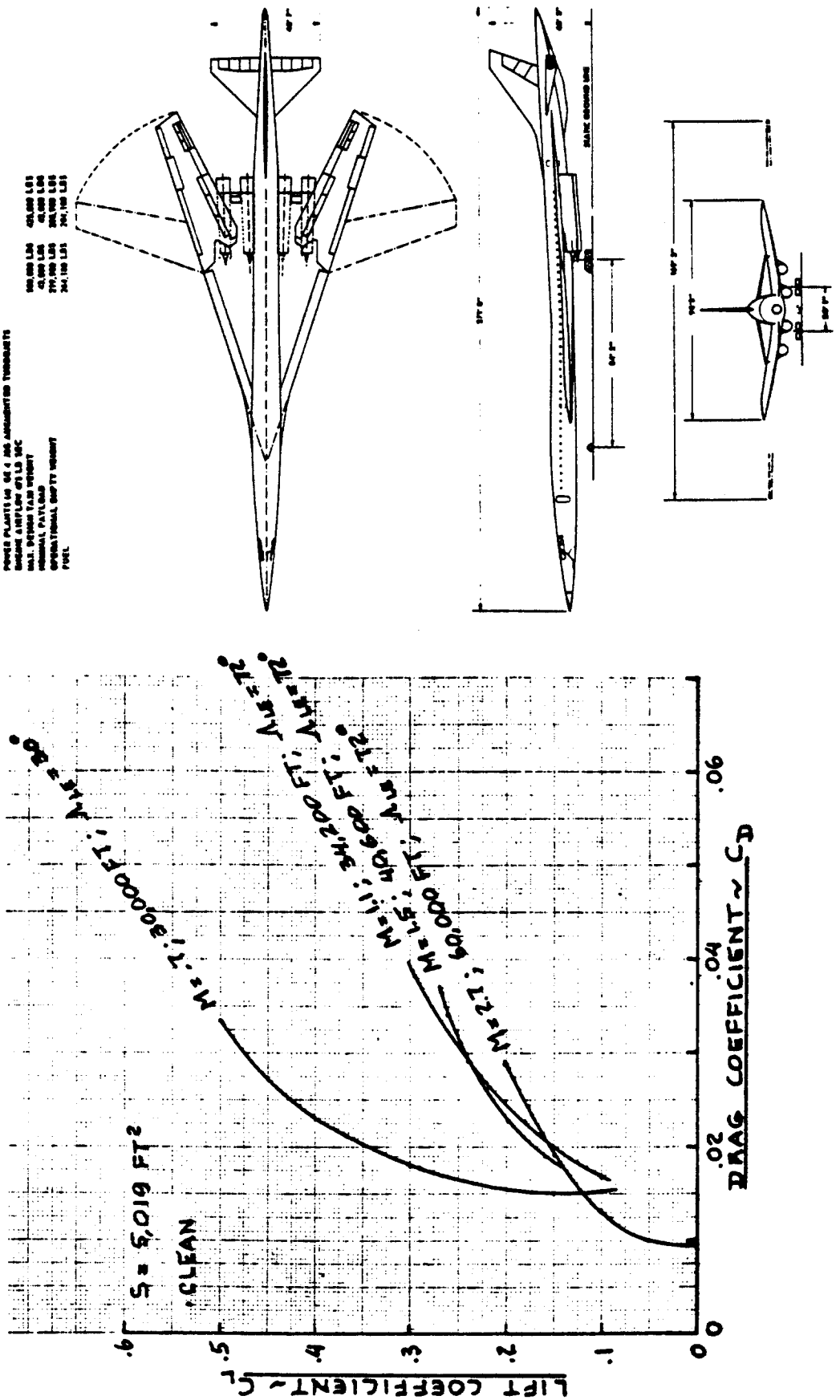

Figure 5.19 Drag Polars: Boeing SST Design

5.2 EQUIVALENT PARASITE AREAS

Figures 5.20 through 5.22 provide data on the relationship between total airplane equivalent parasite area, 'f', the equivalent skin friction coefficient, C_f and the total airplane wetted area, S_{wet}. The zero-lift airplane drag coefficient C_{D_o} is related to the equivalent parasite area, 'f' and to airplane wing area, S by:

$$C_{D_o} = f/S \qquad (5.1)$$

The airplanes for which data are included in Figures 5.20-5.22 are described in some detail in various issues of Reference 31. Wing areas, S, are also given in Reference 31,

5.3 OSWALD'S EFFICIENCY FACTORS

Table 5.1 provides data for Oswald's efficiency factor 'e' in the simplified airplane drag polar equation:

$$C_D = C_{D_o} + (C_L^2)/\pi Ae \qquad (5.2)$$

Note that high values of 'e' are rare, but they do occur. The reader may 'reconstruct' a value for 'e' from any drag polar by matching the polar to Equation 5.2.

5.4 EXAMPLES OF WETTED AREA BREAKDOWNS

Tables 5.2 and 5.3 present example data for wetted area breakdowns of fighters, commuters, transports and a business jet. Table 5.3 also includes data on the breakdown of equivalent parasite area with the corresponding value of average skin friction coefficient.

The reader should always verify any computed wetted area breakdown with known breakdowns for similar airplanes. Any significant differences should be explained!

The reader is also reminded of the correlations between total airplane wetted area and airplane take-off weight, provided in Chapter 3 of Part I. These data should be regarded as a source of comparative information.

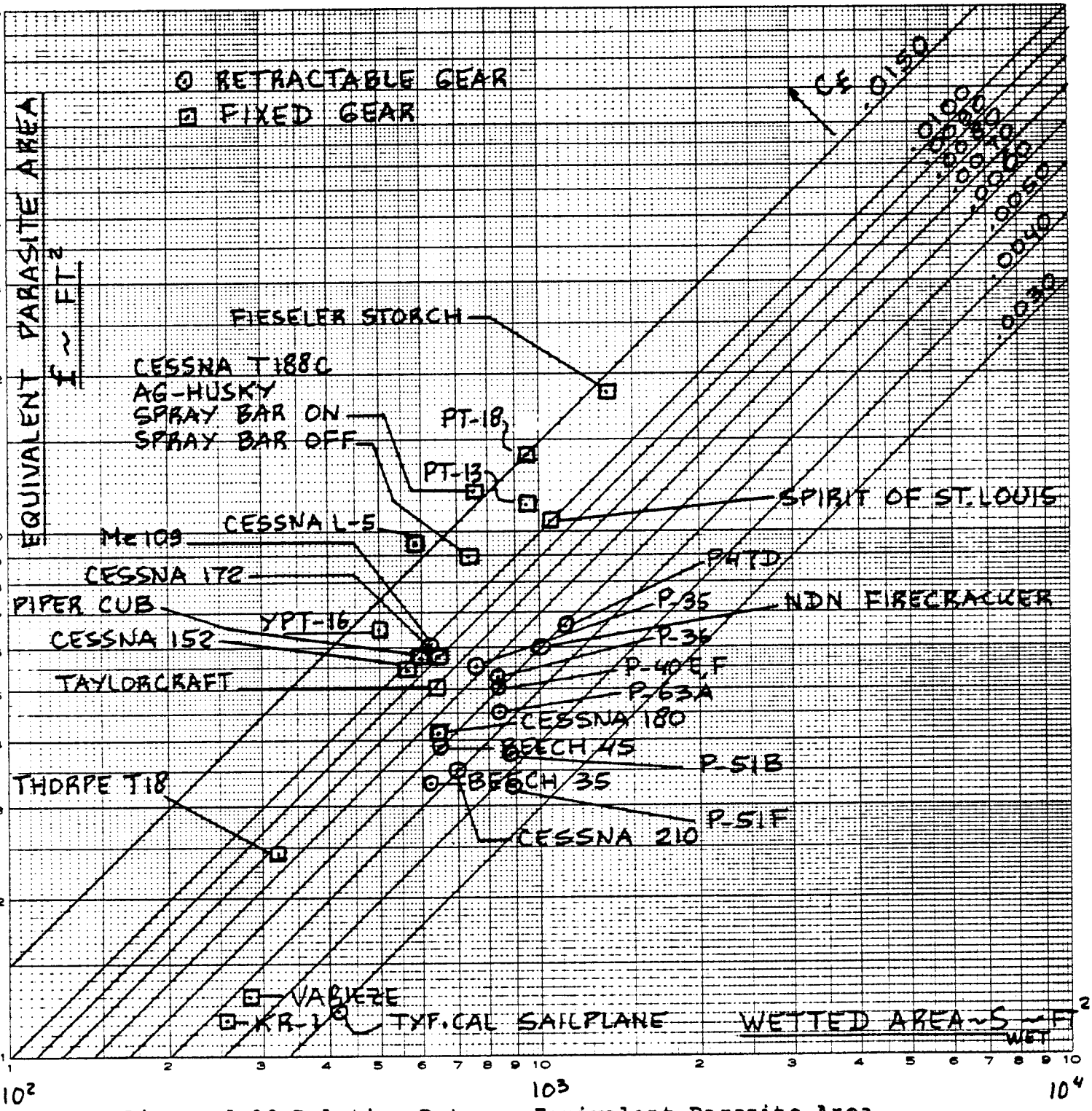

Figure 5.20 Relation Between Equivalent Parasite Area, Equivalent Skin Friction and Wetted Area for Single Engine Propeller Driven Airplanes

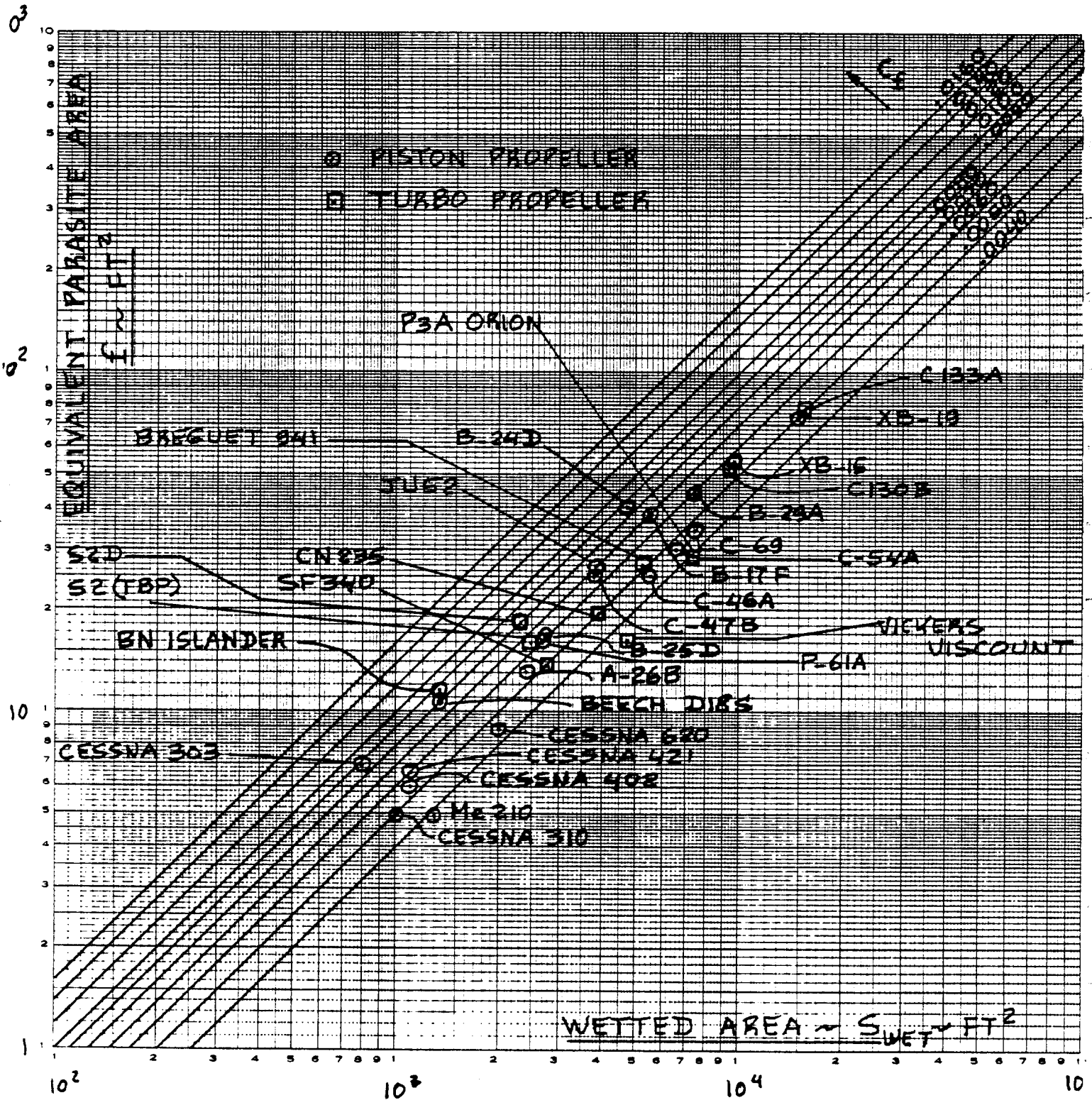

Figure 5.21 Relation Between Equivalent Parasite Area, Equivalent Skin Friction and Wetted Area for Multi-engine Propeller Driven Airplanes

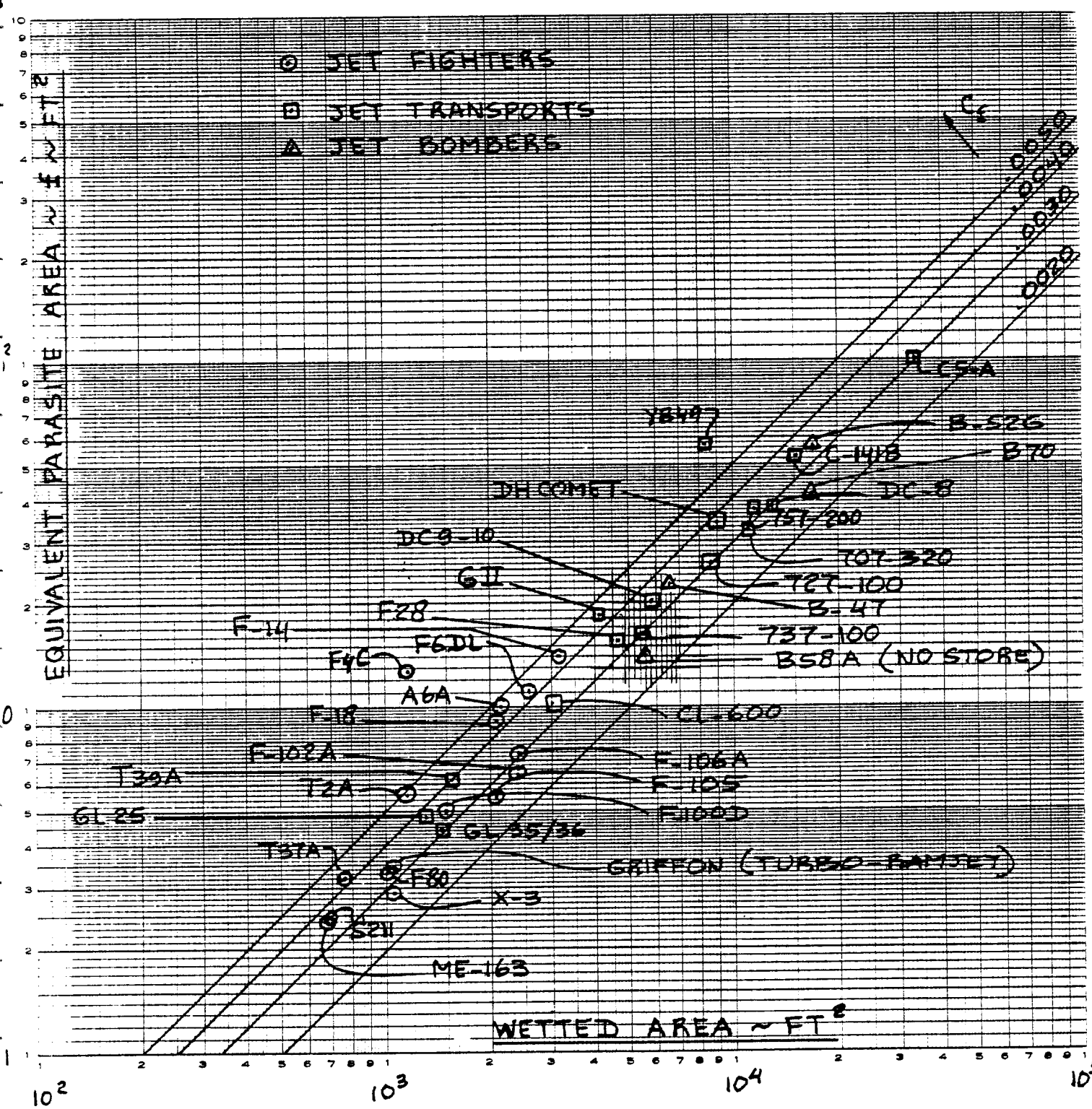

Figure 5.22 Relation between Equivalent Parasite Area, Equivalent Skin Friction and Wetted Area for Jets: Fighters, Bombers and Transports

Table 5.1 Oswald's Efficiency Factor 'e' for Several Airplanes

Single Engine Propeller	'e'		'e'	Four Engine Prop.	'e'
PT-18	0.75	Cessna 150	0.77	C-54A	0.81
AT-7	0.74	Cessna 172	0.77	C-60A	0.63
AT-8	0.61	Cessna 182	0.84	C-64	0.97
Cessna L-5	1.02	Cessna 185	0.86	C-69	0.82
O-46A	0.80	Cessna 177	0.57	XB-19	0.76
OE-2	0.70			B-24D	0.78
Cessna 180	0.75			B-24G	0.84
Beech 35	0.82			B-29A,B	0.94

Prop. Fighters	'e'	Jet Fighter/Trainers	'e'
P-38J	0.76	P-63A	0.86
P-40F	0.70	T-37	0.78
P-47D	1.02	NAA T2C	0.816
P-49	0.80		
P-51B	0.86	Jet Bombers	
P-51F	0.80		'e'
XP-60C	0.66	Boeing B-47B	0.84
P-61A	0.86	Boeing B-52A	0.924

Twin Engine Prop.	'e'	Jet Transports	'e'
A-26B	0.79	Learjet M 25	0.721
C-46A	0.88	Gulfstr.GII	0.950
C-47B	0.89	F-28-2000	0.818
B-25D	0.78	B 707-320B	0.983
B-26F	0.76	L C-141B	1.067
Cessna 310	0.73	L C-5A	1.091
Gulfstream GI	0.78		
SAAB SF 340	0.80		

Table 5.2 Wetted Area Breakdowns for Fighters, Commuters and Transports

Type:	AV-8B	F-4E	F-15C	F/A-18A	SDS330	SC7	F-27
Wing area, S, ft^2	230	530	608	400	453	373	754
Wing aspect ratio, A	4.0	2.82	3.0	3.5	12.3	11.0	12.0
Wetted Areas (ft^2):							
Wing	379	730	691	562	788	477	1,507
Wing strake/LEX				210			
Fuselage	597	1,124	1,468	890	1,543	1,034	1,614
Horizontal tail	86	154	216	176	98	98	344
Vertical tail	56	116	257	208	173	155	387
Nacelles					163	115	in fus.
Ventral	11						
Miscellaneous	45	(outriggers)			114	81	(wing struts)
					45	48	(stub wings)
					126	(gear fairing)	
TOTALS	1,174	2,123	2,632	2,046	3,049	2,008	3,852

Type:	B-757	F-28 1000	F-28 4000	VFW 614	GL M26	
Wing area, S, ft^2	1,951	822	850	689	253	
Wing aspect ratio, A	7.95	7.3	7.96	7.21	5.74	
Wetted areas (ft^2)						
Wing	3,358	1,334	1,399	1,077	402	
Fuselage	5,601	2,217	2,453	1,682	520	
Horizontal tail	893	430	430	342	108	
Vertical tail	762	269	269	202	75	
Nacelles	662	323	323	77	140	
Pylons	127	75	75	74	25	
Flap tracks	225			87	11	(ventral)
Miscellaneous			(antennas) 5		132	(tiptanks)
TOTALS	11,588	4,648	4,950	3,547	1,413	

Table 5.3 Wetted Area and Parasite Area Breakdowns for Jet Transports (ft^2)

Type:	B-47B			B-52A			KC-135		
Component:	S_{wet}	c_f	f	S_{wet}	c_f	f	S_{wet}	c_f	f
Fuselage	2,611	.00167	5.552	4,260	.00168	8.489	3,830	.00169	7.976
Wing	2,580	.00229	7.953	7,710	.00224	23.594	4,332	.00224	13.819
Horiz. tail	508	.00243	1.617	1,650	.00232	4.831	875	.00236	2.655
Vert. tail	450	.00229	1.356	930	.00235	2.755	622	.00230	1.842
Trim			.170			1.000			.380
Nacelles	782	.00223	4.510	1,320	.00235	8.437	632	.00231	3.640
Nac. interf.			.541						
Pylons	139	.00232	.376	310	.00234	.843	304	.00227	.803
Aircon. noz.									.650
Roughness			.438			1.029			.658
Miscellaneous							refuel boom:		1.250
TOTALS	7,070		22.513	16,180		50.978	10,595		33.673

Type:	720			707-320B			727-100		
Component	S_{wet}	c_f	f	S_{wet}	c_f	f	S_{wet}	c_f	f
Fuselage	3,971	.00171	8.453	4,590	.00165	9.400	3,838	.00167	8.080
Wing	4,451	.00226	14.693	5,463	.00222	17.246	2,800	.00223	9.490
Horiz. tail	875	.00239	2.685	1,050	.00236	3.186	720	.00233	2.170
Vert. tail	684	.00235	2.066	684	.00234	2.057	685	.00210	1.860
Trim			.380			.550			.200
Nacelles	660	.00234	4.301	368	.00265	2.696	432	.00219	2.270
						center:	130	.00226	.700
Nacelle interf.			.308			.572			.150
Noise suppr.	140	.00311	.435						
Thrust rev.			1.063						
Pylons	304	.00230	.813	304	.00230	.813	108	.00219	.290
Aircond. nozzle			1.300			.350			.250
Roughness			.700			.765			.530
Miscellaneous				scrubbing drag:		4.238	fl.track fair.:		1.000
TOTALS	11,085		37.197	12,459		41.873	8,713		26.990

5.5 VERIFICATION OF REALISM OF COMPUTED DRAG POLARS

After estimating the drag polar of a new airplane with the methods of Chapter 4, the following procedure should always be followed to verify that the computed drag data are indeed 'in-the-ball-park':

Step 1: Determine for which flight condition and for which external configuration the drag polars need to be determined.

The reader should recognize the fact that airplane drag polars depend upon the following factors:

A) Flight condition:

Mach Number, altitude, lift coefficient (or angle of attack) and Reynold's number which also depends on a characteristic length.

B) External configuration:

The external airplane configuration may be influenced by:

1) flap deflection (take-off, climb, cruise, landing or maneuvering
2) landing gear position: up or down (gear well doors open or not?)
3) speed brake position: open or closed
4) external store disposition
5) loading door position: open or closed
6) weapons door position: open or closed
7) cooling flap position: open for take-off, open for climb, or closed
8) propeller control position: feathered, windmilling or normal
9) jet engine condition: windmilling or normal
10) inlet configuration: blow-down doors, ramps, spikes, bleed- and bypass doors
11) control surface deflection for trim (trim drag), with AEO or OEI

Drag polars can differ significantly depending on how these factors are selected for any given airplane in any given flight condition.

Step 2: Plot the C_D versus α data from the calculations performed with Chapter 4.

Step 3: Plot the C_L versus α data for the airplane with the method of Chapter 10.

Step 4: From steps 2 and 3 crossplot the C_D versus C_L polar.

Figure 5.23 shows an example of how Steps 2, 3 and 4 are carried out.

Step 5: A) From step 4, determine C_{D_o} and compute:

$$f = C_{D_o} S \qquad (5.3)$$

B) Determine the wetted area of your airplane. The data for doing this are already available from the drag polar calculations performed in Chapter 4.

'Verify' the computed wetted area breakdown with the data of Tables 5.2 or 5.3. Also check the total wetted area against the trend data of Figures 3.22 in Part I.

C) Plot the 'f' and S_{wet} data on one of the graphs in Figures 5.20-5.22, whichever is applicable. Determine the C_f value for the airplane and judge whether or not the value of C_f is a reasonable one from an 'aerodynamics technology' viewpoint. This is done by comparison to other airplanes in the same figure.

Step 6: Plot $(C_L)^2$ versus C_D, and determine $dC_D/d(C_L)^2$ as indicated in Figure 5.23.

Compute: $e = [\pi A(dC_D/dC_L)^2$ (5.4)

Compare this value of 'e' with that for similar airplanes in Table 5.1. If there is a large difference, check the calculations or explain why the airplane might be different!

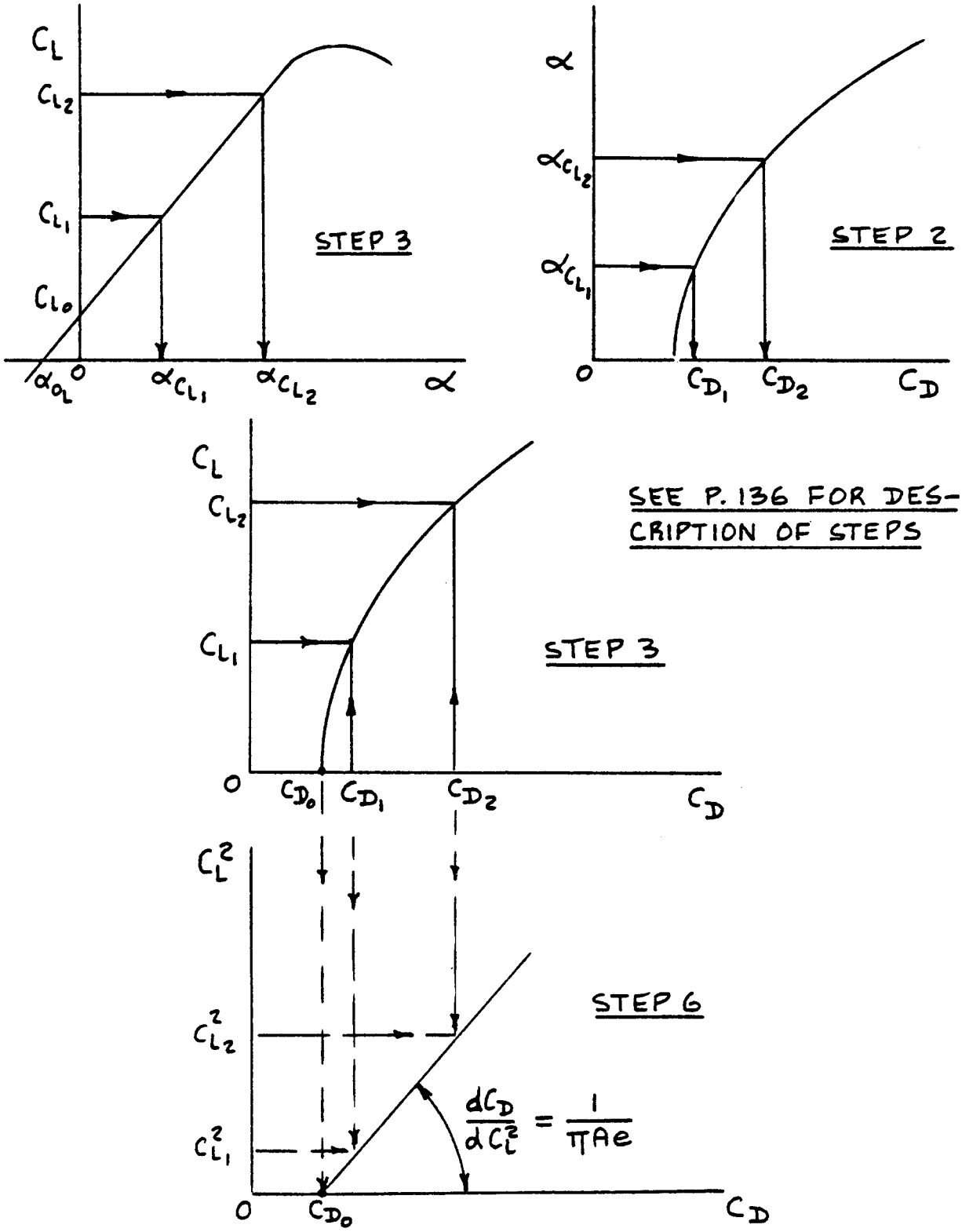

Figure 5.23 Drag Polar Construction from Lift and Drag Data with Angle of Attack

AV-8B Harrier II

MCDONNELL DOUGLAS

The United States Marine Corps AV-8B Harrier II V/STOL Light Attack aircraft built by the McDonnell Douglas Corporation is a vastly improved derivative of the British Aerospace AV-8A Harrier currently in service with the USMC. The Marines have, with ten years of operational experience in the AV-8A, proven the effectiveness advantages of V/STOL for the close air support mission. With the AV-8B Harrier II, the Marines will have a V/STOL aircraft with payload/radius capability comparable to any modern, conventional, light attack aircraft.

The AV-8B will provide:

- Double the payload/radius,
- Accurate, first pass weapon delivery.
- Improved VTO and STO capability.
- Greatly reduced pilot workload,

and will be

- More reliable and more maintainable.

The key to the V/STOL capability of the AV-8B is found in the vectored, 21,180 lb thrust Rolls-Royce Pegasus 11 engine. The pilot can control the direction of engine thrust by positioning the four exhaust nozzles; aft for wingborne flight, down for vertical flight and at intermediate positions for short takeoff and short landing. Aircraft attitude control during V/STOL and hover is accomplished through the reaction control system which directs engine bleed air through reaction nozzles located at the wing tips, the nose and the tail.

Performance Tropical Day (90°F)

- STO distance at max TOGW ..... 1,200 ft
- VTO Weight ..... 19,185 lb
- VL Weight ..... 17,500 lb
- Vmax at altitude ..... 0.91 M
- Vmax at sea level ..... 585 Kts
- Load factor ..... +7 g, −3 g

Interdiction Mission
Hi-Lo-Hi

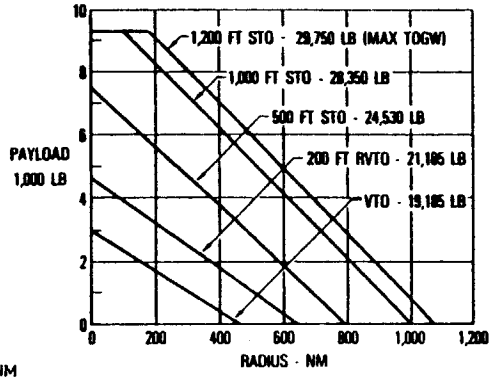

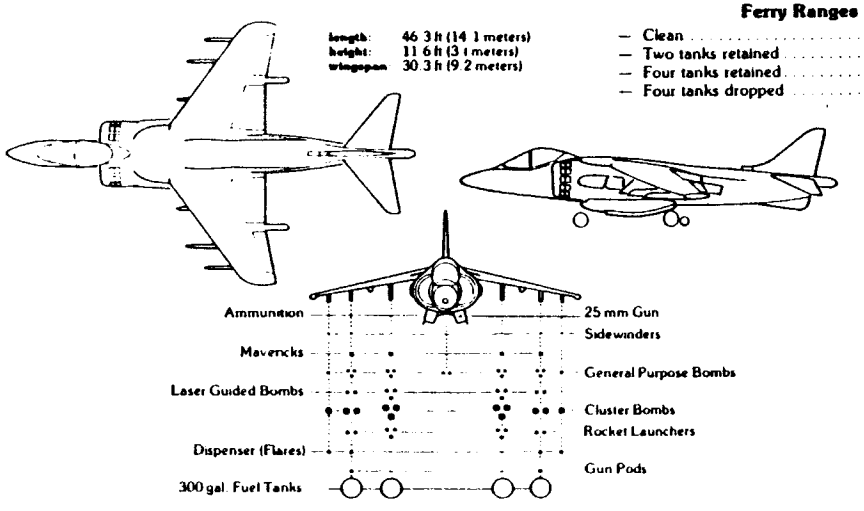

Ferry Ranges

- Clean ..... 1500+ NM
- Two tanks retained ..... 1800+ NM
- Four tanks retained ..... 2000+ NM
- Four tanks dropped ..... 2400+ NM

Weights

- Max design TOGW ..... 29,750 lb
- Operating weight empty ..... 12,750 lb
- Internal fuel ..... 7,500 lb
- Internal and external fuel ..... 15,829 lb
- Max external load ..... 9,200 lb

Major AV-8B Changes from the AV-8A

- Supercritical/composite material wing
- Lift improvement devices
- Large, positive circulation flaps
- Narrowed outrigger tread
- High recovery engine inlets
- Raised, high visibility cockpit
- Stability augmentation and attitude hold system
- Angle rate bombing set
- Inertial navigation set
- Integrated crew station
- Onboard oxygen generation system
- Zero scarf front engine nozzles
- Lengthened aft fuselage

6. INSTALLED POWER AND THRUST PREDICTION METHODS

The purpose of this chapter is to present rapid methods for the prediction of installed power and/or thrust in airplanes. The assumption will be made that the following characteristics of the engine are known:

1. For piston engines: manufacturers shaft horsepower data for a range of altitudes and throttle settings.

2. For gas generators: manufacturers shaft horsepower and thrust data for a range of altitudes, Mach numbers and throttle settings.

3. For jet engines: manufacturers thrust data for a range of altitudes, Mach numbers and throttle settings.

These engine manufacturers data (also called uninstalled data) are based on ideal (teststand) conditions and do <u>not</u> normally include the following effects:

A. Effect of the inlet (air induction system) on pressure recovery, on drag and therefore on engine performance.

   <u>Note:</u> A bellmouth inlet system, assuring very high inlet pressure recovery, is frequently used to determine engine manufacturers data. Fig.6.1 shows a typical teststand arrangement.

B. Effect of power extraction (needed to run essential airplane services) on engine performance.

   <u>Note:</u> Power extraction to run essential engine services ARE normally included in engine manufacturers data.

C. Effect of the exhaust or nozzle configuration on drag and on engine performance.

   <u>Note:</u> The engine manufacturer uses a nozzle configuration which is usually different from that preferred by the airframer. See Figure 6.1.

The methods presented in this chapter are organized as follows:

6.1 Power extraction requirements

6.2 Inlet sizing and integration

6.3 Exhaust or nozzle sizing and integration

6.4 Prediction of installed power and thrust

For a detailed and concise methodology of inlet design and analysis the reader should consult Reference 32. For considerations of design and analysis of inlet and exhaust systems both, Reference 33 is recommended.

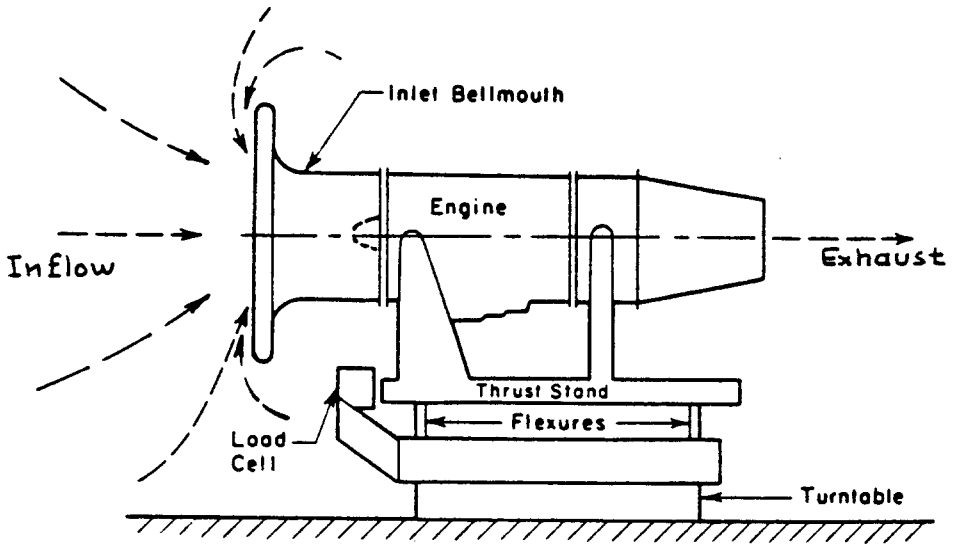

Figure 6.1 Engine Test Stand with Bellmouth Inlet

6.1 POWER EXTRACTION REQUIREMENTS

To operate an airplane in any phase of its mission a certain amount of electrical, mechanical and pneumatic power may be required. These power requirements are normally satisfied by the engines. For that reason they are referred to as power extraction requirements. In some cases power sources other than the propulsion system (for example an APU) are used.

The magnitude of power extraction requirements differs from one airplane to another and from one mission phase to another.

In this section a rapid method for estimating power extraction requirements is presented for:

6.1.1 Piston-propeller driven airplanes

6.1.2 Turbopropeller and jet driven airplanes

6.1.1 Piston-propeller Driven Airplanes

In this type of airplane the following power extraction requirements may be present:

$$P_{extr} = P_{el} + P_{mech} \qquad (6.1)$$

where: P_{el} = the electrical power extraction in shp

P_{mech} = the mechanical power extraction in shp

Electrical power extraction requirements, P_{el} follow from the essential electrical services which are required during any given mission phase. To determine electrical power requirements, an 'electric power load profile' must be prepared. Using p.320 of Part IV as an example, the reader should prepare an electric power load profile for his airplane.

From this electric power load profile the electrical power extraction requirement, P_{el} is determined as:

$$P_{el} = .00134(VA_{plp})/\eta_{gen} \text{ in shp} \qquad (6.2)$$

where: VA_{plp} = the maximum required electrical power in Volt-amperes as obtained from the electric power load profile.

η_{gen} = 0.9 is the efficiency of the electric power generator(s) which are assumed to be driven off the engine accessory drive pad. Modern generators can achieve efficiencies of 0.90 to 0.95.

Lacking a detailed electric power load profile, the P_{el} values suggested in Table 6.1 may be used. The reader should also consult Chapter 6 in Part IV for more information on electrical system power capabilities.

Mechanical power extraction requirements, P_{mech} depend on the systems which are required for the operation of the airplane in a given mission phase. Examples of such system may be:

fuel pumps, hydraulic pumps, cooling fans, heating/airconditioning system, pressurization system, spray system (in agricultural airplanes).

The reader should prepare a list of those systems which require the generation of mechanical power. The total mechanical power required can be written as:

$$P_{mech} = P_{fp} + P_{hydr} + P_{other} \qquad (6.3)$$

where: P_{fp} = the mechanical power required to drive the fuel pumps. This may be found from:

$$P_{fp} = 0.00014(c_p)(SHP)/\eta_{fp} \qquad (6.4)$$

where: c_p is the engine sfc in lbs/shp/hr

SHP is the engine shaft horsepower required in the flight condition being analyzed

η_{fp} = 0.65 is the fuel pump efficiency.

The assumption has been made here that the fuel pumps are operating on a pressure differential of 50 psi. Information on pumps may be found in Ref.34. Data on fuel systems is provided in Chapter 5 of Part IV.

Note: power required to drive electric fuel pumps should be included in P_{el}.

P_{hydr} = the mechanical power required to drive

the hydraulic pumps. The magnitude of P_{hydr} depends on the hydraulic flow and pressure differential needs of the airplane hydraulic system. Section 6.2 of Part IV contains a discussion on the sizing of hydraulic systems. As indicated in Part IV, a hydraulic system load analysis must be performed to find the total hydraulic fluid flow which is required. Having also selected the hydraulic system operating pressure (Part IV, Ch.6), the hydraulic system shaft horsepower requirements are found from:

$$P_{hydr} = 0.0006(\Delta p_{hydr})(\dot{V}_{hydr})/\eta_{hp} \qquad (6.5)$$

where: Δp_{hydr} = the pressure differential (psi), over which the hydraulic system operates. This is roughly equal to the system operating pressure which ranges from 1,500 to 5000 psi. See Chapter 6 in Part IV.

$\dot{V}_{hydr}$ = the hydraulic fluid flow rate in gallons/min (gpm). Page 308 in Part IV provides some guidance for estimating hydraulic fluid flow rates.

η_{hp} = the hydraulic pump(s) operating efficiency. This may be taken to be 0.75 in modern systems.

Note: the power required for electrically driven hydraulic pumps should be included in P_{el}.

P_{other} = the sum of all 'other' mechanical power extraction requirements. Determination of these 'other' mechanical power extraction needs is left to the reader. The best way to proceed is to make a complete list of all 'other' mechanical power requirements for on-board systems. By using appropriate efficiency values, the required value of 'to be extracted' engine shaft horsepower, P_{other} can then be estimated. Ref.34 is a good source for general mechanical system data. Part IV contains discussions of various 'other' types of

system which may be required in airplanes.

Lacking a detailed listing of mechanical power extraction requirements, the values suggested for P_{mech} in Table 6.1 may be used.

The effect of P_{extr} as determined from Eqn. 6.1 on installed engine performance is discussed in Section 6.4.

Table 6.1 Summary of Power Extraction Requirements

Power Extraction Type:	Electrical shp, P_{el}	Mechanical shp, P_{mech}	Pneumatic Bleed slugs/sec
Airplane Type:			
Piston Propeller Driven:			
Single engine, light airplanes	1-2	1-2	0
Single engine, military trainers	2-4	2-4	0
Twin engine, light airplanes	4-6	5-10	0
Multi-engine transports	20-40	30-50	0
Turboprop and Jet Airplanes:			
Single engine, light airplanes	2-4	3-5	$0.01\dot{m}_a$
Single engine, military trainers	5-7	6-10	$0.015\dot{m}_a$
Twin engine turboprops	6-8	7-9	$0.015\dot{m}_a$
Twin engine turbojets or fans	8-10	9-11	$0.025\dot{m}_a$
Twin jet military trainers	10-15	15-20	$0.03\dot{m}_a$
Jet Fighters, air-superiority	50-100	50-100	$0.03\dot{m}_a$
Jet Fighters, attack	100-200	100-200	$0.04\dot{m}_a$
Jet Transports, civil	$0.00070W_{TO}$	$0.00060W_{TO}$	$0.03\dot{m}_a$
Jet Transports, military	$0.00100W_{TO}$	$0.00080W_{TO}$	$0.04\dot{m}_a$

6.1.2 Turbopropeller and Jet Driven Airplanes

For this class of airplanes the power extraction requirements may be determined from:

$$P_{extr} = P_{el} + P_{mech} + P_{pneum} \qquad (6.6)$$

where: P_{el} = the electrical power extraction in shp

P_{mech} = the mechanical power extraction in shp

P_{pneum} = the pneumatic (also called bleed air) power extraction in shp

Electrical power extraction requirements. P_{el} may be determined with the method of Sub-section 6.1.1, via preparation of an electric power load profile as shown on p.320 of Part IV. Lacking such detailed information the P_{el} values suggested in Table 6.1 may be used.

Some airplanes may require extensive radar and electronic warfare equipment. Examples are the Boeing E-3A, the Boeing E-6, the Grumman E-2C and the Lockheed P3V. In those cases large electrical power requirements may exist: 600 kVA in the case of the Boeing E-6!

Normally, these power requirements are satisfied by the installation of directly driven generators on the propulsion installation. If these power requirements cannot be satisfied by power extraction from the regular propulsion system separate power sources may have to be installed.

Mechanical power extraction requirements. P_{mech} may be determined with the method of Sub-section 6.1.1, via a listing of all required mechanical services. Lacking a detailed power extraction calculation, the values suggested in Table 6.1 may be used.

Pneumatic power extraction requirements. P_{pneum} are determined by those systems which are driven by bleed air form the main engines. Typical of such services are:

de-icing and anti-icing systems, heating and airconditioning systems, engine starting systems (for ground start and for air restart), pressurization of fuel tanks, for flap deployment (For example, the B-747 leading edge devices) and for water system pressurization.

A list of airplane services which require bleed air as the source of power must be prepared. Next, the required bleed airflows, $\dot{m}_{bleed}$ (in slugs/sec) must be estimated for each flight situation. From this the total engine bleed airflow can be computed. As a general rule, engine bleed airflow should not exceed 5 percent of the total engine massflow requirement in any given flight condition, $\dot{m}_a$, or major degradation of thrust will occur:

$$\dot{m}_{bleed} < 0.05\dot{m}_a \text{ in slugs/sec} \qquad (6.7)$$

Lacking a detailed evaluation of bleedair requirements, the data of Table 6.1 may be used.

As long as Eqn.(6.7) is satisfied, a first order estimate for P_{pneum} is:

$$P_{pneum} = (\dot{m}_{bleed}/\dot{m}_a)P_{reqd} \text{ for turboprops} \qquad (6.8)$$

and:

$$P_{pneum} = (\dot{m}_{bleed}/\dot{m}_a)(T_{reqd}U_1/550) \text{ for jets} \qquad (6.9)$$

where: P_{reqd} = power required in some flight condition

T_{reqd} = thrust required in some flight condition.

Methods for estimating the power required, P_{reqd} or the thrust required, T_{reqd} are discussed in Part VII.

The effect of P_{extr} as determined form Eqn.(6.6) on installed power or thrust is discussed in Section 6.4.

6.2 INLET SIZING AND INTEGRATION

In preliminary design the process of inlet sizing consists of the determination of the inlet area and the shaping of the duct leading from the inlet area to the engine compressor face.

The inlet must be sized in such a way that it is 'matched' to the airflow requirements of the engine. Figure 6.2 shows a generalized inlet flow situation. Note the following important areas:

A_∞: streamtube cross section at infinity, also called the inlet capture area

A_c: streamtube cross section at the inlet, also called inlet area or cowl capture area

A_f: streamtube cross section at the engine station, also called internal area (note that this cross section is determined by the maximum cross section of the engine plus tolerances for cooling and for installation)

A_e: streamtube cross section at the exit or exhaust, also called the nozzle area

Inlet operation is often characterized by the inlet flow ratio, A_∞/A_c.

During static ground operation, the inlet flow ratio is infinite. Inlet lip flow separation is a major problem in such a case. Figure 6.3a shows such a situation. Frequently an auxiliary inlet is required to allow enough air into the inlet. This is done with a variable inlet geometry feature. Figure 6.3a shows several options.

In the design cruise condition, the inlet is normally matched so that the flow ratio is in the range of 0.5 to 0.8. The inlet operates at its peak performance (high pressure recovery). Figure 6.3b shows this situation.

In some inlets, external surface area is present at points ahead of the inlet: see Figure 6.3c. If external surface area exists ahead of the inlet, the flow ratio is selected to be closer to 1.0 to prevent inlet separation. If no wetted surface area exists ahead of the inlet, the flow ratio is in the 0.5 - 0.8 range.

In a climb, the inlet delivers more air than the engine requires, excess air will be spilled, resulting in

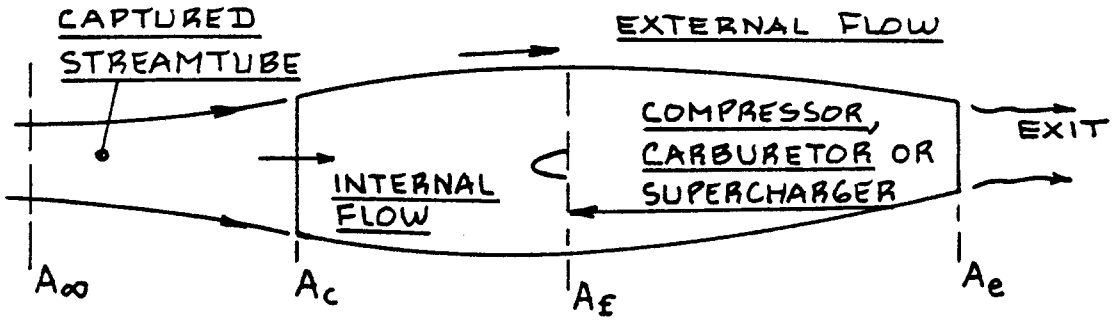

Figure 6.2 Generalized Engine Flow Stations

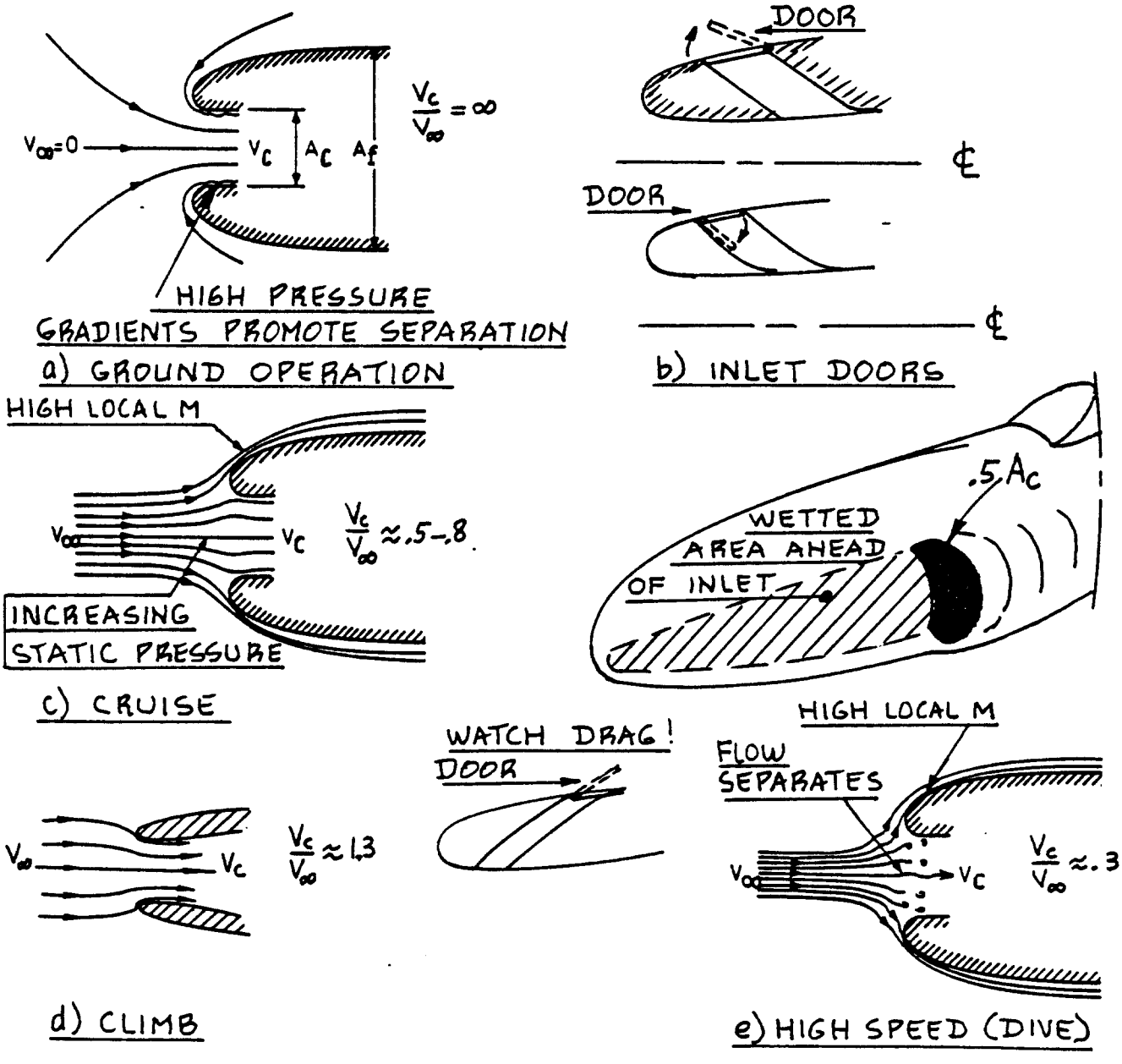

Figure 6.3 Flow Conditions for Subsonic Inlets

extra drag. The flow ratio is in excess of 1.0. Such a situation is shown in Figure 6.3d. If spillage drag becomes too high, bleedair doors may be required: Fig.6.3d shows one such option.

At very high speeds, such as occur in a high speed dive, the flow ratio is much smaller than 1.0. Such low flow ratios, particularly in the presence of large wetted areas in front of the inlet can lead to inlet flow separation resulting in compressor surge. Figure 6.3e shows such a situation.

If an inlet is undersized (such that it does not deliver enough air to the engine), unsatisfactory engine operation may result, causing deficiencies in thrust and/or power.

The objective of an inlet is to deliver air to the engine such that:

1. The correct amount of airflow is delivered to the engine

2. Pressure losses are minimized: pressure losses reduce thrust

3. Inlet flow distortion is minimized (i.e. as much as possible uniform flow is realized)

4. Inlet flow swirl is minimized or matched to the compressor requirements

Fundamentally, two types of inlets exist:

1. Straight through inlets: see Figure 6.4a
   This inlet type is used for engines with axial flow compressors, one-sided centrifugal flow compressors and supercharged piston engines.

2. Plenum chamber inlets: see Figure 6.4b
   This inlet type is used for engines with two-sided centrifugal flow compressors and with normally aspirated piston engines.

The detailed design of inlets is a strong function of how the engine (s) is (are) being integrated into the airframe.

The following subjects will be discussed:

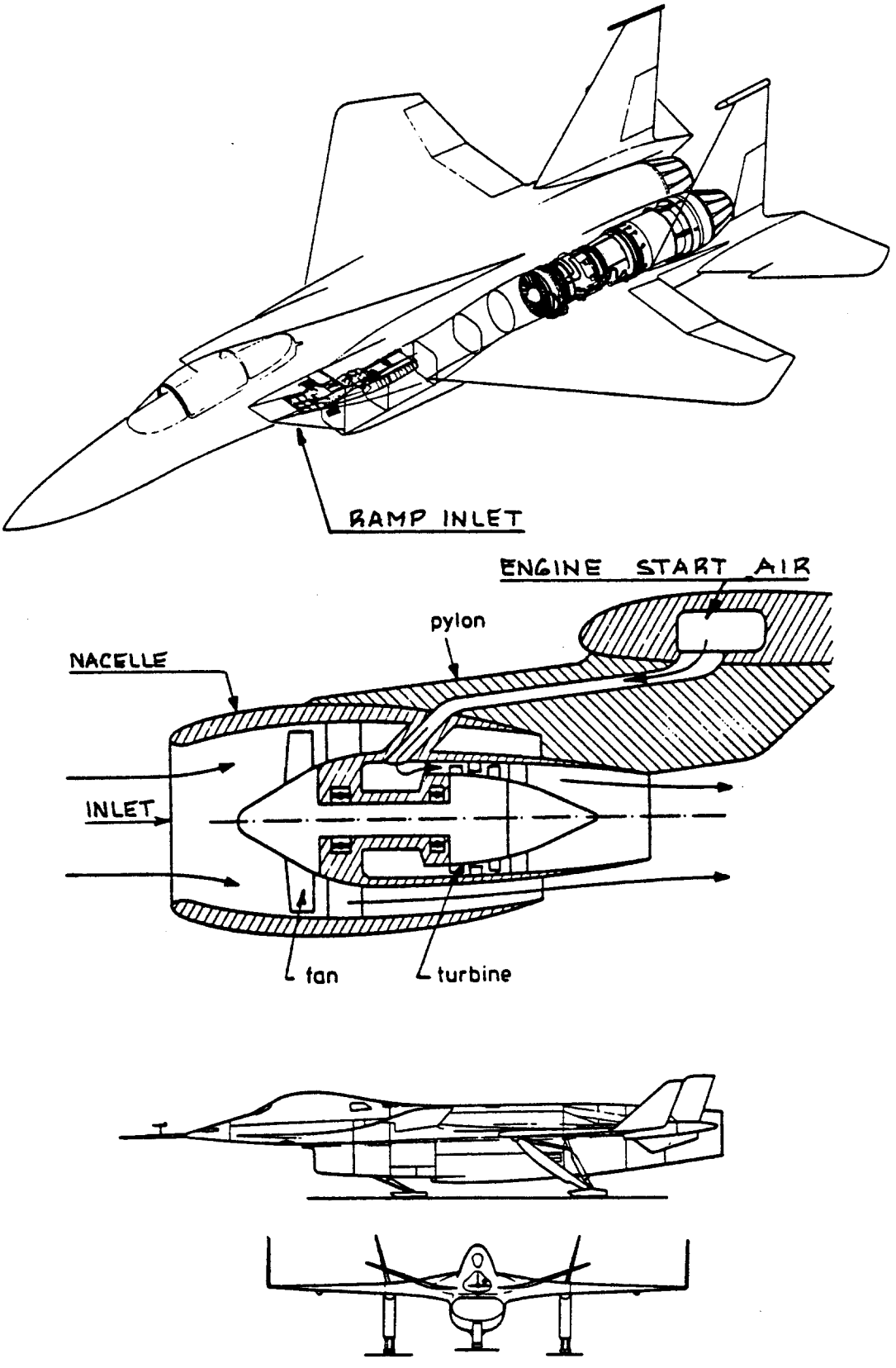

Figure 6.4a Examples of Straight Through Inlets

6.2.1 General inlet arrangements: presents a discussion of different types of inlet arrangement

6.2.2 Inlet sizing: presents a rapid method for estimating the required inlet area, A_c

6.2.3 Inlet pressure loss estimation: presents a rapid method for estimating inlet pressure losses

6.2.4 Inlet drag estimation: presents a rapid method for estimating inlet drag

Selection of the correct type of inlet and the associated inlet geometry has important consequences to the realism of any proposed airplane design. For that reason, inlet design should receive considerable attention in the early design phases of an airplane.

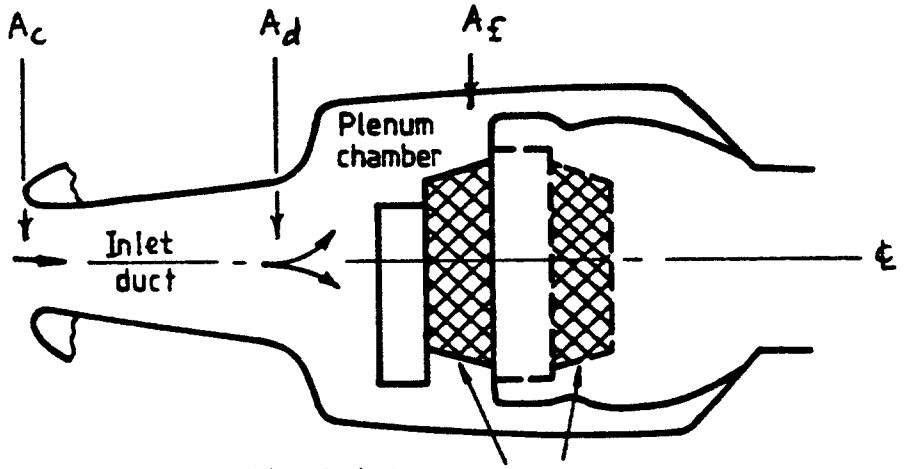

Double Sided Engine Intakes

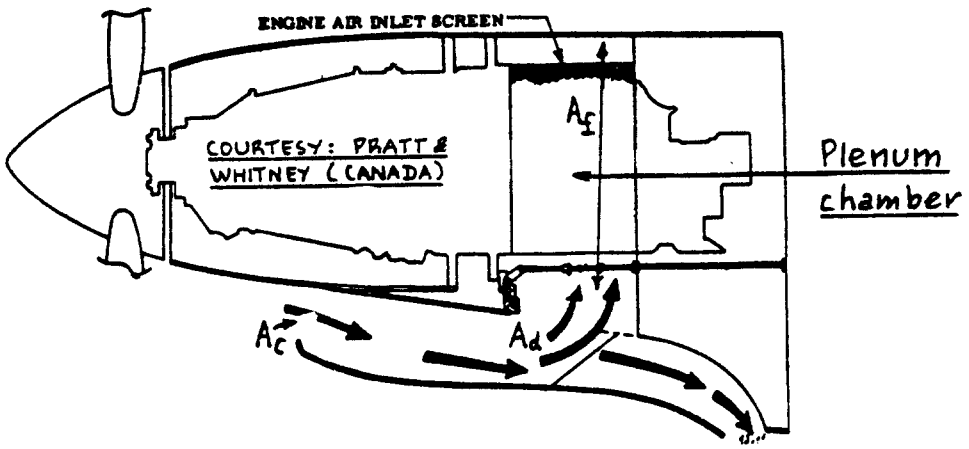

Figure 6.4b Examples of Plenum Inlets

6.2.1 General Inlet Arrangements

The purpose of this sub-section is to present a number of example inlet arrangements as well as comments regarding their applications.

The information is organized as follows:

6.2.1.1 Piston engine inlets
6.2.1.2 Turbopropeller inlets
6.2.1.3 Jet engine inlets: subsonic
6.2.1.4 Jet engine inlets: supersonic

6.2.1.1 Piston engine inlets

Figures 6.5a and 6.5b show several examples of piston engine inlet arrangements.

Figures 6.5a show that inlets for normally aspirated piston engines are of the plenum type. Most plenum installations do not completely seal off all air: cooling air must be routed to those engine components which need cooling for proper operation. After taking care of the cooling function the air is dumped overboard, preferably such that drag is not increased.

Engines with turbochargers tend to have straight through type inlets as shown in Figures 6.5b.

6.2.1.2 Turbopropeller inlets

Figure 6.6 shows several examples of turbopropeller engine (gas generator) inlets. Those shown are all of the straight through type. An example of a plenum type inlet for a turbopropeller installation was shown in Figure 6.4b.

The pressure recovery of the so-called concentric inlet (Figure 6.6d) can be strongly influenced by the design of the propeller airfoils which are in front of the inlet. Icing of such inlets is a major problem and requires detailed attention in the development of inlet anti- and de-icing systems. See Part IV, Chapter 10 for a general discussion of the icing problem.

6.2.1.3 Jet engine inlets: subsonic

Figures 6.7 show several example inlets for subsonic jet engine installations. Note the following types:

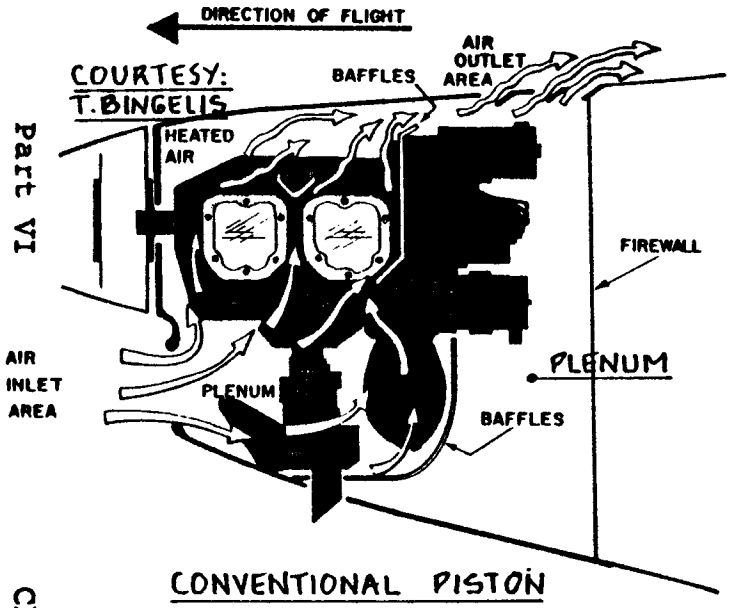

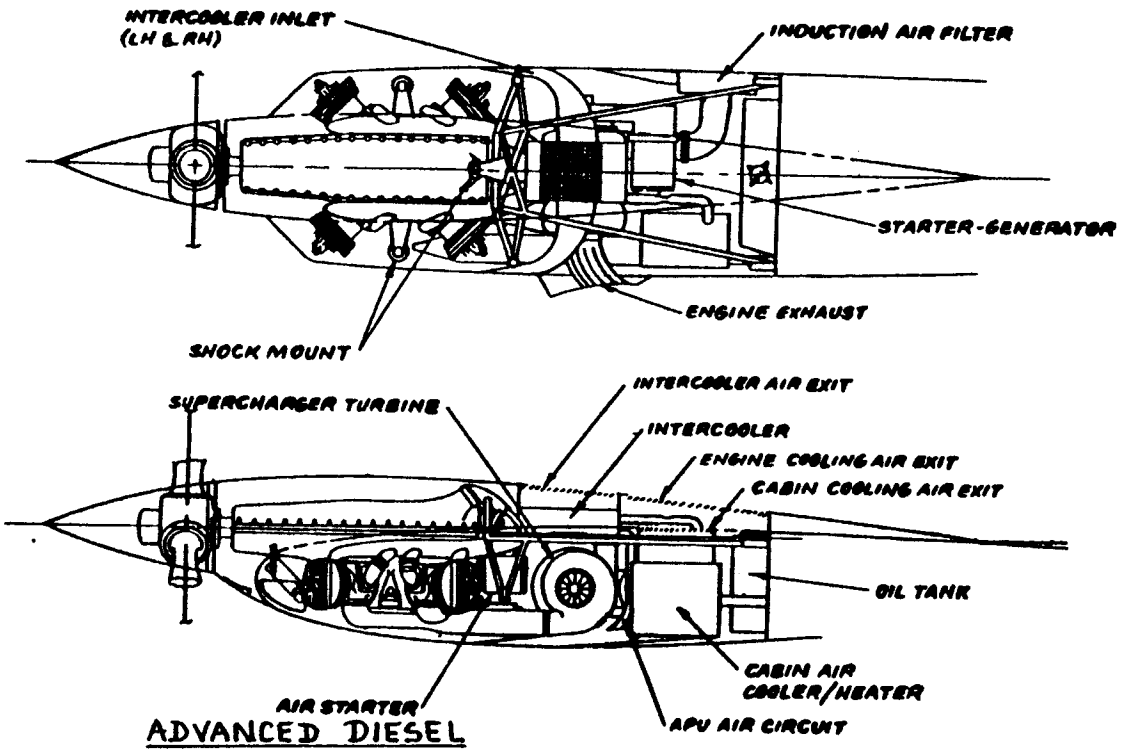

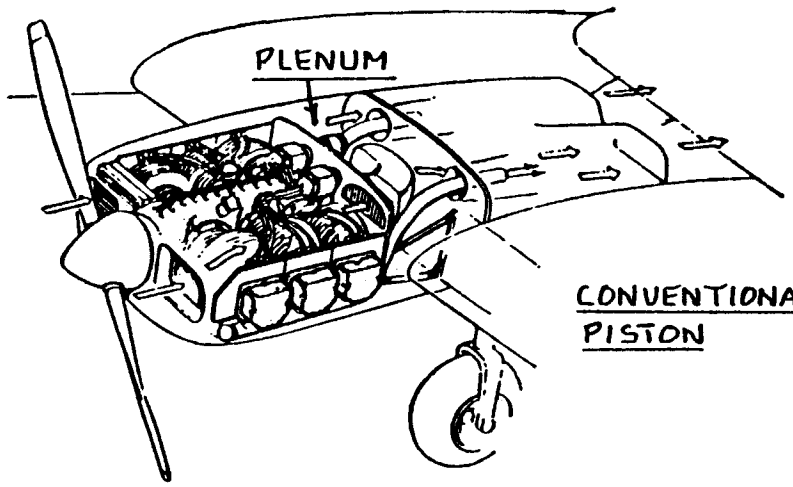

Figure 6.5a Inlets for Normally Aspirated Piston Engines

COURTESY:
CESSNA

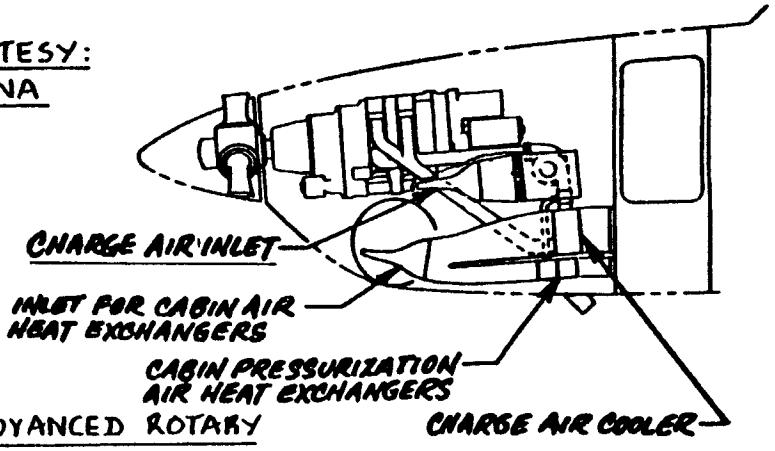

Figure 6.5b Inlets for Supercharged Piston Engines

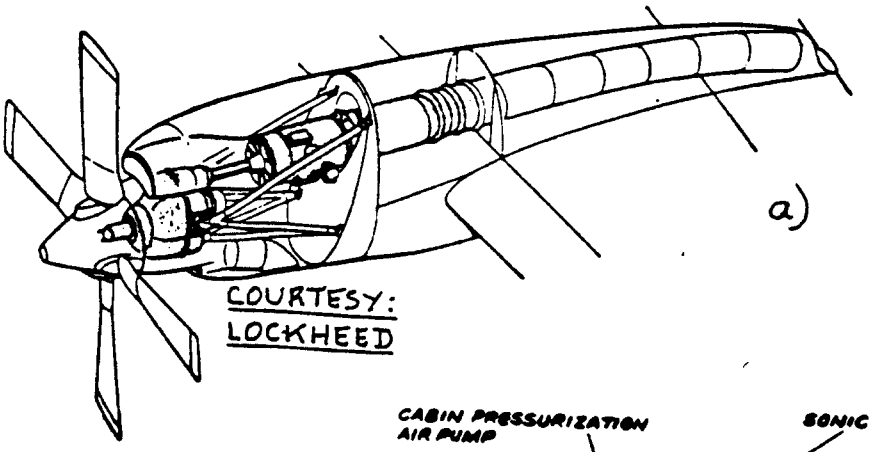

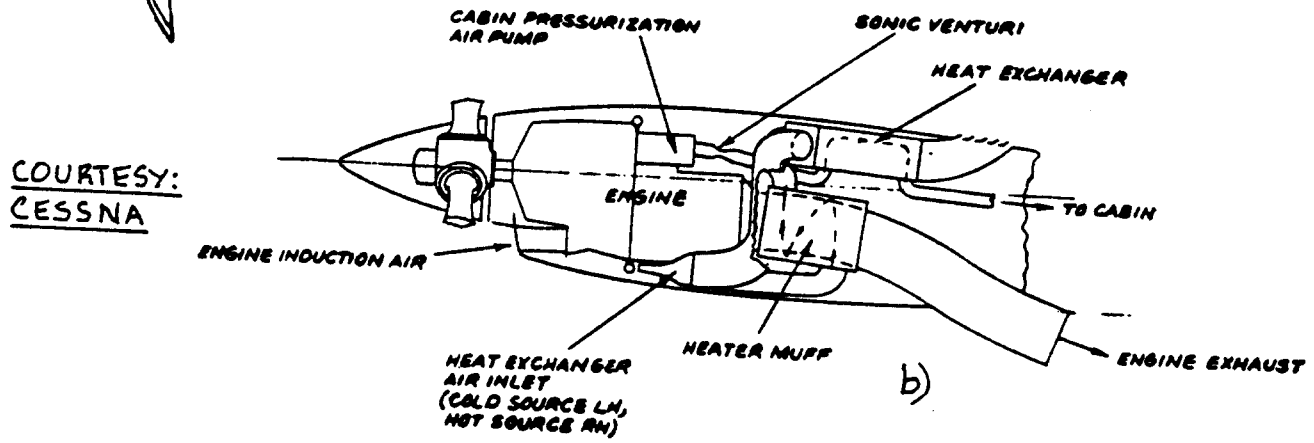

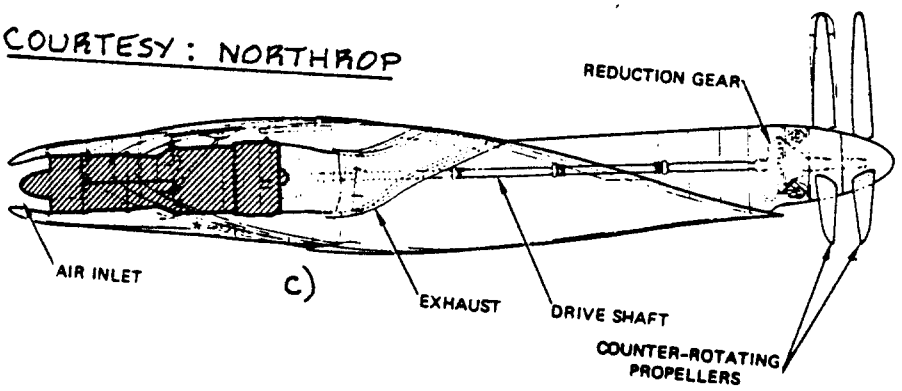

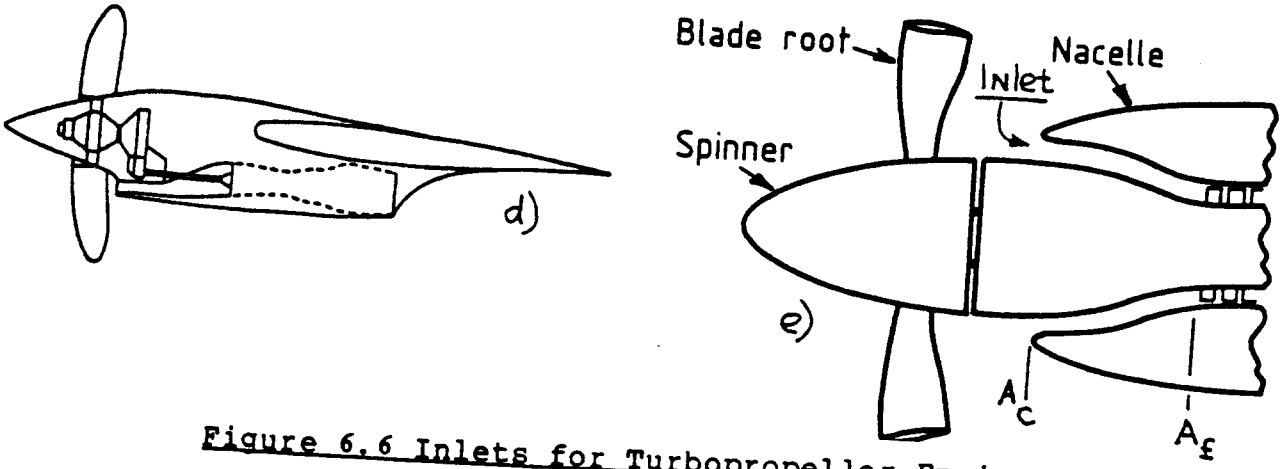

Figure 6.6 Inlets for Turbopropeller Engines

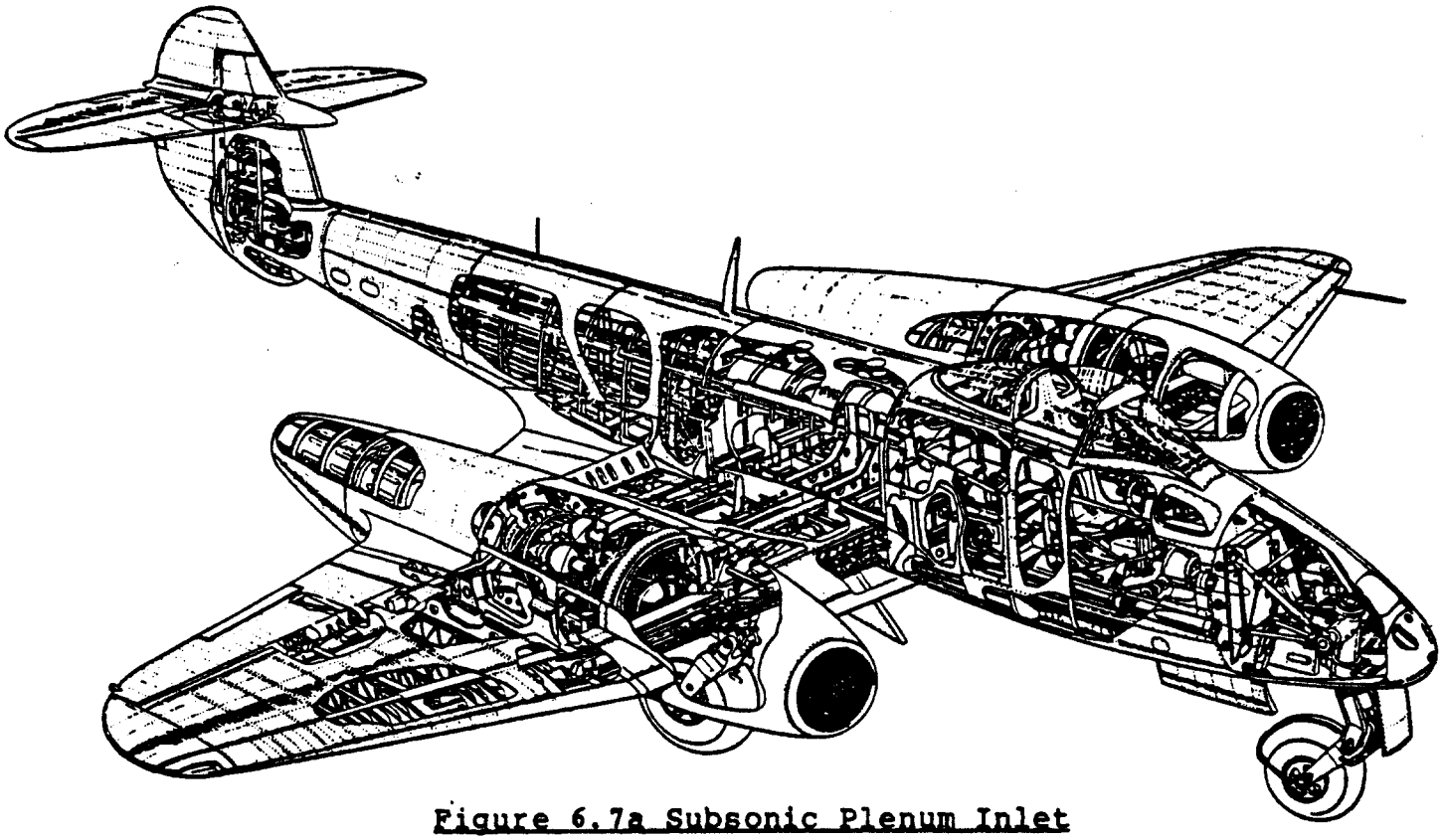

Figure 6.7a Subsonic Plenum Inlet

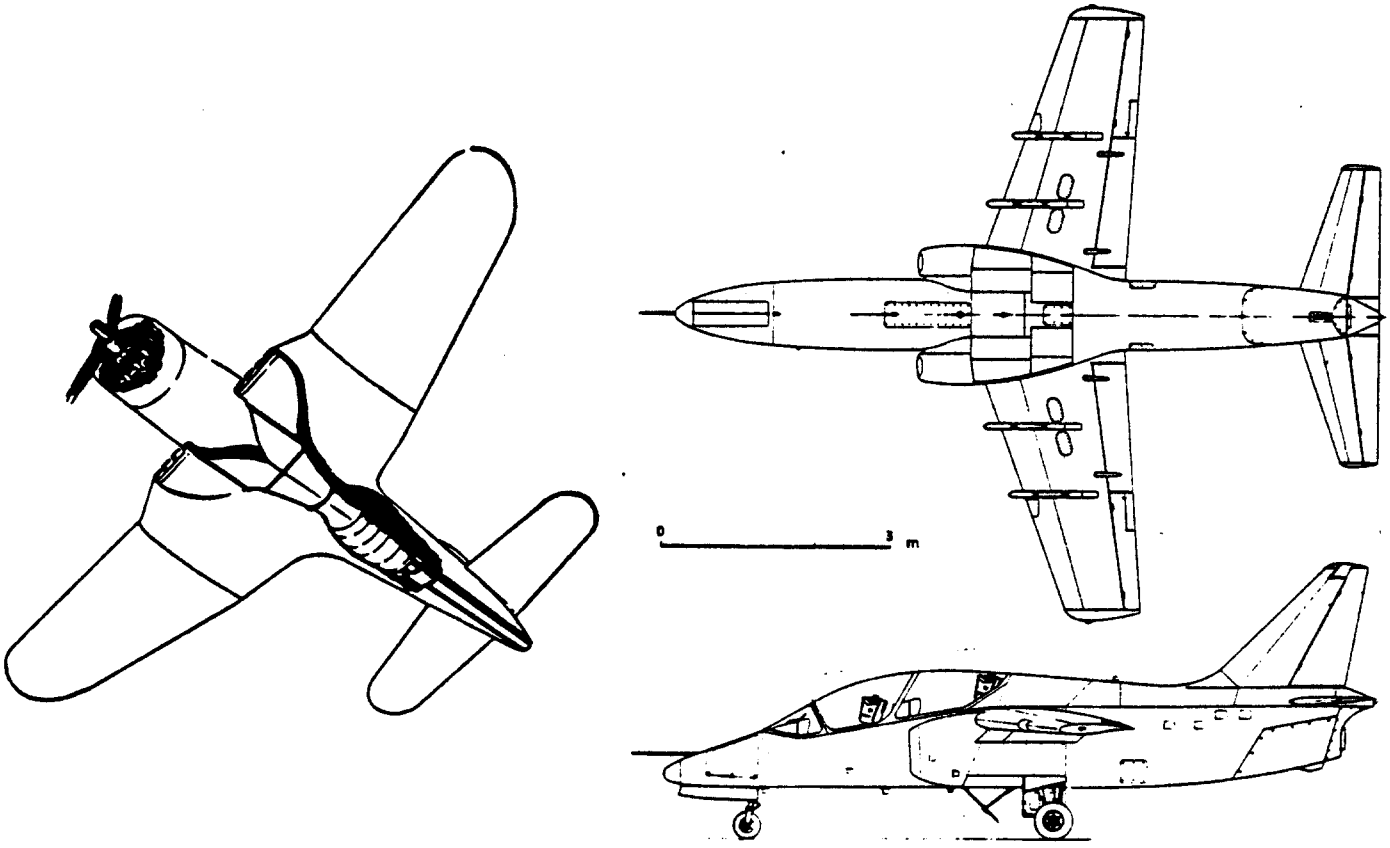

Figure 6.7b Subsonic Bifurcated Inlet

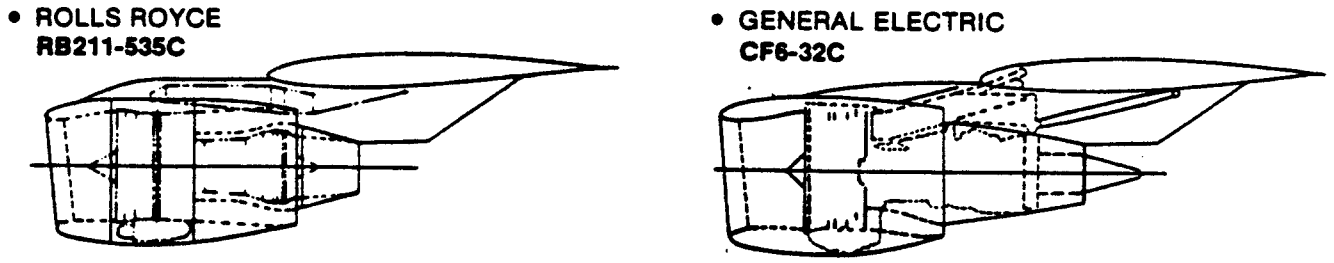

Figure 6.7c Subsonic Podded Nacelle Inlet

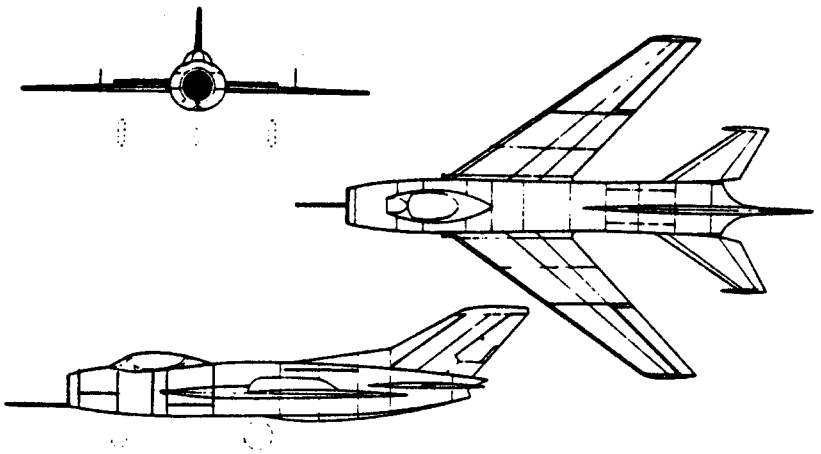

Figure 6.7d Subsonic Pitot Inlet

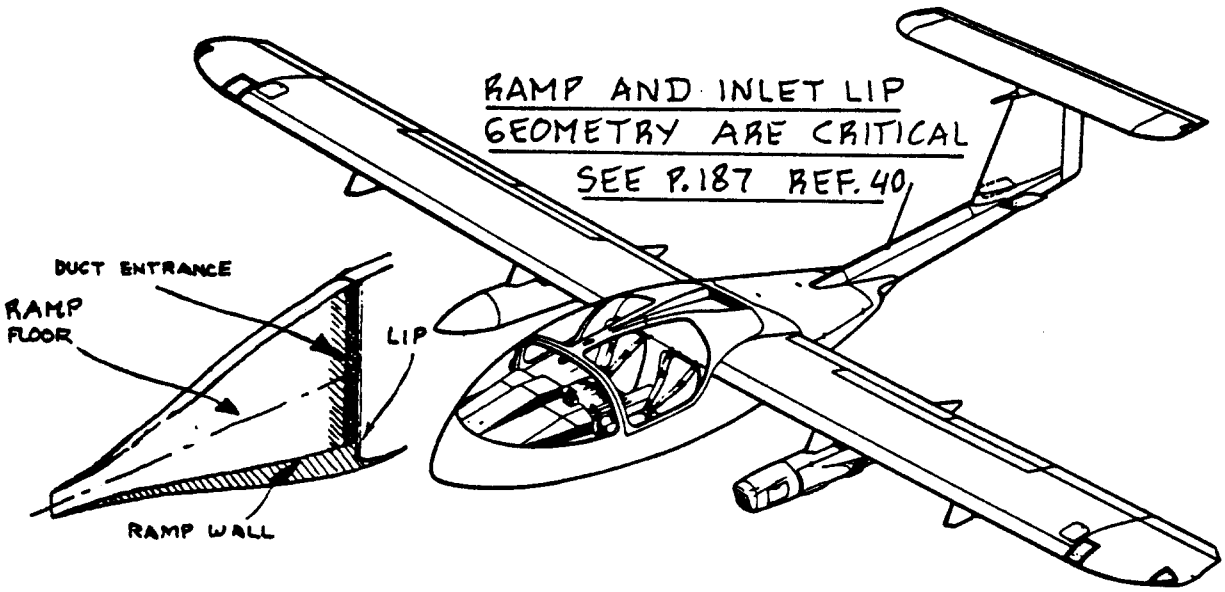

Figure 6.7e Subsonic NACA Submerged Inlet

Figure 6.7a: plenum inlet
Figure 6.7b: bifurcated, straight through inlet
Figure 6.7c: podded nacelle inlet
Figure 6.7d: pitot inlet
Figure 6.7e: NACA submerged inlet

Plenum inlets (Figure 6.7a) are used mainly in combination with double-sided centrifugal flow compressors.

Bifurcated inlets (Figure 6.7b) are used primarily in single engine installations with side inlets. Flow characteristics of bifurcated inlets are complicated, especially at high sideslip angles: inlet buzz and reversed flow on one side are phenomena which need to be 'designed out' of such inlets. Ref.32 contains more information.

Podded nacelle type inlets (Figure 6.7c) have become popular because of easy engine access. When using wing mounted engine pods there is an additional wing weight advantage due to inertial relief.

Pitot type inlets (Figure 6.7d) have been applied to many fighter airplanes. They are not influenced by the flowfield of other airplane components. However, they require very long ducts which causes extra weight and loss in pressure recovery.

The NACA submerged type inlet shown in Figure 6.7e is not very efficient for use with propulsion installations. However, when used for inlets of auxiliary systems (APU, heating and avionics bay cooling) they are quite acceptable and frequently used.

Important Note: Except for pitot and podded nacelle type inlets, all jet engine inlets must be equipped with so-called boundary layer diverters (or b.l. splitters). Figure 6.8 shows two b.l. diverter installations in some detail. If such boundary layer diverters are not used, large pressure recovery losses (thus losses in thrust) will be incurred.

A major consideration in jet fighter inlet design is the behavior of the inlet at very high angles of attack and sideslip. Compressor stall and engine surging are easily induced in such conditions. Ref.32 should be consulted for data on high angle of attack operation.

In subsonic installations it is usually best to keep the inlet as short as possible: long ducts translate into weight and pressure recovery losses. In jet fighters and in jet trainers long ducts cannot always be avoided.

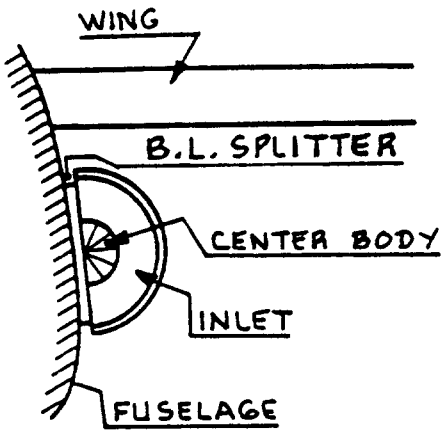

SEE REF. 32 FOR DETAILS ON B.L. SPLITTERS (DIVERTERS)

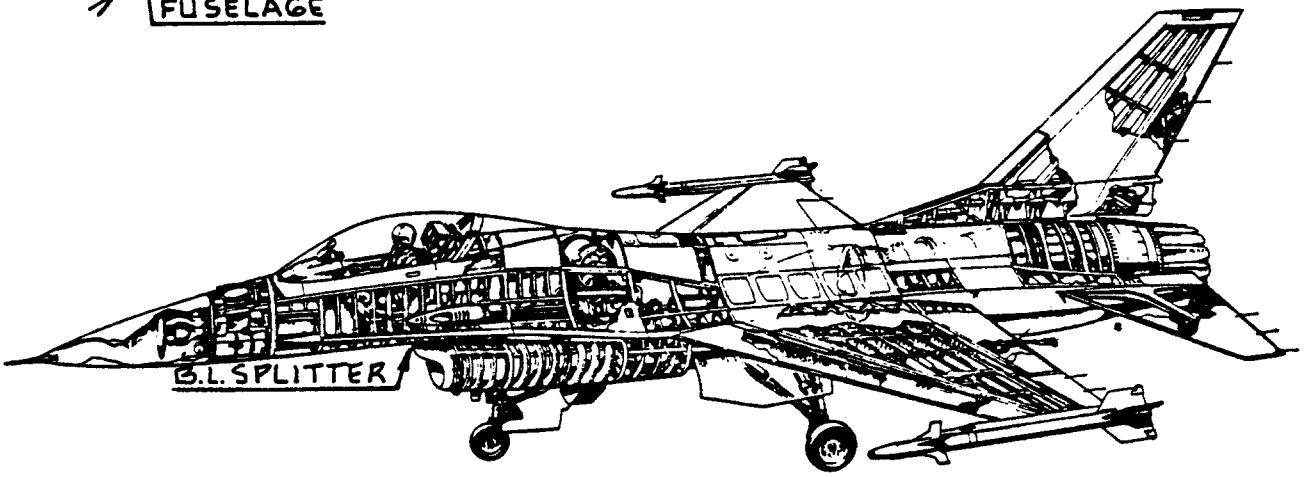

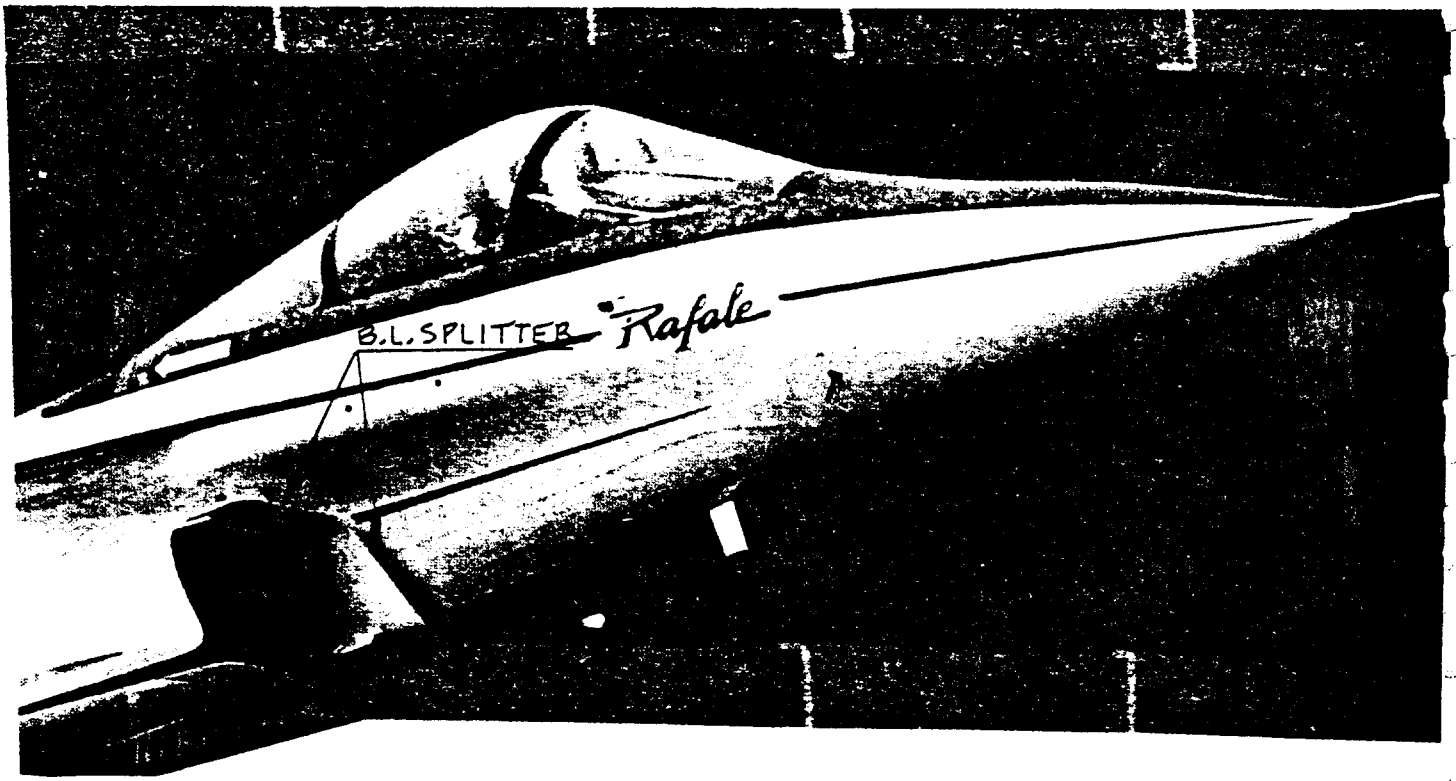

Figure 6.8 Boundary Layer Diverter Examples

6.2.1.4 Jet engine inlets: supersonic

Figures 6.9 show various types of supersonic inlets. Note the boundary layer splitters!

Figure 6.10 shows three fundamentally different types of supersonic inlet:

Fig.6.10a Pitot inlet
Fig.6.10b External compression inlet
Fig.6.10c Mixed (or external/internal) compression inlet

Pressure recovery in supersonic inlets is a strong function of the number and types of shock employed. The theoretical pressure recovery attainable with oblique and with conical shocks are shown in Figure 6.11.

Proper inlet design is extremely critical to supersonic installations as illustrated in Figure 6.12. Note that the inlet is responsible for 75 percent of the total installed thrust! A long inlet duct in supersonic engine installations is often needed to assure smooth flow deceleration (to around M=0.4 at the compressor face) and to assure full use of the favorable pressure distribution in the inlet duct. Figure 6.13 shows the effect of Mach number on thrust distribution. Note that at subsonic speeds, the engine itself (including a convergent nozzle) produces virtually all the thrust. Note also, that at supersonic Mach numbers the engine contribution itself can become negative!

Supersonic inlets frequently require a considerable amount of variable geometry devices. Examples are shown in Figures 6.13. For more information on the operation of such inlets, see References 12 and 32.

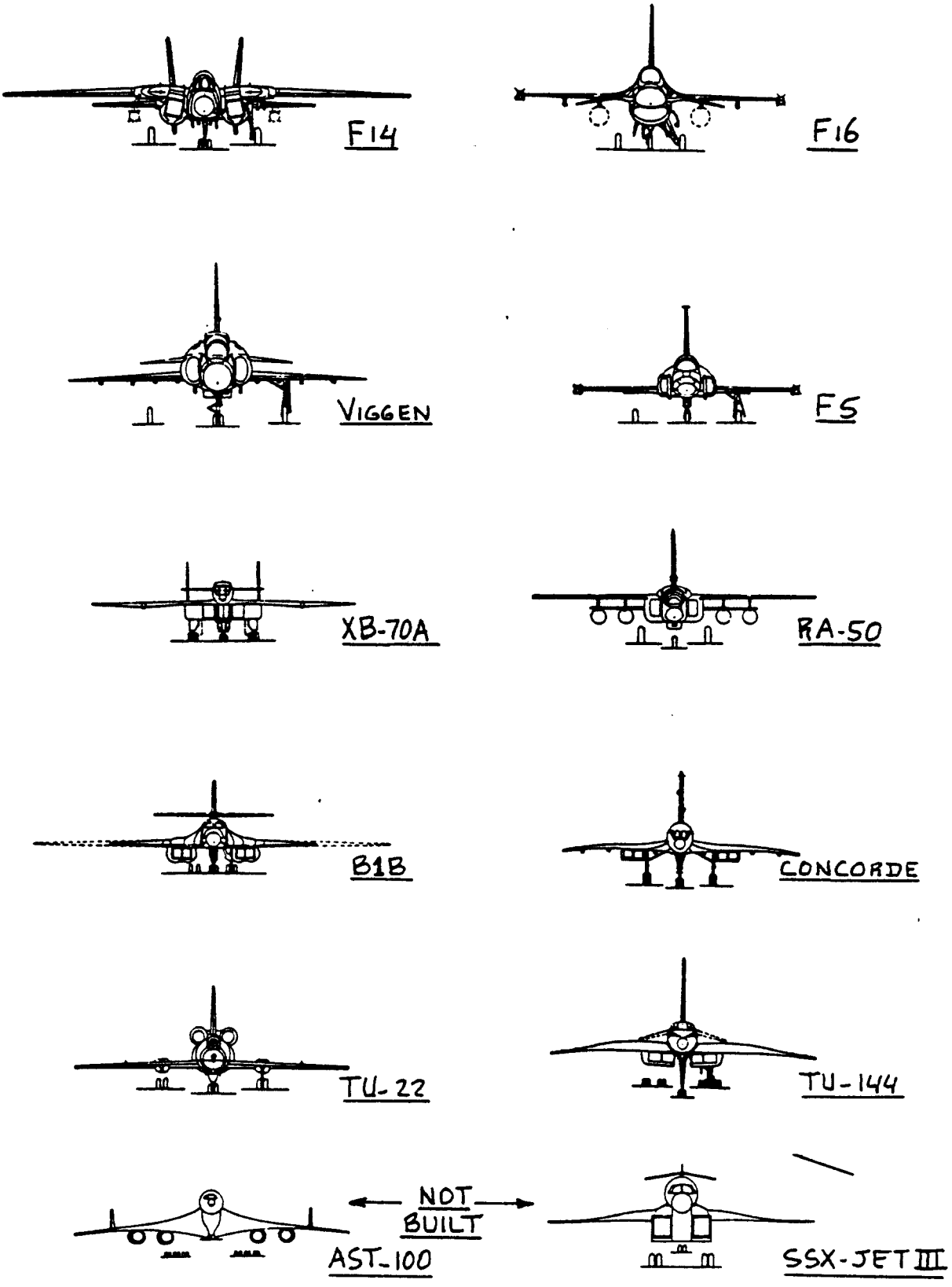

Figure 6.9 Supersonic Inlet Examples

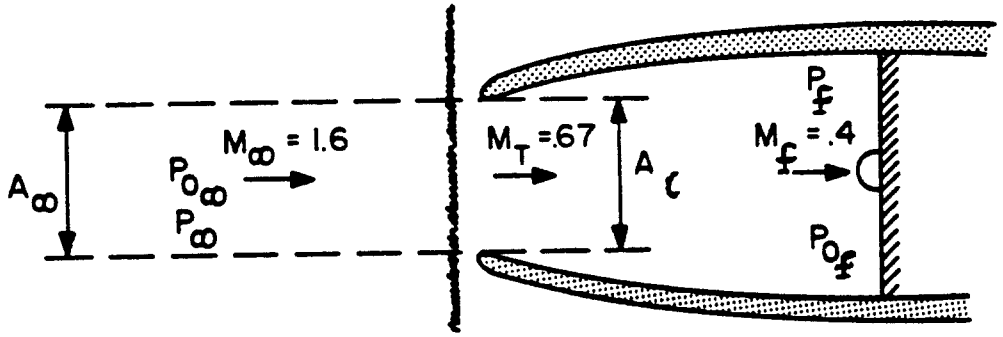

Figure 6.10a Supersonic Pitot Inlet

COPIED FROM REF. 12, COURTESY: L. NICOLAI

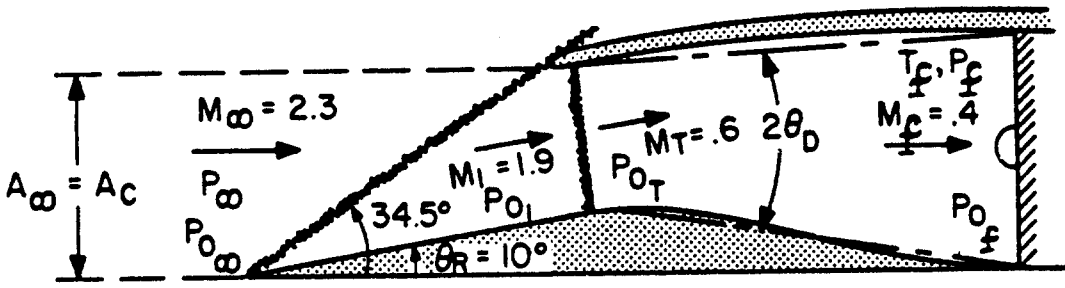

Figure 6.10b Supersonic External Compression Inlet

COPIED FROM REF. 12, COURTESY: L. NICOLAI

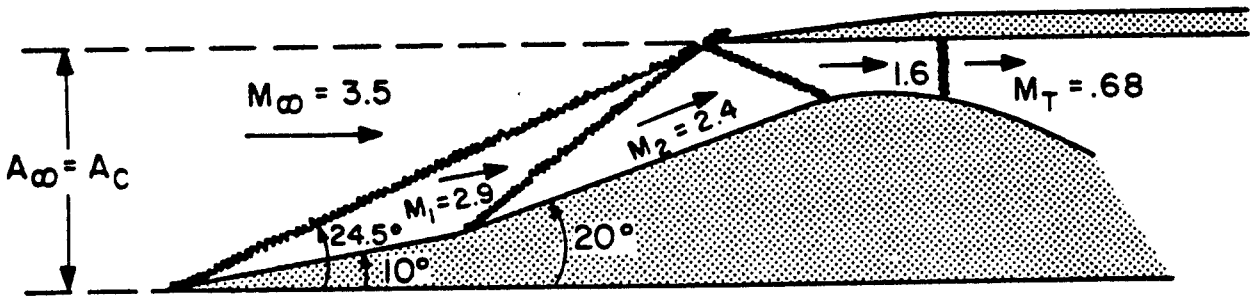

Figure 6.10c Supersonic Mixed Compression Inlet

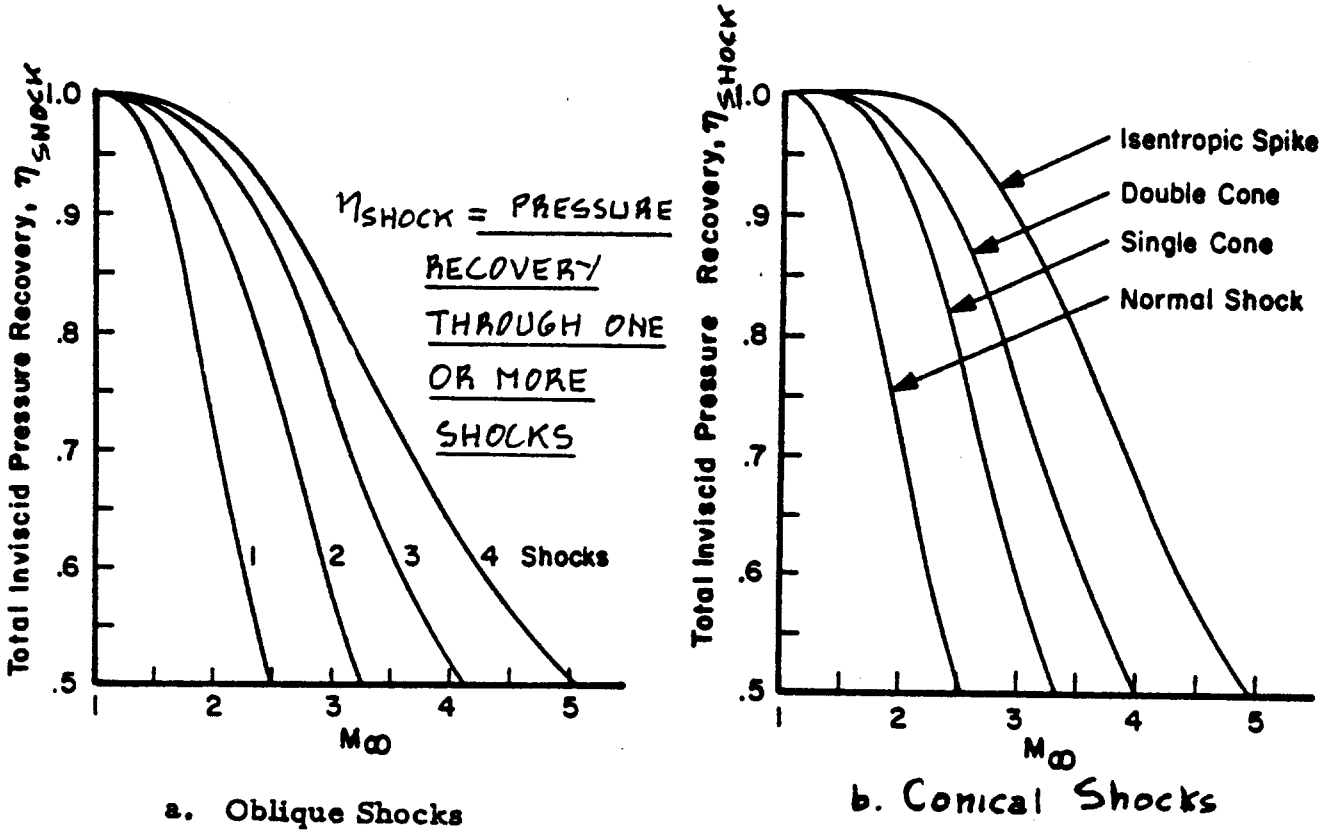

COPIED FROM REF. 12, COURTESY: L. NICOLAI

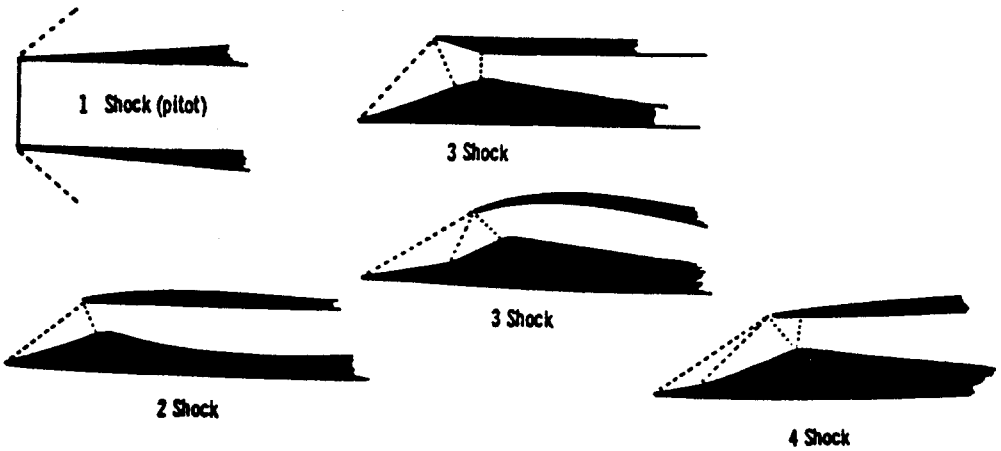

Figure 6.11 Ideal Pressure Recoveries for Oblique and for Conical Shocks

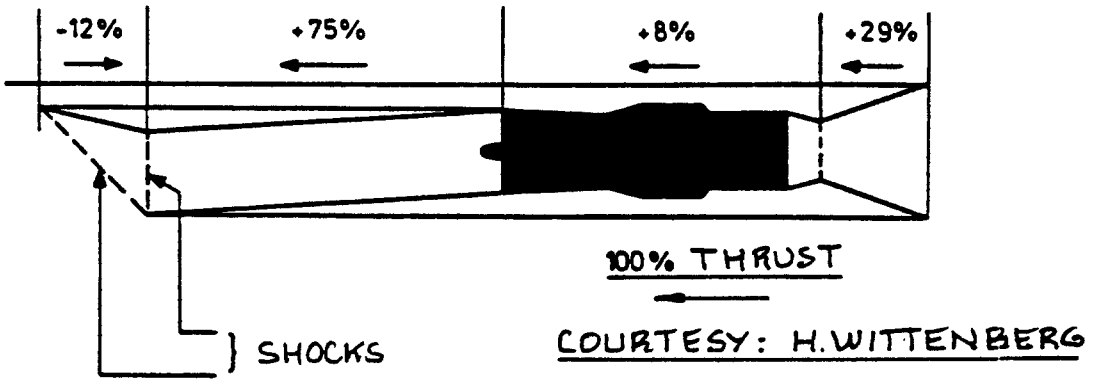

Figure 6.12 Example of the Thrust Distribution over a Supersonic Engine Installation at M=2.2

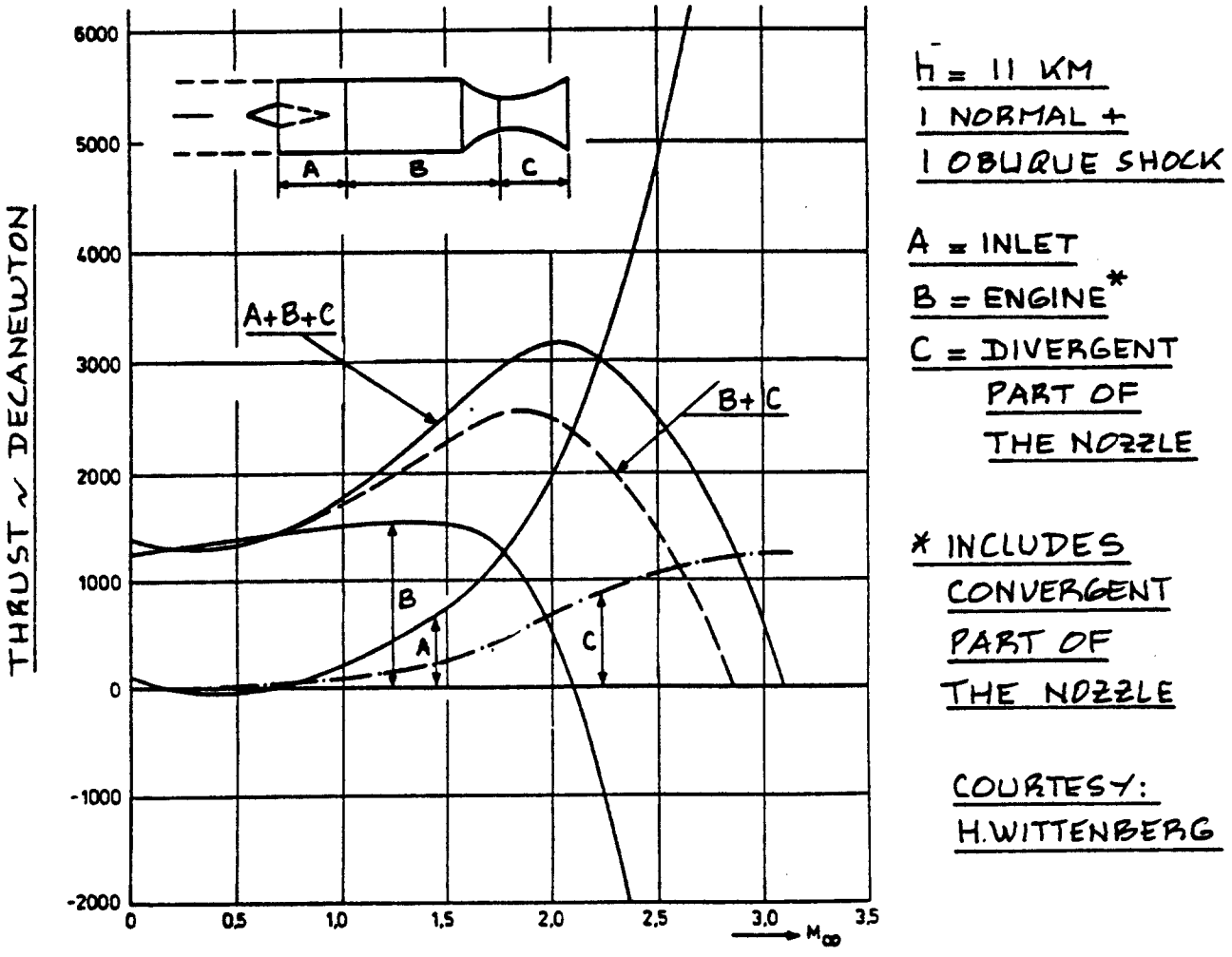

Figure 6.13 Effect of Mach Number on Thrust Distribution of a Supersonic Engine Installation

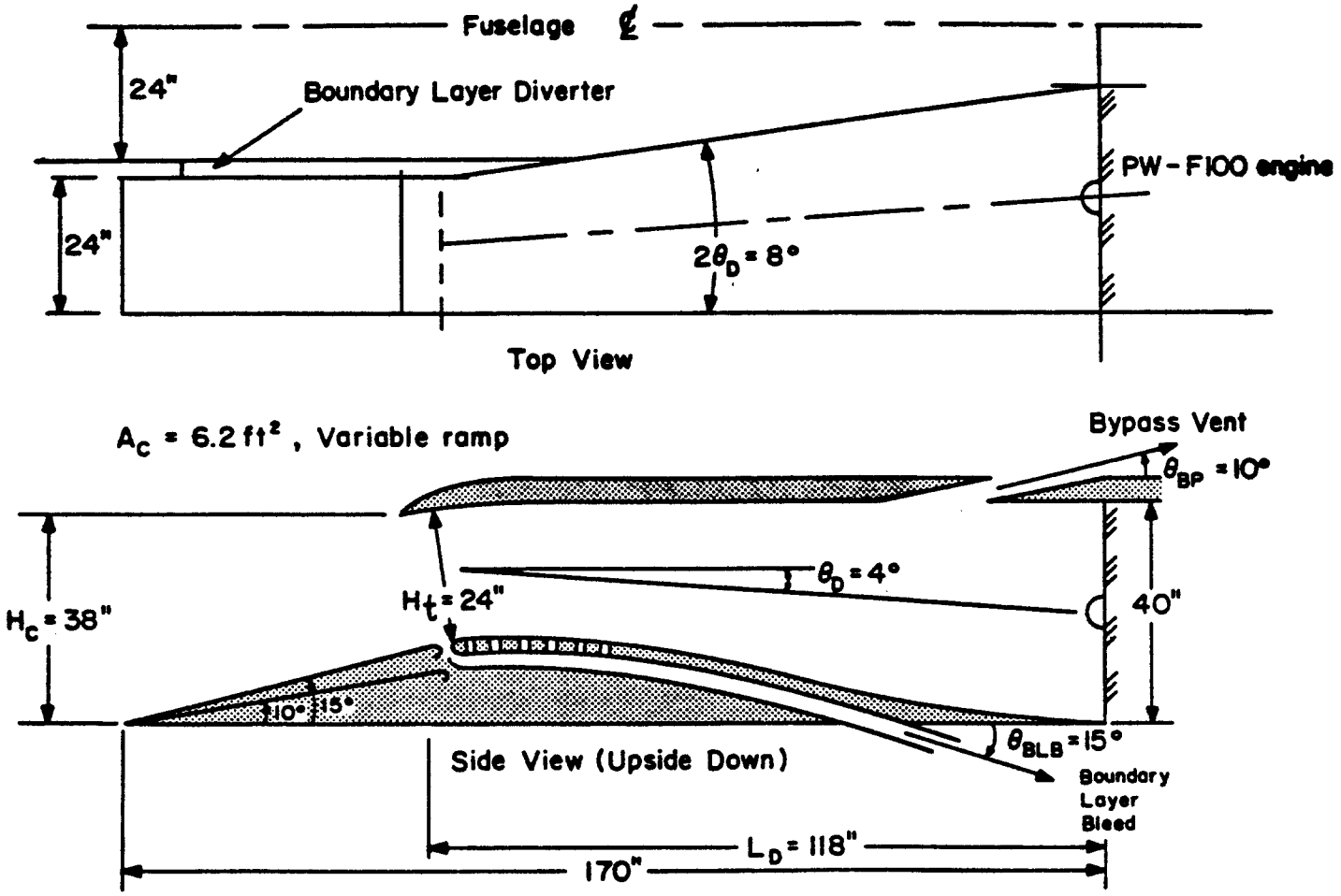

Mach 2.3 Two-Dimensional External Compression Inlet

COPIED FROM REF.12
COURTESY: L.NICOLAI

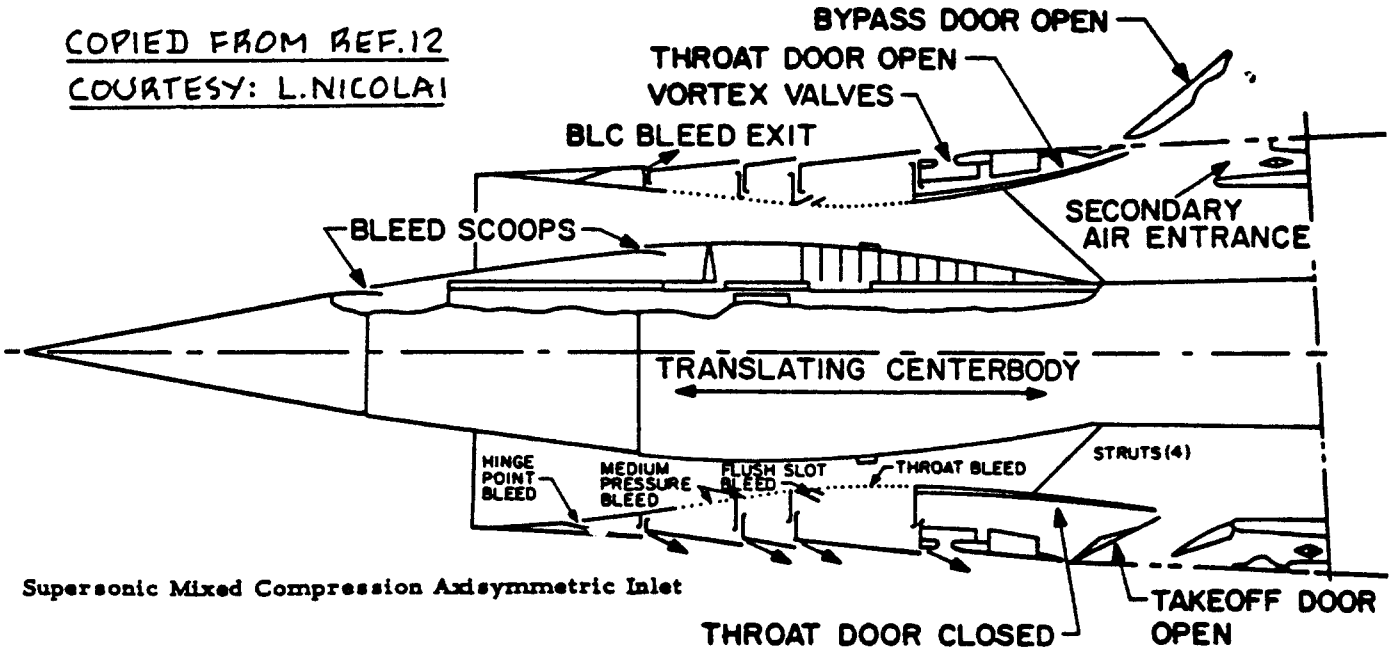

Supersonic Mixed Compression Axisymmetric Inlet

Figure 6.14 Examples of Variable Geometry in Supersonic Engine Installations

6.2.2 Inlet Sizing

The purpose of this sub-section is to present inlet sizing methods for:

6.2.2.1 Piston engine installations
6.2.2.2 Turbopropeller installations
6.2.2.3 Jet engine installations: subsonic
6.2.2.4 Jet engine installations: supersonic

For each of these inlet installations, the general flow picture of Figure 6.2 will be used to identify the required inlet area, A_c.

6.2.2.1 Piston engine installations

Figure 6.5 shows typical inlet configurations for piston engine installations. To determine the required inlet area, A_c it is first required that the engine air flow requirements be determined.

Inlet air for piston engines is required for:

1. Combustion
2. Cooling

The mass flow rate required for a piston engine may be estimated as follows:

$$\dot{m}_a = \dot{m}_{comb} + \dot{m}_{cool} \quad \text{(in slugs/sec)} \tag{6.10}$$

where: $\dot{m}_{comb}$ = the mass flow rate required for combustion. It may be estimated from:

$$\dot{m}_{comb} = (0.000062)(SHP)_{reqd} \tag{6.11}$$

$$\text{where: } (SHP)_{reqd} = P_{reqd}/\eta_p \tag{6.12}$$

where: P_{reqd} is the horsepower required for the flight condition being analyzed. Part VII contains methods for determining P_{reqd} for a variety of flight conditions.

η_p is the propeller efficiency.

Section 6.4 and Ref.15 show how to obtain data for

propeller efficiency. In preliminary design, first approximations are:

η_p = 0.85 for cruise
0.80 for climb
0.70 for take-off

In Equation (6.11) it is assumed that:

1. that the engine efficiency in converting chemical energy in the fuel to shafthorsepower (SHP) is 30 percent.
2. that the fuel/air ratio used is the stochiometrically required value.

$\dot{m}_{cool}$ = the mass flow rate required for cooling.

Its magnitude depends on the type of engine:

<u>For aircooled</u> airplane engines the mass flow rate required for engine cooling may be estimated from:

$$\dot{m}_{cool} = 0.00056(SHP)_{reqd} \quad \text{in slugs/sec} \qquad (6.13)$$

where: $(SHP)_{reqd}$ follows from Eqn.(6.12).

In preliminary design, SHP_{TO} may be used for $(SHP)_{reqd}$.

Detailed methods for estimating $\dot{m}_{cool}$ for aircooled engines are given in References 35 and 36.

<u>For liquid cooled</u> airplane engines the required mass flow rate for the radiator depends strongly on the type of liquid cooling used. Chapter 9 in Reference 8 and Reference 37 should be consulted.

For preliminary design purposes it is suggested to use Eqn.(6.10) for liquid cooled engines also.

Considerable experience with liquid cooled engine installations was obtained in WWII. In many cases it proved possible to design the radiator system in such a way that negligible losses were incurred. However, this was achieved at a considerable increase in weight and complexity.

Knowing the total air mass flow rate, the size of the required inlet area may be estimated from:

$$A_c = \dot{m}_a / \rho U_1 \qquad (6.14)$$

where: $\dot{m}_a$ follows from Eqn.(6.10),

ρ is the air density in slugs/ft^3 and

U_1 is the steady state airspeed in fps.

Note: Eqn.(6.14) is valid for incompressible flow!

The reader must determine which conditions for air density, ρ and airspeed, U_1, yield the largest value for inlet area, A_c. Since zero airspeed represents an anomalie, lift-off speed or climbout speeds are normally used. Extra inlet doors (or cowl flaps) may be required for prolonged static and taxi operations.

To minimize the drag caused by momentum loss in the cooling air, careful design of the ducting leading from the inlet to the overboard dumping point is required. References 8 and 38 should be consulted for more details. Reference 39 contains example calculations for inlet area sizing for piston engines.

6.2.2.2 Turbopropeller installations

Figure 6.6 shows typical inlet configurations for turbopropeller engines.

To determine the required inlet area, A_c it is first necessary to determine the engine air flow requirements.

Inlet air for turbopropeller engines (also called: gas generators) is required for:

1. combustion and mass flow
2. cooling

The mass flow rate for turbopropeller engines may be estimated from:

$$\dot{m}_a = \dot{m}_{gas} + \dot{m}_{cool} \qquad (6.15)$$

where: $\dot{m}_{gas}$ = the air flow rate required by the engine for combustion and for mass flow. In a gas generator the mass flow rate is much larger than the air flow required for combustion. Manufacturers engine data normally include the maximum mass flow rate. Reference 31 also lists required mass flow rates for gas generators. Tables 6.6 and 6.7 in Part III list take-off mass flow rates in lbs/sec for a range of turbopropeller engines.

In preliminary design, a good approximation is:

$$\dot{m}_{gas} = (0.00028)(SHP)_{reqd} \quad \text{(in slugs/sec)} \quad (6.16)$$

where: $(SHP)_{reqd}$ is given by Eqn.(6.12).

$\dot{m}_{cool}$ = the mass flow rate needed for cooling.

For gasgenerators this may be taken as 5 percent of $\dot{m}_{gas}$ for most turboprop installations:

$$\dot{m}_{cool} = 0.05\dot{m}_{gas} \quad (6.17)$$

The required inlet area may be estimated from:

$$A_c = \dot{m}_a/\rho U_1 \quad (6.18)$$

where: $\dot{m}_a$ is found from Eqn.(6.15).

Note: Eqn.(6.18) is valid for incompressible flow!

The reader must determine which conditions for air density, ρ and airspeed, U_1 yield the largest value for inlet area A_c.

Since zero airspeed represents an anomalie, lift-off speed or climbout speeds are normally used. Extra inlet doors (variable inlet geometry) may be needed for prolonged static and taxi operations.

6.2.2.3 Jet engine installations: subsonic

Figure 6.7 shows examples of subsonic jet engine inlets.

To determine the required inlet area, A_c it is first

necessary to determine the engine airflow requirements.

Inlet air for jet engines is required for:

1. combustion and mass flow 2. cooling

The mass flow rate required for a subsonic jet engine installation may be found from:

$$\dot{m}_a = \dot{m}_{gas} + \dot{m}_{cool} \qquad (6.19)$$

where: $\dot{m}_{gas}$ = the air flow rate required for the engine.

In jet engines the flow rate required for combustion is much less than that needed for mass flow. Manufacturers engine data normally include the maximum mass flow $\dot{m}_{gas}$ required by the engine.

Reference 31 also lists those flow rates. Tables 6.8 - 6.11 in Part III list take-off mass flows for a range of jet engines. In preliminary design the following approximation may be used:

$$\dot{m}_{gas} = k_{gas} T_{TO} \qquad (6.20)$$

where: k_{gas} = 0.0003 for BPR values of 0 to 1.0

= 0.0007 for BPR values of 1.0 to 2.0

= 0.0009 for BPR values of 2.0 to 4.0

= 0.0011 for BPR values of 4.0 to 6.0

$\dot{m}_{cool}$ = the air flow rate needed for cooling.

In preliminary design it may be assumed that:

$$\dot{m}_{cool} = 0.06\dot{m}_{gas} \qquad (6.21)$$

The required inlet area, A_c may be estimated from:

$$A_c = \dot{m}_a/\rho U_1 \qquad (6.22)$$

where: $\dot{m}_a$ is found from Eqn. (6.19)

ρ and U_1 are determined by the flight condition.

Note: Eqn. (6.22) is valid for compressible flow.

The inlet size for most subsonic airplanes is dictated by low speed requirements. For that reason, Eqn.(6.22) is applicable to preliminary inlet sizing for subsonic jets.

6.2.2.4 Jet engine installations: supersonic

Figures 6.9 and 6.10 show examples of supersonic jet engine inlet installations.

Inlet air for jet engines in supersonic installations is required for:

1. combustion and mass flow
2. cooling
3. inlet boundary layer bleed

The mass flow rate required for a jet engine in a supersonic installation may be estimated from:

$$\dot{m}_a = \dot{m}_{gas} + \dot{m}_{cool} + \dot{m}_{blb} \qquad (6.23)$$

where: $\dot{m}_{gas}$ = the air flow rate required for the engine.

In jet engines the air flow rate required for combustion is much less than that for mass flow. Manufacturers engine data normally include the maximum mass flow, $\dot{m}_{gas}$ required by the engine.

Reference 31 also lists those flow rates. Tables 6.8 - 6.11 list mass flow rate values for a range of engines. Since most supersonic inlets must also operate at subsonic speeds, the take-off mass flow rates normally size the inlet area. For this reason, Eqn.(6.20) may be used for computing $\dot{m}_{gas}$.

$\dot{m}_{cool}$ = the air flow rate needed for cooling.

In preliminary design it is acceptable to use:

$$\dot{m}_{cool} = 0.08\dot{m}_{gas} \qquad (6.24)$$

$\dot{m}_{blb}$ = the air flow rate needed for boundary layer bleed in the inlet. Because of the fact that supersonic installations require fairly long inlets, the resulting build-up of boundary layer air must be bled away before it reaches the compressor. Figure 6.14 shows such a boundary layer bleed system. The need for boundary layer bleed

translates into a need for extra inlet capture area as shown in Eqn.(6.25).

The inlet area, A_c for a supersonic inlet is as defined in Figure 6.15. The required inlet area, A_c for a supersonic jet engine installation may be estimated from:

$$A_c = (1.08\dot{m}_{gas}/\rho U_1)\{1 + k_{bl}(M_1 - 0.8)\} \qquad (6.25)$$

where: $\dot{m}_{gas}$ follows from Eqn.(6.20)

ρ and U_1 are determined by the flight condition

which in the case of a supersonic installation is taken to be the design supersonic cruise condition or the take-off condition. If the latter results in a larger inlet area than the former, the possibility of using extra inlet doors for subsonic operation must be weighed against 'oversizing' the inlet for supersonic conditions.

$$M_1 = U_1/a \qquad (6.26)$$

where: a is the speed of sound in the design cruise flight condition

k_{bl} is a constant which depends on the type of inlet used:

$k_{bl} = 0$ for pitot inlets and for $M_1 < 0.8$

$k_{bl} = 0.028$ for external compression inlets

$k_{bl} = 0.041$ for mixed external/internal compression inlets

The inlet throat area, A_{throat} in Figure 6.15 must be carefully sized to assure that it can handle the required engine mass flow rate. References 12 and 32 contain methods for determining the throat size.

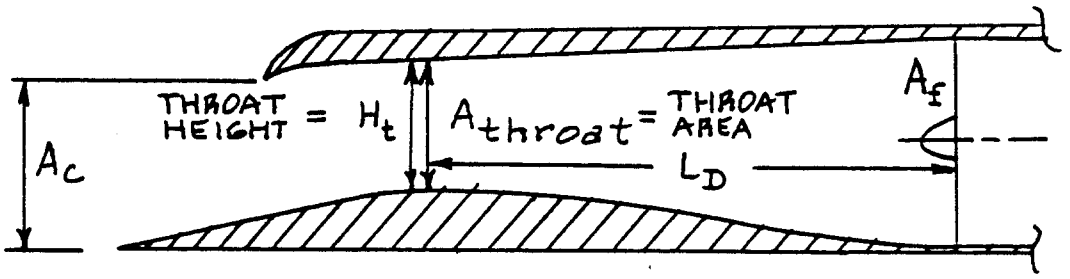

Figure 6.15 Geometry Definition for a Supersonic Inlet

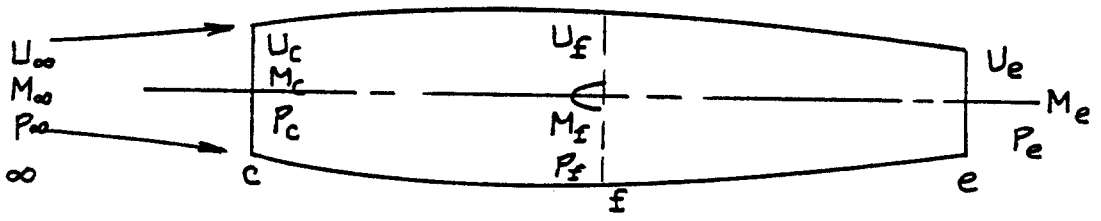

Figure 6.16 Definition of Flow Parameters for Figure 2

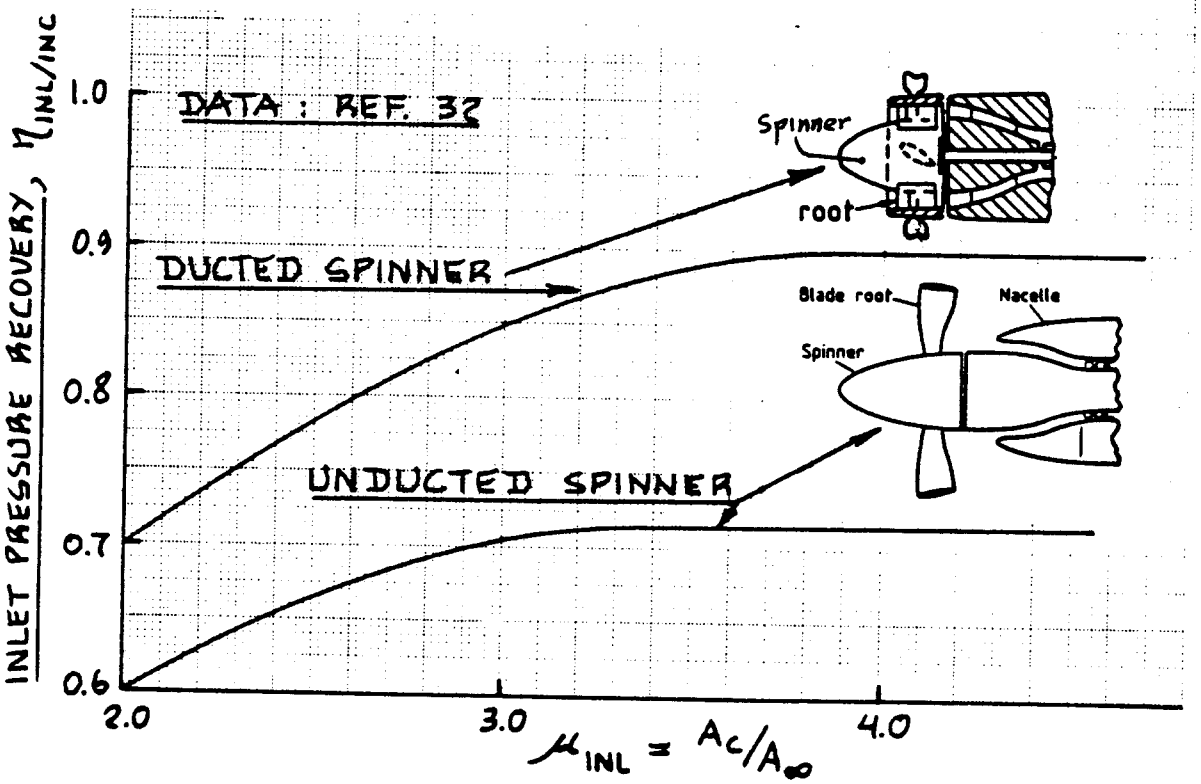

Figure 6.17 Pressure Recovery for Turbopropeller Inlets

6.2.3 Inlet Pressure Loss Estimation

The generalized flow situation shown in Figure 6.2 is repeated in Figure 6.16 with the addition of speed, U, Mach number, M and static pressure, p at each station.

The total pressure at each station is defined as:

$$p_{tot} = p + 0.5\rho U^2 = p + \bar{q} \qquad (6.27)$$

where: p is the local static pressure,

ρ is the local air density and

U is the local air velocity.

The inlet pressure loss is defined as:

$$\Delta p_{inl} = p_{tot_\infty} - p_{tot_f} \qquad (6.28)$$

Inlet pressure loss is frequently compared to free stream dynamic pressure or to free stream total pressure, in which cases it is referred to as the inlet efficiency or inlet pressure recovery, η_{inl}:

For incompressible flow:

$$\eta_{inl/inc} = (p_{tot_f} - p_\infty)/\bar{q}_\infty \qquad (6.29)$$

which can be written as:

$$\eta_{inl/inc} = 1 - \Delta p_{inl}/\bar{q}_\infty \qquad (6.30)$$

For compressible flow:

$$\eta_{inl/com} = p_{tot_f}/p_{tot_\infty} \qquad (6.31)$$

which can be written as:

$$\eta_{inl/com} = 1 - \Delta p_{inl}/p_{tot_\infty} \qquad (6.32)$$

The purpose of this sub-section is to present rapid methods for the calculation of inlet pressure losses in terms of either Δp_{inl} or η_{inl}.

Inlet pressure losses in turn have a detrimental effect on installed engine power or thrust. Methods for determining the effect of inlet pressure losses on installed power or thrust are presented in Section 6.4.

The information is organized as follows:

6.2.3.1 Piston engine inlets
6.2.3.2 Turbopropeller inlets
6.2.3.3 Jet engine inlets: subsonic
6.2.3.4 Jet engine inlets: supersonic

6.2.3.1 Piston engine inlets

For plenum inlets:

Figure 6.5a shows plenum inlets for piston engines.

In well designed piston engine plenum installations, the inlet losses may be held to less than 2 percent. For preliminary design purposes it is acceptable to use:

$$\eta_{inl/inc} = 0.98 \qquad (6.33)$$

For 'straight through' inlets:

Figure 6.5b shows 'straight through' inlets for piston engine applications. The method of 6.2.3.3 for subsonic jet inlets may be used to estimate pressure losses.

6.2.3.2 Turbopropeller inlets

For plenum inlets:

For turbopropellers with plenum inlet installations (See Figure 6.6), the pressure losses may be estimated with the plenum inlet method of 6.2.3.3.

For 'straight through' inlets:

As shown in Figure 6.6, many turbopropeller installations utilize 'straight through' inlets. For such inlets the pressure recovery may be estimated from:

$$\eta_{inl/inc} = f(\mu_{inl}) \qquad (6.34)$$

where: $f(\mu_{inl})$ is established in Figure 6.17 for inlets with unducted spinners as well as ducted spinners.

$$\mu_{inl} = A_c/A_\infty \qquad (6.35)$$

Note that μ_{inl} is the inverse of the inlet flow ratio as defined on page 147.

6.2.3.3 Jet engine inlets: subsonic

For plenum inlets:

Figure 6.7a shows a plenum inlet for a subsonic jet. Pressure losses may be estimated from:

$$\Delta p_{inl}/\bar{q}_\infty = \{1/(\mu_{inl}^2)\}(A_c/A_d)^2(1 - A_d/A_f)^2 \quad (6.36)$$

where: A_c, A_d and A_f for a plenum installation are as defined in Figure 6.18. Ref. 32 should be consulted for more details on jet engine plenum inlets.

For straight through inlets:

Figures 6.7b-d show subsonic, 'straight through' jet inlet examples. The pressure loss in such inlets is a strong function of the absence or presence of boundary layer diverters. Figure 6.8 shows examples of boundary layer diverters.

Without a boundary layer diverter, the pressure loss of a subsonic jet engine inlet may be estimated from:

$$\Delta p_{tot}/\bar{q}_\infty = IC_{Fd}/(\mu_{inl})^2 + HC_{Fa}\mu_{inl} \quad (6.37)$$

where: I is the so-called duct integral, defined as:

$$I = \int_{l_c}^{l_f} (A_c/A)^2 (per_A/A)dl \quad (6.38)$$

where: A is the duct area at station 1,

per_A is the duct perimeter at station 1

l_c is the duct station at the inlet area, A_c: see Figure 6.19

l_f is the duct station at the engine compressor face: see Figure 6.19.

$$C_{Fd} = fC_f \quad (6.39)$$

where: the factor f is given in Figure 6.20

C_f is the equivalent flat plate friction coefficient based on the duct Reynold's Number with the characteristic length taken as $(l_f - l_c)$. Figure 4.3 may

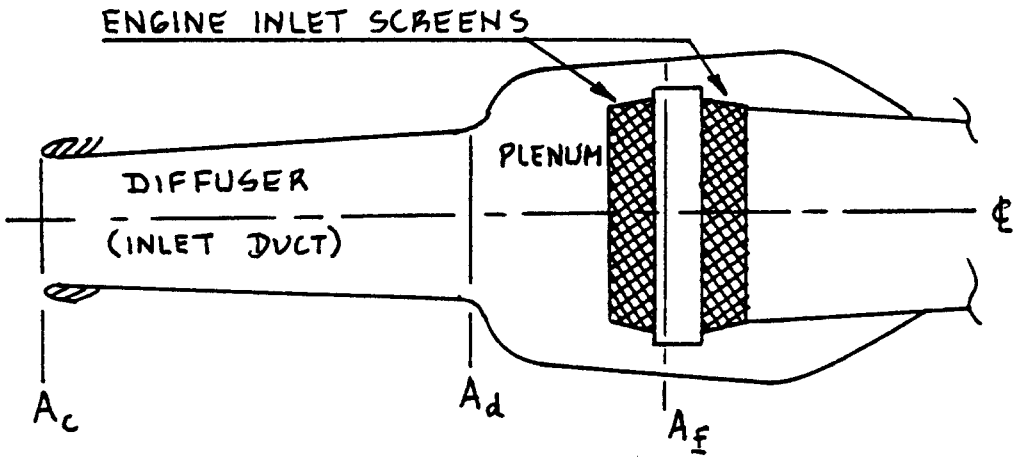

Figure 6.18 Geometry Definition for a Plenum Inlet

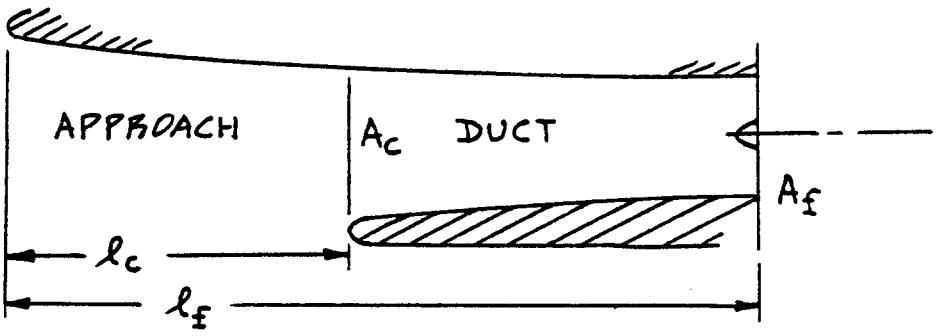

Figure 6.19 Duct Geometry with External Wetted Area

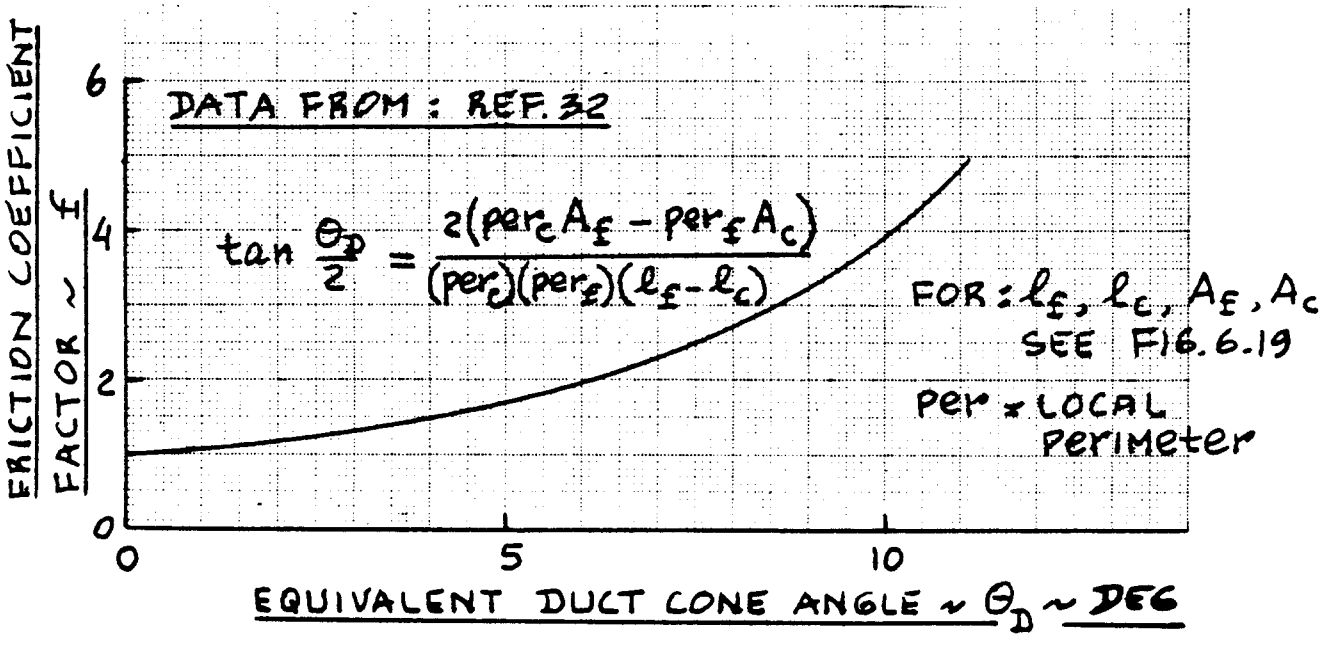

Figure 6.20 Friction Coefficient Factor for Inlet Ducts

be used to find C_f.

μ_{inl} is defined in Eqn.(6.35)

H is the corrected position ratio, defined as:

$$H = (0.8S_{wet\ appr})/A_c \qquad (6.40)$$

where: $S_{wet\ appr}$ is the wetted area of the inlet 'approach' as indicated by the cross-hatched area in Figure 6.21. Observe that for podded nacelle inlets and for pitot inlets: $S_{wet\ appr} = 0$!

C_{Fa} is the overall approach friction coefficient.

It may be set equal to the flat plate friction coefficient corresponding to a Reynolds Number based on l_{appr} as the characteristic length.

Figure 6.21 shows how l_{appr} is defined. Note that $l_{appr} = 0$ for podded nacelle inlets and for pitot inlets!

With a boundary layer diverter, the pressure loss of a subsonic jet engine inlet may be estimated from Eqn.(6.37) by setting H = 0.

The reader should consult Reference 32 for further details.

6.1.3.4 Jet engine inlets: supersonic

Figures 6.9, 6.10 and 6.14 give examples of supersonic inlet configurations. Note that all are of the so-called 'straight through' type. The pressure recovery of a supersonic inlet system is defined as:

$$\eta_{inl/com} = (\eta_{shock})(\eta_{diff}) \qquad (6.41)$$

where: η_{shock} is the pressure recovery through the inlet shock system. It is found from Fig.6.11 depending on the type on inlet.

η_{diff} is the pressure recovery through the subsonic diffuser which follows the system of shocks in the inlet. It may be found from:

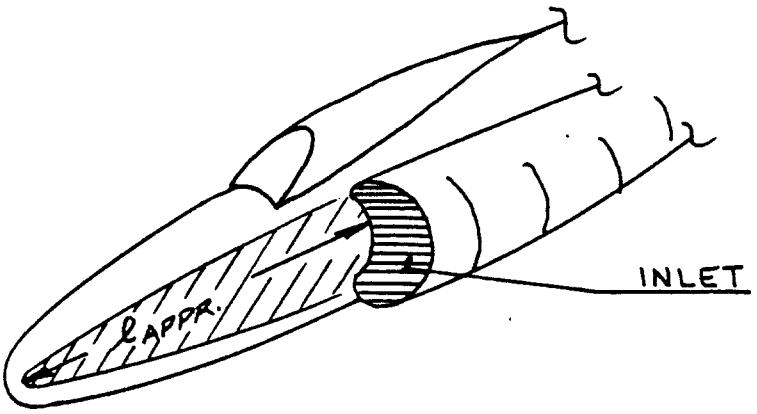

Figure 6.21 Definition of Approach Length

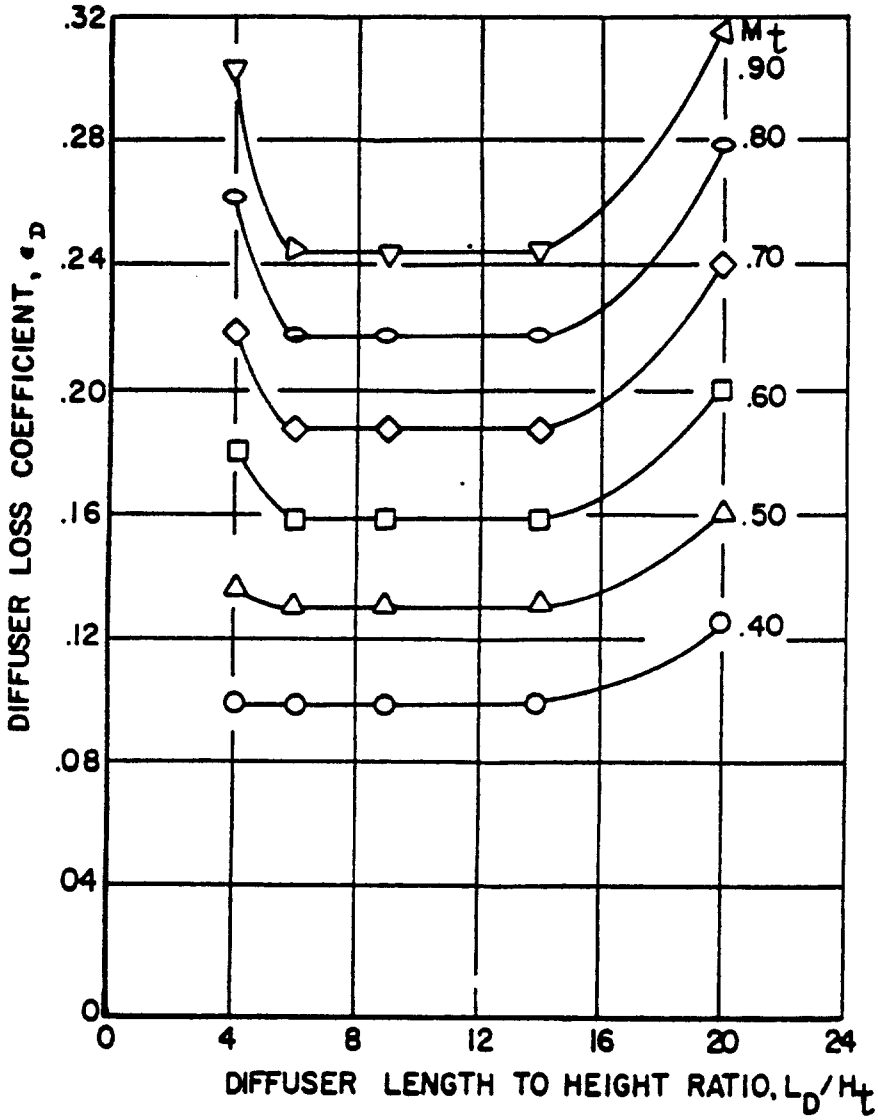

COPIED FROM:
REF. 12
COURTESY:
L. NICOLAI

SEE FIG. 6.15
FOR L_D AND H_t

Figure 6.22a Effect of Diffuser Geometry on Diffuser Loss Coefficient (Shock Ahead of Entrance)

$$\eta_{diff} = 1 - \varepsilon_D\{1 - (1 + 0.2M_T^2)^{-3.5}\} \qquad (6.42)$$

where: ε_D is the diffuser loss coefficient found from Figure 6.22. It depends on the subsonic diffuser geometry!

M_T is the diffuser entry Mach number. This Mach number is equal to the Mach number of the flow through the last shock in the inlet shock system. It can range from 0.4 to 0.9 in practical applications. Usually a number of 0.6 to 0.7 is found in such inlets. In preliminary design it is suggested to 'pick' a suitable number in this range.

M_T must be computed from the system of shocks. A method for doing this may be found in Appendix D of Ref.12.

Methods for determining the effect of inlet pressure losses on installed engine power or thrust are presented in Section 6.4.

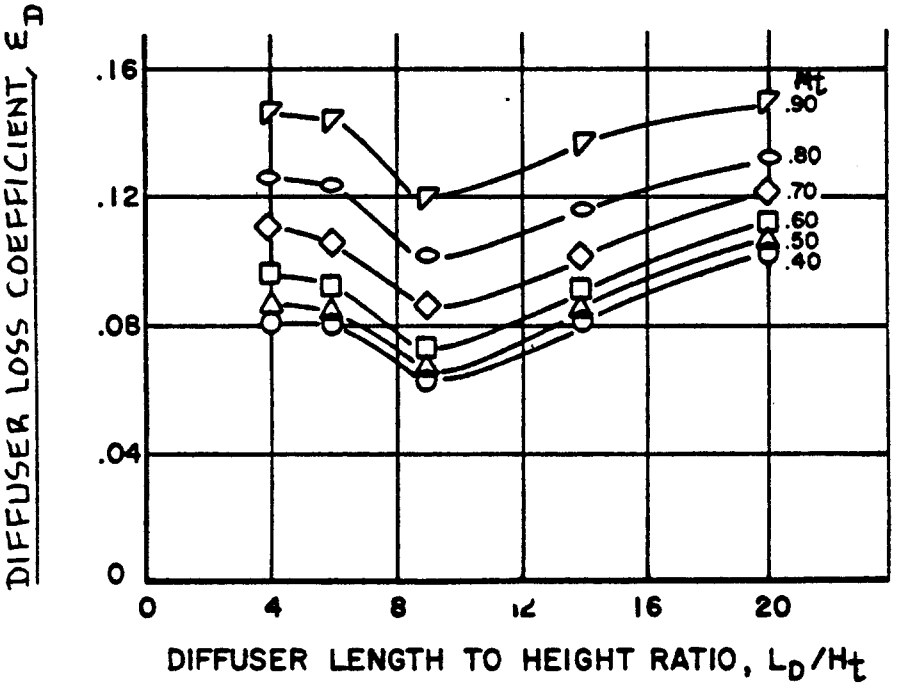

COPIED FROM:
REF. 12
COURTESY:
L. NICOLAI

SEE FIG. 6.15
FOR L_D AND H_t

Figure 6.22b Effect of Diffuser Geometry on Diffuser Loss Coefficient (Subsonic Entrance)

6.2.4 Inlet Extra Drag Estimation

The purpose of this sub-section is to present rapid methods for estimation of the so-called inlet extra drag, $C_{D_{inlextra}}$, which was considered a part of $C_{D_{misc}}$ in Sub-section 4.12.3. The inlet extra drag considered here is that contribution of inlet drag not accounted for in Ch.4 as a result of wetted areas or as a result of cross sectional area distribution.

Inlet pressure recovery and any associated loss in inlet pressure have been discussed in Sub-section 6.2.3. The effect of these losses on installed power and thrust is discussed in Section 6.4.

The extra inlet drag discussion is organized as in the following manner:

6.2.4.1 Piston engine inlets
6.2.4.2 Turbopropeller inlets
6.2.4.3 Jet engine inlets: subsonic
6.2.4.4 Jet engine inlets: supersonic

6.2.4.1 Piston engine inlet extra drag

In well designed piston engine installations, the inlet extra drag should be negligible. If the inlet is undersized, spillage drag may result. Estimation of inlet spillage drag is discussed in 6.2.4.3.

6.2.4.2 Turbopropeller inlet extra drag

In properly designed turbopropeller inlets the inlet extra drag should be negligible. If the inlet is undersized, spillage drag may result. Estimation of inlet spillage drag is discussed in 6.2.4.3.

6.2.4.3 Jet engine inlet extra drag: subsonic

For properly designed subsonic jet inlets the inlet extra drag should be negligible. However, if the inlet is undersized for some flight condition, spillage drag may result. The inlet extra drag due to spillage may be estimated from:

$$C_{D_{inlextra}} = C_f[1 + 0.33\{(d_m - \bar{d}_c)/l_{mc}\}F_{inl}]^{1.667} \quad (6.43)$$

with:

$$F_{inl} = [1 + 1.75(\mu_{inl} - 1)/\mu_{inl}\{(A_m/\bar{A}_c) - 1\}]\bar{A}_c/S \quad (6.44)$$

where: C_f is the equivalent flat plate friction coefficient at a Reynold's Number based on a characteristic length equal to l_{mc}: see Figure 6.23.

d_m is the maximum cowl diameter for the inlet

$\bar{d}_c$ is the cowl diameter at the inlet area position

A_m is the cowl cross section area at d_m

$\bar{A}_c$ is the cowl cross section area at $\bar{d}_c$

μ_{inl} is defined in Eqn.(6.35).

Equation (6.43) applies up to the critical Mach number. To reduce inlet drag above M_{crit}, it is necessary to shape the inlet lips so that they in fact have properties similar to high speed airfoils. Reference 32 contains discussions on inlet lip design at high subsonic Mach numbers.

6.2.4.4 Jet engine inlet extra drag: supersonic

In the supersonic case there are three sources for extra inlet drag:

1. Spillage drag (called additive drag)
2. Bypass drag
3. Boundary layer diverter drag
4. Boundary layer bleed drag

Figure 6.24 shows where these drag types are caused in a supersonic inlet. All three drag types depend on the state of the shock systems in the inlet. Detailed presentations of methods for estimating these drag contributions are beyond the scope of this text. Ref.12 contains methods for estimating these drag increments. Since Ref.12 uses A_c as the inlet drag reference area, all results must be multiplied by A_c/S.

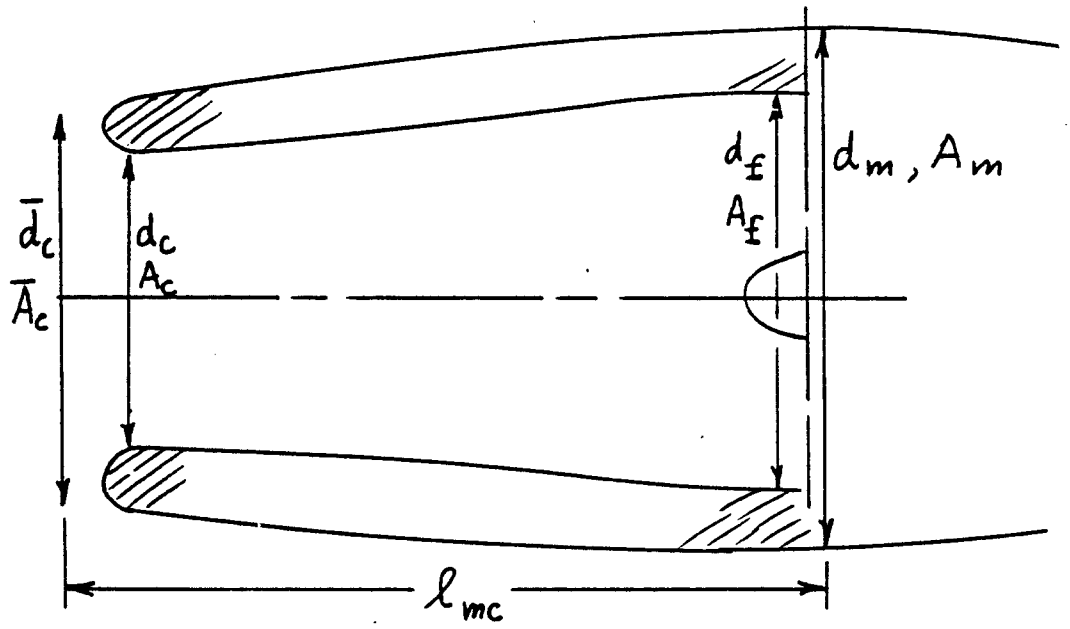

Figure 6.23 Duct Geometry for Inlet Extra Drag Evaluation

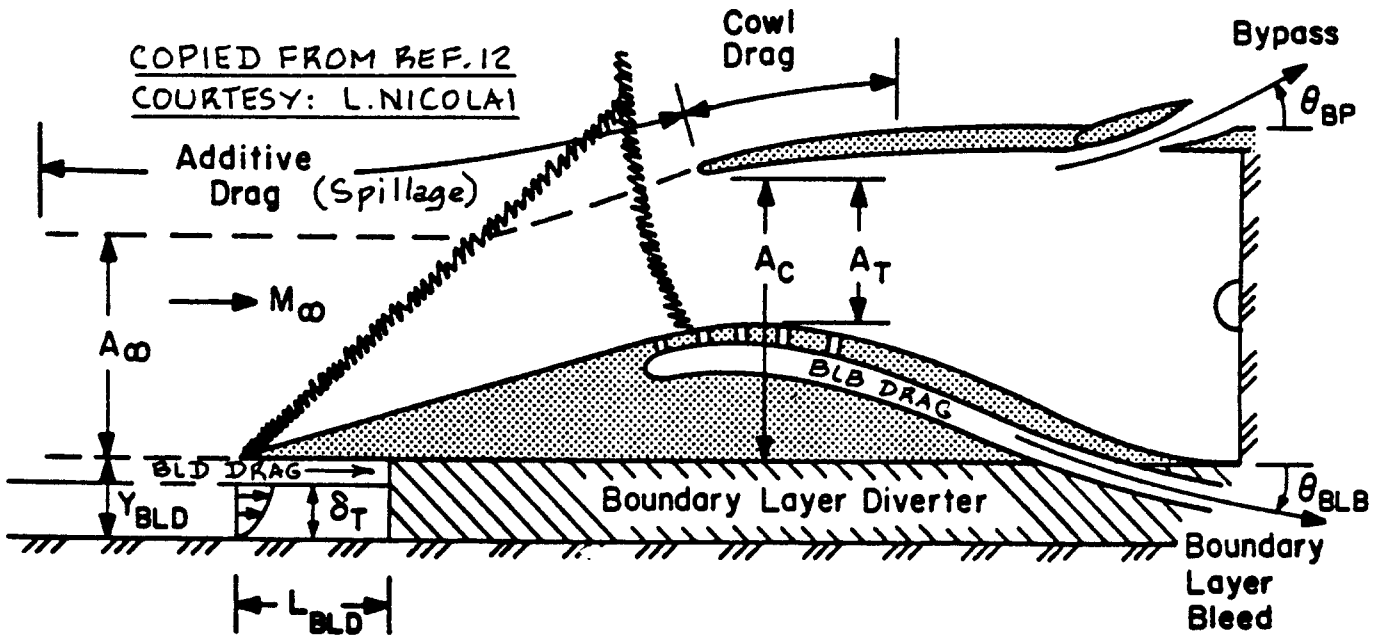

Figure 6.24 Visualization of Extra Drag Types in a Supersonic Inlet

6.3 EXHAUST OR NOZZLE SIZING AND INTEGRATION

In preliminary design the process of exhaust or nozzle sizing and integration consists of:

1. the determination of exhaust and/or nozzle areas

2. the integration of the exhausts and/or nozzles into the airplane

Figure 6.2 defines the nozzle exit area, A_e. Note from Fig.6.77 in Part III that in turbofan engines the nozzle area consists of two concentric areas, located at different longitudinal stations.

Integration of exhausts and/or nozzles into the airplane configuration must be done with care! Without such care, major increases in drag can be the result.

The information in this section is presented as:

6.3.1 General exhaust/nozzle arrangements

6.3.2 Exhaust/nozzle sizing

6.3.3 Estimation of exhaust/nozzle extra drag

The reader should also refer to Part III, Chapter 6 for examples of engine exhaust/nozzle installations.

6.3.1 General Exhaust/Nozzle Arrangements

The purpose of this sub-section is to present examples of exhaust/nozzle configurations which are being used in a number of airplanes.

The information is organized as follows:

6.3.1.1 Piston engine exhausts
6.3.1.2 Turbopropeller exhausts
6.3.1.3 Jet engine nozzles: subsonic
6.3.1.4 Jet engine nozzles: supersonic

6.3.1.1 Piston engine exhausts

Figure 6.5 shows several examples of piston engine exhaust configurations. In many older installations the engine exhaust is 'dumped' overboard in the manner shown in the 'upper' Figure 6.5a: this is very inefficient and causes extra drag. A lower drag installation is the one

shown in the 'lower' Figure 6.5a. Figure 6.25 shows the difference between a 'low drag' and 'high drag' case.

The reader must keep in mind that lowering drag is not always good. If the lower drag is obtained at the cost of increased weight and complexity, a 'design trade study must provide the information on basis of which the decision is made to proceed one way or the other.

The installations of Figures 6.5b represent modern concepts which take maximum advantage of the momentum exchange between inlet, combustion process, cooling requirements and exhaust.

6.3.1.2 Turbopropeller nozzles

Figure 6.6 shows several examples of turbopropeller engine (gas generator) exhaust installations. Note the trend toward exhausting 'parallel' to the local stream.

In many contemporary installations the exhaust pipes are arranged as shown in Figure 6.26. This creates much extra drag. The 'design trade study' comments made under 6.3.1.1 also apply here!

6.3.1.3 Jet engine nozzles: subsonic

Figure 6.7 shows several example of nozzle installations for subsonic jet engines. Note that all nozzles are of the convergent type. In subsonic flow, convergent nozzles are the only efficient nozzle configuration.

6.3.1.4 Jet engine nozzles: supersonic

Figure 6.27 shows a typical supersonic exhaust configuration. Depending on the flight Mach number of the airplane the nozzle should have a different geometry. Figure 6.28 illustrates the effect of flight condition on desired nozzle configuration. Note the convergent/divergent shape of nozzles at supersonic speeds.

The integration of nozzles into the after body of a supersonic airplane is particularly critical to drag. Figure 6.29 shows a number of nozzle/airframe integration concepts with commentary about the effect on drag. Here also, the consequence of weight, cost and complexity must be weighed against aerodynamic efficiency.

6.3.2 Exhaust/Nozzle Sizing

The purpose of this sub-section is to present rapid

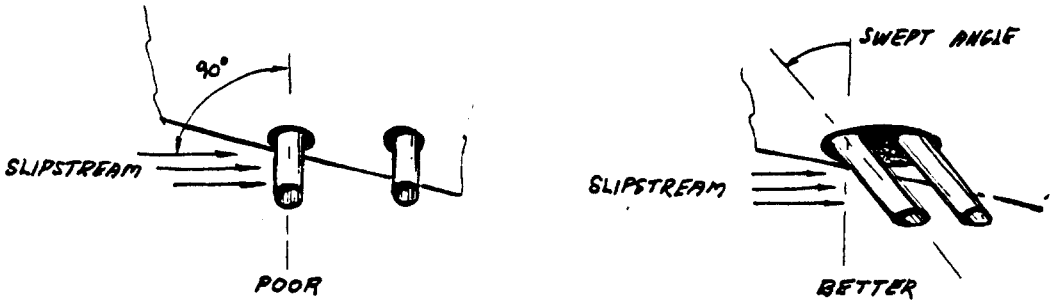

COPIED FROM REF. 38 COURTESY: T.BINGELIS

Figure 6.25 Example of High Drag and Lower Drag Exhaust Stack Installation

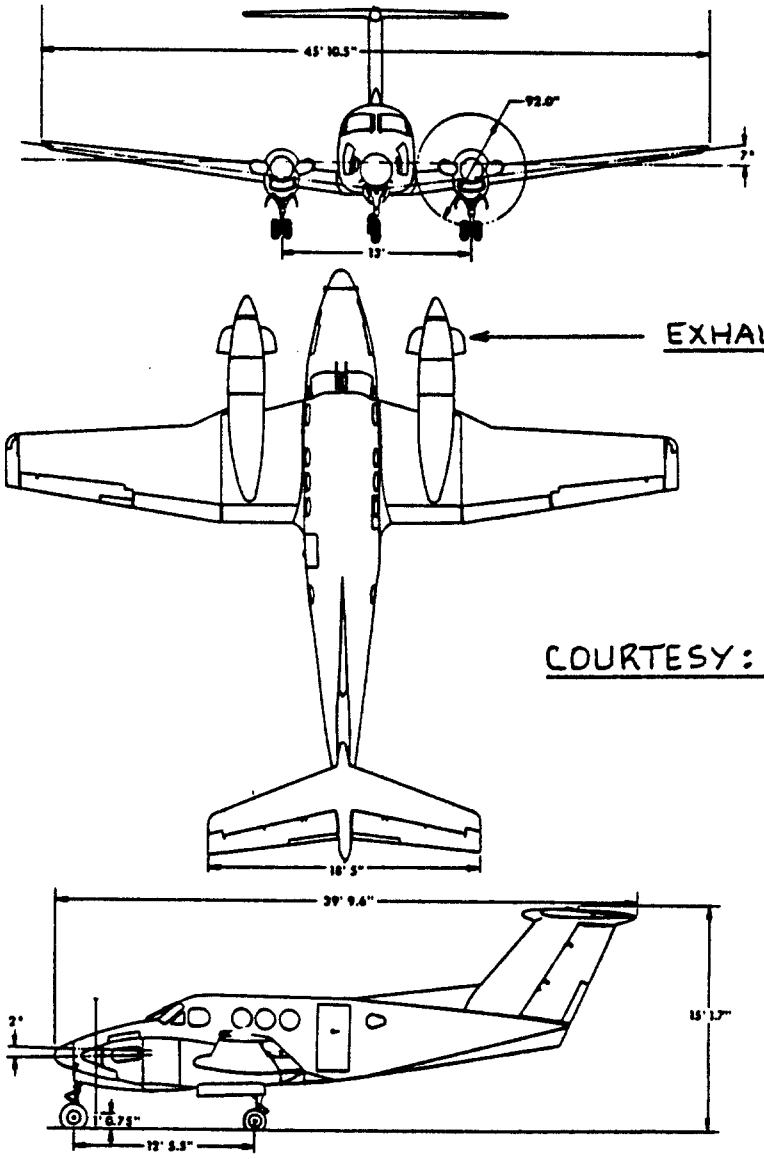

COURTESY: BEECH

Figure 6.26 Example of a High Drag Exhaust Installation as Seen on Contemporary Turboprops

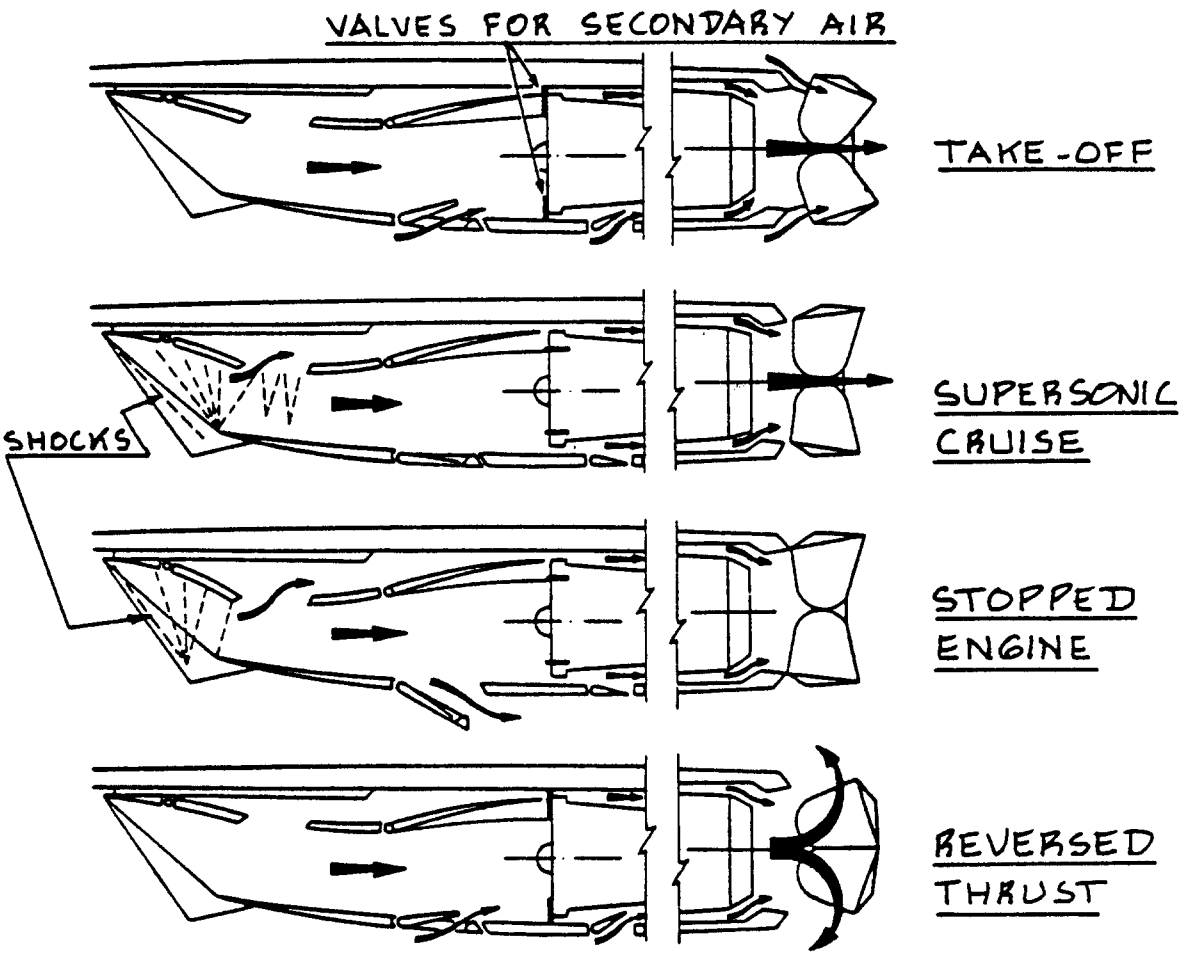

Figure 6.27 Examples of Supersonic Exhaust Configurations

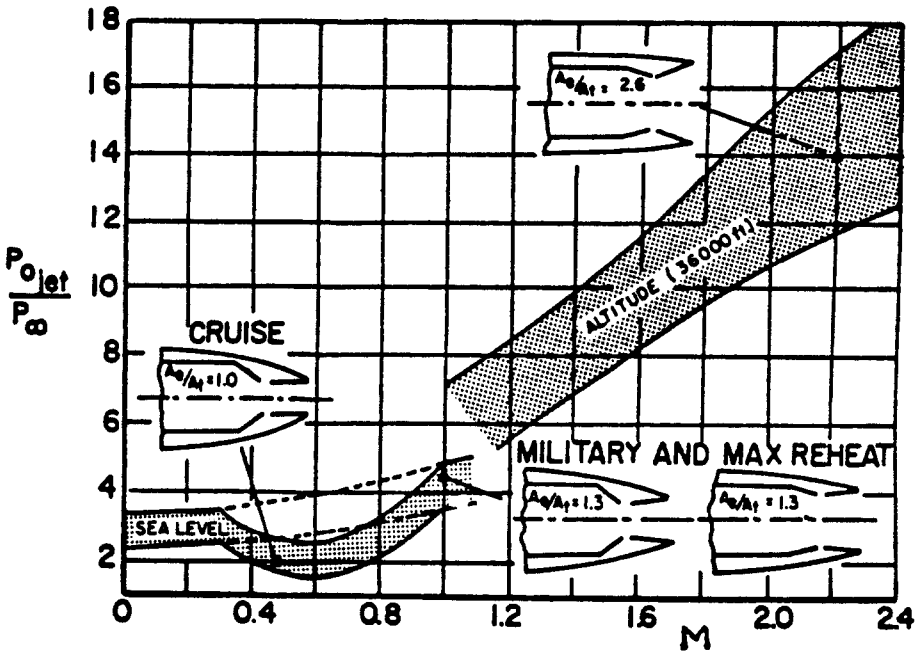

COPIED FROM REF. 12
COURTESY: L. NICOLAI

SEE FIG. 6.30 FOR A_e AND A_t DEFINITION

Figure 6.28 Variation of Nozzle Geometry with Mach Number

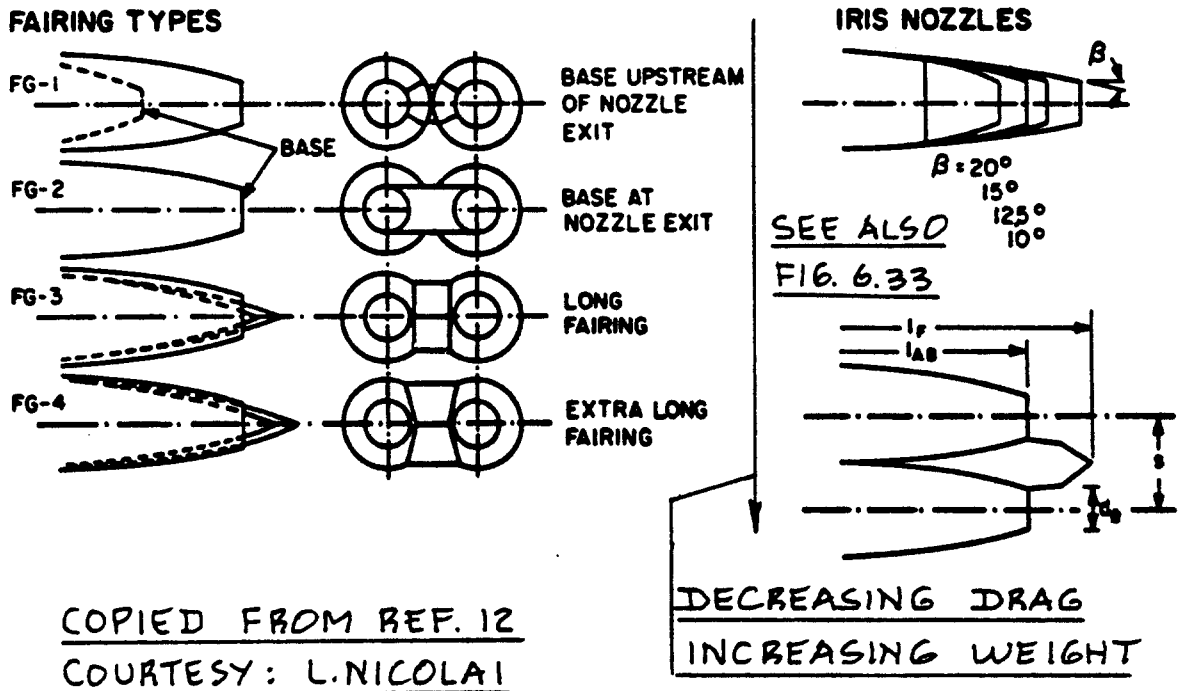

Figure 6.29 Examples of Nozzle/Airframe Integration

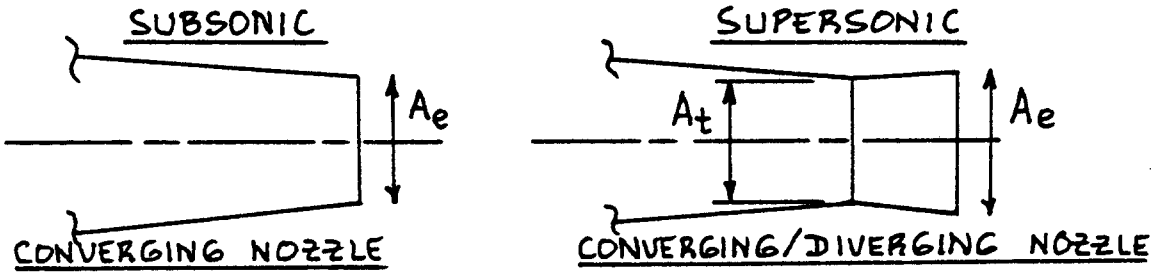

Figure 6.30 Definition of Nozzle Exit and Throat Areas

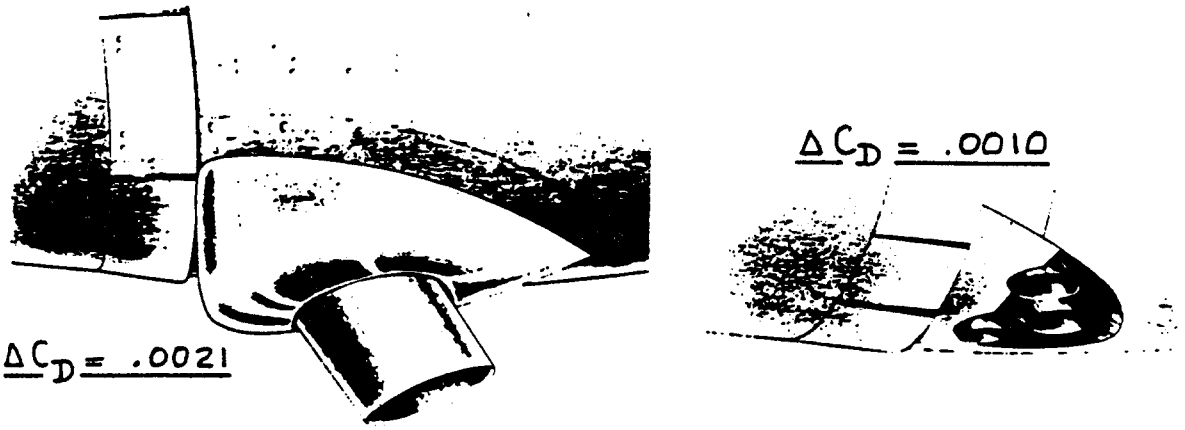

Figure 6.31 Effect of Exhaust Stack Configuration on Drag

methods for the 'sizing' of exhausts and/or nozzle exit areas. Figure 6.30 shows the definition of important nozzle exit and throat areas.

The material in this sub-section is presented as:

6.3.2.1 Piston engine exhausts
6.3.2.2 Turbopropeller nozzles
6.3.2.3 Jet engine nozzles: subsonic
6.3.2.4 Jet engine nozzles: supersonic

6.3.2.1 Piston engine exhausts

The exit size of piston engine exhausts is normally defined by the engine manufacturer. The exit area of the exhaust(s) are dependent on the cross sectional areas of the engine exhaust valve ports. Reference 37 contains detailed descriptions of this aspect of engine design.

The airframer may wish to use the exhaust manifold for purposes of heat extraction (by routing cabin air through a heat exchanger which is wrapped around the exhaust manifold). The airframer may also add noise suppressors and/or ejectors to the exhaust stack(s).

Refs 38 and 40 as well as Section 6.9 in Part III should be consulted for more details on piston engine exhaust configurations.

As a first approximation to the sizing of the total exit area, it is suggested to use an exhaust stack diameter given by:

$$d_{exhst} = (0.0038)SHP_{TO} \text{ in inches} \qquad (6.45)$$

If this diameter becomes too large, it is best to split the exhaust manifold into two or more small stacks.

6.3.2.2 Turbopropeller nozzles

Because turbopropellers are used only in subsonic flight conditions, the nozzles are always of the convergent type as seen in Figure 6.28.

As a first approximation to the sizing of the nozzle exit area, it is suggested to use:

$$d_{exhnoz} = (0.016)SHP_{TO} \text{ in inches} \qquad (6.46)$$

In many turboprop engines the nozzle area is divided over two exhausts. Engine manufacturers specify the ex-

haust area on the basis of their performance guarantees.

6.3.2.3 Jet engine nozzles: subsonic

In subsonic applications the exhaust nozzle is nearly always of the convergent type as shown in Figure 6.28.

The exhaust nozzle size and its configuration depend strongly on the following factors:

1. maximum take-off thrust
2. by-pass ratio
3. need for afterburning
4. design Mach number

The reader should use engine manufacturers data for exhaust nozzle areas. References 12, 33 and 41 provide more details on the subject of nozzle design.

6.3.2.4 Jet engine nozzles: supersonic

The exhaust nozzle size and its configuration depend strongly on the following factors:

1. maximum take-off thrust
2. by-pass ratio
3. need for afterburning
4. design Mach number

The usual nozzle configuration employs variable geometry: convergent for subsonic flight and convergent/divergent for supersonic flight: see Fig.6.28.

Engine manufacturers data should be used to find the size of the subsonic nozzle exit area. Figure 6.28 can be used to estimate the required exit area of the divergent part of the nozzle in its supersonic position.

Sizing of the length of the convergent part of the nozzle is not critical as long as it is not too short: a length of twice the entry diameter should be sufficient.

Sizing of the length of the diverging part of the nozzle is critical if separation is to be prevented. In preliminary design, a length of at least three times the nozzle throat diameter should be adequate.

References 12, 33 and 41 provide more details on the subject of nozzle design.

6.3.3 Estimation of Exhaust/Nozzle Extra Drag

In this sub-section rapid methods for estimating the extra drag caused by exhaust and/or nozzle installations. The material is organized as follows:

6.3.3.1 Piston engines
6.3.3.2 Turbopropeller engines
6.3.3.3 Jet engines: subsonic
6.3.3.4 Jet engines: supersonic

6.3.3.1 Piston engines

Figure 6.31 illustrates the drag increments associated with two piston engine exhaust configurations. In preliminary design it is suggested to use drag increments on the basis of similarity of the proposed installation with those of Figure 6.31.

6.3.3.2 Turbopropeller engines

If the exhaust configuration of a turbopropeller is similar to the one shown in Figure 6.26, the drag increments of 6.3.3.1 may be used as a guide.

If the exhaust configuration is similar to those of Figure 6.6, the additional drag penalty caused by the exhaust may be negligible.

6.3.3.3 Jet engines: subsonic

For engines mounted in nacelle pods, no additional drag increment is incurred: the nacelle drag is accounted for separately.

For engines mounted in a fuselage and exhausting in the rear, extra drag may be incurred. Figure 6.32 shows several nozzle concepts used for subsonic applications. Each concept has a drag penalty associated with it. The drag penalty may be found with the help of Table 6.2.

The airplane drag increment due to the nozzle may be found from:

$$\Delta C_{D_{noz}} = (\Delta C_{D_{noztype}}) S_{fus}/S \qquad (6.47)$$

Note: Eqn.(6.47) assumes that only ONE nozzle is at the rear of the fuselage. If more are present, the drag increases accordingly.

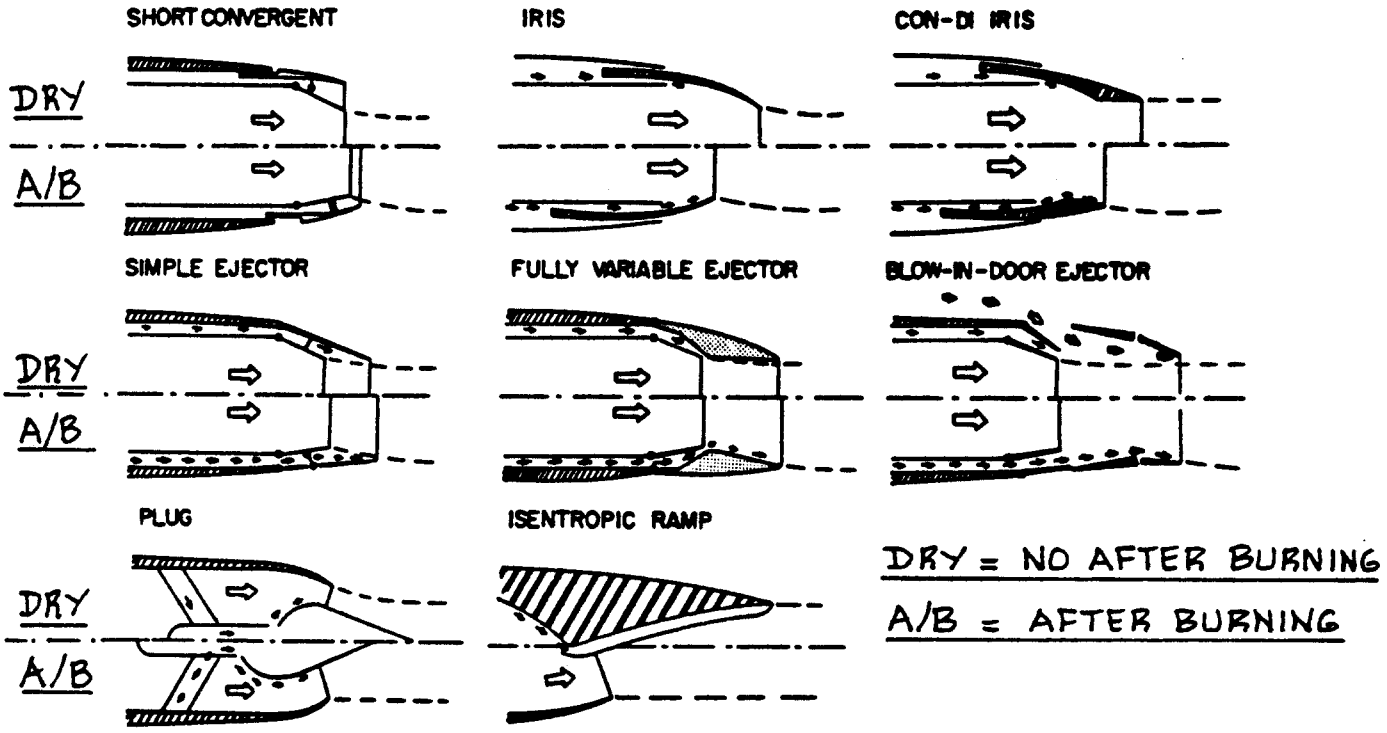

COPIED FROM REF. 12, COURTESY: L. NICOLAI

Figure 6.32 Typical Subsonic Nozzle Concepts

Table 6.2 Drag Penalties for Nozzles Mounted in the Rear of a Fuselage, for Subsonic Flight

Nozzle Type	Drag Increment $\Delta C_{D_{noztype}}$
Short convergent	0.036 - 0.042
Blow-in-door ejector	0.025 - 0.035
Plug	0.015 - 0.020
Fully variable ejector	0.010 - 0.020
Iris	0.010 - 0.020
Ramp	0.010

Notes: 1. these data apply in the M = 0.8 - 0.95 range
2. these data apply to nozzle pressure ratios of 2.5 to 3.0

If more than one engine exhausts at the rear of the fuselage, a difficult 'aerodynamic fairing' problem between the engines can arise. Figure 6.33 shows a number of possibilities. The drag increments due to such 'faired' nozzle arrangements may be estimated from Fig.6.33. Note that longer fairings reduce the drag of the installation. However: a longer fairing also implies a weight increase: as usual, a trade study must be performed to arrive at the correct decision.

6.3.3.4 Jet engines: supersonic

The supersonic drag increment of nozzles is strongly dependent on the method used to 'fair' the rear end of the airplane, especially in the area of the variable geometry nozzle. No simple method can be given for the estimation of nozzle drag increment. References 9, 12, 33 and 41 should be consulted for details.

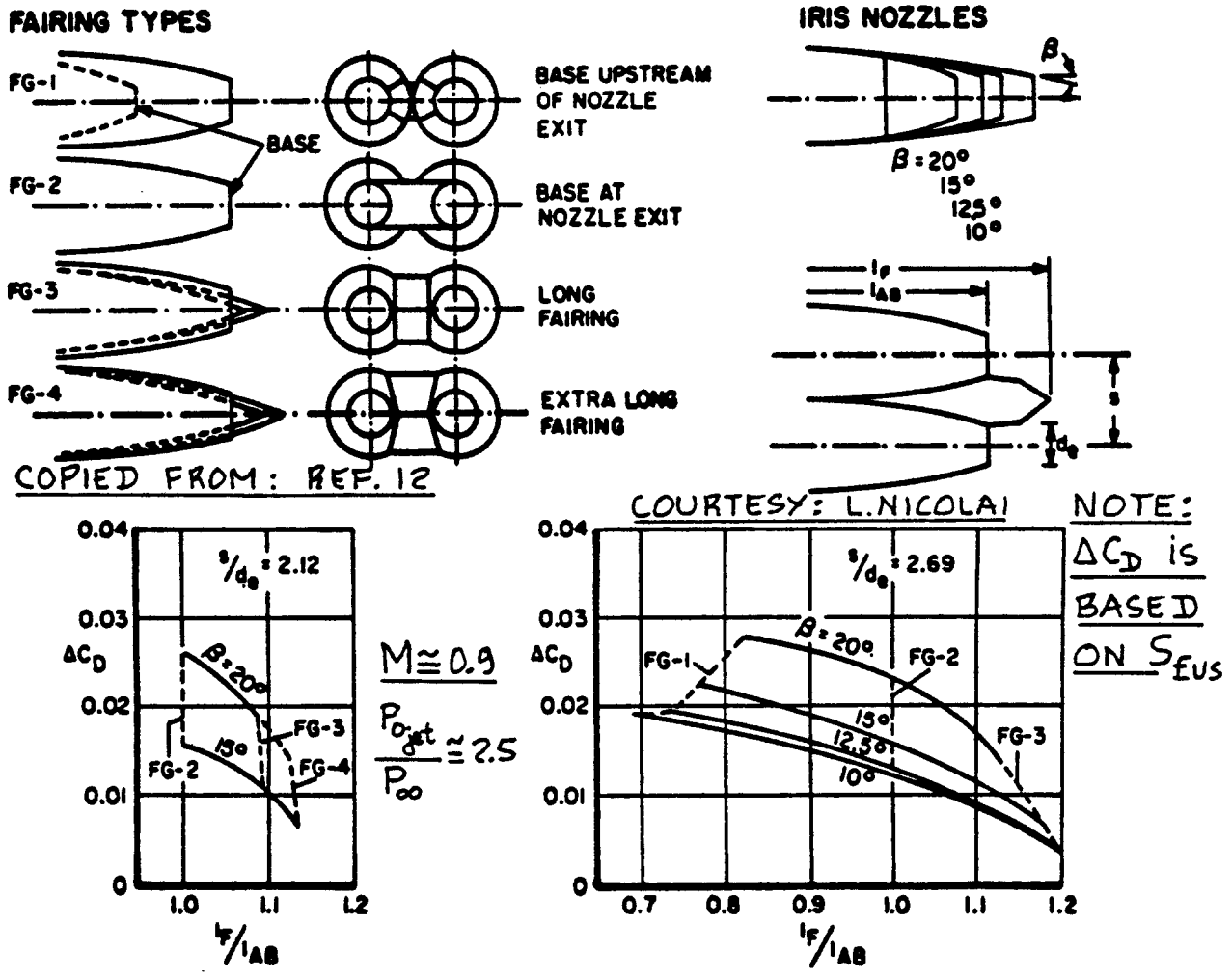

Figure 6.33 Effect of Nozzle Fairing Concept on Drag

6.4 PREDICTION OF INSTALLED POWER AND THRUST

The purpose of this section is to present rapid methods for estimating the installed performance of engines in airplanes. The material is presented as follows:

6.4.1 Propeller Driven Airplanes
6.4.2 Jet Driven Airplanes

6.4.1 Propeller Driven Airplanes

Propeller driven airplanes can use different methods for driving the propeller. In this text the following possibilities will be presented:

6.4.1.1 Piston propeller driven airplanes
6.4.1.2 Turbopropeller driven airplanes

6.4.1.1 Piston propeller driven airplanes

The installed performance of piston engines is normally stated in terms of available, installed power, P_{av}.

In some applications, the static thrust obtainable from a propeller may be important. Methods for finding static propeller thrust for a given amount of available shaft-horse-power are given in Reference 15.

The following step-by-step procedure is suggested for finding available, installed power, P_{av}.

Step 1: Determine the flight conditions for which the installed power available calculation is to be made. This consists of the selection of altitude, temperature and airspeed.

Step 2: From engine manufacturers data determine the available shaft horse power, SHP_{av} for each flight condition. Figure 6.34 shows a typical example of such data.

Step 3: Find the installed, available power, P_{av} from:

$$P_{av} = (SHP_{av} - P_{extr})(\eta_{inl/inc})\eta_p\eta_{gear} \qquad (6.48)$$

where: SHP_{av} follows from Step 2,

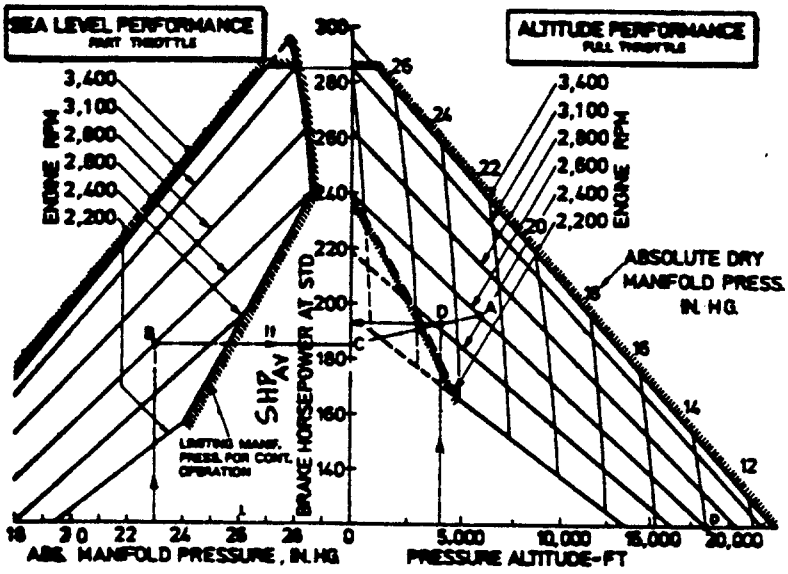

NOTE:

To find the actual horsepower from altitude, rpm, manifold pressure and air inlet temperature:

1. Locate A on full throttle altitude curve for given rpm and manifold pressure
2. Locate B on sea level curve for rpm and manifold pressure and transfer to C
3. Connect A and C by a straight line and read horsepower at given altitude: D
4. Modify horsepower at D for variation of air inlet temperature T from standard altitude temperature T_s by the formula:

Actual hp = hp at D x $\sqrt{\frac{T_s}{T}}$

where T and T_s are absolute temperatures

NORMALLY ASPIRATED

SUPERCHARGED

COPIED FROM REF. 13
COURTESY: E. TORENBEEK

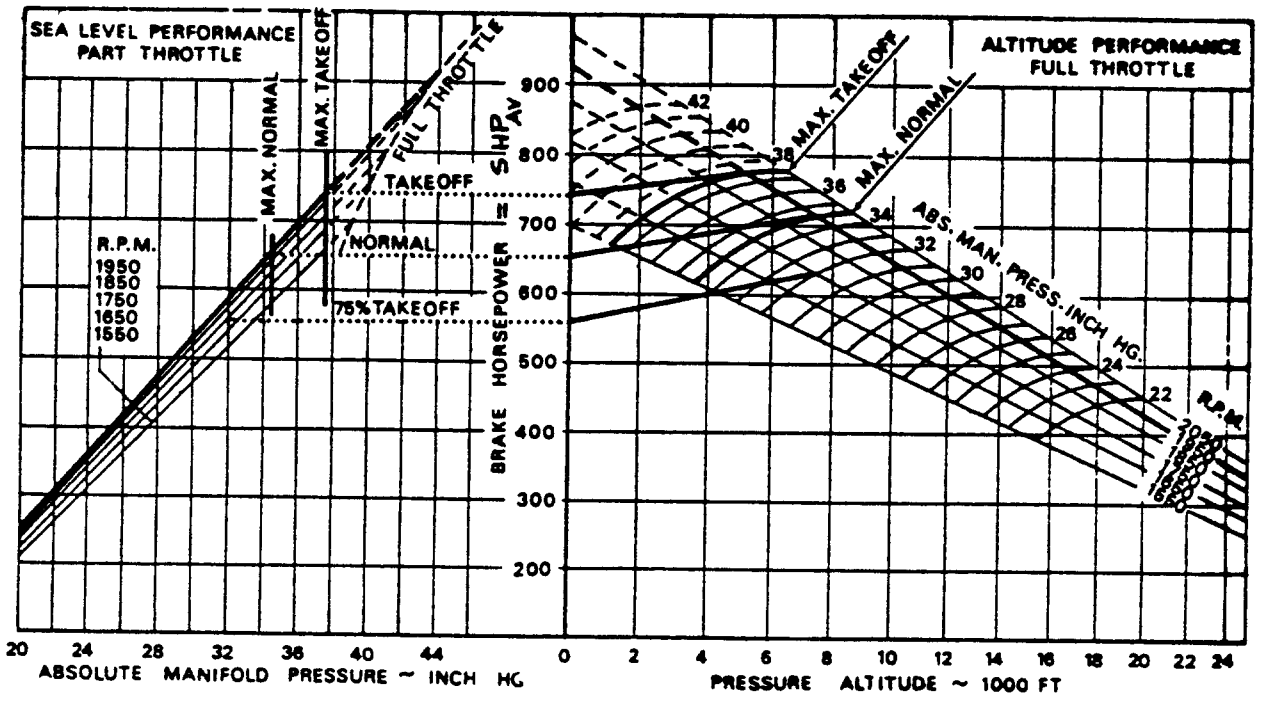

Figure 6.34 Example of Manufacturers Uninstalled Engine Performance Data for a Piston Engine

P_{extr} follows from sub-section 6.1.1.

η_p, the propeller efficiency, may be found from propeller data. Methods to compute propeller efficiency for conventional propellers are provided in References 15, 42, 43, 44 and 45.

NOTE: a rapid method for the determination of the diameter of propellers was given in Chapter 5 of Part II. External noise considerations were not a part of that method. To assure that a propeller meets FAR 36 noise requirements, the method of References 46, 47 and 48 may be used. For preliminary design purposes, as long as the propeller tip speed is kept below a Mach number of 0.85, noise certification should not be a problem.

η_{gear} is the gearbox efficiency.

For direct drive installations use:

$\eta_{gear} = 1.0$

For geared installations with a well designed gearbox, use:

$\eta_{gear} = 0.98$

Step 4: Plot P_{av} versus speed and altitude. Refer to Figure 7.1 in Chapter 7 for an example.

6.4.1.2 Turbopropeller driven airplanes

Installed turbopropeller performance is presented in terms of installed, available power P_{av}.

Most turboprops also deliver a remnant thrust, T_r which varies with the flight condition. For performance calculations this remnant thrust is usually converted to power. This will be done in this text also.

For some applications it is necessary to know the static thrust available from a turboprop installation. For such cases the static remnant thrust is added to the static propeller thrust. Methods for determining static propeller thrust are given in Reference 15.

The following step-by-step procedure is suggested to find

installed, available power, P_{av}:

Step 1: Determine the flight conditions for which the calculation of available installed power and thrust is to be made. This consists of the selection of altitude, temperature and airspeed.

Step 2: From engine manufacturers data determine the available shaft horsepower, SHP_{av} as well as the available remnant thrust, T_r for each flight condition. An example of such data is shown in Figure 6.35.

Step 3: Find the available, installed power, P_{av} from:

$$P_{av} = (\eta_{inl/inc} SHP_{av} - P_{extr})\eta_p + (\eta_{inl/inc})T_r U_1/550 \qquad (6.49)$$

where: $\eta_{inl/inc}$ follows from 6.2.3.2

SHP_{av} and T_r follow from Step 2

P_{extr} follows from sub-section 6.1.2

η_p, the propeller efficiency follows from Step 3 in 6.4.1.1.

Note 1: Eqn.(6.49) assumes that T_r is not affected by power extraction. Actually, this is not correct. Because the contribution of T_r to total available power is usually very small, the error made by this assumption is negligible.

Note 2: Eqn.(6.49) is not valid for $U_1 = 0$.

Note 3: Most turbopropeller engines already have a gearbox installed. The engine manufacturers data include the gearbox losses.

Step 4: Plot P_{av} versus speed and altitude. Refer to Figure 7.2 in Chapter 7 for an example.

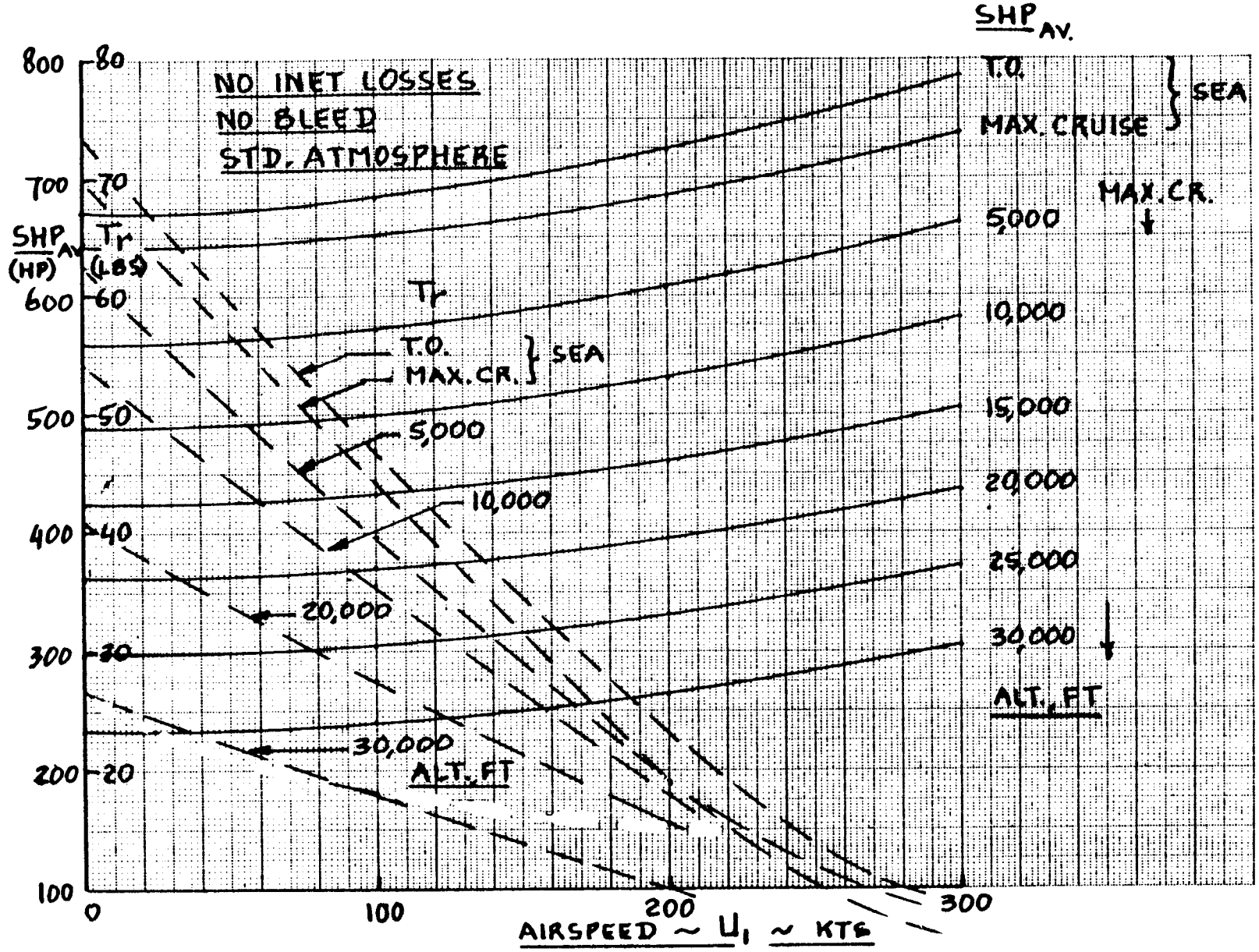

Figure 6.35 Example of Manufacturers Uninstalled Engine Performance Data for a Turboprop Engine

6.4.2 Jet Driven Airplanes

For jet driven airplanes, engine performance is given in terms of available, installed thrust, T_{av}.

Step-by-step procedures for determining T_{av} are presented as follows:

6.4.2.1 Subsonic operations
6.4.2.2 Supersonic operations

6.4.2.1 Subsonic operations:

Step 1: Determine the flight condition for which the installed thrust must be determined. This consists of the selection of altitude, temperature and airspeed.

Step 2: From engine manufacturers data, determine the available uninstalled thrust, $T_{tst/av}$.

Figure 6.36 shows an example of such data.

Step 3: Find the available installed thrust from:

$$T_{av} = \quad (6.50)$$

$$[(T_{tst/av})\{1 - 0.35K_tM_1(1 - \eta_{inl/inc})\} - 550(P_{extr}/U_1)]$$

where: $T_{tst/av}$ follows from Step 2

M_1 is the flight Mach number

$\eta_{inl/inc}$ may be found from 6.2.3.3

P_{extr} follows from Sub-section 6.1.2

K_t is determined from Figure 6.37

Step 4: Plot T_{av} versus speed and altitude. Refer to Figure 7.3 in Chapter 7 for an example.

6.4.2.2 Supersonic operations:

Step 1: Determine the flight conditions for which the available thrust, T_{av} must be found.

This consists of the selection of altitude, temperature and airspeed.

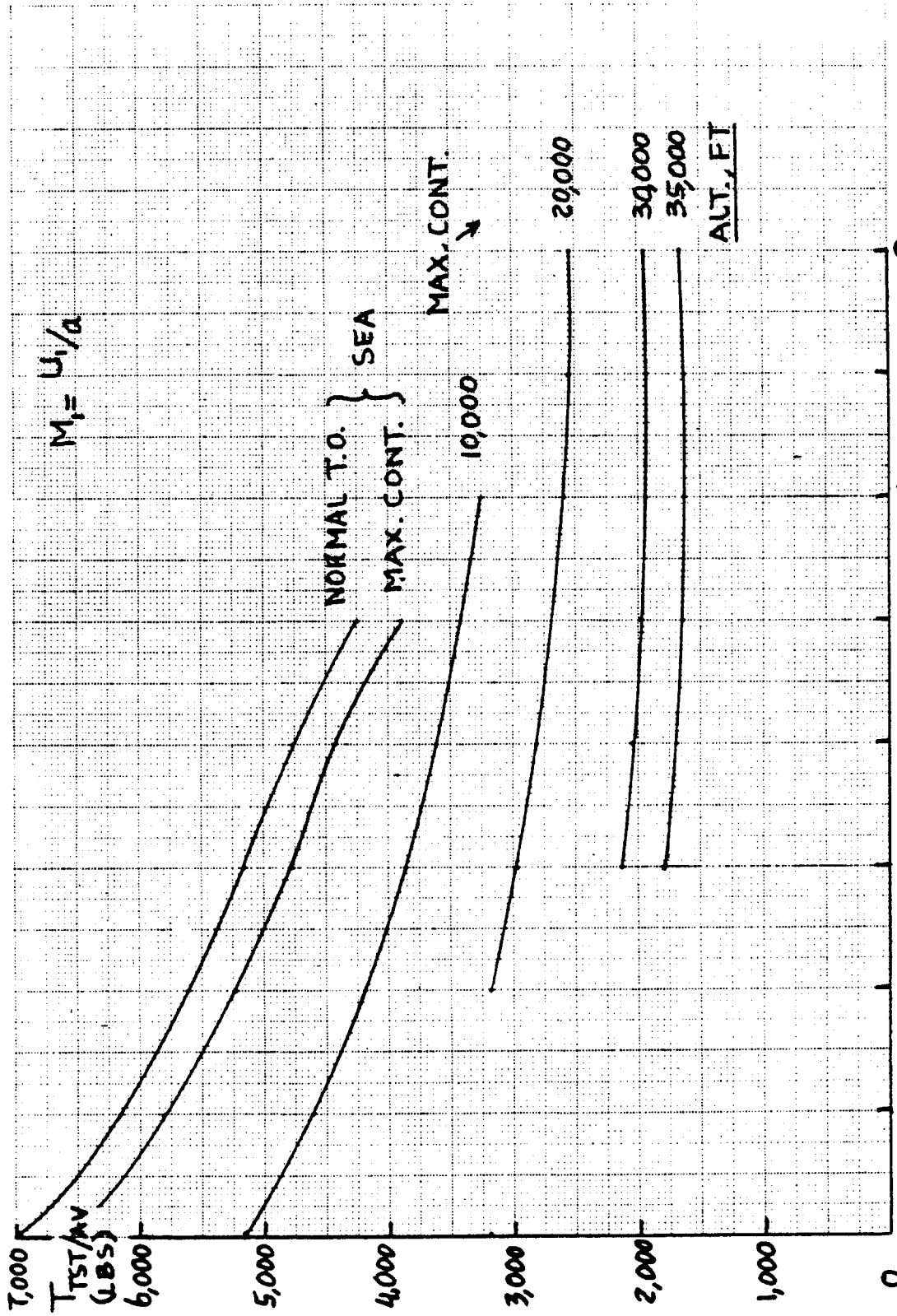

Figure 6.36 Example of Manufacturers Uninstalled Engine Performance Data for a Subsonic Turbofan

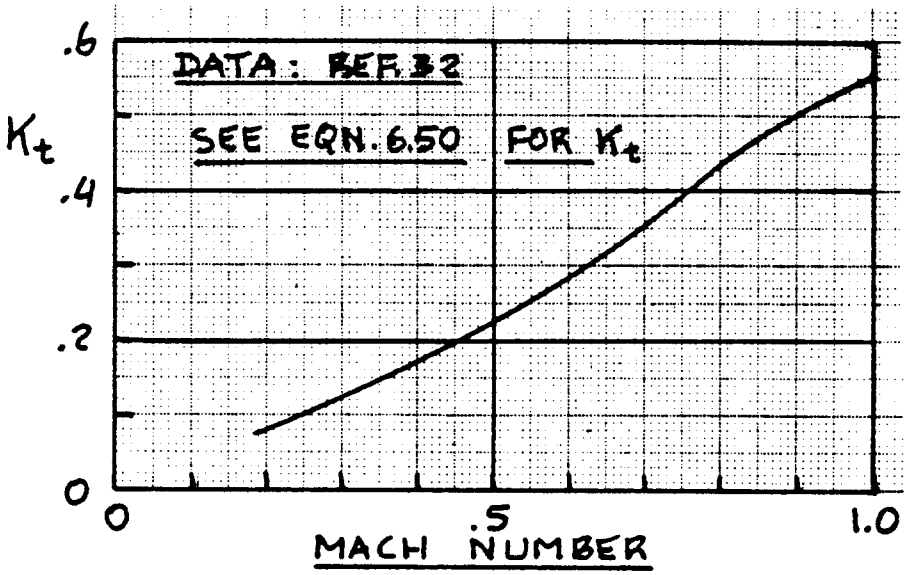

Figure 6.37 Effect of Mach Number on K_t

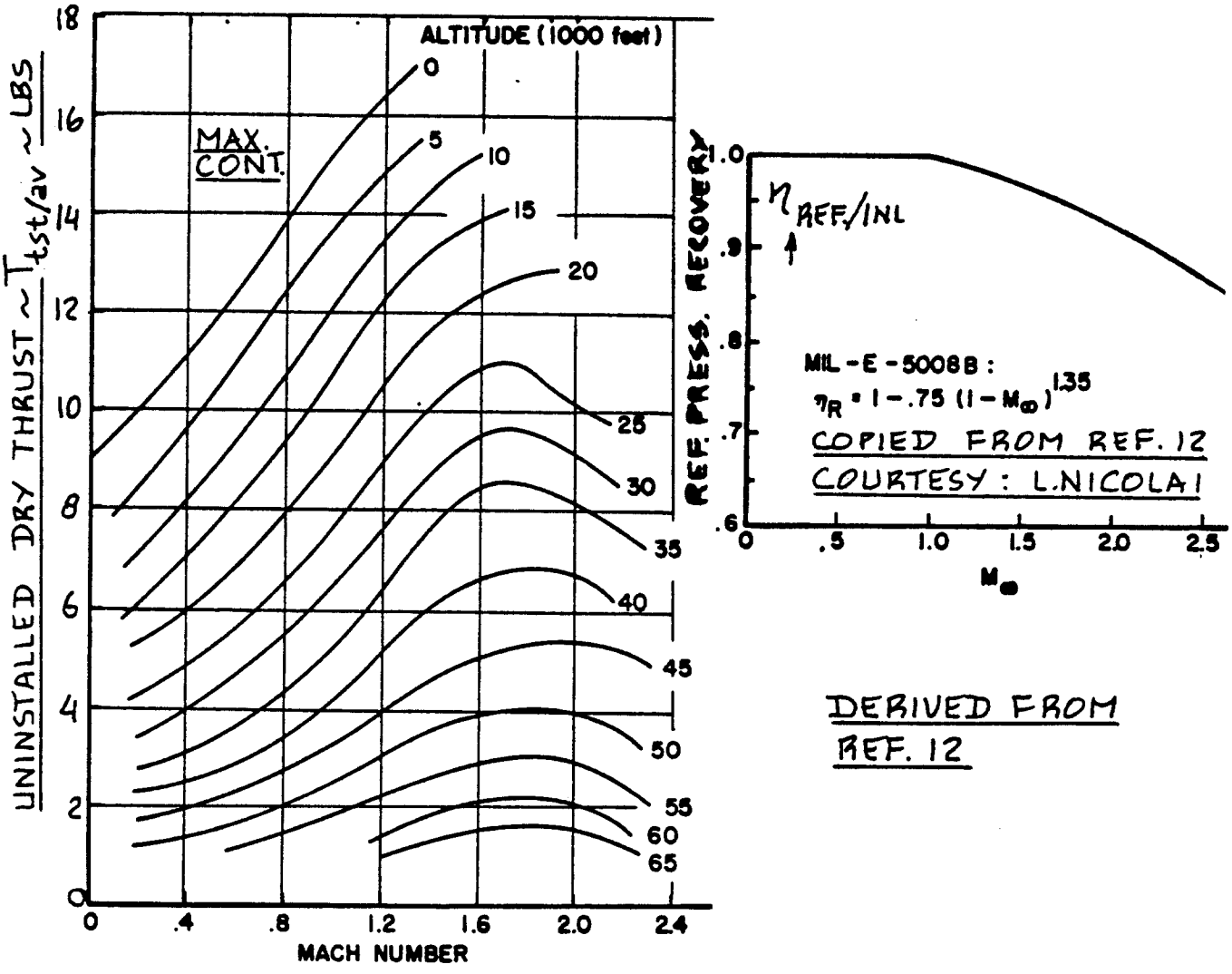

Figure 6.38 Example of Manufacturers Uninstalled Engine Performance Data for a Supersonic Turbofan

Step 2: From engine manufacturers data find the uninstalled, available thrust, $T_{tst/av}$.

Figure 6.38 gives an example of such data.

Note: These data are normally given for an assumed pressure recovery schedule with free stream Mach number: $\eta_{ref/inl}$. Figure 6.38 shows a typical pressure recovery schedule used by engine manufacturers for military engines.

Step 3: Compute the installed, available thrust, T_{av} from:

$$T_{av} = T_{tst/av}(1 - F_t - P_t) - 550P_{extr}/U_1 \qquad (6.51)$$

where: F_t accounts for actual inlet pressure recoveries and is found from:

$$F_t = C_R(\eta_{ref/inl} - \eta_{inl/com}) \qquad (6.52)$$

with: C_R is the ram recovery correction factor found from Figure 6.39.

$\eta_{inl/com}$ is the actual inlet pressure recovery which may be determined from Eqn. (6.41).

$\eta_{ref/inl}$ is found either from Fig. 6.38 or from engine manufacturers data

$$P_t = 2\dot{m}_{bleed}/\dot{m}_a \qquad (6.53)$$

with: $\dot{m}_{bleed}$ found from Eqn. (6.7)

$\dot{m}_a$ determined from engine manufacturers data

P_{extr} follows from Sub-section 6.1.2

NOTE: The installed, available thrust, T_{av} is the

total thrust available from the entire installation. In other words, the effect of the thrust distribution over the various installation components as shown in Fig.6.12 has already been accounted for in the uninstalled engine manufacturers data albeit based on a reference pressure recovery and a reference nozzle.

Step 4: Plot T_{av} versus speed and altitude. Refer to Figure 7.5 in Chapter 7 for an example.

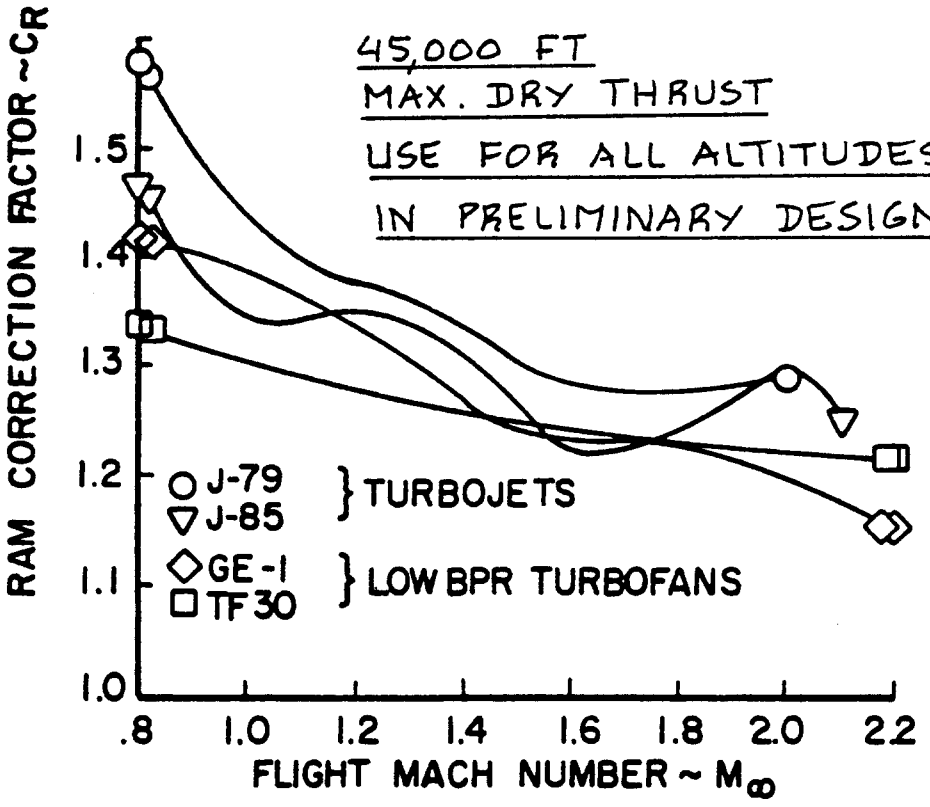

COPIED FROM:
REF. 12, COURTESY:
L. NICOLAI

Figure 6.39 Effect of Mach Number on the Ram Recovery Factor of Several Jet Engines

7. INSTALLED POWER AND THRUST DATA

The purpose of this chapter is to present example data for installed power and thrust. The information is presented as follows:

7.1 Propeller driven airplanes
7.2 Jet driven airplanes

7.1 PROPELLER DRIVEN AIRPLANES

In this section, two examples will be given for the determination of installed power data for propeller driven airplanes:

7.1.1 Piston propeller driven airplanes
7.1.2 Turbopropeller driven airplanes

7.1.1 Piston Propeller Driven Airplanes

The step-by-step procedure of 6.4.1.1 will be used.

Step 1: It will be assumed that installed, available power data must be provided for the following flight conditions:

altitude:	0 - 20,000 ft in increments of 5,000 ft
speed:	from 0 - 200 kts
temperature:	standard atmosphere

Note: the flight condition range must be compatible with the stated mission objectives of the airplane. Such mission objectives are normally defined in the airplane mission specification. Examples of airplane mission specifications are discussed in Part I.

The airplane used in this example is assumed to be a single engine airplane. It has an engine with the uninstalled characteristics of Figure 6.34.

Step 2: Figure 6.34 provides typical engine manufacturers data for a small piston engine. Notice that the data are given in terms of SHP_{av} for various altitudes, engine rpm (throttle) and inlet manifold pressure.

Step 3: The following input information is required before Eqn.(6.48) can be used:

P_{extr}, $\eta_{inl/inc}$, η_{gear} and η_p

This input information must be determined for each individual installation. In preliminary design the methods suggested in 6.4.1.1 may be used.

For the current example the following data will be assumed:

$P_{extr} = 4$ hp $\qquad \eta_{inl/inc} = 0.98$

$\eta_{gear} = 1.0$ (direct drive) $\qquad \eta_p = 0.88$

Warning: propeller efficiency for a fixed pitch propeller can be this high for only one flight condition. In this example a variable pitch propeller has been used.

Step 4: The determination of P_{av} now proceeds as follows:

For a given altitude and engine rpm, Figure 6.34 is used to find the SHP_{av}. Using Equation (6.48) it is then possible to compute P_{av} for each flight condition.

Figure 7.1 shows the results of these calculations for the required range of altitudes and flight speeds.

Note: for the effect of atmospheric temperature on engine performance, engine manufacturers data should be consulted. In the absence of such data, the following approximation may be used:

$$SHP_{av_{at\ T}} = SHP_{av_{at\ std\ T}} (T_{std}/T)^{1/2} \qquad (7.1)$$

7.1.2 Turbopropeller Driven Airplanes

The step-by-step procedure of 6.4.1.2 will be used.

Step 1: It will be assumed that installed, available power data must be provided for the following flight conditions:

altitude:	0 - 40,000 ft in increments of 10,000 ft
speed:	0 - 400 kts
temperature:	standard sealevel

Note: the flight condition range must be compatible

The data in this Figure were arrived at with the assumptions listed in Sub-section 7.1.1.

Eqn.(6.48):

$$P_{av} = (SHP_{av} - P_{extr})\eta_{inl/inc}\eta_p\eta_{gear}$$

$$= (SHP_{av} - 4)(0.98)(0.88)(1.0)$$

<From Fig.6.34> <from Step 3, p.203/204>

3,400 RPM, max. allow.	Sea	5K	10K	15K	20K
SHP_{av}	285	248	206	172	140
$- P_{extr}$	281	244	202	168	136
P_{av}	242	210	174	145	117

Note that P_{av} is not a function of speed in these calculations. The reason is: propeller efficiency was assumed to be constant. This is not always the case!

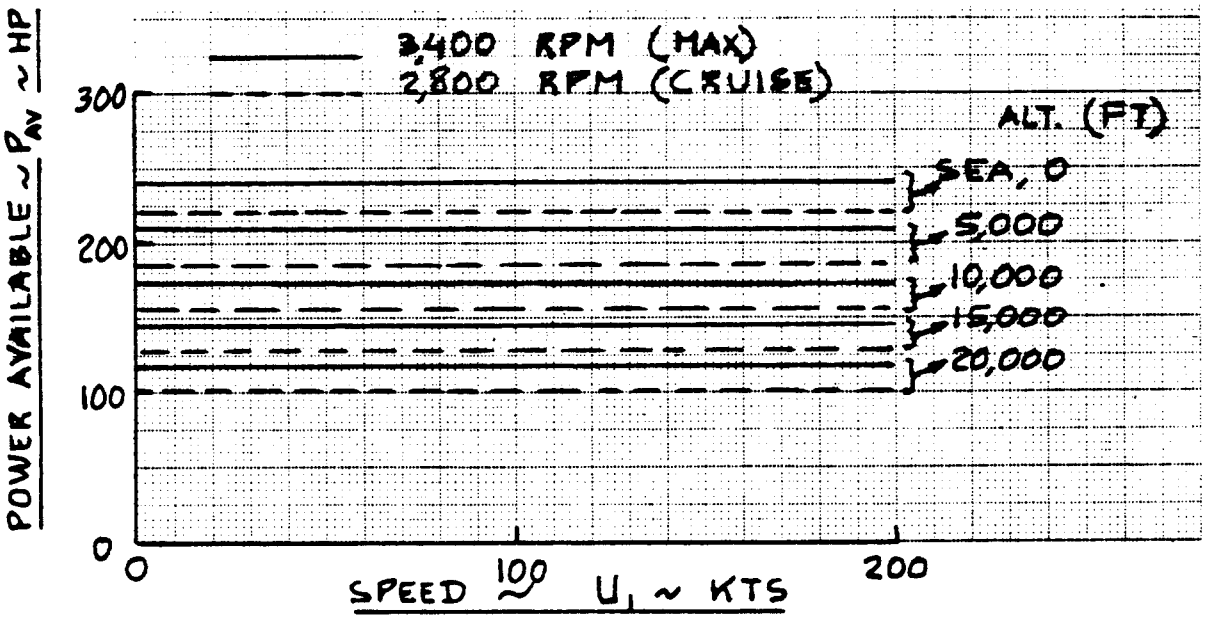

Figure 7.1 Installed Available Horsepower Data for a Single Engine Piston Propeller Airplane

with the stated mission objectives of the airplane. Such mission objectives are normally defined in the airplane mission specification. Examples of airplane mission specifications are discussed in Part I.

The airplane used in this example is assumed to be a twin engine turbopropeller driven airplane. The engines have the uninstalled characteristics of Figure 6.35.

Step 2: Figure 6.35 defines the engine manufacturers data for this example calculation. Note that these data are given in terms of SHP_{av} and T_r.

Step 3: The following input information is required before Equation (6.49) can be used:

P_{extr}, $\eta_{inl/inc}$, U_1 and η_p

This input information must be determined for each individual installation. In preliminary design the methods suggested in 6.4.1.2 may be used.

For the current example the following data will be assumed:

P_{extr} = 10 shp

Plenum inlet with bypass duct: $\eta_{inl/inc}$ = 0.89

η_p = 0.92

U_1 is selected in increments of kts airspeed

Warning: propeller efficiency varies considerably with Mach number. The assumption has been made here that the propeller blades have supercritical airfoil sections and that a propeller pitch angle schedule is used which allows the propeller efficiency to be optimized at all speeds.

Step 4: The determination of installed, available power, P_{av} proceeds as follows:

For any given altitude, Figure 6.35 is used to find SHP_{av} and T_r. Using Equation (6.49) it is now possible to compute P_{av} for each flight condition. Figure 7.2 shows the installed engine performance for the airplane with both engines operating.

Note: for the effect of atmospheric temperature on engine performance, engine manufacturers data should be consulted. In the absence of such data, the following approximation may be used for sealevel performance:

$$SHP_{av_{at\ T}} = SHP_{av_{at\ std\ T}} - 2.33(T - T_{std}) \qquad (7.2)$$

where: T is the actual atmospheric temperature in degrees F.

T_{std} is the atmospheric temperature in the standard atmosphere in degrees F.

Observe that Eqn.(7.2) implies that for each degree of temperature increase above standard, 2.33 hp will be lost!

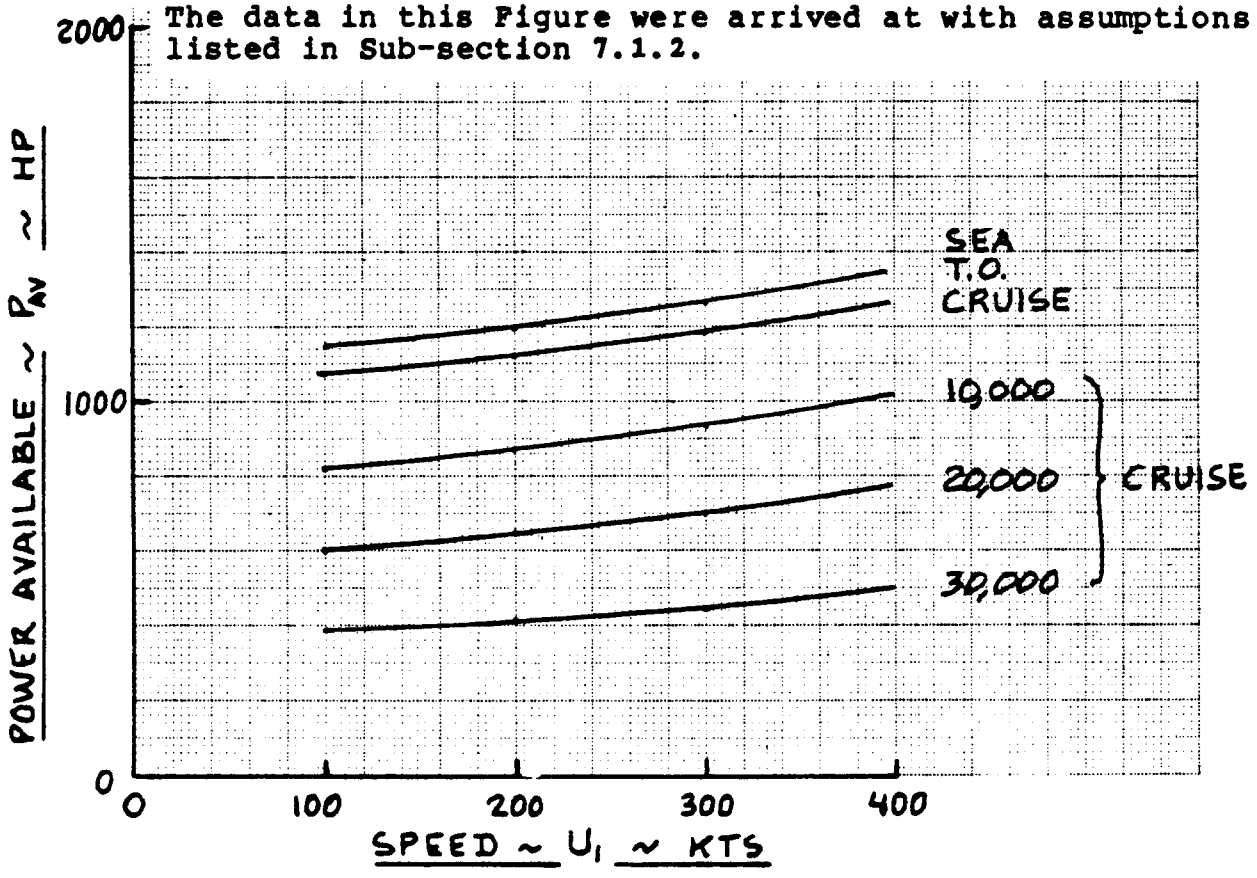

Figure 7.2 Installed Available Horsepower Data for a Twin Engine Turbopropeller Airplane

7.2 JET DRIVEN AIRPLANES

In this section, two examples will be given for the determination of installed thrust for jet driven airplanes:

7.2.1 Subsonic operations

7.2.2 Supersonic operations

7.2.1 Subsonic Operations

The step-by-step procedure of 6.4.2.1 will be used.

Step 1: It will be assumed that installed, available thrust data must be provided for the following flight conditions:

altitude:	0 - 50,000 ft in increments of 10,000 ft
speed:	0 - 500 kts
temperature:	standard atmosphere

Note: the flight condition range must be compatible with the stated mission objectives of the airplane. Such mission objectives are normally defined in the airplane mission specification. Examples of airplane mission specifications are discussed in Part I.

The airplane used in this example is assumed to be a twin engine airplane. It has engines with the uninstalled characteristics of Figure 6.36.

The airplane will be assumed to have a straight-through inlet.

Step 2: Figure 6.36 defines the engine manufacturers data for this example calculation. Note that these data are in terms of $T_{tst/av}$ for a range of flight conditions.

Step 3: The following input information is required before Eqn.(6.50) can be used:

K_t, M_1, $\eta_{inl/inc}$, P_{extr} and U_1

This input information must be determined for each individual installation. In preliminary design the methods suggested in 6.4.2.1 may be used.

For the current example, the following data will be assumed:

K_t from Figure 6.37 at each value of M_1

M_1 follows from the speed and altitude for which the calculations are made.

$\eta_{inl/inc}$ follows from Eqns (6.30) and (6.37).

Note: the inlet geometry must be available before the inlet pressure recovery can be computed! In this example it will be assumed that $\eta_{inl/inc} = 0.95$.

P_{extr} follows from Sub-section 6.1.2. In this example it will be assumed that $P_{extr} = 60$ hp.

U_1 is selected in increments of kts airspeed.

Step 4: The determination of T_{av} now proceeds as follows:

For each speed and altitude combination, Eqn.(6.50) is now used to determine T_{av}. This information is then plotted as in Figure 7.3.

Note: for the effect of atmospheric temperature on engine performance, engine manufacturers data should be consulted.

7.2.2 Supersonic Operations

The step-by-step procedure of 6.4.2.2 will be used.

Step 1: It will be assumed that installed, available thrust must be provided for the following range of flight conditions:

altitude:	0 - 60,000 ft in increments of 10,000 ft
speed:	M = 0 to 2.5
temperature:	standard atmosphere

Note: the flight condition range must be compatible with the stated mission objectives of the airplane. Such mission objectives are normally defined in the airplane mission specification. Examples of airplane mission specifications are discussed in Part I.

The airplane used in this example is assumed to be a

The data in this Figure were arrived at with assumptions listed in Sub-section 7.1.3.

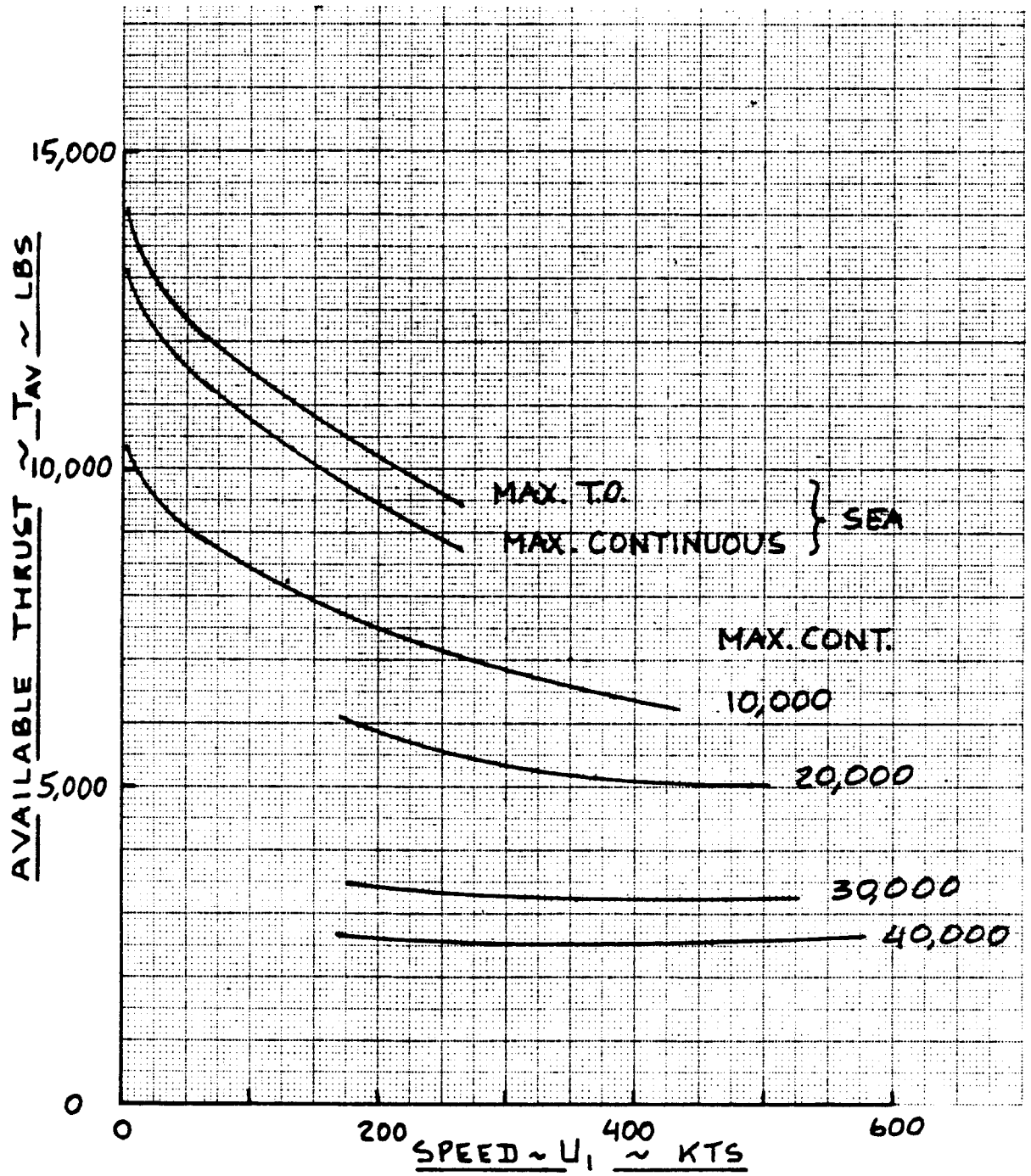

Figure 7.3 Installed Available Thrust Data for a Subsonic Twin Engine Jet Transport

twin engined, supersonic business jet. The inlets are assumed to be of the mixed compression type (Fig.6.10c) with four shocks.

The uninstalled engine performance characteristics are assumed to be those of Figure 6.38.

Step 2: Figure 6.38 defines the engine manufacturers data for this installation in terms of $T_{tst/av}$. Note the reference pressure recovery schedule.

Step 3: The following input information is required before Eqn.(6.51) can be used:

F_t: which depends on C_R, $\eta_{inl/com}$ and $\eta_{ref/inl}$,

P_t: which depends on $\dot{m}_{bleed}$ and $\dot{m}_a$,

P_{extr} and U_1

For the current example it will be assumed that F_t has been determined to vary with Mach number as shown in Figure 7.4, that $P_t = 0.07$ and that $P_{extr} = 20$ hp

Step 4: The determination of T_{av} now proceeds as follows:

For any given speed and altitude, Eqn.(6.51) is used to compute T_{av}. The result is plotted in Figure 7.5.

Note: for the effect of atmospheric temperature on engine performance, engine manufacturers data should be consulted.

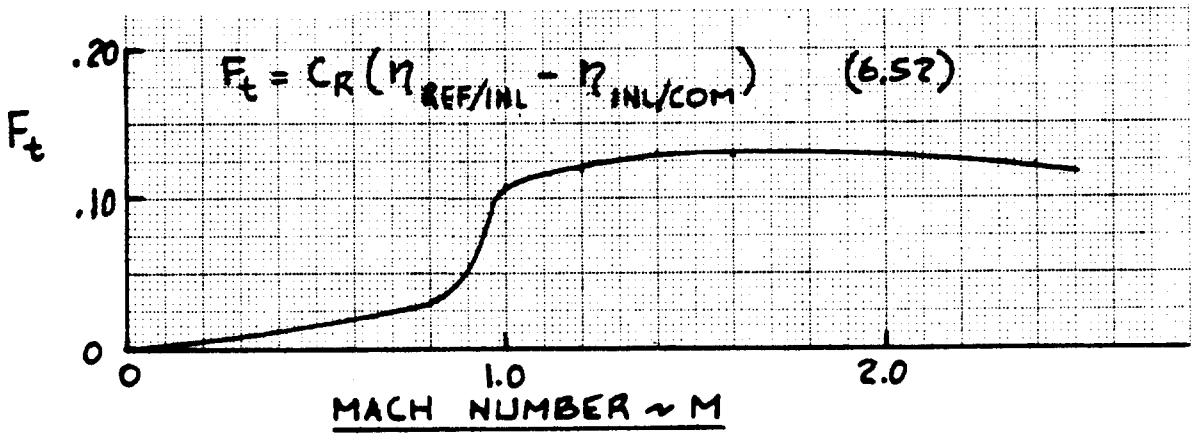

Figure 7.4 Effect of Mach Number on F_t for an Example Supersonic Twin Engine Business Jet

The data in this Figure were arrived at with assumptions listed in Sub-section 7.1.4 and the F_t data of Fig.7.4.

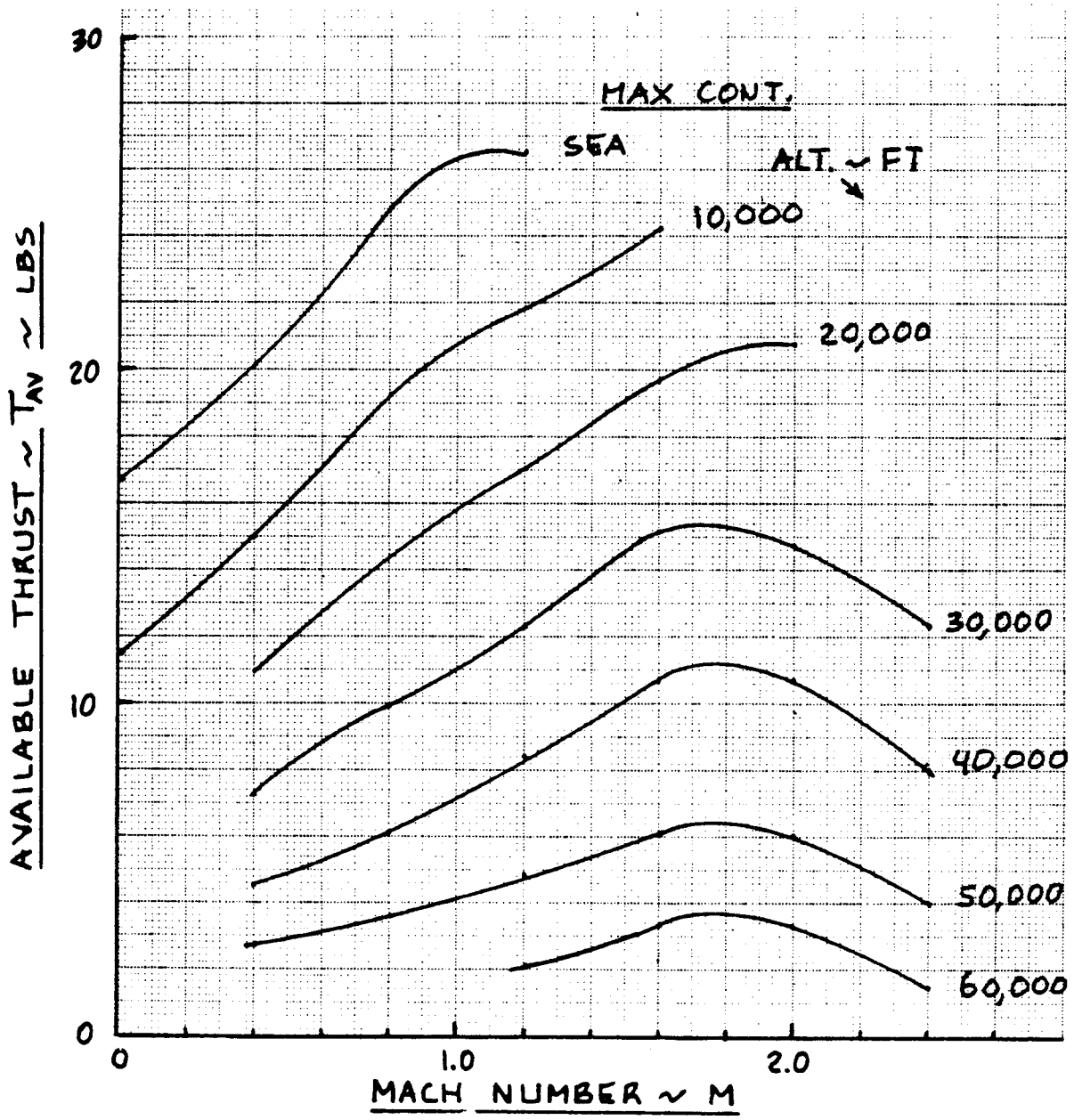

Figure 7.5 Installed Available Thrust Data for a Supersonic Twin Engine Business Jet

8. LIFT AND PITCHING MOMENT PREDICTION METHODS

The purpose of this chapter is to present rapid methods for the prediction of lift and pitching moment characteristics of airplanes. These characteristics are expressed in terms of the following relationships:

*Lift coefficient versus angle of attack

*Pitching moment coefficient versus lift coefficient

The reason for combining these relationships is the fact that unless an airplane can be trimmed (i.e. flown at zero pitching moment coefficient), it is not useful.

Figure 8.1 shows the fundamental C_L-α and C_m-C_L relationships which must be determined for any new design. Note the following maximum lift coefficients:

Clean airplane (flaps up): $C_{L_{max}}$

Flaps down: take-off: $C_{L_{max_{TO}}}$

landing: $C_{L_{max_L}}$

} Trimned with: $\bar{x}_{cg} = \bar{x}_{ref}$

Methods for determining the magnitude of these maximum lift coefficients required to satisfy performance objectives are discussed in Part I as part of the overall sizing process of airplanes.

Class I methods for determining whether or not any given airplane design can achieve certain required maximum lift coefficients are given in Chapter 7 of Part II. The reader must take note of the fact that the effect of trim requirements was accounted for in Ch.7 of Pt.II by subtracting a 'token' increment from the untrimmed maximum lift coefficients. In <u>this</u> chapter Class II methods for estimating trimmed lift coefficients and trimmed maximum lift coefficients are presented. The material is organized as follows:

8.1 Prediction of lift coefficient versus angle of attack
8.2 Prediction of pitching moment versus lift coefficient
8.3 Prediction of trimmed lift and trimmed maximum lift coefficient

The methods are presented for the subsonic flow range. The reader is referred to specific sections of Ref.9 for those transonic and supersonic effects which are considered beyond the scope of this text.

8.1 PREDICTION OF LIFT COEFFICIENT VERSUS ANGLE OF ATTACK

In this section methods for predicting the variation of lift coefficient with angle of attack will be presented as follows:

8.1.1 Airfoil lift and maximum lift: flaps up
8.1.2 Airfoil lift and maximum lift: flaps down
8.1.3 Wing lift and maximum lift: flaps up
8.1.4 Wing lift and maximum lift: flaps down
8.1.5 Airplane lift and maximum lift: flaps up
8.1.6 Airplane lift and maximum lift: flaps down
8.1.7 Airplane lift in ground effect
8.1.8 Power effects on airplane lift

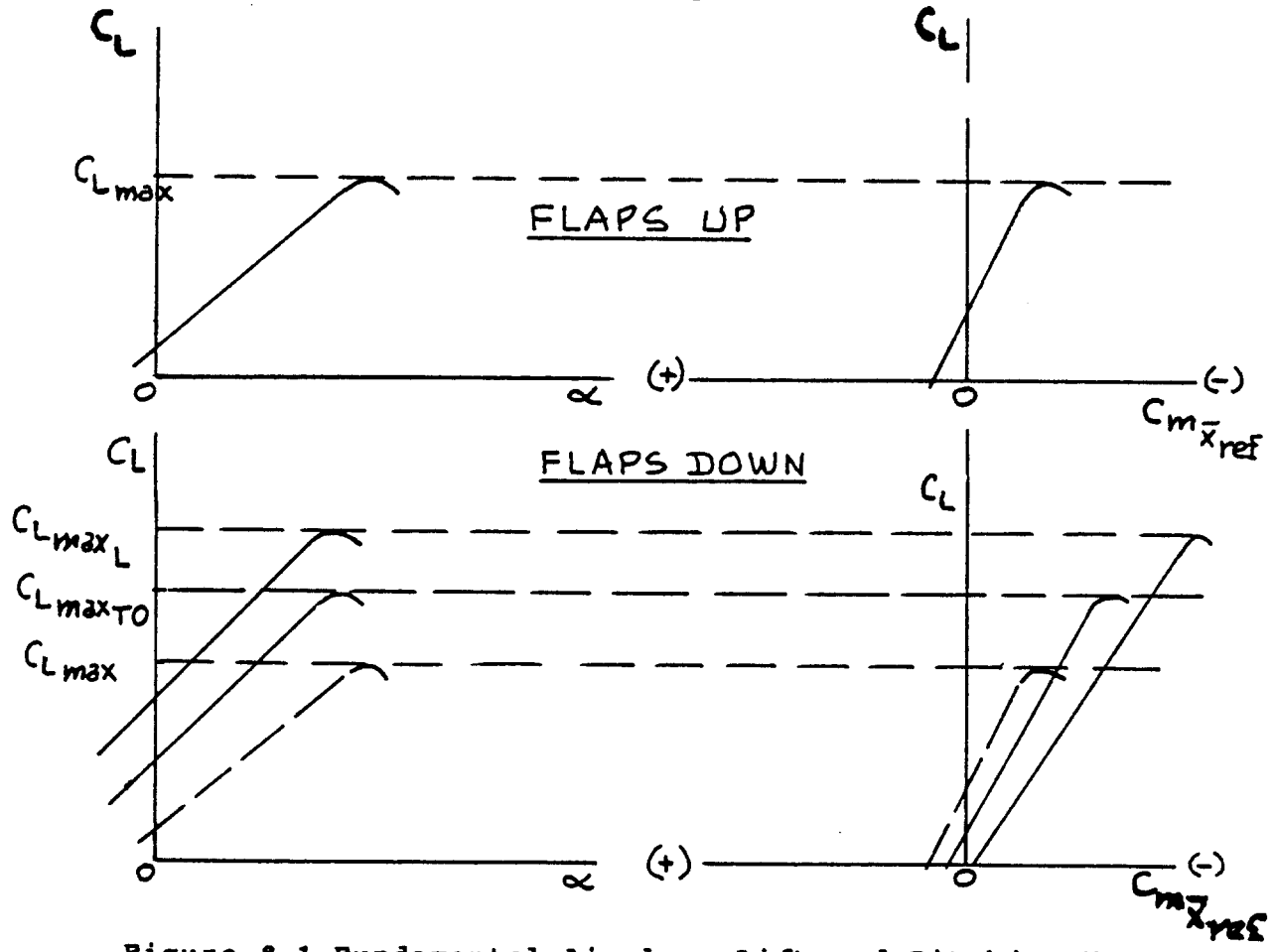

Figure 8.1 Fundamental Airplane Lift and Pitching Moment Characteristics

8.1.1 Airfoil Lift and Maximum Lift: Flaps Up

Figure 8.2 shows the relationship between airfoil lift coefficient and airfoil angle of attack which must be be determined with the methods to be presented in this Section. Key quantities needed in the construction of the airfoil c_l versus α curve are listed, with an indication of where methods for their estimation may be found.

8.1.1.1 Airfoil zero-lift angle of attack: α_{0_l}

Table 8.1 provides a summary of basic airfoil data from which α_{0_l} may be determined. Whenever possible, actual airfoil data should be used.

The airfoil zero-lift angle of attack may be estimated from Ref.9 (4.1.1.1) for arbitrary airfoils.

Experience shows that the airfoil zero-lift angle of attack is NOT a function of Reynold's number or Mach number in the subsonic speed range.

8.1.1.2 Airfoil lift curve slope: c_{l_α}

Table 8.1 provides a summary of basic airfoil data from which c_{l_α} may be determined. Whenever possible, actual airfoil data should be used.

The airfoil lift curve slope may be estimated from Ref.9 (4.1.1.2) for arbitrary airfoils.

Experience shows that the airfoil lift curve slope is dependent on Mach number in accordance with the Prandt-Glauert transformation:

For subsonic speeds:

$$c_{l_\alpha}\ \text{at M} = (c_{l_\alpha}\ \text{at M=0})/(1 - M^2)^{1/2} \qquad (8.1)$$

For supersonic speeds:

$$c_{l_\alpha}\ \text{at M} = 4/(M^2 - 1)^{1/2} \qquad (8.2)$$

For transonic speeds: use tunnel data.

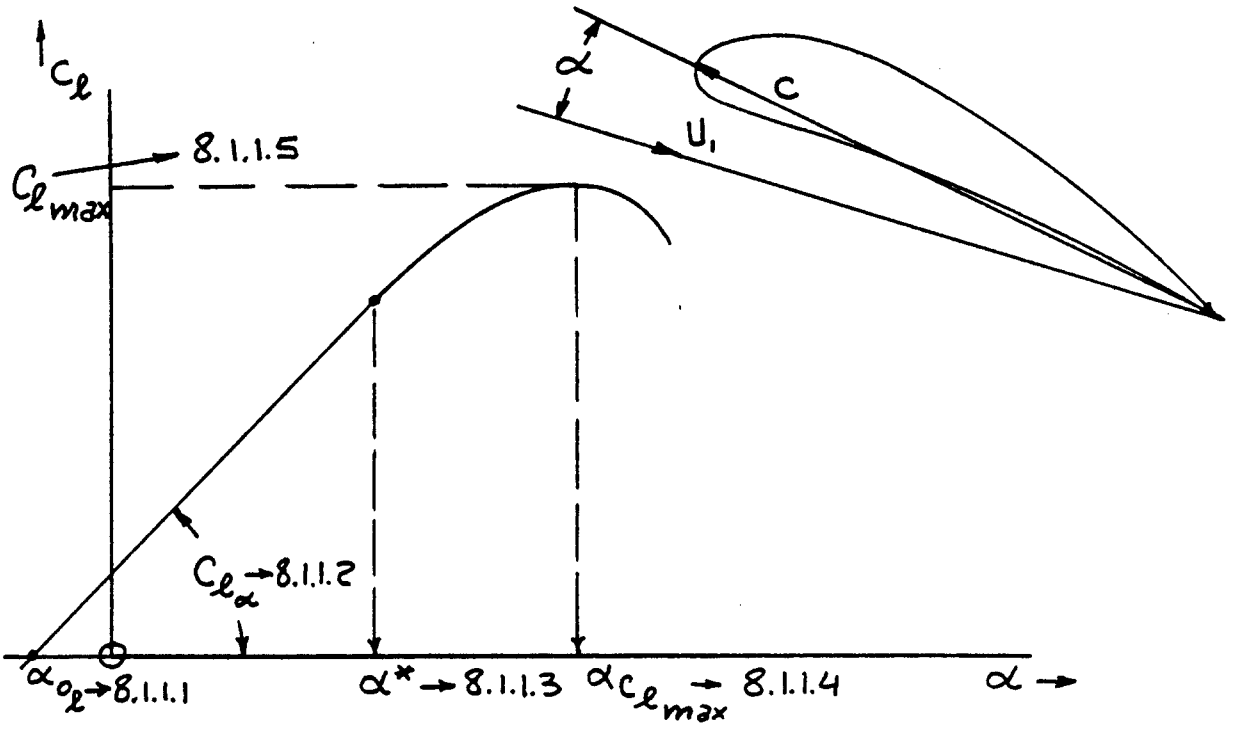

Figure 8.2 Airfoil Lift Coefficient Versus Angle of Attack Curve

Table 8.1a Experimental Low Speed Data for 4- and 5- Digit NACA Airfoils with a Smooth Leading Edge and for $R_N = 9 \times 10^6$ (Ref. 16)

Airfoil	α_{o_ℓ} (deg)	c_{m_o}	c_{l_α} (deg^{-1})	a.c. (tenths c)	$\alpha_{c_{l_{max}}}$ (deg)	$c_{l_{max}}$	α^* (deg)
0006	0	0	.108	.250	9.0	.92	9.0
0009	0	0	.109	.250	13.4	1.32	11.4
1408	0.8	-.023	.109	.250	14.0	1.35	10.0
1410	-1.0	-.020	.108	.247	14.3	1.50	11.0
1412	-1.1	-.025	.108	.252	15.2	1.58	12.0
2412	-2.0	-.047	.105	.247	16.8	1.68	9.5
2415	-2.0	-.049	.106	.246	16.4	1.63	10.0
2418	-2.3	-.050	.103	.241	14.0	1.47	10.0
2421	-1.8	-.040	.103	.241	16.0	1.47	8.0
2424	-1.8	-.040	.098	.231	16.0	1.29	8.4
4412	-3.8	-.093	.105	.247	14.0	1.67	7.5
4415	-4.3	-.093	.105	.245	15.0	1.64	8.0
4418	-3.8	-.088	.105	.242	14.0	1.53	7.2
4421	-3.8	-.085	.103	.238	16.0	1.47	6.0
4424	-3.8	-.082	.100	.239	16.0	1.38	4.8
23012	-1.4	-.014	.107	.247	18.0	1.79	12.0
23015	-1.0	-.007	.107	.243	18.0	1.72	10.0
23018	-1.2	-.005	.104	.243	16.0	1.60	11.8
23021	-1.2	0	.103	.238	15.0	1.50	10.3
23024	-0.8	0	.097	.231	15.0	1.40	9.7

Table 8.1b Experimental Low Speed Data for 6- Digit NACA Airfoils with a Smooth Leading Edge and for $R_N = 9 \times 10^6$ (Ref.16)

Airfoil	α_{o_ℓ} (deg)	c_{m_o}	c_{l_α} (deg^{-1})	a.c. (tenths c)	$\alpha_{c_{l_{max}}}$ (deg)	$c_{l_{max}}$	α^* (deg)
63-006	0	.005	.112	.258	10.0	.87	7.7
63-009	0	0	.111	.258	11.0	1.15	10.7
63-206	-1.9	-.037	.112	.254	10.5	1.06	6.0
63-209	-1.4	-.032	.110	.262	12.0	1.40	10.8
63-210	-1.2	-.035	.113	.261	14.5	1.56	9.6
63_1-012	0	0	.116	.265	14.0	1.45	12.8
63_1-212	-2.0	-.035	.114	.263	14.5	1.63	11.4
63_1-412	-2.8	-.075	.117	.271	15.0	1.77	9.6
64-006	0	0	.109	.256	9.0	.8	7.2
64-009	0	0	.110	.262	11.0	1.17	10.0
64-206	-1.0	-.040	.110	.253	12.0	1.03	8.0
64-209	-1.5	-.040	.107	.261	13.0	1.40	8.9
64-210	-1.6	-.040	.110	.258	14.0	1.45	10.8
64_1-012	0	0	.111	.262	14.5	1.45	11.0
64_1-212	-1.3	-.027	.113	.262	15.0	1.55	11.0
64_1-412	-2.6	-.065	.112	.267	15.0	1.67	8.0

Table 8.1c Experimental Low Speed Data for 6- Digit NACA Airfoils with a Smooth Leading Edge and for $R_N = 9 \times 10^6$ (Ref.16)

Airfoil	α_{o_ℓ} (deg)	c_{m_o}	c_{l_α} (deg^{-1})	a.c. (tenths c)	$\alpha_{c_{l_{max}}}$ (deg)	$c_{l_{max}}$	α^* (deg)
65-006	0	0	.105	.258	12.0	.92	7.6
65-009	0	0	.107	.264	11.0	1.08	9.8
65-206	-1.6	-.031	.105	.257	12.0	1.03	6.0
65-209	-1.2	-.031	.106	.259	12.0	1.30	10.0
65-210	-1.6	-.034	.108	.262	13.0	1.40	9.6
65_1-012	0	0	.110	.261	14.0	1.36	10.0
65_1-212	-1.0	-.032	.108	.261	14.0	1.47	9.4
65_1-412	-3.0	-.070	.111	.265	15.5	1.66	10.5
63A010	0	.005	.105	.254	13.0	1.20	10.0
63A210	-1.5	-.040	.103	.257	14.0	1.43	10.0
64A010	0	0	.110	.253	12.0	1.23	10.0
64A210	-1.5	-.040	.105	.251	13.0	1.44	10.0
64A410	-3.0	-.080	.100	.254	15.0	1.61	10.0
64_1A212	-2.0	-.040	.100	.252	14.0	1.54	11.0
64_2A215	-2.0	-.040	.095	.252	15.0	1.50	12.0

8.1.1.3 Airfoil linear range angle of attack: α^*

Table 8.1 provides a summary of basic airfoil data from which α^* may be determined. Whenever possible, actual airfoil data should be used.

The airfoil linear range angle of attack may also be estimated from Ref.9 (4.1.1.3) for existing airfoils.

8.1.1.4 Airfoil angle of attack for maximum lift: $\alpha_{c_{l_{max}}}$

Table 8.1 provides a summary of basic airfoil data from which $\alpha_{c_{l_{max}}}$ may be determined. Whenever possible, actual airfoil data should be used.

The airfoil angle of attack for maximum lift may be estimated from Ref.9 (4.1.1.4) for existing airfoils.

8.1.1.5 Airfoil maximum lift coefficient: $c_{l_{max}}$

It has been found that airfoil maximum lift coefficient, $c_{l_{max}}$ depends upon the following parameters:

1. Leading edge shape as quantified by the so-called Δy parameter.
2. Maximum thickness and position of maximum thickness.
3. Maximum camber and position of maximum camber.
4. Reynold's number: $\rho c U_1 / \mu$
5. Mach number.

Figure 8.3 defines these parameters for an arbitrary airfoil.

The method is valid for a 'base Reynold's number' of 9×10^6 and for Mach numbers below 0.2. The effect of variations in Reynold's number and Mach number relative to this 'base' is accounted for in the method.

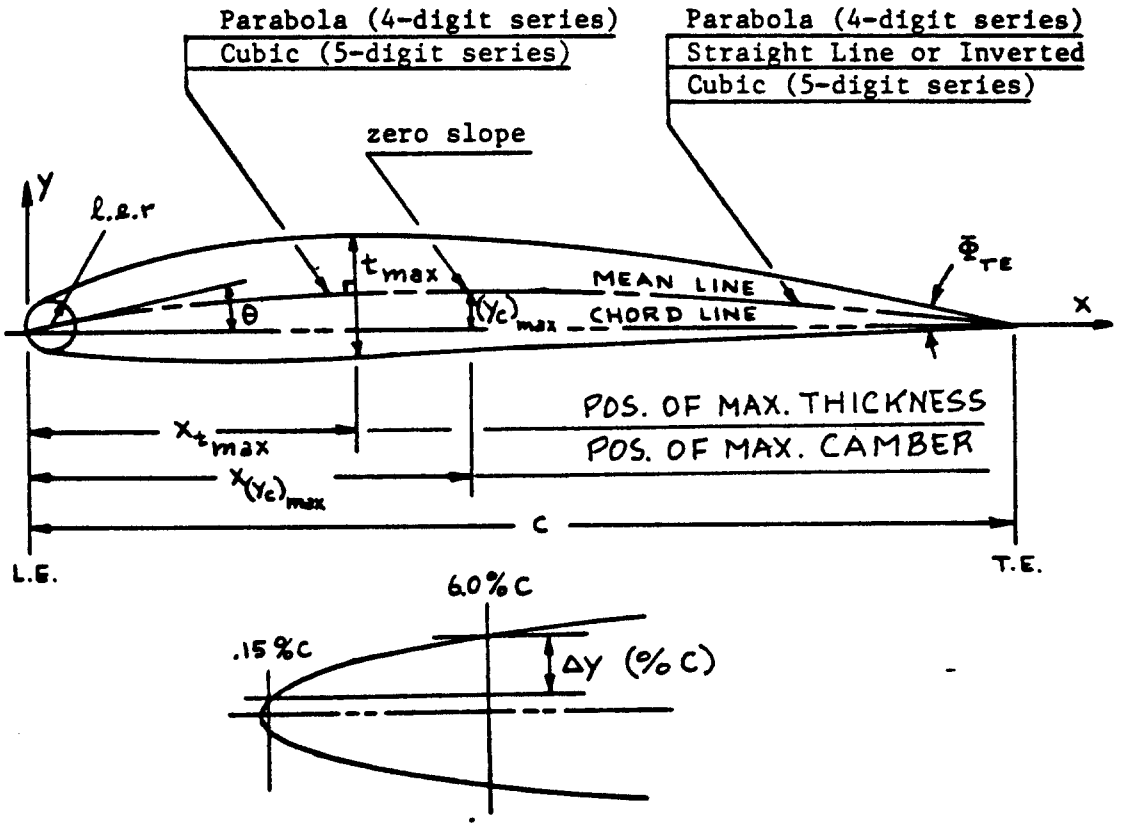

Figure 8.3 Airfoil Geometric Characteristics

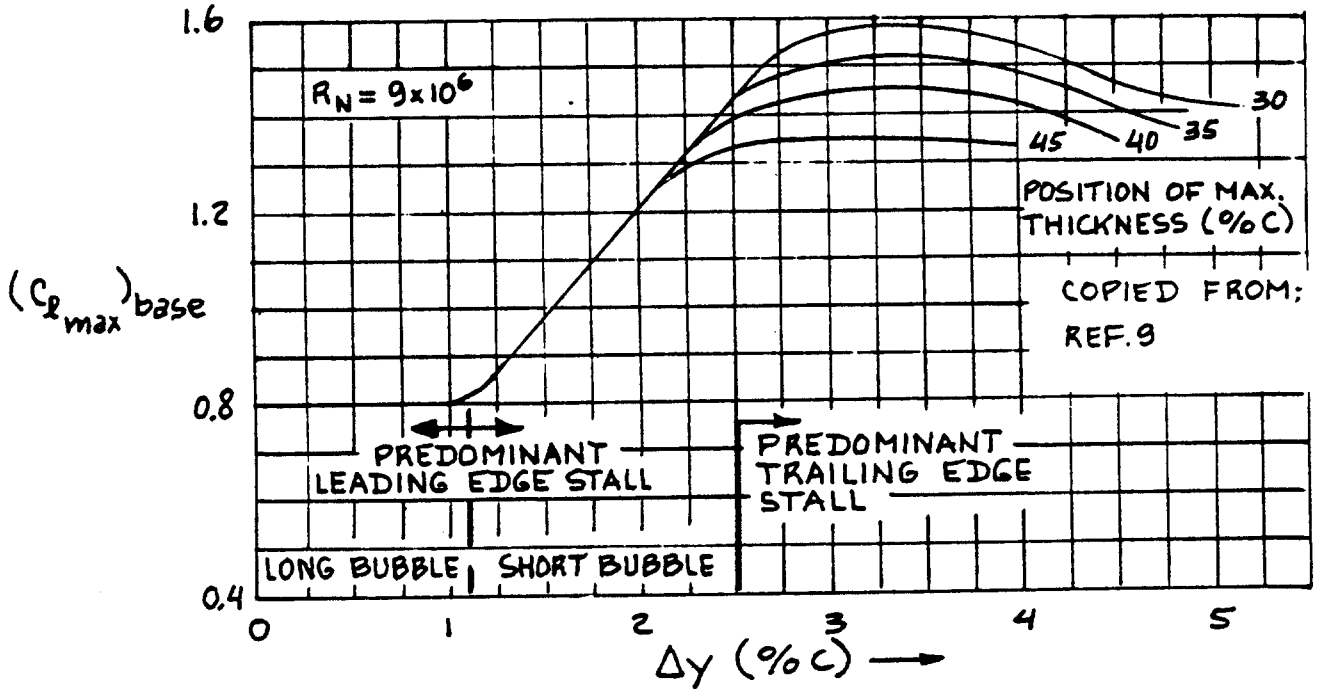

Figure 8.4 Basic Airfoil Maximum Lift Coefficient for Uncambered Airfoils

The maximum lift coefficient of an airfoil may be estimated from:

$$c_{l_{max}} = (c_{l_{max}})_{base} + \Delta_1 c_{l_{max}} + \Delta_2 c_{l_{max}} + \Delta_3 c_{l_{max}} + \Delta_3 c_{l_{max}} + \Delta_4 c_{l_{max}} + \Delta_5 c_{l_{max}} \quad (8.3)$$

where: $(c_{l_{max}})_{base}$ is the basic airfoil maximum lift coefficient, found from Figure 8.4 as a function of airfoil geometry. The parameter Δy in Figure 8.4 is defined in Figure 8.3. Table 8.2 lists example data for Δy.

$\Delta_1 c_{l_{max}}$ is the airfoil maximum lift increment due to camber and due to position of maximum camber. See Figure 8.5.

$\Delta_2 c_{l_{max}}$ is the airfoil maximum lift increment due position of maximum thickness. This increment is obtained from Figure 8.6. NOTE: when the position of maximum thickness is at 30 percent chord, this increment is ZERO.

$\Delta_3 c_{l_{max}}$ is the airfoil maximum lift increment due to Reynold's number: see Figure 8.7.

$\Delta_4 c_{l_{max}}$ is the airfoil maximum lift increment due to airfoil roughness. The basic roughness used is the so-called standard NACA roughness of 0.011 inch grit applied over the first 8 percent chord. Actual airplane roughness is much less severe. For airplanes with 'smooth' and 'clean' leading edges this increment is ZERO. Figure 8.8 provides data for finding this increment.

$\Delta_5 c_{l_{max}}$ is the section maximum lift increment due to Mach number (compressibility) Fig. 8.9 gives data for finding this increment

Whenever possible, actual data should be used. References 49, 50 and 51 should be consulted for specific data on airfoil maximum lift coefficients.

Table 8.1 contains $c_{l_{max}}$ data for a range of airfoils at the base Reynold's number of 9×10^6.

Table 8.2 Example Data for the Leading Edge Δy Parameter

Airfoil NACA	Position of max t/c perc. of c	Camber perc. of c	Position of max camber perc. of c	Δy perc. of c
0009	30	0	not appl.	2.35
1410	30	1.0	40	2.60
2415	30	2.0	40	3.80
4412	30	4.0	40	3.08
4315	30	4.0	30	3.30
4321	30	4.0	30	5.24
23012	30	1.8	13	3.03
23021	30	1.8	15	5.24
43012	30	3.7	15	3.08
63012	30	5.5	15	3.08
63-009	35	0	not appl.	2.00
63-209	35	1.1	50	2.00
63_1-012	35	0	not appl.	2.65
63_1-212	35	1.1	50	2.65
63_1-412	35	2.2	50	2.65
63_1-018	35	0	not appl.	3.95
63_1-618	35	3.3	40	3.95
64-108	40	0.55	50	1.70
64_1-112	40	0.55	50	2.52
64_3-013	40	0	not appl.	3.75
64_3-412	40	2.2	50	3.75
66-009	45	0	not appl.	1.65
66-205	45	1.1	50	1.65
66_2-018	45	0	not appl.	3.30
66_2-416	45	3.2	50	3.30

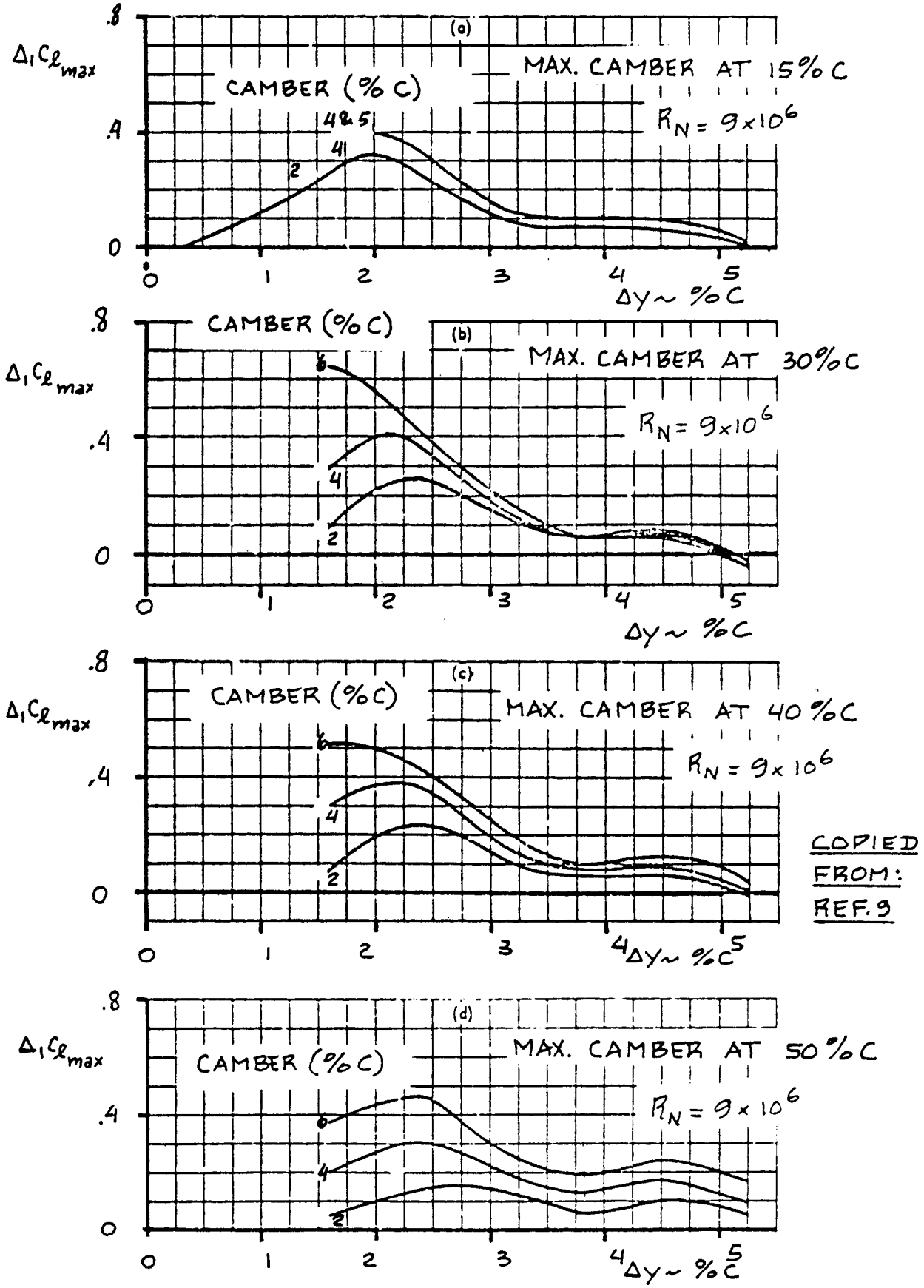

COPIED FROM: REF. 9

Figure 8.5 Effect of Camber on Maximum lift

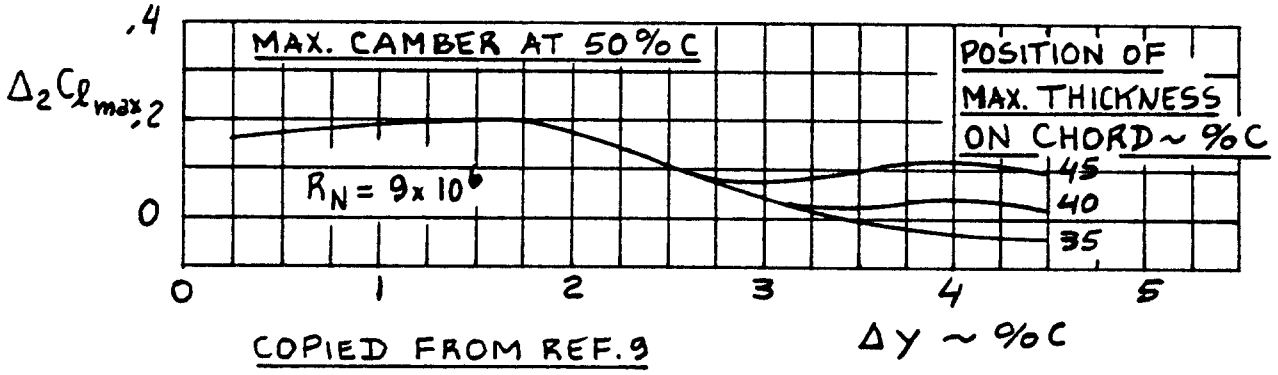

Figure 8.6 Effect of Maximum Thickness Position on Maximum Lift

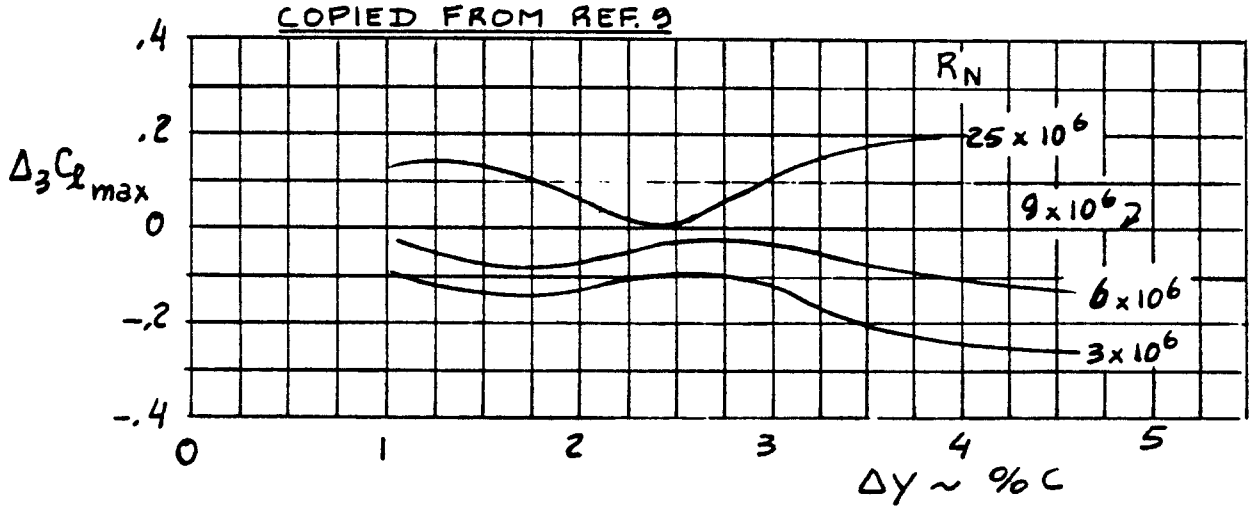

Figure 8.7 Effect of Reynold's Number on Maximum Lift

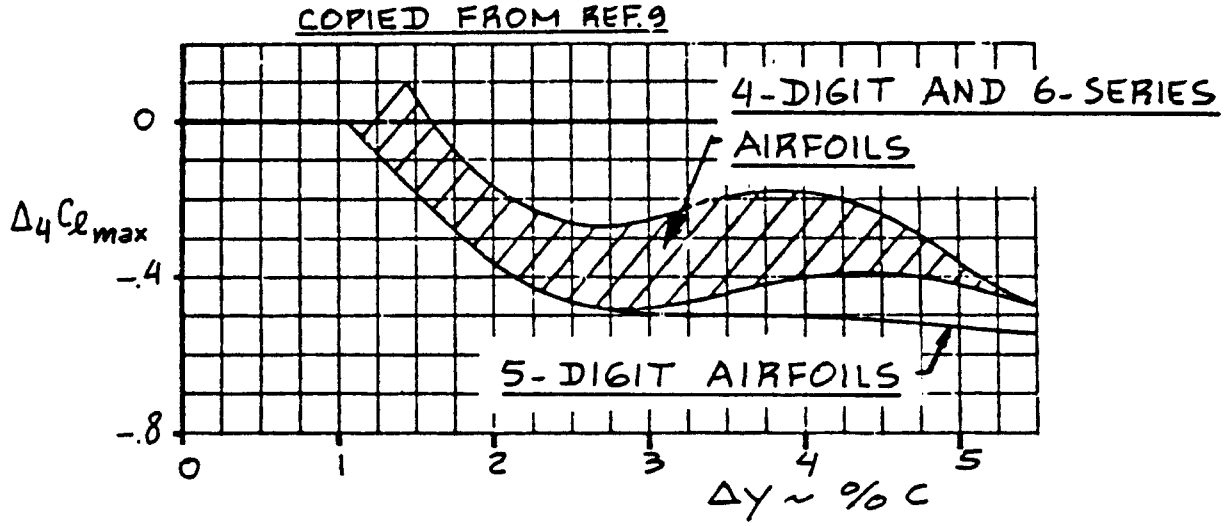

Figure 8.8 Effect of Surface Roughness on Maximum Lift

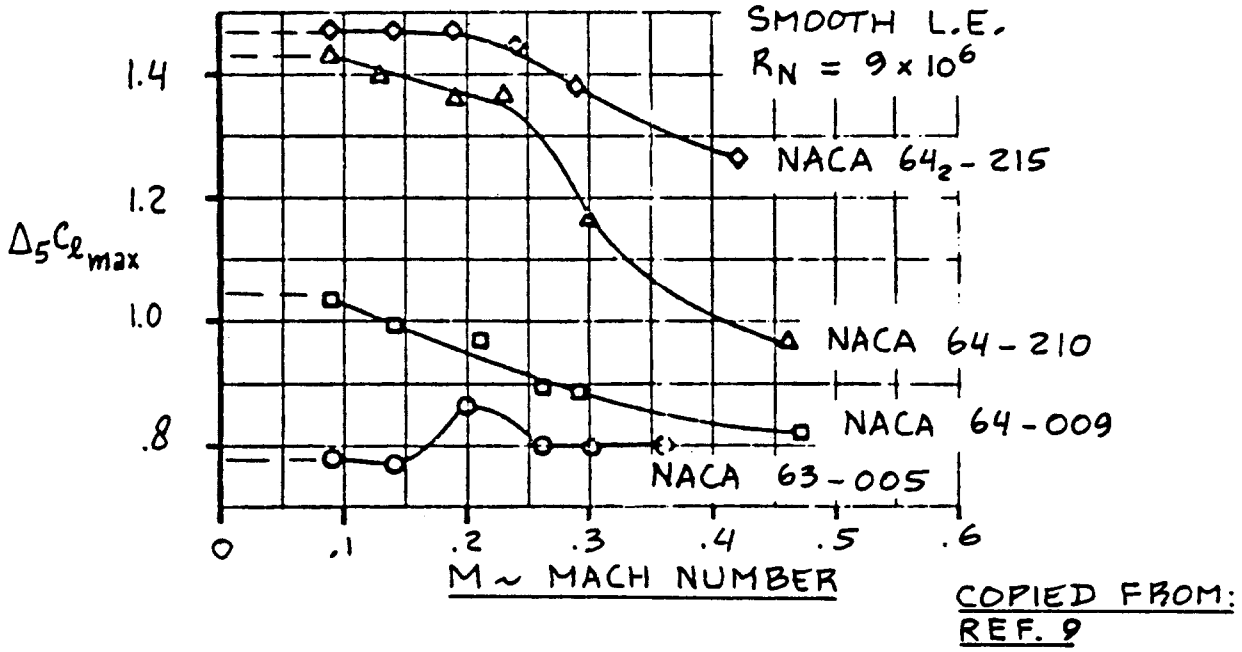

Figure 8.9 Effect of Mach Number on Maximum Lift

8.1.1.6 Construction of airfoil lift curve: flaps up

All ingredients needed to construct the flaps-up airfoil c_l versus α curve are now available. The flaps-up curve in Figure 8.2 can therefore be constructed. Figure 8.10 shows how this is done in a step-by-step manner. The fairing between α^* and $\alpha_{c_{l_{max}}}$ is done with the help of a french curve. The behavior of the lift curve just before and just after stall depends on Reynold's number. Reference 49 and Ref.9 (4.1.1.3) contain more information.

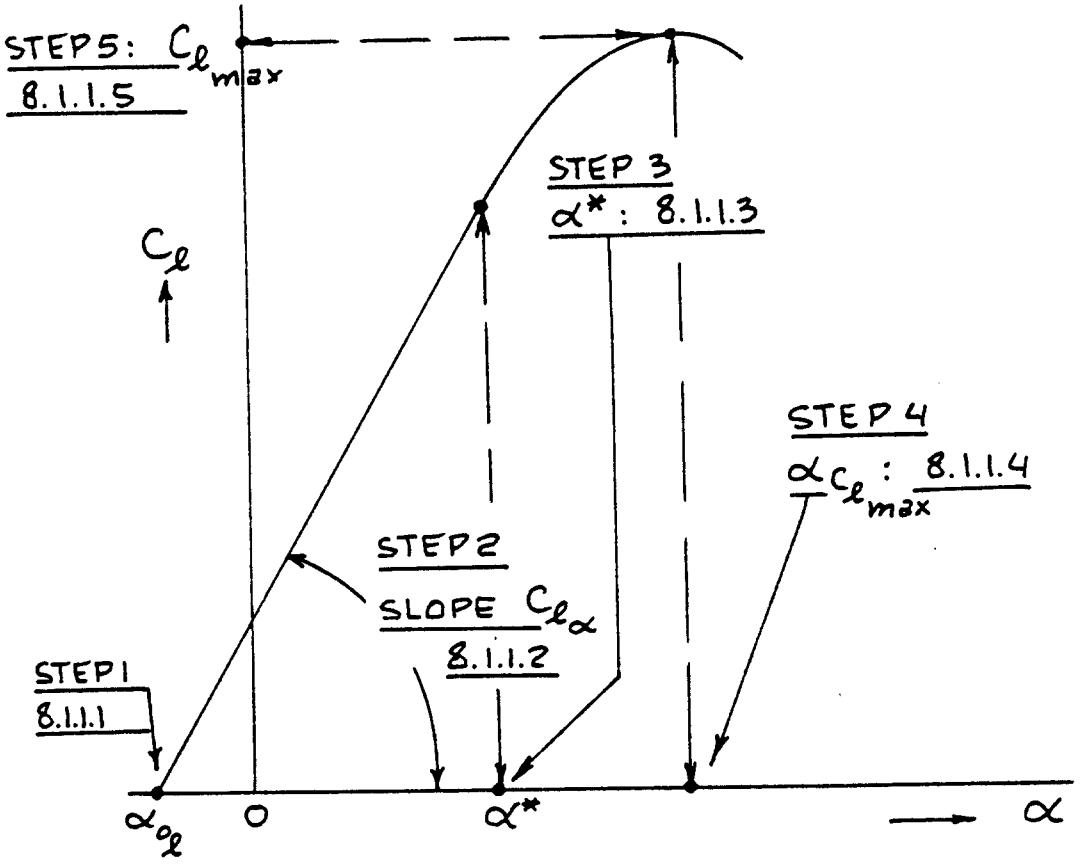

Figure 8.10 Construction of Airfoil Lift Versus α Curve

8.1.2 Airfoil Lift and Maximum Lift: Flaps Down

Figure 8.11 shows the comparison between flaps-up and flaps-down airfoil lift characteristics. Key quantities which are required to determine the flaps-down airfoil lift characteristics are listed with an indication of where methods for their estimation may be found.

8.1.2.1 Airfoil lift increment due to flaps: Δc_l

The airfoil incremental lift coefficient increment due to flaps, Δc_l depends on the type of flaps used.

Methods are presented for the following flap types:

A) Trailing Edge Flaps

a) Plain flaps
b) Single-slotted flaps
c) Fowler flaps
d) Double slotted flaps
e) Split flaps

B) Leading Edge Flaps

a) Nose flaps
b) Krueger flaps
c) Leading edge slats
d) Spoilers

Note: If a wing is equipped with any combination of flaps as defined under A) or B) it is acceptable in preliminary design to add the increments due to each individual flap type. The reader should be aware that this can result in over-prediction of high lift capability!

A) Trailing Edge Flaps

a) Plain flaps

Figure 8.12 defines the geometry of a plain flap. The airfoil incremental lift coefficient due to a plain flap deflection with a sealed gap is given by:

$$\Delta c_l = (\delta_f)\{c_{l_\delta}/(c_{l_\delta})_{theory}\}(c_{l_\delta})_{theory} k' \qquad (8.4)$$

where: k' is a correction factor which accounts for non-linearities at high flap deflections: see Figure 8.13.

$(c_{l_\delta})_{theory}$ is found from Figure 8.14. It accounts for flap size and for thickness ratio.

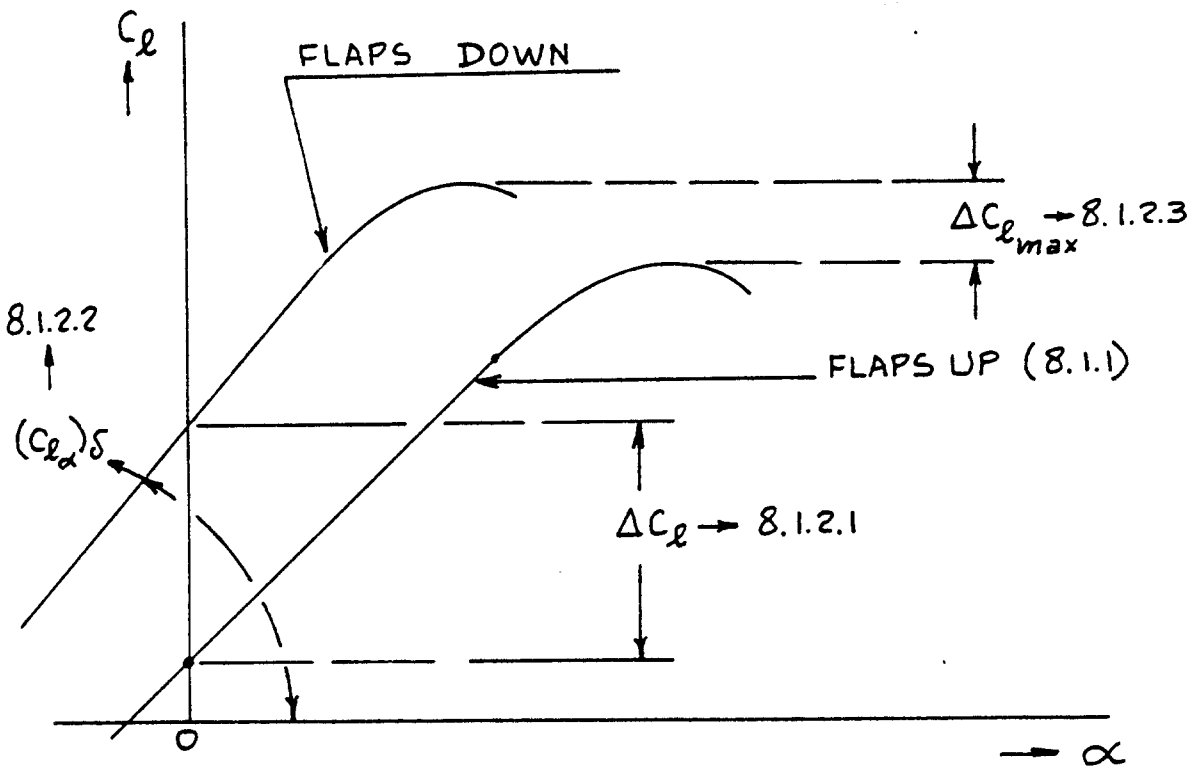

Figure 8.11 Fundamental Airfoil Lift Versus α Curve with the Flaps Down

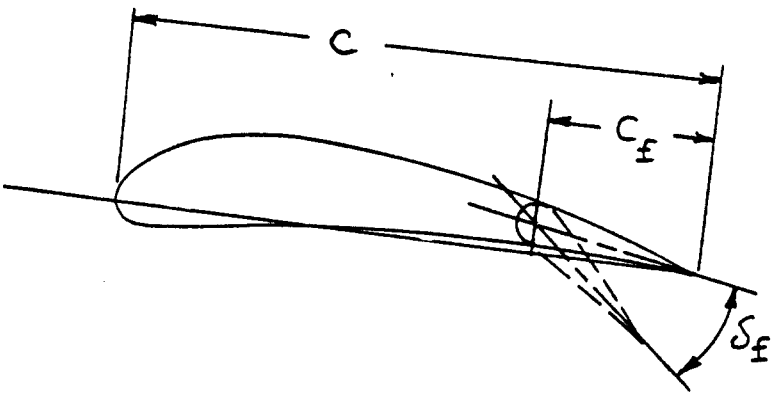

Figure 8.12 Plain Flap Geometry

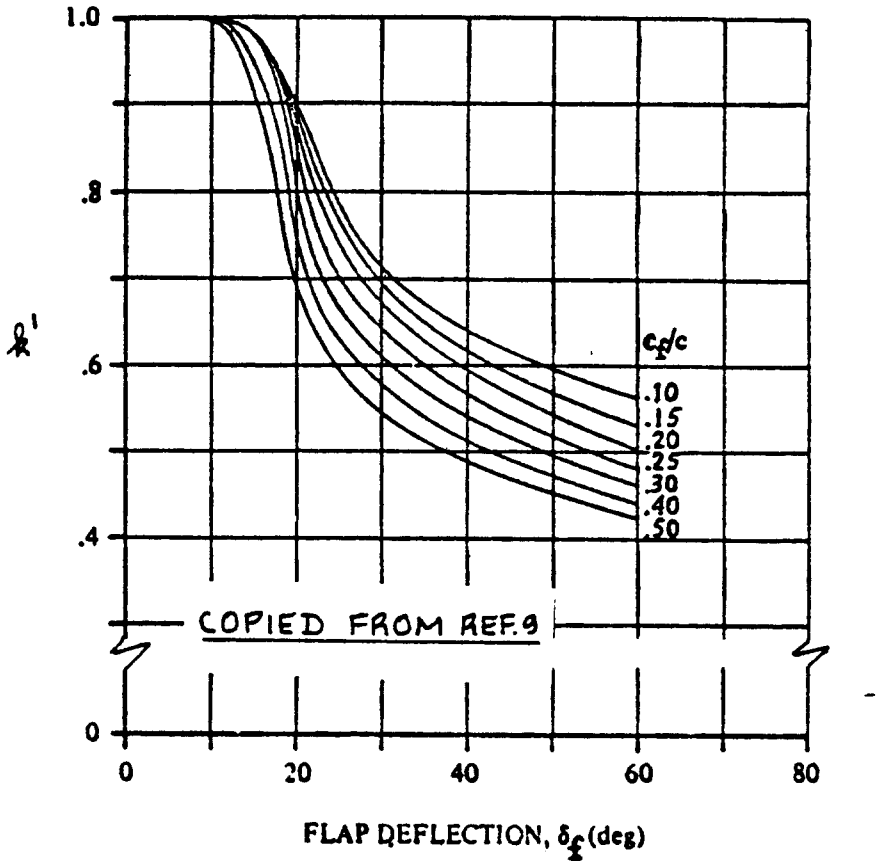

Figure 8.13 Correction Factor for Nonlinear Lift Behavior of Plain Flaps

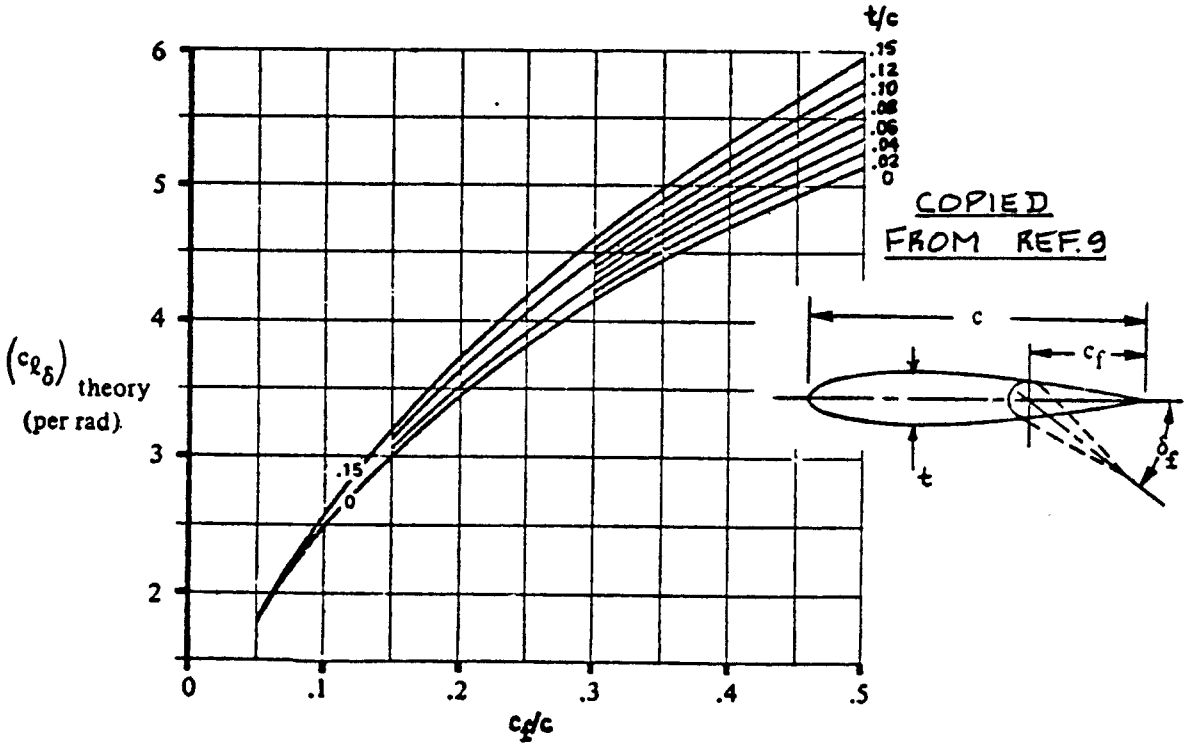

Figure 8.14 Lift Effectiveness of a Plain Flap

$(c_{l_\delta}/(c_{l_\delta})_{theory}$ is found from Figure 8.15.

δ_f is the flap deflection in rad.

Note: for plain flaps with open gaps (not sealed) Reference 49 should be consulted.

b) Single-slotted flaps

Figure 8.16 defines the geometry of a single-slotted flap. The airfoil incremental lift coefficient due to a single-slotted flap deflection is given by:

$$\Delta c_l = (c_{l_\alpha})(\alpha_\delta)(\delta_f) \qquad (8.5)$$

where: c_{l_α} is the airfoil lift-curve-slope with the flaps up. It is found from 8.1.1.2.

α_δ is the airfoil lift effectiveness parameter found from Figure 8.17.

c) Fowler flaps

Figure 8.18 defines the geometry of a Fowler flap. The airfoil incremental lift coefficient due to a Fowler flap deflection is given by:

$$\Delta c_l = (c_{l_\alpha})(\alpha_\delta)(c'/c)(\delta_f) \qquad (8.6)$$

where: (c'/c) is defined in Figure 8.18. All other quantities in Eqn.(8.6) are those listed under b) Single-slotted flaps.

d) Double slotted flaps

Figure 8.19 defines the geometry of double slotted flaps: Types I and II.

Type I:

The airfoil incremental lift coefficient due to a Type I double slotted flap deflection is given by:

$$\Delta c_l = \eta_1 (c_{l_{\delta_{f_1}}})(\delta_1)\{(c + c_1)/c\} + \eta_2 (c_{l_{\delta_{f_2}}})(\delta_{f_1} + \delta_{f_2})(c'/c) \qquad (8.7)$$

where: η_1 and η_2 are found from Figure 8.20 using c_1/c

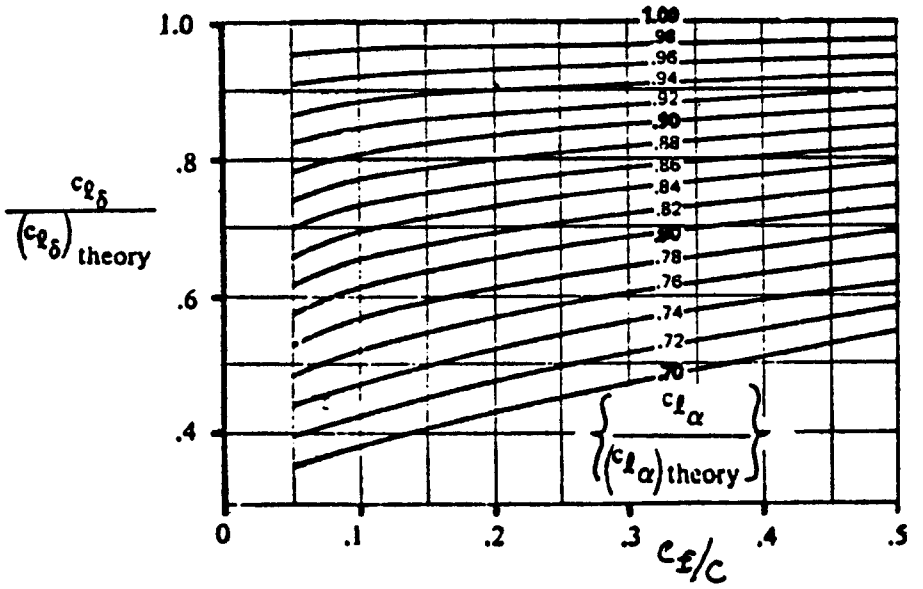

COPIED FROM: REF. 9

FOR C_{ℓ_α} SEE: 8.1.1.2

FOR $(C_{\ell_\alpha})_{theory}$ SEE: REF. 9 SECTION 4.1.1.2 OR USE 2π

Figure 8.15 Correction Factor for Plain Flap Lift

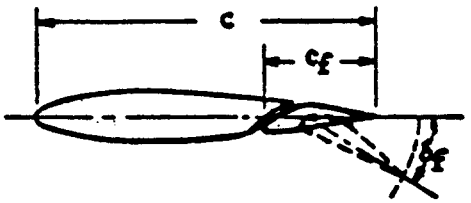

Figure 8.16 Single Slotted Flap Geometry

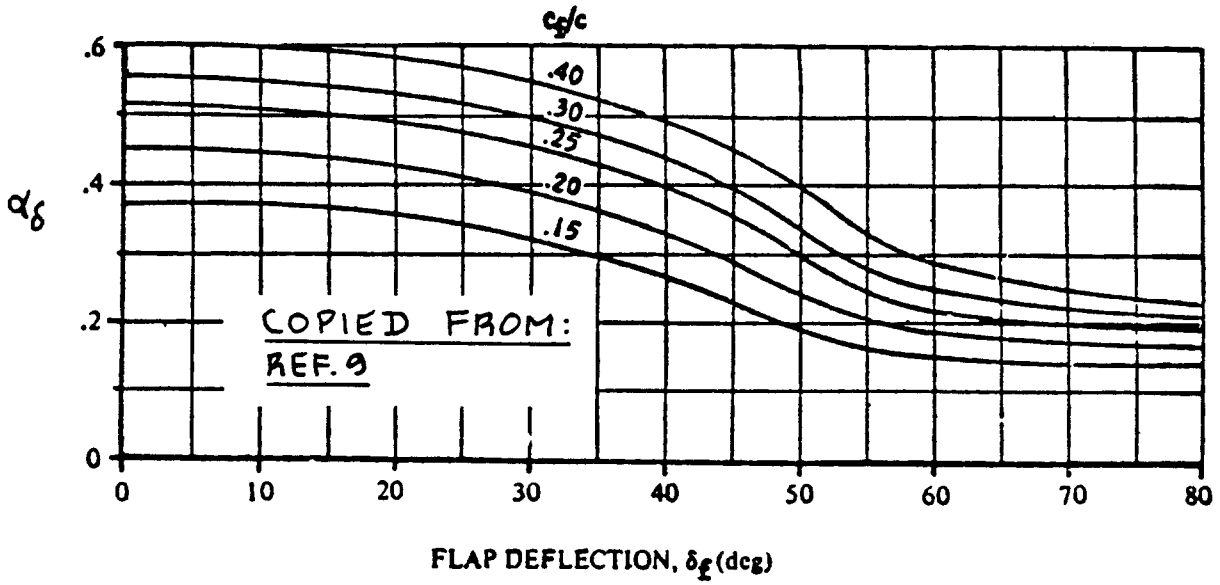

Figure 8.17 Lift Effectiveness of a Single Slotted Flap

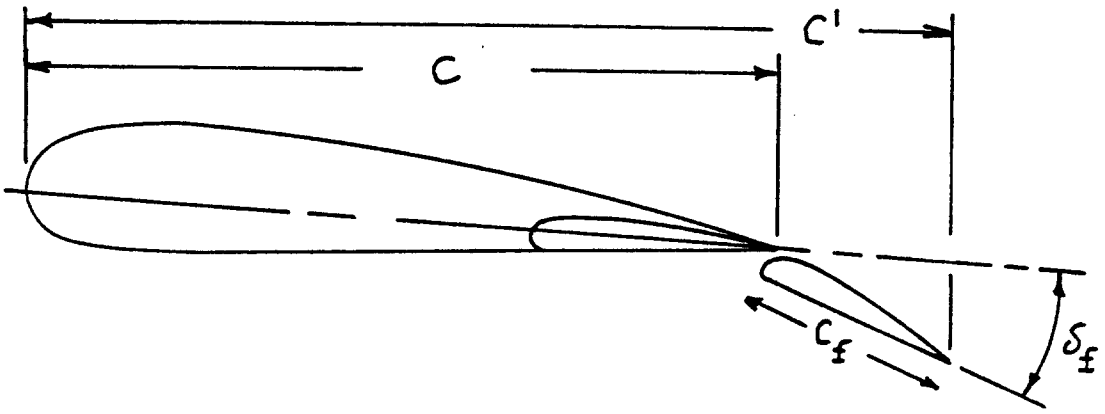

Figure 8.18 Fowler Flap Geometry

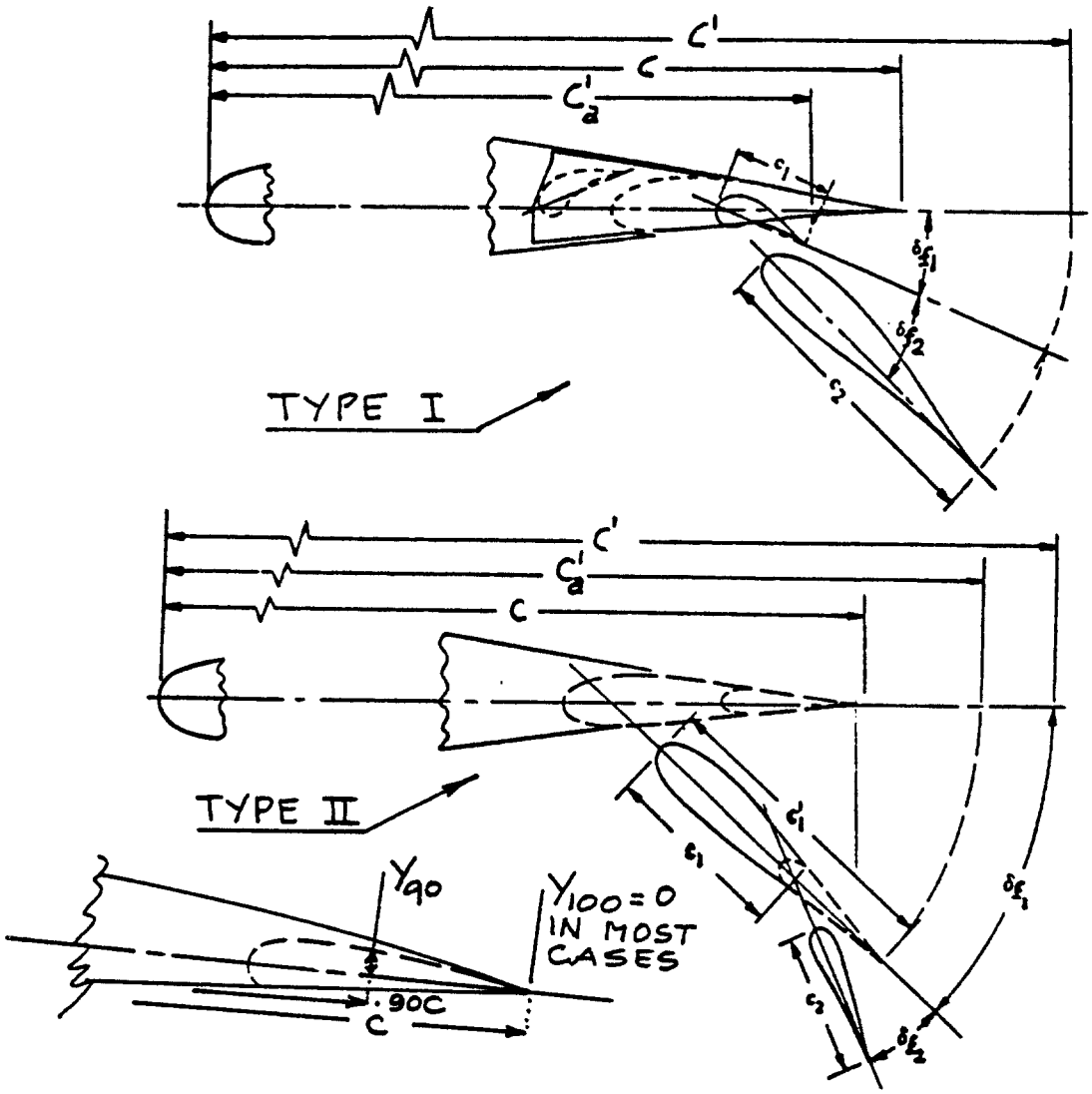

Figure 8.19 Double Slotted Flap Geometry

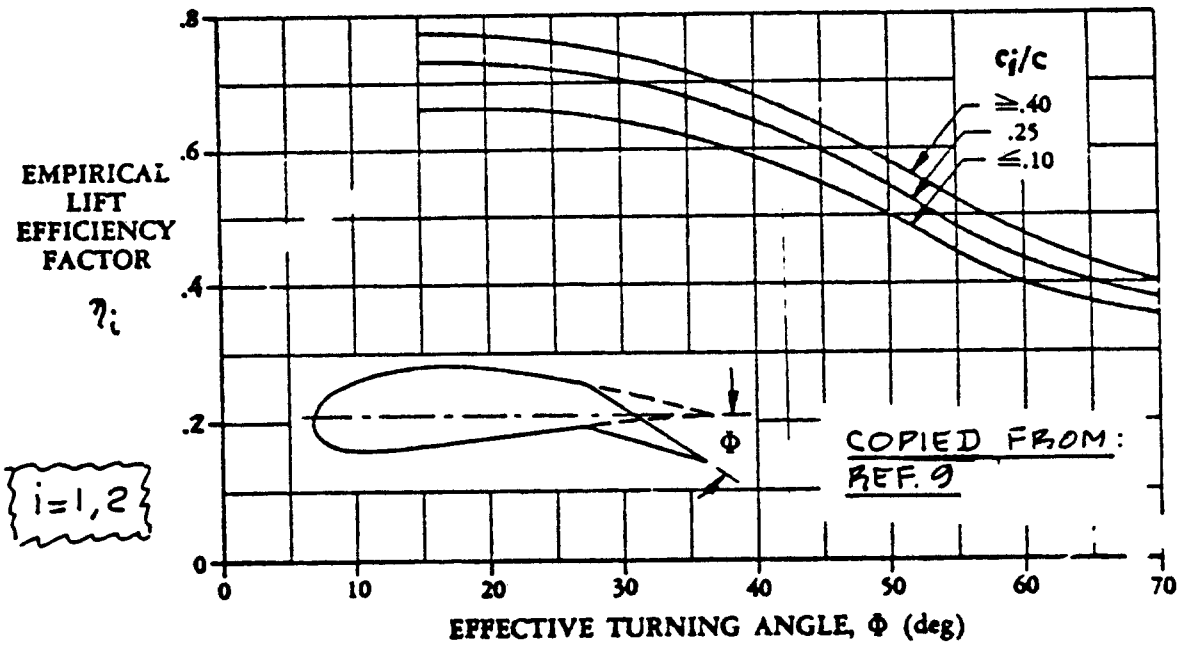

Figure 8.20 Lift Effectiveness for Slotted Flaps

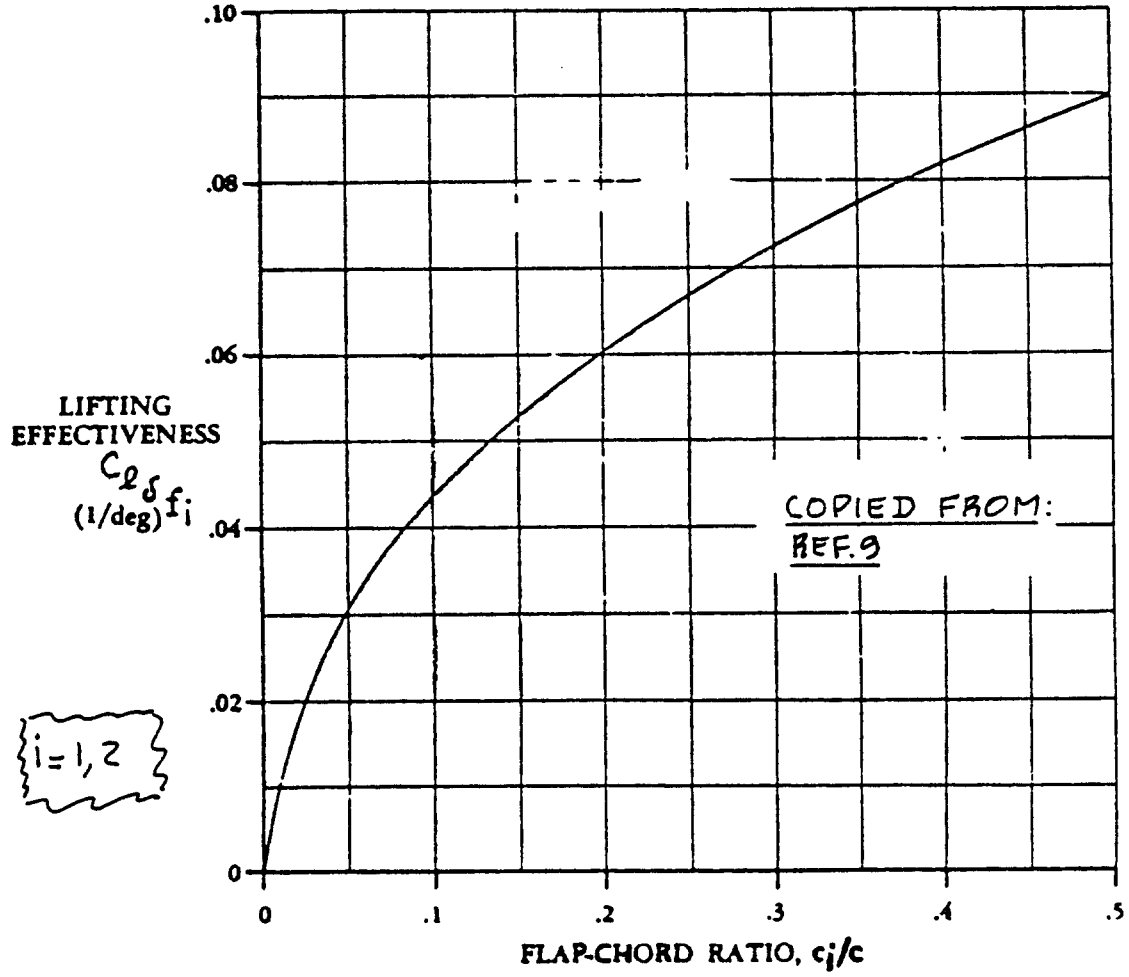

Figure 8.21 Lift Effectiveness for Trailing Edge Flaps

and c_2/c respectively. The effective turning angle, $\bar{\phi}$ is defined as:

for vane: $$\bar{\phi} = \delta_{f_1} + \bar{\phi}_{TE_{upper}} \quad (8.8)$$

for flap segment: $$\bar{\phi} = \delta_{f_1} + \delta_{f_2} + \bar{\phi}_{TE_{upper}} \quad (8.9)$$

with: $$\bar{\phi}_{TE_{upper}} = \arctan\{(10)(y_{90} - y_{100})\} \quad (8.10)$$

where: y_{90} and y_{100} are also defined in Figure 8.19.

$c_{l_{\delta_{f_1}}}$ and $c_{l_{\delta_{f_2}}}$ are found from Figure 8.21 for c_1/c and c_2/c respectively.

Type II:

The incremental lift coefficient due to a Type II double-slotted flap is given by:

$$\Delta c_l = \eta_1 (c_{l_{\delta_{f_1}}})(\delta_{f_1})(c_a'/c) + \eta_2 \eta_t (c_{l_{\delta_{f_2}}})(\delta_{f_2})\{1 + (c'-c_a')/c\} \quad (8.11)$$

where: η_t is found from Figure 8.22.

c' and c_a' are defined in Figure 8.19.

all other quantities are defined under Type I.

e) Split flaps

Figure 8.23 defines the geometry for a split flap. The incremental lift coefficient due to a split flap is given by:

$$\Delta c_l = (c_{l_\alpha})(\alpha_{\delta_{sf}})(\delta_f) \quad (8.12)$$

where: c_{l_α} is found from 8.1.1.2.

$\alpha_{\delta_{sf}}$ is found from Figure 8.24.

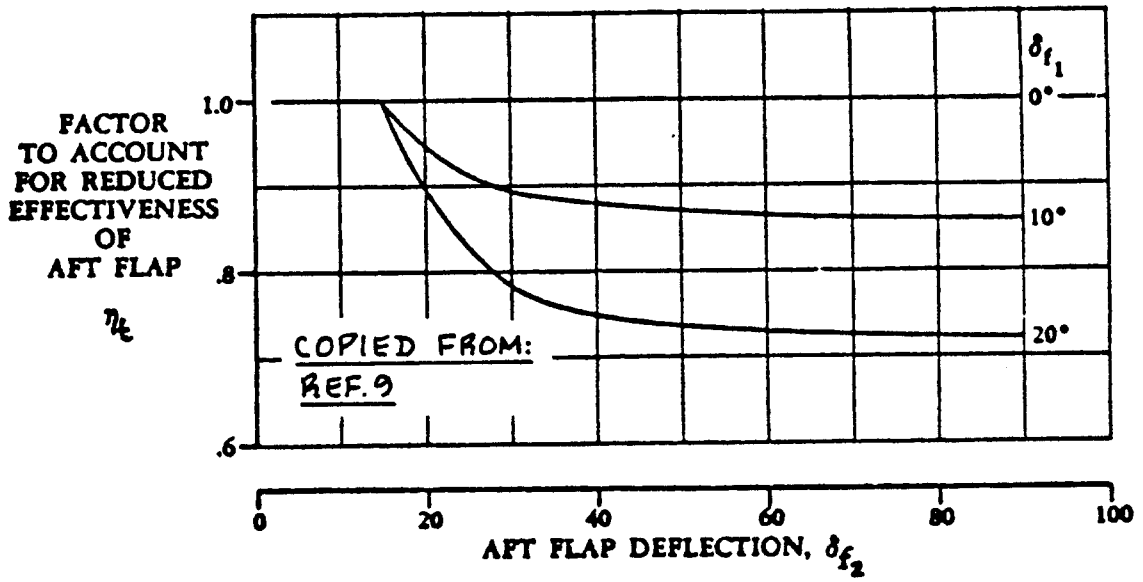

Figure 8.22 Correction Factor for Aft Flap

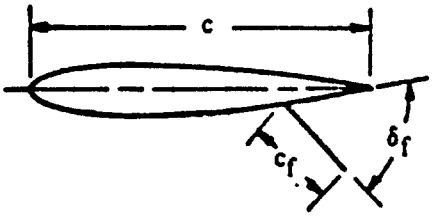

Figure 8.23 Split Flap Geometry

Figure 8.24 Lift Effectiveness of a Split Flap

B) Leading Edge Flaps

a) Nose flaps

Figure 8.25 defines the geometry for a nose flap. The airfoil incremental lift coefficient due to a nose flap deflection is given by:

$$\Delta c_l = c_{l_\delta} \delta_f \qquad (8.13)$$

where: c_{l_δ} is the leading edge flap effectiveness parameter for a nose flap: see Figure 8.26. Use c_f/c as the flap-chord to wing-chord ratio.

δ_f is the nose flap deflection in degrees as defined in Figure 8.25.

b) Krueger Flaps

Figure 8.27 defines the geometry for a Krueger flap. The airfoil incremental lift coefficient due to a Krueger flap is given by:

$$\Delta c_l = c_{l_\delta} \delta_f (c'/c) \qquad (8.14)$$

where: c_{l_δ} is the leading edge flap effectiveness parameter for a Krueger flap: see Figure 8.26. Use c_f/c' as the flap-chord to wing-chord ratio.

δ_f is the Krueger flap deflection in degrees as defined in Figure 8.27.

c'/c is as defined in Figure 8.27.

c) Leading Edge Slats

Figure 8.28 defines the geometry of a leading edge slat. The airfoil incremental lift coefficient due to a leading edge slat is given by:

$$\Delta c_l = c_{l_\delta} \delta_f (c'/c) \qquad (8.15)$$

where: c_{l_δ} is the leading edge flap effectiveness parameter for a leading edge slat as found from Figure 8.26 by using c_f/c' as the leading-edge-slat-chord to wing-chord ratio.

δ_f is the slat deflection in deg.: see Fig. 8.28.

c'/c is as defined in Figure 8.28.

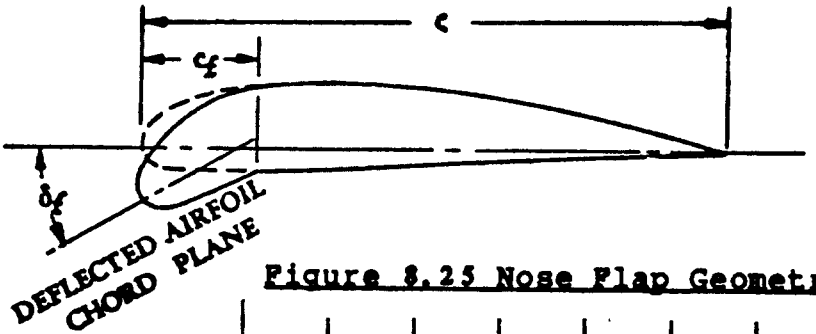

Figure 8.25 Nose Flap Geometry

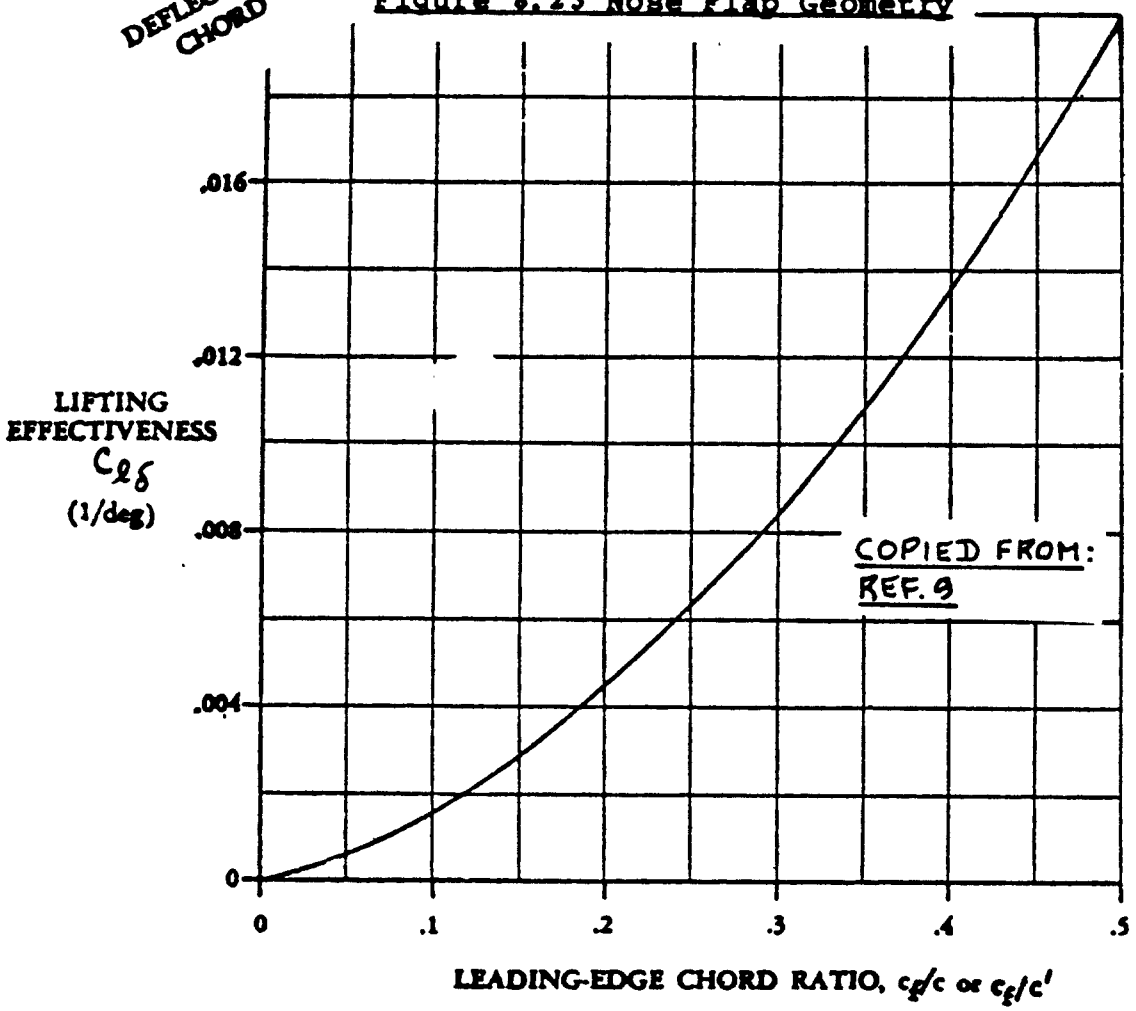

Figure 8.26 Lift Effectiveness of a Leading Edge Flap

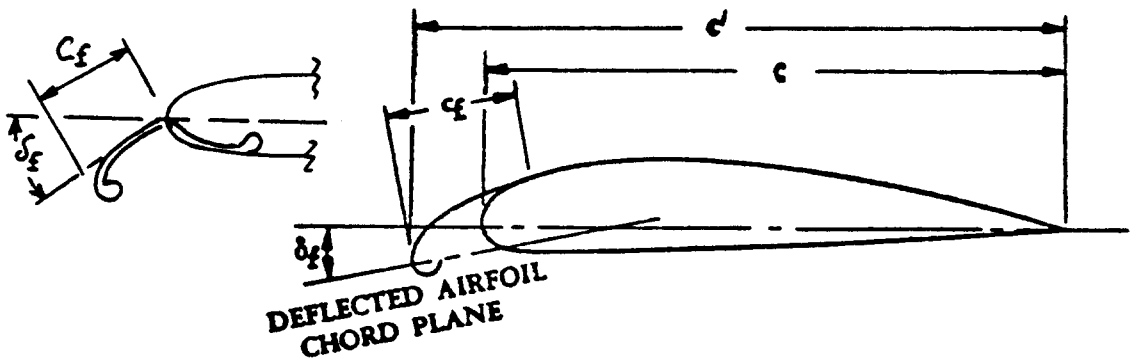

Figure 8.27 Krueger Flap Geometry

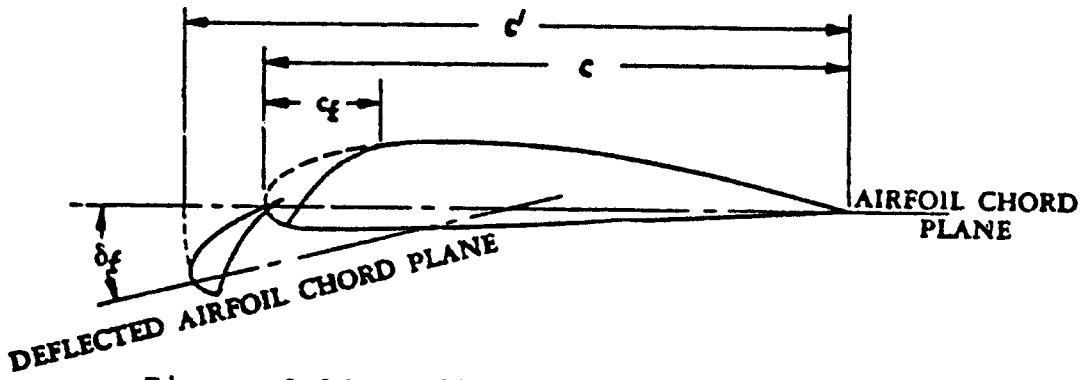

Figure 8.28 Leading Edge Slat Geometry

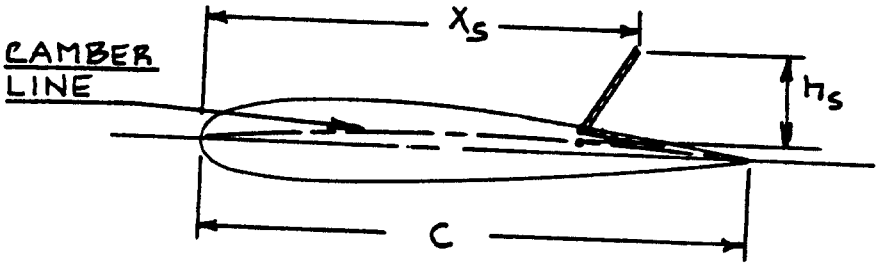

Figure 8.29 Spoiler Geometry

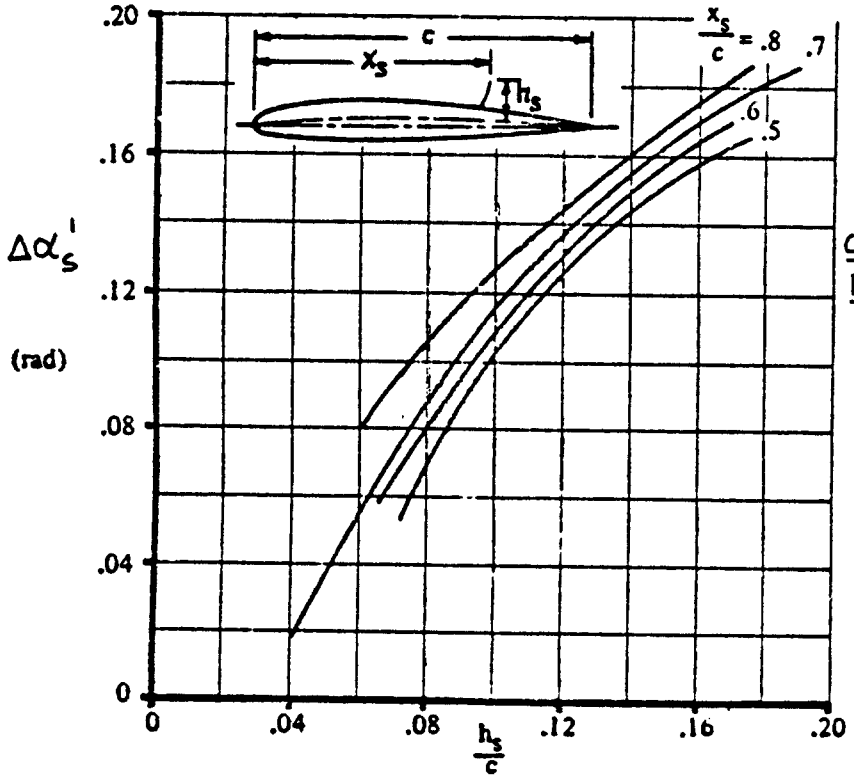

COPIED FROM: REF. 9

Figure 8.30 Lift Effectiveness of a Spoiler

d) Spoilers

Figure 8.29 defines the geometry of a spoiler. Observe that the spoiler is defined by chord position and by vertical position of the spoiler trailing edge. The location of the spoiler hinge line is not important.

The airfoil incremental lift coefficient due to a spoiler deflection is given by:

$$\Delta c_l = -c_{l_\alpha} \Delta\alpha_s' \qquad (8.16)$$

where: c_{l_α} is the unflapped airfoil lift curve slope as found from 8.1.1.2

$\Delta\alpha_s'$ is the spoiler lift effectiveness parameter as found from Figure 8.30.

8.1.2.2 Airfoil lift curve slope due to flaps: $(c_{l_\alpha})_\delta$

As long as the chord length of a flapped airfoil does not change, its lift curve slope does not change either. However, as seen from Figures 8.12, 8.16, 8.19, 8.23, 8.27, 8.28 and 8.29 the flapped airfoil chord is normally larger than the unflapped airfoil chord. For that reason, the flapped airfoil lift curve slope is given by:

$$(c_{l_\alpha})_\delta = (c'/c)c_{l_\alpha} \qquad (8.17)$$

where: c is the chord of the unflapped airfoil

c' is the chord of the flapped airfoil as defined in Figs 8.12, 8.16, 8.23, 8.27, 8.28 or 8.30.

c_{l_α} is the unflapped airfoil lift curve slope as found from 8.1.1.2.

Note: spoiler deflections will be assumed not to alter the lift curve slope of an airfoil.

8.1.2.3 Airfoil maximum lift increment due to flaps: $\Delta c_{l_{max}}$

The magnitude of the maximum lift increment due to flaps depends on the type of flaps used. Methods are presented for trailing edge flaps as well as for leading edge flaps.

A. Trailing Edge Flaps

The airfoil incremental, maximum lift coefficient due to trailing edge flaps is given by:

$$\Delta c_{l_{max}} = k_1 k_2 k_3 (\Delta c_{l_{max}})_{base} \qquad (8.18)$$

where: $(\Delta c_{l_{max}})_{base}$ is the airfoil incremental, maximum lift coefficient due to flaps as determined from Figure 8.31. Note that the data in Figure 8.31 are based on a 25 percent reference flap-chord to airfoil chord ratio AND on a reference flap deflection angle defined in Figure 8.33.

k_1 is a factor which accounts for flap-chord to airfoil chord ratios different from 25 percent. It can be found from Figure 8.32.

k_2 is a factor which accounts for flap angles different from the reference flap angle. It can be found from Figure 8.33.

k_3 is a factor which accounts for flap motion as a function of flap deflection. It can be found from Figure 8.34.

B) Leading Edge Flaps

The airfoil incremental, maximum lift coefficient due to leading edge flaps is given by:

$$\Delta c_{l_{max}} = (c_{l_{\delta_{max}}}) \eta_{max} \delta_f (c'/c) \qquad (8.19)$$

where: $c_{l_{\delta_{max}}}$ is the theoretical maximum lifting effectiveness as found from Figure 8.35.

η_{max} is an empirical factor which accounts for the ratio of airfoil leading edge radius to airfoil thickness of the unflapped airfoil. It is obtained from Figure 8.36.

η_δ is an empirical factor which accounts for the difference between the actual leading edge flap deflection and the reference deflection. It is found from Figure 8.37.

δ_f is the leading edge flap deflection angle in

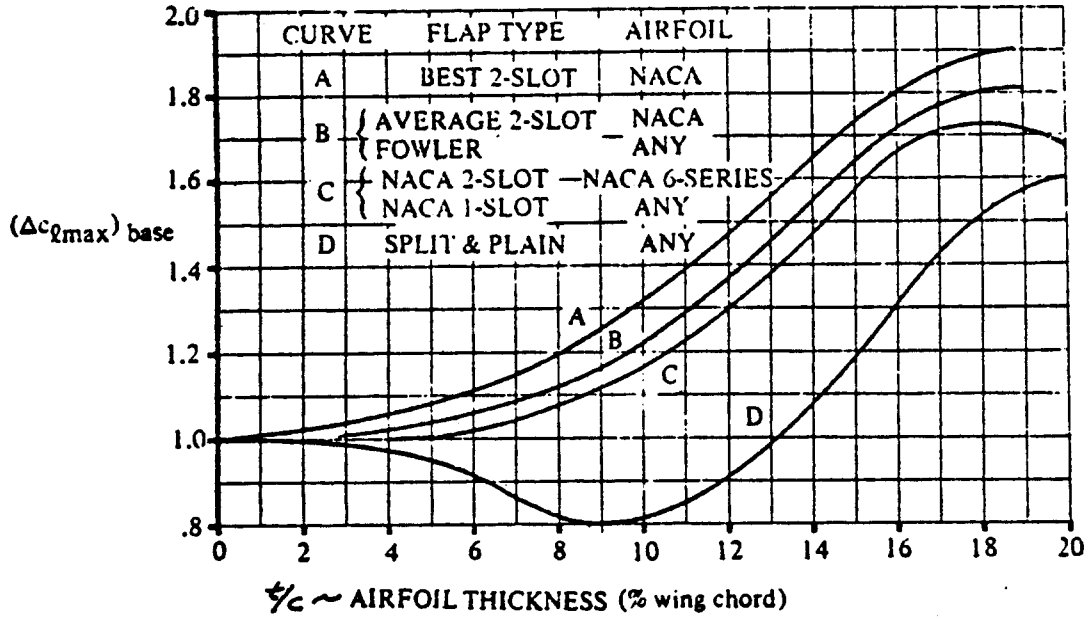

COPIED FROM REF.9

Figure 8.31 Basic Airfoil Maximum Lift Increment due to Trailing Edge Flaps

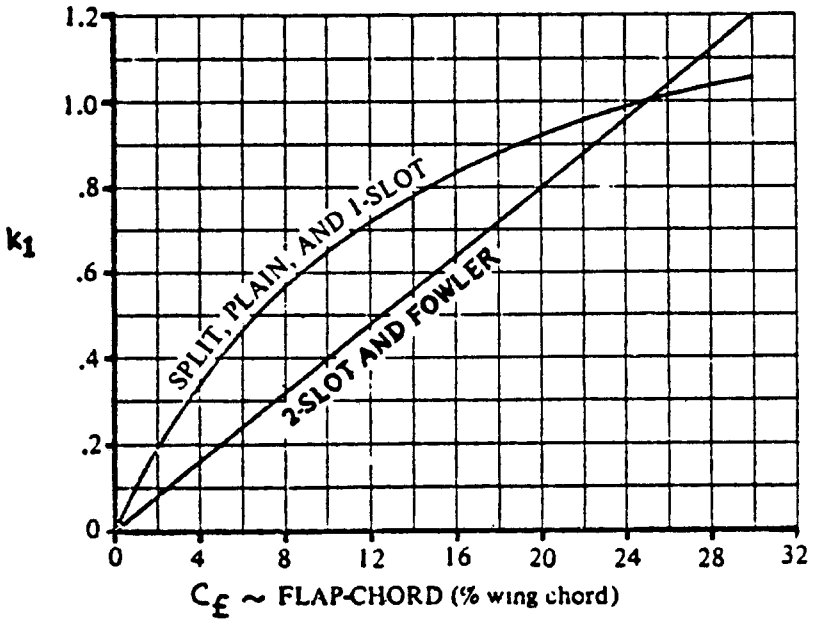

COPIED FROM: REF.9

Figure 8.32 Flap Chord Correction Factor

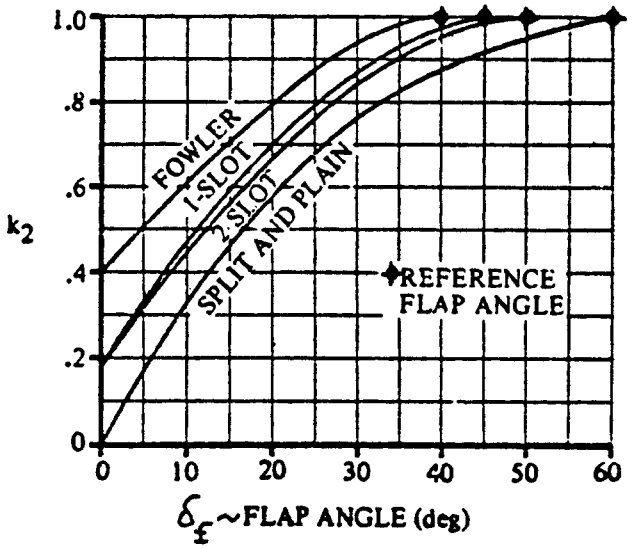

Figure 8.33 Flap Angle Correction Factor

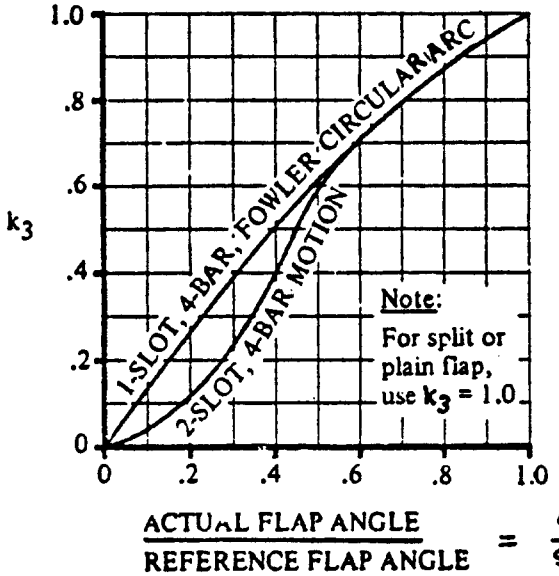

COPIED FROM: REF. 9

Figure 8.34 Flap Motion Correction Factor

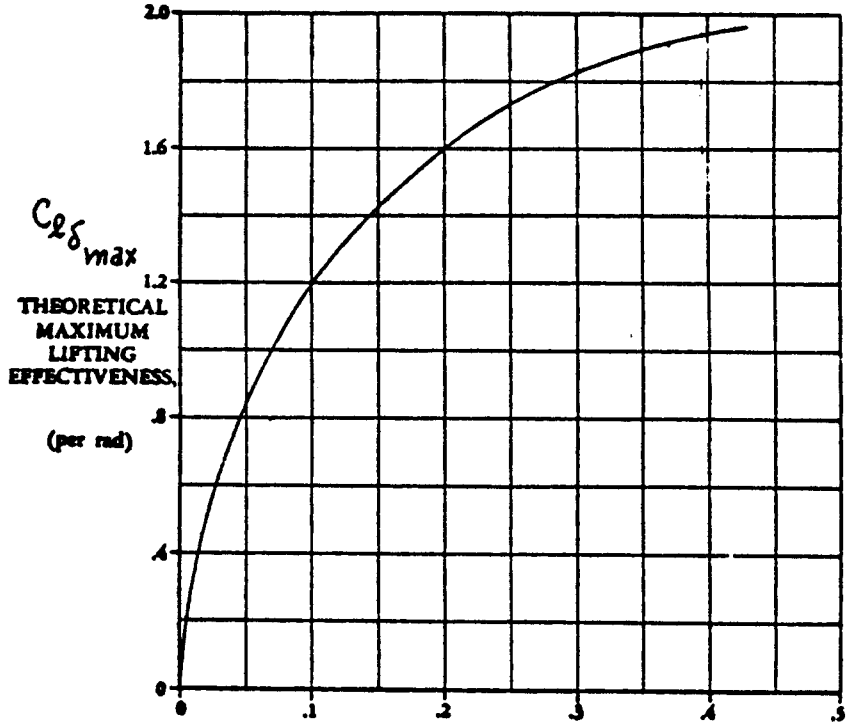

COPIED FROM: REF. 9

Figure 8.35 Maximum Lift Effectiveness for Leading Edge Flaps

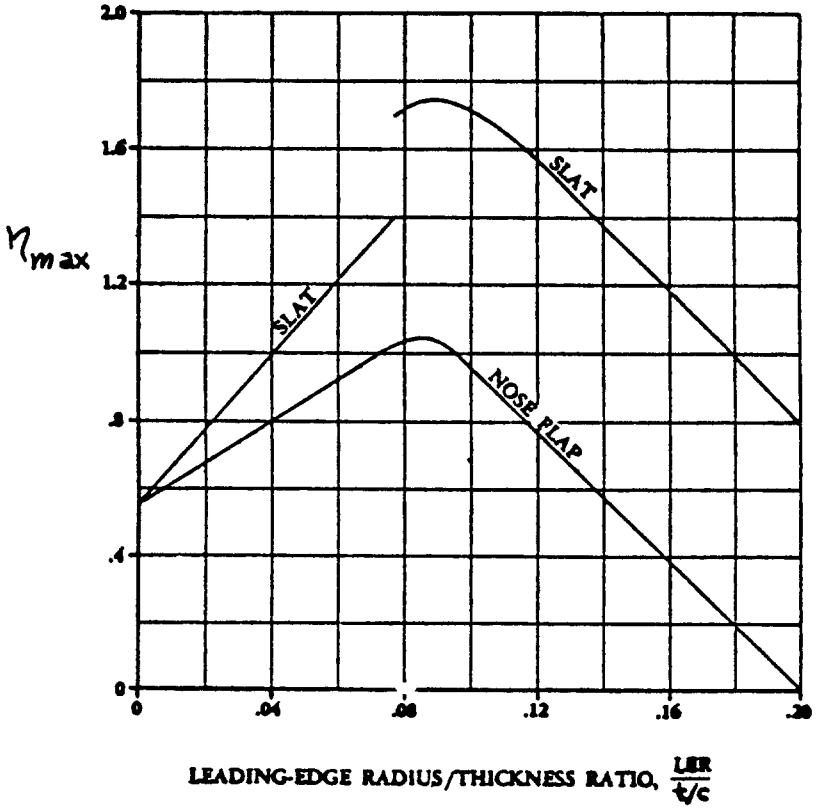

COPIED FROM: REF. 9

Figure 8.36 Effect of Leading Edge Radius and Thickness Ratio on Maximum Lift of Leading Edge Flaps

radians as shown in Figure 8.25, 8.27 or 8.28.

c'/c is the ratio of the airfoil chord with leading edge flaps extended to the basic airfoil chord.

8.1.2.4 Construction of airfoil lift curve: flaps down

All ingredients needed to construct the flaps-down airfoil c_l versus α curve are now available. The flaps-down curve in Figure 8.2 can therefore be constructed. Figure 8.38 shows how this is done in a step-by-step manner. Since no empirical method for the determination of α^* has been presented, the fairing between the linear range and the maximum lift point must be done by guestimation.

The following groundrules are useful:

Trailing edge flaps: the angle of attack for maximum lift with trailing edge flaps down is normally below that for the basic airfoil.

Leading edge flaps: the angle of attack for maximum lift with leading edge flaps down is normally above that for the basic airfoil.

All flaps: the flap deflection angle beyond which the flap lift increment Δc_l ceases to be linear depends on detailed attention paid to flap contour and flap gap design. Table 8.3 provides some guidelines for flap deflection ranges for which linear behavior is expected.

Table 8.3 Linear Flap Effectiveness Range at Low Angles of Attack for Trailing Edge Flaps

Flap Type	δ_f (deg)	
	Poor Design	Good Design
Plain	0 to 10	0 to 20
Single Slotted and Fowler	0 to 20	0 to 30
Double Slotted	0 to 30	0 to 60
Split	0 to 30 or 45	

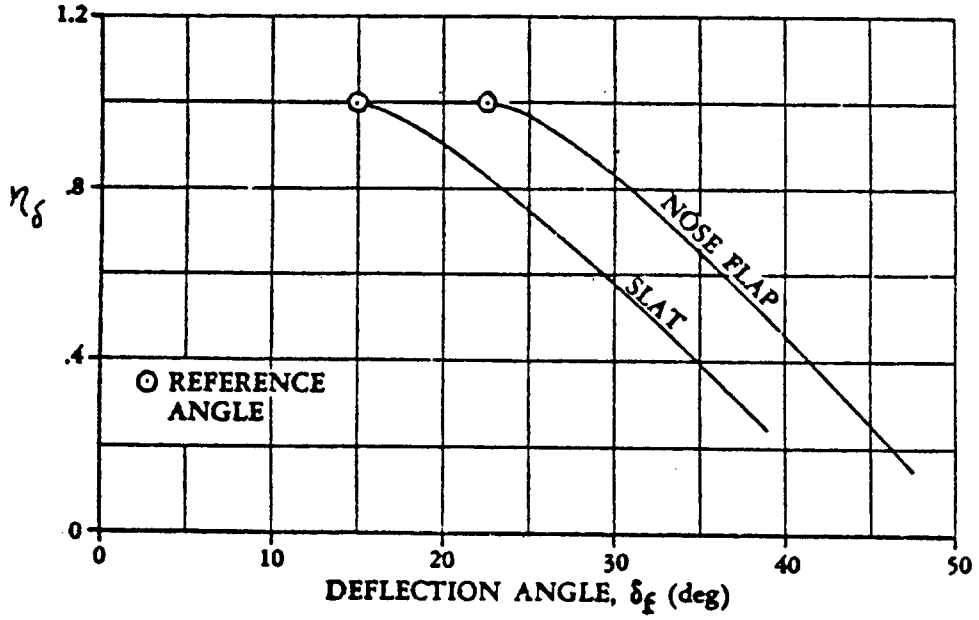

Figure 8.37 Effect of Leading Edge Flap Deflection on Maximum Lift

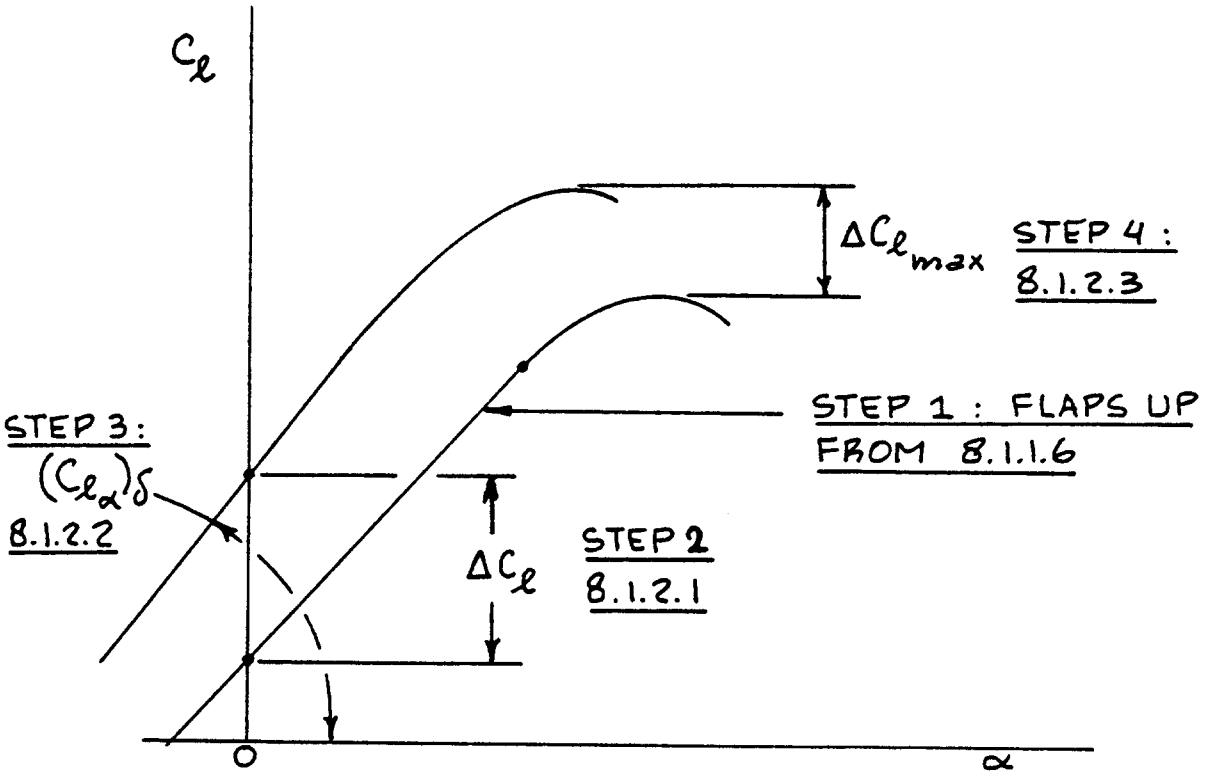

Figure 8.38 Construction of Flaps Down Airfoil Lift Versus α Curve

8.1.3 Wing Lift and Maximum Lift: Flaps Up

Figure 8.39 shows the relationship between wing lift coefficient and wing angle of attack which must be determined with the methods to be presented in this section. Key quantities needed in the construction of the wing C_{L_w} versus α_w curve are listed, with an indication of where methods for their estimation may be found.

8.1.3.1 Wing zero-lift angle of attack: $\alpha_{o_{L_w}}$

The wing angle of attack, α_w is defined as follows:

$$\alpha_w = \alpha - i_w \qquad (8.20)$$

where: α is the airplane angle of attack and

i_w is the wing incidence angle

Figure 8.40 shows how these quantities relate to each other on an airplane. Criteria for the selection of the wing incidence angle, i_w are discussed in Part III, p.195.

For subsonic speeds:

For wings with constant airfoil sections and linear twist distributions the wing zero-lift angle of attack may be estimated from:

$$\alpha_{o_{L_w}} = \{\alpha_{o_l} + (\Delta\alpha_o/\varepsilon_t)\varepsilon_t\}\{(\alpha_{o_l})_{\text{at } M}\}/\{(\alpha_{o_l})_{\text{at } M=0.3}\} \qquad (8.21)$$

where: α_{o_l} is found from 8.1.1.1

$(\Delta\alpha_o/\varepsilon_t)$ is the change in wing zero-lift angle of attack per degree of linear wing twist: See Figure 8.41.

ε_t is the wing twist angle: see Figure 8.41. Criteria for the selection of wing twist angle are presented in Part III, p.193.

$\{(\alpha_{o_l})_{\text{at } M}\}\{(\alpha_{o_l})_{\text{at } M=0.3}\}$ is found from Fig. 8.42.

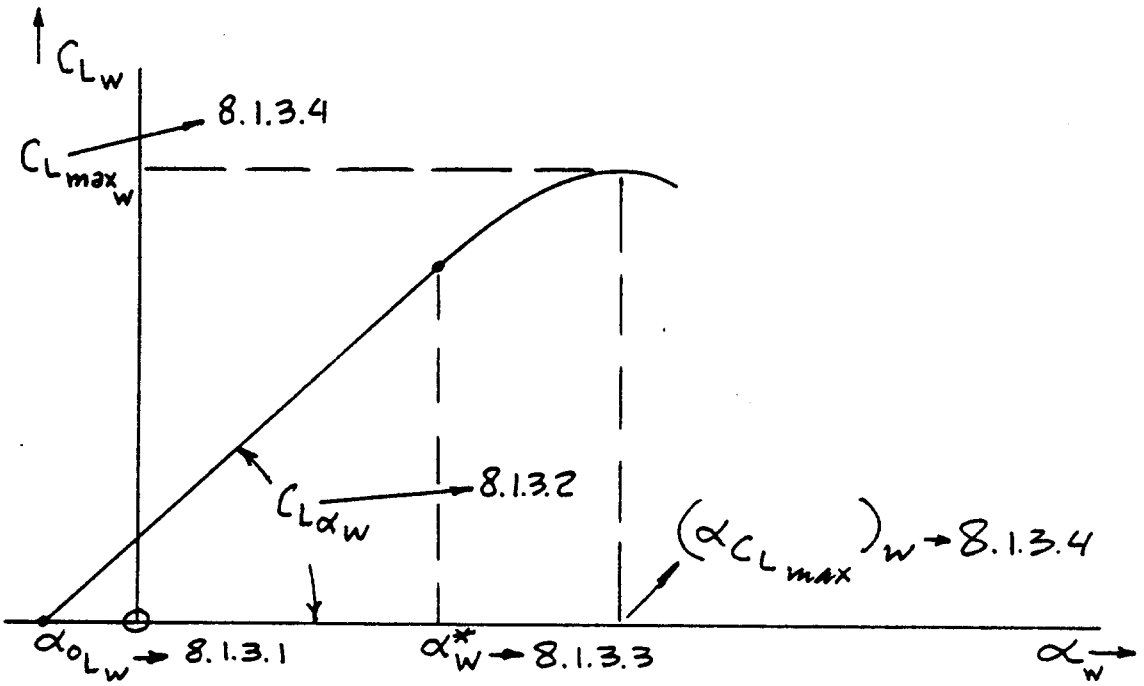

Figure 8.39 Wing Lift Coefficient Versus Angle of Attack Curve

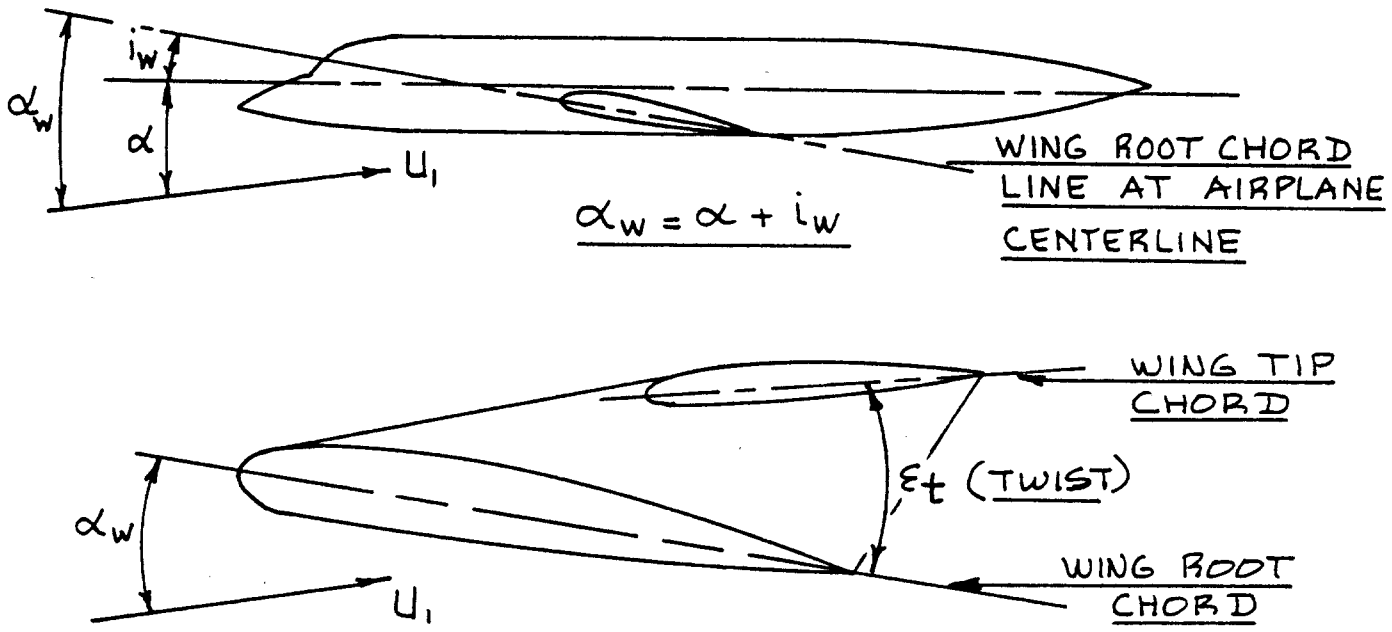

Figure 8.40 Relationship Between Wing Incidence, Wing Angle of Attack and Airplane Angle of Attack

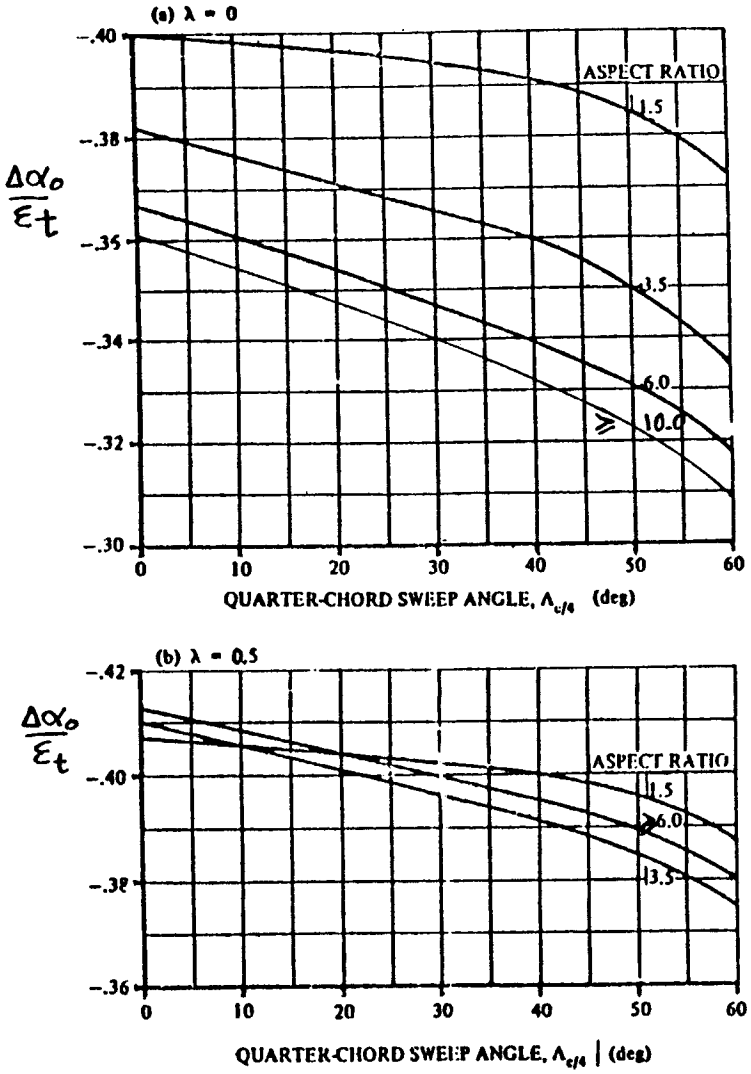

COPIED FROM REF. 9

Figure 8.41 Effect of Linear Twist on Wing Angle of Attack for Zero Lift

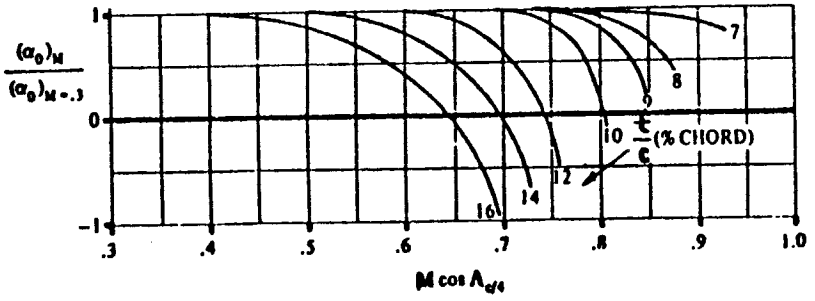

Figure 8.42 Mach Number Correction for Zero-Lift Angle of Attack of Cambered Airfoils

For transonic and supersonic speeds:

In the transonic and supersonic speed ranges experimental data should be used.

8.1.3.2 Wing lift curve slope: $C_{L_{\alpha_W}}$

For subsonic speeds:

For conventional, straight tapered wings, with 'moderate' sweep angles, the lift curve slope may be estimated from Figures 8.43 or from:

$$C_{L_{\alpha_W}} = 2\pi A/[2 + \{A^2\beta^2/k^2(1 + \tan^2\Lambda_{c/2}/\beta^2) + 4\}^{1/2}] \quad (8.22)$$

where: $A = b^2/S$ is the wing aspect ratio - (8.23)

Wing aspect ratio may have to be computed for the so-called 'equivalent' wing planform: See Figure 8.44.

$$\beta = (1 - M^2)^{1/2} \quad (8.24)$$

$$k = (c_{l_\alpha})_{at\ M}/2\pi \quad (8.25)$$

where $(c_{l_\alpha})_{at\ M}$ follows from Eqn.(8.1).

$\Lambda_{c/2}$ is the semi-chord sweep angle. Relations between semi-chord, quarter-chord and leading edge sweep angles are defined in Figures 8.45 and 8.46.

For transonic speeds: see Reference 9.

For supersonic speeds: See Figures 8.47. Note: these figures apply only for low angles of attack.

Methods for estimating wing lift curve slopes for arbitrary wing planforms are presented in Reference 9.

8.1.3.3 Wing linear range of angle of attack: α_W^*

In preliminary design it is acceptable to use:

$\alpha_W^* = \alpha^*$ as found from 8.1.1.3.

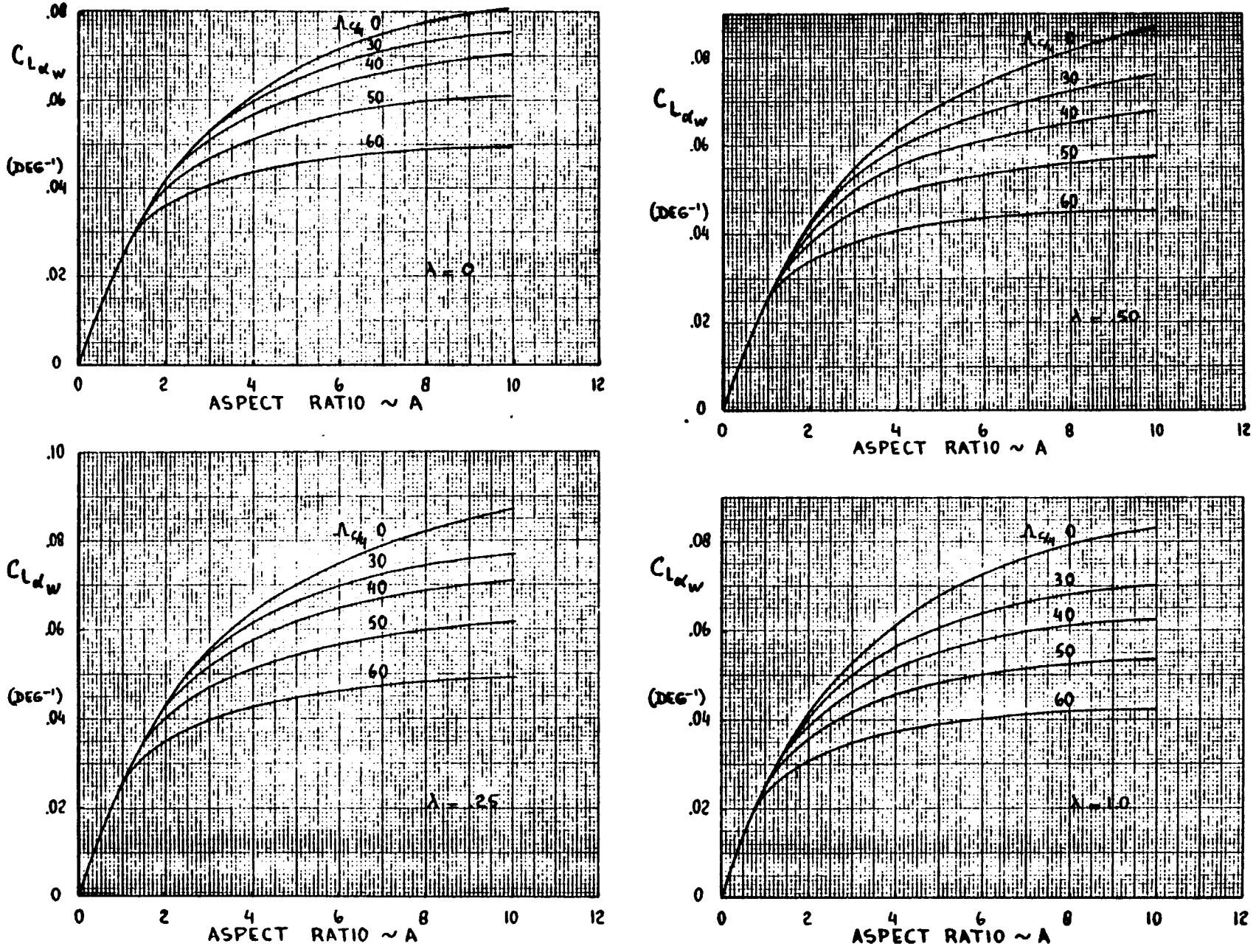

Figure 8.43 Wing Lift Curve Slope at Low Mach Numbers

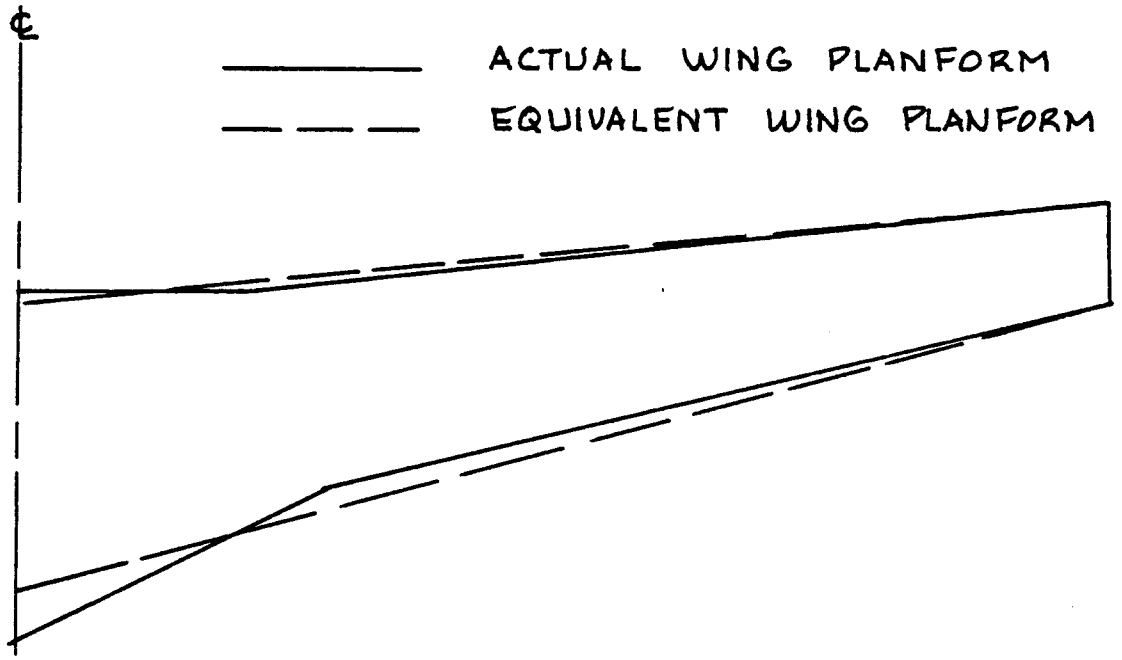

Figure 8.44 Example of an Equivalent Wing Planform

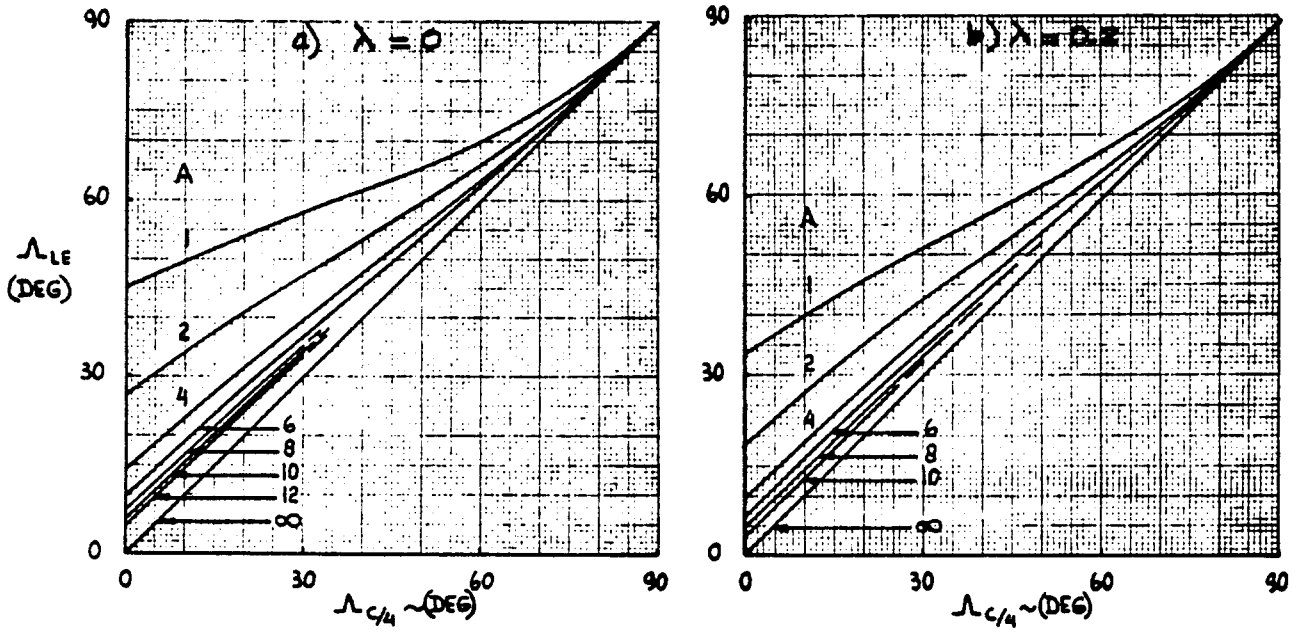

Figure 8.45 Leading Edge Sweep Angle Versus Quarter Chord Sweep Angle for Straight Tapered Wings

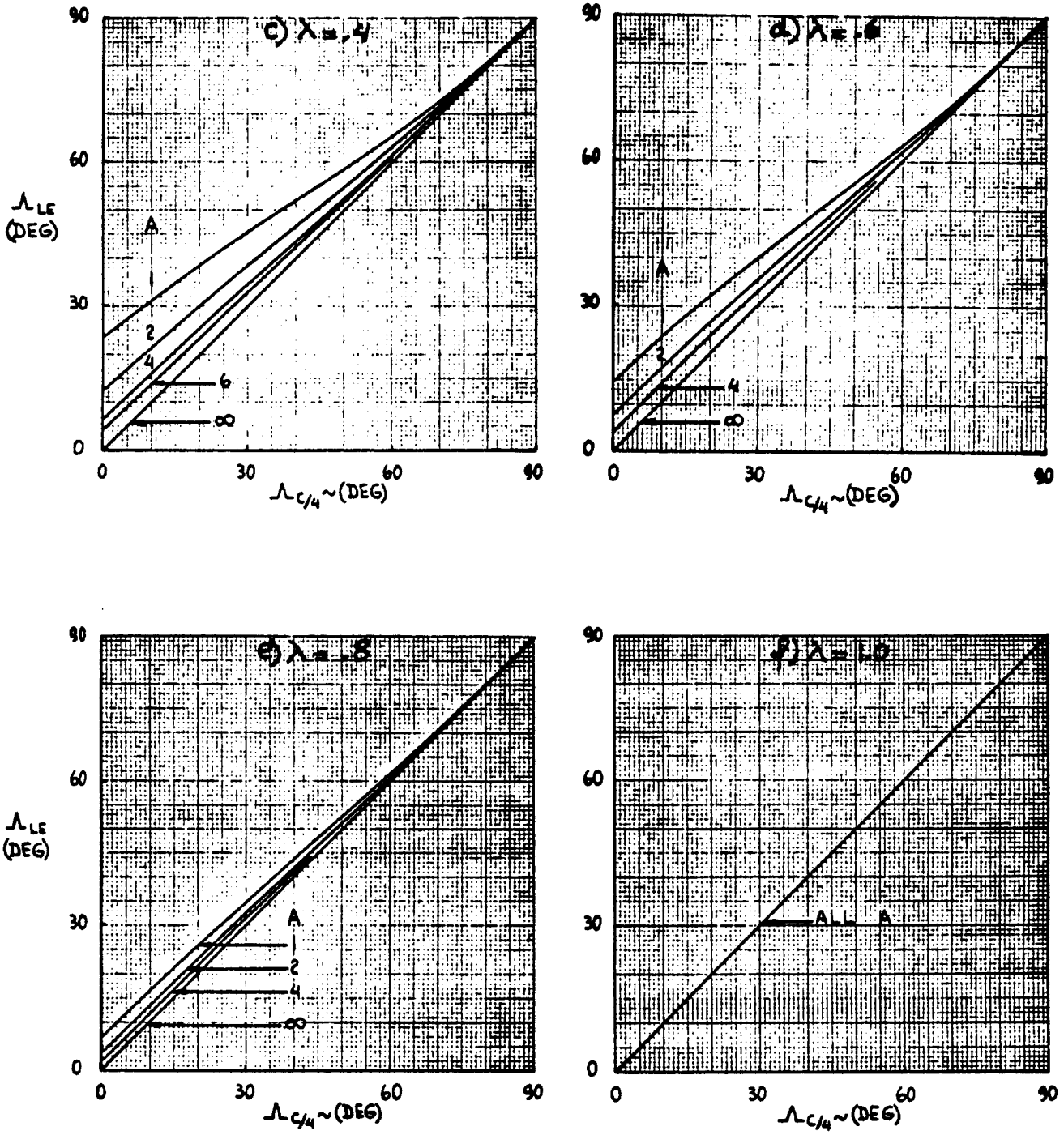

Figure 8.45 (Cont'd) Leading Edge Sweep Angle Versus Quarter Chord Sweep Angle for Straight Tapered Wings

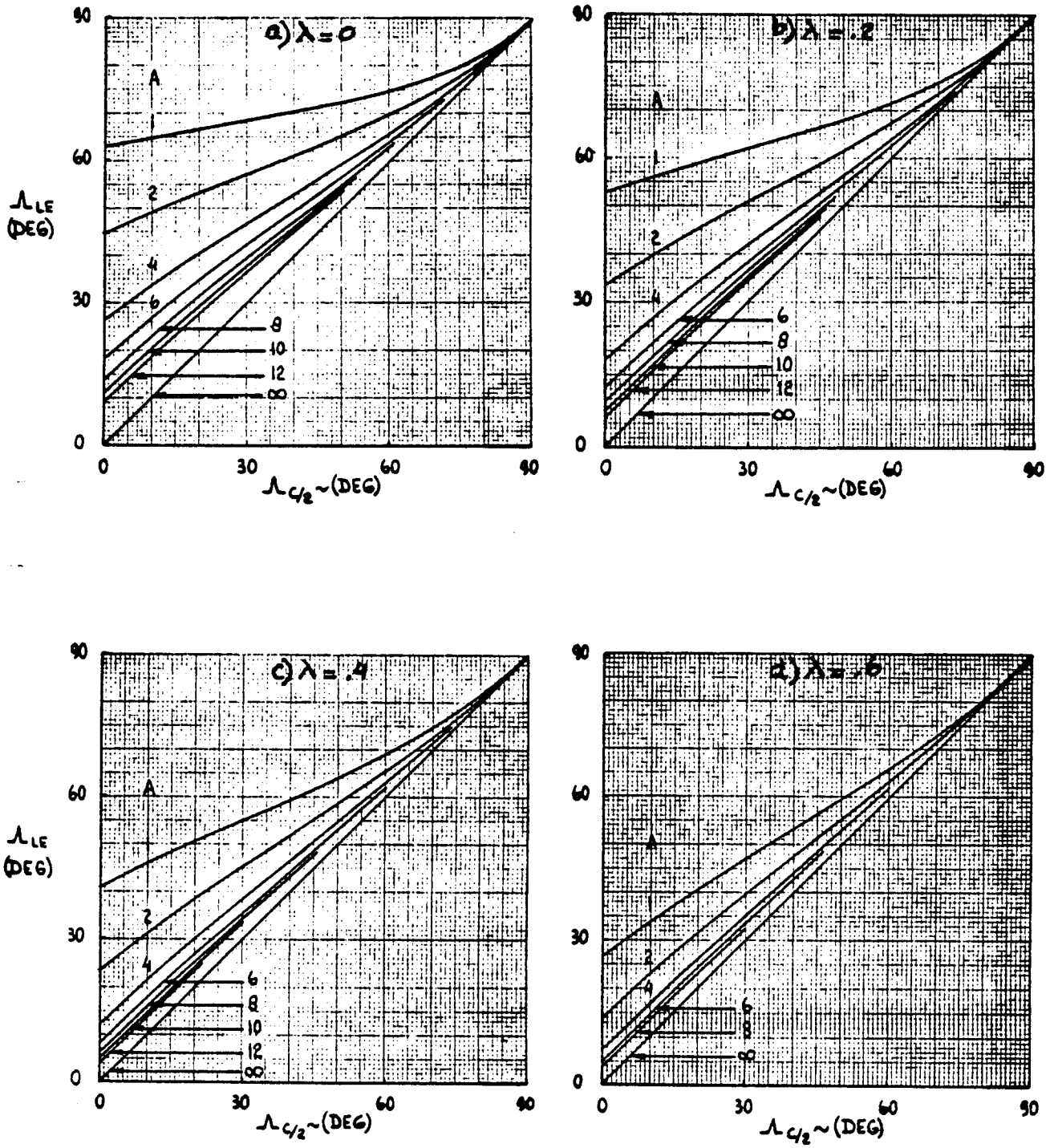

Figure 8.46 Leading Edge Sweep Angle Versus Semi-chord Sweep Angle for Straight Tapered Wings

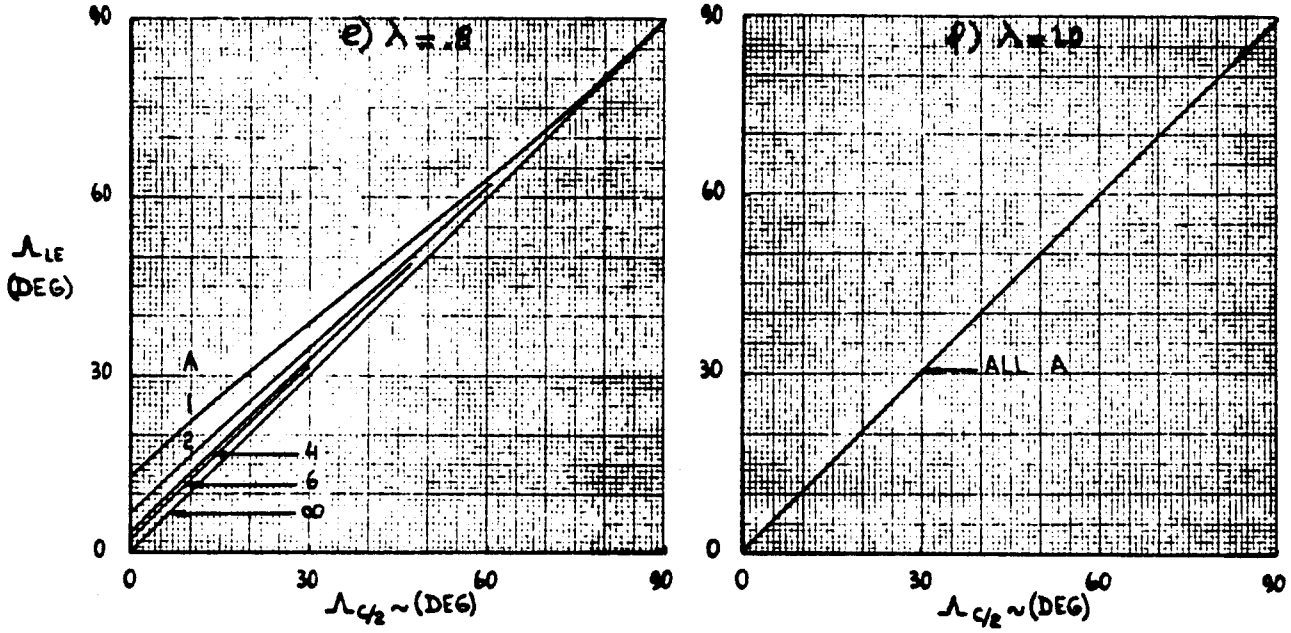

Figure 8.46 (Cont'd) Leading Edge Sweep Angle Versus Semi-chord Sweep Angle for Straight Tapered Wings

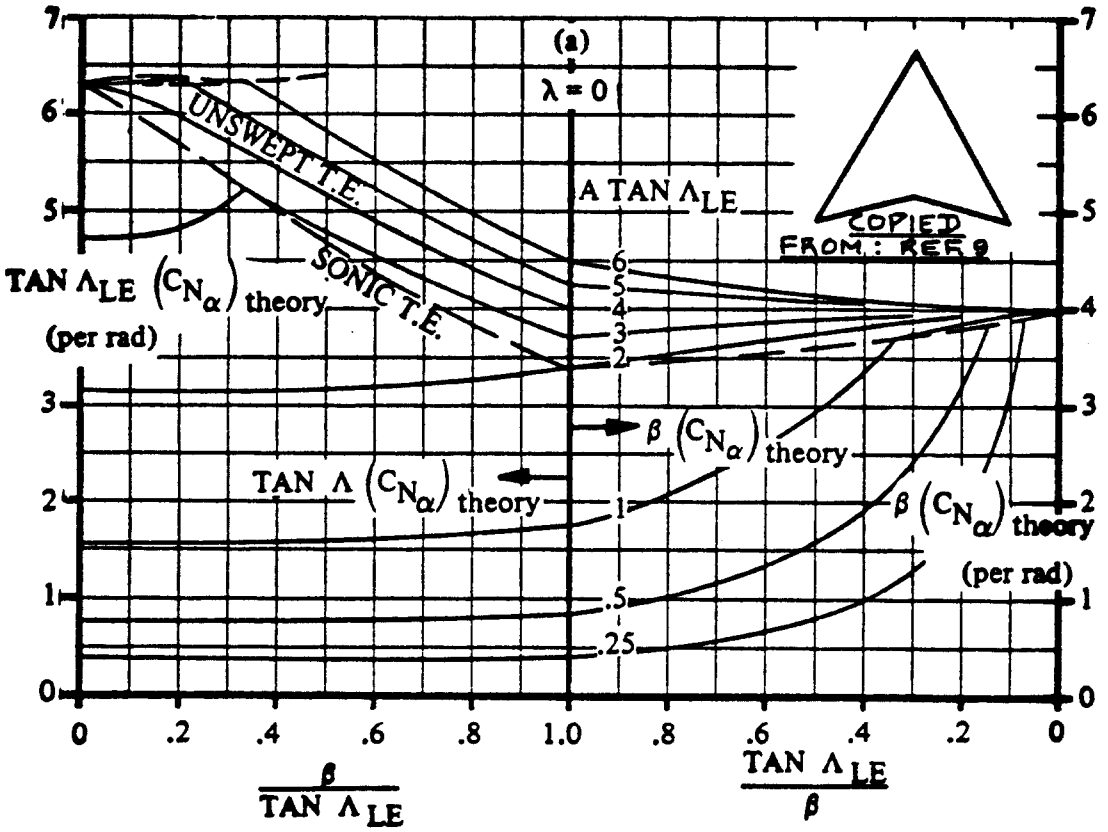

Figure 8.47a Wing Lift Curve Slope for Supersonic Mach Numbers and Low Angle of Attack

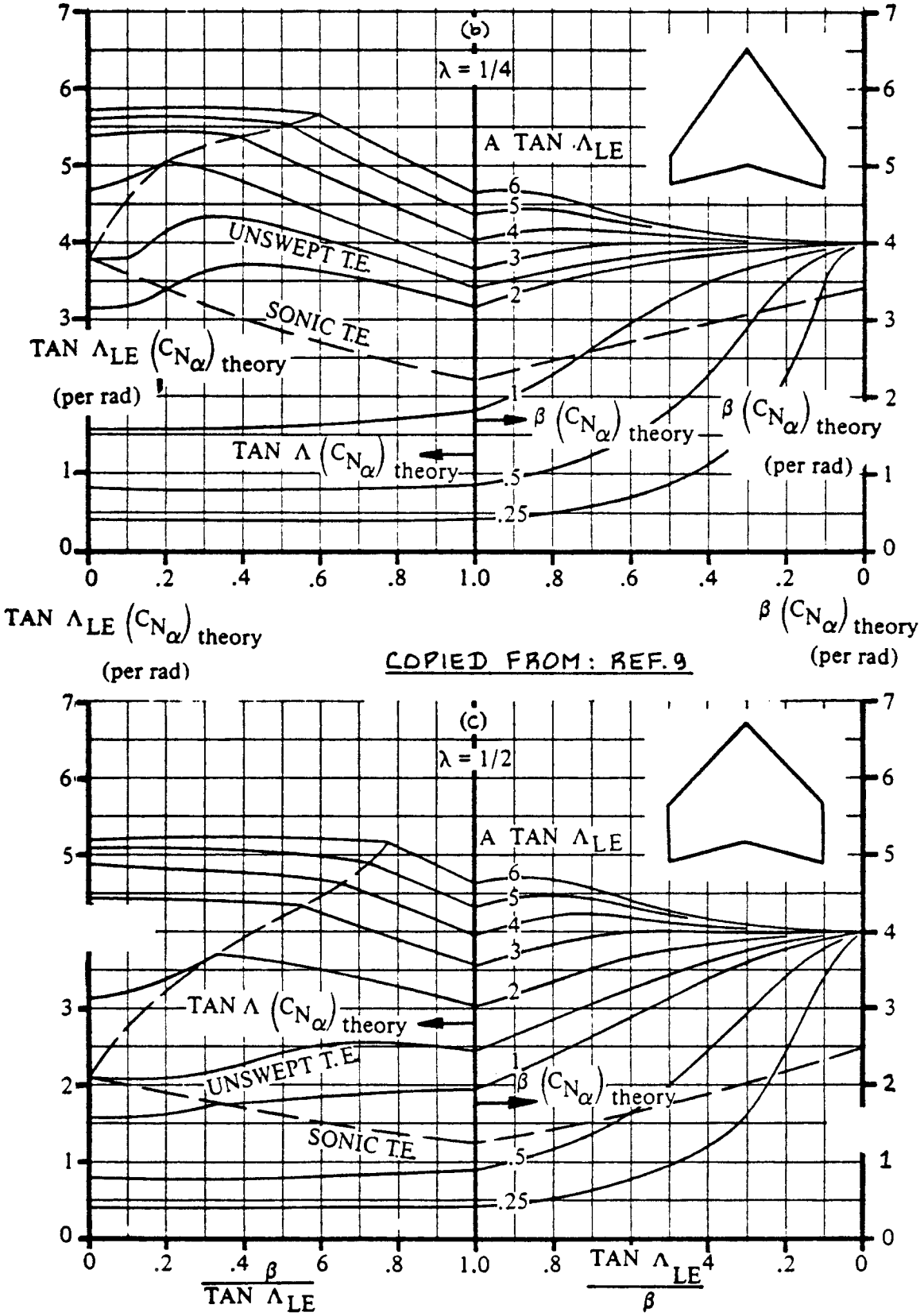

COPIED FROM: REF. 9

Figure 8.47b Wing Lift Curve Slope for Supersonic Mach Numbers and Low Angle of Attack

HINTS FOR USING FIGURES 8.47 a, b, AND c:

Note: for low angles of attack:

$$C_{L_\alpha} = C_{N_\alpha}$$

Note: $C_{N_\alpha} = (C_{N_\alpha})_{theory}\{(C_{N_\alpha})/(C_{N_\alpha})_{theory}\}$,

where: $(C_{N_\alpha})_{theory}$ follows from Figures 8.47a or 8.47b

$\{(C_{N_\alpha})/(C_{N_\alpha})_{theory}\}$ follows from Figure 8.47c

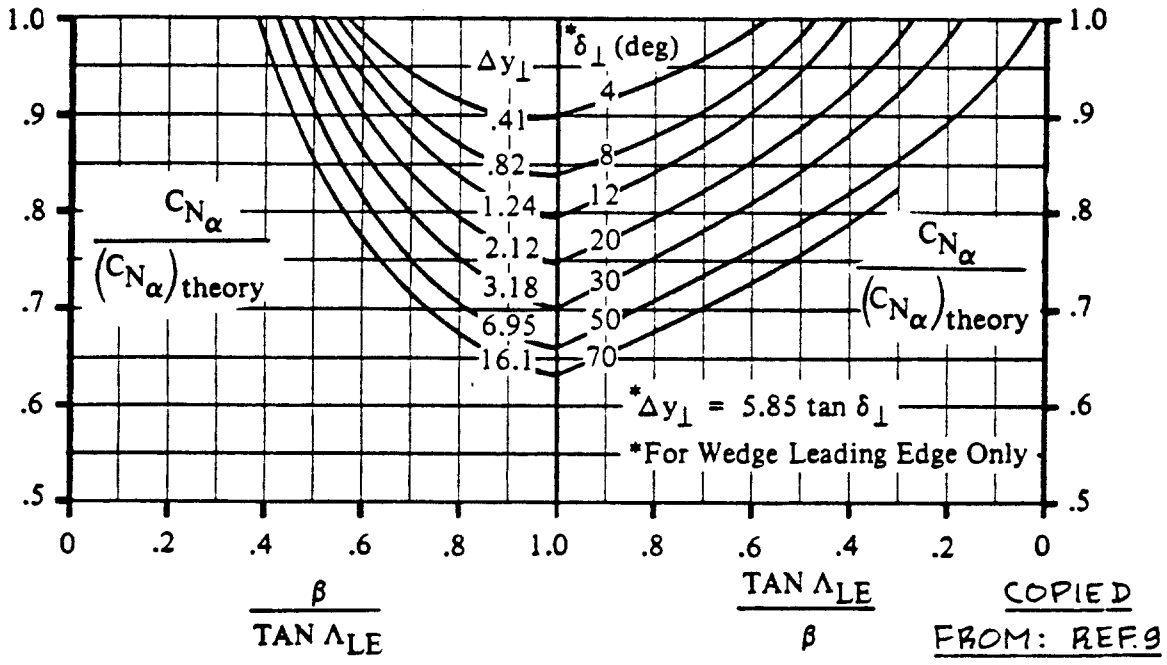

COPIED FROM: REF.9

Figure 8.47c Wing Lift Curve Slope Correction Factor for Wings with Sonic Leading Edge Regions

8.1.3.4 Wing maximum lift coefficient: $C_{L_{max_w}}$ and wing angle of attack for maximum lift: $(\alpha_{C_{L_{max}}})_w$

In this section, the assumption is made that the reader has available a computer program for the calculation of the spanwise lift coefficient distribution for a given wing angle of attack, α_w as defined by Eqn.(8.20).

Methods for finding spanwise distributions of lift coefficient with angle of attack can be found in:

Reference 49: Chapter 1: this method applies to unswept wings at subsonic Mach numbers. However, by using the cosine rule, this method will work for sweep angles up to 35 degrees.

Reference 52: this method applies to arbitrary wing planforms at subsonic speeds.

To estimate the maximum wing (flaps-up) lift coefficient, the following step-by-step procedure is suggested:

Step 1: Determine the spanwise distribution of section maximum lift coefficient. Plot this as shown in Figure 8.48. Note: the section maximum lift coefficient at each spanwise station is found from Section 8.1.1.5 or from airfoil data.

NOTE: at each spanwise station the Reynold's number will be different!

Step 2: With the help of either Ref.49, Ref.52 or with the help of a spanwise-lift computer program, plot the spanwise variation in local section lift coefficient for increasing values of wing angle of attack. Note that at some value of α_w the spanwise plot of

of c_l is tangent to the spanwise plot of

$c_{l_{max}}$ as obtained from Step 1. That value of wing angle of attack is: $(\alpha_{C_{L_{max}}})_w$.

Fig.8.48 also shows the resulting plot(s).

Step 3: Calculate the wing maximum lift coefficient from:

$$C_{L_{max_w}} = (1/S)\int_0^{1.0} bc(c_{l_{w_{stall}}})d\eta \qquad (8.26)$$

where $c_{l_{w_{stall}}}$ is the spanwise value of the local section lift coefficient at:

$$\alpha_w = (\alpha_{C_{L_{max}}})_w$$

Important note: the magnitude of $C_{L_{max_w}}$ is always below that of the magnitude of $c_{l_{max}}$ of any wing airfoil.

8.1.3.5 Construction of wing lift curve: flaps up

All ingredients for constructing the wing lift curve are now available. Figure 8.49 shows how this can be done in a stepwise manner.

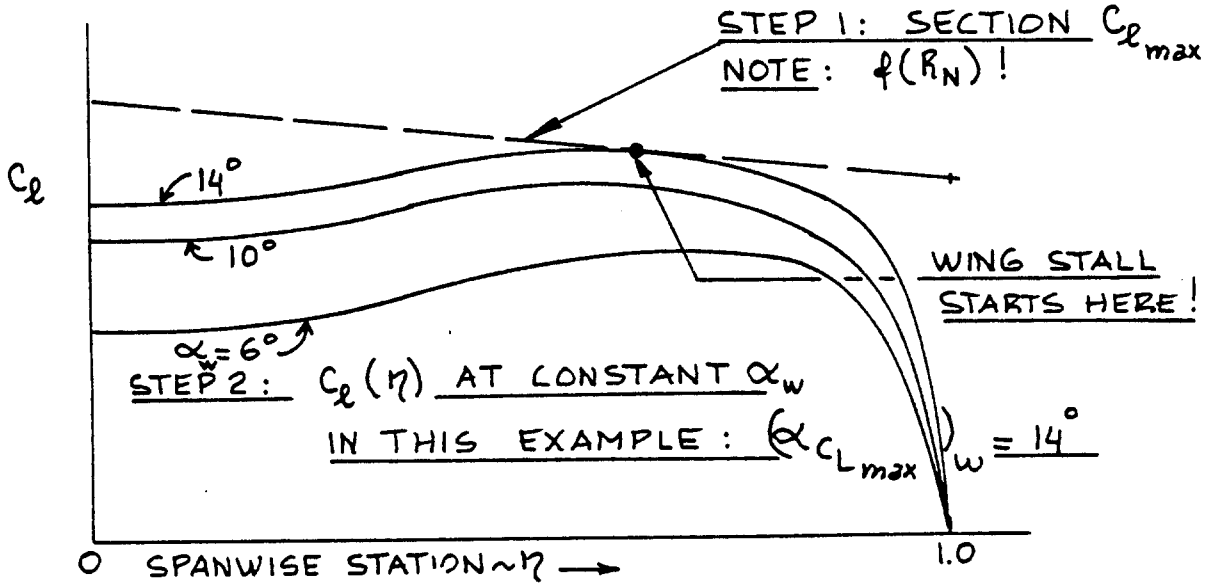

Figure 8.48 Section Maximum Lift Coefficient and Section Lift Coefficient at a Given Angle of Attack Versus Spanwise Position on a Wing

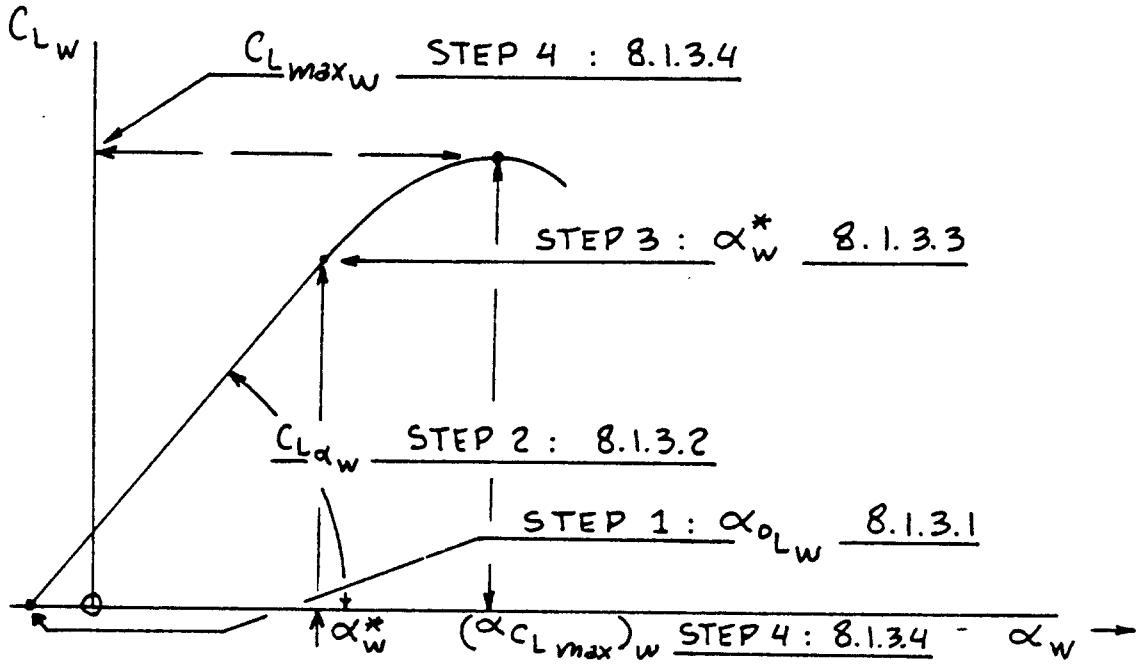

Figure 8.49 Construction of Flaps Up Wing Lift Versus Angle of Attack Curve

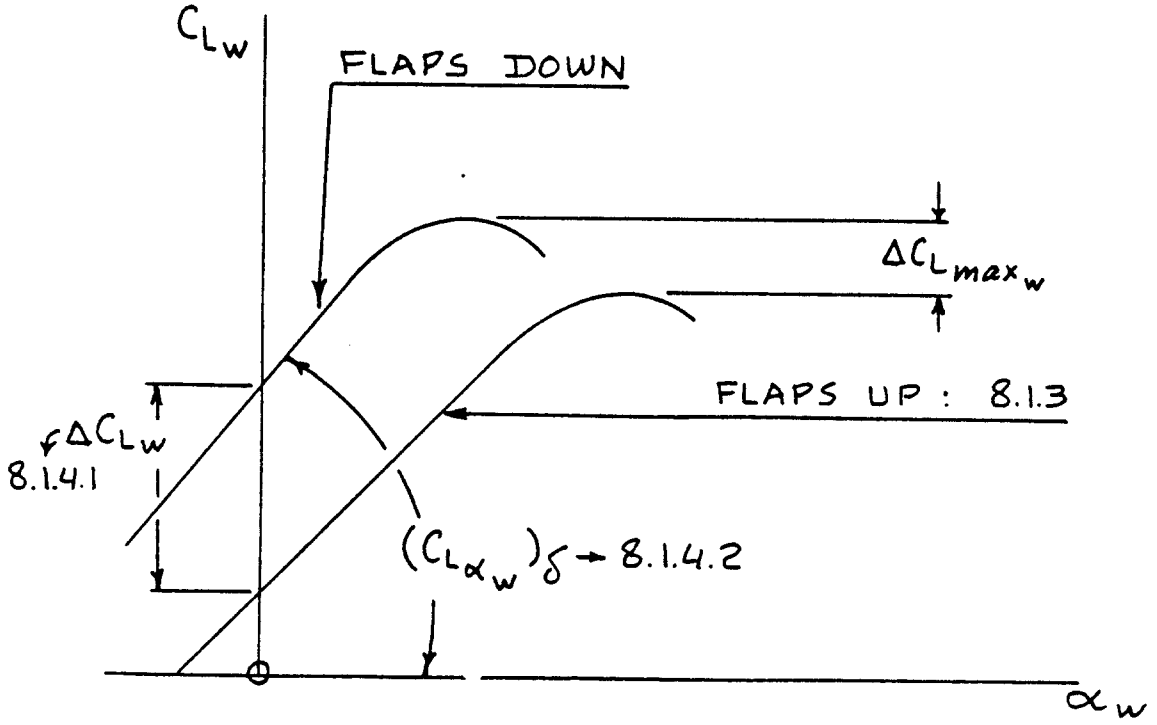

Figure 8.50 Fundamental Wing Lift Versus α Curve with the Flaps Down

8.1.4 Wing Lift and Maximum Lift: Flaps Down

Figure 8.50 shows the relationship between flaps up and flaps down wing lift characteristics. Key quantities needed in the construction of the flaps down wing C_{L_w} versus α_w curve are listed, with an indication of where methods for their estimation may be found.

8.1.4.1 Wing lift increment due to flaps: ΔC_{L_w}

The wing lift increment due to trailing edge and/or leading edge flaps may be estimated from:

$$\Delta C_{L_w} = K_b (\Delta c_l)(C_{L_{\alpha_w}}/c_{l_\alpha}) \left[\{(\alpha_\delta)_{C_L}\}/\{(\alpha_\delta)_{c_l}\}\right] \qquad (8.27)$$

where: K_b is the flap-span factor as obtained from the procedure suggested in Figure 8.51 but with the data from Figure 8.52.

Δc_l is the airfoil lift increment due to flaps as obtained from 8.1.2.1.

$C_{L_{\alpha_w}}$ is the wing lift curve slope as obtained from 8.1.3.2.

c_{l_α} is the wing airfoil lift curve slope as obtained from 8.1.1.2.

$\frac{(\alpha_\delta)_{C_L}}{(\alpha_\delta)_{c_l}}$ is the ratio of the three-dimensional flap-effectiveness parameter to the two-dimensional flap-effectiveness parameter as found in Figure 8.53.

Note: If a mechanical high lift system consists of a combination of leading and trailing edge high lift devices, the method should be applied to each type of device separately. The resulting increments in lift coefficients can then be added.

8.1.4.2 Wing lift curve slope due to flaps: $(C_{L_{\alpha_w}})_\delta$

Wings with NON-TRANSLATING flap systems:

For wings with NON-TRANSLATING flap systems (such as split flaps, plain flaps and nose flaps), the wing lift curve slope flaps-down is considered to be the same as

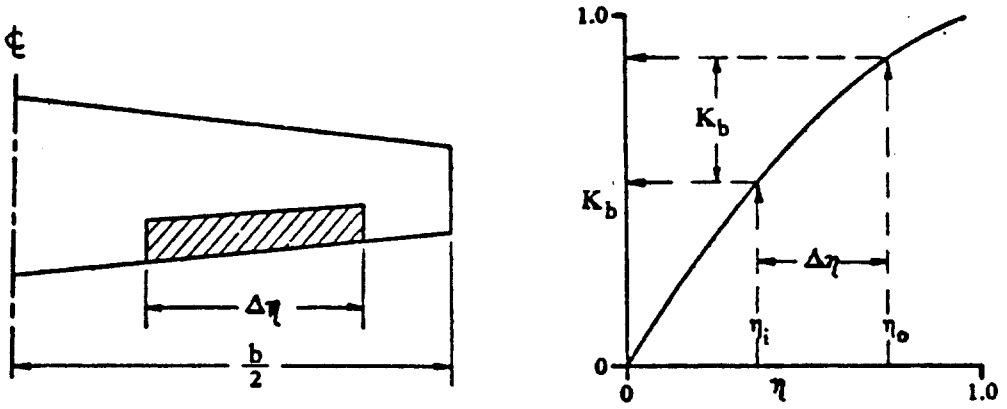

Figure 8.51 Procedure for Estimating K_b

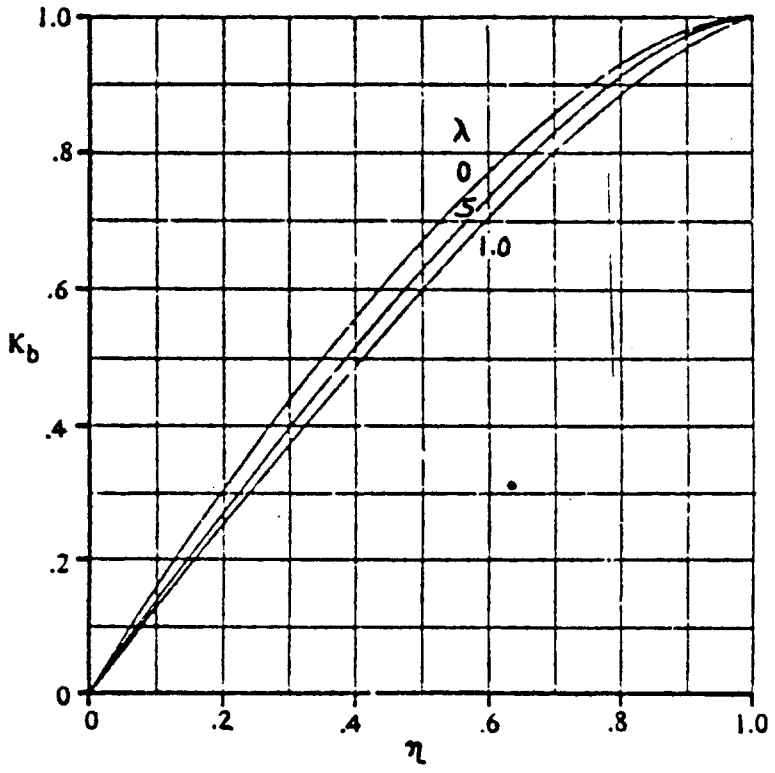

COPIED FROM: REF. 9

Figure 8.52 Effect of Taper Ratio and Flap Span on K_b

COPIED FROM: REF. 9

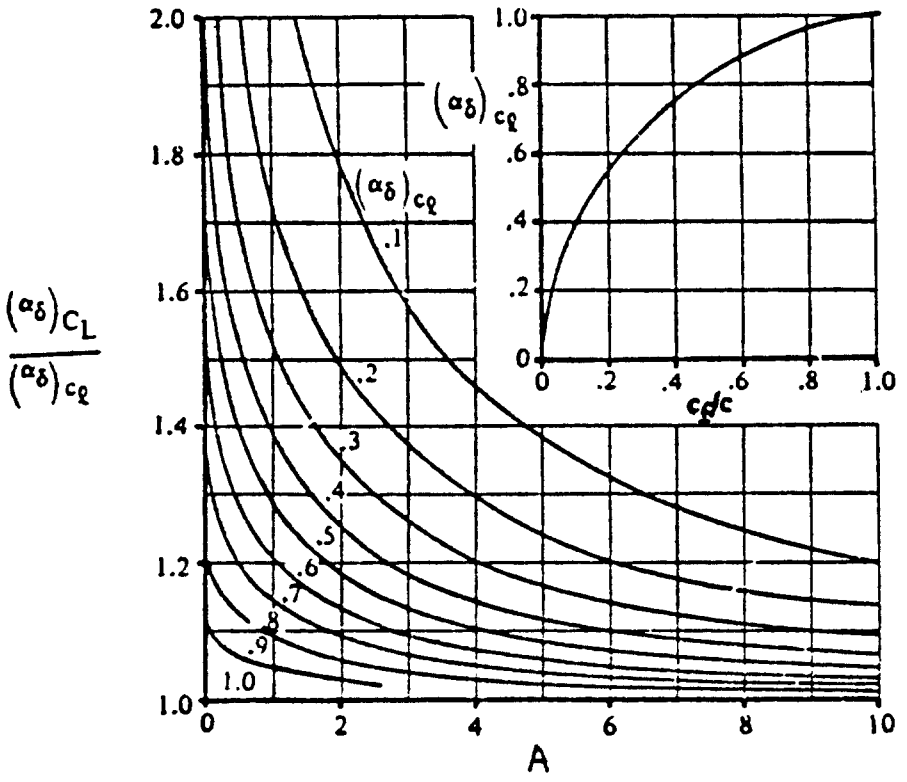

Figure 8.53 Effect of Aspect Ratio and Flap-Chord Ratio on the Three-Dimensional Flap Effectiviness

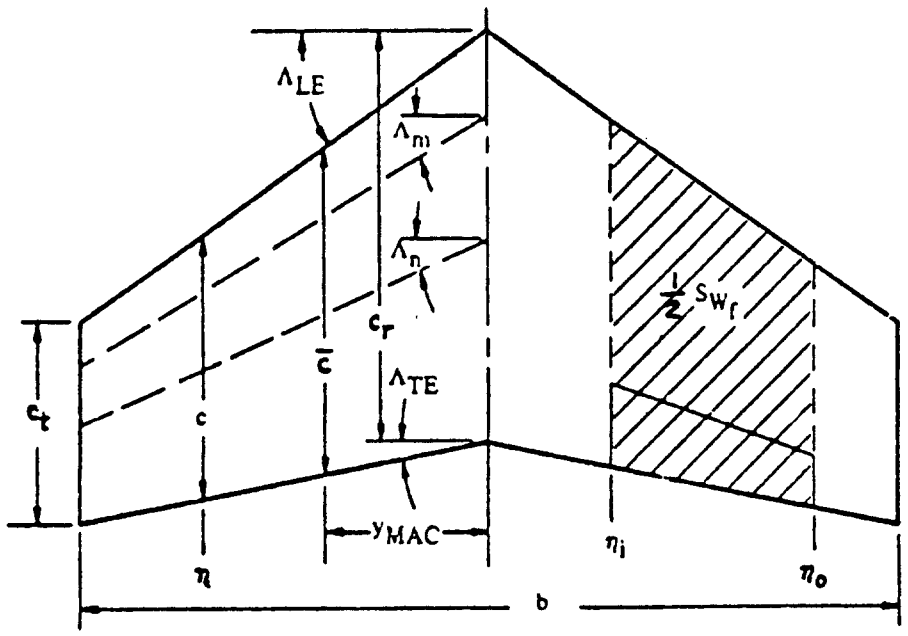

Figure 8.54 Definition of 'Flapped' Wing Area

that for the flaps-up: the method of 8.1.4.1 may be used.

Wings with TRANSLATING flap systems:

For wings with translating flaps (such as Fowler flaps, most slotted flaps, slats and Krueger flaps), the flaps-down lift curve slope may be estimated from:

$$(C_{L_{\alpha_w}})_\delta = C_{L_{\alpha_w}} \{1 + (c'/c - 1)(S_{w_f}/S)\} \qquad (8.28)$$

where: $C_{L_{\alpha_w}}$ is found from 8.1.4.1

c'/c is the ratio of extended wing chord to the chord of the flaps-up wing. Figures 8.18, 8.19 and 8.27 show definitions for these chords depending on the type of flap used.

S_{w_f}/S is the ratio of the 'flapped' wing area to that of the area of the flaps-up wing. Figure 8.54 shows how this is defined.

8.1.4.3 Wing maximum lift increment due to flaps: $\Delta C_{L_{max_w}}$

A) Trailing Edge Flaps

The maximum wing incremental lift coefficient due to trailing edge flaps is found from:

$$\Delta C_{L_{max_w}} = (\Delta c_{l_{max}})(S_{w_f}/S)K_\Delta \qquad (8.29)$$

where: $(\Delta c_{l_{max}})$ is the airfoil incremental lift coefficient due to trailing edge flaps as found from 8.1.2.3.

S_{w_f}/S is defined in Figure 8.54

K_Δ is a planform correction factor found from Figure 8.55.

B) Leading Edge Flaps

The maximum wing incremental lift coefficient due to leading edge flaps (slats and/or Kruegers) is found from:

$$\Delta C_{L_{max_w}} = 7.11(c_{lef}/c)(b_{lef}/b_e)^2\cos^2\Lambda_{c/4} \qquad (8.30)$$

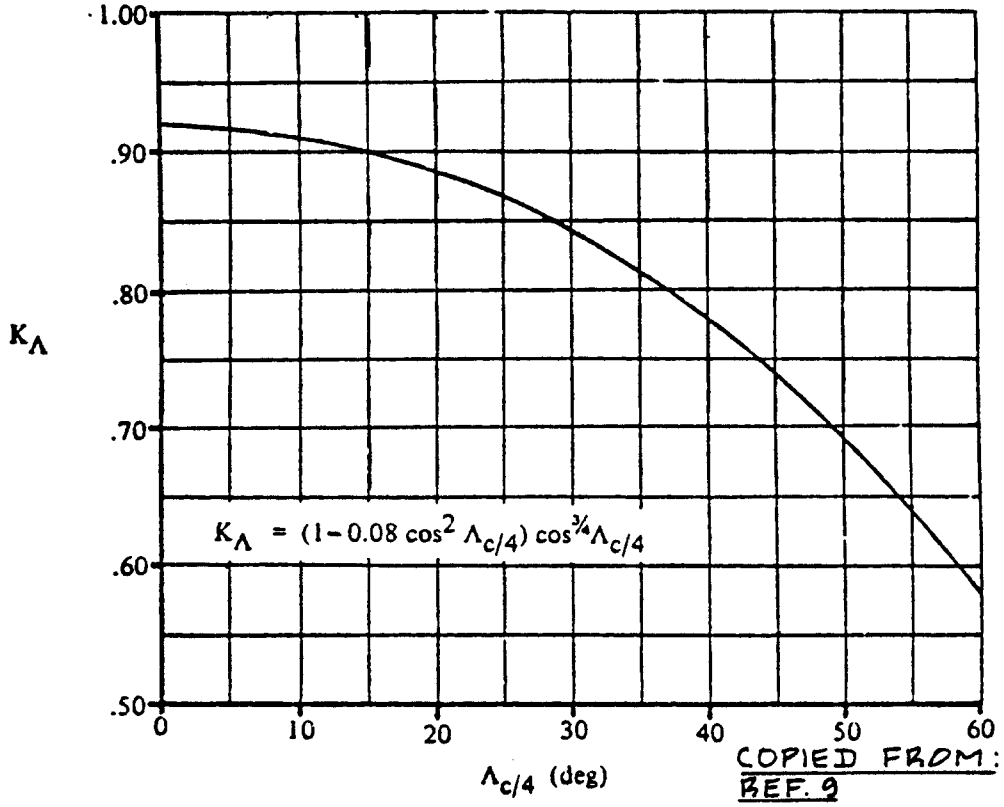

Figure 8.55 Effect of Sweep on Planform Correction Factor

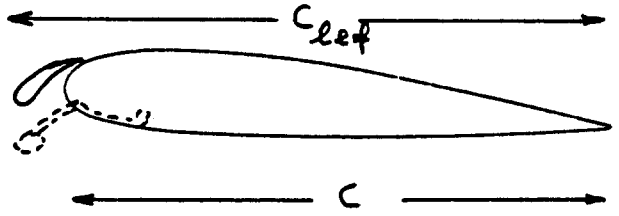

Figure 8.56 Definition of Leading Edge Flap Chord Ratio

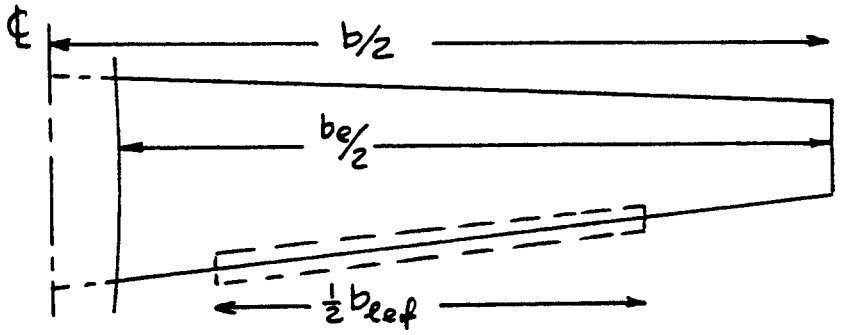

Figure 8.57 Definition of Leading Edge Flap Span Ratio

where: c_{lef}/c is defined in Figure 8.56.

b_{lef}/b_e is defined in Figure 8.57.

8.1.4.4 Construction of the wing lift curve: flaps down

All ingredients necessary to construct the flaps down wing lift curve are now available. Figure 8.58 shows the step-by-step manner in which this can be done.

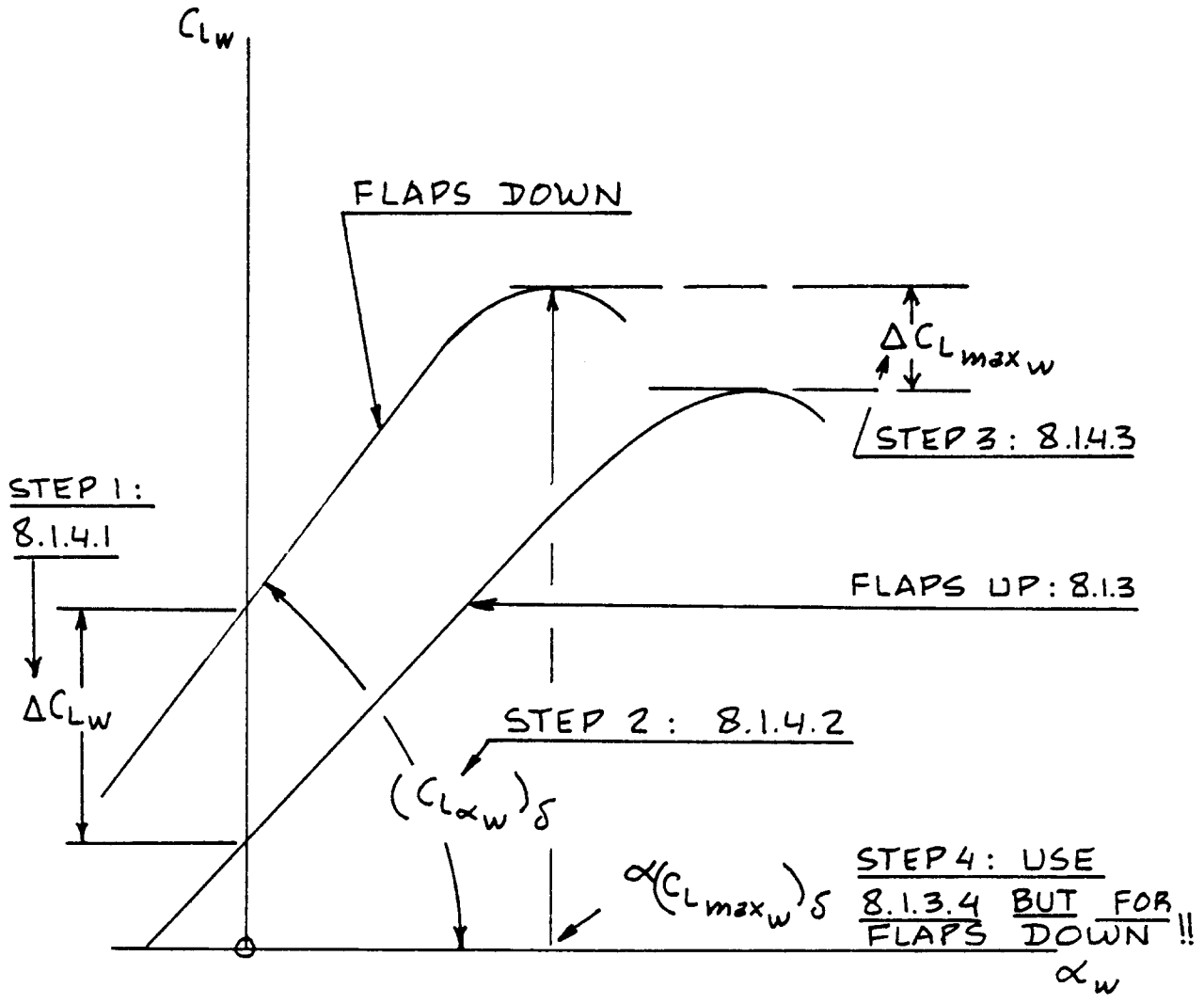

Figure 8.58 Construction of Flaps Down Wing Lift Versus Angle of Attack Curve

8.1.5 Airplane Lift and Maximum Lift: Flaps Up

Figure 8.59 shows the relationship between airplane lift coefficient and airplane angle of attack which must be determined with the methods to be presented in this section. Key quantities needed in the construction of airplane C_L versus α curve are listed, with an indication of where methods for their estimation may be found.

The assumption will be made, that an airplane can be considered to consist of three components:

a) wing + fuselage b) horizontal tail c) canard

Figure 8.60 shows the relative arrangement of these three major components. If an airplane is equipped with pylon mounted nacelles (such as the B-727 and the DC-9), the pylon + nacelle combination should be 'counted' as an additional horizontal tail. Figure 8.61 indicates the 'equivalent' geometries which should then be used.

Figure 8.62 shows a number of important geometric parameters which are used in the calculation of overall airplane lift characteristics.

IMPORTANT CONSIDERATIONS:

In this chapter the following incidence angles are accounted for:

Canard: i_c Wing: i_w Horizontal Tail: i_h

These incidence angle are defined in Figure 8.60. In this sub-section, these incidence angles are assumed to be CONSTANT. The effect of trim requirements is considered in Section 8.3.

A horizontal tail and a canard may be equipped with a trailing edge control surface:

Horizontal tail with elevator, deflection: δ_e

Canard with canardvator, deflection: δ_c

In this sub-section, the assumption will be made that all control surface deflection angles are ZERO. The effect of trim requirements which would cause these control surface deflections to be non-zero is considered in Section 8.3.

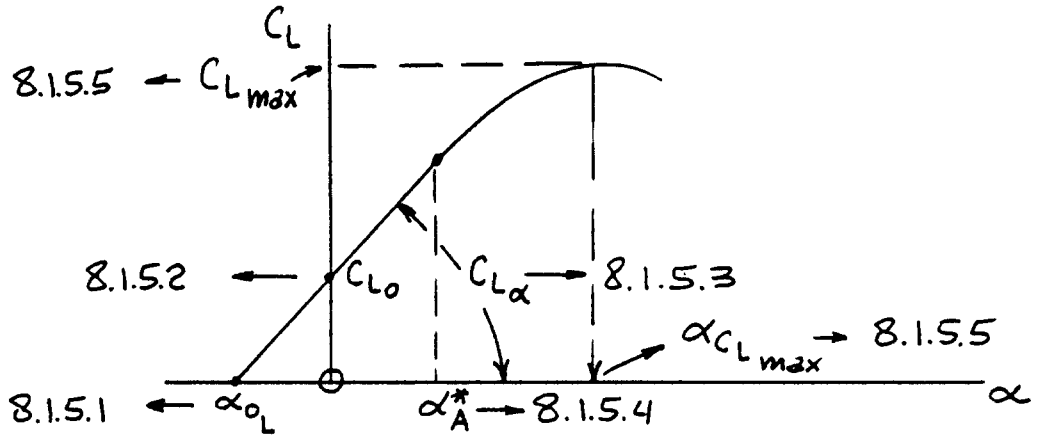

Figure 8.59 Airplane Lift Coefficient Versus Angle of Attack Curve

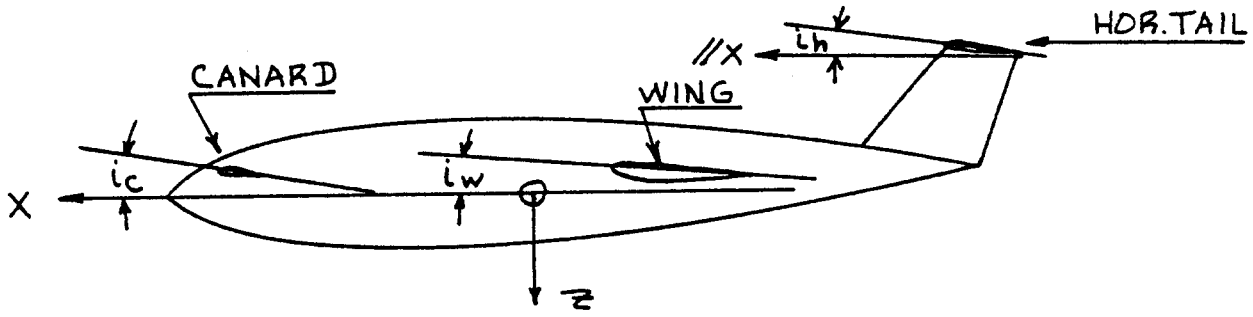

Figure 8.60 Relative Arrangement of Canard, Wing and Horizontal Tail

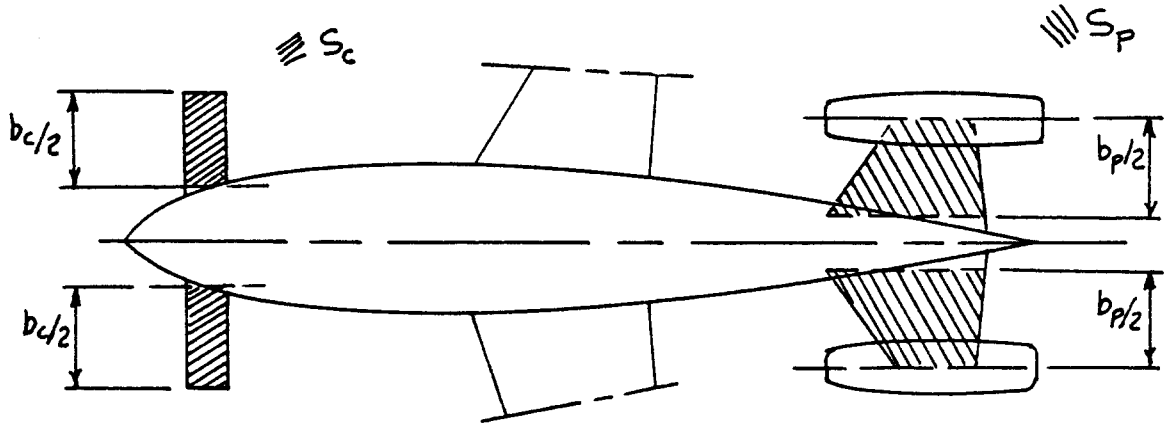

Figure 8.61 Equivalent Geometries for Pylon Engine Mounts

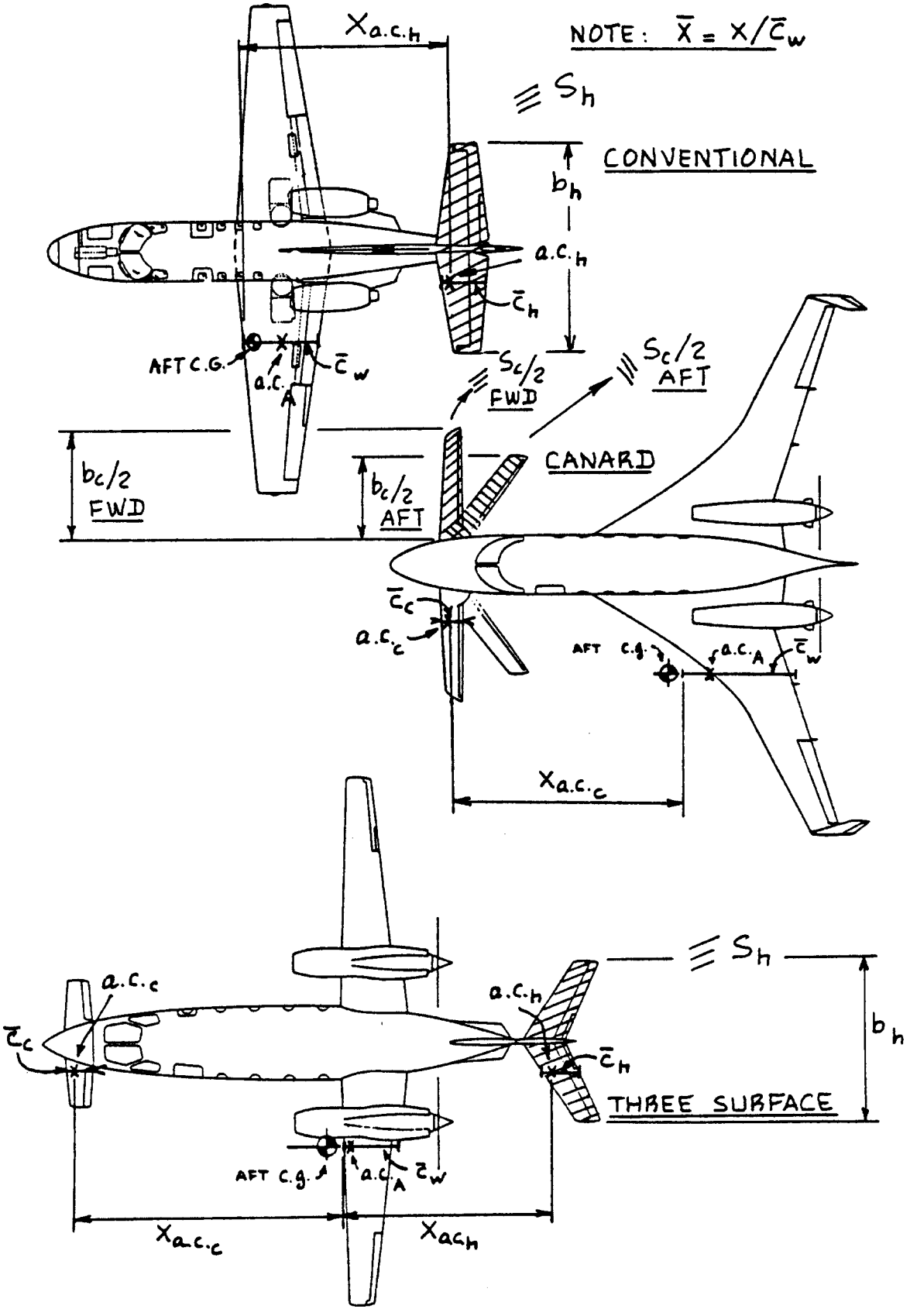

Figure 8.62 Geometric Parameters Required for Computing Overall Airplane Lift

8.1.5.1 Airplane zero-lift angle of attack: α_{o_L}

The airplane zero-lift angle of attack may be estimated from:

$$\alpha_{o_L} = (-C_{L_o})/C_{L_\alpha} \qquad (8.31)$$

where: C_{L_o} is the zero-angle-of-attack lift coefficient which is found from 8.1.5.2.

C_{L_α} is the airplane lift curve slope which may be found from 8.1.5.3.

8.1.5.2 Airplane zero-angle-of-attack lift coefficient: C_{L_o}

The airplane zero-angle-of-attack lift coefficient may be estimated from:

$$C_{L_o} = C_{L_{o_{wf}}} + C_{L_{\alpha_h}} \eta_h (S_h/S)(i_h - \varepsilon_{o_h}) + C_{L_{\alpha_c}} \eta_c (S_c/S)(i_c + \varepsilon_{o_c}) \qquad (8.32)$$

where: $C_{L_{o_{wf}}}$ is the zero-angle-of-attack lift coefficient of the wing-fuselage combination. Unless the fuselage is severely cambered:

$$C_{L_{o_{wf}}} = (i_w - \alpha_{o_{L_w}}) C_{L_{\alpha_{wf}}} \qquad (8.33)$$

where: $\alpha_{o_{L_w}}$ is found from 8.1.3.1.

$C_{L_{\alpha_{wf}}}$ is the wing-fuselage lift curve slope as found from 8.1.5.3.

Note: the subscripts wf (wing-fuselage) and wb (wing-body) are interchangeable.

$C_{L_{\alpha_h}}$ is the horizontal tail lift curve slope as found from 8.1.3.2 with appropriate substitution of tail parameters for wing parameters.

$C_{L_{\alpha_c}}$ is the canard lift curve slope as found from 8.1.3.2 with appropriate substitution of canard parameters for wing parameters.

NOTE: Figure 8.62 defines the necessary geometric parameters needed to compute horizontal tail and canard lift curve slopes.

$$\eta_h = \bar{q}_h/\bar{q} \tag{8.34}$$

$$\eta_c = \bar{q}_c/\bar{q} \tag{8.35}$$

The dynamic pressures $\bar{q}_h$ and $\bar{q}_c$ seen by a horizontal tail and a canard differ from the free stream dynamic pressure $\bar{q}$ for the following reasons:

a) as the air passes over a wing-fuselage combination it gradually looses some of its kinetic energy. This energy loss is proportional to the friction drag of the wing-fuselage.

b) when a horizontal tail or a canard surface are placed in the slipstream of a propeller, the local dynamic pressure depends on the power absorbed by the propeller and on the distance of the surface from the propeller.

In preliminary design it is acceptable to use:

For jet airplanes:

$$\eta_c = 1.0 \tag{8.36}$$

$$\eta_h = \tag{8.37}$$

$$[1 - \{\cos^2(\pi z_h/2z_w)\}\{2.42(C_{D_{o_w}})^{1/2}\}/(x_h/\bar{c} + 0.30)]$$

where: $z_h = x_h \tan(\gamma_h + \varepsilon_{cl} - \alpha_w)$ (8.38)

with x_h, γ_h, ε_{cl} and α_w shown in Fig. 8.63.

$$\varepsilon_{cl} = 1.62C_{L_w}/\pi A \tag{8.39}$$

$$z_w = 0.68\bar{c}\{C_{D_{o_w}}(x_h/\bar{c} + 0.15)\}^{1/2} \tag{8.40}$$

$C_{D_{o_w}}$ is the wing zero-lift drag coefficient as found from 4.2.1.1.

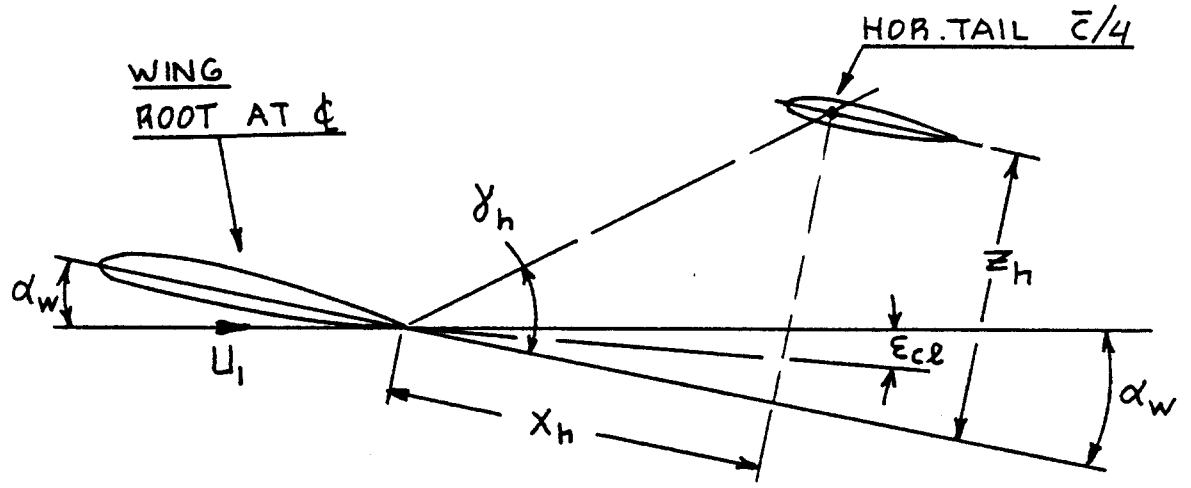

Figure 8.63 Geometric Parameters Required for Computing Dynamic Pressure Ratios

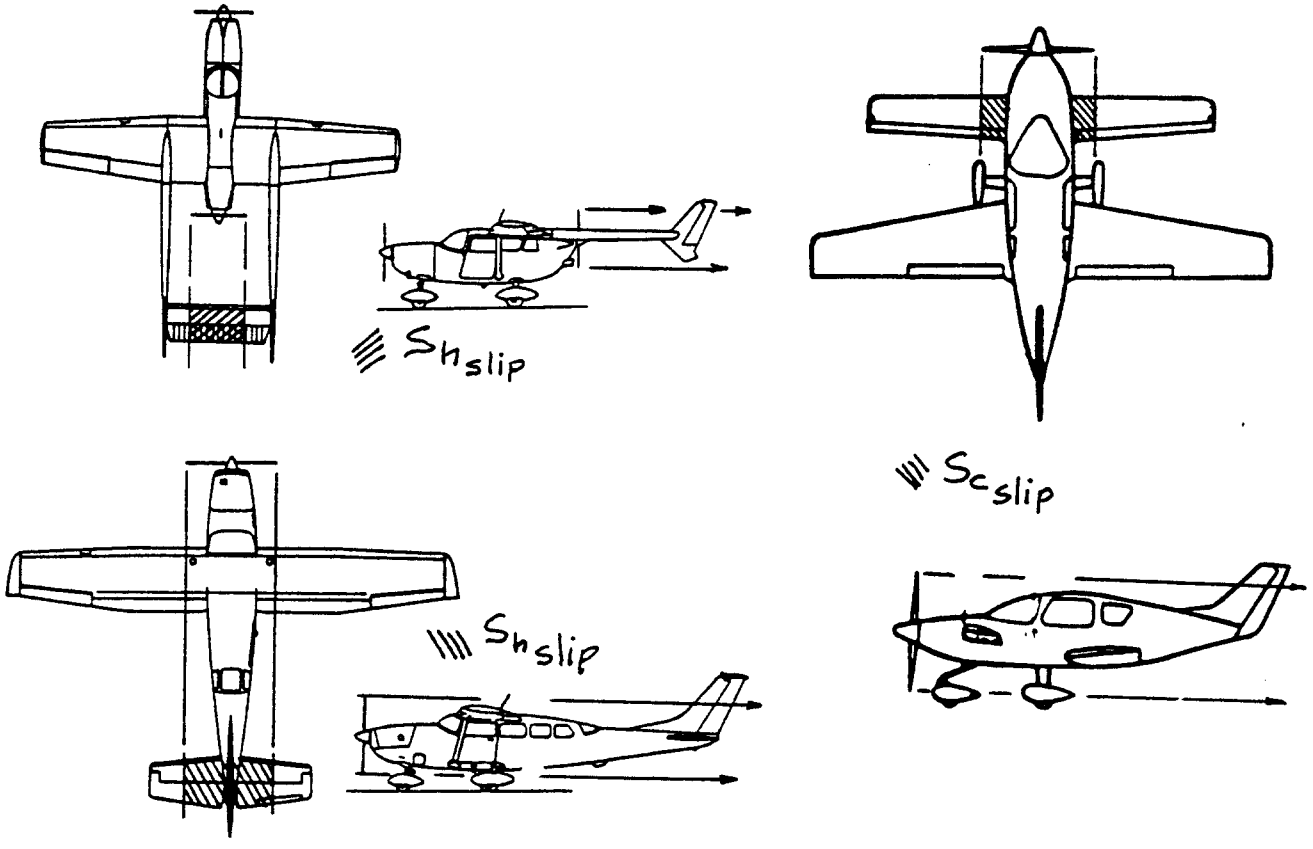

Figure 8.64 Definition of Canard and Tail Areas which are Submerged in Propeller Slipstream

For propeller driven airplanes:

The dynamic pressure ratios depend on where the canard and/or the horizontal tail are located relative to the propeller. The following approximation is suggested:

$$\eta_{h \text{ or } c} = 1 + \{(S_{h \text{ or } c})_{slip}/(S_{h \text{ or } c})\}x$$

$$x[(2200P_{av})/\{\bar{q}U_1\pi(D_p)^2\}] \qquad (8.41)$$

where: $(S_{h \text{ or } c})_{slip}$ is the area of the tail or canard which is submerged in the propeller slipstream: see Figure 8.64.

U_1 is the steady state speed of the airplane

P_{av} is the available horsepower, see Section 6.4.

D_p is the propeller diameter in ft

S_h is the horizontal tail area: see Figure 8.62.

S_c is the canard area: see Figure 8.62.

ε_{o_h} is the horizontal tail downwash angle for zero airplane angle of attack

ε_{o_c} is the canard upwash angle for zero airplane angle of attack

NOTE: the magnitudes of tail downwash angle and canard upwash angle at zero airplane angle of attack are dependent on the wing lift distribution at zero airplane angle of attack. For most airplanes (flaps up) it is acceptable to use: $\varepsilon_{o_h} = \varepsilon_{o_c} = 0$.

In Section 8.1.6 it is seen that with the flaps down this approximation is not valid. In that case, an incremental downwash angle, $\Delta\varepsilon_f$ must be accounted for.

8.1.5.3 Airplane lift curve slope: C_{L_α}

The airplane lift curve slope may be estimated from:

$$C_{L_\alpha} = C_{L_{\alpha_{wf}}} + C_{L_{\alpha_h}} \eta_h (S_h/S)(1 - d\varepsilon/d\alpha) + C_{L_{\alpha_c}} \eta_c (S_c/S)(1 + d\varepsilon_c/d\alpha) \quad (8.42)$$

where: $C_{L_{\alpha_{wf}}}$ is the wing-fuselage (wing-body) lift curve slope, given by:

$$C_{L_{\alpha_{wf}}} = K_{wf} C_{L_{\alpha_w}} \quad (8.43)$$

where: K_{wf} is the wing-fuselage interference factor given by:

$$K_{wf} = 1 + 0.025(d_f/b) - 0.25(d_f/b)^2 \quad (8.44)$$

$C_{L_{\alpha_w}}$ is found from 8.1.3.2.

$d\varepsilon/d\alpha$ = downwash gradient at the horizontal tail =

$$4.44[\{K_A K_\lambda K_h (\cos\Lambda_{c/4})^{1/2}\}^{1.19}]x \; x\{(C_{L_{\alpha_w}})_{\text{at } M}\}/\{(C_{L_{\alpha_w}})_{\text{at } M=0}\} \quad (8.45)$$

where: $K_A = (1/A) - 1/(1 + A^{1.7})$ (8.46)

as shown in Figure 8.65a.

$K_\lambda = (10 - 3\lambda)/7$ (8.47)

as shown in Figure 8.65b.

$K_h = (1 - h_h/b)/(2l_h/b)^{1/3}$ (8.48)

as shown in Figure 8.65c with the parameters h_h, l_h defined in Fig. 8.66.

$d\varepsilon_c/d\alpha$ is the upwash gradient at the canard. It may be found from Figure 8.67 for wings of quarter chord sweep angles up to 35 deg.

All other quantities in Eqn. (8.42) are defined in 8.1.5.2.

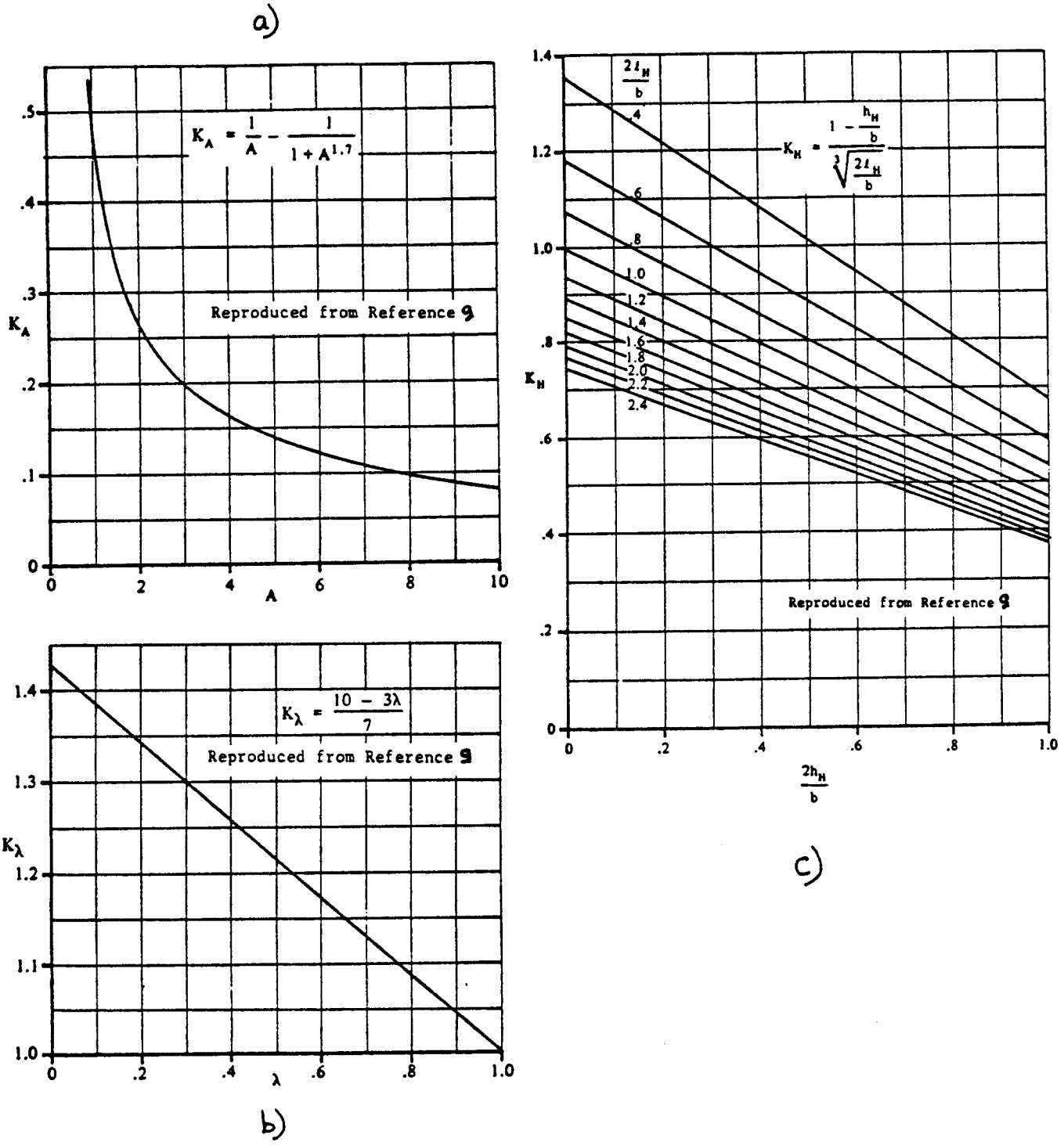

Figure 8.65 Factors for Computing Downwash

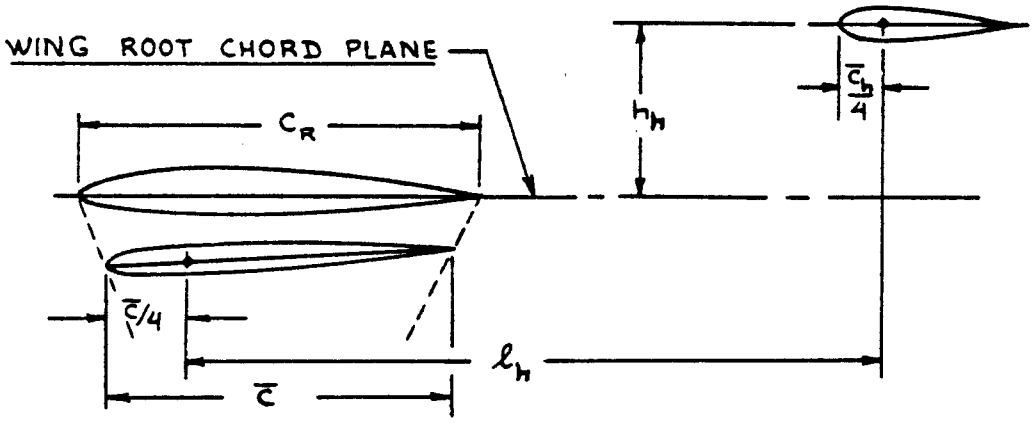

Figure 8.66 Geometric Parameters for Horizontal Tail Location

COPIED FROM: REF. 9

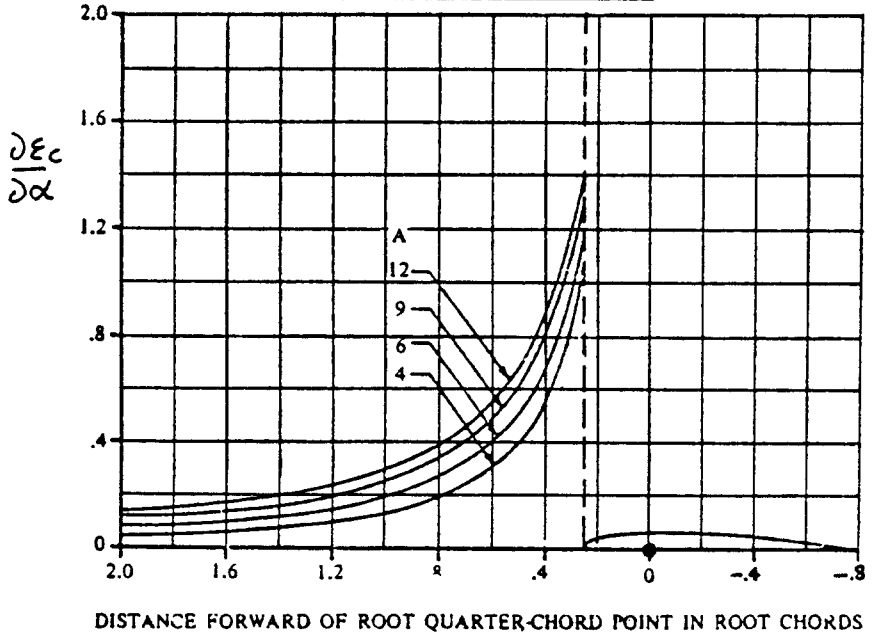

Figure 8.67 Wing Upwash Gradient

8.1.5.4 Airplane linear range of angle of attack: α_A^*

In preliminary design it is acceptable to use:

$$\alpha_A^* = \alpha_w^* - i_w \qquad (8.49)$$

where: α_w^* is found from 8.1.3.3.

8.1.5.5 Airplane maximum lift coefficient: $C_{L_{max}}$ and airplane angle of attack for maximum lift: $\alpha_{C_{L_{max}}}$

The airplane maximum lift coefficient is found from:

$$C_{L_{max}} = C_{L_{max_w}} - (C_{L_{\alpha_{wf}}})\Delta\alpha_{w/c} + \qquad (8.50)$$

$$+ (C_{L_{\alpha_h}})(S_h/S)\{(\alpha_{C_{L_{max}}})(1 - d\varepsilon/d\alpha - \varepsilon_{o_h}) + i_h\} +$$

$$+ (C_{L_{\alpha_c}})(S_c/S)\{(\alpha_{C_{L_{max}}})(1 + d\varepsilon_c/d\alpha) + \varepsilon_{o_c} + i_c\}$$

where: $C_{L_{max_w}}$ is found from 8.1.3.4.

$C_{L_{\alpha_{wf}}}$ is found from Eqn. (8.43)

$\Delta\alpha_{w/c}$ is the difference between the airplane angles of attack for canard stall and for wing stall. In a canard airplane, the canard must always stall before the wing! In preliminary design it is suggested to use: $\Delta\alpha_{w/c} = 3$ deg.

$$\alpha_{C_{L_{max}}} = \alpha_{C_{L_{max_w}}} - i_w - \Delta\alpha_{w/c} \qquad (8.51)$$

where: $\alpha_{C_{L_{max_w}}}$ is found from 8.1.3.4.

All other quantities are defined in 8.1.5.2.

8.1.5.6 Construction of airplane lift curve: flaps-up

All ingredients necessary to construct the airplane C_L versus α curve are now available. Figure 8.68 shows how this can be done in a step-by-step manner.

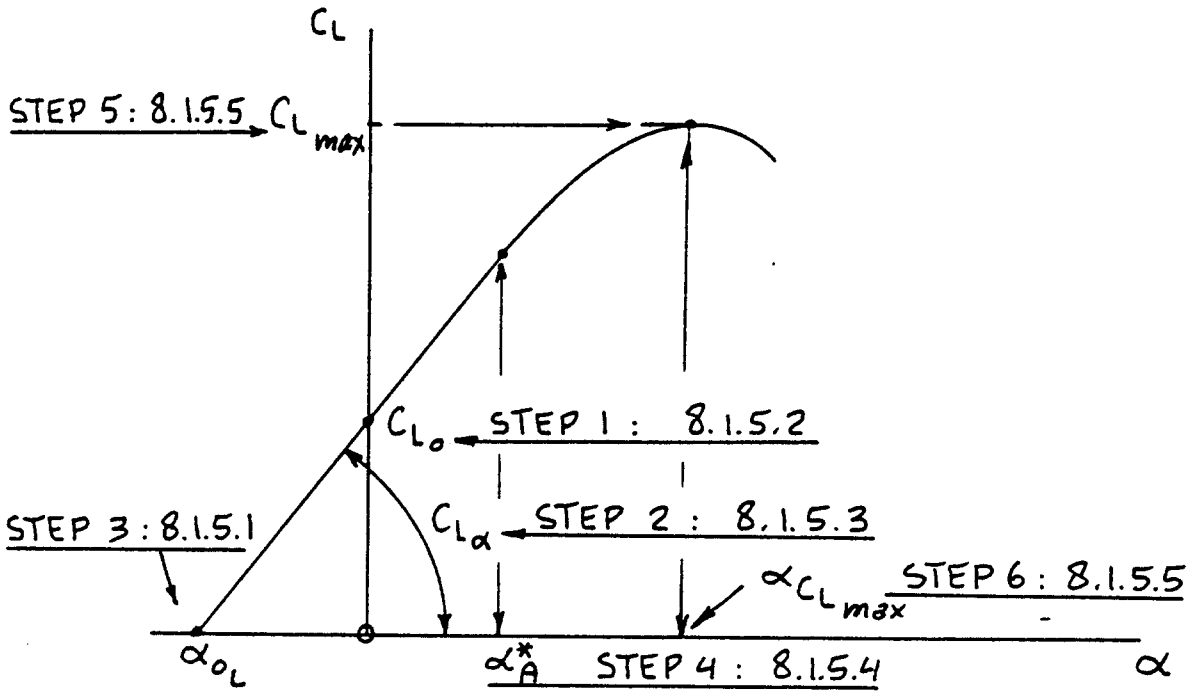

Figure 8.68 Construction of Airplane Lift Versus α Curve

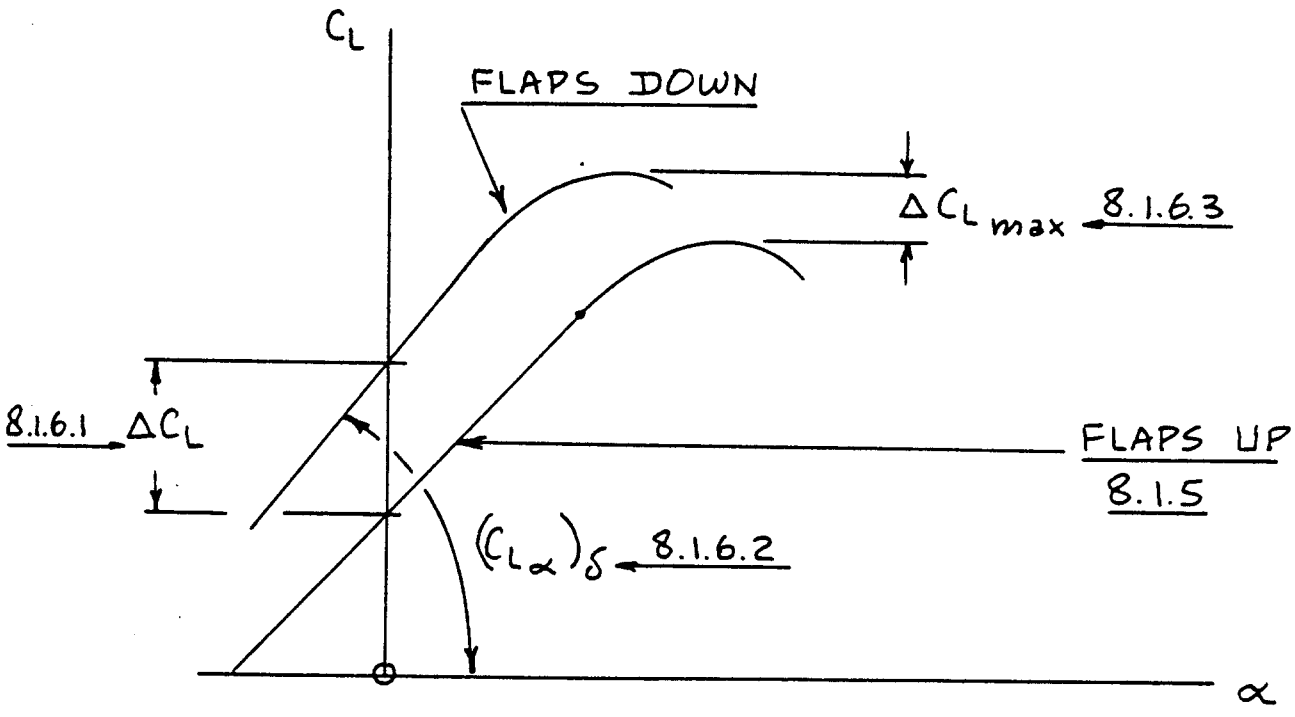

Figure 8.69 Fundamental Airplane Lift Versus α Curve with the Flaps Down

8.1.6 Airplane Lift and Maximum Lift: Flaps Down

Figure 8.69 shows the relationship between airplane lift coefficient in the flaps down configuration and airplane angle of attack which must be determined with the methods to be presented in this section. Key quantities needed in the construction of the flaps down airplane C_L versus α curve are listed, with an indication of where methods for their estimation may be found.

8.1.6.1 Airplane lift increment due to flaps: ΔC_L

The airplane lift increment due to flaps may be estimated from:

$$\Delta C_L = k_{cw}\Delta C_{L_w} + k_{wc}(S_c/S)\Delta C_{L_c} + \quad (8.52)$$

$$+ k_{wh}(S_h/S)\Delta C_{L_h} - C_{L_{\alpha_h}}\eta_h(S_h/S)\Delta\varepsilon_f$$

where: ΔC_{L_w} is found from 8.1.4.1

k_{cw} is a canard-on-wing interference factor. If the canard is small relative to the wing and if the canard is far enough forward of the wing, $k_{cw} = 1.0$ may be used in early design.

Whenever one or both of these conditions are not met, a finite element aerodynamic analysis of the canard-on-wing effect is needed. Such methods are beyond the scope of this text.

k_{wc} is the wing-on-canard interference factor. It is similar to (albeit not the same as) k_{cw}.

In early design it is acceptable to use: $k_{wc} = 1.0$.

S_c is the canard area: see Figure 8.62.

ΔC_{L_c} is found from 8.1.4.1 with appropriate substitution of canard parameters for wing parameters. If a canardvator deflection is present, it should be treated as a plain flap and its lift increment must be added.

Note: In airplanes such as the Piaggio P 180 Avanti, the canard is equipped with a Fowler

flap which is geared to the wing flap. The effect of such a flap must be accounted for! A detailed treatment of such a system is beyond the scope of this text.

k_{wh} is the wing-on-horizontal-tail interference factor. It is similar to (albeit not the same as) k_{cw}. In early design it is acceptable to use: $k_{wh} = 1.0$.

S_h is the horizontal tail area: see Figure 8.62.

ΔC_{L_h} is found from 8.1.4.1 with appropriate substitution of horizontal tail parameters for wing parameters. If an elevator is present, its deflection can be accounted for by considering the elevator to be a plain flap.

$C_{L_{\alpha_h}}$ is the horizontal tail lift-curve-slope which may be found from Eqn. (8.22) with appropriate substitution of horizontal tail parameters for wing parameters.

$\Delta\varepsilon_f$ is the increase in tail downwash angle due to wing flap deflection. It may be estimated from Figure 8.70.

<u>8.1.6.2 Airplane lift curve slope due to flaps:</u> $(C_{L_\alpha})_\delta$

The airplane lift curve slope with the flaps down may be estimated from:

$$(C_{L_\alpha})_\delta = K_{wf}(C_{L_{\alpha_w}})_\delta + C_{L_{\alpha_h}}\eta_h(S_h/S)\{1 - (d\varepsilon/d\alpha)_\delta\} + C_{L_{\alpha_c}}\eta_c(S_c/S)\{1 - (d\varepsilon_c/d\alpha)_\delta\} \quad (8.53)$$

where: $(C_{L_{\alpha_w}})_\delta$ is the wing lift-curve-slope with the flaps down. It is found from Eqn. (8.28).

where: $(d\varepsilon/d\alpha)_\delta$ is the flaps-down downwash gradient at the horizontal tail.

$(d\varepsilon_c/d\alpha)_\delta$ is the flaps-down upwash gradient at the canard.

<u>Note:</u> in preliminary design it is acceptable to set these flaps-down downwash and upwash gradients equal to those with the flaps up. The latter may be determined

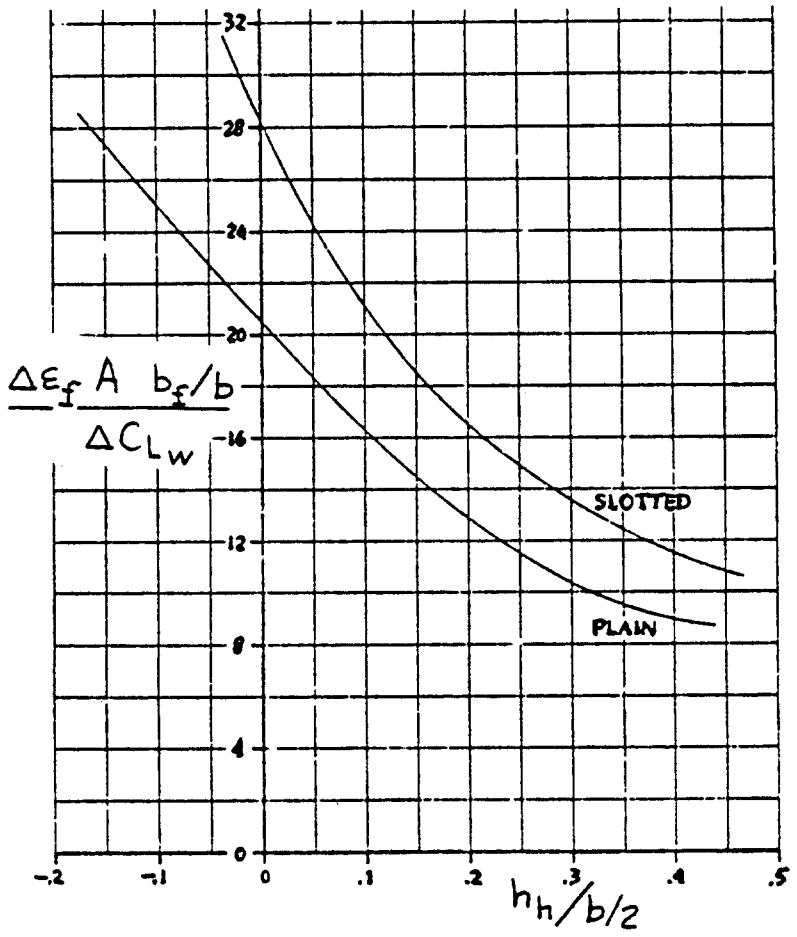

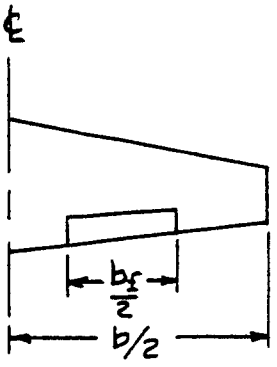

COPIED FROM:
REF. 9

FOR h_h SEE FIG. 8.66

Figure 8.70 Incremental Downwash Angle at the Horizontal Tail due to Flaps

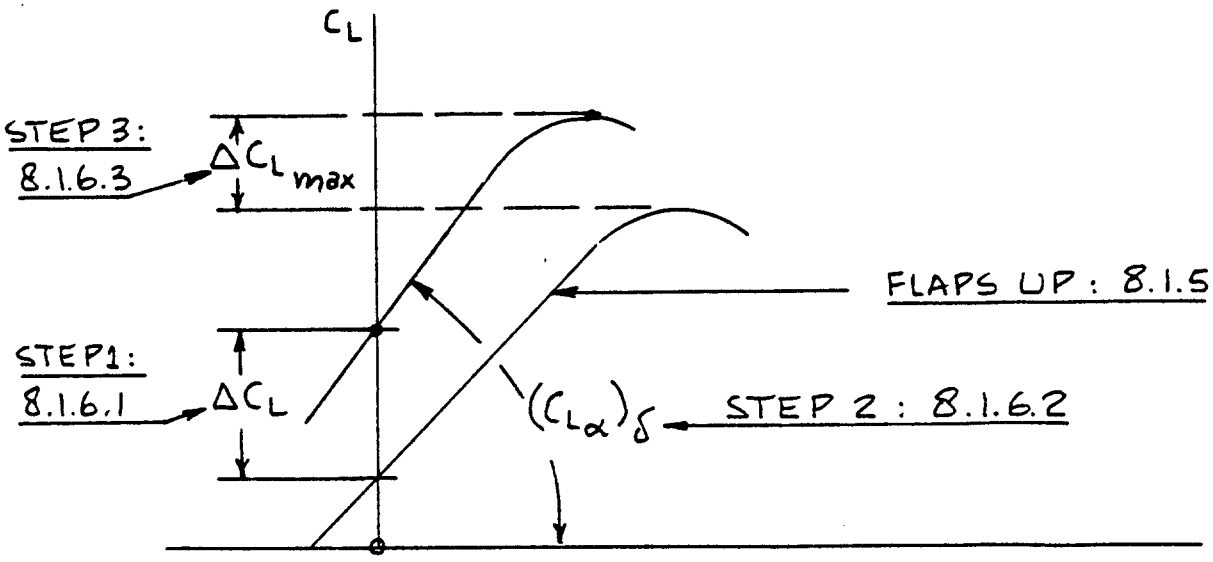

Figure 8.71 Construction of Airplane Lift Versus α Curve with the Flaps Down

from 5.3.

l other quantities were defined in 8.1.5.2 and 8.1.5

8.1.6 irplane maximum lift increment due to flaps: $C_{L_{max}}$

Tairplane maximum lift increment due to flaps may be estted from:

$$\Delta_{max} = k_{cw}\Delta C_{L_{max_w}} - (C_{L_{\alpha_w}})_{\delta}\Delta\alpha_{w/c} + (S_c/S)\Delta C_{L_{max_c}} + (S_h/S)C_{L_{\alpha_h}}\{(1 - d\varepsilon/d\alpha) + i_h - \Delta\varepsilon_f\} \quad (8.54)$$

where: $_c$ is the canard-on-wing interference factor. If the canard is small relative to the wing and if the canard is far enough forward of the wing, $k_{cw} = 1.0$ may be used in early design.

Whenever one or both of these conditions are not met, a finite element aerodynamic analysis of the canard-on-wing effect is needed. Such methods are beyond the scope of this text.

$\Delta\alpha_{wc}$ is the difference between the airplane angles of attack for canard stall and for wing stall. In a canard airplane, the canard must always stall before the wing! In In preliminary design, use:
$\Delta\alpha_{w/c} = 3$ deg.

$\Delta\varepsilon_f$ is the increase in tail downwash angle due to flaps. It may be found from Figure 8.70.

All other quantities in Eqn.(8.51) are defined in 8.1.6.1 anc 8.1.6.2.

8.1.6.4 Construction of airplane lift curve: flaps down

All ingredients necessary to construct the flaps down airplane lift curve are now available. Figure 8.71 shows the step-by-step manner in which this can be done.

8.1.7 Airplane Lift in Ground Effect

When an airplane operates close to the ground, the downwash and the upwash patterns around its lifting surfaces change. References 9 and 14 contain physical explanations for these effects. In this section, the position is taken that the effect of the ground on the C_L versus α behavior of an airplane is a change in angle of attack at constant lift coefficient (or, vice versa, a change in lift coefficient at constant angle of attack). Figure 8.72 shows this in terms of the ground induced change in angle of attack at constant lift coefficient: $\Delta\alpha_g$. Note the difference in ground effect on high and on low aspect ratio configurations. This difference is accounted for as follows:

8.1.7.1 High aspect ratio configurations: transports
8.1.7.2 Low aspect ratio configurations: fighters

NOTE: it will be assumed that the effect of the ground on tail downwash and canard upwash can be neglected as far as overall airplane lift is concerned. The effect of the ground on tail downwash does alter tail lift and because of that the airplane pitching moment is affected: this is accounted for in Section 8.2.

8.1.7.1 High aspect ratio configurations: transports

Figure 8.72a shows the ground induced change in angle of attack at constant lift coefficient: $\Delta\alpha_g$.

For high aspect ratio configurations the change in angle of attack at constant lift coefficient in ground effect may be found from:

$$\Delta\alpha_g = -F_{tv}\{(9.12/A) + 7.16(c_r/b)\}(C_{L_{wf}}) + \qquad (8.55)$$

$$- \{A/(2C_{L_{\alpha_{wf}}})\}(c_r/b)\{(L/L_o) - 1\}(C_{L_{wf}})r +$$

$$- \{(\delta_f/50)^2/(C_{L_{\alpha_{wf}}})\}A(\Delta C_L)_f$$

where: F_{tv} is a factor which accounts for the effect on lift due to the image trailing vortex. It is found from Figure 8.73.

A is the wing aspect ratio

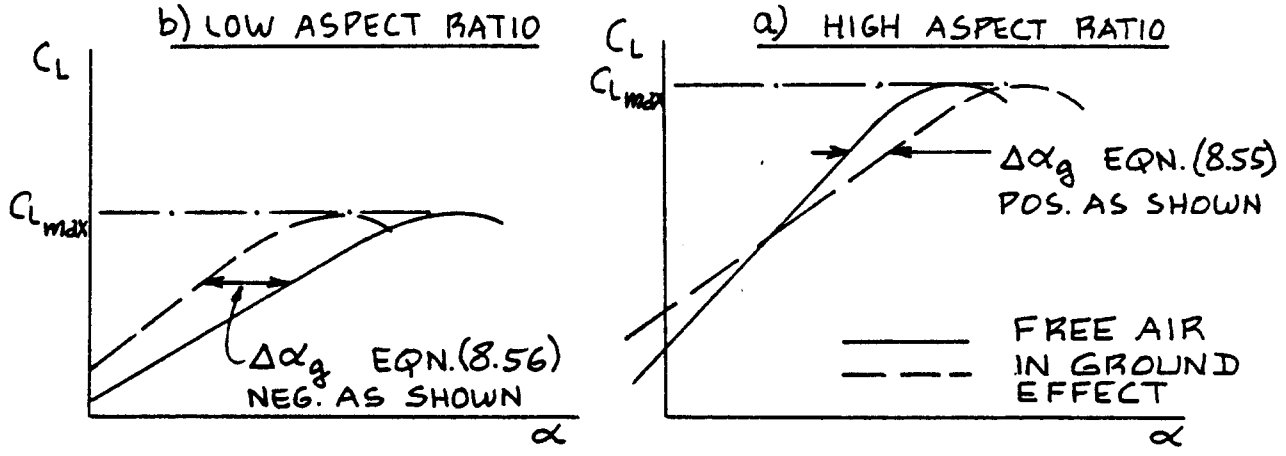

Figure 8.72 Ground Effect on Lift Curves

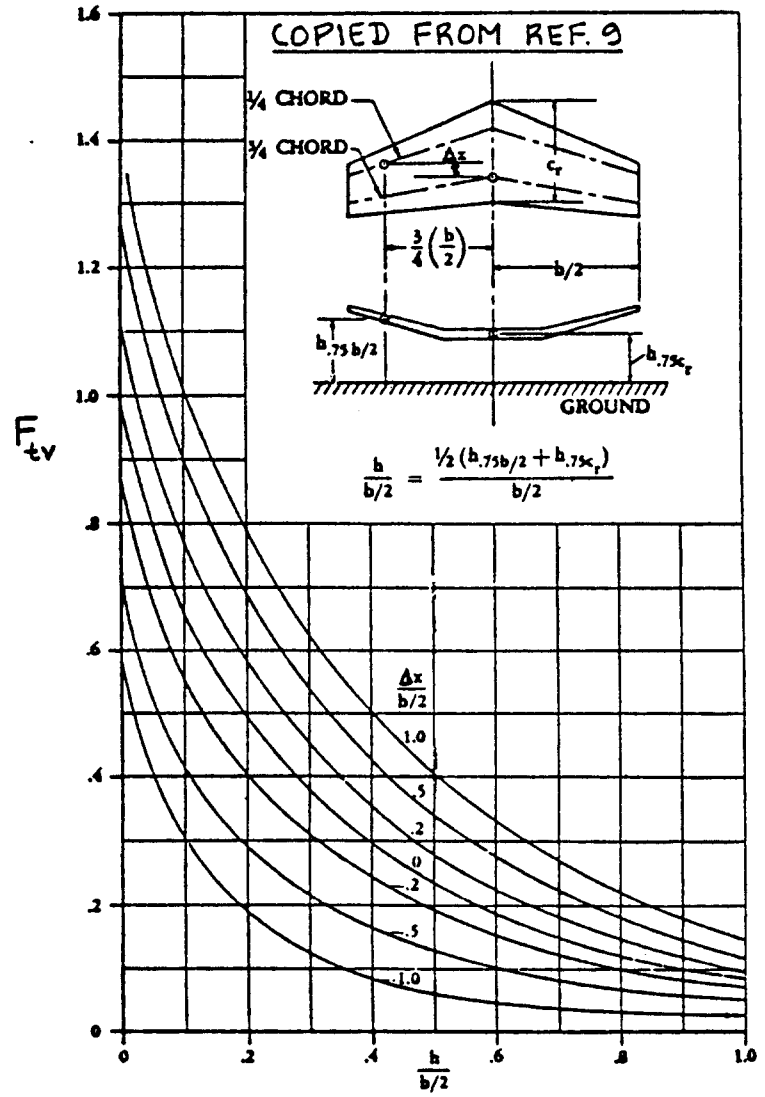

Figure 8.73 Factor Due to Image Trailing Vortex

c_r/b is the ratio of wing root chord to wing

$C_{L_{wf}}$ is the wing-fuselage lift coefficient e ground effect. This is found from Sect 8.1.5 or from Section 8.1.6 (depending e flap deflection) by setting $S_h = S_c =$ (

$C_{L_{\alpha_{wf}}}$ is the wing-fuselage lift-curve-slope determined from Eqn.(8.43), in 1/deg.

$(L/L_o - 1)$ accounts for the effect on lift o the image bound vortex. It is f from Figure 8.74.

r_g is a factor which accounts for the effec finite span. It may be found from Figur 8.

δ_f is the flap deflection in degrees

$\Delta(\Delta C_L)_f$ is a factor which accounts for the e of flaps in ground effect. It is f from Figure 8.76.

Equation (8.55) is used to estimate $\Delta\alpha_g$ for t values of $C_{L_{wf}}$ after which the airplane C_L versus e is modified as indicated in Figure 8.72a. This pr e neglects the effect of the horizontal tail and the d on airplane lift in ground effect. In Section 8.2 will be seen that the effect of the horizontal tai the canard on airplane pitching moment in ground e is NOT neglected.

8.1.7.2 Low aspect ratio configurations: fighters

Figure 8.72b shows the ground induced change gle of attack at constant lift coefficient: $\Delta\alpha_g$. w aspect ratio configurations, this quantity follows

$$\Delta\alpha_g = \qquad (5)$$

$$-18.24(C_{L_{wf}})\sigma_g/A + r_g T_g (C_{L_{wf}})^2/57.3(C_{L_\alpha})_{wf} -$$

where: $C_{L_{wf}}$ is the wing-fuselage lift coefficient free air. This follows from Section or from Section 8.1.6 (depending on tip state) by setting $S_h = S_c = 0$.

BOTH COPIED FROM REF. 9

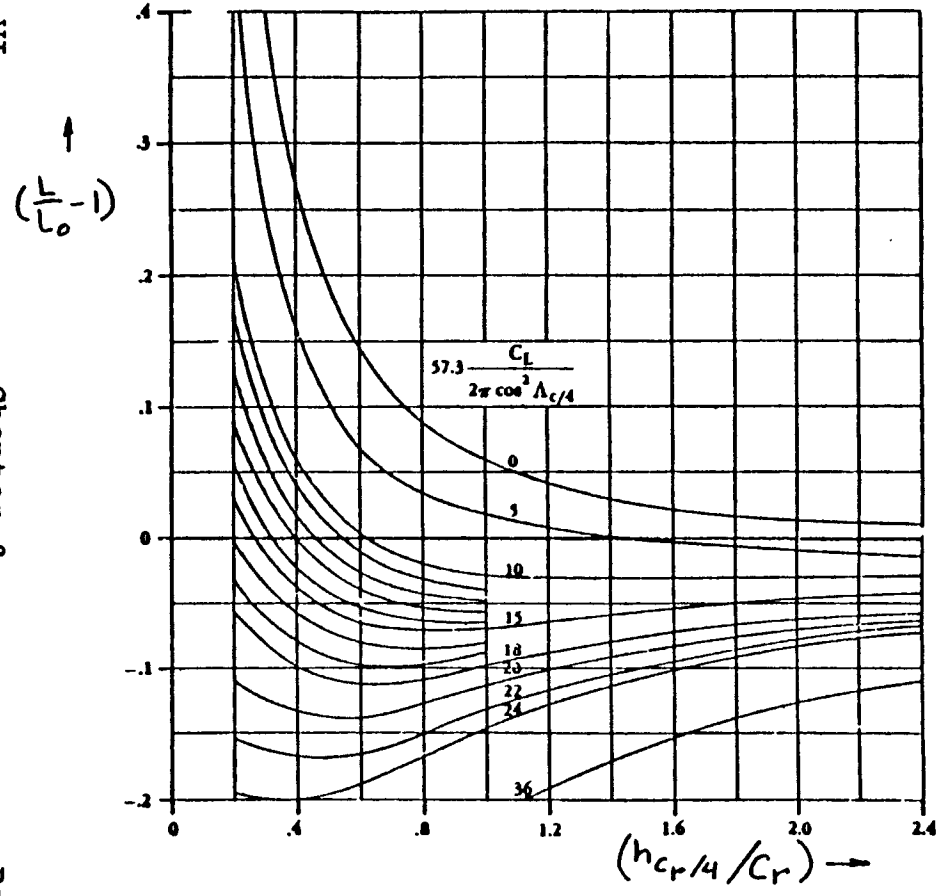

Figure 8.74 Factor Due to Image Bound Vortex

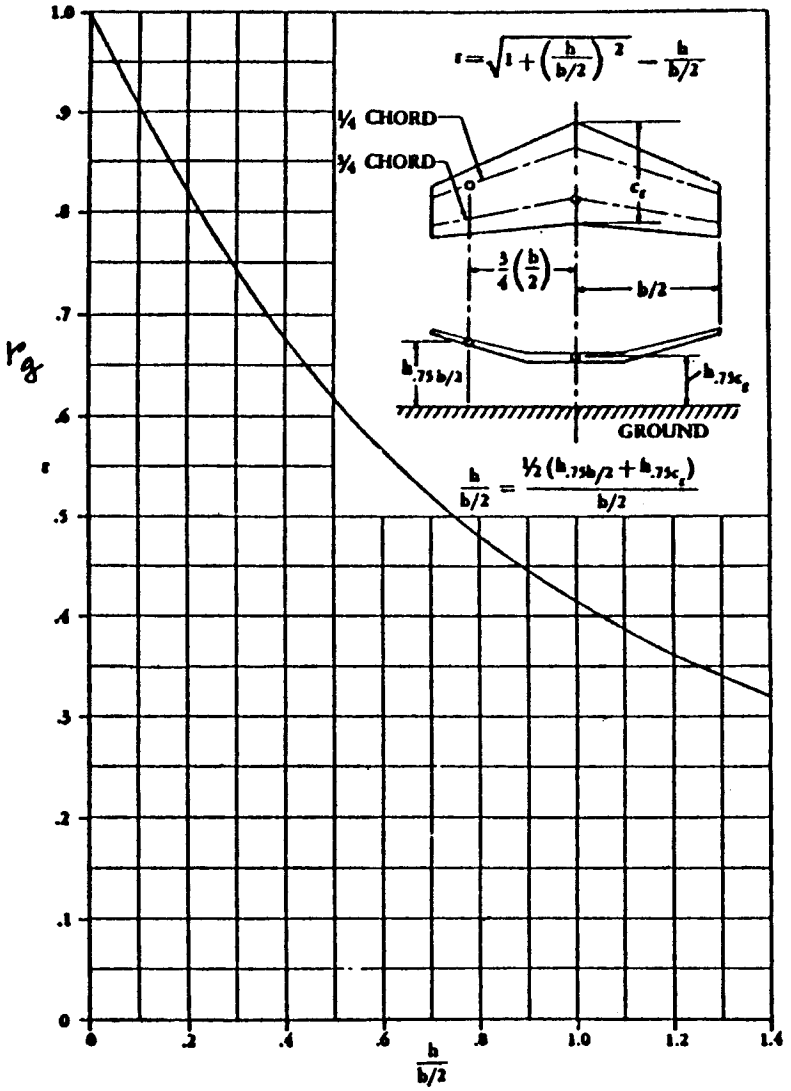

Figure 8.75 Factor Due to Finite Span

BOTH COPIED FROM REF. 9

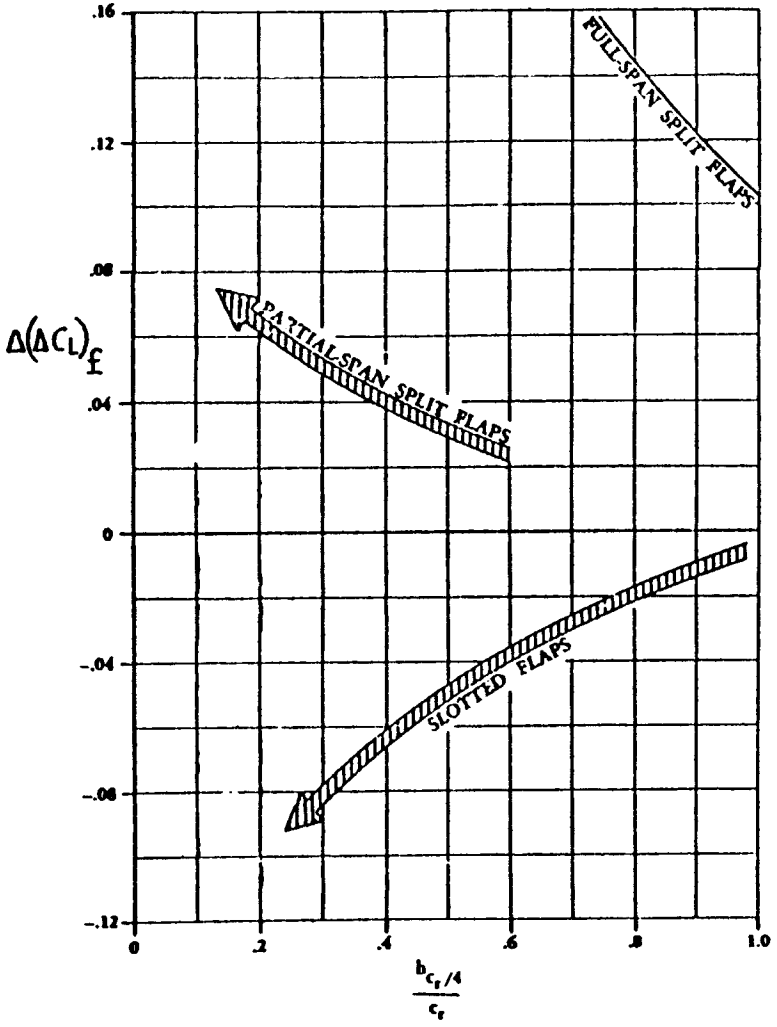

Figure 8.76 Ground Effect on Lift Due to Flaps

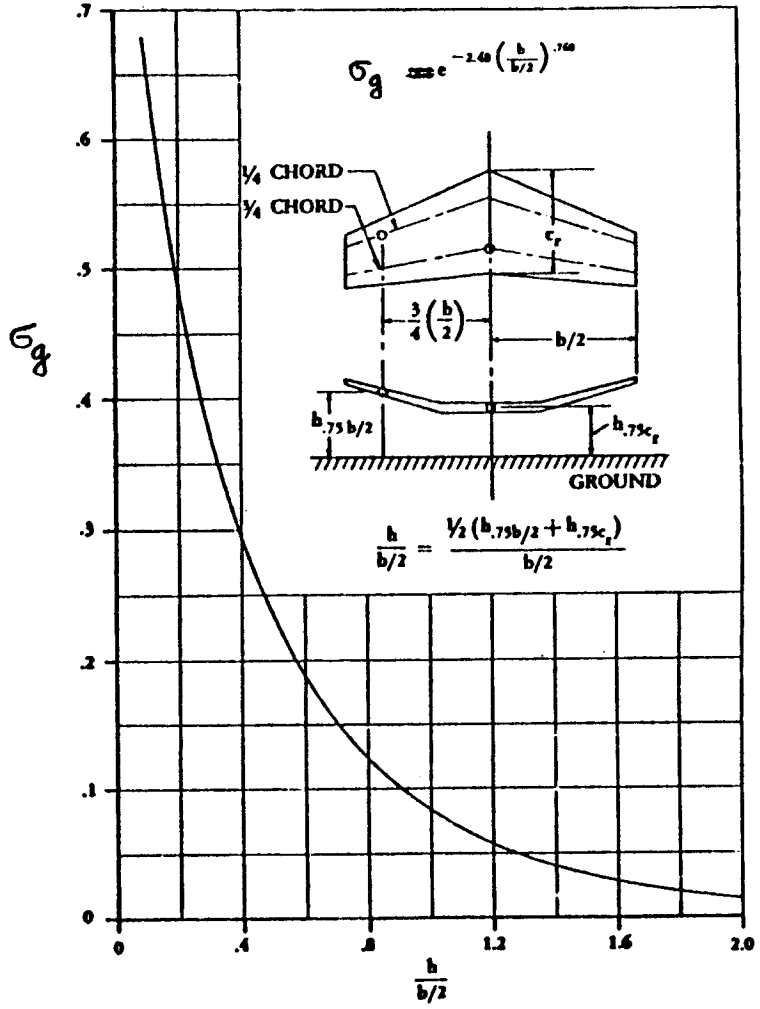

Figure 8.77 Factor Due to Vertical Induced Velocity

σ_g is found from Figure 8.77.

A is the wing aspect ratio.

r_g is found from Figure 8.75.

T_g is found from Figure 8.78.

$(C_{L_\alpha})_{wf}$ is found from Eqn.(8.43), in 1/deg.

B_g is found from Figure 8.79.

Equation (8.56) neglects the effect of wing thickness which is small except for very thick wings close to the ground.

Equation (8.56) is used to estimate $\Delta\alpha_g$ for two values of $C_{L_{wf}}$ after which the airplane C_L versus α curve is modified as indicated in Figure 8.72b. This procedure neglects the effect of the horizontal tail and the canard on airplane lift in ground effect. In Section 8.2.7 it will be seen that the effect of the horizontal tail and the canard on airplane pitching moment in ground effect is NOT neglected.

8.1.8 Power Effects on Airplane Lift

The only power effect on lift which will be considered here is that due to propeller slipstream acting on a wing. Figure 8.80 shows the basic propeller-on-wing geometry. The effect of the propeller is to increase the dynamic pressure over the wing behind the propeller. In turn, this causes an increase in wing lift (and thus in airplane lift) which may be estimated from:

$$\Delta C_{L_w} = \sum_{i=1}^{i=n} \left[(S_{p_i}/S)(C_{L_w}) \left[(2200 P_{av_i}) / \{ \bar{q} U_1 \pi (D_{p_i})^2 \} \right] \right] \quad (8.57)$$

where: S_{p_i} is the wing area affected by the slipstream, see Figure 8.80.

C_{L_w} is the lift coefficient at which the wing is operating. It follows from Sub-sections 8.1.3 or 8.1.4.

BOTH COPIED FROM REF. 9

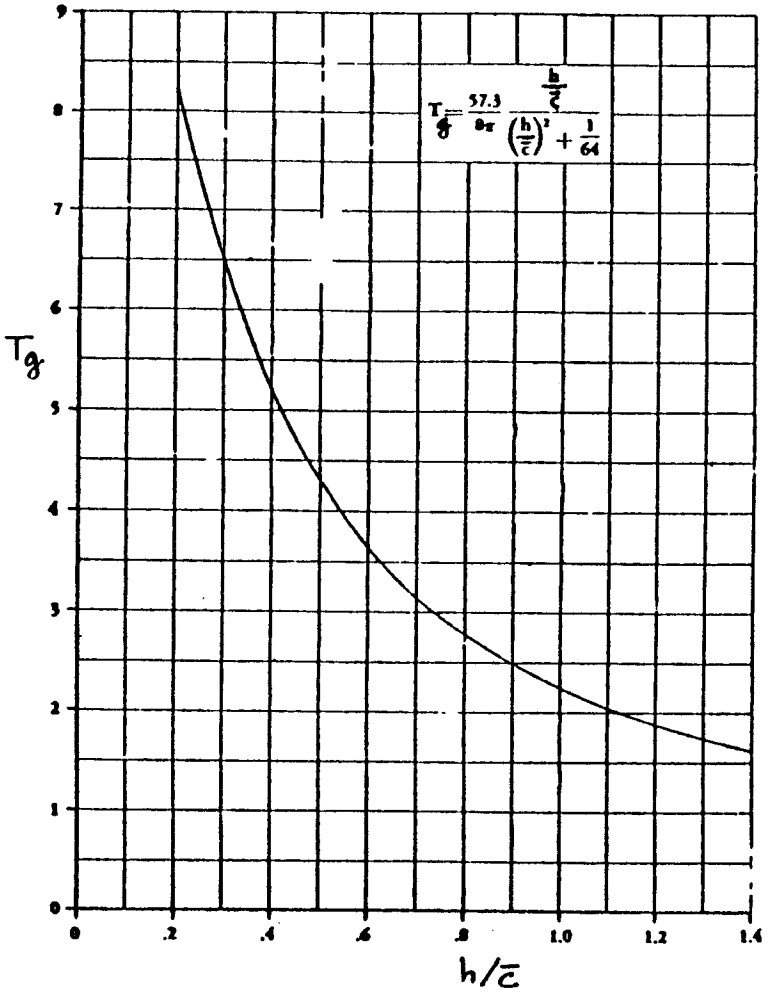

Figure 8.78 Factor Due to Horizontal Induced Velocity

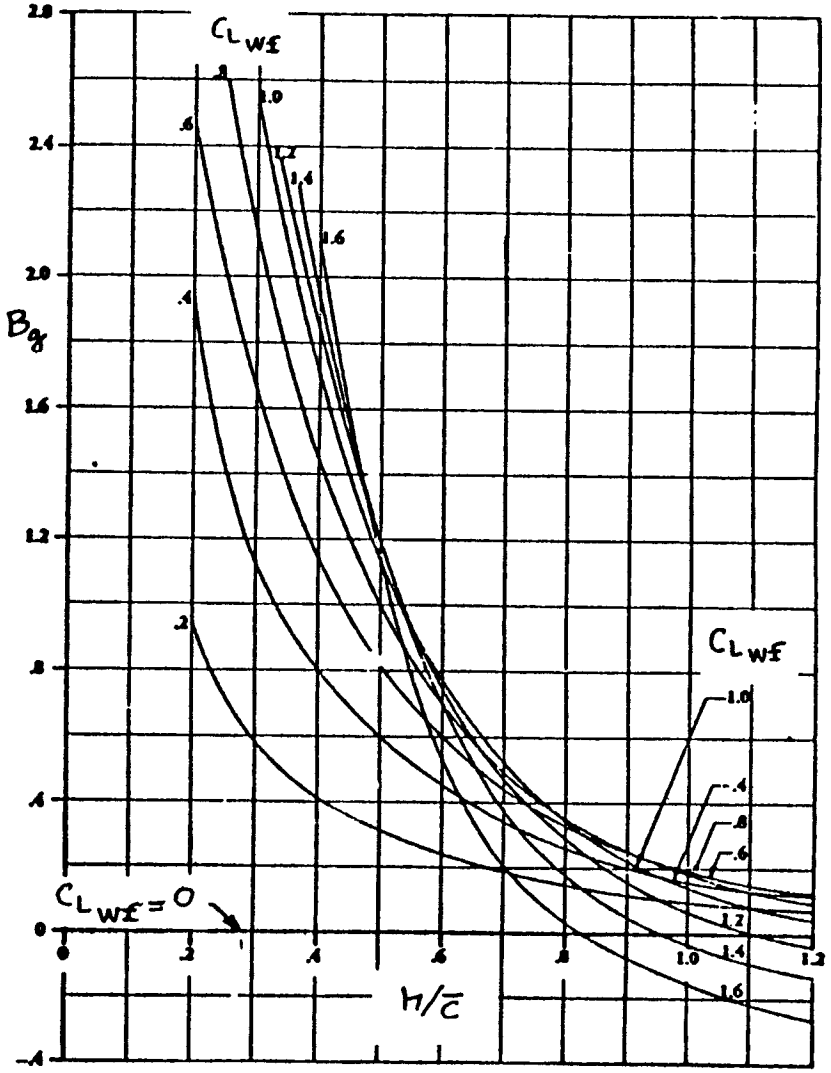

Figure 8.79 Factor Due to Circulation Change

P_{av_i} is the available horsepower, see Section 6.4.

U_1 is the steady state speed of the airplane

D_{p_i} is the propeller diameter in ft.

A more detailed treatment of power effects on lift is considered beyond the scope of this text. Reference 9 addresses this topic.

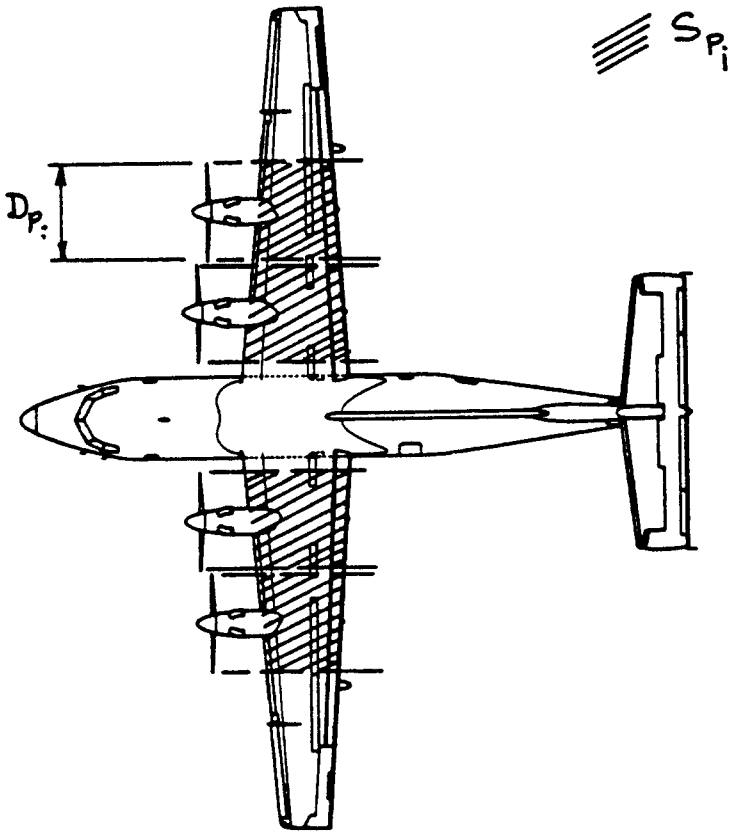

Figure 8.80 Wing Area Affected by Propeller Slipstream

8.2. PREDICTION OF PITCHING MOMENT COEFFICIENT VERSUS LIFT COEFFICIENT

In this section methods for predicting the variation of pitching moment coefficient with lift coefficient will be presented as follows:

8.2.1 Airfoil pitching moment: flaps up
8.2.2 Airfoil pitching moment: flaps down
8.2.3 Wing pitching moment: flaps up
8.2.4 Wing pitching moment: flaps down
8.2.5 Airplane pitching moment: flaps up
8.2.6 Airplane pitching moment: flaps down
8.2.7 Airplane pitching moment in ground effect
8.2.8 Power effects on airplane pitching moment

8.2.1 Airfoil Pitching Moment: Flaps Up

Figure 8.81 shows the relationship between airfoil pitching moment coefficient and airfoil lift coefficient which must be determined with the methods presented in this Section. Key quantities needed in the construction of the airfoil c_m versus c_l curve are listed, with an indication of where methods for their estimation are found. Note that c_m has meaning only when taken about a known reference point. The location of this reference point is defined in 8.2.1.3.

8.2.1.1 Airfoil zero-lift pitching moment coefficient: c_{m_o}

IMPORTANT NOTES:

1. In Chapter 4 the subscript 'o' indicates a drag coefficient at zero lift coefficient.
2. In Section 8.1 the subscript 'o' indicates a lift coefficient at zero angle of attack.
3. In this section (8.2) the subscript 'o' indicates a pitching moment coefficient at zero lift coefficient.

Reference 49 contains a large data base for finding c_{m_o} for many airfoils. This data base applies to the so-called NACA airfoils.

Table 8.1 (p.216-217) provides a summary of airfoil

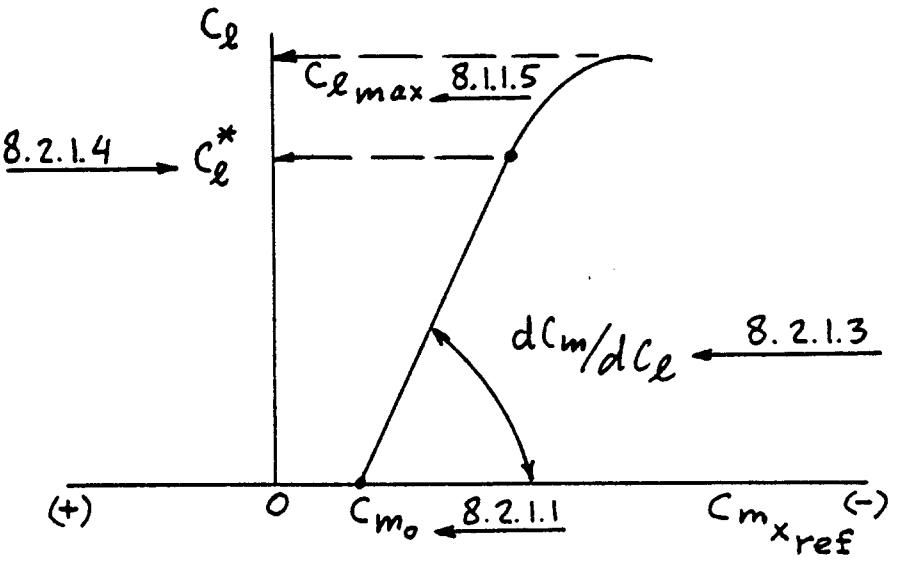

Figure 8.81 Airfoil Pitching Moment Coefficient Versus Lift Coefficient

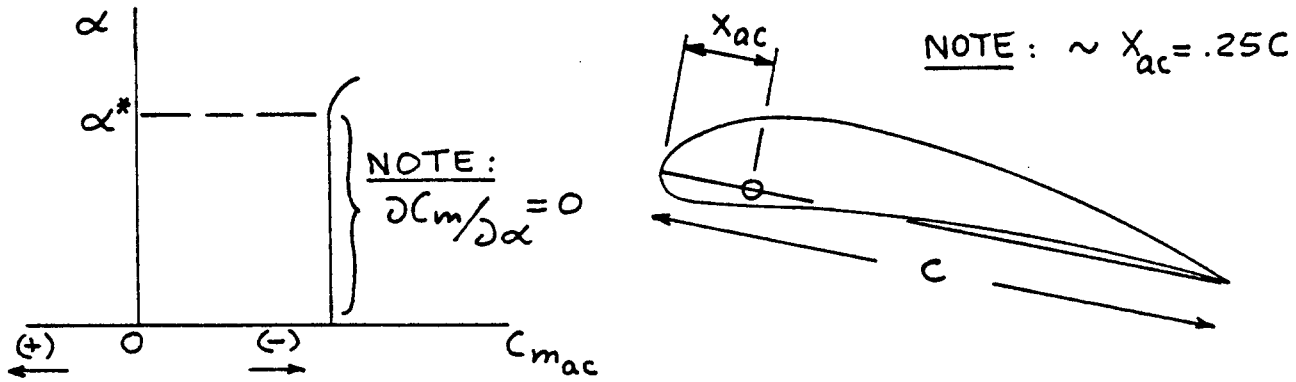

Figure 8.82 Location of Airfoil Aerodynamic Center

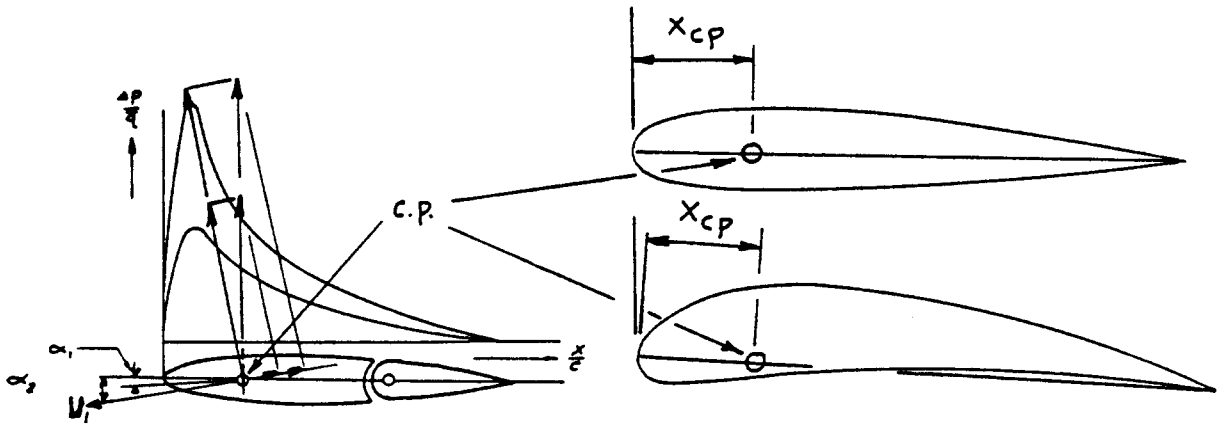

Figure 8.83 Airfoil Center of Pressure: Origin and Location

data from which c_{m_o} may be determined. Where possible, actual airfoil data should be used. Such data may be obtained either from windtunnel data or from theoretical predictions obtained with a modern airfoil code.

Note from Table 8.1 that these c_{m_o} values are zero for symmetrical sections and negative (i.e. nose-down!) for positively cambered airfoils. This will have important consequences to airplane trim!

8.2.1.2 Airfoil aerodynamic center: x_{ac} and airfoil center of pressure: x_{cp}

Definition: The aerodynamic center is that point about which the variation of pitching moment coefficient with angle of attack is zero.

Figure 8.82 shows how the aerodynamic center for an airfoil is located.

Note that this concept implies also that the variation of pitching moment coefficient with lift coefficient is zero, when:

$$\alpha < \alpha^* \tag{8.58}$$

Definition: The center of pressure is that point where the resultant force caused by the pressure distribution acts.

Figure 8.83 shows how the center of pressure arises from the airfoil pressure distribution and how the center of pressure is located.

Evidently, there are two methods to represent forces and moments acting on an airfoil. Figure 8.84 shows both methods. The following relationship exists between the two methods:

$$x_{cp} = x_{ac} - (c_{m_{ac}})c/c_l \tag{8.59}$$

This can also be written as:

$$c_{m_{ac}} = -c_l(x_{cp} - x_{ac})/c \tag{8.60}$$

Note from this that:

$$c_{m_{ac}} = c_{m_o} \tag{8.61}$$

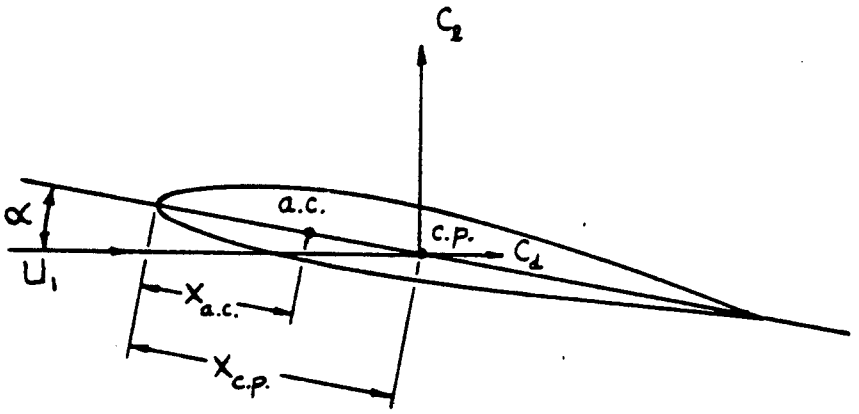

a. Forces at the Center of Pressure

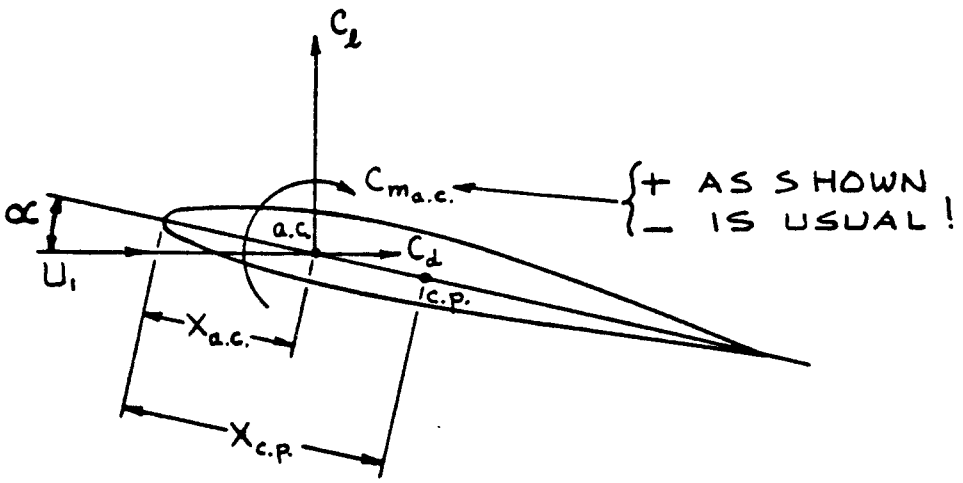

b. Forces at the Aerodynamic Center

Figure 8.84 Methods for Resolving Airfoil Forces and Moments

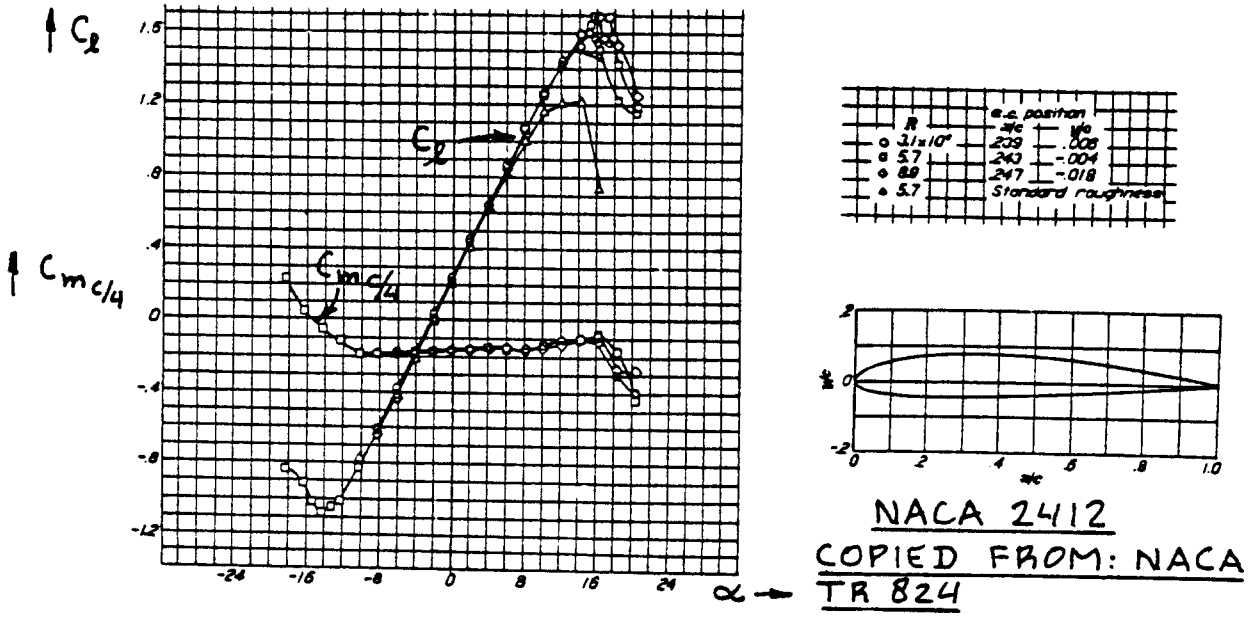

Figure 8.85 Typical Airfoil Lift and Pitching Moment Behavior at Subsonic Speeds

Subsonic:

Figure 8.85 shows typical variations of airfoil pitching moment coefficient with airfoil lift coefficient and with airfoil angle of attack in the subsonic flow range. Such data may be obtained from Reference 49.

Modern airfoil theory is capable of estimating airfoil lift, drag and pitching moment data very accurately. In the absence of experimental data, such theoretically obtained airfoil data may be used.

Table 8.1 (p.216-217) lists values for x_{ac} for several airfoils. Fig.8.86 shows how airfoil a.c. location changes with the thickness ratio, t/c and with the trailing edge angle, $\bar{\varphi}_{te}$.

Transonic:

Airfoil pitching moment behavior changes markedly above the so-called critical Mach number. Experimental data or data obtained from modern airfoil codes should be used to predict the airfoil pitching moment behavior above M_{crit}. The critical Mach number of an airfoil at any lift coefficient may be estimated from:

For NACA airfoils:

$$M_{crit} = 0.86 - 0.1c_l - t/c \qquad (8.62)$$

For supercritical airfoils:

$$M_{crit} = 0.91 - 0.1c_l - t/c \qquad (8.63)$$

Supersonic:

Theoretically, for very thin airfoils at low lift coefficients, the center of pressure moves toward the 50 percent chord point. Figure 8.87 indicates how the centers of pressure vary with thickness ratio, t/c and with angle of attack for symmetrical airfoils. For symmetrical airfoils it is noted that: $x_{cp} = x_{ac}$!

Note: this aft shift of the center of pressure in the supersonic speed range has very significant implications to airplane trim and drag in this speed range!

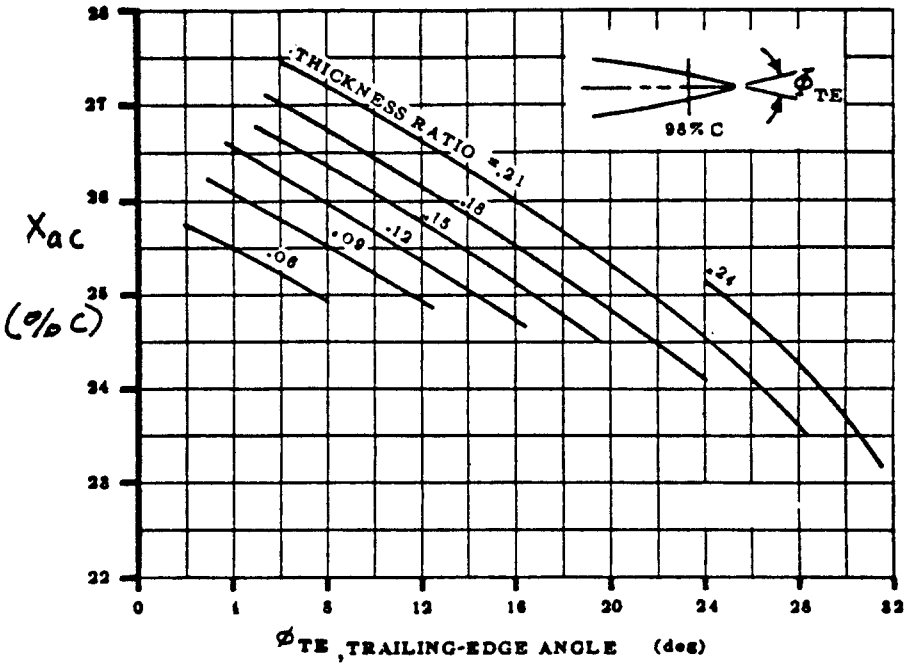

COPIED FROM:
REF. 9

Figure 8.86 Effect of Trailing Edge Angle and Thickness Ratio on Airfoil Aerodynamic Center Location at Subsonic Speeds

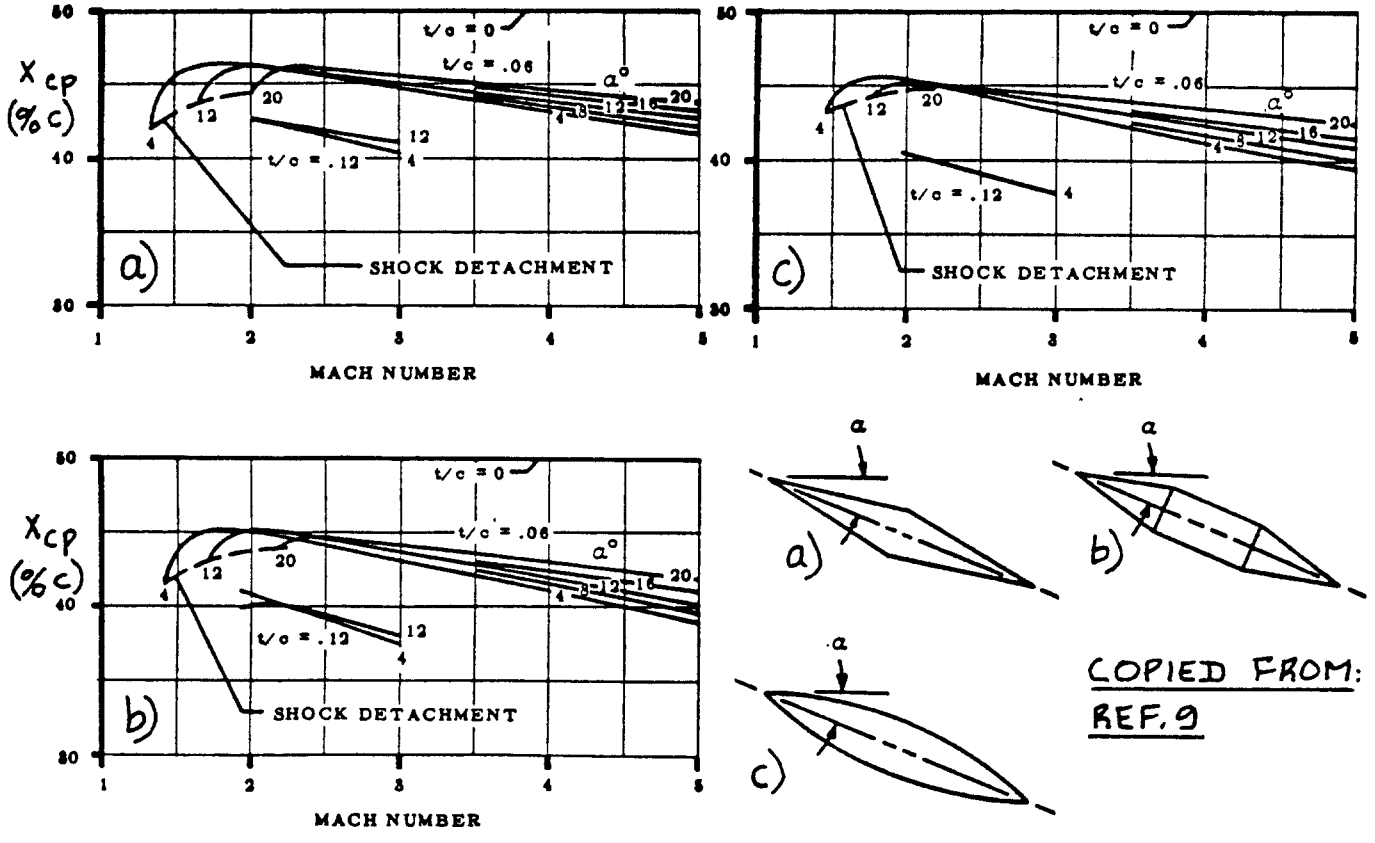

COPIED FROM:
REF. 9

Figure 8.87 Effect of Thickness Ratio and Angle of Attack on Airfoil Center of Pressure Location at Supersonic Speeds

8.2.1.3 Airfoil pitching moment variation with lift coefficient: dc_m/dc_l

To determine the variation of airfoil pitching moment coefficient with lift coefficient it is necessary to first select a so-called reference center: Figure 8.88 shows such a reference center. The pitching moment coefficient is defined relative to this reference center:

$$c_m = c_{m_0} + c_l(x_{ref} - x_{ac})/c \qquad (8.64)$$

The variation of pitching moment coefficient with lift coefficient follows by differentiation:

$$dc_m/dc_l = (x_{ref} - x_{ac})/c = \bar{x}_{ref} - \bar{x}_{ac} \qquad (8.65)$$

8.2.1.4 Airfoil linear range for pitching moment: c_l^*

The range of lift coefficients for which the variation of airfoil pitching moment coefficient with lift coefficient is linear follows from:

$$c_l^* = (c_{l_\alpha})(\alpha^* - \alpha_{o_l}) \qquad (8.66)$$

where all quantities are defined in 8.1.1.

8.2.1.5 Construction of airfoil pitching moment curve: flaps up

All ingredients necessary to construct the airfoil pitching moment curve about a reference center x_{ref} are now available. Figure 8.89 shows how this may be done in a step-by-step manner. Whether or not the pitching moment coefficient breaks in a stable or in an unstable manner depends on the separation behavior of the airfoil. Reference 49 contains experimental data which defines the pitching moment 'break' behavior of airfoils. Many (in fact, most) airfoils have stable pitching moment breaks.

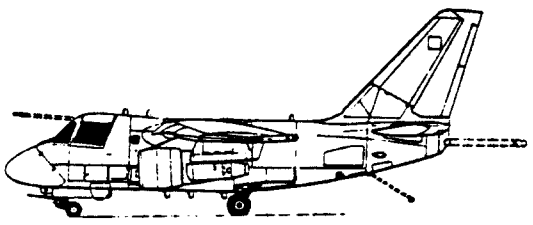

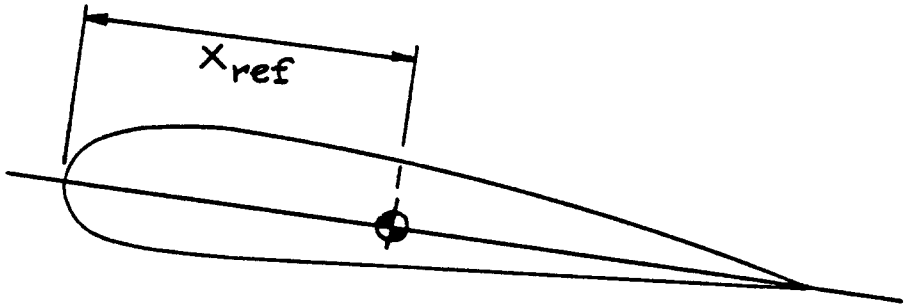

Figure 8.88 Example Location of Reference Center

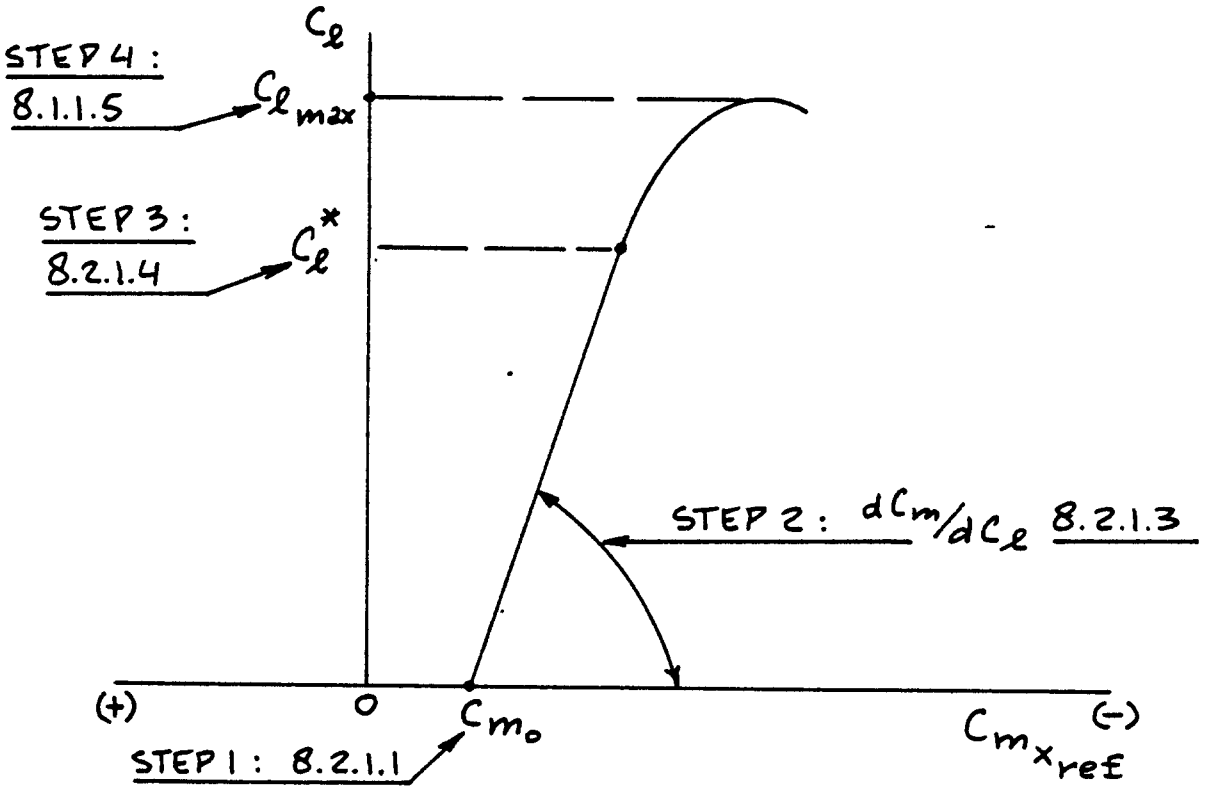

Figure 8.89 Construction of Airfoil Pitching Moment Versus Lift Curve

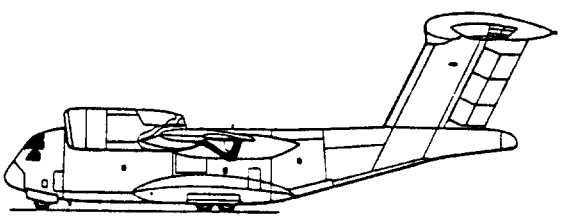

8.2.2 Airfoil Pitching Moment: Flaps Down

Figure 8.90 shows the comparison between flaps-up and flaps-down pitching moment characteristics for an airfoil. Key quantities which are required in the estimation of flap-down behavior are listed with an indication of where methods for their estimation may be found.

Note that the assumption is made that the dc_m/dc_l slope of the airfoil with the flaps down is the same as that for the airfoil with the flaps up. This is reasonable because in the linear angle of attack range, a change in airfoil camber (read flap deflection) has no effect on the c_m-c_l slope.

8.2.2.1 Airfoil pitching moment increment due to flaps: Δc_m

The airfoil incremental pitching moment coefficient due to flaps, Δc_m depends on the type of flaps used.

Methods are presented for trailing edge and for leading edge flaps.

A. Trailing Edge Flaps

For Split, Slotted and Fowler Flaps:

The following method applies to all types of trailing edge flaps, except for plain flaps:

$$\Delta c_m = \Delta c_l \{x_{ref}/c - (x_{cp}/c')(c'/c)\} \qquad (8.67)$$

where: Δc_l is the lift increment due to flaps as found from 8.1.2.

x_{ref} is defined in Figures 8.88 and 8.91.

x_{cp}/c' is found from Figure 8.91.

c' is defined in Figures 8.18 and 8.19. For a split flap and for a plain flap: $c' = c$.

Note: since Δc_l due to flaps as used in Eqn. (8.64) depends on the flap type and on the flap deflection, the latter is inherently accounted for in this method.

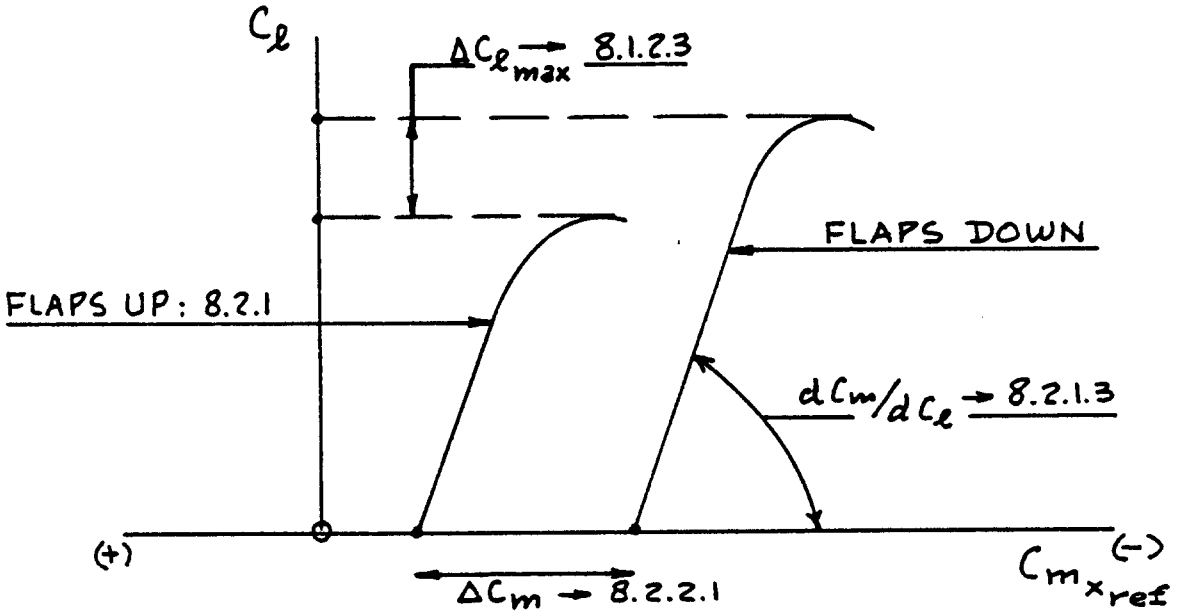

Figure 8.90 Airfoil Pitching Moment Coefficient Versus Lift Coefficient with the Flaps Down

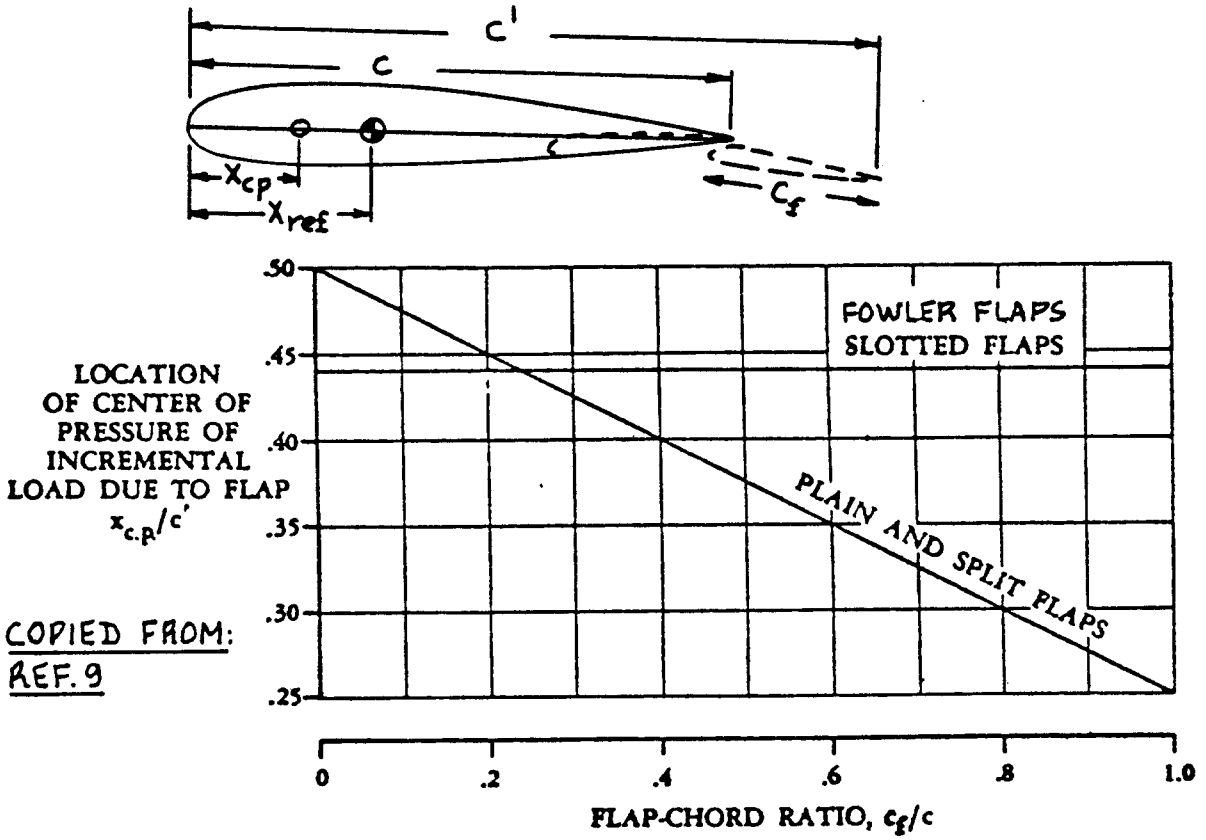

COPIED FROM: REF. 9

Figure 8.91 Location of Center of Pressure due to Incremental Flap Load

For Plain Flaps:

Δc_m is found from Figure 8.92. Observe that this is a pure moment coefficient: its lift dependence is expressed through the plain flap deflection.

B. Leading Edge Flaps:

$$\Delta c_{m_{le}} = (c_{m_{\delta le}})'(c'/c)^2 \delta_{f_{le}} + \{(x_{ref}/c) + (c' - c)/c\}\Delta c_{l_{le}} + c_m\{(c'/c)^2 - 1\} + 0.75 c_l (c'/c)\{(c'/c) - 1\} \quad (8.68)$$

where: $(c_{m_{\delta le}})'$ is found from Figure 8.93.

c'/c is defined in Figures 8.27, 8.28 and 8.93.

δ_{fle} is defined in Figures 8.25, 8.27 and 8.28, where it is called δ_f (in deg).

$\Delta c_{l_{le}}$ is the lift coefficient increment due to leading edge flaps as found from 8.1.2.

c_m is the airfoil pitching moment coefficient with the flaps-up, taken about x_{ref} and as found from 8.2.1.

c_l is the airfoil lift coefficient with the flaps-up as determined from the flight condition.

8.2.2.2 Construction of the flaps-down airfoil pitching moment curve

Figure 8.94 shows how the flaps-down pitching moment curve is obtained from the corresponding flaps-up curve.

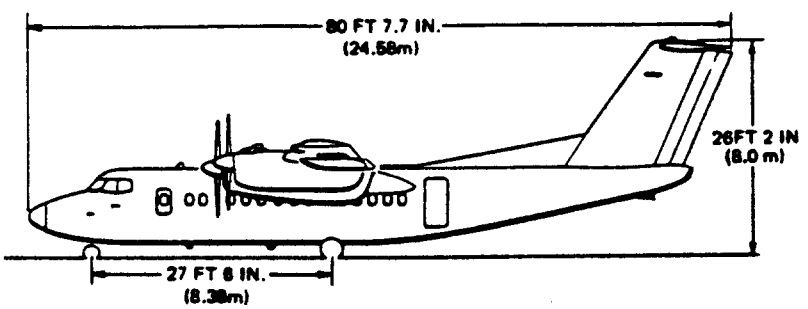

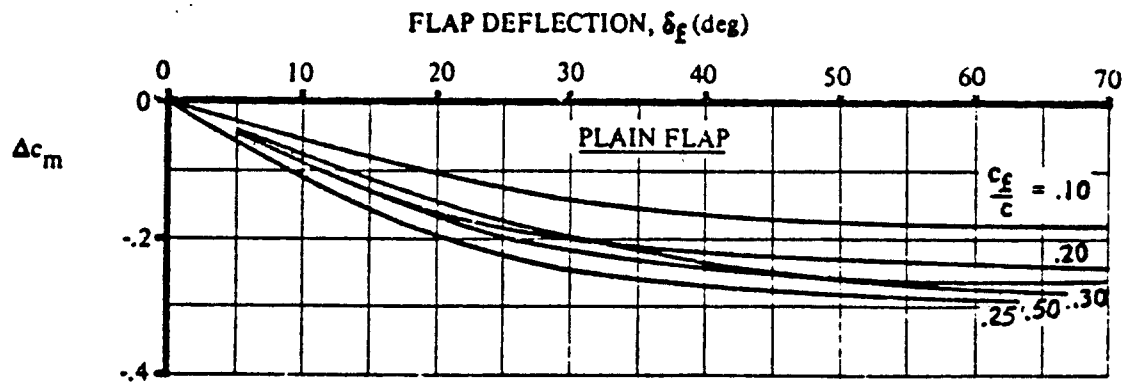

COPIED FROM: REF. 9

Figure 8.92 Incremental Pitching Moment Coefficient due to Plain Flaps

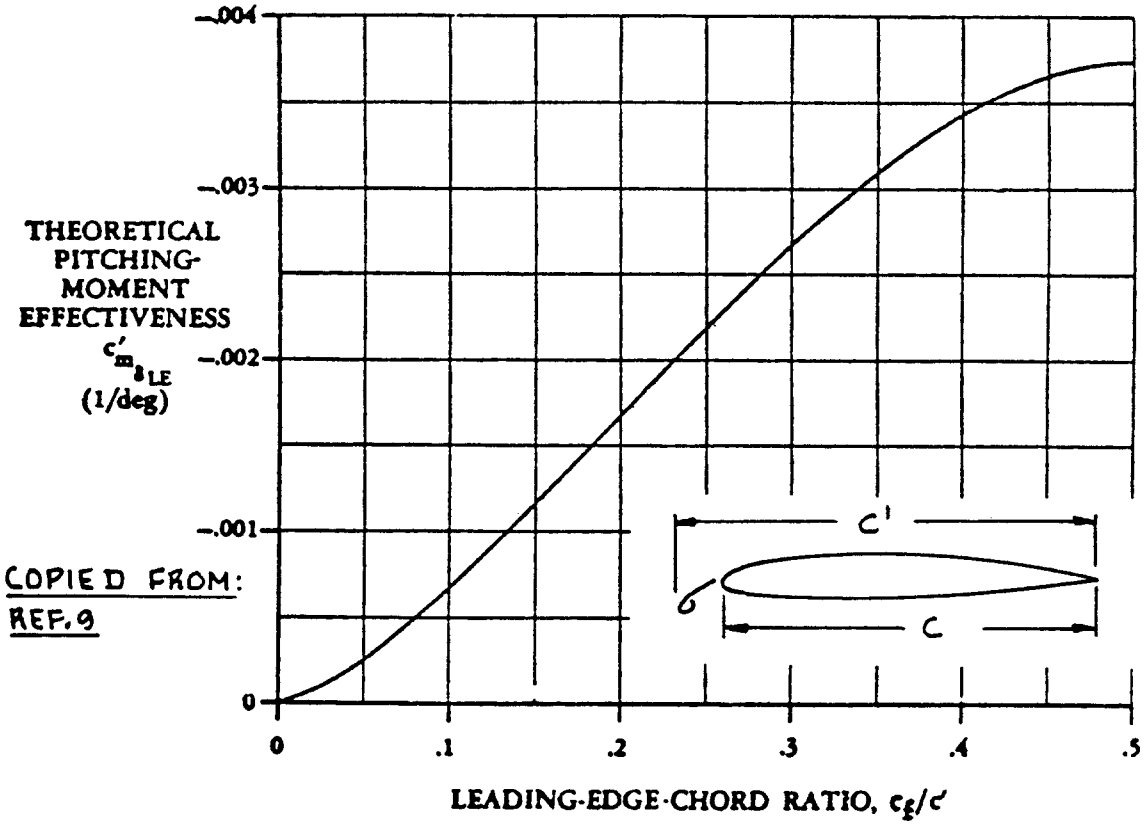

COPIED FROM: REF. 9

Figure 8.93 Pitching Moment Effectiveness due to Leading Edge Flaps

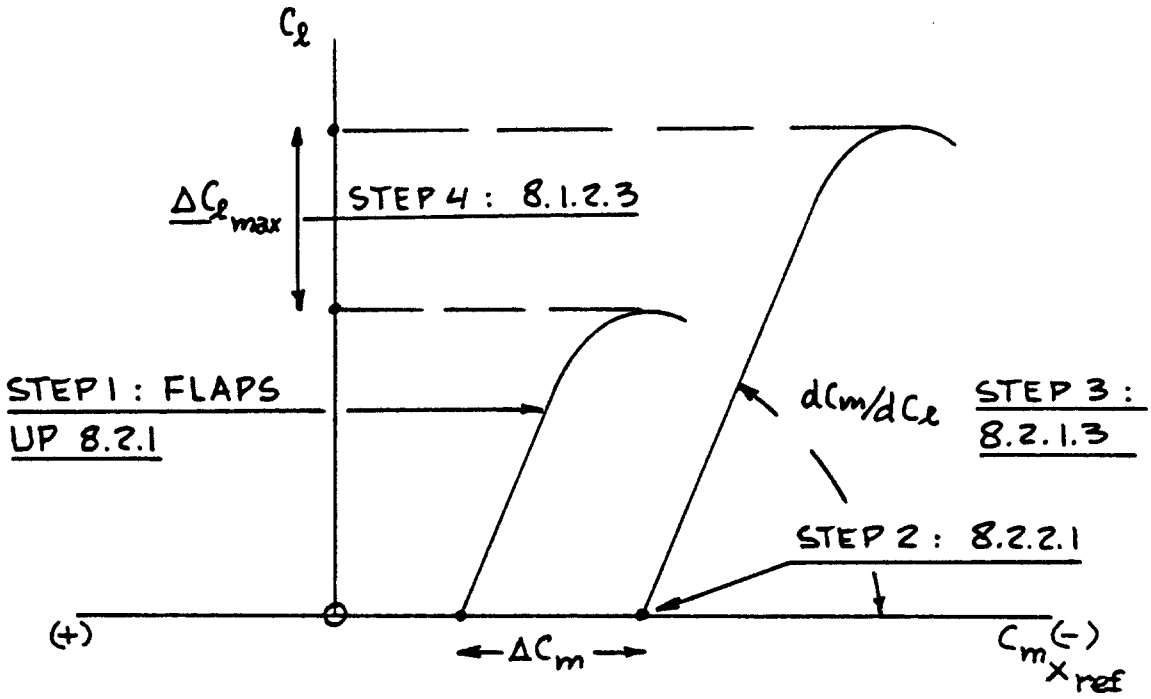

Figure 8.94 Construction of Flaps Down Airfoil Pitching Moment Versus Lift Curve

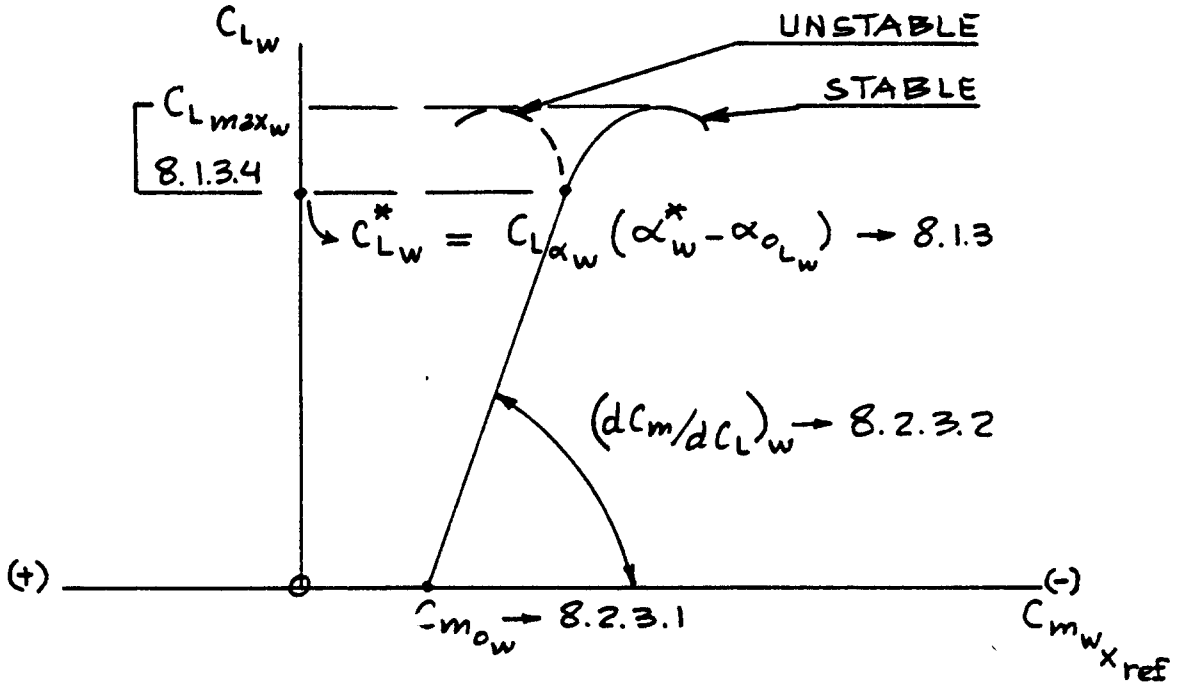

Figure 8.95 Wing Pitching Moment Coefficient Versus Lift Coefficient Curve

8.2.3 Wing Pitching Moment: Flaps-Up

Figure 8.95 shows the flaps-up pitching moment behavior which needs to be predicted with the methods of this section. Key quantities which are required in the estimation of flaps-up behavior are listed with an indication of where methods for their estimation may be found.

A key parameter in estimating wing pitching moment behavior is the mean geometric chord of the wing (mgc), $\bar{c}$ and its location on the planform. Figure 8.96 defines these quantities for two types of straight tapered wing as well as for a more general wing.

Since pitching moments are defined relative to a reference point, it is mandatory to locate such a reference point (also called moment reference center) on the wing planform. Figures 8.97 shows two methods used do this.

Observe that:

$$n_{ref} = x_{ref} + n_{mgc} \tag{8.69}$$

The method labelled as 2 is the preferred method.

8.2.3.1 Wing zero-lift pitching moment coefficient: $C_{m_{o_w}}$

Subsonic:

$$C_{m_{o_w}} = \{(A\cos^2\Lambda_{c/4})/(A + 2\cos\Lambda_{c/4})\}(c_{m_{o_r}} + c_{m_{o_t}})/2 + (\Delta C_{m_o}/\varepsilon_t)\varepsilon_t \tag{8.70}$$

where: $c_{m_{o_r}}$ and $c_{m_{o_t}}$ are the zero-lift pitching moment coefficients of the root and tip airfoils respectively. These follow from 8.2.1.1.

$\Delta C_{m_o}/\varepsilon_t$ is found from Figure 8.98.

Note: This method applies to conventional straight tapered wings with sweep angles below 45 degrees and aspect ratios above 2.5. For other wing types, Reference 9 should be consulted.

Transonic:

Up to the critical Mach number, use:

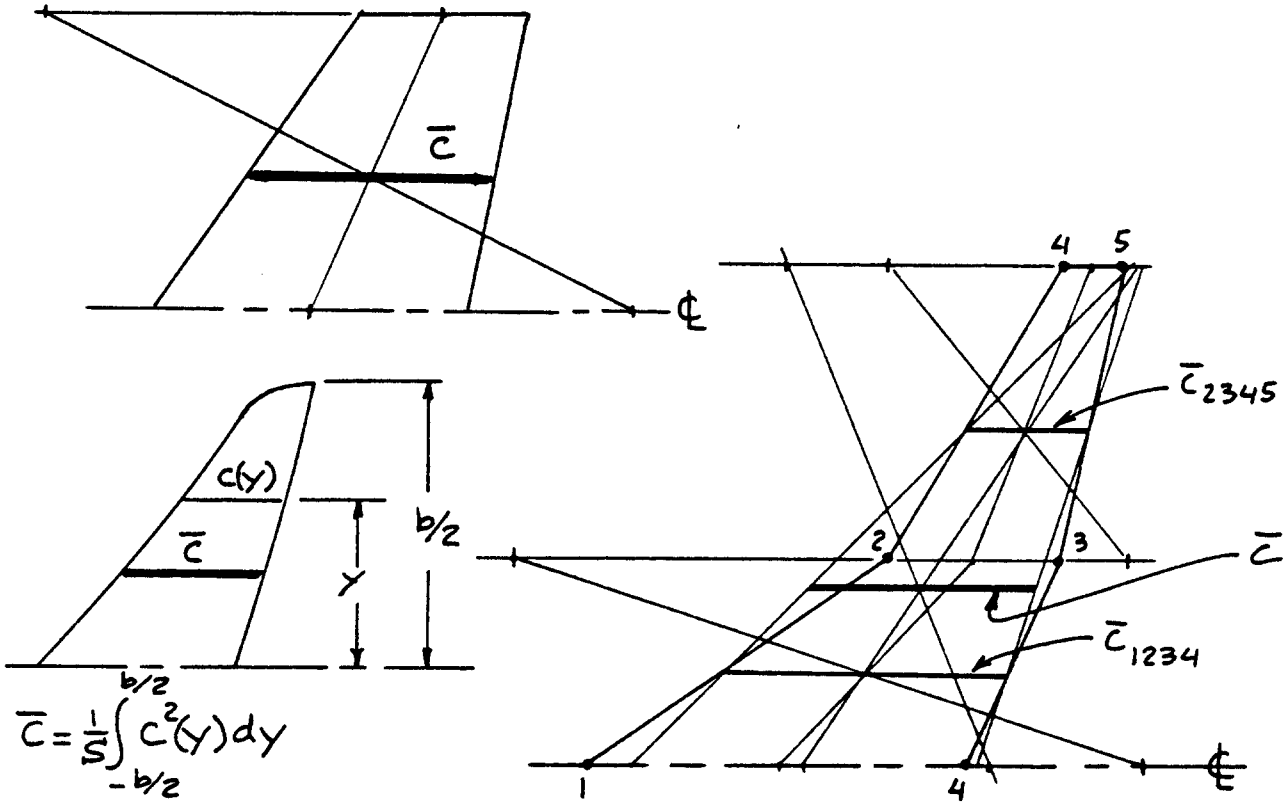

Figure 8.96 Methods for Determining the Wing Mean Geometric Chord

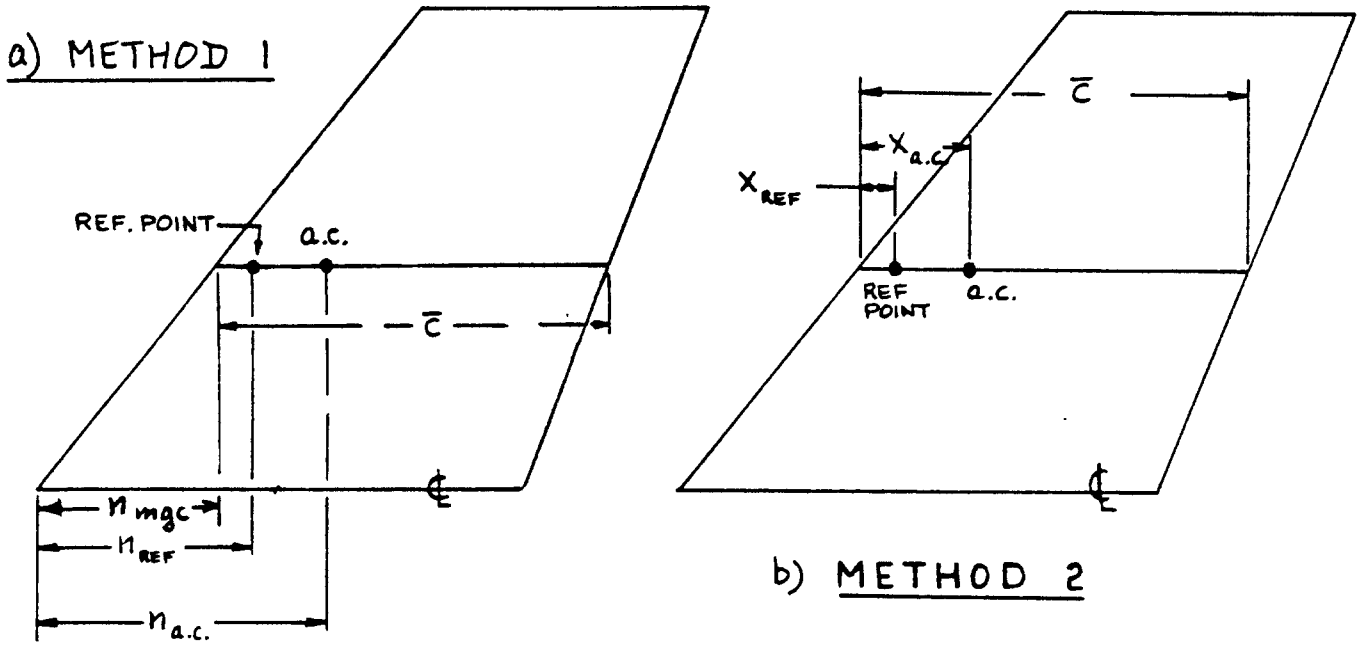

Figure 8.97 Methods for Locating a Wing Reference Point and the Wing Aerodynamic Center

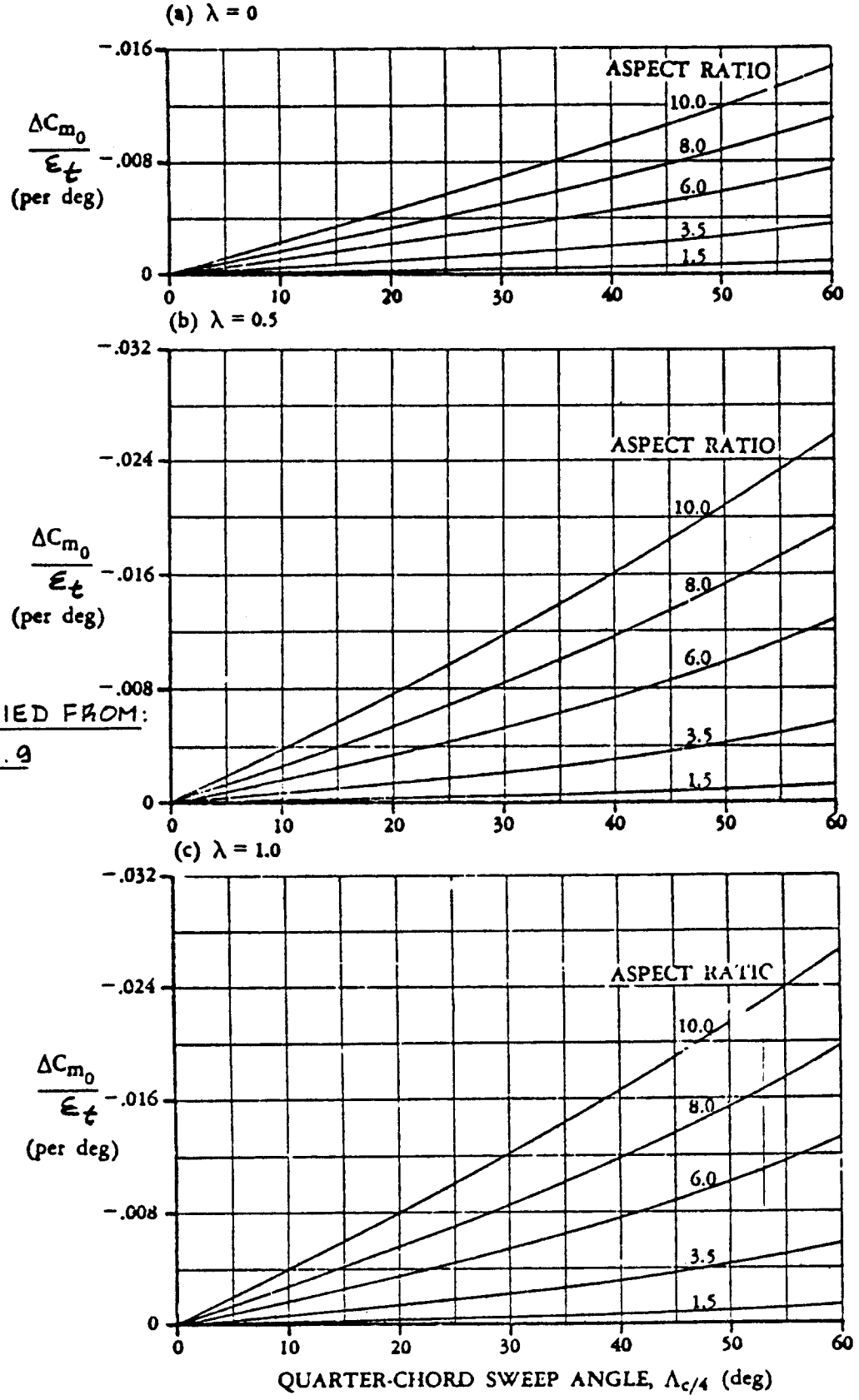

COPIED FROM:
REF. 9

Figure 8.98 Effect of Linear Twist on Wing Zero-lift Pitching Moment Coefficient

$$C_{m_{o_{w_{at\ M}}}} = C_{m_{o_{w_{at M=0}}}} \{(C_{m_o})_M/(C_{m_o})_{M=0}\} \quad (8.71)$$

where: $\{(C_{m_o})_M/(C_{m_o})_{M=0}\}$ is given in Figure 8.99.

$C_{m_{o_{w_{at\ M=0}}}}$ is found from Eqn.(8.70).

Supersonic:

For supersonic Mach numbers it is suggested to use experimental data. Since supersonic wings frequently have little camber, their $C_{m_{o_w}}$ values tend to be small.

8.2.3.2 Slope of the wing pitching moment curve: $(dC_m/dC_L)_w$

The method which follows applies only to straight, tapered planforms. For very highly swept wings and for cranked wings the method of Reference 9 should be used.

Subsonic:

The subsonic slope of the wing pitching moment curve may be found from:

$$(dC_m/dC_L)_w = \{(n_{ref} - n_{ac})/c_r\}(c_r/\bar{c}) \quad (8.72)$$

where: n_{ref} is the location of the moment reference center relative to the wing apex: see Fig.8.97a.

n_{ac} is the location of the wing aerodynamic center relative to the wing apex: see Figure 8.97a.

For wings of aspect ratios above 5 and sweep angles below 35 degrees it is usually acceptable to use:

$$n_{ac} = n_{mgc} + 0.\bar{2}5c \quad (8.73)$$

For other wings, Figure 8.100 should be used.

Transonic:

For transonic Mach numbers, see Reference 9.

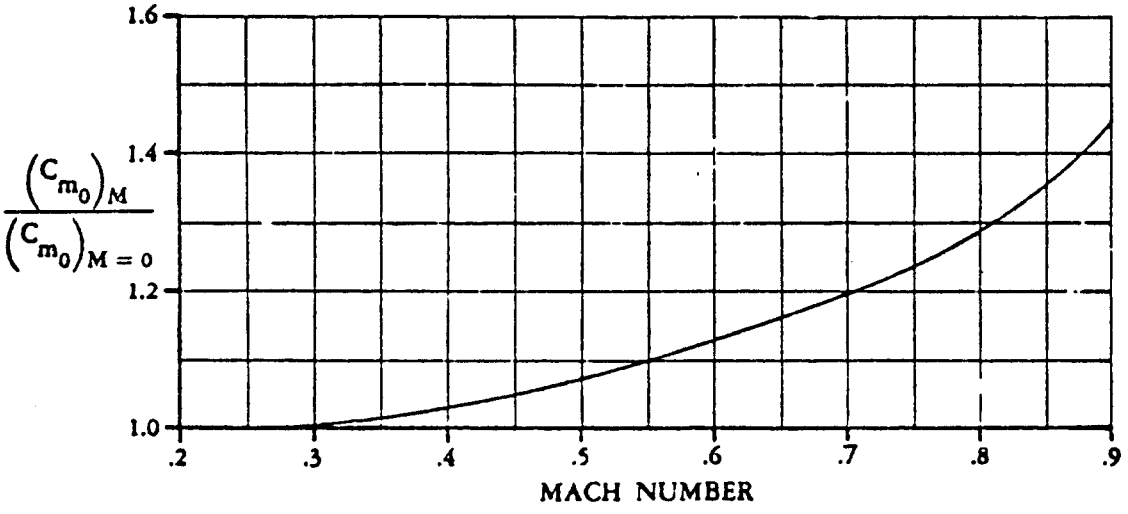

COPIED FROM : REF. 9

Figure 8.99 Effect of Mach Number on Wing Zero-lift Pitching Moment Coefficient

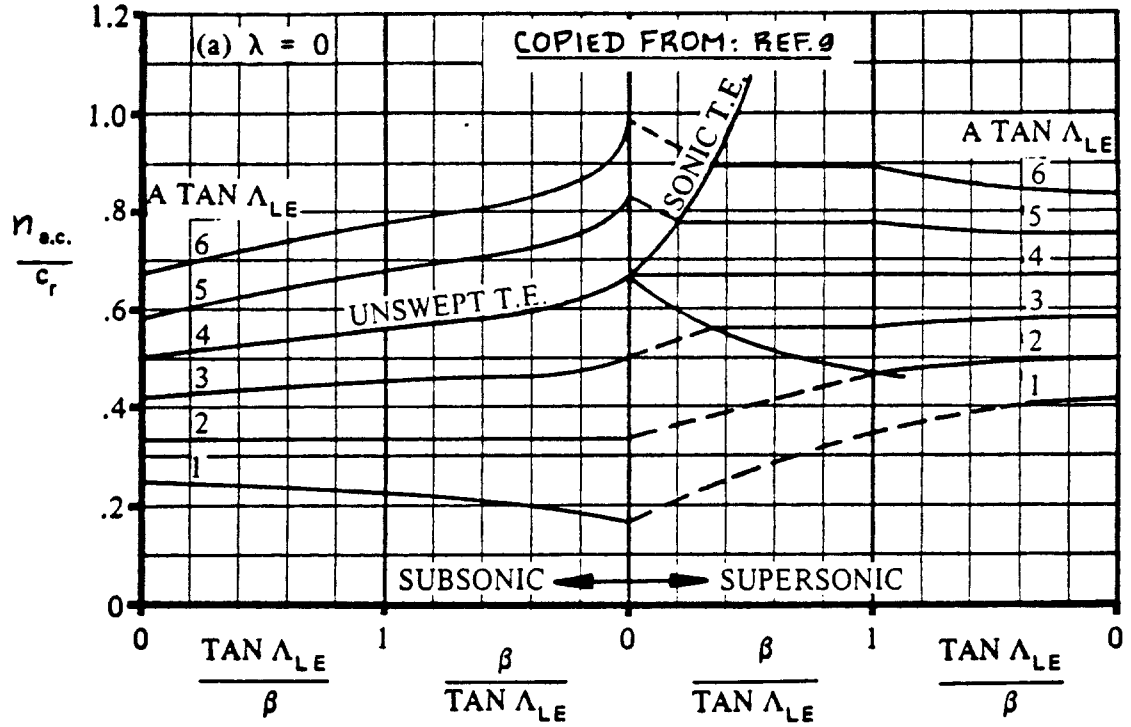

Figure 8.100 Effect of Aspect Ratio, Sweep Angle and Taper Ratio on Wing Aerodynamic Center

COPIED FROM: REF.9

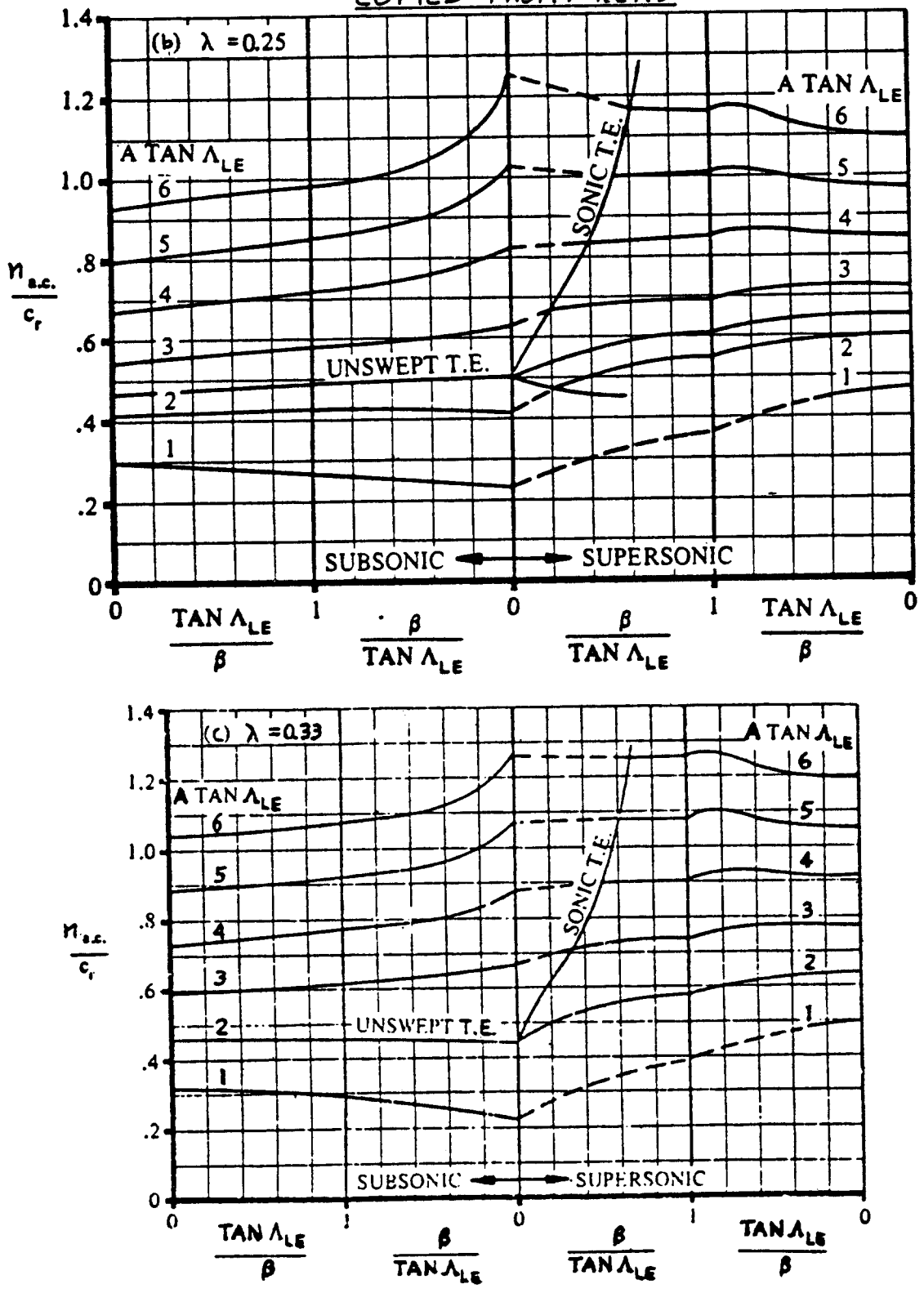

Figure 8.100 (Cont'd) Effect of Aspect ratio, Sweep Angle and Taper Ratio on Wing Aerodynamic Center

COPIED FROM REF.9

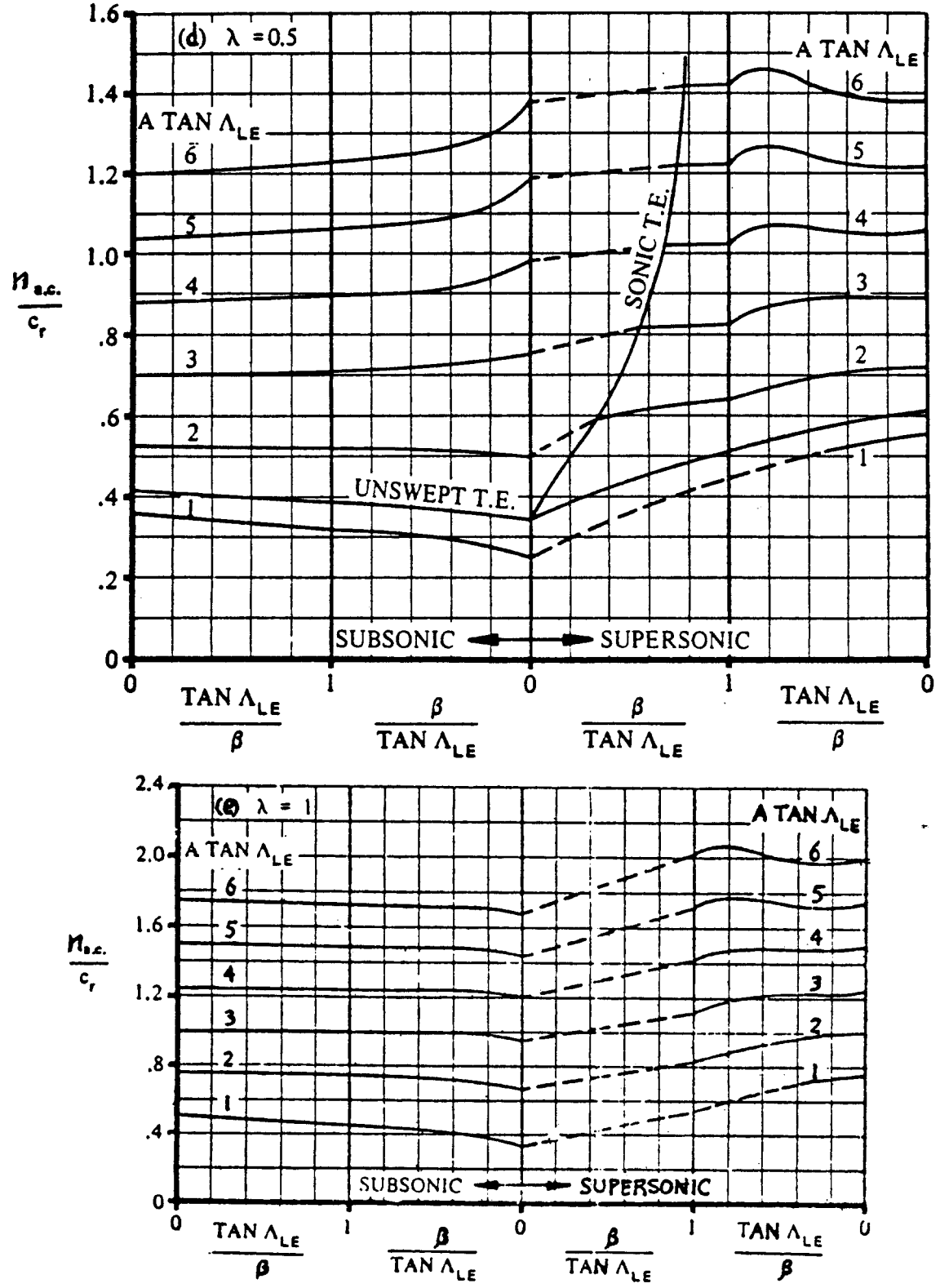

Figure 8.100 (Cont'd) Effect of Aspect Ratio, Sweep Angle and Taper Ratio on Wing Aerodynamic Center

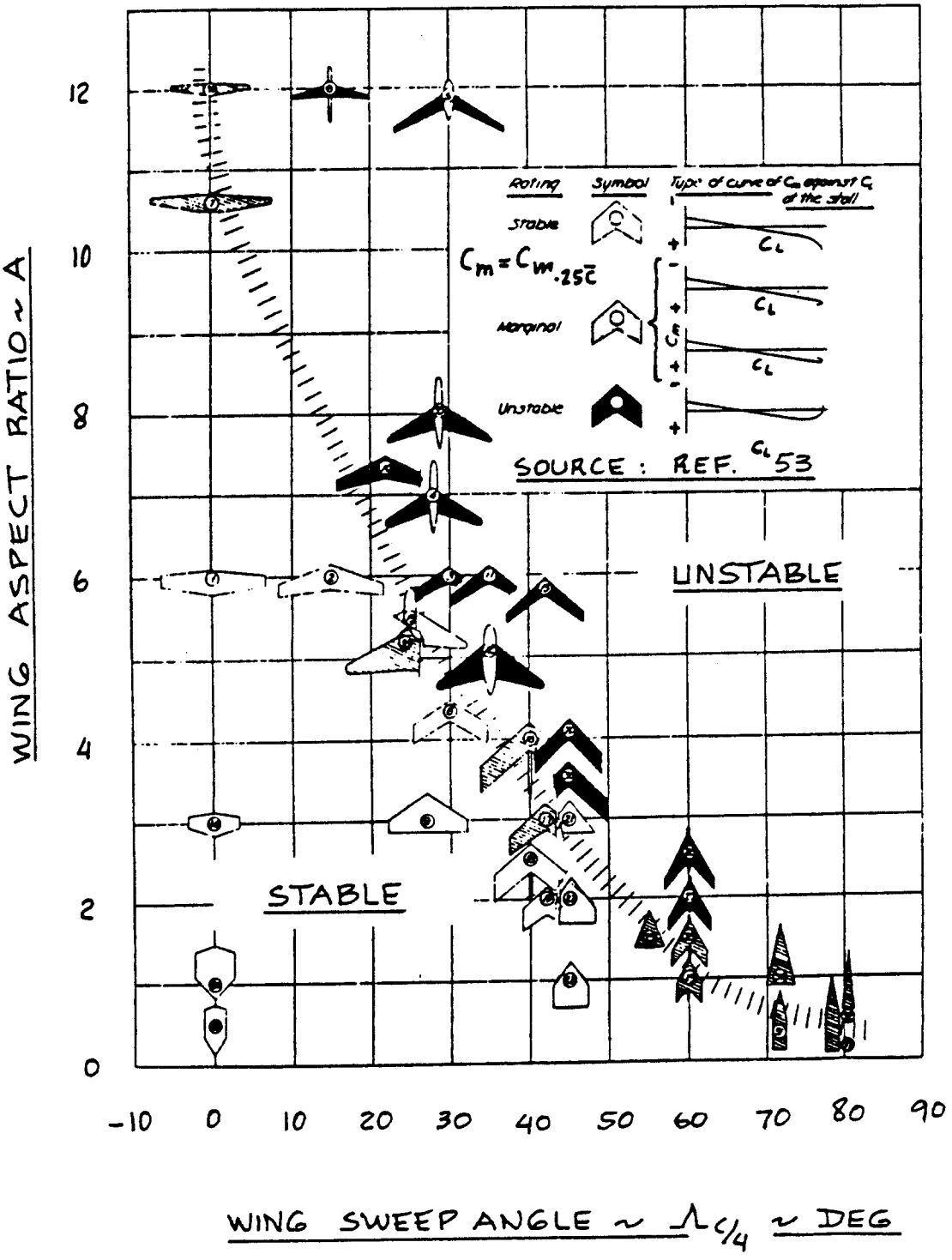

Figure 8.101 Wing Alone Pitch Break Stability Boundary

Supersonic:

For supersonic Mach numbers, see Reference 9.

8.2.3.3 Prediction of stable or unstable pitch break

Whether a wing has stable or unstable pitch break behavior depends on the type of airfoil(s) used as well as on the wing planform. Figure 8.101 may be used as an initial guide in the prediction of pitch break behavior. The reader should refer to Part III, p.266-269 for a more detailed discussion of the pitch break phenomenon. As pointed out in Part IV (p.269) wings with highly swept strakes should be expected to have severely unstable pitch breaks.

8.2.3.4 Construction of the wing pitching moment curve: flaps-up

All ingredients needed for the construction of the flaps-up wing pitching moment curve are now available. Figure 8.102 shows how this can be done in a stepwise manner.

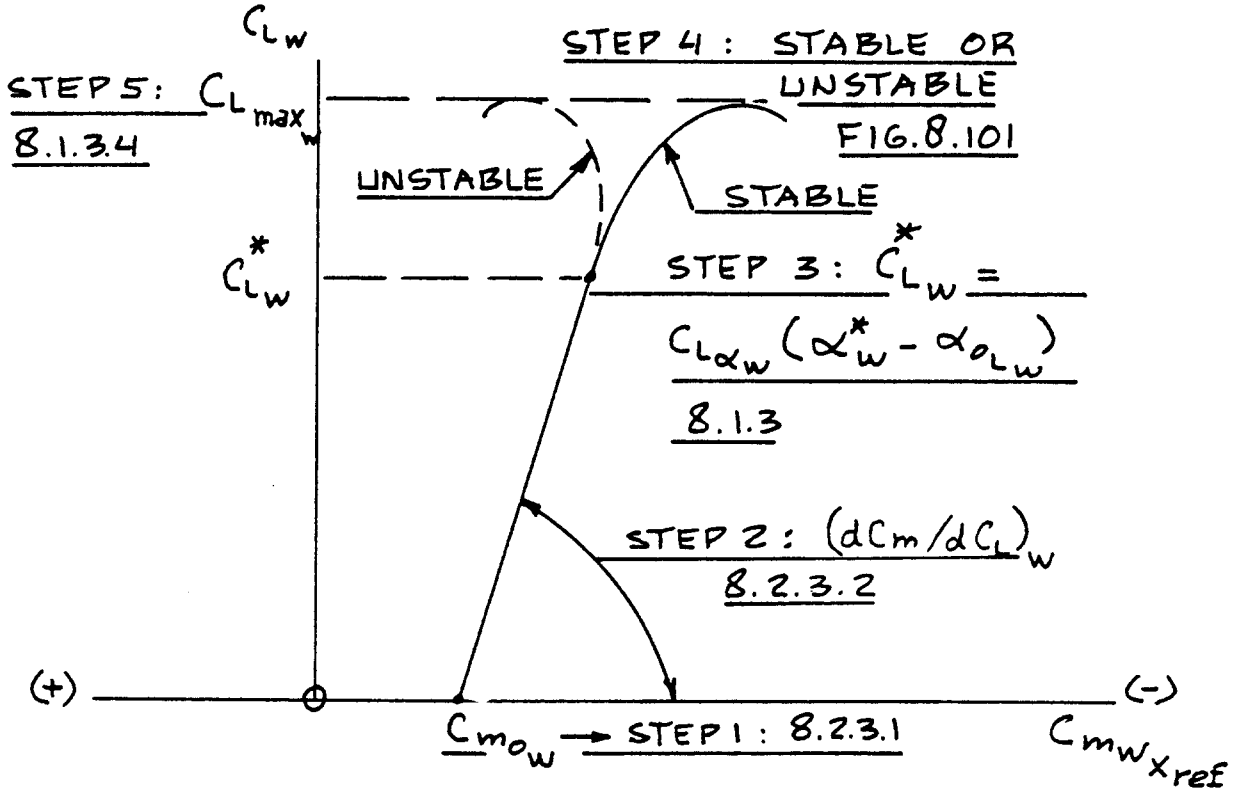

Figure 8.102 Construction of Flaps Up Wing Pitching Moment Versus Lift Curve

8.2.4 Wing Pitching Moment: Flaps-Down

Figure 8.103 shows the flaps-down pitching moment behavior which must be predicted with the methods of this section. Key quantities which are required in the estimation of flaps-down behavior are listed with an indication of where methods for their estimation may be found.

The method given here does not apply to wings with sweep angles in excess of 45 degrees. The method is also not applicable to wings with aspect ratios: A < 2.5.

8.2.4.1 Wing pitching moment increment due to flaps: ΔC_{m_w}

The wing incremental pitching moment coefficient due to flaps depends on the type of flaps used. Methods are presented for trailing edge flaps and for leading edge flaps.

A. Trailing Edge Flaps

In the low angle of attack range, the incremental wing pitching moment coefficient due to trailing edge flaps (taken relative to x_{ref}) may be found from:

$$\Delta C_{m_w} = \tag{8.74}$$

$$(\bar{x}_{ref} - 0.25)(C_{L_w})_\delta + K_\Lambda (A/1.5)(\Delta C_{L_{ref_w}}) \tan\Lambda_{c/4} +$$

$$+ K_p[(\Delta C'_m/\Delta C_{L_{ref_w}})\Delta C_{L_{ref_w}} (c'/c)^2] +$$

$$- K_p[0.25 C_{L_w}\{(c'/c)^2 - (c'/c)\}] + K_p C_{m_w}\{(c'/c)^2 - 1\}$$

where: x_{ref} is defined in Figure 8.97.

$(C_{L_w})_\delta$ is the wing lift coefficient with the flaps down. It follows from 8.1.4.

C_{L_w} is the flaps-up wing lift coefficient as determined from 8.1.3.

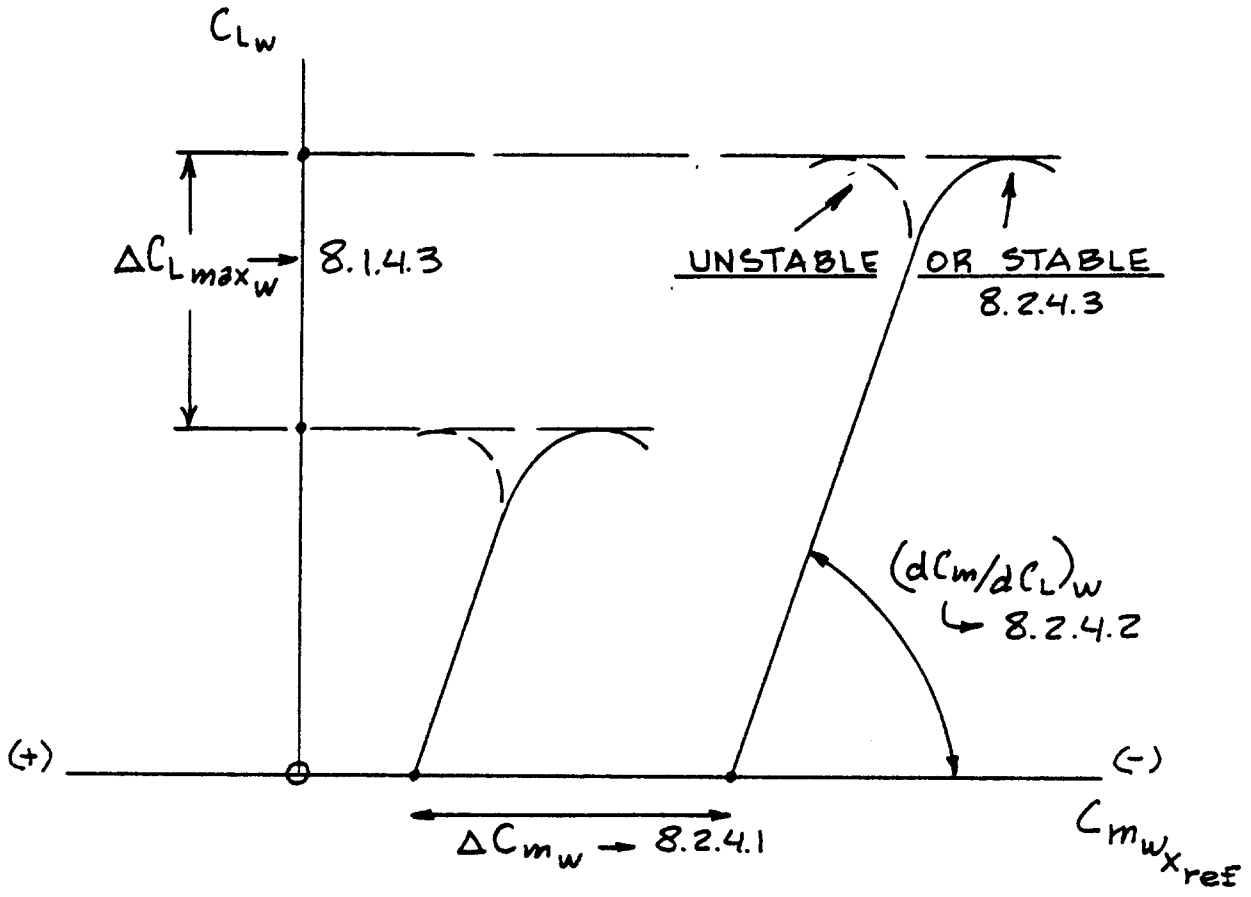

Figure 8.103 Wing Pitching Moment Versus Lift Curve with the Flaps Down

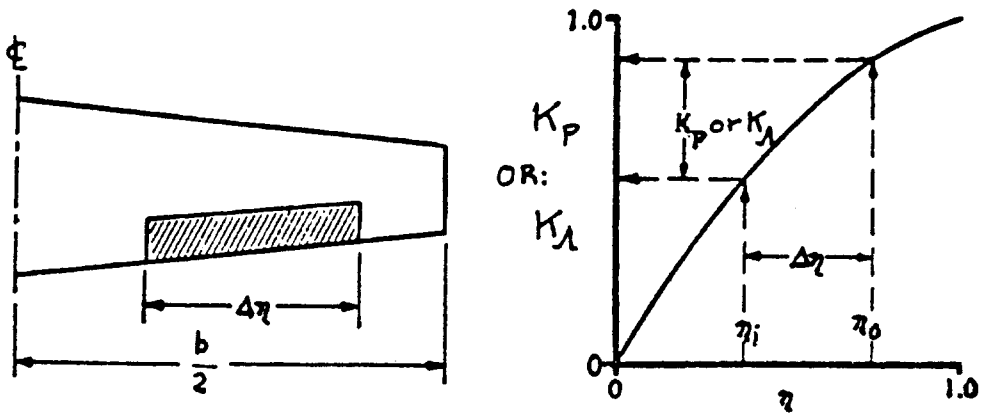

Figure 8.104 Method to Account for Partial Span Flaps

$\Delta C_{L_{ref_w}}$ is the lift increment due to flaps for a reference wing defined by the following geometry:

*full span flap *A = 6 *$\Lambda_{c/2}$ = 0

This quantity can be determined with the methods of 8.1.4.

K_p is the flap span factor which is obtained as shown in Fig. 8.104 with the data of Fig. 8.105.

c'/c is the ratio of the flaps extended wing chord to that with the flaps retracted. Fig. 8.106 shows typical definitions.

$(\Delta C'_m/\Delta C_{L_{ref_w}})$ is obtained from Figure 8.106.

K_Λ is a conversion factor which accounts for a partial-span flap on a swept wing. It is obtained from Fig. 8.107 using the procedure of Figure 8.104.

A is the wing aspect ratio

$\Lambda_{c/4}$ is the wing quarter chord sweep angle.

C_{m_w} is the wing pitching moment coefficient with the flaps retracted as obtained from 8.2.3.

B. Leading Edge Flaps

In the low angle of attack range, the incremental wing pitching moment coefficient due to leading edge flaps (taken relative to $\bar{n}_{ref}$) may be found from:

$$\Delta C_{m_w} = \{(c_{m_{\delta le}})'(c'/c) + (\bar{n}_{ref} - \bar{n}_{le})c_{l_\delta}\}(S_{w_f}/S)\delta_f + \quad (8.75)$$

$$+ [C_{m_w}\{(\bar{c}'/c)^2 - 1\} + 0.75C_{L_w}\{(\bar{c}'/c)(\bar{c}'-c)/c)\}](b_{lef}/b)$$

where: $(c_{m_{\delta le}})'$ is found from Figure 8.93.

$\bar{c}'$ is the mgc of that wing segment affected by the leading edge devices as shown in Figure 8.108.

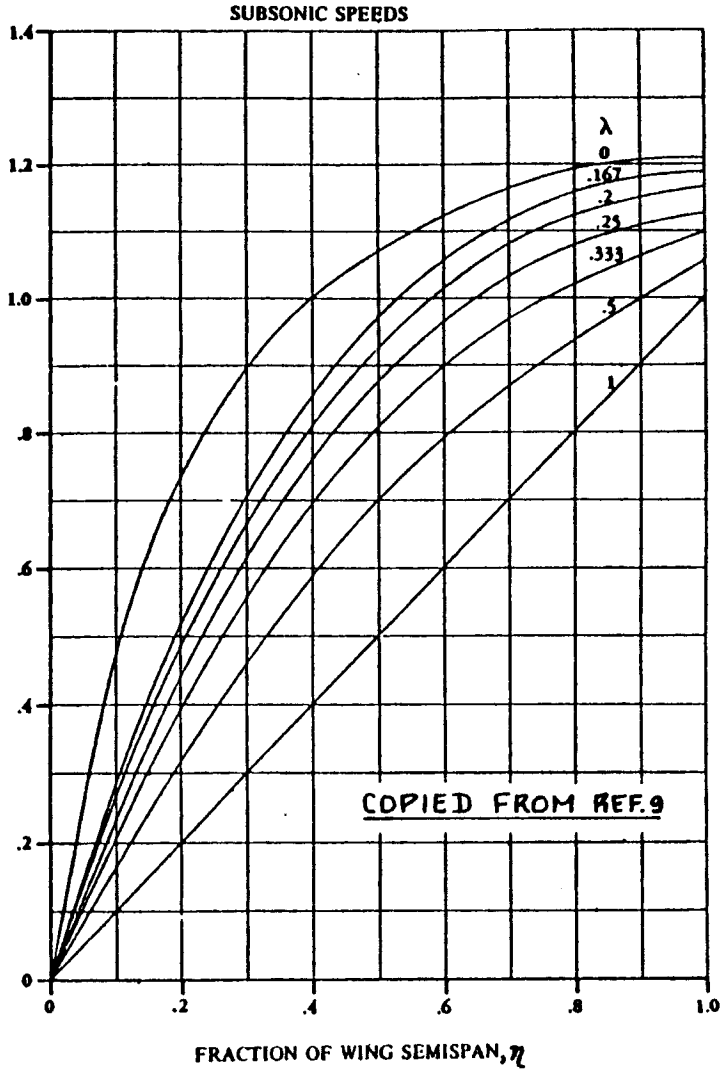

Figure 8.105 Partial Flap Span Factor

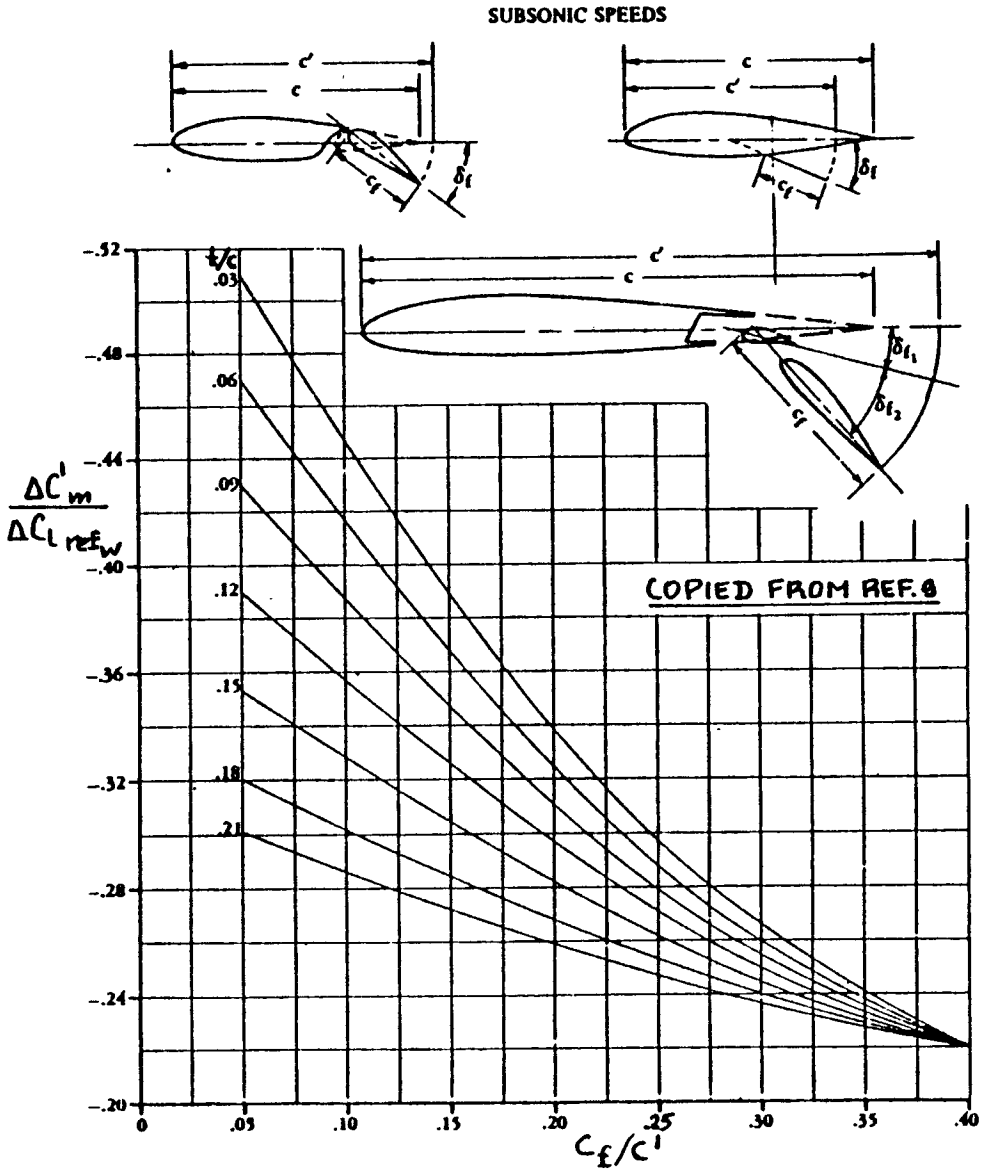

Figure 8.106 Effect of Lift on Pitching Moment for the Reference Wing

COPIED FROM REF. 9

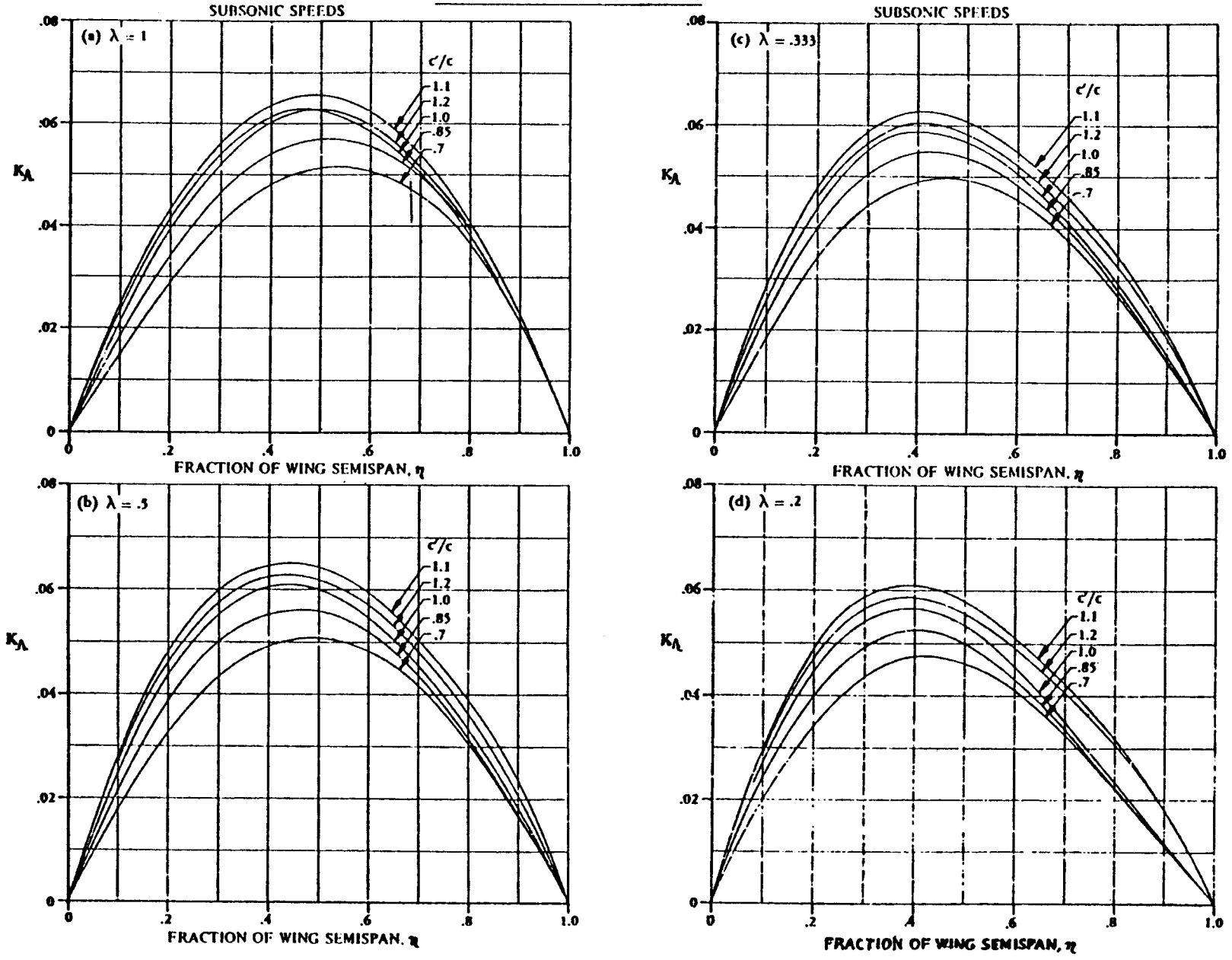

Figure 8.107 Conversion Factor which Accounts for Partial Span Flaps on a Swept Wing

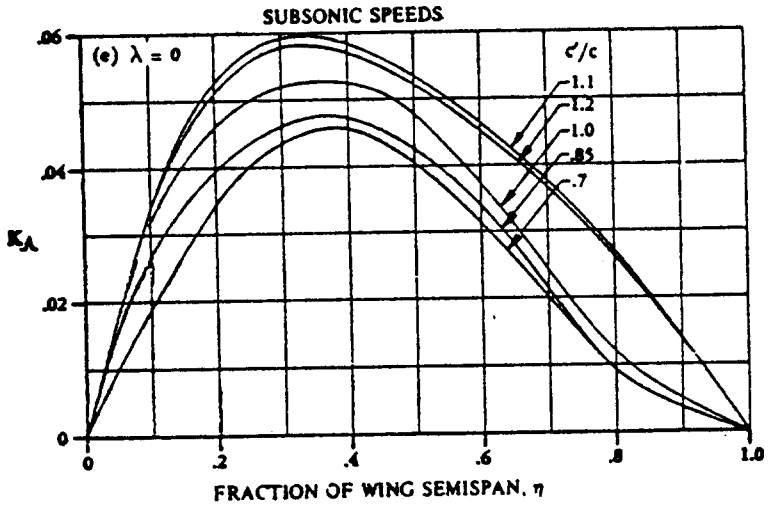

COPIED FROM REF. 9

Figure 8.107 (Cont'd) Conversion Factor which Accounts for Partial Span Flaps on a Swept Wing

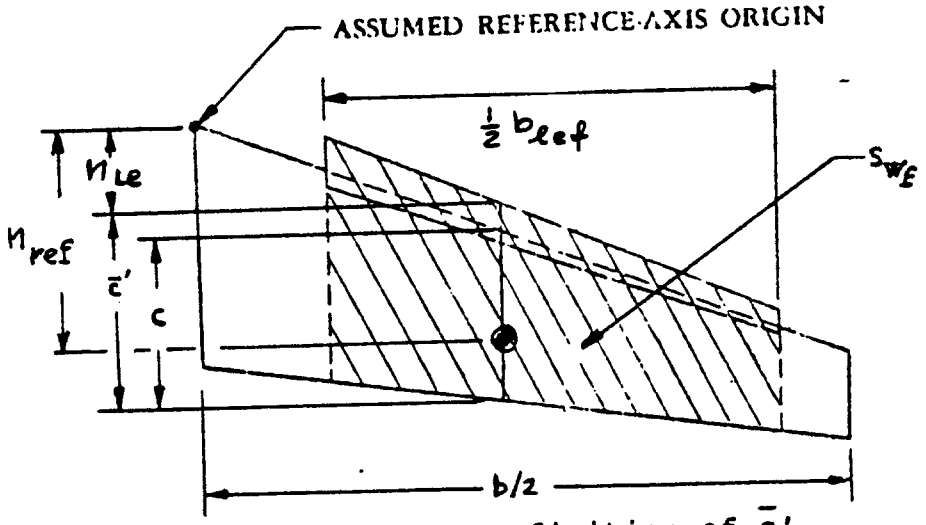

Figure 8.108 Definition of $\bar{c}'$

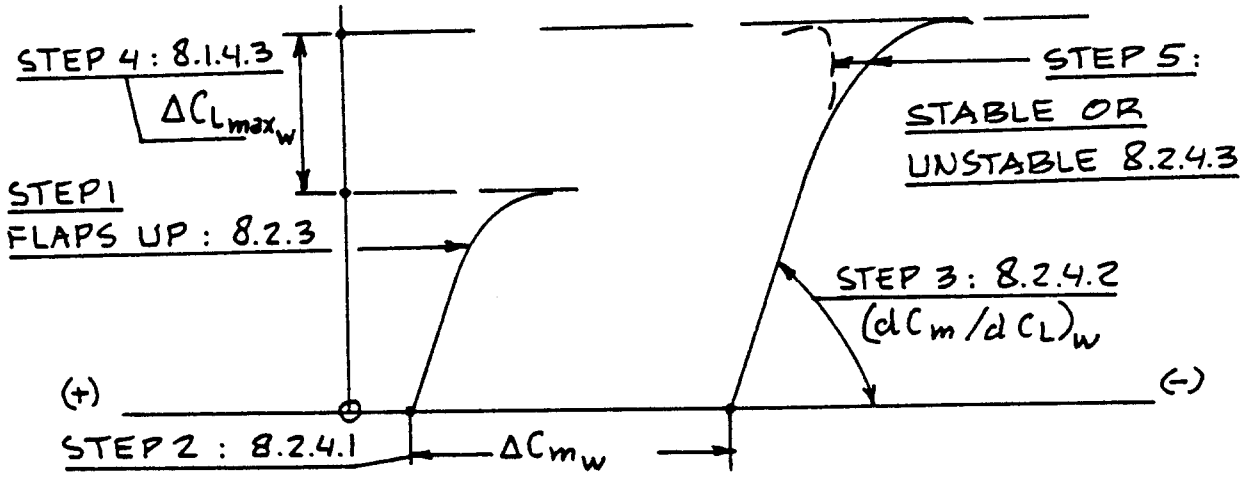

Figure 8.109 Construction of the Flaps Down Wing Pitching Moment Versus Lift Curve

c is the wing chord at $\bar{c}'$, see Figure 8.108.

$\bar{n}_{ref}$ and $\bar{n}_{le}$ are defined in Figure 8.108.

b_{lef} is defined in Figure 8.108.

S_{wf} is the flapped wing area: see Figure 8.108.

C_{m_w} is the wing pitching moment coefficient with the flaps retracted as obtained from 8.2.3.

C_{L_w} is the wing lift coefficient with flaps-up.

8.2.4.2 Slope of the wing pitching moment curve, flaps-down: $(dC_m/dC_L)_{w\delta}$

It may be assumed, that the slope of the wing pitching moment curve with the flaps-down is identical to that with the flaps-up: see 8.2.3.2.

8.2.4.3 Prediction of stable or unstable pitch break: flaps-down

It will be assumed that the pitch break behavior of the wing with the flaps down is similar to that with the flaps up: see 8.2.3.3.

8.2.4.4 Construction of the wing pitching moment curve: flaps-down

All ingredients necessary to construct the flaps-down wing pitching moment curve are now available. Figure 8.109 shows how this may be done in a step-by-step manner.

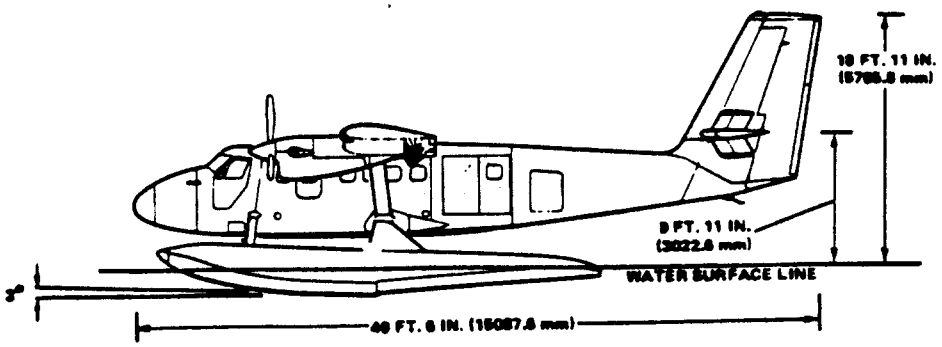

8.2.5 Airplane Pitching Moment: Flaps Up

Figure 8.110 shows the relationship between airplane pitching moment coefficient and airplane lift coefficient which is to be determined with the methods presented in this section. Key quantities needed in the construction of airplane C_m versus C_L curve are listed, with an indication of where methods for their estimation are found.

The assumption will be made, that an airplane can be considered to consist of three components:

a) wing + fuselage b) horizontal tail c) canard

Figure 8.60 shows the relative arrangement of these three major components. If an airplane is equipped with pylon mounted nacelles (such as the B-727 and the DC-9), the pylon + nacelle combination should be 'counted' as an additional horizontal tail. Figure 8.61 indicates the 'equivalent' geometries which should then be used.

Figure 8.62 shows a number of important geometric parameters which are used in the calculation of overall airplane pitching moment characteristics.

IMPORTANT CONSIDERATIONS:

In this chapter the following incidence angles are accounted for:

Canard: i_c Wing: i_w Horizontal Tail: i_h

These incidence angle are defined in Figure 8.60. In this sub-section, these incidence angles are assumed to be CONSTANT. The effect of trim requirements is considered in Section 8.3.

A horizontal tail and a canard may be equipped with a trailing edge control surface:

Horizontal tail with elevator, deflection: δ_e

Canard with canardvator, deflection: δ_c

In this sub-section, the assumption will be made that all control surface deflection angles are ZERO. The effect of trim requirements which would cause these control surface deflections to be non-zero is considered in Section 8.3.

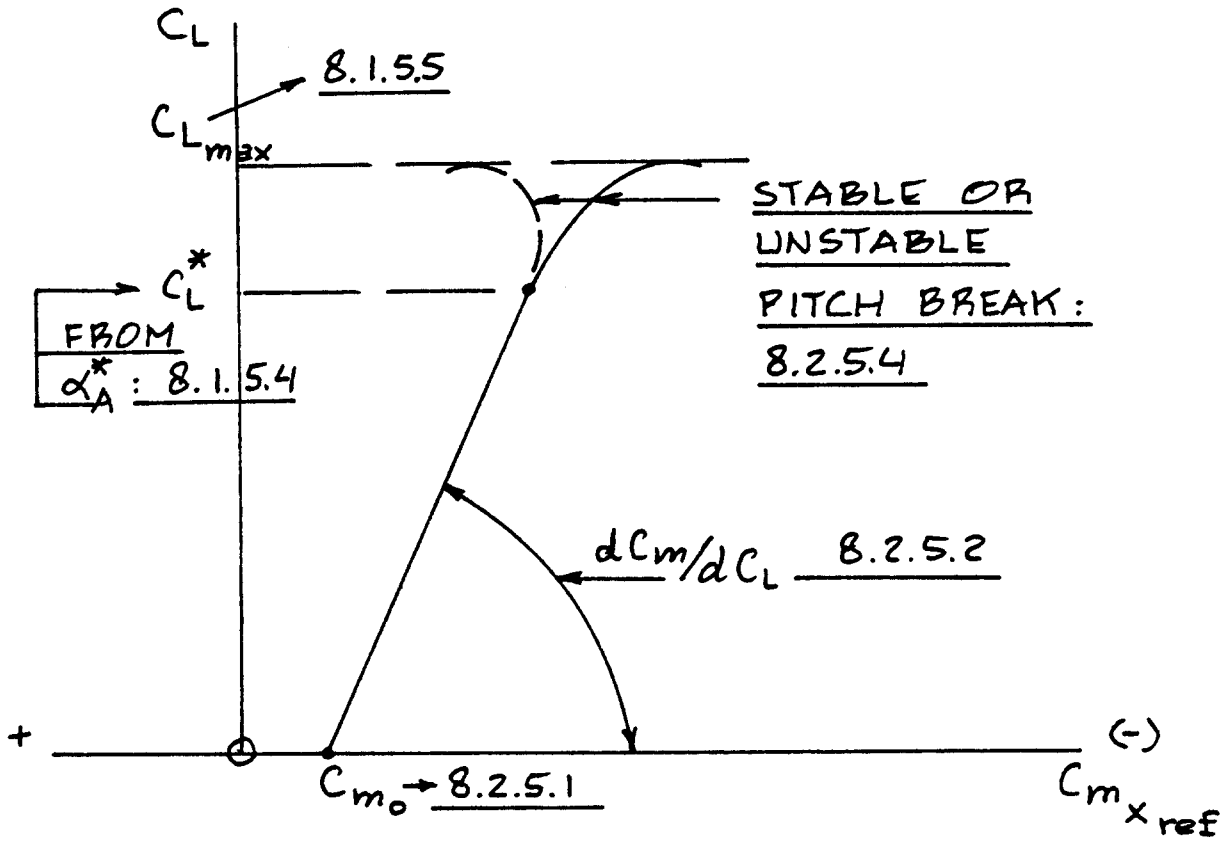

Figure 8.110 Airplane Pitching Moment Versus Lift Curve with the Flaps Up

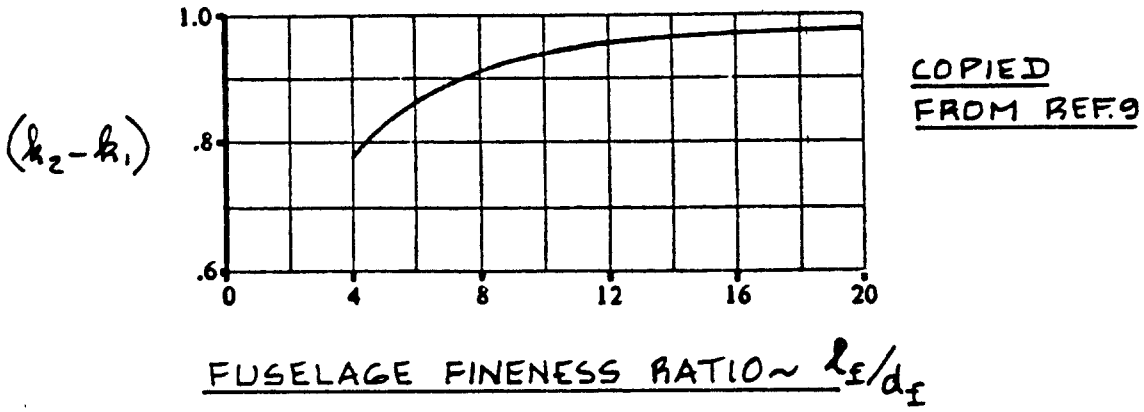

Figure 8.111 Effect of Fuselage Slenderness on the Apparent Mass Factor

8.2.5.1 Airplane zero-lift pitching moment coefficient: C_{m_o}

Subsonic:

The airplane zero-lift pitching moment coefficient may be estimated from:

$$C_{m_o} = C_{m_{o_{wf}}} + C_{m_{o_c}} + C_{m_{o_h}} \quad (8.76)$$

where: $C_{m_{o_{wf}}}$ is the zero-lift pitching moment coefficient of the wing-fuselage combination. It may be computed from:

$$C_{m_{o_{wf}}} = \{(C_{m_{o_w}}) + (C_{m_{o_f}})\}\{(C_{m_o})_M/(C_{m_o})_{M=0}\} \quad (8.77)$$

where: $C_{m_{o_w}}$ is found from Eqn.(8.70)

$$C_{m_{o_f}} = \quad (8.78)$$

$$\{(k_2 - k_1)/36.5\bar{S}c\}[\text{Sum}_{i=1}^{i=13}\{(w_{f_i}^2)(i_w + \alpha_{o_{L_w}} + i_{cl_f})\Delta x_i\}]$$

where: $(k_2 - k_1)$ is found from Figure 8.111.

w_{f_i} is the average width of a fuselage segment as shown in Figure 8.112.

Δx_i is the length of a fuselage segment as shown in Figure 8.112.

i_w is the wing incidence angle as defined in Figure 8.60.

$\alpha_{o_{L_w}}$ is found from Eqn.(8.21)

i_{cl_f} is the incidence angle of the fuselage camber line RELATIVE to the fuselage reference plane (FRP) at the center of each fuselage increment. The sign convention for this angle is illustrated in Figure 8.112. Note that this angle is NEGATIVE for down-camber at the fuselage nose as well as for up-camber at the fuselage tailcone.

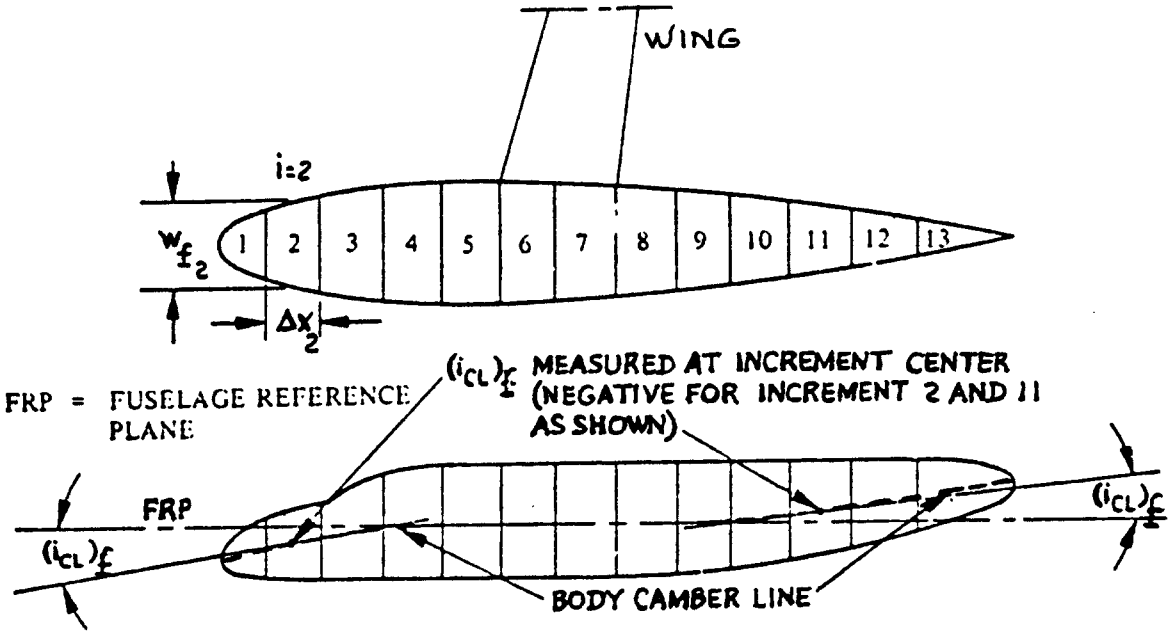

COPIED FROM REF. 9

Figure 8.112 Fuselage Segmentation and Fuselage Camber

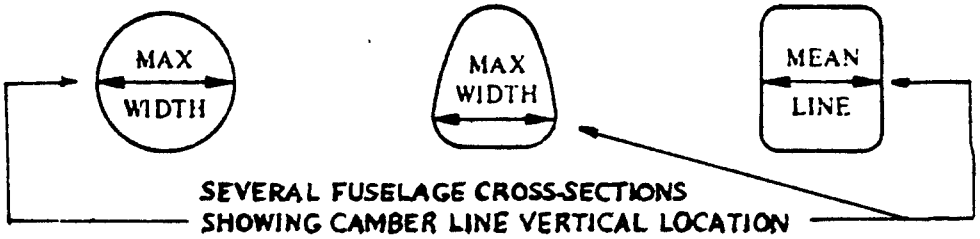

COPIED FROM REF. 9

Figure 8.113 Definition of Maximum Fuselage Width for Several Fuselage Cross Sections

The fuselage camber line is determined in the fuselage sideview by the so-called maximum width locus which in turn arises from the fuselage cross section distribution. It is shown in Figure 8.113 how the maximum fuselage width is defined for three types of fuselage cross sections.

$C_{m_{o_c}}$ and $C_{m_{o_h}}$ are the zero-lift pitching moment coefficient due to the canard and due to the horizontal tail respectively. Their sum may be computed from:

$$C_{m_{o_c}} + C_{m_{o_h}} = \quad (8.79)$$

$$(\bar{x}_{ac_c} + \bar{x}_{ref})C_{L_{o_c}} - (\bar{x}_{ac_h} - \bar{x}_{ref})C_{L_{o_h}}$$

where: x_{ac_c} and x_{ac_h} are defined in Figure 8.114, POSITIVE as shown in that Figure! Note that this is an inconsistent sign convention!!

x_{ref} is the reference (or c.g.) location about which the airplane pitching moment is to be determined: see Figures 8.114 and 8.97b. NOTE: this quantity is POSITIVE when behind the leading edge of the wing m.g.c. and NEGATIVE when forward of the leading edge of the wing m.g.c.!

Observe that:
$$\bar{x}_{ref} = (x_{ref})/c \quad (8.80a)$$
$$\bar{x}_{ac_c} = (x_{ac_c})/c \quad (8.80b)$$
$$\bar{x}_{ac_h} = (x_{ac_h})/c \quad (8.80c)$$

NOTE: for the entire airplane, x_{ref} is normally selected to be a c.g. location in between the most forward and the most aft center of gravity location as found from Chapter 10 in Part II.

$C_{L_{o_c}}$ and $C_{L_{o_h}}$ are the lift coefficients at

zero angle of attack of the canard and of the horizontal tail respectively. These quantities are the third and second term respectively in Eqn.(8.32).

Transonic:

For Mach numbers between 0.6 and 0.9 the subsonic method may be used. Above M=0.9 experimental data should be employed.

Supersonic:

Experimental methods should be used. For slender configurations such as fighter aircraft, Ref.9 presents a reasonable procedure for estimating C_{m_o}.

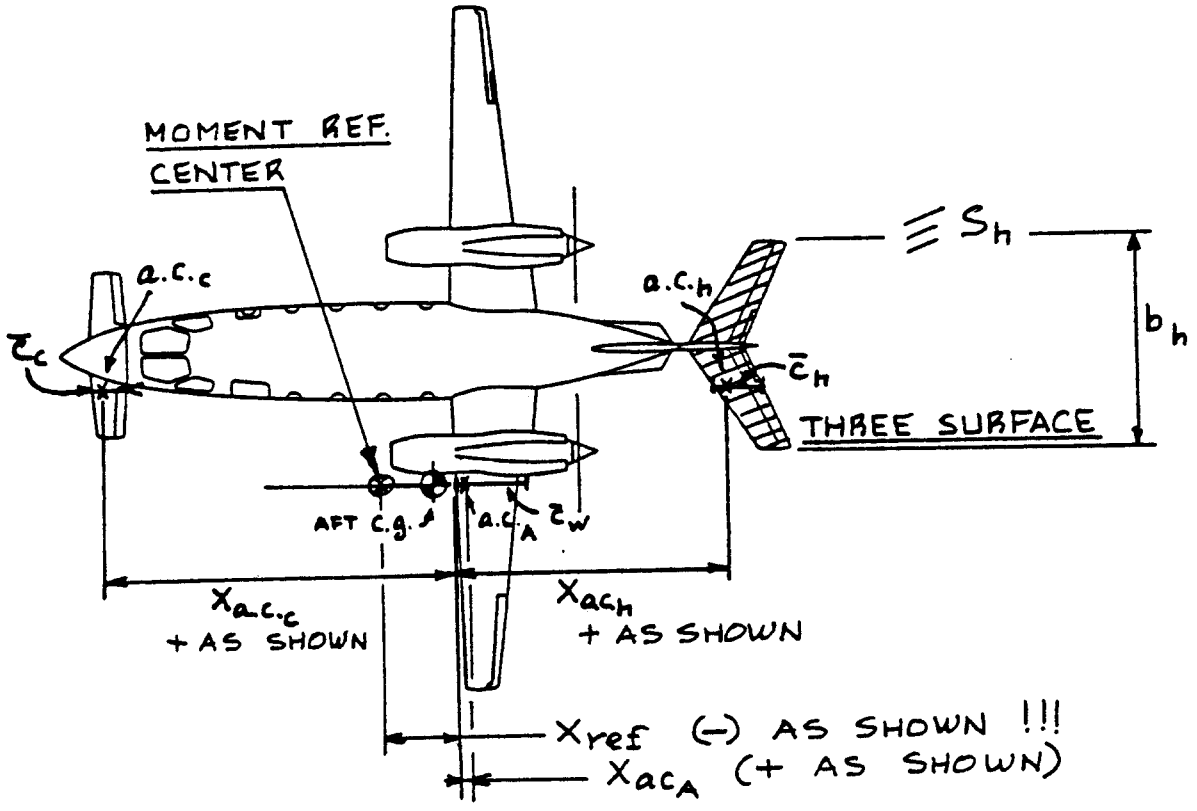

Figure 8.114 Definition of Aerodynamic Center Location Parameters and Moment Reference Center

8.2.5.2 Airplane pitching moment variation with lift coefficient: dC_m/dC_L

Subsonic:

The variation of airplane pitching moment coefficient with lift coefficient may be estimated from:

$$dC_m/dC_L = \bar{x}_{ref} - \bar{x}_{ac_A} \quad (8.81)$$

where:

$\bar{x}_{ref}$ is the location of the moment reference center in fractions of the m.g.c. It is defined in Figures 8.97b and 8.114.

NOTE: for the entire airplane, x_{ref} is normally selected to be a c.g. location in between the most forward and the most aft center of gravity location as determined from Chapter 10 in Part II.

$\bar{x}_{ac_A}$ is the location of the airplane aerodynamic center in fractions of the m.g.c. Fig. 8.114 defines its location on the m.g.c. The following equation may be used to compute it:

$$\bar{x}_{ac_A} = \quad (8.82)$$

$$[(\bar{x}_{ac_{wf}})C_{L_{\alpha_{wf}}} + \{\eta_h C_{L_{\alpha_h}} (1 - d\varepsilon/d\alpha)(S_h/S)\bar{x}_{ac_h} + \eta_c C_{L_{\alpha_c}} (1 + d\varepsilon_c/d\alpha)(S_c/S)\bar{x}_{ac_c}\}]/C_{L_\alpha}$$

where: $\bar{x}_{ac_{wf}} = \bar{x}_{ac_w} + \Delta\bar{x}_{ac_f}$, (8.83)

both being given as fractions of the m.g.c. Note that in terms of their actual lengths:

$$x_{ac_w} = n_{ac} - n_{mgc}, \quad (8.84)$$

both of which are defined in Figure 8.97a.

n_{ac} may be determined from Figure 8.100 or from Eqn. (8.73), depending on the wing type used.

$\Delta\bar{x}_{ac_f}$ is the shift in aerodynamic center caused by adding the fuselage to the wing: it is determined with the method of 8.2.5.3.

η_h and η_c may be found from 8.1.5.2.

$C_{L_{\alpha_{wf}}}$ is found from Eqn.(8.43)

$C_{L_{\alpha_h}}$ and $C_{L_{\alpha_c}}$ are found from Eqn.(8.22) with appriate substitution of parameters.

$d\varepsilon/d\alpha$ and $d\varepsilon_c/d\alpha$ are found from 8.1.5.3.

C_{L_α} is the total airplane liftcurve slope which follows from Eqn.(8.42).

Transonic:

In the transonic speed range, the airplane undergoes an aft shift in aerodynamic center location. In preliminary design it may be assumed that this aft shift is the same as that due to the wing alone. The latter may be determined from Figure 8.100. Note that this figure applies only to straight tapered wings. For other wings, use Ref.9.

Supersonic:

In the supersonic speed range, the airplane undergoes an aft shift in aerodynamic center location. In preliminary design it may be assumed that this aft shift is the same as that due to the wing alone. The latter can be found from Figure 8.100. Note that this figure applies only to straight tapered wings. For other wings, use Ref.9.

8.2.5.3 Calculation of the aerodynamic center shift due to the fuselage: $\Delta\bar{x}_{ac_f}$

The following method may be used up to a Mach number of 0.9. Beyond this Mach number, the fuselage induced shift in a.c. location is assumed constant throughout the transonic and supersonic speed range.

The method presented here is due to Munk, as reported in Reference 54:

$$\Delta x_{ac_f} = -(dM/d\alpha)/(\bar{q}S\bar{c}C_{L_{\alpha_w}}) \qquad (8.85)$$

where: $C_{L_{\alpha_w}}$ is found from Eqn.(8.22) in 1/deg.

$$(dM/d\alpha) = \qquad (8.86)$$

$$(\bar{q}/36.5)(C_{L_{\alpha_w}}/0.08)\left[\sum_{i=1}^{i=13}\left[(w_{f_i})^2(d\bar{\varepsilon}/d\alpha)_i \Delta x_i\right]\right]$$

where: w_{f_i} and Δx_i are defined in 8.2.5.1.

$C_{L_{\alpha_w}}$ is found from Eqn.(8.22) in 1/deg.

$(d\bar{\varepsilon}/d\alpha)_i$ takes on values which depend on the fuselage segment under consideration:

for i=1,2,3,4, use curve 1 in Figure 8.115

for i=5 use curve 2 in Figure 8.115.

for i=6,7,8,9,10,11,12,13, use:

$$(d\bar{\varepsilon}/d\alpha)_i = (x_i/x_h)(1 - d\varepsilon/d\alpha) \qquad (8.87)$$

where: x_i and x_h are defined in Fig.8.116,

and $d\varepsilon/d\alpha$ is found from Eqn.(8.45), but with: $h_h = 0$.

IMPORTANT NOTE: if the airplane has wing mounted nacelles forward of the wing or wing mounted stores forward of the wing, this method should be used to compute the additional a.c. shift. In such cases only segments 1-5 need to be accounted for.

8.2.5.4 Prediction of stable or unstable pitch break

Whether or not an entire airplane has an unstable or a stable pitch break depends on the overall configuration as well as on the sequence with which separated wakes arrive from the wing at aft mounted pylon/nacelle combinations and/or at horizontal tails. The reader should con-

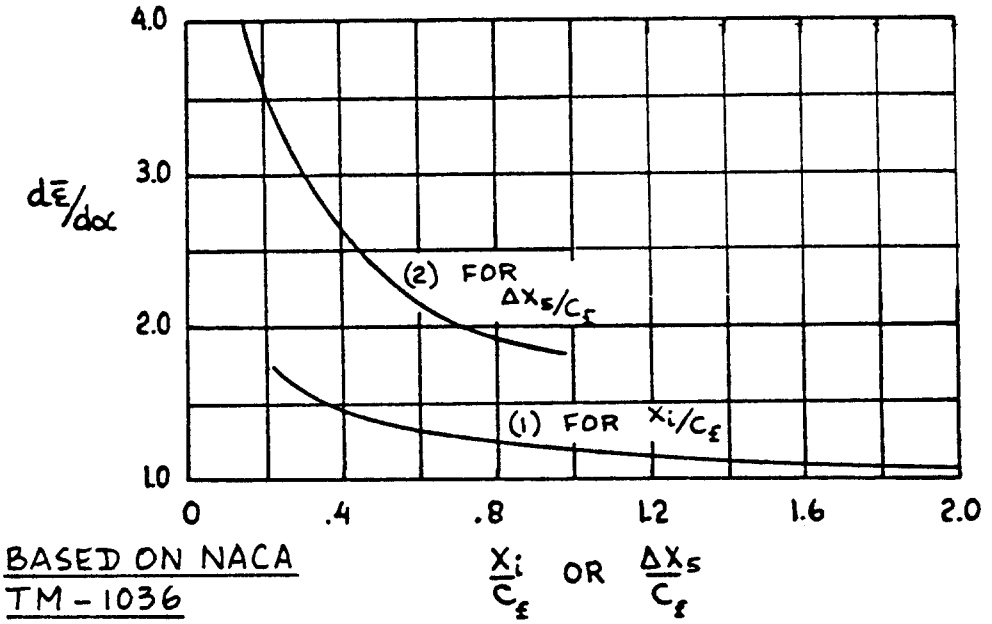

Figure 8.115 Effect of Fuselage (or Nacelle) Segment Location on Upwash Gradient

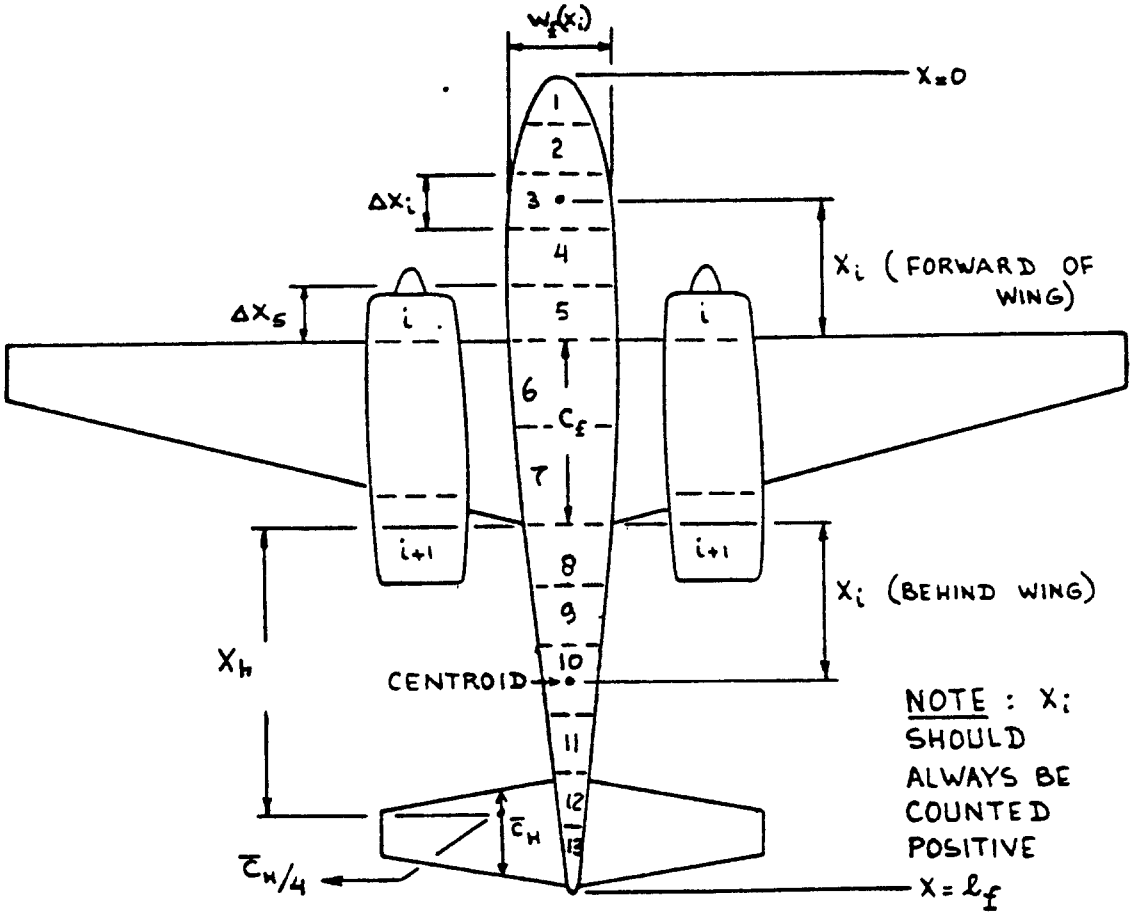

Figure 8.116 Layout for Computing Fuselage and (or) Nacelle Contribution to Airplane Aerodynamic Center Location

sult the discussion of pitch break behavior found in Subsection 5.1.4 of Part III, pages 263-272. As a result of applying this material to a given design, a determination of stable or unstable pitch break behavior can be made.

8.2.5.5 Construction of airplane pitching moment coefficient versus lift coefficient

All ingredients needed to construct the overall airplane C_m versus C_L curve are now available. A step-by-step procedure for doing this is given in Fig. 8.117.

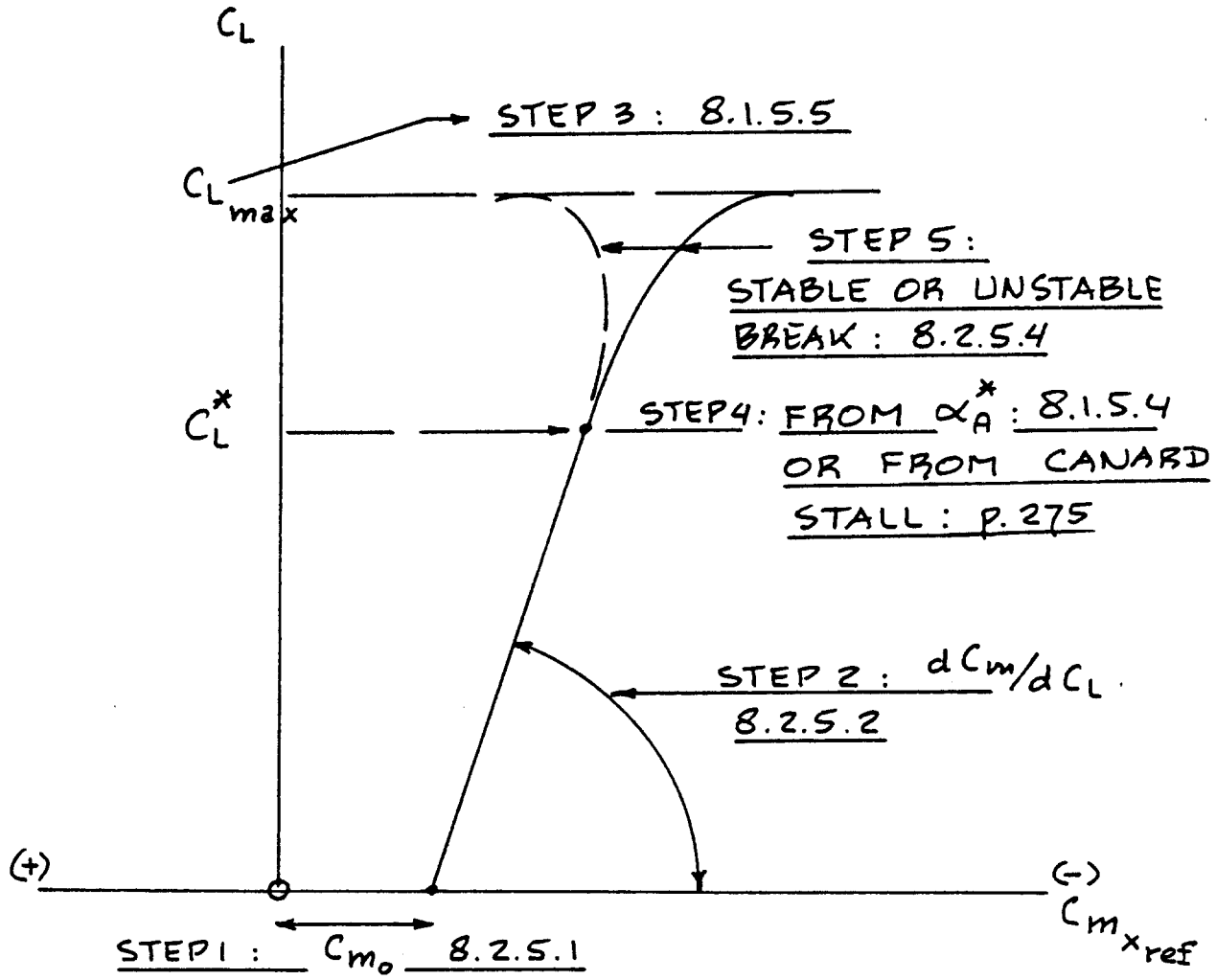

Figure 8.117 Construction of the Flaps Up Airplane Pitching Moment Versus Lift Curve

8.2.6 Airplane Pitching Moment: Flaps Down

Figure 8.118 shows the relationship between airplane pitching moment coefficient and airplane lift coefficient in the flaps down configuration. This relationship will be determined with the methods presented in this section. Key quantities needed in the construction of the airplane C_m versus C_L curve are listed, with an indication of where methods for their estimation are found.

8.2.6.1 Airplane pitching moment coefficient increment due to flaps: ΔC_m

The airplane pitching moment increment due to flaps may be estimated from:

$$\Delta C_m = \Delta C_{m_w} + \Delta C_{m_c} \eta_c (S_c \bar{c}_c / S\bar{c}) + \Delta C_{L_c} (\bar{x}_{ac_c} + \bar{x}_{ref}) +$$

$$+ C_{L_{\alpha_h}} \eta_h (S_h/S)(\bar{x}_{ac_h} - \bar{x}_{ref}) \Delta\varepsilon_f \qquad (8.88)$$

where: ΔC_{m_w} accounts for the pitching moment change due to wing flaps (leading edge and/or trailing edge) and is found from 8.2.4.1

ΔC_{m_c} accounts for the pitching moment change due to canard flaps (usually trailing edge only) and is found from 8.2.4.1 with appropriate substitution of canard parameters for wing parameters. If the canard has no flaps, this quantity is equal to zero.

ΔC_{L_c} is found from 8.1.4.1 with appropriate substitution of canard parameters for wing parameters. The comments made on p.277 apply!

x_{ref}, x_{ac_c} and x_{ac_h} are defined in Figure 8.114.

NOTE: the reader should carefully observe the inconsistent sign convention used for these quantities!

$C_{L_{\alpha_h}}$ is found from 8.1.3.2 with appropriate substitution of horizontal tail parameters for wing parameters.

η_c and η_h are found from 8.1.5.2.

$\Delta\varepsilon_f$ is found from Figure 8.70.

8.2.6.2 Slope of the airplane pitching moment curve flaps down: $(dC_m/dC_L)_\delta$

It may be assumed that the slope of the flaps down pitching moment curve is the same as that of the flaps up pitching moment curve:

$$(dC_m/dC_L)_\delta = dC_m/dC_L \qquad (8.89)$$

8.2.6.3 Prediction of stable or unstable pitch break: flaps down

It will be assumed that the pitch break behavior of the airplane with the flaps down is similar to that with the flaps up. The reader is referred to 8.2.5.4.

8.2.6.4 Construction of the airplane flaps down pitching moment curve

All items needed in the construction of the total airplane pitching moment curve with the flaps down are now available. Figure 8.119 shows a step-by-step procedure to accomplish this.

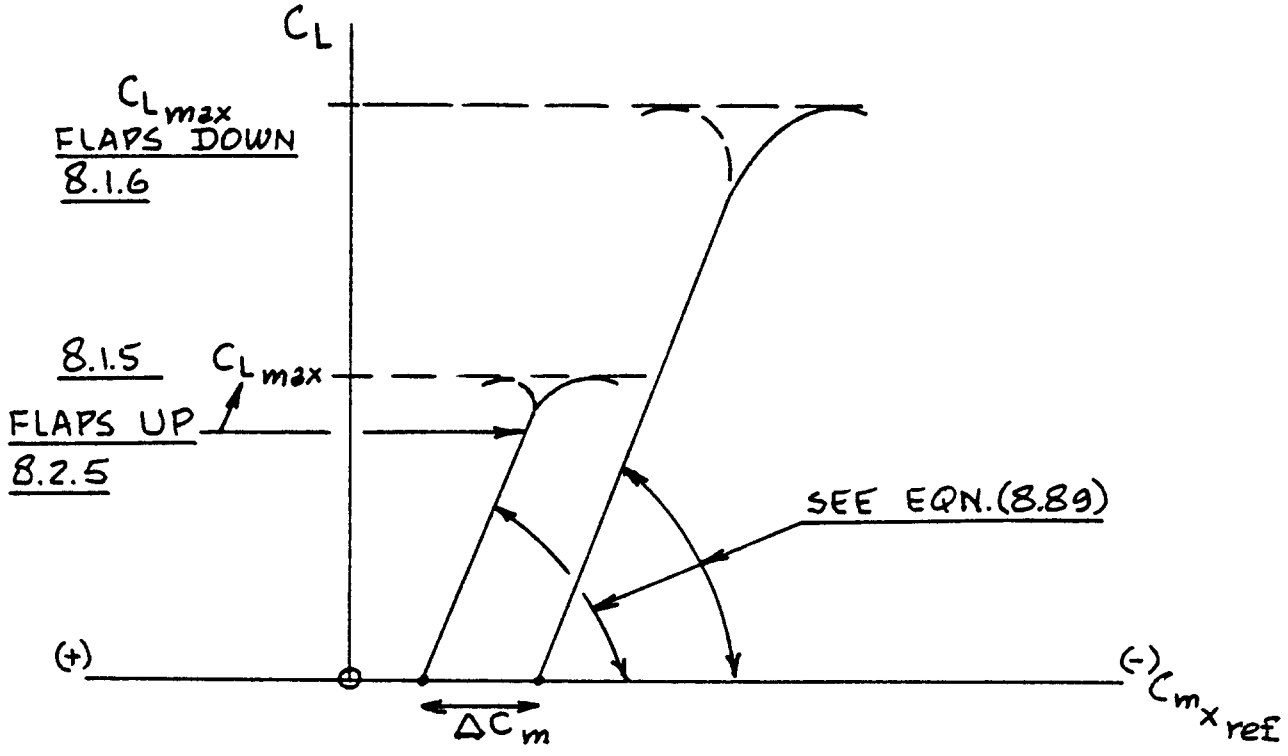

Figure 8.118 Airplane Pitching Moment Versus Lift Curve with the Flaps Down

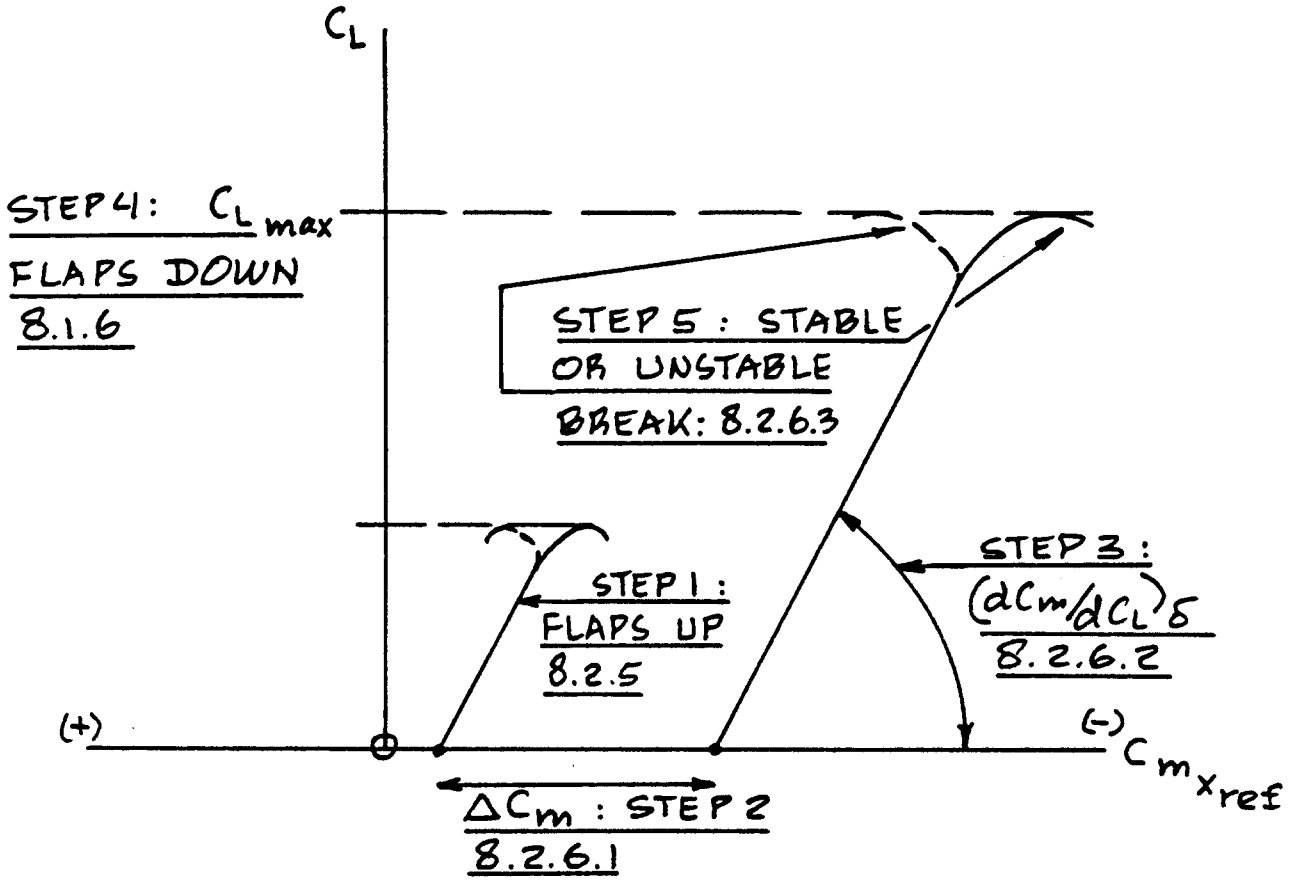

Figure 8.119 Construction of the Flaps Down Airplane Pitching Moment Versus Lift Curve

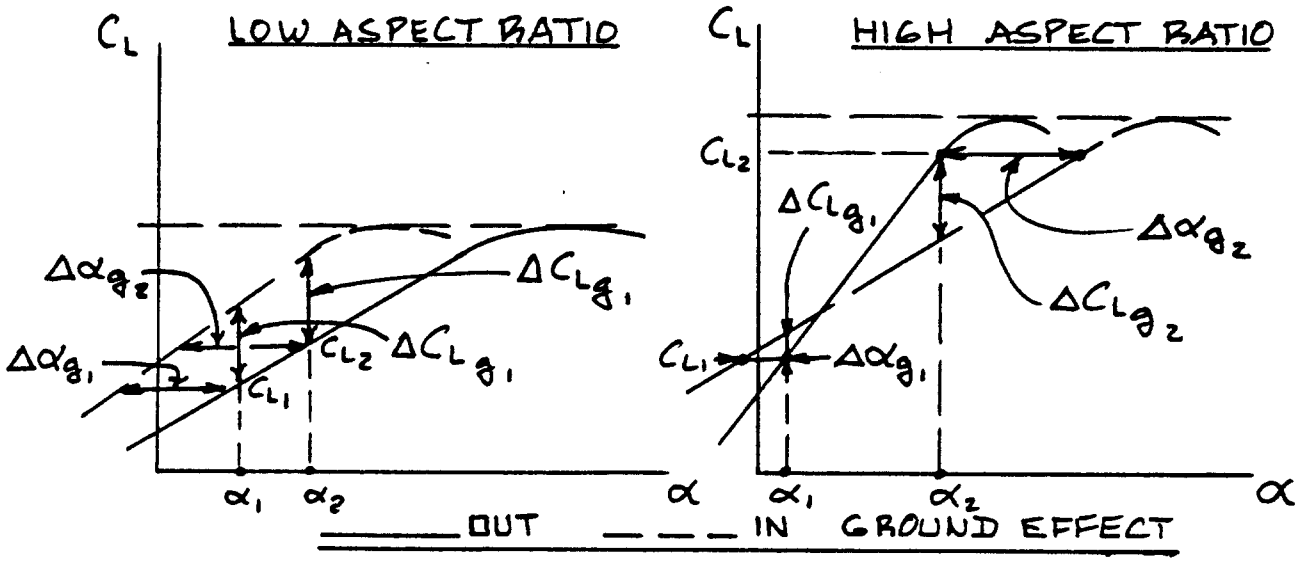

Figure 8.120 Ground Effect on Lift Curves: Revisited

8.2.7 Airplane Pitching Moment in Ground Effect

Figure 8.120 shows a re-interpretation of the airplane lift versus angle of attack curve in and out of ground attack. Figure 8.120 is a different way of looking at Figure 8.72. In Figure 8.72 the assumption was made that the tail lift (and/or the canard lift) do not contribute significantly to airplane lift change due to ground effect. Although this is usually true to a first order of approximation, that does not mean that the pitching moments due to ground induced lift changes on these surfaces are also negligible.

It will be assumed that the aerodynamic center of the airplane does not change due to ground effect. In that case, the pitching moment increment due to ground effect on the entire airplane may be estimated from:

$$(\Delta C_m)_g = \tag{8.90}$$

$$(\Delta C_{m_{wf}})_g + (\Delta C_{m_c})_g + (\Delta C_{m_h})_g$$

where: $$(\Delta C_{m_{wf}})_g = (\bar{x}_{ref} - \bar{x}_{ac_A})(\Delta C_{L_{wf}})_g \tag{8.91}$$

with: x_{ref} and x_{ac_A} defined in Section 8.2.5: observe the inconsistent sign convention!

$(\Delta C_{L_{wf}})_g = (\Delta C_L)_g$ as shown in Figure 8.120.

$(\Delta C_L)_g$ in turn is found at two values of angle of attack, α, from Section 8.1.7 and plotted as shown in Figure 8.120. Note from Section 8.1.7 the difference between high and low aspect ratio configurations!

$$(\Delta C_{m_c})_g = (\Delta C_{L_c})_g \eta_c (\bar{x}_{ac_c} + \bar{x}_{ref}) \tag{8.92}$$

with: x_{ac_c} and x_{ref} defined in Section 8.2.5: observe the inconsistent sign convention!

η_c is found from 8.1.5.2 and:

$$(\Delta C_{L_c})_g = -C_{L_{\alpha_c}} (S_c/S)(\Delta \varepsilon_c)_g \tag{8.93}$$

where: $C_{L_{\alpha_c}}$ is found from 8.1.3.2 with appropriate substitution of canard parameters for wing parameters.

$(\Delta\varepsilon_c)_g$, the ground induced change in upwash angle at the canard is found from 8.2.7.1.

$$(\Delta C_{m_h})_g = -(\Delta C_{L_h})_g \eta_h (\bar{x}_{ac_h} - \bar{x}_{ref}) \qquad (8.94)$$

with: x_{ac_h} and x_{ref} defined in Section 8.2.5: observe the inconsistent sign convention!

η_h is found from 8.1.5.2 and:

$$(\Delta C_{L_h})_g = -C_{L_{\alpha_h}} (S_h/S)(\Delta\varepsilon)_g \qquad (8.95)$$

where: $C_{L_{\alpha_h}}$ is found from 8.1.3.2 with appropriate substitution of horizontal tail parameters for wing parameters.

$(\Delta\varepsilon)_g$ the ground induced change in tail downwash angle is found from 8.2.7.1.

Equation (8.90) is used to find ΔC_m for two angles of attack. The C_m-C_L curve of the airplane in ground effect can now be replotted as shown in Figure 8.121. Note that this in effect causes a slight change in airplane stability due to ground effect despite the assumption of constant a.c. location which was made in Eqn.(8.91).

8.2.7.1 Ground effect on downwash and on upwash

Ground Effect on Downwash

The decrease in tail downwash due to ground effect may be computed from:

$$(\Delta\varepsilon)_g = \qquad (8.96)$$

$$\varepsilon[\{b_{eff}^2 + 4(H_h - H_w)^2\}/\{b_{eff}^2 + 4(H_h + H_w)^2\}]$$

where: $\varepsilon = \alpha(d\varepsilon/d\alpha)$ (8.97)

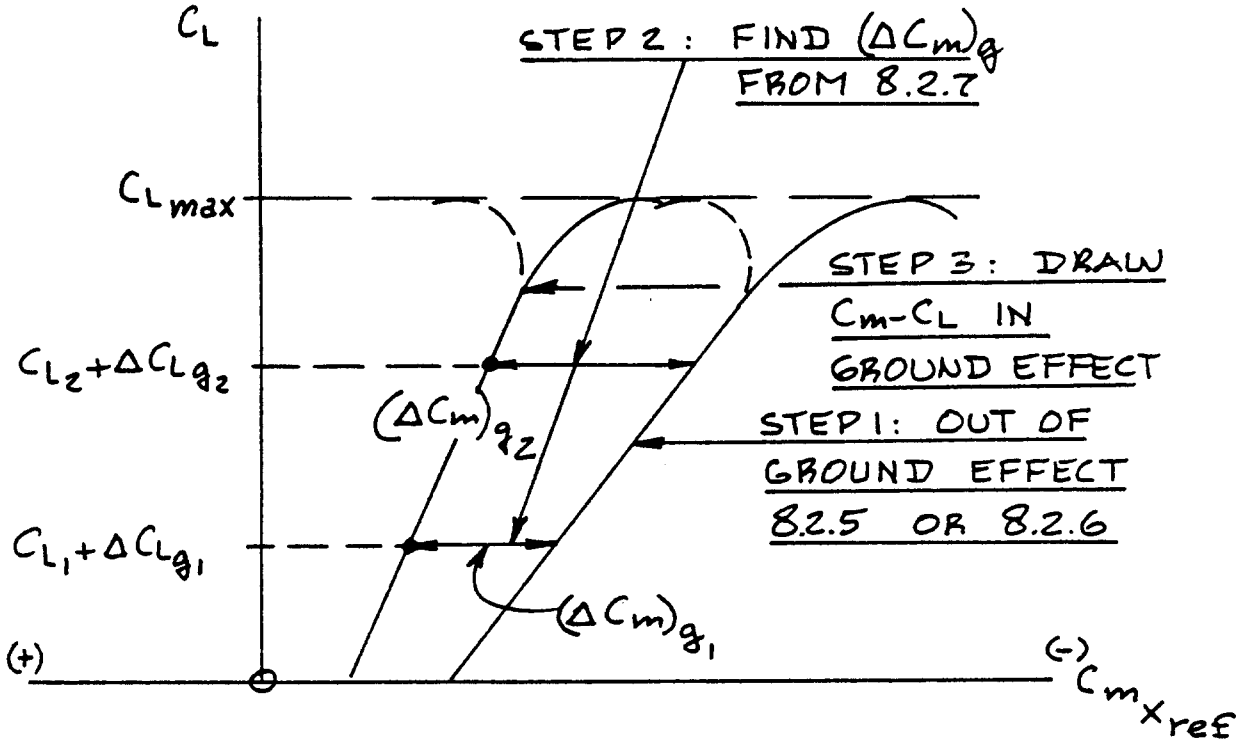

Figure 8.121 Construction of Airplane Pitching Moment Versus Lift Curve in Ground Effect

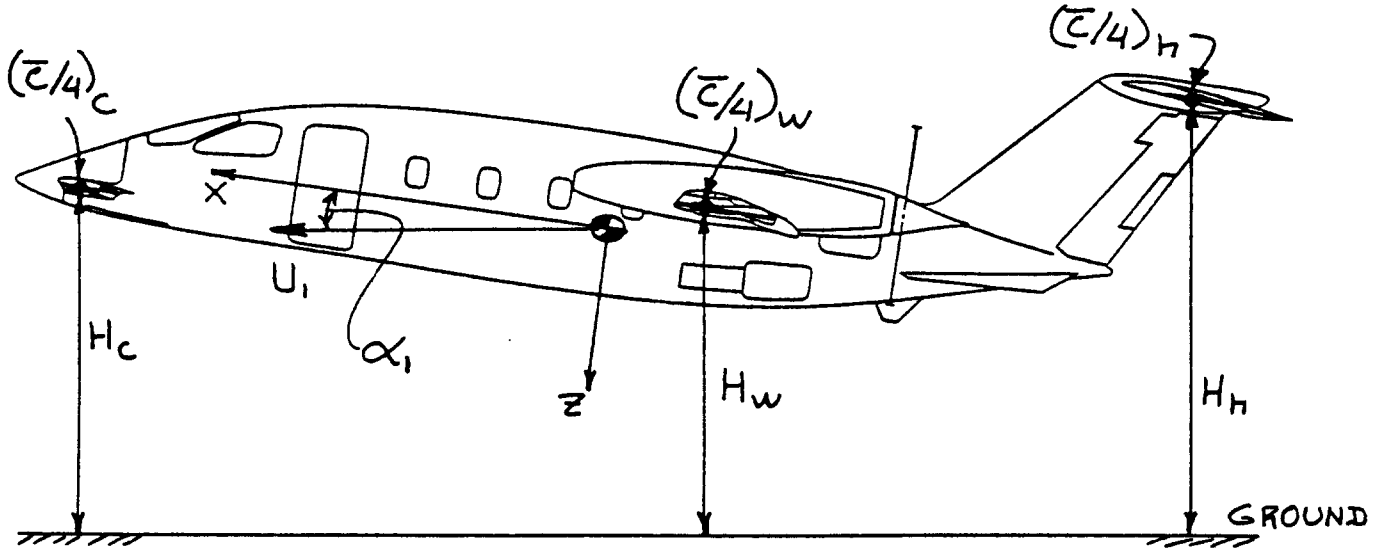

Figure 8.122 Definition of Canard, Wing and Tail Height Above the Ground

with $d\varepsilon/d\alpha$ found from Eqn.(8.45).

H_h is the height of the horizontal tail $\bar{c}_h/4$ above the ground: see Figure 8.122.

H_w is the height of the wing $\bar{c}/4$ above the ground: see Figure 8.122.

$$b_{eff} = \qquad (8.98a)$$

$$(C_{L_{wf}} + \Delta C_L)/\{(C_{L_{wf}}/b'_w) + (\Delta C_L)/b'_f\}$$

where: $C_{L_{wf}}$ is the wing-fuselage lift coefficient flaps up, out of ground effect as found from 8.1.5.

ΔC_L is the lift increment due to flaps out of ground effect as found from 8.1.6.

$$b'_w = b(b'_w/b) \qquad (8.98b)$$

with: (b'_w/b) given in Figure 8.123.

$$b'_f = b(b'_f/b'_w)(b'_w/b) \qquad (8.98c)$$

with: (b'_f/b'_w) given in Figure 8.124.

Ground Effect on Upwash

The decrease in canard upwash due to ground effect may be computed from:

$$(\Delta\varepsilon_c)_g = \varepsilon_c\{(H_c - H_w)^2/(H_c + H_w)^2\} \qquad (8.99)$$

where: $$\varepsilon_c = (\alpha + i_c)(d\varepsilon_c/d\alpha) \qquad (8.100)$$

with: α being the airplane angle of attack and

i_c being the canard incidence angle, while

$d\varepsilon_c/d\alpha$ is found from Figure 8.67

H_c is the height of the canard $\bar{c}_c/4$ above the ground: see Figure 8.122.

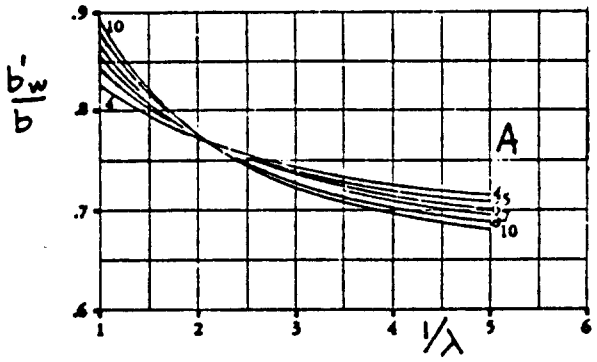

COPIED FROM: REF. 9

Figure 8.123 Effective Wing Span Close to the Ground

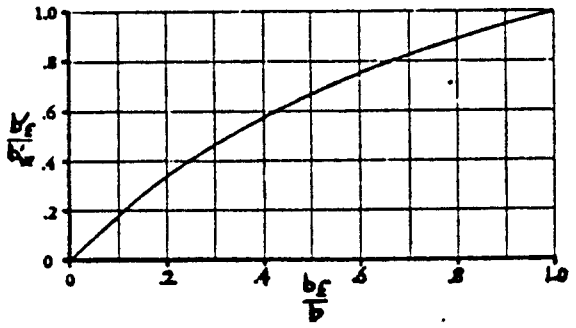

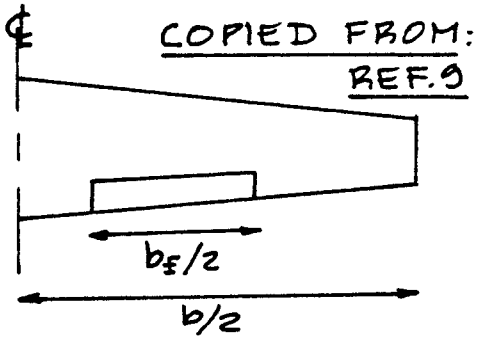

Figure 8.124 Effective Flap Span Close to the Ground

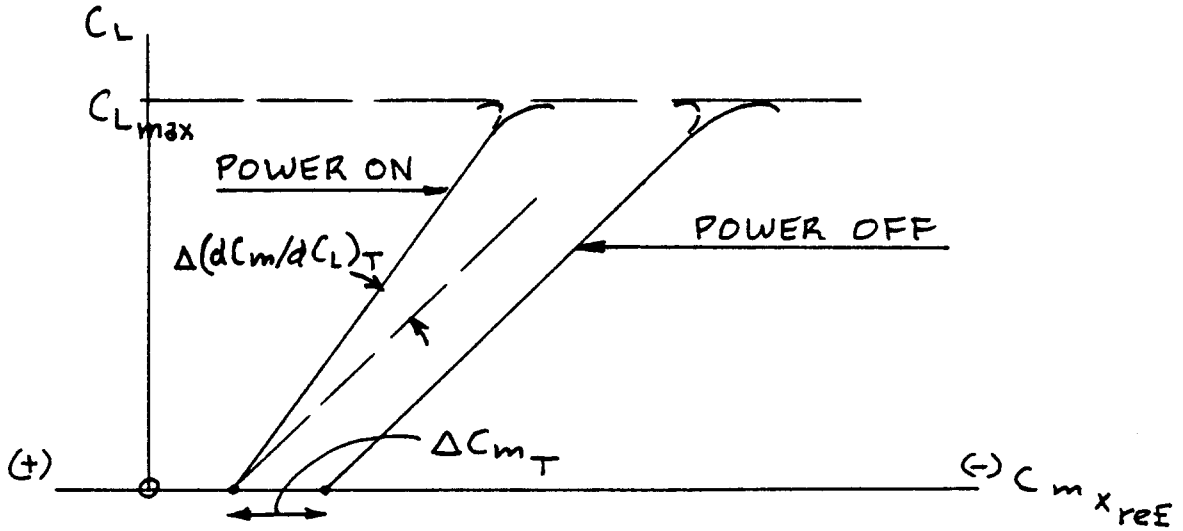

Figure 8.125 Power Effects on Airplane Pitching Moment

8.2.8 Power Effects on Airplane Pitching Moment

For a detailed treatment of power effects on pitching moment the reader should consult Reference 9.

Figure 8.125 shows that two types of power effect on the airplane C_m-C_L curve must be accounted for:

1. A shift in pitching moment at zero lift coefficient: ΔC_{m_T}

   This type of power effect is caused by thrustline offset and/or by the effect of propeller slipstream.

2. A change in slope: $\Delta(dC_m/dC_L)_T$

   The change in slope must be interpreted as a change in apparent static longitudinal stability. This type of power effect is caused by thrustline offset and/or by propeller/inlet normal forces.

These effects are accounted for as follows:

8.2.8.1 Power effect on pitching moment at zero lift coefficient

8.2.8.2 Power effect on longitudinal stability

8.2.8.1 Power effect on pitching moment at zero lift coefficient: ΔC_{m_T}

The effect of power on the pitching moment coefficient at zero lift coefficient may be estimated from:

$$\Delta C_{m_T} = \Delta C_{m_{TL}} + \Delta C_{m_{TS}} \qquad (8.101)$$

where: $\Delta C_{m_{TL}}$ is the pitching moment increment due to thrustline offset

$\Delta C_{m_{TS}}$ is the pitching moment increment due to propeller slipstream

Effect of Thrustline Offset: $\Delta C_{m_{TL}}$

Figure 8.126 illustrates the geometry of thrustline offset as it affects the pitching moment of an airplane.

Since multi-engine airplanes can have the engines

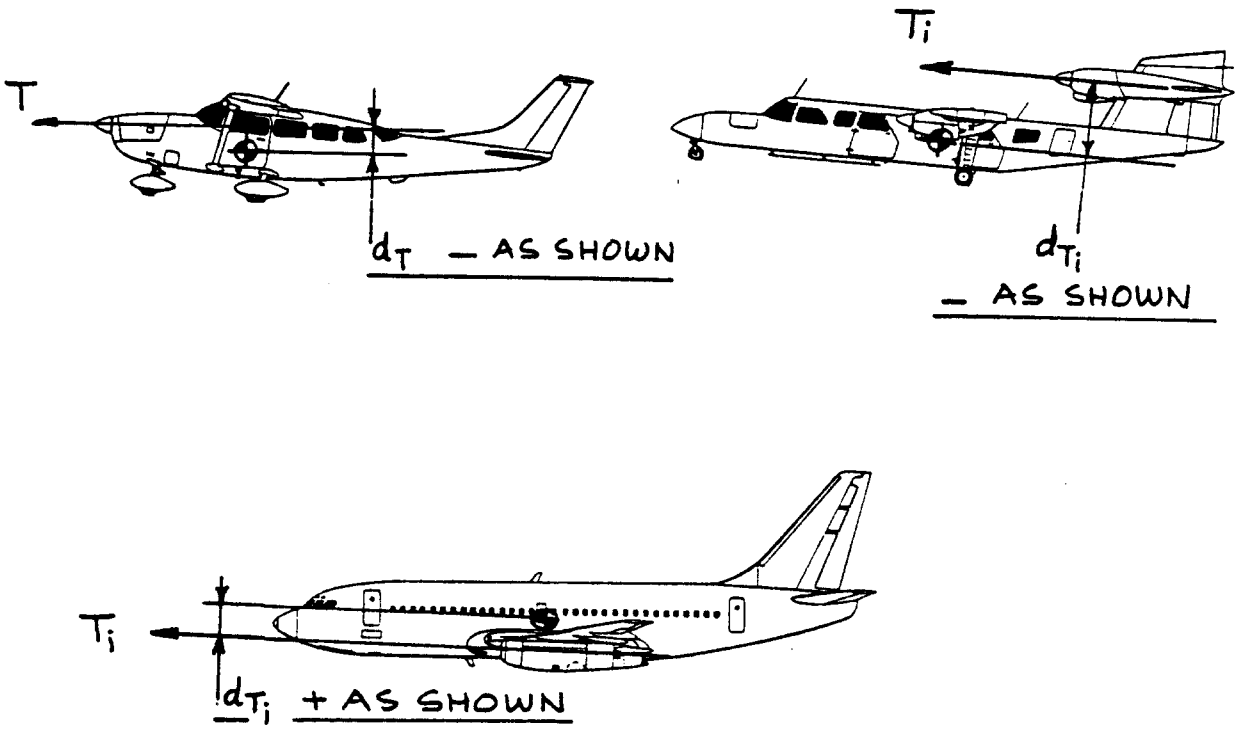

Figure 8.126 Geometry of Thrustline Offset

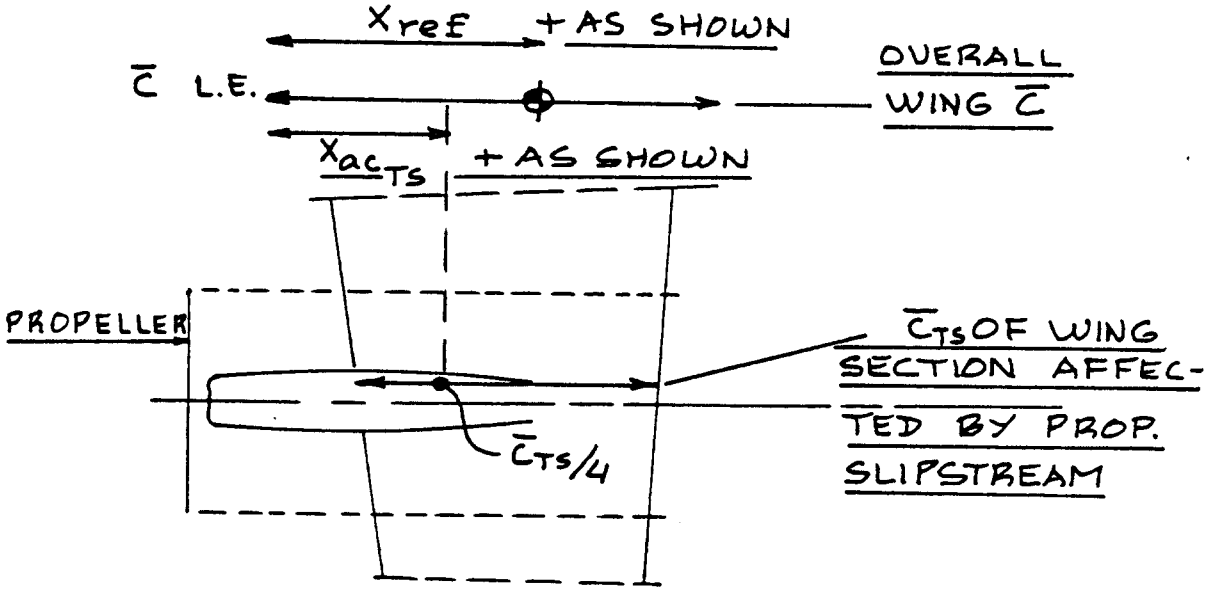

Figure 8.127 Geometric Parameters Affecting Slipstream Effect on a Wing

installed in relationsship to the moment reference point, x_{ref} in a variety of ways, a summation of the effect of individual engines will be required. The incremental pitching moment due to thrustline offset is found from:

$$\Delta C_{m_{TL}} = \sum_{i=1}^{i=n} (T_{av_i} d_{T_i} / \bar{q}S\bar{c}) \qquad (8.102)$$

where: T_{av_i} is the available installed thrust from a propeller or from a jet engine

d_{T_i} is the thrustline offset relative to x_{ref}

Note from Figure 8.126, that d_{T_i} is counted as positive if the thrust line is located beneath the reference point.

Effect of Propeller Slipstream:

There are two types of slipstream effect which can alter the pitching moment of an airplane:

1. Effect of slipstream on a canard or on a horizontal tail
2. Effect of slipstream on a wing

1. Effect of slipstream on a canard or on a horizontal tail

The effect of (propeller) slipstream on the local dynamic pressure at the canard or at the horizontal tail has already been accounted for through the dynamic pressure ratios, η_c and η_h as found from 8.1.5.2.

In all previous calculations for pitching moment, the effect of power can be left out by using $\eta_{h \text{ or } c} = 0$.

2. Effect of slipstream on a wing

The effect of propeller slipstream on a wing may be accounted for from:

$$\Delta C_{m_{TS}} = (\bar{x}_{ac_{TS}} - \bar{x}_{ref}) \Delta C_{L_w} \qquad (8.103)$$

where: $x_{ac_{TS}}$ and x_{ref} are defined in Figure 8.127.

ΔC_{L_w} is found from Eqn. (8.57)

8.2.8.2 Power effect on longitudinal stability: $\Delta(dC_m/dC_L)_T$

The following method to account for power effect on stability is adapted from Reference 54:

$$\Delta(dC_m/dC_L)_T = (dC_m/dC_L)_{TL} + (dC_m/dC_L)_N \qquad (8.104)$$

where: $(dC_m/dC_L)_{TL}$ is the effect of thrustline offset on longitudinal stability

$(dC_m/dC_L)_N$ is the effect of propeller or inlet normal force on longitudinal stability

Methods for estimating these stability effects are now given for:

1. Propeller driven airplanes

2. Jet driven airplanes

1. Propeller driven airplanes:

The effect of thrustline offset on longitudinal stability for propeller driven airplanes is:

$$(dC_m/dC_L)_{TL} = \text{Sum}_{i=1}^{i=n}[(dT_{c_i}/dC_L)\{2(D_{p_i})^2 d_{T_i}/S\bar{c}\}] \qquad (8.105)$$

where: D_{p_i} is the diameter of propeller i.

d_{T_i} is the thrustline offset for propeller i, see Figure 8.126.

$$dT_{c_i}/dC_L = (3/2)K_{T_i}\eta_{p_i}(C_L)^{1/2} \qquad (8.106)$$

with: η_{p_i} is the efficiency of propeller i, and:

$$K_{T_i} = \{550(SHP_{av_i})(\rho)^{1/2}\}/\{(2W/S)^{3/2}(D_{p_i})^2 \qquad (8.107)$$

Note: The effect of thrustline offset on longitudinal stability can be used by the designer to obtain minor changes in static margin by tilting the thrustline relative to the c.g. or relative to x_{ref}. Figure 8.128 shows an example of thrustline tilt angle used in a light air-

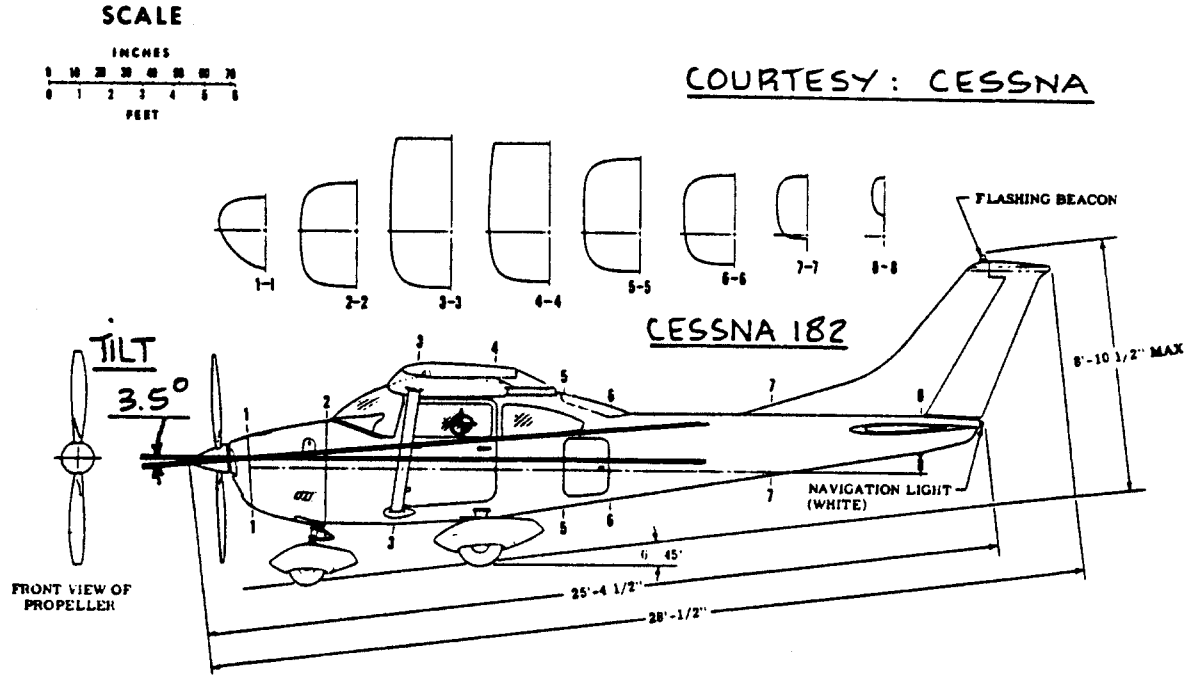

Figure 8.128 Example of Thrustline Tilt

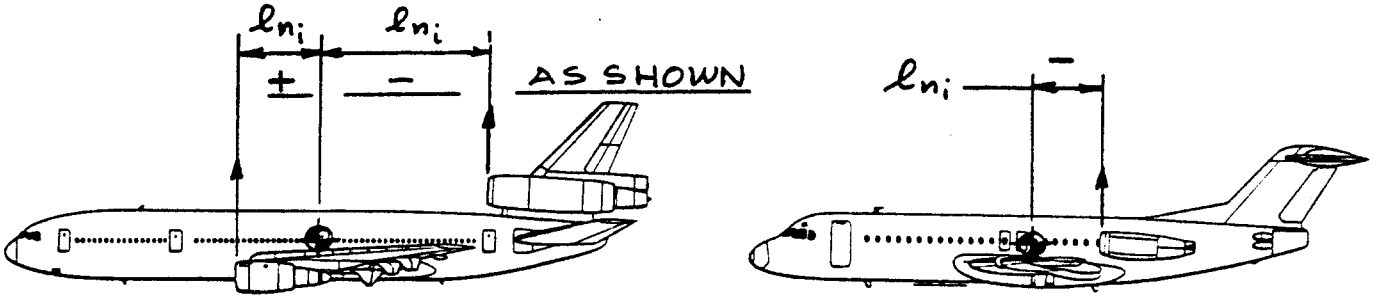

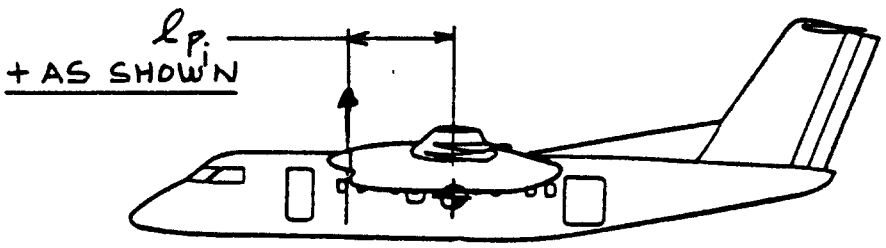

Figure 8.129 Moment Arms for Normal Forces

plane to achieve such an effect.

The effect of propeller normal force on longitudinal stability may be found from:

$$(dC_m/dC_L)_N = \text{Sum}_{i=1}^{i=n}\left[\{(dC_N/d\alpha)_{p_i}(1 + d\bar{\varepsilon}_{p_i}/d\alpha)(l_{p_i})(0.79)(D_{p_i})^2\}/S\bar{c}C_{L_{\alpha_w}}\right] \quad (8.108)$$

where: l_{p_i} is the moment arm of the propeller normal force to the reference point: see Fig. 8.129.

$d\bar{\varepsilon}_{p_i}/d\alpha$ is found from Figure 8.115.

$(dC_N/d\alpha)_{p_i}$ is the change in propeller normal force coefficient with angle of attack. It may be computed from:

$$(dC_N/d\alpha)_{p_i} = [\{(C_{N_\alpha})_{p_i}\}_{K_{N_i}=80.7}][1 + 0.8\{(K_{N_i}/80.7) - 1\}] \quad (8.109)$$

with: $\{(C_{N_\alpha})_{p_i}\}_{K_{N_i}=80.7}$ found from Figure 8.130,

and with:

$$K_{N_i} = 262\{(w_{p_i}/R_{p_i})_{0.3R_{p_i}}\} + 262(w_{p_i}/R_{p_i})_{0.6R_{p_i}} + 135(w_{p_i}/R_{p_i})_{0.9R_{p_i}} \quad (8.110)$$

where: w_{p_i} is the propeller blade width at the radius station indicated in the subscript

R_{p_i} is the propeller blade radius $(0.5D_{p_i})$

2. Jet driven airplanes:

The effect of thrustline offset on the longitudinal stability of most jet driven airplanes is negligible. The reason is the relatively small change in thrust with small changes in speed.

The effect of inlet normal force on longitudinal stability of a jet airplane may be estimated from:

$$(dC_m/dC_L)_N = \sum_{i=1}^{i=n} \left[\frac{\{0.035(\dot{m}_{a_i})(d\bar{\varepsilon}/d\alpha)_i(l_{n_i})\}}{\{Sc\rho U_i(C_{L_{\alpha_w}})\}}\right] \qquad (8.111)$$

where: $\dot{m}_{a_i}$ is the mass flow rate through engine i
This mass flow rate follows from Chapter 6.

$(d\bar{\varepsilon}/d\alpha)_i$ is obtained from Figure 8.115 for inlet i

l_{n_i} is the moment arm of the inlet lip as illustrated in Figure 8.129.

COPIED FROM: REF. 9

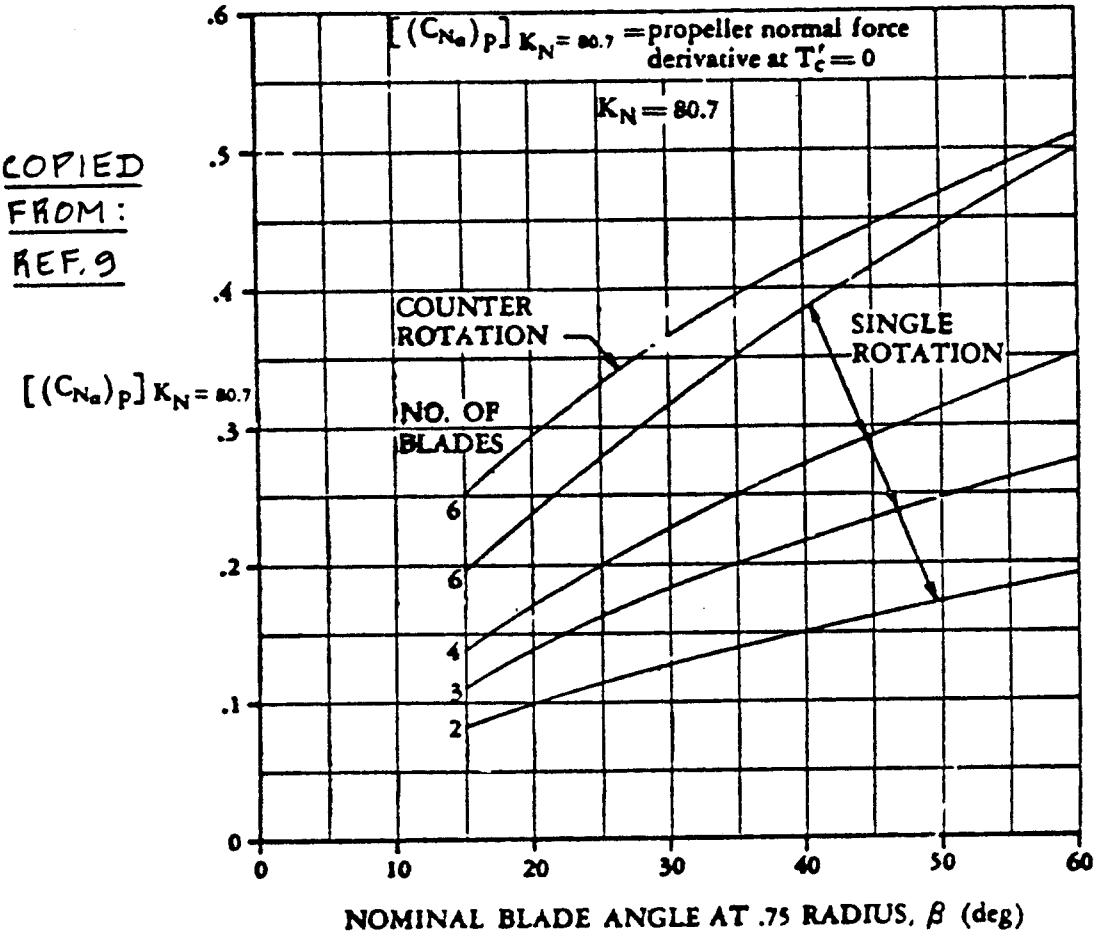

Figure 8.130 Propeller Normal Force Parameter

8.3 PREDICTION OF TRIMMED LIFT AND TRIMMED MAXIMUM LIFT COEFFICIENT

In Sections 8.1 and 8.2 methods are presented for the construction of airplane lift and pitching moment curves. The position was taken that all longitudinal control surface deflections were set at zero.

In any equilibrium flight condition the airplane must also be in moment equilibrium. The effect of pitching moment equilibrium (also known as longitudinal moment trim, or simply: trim) on airplane lift at different center of gravity locations will be accounted for in this Section. The following condition must be satisfied in a trimmed flight condition:

$$C_m = 0 \qquad (8.112)$$

The pitching moment coefficient C_m takes on values which depend on:

1. the lift coefficient at which the airplane is flying,
2. the location of the center of gravity and
3. the power setting.

Methods for computing C_m are given in Section 8.2.

The trim condition as expressed by Eqn.(8.112) is achieved by deflection of one or more control surfaces. In this Section, the following control surfaces will be accounted for:

1. Stabilizer incidence, i_h
2. Elevator deflection, δ_e
3. Canard incidence, i_c
4. Canardvator deflection, δ_c

Figure 8.131 shows typical examples of these control surfaces and their typical arrangement on an airplane. Different types of longitudinal controls may be required on certain airplanes. Examples are: elevons on delta wings (as on the F-106) or symmetrically deflected ailerons (as on the Starship). In this section only types 1-4 will be considered.

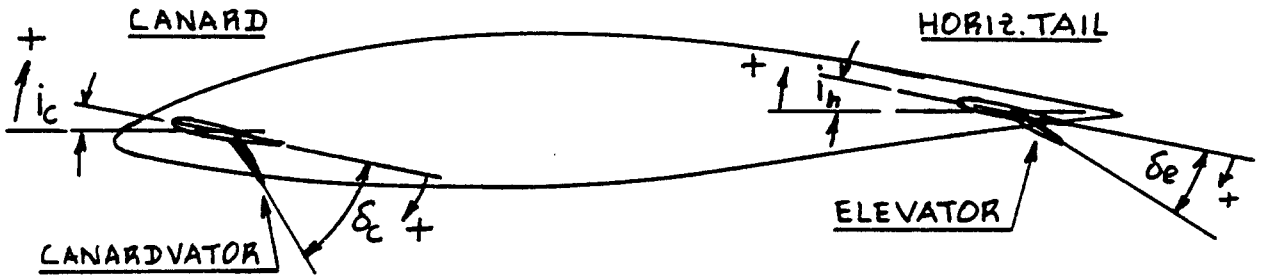

Figure 8.131 Example of Control Surface Arrangements

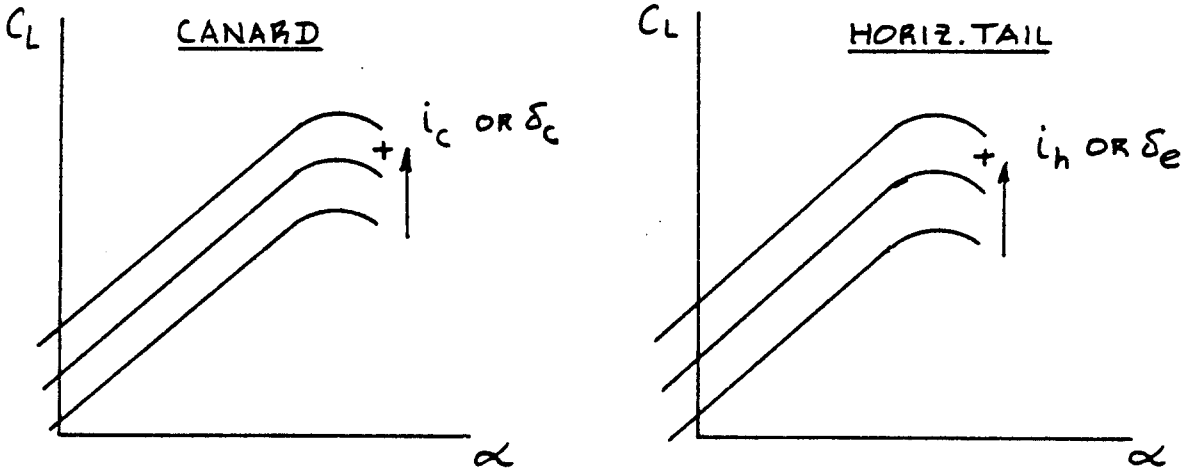

Figure 8.132 Effect of Control Surface Deflection on Airplane Lift

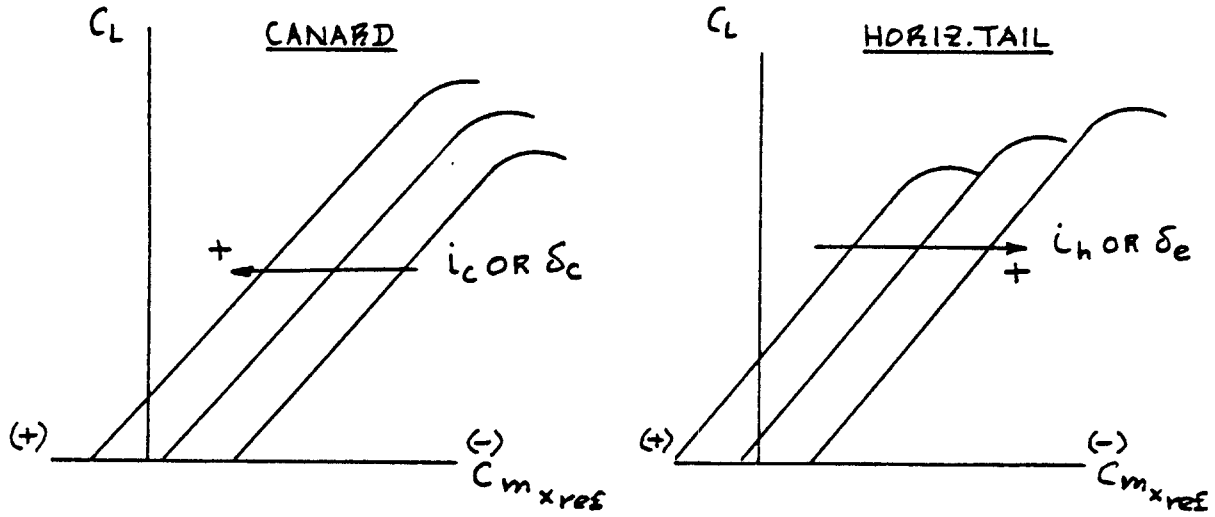

Figure 8.133 Effect of Control Surface Deflection on Airplane Pitching Moment

Deflection of a control surface (which effectively can be thought of as a plain flap) causes changes in airplane lift and in airplane pitching moment in the following ways:

1. Effect of control surface deflection on lift
2. Effect of control surface deflection on pitching moment

1. Effect of Control Surface Deflection on Lift:

$$\Delta C_{L_{ctl}} = \quad (8.113)$$

$$(C_{L_{i_h}})i_h + (C_{L_{\delta_e}})\delta_e + (C_{L_{i_c}})i_c + (C_{L_{\delta_c}})\delta_c$$

where: $C_{L_{i_h}}$, $C_{L_{\delta_e}}$, $C_{L_{i_c}}$ and $C_{L_{\delta_c}}$ are the control surface lift derivatives. They are computed with the methods given in Chapter 10.

Figure 8.132 shows how a control surface deflection affects the airplane lift versus angle of attack curve. Note the control surface sign conventions in Fig. 8.131!

2. Effect of Control Surface Deflection on Pitching Moment:

$$\Delta C_{m_{ctl}} = \quad (8.114)$$

$$(C_{m_{i_h}})i_h + (C_{m_{\delta_e}})\delta_e + (C_{m_{i_c}})i_c + (C_{m_{\delta_c}})\delta_c$$

where: $C_{m_{i_h}}$, $C_{m_{\delta_e}}$, $C_{m_{i_c}}$ and $C_{m_{\delta_c}}$ are the control power derivatives. They may be computed with the methods given in Chapter 10.

Figure 8.133 shows how a control surface deflection affects the airplane pitching moment versus lift curve. Note the control surface sign conventions in Fig. 8.131!

Next, methods are presented for determining the trimmability of airplanes. This is accomplished using so-called trim diagrams.

A method for determining trimmed lift and trimmed maximum lift capability of an airplane is presented for the following cases:

8.3.1 Stable airplane with stable pitchbreak
8.3.2 Unstable airplane with stable pitchbreak
8.3.3 Stable airplane with unstable pitchbreak
8.3.4 Unstable airplane with unstable pitchbreak

In the case of military airplanes with external stores and/or with deployed speedbrakes, significant additional pitching moments may be introduced due to these devices. Such 'drag-induced' pitching moments can be accounted for through a shift of the origin of the C_m-C_L plot. This shift is computed from:

$$\Delta C_{m_{store/speedbrake}} = (\Delta C_{D_{store/speedbrake}}) d_D/\bar{c} \quad (8.115)$$

where: $\Delta C_{D_{store/speedbrake}}$ is the drag increment due to the store or speedbrake. This increment follows from Section 4.9 or from 4.12.

d_D is the moment arm, positive if the drag increment acts ABOVE the c.g.

8.3.1 Stable Airplane with Stable Pitch Break

Figures 8.134a,b present trim diagrams for a stable airplane with a stable pitch break:

Fig. 8.134a is for a conventional (tail-aft) airplane
Fig. 8.134b is for a canard airplane.

The C_L-α and C_L-C_m curves for ZERO control surface deflections are obtained with the methods of Sections 8.1 and 8.2 respectively. The effect of control surface deflections on these curves is determined with the method indicated in Figures 8.132 and 8.133.

Note that the C_m axis is labelled: $C_{m_{x_{ref}}}$. The location of the moment reference center, x_{ref} is normally selected somewhere between the most forward and the most aft locations of the airplane center of gravity. Methods for determining the center of gravity location of any airplane are discussed in Part II, Chapter 10.

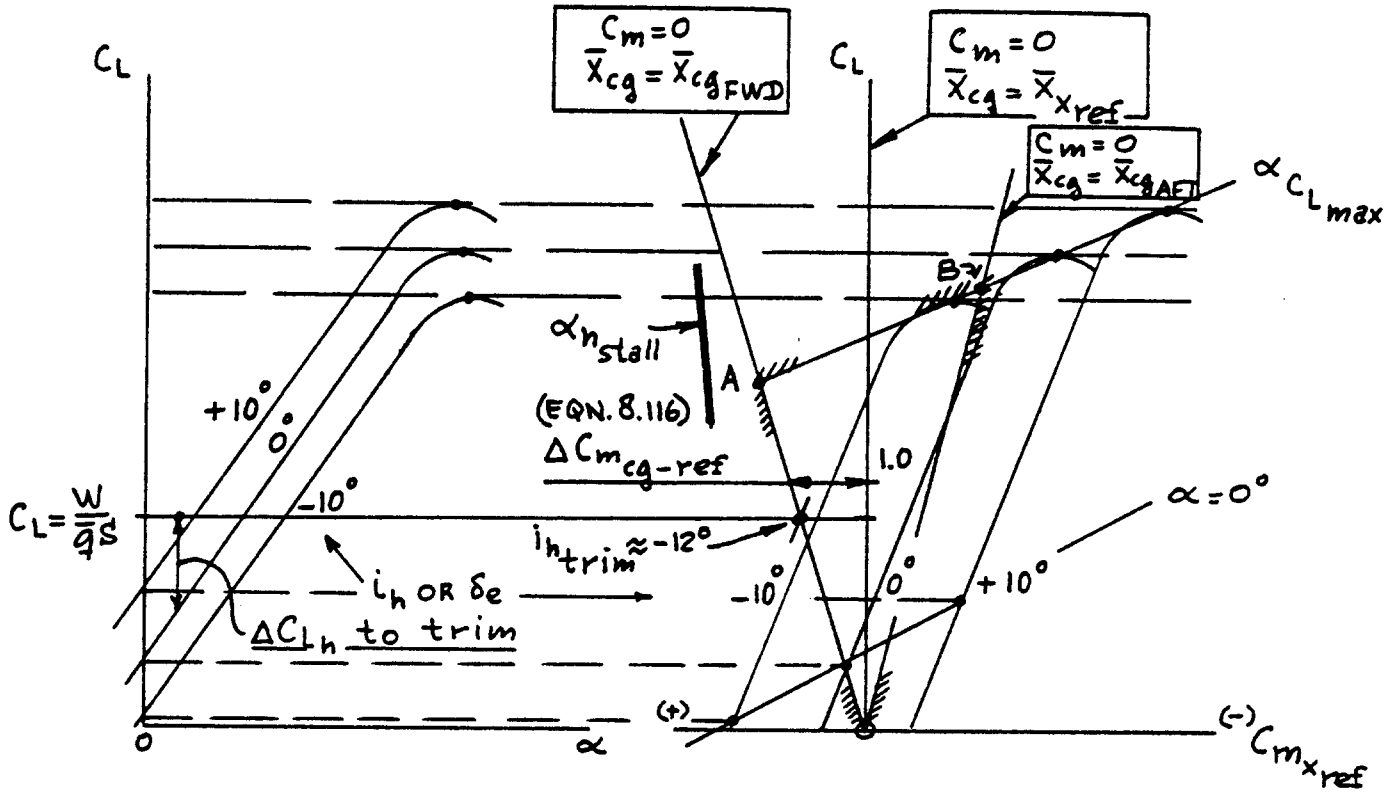

Figure 8.134a Trim Diagram: Stable, Conventional with Stable Pitch Break

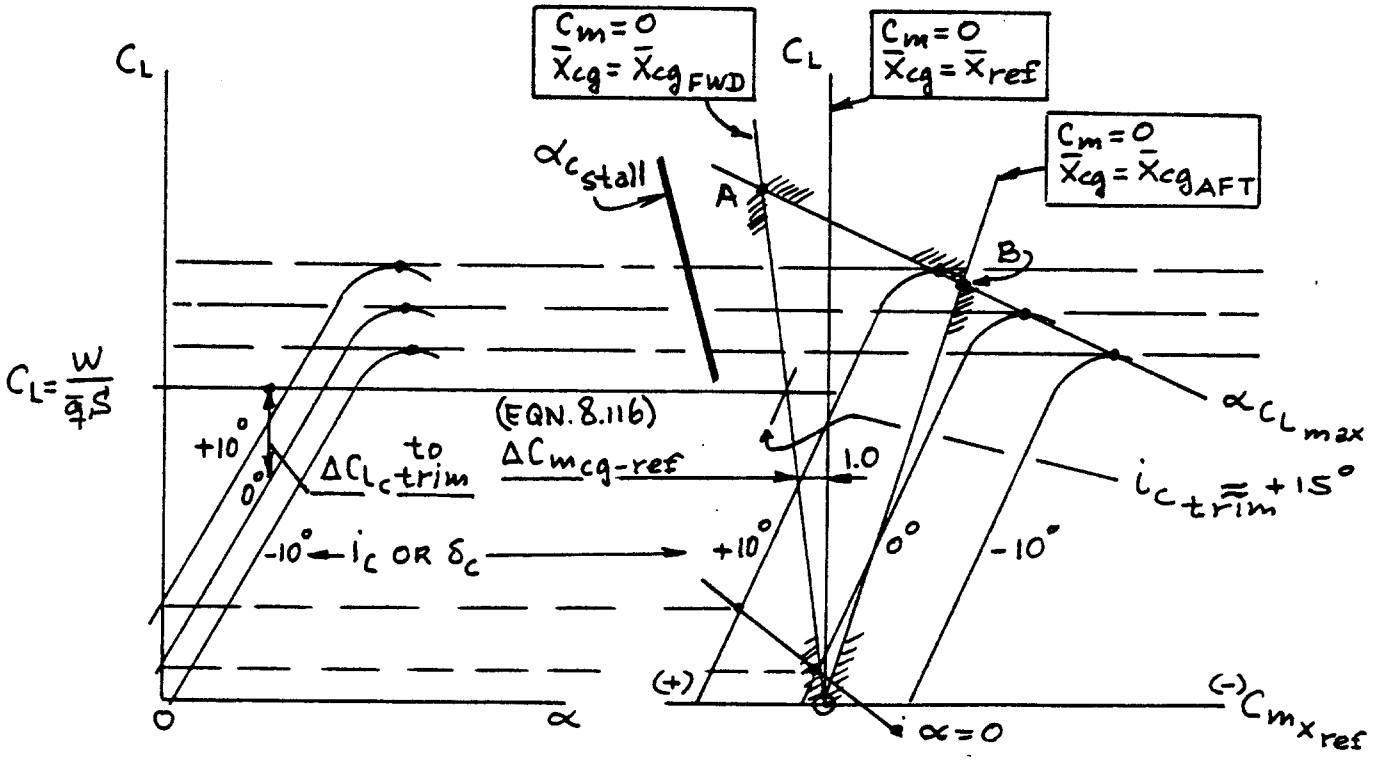

Figure 8.134b Trim Diagram: Stable, Canard with Stable Pitch Break

Observe in Figures 8.134a,b that C_m=0 lines at different centers of gravity have slopes different from that of the C_m=0 line with x_{cg}=x_{ref}. These different slopes may be determined with the help of Procedure 1.

PROCEDURE 1: Determination of Slopes of C_m=0 Lines at Different C.G. Locations

1. Determine the most forward and the most aft c.g. locations of the airplane. This is done with the method of Chapter 10 in Part II.
2. Compute $\bar{x}_{cg} - \bar{x}_{ref}$
3. At C_L=1.0 determine:

$$\Delta C_{m_{cg-ref}} = -1.0(\bar{x}_{cg} - \bar{x}_{ref}) \qquad (8.116)$$

4. Plot $\Delta C_{m_{cg-ref}}$ as shown in Figures 8.134a,b and connect that point with the origin. The line so obtained is the C_m = 0 locus for the new c.g. location.

Note: the proof for this procedure is found in Chapter 5 of Reference 16.

The determination of trimmed lift and maximum lift now proceeds according to Procedure 2.

PROCEDURE 2: Determination of Trimmed Lift and Trimmed Maxiximum Lift

1. Construct the trim diagram as shown in Figures 8.134a or 8.134b. This includes a number of α = constant lines up to α_{stall}
2. Construct the C_m=0 lines for the most aft and for the most forward c.g. locations, with the help of Procedure 1.
3. Identify the trim-triangle: OAB.
4. Draw in the tail or canard stall locus with the

following considerations. For a stalled tail:

$$\alpha_h = \alpha_{h_{stall}} = \alpha + i_h - \varepsilon_{o_h} - \alpha(d\varepsilon/d\alpha) \quad (8.117)$$

where: ε_{o_h} follows from 8.1.5.2

$d\varepsilon/d\alpha$ follows from 8.1.5.3

A value for the tail stall angle, $\alpha_{h_{stall}}$ is found from 8.1.3.4 by substitution of appropriate tail parameters for wing parameters.

For any value of airplane angle of attack, α, Eqn.(8.116) can be used to solve for the corresponding value of i_h which will cause the tail to stall. By repeating this for a range of angles of attack, a tail stall locus can be drawn into Figure 8.134a.

Note: for a canard airplane, the canard stall locus is found in a similar manner by using the following equation:

$$\alpha_c = \alpha_{c_{stall}} = \alpha + i_c + \varepsilon_{o_c} + \alpha_c(d\varepsilon_c/d\alpha) \quad (8.118)$$

where: ε_{o_c} follows from 8.1.5.2

$d\varepsilon_c/d\alpha$ follows from 8.1.5.3

IMPORTANT OBSERVATION: the tail stall and/or the canard stall loci MUST be outside the so-called trim triangle identified in Step 3. If this condition is not satisfied, severe restrictions on the performance of the airplane may result.

5. Compute $C_L = W/qS$ for significant points in the airplane flight envelope. Figure 8.135 shows examples of significant trim points in the flight envelope of low and high speed airplanes. These points depend on the mission requirements

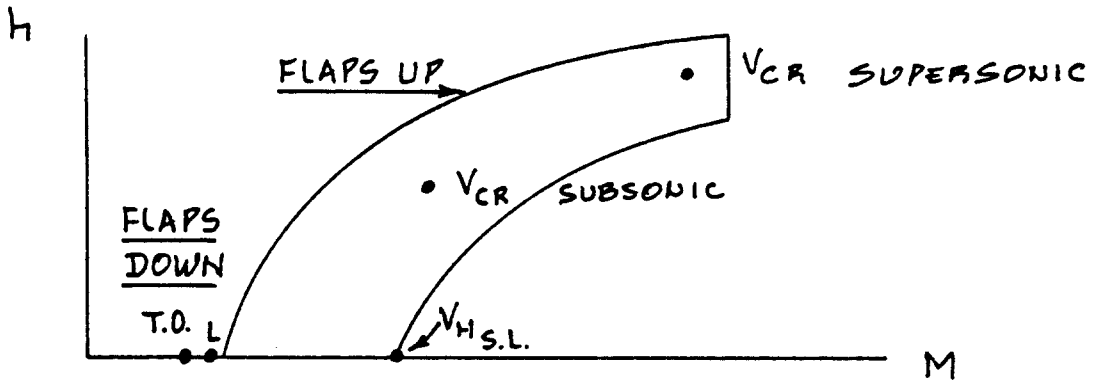

Figure 8.135 Significant Trim Points in Flight Envelope

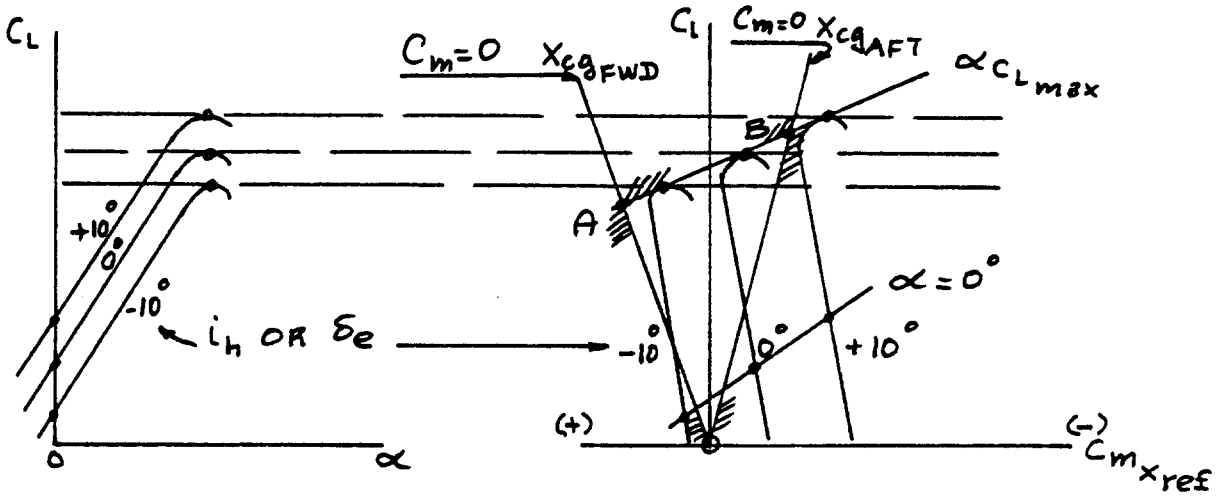

Figure 8.136a Trim Diagram: Unstable, Conventional with Stable Pitch Break

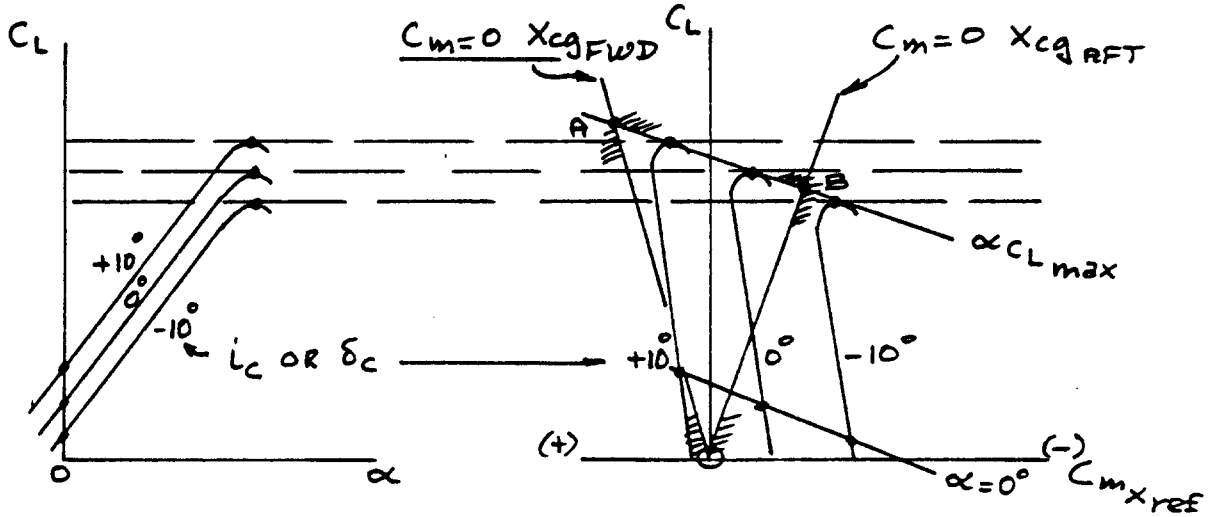

Figure 8.136b Trim Diagram: Unstable, Canard with Stable Pitch Break

placed on the airplane.

6. Determine the c.g. location(s) at which the trim needs to be investigated. Combinations of weight and c.g. locations follow from the weight-c.g. excursion diagram discussed in detail in Ch.10 of Part II.

7. Plot the C_L points on the appropriate C_m=0 line (corresponding to its c.g. location) in Figures 8.134a,b and determine the amount of control surface deflection required to trim. From these control deflections required for trim it is posble to compute the tail or canard lift increments to trim, needed in the trim drag calculations on p.104:

$$\Delta C_{L_{h \text{ or } c}} = (C_{L_{i_{h \text{ or } c}}}) i_{h \text{ or } c} \qquad (8.119)$$

or:

$$\Delta C_{L_{h \text{ or } c}} = (C_{L_{\delta_{e \text{ or } c}}}) \delta_{e \text{ or } c} \qquad (8.120)$$

8. Points A and B in Figures 8.134a,b represent the trimmed maximum lift coefficients at the corresponding c.g. locations of the airplane.

==========

SPECIAL CASE: Three-surface Airplane Trim

In the case of a three surface configuration the designer can choose how to deflect control surfaces on the canard, the wing and the tail in conjunction with each other. Several possible optimization schemes are now possible:

1. Minimize trimmed drag
2. Maximize trimmed maximum lift
3. Maximize maneuvering capability

The construction of a trim diagram for a three surface airplane is left to the reader. The Grumman X-29 and the Piaggio Avanti are examples of three surface airplanes.

8.3.2 Unstable Airplane with Stable Pitch Break

Figures 8.136a,b present example trim diagrams for an unstable airplane with a stable pitch break. The pro-

cedures outlined in 8.3.1 for determining trimmed lift and trimmed maximum lift also apply in this case.

8.3.3 Stable Airplane with Unstable Pitch Break

Figures 8.137a,b present example trim diagrams for a stable airplane with an unstable pitch break. The method of 8.3.1 for determining trimmed lift can be used without modification.

However, to determine the allowable trimmed maximum lift coefficient now is not very straightforward. Depending on the number of pitch curve 'wiggles' and depending on the change in control power at high angle of attack, the trimmed maximum lift coefficient may be limited for reasons other than aerodynamic stall. If handling quality problems or severity of pitch divergence so dictate, the airplane may have to be equipped with stick-shakers and/or with stick-pushers. In such cases the maximum trimmable lift coefficient which can be used in the normal performance envelope of the airplane is predicated on the lift coefficient corresponding to stick-pusher operation. Figures 8.137a,b indicate such an artificial limit.

In the case of airplanes equipped with digital flight control systems a control-limiting scheme may be added to the flight control laws. Such a control limiting scheme may limit the angle of attack which actually can be reached by the airplane. The limiting value of trimmed maximum lift coefficient must then be the one which corresponds to the limit set by the flight control law and not by any inherent aerodynamic limit.

8.3.4 Unstable Airplane with Unstable Pitch Break

Figures 8.138a,b show examples of trim diagrams for an unstable airplane with an unstable pitch break. The comments made under 8.3.2 apply to this case.

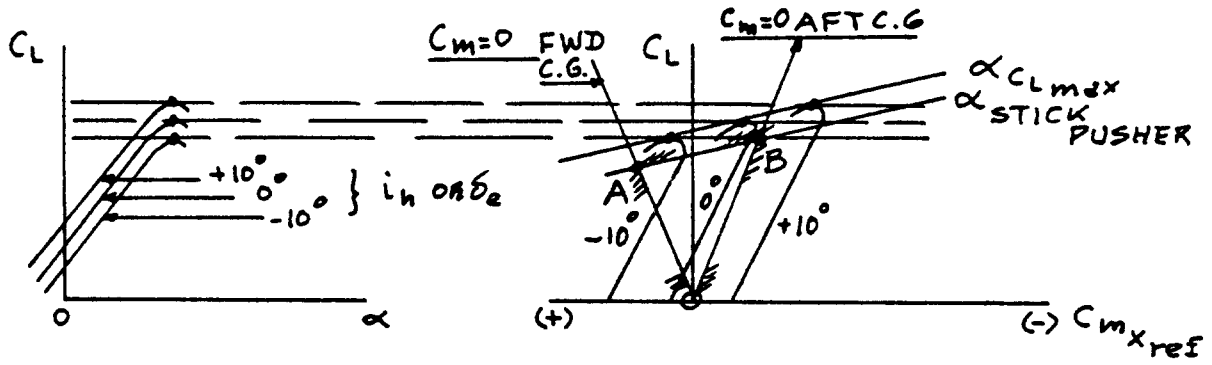

Figure 8.137a Trim Diagram: Stable, Conventional with Unstable Pitch Break

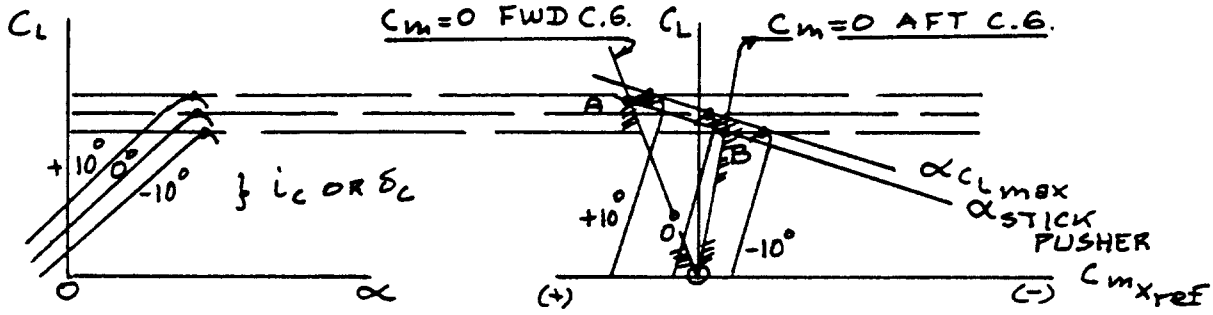

Figure 8.137b Trim Diagram: Stable, Canard with Unstable Pitch Break

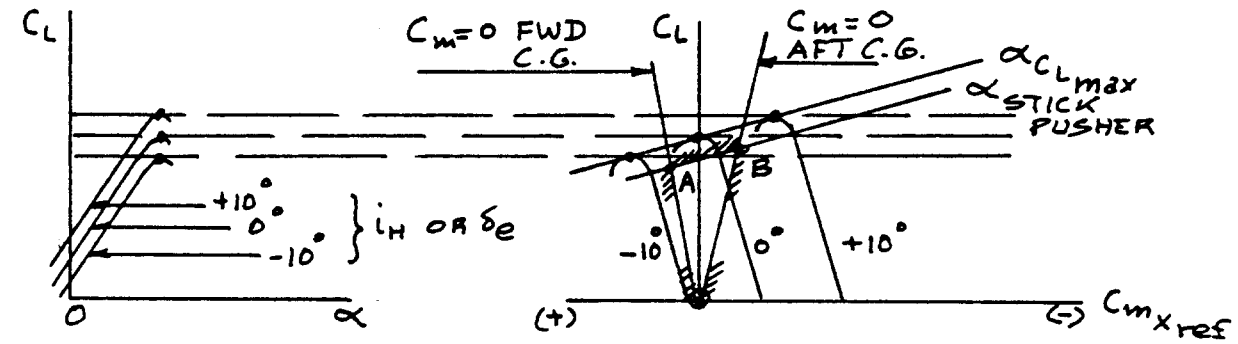

Figure 8.138a Trim Diagram: Unstable, Conventional with Unstable Pitch Break

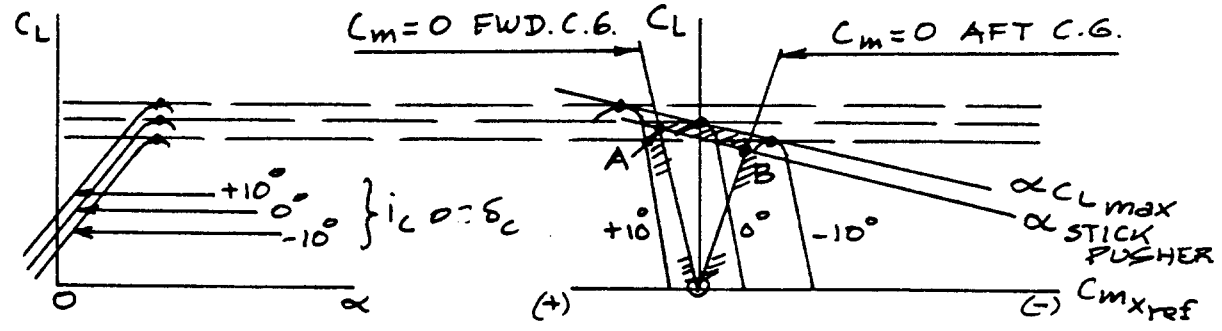

Figure 8.138b Trim Diagram: Unstable, Canard with Unstable Pitch Break

9. AIRPLANE HIGH LIFT DATA

The purpose of this chapter is to present a range of high lift (and some pitching moment) data. These data are presented in the following form:

9.1. Airfoil high lift data: flaps up and down

9.2. Airplane high lift data: flaps up and down

9.3. Mach number effects on high lift

9.1 AIRFOIL HIGH LIFT DATA: FLAPS UP AND FLAPS DOWN

A summary of NACA airfoil high lift and pitching moment data is provided in Table 9.1 for flaps up.

Tables 9.2, 9.3 and 9.4 provide data on airfoil high lift and pitching moment for flaps down.

The reader should carefully note the effect of Reynold's Number on the maximum lift coefficient. This effect must not be neglected in preliminary design. A summary of the effect of Reynold's Number on airfoil maximum lift is provided in Figures 9.1 and 9.2.

References 49 and 51 provide much additional data on airfoil maximum lift and pitching moment as well as on the effect of Reynold's Number.

9.2 AIRPLANE HIGH LIFT DATA: FLAPS UP AND FLAPS DOWN

In this section some examples of actual airplane high lift data are presented.

Tables 9.5 present a summary of airplane trimmed maximum lift coefficient data, flaps up anf flaps down.

Actual airplane high lift versus angle of attack data are presented as follows:

Figure 9.3 N.A.Rockwell T2C
Figure 9.4 N.A.Rockwell S-60 Sabreliner
Figure 9.5 Raisbeck Modification, S-65 Sabreliner
Figure 9.6 Canadair Challenger
Figure 9.7 Learjet M55
Figure 9.8 Boeing 767-300
Figure 9.9 Boeing 737-300

9.3 MACH NUMBER EFFECTS ON HIGH LIFT

At high subsonic Mach numbers the magnitude of maximum lift coefficient tends to decrease as a result of shock induced separations. This decrease in maximum lift manifests itself as buffet (below maximum lift) and as a reduction in maneuvering capability of the airplane. This effect is strongly influenced by:

1. wing sweep angle
2. airfoil thickness
3. airfoil camber

Figure 9.10 shows some early data indicating the effect of planform and Mach number on the maximum lift of wings with a 6 percent thick airfoil.

With modern airfoil design it is possible to achieve significant improvements in high lift at all Mach numbers and do so at much higher airfoil thickness ratios. (This also results in lower structural weights!) Figure 9.11 illustrates this on the Rockwell T2C: the basic airfoil has t/c = 0.12, the modified airfoil has t/c = 0.17.

A penalty which accompanies almost any increase in high lift is an increase in pitching moment. Since this needs to be trimmed out, the net gain in lift is not as high as untrimmed data would indicate. Figure 9.12 shows the effect of airfoil change on the T2C on its pitching moment behavior: note the rather large negative increase in pitching moment.

An example of the buffet boundary ($C_{L_{buffet}} < C_{L_{max}}$) for a modern business jet airplane with an advanced airfoil is given in Figure 9.13.

Most high lift data are obtained for steady state conditions. In flight test such conditions are simulated by accepting high lift data only when the rate of reduction of airspeed is not greater than 1 kt/sec.

In addition to the effect of speed changes on high lift, there are strong effects of rate of change of angle of attack on high lift. The data in Figs 9.14 and 9.15 indicate this! In determining the performance of fighter aircraft these unsteady effects are very important.

Table 9.1 Experimental Low Speed Data for 4- and 5- Digit NACA Airfoils with a Smooth Leading edge and for $R_N = 9 \times 10^6$ (Ref.49)

Airfoil	α_{0_ℓ} (deg)	c_{m_o}	c_{l_α} (deg^{-1})	a.c. (tenths c)	$\alpha_{c_{l_{max}}}$ (deg)	$c_{l_{max}}$	α^* (deg)
0006	0	0	.108	.250	9.0	.92	9.0
0009	0	0	.109	.250	13.4	1.32	11.4
1408	0.8	-.023	.109	.250	14.0	1.35	10.0
1410	-1.0	-.020	.108	.247	14.3	1.50	11.0
1412	-1.1	-.025	.108	.252	15.2	1.58	12.0
2412	-2.0	-.047	.105	.247	16.8	1.68	9.5
2415	-2.0	-.049	.106	.246	16.4	1.63	10.0
2418	-2.3	-.050	.103	.241	14.0	1.47	10.0
2421	-1.8	-.040	.103	.241	16.0	1.47	8.0
2424	-1.8	-.040	.098	.231	16.0	1.29	8.4
4412	-3.8	-.093	.105	.247	14.0	1.67	7.5
4415	-4.3	-.093	.105	.245	15.0	1.64	8.0
4418	-3.8	-.088	.105	.242	14.0	1.53	7.2
4421	-3.8	-.085	.103	.238	16.0	1.47	6.0
4424	-3.8	-.082	.100	.239	16.0	1.38	4.8
23012	-1.4	-.014	.107	.247	18.0	1.79	12.0
23015	-1.0	-.007	.107	.243	18.0	1.72	10.0
23018	-1.2	-.005	.104	.243	16.0	1.60	11.8
23021	-1.2	0	.103	.238	15.0	1.50	10.3
23024	-0.8	0	.097	.231	15.0	1.40	9.7

Airfoil	α_{0_ℓ} (deg)	c_{m_o}	c_{l_α} (deg^{-1})	a.c. (tenths c)	$\alpha_{c_{l_{max}}}$ (deg)	$c_{l_{max}}$	α^* (deg)
63-006	0	.005	.112	.258	10.0	.87	7.7
63-009	0	0	.111	.258	11.0	1.15	10.7
63-206	-1.9	-.037	.112	.254	10.5	1.06	6.0
63-209	-1.4	-.032	.110	.262	12.0	1.40	10.8
63-210	-1.2	-.035	.113	.261	14.5	1.56	9.6
63_1-012	0	0	.116	.265	14.0	1.45	12.8
63_1-212	-2.0	-.035	.114	.263	14.5	1.63	11.4
63_1-412	-2.8	-.075	.117	.271	15.0	1.77	9.6
64-006	0	0	.109	.256	9.0	.8	7.2
64-009	0	0	.110	.262	11.0	1.17	10.0
64-206	-1.0	-.040	.110	.253	12.0	1.03	8.0
64-209	-1.5	-.040	.107	.261	13.0	1.40	8.9
64-210	-1.6	-.040	.110	.258	14.0	1.45	10.8
64_1-012	0	0	.111	.262	14.5	1.45	11.0
64_1-212	-1.3	-.027	.113	.262	15.0	1.55	11.0
64_1-412	-2.6	-.065	.112	.267	15.0	1.67	8.0

Airfoil	α_{0_ℓ} (deg)	c_{m_o}	c_{l_α} (deg^{-1})	a.c. (tenths c)	$\alpha_{c_{l_{max}}}$ (deg)	$c_{l_{max}}$	α^* (deg)
65-006	0	0	.105	.258	12.0	.92	7.6
65-009	0	0	.107	.264	11.0	1.08	9.8
65-206	-1.6	-.031	.105	.257	12.0	1.03	6.0
65-209	-1.2	-.031	.106	.259	12.0	1.30	10.0
65-210	-1.6	-.034	.108	.262	13.0	1.40	9.6
65_1-012	0	0	.110	.261	14.0	1.36	10.0
65_1-212	-1.0	-.032	.108	.261	14.0	1.47	9.4
65_1-412	-3.0	-.070	.111	.265	15.5	1.66	10.5
63A010	0	.005	.105	.254	13.0	1.20	10.0
63A210	-1.5	-.040	.103	.257	14.0	1.43	10.0
64A010	0	0	.110	.253	12.0	1.23	10.0
64A210	-1.5	-.040	.105	.251	13.0	1.44	10.0
64A410	-3.0	-.080	.100	.254	15.0	1.61	10.0
64_1A212	-2.0	-.040	.100	.252	14.0	1.54	11.0
64_2A215	-2.0	-.040	.095	.252	15.0	1.50	12.0

Table 9.2 Effect of Airfoil, Flap Type and Flap Deflection on Drag and on High Lift

ADAPTED FROM REF. 51

FLAP TYPE	FLAP GEOMETRY	NACA AIRFOIL	FLAP CHORD %C	R_N	$C_{l_{max}}$ t.o.	δ_f (DEG) t.o.	C_{d_o} for $C_{l_{max}}$ t.o.	C_{d_o} for δ_f at t.o. with C_l = 1,5	2,0	2,5	$C_{l_{max}}$ LAND.	δ_f (DEG) LAND.	C_{d_o} for $\delta_f=0$	SOURCE:
DOUBLE SLOTTED FLAP	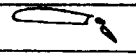	23012	0,1467 0,2500	$3,6.10^6$	3,08	55,65	0,20	—	0,072	0,096	3,55	55,70	0,0085	NACA ARR 3L10
✓	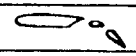	"	0,2270 0,2566	"	3,15	50,60	0,17	—	0,055	0,076	3,46	50,70	"	NACA Rep. 723
✓	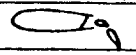	23021	0,1467 0,2566	"	3,06	20,60	0,28	—	0,148	0,178	3,32	"	0,0128	NACA ARR L4J05
✓	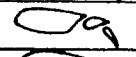	"	0,2267 0,2566	"	3,00	20,50	0,18	0,048	0,066	0,095	3,66	30,60	"	NACA Rep. 723
✓		23020	0,2600 0,2566	"	3,30	"	0,22	0,108	0,110	0,122	3,70	40,80	0,0175	" "
✓		65,3-118	0,309	$6,0.10^6$	2,88	35	0,026	0,009	0,017	0,028	3,40	65	0,0047	NACA ACR 3120
✓		65_3-418	0,29	$1,9.10^6$	2,92	40	—	0,0248	—	—	3,81	"	0,0061	NACA TN 1071
SINGLE SLOTTED FLAP		23012	0,40	$3,5.10^6$	2,80	40	0,16	0,018	0,043	0,092	2,91	50	0,0100	NACA TN 715
✓		23021	"	"	2,62	20	0,13	0,43	0,034	0,075	2,87	"	0,0140	NACA TN 728
✓		23030	0,40	"	2,48	"	0,14	0,052	0,037	—	2,80	"	0,0230	NACA TN 755
✓		63,4-420	0,28	$6,0.10^6$	2,83	30	0,0295	0,0118	0,0173	0,0232	3,00	40	0,0088	NACA ACR 3121
VANED SLOTTED FLAP		23012	0,25	$3,8.10^6$	2,70	50	0,13	0,074	0,099	0,110	2,70	50	0,0150	NACA TN 698
SLOTTED FLAP + .05C SPLIT FLAP		"	0,2566	"	2,74	50,60	0,12	0,036	0,050	0,074	2,89	40,70	0,0250	NACA Rep. 679
SLOTTED FLAP + .10C SL. FLAP		"	"	"	2,96	40,60	0,158	—	0,083	0,114	2,99	"	0,0120	" "
PLAIN FLAP	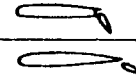	"	0,20	"	2,38	60	0,19	0,152	0,154	—	2,40	75	0,0090	NACA Rep. 664
JUNKERS FLAP	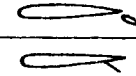	"	0,2667	"	2,28	30,2	0,038	0,028	0,046	—	2,37	40,5	0,0100	" "
SPLIT FLAP		"	0,20	"	2,29	30	0,115	0,080	0,083	—	2,54	75	0,0090	" "
FOWLER FLAP	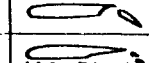	"	0,30	"	3,30	40	0,17	"	0,096	0,113	3,30	40	"	NACA TN 808
QUAD. SLOTTED FOWLER FLAP	 .10C EACH	"	0,40	"	3,28	30	0,14	0,028	0,031	0,050	3,60	40,50 50,70	"	NACA Rep. 689
QUAD SLOTTED FOWLER FLAP	 .075C EACH	"	0,30	"	3,40	30,30 40,50	0,17	—	0,068	0,090	3,40	30,30 40,50	"	NACA Rep. 742

Table 9.3 Effect of Flap Type and Flap Deflection on High Lift

ADAPTED FROM REF. 51

FLAP TYPE	FLAP GEOMETRY	AIRFOIL	R_N	FLAP CHORD %C	FLAP ANGLE (DEG)	A	$C_{L_{MAX}}$	$\Delta C_{L_{MAX}}$	(DEG) $\alpha_{AT\ C_{L_{MAX}}}$	SOURCE:
FIXED SLOT		Clark y	$1,03.10^6$	—	—	6	1,77	0,48	24°	TR 427, TR 554
✓		"	"	—	—	"	1,44	0,15	17°	" "
FIXED SLAT		"	"	0,145	0°	"	1,70	0,41	24°	TR 428, TR 554
TRIPLE SLOTTED WING		"	"	—	—	"	1,93	0,64	25°	TR 427, TR 554
HANDLEY PAGE SLAT	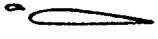	"	"	0,147	—	"	1,84	0,56	28°	TR 400, TR 554 TN 423, TN 443
MAXWELL SLAT	 closed .open	"	$0,85.10^6$	—	—	"	2,07	0,82	28°	TN 598, TR 544
PLAIN FLAP + FIXED SLOT		"	$1,03.10^6$	0,30	45°	"	2,18	0,89	19°	TR 427, TR 554
✓ (S)	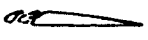	"	"	"	"	"	2,24	0,95	20°	" "
SPLIT FLAP + MAXWELL SLAT	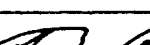	"	$0,85.10^6$	0,211	60°	"	2,33	1,28	21,6°	TR 598, TR 544
SLOTTED FLAP+ FIXED SLOT		"	$1,03.10^6$	0,30	45°	"	2,26	0,97	19°	TR 427, TR 554, TN 702
✓		"	"	"	"	"	2,44	1,15	16°	TR 427, TR 554, TN 702
SLOTTED FLAP+ 2 FIXED SLOTS	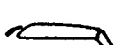	"	"	"	"	"	2,60	1,31	20°	TR 427, TR 554

Table 9.4 Effect of Flap Type on High Lift, on Pitching Moment and on Drag

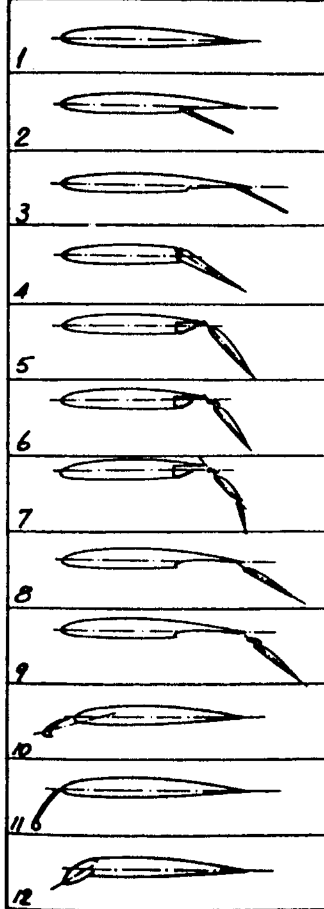

High-lift configuration	High-lift device type	$\delta_{f_{opt}}$ for $C_{l_{max}}$ (deg)	$\Delta C_{l_{max}}$	$\frac{\Delta C_{m_{c/4}}}{\Delta C_l}$	$\frac{\partial C_m}{\partial \delta}$	$\Delta C_{d_{min}}$ @ δ_{opt}	Reyn. No. of test	References
1	Basic wing section 64A010	-	$C_{l_{max}} = 1.0$ (standard roughness)	$C_{m_{c/4}} = 0$	-	$C_{d_{min}} = .009$ (standard roughness)	6×10^6	NACA TN 3007 NACA REP 824
2	Split flap	60	.8	-.275	-.0067	.23	6×10^6	NACA TN 3007 NACA, TN 4040
3	Zap flap	45	1.15	-.30		.21		W.S. Diehl, Engg. Aero. NACA TN 422 A.S.M.E. Transactions April 1934
4	Plain flap	60	.9	-.275	-.0125	.12	6×10^6	NACA REP. 938 NACA TN. 4040 ARC. R&M 2622
5	Single slotted flap	40	1.18	-.33	-.01	.13	35×10^6	NACA REP. 938 NACA TN. 4040 ARC. R&M. 2622
6	Double slotted flap	30/55	1.4	-.41	-.0125	.23	6×10^6	NACA TN 3007 NACA TN. 4040
7	Triple slotted flap	30/44/55	1.6	-.44		.23	6×10^6	NACA WR. L-641
8	Fowler flap	30	1.67	-.42		.10	$\sim3.5\times10^6$	1st IAS-RAS Intl. Conf. 1947, Morgan Abbott-Doenhoff, Theory of Wing Sections NACA REP. 664 (K.D. Wood 1947 Ed. p 170) ARC. R&M 2622 H.D. Fowler, The Fowler Flap
9	Double slotted Fowler flap	15/30	2.25	-.44		~.15	$\sim3.5\times10^6$	1st IAS-RAS. Intl. Conf. 1947, Morgan
10	Leading edge slat	26 (straight wings) 30 with [illegible] 45-60 (swept wings)	~.93	+.11		~0	6×10^6	NACA TN 3007 Journ. of Aircr. Nov-Dec 1966 p [illegible]
11	Krueger flap	40-45 (straight wings) 60 (swept wings)	~.5	-.10		~0	8.2×10^5	NACA TM 1119 Journ. of Aircr. Nov-Dec 1966
12	Leading edge flap (droop nose)	30	[illegible]	[illegible]		~0	6×10^6	NACA TN 3007 NACA TN. 2228

NOTE: ALL DATA FOR:

$A = 12 \quad \lambda = 1.0$

$t/c = 0.10$

$\Lambda_{c/4} = 0°$

$b_f/b = 1.0$

$c_f/c = 0.30$ T.E.

0.15 L.E.

COPIED FROM: REF. 56

Table 9.5a Experimental Trimmed Maximum Lift Coefficients for Several Airplanes

COPIED FROM: REF. 56

MODEL	A	$\Lambda_{c/4}$	$b_{f/b}$	HLD TYPE	TEST TYPE	$C_{L_{max}}$*		REFERENCE
						CLEAN	ALL HLD	
Grumman A6A	6.0	25	~0.8	Fowler Flaps + LE Flaps	F	1.25	2.00	Flight Manual Data
North Am. A5A	4.0	37.5	.765	Plain Flaps + LE Flaps	F	1.05	1.5	Flight Manual Data
North Am. RA-5C	4.0	37.5	.7	Plain Flaps + Blown Outbd. LE Flaps	F		1.8	AIAA Paper 65-751
Douglas A4D	2.91	33	.57	Split Flaps + LE Autoslats	F	.901	1.45	Flight Manual Data
McDonnell F4	2.75	45	.65	Plain Blown Flaps + Inbd. LE Flaps + Outbd. Blown LE Flaps	F	1.05	1.40	Canad. Aeron & Space Journ. March 1966
Fiat G91	4.5	37	.52	Single Slotted Flaps	F	1.0	1.18	Calculated
Republic F105D	3.18	43	.705	Single Slotted Flaps + LE Flaps	F	1.1	1.38	Pilot Handbk. Data
Lockheed F104G	2.45	18.6	.65	Plain Flaps, Droop Ailerons, LE Flaps	F	.75	1.12	Pilot Handbk. Data
Northrop F5	3.7	25	.55	Single Slotted Flaps + LE Flaps	F	1.0	1.4	Pilot Handbk. Data
Hawker Siddeley Buccaneer	3.58	34	1.00	Blown Plain Flaps + Blown LE	F	.96	2.2	Aviation Week 7 Aug 1961 Flight Int'l 3 Nov 1966
Gen. Dynamics F-111	6.0	13	.665	Blown Plain Flaps + Blown Center & Outer LE Flaps	F	1.55	2.45	NASA 1964 SST Conference
North Am. F-100 A (Exp.)	3.72	45	.8	Blown Plain Flaps + Blown LE Flaps	F	1.2	1.5	NASA TN D-321
Douglas F5D-1 (Tailless, NASA OGEE Wing Mod.)	1.7	46	1.0	Plain Elevons + Partial LE Slats	F	1.0	~1.0	NASA TN D-3071
Lockheed XV-4A	6.0	0	.76	Plain Flaps	Full Scale WT	1.15	1.5	NASA TN D-3725
Boeing 727	7.1	30	.75	Triple Slotted Fowler Flaps + LE Slats Outbd. + Kruger Flaps Inbd.	F		2.62	Journ of Aircr. March 65, The Aeroplane Feb. 21, 1963
Boeing 707-320C	7.0	35	.665	Triple Slotted Fowler Flaps + Split Fillet Flaps + LE Flaps	F		1.9	Journ. of Aircr. Mar - Apr. 1965.
Boeing 707-120	7.0	35	.665	Double Slotted Fowler Flaps + Split Fillet Flaps + LE Flaps	F	~1.37 (WT)	1.75	Journ. of Aircr. Mar-Apr. 1965. NACA RM A58H12
Boeing 707-120 (Exp)	7.0	35	.665	Blown Plain Flaps + LE Flaps	F		2.34	NASA TN D-4804

F = Flight; WT = Wind Tunnel; HLD = High Lift Device(s) Down * TRIMMED, GEAR-UP

Table 9.5b Experimental Trimmed Maximum Lift Coefficients for Several Airplanes

COPIED FROM: REF. 56

MODEL	A	$\Lambda_{C/4}$	$b_{f/b}$	HLD TYPE	TEST TYPE	$C_{L_{max}}$* CLEAN	$C_{L_{max}}$* ALL HLD	REFERENCE
Breguet 941 **	6.52	0	~1.0	Double & Triple-Slotted Flaps (Droop Ailerons)	F	1.15	2.8	Journ. of Aircr. May-June 1968 NASA TN D-2231
Lockheed Electra **	7.5	0	.64	Fowler Flaps	F	1.5	2.5	Journ. of Aircr. May-June 1968 NASA TN D-2231
Sud. Caravelle	6.2	20	.63	Double Slotted Flaps	F	1.5	2.25	Journ. of Aircr. May-June 1968 NASA TN D-2231
Lockheed C5A	8	25	.715	Single Slotted Fowler & LE Slats	WT F	1.2 1.45	2.55 2.60	Aircr. Engg. June 1968 LOCKHEED
			.74	Double Slotted Flaps + LE Kruger Flaps + External Jet Blowing	WT		3.8	NASA TN D-4928
Mitsubishi/Mooney MU-2S **	6.8	~0	.93	Double Slotted Flaps + Droop Ailerons	F	1.77	3.13	Vertic. World July 1968 Flight Magaz. Febr. 1964.
Cessna 177 **	7.4	0	.65	Plain Flaps	F	.95	1.55	SAE Paper 680199
Ryan Model 143 (XV-5A) **	3.42	20/37	1.0	Single-Slotted Flaps + Droop Ailerons	F	1.05	1.63	Ryan UP-108 (1965) (Ryan Rep. 29466-2 Vol. II)
Ryan Model 92 (VZ-3RY) **	4.4	0	1.0	Double-Slotted Flaps (Slipstream Deflection) + Fixed LE Slats	WT	1.15	1.5	NASA TN D-89
Douglas A3D	6.75	35.9	.575	Single-Slotted Flaps + LE Slats	Full Scale WT	1.37	1.9	NACA RM A57A24
Douglas A3D	6.75	35.9	.575	Blown, Single-Slotted Flaps + LE Slats	Full Scale WT	1.37	2.7	NACA RM A57D11
North Am. F-86	4.79	35.2	.50	Plain Flaps + LE Autoslats	Full Scale WT	1.09	1.64	NACA RM A52B05
Dornier Do-27 **	7.4	0	.71	Double-Slotted Flaps (Partial Droop Ailerons) + LE Fixed Slots	F	1.3	2.95	Luftfahrttechnik No. 3, 1962
DeHavilland DHC-4 Caribou **	9.9	~0	1.0	Double-Slotted Flaps (Droop Ailerons)	F	1.37	2.63	Calcul. from Pilot Hdbk. Data
Lockheed 49 Constellation **	8.2	0	.62	Fowler Flaps + Split-Fillet Flap	F		2.88	The Fowler Flap
Boeing B-17 **	7.3	0	.57	Zap Flaps	F		2.95	Neville, Aircr. Designers Data Book
Douglas DC-9	8.5	24	.66	Double-slotted Flaps + LE Slat	F	1.5	3.0	SAE Paper 670846
Piper PA-30-160 **	7.3	0	.62	Plain Flaps	Full Scale WT	1.24	1.6	NASA TN D-4983

F = FLIGHT WT = WINDTUNNEL HLD = HIGH LIFT DEVICES DOWN
* TRIMMED, GEAR UP ** PROPELLER(S) OFF

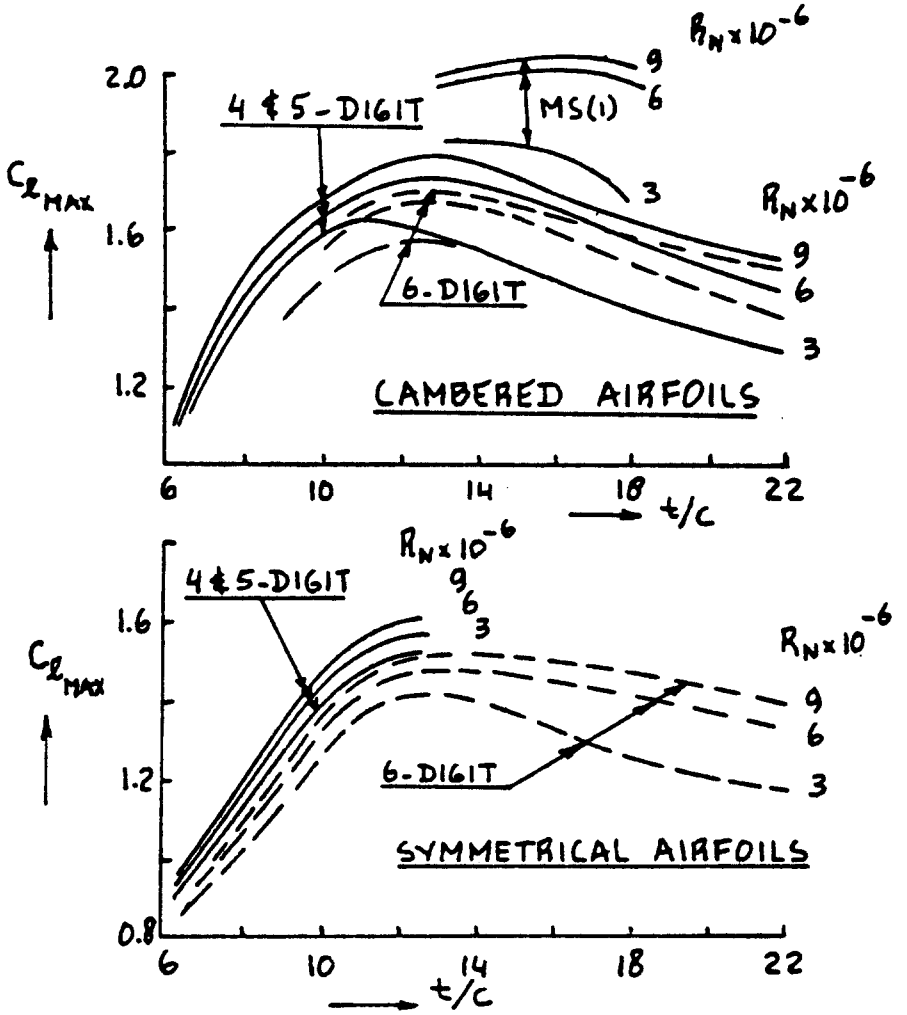

Figure 9.1 Effect of Thickness Ratio and Reynold's Number on NACA Airfoil Maximum Lift Coefficient

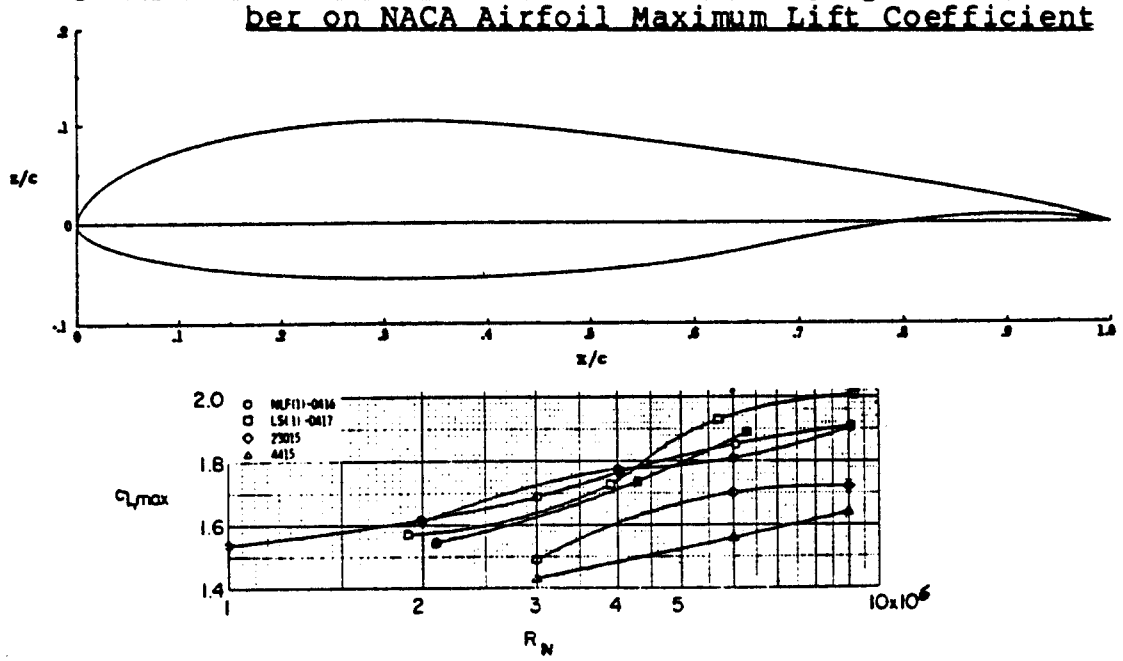

Figure 9.2 Effect of Thickness Ratio and Reynold's Number on Modern Airfoil Maximum Lift Coefficient

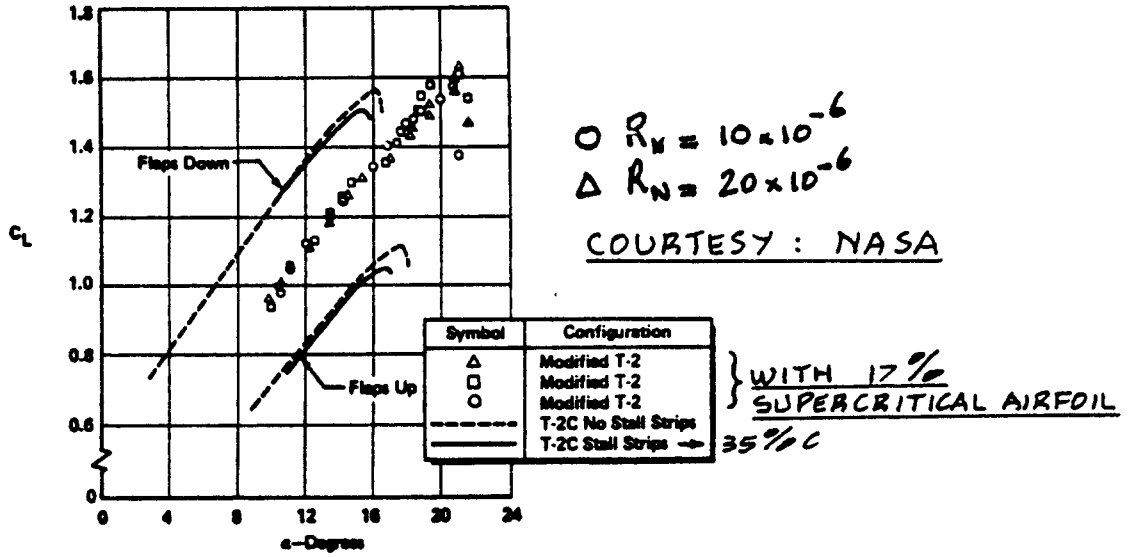

Figure 9.3 Airplane Lift Curve: N.A.Rockwell T2C

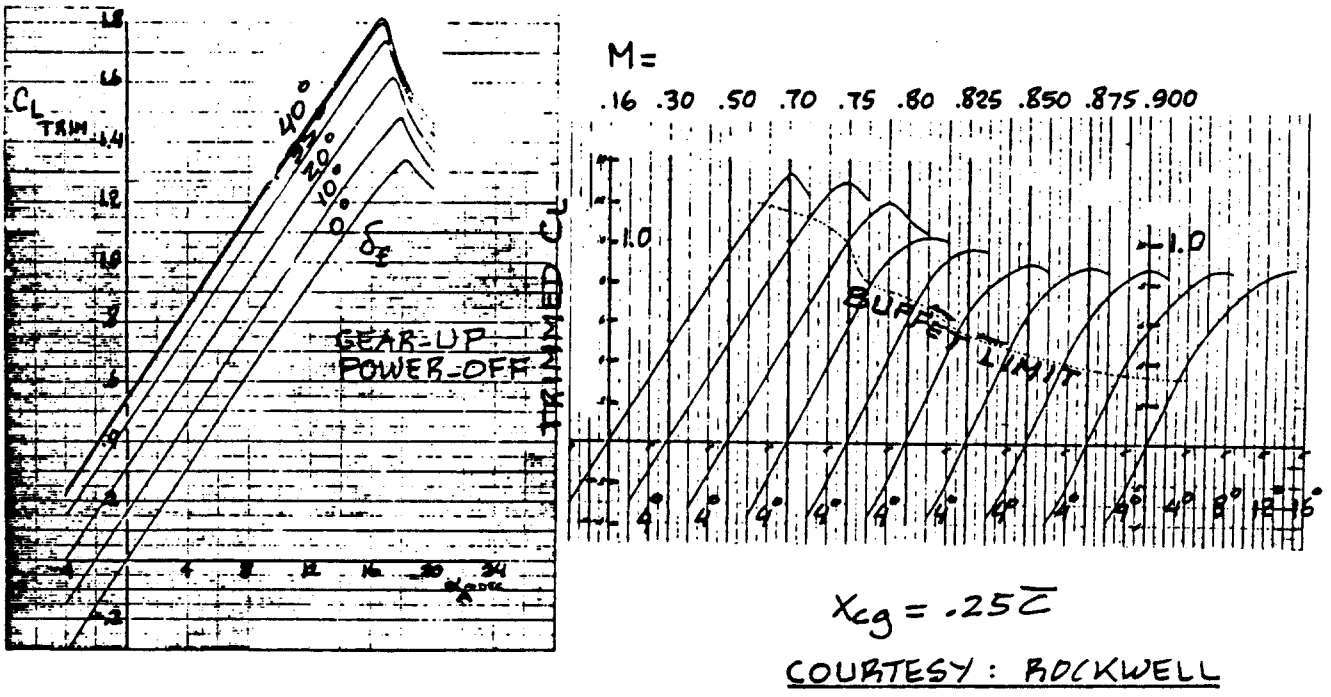

Figure 9.4 Airplane Lift Curve: N.A.Rockwell S-60

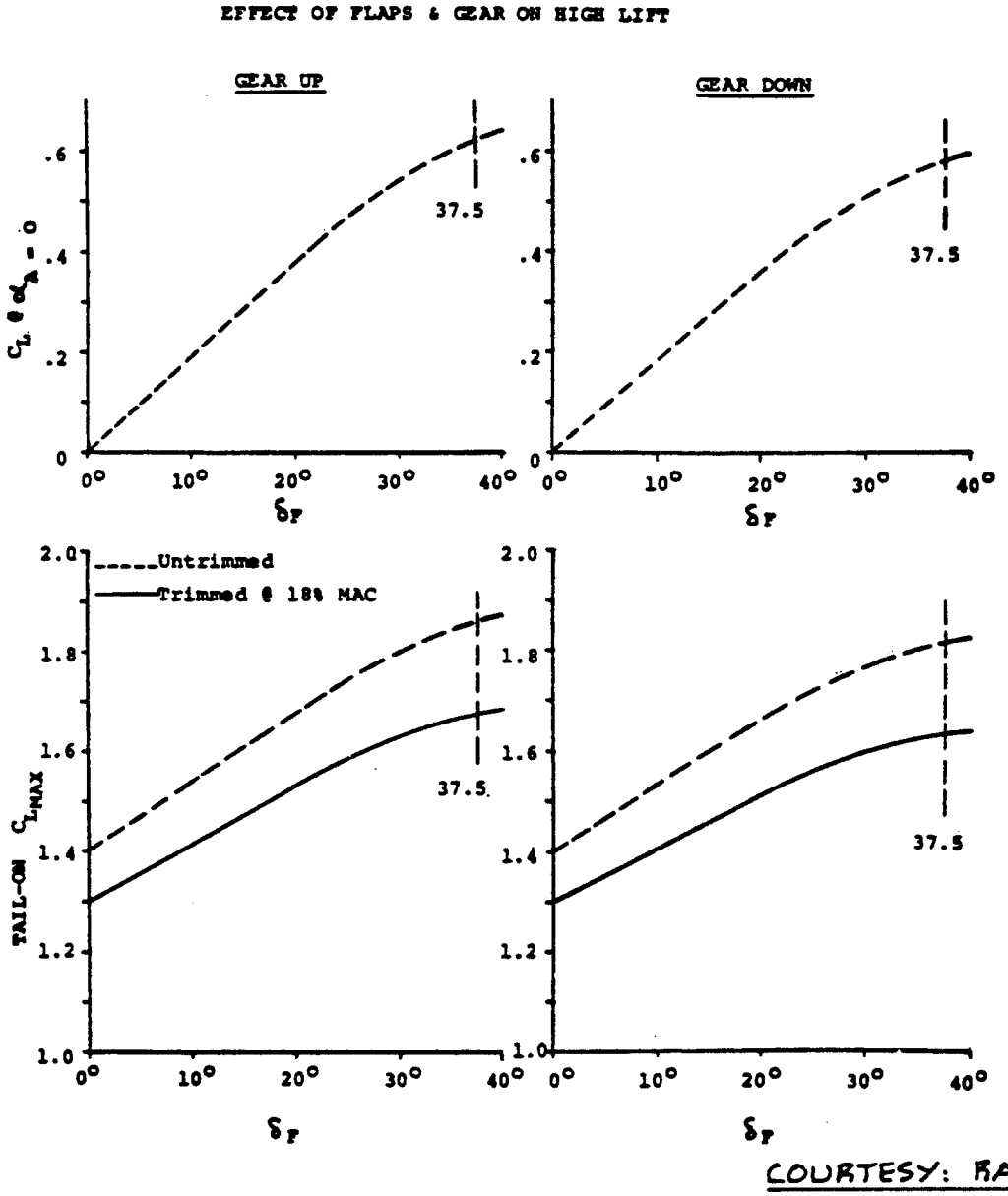

COURTESY: RAISBECK

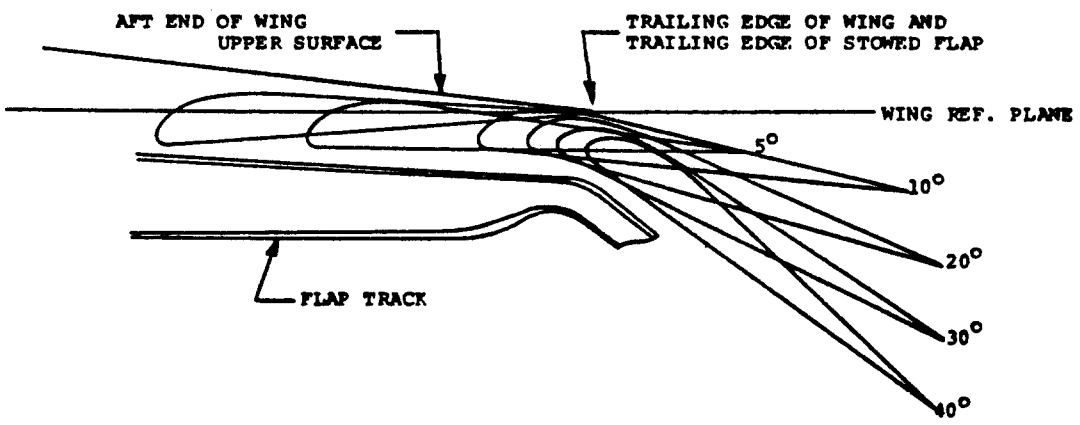

Figure 9.5 Airplane Lift Curve: Raisbeck/Rockwell S-65

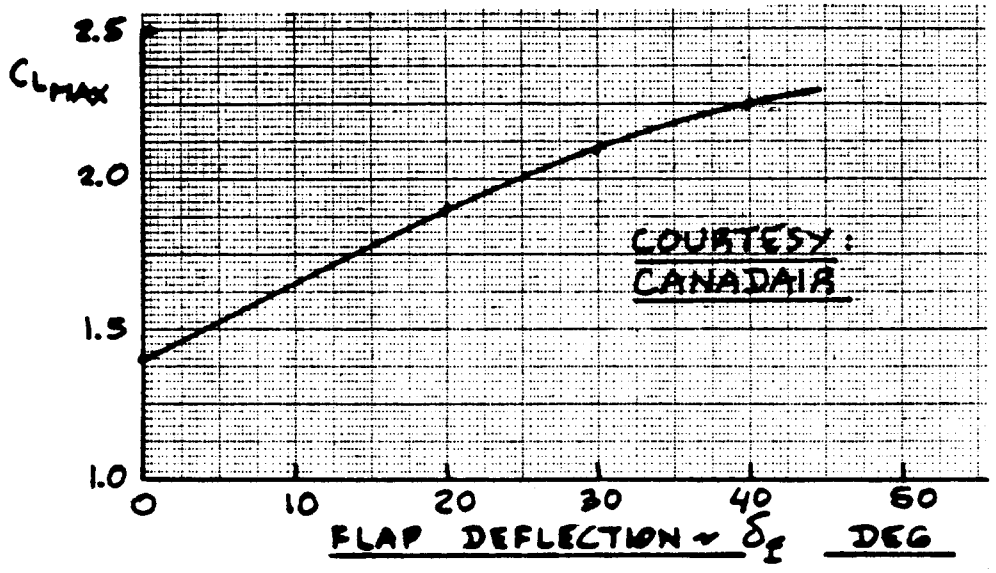

Figure 9.6 Airplane Lift Curve: Canadair Challenger

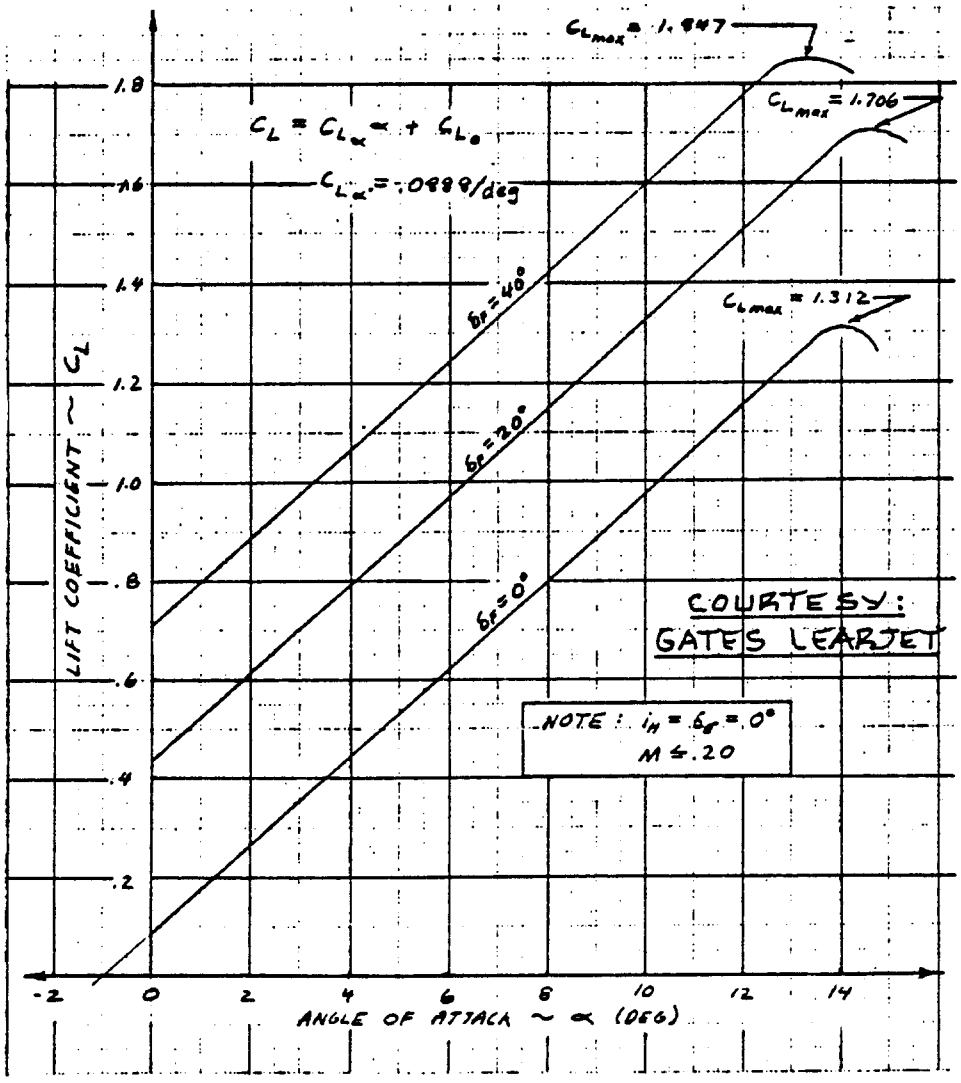

Figure 9.7 Airplane Lift Curve: Gates-Learjet M55

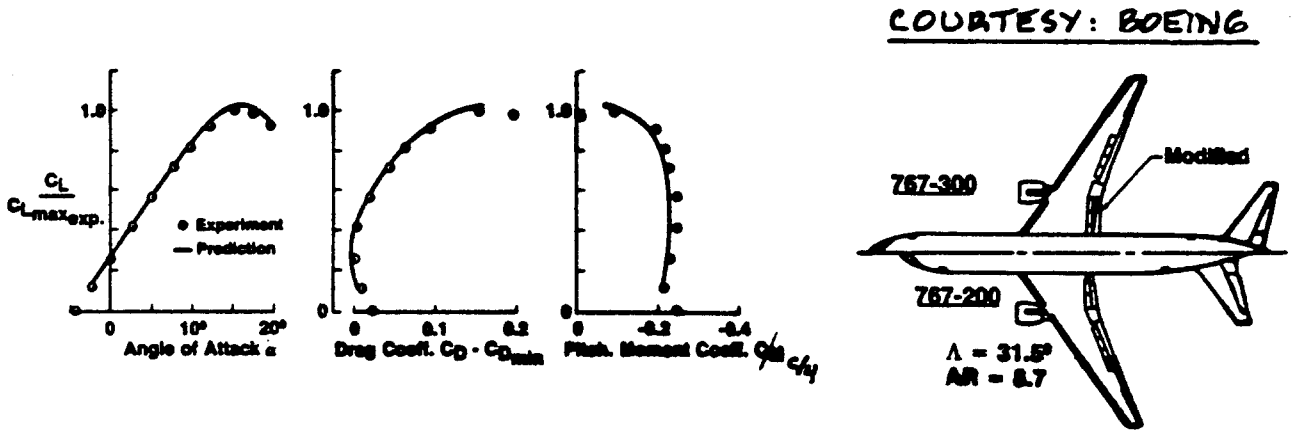

Figure 9.8 Airplane Lift Curve: Boeing 767-300

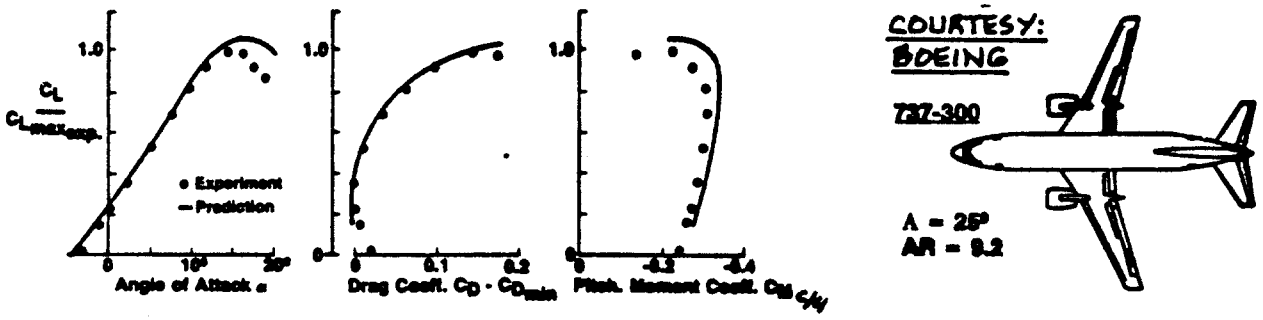

Figure 9.9 Airplane Lift Curve: Boeing 737-300

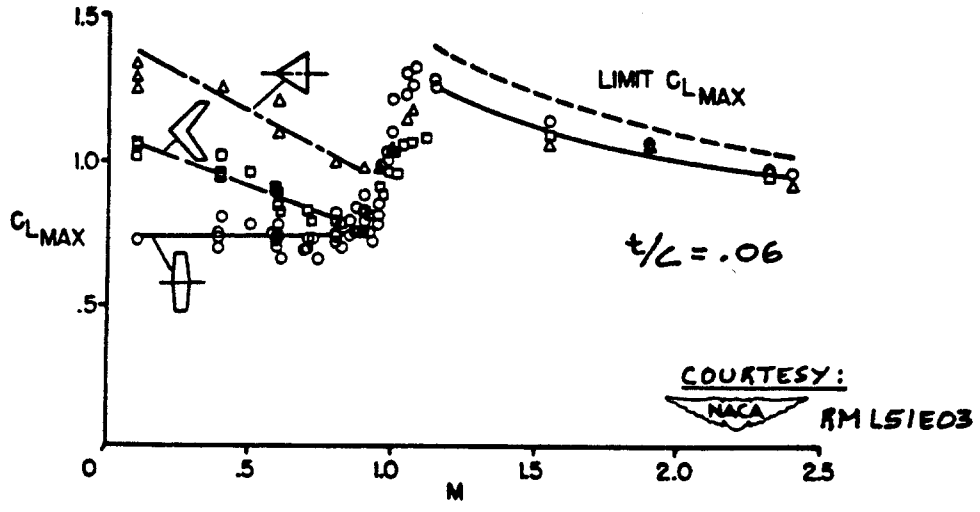

Figure 9.10 Effect of Wing Planform on the Variation of Maximum Lift Coefficient with Mach Number

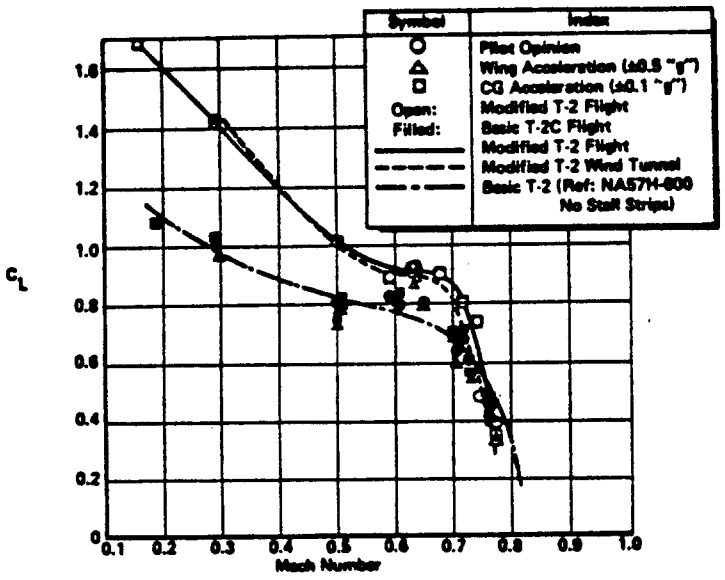

COURTESY:
NASA

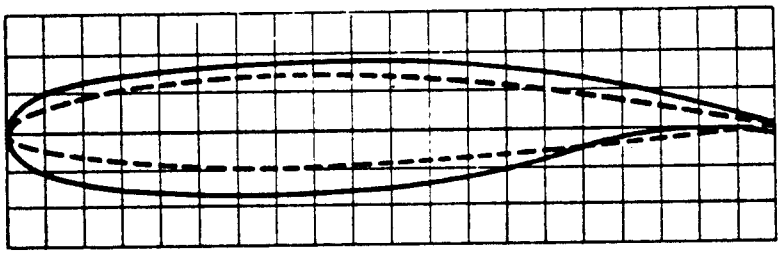

Figure 9.11 Effect of Mach Number on Buffet Onset for a NACA and for and Advanced Airfoil

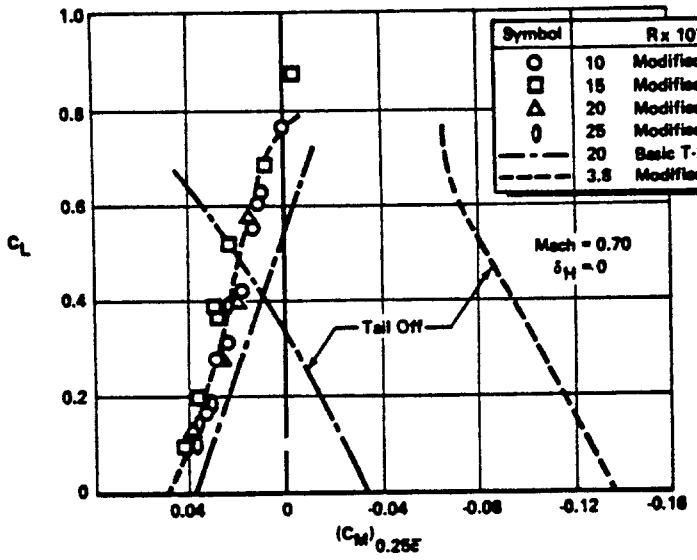

COURTESY:
NASA

Figure 9.12 Effect of Airfoil Change on Pitching Moment

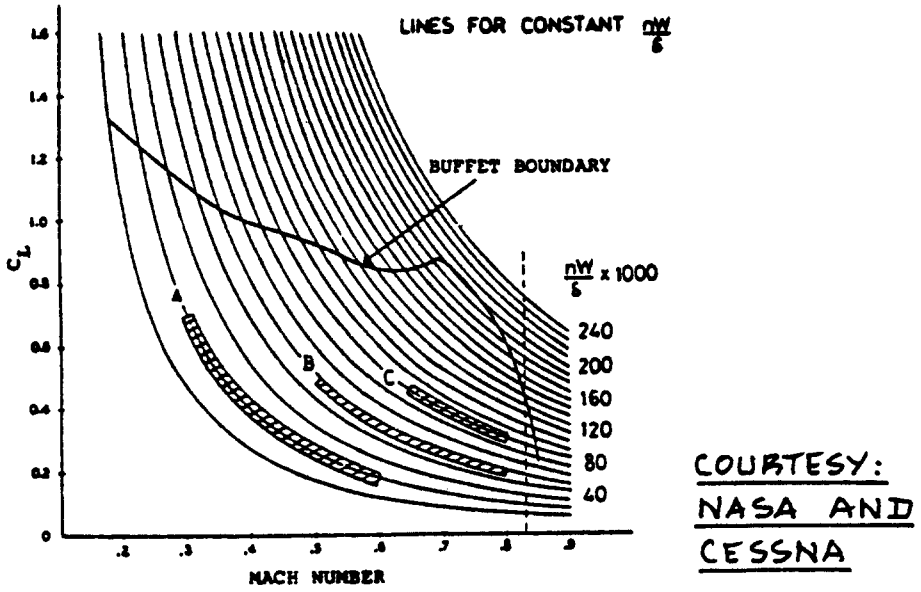

Figure 9.13 Buffet Boundary for the Cessna Citation III

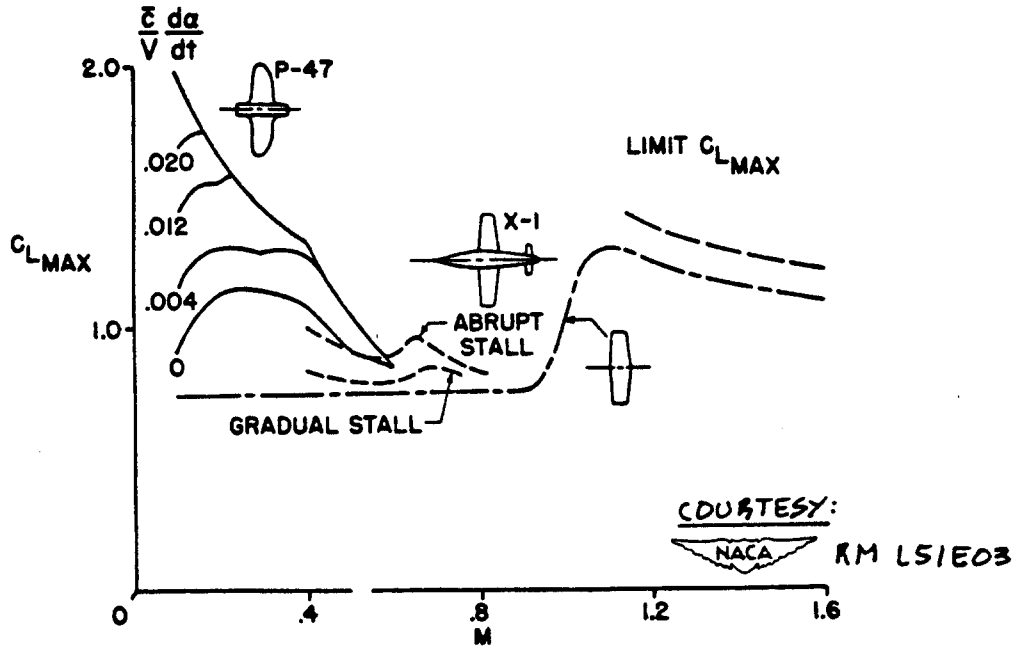

Figure 9.14 Effect of Angle of Attack Rate on the Variation of Maximum Lift with Mach Number

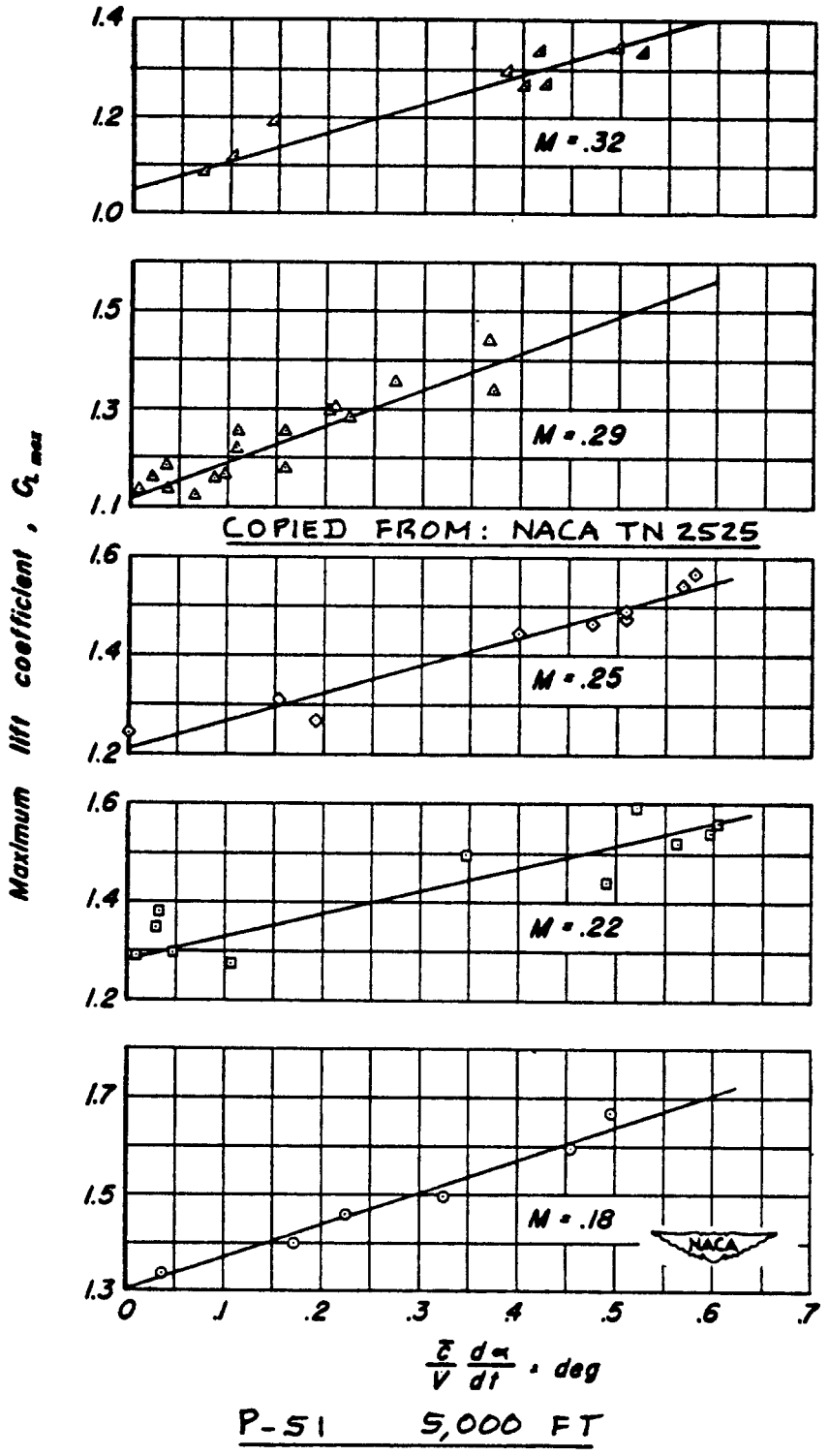

Figure 9.15 Effect of Angle of Attack Rate and Mach Number on Maximum Lift Coefficient

10. STABILITY, CONTROL AND HINGEMOMENT DERIVATIVES

The purpose of this chapter is to present preliminary design methods for the calculation of stability, control and hingemoment derivatives. These derivatives are required as input to the determination of static and dynamic stability and control behavior (handling qualities) of airplanes. Methods for computing static and dynamic stability and control behavior of airplanes are given in Part VII of this text.

Table 10.1 presents the mathematical model used in representing aerodynamic and thrust forces and moments as well as cockpit control forces: Eqns 10.1 through 10.5.

The equations of Table 10.1 are discussed and justified in Chapter 4 of Reference 16. The coefficients and derivatives shown in Table 10.1 may be estimated with the methods of this chapter. These methods are presented in the following manner:

10.1 Steady state coefficients
10.2 Stability Derivatives
10.3 Control derivatives
10.4 Hingemoment Derivatives.

IMPORTANT NOTES:

1.) The methods presented in this chapter apply to rigid airplanes only. Methods which account for aeroelastic effects are discussed in Chapter 8 of Ref.16.

2.) The methods presented in this chapter do not always apply to all speed regimes. Restrictions on applicability to certain speed regimes are given in the text.

3.) All derivatives are in rad^{-1}.

4.) All coefficients and derivatives are defined in the stability axes system, see Table 10.1.

10.1 STEADY STATE COEFFICIENTS

In Table 10.1 there appear a number of steady state coefficients: C_{D_1}, C_{L_1}, C_{m_1}, $C_{T_{x_1}}$ and $C_{m_{T_1}}$.

In the following, definitions are given from which these coefficients may be determined.

Table 10.1a Longitudinal Aerodynamic and Thrust Forces and Moments and Cockpit Control Forces

Forces and Moments

AERODYNAMIC

$$\begin{Bmatrix} \frac{f_{A_x}}{\bar{q}S} \\ \frac{f_{A_z}}{\bar{q}S} \\ \frac{m_A}{\bar{q}S} \end{Bmatrix} = \left[\begin{array}{c|c|c|c|c} -(C_{D_u}+2C_{D_1}) & (-C_{D_\alpha}+C_{L_1}) & -C_{D_{\dot\alpha}} & -C_{D_q} & -C_{D_{\delta_E}} \\ \hline -(C_{L_u}+2C_{L_1}) & (-C_{L_\alpha}-C_{D_1}) & -C_{L_{\dot\alpha}} & -C_{L_q} & -C_{L_{\delta_E}} \\ \hline (C_{m_u}+2C_{m_1}) & C_{m_\alpha} & C_{m_{\dot\alpha}} & C_{m_q} & C_{m_{\delta_E}} \end{array}\right] \begin{Bmatrix} \frac{u}{U_1} \\ \alpha \\ \frac{\dot\alpha \bar{c}}{2U_1} \\ \frac{q\bar{c}}{2U_1} \\ \delta_E \end{Bmatrix} \quad (10.1)$$

(3x1) (3x5) (5x1)

THRUST

$$\begin{Bmatrix} \frac{f_{T_x}}{\bar{q}_1 S} \\ \frac{f_{T_z}}{\bar{q}_1 S} \\ \frac{m_T}{\bar{q}_1 S\bar{c}} \end{Bmatrix} = \left[\begin{array}{c|c} (C_{T_{x_u}} + 2C_{T_{x_1}}) & 0 \\ \hline 0 & 0 \\ \hline (C_{m_{T_u}} + 2C_{m_{T_1}}) & C_{m_{T_\alpha}} \end{array}\right] \begin{Bmatrix} \frac{u}{U_1} \\ \hline \alpha \end{Bmatrix} \quad (10.2)$$

3x1 3x2 2x1

$$F_{S_e} = G_e \cdot HM_e = G_e \cdot \bar{q}_h \cdot S_e \bar{c}_e C_{h_e} \quad (10.3a)$$

$$C_{h_e} = C_{h_o} + C_{h_\alpha}\alpha_h + C_{h_{\delta_e}}\delta_e + C_{h_{\delta_t}}\delta_t \quad (10.3b)$$

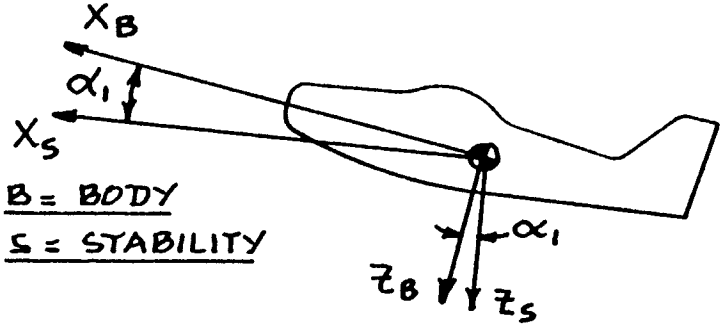

B = BODY

S = STABILITY

Table 10.1b Lateral-Directional Aerodynamic and Thrust Forces and Moments and Cockpit Control Forces

Forces and Moments

$$\begin{Bmatrix} \frac{f_{A_y}}{\bar{q}S} \\ \frac{\ell_A}{\bar{q}Sb} \\ \frac{n_A}{\bar{q}Sb} \end{Bmatrix}_{(3\times1)} = \underbrace{\begin{bmatrix} C_{y_\beta} & C_{y_{\dot\beta}} & C_{y_p} & C_{y_r} & C_{y_{\delta_A}} & C_{y_{\delta_R}} \\ C_{\ell_\beta} & C_{\ell_{\dot\beta}} & C_{\ell_p} & C_{\ell_r} & C_{\ell_{\delta_A}} & C_{\ell_{\delta_R}} \\ C_{n_\beta} & C_{n_{\dot\beta}} & C_{n_p} & C_{n_r} & C_{n_{\delta_A}} & C_{n_{\delta_R}} \end{bmatrix}}_{\text{AERODYNAMIC}\ (3\times6)} \begin{Bmatrix} \beta \\ \frac{\dot\beta b}{2U_1} \\ \frac{pb}{2U_1} \\ \frac{rb}{2U_1} \\ \delta_A \\ \delta_R \end{Bmatrix}_{(6\times1)} \quad (10.4)$$

$$\begin{Bmatrix} \frac{f_{T_y}}{\bar{q}_1 S} \\ \frac{\ell_T}{\bar{q}_1 Sb} \\ \frac{n_T}{\bar{q}_1 Sb} \end{Bmatrix}_{(3\times1)} = \underbrace{\begin{bmatrix} 0 \\ 0 \\ C_{n_{T_\beta}} \end{bmatrix}}_{\text{THRUST}\ (3\times1)} \beta_{(1\times1)} \quad (10.5)$$

AILERON

$$F_{s_a} = G_a \cdot HM_a = G_a \bar{q} \cdot S_a \bar{c}_a C_{h_a} \quad (10.3c)$$

$$C_{h_a} = C_{h_{\delta_a}} \delta_a + C_{h_{\delta_{a_t}}} \delta_{a_t} \quad (10.3d)$$

RUDDER

$$F_{s_r} = G_r \cdot HM_r = G \cdot \bar{q}_v \cdot S_r \bar{c}_r C_{h_r} \quad (10.3e)$$

$$C_{h_r} = C_{h_\beta} \beta + C_{h_{\delta_r}} \delta_r + C_{h_{\delta_{r_t}}} \delta_{r_t} \quad (10.3f)$$

C_{D_1} is the airplane steady state drag coefficient. It is found with the methods of Chapter 4 and is tied uniquely to a specific value of the steady state lift coefficient, C_{L_1}. Figure 10.1 illustrates this.

C_{L_1} is the airplane steady state lift coefficient:

$$C_{L_1} = nW/\bar{q}S \qquad (10.6)$$

where: n is the airplane load factor. Note that for 1g flight, n=1.

C_{m_1} is the airplane steady state pitching moment coefficient. It is determined with the methods of Chapter 8 (8.2.5 and 8.2.6) and is tied uniquely to a specific value of the steady state lift coefficient, C_{L_1}. Figure 10.2 shows this.

$C_{T_{x_1}}$ is the airplane steady state thrust coefficient component in the direction of the stability X-axis. It is determined from:

$$C_{T_{x_1}} = T_{reqd}/\bar{q}S \qquad (10.7)$$

where: T_{reqd} is the thrust required in the steady state. The condition:

$$C_{T_{x_1}} = -C_{D_1} \qquad (10.8)$$

is normally satisfied in the steady state.

$C_{m_{T_1}}$ is the airplane steady state pitching moment coefficient due to thrust. It is found from:

$C_{m_{T_1}} = \Delta C_{m_{TL}}$, see: Eqn.(8.102)

The trim condition:

$$C_{m_1} = -C_{m_{T_1}} \qquad (10.9)$$

is normally satisfied in the steady state.

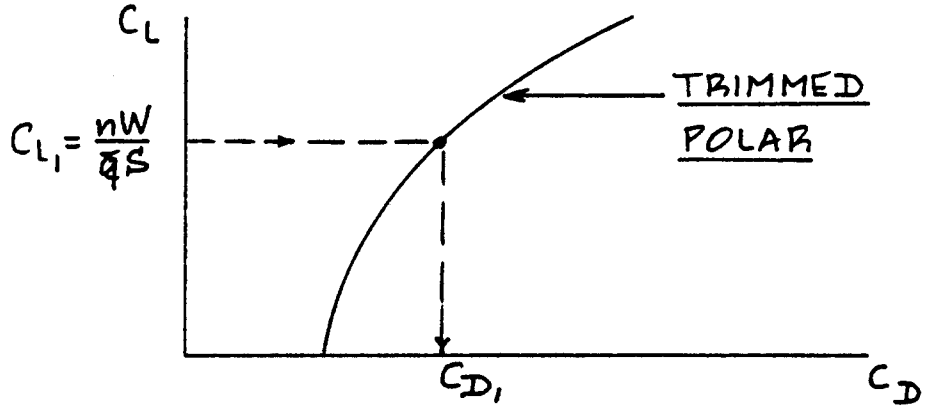

Figure 10.1 Determination of Drag Coefficient from a Known Value of the Lift Coefficient

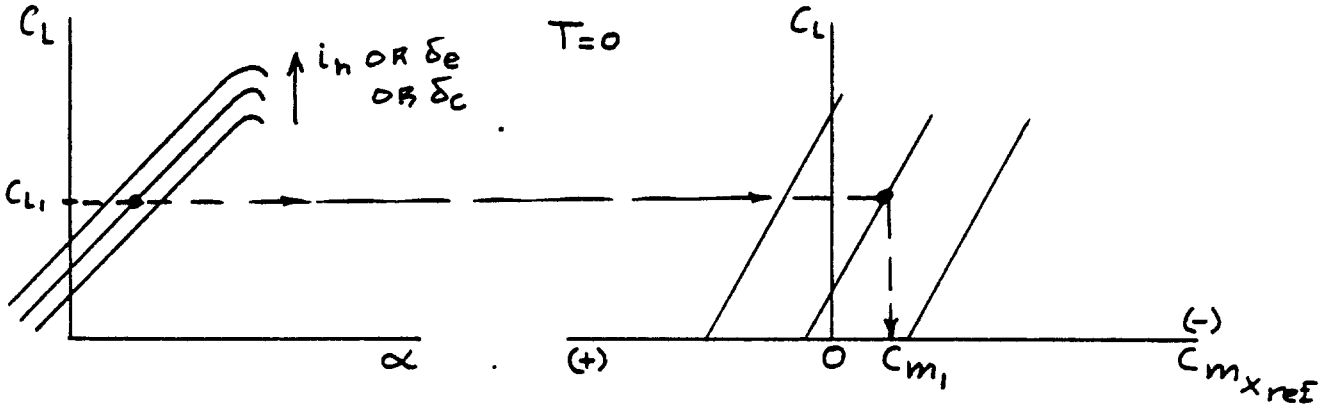

Figure 10.2 Determination of the Value of the Pitching Moment Coefficient

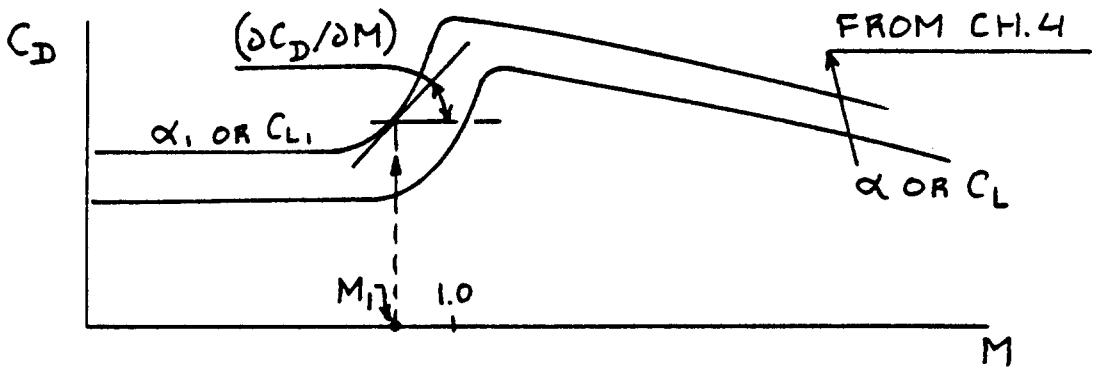

Figure 10.3 Determination of: $\partial C_D / \partial C_m$

10.2 STABILITY DERIVATIVES

In this section, methods for computing the following stability derivatives will be presented:

10.2.1 Speed derivatives
10.2.2 Angle-of-attack derivatives
10.2.3 Rate of angle-of-attack derivatives
10.2.4 Angle of sideslip derivatives
10.2.5 Rate of angle of sideslip derivatives
10.2.6 Roll rate derivatives
10.2.7 Pitch rate derivatives
10.2.8 Yaw rate derivatives

10.2.1 Speed Derivatives: C_{D_u}, C_{L_u}, C_{m_u}, $C_{T_{x_u}}$ and $C_{m_{T_u}}$

Table 10.1 lists the required speed derivatives: note the existence of aerodynamic as well as thrust derivatives.

10.2.1.1 Aerodynamic speed derivatives: C_{D_u}, C_{L_u} and C_{m_u}

1.) C_{D_u}

The drag-due-to-speed derivative, C_{D_u} may be determined in all speed regimes from:

$$C_{D_u} = M_1(\partial C_D/\partial M) \qquad (10.10)$$

where: M_1 is the Mach number in steady state flight

$\partial C_D/\partial M$ is the derivative of the airplane drag coefficient with respect to Mach number. This derivative is found from Figure 10.3.

2.) C_{L_u}

The lift-due-to-speed derivative, C_{L_u} may be determined as follows:

Subsonic:

$$C_{L_u} = \{M_1^2(\cos\Lambda)^2_{c/4}C_{L_1}\}/\{1 - M_1^2(\cos\Lambda)^2_{c/4}\} \qquad (10.11)$$

Transonic: Fair from M=0.8 to M=1.2 as in Fig.10.4

Supersonic: use Eqn.(10.11) also!

3.) C_{m_u}

The pitching-moment-due-to-speed derivative, C_{m_u} may be determined in all speed regimes from:

$$C_{m_u} = - C_{L_1} (\partial \bar{x}_{ac_A} / \partial M) \qquad (10.12)$$

where: C_{L_1} is the airplane lift coefficient in the steady state as found from Eqn. (10.6).

$\bar{x}_{ac_A}$ is the location of the airplane aerodynamic center in fractions of the wing m.g.c. as determined from 8.2.5.2.

10.2.1.2 Thrust versus speed derivatives: $C_{T_{x_u}}$ and $C_{m_{T_u}}$

These derivatives are equal to zero in all speed regimes for gliders and for airplanes equipped with rocket powerplants only.

For propeller-driven airplanes and for jet-driven airplanes these derivatives depend on the characteristics of the propulsion installation.

1.) $C_{T_{x_u}}$

The thrust-due-to-speed derivative, $C_{T_{x_u}}$ may be computed in all speed regimes from:

For Propeller Driven Airplanes:

Fixed pitch propellers:

$$C_{T_{x_u}} = (1/\bar{q}S)(\partial P_{reqd}/\partial u) - 2C_{T_{x_1}} \qquad (10.13)$$

where: P_{reqd} is the installed power required for the flight condition being studied: see Ch. 6.

Variable pitch (constant speed) propellers:

$$C_{T_{x_u}} = - 3C_{T_{x_1}} \qquad (10.14)$$

For Jet Driven Airplanes:

$$C_{T_{x_u}} = (M_1/\bar{q}S)(\partial T_{reqd}/\partial M) - 2C_{T_{x_1}} \qquad (10.15)$$

where: M_1 is the steady state Mach number

$\partial T_{reqd}/\partial M$ is the derivative of installed thrust required with respect to Mach number. It is determined from plots of installed thrust versus Mach number: see Ch.6.

2.) $C_{m_{T_u}}$

The thrust-moment-due-to-speed derivative, $C_{m_{T_u}}$ may be computed in all speed regimes from:

$$C_{m_{T_u}} = (d_T/\bar{c})C_{T_{x_u}} \qquad (10.16)$$

where: d_T is the thrust moment arm relative to the center of gravity as indicated in Figure 8.126. Note: the sign of d_T depends on the location of the thrust line relative to the c.g.

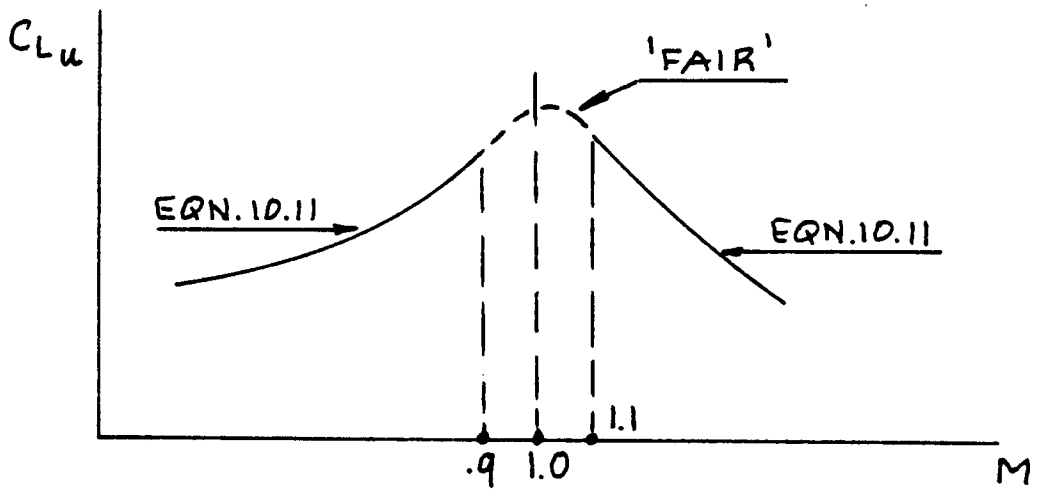

Figure 10.4 Example of Transonic Fairing for: C_{L_u}

10.2.2 Angle-of-Attack Derivatives: C_{D_α}, C_{L_α}, C_{m_α} and $C_{m_{T_\alpha}}$

Table 10.1 identifies the required angle-of-attack derivatives: note that there are aerodynamic as well as thrust derivatives.

10.2.2.1 Aerodynamic angle-of-attack derivatives: C_{D_α}, C_{L_α} and C_{m_α}

1.) C_{D_α}

The drag-due-to-angle-of-attack derivative, C_{D_α} may be found in all speed regimes from:

$$C_{D_\alpha} = (\partial C_D/\partial C_L)C_{L_\alpha} \qquad (10.17)$$

where: $(\partial C_D/\partial C_L)$ is determined as shown in Figure 10.5. Note that this slope must be obtained at the appropriate value of the lift coefficient, C_{L_1} AND at the appropriate value of Mach number, M_1.

C_{L_α} is the overall airplane lift curve slope as found from Eqn.(8.42): see the note of caution under 2.) C_{L_α}.

For airplanes with parabolic drag polars it is often more convenient to use:

$$C_{D_\alpha} = (2C_{L_1}/\pi Ae)C_{L_\alpha} \qquad (10.18)$$

2.) C_{L_α}

The lift-due-to-angle-of-attack derivative (also called lift curve slope), C_{L_α} is found from Eqn.(8.42).

NOTE OF CAUTION: Equation (8.42) applies to all speed regimes, provided the values for upwash and for downwash are valid for the appropriate speed regimes. The method of page 272 for computing downwash is valid only below M=0.9. For the transonic and for the supersonic speed regime Ref.[must be consulted.

3.) C_{m_α}

The pitching-moment-due-to-angle-of-attack derivati-

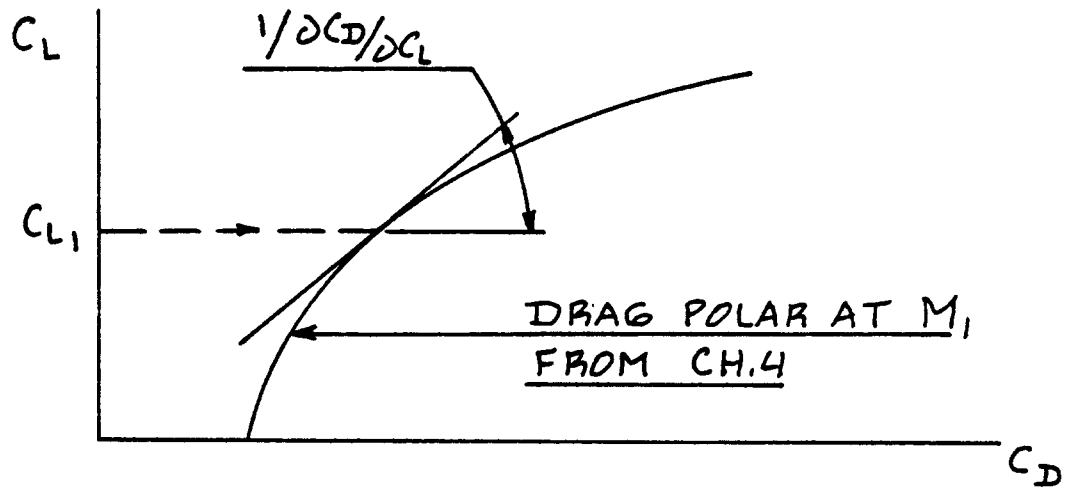

Figure 10.5 Determining $\partial C_D / \partial C_L$ From the Drag Polar

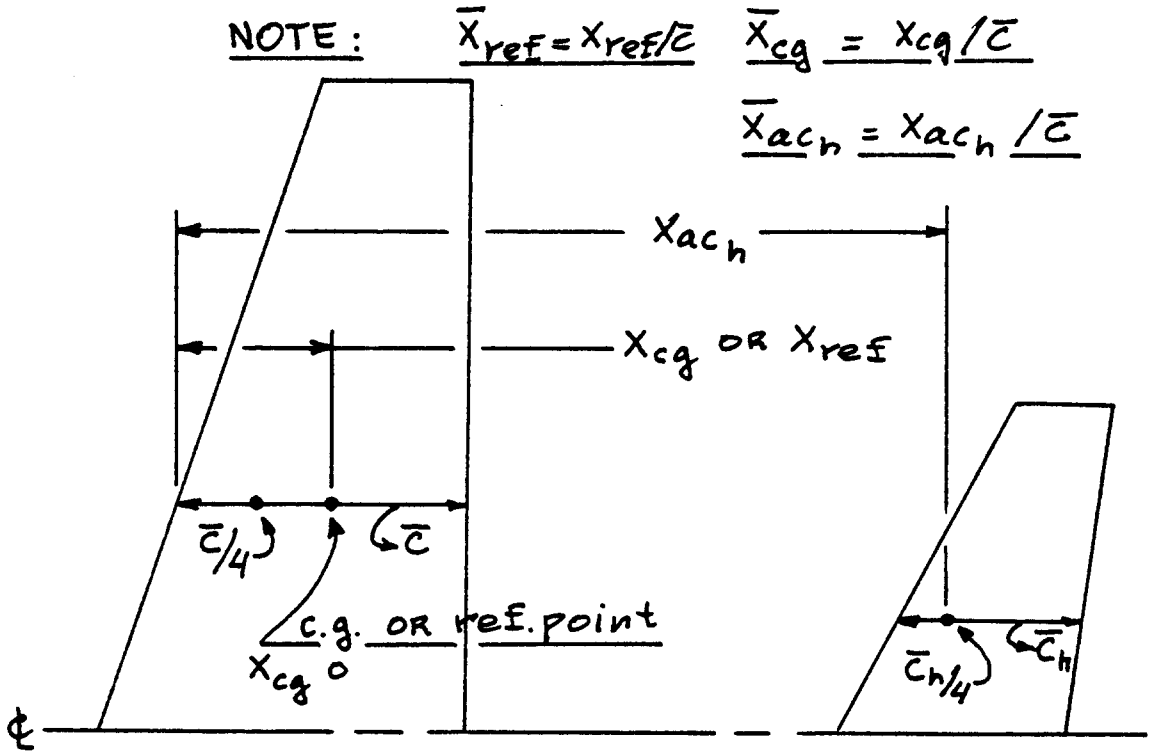

Figure 10.6 Definition of Geometric Parameters for Volume Coefficient

ve (also called static longitudinal stability), C_{m_α} is computed in all speed regimes from:

$$C_{m_\alpha} = (dC_m/dC_L)C_{L_\alpha} \qquad (10.19)$$

where: dC_m/dC_L is found from Eqn.(8.81) with possible corrections for power effects as given in 8.2.8.

C_{L_α} is determined from Eqn.(8.42). The note of caution given before, applies here also!

10.2.2.2 Thrust versus angle-of-attack derivative: $C_{m_{T_\alpha}}$

The only thrust versus angle-of-attack derivative which appears in Table 10.1 is $C_{m_{T_\alpha}}$. This derivative may be found from:

$$C_{m_{T_\alpha}} = \{\Delta(dC_m/dC_L)_T\}C_{L_\alpha} \qquad (10.20)$$

where: $\{\Delta(dC_m/dC_L)_T\}$ is found from Eqn.(8.104).

C_{L_α} is found from Eqn.(8.42). The note of caution given before, applies here also!

10.2.3 Rate of Angle-of-attack Derivatives: $C_{D_{\dot\alpha}}$, $C_{L_{\dot\alpha}}$ and $C_{m_{\dot\alpha}}$

Except for $C_{m_{\dot\alpha}}$, these derivatives are usually not important. The reader should consult Ref.9 for detailed methods covering all speed regimes. The methods given here apply only in the subsonic speed range.

1.) $C_{D_{\dot\alpha}}$

The drag-due-to-rate-of-angle-of-attack derivative, $C_{D_{\dot\alpha}}$ is normally neglected:

$$C_{D_{\dot\alpha}} = 0 \qquad (10.21)$$

2.) $C_{L_{\dot\alpha}}$

The lift-due-to-rate-of-angle-of-attack derivative, $C_{L_{\dot\alpha}}$ may be computed from:

$$C_{L_{\dot\alpha}} = 2(C_{L_{\alpha_h}})\eta_h(\bar{V}_h)(d\varepsilon/d\alpha) \qquad (10.22)$$

where: $C_{L_{\alpha_h}}$ is found from 8.1.3.2 with appropriate substitution of horizontal tail parameters for wing parameters.

η_h is found from 8.1.5.2

$d\varepsilon/d\alpha$ is found from Eqn.(8.45)

$\bar{V}_h$ is the horizontal tail volume coefficient:

$$\bar{V}_h = (\bar{x}_{ac_h} - \bar{x}_{cg})(S_h/S) \qquad (10.23)$$

where: $\bar{x}_{ac_h}$ and $\bar{x}_{cg}$ (or $\bar{x}_{ref}$) are defined in Figure 10.6.

3.) $C_{m_{\dot{\alpha}}}$

The pitching-moment-due-to-rate-of-angle-of-attack, $C_{m_{\dot{\alpha}}}$ may be computed from:

$$C_{m_{\dot{\alpha}}} = -2(C_{L_{\alpha_h}})\eta_h(\bar{V}_h)(\bar{x}_{ac_h} - \bar{x}_{cg})(d\varepsilon/d\alpha \qquad (10.24)$$

where: all quantities are defined before.

NOTE: the reader will observe that Equations (10.23) and (10.24) are based on the assumption that the contribution of the horizontal tail is the only important contribution to these derivatives. This assumption is frequently satisfied. If not, Ref.9 should be used.

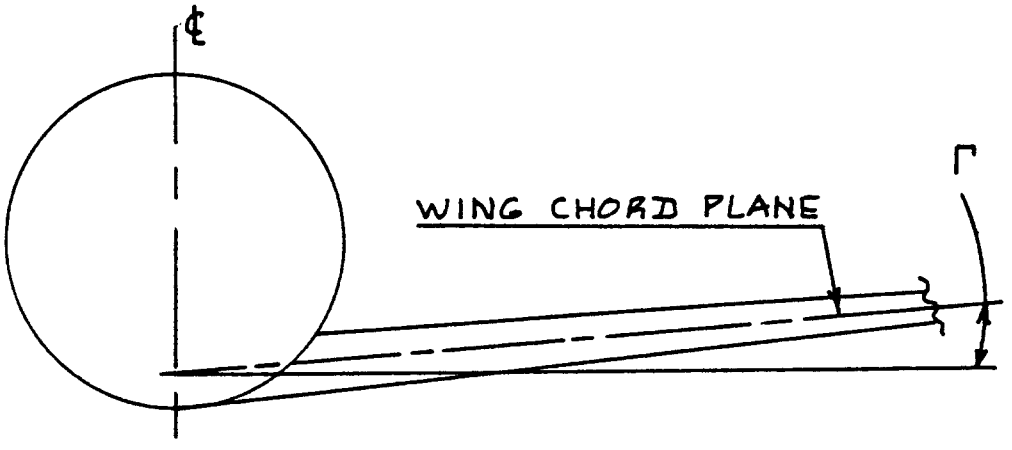

Figure 10.7 Definition of Wing Geometric Dihedral

10.2.4 Angle-of-Sideslip Derivatives: C_{y_β}, C_{l_β}, C_{n_β} and $C_{n_{T_\beta}}$

Table 10.1 identifies the required angle-of-sideslip derivatives: note that there are aerodynamic as well as thrust derivatives.

NOTE: All methods presented for the sideslip derivatives apply to the subsonic speed regime only. For other speed ranges, Ref.9 should be used.

10.2.4.1 Aerodynamic angle-of-sideslip derivatives: C_{y_β}, C_{l_β} and C_{n_β}

1.) C_{y_β}

The sideforce-due-to-sideslip derivative, C_{y_β} may be found from:

$$C_{y_\beta} = C_{y_{\beta_w}} + C_{y_{\beta_f}} + C_{y_{\beta_v}} \qquad (10.25)$$

where: the wing contribution is given by:

$$C_{y_{\beta_w}} = -0.00573(|\Gamma|) \qquad (10.26)$$

with: Γ the wing geometric dihedral angle in deg. Figure 10.7 defines this angle.

the fuselage contribution is given by:

$$C_{y_{\beta_f}} = -2K_i(S_o/S) \qquad (10.27)$$

with: K_i defined in Figure 10.8. The quantities z_w and d_f are defined in Figure 10.9

S_o is the cross-sectional area of the fuselage at station x_o, where the flow ceases to be potential. The distance x_o depends on the distance x_1. The latter is equal to that fuselage station where the derivative dS_x/dx first reaches its maximum negative value: see Figure 10.10. The

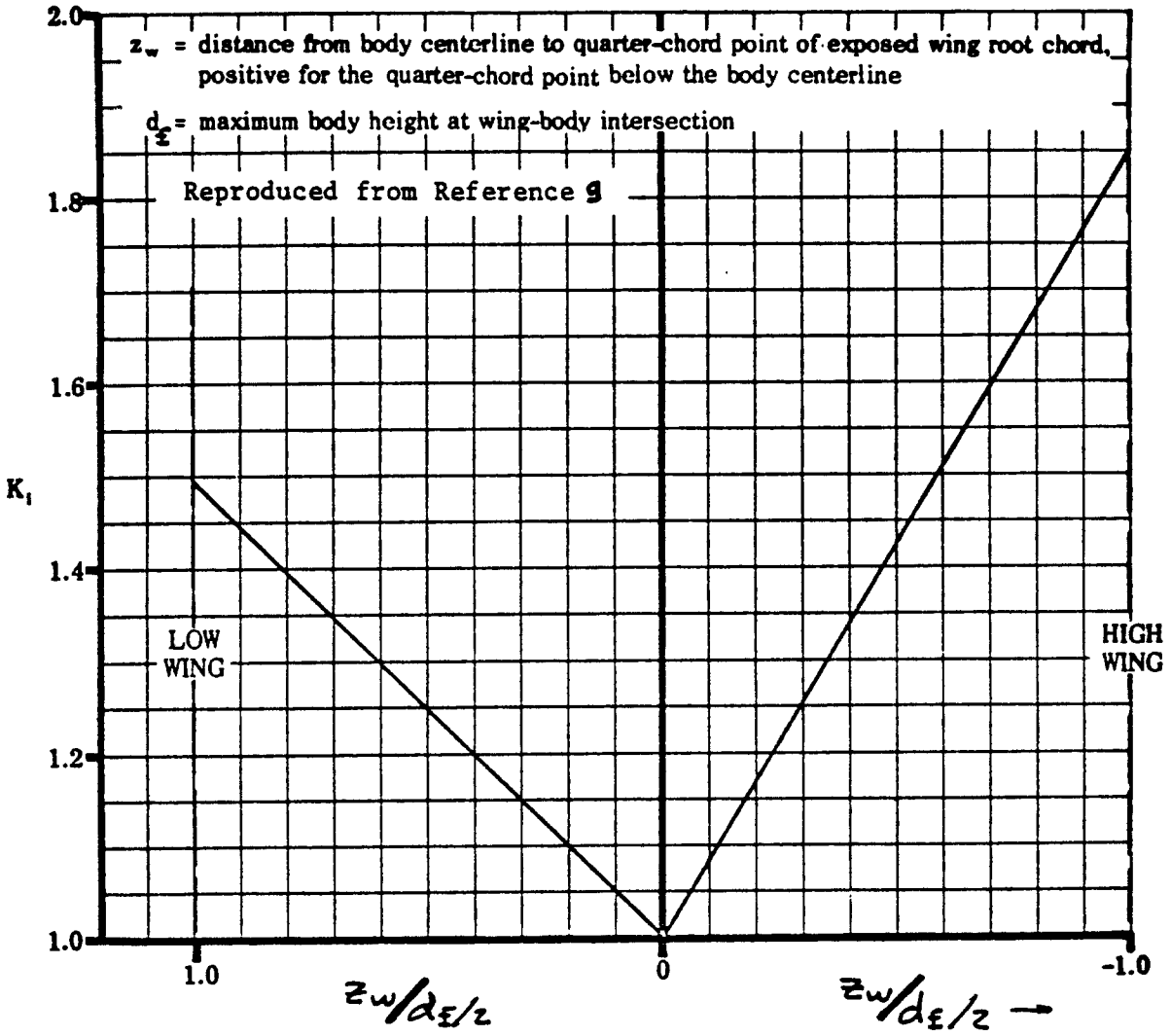

Figure 10.8 Wing-Fuselage Interference Factor, K_i

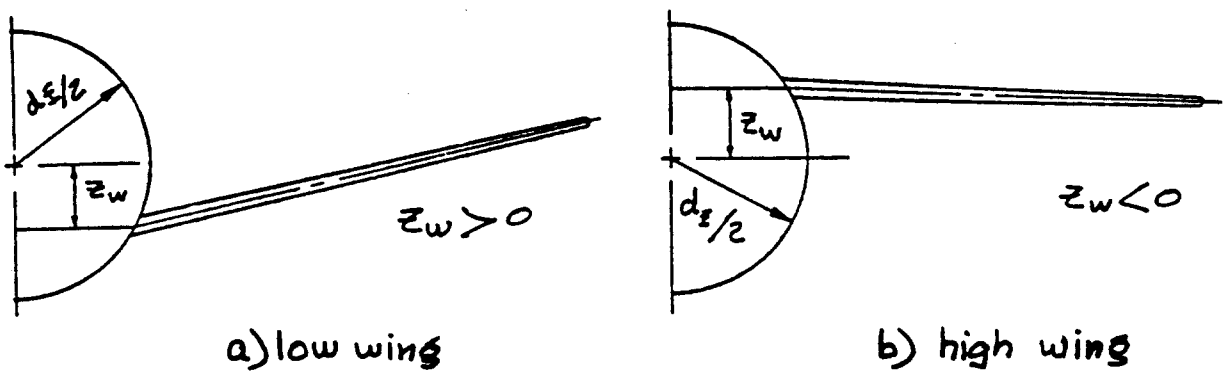

Figure 10.9 Definition of Wing-Fuselage Parameters: z_w and d_f

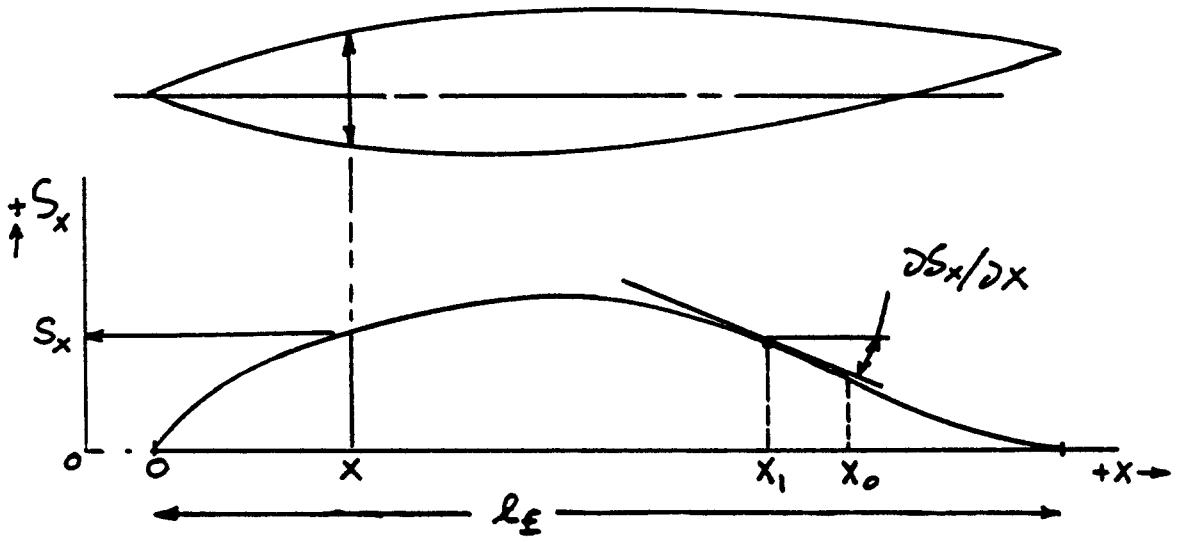

Figure 10.10 Determination of S_o

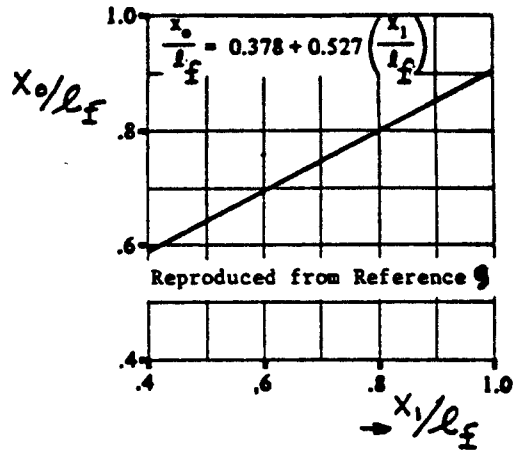

Figure 10.11 Fuselage Station Where Flow Becomes Viscous

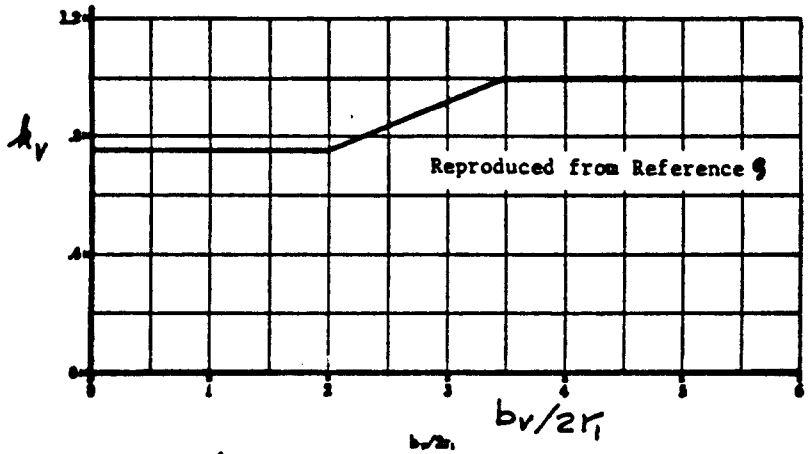

(For definition of $2r_1$ see Figure 10.17)

Figure 10.12 Empirical Factor for Estimating Side-force due to Sideslip of a Single Vertical Tail

distances x_o and x_1 are correlated in Figure 10.11. The fuselage contribution is virtually independent of Mach number.

the vertical tail contribution is given by:

1. For Single Vertical Tails:

$$C_{y_{\beta_v}} = -k_v(C_{L_{\alpha_v}})(1 + d\sigma/d\beta)\eta_v(S_v/S) \qquad (10.28)$$

with: k_v given by Figure 10.12.

$C_{L_{\alpha_v}}$ found from 8.1.3.2 with appropriate substitution of vertical tail parameters for wing parameters. The vertical tail aspect ratio, $A_{v_{eff}}$ must be substituted for A in the method of 8.1.3.2. The effective aspect ratio of the vertical tail may be estimated from:

$$A_{v_{eff}} = (A_{v(f)}/A_v)A_v\{1 + K_{vh}\{(A_{v(hf)}/A_{v(f)}) - 1\} \qquad (10.29)$$

with: $$A_v = (b_v)^2/S_v \qquad (10.30)$$

where: b_v and S_v depend on the vertical tail configuration as shown in Figure 10.13 for a range of vertical tail configurations.

$(A_{v(f)}/A_v)$ is the ratio of the vertical tail aspect ratio in the presence of the fuselage to that of an isolated vertical tail. This ratio can be determined from Figure 10.14.

$(A_{v(hf)}/A_{v(f)})$ is the ratio of the vertical tail aspect ratio in the presence of the horizontal tail and the fuselage to that in the presence of the fuselage alone. This ratio can be determined from Figure 10.15.

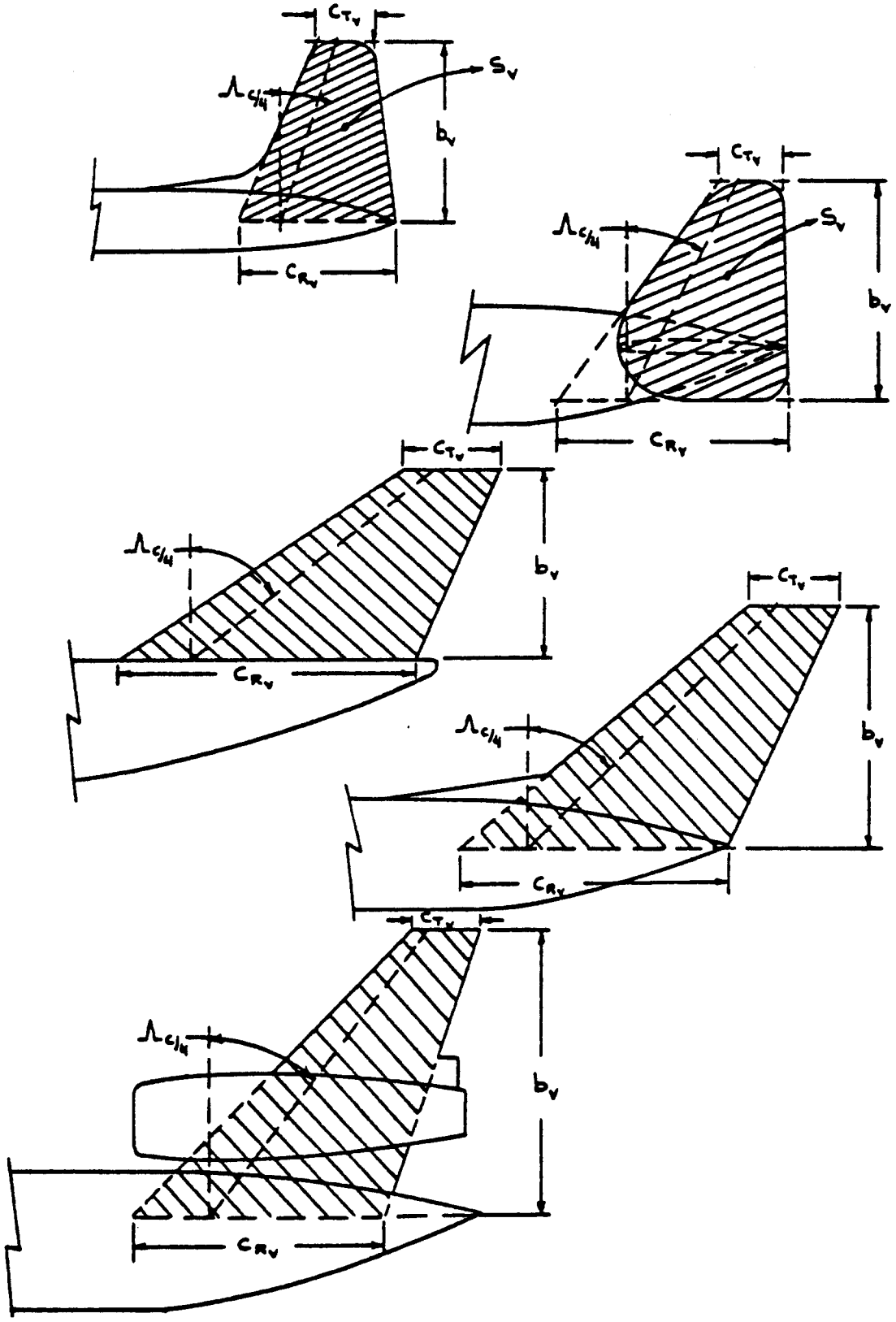

Figure 10.13 Examples of Effective Vertical Tail Geometry

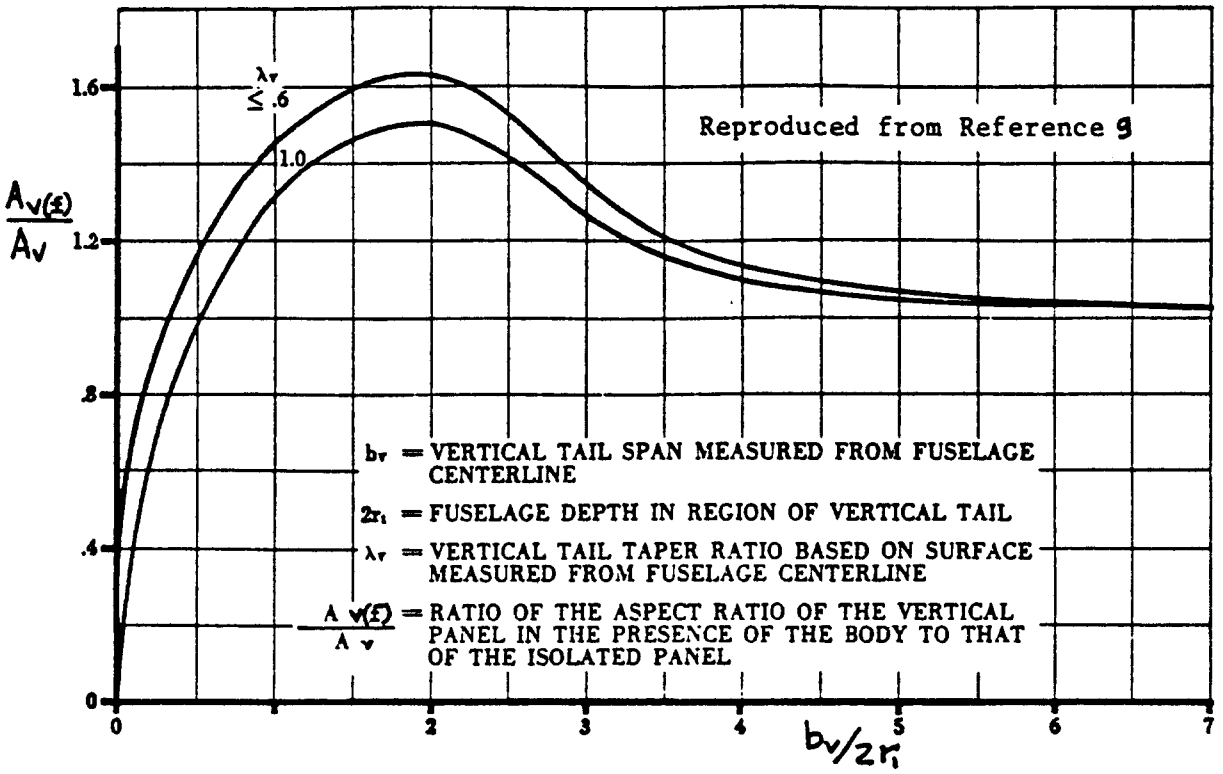

Figure 10.14 Ratio of Vertical Tail Aspect Ratio in Presence of Fuselage to that of Isolated Tail

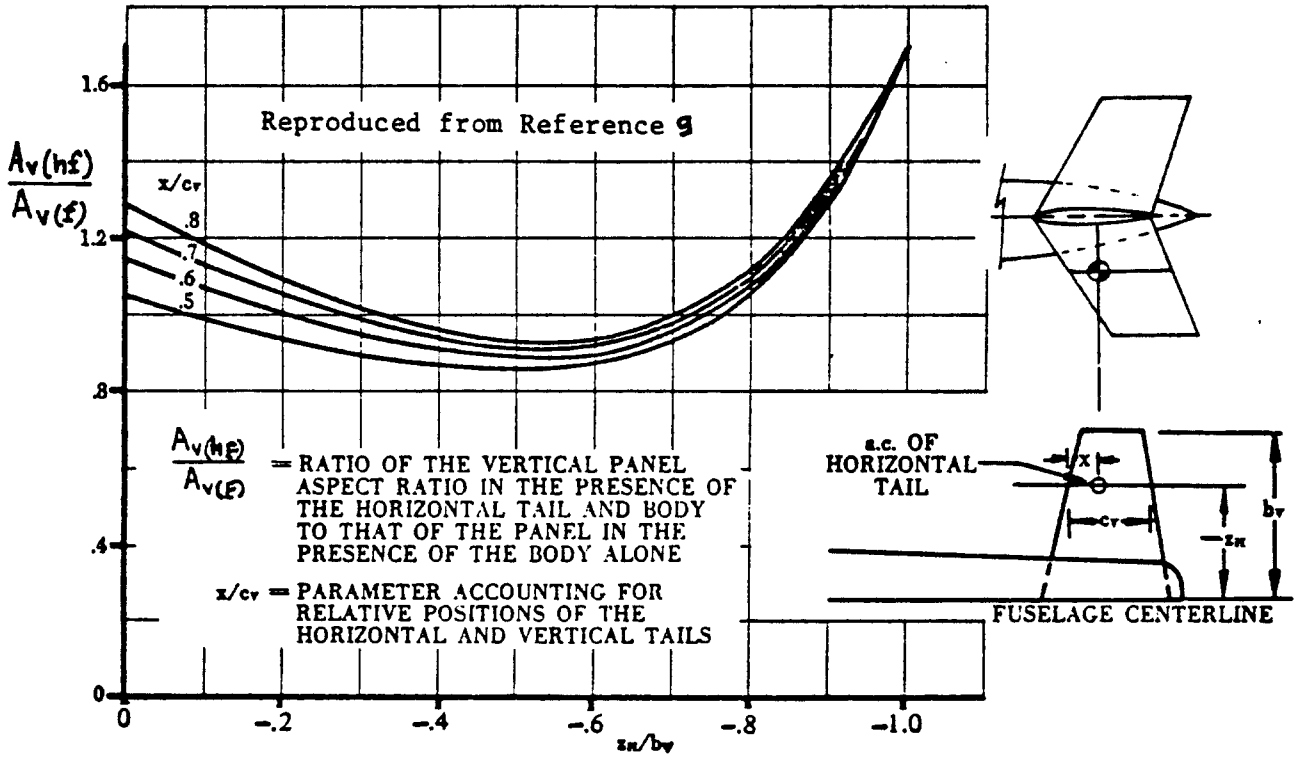

Figure 10.15 Ratio of Vertical Tail Aspect Ratio in Presence of Fuselage and Horizontal Tail to that in Presence of Fuselage Alone

K_{vh} is a factor which accounts for the relative size of the horizontal and the vertical tail. It may be determined from Figure 10.16.

$$(1 + d\sigma/d\beta)\eta_v = \quad (10.31)$$

$$0.724 + 3.06\{(S_v/S)/(1 + \cos\Lambda_{c/4})\} + 0.4z_w/z_f + 0.009A$$

S_v is the effective vertical tail area as defined in Figure 10.13 for several example configurations.

$\Lambda_{c/4}$ is the wing quarter chord sweep angle

A is the wing aspect ratio

2. For Twin Vertical Tails:

$$C_{y_{\beta_v}} = \quad (10.32)$$

$$-2\{C_{y_{\beta_{v(wfh)}}}/C_{y_{\beta_{v_{eff}}}}\}(C_{y_{\beta_{v_{eff}}}})(S_v/S)$$

with: $\{C_{y_{\beta_{v(wfh)}}}/C_{y_{\beta_{v_{eff}}}}\}$ determined from Figure 10.17.

$C_{y_{\beta_{v_{eff}}}}$ determined from Figure 10.18 with the corresponding value of $A_{v_{eff}}$ found from Figure 10.19.

S_v is the area of a single vertical tail panel as defined in Figure 10.13.

2.) C_{l_β}

The rolling-moment-due-to-sideslip derivative, C_{l_β} (also called dihedral effect) may be found from:

$$C_{l_\beta} = C_{l_{\beta_{wf}}} + C_{l_{\beta_h}} + C_{l_{\beta_v}} \quad (10.33)$$

where: the wing-fuselage contribution is given by:

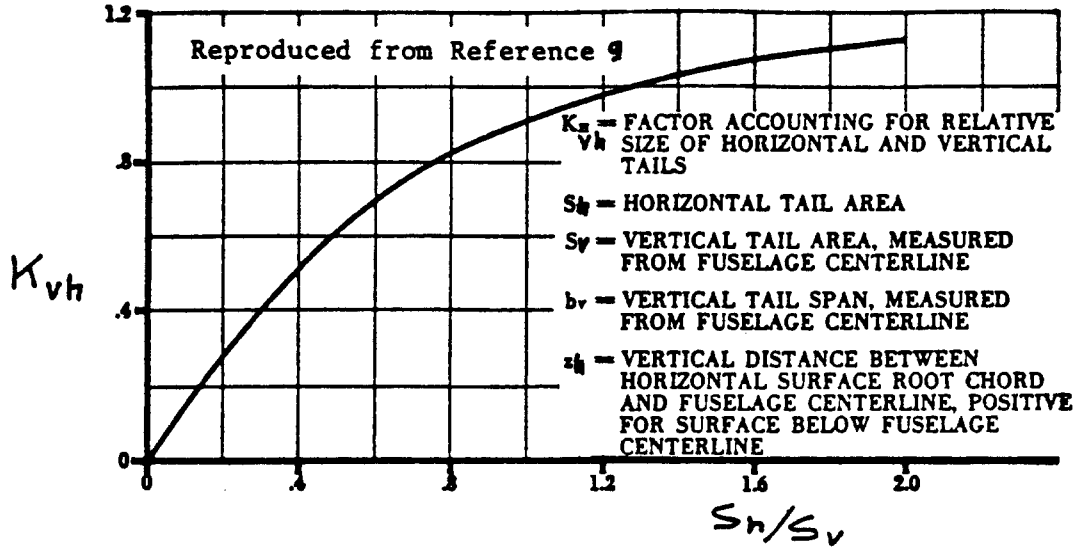

Figure 10.16 Factor which Accounts for Relative Size of Horizontal and Vertical Tail

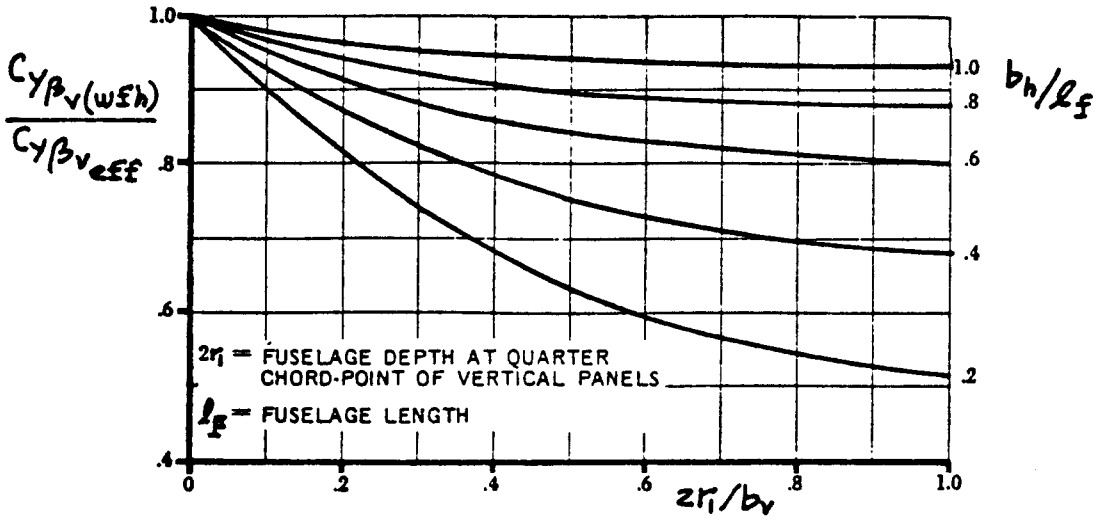

Reproduced from Reference 9

Figure 10.17 Wing-Fuselage-Horizontal-Tail Interference on Side-force due to Sideslip of Twin Vertical Tails

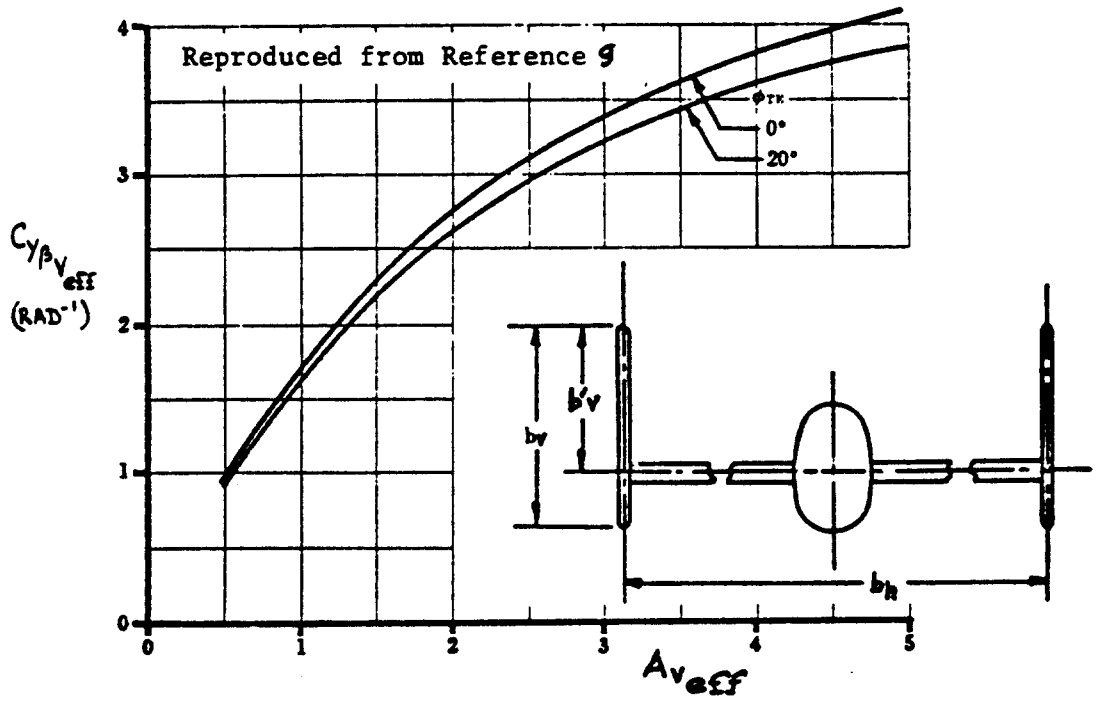

Figure 10.18 Effective Value of the Side-force due to Sideslip Derivative for Twin Vertical Tails

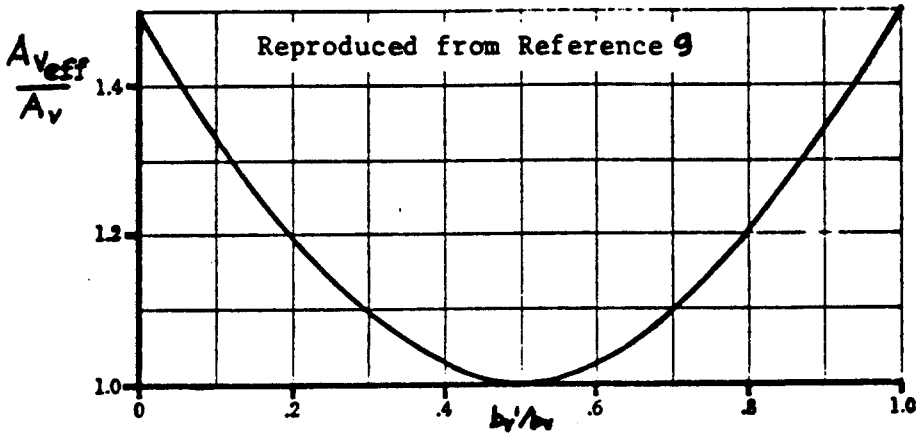

For definition of b'_V see Figure 10.18

Figure 10.19 Effective Value of Vertical Tail Aspect Ratio Used with Figure 10.18

$$C_{l_{\beta_{wf}}} = 57.3[C_{L_{wf}}\{(C_{l_\beta}/C_L)_{\Lambda_{c/2}}(K_{M_\Lambda})(K_f) + (C_{l_\beta}/C_L)_A\} +$$

$$+ \Gamma\{(C_{l_\beta}/\Gamma)K_{M_\Gamma} + (\Delta C_{l_\beta}/\Gamma)\} + (\Delta C_{l_\beta})_{z_w} +$$

$$+ (\varepsilon_t \tan\Lambda_{c/4})\{(\Delta C_{l_\beta})/\varepsilon_t \tan\Lambda_{c/4}\}] \qquad (10.34)$$

with: $C_{L_{wf}}$ is the lift coefficient of the wing-fuselage combination. For any given value of airplane lift coefficient, this may be computed by subtracting the tail and/or the canard lift coefficients (but based on wing area!). For preliminary design purposes it seems acceptable to set: $C_{L_{wf}} = C_{L_1}$.

$(C_{l_\beta}/C_L)_{\Lambda_{c/2}}$ is the wing sweep contribution which may be found from Figure 10.20.

K_{M_Λ} is the compressibility correction to sweep. It is found from Figure 10.21.

K_f is a fuselage correction factor obtained from Figure 10.22.

$\Lambda_{c/2}$ is the wing semi-chord sweep angle

$\Lambda_{c/4}$ is the wing quarter-chord sweep angle

$(C_{l_\beta}/C_L)_A$ is the aspect ratio contribution obtained from Figure 10.23.

Γ is the geometric dihedral angle of the wing as defined in Figure 10.7.

(C_{l_β}/Γ) is the wing dihedral effect found from Figure 10.24.

K_{M_Γ} is the compressibility correction to dihedral as obtained from Figure 10.25.

$(\Delta C_{l_\beta}/\Gamma)$ is the fuselage induced effect on the wing height and is found from:

$$(\Delta C_{l_\beta}/\Gamma) = -0.0005A(d_{f_{ave}}/b)^2 \qquad (10.35)$$

where: A is the wing aspect ratio

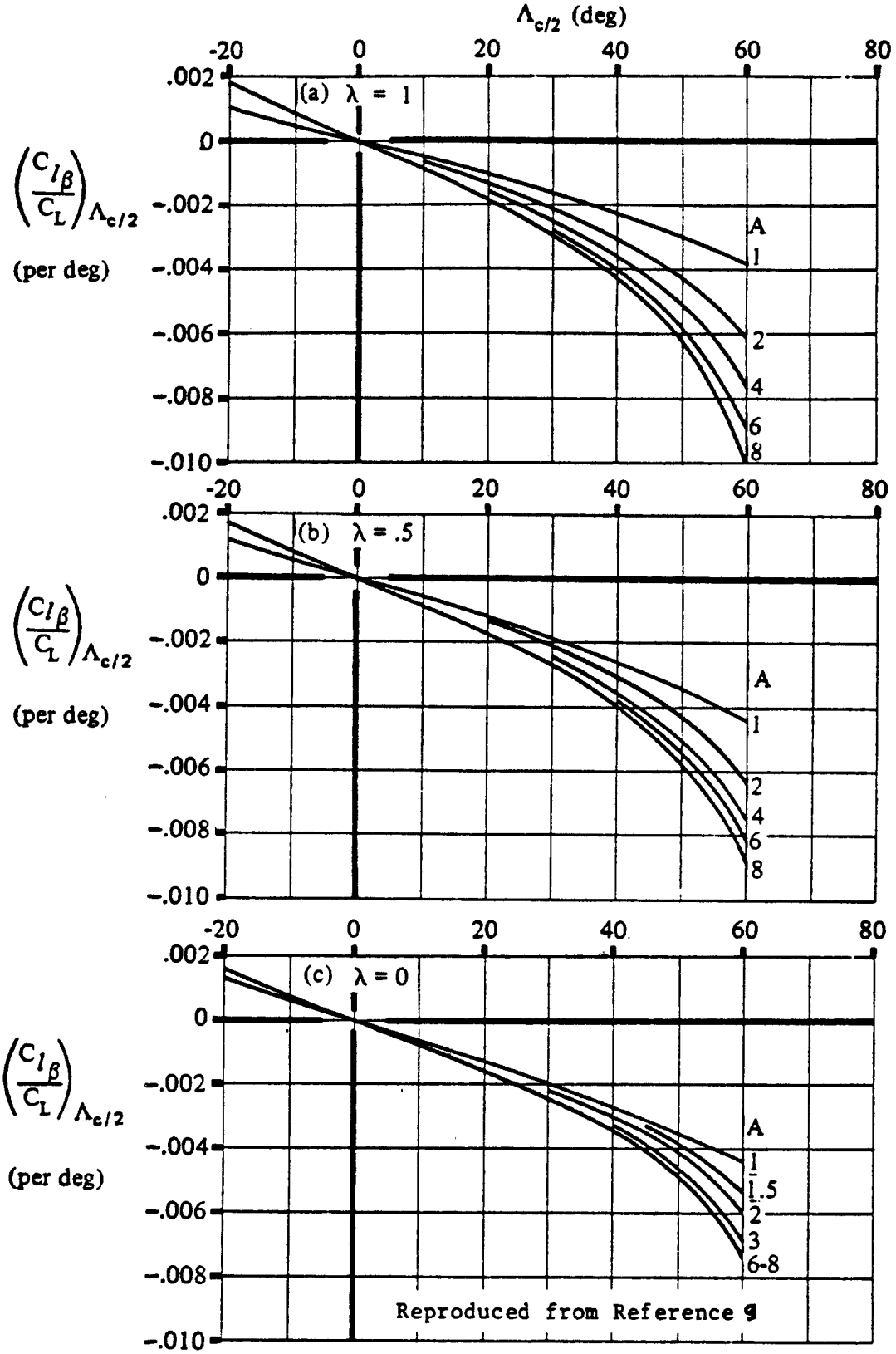

Figure 10.20 Wing Sweep Contribution to Rolling Moment due to Sideslip

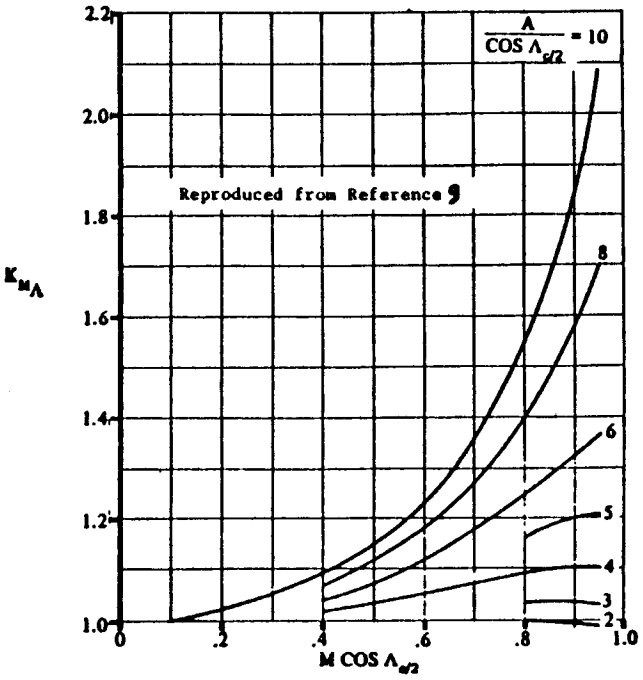

Figure 10.21 Compressibility Correction to Wing Sweep

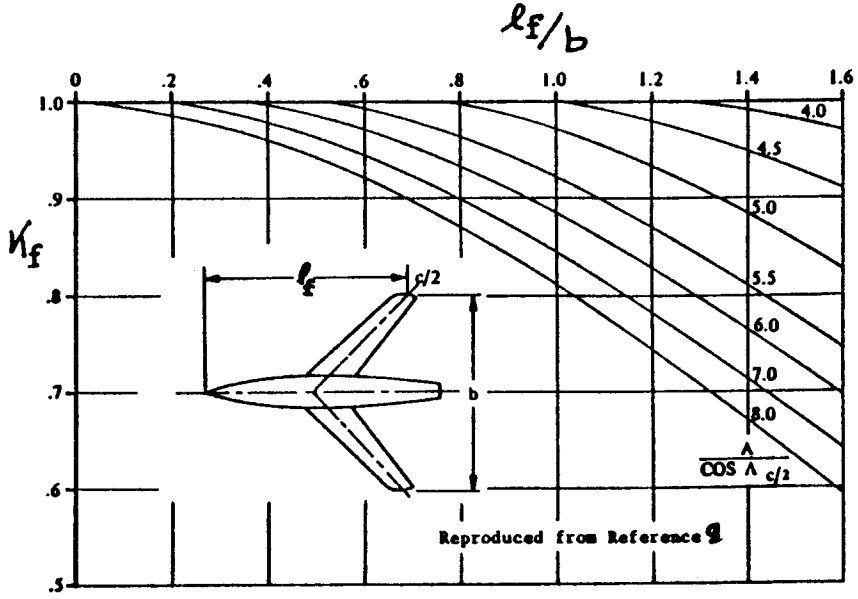

Figure 10.22 Fuselage Correction Factor

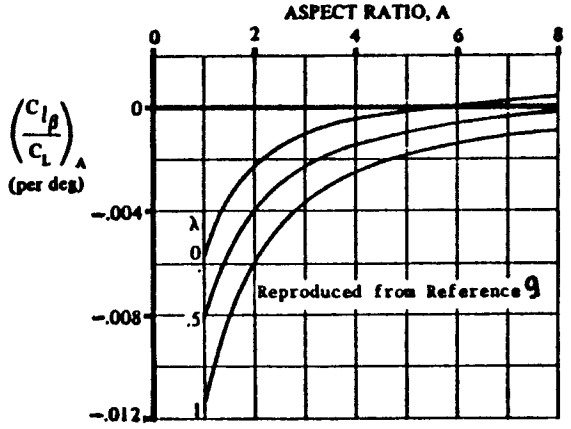

Figure 10.23 Wing Aspect Ratio Contribution to Rolling Moment due to Sideslip

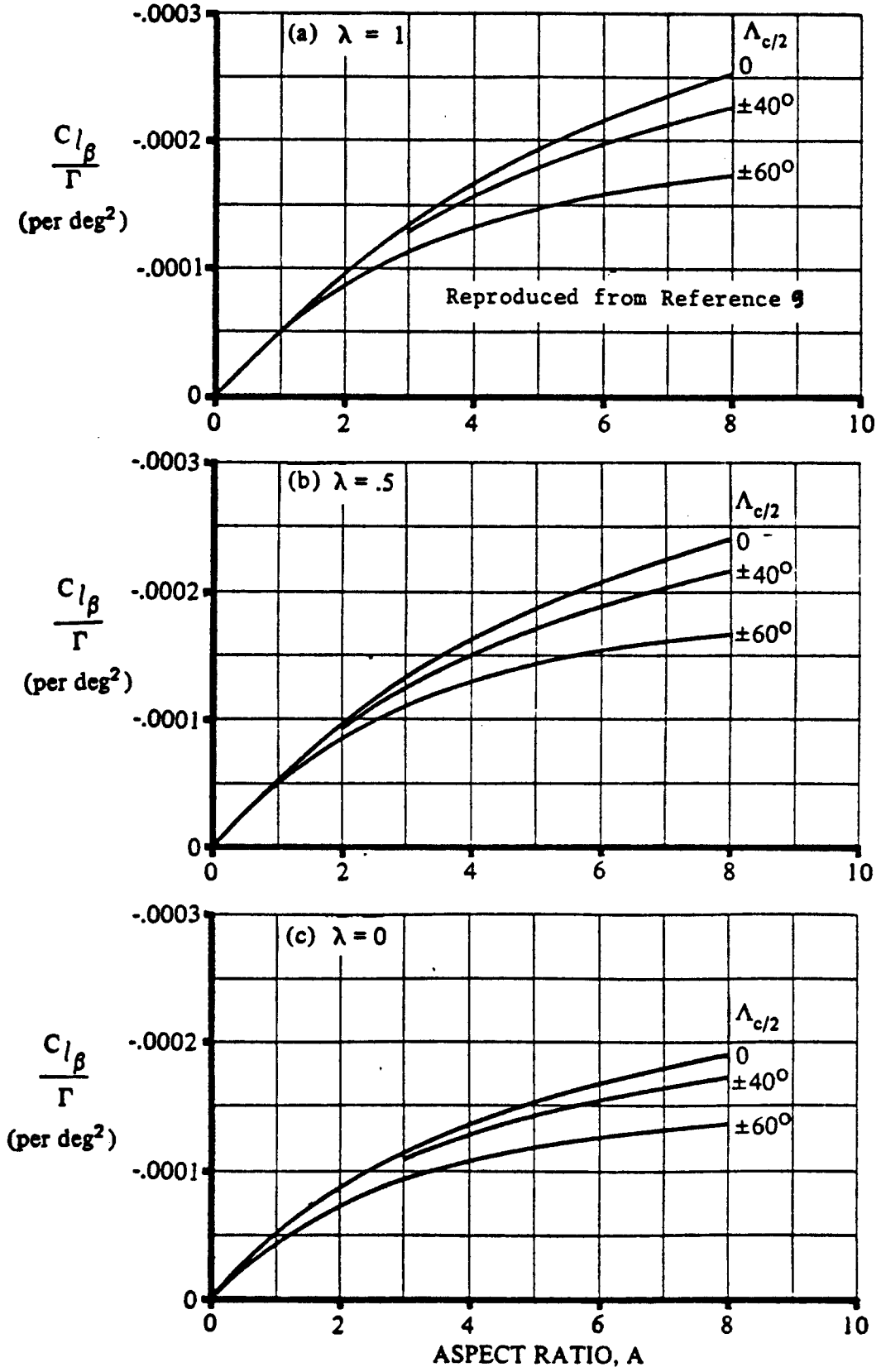

Figure 10.24 Wing Geometric Dihedral Contribution to Rolling Moment due to Sideslip

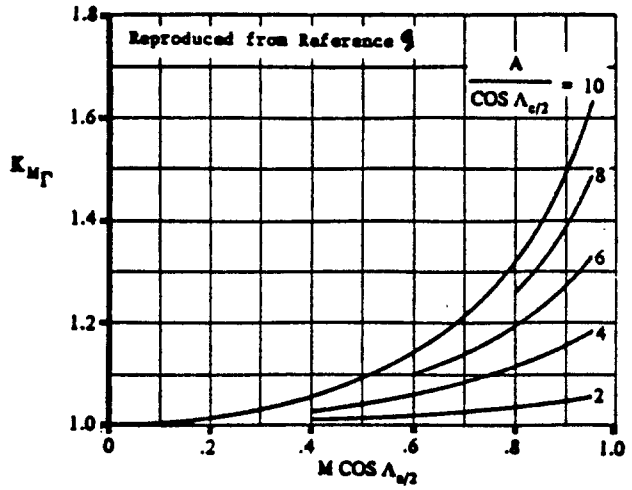

Figure 10.25 Compressibility Correction to Wing Dihedral

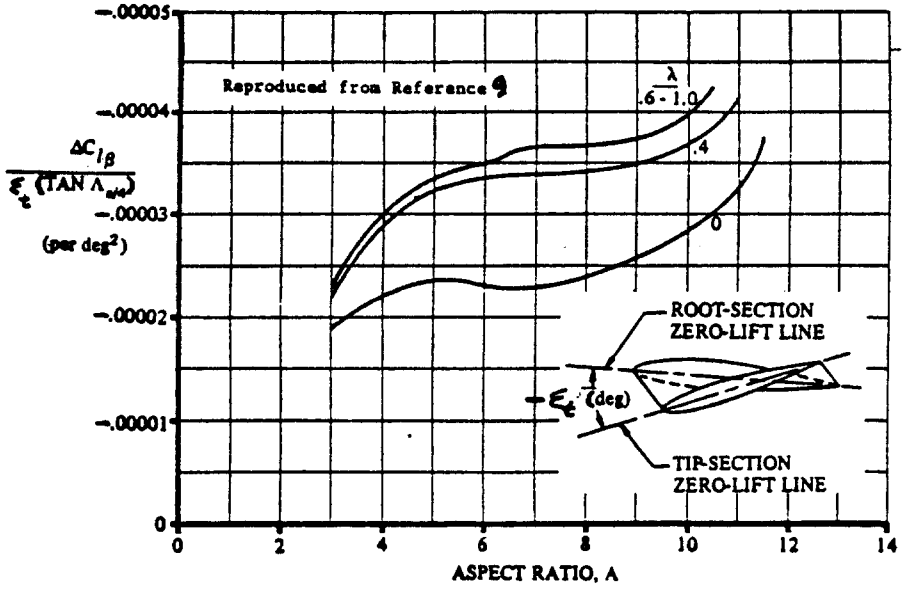

Figure 10.26 Contribution of Wing Twist to Rolling Moment due to Sideslip

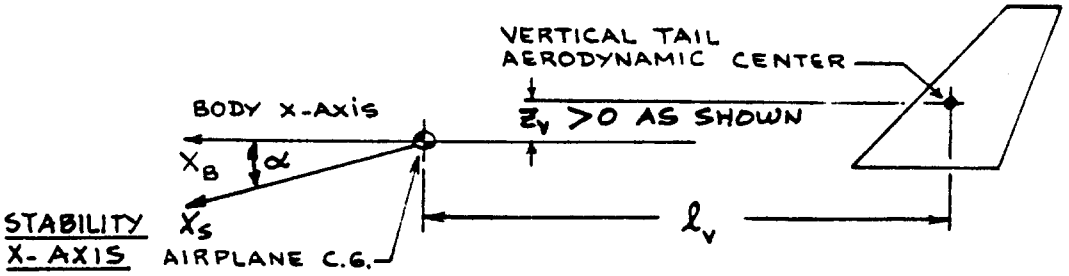

Figure 10.27 Geometry for Locating Vertical Tail(s)

b is the wing span

$$d_{f_{ave}} = \{(\text{ave. fusel. cross-section area})/0.7854\}^{1/2} \quad (10.36)$$

$$(\Delta C_{l_\beta})_{z_w} = 0.042(A)^{1/2}(z_w/b)(d_{f_{ave}}/b) \quad (10.37)$$

where: z_w is defined in Figure 10.9

$d_{f_{ave}}$ is given by Eqn.(10.36)

$\{(\Delta C_{l_\beta})/\varepsilon_t \tan\Lambda_{c/4}\}$ is a wing twist correction factor which is obtained from Fig.10.26.

the horizontal tail contribution is given by:

$$C_{l_{\beta_h}} = (C_{l_{\beta_{hf}}})(S_h b_h/Sb) \quad (10.38)$$

with: $C_{l_{\beta_{hf}}}$ the horizontal tail dihedral effect as computed from Equation (10.34) with appropriate substitution of tail-fuselage for wing-fuselage parameters.

S_h is the horizontal tail area

b_h is the horizontal tail span

the vertical tail contribution is given by:

$$C_{l_{\beta_v}} = (C_{y_\beta})\{z_v\cos\alpha - l_v\sin\alpha)/b\} \quad (10.39)$$

with: C_{y_β} given by Eqn.(10.28)

z_v and l_v defined in Figure (10.27)

3.)C_{n_β}

The yawing-moment-due-to-sideslip derivative, C_{n_β} (also called static directional stability) may be computed from:

$$C_{n_\beta} = C_{n_{\beta_w}} + C_{n_{\beta_f}} + C_{n_{\beta_v}} \quad (10.40)$$

where: the wing contribution is important only at high angles of attack. Ref.9 contains a method for estimating this contribution in such cases. For preliminary design purposes:

$$C_{n_{\beta_w}} = 0 \qquad (10.41)$$

the fuselage contribution is found from:

$$C_{n_{\beta_f}} = -57.3 K_N K_{R_l} (S_{f_s} l_f / Sb) \qquad (10.42)$$

with: K_N an empirical factor determined from Figure 10.28

K_{R_l} a factor dependent on Reynold's Number and obtained from Figure 10.29

S_{f_s} and l_f are defined in Figure 10.28.

the vertical tail contribution is found from:

$$C_{n_{\beta_v}} = -(C_{Y_{\beta_v}})(l_v \cos\alpha + z_v \sin\alpha)/b \qquad (10.43)$$

where: $C_{Y_{\beta_v}}$ is found from Eqn.(10.28)

l_v and z_v are given in Figure 10.27.

10.2.4.2 Thrust versus sideslip derivative: $C_{n_{T_\beta}}$

As suggested in Table 10.1, the only contribution which is of some significance is the yawing-moment-due-to-thrust-in-sideslip derivative, $C_{n_{T_\beta}}$.

For Propeller Driven Airplanes:

$$C_{n_{T_\beta}} = \qquad (10.44)$$

$$\sum_{i=1}^{i=n} \left[\left(\left(dC_N/d\alpha \right)_{p_i} \right) (0.79) (D_{p_i})^2 (l_{p_i}) \right] / Sb$$

where: all terms are as defined on page 342.

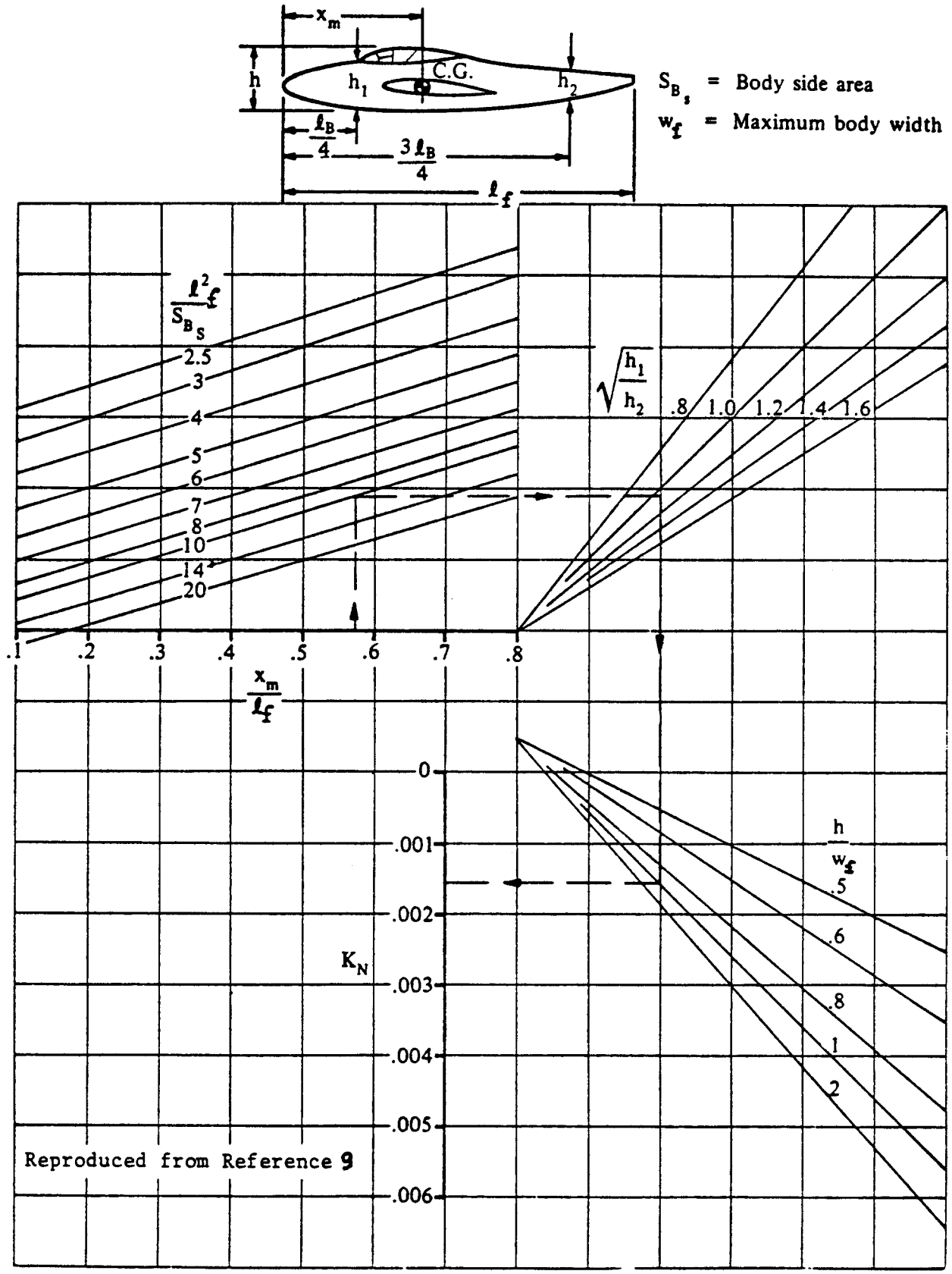

Figure 10.28 Factor Accounting for Wing-Fuselage Interference with Directional Stability

For Jet Driven Airplanes:

$$C_{n_{T_\beta}} = \sum_{i=1}^{i=n} [\{0.035(m_{a_i})(l_{n_i})\}/Sb\rho U_1] \qquad (10.45)$$

where: all terms are as defined on page 343.

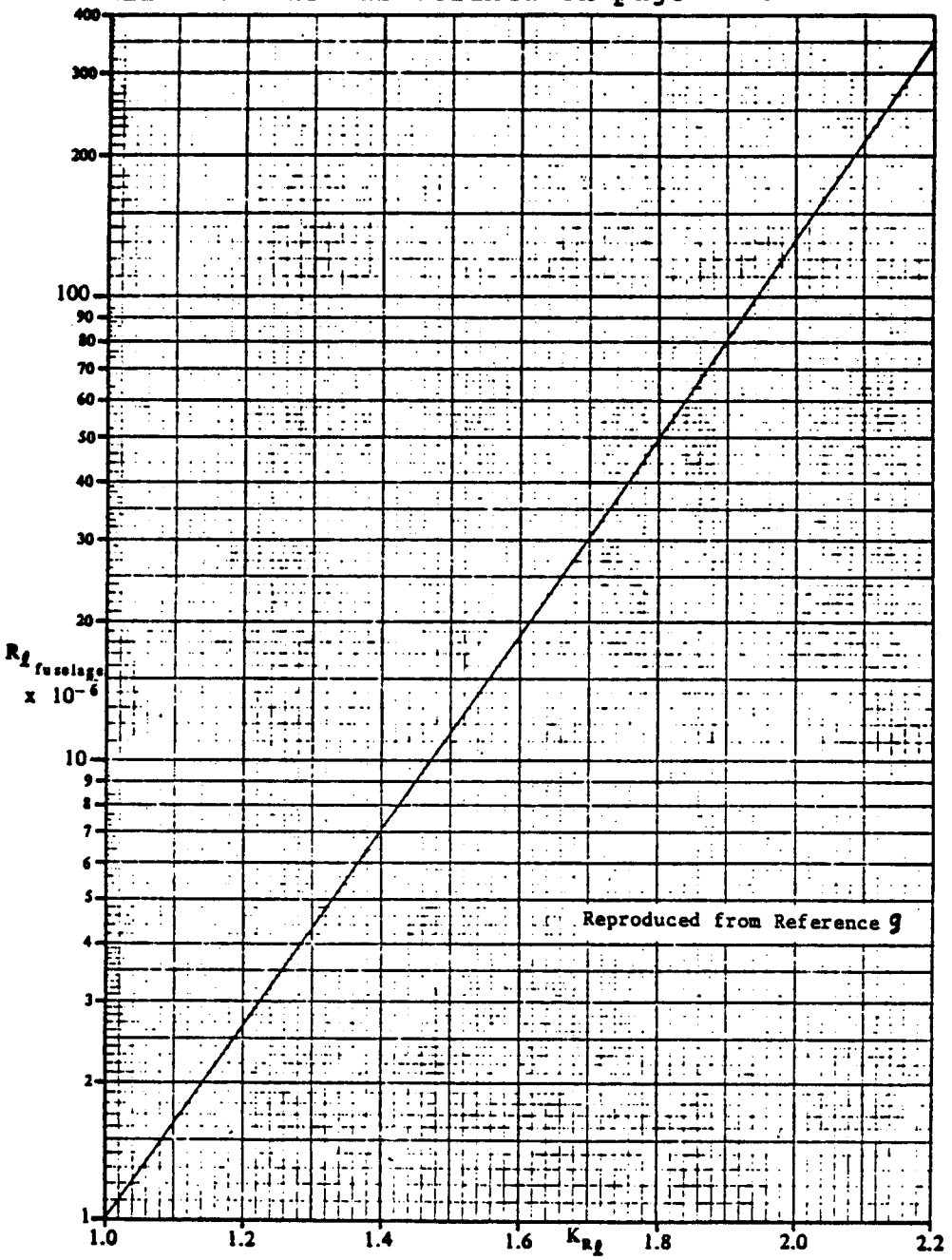

Figure 10.29 Effect of Fuselage Reynold's Number on Wing-Fuselage Directional Stability

10.2.5. Rate of Angle-of-Sideslip Derivatives: $C_{y_{\dot{\beta}}}$, $C_{l_{\dot{\beta}}}$ and $C_{n_{\dot{\beta}}}$

Table 10.1 identifies the required rate-of-angle-of-sideslip derivatives. According to Reference 9, only the vertical tail contributes significantly to these rate derivatives.

NOTE: All methods presented for the rate-of-sideslip derivatives are valid only for the subsonic speed regime. For other speed ranges the reader should consult Ref.9.

1. $C_{y_{\dot{\beta}}}$

The sideforce-due-to-rate-of-sideslip derivative, $C_{y_{\dot{\beta}}}$ may be estimated from:

$$C_{y_{\dot{\beta}}} = \qquad (10.46)$$

$$2(C_{L_{\alpha_v}})(d\sigma/d\beta)(S_v/S)(l_p\cos\alpha_f + z_p\sin\alpha_f)/b$$

where: $C_{L_{\alpha_v}}$ is found with the method indicated under Equation (10.28)

$$d\sigma/d\beta = \qquad (10.47)$$

$$(\sigma_{\beta_\alpha})\alpha_f + (\sigma_{\beta_\Gamma})(\Gamma/57.3) - (\sigma_{\beta_{\varepsilon_t}})\varepsilon_t + (\sigma_{\beta_{wf}})$$

where: σ_{β_α} is the sidewash contribution due to angle of attack. It is found from Figures 10.30.

α_f is the angle of attack of the fuselage

σ_{β_Γ} is the sidewash contribution due to wing dihedral. It is found from Figures 10.31.

Γ is the wing dihedral angle as defined in Figure 10.7.

$\sigma_{\beta_{\varepsilon_t}}$ is the sidewash contribution due to wing twist as obtained from Figures 10.32.

ε_t is the wing twist angle as shown in Figure 10.26.

$\sigma_{\beta_{wf}}$ is the sidewash effect due the fuselage as

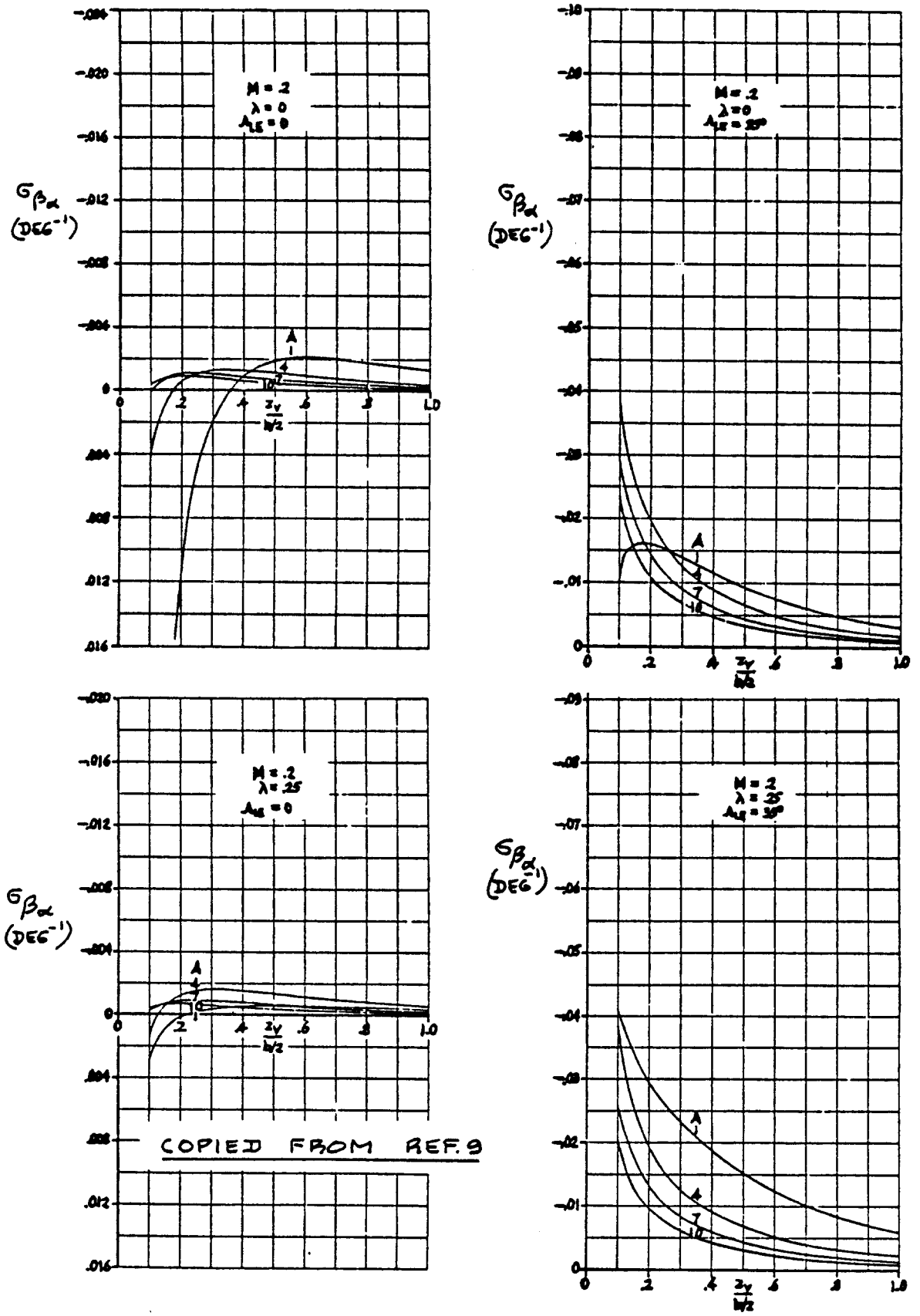

COPIED FROM REF. 9

Figure 10.30a Sidewash Contribution due to Angle of Attack

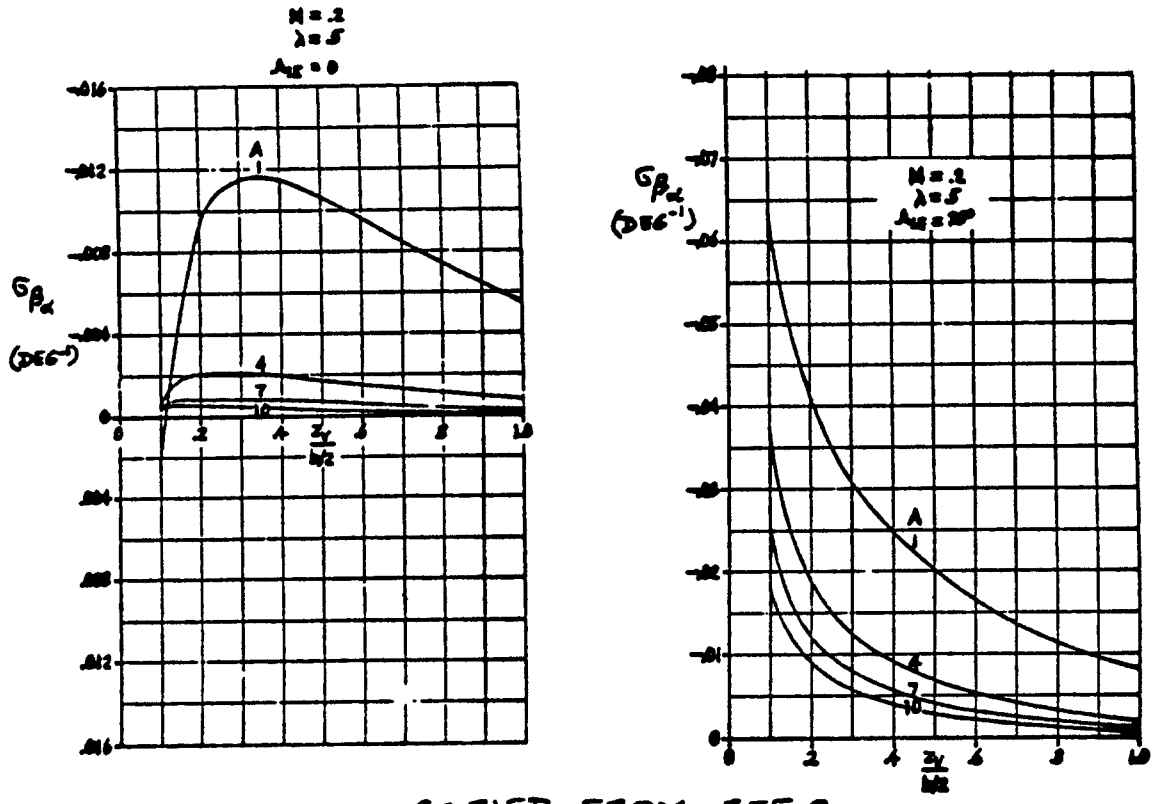

COPIED FROM REF. 9

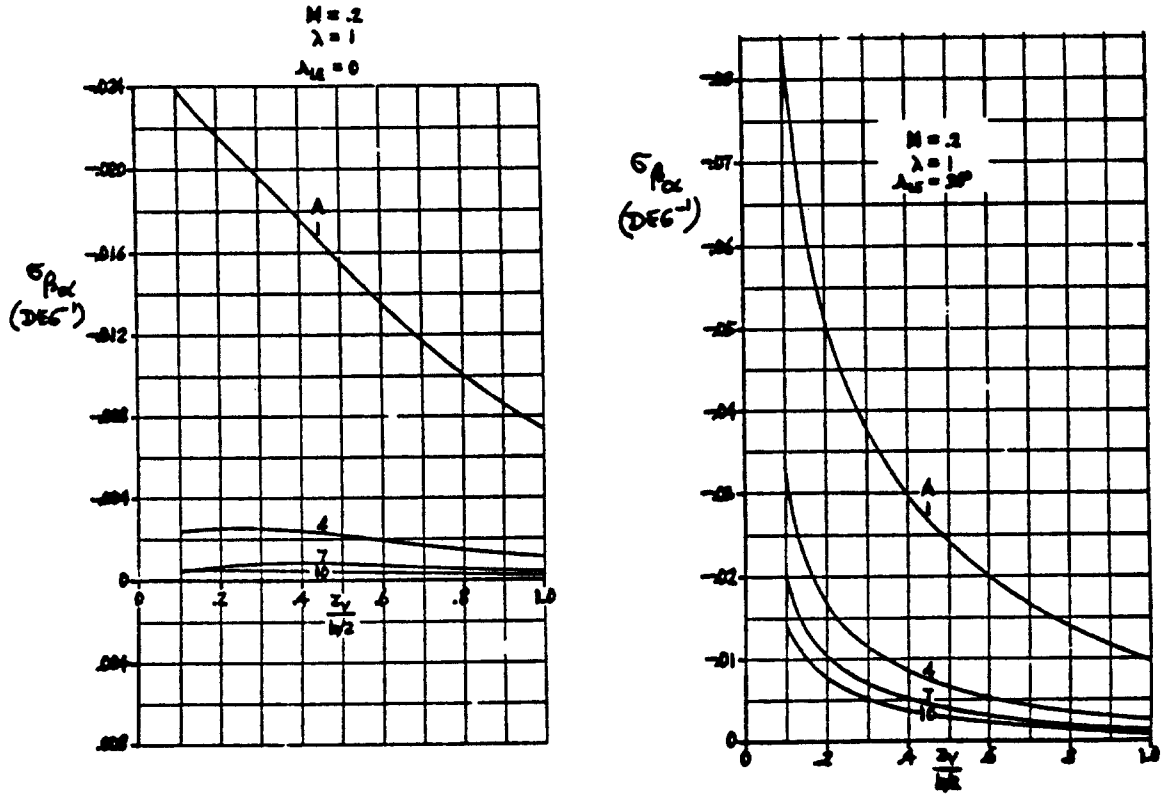

Figure 10.30b Sidewash Contribution due to Angle of Attack

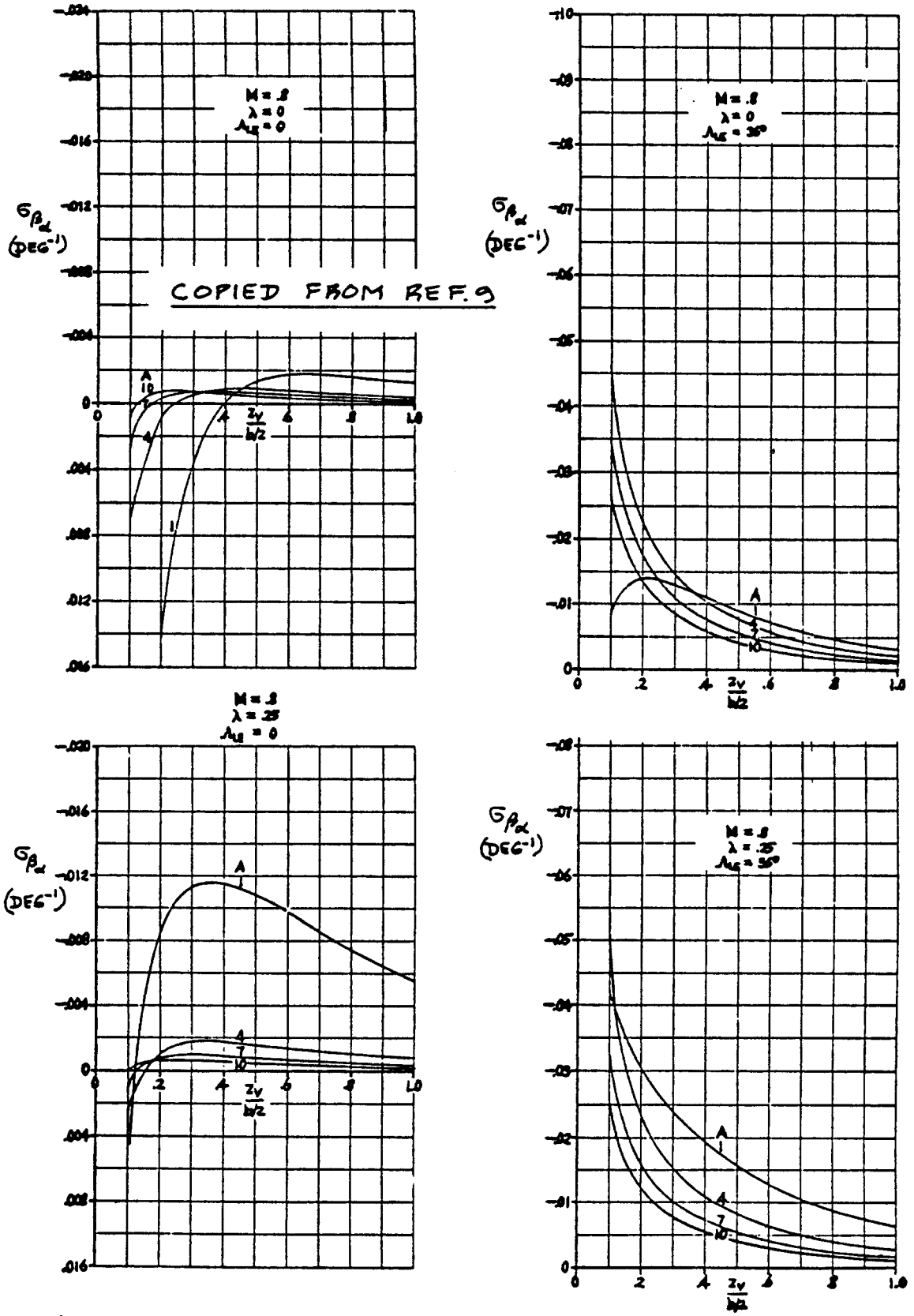

COPIED FROM REF. 9

Figure 10.30c Sidewash Contribution due to Angle of Attack

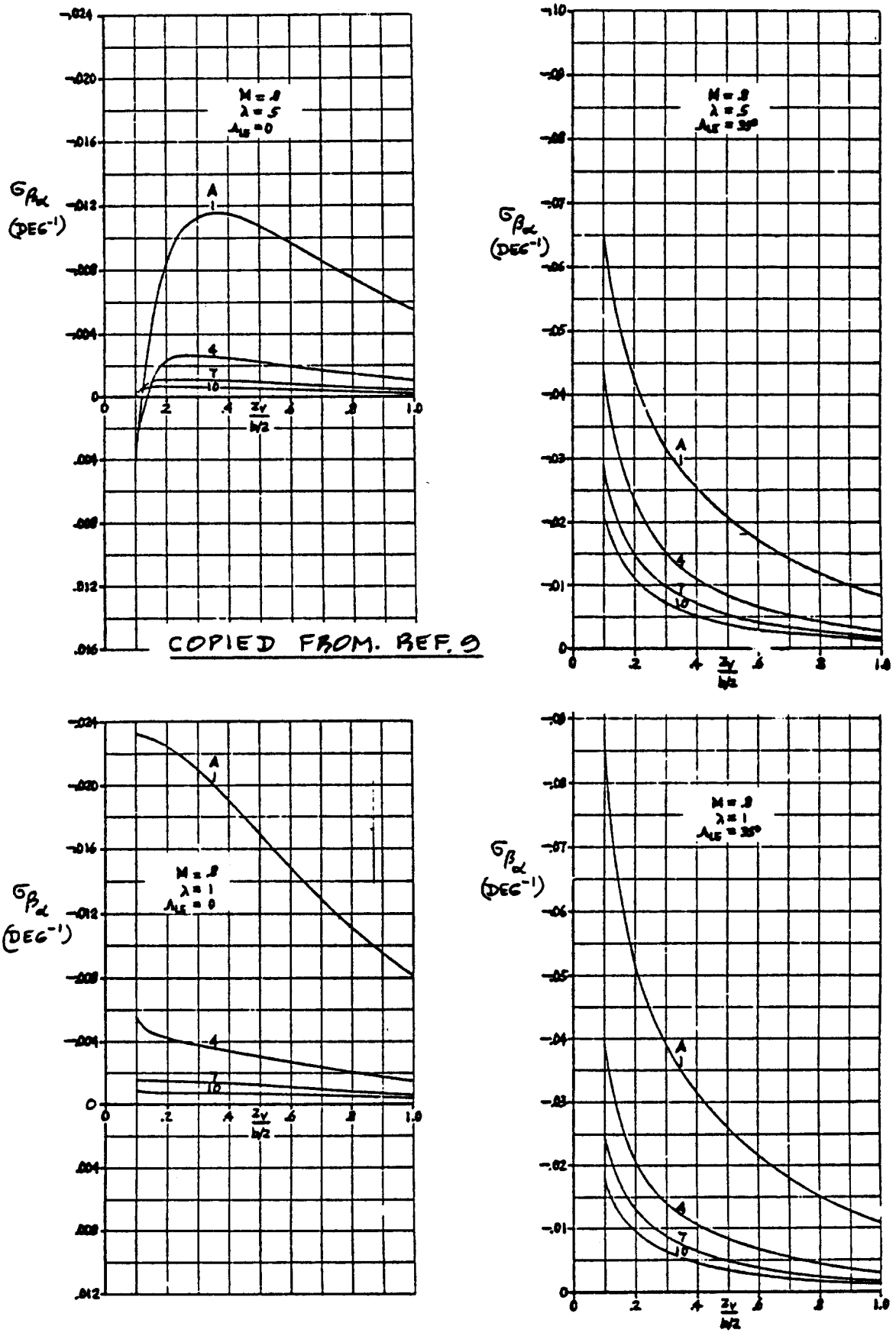

Figure 10.30d Sidewash Contribution due to Angle of Attack

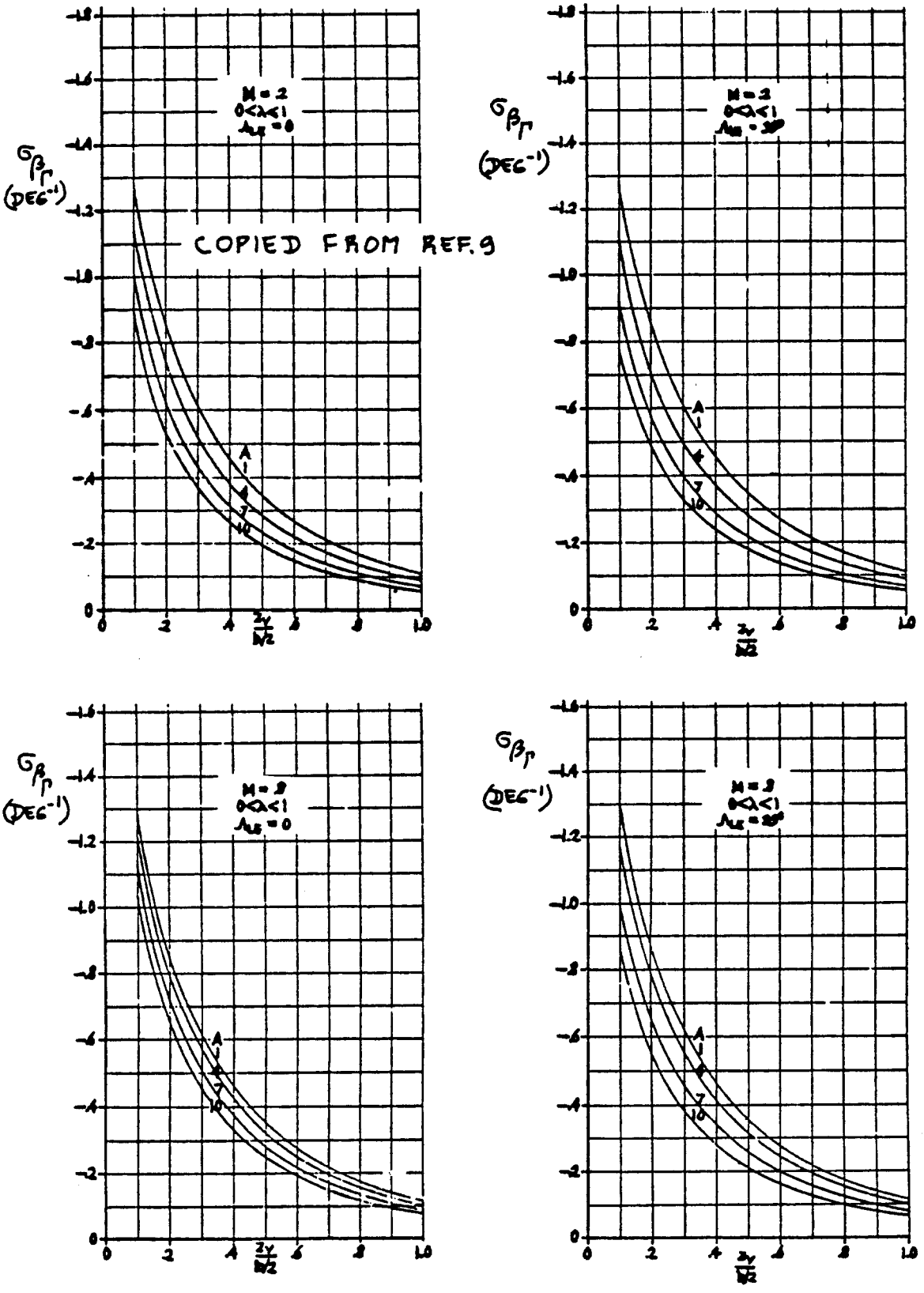

Figure 10.31 Sidewash Contribution due to Wing Dihedral

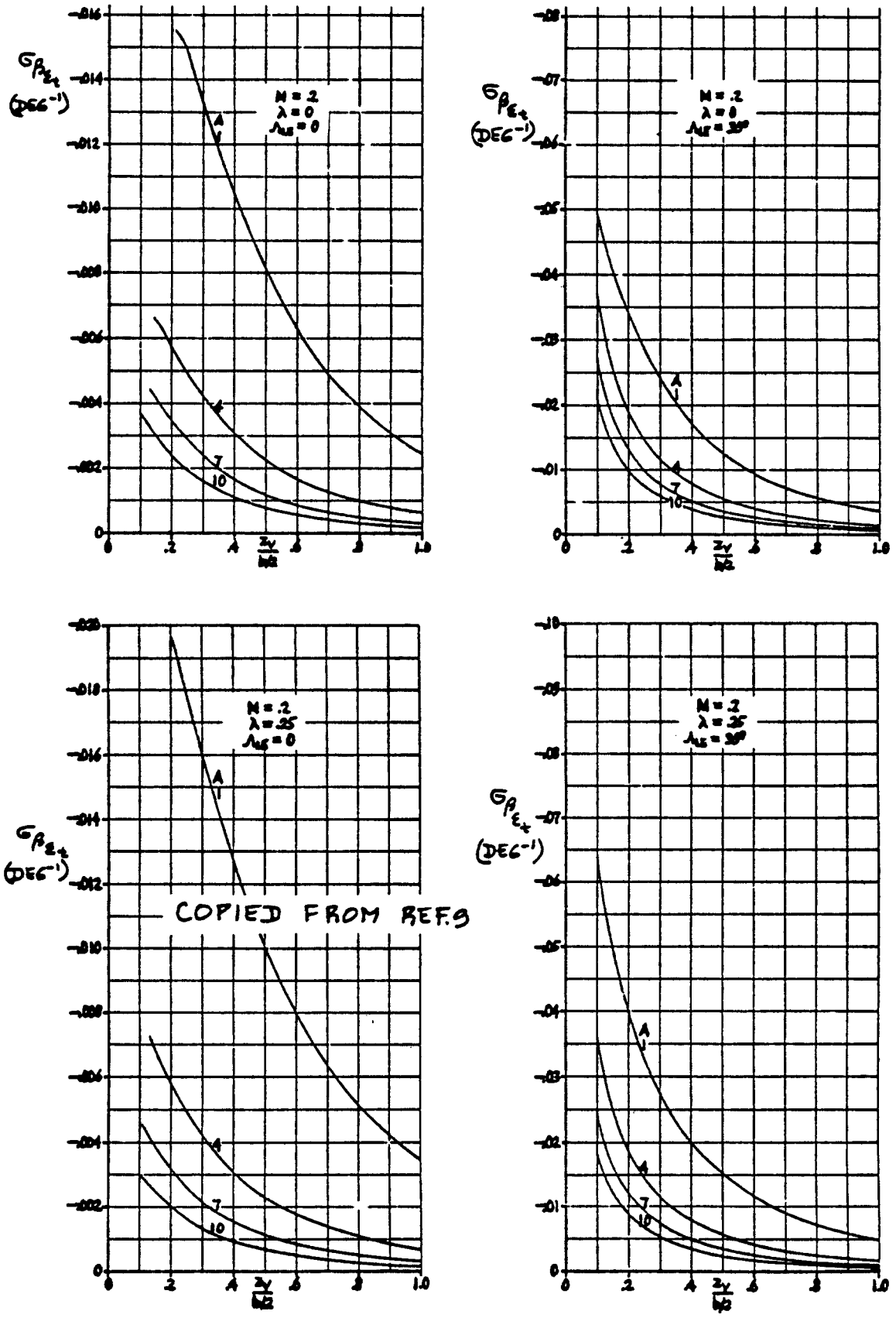

Figure 10.32a Sidewash Contribution due to Wing Twist

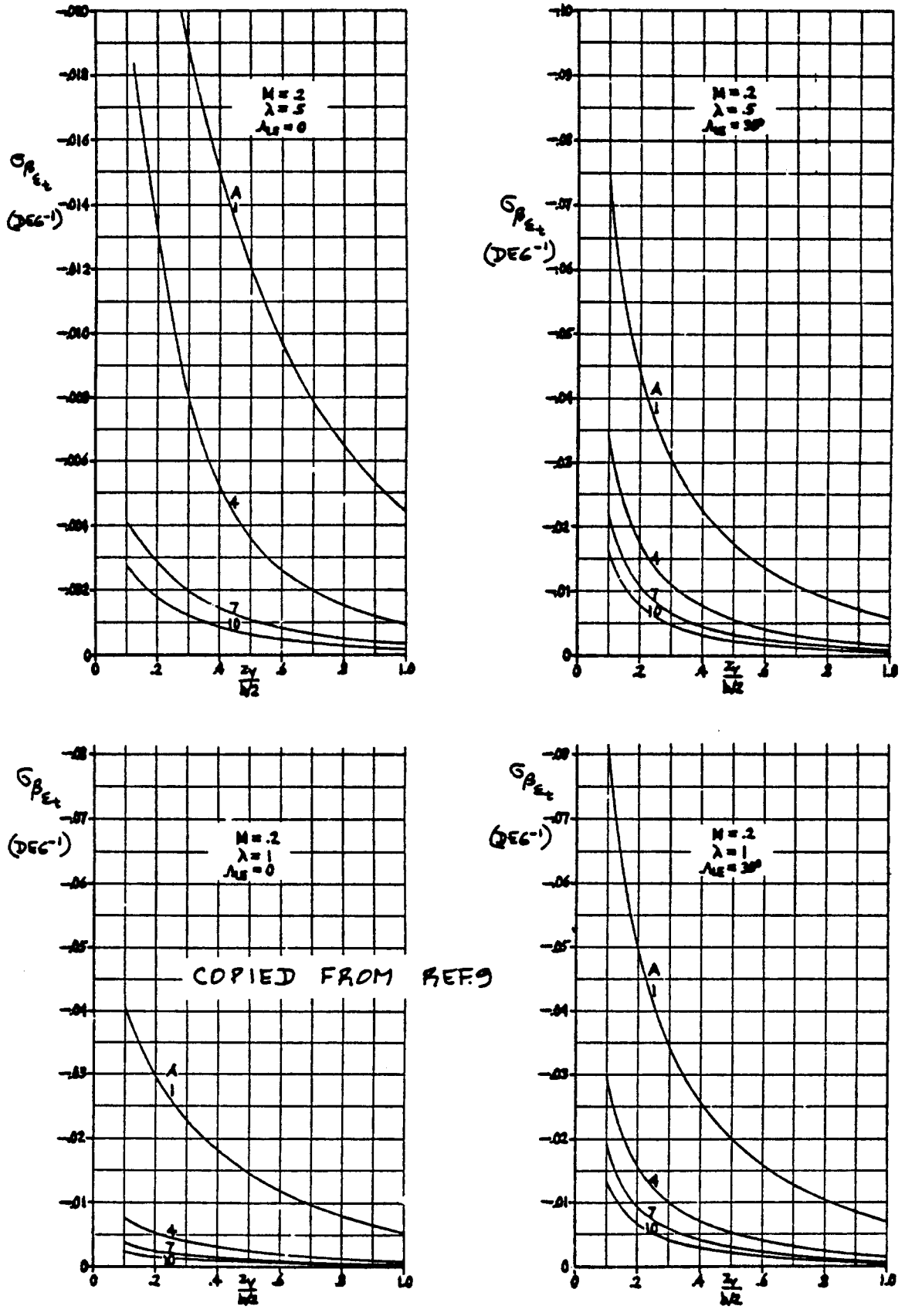

Figure 10.32b Sidewash Contribution due to Wing Twist

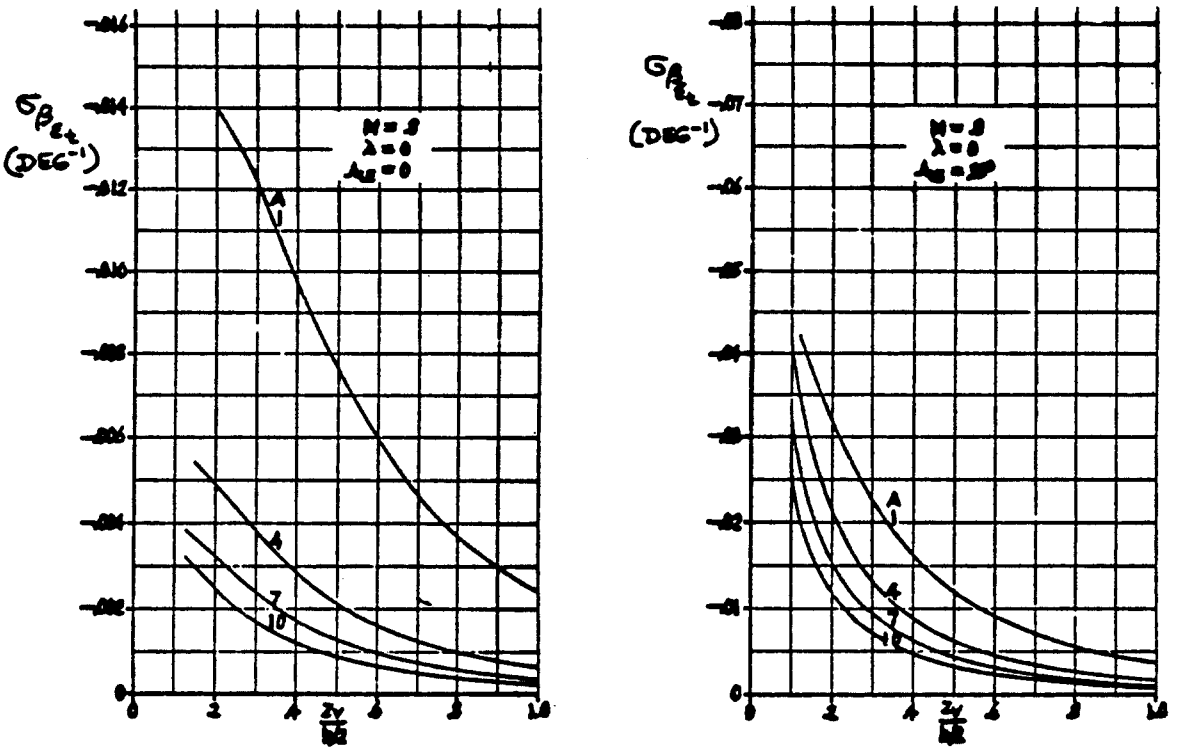

COPIED FROM REF. 9

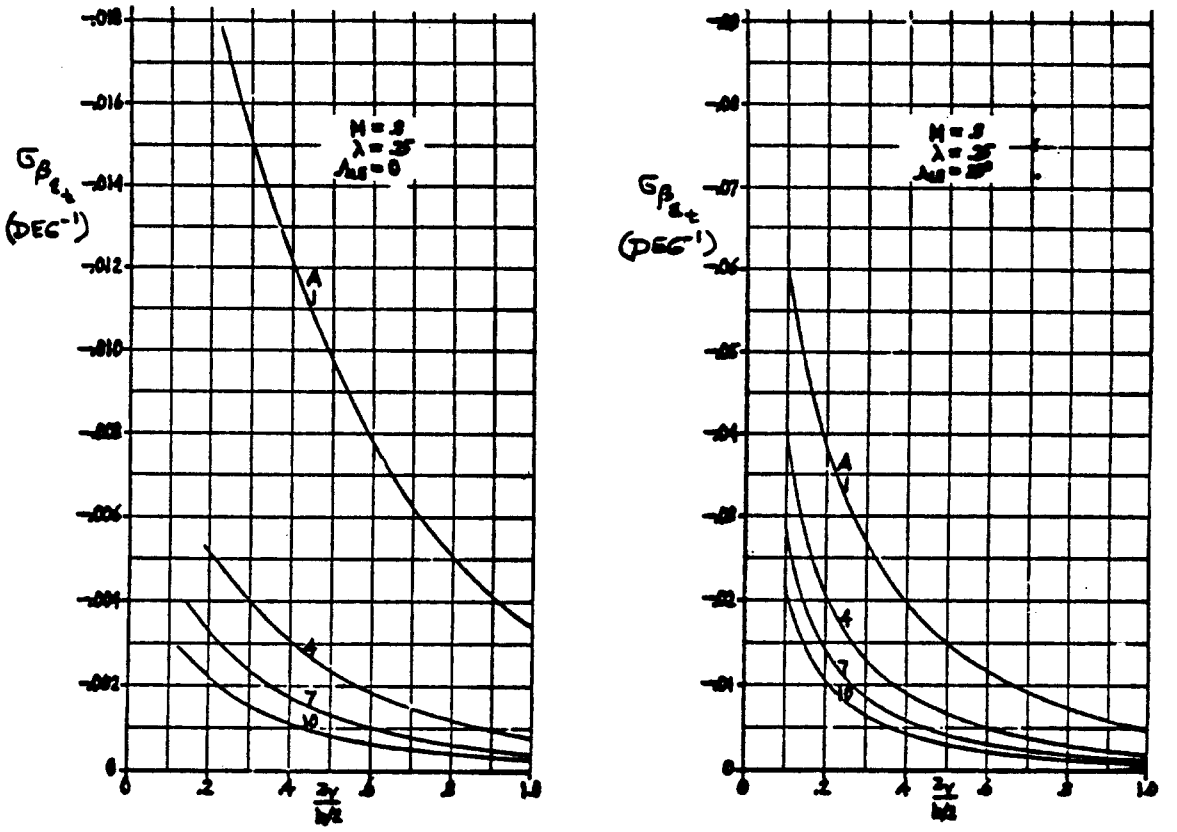

Figure 10.32c Sidewash Contribution due to Wing Twist

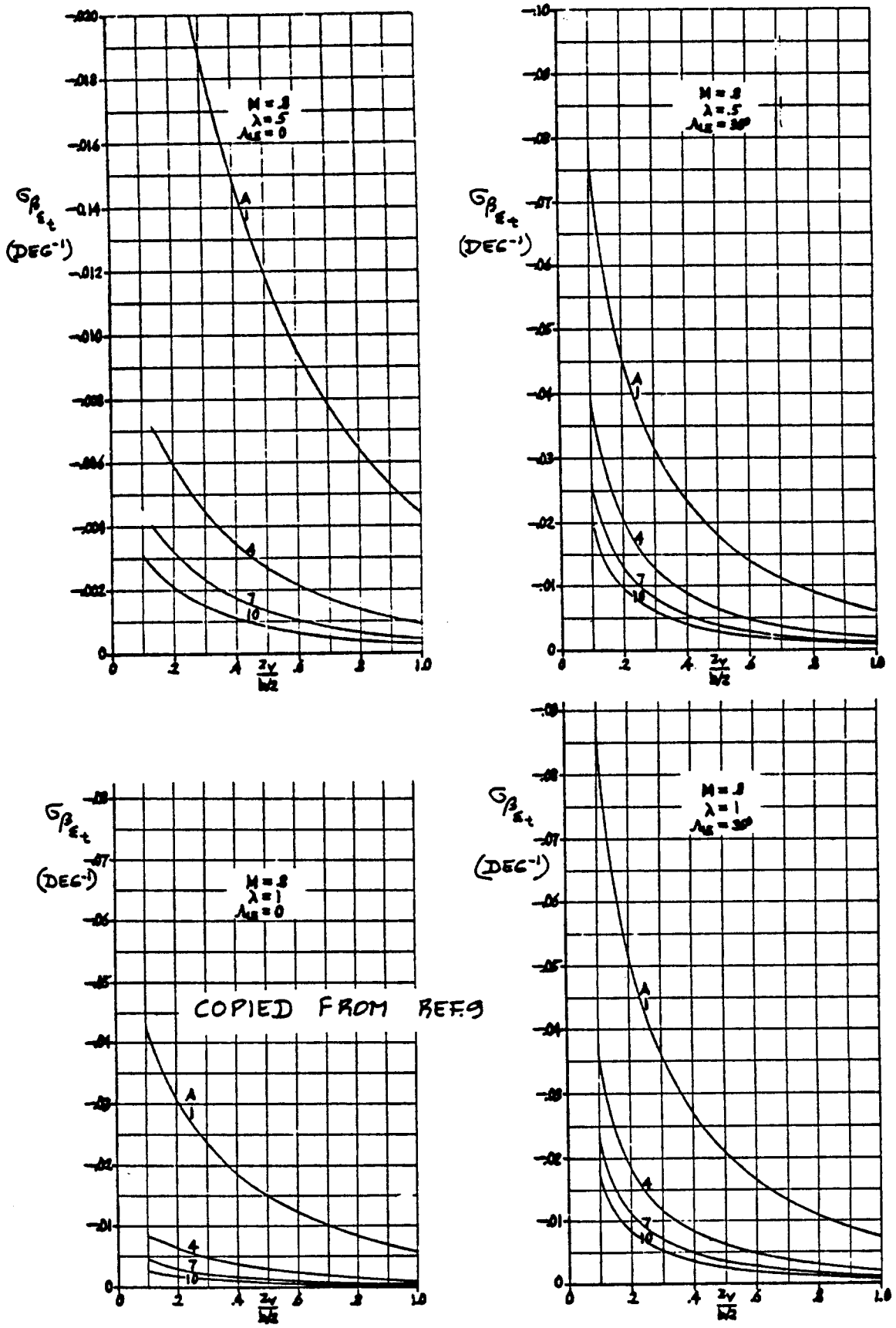

Figure 10.32d Sidewash Contribution due to Wing Twist

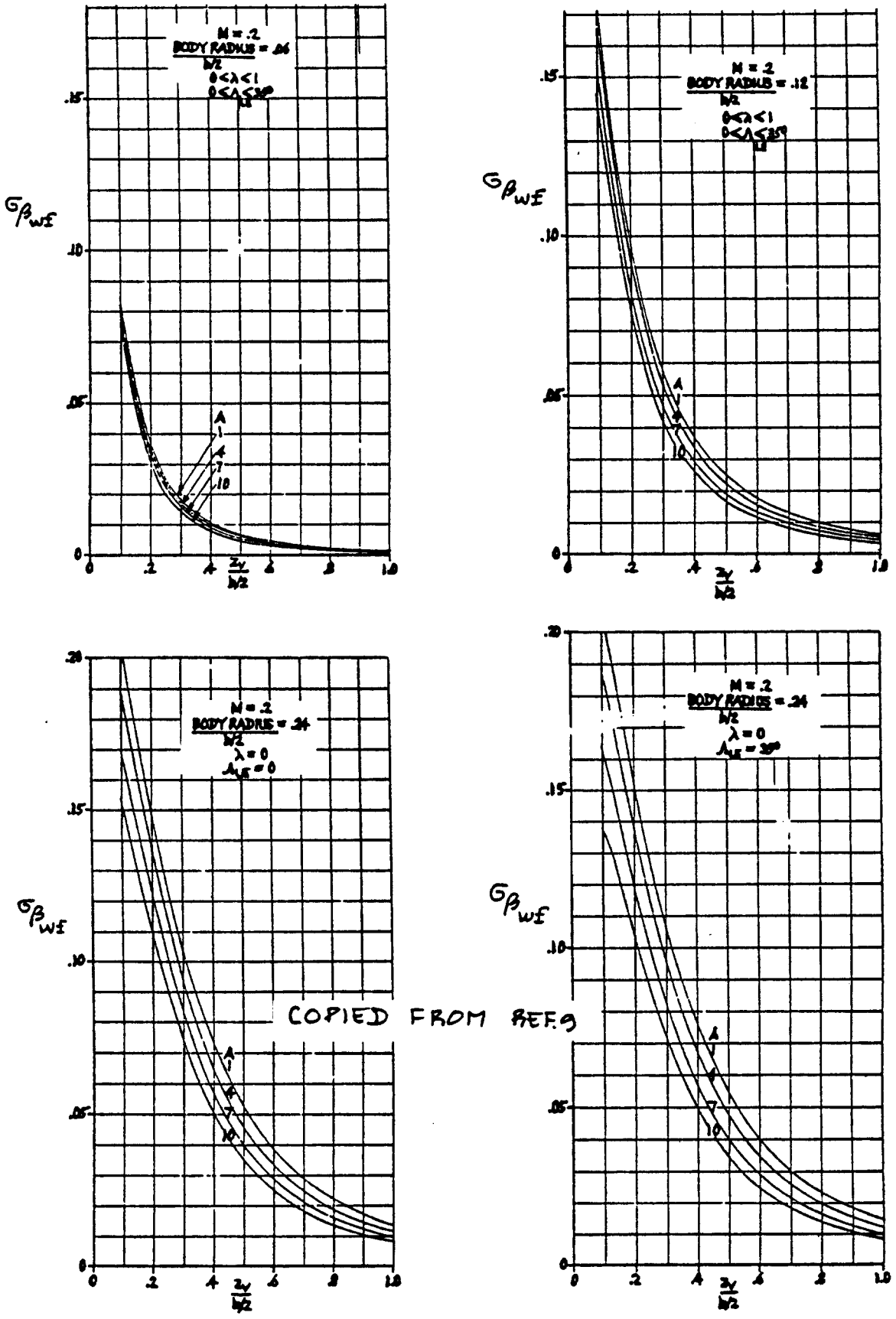

COPIED FROM REF.9

Figure 10.33a Sidewash Contribution due to the Fuselage

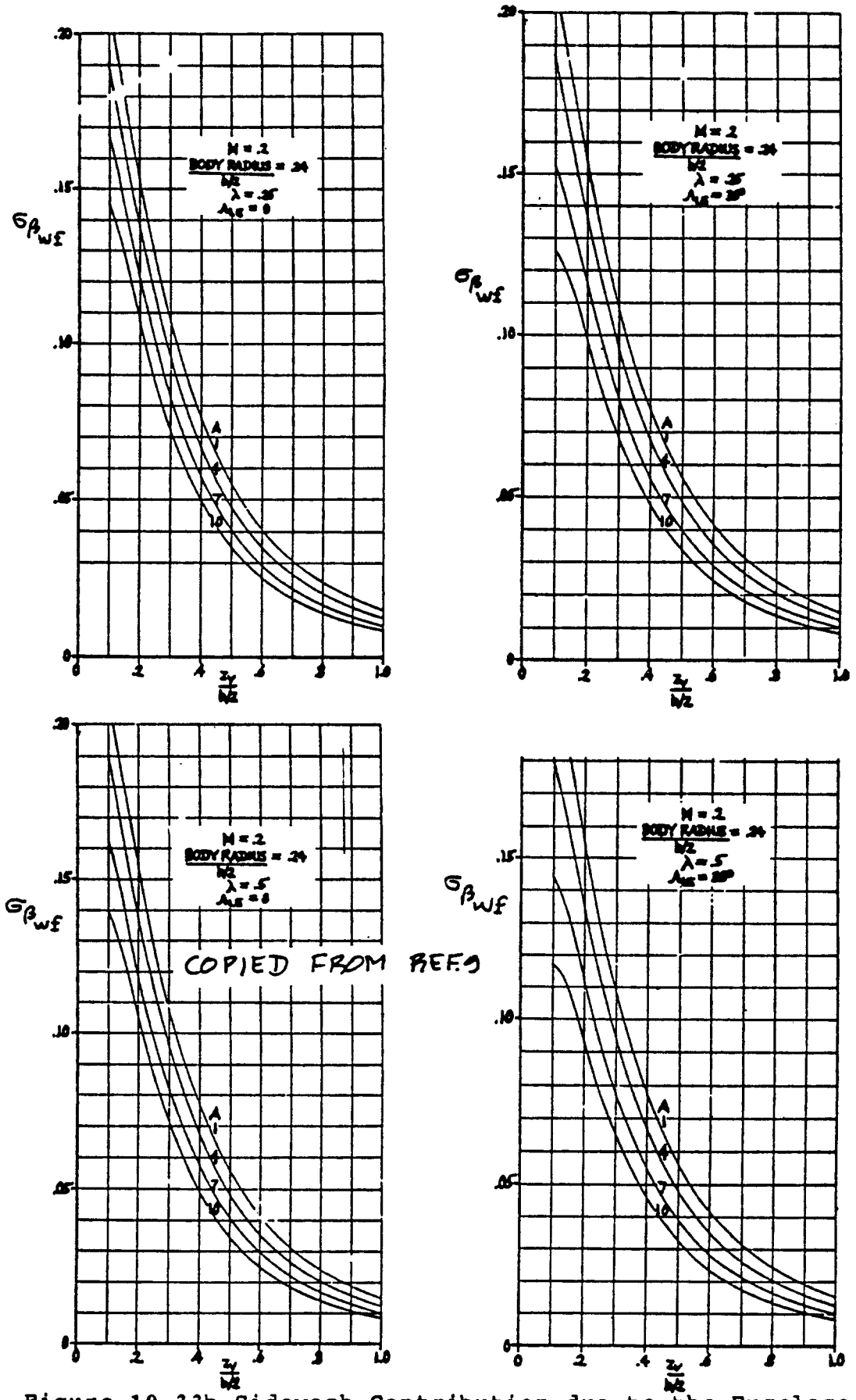

Figure 10.33b Sidewash Contribution due to the Fuselage

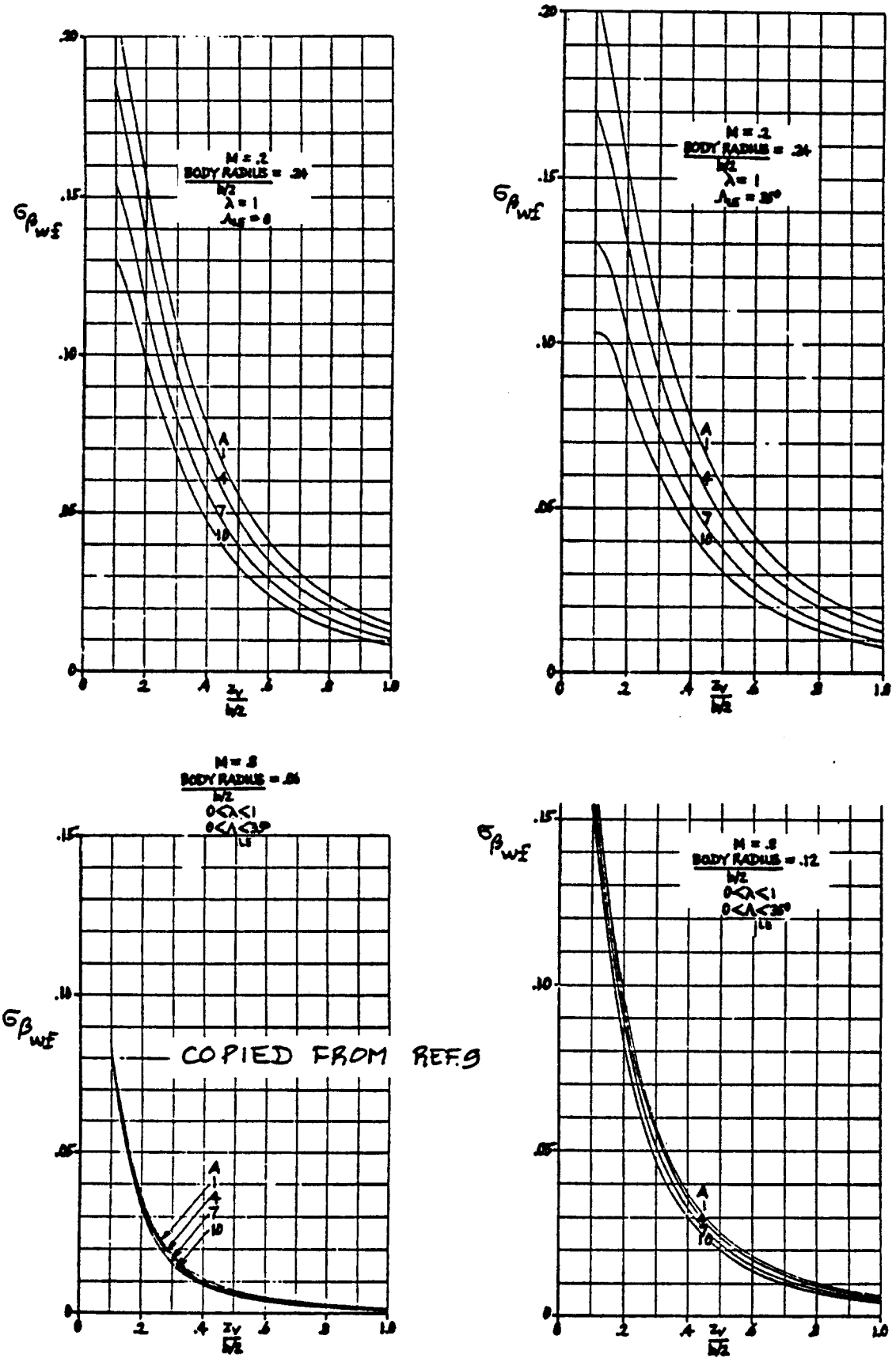

Figure 10.33c Sidewash Contribution due to the Fuselage

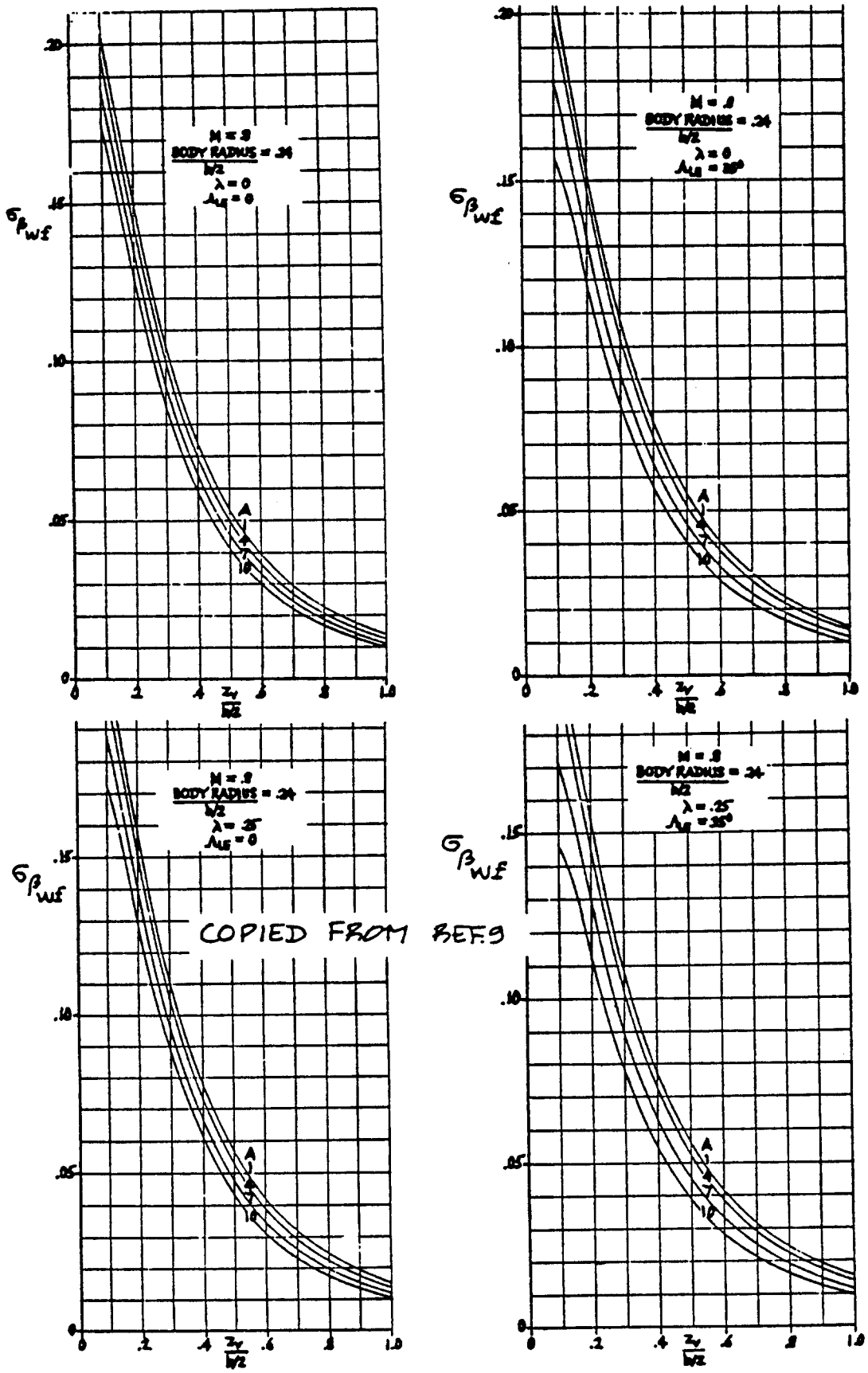

Figure 10.33d Sidewash Contribution due to the Fuselage

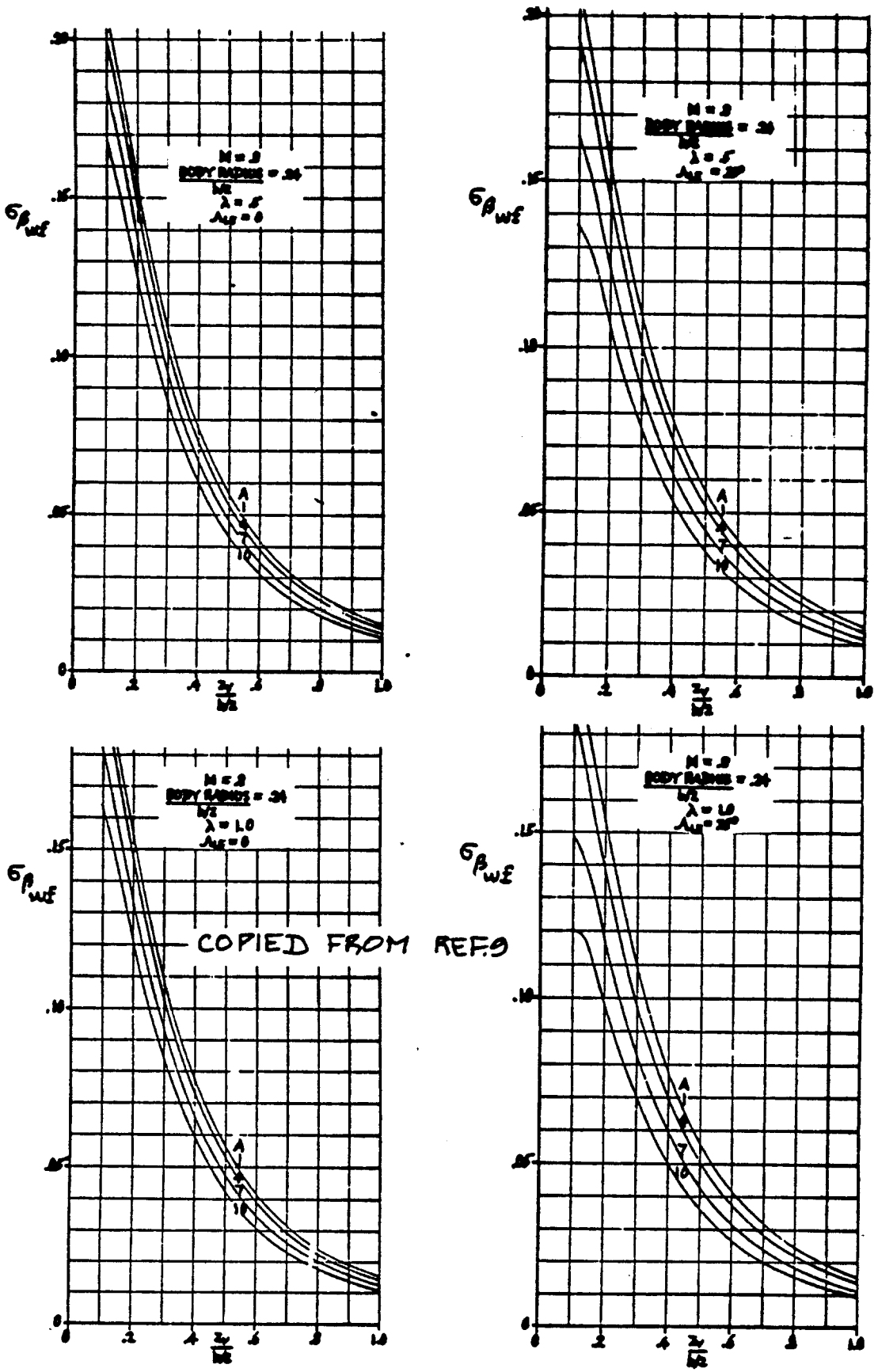

Figure 10.33e Sidewash Contribution due to the Fuselage

obtained from Figures 10.33. Note that the data are presented for a low wing as shown in Figure 10.9a. For a high wing (Fig.10.9b) this term becomes negative because z_w changes sign.

z_p and l_p are defined in Figure 10.34.

2.) $C_{l_{\dot{\beta}}}$

The rolling-moment-due-to-rate-of-sideslip derivative, $C_{l_{\dot{\beta}}}$ may be estimated from:

$$C_{l_{\dot{\beta}}} = C_{y_{\dot{\beta}}}(z_p \cos\alpha_f - l_p \sin\alpha_f)/b \qquad (10.48)$$

where: $C_{y_{\dot{\beta}}}$ is found from Eqn.(10.46)

3.) $C_{n_{\dot{\beta}}}$

The yawing-moment-due-to-rate-of-sideslip derivative, $C_{n_{\dot{\beta}}}$ may be estimated from:

$$C_{n_{\dot{\beta}}} = C_{y_{\dot{\beta}}}(l_p \cos\alpha_f + z_p \sin\alpha_f)/b \qquad (10.49)$$

where: $C_{y_{\dot{\beta}}}$ is found from Eqn.(10.46)

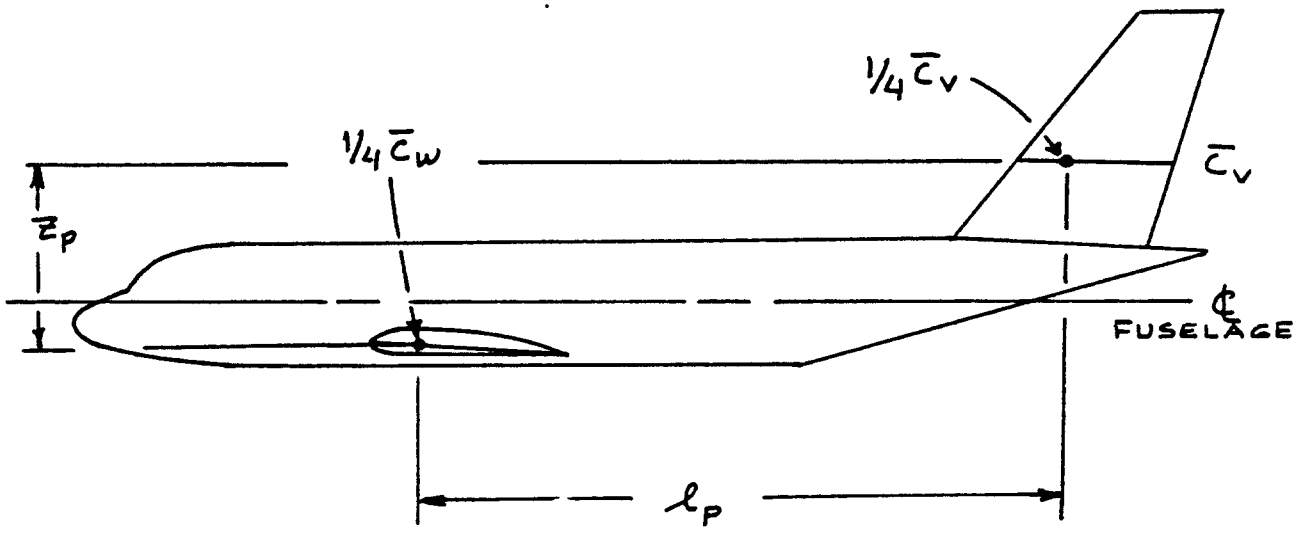

Figure 10.34 Definition of z_p and l_p in Eqn.(10.46)

10.2.6 Roll Rate Derivatives: C_{y_p}, C_{l_p} and C_{n_p}

Table 10.1 identifies the required roll rate derivatives.

NOTE: All methods presented for estimation of the roll rate derivatives apply only in the subsonic speed range. For other speed ranges Ref.9 should be used.

1.) C_{y_p}

The side-force-due-to-roll-rate derivative, C_{y_p} is primarily influenced by the vertical tail and may be determined from:

$$C_{y_p} = 2(C_{y_{\beta_v}})(z_v\cos\alpha - l_v\sin\alpha)/b \qquad (10.50)$$

where: $C_{y_{\beta_v}}$ is found from Eqns (10.28) or (10.32).

z_v and l_v are defined in Figure 10.27.

2.) C_{l_p}

The rolling-moment-due-to-roll-rate derivative, C_{l_p} (also called the roll damping derivative) may be found from:

$$C_{l_p} = C_{l_{p_w}} + C_{l_{p_h}} + C_{l_{p_v}} \qquad (10.51)$$

where: the wing contribution is given by:

$$C_{l_{p_w}} = (\beta C_{l_p}/k)_{C_L=0}(k/\beta) * \qquad (10.52)$$

$$* \{(C_{L_{\alpha_w}})_{C_L}/(C_{L_{\alpha_w}})_{C_L=0}\} * \{(C_{l_p})_{\Gamma}/(C_{l_p})_{\Gamma=0}\} + (\Delta C_{l_p})_{drag}$$

where: $(\beta C_{l_p}/k)_{C_L=0}$ is the roll damping parameter at zero lift which is obtained from Figures 10.35

Note: the parameter β in Eqn.(10.52) is NOT sideslip! In this case:

$$\beta = (1 - M^2)^{1/2} \qquad (10.53)$$

β : EQN. (10.53)

K : EQN. (10.54)

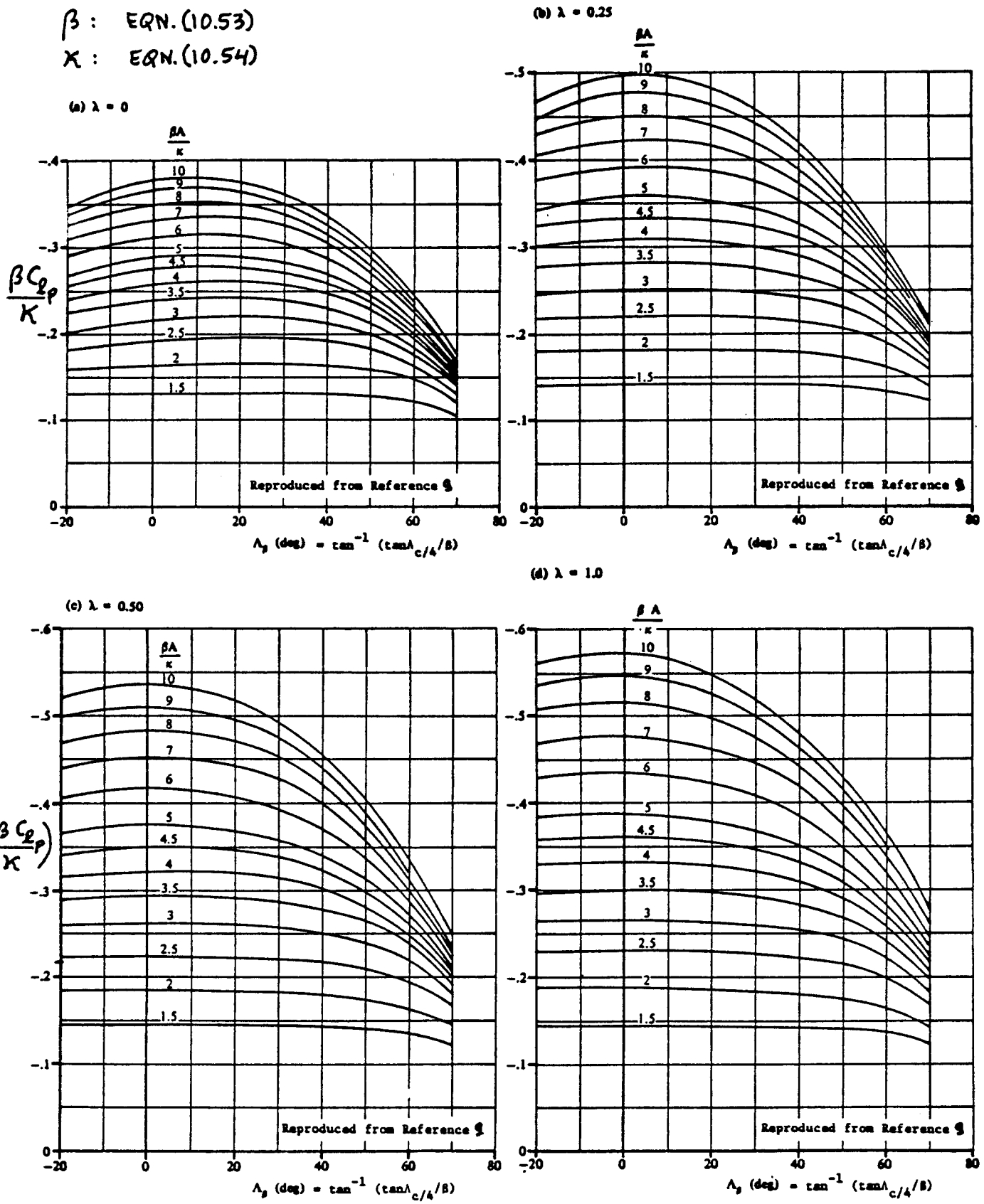

Figure 10.35 Roll Damping Parameter

$$k = (C_{l_\alpha})_M \beta/2\pi \qquad (10.54)$$

$(C_{L_{\alpha_w}})_{C_L=0}$ is the wing lift-curve slope at zero lift as obtained from Equation (8.22).

$(C_{L_\alpha})_{C_L}$ is the wing lift-curve slope at any lift coefficient. It is obtained as the local slope of the wing C_L versus α curve as obtained from 8.1.3.5 or from 8.1.4.4.

$\{(C_{l_p})_\Gamma/(C_{l_p})_{\Gamma=0}\}$ is the dihedral effect parameter which may be obtained from:

$$\{(C_{l_p})_\Gamma/(C_{l_p})_{\Gamma=0}\} =$$

$$\{1 - 4z_w/b\sin\Gamma + 12(z_w/b)^2(\sin\Gamma)^2 \qquad (10.55)$$

with: Γ defined in Figure 10.7

z_w defined in Figure 10.9

The wing drag contribution to roll damping is given by:

$$(\Delta C_{l_p})_{drag} = \qquad (10.56)$$

$$\{(C_{l_p})_{C_{D_L}}/(C_{L_w})^2\}(C_{L_w})^2 - 0.125C_{D_{o_w}}$$

with: $\{(C_{l_p})_{C_{D_L}}/(C_L)^2\}$, the drag-due-to-lift roll damping parameter as found from Figure 10.36

C_{L_w} is the wing lift coefficient as obtained from:

$$C_{L_w} = C_{L_1} - C_{L_h} - C_{L_c} \qquad (10.57)$$

In preliminary design it is acceptable to set:

$$C_{L_1} = C_{L_w} \qquad (10.58)$$

$C_{D_{o_w}}$ is the wing zero-lift drag coefficient as obtained from Chapter 4.

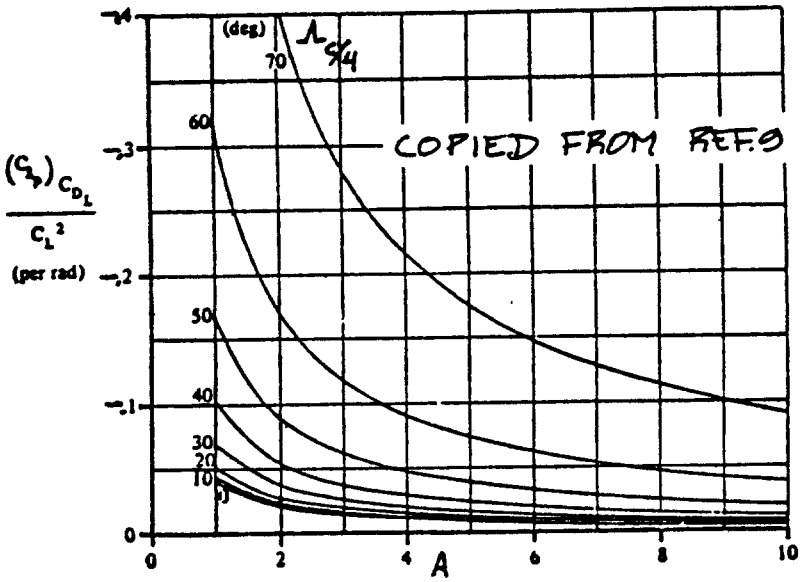

Figure 10.36 Drag-due-to-lift Roll Damping Parameter

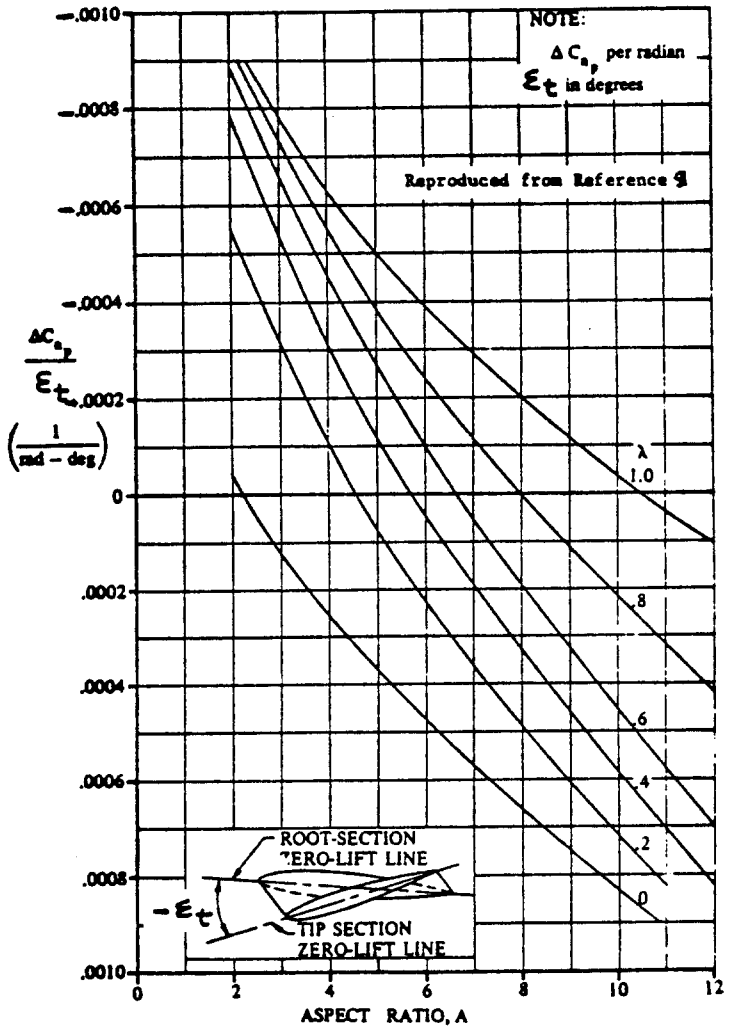

Figure 10.37 Effect of Wing Twist on C_{n_p}

The fuselage contribution to C_{l_p} tends to be negligible for airplanes for which $d_f/b<0.3$. Most airplane configurations satisfy this criterion.

the horizontal tail contribution is given by:

$$C_{l_{p_h}} = 0.5(C_{l_p})_h(S_h/S)(b_h/b)^2 \qquad (10.59)$$

where: $(C_{l_p})_h$ is the roll-damping derivative of the horizontal tail based on its own reference geometry. It is obtained from Eqn. (10.52) with appropriate substitution of horizontal tail parameters for wing parameters.

the vertical tail contribution is given by:

$$C_{l_{p_v}} = 2(z_v/b)^2 C_{y_{\beta_v}} \qquad (10.60)$$

where: z_v is defined in Figure 10.27

$C_{y_{\beta_v}}$ is found from Eqn. (10.28) or from Eqn. (10.32)

3.) C_{n_p}

The yawing-moment-due-to-roll-rate derivative, C_{n_p} may be determined from:

$$C_{n_p} = C_{n_{p_w}} + C_{n_{p_v}} \qquad (10.61)$$

where: the wing contribution is given by:

$$C_{n_{p_w}} = -\{(C_{n_p}/C_L)_{\substack{C_L=0 \\ M}}\}C_L + (C_{n_p}/\varepsilon_t)\varepsilon_t + \{(\Delta C_{n_p}/\alpha_{\delta_f})(\delta_f)\}(\alpha_{\delta_f})\delta_f \qquad (10.62)$$

with:

$$\left(\frac{C_{n_p}}{C_L}\right)_{\substack{C_L=0 \\ M}} = \left(\frac{A+4\cos\Lambda_{c/4}}{AB+4\cos\Lambda_{c/4}}\right)\left[\frac{AB+\frac{1}{2}(AB+\cos\Lambda_{c/4})\tan^2\Lambda_{c/4}}{A+\frac{1}{2}(A+\cos\Lambda_{c/4})\tan^2\Lambda_{c/4}}\right]\left(\frac{C_{n_p}}{C_L}\right)_{\substack{C_L=0 \\ M=0}} \qquad (10.63)$$

where: $B = \{1 - M^2(\cos\Lambda_{c/4})^2\}^{1/2}$ (10.64)

and with:

$$\left(\frac{C_{n_p}}{C_L}\right)_{\substack{C_L=0 \\ M=0}} = -\frac{1}{6}\,\frac{A+6(A+\cos\Lambda_{c/4})\left(\frac{\bar{x}}{c}\,\frac{\tan\Lambda_{c/4}}{A} + \frac{\tan^2\Lambda_{c/4}}{12}\right)}{A+4\cos\Lambda_{c/4}} \quad (\text{rad}^{-1}) \qquad (10.65)$$

C_{n_p}/ε_t is the wing twist contribution as given by Figures 10.37.

ε_t is the wing twist angle defined in Fig.10.37.

$(\Delta C_{n_p}/\alpha_{\delta_f}\delta_f)$ is the contribution due to symmetrical flap deflection as found from Figures 10.38.

$$\alpha_{\delta_f} = \Delta c_l / c_{l_\alpha}\,\delta_f \qquad (10.66)$$

with: Δc_l determined from 8.1.2.1 for the type of flap used

c_{l_α} is the airfoil (flaps-up) lift-curve-slope as found from 8.1.1.2

δ_f is the flap deflection employed

<u>the vertical tail contribution</u> is given by:

$$C_{n_{p_v}} = \qquad (10.67)$$

$$-(2/b^2)(l_v\cos\alpha + z_v\sin\alpha)(z_v\cos\alpha - l_v\sin\alpha - z_v)C_{y_{\beta_v}}$$

where: z_v and l_v are defined in Figure 10.27

$C_{y_{\beta_v}}$ is found from Eqns (10.28) or (10.32)

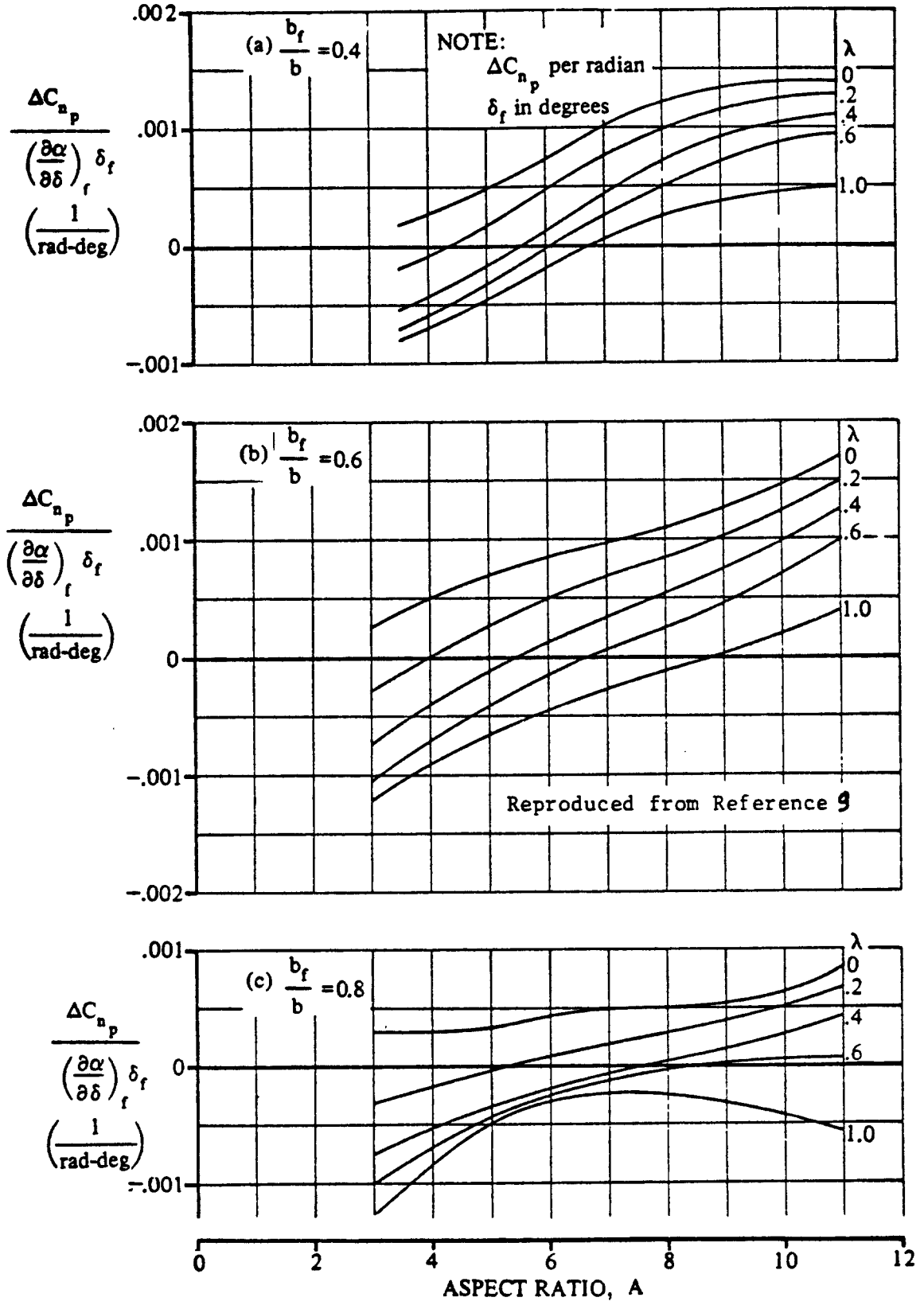

Figure 10.38 Effect of Symmetrical Flap Deflection on C_{n_p}

10.2.7 Pitch Rate Derivatives: C_{D_q}, C_{L_q} and C_{m_q}

Table 10.1 identifies the required pitch rate derivatives.

NOTE: All methods presented for the pitch rate derivatives are valid only for the subsonic speed regime. For other speed ranges the reader should consult Ref.9.

1.) C_{D_q}

The drag-due-to-pitch-rate derivative, C_{D_q} is negligible for almost all airplanes:

$$C_{D_q} = 0 \qquad (10.68)$$

2.) C_{L_q}

The lift-due-to-pitch-rate derivative, C_{L_q} may be estimated from:

$$C_{L_q} = C_{L_{q_w}} + C_{L_{q_h}} + C_{L_{q_c}} \qquad (10.69)$$

where: the wing contribution is given by:

$$C_{L_{q_w}} = \qquad (10.70)$$

$$\{(A + 2\cos\Lambda_{c/4})/(AB + 2\cos\Lambda_{c/4})\}(C_{L_{q_w}})_{M=0}$$

where: B is given by Eqn.(10.64)

$$(C_{L_{q_w}})_{M=0} = (0.5 + 2x_w/\bar{c})c_{l_{\alpha_w}} \qquad (10.71)$$

with: x_w defined in Figure 10.39

$c_{l_{\alpha_w}}$ is the average wing airfoil lift-curve-slope. The wing airfoil lift curve slope at the $\bar{c}$ may be used.

the horizontal tail contribution is given by:

$$C_{L_{q_h}} = 2(C_{L_{\alpha_h}})\eta_h \bar{V}_h \qquad (10.72)$$

where: $C_{L_{\alpha_h}}$ is found from Eqn.(8.22) with appropriate substitution of horizontal tail parameters for wing parameters.

η_h is found from 8.1.5.2

$\bar{V}_h$ is found from Eqn.(10.23)

the canard contribution is found from:

$$C_{L_{q_c}} = -2(C_{L_{\alpha_c}})\eta_c \bar{V}_c \qquad (10.73)$$

where: $C_{L_{\alpha_c}}$ is found from Eqn.(8.22) with appropriate substitution of canard parameters for wing parameters.

η_c is found from 8.1.5.2

$$\bar{V}_c = (\bar{x}_{ac_c} + \bar{x}_{cg})S_c/S \qquad (10.74)$$

where: x_{ac_c} and x_{cg} are shown in Fig.10.39. Note that x_{ac_c} is positive, while x_{cg} is negative as shown!!!

3.) C_{m_q}

The pitching-moment-due-to-pitch-rate derivative, C_{m_q} (also called pitch damping derivative) may be estimated from:

$$C_{m_q} = C_{m_{q_w}} + C_{m_{q_h}} + C_{m_{q_c}} \qquad (10.75)$$

where: the wing contribution is found from:

$$C_{m_{q_w}} = \qquad (10.76)$$

with:

$$(C_{m_{q_w}})_{M=0} = \qquad (10.77)$$

where: K_w is found from Figure 10.40.

the horizontal tail contribution is given by:

$$C_{m_{q_h}} = -2(C_{L_{\alpha_h}})\eta_h \bar{V}_h (\bar{x}_{ac_h} - \bar{x}_{cg}) \qquad (10.78)$$

where: x_{ac_h} is defined in Figure 10.40

All other quantities were defined before!

the canard contribution is given by:

$$C_{m_{q_c}} = -2(C_{L_{\alpha_c}})\eta_c \bar{V}_c (\bar{x}_{ac_c} + \bar{x}_{cg}) \qquad (10.79)$$

where: all quantities have been defined before!

NOTE: many airplanes have pylon mounted nacelles. These pylons contribute to the pitch rate derivatives in the same manner as any empennage surface.

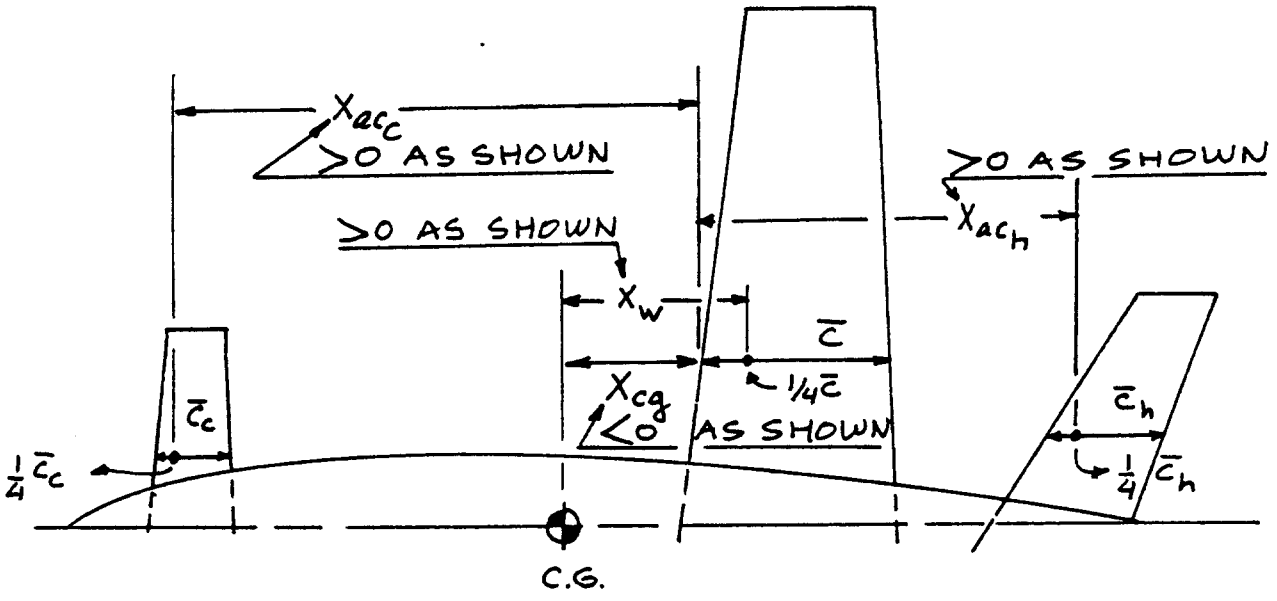

Figure 10.39 Definition of Geometric Parameters

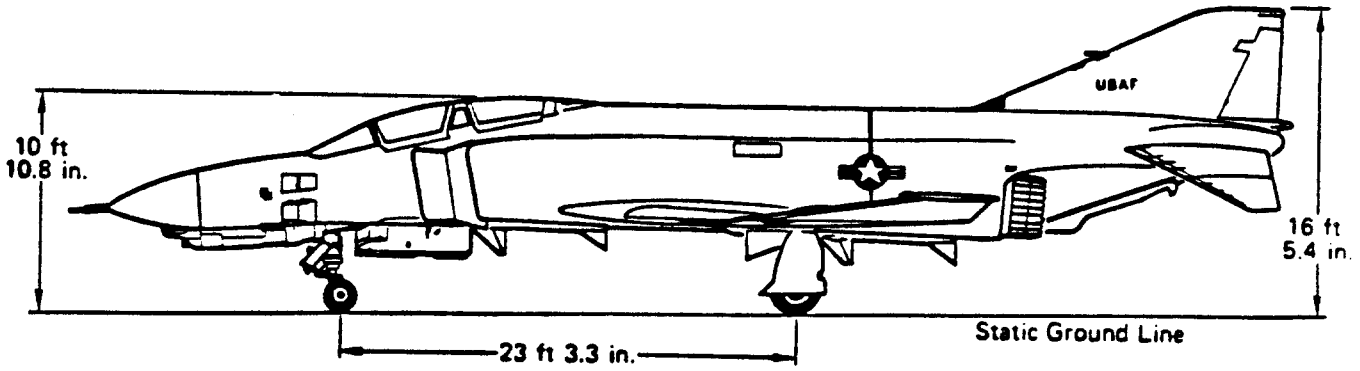

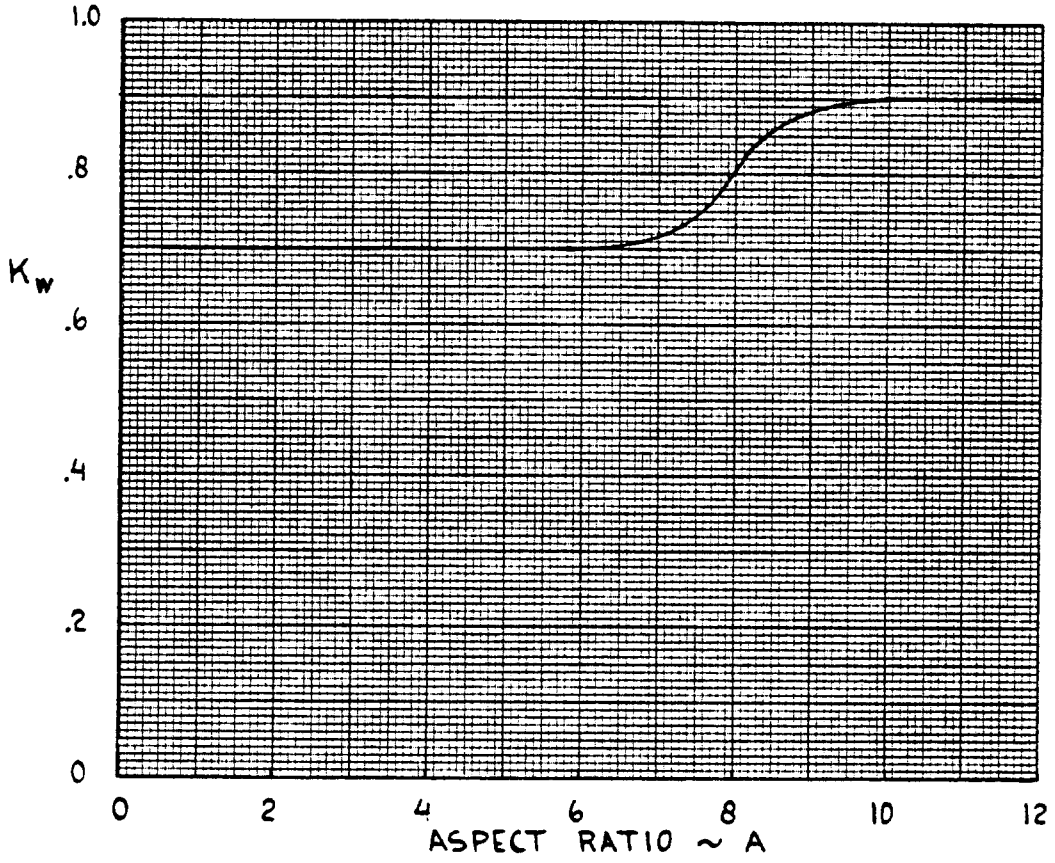

Figure 10.40 Correction Constant for Wing Contribution to Pitch Damping

10.2.8 Yaw Rate Derivatives: C_{y_r}, C_{l_r} and C_{n_r}

Table 10.1 identifies the required yaw rate derivatives.

NOTE: All methods presented for the yaw rate derivatives are valid only for the subsonic speed regime. For other speed ranges the reader should consult Ref.9.

1.) C_{y_r}

The side-force-due-to-yaw-rate derivative, C_{y_r} is primarily influenced by the vertical tail and may be determined from:

$$C_{y_r} = -2(C_{y_{\beta_v}})(l_v \cos\alpha + z_v \sin\alpha)/b \qquad (10.80)$$

where: $C_{y_{\beta_v}}$ is found from Eqns (10.28) or (10.32).

l_v and z_v are defined in Figure 10.27.

2.) C_{l_r}

The rolling-moment-due-to-yaw-rate derivative, C_{l_r} may be estimated from:

$$C_{l_r} = C_{l_{r_w}} + C_{l_{r_v}} \qquad (10.81)$$

where: the wing contribution is found from:

$$C_{l_{r_w}} = (C_{L_w})(C_{l_r}/C_L)_{\substack{C_L=0 \\ M}} + (\Delta C_{l_r}/\Gamma)\Gamma +$$

$$+ (\Delta C_{l_r}/\varepsilon_t)\varepsilon_t + (\Delta C_{l_r}/\alpha_{\delta_f})(\alpha_{\delta_f})\delta_f \qquad (10.82)$$

where: $(C_{l_r})_{\substack{C_L=0 \\ M}}$, the slope of the rolling moment due to roll rate at zero lift is found from:

$$\left(\frac{C_{\ell_r}}{C_L}\right)_{\substack{C_L=0 \\ M}} = \frac{1 + \frac{A(1-B^2)}{2B(AB+2\cos\Lambda_{c/4})} + \frac{AB+2\cos\Lambda_{c/4}}{AB+4\cos\Lambda_{c/4}} \frac{\tan^2\Lambda_{c/4}}{8}}{1 + \frac{A+2\cos\Lambda_{c/4}}{A+4\cos\Lambda_{c/4}} \frac{\tan^2\Lambda_{c/4}}{8}} \left(\frac{C_{\ell_r}}{C_L}\right)_{\substack{C_L=0 \\ M=0}} \qquad (10.83)$$

with B determined by Eqn.(10.64)

and $(C_{l_r}/C_L)_{C_L=0}$ is the slope of the low-speed rolling moment due to yaw rate at zero lift found from Figure 10.41.
M=0

C_{L_w} is the wing lift coefficient as in Eqn.(10.57) or (10.58)

$$(\Delta C_{l_r}/\Gamma) = 0.083(\pi A \sin\Lambda_{c/4})/(A + 4\cos\Lambda_{c/4}) \quad (10.84)$$

Γ is defined in Figure 10.7

$\Delta C_{l_r}/\varepsilon_t$ is the increment in C_{l_r} due to twist and may be determined from Figure 10.42

ε_t is the wing twist angle defined in Figure 10.42

$\Delta C_{l_r}/\alpha_{\delta_f}\delta_f$ is the effect of symmetric flap deflection on the rolling moment due to roll rate and is found from Figure 10.43.

α_{δ_f} is found from Eqn.(10.66)

δ_f is the flap deflection used

<u>the vertical tail contribution is found from:</u>

$$C_{l_{r_v}} = \quad (10.85)$$

$$-(2/b^2)(l_v\cos\alpha + z_v\sin\alpha)(z_v\cos\alpha - l_v\sin\alpha)C_{Y_{\beta_v}}$$

where: z_v and l_v are defined in Figure 10.27

$C_{Y_{\beta_v}}$ is found from Eqn.(10.28) or (10.32)

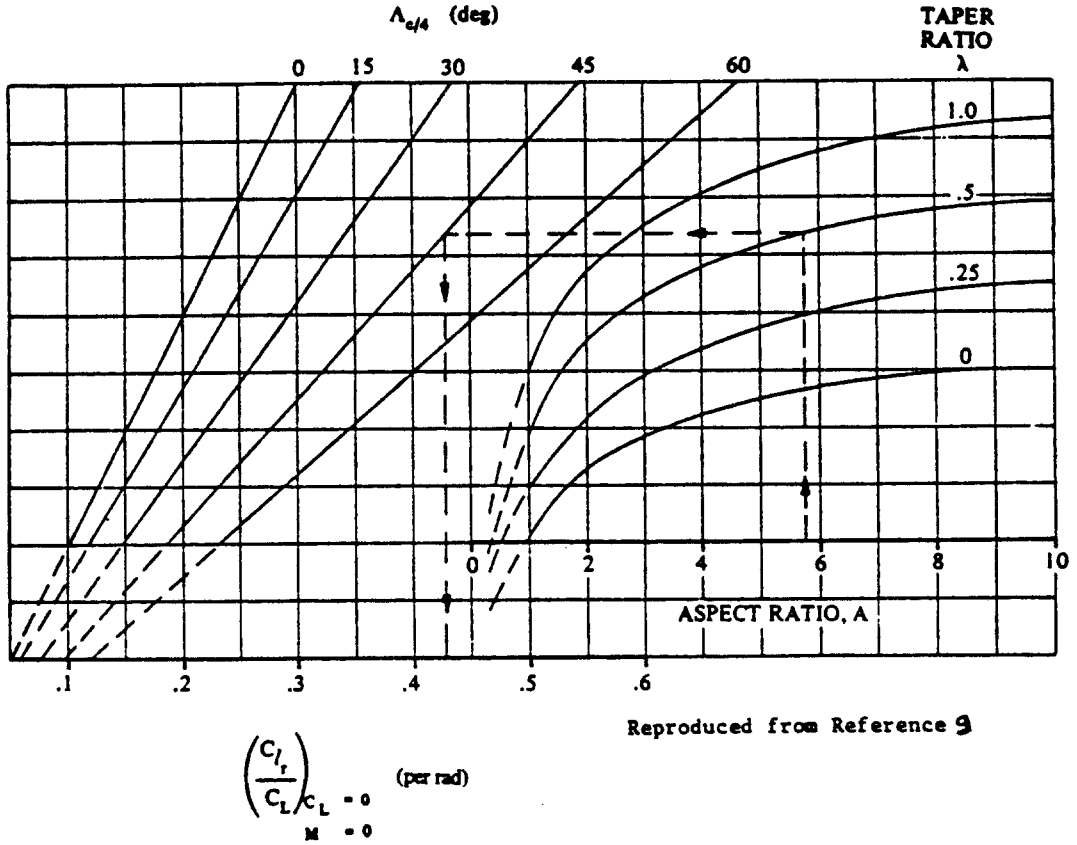

Figure 10.41 Wing Rolling Moment due to Yaw Rate Derivative: Lifting Effect

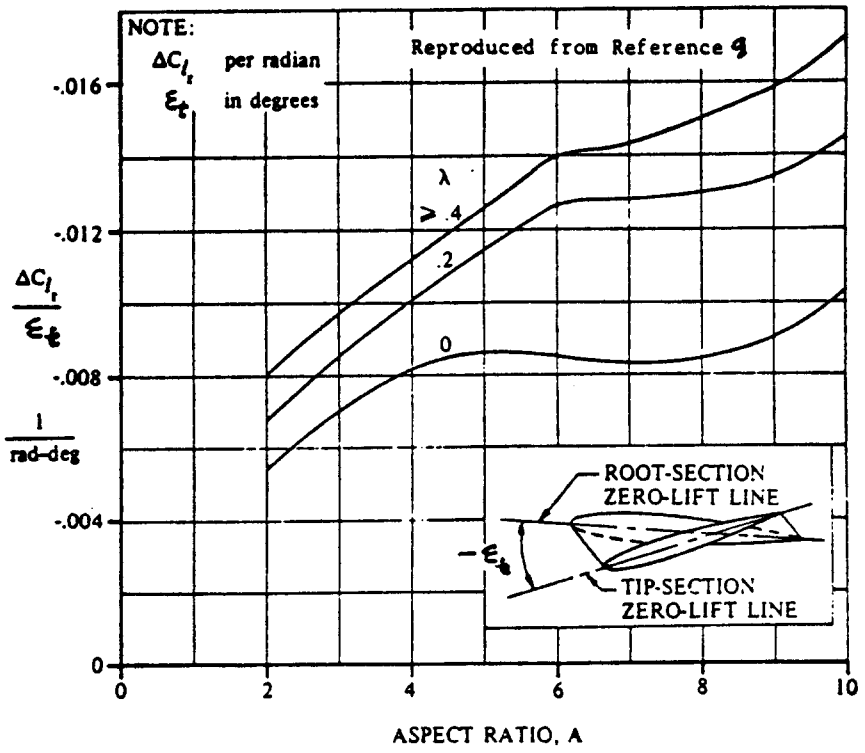

Figure 10.42 Effect of Wing Twist on C_{l_r}

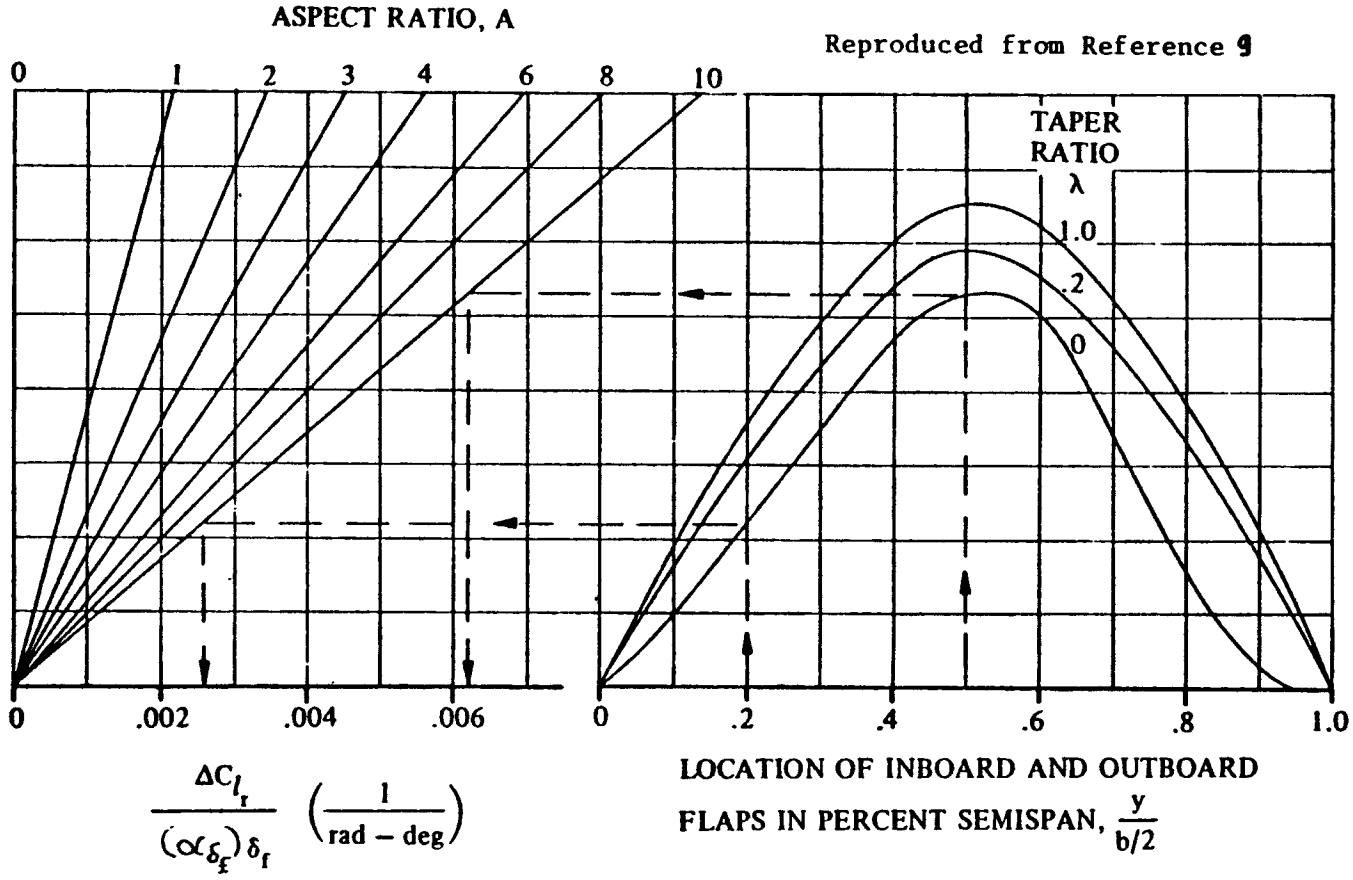

NOTE:

ΔC_{l_r} per radian

δ_f in degrees

NOTE: $\dfrac{\Delta C_{l_r}}{(\alpha_{\delta_f})\,\delta_f} = \left[\dfrac{\Delta C_{l_r}}{(\alpha_{\delta_f})\,\delta_f}\right]_{\text{outboard}} - \left[\dfrac{\Delta C_{l_r}}{(\alpha_{\delta_f})\,\delta_f}\right]_{\text{inboard}}$

Figure 10.43 Effect of Symmetric Flap Deflection on C_{l_r}

3.) C_{n_r}

The yawing-moment-due-to-yaw-rate derivative, C_{n_r} (also called yaw-damping derivative) follows from:

$$C_{n_r} = C_{n_{r_w}} + C_{n_{r_v}} \qquad (10.86)$$

where: <u>the wing contribution is found from:</u>

$$C_{n_{r_w}} = \qquad (10.87)$$

$$(C_{n_r}/C_L^2)(C_{L_w})^2 + (C_{n_r}/C_{D_o})C_{D_{o_w}}$$

where: (C_{n_r}/C_L^2) follows from Figure 10.44

C_{L_w} is given by Eqn.(10.57) or (10.58)

(C_{n_r}/C_{D_o}) is found from Figure 10.45

$C_{D_{o_w}}$ is the zero-lift drag coefficient of the wing as found from Chapter 4.

<u>the vertical tail contribution is found from:</u>

$$C_{n_{r_v}} = (2/b^2)(l_v\cos\alpha + z_v\sin\alpha)^2 C_{y_{\beta_v}} \qquad (10.88)$$

where: l_v and z_v are defined in Figure 10.27

$C_{y_{\beta_v}}$ is found from Eqnn.(10.20) or (10.32)

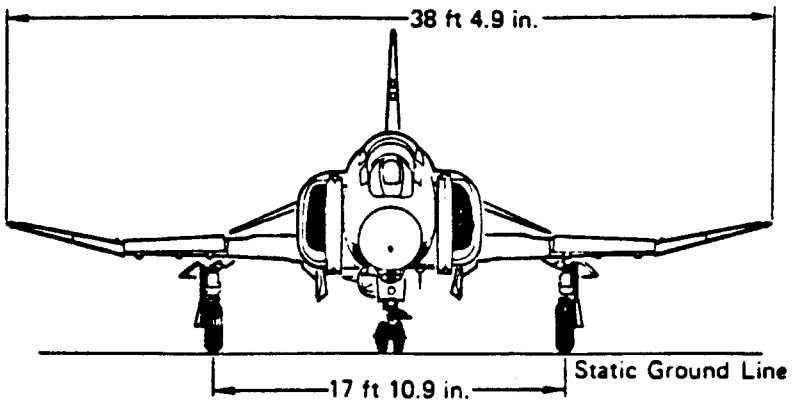

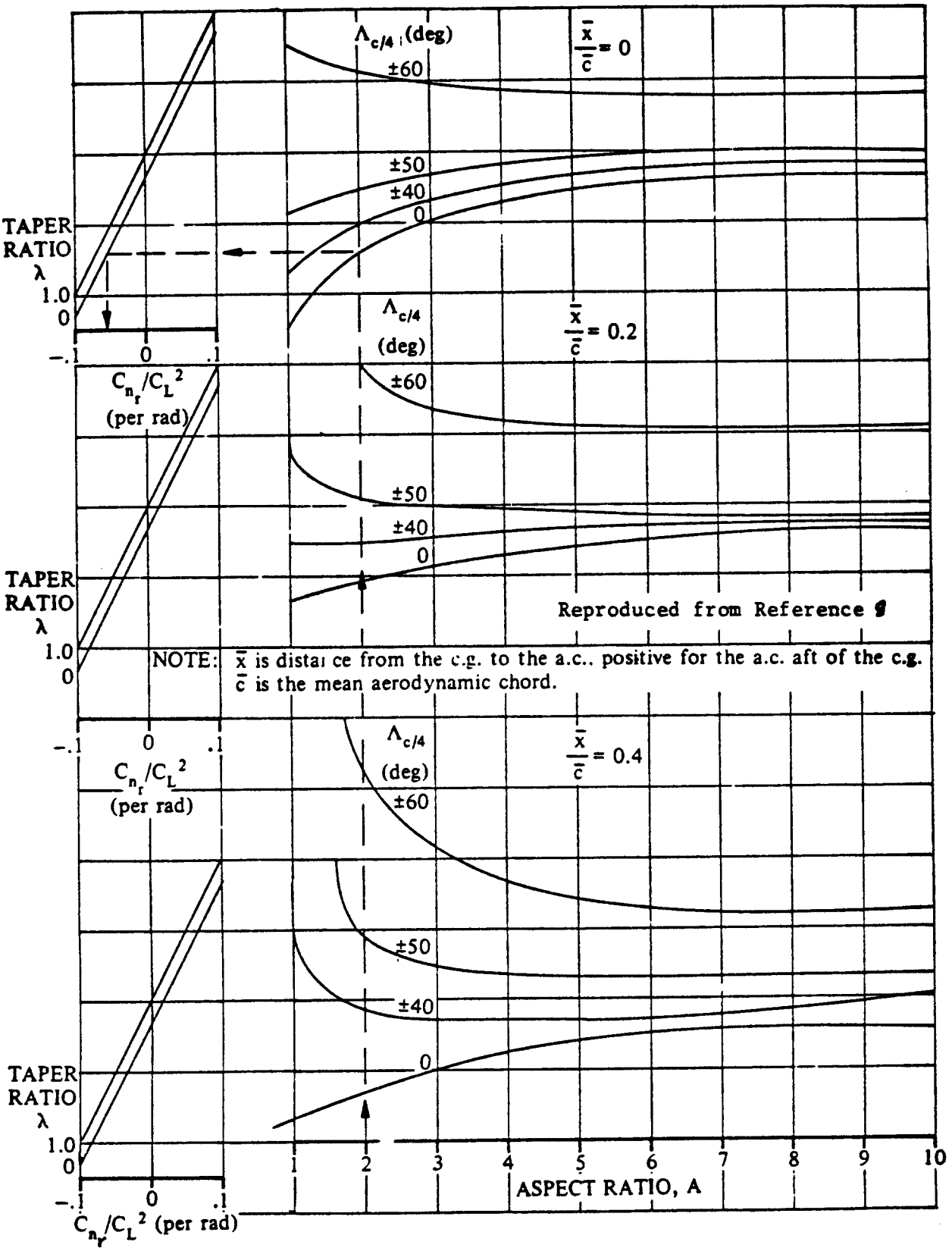

Figure 10.44 Wing Yaw Damping Derivative: Lifting Effect

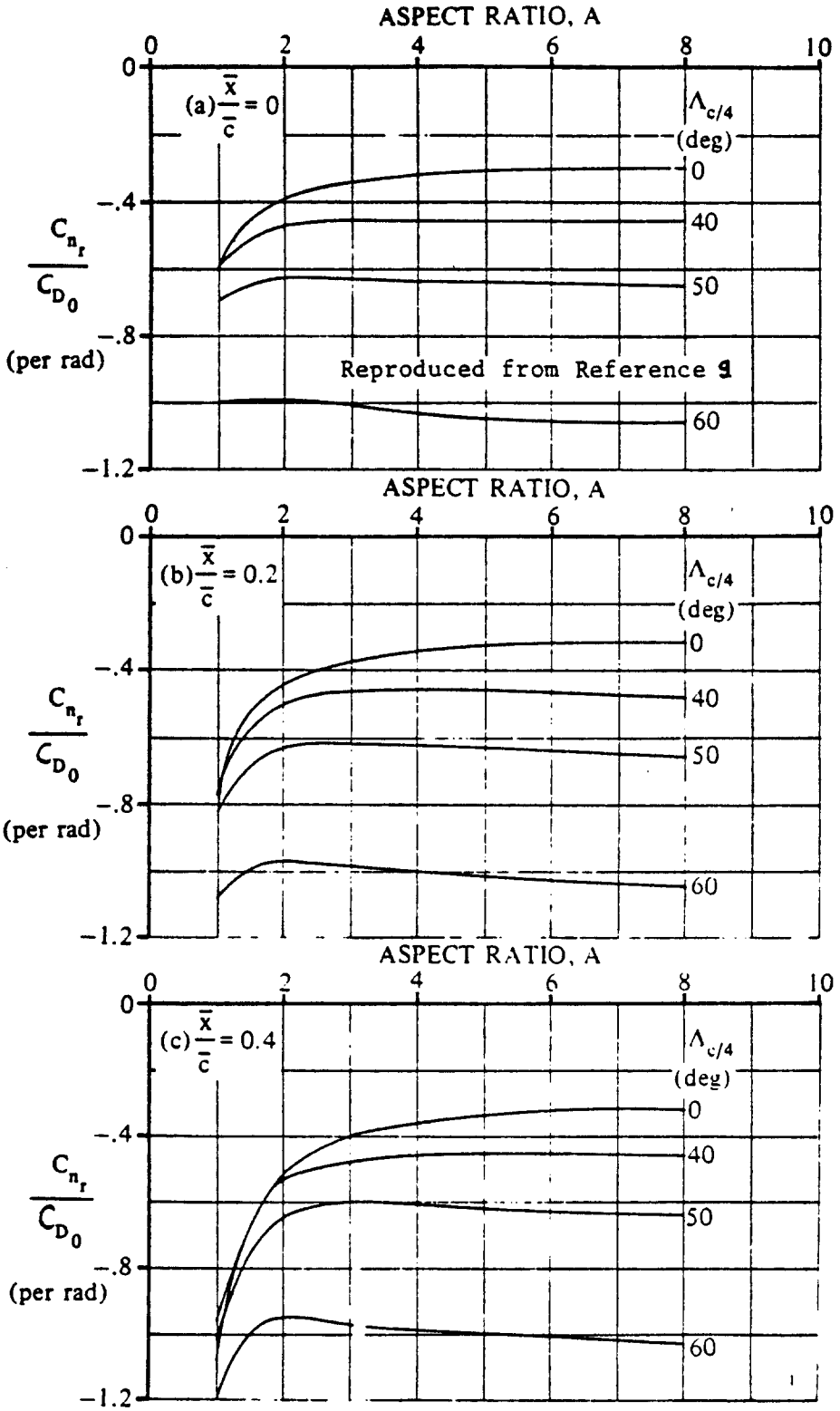

NOTE: $\bar{x}$ is the distance from the c.g. to the a.c., positive for the a.c. aft of the c.g.
$\bar{c}$ is the wing mean aerodynamic chord.

Figure 10.45 Wing Yaw Damping Derivative: Drag Effect

10.3 CONTROL DERIVATIVES

In Table 10.1 the following control derivatives are identified: elevator, aileron and rudder. Because in most airplanes the horizontal stabilizer itself is used as a control device, its derivatives must also be considered. In addition, many recent fighter airplanes and several small commercial airplanes sprout canards, with or without a separate control surface. Many airplanes use spoilers and differential stabilizers as well as ailerons for lateral control.

For these reasons, the following control (power) derivatives are considered in this Section:

10.3.1 Stabilizer Control Derivatives
10.3.2 Elevator Control Derivatives
10.3.3 Canard Control Derivatives
10.3.4 Canardvator Control Derivatives
10.3.5 Aileron Control Derivatives
10.3.6 Spoiler Control Derivatives
10.3.7 Differential Stabilizer Control Derivatives
10.3.8 Rudder Control Derivatives

The methods presented in this section apply only to the subsonic speed regime. For other speed regimes Ref.9 should be consulted.

10.3.1 Stabilizer Control Derivatives: $C_{D_{i_h}}$, $C_{L_{i_h}}$ and $C_{m_{i_h}}$

For a discussion of preliminary sizing of the horizontal stabilizer the reader is referred to Chapters 8 and 11 of Part II.

The methods to be presented apply to cases where the ratio of stabilizer span to local fuselage width is larger than 4.0.

1.) $C_{D_{i_h}}$

The drag-due-to-stabilizer-incidence derivative, $C_{D_{i_h}}$ may be estimated from:

$$C_{D_{i_h}} = 2\{(C_{L_h})/\pi A_h e_h\}(C_{L_{\alpha_h}})\eta_h \qquad (10.89)$$

where: C_{L_h} is the lift coefficient carried by the hori-

zontal stabilizer, based on wing area, S. In preliminary design it is acceptable to set:

$$C_{L_h} = \Delta C_{L_h}, \qquad (10.90)$$

the tail lift increment (based on S) required for trim as defined on p.104. It may be determined with Eqn.(8.119)

A_h is the horizontal tail aspect ratio

e_h is found from p.69.

$C_{L_{\alpha_h}}$ is found from Eqn.(8.22) with appropriate substitution of horizontal tail parameters for wing parameters

η_h is found from p.269 or p.271.

2.) $C_{L_{i_h}}$

The lift-due-to-stabilizer-incidence derivative may be estimated from:

$$C_{L_{i_h}} = \eta_h (S_h/S) C_{L_{\alpha_h}} \qquad (10.91)$$

where: all quantities have been defined before.

3.) $C_{m_{i_h}}$

The pitching-moment-due-to-stabilizer-incidence derivative, $C_{m_{i_h}}$ (also called stabilizer control power) may be found from:

$$C_{m_{i_h}} = -(C_{L_{\alpha_h}}) \eta_h \bar{V}_h \qquad (10.92)$$

where: $\bar{V}_h$ is defined by Eqn.(10.23)

all other quantities were defined before.

10.3.2 Elevator Control Derivatives: $C_{D_{\delta_e}}$, $C_{L_{\delta_e}}$ and $C_{m_{\delta_e}}$

For a discussion of preliminary sizing of the elevator the reader is referred to Chapter 8 of Part II.

Although many airplanes carry approximately full span elevators on the horizontal stabilizer, exceptions do occur. For that reason the elevator should be thought of as a partial span, plain flap.

1.) $C_{D_{\delta_e}}$

The drag-due-to-elevator derivative, $C_{D_{\delta_e}}$ may be estimated from:

$$C_{D_{\delta_e}} = (\alpha_{\delta_e})C_{D_{i_h}} \qquad (10.93)$$

where: $C_{D_{i_h}}$ follows from Eqn. (10.89)

$$(\alpha_{\delta_e}) = \qquad (10.94)$$

$$K_b\{c_{l_\delta}/(c_{l_\delta})_{theory}\}(c_{l_\delta})_{theory}*$$

$$*(k'/c_{l_{\alpha_h}})[\{(\alpha_\delta)_{C_L}\}/\{(\alpha_\delta)_{c_l}\}]$$

where: K_b is the elevator (= plain flap) span factor as obtained from page 259

$\{c_{l_\delta}/(c_{l_\delta})_{theory}\}$ is found from Figure 8.15

$(c_{l_\delta})_{theory}$ is found from Figure 8.14

k' is a correction factor which accounts for nonlinearities at high elevator deflection angles. It is found from Figure 8.13

$[\{(\alpha_\delta)_{C_L}\}/\{(\alpha_\delta)_{c_l}\}]$ is found from Figure 8.53.

Note: in Figs 8.13, 8.14, 8.15 and 8.53 use c_e/c_h for c_f/c

$c_{l_{\alpha_h}}$ is the airfoil lift curve slope of the horizontal stabilizer as obtained from 8.1.1.2.

2.) $C_{L_{\delta_e}}$

The lift-due-to-elevator derivative, $C_{L_{\delta_e}}$ may be found from:

$$C_{L_{\delta_e}} = (\alpha_{\delta_e})C_{L_{i_h}} \qquad (10.95)$$

where: (α_{δ_e}) is found from Eqn.(10.94)

$C_{L_{i_h}}$ is found from Eqn.(10.91)

3.) $C_{m_{\delta_e}}$

The pitching-moment-due-to-elevator derivative, $C_{m_{\delta_e}}$ (also called elevator control power) may be found from:

$$C_{m_{\delta_e}} = (\alpha_{\delta_e})C_{m_{i_h}} \qquad (10.96)$$

where: (α_{δ_e}) is found from Eqn.(10.94)

$C_{m_{i_h}}$ is found from Eqn.(10.92)

10.3.3 Canard Control Derivatives: $C_{D_{i_c}}$, $C_{L_{i_c}}$ and $C_{m_{i_c}}$

For a discussion of preliminary canard sizing the reader is referred to Chapter 11 of Part II.

The methods to be presented apply to cases where the ratio of canard span to local fuselage width is larger than 3.0.

1.) $C_{D_{i_c}}$

The drag-due-to-canard-incidence derivative, $C_{D_{i_c}}$ may be estimated from:

$$C_{D_{i_c}} = 2\{(C_{L_c})/\pi A_c e_c\}(C_{L_{\alpha_c}})\eta_c \qquad (10.97)$$

where: C_{L_c} is the lift coefficient carried by the canard, based on wing area, S. In preliminary design it acceptable to set:

$$C_{L_c} = \Delta C_{L_c}, \qquad (10.98)$$

the canard lift increment (based on S) required for trim as defined on p.104. It may be determined with Eqn.(8.120)

A_c is the canard aspect ratio

e_c is found from p.69.

$C_{L_{\alpha_c}}$ is found from Eqn.(8.22) with appropriate substitution of canard parameters for wing parameters

η_c is found from p.269 or p.271.

2.) $C_{L_{i_c}}$

The lift-due-to-canard-incidence derivative may be estimated from:

$$C_{L_{i_c}} = \eta_c(S_c/S)C_{L_{\alpha_c}} \qquad (10.99)$$

where: all quantities have been defined before.

3.) $C_{m_{i_c}}$

The pitching-moment-due-to-canard-incidence derivative, $C_{m_{i_c}}$ (also called canard control power) may be found from:

$$C_{m_{i_c}} = -(C_{L_{\alpha_c}})\eta_c\bar{V}_c \qquad (10.100)$$

where: $\bar{V}_c$ is defined by Eqn.(10.74)

all other quantities were defined before.

10.3.4 Canardvator Control Derivatives: $C_{D_{\delta_c}}$, $C_{L_{\delta_c}}$ and $C_{m_{\delta_c}}$

Because of a lack of statistical data on canard equipped airplanes, no simple, preliminary design methods are available for the sizing of a canardvator. If the canard is used for trim and control purposes, the trim considerations of Section 8.3 should be used.

Although several canard equipped airplanes carry full span canardvators on the canard, exceptions do occur. For that reason the canardvator should be thought of as a partial span, plain flap.

1.) $C_{D_{\delta_c}}$

The drag-due-to-canardvator derivative, $C_{D_{\delta_c}}$ may be estimated from:

$$C_{D_{\delta_c}} = (\alpha_{\delta_c})C_{D_{i_c}} \qquad (10.101)$$

where: $C_{D_{i_c}}$ follows from Eqn.(10.97)

$$(\alpha_{\delta_c}) = \qquad (10.102)$$

$$K_b\{c_{l_\delta}/(c_{l_\delta})_{theory}\}(c_{l_\delta})_{theory}*$$

$$*(k'/c_{l_{\alpha_h}})[\{(\alpha_\delta)_{C_L}\}/\{(\alpha_\delta)_{c_l}\}]$$

where: K_b is the canardvator (= plain flap) span factor as obtained from page 259

$\{c_{l_\delta}/(c_{l_\delta})_{theory}\}$ is found from Figure 8.15

$(c_{l_\delta})_{theory}$ is found from Figure 8.14

k' is a correction factor which accounts for nonlinearities at high canardvator deflection angles. It is found from Figure 8.13

$[\{(\alpha_\delta)_{C_L}\}/\{(\alpha_\delta)_{c_l}\}]$ is found from Figure 8.53

Note: in Figs 8.13, 8.14, 8.15 and 8.53 use c_{δ_c}/c_c for c_f/c

$c_{l_{\alpha_c}}$ is the airfoil lift curve slope of the canard as obtained from 8.1.1.2.

2.) $C_{L_{\delta_c}}$

The lift-due-to-canardvator derivative, $C_{L_{\delta_c}}$ may be found from:

$$C_{L_{\delta_c}} = (\alpha_{\delta_c})C_{L_{i_c}} \qquad (10.103)$$

where: (α_{δ_c}) is found from Eqn.(10.102)

$C_{L_{i_c}}$ is found from Eqn.(10.99)

3.) $C_{m_{\delta_c}}$

The pitching-moment-due-to-canardvator derivative, (also called canardvator control power) may be found $C_{m_{\delta_c}}$ from:

$$C_{m_{\delta_c}} = (\alpha_{\delta_c})C_{m_{i_c}} \qquad (10.104)$$

where: (α_{δ_c}) is found from Eqn.(10.102)

$C_{m_{i_c}}$ is found from Eqn.(10.100)

10.3.5 Aileron Control Derivatives: $C_{y_{\delta_a}}$, $C_{l_{\delta_a}}$ and $C_{n_{\delta_a}}$

For a discussion of preliminary aileron sizing the reader is referred to Chapter 6 of Part II.

1.) $C_{y_{\delta_a}}$

The side-force-due-to-aileron derivative, $C_{y_{\delta_a}}$ is negligible for most conventional aileron arrangements:

$$C_{y_{\delta_a}} = 0 \qquad (10.105)$$

If ailerons are located in close proximity to a vertical tail (F-106!) a significant side-force due to aileron deflection may arise. Windtunnel data are recommended to determine such aileron induced side forecs.

2.) $C_{l_{\delta_a}}$

The rolling-moment-due-to-aileron derivative, $C_{l_{\delta_a}}$ (also called roll control power) can be estimated with the following procedure:

Step 1: Determine the inboard span location η_i and the outboard span location η_o for the aileron(s) as fractions of the semi-span of the wing. These data follow from the Class I threeview obtained from Chapter 13, Part II.

Step 2: For full chord ailerons ($c_a/c = 1.0$), antisymmetrically deflected, and running from: η=0 to η_i and to η_o respectively, determine the rolling moment effectiveness parameter: $\beta C'_{l_\delta}/k$ from Figures 10.46, with:

β found from Eqn.(10.53)

k found from Eqn.(10.54), where $(c_{l_\alpha})_M$ is

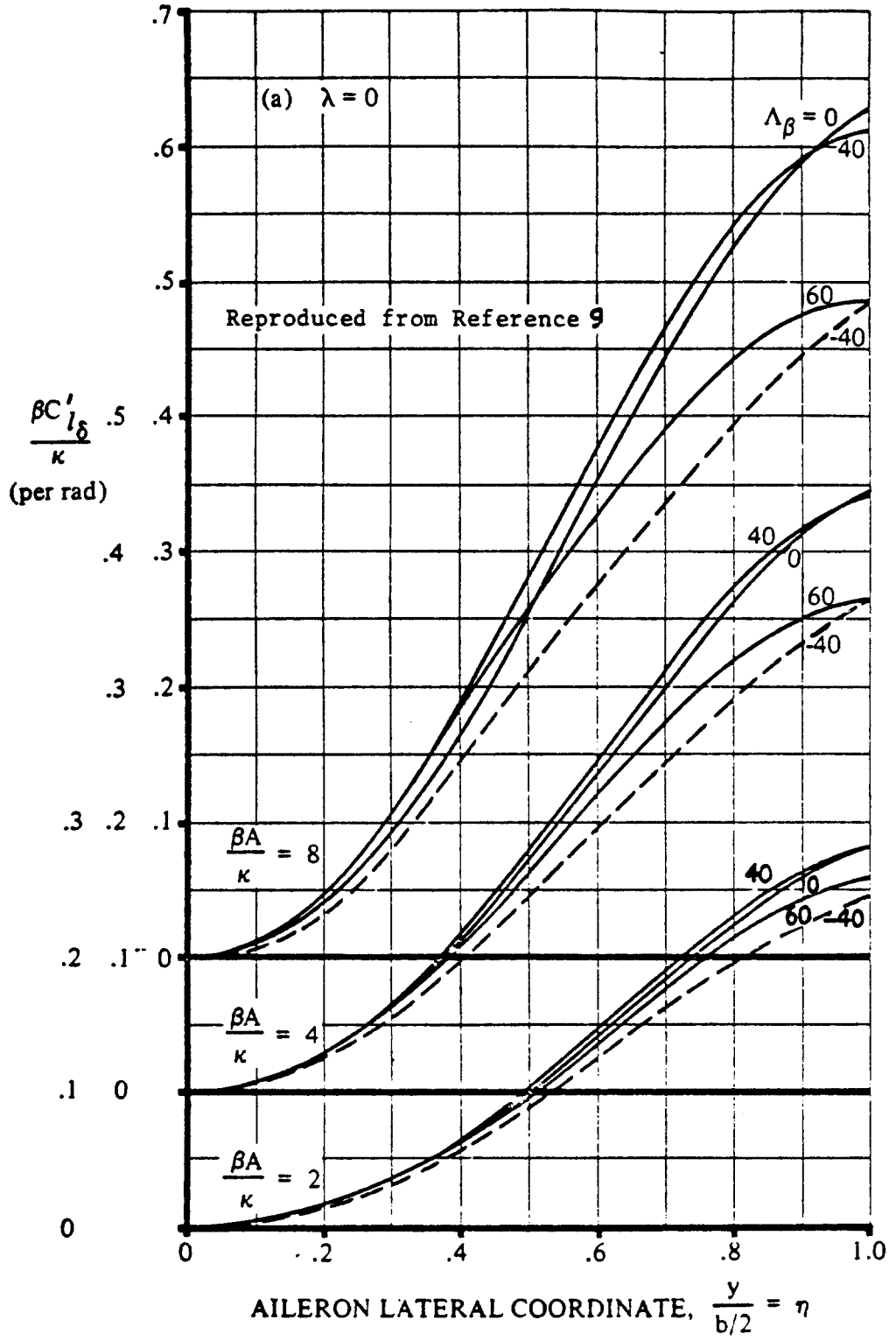

Figure 10.46a Aileron Rolling Moment Parameter

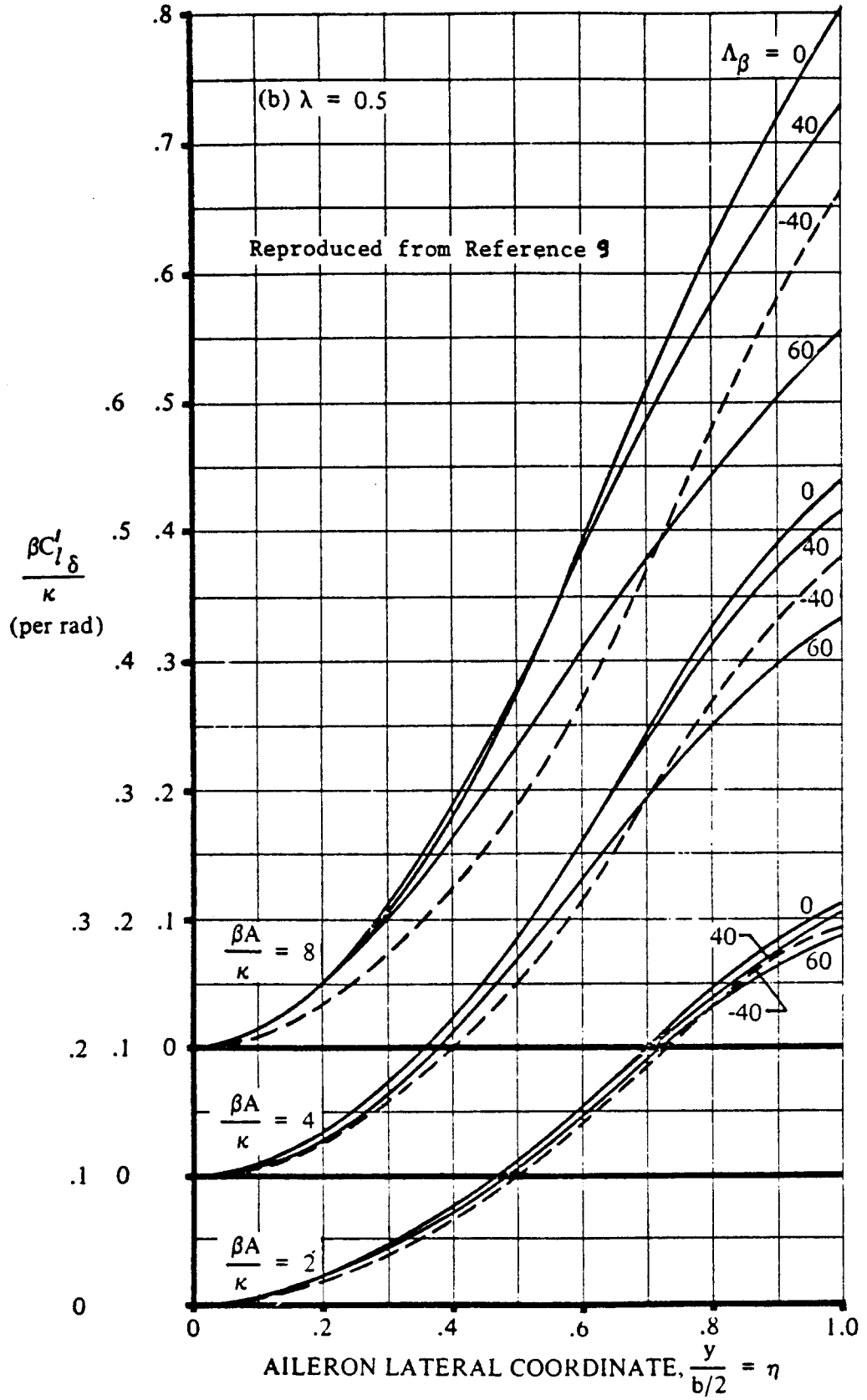

Figure 10.46b Aileron Rolling Moment Parameter

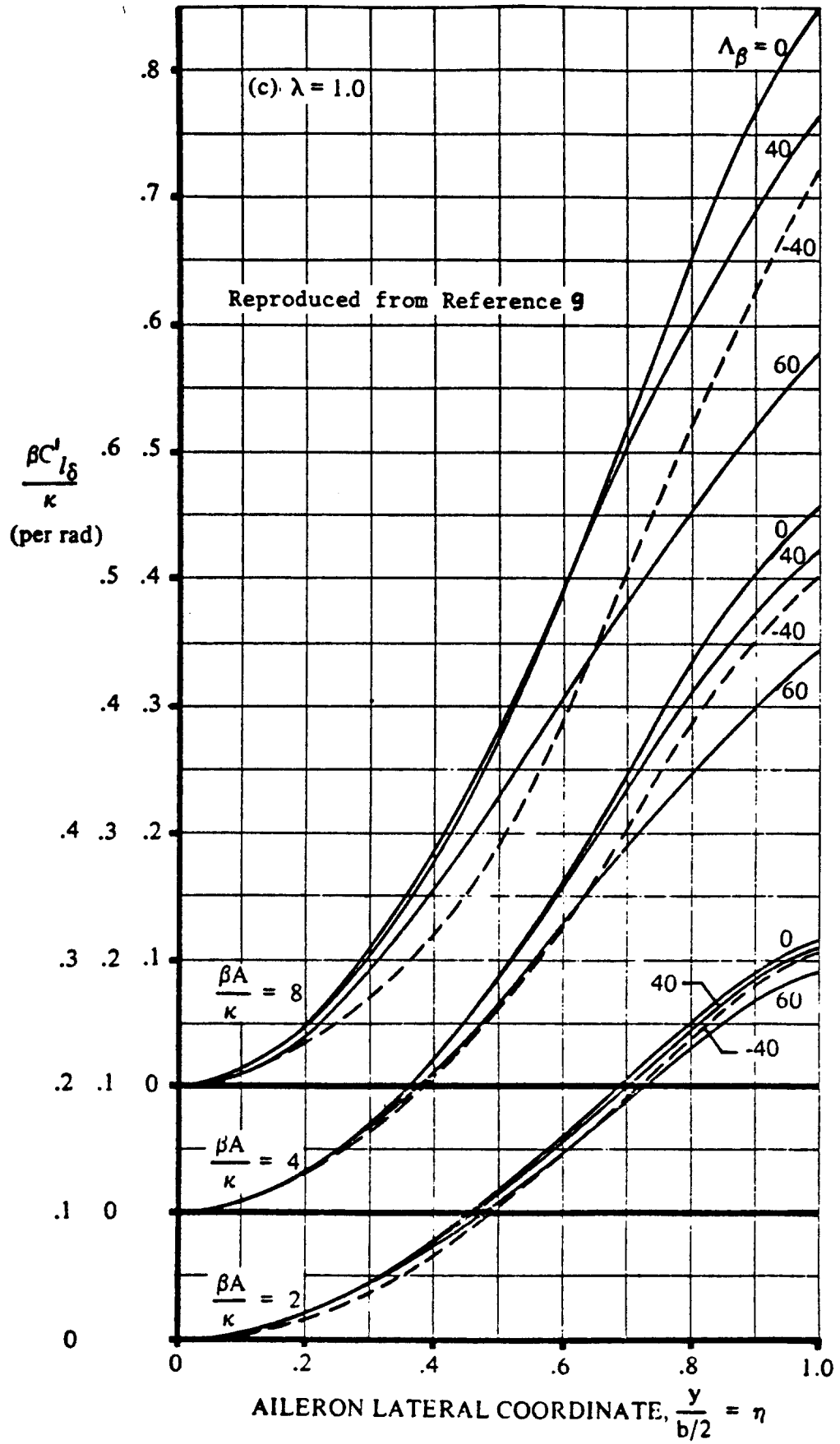

Figure 10.46c Aileron Rolling moment Parameter

determined for the airfoil at the m.g.c of the part of the wing covered by the aileron(s)

A is the wing aspect ratio

$$\Lambda_\beta = \arctan(\tan\Lambda_{c/4}/\beta) \qquad (10.106)$$

Figures 10.46 give the control effectiveness parameter for control spans measured from the plane of symmetry (η=0) outboard. For partial span controls running from η_i to η_o the actual effectiveness parameter is obtained as the difference between the two full span controls. This is illustrated in Figure 10.47.

Step 3: Determine the rolling effectiveness of two full-chord controls anti-symmetrically deflected by:

$$C'_{l_\delta} = (k/\beta)(\beta C'_{l_\delta}/k) \qquad (10.107)$$

Step 4: Determine the rolling effectiveness of the partial-chord controls ($c_a/c < 1.0$), anti-symmetrically deflected from:

$$C_{l_\delta} = (\alpha_{\delta_a})C'_{l_\delta} \qquad (10.108)$$

where:

$$\alpha_{\delta_a} = c_{l_\delta}/(c_{l_\alpha})_a \qquad (10.109)$$

with: c_{l_δ} =

$$\{c_{l_\delta}/(c_{l_\delta})_{theory}\}(c_{l_\delta})_{theory} \qquad (10.110)$$

where: $\{c_{l_\delta}/(c_{l_\delta})_{theory}\}$ is found from Figure 8.15

$(c_{l_\delta})_{theory}$ is found from Figure 8.14

Note: in Figures 8.14 and 8.15, use c_a/c for c_f/c

and where: $(c_{l_\alpha})_a$ is the average airfoil lift-curve-slope of that part of the wing covered by the ailerons. The airfoil at the wing span station corresponding to that of the aileron m.g.c. may be used to compute this.

Step 5: The effect of differential aileron control deflection (for an example, see Part IV, pgs 217 and 220) is taken into account by considering C_{l_δ} of each control as ONE-HALF the anti-symmetric value determined with the aid of Eqn(10.108). The total rolling moment coefficient for differential aileron control deflection is the found from:

$$C_{l_a} = \{(C_{l_\delta}/2)_{left} + (C_{l_\delta}/2)_{right}\}(\delta a_{left} - \delta a_{right}) \qquad (10.111)$$

where it must be kept in mind, that a trailing edge down deflection is a positive control deflection!

THE aileron delfection, δ_a of the airplane is defined as:

$$\delta_a = 0.5(\delta a_{left} - \delta a_{right}) \qquad (10.112)$$

Step 6: The aileron roll control power derivative now follows from:

$$C_{l_{\delta_a}} = (C_{l_\delta})_{left} + (C_{l_\delta})_{right} \qquad (10.113)$$

3.) $C_{n_{\delta_a}}$

The yawing-moment-due-to-aileron derivative, $C_{n_{\delta_a}}$ (also called adverse aileron yaw) may be computed from:

$$C_{n_{\delta_a}} = K_a C_{L_w} C_{l_{\delta_a}} \qquad (10.114)$$

where: K_a is found from Figure 10.48

C_{L_w} is found from Eqns (10.57) or (10.58)

$C_{l_{\delta_a}}$ is given by Eqn.(10.113)

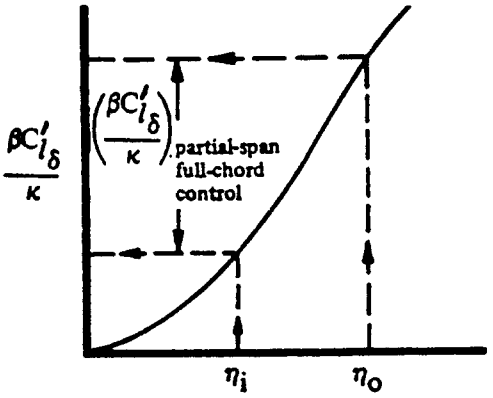

Reproduced from Reference 9

Figure 10.47 Finding the Partial Span Aileron Parameter

Reproduced from Reference 9

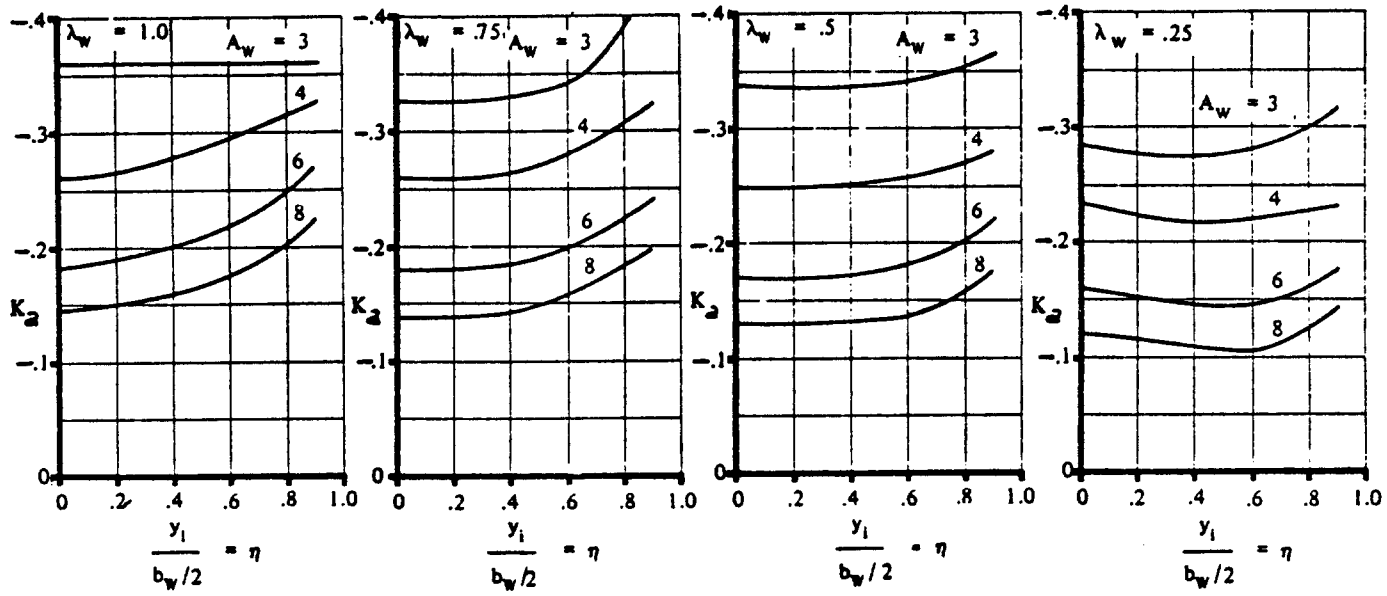

Figure 10.48 Correlation Constant for Yawing Moment due to Aileron Deflection

10.3.6 Spoiler Control Derivatives: $C_{y_{\delta_s}}$, $C_{l_{\delta_s}}$ and $C_{n_{\delta_s}}$

For a discussion of preliminary spoiler sizing the reader is referred to Chapter 6 of Part II.

In this sub-section the following two types of spoilers will be considered:

A) Plug or Flap-Type Spoilers

B) Spoiler-Slot-Deflector Arrangements

Figures 10.49A and B show typical layouts for these spoiler types. Dimensions needed in the determination of spoiler derivatives are also given.

Definition: a positive spoiler deflection is one which results in a positive rolling moment i.e. a roll to the right.

1.) $C_{y_{\delta_s}}$

The side-force-due-to-spoiler derivative, $C_{y_{\delta_s}}$ is negligible for most conventional spoiler arrangements, regardless of spoiler type:

$$C_{y_{\delta_s}} = 0 \qquad (10.115)$$

If spoilers are located in close proximity to a vertical surface a significant side-force due to spoiler deflection may arise. Windtunnel data are recommended to determine such spoiler induced side forces.

2.) $C_{l_{\delta_s}}$

The rolling-moment-due-to-spoiler derivative $C_{l_{\delta_s}}$ (also called spoiler roll control power) depends on the type of spoiler used.

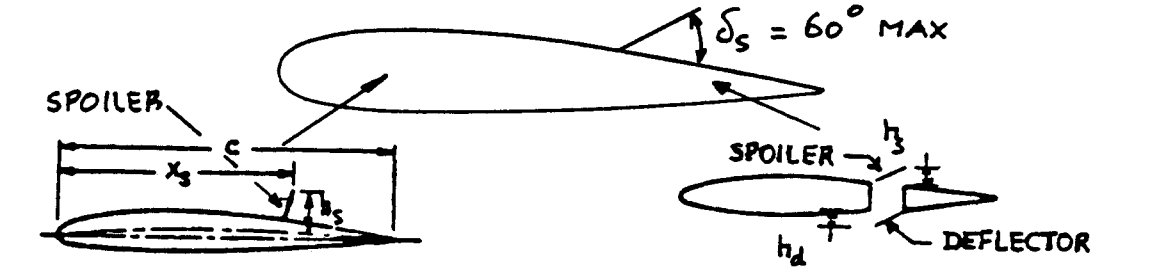

A) PLUG OR FLAP-TYPE B) SPOILER-SLOT-DEFLECTOR

Figure 10.49 General Arrangement for Two Types of Spoiler

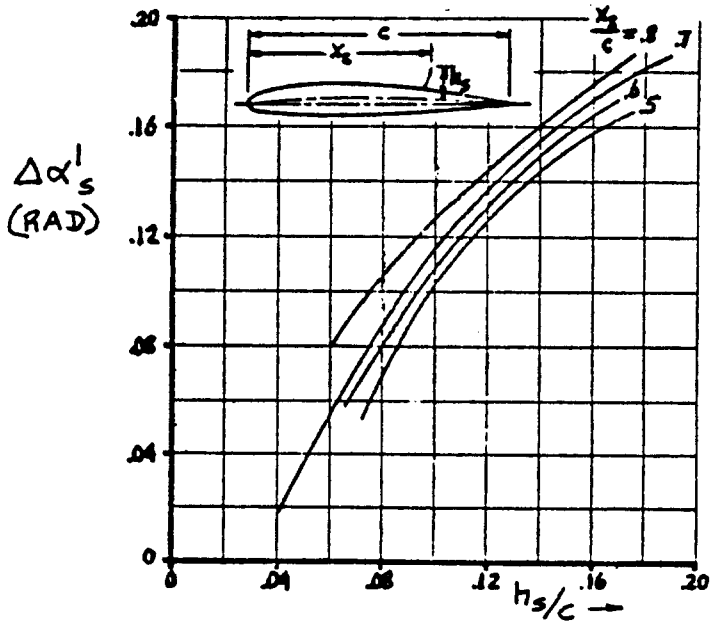

COPIED FROM REF. 9

Figure 10.50 Spoiler Lift Effectiveness

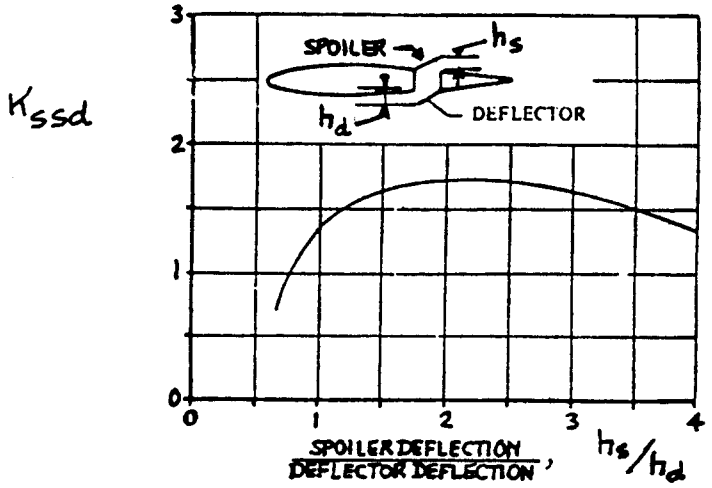

COPIED FROM REF.9

Figure 10.51 Effect of Spoiler Slot and Deflector on Spoiler Rolling Moment Effectiveness

A) Plug or Flap-Type Spoilers

The rolling-moment-due-to-spoiler derivative, $C_{l_{\delta_s}}$ for a plug or flap-type spoiler can be estimated with the following procedure:

Step 1: Determine the inboard span location η_i and the outboard span location η_o for the spoiler panels as fractions of the semi-span and as fractions of the chord of the wing. These data follow from the Class I three-view obtained from Chapter 13, Part II.

Step 2: Assuming a maximum spoiler plate deflection of 60 degrees, translate the spoiler geometry of Step 1 into one consistent with the spoiler geometry of Figure 10.49A: in other words, determine values for h_s/c and x_s/c.

These quantities may be averaged over the span of the spoiler.

Step 3: From Figure 10.50 find the corresponding value of $\Delta\alpha'_s$.

Step 4: Find the spoiler roll control derivative from:

$$c_{l_{\delta_s}} = (1/120)(C'_{l_\delta})\Delta\alpha'_s \cos\Lambda_{c/4} \qquad (10.116)$$

where: C'_{l_δ} is the rolling-moment effectiveness parameter for full chord, antisymmetrically deflected controls as obtained from Eqn.(10.107). The inboard and outboard ends of these controls are taken to be the same as the inboard and outboard ends of the hinge line of the spoiler.

$\Lambda_{c/4}$ is the wing quarter chord sweep angle.

NOTE: this method is valid only for sweep angles up to 40 degrees. For higher sweep angles, see the method of Ref.9.

B) Spoiler-Slot Deflector Arrangements

For a spoiler-slot-deflector arrangement the roll control power derivative may be determined from:

$$C_{l_{\delta_{ssd}}} = K_{ssd} C_{l_{\delta_s}} \qquad (10.117)$$

where: K_{ssd} follows from Figure 10.51 for a given ratio of spoiler angle to deflector angle, δ_s/δ_d

$C_{l_{\delta_s}}$ is determined from Eqn.(10.116).

3.) $C_{n_{\delta_s}}$

The yawing-moment-due-to-spoiler derivative, $C_{n_{\delta_s}}$ (also called proverse yawing moment due to spoiler) also depends on the type of spoiler used.

A) Plug and Flap Type Spoilers

$$C_{n_{\delta_s}} = (1/60) C_{n_s} \qquad (10.118)$$

where: C_{n_s} is found from Figures 10.52 and 10.53 for straight and for swept wings respectively.

B) Spoiler-Slot-Deflector Arrangements

$$C_{n_{\delta_{ssd}}} = K_{ssd} C_{n_{\delta_s}} \qquad (10.119)$$

where: K_{ssd} is found from Figure 10.54

$C_{n_{\delta_s}}$ follows from Eqn.(10.118).

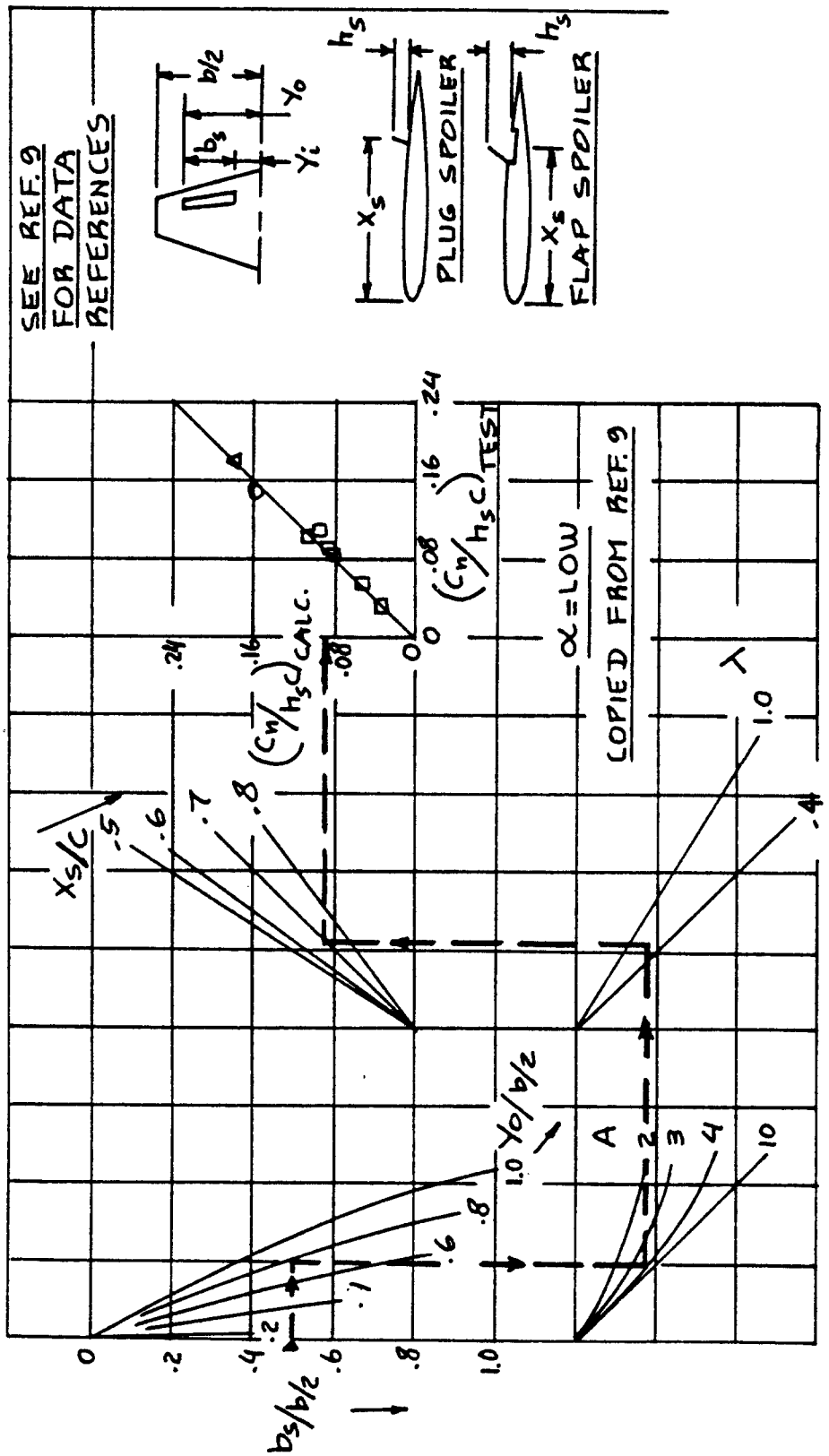

Figure 10.52 Yawing Moment due to Spoiler for Straight Wings at Low Angles of Attack

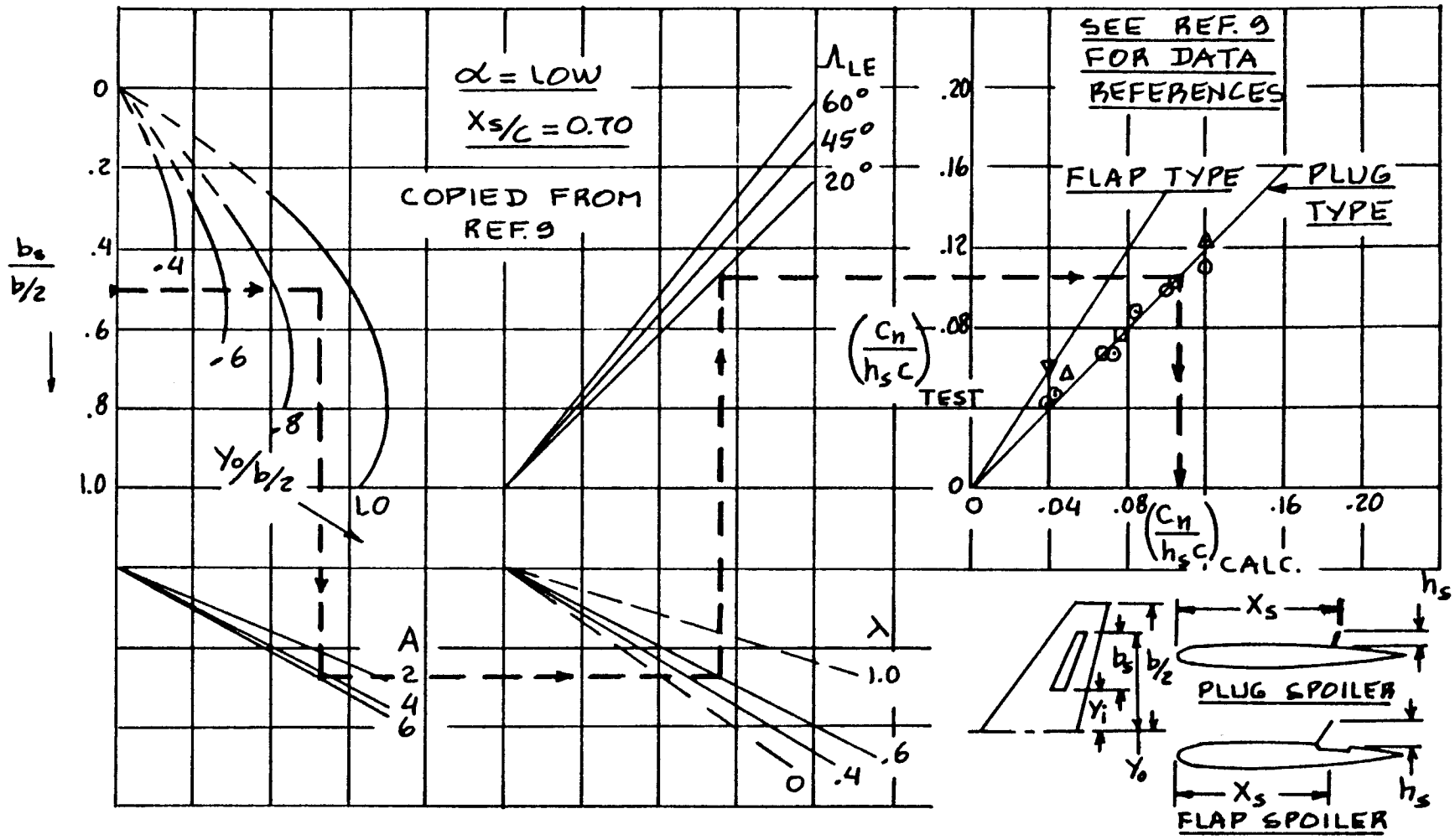

Figure 10.53 Yawing Moment due to Spoiler for Swept Wings at Low Angles of Attack

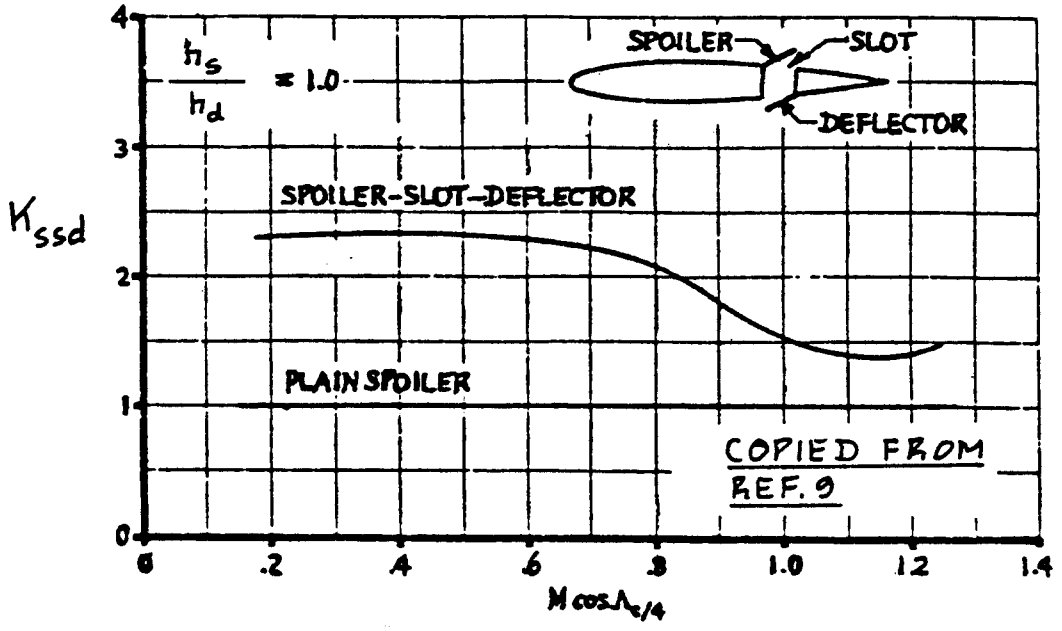

Figure 10.54 Effect of Slot and Deflector on Spoiler Yawing Moment

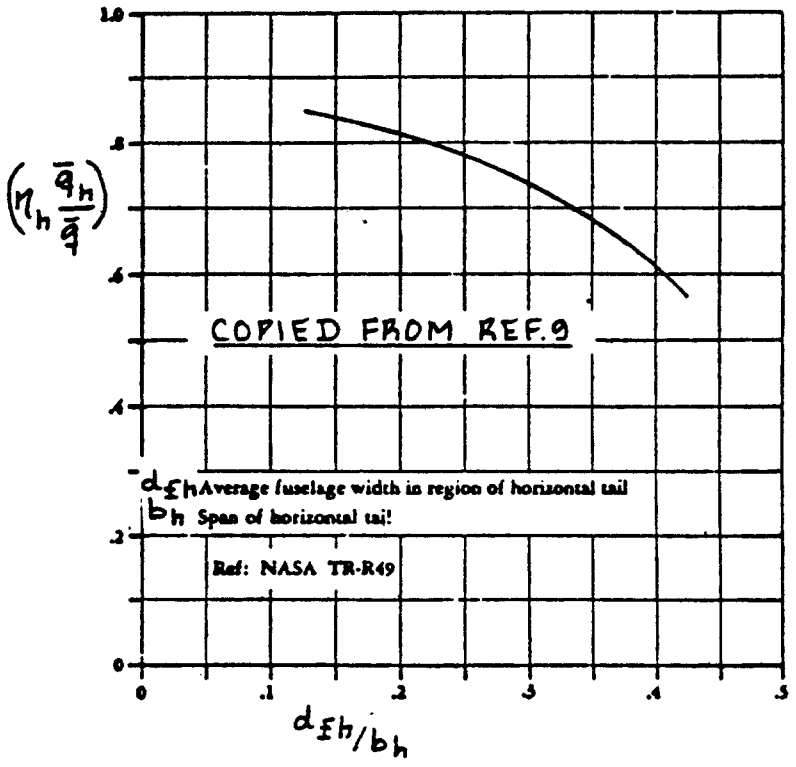

Figure 10.55 Tail Effectiveness Parameter for Fuselage Mounted Horizontal Stabilizers

10.3.7 Differential Stabilizer Control Derivatives: $C_{y_{i_h}}$, $C_{l_{i_h}}$ and $C_{n_{i_h}}$

Many fighter airplanes require so much lateral control power to meet combat roll requirements that differentially controlled horizontal stabilizers are used in addition to wing mounted lateral control devices. The sizing of the horizontal tail (stabilizer) is normally based on requirements for longitudinal stability and control. The reader should refer to Chapter 8 of Part II for preliminary horizontal tail sizing methods.

In this sub-section it will be assumed that the geometry of the horizontal tail surfaces is known.

Definition: a positive differential stabilizer deflection is one resulting in a positive rolling moment: 1.e. left stabilizer up AND 1.e. right stabilizer down).

1.) $C_{y_{i_h}}$

The side-force-due-to-differential stabilizer derivative, $C_{y_{i_h}}$ is negligible for many airplanes:

$$C_{y_{i_h}} = 0 \qquad (10.120)$$

If the stabilizers are located in close proximity to to a vertical surface a significant side-force due to differential stabilizer deflection may arise. Windtunnel data must be used to determine these side forces.

2.) $C_{l_{i_h}}$

The rolling-moment-due-to-differential stabilizer derivative $C_{l_{i_h}}$ (also called differential stabilizer roll control power) may be found from:

$$C_{l_{i_h}} = 0.5\{1 - (\pi A/57.3)(d\varepsilon/d\alpha)\}(\eta_h \bar{q}_h/\bar{q})* \\ *\{(y_{h_e} S_{h_e})/Sb\}(C_{L_{\alpha_h}})_e \qquad (10.121)$$

where: $d\varepsilon/d\alpha$ is found from Eqn. (8.45)

$(\eta_h \bar{q}_h / \bar{q})$ is found from Figure 10.55)

y_{h_e} is the distance from the exposed stabilizer center of pressure to the airplane centerline, and may be determined from:

$$y_{h_e} = (\eta_{cp} b_{h_e}/2) + r_{fh} \qquad (10.122)$$

where: η_{cp} is found from Figure 10.56. In Figure 10.16, A_{h_e} is the aspect ratio of the exposed horizontal tail

b_{h_e} is the semispan of the exposed horizontal stabilizer

r_{fh} is the radius or one half of the equivalent fuselage width at the point of stabilizer attachment

S_{h_e} is the exposed stabilizer area

$(C_{L_{\alpha_h}})_e$ is the lift-curve slope of the exposed horizontal tail. It is obtained by using the exposed horizontal tail aspect ratio, A_{h_e} in Eqn.(8.22) and substituting other appropriate horizontal tail parameters for wing parameters.

NOTE: This method is valid only for angles of attack below roughly six degrees. At higher angles of attack body shed vortices will interfere with the flow over the horizontal tail A method to account for these vortices is given in Ref.9.

3.) $C_{n_{i_h}}$

No reliable preliminary design methods are available for the estimation of this derivative. The qualitative discussion which follows has been adapted from Ref.9.

Figure 10.57 shows typical relations between aileron and differential tail induced yawing moments. The magnitude of the differential tail induced yawing moment is a strong function of tail height (relative to the vertical tail and relative to the wing): Figure 10.58 illustrates

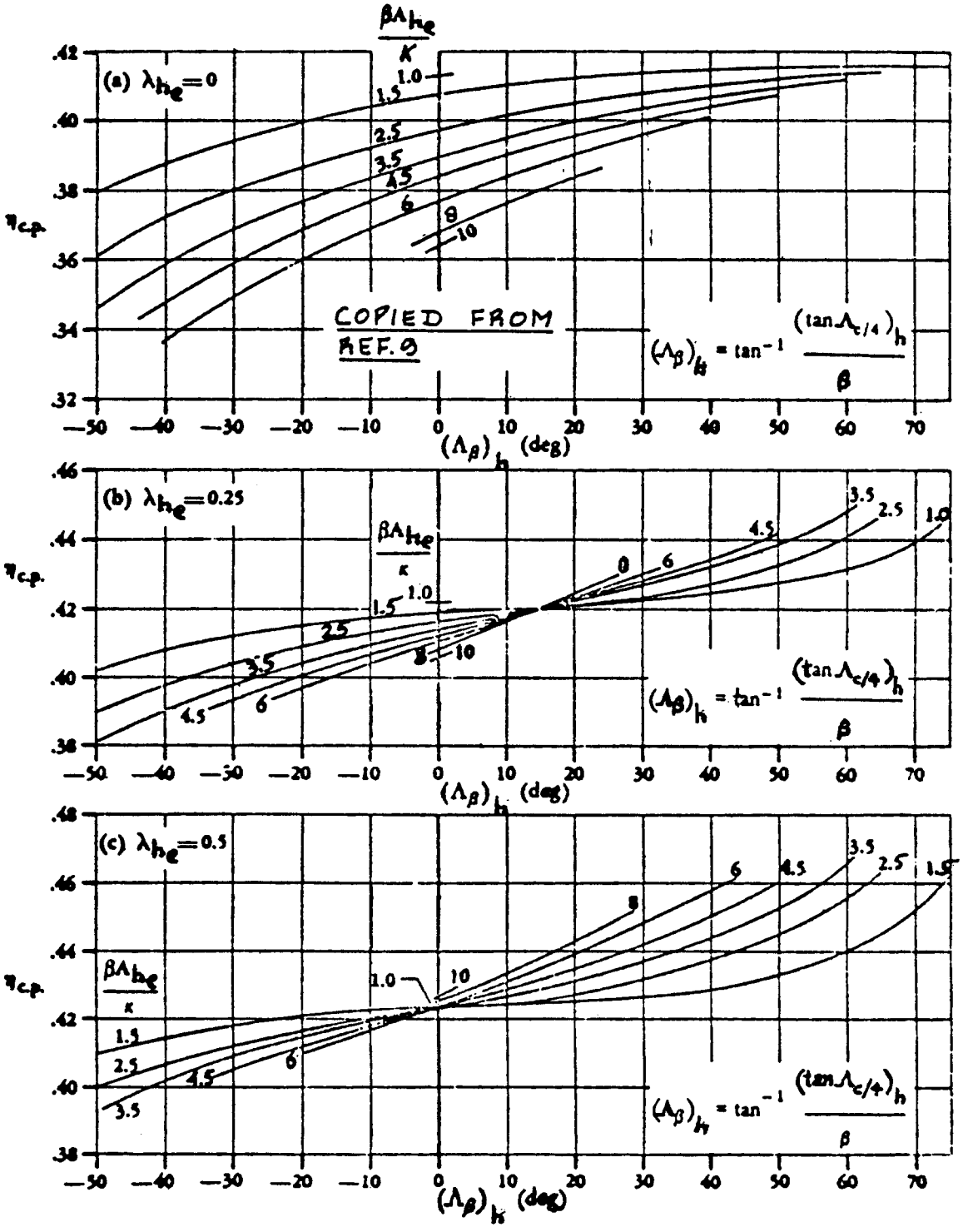

Figure 10.56 Exposed Stabilizer Center of Pressure Location as Affected by Aspect Ratio, Sweep Angle and Taper Ratio

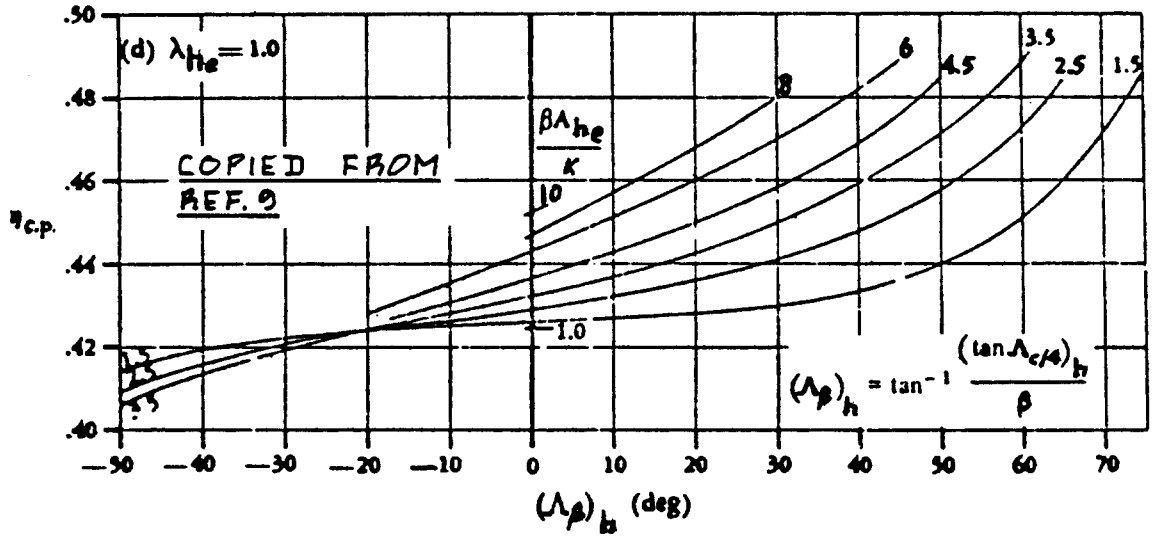

Figure 10.56 (Cont'd) Exposed Stabilizer Center of Pressure Location as Affected by Aspect Ratio, Sweep Angle and Taper Ratio

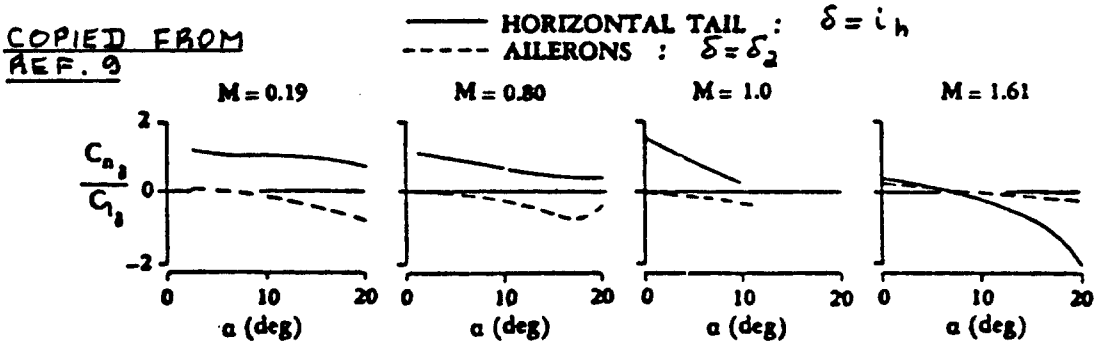

Figure 10.57 Effect of Mach Number on the Yaw-to Roll Ratio of Differential Stabilizers

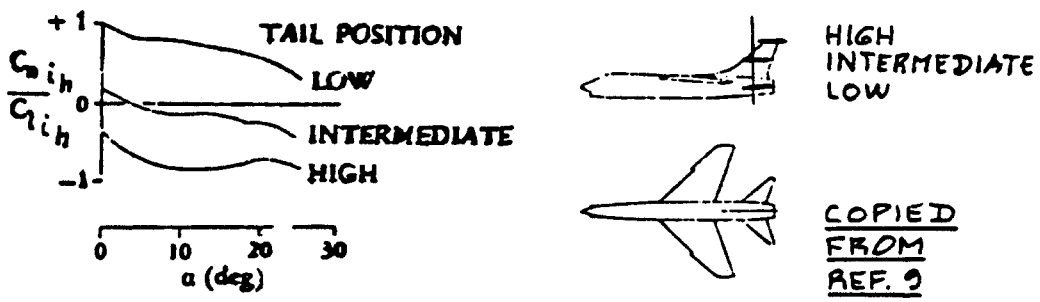

Figure 10.58 Effect of Tail Location on the Yaw-to-Roll Ratio of Differential Stabilizers

typical trends. In addition, the dihedral angle of the horizontal tail can be significant as shown in Fig.10.59.

Finally, the deflection of wing flaps can have significant influence as well. This is shown in Fig.10.60.

For purposes of preliminary design the reader may wish to 'guestimate' a value of $C_{n_{i_h}}/C_{l_{i_h}}$ from Figs 10.57 through 10.60. Where possible windtunnel data should be used.

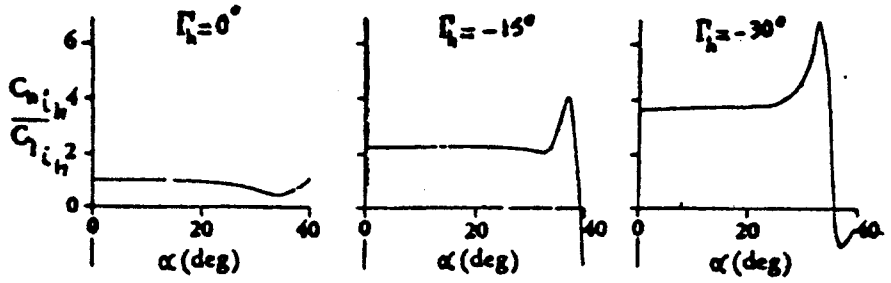

Figure 10.59 Effect of Tail Dihedral on the Yaw-to-Roll Ratio of Differential Stabilizers

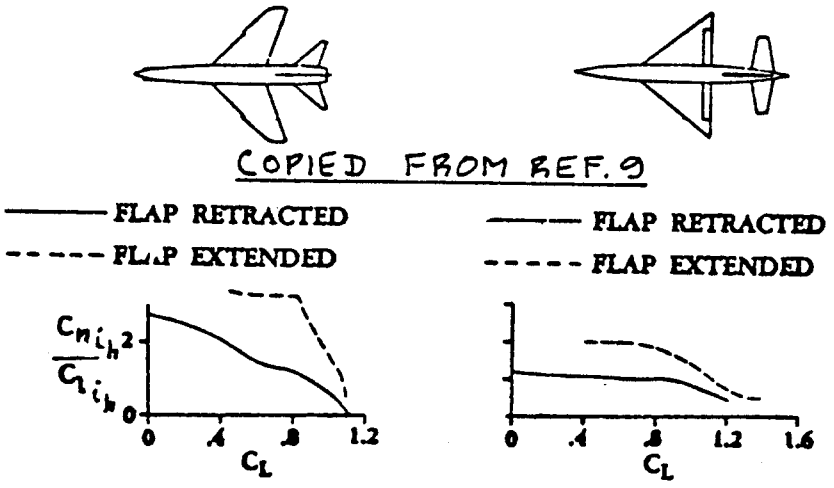

Figure 10.60 Effect of Flaps on the Yaw-to-Roll Ratio of Differential Stabilizers

10.3.8 Rudder Control Derivatives: $C_{y_{\delta_r}}$, $C_{l_{\delta_r}}$ and $C_{n_{\delta_r}}$

For a discussion of vertical tail sizing and rudder sizing the reader is referred to Chapters 8 and 11 in Part II.

Definition: a positive rudder deflection is one resulting in a negative yawing moment (t.e. rudder to the left)

1.) $C_{y_{\delta_r}}$

The side-force-due-to-rudder derivative, $C_{y_{\delta_r}}$ may be computed from:

$$C_{y_{\delta_r}} = (C_{L_{\alpha_v}})(k'K_b)* \qquad (10.123)$$

$$*\{c_{l_\delta}/(c_{l_\delta})_{theory}\}(c_{l_\delta})_{theory}(S_v/S)$$

where: $C_{L_{\alpha_v}}$ is found from p.386

k' is found from Figure 8.53

K_b is found from page 259

$\{c_{l_\delta}/(c_{l_\delta})_{theory}\}$ is found from Figure 8.15

$(c_{l_\delta})_{theory}$ is found from Figure 8.14

S_v is the effective vertical tail area as defined in Figure 10.13.

2. $C_{l_{\delta_r}}$

The rolling-moment-due-to-rudder derivative, $C_{l_{\delta_r}}$ is found from:

$$C_{l_{\delta_r}} = \{(z_v\cos\alpha - l_v\sin\alpha)/b\}C_{y_{\delta_r}} \qquad (10.124)$$

where: z_v and l_v are defined in Figure 10.27

$C_{y_{\delta_r}}$ is found from Eqn.(10.122)

3. $C_{n_{\delta_r}}$

The yawing-moment-due-to-rudder derivative, $C_{n_{\delta_r}}$ (also called rudder control power) may be estimated from:

$$C_{n_{\delta_r}} = -C_{y_{\delta_r}} (l_v \cos\alpha + z_v \sin\alpha)/b \qquad (10.125)$$

where: l_v and z_v are defined in Figure 10.27

$C_{y_{\delta_r}}$ is given by Eqn.(10.122).

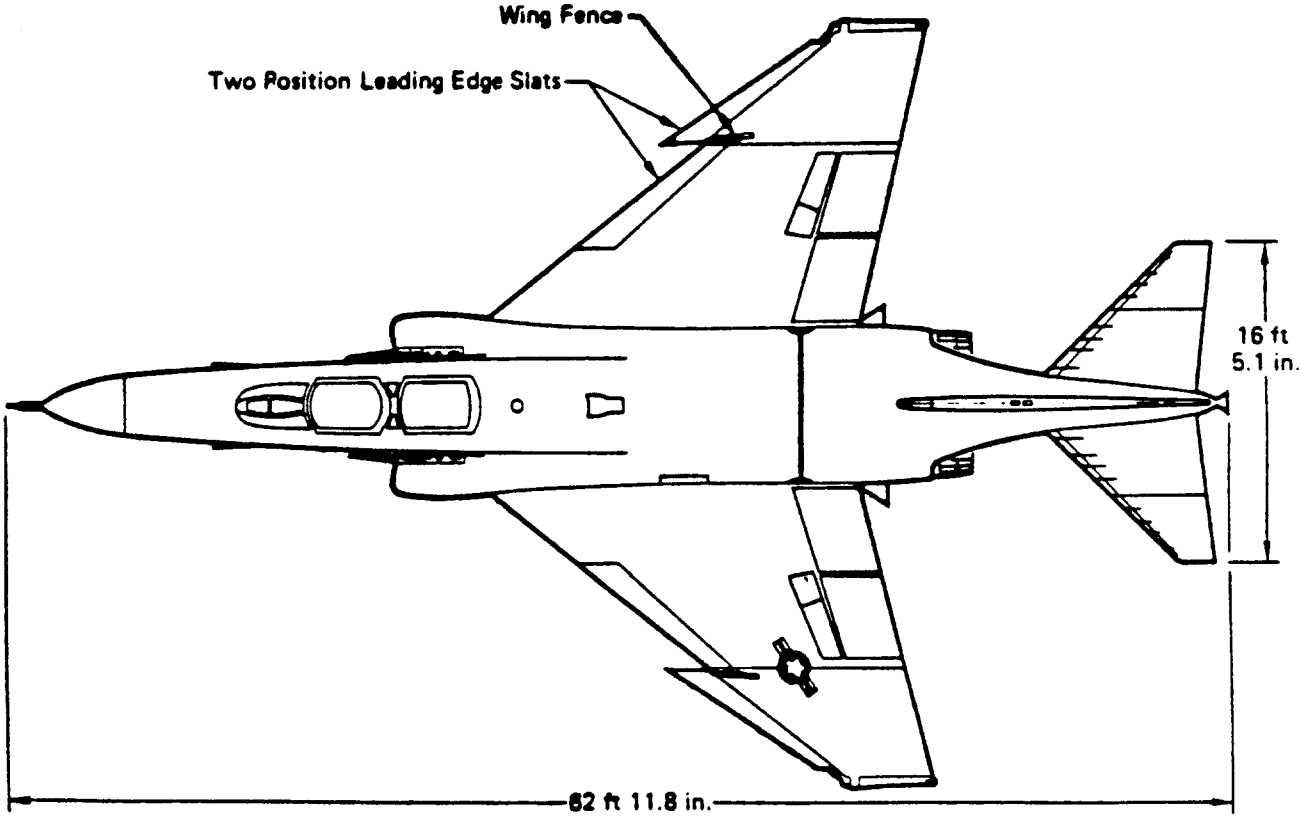

10.4 HINGEMOMENT DERIVATIVES OF CONTROL SURFACES

The purpose of this section is to present rapid methods for the estimation of hingemoment derivatives of control surfaces and tabs in the subsonic speed range. For methods which apply in the transonic and supersonic speed ranges the reader should consult Reference 9.

The methods to be presented apply only in the linear range of control surface deflections (< 20 degrees at best) and in the linear range of angles of attack (roughly 12 degrees). For nonlinear effects the reader should consult Ref.9 and use windtunnel data wherever possible.

Hingemoment derivatives are used for two purposes:

1. Computing stick, wheel and pedal cockpit control forces so they can be checked against airworthiness requirements.

   Part VII contains methods for computing the cockpit control forces as well as methods for checking with airworthiness standards.

2. Computing actuator force levels so that hydraulic or electro-mechanical actuators can be properly sized.

   Chapter 4 in Part IV contains a discussion of actuator sizing criteria.

Figure 10.61 shows a basic control surface and tab arrangement with the necessary geometric parameters identified. Note the use of the following nomenclature: main surface, control surface and tab, shown in Figure 10.61. This nomenclature applies to the following combinations:

1. horizontal tail + elevator + elevator tab

2. canard + canardvator + canardvator tab

3. wing + aileron + aileron tab

4. vertical tail + rudder + rudder tab

For a detailed discussion of the purpose of various combinations of tabs and control surfaces, the reader should consult Chapter 4 of Part IV.

In most cases, hingemoments are taken about the control surface hingeline: corresponding hingemoment coeffi-

cients and derivatives are denoted:

c_h and c_{h_x} respectively.

In some cases, hingemoments need to be considered about the tab hinge line: for example in servo-tab systems. The corresponding hingemoment coefficients and derivatives in that case are denoted:

c^t_h and $c^t_{h_y}$ respectively.

The material in this sub-section is organized as follows:

10.4.1 Two-Dimensional Control Surface and Tab Hingemoment Derivatives about the Control Surface Hingeline

10.4.2 Three-Dimensional Control Surface and Tab Hingemoment Derivatives about the Control Surface Hingeline

10.4.3 Two-Dimensional Tab Hingemoment Derivatives about the Tab Hingeline

10.4.4 Three-Dimensional Tab Hingemoment Derivatives about the Tab Hingeline

The methods apply as long as the airflow over the control surface is attached.

NOTES: 1.) All Two-D hingemoment derivatives are based on c_f^2, where c_f is the plain flap chord defined in Figure 10.61. The plain flap is either the control surface or the tab, depending on the point about which the hingemoments are taken.

2.) All Three-D hingemoment derivatives are based on $(S_{surface})*(\bar{c}_{surface})$, where the area and chord depend on the type of control surface considered: rudder, aileron, elevator, tab, etc.

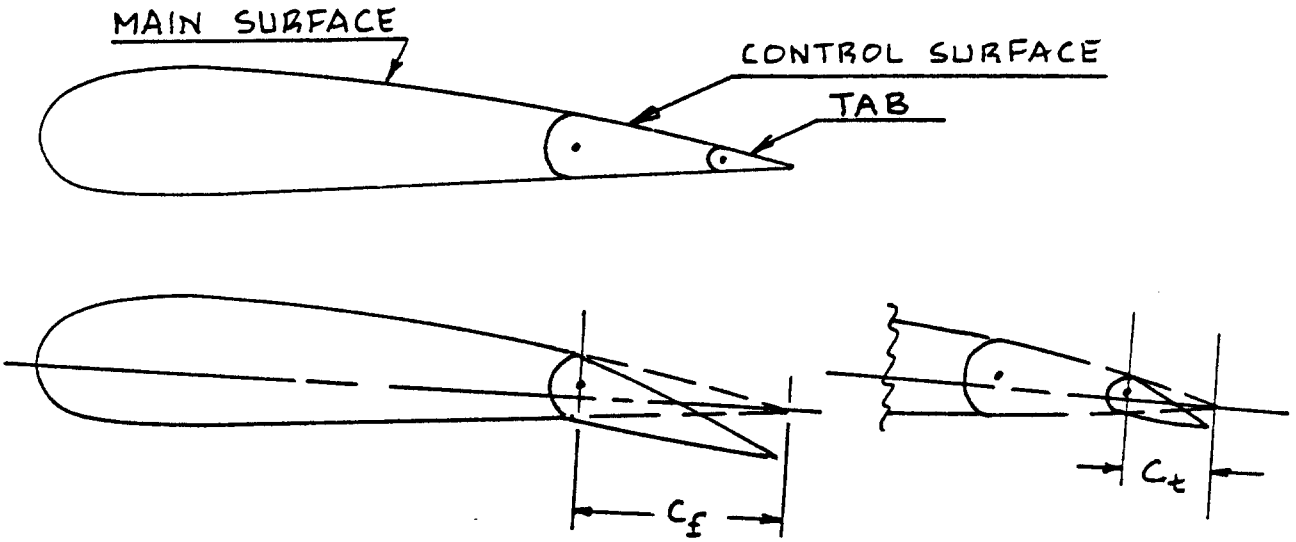

Figure 10.61 Geometry and Nomenclature Used with Control Surfaces and Tabs

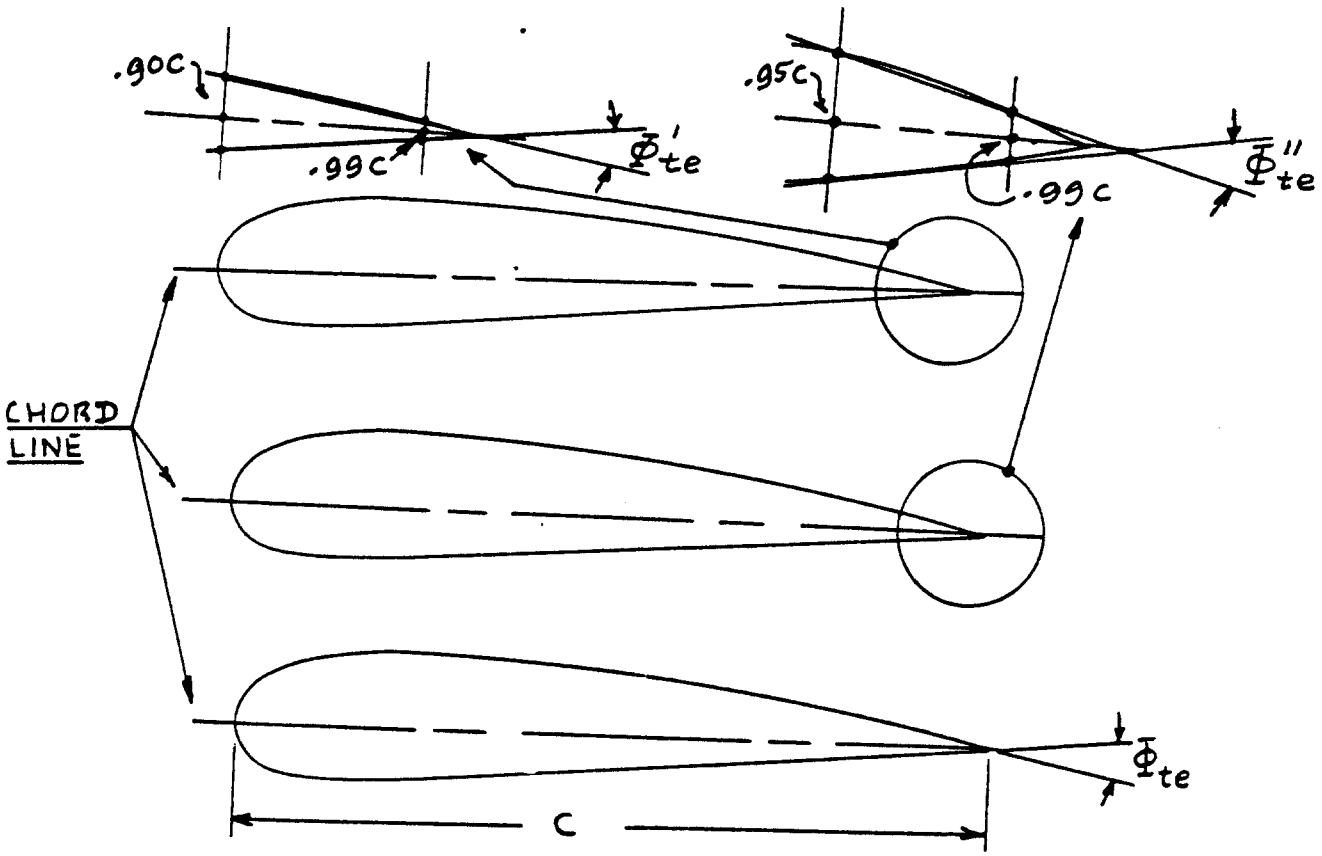

Figure 10.62 Definitions of Trailing Edge Angles

10.4.1 Two-Dimensional Control Surface and Tab Hingemoment Derivatives about the Control Surface Hingeline

The two-dimensional (=airfoil) hingemoment coefficient for a control surface is estimated from:

$$c_h = c_{h_o} + c_{h_\alpha}\alpha + c_{h_\delta}\delta + c_{h_{\delta_t}}\delta_t \qquad (10.126)$$

where: c_{h_o} is the zero-angle-of-attack, zero-control-surface-deflection, zero-tab-angle-deflection hingemoment coefficient. For main surfaces with symmetrical airfoils:

$$c_{h_o} = 0 \qquad (10.127)$$

For main surfaces with cambered airfoils, experimental data should be used.

c_{h_α} is the control surface hingemoment derivative due to angle of attack. It is estimated from 10.4.1.1, where it is called: $c_{h_{\alpha_{bal}}}$

c_{h_δ} is the control surface hingemoment derivative due to control surface deflection. It is obtained from 10.4.1.2

$c_{h_{\delta_t}}$ is the control surface hingemoment derivative due to a tab deflection. It is estimated from 10.4.1.3.

NOTE: The reader should recognize, that depending on the application, the following substitutions must be made in Equation (10.126):

for a wing: $\alpha = \alpha_w$ and $\delta = \delta_a$ or δ_{flap}

for a horizontal tail: $\alpha = \alpha_h$ and $\delta = \delta_e$

for a canard: $\alpha = \alpha_c$ and $\delta = \delta_c$

for a vertical tail: $\alpha = \beta$ and $\delta = \delta_r$

10.4.1.1 Two-D control surface hingemoment derivative due to angle of attack: c_{h_α}

The Two-D control surface hingemoment due to angle of attack derivative, c_{h_α} is determined with the following procedure:

Step 1: Check whether or not the following trailing edge angle condition is satisfied:

$$\tan(\Phi'_{te}/2) = \tan(\Phi''_{te}/2 = \tan(\Phi_{te}/2) = t/c \qquad (10.128)$$

where: Φ'_{te} is the trailing-edge angle defined as the angle between straight lines passing through points at 90 and 99 percent of the chord on the upper and lower airfoil surfaces

Φ''_{te} is the trailing-edge angle defined as the angle between straight lines passing through points at 95 and 99 percent of the chord on the upper and lower airfoil surfaces

Φ_{te} is the trailing-edge angle defined as the angle between tangents to the upper and lower airfoil surfaces at the trailing-edge

Figure 10.62 illustrates these angles.

Condition (10.128) is satisfied whenever the upper and lower surface lines of the control surface are straight.

Step 2: Determine c'_{h_α} from:

$$c'_{h_\alpha} = \qquad (10.129)$$

$$\{c'_{h_\alpha}/(c_{h_\alpha})_{theory}\}(c_{h_\alpha})_{theory}$$

where: $\{c'_{h_\alpha}/(c_{h_\alpha})_{theory}\}$ is found from Fig.10.63a which applies only to radius nose, sealed gap, plain flap type control surfaces

$(c_{h_\alpha})_{theory}$ is found from Figure 10.63b. The parameter $\{c_{l_\alpha}/(c_{l_\alpha})_{theory}\}$ in Fig.10.63a is itself found from Figure 10.64a.

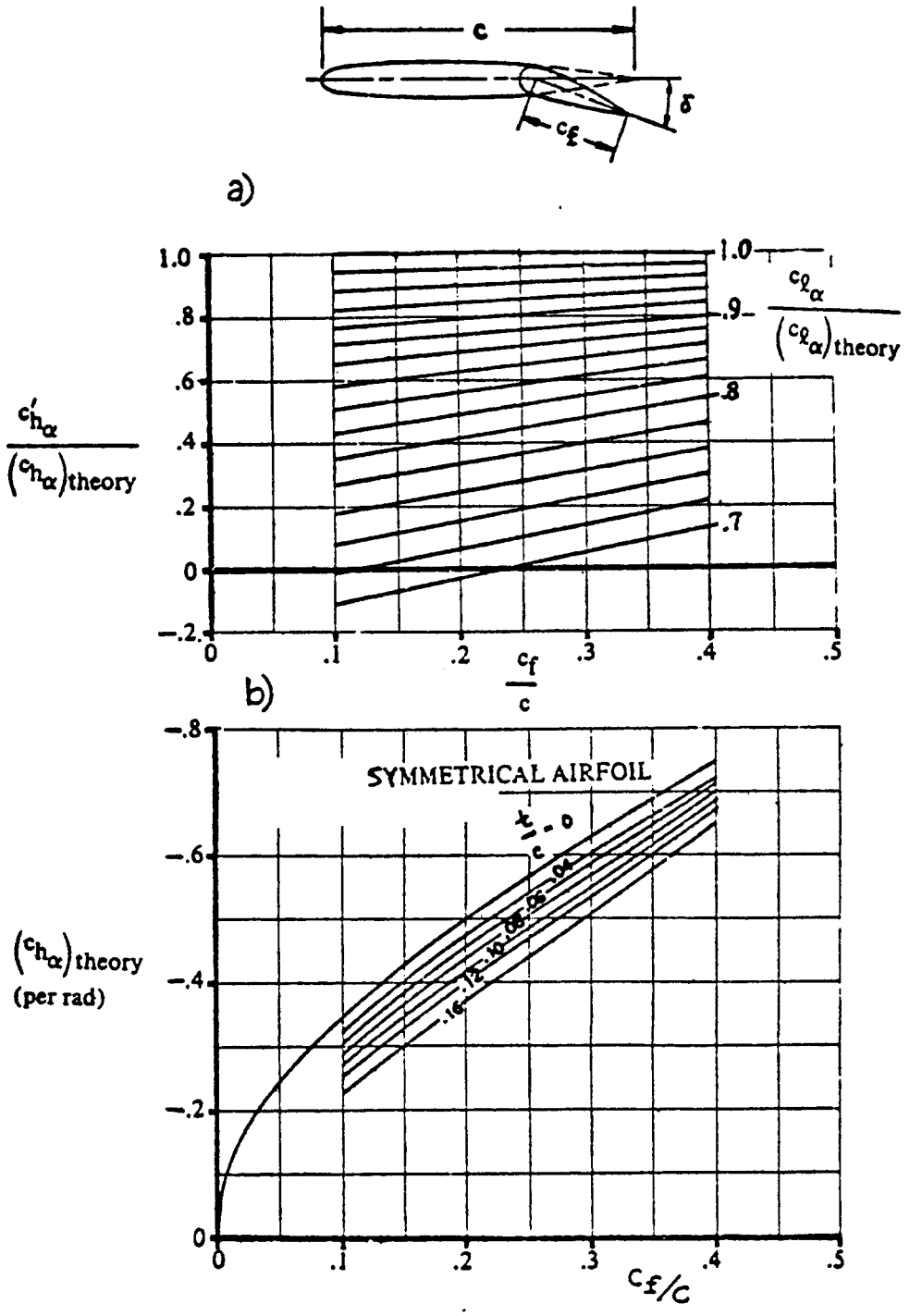

COPIED FROM: REF. 9

Figure 10.63 Two-Dimensional Control Surface Hingemoment Derivative due to Angle of Attack

COPIED FROM REF. 9

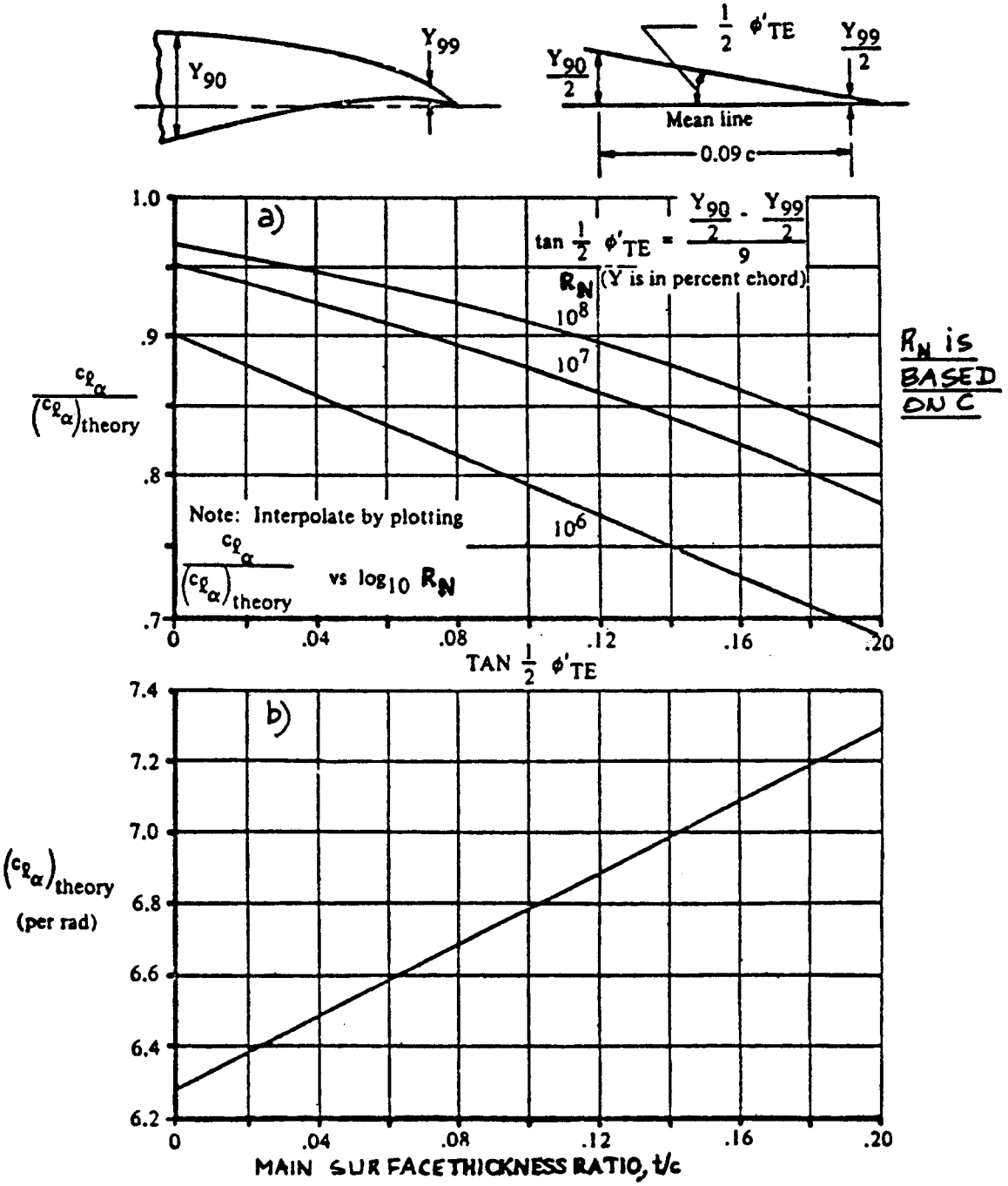

R_N is BASED ON C

Figure 10.64 Effect of Airfoil Thickness and Trailing Edge Angle on Lift Curve Slope

Step 3: If condition (10.126) is not satisfied, compute c''_{h_α} from:

$$c''_{h_\alpha} = (c'_{h_\alpha}) + \qquad (10.130)$$

$$+ 2(c_{l_\alpha})_{theory}[1 - \{c_{l_\alpha}/(c_{l_\alpha})_{theory}\}] *$$

$$*\{\tan(\bar{\Phi}''_{te}/2) - (t/c)\}$$

where: (c'_{h_α}) is obtained from Eqn.(10.129)

$(c_{l_\alpha})_{theory}$ is obtained from Figure 10.64b at the appropriate thickness ratio, t/c

$\{c_{l_\alpha}/(c_{l_\alpha})_{theory}\}$ is obtained from Figure 10.64a

$\bar{\Phi}''_{te}$ is defined under Step 1.

Note that if condition (10.128) is satisfied, and only in that case:

$$c''_{h_\alpha} = c'_{h_\alpha} \qquad (10.131)$$

Step 4: Since the value for c'_{h_α} or c''_{h_α} as found from either Step 2 or Step 3 applies only to round-nose control surfaces, corrections must be made which account for different nose shapes and for aerodynamic balance.

The corrected value for c_{h_α} is found from:

$$(c_{h_\alpha})_{bal} = \qquad (10.132)$$

$$(c''_{h_\alpha})\{(c_{h_\alpha})_{bal}/c''_{h_\alpha}\}$$

where: c''_{h_α} is obtained from Step 3.

$\{(c_{h_\alpha})_{bal}/c''_{h_\alpha}\}$ is found from Figure 10.65a for various nose shapes and

c_b/c_f IS CALLED THE OVERHANG

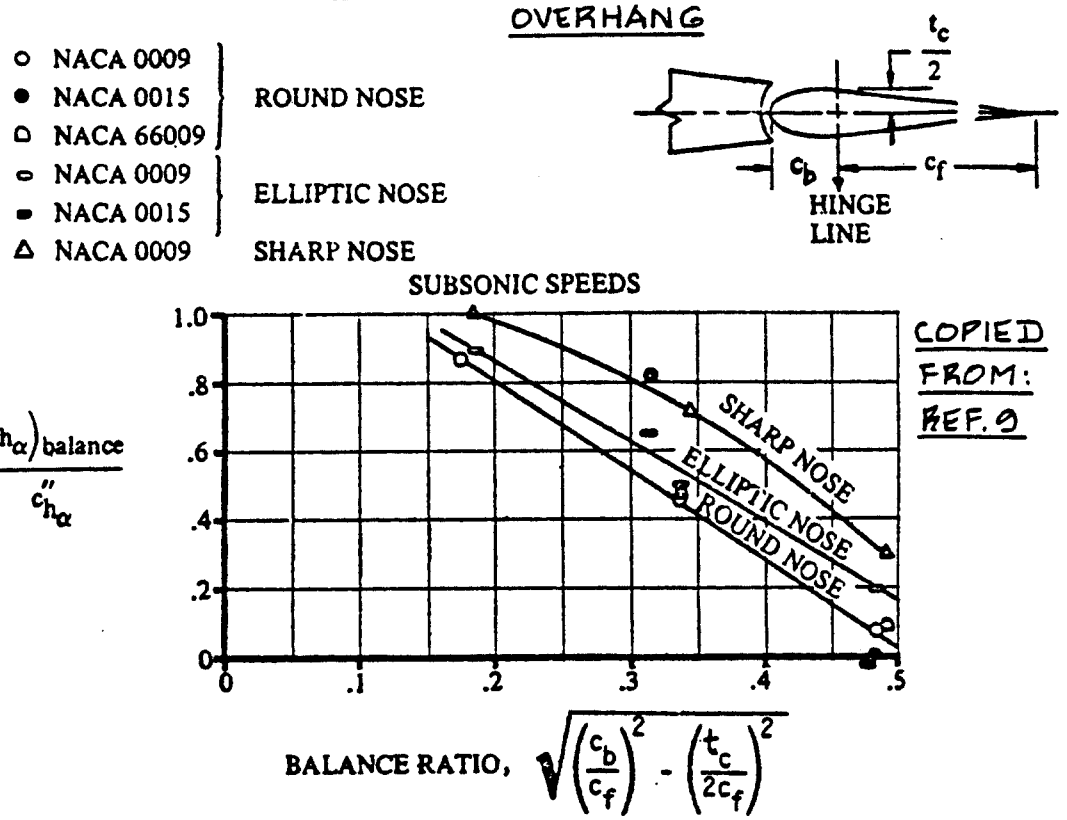

COPIED FROM: REF. 9

Figure 10.65a Effect of Nose Shape and Balance on the Two-Dimensional Hingemoment Derivative due to Angle of Attack

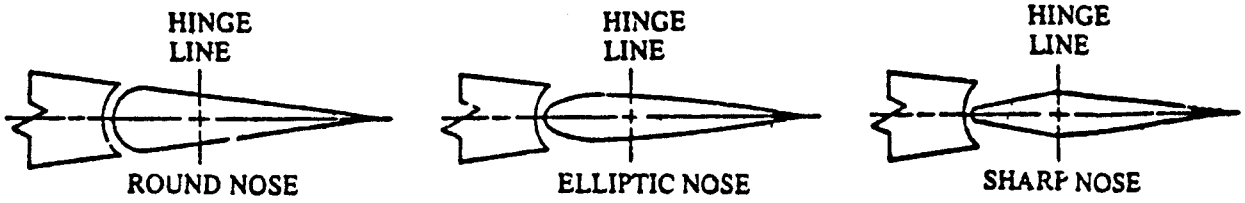

COPIED FROM REF. 9

Figure 10.65b Nose Shape Examples for 35 Percent Balance

at the proper balance ratio. Nose shapes and balance ratio are illustrated and defined in Figure 10.65b.

Step 5: Correct the hingemoment derivative for the effect of Mach Number:

$$(c_{h_\alpha})_M = (c_{h_\alpha})_{bal}/(1 - M^2)^{1/2} \qquad (10.133)$$

Step 6: Hingemoments also depend on whether or not the control surface and/or tab gaps are closed (i.e sealed). Figure 10.66 illustrates the difference between open and closed gaps.

Figure 10.67 may be used to introduce corrections for open gaps, depending on gap-size for the control surface.

Figure 10.68a may be used to correct for the effect of gap-size in the case of an unsealed tab.

NOTE: the Step 6 corrections are applied to $(c_{h_\alpha})_M$ by using ratios obtained from Figures 10.67 or 10.68a as appropriate.

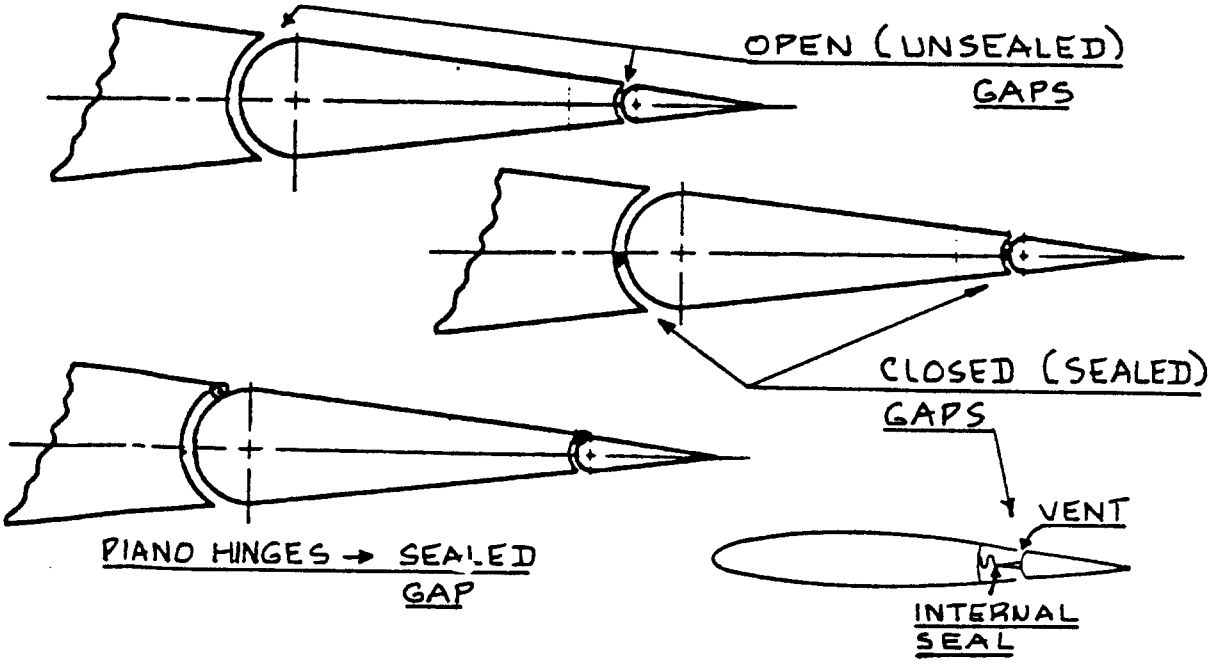

Figure 10.66 Examples of Closed (Sealed) and Open (Unsealed) Control Surface and Tab Gaps

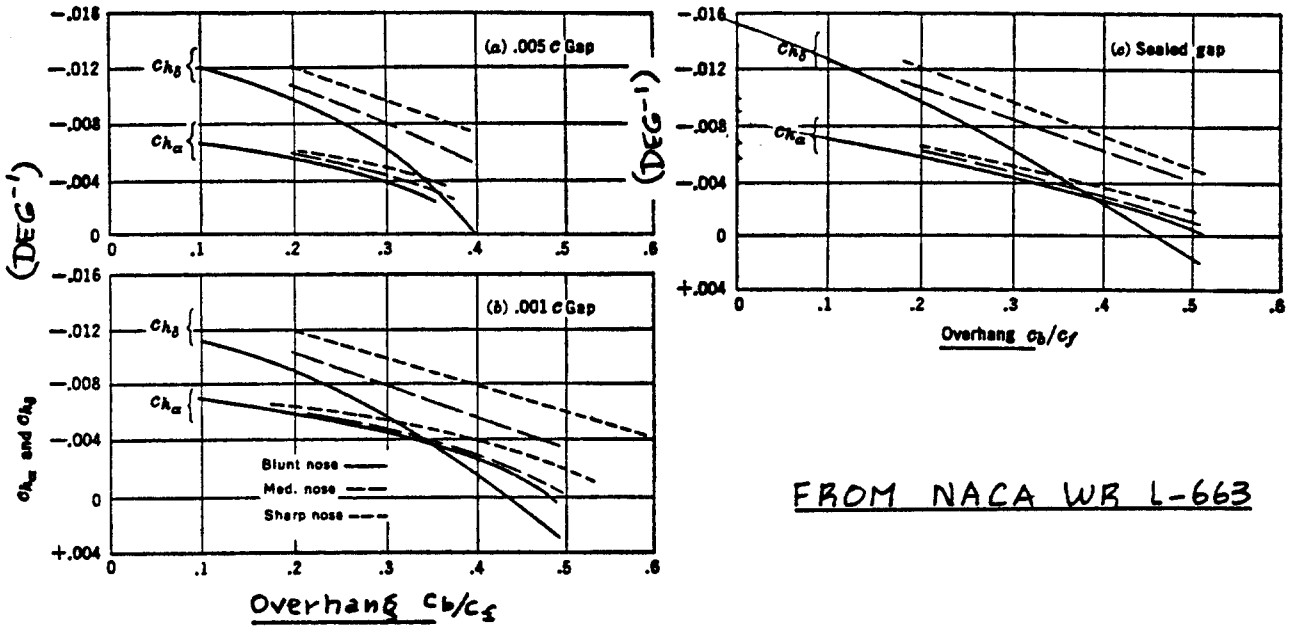

Figure 10.67 Effect of Gap Size and Overhang on Two-Dimensional Hingemoment Derivatives

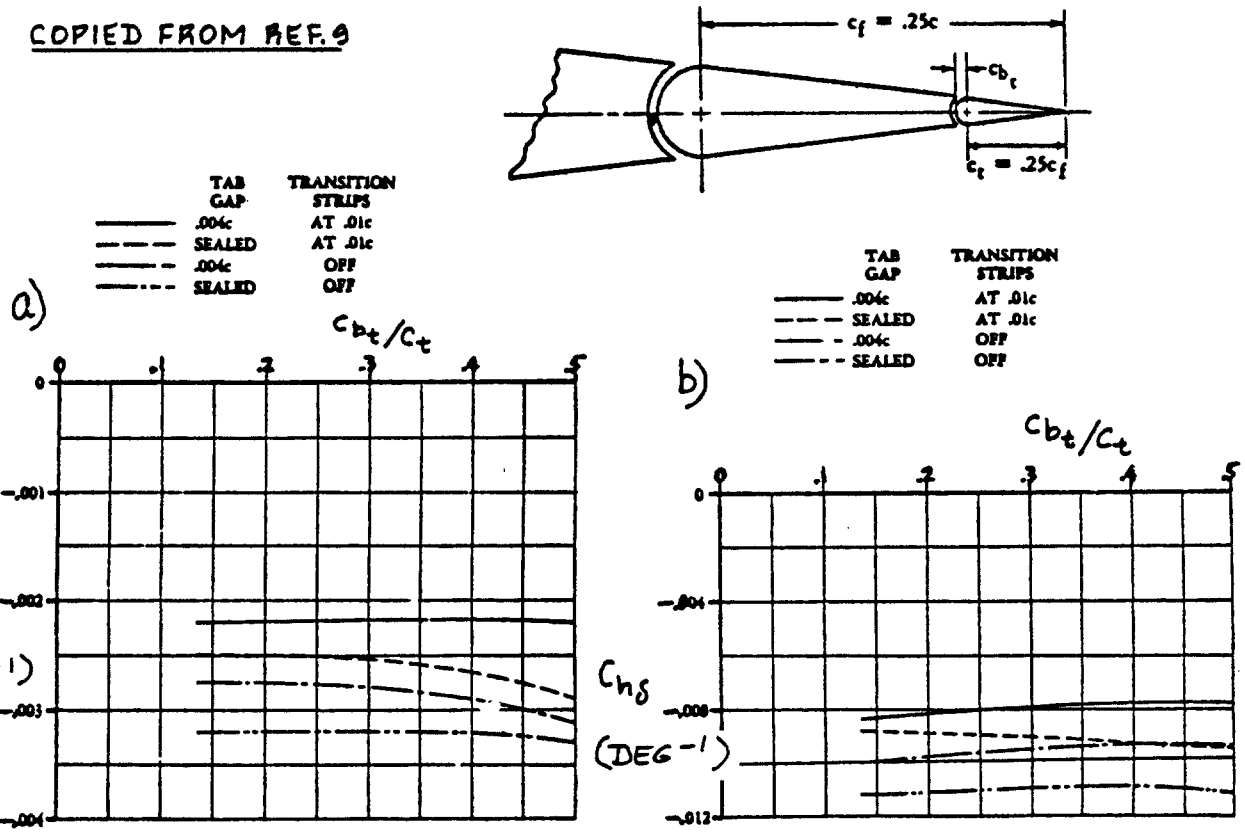

Figure 10.68 Effect of Tab Gap Size and Tab Overhang On Two-Dimensional Hingemoment Derivatives

10.4.1.2 Two-D control surface hingemoment derivative due to control surface deflection: c_{h_δ}

The Two-D control surface hingemoment due to control surface deflection derivative, c_{h_δ} is determined with the following procedure:

Step 1: This is a repeat of Step 1 in 10.4.1.1.

Step 2: Determine c'_{h_δ} from:

$$c'_{h_\delta} = \{c'_{h_\delta}/(c_{h_\delta})_{theory}\}(c_{h_\delta})_{theory} \quad (10.134)$$

where: $\{c'_{h_\delta}/(c_{h_\delta})_{theory}\}$ is found from Fig.10.69a which applies only to radius nose, sealed gap, plain flap type control surfaces

$(c_{h_\delta})_{theory}$ is found from Figure 10.69b. The parameter $\{c_{l_\alpha}/(c_{l_\alpha})_{theory}\}$ in Fig.10.69a is itself found from Figure 10.64a.

Step 3: If condition (10.128) is not satisfied, compute c''_{h_δ} from:

$$c''_{h_\delta} = (c'_{h_\delta}) + 2(c_{l_\delta})_{theory}* \quad (10.135)$$

$$*[1 - \{c_{l_\delta}/(c_{l_\delta})_{theory}\}]\{\tan(\Phi''_{te}/2) - (t/c)\}$$

where: (c'_{h_δ}) is obtained from Eqn.(10.134)

$(c_{l_\delta})_{theory}$ is obtained from Figure 8.14 at the appropriate thickness ratio, t/c

$\{c_{l_\delta}/(c_{l_\delta})_{theory}\}$ is obtained from Figure 8.15

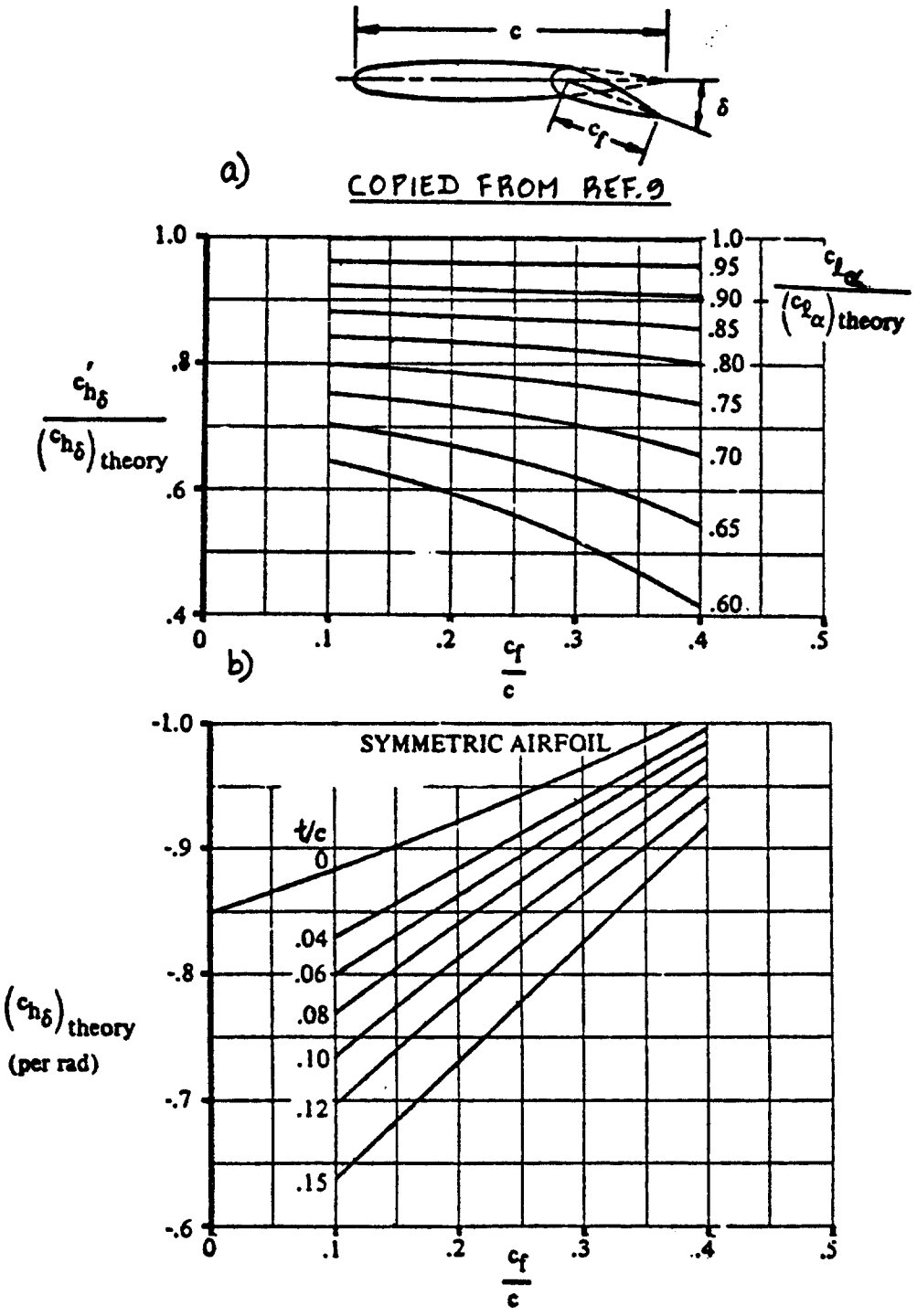

Figure 10.69 Two-Dimensional Control Surface Hingemoment Derivative due to Control Surface Deflection

$\bar{\Phi}''_{te}$ is defined under Step 1 in 10.4.1.1.

NOTE: If the control surface trailing edge is beveled as in Fig.10.70, the value of $\bar{\Phi}''_{te}$ should be set equal to the angle of the bevel!

Note that if condition (10.128) is satisfied, any in that case:

$$c''_{h_\delta} = c'_{h_\delta} \qquad (10.136)$$

ep 4: Since the value for c_{h_δ} obtained under either Step 2 or Step 3 applies only to round-nose control surfaces, corrections must be made which account for different nose shapes and for aerodynamic balance.

The corrected value for c_{h_δ} is found from:

$$(c_{h_\delta})_{bal} = \qquad (10.137)$$

$$(c''_{h_\delta})\{(c_{h_\delta})_{bal}/c''_{h_\delta}\}$$

ere: c''_{h_δ} is obtained from Step 3.

$\{(c_{h_\delta})_{bal}/c''_{h_\delta}\}$ is found from Figure 10.71 for various nose shapes and at the proper balance ratio. Nose shapes and balance ratio are illustrated and defined in Figure 10.65b.

ep 5: Correct the hingemoment derivative for the effect of Mach Number:

$$(c_{h_\delta})_M = (c_{h_\delta})_{bal}/(1 - M^2)^{1/2} \qquad (10.138)$$

ep 6: Hingemoments also depend on whether or not the control surface gaps are closed (i.e. i.e sealed). Figure 10.66 illustrates the the difference between open and closed gaps.

Figures 10.67 and 10.68b may be used to introduce corrections for open gaps, depending on gap size for the control surface and for the tab.

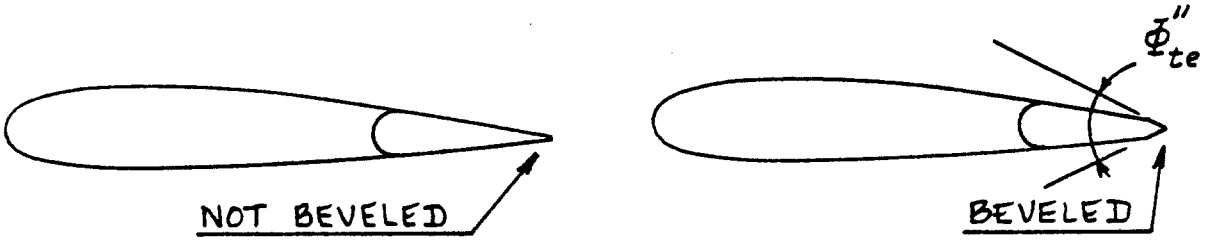

Figure 10.70 Example of Control Surface Beveling

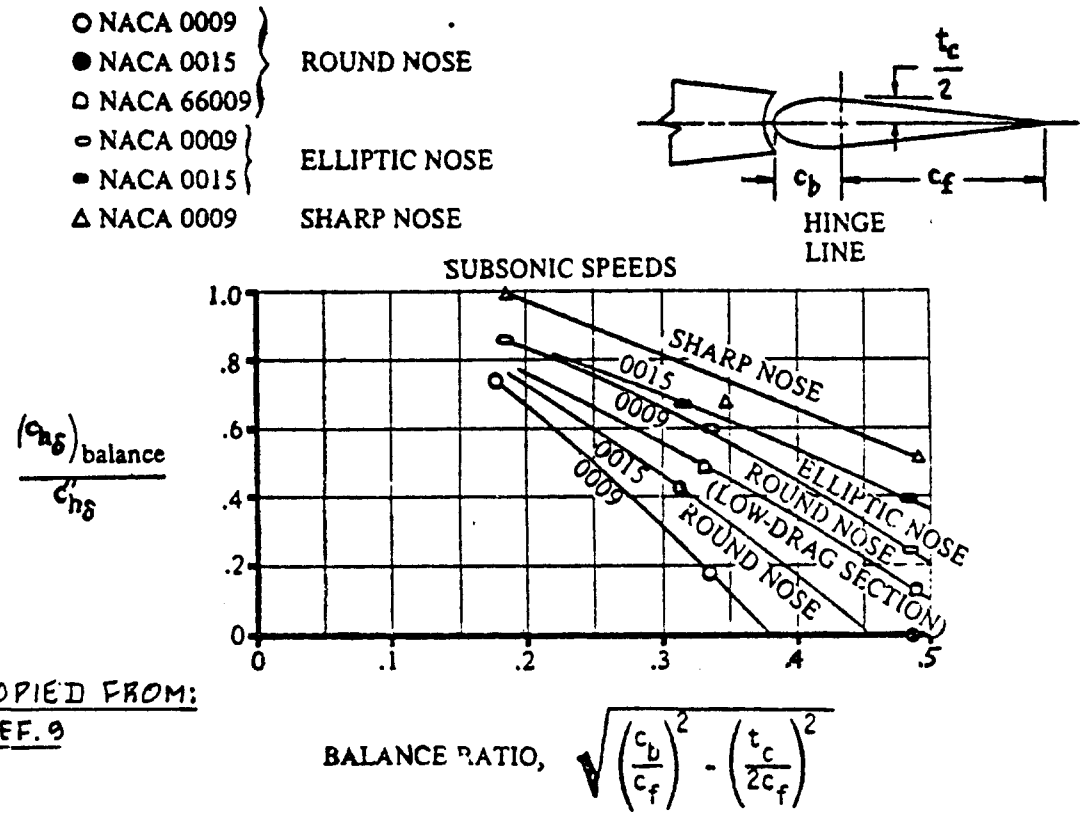

COPIED FROM: REF. 9

Figure 10.71 Effect of Nose Shape and Balance on the Two-Dimensional Control Surface Hingemoment Derivative due to Control Surface Deflection

10.4.1.3 Two-D control surface hingemoment derivative due to tab deflection: $c_{h_{\delta_t}}$

The Two-D control surface hingemoment derivative due to tab deflection, $c_{h_{\delta_t}}$, measured at constant angle of attack and at constant control surface deflection is found from:

$$c_{h_{\delta_t}} = (c_{h_{\delta_t}})_{c_l,\delta} + \quad (10.139)$$
$$- \{(c_{h_{c_l}})_{\delta_t,\delta}\} * \{(c_{l_\alpha})_{\delta_t,\delta}\} * \{(\alpha_{\delta_t})_{c_l,\delta}\}$$

where: $(c_{h_{\delta_t}})_{c_l,\delta}$ is the change in control surface hingemoment coefficient due to tab deflection at constant lift and at constant control surface deflection. It is obtained from Figure 10.72.

$(c_{h_{c_l}})_{\delta_t,\delta}$ is the change in control surface hingemoment due to lift at constant tab deflection and at constant control surface deflection. It is obtained from Figure 10.73.

$(c_{l_\alpha})_{\delta_t,\delta}$ is the airfoil lift curve slope of the main surface to which the control surface is attached. It is found in 8.1.1.2.

$(\alpha_{\delta_t})_{c_l,\delta}$ is the change in angle of attack due to a change in tab deflection. It is found from Figure 10.74.

The derivatives in Equation (10.139) do not account for the effects of tab nose shape and tab gaps: they apply to round nose tabs with sealed gaps only! To account for the effect of differing tab nose shapes and for unsealed tab gaps, the reader should correct $c_{h_{\delta_t}}$ by using appropriate ratios obtained from Figs 10.75 and 10.76.

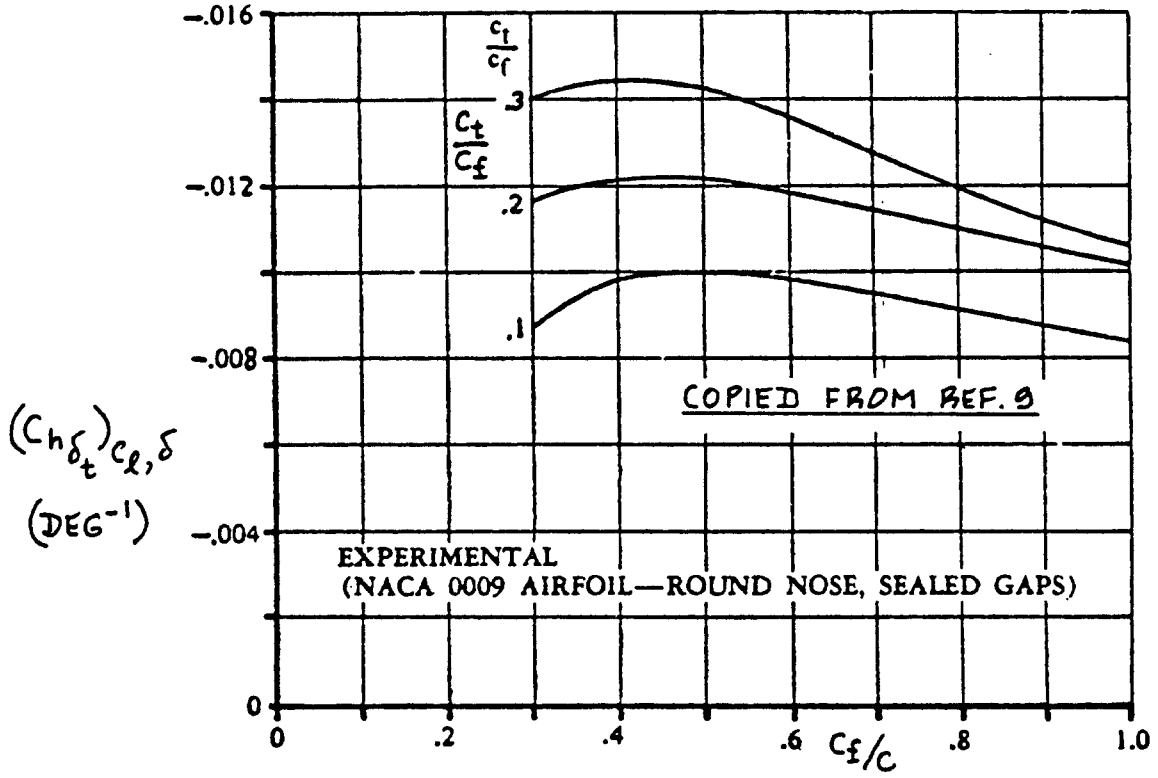

Figure 10.72 Effect of Control Surface Size and Tab Size on the Change in Control Surface Hingemoment Coefficient due to Tab Deflection at Constant Lift Coefficient and at Constant Control Surface Deflection

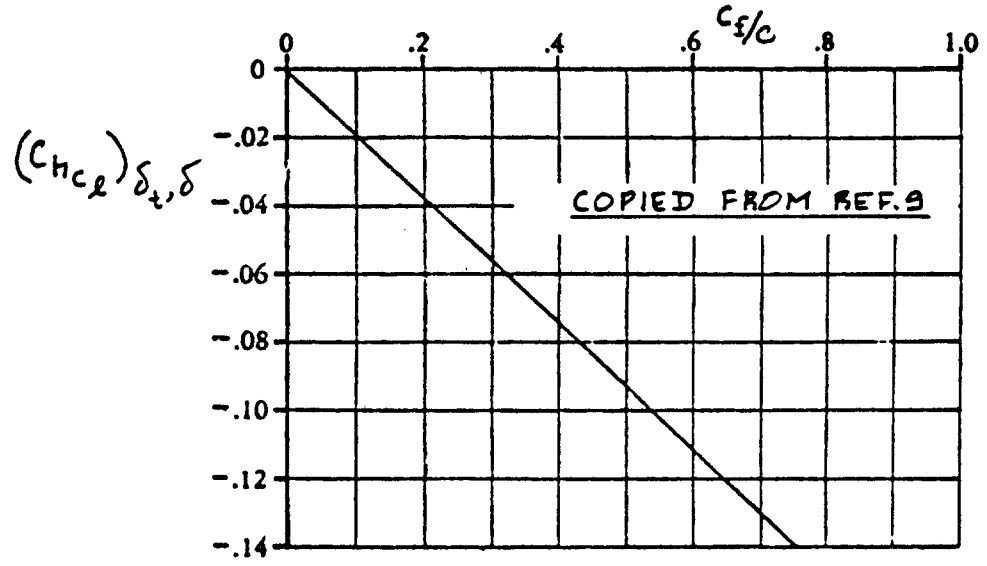

Figure 10.73 Effect of Control Surface Size on the Change in Control Surface Hingemoment due to Lift at Constant Tab Deflection and at Constant Control Surface Deflection

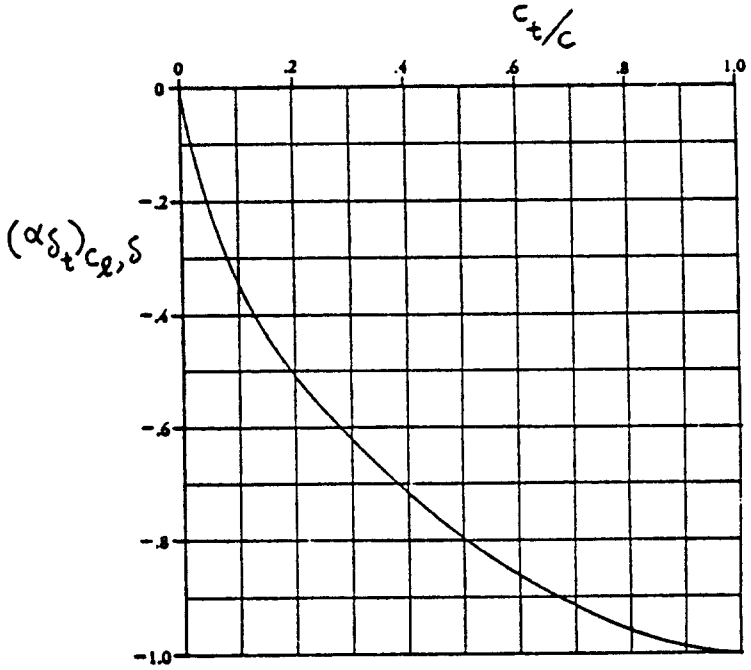

COPIED FROM:
REF. 9

Figure 10.74 Change in Angle of Attack due to a Change in Tab Deflection

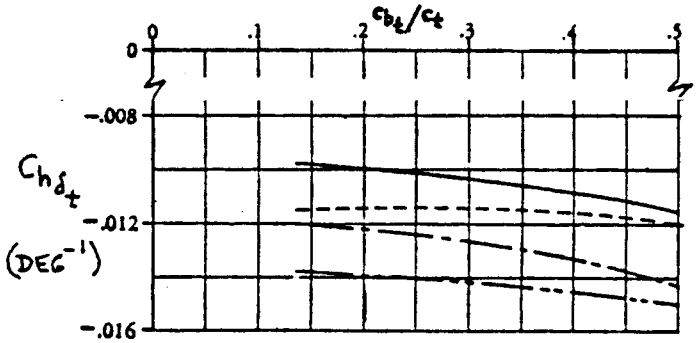

COPIED FROM:
REF. 9

TAB GAP	TRANSITION STRIPS
.004c	AT .01c
SEALED	AT .01c
.004c	OFF
SEALED	OFF

Figure 10.75 Effect of Tab Nose Shape and Tab Overhang on the Control Surface Hingemoment Derivative due to Tab Deflection

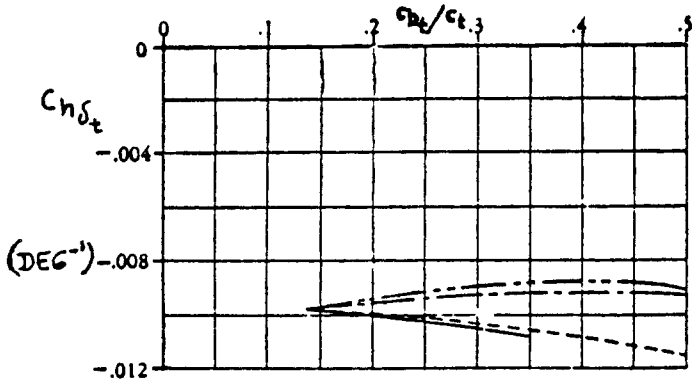

BLUNT
ROUND
ELLIPTICAL
SHARP

COPIED FROM:
REF. 9

Figure 10.76 Effect of Tab Gap Size and Tab Overhang on the Control Surface Hingemoment Derivative due to Tab Deflection

10.4.2 Three-Dimensional Control Surface and Tab Hingemoment Derivatives

The three-dimensional hingemoment coefficient for a control surface is estimated from:

$$C_h = C_{h_o} + C_{h_\alpha}\alpha + C_{h_\delta}\delta + C_{h_{\delta_t}}\delta_t \qquad (10.140)$$

where: C_{h_o} is the zero-angle-of-attack, zero-control-surface-deflection and zero-tab-deflection hingemoment coefficient. For main surfaces with symmetrical airfoils:

$$C_{h_o} = 0 \text{ (symmetrical airfoils only)} \qquad (10.141)$$

For main surfaces with cambered airfoils, experimental data should be used to determine this quantity.

C_{h_α} is the Three-D control surface hingemoment derivative due to angle of attack. It is found from 10.4.2.1

C_{h_δ} is the Three-D control surface hingemoment derivative due to control surface deflection. It is estimated from 10.4.2.2

$C_{h_{\delta_t}}$ is the Three-D control surface hingemoment derivative due to a tab deflection. It is estimated from 10.4.2.3.

10.4.2.1 Three-D control surface hingemoment derivative due to angle of attack: C_{h_α}

The Three-D control surface hingemoment due to angle of attack derivative, C_{h_α} is determined from:

$$C_{h_\alpha} = \qquad (10.142)$$

$$\{(A\cos\Lambda_{c/4})/(A + 2\cos\Lambda_{c/4})\}(c_{h_\alpha})_M + \Delta C_{h_\alpha}$$

where: $(c_{h_\alpha})_M$ is obtained from Eqn. (10.133)

$$\Delta C_{h_\alpha} = \qquad (10.143)$$

$$\{\Delta C_{h_\alpha}/(c_{l_\alpha} B_2 K_\alpha \cos\Lambda_{c/4})\} * (c_{l_\alpha} B_2 K_\alpha \cos\Lambda_{c/4})$$

with: $\{\Delta C_{h_\alpha} / (c_{l_\alpha} B_2 K_\alpha \cos\Lambda_{c/4})\}$ a factor obtained from Figure 10.77a

c_{l_α} is the airfoil lift-curve-slope of the surface to which the control surface is attached. The main surface airfoil at the m.g.c. of the control surface may be used. The method of 8.1.1.2 can be employed to estimate this quantity.

B_2 accounts for control surface and balance chord ratios. It may be determined from Figure 10.77c. The primed values of control surface and balance chord ratios in Figure 10.77c refer to measurements normal to the quarter chord line of the main surface.

K_α accounts for the effect of control surface span. It is found from:

$$K_\alpha = \{(K_\alpha)_{\eta_i}(1 - \eta_i) - (K_\alpha)_{\eta_o}(1 - \eta_o)\}/(\eta_o - \eta_i) \qquad (10.144)$$

where: η_i is the inboard span station of the control surface as a fraction of the main surface semi-span

$(K_\alpha)_{\eta_i}$ is found from Figure 10.77b

η_o is the outboard span station of the control surface as a fraction of the main surface semi-span

$(K_\alpha)_{\eta_o}$ is found from Figure 10.77b

NOTE: Control surface hingemoments are also affected by items such as horns, internal balance plates and various types of tab configurations. A discussion of these items is found in Chapter 3 of Part IV and in Chapter 5 of Reference 16. A detailed treatment of methods for estimating hingemoment derivatives due to these effects is beyond the scope of this text.

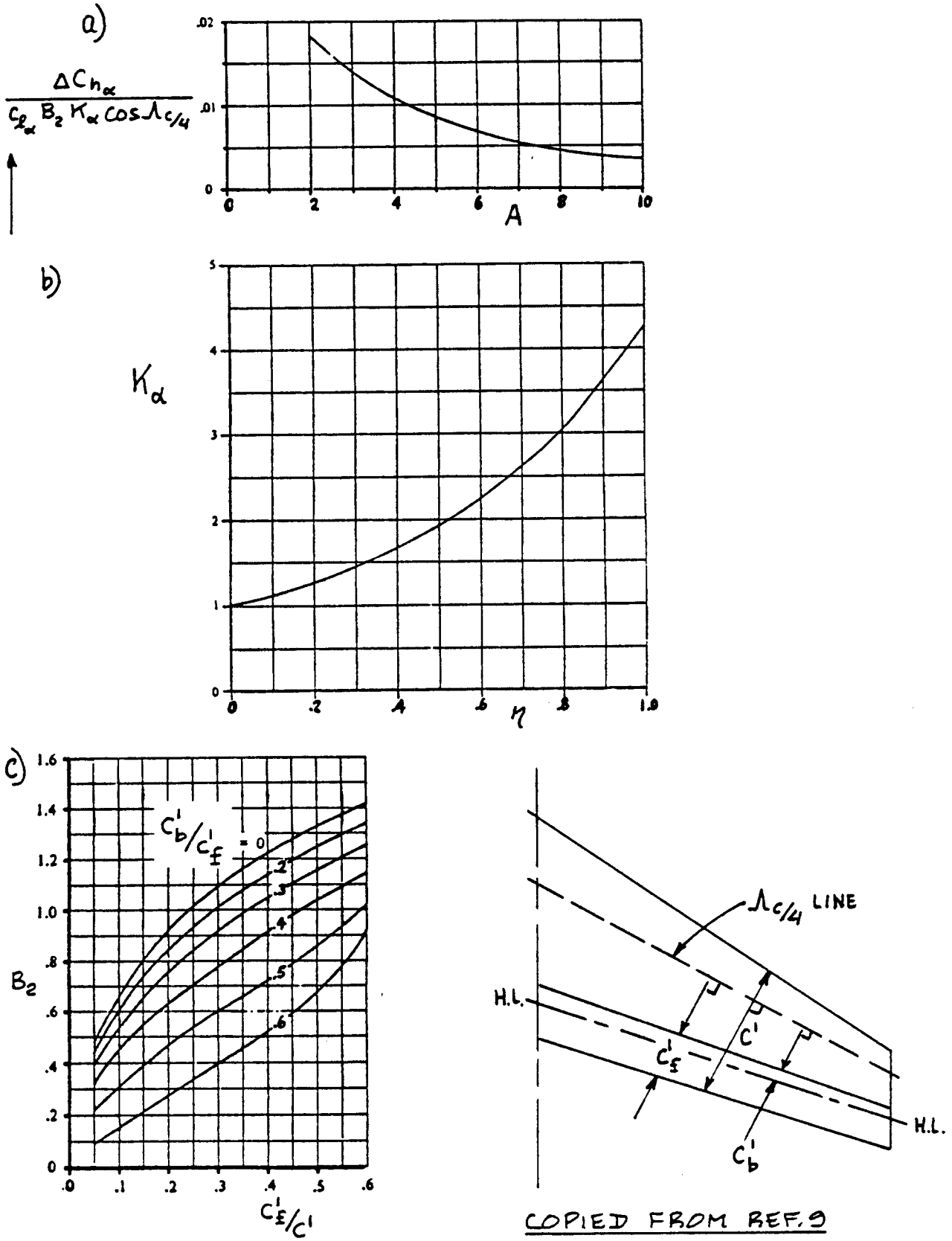

COPIED FROM REF. 9

Figure 10.77 Three-Dimensional Correction Factors for the Control Surface Hingemoment Derivative due to Angle of Attack

10.4.2.2 Three-D control surface hingemoment derivative due to control surface deflection: C_{h_δ}

The Three-D control surface hingemoment due to control surface deflection derivative, C_{h_δ} is found from:

$$C_{h_\delta} = (\cos\Lambda_{c/4})(\cos\Lambda_{hl})^* \qquad (10.145)$$

$$^*[(c_{h_\delta})_M + \alpha_\delta (c_{h_\alpha})_M \{(2\cos\Lambda_{c/4})/(A + 2\cos\Lambda_{c/4})\} + \Delta C_{h_\delta}$$

where: $(c_{h_\alpha})_M$ is found from Equation (10.133)

$(c_{h_\delta})_M$ is found from Equation (10.138)

α_δ is obtained from Figure 8.17

$$\Delta C_{h_\delta} = \qquad (10.146)$$

$$\{\Delta C_{h_\delta}/(c_{l_\delta} B_2 K_\delta \cos\Lambda_{c/4}\cos\Lambda_{hl})\}^* (c_{l_\delta} B_2 K_\delta \cos\Lambda_{c/4}\cos\Lambda_{hl})$$

with: $\{\Delta C_{h_\delta}/(c_{l_\delta} B_2 K_\delta \cos\Lambda_{c/4}\cos\Lambda_{hl})\}$ a factor obtained from Fig.10.78a

c_{l_δ} is found from Figure 8.14

B_2 is found from Figure 10.77c, where the primed values of the control-surface and the balance-chord ratios refer to measurements normal to the quarter chord line

$$K_\delta = \qquad (10.147)$$

$$\{(K_\delta)_{\eta_i}(1 - \eta_i) - (K_\delta)_{\eta_o}(1 - \eta_o)\}/(\eta_o - \eta_i)$$

where: η_i is defined in 10.4.2.1

$(K_\delta)_{\eta_i}$ is found from Figure 10.78b

η_o is defined in 10.4.2.1

$(K_\delta)_{\eta_o}$ is found from Figure 10.78b

The note at the end of 10.4.2.1 applies here also!

10.4.2.3 Three-D control surface hingemoment derivative due to tab deflection: $C_{h_{\delta_t}}$

The Three-D control surface hingemoment due to tab deflection derivative, $C_{h_{\delta_t}}$ is estimated by employing

Equation (10.145) and its sequel with appropriate substitution of tab parameters for control surface parameters.

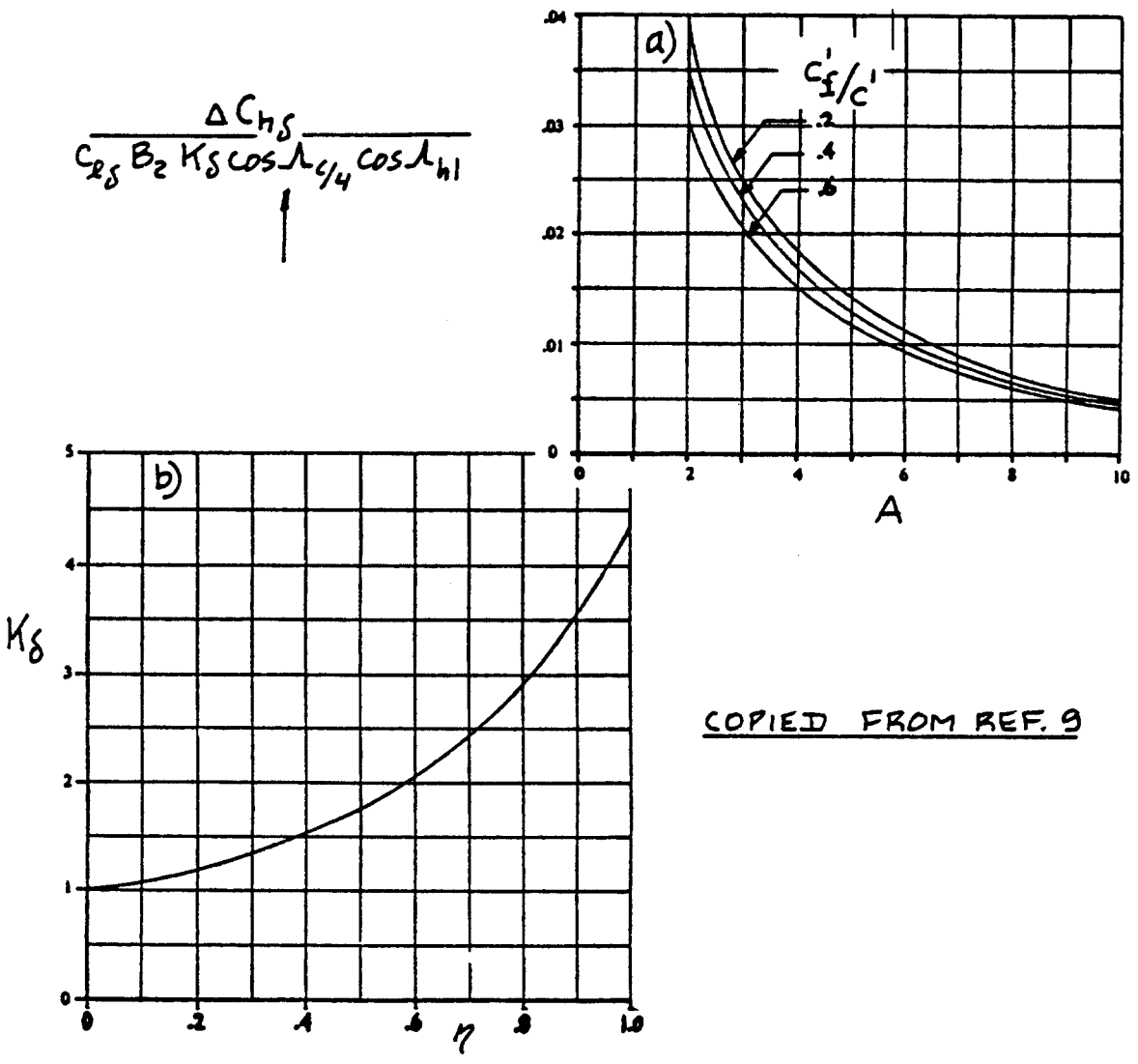

COPIED FROM REF. 9

Figure 10.78 Three Dimensional Correction Factors for the Control Surface Hingemoment Derivative due to Control Surface Deflection

10.4.3 Two-Dimensional Tab Hingemoment Derivatives about the Tab Hingeline

The two-dimensional tab hingemoment coefficient about the tab hingeline can be written as:

$$c^t_h = c^t_{h_o} + c^t_{h_\alpha}\alpha + (c^t_{h_\delta})_{\alpha,\delta_t}\delta + c^t_{h_{\delta_t}}\delta_t \quad (10.148)$$

where: $c^t_{h_o}$ is the zero-angle-of-attack, zero-control-surface-deflection and zero-tab-deflection hingemoment coefficient of the tab about its own hingeline. This quantity is zero for symmetrical airfoils. For cambered airfoils experimental data should be used.

$c^t_{h\alpha}$ is found from 10.4.1.1 by substitution of tab parameters for control surface parameters

$c^t_{h_{\delta_t}}$ is found from 10.4.1.2 by substitution of tab parameters for control surface parameters

$$(c^t_{h_\delta})_{\alpha,\alpha_t} = \quad (10.149)$$

$$(c^t_{h_\delta})_{c_l,\delta_t} - (c^t_{h_{c_l}})_{\delta,\delta_t} * (c_{l_\alpha})_{\delta,\delta_t} * (\alpha_\alpha)_{c_l,\delta_t}$$

with: $(c^t_{h_\delta})_{c_l,\delta_t}$ being the change in tab hingemoment coefficient due to control surface deflection at constant lift and at constant tab deflection. It is found from Figure 10.79a.

$(c^t_{h_{c_l}})_{\delta,\delta_t}$ being the change in tab hingemoment coefficient due to lift at constant control surface deflection and at constant tab deflection. It is found from Figure 10.79b.

$(c_{l_\alpha})_{\delta,\delta_t}$ is the airfoil lift curve slope of the main surface to which the tab (via the control surface) is attached. It is found in 8.1.1.2.

$(\alpha_\delta)_{c_l,\delta_t}$ is the change in angle of attack due to a change in control surface deflection. It is obtained from Figure 10.80 by using the tab-chord to main surface chord ratio.

The derivatives in Equation (10.148) do not account for the effects of tab nose shape and tab gaps: they apply to round nose tabs with sealed gaps only! To account for the effect of differing tab nose shapes and for unsealed tab gaps, the reader should correct $c^t h_y$ by using appropriate ratios obtained from Figs 10.81a,b,c and d.

10.4.4 Three-Dimensional Tab Hingemoment Derivatives about the Tab Hingeline

The three-dimensional tab hingemoment coefficient about the tab hingeline can be determined from:

$$C^t_h = C^t_{h_o} + C^t_{h_\alpha}\alpha + \qquad (10.150)$$

$$(C^t_{h_\delta})_{\alpha,\delta_t}\delta + C^t_{h_{\delta_t}}\delta_t$$

where all coefficients may be determined from their two-dimensional counterparts by using the methods of 10.4.2.1 and 10.4.2.2.

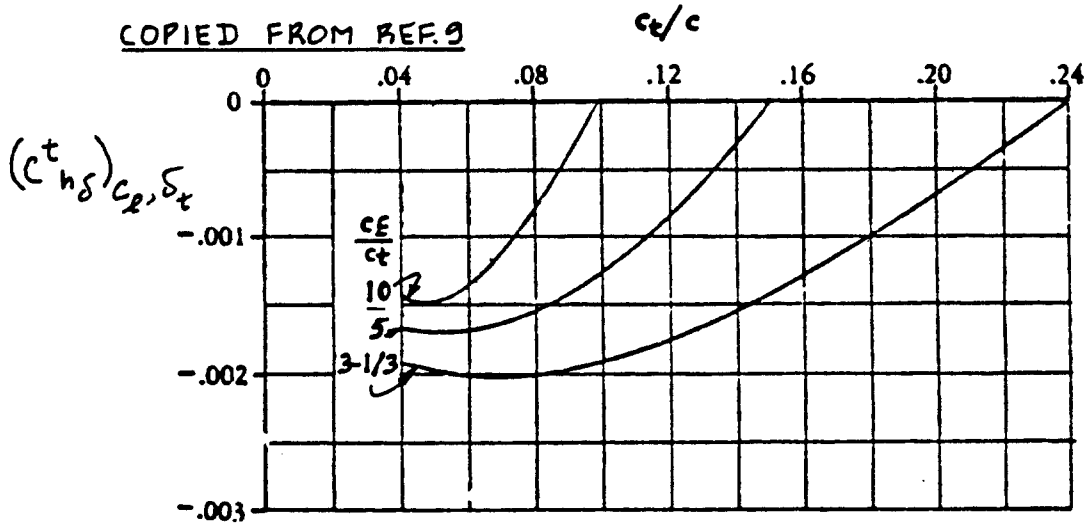

Figure 10.79a Effect of Tab and Control Surface Size on the Change in Tab Hingemoment Coefficient due to Control Surface Deflection at Constant Lift and at Constant Tab Deflection

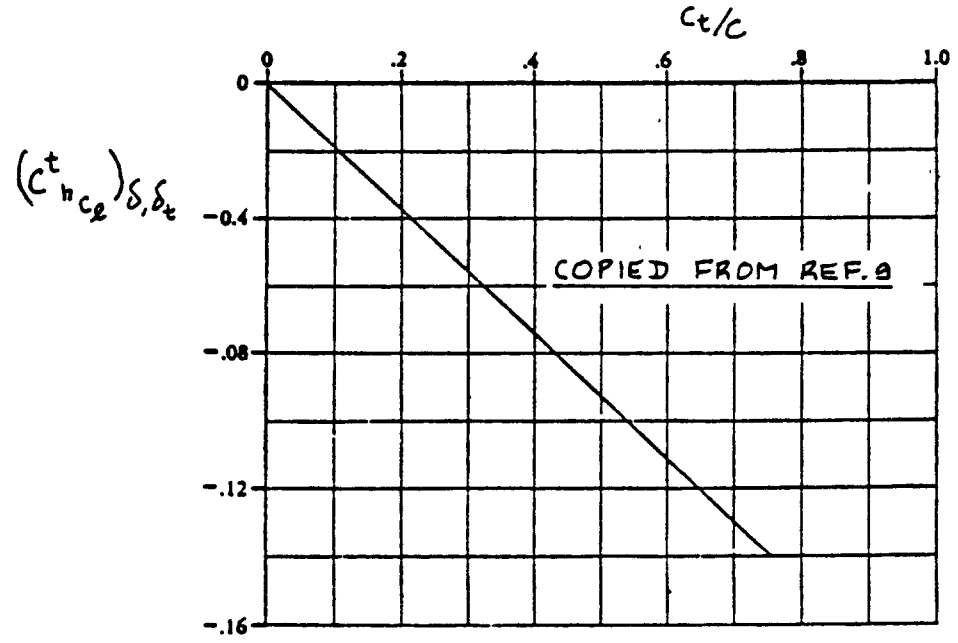

Figure 10.79b Effect of Tab Size on the Change in Tab Hingemoment Coefficient due to Lift at Constant Control Surface Deflection and at Constant Tab Deflection

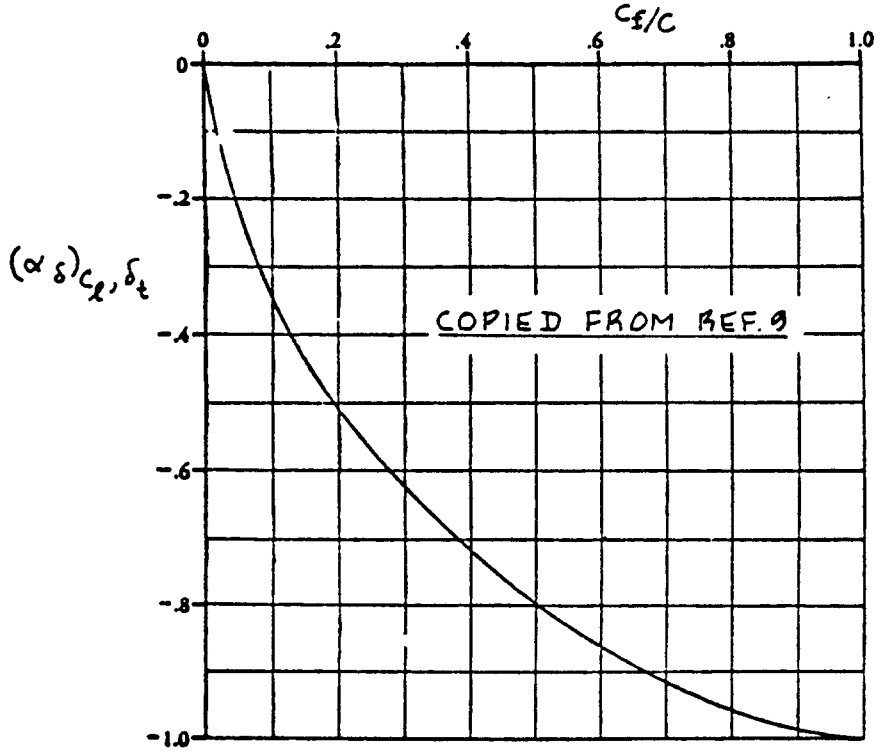

Figure 10.80 Change in Angle of Attack due to a Change in Control Surface Deflection

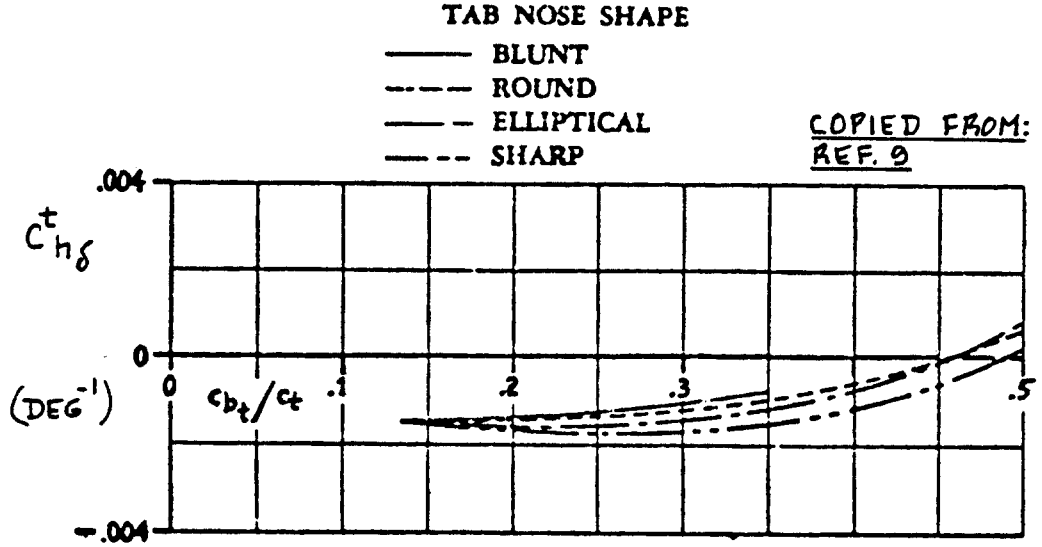

Figure 10.81a Effect of Tab Nose Shape on the Tab Hinge-moment Derivative due to Control Surface Deflection

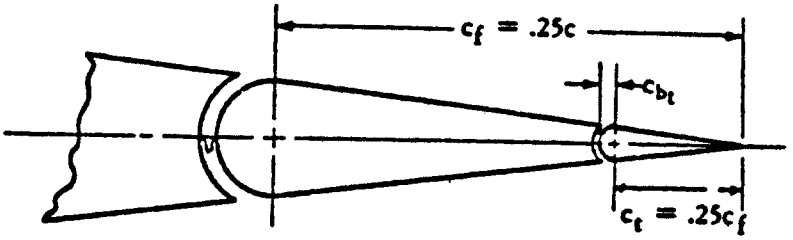

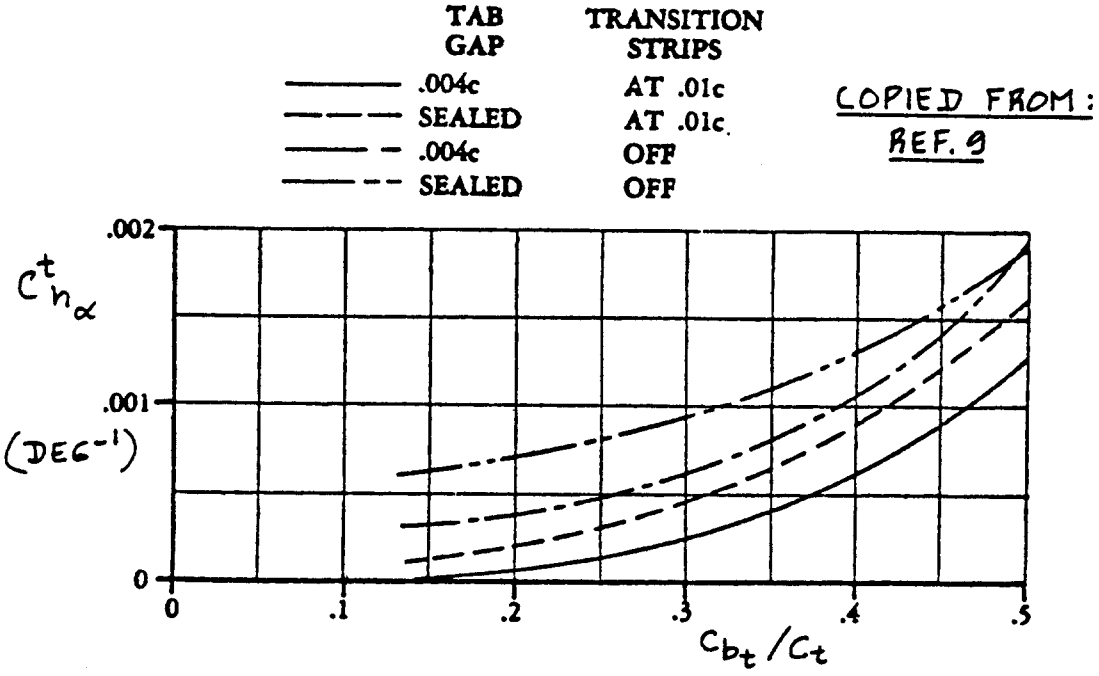

Figure 10.81b Effect of Tab Gap and Tab Size on the Tab Hingemoment Derivative due to Angle of Attack

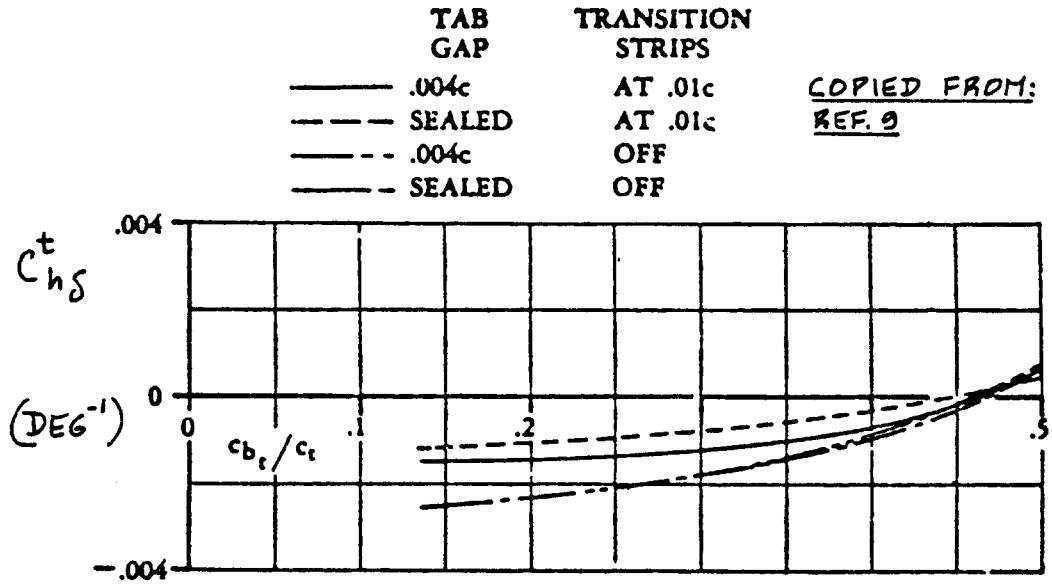

Figure 10.81c Effect of Tab Gap and Tab Size on the Tab Hingemoment Derivative due to Control Surface Deflection

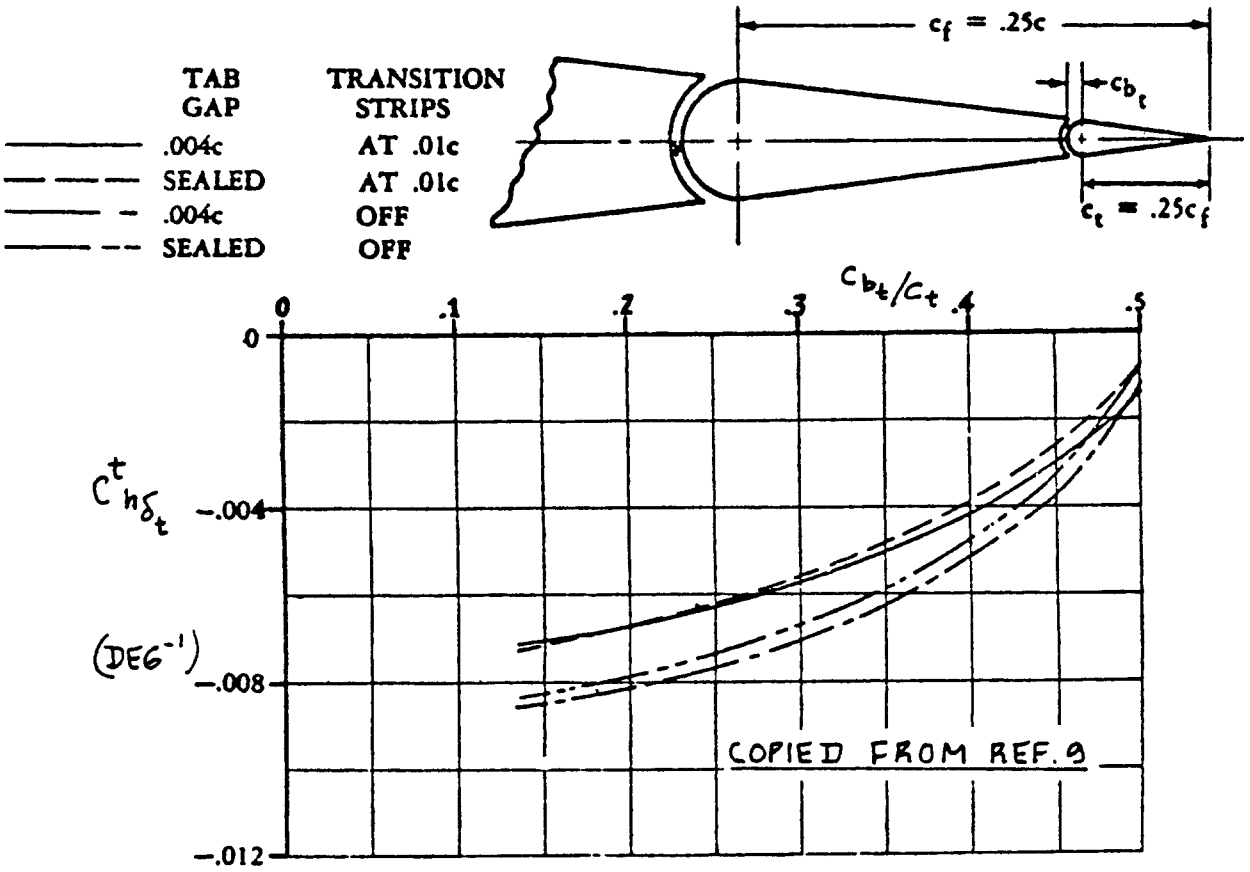

Figure 10.81d Effect of Tab Gap and Tab Size on the Tab Hingemoment Derivative due to Tab Deflection

11. STABILITY AND CONTROL DERIVATIVE DATA

The purpose of this chapter is to provide example data of stability and control derivatives for the following airplanes:

Tables 11.1 Airplane A (representative of a Cessna Model 172 type of airplane)

Tables 11.2 Airplane B (representative of a Beech Model 99 type of airplane)

Tables 11.3 Airplane C (representative of a SIAI-Marchetti S-211 type of airplane)

Tables 11.4 Airplane D (representative of a Gates Learjet Model 24 type of airplane)

Tables 11.5 Airplane E (representative of a McDonnell Douglas F4C type of airplane)

Tables 11.6 Airplane F (representative of a Boeing 747-100 type of airplane)

Except for airplane A, no data were available for hingemoment derivatives. All data are dimensionless.

Table 11.1a Geometry and Derivative Data for Airplane A

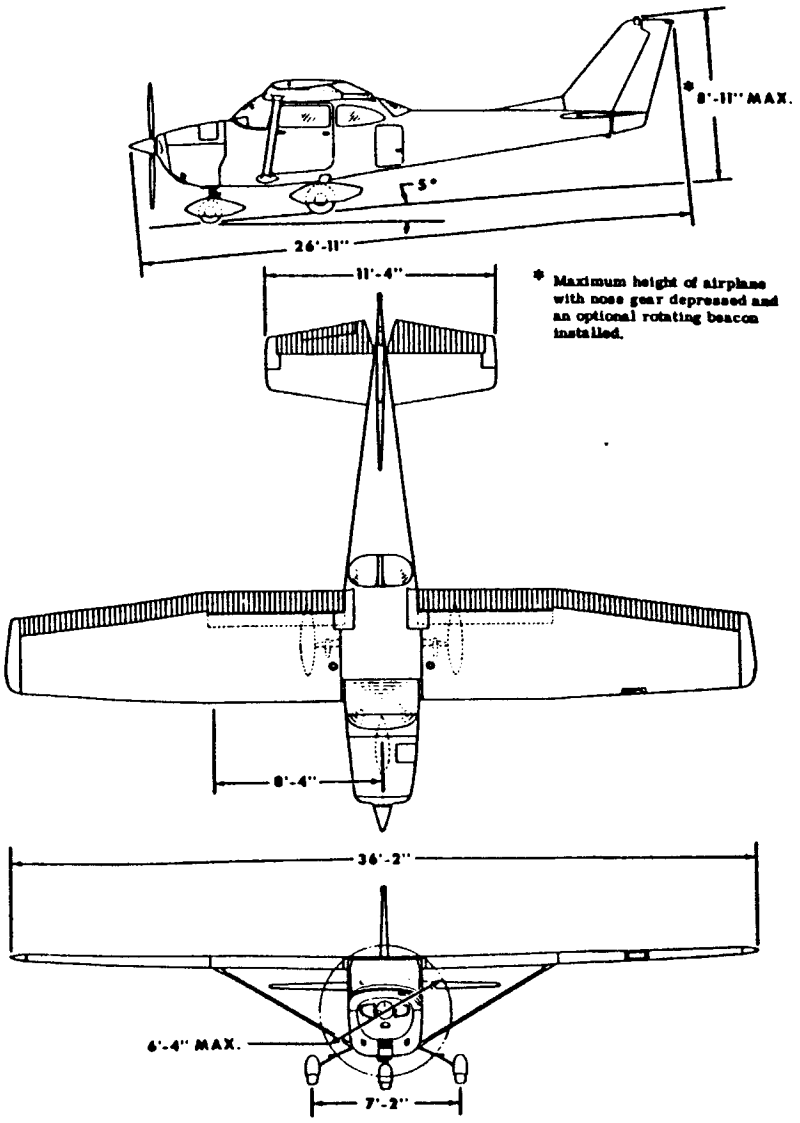

Flight Condition	1
	Cruise
Altitude (ft)	5,000
Air Density (slugs/ft^3)	.002050
Speed (fps)	219
Center of Gravity ($\bar{x}_{cg}$)	.25
Initial Attitude (θ_1 in rad)	0
Geometry and Inertias	
Wing Area (ft^2)	174
Wing Span (ft)	35.8
Wing Mean Geometric Chord (ft)	4.9
Weight (lbs)	2,645
I_{xx} (slug ft^2)	948
I_{yy} (slug ft^2)	1,346
I_{zz} (slug ft^2)	1,967
I_{xz} (slug ft^2)	0
Steady State Coefficients	
C_{L_1}	.31
C_{D_1}	.031
$C_{T_{X_1}}$	.031
C_{m_1}	0
$C_{m_{T_1}}$	0

Table 11.1b Geometry and Derivative Data for Airplane A

Longitudinal Derivatives		Lateral Directional Derivatives	
C_{m_u}	0	C_{ℓ_β}	-.089
C_{m_α}	-.89	C_{ℓ_p}	-.47
$C_{m_{\dot\alpha}}$	-5.2	C_{ℓ_r}	.096
C_{m_q}	-12.4	$C_{\ell_{\delta_A}}$	.178
$C_{m_{T_u}}$	0	$C_{\ell_{\delta_R}}$	.0147
$C_{m_{T_\alpha}}$	0	C_{n_β}	.065
C_{L_u}	0	C_{n_p}	-.03
C_{L_α}	4.6	C_{n_r}	-.099
$C_{L_{\dot\alpha}}$	1.7	$C_{n_{\delta_A}}$	-.053
C_{L_q}	3.9	$C_{n_{\delta_R}}$	-.0657
C_{D_α}	.13	C_{y_β}	-.31
C_{D_u}	0	C_{y_p}	-.037
$C_{T_{X_u}}$	-.093	C_{y_r}	.21
$C_{L_{\delta_E}}$	.43	$C_{y_{\delta_A}}$	0
$C_{D_{\delta_E}}$	.06	$C_{y_{\delta_R}}$	.187
$C_{m_{\delta_E}}$	-1.28		
C_{h_α}	-.050	$C_{h_{\delta_a}}$	-.010
$C_{h_{\delta_e}}$	-.590	$C_{h_{\delta_r}}$	-.570
		C_{h_β}	+.082

Table 11.2a Geometry and Derivative Data for Airplane B

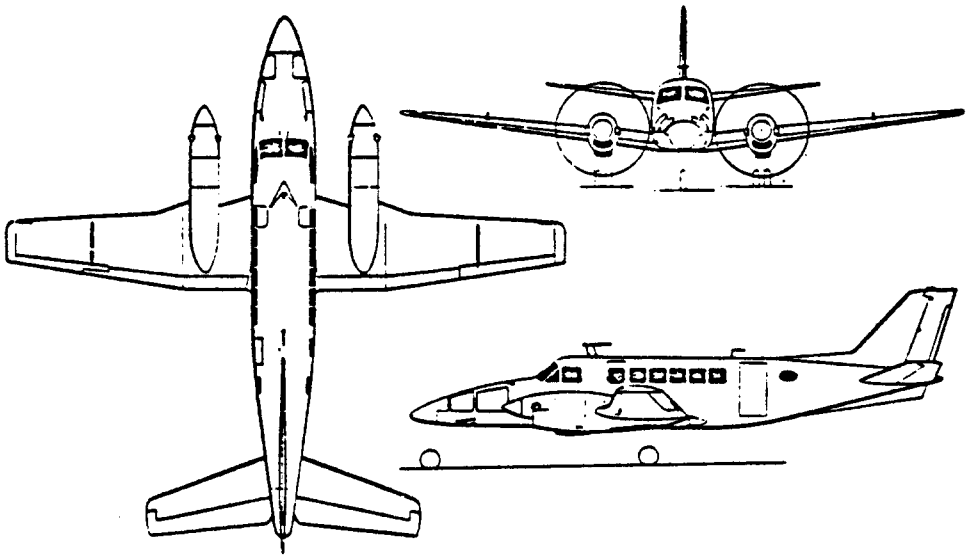

Flight Condition	1	2	3
	Power Approach	Cruise (Low)	Cruise (Normal)
Altitude (ft)	Sealevel	5,000	20,000
Air Density (slugs/ft^3)	.002378	.00205	.001268
Speed (fps)	170	340	450
Center of Gravity ($\bar{x}_{cg}$)	.16	.16	.16
Initial Attitude (θ_1 in rad)	0	0	0
Geometry and Inertias			
Wing Area (ft^2)	280	280	280
Wing Span (ft)	46	46	46
Wing Mean Geometric Chord (ft)	6.5	6.5	6.5
Weight (lbs)	11,000	7,000	11,000
I_{xx} (slug ft^2)	15,189	10,085	15,189
I_{yy} (slug ft^2)	20,250	15,148	20,250
I_{zz} (slug ft^2)	34,141	23,046	34,141
I_{xz} (slug ft^2)	4,371	1,600	4,371
Steady State Coefficients			
C_{L_1}	1.15	.191	.30
C_{D_1}	.162	.0298	.0298
$C_{T_{X_1}}$	.162	.0298	.0298
C_{m_1}	0	0	0
$C_{m_{T_1}}$	0	0	0

Table 11.2b Geometry and Derivative Data for Airplane B

Longitudinal Derivatives	1	2	3
C_{m_u}	0	0	0
C_{m_α}	-2.08	-1.89	-1.89
$C_{m_{\dot{\alpha}}}$	-9.1	-9.1	-9.1
C_{m_q}	-34.0	-34.0	-34.0
$C_{m_{T_u}}$	0	0	0
$C_{m_{T_\alpha}}$	0	0	0
C_{L_u}	.027	.020	.020
C_{L_α}	6.24	5.48	5.48
$C_{L_{\dot{\alpha}}}$	2.7	2.5	2.5
C_{L_q}	8.1	8.1	8.1
C_{D_α}	.933	.131	.131
C_{D_u}	0	0	0
$C_{T_{X_u}}$	-.324	-.0596	-.0596
$C_{L_{\delta_E}}$	.58	.6	.6
$C_{D_{\delta_E}}$	0	0	0
$C_{m_{\delta_E}}$	-1.9	-2.0	-2.0

Lateral-Directional Derivatives	1	2	3
C_{l_β}	-.13	-.13	-.13
C_{l_p}	-.50	-.50	-.50
C_{l_r}	.06	.14	.14
$C_{l_{\delta_A}}$	.156	.156	.156
$C_{l_{\delta_R}}$	.0087	.0109	.0106
C_{n_β}	.120	.080	.080
C_{n_p}	-.005	.019	.019
C_{n_r}	-.204	-.197	-.197
$C_{n_{\delta_A}}$	-.0012	-.0012	-.0012
$C_{n_{\delta_R}}$	-.0763	-.0772	-.0758
C_{y_β}	-.59	-.59	-.59
C_{y_p}	-.21	-.19	-.19
C_{y_r}	.39	.39	.39
$C_{y_{\delta_A}}$	0	0	0
$C_{y_{\delta_R}}$	.144	.148	.144

Table 11.3a Geometry and Derivative Data for Airplane C

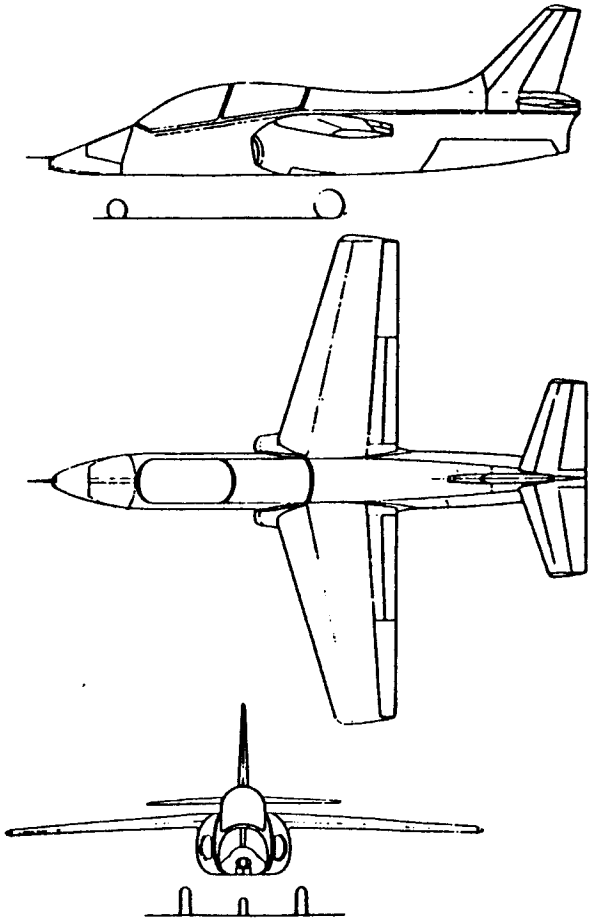

Flight Condition	1	2	3
	Power Approach	Cruise (Normal)	Cruise (High)
Altitude (ft)	Sealevel	25,000	35,000
Air Density (sluge/ft^3)	.002378	.001066	.000739
Speed (fps)	124 (1.2 $V_{S_{PA}}$)	610 (M = .6)	584 (M = .6)
Center of Gravity ($\bar{x}_{cg}$)	.25 (mid)	.25 (mid)	.25 (mid)
Initial Attitude (θ_1 in rad)	0	0	0
Geometry and Inertias			
Wing Area (ft^2)	136	136	136
Wing Span (ft)	26.3	26.3	26.3
Wing Mean Geometric Chord (ft)	5.4	5.4	5.4
Weight (lbs)	3,500	4,000	4,000
I_{xx} (slug ft^2)	750	800	800
I_{yy} (slug ft^2)	4,800	4,800	4,800
I_{zz} (slug ft^2)	5,000	5,200	5,200
I_{xz} (slug ft^2)	200	200	200
Steady State Coefficients			
C_{L_1}	1.4	.15	.23
C_{D_1}	.21	.022	.025
$C_{T_{X_1}}$	.21	.022	.025
C_{m_1}	0	0	0
$C_{m_{T_1}}$	0	0	0

Table 11.3b Geometry and Derivative Data for Airplane C

Longitudinal Derivatives	1	2	3
C_{m_u}	0	0	0
C_{m_α}	-.6	-.24	-.24
$C_{m_{\dot{\alpha}}}$	-7.0	-9.6	-9.6
C_{m_q}	-15.7	-17.7	-17.7
$C_{m_{T_u}}$	0	0	0
$C_{m_{T_\alpha}}$	0	0	0
C_{L_u}	.071	.084	.132
C_{L_α}	5.0	5.5	5.5
$C_{L_{\dot{\alpha}}}$	3.0	4.2	4.2
C_{L_q}	9.0	10.0	10.0
C_{D_α}	1.14	.12	.17
C_{D_u}	0	0	0
$C_{T_{X_u}}$	0	0	0
$C_{L_{\delta_E}}$	.39	.38	.35
$C_{D_{\delta_E}}$	0	0	0
$C_{m_{\delta_E}}$	-.90	-.88	-.82

Lateral-Directional Derivatives	1	2	3
C_{l_β}	-.140	-.110	-.110
C_{l_p}	-.350	-.390	-.390
C_{l_r}	.560	.280	.310
$C_{l_{\delta_A}}$	.110	.100	.100
$C_{l_{\delta_R}}$	.030	.050	.050
C_{n_β}	.160	.170	.170
C_{n_p}	-.030	+.090	+.080
C_{n_r}	-.310	-.260	-.260
$C_{n_{\delta_A}}$	-.030	-.003	-.005
$C_{n_{\delta_R}}$	-.110	-.120	-.120
C_{y_β}	-.94	-1.00	-1.00
C_{y_p}	-.010	-.14	-.12
C_{y_r}	.590	.610	.620
$C_{y_{\delta_A}}$	0	0	0
$C_{y_{\delta_R}}$	.260	.280	.280

Table 11.4a Geometry and Derivative Data for Airplane D

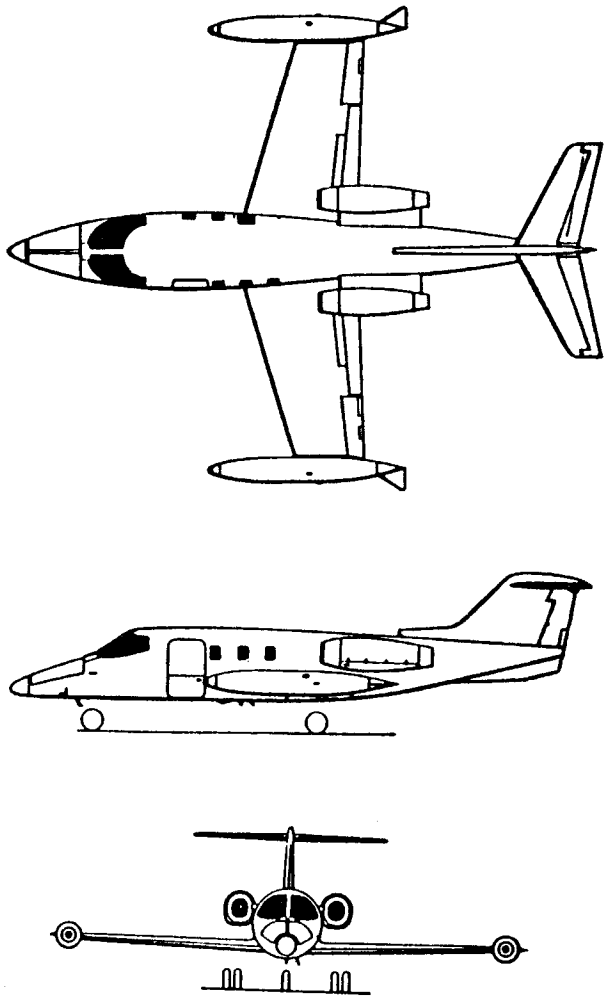

Flight Condition	1	2	3
	Power Approach	Cruise Max. Wht.	Cruise Low Wht.
Altitude (ft)	Sealevel	40,000	40,000
Air Density (slugs/ft^3)	.002378	.000588	.000588
Speed (fps)	170	677 (M = .7)	677 (M = .7)
Center of Gravity ($\bar{x}_{cg}$)	.32 (aft)	.32 (aft)	.32 (aft)
Initial Attitude (deg)	1.8	2.7	1.5
Geometry and Inertias			
Wing Area (ft^2)	230	230	230
Wing Span (ft)	34	34	34
Wing Mean Geometric Chord (ft)	7	7	7
Weight (lbs)	13,000	13,000	9,000
I_{xx_B} (slug ft^2)	28,000	28,000	6,000
I_{yy_B} (slug ft^2)	17,800	18,800	17,800
I_{zz_B} (slug ft^2)	47,000	47,000	25,000
I_{xz_B} (slug ft^2)	1,300	1,300	1,400
Steady State Coefficients			
C_{L_1}	1.64	.41	.28
C_{D_1}	.256	.0335	.0279
$C_{T_{X_1}}$	.256	.0335	.0279
C_{m_1}	0	0	0
$C_{m_{T_1}}$	0	0	0

Table 11.4b Geometry and Derivative Data for Airplane D

Longitudinal Derivatives	1	2	3
C_{m_u}	-.01	.05	.07
C_{m_α}	-.66	-.64	-.64
$C_{m_{\dot{\alpha}}}$	-5.0	-6.7	-6.7
C_{m_q}	-13.5	-15.5	-15.5
$C_{m_{T_u}}$	.006	-.003	-.003
$C_{m_{T_\alpha}}$	0	0	0
C_{L_u}	.04	.40	.28
C_{L_α}	5.04	5.84	5.84
$C_{L_{\dot{\alpha}}}$	1.6	2.2	2.2
C_{L_q}	4.1	4.7	4.7
C_{D_α}	1.06	.30	.22
C_{D_u}	0	.104	.104
$C_{T_{X_u}}$	0	0	0
$C_{L_{\delta_E}}$	.40	.46	.46
$C_{D_{\delta_E}}$	0	0	0
$C_{m_{\delta_E}}$	-.98	-1.24	-1.24

Lateral-Directional Derivatives	1	2	3
C_{l_β}	-.173	-.110	-.100
C_{l_p}	-.39	-.45	-.45
C_{l_r}	.45	.16	.14
$C_{l_{\delta_A}}$	.149	.178	.178
$C_{l_{\delta_R}}$	.014	.019	.021
C_{n_β}	.150	.127	.124
C_{n_p}	-.13	-.008	-.022
C_{n_r}	-.26	-.20	-.20
$C_{n_{\delta_A}}$	-.05	-.02	-.02
$C_{n_{\delta_R}}$	-.074	-.074	-.074
C_{y_β}	-.73	-.73	-.73
C_{y_p}	0	0	0
C_{y_r}	.4	.4	.4
$C_{y_{\delta_A}}$	0	0	0
$C_{y_{\delta_R}}$	.140	.140	.140

Table 11.5a Geometry and Derivative Data for Airplane E

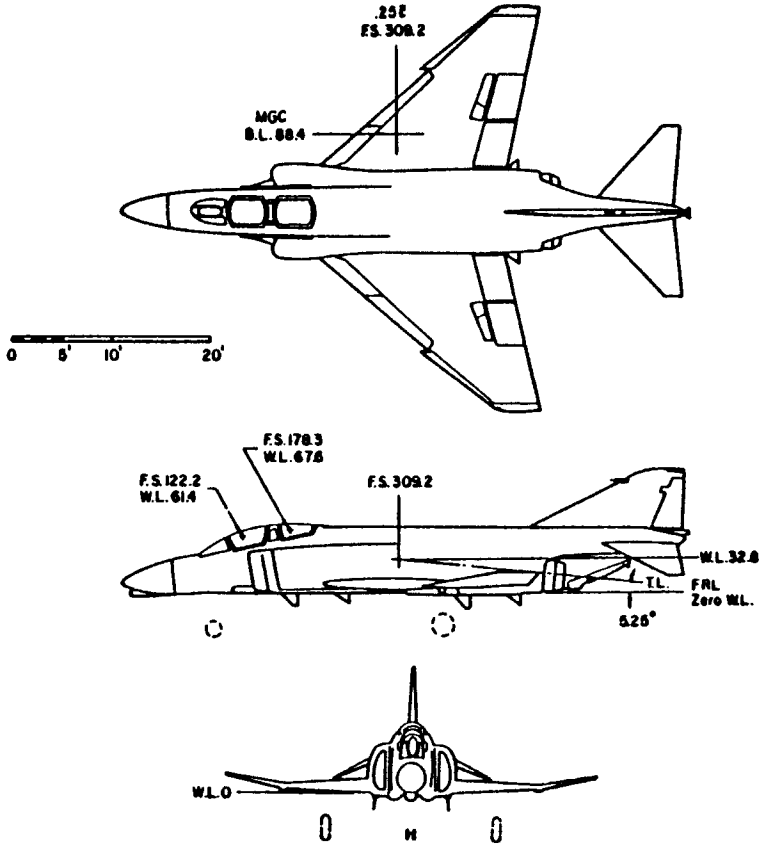

Flight Condition	1	2	3
	Power Approach	Subsonic Cruise	Supersonic Cruise
Altitude (ft)	Sealevel	35,000	55,000
Air Density (sluge/ft^3)	.002378	.000739	.000287
Speed (fps)	230	876	1742
Center of Gravity ($\bar{x}_{cg}$)	.29	.29	.29
Initial Attitude (deg)	11.7	2.6	3.3
Geometry and Inertias			
Wing Area (ft^2)	530	530	530
Wing Span (ft)	38.7	38.7	38.7
Wing Mean Geometric Chord (ft)	16.0	16.0	16.0
Weight (lbs)	33,200	39,000	39,000
I_{xx_B} (slug ft^2)	23,700	25,000	25,000
I_{yy_B} (slug ft^2)	117,500	122,200	122,200
I_{zz_B} (slug ft^2)	133,700	139,800	139,800
I_{xz_B} (slug ft^2)	1,600	2,200	2,200
Steady State Coefficients			
C_{L_1}	1.0	.26	.17
C_{D_1}	.2	.03	.048
$C_{T_{X_1}}$	.2	.03	.048
C_{m_1}	0	0	0
$C_{m_{T_1}}$	0	0	0

Table 11.5b Geometry and Derivative Data for Airplane E

Longitudinal Derivatives	1	2	3
C_{m_u}	0	-.117	+.054
C_{m_α}	-.098	-.40	-.78
$C_{m_{\dot\alpha}}$	-.95	-1.3	-.25
C_{m_q}	-2.0	-2.7	-2.0
$C_{m_{T_u}}$	0	0	0
$C_{m_{T_\alpha}}$	0	0	0
C_{L_u}	0	+.27	-.18
C_{L_α}	2.8	3.75	2.8
$C_{L_{\dot\alpha}}$	0	0	0
C_{L_q}	0	0	0
C_{D_α}	.555	.3	.4
C_{D_u}	0	+.027	-.054
$C_{T_{X_u}}$	0	0	0
$C_{L_{i_H}}$	.24	.40	.25
$C_{D_{i_H}}$	-.14	-.10	-.15
$C_{m_{i_H}}$	-.322	-.58	-.38

(Note: longitudinal control through stabilizer only)

Lateral-Directional Derivatives	1	2	3
C_{l_β}	-.156	-.080	-.025
C_{l_p}	-.272	-.240	-.200
C_{l_r}	.205	.070	.040
$C_{l_{\delta_A}}$	.057	.042	.015
$C_{l_{\delta_R}}$	.0009	.0060	.0030
C_{n_β}	.199	.125	.090
C_{n_p}	.013	-.036	0
C_{n_r}	-.320	-.270	-.260
$C_{n_{\delta_A}}$	+.0041	-.0010	-.0009
$C_{n_{\delta_R}}$	-.072	-.066	-.025
C_{y_β}	-.655	-.68	-.70
C_{y_p}	0	0	0
C_{y_r}	0	0	0
$C_{y_{\delta_A}}$	-.0355	-.016	-.010
$C_{y_{\delta_R}}$	.124	.095	.050

Table 11.6a Geometry and Derivative Data for Airplane F

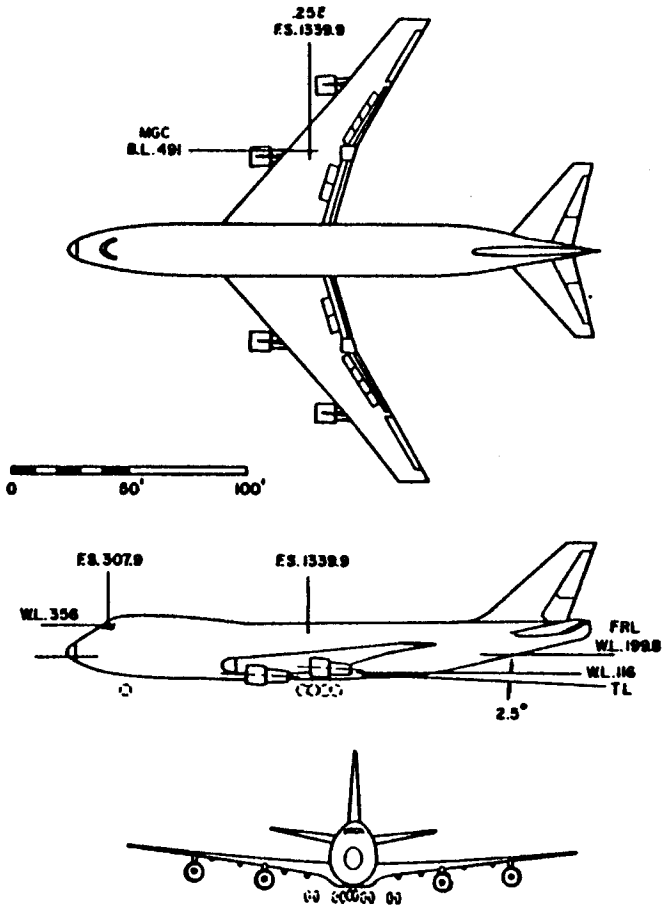

Flight Condition	1	2	3
	Power Approach	Cruise (High)	Cruise (Low)
Altitude (ft)	Sealevel	40,000	20,000
Air Density (sluge/ft^3)	.002389	.000588	.001268
Speed (fps)	221	871	673
Center of Gravity ($\bar{x}_{cg}$)	.25	.25	.25
Initial Attitude (deg)	8.5	2.4	2.5
Geometry and Inertias			
Wing Area (ft^2)	5,500	5,500	5,500
Wing Span (ft)	196	196	196
Wing Mean Geometric Chord (ft)	27.3	27.3	27.3
Weight (lbs)	564,000	636,636	636,636
I_{xx_B} (slug ft^2)	13.7 x 10^6	18.2 x 10^6	18.2 x 10^6
I_{yy_B} (slug ft^2)	30.5 x 10^6	33.1 x 10^6	33.1 x 10^6
I_{zz_B} (slug ft^2)	43.1 x 10^6	49.7 x 10^6	49.7 x 10^6
I_{xz_B} (slug ft^2)	.83 x 10^6	.97 x 10^6	.97 x 10^6
Steady State Coefficients			
C_{L_1}	1.76	.52	.40
C_{D_1}	.263	.045	.025
$C_{T_{X_1}}$	.263	.045	.025
C_{m_1}	0	0	0
$C_{m_{T_1}}$	0	0	0

Table 11.6b Geometry and Derivative Data for Airplane F

Longitudinal Derivatives	1	2	3
C_{m_u}	.071	-.09	+.013
C_{m_α}	-1.45	-1.60	-1.00
$C_{m_{\dot{\alpha}}}$	-3.3	-9.0	-4.0
C_{m_q}	-21.4	-25.5	-20.5
$C_{m_{T_u}}$	0	0	0
$C_{m_{T_\alpha}}$	0	0	0
C_{L_u}	-.22	-.23	+.13
C_{L_α}	5.67	5.5	4.4
$C_{L_{\dot{\alpha}}}$	6.7	8.0	7.0
C_{L_q}	5.65	7.8	6.6
C_{D_α}	1.13	.50	.20
C_{D_u}	0	.22	0
$C_{T_{X_u}}$	0	0	0
$C_{L_{\delta_E}}$	.36	.30	.32
$C_{D_{\delta_E}}$	0	0	0
$C_{m_{\delta_E}}$	-1.40	-1.20	-1.30

Lateral-Directional Derivatives	1	2	3
C_{ℓ_β}	-.281	-.095	-.160
C_{ℓ_p}	-.502	-.320	-.340
C_{ℓ_r}	.195	.200	.130
$C_{\ell_{\delta_A}}$	.053	.014	.013
$C_{\ell_{\delta_R}}$	0	.005	.008
C_{n_β}	.184	.210	.160
C_{n_p}	-.222	+.020	-.026
C_{n_r}	-.36	-.33	-.28
$C_{n_{\delta_A}}$	+.0083	-.0028	+.0018
$C_{n_{\delta_R}}$	-.113	-.095	-.100
C_{y_β}	-1.08	-.90	-.90
C_{y_p}	0	0	0
C_{y_r}	0	0	0
$C_{y_{\delta_A}}$	0	0	0
$C_{y_{\delta_R}}$	.179	.060	.120

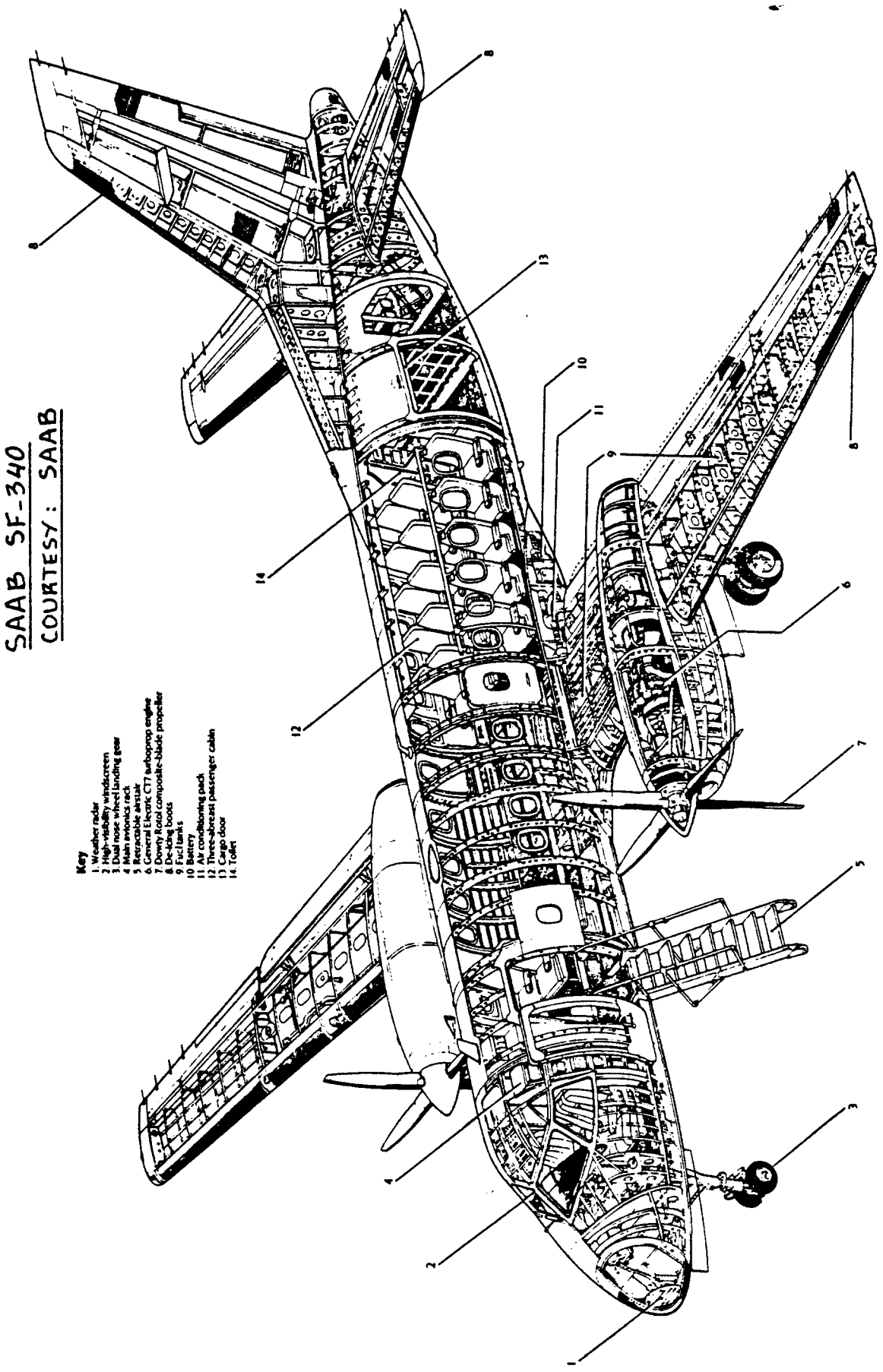
SAAB SF-340
COURTESY: SAAB
Key
1. Weather radar
2. High-visibility windscreen
3. Dual nose wheel landing gear
4. Main engine nacelle
5. Retractable airstair
6. Vertical Electric CT7 turboprop engine
7. Dowty Rotol composite-blade propeller
8. Tailplane de-icing boots
9. Fuel tanks
10. Battery
11. Air conditioning pack
12. Three-abreast passenger cabin
13. Cargo door
14. Toilet

12. USER'S GUIDE

The purpose of this chapter is to present a User's Guide to the prediction methods presented in this part of the eight part series on Airplane Design.

It is assumed that the Preliminary Design Sequence I (see p.11, Part II) has been completed and that the results of the accompanying Class I work have been properly documented. The stage is now set for a more 'in depth' (Class II) analysis of the capabilities of the design. To accomplish this, the following characteristics need to be determined:

1.) Drag polars
2.) Installed thrust or power data
3.) Lift versus angle of attack
4.) Pitching moment versus angle of attack
5.) Stability, control and hingemoment derivatives

The data which are the result of determining items 1.) through 5.) are themselves input data to the calculation and the evaluation of performance, stability, control, handling qualities and airworthiness capabilities of the airplane as outlined in Part VII.

NOTE: The reader should not attempt to perform any of the calculations represented by 1.) through 5.) without a complete geometric definition of the airplane: a dimensioned, Class I threeview MUST be available. This threeview should be of a size large enough so that dimensions needed in predicting items 1.) through 5.) can be 'scaled' directly from this threeview drawing. If a CAD (Computer Aided Design) data base is available for the airplane, so much the better.

12.1 USER'S GUIDE FOR DRAG POLAR DETERMINATION

Step 1: The reader should determine for which conditions drag polars are needed:

Airplane Configuration:
- *Clean
- *Flap position (up, take-off or landing)
- *Landing Gear (up or down)
- *External stores
- *Engine and inlet status

Flight Condition: *Mach Number
*Altitude
*Reynold's Number
*Weight
*Center of Gravity Location

The conditions selected depend on the type of performance calculations which need to be performed with the drag polars. Example of performance capabilities which typically must be determined are:

A) Mission oriented performance such as:

* take-off	* climb	* cruise
* loiter	* descent	* landing
* maneuvering	* high speed dash	* accelerate

B) Airworthiness oriented performance such as:

* climb rate or gradient with failed engine(s)
* balanced fieldlength
* performance following major damage (for example combat damage)

Step 2: Proceed to Chapter 4 to compute the required drag data. Refer to Equation 4.4 and identify which drag components must be determined. Prepare a list of input data needed for the calculation of each drag component.

Plot the results in the form of C_D versus α.

Step 3: Proceed to Section 12.3 and use the resulting C_L versus α plot together with the C_D versus α plot obtained from Step 2 to construct a C_L versus C_D plot (=drag polar).

Step 4: Verify the drag polars with the procedure of Section 5.5, p.135. Also compare the drag polar data with data on similar airplanes: see Section 5.1, p.117.

12.2 USER'S GUIDE FOR DETERMINATION OF INSTALLED THRUST OR POWER

It will be assumed that the Class I powerplant integration has been carried out as indicated in Chapter 5 of Part II. The powerplant installation has therefore been temporarily 'frozen' which means that the following information should be available:

* engine type
* inlet type and inlet size
* number of engines
* exhaust type and nozzle size

Manufacturers uninstalled thrust or power data must also be available at this point.

Finally, it will be assumed that a list of systems required by the airplane including a preliminary determination of the power requirements of these systems, is avalable.

Step 1: Obtain engine manufacturers uninstalled thrust or power data. These data should define uninstalled thrust (or power) as a function of altitude, temperature, airspeed and fuel flow.

If such detailed data are not available, the data in Chapter 6 of Part III may be used to 'guestimate' a set of uninstalled data.

Step 2: Refer to pages 139 and 140 (Chapter 6) and proceed with the preparation of the input data necessary in the calculation of installed thrust or power data.

Step 3: Using the methods of Sections 6.1 through 6.4 estimate the installed power or thrust capabilities of the airplane.

Example data are given in Chapter 7.

12.3 USER'S GUIDE FOR DETERMINATION OF LIFT VERSUS ANGLE OF ATTACK

Step 1: The reader should determine for which flight conditions the lift versus angle of attack data need to be prepared. Refer to Step 1 in Section 12.1 for some guidelines.

Step 2: Proceed to Section 8.1 for the calculation of the required lift versus angle of attack characteristics. Plot the results in the form of C_L versus α.

Step 3: Check the results of Step 2 by comparing with example data on similar airplanes such as given in Chapter 9.

12.4 USER'S GUIDE FOR THE DETERMINATION OF PITCHING MOMENT VERSUS ANGLE OF ATTACK AND THE TRIM DIAGRAM

Step 1: The reader should determine for which flight conditions the pitching moment versus angle of attack data need to be prepared. Refer to Step 1 of Section 12.1 for guidelines.

Step 2: Refer to the weight versus center of gravity diagram (See Chapter 10, Part II) and determine the most forward and aft c.g. location which applies to each flight condition selected in Step 1. Select a suitable c.g. location for use as the reference point in the pitching moment calculations.

Step 3: Proceed to Section 8.2 and determine the pitching moment versus angle of attack characteristics. Plot the results in the form of C_m versus α for the reference point selected in Step 2.

Step 4: Proceed to Section 8.3 and determine the airplane trim diagram in the form of a plot of C_m versus C_L for the reference point selected in Step 2.

Step 5: Verify the results of Step 4 by comparing with data on similar airplanes. Some data are given in Chapter 9.

12.5 USER'S GUIDE FOR THE DETERMINATION OF STABILITY, CONTROL AND HINGEMOMENT DERIVATIVES

Step 1: Determine the flight conditions for which the derivatives need to be determined. Use Step 1 in Section 12.1 for guidelines.

Step 2: Proceed to Chapter 10 and compute the required derivatives.

Step 3: Verify the results of Step 2 by comparing with data on similar airplanes. Example derivative data are given in Chapter 11.

13. REFERENCES

1. Roskam, J., Airplane Design: Part I, Preliminary Sizing of Airplanes.
2. Roskam, J., Airplane Design: Part II, Preliminary Configuration Design and Integration of the Propulsion System.
3. Roskam, J., Airplane Design: Part III, Layout Design of Cockpit, Fuselage, Wing and Empennage: Cutaways and Inboard Profiles.
4. Roskam, J., Airplane Design: Part IV, Layout Design of Landing Gear and Systems.
5. Roskam, J., Airplane Design: Part V, Component Weight Estimation.
6. Roskam, J., Airplane Design: Part VII, Determination of Stability, Control and Performance Characteristics: FAR and Military Requirements.
7. Roskam, J., Airplane Design: Part VIII, Airplane Cost Estimation and Optimization: Design, Development Manufacturing and Operating.

Note: These books are all published by: Roskam Aviation and Engineering Corporation, Rt4, Box 274, Ottawa, Kansas, 66067, Tel. 913-2421624.

8. Hoerner, S.F., Fluid Dynamic Drag, Hoerner Fluid Dynamics, P.O. Box 342, Brick Town, N.J., 08723, '65.
9. Hoak, D.E., et al, USAF Stability and Control Datcom, Flight Control Division, Air Force Flight Dynamics Laboratory, WPAFB, Ohio, 45433-0000, 1978, revised.
10. Nelson and Welsh, Some Examples of the Application of the Transonic and Supersonic Area Rules to the Prediction of Wave Drag, NASA TN D-446, 1960.
11. Kuchemann, D., The Aerodynamic Design of Aircraft, Pergamon Press, England, 1978.
12. Nicolai, L.M., Fundamentals of Aircraft Design, METS Inc., 6520 Kingsland Court, San Jose, CA, 95120.
13. Torenbeek, E., Synthesis of Subsonic Airplane Design, Kluwer Boston inc., Hingham, Maine, 1982.
14. McCormick, B.W., Aerodynamics, Aeronautics and Flight Mechanics, John Wiley and Sons, 1979, N.Y., N.Y.
15. Lan, C.E. and Roskam, J., Airplane Aerodynamics and Performance, Roskam Aviation and Engineering Corp., Route 4, Box 274, Ottawa, Kansas, 66067, 1980.

16. Roskam, J., Airplane Flight Dynamics and Automatic Flight Control Systems, Roskam Aviation and Engineering Corp., Route 4, Box 274, Ottawa, Kansas, 1981.

17. Whitcomb, R.T., A Study of the Zero-lift Drag Rise Characteristics of Wing-Body Combinations Near the Speed of Sound, NACA Report 1273, 1956.

18. Nelson, B.D., Design Scope for Student Supersonic Projects, AIAA Paper 86-2638, Presented at the AIAA/AHS/ASEE Aircraft Systems, Design and Technology Meeting, Dayton, Ohio, 1986.

19. Curry, N.S., Landing Gear Design Handbook, Lockheed Georgia Company, Georgia, 30063, 1982.

20. Royal Aeronautical Society Data Sheets, 1963, London.

21. Anonymous, Aircraft Design, Part III (in Dutch), Dept. of Aeronautical Engineering, Technological University of Delft, Delft, Holland, 1970.

22. Corning, G., Supersonic and Subsonic Airplane Design, Box No.14, College Park, Maryland.

23. Holmes, B.J. et al, Manufacturing Tolerances for Natural Laminar Flow Airframe Surfaces, SAE Paper 850863, 1985.

24. Maddalon, D.V. and McMillin, M.L., Effect of Surface Waviness on a Supercritical Laminar-Flow-Control Airfoil, NASA TM 85705, 1983.

25. Braslow, A.L. and Fischer, M.C., Design Considerations for Application of Laminar Flow Control Systems to Transport Aircraft, Paper presented at the AGARD/FDP VKI Special Course on 'Aircraft Drag Prediction and Reduction', NASA Langley, VA, 1985.

26. Maddalon, D.V. and Wagner, R.D., Operational Considerations for Laminar Flow Aircraft, Paper presented at the NASA/SAE/AIAA/FAA Laminar Flow Aircraft Certification Workshop, Wichita, Kansas, 1985.

27. Schlichting, H., Boundary Layer Theory, Mc Graw-Hill, N.Y., 1955.

28. Vijgen, P.M.H.W., et al, Effects of Compressibility on Design of Subsonic Natural Laminar Flow Fuselages, AIAA Paper 86-1825 CP, 1986.

29. Dodbele, S.S., et al, Shaping of Airplane Fuselages for Minimum Drag, AIAA Paper 86-0316, 1986.

30. Dodbele, S.S. et al, Design of Fuselage Shapes for Natural Laminar Flow, NASA CR-3970, 1986.

31. Taylor, J.W.R., Jane's All The World Aircraft, Published annually by: Jane's Publishing Company' 238 City Road, London EC1V 2PU, England.

32. Seddon, J. and Goldsmith, E.L., Intake Aerodynamics, AIAA Education Series, American Institute of Aeronautics and Astronautics, N.Y., N.Y.

33. Covert, E.E. et al, Thrust and Drag: Its Prediction and Verification, AIAA Education Series, American Institute of Aeronaytics and Astronautics, N.Y., N.Y.

34. Marks, L.S. et al, Mechanical Engineer's Handbook, McGraw Hill Book Company, N.Y., N.Y.

35. Monts, F., The Development of Reciprocating Engine Installation Data for General Aviation Aircraft, SAE Paper 730325, Business Aircraft Meeting, Wichita, Kansas, April, 1973.

36. Corsiglia, V.R. and Katz, J., Full-Scale Study of the Cooling System Aerodynamics of an Operating Piston Engine Installed in a Light Aircraft Wing Panel, SAE Paper 810623, Business Aircraft Meeting, Wichita, Kansas, April, 1981.

37. Taylor, C.F., The Internal Combustion Engine in Theory and Practice, Volumes I and II, MIT Press, 1966.

38. Bingelis, T., Firewall Forward, Engine Installation Methods, Tony Bingelis, 8509 Greenflint Lane, Austin, Texas, 78759, 1974.

39. Thurston, D.B., Design for Flying, McGraw Hill Book Co., N.Y., N.Y., 1978.

40. Bingelis, T., Sportplane Builder, Tony Bingelis, 8509 Greenflint Lane, Austin, Texas, 78759, 1985.

41. Kerrebrock, J.L., Aircraft Engines and Gas Turbines, MIT Press, 1977.

42. Borst, H.V., Propeller Performance and Design as Influenced by the Installation, SAE Paper 810602, Business Aircraft Meeting, Wichita, Kansas, April, 1981.

43. Borst, H.V. et al, Summary of Propeller Design Procedures and Data, Volumes I, II and III, USAAMRL Technical Report 73-34, H.V.Borst Associates, Wayne, Pa, November 1973.

44. McCormick, B.W. et al, The Analysis of Propellers Including Interaction Effects, SAE Paper 790576, Business Aircraft Meeting, Wichita, Kansas, April, 1979.

45. Weick, F.E., Aircraft Propeller Design, McGraw Hill Book Co., N.Y., N.Y., 1930.

46. Smith, M.H., A Prediction Procedure for Propeller Aircraft Flyover Noise Based on Empirical Data, SAE Paper 810604, 1981.

47. Anon., Prediction Procedure for Near-Field and Far-Field Propeller Noise, AIR 1407, SAE Aerospace Information Report, May, 1977.

48. Klatte, R.J., General Aviation Propeller Noise Reduction- Penalties and Potential, SAE Paper 810585, 1981

49. Abbott, I.H. and Von Doenhoff, E., Theory of Wing Sections, Dover Publications, N.Y., 1959.

50. Mueller, T.J. et al, Proceedings of the Conference on Low Reynolds Number Airfoil Aerodynamics, Sponsored by NASA, USNavy and University of Notre Dame, UNDAS CP-77B123, June 1985.

51. Hoerner, S.F. and Borst, H.V., Fluid-Dynamice Lift, Hoerner Fluid Dynamics, Box 342, Brick Town, N.J., 08723, 1975.

52. DeYoung, J., Theoretical Symmetric Span Loading Due To Flap Deflection For Wings Of Arbitrary Planform At Subsonic Speeds, NACA TR 1071, 1952.

53. Shortal, J.A. and Maggin, B., Effect of Sweepback and Aspect Ratio on Longitudinal Stability Characteristics of Wings at Low Speeds, NACA TN 1093, 1946.

54. Perkins, C.D. and Hage, R.E., Airplane Performance, Stability and Control, J.Wiley and Sons, N.Y., 1957.

55. Wittenberg, H., Calculation of Lift and Drag at Low Speeds, Part I: Wing (in Dutch), Technological University Delft, Delft, The Netherlands, 1970.

56. Sanders, K.L., High Lift Devices, A Weight and Performance Trade-off Methodology, T.P.761, Society of Aeronautical Weights Engineers, 1969.

57. Anon., Aeronautical Vestpocket Handbook, United Technologies, Pratt and Whitney Aircraft, PWA Part No. 79500, August 1981.

58. Torenbeek, E., The Computation of Characteristic Areas and Volumes of Major Aircraft Components in Project Design, Memorandum M-189, Delft University of Technology, Dept. of Aerospace Engineering, Delft, The Netherlands, 1973.

14. INDEX

APPENDIX A: STANDARD ATMOSPHERE, SPECIFIC WEIGHTS AND CONVERSION FACTORS

This appendix presents tabulated data for:

The data have been copied from Reference 57.

A1. U.S. Standard Atmosphere, 1962

Definition of Standard Atmosphere

A standard atmosphere is a hypothetical vertical distribution of atmospheric temperature, pressure and density which by international or national agreement is taken to be representative of the atmosphere for the purpose of altimeter calibrations, aircraft design, performance calculations, etc. The internationally accepted standard atmosphere is called the International Civil Aeronautical Organization (ICAO) Standard Atmosphere or the International Standard Atmosphere (ISA). The U.S. Standard Atmosphere, 1962 is in agreement with the ICAO Standard Atmosphere up to 65,000 feet altitude. It is ideal air devoid of moisture, water vapor, and dust, and obeys the perfect gas law. It is based upon accepted standard values of sea level air density, temperature and pressure. Other standard atmosphere models, such as MIL-STD-210A, which represents hot and cold ambient temperature extremes, have also been established.

ICAO and U.S. Standard Atmospheres

Standard Values at Sea Level

	British Units	Metric Units
Pressure, P_o	2116.22 lb/ft² 29.92 in. Hg	1.013250×10^5 N/m² 760 mm Hg
Temperature, T_o	518.67°R 59.0°F	288.15°K 15.0°C
Acceleration due to gravity, g_o	32.1741 ft/sec²	9.80665 m/sec²
Specific weight, $g_o\rho_o$	0.076474 lb/ft³	1.2250 kg/m³
Density, ρ_o	0.0023769 lb-sec²/ft⁴	0.12492 kg sec²/m⁴
Kinematic viscosity, ν_o	1.5723×10^{-4} ft²/sec	1.4607×10^{-5} m²/sec
Absolute viscosity, μ_o	1.2024×10^{-5} lb/ft sec	1.7894×10^{-5} kg/m sec

Standard Values at Altitude

Isothermal altitude, Z_i	36089 ft	11000 m
Isothermal temperature, t	−69.7°F	−56.5°C
Temperature lapse rate (sea level to isothermal)	−3.57°F/ 1000 ft	−6.5°C/km

Temperature Conversion Formulas

$$t\,(°C) = T(°K) - 273.15$$
$$t\,(°C) = [T(°R) - 491.67]/1.8$$
$$t\,(°C) = [t(°F) - 32]/1.8$$
$$T\,(°R) = 1.8\,T(°K)$$
$$t\,(°F) = 1.8[T(°K) - 273.15] + 32$$
$$t\,(°F) = T\,(°R) - 459.67$$
$$t\,(°F) = 1.8\,t(°C) + 32$$

U.S. Standard Atmosphere, 1962
(Geopotential Altitude)
British Units

Altitude feet	Temperature °F	°R	°C	Pressure psia	in. Hg	θ	$\sqrt{\theta}$	δ	σ	$\bar{q}/M^2$ lb/ft²	Sonic Velocity ft/sec	kts
−2000	66.1	525.8	19.0	15.79	32.15	1.0138	1.0069	1.074	1.060	1592.	1124.1	666.0
−1000	62.5	522.2	17.0	15.23	31.02	1.0069	1.0034	1.037	1.030	1536.	1120.2	663.7
0	59.0	518.7	15.0	14.70	29.92	1.0000	1.0000	1.000	1.000	1481.	1116.4	661.5
1000	55.4	515.1	13.0	14.17	28.86	.9932	.9966	.9644	.9710	1429.	1112.6	659.2
2000	51.9	511.6	11.0	13.66	27.82	.9863	.9931	.9298	.9427	1377.	1108.7	656.9
3000	48.3	508.0	9.1	13.17	26.82	.9794	.9897	.8962	.9151	1328.	1104.9	654.6
4000	44.7	504.4	7.1	12.69	25.84	.9725	.9862	.8637	.8881	1279.	1101.0	652.3
5000	41.2	500.9	5.1	12.23	24.90	.9657	.9827	.8321	.8616	1233.	1097.1	650.0
6000	37.6	497.3	3.1	11.78	23.98	.9588	.9792	.8014	.8358	1187.	1093.2	647.7
7000	34.0	493.7	1.1	11.34	23.09	.9519	.9757	.7716	.8106	1143.	1089.2	645.4
8000	30.5	490.2	−0.8	10.92	22.23	.9450	.9721	.7428	.7860	1100.	1085.3	643.0
9000	26.9	486.6	−2.8	10.50	21.39	.9382	.9686	.7148	.7619	1059.	1081.3	640.7
10000	23.3	483.0	−4.8	10.11	20.58	.9313	.9650	.6877	.7385	1019.	1077.4	638.3
11000	19.8	479.5	−6.8	9.720	19.79	.9244	.9615	.6614	.7155	979.8	1073.4	636.0
12000	16.2	475.9	−8.8	9.346	19.03	.9175	.9579	.6360	.6932	942.1	1069.4	633.6
13000	12.6	472.3	−10.7	8.984	18.29	.9107	.9543	.6113	.6713	905.6	1065.4	631.2
14000	9.1	468.8	−12.7	8.633	17.58	.9038	.9507	.5875	.6500	870.2	1061.3	628.8
15000	5.5	465.2	−14.7	8.294	16.89	.8969	.9470	.5644	.6292	836.0	1057.3	626.4
16000	1.9	461.6	−16.7	7.965	16.22	.8900	.9434	.5420	.6089	802.9	1053.2	624.0
17000	−1.6	458.1	−18.7	7.647	15.57	.8831	.9398	.5203	.5892	770.8	1049.2	621.6
18000	−5.2	454.5	−20.7	7.339	14.94	.8763	.9361	.4994	.5699	739.8	1045.1	619.2
19000	−8.8	450.9	−22.6	7.041	14.34	.8694	.9324	.4791	.5511	709.8	1041.0	616.7
20000	−12.3	447.4	−24.6	6.754	13.75	.8625	.9287	.4596	.5328	680.8	1036.8	614.3
21000	−15.9	443.8	−26.6	6.475	13.18	.8556	.9250	.4406	.5150	652.7	1032.7	611.9
22000	−19.5	440.2	−28.6	6.207	12.64	.8488	.9213	.4223	.4976	625.6	1028.5	609.4
23000	−23.0	436.7	−30.6	5.947	12.11	.8419	.9175	.4047	.4806	599.4	1024.4	606.9
24000	−26.6	433.1	−32.5	5.696	11.60	.8350	.9138	.3876	.4642	574.1	1020.2	604.4
25000	−30.2	429.5	−34.5	5.454	11.10	.8281	.9100	.3711	.4481	549.7	1016.0	601.9
26000	−33.7	426.0	−36.5	5.220	10.63	.8213	.9062	.3552	.4325	526.2	1011.7	599.4
27000	−37.3	422.4	−38.5	4.994	10.17	.8144	.9024	.3398	.4173	503.4	1007.5	596.9
28000	−40.9	418.8	−40.5	4.777	9.725	.8075	.8986	.3250	.4025	481.5	1003.2	594.4
29000	−44.4	415.3	−42.4	4.567	9.298	.8006	.8948	.3107	.3881	460.3	988.9	591.9
30000	−48.0	411.7	−44.4	4.364	8.886	.7938	.8909	.2970	.3741	439.9	994.6	589.3
31000	−51.6	408.1	−46.4	4.169	8.489	.7869	.8871	.2837	.3605	420.3	990.3	586.8
32000	−55.1	404.6	−48.4	3.981	8.106	.7800	.8832	.2709	.3473	401.3	986.0	584.2
33000	−58.7	401.0	−50.4	3.800	7.737	.7731	.8793	.2586	.3345	383.1	981.6	581.6
34000	−62.3	397.4	−52.4	3.626	7.383	.7663	.8754	.2467	.3220	365.5	977.3	579.0
35000	−65.8	393.9	−54.3	3.458	7.041	.7594	.8714	.2353	.3099	348.6	972.9	576.4
36000	−69.4	390.3	−56.3	3.297	6.712	.7525	.8675	.2243	.2981	332.3	968.5	573.8
*36089	−69.7	390.0	−56.5	3.282	6.683	.7519	.8671	.2234	.2971	330.9	968.1	573.6
37000	−69.7	390.0	−56.5	3.142	6.397	.7519	.8671	.2138	.2843	316.7	968.1	573.6
38000	−69.7	390.0	−56.5	2.994	6.097	.7519	.8671	.2038	.2710	301.8	968.1	573.6
39000	−69.7	390.0	−56.5	2.854	5.811	.7519	.8671	.1942	.2583	287.7	968.1	573.6
40000	−69.7	390.0	−56.5	2.720	5.538	.7519	.8671	.1851	.2462	274.2	968.1	573.6
41000	−69.7	390.0	−56.5	2.592	5.278	.7519	.8671	.1764	.2346	261.3	968.1	573.6
42000	−69.7	390.0	−56.5	2.471	5.030	.7519	.8671	.1681	.2236	249.0	968.1	573.6
43000	−69.7	390.0	−56.5	2.355	4.794	.7519	.8671	.1602	.2131	237.4	968.1	573.6
44000	−69.7	390.0	−56.5	2.244	4.569	.7519	.8671	.1527	.2031	226.2	968.1	573.6
45000	−69.7	390.0	−56.5	2.139	4.355	.7519	.8671	.1455	.1936	215.6	968.1	573.6
46000	−69.7	390.0	−56.5	2.039	4.151	.7519	.8671	.1387	.1845	205.5	968.1	573.6
47000	−69.7	390.0	−56.5	1.943	3.956	.7519	.8671	.1322	.1758	195.8	968.1	573.6
48000	−69.7	390.0	−56.5	1.852	3.770	.7519	.8671	.1260	.1676	186.7	968.1	573.6
49000	−69.7	390.0	−56.5	1.765	3.593	.7519	.8671	.1201	.1597	177.9	968.1	573.6
50000	−69.7	390.0	−56.5	1.682	3.425	.7519	.8671	.1145	.1522	169.5	968.1	573.6
51000	−69.7	390.0	−56.5	1.603	3.264	.7519	.8671	.1091	.1451	161.6	968.1	573.6
52000	−69.7	390.0	−56.5	1.528	3.111	.7519	.8671	.1040	.1383	154.0	968.1	573.6
53000	−69.7	390.0	−56.5	1.456	2.965	.7519	.8671	.09909	.1318	146.8	968.1	573.6
54000	−69.7	390.0	−56.5	1.388	2.826	.7519	.8671	.09444	.1256	139.9	968.1	573.6
55000	−69.7	390.0	−56.5	1.323	2.693	.7519	.8671	.09000	.1197	133.3	968.1	573.6
56000	−69.7	390.0	−56.5	1.261	2.567	.7519	.8671	.08578	.1141	127.1	968.1	573.6
57000	−69.7	390.0	−56.5	1.201	2.446	.7519	.8671	.08175	.1087	121.1	968.1	573.6
58000	−69.7	390.0	−56.5	1.145	2.321	.7519	.8671	.07792	.1036	115.4	968.1	573.6
59000	−69.7	390.0	−56.5	1.091	2.222	.7519	.8671	.07426	.09877	110.0	968.1	573.6
60000	−69.7	390.0	−56.5	1.040	2.118	.7519	.8671	.07078	.09413	104.8	968.1	573.6
61000	−69.7	390.0	−56.5	.9913	2.018	.7519	.8671	.06746	.08971	99.93	968.1	573.6
62000	−69.7	390.0	−56.5	.9448	1.924	.7519	.8671	.06429	.08550	95.24	968.1	573.6
63000	−69.7	390.0	−56.5	.9005	1.833	.7519	.8671	.06127	.08149	90.77	968.1	573.6
64000	−69.7	390.0	−56.5	.8582	1.747	.7519	.8671	.05840	.07767	86.51	968.1	573.6
65000	−69.7	390.0	−56.5	.8179	1.665	.7519	.8671	.05566	.07402	82.45	968.1	573.6

U.S. Standard Atmosphere, 1962
(Geopotential Altitude)
British Units

Altitude feet	Temperature °F	°R	°C	Pressure psia	in. Hg	θ	$\sqrt{\theta}$	δ	σ	$\bar{q}/M^2$ lb/ft²	Sonic Velocity ft/sec	kts
* 65617	−69.7	390.0	−56.5	.7941	1.617	.7519	.8671	.05403	.07186	80.04	968.1	573.6
70000	−67.3	392.4	−55.2	.6437	1.311	.7565	.8698	.04380	.05789	64.88	971.0	575.3
75000	−64.6	395.1	−53.6	.5073	1.0333	.7618	.8728	.03452	.04532	51.14	974.4	577.3
80000	−61.8	397.9	−52.1	.4005	.8155	.7671	.8759	.02726	.03553	40.37	977.8	579.3
85000	−59.1	400.6	−50.6	.3167	.6449	.7724	.8789	.02155	.02790	31.93	981.2	581.3
90000	−56.3	403.4	−49.1	.2509	.5108	.7777	.8819	.01707	.02195	25.29	984.5	583.3
95000	−53.6	406.1	−47.5	.1990	.4052	.7830	.8849	.01354	.01730	20.06	987.9	585.3
100000	−50.8	408.9	−46.0	.1581	.3220	.7883	.8878	.01076	.01365	15.94	991.2	587.3
*104987	−48.1	411.6	−44.5	.1259	.2563	.7935	.8908	.008567	.010800	12.69	994.5	589.2
150000	21.0	480.7	−6.1	.01893	.03854	.9269	.9627	.001288	.001390	1.908	1074.8	636.8
*154199	27.5	487.2	−2.5	.01609	.03275	.9393	.9692	.0001095	.001165	1.622	1082.0	641.1
*170604	27.5	487.2	−2.5	.00557	.01742	.9393	.9692	.0005823	.0006199	.8626	1082.0	641.1
200000	−4.8	454.9	−20.4	.02655	.005406	.8771	.9365	.0001807	.0002060	.2677	1045.5	619.5
*200131	−4.9	454.8	−20.5	.02641	.005377	.8768	.9364	.0001797	.0002050	.2662	1045.4	619.4

*Boundary between atmosphere layers of constant thermal gradient.

Note: The ICAO atmosphere is identical to the U.S. Standard Atmosphere for altitudes below 65,617 ft.

A2. Specific Weights of Liquids and Gases

Weights of Liquids

Liquid	Specific Gravity at °C		Specific Wt lb/U.S. gal	lb/cu ft
Acetylene tetrabromide ($AcBr_4$)	2.99	25	24.95	186.67
Alcohol (methyl)	0.810	0	6.75	50.5
Benzine	0.899	0	7.5	56.1
Carbon tetrachloride	1.595	20	13.32	99.6
Ethylene glycol	1.12		9.3	69.6
Gasoline	0.72		5.87	44.9
Glycerine	1.261	20	10.52	78.71
JP1 (MIL-L-5616)	0.80		6.65	49.7
JP3 (MIL-J-5624D)	0.775		6.45	48.2
JP4 (MIL-J-5624D)	0.785		6.55	49.0
JP5 (MIL-J-5624D)	0.817	15	6.82	51.1
Kerosene	0.82		6.7	51.2
Mercury	13.546	20	113.0	845.6
Oil (MIL-6082B Grade 1100)	0.89	15	7.4	55.3
Sea water	1.025	15	8.55	63.99
Synthetic oil (MIL-L-7808C-1)	0.928	15	7.74	57.9
Water	1.000	4	8.345	62.43
Jet A fuel (ASTM-D-1655)	.808	15	6.74	50.4

Weights of Gases

Gas	Specific Wt * lb/cu ft
Air	.07651 (at 59.0°F)
Air	.08071
Carbon dioxide	.12341
Carbon monoxide	.07806
Helium	.01114
Hydrogen	.005611
Nitrogen	.07807
Oxygen	.089212

*At atmospheric pressure and 0°C.

A3. Conversion Factors

Multiply	By			To obtain
acre	4.3560	X	10^{4}	square feet
	4.0469	X	10^{-1}	hectares
	4.0469	X	10^{3}	square meters
	1.5625	X	10^{-3}	square miles
	4.8400	X	10^{3}	square yards
atmosphere (atm)(1962)	7.6000	X	10	centimeters of mercury
	2.9921	X	10	inches of mercury
	1.0332	X	10^{4}	kilograms/square meter
	1.0133	X	10^{5}	newtons/square meter
	1.4696	X	10	pounds/square inch
bar	9.8692	X	10^{-1}	atmospheres
	1.0000	X	10^{6}	dynes/square centimeter
	7.5006	X	10^{2}	millimeters of mercury
	1.0000	X	10^{5}	newtons/square meter
	1.4504	X	10	pounds/square inch
barn	1.0000	X	10^{-24}	square centimeters (nuclear cross-section)
barrel, liquid (U.S.)	3.1500	X	10	gallons
	1.1924	X	10^{-1}	cubic meters
British thermal unit (Btu)	2.5180	X	10^{2}	calories(post-1956 IST)
	7.7817	X	10^{2}	foot-pounds
	1.0551	X	10^{10}	ergs
	3.9301	X	10^{-4}	horsepower-hours
	1.0551	X	10^{3}	joules
	1.0551	X	10^{3}	newton-meters
	2.9302	X	10^{-4}	kilowatt-hours
	1.0551	X	10^{3}	watt-seconds
British thermal unit/minute (Btu/min)	4.1999			calories/second
	1.7548	X	10^{8}	ergs/second
	1.2970	X	10	foot-pounds/second
	2.3581	X	10^{-2}	horsepower
	1.7548	X	10	joules/second
	1.7931			kilogram-meters/second
	1.7548	X	10	watts
calorie (cal)	3.9683	X	10^{-3}	British thermal units
	3.0880			foot-pounds
	4.1868	X	10^{7}	ergs
	4.1868			joules
	1.1630	X	10^{-6}	kilowatt-hours
	4.1868			watt-seconds
calorie/second (cal/sec)	2.3810	X	10^{-1}	British thermal units/minute
	4.1868	X	10^{7}	ergs/second
	3.0880			foot-pounds/second
	4.1868			joules/second
centimeter (cm)	3.2808	X	10^{-2}	feet
	3.9370	X	10^{-1}	inches
	1.0000	X	10^{-5}	kilometers
	1.0000	X	10^{-2}	meters
	1.0936	X	10^{-2}	yards
centimeter/second (cm/sec)	3.2808	X	10^{-2}	feet/second
	3.9370	X	10^{-1}	inches/second
	1.0000	X	10^{-2}	meters/second
centipoise	6.7197	X	10^{-4}	pounds(mass)/second-foot
	3.6000			kilograms/hour-meter
cubic centimeter (cm^3)	1.0000	X	10^{-3}	cubic decimeters
	3.5315	X	10^{-5}	cubic feet
	6.1024	X	10^{-2}	cubic inches
	1.0000	X	10^{-6}	cubic meters
	1.3080	X	10^{-6}	cubic yards
cubic decimeter (liter) (dm^3)	1.0000	X	10^{3}	cubic centimeters
	3.5315	X	10^{-2}	cubic feet
	6.1024	X	10	cubic inches
	1.0000	X	10^{-3}	cubic meters
	1.3080	X	10^{-3}	cubic yards
cubic foot (ft^3)	2.8317	X	10^{3}	cubic centimeters
	2.8317	X	10	cubic decimeters
	1.7280	X	10^{3}	cubic inches
	2.8317	X	10^{-2}	cubic meters
	3.7037	X	10^{-2}	cubic yards
cubic inch (in^3)	1.6387	X	10	cubic centimeters
	1.6387	X	10^{-2}	cubic decimeters
	5.7870	X	10^{-4}	cubic feet
	1.6387	X	10^{-5}	cubic meters
	2.1433	X	10^{-5}	cubic yards
cubic meter (m^3)	1.0000	X	10^{6}	cubic centimeters
	1.0000	X	10^{3}	cubic decimeters
	3.5315	X	10	cubic feet
	6.1024	X	10^{4}	cubic inches
	1.3080			cubic yards
curie	3.7000	X	10^{10}	disintegrations/second
degree (deg)	6.0000	X	10	minutes
	1.7453	X	10^{-2}	radians
	2.7778	X	10^{-3}	revolutions
	3.6000	X	10^{3}	seconds
dyne	1.0197	X	10^{-3}	grams
	1.0197	X	10^{-6}	kilograms
	1.0000	X	10^{-5}	newtons
	3.5970	X	10^{-3}	ounces
	2.2481	X	10^{-6}	pounds
dyne/square centimeter	2.9530	X	10^{-5}	inches of mercury
	1.0197	X	10^{-2}	kilograms/square meter
	7.5006	X	10^{-4}	millimeters of mercury
	1.0000	X	10	newtons/square meter
	1.4504	X	10^{-5}	pounds/square inch
electron volt (eV)	3.8268	X	10^{-20}	calories
	1.6022	X	10^{-12}	ergs
	1.0000	X	10^{-6}	MeV(mega electron volts)
erg	9.4782	X	10^{-11}	British thermal units
	2.3885	X	10^{-8}	calories
	1.0000			dyne-centimeters
	7.3756	X	10^{-8}	foot-pounds
	1.0000	X	10^{-7}	joules
erg/second	5.6869	X	10^{-9}	British thermal units/minute
	2.3885	X	10^{-8}	calories/second
	7.3756	X	10^{-8}	foot-pounds/second
	1.0000	X	10^{-7}	joules/second
	1.0000	X	10^{-7}	watts
flow rate, fuel (lb/hr)	4.5359	X	10^{-1}	kilograms/hour
foot (ft)	3.0480	X	10	centimeters
	1.2000	X	10	inches
	3.0480	X	10^{-4}	kilometers
	3.0480	X	10^{-1}	meters
	1.8939	X	10^{-4}	miles
	3.3333	X	10^{-1}	yards
foot-pound (ft-lb)	1.2851	X	10^{-3}	British thermal units
	1.3558	X	10^{7}	ergs
	5.0505	X	10^{-7}	horsepower-hours
	1.3558			joules
	3.7662	X	10^{-7}	kilowatt-hours
	1.3558			newton-meters
foot-pound/second (ft-lb/sec)	7.7104	X	10^{-2}	British thermal units/minute
	3.2383	X	10^{-1}	calories/second
	1.8182	X	10^{-3}	horsepower
	1.3558			joules/second
	1.3826	X	10^{-1}	kilogram-meters/second
	1.3558			watts
foot/second (fps)	3.0480	X	10	centimeters/second
	1.0973			kilometers/hour
	5.9248	X	10^{-1}	knots
	3.0480	X	10^{-1}	meters/second
	6.8182	X	10^{-1}	miles/hour

Conversion Factors (continued)

Multiply	By			To obtain
gallon (U.S.) (gal)	1.3368	X	10^{-1}	cubic feet
	3.7854			liters
	3.7854	X	10^{-3}	cubic meters
	8.0000			pints
	4.0000			quarts
gram (gm)	1.0000	X	10^{-3}	kilograms
	3.5274	X	10^{-2}	ounces
	2.2046	X	10^{-3}	pounds
	9.8067	X	10^{2}	dynes
	9.8067	X	10^{-3}	newtons
hectare	2.4711			acres
	1.0000	X	10^{2}	ares
	1.0000	X	10^{4}	square meters
	3.8610	X	10^{-3}	square miles
horsepower (hp)	4.2436	X	10	British thermal units/minute
	5.5000	X	10^{2}	foot-pounds/second
	3.3000	X	10^{4}	foot-pounds/minute
	7.4570	X	10^{2}	joules/second
	7.6040	X	10	kilogram-meters/second
	7.4570	X	10^{2}	watts
horsepower-hour (hp-hr)	2.5461	X	10^{3}	British thermal units
	1.9800	X	10^{6}	foot-pounds
	2.6845	X	10^{6}	joules
	7.4570	X	10^{-1}	kilowatt-hours
hour (hr)	6.0000	X	10	minutes
	3.6000	X	10^{3}	seconds
	4.1781	X	10^{-2}	sidereal days
	4.1667	X	10^{-2}	solar days
	1.1416	X	10^{-4}	solar years
imperial gallon	2.7742	X	10^{2}	cubic inches
	1.2009			gallons (U.S.)
	4.5460			liters
inch (in)	2.5400			centimeters
	8.3333	X	10^{-2}	feet
	2.5400	X	10^{-2}	meters
	2.7778	X	10^{-2}	yards
inch of mercury at 0°C (in Hg)	3.3421	X	10^{-2}	atmospheres
	3.3864	X	10^{-2}	bars
	3.3864	X	10^{4}	dynes/square centimeter
	1.3595	X	10	inches of water
	2.5400	X	10	millimeters of mercury
	3.3864	X	10^{3}	newtons/square meter
	7.0727	X	10	pounds/square feet
	4.9116	X	10^{-1}	pounds/square inch
inch/second (ips)	8.3333	X	10^{-2}	feet/second
	2.5400			centimeters/second
	2.5400	X	10^{-2}	meters/second
inch of water at 4°C (in H_2O)	2.4584	X	10^{-3}	atmospheres
	7.3556	X	10^{-2}	inches of mercury
	1.8683			millimeters of mercury
	2.4910	X	10^{2}	newtons/square meter
	3.6128	X	10^{-2}	pounds/square inch
joule (J)	9.4771	X	10^{-4}	British thermal units
	2.3889	X	10^{-1}	calories
	1.0000	X	10^{7}	dyne-centimeters
	1.0000	X	10^{7}	ergs
	7.3756	X	10^{-1}	foot-pounds
	1.0000			newton-meters
	1.0000			watt-seconds
kilogram (kg)	1.0000	X	10^{3}	grams
	3.5274	X	10	ounces
	2.2046			pounds
	6.8521	X	10^{-2}	slugs
	9.8067			newtons
	7.9290	X	10	poundals
kilogram/ square meter (kg/m^2)	9.6783	X	10^{-5}	atmospheres
	9.8067	X	10^{-5}	bars
	2.8959	X	10^{-3}	inches of mercury
	9.8067			newtons/ square meter
kilogram/ square meter (kg/m^2)	6.5895			poundals/square foot
	2.0482	X	10^{-1}	pounds/square foot
	1.4223	X	10^{-3}	pounds/square inch
kilogram-meter (kgm)	9.2938	X	10^{-3}	British thermal units
	7.2330			foot-pounds
	9.8067			joules
	9.8067			newton-meters
	2.7232	X	10^{-6}	kilowatt-hours
kilogram-meter/ second (kgm/sec)	3.3458	X	10	British thermal units/hour
	2.3423			calories/second
	7.2330			foot-pounds/second
	9.8067			joules/second
	1.3151	X	10^{-2}	horsepower
	9.8067	X	10^{-3}	kilowatts
kilometer (km)	3.2808	X	10^{3}	feet
	3.9370	X	10^{4}	inches
	1.0000	X	10^{3}	meters
	6.2137	X	10^{-1}	miles
	1.0936	X	10^{3}	yards
kilometer/hour (km/hr)	9.1130	X	10^{-1}	feet/second
	5.3960	X	10^{-1}	knots
	6.2137	X	10^{-1}	miles/hour
	2.7778	X	10^{-1}	meters/second
kilonewton (kN)	2.2481	X	10^{2}	pounds
kilowatt hour (kWh)	3.4128	X	10^{3}	British thermal units
	2.6560	X	10^{6}	foot-pounds
	1.3414			horsepower-hours
	3.6000	X	10^{6}	joules
	3.6721	X	10^{5}	kilogram-meters
	3.6000	X	10^{6}	watt-seconds
knot (kt)	1.6890			feet/second
	1.1516			miles/hour
	1.8532			kilometers/hour
	5.1480	X	10^{-1}	meters/second
light year	3.1040	X	10^{16}	feet
	5.8786	X	10^{12}	miles
	9.4608	X	10^{15}	meters
liter (l)	6.1024	X	10	cubic inches
	3.5315	X	10^{-2}	cubic feet
	2.6417	X	10^{-1}	gallons (U.S. liquid)
	1.0000	X	10^{-3}	cubic meters
	2.1134			pints (U.S. liquid)
	1.0567			quarts (U.S. liquid)
meter (m)	1.0000	X	10^{2}	centimeters
	3.2808			feet
	3.9370	X	10	inches
	1.0000	X	10^{-3}	kilometers
	6.2137	X	10^{-4}	miles
	1.0936			yards
meter/second (m/sec)	3.2808			feet/second
	3.6000			kilometers/hour
	1.9438			knots
	2.2369			miles/hour
metric horsepower	9.8632	X	10^{-1}	horsepower
	7.3550	X	10^{-1}	kilowatts
mile (mi)	5.2800	X	10^{3}	feet
	6.3360	X	10^{4}	inches
	1.6093			kilometers
	1.6093	X	10^{3}	meters
	3.2000	X	10^{2}	rods
	1.7600	X	10^{3}	yards
mile/hour (mph)	1.4667			feet/second
	1.6093			kilometers/hour
	8.6898	X	10^{-1}	knots
	4.4704	X	10^{-1}	meters/second
millimeter of mercury at 0°C (torr) (mm Hg)	1.3332	X	10^{3}	dynes/square centimeter
	3.9370	X	10^{-2}	inches of mercury (0°C)
	5.3526	X	10^{-1}	inches of water (4°C)
	1.3332	X	10^{2}	newtons/square meter
	1.9337	X	10^{-2}	pounds/square inch

Conversion Factors (continued)

Multiply	By			To obtain
minute (angle) (min)	1.6667	X	10^{-2}	degrees
	2.9089	X	10^{-4}	radians
	4.6296	X	10^{-6}	revolutions
	6.0000	X	10	seconds
minute (time) (min)	1.6667	X	10^{-2}	hours
	6.0000	X	10	seconds
	6.9444	X	10^{-4}	solar days
	1.9026	X	10^{-6}	solar years
nautical mile (international) (n mi)	6.0761	X	10^{3}	feet
	1.8520	X	10^{3}	meters
newton (N)	1.0000	X	10^{5}	dynes
	1.0197	X	10^{2}	grams
	1.0197	X	10^{-1}	kilograms
	2.2481	X	10^{-1}	pounds
	7.2330			poundals
newton/ square meter (pascal (Pa)) (N/m^2)	9.8692	X	10^{-6}	atmospheres
	1.0000	X	10	dynes/square centimeter
	2.9530	X	10^{-4}	inches of mercury (0°C)
	1.0197	X	10^{-1}	kilograms/square meter
	6.7200	X	10^{-1}	poundals/square foot
	2.0885	X	10^{-2}	pounds/square foot
	1.4504	X	10^{-4}	pounds/square inch
ounce (oz)	2.8349	X	10	grams
	2.8349	X	10^{-2}	kilograms
	6.2500	X	10^{-2}	pounds
	1.9428	X	10^{-3}	slugs
	2.7801	X	10^{4}	dynes
parsec	1.9163	X	10^{13}	miles
	3.0857	X	10^{16}	meters
pieze	1.0000	X	10^{3}	newtons/square meter
pound(mass) (lb)	4.5359	X	10^{2}	grams
	4.5359	X	10^{-1}	kilograms
	1.6000	X	10	ounces
pound (force) (lbf)	3.1081	X	10^{-2}	slugs
	4.4482			newtons
	4.4482	X	10^{-1}	dekanewtons
	4.4482	X	10^{-3}	kilonewtons
	3.2174	X	10	poundals
pound/ square foot (psf)	4.7254	X	10^{-4}	atmospheres
	4.7880	X	10^{-4}	bars
	4.7880	X	10^{2}	dynes/square centimeter
	1.4139	X	10^{-2}	inches of mercury (0°C)
	4.8824			kilograms/square meter
	4.7880	X	10	newtons/square meter
	3.2174	X	10	poundals/square foot
	6.9444	X	10^{-3}	pounds/square inch
pound/ square inch (psi)	6.8046	X	10^{-2}	atmospheres
	6.8948	X	10^{4}	dynes/square centimeter
	2.0360			inches of mercury (0°C)
	2.7681	X	10	inches of water (4°C)
	7.0307	X	10^{2}	kilograms/square meter
	6.8948	X	10^{3}	newtons/square meter
	4.6333	X	10^{3}	poundals/square foot
	1.4400	X	10^{2}	pounds/square foot
poundal	1.4098	X	10^{-2}	kilograms
	1.3825	X	10^{-1}	newtons
	3.1081	X	10^{-2}	pounds
poundal/ square foot	1.5174	X	10^{-1}	kilograms/square meter
	1.4882	X	10^{-1}	newtons/square meter
	3.1081	X	10^{-2}	pounds/square foot
	2.1583	X	10^{-4}	pounds/square inch
radian (rad)	5.7296	X	10	degrees
	3.4378	X	10^{3}	minutes
	1.5916	X	10^{-1}	revolutions
	2.0626	X	10^{5}	seconds
revolution (rev)	3.6000	X	10^{2}	degrees
	2.1600	X	10^{4}	minutes
	6.2832			radians
	1.2960	X	10^{6}	seconds
second (angle) (sec)	2.7778	X	10^{-4}	degrees
	1.6667	X	10^{-2}	minutes
	4.8481	X	10^{-6}	radians
	7.7160	X	10^{-7}	revolutions
second (time) (sec)	2.7778	X	10^{-4}	hours
	1.6667	X	10^{-2}	minutes
	1.1574	X	10^{-5}	solar days
slug	1.4594	X	10^{4}	grams
	1.4594	X	10	kilograms
	5.1478	X	10^{2}	ounces
	3.2174	X	10	pounds
square centimeter (cm^2)	1.0764	X	10^{-3}	square feet
	1.5500	X	10^{-1}	square inches
	1.0000	X	10^{-4}	square meters
	1.0000	X	10^{2}	square millimeters
square foot (ft^2)	2.2957	X	10^{-5}	acres
	9.2903	X	10^{2}	square centimeters
	1.4400	X	10^{2}	square inches
	9.2903	X	10^{-2}	square meters
	3.5870	X	10^{-8}	square miles
	1.1111	X	10^{-1}	square yards
square inch (in^2)	1.2732	X	10^{6}	circular mils
	6.4516			square centimeters
	6.9444	X	10^{-3}	square feet
	6.4516	X	10^{-4}	square meters
	6.4516	X	10^{2}	square millimeters
	1.0000	X	10^{6}	square mils
	7.7160	X	10^{-4}	square yards
square kilometers (km^2)	2.4711	X	10^{2}	acres
	1.0764	X	10^{7}	square feet
	1.0000	X	10^{6}	square meters
	3.8610	X	10^{-1}	square miles
square meter (m^2)	2.4711	X	10^{-4}	acres
	1.0000	X	10^{-4}	hectares
	1.0000	X	10^{4}	square centimeters
	1.0764	X	10	square feet
	1.5500	X	10^{3}	square inches
	3.8610	X	10^{-7}	square miles
	1.1960			square yards
square mile (mi^2)	6.4000	X	10^{2}	acres
	2.5900	X	10^{2}	hectares
	2.7878	X	10^{7}	square feet
	2.5900			square kilometers
	2.5900	X	10^{6}	square meters
	3.0976	X	10^{6}	square yards
thermie	4.1868	X	10^{6}	joules
thrust specific fuel consumption (TSFC) (lb/hr/lb Fn)	1.0197	X	10^{2}	kilograms/hour/ dekanewton
watt (joule/ second) (W)	3.4121			British thermal units/hour
	5.6869	X	10^{-2}	British thermal units/minute
	2.3900	X	10^{-1}	calories/second
	1.0000	X	10^{7}	ergs/second
	7.3756	X	10^{-1}	foot-pounds/second
	1.3410	X	10^{-3}	horsepower
	1.0197	X	10^{-1}	kilogram-meters/second
watt second (Wsec)	9.4782	X	10^{-4}	British thermal units
	7.3756	X	10^{-1}	foot-pounds
	1.0000			joule
	2.7778	X	10^{-7}	kilowatt-hours

APPENDIX B: METHODS FOR COMPUTING CIRCUMFERENCES, AREAS AND VOLUMES

In the process of airplane project design it is frequently necessary to compute the cross-section circumference, the surface area and/or the volume of components of the airplane such as: fuselages, fuselage boattails, wings, fuel tanks and nacelles.

Reference 58, by Professor E.Torenbeek of Delft University of Technology in Delft, The Netherlands is an excellent source of methods for computing such items. For that reason, Reference 58 has been copied and adapted for incorporation as Appendix B in this book.

Nomenclature

Most symbols are used only occasionaly. Therefore, the nomenclature is mentioned in the text or on the relevant figure or diagram.

Contents page

B1. Introduction

In the calculation of mass properties and aerodynamic coefficients like profile drag coefficients and stability derivatives, reference is made to frontal areas, sideview areas, wetted areas and volumes. Once the detailed shape of the major aircraft components is accurately established by means of lofting processes (e.g. ref.B3), these characteristic areas and volumes can be computed numerically or by means of graphical methods. The present subject, however, is associated with project design studies, where the detailed shape and dimensions are not always accurately known or, in some cases, may have been chosen provisionally. An estimation, accurate within a few percent of the exact value, may be acceptable when emphasis is laid on time saving.

In the present memorandum methods are presented for the calculation of circumferences, areas and volumes, having different degrees of accuracy. The most exact procedure is based on a representation of the surface contour lines by a suitable polynomial with fractional exponents. Such a two-parameter method is explained in ch.B2 and is very simple to use when a three-view drawing of the component is available. Generalized results of the various integrations are presented in diagrams (ch.B3). These are useful not only for accurate computations, but they have been used for the derivation of simplified methods as well.

The reader who is interested in practical results only may omit the reading of chapters B2 and B3. Chapters B4, B5 and B6 deal with applications for fuselages, wings, tailplanes, fuel tanks and engine nacelles. In general, both accurate and simplified methods are presented. For fuselages a review of the various available methods is given on fig. 5.

B2. Approximation of contours by analytical functions

The rigid requirements in aeronautical design have led to the adoption of streamline shapes with smooth, continuous external lines, resulting in a smooth rate of change of curvature along the entire length of the body. For fuselages, the application of a pressurized cabin makes a circular cross section or a section built up from circular sections a very desirable, if not mandatory feature. Extensive areas of double curvature, like saddle surfaces, should be avoided because of the associated costly manufacturing processes. The design criteria for wings are entirely different as the external shape is dictated by aerodynamic requirements, viz. low drag, high maximum lift, favourable characteristics at high incidences and at Mach numbers where compressibility effects are dominant. For subsonic aircraft, leading and trailing edges of wings and tail surfaces are frequently straight lines. Aerofoils have neatly

rounded noses, while sharp trailing edges are used for good lifting properties. For ease of production, intermediate sections are often constructed from tip and root sections by assuming straight lines between corresponding points ("linear lofting").

In general, it will be necessary to subdivide the body, for which the characteristic areas and volumes must be calculated, into several sections. For example, the pressurized fuselage of a transport aircraft is logically split up into a nose section, a cylindrical mid section and a tail section. The more sections are used in non-cylindrical parts, the higher will be the accuracy of prediction. For project-design purposes, however, a method is required, resulting in an error of probably not more than a few percent, using a very limited amount of subdivisions to minimize the computational time.

The general shape of many curves and external lines can be represented in a most satisfactory way by the following two-dimensional convex polynomial:

$$(\frac{x}{a})^n + (\frac{y}{b})^m = 1 \qquad ; \text{ for } n, m \geq 1 \qquad (1)$$

For typical fuselage nose and tail sections examples of this function are plotted in fig. 1 for two combinations of the exponents n and m.

Several special cases of eq. 1 are plotted in fig. 2 and discussed below.

The straight line ($n = m = 1$), used for cones.
Parabola 1 ($n = 2$ and $m = 1$) is representative to some degree for fuselage tail sections.
Parabola 2 ($n = 1$ and $m = 2$). Provided that the base area is not too large, this parabola may occasionally be used for blunt fuselage ends.
The ellipse ($n = m = 2$), appearing as a circle in fig. 2. Many fuselage and wing sections and nacelle noses have near-elliptic shapes.
Quartic 1 ($n = 4$; $m = 2$) and quartic 2 ($n = 2$; $m = 4$), representative for blunt noses and tails.
Lamé's quartic ($n = m = 4$). This curve is of particular interest for the representation of cross-sectional shapes of small aircraft with unpressurized cabins.

It is not suggested that for a particular body the sectional contour should be approximated by any of these special functions; errors of 5 - 10% in volumes and wetted areas may be introduced by doing so. However, several of these special cases can be treated analytically and are therefore useful to check the general solution, in which intermediate (fractional) values for n and m are treated as well.

For a specified contour shape, n and m can be determined readily from the geometric parameters φ and γ, defined in fig. 3. To this end, a suitable choice of the X- and Y-axes must be made.
For fuselages, the X-axis will usually be located in the plane of symmetry, the Y-axis may be on the intersection of the cylindrical part with the nose or tail section.
For wing sections, the effect of camber on the circumferential length of a section is negligible. On the corresponding symmetrical section, the X-axis is the chordline and the Y-axis will be taken at the point of maximum section thickness.

Point S in fig. 3 is determined graphically in the drawing as the intersection of the contourline and the diagonal of the rectangle which encloses the contour. The X-coordinate of S as a fraction of the projected contourlength (a) defines the parameter φ. The intersection of the tangent at S and the X-axis defines the parameter γ. The projected height of the contour is b. Although the graphical construction of a tangent is not always a very accurate procedure, it will be shown later on that the results are not affected to a great deal by errors in γ.

The equations relating combinations (n,m) and (φ,γ) to each other are derived in Ref. 58 ; the results are plotted in diagram 1. Once φ and γ are measured in the drawing, n and m can be found and, if desired, a check on the accuracy of the approximation by eq. 1 can be made by calculation of the contour. However, in ch.B3 it will be demonstrated that for the purpose of calculating volumes and areas, considerable deviations from the actual shape are acceptable, provided that the value of φ is accurate. For example, the parabolae 1 and 2 in fig. 2 have the same value $\varphi = \frac{1}{2}(\sqrt{5}-1)$. The sectional areas for both curves are exactly equal, the circumferential lengths are equal within a few tenths of a percent, while the volumes and wetted areas of corresponding bodies of revolution differ by one or two percent only.

B3. Diagrams for areas, circumferences and volumes

The choice of the polynomial given by eq. 1 provides the tool to calculate areas, circumferences and volumes of body sections. The suitability of the function is confirmed by the fact that all results can be plotted in two-dimensional diagrams, although 4 geometric parameters (φ, γ, a and b) are involved. The diagrams can be used for a very quick calculation, as no integrations are necessary.
For cross sections of pressure cabins a separate diagram is included.

B3.1 Sectional (projected) area - diagram 2

The area enclosed by the contour, the X-axis and the Y-axis is:

$$\text{SECTIONAL AREA} = \int_0^a y\,dx \qquad (2)$$

By substitution of y from eq. 1 and integration, the final result as derived in Ref. 58 is found and plotted in diagram 2. In terms of n and m, the area is determined by Γ-functions, which are symmetrical with respect to n and m. The simple representation in diagram 2 is possible, as the area is not affected by γ.

B3.2 Circumference of a section contour - diagram 3

The expression for the circumferential length is:

$$\text{CIRCUMFERENCE} = \int\sqrt{(dx)^2 + (dy)^2} = \int_0^a \sqrt{1 + \left(\frac{dy}{dx}\right)^2}\,dx \qquad (3)$$

For several special combinations of n and m, this integral can be solved analytically Ref. 58 , resulting in expressions with n, m and the ratio a/b as parameters. As in the case of the sectional area, it appears convenient to use φ and γ instead, but the effect of γ appears to be small. Hence, in diagram 3 only φ and a/b are used as parameters. Although the result is now no longer exact, the error introduced is quite small.
For example:

a) the difference between the exact results for the two parabolae 1 and 2 is indistinguishable in the diagram,
b) the two quartics (n = 4; m = 2 and n = 2; m = 4) are both represented by the dotted line $\varphi = \sqrt{(\sqrt{5}-1)/2} = 0.786$. For a given value of a/b, the error with respect to the exact result, as shown in the diagram, is less than one percent.

In some cases, the calculation of the circumferential length of a cross section is an intermediate step in the computation of wetted area. In those cases, the height/width ratio is always between 0.5 and 2 and, within the corresponding range $0.5 < a/b < 1.0$, the circumference is hardly affected by a/b as well. This property will be used for the simplified calculations of par. 4.2.

B3.3 Volume of bodies of revolution - diagram 4

By rotation of the contour, given by eq. 1, about the X-axis, a body of revolution is formed, with a volume equal to:

$$\text{VOLUME} = \int_0^a \pi y^2\,dx \qquad (4)$$

The complete solution is derived in Ref. 58 in terms of n and m and plotted in diagram 4. The parameters φ and γ may be used instead. The volume, expressed as a fraction of the cylinder volume (length a, radius b), is not affected by a/b. As in the previous cases, the parameter φ is most prominent, γ is of secondary importance. It can be shown that formulae for the sectional shape different from eq. 1 yield essentially the same results, provided that the same value of φ is used.

B3.4 Wetted area of bodies of revolution - diagram 5

The body of revolution as defined in the previous paragraph has the following wetted area:

$$\text{EXTERNAL AREA} = \int 2\pi y \sqrt{(dx)^2 + (dy)^2} = 2\pi \int_0^a y \sqrt{1 + \left(\frac{dy}{dx}\right)^2}\, dx \qquad (5)$$

For special combinations of n and m, analytical expressions for this integral can be derived (see Ref. 58). The wetted area, plotted in diagram 5 as a fraction of the cylinder external area ($2\pi ab$) plus one side area (πb^2), is affected primarily by φ and a/b. In analogy to the case for the circumference, the omission of γ results in errors of not more than 1 or 2%. This is illustrated in the diagram for the two parabolae, both represented by $\varphi = \frac{1}{2}(\sqrt{5} - 1)$ and the two quartics, with $\varphi = \sqrt{(\sqrt{5} - 1)/2}$.

B3.5 Correction factors for double bubble and flattened cross sections- diagram 6

For fuselages with "double bubble" cross sectional shapes, like the DC-8, DC-9, VC-10 and others, or a flattened belly below the cabin floor (e.g. F-27, C-5A), correction factors can be derived, relating the circumference and sectional area to those of a circle. The circle diameter is assumed equal to the max. width of the actual fuselage. The relevant equations are presented in fig. 4 and the results plotted in diagram 6. All parameters used can be measured on a drawing of the cross section or front view.

B4. Fuselages

The methods presented in this chapter refer to the gross wetted area of the streamline body by which most fuselage shapes can be approximated. Cockpit canopies, fillets, wing-fuselage attachments, air scoops, etc., are ignored and must be accounted for seperately.
A choice can be made between several methods. The most accurate of these is described in par.B4.1 and can be used when a complete three-view drawing is available. For substantially non-cylindrical fuselages, several cross sections must be available as well. The simplified methods discussed in par.B4.2 are useful when the fuselage shape or some dimensions are not completely known. A survey of the applicability of the various methods is given in fig. 5.

B4.1 "Accurate" calculations

a. Fuselages with circular cross sections

The nose and tail sections are usually nearly bodies of revolution as well. The planview is used to subdivide the fuselage into a nose section, a cylindrical mid section (if present) and a tail section and the parameters φ and γ are determined (fig. 3). Projected areas in sideview or planview can be derived from diagram 2. Volumes and wetted areas are computed with diagrams 4 and 5.

b. Fuselages with a blunt base or a beaver tail

The approximation for blunt and beaver tails, as presented in diagrams 7 and 8, can be used on the condition that the contour lines are not too different from a parabolic shape. Formulae for ogives can be found in ref.B6.

c. Fuselages with double-bubble or flattened cross sections

The volume and wetted area are computed, assuming that the fuselage is a body of revolution with diameter equal to the maximum width of the fuselage (fig. 4). Similarly to case a., the planview is used. The correction factors in diagram 6 are then applied to the frontal area, the volume and the wetted area.

d. Fuselages with non-circular cross sections

The following procedure is suggested:

1. A subdivision into a suitable number of segments is made.

2. The parallel end faces of the segments are local cross sections; their areas and circumference are calculated with diagrams 2 and 3.
3. The segments are approximated by bodies of type A or B in fig. 7. Their volumes are computed and added.
4. The circumferential lengths of the cross sections are plotted on the longitudinal axis and integrated numerically (e.g. Simpson's rule, ref.B6) or with diagram 3.
5. The integral is corrected by addition of an extra percentage:

$$\frac{\Delta(\text{vetted area})}{\text{vetted area}} = 75 \frac{\text{frontal area}}{(\text{fuselage length})^2} \ \% \qquad (6)$$

This approximate correction accounts for the fact that integration of the circumferential length should take place along the external contour instead of the longitudinal axis.

B4.2 Simplified methods

In many cases the fuselage contour is not completely defined and a certain amount of help from statistical data will be acceptable. The designer can make a choice between the following approximate methods:

a. Three-view drawing is available

In chapters 2 and 3 the parameters φ and γ were introduced to find the fractional exponents n and m. It was found that
- the effect of γ is very small or completely absent,
- for practical cross-sectional shapes the effect of the height/width ratio on the circumference is negligible.

Moreover, by application of the method to practical fuselages, it was concluded that for the most common nose and tail sections the vetted area as a fraction of the cilinder area ($2\pi ab$ in diagram 5) is approximately a function of φ only. Therefore, the procedure of ch.B4.1 can be simplified and the results are summarized in diagram 9.

b. Fuselage length, cross-sectional shape and length of mid section are known

Diagram 10 is composed from the results of calculations of volumes and vetted areas for several actual fuselages with near-circular cross sections, using diagrams 2-6. The dotted line is taken as the mean value and corrections are derived from diagram 2 and 3. This simple diagram may be of use when the actual shape of nose and tail sections are not specified.

c. Axisymmetric streamline bodies of given length and diameter

In fig. 6 the ratio:

$$\frac{\text{vetted area}}{2\sqrt[3]{2\pi\lambda}\,(\text{volume})^{2/3}}, \text{ where } \lambda = \frac{\text{length}}{\text{diameter}},$$

is plotted for cylinders, ellipsoids, paraboloids, double cones and typical streamline shapes with and without a cylindrical center section. This ratio is approximated by a simple function of λ for streamline bodies. Once the volume is known, the wetted area can be calculated in a straight forward manner. The expressions for the volume are based on typical nose and tail section shapes, according to fig. 1.

d. Volume and wetted area based on cabin dimensions

When observing actual fuselage shapes, it is noted that the fuselage length is considerably affected by the detailed shape of the nose and the tail extremities. On the contrary, the volume and wetted area are much less affected. In preliminary design the fuselage tail length may be subject to optimization at a later stage, when accurate data are available on structure weight and afterbody drag, in order to find the most favourable tailplane moment arm.

The dimensions of the passenger cabin and the freighthold volume, however, are established at a very early phase of the design, these being derived mainly from the design specifications. Hence, diagram 11 gives a statistical correlation of gross vetted areas and volumes with the principal dimensions of the pressurized section and with cabin plus freighthold volume. The diagram may be used in different ways:

- for given pressure cabin outside dimensions, the volume and wetted area are found immediately;
- if only the passenger cabin plus freighthold volume are known, the fuselage volume is read from the diagram and the vetted area is computed with the presented formula (based on fig. 6).

For payloads in excess of 30 passengers roughly, the correlation is remarkable in view of the simplicity of the method.

B5. Wings, tailplanes and fuel tanks

B5.1 Wetted area of wings and tailplanes

The wetted area is computed by spanwise integration of the sectional circumference. The net (exposed) area (S_{net}) to be used is the horizontal projection of the area exposed to the airflow.

The circumference of an arbitrary section can be computed from diagram 3, using a suitable subdivision of the contour. For most subsonic sections, the following simple expression is reasonably accurate:

$$\text{circumference} = 2 \times \text{chordlength} \; (1 + 0.25 \cdot t/c) \quad (7)$$

where t/c = thickness/chord ratio (fig. 8)

The vetted area of a linear lofted lifting surface is derived by integration:

$$\text{wetted area} = 2S_{net}\left\{1 + 0.25(t/c)_r \frac{1+\tau\lambda}{1+\lambda}\right\} \qquad (8)$$

λ = tipchord/root chord (taper ratio)

$\tau = (t/c)_t \,/\, (t/c)_r$

r = root; t = tip

In this particular case, the root and tip sections refer to the exposed part of the wing or tailplane.

B5.2 Fuel tank volume

a. Most internal bag-type tanks can be represented by a geometric body with parallel end faces of type A or B in fig. 7.

b. For integral tanks the external shape of the structure will be used to apply fig. 7. In this case, the volume of the structure * should be subtracted. In a completely filled tank roughly 5% of the volume must be available for expansion of the fuel (subsonic aircraft).

c. External fuel tanks can be treated in a similar fashion as the fuselage, e.g. with fig. 6 or diagram 10.

d. In project design a check on the available tank capacity must be made. A first estimate for the integral tank volume is given in fig. 8. Although statistical data were used to derive the constant 0.54, the method is not very accurate. Hence, when the available tank volume appears to be critical, a more precise calculation is necessary, to account for the actual section variation and the location of the spars.

B6. Engine nacelles and air ducts

In the most general case, the engine nacelle group may consist of a fan cowling, a gasgenerator cowling and a plug in the hot flow (fig. 9). The wetted areas of these components can be computed with the data on fig. 9 and diagram 7.

---

* to be derived from the structural weight.

References

B1. Schmidt, A.H. : "A simplified method for estimating the vetted area of aircraft fuselages". S.A.W.E. Technical Paper No. 308, 1962.

B2. Haase, H.H. : "The analytical development of curves and streamline shapes". Republic Aviation Corporation, 1948.

B3. Rehbinder, G. : "Analytical definition of aircraft shape". Journal of Aircraft, Vol. 4 No. 6, nov-dec. 1967, page 544-546.

B4. Granholm, J.W. : "The use of closed-curve equations of variable degree in airplane fuselage lofting". Aeronautical Engineering Review, july 1954, page 52-57.

B5. Abramowitz, M. and Stegun, I.A. : "Handbook of mathematical functions". Dover Publications, Inc., New York, 1965.

B6. An. : "Weight engineers handbook". Society of Aeronautical Weight Engineers Inc., revised ed. december 1968.

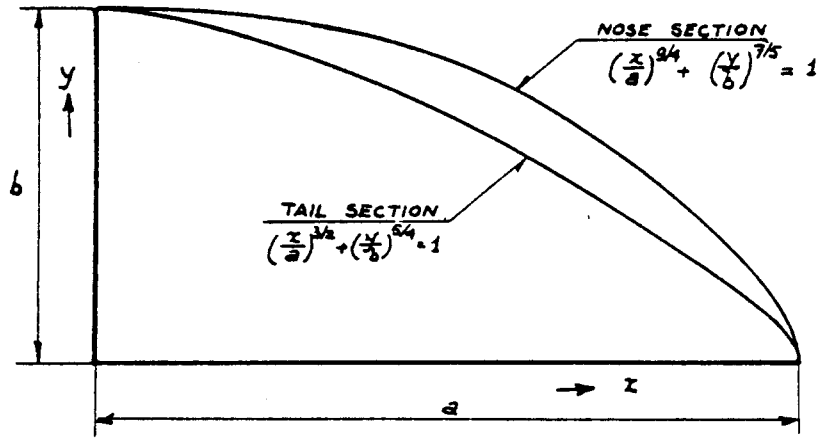

FIG. 1 : REPRESENTATION OF TYPICAL NOSE AND TAIL SECTIONS OF STREAMLINE BODIES BY MATHEMATICAL FUNCTIONS

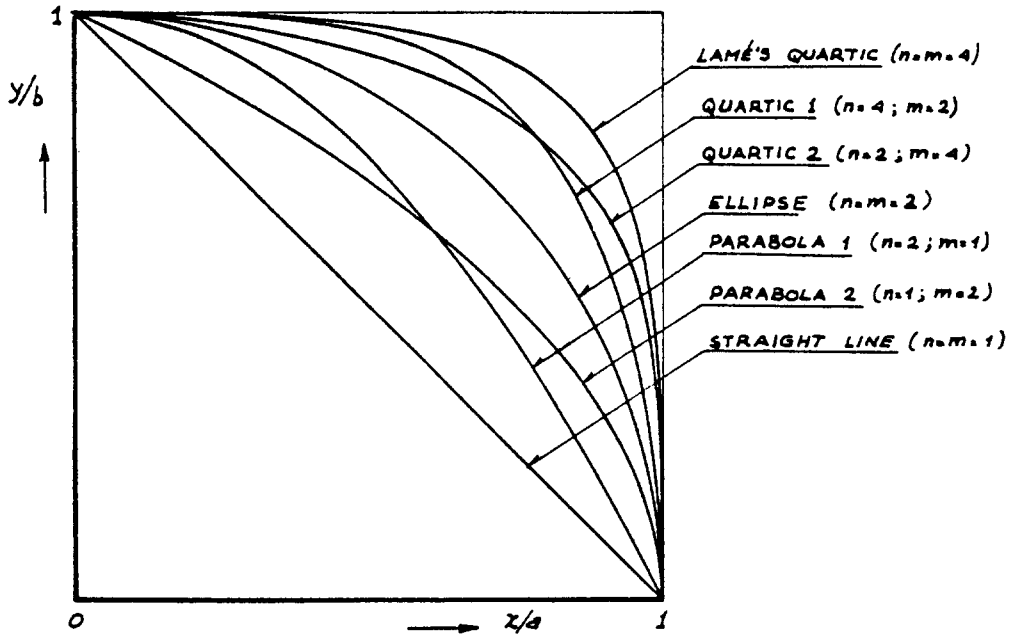

FIG. 2 : SPECIAL CASES OF THE FUNCTION $\left(\frac{x}{a}\right)^n + \left(\frac{y}{b}\right)^m = 1$

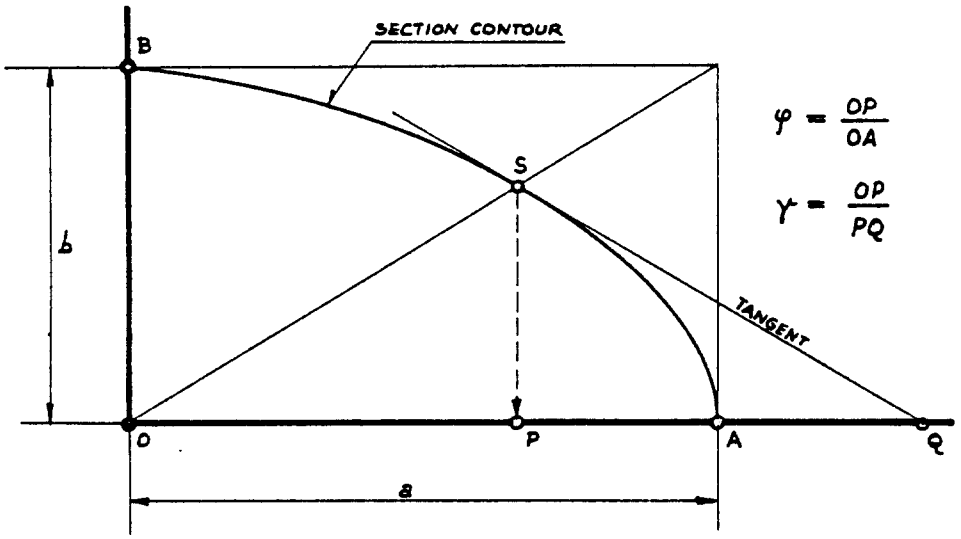

FIG. 3 : GRAPHICAL DETERMINATION OF THE PARAMETERS φ AND γ FROM THE DESIGN DRAWING

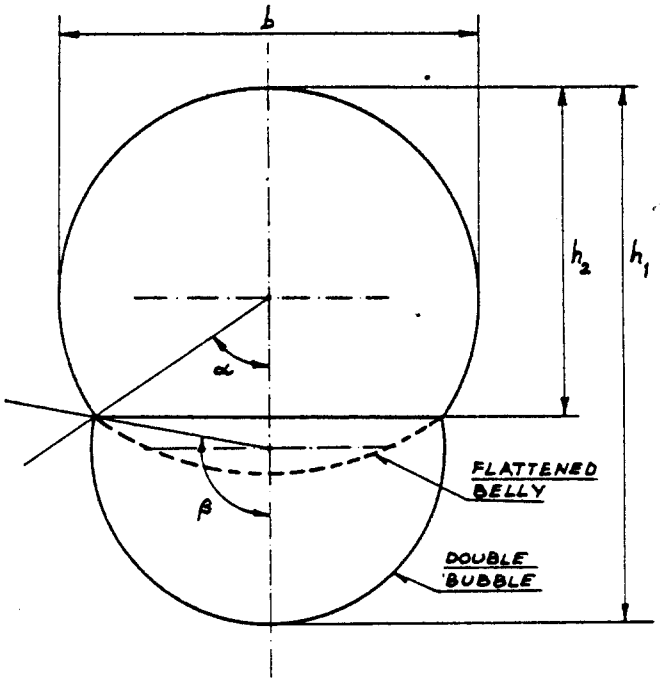

$$\cos\alpha = 2\frac{h_2}{b} - 1$$

$$\cos\beta = \frac{1 - b/h_2 + (h_1/h_2 - 1)^2}{1 - b/h_2 - (h_1/h_2 - 1)^2}$$

NOTE : CIRCUMFERENCE AND AREA ARE PLOTTED IN DIAGRAM 6 IN TERMS OF h_2/b AND h_2/h_1

$$\frac{\text{CIRCUMFERENCE}}{\pi b} = 1 - \frac{\alpha}{\pi} + \frac{\beta}{\pi}\frac{\sin\alpha}{\sin\beta}$$

$$\frac{\text{AREA}}{\frac{\pi}{4}b^2} = 1 - \left(\frac{\alpha}{\pi} - \frac{\sin 2\alpha}{2\pi}\right) + \left(\frac{\beta}{\pi} - \frac{\sin 2\beta}{2\pi}\right)\left(\frac{\sin\alpha}{\sin\beta}\right)^2$$

FIG. 4 : GEOMETRY OF CROSS SECTIONS COMPOSED OF TWO CIRCLE SECTORS

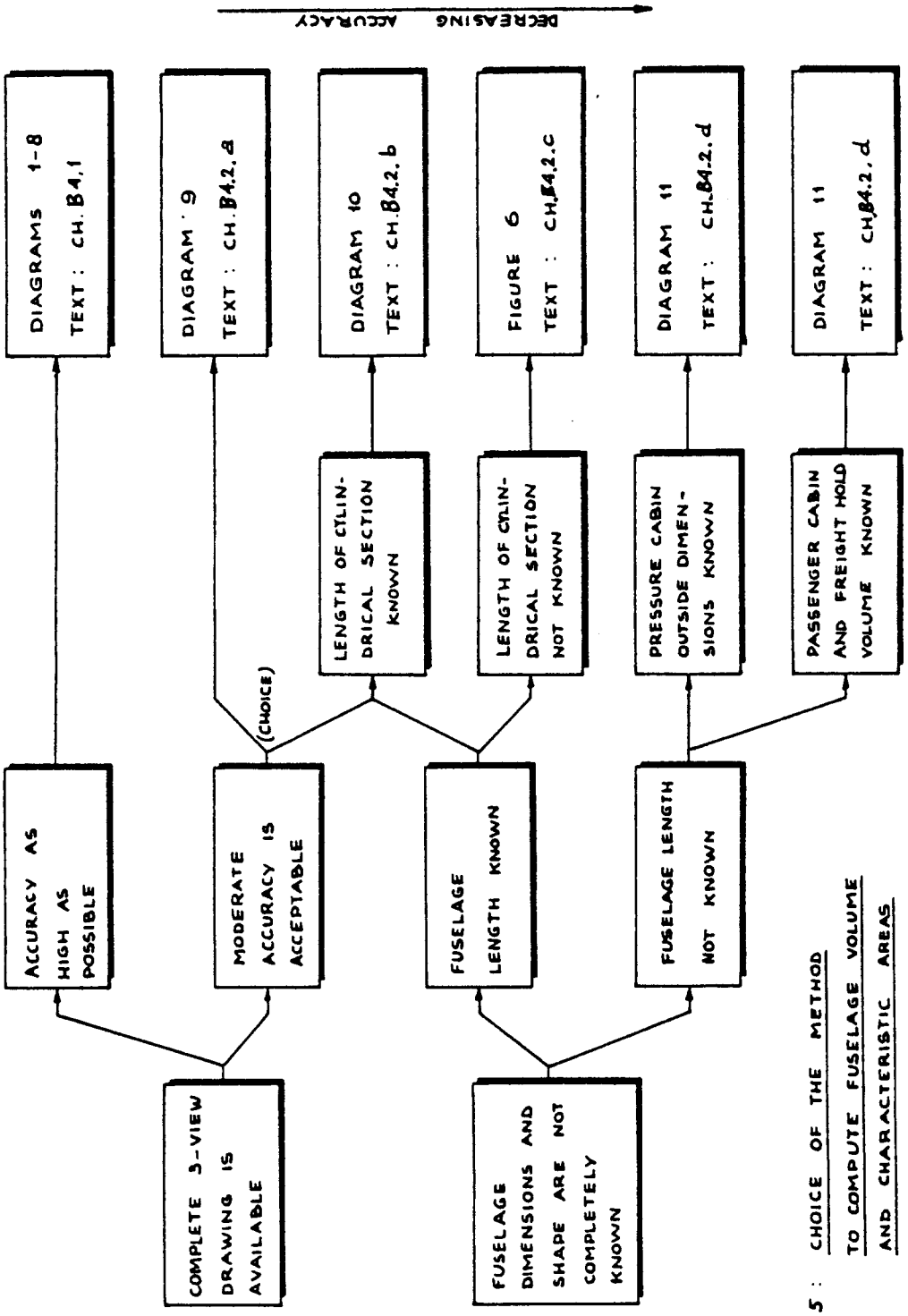

FIG. 5 : CHOICE OF THE METHOD TO COMPUTE FUSELAGE VOLUME AND CHARACTERISTIC AREAS

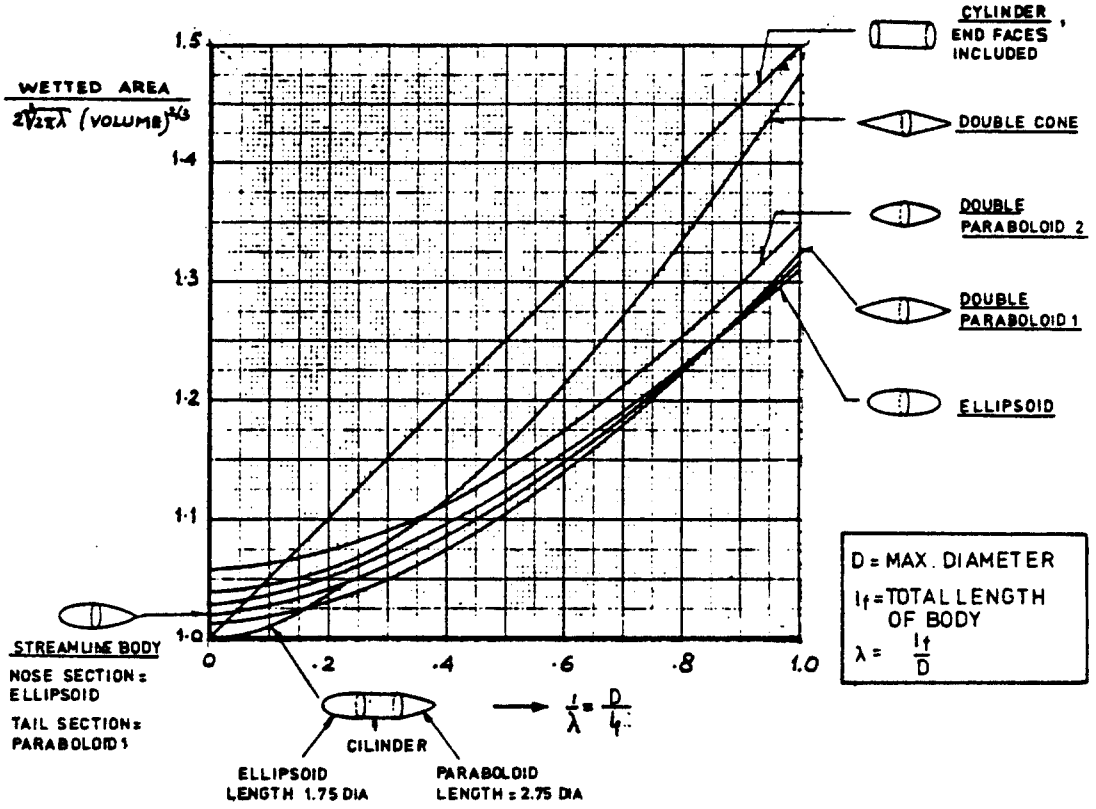

STREAMLINE BODY WITH CYLINDRICAL CENTER SECTION ($\lambda > 4.5$)

FOR FUSELAGES WITH CYLINDRICAL CENTER SECTION, NOSE AND TAIL SECTION SHAPES ACCORDING TO FIG. 1 AND LENGTH/DIAMETER RATIOS EQUAL TO 1.75 AND 2.75 RESP. :

$$\left.\begin{aligned}\text{VOLUME} &= \frac{\pi}{4} D^2 l_f \left(1-\frac{2}{\lambda}\right)\\ \text{WETTED AREA} &= \pi D l_f \left(1-\frac{2}{\lambda}\right)^{2/3}\left(1+\frac{1}{\lambda^2}\right)\end{aligned}\right\} \lambda \geq 4.5$$

FOR STREAMLINE BODIES WITHOUT CYLINDRICAL CENTER SECTION, NOSE AND TAIL SECTION SHAPES ACCORDING TO FIG. 1 :

$$\text{VOLUME} = \frac{\pi}{4} D^2 l_f \left(0.50 + 0.135\,\frac{l_n}{l_f}\right) \qquad (l_n = \text{LENGTH OF BODY NOSE})$$

$$\text{WETTED AREA} = \pi D l_f \left(0.50 + 0.135\,\frac{l_n}{l_f}\right)^{2/3}\left(1.015 + \frac{0.3}{\lambda^{3/2}}\right)$$

FIG. 6 : VOLUME AND WETTED AREA OF AXISYMMETRIC STREAMLINE BODIES.

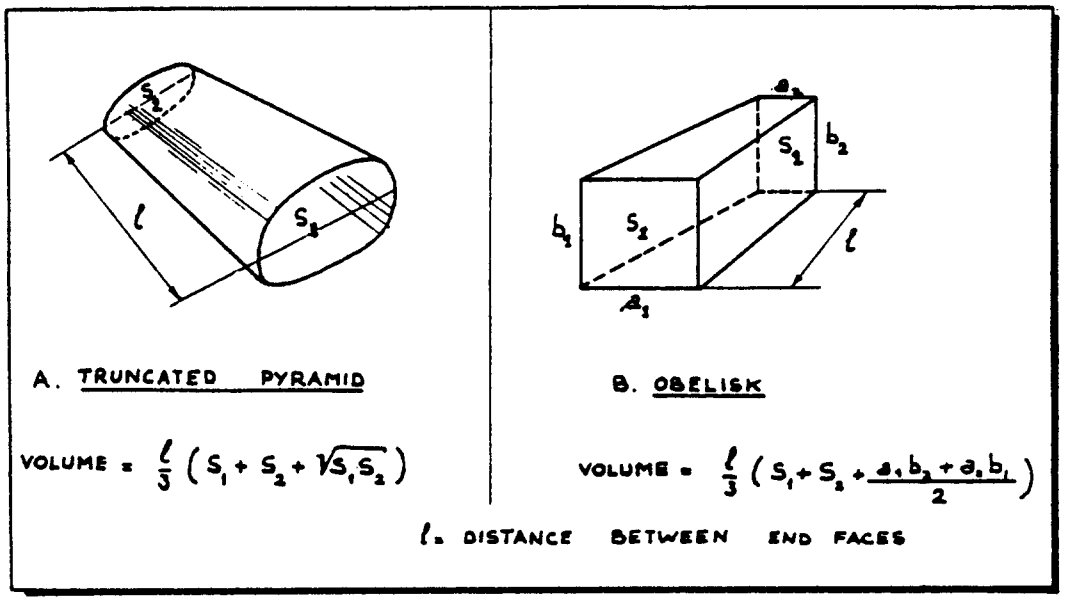

FIG. 7 : VOLUME OF GEOMETRIC BODIES WITH PARALLEL END FACES

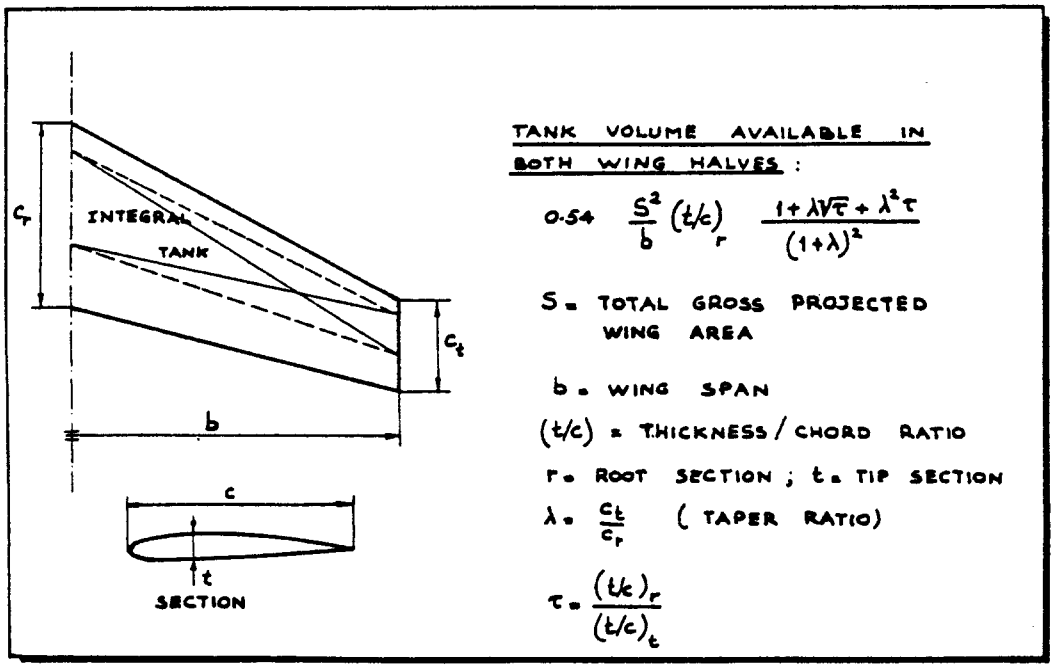

FIG. 8.: APPROXIMATION FOR INTEGRAL FUEL TANK VOLUME, AVAILABLE IN A LINEAR LOFTED WING

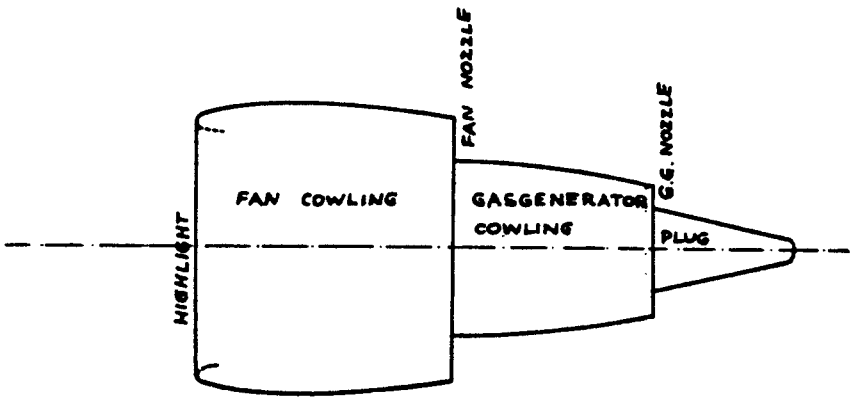

COMPONENTS OF AN ENGINE NACELLE GROUP

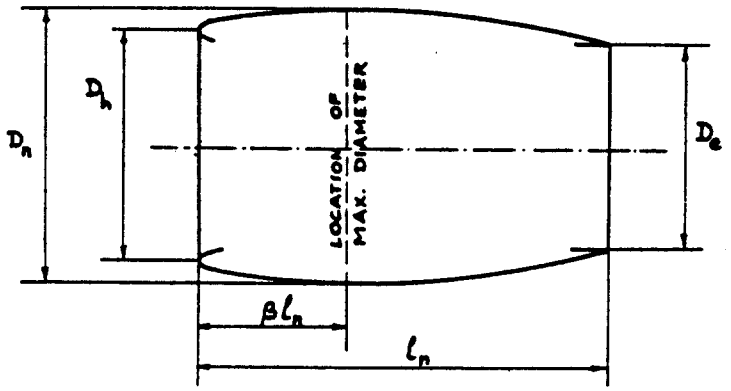

EXTERNAL WETTED AREA OF FAN COWLING :

$$l_n D_n \left\{ 2 + 0.35\beta + 0.80\beta \frac{D_h}{D_n} + 1.15(1-\beta)\frac{D_e}{D_n} \right\}$$

WETTED AREA OF GASGENERATOR COWLING : DIAGRAM 7

WETTED AREA OF PLUG :

2 * PLUG LENGTH * MAX. DIAMETER

FIG. 8 : WETTED AREA OF AN ENGINE NACELLE

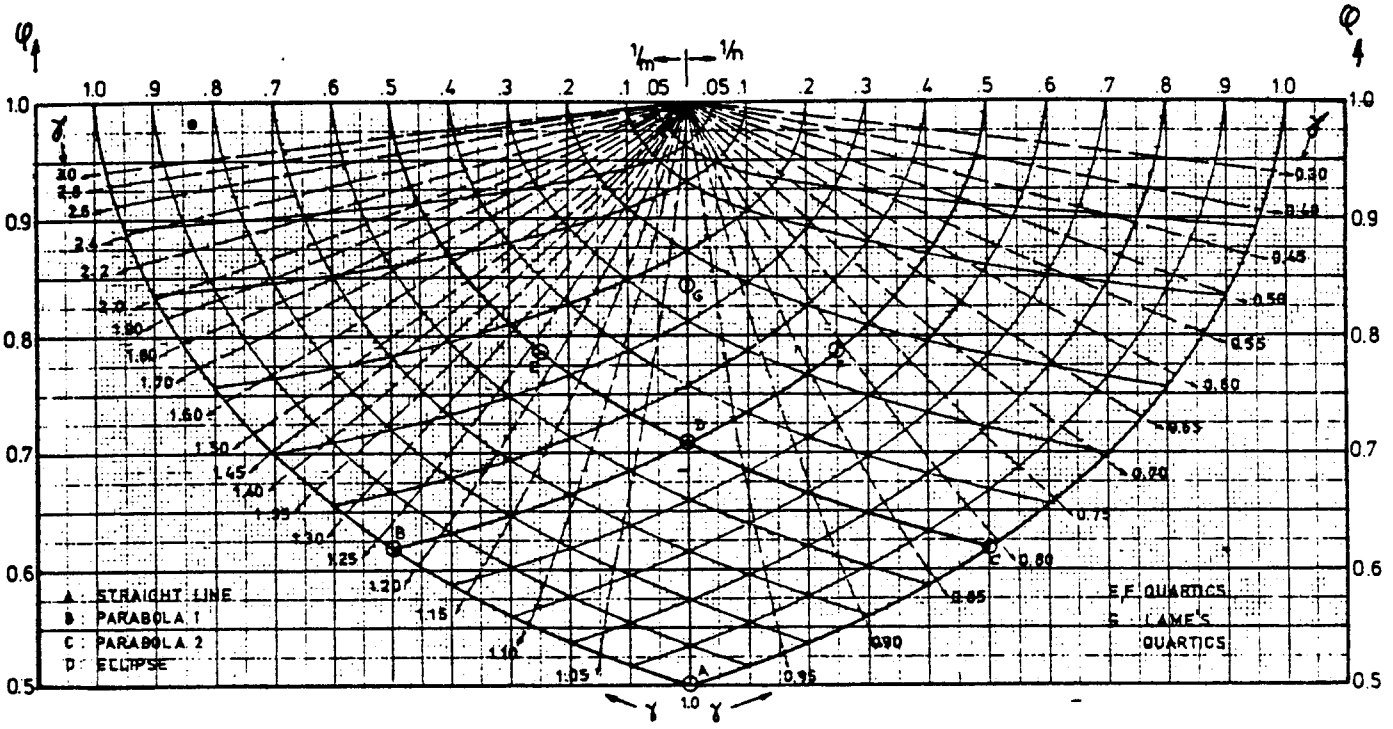

GENERAL EQUATION OF THE CONTOUR : $\left(\frac{x}{a}\right)^n + \left(\frac{y}{b}\right)^m = 1$

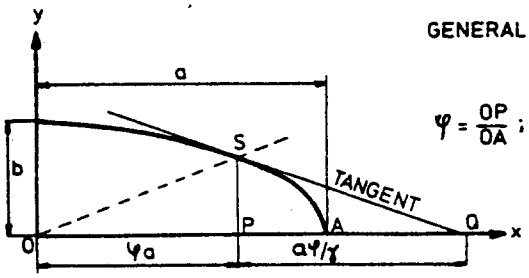

$\varphi = \frac{OP}{OA}$; $\gamma = \frac{OP}{PQ}$

RELATION BETWEEN (φ, γ) AND (n,m) :

$\varphi^n + \varphi^m = 1$; $\gamma = \frac{n}{m}\varphi^{n-m}$

DIAGRAM 1: DETERMINATION OF n AND m FROM KNOWN VALUES OF φ AND γ

AREA / a·b

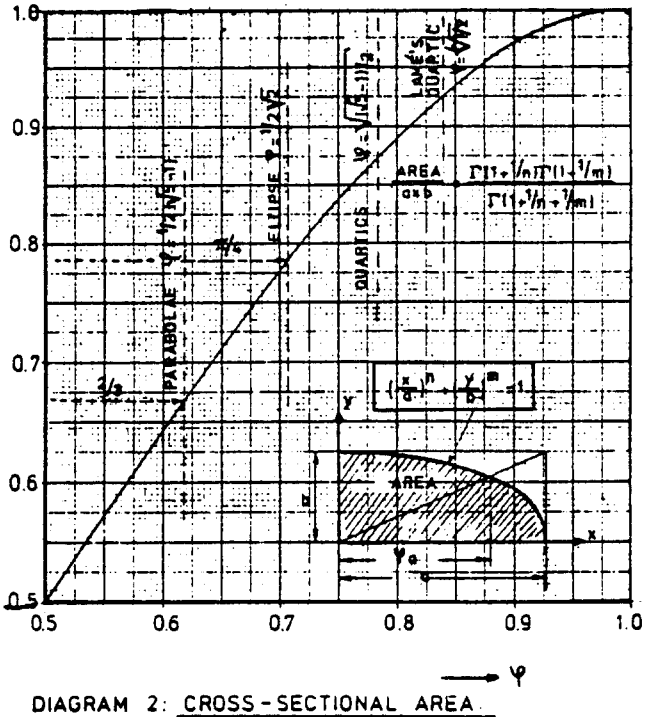

DIAGRAM 2: CROSS-SECTIONAL AREA

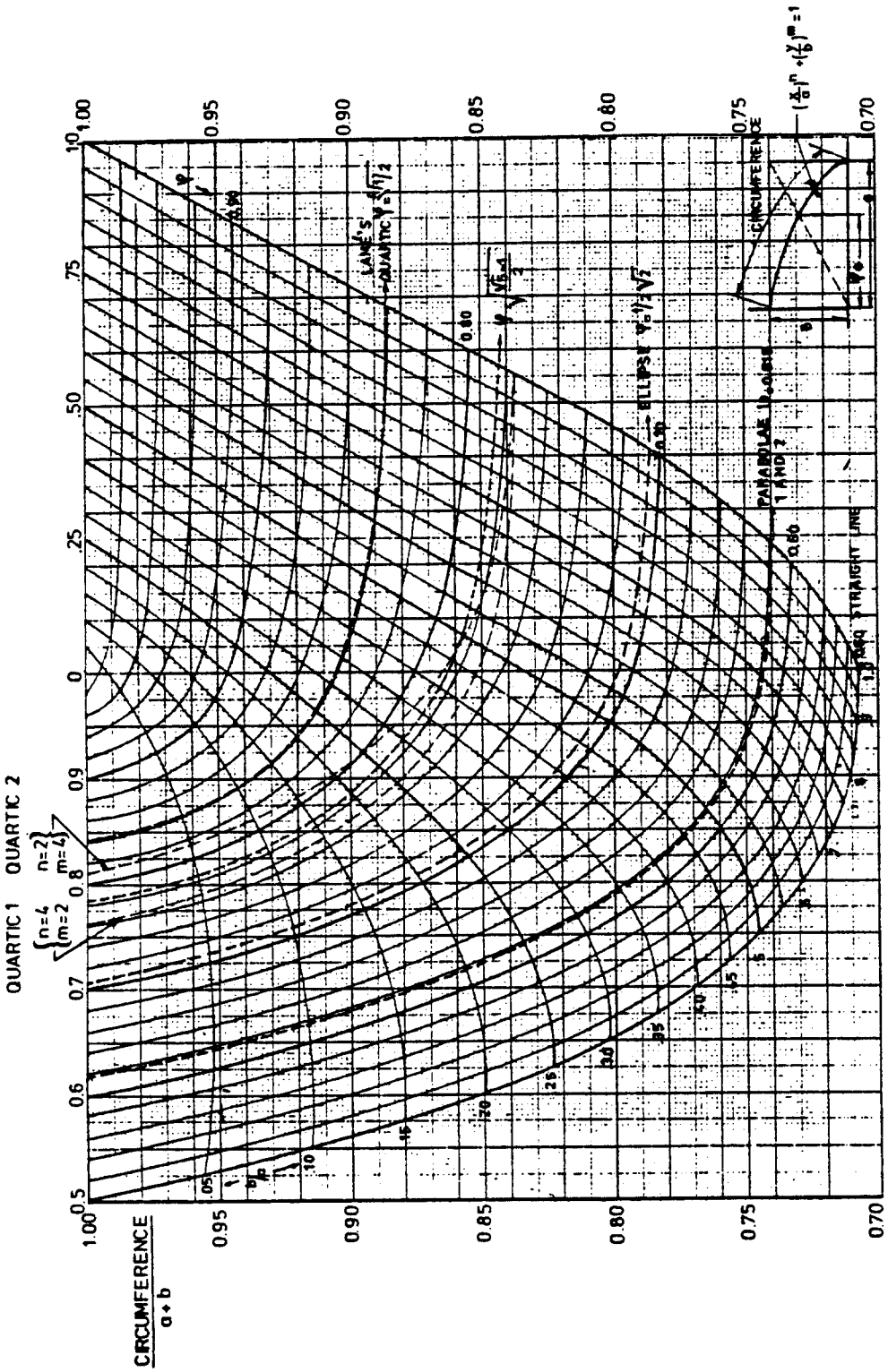

DIAGRAM 3: CIRCUMFERENCE OF A CONTOURLINE

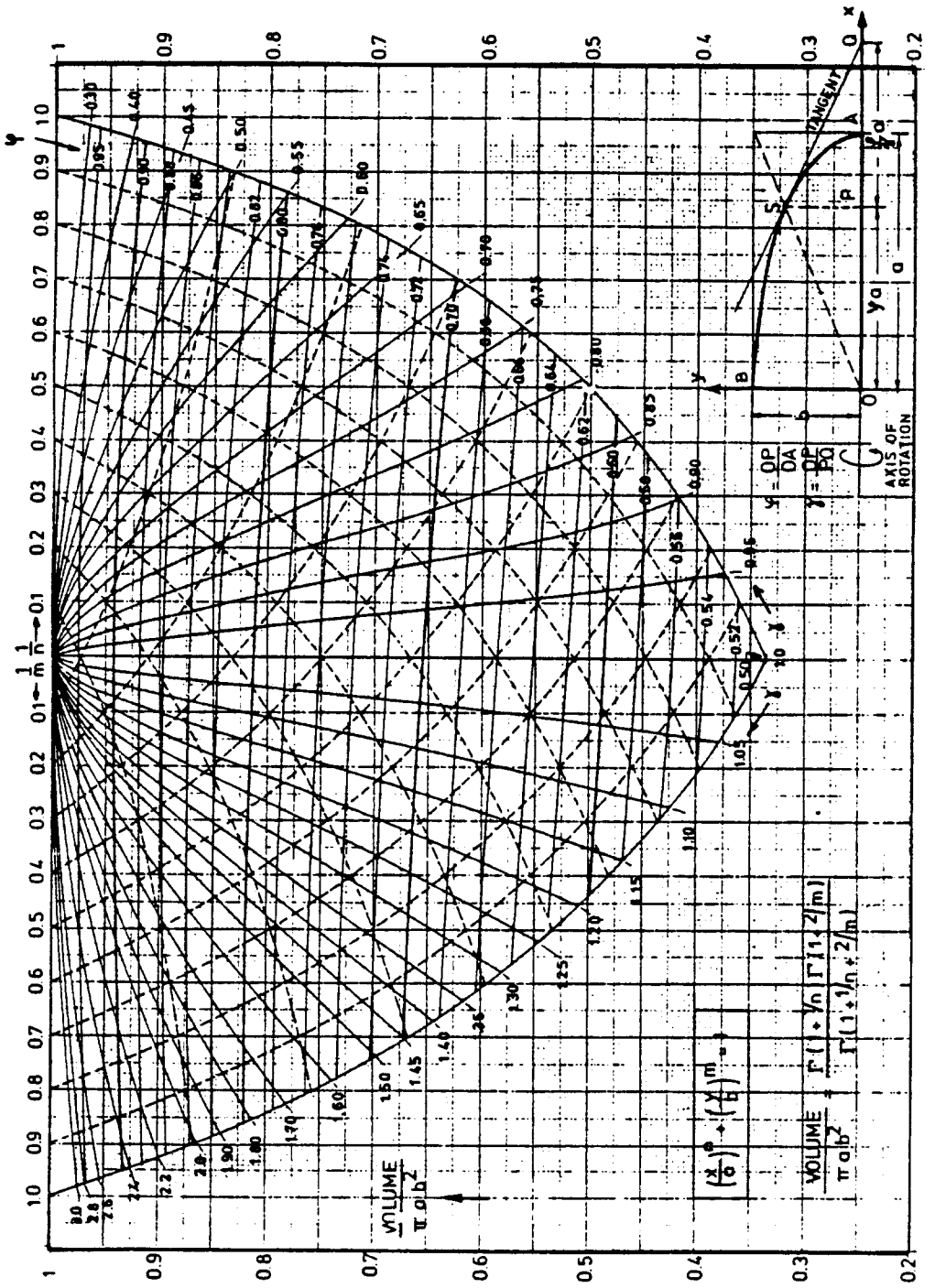

DIAGRAM 4: VOLUME OF A BODY OF REVOLUTION

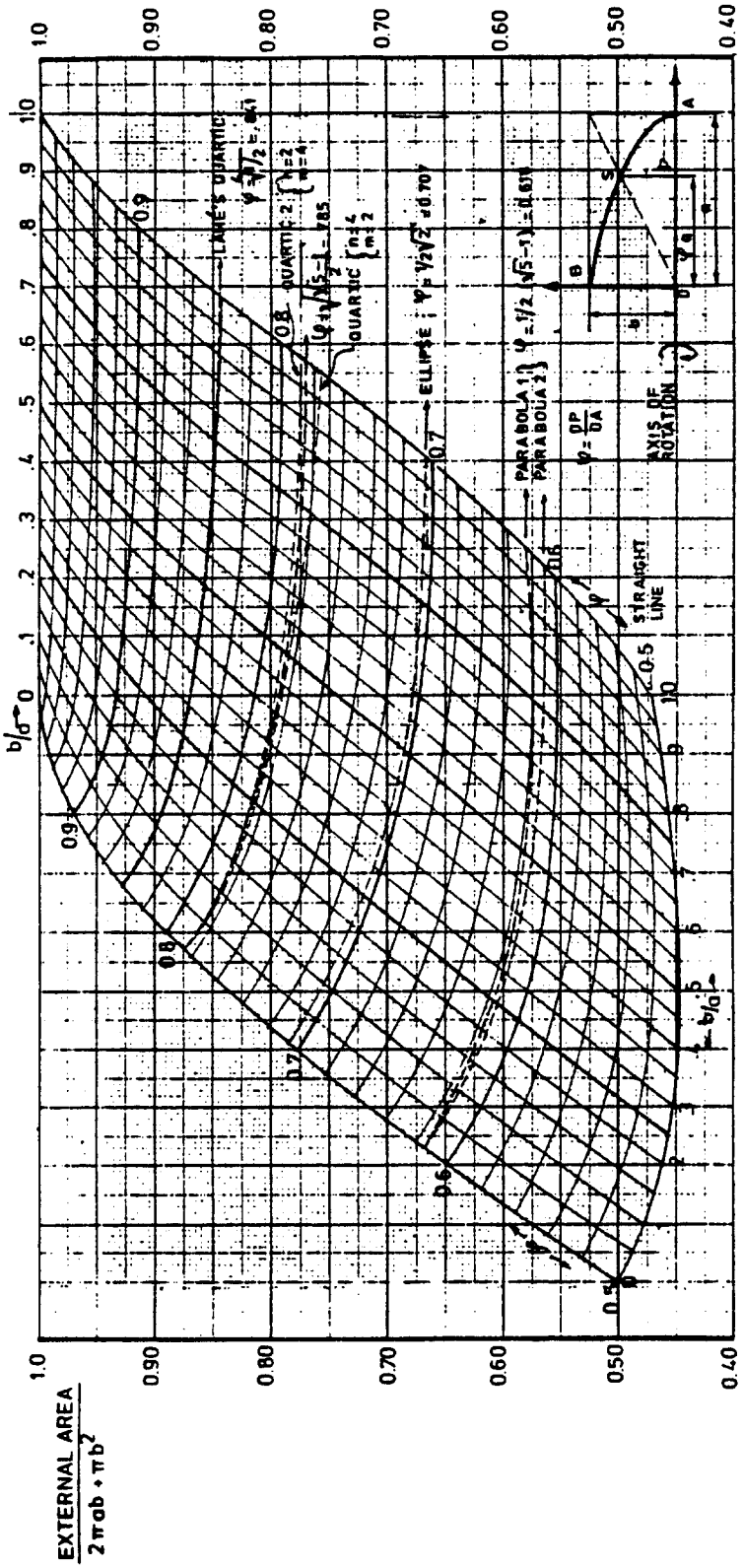

DIAGRAM 5: EXTERNAL AREA OF A BODY OF REVOLUTION.

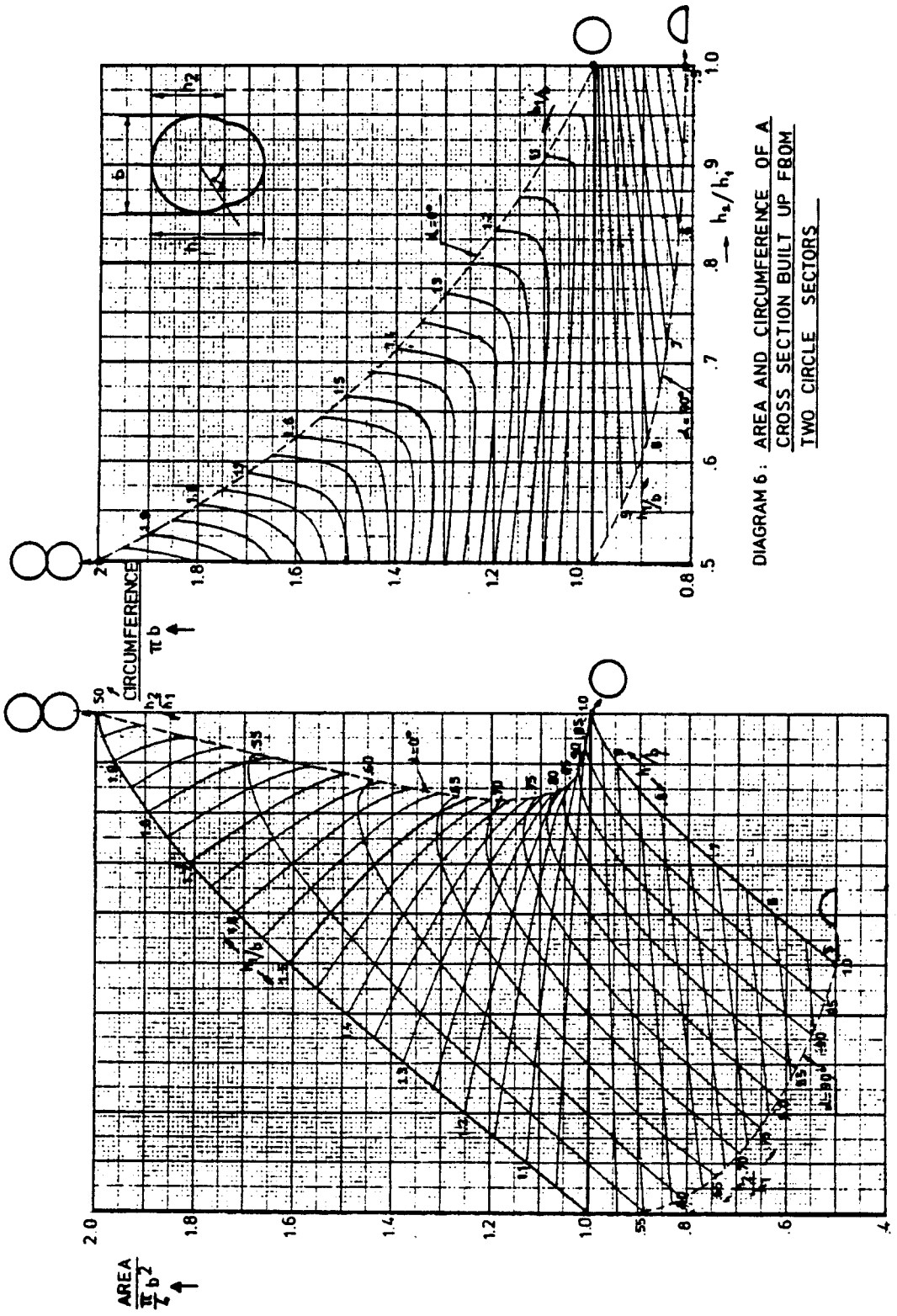

DIAGRAM 6: AREA AND CIRCUMFERENCE OF A CROSS SECTION BUILT UP FROM TWO CIRCLE SECTORS

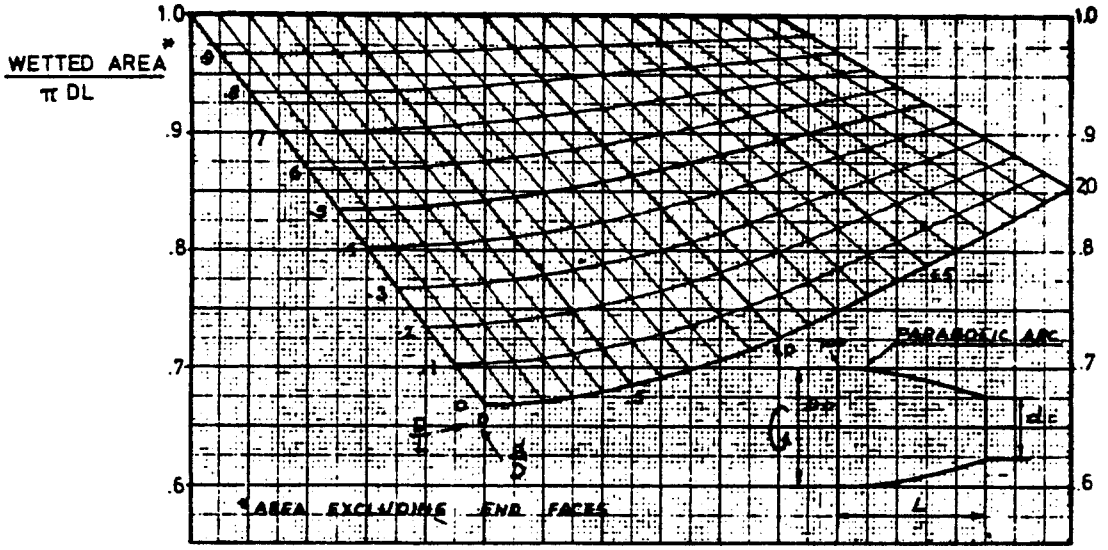

$$\frac{\text{VOLUME}}{\frac{\pi}{4}D^2L} = \frac{1}{15}\left\{8+4\frac{d}{D}+3\left(\frac{d}{D}\right)^2\right\}$$

DIAGRAM 7: GEOMETRIC PROPERTIES OF A FRUSTRUM OF A PARABOLOID

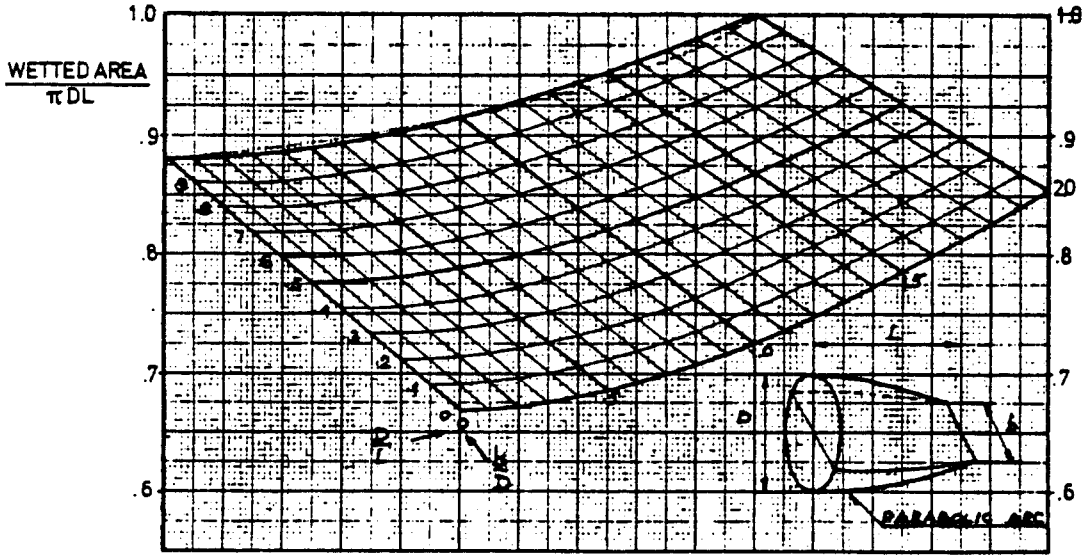

$$\frac{\text{VOLUME}}{\frac{\pi}{4}D^2L} = \frac{1}{15}\left\{8+2\frac{b}{D}\right\}$$

DIAGRAM 8: APROXIMATE WETTED AREA AND VOLUME OF A "BEAVER TAIL"

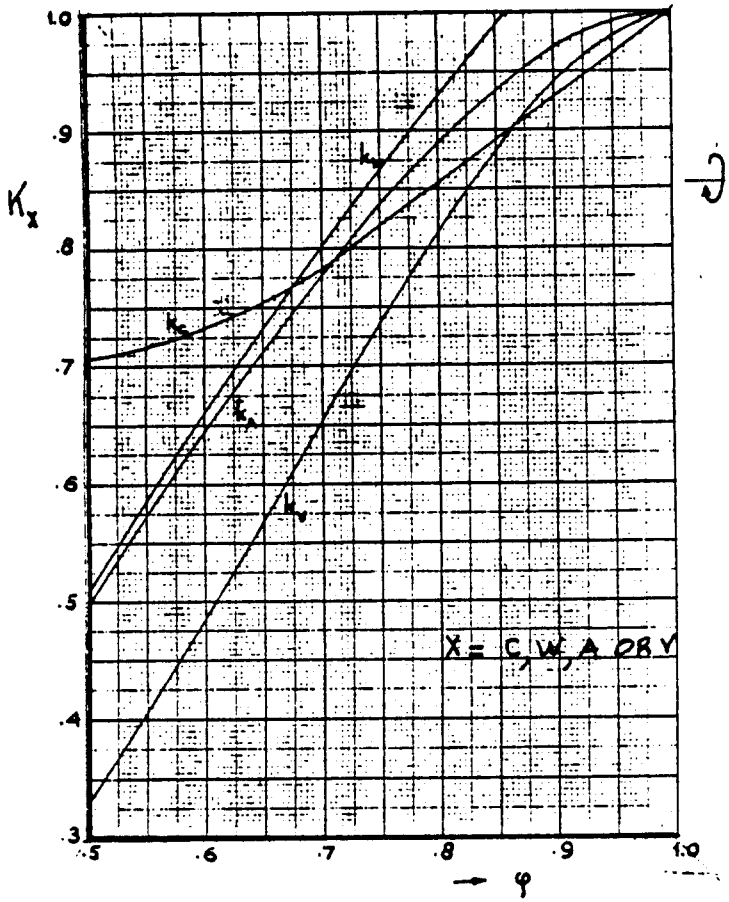

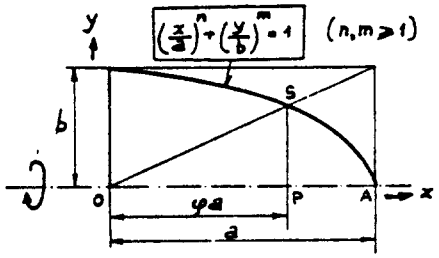

$k_A = \frac{\text{AREA OF SECTION}}{a \cdot b}$

$k_c = \frac{\text{CIRCUMFERENCE}}{a + b}$

$k_v = \frac{\text{VOLUME OF BODY OF REV.}}{\pi a b^2}$

$k_w = \frac{\text{WETTED AREA BODY OF REV.}}{2\pi a b}$

$\varphi = \frac{OP}{OA}$

DIAGRAM 9 :
SIMPLIFIED CALCULATION OF AREAS AND VOLUME

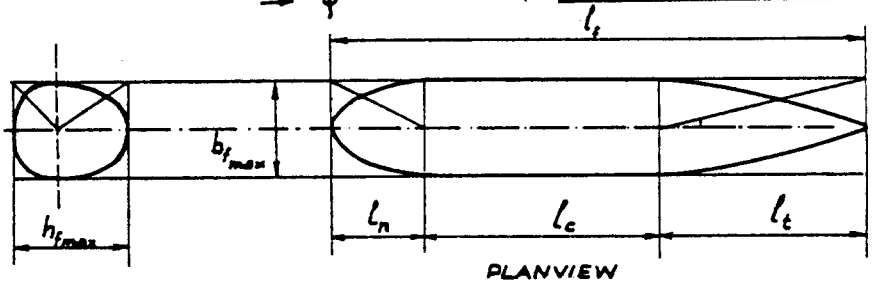

PLANVIEW

FRONT VIEW : AREA $S_f = k_A \cdot b_{f_{max}} \cdot h_{f_{max}}$

CIRCUMFERENCE $C_f = 2\, k_c \,(b_{f_{max}} + h_{f_{max}})$

(IF NECESSARY, THE FRONT VIEW IS SUBDIVIDED INTO SEVERAL PARTS)

VOLUME : $V_f = S_f (l_c + k_{v_n} l_n + k_{v_t} l_t)$

k_v IS DETERMINED FROM THE PLANVIEW FOR THE NOSE SECTION (k_{v_n}) AND THE TAIL SECTION (k_{v_t})

WETTED AREA : $S_{WET} = C_f (l_c + k_{w_n} l_n + k_{w_t} l_t)$

k_w - VALUES ARE DETERMINED FROM THE PLAN VIEW

PLANVIEW AND SIDEVIEW AREAS CAN BE COMPUTED IN SIMILAR FASHION

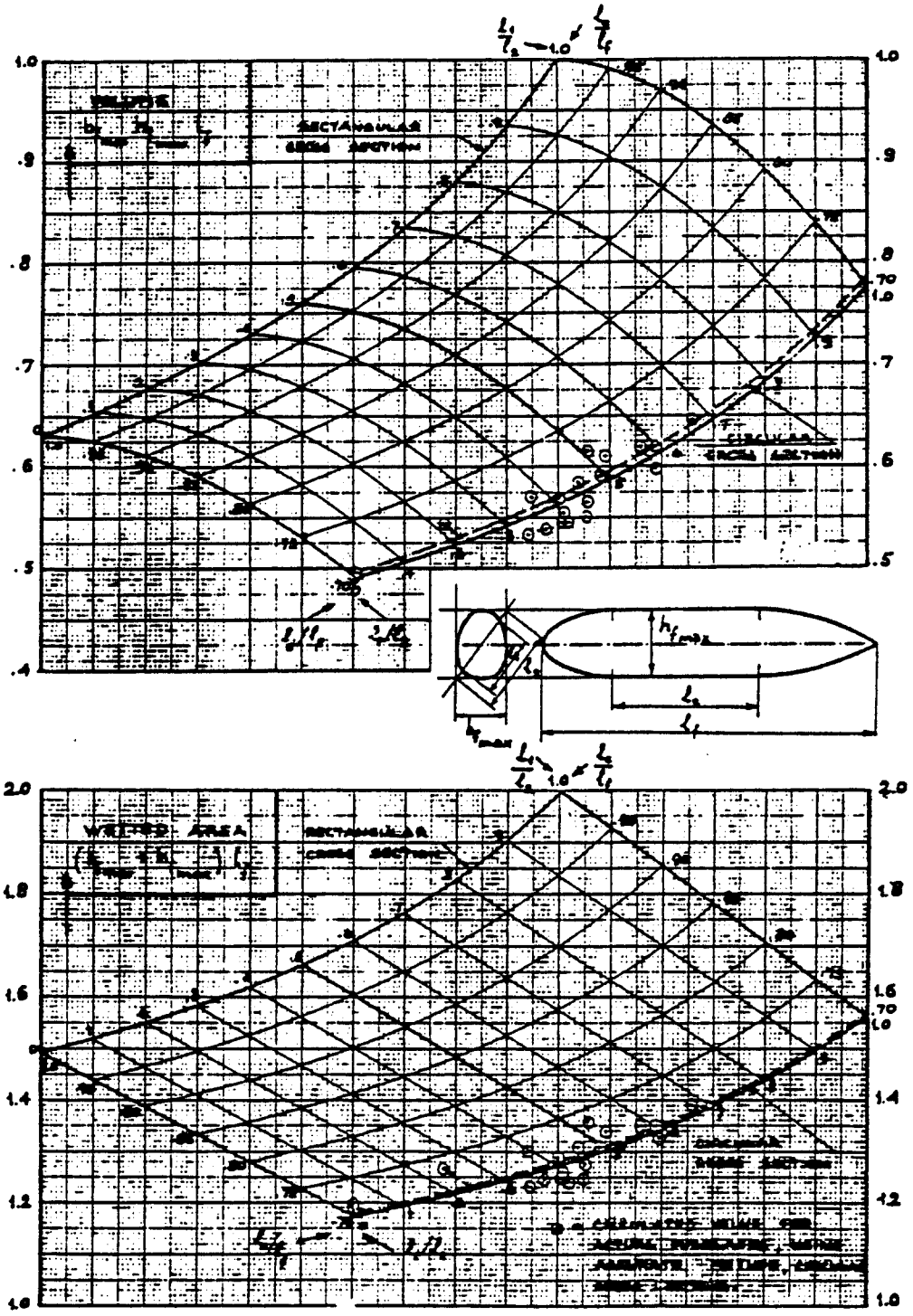

DIAGRAM 10: APPROXIMATE CALCULATION OF FUSELAGE VOLUME AND WETTED AREA (GIVEN: LENGTH OF CYL. SECTION)

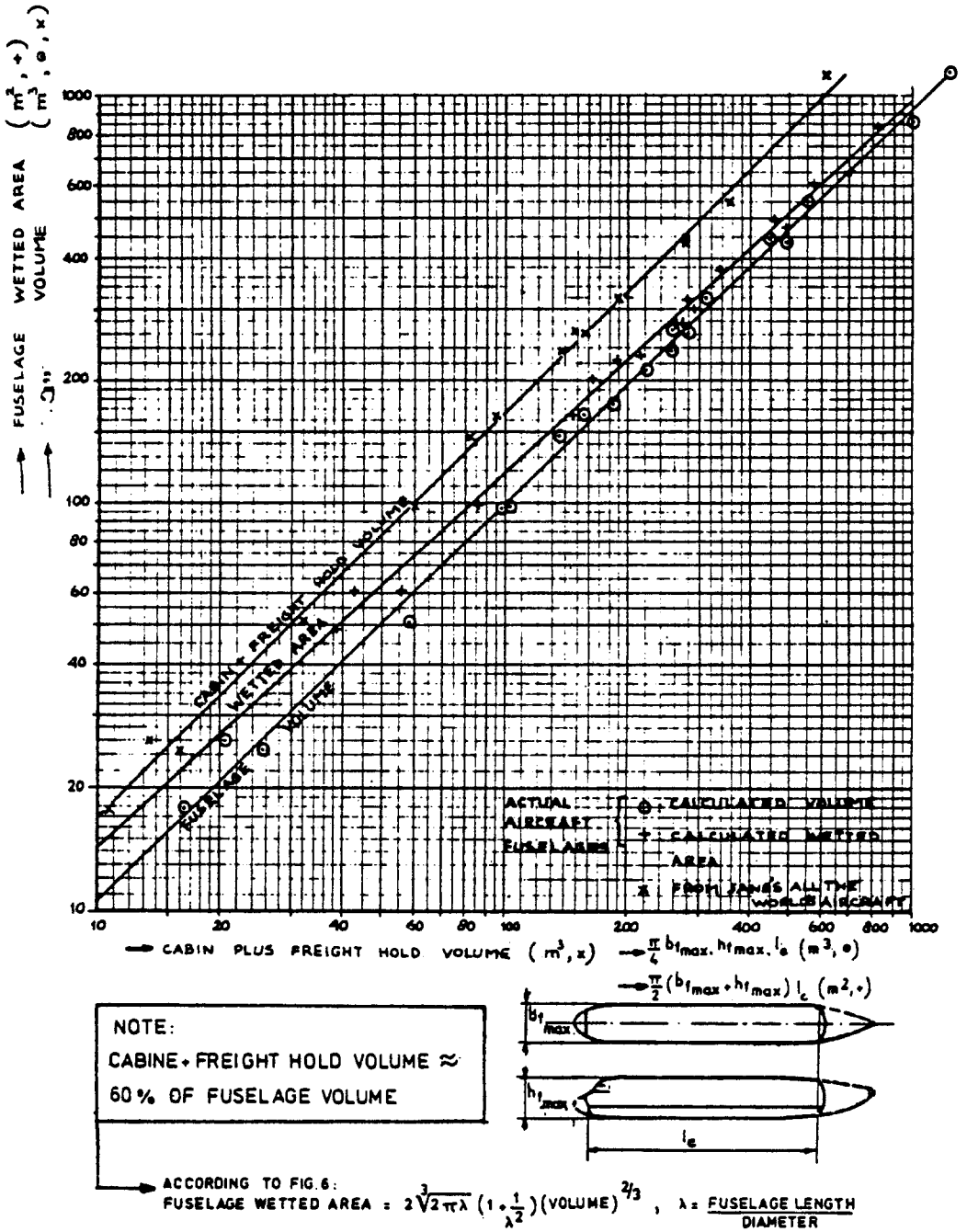

DIAGRAM 11 : STATISTICAL CORRELLATION OF VOLUME AND WETTED AREA BASED ON PRESSURE CABIN DIMENSIONS (VALID FOR FUSELAGES WITH CILINDRICAL SECTION)

CONSTRUCCIONES AERONAUTICAS, S. A.
D. PROYECTOS Y SISTEMAS
2352
BIBLIOTECA
TECNICA
INFORMACION Y DOCUMENTACION
GETAFE (Madrid)

AIRPLANE DESIGN

PART VII: DETERMINATION OF STABILITY, CONTROL AND PERFORMANCE CHARACTERISTICS: FAR AND MILITARY REQUIREMENTS

by

Dr. Jan Roskam
Ackers Distinguished Professor
of Aerospace Engineering
The University of Kansas
Lawrence, Kansas

NO PART OF THIS BOOK MAY BE REPRODUCED WITHOUT
PERMISSION FROM THE AUTHOR

Copyright: Roskam Aviation and Engineering Corporation
Rt4, Box 274, Ottawa, Kansas, 66067
Tel. 913-2421624
First Printing: 1988

TABLE OF CONTENTS

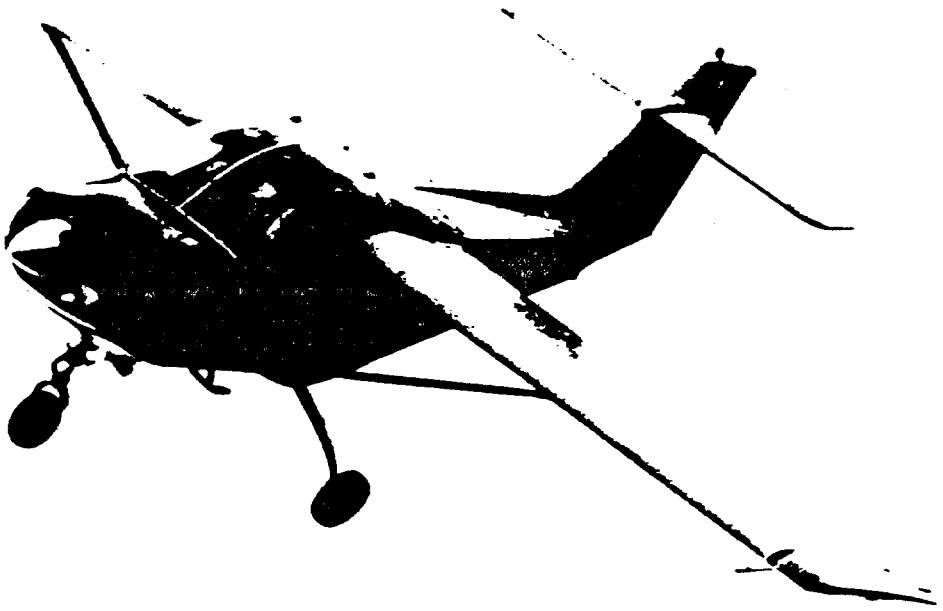

COURTESY : SAAB

TABLE OF SYMBOLS

The Table of Symbols is organized as follows:

IMPORTANT NOTES:

1. All aerodynamic coefficients and derivatives are defined in the stability axis system, unless stated to the contrary!
2. All rate derivatives are with respect to:

   (rate)$\bar{c}/2U_1$ or (rate)$b/2U_1$ depending on

   whether they are longitudinal or lateral-directional derivatives.
3. All speed derivatives are with respect to: u/U_1
4. Appendices contain separate symbol listings.

1. GENERAL SYMBOLS

Symbol	Definition	Dimension
$\bar{a}$	average deceleration during the groundrun	ft/sec^2
a_{lat}	lateral acceleration	ft/sec^2
a_{vert}	vertical acceleration	ft/sec^2
A	Wing aspect ratio	-----
A_h	Horizontal tail aspect ratio	-----
b	wing span	ft
b_f	flapped wing span	ft

$\bar{c}$	wing mean geometric chord, m.g.c.	ft
c_j	specific fuel consumption	lbs/lbs/hr
c_p	specific fuel consumption	lbs/hp/hr
$\bar{c}_{subscript}$	mean geometric chord of the surface corresponding to subscript area	ft
c_β	gear cornering coefficient, see page 47	lbs/deg
C_{D_o}	Zero lift drag coefficient	-----
C_{D_1}	Airplane steady state drag coefficient	-----
C_{D_u}	Airplane drag-due-to-speed derivative	-----
CGR	Climb gradient	rad
C_h	Hingemoment coefficient	-----
C_{h_o}	Hingemoment coefficient at zero angle of attack	-----
C_{h_α}	Hingemoment derivative due to angle of attack	1/rad
C_{h_β}	Hingemoment derivative due to sideslip angle	1/rad
C_{h_δ}	Hingemoment derivative due to control surface defl.	1/rad
C_{l_p}	Rolling moment due to roll rate derivative	1/rad
C_{l_r}	Rolling moment due to yaw rate derivative	1/rad
C_{l_β}	Rolling moment due to sideslip derivative	1/rad
$C_{l_{\beta_B}}$	Rolling moment due to sideslip derivative in the body axis system	1/rad
$C_{l_{\delta_a}}$	Rolling moment due to aileron derivative	1/rad
$C_{l_{\delta_{cpt}}}$	Rolling moment due to cockpit controller derivative, see Eqn.(2.63)	1/rad
$C_{l_{\delta_r}}$	Rolling moment due to rudder derivative	1/rad
$C_{l_{\delta_s}}$	Rolling moment due to spoiler derivative	1/rad

$C_L = W/\bar{q}S$	Airplane lift coefficient level flight	-----
C_{L_o}	Airplane lift coefficient at zero angle of attack	-----
C_{L_1}	Airplane steady state lift coefficient	-----
C_{L_q}	Lift due to pitchrate derivative	1/rad
C_{L_α}	Airplane lift curve slope	1/rad
$C_{L_{\delta_{ctrl}}}$	Airplane lift due to control surface deflection deriv.	1/rad
$C_{L_{\delta_e}}$	Airplane lift due to elevator deflection deriv.	1/rad
$C_{L_{wf}}$	Lift coefficient of the wing + fuselage	-----
$c_{m_{ac_f}}$	section pitching moment coefficient including flaps, about the section a.c.	-----
$C_{m_{ac_{wf}}}$	Pitching moment coefficent about the wing/fuselage aerodynamic center	-----
C_m	Airplane pitching moment coefficient	-----
C_{m_o}	Airplane pitching moment coefficient at zero angle of attack	-----
C_{m_α}	Airplane static longitudinal stability deriv.	1/rad
$C_{m_{\delta_{ctrl}}}$	Airplane pitching moment due to control surface deflection derivative	1/rad
$C_{m_{\delta_e}}$	Airplane pitching moment due to elevator deriv.	1/rad
C_{m_q}	Airplane pitching moment due to pitchrate deriv.	1/rad
C_{n_p}	Yawing moment due to roll-rate derivative	1/rad
C_{n_r}	Yawing moment due to yaw-rate derivative	1/rad
C_{n_β}	Yawing moment due to sideslip derivative	1/rad
$C_{n_{\beta_B}}$	Yawing moment due to sideslip in the body fixed axis system	1/rad
$C_{n_{\delta_a}}$	Yawing moment due to aileron derivative	1/rad

$C_{n_{\delta_r}}$	Yawing moment due to rudder derivative	1/rad
C_{ride}	Ride comfort index	-----
$C_{T_{x_1}}$	Airplane steady state thrust coefficient	-----
$C_{T_{x_u}}$	Airplane thrust-due-to-speed derivative	-----
C_{y_p}	Sideforce due to rollrate derivative	1/rad
C_{y_r}	Sideforce due to yawrate derivative	1/rad
C_{y_β}	Sideforce due to sideslip derivative	1/rad
$C_{y_{\delta_a}}$	Sideforce due to aileron deflection deriv.	1/rad
$C_{y_{\delta_r}}$	Sideforce due to rudder deflection deriv.	1/rad
d_T	thrust moment arm in pitch about the airplane c.g.	ft
$D = C_D \bar{q} S$	Airplane drag	lbs
e	Oswald's efficiency factor	-----
E	Endurance	hrs
f_{mp}	range factor, page 134	-----
f_{TO}	obstacle height factor, see page 119	-----
F_a	Lateral cockpit control force	lbs
F_r	Directional cockpit control force	lbs
F_s	Longitudinal cockpit control force	lbs
F_{T_y}	Sideforce component due to thrust	lbs
g=32.2	acceleration of gravity	ft/sec^2
G	gearing ratio	rad/ft
h	altitude	ft
h_L	obstacle height for landing	ft

h_{TO}	obstacle height for takeoff	ft
HM	Hingemoment	ftlbs
I_{xx}	Rolling moment of inertia about the c.g.	$slugft^2$
I_{yy}	Pitching moment of inertia about the c.g.	$slugft^2$
$I_{yy_{mg}}$	Pitching moment of inertia about the main gear to runway contact point	$slugft^2$
I_{zz}	Yawing moment of inertia about the c.g.	$slugft^2$
K	See Eqn.(4.7), p.109	-----
K_1	Gust parameter, see p.107	-----
K_2	Gust parameter, see pages 107 and 108	-----
K_a, K_r	Proportionality constant for cockpit control force coupling of aileron to rudder and vice versa	lbs/rad
l_h	distance of the horizontal tail aerodynamic center to the airplane c.g.	ft
$L = C_L \bar{q} S$	Airplane lift	lbs
L.E.	Leading Edge	-----
L_h	Lift acting on the horizontal tail at the hor. tail aerodynamic center	lbs
L_v	Gust length in y-dir.	ft
L_w	Gust length in z-dir.	ft
L_{wf}	Lift acting on wing + fuselage at the wing/fuselage aerodynamic center	lbs
L_p	$C_{l_p} \bar{q}_1 Sb^2/2I_{xx}U_1$	1/sec
L_r	$C_{l_r} \bar{q}_1 Sb^2/2I_{xx}U_1$	1/sec
L_T	Rolling moment due to thrust	ftlbs
L_β	$C_{l_\beta} \bar{q}_1 Sb/I_{xx}$	1/sec

$m=W/g$	airplane mass	slugs
$M_{ac_{wf}}$	Pitching moment about the wing/fuselage aerodynamic center	ftlbs
M_q	$C_{m_q}\bar{q}_1 S\bar{c}^2/2I_{yy}U_1$	1/sec
M_α	$C_{m_\alpha}\bar{q}_1 S\bar{c}/I_{yy}$	$1/sec^2$
$M_{\dot{\alpha}}$	$C_{m_{\dot{\alpha}}}\bar{q}_1 S\bar{c}^2/2I_{yy}U_1$	1/sec
n	load factor (L/W)	-----
$\bar{n}$	load factor function, see page 32	-----
n_α	load factor derivative with respect to angle of attack	1/rad
$N_{1,2,3}$	Numerator determinants defined in Table 2.1	
N_D	Yawing moment due to asymmetric drag	ftlbs
N_r	$C_{n_r}\bar{q}_1 Sb^2/2I_{zz}U_1$	1/sec
N_T	Yawing moment due to asymmetric thrust	ftlbs
N_β	$C_{n_\beta}\bar{q}_1 Sb/I_{zz}$	$1/sec^2$
p	roll rate	deg/sec
P_{mg}	Vertical reaction force on the main gear	lbs
P_{ng}	Vertical reaction force on the nose gear	lbs
P_{reqd}	$T_{reqd}U_1/550$, power reqd	hp
P_s	Specific excess power	ft/sec
$\bar{q}$	dynamic pressure	psf

Q_1	Steady state pitch rate	rad/sec
R	Range	nm or sm
RC	Rate of climb	ft/min or ft/sec
RD	Rate of descent	ft/min or ft/sec
R_e/R_r	Rigid-to-elastic ratio	-----
R_L	Loop radius	ft
R_t	Turn radius	ft
s_{AIR}	Air distance in landing	ft
s_{FL}	Landing fieldlength	ft
s_L	Landing distance	ft
s_{LG}	Landing ground distance	ft
s_{TO}	Takeoff distance	ft
s_{TOG}	Takeoff ground distance	ft
S	wing area	ft^2
$S.M._{free}$	Static margin, stick free	-----
$S_{subscript}$	Surface area corresponding to subscript area	ft^2
t	time	sec
T	installed thrust	lbs
$\bar{T}$	Average thrust (p.117)	lbs
T_{reqd}	W/(L/D), Thrust reqd	lbs
T_R	Roll time constant	sec
T_2	Time to double amplitude	sec
$\dot{u}$	airplane forward acceleration, also:	ft/sec^2
$\dot{u}$	bleed rate	ft/sec^2
U	forward speed	ft/sec
$\dot{U}$	forward acceleration	ft/sec^2
U_1	Steady state speed	fps
V	Speed	fps
V_A	Approach speed	fps

V_s	Stall speed	fps
$V_{s_{PA}}$	Stall speed in power approach	fps
V_{TD}	Touchdown speed	fps
W	Airplane weight	lbs
$\dot{W}_F$	Fuel flow rate	lbs/sec
$\bar{x}_{ac_A}$	airplane aerodynamic center location in fractions of wing m.g.c.	-----
x_{ac_h}	horiz. tail aerodynamic center location relative to leading edge of the wing m.g.c.	ft
$x_{ac_{wf}}$	location of wing/fuselage aerodynamic center relative to leading edge of wing m.g.c.	ft
$\bar{x}_{cg}$	airplane center of gravity location in fractions of wing m.g.c.	-----
x_{ng}	distance from nose gear to leading edge of wing m.g.c.	ft
x_{mg}	distance from main gear to leading edge of wing m.g.c.	ft
y_{mg}	lateral distance from the main gear to the c.g.	ft
Y_{ng}	Lateral ground friction force on nose gear	lbs
Y_{mg}	Lateral ground friction force on main gear	lbs
Y_r	$C_{y_r} \bar{q}_1 Sb/2mU_1$	ft/sec
Y_β	$C_{y_\beta} \bar{q}_1 S/m$	ft/sec^2
z_D	vertical distance from drag force to the c.g.	ft
z_{mg}	vertical distance from the c.g. to the main gear to ground contact point	ft

z_T	vertical distance from the thrustline to the c.g.	ft
Z_α	$-\bar{q}_1 S(C_{L_\alpha} + C_{D_1})/m$	ft/sec^2

2. GREEK SYMBOLS

α	angle of attack	deg or rad
α_g	angle of attack on the ground	deg or rad
α_δ	angle of attack effectiveness due to control surface deflection	-----
β	sideslip angle	deg or rad
β_{cross}	crosswind induced sideslip	deg or rad
$\beta_{ng \text{ or } mg}$	gear slip angle	deg or rad
γ	flight path angle	deg or rad
$\dot{\gamma}$	rate of change of flight path angle	rad/sec
γ_2	angle defined on p.121	deg or rad
$\gamma_{2_{min}}$	angle defined on p.122	deg or rad
Λ_{le}	leading edge sweep angle	deg or rad
δ	control surface deflection angle	deg or rad
δ_{cpt}	cockpit control deflection	deg or rad
Δ	Denominator determinant defined in Table 2.1, also: incremental value of ...	
ε	downwash angle at the horizontal tail	deg or rad
η_h	ratio of dynamic pressure at hor. tail to free stream	-----
θ	pitch attitude angle	deg or rad
λ	taper ratio, also engine bypass ratio	-----
μ_g	tire-to-ground friction coefficient	-----
μ'	see p.121	-----
ρ	air density	$slug/ft^3$

σ_v	rms lateral gust velocity	fps
σ_w	rms vert. gust velocity	fps
ζ	damping ratio	-----
τ_R	roll time constant, also: T_R	sec
ϕ	bank angle	deg or rad
ϕ_T	thrust inclination angle	deg or rad
$\dot{\psi}$	Airplane turnrate	deg/sec or rad/sec
ψ_A	Airplane crab angle	deg or rad
ψ_{steer}	Nose gear steering angle	deg or rad
ω_n	undamped natural freq.	rad/sec

3. SUBSCRIPTS

1	Steady state
2	takeoff safety speed
3	speed at obstacle
a	aileron
abs	absolute
cl	climb
cr	cruise
cross	crosswind
e	elevator
end	end
fg	front gear
h	horizontal tail
in	initial
lat	lateral
mc	minimum control
mg	main gear
man	maneuver
max	maximum
min	minimum
ng	nose gear

o	sealevel
r	rudder
reqd	required
rg	rear gear
s	stall, also: stability axes
sb	speedbrake
t	tab
tg	tail gear
v	vertical tail
w	wing
wf	wing + fuselage
A	Approach
B	Body axes
D	Dutch Roll
E	Empty
F	Fuel
GL	Glide
L	Landing, also: Left
P	Phugoid
PL	Payload
R	Roll Also: Right
S	Spiral
SP	Short Period
T	Throttle
TO	Takeoff

4. Acronyms

AEO	All engines operating
ASW	Anti submarine warfare
BFL	Balanced fieldlength
CGR	Climb gradient
LOF	Liftoff
NADC	Naval Air Development Center
OEI	One engine inoperative
P.D.	Preliminary design
rms	root mean square
SHP	Shaft horsepower

ACKNOWLEDGEMENT

Writing a book on airplane design is impossible without the supply of a large amount of data. In this particular volume, the author has used a large number of photographs and threeview data from the following companies:

Aerospatiale
Beech Aircraft Corp.
The Boeing Company
British Aerospace Corp.
Cessna Aircraft Company
Fairchild Republic Co.
Gates Learjet Corporation
Fokker Aircraft Co.
Piper Aircraft Corporation
General Dynamics Corporation
Grumman Aerospace Corp.
Gulfstream Aerospace Corp.
Lockheed Aircraft Corp.
McDonnell Douglas Corp.
SAAB
Rinaldo Piaggio, SpA.

The author wishes to thank these companies for kindly allowing the use of this information: it makes this book much more attractive.

A significant amount of airplane design information has been accumulated by the author over many years from the following magazines:

Interavia (Swiss, monthly)
Flight International (British, weekly)
Business and Commercial Aviation (USA, monthly)
Aviation Week and Space Technology (USA, weekly)
Journal of Aircraft (USA, AIAA, monthly)

The author wishes to acknowledge the important role played by these magazines in his own development as an aeronautical engineer. Aeronautical engineering students and graduates should read these magazines regularly.

1. INTRODUCTION

The purpose of this series of books on Airplane Design is to familiarize aerospace engineering students with the design methodology and design decision making involved in the process of designing airplanes.
The series of books is organized as follows:

Part I:	PRELIMINARY SIZING OF AIRPLANES
Part II:	PRELIMINARY CONFIGURATION DESIGN AND INTEGRATION OF THE PROPULSION SYSTEM
PART III:	LAYOUT DESIGN OF COCKPIT, FUSELAGE, WING AND EMPENNAGE: CUTAWAYS AND INBOARD PROFILES
PART IV:	LAYOUT DESIGN OF LANDING GEAR AND SYSTEMS
PART V:	COMPONENT WEIGHT ESTIMATION
PART VI:	PRELIMINARY CALCULATION OF AERODYNAMIC, THRUST AND POWER CHARACTERISTICS
PART VII:	DETERMINATION OF STABILITY, CONTROL AND PERFORMANCE CHARACTERISTICS: FAR AND MILITARY REQUIREMENTS
PART VIII:	AIRPLANE COST ESTIMATION: DESIGN, DEVELOPMENT, MANUFACTURING AND OPERATING

In this part (Part VII) frequent use is made of most other parts in this series on Airplane Design: Refs 1-7.

In Parts I and II so-called Class I methods for sizing airplanes to performance, stability and control requirements were presented. These methods are compatible with Preliminary Design Sequence I as outlined in Steps 1-16 in Part II. A flowchart which relates Class I methods and P.D. Sequence I to Class II methods and P.D. Sequence II is presented in Table 1.1.

The purpose of Part VII is to present Class II preliminary design methods for determining stability, control and performance characteristics of airplanes. These methods are compatible with Steps 17-36 of Preliminary Design Sequence II as outlined also in Part II.

The objective of these methods is to assure that:

1. the mission requirements of the airplane (as stated in the mission specification) are satisfied

2. the airworthiness regulations (as stated in References 8, 9 and 10) are met

Table 1.1 Flowchart of the Preliminary Design Process

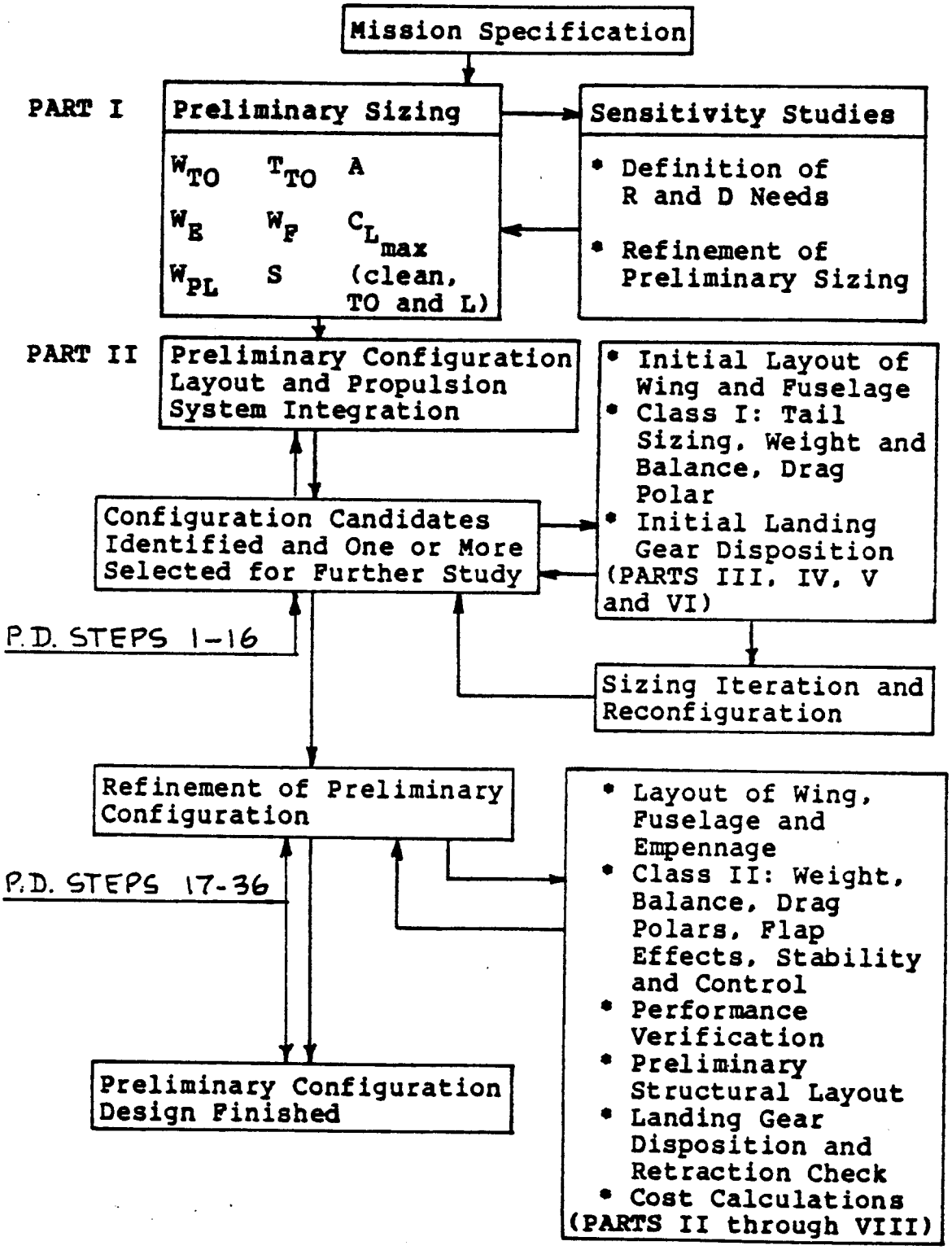

Airplanes must be controllable, maneuverable and trimmable to be safe as well as useful. Chapter 2 presents methods for assessing the controllability, the maneuverability and the trimmability capabilities of new airplane designs.

Stability is a requirement for all airplanes*. Methods for predicting the static and dynamic stability characteristics of airplanes are found in Chapter 3.

To be useful most airplanes must possess ride qualities such that the crew can carry out its functions and such that passengers are not made uncomfortable. The subject of ride qualities is taken up in Chapter 4.

All airplanes must satisfy specific performance objectives which are normally defined in a statement of mission requirements. For an airplane to be airworthy, it must also meet certain safety related performance requirements. Methods for computing the performance capabilities of airplanes are discussed in Chapter 5.

Airworthiness regulations have a major impact on the design and development of airplanes. Therefore, the most important aspects of civil and military stability, control and performance airworthiness requirements (regulations) are presented in Appendices A and B.

Part VII is not intended as a textbook on airplane performance, stability and control. It is designed as a reference manual for students to ascertain that their designs will meet mission performance as well as stability and control requirements. For a detailed presentation of airplane performance, stability and control theory and methods References 11 and 12 are recommended.

Frequently, the mission specification of an airplane will identify which regulations form the certification base for an airplane. If that is not the case it is recommended that Table 1.2 be used to identify the type of airplane which is being designed. With this information, Table 1.3 can then be used to identify which regulations apply to the design.

---

* Stability can be satisfied in an open or closed loop manner. If stability is satisfied 'open loop' it is referred to as 'inherent stability'. If stability is satisfied 'closed loop' it is referred to as 'de facto stability'.

A most important aspect of airplane design is to ensure that the airplane has not only satisfactory performance characteristics but also acceptable flying qualities following one or more failures of flight crucial components. To analyze the effect of failures of flight crucial components, the regulations must be interpreted in terms of the so-called airworthiness code as well as in terms of minimum acceptable levels of flying qualities. Appendix C contains a brief outline of the methodology used in determining the required levels of flying qualities in case of flight crucial failures.

TABLE 1.2 AIRPLANE TYPES

1. Homebuilt Propeller Driven Airplanes
2. Single Engine Propeller Driven Airplanes
3. Twin Engine Propeller Driven Airplanes
4. Agricultural Airplanes
5. Business Jets
6. Regional Turbopropeller Driven Airplanes
7. Transport Jets
8. Military Trainers
9. Fighters
10. Military Patrol, Bomb and Transport Airplanes
11. Flying Boats, Amphibious and Float Airplanes
12. Supersonic Cruise Airplanes

TABLE 1.3 RELATION BETWEEN AIRPLANE TYPE AND APPLICABLE AIRWORTHINESS REQUIREMENTS (REGULATIONS)

Airplane Type (See Table 1.2)	Passenger Limit	Weight Limit	Regulations
1	none	none	Experimental: FAR 21
2,3,4,5,11,12	<9	12,500	Normal Category: FAR 23, Appendix A
3,6,7,12	<19	<19,000	Commuter Category: FAR 23, Appendix A, see page 207
5,6,7,11,12	>19	none	FAR 25: Appendix A
8,9,10	none	none	Military: Appendix B

2. CONTROLLABILITY, MANEUVERABILITY AND TRIM

The purpose of this chapter is to present Class II methods for analyzing the controllability, maneuverability and trimmability of a newly designed airplane. These methods are compatible with Step 24 in Preliminary Design Sequence II as outlined in Chapter 2 of Part II.

The objectives of the methods in this chapter are to assure that:

1. the airplane has sufficient control power to maintain steady state, straight line flight
2. the airplane can be safely maneuvered from one steady state flight condition to another
3. cockpit control force levels are acceptable under all expected conditions, including those caused by configuration changes
4. the airplane can be trimmed in certain flight conditions

The qualitative statements 1-4 are only one component of what constitutes good flying qualities (handling qualities) of airplanes. These qualitative statements are translated in terms of quantitative requirements in the airworthiness requirements of References 8 and 9. These airworthiness requirements will be referred to as the REGULATIONS.

Which regulations apply to a given new airplane design depends on the projected use of that airplane. Certification according to more than one regulation is possible at the option of the designer. Broadly speaking, the regulations are applied as indicated in Table 1.3 of Chapter 1.

The material in this chapter is organized as follows:

It is essential to gain insight into how the various regulatory requirements for control, maneuvering and trim fit into the airplane design process. For that reason, the material in most sections is presented in the following general sequence:

1. identification of the applicable airworthiness regulation(s)

2. relationship to the stability and control checks performed as part of the preliminary layout design steps described in Chapter 2 of Part II: P.D. Sequences I and II (mostly Steps 11 and 24)

3. presentation of a model for analyzing controllability, trimmability and/or maneuverability

4. a step-by-step procedure for determining whether or not the airplane meets the control, trim and/or maneuvering requirements of the regulations

In this chapter, frequent use is made of the following terms:

* control surface
* trim surface
*trim
*trim diagram

Definitions of these terms are as follows:

Definition: A control surface is a surface used by the pilot to attain airplane moment equilibrium and/or to maneuver the airplane from one flight condition to another flight condition.

Definition: A trim surface is a surface used by the pilot to attain zero required cockpit control force while retaining moment equilibrium.

Definition: When an airplane is in moment equilibrium while the cockpit control force is zero, the airplane is trimmed.

Definition: A trim diagram is used to determine the conditions for which moment equilibrium (not necessarily with zero cockpit control forces) can be attained.

For detailed discussion(s) of airplane stability and control characteristics Reference 12 should be consulted.

2.1 LONGITUDINAL CONTROLLABILITY AND TRIM

2.1.1 Applicable Regulations

Civil: FAR 23.143, 23.145, 23.161, FAR 25.143, FAR 25.145, 25.161, see: Appendix A.

Military: Mil-F-8785C, Par.3.2, see Appendix B.

2.1.2 Relationship to Preliminary Design

See Part II, Chapter 2 (in particular Step 24), Chapter 8 and Chapter 11.

2.1.3 Mathematical Model for Analyzing Longitudinal Controllability and Trim

The regulations essentially require that any airplane, when trimmed in a given flight condition at a given airspeed:

A. can be maneuvered safely and easily to another speed

B. can be controlled safely and easily when a configuration change is made

The words 'safely' and 'easily' as used here are defined in the regulations in terms of control forces which may not be exceeded and/or in terms of control power levels which must be available.

The words 'configuration change' are meant to imply any of the following events:

1. Change in center of gravity location
2. Change in thrust (or power) setting (voluntary or failure)
3. Hard-over failure of any control or trim surface
4. Change in landing gear position (up or down)
5. Change in flap position (up, take-off, approach or landing)
6. Change in speed brake position (retracted or deployed)
7. Store release (i.e. bomb or payload drop): symmetrical and asymmetrical
8. Weapons firing (i.e. moment due to recoil force)
9. Combat damage

Whether or not these events must be assumed to occur

simultaneously is stated in the applicable regulations!

For purposes of Class II analyses, longitudinal controllability is considered satisfied if:

1. Sufficient control power is available to cope with all required configuration changes

2. Sufficient control power is available to allow the airplane to be maneuvered from one flight speed to another

3. Cockpit control forces required in the use of control power to satisfy controllability are within the limits prescribed in the regulations

Figure 2.1 depicts the forces and moments which act on an airplane in a symmetrical, wings level, steady state, straight line flight condition.

The following three equations of motion apply to this case:

1. The Drag Equation:

$$C_{L_1}\sin\gamma = C_{D_1} + T\cos(\phi_T + \alpha) \qquad (2.1)$$

2. The (One-g) Lift Equation:

$$C_{L_1}\cos\gamma = \{C_{L_o} + C_{L_\alpha}\alpha + \qquad (2.2)$$

$$+ \sum_{i=n}^{i=1}\left(C_{L_{\delta_{ctrl_i}}}\delta_{ctrl_i}\right\} + (T/\bar{q}S)\sin(\phi_T + \alpha)$$

3. The Pitching Moment Equation:

$$0 = (C_{m_o} + C_{m_\alpha}\alpha + \sum_{i=n}^{i=1}\left(C_{m_{\delta_{ctrl_i}}}\delta_{ctrl_i}\right\} + (Td_T/\bar{q}S\bar{c}) \qquad (2.3)$$

For any given flight condition (i.e. known $\bar{q}$) at any given thrust setting (i.e. known T) the usual variables in these equations are:

α, γ and one of the i control surface deflections, δ_{ctrl_i}.

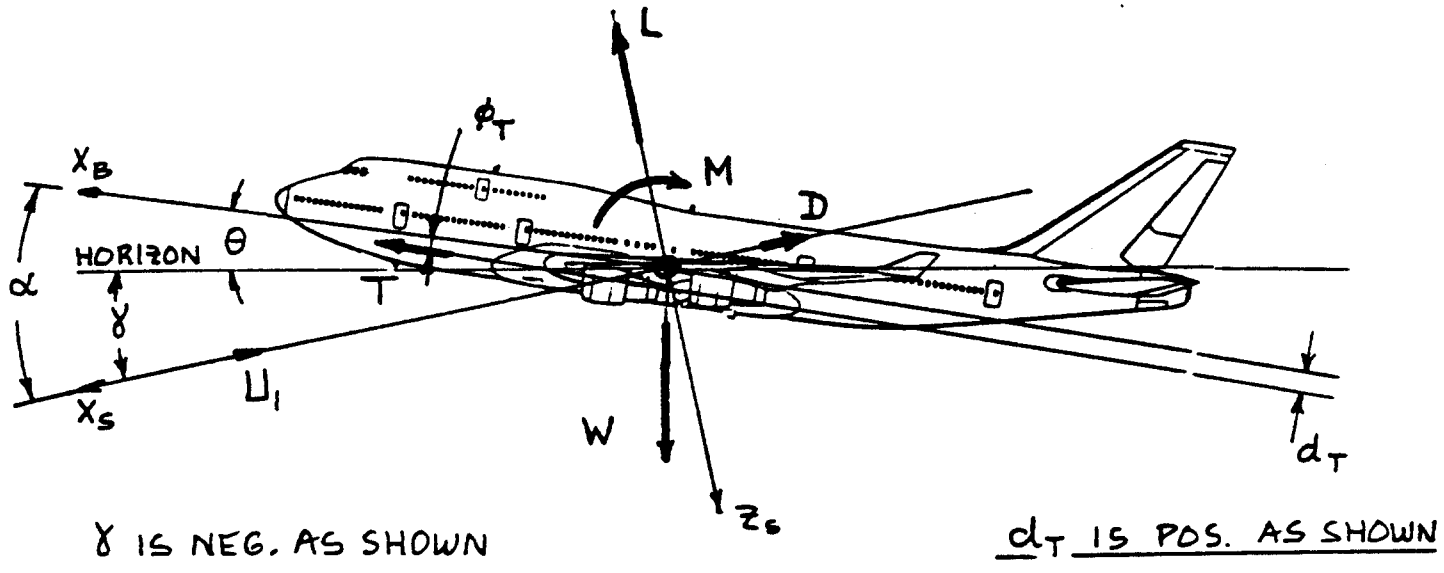

Figure 2.1 Forces and Moments Acting on an Airplane in Symmetrical, Wings Level, Steady State, Straight Line Flight

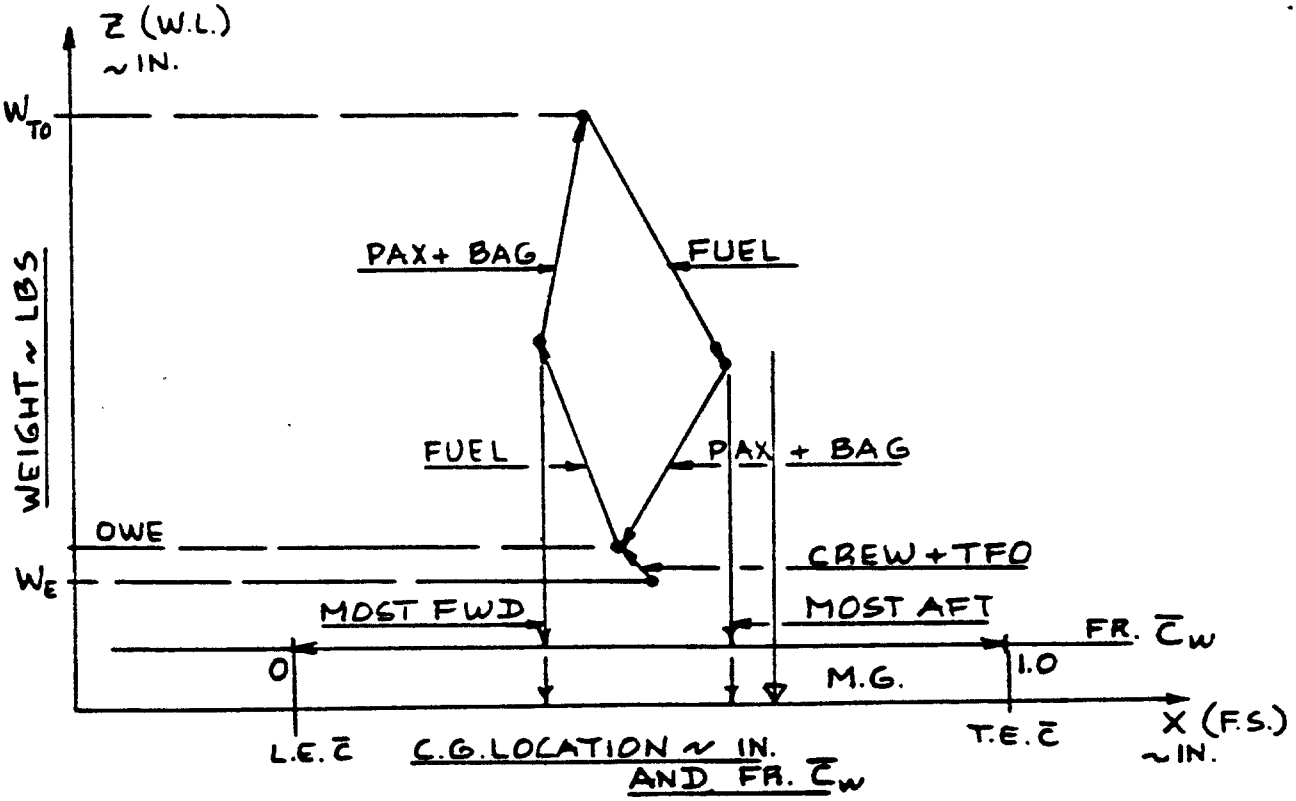

Figure 2.2 Example of a Weight/C.G. Envelope

The numerical solutions for these variables must be 'tested' against acceptability criteria. These acceptability criteria normally consist of allowable bounds on the numerical values of α, γ and δ_{ctrl_i}. Acceptability criteria are presented in Subsection 2.1.4.

Methods for computing airplane drag coefficient, C_D and installed thrust, T in Eqn.(2.1) are given in Chapters 4 and 6 of Part VI. The reader is reminded of the fact that the drag coefficient in Eqn.(2.1) is the so-called 'trimmed' drag coefficient! That means: C_D includes the drag effect of all control surface deflections necessary to achieve moment equilibrium and trim.

Methods for computing the stability and control derivatives in Equations (2.2) and (2.3) are provided in Chapter 10 of Part VI.

The reason for using the 'Sum' terms in Equations (2.2) and (2.3) explicitly is to recognize the fact that many airplanes use two (or more) different types of longitudinal controls. Frequently, one of these controls is used for primary longitudinal control while the other is used for longitudinal trim.

A detailed justification for Equations (2.1) through (2.3) is given in Reference 12 (Chapter 5).

In preliminary design, the following assumptions are made to enable a rapid resolution of the controllability issue:

1. The drag equation (2.1) is inherently satisfied.

   For any given desired flight path angle, γ this means that the throttles are set to balance the drag equation.

2. The flight path angle, γ is small enough to use: $\cos\gamma = 1.0$.

The consequence of these assumptions is that only Equations (2.2) and (2.3) are needed to determine controllability! This can be done with the help of the airplane trim diagram. The trim diagram allows a graphical

solution of Equations (2.2) and (2.3) while accounting for all eight configuration changes mentioned before. A method for constructing airplane trim diagrams is presented in Part VI, Chapter 8.

Class II analysis of longitudinal trim is usually accomplished by writing an equation for the cockpit control force required to hold the aerodynamic controls in a position such that Eqns (2.2) and (2.3) are satisfied. Such an equation is called the stick- (or wheel-) force equation and it takes the following form:

$$F_s = G(HM) + F_{s_{artificial}} \qquad (2.4)$$

where: G is the control system gearing ratio. For a discussion and definition of control system gearing ratios, see Part IV, Chapter 4 and Reference 12, Chapter 5. Typical numerical values for gearing ratios are given in Table 4.1 of Part VI.

HM is the control surface hingemoment, normally expressed in ftlbs and computed from:

$$HM = C_h \bar{q} (\bar{Sc})_{control\ surface} \qquad (2.5)$$

where: C_h is the control surface hingemoment coefficient. This hingemoment coefficient depends on the detail design of the control surfaces of the airplane. Section 10.4 of Part VI contains methods for estimating hingemoment coefficients and their derivatives.

$F_{s_{artificial}}$ is the incremental cockpit control force due to such items as: downsprings, bobweights and other 'feel'-systems. For a discussion of such devices, see Reference 12, Chapter 5 and Part IV, Chapter 4.

In these Class II methods the mathematical coupling which exists between Equations (2.1) through (2.4) is neglected. For an exact approach to the question of controllability and trim the reader is referred to the generalized matrix approach to trim as described in Section 5.6 of Reference 12.

2.1.4 Step-by-Step Procedure for Analyzing Longitudinal Controllability and Trim

The following step-by-step procedure is suggested to determine the longitudinal controllability and trim characteristics of an airplane during preliminary design:

Step 1: Determine which regulations apply to the design: see Table 1.3 and Subsection 2.1.1.

Step 2: The regulations define pairs of flight conditions so that the airplane must be controllable and maneuverable within each pair. Tabulate these flight conditions.

Step 3: The regulations define for which airplane weights the various controllability and trim requirements must be met. Tabulate these weights.

Note: It is important to also determine the airplane configuration and/or change in configuration associated with each pair of flight conditions: see items 1-9 on page 7. Tabulate the airplane configurations and/or the change in configuration as stipulated by the regulations.

Step 4: For the flight conditions and configurations defined in Steps 2 and 3 determine and tabulate: Mach number, M, dynamic pressure, $\bar{q}$ and center of gravity location(s), $\bar{x}_{cg}$.

Note: the center of gravity location associated with any given configuration follows from the weight/c.g. envelope developed with the method of Chapter 10 in Part II. A typical example of such a weight/c.g. envelope is shown in Figure 2.2.

Step 5: For the conditions defined in Steps 2, 3 and 4 construct the airplane trim diagram. This can be done with the help of Section 8.3 in Part VI. Chapter 12 of Part VI should also be consulted. Figure 2.3 shows an example trim diagram for a conventional airplane.

Notes: 1.) Before the trim diagram can be constructed, a decision must have been made relative to the type and size of longitudi-

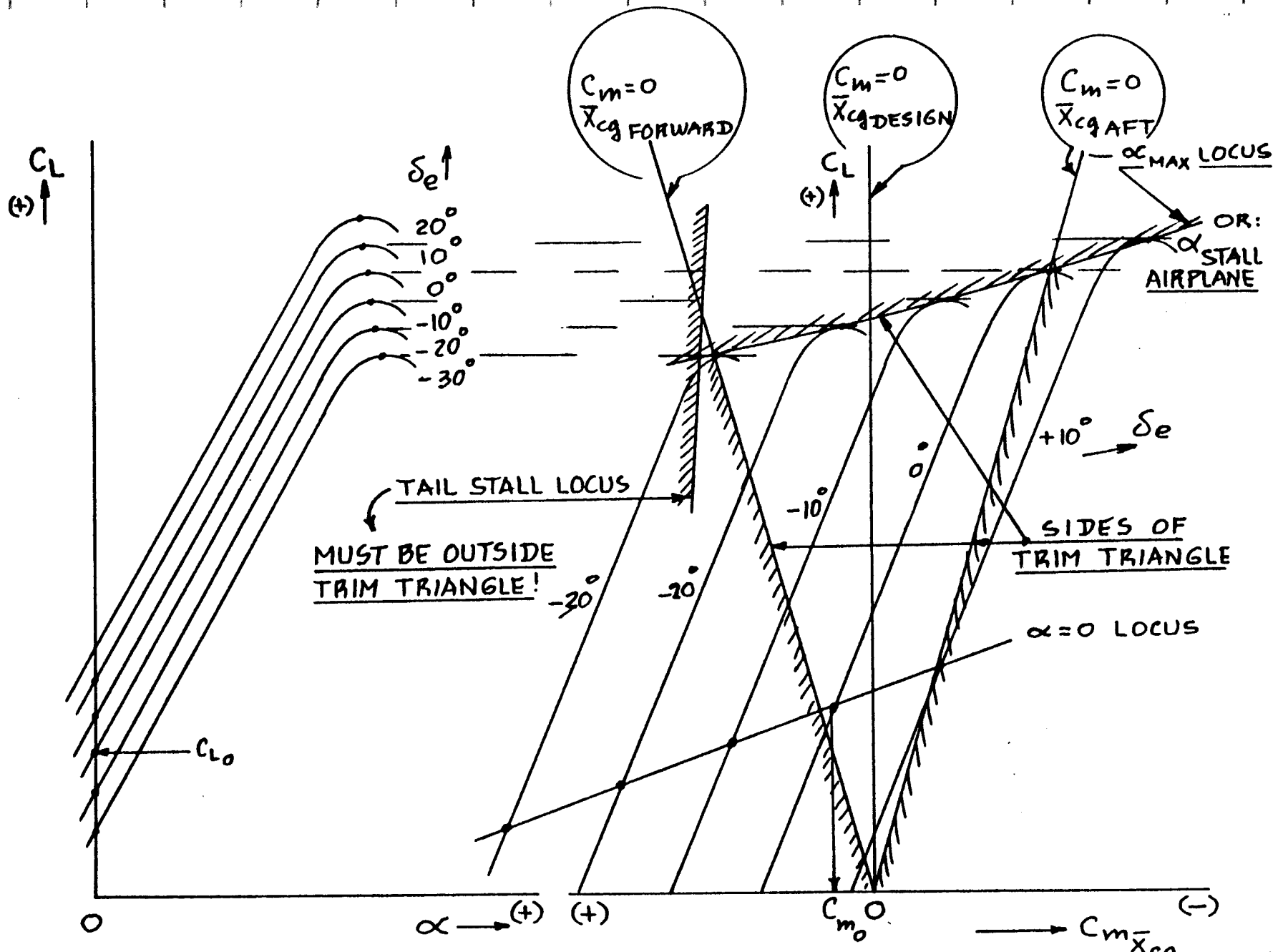

Figure 2.3 Example Trim Diagram for a Conventional (i.e. Tail Aft) Airplane

nal control surfaces to be employed!

2.) The method for constructing airplane trim diagrams in Part VI applies to conventional, pure canard as well as three-surface airplanes.

3.) The c.g. location associated with the vertical $C_m=0$ line in Figure 2.3 is normally selected to be the one for a typical 'design' mission of the airplane.

4.) The boundaries of the trim-triangle as shown in the example of Fig.2.3 are:

a) the $C_m=0$ lines for the most forward and for the most aft c.g. locations which in turn follow from the weight/c.g. envelope of Figure 2.2.

b) the α_{max} locus. This locus follows from either the airplane stall angle of attack or from the airplane angle of attack for which the stick pusher is set to trigger.

5.) Make sure that the effect of configuration changes 2-9 of page 7 are taken into account. This is particularly important in the case of thrust-induced-pitching-moment coefficient $Td_T/\bar{q}S\bar{c}$ and flaps.

Configuration events 2-9 (page 7) can be interpreted as a change in C_{m_o} and/or C_{L_o}.

Step 6: From the trim diagram of Step 5 determine whether or not equilibrium flight is possible within each pair of flight conditions.

This is accomplished by first computing the airplane lift coefficient for the initial and for the end flight condition associated with each pair of flight conditions from:

$$C_{L_{in}} = W/\bar{q}_{in}S \qquad (2.6)$$

and from:

$$C_{L_{end}} = W/\bar{q}_{end}S \qquad (2.7)$$

Second, in Figure 2.3 enter these lift coefficients into the trim diagram at the appropriate center of gravity line.

Step 7: Determine whether or not the results of Step 6 are acceptable. Criteria for acceptability can be:

1. the control surface deflections are within the control power capabilities designed into the airplane. Typical control deflection ranges may be found in various issues of Reference 13.

2. the angle of attack (or the lift coefficient) is below airplane stall.

3. the tail and/or the canard are not stalled inside the 'trim-triangle'.

NOTE: if one or more of these acceptability criteria are violated, the design must be adjusted until they are satisfied. Such design adjustments may consist of increases in control surface sizes, a change in airfoil(s) and/or rebalancing of the configuration.

In marginal cases a decision to scrap the design and start from scratch may be the only good choice!!

Step 8: Determine whether the flight control system of the airplane is of the reversible or irreversible type.

If reversible, proceed to Step 9. If irreversible, proceed to Step 12.

Note: airplanes with irreversible flight control systems usually require artificial control force feel systems. The design and analysis of such systems is beyond the scope of this text. Chapter 5 of Reference 12 may be consulted for further information on this subject.

Step 9: Using Eqns (2.4) and (2.5), compute the trim surface deflection required to set the cockpit control force equal to zero for the initial flight condition.

To do this requires that a preliminary decision as to the sizing and location of trim control surfaces has been made. If not, now is the time to make this decision.

An example of how the trim control surface deflection for $F_s=0$ may be computed will

be given for the case of an airplane with an elevator as the primary control surface and an elevator tab as the trim control surface. The reader will have to adjust this analysis to suit his own control system.

For an airplane with an elevator as the primary control surface and an elevator tab as the trim control surface the stick force equation (2.4) may be specialized to:

$$F_s = F_{s_{artificial}} + G\bar{q}\eta_h S_e \bar{c}_e [C_{h_o} + C_{h_\alpha}\{\alpha(1 - d\varepsilon/d\alpha) + i_h - \varepsilon_o\} + C_{h_{\delta_e}}\delta_e + C_{h_{\delta_t}}\delta_t] \quad (2.8)$$

Setting F_s equal to zero the required tab deflection to trim the airplane is found from:

$$\delta_t = \quad (2.9)$$

$$[\{-F_{s_{artificial}}/(G\bar{q}_{in}\eta_h S_e \bar{c}_e)\} - [C_{h_o} + C_{h_\alpha}\{\alpha\,(1 - d\varepsilon/d\alpha) + i_h - \varepsilon_o\} + C_{h_{\delta_e}}\delta_e]]/C_{h_{\delta_t}}$$

where: α and δ_e both follow from the trim diagram, Figure 2.3 at the appropriate value of $C_{L_{in}}$ and at the appropriate combination of c.g. location and airplane configuration!

G, the gearing ratio depends on the detail design of the flight control system. Ty-

pical values are found in Table 4.1 of Part IV.

i_h is the stabilizer incidence setting, fixed or vaiable, depending on the design of the control system.

all hingemoment coefficients in Eqns (2.8) and (2.9) can be computed with the methods Section 10.4, Part VI.

the value of $F_{s_{artificial}}$ depends on the detail design of the flight control system. In airplanes without artificial feel gadgetry such as a bobweight, a downspring, a springtab or a feel system, this force should be set equal to zero.

Note: The tab deflection magnitude as determined from Eqn.(2.9) should not exceed 25 degrees!

If the airplane is equipped with a different type of flight control system than that assumed in this example, the reader must redevelop Equation (2.8) accordingly. A detailed treatment of the many possible types of flight control systems is beyond the scope of this text. The reader is referred to Part IV, Chapter 4 for many practical examples of different primary and trim control systems. A general analytical treatment of the cockpit control force behavior of various types of systems is given in Reference 12, Chapter 5.

Step 10: For the final (end) flight condition find the cockpit control force with Eqn.(2.8),

PROVIDED: $C_{L_{end}}$ and $\bar{q}_{end}$ are used instead of $C_{L_{in}}$ and $\bar{q}_{in}$, to find α and δ_e!

NOTES: 1.) The value for δ_t in this case is that obtained exactly from Eqn.(2.8) if the regulations do not allow retrimming of the airplane between the two flight conditions!

2.) The cockpit control force required to cope with one or more configuration changes (listed as 2-9

on page 7) may also be computed from Eqn.(2.8).

Step 11: Check the cockpit control force against the magnitude allowed by the regulation(s). If the cockpit control force exceeds the value allowed, a redesign of the flight control system may be required. Methods for 'tailoring control forces by tabs, balances and control surface design are discussed in Part III, Chapter 3 and in Reference 12, Chapter 5.

NOTE: The method presented here neglects coupling between Equations (2.1) through (2.4). For purposes of preliminary design this method is usually adequate. For a more complete approach to the solution of airplane trim problems the reader should consult Section 5.5 of Ref.12.

Step 12: Document the results obtained, including any design changes made as a result of not meeting (or exceeding!) any of the airworthiness regulations.

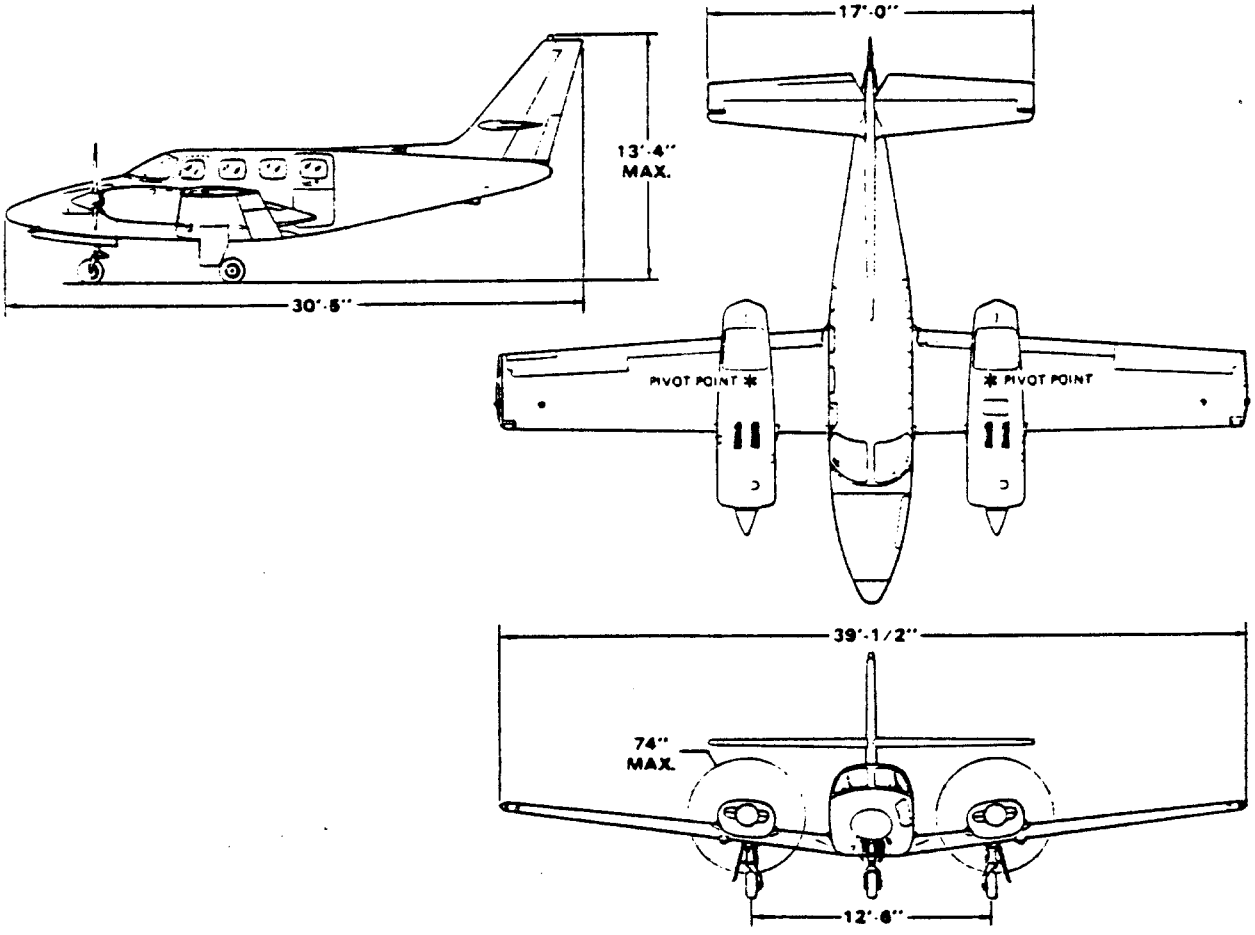

2.2 DIRECTIONAL AND LATERAL CONTROLLABILITY AND TRIM

2.2.1 Applicable Regulations

Civil: FAR 23.143, 23.147, 23.161, FAR 25.143, FAR 25.147, 25.161, see: Appendix A.

Military: Mil-F-8785C, Par.3.3, see Appendix B.

2.2.2 Relationship to Preliminary Design

See Part II, Chapter 2 (in particular Step 24), Chapter 8 and Chapter 11.

2.2.3 Mathematical Model for Analyzing Directional and Lateral Controllability and Trim

The regulations essentially require that any airplane, when trimmed in a given flight condition at a given airspeed:

A. can make turns at a specified bank angle into and away from one or more inoperative engines

B. can make sudden changes in heading while keeping the wings approximately level

The magnitudes of required bank angles and changes in heading angle are specified differently in each regulation, depending on the type of airplane.

In addition, the regulations specify the airplane configuration for which directional and lateral controllability must be satisfied. Configuration definitions usually include such items as:

1. Center of gravity location
2. Thrust or power setting (voluntary or failure)
3. Hard-over failure of any control or trim surface
4. Landing gear position (up or down)
5. Flap position (up, take-off, approach or landing)
6. Speed brake position (retracted or deployed)
7. Weapons loading (mostly asymmetrical loadings)
8. Weapons firing (mostly asymmetrical firing)
9. Combat damage

The regulations determine the various combinations of these configuration items which must be considered.

For purposes of Class II analyses, directional and lateral controllability is considered satisfied if:

1. Sufficient control power is present to perform the required turns and heading changes in all required configurations

2. Cockpit control forces required in the use of control power to satisfy controllability are within the limits prescribed in the regulations

The making of turns and changes of heading is assumed to place at such a slow rate that controllability can be verified by examining:

a. the numerical values of the lateral-directional motion variables: β, δ_a and δ_r

and:

b. the numerical values of the lateral-directional cockpit control forces

for 'before' and 'after' flight conditions (initial and end).

The following three equations of motion apply to this case:

$$-C_L \sin\phi\cos\gamma = (F_{T_Y})/\bar{q}S + C_{Y_\beta}\beta + C_{Y_{\delta_a}}\delta_a + C_{Y_{\delta_r}}\delta_r \qquad (2.10)$$

$$0 = (L_T)/\bar{q}Sb + C_{l_\beta}\beta + C_{l_{\delta_a}}\delta_a + C_{l_{\delta_r}}\delta_r \qquad (2.11)$$

$$0 = (N_T + N_D)/\bar{q}Sb + C_{n_\beta}\beta + C_{n_{\delta_a}}\delta_a + C_{n_{\delta_r}}\delta_r \qquad (2.12)$$

The numerical solutions to these equations must be 'tested' against acceptability criteria. These acceptability criteria normally consist of allowable bounds on the numerical values of the motion variables in these equations. These acceptability criteria are given in Subsection 2.2.4.

For any given flight condition (i.e. known $\bar{q}$) at any given thrust setting (i.e. known F_{Y_T}, L_T, N_T and N_D) the usual variables in these equations are:

β, δ_a and δ_r, which assumes that the bank angle, ϕ is determined by the 'initial' and 'end' conditions of the turns and/or the associated heading changes if the latter are to be made within a specified time.

The numerical solutions to these equations must be 'tested' against acceptability criteria. These acceptability criteria normally consist of allowable bounds on the numerical values of β, δ_a and δ_r. Acceptability criteria are presented in Subsection 2.2.4.

Methods for computing the stability and control derivatives which appear in Equations (2.10) - (2.12) are presented in Chapter 10 of Part VI.

Methods for computing installed thrust (from which F_{y_T}, L_T and N_T may be found) are presented in Chapter 6 of Part VI.

The yawing moment due to drag, N_D is found from the drag due to windmilling powerplants. Drag coefficients for windmilling jet engines and propellers may be computed with the method of Chapter 4, Part VI.

The lateral-directional cockpit control forces may be found from the following equations:

$$F_a = G_a \bar{q} S_a \bar{c}_a (C_{h_{\delta_a}} \delta_a + C_{h_{\delta_{a_t}}} \delta_{a_t}) + K_a \delta_r \qquad (2.13)$$

$$F_r = G_r \bar{q} S_r \bar{c}_r (C_{h_{\delta_r}} \delta_r + C_{h_{\delta_{r_t}}} \delta_{r_t} + C_{h_{r_\beta}} \beta) + K_r \delta_a \qquad (2.14)$$

The hingemoment derivatives in Equations (2.13) and (2.14) may be found with the methods of Ch.10, Part VI.

The reader should assume that the β-hingemoment derivative in Eqn.(2.14) is similar to the α-hingemoment derivatives of Chapter 10, Part VI. Likewise, the δ_a- and δ_r-hingemoment derivatives in Eqns (2.13) and (2.14) are similar to the δ-hingemoment derivatives of Chapter 10, Part VI.

Typical values for the gearing ratios, G_a and G_r may be found in Table 4.1 of Part IV.

The rudder-aileron interconnect terms, K_a and K_r are normally present only in airplanes with unsatisfactory control behavior. Ideally these terms should be zero.

2.2.4 Step-by-Step Procedure for Analyzing Directional and Lateral Controllability and Trim

Directional and lateral controllability can be verified with the following step-by-step procedure:

Step 1: Determine which regulations apply to the design: see Table 1.3 and Subsection 2.2.1.

Step 2: The regulations define flight conditions for which it must be possible to carry out turning and sudden heading change maneuvers. Identify these flight conditions.

When changes of bank angle are involved from positive to negative (right to left) values, identify one as the 'initial' and the other as the 'end' flight condition.

Note: It is important to also determine the airplane configuration and/or change in configuration associated with each flight condition: see items 1-9 on page 19.

Tabulate the flight condition and airplane configuration data as stipulated by the regulations.

Step 3: For the flight conditions defined in Step 2, determine: Mach number, M, dynamic pressure, $\bar{q}$ and center of gravity location, $\bar{x}_{cg}$. See the note under Step 4 in Subsection 2.1.4.

Step 4: For the conditions defined in Steps 2 and 3 determine the stability, control and other airplane characteristics required to solve the lateral-directional equations of motion: (2.10) - (2.12).

Notes: 1) methods for calculating stability and control derivatives are given in Ch.10 of Part VI. Methods for determining installed thrust (or power) are given in Ch.6 of Part VI.

2) which engines are to be considered inoperative is defined in the regulations. The magnitude and sign of F_{Y_T}, L_T, N_T and N_D

depend on which engines are inoperative!!

Step 5: From solutions to Eqns (2.10) - (2.12) as defined by Eqns (2.15) - (2.17) in Table 2.1 determine whether or not turning maneuvers can be made which satisfy the regulations.

Note: The regulations may be considered to be satisfied if the magnitudes of the following variables are within acceptable bounds:

1. lateral control surface deflection(s), δ_a
2. directional control surface deflection(s), δ_r
3. sideslip angle, β

For a control surface deflection to be 'acceptable' means that it must be within the stall limits of that surface. Typical acceptability criteria are:

Lateral: $|\delta_a| < 25$ deg.

Directional: $|\delta_r| < 25$ deg. for single hinge rudder
< 35 deg. for double hinge rudder

For a sideslip angle to be 'acceptable' it must be sufficiently small so that the airplane drag is not significantly increased and so that the directional stability of the airplane has not significantly deteriorated due to vertical tail stall. Typical acceptability criteria are:

Sideslip angle for drag: $|\beta| < 5$ deg.

Sideslip angle for directional stability: $|\beta| < 12$ deg.

NOTE: If one or more of these acceptability criteria are violated, the design must be adjusted until they are satisfied. Such design adjustments may consist of increases in control surface sizes, addition of other types of control surfaces and/or a change (size and/or location) of the vertical tail.

In marginal cases a decision to scrap the design and start from scratch may be the only good choice!

Step 6: Determine whether the flight control system of the airplane is of the reversible or irreversible type.

Table 2.1 Solutions for Eqns.(2.10) - (2.12) of Page 20

$\beta = N_1/\Delta$ (2.15) $\qquad \delta_a = N_2/\Delta$ (2.16) $\qquad \delta_r = N_3/\Delta$ (2.17)

with:

$$N_1 = \begin{vmatrix} -(C_{L_1}\sin\phi\cos\gamma + F_{T_{y_1}}/\bar{q}_1 S) & C_{y_{\delta_a}} & C_{y_{\delta_r}} \\ -L_{T_1}/\bar{q}_1 Sb & C_{l_{\delta_a}} & C_{l_{\delta_r}} \\ (-N_{T_1} - N_{D_1})/\bar{q}_1 Sb & C_{n_{\delta_a}} & C_{n_{\delta_r}} \end{vmatrix} \qquad (2.18)$$

$$N_2 = \begin{vmatrix} C_{y_\beta} & -(C_{L_1}\sin\phi\cos\gamma + F_{T_{y_1}}/\bar{q}_1 S) & C_{y_{\delta_r}} \\ C_{l_\beta} & -L_{T_1}/\bar{q}_1 Sb & C_{l_{\delta_r}} \\ C_{n_\beta} & -(N_{T_1} + N_{D_1})/\bar{q}_1 Sb & C_{n_{\delta_r}} \end{vmatrix} \qquad (2.19)$$

$$N_3 = \begin{vmatrix} C_{y_\beta} & C_{y_{\delta_a}} & -(C_{L_1}\sin\phi\cos\gamma + F_{T_{y_1}}/\bar{q}_1 S) \\ C_{l_\beta} & C_{l_{\delta_a}} & -L_{T_1}/\bar{q}_1 Sb \\ C_{n_\beta} & C_{n_{\delta_a}} & -(N_{T_1} + N_{D_1})/\bar{q}_1 Sb \end{vmatrix} \qquad (2.20)$$

$$\Delta = \begin{vmatrix} C_{y_\beta} & C_{y_{\delta_a}} & C_{y_{\delta_r}} \\ C_{l_\beta} & C_{l_{\delta_a}} & C_{l_{\delta_r}} \\ C_{n_\beta} & C_{n_{\delta_a}} & C_{n_{\delta_r}} \end{vmatrix} \qquad (2.21)$$

NOTE: The subscript 1 indicates steady state flight!

If reversible, proceed to Step 7. If irreversible, proceed to Step 10.

Note: airplanes with irreversible flight control systems usually require artificial control force feel systems. The design and analysis of such systems is beyond the scope of this text. Chapter 5 of Reference 12 may be consulted for further information on this subject.

Step 7: Using Eqns (2.13) and (2.14), compute the trim surface deflections, δ_{a_t} and δ_{r_t} required to set both cockpit control forces, F_a and F_r equal to zero for the 'initial' flight condition.

Acceptable values for the trim-tab deflections are:

$$|\delta_{(a \text{ or } r)_t}| < 20 \text{ degrees}$$

Step 8: For the 'end' flight condition(s), use Eqns (2.13) and (2.14) to compute the cockpit control forces, F_a and F_r.

Note: be sure to use the trim surface values obtained from Step 7!

Step 9: Check the cockpit control force values against the magnitudes allowed by the regulation.

If any cockpit control force exceeds the value allowed, a redesign of the flight control system may be required. Methods for tailoring control forces by tabs, balances and control surface design are discussed in Part III, Chapter 3 and in Reference 12, Chapter 5.

Step 10: Document the results obtained, including any design changes made as a result of not meeting (or exceeding!) any of the airworthiness regulations.

NOTE: The method presented here neglects coupling between Equations (2.10) through (2.14). A generalized approach to the solution of airplane trim problems is presented in Chapter 5 of Reference 12.

2.3 MINIMUM CONTROL SPEED

2.3.1 Applicable Regulations

Civil: FAR 23.149, FAR 25.149, see Appendix A.

Military: Mil-F-8785C, Par. 3.3.9.2, see Appendix B.

2.3.2 Relationship to Preliminary Design

See Part II, Chapter 2 (in particular Step 24), Chapter 8 and Chapter 11.

2.3.3 Mathematical Model for Analyzing Minimum Control Speed

The regulations essentially require that any airplane, when experiencing failure of its most critical engine:

1. can be brought under control in such a manner that straight line flight is possible with zero sideslip or with a bank angle of no more than five degrees toward the operating engine

2. does not require more than:

   civil airplanes: 150 lbs of rudder pedal force

   military airplanes: a) 180 lbs of rudder pedal force
   b) the roll control force specified in Table X of Par.3.3.4.3, Appendix B

3. can do so at a speed called the minimum control speed, V_{mc} which must satisfy the following conditions:

   For take-off with one engine inoperative

   civil airplanes: $V_{mc} < 1.2V_s$

   military airplanes: $V_{mc} < V_{min_{TO}}$, where in

   preliminary design: $V_{min_{TO}} = 1.1V_{s_{TO}}$

   For landing with one or two engines inoperative

   civil airplanes: $V_{mc} > V_A$

military airplanes: $V_{mc} > 1.4V_{min}$, where V_{min} is defined in Section 6.2 of Appendix B

In addition, the regulations specify the airplane configuration for which the minimum control speed capability must be satisfied. As a general rule, configuration changes and/or power (thrust) changes are not allowed.

For purposes of Class II analyses, controllability is considered satisfied if:

1. Sufficient control power is present to cope with the stated requirements

2. Cockpit control forces required in the use of control power to satisfy controllability are within the limits prescribed in the regulations

Equations (2.15) through (2.17), see Table 2.1, are normally used to determine the magnitude of sideslip angle, rudder angle and aileron angle needed to keep the airplane in straight line flight and with a favorable bank angle of 5 degrees.

Equations (2.13) and (2.14) are used next to determine the cockpit control forces needed to keep the rudder and aileron deflections at the values required by Equations (2.15) through (2.17).

2.3.4 Step-by-Step Procedure for Determining the Minimum Control Speed

In preliminary design the minimum control speed capability of an airplane can be verified with the following step-by-step procedure:

Step 1: Determine which regulations apply to the design: see Table 1.3 and Subsection 2.3.1.

Step 2: The regulations define flight conditions and airplane configurations for which the regulations apply. Identify these flight conditions and configurations and determine the corresponding airplane weight, W.

Step 3: For the flight conditions and configurations of Step 2, determine: Mach Number, M, dynamic pressure, $\bar{q}$, lift coefficient, C_L

and center of gravity location, $\bar{x}_{cg}$.

Step 4: For the conditions defined in Steps 2 and 3, determine the required stability and control derivatives as well as the asymmetric engine side force, rolling moment and yawing moment (including any drag induced effects): see Equations (2.10) - (2.12).

Step 5: Using Equations (2.15) through (2.17), find the values of sideslip angle, aileron angle and rudder angle required at V_{mc}. The regulations allow the use of a bank angle of no more than 5 degrees toward the operating engine(s).

Step 6: Determine whether or not the results of Step 5 are acceptable.

Criteria for acceptability can be:

1. The sideslip angle, β must not be so large that the added drag due to sideslip would cause the airplane to violate the minimum climb requirements of Section 5.3

2. The aileron and/or rudder deflection angles are less than those values for which wing and/or vertical tail stall might result. Typical maximum acceptable angles are:

   Ailerons: < 25 degrees or whatever corresponds to no more than 75 percent of available lateral control power in the flight condition and airplane configuration being considered

   Rudder: < 25 degrees for single hingeline rudders
   < 35 degrees for double hingeline rudders

If the airplane violates any of these acceptability criteria, the design must be adjusted until the regulatory requirements are satisfied. This may involve changing control surface sizes, changing vertical tail size and location and/or re-arranging the most critical engines.

In marginal cases the decision to scrap the design and start from scratch may be the appropriate choice!!

If the airplane is equipped with a reversible flight control system in the roll and yaw axes proceed to Step 7. If not, proceed to Step 10.

Step 7: Determine the hingemoment coefficients and derivatives contained in Equations (2.13) and (2.14).

Step 8: Calculate the lateral and directional cockpit control forces needed to hold the aileron and rudder surfaces at deflection values corresponding to those obtained in Step 5. Use Equations (2.13) and (2.14).

Note: the values for the trim-tab deflections must be those corresponding to the trimmed flight condition prior to engine failure.

Step 9: Determine whether or not the roll control and rudder control forces of Step 8 are acceptable. The rudder control forces are normally the most critical ones!

Criteria for acceptability are given in the applicable regulations. A summary of the allowable rudder pedal forces is given under Subsection 2.3.3.

Step 10: Document the results obtained, including any design changes made as a result of not meeting (or exceeding!) any of the airworthiness regulations.

NOTE: The method presented here neglects coupling between Equations (2.10) through (2.14). A generalized approach to the solution of the lateral-directional trim problem is given in Chapter 5 of Reference 12.

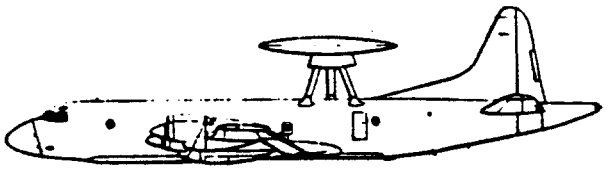

2.4 MANEUVERING FLIGHT

2.4.1 Applicable Regulations

Civil: FAR 23.151 (acrobatic and utility category only), FAR 23.155, see Appendix A.
Note: there are no sustained maneuvering requirements in FAR 25!

Military: Mil-F-8785C, Par. 3.2.2.2, see Appendix B.

2.4.2 Relationship to Preliminary Design

Maneuvering flight requirements are accounted for in the initial sizing process to assure that:

1. The powerplant installation can overcome the extra drag incurred during maneuvers: see Part I, Chapter 3.

2. The maximum trimmed lift capability of the airplane is consistent with the maneuvering demands. See Part I, Chapter 3 and Part II, Chapter 7.

Note: these maneuvering requirements are of great importance to the design of fighters and acrobatic and utility category airplanes.

2.4.3 Mathematical Model for Analyzing Maneuvering Flight

The regulations essentially require that:

1. the airplane must be able to attain certain specified load factors: instantaneous or sustained.

2. the longitudinal cockpit control force per unit load factor increase (stick-force per 'g') shall be bounded by maximum as well as by minimum allowable values. Reversal in the stick-force per 'g' gradient is not allowed.

To satisfy the first item requires that the airplane be capable of achieving a value of maximum lift coefficient which is consistent with the required load factor. There are two types of required load factors:

A) Instantaneous load factors
and
B) Sustained load factors.

A) Instantaneous load factors

Three conditions must be satisfied to achieve a specified instantaneous load factor, n_{reqd}:

A1) The available lift condition,
A2) The available control power condition
and
A3) The cockpit control force condition.

A1) The available lift condition

The available lift condition is:

$$n_{reqd} < C_{L_{max}} \bar{q} S / W \qquad (2.22)$$

where: n_{reqd} is the load factor which must be attained according to the mission specification and/or according to the applicable regulation.

$C_{L_{max}}$ must be interpreted as the maximum trimmed lift coefficient of which the airplane is capable in the given flight condition. The magnitude of $C_{L_{max}}$ depends on the wing design and on the type and size of flaps used, on the type of longitudinal control used and on the center of gravity location. Methods to estimate maximum trimmed lift coefficients are given in Section 8.3 of Part VI.

A2) The available control power condition

The available control power condition is:

$$\delta_{e_{reqd}} = \delta_{e_{trim}} + (\partial \delta_e / \partial n) n_{reqd} \qquad (2.23)$$

where: $\delta_{e_{trim}}$ is the elevator deflection required to trim the airplane in the steady state flight condition before the maneuver was initiated. It is computed with the procedure of sub-section 2.1.4.

$\partial \delta_e / \partial n$ is the elevator versus load-factor gradient. It may be computed from:

$$\partial \delta_e / \partial n = \qquad (2.24)$$

$$\{-C_{L_\alpha} C_{m_q} (\bar{c} g / 2 U_1^2) \bar{n} - C_{m_\alpha} C_{L_1}\} / (C_{L_\alpha} C_{m_{\delta_e}} - C_{L_{\delta_e}} C_{m_\alpha})$$

with: $\bar{n} = n$ for symmetrical pull-up maneuvers

$\bar{n} = (1 + 1/n^2)$ for turning maneuvers

The stability and control derivatives in Eqn.(2.24) may be computed with the methods of Chapter 10, Part VI.

n_{reqd} is defined under Eqn.(2.22)

Note: the condition: $\delta_{e_{reqd}} < \delta_{e_{available}}$ must always be satisfied, where: $\delta_{e_{available}}$ is that value of elevator deflection which is geometrically available: also called the maximum available elevator throw.

A3) The cockpit control force condition

This condition demands that the level of required cockpit control force needed to perform an instantaneous maneuver must be less than values specified in the regulations:

$$F_s = F_{s_1} + (\partial F_s/\partial n) n_{reqd} \qquad (2.25)$$

where: F_{s_1} is the cockpit control force required to 'hold' the steady state. If the airplane is in complete trim in the steady state, $F_{s_1} = 0$.

n_{reqd} is defined under Eqn.(2.22)

The 'stick-force-per-g', $\partial F_s/\partial n$ is found from

an equation, the terms in which depend strongly on the type of control system employed. For an airplane which uses an elevator for primary control, and no bobweight, Ref.12 shows that the following equation determines the stick-force per 'g':

$$\partial F_{s_e}/\partial n = \eta_h \bar{q} S_e \bar{c}_e G_e^* \qquad (2.26)$$

$$*\{C_{L_1} (C_{h_{\delta_e}}/C_{m_{\delta_e}})(SM_{free}) + (gl_h/U_1^2)(C_{h_\alpha} - C_{h_{\delta_e}}/\alpha_{\delta_e})\}$$

where: l_h is the distance of the horizontal tail aerody-

namic center to the airplane center of gravity

SM_{free} is the static margin stick free which may be determined from:

$$SM_{free} = \bar{x}_{ac_A} - \bar{x}_{cg} + \qquad (2.27)$$

$$+ \{(C_{m_{\delta_e}} C_{h_\alpha})/(C_{L_{\alpha_A}} C_{h_{\delta_e}})\}(1 - d\varepsilon/d\alpha)$$

where: all terms are defined in the list of symbols. They may be determined with the help of Part VI.

Note: For an airplane which uses another type of primary longitudinal controller (other than an elevator), the reader should re-develop the appropriate equations in this Section to reflect the actual control system used.

B) Sustained load factors

Four conditions must be satisfied to achieve a specified magnitude of sustained load factor:

B1) The available lift condition,
B2) The available control power condition,
B3) The cockpit control force condition
and
B4) The available thrust condition.

Conditions B1 through B3 are identical to conditions A1 through A3 which were discussed before.

B4) The available thrust condition

This condition is discussed in Section 5.7.

2.4.4 Step-by-step Procedure for Determining Maneuvering Flight Ability

The following step-by-step procedure is suggested to check maneuvering flight ability in preliminary design.

Step 1: Read the regulations and determine which regulations apply to the design.

Step 2: The regulations define flight conditions and airplane configurations for which the regulations apply. Identify these flight conditions and configurations and determine the corresponding airplane weight, W.

Step 3: For the flight conditions and configurations of Step 2, determine: Mach Number, M, dynamic pressure, $\bar{q}$, lift coefficient, C_L and center of gravity location, $\bar{x}_{cg}$.

Step 4: This step concerns the available lift condition as given by A1) or B1) in sub-section 2.4.3.

For the flight conditions and for the configurations of Steps 2 and 3 determine the maximum achievable load factor from:

$$n_{max} = C_{L_{max}} \bar{q}S/W \qquad (2.28)$$

The maximum lift coefficient, $C_{L_{max}}$ in Eqn.(2.28) is that 'trimmed' value which applies to the airplane configuration (flaps up or down) as well as to the flight condition (particularly the Mach number) being analyzed. Methods for determining trimmed maximum lift coefficients are presented in Section 8.3 of Part VI.

Compare n_{max} from Eqn.(2.28) with n_{reqd} from Eqn.(2.22) and determine whether or not the airplane can satisfy its maneuvering requirements from a maximum lift viewpoint.

Step 5: This step concerns the available control power condition, as given in A2) or B2) in sub-section 2.4.3.

For the conditions defined in Steps 2 and 3, determine the required stability, control and hingemoment derivatives as well as other terms identified in Eqns (2.23) and (2.24).

Part VI contains methods for estimating all required parameters.

Compute the amount of elevator required to attain the specified load factor from Eqns (2.23) and (2.24).

The amount of elevator deflection required to attain the specified load factor should not exceed the available elevator travel, nor should it exceed that amount which would cause the tail to stall.

Step 6: This step concerns the required cockpit control force level as given in A3) or B3) in sub-section 2.4.3.

For the conditions defined in Steps 2 and 3, determine the required stability, control, hingemoment derivatives as well as other terms identified in Eqns (2.25) and (2.26).

Compute the stick-force required to pull the specified load factor from Eqns (2.25) and (2.26). Compare the computed magnitude of stick-force with those specified in the regulations.

Step 7: This step concerns the available thrust condition of B4) in sub-section 2.4.3.

Using the methods of Section 5.7, determine whether sufficient thrust is available to maintain (sustain) the required load factor.

Step 8: Determine whether or not the results of Steps 4, 5, 6 and 7 are acceptable. If not, inspect the applicable equations for 'clues' as to what design changes may be needed to 'fix' the problem. It may very well be that major changes in the design of the wing and/or the flight control system are required!

If the available thrust condition of Step 7 is not met, an increase in thrust may be required. This could cause a major change in the design of the airplane!

Step 9: Document the results obtained, including any design changes made as a result of not meeting (or exceeding!) any of the mission specifications and/or regulations.

2.5 CONTROL DURING THE TAKEOFF GROUNDRUN

2.5.1 Applicable Regulations

Civil: FAR 23.143, 23.51, 23.231, 23.233 and 23.235, see Appendix A.

FAR 25.107, 25.143, 25.149, 25.231, 25.233, 25.235 and 25.237, see Appendix A.

Military: MIL-F-8785C, Section 3.3 (in particular 3.3.7 and 3.2.3.3), see Appendix B.

2.5.2 Relationship to Preliminary Design

See Chapter 11, Part II.

2.5.3 Mathematical Model for Analyzing Control During the Takeoff Groundrun

The regulations essentially require that any airplane shall be safely controllable and maneuverable during take-off ground operations.

The words 'safely' and 'easily' as used here imply the following:

1. Sufficient control power must exist to effect take-off rotation: this applies to airplanes with tricycle as well well as to airplanes with tail-dragger landing gears.

2. Sufficient control power must exist to lift the tail early in the takeoff run for airplanes with tailwheels. Following this, there must be sufficient control power to effect lift-off.

3. Directional control and lateral control must be sufficient to allow for straight line taxiing as well as for straight line takeoff runs in cross winds as specified in the regulations.

4. The control forces required to accomplish 1,2 and 3 shall be sufficiently small. Also, nu unusual pilot control technique shall be required.

The regulations also imply that these characteristics be satisfied under the most adverse conditions of:

1. center of gravity location
2. power setting (voluntary or failure)

3. flap position as required for takeoff
4. weapons or payload disposition as required by the airplane mission

Class II analysis of control during takeoff is normally accomplished by uncoupling the longitudinal control problem from the directional/lateral control problem:

2.5.3.1 Mathematical model for analyzing longitudinal control during the takeoff groundrun

2.5.3.2 Mathematical model for analyzing directional and lateral control during the takeoff groundrun

2.5.3.1 Mathematical model for analyzing longitudinal control during the takeoff groundrun

Figure 2.4 shows the forces and moments which act on an airplane during the take-off run. Note the difference between:

a) Tricycle Gear Configurations
b) Taildragger Gear Configurations
c) Tandem Gear Configurations

The following mathematical model is presented for airplanes with conventional (that is tail-aft) configurations and with a tricycle landing gear.

NOTA BENE: The reader should modify this mathematical model to reflect the actual airplane configuration and landing gear layout of his airplane.

The following example applies to conventional airplanes equipped with a tricycle landing gear. Figure 2.5 defines all forces, moments and moment arms.

NOTA BENE: All aerodynamic quantities in Figure 2.5 must be determined in the presence of ground effect! See Part VI for methods to do this.

The longitudinal equations of motion which govern the controllability of the airplane on the ground are:

$$T\cos(\alpha_g + \phi_T) - \mu_g(P_{mg} + P_{ng}) - D = (W/g)\dot{u} \qquad (2.29)$$

$$T\sin(\alpha_g + \phi_T) + L_{wf} + L_h + P_{mg} + P_{ng} - W = 0 \qquad (2.30)$$

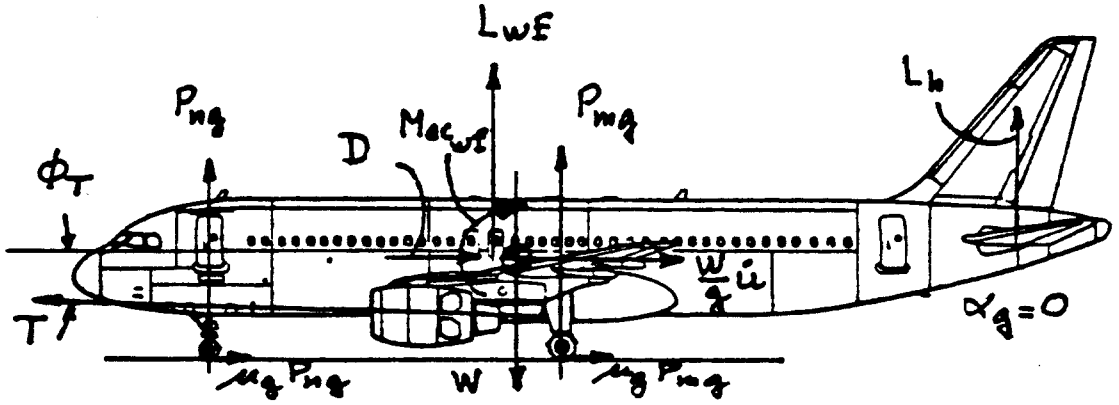

2.4a Tricycle Landing Gear

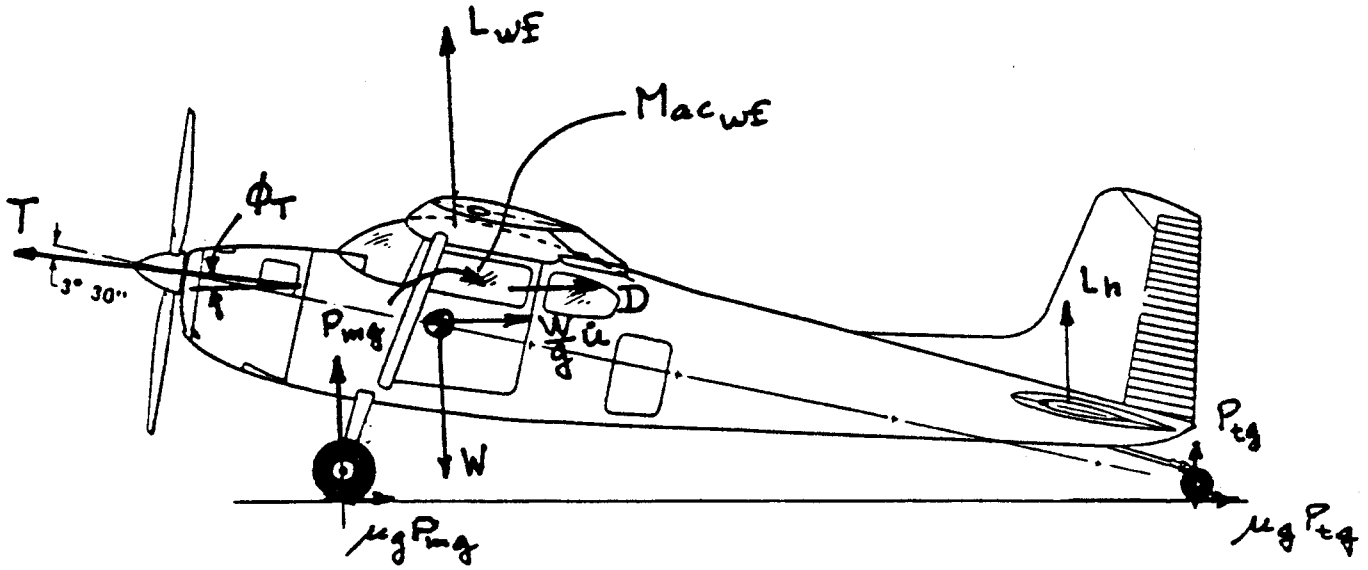

2.4b Taildragger Landing Gear

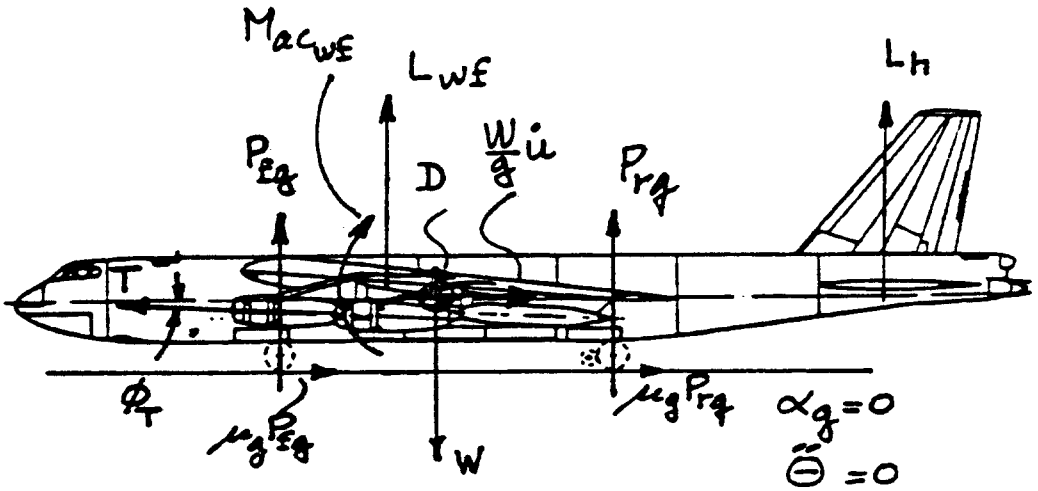

2.4c Tandem Landing Gear

Figure 2.4 Longitudinal Forces and Moments Acting on an Airplane During the Takeoff Groundrun

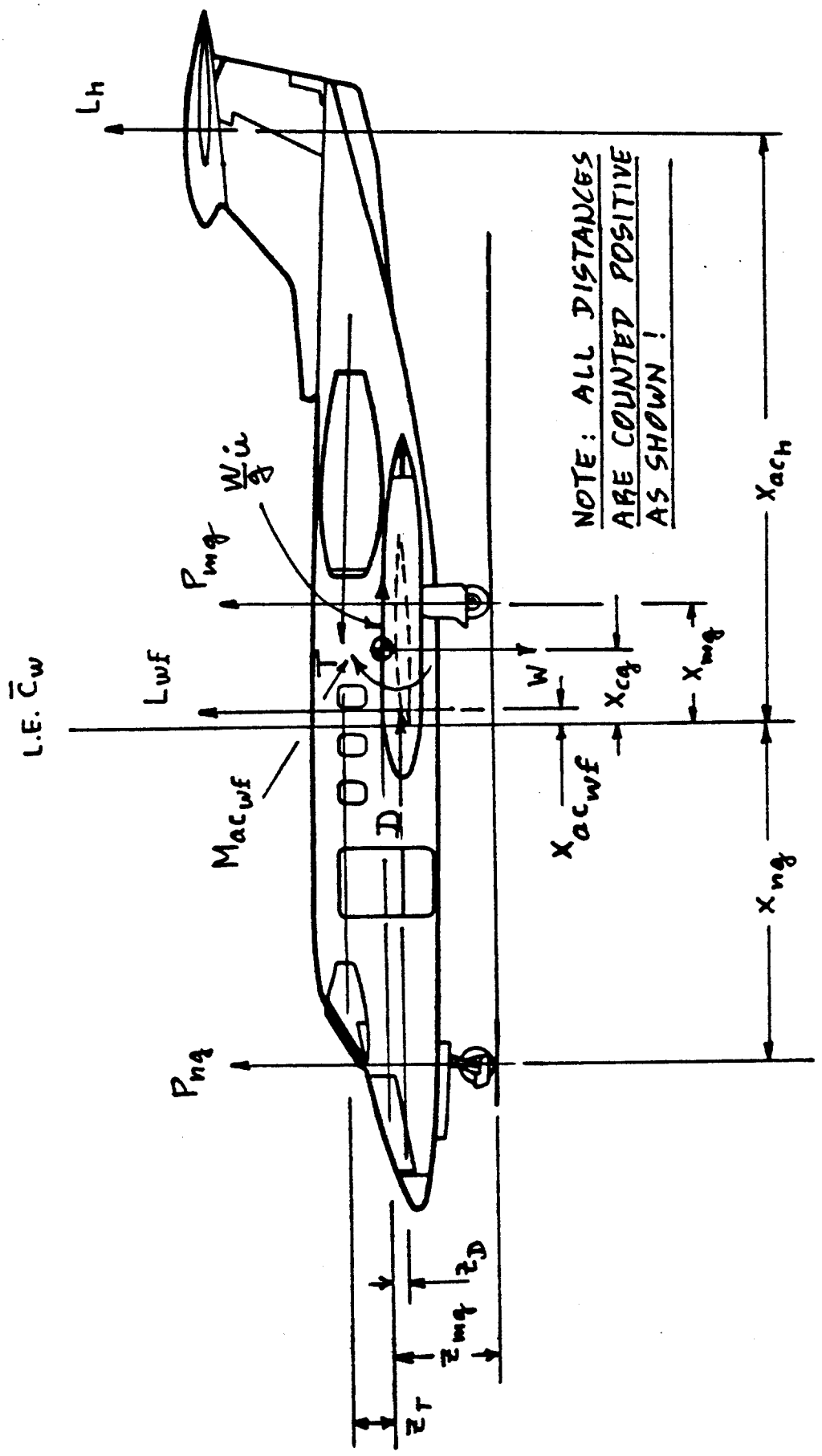

Figure 2.3 Forces, Moments and Moment Arms for Longitudinal Control During the Takeoff Groundrun

$$M_{ac_{wf}} - T(z_{mg} - z_T) - W(x_{mg} - x_{cg}) + P_{ng}(x_{ng} + x_{cg}) +$$

$$+ L_{wf}(x_{mg} - x_{ac_{wf}}) + D(z_{mg} - z_D) + (W/g)\dot{u}z_{mg} +$$

$$- L_h(x_{ac_h} - x_{mg}) = I_{yy_{mg}}\ddot{\theta} \qquad (2.31)$$

where: T is the installed thrust during the take-off run. It varies with speed during the take-off run and is determined with the method of Part VI, Ch.6.

α_g is the angle of attack during the groundrun. This angle is usually very small except at the instant before liftoff.

ϕ_T is the thrust inclination angle

μ_g is the wheel-ground rolling friction coefficient. During take-offs use:

for concrete or asphalt:	$\mu_g = 0.02$
for hard turf:	$\mu_g = 0.04$
for short grass:	$\mu_g = 0.05$
for long grass:	$\mu_g = 0.10$
for soft ground:	$\mu_g = 0.10$ to 0.30

Note: these values are recommended for use on civil airplanes. For military airplanes consult Appendix B.

P_{mg} and P_{ng} are the ground reaction forces. It is assumed that the nosewheel is no longer in touch with the ground (i.e. $P_{ng}=0$), at the instant that the rotation has been initiated.

D is the airplane drag in ground effect:

$$D = (C_D)\bar{q}S \qquad (2.32)$$

with: C_D the drag coefficient on the ground. This drag coefficient follows from

the airplane drag polar on the ground as discussed in Part VI, Chapter 4.

$\bar{q}$ is the dynamic pressure. It varies during the take-off run.

W is the weight. This is not necessarily the airplane maximum take-off weight. It is up to the designer to determine the most critical combination of weight and center of gravity location, x_{cg}. The weight versus c.g. diagram of Ch.10 of Part II should be used.

$\dot{u}$ is the forward acceleration along the runway.

L_{wf} is the wing-fuselage lift in ground effect:

$$L_{wf} = C_{L_{wf}} \bar{q} S \qquad (2.33)$$

with: $C_{L_{wf}}$ the airplane lift coefficient during the ground roll, in ground effect. Its value will be constant before initiation of the rotation. The methods of Pt VI, Chapter 8 can be used to determine this lift coefficent.

NOTE: The relative location of L_{wf} to the main landing gear is important. If it too far forward, the airplane will have a tendency to rapidly autorotate after the pilot has initiated the rotation by pulling the cockpit control aft. This autorotation is caused by the rapid increase in L_{wf} as the angle of attack begins to increase. The designer should attempt to locate L_{wf} as close as possible to but forward of the main gear!

L_h is the tail lift during the ground roll:

$$L_h = C_{L_h} \bar{q}_h S_h \qquad (2.34)$$

with: C_{L_h} the horizontal tail lift coefficient during the ground roll. It must be evaluated in ground effect. It will be constant (and usually negative due to the preset negative incidence angle on the stabilizer) before initiation of rotation.

Upon initiation of rotation the tail lift coefficient becomes large and negative. The negative tail lift in ground effect may be computed with the methods of Part VI, Chapter 8.

$\bar{q}_h$ is the dynamic pressure at the horizontal tail. It varies during the take-off roll and is related to $\bar{q}$ by: $\bar{q}_h = \eta_h \bar{q}$ (2.35)

The dynamic pressure ratio at the tail, η_h is found from Part VI, p.269.

$M_{ac_{wf}}$ is the wing-fuselage pitching moment about the wing-fuselage aerodynamic center in ground effect and with the flaps in the take-off position:

$$M_{ac_{wf}} = C_{m_{ac_{wf}}} \bar{q} S \bar{c} \qquad (2.36)$$

with: $C_{m_{ac_{wf}}}$ the wing-fuselage pitching moment coefficient about the wing-fuselage aerodynamic center and with the flaps in the take-off position. This coefficient may be determined with the methods of Part VI, Chapter 8. It must be computed in ground effect.

If the reader does not wish to employ the rather laborious methods of Part VI, the following approximation may be employed:

$$C_{m_{ac_{wf}}} = 1.1(b_f/b) c_{m_{ac_f}} \qquad (2.37)$$

where: the factor 1.1 accounts for ground effect

b_f/b is the flap-span to wing-span ratio

$c_{m_{ac_f}}$ is the airfoil pitching moment coefficient with the flap down (in this case in the take-off position). Methods for determining the effect of flaps on airfoil $c_{m_{ac}}$ are given in subsection 8.2.2.1 of Part VI.

z_{mg} is defined in Figure 2.5.

z_T is defined in Figure 2.5.

x_{mg} is defined in Figure 2.5.

x_{cg} is defined in Figure 2.5.

$x_{ac_{wf}}$ is defined in Figure 2.5.

z_D is defined in Figure 2.5. It is usually taken at the wing-fuselage aerodynamic center.

x_{ac_h} is defined in Figure 2.5.

$I_{yy_{mg}}$ is the pitching moment of inertia about the main gear contact point. It may be computed from:

$$I_{yy_{mg}} = I_{yy} + (W/g)\{z_{mg}^2 + (x_{mg} - x_{cg})^2\} \quad (2.38)$$

with: I_{yy} the airplane moment of inertia as determined from Part V, Chapter 3 or, more appropriately for Class II methods from Part V, Chapter 10

$\ddot{\theta}$ is the pitch angular acceleration at the instant of initiation of rotation. In preliminary design it is suggested to use:

For large transports: $\ddot{\theta} = 6$ to 8 deg/sec^2

For small transports: $\ddot{\theta} = 8$ to 10 deg/sec^2

For light airplanes and for fighters: $\ddot{\theta} = 10$ to 12 deg/sec^2

Equations (2.29) through (2.31) are normally solved for the amount of horizontal tail area required to achieve take-off rotation at the rotation speed, V_{rot}:

$$S_h = \{-z_T T + z_D D + W(x_{mg} - x_{cg} + \mu_g z_{mg}) - L_{wf}(x_{mg} + \\ - x_{ac_{wf}} + \mu_g z_{mg}) - C_{m_{ac_{wf_g}}} \bar{q}_{rot} S\bar{c} - I_{yy_{mg}} \ddot{\theta}\} / \\ \{\bar{q}_{rot}(x_{ac_h} - x_{mg} + \mu_g z_{mg}) C_{L_{h_{max}}}\} \qquad (2.39)$$

The rotation speed is defined relative to the stall speed in the regulations: Appendix A or Appendix B.

Values for maximum lift coefficient for the horizontal tail depend on the tail design and on the ground effect (ground proximity) of the tail during the rotation process. If the reader does not wish to employ the rather laborious methods of Part VI to estimate $C_{L_{h_{max}}}$ it is suggested to use:

$C_{L_{h_{max}}} = -0.35(A_h)^{1/3}$ for fixed stabilizer with 30 percent chord elevator

$= -0.8$ for a controllable stabilizer with a fixed elevator at zero deflection

$= -1.2$ for a controllable stabilizer with a 30 percent chord elevator deflected for maximum down lift

Note: higher values for maximum downlift on the tail are possible with negative camber, negative slots and/or blowing over the lower surface.

2.5.3.2 Mathematical model for analyzing lateral-directional control during the take-off groundrun

The regulations essentially require that controllability during the take-off run is such as to ensure that:

1) Positive steering is possible
2) Wing-over is impossible
3) The airplane does not slide off the runway

Wet and/or slick runway surfaces coupled with strong crosswinds can cause anyone of these problems. The regulations specify the magnitude of crosswinds which each airplane category must be able to cope with.

Figure 2.6 shows the forces and moments which are important to these ground operation problems. To satisfy items 1), 2) and 3) it is necessary for the designer to show that the following three runway constraints are satisfied:

Runway Constraint 1:

The lateral ground friction force on the nosegear should not reverse sign. For positive sideslip due to crosswind (as shown in Figure 2.6), it is required that:

$$Y_{ng} > 0 \qquad (2.40)$$

If condition (2.40) is violated, nosewheel steering becomes ineffective.

Runway Constraint 2:

The normal force (= vertical ground reaction) on either main gear should not become zero. For positive sideslip due to crosswind it is required that:

$$P_{mg_L} > 0 \text{ and } P_{mg_R} > 0, \qquad (2.41)$$

where:

$$P_{mg_L} + P_{mg_R} = P_{mg} \qquad (2.42)$$

If either of the conditions (2.41) is violated, the airplane will start to 'wing-over'.

Runway Constraint 3:

The sum of all lateral ground friction forces should

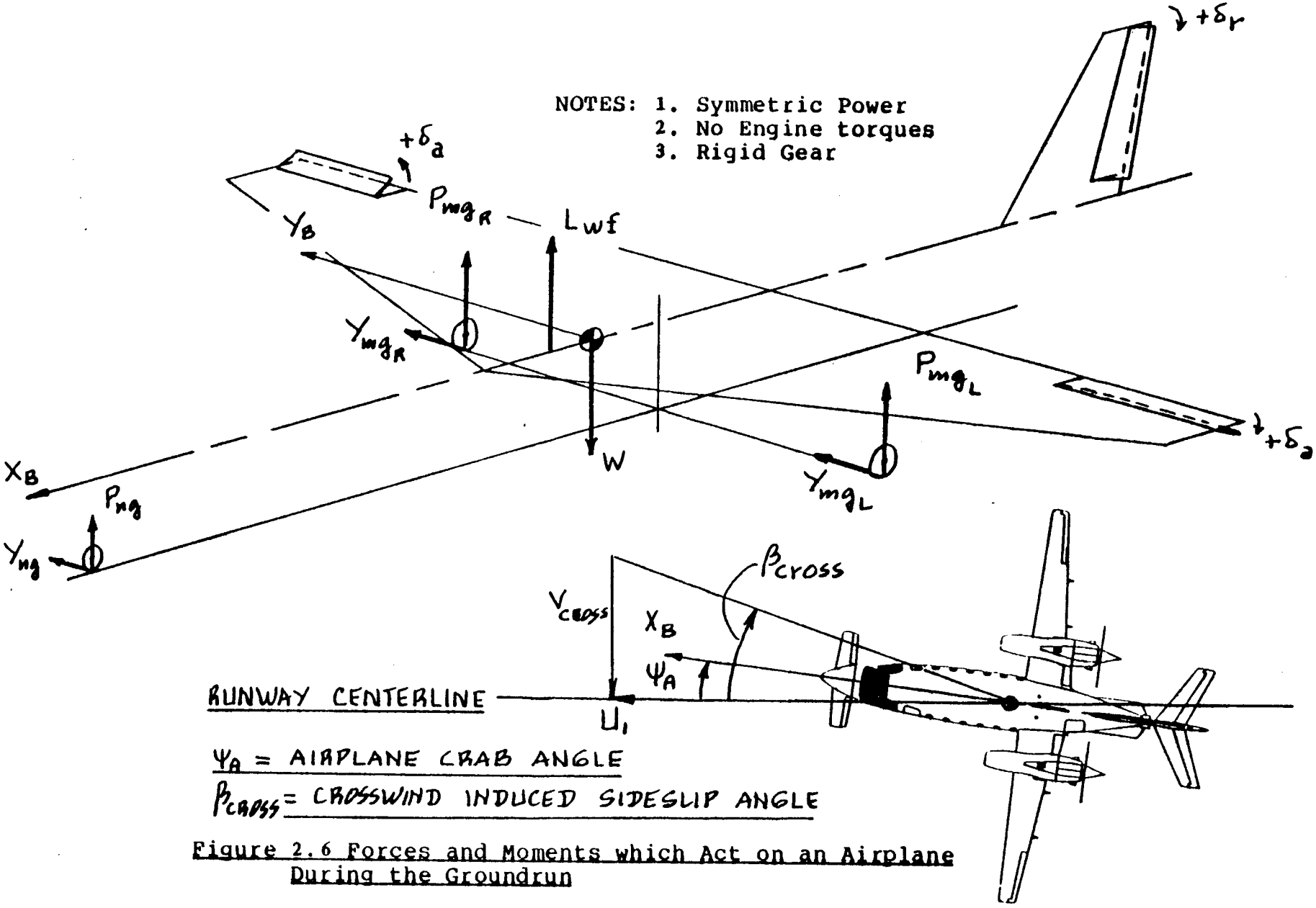

Ψ_A = AIRPLANE CRAB ANGLE

β_{CROSS} = CROSSWIND INDUCED SIDESLIP ANGLE

Figure 2.6 Forces and Moments which Act on an Airplane During the Groundrun

not reverse sign. For positive sideslip due to crosswind it is required that:

$$Y_{ng} + Y_{mg_L} + Y_{mg_R} > 0 \qquad (2.43)$$

If condition (2.43) is violated, the airplane will begin to slide off the runway.

Note: As soon as the take-off rotation process as described in sub-section 2.5.3.1 is completed, the runway constraints loose their validity: the airplane is flying.

The magnitudes of the lateral gear forces, Y_{ng} and $Y_{mg_{(L \text{ or } R)}}$, depend on the values of the vertical gear reactions: P_{ng} and $P_{mg_{(L \text{ or } R)}}$ and on the so-called gear cornering coefficient.

The vertical gear reactions, P_{ng} and P_{mg} (and the airplane forward acceleration, $\dot{u}$) may be computed from from Equations (2.29) through (2.31) by setting:

a) Thrust equal to takeoff thrust

b) L_h to a value corresponding to the primary longitudinal control deflection used during the take-off roll (prior to initiation of rotation!).

c) $\ddot{\theta} = 0$

The relationship between the lateral gear forces, Y_{ng} and $Y_{mg_{(L \text{ or } R)}}$, the so-called cornering coefficient, c_β and the vertical gear reactions, P_{ng} and $P_{mg_{(L \text{ or } R)}}$ are normally writtent as follows:

$$Y_{ng} = c_\beta P_{ng} \qquad (2.44)$$

$$Y_{mg_{(L \text{ or } R)}} = c_\beta P_{mg_{(L \text{ or } R)}} \qquad (2.45)$$

The cornering coefficient itself is a function of the gear slip angles, $\beta_{ng \text{ or } mg}$ which are defined in

Figure 2.7. They can be expressed as:

for the main gear: $\beta_{mg} = \psi_A$ (2.46)

for the nose gear: $\beta_{ng} = \psi_A + U_{steer}$ (2.47)

where: ψ_A is the airplane crab angle.

ψ_{steer} is the nosegear steering angle.

Note: These relations assume a steerable nosegear and a non-steerable main gear!

In preliminary design it is conservative to write:

For dry surfaces:

for the main gear: $c_\beta = 0.025\psi_A$ (2.48)

for the nose gear: $c_\beta = 0.025(\psi_A + \psi_{steer})$ (2.49)

For slick surfaces:

for the main gear: $c_\beta = 0.005\psi_A$ (2.50)

for the nose gear: $c_\beta = 0.005(\psi_A + \psi_{steer})$ (2.51)

For purposes of preliminary design it is acceptable to assume that the maximum possible value for the cornering coefficients are:

$c_\beta = 0.70$ for dry surfaces

$= 0.15$ for slick surfaces

In checking the runway constraint conditions (2.40) and (2.43) these maximum allowable values should be kept in mind!

Figure 2.7 illustrates the relationships between the cornering coefficients and the gear slip angle.

To find the actual values of the lateral gear forces, the lateral-directional equations of motion are needed. The steady state lateral-directional equations of motion for a straight line track along the runway are:

$$\{(C_{y_\beta})(\beta_{cross} - \psi_A) + C_{y_{\delta_a}}\delta_a + C_{y_{\delta_r}}\delta_r\}\bar{q}S + Y_{ng} +$$

$$+ Y_{mg_L} + Y_{mg_R} = 0 \qquad (2.52)$$

$$\{(C_{l_\beta})(\beta_{cross} - \Psi_A) + C_{l_{\delta_a}}\delta_a + C_{l_{\delta_r}}\delta_r\}\bar{q}Sb + P_{mg_L}y_{mg} +$$

$$- P_{mg_R}y_{mg} - Y_{ng}z_{ng} - (Y_{mg_L} + Y_{mg_R})z_{mg} = 0 \qquad (2.53)$$

$$\{(C_{n_\beta})(\beta_{cross} - \Psi_A) + C_{n_{\delta_a}}\delta_a + C_{n_{\delta_r}}\delta_r\}\bar{q}Sb +$$

$$+ Y_{ng}(x_{ng} - x_{cg}) - (Y_{mg_L} + Y_{mg_R})(x_{mg} - x_{cg}) = 0 \qquad (2.54)$$

The x- and z- distances in these equations are defined in Figure 2.6. They are consistent with Figure 2.5.

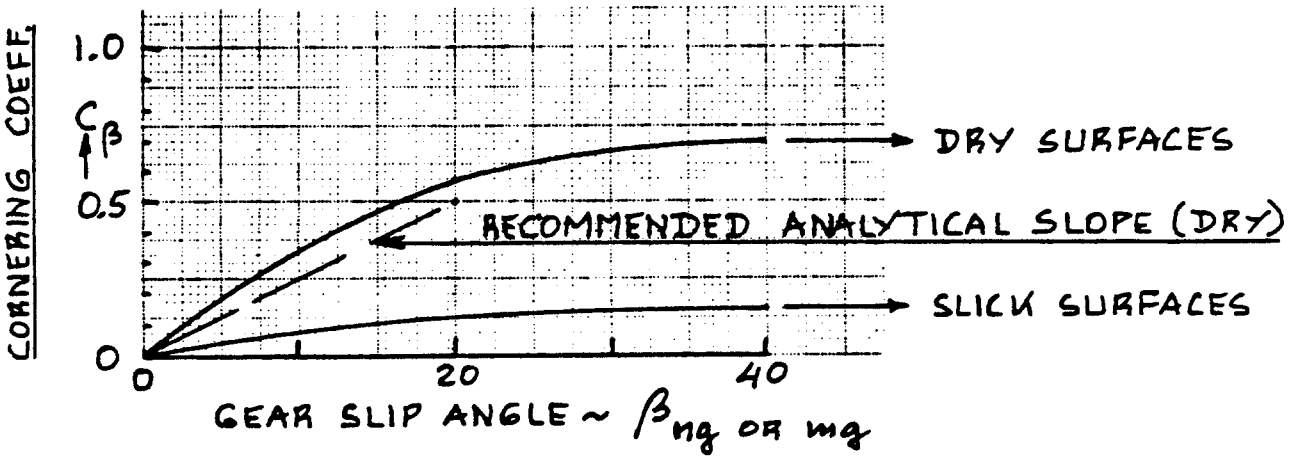

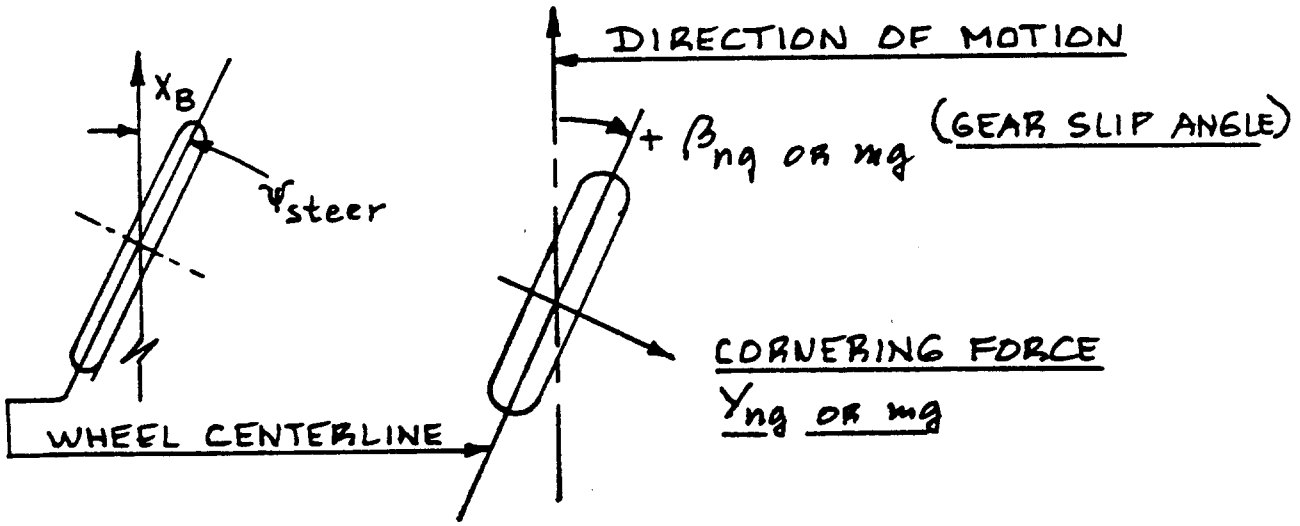

Figure 2.7 Gear Slip Angle, Gear Steering Angle, and Cornering Coefficients

Assumptions made in setting up these equations are:

1. The airplane does not bank (gear is rigid in the vertical direction).

2. All gears are rigid in torsion.

3. The tire induced torque on the gears can be neglected.

4. The engine induced torque in roll and in yaw can be neglected.

5. The dynamic pressure is a constant value between zero and that value corresponding to liftoff.

   The change in dynamic pressure during the takeoff groundrun is accounted for by solving Equations (2.52) - (2.54) for a range of values of dynamic pressure.

By using Equations (2.42), and (2.44) through (2.49) it is possible to cast Equations (2.52) - (2.54) in the following, more tractable form:

$$\{(C_{y_\beta})(\beta_{cross} - \psi_A) + C_{y_{\delta_A}}\delta_a + C_{y_{\delta_r}}\delta_r\}\bar{q}S +$$

$$+ 0.025(\psi_A + \psi_{steer})P_{ng} + 0.025\psi_A P_{mg} = 0 \qquad (2.55)$$

$$\{(C_{l_\beta})(\beta_{cross} - \psi_A) + C_{l_{\delta_a}}\delta_a + C_{l_{\delta_r}}\delta_r\}\bar{q}Sb +$$

$$+ 2P_{mg_L}y_{mg} - P_{mg}y_{mg} - 0.025(\psi_A + \psi_{steer})P_{ng}z_{ng} +$$

$$- 0.025\psi_A P_{mg}z_{mg} = 0 \qquad (2.56)$$

$$\{(C_{n_\beta})(\beta_{cross} - \psi_A) + C_{n_{\delta_a}}\delta_a + C_{n_{\delta_r}}\delta_r\}\bar{q}Sb +$$

$$+ 0.025(\psi_A + \psi_{steer})P_{ng}(x_{ng} - x_{cg}) +$$

$$- 0.025\psi_A P_{mg}(x_{mg} - x_{cg}) = 0 \qquad (2.57)$$

The following observations are in order:

A. The crosswind, V_{cross}, is specified by the mission specification and/or by the regulations. From the crosswind and the airplane speed along the runway, U_1:

$$\beta_{cross} = \arctan(V_{cross}/U_1) \qquad (2.58)$$

B. The variables in Equations (2.55) - (2.57) are:

1. The runway crab angle, ψ_A
2. The left vertical main gear reaction, P_{mg_L}
3. The lateral control deflection angle, δ_a
4. The rudder deflection angle, δ_r
5. The nosegear steering angle, ψ_{steer}

There are five variables and three equations. Thus, two variables must be specified. Usually the assumption is made that the pilot will select the nosegear steering angle, ψ_{steer} and the aileron deflection angle, δ_a to obtain the desired straight line track along the runway without winging over. The other variables are then completely determined by Eqns (2.55)-(2.57). Based on assumed values for ψ_{steer} and δ_a, and the solved variables ψ_A, P_{mg_L} and δ_r the designer must then make sure that the constraints 1 - 3 are not violated. Subsection 2.5.4 contains a procedure for these calculations.

2.5.4 Step-by-Step Procedure for Analyzing Control During the Take-off Groundrun

2.5.4.1 Step-by-step procedure for analyzing longitudinal control during the take-off groundrun

The following step-by-step procedure is suggested to verify the longitudinal controllability of an airplane during take-off:

Step 1: Read the regulations and determine which regulations apply to the design.

Step 2: The regulations define the speeds at which take-off rotation must be possible. Determine these speeds.

Step 3: The mission of the airplane defines the most severe field conditions in terms of altitude, temperature and surface conditions. This determines the atmospheric density to be used in the analysis. The field condition also deter mines the wheel-ground rolling friction coefficient, μ_g which should be used: see page 40 for guidelines.

Step 4: Determine the most critical weight versus c.g. locations for which take-off rotation must be possible.

Step 5: Determine all forces and coefficients needed to find the horizontal tail area required to rotate, from Eqn.(2.39). Make sure that ground effect is accounted for!

NOTE: If the airplane is not a conventional tricycle gear airplane it will be necessary to rewrite Equations (2.29) through (2.31)!

Step 6: Using Eqn.(2.39), find S_h as a function of speed, plot this relationship and mark the desired take-off rotation speed. Next, perform a sensitivity analysis to determine the sensitivity of the solution to such parameters as:

z_T, the vertical thrustline location.

$C_{m_{ac_{wf}}}$, the pitching moment coefficient of wing-fuselage with flaps in the take-off position. Determine the effect of flap type and flap size on the solution for S_h.

$C_{L_{h_{max}}}$, the maximum available lift coefficient of the horizontal tail.

Compare the value of S_h required for takeoff rotation with the value required from other considerations such as: control, trim and

stability). Decide on a course of action.

IMPORTANT NOTE: It turns out that the horizontal tail of many airplanes is determined by the take-off rotation requirement rather than by stability or by trim requirements. If that is the case a sensitivity analysis will allow for rapid decision making relative to changes in the design to bring this tail sizing requirement in better balance with the other tail sizing requirements.

Step 7: Document the results obtained, including any design changes made.

2.5.4.2 Step-by-step procedure for analyzing lateral-directional control during the take-off groundrun

Step 1: Read the regulations and determine which regulations apply to the design.

Step 2: The regulations define the crosswind magnitudes which the airplane must be able to cope with. Note these!

Step 3: Compute the stability and control derivatives identified in Eqns (2.55) - (2.57). The methods of Part VI can be used to do this.

Step 4: For a range of speeds between zero and V_{rot} determine the vertical gear reactions, P_{ng} and P_{mg} from Eqns (2.29) - (2.31) but using conditions a,b and c as stated on page 47.

Note: The nosegear reaction depends strongly on the longitudinal control deflections used during the take-off roll. The longitudinal trim control (usually the stabilizer incidence angle) must be set at an angle consistent with the requirement for take-off rotation: this usually means a negative angle!! The primary longitudinal control deflection may be assumed to be that giving the most favorable steering (usually full nose down).

Step 5: With the help of the specified crosswind determine the crosswind angle, β_{cross} from Equation (2.58). This must be done for a range of speeds consistent with Step 4.

Step 6: Select values for the nosegear steering angle, ψ_{steer} and for the aileron angle, δ_a.

With the help of Eqns (2.55) - (2.57) determine the airplane crab angle, ψ_A, the left vertical gear reaction, P_{mg_L} and the rudder angle, δ_r.

Step 7: With the results of Step 6, compute all gear reactions which appear in the runway constraint conditions 1, 2 and 3. See whether or not these constraints are satisfied. If not, different initial assumptions for ψ_A and δ_a may be tried as long as these new values are feasible. It may be, that the airplane cannot cope with the required cross wind conditions. In that case, possible design solutions are:

1. A larger vertical tail: more directional stability and perhaps more rudder control power.
2. Larger values for y_{mg} (larger distance between the main gears. This can have major redesign implications!
3. Incorporate a crosswind main gear into the airplane. See Part IV, Chapter 2 for implications!
4. Sometimes a smaller crosswind capability has to be accepted despite the fact that this will hurt the operational flexibility of the airplane.

Step 8: Document the results obtained, including any design changes made.

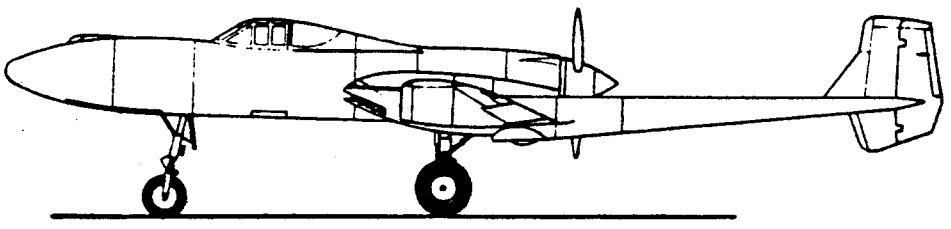

2.6 CONTROL DURING THE LANDING GROUNDRUN

2.6.1 Applicable Regulations:

Civil: FAR 23.231, see Appendix A.

FAR 25.231, 233, 237, see Appendix A.

Military: MIL-F-8785C, Section 3.3 (inparticular 3.2.3.3), see Appendix B.

2.6.2 Relationship to Preliminary Design

See Chapter 11, Part II.

2.6.3 Mathematical Model for Analyzing Control During the Landing Groundrun

The mathematical model to be used in this case is essentially that of Section 2.5.3 with the following additions:

1. The thrust, T should be investigated for flight idle as well as for reversed thrust if the airplane is equipped with a thrust reverser system.

2. Application of brakes should now be considered. The rolling friction coefficient, μ_g encountered during braking depends on brake design. For typical values, consult Part IV, pages 60 and 61.

3. Application of wing mounted spoilers can reduce the wing-fuselage lift very considerably thus changing L_{wf} in Eqns. (2.30) and (2.31).

4. The airplane may touch down in a 'crabbed' position. The crab-angle, Ψ_A depends on the value of crosswind and on the touchdown speed, V_L:

$$\Psi_A = \arctan(V_{cross}/V_L) \qquad (2.59)$$

5. The longitudinal control deflections are those most favorable for positive nosegear steering.

2.6.4 Step-by-Step Procedure for Analyzing Control During the Landing Groundrun

Use the procedures of Section 2.5.4 with the exception, that airplane speed ranges from V_L down to zero.

2.7 ROLL PERFORMANCE

2.7.1 Applicable Regulations

Civil: FAR 23.157 and FAR 25.147, see Appendix A.

Military: MIL-F-8785C, Section 3.3, see Appendix B.

2.7.2 Relationship to Preliminary Design

Part II, Chapter 2 (see Step 24), and Chapter 6.

2.7.3 Mathematical Model for Analyzing Roll Performance

The regulations essentially require that any airplane, when trimmed in a given flight condition at a given airspeed and in a given configuration:

1. can be maneuvered safely and easily from one bank angle to another (rolled) within some specified time period (Except FAR 25.147)

2. has roll time constant values which are within certain limits (Military only)

The words 'safely' and 'easily' as used here are defined in the regulations in terms of lateral cockpit control forces which may not be exceeded while achieving the bank angles and roll rates which must be obtained within some specified amount of time. In addition, the regulations imply that reversals in bank angle and roll rate may not occur outside well defined boundaries.

The words 'airplane configuration' imply one or more of the following as defined in the regulations:

1. center of gravity location
2. power setting (voluntary or failure)
3. landing gear position (up or down)
4. flap position (up, take-off, approach or landing)
   Note: in some instances asymmetric flap deployment has to be considered.
5. asymmetric fuel distribution
6. asymmetric weapons or payload disposition

When in doubt about the specific meaning of civil roll performance requirements, the author suggests to use the corresponding military specification.

Class II analysis of roll performance is normally accomplished with solutions of the so-called single-de-

gree-of-freedom differential rolling equation:

$$\ddot{\phi} = L_p\dot{\phi} + L_{\delta_{cpt}}\delta_{cpt} \qquad (2.60)$$

where: ϕ is the bank angle in rad

$\dot{\phi} = p$ is the roll rate in rad/sec

L_p is the dimensional roll damping derivative, which is defined as:

$$L_p = (C_{l_p}\bar{q}Sb^2)/(2I_{xx_s}U_1) \qquad (2.61)$$

in which: C_{l_p} is the dimensionless roll damping derivative. Part VI, Chapter 10 gives a method for estimating C_{l_p}

S is the wing area in ft^2

b is the wing span in ft

U_1 is the steady state speed in fps

I_{xx_s} is the rolling moment of inertia in $slugft^2$ in the stability axis system. Methods for computing the moments of inertia in an arbitrary body axis system are provided in Chapters 3 and 10 of Part V. Transformation of airplane moments of inertia to the stability axes system can be accomplished with the help of Appendix D.

$L_{\delta_{cpt}}$ is the dimensional roll control power derivative. It is defined as:

$$L_{\delta_{cpt}} = (C_{l_{\delta_{cpt}}}\bar{q}Sb)/I_{xx_s} \qquad (2.62)$$

$C_{l_{\delta_{cpt}}}$ is the lateral control power derivative. Read on to see how it may be computed.

δ_{cpt} is the lateral cockpit control deflection in degrees, in radians or in inches depending on the type of cockpit controller in use. The cockpit controller is normally geared to the

lateral control surfaces. Many airplanes employ more than one type of lateral control surface. If an airplane uses both ailerons and spoilers and if a linear gearing is assumed between the cockpit controller and the lateral control surface it is possible to write:

$$C_{l_{\delta_{cpt}}} \delta_{cpt_{max}} = C_{l_{\delta_a}} \delta_{a_{max}} + C_{l_{\delta_s}} \delta_{s_{max}} \qquad (2.63)$$

where: $C_{l_{\delta_a}}$ is the aileron control power derivative in 1/deg or in 1/rad. It may be computed with the method of Chapter 10 in Part VI.

$\delta_{a_{max}}$ is the maximum available aileron deflection in degrees or in radians

$C_{l_{\delta_s}}$ is the spoiler control power derivative in 1/deg or in 1/rad. It may be computed with the method of Chapter 10 in Part VI.

δ_s is the maximum available spoiler deflection in degrees or in radians.

$\delta_{cpt_{max}}$ represents the maximum available deflection of the lateral cockpit controller in inches or in radians. This quantity follows from the detail design of the cockpit as discussed in Chapter 2 of Part III. Maximum allowable deflections for sticks and wheels are defined in Chapter 2, Part III. Once $\delta_{cpt_{max}}$ has been determined, Eqn.(2.63) can be used to solve for $C_{l_{\delta_{cpt}}}$.

It must be possible for the pilot to move the lateral cockpit controller (stick, wheel or other) to a position consistent with the required roll performance. This means that the accompanying cockpit control force should not exceed the capabilities of the pilot. The magnitudes of allowable lateral control forces are defined in the regulations. The lateral cockpit control force may be estimated from:

$$F_{s_{lat}} = \text{Sum}\ (G_i HM_i) + F_{s_{lat_{artificial}}} \qquad (2.64)$$

where: G_i is the gearing ratio in rad/in or in rad/ft associated with the i^{th} lateral control surface

HM_i is the hingemoment in ftlbs associated with the i^{th} lateral control surface. Such hingemoments may be estimated from:

$$HM_i = C_{h_i} \bar{q} S_i \bar{c}_i \qquad (2.65)$$

where: C_{h_i} is the hingemoment coefficient associated with the i^{th} lateral control surface. Methods for estimating hingemoment coefficients are given in Chapter 10 of Part VI.

S_i is the reference area of the ith lateral control surface

$\bar{c}_i$ is the m.g.c. of the ith lateral control surface

$F_{s_{lat_{artificial}}}$ is the lateral cockpit controller force produced by the lateral force-feel system. For a discussion of force-feel systems, see Ref.12, Chapter 5.

2.7.4 Step-by-Step Procedure for Analyzing Roll Performance

In preliminary design, the roll performance capabilities of an airplane can be verified with the following step-by-step procedure:

Step 1: Read the regulations and determine which regulations apply to the design.

Step 2: The regulations define flight conditions and airplane configurations for which certain roll performance standards are to be met. Identify these flight conditions.

Note: Also determine the airplane configu-

ration for which the regulations apply.

Step 3: For the flight conditions defined in Step 2, determine: Mach number, M, dynamic pressure, $\bar{q}$ and the rolling moment of inertia (in stability axes!).

Step 4: For the conditions defined in Steps 2 and 3 determine the roll damping derivative, C_{l_p}.

NOTE: for airplanes subject to aeroelastic deformations, read Section 2.9!

Step 5: For the conditions defined in Steps 2 and 3 determine the roll control power derivative due to lateral cockpit control, $C_{l_{\delta_{cpt}}}$.

This derivative depends on the type of roll control system used. For an airplane which uses ailerons and/or spoilers, Eqn.(2.63) may be used. If a differential stabilizer is used, the appropriate term must be added to Eqn.(2.63). Methods for estimating control power derivatives due to ailerons, spoilers and differential stabilizer are given in Chapter 10 of Part VI.

Acceptable values for control surface deflections depend on aerodynamic considerations. Suggested 'not-to-exceed' values for lateral control surface deflections are:

Ailerons: $\delta_{a_{max}} < 25$ degrees

Spoilers: $\delta_{s_{max}} < 60$ degrees

Differential stabilizer: $\delta_{i_h} < 15$ degrees

NOTE: for airplanes subject to aeroelastic deformations, read Section 2.9!

Step 6: Determine the roll angle performance capability of the airplane from:

$$\phi(t) = \{(-L_{\delta_{cpt}}\delta_{cpt})t/L_p\} + [(L_{\delta_{cpt}}\delta_{cpt})/\{(L_p)^2\}](e^{L_p t} - 1) \qquad (2.66)$$

where: $\phi(t)$ is the bank angle reached at t seconds after full movement of the lateral cockpit controller, δ_{cpt}. Note that Eqn. (2.66) is based on the assumption that the control input can be thought of as a 'perfect' step input.

t is the time elapsed from full movement of the cockpit controller, δ_{cpt} to the time at which the bank angle is to be measured.

IMPORTANT NOTE: in most regulations, the values for $\phi(t)$ and the corresponding value of t are given. Therefore, Eqn. (2.66) can be used by the designer to solve for that value of the control power derivative, $L_{\delta_{cpt}}$ which is needed to satisfy the regulation. With that information the designer can decide how to change the lateral control surface sizes and locations until the regulation is satisfied.

Step 7: Calculate the airplane roll time constant, τ_R from:

$$\tau_R = -1/L_p \qquad (2.67)$$

where L_p is found from Equation (2.61).

If the airplane is to have acceptable roll performance, the roll time constant must be below some maximum allowable value. Maximum allowable values for the roll time constant are presented in the military regulations: Appendix B, Table VII, page 297.

Important Note: The civil regulations do not require specific values of the roll time constant. Accepted design practice in the U.S.A. is to use the appropriate military specifications (Airplane class, flight phase and handling quality level) whenever the civil regulations fail to provide specific design guidance.

Step 8: Document the results obtained, including any design changes made.

2.8 HIGH SPEED CHARACTERISTICS

2.8.1 Applicable Regulations

Civil: FAR 23.253 and FAR 25.253, see Appendix A.

Military: MIL-F-8785C, Section 3.2, in particular Sub-sections 3.2.3.6 and 3.2.3.7, see Appendix B.

2.8.2 Relationship to Preliminary Design

Part II, Chapter 8, in particular Step 8.4.

2.8.3 Mathematical Model for Analyzing High Speed Characteristics

The regulations essentially require that any airplane, when inadvertently placed in a flight condition between the maximum allowable operating speed and the design dive speed, must be able to be recovered to a normal operating flight condition without the use of exceptional pilot skills and without exceeding reasonable cockpit control force levels.

To satisfy these requirements it is usually sufficient in preliminary design to show that no reversals occur in control force versus speed gradients within the speed range prescribed in the regulations.

Calculation of the control force versus speed gradients can be done with the method of Section 3.1.3 with the proviso that all derivatives and coefficients must be evaluated at the high Mach numbers required by the regulations. This cannot normally be done without the availability of windtunnel data and/or advanced aerodynamic panel codes.

Note: Another way around the high speed handling problem is to prevent the airplane from becoming exposed to certain Mach number ranges. This can be done by the addition of 'flight envelope protection' systems, such as on the Airbus 320.

2.8.4 Step-by-Step Procedure for Analyzing High Speed Characteristics

The step-by-step procedure for analyzing high speed characteristics is similar to that of Section 3.1.4. All stability derivatives and coefficients must be evaluated at the high Mach numbers required by the regulations.

2.9 AEROELASTIC CONSIDERATIONS

The analysis methods and procedures presented in Sections 2.1 through 2.8 are based on the assumption that designer has available ALL values for aerodynamic coefficients, control power derivatives and stability derivatives which reflect the ACTUAL airplane behavior in a particular flight condition.

In Sections 2.1 through 2.8 frequent reference is made to the methods for estimating aerodynamic coefficients, control power derivatives and stability derivatives in Part VI. The reader MUST keep in mind that these methods are VALID ONLY for RIGID airplanes. Most high performance airplanes, including fighters and transports are often far from rigid: they exhibit significant aeroelastic behavior!

Therefore it becomes necessary to evaluate the aerodynamic coefficients, the control power derivatives and the stability derivatives not only as a function of Mach number, but also as a function of dynamic pressure. It is the dynamic pressure which (at any combination of angle of attack and Mach number) determines the severity of aeroelastic distortions.

Calculating aeroelastic effects requires rather detailed knowledge of the airplane structural properties: in particular the EI (bending stiffness) and GJ (torsional stiffness) distribution about the airplane elastic axes. In the early design phase such knowledge may not yet be available. Therefore, in the early preliminary design phase, use is made of so-called elastic-to-rigid ratios. These ratios are used to 'guestimate' the ELASTIC AIRPLANE value of a coefficient (or derivative) from a known value of that coefficient (or derivative) for the corresponding RIGID AIRPLANE. A typical example is:

$$C_{L_\alpha}{}_{elastic} = (R_e/R_r)C_{L_\alpha}{}_{rigid} \qquad (2.68)$$

where: $C_{L_\alpha}{}_{rigid}$ is the lift-curve slope of the rigid airplane as computed with the methods of Part VI.

R_e/R_r is the elastic-to-rigid ratio which may be computed with the methods of Ch. 8, Reference 12, provided the required structural stiffness information and elastic axes locations are available.

In preliminary design, these ratios are frequently 'guestimated' on the basis of computed data on similar configurations. Chapter 8 of Reference 12 provides examples of elastic airplane versus rigid airplane derivatives. The reader may use these to arrive at an 'educated' guestimate of R_e/R_r for a newly designed airplane. Care must be exercised in doing this: the data in Reference 12 apply to transport airplanes only!

Figure 2.8 shows an example application of these ideas.

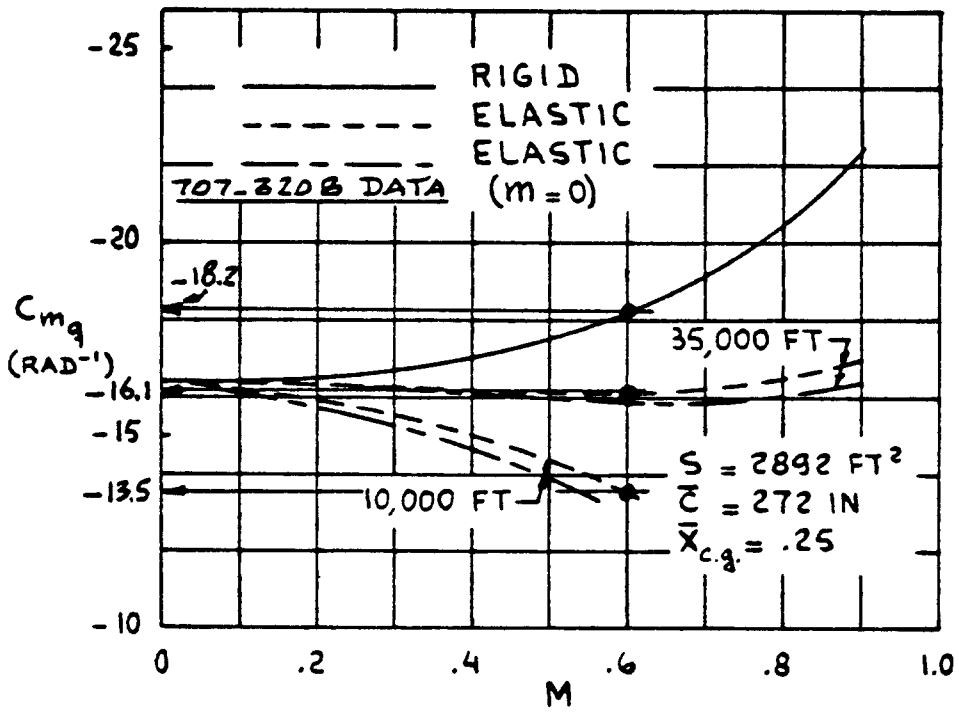

AT M = 0.6 AND 10,000 FT $R_e/R_r = -13.5/-18.2 = 0.74$

" " AND 35,000 FT $R_e/R_r = -16.1/-18.2 = 0.88$

Figure 2.8 Example of Extraction of R_e/R_r Values from Elastic Airplane Derivative Data

3. STABILITY: STATIC AND DYNAMIC

The purpose of this chapter is to present Class II methods for analyzing the static and dynamic stability characteristics of airplanes. These methods are compatible with Step 24 in Preliminary Design Sequence II as outlined in Chapter 2 of Part II.

The designer must decide at the outset whether his airplane should be designed with:

1. Inherent stability OR WITH: 2. De-facto stability.

Definition 1: Airplanes with 'inherent stability' do not require any form of 'closed loop' stability augmentation.

The Cessna 172 and the Fokker F-50 are examples of such airplanes.

As a general rule, low to moderate performance airplanes are designed with inherent stability.

Definition 2: Airplanes with 'de-facto stability' require static and/or dynamic stability augmentation.

The F-18 and the X-29 are examples of such airplanes. Both are inherently unstable and rely on a feedback system to achieve theirs de-facto stability: they cannot be controlled without feedback!

As a general rule very high performance airplanes are designed with de-facto stability.

Most moderate to high performance airplanes (B-727, DC-10, C- 141) have inherent static stability but are deficient in inherent dynamic stability. Such airplanes are typically equipped with feedback systems to assure that they have de-facto dynamic stability.

The B-727 and the DC-10 have yaw dampers to assure that the dutch roll damping ratio is sufficiently large. The C-141 also has a pitch damping system to assure that the short period damping ratio is sufficiently large.

QUESTION: What drives airplane designers toward de-facto (or artificial) stability?

ANSWERS: 1. For fighters: Enhanced maneuverability!

2. For transports: Savings in tail areas and weight as well as savings in drag! These savings must be traded against greater complexity of the flight control system and its sensors.

Reliability and maintainability issues also play an important role in the design decision making process between inherent and de-facto stability.

IMPORTANT COMMENT: The choice between inherent stability and de-facto stability is made by the designer (together with the customer) and NOT by the regulations!

The objective of the methods in this chapter is to assure that the airplane meets all the regulatory static and dynamic stability requirements which are placed on an airplane. These regulatory requirements are placed on an airplane to ensure that it is airworthy. Airworthiness in this case implies that the airplane possesses safe, 'minimum' handling characteristics.

To ensure safe, minimum handling characteristics the civil and the military regulations specify certain minimum allowable frequency, damping, time constant and response parameters.

A problem with many civil stability regulations (see (Appendix A) is that they are frequently cast in language which is not easily translated in numerical statements. This makes them difficult to use by designers!

However, the military regulations (see Appendix B) are written in terms of very specific numerical design objectives. For that reason, the military regulations are commonly used in the preliminary design process of BOTH civil and military airplanes.

The military regulations (Appendix B) define static, dynamic and control-response characteristics in three levels. These levels can be summarized as follows:

LEVEL 1: Flying qualities which are clearly adequate for any given mission flight phase.

LEVEL 2: Flying qualities which are adequate to complete the mission flight phase but some increase in pilot workload or degradation in mission effectiveness, or both, exists.

LEVEL 3: Flying qualities such that the airplane can

be controlled safely, but pilot workload is excessive or mission effectiveness is inadequate, or both. HOWEVER: the airplane can be safely landed.

IMPORTANT DESIGN GUIDELINES FOR CIVIL AND FOR MILITARY AIRPLANES:

1. Inherently stable airplanes must be designed to LEVEL 1 requirements.

2. De-facto stable airplanes must be designed to LEVEL 1 requirements with the feedback augmentation system in the normal state.

3. After failures occur in the flight control system the degraded handling quality levels which are tolerated depend on the probability, P (per flight) with which the failures occur.

HANDLING QUALITY LEVEL which is tolerated:	Civil Airplanes	Military Airplanes
LEVEL 2	$P < 10^{-4}$	for $P < 10^{-2}$
LEVEL 3	$P < 10^{-6}$	for $P < 10^{-4}$

The airplane designer must be aware of the fact that a penalty paid for 'de-facto' stability is that stability augmentation systems use control power to achieve their objective. It is up to the designer to assure that the required levels of control power are indeed designed into the airplane during the preliminary design process.

The material in this chapter is organized as follows:

3.1 Static longitudinal stability
3.2 Static lateral and directional stability
3.3 Dynamic longitudinal stability
3.4 Dynamic lateral-directional stability
3.5 Dynamic coupling
3.6 Stall characteristics
3.7 Spinning
3.8 Aeroelastic considerations

Reference 12 can be used as a source for derivations and applications of the theory of airplane static and dynamic stability and control: open and closed loop.

3.1 STATIC LONGITUDINAL STABILITY

3.1.1 Applicable Regulations

Civil: FAR 23.171, 23.173, 23.175, and 23.253, see Appendix A.

FAR 25.171, 25.173, 25.175, 25.253, and 25.255, see Appendix A.

Military: Mil-F-8785C, Sub-section 3.2.1 and Paragraph 3.2.2.2, see Appendix B.

3.1.2 Relationship to Preliminary Design

See Part II, Chapter 11.

3.1.3 Mathematical Model for Analyzing Static Longitudinal Stability

The regulations essentially require that the airplane must possess the following characteristics:

1.) With the airplane trimmed at speeds which are specified in the regulations, a PULL must be required to obtain AND maintain speeds below the trim speed. Conversely, a PUSH must be required to obtain AND maintain speeds above the trim speed.

2.) The speed must return to within some specified percentage of the trim speed if the cockpit control is released from the push or pull condition(s) implied by 1.).

3.) The stick-force speed gradient must not be less than that specified in the regulations.

Figure 3.1 illustrates these concepts.

It is clear that a mathematical model for analysis of these characteristics must relate the stick force to speed relative to any given trim speed. Since the mathematical relationship between stick force and speed depends on the type of control system employed (as shown in Eqn.(2.8)) the designer must decide on the type of flight control system to be used in his airplane.

In the following it is assumed that the airplane is equipped with an elevator as the primary longitudinal controller. The stabilizer angle is assumed to have the

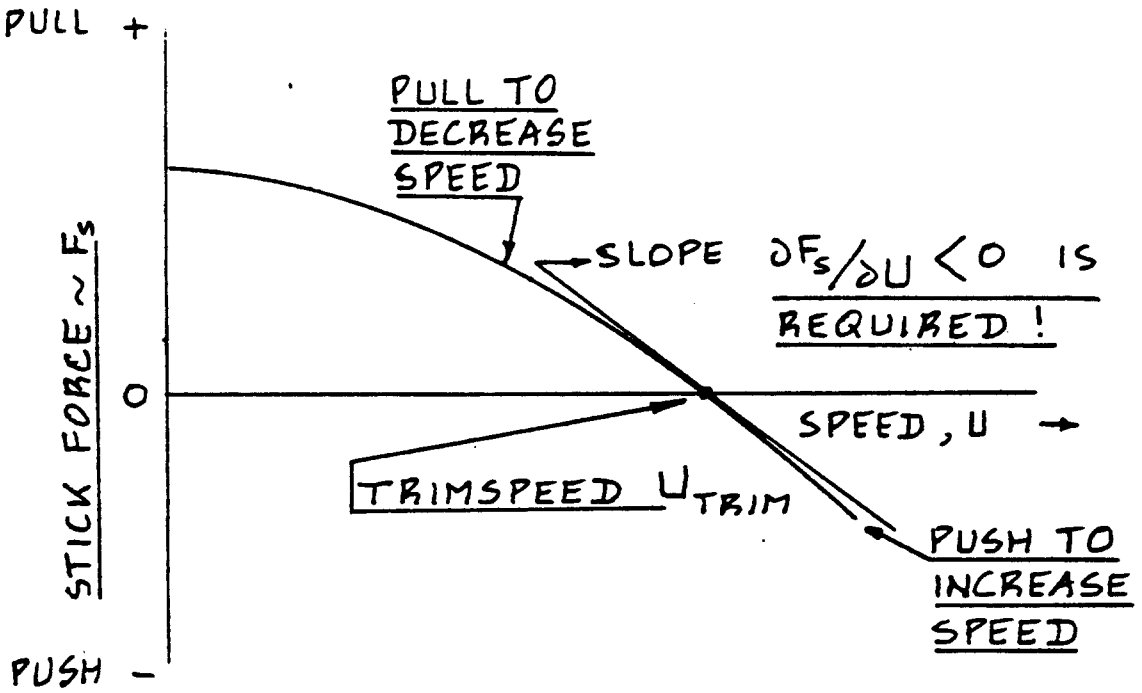

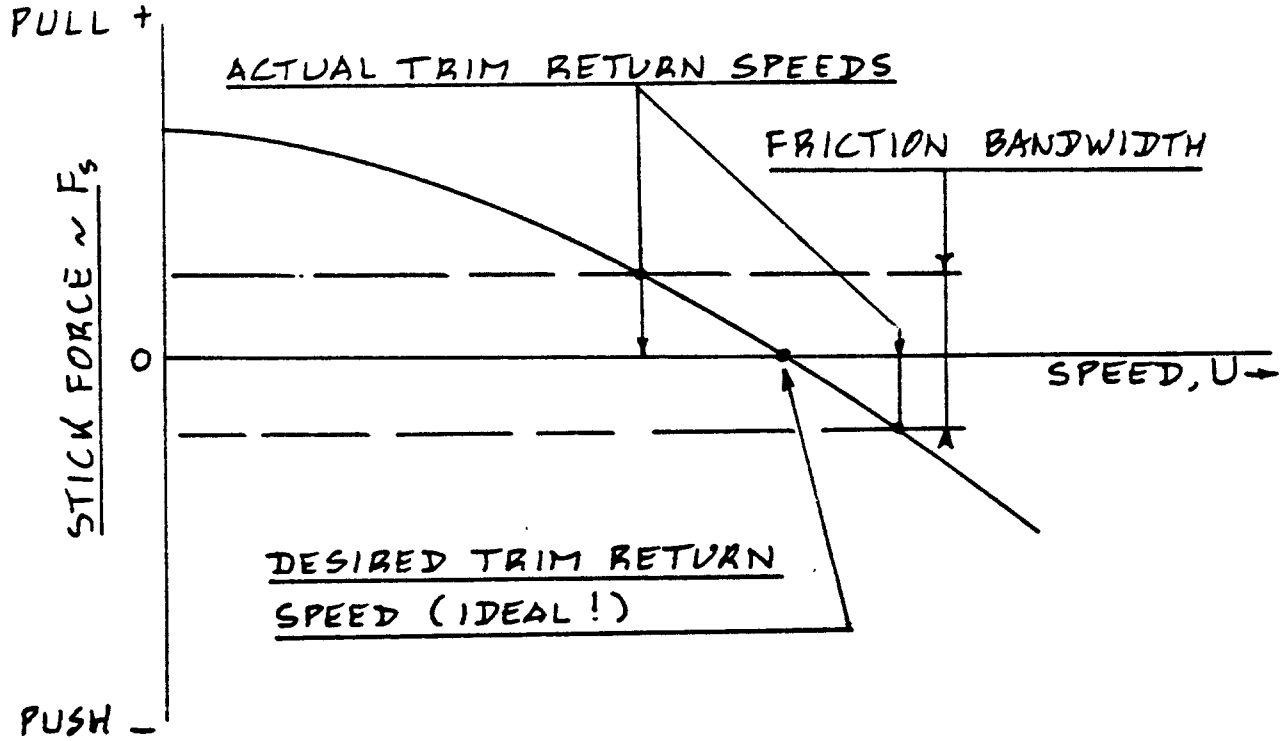

Figure 3.1 Stick-force Versus Speed and Return-to-Trim-Speed Characteristics

stick force trim function. In that case, Reference 12, Chapter 5 shows that the following relations hold:

1. For the stick force needed to maintain a speed U, relative to a given trimspeed, U_{trim}:

$$F_s = \eta_h G S_e \bar{c}_e (W/S) x \qquad (3.1)$$

$$x (C_{h_{\delta_e}} / C_{m_{\delta_e}}) (S.M._{free}) \{1 - (U/U_{trim})^2$$

2. For the stick-force-speed-gradient at the trim-speed:

$$(\partial F_s / \partial U)_{trim} = -(2/U_{trim}) x \qquad (3.2)$$

$$x \eta_h G S_e \bar{c}_e (W/S) (C_{h_{\delta_e}} / C_{m_{\delta_e}}) (S.M._{free})$$

where: $S.M._{free}$ is the stick-free static margin of the airplane. This quantity may be found from the following approximation:

$$S.M._{free} = \bar{x}_{ac_A} - \bar{x}_{cg} + \qquad (3.3)$$

$$+ (C_{m_{\delta_e}} / C_{L_\alpha}) (C_{h_\alpha} / C_{h_{\delta_e}}) (1 - d\varepsilon/d\alpha)$$

with: $\bar{x}_{ac_A}$ the airplane aerodynamic center as found from Part VI, Sub-section 8.2.5.2

$\bar{x}_{cg}$ the airplane c.g. location in fractions of the wing m.g.c.

All other quantities have been previously defined.

NOTE 1: As long as the hingemoment derivative $C_{h_{\delta_e}}$ has the normal (negative) sign, the stick-force as found from Equation (3.1) and the stick-force-speed-gradient as found from Equation (3.2) have the correct sign, provided the airplane has a POSITIVE STATIC MARGIN!

NOTE 2: The reader should modify these equations if the flight control system of his airplane is different

than the one assumed here. For guidance on how to do this the reader should consult Chapter 5 of Reference 12.

3.1.4 Step-by-Step Procedure for Analyzing Static Longitudinal Stability

Step 1: Determine which regulations apply to the design: see Table 3.1 and Subsection 3.1.1.

Step 2: The regulations define the flight conditions and the airplane configurations for which the stability requirements must be met. Tabulate these flight conditions and these configurations.

Step 3: For the flight conditions and for the airplane configurations of Step 2 determine the Mach number, the dynamic pressure and the center of gravity locations.

Step 4: For the flight conditions and for the airplane configurations of Steps 2 and 3 determine all derivatives and coefficients used in Equations (3.1) through (3.3).

Step 5: Calculate the stick-force-speed gradient from Eqn.(3.2) and check its value against that allowed in the applicable regulation. If the required gradient is not achieved, determine which parameters need to be adjusted. Note: in many cases a satisfactory gradient can be achieved only by moving the aft allowable center of gravity forward! This has obvious implications to the utility of the airplane!

Step 6: Document the results obtained, including any design changes made.

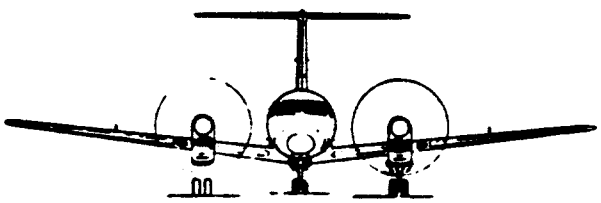

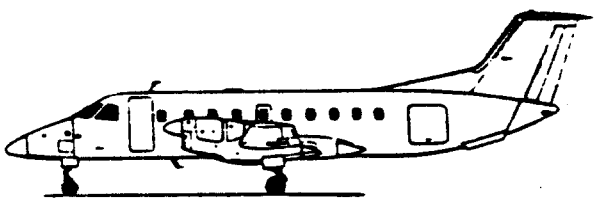

3.2 STATIC LATERAL AND DIRECTIONAL STABILITY

3.2.1 Applicable Regulations

Civil: FAR 23.171 and FAR 23.177, see Appendix A.

FAR 25.171 and FAR 25.177, see Appendix A.

Military: Mil-F-8785C, Sub-section 3.3.6, see Appendix B.

3.2.2 Relationship to Preliminary Design

See Part II, Chapter 11.

3.2.3 Mathematical Model for Analyzing Static Lateral and Directional Stability

The regulations essentially require that the airplane must possess the following characteristics:

1.) When the airplane is put in a sideslip (skid) condition it shall have the tendency to return to the original (zero sideslip) condition.

2.) The rudder pedal force required to put the airplane in a sideslip condition shall be such that the pedal-force-gradient is does not reverse its sign.

3.) When the airplane is put in a positive sideslip (skid), it must have the tendency to raise the left wing.

Figure 3.2 illustrates these concepts. The conditions for which these requirements are satisfied are now presented.

1.) This condition is referred to as the condition for positive directional stability:

a) For irreversible control systems:

$$C_{n_\beta} > 0 \qquad (3.4)$$

The directional stability derivative, C_{n_β} may be computed with the method of Section 10.2.4 of Part VI. From those methods it will be clear that directional stability strongly de-

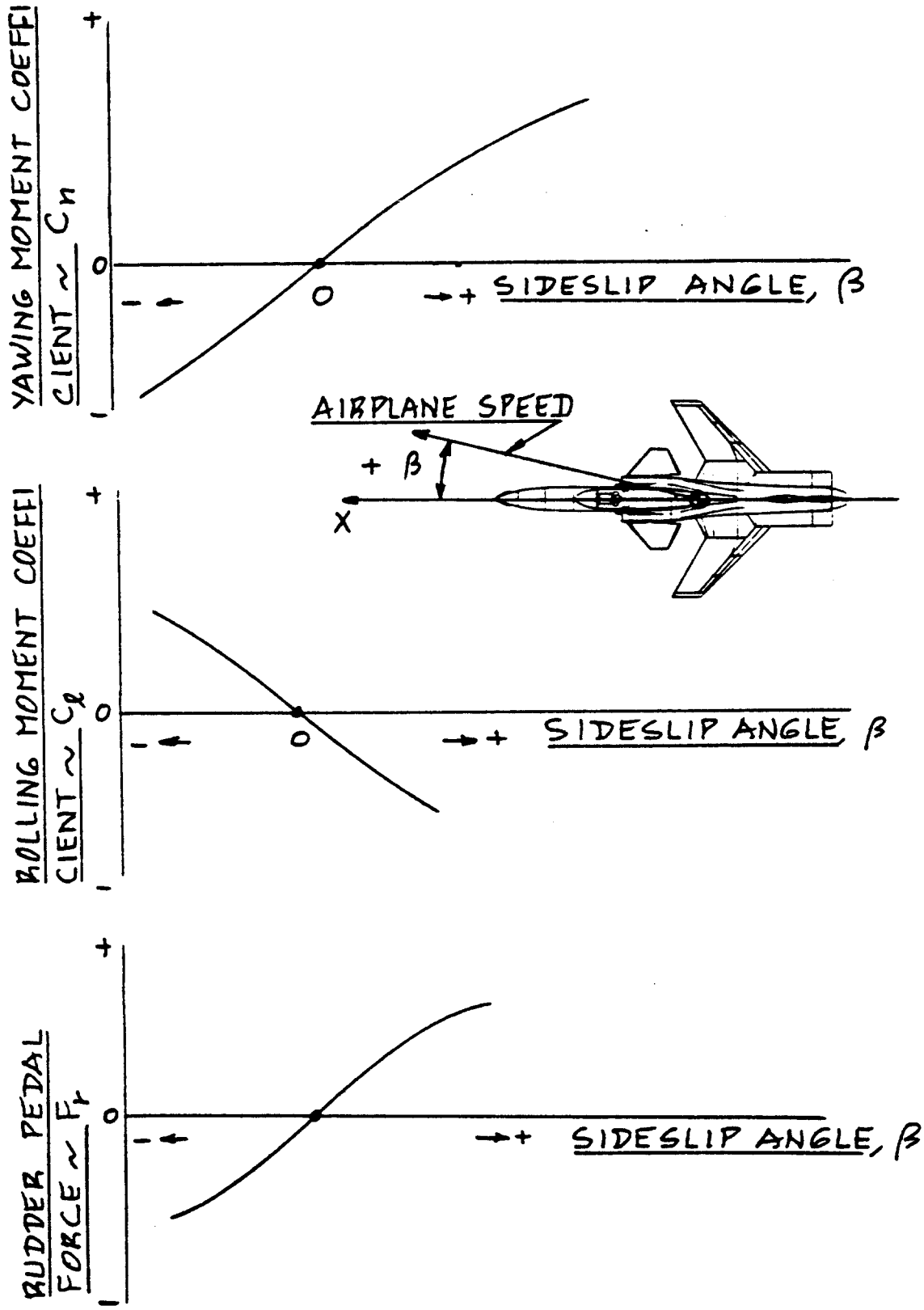

Figure 3.2 Requirements for Lateral and Directional Static Stability

pends on the size and shape of the fuselage and on the size, shape and location of the vertical tail.

b) For reversible control systems:

$$C_{n_{\beta_{free}}} = C_{n_{\beta_{fixed}}} + C_{n_{\delta_r}} (C_{h_{\beta_v}} / C_{h_{\delta_r}}) \quad (3.5)$$

where: $C_{n_{\beta_{fixed}}} = C_{n_\beta}$ of Eqn.(3.4)

$C_{n_{\delta_r}}$ is the rudder control power derivative. It may be computed with the method of Section 10.3.8 of Part VI.

$C_{h_{\beta_v}}$ is the rudder hingemoment derivative due to sideslip. It is physically equivalent to the elevator hingemoment derivative due to elevator deflection, $C_{h_{\delta_e}}$ and may be computed with the help of Sect.10.4 of Pt VI.

$C_{h_{\delta_r}}$ is the rudder hingemoment derivative due to rudder deflection. It is physically equivalent to the elevator hingemoment derivative due to elevator deflection, $C_{h_{\delta_e}}$ and may be computed with the method of Section 10.4 of Pt VI.

2.) This condition is satisfied if:

$$\partial F_r / \partial \beta > 0 \quad (3.6)$$

It is shown in Chapter 5 of reference 12 that this in turn is satisfied if:

$$C_{n_{\beta_{free}}} > 0 \quad (3.7)$$

Note therefore that for this type of airplane the detail design of the flight control system becomes (again) important!

3.) This condition is satisfied as long as:

$$C_{l_\beta} < 0 \qquad (3.8)$$

The lateral stability derivative, C_{l_β} may be determined with the method of Section 10.2.4 of Part VI. The method makes it clear that this derivative depends mainly on three factors:

a) wing geometric dihedral angle
b) wing position on the fuselage (high or low)
c) wing sweep angle and lift coefficient

3.2.4 Step-by-Step Procedure for Analyzing Static Lateral and Directional Stability

Step 1: Determine which regulations apply to the design: see Table 1.3 and Subsection 3.2.1.

Step 2: The regulations define the flight conditions and the airplane configurations for which the static lateral-directional stability requirements must be satisfied. Tabulate these flight conditions and these configurations.

Step 3: For the flight conditions and for the airplane configurations of Step 2 determine the Mach number, the dynamic pressure and the center of gravity locations.

Step 4: For the conditions and configurations of Steps 2 and 3 determine the derivatives used in Equations (3.4) through (3.8).

Step 5: Using Equations (3.4) through (3.8) determine whether or not these stability conditions are satisfied. If not, determine how the design must be modified to meet the requirements.

NOTE: It may very well be that the airplane needs a larger vertical tail or that the geometric dihedral angle of the wing will have to be changed to meet the regulations.

Step 6: Document the results obtained, including any design changes made.

3.3 DYNAMIC LONGITUDINAL STABILITY

3.3.1 Applicable Regulations

Civil: FAR 23.181 and FAR 25.181, see Appendix A.

Military: Mil-F-8785C, Par.3.2.2, see Appendix B.

3.3.2 Relationship to Preliminary Design

See Part II, Step 24 in Chapter 2. Also, read Chapter 11 in Part II.

3.3.3 Mathematical Model for Analyzing Dynamic Longitudinal Stability

The civil regulations in Appendix A are vague about specific requirements for frequency and damping characteristics. For that reason the military regulations of Appendix B are used to check whether or not a civil airplane design meets the intent of the civil regulations.

The civil and military requirements for dynamic stability must be met with the cockpit controls held fixed as well as with the cockpit controls kept free. The analysis of dynamic stability with the controls held free is beyond the scope of preliminary design since it requires detailed design data on the flight control system. For that reason, only the 'controls fixed' case is considered here. An analytical approach to the analysis of dynamic stability with controls free is given in Reference 12.

The military regulations (Appendix B) specify ranges of acceptable values for the following dynamic stability parameters of the airplane phugoid (P) and short-period (SP) modes of perturbed motion:

1. Undamped natural frequency: $\omega_{n_{SP}}$
2. Damping ratio: ξ_P and ξ_{SP}

Because phugoid frequency is primarily determined by airplane speed, there is no requirement for it.

The required numerical magnitudes for frequency and damping behavior of airplanes depends on:

1. Airplane Type: this is recognized by classifying airplanes in four classes:

   Class I, II, III or IV: see Appendix B.

2. Flight Phase: this is recognized by classifying flight conditions into three flight phases:

Phase: A, B, and C: see Appendix B.

The following characterization is typical of the modal breakdown for most airplanes in most flight conditions:

Mode	Undamped Natural Frequency	Damping Ratio	Most Important Motion Variables
Phugoid	Low	Low	Speed and Pitch Attitude Angle
Short Period	High	Moderately High	Angle of Attack, Pitch Attitude Angle

The damping characteristics of the phugoid mode of motion primarily affects the pilot's ability to control airspeed with the longitudinal controls. The phugoid damping ratio must not be too low.

The frequency and damping characteristics of the short period mode of motion primarily affects the pilot's ability to control pitch attitude angle. The short period frequency must not be too low, nor too high. The short period damping ratio must not be too low.

The phugoid and short period frequencies and damping ratios can be found from a solution of the three-degree-of-freedom, small perturbation equations of motion of an airplane. General methods (so-called Class III methods) for solving such equations are presented in Chapter 6 of Reference 12. In preliminary design it is acceptable to employ approximations for the phugoid and for the short-period behavior of an airplane. The Class II methods to be presented next are based on such approximate methods. The justification for these Class II methods is also discussed in Chapter 6 of Reference 12.

3.3.3.1 Class II method for analysis of phugoid characteristics

The following Class II method is suggested for determining phugoid undamped natural frequency and damping ratio:

$$\omega_{n_p} = (1.414g/U_1) \tag{3.9}$$

$$\xi_p = \{g/(2C_{L_1}U_1\omega_{n_p})\}(C_{D_u} + 2C_{D_1} - C_{T_{x_u}} - 2C_{T_{x_1}}) \tag{3.10}$$

where: U_1 is the steady state speed for the flight condition for which the dynamic stability of the airplane is being analyzed.

ρ is the air density for the flight condition being analyzed.

C_{L_1} is the steady state lift coefficient in the flight condition being analyzed.

C_{D_u} and $C_{T_{x_u}}$ are the drag-due-to-speed and thrust-due-to-speed derivatives. These derivatives may be computed with the methods of Ch.10 of Part VI.

C_{D_1} and $C_{T_{x_1}}$ are the steady state drag and thrust coefficients. These may be computed with the methods of Ch.10 of Part VI.

Observe that the phugoid frequency depends only on airplane speed! The phugoid damping ratio depends on the steady state drag and thrust as well as on the variation of drag and thrust with speed (Mach number!). Also observe, that the phugoid damping ratio is inversely proportional to the airplane lift-to-drag ratio, C_{L_1}/C_{D_1}.

3.3.3.2 Class II method for analysis of short period characteristics

The following Class II method is suggested for determination of the short period undamped natural frequency and damping ratio:

$$\omega_{n_{SP}} = \{(Z_\alpha M_q/U_1) - M_\alpha\}^{1/2} \tag{3.11}$$

$$\xi_{SP} = -\{M_q + (Z_\alpha/U_1) + M_{\dot{\alpha}}\}/2\omega_{n_{SP}} \tag{3.12}$$

where: the dimensional derivatives: Z_α, M_α, $M_{\dot{\alpha}}$ and M_q are all defined in the list of symbols. These de-

rivatives are functions of several dimensional derivatives which can be determined with the methods of Chapter 10, Part VI.

U_1 is the steady state speed corresponding to the flight condition for which dynamic stability is being analyzed.

It turns out that for many airplanes, in many flight conditions, the combination $(Z_\alpha M_q / U_1)$ in Eqn.(3.11) is small compared to M_α. The significance of this is that the short period undamped natural frequency is determined mostly by the magnitude of the derivative M_α.

IMPORTANT OBSERVATION ON EQN.(3.11):

The derivative M_α depends directly on the center of gravity location of the airplane, because:

$$C_{m_\alpha} = C_{L_\alpha} (\bar{x}_{cg} - \bar{x}_{ac_A}) \qquad (3.13)$$

Therefore: the short period undamped natural frequency of an airplane depends primarily on the distance between the center of gravity and the airplane aerodynamic center (stick-fixed neutral point!).

The reader is reminded of the fact that the c.g. location at any given airplane weight depends on the loading state of the airplane as reflected by the airplane weight-c.g. excursion diagram of Chapter 10 in Part II.

IMPORTANT OBSERVATION ON EQN.(3.12):

This equation predicts that the short period damping ratio of an airplane will always be positive! This is NOT correct. If this equation predicts the damping ratio to be less than 0.1, the reader is advised to use the Class III method of Chapter 6 of Reference 12.

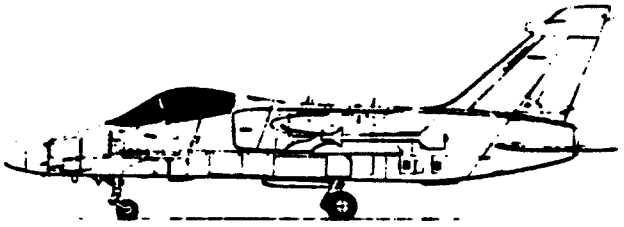

3.3.4 Step-by-Step Procedure for Analyzing Dynamic Longitudinal Stability

Step 1: Determine which regulations apply to the design: see Table 1.3 and Subsection 3.3.1.

Step 2: Determine from the description of airplane Classes in Appendix B which airplane Class (I, II, III or IV) best 'fits' the design.

Step 3: Determine for which flight conditions and for which airplane configurations the dynamic stability must be verified. Determine which flight phase category (A, B or C) is associated with each flight condition. The definition of flight phase categories is given in Appendix B.

Tabulate this information.

For inexperienced readers the following guidelines may be useful:

Flight conditions:

For purposes of preliminary design, the most critical flight conditions may be determined from the 'design' flight envelope. Figure 3.3 gives examples of 'design' flight envelopes for a civil and for a military airplane. The 'design' flight envelope normally follows from the airplane mission specification and from the Class II performance calculations which have been performed as part of Step 28 as described in Chapter 2 of Part II. Methods for Class II performance calculations are presented in Chapter 5.

Figure 3.3 shows the most critical flight conditions for which the dynamic stability should be verified at the early design stage.

Airplane configurations:

For purposes of preliminary design, the most critical airplane configurations occur at the most forward and at the most aft center of gravity locations. These c.g. locations follow from the weight-c.g. excursion diagram of Chapter 10 in Part II.

To decide on other critical configuration effects, the reader should check items 1-9 on page 7 and determine which of these effects apply to his design.

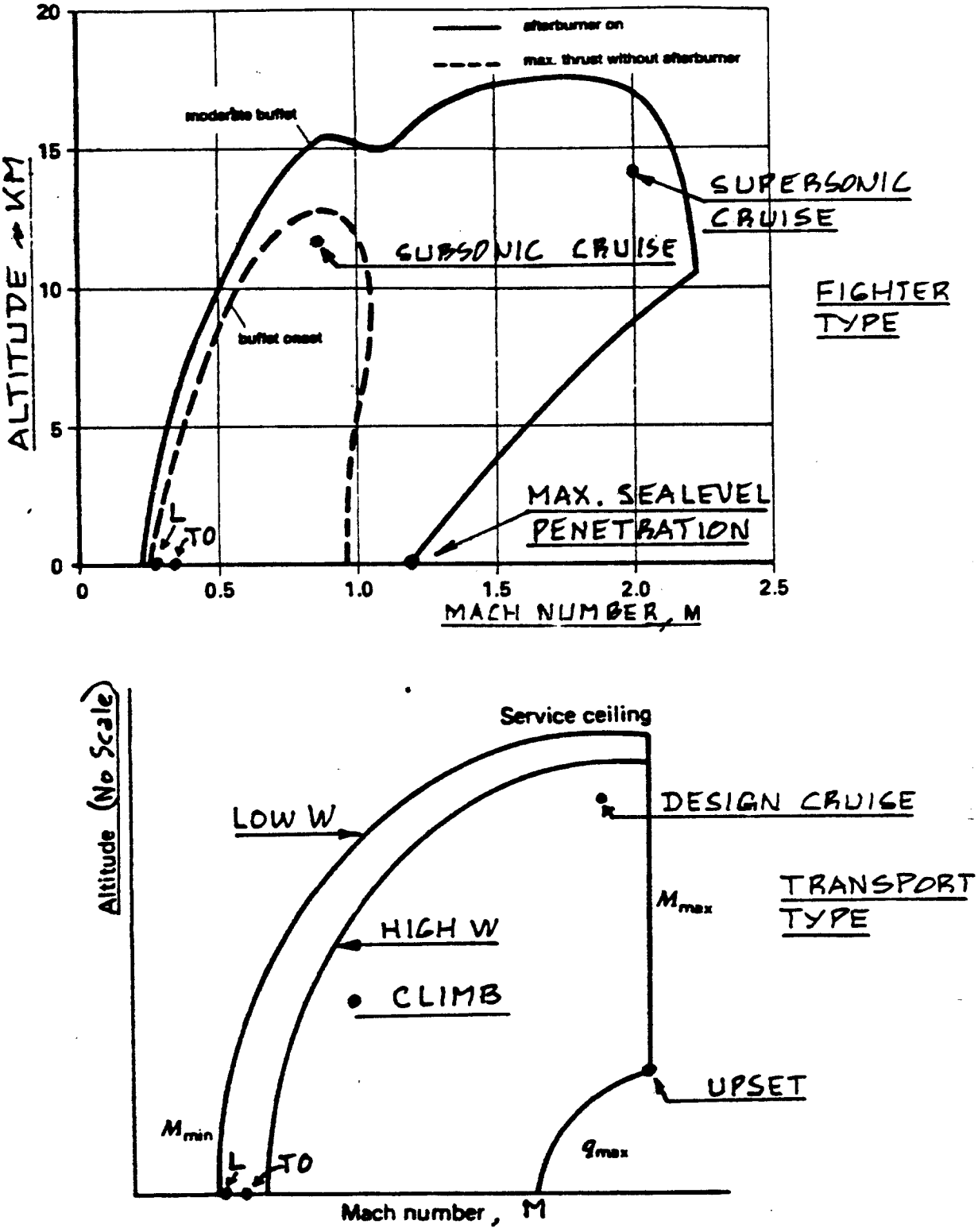

Figure 3.3 Examples of Civil Transport and Military Fighter Flight Envelopes with Indication of Flight Conditions Requiring Static and Dynamic Stability Calculations in Preliminary Design

Step 4: For the flight conditions and for the airplane configurations defined in Step 3, calculate the derivatives and other parameters which appear in Eqns (3.9) through (3.12).

Since the allowable short-period frequency ranges in Appendix B depend on the load-factor-to-angle-of-attack derivative n_α, also compute:

$$n_\alpha = \bar{q}SC_{L_\alpha}/W \qquad (3.14)$$

These 'input' data should all be tabulated!

Step 5: Decide whether the airplane being designed is to be 'inherently stable' or 'de-facto' stable.

Definitions for these types of stability are given on page 65.

If the airplane is to be 'inherently stable' proceed to Step 6.

If the airplane is to be 'de-facto stable' proceed to Step 8.

The choice between 'inherent' and 'de-facto' stability is made by the designer and not by the regulations!

Step 6: Determine the phugoid damping ratios associated with the flight conditions and airplane configurations of Step 3. Use Eqn.(3.10).

Determine the LEVEL 1 phugoid damping ratio requirements from Paragraph 3.2.1.2, in Appendix B.

Decide whether or not the airplane meets the LEVEL 1 requirements. If not, determine from Eqn.(3.10) what (if any) design changes should be made to satisfy the LEVEL 1 requirements OR put the airplane in the 'de-facto' stable category and proceed to Step 8.

Note: in most cases it will be found to be impractical to modify airplane phugoid damping through airplane design changes. The reasons are that phugoid damping depends mostly on drag and on installed thrust characteris-

tics. These in turn are normally dictated by performance considerations! Therefore, airplanes with deficient inherent phugoid damping are usually equipped with speed-to-thrust-feedback, speed-to-speedbrake feedback and/or with pitch-attitude-feedback. Chapter 13 of Reference 12 contains detailed discussions of such systems.

Step 7: Determine the short period frequencies and damping ratios associated with the flight conditions and airplane configurations of Step 3. Use Eqns.(3.11) and (3.12).

Determine the LEVEL 1 short period frequency and damping ratio requirements with the help of Figures B1 through B3 and Table IV in Appendix B. Compute n_α with Eqn.(3.14).

Decide whether or not the airplane meets the LEVEL 1 requirements. If not, use Eqns (3.11) and (3.12) to determine what design changes should be made to the airplane.

Note 1: By performing a derivative sensitivity analysis on Equations (3.11) and (3.12) the reader will find that the short period frequency is very sensitive to C_{m_α} (thus, according to Eqn.(3.13) to c.g. location!). It is also found that for a given short period frequency, the short period damping ratio is very sensitive to C_{m_q} (in other words to tail moment arm as shown in Section 10.2.7 of Part VI!).

Note 2: From a practical viewpoint, the only derivative over which the designer has much influence at this stage of the design is C_{m_α}. Eqn.(3.13) shows that this derivative may be altered by changes in the center of gravity location. The designer may therefore wish to 'taylor' the c.g. range of the airplane such as to bring the short period frequency range 'in line' with the requirements. Such c.g. range 'tailoring' will result in modification of the weight and balance of the airplane as discussed in Chapter 10 of Part II.

Another option is to put the airplane in the 'de-facto stable' category and proceed to Step 9.

Step 8: Carry out the instructions in the first two paragraphs of Step 6: the result is the inherent phugoid damping ratio, ζ_p. Note from Appendix B, Par.3.2.1.2 that the Level 1, minimum required phugoid damping ratio is: $\zeta_p = 0.04$. If the inherent phugoid damping ratio is insufficient, augmentation can be accomplished with speedbrake or throttle (i.e. thrust) feedback to speed. The required feedback gains can be found as follows:

1. For speed feedback to a speedbrake:

Compute the required increment in the speed-damping derivative, C_{D_u} from:

$$\Delta C_{D_u} = \{(0.08 C_{L_1} U_1 \omega_{n_p})/g\} - C_{D_u} - 2C_{D_1} + C_{T_{x_u}} + 2C_{T_{x_1}} \qquad (3.15)$$

Compute the speedbrake feedback gain from:

$$k_{u/\delta_{sb}} = \Delta C_{D_u} / (U_1 C_{D_{\delta_{sb}}}) \qquad (3.16)$$

The magnitude of this gain should not exceed a value of 150 degrees of speedbrake deflection per unit of u/U_1.

The drag-due-to-speedbrake derivative $C_{D_{\delta_{sb}}}$ may be computed using the 'spoiler drag' method of Sub-section 4.12.1 in Part VI.

For speed feedback to throttle:

Compute the required increment in $C_{T_{x_u}}$ from:

$$\Delta C_{T_{x_u}} = -\{(0.08 C_{L_1} U_1 \omega_{n_p})/g\} - C_{D_u} - 2C_{D_1} + C_{T_{x_u}} + 2C_{T_{x_1}} \qquad (3.17)$$

Compute the throttle feedback gain from:

$$k_{u/\delta_T} = \Delta C_{T_{x_u}} / (U_1 C_{T_{\delta_T}}) \qquad (3.18)$$

The magnitude of this feedback gain should not exceed a value which corresponds to more than 15 percent increase in thrust for a sheargust of 25 fps.

The thrust-coefficient-due-to-throttle derivative, $C_{T_{\delta_T}}$ follows from taking the slope of thrust coefficient versus throttle position of the engine, remembering that:

$$C_T = T/\bar{q}S \qquad (3.19)$$

where: T is the installed thrust of the engine. It may be found with the method of Chapter 6 in Part VI.

For more detailed methods of synthesizing speed-damping feedback systems, refer to Chapter 13 of Reference 12.

Step 9: For the appropriate flight conditions and for the airplane configurations of Step 2 AND for the n_a values of Step 3, find the allowable short period frequency values from Figures B.1 through B.3 in Appendix B.

Decide which frequency levels the airplane should have for each flight condition. Such a frequency level is called: $\omega_{n_{SP_{de\text{-}facto}}}$.

Compute the 'de-facto' level of static stability at which the airplane should operate from:

$$(C_{m_\alpha})_{de\text{-}facto} = \qquad (3.20)$$

$$\{(Z_\alpha M_q/U_1) - (\omega_{n_{SP_{de\text{-}facto}}})^2\}(I_{yy}/\bar{q}S\bar{c})$$

Find the angle-of-attack feedback gain, k_α from:

$$k_\alpha = \{(C_{m_\alpha})_{\text{de-facto}} - C_{m_\alpha}\}/C_{m_{\delta_e}} \qquad (3.21)$$

where: C_{m_α} is the inherent value of the static longitudinal stability derivative of the airplane. This value will normally be positive (unstable) for a 'de-facto' stable airplane!

The value for k_α should not be larger than 5 degrees of elevator deflection per degree of angle of attack. If k_α does not satisfy this condition, the longitudinal control power level, $C_{m_{\delta_e}}$ must be increased until it does.

Note: if the feedback is around the stabilizer instead of around the elevator, replace the elevator derivative by the stabilizer derivative in Equation (3.16).

Step 10: For the appropriate flight conditions and for the airplane configurations of Step 3, find the minimum allowable damping ratios at which the airplane should operate by using Table IV in Appendix B. This damping ratio level is called: $\xi_{SP_{\text{de-facto}}}$.

Compute the 'de-facto' level of C_{m_q} at which the airplane should operate from:

$$C_{m_{q_{\text{de-facto}}}} = -(2\omega_{n_{SP_{\text{de-facto}}}} \xi_{SP_{\text{de-facto}}}) + -(Z_\alpha/U_1) - M_\alpha \qquad (3.22)$$

Compute the pitchrate feedback gain from:

$$k_q = \{(C_{m_{q_{\text{de-facto}}}} - C_{m_q})(\bar{c}/2U_1)\}/C_{m_{\delta_e}} \qquad (3.23)$$

The magnitude of this gain should not exceed 2 deg/deg/sec. If it does, the airplane needs more control power.

Step 11: Document the results obtained, including any design changes made.

3.4 DYNAMIC LATERAL-DIRECTIONAL STABILITY

3.4.1 Applicable Regulations

Civil: FAR 23.181 and FAR 25.181, see Appendix A.

Military: Mil-F-8785C, Par.3.3.1, see Appendix B.

3.4.2 Relationship to Preliminary Design

See Part II, Step 24 in Chapter 2.

3.4.3 Mathematical Model for Analyzing Lateral-Directional Dynamic Stability

Because the civil regulations in Appendix A are vague about specific requirements of frequency, damping and time-constant characteristics it is customary to use the military regulations of Appendix B to verify whether or not a new civil airplane design meets the intent of the regulations.

The civil and military requirements for dynamic stability must be met with the cockpit controls held fixed as well as with the cockpit controls kept free. The analysis of dynamic stability with the controls held free is beyond the scope of preliminary design since it requires detailed design data on the flight control system. For that reason, only the 'controls fixed' case is considered here. An analytical approach to the analysis of dynamic stability with controls free is given in Reference 12.

The military regulations (Apppendix B) specify ranges of acceptable values for the following dynamic stability parameters:

For the spiral mode: minimum allowable time-to-double the amplitude, T_{2_S}

For the dutch roll mode: minimum allowable undamped natural frequency, ω_{n_D}

minimum allowable damping ratio, ζ_D

minimum allowable real root part value: $\omega_{n_D}\zeta_D$

For the roll mode: see Section 2.7.

The following characterization is typical of the

modal breakdown for most airplanes in most flight conditions:

Mode	Undamped Natural Frequency	Damping Ratio	Time Constant	Most Important Motion Variables
Spiral	N.A.	N.A.	Large, Unstable	Heading and bank angles
Dutch Roll	Moderately High	Low	N.A.	Sideslip and bank angles
Roll	N.A.	N.A.	Small	Bank angle

Note: Roll mode requirements are discussed in Section 2.7

The spiral behavior primarily affects the pilot's ability to maintain wings level flight, particularly when in IFR conditions.

The dutch roll behavior tends to make passengers sick if it is undamped. If the dutch roll mode has a high degree of bank angle participation, it can interfere with a pilot's ability to carry out rapid rolling maneuvers and/or bank angle tracking maneuvers.

The spiral and dutch roll mode behavior can be obtained from a solution of the three-degree-of-freedom, small perturbation equations of motion of an airplane. General methods (so-called Class III methods) for solving such equations are given in Chapter 6 of Reference 12. In preliminary design it is acceptable to employ approximations for the spiral and for the dutch roll behavior of an airplane. The Class II methods to be presented in Subsections 3.4.3.1 and 3.4.3.2 are based on such approximate methods. The justification for these Class II methods is also discussed in Chapter 6 of Reference 12.

3.4.3.1 Class II method for analysis of the spiral characteristics

There is no requirement for a stable spiral root. In fact, too much spiral stability is considered undesirable in most airplanes. An acceptable Class II condition for spiral stability is:

$$L_\beta N_r - N_\beta L_r > 0 \qquad (3.24)$$

If this spiral stability condition is violated (as

is often the case), an acceptable Class II method for predicting the time-to-double the amplitude in the spiral mode is:

$$T_{2_S} = (L_\beta \ln 2)/(N_\beta L_r - L_\beta N_r) \qquad (3.25)$$

All dimensional stability derivatives in Equations (3.24) and (3.25) are defined in the list of symbols. The corresponding dimensionless derivatives may be computed with the methods of Chapter 10 in Part VI.

3.4.3.2 Class II method for analysis of the dutch roll characteristics

The following Class II method is suggested for the calculation of the dutch roll undamped natural frequency and damping ratio:

$$\omega_{n_D} = [\{Y_\beta N_r + N_\beta (U_1 - Y_r)\}/U_1]^{1/2} \qquad (3.26)$$

$$\zeta_D = -\{N_r + (Y_\beta/U_1)\}/2\omega_{n_D} \qquad (3.27)$$

All dimensional stability derivatives in Equations (3.26) and (3.27) are defined in the list of symbols. The corresponding dimensionless derivatives may be computed with the methods of Chapter 10, Part VI.

IMPORTANT OBSERVATION ON EQUATION (3.27):

This equation predicts that the dutch roll damping ratio will always be positive. This is NOT correct! The problem is that this dutch roll approximation ignores the effects of the derivatives C_{l_β}, C_{l_p} and C_{n_p}.

If this equation predicts the damping ratio to be less than 0.05, it is suggested that the reader use the Class III method of Chapter 6, Reference 12 to predict the actual dutch roll damping ratio.

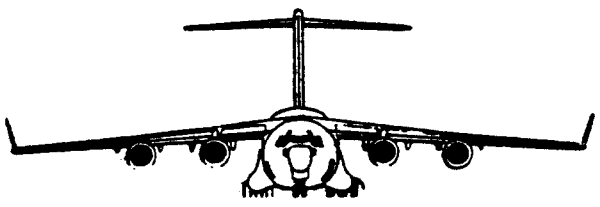

3.4.4 Step-by-Step Procedure for Analyzing Dynamic Lateral-Directional Stability

Step 1: Determine which regulations apply to the design: see Table 1.3 and Subsection 3.4.1.

Step 2: Determine from the description of airplane Classes in Appendix B which airplane Class (I, II, III or IV) best 'fits' the design.

Step 3: Determine for which flight conditions and for which airplane configurations the dynamic stability must be verified. Determine which flight phase category (A, B or C) is associated with each flight condition. The definition of flight phase categories is given in Appendix B.

Tabulate this information.

NOTE: Be sure to read the guidelines stated under Step 3 in Subsection 3.3.4 (pages 80-81)!

Step 4: For the flight conditions and for the airplane configurations defined in Step 3, calculate the derivatives and other parameters which appear in Eqns. (3.24) through (3.27).

Step 5: Decide whether the airplane is to be 'inherently' stable or 'de-facto' stable.

Definitions for these types of stability are given on pages 65-67.

If the airplane is to be 'inherently stable' proceed to Step 6.

If the airplane is to be 'de-facto' stable, proceed to Step 8.

The choice between 'inherent' and 'de-facto' stability is made by the designer and not by the regulations!

Step 6: Determine whether or not the airplane is spirally stable with the help of Eqn.(3.24).

Case 1: Stable spiral

If the airplane is found to be spirally stable, it may in fact be too spirally stable!

Since specific levels of spiral stability are not required by the regulations, the designer should check how much of a change in the derivative L_β (i.e. C_{l_β}) is needed to obtain neutral spiral stability. The required change in L_β can normally be achieved through a change in the wing geometric dihedral angle. The required change in the wing geometric dihedral angle can be obtained with Eqn.(10.34) on p.392 of Part VI. Recalculate L_β as required!

Case 2: Unstable spiral

If the airplane is found to be unstable in the spiral mode, use Eqn.(3.25) to find the spiral 'time-to-double' the amplitude.

From the regulations determine whether or not the Level 1 requirements are met. If not, use Eqn.(3.25) to determine that value of L_β (and C_{l_β}) for which the Level 1 requirement is met. Use Eqn.(10.34) on p.392 of Part VI to determine the change in wing geometric dihedral angle needed to get the required Level 1 value of T_{2_S}. Recalculate L_β as required!

IMPORTANT NOTE: When it is decided to change the wing geometric dihedral angle, make sure that the lateral landing gear clearance criterion of Figure 9.1b, page 221 of Part II is not violated!

Step 7: Use Equations (3.26) and (3.27) to find the dutch roll characteristics of the airplane.

From the regulations determine whether or not Level 1 requirements are met. If not, use Eqns.(3.26) and (3.27) to find 'compatible' values for N_r and N_β so that the Level 1 requirements are met.

NOTE 1: The reader will usually find that the undamped natural frequency of Eqn.(3.26) is 'driven' by N_β, while the damping ratio of Eqn. (3.27) is 'driven' by N_r.

NOTE 2: from Part VI, Equations (10.43) and (10.88) the reader will be able to verify that N_r and N_β BOTH depend on:

1. Vertical tail size
2. Vertical tail moment arm
3. Vertical tail lift-curve-slope and therefore on vertical tail planform geometry

'Compatible' values for N_r and N_β are required because of these relationships.

Make the necessary changes in the design and check that the spiral condition has not been significantly affected. If it has, an iteration between Steps 6 and 7 will be needed.

Step 8: Using Equations (3.25) - (3.27) determine the spiral and dutch roll characteristics of the airplane. Check these characteristics against the requirements of Appendix B, Tables VI and VIII and determine the level of handling qualities for the airplane.

It will now be necessary to determine what type of feedback is required to 'augment' the airplane such that it meets the Level 1 requirements. When it does, it is referred to as a 'de-facto' stable airplane. The following requirements for feedback may arise:

1) sideslip angle feedback: this changes C_{y_β}, C_{l_β} and C_{n_β}

2) yawrate feedback: this changes C_{y_r}, C_{l_r} and C_{n_r}

3) rollrate feedback: this changes C_{y_p}, C_{l_p} and C_{n_p}

The usual procedure is:

Step 8.1: Find those values of N_r, N_β and L_β which meet Level 1 requirements for the dutch roll and spiral characteristics as expressed by Equations (3.25) - (3.27).

NOTES: 1) Use Eqn.(3.26) to find the value of N_β which

meets Level 1 frequency requirement

2) Use Eqn.(3.27) to find the value of N_r which meets Level 1 damping requirements: using the 'new' frequency value!

3) Use Eqn.(3.25) to find the value of L_β which meets Level 1 time-to-double-spiral-amplitude.

Step 8.2: By subtraction, determine the 'increment', (Δ = de-facto - inherent) in each derivative which must be generated by the feedback system.

Step 8.3: Estimate the feedback gains and judge them by an acceptability criterion.

The feedback gains may be estimated from:

$$k_{\beta/\delta_r} = (C_{n_\beta}{}_{\text{de-facto}} - C_{n_\beta}{}_{\text{inherent}})/C_{n_{\delta_r}} \quad (3.28)$$

$$k_{r/\delta_r} = (C_{n_r}{}_{\text{de-facto}} - C_{n_r}{}_{\text{inherent}})b/(2U_1 C_{n_{\delta_r}}) \quad (3.29)$$

$$k_{\beta/\delta_a} = (C_{l_\beta}{}_{\text{de-facto}} - C_{l_\beta}{}_{\text{inherent}})/C_{l_{\delta_a}} \quad (3.30)$$

Gains estimated from Eqns.(3.28) - (3.30) are judged acceptable in preliminary design if they satisfy the following inequalities:

$$(k_{\beta/\delta_r})_{\beta\,\text{expected}} < 0.3\delta_{r\,\text{available}} \quad (3.31)$$

$$(k_{r/\delta_r})_{r\,\text{expected}} < 0.3\delta_{r\,\text{available}} \quad (3.32)$$

$$(k_{\beta/\delta_a})_{\beta\,\text{expected}} < 0.3\delta_{a\,\text{available}} \quad (3.33)$$

The 'expected values of the sideslip and yawrate perturbations in Equations (3.29) - (3.32) depend on the type of airplane being designed. The following guidelines are suggested:

Airplane Type	$\beta_{expected}$	$r_{expected}$
Transports	5 deg	10 deg/sec
Fighters	10 deg	20 deg/sec
Light airplanes	10 deg	20 deg/sec

The reader is referred to Chapter 6 of Reference 12 for the development of the theory behind these gain estimations.

If the gain acceptability criteria are violated, the airplane does not have sufficient control power to be augmented to Level 1 requirements. The designer should incorporate the necessary design changes to increase the appropriate control power levels. Control power equations in Section 10.3 of Part VI should be used to determine which design changes are feasible. In some cases it will be found necessary to introduce new control surfaces and/or to scrap the design and start from scratch!

Step 9: Document the results obtained, including any design changes made.

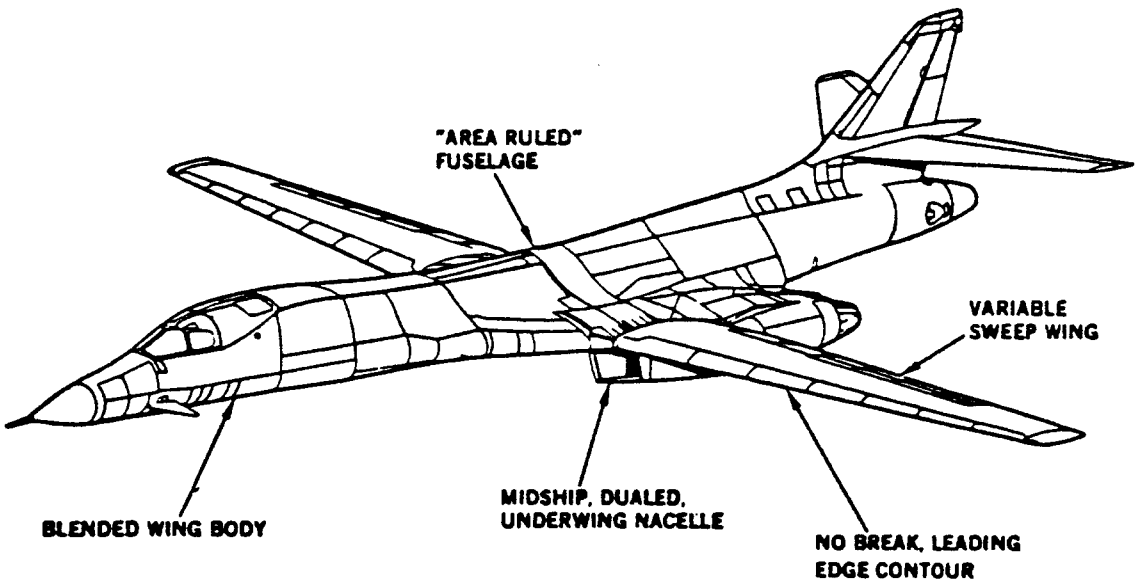

3.5 DYNAMIC COUPLING

3.5.1 Applicable Regulations

Civil: There are no specific regulations governing dynamic coupling phenomena. However, the FAR's can be interpreted as requiring that no dynamic coupling phenomena may exist which make normal piloting difficult.

Note: the only type of civil airplanes which conceivably might encounter dynamic coupling phenomena are aerobatic type airplanes.

Military: Mil-F-8785C, Par.3.4.3, see Appendix B

Notes: 1) Roll-rate coupling into pitch and yaw degrees of freedom occurs in fighter type airplanes during combat roll rate maneuvers.

2) Pitch-rate coupling into the lateral-directional degrees of freedom occurs in fighter type airplanes during rolling pull-up or during rolling push-over maneuvers.

3.5.2 Relationship to Preliminary Design

Dynamic coupling was not addressed in Part II.

3.5.3 Mathematical Model for Analyzing Dynamic Coupling

Two types of dynamic coupling phenomena will be addressed:

3.5.3.1 Roll-rate coupling

3.5.3.2 Pitch-rate coupling

3.5.3.1 Roll-rate coupling

As shown in Chapter 7 of Reference 12, when roll-rate coupling is divergent, violent excursions in angle of attack and/or in sideslip angle may occur during combat roll-rate maneuvers. These excursions can be so violent, that structural failure occurs.

A theoretical model for determining whether or not an airplane will experience roll-rate coupling induced instabilities is discussed in Chapter 7 of Reference 12. Based on this mathematical model the following condition for stability can be derived:

$$[[(M_q N_r/M_\alpha) + D_1 + (N_\beta/M_\alpha)C_1]^2 +$$

$$- 4C_1 D_1 (N_\beta/M_\alpha)] < 0 \qquad (3.34)$$

where: all dimensional derivatives are defined in the list of symbols.

$$C_1 = (I_{xx} - I_{zz})/I_{yy} \qquad (3.35)$$

$$D_1 = (I_{yy} - I_{xx})/I_{zz} \qquad (3.36)$$

The moments of inertia in Eqns (3.35) and (3.36) must be determined in the airplane stability axes system!!

3.5.3.2 Pitch-rate coupling

No suitable Class II mathematical model is available for the analysis of pitch-rate coupling into the lateral-directional degrees of freedom. For a Class III method, the reader is referred to Chapter 7 of Reference 12.

3.5.4 Step-by-Step Procedure for Analyzing Roll-rate Coupling

Step 1: Read the applicable regulation, see 3.5.1.

Step 2: From the operational flight envelope of the airplane, determine the flight conditions and airplane configurations for which roll-rate coupling must be analyzed.

Note: flight conditions which are critical for roll coupling are usually those at moderate to high altitude.

Step 3: For the flight conditions and airplane configurations of Step 2 determine the dimensional derivatives which occur in Eqn.(3.34)

Note: for a highly augmented airplane, these derivatives must include the effect of the stability augmentation system.

Step 4: Using Eqn.(3.34) determine whether or not the airplane has roll-rate coupling instability. If not, proceed to Step 8, otherwise proceed to Step 5.

Step 5: Determine the minimum roll-rate for which roll-rate coupling instability instability occurs from the method of Chapter 7, Ref.12.

Step 6: Determine the maximum roll rate of which the airplane is capable from:

$$|p_{max}| = |-(L_{\delta_a} \delta_{a_{max}})/L_p| \qquad (3.37)$$

where: all dimensional stability derivatives are defined in the list of symbols.

If the airplane maximum roll rate from Eqn.(3.37) is less than that of Step 5, proceed to Step 8, if not, proceed to Step 7.

Step 7: Investigate with the help of Eqn.(3.34) what values the derivatives must have to assure that the airplane is stable against roll-rate coupling. These new values are the so-called 'augmented' (or 'de-facto') values which these derivatives must have to prevent roll coupling instability.

With the help of Equations (3.28) - (3.30), determine the required feedback gains.

Next, using the acceptability criteria as expressed by Eqns (3.31) - (3.33) determine whether or not sufficient control power is available in the airplane. If not, introduce the necessary design changes.

Step 8: Document the results obtained as well as any design changes made.

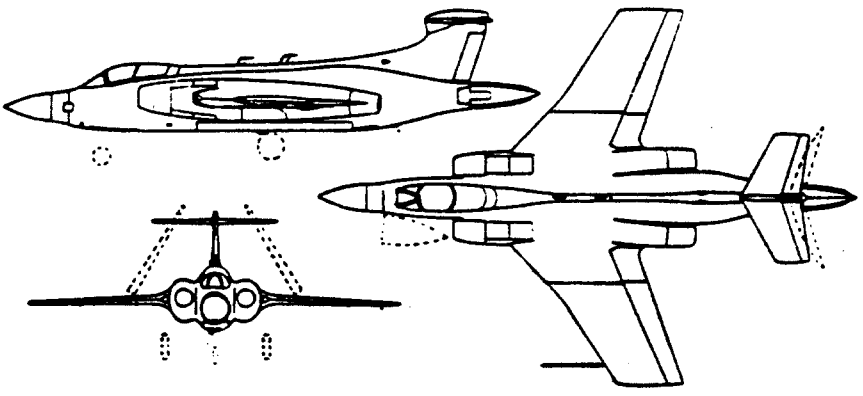

3.6 STALL CHARACTERISTICS

3.6.1 Applicable Regulations

Civil: FAR 23.201, 23.203, 23.305 and 23.207, see Appendix A.

FAR 25.201, 25.203, 25.205 and 25.207, see Appendix A.

Military: Mil-F-8785C, Par.3.4.2, see Appendix B

3.6.2 Relationship to Preliminary Design

See Step 6 in Preliminary Design Sequence I, p.12, Chapter 2 in Part II. Also see Chapter 7 in Part II and Subsection 5.1.4 in Part III.

3.6.3 Mathematical Model for Analyzing Stall Characteristics

Stall characteristics must be shown to satisfy the regulations for stalls starting from the following types of flight condition:

1. Wings level flight

2. Turning flight, including accelerated stalls

3. Engine-out stalls

The regulations essentially require that the airplane possess the following desirable tendencies when put in an approach to any of these stalls:

A. No sudden, uncontrollable pitch-up

B. Adequate roll control and no more wing drop than specified in the regulations

C. Adequate directional control

D. Adequate stall warning

E. Resistance to spin departure.

There are no closed form Class II methods for assuring satisfactory stall characteristics, with the exception of item E.

The following fundamental characteristics will nor-

mally lead to acceptable stall behavior relative to A-D.

1. Spanwise lift distributions which are conducive to wing root stall instead of to wing tip stall. Read the suggestions on wing design in Chapter 4 of Part III.

2. Wingtip mounted roll control devices when used to 25 percent of maximum available should not produce wing tip stall.

3. The location of the horizontal tail relative to the wing should satisfy the 'no-pitch-up' design criteria of Subsection 5.1.4 in Part III, or if not, the appropriate stick-shaker and stick pusher systems must be installed.

4. The rudder should not be blanked by a stalled wing wake emanating from the wing root or from any other sources of separated flow (such as from nacelles or from leading edge strakes). Read the suggestions on empennage design in Chapter 5 of Part III.

Methods for determining spanwise lift distributions are presented in References 14 and 15.

As for item E, an airplane has been found to be resistant to spin departure as long as its so-called $C_{n_{\beta_{dyn}}}$ is positive:

$$C_{n_{\beta_{dyn}}} = \{C_{n_{\beta_B}} + - (I_{zz_B}/I_{xx_B})C_{l_{\beta_B}} (\tan\alpha)\}\cos\alpha > 0 \qquad (3.38)$$

3.6.4 Step-by-Step Procedure for Analyzing Stall Characteristics

Step 1: Read the applicable regulations, see Table 1.3 and Section 3.6.1.

Step 2: From the regulations determine the flight conditions and airplane configurations for which satisfactory stall characteristics must be shown.

Step 3: For the flight conditions and airplane configurations of Step 2 determine the spanwise

lift distribution for a range of angles of attack. Also determine the spanwise variation of section (= airfoil) maximum lift coefficient. Be sure to account for the effect of Reynold's Number!!

This is readily done with the method of Sub-sub-section 8.1.3.4 (pages 256-257), Pt VI.

1. The span location where tangency occurs between the two spanwise distributions is the span location where the wing will begin to stall. This span location must be close to the wing root for satisfactory stall characteristics.

   If stall occurs close to the tip, the wing design should be changed. Possible design changes are:

   a) addition of twist (or wash-out)
   b) change to airfoils capable of higher maximum lift coefficient values at the appropriate Reynold's Numbers.
   c) a variation of b) is to add leading edge droop to the outboard wing.

2. The angle of attack where tangency of item one first occurs is the value of WING angle of attack for which the stall will occur. Remember that the airplane angle of attack differs from the wing angle of attack by the wing incidence angle!

3. If the decision is made to 'live' with outboard wing stall, a stick-shaker and/or a stick-pusher may have to be installed. In such an event, the value of lift coefficient corresponding to that at which the stick-pusher is triggered must be used as the effective value of wing maximum lift coefficient.

Step 4: Determine the airplane pitch-up characteristics with the guidelines of Subsection 5.1.4 of Part III. If a stick-pusher is required, see item 3.) under Step 3.

Step 5: Determine whether directional control at the stall is available by sketching in the location of the separated wing-root wake at the

tail location of the airplane: see Fig.5.13 in Part III.

Step 6: For the conditions of Step 2, compute the body axis directional and lateral stability derivatives as well as the moments of inertia in Eqn.(3.38) and verify whether the corresponding spin departure resistance criterion is met. If not, introduce the required design changes.

Note: these design changes can take the form of a larger or relocated vertical tail (or tails), a change in wing geometric dihedral and/or a change in mass distribution.

Step 7: Document the results obtained as well as any design changes made.

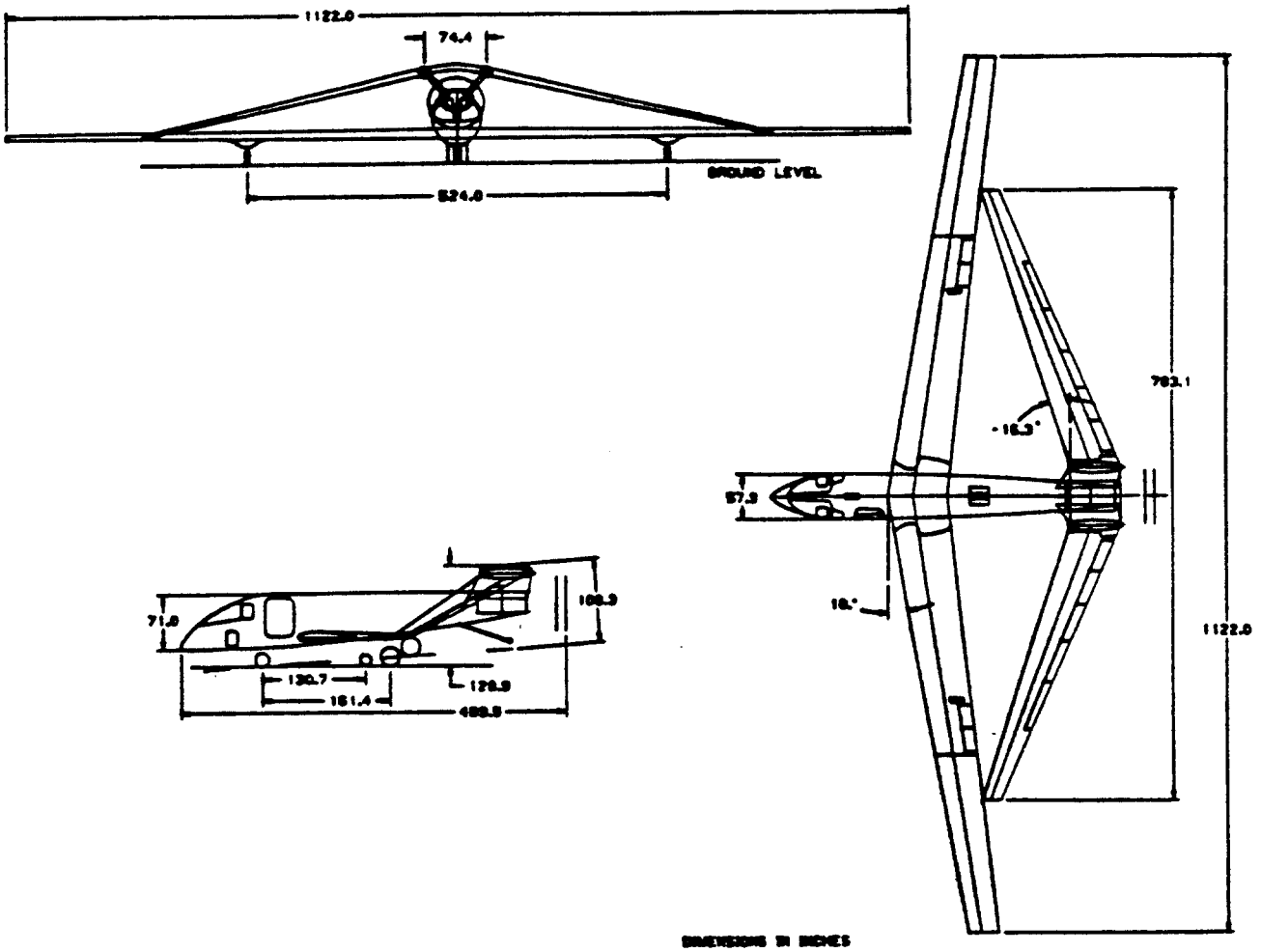

3.7 SPIN CHARACTERISTICS

3.7.1 Applicable Regulations

Civil: FAR 23.221, see Appendix A.

Military: Mil-F-8785C, Par.3.4.2.2, see Appendix B

3.7.2 Relationship to Preliminary Design

See Chapter 5 in Part III!

3.7.3 Mathematical Model for Analyzing Spin Characteristics

There is no suitable mathematical model for Class I design analysis purposes. A method for predicting aerodynamic forces and moments on a spinning airplane is given in Reference 16.

3.7.4 Step-by-Step Procedure for Analyzing Spin Characteristics

Step 1: Read the applicable regulations, see Table 1.3 and Section 3.7.1.

Step 2: From the regulations determine the flight conditions and airplane configurations for which satisfactory spin characteristics must be shown.

Step 3: Read the sections on aircraft spin and corresponding design guidelines in Stinton, Reference 17, pages 464 - 490. Check the design of the airplane in terms of the 'Stinton' approach and make design adjustments where required.

Step 4: Document the results obtained as well as any design changes made.

3.8 AEROELASTIC CONSIDERATIONS

All stability derivatives used in determining dynamic stability characteristics in this chapter are subject to aeroelastic effects. The method of Section 2.9 can be applied to all stability and control derivatives of Ch.3. Highly elastic airplanes, such as very large transport airplanes, are also subject to acceleration/mass induced aeroelastic effects. Acceleration/mass effects are discussed in detail in Chapter 8 of Reference 12.

4. RIDE AND COMFORT CHARACTERISTICS

The purpose of this chapter is to provide methods and guidelines for the analysis and selection of those design aspects which influence the ride and comfort characteristics of airplanes. These characteristics are important for the following reasons:

1. If ride and comfort are not acceptable to passengers, they are unlikely to return for another flight. This hurts the commercial viability of an airplane!

2. If ride and comfort are not acceptable to crewmembers, they may not be able to carry out their duties thus negatively affecting safety and/or mission effectiveness!

The following aspects of ride and comfort can be important, depending on such factors as time exposure and the requirement to perform duties:

1. Airplane response to atmospheric turbulence:

   High levels of vertical and lateral accelerations are uncomfortable to passengers and may make it difficult (sometimes impossible) for crew members to carry out their duties.

   Additional factors to be considered here are:

   a) distance to the center of gravity
   b) flexible (elastic) behavior of the structure

2. Cabin interior noise and temperature

3. Cabin (or cockpit) interior dimensions

4. Seat dimensions and seat comfort

References 18 through 23 should be consulted for detailed information (and further references) on the importance of these factors to ride and comfort.

Neither military nor civil regulations contain specific numerical design guidelines for the above factors. The design guidelines given in this chapter cover only turbulence induced accelerations as experienced by the crew and by the passengers. These design guidelines,

augmented with the use of 'common sense' and the use of 'standard' design practice in the other areas should suffice during the preliminary design evaluation of a new airplane.

The material in this chapter is organized as follows:

4.1 Relationship to preliminary design
4.2 Mathematical model for analyzing ride characteristics
4.3 Step-by-step procedure for analyzing ride characteristics

4.1 RELATIONSHIP TO PRELIMINARY DESIGN

Selection of wing loading (W/S), wing planform (A, Λ_{le}, λ), fuselage and cockpit interior dimensions and seating arrangement all affect the ride and comfort of passengers and crew members. Having said that, it is sobering to reflect on the following statements:

1. The airplane sizing process described in Part I results in a choice of wing-loading without even considering ride characteristics!

2. The decisions made in P.D. Sequence I, Steps 4 and 6 (Part II) came about without specific reference to comfort and ride!

As a result of the ride analysis and ride criteria presented in Section 4.2, the designer may wish to modify some of these early design decisions. However, the effect of such design changes on performance and/or on stability and control must be assessed!

For some airplane missions, flight through moderate to severe turbulence may be necessary. Examples are:

1. Low altitude attack missions
2. Pipeline spotting missions

In such cases, designing the basic airplane and its wing for reasonable ride quality levels at the crew station, turns out to be not feasible. In such cases it may become necessary to employ a so-called 'ride-control system'. The B-1 bomber has such a ride control system. A schematic of this type of system is shown in Figure 4.1.

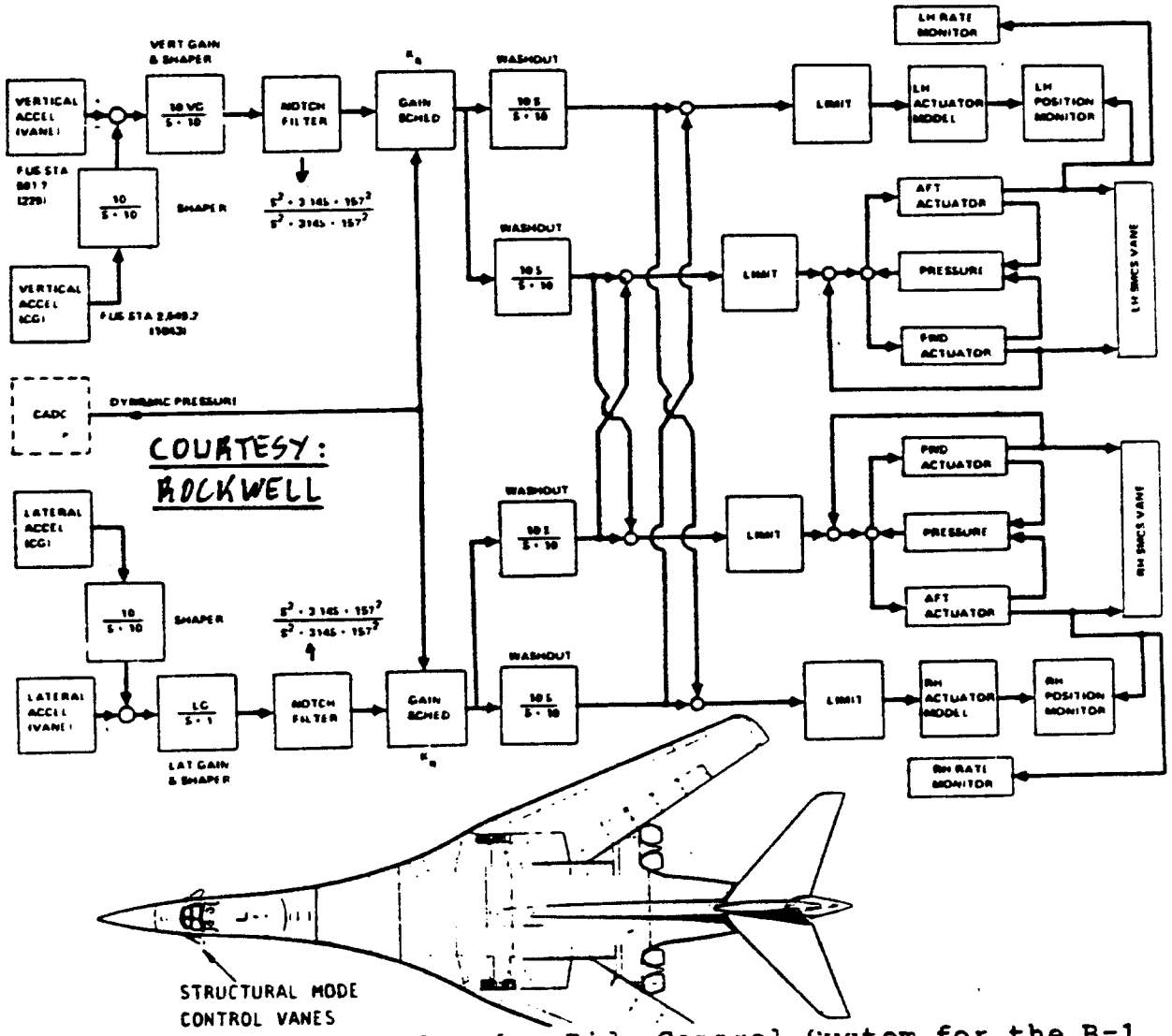

Figure 4.1 Example of a Ride Control System for the B-1

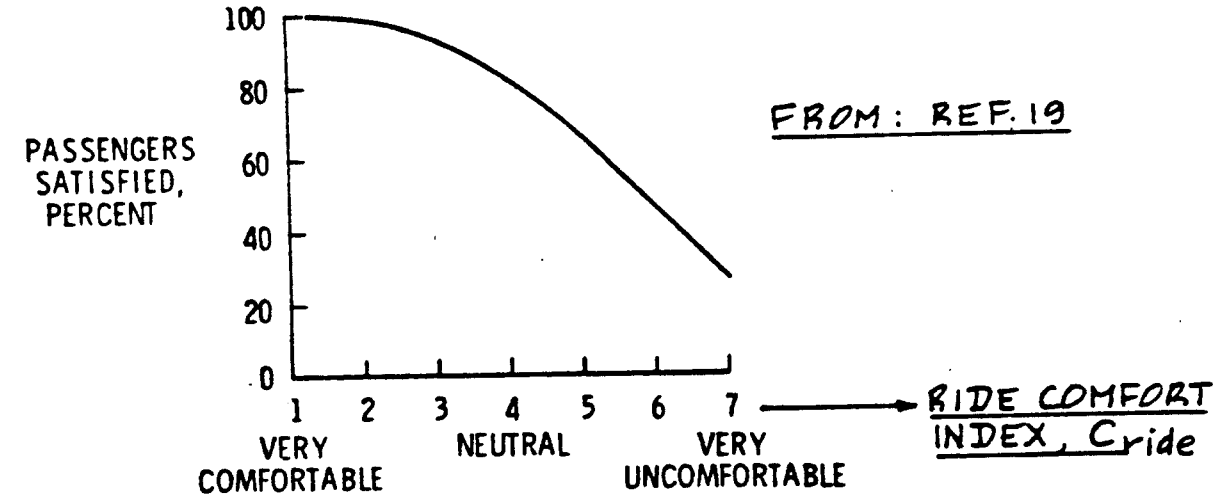

Figure 4.2 Effect of Ride Comfort Rating on Percentage of Passengers Satisfied with the Ride

4.2 MATHEMATICAL MODEL FOR ANALYZING RIDE AND COMFORT CHARACTERISTICS

Two ingredients are required for analyzing the ride characteristics of a new design:

1. A ride characteristic rating scale (metric)
2. A formula which relates vehicle design parameters to that metric.

Two models will be presented:

4.2.1 A model for the prediction of ride comfort from a passenger viewpoint (civil and military)

4.2.2 A model for the prediction of ride comfort from a crew station viewpoint (civil or military)

4.2.1 A Model for the Prediction of Ride Comfort from a Passenger Viewpoint (Civil or Military)

The following model was distilled from Reference 18.

The relative ride-comfort will be measured in terms of a ride comfort index, C_{ride} which is related to passenger satisfaction in Figure 4.2. In this section, only the effect of vertical and lateral accelerations on this ride comfort index will be accounted for.

The effect of airplane vertical and lateral accelerations (in response to atmospheric turbulence) on the ride comfort index, C_{ride} may be estimated from:

$$C_{ride} = 2 + 18.9a_{vert} + 12.1a_{lat} \qquad (4.1a)$$

which applies for $a_{vert} > 1.6a_{lat}$, and:

$$C_{ride} = 2 + 1.62a_{vert} + 38.9a_{lat} \qquad (4.1b)$$

which applies for $a_{vert} < 1.6a_{lat}$

where: the accelerations a_{vert} and a_{lat} are measured in relative 'g'-level ('g'/fps of vertical or lateral rms gust). They are measured at the center of

gravity of the airplane and can be found from:

$$a_{vert} = (0.5\rho U_1)(C_{L_\alpha})(\sigma_w)/(W/S) \qquad (4.2)$$

and:

$$a_{lat} = (0.5\rho U_1)(C_{y_\beta})(\sigma_v)/(W/S) \qquad (4.3)$$

where: the derivatives C_{L_α} and C_{y_β} are for the entire airplane (in 1/rad). Part VI contains methods for their estimation. For elastic airplanes, the method of Section 3.8 should be used.

σ_w and σ_v are the rms of gust (or turbulence) velocities induced by the atmosphere. Their values depend on altitude, terrain and probability of occurrence. Figure 4.3 can be used to determine these gust values.

4.2.2 A Model for the Prediction of Ride Comfort from a Crew Station Viewpoint (Civil or Military)

In preliminary design it is acceptable to use the following criterion for the acceptability of turbulence response at the crew station:

$$\bar{A} < 0.005 \qquad (4.4)$$

where: $\bar{A}$ is the 'rms g-level' per fps gust input at the crew station. This gust (or turbulence) response may be computed from:

$$\bar{A} = (0.5\rho U_1 C_{L_\alpha})K_1K_2/(W/S) \qquad (4.5)$$

$$\text{with: } K_1 = 0.66 + (0.39/\bar{c})l_{crew} \qquad (4.6)$$

where: $\bar{c}$ is the wing m.g.c. in ft

l_{crew} is the distance from the crew station to the leading edge of the wing m.g.c., in ft

C_{L_α} is the airplane liftcurve slope in 1/rad. Aeroelastic effects on

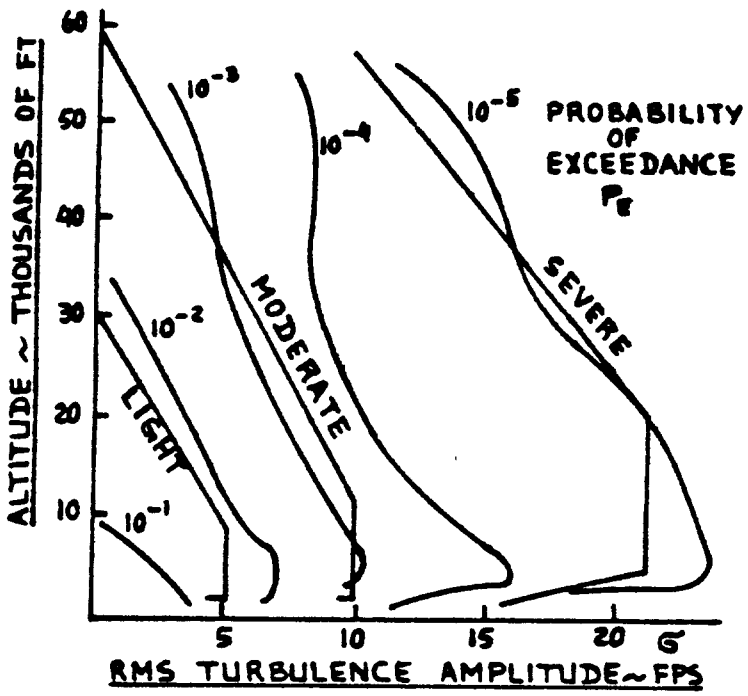

FROM: FIG. B7, APPENDIX B

Figure 4.3 Root Mean Square (RMS) Gust or Turbulence Amplitudes as Related to Altitude and Probability of Exceedance

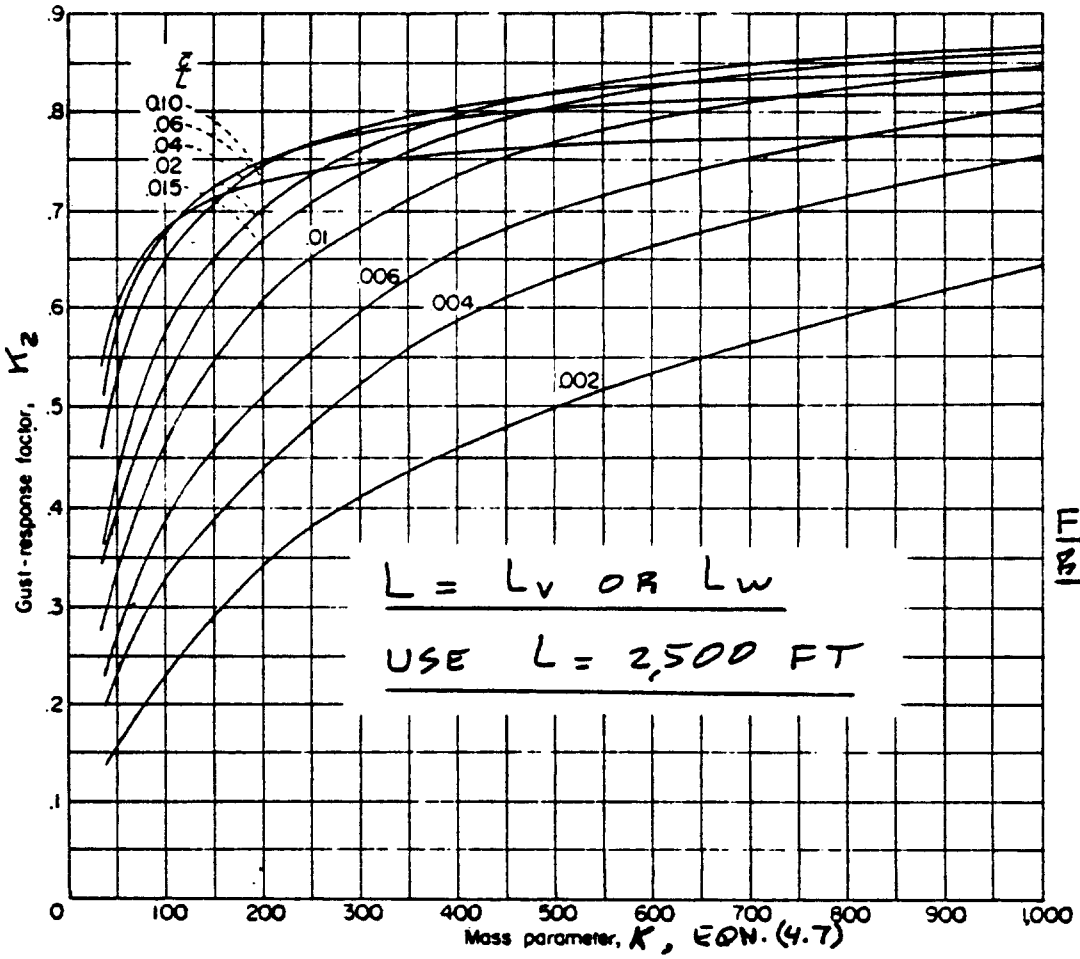

FROM: REF. 25

Figure 4.4 Effect of Gust Length and Mass Parameter on Gust Response Factor

this derivative may have to be accounted for: see Section 3.8.

K_2, the gust response factor, is found from: Figure 4.4.

Notes: 1.) In Figure 4.4, $L_{v \text{ or } w}$ is the so-called gust length. In preliminary design it is acceptable to use: $L_{v \text{ or } w} = 2{,}500$ ft

2. Also in Figure 4.4:

$$K = 4W/(32.2\pi\rho S\bar{c}) \qquad (4.7)$$

To give the reader a 'feel' for the meaning of ride criterion (4.4), consider the following. Table 4.1 lists a subjective crew rating of how rms vertical accelerations are perceived by pilots.

If an airplane with an $\bar{A}$ value of 0.005 at sealevel, encounters a rms vertical gust at sealevel of 10 fps (P = 0.001), the crew would feel a 0.05 rms 'g' level.

Table 4.1 Subjective Ratings of Vertical Acceleration

Pilot's Description of Turbulence		RMS Vertical Acceleration in 'g'
Negligible	(Data from:	0.05
Slight	Ref.20)	0.10
Moderate		0.10 - 0.15
Moderately Heavy		0.20 - 0.30
Severe		0.30 - 0.60
Extreme		0.60

4.3 STEP-BY-STEP PROCEDURE FOR ANALYZING RIDE AND COMFORT CHARACTERISTICS

Step 1: For those flight conditions and configurations for which ride qualities are a concern, list:

Weight, Mach Number (and Speed), altitude and configuration (flaps, power, loading, etc.).

Step 2: For the flight conditions of Step 1, determine:

a) the derivatives C_{y_β} and C_{L_α}

Note: include the effect of aeroelasticity

when necessary!

b) the atmospheric density

c) the wing loading, W/S

d) the gust (turbulence) rms values from Figure 4.3. In preliminary design a probability level of 0.01 or 0.001 is usually appropriate.

Step 3: Using Eqns.(4.2) and (4.3) compute the relative accelerations and using Eqn.(4.1) determine the comfort index. Use Figure 4.1 to determine the percentage of satisfaction with the ride.

This percentage of satisfaction should be about 80. If it is less, a design change should be considered.

From Eqns.(4.1)-(4.3) it is evident that the wing loading, W/S and the vertical tail size and shape are the only available design parameters. The real problem is, that these parameters are probably already 'fixed' on the basis of previous design considerations. If that is the case, a ride control system should be considered. For the design of such systems, References 26 and 27 are suggested. Figure 4.1 shows an example of such a system.

Step 4: Determine the additional parameters needed to estimate $\bar{A}$ in Equation (4.4), then compute $\bar{A}$.

If $\bar{A}$ does not meet criterion (4.4) a design change is in order. Most likely, the only practical alternative is a ride control system, such as shown in Figure 4.1. For synthesis methods of such systems, see References 26 and 27.

Step 5: Document the results obtained, including any design changes made.

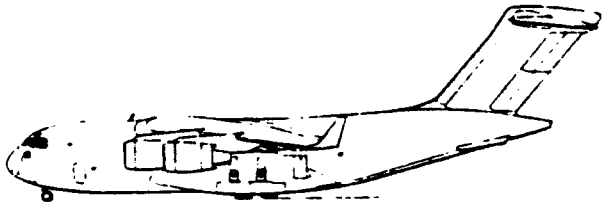

5. PERFORMANCE

The purpose of this chapter is to present Class II methods for predicting the performance characteristics of airplanes. These methods are compatible with Step 24 in Preliminary Design Sequence II as outlined in Chapter 2 of Part II.

The performance characteristics of airplanes must meet the following requirements:

1) Mission performance requirements

2) Airworthiness performance requirements (performance regulations)

The mission performance requirements are normally dictated by the customer, civil or military. The airworthiness performance requirements (referred to in this text as the REGULATIONS) are set by government agencies such as the FAA (civil) or one of the armed forces: USAF, USNavy, USMC or USArmy (military).

To provide the reader with insight into where a given performance characteristic fits into the airplane preliminary design process, the material in each section is organized to provide the following information:

1) identification of the applicable airworthiness regulation(s)

2) relationship to the performance sizing process of Part I of this series of books

3) presentation of a model for analyzing the performance

4) a step-by-step procedure for determining whether or not an airplane meets the mission and airworthiness performance requirements

An important assumption made in this chapter is that the airplane can be considered to be a so-called point-mass model. For the point-mass model to be valid, the stability and control characteristics of the airplane (as discussed in Chapters 3 and 4) must satisfy the corresponding regulations. In addition, the airplane is assumed to be in complete moment equilibrium: any drag polars used in this chapter MUST be the TRIMMED DRAG POLARS!

The material in this chapter is organized in the following manner:

5.1 Stall
5.2 Takeoff
5.3 Climb
5.4 Cruise, range and payload-range
5.5 Endurance and loiter
5.6 Dive
5.7 Maneuvering
5.8 Descent and glide
5.9 Landing
5.10 Mission profile analysis
5.11 Productivity
5.12 Presentation of airplane performance data

COURTESY: CANADAIR

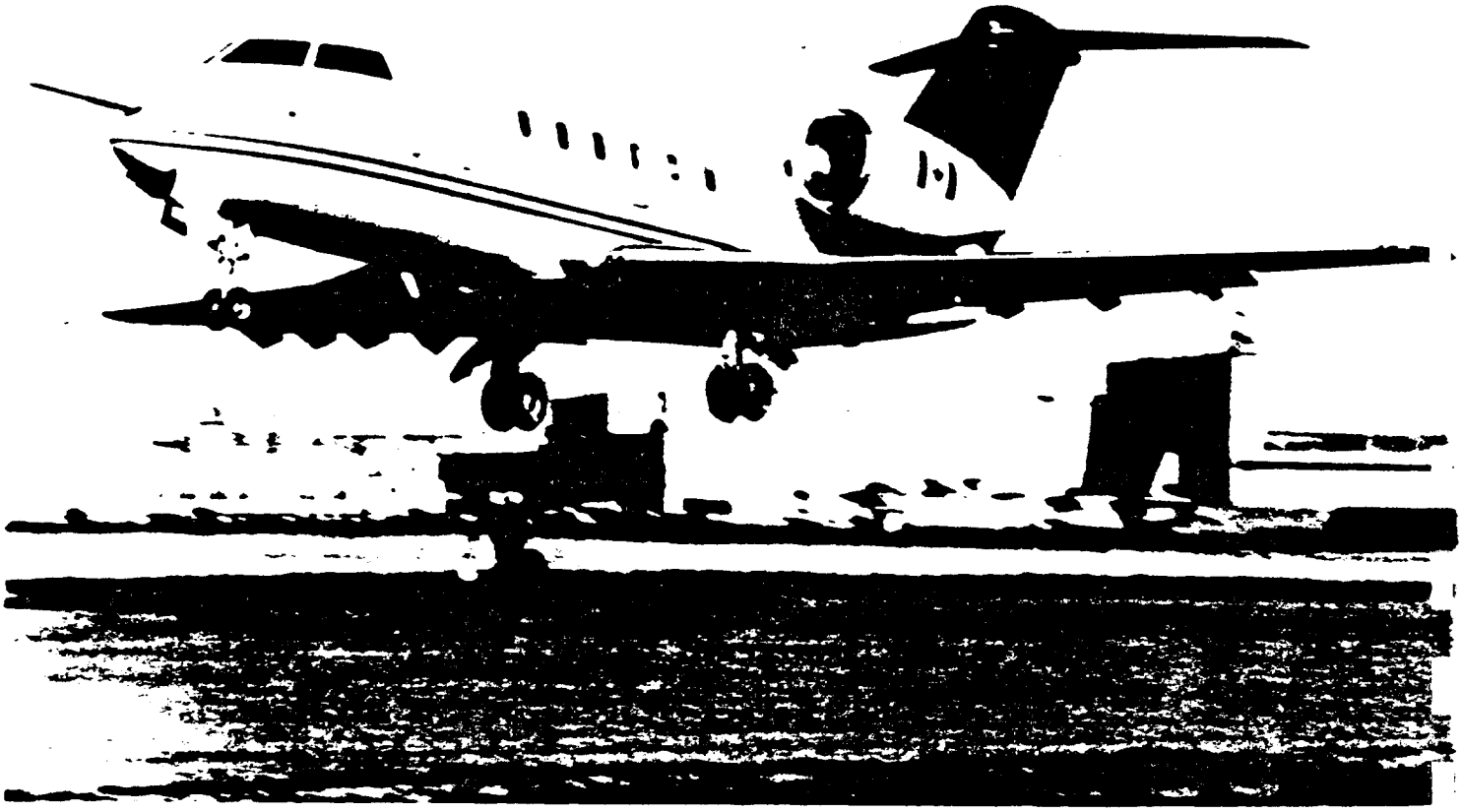

5.1 STALL

5.1.1 Applicable Regulations

Civil: FAR 23.45, 23.49, FAR 25.101 and 25.103, see Appendix A.

Military: MIL-C-005011B, Par.3.4.2.3 or AS-5263, Par.3.5.2.3, see Appendix B.

5.1.2 Relationship to Preliminary Design

See Part I, Section 3.1 and Chapter 7, Part II.

5.1.3 Mathematical Model for Analyzing Stall

Figure 5.1 depicts the forces acting on the airplane in a 1-g stall in steady, level, symmetrical flight. The following equations of motion apply:

$$T\sin(\alpha + \phi_T) + L = W \tag{5.1}$$

$$T\cos(\alpha + \phi_T) = D \tag{5.2}$$

At the stall, the airplane is flying at:

$C_L = C_{L_{max}}$ and $\alpha = \alpha_{C_{L_{max}}}$. Therefore, the stall speed follows from:

$$V_s = [2\{W - T\sin(\alpha_{C_{L_{max}}} + \phi_T)\}/\{\rho C_{L_{max}} S\}]^{1/2} \tag{5.3}$$

where: W is the weight at which the stall speed is to be determined

T is the thrust setting used in the stall maneuver. This will normally be equal to zero (power-off stall). Since thrust does depend on speed, an iterative solution to Eqn.(5.3) is required if T is not zero.

Note: If the thrust is derived from a propeller instead of from a jet engine, it may be computed from:

$$T = (550\eta_p SHP)/V_s \tag{5.4}$$

where: η_p is the propeller efficiency

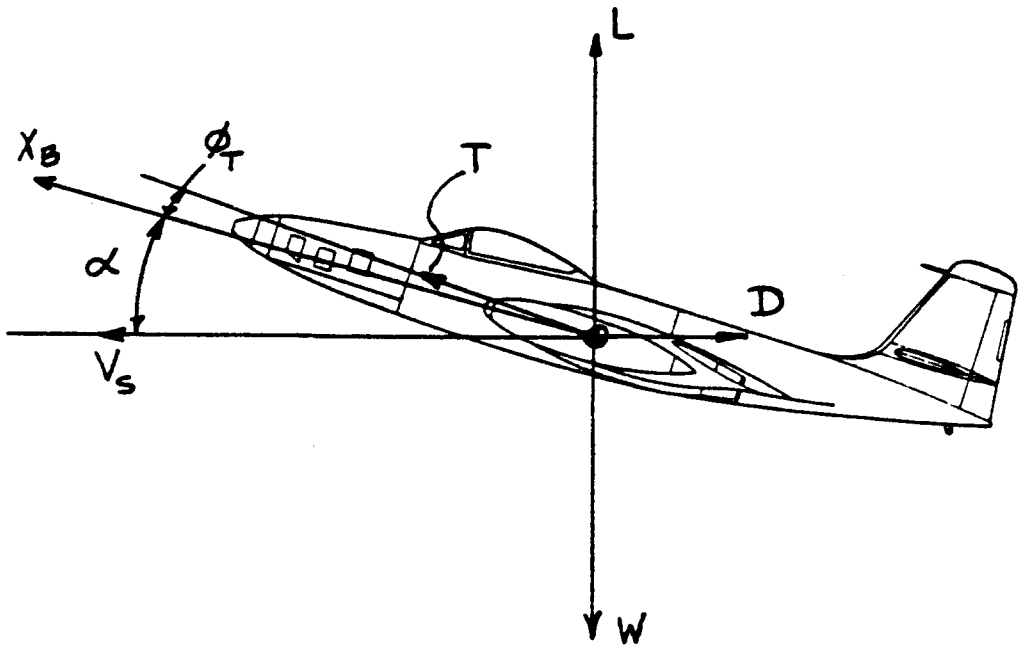

Figure 5.1 Forces Acting on an Airplane in a 1-g Stall In Steady, Level symmetrical Flight

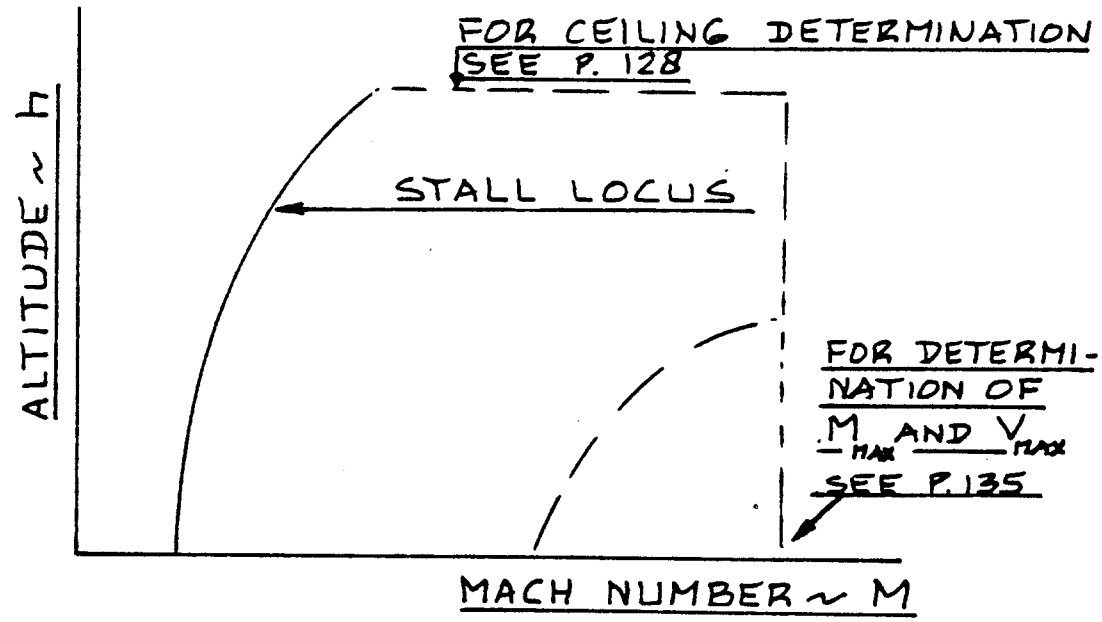

Figure 5.2 Example Flight Envelope

SHP is the shaft horsepower delivered by the engine(s)

V_s is the stall speed as found from Equation (5.3). Note that an iterative solution of Eqn.(5.3) is required if SHP is not zero.

$\alpha_{C_{L_{max}}}$ is the angle of attack at the stall

ϕ_T is the thrustline inclination, see Fig.5.1

Therefore, Eqn.(5.3) applies to vectorable thrust airplanes. For most airplanes it is acceptable to assume $\phi_T = 0$.

ρ is the air density corresponding to the altitude at which the stall is to be done

$C_{L_{max}}$ is the trimmed maximum lift coefficient of the airplane. As explained in Ch.2 of this text as well as in Section 8.3 of Part VI, its value depends strongly on center of gravity location AND on controllability and pitch-up behavior.

NOTE WELL: For high speed airplanes the maximum lift coefficient is also dependent on Mach number. This dependency is discussed in Chapter 9 of Part VI.

The dependency of maximum lift coefficient on Mach number is very important in defining the stall boundary of the airplane flight envelope. This is discussed further in Section 5.11.

S is the (reference) wing area

If T = 0 and $\phi_T = 0$, Equation (5.3) reduces to its classical form:

$$V_s = \{(2W)/(\rho C_{L_{max}} S)\}^{1/2} \qquad (5.5)$$

IMPORTANT COMMENT: The 1-g stall speed as determined from this method is somewhat conservative in view of the manner in which the regulations define the stall speed as determined by certification flight tests. The conservatism usually amounts to about 6 percent. For a more dis-

cussion of this, see Reference 11, pages 482-486.

5.1.4 Step-by-Step Procedure for Analyzing Stall

The following step-by-step procedure is suggested to calculate the airplane stall speed.

Step 1: Determine which regulations apply to the design: see Table 1.3 and Sub-section 2.1.1. READ the regulations!

Step 2: Tabulate the flight conditions, configurations, loading conditions and c.g. locations for which the stall speed of the airplane must be determined. This information comes from the regulations AND from the mission performance requirements. The reader should consult the list of items 1-9 on page 7!

Step 3: For the flight conditions and configurations defined in Step 2, determine the value(s) of the maximum lift coefficient. Be sure to account for the effects of Mach number and c.g. location on $C_{L_{max}}$!

Step 4: For the conditions of Step 2 find the values of all other terms in Equation 5.3.

Step 5: Compute the stall speed(s) from Eqn.(5.3), and record in kts, fps and in Mach number.

Step 6: Check the stall speed(s) of Step 5 against the regulatory requirements and against the mission performance requirements. If a discrepancy is found, determine what (if any) redesign action needs to be taken.

Discrepancies occur usually as a result of not being able to generate the required magnitude of $C_{L_{max}}$ (TRIMMED!!). This in turn can be remedied usually by a change in wing and/or flap design!

Step 7: Plot the variation of Mach number at the stall with altitude. This constitutes the left side of the airplane operational flight envelope. Figure 5.2 shows an example.

Step 8: Document the results obtained, including any design changes made.

5.2 TAKE-OFF

5.2.1 Applicable Regulations

Civil: FAR 23.45, 23.51, FAR 25.101, and 25.107, see Appendix A.

Military: MIL-C-005011B, par. 3.4.2.4 and 3.4.5 or AS-5263, par. 3.5.2.4, 3.5.2.5 and 3.5.5, see Appendix B.

5.2.2 Relationship to Preliminary Design

See Part I, Section 3.2.

5.2.3 Mathematical Model for Analyzing Takeoff Performance

The definition of take-off distance and the associated reference speeds depends on which regulation is used to certify the airplane: FAR 23, FAR 25 or Military.

Figure 5.3 shows the differences in the definitions for takeoff distances and the associated reference speeds.

The following method for computing the takeoff distance, s_{TO} is due to Torenbeek (Reference 26). The takeoff distance, s_{TO} equals the takeoff field length, s_{TOFL} when the landing distance, s_L or s_{FL} (See Section 5.9) is less than or equal to s_{TO}.

$$s_{TO} = f_{TO} h_{TO} \left[(1/\gamma_{LOF}) + \frac{(V_3/V_{s_{TO}})^2 (W/S)_{TO} \{ (\bar{T}/W)_{TO} - \mu' \}^{-1} + 1.414\}}{(h_{TO} \rho g C_{L_{max_{TO}}})(1 + 1.414\gamma_{LOF})} \right] \quad (5.6)$$

where: f_{TO} depends on the obstacle height: see Table 5.1.

h_{TO} is the obstacle height, see Table 5.1.

$(V_3/V_{s_{TO}})$ is the ratio of the speed at the obstacle height, V_3 to the stall speed in

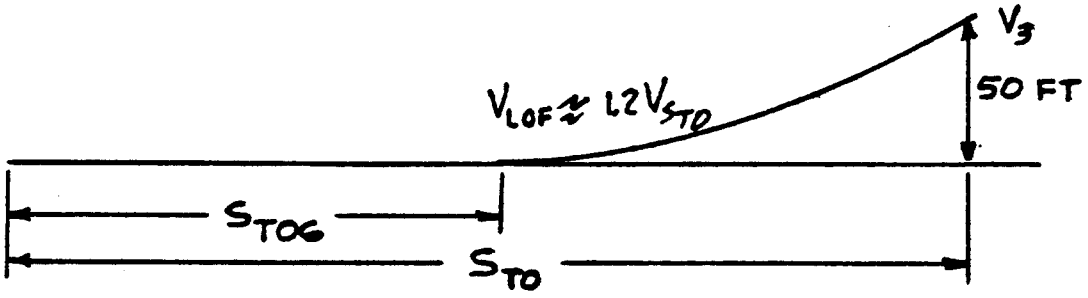

Definition of FAR 23 Take-off Distance

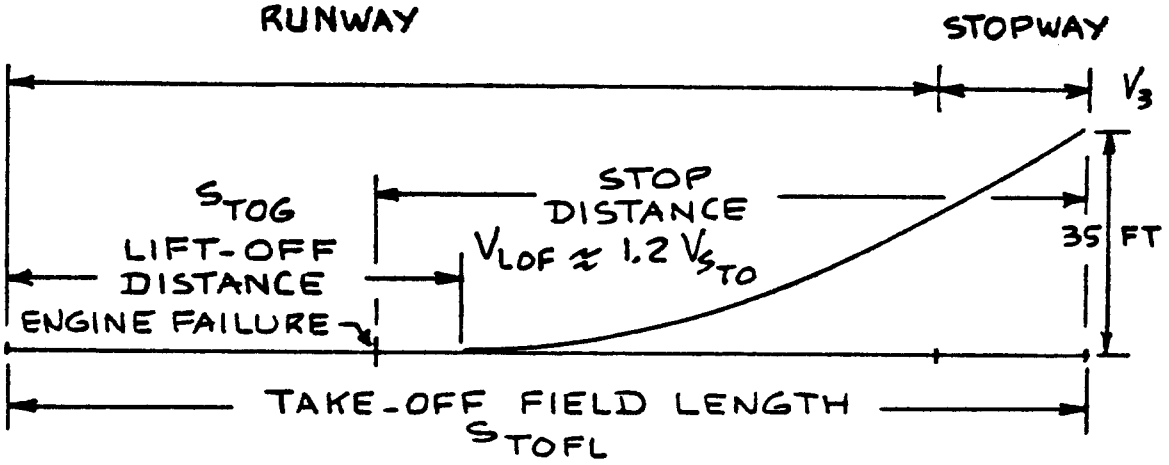

Definition of FAR 25 Take-off Distance

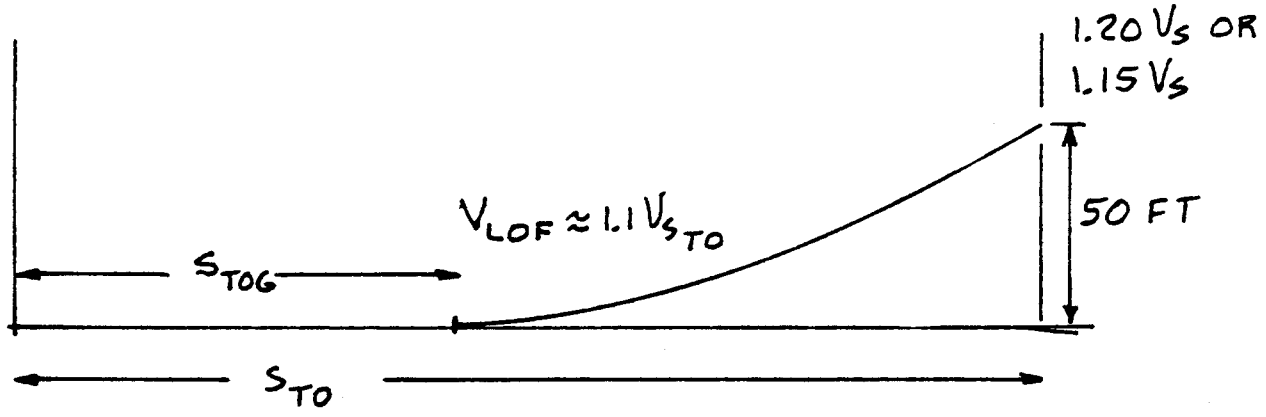

Definition of Military Takeoff Distance

Figure 5.3 Definition of Takeoff Distances According to the Regulations

the takeoff configuration, $V_{s_{TO}}$. This ratio is defined in Table 5.1.

Table 5.1 Parameter Values for Equation (5.6)

Regulation	$V_3/V_{s_{TO}}$	f_{TO}	h_{TO}
FAR 23	1.3	1.0	50 ft
FAR 25	1.25 to 1.3 (no requirement)	1.15	35 ft
AS-5263	1.2	1.0	50
MIL-C-005011B	1.15	1.0	50 ft

$(W/S)_{TO}$ is the takeoff wing loading

$(\bar{T}/W)_{TO}$ is the mean thrust-to-weight ratio taken at a speed of $0.707V_{LOF}$. The value of T may be computed from:

For Jet Driven Airplanes:

$$\bar{T} = 0.75T_{TO}(5 + \lambda)/(4 + \lambda) \qquad (5.7)$$

where: $T_{TO_{max}}$ is the maximum static thrust at takeoff

λ is the engine bypass ratio

For Propeller Driven Airplanes:

$$\bar{T} = 5.75P_{TO}\{(\sigma ND_p^2)/P_{TO}\}^{1/3} \qquad (5.8)$$

where: P_{TO} is the maximum shaft horsepower at takeoff (static), all engines operating

NOTE:
FACTOR 5.75 IN EQN. (5.8) APPLIES TO VARIABLE PITCH PROPELLERS ONLY! FOR FIXED PITCH USE 4.60.

$(P_{TO}/ND_p^2$ is the propeller diskloading at takeoff (static). Its Class I determined value (Step 5.6 in Chapter 5 of Part II) may be checked for acceptability by referring to Figure 5.4.

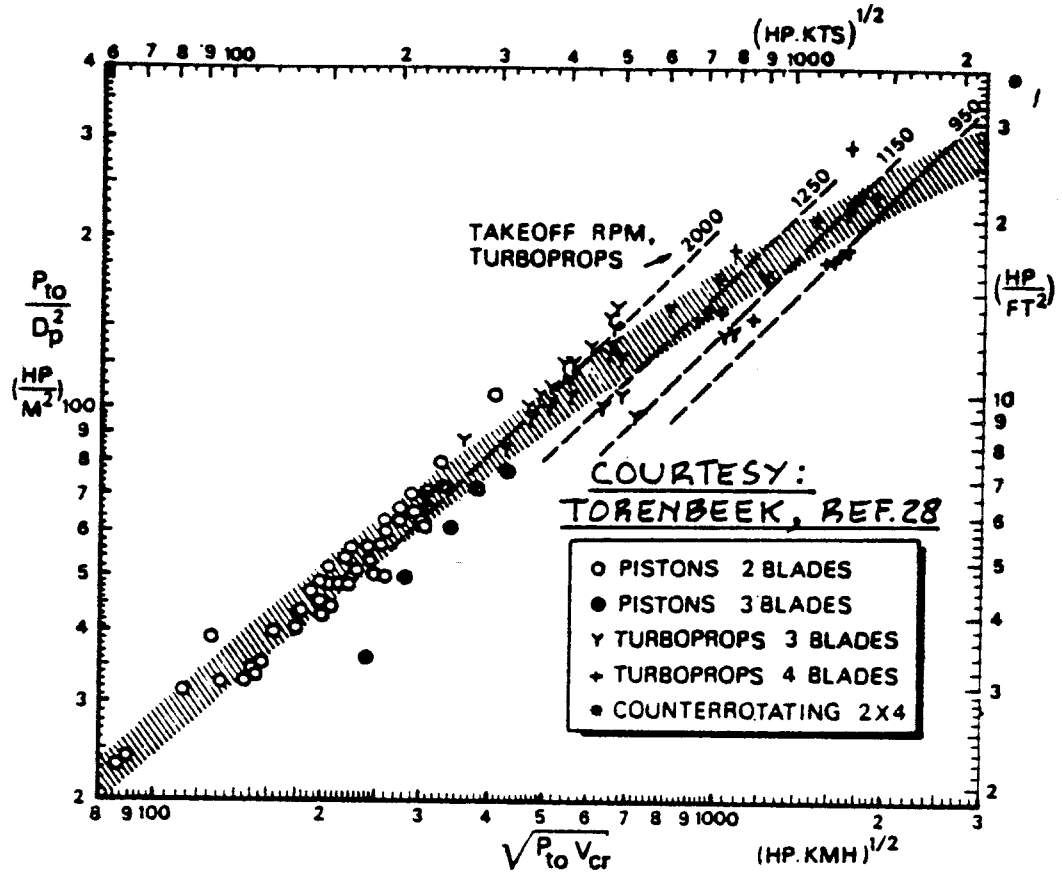

Figure 5.4 Method for Selecting Propeller Disk Loading During Preliminary Design

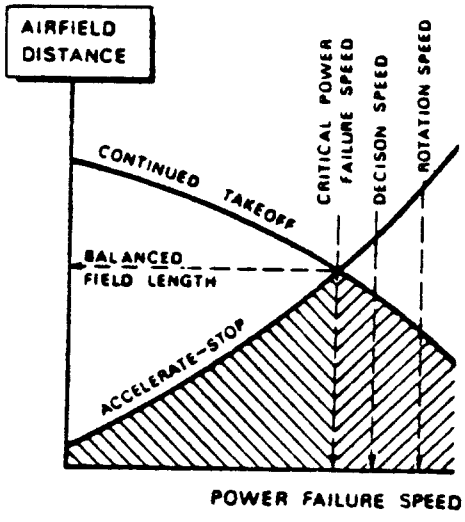

COURTESY:
TORENBEEK, REF. 28

Figure 5.5 Sketch of the Meaning of Balanced Field Length

N is the number of engines

$$\mu' = \mu_g + 0.72(C_{D_o}/C_{L_{max_{TO}}}) \quad (5.9)$$

where: μ_g is the friction coefficient as determined from page 40

C_{D_o} is the zero-lift drag coefficient in the takeoff configuration

$C_{L_{max_{TO}}}$ is the maximum lift coefficient in the takeoff configuration. It is determined from Part VI, Section 8.3. Ground effect must be accounted for.

$$\gamma_{LOF} = \{(T - D)/W\}_{LOF} \quad (5.10)$$

but this may be approximated by:

$$\gamma_{LOF} = 0.9(\bar{T}/W)_{TO} - 0.3/(A^{1/2}) \quad (5.11)$$

In the design of commercial transports and certain military transports the concept of balanced fieldlength, (BFL) is often used. In the case of military airplanes, BFL is normally called the Critical Field Length.

The definition of balanced fieldlength is illustrated in Figure 5.5. Torenbeek (Reference 28) shows that:

$$BFL = [\{655/(\sigma)^{1/2}\}] + \quad (5.12)$$

$$+ \{0.863/(1 + 2.3(\gamma_2 - \gamma_{2_{min}}))\}*$$

$$*\{(W/S)_{TO}/(0.694\rho g C_{L_{max_{TO}}}) + h_{TO}\}\{1/((\bar{T}/W_{TO}) - \mu') + 2.7\}$$

where: $\gamma_2 = (T/W)_{TO_{OEI}} - \{(C_L/C_D)_{TO_{OEI}}\}^{-1}$ (5.13)

which is called the second-segment climb gradient with one engine inoperative.

with: $(T/W)_{TO_{OEI}}$ is the thrust-to-weight ratio in the takeoff configuration, but with one engine inoperative and at $1.2V_{s_{TO}}$.

$\{(C_L/C_D)_{TO_{OEI}}\}^{-1}$ is the lift-to-drag ratio in the takeoff configuration, with one engine inoperative (this does cause extra drag!!) and at $1.2V_{s_{TO}}$

γ_{2min} = 0.024 for N=2

0.027 for N=3

0.030 for N=4

All other parameters were previously defined.

In several instances a takeoff specification will call merely for a groundrun during takeoff to be less than some specified value. In such cases the following equation for the groundrun only is useful:

$$s_{TOG} = \{(V_{LOF})^2/2g\}/\{(\bar{T}/W)_{TO} - \mu'\} \qquad (5.14)$$

where: $V_{LOF} = 1.2V_{s_{TO}}$ for commercial airplanes, and

$1.1V_{s_{TO}}$ for military airplanes

all other parameters have been previously defined.

Important Note:

Airplanes which are also carrier based must be compatible with the performance restrictions inherent in each catapult system. A suitable mathematical model for determining airplane compatibility with USNavy catapult systems is given in Sub-sub-section 3.2.5.2, page 103, in Part I.

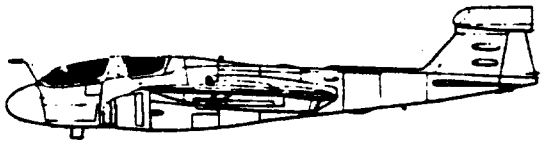

5.2.4 Step-by-Step Procedure for Analyzing Takeoff Performance

The following step-by-step procedure is suggested for determining the takeoff distance of a new airplane:

Step 1: Determine which regulation applies to the design and read that regulation. See Table 1.3 and Sub-section 2.1.1.

Determine the takeoff distance requirements from the mission specification.

Step 2: Determine whether Eqn.(5.6), Eqn.(5.12) or Eqn.(5.14) govern the takeoff distance calculation and prepare the required input data.

If the airplane has a catapulting requirement, such as carrier based airplanes, the reader should use the method of Sub-sub-section 3.2.5.2 of page 103 in Part I to determine the compatibility of the airplane with catapult performance capability.

Step 3: Compute the takeoff distance with either Eqn. (5.6), (5.12) or (5.14). Compare the result with the mission fieldlength requirements. If there is more than a 5 percent discrepancy, a design adjustment to the airplane is in order.

Note: The parameters which affect the takeoff distance most strongly are:

1. The takeoff thrust-to-weight ratio $(T/W)_{TO}$
2. The takeoff wing loading, $(W/S)_{TO}$
3. The takeoff maximum lift coefficient, $C_{L_{max_{TO}}}$

Remember: there is little value in significantly exceeding a mission requirement AND:

not meeting a mission requirement may lead to rejection of the design

Step 4: Document the results obtained, including any design changes made.

5.3 CLIMB

5.3.1 Applicable Regulations

Civil: FAR 23.45, 23.65, 23.67, and 23.77, see Appendix A.

FAR 25.101, 25.111, 25.115, 25.117, 25.119, 25.121 and 25.123, see Appendix A.

Military: MIL-C-005011B, Par.3.4.2.4 and 3.4.2.5 or AS-5263, Par.3.5.2.4.1 and 3.5.2.6, see Appendix B.

5.3.2 Relationship to Preliminary Design

See Part I, Chapter 3, Section 3.4. In addition, see Part II, Chapter 2, Step 14 and Step 27.

5.3.3 Mathematical Model for Analyzing Climb Performance

Figure 5.6 depicts the forces which act on an airplane in an accelerated, symmetrical flight condition. The corresponding equations of motion are:

$$T\cos(\alpha + \phi_T) - C_D\bar{q}S - W\sin\gamma = (W/g)\dot{U} \qquad (5.15)$$

$$T\sin(\alpha + \phi_T) + C_L\bar{q}S - W\cos\gamma = (W/g)U\dot{\gamma} \qquad (5.16)$$

The reader is reminded of the fact, that these equations assume that moment equilibrium exists. This implies, that the drag polar, which defines the relation between C_L and C_D is the 'trimmed' drag polar. See Part VI, Section 4.10 for a discussion of trim drag.

Equations (5.15) and (5.16) are used to determine the rate of climb and the climb gradient of which an airplane is capable in a range of flight conditions.

In preliminary design, the effect of acceleration normal to the flight path as expressed by the $\dot{\gamma}$-term will be neglected. Furthermore, other than for fighters, the climb angle, γ is usually smaller than about 15 degrees so that $\cos\gamma=1.0$ and $\sin\gamma=\gamma$ can be used.

The rate-of-climb, RC (for any flight path angle) is

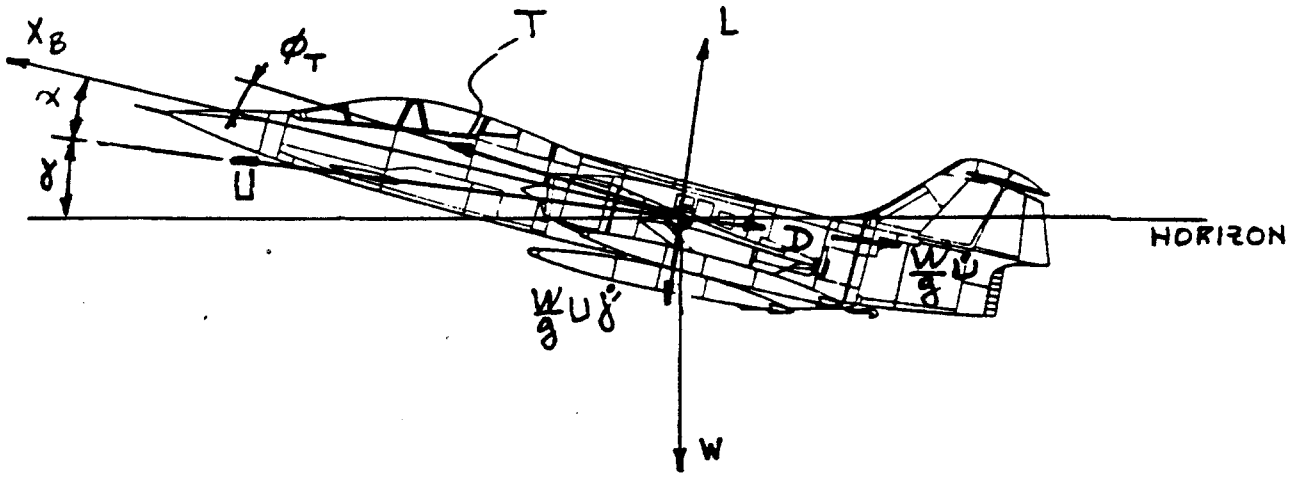

Figure 5.6 Forces Acting on an Airplane in Accelerated, Symmetrical Flight

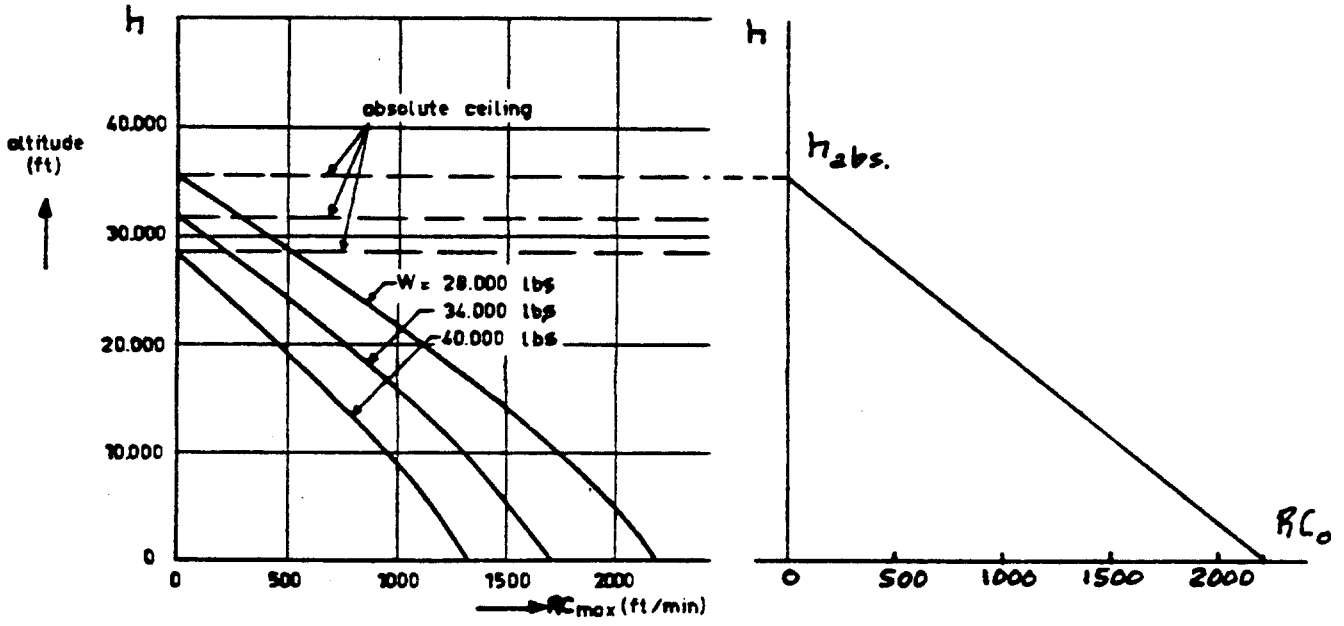

ACTUAL

LINEARIZED

Figure 5.7 Variations of Rate-of-Climb with Altitude

defined as:

$$RC = dh/dt = U\sin\gamma \tag{5.17}$$

With the help of Eqns.(5.16) - (5.17) it is shown in Reference 11, page 384, that:

$$RC = \{(T - D)U/W\}/\{1 + (U/g)dU/dh\} \tag{5.18}$$

The term (U/g)dU/dh is called the acceleration factor. It has a significant effect on fighter performance. It also has a significant effect on climb performance at high altitude. Since most regulations which deal with climb performance apply close to the ground, it is usually acceptable to consider only climb at constant true airspeed, in which case the acceleration factor is zero.

Therefore, for steady, symmetrical flight the rate-of-climb is:

$$RC = (T - D)U_1/W \tag{5.19}$$

From this, the climb gradient, CGR follows as:

$$CGR = RC/U_1 = (T - D)/W \tag{5.20}$$

The regulations specify either a minimum required rate-of-climb, RC or a minimum required climb gradient, CGR. The reader should read the applicable regulations to determine which values for CR and/or CGR apply to a given airplane.

For Class II climb performance analysis it is acceptable to use the equations of Chapter 3, Part I. These equations will be stated here in general. The reader must realize that the parameters in these equations are different for each particular flight condition and for each particular airplane configuration!

1. For propeller-driven airplanes:

$$RC\ (fpm) = 33{,}000[\eta_p/(W/P) + \tag{5.21}$$

$$- \{(W/S)^{1/2}/19(C_L^{3/2}/C_D)\sigma^{1/2}\}]$$

$$CGR = -(L/D)^{-1} + \tag{5.22}$$

$$+ \{(C_L)^{1/2}18.97\eta_p\sigma^{1/2}\}/\{(W/P)(W/S)^{1/2}\}$$

2. For jet-driven airplanes:

$$RC\ (fpm) = 60U_1[(T/W) - (L/D)^{-1}] \qquad (5.23)$$

$$CGR = (T/W) - (L/D)^{-1} \qquad (5.24)$$

Many airplane mission specifications require mission specific climb capabilities such as:

1. Minimum climb rate at some altitude (such as sea level)
2. Minimum time-to-climb to some altitude
3. Ceiling
4. Specific excess power

1. Minimum climb rate at some altitude

The climb rate at any altitude can be estimated with Equations (5.21) and (5.23).

2. Minimum time-to-climb to some altitude

The time to climb to any altitude can be estimated from:

$$t_{cl} = \int_0^h (1/RC)dh \qquad (5.25)$$

This equation can be solved by integration over several increments of altitude. Increments of 5,000 ft provide sufficient accuracy in preliminary design. The average value of the rate-of-climb, RC in Eqn.(5.25) at some altitude increment can be estimated from Eqn.(5.21) or (5.23). Figure 5.7 shows typical variations of rate-of-climb with altitude.

If an estimate is available for the absolute ceiling of an airplane (see next item 3.), AND if the RC varies approximately linearly with altitude, then it is possible to find the time-to-climb to any altitude between sealevel and the absolute ceiling from:

$$t_{cl} = (h_{abs}/RC_o)\ln((1 - h/h_{abs})^{-1} \qquad (5.26)$$

where: RC_o is the maximum rate-of-climb at sealevel, found from either Equation (5.21) or (5.23). Figure 5.7 also shows the linearized variation of rate-of-climb with altitude.

3. Ceiling

Equation (5.21) or (5.23) can be used to find that altitude for which the rate of climb corresponds to one of the ceiling definitions of Table 5.2. The ceiling is the upper side of the flight envelope: see Figure 5.2.

4. Specific excess power

The specific excess power of an airplane is computed from:

$$P_s = (T - D)U/W \qquad (5.27)$$

Note that this equation is similar to Eqn.(5.18).

More accurate and specialized mathematical models for the computation of climb performance are presented in Reference 11. They will not be repeated here.

To help the reader find specific models for the computation of climb performance, the following guide is presented:

1. For Propeller Driven Airplanes:

   See Reference 11, Section 9.2, pages 384-395.

2. For Jet Powered Airplanes:

   See Reference 11, Section 9.3, pages 395-400.

3. For Fighters (Steep Climbs):

   See Reference 11, Section 9.4, pages 400-401.

4. For Ceilings and Time-to-Climb:

   See Reference 11, pages 405-407

5. For Specific Excess Power:

   See Reference 11, pages 510-516.

Table 5.2 Definition of Airplane Ceilings

Ceiling Type	Minimum Required Climb Rate
Absolute ceiling	0 fpm
Service ceiling	
Commercial/Piston-propeller	100 fpm
Commercial/jet	500 fpm
Military at maximum power	100 fpm
Combat ceiling	
Military/Subsonic/maximum power	500 fpm at M<1
Military/Supersonic/maximum power	1,000 fpm at M>1
Cruise ceiling	
Military/Subsonic/max.cont. power	300 fpm at M<1
Military/Supersonic/max.cont. power	1,000 fpm at M>1

Table 5.3 Summary of Regulatory Climb Requirements for FAR 25 Transports

PHASE OF FLIGHT		AIRPLANE CONFIGURATION: FLAPS	U.C.	ENGINES		FLIGHT SPEED	MINIMUM, CLIMB GRADIENT, %: N=1	N=2	N=3
LIFTOFF	1ST SEGMENT	TAKE OFF	+	ONE ENGINE OUT	TAKE OFF	LIFT-OFF	0	.3	.5
TAKEOFF FLIGHT PATH	2ND SEGMENT	TAKE OFF	+		TAKE OFF	V_2	2.4	2.7	3.0
	FINAL TAKEOFF	EN ROUTE	+		MAX. CONT.	$\geq 1{,}25V_s$	1.2	1.5	1.7
APPROACH CLIMB		APPR.	+		TAKEOFF	$\leq 1{,}5V_s$	2.1	2.4	2.7
LANDING CLIMB		LAND.	+	ALL ENGINES TAKEOFF		$\leq 1{,}3V_s$	3.2	3.2	3.2

COURTESY: TORENBEEK, REF. 28

V_s = Stalling speed

V_2 = Takeoff safety speed ($\geq 1.2V_s$)

* Summary only

5.3.4 Step-by-Step Procedure for Determining Climb Performance

Step 1: Determine which regulations apply to the design and read that regulation.

Tabulate the regulatory climb requirements in a manner similar to that shown in Table 5.3.

Determine the climb performance requirements stated in the airplane mission requirements.

Tabulate all mission climb requirements in a manner similar to Table 5.3.

Note from Table 5.3 that the prescribed configuration of the airplane is carefully listed! This has significant consequences for the drag polars!

Step 2: Using the guidelines of Sub-section 5.3.3 determine which methods and/or equations apply to the analysis of the climb requirements of Step 1.

Prepare the necessary input data for all flight conditions and airplane configurations for which climb performance must be assessed.

Step 3: Carry out the climb performance calculations and compare the results against the regulations and/or the mission climb requirements. Note any discrepancies.

Step 4: Analyze what changes are required to eliminate the discrepancies in climb performance noted in Step 3.

Typical changes which may be contemplated are:

a) Increase or decrease in thrust or power

b) Change in aerodynamic design to lower the drag

Note that major changes in these areas may have repercussions for most other aspects of the design and may therefore require an iteration!

Step 5: Document the results, including any design changes made.

5.4 CRUISE, RANGE AND PAYLOAD-RANGE

5.4.1 Applicable Regulations

Civil: There are no airworthiness regulations which deal specifically with cruise performance. Fuel reserve regulations are specified in FAR 91. Most commercial operations are conducted with fuel reserve rules which are more conservative than those of FAR 91.

Military: MIL-C-005011C (USAF) and AS-5263 (USN and USMC), give definitions, see Appendix B.

5.4.2 Relationship to Preliminary Design

See Part I, Chapter 2. In addition, see Part II, Chapter 2, Step 14, Step 27 and Step 28.

5.4.3 Mathematical Model for Analyzing Cruise and Range Performance

Figure 5.8 depicts the forces which act on an airplane in a horizontal, steady, symmetrical, 1-g cruise flight condition. The equations of motion are:

$$T\cos(\alpha + \phi_T) - C_D\bar{q}S = 0 \qquad (5.28)$$

$$T\sin(\alpha + \phi_T) + C_L\bar{q}S = W \qquad (5.29)$$

The reader is reminded of the fact, that these equations assume that moment equilibrium exists. This implies, that the airplane drag polar, which defines the relationship between C_L and C_D is the 'trimmed' drag polar. Part VI, Section 4.10 presents a method for computing trim drag.

There also exists a unique relationship between the angle of attack, α and the lift coefficient, C_L. A method for determining C_L versus α is given in Part VI, Chapter 8.

The quantity T in Equations (5.28) and (5.29) is the so-called <u>installed thrust.</u> Methods for determining the installed thrust capability of an airplane are presented in Part VI, Chapter 6.

For most conventional airplanes, the angle $(\alpha + \phi_T)$

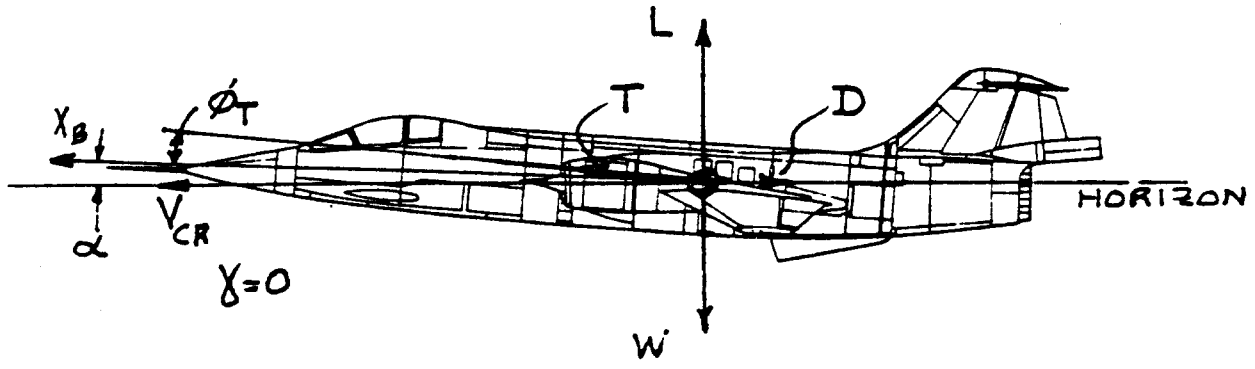

Figure 5.8 Forces Acting on an Airplane in Level, Steady, Symmetrical Flight

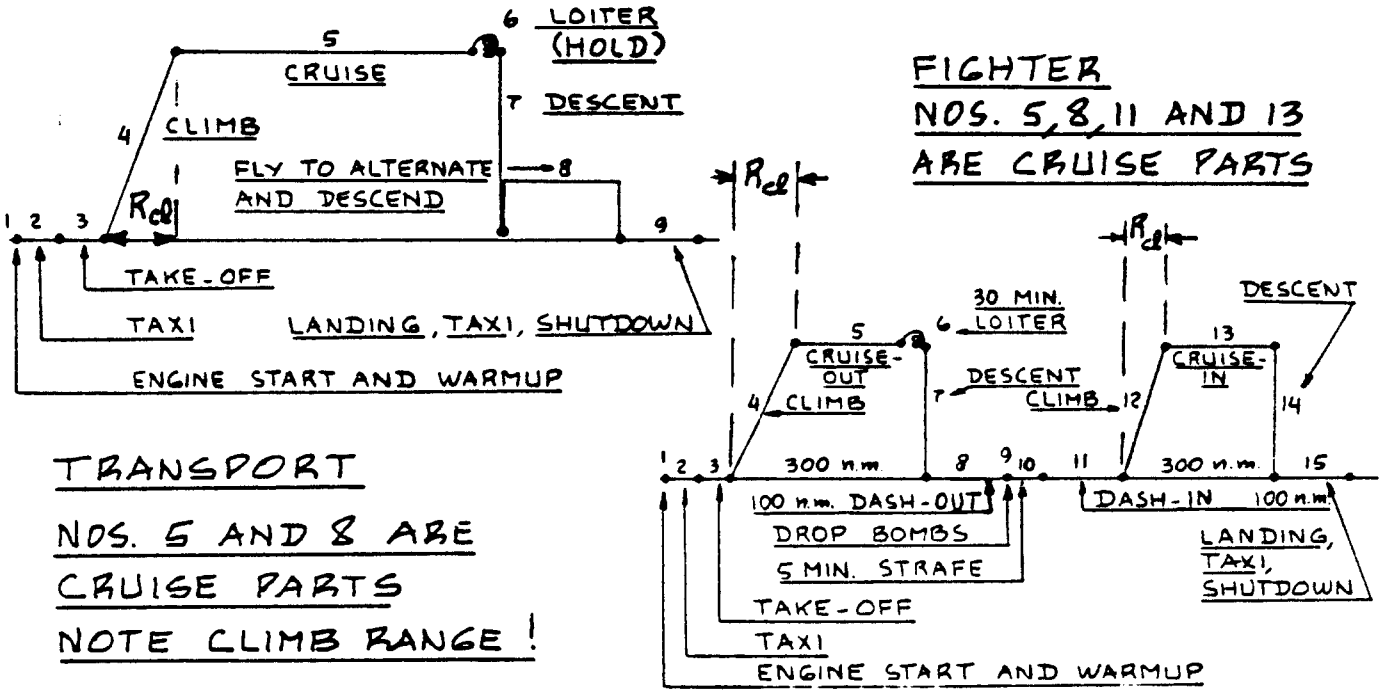

Figure 5.9 Example Mission Profiles for a Transport and for a Fighter

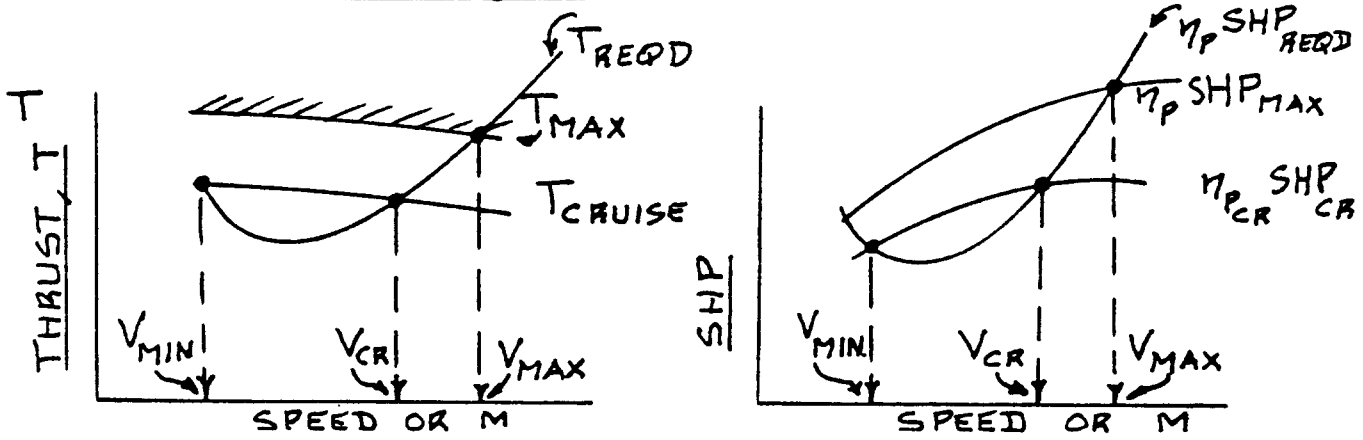

Figure 5.10 Determination of Cruise Speed and Maximum Level Flight Speed

is so small that it can be neglected. In that case, the cruise lift coefficient follows from:

$$C_{L_{cr(uise)}} = W/\bar{q}S \qquad (5.30)$$

The required cruise thrust-to-weight ratio then is:

$$(T/W)_{cr} = 1/(L/D)_{cr} \qquad (5.31)$$

If $(\alpha + \phi_T)$ is not negligibly small, Eqn.(5.30) is used to find a first approximation for the cruise lift coefficient. This value of C_L is then used to find C_D from the trimmed drag polar and also to find α from the C_L versus α curve. Since the thrust inclination angle, ϕ_T is assumed to be known, Eqn.(5.28) can now be used to find the required installed thrust. This thrust value must be less than the maximum installed thrust available in that flight condition! This thrust value is then substituted into Eqn.(5.29) and a new value for C_L is determined, etc., etc. until the process converges. Convergence may be assumed to have been reached when the lift-to-drag ratio is within 1 percent. This determines the cruise lift-to-drag ratio, $(L/D)_{cr}$.

IMPORTANT NOTE: The reader will find that in nearly all cruise flight conditions:

$$(L/D)_{cr} < (L/D)_{max} \qquad (5.32)$$

In a 'cruise matched' airplane, the cruise lift-to-drag ratio is roughly 90 percent of the maximum lift-to-drag ratio.

Most airplane missions specify cruise requirements in the following manner:

1. Cruise speed and cruise altitude
2. Range and payload (Requirement for a specific Range-Payload Diagram)
3. Fuel reserves at the end of the design mission as a fraction of fuel used up to that point or in terms of a so-called reserve mission.

4. Maximum cruise speed, altitude and payload (some of which may be external)

5. Payload expended, as in military airplanes which expend ammunition and release weapons and stores.

It is always useful to translate airplane mission requirements into a mission profile. Figure 5.9 shows examples for a civil and for a military airplane.

For Class II analysis of cruise range performance it is acceptable to use the following Breguet equations, PROVIDED the procedure of Step 5 in Sub-section 5.4.4 is used:

For Propeller Driven Airplanes:

For constant altitude cruise:

$$R = f_{mp}(\eta_p/c_p)(L/D)\ln(W_{initial}/W_{end}) \qquad (5.33)$$

Note that: when $f_{mp} = 326$, R is in nautical miles!

when $f_{mp} = 375$, R is in statue miles!

For constant speed cruise:

$$R = f_{mp}(\eta_p/c_p)(L/D)\ln(W_{initial}/W_{end}) \qquad (5.34)$$

Note that this equation is identical to Eqn. (5.33)! This works only if the assumption is made that the airplane cruises roughly at the same values of η_p, c_p and L/D, regardless of the type of cruise. That assumption is usually valid.

For Jet Driven Airplanes:

For constant altitude cruise:

$$R = (f_{mj}/c_j)(\rho S)^{-1/2}\{(C_L)^{1/2}/C_D\}\{(W_{initial})^{1/2} - (W_{end})^{1/2}\} \qquad (5.35)$$

Note that: when $f_{mj} = 1.677$, R is in nautical miles!

when $f_{mj} = 1.929$, R is in statute miles!

For constant speed cruise:

$$R = (V/c_j)(L/D)\ln(W_{initial}/W_{end}) \quad (5.36)$$

Note that if V is expressed in sm/hr, R is in sm, but, if V is expressed in nm/hr, R is in nm!

In many missions (see Figure 5.9!) range credit may be taken for the climb and/or for the descent part of a mission. If that is the case, the following equations may be used to determine these range increments:

$$R_{cl} = V_{cl}t_{cl} \quad (5.37)$$

where: V_{cl} is the speed at which the climb is conducted. For high performance airplanes, 250 kts is a good guess!

$$t_{cl} = h_{cl}/RC_{ave} \quad (5.38)$$

with: RC_{ave} being determined by one of the climb equations in Section 5.3.

For descent range, Equations (5.37) and (5.38) must be changed to reflect the appropriate descent terms.

The construction of the payload-range diagram for airplanes is discussed in Sub-section 5.4.4.

If part of a mission profile requires a given cruise speed or a given maximum speed, this can be determined graphically from Figure 5.10. At a given thrust (or power) setting the corresponding speed is found from the intersection of the thrust (or power) available and the thrust (or power) required curves. Maximum speed corresponds to the right hand side of the flight envelope as shown in Figure 5.2.

More detailed methods for determining cruise range and cruise speed are presented in Ref.11, Chapter 11. These will not be repeated here. To help the reader find specific models for the computation of range performance, the following guide is presented:

For Propeller Driven Airplanes:

See Reference 11, Section 11.1, pages 454-464.

For Jet Driven Airplanes:

See Reference 11, Section 11.2, pages 464-478.

5.4.4 Step-by-Step Procedure for Analyzing Cruise and Range Performance

Step 1: From the mission requirements of the airplane determine the cruise and range requirements for the airplane. This is most readily done with the help of a mission profile which can be constructed from the airplane mission specification.

Figure 5.9 shows examples of mission profiles for a transport and for a fighter, with the cruise portions indicated.

Tabulate all cruise altitude, cruise speed, range and payload requirements. Also note the configuration the airplane is supposed to be in! For military airplanes, external stores and weapons can have a major effect on the drag polar!

NOTE: Certain military airplanes are required to fly several cruise segments under different speed and altitude conditions!

Step 2: For all flight conditions and configurations defined in Step 1, determine the airplane trimmed drag polars. This can be done with the method of Section 4.10 in Part VI.

Step 3: Using installed engine data, obtain the numerical values for the engine efficiency parameters: c_j (for jets) and/or c_p and η_p (for props).

These parameters depend on speed and altitude which are normally prescribed in the mission requirements.

Chapter 6 in Part VI contains methods for computing installed thrust and/or power characteristics, including efficiencies and s.f.c.'s.

Step 4: Determine the range capability of the airplane in each of the range portions of the mission profile. This is done as follows:

Decide whether the range is to be at constant altitude or at constant speed. Identify which of the Breguet equations (5.33)-(5.36) apply.

For airplanes with short ranges (about 500 nm) it is reasonable to assume that all parameters in

the Breguet range equations are constant during the intended cruise operation. For airplanes with medium to long ranges this is not acceptable. For such airplanes it is suggested to break the cruise part of the mission into segments of approximately 500 nm each. The parameters in the Breguet range equations can be assumed constant but different for each cruise segment!

Now proceed as follows:

For the first range segment, estimate the average cruise lift coefficient from:

$$C_{L_{cr_1}} = (W_{begin} - 0.5W_{fuel_1})/\bar{q}_1 S \qquad (5.39)$$

where for propeller driven airplanes:

$$W_{fuel_1} = (R_1/V_{cr_1})\{(c_p/\eta_p)P_{reqd}\}_1 \qquad (5.40)$$

and where for jet driven airplanes:

$$W_{fuel_1} = (R_1/V_{cr_1})\{c_j W/(L/D)\}_1 \qquad (5.41)$$

Note: the subscript '1' here means that the particular quantity applies to cruise segment 1.

The average value of cruise lift coefficient (in Eqn.(5.39)) is entered into the trimmed drag polar to determine the corresponding value of the drag coefficient. This information in turn is used to compute the values of (L/D) and/or of $\{(C_L)^{1/2}/C_D\}$ which are needed in the Breguet range Eqns.(5.33)-(5.36).

This procedure is repeated as many times as needed until the required total range is met or until the fuel available is exhausted.

Step 5: Note any discrepancies between the computed range and the required range. Decide what design changes (if any) must be made.

Possible design changes which can be contemplated at this stage are:

1. Improve L/D by lowering wetted area or increasing the wing loading and/or the aspect ratio.

2. Switch to engines with lower fuel consumption.

3. Switch to a more efficient propeller.

4. Try to design a more efficient structure so that the fuel-to-weight ratio can be improved.

5. Carry more or less fuel, as required.

Any of these design changes may have repercussions for other areas of the design. Design iterations may have to be performed.

Step 6: Prepare a payload range diagram.

This step normally applies only to transport type airplanes. Figure (5.11) shows an example of a payload-range diagram. The important points A, B, C and D are indicated. These points can be determined in the following manner:

Point A: At this point the airplane weight is equal to the sum of the operating weight empty, (W_{OE}) and the maximum payload weight, W_{PL}. There is no fuel on board and thus the range is zero.

Point B: At this point the range is that for maximum payload. This is sometimes called the harmonic range of the airplane. The weight of the airplane at takeoff is equal to the sum of the operating weight empty, W_{OE}, the maximum payload weight, W_{PL} and that fuel weight which causes the airplane to be at its maximum allowable takeoff weight.

The range corresponding to point B is computed with the procedure of Step 4.

Point C: Between points B and C, payload has to be traded for fuel. This can be done until the maximum volumetric capacity (in terms of fuel) of the airplane has been reached. That is the case at point C. The takeoff weight of the airplane is still at its maximum allowable value.

The range corresponding to point C is computed

with the procedure of Step 4. Make sure that the payload weight is computed correctly!

Note: fuel volume limits are normally reached first due to wing fuel volume limitations. In many airplanes additional fuel can be stored in 'safe' parts of the fuselage, in horizontal and /or vertical tails and sometimes in external containers.

Point D: Beyond point C, the only way to get more range out of the airplane is to unload payload weight. At point D, the takeoff weight of the airplane is the sum of its operating weight empty, W_{OE} and its maximum fuel capability (on basis of volumetric capacity). The range corresponding to point D is called the ferry range.

The range corresponding to point D is computed with the procedure of Step 4. Make sure that NO payload is included and that the takeoff weight is no more than the maximum allowable weight. If there is no fuel volume limit, then the maximum allowable takeoff weight is the limit.

Step 7: Document all the results, including any design changes made.

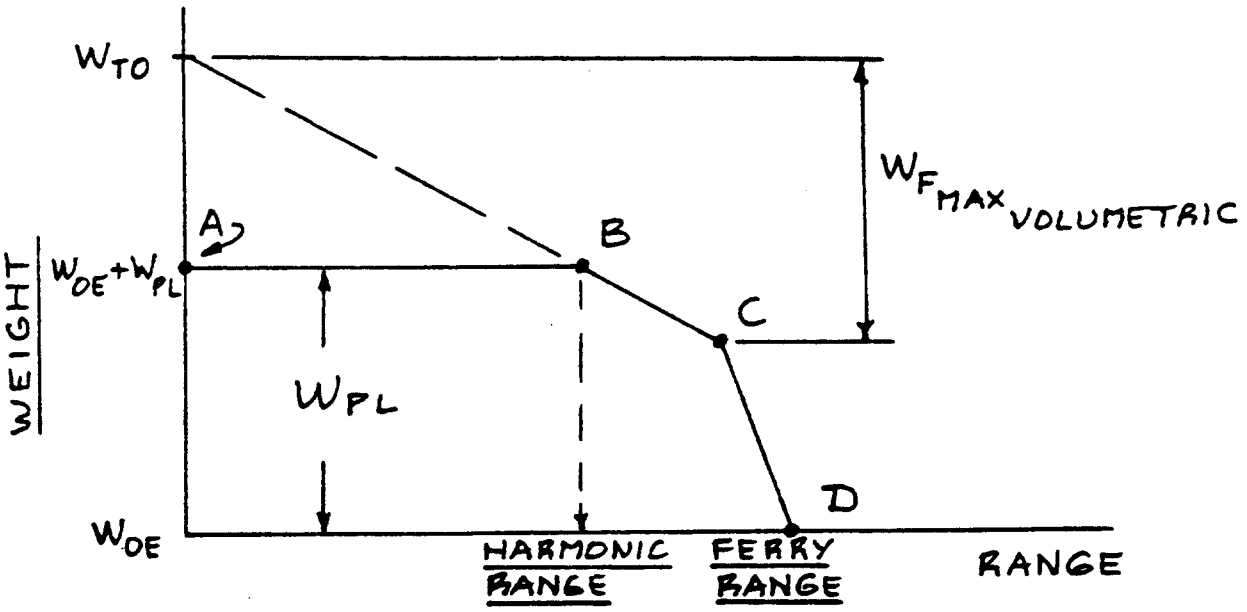

Figure 5.11 Example of a Payload-Range Diagram

5.5 ENDURANCE AND LOITER

5.5.1 Applicable Regulations

Civil: There are no airworthiness regulations which deal specifically with endurance and loiter. Fuel reserve regulations are specified in FAR 91. Most commercial operations are conducted with fuel reserve rules which are more conservative than those of FAR 91.

Military: MIL-C-005011C (USAF) and AS-5263 (USN and USMC), give definitions, see Appendix B.

5.5.2 Relationship to Preliminary Design

See Part I, Chapter 2. In addition, see Part II, Chapter 2, Step 14, Step 27 and Step 28.

5.5.3 Mathematical Model for Analyzing Endurance and Loiter

Figure 5.8 depicts the forces which act on an airplane in a horizontal, steady, symmetrical, 1-g loiter flight condition. The equations of motion are the same as those for range in Sub-section 5.4.3: Eqns.(5.28) and (5.29).

The reader is reminded of the fact, that these equations assume that moment equilibrium exists. This implies, that the airplane drag polar, which defines the relationship between C_L and C_D is the 'trimmed' drag polar. Part VI, Section 4.10 presents a method for computing trim drag.

There also exists a unique relationship between the angle of attack, α and the lift coefficient, C_L. A method for determining C_L versus α is given in Part VI, Chapter 8.

The quantity T in Equations (5.28) and (5.29) is the so-called installed thrust. Methods for determining the installed thrust capability of an airplane are presented in Part VI, Chapter 6.

For most conventional airplanes, the angle $(\alpha + \phi_T)$ is so small that it can be neglected. This, despite the fact that endurance or loitering flights are normally carried out at fairly low speeds and thus at relatively

high angles of attack. The lift coefficient for endurance or loiter can be computed from:

$$C_{L_{ltr}} = W/\bar{q}S \qquad (5.42)$$

where: W is that weight value appropriate to the endurance/loiter flight condition being analyzed.

The required loiter thrust-to-weight ratio then is:

$$(T/W)_{ltr} = 1/(L/D)_{ltr} \qquad (5.43)$$

If $(\alpha + \phi_T)$ is not negligibly small, Eqn.(5.42) is used to find a first approximation for the loiter lift coefficient. This value of C_L is then used to find C_D from the trimmed drag polar and also to find α from the C_L versus α curve. Since the thrust inclination angle, ϕ_T is assumed to be known, Eqn.(5.28) can now be used to find the required installed thrust. This thrust value must be less than the maximum installed thrust available in that flight condition! This thrust value is then substituted into Eqn.(5.29) and a new value for C_L is determined, etc., etc. until the process converges. Convergence may be assumed to have been reached when the lift-to-drag ratio is within 1 percent. This determines the loiter lift-to-drag ratio, $(L/D)_{ltr}$.

IMPORTANT NOTE: The reader will find that in nearly all loiter flight conditions:

$$(L/D)_{ltr} \approx (L/D)_{max} \qquad (5.44)$$

Most airplane missions specify loiter or endurance requirements in the following manner:

1. Loiter speed and loiter altitude.

   In high altitude observation airplanes it is essential that the loiter speed be at least equal to that of prevailing winds at loiter altitude.

   In civil airplanes there normally is a requirement to 'hold' at the end of a cruise mission. This is in fact a requirement to loiter. The

loiter speed must be compatible with air traffic control requirements.

In military airplanes there often is a requirement to loiter over a given location to wait for attack or engagement instructions.

2. Payload to be carried while loitering.

It is always useful to translate airplane mission requirements and into a mission profile. Figure 5.9 shows examples for a civil and for a military airplane.

For Class II analysis of loiter/endurance performance it is acceptable to use the following Breguet equations PROVIDED the procedure of Step 4 in Sub-section 5.5.4 is used:

For Propeller Driven Airplanes:

For constant altitude endurance/loiter:

$$E = 778(\eta_p/c_p)(\rho S)^{1/2}\{(C_L)^{3/2}/C_D\}*$$

$$*\{(W_{end})^{-1/2} - (W_{initial})^{-1/2}\} \qquad (5.45)$$

Note that E is in hours!

For constant speed endurance/loiter:

$$E = 928(\eta_p/c_p)(1/V)(L/D)\ln(W_{initial}/W_{end}) \qquad (5.46)$$

Note that E is in hours and V is in kts!

For Jet Driven Airplanes:

For constant altitude endurance/loiter:

$$E = (1/c_j)(L/D)\ln(W_{initial}/W_{end}) \qquad (5.47)$$

Note that E is in hours!

For constant speed endurance/loiter:

$$E = (1/c_j)(L/D)\ln(W_{initial}/W_{end} \qquad (5.48)$$

Note that this equation is identical to Eqn.(5.47)!

If part of a mission profile requires a given loiter speed, this can be determined graphically from Figure 5.10. At a given thrust (or power) setting the corresponding speed is found from the intersection of the thrust (or power) available and the thrust (or power) required curves. Note that loiter usually represents the low speed intersection while cruise was represented by the high speed intersection.

More detailed methods for determining endurance/loiter performance are presented in Ref.11, Chapter 11. These will not be repeated here. To help the reader find specific models for the computation of range performance, the following guide is presented:

For Propeller Driven Airplanes:

See Reference 11, Section 11.1, pages 454-464.

For Jet Driven Airplanes:

See Reference 11, Section 11.2, pages 464-478.

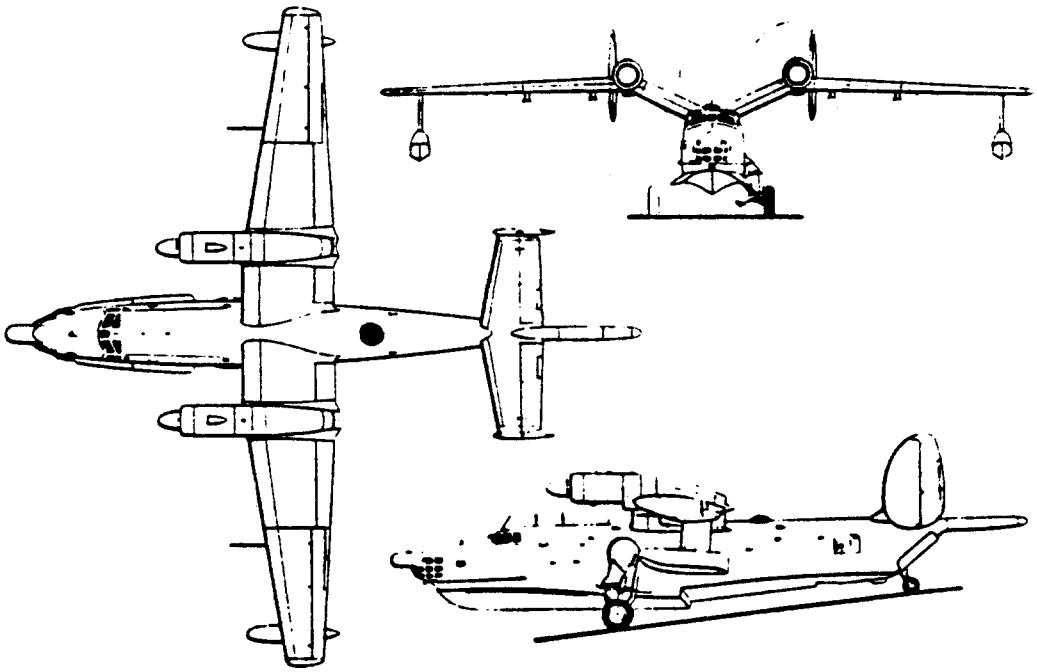

5.5.4 Step-by-Step Procedure for Analyzing Endurance and Loiter

Step 1: From the mission requirements of the airplane determine the endurance and/or loiter requirements. This is most readily done with the help of a mission profile which can be constructed from the airplane mission specification.

Figure 5.9 shows examples of mission profiles for a transport and for a fighter. In Figure 5.9 the loiter requirements are items 6.

Tabulate all endurance/loiter altitude, speed and payload requirements. Also note the configuration the airplane is supposed to be in! For military airplanes, external stores and weapons can have a major effect on the drag polar!

Step 2: For all flight conditions and configurations defined in Step 1, determine the airplane trimmed drag polars. This may be done with the method of Section 4.10 in Part VI.

Step 3: Using installed engine data, obtain the numerical values for the engine efficiency parameters: c_j (for jets) and/or c_p and η_p (for props).

These parameters depend on speed and altitude which are normally prescribed in the mission specification.

Methods for determining installed engine characteristics are given in Chapter 6 of Part VI.

Step 4: Determine the endurance and/or loiter capability of the airplane for each of the endurance or loiter portions of the mission profile. This is done as follows:

Decide whether the endurance and/or loiter is to be performed at constant altitude or at constant speed. Identify which of the Breguet equations (5.45)-(5.48) apply.

For airplanes with short endurance or loiter segments (approximately 0.5 hours) it is reasonable to assume that all parameters in the Breguet equations are constant during the intended opera-

tion. For airplanes with longer endurance or loiter requirements this is not acceptable. For such airplanes it is suggested to break the endurance or loiter part of the mission into segments of approximately 0.5 hours each. The parameters in the Breguet endurance/loiter equations can be assumed constant but different for each segment!

Now proceed as follows:

For the first endurance/loiter segment, estimate the average loiter lift coefficient from:

$$C_{L_{ltr_1}} = (W_{begin} - 0.5W_{fuel_1})/\bar{q}_1 S \qquad (5.49)$$

where for propeller driven airplanes:

$$W_{fuel_1} = E_1\{(c_p/\eta_p)P_{reqd}\}_1 \qquad (5.50)$$

and where for jet airplanes:

$$W_{fuel_1} = E_1\{c_j W/(L/D)\}_1 \qquad (5.51)$$

Note: the subscript '1' here means that the particular quantity applies to endurance/loiter segment 1.

The average value of endurance/loiter lift coefficient (in Eqn.(5.49)) is entered into the trimmed drag polar to determine the corresponding value of the drag coefficient. This information in turn is used to compute the values of (L/D) or $\{(C_L)^{3/2}/C_D\}$ or $\{(C_L)^{1/2}/C_D\}$ which are needed in the Breguet endurance/loiter Eqns.(5.45)-(5.48).

This procedure is repeated as many times as needed until the required total endurance/loiter time is met or until the fuel is exhausted.

Step 5: Note any discrepancies between the computed endurance/loiter times and those required by the mission specification. Decide what design changes (if any) must be made.

Possible design changes are discussed in Step 5 in Sub-section 5.4.4.

Step 6: Document all the results, including any design changes made.

5.6 DIVE

5.6.1 Applicable Regulations

Civil: There are no airworthiness regulations which deal specifically with dives from a performance viewpoint. The following FAR's define the required load factors at the dive speed for civil airplanes:

FAR 23.333, 23.335, 25.333 and 25.335, see Appendix A and also Part V, pages 31-38.

Military: There are no performance related requirements placed on the dive speed. For load factor definitions, see Part V, pages 38 and 39.

5.6.2 Relationship to Preliminary Design

See Part II, Chapter 2, Step 20.

5.6.3 Mathematical Model for Analyzing Dives

Figure 5.12 depicts the forces which act on an airplane in a straight line dive. The equations of motion for a straight line dive at constant speed are:

$$T\cos(\alpha + \phi_T) - C_D\bar{q}S - W\sin\gamma = 0 \qquad (5.52)$$

$$T\sin(\alpha + \phi_T) + C_L\bar{q}S - W\cos\gamma = 0 \qquad (5.53)$$

These equations represent a 'snapshot' taken at constant altitude. The flight path (here: dive) angle, γ is negative in these equations and is negative as shown in Figure 5.12.

In these equations, which assume that moment equilibrium exists, the airplane drag coefficient comes from a 'trimmed' drag polar. Part VI, Section 4.10 presents a method for computing trim drag.

The stability and control characteristics of the airplane in dives (high speed) were already discussed in Chapter 4: Sections 2.1, 2.8 and 2.9.

There also exists a unique relationship between the angle of attack, α and the lift coefficient, C_L. A method for determining C_L versus α is given in Part VI, Chapter 8.

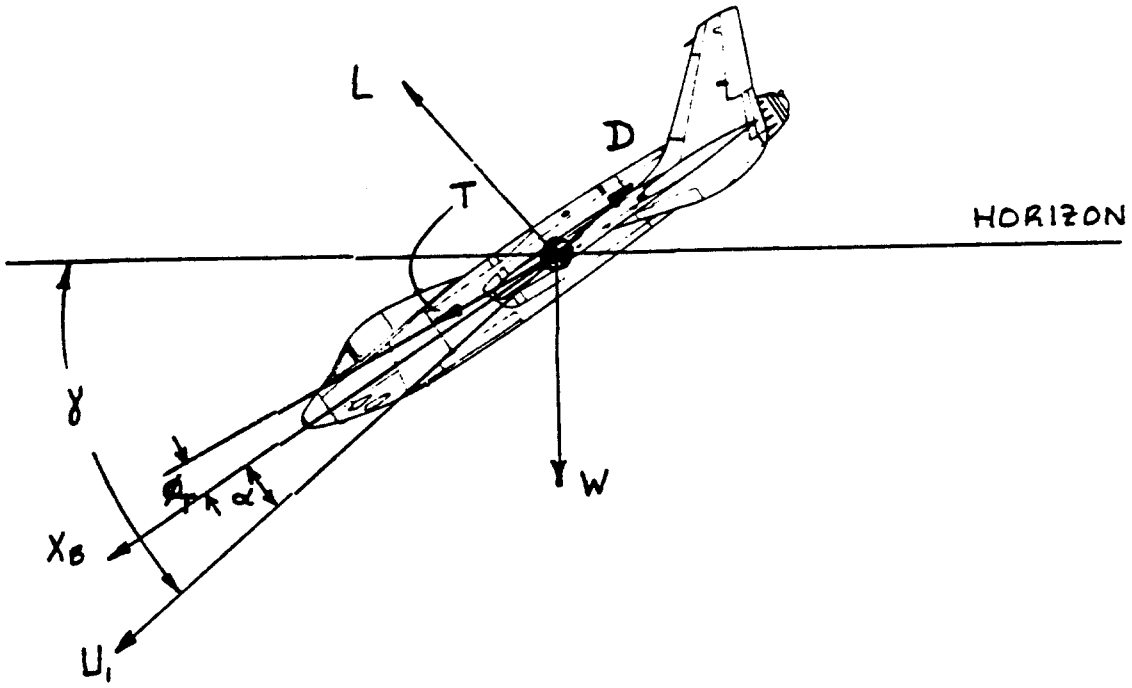

Regular Dive

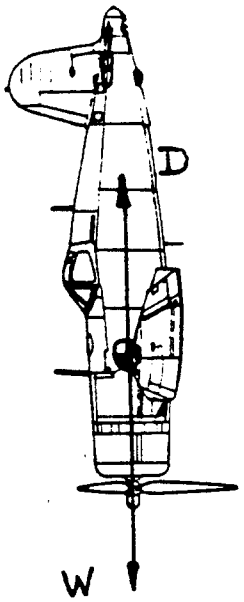

Vertical Dive

Figure 5.12 Forces Acting on an Airplane in a Dive

The quantity T in Equations (5.52) and (5.53) is the so-called installed thrust. Methods for determining the installed thrust capability of an airplane are presented in Part VI, Chapter 6.

The following quantities in Eqns.(5.52) and (5.53) are to be considered as variables: speed or dynamic pressure, $\bar{q}$, angle of attack, α and flight path angle, γ. The thrust (or power) setting, T, the weight, W and the thrust inclination angle ϕ_T are assumed to be known. Obviously one of the variables will have to be preselected!

Usually a dive is considered at some known dive angle or at some known speed.

1. Dive for known speed.

In this case, the dynamic pressure, $\bar{q}$ is known. The solution process goes as follows:

Assume a value for angle of attack, α. This is used to find C_D and C_L. Equation (5.52) is then used to solve for the flight path angle, γ. Next, Equation (5.53) is used to solve for α. This value of α is compared with the first one and an iteration is performed until there is agreement to within 0.1 degrees.

2. Dive for known dive angle.

In this case, the flight path angle, γ is known. The solution process goes as follows:

Assume a value for angle of attack, α. This is used to find C_D and C_L. Equation (5.52) is then used to solve for the dynamic pressure, $\bar{q}$. Next, Equation (5.53) is used to solve for α. This value of α is compared with the first one and an iteration is performed until there is agreement to within 0.1 degrees.

NOTE: in certain applications a speed brake may be employed. The effect of speedbrakes on the drag polar is discussed in Section 4.12 in Part VI.

In extreme cases an airplane may be required to dive vertically. The equilibrium dive speed in such a case is called the 'terminal dive speed'.

Figure 5.12 also shows the forces which act on the airplane in that case. Since no lift is required in a vertical dive, the drag coefficient is equal to the zero-lift drag coefficient, C_{D_o} and the equation of motion is:

$$T - W = C_{D_o} \bar{q} S \qquad (5.54)$$

Since T and C_{D_o} both depend on speed, this equation must be solved also with an iteration. Assume a terminal Mach number at some altitude. Find C_{D_o} and the installed thrust (for whatever thrust setting has been assumed) and see if the equation is satisfied. If not, iterate until the terminal dive speed is within 0.5 percent.

5.6.4 Step-by-Step Procedure for Analyzing Dives

Step 1: Determine the flight conditions and airplane configurations for which dives must be performed. This information is normally contained in the mission specification.

Step 2: For the flight conditions and configurations defined in Step 1, determine the trimmed drag polars of the airplane. Also determine the installed thrust (or power) characteristics.

Trimmed drag polars are determined with the method of Chapter 4, Part VI. Installed thrust (or power) characteristics are determined with the method of Chapter 6, Part VI.

Step 3: Use the iteration process defined in Sub-section 5.6.3 to determine the dive performance of the airplane. Compare the results with the requirements and decide whether or not design adjustments are in order.

Step 4: Document the results, including any design changes made.

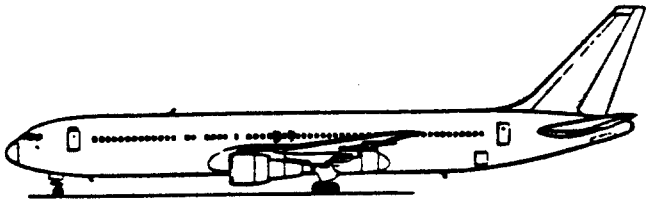

5.7 MANEUVERING

5.7.1 Applicable Regulations

Civil: There are no airworthiness regulations which deal specifically with maneuvering performance. The load factors which an airplane must be able to withstand from a structural viewpoint are covered in:

FAR 23.333, 23.335, 23.337, 25.333, 25.335 and 25.337.

Military: MIL-F-8785C, Pars. 3.1.7 and 3.2.3.5-6.

5.7.2 Relationship to Preliminary Design

See Part I, Section 3.5 and Step 27, Part II.

5.7.3 Mathematical Model for Analyzing Maneuvering Flight

The following maneuvers will be considered:

1. Instantaneous maneuvers: pull-up (push-over) and level turns

2. Sustained maneuvers: pull-up (push-over) and level turns.

Figures 5.13 and 5.14 show the forces which act on an airplane in pull-ups and in level turns.

The equations of motion for the situation of Figure 5.13, which represents a steady, symmetrical pullup are:

$$T\cos(\alpha + \not{\beta}_T) - C_D\bar{q}S - W\sin\gamma = 0 \qquad (5.55)$$

$$T\sin(\alpha + \not{\beta}_T) + C_L\bar{q}S - (W/g)U_1Q_1 - W\cos\gamma = 0 \qquad (5.56)$$

Note that at the bottom of the pullup: $\gamma = 0$.

These equations represent a 'snapshot' taken at constant altitude. The flight path (here: dive) angle, γ is negative in these equations and as shown in Figure 5.13.

In these equations, which assume that moment equilibrium exists, the airplane drag coefficient comes from a 'trimmed' drag polar. Part VI, Section 4.10 presents a method for computing trim drag.

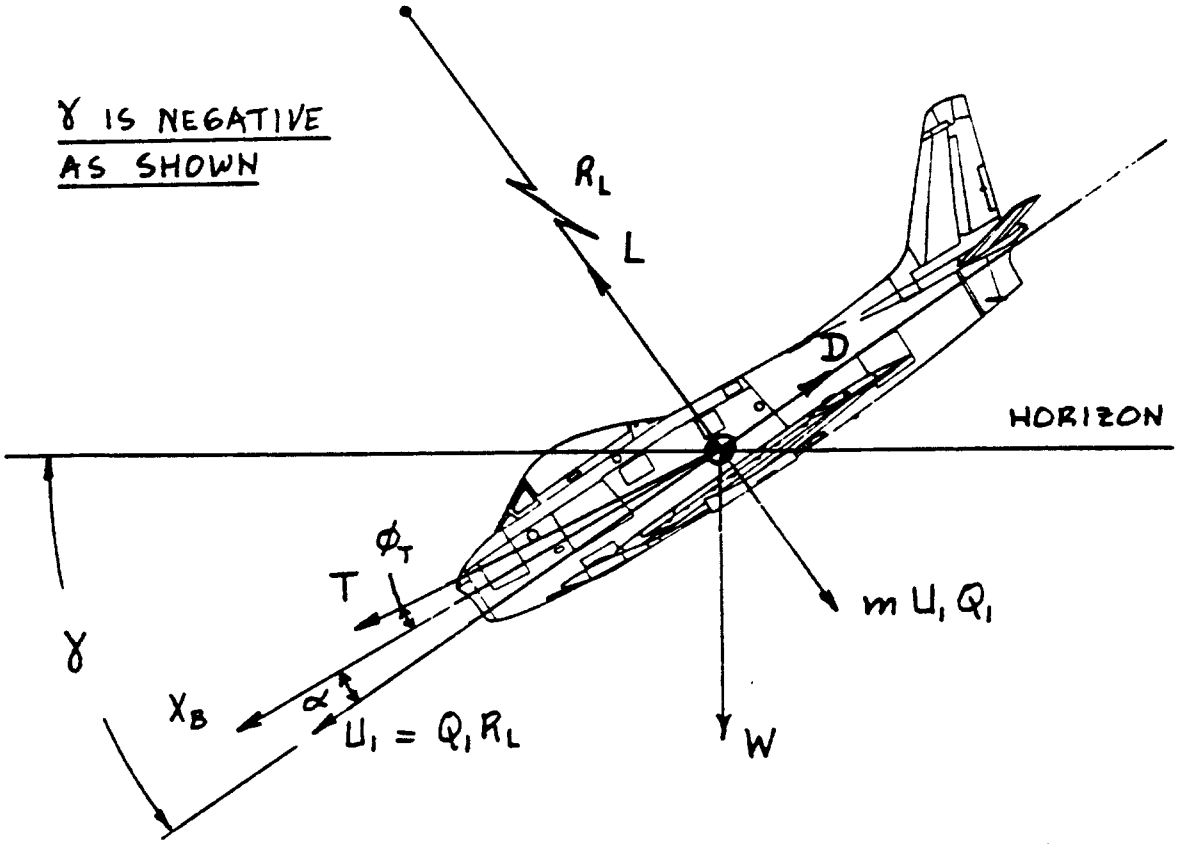

Figure 5.13 Forces Acting on an Airplane in a Pullup

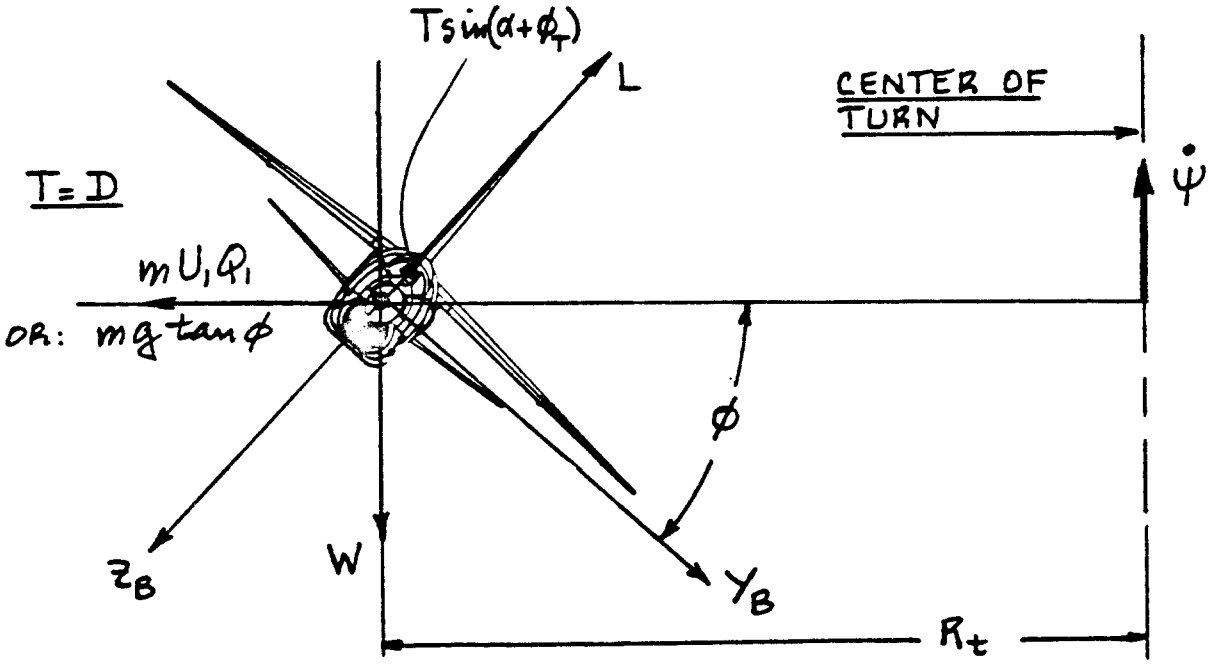

Figure 5.14 Forces Acting on an Airplane in a Level Turn

The stability and control characteristics of the airplane in dives (high speed) were already discussed in Chapter 4: Sections 2.1, 2.8 and 2.9.

There also exists a unique relationship between the angle of attack, α and the lift coefficient, C_L. A method for determining C_L versus α is given in Part VI, Chapter 8. The lift coefficient in this case is also dependent on pitchrate, Q_1 through the stability derivative: C_{L_q}. The reader is referred to Chapter 5 of Reference 12 for a discussion of this effect.

The pitchrate, Q_1 in a pullup is:

$$Q_1 = (g/U_1)(n - 1) \tag{5.57}$$

where: n is the load factor in the maneuver.

The quantity T in Equations (5.55) and (5.56) is the so-called <u>installed thrust.</u> Methods for determining the installed thrust capability of an airplane are presented in Part VI, Chapter 6.

The equations of motion for the situation depicted in Figure 5.14 (steady level turn) are:

$$T\cos(\alpha + \phi_T) - C_D\bar{q}S = 0 \tag{5.58}$$

$$T\sin(\alpha + \phi_t) + C_L\bar{q}S - W\cos\phi - (W/g)U_1Q_1 = 0 \tag{5.59}$$

All comments made for Equations (5.55) and (5.56) apply also to these equations. The pitchrate, Q_1 in a level turn is:

$$Q_1 = (g/U_1)(n - 1/n) \tag{5.60}$$

The <u>turnrate</u> in a level turn is:

$$\dot{\psi}_1 = (g\tan\phi)/U_1 = (g/U_1)(n^2 - 1)^{1/2} \tag{5.61}$$

The <u>turn radius</u> in a level turn is:

$$R_t = \{(U_1)^2/g\}/\tan\phi = \{(U_1)^2/g\}/(n^2 - 1)^{1/2} \quad (5.62)$$

As a help to the reader, Figure 5.15 has been included. It allows rapid determination of turnrate and turn radius.

In the case of acrobatic airplanes and certain military airplanes the mission specification may contain specific numerical requirements for 'pulling g's or for specific turnrates and /or turn radii.

To meet these requirements on an <u>instantaneous</u> basis, all that is required is to show that the maximum trimmed lift capability of the airplane in a given flight condition and airplane configuration is not exceeded:

$$C_{L_{maneuver}} < C_{L_{max}} \text{ or } C_{L_{buffet}} \quad (5.63)$$

To meet these requirements on a <u>sustained</u> basis, condition (5.63) must still be satisfied. However, in addition, the following condition must be satisfied:

$$T_{reqd} < T_{max} \text{ or } P_{reqd} < P_{max} \quad (5.64)$$

At this stage in the preliminary design process it suffices to verify the sustained capability by showing that:

<u>for jet airplanes:</u>

$$T_{reqd} = \{C_{D_o} + (C_{L_{man}})^2/\pi Ae\} < T_{max} \quad (5.65)$$

<u>for propeller driven airplanes:</u>

$$P_{reqd} = \{C_{D_o} + (C_{L_{man}})^2/\pi Ae\}U_1/550 < P_{max} \quad (5.66)$$

The lift coefficient in Equations (5.65) and (5.66) is to be found from:

$$C_{L_{man}} = nC_{L_1} \quad (5.67)$$

where: n is the loadfactor in the maneuver and

$$C_{L_1} = W/\bar{q}S \quad (5.68)$$

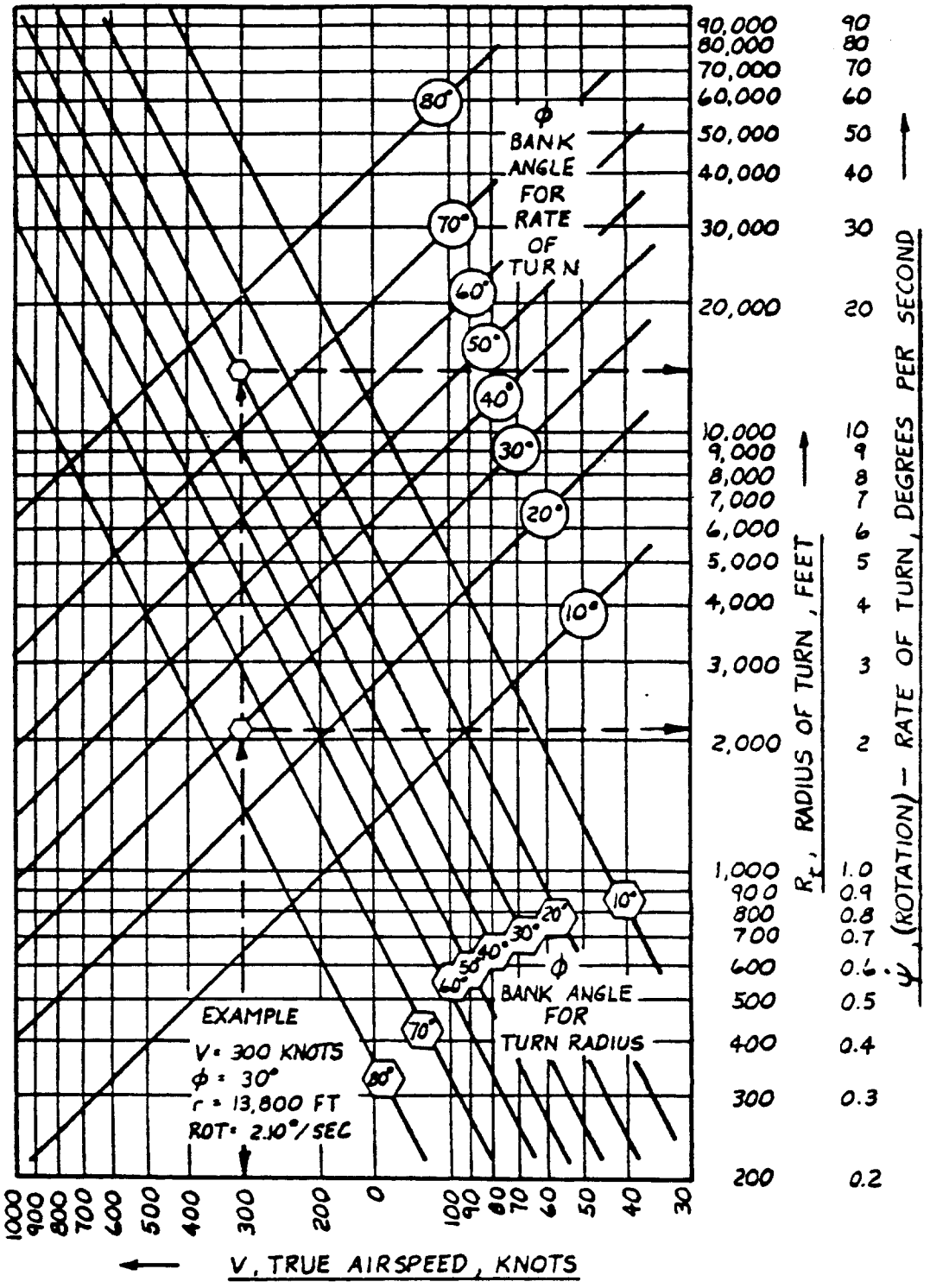

Figure 5.15 Generalized Turning Performance in a Level Turn

Taken from: Hurt, H.H.Jr., Aerodynamics for Pilots, ATC Manual 51-3, 1963.

IMPORTANT NOTE:

Whenever sufficient thrust (or power) IS NOT available to keep the speed constant in a pullup or turn, the speed will begin to bleed off. The rate at which this occurs is called the 'Bleed Rate'. See Appendix B for further information on bleed rate. Modern fighters may have to be designed to have certain minimum bleed rate values in certain combat situations. The equations of motion which govern the airplane behavior in such cases is too complex for Class II methods. Reference 12 in Chapter 2, page 43 shows a development of the general equations of motion. The bleed rate can be determined from these equations by integration.

An approximation for the bleed rate is given in Subsection 5.7.4.

The reader is encouraged to read Reference 29 for some interesting views on fighter agility.

5.7.4 Step-by-Step Procedure for Analyzing Maneuvering Flight

Step 1: From the mission specification of the airplane determine the required maneuvering capabilities.

Typically these are stated in terms of:

1. Instantaneous g's
2. Sustained g's
3. Turn radius
4. Turnrate
5. Bleedrate

Tabulate the flight conditions and airplane configurations for which maneuvering requirements must be met.

Step 2: Match each maneuvering requirement with the appropriate equation in Sub-section 5.7.3 and determine the required input information.

This input information generally will consist of:

1. Trimmed drag polars for the appropriate Mach number and configuration.

2. Installed thrust (or power) data for the ap-

propriate Mach number and throttle setting.

3. Maximum trimmed lift capability and buffet boundary data.

NOTE: In sub-section 5.7.3 no equation was given for bleed rate. As a first and rough approximation it is suggested to use:

$$\text{Bleed rate} = \dot{u} = C_D \bar{q} S - T\cos(\alpha + \phi_T) \qquad (5.69)$$

where: $$C_D = C_{D_o} + (C_{L_{man}})^2/\pi Ae \qquad (5.70)$$

with: $C_{L_{man}}$ given by Eqn.(5.67).

Step 3: With the data and equations from Steps 1 and 2 determine whether the airplane meets the maneuvering requirements.

If discrepancies are evident, identify the reason(s). Typical reasons for not meeting maneuvering requirements are:

1. Deficiency in maximum lift capability: this requires adjustments in wing design

2. Deficiencies in thrust (or power) capability: this requires adjustments in powerplant choice or powerplant installation design.

Decide on any design adjustments required and see whether the design needs to be iterated.

Note: For fighter airplanes the maneuvering and specific excess power (specific energy) capabilities are often plotted as a function of speed and altitude. Figures 5.16 and 5.17 represent typical examples.

Step 4: Document the results, including any design changes made.

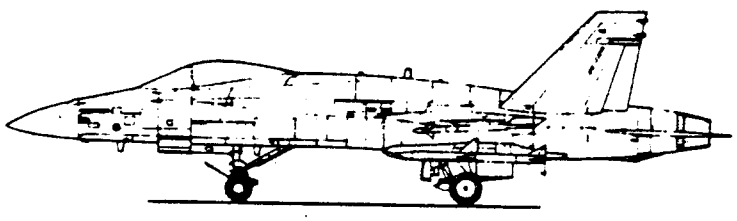

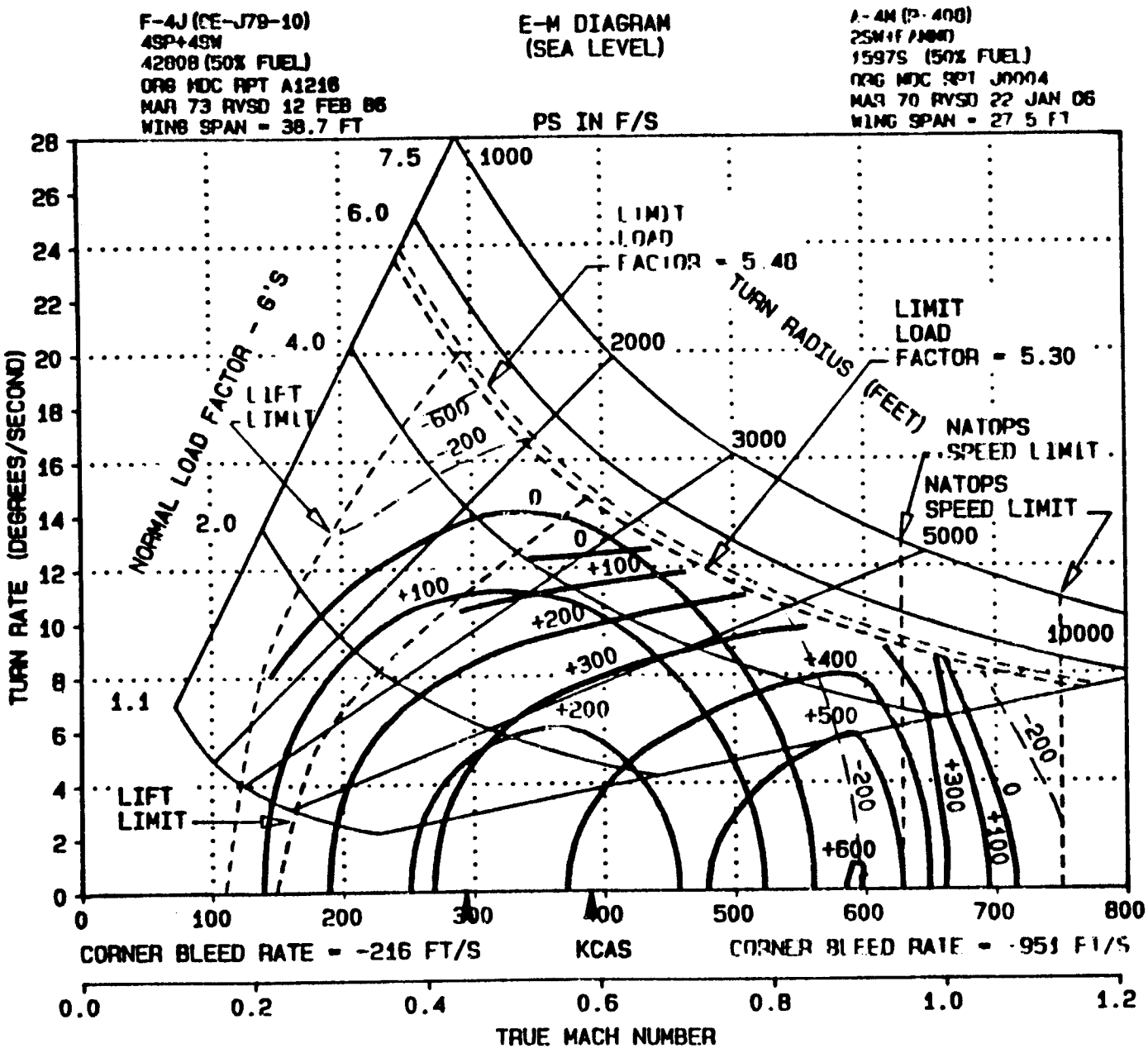

COURTESY: NADC

Figure 5.16 Maneuvering Performance: F-4J Versus A-4M

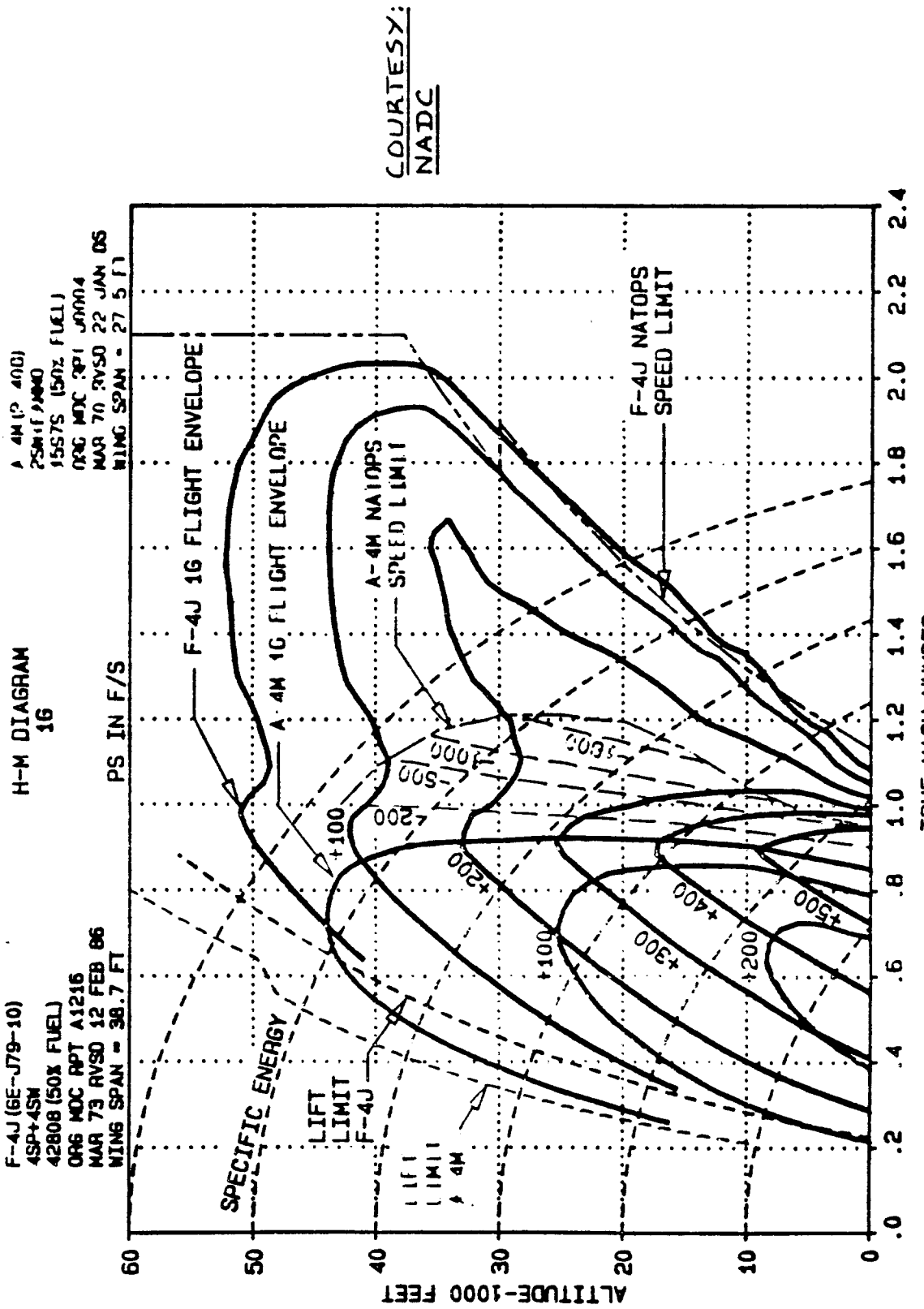

Figure 5.17 Flight Envelopes and Specific Energy: F-4J Versus A-4M

5.8 DESCENT AND GLIDE

5.8.1 Applicable Regulations

Civil: There are no regulations which deal with descents and glides from a performance viewpoint. The descent flight phase normally terminates in an approach to landing. During that phase the climb regulations are in effect: see Section 3.5.

Military: The only regulation in force is that which disallows range credit for descents by subsonic airplanes. For supersonic airplanes descent range credit may be taken in certain instances. See: MIL-C-005011B, par.3.5.3.4. The USNavy AS-5263 does not allow range credit for descent at all. See Appendix B.

5.8.2 Relationship to Preliminary Design

This performance item was not included in the airplane sizing process, except to account for fuel used: see Part I, Section 2.4.

5.8.3 Mathematical Model for Analyzing Descent and Glide

Descents and glides are closely related to climbs and dives. The differences are subtle. In a descent the flight path angle is normally shallow and thrust (or power) is reduced. In a glide the flight path angle is still shallow (the Space Shuttle is an exception!) but the thrust (or power) is at flight idle, zero or absent (such as in gliders!).

Figure 5.18 depicts the forces which act on an airplane in a descent, Figure 5.19 for a glide.

For a (partial) power descent, the equations of motion are:

$$T\cos(\alpha + \phi_T) - C_D\bar{q}S - W\sin\gamma = 0 \qquad (5.71)$$

$$T\sin(\alpha + \phi_T) + C_L\bar{q}S - W\cos\gamma = 0 \qquad (5.72)$$

These equations are identical to Eqns.(5.52) and (5.53), with the flight path angle, γ being NEGATIVE again. Solutions to these equations are discussed in Subsection 5.6.3 on pages 146-148.

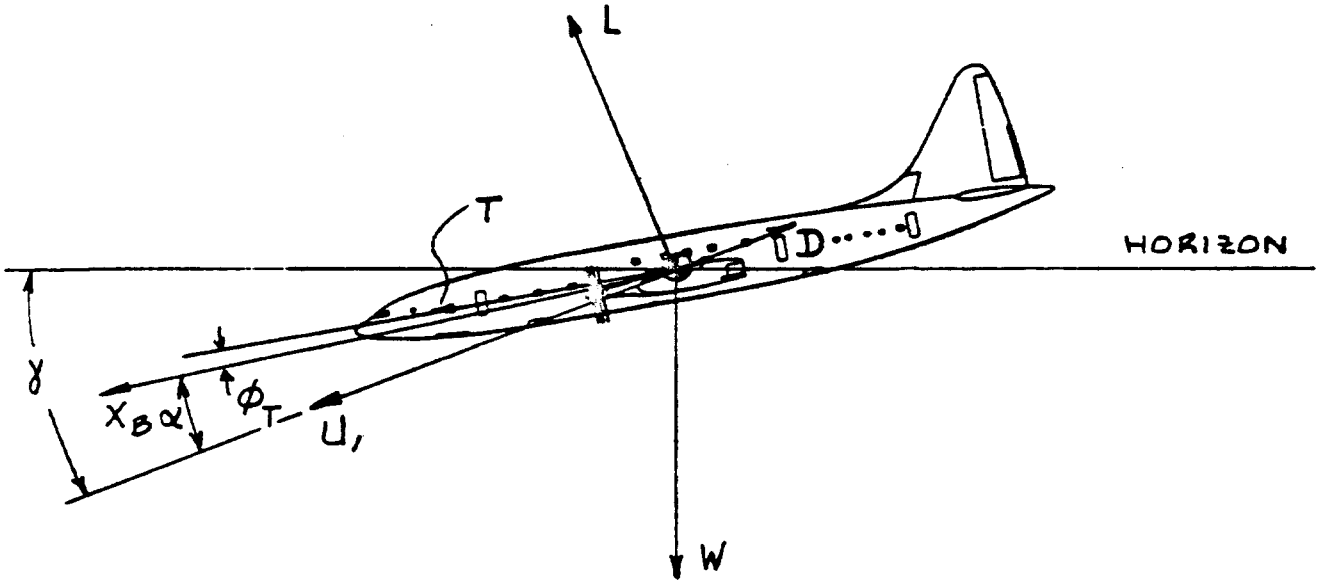

Figure 5.18 Forces Acting on an Airplane in a Descent

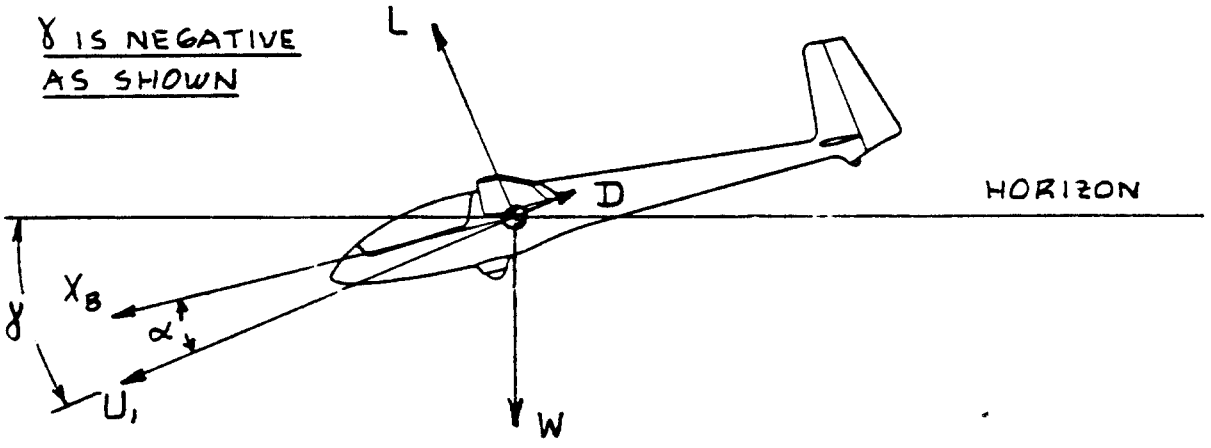

Figure 5.19 Forces Acting on an Airplane in a Glide

Once the flight path angle is known, the rate of descent, RD is found from:

$$RD = -U_1 \sin\gamma, \text{ with } \gamma \text{ being negative} \qquad (5.73)$$

For a glide (power off), the equations of motion are:

$$C_D \bar{q} S + W \sin\gamma = 0 \qquad (5.74)$$

$$C_L \bar{q} S - W \cos\gamma = 0 \qquad (5.75)$$

In this case the flight path angle, γ follows from:

$$\tan\gamma = -(C_D/C_L) = -1/(C_L/C_D) \qquad (5.76)$$

The rate of descent follows from:

$$RD = \{(W/S)(2/\rho)(C_D^{\,2}/C_L^{\,3/2})(\cos\gamma)^3\}^{1/2} \qquad (5.77)$$

If the glide is conducted at constant lift-to-drag ratio, the glide range is:

$$R_{GL} = -h/\tan\gamma \qquad (5.78)$$

Similarly, the time-in-the-air follows from:

$$t_{GL} = h/RD \qquad (5.79)$$

5.8.4 Step-by-Step Procedure for Analyzing Descent and Glide

Step 1: Determine the descent and/or glide requirements for the airplane from the mission specification.

Note: Except for gliders, most airplane specifications do not contain requirements for descents and/or glides.

Step 2: Determine which of equations (5.71)-(5.79) apply to and obtain the required input information.

Step 3: Compute the descent and/or glide flight path angle, speed, rate-of-descent, range and time-in-the-air. Compare these data with the requirements (if any). Determine what (if any) design adjustments must be made.

If the deficiency is in glide range or time-in-the-air, the problem is usually too much drag.

Step 4: Document the results of all calculations, including any design adjustments made.

5.9 LANDING

5.9.1 Applicable Regulations

Civil: FAR 23.75 and FAR 25.125, see Appendix A.

Military: MIL-C-005011B, par. 3.4.2.11, 3.4.2.12 and 3.4.7 and:
AS-5263, par. 3.5.2.12-13, and 3.5.7, see Appendix B.

5.9.2 Relationship to Preliminary Design

See Part I, Section 3.3.

5.9.3 Mathematical Model for Analyzing Landing Performance

The definition of landing distance and the associated reference speeds depends on which regulation is used to certify the airplane: FAR 23, FAR 25 or Military.

Figure 5.20 shows the differences in the definitions for landing distances and the associated reference speeds.

The following method for computing the landing distance, s_L and the landing fieldlength, s_{FL} is due to Torenbeek (Reference 28):

For FAR 25:

$$s_{FL} = s_L/0.6 \tag{5.80}$$

For FAR 23 and for Military:

$$s_L = s_{AIR} + s_{LG} \tag{5.81}$$

where: s_{AIR} is the distance from the obstacle height, h_L to the point of touchdown:

$$s_{AIR} = (1/\bar{\gamma})\{(V_A^2 - V_{TD}^2)/2g + h_L\} \tag{5.82}$$

$$\text{with: } \bar{\gamma} = \{(D - T)/W\}_{ave}, \tag{5.83}$$

for which an average value of 0.10 is often used. This quantity actually ranges from about 0.05 (transports) at the obstacle, to a value of C_D/C_L in ground effect at touch-

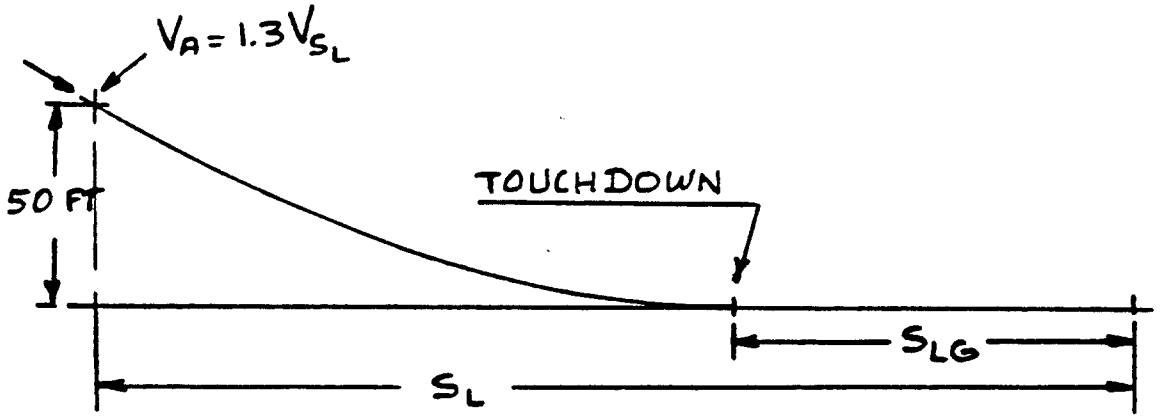

Definition of FAR 23 Landing Distance

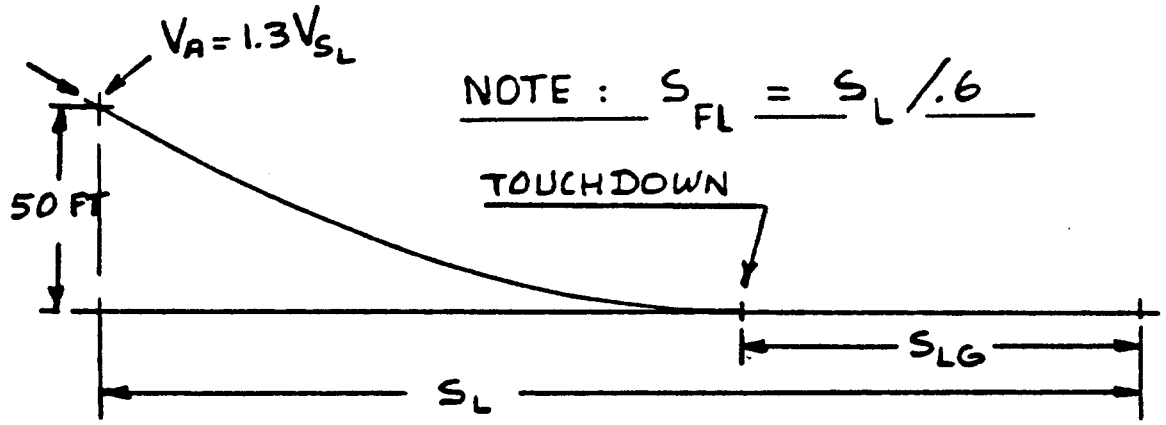

Definition of FAR 25 landing Distance

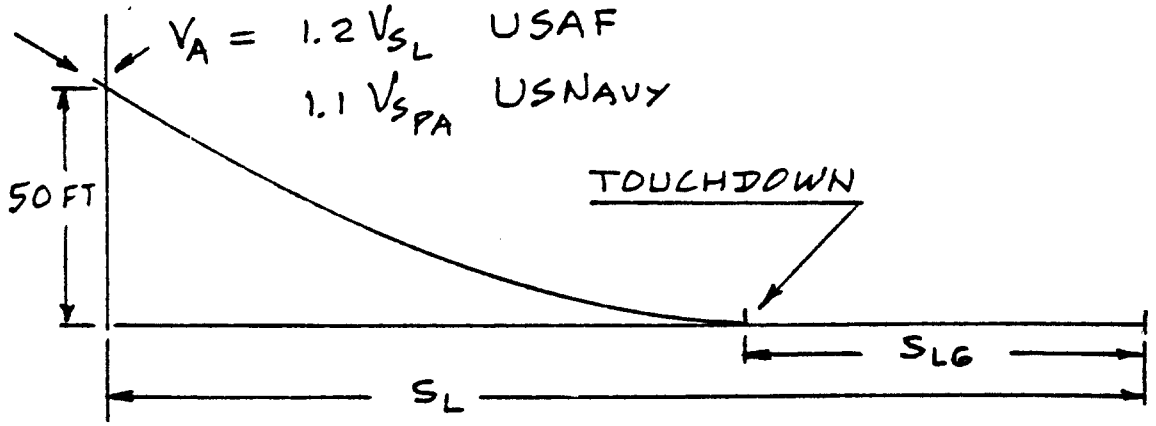

Definition of Military Landing Distance

Figure 5.20 Definition of Landing Distances According to the Regulations

down which assumes that T=0 at touchdown.

V_A is the approach speed at the obstacle:

FAR 23 and 25: $V_A = 1.3V_{s_L}$ (5.84)

MIL-C-005011B: $V_A = 1.2V_{s_L}$ (5.85)

AS-5263: $V_A = 1.1V_{s_{PA}}$ (5.86)
but with thrust required for level flight at $1.15V_{s_{PA}}$

$$V_{TD} = V_A[1 - \{(\bar{\gamma})^2/\Delta n\}]^{1/2} \quad (5.87)$$

with: Δn = 0.10 as a reasonable average: this quantity depends on pilot technique and on airplane handling qualities!

h_L = 50 feet in all regulations

s_{LG} is the landing ground run to zero speed on the runway:

$$s_{LG} = \{(V_{TD})^2\}/2\bar{a} \quad (5.88)$$

with: $\bar{a}$, the average deceleration for the ground-run. In preliminary design it is acceptable to use:

For light airplanes with simple brake systems:

$\bar{a}/g$ = 0.30 to 0.35

For turboprops without use of reversible propellers:

$\bar{a}/g$ = 0.35 to 0.45

For turbojets and turbofans with ground-spoilers, antiskid devices and speed brakes (but no reverse thrust):

$\bar{a}/g$ = 0.40 to 0.50

For the latter, including nosewheel braking:

$\bar{a}/g$ = 0.50 to 0.60

Important Note:

Airplanes which are carrier based must be compatible with the performance restrictions inherent in each arresting system. A suitable mathematical model for determining compatibility with USNavy arresting gear systems is given in Sub-sub-section 3.3.5.2, page 115, Part I.

5.9.4 Step-by-Step Procedure for Analyzing Landing Performance

The following step-by-step procedure is suggested for determining the landing distance(s) of an airplane:

Step 1: Determine which regulation applies to the design and read that regulation. See Table 1.3 and Subsection 2.1.1.

Determine the landing distance requirements from the mission specification.

Step 2: Determine whether Eqn.(5.80) or Eqn.(5.81) govern the landing distance calculation and prepare the necessary input data.

IMPORTANT NOTES:

1. Military airplanes may have to land with a variety of stores on board. Their effect on weight and on the drag polar must be accounted for.

2. The weight at landing is the so-called landing weight, W_L. The regulations require the designer to identify what that landing weight is in relationship to the takeoff weight, W_{TO}.

   Table 3.3, page 107 of Part I provides typical ranges of landing-weight-to-takeoff-weight ratios.

Step 3: Compute the landing distance(s) with the appropriate equation of Step 2 and compare the results

with the requirements of Step 1. If there is a discrepancy of more than 5 percent, design changes are warranted.

Step 4: Decide what (if any) design changes are warrented. Typical design changes which can be contemplated are:

1. Lower wing loading, W/S

2. Higher maximum landing lift coefficient, $C_{L_{max_L}}$. This can be achieved with a change in wing flap design. The effect on weight, complexity and lateral control space must be accounted for!

Step 5: Document the results obtained, including any design changes made.

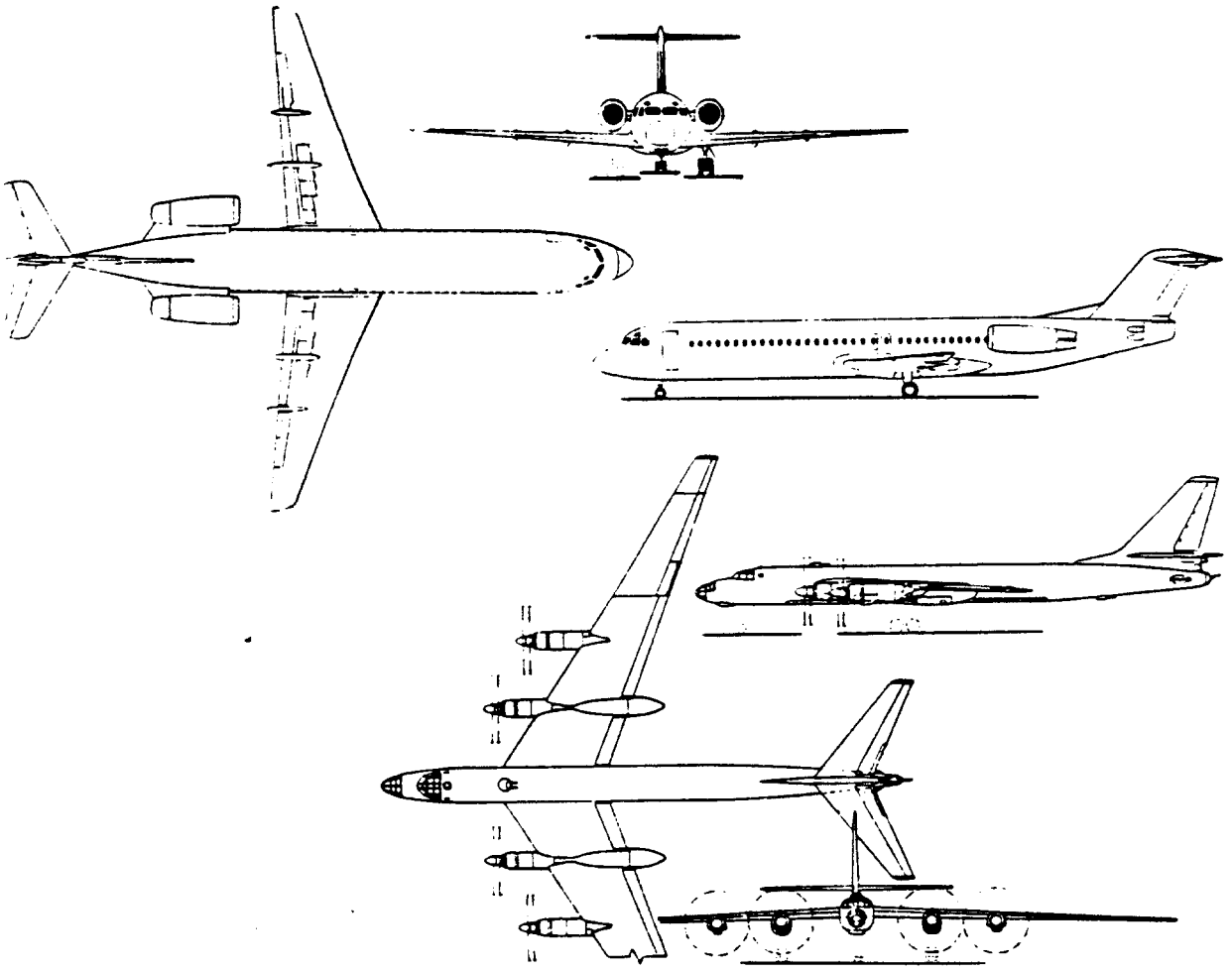

5.10 MISSION PROFILE ANALYSIS

Particularly in the case of military airplanes, but also for civil airplanes it is useful to prepare mission profiles for all intended missions of the airplane.

Two examples mission profiles are given in Fig.5.21. These mission profiles were used in the early sizing process as outlined in Chapter 2 of Part I. The initial mission performance verification was done as part of P.D. Sequence I, see Step 14, page 16, Part II.

These mission profiles are used again in the final mission performance verification process as outlined in Sections 5.1-5.9 of this chapter. This corresponds to Step 24 in P.D. Sequence II, see page 20, Part II.

For military airplanes various military missions have been given 'standardized' mission profiles. Detailed examples of these may be found in Appendix B.

It will be seen that these mission profiles consist of mission segments which are typically labelled as:

Takeoff, Climb, Cruise, Loiter,

Descent, Landing, Combat, etc.

The methods of Sections 5.1 - 5.9 can be used to perform almost any mission profile analysis.

A typical mission profile analysis will produce the following results:

1. Verification of stall speed requirements: see Section 5.1 for the method.

2. Verification of takeoff fieldlength requirements: see Section 5.2 for the method.

3. Verification of climb requirements: see Section 5.3 for the method.

4. Verification of cruise, range and payload-range requirements: see Section 5.4 for the method.

5. Verification of endurance/loiter requirements: see Section 5.5 for the method.

6. Verification of dive requirements: see Section 5.6 for the method.

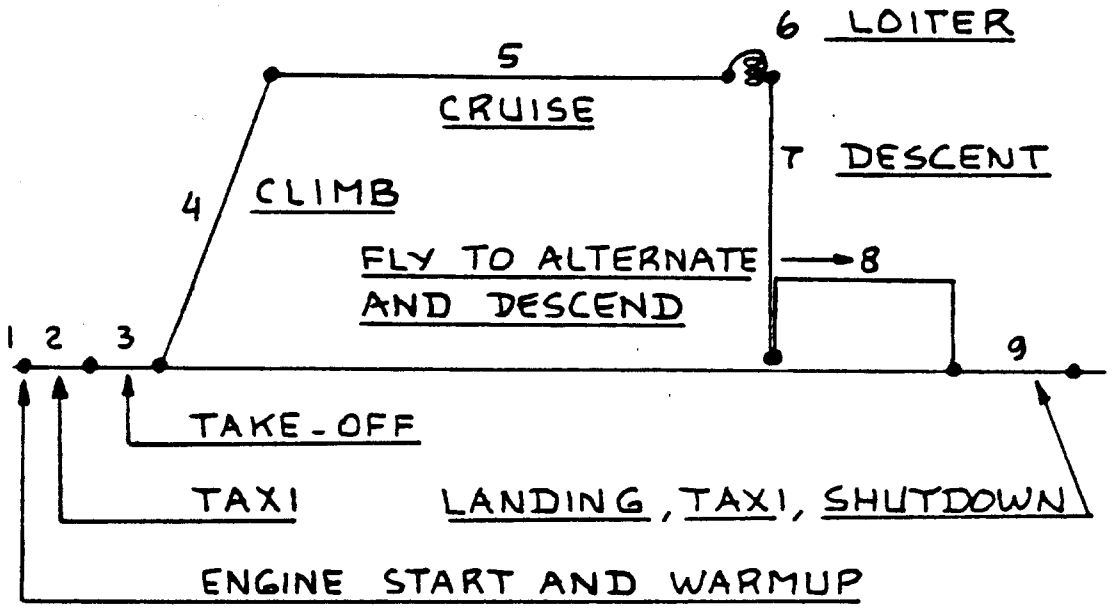

Transport

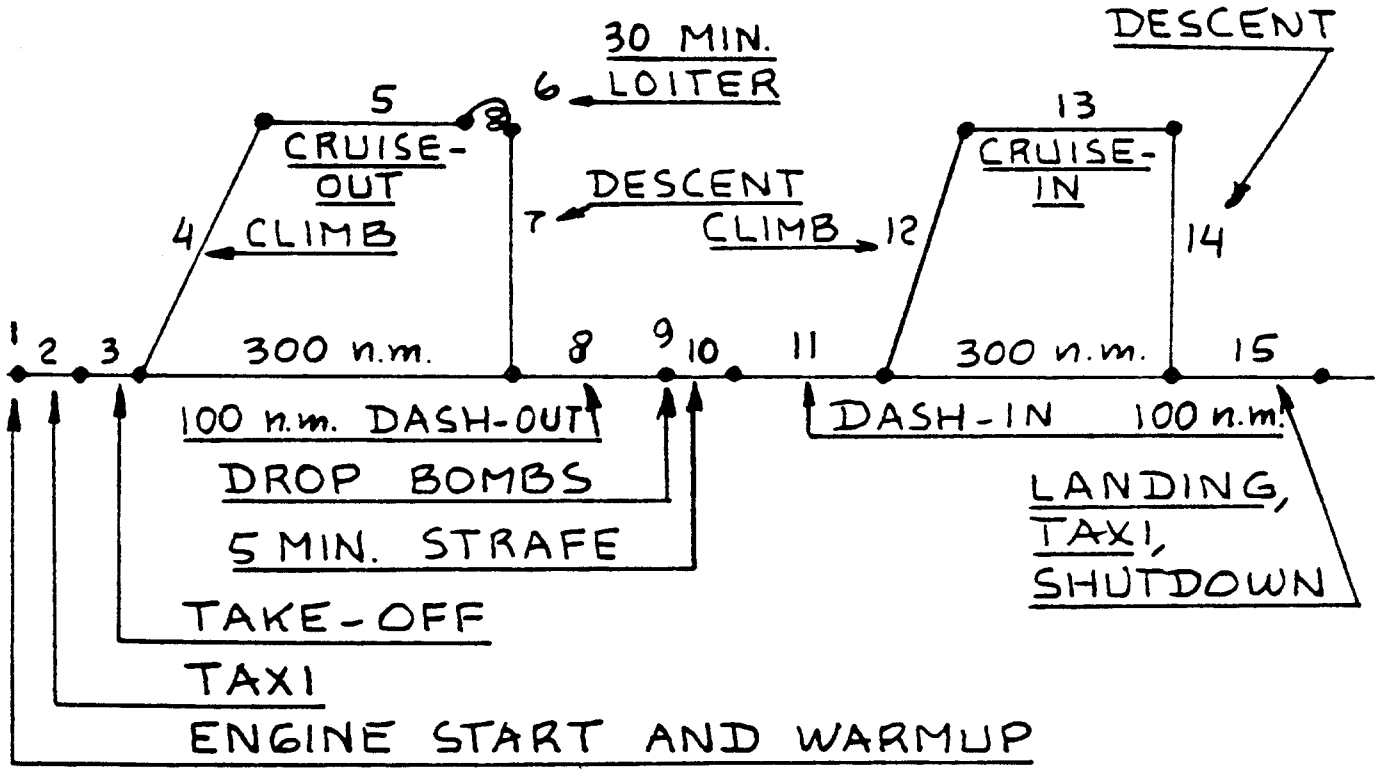

Fighter

Figure 5.21 Example Mission Profiles

7. Verification of maneuvering requirements: see Section 5.7 for the method.

8. Verification of descent and glide requirements: see Section 5.8 for the method.

9. Verification of landing fieldlength requirements: see Section 5.9 for the method.

10. Verification of fuel used during each segment of the intended mission profile:

    For each mission profile segment, i the fuel used can be estimated from:

$$(W_{F_{used}})_i = (\dot{W}_F)_i t_i \qquad (5.89)$$

    where: $(\dot{W}_F)_i$ is the average fuel flow rate in pounds per second for segment i.

    t_i is the time to complete segment i.

    Notes: 1. for climb, cruise, loiter, and descent mission phases values for t_i are easily obtained. For other mission phases these times have to be based on the operational environment. For example, taxi-fuel will be more for Chicago O'Hare than for Kansas City International.

    2. for military airplanes the method used to compute 'fuel'used' in specific mission segments is outlined in Appendix B!

    3. lacking data on the operational environment of a civil airplane, use the military method of Appendix B.

11. Preparation of a payload-range diagram: see Section 5.4 for the methodology.

12. Mission performance critique: this consists of a list of performance shortcomings AND performance excesses PLUS a list of suggested 'fixes'

The effect of performance demands during each individual mission profile segment on the takeoff weight of an airplane is easily evaluated with the so-called 'Breguet-Partials' method of Section 2.7 in Part I.

5.11 PRODUCTIVITY

When the technical aspects of the design of a new airplane have been decided on and the configuration is frozen, the important question is:

IS THE PRODUCTIVITY OF THE AIRPLANE SUFFICIENTLY HIGH TO WARRANT ITS FULL SCALE DEVELOPMENT?

To give an answer to this question, two tasks must be performed:

1. An analysis of the COST of the airplane.

   This corresponds to Step 36, page 23 of Part II. Methods for cost analysis are given in Part VIII.

2. A set of productivity evaluation criteria must be agreed upon so that the new design can be judged in a fair and understood manner.

   A number of possible evaluation criteria are given in this section.

The methods of Parts I through VII are aimed at designing an airplane to a set of stated mission requirements, while meeting all applicable airworthiness regulations. Along the way a large number of 'arbitrary' design decisions are made. The impact of these design decisions on the productivity of the airplane are not always clear. One example of such an 'arbitrary' decision was the selection of the overall configuration: Step 3 in Preliminary Design Sequence I, page 11, Part II.

That such an important decision as the selection of the overall configuration is labelled as 'arbitrary' may surprise the reader, but it should not. Refer to Figure 1.1, page 5 of Part II and to Note 1 at the bottom of page 3 of Part II!!!

In many instances, the red-white-and-blue team approach will have been used and as a result several airplane designs have evolved, all of which meet the mission and airworthiness requirements. Which is 'best'?

Again, it will be necessary to establish a set of evaluation criteria before this question can be answered.

Typical evaluation criteria which are used to judge the productivity of airplane designs are:

1. Performance Related Criteria such as:

1.1 Takeoff weight (mostly because of a historical relationship between acquisition cost and weight)

All else being the same, a low takeoff weight is judged to be 'good'.

1.2 Volume of the payload-range diagram. Examples of payload-range diagrams with different 'volumes' are given in Figures 5.22 and 5.23.

All else being the same, a large payload-range volume is judged to be 'good'.

1.3 Specific range, nm/lbs of fuel: U_1/c_jT_{reqd} or U_1/c_pP_{reqd}.

All else being the same, a large specific range is judged to be 'good'.

1.4 Seat-miles per pound of fuel:

U_1N_{seats}/c_jT_{reqd} or U_1N_{seats}/c_pP_{reqd}

All else being the same a high value of seat-miles per pound of fuel is judged to be 'good'.

1.5 Available sortie rate: high sortie rates are judged 'good'.

2. Cost Related Criteria such as:

2.1 Acquisition Cost (Also referred to as cost of ownership.

All else being the same this cost must be small for the airplane to be judged 'good'.

2.2 Profit potential: Payload available MINUS payload to break-even of operating costs.

All else being the same, the larger the profit potential, the 'better' the airplane.

2.3 (Speed times payload)/(Acquisition Cost), used in judging general aviation airplanes.

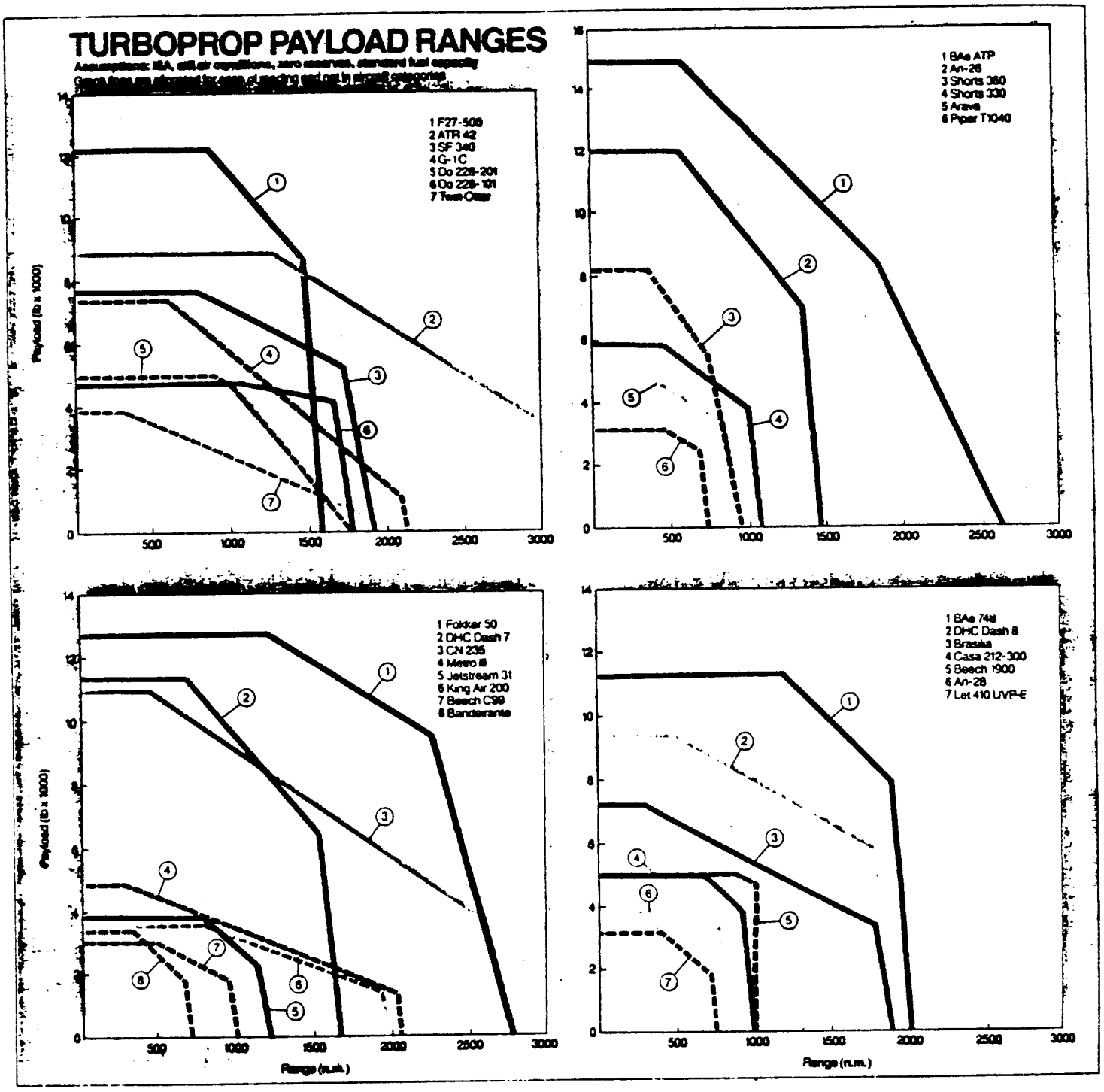

FROM: FLIGHT INTERNATIONAL*, MAY 10 1986

*BRITISH AEROSPACE WEEKLY

Figure 5.22 Payload-Range Diagrams for Turboprops

Figure 5.23 Payload-Range Diagrams for Jet Transports

Payload range – Boeing 747 family

- Long-range cruise
- Standard day
- International reserves

747SR	BRGW 520,000lb to 600,000lb
747-100B/-300	BRGW 710,000lb to 750,000lb
747-200B/-300	BRGW 775,000lb to 833,000lb
747SP	BRGW 630,000lb to 700,000lb
747-400	BRGW 800,000lb to 850,000lb

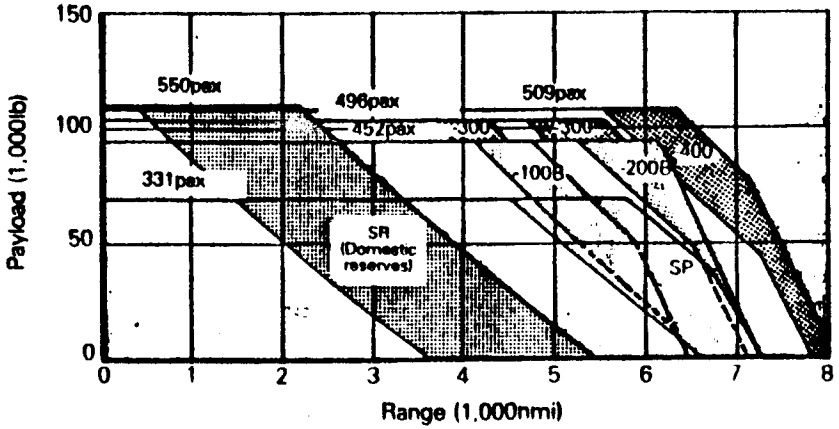

Payload range – McDonnell Douglas MD-11

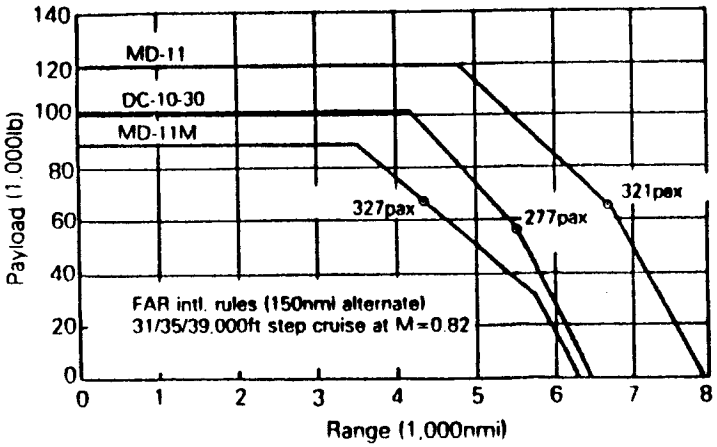

Payload range – Boeing 767

- Mixed-class interiors
- Passengers at 200lb each

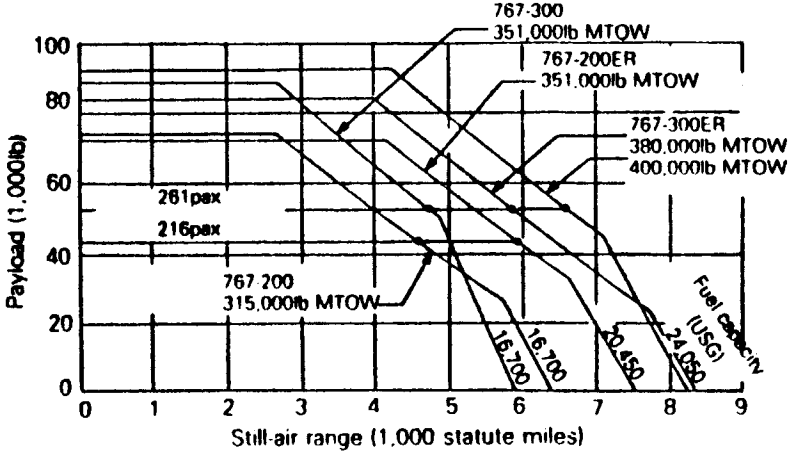

Payload range – Airbus A300/A310

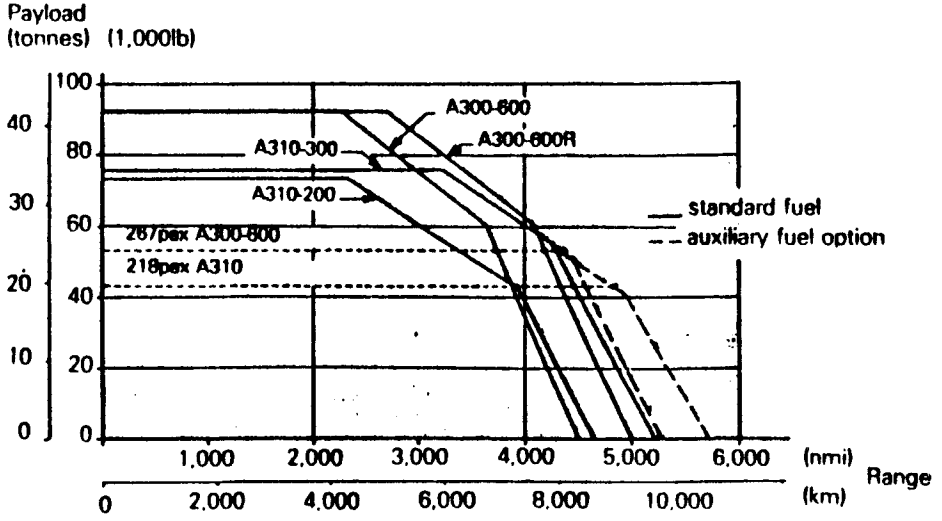

FROM: INTERAVIA* MAY 1986

*SWISS MONTHLY

All else being the same, when this parameter is larger, the airplane is judged to be better.

2.4 Direct Operating Cost (DOC).

All else being the same, low DOC is judged to be 'good'.

2.5 Return on Investment (ROI).

All else being the same, high ROI is judged to be 'good'.

2.6 Life Cycle Cost (LCC).

All else being the same, low LCC is judged to be 'good'.

2.7 Maintenance manhours required per flight hour or per sortie.

This quantity should be low for the airplane to be judged 'good'.

The 'performance' related criteria, 1.1-1.6 can be evaluated with the methods of Sections 5.1-5.10.

The 'cost' related criteria, 2.1-2.7 require a method to relate airplane design parameters to cost.

Part VIII specifically addresses the problem of estimating airplane cost. Once cost relationships are established it is possible to iterate certain influential (to cost) design parameters with as goal to 'minimize' certain costs. Reference 30 deals specifically with these design optimization problems.

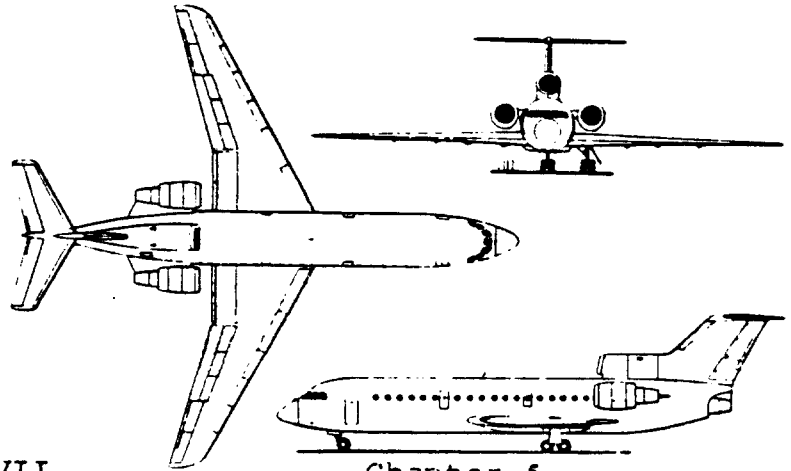

5.12 PRESENTATION OF AIRPLANE PERFORMANCE DATA

Once a new airplane design is 'finished' it is advisable to present the performance capabilities of the airplane in a generally understandable format AND to include the basic aerodynamic and installed thrust (or power) data on which all performance is based.

Since this type of documentation is not regulated by the FAA, there are no guidelines for the preparation of such data for civil airplanes. Each airplane manufacturer has evolved his own method of doing so.

For military airplanes the situation is different. The USAF, but in particular the USNAVY has standardized the required documentation of aerodynamic, thrust and performance data in the following manner:

For Aerodynamic and Thrust data: See Appendix B1.2, pages 265-271.

For Performance data: See Appendix B1.2, pages 272-279.

The author suggests that, when lacking a given format for the documentation of aerodynamic, thrust and performance data, this USNAVY method be used.

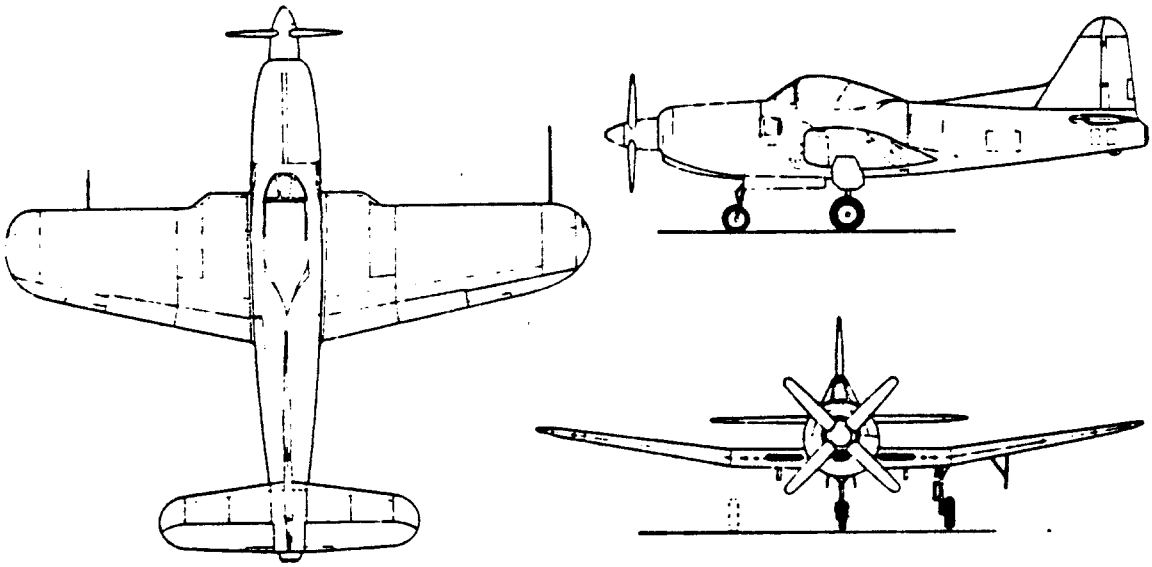

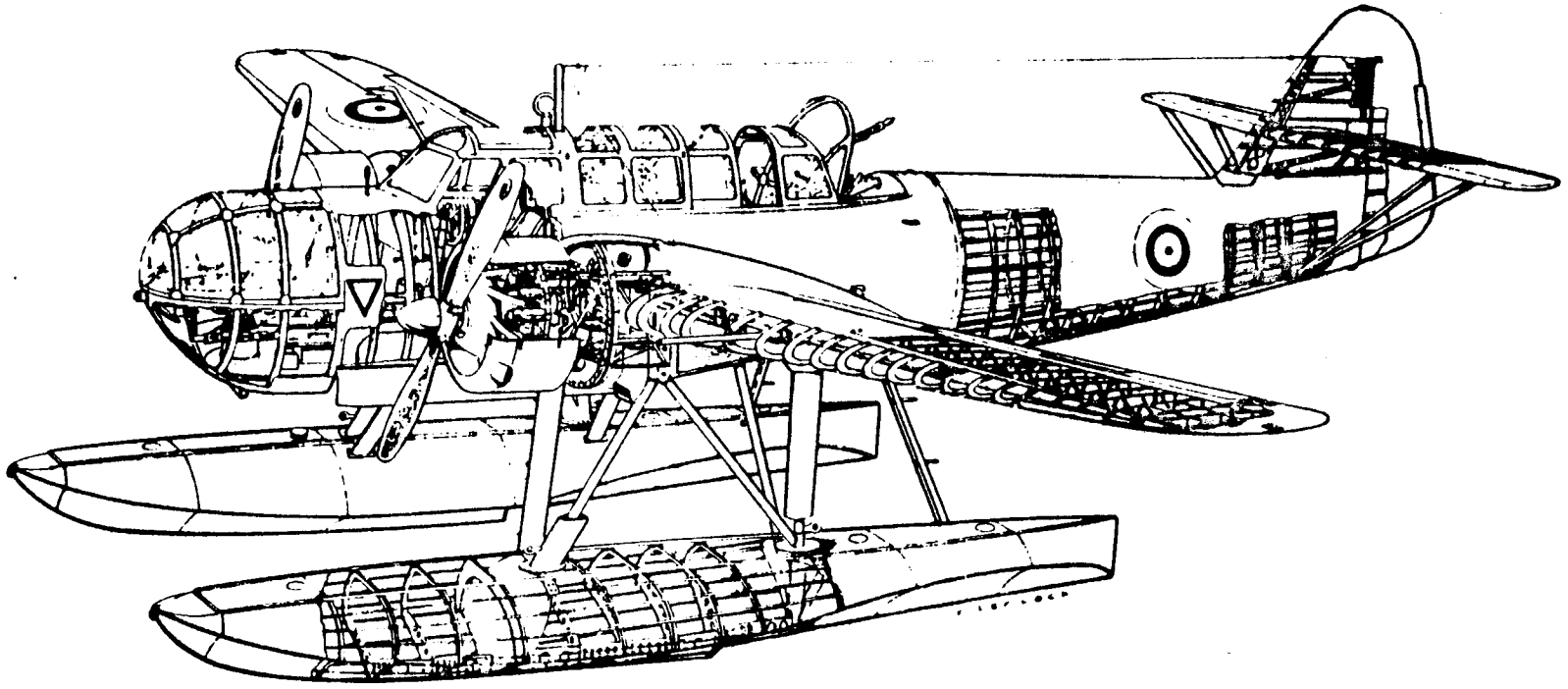

COURTESY: FOKKER

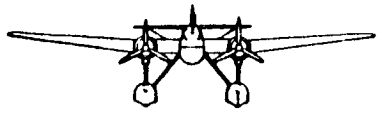

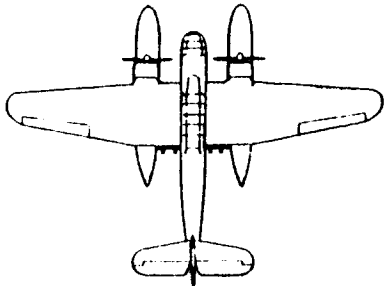

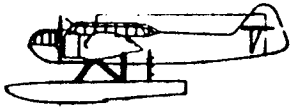

FOKKER T. VIII-W

6. REFERENCES

1. Roskam, J., Airplane Design: Part I, Preliminary Sizing of Airplanes.

2. Roskam, J., Airplane Design: Part II, Preliminary Configuration Design and Integration of the Propulsion System.

3. Roskam, J., Airplane Design: Part III, Layout Design of Cockpit, Fuselage, Wing and Empennage: Cutaways and Inboard Profiles.

4. Roskam, J., Airplane Design: Part IV, Layout Design of Landing Gear and Systems.

5. Roskam, J., Airplane Design: Part V, Component Weight Estimation.

6. Roskam, J., Airplane Design: Part VI, Preliminary Calculation of Aerodynamic, Thrust and Power Characteristics.

7. Roskam, J., Airplane Design: Part VIII, Airplane Cost Estimation and Optimization: Design, Development Manufacturing and Operating.

Note: These books are all published by: Roskam Aviation and Engineering Corporation, Rt4, Box 274, Ottawa, Kansas, 66067, Tel. 913-2421624.

8. Anon., Code of Federal Regulations, Aeronautics and Space, Parts 1- 59, January 1987, Superintendent of Documents, U.S. Government Printing Office, Washington, D.C., 20402.

9. Anon., MIL-F-8785C, Military Specification, Flying Qualities of Piloted Airplanes, November, 1980.

10a. Anon., MIL-C-005011B(USAF), Military Specification, Charts: Standard Aircraft Characteristics and Performance, Piloted Aircraft (Fixed Wing), June, 1977.

10b. Anon., AS-5263(USNavy), Guidelines for the Preparation of Standard Aircraft Characteristic Charts and Performance Data, Piloted Aircraft (Fixed Wing), October 1986.

11. Lan, C.E. and Roskam, J., Airplane Aerodynamics and

Performance, Roskam Aviation and Engineering Corp., Route 4, Box 274, Ottawa, Kansas, 66067, 1980.

12. Roskam, J., Airplane Flight Dynamics and Automatic Flight Control Systems, Roskam Aviation and Engineering Corp., Route 4, Box 274, Ottawa, Kansas, 1981.

13. Taylor, J.W.R., Jane's All The World's Aircraft, Jane's Publishing Company, London, England. (This book is reprinted annually)

14. Abbott, I.H. and Von Doenhoff, E., Theory of Wing Sections, Dover Publications, N.Y., 1959.

15. DeYoung, J., Theoretical Symmetric Span Loading Due To Flap Deflection For Wings of Arbitrary Planform At Subsonic Speeds, NACA TR 1071, 1952.

16. Pamadi, B.N. and Taylor, L.W., Jr., Semi-empirical Method for Prediction of Aerodynamic Forces and Moments on a Steadily Spinning Light Airplane, NASA TM 4009, December 1987.

17. Stinton, D., The Design of the Aeroplane, Granada, London, England, 1983.

18. Conner, D.W. and Jacobsen, I.D., Passenger Ride Comfort Technology for Transport Aircraft Situations, NASA TM X-73953, October 1976.

19. Conner, D.W., Passenger Comfort Technology for System Decision Making, NASA TM 81875, August 1980.

20. Notess, B., A Triangle, Flexible Airplanes, Gusts and Crew, Cornell Aero Lab., Inc., Memorandum No.343, May 1963.

21. Rex, H.R. and Magdaleno, R.E., Biomechanical Models for Vibration Feedthrough to Hands and Head for a Semisupine Pilot, Aviation, Space and Environmental Medicine, January 1978.

22. Dempsey, T.K., and Leatherwood, J.D., Discomfort Criteria for Single-Axis Vibration, NASA TP 1422, May 1979.

23. Rupf, J.A., Noise Effects on Passenger Communications in Light Aircraft, SAE Paper 770446, April 1977.

24. Roskam, J., Forward Swept Wings and Commuter Airplanes, Proceedings of the International Conference on

Forward Swept Wing Aircraft, University of Bristol, England, March 1982.

25. Press, H., Meadows, M.T. and Hadlock, I., A Reevaluation of Data on Atmospheric Turbulence and Airplane Gust Loads for Application in Spectral Calculations, NACA TR 1272, 1956.

26. Hammond, T.A., Amin, S.P. and Downing, D.R., Ride Quality Systems for Commuter Aircraft, SAE Paper 830744, April 1983.

27. Oehman, W.I., Optimum Design Considerations of a Gust Alleviator for Aircraft, NASA TN D-8152, March 1976.

28. Torenbeek, E., Synthesis of Subsonic Airplane Design, Delft University Press, Martinus Nijhoff Publishers, Kluwer Boston, Inc., Hingham, MA, 02043, 1982.

29. McAtee, T.P., Agility in Demand, Aerospace America, May, 1988.

30. Johnson, V.S., Life Cycle Cost in the Conceptual Design of Subsonic Commercial Aircraft, Ph.D. Dissertation, University of Kansas, May 1989.

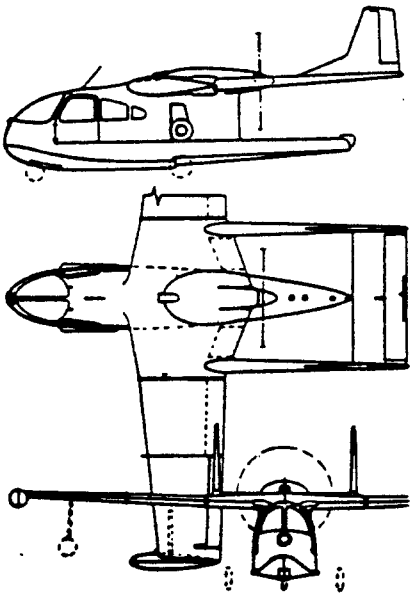

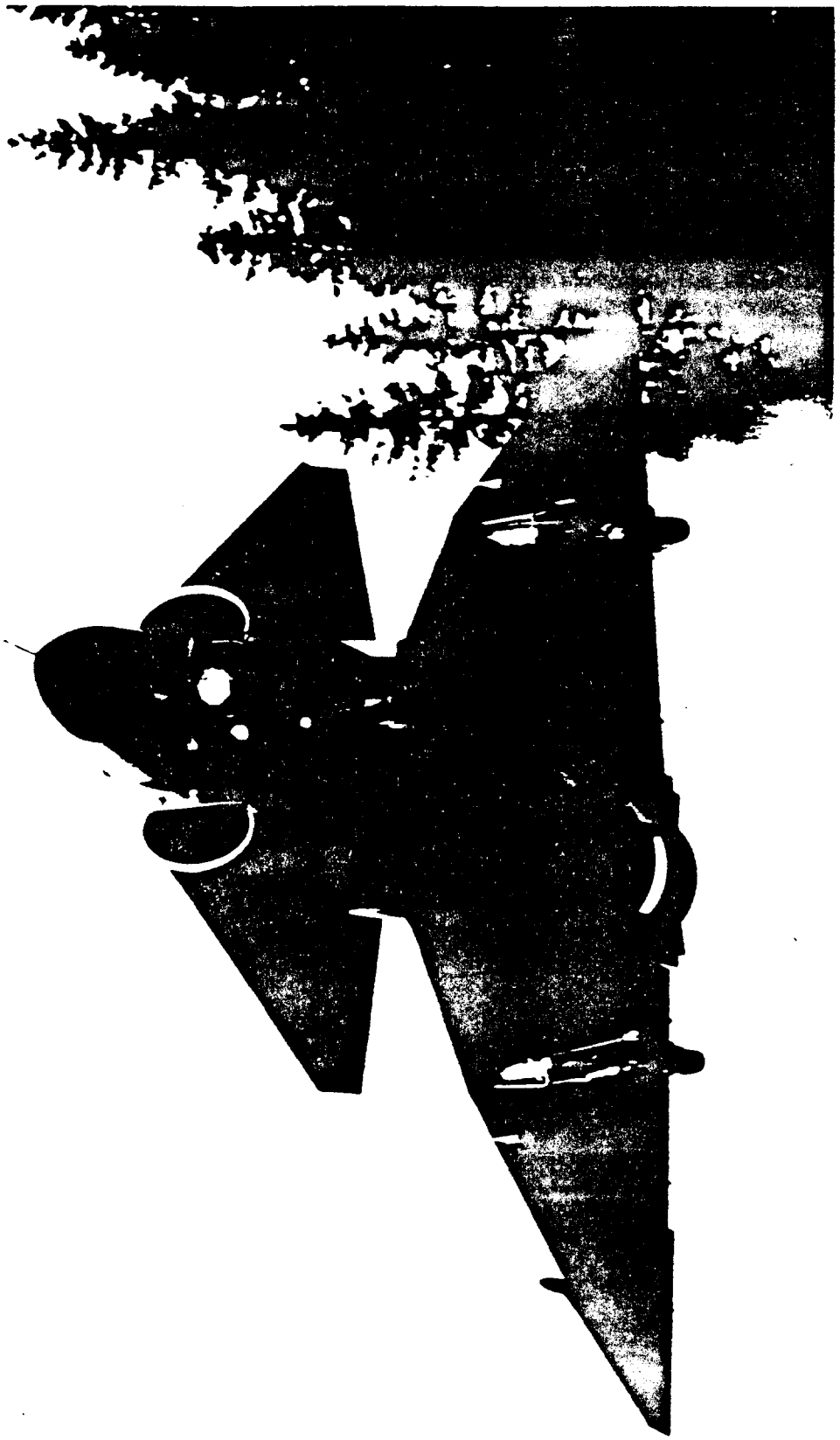

COURTESY: SAAB

7. INDEX

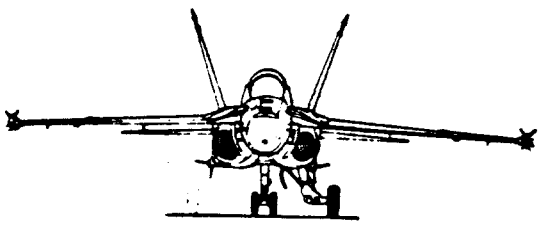

APPENDIX A: CIVIL AIRWORTHINESS REGULATIONS FOR AIRPLANE PERFORMANCE, STABILITY AND CONTROL

Before a civil airplane can be sold to the public, to corporations or to airlines a type certificate must have been issued. This type certificate ensures that the airplane has been designed and built in accordance with federally enforced minimum airworthiness standards. These minimum airworthiness standards are incorporated in the Federal Aviation Regulations (FAR's) of Reference 8. These regulations have a major impact on the design of airplanes. For that reason it is essential that airplane designers are aware of content and meaning of these regulations.

To obtain a type certificate for a new airplane design the procedures laid down in FAR 21 (Reference 8) must be followed.

The purpose of this appendix is to present copies of those federal aviation regulations which pertain to the minimum required performance, stability and control characteristics of airplanes. In the regulations, the minimum required performance characteristics are listed under the heading: 'performance'. The minimum required stability and control characteristics are listed under the heading: 'flight characteristics'.

Complete versions of the federal aviation regulations may be found in Reference 8. This appendix is organized as follows:

A1. Definitions and Abbreviations

In this Section a summary is given of those definitions which are needed for proper interpretation of those FAR 23 and 25 Parts which deal with performance and with flight characteristics.

PART 1—DEFINITIONS AND ABBREVIATIONS

Sec.
1.1 General definitions.
1.2 Abbreviations and symbols.
1.3 Rules of construction.

AUTHORITY: 49 U.S.C. 1347, 1348, 1354(a), 1357(d)(2), 1372, 1421 through 1430, 1432, 1442, 1443, 1472, 1510, 1522, 1652(e), 1655(c), 1657(f), 49 U.S.C. 106(g) (Revised Pub. L. 97-449, January 12, 1983).

§ 1.1 General definitions.

As used in Subchapters A through K of this chapter, unless the context requires otherwise:

"Aerodynamic coefficients" means non-dimensional coefficients for aerodynamic forces and moments.

"Aircraft" means a device that is used or intended to be used for flight in the air.

"Aircraft engine" means an engine that is used or intended to be used for propelling aircraft. It includes turbosuperchargers, appurtenances, and accessories necessary for its functioning, but does not include propellers.

"Airframe" means the fuselage, booms, nacelles, cowlings, fairings, airfoil surfaces (including rotors but excluding propellers and rotating airfoils of engines), and landing gear of an aircraft and their accessories and controls.

"Airplane" means an engine-driven fixed-wing aircraft heavier than air, that is supported in flight by the dynamic reaction of the air against its wings.

"Brake horsepower" means the power delivered at the propeller shaft (main drive or main output) of an aircraft engine.

"Calibrated airspeed" means the indicated airspeed of an aircraft, corrected for position and instrument error. Calibrated airspeed is equal to true airspeed in standard atmosphere at sea level.

"Category":

(1) As used with respect to the certification, ratings, privileges, and limitations of airmen, means a broad classification of aircraft. Examples include: airplane; rotorcraft; glider; and lighter-than-air; and

(2) As used with respect to the certification of aircraft, means a grouping of aircraft based upon intended use or operating limitations. Examples include: transport, normal, utility, acrobatic, limited, restricted, and provisional.

"Category A," with respect to transport category rotorcraft, means multiengine rotorcraft designed with engine and system isolation features specified in Part 29 and utilizing scheduled takeoff and landing operations under a critical engine failure concept which assures adequate designated surface area and adequate performance capability for continued safe flight in the event of engine failure.

"Category B," with respect to transport category rotorcraft, means single-engine or multiengine rotorcraft which do not fully meet all Category A standards. Category B rotorcraft have no guaranteed stay-up ability in the event of engine failure and unscheduled landing is assumed.

"Category II operations", with respect to the operation of aircraft, means a straight-in ILS approach to the runway of an airport under a Category II ILS instrument approach procedure issued by the Administrator or other appropriate authority.

"Category III operations," with respect to the operation of aircraft, means an ILS approach to, and landing on, the runway of an airport using a Category III ILS instrument approach procedure issued by the Administrator or other appropriate authority.

"Clearway" means:

(1) For turbine engine powered airplanes certificated after August 29, 1959, an area beyond the runway, not less than 500 feet wide, centrally located about the extended centerline of the runway, and under the control of the airport authorities. The clearway is expressed in terms of a clearway plane, extending from the end of the runway with an upward slope not exceeding 1.25 percent, above which no object nor any terrain protrudes. However, threshold lights may protrude above the plane if their height above the end of the runway is 26 inches or

less and if they are located to each side of the runway.

(2) For turbine engine powered airplanes certificated after September 30, 1958, but before August 30, 1959, an area beyond the takeoff runway extending no less than 300 feet on either side of the extended centerline of the runway, at an elevation no higher than the elevation of the end of the runway, clear of all fixed obstacles, and under the control of the airport authorities.

"Climbout speed," with respect to rotorcraft, means a referenced airspeed which results in a flight path clear of the height-velocity envelope during initial climbout.

"Critical altitude" means the maximum altitude at which, in standard atmosphere, it is possible to maintain, at a specified rotational speed, a specified power or a specified manifold pressure. Unless otherwise stated, the critical altitude is the maximum altitude at which it is possible to maintain, at the maximum continuous rotational speed, one of the following:

(1) The maximum continuous power, in the case of engines for which this power rating is the same at sea level and at the rated altitude.

(2) The maximum continuous rated manifold pressure, in the case of engines, the maximum continuous power of which is governed by a constant manifold pressure.

"Critical engine" means the engine whose failure would most adversely affect the performance or handling qualities of an aircraft.

"Decision height," with respect to the operation of aircraft, means the height at which a decision must be made, during an ILS or PAR instrument approach, to either continue the approach or to execute a missed approach.

"Equivalent airspeed" means the calibrated airspeed of an aircraft corrected for adiabatic compressible flow for the particular altitude. Equivalent airspeed is equal to calibrated airspeed in standard atmosphere at sea level.

"Flap extended speed" means the highest speed permissible with wing flaps in a prescribed extended position.

"Flightcrew member" means a pilot, flight engineer, or flight navigator assigned to duty in an aircraft during flight time.

"Flight level" means a level of constant atmospheric pressure related to a reference datum of 29.92 inches of mercury. Each is stated in three digits that represent hundreds of feet. For example, flight level 250 represents a barometric altimeter indication of 25,000 feet; flight level 255, an indication of 25,500 feet.

"Flight time" means the time from the moment the aircraft first moves under its own power for the purpose of flight until the moment it comes to rest at the next point of landing. ("Block-to-block" time.)

"Flight visibility" means the average forward horizontal distance, from the cockpit of an aircraft in flight, at which prominent unlighted objects may be seen and identified by day and prominent lighted objects may be seen and identified by night.

"Glider" means a heavier-than-air aircraft, that is supported in flight by the dynamic reaction of the air against its lifting surfaces and whose free flight does not depend principally on an engine.

"Ground visibility" means prevailing horizontal visibility near the earth's surface as reported by the United States National Weather Service or an accredited observer.

"Idle thrust" means the jet thrust obtained with the engine power control level set at the stop for the least thrust position at which it can be placed.

"IFR conditions" means weather conditions below the minimum for flight under visual flight rules.

"Indicated airspeed" means the speed of an aircraft as shown on its pitot static airspeed indicator calibrated to reflect standard atmosphere adiabatic compressible flow at sea level uncorrected for airspeed system errors.

"Landing gear extended speed" means the maximum speed at which an aircraft can be safely flown with the landing gear extended.

"Landing gear operating speed" means the maximum speed at which the landing gear can be safely extended or retracted.

"Large aircraft" means aircraft of more than 12,500 pounds, maximum certificated takeoff weight.

"Load factor" means the ratio of a specified load to the total weight of the aircraft. The specified load is expressed in terms of any of the following: aerodynamic forces, inertia forces, or ground or water reactions.

"Mach number" means the ratio of true airspeed to the speed of sound.

"Manifold pressure" means absolute pressure as measured at the appropriate point in the induction system and usually expressed in inches of mercury.

"Minimum descent altitude" means the lowest altitude, expressed in feet above mean sea level, to which descent is authorized on final approach or during circle-to-land maneuvering in execution of a standard instrument approach procedure, where no electronic glide slope is provided.

"Pitch setting" means the propeller blade setting as determined by the blade angle measured in a manner, and at a radius, specified by the instruction manual for the propeller.

"Propeller" means a device for propelling an aircraft that has blades on an engine-driven shaft and that, when rotated, produces by its action on the air, a thrust approximately perpendicular to its plane of rotation. It includes control components normally supplied by its manufacturer, but does not include main and auxiliary rotors or rotating airfoils of engines.

"Rated maximum continuous augmented thrust", with respect to turbojet engine type certification, means the approved jet thrust that is developed statically or in flight, in standard atmosphere at a specified altitude, with fluid injection or with the burning of fuel in a separate combustion chamber, within the engine operating limitations established under Part 33 of this chapter, and approved for unrestricted periods of use.

"Rated maximum continuous power," with respect to reciprocating, turbopropeller, and turboshaft engines, means the approved brake horsepower that is developed statically or in flight, in standard atmosphere at a specified altitude, within the engine operating limitations established under Part 33, and approved for unrestricted periods of use.

"Rated maximum continuous thrust", with respect to turbojet engine type certification, means the approved jet thrust that is developed statically or in flight, in standard atmosphere at a specified altitude, without fluid injection and without the burning of fuel in a separate combustion chamber, within the engine operating limitations established under Part 33 of this chapter, and approved for unrestricted periods of use.

"Rated takeoff augmented thrust", with respect to turbojet engine type certification, means the approved jet thrust that is developed statically under standard sea level conditions, with fluid injection or with the burning of fuel in a separate combustion chamber, within the engine operating limitations established under Part 33 of this chapter, and limited in use to periods of not over 5 minutes for takeoff operation.

"Rated takeoff power", with respect to reciprocating, turbopropeller, and turboshaft engine type certification, means the approved brake horsepower that is developed statically under standard sea level conditions, within the engine operating limitations established under Part 33, and limited in use to periods of not over 5 minutes for takeoff operation.

"Rated takeoff thrust", with respect to turbojet engine type certification, means the approved jet thrust that is developed statically under standard sea level conditions, without fluid injection and without the burning of fuel in a separate combustion chamber, within the engine operating limitations established under Part 33 of this chapter, and limited in use to periods of not over 5 minutes for takeoff operation.

Rated "30-minute power", with respect to helicopter turbine engines, means the maximum brake horsepower, developed under static conditions at specified altitudes and atmospheric temperatures, under the maximum conditions of rotor shaft rotational speed and gas temperature, and limited in use to periods of not over 30 minutes as shown on the engine data sheet.

Rated "2½ minute power", with respect to helicopter turbine engines, means the brake horsepower, developed statically in standard atmosphere at sea level, or at a specified altitude, for one-engine-out operation of multiengine helicopters for 2½ minutes at rotor shaft rotation speed and gas temperature established for this rating.

"Rating" means a statement that, as a part of a certificate, sets forth special conditions, privileges, or limitations.

"Small aircraft" means aircraft of 12,500 pounds or less, maximum certificated takeoff weight.

"Standard atmosphere" means the atmosphere defined in U.S. Standard Atmosphere, 1962 (Geopotential altitude tables).

"Stopway" means an area beyond the takeoff runway, no less wide than the runway and centered upon the extended centerline of the runway, able to support the airplane during an aborted takeoff, without causing structural damage to the airplane, and designated by the airport authorities for use in decelerating the airplane during an aborted takeoff.

"Takeoff power":

(1) With respect to reciprocating engines, means the brake horsepower that is developed under standard sea level conditions, and under the maximum conditions of crankshaft rota-

tional speed and engine manifold pressure approved for the normal takeoff, and limited in continuous use to the period of time shown in the approved engine specification; and

(2) With respect to turbine engines, means the brake horsepower that is developed under static conditions at a specified altitude and atmospheric temperature, and under the maximum conditions of rotor shaft rotational speed and gas temperature approved for the normal takeoff, and limited in continuous use to the period of time shown in the approved engine specification.

"Takeoff safety speed" means a referenced airspeed obtained after lift-off at which the required one-engine-inoperative climb performance can be achieved.

"Takeoff thrust", with respect to turbine engines, means the jet thrust that is developed under static conditions at a specific altitude and atmospheric temperature under the maximum conditions of rotorshaft rotational speed and gas temperature approved for the normal takeoff, and limited in continuous use to the period of time shown in the approved engine specification.

"Time in service", with respect to maintenance time records, means the time from the moment an aircraft leaves the surface of the earth until it touches it at the next point of landing.

"True airspeed" means the airspeed of an aircraft relative to undisturbed air. True airspeed is equal to equivalent airspeed multiplied by $(\rho 0/\rho)^{1/2}$.

§ 1.2 Abbreviations and symbols.

In Subchapters A through K of this chapter:

"AGL" means above ground level.

"ALS" means approach light system.

"ASR" means airport surveillance radar.

"ATC" means air traffic control.

"CAS" means calibrated airspeed.

"CAT II" means Category II.

"CONSOL or CONSOLAN" means a kind of low or medium frequency long range navigational aid.

"DH" means decision height.

"DME" means distance measuring equipment compatible with TACAN.

"EAS" means equivalent airspeed.

"FAA" means Federal Aviation Administration.

"FM" means fan marker.

"GS" means glide slope.

"HIRL" means high-intensity runway light system.

"IAS" means indicated airspeed.

"ICAO" means International Civil Aviation Organization.

"IFR" means instrument flight rules.

"ILS" means instrument landing system.

"IM" means ILS inner marker.

"INT" means intersection.

"LDA" means localizer-type directional aid.

"LFR" means low-frequency radio range.

"LMM" means compass locator at middle marker.

"LOC" means ILS localizer.

"LOM" means compass locator at outer marker.

"*M*" means mach number.

"MAA" means maximum authorized IFR altitude.

"MALS" means medium intensity approach light system.

"MALSR" means medium intensity approach light system with runway alignment indicator lights.

"MCA" means minimum crossing altitude.

"MDA" means minimum descent altitude.

"MEA" means minimum en route IFR altitude.

"MM" means ILS middle marker.

"MOCA" means minimum obstruction clearance altitude.

"MRA" means minimum reception altitude.

"MSL" means mean sea level.

"NDB(ADF)" means nondirectional beacon (automatic direction finder).

"NOPT" means no procedure turn required.

"OM" means ILS outer marker.

"PAR" means precision approach radar.

"RAIL" means runway alignment indicator light system.

"RBN" means radio beacon.

"RCLM" means runway centerline marking.

"RCLS" means runway centerline light system.

"REIL" means runway end identification lights.

"RR" means low or medium frequency radio range station.

"RVR" means runway visual range as measured in the touchdown zone area.

"SALS" means short approach light system.

"SSALS" means simplified short approach light system.

"SSALSR" means simplified short approach light system with runway alignment indicator lights.

"TACAN" means ultra-high frequency tactical air navigational aid.

"TAS" means true airspeed.
"TDZL" means touchdown zone lights.
"TVOR" means very high frequency terminal omnirange station.

V_A means design maneuvering speed.
V_B means design speed for maximum gust intensity.
V_C means design cruising speed.
V_D means design diving speed.
V_{DF}/M_{DF} means demonstrated flight diving speed.
V_F means design flap speed.
V_{FC}/M_{FC} means maximum speed for stability characteristics.
V_{FE} means maximum flap extended speed.
V_H means maximum speed in level flight with maximum continuous power.
V_{LE} means maximum landing gear extended speed.
V_{LO} means maximum landing gear operating speed.
V_{LOF} means lift-off speed.
V_{MC} means minimum control speed with the critical engine inoperative.
V_{MO}/M_{MO} means maximum operating limit speed.
V_{MU} means minimum unstick speed.
V_{NE} means never-exceed speed.
V_{NO} means maximum structural cruising speed.
V_R means rotation speed.

V_S means the stalling speed or the minimum steady flight speed at which the airplane is controllable.
V_{S0} means the stalling speed or the minimum steady flight speed in the landing configuration.
V_{S1} means the stalling speed or the minimum steady flight speed obtained in a specific configuration.
V_{TOSS} means takeoff safety speed for Category A rotorcraft.
V_X means speed for best angle of climb.
V_Y means speed for best rate of climb.
V_1 means takeoff decision speed (formerly denoted as critical engine failure speed).
V_2 means takeoff safety speed.
V_2 min means minimum takeoff safety speed.

"VFR" means visual flight rules.
"VHF" means very high frequency.
"VOR" means very high frequency omnirange station.
"VORTAC" means collocated VOR and TACAN.

[Doc. No. 1150, 27 FR 4590, May 15, 1962]

EDITORIAL NOTE: For FEDERAL REGISTER citations affecting § 1.2, see the List of CFR Sections Affected appearing in the Finding Aids, section of this volume.

§ 1.3 Rules of construction.

(a) In Subchapters A through K of this chapter, unless the context requires otherwise:
(1) Words importing the singular include the plural;
(2) Words importing the plural include the singular; and
(3) Words importing the masculine gender include the feminine.
(b) In Subchapters A through K of this chapter, the word:
(1) "Shall" is used in an imperative sense;
(2) "May" is used in a permissive sense to state authority or permission to do the act prescribed, and the words "no person may * * *" or "a person may not * * *" mean that no person is required, authorized, or permitted to do the act prescribed; and
(3) "Includes" means "includes but is not limited to".

[Doc. No. 1150, 27 FR 4590, May 15, 1962, as amended by Amdt. 1-10, 31 FR 5055, Mar. 29, 1966]

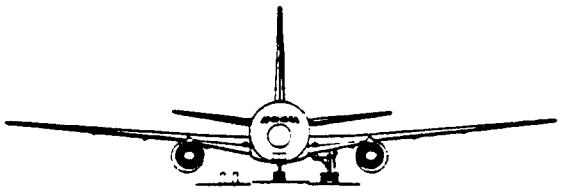

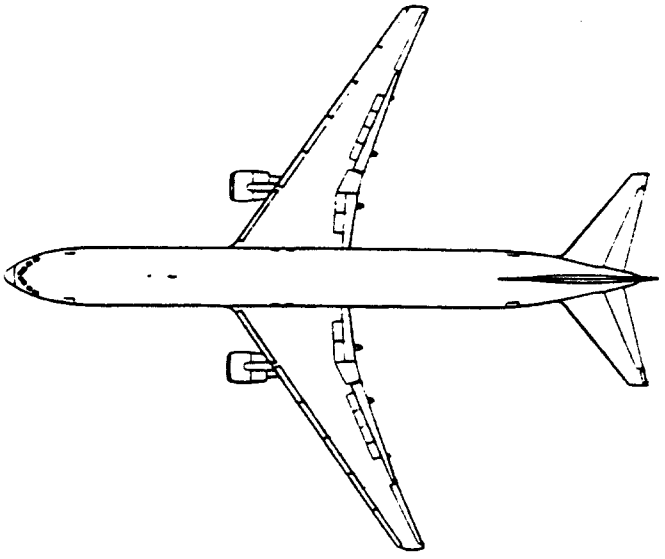

A2. Federal Aviation Regulation: FAR 23 with 1987 Amendments

In this Section a summary is given of that part of FAR 23 which deals with performance and with flight characteristics.

Subpart A—General

§ 23.1 Applicability.

(a) This part prescribes airworthiness standards for the issue of type certificates, and changes to those certificates, for small airplanes in the normal, utility, and acrobatic categories that have a passenger seating configuration, excluding pilot seats, of nine seats or less.

(b) Each person who applies under Part 21 for such a certificate or change must show compliance with the applicable requirements of this part.

[Doc. No. 4080, 29 FR 17955, Dec. 18, 1964, as amended by Amdt. 23-10, 36 FR 2864, Feb. 11, 1971]

§ 23.2 Special retroactive requirements.

Notwithstanding §§ 21.17 and 21.101 of this chapter and irrespective of the type certification basis, each normal, utility, and acrobatic category airplane having a passenger seating configuration, excluding pilot seats, of nine or less, manufactured one year after December 12, 1985, or any such foreign manufactured airplane for entry into the U.S., must meet the requirements of § 23.785 (g) and (h). For the purpose of this paragraph, the date of manufacture is:

(a) The date the inspection acceptance records, or equivalent, reflect that the airplane is complete and meets the FAA Approved Type Design Data; or

(b) In the case of a foreign manufactured airplane, the date the foreign civil airworthiness authority certifies the airplane is complete and issues an original standard airworthiness certificate, or the equivalent in that country.

[Doc. No. 23-32, 50 FR 46877, Nov. 13, 1985]

§ 23.3 Airplane categories.

(a) The normal category is limited to airplanes intended for nonacrobatic operation. Nonacrobatic operation includes—

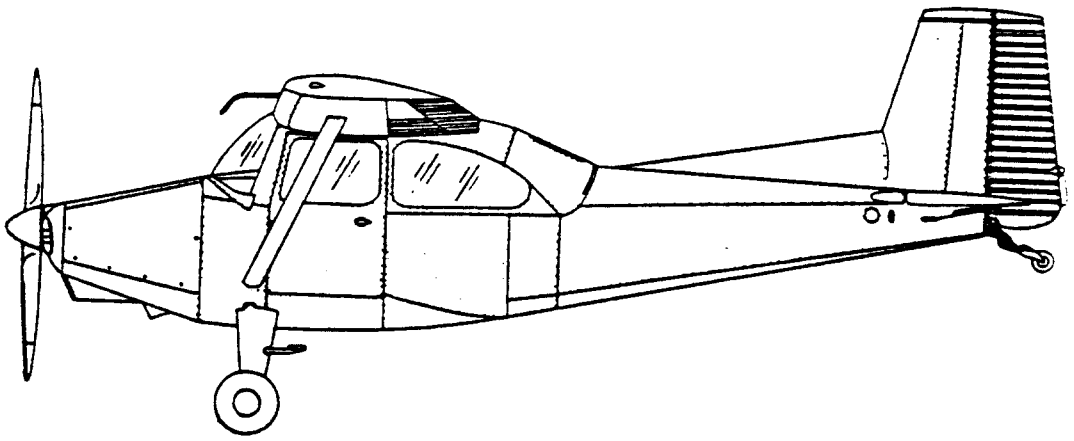

(1) Any maneuver incident to normal flying;

(2) Stalls (except whip stalls); and

(3) Lazy eights, chandelles, and steep turns, in which the angle of bank is not more than 60 degrees.

(b) The utility category is limited to airplanes intended for limited acrobatic operation. Airplanes certificated in the utility category may be used in any of the operations covered under paragraph (a) of this section and in limited acrobatic operations. Limited acrobatic operation includes—

(1) Spins (if approved for the particular type of airplane); and

(2) Lazy eights, chandelles, and steep turns, in which the angle of bank is more than 60 degrees.

(c) The acrobatic category is limited to airplanes intended for use without restrictions other than those shown to be necessary as a result of required flight tests.

(d) Small airplanes may be certificated in more than one category if the requirements of each requested category are met.

[Doc. No. 4080, 29 FR 17955, Dec. 18, 1964, as amended by Amdt. 23-4, 32 FR 5934, Apr. 14, 1967]

Subpart B—Flight

General

§ 23.21 Proof of compliance.

(a) Each requirement of this subpart must be met at each appropriate combination of weight and center of gravity within the range of loading conditions for which certification is requested. This must be shown—

(1) By tests upon an airplane of the type for which certification is requested, or by calculations based on, and equal in accuracy to, the results of testing; and

(2) By systematic investigation of each probable combination of weight and center of gravity, if compliance cannot be reasonably inferred from combinations investigated.

(b) The following general tolerances are allowed during flight testing. However, greater tolerances may be allowed in particular tests:

Item	Tolerance
Weight	+5%, -10%.
Critical items affected by weight	+5%, -1%.
C.G.	±7% total travel.

§ 23.23 Load distribution limits.

Ranges of weight and centers of gravity within which the airplane may be safely operated must be established and must include the range for lateral centers of gravity if possible loading conditions can result in significant variation of their positions. If low fuel adversely affects balance or stability, the airplane must be tested under conditions simulating those that would exist when the amount of usable fuel does not exceed one gallon for each 12 maximum continuous horsepower of the engine or engines.

[Doc. No. 4080, 29 FR 17955, Dec. 18, 1964, as amended by Amdt. 23-17, 41 FR 55463, Dec. 20, 1976]

§ 23.25 Weight limits.

(a) *Maximum weight.* The maximum weight is the highest weight at which compliance with each applicable requirement of this part (other than those complied with at the design landing weight) is shown. The maximum weight must be established so that it is—

(1) Not more than—

(i) The highest weight selected by the applicant;

(ii) The design maximum weight, which is the highest weight at which compliance with each applicable structural loading condition of this part (other than those complied with at the design landing weight) is shown; or

(iii) The highest weight at which compliance with each applicable flight requirement is shown, except for airplanes equipped with standby power rocket engines, in which case it is the highest weight established in accordance with Appendix E of this part; or

(2) Assuming a weight of 170 pounds for each occupant of each seat for normal category airplanes and 190 pounds (unless otherwise placarded) for utility and acrobatic category airplanes, not less than the weight with—

(i) Each seat occupied, oil at full tank capacity, and at least enough fuel for one-half hour of operation at rated maximum continuous power; or

(ii) The required minimum crew, and fuel and oil to full tank capacity.

(b) *Minimum weight.* The minimum weight (the lowest weight at which compliance with each applicable requirement of this part is shown) must be established so that it is not more than the sum of—

(1) The empty weight determined under § 23.29;

(2) The weight of the required minimum crew (assuming a weight of 170 pounds for each crewmember); and

(3) The weight of—

(i) For turbojet powered airplanes, 5 percent of the total fuel capacity of that particular fuel tank arrangement under investigation, and

(ii) For other airplanes, the fuel necessary for one-half hour of operation at maximum continuous power.

[Doc. No. 4080, 29 FR 17955, Dec. 18, 1964, as amended by Amdt. 23-7, 34 FR 13086, Aug. 13, 1969; Amdt. 23-21, 43 FR 2317, Jan. 16, 1978]

§ 23.29 Empty weight and corresponding center of gravity.

(a) The empty weight and corresponding center of gravity must be determined by weighing the airplane with—

(1) Fixed ballast;

(2) Unusable fuel determined under § 23.959; and

(3) Full operating fluids, including—

(i) Oil;

(ii) Hydraulic fluid; and

(iii) Other fluids required for normal operation of airplane systems, except potable water, lavatory precharge water, and water intended for injection in the engines.

(b) The condition of the airplane at the time of determining empty weight must be one that is well defined and can be easily repeated.

[Doc. No. 4080, 29 FR 17955, Dec. 18, 1964; 30 FR 258, Jan. 9, 1965, as amended by Amdt. 23-21, 43 FR 2317, Jan. 16, 1978]

§ 23.31 Removable ballast.

Removable ballast may be used in showing compliance with the flight requirements of this subpart, if—

(a) The place for carrying ballast is properly designed and installed, and is marked under § 23.1557; and

(b) Instructions are included in the airplane flight manual, approved manual material, or markings and placards, for the proper placement of the removable ballast under each loading condition for which removable ballast is necessary.

[Doc. No. 4080, 29 FR 17955, Dec. 18, 1964; 30 FR 258, Jan. 9, 1965, as amended by Amdt. 23-13, 37 FR 20023, Sept. 23, 1972]

§ 23.33 Propeller speed and pitch limits.

(a) *General.* The propeller speed and pitch must be limited to values that will assure safe operation under normal operating conditions.

(b) *Propellers not controllable in flight.* For each propeller whose pitch cannot be controlled in flight—

(1) During takeoff and initial climb at $V^{\prime}$, the propeller must limit the engine r.p.m., at full throttle or at maximum allowable takeoff manifold pressure, to a speed not greater than the maximum allowable takeoff r.p.m.; and

(2) During a closed throttle glide at the placarded "never-exceed speed", the propeller may not cause an engine speed above 110 percent of maximum continuous speed.

(c) *Controllable pitch propellers without constant speed controls.* Each propeller that can be controlled in flight, but that does not have constant speed controls, must have a means to limit the pitch range so that—

(1) The lowest possible pitch allows compliance with paragraph (b)(1) of this section; and

(2) The highest possible pitch allows compliance with paragraph (b)(2) of this section.

(d) *Controllable pitch propellers with constant speed controls.* Each controllable pitch propeller with constant speed controls must have—

(1) With the governor in operation, a means at the governor to limit the maximum engine speed to the maximum allowable takeoff r.p.m.; and

(2) With the governor inoperative, a means to limit the maximum engine speed to 103 percent of the maximum allowable takeoff r.p.m. with the pro-

peller blades at the lowest possible pitch and with takeoff manifold pressure, the airplane stationary, and no wind.

PERFORMANCE

§ 23.45 General.

(a) Unless otherwise prescribed, the performance requirements of this subpart must be met for still air and a standard atmosphere.

(b) The performance must correspond to the propulsive thrust available under the particular ambient atmospheric conditions, the particular flight condition, and the relative humidity specified in paragraph (d) or (e) of this section, as appropriate.

(c) The available propulsive thrust must correspond to engine power or thrust, not exceeding the approved power or thrust, less—

(1) Installation losses; and

(2) The power or equivalent thrust absorbed by the accessories and services appropriate to the particular ambient atmospheric conditions and the particular flight condition.

(d) For reciprocating engine-powered airplanes, the performance, as affected by engine power, must be based on a relative humidity of 80 percent in a standard atmosphere.

(e) For turbine engine-powered airplanes, the performance, as affected by engine power or thrust, must be based on a relative humidity of—

(1) 80 percent, at and below standard temperature; and

(2) 34 percent, at and above standard temperature plus 50 degrees F.

Between these two temperatures, the relative humidity must vary linearly.

[Amdt. 23-21, 43 FR 2317, Jan. 16, 1978]

§ 23.49 Stalling speed.

(a) V_{s_0} is the stalling speed, if obtainable, or the minimum steady speed, in knots (CAS), at which the airplane is controllable, with the—

(1) Applicable power or thrust condition set forth in paragraph (e) of this section;

(2) Propellers in the takeoff position;

(3) Landing gear extended;

(4) Wing flaps in the landing position;

(5) Cowl flaps closed;

(6) Center of gravity in the most unfavorable position within the allowable landing range; and

(7) Weight used when V_{s_0} is being used as a factor to determine compliance with a required performance standard.

(b) V_{s_0} at maximum weight may not exceed 61 knots for—

(1) Single-engine airplanes; and

(2) Multiengine airplanes of 6,000 pounds or less maximum weight that cannot meet the minimum rate of climb specified in § 23.67(b) with the critical engine inoperative.

(c) V_{s_1} is the calibrated stalling speed, if obtainable, or the minimum steady speed, in knots, at which the airplane is controllable, with the—

(1) Applicable power or thrust condition set forth in paragraph (e) of this section;

(2) Propellers in the takeoff position;

(3) Airplane in the condition existing in the test in which V_{s_1} is being used; and

(4) Weight used when V_{s_1} is being used as a factor to determine compliance with a required performance standard.

(d) V_{s_0} and V_{s_1} must be determined by flight tests, using the procedure specified in § 23.201.

(e) The following power or thrust conditions must be used to meet the requirements of this section:

(1) For reciprocating engine-powered airplanes, engines idling, throttles closed or at not more than the power necessary for zero thrust at a speed not more than 110 percent of the stalling speed.

(2) For turbine engine-powered airplanes, the propulsive thrust may not be greater than zero at the stalling speed, or, if the resultant thrust has no appreciable effect on the stalling speed, with engines idling and throttles closed.

[Doc. No. 4080, 29 FR 17955, Dec. 18, 1964, as amended by Amdt. 23-7, 34 FR 13086, Aug. 13, 1969; Amdt. 23-21, 43 FR 2317, Jan. 16, 1978]

§ 23.51 Takeoff.

(a) For each airplane (except a skiplane for which landplane takeoff data has been determined under this paragraph and furnished in the Airplane Flight Manual) the distance required to takeoff and climb over a 50-foot obstacle must be determined with—

(1) The engines operating within approved operating limitations; and

(2) The cowl flaps in the normal takeoff position.

(b) For multiengine airplanes, the lift-off speed, V_{LOF}, may not be less than V_{MC} determined in accordance with § 23.149.

(c) Upon reaching a height of 50 feet above the takeoff surface level, the airplane must have reached a speed of not less than the following:

(1) For multiengine airplanes, the higher of—

(i) 1.1 V_{MC}; or

(ii) 1.3 V_{S_1}, or any lesser speed, not less than Vx plus 4 knots, that is shown to be safe under all conditions, including turbulence and complete engine failure.

(2) For single engine airplanes—

(i) 1.3 V_{S_1}; or

(ii) Any lesser speed, not less than Vx plus 4 knots, that is shown to be safe under all conditions, including turbulence and complete engine failure.

(d) The starting point for measuring seaplane and amphibian takeoff distance may be the point at which a speed of not more than three knots is reached.

(e) Takeoffs made to determine the data required by this section may not require exceptional piloting skill or exceptionally favorable conditions.

[Amdt. 23-21, 43 FR 2317, Jan. 16, 1978]

§ 23.65 Climb: All engines operating.

(a) Each airplane must have a steady rate of climb at sea level of at least 300 feet per minute and a steady angle of climb of at least 1:12 for landplanes or 1:15 for seaplanes and amphibians with—

(1) Not more than maximum continuous power on each engine;

(2) The landing gear retracted;

(3) The wing flaps in the takeoff position; and

(4) The cowl flaps or other means for controlling the engine cooling air supply in the position used in the cooling tests required by §§ 23.1041 through 23.1047.

(b) Each airplane with engines for which the takeoff and maximum continuous power ratings are identical and that has fixed-pitch, two-position, or similar propellers, may use a lower propeller pitch setting than that allowed by § 23.33 to obtain rated engine r.p.m. at Vx, if—

(1) The airplane shows marginal performance (such as when it can meet the rate of climb requirements of paragraph (a) of this section but has difficulty in meeting the angle of climb requirements of paragraph (a) of this section or of § 23.77); and

(2) Acceptable engine cooling is shown at the lower speed associated with the best angle of climb.

(c) Each turbine engine-powered airplane must be able to maintain a steady gradient of climb of at least 4 percent at a pressure altitude of 5,000 feet and a temperature of 81 degrees F (standard temperature plus 40 degree F) with the airplane in the configuration prescribed in paragraph (a) of this section.

[Amdt. 23-21, 43 FR 2317, Jan. 16, 1978]

§ 23.67 Climb: one engine inoperative.

(a) Each reciprocating engine-powered multiengine airplane of more than 6,000 pounds maximum weight must be able to maintain a steady rate of climb of at least 0.027 $V_{S_0}^2$ (that is, the number of feet per minute is obtained by multiplying the square of the number of knots by 0.027 at an altitude of 5,000 feet with the—

(1) Critical engine inoperative, and its propeller in the minimum drag position;

(2) Remaining engines at not more than maximum continuous power;

(3) Landing gear retracted;

(4) Wing flaps in the most favorable position; and

(5) Cowl flaps in the position used in the cooling tests required by §§ 23.1041 through 23.1047.

(b) For reciprocating engine-powered multiengine airplanes of 6,000 pounds or less maximum weight, the following apply:

(1) Each airplane with a V_{S_0} of more than 61 knots must be able to maintain a steady rate of climb of at least 0.027 $V_{S_0}^2$ (that is, the number of feet per minute is obtained by multiplying the square of the number of knots by 0.027), at an altitude of 5,000 feet with the—

(i) Critical engine inoperative and its propeller in the minimum drag position;

(ii) Remaining engines at not more than maximum continuous power;

(iii) Landing gear retracted;

(iv) Wing flaps in the most favorable position; and

(v) Cowl flaps in the position used in the cooling tests required by §§ 23.1041 through 23.1047.

(2) For each airplane with a stalling speed of 61 knots or less, the steady rate of climb at 5,000 feet must be determined with the—

(i) Critical engine inoperative and its propeller in the minimum drag position;

(ii) Remaining engines at not more than maximum continuous power;

(iii) Landing gear retracted;

(iv) Wing flaps in the most favorable position; and

(v) Cowl flaps in the position used in the cooling tests required by §§ 23.1041 through 23.1047.

(c) For turbine-powered multiengine airplanes the following apply:

(1) The steady gradient of climb must be determined at each weight, altitude, and ambient temperature within the operational limits established by the applicant, with the—

(i) Critical engine inoperative, and its propeller in the minimum drag position;

(ii) Remaining engines at not more than maximum continuous power or thrust;

(iii) Landing gear retracted;

(iv) Wing flaps in the most favorable position; and

(v) The means for controlling the engine cooling air supply in the position used in the engine cooling tests required by §§ 23.1041 through 23.1047.

(2) Each airplane must be able to maintain the following climb gradients with the airplane in the configuration prescribed in paragraph (c)(1) of this section:

(i) 1.2 percent (or, if greater, a gradient equivalent to a rate of climb of 0.027 Vs_o^2) at a pressure altitude of 5,000 feet and standard temperature (41 degrees F).

(ii) 0.6 percent (or, if greater, a gradient equivalent to a rate of climb of 0.014 Vs_o^2) at a pressure altitude of 5,000 feet and 81 degrees F (standard temperature plus 40 degrees F).

(3) The minimum climb gradient specified in paragraphs (c)(2) (i) and (ii) of this section must vary linearly between 41 degrees F and 81 degrees F and must change at the same rate up to the maximum operating termperature approved for the airplane.

(4) In paragraphs (c)(2) (i) and (ii) of this section, rate of climb is expressed in feet per minute and Vs_o is expressed in knots.

(d) For all multiengine airplanes, the speed for best rate of climb with one engine inoperative must be determined.

[Doc. No. 4080, 29 FR 17955, Dec. 18, 1964, as amended by Amdt. 23-7, 34 FR 13086, Aug. 13, 1969; Amdt. 23-21, 43 FR 2317, Jan. 16, 1978]

§ 23.75 Landing.

For airplanes (except skiplanes for which landplane landing data have been determined under this section and furnished in the Airplane Flight Manual), the horizontal distance necessary to land and come to a complete stop (or to a speed of approximately 3 knots for water landings of seaplanes and amphibians) from a point 50 feet above the landing surface must be determined as follows:

(a) A steady gliding approach with a calibrated airspeed of at least 1.3 Vs_1 must be maintained down to the 50-foot height.

(b) The landing may not require exceptional piloting skill or exceptionally favorable conditions.

(c) The landing must be made without excessive vertical acceleration or tendency to bounce, nose over, ground loop, porpoise, or water loop.

(d) It must be shown that a safe transition to the balked landing conditions of § 23.77 can be made from the conditions that exist at the 50-foot height.

(e) The pressures on the wheel braking system may not exceed those specified by the brake manufacturer.

(f) Means other than wheel brakes may be used if that means—

(1) Is safe and reliable;

(2) Is used so that consistent results can be expected in service; and

(3) Is such that exceptional skill is not required to control the airplane.

[Amdt. 23-21, 43 FR 2318, Jan. 16, 1978]

§ 23.77 Balked landing.

(a) For balked landings, each airplane must be able to maintain a steady angle of climb at sea level of at least 1:30 with—

(1) Takeoff power on each engine;

(2) The landing gear extended; and

(3) The wing flaps in the landing position, except that if the flaps may safely be retracted in two seconds or less without loss of altitude and without sudden changes of angle of attack or exceptional piloting skill, they may be retracted.

(b) Each turbine engine-powered airplane must be able to maintain a steady rate of climb of at least zero at a pressure altitude of 5,000 feet at 81 degrees F (standard temperature plus 40 degrees F), with the airplane in the configuration prescribed in paragraph (a) of this section.

[Amdt. 23-21, 43 FR 2318, Jan. 16, 1978]

Flight Characteristics

§ 23.141 General.

The airplane must meet the requirements of §§ 23.143 through 23.253 at the normally expected operating altitudes without exceptional piloting skill, alertness, or strength.

[Amdt. 23-17, 41 FR 55464, Dec. 20, 1976]

Controllability and Maneuverability

§ 23.143 General.

(a) The airplane must be safely controllable and maneuverable during—

(1) Takeoff;

(2) Climb;

(3) Level flight;

(4) Dive; and

(5) Landing (power on and power off with the wing flaps extended and retracted).

(b) It must be possible to make a smooth transition from one flight condition to another (including turns and slips) without danger of exceeding the limit load factor, under any probable operating condition (including, for multiengine airplanes, those conditions normally encountered in the sudden failure of any engine).

(c) If marginal conditions exist with regard to required pilot strength, the "strength of pilots" limits must be shown by quantitative tests. In no case may the limits exceed those prescribed in the following table:

Values in pounds of force as applied to the control wheel or rudder pedals	Pitch	Roll	Yaw
(a) For temporary application:			
Stick	60	30	.....
Wheel (applied to rim)	75	60	.....
Rudder pedal	.....	.....	150
(b) For prolonged application	10	5	20

[Doc. No. 4080, 29 FR 17955, Dec. 18, 1964, as amended by Amdt. 23-14, 38 FR 31819, Nov. 19, 1973; Amdt. 23-17, 41 FR 55464, Dec. 20, 1976]

§ 23.145 Longitudinal control.

(a) It must be possible, at speeds below the trim speed, to pitch the nose downward so that the rate of increase in airspeed allows prompt acceleration to the trim speed with—

(1) Maximum continuous power on each engine and the airplane trimmed at V_X;

(2) Power off and the airplane trimmed at a speed determined in accordance with § 23.161(c)(3) or (4) as appropriate or at the minimum trim speed, whichever is higher; and

(3) Wing flaps and landing gear (i) retracted, and (ii) extended.

(b) With the landing gear extended no change in trim or exertion of more control force than can be readily applied with one hand for a short period of time may be required for the following maneuvers:

(1) With power off, flaps retracted, and the airplane trimmed at $1.4V_{s_1}$ or the minimum trim speed, whichever is higher, extend the flaps as rapidly as possible and allow the airspeed to transition from $1.4V_{s_1}$ to $1.4V_{s_0}$, or if appropriate from the minimum trim speed to a speed equal to V_{s_0} increased by the same percentage that the minimum trim speed at the initial condition was greater than V_{s_1}.

(2) With power off, flaps extended, and the airplane trimmed at $1.4V_{s_0}$ or the minimum trim speed, whichever is higher, retract the flaps as rapidly as possible and allow the airspeed to transition from $1.4V_{s_0}$ to $1.4V_{s_1}$, or if appropriate, from the minimum trim speed to a speed equal to $1.4V_{s_1}$ increased by the same percentage that the minimum trim speed at the initial condition was greater than V_{s_0}.

(3) Repeat paragraph (b)(2) of this section except with maximum continuous power.

(4) With power off, flaps retracted, and the airplane trimmed at a speed determined in accordance with § 23.161 (c)(3) or (4), as appropriate or at the minimum trim speed, whichever is higher, apply takeoff power rapidly while maintaining the same airspeed.

(5) Repeat subparagraph (4) of this paragraph, except with the flaps extended.

(6) With power off, flaps extended, and the airplane trimmed at a speed determined in accordance with § 23.161 (c)(3) or (4), as appropriate or at the minimum trim speed, whichever is higher, obtain and maintain airspeeds between 1.1 V_{s_1} and either 1.7 V_{s_1} or V_F, whichever is lower.

(c) It must be possible to maintain approximately level flight when flap retraction from any position is made during steady horizontal flight at 1.1 V_{s_1} with simultaneous application of not more than maximum continuous power.

(d) It must be possible, with a pilot control force of not more than 10 pounds, to maintain a speed of not more than the speed determined in accordance with § 23.161(c)(4), during a power-off glide with landing gear and wing flaps extended.

(e) By using normal flight and power controls, except as otherwise noted in paragraphs (e)(1) and (e)(2), it must be possible in the following airplanes to establish a zero rate of descent at an attitude suitable for a controlled landing without exceeding the operational and structural limitations of the airplane:

(1) For single engine and multiengine airplanes, without the use of the primary longitudinal control system.

(2) For multiengine airplanes—

(i) Without the use of the primary directional control; and

(ii) If a single failure of any one connecting or transmitting link would affect both the longitudinal and directional primary control system, without the primary longitudinal and directional control system.

[Doc. No. 4080, 29 FR 17955, Dec. 18, 1964, as amended by Amdt. 23-7, 34 FR 13086, Aug. 13, 1969; Amdt. 23-14, 38 FR 31819, Nov. 19, 1973; Amdt. 23-17, 41 FR 55464, Dec. 20, 1976]

§ 23.147 Directional and lateral control.

(a) For each multiengine airplane, it must be possible to make turns with 15 degrees of bank both towards and away from an inoperative engine, from a steady climb at 1.4 V_{s_1} or V_Y with—

(1) One engine inoperative and its propeller in the minimum drag position;

(2) The remaining engines at not more than maximum continuous power;

(3) The rearmost allowable center of gravity;

(4) The landing gear (i) retracted, and (ii) extended;

(5) The flaps in the most favorable climb position; and

(6) Maximum weight.

(b) For each multiengine airplane, it must be possible, while holding the wings level within five degrees, to make sudden changes in heading safely in both directions. This must be shown at 1.4 V_{s_1} or V_Y with heading changes up to 15 degrees (except that the heading change at which the rudder force corresponds to the limits specified in § 23.143 need not be exceeded), with the—

(1) Critical engine inoperative and its propeller in the minimum drag position;

(2) Remaining engines at maximum continuous power;

(3) Landing gear (i) retracted, and (ii) extended;

(4) Flaps in the most favorable climb position; and

(5) Center of gravity at its rearmost allowable position.

§ 23.149 Minimum control speed.

(a) V_{MC} is the calibrated airspeed, at which, when the critical engine is suddenly made inoperative, it is possible to recover control of the airplane with that engine still inoperative and maintain straight flight either with zero yaw or, at the option of the applicant, with an angle of bank of not more than five degrees. The method used to simulate critical engine failure must represent the most critical mode of powerplant failure with respect to controllability expected in service.

(b) For reciprocating engine-powered airplanes, V_{MC} may not exceed 1.2 V_S, (where V_S, is determined at the maximum takeoff weight with—

(1) Takeoff or maximum available power on the engines;

(2) The most unfavorable center of gravity;

(3) The airplane trimmed for takeoff;

(4) The maximum sea level takeoff weight (or any lesser weight necessary to show V_{MC});

(5) Flaps in the takeoff position;

(6) Landing gear retracted;

(7) Cowl flaps in the normal takeoff position;

(8) The propeller of the inoperative engine—

(i) Windmilling;

(ii) In the most probable position for the specific design of the propeller control; or

(iii) Feathered, if the airplane has an automatic feathering device; and

(9) The airplane airborne and the ground effect negligible.

(c) For turbine engine-powered airplanes, V_{MC} may not exceed 1.2 V_S, (where V_S, is determined at the maximum takeoff weight) with—

(1) Maximum available takeoff power or thrust on the engines;

(2) The most unfavorable center of gravity;

(3) The airplane trimmed for takeoff;

(4) The maximum sea level takeoff weight for any lesser weight necessary to show V_{MC});

(5) The airplane in the most critical takeoff configuration except with the landing gear retracted; and

(6) The airplane airborne and the ground effect negligible.

(d) At V_{MC}, the rudder pedal force required to maintain control may not exceed 150 pounds, and it may not be necessary to reduce power or thrust of the operative engines. During recovery, the airplane may not assume any dangerous attitude and it must be possible to prevent a heading change of more than 20 degrees.

[Amdt. 23-21, 43 FR 2318, Jan. 16, 1978]

§ 23.151 Acrobatic maneuvers.

Each acrobatic and utility category airplane must be able to perform safely the acrobatic maneuvers for which certification is requested. Safe entry speeds for these maneuvers must be determined.

§ 23.153 Control during landings.

For an airplane that has a maximum weight of more than 6,000 pounds, it must be possible, while in the landing configuration, to safely complete a landing without encountering forces in excess of those prescribed in § 23.143(c) following an approach to land:

(a) At a speed 5 knots less than the speed used in complying with § 23.75 and with the airplane in trim or as nearly as possible in trim;

(b) With neither the trimming control being moved throughout the maneuver nor the power being increased during the landing flare; and

(c) With the thrust settings used in demonstrating compliance with § 23.75.

[Amdt. 23-14, 38 FR 31819, Nov. 19, 1973]

§ 23.155 Elevator control force in maneuvers.

(a) The elevator control force needed to achieve the positive limit maneuvering load factor may not be less than:

(1) For wheel controls, W/100 (where W is the maximum weight) or 20 pounds, whichever is greater, except that it need not be greater than 50 pounds; or

(2) For stick controls, W/140 (where W is the maximum weight) or 15 pounds, whichever is greater, except that it need not be greater than 35 pounds.

(b) The requirement of paragraph (a) of this section must be met with wing flaps and landing gear retracted under each of the following conditions:

(1) At 75 percent of maximum continuous power for reciprocating engines, or the maximum power or thrust selected by the applicant as an operating limitation for use during cruise for reciprocating or turbine engines.

(2) In a turn, after the airplane is trimmed with wings level at the minimum speed at which the required normal acceleration can be achieved without stalling, and at the maximum level flight trim speed except that the speed may not exceed V_{NE} or V_{MO}/M_{MO}, whichever is appropriate.

(c) Compliance with the requirements of this section may be demonstrated by measuring the normal acceleration that is achieved with the limiting stick force or by establishing the stick force per g gradient and extrapolating to the appropriate limit.

[Amdt. 23-14, 38 FR 31819, Nov. 19, 1973; 38 FR 32784, Nov. 28, 1973]

§ 23.157 Rate of roll.

(a) *Takeoff.* It must be possible, using a favorable combination of controls, to roll the airplane from a steady 30-degree banked turn through an angle of 60 degrees, so as to reverse the direction of the turn within:

(1) For an airplane of 6,000 pounds or less maximum weight, 5 seconds from initiation of roll; and

(2) For an airplane of over 6,000 pounds maximum weight,

$$(W+500)/1,300$$

seconds, where W is the weight in pounds.

(b) The requirement of paragraph (a) must be met when rolling the airplane in either direction in the following condition:

(1) Flaps in the takeoff position;

(2) Landing gear retracted;

(3) For a single engine airplane, at maximum takeoff power or thrust; and for a multiengine airplane, with the critical engine inoperative, the propeller in the minimum drag position, and the other engines at maximum continuous power or thrust; and

(4) The airplane trimmed at $1.2V_{S_1}$, or as nearly as possible in trim for straight flight.

(c) *Approach.* It must be possible, using a favorable combination of controls, to roll the airplane from a steady 30-degree banked turn through an angle of 60 degrees, so as to reverse the direction of the turn within:

(1) For an airplane of 6,000 pounds or less maximum weight, 4 seconds from initiation of roll; and

(2) For an airplane of over 6,000 pounds maximum weight,

$$(W+2,800)/2,200$$

seconds, where W is the weight in pounds.

(d) The requirement of paragraph (c) must be met when rolling the airplane in either direction in the following conditions:

(1) Flaps extended;

(2) Landing gear extended;

(3) All engines operating at idle power or thrust and with all engines operating at the power or thrust for level flight; and

(4) The airplane trimmed at the speed that is used in determining compliance with § 23.75.

[Amdt. 23-14, 38 FR 31819, Nov. 19, 1973]

TRIM

§ 23.161 Trim.

(a) *General.* Each airplane must meet the trim requirements of this section after being trimmed, and without further pressure upon, or movement of, the primary controls or their corresponding trim controls by the pilot or the automatic pilot.

(b) *Lateral and directional trim.* The airplane must maintain lateral and directional trim in level flight at 0.9 V_H or V_C, whichever is lower, with

the landing gear and wing flaps retracted.

(c) *Longitudinal trim.* The airplane must maintain longitudinal trim under each of the following conditions:

(1) A climb with maximum continuous power at a speed between Vx and 1.4 Vs_1, with—

(i) The landing gear and wing flaps retracted; and

(ii) The landing gear retracted and the wing flaps in the takeoff position.

(2) A power approach with a 3 degree angle of descent, the landing gear extended, and with—

(i) The wing flaps retracted and at a speed of 1.4 Vs_1; and

(ii) The applicable airspeed and flap position used in showing compliance with § 23.75.

(3) Level flight at any speed from 0.9 VH to either Vx or 1.4 Vs_1, with the landing gear and wing flaps retracted.

(d) In addition, each multiengine airplane must maintain longitudinal and directional trim at a speed between V_Y and 1.4 V_{S_1}, with—

(1) The critical engine inoperative;

(2) The remaining engines at maximum continuous power;

(3) The landing gear retracted;

(4) The wing flaps retracted; and

(5) An angle of bank of not more than five degrees.

[Doc. No. 4080, 29 FR 17955, Dec. 18, 1964, as amended by Amdt. 23-21, 43 FR 2318, Jan. 16, 1978]

STABILITY

§ 23.171 General.

The airplane must be longitudinally, directionally, and laterally stable under §§ 23.173 through 23.181. In addition, the airplane must show suitable stability and control "feel" (static stability) in any condition normally encountered in service, if flight tests show it is necessary for safe operation.

§ 23.173 Static longitudinal stability.

Under the conditions specified in § 23.175 and with the airplane trimmed as indicated, the characteristics of the elevator control forces and the friction within the control system must be as follows:

(a) A pull must be required to obtain and maintain speeds below the specified trim speed and a push required to obtain and maintain speeds above the specified trim speed. This must be shown at any speed that can be obtained, except that speeds requiring a control force in excess of 40 pounds or speeds above the maximum allowable speed or below the minimum speed for steady unstalled flight, need not be considered.

(b) The airspeed must return to within plus or minus 10 percent of the original trim speed when the control force is slowly released at any speed within the speed range specified in paragraph (a) of this section.

(c) The stick force must vary with speed so that any substantial speed change results in a stick force clearly perceptible to the pilot.

[Doc. No. 4080, 29 FR 17955, Dec. 18, 1964, as amended by Amdt. 23-14, 38 FR 31820 Nov. 19, 1973]

§ 23.175 Demonstration of static longitudinal stability.

Static longitudinal stability must be shown as follows:

(a) *Climb.* The stick force curve must have a stable slope, at speeds between 85 and 115 percent of the trim speed, with—

(1) Flaps in the climb position;

(2) Landing gear retracted;

(3) 75 percent of maximum continuous power for reciprocating engines or the maximum power or thrust selected by the applicant as an operating limitation for use during a climb for turbine engines; and

(4) The airplane trimmed for V_Y, except that the speed need not be less than 1.4 V_{S_1}.

(b) *Cruise—Landing gear retracted (or fixed gear).* (1) For the cruise conditions specified in paragraphs (b) (2) and (3) of this section, the following apply:

(i) The speed need not be less than 1.3 V_{S_1}.

(ii) For airplanes with V_{NE} established under § 23.1505(a), the speed need not be greater than V_{NE}.

(iii) For airplanes with V_{MO}/M_{MO} established under § 23.1505(c), the speed need not be greater than a speed midway between V_{MO}/M_{MO} and the lesser of V_D/M_D or the speed demon-

strated under § 23.251, except that for altitudes where Mach number is the limiting factor, the speed need not exceed that corresponding to the Mach number at which effective speed warning occurs.

(2) *High speed cruise.* The stick force curve must have a stable slope at all speeds within a range that is the greater of 15 percent of the trim speed plus the resulting free return speed range, or 40 knots plus the resulting free return speed range, above and below the trim speed, with—

(i) Flaps retracted.

(ii) Seventy-five percent of maximum continuous power for reciprocating engines or, for turbine engines, the maximum cruising power or thrust selected by the applicant as an operating limitation, except that the power need not exceed that required at V_{NE} for airplanes with V_{NE} established under § 23.1505(a), or that required at V_{MO}/M_{MO} for airplanes with V_{MO}/M_{MO} established under § 23.1505(c).

(iii) The airplane trimmed for level flight.

(3) *Low speed cruise.* The stick force curve must have a stable slope under all the conditions prescribed in paragraph (b)(2) of this section, except that the power is that required for level flight at a speed midway between 1.3 V_{S_1} and the trim speed obtained in the high speed cruise condition under paragraph (b)(2) of this section.

(c) *Landing gear extended (airplanes with retractable gear).* The stick force curve must have a stable slope at all speeds within a range from 15 percent of the trim speed plus the resulting free return speed range below the trim speed, to the trim speed (except that the speed range need not include speeds less than 1.4 V_{S_1} nor speeds greater than V_{LE}, with—

(1) Landing gear extended;

(2) Flaps retracted;

(3) 75 percent of maximum continuous power for reciprocating engines, or for turbine engines, the maximum cruising power or thrust selected by the applicant as an operating limitation, except that the power need not exceed that required for level flight at V_{LE}; and

(4) The airplane trimmed for level flight.

(d) *Approach and landing.* The stick force curve must have a stable slope at speeds between 1.1 V_{S_1} and 1.8 V_{S_1} with—

(1) Wing flaps in the landing position;

(2) Landing gear extended;

(3) The airplane trimmed at a speed in compliance with § 23.161(c)(4).

(4) Both power off and enough power to maintain a 3° angle of descent.

[Amdt. 23-7, 34 FR 13087, Aug. 13, 1969, as amended by Amdt. 23-14, 38 FR 31820, Nov. 19, 1973; Amdt. 23-17, 41 FR 55464, Dec. 20, 1976]

§ 23.177 Static directional and lateral stability.

(a) *Three-control airplanes.* The stability requirements for three-control airplanes are as follows:

(1) The static directional stability, as shown by the tendency to recover from a skid with the rudder free, must be positive for any landing gear and flap position appropriate to the takeoff, climb, cruise, and approach configurations. This must be shown with symmetrical power up to maximum continuous power, and at speeds from 1.2 V_{S_1} up to the maximum allowable speed for the condition being investigated. The angle of skid for these tests must be appropriate to the type of airplane. At larger angles of skid up to that at which full rudder is used or a control force limit in § 23.143 is reached, whichever occurs first, and at speeds from 1.2 V_{S_1} to V_A, the rudder pedal force must not reverse.

(2) The static lateral stability, as shown by the tendency to raise the low wing in a slip, must be positive for any landing gear and flap positions. This must be shown with symmetrical power up to 75 percent of maximum continuous power at speeds above 1.2 V_{S_1}, up to the maximum allowable speed for the configuration being investigated. The static lateral stability may not be negative at 1.2 V_{S_1}. The angle of slip for these tests must be appropriate to the type of airplane, but in no case may the slip angle be less than that obtainable with 10 degrees of bank.

(3) In straight, steady slips at 1.2 V_{S1} for any landing gear and flap positions, and for any symmetrical power conditions up to 50 percent of maximum continuous power, the aileron and rudder control movements and forces must increase steadily (but not necessarily in constant proportion) as the angle of slip is increased up to the maximum appropriate to the type of airplane. At larger slip angles up to the angle at which the full rudder or aileron control is used or a control force limit contained in § 23.143 is obtained, the rudder pedal force may not reverse. Enough bank must accompany slipping to hold a constant heading. Rapid entry into, or recovery from, a maximum slip may not result in uncontrollable flight characteristics.

(b) *Two-control (or simplified control) airplanes.* The stability requirements for two-control airplanes are as follows:

(1) The directional stability of the airplane must be shown by showing that, in each configuration, it can be rapidly rolled from a 45 degree bank in one direction to a 45 degree bank in the opposite direction without showing dangerous skid characteristics.

(2) The lateral stability of the airplane must be shown by showing that it will not assume a dangerous attitude or speed when the controls are abandoned for two minutes. This must be done in moderately smooth air with the airplane trimmed for straight level flight at 0.9 V_H or V_C, whichever is lower, with flaps and landing gear retracted, and with a rearward center of gravity.

[Doc. No. 4080, 29 FR 17955, Dec. 18, 1964; 30 FR 258, Jan. 9, 1965, as amended by Amdt. 23-21, 43 FR 2318, Jan. 16, 1978]

§ 23.179 Instrumented stick force measurements.

Instrumented stick force measurements must be made unless—

(a) Changes in speed are clearly reflected by changes in stick forces; and

(b) The maximum forces obtained under §§ 23.173 and 23.175 are not excessive.

§ 23.181 Dynamic stability.

(a) Any short period oscillation not including combined lateral-directional oscillations occurring between the stalling speed and the maximum allowable speed appropriate to the configuration of the airplane must be heavily damped with the primary controls—

(1) Free; and

(2) In a fixed position.

(b) Any combined lateral-directional oscillations ("Dutch roll") occurring between the stalling speed and the maximum allowable speed appropriate to the configuration of the airplane must be damped to 1/10 amplitude in 7 cycles with the primary controls—

(1) Free; and

(2) In a fixed position.

[Amdt. 23-21, 43 FR 2318, Jan. 16, 1978]

STALLS

§ 23.201 Wings level stall.

(a) For an airplane with independently controlled roll and directional controls, it must be possible to produce and to correct roll by unreversed use of the rolling control and to produce and to correct yaw by unreversed use of the directional control, up to the time the airplane pitches.

(b) For an airplane with interconnected lateral and directional controls (2 controls) and for an airplane with only one of these controls, it must be possible to produce and correct roll by unreversed use of the rolling control without producing excessive yaw, up to the time the airplane pitches.

(c) The wing level stall characteristics of the airplane must be demonstrated in flight as follows: The airplane speed must be reduced with the elevator control until the speed is slightly above the stalling speed, then the elevator control must be pulled back so that the rate of speed reduction will not exceed one knot per second until a stall is produced, as shown by an uncontrollable downward pitching motion of the airplane, or until the control reaches the stop. Normal use of the elevator control for recovery is allowed after the pitching motion has unmistakably developed.

(d) Except where made inapplicable by the special features of a particular type of airplane, the following apply

to the measurement of loss of altitude during a stall:

(1) The loss of altitude encountered in the stall (power on or power off) is the change in altitude (as observed on the sensitive altimeter testing installation) between the altitude at which the airplane pitches and the altitude at which horizontal flight is regained.

(2) If power or thrust is required during stall recovery the power or thrust used must be that which would be used under the normal operating procedures selected by the applicant for this maneuver. However, the power used to regain level flight may not be applied until flying control is regained.

(e) During the recovery part of the maneuver, it must be possible to prevent more than 15 degrees of roll or yaw by the normal use of controls.

(f) Compliance with the requirements of this section must be shown under the following conditions:

(1) *Wing flaps:* Full up, full down, and intermediate, if appropriate.

(2) *Landing gear:* Retracted and extended.

(3) *Cowl flaps:* Appropriate to configuration.

(4) *Power:* Power or thrust off, and 75 percent maximum continuous power or thrust.

(5) *Trim:* 1.5 V_{S_1} or at the minimum trim speed, whichever is higher.

(6) *Propeller:* Full increase rpm position for the power off condition.

[Amdt. 23-14, 38 FR 31820, Nov. 19, 1973]

§ 23.203 Turning flight and accelerated stalls.

Turning flight and accelerated stalls must be demonstrated in flight tests as follows:

(a) Establish and maintain a coordinated turn in a 30 degree bank. Reduce speed by steadily and progressively tightening the turn with the elevator until the airplane is stalled or until the elevator has reached its stop. The rate of speed reduction must be constant, and:

(1) For a turning flight stall, may not exceed one knot per second; and

(2) For an accelerated stall, be 3 to 5 knots per second with steadily increasing normal acceleration.

(b) When the stall has fully developed or the elevator has reached its stop, it must be possible to regain level flight without:

(1) Excessive loss of altitude;

(2) Undue pitchup;

(3) Uncontrollable tendency to spin;

(4) Exceeding 60 degree of roll in either direction from the established 30 degree bank; and

(5) For accelerated entry stalls, without exceeding the maximum permissible speed or the allowable limit load factor.

(c) Compliance with the requirements of this section must be shown with:

(1) *Wing flaps:* Retracted and fully extended for turning flight and accelerated entry stalls, and intermediate, if appropriate, for accelerated entry stalls;

(2) *Landing gear:* Retracted and extended;

(3) *Cowl flaps:* Appropriate to configuration;

(4) *Power:* 75 percent maximum continuous power; and

(5) *Trim:* 1.5 V_{S_1} or minimum trim speed, whichever is higher.

[Amdt. 23-14, 38 FR 31820, Nov. 19, 1973]

§ 23.205 Critical engine inoperative stalls.

(a) A multiengine airplane may not display any undue spinning tendency and must be safely recoverable without applying power to the inoperative engine when stalled. The operating engines may be throttled back during the recovery from stall.

(b) Compliance with paragraph (a) of the section must be shown with:

(1) *Wing flaps:* Retracted.

(2) *Landing gear:* Retracted.

(3) *Cowl flaps:* Appropriate to level flight critical engine inoperative.

(4) *Power:* Critical engine inoperative and the remaining engine(s) at 75 percent maximum continuous power or thrust or the power or thrust at which the use of maximum control travel just holds the wings laterally level in the approach to stall, whichever is lesser.

(5) *Propeller:* Normal inoperative position for the inoperative engine.

(6) *Trim:* Level flight, critical engine inoperative, except that for an air-

plane of 6,000 pounds or less maximum weight that has a stalling speed of 61 knots or less and cannot maintain level flight with the critical engine inoperative, the airplane must be trimmed for straight flight, critical engine inoperative, at a speed not greater than $1.5V_{S1}$.

[Amdt. 23-14, 38 FR 31820, Nov. 19, 1973]

§ 23.207 Stall warning.

(a) There must be a clear and distinctive stall warning, with the flaps and landing gear in any normal position, in straight and turning flight.

(b) The stall warning may be furnished either through the inherent aerodynamic qualities of the airplane or by a device that will give clearly distinguishable indications under expected conditions of flight. However, a visual stall warning device that requires the attention of the crew within the cockpit is not acceptable by itself.

(c) The stall warning must begin at a speed exceeding the stalling speed by a margin of not less than 5 knots, but not more than the greater of 10 knots or 15 percent of the stalling speed, and must continue until the stall occurs.

[Amdt. 23-7, 34 FR 13087, Aug. 13, 1969]

SPINNING

§ 23.221 Spinning.

(a) *Normal category.* A single-engine, normal category airplane must be able to recover from a one-turn spin or a 3-second spin, whichever takes longer, in not more than one additional turn, with the controls used in the manner normally used for recovery. In addition—

(1) For both the flaps-retracted and flaps-extended conditions, the applicable airspeed limit and positive limit maneuvering load factor may not be exceeded;

(2) There may be no excessive back pressure during the spin or recovery; and

(3) It must be impossible to obtain uncontrollable spins with any use of the controls.

For the flaps-extended condition, the flaps may be retracted during recovery.

(b) *Utility category.* A utility category airplane must meet the requirements of paragraph (a) of this section or the requirements of paragraph (c) of this section.

(c) *Acrobatic category.* An acrobatic category airplane must meet the following requirements:

(1) The airplane must recover from any point in a spin, in not more than one and one-half additional turns after normal recovery application of the controls. Prior to normal recovery application of the controls, the spin test must proceed for six turns or 3 seconds, whichever takes longer, with flaps retracted, and one turn or 3 seconds, whichever takes longer, with flaps extended. However, beyond 3 seconds, the spin may be discontinued when spiral characteristics appear with flaps retracted.

(2) For both the flaps-retracted and flaps-extended conditions, the applicable airspeed limit and positive limit maneuvering load factor may not be exceeded. For the flaps-extended condition, the flaps may be retracted during recovery, if a placard is installed prohibiting intentional spins with flaps extended.

(3) It must be impossible to obtain uncontrollable spins with any use of the controls.

(d) *Airplanes "characteristically incapable of spinning".* If it is desired to designate an airplane as "characteristically incapable of spinning", this characteristic must be shown with—

(1) A weight five percent more than the highest weight for which approval is requested;

(2) A center of gravity at least three percent aft of the rearmost position for which approval is requested;

(3) An available elevator up-travel four degrees in excess of that to which the elevator travel is to be limited for approval; and

(4) An available rudder travel seven degrees, in both directions, in excess of that to which the rudder travel is to be limited for approval.

[Doc. No. 4080, 29 FR 17955, Dec. 18, 1964, as amended by Amdt. 23-7, 34 FR 13087, Aug. 13, 1969]

GROUND AND WATER HANDLING CHARACTERISTICS

§ 23.231 Longitudinal stability and control.

(a) A landplane may have no uncontrollable tendency to nose over in any reasonably expected operating condition, including rebound during landing or takeoff. Wheel brakes must operate smoothly and may not induce any undue tendency to nose over.

(b) A seaplane or amphibian may not have dangerous or uncontrollable porpoising characteristics at any normal operating speed on the water.

§ 23.233 Directional stability and control.

(a) There may be no uncontrollable ground or water looping tendency in 90 degree cross winds, up to a wind velocity of 0.2 V_{SO}, at any speed at which the airplane may be expected to be operated on the ground or water.

(b) A landplane must be satisfactorily controllable, without exceptional piloting skill or alertness, in power-off landings at normal landing speed, without using brakes or engine power to maintain a straight path.

(c) The airplane must have adequate directional control during taxiing.

§ 23.235 Taxiing condition.

The shock-absorbing mechanism may not damage the structure of the airplane when the airplane is taxied on the roughest ground that may reasonably be expected in normal operation.

§ 23.239 Spray characteristics.

Spray may not dangerously obscure the vision of the pilots or damage the propellers or other parts of a seaplane or amphibian at any time during taxiing, takeoff, and landing.

MISCELLANEOUS FLIGHT REQUIREMENTS

§ 23.251 Vibration and buffeting.

Each part of the airplane must be free from excessive vibration under any appropriate speed and power conditions up to at least the minimum value of V_D allowed in § 23.335. In addition, there may be no buffeting, in any normal flight condition, severe enough to interfere with the satisfactory control of the airplane, cause excessive fatigue to the crew, or result in structural damage. Stall warning buffeting within these limits is allowable.

§ 23.253 High speed characteristics.

If a maximum operating speed V_{MO}/M_{MO} is established under § 23.1505(c), the following speed increase and recovery characteristics must be met:

(a) Operating conditions and characteristics likely to cause inadvertent speed increases (including upsets in pitch and roll) must be simulated with the airplane trimmed at any likely cruise speed up to V_{MO}/M_{MO}. These conditions and characteristics include gust upsets, inadvertent control movements, low stick force gradient in relation to control friction, passenger movement, leveling off from climb, and descent from Mach to airspeed limit altitude.

(b) Allowing for pilot reaction time after effective inherent or artificial speed warning occurs, it must be shown that the airplane can be recovered to a normal attitude and its speed reduced to V_{MO}/M_{MO}, without—

(1) Exceptional piloting strength or skill;

(2) Exceeding V_D/M_D, the maximum speed shown under § 23.251, or the structural limitations; or

(3) Buffeting that would impair the pilot's ability to read the instruments or to control the airplane for recovery.

(c) There may be no control reversal about any axis at any speed up to the maximum speed shown under § 23.251. Any reversal of elevator control force or tendency of the airplane to pitch, roll, or yaw must be mild and readily controllable, using normal piloting techniques.

[Amdt. 23-7, 34 FR 13087, Aug. 13, 1969; as amended by Amdt. 23-26, 45 FR 60170, Sept. 11, 1980]

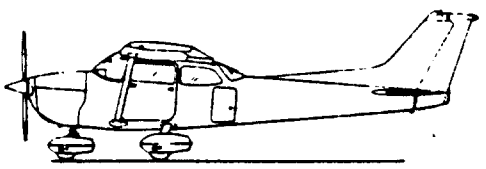

Adoption of the Amendments

Accordingly, Parts 21, 23, 36, 91, and 135 of the Federal Aviation Regulations (14 CFR Parts 21, 23, 36, 91, and 135) are amended, as follows:

1. By amending Part 23 by revising the title to read as follows:

PART 23—AIRWORTHINESS STANDARDS: NORMAL, UTILITY, ACROBATIC, AND COMMUTER CATEGORY AIRPLANES

2. The authority citation for Part 23 continues to read as follows:

Authority: 49 U.S.C. 1344, 1354(a), 1355, 1421, 1423, 1425, 1428, 1429, 1430, and 1502; and 49 U.S.C. 106(g) (Revised, Public L. 97-449, January 12, 1983).

3. By amending § 23.1 by revising paragraph (a) to read as follows:

§ 23.1 Applicability.

(a) This part prescribes airworthiness standards for the issue of type certificates, and changes to those certificates, for airplanes in the normal, utility, acrobatic, and commuter categories.

• • • • •

4. By amending § 23.3 by revising paragraphs (a) introductory text, (b) introductory text, and (c); by revising and redesignating paragraph (d) as (e), and by adding a new paragraph (d) to read as follows:

§ 23.3 Airplane categories.

(a) The normal category is limited to airplanes that have a seating configuration, excluding pilot seats, of nine or less, a maximum certificate takeoff weight of 12,500 pounds or less, and intended for nonacrobatic operation. Nonacrobatic operation includes:

• • • • •

(b) The utility category is limited to airplanes that have a seating configuration, excluding pilot seats, of nine or less, a maximum certificated takeoff weight of 12,500 pounds or less, and intended for limited acrobatic operation. Airplanes certificated in the utility category may be used in any of the operations covered under paragraph (a) of this section and in limited acrobatic operations. Limited acrobatic operation includes:

• • • • •

(c) The acrobatic category is limited to airplanes that have a seating configuration, excluding pilot seats, of nine or less, a maximum certificated takeoff weight of 12,500 pounds or less, and intended for use without restrictions, other than those shown to be necessary as a result of required flight tests.

(d) The commuter category is limited to propeller-driven, multiengine airplanes that have a seating configuration excluding pilot seats, of 19 or less, and a maximum certificated takeoff weight of 19,000 pounds or less, intended for nonacrobatic operation as described in paragraph (a) of this section.

(e) Airplanes may be type certificated in more than one category of this part if the requirements of each requested category are met.

5. By amending § 23.25(a)(2) by inserting the words "and commuter" after the word "normal"; and by revising paragraph (a) introductory text to read as follows:

§ 23.25 Weight limits.

(a) *Maximum weight.* The maximum weight is the highest weight at which compliance with each applicable requirement of this Part (other than those complied with at the design landing weight) is shown. In addition, for commuter category airplanes, the applicant must establish a maximum zero fuel weight. The maximum weight must be established so that it is—

• • • • •

6. By amending § 23.45 by revising paragraph (a) and by adding a new paragraph (f) to read as follows:

§ 23.45 General.

(a) Unless otherwise prescribed, the performance requirements of this subpart must be met for still air; and

(1) Standard atmospheric conditions for normal, utility, and acrobatic category airplanes; or

(2) Ambient atmospheric conditions for commuter category airplanes.

• • • • •

(f) For commuter category airplanes, the following also apply:

(1) Unless otherwise prescribed, the applicant must select the takeoff, en route, approach, and landing configurations for the airplane;

(2) The airplane configuration may vary with weight, altitude, and temperature, to the extent they are compatible with the operating procedures required by paragraph (f)(3) of this section;

(3) Unless otherwise prescribed, in determining the critical-engine-inoperative takeoff performance, takeoff flight path, the accelerate-stop distance, takeoff distance, and landing distance, changes in the airplane's configuration, speed, power, and thrust must be made in accordance with procedures established by the applicant for operation in service;

(4) Procedures for the execution of missed approaches and balked landings associated with the conditions prescribed in §§ 23.67(e)(3) and 23.77(c) must be established; and

(5) The procedures established under paragraphs (f)(3) and (f)(4) of this section must—

(i) Be able to be consistently executed by a crew of average skill;

(ii) Use methods or devices that are safe and reliable; and

(iii) Include allowance for any reasonably expected time delays in the execution of the procedures.

7. By amending § 23.51 by removing paragraphs (b) and (c); by redesignating paragraphs (d) and (e) as (b) and (c) respectively; and by adding a new paragraph (d) to read as follows:

§ 23.51 Takeoff.

• • • • •

(d) For commuter category airplanes, takeoff performance and data as required by §§ 23.53 through 23.59 must be determined and included in the Airplane Flight Manual—

(1) For each weight, altitude, and ambient temperature within the operational limits selected by the applicant;

(2) For the selected configuration for takeoff;

(3) For the most unfavorable center of gravity position;

(4) With the operating engine within approved operating limitations;

(5) On a smooth, dry, hard surface runway; and

(6) Corrected for the following operational correction factors:

(i) Not more than 50 percent of nominal wind components along the takeoff path opposite to the direction of takeoff and not less than 150 percent of nominal wind components along the takeoff path in the direction of takeoff; and

(ii) Effective runway gradients.

8. By adding a new § 23.53 to read as follows:

§ 23.53 Takeoff speeds.

(a) For multiengine airplanes, the lift-off speed, V_{LOF}, may not be less than V_{MC} determined in accordance with § 23.149.

(b) Each normal, utility, and acrobatic category airplane, upon reaching a height of 50 feet above the takeoff surface level, must have reached a speed of not less than the following:

(1) For multiengine airplanes, the higher of—

(i) 1.1 V_{MC}; or

(ii) 1.3 V_{S_1}, or any lesser speed, not less than V_X plus 4 knots, that is shown to be safe under all conditions, including turbulence and complete engine failure.

(2) For single engine airplanes—

(i) 1.3 V_{S_1}; or

(ii) Any lesser speed, not less than V_X plus 4 knots, that is shown to be safer

under all conditions, including turbulence and complete engine failure.

(c) For commuter category airplanes, the following apply:

(1) The takeoff decision speed, V_1, is the calibrated airspeed on the ground at which, as a result of engine failure or other reasons, the pilot is assumed to have made a decision to continue or discontinue the takeoff. The takeoff decision speed, V_1, must be selected by the applicant but may not be less than the greater of the following:

(i) 1.10 V_{S1};

(ii) 1.10 V_{MC} established in accordance with § 23.149;

(iii) A speed at which the airplane can be rotated for takeoff and shown to be adequate to safely continue the takeoff, using normal piloting skill, when the critical engine is suddenly made inoperative; or

(iv) V_{EF} plus the speed gained with the critcial engine inoperative during the time interval between the instant that the critical engine is failed and the instant at which the pilot recognizes and reacts to the engine failure as indicated by the pilot's application of the first retarding means during the accelerate-stop determination of § 23.55.

(2) The takeoff safety speed, V_2, in terms of calibrated airspeed, must be selected by the applicant so as to allow the gradient of climb required in § 23.67 but must not be less than V_1 or less than 1.2V_{S1}.

(3) The critical engine failure speed, V_{EF}, is the calibrated airspeed at which the critical engine is assumed to fail. V_{EF} must be selected by the applicant but not less than V_{MC} determined in accordance with § 23.149.

(4) The rotation speed, V_R in terms of calibrated airspeed, must be selected by the applicant and may not be less than the greater of the following:

(i) V_1; or

(ii) The speed determined in accordance with § 23.57(c) that allows attaining the initial climb out speed, V_2, before reaching a height of 35 feet above the takeoff surface.

(5) For any given set of conditions, such as weight, altitude, configuration, and temperature, a single value of V_R must be used to show compliance with both the one-engine-inoperative takeoff and all-engines-operating takeoff requirements:

(i) One-engine-inoperative takeoff determined in accordance with § 23.57; and

(ii) All-engines-operating takeoff determined in accordance with § 23.59.

(6) The one-engine-inoperative takeoff distance, using a normal rotation rate at a speed of 5 knots less than V_R established in accordance with paragraphs (c)(4) and (5) of this section, must be shown not to exceed the corresponding one-engine-inoperative takeoff distance determined in accordance with § § 23.57 and 23.59 using the established V_r. The take off distance determined in accordance with § 23.59 and the takeoff must be safely continued from the point at which the airplane is 35 feet above the takeoff surface at a speed not less than 5 knots less than the established V_2 speed.

(7) The applicant must show, with all engines operating, that marked increases in the scheduled takeoff distances determined in accordance with § 23.59 do not result from over-rotation of the airplane and out-of-trim conditions.

9. By adding a new § 23.55 to read as follows:

§ 23.55 Accelerate-stop distance.

For each commuter category airplane, the accelerate-stop distance must be determined as follows:

(a) The accelerate-stop distance is the sum of the distances necessary to—

(1) Accelerate the airplane from a standing start to V_1; and

(2) Come to a full stop from the point at which V_1 is reached assuming that in the case of engine failure, the pilot has decided to stop as indicated by application of the first retarding means at the speed V_1.

(b) Means other than wheel brakes may be used to determine the accelerate-stop distance if that means is available with the critical engine inoperative and if that means—

(1) Is safe and reliable;

(2) Is used so that consistent results can be expected under normal operating conditions; and

(3) Is such that exceptional skill is not required to control the airplane.

10. By adding a new § 23.57 to read as follows:

§ 23.57 Takeoff path.

For each commuter category airplane, the takeoff path is as follows:

(a) The takeoff path extends from a standing start to a point in the takeoff at which the airplane is 1,500 feet above the takeoff surface or at which the transition from the takeoff to the en route configuration is completed, whichever point is higher; and

(1) The takeoff path must be based on the procedures prescribed in § 23.45;

(2) The airplane must be accelerated on the ground to V_{EF} at which point the critical engine must be made inoperative and remain inoperative for the rest of the takeoff; and

(3) After reaching V_{EF}, the airplane must be accelerated to V_2.

(b) During the acceleration to speed V_2, the nose gear may be raised off the ground at a speed not less than V_R. However, landing gear retraction may not be initiated until the airplane is airborne.

(c) During the takeoff path determination, in accordance with paragraphs (a) and (b) of this section—

(1) The slope of the airborne part of the takeoff path must be positive at each point;

(2) The airplane must reach V_2 before it is 35 feet above the takeoff surface, and must continue at a speed as close as practical to, but not less than V_2, until it is 400 feet above the takeoff surface;

(3) At each point along the takeoff path, starting at the point at which the airplane reaches 400 feet above the takeoff surface, the available gradient of climb may not be less than—

(i) 1.2 percent for two-engine airplanes;

(ii) 1.5 percent for three-engine airplanes;

(iii) 1.7 percent for four-engine airplanes; and

(4) Except for gear retraction and automatic propeller feathering, the airplane configuration may not be changed, and no change in power or thrust that requires action by the pilot may be made, until the airplane is 400 feet above the takeoff surface.

(d) The takeoff path must be determined by a continuous demonstrated takeoff or by synthesis from segments. If the takeoff path is determined by the segmental method—

(1) The segments must be clearly defined and must be related to the distinct changes in the configuration, power or thrust, and speed;

(2) The weight of the airplane, the configuration, and the power or thrust must be constant throughout each segment and must correspond to the most critical condition prevailing in the segment;

(3) The flight path must be based on the airplane's performance without ground effect;

(4) The takeoff path data must be checked by continuous demonstrated takeoffs up to the point at which the airplane is out of ground effect and its speed is stabilized to ensure that the path is conservative relative to the continuous path; and

(5) The airplane is considered to be out of the ground effect when it reaches a height equal to its wing span.

11. By adding a new § 23.59 to read as follows:

§ 23.59 Takeoff distance and takeoff run.

For each commuter category airplane—

(a) Takeoff distance is the greater of—

(1) The horizontal distance along the takeoff path from the start of the takeoff to the point at which the airplane is 35 feet above the takeoff surface as determined under § 23.57; or

(2) With all engines operating, 115 percent of the horizontal distance along the takeoff path, with all engines operating, from the start of the takeoff to the point at which the airplane is 35 feet above the takeoff surface, as determined by a procedure consistent with § 23.57.

(b) If the takeoff distance includes a clearway, the takeoff run is the greater of—

(1) The horizontal distance along the takeoff path from the start of the takeoff to a point equidistant between the point at which V_{LOF} is reached and the point at which the airplane is 35 feet above the takeoff surface as determined under § 23.57; or

(2) With all engines operating, 115 percent of the horizontal distance along the takeoff path, with all engines operating, from the start of the takeoff to a point equidistant between the point at which V_{LOF} is reached and the point at which the airplane is 35 feet above the takeoff surface determined by a procedure consistent with § 23.57.

12. By adding a new § 23.61 to read as follows:

§ 23.61 Takeoff flight path.

For each commuter category airplane, the takeoff flight path must be determined as follows:

(a) The takeoff flight path begins 35 feet above the takeoff surface at the end of the takeoff distance determined in accordance with § 23.59.

(b) The net takeoff flight path data must be determined so that they represent the actual takeoff flight paths, as determined in accordance with § 23.57 and with paragraph (a) of this section, reduced at each point by a gradient of climb equal to—

(1) 0.8 percent for two-engine airplanes;

(2) 0.9 percent for three-engine airplanes; and

(3) 1.0 percent for four-engine airplanes.

(c) The prescribed reduction in climb gradient may be applied as an equivalent reduction in acceleration along that part of the takeoff flight path at which the airplane is accelerated in level flight.

13. By amending § 23.65 by adding a new paragraph (d) to read as follows:

§ 23.65 Climb: All engines operating.

* * * * *

(d) In addition for commuter category airplanes, performance data must be determined for variations in weight, altitude, and temperatures at the most critical center of gravity for which approval is requested.

14. By amending § 23.67 by inserting the words "normal, utility, and acrobatic category" before the word "reciprocating" in both paragraphs (a) and (b) and before the word "turbine" in paragraph (c); and by adding a new paragraph (e) to read as follows:

§ 23.67 Climb: One engine inoperative.

* * * * *

(e) For commuter category airplanes, the following apply:

(1) *Takeoff climb:* The maximum weight at which the airplane meets the minimum climb performance specified in paragraphs (i) and (ii) must be determined for each altitude and ambient temperature within the operating limitations established for the airplane, out of ground effect in free air, with the airplane in the takeoff configuration, with the most critical center of gravity, the critical engine inoperative, the remaining engines at the maximum takeoff power or thrust, and the propeller of the inoperative engine windmilling with the propeller controls in the normal position, except that, if an approved automatic propeller feathering system is installed, the propeller may be in the feathered position:

(i) *Takeoff, landing gear extended.* The minimum steady gradient of climb between the lift-off speed, V_{LOF}, and until the landing gear is retracted must be measurably positive for two-engine airplanes, not less than 0.3 percent for three-engine airplanes, or 0.5 percent for four-engine airplanes at all points along the flight path; and

(ii) *Takeoff, landing gear retracted.* The minimum steady gradient of climb must not be less than 2 percent for two-engine airplanes, 2.3 percent for three-engine airplanes, and 2.6 percent for four-engine airplanes at the speed V_2, until the airplane is 400 feet above the takeoff surface. For airplanes with fixed landing gear, this requirement must be met with the landing gear extended.

(2) *En route climb:* The maximum weight must be determined for each altitude and ambient temperature within the operational limits established for the airplane, at which the steady gradient of climb is not less than 1.2 percent for two-engine airplanes, 1.5 percent for three-engine airplanes, and 1.7 percent for four-engine airplanes at an altitude of 1,500 feet above the takeoff surface, with the airplane in the en route configuration, the critical engine inoperative, the remaining engine at the maximum continuous power or thrust, and the most unfavorable center of gravity.

(3) *Approach:* In the approach configuration corresponding to the normal all-engines-operating procedure in which V_{S_1} for this configuration does not exceed 110 percent of the V_{S_1} for the related landing configuration, the steady gradient of climb may not be less than 2.1 percent for two-engine airplanes, 2.4 percent for three-engine airplanes, and 2.7 percent for four-engine airplanes, with—

(i) The critical engine inoperative and the remaining engines at the available takeoff power or thrust;

(ii) The maximum landing weight; and

(iii) A climb speed established in connection with the normal landing procedures but not exceeding 1.5 V_{S_1}.

15. By amending § 23.75 by adding a new paragraph (g) to read as follows:

§ 23.75 Landing.

* * * * *

(g) In addition, for commuter category airplanes, the following apply:

(1) The landing distance must be determined for standard temperatures at each weight, altitude, and wind condition within the operational limits established by the applicant;

(2) A steady gliding approach, or a steady approach at a gradient of descent not greater than 5.2 percent (3°), at a calibrated airspeed not less than 1.3V_{S_1}, must be maintained down to the 50-foot height; and

(3) The landing distance data must include correction factors for not more than 50 percent of the nominal wind components along the landing path opposite to the direction of landing and not less than 150 percent of the nominal wind components along the landing path in the direction of landing.

16. By amending § 23.77 by inserting the words "normal, utility, and acrobatic category" before the word "airplane"; and by adding an "s" to the word "airplane" in paragraph (a); by inserting the words "normal, utility, and acrobatic category" before the word "turbine"; by adding an "s" to the word "airplane" in the first part of the sentence in paragraph (b); and by adding a new paragraph (c) to read as follows:

§ 23.77 Balked landing.

* * * * *

(c) For each commuter category airplane, with all engines operating, the maximum weight must be determined with the airplane in the landing configuration for each altitude and ambient temperature within the operational limits established for the airplane, with the most unfavorable center of gravity and out-of-ground effect in free air, at which the steady gradient of climb will not be less than 3.3 percent with—

(1) The engines at the power or thrust that is available 8 seconds after initiation of movement of the power or thrust controls from the minimum flight-idle position to the takeoff position.

(2) A climb speed not greater than the approach speed established under § 23.75 and not less than the greater of 1.05 V_{MC} or 1.10V_{S_1}.

17. By amending § 23.161 by revising paragraphs (b), (c) introductory test, and (c)(3) to read as follows:

§ 23.161 Trim.

• • • • •

(b) *Lateral and directional trim.* The airplane must maintain lateral and directional trim in level flight with the landing gear and wing flaps retracted as follows:

(1) For normal, utility, and acrobatic category airplanes, at a speed of $0.9V_H$ or V_C, whichever is lower; and

(2) For commuter category airplanes, at a speed of V_H or V_{MO}/M_{MO}, whichever is lower.

(c) *Longitudinal trim.* The airplane must maintain longitudinal trim under each of the following conditions, except that it need not maintain trim at a speed greater than V_{MO}/M_{MO}:

• • • • •

(3) Level flight at any speed with the landing gear and wing flaps retracted as follows:

(i) For normal, utility, and acrobatic category airplanes, at any speed from $0.9V_H$ to either V_X or $1.4V_{S_1}$; and

(ii) For commuter category airplanes, at a speed of V_H or V_{MO}/M_{MO}, whichever is lower, to either V_X or $1.4V_{S_1}$.

• • • • •

18. By amending § 23.173 by revising paragraph (b) to read as follows:

§ 23.173 Static longitudinal stability.

• • • • •

(b) The airspeed must return to within the tolerances specified for applicable categories of airplanes when the control force is slowly released at any speed within the speed range specified in paragraph (a) of this section. The applicable tolerances are—

(1) The airspeed must return to within plus or minus 10 percent of the original trim airspeed; and

(2) For commuter category airplanes, the airspeed must return to within plus or minus 7.5 percent of the original trim airspeed for the cruising condition specified in § 23.175(b).

• • • • •

19. By amending § 23.175 by revising paragraph (b)(2) introductory text to read as follows:

§ 23.175 Demonstration of static longitudinal stability.

• • • • •

(b) *Cruise—Landing gear retracted (or fixed gear).*

• • • • •

(2) *High speed cruise.* The stick force curve must have a stable slope at all speeds within a range that is the greater of 15 percent of the trim speed plus the resulting free return speed range or 40 knots plus the resulting free return speed range for normal, utility, and acrobatic category airplanes, above and below the trim speed. For commuter category airplanes, the stick force curve must have a stable slope for a speed range of 50 knots from the trim speed, except that the speeds need not exceed V_{FC}/M_{FC} or be less than $1.4\ V_{S_1}$ and this speed range is considered to begin at the outer extremes of the friction band with a stick force not to exceed 50 pounds. In addition, for commuter category airplanes, V_{FC}/M_{FC} may not be less than a speed midway between V_{MO}/M_{MO} and V_{DF}/M_{DF}, except that, for altitudes where Mach number is the limiting factor, M_{FC} need not exceed the Mach number at which effective speed warning occurs. These requirements for all categories of airplane must be met with—

• • • • •

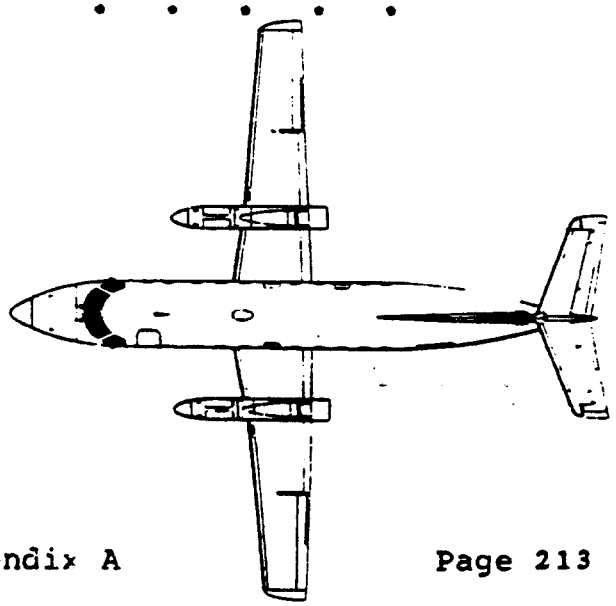

A3. Federal Aviation Regulation: FAR 25

In this Section a summary is given of that part of FAR 25 which deals with performance and with flight characteristics.

Subpart A—General

§ 25.1 Applicability.

(a) This part prescribes airworthiness standards for the issue of type certificates, and changes to those certificates, for transport category airplanes.

(b) Each person who applies under Part 21 for such a certificate or change must show compliance with the applicable requirements in this part.

§ 25.2 Special retroactive requirements.

Notwithstanding §§ 21.17 and 21.101 of this chapter and irrespective of the date of application, each applicant for a type certificate and each applicant for a supplemental-type certificate (or an amendment to a type certificate) involving an increase in passenger seating capacity to a total greater than that for which the airplane has been type certificated, must show:

(a) After October 23, 1967, that the airplane concerned meets the requirements of §§ 25.783(g), 25.803(c) (2) through (9), 25.803(d), 25.807 (a), (c), and (d), 25.809 (f), and (h), 25.811 (a), (b), (d), (e), (f), and (g), 25.812(a)(1), (b), (c), (d), (e), (h), (i), (j), and (k) (1) and (2), 25.813 (a), (b), and (c), 25.815, 25.817, 25.853 (a) and (b), 25.855(a), 25.993(f), and 25.1359(c), in effect on October 24, 1967, or June 20, 1968, and

(b) After April 24, 1969, that the airplane concerned meets the requirements of §§ 25.721(d), 25.803(e), 25.811(c), 25.812 (a)(2), (f), (g), and (k)(3) in effect on October 24, 1967; and

(c) After April 23, 1969, that the airplane concerned meets the requirements of § 25.785(c) in effect either prior to or on that date; and

(d) After April 23, 1969, that the airplane concerned meets the requirements of §§ 25.803(b) and 25.803(c)(1) in effect on that date.

(Sec. 604, 72 Stat. 778; (49 U.S.C. 1424)

[Amdt. 25-15, 32 FR 13262, Sept. 20, 1967; 32 FR 13635, Sept. 29, 1967; Amdt. 25-17, 33 FR 9066, June 20, 1968; Amdt. 25-20, 34 FR 5544, Mar. 22, 1969]

Subpart B—Flight

General

§ 25.21 Proof of compliance.

(a) Each requirement of this subpart must be met at each appropriate combination of weight and center of gravity within the range of loading conditions for which certification is requested. This must be shown—

(1) By tests upon an airplane of the type for which certification is requested, or by calculations based on, and equal in accuracy to, the results of testing; and

(2) By systematic investigation of each probable combination of weight and center of gravity, if compliance cannot be reasonably inferred from combinations investigated.

(b) If there is less than a 2 knot difference in the forward and rearward c.g. stalling speeds, the flying qualities may be based upon the forward c.g. stalling speeds.

(c) The controllability, stability, trim, and stalling characteristics of the airplane must be shown for each altitude up to the maximum expected in operation.

(d) The following general tolerances from specified values are allowed during flight testing. However, greater tolerances may be allowed in particular tests. These tolerances are plus or minus variations unless otherwise noted in the particular test:

Item	Tolerance
Weight	+5%, −10%.
Critical items affected by weight.	+5%, −1%.
C.G.	7% total travel.
Airspeed	3 knots or 3%, whichever is higher.
Power	5%.
Wind (takeoff and landing tests).	As low as possible but not to exceed approximately 12% V_{s_1} or 10.0 knots, whichever is lower, along the runway surface.

(e) If compliance with the flight characteristics requirements is dependent upon a stability augmentation system or upon any other automatic or power-operated system, compliance must be shown with §§ 25.671 and 25.672.

(f) In meeting the requirements of §§ 25.105(d), 25.125, 25.233, and 25.237, the wind velocity must be measured at a height of 10 meters above the surface, or corrected for the difference between the height at which the wind velocity is measured and the 10-meter height.

(Secs. 313(a), 601, 603, 604, and 605 of the Federal Aviation Act of 1958 (49 U.S.C. 1354(a), 1421, 1423, 1424, and 1425); and sec. 6(c) of the Dept. of Transportation Act (49 U.S.C. 1655(c)))

[Doc. No. 5066, 29 FR 18291, Dec. 24, 1964, as amended by Amdt. 25-23, 35 FR 5671, Apr. 8, 1970; Amdt. 25-42, 43 FR 2320, Jan. 16, 1978]

§ 25.23 Load distribution limits.

(a) Ranges of weights and centers of gravity within which the airplane may be safely operated must be established. If a weight and center of gravity combination is allowable only within certain load distribution limits (such as spanwise) that could be inadvertently exceeded, these limits and the corresponding weight and center of gravity combinations must be established.

(b) The load distribution limits may not exceed—

(1) The selected limits;

(2) The limits at which the structure is proven; or

(3) The limits at which compliance with each applicable flight requirement of this subpart is shown.

§ 25.25 Weight limits.

(a) *Maximum weights.* Maximum weights corresponding to the airplane operating conditions (such as ramp, ground or water taxi, takeoff, en route, and landing), environmental conditions (such as altitude and temperature), and loading conditions (such as zero fuel weight, center of gravity position and weight distribution) must be established so that they are not more than—

(1) The highest weight selected by the applicant for the particular conditions; or

(2) The highest weight at which compliance with each applicable structural loading and flight requirement is shown, except that for airplanes equipped with standby power rocket engines the maximum weight must not be more than the highest weight established in accordance with Appendix E of this part.

(b) *Minimum weight.* The minimum weight (the lowest weight at which compliance with each applicable requirement of this part is shown) must be established so that it is not less than—

(1) The lowest weight selected by the applicant;

(2) The design minimum weight (the lowest weight at which compliance with each structural loading condition of this part is shown); or

(3) The lowest weight at which compliance with each applicable flight requirement is shown.

[Doc. No. 5066, 29 FR 18291, Dec. 24, 1964, as amended by Amdt. 25-23, 35 FR 5671, Apr. 8, 1970]

§ 25.27 Center of gravity limits.

The extreme forward and the extreme aft center of gravity limitations must be established for each practicably separable operating condition. No such limit may lie beyond—

(a) The extremes selected by the applicant;

(b) The extremes within which the structure is proven; or

(c) The extremes within which compliance with each applicable flight requirement is shown.

§ 25.29 Empty weight and corresponding center of gravity.

(a) The empty weight and corresponding center of gravity must be determined by weighing the airplane with—

(1) Fixed ballast;

(2) Unusable fuel determined under § 25.959; and

(3) Full operating fluids, including—

(i) Oil;

(ii) Hydraulic fluid; and

(iii) Other fluids required for normal operation of airplane systems, except potable water, lavatory precharge water, and water intended for injection in the engines.

(b) The condition of the airplane at the time of determining empty weight must be one that is well defined and can be easily repeated.

(Secs. 313(a), 601, 603, 604, and 605 of the Federal Aviation Act of 1958 (49 U.S.C. 1354(a), 1421, 1423, 1424, and 1425); and sec. 6(c) of the Dept. of Transportation Act (49 U.S.C. 1655(c)))

[Doc. No. 5066, 29 FR 18291, Dec. 24, 1964, as amended by Amdt. 25-42, 43 FR 2320, Jan. 16, 1978]

§ 25.31 Removable ballast.

Removable ballast may be used on showing compliance with the flight requirements of this subpart.

§ 25.33 Propeller speed and pitch limits.

(a) The propeller speed and pitch must be limited to values that will ensure-

(1) Safe operation under normal operating conditions; and

(2) Compliance with the performance requirements of §§ 25.101 through 25.125.

(b) There must be a propeller speed limiting means at the governor. It must limit the maximum possible governed engine speed to a value not exceeding the maximum allowable r.p.m.

(c) The low pitch blade stop, or other means used to limit the low pitch position of the propeller blades, must be set so that the engine speed does not exceed 103 percent of the maximum allowable engine r.p.m. with—

(1) The propeller blades at the low pitch limit and governor inoperative; and

(2) Takeoff manifold pressure with the airplane stationary under standard atmospheric conditions.

[Doc. No. 5066, 29 FR 18291, Dec. 24, 1964, as amended by Amdt. 25-57, 49 FR 6848, Feb. 23, 1984]

PERFORMANCE

§ 25.101 General.

(a) Unless otherwise prescribed, airplanes must meet the applicable performance requirements of this subpart for ambient atmospheric conditions and still air.

(b) The performance, as affected by engine power or thrust, must be based on the following relative humidities;

(1) For turbine engine powered airplanes, a relative humidity of—

(i) 80 percent, at and below standard temperatures; and

(ii) 34 percent, at and above standard temperatures plus 50° F.

Between these two temperatures, the relative humidity must vary linearly.

(2) For reciprocating engine powered airplanes, a relative humidity of 80 percent in a standard atmosphere. Engine power corrections for vapor pressure must be made in accordance with the following table:

Altitude H (ft.)	Vapor pressure e (in. Hg.)	Specific humidity w (Lb. moisture per lb. dry air)	Density ratio $\rho/\sigma = 0.0023769$
0	0.403	0.00849	0.99508
1,000	.354	.00773	.96672
2,000	.311	.00703	.93895
3,000	.272	.00638	.91178
4,000	.238	.00578	.88514
5,000	.207	.00523	.85910
6,000	.1805	.00472	.83361
7,000	.1566	.00425	.80870
8,000	.1356	.00382	.78434
9,000	.1172	.00343	.76053
10,000	.1010	.00307	.73722
15,000	.0463	.001710	.62868
20,000	.01978	.000696	.53263
25,000	.00778	.000436	.44806

(c) The performance must correspond to the propulsive thrust available under the particular ambient atmospheric conditions, the particular flight condition, and the relative humidity specified in paragraph (b) of this section. The available propulsive thrust must correspond to engine

power or thrust, not exceeding the approved power or thrust less—

(1) Installation losses; and

(2) The power or equivalent thrust absorbed by the accessories and services appropriate to the particular ambient atmospheric conditions and the particular flight condition.

(d) Unless otherwise prescribed, the applicant must select the takeoff, en route, approach, and landing configurations for the airplane.

(e) The airplane configurations may vary with weight, altitude, and temperature, to the extent they are compatible with the operating procedures required by paragraph (f) of this section.

(f) Unless otherwise prescribed, in determining the accelerate-stop distances, takeoff flight paths, takeoff distances, and landing distances, changes in the airplane's configuration, speed, power, and thrust, must be made in accordance with procedures established by the applicant for operation in service.

(g) Procedures for the execution of balked landings and missed approaches associated with the conditions prescribed in §§ 25.119 and 25.121(d) must be established.

(h) The procedures established under paragraphs (f) and (g) of this section must—

(1) Be able to be consistently executed in service by crews of average skill;

(2) Use methods or devices that are safe and reliable; and

(3) Include allowance for any time delays, in the execution of the procedures, that may reasonably be expected in service.

[Doc. No. 5066, 29 FR 18291, Dec. 24, 1964, as amended by Amdt. 25-38, 41 FR 55466, Dec. 20, 1976]

§ 25.103 Stalling speed.

(a) V_S is the calibrated stalling speed, or the minimum steady flight speed, in knots, at which the airplane is controllable, with—

(1) Zero thrust at the stalling speed, or, if the resultant thrust has no appreciable effect on the stalling speed, with engines idling and throttles closed;

(2) Propeller pitch controls (if applicable) in the position necessary for compliance with paragraph (a)(1) of this section and the airplane in other respects (such as flaps and landing gear) in the condition existing in the test in which V_S is being used;

(3) The weight used when V_S is being used as a factor to determine compliance with a required performance standard; and

(4) The most unfavorable center of gravity allowable.

(b) The stalling speed V_S is the minimum speed obtained as follows:

(1) Trim the airplane for straight flight at any speed not less than 1.2 V_S or more than 1.4 V_S At a speed sufficiently above the stall speed to ensure steady conditions, apply the elevator control at a rate so that the airplane speed reduction does not exceed one knot per second.

(2) Meet the flight characteristics provisions of § 25.203.

§ 25.105 Takeoff.

(a) The takeoff speeds described in § 25.107, the accelerate-stop distance described in § 25.109, the takeoff path described in § 25.111, and the takeoff distance and takeoff run described in § 25.113, must be determined—

(1) At each weight, altitude, and ambient temperature within the operational limits selected by the applicant; and

(2) In the selected configuration for takeoff.

(b) No takeoff made to determine the data required by this section may require exceptional piloting skill or alertness.

(c) The takeoff data must be based on—

(1) A smooth, dry, hard-surfaced runway, in the case of land planes and amphibians;

(2) Smooth water, in the case of seaplanes and amphibians; and

(3) Smooth, dry snow, in the case of skiplanes.

(d) The takeoff data must include, within the established operational limits of the airplane, the following operational correction factors:

(1) Not more than 50 percent of nominal wind components along the takeoff path opposite to the direction of takeoff, and not less than 150 per-

cent of nominal wind components along the takeoff path in the direction of takeoff.

(2) Effective runway gradients.

§ 25.107 Takeoff speeds.

(a) V_1 must be established in relation to V_{EF} as follows:

(1) V_{EF} is the calibrated airspeed at which the critical engine is assumed to fail. V_{EF} must be selected by the applicant, but may not be less than V_{MCG} determined under § 25.149(e).

(2) V_1, in terms of calibrated airspeed, is the takeoff decision speed selected by the applicant; however, V_1 may not be less than V_{EF} plus the speed gained with the critical engine inoperative during the time interval between the instant at which the critical engine is failed, and the instant at which the pilot recognizes and reacts to the engine failure, as indicated by the pilot's application of the first retarding means during accelerate-stop tests.

(b) V_{2MIN}, in terms of calibrated airspeed, may not be less than—

(1) 1.2 V_S for—

(i) Two-engine and three-engine turbopropeller and reciprocating engine powered airplanes; and

(ii) Turbojet powered airplanes without provisions for obtaining a significant reduction in the one-engine-inoperative power-on stalling speed;

(2) 1.15 V_S for—

(i) Turbopropeller and reciprocating engine powered airplanes with more than three engines; and

(ii) Turbojet powered airplanes with provisions for obtaining a significant reduction in the one-engine-inoperative power-on stalling speed; and

(3) 1.10 times V_{MC} established under § 25.149.

(c) V_2, in terms of calibrated airspeed, must be selected by the applicant to provide at least the gradient of climb required by § 25.121(b) but may not be less than—

(1) V_{2MIN}, and

(2) V_R plus the speed increment attained (in accordance with § 25.111 (c)(2)) before reaching a height of 35 feet above the takeoff surface.

(d) V_{MU} is the calibrated airspeed at and above which the airplane can safely lift off the ground, and continue the takeoff. V_{MU} speeds must be selected by the applicant throughout the range of thrust-to-weight ratios to be certificated. These speeds may be established from free air data if these data are verified by ground takeoff tests.

(e) *VR*, in terms of calibrated airspeed, must be selected in accordance with the conditions of paragraphs (e)(1) through (4) of this section:

(1) V_R may not be less than—

(i) V_1;

(ii) 105 percent of V_{MC};

(iii) The speed (determined in accordance with § 25.111(c)(2)) that allows reaching V_2 before reaching a height of 35 feet above the takeoff surface; or

(iv) A speed that, if the airplane is rotated at its maximum practicable rate, will result in a V_{LOF} of not less than 110 percent of V_{MU} in the all-engines-operating condition and not less than 105 percent of V_{MU} determined at the thrust-to-weight ratio corresponding to the one-engine-inoperative condition.

(2) For any given set of conditions (such as weight, configuration, and temperature), a single value of V_R, obtained in accordance with this paragraph, must be used to show compliance with both the one-engine-inoperative and the all-engines-operating takeoff provisions.

(3) It must be shown that the one-engine-inoperative takeoff distance, using a rotation speed of 5 knots less than V_R established in accordance with paragraphs (e)(1) and (2) of this section, does not exceed the corresponding one-engine-inoperative takeoff distance using the established V_R. The takeoff distances must be determined in accordance with § 25.113(a)(1).

(4) Reasonably expected variations in service from the established takeoff procedures for the operation of the airplane (such as over-rotation of the airplane and out-of-trim conditions) may not result in unsafe flight characteristics or in marked increases in the scheduled takeoff distances established in accordance with § 25.113(a).

(f) V_{LOF} is the calibrated airspeed at which the airplane first becomes airborne.

(Secs. 313(a), 601, 603, 604, and 605 of the Federal Aviation Act of 1958 (49 U.S.C. 1354(a), 1421, 1423, 1424, and 1425); and sec. 6(c) of the Dept. of Transportation Act (49 U.S.C. 1655(c)))

[Doc. No. 5066, 29 FR 18291, Dec. 24, 1964, as amended by Amdt. 25-38, 41 FR 55466, Dec. 20, 1976; Amdt. 25-42, 43 FR 2320, Jan. 16, 1978]

§ 25.109 Accelerate-stop distance.

(a) The accelerate-stop distance is the greater of the following distances:

(1) The sum of the distances necessary to—

(i) Accelerate the airplane from a standing start to V_{EF} with all engines operating;

(ii) Accelerate the airplane from V_{EF} to V_1 and continue the acceleration for 2.0 seconds after V_1 is reached, assuming the critical engine fails at V_{EF}; and

(iii) Come to a full stop from the point reached at the end of the acceleration period prescribed in paragraph (a)(1)(ii) of this section, assuming that the pilot does not apply any means of retarding the airplane until that point is reached and that the critical engine is still inoperative.

(2) The sum of the distances necessary to—

(i) Accelerate the airplane from a standing start to V_1 and continue the acceleration for 2.0 seconds after V_1 is reached with all engines operating; and

(ii) Come to a full stop from the point reached at the end of the acceleration period prescribed in paragraph (a)(2)(i) of this section, assuming that the pilot does not apply any means of retarding the airplane until that point is reached and that all engines are still operating.

(b) Means other than wheel brakes may be used to determine the accelerate-stop distance if that means—

(1) Is safe and reliable;

(2) Is used so that consistent results can be expected under normal operating conditions; and

(3) Is such that exceptional skill is not required to control the airplane.

(c) The landing gear must remain extended throughout the accelerate-stop distance.

(d) If the accelerate-stop distance includes a stopway with surface characteristics substantially different from those of a smooth hard-surfaced runway, the takeoff data must include operational correction factors for the accelerate-stop distance. The correction factors must account for the particular surface characteristics of the stopway and the variations in these characteristics with seasonal weather conditions (such as temperature, rain, snow, and ice) within the established operational limits.

(Secs. 313(a), 601, 603, 604, and 605 of the Federal Aviation Act of 1958 (49 U.S.C. 1354(a), 1421, 1423, 1424, and 1425); and sec. 6(c) of the Dept. of Transportation Act (49 U.S.C. 1655(c)))

[Doc. No. 5066, 29 FR 18291, Dec. 24, 1964, as amended by Amdt. 25-42, 43 FR 2321, Jan. 16, 1978]

§ 25.111 Takeoff path.

(a) The takeoff path extends from a standing start to a point in the takeoff at which the airplane is 1,500 feet above the takeoff surface, or at which the transition from the takeoff to the en route configuration is completed and a speed is reached at which compliance with § 25.121(c) is shown, whichever point is higher. In addition—

(1) The takeoff path must be based on the procedures prescribed in § 25.101(c);

(2) The airplane must be accelerated on the ground to V_{EF}, at which point the critical engine must be made inoperative and remain inoperative for the rest of the takeoff; and

(3) After reaching V_{EF}, the airplane must be accelerated to V_2.

(b) During the acceleration to speed V_2, the nose gear may be raised off the ground at a speed not less than V_R. However, landing gear retraction may not be begun until the airplane is airborne.

(c) During the takeoff path determination in accordance with paragraphs (a) and (b) of this section—

(1) The slope of the airborne part of the takeoff path must be positive at each point;

(2) The airplane must reach V_2 before it is 35 feet above the takeoff surface and must continue at a speed as close as practical to, but not less than V_2, until it is 400 feet above the takeoff surface;

(3) At each point along the takeoff path, starting at the point at which the airplane reaches 400 feet above the takeoff surface, the available gradient of climb may not be less than—

(i) 1.2 percent for two-engine airplanes;

(ii) 1.5 percent for three-engine airplanes; and

(iii) 1.7 percent for four-engine airplanes; and

(4) Except for gear retraction and propeller feathering, the airplane configuration may not be changed, and no change in power or thrust that requires action by the pilot may be made, until the airplane is 400 feet above the takeoff surface.

(d) The takeoff path must be determined by a continuous demonstrated takeoff or by synthesis from segments. If the takeoff path is determined by the segmental method—

(1) The segments must be clearly defined and must be related to the distinct changes in the configuration, power or thrust, and speed;

(2) The weight of the airplane, the configuration, and the power or thrust must be constant throughout each segment and must correspond to the most critical condition prevailing in the segment;

(3) The flight path must be based on the airplane's performance without ground effect; and

(4) The takeoff path data must be checked by continuous demonstrated takeoffs up to the point at which the airplane is out of ground effect and its speed is stabilized, to ensure that the path is conservative relative to the continous path.

The airplane is considered to be out of the ground effect when it reaches a height equal to its wing span.

(e) For airplanes equipped with standby power rocket engines, the takeoff path may be determined in accordance with section II of Appendix E.

(Secs. 313(a), 601, 603, 604, and 605 of the Federal Aviation Act of 1958 (49 U.S.C. 1354(a), 1421, 1423, 1424, and 1425); and sec. 6(c) of the Dept. of Transportation Act (49 U.S.C. 1655(c)))

[Doc. No. 5066, 29 FR 18291, Dec. 24, 1964, as amended by Amdt. 25-6, 30 FR 8468, July 2, 1965; Amdt. 25-42, 43 FR 2321, Jan. 16, 1978; Amdt. 25-54, 45 FR 60172, Sept. 11, 1980]

§ 25.113 Takeoff distance and takeoff run.

(a) Takeoff distance is the greater of—

(1) The horizontal distance along the takeoff path from the start of the takeoff to the point at which the airplane is 35 feet above the takeoff surface, determined under § 25.111; or

(2) 115 percent of the horizontal distance along the takeoff path, with all engines operating, from the start of the takeoff to the point at which the airplane is 35 feet above the takeoff surface, as determined by a procedure consistent with § 25.111.

(b) If the takeoff distance includes a clearway, the takeoff run is the greater of—

(1) The horizontal distance along the takeoff path from the start of the takeoff to a point equidistant between the point at which V_{LOF} is reached and the point at which the airplane is 35 feet above the takeoff surface, as determined under § 25.111; or

(2) 115 percent of the horizontal distance along the takeoff path, with all engines operating, from the start of the takeoff to a point equidistant between the point at which V_{LOF} is reached and the point at which the airplane is 35 feet above the takeoff surface, determined by a procedure consistent with § 25.111.

[Doc. No. 5066, 29 FR 18291, Dec. 24, 1964, as amended by Amdt. 25-23, 35 FR 5671, Apr. 8, 1970]

§ 25.115 Takeoff flight path.

(a) The takeoff flight path begins 35 feet above the takeoff surface at the end of the takeoff distance determined in accordance with § 25.113(a).

(b) The net takeoff flight path data must be determined so that they represent the actual takeoff flight paths (determined in accordance with § 25.111 and with paragraph (a) of this section) reduced at each point by a gradient of climb equal to—

(1) 0.8 percent for two-engine airplanes;

(2) 0.9 percent for three-engine airplanes; and

(3) 1.0 percent for four-engine airplanes.

(c) The prescribed reduction in climb gradient may be applied as an equivalent reduction in acceleration along that part of the takeoff flight path at which the airplane is accelerated in level flight.

§ 25.117 Climb: general.

Compliance with the requirements of §§ 25.119 and 25.121 must be shown at each weight, altitude, and ambient temperature within the operational limits established for the airplane and with the most unfavorable center of gravity for each configuration.

§ 25.119 Landing climb: All-engine-operating.

In the landing configuration, the steady gradient of climb may not be less than 3.2 percent, with—

(a) The engines at the power or thrust that is available eight seconds after initiation of movement of the power or thrust controls from the minimum flight idle to the takeoff position; and

(b) A climb speed of not more than 1.3 V_S.

§ 25.121 Climb: One-engine-inoperative.

(a) *Takeoff; landing gear extended.* In the critical takeoff configuration existing along the flight path (between the points at which the airplane reaches V_{LOF} and at which the landing gear is fully retracted) and in the configuration used in § 25.111 but without ground effect, the steady gradient of climb must be positive for two-engine airplanes, and not less than 0.3 percent for three-engine airplanes or 0.5 percent for four-engine airplanes, at V_{LOF} and with—

(1) The critical engine inoperative and the remaining engines at the power or thrust available when retraction of the landing gear is begun in accordance with § 25.111 unless there is a more critical power operating condition existing later along the flight path but before the point at which the landing gear is fully retracted; and

(2) The weight equal to the weight existing when retraction of the landing gear is begun, determined under § 25.111.

(b) *Takeoff; landing gear retracted.* In the takeoff configuration existing at the point of the flight path at which the landing gear is fully retracted, and in the configuration used in § 25.111 but without ground effect, the steady gradient of climb may not be less than 2.4 percent for two-engine airplanes, 2.7 percent for three-engine airplanes, and 3.0 percent for four-engine airplanes, at V_2 and with—

(1) The critical engine inoperative, the remaining engines at the takeoff power or thrust available at the time the landing gear is fully retracted, determined under § 25.111, unless there is a more critical power operating condition existing later along the flight path but before the point where the airplane reaches a height of 400 feet above the takeoff surface; and

(2) The weight equal to the weight existing when the airplane's landing gear is fully retracted, determined under § 25.111.

(c) *Final takeoff.* In the en route configuration at the end of the takeoff path determined in accordance with § 25.111, the steady gradient of climb may not be less than 1.2 percent for two-engine airplanes, 1.5 percent for three-engine airplanes, and 1.7 percent for four-engine airplanes, at not less than 1.25 V_S and with—

(1) The critical engine inoperative and the remaining engines at the available maximum continuous power or thrust; and

(2) The weight equal to the weight existing at the end of the takeoff path, determined under § 25.111.

(d) *Approach.* In the approach configuration corresponding to the normal all-engines-operating procedure in which V_S for this configuration does not exceed 110 percent of the V_S for the related landing configuration, the steady gradient of climb may not be less than 2.1 percent for two-engine airplanes, 2.4 percent for three-engine airplanes, and 2.7 percent for four-engine airplanes, with—

(1) The critical engine inoperative, the remaining engines at the available takeoff power or thrust;

(2) The maximum landing weight; and

(3) A climb speed established in connection with normal landing procedures, but not exceeding 1.5 V_s.

§ 25.123 En route flight paths.

(a) For the en route configuration, the flight paths prescribed in paragraphs (b) and (c) of this section must be determined at each weight, altitude, and ambient temperature, within the operating limits established for the airplane. The variation of weight along the flight path, accounting for the progressive consumption of fuel and oil by the operating engines, may be included in the computation. The flight paths must be determined at any selected speed, with—

(1) The most unfavorable center of gravity;

(2) The critical engines inoperative;

(3) The remaining engines at the available maximum continuous power or thrust; and

(4) The means for controlling the engine-cooling air supply in the position that provides adequate cooling in the hot-day condition.

(b) The one-engine-inoperative net flight path data must represent the actual climb performance diminished by a gradient of climb of 1.1 percent for two-engine airplanes, 1.4 percent for three-engine airplanes, and 1.6 percent for four-engine airplanes.

(c) For three- or four-engine airplanes, the two-engine-inoperative net flight path data must represent the actual climb performance diminished by a gradient of climb of 0.3 percent for three-engine airplanes and 0.5 percent for four-engine airplanes.

§ 25.125 Landing.

(a) The horizontal distance necessary to land and to come to a complete stop (or to a speed of approximately 3 knots for water landings) from a point 50 feet above the landing surface must be determined (for standard temperatures, at each weight, altitude, and wind within the operational limits established by the applicant for the airplane) as follows:

(1) The airplane must be in the landing configuration.

(2) A steady gliding approach, with a calibrated airspeed of not less than 1.3 V_s, must be maintained down to the 50 foot height.

(3) Changes in configuration, power or thrust, and speed, must be made in accordance with the established procedures for service operation.

(4) The landing must be made without excessive vertical acceleration, tendency to bounce, nose over, ground loop, porpoise, or water loop.

(5) The landings may not require exceptional piloting skill or alertness.

(b) For landplanes and amphibians, the landing distance on land must be determined on a level, smooth, dry, hard-surfaced runway. In addition—

(1) The pressures on the wheel braking systems may not exceed those specified by the brake manufacturer;

(2) The brakes may not be used so as to cause excessive wear of brakes or tires; and

(3) Means other than wheel brakes may be used if that means—

(i) Is safe and reliable;

(ii) Is used so that consistent results can be expected in service; and

(iii) Is such that exceptional skill is not required to control the airplane.

(c) For seaplanes and amphibians, the landing distance on water must be determined on smooth water.

(d) For skiplanes, the landing distance on snow must be determined on smooth, dry, snow.

(e) The landing distance data must include correction factors for not more than 50 percent of the nominal wind components along the landing path opposite to the direction of landing, and not less than 150 percent of the nominal wind components along the landing path in the direction of landing.

(f) If any device is used that depends on the operation of any engine, and if the landing distance would be noticeably increased when a landing is made with that engine inoperative, the landing distance must be determined with that engine inoperative unless the use of compensating means will result in a landing distance not more than that with each engine operating.

CONTROLLABILITY AND MANEUVERABILITY

§ 25.143 General.

(a) The airplane must be safely controllable and maneuverable during—

(1) Takeoff;

(2) Climb;

(3) Level flight;

(4) Descent; and

(5) Landing.

(b) It must be possible to make a smooth transition from one flight condition to any other flight condition without exceptional piloting skill, alertness, or strength, and without danger of exceeding the airplane limit-load factor under any probable operating conditions, including—

(1) The sudden failure of the critical engine;

(2) For airplanes with three or more engines, the sudden failure of the second critical engine when the airplane is in the en route, approach, or landing configuration and is trimmed with the critical engine inoperative; and

(3) Configuration changes, including deployment or retraction of deceleration devices.

(c) If, during the testing required by paragraphs (a) and (b) of this section, marginal conditions exist with regard to required pilot strength, the "strength of pilots" limits may not exceed the limits prescribed in the following table:

Values in pound of force as applied to the control wheel or rudder pedals	Pitch	Roll	Yaw
For temporary application	75	60	150
For prolonged application	10	5	20

(d) In showing the temporary control force limitations of paragraph (c) of this section, approved operating procedures or conventional operating practices must be followed (including being as nearly trimmed as possible at the next preceding steady flight condition, except that, in the case of takeoff, the airplane must be trimmed in accordance with approved operating procedures).

(e) For the purpose of complying with the prolonged control force limitations of paragraph (c) of this section, the airplane must be as nearly trimmed as possible.

(Secs. 313(a), 601 603, 604, and 605 of the Federal Aviation Act of 1958 (49 U.S.C. 1354(a), 1421, 1423, 1424, and 1425); and sec. 6(c) of the Dept. of Transportation Act (49 U.S.C. 1655 (c)))

[Doc. No. 5066, 29 FR 18291, Dec. 24, 1964, as amended by Amdt. 25-42, 43 FR 2321, Jan. 16, 1978]

§ 25.145 Longitudinal control.

(a) It must be possible at any speed between the trim speed prescribed in § 25.49(c)(2)(i) and V_{s1} (for reciprocating engine powered airplanes), or at any speed between the trim speed prescribed in § 25.103(b)(1) and V_s (for turbine engine powered airplanes), to pitch the nose downward so that the acceleration to this selected trim speed is prompt with—

(1) The airplane trimmed at the trim speed prescribed in § 25.49(c)(2)(i) (for reciprocating engine powered airplanes), or in § 25.103(b)(1) (for turbine engine powered airplanes);

(2) The landing gear extended;

(3) The wing flaps (i) retracted and (ii) extended; and

(4) Power (i) off and (ii) at maximum continuous power on the engines.

(b) With the landing gear extended, no change in trim control, or exertion of more than 50 pounds control force (representative of the maximum temporary force that readily can be applied by one hand) may be required for the following maneuvers:

(1) With power off, flaps retracted, and the airplane trimmed at 1.4 V_{s1}, extend the flaps as rapidly as possible while maintaining the airspeed at approximately 40 percent above the stalling speed existing at each instant throughout the maneuver.

(2) Repeat paragraph (b)(1) except initially extend the flaps and then retract them as rapidly as possible.

(3) Repeat paragraph (b)(2) except with takeoff power.

(4) With power off, flaps retracted, and the airplane trimmed at 1.4 V_{s1}, apply takeoff power rapidly while maintaining the same airspeed.

(5) Repeat paragraph (b)(4) except with flaps extended.

(6) With power off, flaps extended, and the airplane trimmed at 1.4 V_{s_1}, obtain and maintain airspeeds between 1.1 V_{s_1}, and either 1.7 V_{s_1}, or V_{fe}, whichever is lower.

(c) It must be possible, without exceptional piloting skill, to prevent loss of altitude when complete retraction of the high lift devices from any position is begun during steady, straight, level flight at 1.1 V_{s_1} for propeller powered airplanes, or 1.2 V_{s_1} for turbojet powered airplanes, with—

(1) Simultaneous application of not more than takeoff power taking into account the critical engine operating conditions;

(2) The landing gear extended; and

(3) The critical combinations of landing weights and altitudes.

If gated high-lift device control positions are provided, retraction must be shown from any position from the maximum landing position to the first gated position, between gated positions, and from the last gated position to the full retraction position. In addition, the first gated control position from the landing position must correspond with the high-lift devices configuration used to establish the go-around procedure from the landing configuration. Each gated control position must require a separate and distinct motion of the control to pass through the gated position and must have features to prevent inadvertent movement of the control through the gated position.

[Doc. No. 5066, 29 FR 18291, Dec. 24, 1964, as amended by Amdt. 25-23, 35 FR 5671, Apr. 8, 1970]

§ 25.147 Directional and lateral control.

(a) *Directional control; general.* It must be possible, while holding the wings approximately level, to safely make reasonably sudden changes in heading in both directions. This must be shown at 1.4 V_{s_1} for heading changes up to 15° (except that the heading change at which the rudder pedal force is 150 pounds need not be exceeded), and with—

(1) The critical engine inoperative and its propeller in the minimum drag position;

(2) The power required for level flight at 1.4 V_{s_1}, but not more than maximum continuous power;

(3) The most unfavorable center of gravity;

(4) Landing gear retracted;

(5) Flaps in the approach position; and

(6) Maximum landing weight.

(b) *Directional control; airplanes with four or more engines.* Airplanes with four or more engines must meet the requirements of paragraph (a) of this section except that—

(1) The two critical engines must be inoperative with their propellers (if applicable) in the minimum drag position;

(2) The center of gravity must be in the most forward position; and

(3) The flaps must be in the most favorable climb position.

(c) *Lateral control; general.* It must be possible to make 20° banked turns, with and against the inoperative engine, from steady flight at a speed equal to 1.4 V_{s_1}, with—

(1) The critical engine inoperative and its propeller (if applicable) in the minimum drag position;

(2) The remaining engines at maximum continuous power;

(3) The most unfavorable center of gravity;

(4) Landing gear (i) retracted and (ii) extended;

(5) Flaps in the most favorable climb position; and

(6) Maximum takeoff weight.

(d) *Lateral control; airplanes with four or more engines.* Airplanes with four or more engines must be able to make 20° banked turns, with and against the inoperative engines, from steady flight at a speed equal to 1.4 V_{s_1}, with maximum continuous power, and with the airplane in the configuration prescribed by paragraph (b) of this section.

(e) *Lateral control; all engines operating.* With the engines operating, roll response must allow normal maneuvers (such as recovery from upsets produced by gusts and the initiation of evasive maneuvers). There must be enough excess lateral control in sideslips (up to sideslip angles that might be required in normal operation), to allow a limited amount of maneuver-

ing and to correct for gusts. Lateral control must be enough at any speed up to V_{FC}/M_{FC} to provide a peak roll rate necessary for safety, without excessive control forces or travel.

(Secs. 313(a), 601, 603, 604, and 605 of the Federal Aviation Act of 1958 (49 U.S.C. 1354(a), 1421, 1423, 1424, and 1425); and sec. 6(c) of the Dept. of Transportation Act (49 U.S.C. 1655 (c)))

[Doc. No. 5066, 29 FR 18291, Dec. 24, 1964, as amended by Amdt. 25-42, 43 FR 2321, Jan. 16, 1978]

§ 25.149 Minimum control speed.

(a) In establishing the minimum control speeds required by this section, the method used to simulate critical engine failure must represent the most critical mode of powerplant failure with respect to controllability expected in service.

(b) V_{MC} is the calibrated airspeed, at which, when the critical engine is suddenly made inoperative, it is possible to recover control of the airplane with that engine still inoperative, and maintain straight flight either with zero yaw or, at the option of the applicant, with an angle of bank of not more than five degrees.

(c) V_{MC} may not exceed 1.2 V_S with—

(1) Maximum available takeoff power or thrust on the engines;

(2) The most unfavorable center of gravity;

(3) The airplane trimmed for takeoff;

(4) The maximum sea level takeoff weight (or any lesser weight necessary to show V_{MC});

(5) The airplane in the most critical takeoff configuration existing along the flight path after the airplane becomes airborne, except with the landing gear retracted;

(6) The airplane airborne and the ground effect negligible; and

(7) If applicable, the propeller of the inoperative engine—

(i) Windmilling;

(ii) In the most probable position for the specific design of the propeller control; or

(iii) Feathered, if the airplane has an automatic feathering device acceptable for showing compliance with the climb requirements of § 25.121.

(d) The rudder forces required to maintain control at V_{MC} may not exceed 150 pounds nor may it be necessary to reduce power or thrust of the operative engines. During recovery, the airplane may not assume any dangerous attitude or require exceptional piloting skill, alertness, or strength to prevent a heading change of more than 20 degrees.

(e) V_{MCG}, the minimum control speed on the ground, is the calibrated airspeed during the takeoff run, at which, when the critical engine is suddenly made inoperative, it is possible to recover control of the airplane with the use of primary aerodynamic controls alone (without the use of nosewheel steering) to enable the takeoff to be safely continued using normal piloting skill and rudder control forces not exceeding 150 pounds. In the determination of V_{MCG}, assuming that the path of the airplane accelerating with all engines operating is along the centerline of the runway, its path from the point at which the critical engine is made inoperative to the point at which recovery to a direction parallel to the centerline is completed may not deviate more than 30 feet laterally from the centerline at any point. V_{MCG} must be established with—

(1) The airplane in each takeoff configuration or, at the option of the applicant, in the most critical takeoff configuration;

(2) Maximum available takeoff power or thrust on the operating engines;

(3) The most unfavorable center of gravity;

(4) The airplane trimmed for takeoff; and

(5) The most unfavorable weight in the range of takeoff weights.

(f) V_{MCL}, the minimum control speed during landing approach with all engines operating, is the calibrated airspeed at which, when the critical engine is suddenly made inoperative, it is possible to recover control of the airplane with that engine still inoperative, and maintain straight flight either with zero yaw or, at the option of the applicant, with an angle of bank of not more than 5 degrees. V_{MCL} must be established with—

(1) The airplane in the most critical configuration for approach with all engines operating;

(2) The most unfavorable center of gravity;

(3) The airplane trimmed for approach with all engines operating;

(4) The maximum sea level landing weight (or any lesser weight necessary to show V_{MCL}); and

(5) Maximum available takeoff power or thrust on the operating engines.

(g) For airplanes with three or more engines, V_{MCL-2}, the minimum control speed during landing approach with one critical engine inoperative, is the calibrated airspeed at which, when a second critical engine is suddenly made inoperative, it is possible to recover control of the airplane with both engines still inoperative and maintain straight flight either with zero yaw or, at the option of the applicant, with an angle of bank of not more than 5 degrees. V_{MCL-2}, must be established with—

(1) The airplane in the most critical configuration for approach with the critical engine inoperative;

(2) The most unfavorable center of gravity;

(3) The airplane trimmed for approach with the critical engine inoperative;

(4) The maximum sea level landing weight (or any lesser weight necessary to show V_{MCL-2});

(5) The power or thrust on the operating engines required to maintain an approach path angle of 3 degrees when one critical engine is inoperative; and

(6) The power or thrust on the operating engines rapidly changed, immediately after the second critical engine is made inoperative, from the power or thrust prescribed in paragraph (g)(5) of this section to—

(i) Minimum available power or thrust; and

(ii) Maximum available takeoff power or thrust.

(h) The rudder control forces required to maintain control at V_{MCL} and V_{MCL-2} may not exceed 150 pounds, nor may it be necessary to reduce the power or thrust of the operating engines. In addition, the airplane may not assume any dangerous attitudes or require exceptional piloting skill, alertness, or strength to prevent a divergence in the approach flight path that would jeopardize continued safe approach when—

(1) The critical engine is suddenly made inoperative; and

(2) For the determination of V_{MCL-2}, the power or thrust on the operating engines is changed in accordance with paragraph (g)(6) of this section.

(Secs. 313(a), 601, 604, and 605 of the Federal Aviation Act of 1958 (49 U.S.C. 1354(a), 1421, 1423, 1424, and 1425); and sec. 6(c) of the Dept. of Transportation Act (49 U.S.C. 1655(c)))

[Doc. No. 5066, 29 FR 18291, Dec. 24, 1964, as amended by Amdt. 25-42, 43 FR 2321, Jan. 16, 1978]

TRIM

§ 25.161 Trim.

(a) *General.* Each airplane must meet the trim requirements of this section after being trimmed, and without further pressure upon, or movement of, either the primary controls or their corresponding trim controls by the pilot or the automatic pilot.

(b) *Lateral and directional trim.* The airplane must maintain lateral and directional trim with the most adverse lateral displacement of the center of gravity within the relevant operating limitations, during normally expected conditions of operation (including operation at any speed from 1.4 V_{S1} to V_{MO}/M_{MO}).

(c) *Longitudinal trim.* The airplane must maintain longitudinal trim during—

(1) A climb with maximum continuous power at a speed not more than 1.4 V_{S1}, with the landing gear retracted, and the flaps (i) retracted and (ii) in the takeoff position;

(2) A glide with power off at a speed not more than 1.4 V_{S1}, with the landing gear extended, the wing flaps (i) retracted and (ii) extended, the most unfavorable center of gravity position approved for landing with the maximum landing weight, and with the most unfavorable center of gravity position approved for landing regardless of weight; and

(3) Level flight at any speed from 1.4 V_{s_1}, to V_{MO}/M_{MO}, with the landing gear and flaps retracted, and from 1.4 V_{s_1} to V_{LE} with the landing gear extended.

(d) *Longitudinal, directional, and lateral trim.* The airplane must maintain longitudinal, directional, and lateral trim (and for the lateral trim, the angle of bank may not exceed five degrees) at 1.4 V_{s_1} during climbing flight with—

(1) The critical engine inoperative;

(2) The remaining engines at maximum continuous power; and

(3) The landing gear and flaps retracted.

(e) *Airplanes with four or more engines.* Each airplane with four or more engines must maintain trim in rectilinear flight—

(1) At the climb speed, configuration, and power required by § 25.123(a) for the purpose of establishing the rate of climb;

(2) With the most unfavorable center of gravity position; and

(3) At the weight at which the two-engine-inoperative climb is equal to at least 0.013 $V_{s_{01}}$ at an altitude of 5,000 feet.

[Doc. No. 5066, 29 FR 18291, Dec. 24, 1964, as amended by Amdt. 25-23, 35 FR 5671, Apr. 8, 1970; Amdt. 25-38, 41 FR 55466, Dec. 20, 1976]

Stability

§ 25.171 General.

The airplane must be longitudinally, directionally, and laterally stable in accordance with the provisions of §§ 25.173 through 25.177. In addition, suitable stability and control feel (static stability) is required in any condition normally encountered in service, if flight tests show it is necessary for safe operation.

[Doc. No. 5066, 29 FR 18291, Dec. 24, 1964, as amended by Amdt. 25-7, 30 FR 13117, Oct. 15, 1965]

§ 25.173 Static longitudinal stability.

Under the conditions specified in § 25.175, the characteristics of the elevator control forces (including friction) must be as follows:

(a) A pull must be required to obtain and maintain speeds below the specified trim speed, and a push must be required to obtain and maintain speeds above the specified trim speed. This must be shown at any speed that can be obtained except speeds higher than the landing gear or wing flap operating limit speeds or V_{FC}/M_{FC}, whichever is appropriate, or lower than the minimum speed for steady unstalled flight.

(b) The airspeed must return to within 10 percent of the original trim speed for the climb, approach, and landing conditions specified in § 25.175 (a), (c), and (d), and must return to within 7.5 percent of the original trim speed for the cruising condition specified in § 25.175(b), when the control force is slowly released from any speed within the range specified in paragraph (a) of this section.

(c) The average gradient of the stable slope of the stick force versus speed curve may not be less than 1 pound for each 6 knots.

(d) Within the free return speed range specified in paragraph (b) of this section, it is permissible for the airplane, without control forces, to stabilize on speeds above or below the desired trim speeds if exceptional attention on the part of the pilot is not required to return to and maintain the desired trim speed and altitude.

[Amdt. 25-7, 30 FR 13117, Oct. 15, 1965]

§ 25.175 Demonstration of static longitudinal stability.

Static longitudinal stability must be shown as follows:

(a) *Climb.* The stick force curve must have a stable slope at speeds between 85 and 115 percent of the speed at which the airplane—

(1) Is trimmed, with—

(i) Wing flaps retracted;

(ii) Landing gear retracted;

(iii) Maximum takeoff weight; and

(iv) 75 percent of maximum continuous power for reciprocating engines or the maximum power or thrust selected by the applicant as an operating limitation for use during climb for turbine engines; and

(2) Is trimmed at the speed for best rate-of-climb except that the speed need not be less than 1.4 V_{s_1}.

(b) *Cruise.* Static longitudinal stability must be shown in the cruise condition as follows:

(1) With the landing gear retracted at high speed, the stick force curve must have a stable slope at all speeds within a range which is the greater of 15 percent of the trim speed plus the resulting free return speed range, or 50 knots plus the resulting free return speed range, above and below the trim speed (except that the speed range need not include speeds less than 1.4 V_{S1}, nor speeds greater than V_{FC}/M_{FC}, nor speeds that require a stick force of more than 50 pounds), with—

(i) The wing flaps retracted;

(ii) The center of gravity in the most adverse position (see § 25.27);

(iii) The most critical weight between the maximum takeoff and maximum landing weights;

(iv) 75 percent of maximum continuous power for reciprocating engines or for turbine engines, the maximum cruising power selected by the applicant as an operating limitation (see § 25.1521), except that the power need not exceed that required at V_{MO}/M_{MO}; and

(v) The airplane trimmed for level flight with the power required in paragraph (b)(1)(iv) of this section.

(2) With the landing gear retracted at low speed, the stick force curve must have a stable slope at all speeds within a range which is the greater of 15 percent of the trim speed plus the resulting free return speed range, or 50 knots plus the resulting free return speed range, above and below the trim speed (except that the speed range need not include speeds less than 1.4 V_{S1}, nor speeds greater than the minimum speed of the applicable speed range prescribed in paragraph (b)(1), nor speeds that require a stick force of more than 50 pounds), with—

(i) Wing flaps, center of gravity position, and weight as specified in paragraph (b)(1) of this section;

(ii) Power required for level flight at a speed equal to V_{MO} + 1.4 $V_{S1}/2$; and

(iii) The airplane trimmed for level flight with the power required in paragraph (b)(2)(ii) of this section.

(3) With the landing gear extended, the stick force curve must have a stable slope at all speeds within a range which is the greater of 15 percent of the trim speed plus the resulting free return speed range, or 50 knots plus the resulting free return speed range, above and below the trim speed (except that the speed range need not include speeds less than 1.4 V_{S1}, nor speeds greater than V_{LE}, nor speeds that require a stick force of more than 50 pounds), with—

(i) Wing flap, center of gravity position, and weight as specified in paragraph (b)(1) of this section;

(ii) 75 percent of maximum continuous power for reciprocating engines or, for turbine engines, the maximum cruising power selected by the applicant as an operating limitation, except that the power need not exceed that required for level flight at V_{LE}; and

(iii) The aircraft trimmed for level flight with the power required in paragraph (b)(3)(ii) of this section.

(c) *Approach.* The stick force curve must have a stable slope at speeds between 1.1 V_{S1} and 1.8 V_{S1}, with—

(1) Wing flaps in the approach position;

(2) Landing gear retracted;

(3) Maximum landing weight; and

(4) The airplane trimmed at 1.4 V_{S1} with enough power to maintain level flight at this speed.

(d) *Landing.* The stick force curve must have a stable slope, and the stick force may not exceed 80 pounds, at speeds between 1.1 V_{S0} and 1.3 V_{S0} with—

(1) Wing flaps in the landing position;

(2) Landing gear extended;

(3) Maximum landing weight;

(4) Power or thrust off on the engines; and

(5) The airplane trimmed at 1.4 V_{S0} with power or thrust off.

[Doc. No. 5066, 29 FR 18291, Dec. 24, 1964, as amended by Amdt. 25-7, 30 FR 13117, Oct. 15, 1965]

§ 25.177 Static directional and lateral stability.

(a) The static directional stability (as shown by the tendency to recover from a skid with the rudder free) must be positive for any landing gear and flap position and symmetrical power condition, at speeds from 1.2 V_{S1} up to V_{FE}, V_{LE}, or V_{FC}/M_{FC} (as appropriate).

(b) The static lateral stability (as shown by the tendency to raise the

low wing in a sideslip with the aileron controls free and for any landing gear and flap position and symmetrical power condition) may not be negative at any airspeed (except speeds higher than V_{FE} or V_{LE}, when appropriate) in the following airspeed ranges:

(1) From 1.2 V_{S1} to V_{MO}/M_{MO}.

(2) From V_{MO}/M_{MO} to V_{FC}/M_{FC} unless the Administrator finds that the divergence is—

(i) Gradual;

(ii) Easily recognizable by the pilot; and

(iii) Easily controllable by the pilot.

(c) In straight, steady, sideslips (unaccelerated forward slips) the aileron and rudder control movements and forces must be substantially proportional to the angle of sideslip, and the factor of proportionality must lie between limits found necessary for safe operation throughout the range of sideslip angles appropriate to the operation of the airplane. At greater angles, up to the angle at which full rudder control is used or a rudder pedal force of 180 pounds is obtained, the rudder pedal forces may not reverse and increased rudder deflection must produce increased angles of sideslip. Unless the airplane has a yaw indicator, there must be enough bank accompanying sideslipping to clearly indicate any departure from steady unyawed flight.

(Secs. 313(a), 601, 603, 604, and 605 of the Federal Aviation Act of 1958 (49 U.S.C. 1354(a), 1421, 1423, 1424, and 1425); and sec. 6(c) of the Dept. of Transportation Act (49 U.S.C. 1655(c)))

[Doc. No. 5066, 29 FR 18291, Dec. 24, 1964, as amended by Amdt. 25-42, 43 FR 2322, Jan. 16, 1978]

§ 25.181 Dynamic stability.

(a) Any short period oscillation, not including combined lateral-directional oscillations, occurring between stalling speed and maximum allowable speed appropriate to the configuration of the airplane must be heavily damped with the primary controls—

(1) Free; and

(2) In a fixed position.

(b) Any combined lateral-directional oscillations ("Dutch roll") occurring between stalling speed and maximum allowable speed appropriate to the configuration of the airplane must be positively damped with controls free, and must be controllable with normal use of the primary controls without requiring exceptional pilot skill.

(Secs. 313(a), 601, 603, 604, and 605 of the Federal Aviation Act of 1958 (49 U.S.C. 1354(a), 1421, 1423, 1424, and 1425); and sec. 6(c) of the Dept. of Transportation Act (49 U.S.C. 1655(c)))

[Amdt. 25-42, 43 FR 2322, Jan. 16, 1978]

Stalls

§ 25.201 Stall demonstration.

(a) Stalls must be shown in straight flight and in 30 degree banked turns with—

(1) Power off; and

(2) The power necessary to maintain level flight at 1.6 V_{S1} (where V_{S1} corresponds to the stalling speed with flaps in the approach position, the landing gear retracted, and maximum landing weight).

(b) In either condition required by paragraph (a) of this section, it must be possible to meet the applicable requirements of § 25.203 with—

(1) Flaps and landing gear in any likely combination of positions;

(2) Representative weights within the range for which certification is requested; and

(3) The most adverse center of gravity for recovery.

(c) The following procedure must be used to show compliance with § 25.203:

(1) With the airplane trimmed for straight flight at the speed prescribed in § 25.103(b)(1), reduce the speed with the elevator control until it is steady at slightly above stalling speed. Apply elevator control so that the speed reduction does not exceed one knot per second until (i) the airplane is stalled, or (ii) the control reaches the stop.

(2) As soon as the airplane is stalled, recover by normal recovery techniques.

(d) Occurrence of stall is defined as follows:

(1) The airplane may be considered stalled when, at an angle of attack measurably greater than that for maximum lift, the inherent flight characteristics give a clear and distinctive indication to the pilot that the airplane is stalled. Typical indications of a stall,

occurring either individually or in combination, are—

(i) A nose-down pitch that cannot be readily arrested;

(ii) A roll that cannot be readily arrested; or

(iii) If clear enough, a loss of control effectiveness, an abrupt change in control force or motion, or a distinctive shaking of the pilot's controls.

(2) For any configuration in which the airplane demonstrates an unmistakable inherent aerodynamic warning of a magnitude and severity that is a strong and effective deterrent to further speed reduction, the airplane may be considered stalled when it reaches the speed at which the effective deterrent is clearly manifested.

(Secs. 313(a), 601, 603, 604, and 605 of the Federal Aviation Act of 1958 (49 U.S.C. 1354(a), 1421, 1423, 1424, and 1425); and sec. 6(c) of the Dept. of Transportation Act (49 U.S.C. 1655(c)))

[Doc. No. 5066, 29 FR 18291, Dec. 24, 1964, as amended by Amdt. 25-38, 41 FR 55466, Dec. 20, 1976; Amdt. 25-42, 43 FR 2322, Jan. 16, 1978]

§ 25.203 Stall characteristics.

(a) It must be possible to produce and to correct roll and yaw by unreversed use of the aileron and rudder controls, up to the time the airplane is stalled. No abnormal nose-up pitching may occur. The longitudinal control force must be positive up to and throughout the stall. In addition, it must be possible to promptly prevent stalling and to recover from a stall by normal use of the controls.

(b) For level wing stalls, the roll occurring between the stall and the completion of the recovery may not exceed approximately 20 degrees.

(c) For turning flight stalls, the action of the airplane after the stall may not be so violent or extreme as to make it difficult, with normal piloting skill, to effect a prompt recovery and to regain control of the airplane.

§ 25.205 Stalls: Critical engine inoperative.

(a) It must be possible to safely recover from a stall with the critical engine inoperative—

(1) Without applying power to the inoperative engine;

(2) With flaps and landing gear retracted; and

(3) With the remaining engines at up to 75 percent of maximum continuous power, or up to the power at which the wings can be held level with the use of maximum control travel, whichever is less.

(b) The operating engines may be throttled back during stall recovery from stalls with the critical engine inoperative.

§ 25.207 Stall warning.

(a) Stall warning with sufficient margin to prevent inadvertent stalling with the flaps and landing gear in any normal position must be clear and distinctive to the pilot in straight and turning flight.

(b) The warning may be furnished either through the inherent aerodynamic qualities of the airplane or by a device that will give clearly distinguishable indications under expected conditions of flight. However, a visual stall warning device that requires the attention of the crew within the cockpit is not acceptable by itself. If a warning device is used, it must provide a warning in each of the airplane configuations prescribed in paragraph (a) of this section at the speed prescribed in paragraph (c) of this section.

(c) The stall warning must begin at a speed exceeding the stalling speed (i.e., the speed at which the airplane stalls or the minimum speed demonstrated, whichever is applicable under the provisions of § 25.201(d)) by seven percent or at any lesser margin if the stall warning has enough clarity, duration, distinctiveness, or similar properties.

(Secs. 313(a), 601, 603, 604, and 605 of the Federal Aviation Act of 1958 (49 U.S.C. 1354(a), 1421, 1423, 1424, and 1425); and sec. 6(c) of the Dept. of Transportation Act (49 U.S.C. 1655(c)))

[Doc. No. 5066, 29 FR 18291, Dec. 24, 1964, as amended by Amdt. 25-7, 30 FR 13118, Oct. 15, 1965; Amdt. 25-42, 43 FR 2322, Jan. 16, 1978]

GROUND AND WATER HANDLING CHARACTERISTICS

§ 25.231 Longitudinal stability and control.

(a) Landplanes may have no uncontrollable tendency to nose over in any reasonably expected operating condition or when rebound occurs during landing or takeoff. In addition—

(1) Wheel brakes must operate smoothly and may not cause any undue tendency to nose over; and

(2) If a tail-wheel landing gear is used, it must be possible, during the takeoff ground run on concrete, to maintain any altitude up to thrust line level, at 80 percent of V_{s_1}.

(b) For seaplanes and amphibians, the most adverse water conditions safe for takeoff, taxiing, and landing, must be established.

§ 25.233 Directional stability and control.

(a) There may be no uncontrollable ground-looping tendency in 90° cross winds, up to a wind velocity of 20 knots or 0.2 V_{s_0}, whichever is greater, except that the wind velocity need not exceed 25 knots. At any speed at which the airplane may be expected to be operated on the ground. This may be shown while establishing the 90° cross component of wind velocity required by § 25.237.

(b) Landplanes must be satisfactorily controllable, without exceptional piloting skill or alertness, in power-off landings at normal landing speed, without using brakes or engine power to maintain a straight path. This may be shown during power-off landings made in conjunction with other tests.

(c) The airplane must have adequate directional control during taxiing. This may be shown during taxiing prior to takeoffs made in conjunction with other tests.

(Secs. 313(a), 601, 603, 604, and 605 of the Federal Aviation Act of 1958 (49 U.S.C. 1354(a), 1421, 1423, 1424, and 1425); and sec. 6(c) of the Dept. of Transportation Act (49 U.S.C. 1655(c)))

[Doc. No. 5066, 29 FR 18291, Dec. 24, 1964, as amended by Amdt. 25-23, 35 FR 5671, Apr. 8, 1970; Amdt. 25-42, 43 FR 2322, Jan. 16, 1978]

§ 25.235 Taxiing condition.

The shock absorbing mechanism may not damage the structure of the airplane when the airplane is taxied on the roughest ground that may reasonably be expected in normal operation.

§ 25.237 Wind velocities.

(a) For landplanes and amphibians, a 90-degree cross component of wind velocity, demonstrated to be safe for takeoff and landing, must be established for dry runways and must be at least 20 knots or 0.2 V_{s_0}, whichever is greater, except that it need not exceed 25 knots.

(b) For seaplanes and amphibians, the following applies:

(1) A 90-degree cross component of wind velocity, up to which takeoff and landing is safe under all water conditions that may reasonably be expected in normal operation, must be established and must be at least 20 knots or 0.2 V_{s_0}, whichever is greater, except that it need not exceed 25 knots.

(2) A wind velocity, for which taxiing is safe in any direction under all water conditions that may reasonably be expected in normal operation, must be established and must be at least 20 knots or 0.2 V_{s_0}, whichever is greater, except that it need not exceed 25 knots.

(Secs. 313(a), 601, 603, 604, and 605 of the Federal Aviation Act of 1958 (49 U.S.C. 1354(a), 1421, 1423, 1424, and 1425); and sec. 6(c) of the Dept. of Transportation Act (49 U.S.C. 1655(c)))

[Amdt. 25-42, 43 FR 2322, Jan. 16, 1978]

§ 25.239 Spray characteristics, control, and stability on water.

(a) For seaplanes and amphibians, during takeoff, taxiing, and landing, and in the conditions set forth in paragraph (b) of this section, there may be no—

(1) Spray characteristics that would impair the pilot's view, cause damage, or result in the taking in of an undue quantity of water;

(2) Dangerously uncontrollable porpoising, bounding, or swinging tendency; or

(3) Immersion of auxiliary floats or sponsons, wing tips, propeller blades,

or other parts not designed to withstand the resulting water loads.

(b) Compliance with the requirements of paragraph (a) of this section must be shown—

(1) In water conditions, from smooth to the most adverse condition established in accordance with § 25.231;

(2) In wind and cross-wind velocities, water currents, and associated waves and swells that may reasonably be expected in operation on water;

(3) At speeds that may reasonably be expected in operation on water;

(4) With sudden failure of the critical engine at any time while on water; and

(5) At each weight and center of gravity position, relevant to each operating condition, within the range of loading conditions for which certification is requested.

(c) In the water conditions of paragraph (b) of this section, and in the corresponding wind conditions, the seaplane or amphibian must be able to drift for five minutes with engines inoperative, aided, if necessary, by a sea anchor.

Miscellaneous Flight Requirements

§ 25.251 Vibration and buffeting.

(a) The airplane must be designed to withstand any vibration and buffeting that might occur in any likely operating condition. This must be shown by calculations, resonance tests, or other tests found necessary by the Administrator.

(b) Each part of the airplane must be shown in flight to be free from excessive vibration, under any appropriate speed and power conditions up to at least the minimum value of V_D allowed in § 25.335. The maximum speeds shown must be used in establishing the operating limitations of the airplane in accordance with § 25.1505. In addition, it must be shown by analysis or tests, that the airplane is free from such vibration that would prevent safe flight under the conditions in § 25.629(d).

(c) Except as provided in paragraph (d) of this section, there may be no buffeting condition, in normal flight, including configuration changes during cruise, severe enough to interfere with the control of the airplane, to cause excessive fatigue to the crew, or to cause structural damage. Stall warning buffeting within these limits is allowable.

(d) There may be no perceptible buffeting condition in the cruise configuration in straight flight at any speed up to V_{MO}/M_{MO}, except that stall warning buffeting is allowable.

(e) With the airplane in the cruise configuration, the positive maneuvering load factors at which the onset of perceptible buffeting occurs must be determined for the ranges of airspeed or Mach Number, weight, and altitude for which the airplane is to be certificated. The envelopes of load factor, speed, altitude, and weight must provide a sufficient range of speeds and load factors for normal operations. Probable inadvertent excursions beyond the boundaries of the buffet onset envelopes may not result in unsafe conditions.

[Doc. No. 5066, 29 FR 18291, Dec. 24, 1964, as amended by Amdt. 25-23, 35 FR 5671, Apr. 8, 1970]

§ 25.253 High-speed characteristics.

(a) *Speed increase and recovery characteristics.* The following speed increase and recovery characteristics must be met:

(1) Operating conditions and characteristics likely to cause inadvertent speed increases (including upsets in pitch and roll) must be simulated with the airplane trimmed at any likely cruise speed up to V_{MO}/M_{MO}. These conditions and characteristics include gust upsets, inadvertent control movements, low stick force gradient in relation to control friction, passenger movement, leveling off from climb, and descent from Mach to airspeed limit altitudes.

(2) Allowing for pilot reaction time after effective inherent or artificial speed warning occurs, it must be shown that the airplane can be recovered to a normal attitude and its speed reduced to V_{MO}/M_{MO}, without-

(i) Exceptional piloting strength or skill;

(ii) Exceeding V_D/M_D, V_{DF}/M_{DF}, or the structural limitations; and

(iii) Buffeting that would impair the pilot's ability to read the instruments or control the airplane for recovery.

(3) There may be no control reversal about any axis at any speed up to V_{DF}/M_{DF}. Any reversal of elevator control force or tendency of the airplane to pitch, roll, or yaw must be mild and readily controllable, using normal piloting techniques.

(b) *Maximum speed for stability characteristics, V_{FC}/M_{FC}.* V_{FC}/M_{FC} is the maximum speed at which the requirements of §§ 25.147(e), 25.175(b)(1), 25.177, and 25.181 must be met with flaps and landing gear retracted. It may not be less than a speed midway between V_{MO}/M_{MO} and V_{DF}/M_{DF}, except that, for altitudes where Mach number is the limiting factor, M_{FC} need not exceed the Mach number at which effective speed warning occurs.

[Doc. No. 5066, 29 FR 18291, Dec. 24, 1964, as amended by Amdt. 25-23, 35 FR 5671, Apr. 8, 1970; Amdt. 25-54, 45 FR 60172, Sept. 11, 1980]

§ 25.255 Out-of-trim characteristics.

(a) From an initial condition with the airplane trimmed at cruise speeds up to V_{MO}/M_{MO}, the airplane must have satisfactory maneuvering stability and controllability with the degree of out-of-trim in both the airplane nose-up and nose-down directions, which results from the greater of—

(1) A three-second movement of the longitudinal trim system at its normal rate for the particular flight condition with no aerodynamic load (or an equivalent degree of trim for airplanes that do not have a power-operated trim system), except as limited by stops in the trim system, including those required by § 25.655(b) for adjustable stabilizers; or

(2) The maximum mistrim that can be sustained by the autopilot while maintaining level flight in the high speed cruising condition.

(b) In the out-of-trim condition specified in paragraph (a) of this section, when the normal acceleration is varied from +1 g to the positive and negative values specified in paragraph (c) of this section—

(1) The stick force vs. g curve must have a positive slope at any speed up to and including V_{FC}/M_{FC}; and

(2) At speeds between V_{FC}/M_{FC} and V_{DF}/M_{DF} the direction of the primary longitudinal control force may not reverse.

(c) Except as provided in paragraphs (d) and (e) of this section, compliance with the provisions of paragraph (a) of this section must be demonstrated in flight over the acceleration range—

(1) −1 g to +2.5 g; or

(2) 0 g to 2.0 g, and extrapolating by an acceptable method to −1 g and +2.5 g.

(d) If the procedure set forth in paragraph (c)(2) of this section is used to demonstrate compliance and marginal conditions exist during flight test with regard to reversal of primary longitudinal control force, flight tests must be accomplished from the normal acceleration at which a marginal condition is found to exist to the applicable limit specified in paragraph (b)(1) of this section.

(e) During flight tests required by paragraph (a) of this section, the limit maneuvering load factors prescribed in §§ 25.333(b) and 25.337, and the maneuvering load factors associated with probable inadvertent excursions beyond the boundaries of the buffet onset envelopes determined under § 25.251(e), need not be exceeded. In addition, the entry speeds for flight test demonstrations at normal acceleration values less than 1 g must be limited to the extent necessary to accomplish a recovery without exceeding V_{DF}/M_{DF}.

(f) In the out-of-trim condition specified in paragraph (a) of this section, it must be possible from an overspeed condition at V_{DF}/M_{DF} to produce at least 1.5 g for recovery by applying not more than 125 pounds of longitudinal control force using either the primary longitudinal control alone or the primary longitudinal control and the longitudinal trim system. If the longitudinal trim is used to assist in producing the required load factor, it must be shown at V_{DF}/M_{DF} that the longitudinal trim can be actuated in the airplane nose-up direction with the primary surface loaded to correspond to the least of the following airplane nose-up control forces:

(1) The maximum control forces expected in service as specified in §§ 25.301 and 25.397.

(2) The control force required to produce 1.5 g.

(3) The control force corresponding to buffeting or other phenomena of such intensity that it is a strong deterrent to further application of primary longitudinal control force.

(Secs. 313(a), 601, 603, 604, and 605 of the Federal Aviation Act of 1958 (49 U.S.C. 1354(a), 1421, 1423, 1424, and 1425); and sec. 6(c) of the Dept. of Transportation Act (49 U.S.C. 1655(c)))

[Amdt. No. 25-42, 43 FR 2322, Jan. 16, 1978]

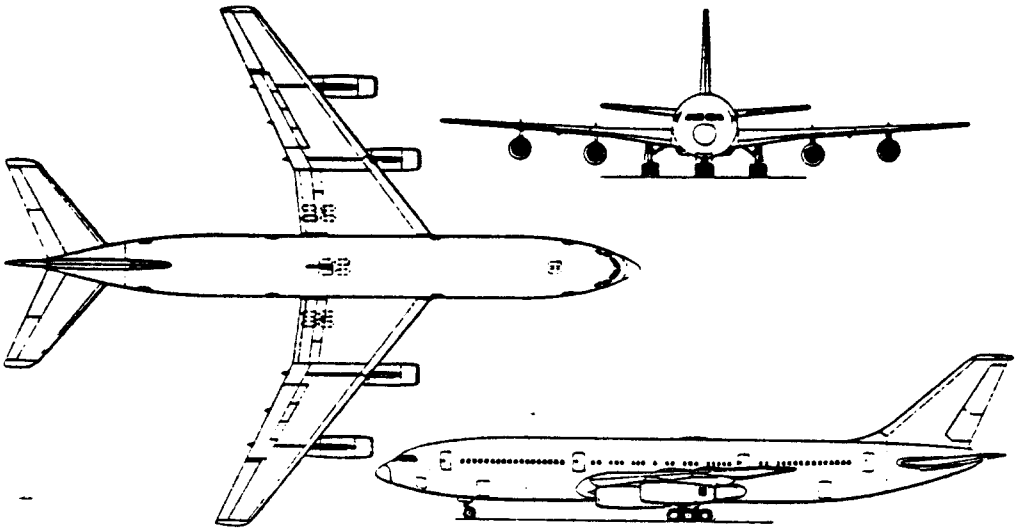

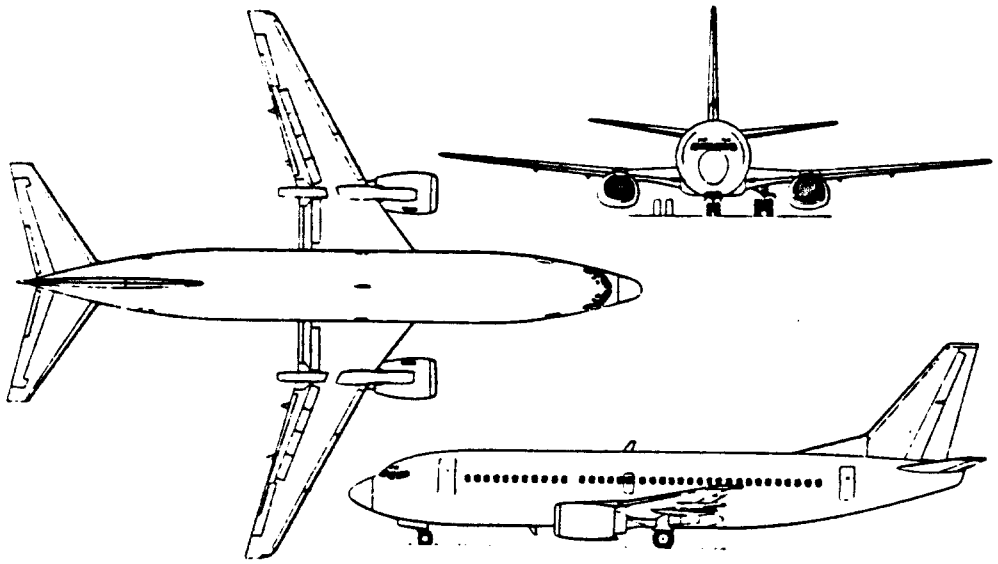

APPENDIX B: MILITARY AIRWORTHINESS REGULATIONS FOR AIRPLANE PERFORMANCE, STABILITY AND CONTROL

Before a military airplane is accepted for service in the US Air Force, the US Navy, the US Marine Corps or the US Army it must meet a number of safety and airworthiness standards which are spelled out in so-called Military Specifications. For purposes of airplane preliminary design, the following specifications are important:

B1. Airplane Performance

B1.1 MIL-C-005011B(USAF): Military Specification, Charts: Standard Aircraft Characteristics and Performance, Piloted Aircraft (Fixed Wing), June 1977.

B1.2 AS-5263(USNAVY): Naval Air Systems Command Specification, Guidelines for the Preparation of Standard Aircraft Characteristics Charts and Performance Data, Piloted Aircraft (Fixed Wing), October 1986.

B2. Airplane Stability, Control and Flying Qualities

B2.1 MIL-F-8785C: Military Specification, Flying Qualities of Piloted Airplanes, November 1980.

IMPORTANT NOTE: Only those parts of the specifications which are of importance to the preliminary designer are reproduced in this Appendix and organized as follows:

B1. Airplane Performance

B1.1 MIL-C-005011B(USAF): Military Specification, Charts: Standard Aircraft Characteristics and Performance, Piloted Aircraft (Fixed Wing), June 1977.

This limited coordination Military Specification has been prepared by the Air Force based upon currently available technical information, but it has not been approved for promulgation as a coordinated revision of Military Specification MIL-C-5011A. It is subject to modification. However, pending its promulgation as a coordinated Military Specification, it may be used in procurement.

1. SCOPE

1.1 Scope. This specification governs the definitions of requirements for, and methods of presenting characteristics and performances for military piloted airplanes. This specification while primarily oriented to conventional take-off and landing (CTOL) aircraft may be applied to STOL and VTOL airplanes if the design criteria established by requirements for specific designs are substituted for the CTOL criteria established herein.

1.2 Application. This specification is applicable to the preparation and presentation of characteristics and performance data. It is also applicable, when appropriate, as an outline of design requirements and mission rules for use in contractual documents and specifications.

1.3 Classification. Characteristics and performance data shall be presented on the following types of charts as required by the procuring agency, and utilizing format as provided. Unauthorized reproduction of such charts bearing the (by authority of the Secretary of the Air Force) statement is prohibited; however no restriction is placed upon use of the format.

1.3.1 Standard aircraft characteristics charts. The standard aircraft characteristics charts are intended to provide a concise, accurate compilation of physical characteristics and performance capabilities of a weapon system.

1.3.1.1 Arrangement. The standard aircraft characteristics chart is basically composed of 10 pages with provisions for supplemental pages as required by the procuring agency. Pages 1, 2, 3, 4, 6 and 9 are mandatory. Pages 5, 7 and 8 are optional as determined by the procuring agency. If certain pages are not required for a specific weapon system, and are omitted, the remaining pages shall be numbered consecutively.

1.3.1.1.1 Basic. The arrangement of the standard aircraft characteristics chart shall be as follows:

a. Page 1 -- Cover sheet which shall include a photograph or perspective drawing of the aircraft model in flight.

b. Page 2 -- Drawings showing descriptive details of the aircraft, such as: Three-view, fuel and oil tankage, armament, inboard profile, etc.

c. Page 3 -- Mission, description, and principal characteristics of the aircraft.

d. Page 4 -- Performance data for the aircraft in tabulated form.

e. Page 5 -- Supplemental tabulated performance data.

f. Page 6 -- Performance graphs.

g. Page 7 -- Supplemental performance graphs.

h. Page 8 -- External store loadings.

i. Page 9 -- Notes. Mission profiles, applicable allowances, and explanatory notes.

Specific requirements are detailed in 3.6.2.

1.3.1.1.2 Supplemental pages. Aircraft characteristics and performance data not coming within the scope of the standard aircraft characteristics charts shall be presented on supplemental pages. Reasons for preparing supplemental pages may be as follows:

a. Possible special loadings or conditions which may:

(1) Be used in restricted tactical operations

(2) Involve non-standard procedures and special operating techniques

(3) Show the maximum potential use of certain aircraft in special missions.

b. Special loadings that may involve equipment, which, for security reasons are only suitable for limited distribution.

c. Theater operations involving non-standard atmospheric conditions.

d. To show additional drawings, illustrations, and graphs. The supplemental page format should be the same as the standard aircraft characteristics chart but may consist of a special design suitable for binding along with the corresponding pages.

1.3.2 Characteristics summary. The characteristics summary is intended to present a summary of performance capabilities on the design mission and principal features in an abbreviated format. Data shown on the characteristics summary shall be in agreement with similar data shown on the standard aircraft characteristics chart. The standard format for the characteristics summary of each model, shall consist basically of a two-page, single-sheet, and shall be 8 by 10-1/2 inches in size after reproduction.

1.4 Categories. The foregoing charts shall be identified by categories to show the development status of the aircraft or data involved.

1.4.1 Development. Charts in this category provide information on new designs during the detail design development after the design becomes stabilized and only minor configuration changes are anticipated.

1.4.2 Service. Charts in this category provide information of aircraft during production and operational use.

1.5 Markings. Each of the foregoing chart types shall be marked as follows:

1.5.1 Designation. The military model designation shall be shown on the lower outer corner.

1.5.2 Category. The chart category as defined in 1.4 shall be shown on the upper outer corner.

1.5.3 Date. The date of publication will be inserted by the procuring agency on the lower inner corner.

1.5.4 Security. The security classification shall be marked as specified by the current DOD Security Regulations. For security purposes each block or graph shall be considered as a paragraph.

1.5.5 Reserved. The upper inner corner is reserved for the use of the procuring agency.

1.6 Submittal. Initial submittal of charts in the development category shall be accomplished after the design has stabilized as determined by the procuring agency. Charts in the service category shall be submitted after the system has been approved for production.

2. APPLICABLE DOCUMENTS

2.1 Issues of documents. The following documents, (effective on the date of invitation for request for proposal) form a part of this specification to the extend specified herein:

SPECIFICATIONS

MILITARY

MIL-G-5572	Gasoline, Aviation, Grades 80/87, 100/130, 115/145
MIL-T-5624	Turbine Fuel, Aviation, Grades JP-4 and JP-5
MIL-M-7700	Manuals, Flight
MIL-F-8785	Flying Qualities of Piloted Airplanes
MIL-A-008860	Airplane Strength and Rigidity, General Specification for
MIL-W-25140	Weight and Balance Control System (For Airplanes and Rotorcraft)
MIL-T-83133	Turbine Fuel, Aviation, Kerosene Type, Grade JP-8

STANDARDS

MILITARY

MIL-STD-210	Climatic Extremes for Military Equipment
MIL-STD-1374	Weight and Balance Data Reporting Forms for Aircraft (Including Rotorcraft)

MANUAL

AFM 60-16	General Flight Rules

(Copies of specifications, standards, drawings, and publications required by contractors in connection with specific procurement functions should be obtained from the procuring activity or as directed by the contracting officer.)

3. REQUIREMENTS

3.1 General. Unless otherwise specified by the procuring agency, preparation by contractors of charts (and revision thereto) for each model shall include the preparation of photographically reproducible copy in the required types and categories. Substantiating reports containing supporting characteristics and performance data are required.

3.1.1 Revisions. Revisions to the charts, shall be prepared and submitted by the contractor. Unless otherwise specified by the procuring agency, revisions are required whenever significant changes in vehicle configuration or data occur, as for:

a. A change in vehicle dimensions
b. An accumulation of changes resulting in a significant performance change. (See 3.1.1.1).

c. A change in propulsion system designation, augmentation, or rating.
d. The addition of external stores.
e. The availability of test data showing significant performance change. (See 3.1.1.1).
f. When specifically directed by the procuring agency.

3.1.1.1 Criteria. The following criteria will be used in forming a judgment as to whether a significant change in performance exists:

a. A change of 5 percent or more in drag.
b. A change of 5 percent or more in installed thrust.
c. A change of 5 percent or more in specific fuel consumption.
d. A change in weight which in itself results in a 5 percent or greater change in mission radius or range.
e. Any combination of two or more of the above resulting in a change of 5 percent or more in any performance parameter.

3.1.1.2 Number. Each chart shall cover only one aircraft model. The probable number of charts and revisions which are required throughout the life of the aircraft model will depend on the number of aircraft changes experienced.

3.2 Substantiating report. All data presented on the charts shall be substantiated by reports submitted with the charts. The reports may be legible rough draft copies of the contractor's work sheets. They shall be complete and shall present in detail the contractor's build up of aerodynamic and propulsive data and shall contain a listing of adequate references, authority, and justification for all data used. Contractors are free to use calculation methods of their own selection, but such methods shall be explained in detail so as to permit a ready understanding of aerodynamic, propulsive and weights bookkeeping methods. Calculations shall be presented in sufficient detail as to permit ready review and check of conclusions.

3.2.1 Basic aerodynamic data. Prior to proceeding with the initial performance calculations for the Standard Aircraft Characteristics charts mutual agreement shall be established between the contractor and the procuring agency relative to the aerodynamic and propulsive and weight data to be used for performance data. This agreement shall be accomplished through normal review and reporting procedures.

3.2.2 Report. The basic aerodynamic propulsive and weight data (see 3.2.1) shall, after review and acceptance by the procuring agency, form the basis for the detailed preparation of the substantiating data report. These data shall be expanded as necessary and used to prepare the detailed performance data required to substantiate the Standard Aircraft Characteristics.

3.2.3 Revisions. The substantiating data report shall be revised under the same criteria as the charts (see 3.1.1).

3.2.4 Text. The required data and the arrangement of the substantiating data report is contained in Appendix IA.

3.3 Standards. Characteristics and performance data shall be based on engineering analysis which produce results consistent with flight test results.

3.3.1 Basis for data. All characteristics and performance data shall be based on the latest reliable aerodynamic, propulsion system, and weight information. The information given shall include the effects on weight and performance of all authorized contract and service changes, together with important changes assured of authorization but pending at the date of chart issue.

3.3.1.1 Changes in characteristics. Changes in aircraft characteristics which do not result in a significant performance change (see 3.1.1.1) do not require a revision by the contractor. However, the procuring agency shall be notified by correspondence so that proper notat on may be appended to the published chart.

3.3.1.2 Flight test. The latest flight test data approved by the procuring agency shall be used as a basis for performance.

3.3.2 Limitations. Performance data shall fall within all established limitations on the vehicle and its components.

3.3.3 Aircraft condition. Performance shall be presented in such a manner as to show clearly the applicable aerodynamic configuration, propulsion system, and loading information. Aircraft configurations shall include the installation of complete service equipment applicable to that particular aircraft model for the mission concerned. Flight performance shall be presented with guns, rotable enclosures, bomb bay doors, etc., in position of least drag, and external bombs or other armament in position for each loading condition, as noted.

3.3.4 Atmosphere. Performance shall be based on the latest approved standard atmospheric tables as specified by the procuring agency.

3.3.4.1 Standard day. Unless otherwise specified, performance shall be based on the standard atmosphere as tabulated and described in Appendix IC.

3.3.4.2 Non-standard day. Tropical and Hot day properties must conform to Appendix IC.

3.4 Definitions. The following definitions are used for the various data on the charts and shall be strictly adhered to.

3.4.1 Weights. Weights given on the charts shall comply with the following definitions derived from, and consistent with, MIL-STD-1374, MIL-W-25140 and T.O.AN 01-1B-50 (see 6.2).

3.4.1.1 Empty weight. The weight of the structure, propulsion system, equipment, etc., in the configuration defined in current system specification.

3.4.1.2 Basic weight. The empty weight adjusted for non-expendable operational items. (Weight empty plus unusable fuel and oil and all fixed armament and equipment for normal operation.)

3.4.1.3 Operating weight. Mission take-off weight less payload and usable fuel. (Basic weight plus usable oil, crew, crew baggage, steward equipment, emergency equipment, special mission fixed equipment, pylon and racks not in basic weight, and other nonexpendable items not in basic weight.)

3.4.1.4 Design weight. Weight at which specified structural design requirements are met or are required to be met.

3.4.1.5 Take-off weight. Take-off weight is the total weight of the aircraft with the fuel and payload (see 3.4.1.10) for the mission presented. The take-off weight normally shall be determined prior to start of engines except in specially approved cases when weight expended during taxi and take-off are excluded (see 3.4.1.5.1.b).

3.4.1.5.1 Maximum. Maximum take-off weight is the greatest weight for take-off established by Technical Orders, design requirements, or other specific recommendations of the procuring agency and is the least weight determined by the following criteria:

a. The weight of the vehicle fully loaded with fuel, oil, armament or cargo to the capacity for which space or tankage is normally provided. The bearing load for the floor and supporting structure shall not be exceeded.
b. The aircraft and its components (wings, landing gear, supporting structures for ordnance, cargo, etc.) shall be capable of sustaining the authorized load factor and shall not violate the minimum criteria of applicable specifications for taxi and ground handling. When ground handling criteria permits a higher weight than does the flight limit, those items expended during take-off, (water, ATO, etc.) may be added to the quoted maximum take-off weight for mission computations, and proper notation thereof will be carried in qualifying note on the performance charts.
c. Throughout the mission profile the center of gravity shall remain within design limits.
d. The maximum tow force, shall not be exceeded.

3.4.1.5.2 Typical design criteria. For design purposes consideration may be made of alternate definitions of maximum take-off weight such as: Specifying the critical field length and ground run associated with the operational concept of the design, including the effects of such items as runway surface (hard, sod, etc.), ambient runway temperature and pressure altitudes.

3.4.1.6 Maximum inflight weight. The maximum weight at which the aircraft is authorized to be airborne. This weight may be greater than maximum take-off weight if in-flight refueling is utilized.

3.4.1.7 Maximum ramp weight. Maximum in-flight weight unrefueled plus fuel, water, etc., used during engine start, taxi, and take-off, shall not exceed other limits such as those for taxiing, ground handling, wheel jacking, etc., as specified in MIL-A-008860.

3.4.1.8 Combat weight. Weight over the target for the mission presented with fuel and oil but without bombs, missiles, mines, cargo or droppable tanks unless otherwise noted.

3.4.1.8.1 Fuel load is determined as follows:

a. Bomber, Fighter Bomber, Missile Carrier (for ground attack) - Immediately after dropping the offensive ordnance, but prior to escape.

b. Fighter (interceptor, air superiority) - Immediately prior to combat.

c. Tanker - Immediately after completion of fuel transfer.

d. Reconnaissance - Immediately after arrival at target (after drop of photo flash bombs if carried).

e. Others (cargo-trainers) - Prior to start of return flight for resupply (radius mission) and prior to landing for range missions.

f. Ferry Mission (all vehicle types) - Reserve fuel only.

3.4.1.8.1.1 Typical design criteria. For design purposes, consideration of alternate definitions of combat fuel load such as: with 50 percent of combat fuel allowance consumed, with 100 percent of combat fuel allowance consumed, or any other criteria selected to optimize the aircraft design.

3.4.1.9 Landing weight

3.4.1.9.1 Maximum. Maximum landing weight is the greatest weight established for landing by structural criteria.

3.4.1.9.2 Mission. The weight at the end of the mission as determined by the mission ground rules. It shall include the fuel reserve as specified by the mission.

3.4.1.10 Payload. The load which justifies the mission. Payload includes cargo, personnel other than crew, bombs, chaff, missiles, reconnaissance cameras, electronic countermeasures pods, photo flash flares, fuel carried for transfer by tankers, and ammunition.

Special equipment required for the mission such as winterization, rescue equipment, except that carried for drop by (H) type vehicles (search-rescue), cargo handling, etc., shall not be included in payload.

3.4.1.11 Fuel. Standard fuel weight of fuel in pounds per U. S. gallon shall be as follows:

a. MIL-F-5572 (Gasoline in all grades) – 6.0 lbs/gal.
b. MIL-F-5624 (JP-4) Jet fuel – 6.5 lbs/gal.
c. MIL-F-5624C (JP-5) Jet fuel – 6.8 lbs/gal.
d. MIL-T-83133 (JP-8) Jet fuel – 6.7 lbs/gal.
e. If design requires special fuels of specified densities or BTU content, such shall be used and specified in the chart notes.

3.4.2 Speeds. All speeds shall be level flight true airspeeds in knots and mach number as applicable.

3.4.2.1 Maximum speed. The highest speed obtainable for configuration and weight in level flight. The altitude at which this speed occurs shall be stated. It shall be the lesser of the speeds determined by the intersection of the thrust (power) available and required curves or the speed limit imposed through structural or heating consideration.

3.4.2.2 Penetration speed. A specified speed ( ) at which the aircraft shall conduct the final run in to the target at a specified altitude. This speed shall be specified by design requirements.

3.4.2.2.1 Combat speed. Maximum speed at combat weight and combat altitude with maximum power.

3.4.2.3 Stall speed. The stall speed shall be computed on the basis of 1.0g flight with the maximum trimmed lift coefficient established by computation or wind tunnel testing. Upon availability of flight test results, stall speed shall be changed to the highest of the speeds for steady straight 1.0g flight at $C_{L\ max.}$, the speed at which abrupt loss of control occurs about any of the pitch, roll or yaw axes, the speed at which intollerable buffet or structural vibration is encountered, or other minimum permissible speed as defined in MIL-F-8785.

3.4.2.3.1 Power-off. The stall speed without power.

3.4.2.4 Take-off speed

3.4.2.4.1 Take-off speed shall be the highest of the speeds specified below:

a. A speed corresponding to 110 percent of power off stall speed in the take-off configuration.
b. A speed determined by the lift coefficient, in ground effect, for the maximum angle of attack attainable with the main landing gear oleo in the static position with aircraft on ground.
c. Minimum speed at which the aircraft has a climb gradient potential of 1/2 percent (0.005), with maximum power, in the take-off configuration, out of ground effect. For multi-engine aircraft this potential shall be obtainable with the most critical engine inoperative. Where;

$$\text{gradient} = \frac{[\text{Vertical Height in climb (ft)}]}{[\text{Horizontal distance in climb (ft)}]} \qquad (1)$$

d. Air minimum control speed as specified in 3.4.2.8.2.
e. The speed which permits attaining obstacle climb-out speed, as defined in 3.4.2.5, at or before reaching 50 ft. height above the runway.

3.4.2.4.1.1 Typical design criteria. For design purposes, consideration may be made of alternate definitions of take-off speed such as: a higher or lower percentage of stall speed, a higher climb gradient potential or other criteria which optimizes the design.

3.4.2.5 Obstacle climb-out speed. The climb speed at the 50-foot obstacle shall not be less than the highest of the speeds specified below.

a. One hundred fifteen percent of power off, 1.0g, stall speed. 1.15 Vs
b. Air minimum control speed.
c. Speed at which the aircraft has a climb gradient of 2.5 percent (0.025) with gear up, flaps in take-off position, with maximum power, out-of-ground effect. For multi-engine aircraft this potential shall be obtainable with the most critical engine inoperative.
d. If gear retraction results in a transient drag increase over that for gear down, the speed at which the aircraft has a 1/2 percent (0.005) climb gradient potential with flaps in take-off setting, gear in transit, with maximum thrust out-of-ground effect. For multi-engine aircraft, the most critical engine shall be inoperative.

3.4.2.5.1 Typical design criteria. For design purposes, consideration may be made of alternative limitations to the obstacle climb-out speed such as: a higher or lower percentage of the stall speed, an increase in climb gradient potential or any criteria which is in keeping with the operational concept of the design.

3.4.2.6 Climb speed. The climb speed shall be the airspeed at which the maximum rate-of-climb is attained for the given configuration, weight, altitude, and power. Consideration shall be made for kinetic energy corrections in optimizing the climb speed schedule. When authorized in the applicable flight manual, a simplified, non-optimum speed schedule may be used.

3.4.2.7 Critical engine failure speed. The critical engine failure speed shall be the speed at which the most critical engine can fail and the same distance be required to either continue the take-off or abort. See 3.4.5.4.

3.4.2.8 Minimum engine-out control speed

3.4.2.8.1 Ground. The minimum control speed, ground, shall be the minimum speed during the take-off run where the engine, most critical to directional control, can fail and directional control can be maintained as defined in MIL-F-8785.

3.4.2.8.2 Air. The minimum control speed, air, shall be the minimum airborne speed with maximum thrust where the engine, most critical to control, can fail and directional control can be maintained.

3.4.2.9 Cruise speed

3.4.2.9.1 Maximum range cruise speed. The speed for maximum range operation shall be the speed at which maximum nautical miles per pound of fuel are attainable at the momentary weight and altitude.

3.4.2.9.2 Long range cruise speed. The higher of the two airspeeds which give nautical miles per pound of fuel equal to 99 percent of the maximum nautical miles per pound of fuel for momentary weight and altitude. This speed may be used to decrease mission time without severe penalty to range.

3.4.2.9.3 Maximum cruise speed. The highest speed that can be maintained with maximum continuous power at stated altitude, weight and configuration.

3.4.2.9.4 Average cruise speed. Total distance covered in cruise divided by the time for cruise (distance and time for climb, acceleration to combat speed, combat time, loiter time etc. are not included).

3.4.2.10 Maximum endurance (loiter) speed. The airspeed for maximum endurance shall correspond to the speed for minimum fuel flow attainable at momentary weight and altitude except as limited by acceptable flying qualities.

3.4.2.10.1 Combat loiter speed. The airspeed for maximum endurance shall correspond to the speed for minimum fuel flow attained at momentary weight and attitude except that the airspeed must be adequate to allow an instantaneous load factor of a specified value.

3.4.2.11 Approach speed. The approach speed down to the 50-foot obstacle shall be the higher of:

a. Air minimum control speed, gear down, flaps in approach configuration and lift augmentation operable.
b. A speed of 120 percent of 1.0g power-off stall speed, out-of-ground effect, gear down, flaps in approach configuration.

c. A speed at which the aircraft has a climb gradient potential of 2.5 percent (0.025) with gear retracted, flaps in approach configuration, and with maximum dry take-off power. For multi-engine aircraft the most critical engine shall be inoperative.

Note: If other than landing flap is selected for approach, it's characteristics shall be specified i.e., approach flap develops a stall -- percent higher than does landing flap.

3.4.2.11.1 Typical design criteria. For design purposes, consideration may be made of alternate definitions of approach speed such as: higher or lower percentage of stall speed, a higher climb gradient potential, alternate go-around power settings or any other criteria which might optimize the design.

3.4.2.12 Landing speed. The landing speed shall be the greater of:

a. A speed determined by the lift coefficient, in ground effect, for the maximum angle attainable with the main landing gear oleo in the static compressed position with aircraft on ground.
b. One hundred fifteen percent (115 percent) of 1.0g power-off stall speed in the landing configuration.

3.4.2.12.1 Typical design criteria. For design purposes, consideration may be given to alternate definitions of landing speed such as: geometry-limited with oleos in full or partial extended position, changes in percentage of stall speed and climb gradient potential or any other criteria which would optimize the design.

3.4.3 Ceiling

3.4.3.1 Service ceiling. The altitude at which the maximum rate of climb at subsonic speed is 100 ft/min at stated weight and engine power.

3.4.3.2 Combat ceiling

3.4.3.2.1 Subsonic. The altitude at which the max subsonic rate of climb is 500 ft/min at stated weight and power.

3.4.3.2.2 Supersonic. The highest altitude at which the vehicle can fly supersonically and have a climb potential of 1000 fpm at stated power and weight.

3.4.3.3 Cruise ceiling

3.4.3.3.1 Subsonic. The altitude at which the maximum rate-of-climb potential is 300 ft/min at maximum continuous engine rating at momentary weight.

3.4.3.3.2 Supersonic. The highest altitude at which the vehicle can fly supersonic at maximum continuous power with a climb potential of 1000 fpm at momentary weight.

3.4.4 Altitude

3.4.4.1 Cruise altitude. The altitude at which the cruise portion of the missions is computed. Depending on the mission ground rules, the cruise altitude may be assigned or it may be otherwise governed by limitations such as terrain clearance, mission length, ceilings, oxygen or other crew/aircraft restrictions. In no case shall cruise altitude exceed cruise ceiling.

3.4.4.2 Optimum cruise altitude. The altitude at which the aircraft attains the maximum nautical miles per pound of fuel for the momentary weight and configuration. If this altitude exceeds cruise ceiling the latter shall be used for cruise.

3.4.4.3 Combat altitude. The altitude at the target for the specific mission shown.

3.4.5 Take-off. Criteria for conventional take-off aircraft shall comply with the following: (for STOL aircraft the criteria shall be determined by design criteria.) (Vertical components of thrust may be used in take-off computation.)

3.4.5.1 Ground run distance (i.e. take-off distance). Take-off ground run distance shall be that normally obtainable in service operation at Sea Level with standard atmospheric conditions, zero wind, no runway slope on hard (concrete or asphalt) surfaced runways. The take-off speed criteria of 3.4.2.4 shall be used.

3.4.5.1.1 Typical design criteria. For design purposes, consideration may be made of alternate definitions of take-off ground run such as: non-standard atmospheric conditions, higher pressure altitudes, alternate runway surfaces (hard, sod etc.), head or tail-wind or other criteria in keeping with the operational concept of the design.

3.4.5.2 Distance to 50 ft. The distance to clear a 50-foot obstacle shall be the sum of take-off ground run distance of 3.4.5.1 plus the airborne distance needed to accelerate and climb to arrive at the 50-foot height at the speed specified in 3.4.2.5.

3.4.5.3 Take-off time. The take-off time shall be that normally obtainable in service operation at sea level under standard day atmospheric conditions with no wind. The time is measured from start of take-off (brake release) to start of enroute climb (attainment of climb speed).

3.4.5.4 Critical field length. Critical field length is the sum of the distance required to accelerate with all engines operative to critical engine failure speed (3.4.2.7) plus the distance to accelerate with the critical engine inoperative to take-off or to decelerate to a stop from critical engine failure speed in the same distance.

3.4.5.4.1 Data basis. The data basis for the computation of the stopping distance for the chart for critical field length shall be as follows:

a. At engine failure speed the aircraft continues to accelerate for 3 seconds pilot reaction time with remaining engines at maximum power and zero thrust on the inoperative engine.
b. At the end of the 3-second acceleration time, power on all engines is instantaneously reduced to idle, brakes applied, and deceleration devices deployed.
c. Sufficient time, after, b, above, shall be allowed for deployment of the deceleration device(s) or for reverse thrust to reach maximum before including its effect on deceleration.

3.4.5.5 Coefficient of friction. The coefficient μ, as used in this document is defined as the ratio of the total retardation force attributable to the braking system to the momentary gross weight of the aircraft. The following values will be used unless ground or flight test data are available.

3.4.5.5.1 Rolling μ. The rolling (unbraked) coefficient of friction for a dry, hard surface runway shall be assumed equal to 0.025.

3.4.5.5.2 Braking μ. The total braking coefficient of friction for a dry hard surface runway shall be assumed equal to 0.30.

3.4.5.5.3 Test data. Test μ values may be either the results of tests conducted on the specific aircraft or similar types, i.e. commercial aircraft.

3.4.5.5.4 Typical design criteria. For design purposes, consideration may be given to the effects of new and improved methods of increasing the total retardation force such as by anti-skid devices.

3.4.6 Climb. Climb after take-off may be divided into two segments as specified by the procuring agency: Initial climb-out and enroute climb.

3.4.6.1 Initial climb-out. Climb-out shall be at a speed which shall not be less than that limited by the criteria of 3.4.2.5. Gear retraction shall be initiated as soon as an adequate positive climb gradient (3.4.2.5c and d), using applicable power, has been established and maintained while accelerating to climb-out speed. Flaps shall be in the take-off position.

3.4.6.1.1 All engines operating. Initial climb-out with all engines operating shall be based on all engines operating from brake release to take-off. Acceleration to climb-out speed and climb-out shall be based on the thrust (power) available with all available engines.

3.4.6.1.2 One engine inoperative. Initial climb-out with one engine inoperative shall be based on all engines operating from brake release to critical engine failure speed and with the critical engine inoperative from critical engine failure speed to take-off. Acceleration to climb-out speed and climb-out shall be based upon the thrust (power) available with the remaining engines at take-off thrust and the drag of the inoperative engine. If means of reducing drag of the inoperative engine are a design feature, such drag reduction shall be utilized with a time allowance for activation.

3.4.6.2 Climb path angle. The climb flight path angle shall be expressed in terms of a gradient (vertical feet per 100 horizontal feet). This path shall be determined from the 50-foot height point and at the 50-foot height climb-out speed as determined in 3.4.2.5. Conditions shall be with gear up, flaps in take-off position, out of ground effect and with appropriate configuration, power and weight. For multi-engine aircraft the climb flight path with the critical engine inoperative shall be included.

3.4.6.3 Enroute climb. Enroute climb data shall be based on the appropriate configuration, power and weight. The aircraft shall have the landing gear and flaps retracted and have attained the airspeed for best climb for the applicable condition.

3.4.6.4 Time to climb. The time to climb to specified altitude(s) shall be expressed in minutes from start of enroute climb. Weight reduction as a result of fuel consumption shall be applied to the calculations.

3.4.6.5 Combat climb. Combat climb is the instantaneous maximum vertical speed capability in feet per minute at combat conditions, such as, weight, configuration, altitude, and power.

3.4.7 Landing distance. The following criteria are for conventional aircraft. (For STOL aircraft the criteria shall be as established by design requirements.) Landing distance includes: (a) landing ground roll and (b) distance over a 50 foot height. Distances shall be for the landing configuration and weight and shall be based on the landing speeds defined in 3.4.2.12. Unless otherwise specified, ground roll deceleration shall be based on operation at Sea Level, standard day, zero wind, no runway slope, idle power and a braking coefficient as defined in 3.4.5.5.2.

3.4.7.1 Typical design criteria. For design purposes, consideration may be given to alternate definitions of landing distance such as: reverse thrust, atmospheric conditions, runway slopes and winds of a non-standard nature, a rigid computer analysis of the air distance and other similar criteria selected to optimize the design of the airplane.

3.4.8 Power. The term (power) is used to mean brake horsepower or thrust as applicable with due consideration for installation effects and limitations. Engine and assisted takeoff ratings as defined in 3.6.2.1.5 c and 3.6.3.1.4 shall be those which appear in the approved engine model specification without regard to installation effects or limitations.

3.4.8.1 Maximum power. Maximum engine power output. This condition of operation may have an incremental duration time limit. This term is used for both augmented and non-augmented engines.

3.4.8.2 Intermediate power. Maximum engine power output without augmentation. This condition may be time limited. This term is used only for augmented engines.

3.4.8.3 Maximum continuous power. Maximum engine power output which may be used continuously, no time limit is imposed.

3.4.8.4 Cruise power. The power required to fly the aircraft at cruise speed for the configuration, altitude and weight designated.

3.4.8.5 Minimum augmented. Lowest power at which the engine will operate with augmentation at any point specified within the augmented operating envelope.

3.4.9 Fuel. Unless otherwise specified, fuel for gas turbine engines shall be JP-4. Weights shall be obtained from 3.4.1.11.

3.4.9.1 Fuel consumption corrections. Corrections or allowances to engine fuel flow shall be made for all propulsion system installation losses such as accessory drives, BLC bleed, environmental system bleed, nozzle losses, pressure recovery, etc.

3.4.10 Mission types. Representative operational missions for various types of aircraft are specified in table I. Typical maximum effort missions are shown in Appendix IB to this specification. These maximum effort missions specify the exact fuel allowances for take-off and climb, combat, and landing reserves and are included since they are often used to compare USAF aircraft and foreign aircraft performance capabilities on a common basis.

3.4.10.1 Design mission. The design mission is defined as the primary mission for which the aircraft was specifically procured. This mission will normally be defined in procurement documents such as the statement of work and will include the flight profile, allowances, fuel (clean or external tanks) and payload. Ground rules and allowances for the design mission are dictated by the specific operational requirements and will be used in describing the mission capabilities in the Standard Aircraft Characteristics charts. Some useful alternate design criteria are discussed in 3.5.3 and in other applicable parts of this specification.

3.4.10.2 Ferry mission (ferry range). The greatest distance attainable on a practical one-way mission with maximum authorized fuel and no payload.

3.4.10.3 Typical missions. Any missions, preferably from table I, which would present the additional capabilities of the aircraft. Normally these will include at least one mission at the maximum take-off weight (3.4.1.5.1) with the ground rules corresponding to the design mission.

3.4.10.4 Inflight refueled mission. For aircraft capable of inflight refueling, a refueled mission is the distance (radius or range) attainable through receipt of replacement fuel during flight. A single refueling operation is required although multiple refueling operations may be added if considered to be feasible. Basic profiles from table I shall apply with special allowance from table II considered.

3.4.10.5 Combat range. Combat range is the distance (including distance covered in climb) attainable on a one-way flight carrying payload (bombs, cargo, personnel) the entire distance. Droppable fuel tanks are dropped when empty. Allowances for take-off, climb, cruise are taken from the design mission. Combat range for bomber, fighter, and attack aircraft should be computed without landing reserves. Landing reserves should be included for aircraft.

3.4.10.6 Combat radius. Combat radius is the distance [including distance covered in climb(s)] to the mid-point of a equal legged mission from base to target and return. Specific mission profile actions, allowances and reserves shall be as set forth in table I and in the mission being considered.

3.4.10.6.1 Typical design criteria. For design purposes, consideration may be given to the requirement for missions containing unequal legs (offset). Significant design impact could result from a mission where the aircraft is recovered at a remote base without the requirement of returning to home base.

3.5 Mission detailed requirements

3.5.1 General mission requirements. Unless otherwise specified, the following general ground rules shall apply:

3.5.1.1 Standard atmosphere. Data shall be presented for standard day atmosphere.

3.5.1.2 Wind. Data shall be for a no-wind condition.

3.5.1.3 Formation flight. Data shall be for a single aircraft only.

3.5.1.4 Ordnance expenditure. All ordnance shall be expended at the start of combat unless otherwise specified.

3.5.1.5 Off-loading fuel. Fuel may be off-loaded to avoid exceeding the maximum allowable take-off weight.

3.5.1.6 External fuel tanks. External fuel tanks on combat aircraft, shall be dropped when empty or prior to combat unless such tanks are designed to be carried during combat. Unless otherwise restricted (Center of Gravity etc.), dropping of external tanks shall be sequenced to provide maximum range. Cargo and tanker aircraft shall not drop empty external tanks.

3.5.1.7 Pylons/Racks. In the computation of range/radius performance, pylons and racks shall be retained unless required to be dropped by design requirements

3.5.1.8 Reduced engine operation. When applicable, a minimum number of engines may be used to increase range if such operation would represent normal service usage. However, such action shall conform to 3.5.1.9.

3.5.1.9 Authorized operation. No operational technique, see 3.5.1.8, shall be utilized that is not included, or is not intended to be included as recommended procedure in the applicable flight manual.

3.5.1.10 Trainer aircraft. The trainer mission as defined by table I is applicable to basic and advanced trainer airplanes. Combat and tactical trainer airplanes fly the design mission for the appropriate parent-type airplane.

3.5.1.11 Variable geometry wing (VGW) aircraft. Normally VGW aircraft will have wings in unswept position for take-off and subsonic flight and swept for supersonic dash and chase profile segment unless footnoted otherwise.

3.5.2 Mission loading requirements. In order to facilitate and expedite the submittal of the charts, the contractor should contact the procuring agency to discuss the various mission loadings prior to submittal. In the absence of special instructions, the following shall apply.

3.5.2.1 Design mission loading. The fuel and payload loading for the design mission shall be the primary loading condition as defined in the system specification for the aircraft.

3.5.2.2 Typical missions loading. Loadings shall be selected from those included in the system specification or other approved loadings which depict a particular capability of the aircraft. At least one mission shall conform to the maximum gross weight specified in 3.4.1.5.1.

3.5.2.3 Ferry mission loading. Loading shall consist of the maximum authorized fuel and no payload.

3.5.2.4 Inflight refueled mission loading. One mission shall be for the same loading as the design mission. Other loadings may be selected from the typical missions.

3.5.2.5 Combat range mission loading. Identical to the loading of the associated combat radius mission.

3.5.3 Mission segments. Rationale for mission segments is presented below.

3.5.3.1 Take-off. Fuel allowances for ground operation including starting engines warm-up, taxi, take-off and acceleration to climb speed, are as defined in the requirements for the design mission.

3.5.3.1.1 Typical design criteria. For design purposes, consideration may be given to defining the take-off allowance to fully utilize the state-of-the-art. Some typical examples are:

a. Specify engine operation for specific time periods at specified powers. Such as, fuel used during 5 minutes of maximum continuous power operation at Sea Level on a standard day plus 1 minute of maximum power operation if afterburner is used during take-off.
b. Estimate fuel required to start the engine(s), run-up, taxi a specified distance at a specified power setting and to accelerate from brake release to climb speed at a specified power.
c. Estimate fuel for a specified time at a specified thrust/weight ratio to account for starting and taxi plus fuel for take-off and acceleration to climb speed computed from the following:

$$W_{f_{TO}} = \frac{V_c W_{TO}}{2g} \cdot \frac{(\dot{W}_o \cdot \dot{W}_c)}{T-D}$$

When: $W_{f_{TO}}$ = Take-off and acceleration fuel, lbs

V_c = initial climb speed, ft/sec

W_{TO} = take-off weight, lbs

$\dot{W}_o$ = static fuel flow at take-off power, lbs/sec

$\dot{W}_c$ = fuel flow at initial climb speed at take-off power, lbs/sec

T-D = thrust minus drag at V_c, lbs

g = acceleration of gravity, S.L., ft/sec^2 (2)

Note: If power is to be varied between lift-off and climb speed this equation can be so modified.

d. Other specific criteria may be selected to more accurately portray the operational characteristics of the specific design.

3.5.3.2 Climb. Except for point intercept missions, all climbs shall be enroute with power and speed schedules optimized to maximize mission range. Point intercept missions shall be optimized to obtain minimum time to combat altitude.

3.5.3.2.1 Typical design criteria. For design purposes, consideration may be given to alternate climb schedules to more adequately portray the desired operational capability of the design. For example the following schedules could apply: minimum time, minimum fuel, maximum range, specified power or speed, accelerate during climb, etc.

3.5.3.3 Cruise. Unless specifically assigned, aircraft shall cruise at the speed and altitude for maximum or long range for the applicable configuration, power and weight. Except where the altitude is specified, the aircraft may utilize a cruise climb to optimize cruise distance. This altitude shall not exceed cruise ceiling.

3.5.3.3.1 Typical design criteria. For design purposes, consideration may be given to specifying a cruise technique selected to optimize the desired characteristics of the design. Techniques to be considered include: constant altitude cruise, constant speed cruise, cruise climb profile, step climb, cruise at specified power, cruise with reduced number of engines, cruise altitude in excess of cruise ceiling, fixed distance segment, headwinds or tail winds, non-standard temperatures, etc.

3.5.3.4 Combat. Combat shall be considered by setting aside a quantity of fuel based upon a specified measure of combat performance. For task-oriented fuel allowances, computation shall be based upon weight at start of combat period with benefit due to weight reduction cridited; change in speed due to weight reduction shall be ignored.

3.5.3.4.1 Escape and evasion. Escape and evasion shall be considered by setting aside a quantity of fuel based upon a specified measure of performance.

3.5.3.4.2 Typical design criteria. For design purposes, consideration may be given to various methods of accounting for the fuel to be used during combat or escape and evasion action. Some examples of methods are:

a. Fuel required for a specified time with a specified power at a specified speed and a specified altitude.
b. Fuel consumed in expending a specified quantity of energy. For example:

$$\text{Combat fuel} = \frac{E_s \dot{W}_f}{P_s}$$

When: E_s = Specific energy, ft

$\dot{W}_f$ = fuel flow at combat speed, power, and altitude, lbs/sec

P_s = excess energy or $\frac{(T-D)V_c}{W_{T_c}}$, ft/sec

V_c = combat true airspeed, ft/sec

W_{T_c} = combat weight, lbs

(T-D) = thrust minus drag, lbs (3)

c The quantity of fuel determined as the sum of the fuel required to accelerate from cruise speed to a specified speed, plus fuel required to make a specified number of sustainable turns at a specified speed or speeds. These operations shall be performed at a selected power(s) and altitude(s).
d. All or a portion of the armament may be expended.
e. Other specific criteria selected to more accurately portray the operational characteristics of the specific design.

3.5.3.4 Descent. For vehicles whose best cruise is subsonic, no time, fuel or distance shall be credited for descent. For supersonic cruise vehicles, credit shall be taken for descent and deceleration to a specified altitude and speed. Vehicles which conduct a supersonic run out from the target may, if the cruise altitude and speed are lower than the run out altitude and speed, account for distance in descent and deceleration to cruise.

3.5.3.5 Typical design criteria. For design purposes, consideration may be given to alternate definitions of descent. For example: Time, fuel and distance could be credited, descent could be a long range (airline) approach, use of power could vary from none to full, speeds could vary from near stall to redline, altitudes could be reduced in step increments, etc.

3.5.3.6 Landing reserve. Since the mission profiles of table I are generalized, no compliance with the alternate landing destination of AFM 60-16 is possible. Instead, a landing reserve is required which would be typical of operational use.

3.5.3.6.1 Typical design criteria. For design purposes, consideration may be given to defining the landing reserves to fully utilize the state-of-the-art. Some examples are:

a. The fuel required for a ground controlled approach; a wave-off, go-around and a second, successful landing. This could be approximated by using the equivalent of fuel consumed during a specified time at maximum endurance at Sea Level with all engines operating.
b. A specified percentage of initial fuel load.
c. Fuel consumed during a specified time of operation at a specified power at a specified altitude.
d. The greater of the fuel required for 10 percent of mission time or 20 minutes at maximum endurance speed at 10,000 feet (AFM 60-16).
e. Fuel required to fly to an alternate field (specify distance) plus a specified time at a specified speed at a specified altitude to account for landing.
f. Combinations of the above or other criteria selected to optimize the design.

3.5.4 Mission time. Time in air excluding the time before the start of initial climb and reserve unless otherwise specified and noted. For interceptors only: includes actual time required for take-off and acceleration to climb speed.

3.5.5 Cycle time. The time of flight from the start of initial climb (omitting take-off time) to the time when the engines are stopped after landing.

3.5.6 Block time. The total time of flight from engine start to engine stop after landing.

3.5.7 Intercept time. The time from engine start until initiation of combat at the intercept altitude. This time includes the period required for take-off and acceleration to climb speed.

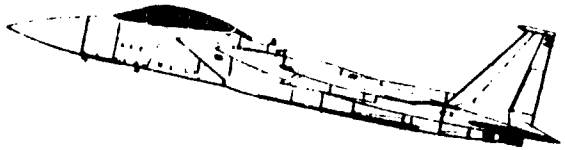

TABLE I

STANDARD MISSIONS

ATTACK

*	A-1	Hi-Hi-Hi
	A-2	Hi-Lo-Hi
*	A-3	Hi-Lo-Lo-Hi
	A-4	Lo-Lo-Lo-Hi
*	A-5	Lo-Lo-Lo-Lo
*	A-6	CAP

BOMBER

*	B-1	Hi-Hi-Hi-Hi
	B-2	Hi-Lo-Lo-Hi

CARGO

	C-1	Supply
*	C-2	Assault

FIGHTER

*	F-1	Air Superiority
	F-2	Point Intercept
	F-3	Area Intercept
	F-4	CAP
	F-5	Hi-Hi-Hi
	F-6	Hi-Lo-Hi
	F-7	Hi-Lo-Lo-Hi
	F-8	Lo-Lo-Lo-Hi
	F-9	Lo-Lo-Lo

TANKER

	T-1	Buddy Refuel
*	T-2	Rendezvous Refuel

GENERAL

	G-1	Airborne Warning and Control
	G-2	Rescue
	G-3	Forward Air Controller
	G-4	Trainer
	G-5	ASW Search
*	G-6	Ferry Mission

* MISSION PROFILES INCLUDED IN THIS TEXT. FOR OTHERS SEE MIL-C-005011B

TABLE I. STANDARD MISSIONS (Continued)

MISSION A-1

HI-HI-HI - ATTACK

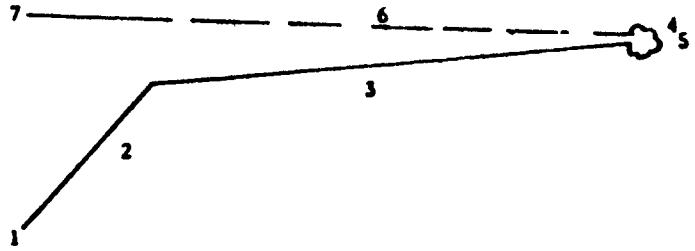

SEGMENT	ALLOWANCE
1. Take-off and accelerate to climb speed ( )	1. See 3.5.3.1
2. Climb on course to cruise altitude ( )	2. Speed and power for maximum range
3. Cruise to target ( )	3. Speed and altitude for maximum range
4. Drop Stores ( )	4. Weight reduction equal to store weight
5. Escape and evasion ( )	5. See 3.5.3.4.1
6. Cruise to base ( )	6. Same as 3
7. Arrive over base with reserve fuel ( )	7. See 3.5.3.6

NOTES

1. For segment details and rationale - see 3.5.3
2. For each segment, enter incremental values: (Time; hours; Fuel; pounds; Distance; n. miles)
3. For tanker missions with a specified receiver - See table III

TABLE I. STANDARD MISSIONS (Continued)

MISSION A-3

HI-LO-LO-HI - ATTACK

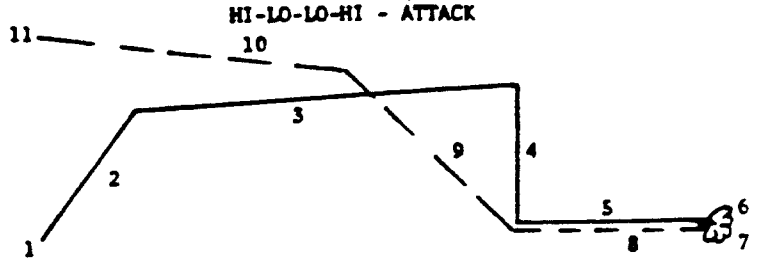

SEGMENT	ALLOWANCE
1. Take-off and accelerate to climb speed ( )	1. See 3.5.3.1
2. Climb on course to cruise altitude ( )	2. Speed and power for maximum range
3. Cruise to start of penetration ( )	3. Speed and altitude for maximum range
4. Descend to Sea Level	4. No time, fuel or distance credited except where specified
5. Run-in specified distance at Sea Level to target ( )	5. At penetration speed at Sea Level with power as required
6. Drop Stores ( )	6. Weight reduction equal to store weight
7. Attack target ( )	7. See 3.5.3.4
8. Run-out specified distance at Sea Level from target ( )	8. Same as 5
9. Climb on course to cruise	9. Same as 2
10. Cruise to base ( )	10. Same as 3
11. Arrive over base with reserve fuel ( )	11. See 3.5.3.6

TABLE I. STANDARD MISSIONS (Continued)

MISSION A-5

LO-LO-LO-LO - ATTACK

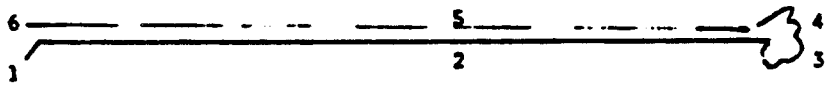

SEGMENT	ALLOWANCE
1. Take-off and accelerate to cruise speed ( )	1. See 3.5.3.1
2. Cruise at Sea Level to target ( )	2. Speed and power for maximum range
3. Drop stores ( )	3. Weight reduction equal to store weight
4. Attack target ( )	4. See 3.5.3.4
5. Cruise to base at Sea Level	5. Same as 2
6. Arrive over base with reserve fuel ( )	6. See 3.5.3.6

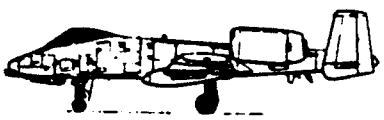

TABLE I. STANDARD MISSIONS (Continued)

MISSION A-6

COMBAT AIR PATROL - ATTACK

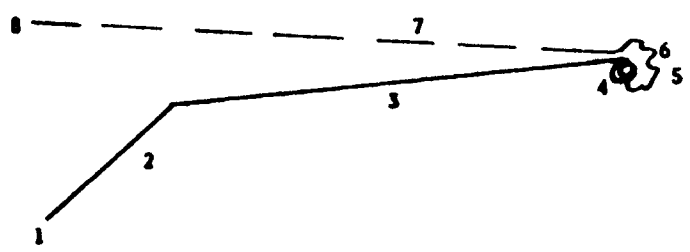

SEGMENT	ALLOWANCE
1. Take-off and accelerate to climb speed ( )	1. See 3.5.3.1
2. Climb on course to cruise altitude ( )	2. Speed and power for maximum range
3. Cruise to target area specified distance from base ( )	3. Speed and altitude for maximum range
4. Loiter at specified altitude awaiting target assignment ( )	4. Speed and power for combat loiter at specified altitude
5. Drop stores ( )	5. Weight reduction equal to store weight
6. Attack target, escape and evade ( )	6. See 3.5.3.4
7. Cruise to base ( )	7. Same as 3
8. Arrive over base with reserve fuel ( )	8. See 3.5.3.6

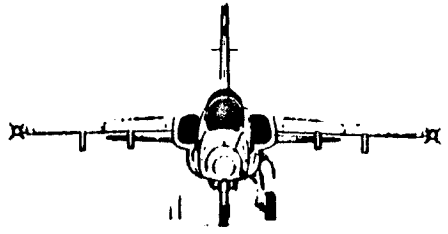

TABLE I. STANDARD MISSIONS (Continued)

MISSION B-1

HI-HI-HI-HI - BOMBER

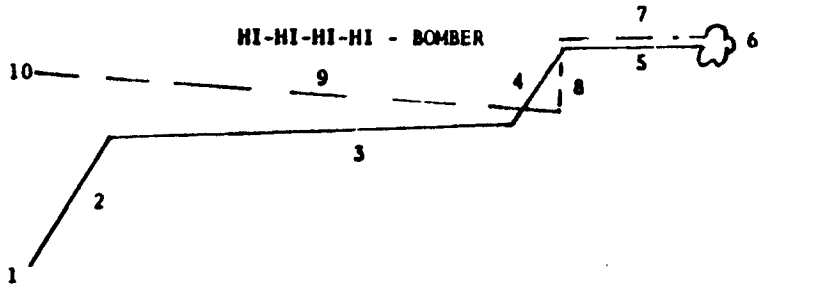

SEGMENT	ALLOWANCE
1. Take-off and accelerate to climb speed ( )	1. See 3.5.3.1
2. Climb on course to cruise altitude ( )	2. Power and speed to maximize range
3. Cruise ( )	3. Speed and altitude for max range
4. Climb to combat altitude	4. Power and speed to maximize range
5. Run-in specified distance at speed for maximum continuous power at combat ceiling ( )	5. Maximum continuous power. If this results in supersonic speeds, include time fuel and distance to accelerate as part of the penetration.
6. Drop stores and conduct evasive and turn action ( )	6. Weight reduction includes store weight plus combat fuel allowance. See 3.5.3.4.
7. Run-out specified distance at speed for maximum continuous power at combat ceiling ( )	7. Same as 5
8. Descend to cruise altitude ( )	8. No time, fuel or distance is credited for subsonic vehicles. If segment 7 is supersonic, credit may be taken for time, fuel and distance to decelerate and descent to cruise altitude
9. Cruise back to base ( )	9. Same as 3
10. Arrive over base with reserve fuel ( )	10. See 3.5.3.6

TABLE I. STANDARD MISSIONS (Continued)

MISSION F-1

AIR SUPERIORITY - FIGHTER

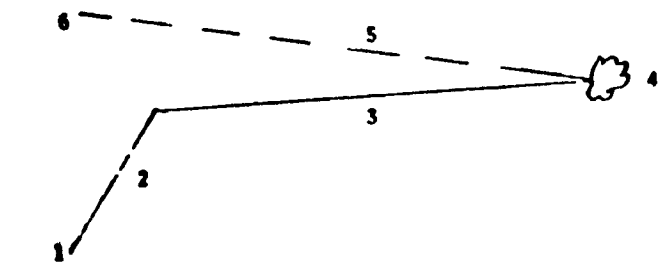

SEGMENT	ALLOWANCE
1. Take-off and accelerate to climb speed ( )	1. See 3.5.3.1
2. Climb on course to cruise altitude ( )	2. Speed and power for maximum range
3. Cruise to combat area ( )	3. Speed and altitude for maximum range
4. Engage enemy aircraft and expend ordnance at start of combat ( )	4. See 3.5.3.4
5. Cruise to base ( )	5. Same as 3. The aircraft is assumed to be at cruise altitude, speed and heading at the completion of combat
6. Arrive over base with reserve fuel ( )	6. See 3.5.3.6

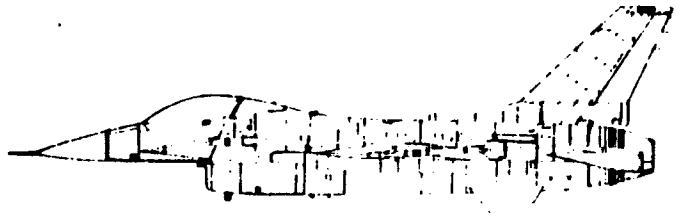

TABLE I. STANDARD MISSIONS (Continued)

MISSION C-2

CARGO-ASSAULT

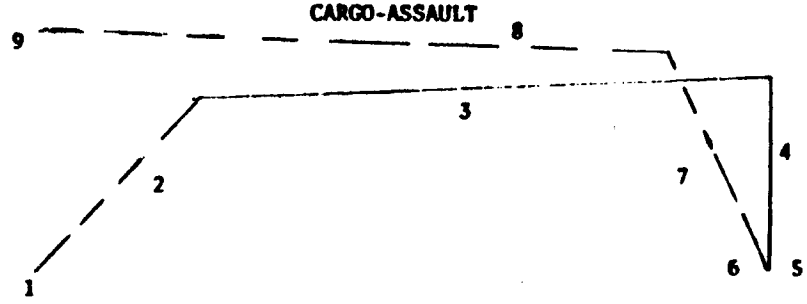

SEGMENT	ALLOWANCE
1. Take-off and accelerate to climb speed ( )	1. See 3.5.3.1
2. Climb on course to cruise altitude ( )	2. Speed and power for maximum range
3. Cruise to combat area ( )	3. Speed and altitude for maximum range
4. Descend to Sea Level	4. No time, fuel or distance credited except where specified
5. Land off-load payload and reload one half payload of casualties etc ( )	5. No time, fuel or distance credited. Payload is reduced by one-half.
6. Take-off and accelerate to climb speed ( )	6. See 3.5.3.1
7. Climb on course to cruise altitude ( )	7. Same as 2
8. Cruise to base ( )	8. Same as 3
9. Arrive over base with fuel reserve ( )	9. See 3.5.3.6

TABLE I. STANDARD MISSIONS (Continued)

MISSION T-2

TANKER - RENDEZVOUS

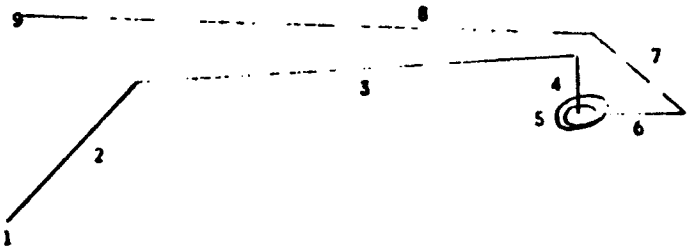

SEGMENT	ALLOWANCE
1. Take-off and accelerate to climb speed ( )	1. See 3.5.3.1
2. Climb on course to cruise altitude ( )	2. Speed and power for maximum range
3. Cruise to refuel point ( )	3. Speed and altitude for maximum range
4. Descend to specified altitude	4. No fuel, time or distance credited except where specified
5. Loiter 1 hour for rendezvous ( )	5. Fuel for 1 hour maximum endurance. No distance credited
6. Transfer fuel at speed for maximum continuous power ( )	6. Credit time, fuel and distance while transferring fuel at maximum rate. Segment performed at maximum continuous power
7. Climb on course to return cruise altitude ( )	7. Same as 2
8. Cruise to base	8. Same as 3
9. Arrive over base with reserve fuel ( )	9. See 3.5.3.6

Note: This mission is to present tanker capability without cons deration of a specific receiver.

TABLE I. STANDARD MISSIONS (Continued)

MISSION G-6

FERRY MISSION

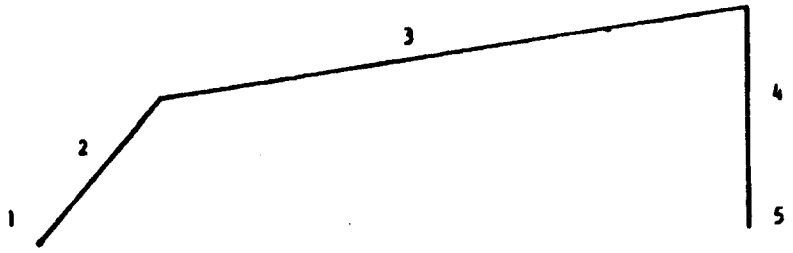

SEGMENT	ALLOWANCE
1. Take-off and accelerate to climb speed ( )	1. See 3.5.3.1
2. Climb on course to cruise altitude ( )	2. Speed and power for maximum range
3. Cruise to remote base	3. Speed and altitude for maximum range. Normally external fuel tanks shall be retained if carried.
4. Descent to sea level	4. No time, fuel or distance credited unless otherwise specified
5. Arrive over remote base with reserve fuel ( )	5. See 3.5.3.6

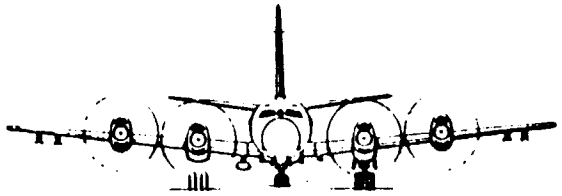

B1.2 AS-5263(USNAVY): Naval Air Systems Command Specification, Guidelines for the Preparation of Standard Aircraft Characteristics Charts and Performance Data, Piloted Aircraft (Fixed Wing), October 1986.

THIS SPECIFICATION HAS BEEN APPROVED BY THE
NAVAL AIR SYSTEMS COMMAND, DEPARTMENT OF THE NAVY

1. SCOPE.

1.1 SCOPE. This specification governs the definition of requirements for and methods of presenting characteristics and performance for Navy piloted fixed wing aircraft.

1.2 APPLICATION. For all piloted fixed wing aircraft proposed or contracted for subsequent to the effective date of this specification, characteristics and performance data shall be prepared and presented in accordance with the provisions of this specification and submitted to the Naval Air Systems Command for acceptance, unless specifically exempted by the Navy. Deviations from the provisions of this specification to portray more adequately the capability of certain aircraft are permissible, but shall in all cases be approved by the Naval Air Systems Command. Authorized deviations shall be fully explained through proper annotations on the data charts.

1.3 TYPES OF CHARTS. Characteristics and performance data shall be presented on the following types of charts as required by the Navy and utilizing formats as provided. Unauthorized reproduction of such charts is prohibited.

1.3.1 Standard Aircraft Characteristics Charts. The Standard Aircraft Characteristics (SAC) Charts are intended to provide Navy technical and staff personnel with a concise, accurate compilation of physical characteristics and performance capabilities of a weapon system. Standardization is required for convenience and to allow direct comparison with other weapon systems intended for a similar mission.

1.3.1.1 Arrangement. The Standard Aircraft Characteristics Chart is basically composed of ten pages with provisions for supplemental pages as required by the Naval Air Systems Command. If certain pages are not required for a specific weapon system, they shall be omitted and the remaining pages renumbered consecutively.

1.3.1.1.1 Basic. The normal arrangement of the Standard Aircraft Characteristics Chart shall be as follows (Refer to Sample SAC Chart in Appendix I):

a. Page 1. Cover sheet, which shall include a photograph or perspective drawing of the aircraft model in flight.

b. Page 2. A drawing showing a descriptive arrangement of the aircraft and a drawing showing the armament installations, the tankage installation, cargo space or interior arrangements as required by the Navy.

c. Page 3. Mission, description and principal characteristics of the aircraft.

d. Page 4. Performance data for the aircraft in tabulated form, with applicable notes.

e. Page 5. Auxiliary performance page, giving alternate loadings and the respective radii and associated performance, where applicable.

f. Page 6. Performance graphs. Speed, takeoff and landing distance, rates of climb, maneuverability, etc.

g. Page 7. Performance graphs. Trade-off curves as applicable.

h. Page 8. Carrier suitability graphs. Performance curves for catapulting, arresting, single engine climb, accelerations, approach speeds, and required Wind over Deck.

i. Page 9. External store loadings. Tabulated stores and stations on which they may be carried.

j. Page 10. Notes. Mission profiles, applicable allowances and explanatory notes.

1.3.1.1.2 Supplemental Pages. Aircraft characteristics and performance data not coming within the scope of the Standard Aircraft Characteristics Charts shall be presented on supplemental pages. Reasons for preparing supplemental pages may be as follows:

a. Possible special loadings or extreme overload conditions which may:

1. Be used in restricted tactical operations.

2. Involve non-standard procedures and special operating techniques.

3. Show the maximum potential use of certain aircraft in special missions.

b. Such loadings that may involve equipment which for security reasons are only suitable for limited distribution.

c. Theater operations involving non-standard atmospheric conditions.

d. To show inboard profiles, additional drawings, illustrations and graphs.

The supplemental page format should be the same as the Standard Aircraft Characteristics Chart or may consist of a special design suitable for binding along with the corresponding basic Standard Aircraft Characteristics Charts.

1.4 CATEGORIES. The foregoing charts shall be identified by categories to show the development status of the aircraft or data involved. All chart format shall be completed in full detail.

1.4.1 Proposal. Proposal data charts are intended to provide information during the evaluation of new designs, design studies and proposed modifications of existing designs and are primarily for limited distribution within the Navy.

1.4.2 Mock-Up. Mock-up charts are intended to provide information on new designs during the initial period from source selection to completion of mock-up. The initial mock-up chart need not include the effect of all design changes recommended by the Navy, but should contain under notes a complete list of major design changes.

1.4.3 Pre-Service. Pre-service charts are intended to provide information on new designs from the period of time from completion of mock-up to roll out of flight test article. Initial pre-service chart will normally be issued as soon after mock-up as the configuration and weight have stabilized to define the initial test article to be fabricated.

1.4.4 Service. Service data charts are intended to provide information on service models. Preparation of the initial issue of a chart on a service model shall normally be initiated not later than when the configuration and weight have stabilized following mock-up inspection. Thus, it may take the place of pre-service charts or may be delayed until after initial flight test if design changes are anticipated therefrom.

1.5 MARKINGS. Each of the foregoing chart types shall be marked as follows (Refer to Sample SAC Chart in Appendix I):

1.5.1 Designation. The military model designation or the contractor's model designation (in the case of charts in the proposal category) shall be shown on the lower outer corner.

1.5.2 Category. The chart category as defined in Paragraph 1.4 shall be shown on the upper outer corner.

1.5.3 Date. The date of publication will be inserted by the Navy on the lower inner corner.

1.5.4 Security. The security classification shall be specified by the Navy and shall be shown on center at top and bottom.

1.5.5 Chart Identification. The upper inner corner is to be used for chart identification. Identification number shall be obtained from the Navy prior to submission of the charts for approval.

2. APPLICABLE SPECIFICATIONS AND OTHER PUBLICATIONS.

The following publications (effective on the date of invitation for request for proposal) shall form a part of this specification to the extent specified herein:

2.1 SPECIFICATIONS AND PRIMARY PUBLICATIONS.

MILITARY

MIL-D-7822	DRAWINGS: FOR STANDARD AIRCRAFT CHARACTERISTICS AND PERFORMANCE CHARTS, PILOTED AIRCRAFT.
MIL-A-08860	AIRPLANE STRENGTH AND RIGIDITY; GENERAL SPECIFICATION FOR.
MIL-G-5572	FUEL; AVIATION GRADES 80/87, 100/130, 115/145 - 6.0 LBS/GAL.
MIL-T-5624	FUEL; AIRCRAFT TURBINE AND JET ENGINE, GRADES JP-4 - 6.5 LBS/GAL. AND JP-5 - 6.8 LBS/GAL.
MIL-T-83133	TURBINE FUEL, AVIATION, KEROSENE TYPE, GRADE JP-8 - 6.7 LBS/GAL.

MILITARY

MIL-F-8785C	FLYING QUALITIES OF PILOTED AIRPLANES.
MIL-M-85025(AS)	MANUALS, NATOPS FLIGHT; REQUIREMENTS FOR PREPARATION OF.
MIL-STD-210	CLIMATIC EXTREMES FOR MILITARY EQUIPMENT.
MIL-F-22203(AER)	PERFORMANCE DATA REPORT FOR STANDARD AIRCRAFT CHARACTERISTICS CHARTS FOR PILOTED AIRCRAFT.
MIL-STD-1374	WEIGHT AND BALANCE DATA REPORTING FORMS FOR AIRCRAFT (INCLUDING ROTORCRAFT).
MIL-W-25140	WEIGHT AND BALANCE CONTROL SYSTEM. (FOR AIRPLANES AND ROTORCRAFT).
OPNAVINST 3710.7	NATOPS GENERAL FLIGHT AND OPERATING INSTRUCTIONS.
NAVAIR 01-1B-40	NAVY TECHNICAL MANUAL OF WEIGHT AND BALANCE DATA.
NAVAIR 01-1B-50	NAVY TECHNICAL MANUAL, USN AIRCRAFT WEIGHT AND BALANCE CONTROL.
TECHNICAL ORDER 01-1B-40	AIR FORCE TECHNICAL MANUAL OF WEIGHT AND BALANCE DATA.

2.2 OTHER PUBLICATIONS. AS 2694. Engines, Aircraft, Turboshaft and Turboprop, General Specification for.

(Copies of specifications, standards and drawings required by contractors in connection with specific procurement functions should be obtained from the procuring agency or as directed by the contracting officer).

3. REQUIREMENTS.

3.1 GENERAL. Unless otherwise specified by the Navy, preparation by contractors of charts (and revision thereto) for each model shall include the preparation of photographically reproducible copy in the required types and categories, and, in addition, satisfactory reports containing supporting characteristics and performance data.

3.1.1 Revisions. Revisions to the charts shall be prepared and submitted by the contractor throughout the life of the contract unless specified otherwise by the Navy. Revisions are required whenever significant changes in vehicle configuration or data occur, as for example:

1. A change in vehicle dimensions.
2. An accumulation of weight changes resulting in a significant performance change (Paragraph 3.1.1.1).
3. A change in power plant designation, augmentation, or power plant rating.
4. The addition of external stores.
5. The availability of test data or new test data showing significant performance change (Paragraph 3.1.1.1).
6. When specifically directed by the Navy.

3.1.1.1 Criteria. The following criteria will be used in forming a judgement as to whether a significant change in performance exists:

1. A change of 5 percent or more in drag.
2. A change of 5 percent or more in installed thrust (power).
3. A change of 5 percent or more in specific fuel consumption.
4. A change in weight which in itself results in a 5 percent or greater change in mission radius or range.
5. Any combination of two or more of the above resulting in a change of 5 percent or more in mission radius or range.

3.1.1.2 Number. Each chart shall cover only one aircraft model. For the information of the contractor, the following guide is given regarding the probable number of charts and revisions thereto which are required throughout the life of the aircraft model. The exact number of revisions required will depend on the number of aircraft changes experienced.

CATEGORY OF CHART	REASON	BASIS FOR DATA
PROPOSAL	NEW DESIGN	ESTIMATED
MOCK-UP	CONTRACT FOR NEW AIRCRAFT	ESTIMATED
PRE-SERVICE	BETWEEN MOCK-UP AND FIRST FLIGHT	ESTIMATED
SERVICE	FLIGHT TEST	FLIGHT TEST
SERVICE (REVISION)	OPERATIONAL OR FLEET INTRODUCTION	FLIGHT TEST

3.2 STANDARD AIRCRAFT CHARACTERISTICS CHARTS.

3.2.1 Required Characteristic Data (Including Descriptive Detail). A sample Standard Aircraft Characteristics Chart is provided for reference in Appendix I.

3.2.1.1 Page 1. Cover Sheet. The cover sheet shall include a picture of the aircraft. In order of preference: A photograph of the aircraft in flight, a photograph of the aircraft on the ground, a photograph of a model, or an artist's conceptual drawing of the aircraft in flight. The photograph or drawing shall be of good contrast or permit satisfactory reproduction and should portray the distinguishing features of the aircraft. The photograph shall be glossy black and white and have dimensions not less than 5" x 8" and not greater than 7" x 11 1/2", not including the border. The aircraft model designation and the approved popular name shall be typeset using 24 point Futura Demibold or equivalent, centered below the title leaving a 1/2 inch space. One-half inch below the aircraft designation, center the contractor's name using 18 point Futura Demibold or equivalent.

3.2.1.2 Page 2. Drawings. The three-view drawings shall be drawn in ink on suitable drawing material and may be made oversize at whatever scale the manufacturer deems suitable. This over-size ink drawing shall then be photographically reduced and inserted on the appropriate block within the format sheet. Full advantage shall be taken of the space allotted so as to provide the largest three-view arrangement attainable within the 7 1/8" x 10 7/8" block in keeping with the positioning guidelines of paragraph 3.2.1.2.a and 3.2.1.2.b. The line weights used on the three-view drawings must be suitable to provide reproductionof the format page when reduced to 9 1/2" wide. All dimensions and text entered on this format page shall be typeset using 10 point Futura Medium or equivalent.

a. Descriptive arrangement drawing. In top of block give top view drawing; in middle of block give front view drawing; in bottom of block give side view drawings. Folded wings and extended tail hook shall be shown with dotted lines. Dimension in feet and fractions: wing span extended and folded, horizontal tail span, length, height, wheel base, wheel tread. A scale should be included. Describe wing airfoil shape at wing root and wing tip. Give wing planform area, mean aerodynamic chord (M.A.C.) and aspect ratio.

b. Armament and tankage drawing. In top of block give top view drawing; in middle of block give front view drawing; in bottom of block give side view drawing. Drawings shall be shown with external fuel tanks mounted. Internal fuel tank locations shall be shown by means of cross hatching. Tanks with survivability enhancements, i.e. foam, should be designated. Tank capacities shall be given. A scale should be included.

3.2.1.3 Page 3. Mission, Description and Principal Characteristics. The mission and description page shall include the information given below.

a. Mission and Description. The first paragraph in this block shall describe the primary and secondary missions of the aircraft. The second paragraph shall describe general design features, such as configuration, type of structure (use of composites, etc.), powered wing fold mechanism, etc. The third paragraph shall describe features of the propulsion and fuel systems, such as turbofan engine bypass ratio, number and capacity of external fuel tanks, self sealing fuel tanks, retractable refueling probe, etc. The fourth paragraph shall describe armament features, such as number of external store stations, gun caliber, forward looking IR, chaff dispensers, etc. The fifth paragraph shall describe control system features, such as type of high lift system, digital fly-by-wire, mechanical backup to primary control surfaces, rudder aileron interconnect, etc. The sixth paragraph shall describe avionic suite features, such as multi-mode radar, central digital computer, inertial navigation, etc. The seventh paragraph shall describe crew system features, such as ejection seat, anti-G system, etc.; if cabin is pressurized, the airplane altitude at which a 10,000 foot cabin altitude is reached shall be stated. Following the above descriptions, a sub-heading DEVELOPMENT shall give important dates: contract date, first flight, initial carrier sea trials, initial service date, etc.

b. Power Plant. Data to be listed shall include: number and model of engines, manufacturer, engine specification number, type, augmentation, length with afterburner, inlet diameter, dry weight, etc. If propellers are used, give the following data: manufacturer, propeller specification number, diameter, number of blades, gear ratio.

c. Ratings. Engine ratings shall include thrust or power, rpm, altitude(s) and time limits or deviations, as applicable. Engine ratings and auxiliary thrust device (ATD) ratings shall conform to those established in the officially approved engine specifications. Ratings with an augmentation shall be identified by note. If performance items are based on thrusts (powers) which differ appreciably from the listed specification ratings due to flight or engine laboratory test results or restrictions, such thrusts (powers) with explanations will be listed under notes. Reference to source of such thrust (power) shall be clearly stated in the performance data report.

d. Weight and Load Factors. The gross weights and the corresponding allowable load factors shall not exceed the limits established by the latest applicable technical orders, design requirements, or other specific recommendation of the Naval Air Systems Command. Maximum weights for which a mission is shown on the Standard Aircraft Characteristics Charts to illustrate maximum combat capabilities, but which may involve non-standard operating procedure and/or special operating techniques associated with such weight may be given, provided such weights are clearly identified with a note defining the limitations on usage. The following weights with corresponding load factors for both land based and carrier based aircraft as applicable, shall be given:

LOADING	POUNDS	LOAD FACTOR	REFERENCE
EMPTY			3.5.1.1
BASIC			3.5.1.2
DESIGN			3.5.1.4
COMBAT (BASIC MISSION)			3.5.1.6
MAXIMUM TAKEOFF			3.5.1.7.1
OVERLOAD MAXIMUM TAKEOFF			3.5.1.7.2
MAXIMUM IN-FLIGHT			3.5.1.8
MAXIMUM LANDING			3.5.1.9.2

NOTE:

Basis of Weight Data. The weights given shall correspond to the definitions of Paragraph 3.5.1. Weight empty shall be identified by the symbols "E": (estimated), "C": (calculated), or "A": (actual). As applicable, notation shall be made immediately below the takeoff weight of the immediate factor(s) limiting takeoff weight.

e. Fuel and Oil. The number of fuel and oil tanks, their usable capacities and locations, extent of self sealing provisions, together with grade and specification of fuel and oil used, shall be listed. Fuel tanks shall be grouped by fuel system.

f. Electronics. Sub-headings for airborne weapons control, electronic warfare, navigation and flight aids, communication and identification, control and display, and flight control shall be given. Under each sub-heading, list item and military model number in tabular form.

g. Ordnance. Data concerning the standard size and number of each type of droppable ordnance items such as bombs, torpedoes, mines, rockets, missiles and the maximum bomb load which may be accommodated by the aircraft. Ordnance carried externally shall be identified. The number and caliber of guns, the number of turrets, rounds of ammunition per gun, and the gun stations shall be listed.

h. Cargo. Maximum cargo load, clear space dimensions, limit floor loads, door size and location, usable cubage, etc. are to be given as applicable. Additional cargo information may be entered on a supplemental "NOTES" page.

i. Dimensions. Overall dimensions, in agreement with the general arrangement drawings of the basic aircraft in the three point position, such as length, height, width, maximum tread, and propeller ground clearance shall be given. Dimensions should be given in the wings folded and flight condition. Also include wing area and Aspect Ratio. Dimensions shall be given in feet and tenths of a foot.

3.2.1.4 Page 4. Performance Summary. Tabulated performance for the clean mission, basic mission, ferry mission, other typical missions (Paragraphs 3.5.10 to 3.5.10.4) shall include applicable loading and performance items. (See Page 4 of sample chart in Appendix I). Columns 1 and 2 of Page 4 are restricted to the clean and basic missions, as defined in Paragraph 3.5.10.1 and 3.5.10.2, respectively. Other columns, except the last column are restricted for the contractor's use in presenting performance data depicting the mission for which the vehicle was designed; requirement for compliance with ground rules outlined in this specification is waived for presentation of data on these typical missions (See Paragraph 3.5.10.5). Criteria (ground rules) for the typical missions shall be presented on Page 9. The last column used is restricted for use in depicting data for the Ferry Mission (See Paragraph 3.5.10.4).

a. The format of the performance summary page is shown on page I-4 in Appendix I. Show tabulated performance data for no more than six missions on each page. Data for all missions for which Navy requests are submitted shall be placed on the performance summary. A second performance summary page shall be used if the Navy requests data for more than 6 missions.

b. For each mission, divide the takeoff loading condition block into upper and lower sections; in the upper section give the name of the mission, in the lower section on the left side give the loading number in a circle, and to the right of that, show the missile, bomb and external tank loadings with the number of each item in parentheses. In the combat loading condition block on the left side, show the loading number in a circle, and to the right of that, describe the armament and external tank configuration (tanks off, missiles, retained, etc.). The takeoff loading condition for mission 1 is loading number 1; the combat loading condition for mission 1 is loading number 2; the takeoff loading condition for mission 2 is loading number 3; the combat loading condition for mission 2 is loading number 4; etc.

c. The space at the bottom of the page shall be used for footnotes lettered (A), (B), (C) etc. The applicability of the notes shall be shown by placing the appropriate letter behind the wording of the item affected; for example, the letter (A) placed behind the words "Takeoff Run at S.L." could be used along with the footnote, "(A) Intermediate Thrust (Power), Standard Day," to denote the thrust (power) setting for takeoff data. The last footnote shall be, "( ) Performance Basis: wind tunnel or flight test (as appropriate) followed by contractor's report number for the substantiating performance data report."

3.2.1.5 Page 5. Mission Summary - Alternate Loadings. For the basic mission and several secondary missions, show external store loading, takeoff gross weight, combat radius and mission time in tabular form. Data for various combinations of missiles, bombs, rocket packages and external fuel tanks shall be shown. Data should be given to demonstrate the capabilities of fighter, attack, patrol and anti-submarine warfare aircraft across a broad spectrum of loadings. Data may be given for missions not covered in the Performance Summary (Paragraph 3.2.1.4).

3.2.1.6 Page 6. Performance Graphs. Performance data shall be shown graphically on the appropriate grids provided. Curves shall not extend beyond any applicable limit.

a. Speed. As a function of altitude, plot maximum speed at basic mission combat weight with maximum, intermediate, and normal thrust (power), as applicable. Show maximum speed for several alternate mission loadings at the same power settings to show the effects of drag of significant external stores and/or important weight changes.

b. Climb. As a function of altitude, plot rate of climb at basic mission combat weight with maximum, intermediate, or normal thrust (power), as applicable. Show rates of climb for alternate loadings in order to show the effects of drag changes with various external stores and/or important weight changes. The effects of weight reduction during climb shall not be considered.

c. Takeoff. Plot gross weight versus takeoff distance for sea level, zero wind, standard day and tropical day. Show lines for ground run distance, total distance over 50-foot obstacle and critical field length.

d. Fourth Block. Data shown here should depend on type of aircraft. For fighter aircraft, show maneuverability; i.e. Mach number versus load factor in a constant altitude turn for the basic mission at a typical combat altitude; show load factor at various rates of longitudinal acceleration. For attack aircraft, patrol aircraft, anti-submarine aircraft, early warning aircraft and mission-dedicated electronic aircraft, show search time; i.e., radius versus time on station; show lines for basic mission and for several typical missions. For trainer aircraft, plot range versus cruise altitude; show lines for basic mission and for several typical missions. For cargo aircraft, plot range versus cargo weight; show lines for normal and overload takeoff gross weights. For tanker aircraft, plot radius versus pounds of fuel transferred; show data for loiter times of 0.5, 1.0, 1.5 hours, etc.

3.2.1.7 Page 7. Trade-Off Graphs.

a. This page shall contain up to four graphs, showing performance trade-offs for fighter, attack, patrol and anti-submarine warfare aircraft (See page I-7 of Appendix I).

b. The trade-offs shown may be selected from the following or be special graphs designed by the contractor to more aptly display the capabilities of the aircraft: combat radius versus combat time, combat radius versus combat patrol time, combat radius versus dash radius, combat radius versus combat loiter time. On each graph, lines for several loadings from the Performance Summary (Paragraph 3.2.1.4) shall be given.

3.2.1.8 Page 8. Carrier Suitability Graphs.

a. For carrier based aircraft, performance graphs are required as follows: gross weight versus minimum wind over deck required for catapulting shown for catapult gear selected by the Navy, gross weight versus minimum wind over deck required for arrestment shown for arresting gear selected by the Navy, gross weight versus single engine rate of climb at V_{PA} approach speed, gross weight versus V_{PA} and versus V_{SPA} stall speed at approach power. Both standard and tropic day values shall be shown.

3.2.1.9 Page 9. External Store Loadings.

a. This page shall contain a simplified front view drawing of the aircraft with landing gear retracted showing external store stations. Under the drawing, a table shall be given with columns numbered corresponding to external store stations. The left hand column of the table shall contain a list of all possible external stores. Within the table, the number of each external store that can be carried at each external store station shall be given with the number 1, 2, etc.

3.2.1.10 Page 10. Notes.

a. For each mission, a sketch shall be given showing combat radius versus altitude with lines drawn showing climb, cruise to target, action over target, return cruise and descent. Altitude at significant points shall be called out in feet.

b. Above each sketch, the name of the mission shall be given with notes underneath. Notes for a typical mission are as follows:

1. For Taxi, warmup, takeoff and acceleration to best climb speed: Fuel allowance equal to 4.6 minutes at intermediate thrust plus 30 seconds afterburner thrust if afterburner is used for takeoff.

2. CLIMB: On course at best climb speed at intermediate thrust to best cruise altitude (not to exceed cruise ceiling).

3. CRUISE OUT: At speeds and altitudes for best range, using a cruise climb flight path (not to exceed cruise ceiling).

4. DESCENT: Descend to sea level (no fuel used, no distance gained).

5. COMBAT: Fuel allowance equal to 5 minutes at maximum speed with intermediate thrust at sea level. No distance is credited (drop bombs, retain mounting hardware and missiles after combat).

6. CLIMB: On course at best climb speed at intermediate thrust from sea level to best cruise altitude (not to exceed cruise ceiling).

7. CRUISE BACK: At speeds and altitudes for best range, using a cruise climb flight path (not to exceed cruise ceiling).

8. DESCENT: Descend to sea level (no fuel used, no distance gained).

9. RESERVE: Fuel allowance equal to 20 minutes loiter at sea level at speeds for maximum endurance with all engines operating plus 5% of initial total fuel (internal plus external).

a. Mission Time: Items 2 through 8.
b. Cycle Time: Items 2 through 9.

3.3 SUBSTANTIATING DATA. All data presented on the charts shall be substantiated by reports which shall be submitted with the charts. The reports may be in legible rough draft form utilizing the contractor's worksheet copy, but they shall be complete and shall contain a list of adequate references, authority and justification for all data used. Contractors are free to use calculation methods of their own selection, but such methods shall be fully explained and sample calculations shall be given. Calculations shall be presented in sufficient detail to permit ready review and check of conclusions and to enable additional calculations to be made by the Navy as required.

3.3.1 Basic Aerodynamic Data Report. Prior to preparation of the formal Substantiating Data Report, the approval of the Navy shall be obtained for the data which will form the basis for the Standard Aircraft Characteristics Charts. These basic data, including adequate calculations and material for verification shall include those data described in Appendix II of this report. Data not accepted by the Navy shall be replaced after conference with the contractor by similar data to be designated by the Navy.

3.3.1.1 Revisions. The Basic Aerodynamic Data Report shall be revised under the same criteria as the charts (Paragraph 3.1.1).

3.3.2 Substantiating Performance Data Report. The Basic Aerodynamic Data (Paragraph 3.3.1) shall, after verification and approval by the Navy, form the basis for the detailed preparation of the formal Substantiating Data Report. These data shall be expanded as necessary and used to prepare the detailed performance data required to substantiate the validity of the Standard Aircraft Characteristics Charts. The Substantiating Data Report also serves as the data base for the Naval Air Training and Operating Procedures Standardization (NATOPS) Flight Manual.

3.3.2.1 Revisions. The substantiating data report shall be revised under the same criteria as the charts (Paragraph 3.1.1).

3.3.2.2 Text. The arrangement of the substantiating data report shall be arranged as shown in Appendix III.

3.4 STANDARDS. Characteristics and performance data shall be based on practical engineering analysis which produce results consistent with flight test results of vehicles of like types using standard operating procedures.

3.4.1 Basis for Data. All characteristics and performance data shall be based on the latest reliable aerodynamic, power plant and weight information available. The information given shall include the effect on weight and/or performance of all authorized contract and service changes, together with important changes assured of authorization but pending at the date of chart issue.

3.4.1.1 Changes in Characteristics. Changes in aircraft characteristics which do not result in a significant performance change (Paragraph 3.1.1) need not be justification for a revision by the contractor. However, the Navy shall be notified by correspondence so that proper notation may be appended to the published chart.

3.4.1.2 Flight Tests. Latest approved flight test data shall be used, as soon as available, as a basis for performance. While official military flight test results are to be preferred, contractor flight test results shall be considered, provided:

1. The contractor submits his method of flight test, instrumentation used and analysis leading to reduction of test results to standard conditions for review and approval by the Navy.

2. Specific "raw" test data and data reduced to standard conditions are provided to the Navy for approval prior to use in chart preparation.

3.4.1.3 Guarantees. The data quoted need not necessarily reflect contractor's aircraft performance guarantees.

3.4.2 Limitations. Performance data shall fall within all established limitations on the vehicle and its components, except as specifically provided herein.

3.4.3 Aircraft Condition. Performance shall be presented in such a manner as to show clearly the applicable aerodynamic configuration, power plant and loading information. Aircraft configurations shall include the installation of complete service equipment applicable to that particular aircraft model for the mission concerned. No special sealing of doors or cracks, filling of seams, waxing, or polishing shall be allowed, unless this is standard practice and is so stated on the charts. Flight performance shall be presented with guns, rotatable enclosures, bomb bay doors, etc., in position of least drag, retractable enclosures and wheels in retracted or closed position and external bombs or other armament in position for each condition, as noted. Fuel loadings shall comprise only those for which service approval has been obtained.

3.4.4 Atmosphere. Performance shall be based on the latest approved standard atmospheric tables as specified by the Navy.

3.4.4.1 Standard Day. Unless otherwise specified, performance shall be based on the latest approved ICAO standard atmosphere (59°F @ S.L.) as tabulated and described in Appendix IV.

3.4.4.2 Non-Standard Day. Unless otherwise specified, non-standard day performance shall be based on MIL-STD-210 Tropical (89.8°F @ S.L.) and Hot (103°F @ S.L.) conditions tabulated and described in Appendix IV.

3.5 DEFINITIONS. The following definitions are used for the various data on the charts and shall be strictly adhered to.

3.5.1 Weights. Weights used in preparation of and presented on the charts shall conform with the following definitions and be consistent with MIL-STD-1374, MIL-W-25140 and Technical Manual 01-1B-40.

3.5.1.1 Weight Empty. The weight empty condition shall be as defined in the latest model detail specification (does not include crew, fuel, armament, cargo, bombs, disposable or special equipment). The empty weight to be used in preparation of the SAC Chart shall be, in order of preference, the actual empty weight, the latest available calculated or estimated empty weight.

3.5.1.2 Basic Weight. Configuration for operating purposes, as defined in Technical Manual of Weight and Balance Data, NAVAIR 01-1B-40 and AIR FORCE Technical Order 01-1B-40 (empty weight plus trapped fuel and all fixed armament and equipment for normal operation).

3.5.1.3 Operating Weight. Zero fuel and zero payload weight - a convenience weight to which operators need add only fuel and payload for gross weight. (Basic weight plus crew and any special equipment that may be required. Does not include usable fuel, ammo, bombs, or auxiliary fuel tanks if such tanks are to be dropped in flight).

3.5.1.4 Design Weight. Weight at which specified flight structural design requirements are met or are required to be met.

3.5.1.5 Ramp Weight. Maximum in-flight weight unrefueled plus fuel, water, etc., used during takeoff. Shall not exceed other limits, such as maximum taxi weight, ground handling, wheel jacking, etc.; as specified in MIL-A-008860.

3.5.1.6 Combat Weight. Weight over the target for the mission presented with fuel, ammunition (including missile ordnance) used for air-to-air combat but without bombs, missiles (used for attack of surface targets), torpedoes, mines, cargo or droppable tanks unless otherwise noted.

1. For aircraft without external tanks, fuel load shall be 60 percent of initial usable fuel.

2. For aircraft with external drop tanks, fuel load shall be 60 percent of initial usable fuel load, or full internal fuel, whichever is less.

3.5.1.7 Takeoff Weight. Takeoff weight is the total weight of the aircraft with the fuel and payload for the mission presented. The takeoff weight normally shall be determined prior to start of engines, except in specially approved cases when weight expended during taxi and takeoff are excluded (Paragraph 3.5.1.5). Takeoff weight shall not exceed maximum takeoff weight.

3.5.1.7.1 Maximum Takeoff Weight. Maximum takeoff weight is the greatest weight for takeoff established by Technical Orders, design requirements, or other specific recommendations of the Navy.

3.5.1.7.2 Overload. Unless otherwise specified by the Navy, the maximum (overload) takeoff weight shall not exceed the least determined by the following:

CONSTRUCCIONES AERONAUTICAS S.A. - D. PROYECTOS Y ESTUDIOS

a. The weight of the aircraft fully loaded with fuel, bombs and cargo to capacity for which space and/or tankage is normally provided. Bearing capacity for the floor and/or supporting structure shall not be exceeded. The expendable weight of ATD and water used for takeoff may be added to the quoted maximum takeoff weight provided the criteria of Paragraph 3.5.1.7.2.b is satisfied and a qualifying note appears on the chart.

b. The aircraft and its components (wing, landing gear, supporting structure for ordnance, cargo, etc.) shall sustain at least a 2.0g normal load factor for each phase of operation and shall meet the minimum criteria of the applicable specifications for taxi and ground handling (MIL-A-008860).

c. The maximum rate of climb at Sea Level altitude under standard atmospheric conditions shall not be less than 500 ft/min with all engines operating at normal (maximum continuous) rating.

d. For multi-engine aircraft without ejection seats, the rate of climb with one engine inoperative at Sea Level altitude under standard atmospheric conditions shall not be less than 100 ft/min at the 50 feet obstacle, out of ground effect, in takeoff configuration and at maximum takeoff engine rating minus easily jettisonable items (i.e., external fuel tanks and bombs). For multi-engine aircraft with ejection seats, the required rate of climb will depend on the mission and will be specified by the Naval Air Systems Command.

e. Throughout the flight, the center of gravity shall remain within the limits for satisfactory ground handling and flight.

f. Such other criteria as may be specified by the Navy for the specific aircraft model presented.

g. The following takeoff criteria will be based on Sea Level altitude and standard atmospheric conditions:

1. For all vehicles (single and multi-engine), critical field length shall not exceed 8,000 feet.
2. The maximum tow force for carrier operation and maximum acceptable wind-over-deck, as defined by the Naval Air Systems Command, shall not be exceeded.

3.5.1.7.3 Normal. The maximum (normal takeoff weight) shall not exceed the least weight determined by criteria of Paragraph 3.5.1.7.2 and the following additional criteria:

a. For multi-engine aircraft without ejection seats, the maximum thrust (power) rate of climb with one engine inoperative (propeller feathered or rotor windmilling) shall not be less than 100 ft/min at takeoff speed, in takeoff configuration at sea level under a 103°F atmospheric temperature minus easily jettisonable items (i.e., external fuel tanks and bombs). For multi-engine aircraft with ejection seats, the required rate of climb will depend on the mission and will be specified by the Naval Air Systems Command.

b. The aircraft shall be capable of cruising at airspeeds of maximum range at 5,000 feet altitude (pressure) on a 103°F day with power not exceeding 70 percent of normal (maximum continuous) rating for reciprocating engines and 85 percent for gas turbine engines.

c. The takeoff distance over 50 feet height at sea level on a 103°F day shall not exceed 10,000 feet.

3.5.1.8 Maximum In-Flight Weight. Weight at which the aircraft is authorized to be airborne. It is possible to be greater than maximum takeoff weight if in-flight refueling is utilized.

3.5.1.9 Landing Weight.

3.5.1.9.1 Normal. The weight as determined by the computation of the mission ground rules. It shall include the fuel reserve as specified in Paragraph 3.6.4.

3.5.1.9.2 Maximum. Maximum landing weight is the greatest weight established for landing by flight restrictions, detailed specifications, or specific recommendations of the Navy.

3.5.1.10 Payload. The load which justifies the mission. Payload includes cargo, personnel other than crew (passengers), bombs, chaff, missiles (offensive and decoy), reconnaissance cameras, photo flash flares, bombs, fuel carried for transfer by tankers, ammunition and air-to-air missiles carried by fighter aircraft and gunnery trainers. Special equipment required for the mission, such as winterization, rescue equipment (except that carried for drop by "H" type aircraft [search-rescue]), cargo handling, etc., shall not be included in payload. The maximum zero fuel weight limitations must be observed when selecting payload.

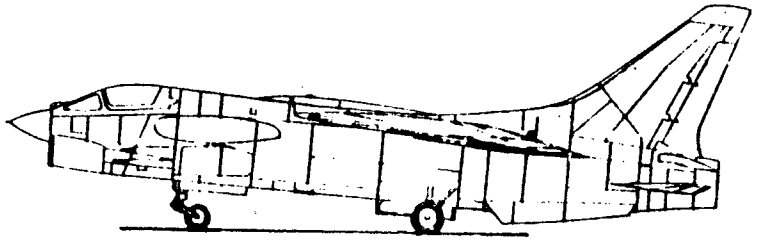

3.5.1.11 Weight Definition Guide. For the information of the contractor, the following guide (ref. MIL-W-25140) is given to the above weight definitions:

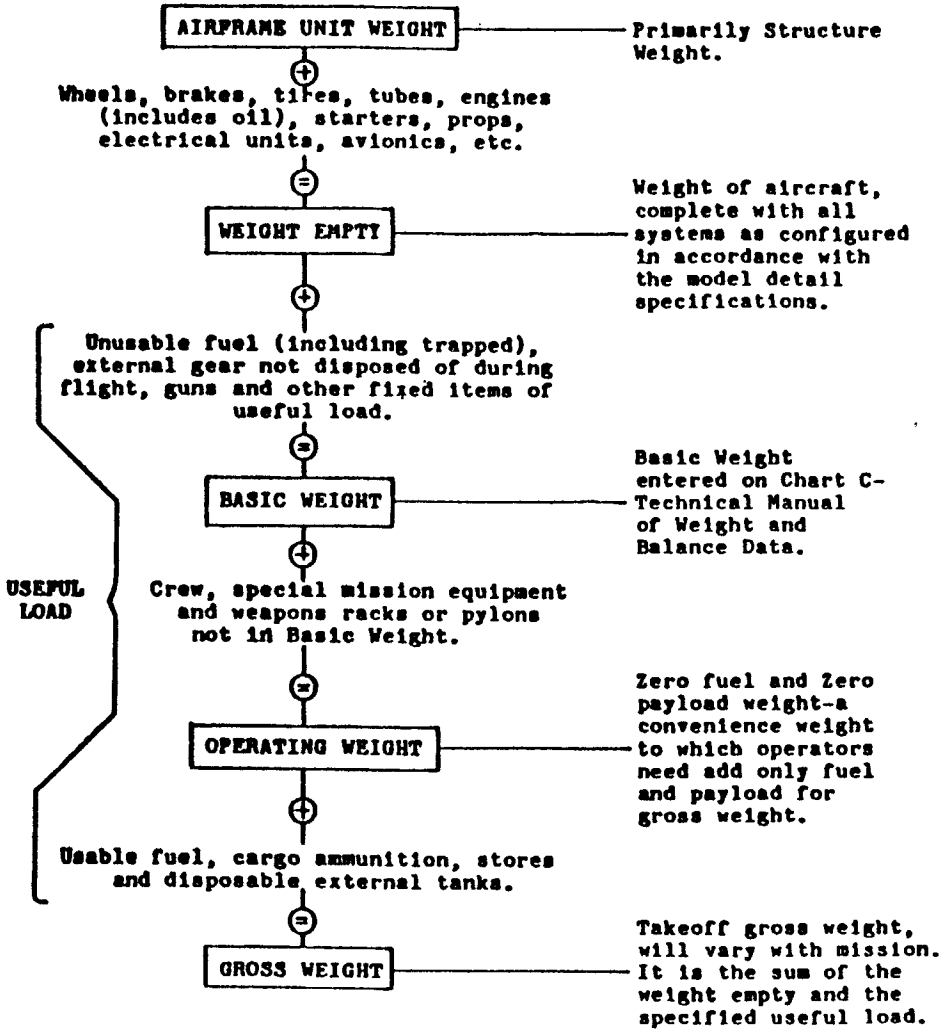

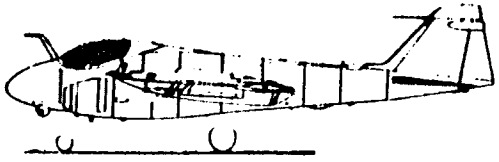

3.5.1.12 Fuel. Standard weight of fuel in pounds per U.S. gallon shall be as follows:

a. MIL-G-5572, Gasoline in all grades - 6.0 lbs/gal.

b. MIL-T-5624, JP-4, Jet Fuel - 6.5 lbs/gal.

c. MIL-T-5624, JP-5, Jet Fuel - 6.8 lbs/gal.

d. MIL-T-83133, JP-8, Jet Fuel - 6.7 lbs/gal.

3.5.2 Speed. All speeds shall be true airspeeds in knots and Mach number as applicable (Mach number for jet aircraft, true airspeed for propeller aircraft).

3.5.2.1 Maximum Speed. Highest speed obtainable in level flight. State the weight, altitude and engine-power rating. Such maximum speed shall be within all operating restrictions (i.e., thrust, structural, heating limitations), with the limiting restriction noted. For the Performance Summary, maximum speed shall be at specified weight, maximum thrust (power) and the altitude for best speed (or Navy designated conditions).

3.5.2.1.1 Level Flight Maximum Speed (V_H). The maximum speed attainable at the basic flight design gross weight in the basic configuration in level flight with maximum available thrust (power) including use of afterburners, rocket thrust augmentation considering engine limitations, or afterburners and rocket thrust augmentation considering engine limitations, whichever is applicable.

3.5.2.1.2 Limit Speed (V_L). For the basic and high drag configurations, the maximum attainable speed commensurate with the operational use of the airplane considering shallow and steep dive angles, thrust, operation and nonoperation of speed brakes, and inadvertent upsets from gusts.

3.5.2.2 Combat Speed. Highest speed obtainable in level flight at combat weight with maximum thrust (power) at combat altitude.

3.5.2.3 Stall Speed. The stall speed shall be computed on the basis of 1.0g flight with the maximum trimmed lift coefficient established by computation or wind tunnel testing. Upon availability of flight test results, stall speed shall be changed to the highest of the speeds for steady straight 1.0g flight at C_L maximum, the speed at which abrupt loss of control occurs about any of the pitch, roll or yaw axes, the speed at which intolerable buffet or structural vibration is encountered, or other minimum permissible speed as defined in MIL-F-8785.

3.5.2.3.1 Power-Off. The stall speed without thrust (power) or, if significantly affected, with flight idle thrust (power).

3.5.2.3.2 Power-On. The stall speed using approach power which is defined as the thrust (power) required for level flight at 1.15 times the power-off stall speed in the landing configuration (Reference MIL-P-8785C).

3.5.2.4 Takeoff Speed

3.5.2.4.1 Takeoff Speed Criteria. Takeoff speed shall be the highest of the speeds specified by the following:

a. 1.1 times the speed represented by 90 percent maximum lift coefficient, power-on, including ground effects in the takeoff configuration.

b. A speed determined by the lift coefficient, in ground effect, for the maximum angle of attack attainable with the main landing gear oleo in the static position with aircraft on ground.

c. Minimum speed at which the aircraft has a climb gradient potential of 1/2 percent (0.005), with takeoff thrust (power), in the takeoff configuration, out-of-ground effect. For multi-engine aircraft, this potential shall be obtainable with the most critical engine inoperative (with rotor windmilling or propeller feathered). Where;

$$\text{gradient} = \frac{[\text{Vertical Height in Climb (ft)}]}{[\text{Horizontal Distance in Climb (ft)}]} \qquad (1)$$

d. 1.05 times air minimum control speed as specified in Paragraph 3.5.2.8.2.

e. The speed which permits attaining obstacle climb-out speed, as defined in Paragraph 3.5.2.6, at or before reaching 50 feet height above the runway.

3.5.2.4.1.1 Typical Design Criteria. For design purposes, consideration may be made of alternate definitions of takeoff speed such as: a higher or lower percentage of stall speed, a higher climb gradient potential or other criteria which optimizes the design.

3.5.2.4.2 Refusal Speed. The maximum speed during takeoff which will allow the aircraft to stop within the available remaining runway length.

3.5.2.5 Catapult End Airspeed (V_C). The airspeed required at the end of the catapult stroke to support the airplane under the conditions of attitude, lift, and longitudinal acceleration specified for catapulting. An example would be where the c.g. position of the aircraft shall sink no more than 10 feet from its position at the end of the power stroke, with a deck run not to exceed 32 feet (distance from the end of the power stroke to round-down), without exceeding the angle of attack for 0.9 $C_{L_{max}}$, power off, and with cockpit control position fixed for a specified loading, weight and thrust (power) setting. The aircraft is also required to have a longitudinal acceleration of $a/g > .065$ at zero flight path angle at the catapult end airspeed.

3.5.2.6 Obstacle Climb-Out Speed. The climb speed at the 50-foot obstacle shall not be less than the highest of the speeds specified below.

a. 1.2 times power-off stall speed with flaps in takeoff position, landing gear retracted.

b. 1.1 times air minimum control speed.

c. Speed at which the aircraft has a climb gradient of 2.5 percent (0.025) with gear up, flaps in takeoff position, with maximum thrust (power), out-of-ground effect. For multi-engine aircraft, this potential shall be obtainable with the most critical engine inoperative (rotor windmilling or propeller feathered).

d. If gear retraction results in a transient drag increase over that for gear down, the speed at which the aircraft has a 1/2 percent (0.005) climb gradient potential with flaps in takeoff setting, gear in transit, with maximum thrust (power) out-of-ground effect. For multi-engine aircraft, the most critical engine shall be inoperative (with propeller feathered or rotor windmilling).

3.5.2.7 Climb Speed. The climb speed shall be the airspeed at which the optimum rate-of-climb is attained for the given configuration, weight, altitude and power. Consideration shall be made for kinetic energy corrections in optimizing the climb speed schedule. When authorized in the applicable Flight Manual, a simplified, non-optimum speed schedule may be used.

3.5.2.8 Critical Engine Failure Speed. The critical engine failure speed shall be the speed occurring during the takeoff run at which an engine can fail and the same distance is required to either continue the takeoff to lift off or to stop the aircraft.

3.5.2.9 Minimum Engine-Out Control Speed.

3.5.2.9.1 Ground. The minimum control speed, ground, shall be the minimum speed during the takeoff run where the engine most critical to directional stability can fail and directional control can be maintained.

3.5.2.9.2 Air. The minimum control speed, air, shall be the minimum airborne speed with maximum thrust (power) where the engine most critical to stability can fail and control can be maintained under the conditions specified in MIL-P-8785.

3.5.2.10 Cruise Speed.

3.5.2.10.1 Maximum Range Cruise Speed. The speed for maximum range operation shall be the speed at which maximum nautical miles per pound of fuel are attainable at the momentary weight and altitude conditions.

3.5.2.10.2 Long Range Cruise Speed. The higher of the two airspeeds which give nautical miles per pound of fuel equal to 99 percent of the maximum nautical miles per pound of fuel for momentary weight and altitude unless otherwise limited by handling characteristics. For propeller driven aircraft, long range cruise speed is used in lieu of maximum range cruise speed.

3.5.2.10.3 Maximum Cruise Speed. The highest speed that can be maintained with stated thrust (power), altitude, weight and configuration.

3.5.2.10.4 Average Cruise Speed. Total distance covered in cruise divided by time for cruise (distance and time for climb, acceleration to combat speed, combat time and loiter time are not included).

3.5.2.11 Loiter Speed

3.5.2.11.1 Maximum Endurance (Loiter) Speed. The airspeed for maximum endurance shall correspond to the speed for minimum fuel flow attainable at momentary weight and altitude, except as limited by acceptable handling characteristics of the aircraft.

3.5.2.11.2 Combat Loiter Speed. The airspeed for combat loiter shall correspond to the speed for minimum fuel flow attained at momentary weight and altitude, except that the airspeed must be adequate to allow an instantaneous load factor of a specified value.

3.5.2.11.3 Corner Speed. The lowest airspeed at which the lift and structural lines intersect. This is the speed at which the maximum turn rate and minimum turn radius exists for the specified altitude.

3.5.2.12 Landing Speed. The landing speed shall be determined by the maximum angle of attack attainable with the main landing gear oleo strut positioned for the static condition. The landing speed shall not be less than 110 percent of power-off stall speed for the landing configuration. The speed over a 50-foot height shall be at least 120 percent of power-off stall speed in the landing configuration.

3.5.2.13 Landing Touchdown Speed. For design purposes landing touchdown speed is that speed equal to 1.05 times approach speed. For operational aircraft, landing touchdown speed will be determined using fleet survey data.

3.5.2.13.1 Approach Speed. With the aircraft in the landing configuration and on a 4° glide slope on a 89.8°F day, the minimum usable approach speed $V_{PA_{MIN}}$, shall be the highest of the airspeeds defined by the following:

a. The lowest speed at which it is possible to achieve a level flight longitudinal acceleration of 5 ft/sec^2 within 2.5 seconds after initiation of throttle movement and speed brake retraction.

b. $V_{S_{PA}}$ x 1.1 where $V_{S_{PA}}$ is the power-on stall speed using the thrust (power) required for level flight at 1.15 V_{S_L}, the power-off stall speed.

c. The lowest level flight speed at which the pilot, at the design eye position, can see the stern of the carrier at the waterline when intercepting a 4° glide slope at an altitude of 600 feet. The origin of the glide slope is 500 feet forward of the stern and 63 feet above the waterline.

d. The lowest speed at which all stability and control requirements are satisfied (MIL-F-8785).

e. The lowest speed at which the aircraft is capable of making a glide path correction from stabilized flight at $V_{PA_{MIN}}$ to a new glide path 50 feet above the original glide path within five (5) seconds after initiation of the maneuver. The maneuver shall be performed without change in thrust settings, and the aircraft angle of attack during the maneuver shall not exceed that necessary to achieve 50 percent of the maximum positive delta load factor available, based on static lift coefficient, at the initiation of the maneuver. Control rate input for simulation of $V_{PA_{MIN}}$ shall not exceed control system limits. The maneuver shall be considered complete when a glide path correction of 50 feet has been reached. After completion of this maneuver, the aircraft shall be capable of maintaining a new glide path at least 50 feet above and parallel to the initial glide path, with the pilot permitted to change thrust setting as required.

f. To insure rapid aircraft response to step throttle commands corresponding to + 3.86 ft/sec^2 longitudinal acceleration, such throttle inputs shall result in achieving 90 percent of the commanded acceleration within 1.2 seconds. This requirement shall apply in the approach configuration throughout the range of all throttle settings required for operations over the usable approach configuration weight/drag levels while trimmed on a 4° glide slope.

Note: Control rate input for simulation of $V_{PA_{MIN}}$ shall not exceed control system limits. Calculation of $V_{PA_{MIN}}$ shall be based on static lift coefficient.

3.5.3 Ceiling

3.5.3.1 Service Ceiling. Service ceiling is that altitude at which the rate of climb at subsonic speed is 100 ft/min at stated loading, weight and engine thrust (power).

3.5.3.2 Combat Ceiling.

3.5.3.2.1 Subsonic Vehicles. Combat ceiling for subsonic vehicles is that altitude at which the rate of climb is 500 ft/min at the stated loading, weight and thrust (power).

3.5.3.2.2 Supersonic Vehicles. Combat ceiling for supersonic vehicles is the highest altitude at which the vehicle can fly supersonically and have a 500 ft/min rate of climb at the stated loading, weight and thrust (power).

3.5.3.3 Cruise Ceiling

3.5.3.3.1 Subsonic Vehicles. Cruise ceiling for subsonic cruise vehicles is that altitude at which the rate of climb is 300 ft/min at normal (maximum continuous) engine rating at stated weight and loading.

3.5.3.3.2 Supersonic Vehicles. Cruise ceiling for supersonic cruise vehicles is that altitude at which the rate of climb is 300 ft/min at normal (maximum continuous) engine rating at stated weight and loading.

3.5.4 Altitude.

3.5.4.1 Cruise Altitude. The cruise altitude is the altitude at which the cruise portion of the missions is computed. Depending on the mission ground rules, the cruise altitude may be

assigned. Otherwise, it is governed by the following limitations: for pressurized aircraft, cruise ceiling shall not exceed the altitude where cabin altitude is 10,000 feet. For unpressurized aircraft with oxygen masks, cruise ceiling shall not exceed 20,000 feet (Reference OPNAVINST 3710.7K Paragraph 714). In no case shall cruise altitude exceed cruise ceiling.

3.5.4.2 Optimum Cruise Altitude. The altitude at which the aircraft attains the maximum nautical miles per pound of fuel for the momentary weight and configuration. If this altitude exceeds cruise ceiling, the latter shall be used for cruise.

3.5.4.3 Combat Altitude. Combat altitude is the altitude at the target for the specific mission shown.

3.5.5 Takeoff. Criteria for conventional takeoff aircraft shall comply with the following: (For STOL aircraft the criteria shall be determined by design criteria.) (Vertical components of thrust may be used in takeoff computation.)

3.5.5.1 Ground Run Distance (i.e., Takeoff Distance). Takeoff ground run distance shall be that normally obtainable in service operation at Sea Level with standard atmospheric conditions, zero wind, no runway slope on hard (concrete or asphalt) surfaced runways. For estimated data, the takeoff speed criteria of Paragraph 3.5.2.4 shall be used.

3.5.5.1.1 Typical Design Criteria. For design purposes, consideration may be made of alternate definitions of takeoff ground run such as: non-standard atmospheric conditions, higher pressure altitudes, alternate runway surfaces (hard, sod, etc.), head or tail-wind or other criteria in keeping with the operational concept of the design.

3.5.5.2 Distance To 50 Feet. The distance to clear a 50-foot obstacle shall be the sum of takeoff ground run distance of 3.5.5.1 plus the airborne distance required to accelerate and climb to arrive at the 50-foot height at the speed specified in 3.5.2.6.

3.5.5.3 Takeoff Time. The takeoff time shall be that normally obtainable in service operation at Sea Level under standard day atmospheric conditions with no wind. The time is measured from start of takeoff (brake release) to start of enroute climb (attainment of climb speed).

3.5.5.4 Critical Field Length. Critical field length is defined as the total length of runway required to accelerate on all engines to the critical engine failure speed, experience an engine failure, and either continue to takeoff or stop.

3.5.5.4.1 Data Basis. The data basis for the computation of the stopping distance for critical field length shall be as follows:

a. At engine failure speed, the aircraft continues to accelerate for 3 seconds with remaining engine(s) operating at maximum thrust (power) and with zero thrust on the inoperative engine.

b. At the end of the 3-second acceleration time, thrust (power) on all engines is instantaneously reduced to idle, brakes applied and deceleration devices deployed.

c. Sufficient time after b, above, shall be allowed for deployment of the deceleration device(s) or for reverse thrust to reach maximum before including its effect on deceleration.

3.5.5.5 Coefficient of Friction. The coefficient, μ, as used in this document is defined as the ratio of the total retardation force attributable to the braking system to the momentary gross weight of the aircraft (momentary gross weight defined as weight on wheels which is weight minus lift). The following values will be used unless ground or flight test data are available.

3.5.5.5.1 Rolling. The rolling (unbraked) coefficient of friction for a dry, hard runway shall be equal to 0.025.

3.5.5.5.2 Braking. The braking coefficient of friction for a dry, hard runway shall be equal to 0.3. Application of anti-skid criteria will be specified by the Navy.

3.5.5.5.3 Test Data. Test μ values may be either the results of tests conducted on the specific aircraft or similar types, i.e. commerical aircraft.

3.5.5.5.4 Typical Design Criteria. For design purposes, the following coefficient of friction values should be used for the conditions specified on a hard surfaced runway:

RUNWAY CONDITION	ROLLING UNBRAKED	BRAKES	ANTI-SKID BRAKES
Dry	.025	.30	.38
Wet (Rain)	.05	.14	.20
Snow	.09	.10	.15
Ice	.05	.07	.09

3.5.6 Climb. Climb after takeoff may be divided into two segments: initial climbout and enroute climb.

3.5.6.1 Initial Climb-Out. Climb-out shall be at a speed which shall not be less than that limited by the criteria of 3.5.2.6. Gear retraction shall be initiated as soon as an adequate positive climb gradient (3.5.2.6.c and d), using applicable power, has been established and maintained while accelerating to climb-out speed. Flaps shall be in the takeoff position. Enroute climb speed shall be reached at a height no greater than 1,000 feet above ground.

3.5.6.1.1 All Engines Operating. Initial climb-out with all engines operating shall be based on all engines operating from brake release to takeoff. Acceleration to climb-out speed and climb-out shall be based on the thrust (power) available with all available engines.

3.5.6.1.2 One Engine Inoperative. Initial climb-out with one engine inoperative shall be based on all engines operating from brake release to critical engine failure speed and with the

critical engine inoperative from critical engine failure speed to takeoff. Acceleration to climb-out speed and climb-out shall be based upon the thrust (power) available with the remaining engines at takeoff thrust (power) and the drag of the inoperative engine. If means of reducing drag of the inoperative engine are a design feature, such drag reduction shall be utilized with a time allowance for activation.

3.5.6.2 Enroute Climb. Except for point intercept missions, all climbs shall be enroute with thrust (power) and speed schedules optimized to maximize mission range. Point intercept missions shall be optimized to obtain minimum time to combat altitude.

3.5.6.2.1 Enroute Climb Data. Enroute climb data shall be based on the appropriate configuration, thrust (power) and weight. The aircraft shall have the landing gear and flaps retracted and have attained the airspeed for best climb for the applicable condition.

3.5.6.2.2 Enroute Climb Power. For jet (fighter, attack, trainers, etc.) aircraft enroute climb to cruise altitude shall be at intermediate (military) thrust. For propeller (patrol, transport, etc.) aircraft use maximum continuous power.

3.5.6.2.3 Typical Design Criteria. For design purposes, consideration may be given to alternate climb schedules to more adequately portray the desired operational capability of the design. For example, the following schedules could apply: minimum time, minimum fuel, maximum range, specified thrust (power) or speed, accelerate during climb, etc.

3.5.6.3 Time to Climb. The time to climb to a specified altitude(s) shall be expressed in minutes from start of enroute climb. Weight reduction as a result of fuel consumption shall be applied to the calculations.

3.5.6.4 Combat Climb. Combat climb is the instantaneous maximum vertical speed capability in feet per minute at combat conditions, such as, weight, configuration, altitude, and thrust (power).

3.5.7 Landing Distance. The following criteria are for conventional aircraft. (For STOL aircraft, the criteria shall be as established by design requirements). Landing distance includes: (a) landing ground roll and (b) distance over a 50-foot height. Distances shall be for the landing configuration and weight and shall be based on the landing speeds defined in 3.5.2.12. Unless otherwise specified, ground roll deceleration shall be based on operation at Sea Level, standard day, zero wind, no runway slope, on hard (concrete or asphalt) surfaced runways, idle thrust (power) and a braking coefficient as defined in 3.5.5.5.2. Factors that should be considered are pilot reaction time, thrust decay, aerodynamic and mechanical braking, and maximum brake capacity.

3.5.7.1 Typical Design Criteria. For design purposes, consideration may be given to alternate definitions of landing distance such as: reverse thrust, atmospheric conditions alternate runway surfaces, runway slopes and winds of a non-standard nature, a rigid computer analysis of the air distance and other similar criteria selected to optimize the design of the airplane.

3.5.8 Thrust (Power). The term thrust (power) is used to mean thrust (jet engine) and/or brake horsepower (shaft engines) as applicable with due consideration for installation effects and limitations. Engine and ATD ratings as defined in Paragraph 3.2.1.3.c shall be those which appear in the approved engine model specification without regard to installation effects or limitations.

3.5.8.1 Maximum Thrust (Power). Maximum thrust (power) is the highest thrust (power) which the engine will consistently deliver at specific ground or flight conditions for the durations (incremental and total) specified in the model specification for demonstration during the qualification or preliminary flight rating tests.

3.5.8.2 Intermediate Thrust (Power). Intermediate thrust (power) is the highest thrust (power) which the engine will consistently deliver at specific ground or flight conditions for an incremental duration of at least 30 minutes, and a total duration as specified in the engine model specification for demonstration during qualification or preliminary flight rating tests. Intermediate thrust is equivalent to the old term military thrust.

3.5.8.3 Maximum Continuous Thrust (Power). Maximum continuous thrust (power) is the highest thrust (power) which the engine will consistently deliver at specific ground or flight conditions for an unlimited time period.

3.5.8.4 Cruise Thrust (Power). The thrust (power) required to fly the aircraft at cruise speed for the configuration, altitude and weight designated.

3.5.8.5 Idle Thrust (Power). Idle thrust (power) is the lowest thrust (power) which the engine will consistently deliver at specific ground or flight conditions for an unlimited duration or as defined in the engine model specification for demonstration during qualification or preliminary flight rating tests.

3.5.9 Fuel Consumption Service Tolerance. Unless authorized otherwise, for proposal aircraft, all fuel consumption data, regardless of source, shall be increased by 5 percent for all engine thrust (power) conditions as a service tolerance to allow for practical operation. In addition, corrections or allowances to engine fuel flow shall be made for all power plant installation losses such as accessory drives, ducts, fans, cabin pressure bleed, etc. Fuel consumption data will not be increased by 5 percent for service aircraft, if verified by Navy approved flight test.

3.5.10 Mission Types. For pre-service and service SAC Charts (1.4.3 and 1.4.4), the tabulated performance data of SAC Chart page 4 shall show performance data for missions designated by the Navy. Typical missions for various types of aircraft are

shown in Appendix V for use in Proposal SAC Charts (1.4.1). Unless otherwise specified, reserve fuel shall conform to the allowances shown in Appendix V.

3.5.10.1 Clean Mission. The first mission to be described in the Standard Aircraft Characteristics Charts will be the Clean Mission. This mission is intended to show the maximum capabilities of the aircraft (usually a high-high-high profile).

3.5.10.2 Basic Mission. The basic mission is the mission profile detailed in Appendix V which most nearly depicts the primary intended operational use of the aircraft. To maintain the capability of presenting a direct comparison between similar type aircraft, no deviation from the ground rules of Appendix V can be allowed.

3.5.10.3 Design Mission. The design mission is defined as the primary mission for which the aircraft was specifically procured. This mission will normally be defined in procurement documents such as the statement of work and will include the flight profile, allowances, fuel (clean or external tanks) and payload. Ground rules and allowances for the design mission are dictated by the specific operational requirements and will be used in describing the mission capabilities in the Standard Aircraft Characteristics Charts.

3.5.10.4 Ferry Mission. Ferry range is the greatest distance attainable on a practicable one-way mission with maximum authorized fuel and no pay load according to a specified sequence of operations, allowances and reserves. External fuel tanks may be carried and must be retained for the duration of the flight.

3.5.10.5 Typical Missions. Any missions, preferably from Appendix V, which would present the additional capabilities of the aircraft. If different from Appendix V, the mission definitions should be coordinated with the Navy.

3.5.10.6 In-Flight Refueled Mission. For aircraft capable of in-flight refueling, a refueled mission is the greatest distance (radius or range) attainable through receipt of replacement fuel during flight. A single refueling operation is required although multiple refueling operations may be used if considered to be feasible. Basic ground rules from Appendix V shall apply.

3.5.11 Combat Radius. Combat radius is the distance (including distance covered in climb) attainable on a practicable flight to the target and return a distance equal to that flown out, carrying a specific load (bombs, cargo, personnel, etc.), to or from the target according to a sequence of operations specified under "Mission Types" (Paragraph 3.5.10). Droppable fuel tanks are discussed in Paragraph 3.6.1.6.

3.5.12 Combat Range. Combat range is the distance (including distance covered in climb) attainable on a practicable one-way flight carrying payload (bombs, cargo, personnel) the entire distance. Droppable fuel tanks are not dropped when empty.

3.6 MISSION DETAILED REQUIREMENTS.

3.6.1 General Mission Requirements. Unless otherwise specified, the following general ground rules shall apply:

3.6.1.1 Standard Atmosphere. Data shall be presented for standard day atmosphere.

3.6.1.2 Wind. Data shall be for a no-wind condition.

3.6.1.3 Formation Flight. Data shall be for a single aircraft only.

3.6.1.4 Ordnance Expenditure. Ammunition and air-to-air missiles shall not be expended during the mission.

3.6.1.5 Off-Loading Fuel. Fuel may be off-loaded to avoid exceeding the maximum allowable takeoff weight.

3.6.1.6 External Fuel Tanks. For combat radius missions only, external fuel tanks shall be dropped when empty or prior to combat unless such tanks are designed to be carried during combat. Unless otherwise restricted (e.g. CG, etc.), dropping of external tanks shall be sequenced to provide maximum range. Cargo, tanker and training missions for Attack and Fighter aircraft shall not drop external tanks.

3.6.1.7 Pylons/Racks. Bomb racks, etc. shall not be jettisoned with the external stores. Pylons shall be retained during return to base.

3.6.1.8 Reduced Engine Operation. When applicable, a minimum number of engines may be used to increase range or loiter time if such operation would represent normal service usage. However, such action shall conform to Paragraph 3.6.1.9.

3.6.1.9 Authorized Operation. No operational technique shall be utilized that is not, or is not intended to be included as a recommended procedure in the applicable flight manual.

3.6.1.10 Trainer Aircraft. The trainer basic missions, as defined in Appendix V is applicable to basic and advanced trainer airplanes. Combat and tactical trainer airplanes fly the basic mission for the appropriate parent-type airplane.

3.6.1.11 Variable Geometry Wing (VGW) Aircraft. For VGW aircraft, the automatic sweep program will be clearly defined and used unless otherwise noted. If not automatic, the VGW aircraft will be assumed to have wings in the unswept position for takeoff and subsonic flight and swept for supersonic dash unless footnoted otherwise.

3.6.2 Mission Loading Requirements. In order to facilitate and expedite the make-up and delivery of the charts, it is suggested that the contractor contact the procuring service to discuss the various mission loadings prior to submission. In the absence of special instructions, the following shall apply:

3.6.2.1 Basic Mission Loading. The fuel and payload loading for the basic mission shall be the basic loading condition as defined by the first load condition given in the detail specification weight statement for the aircraft.

3.6.2.2 Typical Mission Loadings. Loadings shall be selected from those included in the detail specification or other approved loadings which depict a particular capability of the

aircraft. At least one mission shall conform to the maximum (overload) gross weight (Paragraph 3.5.1.7.2).

3.6.2.3 Ferry Mission Loadings. Loading shall consist of maximum authorized fuel and no payload.

3.6.2.4 In-Flight Refueling Mission Loading. One mission shall be for the same loading as the basic mission. Other loadings may be selected by the typical missions.

3.6.2.5 Combat Range Mission Loading. Identical to the loading of the associated combat radius mission.

3.6.3 Mission Segments. Rationale for mission segments is presented in the following:

3.6.3.1 Takeoff. Ground operation, including starting engines, warm-up, taxi, takeoff and acceleration to climb speed are variable. An arbitrary fuel allowance, based on statistical analysis, must be used. The takeoff fuel allowance used for gas turbine engine and turboprop powered aircraft is a quantity of fuel equal to the fuel used during 4.6 minutes of intermediate thrust operation at Sea Level Standard Day (10 minutes maximum continuous power for reciprocating engines). If afterburners are required for use during takeoff, a fuel allowance equal to 30 seconds of operation at maximum thrust at Sea Level Standard Day must be used along with fuel for 4.6 minutes operation at intermediate thrust.

3.6.3.2 Climb. See Paragraph 3.5.6.

3.6.3.2.1 Typical Design Criteria. For design purposes, consideration may be given to defining the takeoff allowance to fully utilize the state-of-the-art. Some typical examples are:

a. Specify engine operation for specific time periods at specified powers. Such as, fuel used during 4.6 minutes of intermediate thrust operation at Sea Level, on a standard day plus 30 seconds of maximum thrust operation if afterburner is used during takeoff.

b. Estimate fuel required to start the engine(s), run-up, taxi a specified distance at a specified thrust (power) setting and to accelerate from brake release to climb speed at a specified power.

c. Estimate fuel for a specified time at a specified thrust (power)/weight ratio to account for starting and taxi plus fuel for takeoff and acceleration to climb speed computed from the following:

$$W_{f_{TO}} = \frac{V_c W_{TO}}{2g} \cdot \frac{(\dot{W}_o + \dot{W}_c)}{T-D} \qquad (2)$$

When:

$W_{f_{TO}}$ = takeoff and acceleration fuel, lbs.

V_c = initial climb speed, ft/sec.

W_{TO} = takeoff weight, lbs.

$\dot{W}_o$ = static fuel flow at takeoff power, lbs/sec.

$\dot{W}_c$ = fuel flow at initial climb speed at takeoff power, lbs/sec.

T-D = thrust minus drag at V_c, lbs.

g = acceleration of gravity, Sea Level, ft/sec^2

NOTE:

If thrust (power) is to be varied between lift-off and climb speed, this equation can be so modified.

d. Other specific criteria may be selected to more accurately portray the operational characteristics of the specific design.

3.6.3.3 Cruise. Unless specifically assigned, aircraft shall cruise at the speed and altitude for maximum specific range (optimum cruise altitude) for the applicable configuration, thrust (power) and weight. This altitude shall not exceed cruise ceiling. For aircraft having a low optimum altitude (e.g.: Reciprocating Engine Aircraft), the cruise altitude shall not be less than 5,000 feet for terrain clearance over land or 1,500 feet over water. Except where the altitude is specified, the aircraft may utilize a cruise climb to optimize cruise distance. Turbojet and turbofan driven aircraft shall cruise at maximum range cruise speed (Paragraph 3.5.2.10.1) and propeller driven aircraft shall cruise at long range cruise speed (Paragraph 3.5.2.10.2).

3.6.3.3.1 Typical Design Criteria. For design purposes, consideration may be given to specifying a cruise technique selected to optimize the desired characteristics of the design. Techniques to be considered include: constant altitude cruise, constant speed cruise, cruise climb profile, step climb, cruise at specified power, cruise with reduced number of engines, cruise altitude in excess of cruise ceiling, fixed distance segment, headwinds or tail winds, non-standard temperatures, etc.

3.6.3.4 Combat. Combat shall be considered by setting aside a quantity of fuel to be used for that purpose if required. Normally, fuel flow for this allowance shall be based on the level flight stabilized speeds for the altitude and thrust (power) stated in Appendix V. The change in speed due to weight reduction during the combat period shall be ignored. When more than one thrust (power) setting is used, the lesser thrust (power) will be used first and each treated independently. For task-oriented fuel allowances, computation shall be based upon weight at start of combat period with benefit due to weight reduction credited; change in speed due to weight reduction shall be ignored.

3.6.3.4.1 Escape and Evasion. Escape and evasion shall be considered by setting aside a quantity of fuel based upon a specified measure of performance.

3.6.3.4.2 Typical Design Criteria. For design purposes, consideration may be given to various methods of accounting for the fuel to be used during combat or escape and evasion action. Some examples of methods are:

a. Fuel required for a specified time with a specified thrust (power) at a specified speed and a specified altitude.

b. Fuel consumed in expending a specified quantity of energy. For example:

$$\text{Combat Fuel} = \frac{E_s \dot{W}_f}{P_s} \qquad (3)$$

When:

E_s = specific energy, feet.

W_f = fuel flow at combat speed, power, and altitude, lbs/sec.

P_s = excess energy or $\frac{(T-D)V_c}{W_{T_c}}$, ft/sec.

V_c = combat true airspeed, ft/sec.

W_{T_c} = combat weight, lbs.

(T-D) = thrust minus drag, lbs.

c. The quantity of fuel determined as the sum of the fuel required to accelerate from cruise speed to a specified speed, plus fuel required to make a specified number of sustainable turns at a specified speed or speeds. These operations shall be performed at a selected thrust (power)(s) and altitude(s).

d. All or a portion of the armament may be expended.

e. Other specific criteria selected to more accurately portray the operational characteristics of the specific design.

3.6.3.5 Search and Loiter. Speed shall be as given in Paragraph 3.5.2.11.

3.6.3.6 Descent. For vehicles whose best cruise is subsonic, no time, fuel or distance will be credited for descent. For supersonic cruise vehicles, credit may be taken for descent and deceleration to an altitude of 25,000 feet and a specified speed. Aircraft which conduct a supersonic runout from the target may, if the cruise altitude and speed are lower than the runout altitude and speed, account for distance in descent and deceleration to cruise.

3.6.3.6.1 Typical Design Criteria. For design purposes, consideration may be given to alternate definitions of descent. For example: time, fuel and distance could be credited, descent could be a long range (airline) approach, use of thrust (power) could vary from none to full, speeds could vary from near stall to redline, altitudes could be reduced in step increments, etc. For gas turbine powered aircraft, the criteria will usually be idle thrust (power) descent to a given altitude at a given speed, i.e., M=0.8 to Sea Level (outbound leg to target area), 250 KCAS to 20,000 feet (return leg to land).

3.6.4 Landing Reserve. Fuel onboard at landing shall be the greater of the following:

a. Fuel allowance equal to 10 percent of initial usable fuel as required by OPNAVINST 3710.7K Paragraph 326.

b. Fuel allowance equal to 20 minutes loiter (30 minutes for cargo and transport aircraft) at sea level at speeds for maximum endurance with all engines operating plus 5% of initial total usable fuel (internal plus external).

3.6.4.1 Typical Design Criteria. For design purposes, consideration may be given to defining the landing reserves to fully utilize the state-of-the-art. Some examples are:

a. The fuel required for a ground controlled approach; a wave-off, go-around and a second, successful landing. This could be approximated by using the equivalent of fuel consumed during a specified time at maximum endurance at Sea Level with all engines operating.

b. A specified percentage of initial fuel load.

c. Fuel consumed during a specified time of operation at a specified power at a specified altitude.

d. The greater of the fuel required for 10 percent of mission time or 20 minutes at maximum endurance speed at 10,000 feet.

e. Fuel required to fly to an alternate field (specify distance) plus a specified time at a specified speed at a specified altitude to account for landing.

f. Combinations of the above or other criteria selected to optimize the design.

3.6.5 Mission Time. Time in air (excludes time before start of initial climb and reserve).

3.6.6 Cycle Time. The time of flight from the start of enroute climb (omitting takeoff time) to stopping engines after landing.

3.6.7 Block Time. The total time of flight from start engines to stop engines after landing.

3.6.8 Intercept Time. The time from engine start until initiation of combat at the intercept altitude. This time includes the period required for takeoff and acceleration to climb speed.

SECTION 1

BASIC AERODYNAMIC DATA REPORT

INTRODUCTION

SECTION 1. INTRODUCTION
2. THRUST/LIFT/DRAG BOOKKEEPING PROCEDURE FOR PERFORMANCE CALCULATIONS
3. EXAMPLE TABLE OF CONTENTS
4. EXAMPLE PLOTS

INTRODUCTION

Prior to proceeding with the initial performance calculations for the Standard Aircraft Characteristics Charts, the following basic data, including all calculations and materials necessary to substantiate these data, shall be submitted to NAVAIR (AIR-53012) for acceptance [normally not later than sixty (60) days following receipt of Authority to Proceed unless specifically extended by NAVAIR (AIR-53012)]. The aerodynamic and propulsion system thrust/drag bookkeeping procedures for performance calculations are outlined in Section 2 of this Appendix and shall be utilized, where applicable to the particular design, in the presentation of basic data and for performance calculations. Prior to subsequent performance calculations, these basic data shall be submitted.

1. Low speed drag analysis itemized according to various aircraft components (wing, fuselage, drag devices, etc.).

2. Plots of parasitic drag coefficient, $C_{D_{min}}$; incremental skin friction drag coefficient due to variation of flat plate skin friction drag with Reynolds number (fully turbulent boundary layer case adjusted for the effects of compressibility should be utilized); lift coefficient for minimum drag, C_{L_B}, as a function of Mach number; and trimmed airplane efficiency factor "e" versus Mach number for various values of lift coefficient. Trimmed airplane drag polars at various values of Mach number may be submitted in lieu of the "e" and C_{L_B} curves. Incremental drag coefficient, ΔC_D, versus Mach number for drag devices and for each required external store and combination of stores shall be presented.

3. Standard Day net thrust available and fuel flow variation with altitude and Mach number for maximum afterburner, intermediate and normal engine operation (including idle power) with all losses (induction system, nozzle, compressor bleed and accessory drive power extraction) indicated. The variation of fuel flow with net thrust as a function of Mach number and altitude for partial thrust operation shall be presented. Also, intermediate and maximum (afterburner) thrust available at Sea Level, 89.8°F, between Mach equal 0 and 0.3. Engine ram drag shall also be presented for all of the above engine conditions. When applicable, one engine inoperative data and partial afterburner net thrust versus fuel flow should be presented at specific altitudes/conditions.

4. Untrimmed lift coefficient plotted against pitching moment, angle-of-attack and drag coefficient for three horizontal tail positions, without thrust effect, in the takeoff and landing configurations, and both in and out of ground effect. Trimmed lift coefficient versus angle-of-attack and drag coefficient, without thrust effect, for the takeoff and approach configuration (in and out of ground effect) and for the clean configuration.

5. Breakout of wetted areas and aircraft dimensional data.

6. Area distribution for MN = 1.0 (Total and broken down by components).

7. Catapult:

   a. Load-stroke data for main and nose gear.

   b. Load-tire deflection data for main and nose gear. For 7.a and 7.b, specify if load is total load, load on one side, or load on one wheel.

   c. Moment of inertia about Y-Y axis (pitch).

   d. CM $\dot{\alpha}$ and CM $\dot{\theta}$.

8. Drawings:

   a. General Arrangement, 1/20 scale dimensioned, including CG and thrust line locations.

   b. Landing gear (side view) showing main and nose gear hub locations (station and waterline) in extended and compressed position; tow bar attachment point and tow bar length.

NOTE: Data not accepted by NAVAIR shall be replaced, after conference with the contractor, by similar data designated by NAVAIR.

Section 3 presents an example "Table of Contents" that illustrates the format for the Basic Aerodynamic Data Report. It is required that this format be used unless exempted by NAVAIR (AIR-53012).

Section 4 presents example plot formats to be used in the graphical presentation of data for the Basic Aerodynamic Data Report. The aircraft and configuration should be noted where applicable. This includes maneuver devices and schedules (Mach and angle-of-attack) for these devices. For maximum lift coefficient, include maximum defensive and offensive limits, maximum tracking and buffet onset. On all external stores show effect of C_L on drag coefficient. Also, effect of speed brakes should be shown, where applicable.

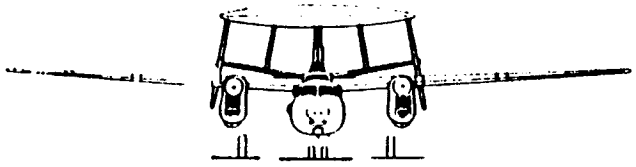

SECTION 2

BASIC AERODYNAMIC DATA REPORT

THRUST/LIFT/DRAG BOOKKEEPING PROCEDURES
FOR PERFORMANCE CALCULATIONS

1. This Appendix discusses the requirements for the presentation and calculation of aircraft performance. These procedures outlined in Figure II-1, are intended for use during design, development and test of the aircraft (whether performance calculations are based on analytical, wind tunnel or flight analysis) and shall be utilized, where applicable to the particular design, (a) in the presentation of basic data, (b) for aircraft performance calculations, and (c) to enhance generalization of aerodynamic data obtained from flight test.

2. The basis for the thrust/lift/drag bookkeeping procedures and attendant list of symbols and definitions is:

a. Realism in the allocation of aerodynamic and propulsion system force components to thrust and drag.

b. The inclusion of all force components independent of engine power setting in the aircraft lift/drag characteristics.

c. The inclusion of all force components which are functions of engine throttle setting and/or induction and exhaust system geometry in installed propulsion system characteristics.

d. The availability of aerodynamic/propulsion system interaction effects and Reynolds number effects to generalize flight-measured lift/drag data for correlation of flight-measured and wind-tunnel-derived full-scale lift/drag characteristics.

3. The "reference" configuration between aerodynamic force and moment and propulsion wind tunnel tests shall be as follows:

Inlet: Inlet(s) operating at the critical mass flow ratio or the Mach number being tested. Inlet drag for this condition will be included in aircraft drag.

Nozzle/Afterbody: The nozzle(s) should be in the full-open position, with $P_{EXIT}/P_{\infty} = 1.0$. Nozzle/afterbody drag for this condition is included in aircraft drag.

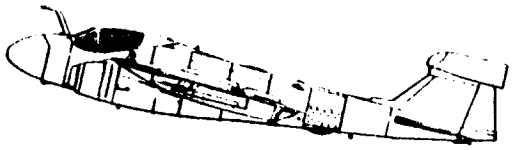

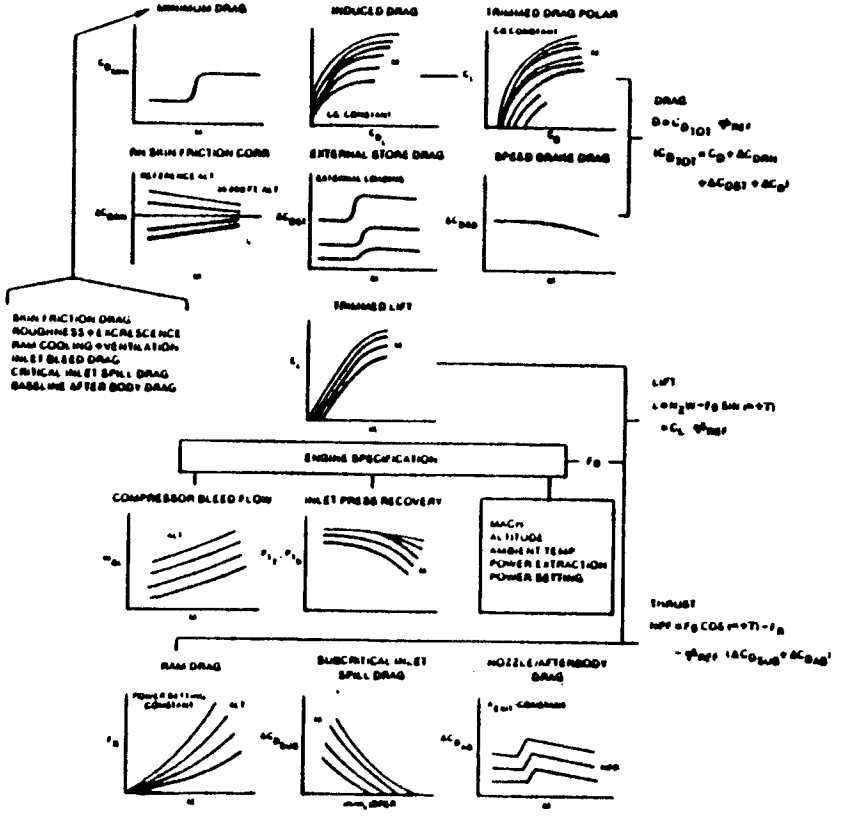

FIGURE II-1. THRUST/LIFT/DRAG BOOKKEEPING PROCEDURES FOR PERFORMANCE CALCULATIONS

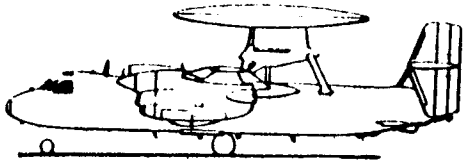

LIST OF SYMBOLS AND DEFINITION OF TERMS

Alt	ALTITUDE
A_{EXIT}	NOZZLE EXIT AREA
C_D	DRAG COEFFICIENT (CLEAN CONFIGURATION)
C_{D_i}	INDUCED DRAG COEFFICIENT
$\Delta C_{D_{AB}}$	INCREMENTAL NOZZLE/AFTERBODY DRAG COEFFICIENT THAT IS A FUNCTION OF ENGINE THROTTLE POSITION
$C_{D_{min}}$	MINIMUM DRAG COEFFICIENT (INCLUDING SEA LEVEL SKIN FRICTION DRAG, ROUGHNESS AND EXCRESCENCE, RAM COOLING AND VENTILATION, INLET BLEED DRAG, SUPERCRITICAL INLET SPILLAGE DRAG AND BASELINE NOZZLE/AFTERBODY DRAG)
$\Delta C_{D_{RN}}$	INCREMENTAL SKIN FRICTION DRAG COEFFICIENT DUE TO VARIATION OF FLAT PLATE SKIN FRICTION DRAG WITH REYNOLDS NUMBER
$\Delta C_{D_{SB}}$	INCREMENTAL DRAG COEFFICIENT DUE TO SPEEDBRAKE DEFLECTION
$\Delta C_{D_{ST}}$	INCREMENTAL DRAG COEFFICIENT DUE TO CARRIAGE OF EXTERNAL STORES
$\Delta C_{D_{SUB}}$	INCREMENTAL SUBCRITICAL INLET SPILLAGE DRAG COEFFICIENT
$C_{D_{TOT}}$	TOTAL DRAG COEFFICIENT (C_D AND $C_{D_{RN}}$ AND $C_{D_{ST}}$ AND $C_{D_{SB}}$)
C_L	LIFT COEFFICIENT
CG	CENTER OF GRAVITY POSITION
D	DRAG
F_g	INSTALLED ENGINE GROSS THRUST
F_R	ENGINE RAM DRAG
L	LIFT
M	MACH NUMBER
$\dot{m}$	INLET MASS FLOW OF OPERATING ENGINE CONDITION

LIST OF SYMBOLS AND DEFINITION OF TERMS

$\dot{m}_o$	THEORETICAL MAXIMUM MASS FLOW FOR REFERENCE INLET CAPTURE AREA
$(\dot{m}/\dot{m}_o)oper$	INLET OPERATING MASS FLOW RATIO
NPF	NET PROPULSIVE FORCE ($F_g \cos(\alpha + \epsilon) - F_R - qS_{REF}(C_{D_{SUB}} + C_{D_{AB}})$
NPR	NOZZLE PRESSURE RATIO (P_{EXIT}/P_a)
N_z	AIRCRAFT ACCELERATION ALONG VERTICAL AXIS
P_a	AMBIENT PRESSURE
P_{EXIT}	NOZZLE EXIT STATIC PRESSURE
$P_{T_{EXIT}}$	NOZZLE EXIT TOTAL PRESSURE
P_{T_o}	FREESTREAM TOTAL PRESSURE
P_{T_2}	TOTAL PRESSURE AT ENGINE COMPRESSOR FACE
P_{T_2}/P_{T_o}	INLET PRESSURE RECOVERY
q	DYNAMIC PRESSURE
RN	REYNOLDS NUMBER
S.L.	SEA LEVEL
S_{REF}	REPERENCE WING AREA FOR AERODYNAMIC COEFFICIENTS
W	AIRPLANE GROSS WEIGHT
W_a	INLET AIRFLOW
W_{BL}	ENGINE COMPRESSOR BLEED AIRFLOW
α	ANGLE-OF-ATTACK
δ	RATIO OF AMBIENT TO STANDARD SEA LEVEL STATIC PRESSURE
θ	RATIO OF AMBIENT TO STANDARD SEA LEVEL STATIC TEMPERATURE
ϵ	LONGITUDINAL THRUST LINE INCLINATION

SECTION 3

BASIC AERODYNAMIC DATA REPORT

EXAMPLE TABLE OF CONTENTS

SECTION 4

BASIC AERODYNAMIC DATA REPORT

EXAMPLE PLOTS

HIGH SPEED LIFT & DRAG CHARACTERISTICS

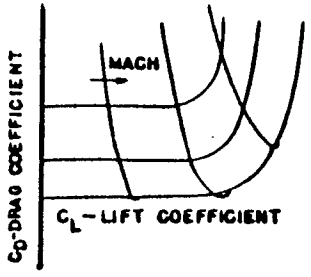

FIGURE - 1

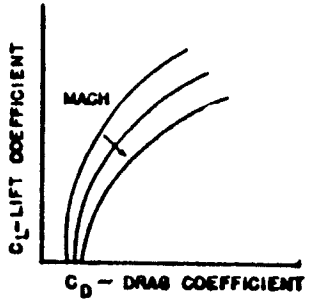

FIGURE - 2

HIGH SPEED LIFT & DRAG CHARACTERISTICS (CONT'D)

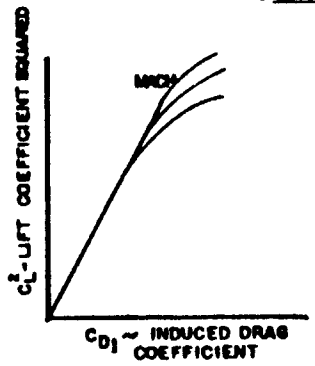

FIGURE - 3

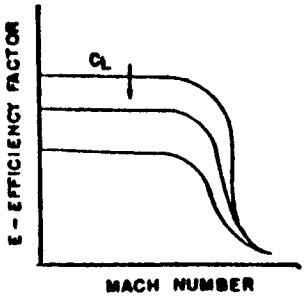

FIGURE - 4

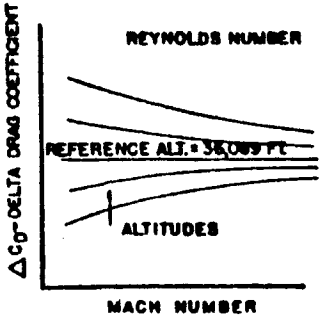

FIGURE - 9

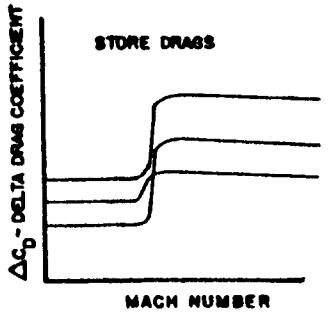

FIGURE - 10

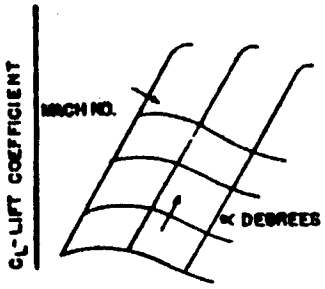

FIGURE - 5

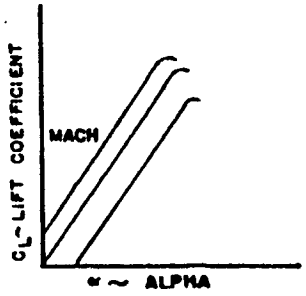

FIGURE - 6

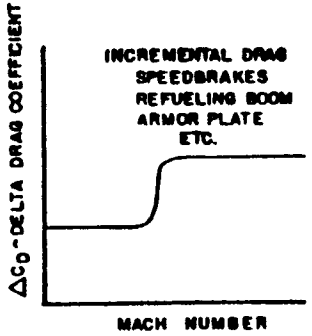

FIGURE - 11

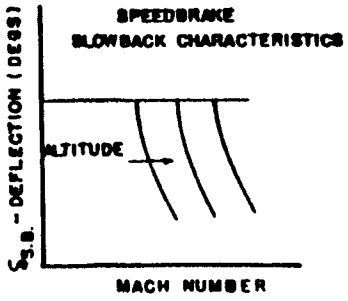

FIGURE - 12

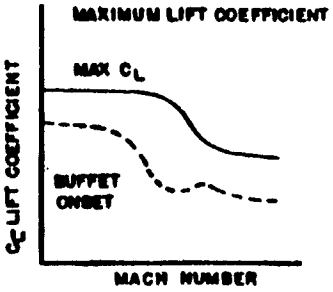

FIGURE - 7

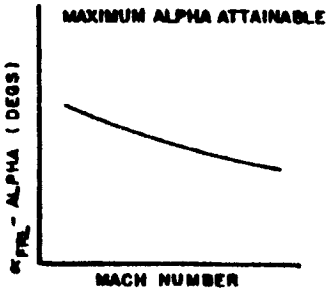

FIGURE - 8

LOW SPEED HIGH LIFT CONFIGURATIONS

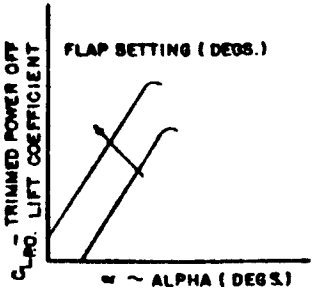

FIGURE - 13

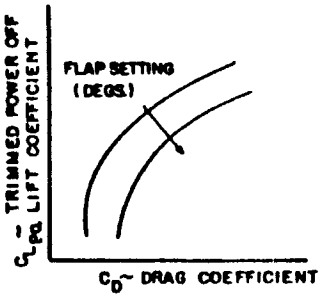

FIGURE - 14

HIGH SPEED LIFT & DRAG CHARACTERISTICS (CONT'D)

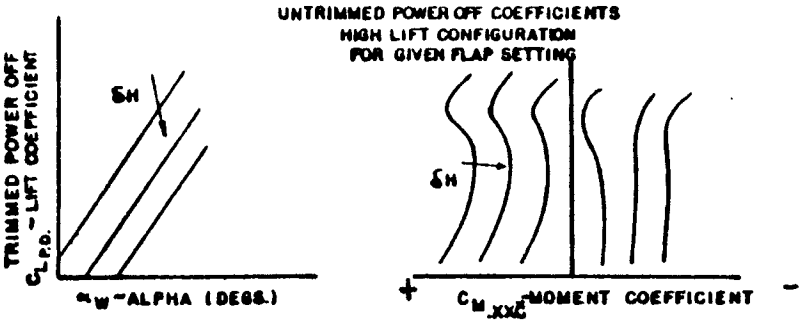

FIGURE - 15

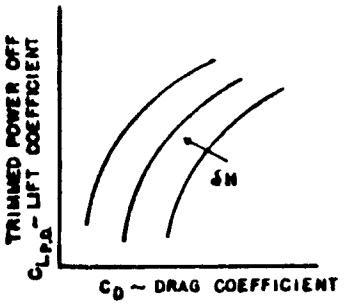

FIGURE - 16

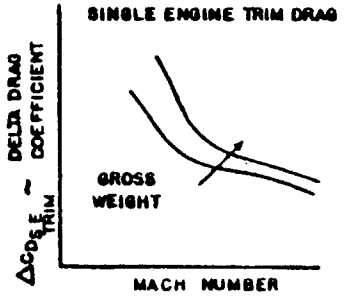

FIGURE - 17

PROPULSION DATA

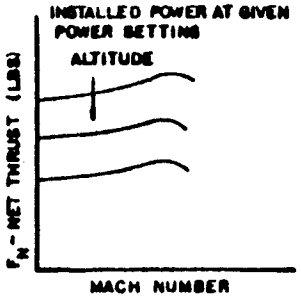

FIGURE - 18

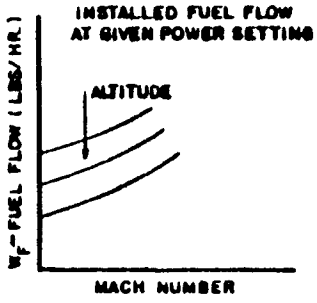

FIGURE - 19

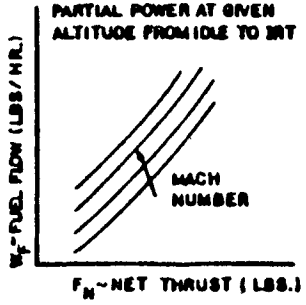

FIGURE - 20

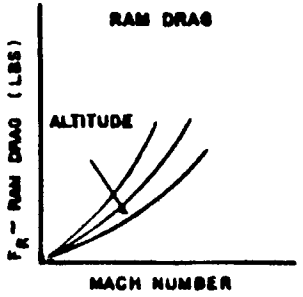

FIGURE - 21

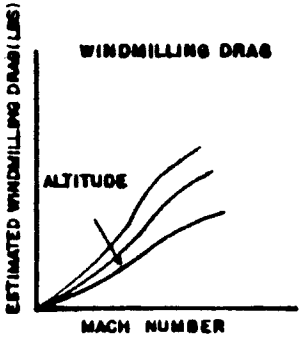

FIGURE - 22

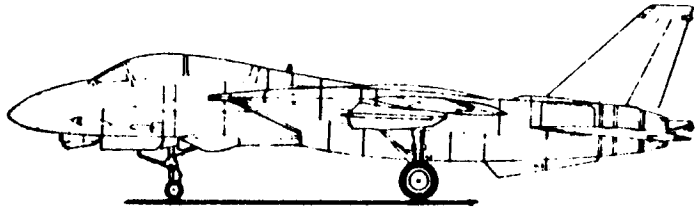

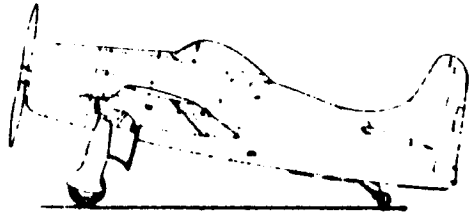

SPECIALIZED PROPELLER AIRCRAFT

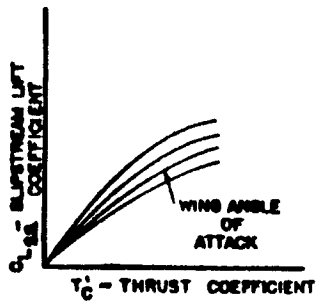

FIGURE - 23

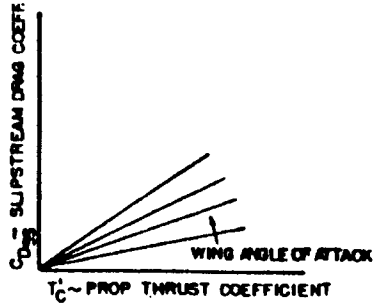

FIGURE - 24

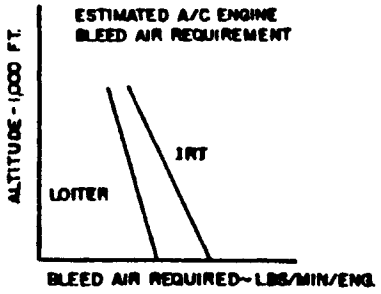

FIGURE - 27

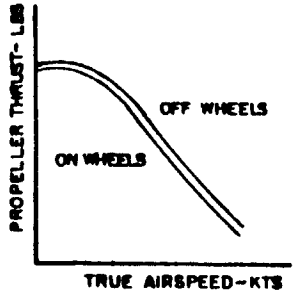

FIGURE - 28

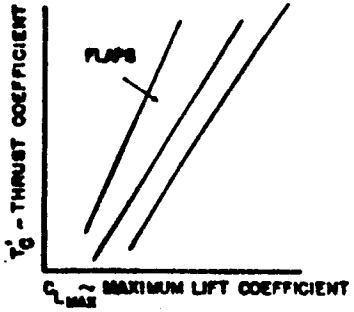

FIGURE - 25

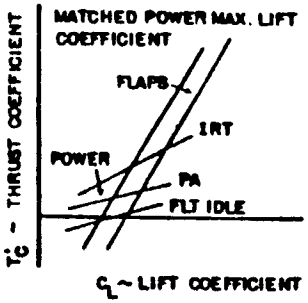

FIGURE - 26

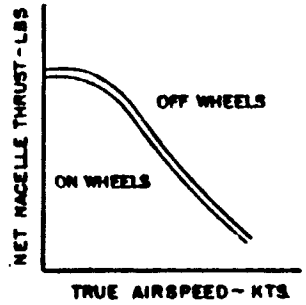

FIGURE - 29

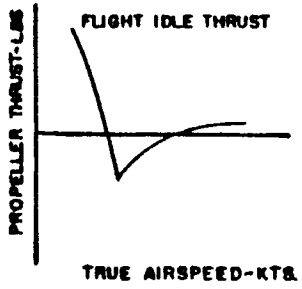

FIGURE - 30

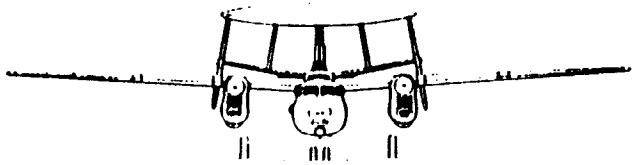

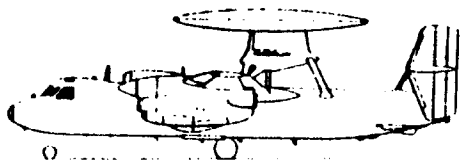

SECTION 1

SUBSTANTIATING DATA REPORT

INTRODUCTION

SECTION 1. INTRODUCTION
2. EXAMPLE TABLE OF CONTENTS
3. EXAMPLE PLOTS

INTRODUCTON

The performance Substantiating Data Report shall be prepared using the data contained in the Basic Aerodynamic Data Report which has been accepted by NAVAIR (AIR-53012). It shall include data to substantiate the information given in the Standard Aircraft Characteristics Charts and must be sufficiently complete to expedite a prompt investigation and review of the derived performance and to permit additional calculations to be made by NAVAIR (AIR-53012). The report also provides the general basis for and should be consistent with the Flight Manual Performance Data.

Section 2 presents an example "Table of Contents" that illustrates the format for the performance Substantiating Data Report. This format outlines the pertinent data to be provided and should be used unless exempted by NAVAIR (AIR-53012).

Section 3 presents example plot formats to be used in the graphical presentation of data for the performance Substantiating Data Report. Where applicable, one engine inoperative data should be provided in addition to the all engines operating condition. In the high lift configuration, data should be provided for all normal and emergency conditions. These include the various flap settings, lift devices (slats, etc.), and drag devices (speed brakes, etc.) available for pilot use. Field stopping/landing distance should be determined with and without reverse thrust, if appropriate.

The graphical presentation should be clear and concise with scales easy to read. Any questions concerning scales or format should be directed to NAVAIR (AIR-53012).

SECTION 2

SUBSTANTIATING DATA REPORT

EXAMPLE TABLE OF CONTENTS

1.0 SUMMARY (INCLUDING SAC CHARTS)

2.0 INTRODUCTION (INCLUDES DATA SOURCE)

3.0 TABULATED DATA

3.1 Aircraft General Arrangement

3.2 Aircraft Dimensional Data

3.3 Weight and Configuration Summary
(Includes tabulation of weight used in SAC Chart)

3.4 Aircraft Basic Useful Load

3.5 Fuel and Oil

3.6 Propulsion System
(Reference Engine Specification) Dimensions, Capture Area, Uninstalled Thrust, RPM (N_2), SFC, Airflow, Time Limit for Various Power Settings

4.0 MISSION AND TRADE-OFF SUMMARIES

5.0 PERFORMANCE DATA PRESENTATION METHOD

6.0 MAXIMUM MACH NUMBER
(Includes V_L, V_H and other limits)

7.0 CEILINGS
(Absolute, Service, Cruise and Combat Ceilings for Applicable Power Settings)

8.0 CLIMB PERFORMANCE

8.1 Climb - Speed Schedule

8.2 Rate-of-Climb

8.3 Time, Distance and Fuel to Climb
(Maximum Range and Minimum Time)

8.3.1 Intermediate Power

8.3.2 Maximum Power

9.0 CRUISE PERFORMANCE

9.1 Optimum Cruise

9.2 Cruise at Constant Mach and Altitude

10.0 ENDURANCE AND LOITER

10.1 Optimum Loiter

10.2 Specific Endurance at Constant Altitude

11.0 SPECIALIZED PERFORMANCE

11.1 Buddy Refueling

11.2 Search Performance (Flat Turning and Orbiting)

11.3 Loiter at Corner Speeds

11.4 Bingo

11.5 Single Engine Cruise

SECTION 3

SUBSTANTIATING DATA REPORT

EXAMPLE PLOTS

PLOTS ARE ARRANGED TO CONFORM WITH SECTION 2:
ITEMS 5, 22 AND 23 OMITTED

4.0 MISSION TRADEOFF SUMMARIES

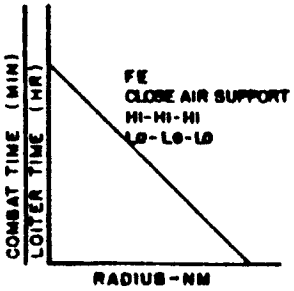

FIGURE - 1

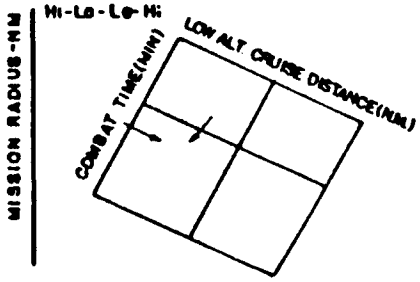

FIGURE - 2

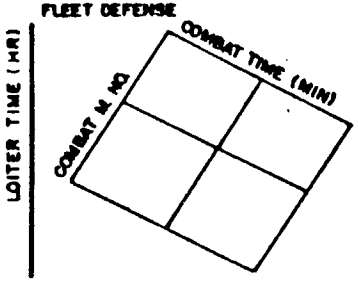

FIGURE - 3

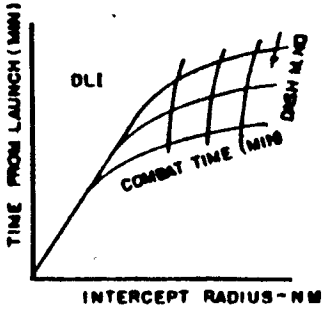

FIGURE - 4

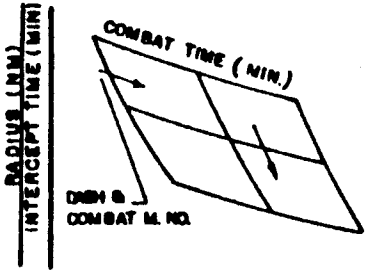

FIGURE - 5

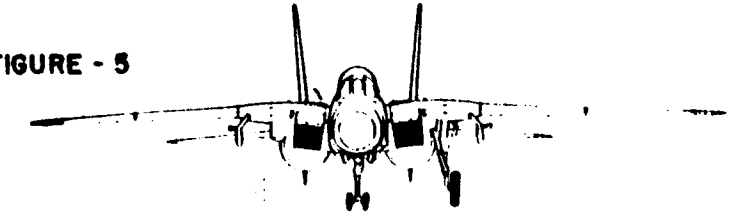

6.0 MAXIMUM MACH NUMBER

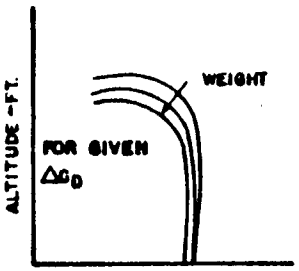

FIGURE-6

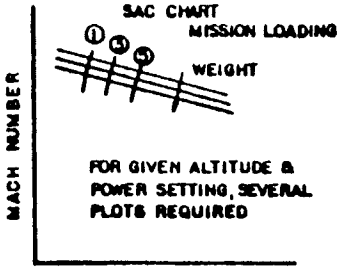

FIGURE - 7

7.0 CEILINGS

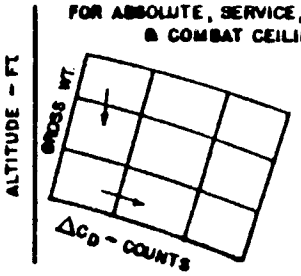

FIGURE-8

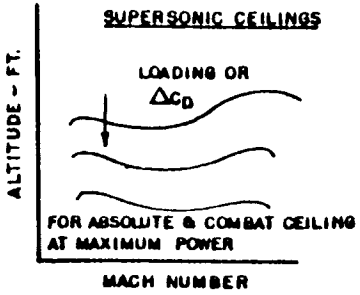

FIGURE - 9

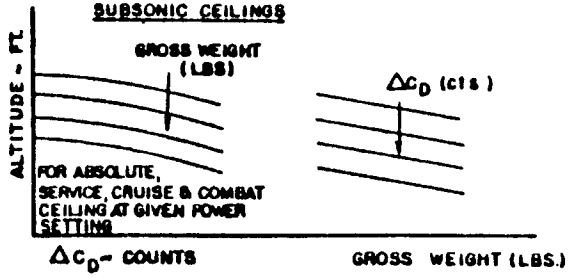

FIGURE - 10

8.0 CLIMB PERFORMANCE

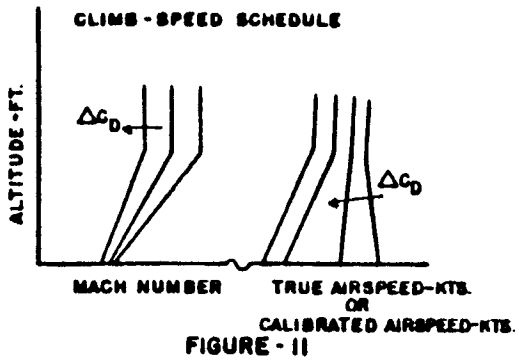

FIGURE - 11

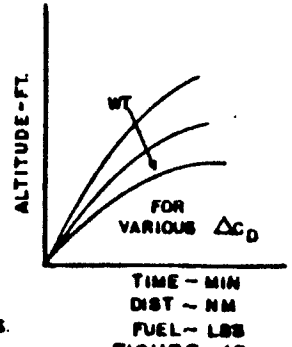

FIGURE - 12

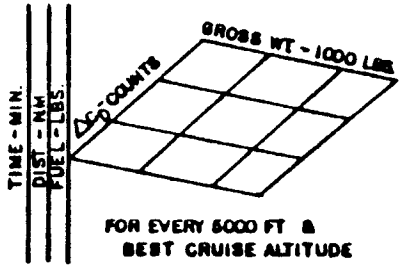

FIGURE - 13

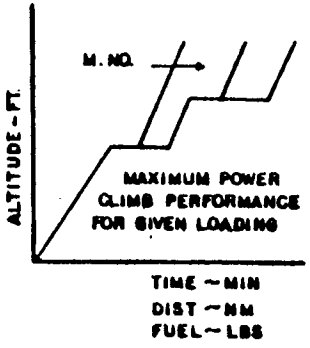

FIGURE - 14

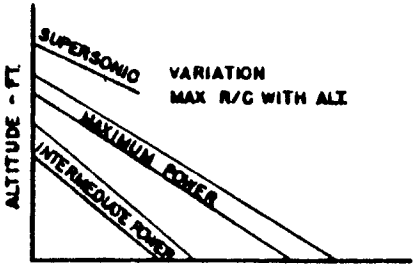

FIGURE - 15

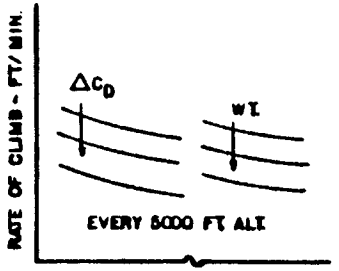

FIGURE - 16

9.0 CRUISE PERFORMANCE

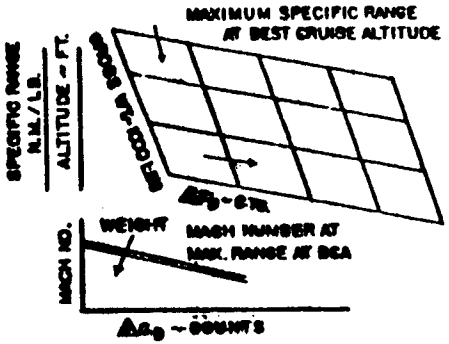

FIGURE - 17

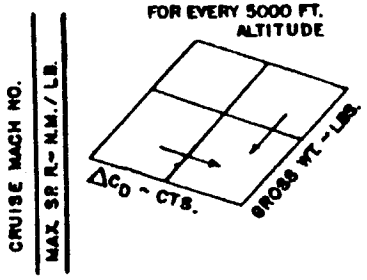

FIGURE - 18

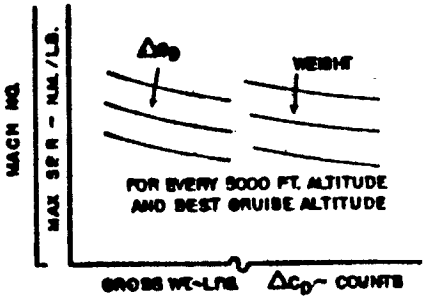

FIGURE - 19

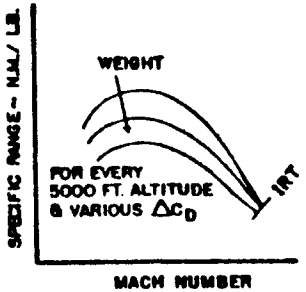

FIGURE - 20

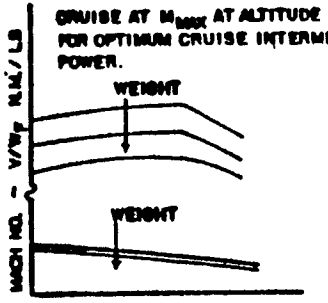

FIGURE - 21

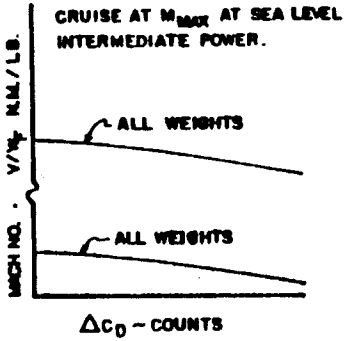

FIGURE - 22

9.0 CRUISE PERFORMANCE CONT'D

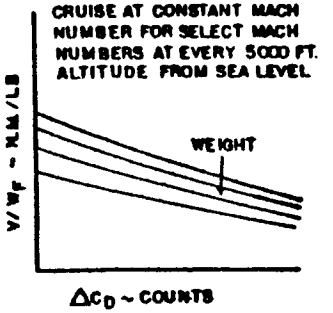

FIGURE - 23

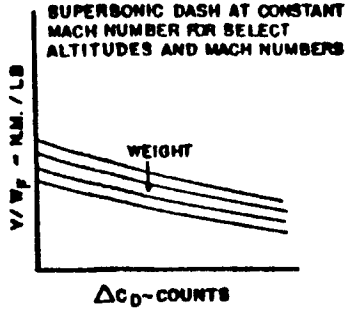

FIGURE - 24

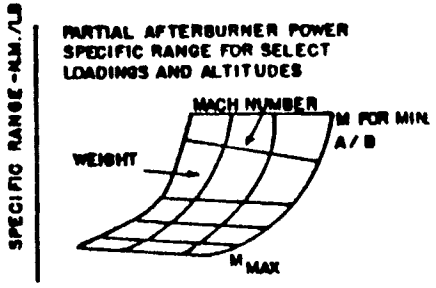

FIGURE - 25

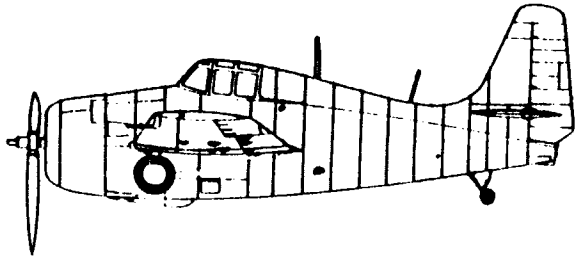

10. ENDURANCE & LOITER

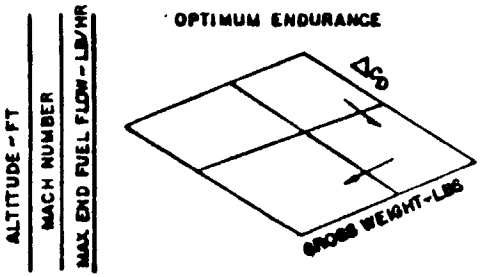

FIGURE - 26

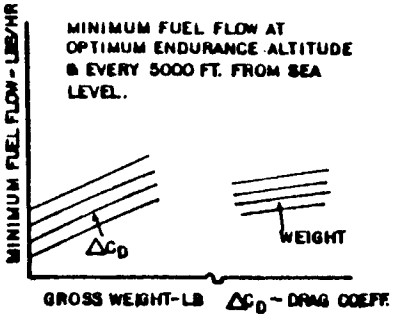

FIGURE - 27

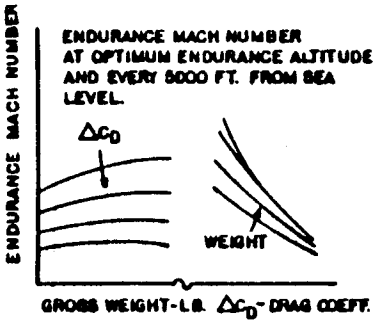

FIGURE - 28

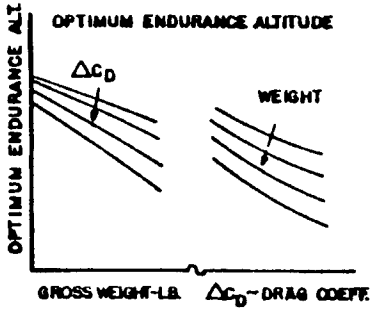

FIGURE - 29

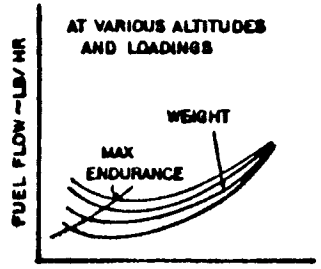

FIGURE - 30

12.0 DESCENT PERFORMANCE

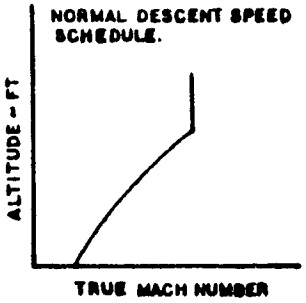

FIGURE - 31

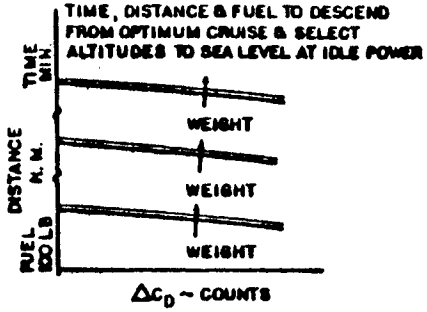

FIGURE - 32

13.0 ACCELERATION PERFORMANCE

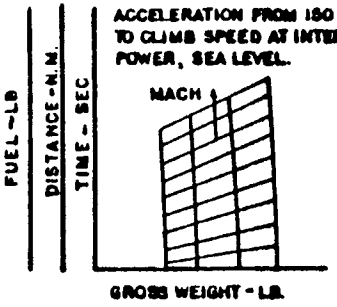

FIGURE - 33

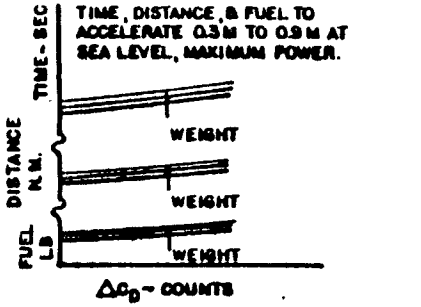

FIGURE - 34

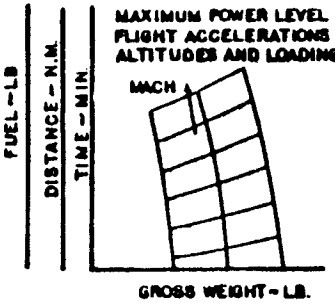

FIGURE - 35

14.0 MANEUVERABILITY COMBAT PERFORMANCE

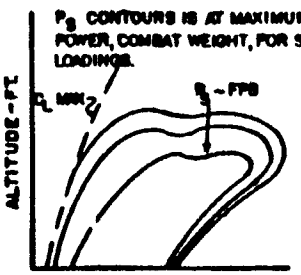

FIGURE - 36

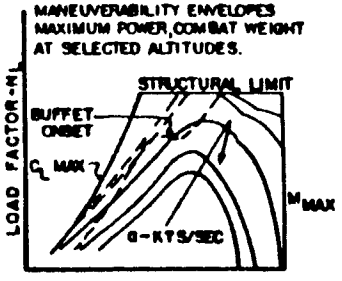

FIGURE - 37

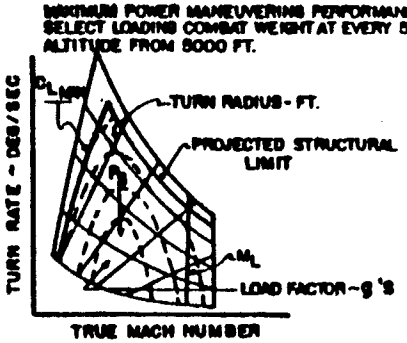

FIGURE - 38

OPERATIONAL ENVELOPES

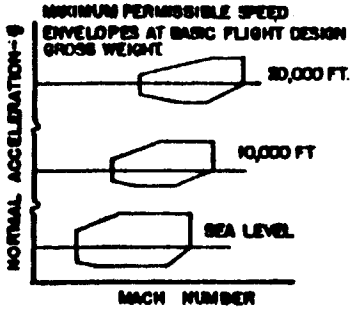

FIGURE - 39

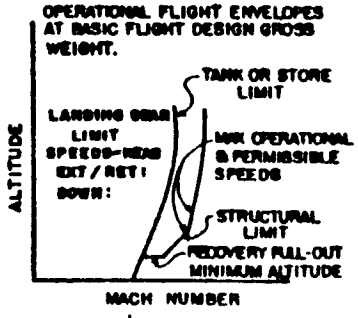

FIGURE - 40

15.0 LONGITUDINAL ACCELERATION

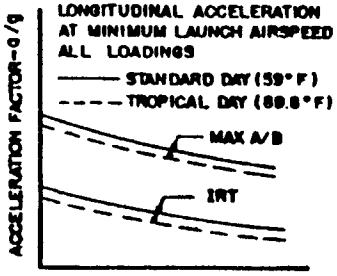

FIGURE - 41

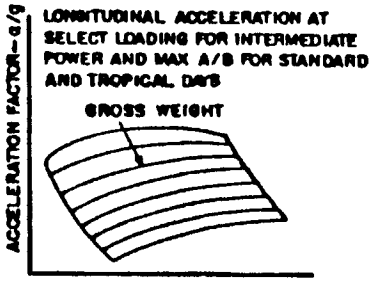

FIGURE - 42

16.0 CATAPULT PERFORMANCE

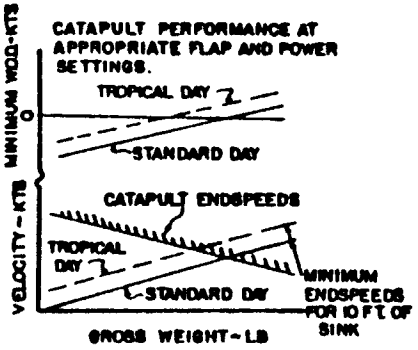

FIGURE - 43

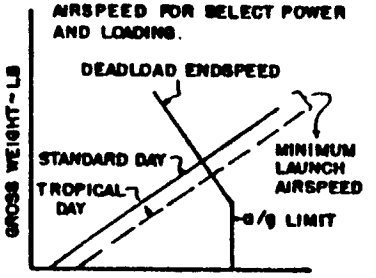

FIGURE - 44

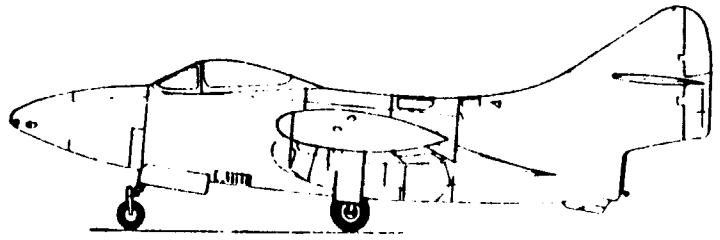

17.0 CARRIER APPROACH SPEED & ARRESTING WIND-OVER-DECK

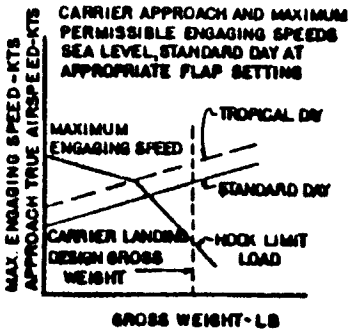

FIGURE-45

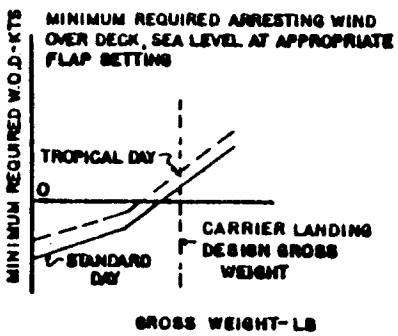

FIGURE-46

18.0 STALL SPEEDS

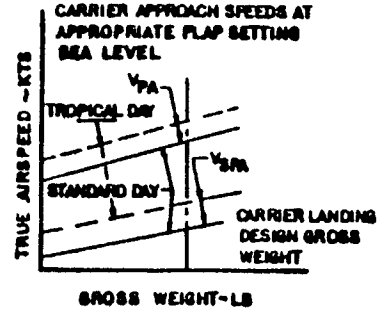

FIGURE-47

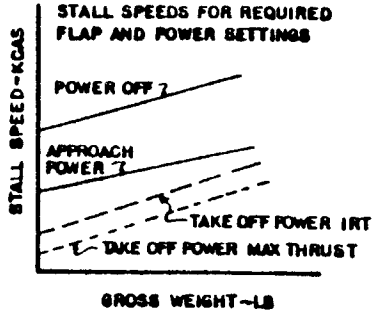

FIGURE-48

19.0 FIELD TAKE-OFF

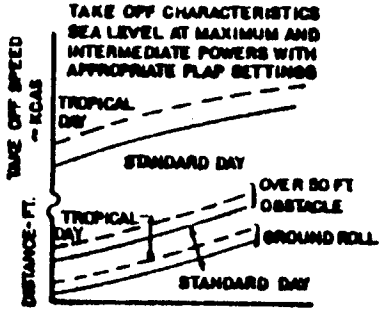

FIGURE-49

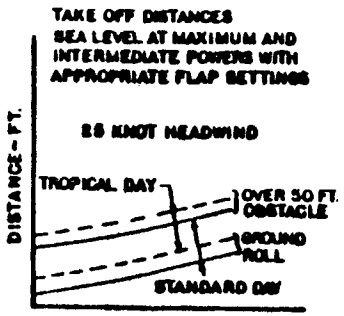

FIGURE-50

20.0 FIELD LANDING

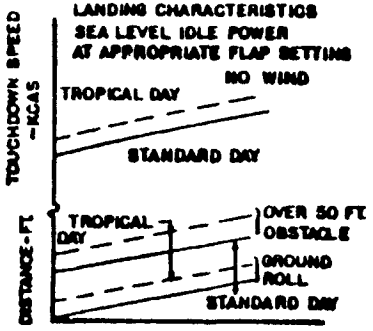

FIGURE-51

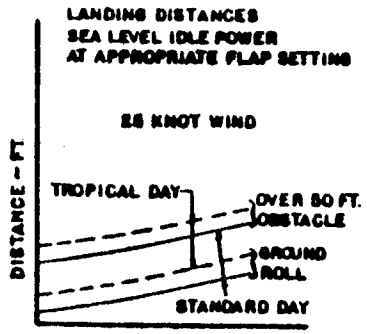

FIGURE-52

21.0 SINGLE ENGINE RATE-OF-CLIMB

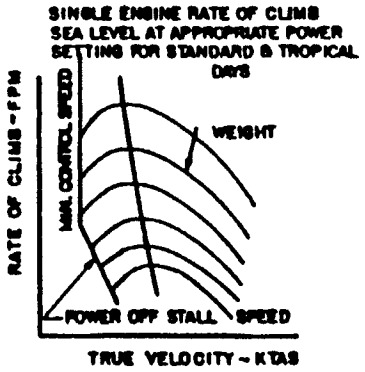

FIGURE - 53

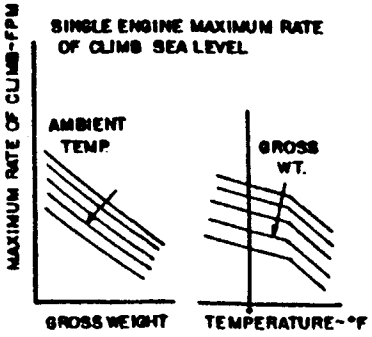

FIGURE - 54

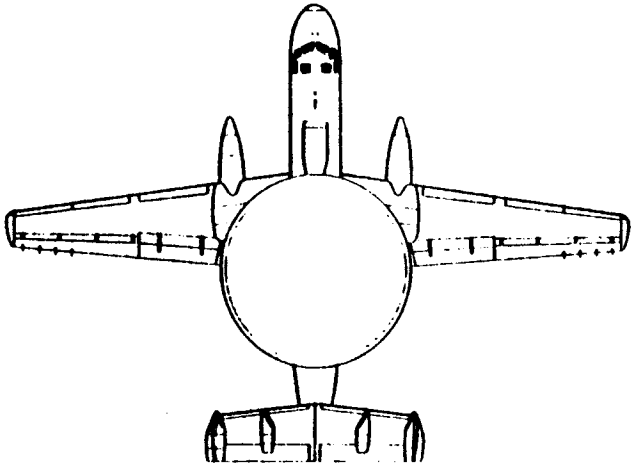

MISCELLANEOUS PROPULSION DATA

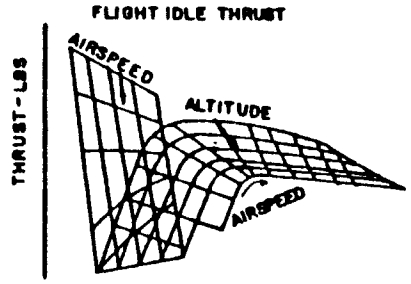

FIGURE - 55

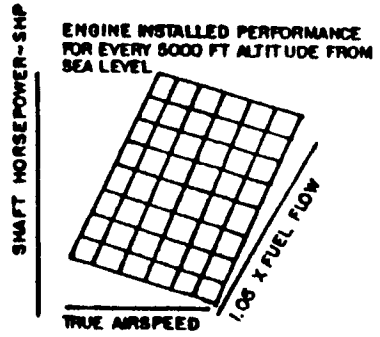

FIGURE - 56

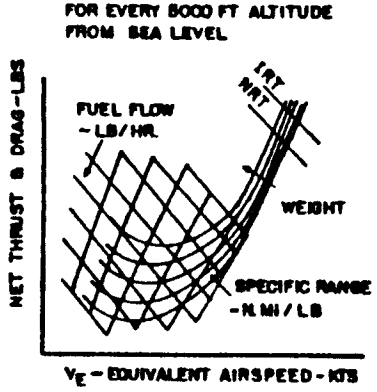

FIGURE - 57

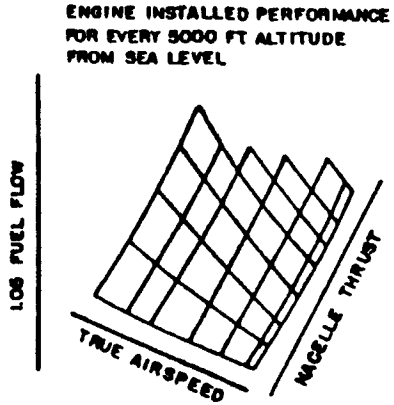

FIGURE - 58

APPENDIX V

MISSION PROFILES

GENERAL MISSIONS

* 1. HI-HI-HI
2. Fighter Escort
3. Fighter Escort (Alternate)
* 4. Deck Launched Intercept
5. Deck Launched Intercept (Alternate)
* 6. Combat Air Patrol
* 7. Close Support
8. Ferry/Cross Country Navigation
* 9. Interdiction (HI-LO-LO-HI)
10. Interdiction (Alternate)
11. HI-LO-HI
12. LO-LO-LO
13. LO-LO-LO-HI
* 14. ASW SEARCH
* 15. ASW
* 16. MINELAYING
* 17. WEAPONS DELIVERY/ GUNNERY (TRAINING)

* MISSION PROFILES INCLUDED IN THIS TEXT. FOR OTHERS SEE AS-5263

HI-HI-HI
(High Altitude Subsonic)

1. For taxi, warmup, takeoff and acceleration to best climb speed: Fuel allowance at sea level static equal to 4.6 minutes at intermediate thrust plus 30 seconds afterburner thrust if afterburner is used for takeoff.

2. Climb: On course at best climb speed at intermediate power to best cruise altitude (not to exceed cruise ceiling).

3. Cruise Out: To target at speed and altitudes for best range, using a cruise climb flight path (not to exceed cruise ceiling).

4. Combat: Fuel allowance equal to 5 minutes at maximum speed with intermediate thrust at best cruise altitude. No distance is credited (drop bombs, retain mounting hardware and missiles after combat).

5. Cruise Back: To base at speed and altitudes for best range, using a cruise climb flight path (not to exceed cruise ceiling).

6. Descent: Descend to sea level (no fuel used, no distance gained).

7. Reserve: Fuel allowance equal to 20 minutes loiter at sea level at speeds for maximum endurance with all engines operating plus 5% of initial total fuel (internal plus external).

(a) Mission Time: Items 2 through 6.
(b) Cycle Time: Items 2 through 7.

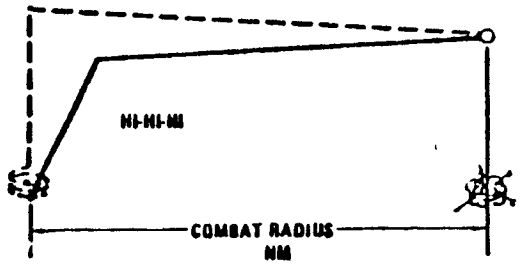

DECK LAUNCHED INTERCEPT

1. For taxi, warmup, takeoff and acceleration to Mach 0.3: Fuel allowance at sea level static equal to 4.6 minutes at intermediate thrust plus 30 seconds afterburner thrust if afterburner is used for takeoff.

2. Acceleration: Maximum power acceleration from Mach 0.3 to Mach 0.9 at sea level.

3. Climb: On course at Mach 0.9 at maximum power to 35,000 feet.

4. Acceleration: Maximum power acceleration from Mach 0.9 to Mach 1.35 at 35,000 feet.

5. Dash Out: Mach 1.35 dash at 35,000 feet.

6. Combat: Fuel allowance equal to 1 minute at maximum power, Mach 1.35 at 35,000 feet (no distance is credited, missiles are retained).

7. Climb: On course at best climb speed at intermediate power to best cruise altitude (not to exceed cruise ceiling).

8. Cruise Back: To base at speed and altitudes for best range, using a cruise climb flight path (not to exceed cruise ceiling).

9. Descent: Descend to sea level (no fuel used, no distance gained).

10. Reserve: Fuel allowance equal to 20 minutes loiter at sea level at speeds for maximum endurance with all engines operating plus 5% of initial total fuel (internal plus external).

(a) Mission Time: Items 2 through 9.
(b) Cycle Time: Items 2 through 10.

NOTE: Dash Mach and Altitude variations should be considered for this mission.

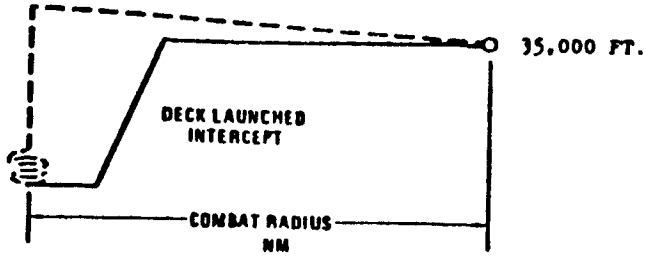

COMBAT AIR PATROL

1. For taxi, warmup, takeoff and acceleration to best climb speed: Fuel allowance at sea level static equal to 4.6 minutes at intermediate thrust plus 30 seconds afterburner thrust if afterburner is used for takeoff.

2. Climb: On course at best climb speed at intermediate thrust to best cruise altitudes (not to exceed cruise ceiling).

3. Cruise Out: To 150 nautical miles at speed and altitudes for best range, using a cruise climb flight path (not to exceed cruise ceiling).

4. Descent: Descend to 35,000 feet (no fuel used, no distance gained).

5. Loiter: Loiter at speed for maximum endurance at 35,000 feet (no distance is credited).

6. Combat: Fuel allowance equals that used to accelerate from loiter speed at 35,000 feet to Mach 1.2 plus 2 minutes at maximum power, Mach 1.2 at 35,000 feet (no distance is credited, missiles are retained).

7. Climb: On course at best climb speed at intermediate thrust to best cruise altitude (not to exceed cruise ceiling).

8. Cruise Back: To base at speed and altitudes for best range, using a cruise climb flight path (not to exceed cruise ceiling).

9. Descent: Descend to sea level (no fuel used, no distance gained).

10. Reserve: Fuel allowance equal to 20 minutes loiter at sea level at speeds for maximum endurance with all engines operating plus 5% of initial total fuel (internal plus external).

(a) Mission Time: Items 2 through 9.
(b) Cycle Time: Items 2 through 10.

NOTE: Loiter altitude and combat variations should be considered for this mission.

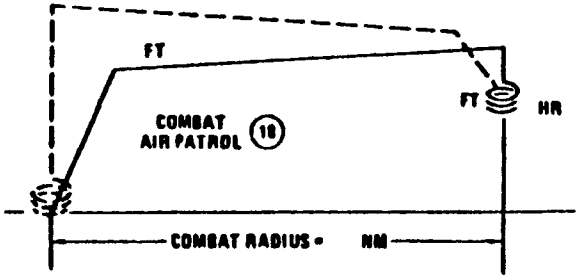

CLOSE SUPPORT

1. For taxi, warmup, takeoff and acceleration to best climb speed: Fuel allowance at sea level static equal to 4.6 minutes at intermediate thrust plus 30 seconds afterburner thrust if afterburner is used for takeoff.

2. Climb: On course at best climb speed at intermediate thrust to best cruise altitude (not to exceed cruise ceiling).

3. Cruise Out: To target at speed and altitudes for best range, using a cruise climb flight path (not to exceed cruise ceiling).

4. Descent: Descend to 5,000 feet (no fuel used, no distance gained).

5. Loiter: Loiter for 1 hour at speed for maximum endurance at 5,000 feet (no distance is credited, drop bombs after loiter, retain mounting hardware and missiles).

6. Climb: On course at best climb speed at intermediate thrust from 5,000 feet to best cruise altitude (not to exceed cruise ceiling).

7. Cruise Back: To base at speed and altitudes for best range, using a cruise climb flight path (not to exceed cruise ceiling).

8. Descent: Descend to sea level (no fuel used, no distance gained).

9. Reserve: Fuel allowance equal to 20 minutes loiter at sea level at speeds for maximum endurance with all engines operating plus 5% of initial total fuel (internal plus external).

(a) Mission Time: Items 2 through 8.
(b) Cycle Time: Items 2 through 9.

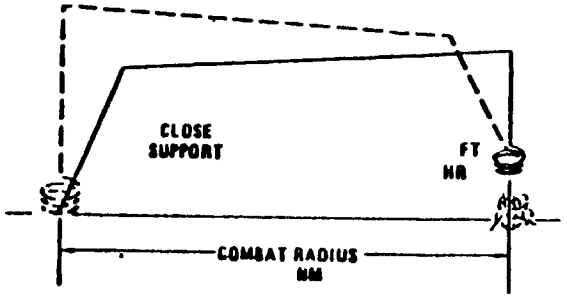

INTERDICTION

1. For taxi, warmup, takeoff and acceleration to best climb speed: Fuel allowance at sea level static equal to 4.6 minutes at intermediate thrust plus 30 seconds afterburner thrust if afterburner is used for takeoff.

2. Climb: On course at best climb speed at intermediate thrust to best cruise altitude (not to exceed cruise ceiling).

3. Cruise Out: At speeds and altitudes for best range, using a cruise climb flight path (not to exceed cruise ceiling).

4. Descent: Descend to sea level (no fuel used, no distance gained).

5. Run-in to Target: Sea level dash for 50 nautical miles at Mach 0.8 (or maximum speed at intermediate thrust if less than Mach 0.8).

6. Combat: Fuel allowance equal to 5 minutes at intermediate thrust, Mach 0.8 (or maximum speed if less than Mach 0.8) at sea level. No distance is credited (drop bombs, retain mounting hardware and missiles after combat).

7. Run-out from Target: Sea level dash for 50 nautical miles at Mach 0.8 (or maximum speed at intermediate thrust if less than Mach 0.8).

8. Climb: On course at best climb speed at intermediate thrust from sea level to best cruise altitude (not to exceed cruise ceiling).

9. Cruise Back: At speeds and altitudes for best range, using a cruise climb flight path (not to exceed cruise ceiling).

10. Descent: Descend to sea level (no fuel used, no distance gained).

11. Reserve: Fuel allowance equal to 20 minutes loiter at sea level at speeds for maximum endurance with all engines operating plus 5% of initial total fuel (internal plus external).

(a) Mission Time: Items 2 through 10.
(b) Cycle Time: Items 2 through 11.

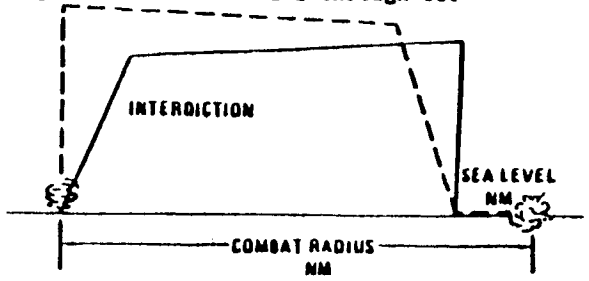

ASW SEARCH

1. For Taxi, warmup, takeoff and acceleration to best climb speed: Fuel allowance at sea level static equal to 4.6 minutes at intermediate thrust (10 minutes for propeller engine aircraft at normal power) plus 30 seconds afterburner thrust if afterburner is used for takeoff.

2. Climb: On course at best climb speed at intermediate thrust (normal power for props) to search altitude (not to exceed cruise ceiling).

3. Cruise Out: At search altitude at speed for maximum endurance (unless otherwise limited by handling qualities).

4. Cruise Back: At search altitude at speed for maximum endurance (unless otherwise limited by handling qualities).

5. Descent: Descend to sea level (no fuel used, no distance gained).

6. Reserve: Fuel allowance equal to 20 minutes (30 minutes for props) loiter at sea level at speeds for maximum endurance (maximum range for props) with all engines operating plus 5% of initial total fuel (internal plus external).

(a) Mission Time: Items 2 through 5.
(b) Cycle Time: Items 2 through 6.

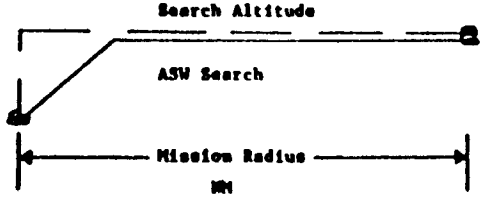

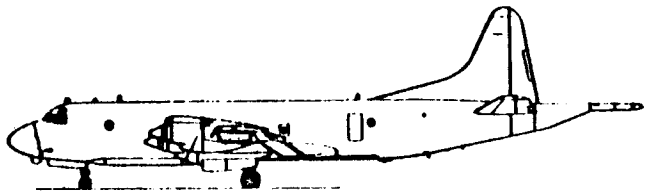

ASW

1. For Taxi, warmup, takeoff and acceleration to best climb speed: Fuel allowance at sea level static equal to 4.6 minutes at intermediate thrust (10 minutes for propeller engine aircraft at normal power) plus 30 seconds afterburner thrust if afterburner is used for takeoff.

2. Climb: On course at best climb speed at intermediate thrust (normal power for props) to best cruise altitude (not to exceed cruise ceiling).

3. Cruise Out: At speeds and altitudes for best range, using a cruise climb flight path (not to exceed cruise ceiling).

4. Descent: Descend to 20,000 feet (no fuel used, no distance gained).

5. Search: Search for 3 hours at speed for maximum endurance at 20,000 feet.

6. Descent: Descend to 200 feet (no fuel used, no distance gained).

7. Search: Search for 1 hour at speed for maximum endurance at 200 feet.

8. Climb: On course at best climb speed at intermediate thrust (normal power for props) to best cruise altitude (not to exceed cruise ceiling).

9. Cruise Back: At speeds and altitudes for best range, using a cruise climb flight path (not to exceed cruise ceiling).

10. Descent: Descend to sea level (no fuel used, no distance gained).

11. Reserve: Fuel allowance equal to 20 minutes (30 minutes for props) loiter at sea level at speeds for maximum endurance (maximum range for props) with all engines operating plus 5% of initial total fuel (internal plus external).

(a) Mission Time: Items 2 through 10.
(b) Cycle Time: Items 2 through 11.

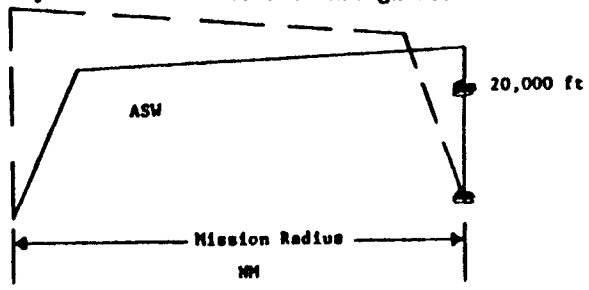

MINELAYING

1. For Taxi, warmup, takeoff and acceleration to best climb speed: Fuel allowance at sea level static equal to 4.6 minutes at intermediate thrust (10 minutes for propeller engine aircraft at normal power) plus 30 seconds afterburner thrust if afterburner is used for takeoff.

2. Climb: On course at best climb speed at intermediate thrust (normal power for props) to best cruise altitude (not to exceed cruise ceiling).

3. Cruise Out: At speeds and altitudes for best range, using a cruise climb flight path (not to exceed cruise ceiling).

4. Descent: Descend to 200 feet (no fuel used, no distance gained).

5. Penetrate: At maximum continuous power for 300 nautical miles at 200 feet.

6. Attack: At maximum continuous power for 100 nautical miles at 200 feet.

7. Release Mines.

8. Escape: On course at maximum continuous power for 300 nautical miles.

9. Climb: On course at best climb speed at intermediate thrust (normal power for props) from 200 feet to best cruise altitude (not to exceed cruise ceiling).

10. Cruise Back: At speeds and altitudes for best range, using a cruise climb flight path (not to exceed cruise ceiling).

11. Descent: Descend to sea level (no fuel used, no distance gained).

12. Reserve: Fuel allowance equal to 20 minutes (30 minutes for props) loiter at sea level at speeds for maximum endurance (maximum range for props) with all engines operating plus 5% of initial total fuel (internal plus external).

(a) Mission Time: Items 2 through 11.
(b) Cycle Time: Items 2 through 12.

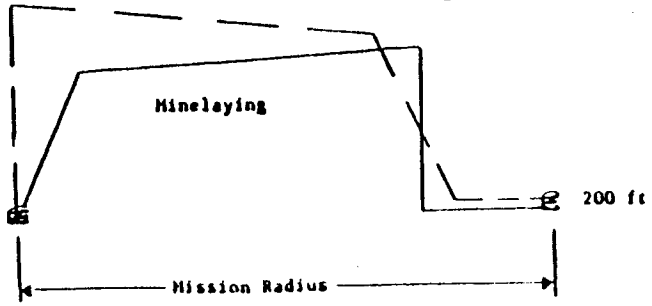

WEAPONS DELIVERY/GUNNERY

1. For Taxi, warmup, takeoff and acceleration to best climb speed: Fuel allowance at sea level static equal to 4.6 minutes at intermediate thrust plus 30 seconds afterburner thrust if afterburner is used for takeoff.

2. Climb: On course at best climb speed at intermediate thrust to 20,000 feet.

3. Cruise Out: 60 nautical miles from initial climb point at speed for best range at 20,000 feet.

4. Descent: Descend to gunnery altitude (10,000 feet) or weapons delivery altitude (sea level), (no fuel used, no distance gained).

5a. Gunnery Option: Time for gunnery shall be allocated as follows: 60% at intermediate thrust (Mach to be designated by NAVAIR), 25% at 80% intermediate thrust fuel flow (Mach to be designated by NAVAIR), and 15% at speed for best range. (no distance gained).

5b. Weapons Delivery Option: Time for weapons delivery shall be allocated as follows: 50% at intermediate thrust (Mach to be designated by NAVAIR), and 50% at 80% intermediate thrust fuel flow (Mach to be designated by NAVAIR). (no distance gained).

6. Climb: On course at best climb speed at intermediate thrust from gunnery (10,000 feet) or weapons delivery (sea level) altitude.

7. Cruise Back: 60 nautical miles from climb point at speed for best range at 20,000 feet.

8. Descent: Descend to sea level (no fuel used, no distance gained).

9. Reserve: Fuel allowance equal to 20 minutes loiter at sea level at speeds for maximum endurance with all engines operating plus 5% of initial total fuel (internal plus external).

(a) Mission Time: Items 2 through 8.
(b) Cycle Time: Items 2 through 9.

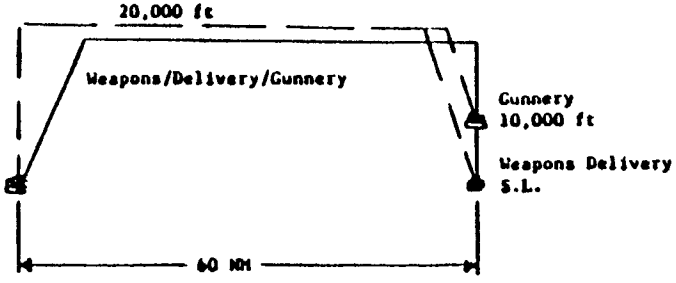

B2. Airplane Stability, Control and Flying Qualities

NOTES: 1. FOR SYMBOLS SEE P. 330-341
2. FOR CONTENTS SEE P. 341-343

B2.1 MIL-F-8785C: Military Specification, Flying Qualities of Piloted Airplanes, November 1980.

This specification is approved for use by all Departments and Agencies of the Department of Defense.

1. SCOPE

1.1 Scope. This specification contains the requirements for the flying and handling qualities, in flight and on the ground, of U.S. Military, manned, piloted airplanes except for flight at airspeeds below V_{con} (MIL-F-83300).

It is intended to assure flying qualities that provide adequate mission performance and flight safety regardless of design implementation or flight control system mechanization. The structure of the specification allows its use to guide these aspects in design tradeoffs, analyses and tests.

1.2 Application. The flying qualities of all airplanes proposed or contracted for shall be in accordance with the provisions of this specification. The requirements apply as stated to the combination of airframe and related subsystems. Stability augmentation and control augmentation are specifically to be included when provided in the airplane. The automatic flight control system is also to be considered to the extent stated in MIL-F-9490 or MIL-C-18244, whichever applies. The requirements are written in terms of cockpit flight controls that produce essentially pitching, yawing and rolling moments. This approach is not meant to preclude other modes of control for special purposes. Additional or alternative requirements may be imposed by the procuring activity in order to fit better the intended use or the particular design.

1.3 Classification of airplanes. For the purpose of this specification, an airplane shall be placed in one of the following Classes:

Class I Small, light airplanes such as:
- Light utility
- Primary trainer
- Light observation

Class II Medium weight, low-to-medium maneuverability airplanes such as:
- Heavy utility/search and rescue
- Light or medium transport/cargo/tanker
- Early warning/electronic countermeasures/airborne command, control or communications relay
- Antisubmarine
- Assault transport
- Reconnaissance
- Tactical bomber
- Heavy attack
- Trainer for Class II

Class III Large, heavy, low-to-medium maneuverability airplanes such as:
- Heavy transport/cargo/tanker
- Heavy bomber
- Patrol/early warning/electronic countermeasures/airborne command, control, or communications relay
- Trainer for Class III

Class IV High-maneuverability airplanes such as:
- Fighter/interceptor
- Attack
- Tactical reconnaissance
- Observation
- Trainer for Class IV

The procuring activity will assign an airplane to one of these Classes, and the requirements for that Class shall apply. When no Class is specified in a requirement, the requirement shall apply to all Classes. When operational missions so dictate, an airplane of one Class may be required by the procuring activity to meet selected requirements ordinarily specified for airplanes of another Class.

1.3.1 Land- or carrier-based designation. The letter -L following a Class designation identifies an airplane as land-based. Carrier-based airplanes are similarly identified by -C. When no such differentiation is made in a requirement, the requirement shall apply to both land-based and carrier-based airplanes.

1.4 Flight Phase Categories. The Flight Phases have been combined into three Categories which are referred to in the requirement statements. These Flight Phases shall be considered in the context of total missions so that there will be no gap between successive Phases of any flight and so that transition will be smooth. In certain cases, requirements are directed at specific Flight Phases identified in the requirement. When no Flight Phase or Category is stated in a requirement, that requirement shall apply to all three Categories. Flight Phases descriptive of most military airplane missions are:

Nonterminal Flight Phases:

Category A: Those nonterminal Flight Phases that require rapid maneuvering, precision tracking, or precise flight-path control. Included in this Category are:

a. Air-to-air combat (CO)
b. Ground Attack (GA)
c. Weapon delivery/launch (WD)
d. Aerial recovery (AR)
e. Reconnaissance (RC)
f. In-flight refuelling (receiver) (RR)
g. Terrain following (TF)
h. Antisubmarine search (AS)
i. Close formation flying (FF)

Category B: Those nonterminal Flight Phases that are normally accomplished using gradual maneuvers and without precision tracking, although accurate flight-path control may be required. Included in this Category are:

a. Climb (CL)
b. Cruise (CR)
c. Loiter (LO)
d. In-flight refueling (tanker) (RT)
e. Descent (D)
f. Emergency descent (ED)
g. Emergency deceleration (DE)
h. Aerial delivery (AD)

Terminal Flight Phases:

Category C: Terminal Flight Phases are normally accomplished using gradual maneuvers and usually require accurate flight-path control. Included in this category are:

a. Takeoff (TO)
b. Catapult takeoff (CT)
c. Approach (PA)
d. Wave-off/go-around (WO)
e. Landing (L)

When necessary, recategorization or addition of Flight Phases or delineation of requirements for special purpose situations, e.g. zoom climbs, will be accomplished by the procuring activity.

1.5 Levels of flying qualities. Where possible, the requirements of Section 3 have been stated in terms of three values of the stability or control parameter being specified. Each value is a minimum condition to meet one of three Levels of acceptability related to the ability to complete operational missions for which the airplane is designed. The Levels are:

Level 1: Flying qualities clearly adequate for the mission Flight Phase.

Level 2: Flying qualities adequate to accomplish the mission Flight Phase, but some increase in pilot workload or degradation in mission effectiveness, or both, exists.

Level 3: Flying qualities such that the airplane can be controlled safely, but pilot workload is excessive or mission effectiveness is inadequate, or both. Category A Flight Phases can be terminated safely, and Category B and C Flight Phases can be completed.

2. APPLICABLE DOCUMENTS

2.1 Issues of documents. The following documents, of the issue in effect on the date of invitation for bids or request for proposal, form a part of this specification to the extent specified herein:

SPECIFICATIONS

MILITARY

MIL-D-8708	Demonstration Requirements for Airplanes
MIL-A-8861	Airplane Strength and Rigidity Flight Loads
MIL-F-9490	Flight Control Systems- Design, Installation and Test of, Piloted Aircraft, General Specification for
MIL-C-18244	Control and Stabilization Systems, Automatic, Piloted Aircraft, General Specification for
MIL-F-18372	Flight Control Systems, Design, Installation and Test of, Aircraft, General Specification for
MIL-W-25140	Weight and Balance Control Data (for Airplanes and Rotorcraft)
MIL-F-83300	Flying Qualities of Piloted V/STOL Aircraft
MIL-S-83691	Stall/Post-Stall/Spin Flight Test Demonstration Requirements for Airplanes

STANDARDS

MIL-STD-756	Reliability Prediction

(Copies of specifications and standards required by contractors in connection with specific procurement functions should be obtained from the procuring activity or as directed by the contracting officer).

3. REQUIREMENTS

3.1 General Requirements

3.1.1 Operational missions. The procuring activity will specify the operational missions to be considered by the contractor in designing the airplane to meet the flying quality requirements of this specification. These missions will include all associated Flight Phases and tasks, such as takeoff, takeoff abort, landing and missed approach. Operational missions include the entire spectrum of intended usage including aircrew upgrade and training.

3.1.2 Loadings. The contractor shall define the envelopes of center-of-gravity and corresponding weights that will exist for each Flight Phase. These envelopes shall include the most forward and aft center-of-gravity positions as defined in MIL-W-25140. In addition, the contractor shall determine the maximum center-of-gravity excursions attainable through failures in systems or components, such as fuel sequencing, hung stores, etc., for each Flight Phase to be considered in the Failure States of 3.1.6.2. Within these envelopes, plus a growth margin to be specified by the procuring activity, and for the excursions cited above, this specification shall apply.

3.1.3 Moments and products of inertia. The contractor shall define the moments and products of inertia of the airplane associated with all loadings of 3.1.2. The requirements of this specification shall apply for all moments and products of inertia so defined.

3.1.4 External stores. The requirements of this specification shall apply for all combinations of external stores required by the operational missions. The effects of external stores on the weight, moments of inertia, center-of-gravity position, and aerodynamic characteristics of the airplane shall be considered for each mission Flight Phase. When the stores contain expendable loads, the requirements of this specification apply throughout the range of store loadings. The external stores and store combinations to be considered for flying qualities design will be specified by the procuring activity. In establishing external store combinations to be investigated, consideration shall be given to asymmetric as well as to symmetric combinations.

3.1.5 Configurations. The requirements of this specification shall apply for all configurations required or encountered in the applicable Flight Phases of 1.4. A (crew-) selected configuration is defined by the positions and adjustments of the various selectors and controls available to the crew except for pitch, roll, yaw, throttle and trim controls. Examples are: the flap control setting and the yaw damper ON or OFF. The selected configurations to be examined must consist of those required for performance and mission accomplishment. Additional configurations to be investigated may be defined by the procuring activity.

3.1.6 State of the airplane. The State of the airplane is defined by the selected configuration together with the functional status of each of the airplane components or systems, throttle setting, weight, moments of inertia, center-of-gravity position, and external store complement. The trim setting and the positions of the pitch, roll and yaw controls are not included in the definition of Airplane State since they are often specified by the requirements.

3.1.6.1 Airplane Normal States. The contractor shall define and tabulate all pertinent items to describe the Airplane Normal (no component or system failure) State(s) associated with each of the applicable Flight Phases. This tabulation shall be in the format and shall use the nomenclature specified in 6.2. Certain items, such as weight, moments of inertia, center-of-gravity position, wing sweep, or thrust setting may vary continuously over a range of values during a Flight Phase. The contractor shall replace this continuous variation by a limited number of values of the parameter in question which will be treated as specific States, and which include the most critical values and extremes encountered during the Flight Phase in question.

3.1.6.2 Airplane Failure States. The contractor shall define and tabulate all Airplane Failure States, which consist of Airplane Normal States modified by one or more malfunctions in airplane components or systems, for example, a discrepancy between a selected configuration and an actual configuration. Those malfunctions that result in center-of-gravity positions outside the center-of-gravity envelope defined in 3.1.2 shall be included. Each mode of failure shall be considered. Failures occurring in any Flight Phase shall be considered in all subsequent Flight Phases.

3.1.6.2.1 Airplane Special Failure States. Certain components, systems, or combinations thereof may have extremely remote probability of failure during a given flight. These failure probabilities may, in turn, be very difficult to predict with any degree of accuracy. Special Failure States of this type need not be considered in complying with the requirements of Section 3 if justification for considering the Failure States as Special is submitted by the contractor and approved by the procuring activity.

3.1.7 Operational Flight Envelopes. The Operational Flight Envelopes define the boundaries in terms of speed, altitude and load factor within which the airplane must be capable of operating in order to accomplish the missions of 3.1.1. Envelopes for each applicable Flight Phase shall be established with the guidance and approval of the procuring activity. In the absence of specific guidance, the contractor shall use the representative conditions of Table I for the applicable flight phases.

TABLE I OPERATIONAL FLIGHT ENVELOPES

Flight Phase Category: A

Flight Phase	Airspeed		Altitude		Load Factor	
	$V_{o_{min}}$ ($M_{o_{min}}$)	$V_{o_{max}}$ ($M_{o_{max}}$)	$h_{o_{min}}$	$h_{o_{max}}$	$n_{o_{min}}$	$n_{o_{max}}$
Air-to-air Combat (CO)	$1.4V_S$	V_{MAT}	MSL	Combat Ceiling	-1.0	n_L
Ground Attack (GA)	$1.3V_S$	V_{MRT}	MSL	Medium	-1.0	n_L
Weapon Delivery/ Launch (WD)	V_{range}	V_{MAT}	MSL	Combat Ceiling	0.5	•
Aerial Recovery (AR)	$1.2V_S$	V_{MRT}	MSL	Combat	0.5	n_L
Reconnaissance (RC)	$1.3V_S$	V_{MAT}	MSL	Combat Ceiling	•	•
In-Flight Refuel (Receiver) (RR)	$1.2V_S$	V_{MRT}	MSL	Combat Ceiling	0.5	2.0
Terrain Following (TF)	V_{range}	V_{MAT}	MSL	10,000 ft	0	3.5
Antisubmarine Search (AS)	$1.2V_S$	V_{MRT}	MSL	Medium	0	2.0
Close Formation Flying (FF)	$1.4V_S$	V_{MAT}	MSL	Combat Ceiling	-1.0	n_L

Flight Phase Category: B

Flight Phase	Airspeed		Altitude		Load Factor	
	$V_{o_{min}}$ ($M_{o_{min}}$)	$V_{o_{max}}$ ($M_{o_{max}}$)	$h_{o_{min}}$	$h_{o_{max}}$	$n_{o_{min}}$	$n_{o_{max}}$
Climb (CL)	$0.85V_{R/C}$	$1.3V_{R/C}$	MSL	Cruise Ceiling	0.5	2.0
Cruise (CR)	V_{range}	V_{NRT}	MSL	Cruise Ceiling	-1.0	2.0
Loiter (LO)	$0.85V_{end}$	$1.3V_{end}$	MSL	Cruise Ceiling	0.5	2.0
In-Flight Refuel (Tanker) (RT)	$1.4V_S$	V_{MAT}	MSL	Cruise Ceiling	0.5	2.0
Descent (D)	$1.4V_S$	V_{MAT}	MSL	Cruise Ceiling	0.5	2.0
Emergency Descent (ED)	$1.4V_S$	V_{max}	MSL	Cruise Ceiling	0.5	2.0
Emergency Deceleration(DE)	$1.4V_S$	V_{max}	MSL	Cruise Ceiling	0.5	2.0
Aerial Delivery (AS)	$1.2V_S$	200 kts	MSL	10,000 ft	0	2.0

TABLE I OPERATIONAL FLIGHT ENVELOPES (Cont'd)

Flight Phase Category: C

Flight Phase	Airspeed		Altitude		Load Factor	
	$V_{o_{min}}$ ($M_{o_{min}}$)	$V_{o_{max}}$ ($M_{o_{max}}$)	$h_{o_{min}}$	$h_{o_{max}}$	$n_{o_{min}}$	$n_{o_{max}}$
Takeoff (TO)	Minimum Normal Takeoff Speed	V_{max}	MSL	10,000 ft	0.5	2.0
Catapult Takeoff (CT)	Min. Catapult End Airspeed	$V_{o_{min}}$ + 30 kts	MSL		0.5	n_L
Approach (PA)	Minimum Normal Approach Speed	V_{max}	MSL	10,000 ft	0.5	2.0
Wave-off/Go-around (WO)	Minimum Normal Approach Speed	V_{max}	MSL	10,000 ft	0.5	2.0
Landing (L)	Minimum Normal Approach Speed	V_{max}	MSL	10,000 ft	0.5	2.0

* Appropriate to the operational mission

3.1.8 Service Flight Envelopes. For each Airplane Normal State the contractor shall establish, subject to the approval of the procuring activity, Service Flight Envelopes showing combinations of speed, altitude and normal acceleration derived from airplane limits as distinguished from mission requirements. For each applicable Flight Phase and Airplane Normal State, the boundaries of the Service Flight Envelopes can be coincident with or lie outside the corresponding Operational Flight Envelopes, but in no case shall they fall inside those Operational boundaries. The boundaries of the Service Flight Envelopes shall be based on considerations discussed in 3.1.8.1, 3.1.8.2, 3.1.8.3 and 3.1.8.4.

3.1.8.1 Maximum service speed. The maximum service speed, V_{max} or M_{max}, for each altitude is the lowest of:

a. The maximum permissible speed

b. A speed which is a safe margin below the speed at which intolerable buffet or structural vibration is encountered

c. The maximum airspeed at MAT, for each altitude, for dives (at all angles) from V_{MAT} at all altitudes, from which recovery can be made at 2,000 ft above MSL or higher without penetrating a safe margin from loss of control, other dangerous behavior or intolerable buffet, and without exceeding structural limits.

3.1.8.2 Minimum service speed. The minimum service speed, V_{min} or M_{min}, for each altitude is the highest of:

a. $1.1V_S$

b. V_S + 10 knots equivalent airspeed

c. The speed below which full airplane-nose-up pitch control power and trim are insufficient to maintain steady, straight flight.

d. The lowest speed at which level flight can be maintained with MRT and, for Category C Flight Phases:

e. A speed limited by reduced visibility or an extreme pitch attitude that would result in the tail or aft fuselage contacting the ground.

3.1.8.3 Maximum service altitude. The maximum service altitude, h_{max} for a given speed is the maximum altitude at which a rate of climb of 100 feet per minute can be maintained in unaccelerated flight with MAT.

3.1.8.4 Service load factors. Maximum and minimum service load factors, n(+) [n(-)], shall be established as a function of speed for several significant altitudes. The maximum [minimum] service load factor, when trimmed for 1g flight at a particular speed and altitude, is the lowest [highest] algebraically of:

a. The positive [negative] structural limit load factor

b. The steady load factor corresponding to the minimum allowable value of lift coefficient for stall warning (3.4.2.1.1.2)

c. The steady load factor at which the pitch control is in the full airplane-nose-up [nose-down] position

d. A safe margin below [above] the load factor at which intolerable buffet or structural vibration is encountered.

3.1.9 Permissible Flight Envelopes. The contractor shall define Permissible Flight Envelopes which encompass all regions in which operation of the airplane is both allowable and possible, consistent with 3.1.10.3.3. These Envelopes define boundaries in terms of speed, altitude and load factor.

3.1.10 Application of Levels. Levels of flying qualities as indicated in 1.5 are employed in this specification in realization of the possibility that the airplane may be required to operate under abnormal conditions. Such abnormalities that may occur as a result of either flight outside the Operational Flight Envelope, failure of airplane components, or both, are permitted to comply with a degraded Level of flying qualities as specified in 3.1.10.1 through 3.1.10.3.3 (see also 4.1.1).

3.1.10.1 Requirements for Airplane Normal States. The minimum required flying qualities for Airplane Normal States (3.1.6.1) are as specified in Table II.

TABLE II LEVELS FOR AIRPLANE NORMAL STATES

Within Operational Flight Envelope	Within Service Flight Envelope
Level 1	Level 2

3.1.10.2 Requirements for Airplane Failure States. When Airplane Failure States exist (3.1.6.2), a degradation in flying qualities is permitted only if the probability of encountering a lower Level than specified in 3.1.10.1 is sufficiently small. At intervals established by the procuring activity, the contractor shall determine, based on the most accurate available data, the probability of occurrence of each Airplane Failure State per flight and the effect of that Failure State on the flying qualities within the Operational and Service Flight Envelopes. These determinations shall be based on MIL-STD-756 except that:

a. All airplane components and systems are assumed to be operating for a time period, per flight, equal to the longest operational mission time to be considered by the contractor in designing the airplane, and

b. Each specific failure is assumed to be present at whichever point in the Flight Envelope being considered is the most critical (in the flying qualities sense). From these Failure State probabilities and effects, the contractor shall determine the overall probability, per flight, that one or more flying qualities are degraded to Level 2 because of one or more failures. The contractor shall also determine the probability that one or more flying qualities are degraded to Level 3. These probabilities shall be less than the values specified in Table III.

In no case shall a Failure State (except an approved Special Failure State) degrade any flying quality parameter outside the Level 3 limit.

TABLE III LEVELS FOR AIRPLANE FAILURE STATES

Probability of Encountering	Within Operational Flight Envelope	Within Service Flight Envelope
Level 2 after failure	$< 10^{-2}$ per flight	
Level 3 after failure	$< 10^{-4}$ per flight	$< 10^{-2}$ per flight

3.1.10.2.1 Requirements for specific failures. The requirements on the effects of specific types of failures, e.g. propulsion or flight control system, shall be met on the basis that the specific type of failure has occurred, regardless of its probability of occurrence.

3.1.10.3 Exceptions

3.1.10.3.1 Ground operation and terminal flight phases. Some requirements pertaining to takeoff, landing and taxiing involve operations outside the Operational, Service and Permissible Flight Envelopes, such as at V_S or on the ground. When requirements are stated at conditions such as these, the Levels shall be applied as if the conditions were in the Operational Flight Envelope.

3.1.10.3.2 When Levels are not specified. Within the Operational and Service Flight Envelopes, all requirements that are not identified with specific Levels shall be met under all conditions of component and system failure except approved Airplane Special Failure States (3.1.6.2.1).

3.1.10.3.3 Flight outside the Service Flight Envelope. From all points in the Permissible Flight Envelopes, it shall be possible readily and safely to return to the Service Flight Envelope without exceptional pilot skill or technique, regardless of component failure or system failures. The requirements on flight at high angle of attack, dive characteristics, dive recovery devices and dangerous flight conditions shall also apply.

3.1.11 Interpretation of subjective requirements. In several instances throughout the specification subjective terms, such as objectionable flight characteristics, realistic time delay, normal pilot technique and excessive loss of altitude or buildup of speed, have been employed to permit latitude where absolute quantitative criteria might be unduly restrictive. Final determination of compliance with requirements so worded will be made by the procuring activity (1.5).

3.1.12 Interpretation of quantitative requirements. The numerical requirements of this specification generally are stated in terms of a linear description of the airplane. Certain factors, for example flight control system nonlinearities and higher-order characteristic or aerodynamic nonlinearities, can cause the aircraft response to differ significantly from that of the linear model. The contractor shall define equivalent classical systems which have responses most closely matching those of the actual aircraft. Then those numerical requirements of section 3 which are stated in terms of linear system parameters (such as frequency, damping ratio and modal phase angles) apply to the parameters of that equivalent system rather than to any particular modes of the actual higher-order system. The procuring activity shall be the judge of the adequacy of the response match between equivalent and actual aircraft.

3.2 Longitudinal flying qualities. For Levels 1 and 2 there shall be no tendency for airspeed to diverge aperiodically when the airplane is disturbed from trim with the cockpit controls fixed and with them free. This requirement will be considered satisfied if the variations of pitch control force and pitch control position with airspeed are smooth and the local gradients stable, with:

a. Trimmer and throttle controls not moved from the trim setting by the crew, and

b. 1g acceleration normal to the flight path, and

c. constant altitude

over a range about the trim speed of +/- 15 percent or +/- 50 knots equivalent airspeed, whichever is less (except where limited by the boundaries of the Service Flight Envelopes). Alternatively, this requirement will be considered satisfied if stability with respect to speed is provided through the flight control system, even though the resulting pitch control force and deflection gradients may be zero. For Level 3 the requirements may be relaxed, subject to approval by the procuring activity of the maximum instability to be allowed for the particular case. In no event shall its time to double amplitude be less than 6 seconds. In the presence of one or more other Level 3 flying qualities, no static longitudinal instability will be permitted unless the flight safety of that combination of characteristics has been demonstrated to the satisfaction of the procuring activity. Stable gradients mean that the pitch controller deflection and force increments required to maintain straight, steady flight at a different speed are in the same sense as those required to initiate the speed change, that is, airplane-nose-down control to fly at a faster speed, airplane-nose-up control to fly at a slower speed. The term gradient does not include that portion of the control force or control position versus airspeed curve within the breakout force range.

3.2.1.1.1 Relaxation in transonic flight. The requirements of 3.2.1.1 may be relaxed in the transonic speed range provided any divergent airplane motions or reversals in slope of pitch control force and position with speed are gradual and not objectionable to the pilot. In no case, however, shall the requirements of 3.2.1.1 be relaxed more than the following:

a. Levels 1 and 2 - For center-stick controllers, no local force gradient shall be more unstable than 3 lbs per 0.01 M nor shall the force change exceed 10 lbs in the unstable direction. The corresponding limits for wheel controllers are 5 lbs per 0.01 M and 15 lbs, respectively.

b. Level 3- For center-stick controllers, no local force gradient shall be more unstable than 6 lbs per 0.01 M nor shall the force ever exceed 20 lbs in the unstable direction. The corresponding limits for wheel controllers are 10 lbs per 0.01 M and 30 lbs respectively.

This relaxation does not apply to Level 1 for any Flight Phase which requires prolonged transonic operation.

3.2.1.1.2 Pitch control force variations during rapid speed changes. When the airplane is accelerated and decelerated rapidly through the operational speed range and through the transonic speed range by the most critical combination of changes in power, actuation of deceleration devices, steep turns and pullups, the magnitude and rate of the associated trim change shall not be so great as to cause difficulty in maintaining the desired load factor by normal pilot techniques.

3.2.1.2 Phugoid stability. The long-period airspeed oscillations which occur when the airplane seeks a stabilized airspeed following a disturbance shall meet the following requirements:

a. Level 1 ----- ζ_p at least 0.04

b. Level 2 ----- ζ_p at least 0

c. Level 3 ----- T_2 at least 55 seconds

These requirements apply with the pitch control free and also with it fixed. They need not be met transonically in cases where 3.2.1.1.1 permits relaxation of the static stability requirement.

3.2.1.3 Flight-path stability. Flight-path stability is defined in terms of flight-path-angle change where the airspeed is changed by the use of pitch control only (throttle setting not changed by the crew). For the landing approach Flight Phase, the curve of flight-path angle versus true airspeed shall have a local slope at $V_{o_{min}}$ which is negative or less positive than:

a. Level 1 ----- 0.06 degrees/knot

b. Level 2 ----- 0.15 degrees/knot

c. Level 3 ----- 0.24 degrees/knot

The thrust setting shall be that required for the normal approach glide path at $V_{o_{min}}$. The slope of the curve of flight-path angle versus airspeed at 5 knots slower than $V_{o_{min}}$ shall not be more than 0.05 degrees/knot more positive than the slope at $V_{o_{min}}$, as illustrated by:

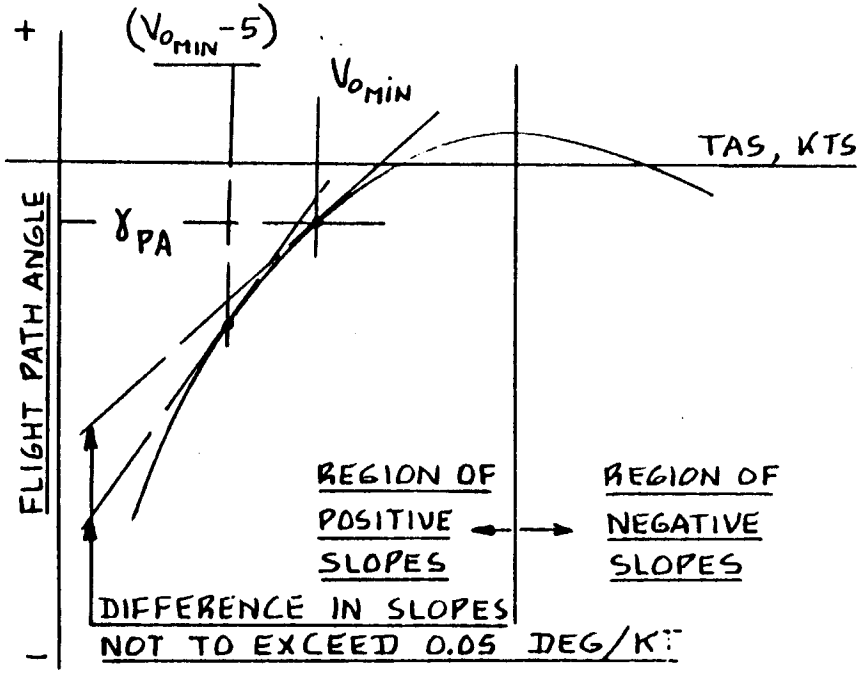

3.2.2 Longitudinal maneuvering characteristics

3.2.2.1 Short-period response. The short-period response of angle-of-attack which occurs at approximately constant speed, and which may be produced by abrupt control inputs, shall meet the requirements of 3.2.2.1.1 and 3.2.2.1.2. These requirements apply, with the cockpit control free and with it fixed, for responses of any magnitude that might be experienced in service use. If oscillations are nonlinear with amplitude, the requirements shall apply to each cycle of the oscillation. In addition to meeting the numerical requirements of 3.2.2.1.1 and 3.2.2.1.2, the contractor shall show that the airplane has suitable response characteristics in atmospheric disturbances (3.7 and 3.8).

3.2.2.1.1 Short-period frequency and acceleration sensitivity. The equivalent short-period undamped natural frequency, $\omega_{n_{sp}}$, shall be within the limits shown on Figures B1, B2 and B3. If suitable means of directly controlling normal force are provided, the lower bounds on $\omega_{n_{sp}}$ and n/α of Figure B3 may be relaxed if approved by the procuring activity.

3.2.2.1.2 Short-period damping. The equivalent short-period damping ratio, ζ_{sp} shall be within the limits of Table IV.

TABLE IV SHORT-PERIOD DAMPING RATIO LIMITS

	Category A and C Flight Phases		Category B Flight Phases	
Level	Minimum	Maximum	Minimum	Maximum
1	0.35	1.30	0.30	2.00
2	0.25	2.00	0.20	2.00
3	0.15*	-	0.15*	-

*May be reduced at altitudes above 20,000 ft if approved by the procuring activity.

3.2.2.1.3 Residual oscillations. Any sustained residual oscillations in calm air shall not interfere with the pilot's ability to perform the tasks required in service use of the airplane. For Levels 1 and 2, oscillations in normal acceleration at the pilot's station greater than +/-0.05g will be considered excessive for any Flight Phase, as will pitch attitude oscillations greater than +/-3 mils for Category A Flight Phases requiring precise control of pitch attitude. These requirements shall apply with the pitch control fixed and with it free.

3.2.2.2 Control feel and stability in maneuvering flight at constant speed. In steady turning flight and in pullups at constant speed, there shall be no tendency for the airplane pitch attitude or angle of attack to diverge aperiodically with controls fixed or with controls free. For the above conditions, the incremental force and control deflection required to maintain a change in normal load factor and pitch rate shall be in the same sense (aft-more positive, forward-more negative) as those required to initiate the change. These requirements apply for all local gradients throughout the range of service load factors defined in 3.1.8.4.

3.2.2.2.1 Control forces in maneuvering flight. At constant speed in steady turning flight, pullups and pushovers, the variation in pitch controller force with steady-state normal acceleration shall have no objectionable non-linearities within the following load factor ranges:

Class	Minimum	Maximum
I, II and III	0.5	$0.5(n_{o}(+) + 1)$ or 3
IV	0	whichever is less

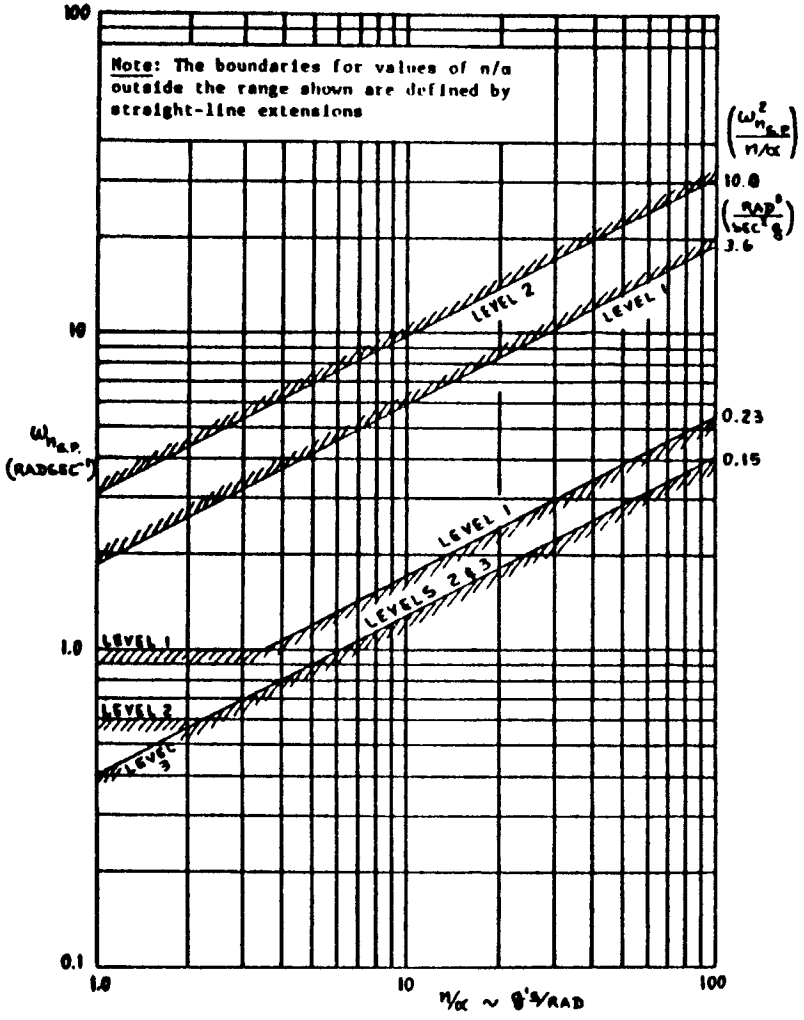

Figure B1 Short-Period Frequency Requirements-Category A Flight Phases

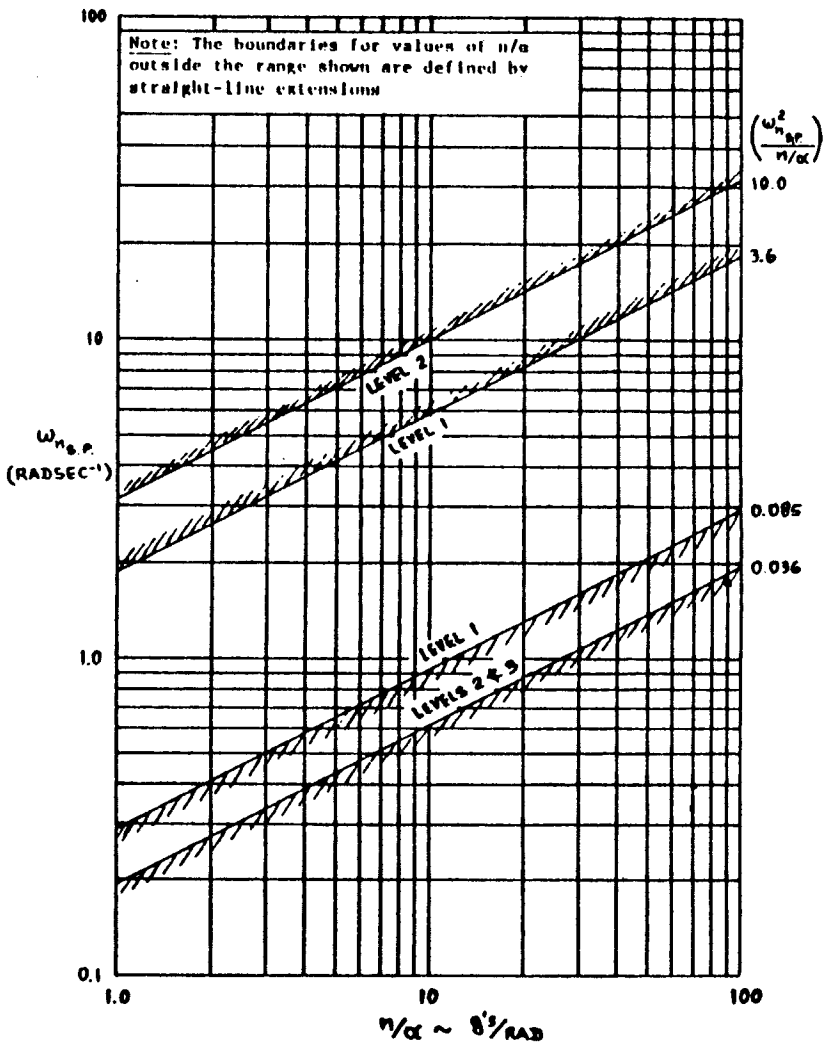

Figure B2 Short-Period Frequency Requirements-Category B Flight Phases

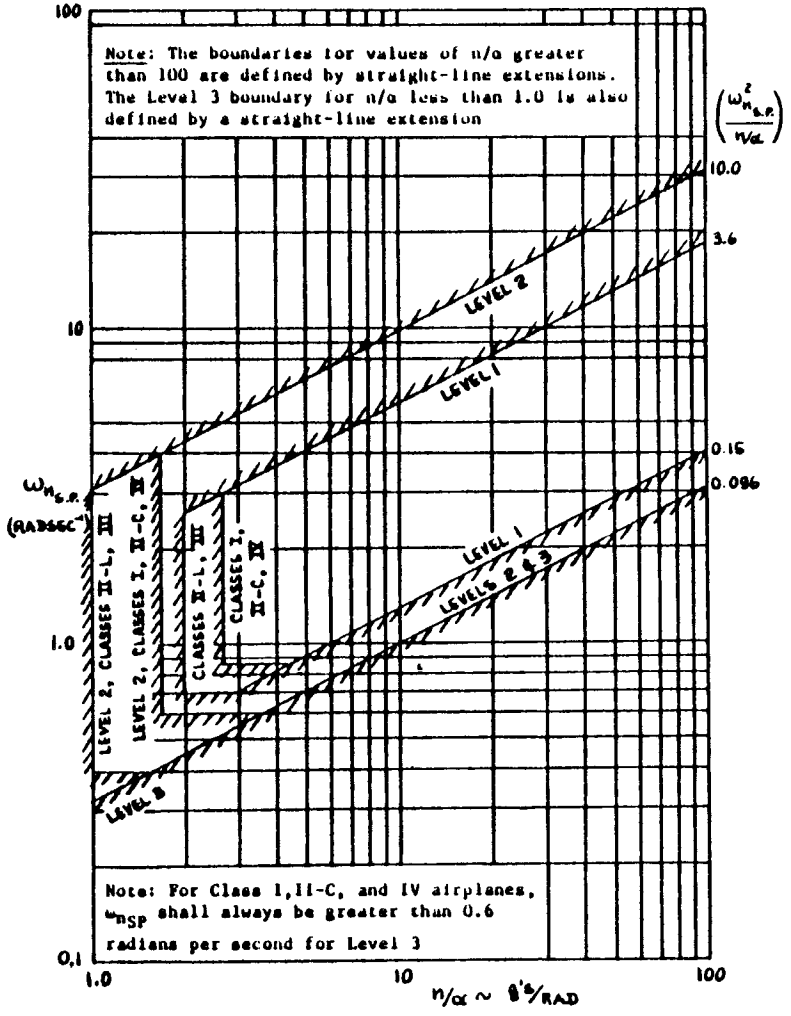

Figure B3 Short-Period Frequency Requirements-Category C Flight Phases

Outside this range, a departure from linearity resulting in a local gradient which differs from the average gradient for the maneuver by more than 50 percent is considered excessive, except that larger increases in force gradient are permissible at load factors greater than $0.85n_L$. All local force gradients shall be within the limits of Table V. In addition, F_s/n_z should be near the Level 1 upper boundaries of Table V for combinations of high frequency and low damping. The term gradient does not include that portion of the force versus n_z curve within the breakout force.

Since the range of acceptable force gradients for side stick controllers varies with the control deflection gradient and the task to be performed, the contractor shall show that the control force gradients will provide suitable flying qualities.

3.2.2.2.2 Control motions in maneuvering flight. For all types of pitch controllers, the control motions in maneuvering flight shall not be so large or so small as to be objectionable. For Category A Flight Phases, the average gradient of pitch-control force per unit of pitch-control deflection at constant speed shall not be less than 3.0 pounds per inch for wheel and center-stick controllers or 2.0 pounds per degree for side-stick controllers for Levels 1 and 2.

3.2.2.3 Longitudinal pilot-induced oscillations. There shall be no tendency for pilot-induced oscillations, that is, sustained or uncontrollable oscillations resulting from the efforts of the pilot to control the airplane. The pitch attitude response dynamics of the airplane plus control system shall not change abruptly with the motion amplitudes of pitch, pitch rate or normal acceleration unless it can be shown that this will not result in a pilot-induced oscillation. The requirements of 3.2.2.3.1 and 3.2.2.3.2 shall be met for all expected airplane motion amplitudes and frequencies, starting at any service load factor.

3.2.2.3.1 Dynamic control forces in maneuvering flight. The frequency response of normal acceleration at the pilot to pitch control force shall be such that the inverse amplitude is greater than the following for all frequencies greater than 1.0 rad/sec. Units are pounds per g.

Controller Type	Level 1	Level 2	Level 3
One-handed Controllers	$14/(n_L - 1)$	$12/(n_L - 1)$	$8/(n_L - 1)$
Two-handed Controllers	$30/(n_L - 1)$	$23/(n_L - 1)$	$17/(n_L - 1)$

3.2.2.3.2 Control feel. The deflection of the pilot's control must not lead the control force throughout the frequency range of pilot control inputs. In addition, the peak control forces developed during abrupt maneuvers shall not be objectionably light, and the buildup of control force during the maneuver entry shall lead the buildup of normal acceleration.

TABLE V PITCH MANEUVERING FORCE GRADIENT LIMITS

For Center Stick Controllers:

Level	Maximum Gradient, $(F_s/n)_{max}$, lbs/g	Minimum Gradient, $(F_s/n)_{min}$, lbs/g
1	240/(n/a) but not more than 28.0 nor less than $56/(n_L - 1)$*	The higher of $21/(n_L - 1)$ and 3.0
2	360/(n/a) but not more than 42.5 nor less than $85/(n_L - 1)$	The higher of $18/(n_L - 1)$ and 3.0
3	56.0	The higher of $12/(n_L - 1)$ and 2.0

*For n_L < 3, $(F_s/n)_{max}$ is 28.0 for Level 1, and 42.5 for Level 2.

For Wheel Controllers:

Level	Maximum Gradient, $(F_s/n)_{max}$, lbs/g	Minimum Gradient, $(F_s/n)_{min}$, lbs/g
1	500/(n/a) but not more than 120.0 nor less than $120/(n_L - 1)$	The higher of $35/(n_L - 1)$ and 6.0
2	775/(n/a) but not more than 182.0 nor less than $182/(n_L - 1)$	The higher of $30/(n_L - 1)$ and 6.0
3	240.0	3.0

3.2.3 Longitudinal control

3.2.3.1 Longitudinal control in unaccelerated flight. In erect unaccelerated flight at all service altitudes, the attainment of speed between V_S and V_{max} shall not be limited by the effectiveness of the longitudinal control or controls.

3.2.3.2 Longitudinal control in maneuvering flight. Within the Operational Flight Envelope, it shall be possible to develop, by use of the pitch control alone, the following range of load factors:

Levels 1 and 2 ----- $n_o(-)$ to $n_o(+)$

Level 3 ----- n = 0.5g to the lower of:

a) $n_o(+)$

b) n = 2.0 for $n_o(+)$ < 3g

= $0.5(n_o(+) + 1)$ for $n_o(+)$ > 3g

This maneuvering capability is required at the 1g trim speed and, with trim and throttle settings not changed by the crew, over a range about the trim speed the lesser of +/-15 percent or +/-50 knots equivalent airspeed (except where limited by the boundaries of the Operational Flight Envelope). Within the Service and Permissible Flight Envelopes, the dive-recovery requirements of 3.2.3.5 and 3.2.3.6, respectively, shall be met.

3.2.3.3 Longitudinal control in takeoff. The effectiveness of the pitch control shall not restrict the takeoff performance of the airplane and shall be sufficient to prevent over-rotation to undesirable attitudes during takeoffs. Satisfactory takeoffs shall not be dependent upon use of the trimmer control during takeoff or on complicated control manipulation by the pilot. For nose-wheel airplanes it shall be possible to obtain, at $0.9V_{min}$, the pitch attitude which will result in takeoff at V_{min}. For tail-wheel airplanes, it shall be possible to maintain any pitch attitude up to that for a level thrust-line at $0.5V_S$ for Class I airplanes and at V_S for Class II, III and IV airplanes. These requirements shall be met on hard-surfaced runways. In the event that an airplane has a mission requirement for operation from unprepared fields, these requirements shall be met on such fields.

3.2.3.3.1 Longitudinal control in catapult takeoff. On airplanes designed for catapult takeoff, the effectiveness of the pitch control shall be sufficient to prevent the airplane from pitching up or down to undesirable attitudes in catapult takeoffs at speeds ranging from the minimum safe launching speed to launching speed 30 knots higher than the minimum. Satisfactory catapult takeoffs shall not depend upon complicated control manipulation by the pilot.

3.2.3.3.2 Longitudinal control force and travel in takeoff. With the trim setting optional but fixed, the pitch-control forces required during all types of takeoffs for which the airplane is designed, including short-field takeoffs and assisted takeoffs such as catapult or rocket-augmented, shall be within the following limits:

Nose-wheel and bicycle-gear airplanes

Classes I, IV-C -------- 20 pounds pull to 10 pounds push

Classes II-C, IV-L ----- 30 pounds pull to 10 pounds push

Classes II-L, III ------ 50 pounds pull to 20 pounds push

Tail-wheel airplanes

Classes I, II-C, IV ---- 20 pounds push to 10 pounds pull

Classes II-L, III ------ 35 pounds push to 15 pounds pull

The pitch-control travel during takeoffs shall not exceed 75 percent of the total travel, stop-to-stop. Here the term takeoff includes the ground run, rotation and lift-off, the ensuing acceleration to V_{max}(TO), and the transient caused by assist cessation. Takeoff power shall be maintained until V_{max}(TO) is reached, with the landing gear and high-lift devices retracted in the normal manner at speeds from $V_{o_{min}}$ (TO) to V_{max}(TO).

3.2.3.4 Longitudinal control in landing. The pitch control shall be sufficiently effective in the landing Flight Phase in close proximity to the ground, that in calm air:

a. The geometry-limited touchdown attitude can be maintained in level flight or

b. The lower of V_S(L) or the guaranteed landing speed can be obtained.

This requirement shall be met with the airplane trimmed for the approach Flight Phase at the recommended approach speed. The requirements of 3.2.3.4 and 3.2.3.4.1 define Levels 1 and 2, and the requirements of 3.4.10 define Level 3.

3.2.3.4.1 Longitudinal control forces in landing. The pitch-control forces required to meet the requirements of 3.2.3.4 shall be pull forces and shall not exceed:

Classes I, II-C ----- 35 pounds

Classes II-L -------- 50 pounds

3.2.3.5 Longitudinal control forces in dives - Service Flight Envelope. With the airplane trimmed for level flight at speeds throughout the Service Flight Envelope, the control forces in dives to all attainable airspeeds within the Service Flight Envelope shall not exceed 50 pounds push or 10 pounds pull for center-stick controllers, nor 75 pounds push or 15 pounds pull for wheel controllers. In similar dives, but with trim optional following the dive entry, it shall be possible with normal piloting techniques to maintain the forces within the limits of 10 pounds push or pull for center-stick controllers, and 20 pounds push or pull for wheel controllers. In event that operation of the trim system requires removal of one hand from a wheel control the force limits shall be as for a center-stick. The forces required for recovery from these dives shall be in accordance with the gradients specified in 3.2.2.2.1 although speed may vary during the pullout.

3.2.3.6 Longitudinal control forces in dives - Permissible Flight Envelope. With the airplane trimmed for level flight at V_{MAT} but with trim optional in the dive, it shall be possible to maintain the pitch control force within the limits of 50 pounds push or 35 pounds pull in dives to all attainable speeds within the Permissible Flight Envelope. The force required for recovery from these dives shall not exceed 120 pounds. Trim and deceleration devices, etc., may be used to assist in recovery if no unusual pilot technique is required.

3.2.3.7 Longitudinal control in sideslips. With the airplane trimmed for straight, level flight with zero sideslip, the pitch-control force required to maintain constant speed in steady sideslips with up to 50 pounds of pedal force in either direction shall not exceed the pitch-control force that would result in a 1g change in normal acceleration. In no case, however, shall the pitch-control force exceed:

Center-stick controllers ----- 10 lbs pull to 3 lbs push

Wheel controllers ------------ 15 lbs pull to 10 lbs push

If a variation of pitch-control force with sideslip does exist, it is preferred that increasing pull force accompany increasing sideslip, and that the magnitude and direction of the force change be similar for right and left sideslips. These requirements define Levels 1 and 2. For Level 3 there shall be no uncontrollable pitching motions associated with the sideslips discussed above.

3.3 Lateral-directional flying qualities

3.3.1 Lateral-directional mode characteristics

3.3.1.1 Lateral-directional oscillations (Dutch roll). The frequency, ω_{n_d}, and damping ratio, ζ_d, of the lateral-directional oscillations following a yaw disturbance input shall exceed the minimum values in Table VI. The requirements shall be met in trimmed and in maneuvering flight with the cockpit controls fixed and with them free, in oscillations of any magnitude that might be expected in operational use. If the oscillation is nonlinear with amplitude, the requirements shall apply to each cycle of the oscillation. In calm air residual oscillations may be tolerated only if the amplitude is sufficiently small that the motions are not objectionable and do not impair mission performance. For Category A Flight Phases, angular deviations shall be less than +/- 3 mils.

3.3.1.2 Roll mode. The roll-mode time constant, T_r, shall be no greater than the appropriate value in Table VII.

TABLE VI MINIMUM DUTCH ROLL FREQUENCY AND DAMPING

Level	Flight Phase Category	Class	Min. ζ_d *	Min. $\zeta_d\omega_{n_d}$ * rad/sec.	Min. ω_{n_d} rad/sec.
1	A (CO and GA)	IV	0.4	-	1.0
	A	I, IV	0.19	0.35	1.0
		II, III	0.19	0.35	0.4**
	B	All	0.08	0.15	0.4**
	C	I, II-C, IV	0.08	0.15	1.0
		II-L, III	0.08	0.10	0.4**
2	All	All	0.02	0.05	0.4**
3	All	All	0	-	0.4**

* The governing damping requirement is that yielding the larger value of ζ_d, except that a ζ_d of 0.7 is the maximum required for Class III.

** Class III airplanes may be excepted from the minimum ω_{n_d} requirement, subject to approval by the procuring activity, if the requirements of 3.3.2 through 3.3.2.4.1, 3.3.5 and 3.3.9.4 are met.

When $(\omega_{n_d})^2|\phi/\beta|_d$ is greater than 20 $(rad/sec)^2$, the minimum $\zeta_d\omega_{n_d}$ shall be increased above the $\zeta_d\omega_{n_d}$ minimums listed in Table VI by:

Level 1 - $\Delta\zeta_d\omega_{n_d} = 0.014((\omega_{n_d})^2|\phi/\beta|_d - 20)$

Level 2 - $\Delta\zeta_d\omega_{n_d} = 0.009((\omega_{n_d})^2|\phi/\beta|_d - 20)$

Level 3 - $\Delta\zeta_d\omega_{n_d} = 0.005((\omega_{n_d})^2|\phi/\beta|_d - 20)$

with ω_{n_d} in rad/sec.

TABLE VII MAXIMUM ROLL-MODE TIME CONSTANT, T_r, SECONDS

Flight Phase Category	Class	Level 1	Level 2	Level 3
A	I, IV	1.0	1.4	
	II, III	1.4	3.0	
B	All	1.4	3.0	10.0
C	I, II-C, IV	1.0	1.4	
	II-L, III	1.4	3.0	

3.3.1.3 Spiral stability. The combined effects of spiral stability, flight-control-system characteristics and rolling moment change with speed shall be such that following a disturbance in bank of up to 20 degrees, the time for the bank angle to double shall be greater than the values in Table VIII. This requirement shall be met with the airplane trimmed for wings-level, zero-yaw-rate flight with the cockpit controls free.

TABLE VIII SPIRAL STABILITY - MINIMUM TIME TO DOUBLE AMPLITUDE, T_{2_s}

Flight Phase Category	Level 1	Level 2	Level 3
A and C	12 sec.	8 sec.	4 sec.
B	20 sec.	8 sec.	4 sec.

3.3.1.4 Coupled roll-spiral oscillation. For Flight Phases which involve more than gentle maneuvering, such as CO and GA, the airplane characteristics shall not exhibit a coupled roll-spiral mode in response to the pilot roll control commands. A coupled roll-spiral mode will be permitted for Category B and C Flight Phases provided the product of frequency and damping ratio exceeds the following requirements:

Level	$\zeta_{rs}\omega_{n_{rs}}$, rad/sec
1	0.5
2	0.3
3	0.15

3.3.2 Lateral-directional dynamic response characteristics. Lateral-directional dynamic response characteristics are stated in terms of response to atmospheric disturbances and in terms of allowable roll rate and bank angle oscillations, sideslip excursions, roll control forces and yaw control forces that occur during specified rolling and turning maneuvers to the right and to the left. The requirements of 3.3.2.2, 3.3.2.3 and 3.3.2.4 apply for roll commands of all magnitudes needed to meet the roll performance requirements of 3.3.4 and 3.3.4.1.

3.3.2.1 Lateral-directional response to atmospheric disturbances. The combined effect of ω_{n_d}, ζ_d, T_r, $|\phi/\beta|_d$, $\angle(p/\beta)$, gust sensitivity, and flight-control-system nonlinearities on response and controllability characteristics in atmospheric disturbances shall be considered (see 3.8.3). In particular, the roll acceleration, rate and displacement responses to side gusts shall be investigated for airplanes with large rolling moment due to sideslip (i.e. large dihedral effect).

3.3.2.2 Roll rate oscillations. Following a yaw-control-free step roll control command, the roll rate at the first minimum following the first peak shall be of the same sign and not less than the following percentage of the roll rate at the first peak:

Level	Flight Phase Category	Percent
1	A and C	60
	B	25
2	A and C	25
	B	0

For all Levels, the change in bank angle shall always be in the direction of the roll control command. The roll command shall be held fixed until the bank angle has changed at least 90 degrees.

3.3.2.2.1 Additional roll rate requirement for small inputs. The value of the parameter p_{osc}/p_{av} following a yaw-control-free step roll command shall be within the limits shown on Figure B4 for Levels 1 and 2. This requirement applies for step roll-control commands up to the magnitude which causes a 60-degree bank angle change in $1.7T_d$ seconds.

3.3.2.3 Bank angle oscillations. The value of the parameter ϕ_{osc}/ϕ_{av} following a yaw-control-free impulse roll control command shall be within the limits as shown on Figure B5 for Levels 1 and 2. The impulse shall be as abrupt as practical within the strength limits of the pilot and the rate limits of the roll control system.

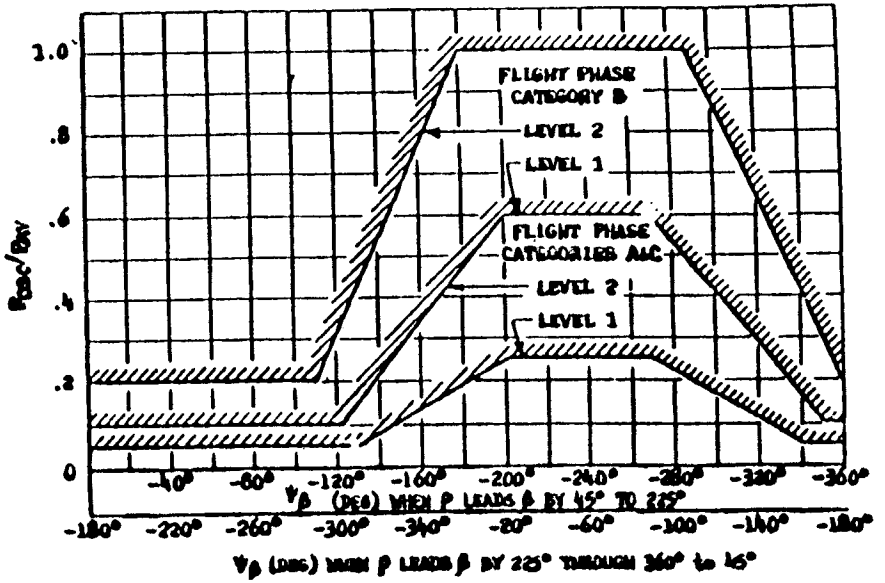

Figure B4 Roll Rate Oscillation Limitations

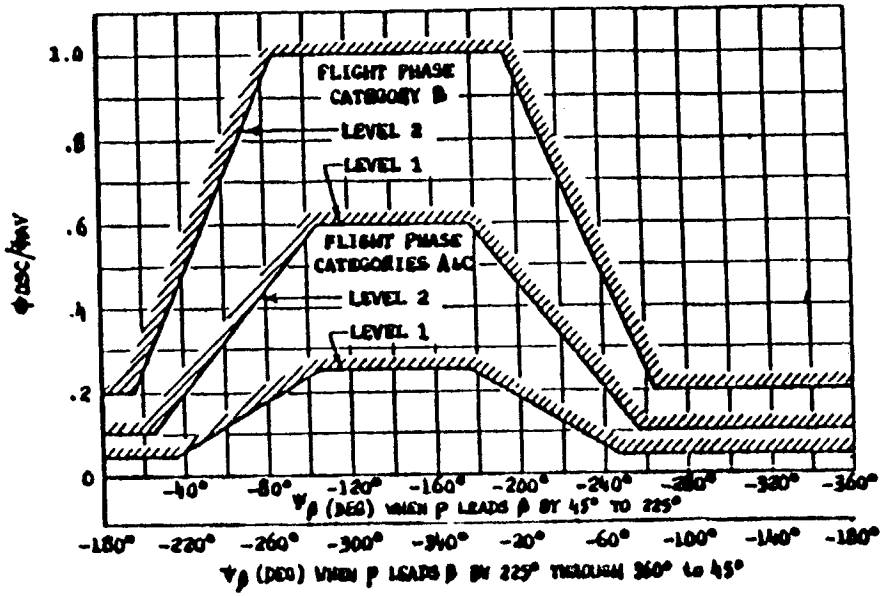

Figure B5 Bank Angle Oscillation Limittions

3.3.2.4 Sideslip excursions. Following a yaw-control-free step roll control command, the ratio of the sideslip increment, $\Delta\beta$ to the parameter k (6.2.6) shall be less than the values specified herein. The roll command shall be held fixed until the bank angle has changed at least 90 degrees.

Level	Flight Phase Category	Adverse Sideslip (Right roll command causes RIGHT sideslip	Proverse Sideslip (Right roll command causes LEFT sideslip
1	A	6 degrees	2 degrees
	B and C	10 degrees	3 degrees
2	All	15 degrees	4 degrees

3.3.2.4.1 Additional sideslip requirement for small inputs. The amount of sideslip following a yaw-control-free step roll control command shall be within the limits shown on Figure B6 for Levels 1 and 2. This requirement shall apply for step roll control commands up to the magnitude which causes a 60-degree bank angle change within T_d or 2 seconds, whichever is longer.

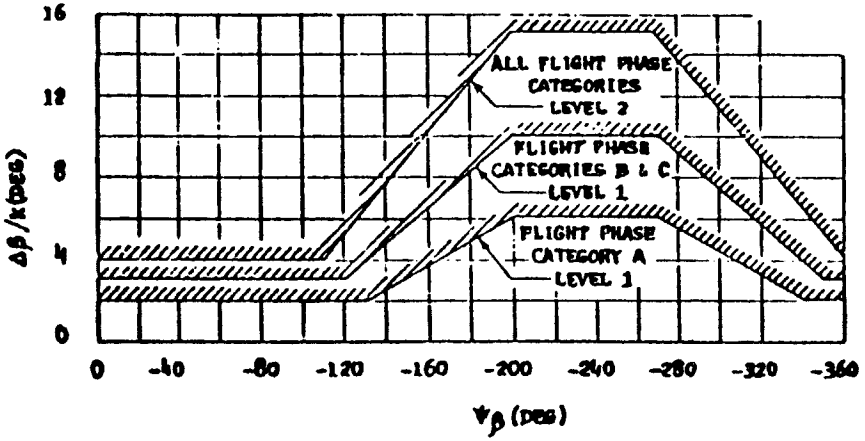

Figure B6 Sideslip Excursion Limitations

3.3.2.5 Control of sideslip in rolls. In the rolling maneuvers described in 3.3.4, but with coordination allowed for all Classes, directional-control effectiveness shall be adequate to maintain zero sideslip with pedal force not greater than 50 pounds for Class IV airplanes in Flight Phase Category A, Level 1, and 100 pounds for all other combinations of Class, Flight Phase Category and Level.

3.3.2.6 Turn coordination. It shall be possible to maintain steady coordinated turns in either direction, using 60 degrees of bank for Class IV airplanes, 45 degrees of bank for Class I and II airplanes, and 30 degrees of bank for Class III airplanes, with a pedal force not exceeding 40 pounds. It shall be possible to perform steady turns at the same bank angles with yaw-controls-free, with a roll-stick force not exceeding 5 pounds or a roll-wheel force not exceeding 10 pounds. These requirements constitute Levels 1 and 2, with the airplane trimmed for wings-level straight flight.

3.3.3 Pilot-induced oscillations. There shall be no tendency for sustained or uncontrollable lateral-directional oscillations resulting from efforts of the pilot to control the airplane.

3.3.4 Roll control effectiveness. Roll performance in terms of a bank angle change in a given time, ϕ_t, is specified in Table IXa for Class I and Class II airplanes, in 3.3.4.1 for Class IV airplanes, and in 3.3.4.2 for Class III airplanes. For rolls from banked flight, the initial condition shall be coordinated, that is, zero lateral acceleration. The requirements apply to roll commands to the right and to the left, initiated both from steady bank angles and from wings-level flight except as otherwise stated. Inputs shall be abrupt, with the time measured from the initiation of control force application. The pitch control shall be fixed throughout the maneuver. Yaw control pedals shall remain free for Class IV airplanes for Level 1, and for all carrier-based airplanes in Category C Flight Phases for Levels 1 and 2, but otherwise, yaw control pedals may be used to reduce sideslip that retards roll rate (not to produce sideslip which augments roll rate) if such control inputs are simple, easily coordinated with roll control inputs and consistent with piloting techniques for the airplane class and mission. For Flight Phase TO, the time required to bank may be increased proportional to the ratio of the rolling moment of inertia at takeoff to the largest rolling moment of inertia at landing, for weights up to the maximum authorized landing weight.

TABLE IXa ROLL PERFORMANCE FOR CLASS I AND II AIRPLANES

Time to Achieve the Following Bank Angle Change (Seconds)

Class	Level	Category A		Category B		Category C	
		60^{o}	45^{o}	60^{o}	45^{o}	30^{o}	25^{o}
I	1	1.3		1.7		1.3	
I	2	1.7		2.5		1.8	
I	3	2.6		3.4		2.6	
II-L	1		1.4		1.9	1.8	
II-L	2		1.9		2.8	2.5	
II-L	3		2.8		3.8	3.6	
II-C	1		1.4		1.9		1.0
II-C	2		1.9		2.8		1.5
II-C	3		2.8		3.8		2.0

TABLE IXb ROLL PERFORMANCE FOR CLASS IV AIRPLANES

Time to Achieve the Following Bank Angle Change (Seconds)

Level	Speed	Category A			Category B	Category C
	Range	30^{o}	50^{o}	90^{o}	90^{o}	30^{o}
1	VL	1.1			2.0	1.1
	L	1.1			1.7	1.1
	M			1.3	1.7	1.1
	H		1.1		1.7	1.1
2	VL	1.6			2.8	1.3
	L	1.5			2.5	1.3
	M			1.7	2.5	1.3
	H		1.3		2.5	1.3
3	VL	2.6			3.7	2.0
	L	2.0			3.4	2.0
	M			2.6	3.4	2.0
	H		2.6		3.4	2.0

3.3.4.1 Roll performance for Class IV airplanes. Roll performance in terms of ϕ_t for Class IV airplanes is specified in Table IXb. Additional or alternate roll performance requirements are specified in 3.3.4.1.1 and 3.3.4.1.2: these requirements take precedence over those in Table IXb. Roll performance for Class IV airplanes is specified over the following ranges of airspeeds:

Speed Range		Equivalent Airspeed Range
VL	Level 1:	$V_{o_{min}} \leq V < V_{min} + 20$ kts
	Levels 2 and 3:	$V_{min} \leq V \leq V_{min} + 20$ kts
L	Level 1:	$V_{min} + 20$ kts$^{(1)} \leq V < 1.4V_{min}$
	Levels 2 and 3:	$V_{min} + 20$ kts $\leq V < 1.4V_{min}$
M	Level 1:	$1.4V_{o_{min}} \leq V < 0.7V_{max}$$^{(2)}$
	Levels 2 and 3:	$1.4V_{min} \leq V < 0.7V_{max}$
H	Level 1:	$0.7V_{max}$$^{(2)} < V \leq V_{o_{max}}$
	Levels 2 and 3:	$0.7V_{max} \leq V \leq V_{max}$

(1) or $V_{o_{min}}$ whichever is greater

(2) or $V_{o_{max}}$ whichever is less

3.3.4.1.1 Roll performance in Flight Phase CO. Roll performance for Class IV airplanes in Flight Phase CO is specified in Table IXc in terms of ϕ_t for 360 degree rolls initiated at 1g, and in Table IXd for rolls initiated at load factors between $0.8n_o(-)$ and $0.8n_o(+)$.

3.3.4.1.2 Roll performance in Flight Phase GA. The roll performance requirements for Class IV airplanes in Flight Phase GA with large complements of external stores may be relaxed from those specified in Table IXb, subject to approval by the procuring activity. For any external loading specified in the contract, however, the roll performance shall not be less than that in Table IXe where the roll performance is specified in terms of ϕ_t for rolls initiated at load factors between $0.8n_o(-)$ and $0.8n_o(+)$.

For any asymmetric loading specified in the contract, roll control power shall be sufficient to hold the wings level at the maximum load factors specified in 3.2.3.2 with adequate control margin (3.4.10).

3.3.4.1.3 Roll response. Stick-controlled Class IV airplanes in Category A Flight Phase shall have a roll response to control force not greater than 15 degrees in 1 second per pound for Level 1, and not greater than 25 degrees in 1 second per pound for Level 2. For Category C

TABLE IXc FLIGHT PHASE CO ROLL PERFORMANCE IN 360° ROLLS

Level	Speed Range	Time to Achieve the Following Bank Angle Change (Seconds) 30°	90°	180°	360°
1	VL	1.0			
	L		1.4	2.3	4.1
	M		1.0	1.6	2.8
	H		1.4	2.3	4.1
2	VL	1.6			
	L	1.3			
	M		1.3	2.0	3.4
	H		1.7	2.6	4.4
3	VL	2.5			
	L	2.0			
	M		1.7	3.0	
	H		2.1		

TABLE IXd FLIGHT PHASE CO ROLL PERFOHMANCE

Level	Speed Range	Time to Achieve the Following Bank Angle Change (Seconds) 30°	50°	90°	180°
1	VL	1.0			
	L		1.1		
	M			1.1	2.2
	H		1.0		
2	VL	1.6			
	L	1.3			
	M			1.4	2.8
	H		1.4		
3	VL	2.5			
	L	2.0			
	M			1.7	3.4
	H		1.7		

Flight Phases. the roll sensitivity shall be not greater than 7.5 degrees in 1 second per pound for Level 1, and not greater than 12.5 degrees in 1 second per pound for Level 2. In case of conflict between the requirements of 3.3.4.1.3 and 3.3.4.3, the requirements of 3.3.4.1.3 shall govern. The term sensitivity does not include breakout force.

TABLE IXe FLIGHT PHASE GA ROLL PERFORMANCE

Level	Speed Range	Time to Achieve the Following Bank Angle Change (Seconds) 30°	50°	90°	180°
1	VL	1.5			
	L		1.7		
	M			1.7	3.0
	H		1.5		
2	VL	2.8			
	L	2.2			
	M			2.4	4.2
	H		2.4		
3	VL	4.4			
	L	3.8			
	M			3.4	6.0
	H		3.4		

TABLE IXf CLASS III ROLL PERFORMANCE

Level	Speed Range	Time to Achieve 30° Bank Angle Change (Seconds) Category A	Category B	Category C
1	L	1.8	2.3	2.5
	M	1.5	2.0	2.5
	H	2.0	2.3	2.5
2	L	2.4	3.9	4.0
	M	2.0	3.3	4.0
	H	2.5	3.9	4.0
3	All	3.0	5.0	6.0

3.3.4.2 Roll performance for Class III airplanes. Roll performance in terms of ϕ_t for Class III airplanes is specified in Table IXf over the following ranges of airspeeds:

Speed Range		Equivalent Airspeed Range
L	Level 1:	$V_{o_{min}} \leq V < 1.8V_{min}$
	Levels 2 and 3:	$V_{min} \leq V < 1.8V_{min}$
M	Level 1:	$1.8V_{min}$ (1) $\leq V < 0.7V_{max}$ (2)
	Levels 2 and 3:	$1.8V_{min} \leq V < 0.7V_{max}$
H	Level 1:	$0.7V_{max}$ (2) $\leq V \leq V_{o_{max}}$
	Levels 2 and 3:	$0.7V_{max} \leq V \leq V_{max}$

(1) or $V_{o_{min}}$ whichever is greater

(2) or $V_{o_{max}}$ whichever is less

3.3.4.3 Roll control forces. The stick or wheel force required to obtain the rolling performance specified in 3.3.4, 3.3.4.1 and 3.3.4.2 shall be neither greater than the maximum in Table X nor less than the breakout force plus:

a. Level 1 ----- one-fourth the values in Table X

b. Level 2 ----- one-eighth the values in Table X

c. Level 3 ----- zero

TABLE X MAXIMUM ROLL CONTROL FORCES

Level	Class	Flight Phase Category	Maximum Stick Force (lbs)	Maximum Wheel Force (lbs)
1	I,II-C, IV	A, B	20	40
		C	20	20
	II-L, III	A, B	25	50
		C	25	25
2	I, II-C, IV	A, B	30	60
		C	20	20
	II-L, III	A, B	30	60
		C	30	30
3	All	All	35	70

3.3.4.4 Linearity of roll response. There shall be no objectionable nonlinearities in the variation of rolling response with roll control deflection or force. Sensitivity or sluggishness in response to small control deflections or force shall be avoided.

3.3.4.5 Wheel control throw. For airplanes with wheel controllers, the wheel throw necessary to meet the roll performance requirements specified in 3.3.4 and 3.3.4.2 shall not exceed 60 degrees in either direction. For completely mechanical systems, the requirement may be relaxed to 80 degrees.

3.3.5 Directional control characteristics. Directional stability and control characteristics shall enable the pilot to balance yawing moments and control yaw and sideslip. Sensitivity to yaw control pedal forces shall be sufficiently high that directional control and force requirements can be met and satisfactory coordination can be achieved without unduly high pedal forces, yet sufficiently low that occasional improperly coordinated control inputs will not seriously degrade the flying qualities.

3.3.5.1 Directional control with speed change. When initially trimmed directionally with symmetric power, the trim change of propeller-driven airplanes with speed shall be such that wings-level straight flight can be maintained over a speed range of +/- 30 percent of the trim speed or +/- 100 knots equivalent airspeed, whichever is less (except where limited by boundaries of the Service Flight Envelope) with yaw-control-pedal forces not greater than 100 pounds for Levels 1 and 2 and not greater than 180 pounds for Level 3, without retrimming. For other airplanes, yaw-control-pedal forces shall not exceed 40 pounds at the specified conditions for Levels 1 and 2 or 180 pounds for Level 3.

3.3.5.1.1 Directional control with asymmetric loading. When initially trimmed directionally with each asymmetric loading specified in the contract at any speed in the Operational Flight Envelope, it shall be possible to maintain a straight flight path throughout the Operational Flight Envelope with yaw-control-pedal forces not greater than 100 pounds for Levels 1 and 2 and not greater than 180 pounds for Level 3, without retrimming.

3.3.5.2 Directional control in wave-off (go-around). For propeller-driven Class IV, and all propeller-driven carrier-based airplanes the response to thrust, configuration and airspeed change shall be such that the pilot can maintain straight flight during wave-off (go-around) initiated at speeds down to V_s (PA) with yaw-control-pedal forces not exceeding 100 lbs when trimmed at $V_{o_{min}}$ (PA).

For other airplanes, yaw-control-pedal forces shall not exceed 40 pounds for the specified conditions. The preceding requirements apply for Levels 1 and 2. For all

airplanes the Level 3 requirement is to maintain straight flight in these conditions with yaw-control-pedal forces not exceeding 180 pounds. For all Levels, bank angles up to 5 degrees are permitted.

3.3.6 Lateral-directional characteristics in steady sideslips. The requirements of 3.3.6.1 through 3.3.6.3.1 and 3.3.7.1 are expressed in terms of characteristics in yaw-control-induced steady, zero-yaw-rate sideslips with the airplane trimmed for wings-level straight flight. Requirements of 3.3.6.1 through 3.3.6.3 apply at sideslip angles up to those produced or limited by:

a. Full yaw-control-pedal deflection, or

b. 250 pounds of yaw-control-pedal force, or

c. Maximum roll control or surface deflection,

except that for single-propeller-driven airplanes during wave-off (go-around), yaw-control-pedal deflection in the direction opposite to that required for wings-level straight flight need not be considered beyond the deflection for a 10-degree change in sideslip from the wings-level straight flight condition.

3.3.6.1 Yawing moments in steady sideslips. For sideslips specified in 3.3.6, right yaw-control-pedal deflection and force shall produce left sideslips and left yaw-control-pedal deflection and force shall produce right sideslips. For Levels 1 and 2 the following requirements shall apply. The variation of sideslip angle with yaw-control-pedal deflection shall be essentially linear for sideslip angles between +15 degrees and -15 degrees. For larger sideslip angles, an increase in yaw-control-pedal deflection shall always be required for an increase in sideslip. The variation of sideslip angle with yaw-control-pedal force shall be essentially linear for sideslip angles between +10 degrees and -10 degrees. Although a lightening of pedal force is acceptable for sideslip angles outside this range, the pedal force shall never reduce to zero.

3.3.6.2 Side forces in steady sideslips. For the sideslips of 3.3.6, an increase in right bank angle shall accompany an increase in right sideslip, and an increase in left bank angle shall accompany an increase in left sideslip.

3.3.6.3 Rolling moments in steady sideslips. For the sideslips of 3.3.6, left roll-control deflection and force shall accompany left sideslips, and right roll-control deflection and force shall accompany right sideslips. For Levels 1 and 2, the variation of roll-control deflection and force with sideslip angle shall be essentially linear.

3.3.6.3.1 Exception for wave-off (go-around). The requirement of 3.3.6.3 may, if necessary, be excepted for wave-off (go-around) if task performance is not impaired and no more than 50 percent of roll control power available to the pilot, and no more than 10 pounds of roll-control force, are required in a direction opposite to that specified in 3.3.6.3.

3.3.6.3.2 Positive effective dihedral limit. For Levels 1 and 2, positive effective dihedral (right roll control for right sideslip and left roll control for left sideslip) shall never be so great that more than 75 percent of roll control power available to the pilot, and no more than 10 pounds of roll-stick force or 20 pounds of roll-wheel force, are required for sideslip angles which might be experienced in service employment.

3.3.7 Lateral-directional control in crosswinds. It shall be possible to take off and land with normal pilot skill and technique in 90-degree crosswinds, from either side, of velocities up to those specified in Table XI. Roll-control force shall be within the limits specified in 3.3.4.2, and yaw-control-pedal forces shall not exceed 100 pounds for Level 1 or 180 pounds for Levels 2 and 3. This requirement can normally be met through compliance with 3.3.7.1 and 3.3.7.2.

TABLE XI CROSSWIND VELOCITY

Level	Class	Crosswind
1 and 2	I	20 knots
	II, III, and IV	30 knots
	Water-based airplanes	20 knots
3	All	One half the values for Levels 1 and 2

3.3.7.1 Final approach in crosswinds. For all airplanes except land-based airplanes equipped with crosswind landing gear, or otherwise constructed to land in a large crabbed attitude, yaw- and roll-control power shall be adequate to develop at least 10 degrees of sideslip (3.3.6) in the power approach with yaw-control-pedal forces not exceeding the values specified in 3.3.7. For Level 1, roll control shall not exceed either 10 pounds of force or 75 percent of control power available to the pilot. For Levels 2 and 3, roll-control force shall not exceed 20 pounds.

3.3.7.2 Takeoff run and landing rollout in crosswinds. Yaw and roll control power, in conjunction with other normal means of control, shall be adequate to maintain a straight flight path on the ground or other landing surface. This requirement applies in calm air and in crosswinds up to the values specified in Table XI with cockpit control forces not exceeding the values specified in 3.3.7.

3.3.7.2.1 Cold- and wet-weather operation. The requirements of 3.3.7.2 apply on wet runways for all airplanes, and on snow-packed and icy runways for airplanes intended to operate under such conditions. If compliance is not demonstrated under these adverse runway conditions, directional control shall be maintained by use of aerodynamic controls alone at all airspeeds above 50 knots for Class IV airplanes and above 30 knots for all others. For very slippery runways, the requirement need not apply for crosswind components at which the force tending to blow the airplane off the runway exceeds the opposing tire-runway frictional force with the tires supporting the entire weight of the airplane.

3.3.7.2.2 Carrier-based airplanes. All carrier-based airplanes shall be capable of maintaining a straight path on the ground without the use of wheel brakes, at airspeeds of 30 knots and above, during takeoffs and landings in a 90-degree crosswind of at least 10 percent $V_S(L)$. Cockpit control forces shall be as specified in 3.3.7.

3.3.7.3 Taxiing wind speed limits. It shall be possible to taxi at any angle to a 35-knot wind for Class I airplanes and to a 45-knot wind for Class II, III and IV airplanes.

3.3.8 Lateral-directional control in dives. Yaw and roll control power shall be adequate to maintain wings level and sideslip zero, without retrimming, throughout the dives and pullouts of 3.2.3.5 and 3.2.3.6. In the Service Flight Envelope, roll control forces shall not exceed 20 pounds for propeller-driven airplanes or 10 pounds for other airplanes. Yaw-control-pedal forces shall not exceed 180 pounds for propeller-driven airplanes or 50 lbs for other airplanes.

3.3.9 Lateral-directional control with asymmetric thrust. Asymmetric loss of thrust may be caused by many factors including engine failure, inlet unstart, propeller failure or propeller-drive failure. Following sudden asymmetric loss of thrust from any factor, the airplane shall be safely controllable in the crosswinds of Table XI from the unfavorable direction. The requirements of 3.3.9.1 through 3.3.9.4 apply for the appropriate Flight Phases when any single failure or malperformance of the propulsive system, including inlet or exhaust, causes loss of thrust on one or more engines or propellers, considering also the effect of the failure or malperformance on all subsystems or driven by the failed propulsive system.

3.3.9.1 Thrust loss during takeoff run. It shall be possible for the pilot to maintain control of an airplane on the takeoff surface following sudden loss of thrust from the most critical factor. Thereafter, it shall be possible to achieve and maintain a straight path on the takeoff surface without a deviaton of more than 30 feet from the path originally intended, with yaw-control-pedal forces not exceeding 180 pounds. For the continued takeoff, the requirement shall be met when thrust is lost at speeds from the refusal speed (based on the shortest runway from which the airplane is designed to operate) to the maximum takeoff speed, with takeoff thrust maintained on the operative engine(s), using only controls not dependent upon friction against the takeoff surface or upon release of the pitch, roll, yaw or throttle controls. For the aborted takeoff, the requirement shall be met at all speeds below the maximum takeoff speed, however, additional controls such as nosewheel steering and differential braking may be used. Automatic devices which normally operate in the event of a thrust failure may be used in either case.

3.3.9.2 Thrust loss after takeoff. During takeoff it shall be possible without a change in selected configuration to achieve straight flight following sudden asymmetric loss of thrust from the most critical factor at speeds from V_{min} (TO) to V_{max} (TO), and thereafter to maintain straight flight throughout the climbout. The yaw-control-pedal force required to maintain straight flight with asymmetric thrust shall not exceed 180 lbs. Roll control shall not exceed either the force limits specified in 3.3.4.3 or 75 percent of available control power, with takeoff thrust maintained on the operative engine(s) and trim at normal setting for takeoff with symmetric thrust. Automatic devices which normally operate in the event of a thrust failure may be used, and the airplane may be banked up to 5 degrees away from the inoperative engine.

3.3.9.3 Transient effects. The airplane motions following sudden asymmetric loss of thrust shall be such that dangerous conditions can be avoided by pilot corrective action. A realistic time delay (3.4.8) of at least 1 second shall be incorporated.

3.3.9.4 Asymmetric thrust - yaw controls free. The static directional stability shall be such that at all speeds above $1.4V_{min}$, with asymmetric loss of thrust from the most critical factor while the other engine(s) develop normal rated thrust, the airplane with yaw-control-pedals free may be balanced directionally in steady straight flight. The trim settings shall be those required for wings-level straight flight prior to the engine failure. Roll-control forces shall not exceed the Level 2 upper limits specified in 3.3.4.2 for Levels 1 and 2 and shall not exceed the Level 3 upper limits for Level 3.

3.3.9.3 Two engines inoperative. At the one-engine-out speed for maximum range with any engine initially failed, it shall be possible upon failure of the most critical remaining engine to stop the transient motion and thereafter to maintain straight flight from that speed to the speed for maximum range with both engines failed. In addition, it shall be possible to effect a safe recovery at any service speed above $V_{o_{min}}$ (CL) following sudden simultaneous failure of the two most critical engines.

3.4 Miscellaneous flying qualities. Dangerous conditions may exist where the airplane should not be flown. When approaching these flight conditions, it shall be possible by clearly discernible means for the pilot to recognize the impending dangers and take corrective action. Final determination of the adequacy of all warning of impending dangerous flight conditions will be made by the procuring activity, considering functional effectiveness and reliability.

3.4.1.1 Warning and indication. Warning and indication of approach to a dangerous condition shall be clear and unambiguous. For example, a pilot must be able to distinguish readily among stall warning (which requires pitching down or increasing speed), Mach buffet (which may indicate a need to decrease speed), and normal airplane vibration (which indicates no need for pilot action).

3.4.1.2 Devices for indication, warning, prevention, recovery. It is intended that dangerous flight conditions be eliminated and the requirements of this specification met by appropriate aerodynamic design and mass distribution, rather than through incorporation of a special device or devices. Such devices may be used only if the procuring activity approves the need, the design criteria, possible Special Failure States (3.1.6.2.1) and the devices themselves. As a minimum, these devices shall perform their function whenever needed but shall not limit flight within the Operational Flight Envelope. Neither normal nor inadvertent operation of such devices shall create a hazard to the airplane. For Levels 1 and 2, nuisance operation shall not be possible. Functional failure of the devices shall be indicated to the pilot.

3.4.2 Flight at high angle of attack. The requirements of 3.4.2 through 3.4.2.2.2 concern stall warning, stalls, departure from controlled flight, post-stall gyrations, spins, recoveries and related characteristics. They apply at speeds and angles of attack which in general are outside the Service Flight Envelope. They are intended to assure safety and the absence of mission limitations due to high angle of attack characteristics.

3.4.2.1 Stalls. The stall is defined in terms of airspeed and angle of attack in 6.2.2 and 6.2.5 respectively. It usually is a phenomenon caused by airflow separation induced by high angle of attack, but it may instead be determined by some limit on usable angle of attack. The stall requirements apply for all Airplane Normal States in straight unaccelerated flight and in turns and pullups with attainable normal accelerations up to n_L. Specifically, the Airplane Normal States associated with the configurations, throttle settings and trim settings of 6.2.2 shall be investigated. Also, the requirements apply to Airplane Failure States that affect stall characteristics.

3.4.2.1.1 Stall approach. The stall approach shall be accompanied by an easily perceptible warning consisting of shaking of the cockpit controls, buffeting or shaking of the airplane, or a combination of both. The onset of this warning shall occur within the ranges specified in 3.4.2.1.1.1 and 3.4.2.1.1.2 but not within the Operational Flight Envelope. The increase in buffeting intensity with further increase in angle of attack shall be sufficiently marked to be noted by the pilot. The warning shall continue until the angle of attack is reduced to a value less than that for warning onset. At all angles of attack up to the stall, the cockpit controls shall remain effective in their normal sense, and small control inputs shall not result in departure from controlled flight. Prior to the stall, uncommanded oscillations shall not be objectionable to the pilot.

3.4.2.1.1.1 Warning speed for stalls at 1g normal to the flight path. Warning onset for stalls at 1g normal to the flight path shall occur between the following limits when the stall is approached gradually:

Flight Phase	Minimum Speed for Onset	Maximum Speed for Onset
Approach	Higher of $1.05V_S$ or V_S + 5 knots	Higher of $1.10V_S$ or V_S + 10 knots
All other	Higher of $1.05V_S$ or V_S + 5 knots	Higher of $1.15V_S$ or V_S + 15 knots

3.4.2.1.1.2 Warning range for accelerated stalls. Onset of stall warning shall occur outside the Operational Flight Envelope associated with the Airplane Normal State and within the following range or fraction of lift at stall at that airspeed, in that Airplane State, when the stall is approached gradually:

Flight Phase	Minimum Lift at Onset	Maximum Lift at Onset
Approach	$0.82C_{L_{stall}}$	$0.90C_{L_{stall}}$
All other	$0.75C_{L_{stall}}$	$0.90C_{L_{stall}}$

3.4.2.1.2 Stall characteristics. In the unaccelerated stalls of 3.4.2.1, the airplane shall not exhibit rolling, yawing or downward pitching at the stall which cannot be controlled to stay within 20 degrees for Classes

I, II and III or 30 degrees for Class IV airplanes. It is desired that no pitchup tendencies occur in unaccelerated or accelerated stalls. In unaccelerated stalls, mild nose-up pitch may be acceptable if no pitch control force reversal occurs and if no dangerous, unrecoverable flight conditions result. A mild nose-up tendency may be acceptable in accelerated stalls if the operational effectiveness of the airplane is not compromised and:

a. The airplane has adequate stall warning

b. Pitch control effectiveness is such that it is possible to stop the pitchup promptly and reduce the angle of attack and

c. At no point during the stall, stall approach or recovery does any portion of the airplane exceed structural limit loads.

The requirements apply for all stalls, including stalls entered abruptly.

3.4.2.1.3 Stall prevention and recovery. It shall be possible to prevent the stall by moderate use of the pitch control alone at the onset of the stall warning. It shall be possible to recover from a stall by simple use of the pitch, roll and yaw controls with cockpit control forces not to exceed those of 3.4.4.1, and to regain level flight without excessive loss of altitude or buildup of speed. Throttles shall remain fixed until speed has begun to increase and an angle of attack below the stall has been regained unless compliance would result in exceeding engine operating limitations. In the straight-flight stalls of 3.4.2.1, with the airplane trimmed at an airspeed not greater than $1.4V_S$, pitch control power

shall be sufficient to recover from any attainable angle of attack.

3.4.2.1.3.1 One-engine-out stalls. On multi-engine airplanes, it shall be possible to recover safely from stalls with the critical engine inoperative. This requirement applies with the remaining engines at up to:

Flight Phase	Thrust
TO	Takeoff
CL	Normal climb
PA	Normal approach
WO	Waveoff

3.4.2.2 Post-stall gyrations and spins. The post-stall gyration and spin requirements apply to all modes of motion that can be entered from upsets, decelerations, and extreme maneuvers appropriate to the Class and Flight Phase Category. Entries form inverted flight shall be included for Class I and IV airplanes. Entry angles of attack and sideslip up to maximum control capability and under dynamic flight conditions are to be included, except as limited by structural considerations. For all Classes and Flight Phase Categories, thrust settings up to and including MAT shall be included, with and without one critical engine inoperative at entry. The requirements hold for all Airplane Normal States and for all states of stability and control augmentation systems, except approved Special Failure States. Store release shall not be allowed during loss of control, spin or gyration, recovery, or subsequent dive pullout. Automatic disengagement of augmentation systems, however, is permissible if it is necessary and does not prevent meeting any other requirements. Re-engagement shall be possible in flight following recovery.

3.4.2.2.1 Departure from controlled flight. All Classes of airplanes shall be extremely resistant to departure from controlled flight, post-stall gyrations and spins. The airplane shall exhibit no uncommanded motion which cannot be arrested promptly by simple appropriate application of pilot control. In addition, the procuring activity may designate that certain training airplanes shall be capable of a developed spin and consistent recovery.

3.4.2.2.2 Recovery from post-stall gyrations and spins. For airplanes which, according to MIL-A-8861 must be structurally designed for spinning, the following requirements apply. The proper recovery technique(s) must be readily ascertainable by the pilot, and simple and easy to apply under the motions encountered. Whatever the motions, safe consistent recovery and pullout shall be possible without exceeding the control forces of 3.4.4.1 and without exceeding structural limitations. A single technique shall provide prompt recovery from all post-stall gyrations and incipient spins, without requiring the pilot to determine the direction of motion and without tendency to develop a spin. The same technique used to recover from post-stall gyrations and incipient spins, or at least a compatible one, is also desired for spin recovery. For all modes of spin that can occur, these recoveries shall be attainable within the number of turns, measured from the initiation of recovery action as follows:

Class	Flight Phase Category	Turns for Recovery
I	A, B	1.5
I	PA	1
Others	PA	1
Others	A, B	2

Avoidance of a spin reversal or an adverse mode change shall not depend upon precise pilot control timing or deflection. It is desired that all airplanes be readily recoverable from all attainable attitudes and motions. The post-stall characteristics of those airplanes not required to comply with requirements of this paragraph shall be determined by analysis and model test.

3.4.3 Cross-axis coupling in roll maneuvers. For Class I and IV airplanes in yaw-control-free, pitch-control-fixed, maximum performance rolls through 360 degrees, entered from straight flight or from turns, pushovers, or pullups ranging from 0g to 0.8n_L, the resulting yaw or pitch motions and sideslip or angle of attack changes shall neither exceed structural limits nor cause other dangerous flight conditions such as uncontrollable motions or roll autorotation.

During combat-type maneuvers involving rolls through angles up to 360 degrees and rolls which are checked at a given bank angle, the yawing and pitching shall not be so severe as to impair the tactical effectiveness of the maneuver. These requirements define Level 1 and 2 operation. For Class II and III airplanes, these requirements apply in rolls through 120 degrees and rolls which are checked at a given bank angle.

3.4.4 Control harmony. The pitch- and roll-control force and displacement sensitivities and breakout forces shall be compatible so that intentional inputs to one control axis will not cause inadvertent inputs to the other.

3.4.4.1 Control force coordination. The cockpit control forces required to perform maneuvers which are normal for the airplane should have magnitudes which are related to the pilot's capability to produce such forces in combination. The following control force levels are considered to be limiting values compatible with pilot's capability to apply simultaneous forces:

Control Type	Pitch	Roll	Yaw
Side-stick or Center-stick	50 lbs	25 lbs	
Wheel	75 lbs	40 lbs	
Pedal			175 lbs

3.4.5 Buffet. Within the boundaries of the Operational Flight Envelope, there shall be no objectionable buffet which might detract from the effectiveness of the airplane in executing its intended missions.

3.4.6 Release of stores. The intentional release of any stores shall not result in objectionable flight characteristics for Levels 1 and 2. However, the intentional release of stores shall never result in dangerous or intolerable flight characteristics. This requirement applies for all flight conditions and store loadings at which normal or emergency store release is permissible.

3.4.7 Effects of armament delivery and special equipment. Operation of moveable parts such as bomb bay doors, cargo doors, armament pods, refueling devices and rescue equipment, or firing of weapons, release of bombs, or delivery or pickup of cargo shall not cause buffet, trim changes, or other characteristics which impair the tactical effectiveness of the airplane under any pertinent flight condition. These requirements shall be met for Level 1 and for Level 2.

3.4.8 Transients following failures. The airplane motions following sudden system or component failures shall be such that dangerous conditions can be avoided by pilot corrective action. A realistic time delay between the failure and initiation of pilot corrective action shall be incorporated when determining compliance. This time delay should include an interval between the occurrence of the failure and the occurrence of a cue such as acceleration, rate, displacement, or sound that will definitely indicate to the pilot that a failure has occurred, plus an additional interval which represents the time required for the pilot to diagnose the situation and initiate corrective action.

3.4.9 Failures. No single failure of any component or system shall result in dangerous or intolerable flying qualities. Special Failure States (3.1.6.2.1) are excepted. The crew member concerned shall be provided with immediate and easily interpreted indications whenever failures occur that require or limit any flight crew action or decision.

3.4.10 Control margin. Control authority, rate and hinge moment capability shall be sufficient to assure safety throughout the combined range of all attainable angles of attack (both positive and negative) and sideslip. This requirement applies to the prevention of loss of control and to recovery from any situation for all maneuvering, including pertinent effects of factors such as regions of control-surface-fixed instability, inertial coupling, fuel slosh, the influence of symmetric and asymmetric stores (3.1.4), stall/post-stall/spin characteristics (3.4.2 through 3.4.2.2.2), atmospheric disturbances (3.8) and Airplane Failure States (3.1.10.1 and 3.1.10.2 with maneuvering flight appropriate to the Failure State to be included). Consideration shall be taken of the degrees of effectiveness and certainty of operation of limiters, c.g. control malfunction or mismanagement, and transients from failures in the propulsion, flight control and other relevant systems.

3.4.11 Direct force controls. Use of devices for direct normal-force control and direct side-force control shall not produce objectionable changes in attitude for any amount of control up to the maximum available. This requirement shall be met for Levels 1 and 2.

3.5 Characteristics of the primary flight control system

3.5.1 General characteristics. As used in this specification, the term primary flight control system includes the pitch, roll and yaw controls, stability augmentation systems, and all mechanisms and devices which they operate. The requirements of this section are concerned with those aspects of the primary flight control system which are directly related to the flying qualities. These requirements are in addition to the requirements of the applicable control system design specifications, e.g.: MIL-F-9490 or MIL-C-18244.

3.5.2 Mechanical characteristics. Some of the important mechanical characteristics of control systems (including servo valves and actuators) are: friction and preload, lost motion, flexibility, mass imbalance and inertia, nonlinear gearing, and rate limiting. Requirements for some of these characteristics are contained in 3.5.2.1 through 3.5.2.4. Meeting these separate requirements, however, will not necessarily ensure that the overall system will be adequate, the mechanical characteristics must be compatible with the nonmechanical portions of the control system as well as with the airframe dynamic characteristics.

3.5.2.1 Control centering and breakout forces. Longitudinal, lateral and directional controls should exhibit positive centering in flight at any normal trim setting. Although absolute centering is not required, the combined effects of centering, breakout force, stability and force gradient shall not produce objectionable flight characteristics, such as poor precision-tracking ability, or permit large departures from trim conditions with controls free. Breakout forces, including friction, preload, etc., shall be within the limits of Table XII. The values in Table XII refer to the cockpit control force required to start movement of the control surface in flight for Levels 1 and 2, the upper limits are doubled for Level 3.

Measurement of breakout forces on the ground will ordinarily suffice in lieu of actual flight measurement, provided that the qualitative agreement between ground measurement and flight observation can be established.

3.5.2.2 Cockpit control free play. The free play in each cockpit control, that is, any motion of the cockpit control which does not move the control surface in flight, shall not result in objectionable flight characteristics, particularly for small-amplitude control inputs.

3.5.2.3 Rate of control displacement. The ability of the airplane to perform the operational maneuvers required of it shall not be limited in the atmospheric disturbances specified in 3.7 by control surface deflection rates (3.8.3.1, 3.8.3.2 and 3.4.10). For powered or boosted controls, the effect of engine speed and the duty cycle

TABLE XII ALLOWABLE BREAKOUT FORCES, POUNDS

Control		Classes I, II-C, IV		Classes II-L, III	
		Min.	Max.	Min.	Max.
Pitch	Stick	0.5	3.0	0.5	5.0
	Wheel	0.5	4.0	0.5	7.0
Roll	Stick	0.5	2.0	0.5	4.0
	Wheel	0.5	3.0	0.5	6.0
Yaw	Pedal	1.0	7.0	1.0	14.0

of both primary and secondary control together with the pilot control technique shall be included when establishing compliance with this requirement.

3.5.2.4 Adjustable controls. When a cockpit control is adjustable for pilot physical dimensions and comfort, the control forces defined in 6.2 refer to the mean adjustment. A force referred to any other adjustment shall not differ by more than 10 percent from the force referred to the mean adjustment.

3.5.3 Dynamic characteristics. A linear or smoothly varying airplane response to cockpit-control deflection and to control force shall be provided for all amplitudes of control input. The response of the control surfaces in flight shall not lag the cockpit-control force inputs by more than the angles specified in Table XIII, for frequencies equal to or less than the frequencies specified in Table XIII.

TABLE XIII ALLOWABLE CONTROL SURFACE LAGS

Level	Allowable Lag, degrees: Flight Phase Category A and C	Flight Phase Category B
1	15	30
2	30	45
3	60	60

Control	Upper Frequency, rad/sec
Pitch	the larger of $\omega_{n_{sp}}$ and 2.0
Roll and Yaw	the largest of ω_{n_d}, $1/T_r$ and 2.0

In addition, the response of the airplane motion shall not exhibit a time delay longer than the values given in Table XIV for a pilot-initiated step control force input.

Further, the values of the equivalent time delay derived from equivalent system match of the aircraft response to cockpit controls shall not exceed the values given in Table XIV.

TABLE XIV ALLOWABLE AIRPLANE RESPONSE DELAY

Level	Allowable Delay, Seconds
1	0.10
2	0.20
3	0.25

3.5.3.1 Damping. All control system oscillations shall be well damped, unless they are of such an amplitude, frequency and phasing that they do not result in objectionable oscillations of the cockpit controls or the airframe during abrupt maneuvers and during flight in atmospheric disturbances.

3.5.4 Augmentation systems. Operation of stability augmentation and control augmentation systems and devices shall not introduce any objectionable flight or ground handling characteristics.

3.5.5 Failures. The following events shall not cause dangerous or intolerable flying qualities:

a. Complete or partial loss of any function of the augmentation system following a single failure

b. Failure-induced transient motions and trim changes either immediately after failure or upon subsequent transfer to alternate control modes

c. Configuration changes required or recommended following failure.

3.5.5.1 Failure transients. With controls free, the airplane motions due to failures described in 3.5.5 shall not exceed the following limits for at least 2 seconds following the failure, as a function of the Level of flying qualities after the failure transient has subsided:

Levels 1 and 2 (after failure)	+/- 0.5g incremental normal or lateral acceleration at the pilot's station and +/- 10 degrees per second roll rate, except that neither stall angle of attack nor structural limits shall be exceeded. In addition for Category A, vertical or lateral excursions of 5 feet, +/- 2 degrees bank angle
Level 3 (after failure)	No dangerous attitude or structural limit is reached, and no dangerous alteration of the flight path results from which recovery is impossible.

3.5.5.2 Trim changes due to failures. The changes in control forces required to maintain attitude and sideslip for the failures described in 3.5.5 shall not exceed the following limits for at least 5 seconds following the failure:

Pitch----------20 pounds
Roll----------10 pounds
Yaw----------50 pounds

3.5.6 Transfer to alternate control modes. The transient motions and trim changes resulting from the intentional engagement or disengagement of any portion of the primary flight control system by the pilot shall be such that dangerous flying qualities never result.

3.5.6.1 Transfer transients. With controls free, the transients resulting from the situations described in 3.5.6 shall not exceed the following limits for at least 2 seconds following the transfer:

Within the Operational Flight Envelope	+/- 0.1g normal or lateral acceleration at the pilot's station and +/- 3 deg/sec roll
Within the Service Flight Envelope	+/- 0.5g at the pilot's station, +/- 5 deg/sec roll, the lesser of +/- 5 degrees sideslip and the structural limits.

These requirements apply only for Airplane Normal States.

3.5.6.2 Trim changes. The changes in control forces required to maintain attitude and sideslip for the situations described in 3.5.6 shall not exceed the following limits for at least 5 seconds following the transfer:

Pitch----------20 pounds
Roll----------10 pounds
Yaw----------50 pounds

These requirements apply only for Airplane Normal States.

3.6 Characteristics of secondary control systems

3.6.1 Trim system. In straight flight, throughout the Operational Flight Envelope the trimming devices shall be capable of reducing all the cockpit control forces to zero for Levels 1 and 2. For Level 3 the untrimmed steady-state cockpit-control forces shall not exceed 10 pounds

in pitch, 5 pounds in roll and 20 pounds in yaw (pedal). The failures to be considered in applying the Level 2 and 3 requirements shall include trim sticking and runaway in either direction. It is permissible to meet the Level 2 and 3 requirements by providing the pilot with alternate trim mechanisms or override capability. Additional requirements on trim rate and authority are contained in Mil-F-9490 and Mil-F-18372.

3.6.1.1 Trim for asymmetric thrust. For all multi-engine airplanes, it shall be possible to trim the cockpit-control forces to zero in straight flight with up to two engines inoperative following asymmetric loss of thrust from the most critical factors (3.3.9). This requirement defines Level 1 in level-flight cruise at speeds from the maximum-range speed for the engine(s)-out configuration to the speed obtainable with normal rated thrust on the functioning engine(s). Systems completely dependent on the failed engine(s) shall also be considered failed.

3.6.1.2 Rate of trim operation. Trim devices shall operate rapidly enough to enable the pilot to maintain low control forces under changing conditions normally encountered in service, yet not so rapidly as to cause oversensitivity or trim precision difficulties under any conditions. Specifically, it shall be possible to trim the pitch control forces to less than +/- 10 pounds for center-stick airplanes and +/- 20 pounds for wheel-control airplanes throughout:

a. dives and ground attack maneuvers required in normal service operation and

b. level-flight acceleration at maximum augmented thrust from 250 knots or $V_{R/C}$, whichever is less, to V_{max} at any altitude when the airplane is trimmed for level flight prior to initiation of the maneuver.

In the event that operation of the trim system requires removal of one hand from the wheel-control, Level 1 force limits shall be as for a center-stick.

3.6.1.3 Stalling of trim systems. Stalling of a trim system due to aerodynamic loads during maneuvers shall not result in an unsafe condition. Specifically, the longitudinal trim system shall be capable of operating during the dive recoveries of 3.2.3.6 at any attainable permissible n, at any possible position of the trimming device.

3.6.1.4 Trim system irreversibility. All trimming devices shall maintain a given setting indefinitely unless changed by the pilot, or by a special automatic interconnect (such as to the landing flaps), or by the operation of an augmentation device. If an automatic interconnect or augmentation device is used in conjunction with a trim device, provision shall be made to ensure the accurate return of the device to its initial trim position on removal of each interconnect or augmentation command.

3.6.2 Speed and flight-path control devices. The effectiveness and response times of the longitudinal controls shall be sufficient to provide adequate control of flight path and airspeed at any flight condition within the Operational Flight Envelope. This requirement may be met by use of devices such as throttles, thrust reversers, auxiliary drag devices and flaps.

3.6.3 Transients and trim changes. The transients and steady-state trim changes for normal operation of secondary control devices (such as throttle, thrust reversers, flaps, slats, speed brakes, deceleration devices, dive recovery devices, wing sweep and landing gear) shall not impose excessive control forces to maintain the desired heading, altitude, attitude, rate of climb, speed or load factor without use of trimmer control. This requirement applies to all in-flight configuration changes and combinations of changes made under service conditions, including the effects of asymmetric operations such as unequal operation of the landing gear, speed brakes, slats or flaps. In no case shall there be any objectionable buffeting or oscillation caused by such devices. More specific requirements on secondary control devices are contained in 3.6.3.1, 3.6.4 and 3.6.5 and in Mil-F-9490 and Mil-F-18372.

3.6.3.1 Pitch trim changes. The pitch trim changes caused by operation of secondary control devices shall not be so large that a peak pitch control force in excess of 10 lbs for center-stick controllers or 20 lbs for wheel controllers is required when such configuration changes are made in flight under conditions representative of operational procedure. Generally, the conditions listed in Table XV will suffice for determination of compliance with this requirement. (For airplanes with variable-sweep wings, additional requirements will be imposed consistent with operational employment of the vehicle). With the airplane trimmed for each specified initial condition, the peak force required to maintain the specified parameter constant following the specified configuration change shall not exceed the stated value for a time interval of at least 5 seconds following the completion of the pilot action initiating the configuration change. The magnitude and rate of trim change subsequent to this time period shall be such that the forces are easily trimmable by use of the normal trimming devices. These requirements define Level 1. For Levels 2 and 3, the allowable forces are increased by 50 percent.

3.6.4 Auxiliary dive recovery devices. Operation of any auxiliary device intended solely for dive recovery shall always produce a positive increment of normal acceleration, but the total normal load factor shall never exceed $0.8n_L$, controls free.

TABLE XV PITCH TRIM CHANGE CONDITIONS

No.	Flight Phase	Initial Trim Condition: Altitude	Speed	Landing Gear	High Lift Devices and Wing Flaps	Thrust	Configuration Change	Parameter held constant
1	Approach	$h_{o_{min}}$	Normal pattern entry speed	Up	Up	TLF	Gear down	Altitude and airspeed*
2	Same	Same	Same	Up	Up	TLF	Gear Down	Altitude
3	Same	Same	Same	Down	Up	TLF	Extend high-lift devices and wing flaps	Altitude and airspeed*
4	Same	Same	Same	Down	Up	TLF	Extend high-lift devices and wing flaps	Altitude
5	Same	Same	Same	Down	Down	TLF	Idle thrust	Airspeed
6	Same	Same	$V_{o_{min}}$	Down	Down	TLF	Extend approach drag device	Airspeed
7	Same	Same	Same	Down	Down	TLF	Takeoff thrust	Airspeed
8	Same	Same	Same	Down	Down	TLF	Takeoff thrust plus normal cleanup for wave-off (go-around)	Airspeed
9	Takeoff	$h_{o_{min}}$	$V_{o_{min}}$	Down	Takeoff	Takeoff thrust	Gear up	Pitch attitude
10	Same	Same	Minimum flap retract speed	Up	Takeoff	Takeoff thrust	Retract high lift devices and wing flaps	Airspeed
11	Cruise and air-to-air combat	$h_{o_{min}}$ and $h_{o_{max}}$	Speed for level flight	Up	Up	MRT	Idle thrust	Pitch Attitude
12	Same	Same	Same	Up	Up	MRT	Actuate deceleration device	Same
13	Same	Same	Same	Up	Up	MRT	Maximum augmented thrust	Same
14	Same	Same	Speed for best range	Up	Up	TLF	Actuate deceleration device	Same

Notes: 1. Auxiliary drag devices are initially retracted, and all details of configuration not specifically mentioned are normal for the Flight Phase.

2. If power reduction is permitted in meeting the deceleration requirements established for the mission, actuation of the deceleration device in Numbers 12 and 14 shall be accompanied by the allowable power reduction.

* Throttle may be changed during the maneuver

3.7 Atmospheric disturbances

3.7.1 Form of the disturbance models. Where feasible, the Von Karman form shall be used for the continuous turbulence model, so that the flying qualities analyses will be consistent with comparable structural analyses. When no comparable structural analysis is performed or when it is not feasible to use the Von Karman form, use of the Dryden form will be permissible. In general, both the continuous turbulence model and the discrete gust model shall be used. The scales and intensities used in determining the gust magnitudes for the discrete gust model shall be the same as those in the continuous model.

3.7.1.1 Continuous turbulence model (Von Karman form). The Von Karman form of the spectra for the turbulence velocities is:

$$\Phi_{u_g}(\Omega) = \frac{(\sigma_u)^2(2L_u/\pi)}{[1 + (1.339L_u\Omega)^2]^{5/6}}$$

$$\Phi_{v_g}(\Omega) = \frac{(\sigma_v)^2(L_v/\pi)[1 + (8/3)(1.339L_v\Omega)^2]}{[1 + (1.339L_v\Omega)^2]^{11/6}}$$

$$\Phi_{w_g}(\Omega) = \frac{(\sigma_w)^2(L_w/\pi)[1 + (8/3)(1.339L_w\Omega)^2]}{[1 + (1.339L_w\Omega)^2]^{11/6}}$$

3.7.1.2 Continuous turbulence model (Dryden form). The Dryden form of the spectra of turbulence velocities is:

$$\Phi_{u_g}(\Omega) = \frac{(\sigma_u)^2(2L_u/\pi)}{[1 + (L_u\Omega)^2]}$$

$$\Phi_{v_g}(\Omega) = \frac{(\sigma_v)^2(L_v/\pi)[1 + 3(L_v\Omega)^2]}{[1 + (L_v\Omega)^2]^2}$$

$$\Phi_{w_g}(\Omega) = \frac{(\sigma_w)^2(L_w/\pi)[1 + 3(L_w\Omega)^2]}{[1 + (L_w\Omega)^2]^2}$$

3.7.1.3 Discrete gust model. The discrete gust model may be used for any of the three gust-velocity components and, by derivation, any of the three angular components. The discrete gust has the '(1 - cosine)' shape given by:

$v = 0$ for $x < 0$

$v = (v_m/2)(1 - \cos(\pi x/d_m))$, for $0 < x < d_m$

$v = v_m$ for $x > d_m$

In graphical form this is:

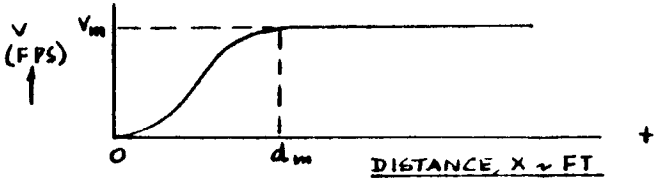

The discrete gust above may be used singly or in multiples to assess airplane response to, or pilot control of, large disturbances. Step function or linear ramp gusts may also be used.

3.7.2 Medium/high-altitude model. The scales and intensities are based on the assumption that turbulence above 2,000 feet is isotropic. Then:

and: $\sigma_u = \sigma_v = \sigma_w$

$L_u = L_v = L_w$

3.7.2.1 Turbulence scale lengths. The scales to be used are:

$L_u = L_v = L_w = 2,500$ feet using the Von Karman form, or

$L_u = L_v = L_w = 1,750$ feet using the Dryden form.

3.7.2.2 Turbulence intensities. Root-mean-square turbulence intensities are shown in Figure B7 as functions of altitude and probability of exceedance. Simplified variations for application to the requirements of this specification are indicated.

3.7.2.3 Gust lengths. Several values of d_m shall be used, each chosen so that the gust is tuned to each of the natural frequencies of the airplane and its flight control system (higher-frequency structural modes may be excepted). The magnitude of v_m shall be determined from Figure B8.

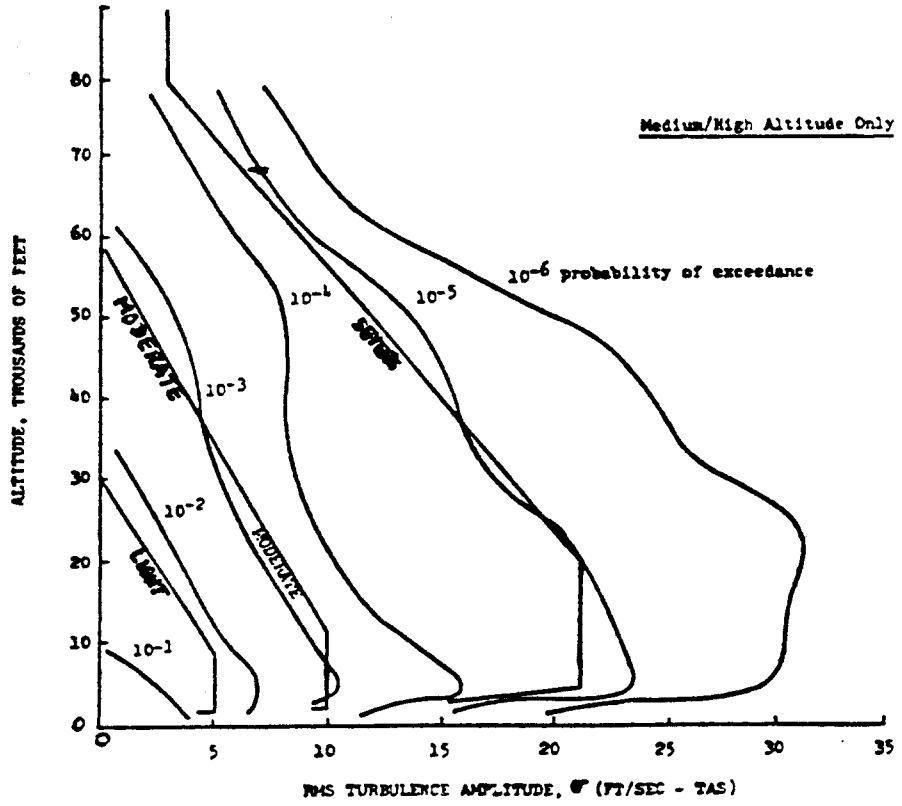

Figure B7 Turbulence Exceedance Probability

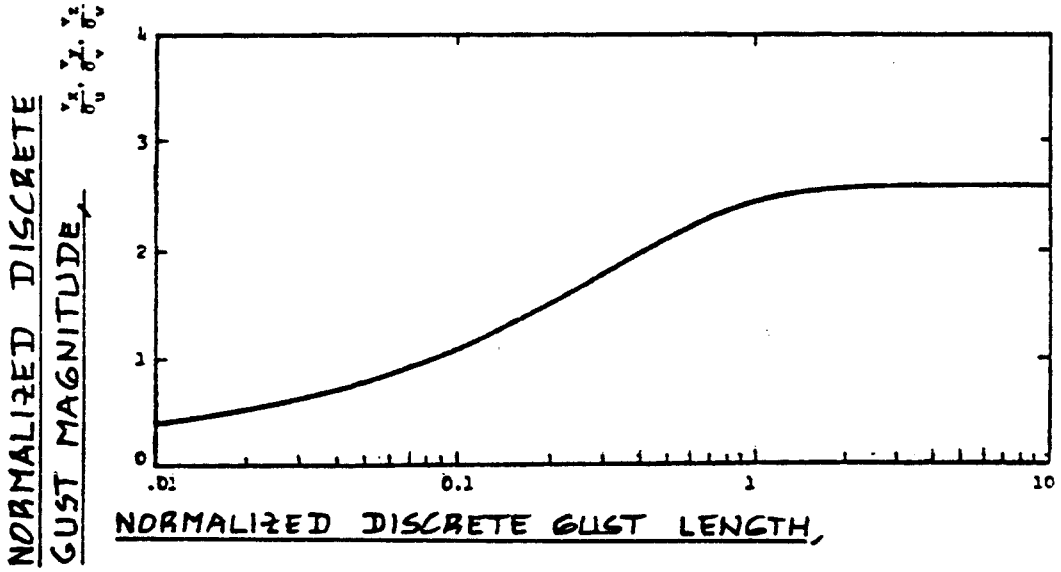

Figure B8 Magnitude of Discrete Gusts

3.7.2.4 Gust magnitudes. The Light and Moderate gust magnitudes u_g, v_g and w_g shall be determined from Figure B8 using the values of d_x, d_y and d_z determined according to 3.7.2.3, and the appropriate RMS turbulence intensities from Figure B7. Severe gusts shall be:

a. 66 ft/sec EAS at V_G, gust penetration speed

b. 50 ft/sec EAS at $V_{O_{max}}$

c. 25 ft/sec EAS at V_{max}

d. 50 ft/sec EAS at speeds up to V_{max} (PA) with the landing gear and other devices which are open or extended in their maximum open or maximum extended positions

e. For altitudes above 20,000 feet the gust magnitudes may be reduced linearly from:

(1) 66 ft/sec EAS at 20,000 feet to 38 ft/sec EAS at 50,000 feet for the V_G condition

(2) 50 ft/sec EAS at 20,000 feet to 25 ft/sec EAS at 50,000 feet for the $V_{O_{max}}$ condition

(3) 25 ft/sec EAS at 20,000 feet to 12.5 ft/sec EAS at 50,000 feet for the V_{max} condition

f. For altitudes above 50,000 feet the equivalent gust velocity specified at 50,000 feet shall be multiplied by the factor $(\rho/\rho_{50})^{1/2}$, the square root of the ratio of air density at altitude to standard atmospheric density at 50,000 feet.

3.7.3 Low-altitude disturbance model. This section specifies the model of atmospheric disturbances to be used for all Category C operations. The effects of wind shear, turbulence and gusts may be analyzed separately. Some analysis and piloted simulation is required considering a complete environmental representation, demonstrating compliance with the requirements with the cumulative effects of wind shear, turbulence and gusts. A non-Gaussian turbulence representation together with a wind model may also be used to represent the patchy, intermittent nature of actual measured turbulence.

3.7.3.1 Wind speeds. The wind speed at 20 feet above the ground, u_{20}, is shown in Figure B9 as a function of probability of occurrence. The values to be used for the different intensities of atmospheric disturbance are indicated.

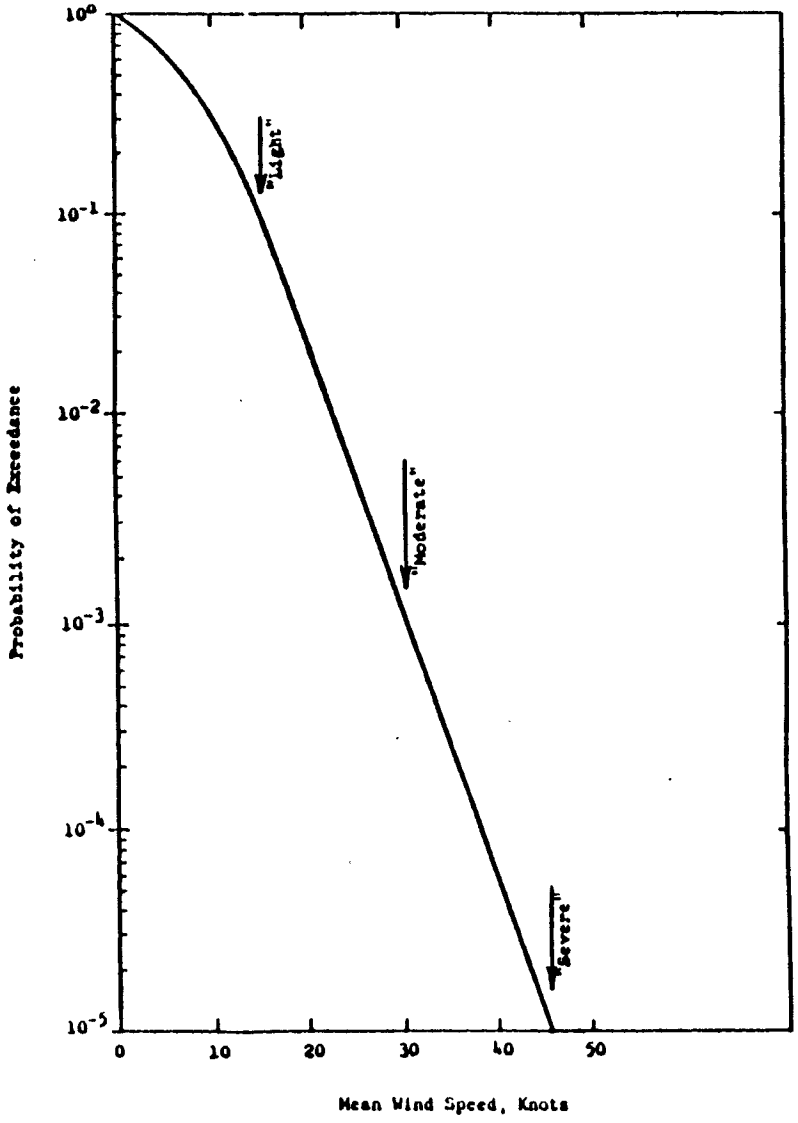

Figure B9 Probability of Exceeding Mean Wind Speed at 20 Feet

3.7.3.2 Wind shear. The magnitude of the wind scalar shear is defined by the use of the following expression for the mean wind profile as a function of altitude:

$$u_w = u_{20}(\ln(h/z_o))/(\ln(20/z_o))$$

where: z_o = 0.15 feet for Category C Flight Phase

= 2.0 feet for other Flight Phases.

3.7.3.3 Vector shear. Different orientations of the mean wind relative to the runway for Category C, or relative to the aircraft flight path for other Flight Phases, shall be considered. In addition, changes in direction of the mean wind speed over a given height change shall be considered as follows:

Disturbance intensity	Change in mean wind heading, degrees	Height of vector shear, feet
LIGHT	0	----
MODERATE	90	600
SEVERE	90	300

A range of values for the initial wind orientation and the initial altitude for onset of the shear shall be considered. Relative to the runway, magnitudes of $u_{20}\sin\psi_w$ greater than the crosswind values in 3.3.7 or tailwind component at 20 feet greater than 10 knots need not be considered. At any altitude other than 20 feet these limits do not apply.

3.7.3.4 Turbulence. The turbulence models of 3.7.1.1 or 3.7.1.2 shall be used. The appropriate scale lengths are shown in Figure B10 as functions of altitude. The turbulence intensities to be used are:

$\sigma_w = 0.1u_{20}$, and σ_u and σ_v given by Figure B11 as functions of σ_w and altitude.

3.7.3.5 Gusts. Discrete gusts of the form specified in 3.7.2.3 shall be used, with both single and double ramps to be considered. Several values of d_m shall be used, each chosen so that the gust is tuned to each of the natural frequencies of the airplane and its flight control system. The gust magnitudes shall be determined from Figure B8 using the appropriate values from Figures B10 and B11. The two halves of a double gust do not have to be the same length or magnitude.

3.7.4 Carrier landing disturbance model. This section specifies the model of atmospheric disturbances to be used for carrier landing operations. This model shall be used in analysis and piloted simulation to determine aircraft control response and path control accuracy during carrier landing. This model supplements but does not replace the low-altitude model of 3.7.3.

The terminal approach carrier landing disturbance model shall be used during simulation of the last 1/2 mile of the carrier approach. The u velocity component is aligned with the wind over the deck. Total disturbance velocities are computed by adding segments caused by random free-air turbulence, u_1, v_1, w_1, steady ship-wake disturbance, u_2, w_2, periodic ship-motion-induced turbulence, u_3, w_3, and random ship-wake disturbance, u_4, v_4, w_4.

The total air disturbance components u_g, v_g and w_g are then computed as:

$$u_g = u_1 + u_2 + u_3 + u_4$$

$$v_g = v_1 + v_4$$

$$w_g = w_1 + w_2 + w_3 + w_4$$

The input to all of the random disturbance filters shall be generated by filtering the wide-band, Gaussian output of zero-mean, unit-variance random-number generators.

3.7.4.1 Free-air turbulence components. The free-air turbulence components which are independent of aircraft relative position are represented by filtering the output of white-noise generators described in 3.7.4 to produce the following spectra:

$$\Phi_{u_1}(\Omega) = \frac{200}{(1 + (1000\Omega)^2)} \quad \text{per radian/ft}$$

$$\Phi_{v_1}(\Omega) = \frac{5900(1 + (4000\Omega)^2)}{(1 + (1000\Omega)^2)(1 + (4000\Omega/3)^2)} \quad \text{per radian/ft}$$

$$\Phi_{w_1}(\Omega) = \frac{71.6}{(1 + (1000\Omega)^2)} \quad \text{per radian/ft}$$

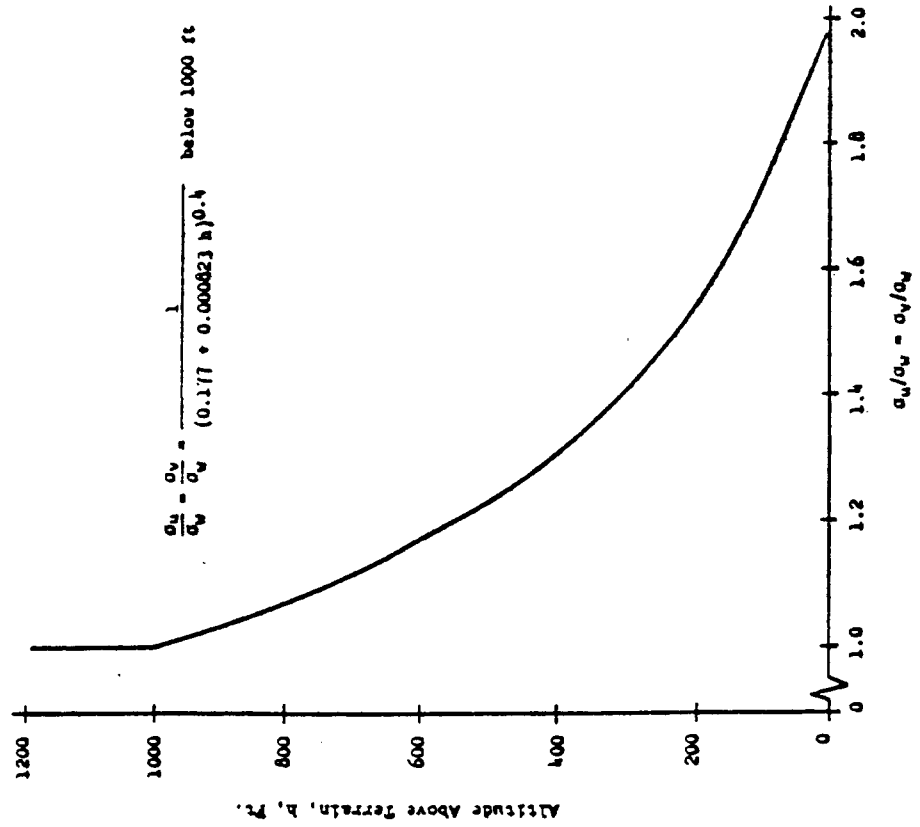

Figure B11 Horizontal Turbulence RMS Intensities

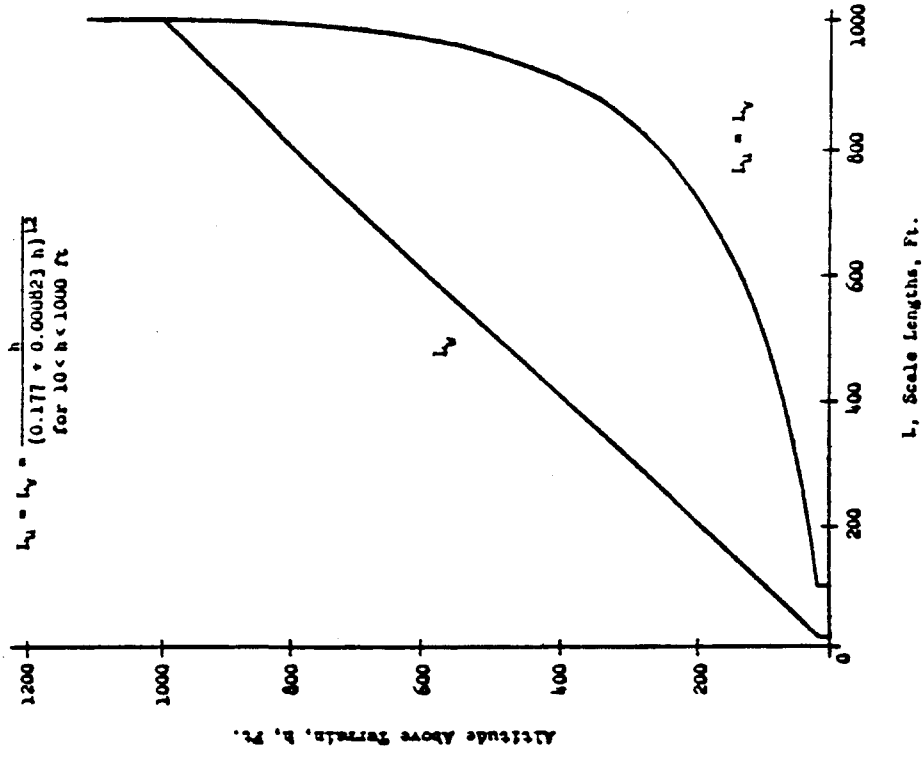

Figure B10 Low Altitude Turbulence Intensity Scales

3.7.4.2 Steady component of carrier airwake. The steady components of the carrier airwake consist of a reduction in the steady wind and a predominant upwash aft of the ship which are functions of range. Figure B12 illustrates the steady wind functions $u_2/V_{w/d}$ and $w_2/V_{w/d}$ as functions of position aft of the ship center of pitch.

3.7.4.3 Periodic component of carrier airwake. The periodic component of the airwake varies with ship pitching frequency, pitch magnitude, wind over deck and aircraft range. These components are computed as follows:

$$u_3 = \theta_s V_{w/d}(2.22 + 0.0009X)C$$

$$w_3 = \theta_s V_{w/d}(4.98 + 0.0018X)C$$

with: C =

$$\cos[\omega_p(t + t(V - V_{w/d})/(0.85V_{w/d}) + X/(0.85V_{w/d})) + P]$$

where: ω_p = Ship pitch frequency, rad/sec.

θ_s = Ship pitch amplitude, rad.

P = Random phase, rad.

X = the distance from the ship center of pitch, in ft, as defined in Figure B12.

Notes from the author: 1. The center of pitch location depends on the type of carrier. In preliminary design, the center of pitch may be assumed to be at one half the length of the carrier.

2. Values for ship pitch frequency, pitch amplitude and random phase must be obtained from the procuring activity. These values depend on ship type and on sea state.

The u component is set to zero for X < -2236 feet, and the w component is set to zero for X < -2536 feet.

3.7.4.4 Random component of carrier air wake. The ship-related random velocity components are computed by filtering white noise (3.7.4) as follows:

$$u_4 = \frac{\sigma(X)(2\tau(X))^{1/2}(\text{Input})}{(\tau(X)j\omega + 1)}$$

$$w_4 = v_4 = \frac{0.035V_{w/d}(6.66)^{1/2}(\text{Input})}{(3.33j\omega + 1)}$$

where:

$\sigma(X)$ = RMS Amplitude in ft/sec., see Figure B13

$\tau(X)$ = Time constant in sec., see Figure B13

Input = (Random number output)$(j\omega/(j\omega + 0.1))\sin(10\pi t)$

3.7.5 Application of the disturbance model in analyses. The gust and turbulence velocities shall be applied to the airplane equations of motion through the aerodynamic terms only, and the direct effect on the aerodynamic sensors shall be included when such sensors are part of the airplane augmentation system. When using the discrete gust model, all significant aspects of the penetration of the gust by the airplane shall be incorporated in the analyses. Application of the disturbance model depends on the range of frequencies of concern in the analyses of the airframe. When structural modes are significant, the exact distribution of turbulence velocities should be considered. For this purpose, it is acceptable to consider u_g and v_g as being one-dimensional functions only of x, but w_g shall be considered two-dimensional, a function of both x and y, for the evaluation of aerodynamic forces and moments.

When structural modes are not significant, airframe rigid-body responses may be evaluated by considering uniform gust or turbulence immersion along with linear gradients of the disturbance velocities. The uniform immersion is accounted for by u_g, v_g and w_g defined at the airplane center of gravity. The angular velocities due to turbulence are equivalent in effect to airplane angular velocities. Approximations for these angular velocities are defined (precisely at very low frequencies only) as follows:

$$\dot{\alpha}_g = q_g = \partial w_g/\partial x,\ p_g = \partial w_g/\partial y,\ r_g = \partial v_g/\partial x$$

The spectra of the angular velocity disturbances due to turbulence are then given by:

$$\Phi_{p_g}(\Omega) = \{(\sigma_w)^2/L_w\}\frac{(0.8(\pi L_w/4b)^{1/3})}{(1 + (4b\Omega/\pi)^2)}$$

$$\Phi_{q_g}(\Omega) = [(\Omega)^2/(1 + (4b\Omega/\pi)^2)]\Phi_{w_g}(\Omega)$$

$$\Phi_{r_g}(\Omega) = [(\Omega)^2/(1 + (3b\Omega/\pi)^2)]\Phi_{v_g}(\Omega)$$

where: b is the wing span.

The turbulence components u_g, v_g, w_g and p_g shall be considered mutually independent (uncorrelated) in a statistical sense. However, q_g is correlated with w_g, and r_g is correlated with v_g. For the discrete gusts the linear gradient gives angular velocity perturbations of the following form:

$$p_g = p_m \sin(\pi x/d_m) \qquad 0 \leq x \leq d_m$$

For the low-altitude model, the turbulence velocity components u_g, v_g and w_g are to be taken along axes with u_g aligned along the relative mean wind vector and with w_g vertical.

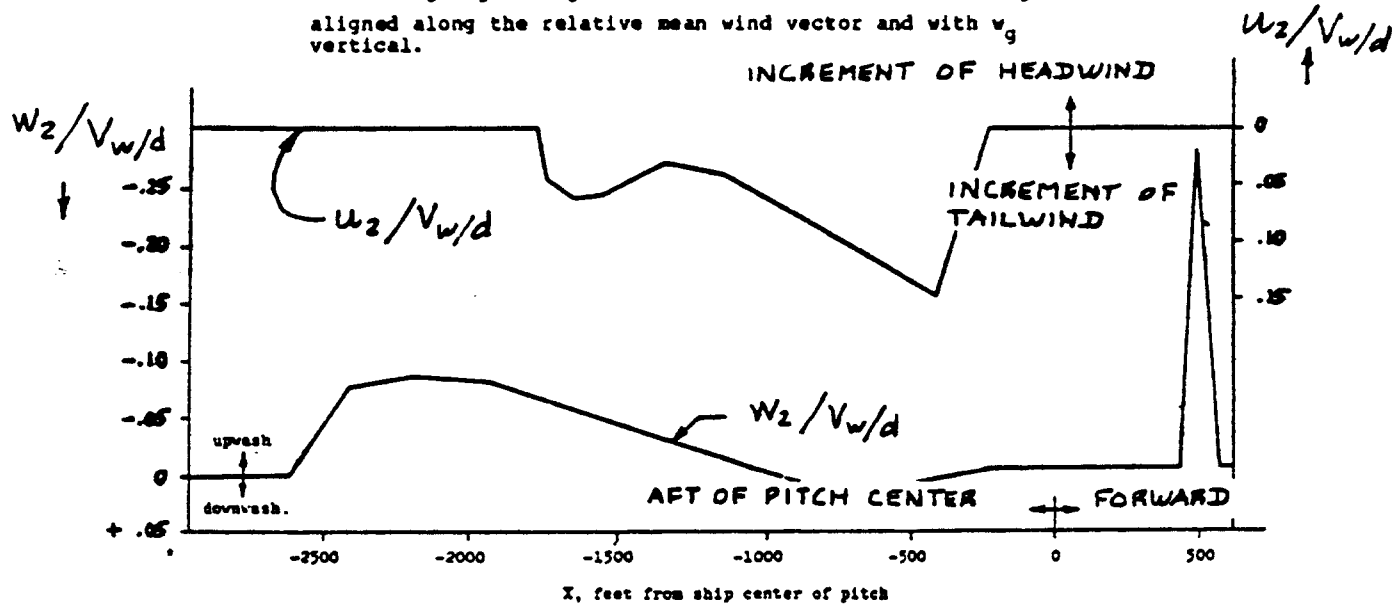

Figure B12 CVA Ship Burble Steady Wind Ratios

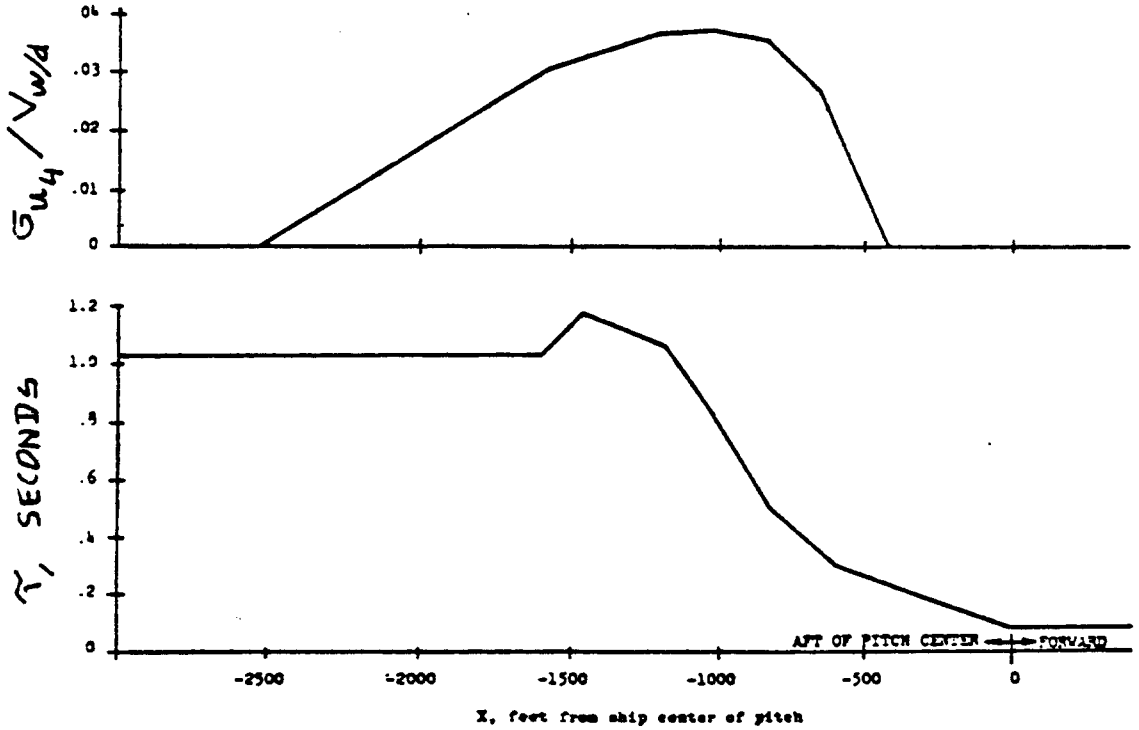

Figure B13 u-Component Burble Time Constant and Variance

3.8 Requirements for use of the disturbance models

Explicit consideration of the effects of disturbances on flying qualities, if required by the procuring activity, shall be in accordance with requirements in 3.8.2 through 3.8.3.2. In particular, 3.8.3.1 will replace 3.1.10.1 and 3.8.3.2 will replace 3.1.10.2.

3.8.1 Use of disturbance models. Paragraphs 3.7.1 through 3.7.4.4 specify models of wind shear, continuous random turbulence and discrete gusts that shall be used to assess:

a. The effects of certain environmental conditions on the flying qualities of the airplane.

b. The ability of the pilot to recover from upsets caused by environmental conditions.

c. Flight path control precision during manual and automatic carrier landing.

For the purpose of this specification the atmosphere shall be considered to consist of three regions:

(1) low-altitude (ground level to approximately 2,000 feet AGL),

(2) medium/high-altitude (above approximately 2,000 feet) and,

for carrier landing only,

(3) terminal approach (0 - 300 feet altitude and 1/2 mile to touchdown).

The low-altitude model shall apply to Category C and any other Flight Phase (e.g. ground attack, terrain following) designated by the procuring activity. The medium/high-altitude model is intended to apply to those Flight Phases where proximity to the ground is not a factor, generally Categories A and B. In application it will be permissible to use conditions at an average altitude for the medium/high-altitude model only. The carrier landing disturbance model will apply to carrier-based aircraft only.

3.8.2 Qualitative degrees of suitability. In assessing the qualitative suitability of flying qualities three intensities and disturbances shall be considered. These intensities are Light, Moderate and Severe as defined in 3.7. The requirements for the effects of these disturbances are contained in 3.8.3.1 and 3.8.3.2 for the different Flight Envelopes and Airplane States.

The qualitative degrees of suitability of flying qualities are categorized as follows:

Satisfactory	Flying qualities clearly adequate for the mission Flight Phase
Acceptable	Flying qualities adequate to accomplish the mission Flight Phase, but some increase in pilot workload or degradation in mission effectiveness, or both, exists
Controllable	Flying qualities such that the airplane can be controlled safely, but pilot workload is excessive or mission effectiveness is inadequate, or both. Category A Flight Phases can be terminated safely, and Category B and C Flight Phases can be completed.
Recoverable	Flying qualities such that control can be maintained long enough to fly out of a disturbance. All Flight Phases can be terminated safely and a wave-off/go-around can be accomplished.

3.8.3 Effects of atmospheric disturbances. Levels of flying qualities as indicated in 1.5 are employed in this specification in realization of the possibility that the airplane may be required to operate under abnormal conditions. Such abnormalities may occur also as a result of extreme atmospheric disturbances, or some combination of conditions. For these factors a degradation of flying qualities is permitted as specified in 3.8.3.1 and in 3.8.3.2 (see also 4.1.1).

3.8.3.1 Requirements for Airplane Normal States. In atmospheric disturbances the minimum required flying qualities for Airplane Normal States (3.1.6.1) are as specified in Table XVI.

3.8.3.2 Requirements for Airplane Failure states. When Airplane Failure States exist (3.1.6.2), a degradation in flying qualities is permitted only if the probability of encountering a lower Level than specified in 3.8.3.1 is sufficiently small. At intervals established by the procuring activity, the contractor shall determine, based on the most accurate available data, the probability of occurrence of each Airplane Failure State per flight and the effect of that Failure State on the flying qualities within the Operational and Service Flight Envelopes. These determinations shall be based on Mil-STD-756 except that:

a. All airplane components and systems are assumed to be operating for a time period, per flight, equal to the longest operational mission time to be considered by the contractor in designing the airplane, and

b. Each specific failure is assumed to be present at whichever point in the Flight Envelope being considered is most critical (in the flying qualities sense).

From these Failure State probabilities and effects, the contractor shall determine the overall probability, per flight, that one or more flying qualities are degraded to Level 2 because of one or more failures. The contractor shall also determine the probability that one or more

flying qualities are degraded to Level 3. Table XVII specifies the requirements as functions of the probability of encountering the degradation in flying qualities.

TABLE XVI LEVELS FOR AIRPLANE NORMAL STATES

Atmospheric Disturbances	Within Operational Flight Envelope	Within Service Flight Envelope
LIGHT to CALM	Quantitative requirements Level 1, Qualitative requirements Satisfactory	Quantitative requirements Level 2, Qualitative requirements Acceptable
MODERATE to LIGHT	Quantitative requirements Level 1, Qualitative requirements Acceptable or better	Quantitative requirements Level 2, Qualitative requirements Controllable or better
SEVERE to MODERATE	Qualitative requirements Controllable or better	Qualitative requirements Recoverable or better

TABLE XVII LEVELS FOR AIRPLANE FAILURE STATES

Atmospheric Disturbances	Failure State I*	Failure State II**
LIGHT to CALM	Quantitative requirements Level 2 and qualitative requirements Acceptable or better	Quantitative requirements Level 3 and qualitative requirements Controllable or better
MODERATE to LIGHT	Quantitative requirements Level 2 and qualitative requirements Controllable or better	Quantitative requirements Level 3 and qualitative requirements Recoverable or better
SEVERE to MODERATE	Qualitative requirements Recoverable or better	

* For flight in the Operational Flight Envelope: Probability of encountering degraded levels of flying qualities due to failure(s) < 1 per 100 flights

** For flight in the Operational Flight Envelope: Probability of encountering degraded levels of flying qualities due to failure(s): < 1 per 10,000 flights, and for flight in the Service Flight Envelope: Probability of encountering degraded levels of flying qualities due to failure(s): < 1 per 100 flights

4. QUALITY ASSURANCE

4.1 Compliance demonstration. Compliance with all requirements of section 3 shall be demonstrated through analysis. In addition, compliance with many of the requirements will be demonstrated by simulation, flight test or both. The methods for demonstrating compliance shall be established by agreement between the procuring activity and the contractor. Representative flight conditions, configurations, external store complements, loadings, etcetera, shall be determined for detailed investigations in order to restrict the number of design and test conditions. The selected design points must be sufficient to allow accurate extrapolation to other conditions at which the requirements apply.

Table XVIII specifies the general guidelines but the peculiarities of the specific airplane design may require additional or alternate test conditions. The required failure analyses shall be thorough, excepting only approved Special Failure States (3.1.6.2.1).

4.1.1 Analytical compliance

4.1.1.1 Effects of Failure States. To determine theoretical compliance with the requirements of 3.1.10.2, the following steps must be performed:

a. Identify those Airplane Failure States which have a significant effect on flying qualities (3.1.6.2)

b. Define the longest flight duration to be encountered during operational missions (3.1.1)

c. Determine the probability of encountering various Airplane Failure States per flight, based on the above flight duration (3.1.10.2)

d. Determine the degree of flying qualities degradation associated with each Airplane Failure State in terms of Levels as defined in the specific requirements

e. Determine the most critical Airplane Failure States (assuming the failures are present at whichever point in the Flight Envelope being considered is most critical in a flying qualities sense), and compute the total probability of encountering Level 2 flying qualities in the Operational Flight Envelope due to equipment failures. Likewise, compute the probability of encountering Level 3 flying qualities in the Operational Flight Envelope, etc.

f. Compare the computed values above with the requirements specified in 3.1.10.2 and 3.1.10.3. An example which illustrates an approximate estimate of the probabilities of encounter follows: if the failures are all statistically independent, determine the sum of the probabilities of encountering all Airplane Failure

States which degrade flying qualities to Level 2 in the Operational Flight Envelope. This sum must be less than 1 per 100 flights.

If the requirements are not met, the designer must consider alternate courses such as:

a. Improve the airplane flying qualities associated with the more probable Failure States, or

b. Reduce the probability of encountering the more probable Failure States through equipment redesign, redundancy, etc.

Regardless of the probability of encountering any given Airplane Failure States (with the exception of Special Failure States) the flying qualities shall not degrade below Level 3.

4.1.1.2 Effects of atmospheric disturbances. Paragraph 4.1.1.1 indicates a procedure for satisfying the requirements on the degrading effects of Airplane Failure States, without consideration of atmospheric disturbances. Atmospheric disturbances also may cause a degradation in pilot opinion as specified in 3.8.2. In application, numerical values of control force and deflection, and of steady-state and dynamic response parameters (for example $n_{o_{max}}$, $\partial F_s/\partial n$, θ_t) are to be considered as mean values in the presence of atmospheric disturbances. These are frequently equivalent to the values in calm air. Numerical values of frequency-response parameters and of control authority are effective values for the airplane in each particular intensity of atmospheric disturbance. The qualitative requirements of 3.8.3.1 and 3.8.3.2 should then be assessed for both Airplane Normal States and critical Failure States identified in 4.1.1.1.

4.1.1.3 Computational assumptions. Assumptions a and b of 3.1.10.2 are somewhat conservative, but they simplify the required computations in 3.1.10.2 and provide a set of workable ground rules for theoretical predictions. The reasons for these assumptions are:

a. '...components and systems are ... operating for a time period per flight equal to the longest operational mission time ...'. Since most component failure data are in terms of failures per flight hour, even though continuous operation may not be typical (e.g. yaw damper ON during supersonic flight only), failure probabilities must be predicted on a per flight basis using 'typical' total flight time. The 'longest operational mission time' as 'typical' is a natural result. If acceptance cycles-to-failure reliability data are available (MIL-STD-756), these data may be used for prediction purposes based on maximum cycles per operational mission, subject to procuring activity approval. In any event, compliance with the requirements of 3.1.10.2, as determined in accordance with Section 4, is based on the probability of encounter per flight.

b. '... failure is assumed to be present at whichever point ... is most critical ...'. This assumption is in keeping with the requirements of 3.1.6.2 regarding Flight Phases subsequent to the actual failure in question. In cases that are unrealistic from the operational standpoint, the specific Airplane Failure States might fall in the Airplane Special Failure State classification (3.1.6.2.1).

4.1.2 Simulation. The danger, extent or difficulty of flight testing may dictate simulation rather than flight test to evaluate some conditions and events, such as the influence of Severe disturbances, events close to the ground (except 3.2.3.4 shall be demonstrated in flight), combined Failure States and disturbances, etc. In addition, by agreement with the procuring activity, piloted simulation shall be performed before first flight of a new airplane design in order to demonstrate compliance with qualitative requirements in atmospheric disturbances and in the critical conditions identified in 4.1.1.1. Where simulation is the ultimate method of demonstrating compliance for a requirement, the simulation model shall be validated with flight test data and approved by the procuring activity.

4.1.3 Flight test demonstration. The required flight tests will be defined by operational, technical and safety considerations as decided jointly by the procuring activity, the test agency and the contractor using results from 4.1.1 and 4.1.2. It is not expected that flight test demonstration of the requirements in Moderate and Severe disturbances will be done unless required by the airplane mission. Some flights can be expected to encounter actual disturbances. Then the qualitative requirements would apply if the disturbance intensity could be categorized.

4.2 Airplane States. The parameters defining Airplane States shall be tabulated. Table XIX illustrates an acceptable format.

4.2.1 Weights and moments of inertia. Terms specified in Table XVIII such as 'heaviest weight' and 'greatest moment of inertia' mean the heaviest and greatest consistent with 3.1.2 and 3.1.3. When a critical center-of-gravity position is identified, the airplane weight and associated moments of inertia shall correspond to the most adverse service loading in which that critical center-of-gravity position is obtained.

4.2.2 Center-of-gravity positions. Terms specified in Table XVIII such as 'most forward c.g.' and 'most aft c.g.' mean the most forward or aft consistent with 3.1.2. When a critical weight or inertia is identified, the center-of-gravity position shall correspond to the most adverse service loading in which that critical weight or moment of inertia is obtained.

4.2.3 Thrust settings. Thrust settings shall be as listed in Table XIX.

TABLE XVIII DESIGN AND TEST CONDITION GUIDELINES

Requirement Number	Title	Critical Loading (4.2.1 and 4.2.2)	Load Factor	Altitude (4.3.1)	Speed	Flight Phase
Section 3.2	Longitudinal Flying Qualities					
3.2.1.1	Longitudinal static stability	Most aft c.g.	1.0	$h_{o_{min}}$, medium, $h_{o_{max}}$	V_{min} to V_{max}, transonic	CO, CR, LO, RR, FF, RT, PA, L, WO TO, CT
3.2.1.1.1	Relaxation in transonic flight	Same	Same	Same	Same	Same
3.2.1.1.2	Elevator control force variations during rapid speed changes	----	As reqd	Same	Same	CO, GA, DE
3.2.1.2	Phugoid stability	Most fwd c.g.*	1.0	Same	V_{min} to V_{max}	CR, LO, PA, RT
3.2.1.3	Flight-path stability	----	Same	Same	$V_{o_{min}}$, $V_{o_{min}}$ - 5 kts	PA
3.2.2.1.1	Short period frequency and acceleration sensitivity	Most fwd* and most aft** c.g.	Same	Same	V_{min} to V_{max}	(*), CR, RT, PA, L, CT
3.2.2.1.2	Short period damping	Most fwd c.g.	1.0	$h_{o_{min}}$, medium, $h_{o_{max}}$	V_{min} to V_{max}	(*), CR, RT, PA, CT
3.2.2.1.3	Residual oscillations	----	Same	Same	$V_{o_{min}}$ to $V_{o_{max}}$	(*), PA
3.2.2.2	Control feel and stability in maneuvering flight	Most aft c.g.	n(-) to n(+)	Same	V_{min} to V_{max}	(*), RT, CR, PA, L, CT
3.2.2.2.1	Control forces in maneuvering flight	Most fwd* and most aft** c.g.	n_o(-) to $n_{(+)}$	Same	Same	Same
3.2.2.2.2	Control motions in maneuvering flight	Most fwd c.g.*	Same	Same	Same	Same
3.2.2.3	Longitudinal pilot-induced oscillations	----	Min. to max. permissible	Same	Same	(*), RT, CR, PA, L, CT
3.2.2.3.1	Dynamic control forces in maneuvering flight	Most fwd c.g.*	1.0	$h_{o_{min}}$, medium, $h_{o_{max}}$	V_{min} to V_{max}	----
3.2.2.3.2	Control feel	Most aft c.g.**	Same	Same	Same	----
3.2.3.1	Longitudinal control in unaccelerated flight	Most fwd c.g.	Same	Same	Same	----

* Combined with heaviest weight ** Combined with lightest weight

TABLE XVIII (CONT'D) DESIGN AND TEST CONDITION GUIDELINES

Requirement Number	Title	Critical Loading (4.2.1 and 4.2.2)	Load Factor	Altitude (4.3.1)	Speed	Flight Phase
3.2.3.2	Longitudinal control in maneuvering flight	Most fwd c.g.*	As reqd	Same	$V_{o_{min}}$ to $V_{o_{max}}$	CO, GA, AR, TF, CR, PA
3.2.3.3	Longitudinal control in takeoff	Most fwd c.g. for nosewheel and most aft c.g. for tailwheel airplanes	1.0	Low	As reqd	TO
3.2.3.3.1	Longitudinal control in catapult takeoff	Most fwd and most aft c.g.	As reqd	Same	Min. safe launch speed to min. + 30 kts	CT
3.2.3.3.2	Longitudinal control force and travel in takeoff	Most fwd and most aft c.g.	As reqd	Low	0 to V_{max} (TO)	TO, CT
3.2.3.4	Longitudinal control in landing	Most fwd c.g.	1.0	Same	V_s(L) or geometric limit	L
3.2.3.4.1	Longitudinal control forces in landing	Same	Same	Same	Same	L
3.2.3.5	Longitudinal control forces in dives (SFE)	Most fwd* and most aft** c.g.	As reqd	2000 ft above MGL to h_{max}	V_{min} to V_{max}	D, ED, CO, CR
3.2.3.6	Longitudinal control forces in dives (PFE)	Same	Same	As reqd	V_{MAT} to max permissible	Same
3.2.3.7	Longitudinal control in sideslips	----	1.0	$h_{o_{min}}$, medium, $h_{o_{max}}$	V_{min} to V_{max}	CO, CR, PA, L
Section 3.3	Lateral-Directional Flying Qualities					
3.3.1.1	Lateral-directional oscillations (Dutch roll)	Greatest yawing moment of inertia	1.0 and n_o(+)	$h_{o_{min}}$, medium, $h_{o_{max}}$	V_{min} to $V_{o_{max}}$	(*), CR, RT, PA, L
3.3.1.2	Roll mode	Greatest rolling moment of inertia	Same	$h_{o_{max}}$	Same	(*), CR, PA, L
3.3.1.3	Spiral stability	----	1.0	Same	Same	(*), CL, CR, LO, RT, DE, PA, L
3.3.1.4	Coupled roll-spiral oscillations	----	1.0 and n_o(+)	Same	Same	(*), CR, PA, L
3.3.2.1	Lateral-directional response to atmospheric disturbances	----	1.0	Same	Same	----
3.3.2.2	Roll rate oscillations	----	1.0 and n_o(+)	Same	Same	(*), CR, PA, L
3.3.2.2.1	Additional roll rate reqm't for small inputs	----	Same	Same	Same	Same

* Combined with heaviest weight
** Combined with lightest weight
SFE - Service Flight Envelope
PFE - Permissible Flight Envelope

TABLE XVIII (CONT'D) DESIGN AND TEST CONDITION GUIDELINES

Requirement Number	Title	Critical Loading (4.2.1 and 4.2.2)	Load Factor	Altitude (4.3.1)	Speed	Flight Phase
3.3.2.3	Bank angle oscillations	----	1.0 and n_o(+)	$h_{o_{min}}$, medium, $h_{o_{max}}$	V_{min} to $V_{o_{max}}$	(*), CR, PA, L
3.3.2.4	Sideslip excursions	Greatest yawing and rolling moment of inertia	1.0	Same	Same	Same
3.3.2.4.1	Additional sideslip reqm't for small inputs	Same	1.0	Same	Same	Same
3.3.2.5	Control of sideslip in rolls	Greatest rolling moment of inertia	As reqd	Same	Same	CO, GA, AR, TF, CR, PA, L
3.3.2.6	Turn coordination	----	Same	Same	$V_{o_{min}}$	CO, CR, LO, PA
3.3.3	Pilot-induced oscillations	----	Min. to max. permissible	MSL to h_{max}	V_{min} to V_{max}	----
3.3.4	Roll control effectiveness	Greatest rolling moment of inertia	As reqd (not above $0.8n_L$)	$h_{o_{min}}$, medium, $h_{o_{max}}$	V_{min} to V_{max}	CO, GA, AR, TF, CR, PA, L
3.3.4.1	Roll performance for Class IV airplanes	Same	Same	Same	Same	Same
3.3.4.1.1	Roll performance in Flight Phase CO	Same	Same	$h_{o_{min}}$	Same	CO
3.3.4.1.2	Roll performance in Flight Phase GA	Same	Same	Same	Same	GA
3.3.4.1.3	Roll response	Smallest rolling moment of inertia	Same	$h_{o_{min}}$ medium $h_{o_{max}}$	Same	----
3.3.4.2	Roll performance for Class III airplanes	Greatest and smallest rolling moment of inertia	Same	Same	Same	CO, GA, AR, TF, CR, PA, L
3.3.4.3	Roll control force	Greatest rolling moment of inertia	As reqd (not above $0.8n_L$)	$h_{o_{min}}$ medium, $h_{o_{max}}$	V_{min} to V_{max}	----
3.3.4.4	Linearity of roll response	Same	Same	Same	Same	CO, GA, AR, TF, CR, PA, L
3.3.4.5	Wheel control throw	Same	Same	Same	Same	Same
3.3.5	Directional control characteristics	----	n(-) to n(+)	Same	Same	(*), CR, PA, L

* Combined with heaviest weight ** Combined with lightest weight

TABLE XVIII (CONT'D) DESIGN AND TEST CONDITION GUIDELINES

Requirement Number	Title	Critical Loading (4.2.1 and 4.2.2)	Load Factor	Altitude (4.3.1)	Speed	Flight Phase
3.3.5.1	Directional control with speed change	----	1.0	Same	Same	CO, GA, CR, D, PA, L
3.3.5.1.1	Directional control with asymmetric loading	----	Same	Same	$V_{o_{min}}$ to $V_{o_{max}}$	----
3.3.5.2	Directional control in wave-off (go-around)	Lightest weight	1.0	Low	V_{min} (PA) or guaranteed landing speed	WO
3.3.6 (3.3.6.1, 3.3.6.2, 3.3.6.3, 3.3.6.3.1, 3.3.6.3.2)	Lateral-directional characteristics in steady sideslips	Same	Same	$h_{o_{min}}$ medium, $h_{o_{max}}$	V_{min} to V_{max}	CO, CR, PA, L
3.3.7	Lateral-directinal control in cross winds	----	Same	Low	As reqd	TO, L
3.3.7.1	Final approach in cross winds	----	Same	Same	V_{min} to V_{max}	PA
3.3.7.2 (3.3.7.2.1, 3.3.7.2.2)	Takeoff run and landing rollout in cross wind	----	As reqd	Same	As reqd	TO, L
3.3.7.3	Taxiing wind speed limits	----	As reqd	Same	All taxiing speeds	TAXI
3.3.8	Lateral-directional control in dives	----	As reqd	2,000 ft above MSL to h_{max}	V_{MAT} to V_{max}	D, ED
3.3.9.1	Thrust loss during takeoff run	Lightest weight	1.0	$h_{o_{min}}$	0 to max. takeoff speed	TO
3.3.9.2	Thrust loss after takeoff	Same	Same	Same	Down to V_{min} (TO)	TO, CT
3.3.9.3	Transient effects	Same	Same	All	V_{min} to V_{max}	CO, GA, TF, CR, CL, TO, CT
3.3.9.4	Asymmetric thrust, rudder pedals free	Same	Same	$h_{o_{min}}$, medium, $h_{o_{max}}$	$1.4V_{min}$	CR
3.3.9.5	Two engines inoperative	----	Same	Same	V_{range} (1 and 2 engines out)	----

• Combined with heaviest weight •• Combined with lightest weight

TABLE XVIII (CONT'D) DESIGN AND TEST CONDITION GUIDELINES

Requirement Number	Title	Critical Loading (4.2.1 and 4.2.2)	Load Factor	Altitude (4.3.1)	Speed	Flight Phase
Section 3.4	Miscellaneous Flying Qualities					
3.4.2	Flight at high angle of attack	See MIL-S-83691 or MIL-D-8708, whichever is applicable for flight demonstration. More severe conditions generally will be investigated by analysis and by model testing. ***				
3.4.2.1	Stalls (3.4.2.1.1 through 3.4.2.1.3.1)	See *** above				
3.4.2.2	Post-stall gyrations and spins (3.4.2.2.1, 3.4.2.2.2)	See *** above				
3.4.3	Cross-axis coupling in roll maneuvers	----	0 to $0.8n_L$	$h_{o_{min}}$, medium $h_{o_{max}}$	$V_{o_{min}}$ to $V_{o_{max}}$	CO, GA, AR, TF
3.4.4 (3.4.4.1)	Control harmony	----	$n_o(-)$ to $n_o(+)$	Same	Same	----
3.4.5	Buffet	----	Same	Same	Same	(*)
3.4.6	Release of stores	----	Same	Same	Same	CO, GA, WD, D
3.4.7	Effects of armament delivery and special equipment	----	Same	Same	Same	(*), RT
3.4.8	Transients following failures	----	All	$h_{o_{min}}$ to $h_{o_{max}}$	All	----
3.4.10	Control margin	----	Same	Same	Same	----
3.4.11	Direct force control	----	1.0 +/- max. DLC authority	Same	$V_{o_{min}}$ to $V_{o_{max}}$	----
Section 3.5	Characteristics of the Primary Flight Control System					
3.5.2 (3.5.2.1, 3.5.2.2, 3.5.2.3)	Mechanical characteristics	----	$n_o(-)$ to $n_o(+)$	$h_{o_{min}}$ and $h_{o_{max}}$	V_{min} to V_{max}	----
3.5.3	Dynamic characteristics	Most fwd c.g. and lowest rolling and yawing moments of inertia	1.0			----
3.5.5 (3.5.5.1, 3.5.5.2)	Failures	----	All			----
3.5.6 (3.5.6.1, 3.5.6.2)	Transfer to alternate control modes	----	1.0	$h_{o_{min}}$, medium, $h_{o_{max}}$		----

NOTES: 1. ---- indicates that no general guidance can be provided.

2. The phrase 'As reqd' means the flight conditions are specified in the requirement or are determined by the nature of the test maneuver.

3. (*) means all applicable Category A Flight Phases.

TABLE XXIII (CONT'D) DESIGN AND TEST CONDITION GUIDELINES

Requirement Number	Title	Critical Loading (4.2.1 and 4.2.2)	Load Factor	Altitude (4.3.1)	Speed	Flight Phase
Section 3.6	Characteristics of Secondary Control Systems					
3.6.1	Trim system	Most fwd and most aft c.g.	1.0	$h_{o_{min}}$, medium, $h_{o_{max}}$	V_{min} to V_{max}	----
3.6.1.1	Trim for asymmetric thrust	Same	Same	$h_{o_{min}}$ and max. attainable	V_{range} to V_{MRT} (with 1 and 2 engines out)	CR
3.6.1.2	Rate of trim operation	----	Same	As reqd	As reqd	CO, GA, D, ED
3.6.1.3	Stalling of trim system	Most fwd c.g. combined with heaviest weight	As reqd	Same	Start of dive recovery to V_{max}	D, ED, CO, CR
3.6.1.4	Trim system irreversibility	----	1.0	MSL to h_{max}	V_{min} to V_{max}	----
3.6.2	Speed and flight-path control devices	----	1.0 to n_o(+)	$h_{o_{min}}$ medium, $h_{o_{max}}$	$V_{o_{min}}$ to $V_{o_{max}}$	(*), RT, ED, DE, PA, WO, GA
3.6.3	Transients and trim changes	----	n_o(-) to n_o(+)	$h_{o_{min}}$, medium, $h_{o_{max}}$	V_{min} to V_{max}	----
3.6.3.1	Pitch trim changes	----	As reqd	As reqd	As reqd	CO, CR, FA TO, CT
3.6.4	Auxiliary dive recovery devices	Most aft c.g. combined with lightest weight	Same	MSL to to h_{max}	$V_{o_{min}}$ to V_{max}	D, ED
Section 3.7	Atmospheric Disturbances	----	1.0	Same	V_{min} to V_{max}	----
Section 3.8	Requirements for Use of the Disturbance Models	----	All	Same	Same	----

NOTES: 1. ---- indicates that no general guidance can be provided.

2. The phrase 'As reqd' means the flight conditions are specified in the requirement or are determined by the nature of the test maneuver.

3. (*) means all applicable Category A Flight Phases.

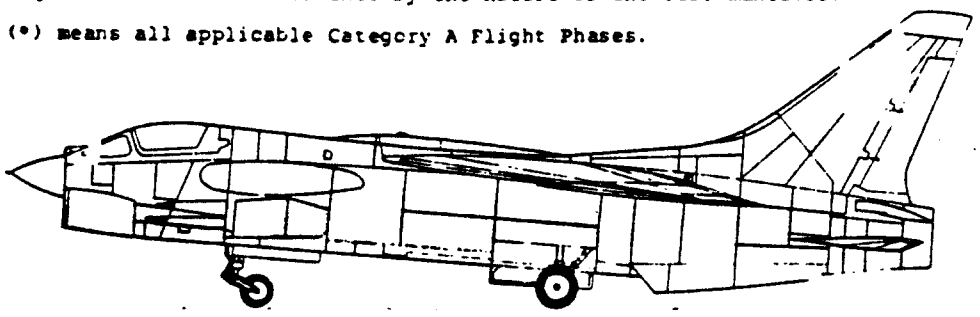

TABLE XIX DEFINITION OF AIRPLANE NORMAL STATES

Flight Phase	Symbol	Weight	C.G.	External Stores	Thrust	Thrust Vector Angle	High Lift Devices	Wing Sweep
Takeoff	TO							
Climb	CL							
Cruise	CR							
Loiter	LO							
Descent	D							
Emergency Descent	ED							
Emergency Deceleration	DE							
Approach	PA							
Wave-off/ Go-around	WO							
Landing	L							
Air-to-air Combat	CO							
Ground Attack	GA							
Weapon Delivery/ Launch	WD							
Aerial Delivery	AD							
Aerial Recovery	AR							
Reconnaissance	RC							
Refuel Receiver	RR							
Refuel Tanker	RT							
Terrain Following	TF							
Antisubmarine Search	AS							
Close Formation Flying	FF							
Catapult Takeoff	CT							

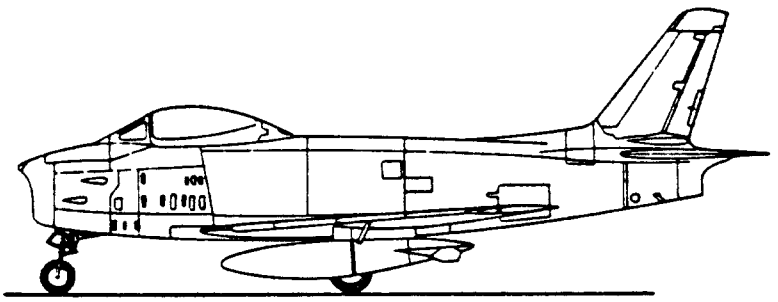

TABLE XIX (CONT'D) DEFINITION OF AIRPLANE NORMAL STATES

Flight Phase	Symbol	Wing Incidence	Landing Gear	Speed Brakes	Bomb Bay or Cargo Doors	Stability Augmen-tation	Other
Takeoff	TO						
Climb	CL						
Cruise	CR						
Loiter	LO						
Descent	D						
Emergency Descent	ED						
Emergency Deceleration	DE						
Approach	PA						
Wave-off/ Go-around	WO						
Landing	L						
Air-to-air Combat	CO						
Ground Attack	GA						
Weapon Delivery/ Launch	WD						
Aerial Delivery	AD						
Aerial Recovery	AR						
Reconnaissance	RC						
Refuel Receiver	RR						
Refuel Tanker	RT						
Terrain Following	TF						
Antisubmarine Search	AS						
Close Formation Flying	FF						
Catapult Takeoff	CT						

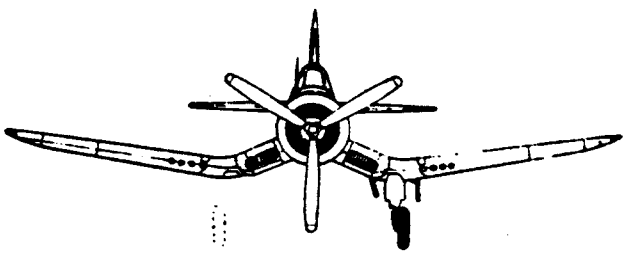

4.3 Design and test conditions

4.3.1 Altitudes. For terminal Flight Phases, it will normally suffice to examine the selected Airplane States at only one altitude below 10,000 feet (low altitude). For nonterminal Flight Phases, it will normally suffice to examine the selected Airplane States at one altitude below 10,000 feet or at the lowest operational altitude (low altitude), the maximum operational altitude ($h_{o_{max}}$), and one intermediate altitude. When the maximum operational altitude is above 40,000 feet or when stability or control characteristics vary rapidly with altitude, more intermediate altitudes than specified in Table XVIII shall be investigated. When the Service Flight Envelope extends far above or below the Operational Flight Envelope, the service-altitude extremes must be considered.

4.3.2 Special conditions. In addition to the flight conditions previously indicated, the speed-altitude combinations that result in the following shall be investigated, where applicable:

a. Maximum normal acceleration response per degree of controller deflection

b. Maximum normal acceleration response per pound of control force

c. Highest dynamic pressure and highest Mach Number.

4.4 Tests at specialized facilities. Certain tests, by their nature can be conducted only at specialized facilities which are not accessible to either the procuring activity or the contractor except at the option of a third organization. In such cases, when an agreement of test support at the specialized facility is obtained by the procuring activity, an analysis of results obtained in the tests, is a necessary part of the analytical compliance demonstration.

5. PREPARATION FOR DELIVERY

5.1 Section 5 is not applicable to this specification.

6. NOTES

6.1 Intended use. This specification contains the flying qualities requirements for piloted airplanes and forms one of the bases for determination by the procuring activity of airplane acceptability. The specification consists of design requirements in terms of criteria for use in stability and control calculations, analysis of wind tunnel test results, simulator evaluations, flight testing, etc. The requirements should be met as far as possible by providing an inherently good basic airframe. Cost, performance, reliability, maintenance, etc. tradeoffs are necessary in determining the proper balance between airframe characteristics and augmented dynamic response characteristics. The contractor should advise the procuring activity of any significant design penalties which may result from meeting any particular requirement.

6.2 Definitions. Terms and symbols used throughout this specification are defined as follows:

6.2.1 General.

S	wing area
s	Laplace operator
$\bar{q}$	dynamic pressure
MSL	mean sea level
T_2	time to double amplitude: $T_2 = -0.693/\zeta\omega_n$ for oscillations; $T_2 = 0.693T_s$ or τ for first order divergences
Airplane Normal States	nomenclature and format of Table XIX shall be used in defining the Airplane Normal States (3.1.6.1)
Service ceiling	altitude at a given airspeed at which the rate of climb is 100 ft/min at the stated weight and engine thrust
Combat ceiling	altitude at a given airspeed at which the rate of climb is 500 ft/min at the stated weight and engine thrust
Cruising ceiling	altitude at a given airspeed at which the rate of climb is 300 ft/min at NRT at the stated weight
h_{max}	maximum service altitude (defined in 3.1.8.3)
$h_{o_{max}}$	maximum operational altitude (3.1.7)
$h_{o_{min}}$	minimum operational altitude (3.1.7)
c.g.	airplane center of gravity

6.2.2 Speeds.

Equivalent airspeed, EAS	true airspeed multiplied by $(\sigma)^{1/2}$, where σ is the ratio of free-stream density at the given altitude to standard sealevel air density
Calibrated airspeed	airspeed-indicator reading corrected for position and instrument error but NOT for compressibility
Refusal speed	the maximum speed to which the airplane can accelerate and then stop in the available runway length

M	Mach number
V	airspeed along the flight path (where appropriate, may be replaced by M in this specification)
V_S	stall speed (equivalent airspeed), at 1g normal to the flight path, defined as the highest of:

a) speed for steady straight flight at $C_{L_{max}}$, the first local maximum of the curve of lift coefficient ($L/\bar{q}S$) versus angle of attack which occurs as C_L is increased from zero

b) speed at which uncommanded pitching, rolling or yawing occurs (3.4.2.1.2)

c) speed at which intolerable buffet or structural vibration is encountered

Conditions for determining V_S.

The airplane shall be initially trimmed at approximately $1.2V_S$ with the following settings, after which the trim and and throttle settings shall be held constant:

Flight Phase	Thrust Settings*	Trim Setting
Climb (CL)	Normal climb	For straight flight
Descent (D)	Normal Descent	For straight flight
Emergency descent (ED)	Idle	For straight flight
Emergency deceleration (DE)	Idle	For straight flight
Takeoff (TO)	Takeoff	Recommended takeoff setting
Approach (PA)	Normal approach	For normal approach
Wave-off/ Go-around (WO)	Takeoff	For normal approach
Landing (L)	Idle	For normal approach
All other	TLP at $1.2V_S$	For straight flight

* Either on all engines or on remaining engines with critical engine inoperative whichever yields the higher value of V_S.

In flight test, it is necessary to reduce speed very slowly (typically 0.5 knot per second or less) to minimize dynamic lift effects. The load factor will generally not be exactly 1g when stall occurs, when this is the case, V_S is defined as follows:

$V_S = V/(n_f)^{1/2}$

where V and n_f are the measured values at stall, n_f being the load factor normal to the flight path.

$V_S(X)$, $V_{min}(X)$, $V_{max}(X)$	short-hand notation for the speeds V_S, V_{min}, V_{max}, for a given configuration, weight, c.g. position, and external store combination associated with some Flight Phase X. For example, the designation $V_{max}(TO)$ is used in 3.2.3.3.2 to emphasize that the speed intended (for the weight, center of gravity, and external store combination under consideration) is V_{max} for the configuration associated with the takeoff Flight Phase. This is necessary to avoid confusion, since the configuration and the Flight Phase change from takeoff to climb during the maneuver.
V_{con}	speed below which control is lost
V_{trim}	trim speed
V_{end}	speed for maximum endurance
$V_{L/D}$	speed for maximum lift-to-drag ratio
$V_{R/C}$	speed for maximum rate of climb
V_{range}	speed for maximum range with zero wind
V_{NRT}	high speed, level flight, normal rated thrust
V_{MRT}	high speed, level flight, military rated thrust
V_{MAT}	high speed, level flight, maximum augmented thrust
V_{max}	maximum service speed (see 3.1.8.1)
V_{min}	minimum service speed (see 3.1.8.2)

$V_{o_{max}}$	maximum operational speed (see 3.1.7)
$V_{o_{min}}$	minimum operational speed (see 3.1.7)
V_G	gust penetration speed

6.2.3 Thrust and power.

Thrust and power	for propeller-driven airplanes the word 'thrust' shall be replaced by the word 'power' throughout this specification
TLF	thrust for level flight
NRT	normal rated thrust, which is the maximum thrust at which the engine can operate continuously
MRT	military rated thrust, which is the maximum thrust at which the engine can be operated for a specified period
MAT	maximum augmented thrust: the maximum thrust, augmented by all means available for the Flight Phase
Takeoff thrust	maximum thrust available for takeoff

6.2.4 Control parameters.

Pitch, roll, yaw controls	the stick or wheel and pedals manipulated by the pilot to produce pitching, rolling and yawing moments respectively, the cockpit controls
Pitch control force, F_S	component of applied force, exerted by the pilot on the cockpit control, in or parallel to the plane of symmetry, acting at the center of the stick grip or wheel in a direction perpendicular to a line between the center of the stick grip and the stick or control column pivot
Roll control force	for a stick control, the component of control force exerted by the pilot in a plane perpendicular to the plane of symmetry, acting at the center of the stick grip in a direction perpendicular to a line between the center of the stick grip and the stick pivot. For a wheel control, the total moment applied by the pilot applied about the wheel axis in the plane of the wheel, divided by the average radius from the wheel pivot to the pilot's grip
Yaw-control pedal force	difference of push-force components of forces exerted by the pilot on the yaw-control pedals, lying in planes parallel to the plane of symmetry, measured perpendicular to the pedals at the normal point of application of the pilot's instep on the respective yaw-control pedals
Direct normal force control	a device producing direct normal force for the primary purpose of controlling the flight path of the airplane. Direct normal force control is the descriptive title given to the concept of directly modulating the normal force on the airplane by changing its lifting capabilities at a constant angle of attack and constant airspeed or by controlling the normal force component of such items as jet exhausts, propellers, and fans
Control power	effectiveness of control surfaces in applying forces or moments to an airplane. For example, 50 percent of available roll control power is 50 percent of the maximum rolling moment that is available to the pilot with allowable roll control force

6.3.5 Longitudinal parameters.

ζ_{sp}	damping ratio of the short-period oscillation
$\omega_{n_{sp}}$	undamped natural frequency of the short-period oscillation
ζ_p	damping ratio of the phugoid oscillation
ω_{n_p}	undamped natural frequency of the phugoid oscillation
n	normal acceleration or normal load factor, measured at the c.g.
n_L	symmetrical flight limit load factor for a given Airplane Normal State, based on structural considerations
n_{max}, n_{min}	maximum and minimum service load factors
n(+), n(-)	for a given altitude, the upper and lower boundaries of n in the V-n diagrams depicting the Service Flight Envelope
$n_{o_{max}}$, $n_{o_{min}}$	maximum and minimum operational load factors

$n_o(+)$, $n_o(-)$ for a given altitude, the upper and lower boundaries of n in the V-n diagrams depicting the Operational Flight Envelope

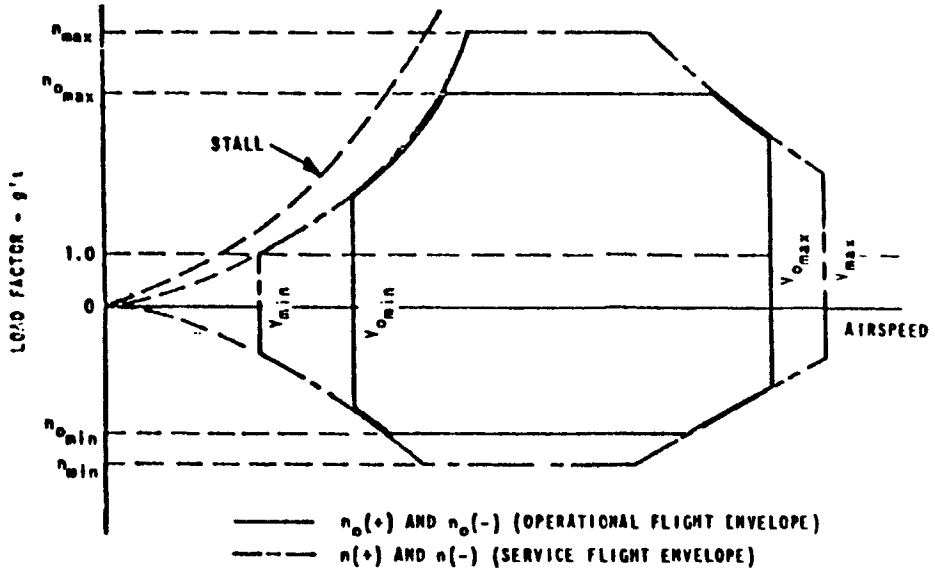

α angle of attack, the angle in the plane of symmetry between the fuselage reference line and the line tangent to the flight path at the airplane c.g.

α_S the stall angle of attack at constant speed for the configuration, weight, c.g. position and external store combination associated with a given Airplane Normal State, defined as the lowest of the following:

a) Angle of attack for the highest steady load factor, normal to the flight path, that can be attained at a given speed or Mach number

b) Angle of attack, for a given speed or Mach number, at which uncommanded pitching, rolling or yawing occurs (3.4.2.1.2)

c) Angle of attack, for a given speed or Mach number, at which intolerable buffeting is encountered.

$C_{L_{stall}}$ lift coefficient at α_S defined above

n/α the steady-state normal acceleration change per unit change in angle of attack for an incremental pitch control deflection at constant speed (airspeed and Mach number)

F_S/n gradient of steady-state pitch control force versus n at constant speed (see 3.2.2.2.1)

γ climb angle, positive for climbing flight:

$\gamma = \sin^{-1}$(vertical speed/true airspeed)

θ pitch attitude, the angle between the fuselage reference line (body x-axis) and the horizontal

' aerodynamic lift plus thrust component normal to the flight path

6.2.6 Lateral-directional parameters.

δ_{AS} displacement of the roll control stick or wheel along its path

T_r first-order roll mode time constant, positive for stable mode

T_s first-order spiral mode time constant, positive for stable mode

λ_r $(-1/T_r)$

λ_s $(-1/T_s)$

ω_ϕ undamped natural frequency of numerator quadratic of ϕ/δ_{AS} transfer function

ζ_ϕ damping ratio of numerator quadratic of ϕ/δ_{AS} transfer function

ω_{n_d} undamped natural frequency of the Dutch roll oscillation

ζ_d damping ratio of the Dutch roll oscillation

T_d damped period of the Dutch roll:

$T_d = 2\pi/(\omega_{n_d}(1 - \zeta_d^2)^{1/2})$

$\omega_{n_{rs}}$ undamped natural frequency of a coupled roll-spiral oscillation

ζ_{rs} damping ratio of a coupled roll-spiral oscillation

ϕ bank angle measured in the y-z plane, between the y-axis and the horizontal (6.3.1)

ϕ_t bank angle change in time t, in response to control deflection of the form given in 3.3.4

p roll rate about the x-axis (6.2.1)

p_{osc}/p_{av} a measure of the ratio of the oscillatory component of roll rate to the average component of roll rate following a yaw-control-free step roll control command:

For $\zeta_d < 0.2$: $p_{osc}/p_{av} = (p_1 + p_3 - 2p_2)/(p_1 + p_3 + 2p_2)$

For $\zeta_d > 0.2$: $p_{osc}/p_{av} = (p_1 - p_2)/(p_1 + p_2)$

where p_1, p_2, and p_3 are roll rates at the first, second and third peaks respectively. (Figures B14 and B15)

ϕ_{osc}/ϕ_{av} a measure of the ratio of the oscillatory component of bank angle to the average component of bank angle following a pedals-free impulse aileron command:

For $\zeta_d < 0.2$: $\phi_{osc}/\phi_{av} = (\phi_1 + \phi_3 - 2\phi_2)/(\phi_1 + \phi_3 + 2\phi_2)$

For $\zeta_d > 0.2$: $\phi_{osc}/\phi_{av} = (\phi_1 - \phi_2)/(\phi_1 + \phi_2)$

where: ϕ_1, ϕ_2 and ϕ_3 are bank angles at the first, second and third peaks respectively. (Figures B14 and B15)

β sideslip angle at the center of gravity, angle between undisturbed flow and plane of symmetry. Positive, or right sideslip corresponds to incident flow approaching from the right side of the plane of symmetry.

$\Delta\beta$ maximum change in sideslip occurring within 2 seconds or one half-period of the Dutch roll, whichever is greater, for a step roll-control command. (Figures B14 and B 15)

k ratio of 'command roll performance' to 'applicable roll performance requirement' of 3.3.4 or 3.3.4.1, with:

$k = (\phi_t)_{command}/(\phi_t)_{requirement}$

where:

a) 'Applicable roll performance requiment', (ϕ_t) requirement, is determined from 3.3.4 and 3.3.4.1 for the Class, Flight Phase Category and Level under consideration

b) 'Commanded roll performance', (ϕ_t) command, is the bank angle attained in the stated time for a given step roll command with yaw control pedals employed as specified in 3.3.4 and 3.3.4.1

t_{n_β} time for the Dutch roll oscillation in the sideslip response to reach the n^{th} local maximum for a right step or pulse roll-control command, or the n^{th} local minimum for a left command. In the event a step control input cannot be accomplished, the control shall be moved as abruptly as practical and, for purposes of this definition, time shall be measured from the instant the cockpit control deflection passes through half the amplitude of the commanded value. For pulse inputs, time shall be measured from a point halfway through the duration of the pulse.

Ψ_β phase angle expressed as a lag for a cosine representation of the Dutch roll oscillation in sideslip, where:

$\Psi_\beta = -(360/T_d)t_{n_\beta} + (n - 1)360$ deg.

with n as in t_n above.

$\angle(p/\beta)$ phase angle between roll rate and sideslip in the free Dutch roll oscillation. This phase angle is positive when p leads β by an angle between 0 and 180 degrees.

$|\phi/\beta|_d$ at any instant, the ratio of amplitudes of the bank-angle and sideslip-angle envelopes in the Dutch roll mode

Examples showing measurement of roll-sideslip coupling parameters are shown on Figure B14 for right rolls and Figure B15 for left rolls. Since several oscillations of the Dutch roll are required to measure these parameters, and since for proper identification large roll rates and bank angle changes must generally be avoided, step roll control inputs should be small. It should be noted that since Ψ_β is the phase angle for the Dutch roll component of sideslip, care must be taken to select a peak far enough downstream that the position of the peak is not influenced by the roll mode. In practice, peaks occurring one or two roll mode time constants after the aileron input will be relatively undistorted. Care must also be taken when there is ramping of the sideslip trace, since ramping will displace the position of a peak of the trace from the corresponding peak of the Dutch roll component. In practice, the peaks of the Dutch roll component of sideslip are located by first drawing a line through the ramping portion of the sideslip trace and then noting the times at which the vertical distance between the line and the sideslip trace is the greatest. (See the following sketch for Case (a) of Figures B14 and B15; p. 359.)

Since the first local maximum of the Dutch roll component of the sideslip response occurs at t = 2.95 seconds,

$$\Psi_\beta = -(360/T_d)t_{n_\beta} + (n - 1)360 =$$

$$= -(360/3.5)(2.95) = -303 \text{ deg.}$$

Level 1 flying qualities of a Class IV airplane in the approach are under examination, so the roll performance requirement from Table IX upon which the parameter 'k' in the sideslip excursion requirement (Figure B6) is based, is ϕ_t = 30 degrees in 1 second with rudder pedals free (as in the rolls of 3.3.2.4). From the definitions, 'k' for this condition is:

$$k = (\phi_1)_{command}/(\phi_1)_{requirement}$$

Therefore from Figures B14 and B15:

Case (a), k = 9.1/30 = 0.30

Case (b), k = 8.1/30 = 0.27

Case (c), k = 6.8/30 = 0.23

Case (d), k = 6.0/30 = 0.20

6.2.7 Atmospheric disturbance parameters.

j	$(-1)^{1/2}$
Ω	spatial (reduced) frequency (radians per foot)
ω	temporal frequency (radians per sec), where: $\omega = \Omega V$
t	time (seconds)
u_g	disturbance velocity along the x-axis, positive forward (ft/sec)
v_g	disturbance velocity along the y-axis, positive to the pilot's right (ft/sec)
w_g	disturbance velocity along the z-axis, positive down (ft/sec)
	Note: Random u_g, v_g and w_g have Gaussian (normal) distributions
$V_{w/d}$	magnitude of wind over the aircraft carrier deck (ft/sec)
σ, RMS	root-mean-square disturbance intensity, where: $\sigma^2 = \int_0^\infty \phi(\Omega)d\Omega = \int_0^\infty \phi(\omega)d\omega$
σ_u	root-mean-square intensity of u_g
σ_v	root-mean-square intensity of v_g
σ_w	root-mean-square intensity of w_g
L_u	scale for u_g (feet)
L_v	scale for v_g (feet)
L_w	scale for w_g (feet)
$\phi_{u_g}(\Omega)$	spectrum for u_g, where: $\phi_{u_g}(\Omega) = V\phi_{u_g}(\omega)$
$\phi_{v_g}(\Omega)$	spectrum for v_g, where: $\phi_{v_g}(\Omega) = V\phi_{v_g}(\omega)$
$\phi_{w_g}(\Omega)$	spectrum for w_g, where: $\phi_{w_g}(\Omega) = V\phi_{w_g}(\omega)$
v_m	generalized discrete gust intensity, positive along the positive axes, m = x, y, z (ft/sec)
d_m	generalized discrete gust length (always positive), m = x, y, z (feet)
u_{20}	wind speed at 20 feet above the ground

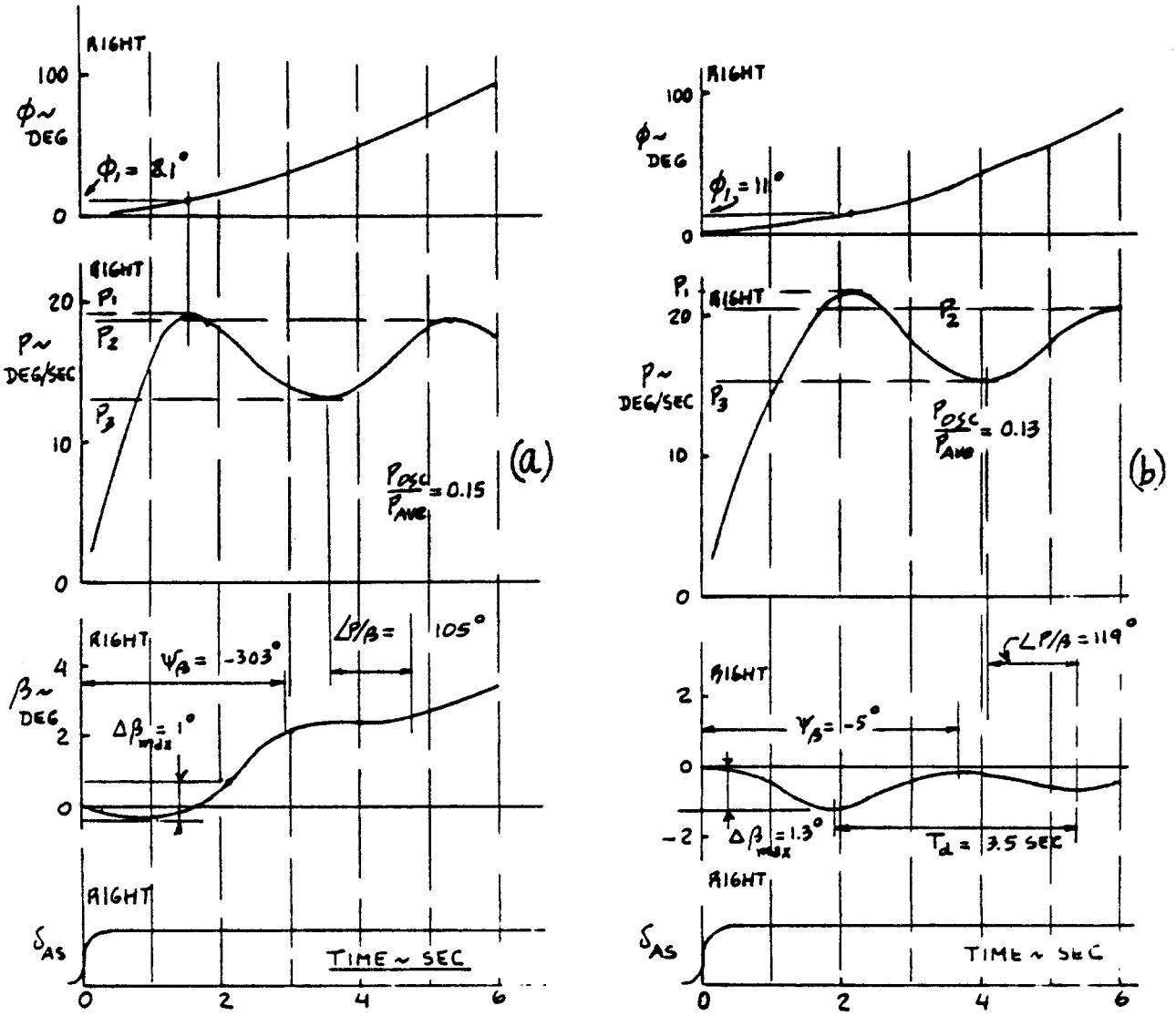

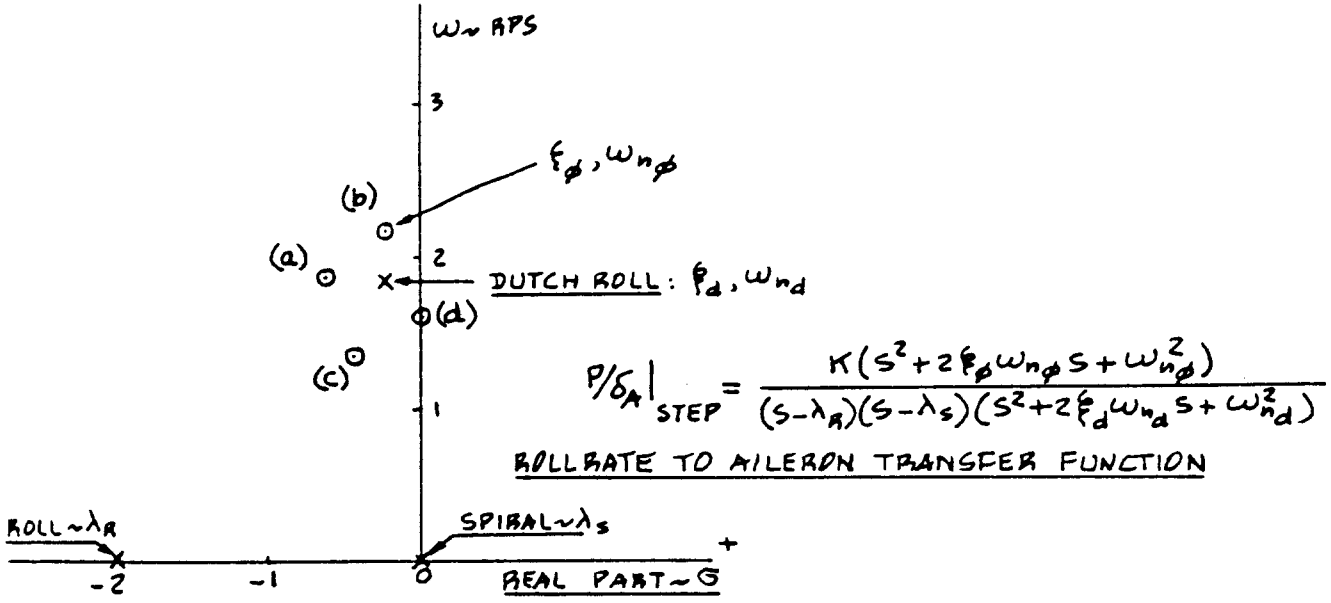

Figure B14 Roll-Sideslip Coupling Parameters: Right Rolls

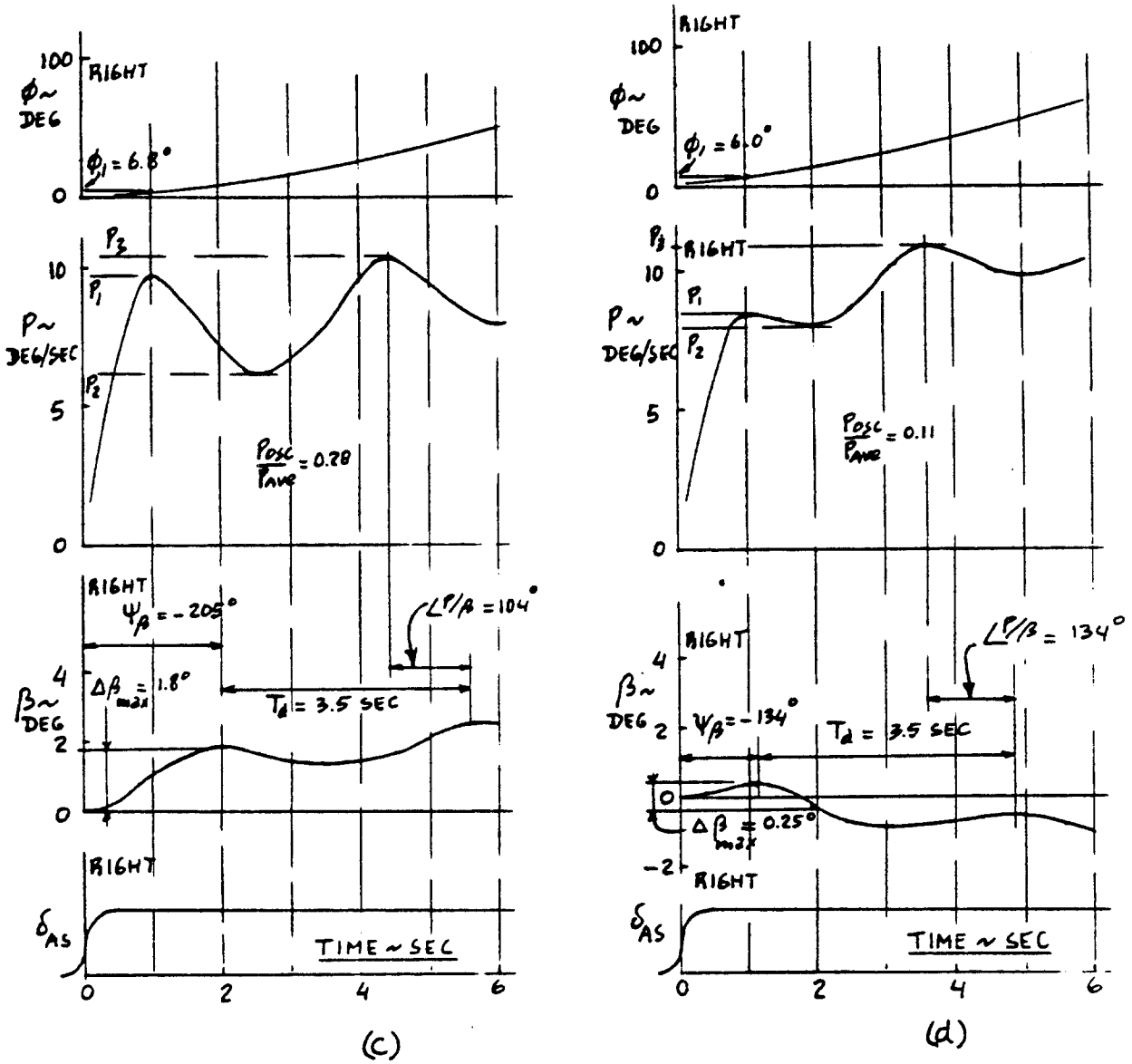

Figure B14 (Cont'd) Roll-Sideslip Coupling Parameters: Right Rolls

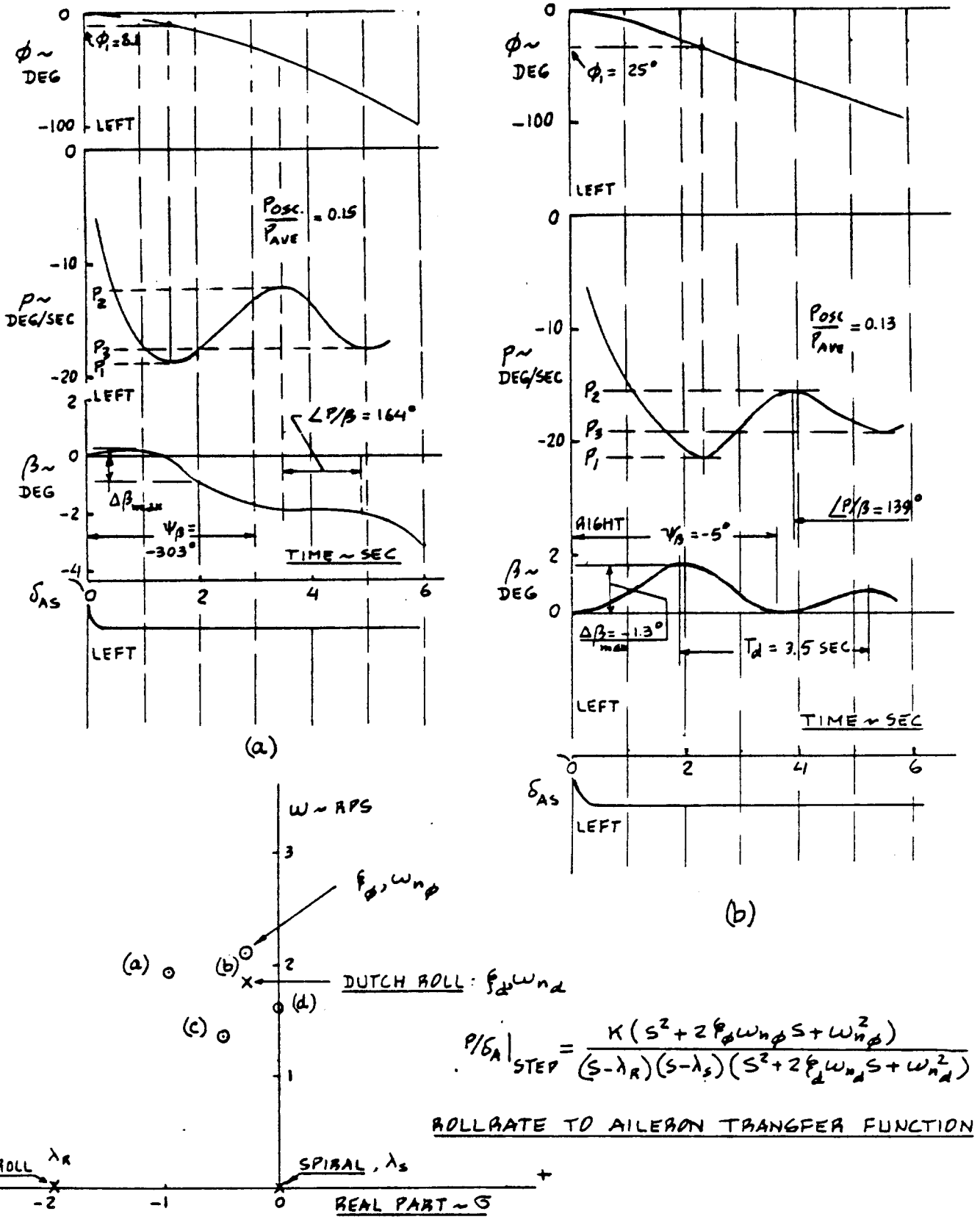

$$p/\delta_A\Big|_{STEP} = \frac{K(s^2 + 2\zeta_\phi\omega_{n\phi}s + \omega_{n\phi}^2)}{(s-\lambda_R)(s-\lambda_s)(s^2 + 2\zeta_d\omega_{nd}s + \omega_{nd}^2)}$$

ROLLRATE TO AILERON TRANSFER FUNCTION

Figure B15 Roll-Sideslip Coupling Parameters: Left Rolls

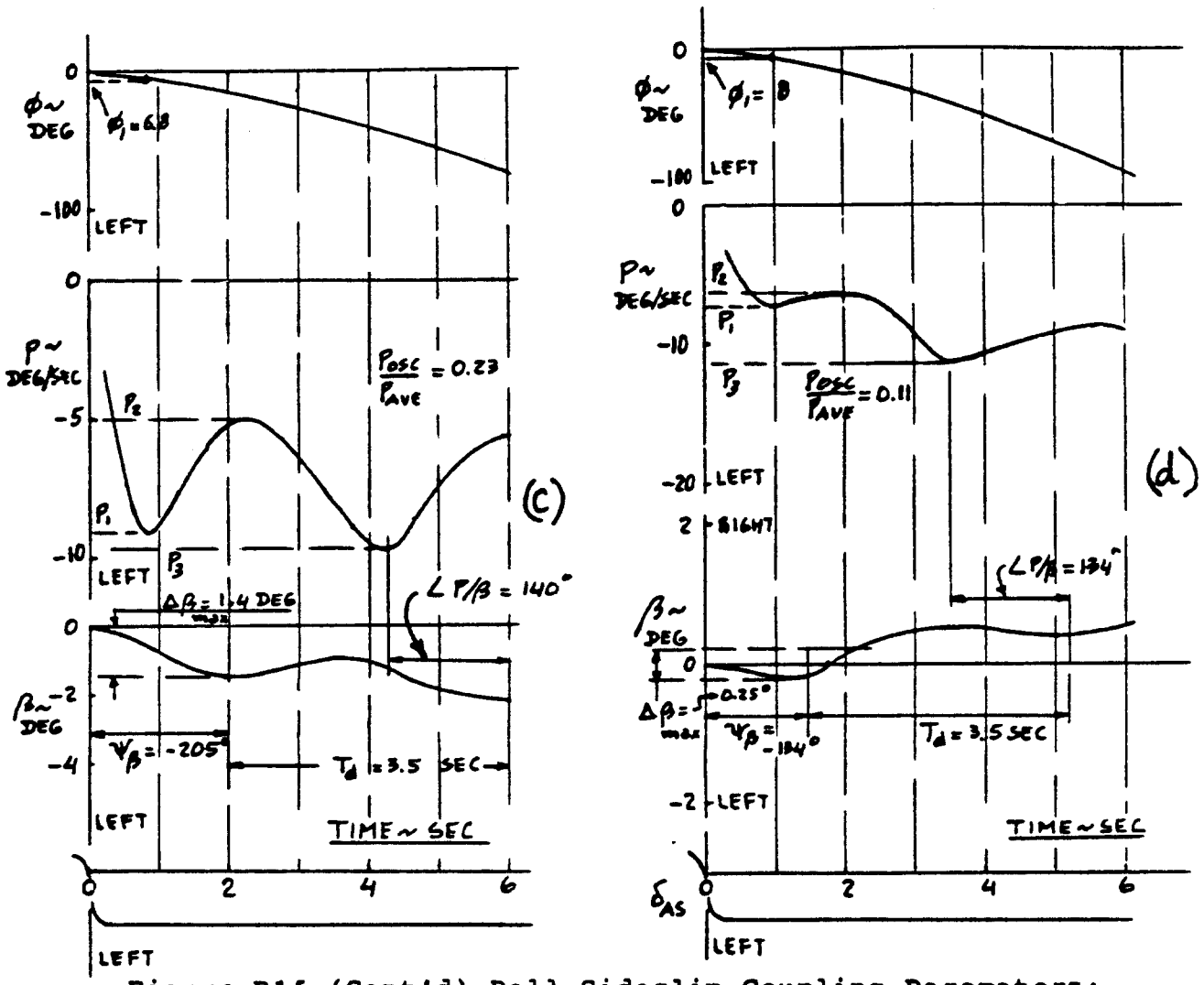

Figure B15 (Cont'd) Roll-Sideslip Coupling Parameters: Left Rolls

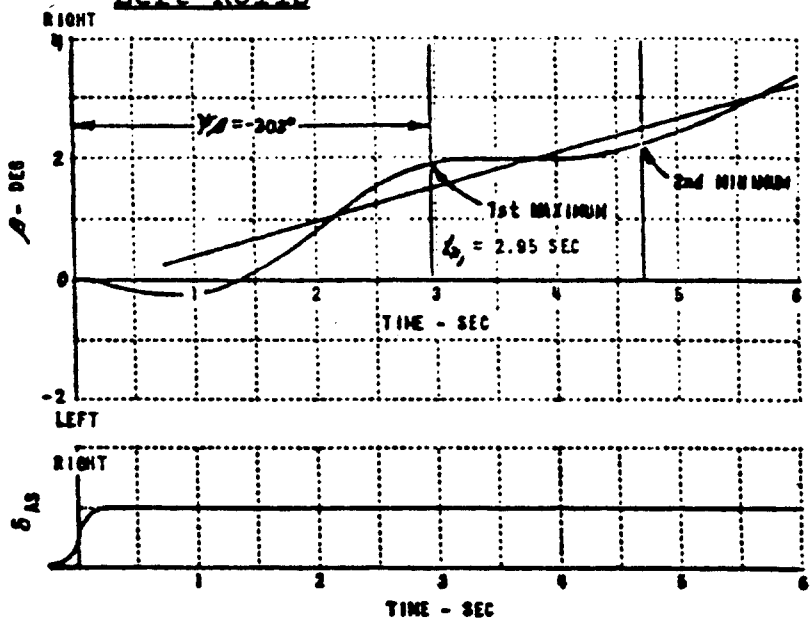

SKETCH CORRESPONDING TO COMMENT ON FIGS B14 AND B15 ON P. 335, LEFT

x	distance from airplane to ship center of pitch, negative aft of ship (feet)
V_w	mean wind direction relative to the runway (3.7.3.3)

6.2.8 Terms used in high angle of attack requirements.

Post-stall: The flight regime involving angles of attack greater than nominal stall angles of attack. The airplane characteristics in the post-stall regime may consist of three more or less distinct consecutive types of airplane motion following departure from controlled flight: post-stall gyration, incipient spin, and developed spin.

Post-stall gyration (PSG): Uncontrolled motions about one or more airplane axes following departure from controlled flight. While this type of airplane motion involves angles of attack higher than the stall angle, lower angles may be encountered intermittently in the course of the motion.

Spin: That part of post-stall airplane motion which is characterized by a sustained yaw rotation. The spin may be erect or inverted, flat (high angle of attack) or steep (low, but still stalled angle of attack) and the rotary motions may have oscillations in pitch, roll and yaw superimposed on them. The incipient spin is the initial, transient phase of the motion during which it is not possible to identify the spin mode, usually followed by the developed spin, the phase during which it is possible to identify the spin mode.

6.3 Interpretation of F_s/n limits of Table V. Because the limits on F_s/n are a function of both n_L and n/α, Table V is rather complex. To illustrate its use, the limits are presented on Figure B16 for an airplane having a center-stick controller and n_L = 7.0.

6.4 Gain scheduling. Changes of mechanical gearings and stability augmentation gains in the primary flight control system are sometimes accomplished by scheduling the changes as a function of the settings of secondary control devices, such as flaps or wing sweep. This practice is generally acceptable, but gearings and gains normally should not be scheduled as a function of trim control settings since pilots do not always keep airplanes in trim.

6.5 Engine considerations. Secondary effects of engine operation may have an important bearing on flying qualities and should not be overlooked in design. These considerations are:

a) the influence of engine gyroscopic moments on airframe dynamic motions

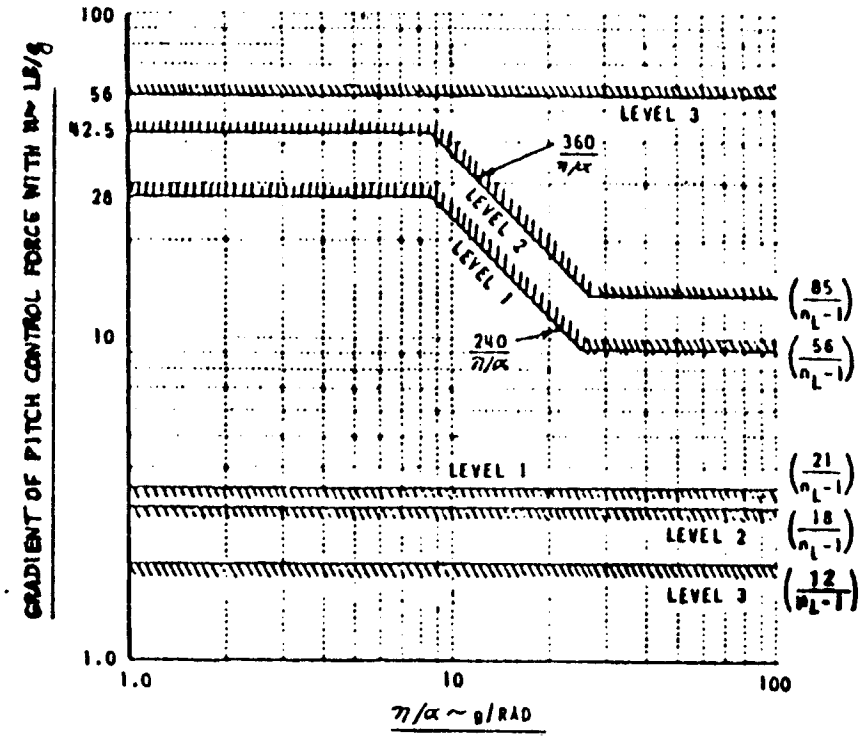

Figure B16 Example of Pitch Maneuvering Force Gradient Limits: Center-stick Controller, n_L = 7.0

b) the effects of engine operation (including flameout and intentional shutdown) on characteristics of flight at high angle of attack (3.4.2)

c) the reduction at low rpm of engine-derived power for operating the flight control system.

6.6 Effects of aeroelasticity, control equipment and structural dynamics. Since aeroelasticity, control equipment and structural dynamics may exert an important influence on the airplane flying qualities, such effects should not be overlooked in calculations or analyses directed toward investigation of compliance with the requirements of this specification.

6.7 Application of Levels. Part of the intent of 3.1.10 is to ensure that the probability of encountering significantly degraded flying qualities because of component

or subsystem failure is small. For example, the probability of encountering very degraded flying qualities (Level 3) must be less than specified values per flight.

6.7.1 Level definitions. To determine the degradation in flying qualities parameters for a given Airplane Failure State the following definitions are provided:

a. Level 1 is better than or equal to the Level 1 boundary, or number, specified in Section 3

b. Level 2 is worse than Level 1, but no worse than the Level 2 boundary, or number

c. Level 3 is worse than Level 2, but no worse than the Level 3 boundary, or number.

When a given boundary, or number, is identified simultaneously as Level 1 and Level 2, this means that the flying qualities outside the boundary conditions shown, or worse than the number given, are at best Level 3 flying qualities. Also, since Level 1 and Level 2 requirements are the same, flying qualities must be within this common boundary, or number, in both the Operational and Service Flight Envelopes for Airplane Normal States (3.1.10.1). Airplane Failure States that do not degrade flying qualities beyond this common boundary are not considered in meeting the requirements of 3.1.10.2. Airplane Failure States that represent degradations to Level 3 must, however, be included in the computation of the probability of encountering Level 3 degradations in both the Operational and Service Flight Envelopes. Again, degradation beyond the Level 3 boundary is not permitted regardless of component failures.

TABLE OF CONTENTS FOR APPENDIX B2: MIL-F-8785C: MILITARY SPECIFICATION, FLYING QUALITIES OF PILOTED AIRPLANES

3.2.3.7	Longitudinal control in sideslips
3.3	Lateral-directional flying qualities
3.3.1	Lateral-directional mode characteristics
3.3.1.1	Lateral-directional oscillations (Dutch roll)
3.3.1.2	Roll mode
3.3.1.3	Spiral stability
3.3.1.4	Coupled roll-spiral oscillation
3.3.2	Lateral-directional dynamic response characteristics
3.3.2.1	Lateral-directional response to atmospheric disturbances
3.3.2.2	Roll rate oscillations
3.3.2.2.1	Additional roll rate requirement for small inputs
3.3.2.3	Bank angle oscillations
3.3.2.4	Sideslip excursions
3.3.2.4.1	Additional sideslip requirement for small inputs
3.3.2.5	Control of sideslip in rolls
3.3.2.6	Turn coordination
3.3.3	Pilot-induced oscillations
3.3.4	Roll control effectiveness
3.3.4.1	Roll performance for Class IV airplanes
3.3.4.1.1	Roll performance in Flight Phase CO
3.3.4.1.2	Roll performance in Flight Phase GA
3.3.4.1.3	Roll response
3.3.4.2	Roll performance for Class III airplanes
3.3.4.3	Roll control forces
3.3.4.4	Linearity of roll response
3.3.4.5	Wheel control throw
3.3.5	Directional control characteristics
3.3.5.1	Directional control with speed change
3.3.5.1.1	Directional control with asymmetric loading
3.3.5.2	Directional control in wave-off (go-around)
3.3.6	Lateral-directional characteristics in steady sideslips
3.3.6.1	Yawing moments in steady sideslips
3.3.6.2	Side forces in steady sideslips
3.3.6.3	Rolling moments in steady sideslips
3.3.6.3.1	Exception for wave-off (go-around)
3.3.6.3.2	Positive effective dihedral limit
3.3.7	Lateral-directional control in crosswinds
3.3.7.1	Final approach in crosswinds
3.3.7.2	Takeoff run and landing rollout in crosswinds
3.3.7.2.1	Cold- and wet-weather operation
3.3.7.2.2	Carrier-based airplanes
3.3.7.3	Taxiing wind speed limits
3.3.8	Lateral-directional control in dives
3.3.9	Lateral-directional control with asymmetric thrust
3.3.9.1	Thrust loss during takeoff run
3.3.9.2	Thrust loss after takeoff
3.3.9.3	Transient effects
3.3.9.4	Asymmetric thrust- yaw controls free
3.3.9.5	Two engines inoperative
3.4	Miscellaneous flying qualities
3.4.1	Dangerous flight conditions
3.4.1.1	Warning and indication
3.4.1.2	Devices for indication, warning, prevention, recovery
3.4.2	Flight at high angle of attack
3.4.2.1	Stalls
3.4.2.1.1	Stall approach
3.4.2.1.1.1	Warning speed for stalls at 1g normal to the flight path
3.4.2.1.1.2	Warning range for accelerated stalls
3.4.2.1.2	Stall characteristics
3.4.2.1.3	Stall prevention and recovery
3.4.2.1.3.1	One-engine-out stalls
3.4.2.2	Post-stall gyrations and spins
3.4.2.2.1	Departure from controlled flight
3.4.2.2.2	Recovery from post-stall gyrations and spins
3.4.3	Cross-axis coupling in roll maneuvers
3.4.4	Control harmony
3.4.4.1	Control force coordination
3.4.5	Buffet
3.4.6	Release of stores
3.4.7	Effects of armament delivery and special equipment
3.4.8	Transients following failures
3.4.9	Failures
3.4.10	Control margin
3.4.11	Direct force control
3.5	Characteristics of the primary flight control system
3.5.1	General characteristics
3.5.2	Mechanical characteristics
3.5.2.1	Control centering and breakout forces
3.5.2.2	Cockpit control free play
3.5.2.3	Rate of control displacement
3.5.2.4	Adjustable controls
3.5.3	Dynamic characteristics
3.5.3.1	Damping
3.5.4	Augmentation systems
3.5.5	Failures
3.5.5.1	Failure transients
3.5.5.2	Trim changes due to failures
3.5.6	Transfer to alternate control modes
3.5.6.1	Transfer transients
3.5.6.2	Trim changes
3.6	Characteristics of secondary control systems
3.6.1	Trim system
3.6.1.1	Trim for asymmetric thrust
3.6.1.2	Rate of trim operation
3.6.1.3	Stalling of trim system
3.6.1.4	Trim system irreversibility
3.6.2	Speed and flight-path control devices
3.6.3	Transients and trim changes
3.6.3.1	Pitch trim changes
3.6.4	Auxiliary dive recovery devices

3.7	Atmospheric disturbances
3.7.1	Form of the disturbance models
3.7.1.1	Turbulence model (von Karman form)
3.7.1.2	Turbulence model (Dryden form)
3.7.1.3	Discrete gust model
3.7.2	Medium/high-altitude model
3.7.2.1	Turbulence scale lengths
3.7.2.2	Turbulence intensities
3.7.2.3	Gust lengths
3.7.2.4	Gust magnitudes
3.7.3	Low-altitude disturbance model
3.7.3.1	Wind speeds
3.7.3.2	Wind shear
3.7.3.3	Vector shear
3.7.3.4	Turbulence
3.7.3.5	Gusts
3.7.4	Carrier landing disturbance model
3.7.4.1	Free-air turbulence components
3.7.4.2	Steady component of carrier airwake
3.7.4.3	Periodic component of carrier airwake
3.7.4.4	Random component of carrier airwake
3.7.5	Application of the disturbance model in analysis
3.8	Requirements for use of the disturbance models
3.8.1	Use of disturbance models
3.8.2	Qualitative degrees of suitability
3.8.3	Effects of atmospheric disturbances
3.8.3.1	Requirements for Airplane Normal States
3.8.3.2	Requirements for Airplane Failure States
4.	QUALITY ASSURANCE
4.1	Compliance demonstration
4.1.1	Analytical compliance
4.1.1.1	Effects of failure states
4.1.1.2	Effects of atmospheric disturbances
4.1.1.3	Computational assumptions
4.1.2	Simulation
4.1.3	Flight test demonstration
4.2	Airplane States
4.2.1	Weights and moments of inertia
4.2.2	Center-of-gravity positions
4.2.3	Thrust settings
4.3	Design and test conditions
4.3.1	Altitudes
4.3.2	Special conditions
4.4	Tests at specialized facilities
5.	PREPARATION FOR DELIVERY
5.1	Not applicable
6.	NOTES
6.1	Intended use
6.2	Definitions
6.2.1	General
6.2.2	Speeds
6.2.3	Thrust and power
6.2.4	Control parameters
6.2.5	Longitudinal parameters
6.2.6	Lateral-directional parameters
6.2.7	Atmospheric parameters
6.2.8	Terms used in high angle of attack requirements
6.3	Interpretation of F_s/n limits of Table V
6.4	Gain scheduling
6.5	Engine considerations
6.6	Effects of aeroelasticity, control equipment and structural dynamics
6.7	Application of Levels
6.7.1	Level definitions

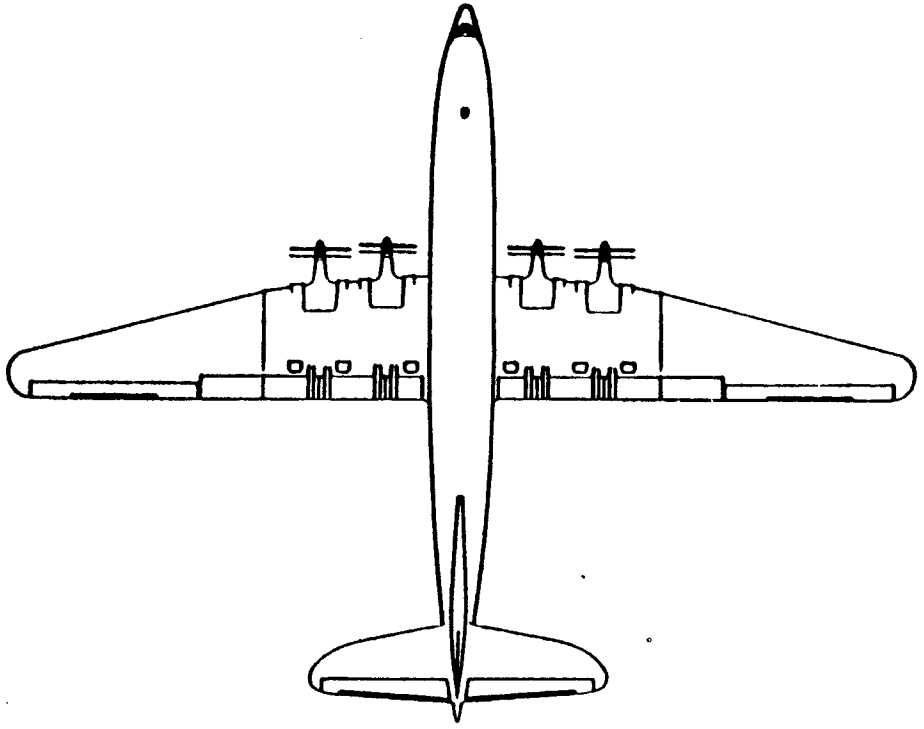

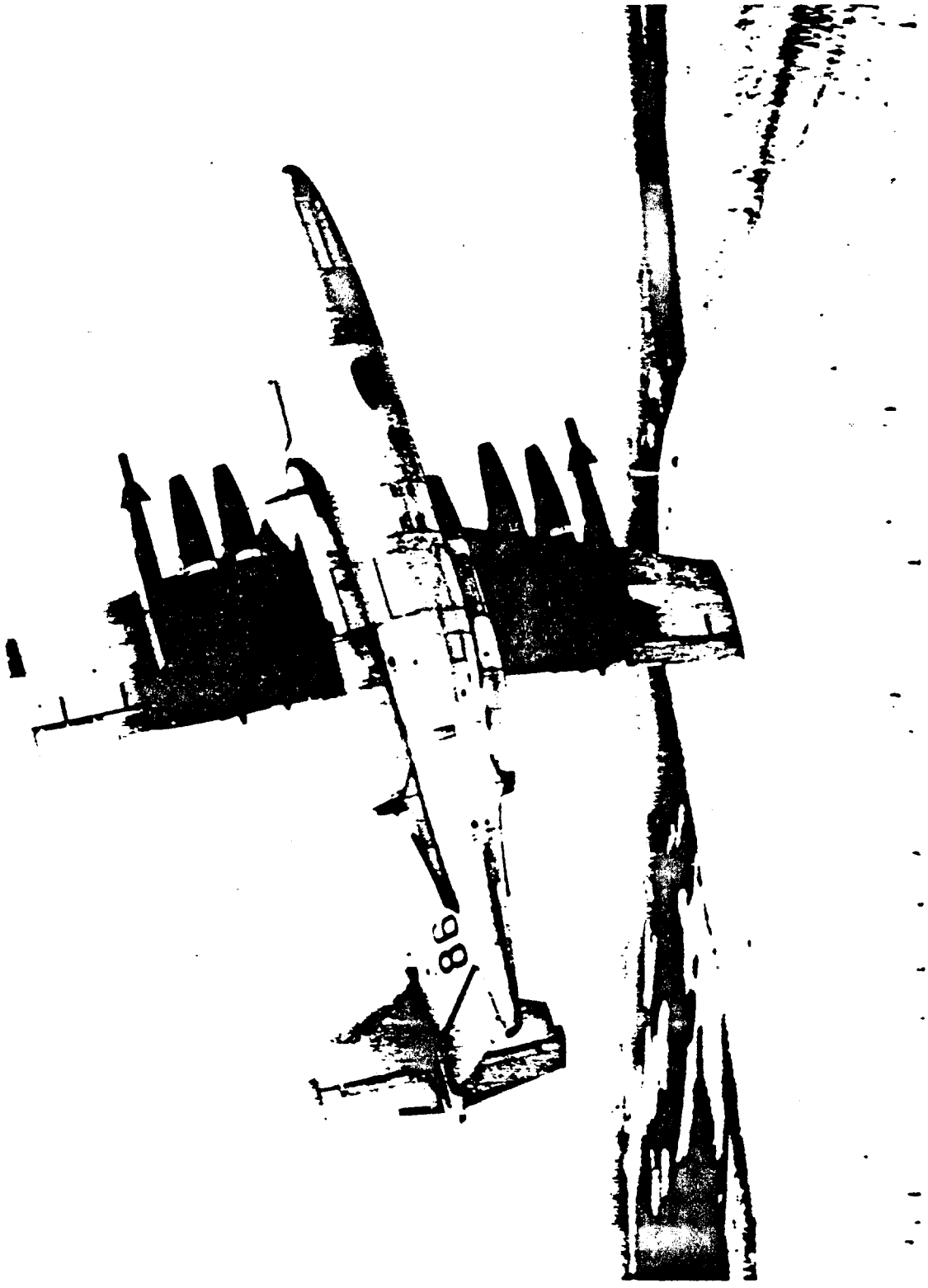

COURTESY : SAAB

APPENDIX C: THE AIRWORTHINESS CODE AND THE RELATIONSHIP BETWEEN FAILURE STATES, LEVELS OF PERFORMANCE AND LEVELS OF FLYING QUALITIES

The purpose of this appendix is to provide airplane designers with a link between the airworthiness regulations, the failure of flight crucial systems and the required level of performance and flying qualities.

LEMMA: It is NOT possible to design an airplane so that the probability of catastrophic failure is zero.

For the airplane designer, the consequence of this Lemma is that:

1. The airplane and all its systems must be designed so that catastrophic failures do not occur above some agreed upon (low) level of probability.

2. The consequences of each flight crucial failure must be understood and the probability of its occurrence must be predicted.

The civil airworthiness code of Figure C1 reflects this design philosophy in a qualitative and quantitative manner. The airworthiness code of Figure C1 reflects the intent of the civil regulations of Appendix A.

The military airworthiness code of Figure C2 reflects this design philosophy in a qualitative and quantitative manner. The airworthiness code of Figure C2 reflects the intent of the military regulations as presented in Appendix B.

There is no formal linkage between the civil and the military airworthiness requirements. However, Figure C2 when compared to Figure C1 infers such a linkage. This inference was made by the author!

The airworthiness codes of Figures C1 and C2 depict the 'level of airplane capability' left, following some failure. The following definitions of capability levels are suggested by the author. They are based on those stated in Appendix B, Section B3:

Level 1: Characteristics clearly adequate for the conduct of the flight.

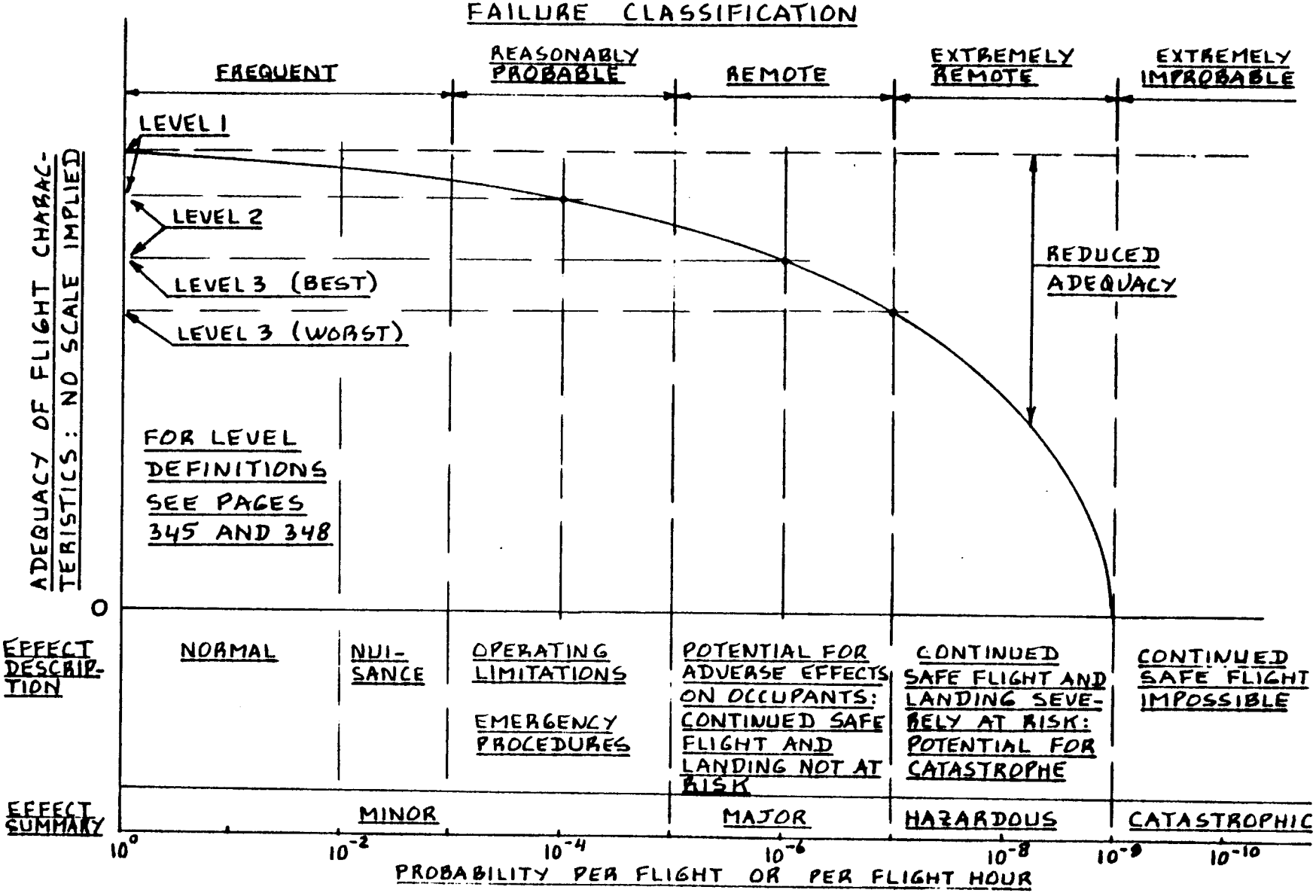

Figure C1 The Civil Airworthiness Code

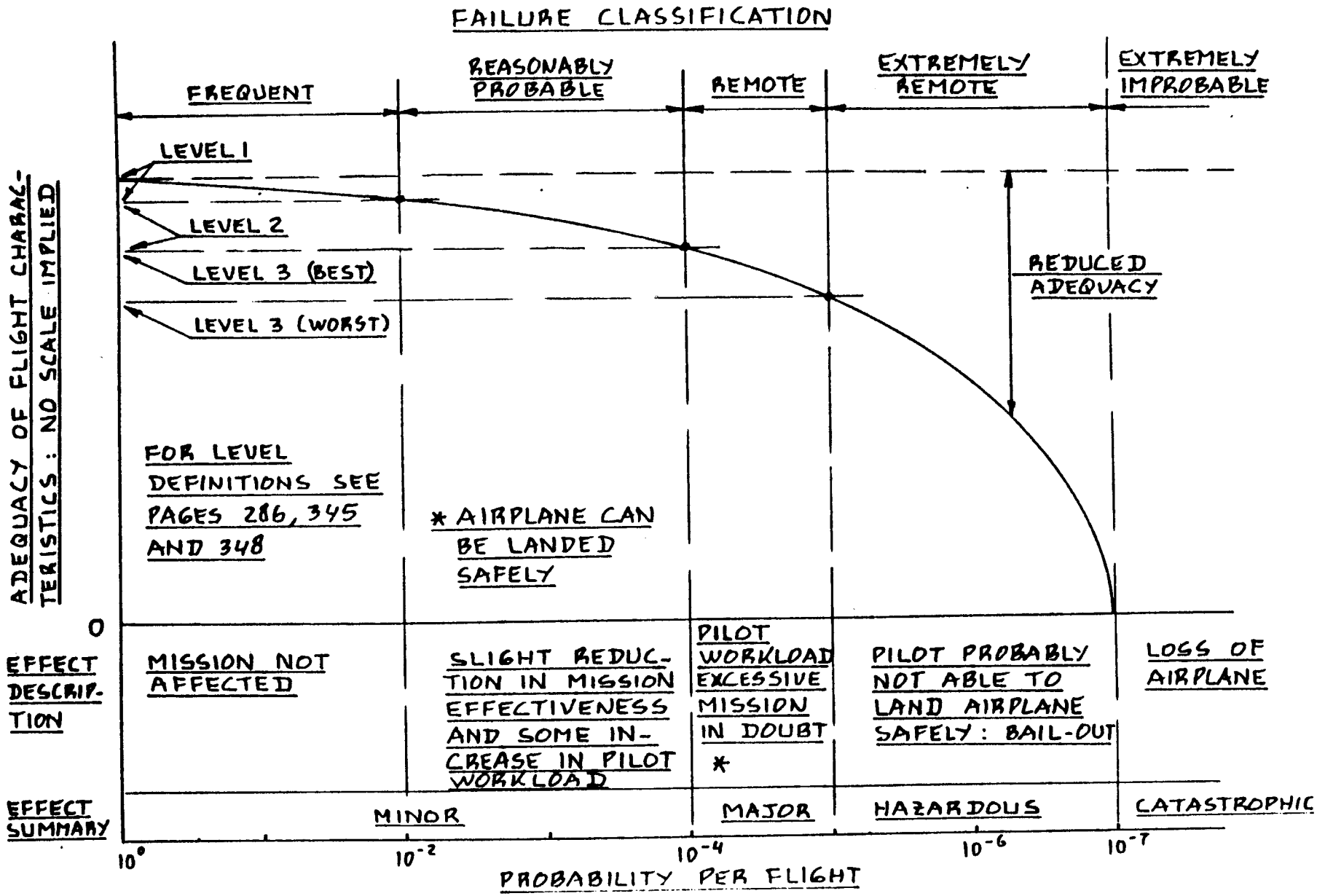

Figure C2 The Military Airworthiness Code

Level 2: Characteristics adequate to conduct the flight, but some increase in pilot workload or some degradation in mission effectiveness, or both, exists.

Level 3: Characteristics such that the flight can be continued and a safe landing conducted, but pilot workload is excessive or mission effectiveness is inadequate, or both.

Note: for flight characteristics worse than Level 3 a catastrophic crash is likely to occur.

The word 'characteristics' as used here implies: performance capabilities and/or flying qualities. Therefore, from a preliminary design viewpoint, two failure aspects are important:

C1: Failures Affecting Performance
C2: Failures Affecting Stability and Control (i.e. flying qualities to the military and flight characteristics to the civilians)

C1: FAILURES AFFECTING PERFORMANCE

The civil and military performance regulations of Appendices A and B cover three failure situations:

Failure Situation:	Level Definition
1. All engines operating (AEO):	Level 1
2. One engine inoperative (OEI):	Level 2
3. Two or more engines inoperative:	Level 3

The Level association given above is suggested by the author: it is NOT found in any of the regulations.

C2 STABILITY AND CONTROL

The civil regulations for stability and control behavior (flight characteristics) as stated in Appendix A apply to the required characteristics with ALL systems functioning normally.

The military regulations for stability and control (flying qualities) as stated in Appendix B allow for three Levels of flying qualities. The definition of these Levels is given on page 286. Each Level of flying qualities is associated with some failure in the flight control system AND with a probability of occurrence: see

Table II on page 290. Appendix B provides numerical values for all pertinent flying qualities at each flying quality Level and for each phase of flight.

The civil regulations do not formally recognize a link between failures and degradation (Level) in flying qualities. However, industry design practice is to use the military flying quality Levels in design, but with failure probabilities which are typically a factor 100 times better than those allowed by the military.

As seen in Figures C1 and C2, the relative level of failure probability in civil airplanes is a factor 100 lower than that for military airplanes.

With regard to flight control system design, it is suggested to consider the following two extremes:

TYPE 1: Airplanes with reversible control systems and inherent stability.

In these airplanes the assumption should be made that all control system components are purely mechanical so that their probability of failure is equal to the probability of failure in the primary airplane structure. Such airplanes should be designed to Level 1 flying qualities when intended for the military: see Appendix B.

For civil airplanes the regulations of Appendix A should be used where possible. In cases where the civil regulations fail to provide numerical design guidelines, the pertinent military regulation of Appendix B should be used.

TYPE 2: Airplanes with irreversible control systems and inherent instability.

With all systems operating, civil and military airplanes should be designed according to the Type 1 philosophy stated before.

With one or more failures, <u>civil and military</u> airplanes should be designed to the appropriate handling quality levels as stated in Appendix B. The failure probability levels associated with civil airplanes should be at least a factor 100 lower than that associated with military airplanes.

For airplanes which fit in between Types 1 and 2, the design philosophy for Type 2 airplanes should be used.

COURTESY : SAAB

APPENDIX D: INERTIA TRANSFORMATIONS

The purpose of this appendix is to provide equations for the transformation of airplane moments and product of inertia from one body fixed axis system to another. The two axis systems are shown in Figure D1. Note that both are centered on the airplane center of gravity.

The transformation equations are as follows:

$$\begin{Bmatrix} I_{xx_s} \\ I_{zz_s} \\ I_{xz_s} \end{Bmatrix} = \begin{bmatrix} \cos^2\alpha_1 & \sin^2\alpha_1 & -\sin 2\alpha_1 \\ \sin^2\alpha_1 & \cos^2\alpha_1 & \sin 2\alpha_1 \\ 0.5\sin 2\alpha_1 & -0.5\sin 2\alpha_1 & \cos 2\alpha_1 \end{bmatrix} \times \begin{Bmatrix} I_{xx_B} \\ I_{zz_B} \\ I_{xz_B} \end{Bmatrix}$$

The angle α_1 represents the steady state angle of attack of the airplane. The subscript 'B' refers to an arbitrarily selected body-fixed axis system. The subscript 's' refers to the so-called stability axis system (its x-axis is aligned with the steady state velocity vector, U_1 of the airplane) which is ALSO a body-fixed axis system!

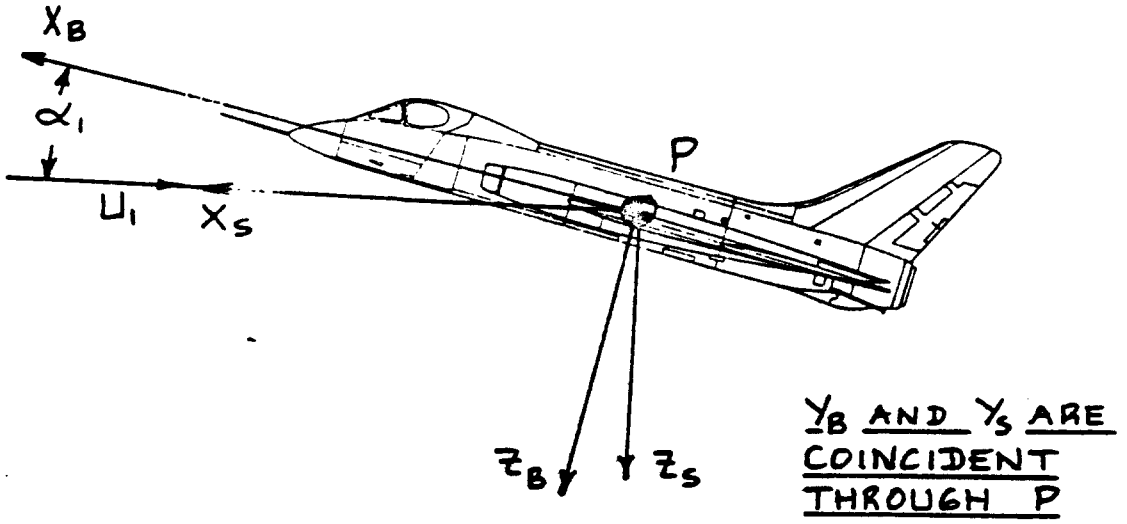

Figure D1 Airplane Axis Systems

AIRPLANE DESIGN

PART VIII: AIRPLANE COST ESTIMATION: DESIGN, DEVELOPMENT, MANUFACTURING AND OPERATING

by

Dr. Jan Roskam
Ackers Distinguished Professor
of Aerospace Engineering
The University of Kansas
Lawrence, Kansas

NO PART OF THIS BOOK MAY BE REPRODUCED WITHOUT
PERMISSION FROM THE AUTHOR

Copyright: Roskam Aviation and Engineering Corporation
Rt4, Box 274, Ottawa, Kansas, 66067, USA
Tel. 913-2421624

First Printing: 1990 (hardbound)

TABLE OF CONTENTS

TABLE OF SYMBOLS

The Table of Symbols is organized as follows:

1. GENERAL SYMBOLS

Symbol	Definition	Dimension
a	speed of sound	ft/sec or kts
A	Aspect ratio (wing)	-----
A (alternate)	Regression coefficient in Equation (8.1)	-----
AEP	Airplane Estimated Price	USD
AFP	Airframe price	USD
AH	Number of flight hours for a crew member, per year	hrs/yr
AMP	Airplane Market Price	USD
ANW	Airplane net worth	USD
ASP	Avionics systems price per airplane	USD
ATF	Airplane type factor	-----
b	wing span	ft
B	Regression coefficient in Equation (8.1)	-----
c_f	skin friction coefficient	-----
c_j	Engine specific fuel consumption (jet)	1/hr
c_p	Engine specific fuel consumption (piston or turboprop)	1/hphr
C	See Eqn. (8.3)	-----
C_{aed}	Airframe engineering and design cost	USD
C_{amb}	Applied maintenance burden	USD/nm
C_{apc}	Airplane production cost	USD
C_{apctrl}	Cost of airplane control	USD/nm
C_{aps}	Cost of airplane service	USD/nm

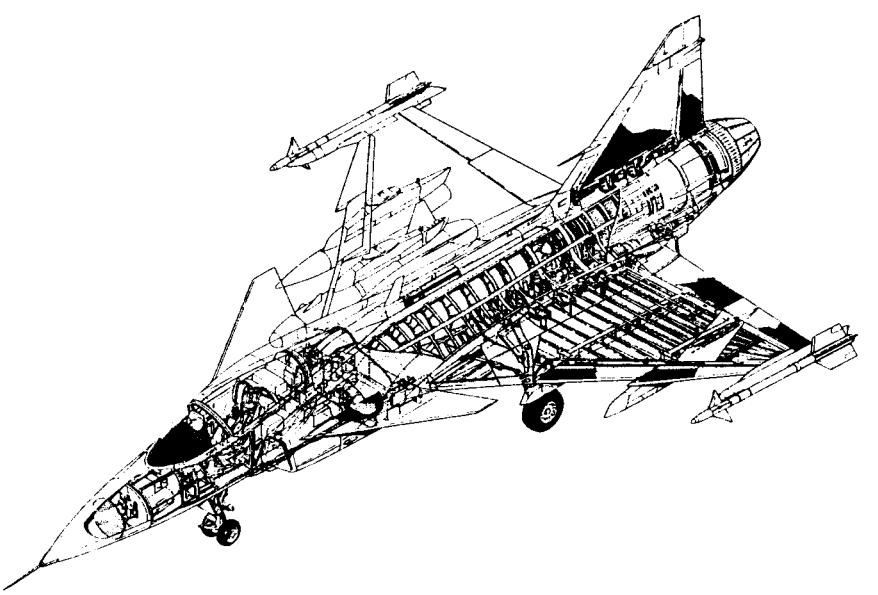

COURTESY : SAAB

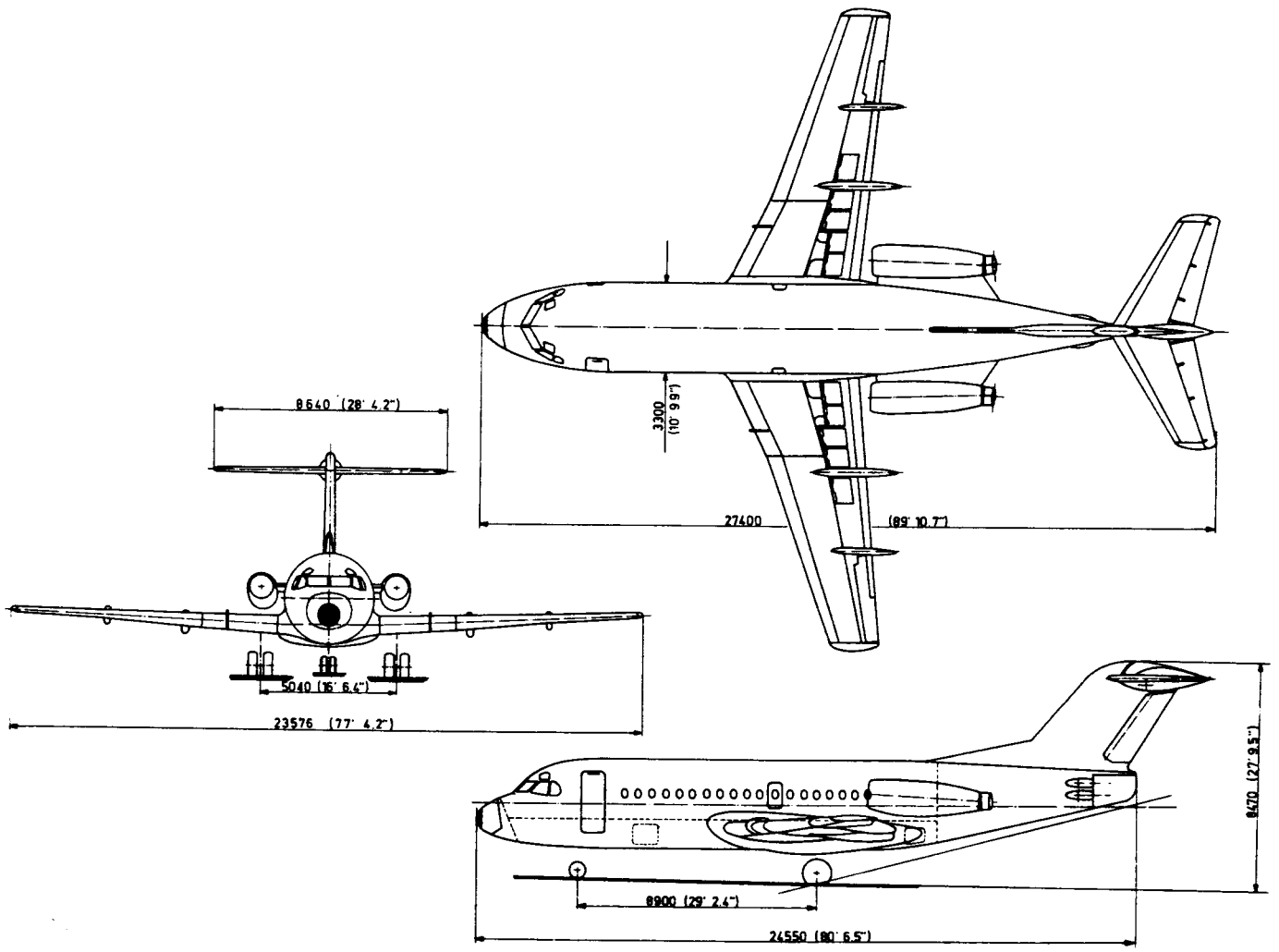

COURTESY: FOKKER

C_{aplf}	Airplane landing fee per landing	USD/landing
C_{apnf}	Navigation fee charged per flight	USD/flight
C_{auc}	Acquisition unit cost	USD/airplane
$C_{avionics}$	Avionics systems cost	USD
C_{cat}	Cost for cabin attendants	USD/nm
C_{crew}	Crew cost	USD/nm
C_{crewpr}	Crew cost for airplane program	USD
C_{dap}	Cost of airframe depreciation	USD/nm
C_{dapsp}	Cost of airplane spare parts depreciation	USD/nm
C_{dav}	Cost of avionics systems depreciation	USD/nm
C_{deng}	Cost of engine depreciation	USD/nm
C_{dengsp}	Cost of engine spare parts depreciation	USD/nm
C_{dgef}	Cost of depreciation of ground facilities and equipment	USD/nm
C_{dprp}	Cost of propeller depreciation	USD/nm
C_{dst}	Development support and test cost	USD
C_{e}	Engine unit cost	USD
$C_{(e + a)}$	Cost of engine and avionics	USD
C_{fin}	Financing cost	USD
C_{frt}	Cost of handling freight	USD/nm
C_{fta}	Cost for flight test airplanes	USD
C_{fto}	Flight test operations cost	USD
C_{ins}	Cost of insurance	USD/nm
C_{int}	Cost of interiors	USD
$C_{lab/ap}$	Labor cost of airframe and systems	USD/nm
$C_{lab/eng}$	Labor cost of engine maintenance	USD/nm

C_{lf}	Direct operating cost due to landing fees	USD/nm
C_{lcuc}	Life cycle unit cost	USD/airplane
C_{man}	Manufacturing labor cost	USD
C_{mat}	Materials cost	USD
$C_{mat/ap}$	Cost of maintenance materials for airplane and systems	USD/nm
$C_{mat/apblhr}$	Cost of airframe and systems maintenance materials	USD/nm
$C_{mat/eng}$	Cost of maintenance materials for engines	USD/nm
$C_{mat/engblhr}$	Cost of engine maintenance materials per block hour	USD/hr
C_{mgef}	Cost of maintaining ground equipment and facilities	USD/nm
C_{mls}	Cost for meal service	USD/nm
$C_{mpersdir}$	Progam cost for direct maintenance personnel	USD
C_{muc}	Manufacturing unit cost	USD/airplane
C_{nf}	Direct operating cost due to navigation fees	USD/nm
$C_{n_{\delta_R}}$	Yawing moment derivative due to rudder deflection	1/rad
$C_{ops_{dir}}$	Direct operating cost for entire airplane program	USD
$C_{ops/hr}$	Operating cost per hour	USD/hr
$C_{ops_{ind}}$	Indirect operating cost for entire airplane program	USD
C_{p}	Propeller unit cost	USD
$C_{pax/gen}$	General passenger cost	USD/nm
$C_{pax/ins}$	Cost of passenger insurance	USD/nm
C_{pol}	Fuel and oil cost	USD/nm
C_{pro}	Profit (cost)	USD
C_{puc}	Program unit cost	USD/airplane
C_{qc}	Quality control cost	USD
C_{rt}	Direct operating cost due to registry taxes	USD/nm

C_{tool}	Tooling cost	USD
C_{ACQ}	Total cost of acquisition	USD
C_{CONMAT}	Program cost of consumable materials	USD
C_D	Drag coefficient	-----
C_{D_o}	Zero-lift drag coefficient	----
C_{DEPOT}	Program cost associated with depots	USD
C_{DISP}	Total cost of the disposal phase	USD
CEF	Cost Escalation Factor	-----
CEF-ratio	See below Eqn.(2.5) for a definition	-----
C_L	Lift coefficient	-----
$C_{L_{max}}$	Maximum lift coefficient	-----
C_{MAN}	Total cost of the manufacturing phase	USD
C_{MISC}	Program miscellaneous cost	USD
C_{OPS}	Total cost of the operations phase	USD
$C_{PERSDIR}$	Program cost of direct personnel	USD
$C_{PERSIND}$	Program cost of indirect personnel	USD
C_{POL}	Program cost of fuel, oil and lubricants	USD
C_{PRO}	Manufacturer's profit in the manufacturing phase	USD
C_{PROT}	Prototype cost	USD
C_{RDTE}	Total cost of the RDTE phases	USD
C_{SPARES}	Program cost of spares	USD
D	See Eqn.(8.4)	lbs
DOC	Direct Operating Cost	USD/nm
DOC_{depr}	Direct operating cost of depreciation	USD/nm
DOC_{fin}	Direct operating cost of financing	USD/nm
DOC_{flt}	Direct operating cost of flying	USD/nm

DOC_{lnr}	Direct operating cost of landing fees, navigation fees and registry taxes	USD/nm
DOC_{maint}	Direct operating cost of maintenance	USD/nm
DP_{ap}	Airplane depreciation period	yrs
DP_{apsp}	Airplane spare parts depreciation period	yrs
DP_{av}	Avionics systems depreciation period	-----
DP_{engsp}	Engine spare parts depreciation period	yrs
DP_{prp}	Propeller depreciation period	yrs
e	Oswald's efficiency factor	----
E	Endurance	hrs
$EP = C_e$	Engine price	USD
ESPPF	Engine spare parts price factor	-----
$f_{amb/lab}$	overhead distribution factor for labor cost	-----
$f_{amb/mat}$	overhead distribution factor for material cost	-----
f_{depot}	depot cost fraction of C_{OPS}	-----
$f_{ins_{hull}}$	annual hull insurance rate	USD/USD/yr
f_{ioc}	indirect operating cost fraction of DOC	-----
f_{lf}	(landing fee) factor which depends on airplane size	-----
f_{misc}	miscellaneous cost fraction of C_{OPS}	-----
$f_{persdir}$	direct personnel cost fraction of C_{OPS}	-----
$f_{persind}$	indirect personnel cost fraction of C_{OPS}	-----
f_{pol}	fuel, oil and lubricant cost fraction of C_{OPS}	-----
f_{rt}	(registry tax) factor which depends on airplane size	-----

f_{spares}	indirect cost of spares as a fraction of C_{OPS}	-----
F_{apsp}	Airplane spare parts factor	---
F_{cad}	Judgement factor of relative company experience with CAD	
F_{dap}	Airframe depreciation factor	--
F_{dapsp}	Airplane spare parts depreciation factor	-----
F_{dav}	Avionics systems depreciation factor	-----
F_{deng}	Engine depreciation factor	----
F_{dengsp}	Engine spare parts depreciation factor	-----
F_{diff}	Judgement factor of relative program difficulty	-----
F_{dprp}	Propeller depreciation factor	-----
F_{engsp}	Engine spare parts factor	-----
F_{fin}	Finance cost fraction	-----
F_{ftoh}	Overhead factor associated with flight test activities	---
F_{int}	Interior cost factor which depends on number of pax	USD/pax
F_{mat}	Judgement factor to account for differing materials cost	-----
F_{obs}	Judgement factor to account for observables characteristics	
F_{pro}	Profit fraction	-----
F_{tsf}	Cost adjustment factor for extra test and simulation facilities	-----
FD	Fuel density	lbs/gallon
F_{OL}	Factor which accounts for cost of oil and lubricants	-----
FP	Fuel price	USD/gallon
H_{em}	Attained number of hours between engine overhaul	hrs
IOC	Indirect Operating Cost	USD/nm
IOC_{ascf}	Indirect operating cost for airplane and traffic servicing, control and freight	USD/nm

V_C	Design cruising speed	kts
V_s	Stall speed	kts
W	Weight	lbs
W_{ampr}	Aeronautical Manufacturers Planning Report Weight	lbs
W_{crew}	Crew weight	lbs
W_{eng}	Weight per engine	lbs
W_{feq}	Fixed equipment weight	lbs
$W_{ol_{bl}}$	Block oil used	lbs
$W_{pwrplt} = W_{pwr}$	Powerplant weight	lbs
W_{struct}	Airplane structural weight	----
W_A	Airframe weight	lbs
W_E	Airplane empty weight	lbs
$W_{F_{bl}}$	Block fuel used	lbs
$W_{F_{used}}$	Mission fuel used	lbs
W_{PL}	Payload weight	lbs
W/S	Wing loading	lbs/ft^2
W_{TO}	Takeoff Weight	lbs
W_{US}	Useful load	lbs
y_T	Engine-out moment arm	ft

2. Greek Symbols

δ_R	rudder deflection	rad
η_p	propeller efficiency	-----
ρ	air density	$slugs/ft^3$

3. Subscripts

aed	airframe engineering and design
api	airconditioning and pressurization

IOC_{gaa}	Indirect operating cost for general administrative expenses	USD/nm
IOC_{pax}	Indirect operating cost for passenger services	USD/nm
IOC_{pse}	Indirect operating cost for promotion, sales and entertainment	USD/nm
IOC_{sta}	Indirect operating cost for maintaining ground equipment and facilities	USD/nm
K_j	Vacation (etc) pay factor	-----
$K_{H_{em}}$	Attained period between overhaul factor	-----
LCC	Life Cycle Cost	USD (United States Dollars)
L/D	Lift-to-drag ratio	-----
L_R	Annual loss rate in number of airplanes lost per 10^5 hrs	1/hrs
M_1	Steady state Mach number	-----
M_{ff}	Overall mission fuel fraction	-----
M_{res}	Reserve fuel fraction	-----
M_{tfo}	Trapped fuel and oil fraction	-----
MHR_{aed}	Engineering manhours	hrs
$MHR_{aed_{program}}$	Engineering manhours for entire program	hrs
MHR_{flthr}	Total maintenance manhours per flight hour	hrs/hr
MHR_{man}	Manufacturing manhours	hrs
$MHR_{map_{bl}}$	Airframe and systems maintenance manhours per block hour	hrs/hr
$MHR_{map_{flt}}$	Airframe and systems maintenance manhours per flight hour	hrs/hr
$MHR_{man_{program}}$	Manufacturing manhours for entire program	hrs

$MHR_{map_{bl}}$	Maintenance manhours for airframe and systems	hrs/blhr
$MHR_{meng_{bl}}$	Maintenance manhours for engines per block hour	hrs/hr
MHR_{tool}	Tooling manhours	hrs
$MHR_{tool_{program}}$	Tooling manhours for entire program	hrs
n	learning curve exponent	-----
n_{c_j}	number of crew members of type j	-----
N_{acq}	Number of airplanes acquired	--
N_{crew}	Number in crew	-----
N_e	Number of engines per airplane	-----
N_{loss}	Number of airplanes lost through accidents over the airplane service life	-----
N_m	Number of airplanes built to production standards	-----
N_{market}	Estimated number of airplanes in a given market	-----
$N_{mission}$	Number of missions flown per year	-----
N_p	Number of propellers per airplane	-----
N_{pax}	Number of passengers	-----
$N_{program}$	Total number of airplanes built in a program	-----
N_{prot}	Number of prototypes	-----
N_{rdte}	Number of airplanes built in rdte phases	-----
N_r	Number of airplanes built per month	-----
N_{res}	Number of airplanes kept in reserve	-----
N_{serv}	Number of airplanes in active service	-----
N_{st}	Number of static test airframes built	-----
N_{yr}	Number of years an airplane is operated	-----

OD	Oil density	lbs/gallon
OHR_{crew}	Overhead rate factor associated with crew pay	-----
OLP	Oil price	USD/gallon
P	P percent learning curve	-----
Pay_{crew}	Annual pay of crew	USD/yr
P_{pot}	Profit potential	USD
$PP = C_p$	Propeller price	USD
$\bar{q}$	dynamic pressure	lbs/ft^2
R	Range	nm
R_{bl}	Block distance	nm
$R_{bl_{ann}}$	Annual block miles flown	nm/yr
R_{cl}	Climb distance	nm
R_{conmat}	Average cost of consumable materials per maintenance manhour	USD/hr
R_{cr}	Crew ratio	-----
R_{de}	Descent distance	nm
R_e	Engineering manhour rate	USD/hr
$R_{l_{ap}}$	Airplane maintenance labor rate	USD/hr
$R_{l_{eng}}$	Engine maintenance labor rate	USD/hr
R_m	Manufacturing manhour rate	USD/hr
R_{man}	Maneuvering distance	nm
$R_{m_{ml}}$	Military maintenance labor rate (incl. overhead)	USD/hr
R_t	Tooling manhour rate	USD/hr
REV	Revenue per nm	USD/nm
ROI	Return on investment	-----
S	Wing (reference) area	ft^2
S_{wet}	Wetted area	ft^2
SAL_j	Annual salary of crew member of type j	USD/yr

t_{bl}	block time	hrs
t_{cl}	climb time	hrs
t_{cr}	cruise time	hrs
t_{de}	descent time	hrs
t_{flt}	average flight time	hrs
t_{gm}	ground maneuver time	hrs
t_{pft}	Number of flight test hours flown by manufacturer	hrs
t_{man}	maneuvering time	hrs
t_{mis}	average mission time	hrs
tx_{inv}	investment tax rate	-----
tx_{rev}	income (revenue) tax rate	-----
T	Thrust	lbs
TEF	Travel expense factor	-----
TOC	Total operating cost	USD/nm
T_{TO}	Total takeoff thrust	lbs
T/W	Thrust to weight ratio	-----
$U_{ann_{bl}}$	Annual utilization in blockhours	hrs
$U_{ann_{flt}}$	Annual utilization in flight hours	hrs
V	Speed	keas
V_{bl}	Block speed	kts
V_{cr}	Cruise speed	kts
V_{de}	Descent speed (forward)	kts
V_{flt}	Average flight speed	kts
V_{man}	Speed while maneuvering	kts
V_{max}	Maximum design speed	kts
V_{mc}	Minimum control speed	kts

apu	auxiliary power unit
arm	armament and fire control
avionics	avionics
AMPR, ampr	Aeronautical Manufacturers Planning Report (Also called DCPR)
cl	climb
clean	clean airplane: gear and flaps up (retracted)
cr	cruise
C	Design Cruise
CAD	Computer Aided Drafting
dst	development support and testing
DCPR	Defense Contractors Planning Report (Also called AMPR)
DISP	Disposal
e	engine
els	electrical system
ess	engine starting system
E	Empty
fin	finance
fta	flight test airplanes
fto	flight test operations
F	Fuel
H	Maximum Level
iae	instruments, avionics and electronics
j	number which indicates type of crew member, j=1, 2, 3
L	Landing
m	manufacturing phase
mat	materials
max	maximum design
OPS	Operations
pro	profit
program	for entire program
PL	Payload
qc	quality control

r	rdte phase
rdte, RDTE	Research, Development, Test and Evaluation
tfo	trapped fuel and oil
tool	tooling
tsf	test and simulation facilities
TO	Takeoff

4. Acronyms and Abbreviations

AAA	Advanced Aircraft Analysis
ANG	Air National Guard
Ch	Chapter
CL	Climb
CR	Cruise
DESC	Descent
ECM	Electronic Counter Measures
FBO	Fixed Base Operator
IFF	Identification Friend or Foe
keas	knots equivalent airspeed
LCC	Life Cycle Cost
LTR	Loiter
Pt	Part
SLS	Sea level standard
TO	Takeoff
USAF	United States Air Force
USMC	United States Marine Corps
USN	United States Navy

COURTESY : PIAGGIO

ACKNOWLEDGEMENT
==========

Writing a book on airplane design is impossible without the supply of a large amount of data. The author is grateful to the following companies for supplying the necessary data to incorporate in this book:

Beech Aircraft Corporation
Boeing Commercial Airplane Company
Learjet Corporation
Lockheed Aircraft Corporation

A significant amount of airplane cost, price and revenue information has been accumulated by the author from the following magazines:

Interavia (Swiss monthly)
Flight International (British weekly)
Business and Commercial Aviation (USA, monthly)
Aviation Week and Space Technology (USA, weekly)

The author is particularly grateful to Mr. John W. Olcott, Publisher/Editor of Commercial and Business Aviation, for his permission to copy material from the 1989 Planning and Purchasing Handbook in Appendix C of this book.

The author also acknowledges the work done by two of his students: Mr. Larry Belmard and Mrs. Donna Gerren in checking calculations and proofreading the material.

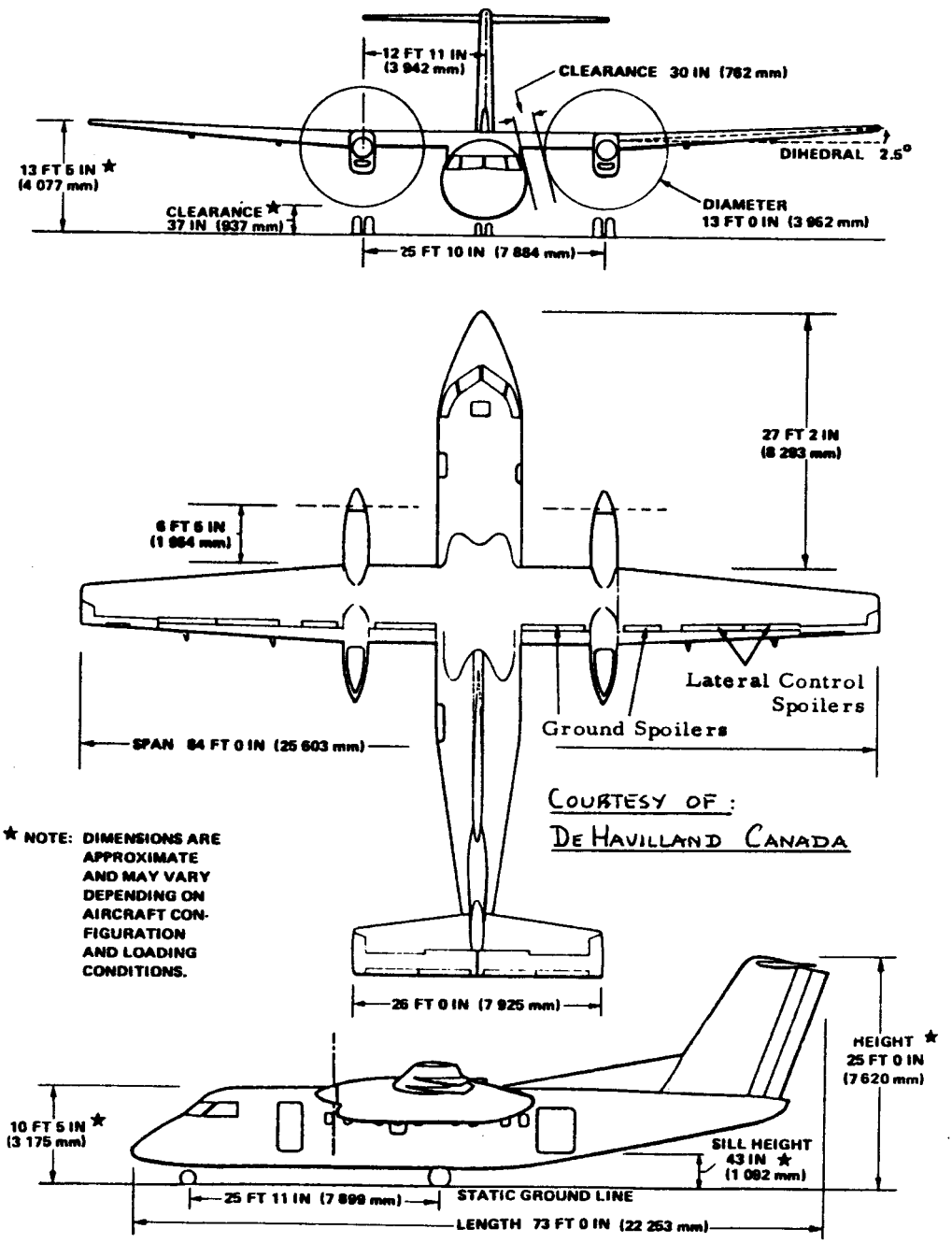
12 FT 11 IN
(3 942 mm)
CLEARANCE 30 IN (762 mm)
DIHEDRAL 2.5°
13 FT 5 IN ★
(4 077 mm)
CLEARANCE ★
37 IN (937 mm)
DIAMETER
13 FT 0 IN (3 962 mm)
25 FT 10 IN (7 884 mm)
27 FT 2 IN
(8 283 mm)
6 FT 6 IN
(1 964 mm)
Lateral Control
Spoilers
Ground Spoilers
SPAN 84 FT 0 IN (25 603 mm)
COURTESY OF :
DE HAVILLAND CANADA
★ NOTE: DIMENSIONS ARE APPROXIMATE AND MAY VARY DEPENDING ON AIRCRAFT CONFIGURATION AND LOADING CONDITIONS.
26 FT 0 IN (7 925 mm)
HEIGHT ★
25 FT 0 IN
(7 620 mm)
10 FT 5 IN ★
(3 175 mm)
SILL HEIGHT
43 IN ★
(1 092 mm)
25 FT 11 IN (7 899 mm)
STATIC GROUND LINE
LENGTH 73 FT 0 IN (22 253 mm)

1. INTRODUCTION

The purpose of this series of textbooks on Airplane Design is to familiarize aerospace engineering students with the design methodology and design decision making involved in the process of designing airplanes. The series of books is organized as follows:

Part I:	PRELIMINARY SIZING OF AIRPLANES
Part II:	PRELIMINARY CONFIGURATION DESIGN AND INTEGRATION OF THE PROPULSION SYSTEM
PART III:	LAYOUT DESIGN OF COCKPIT, FUSELAGE, WING AND EMPENNAGE: CUTAWAYS AND INBOARD PROFILES
PART IV:	LAYOUT DESIGN OF LANDING GEAR AND SYSTEMS
PART V:	COMPONENT WEIGHT ESTIMATION
PART VI:	PRELIMINARY CALCULATION OF AERODYNAMIC, THRUST AND POWER CHARACTERISTICS
PART VII:	DETERMINATION OF STABILITY, CONTROL AND PERFORMANCE CHARACTERISTICS: FAR AND MILITARY REQUIREMENTS
PART VIII:	AIRPLANE COST ESTIMATION: DESIGN, DEVELOPMENT, MANUFACTURING AND OPERATING

In this part (Part VIII) frequent reference is made to other parts in this Airplane Design series: Refs 1-7.

The purpose of Part VII is to present preliminary cost estimating methods for newly designed airplanes. The methods are presented in such a manner that they can be applied to commercial and to military airplanes of all types.

Chapter 2 presents a discussion of cost definitions and concepts. The idea of Life Cycle Cost is defined and its relation to the design decision making process is outlined.

The major cost sources of LCC are treated in some detail in Chapters 3 through 6 in the form of systematic cost estimating procedures and examples for:

* Research, development, technology and evaluation cost in Chapter 3

* Manufacturing and Acquisition cost in Chapter 4

* Operating cost for commercial airplanes in Chapter 5

* Operating cost for military airplanes in Chapter 6

An example of LCC determination for a military airplane is given in Chapter 7.

It is important that students of airplane design understand the role of optimization. Chapter 8 contains some fundamental discussions on this subject. The topic of 'design-to-cost' is also introduced in this chapter. Finally, a list of 88 design guidelines for 'low cost' is included in Chapter 8.

The decision on whether or not to proceed with full scale development of a new design involves a variety of factors. The purpose of Chapter 9 is to give an overview of key factors in airplane program decision making. This includes a list of 19 lessons learned on past programs.

Actual price data for airplanes and airplane components are hard enough to find for practicing engineers. For students this is often a very time consuming problem. To help with the problem of getting 'on track' with price data several appendices are included with specific information on prices:

* Appendix A includes airplane price data

* Appendix B includes engine and propeller price data

* Appendix C includes avionics systems price data

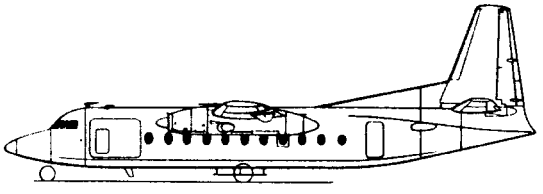

2. COST: DEFINITIONS AND CONCEPTS

The purpose of this chapter is to introduce aerospace engineering students to several important definitions and concepts, all dealing with airplane cost. The material is organized as follows:

2.1 Cost, Price and Profit
2.2 Airplane Program, Life Cycle and Life Cycle Cost
2.3 Examples of Aeronautical Enterprises
2.4 Some Observations on Profit and Cost

2.1 COST, PRICE AND PROFIT

First, it is necessary to define the meaning of the terms: COST, PRICE and PROFIT.

Definition 1: The COST of an airplane is the total amount of expenditure of resources, usually measured in dollars, needed to manufacture that airplane.

Definition 2: The PRICE of an airplane is the amount of dollars paid for the airplane by customers.

Definition 3: Profit = Price - Cost (2.1)

How cost, price and profit are viewed depends on which position is occupied in the economic process. Five examples of different viewpoints are:

Example 1: Position of the airplane manufacturer.

Assume that the cost to produce a certain airplane is USD 100,000. If the selling price is USD 110,000 a profit is made of USD 10,000. In the presence of competition it will be of prime interest to the manufacturer to offer his airplane at the lowest possible price (and still make a profit) while assuring that his airplane will be profitable or affordable to operate by his customer. This means that design, development and manufacturing costs must be kept as low as possible.

Example 2: Position of the commercial airplane operator.

To the commercial airplane operator, the price paid for an airplane is a cost (acquisition cost). Another cost is that incurred to operate the airplane.

The operator hopes to sell enough revenue ton miles (RTM) or revenue passenger miles (RPM) to make the operation of the airplane profitable. To make this possible, the acquisition and the operating cost must be as low as possible.

Example 3: Position of the personal or corporate airplane operator.

To this type of operator the airplane is a tool used to enhance certain aspects of business or to satisfy certain personal needs. Affordability is of prime concern to this type of operator. Affordability usually translates into requirements for low acquisition cost, low operating cost and high resale value.

Government tax policies and tax laws tend to have a significant impact on airplane affordability for this type of operator.

Example 4: Position of the government/military airplane operator.

The government/military airplane operator normally has a limited budget available with which to carry out certain missions. The price paid for an airplane and the cost incurred while operating the airplane all are costs to this operator. What this operator hopes to achieve is to carry out the required missions within the available budget. To make this possible the acquisition cost and the operating cost need to be as low as possible.

Military operators are normally directly involved in the design and development process with the airplane manufacturer. The cost associated with the design and development process can be significant particularly if the production run is small.

Example 5: Position of the consumer/taxpayer.

The consumer/taxpayer is the person who ends up paying for all activities required to design, manufacture, operate and dispose of airplanes. The consumer/taxpayer is ultimately interested in lowering the total cost associated with all aeronautical activities.

At this point it should be observed that all costs mentioned so far are those which can be measured directly

in dollars. Such costs are referred to also as economic costs. There are other types of cost as well: social, psychological and environmental, to name a few. Examples of causes of these costs are:

Social Cost: If a company decides to relocate its operations to another part of the country (or the world) then social costs are incurred because of loss of employment, relocation of families, etc. The burden of carrying the economic costs associated with social costs are normally carried by the taxpayer.

Psychological Cost: Airplanes tend to create a significant amount of noise during takeoff and landing. This can cause distress in people and can be thought of as a psychological cost. The psychological distress can become so severe as to lead to anti-noise legislation. Examples are found in FAR 36 which places the burden of the noise problem on the designer and thus, ultimately on the consumer.

Environmental Cost: Pollution caused by certain airplane operations represents an environmental cost. Examples are: atmospheric pollution due to exhaust gasses, fuel dumping in emergencies and chemical discharges resulting from manufacturing and maintenance processes.

Although these types of cost are important, they are difficult to quantify and will not be considered in this text. Many of these costs are ultimately borne by taxpayers although some of them are borne by the consumer (fare paying passenger) through increased operating cost as in the case of costs incurred by meeting FAR 36.

There is much confusion about the relationship between cost and price. If an airplane manufacturer buys certain equipment for installation in an airplane which is being manufactured, he pays a certain price for that equipment. That price paid then becomes part of his cost to produce that airplane!

What a manufacturer charges in the marketplace for a certain airplane becomes the price charged. That price may or may not have a rational relationship to the actual cost. Example: true or not, it was said that Cessna actually 'lost' money on each Cessna 152 it produced. The reason, true or not, was that it was felt that Cessna 152 customers eventually would 'step-up' to a more expensive airplane model on which a profit was actually made. This is the so-called 'loss-leader' policy which is popular in supermarkets as well!

2.2 AIRPLANE PROGRAM, LIFE CYCLE AND LIFE CYCLE COST

The evolution of an airplane from design to manufacturing, operation and finally, disposal is referred to as an airplane program. A typical airplane program can be divided into the following six phases:

Phase 1: Planning and Conceptual Design.

During this phase the activities depicted in Figure 2.1 take place. Planning here consists primarily of mission requirements research. This eventually leads to a mission specification. Conceptual design here consists of the design activities associated with Preliminary Design Sequence I as outlined in Parts I and II of this text.

Some very preliminary cost studies are also conducted during this phase.

Phase 2: Preliminary Design and System Integration.

During this phase the activities depicted in Figure 2.2 take place. The accompanying design activities are those associated with Preliminary Design Sequence II as outlined in Parts I and II of this text. Design trade studies are conducted to find that combination of technology and cost which might result in a viable airplane program.

Phase 3: Detail Design and Development.

During this phase the airplane and system integration design is finalized for certification flight testing and for production.

Phase 4: Manufacturing and Acquisition.

During this phase the airplane is manufactured and delivered to (acquired by) the customer.

Phase 5: Operation and Support.

During this phase the airplane is being acquired by the user and is being operated with the accompanying support activities.

Note: Phases 4 and 5 normally overlap.

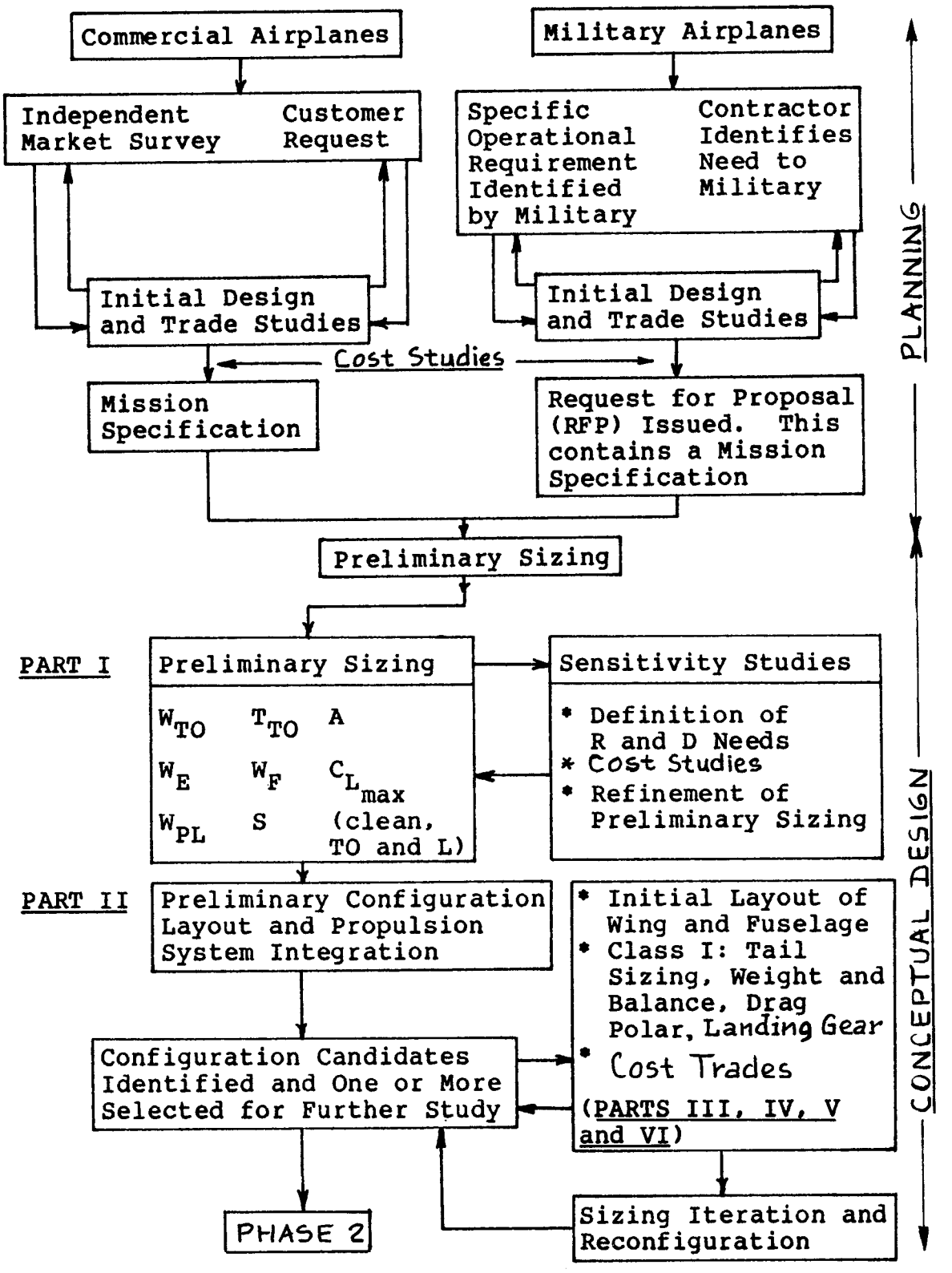

Figure 2.1 Phase 1: Planning and Conceptual Design

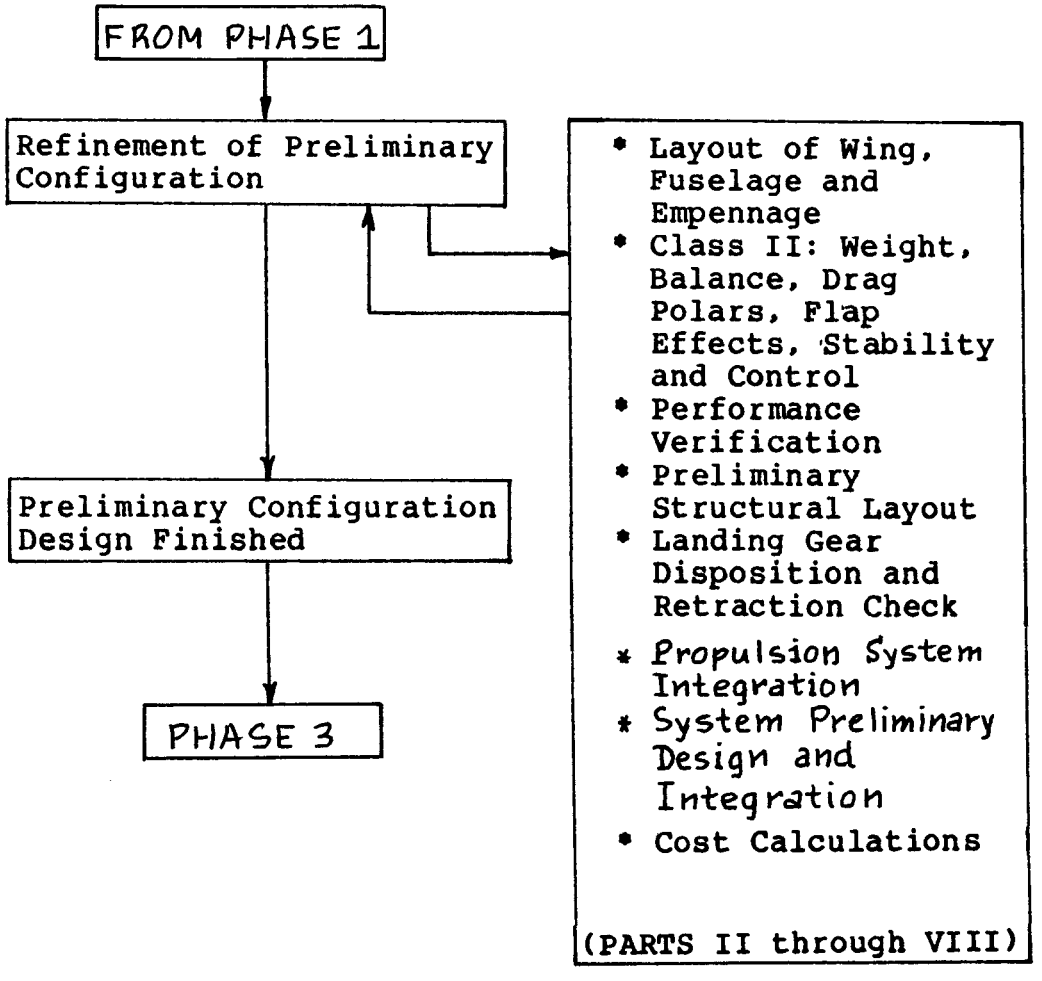

Figure 2.2 Phase 2: Preliminary Design and System Integration

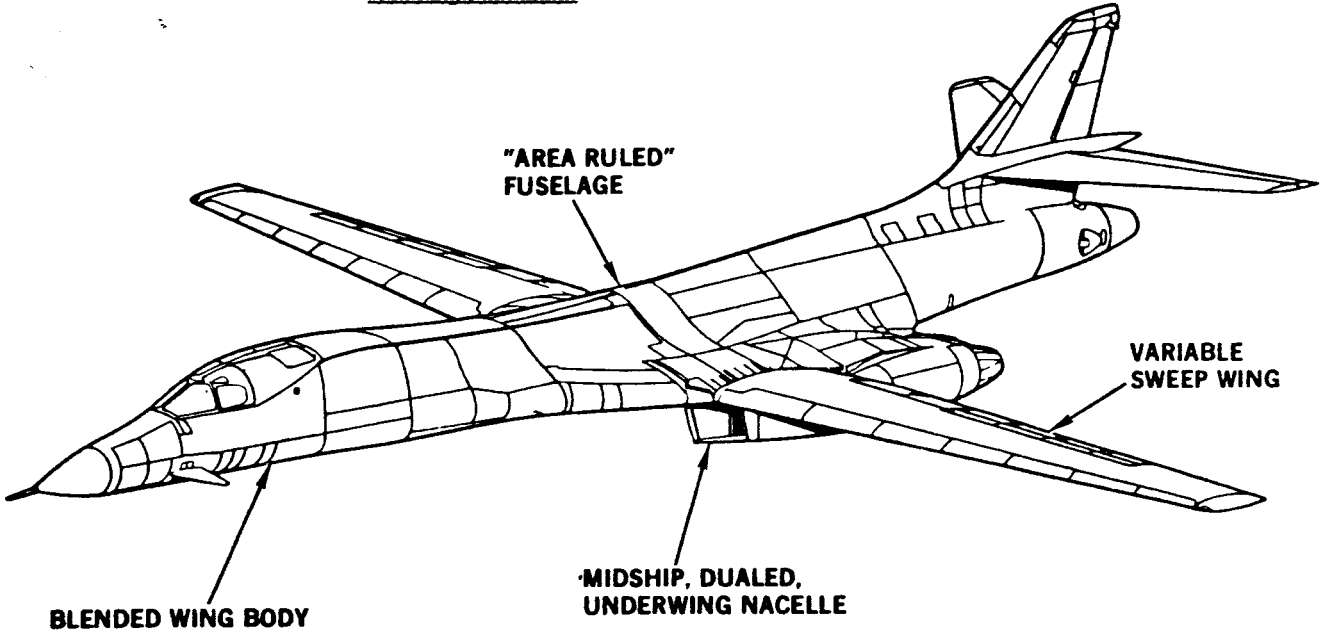

Phase 6: Disposal.

This phase marks the end of the operational life of the airplane. Disposal activities may include destruction of the airplane and disposal of the remaining materials. In case of military airplanes it may also include storage (at Davis-Monthan AFB for example). Disposal becomes necessary when an airplane has reached the limit of its technological or economical life.

Note: Phases 5 and 6 normally overlap.

Figure 2.3 shows these six phases with an indication of their relative impact on costs associated with a typical airplane program. Note the following definitions:

Definition 4: The time elapsed during the six phases of an airplane program (Fig.2.3) is called the Airplane Life Cycle.

Definition 5: The total cost of an airplane program incurred during the airplane life cycle is called the Life Cycle Cost.

Note: the vertical scale in Figure 2.3 indicates the cost associated with each program phase as a percentage of life cycle cost: LCC.

For preliminary cost estimating purposes the life cycle cost of an airplane program is broken down into four cost sources:

1. Research, development, test and evaluation cost: C_{RDTE}.

   This cost source accounts for all costs incurred in phases 1, 2 and 3 in Figure 2.3. A method for estimating C_{RDTE} is presented in Chapter 3.

2. Acquistion cost: C_{ACQ}.

   This cost source includes the manufacturing cost: C_{MAN} and the manufacturer's profit: C_{PRO}. Thus:

   $$C_{ACQ} = C_{MAN} + C_{PRO} \qquad (2.2)$$

   These costs are incurred during Phase 4 in Figure 2.3. A method for estimating C_{ACQ} is presented in Chapter 4.

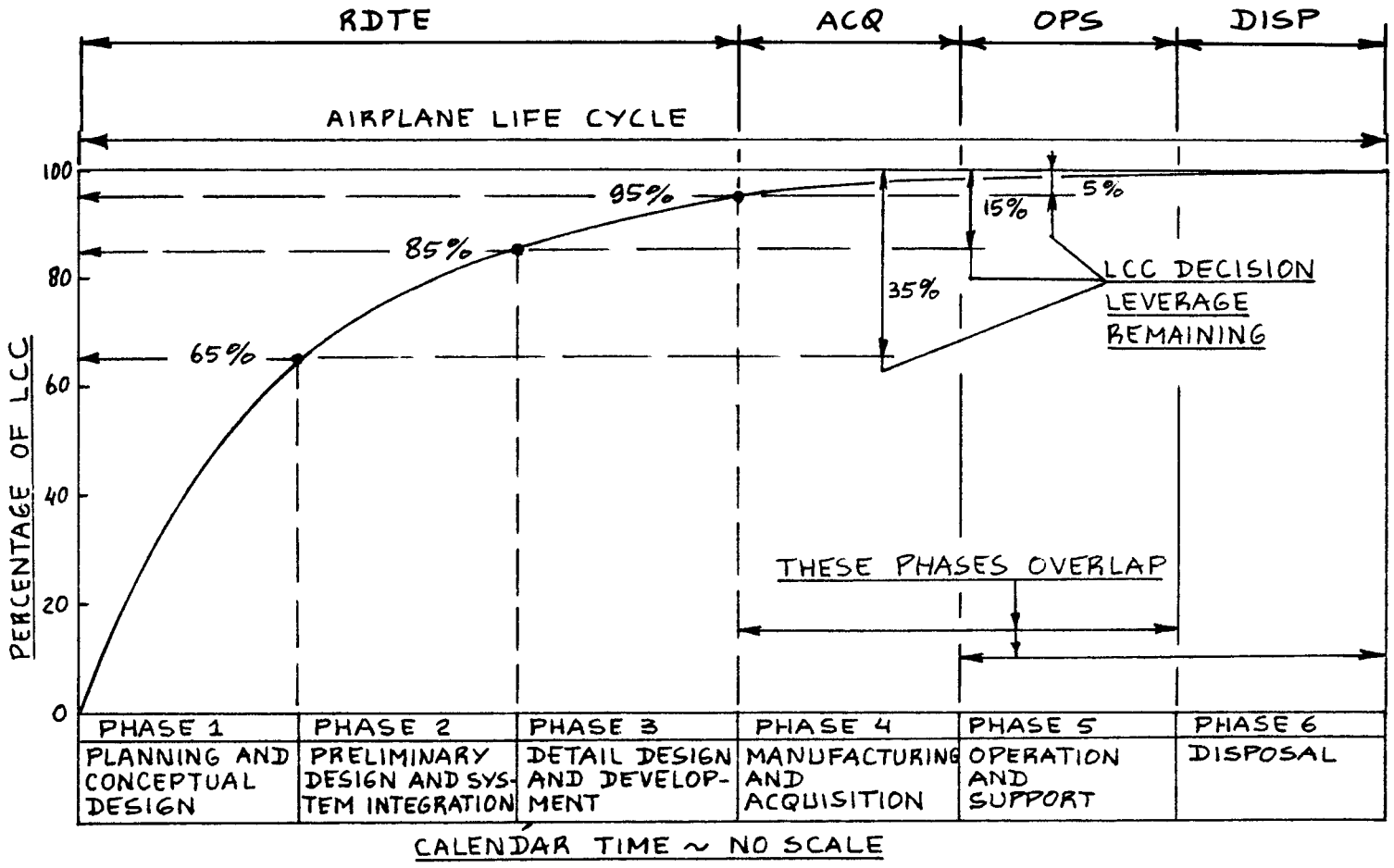

BASED ON AN IDEA IN REF.8

Figure 2.3 Impact of Airplane Program Phases on Life Cycle Cost

3. Operating cost: C_{OPS}.

   This cost source represents the cost incurred while operating the airplane: see Phase 5 in Figure 2.3. The airplane manufacturer and his suppliers (vendors) usually incur certain support costs during this phase. A method for estimating C_{OPS} is given in Chapter 5 for commercial airplanes and in Chapter 6 for military airplanes.

4. Disposal cost: C_{DISP}.

   This is the cost incurred in disposing of the airplane: see Phase 6 in Figure 2.3. Chapter 7 presents an approach to the estimation of C_{DISP}.

The life cycle cost of an airplane program (LCC) can now be expressed as:

$$LCC = C_{RDTE} + C_{ACQ} + C_{OPS} + C_{DISP} \qquad (2.3)$$

Chapter 7 presents an example of LCC estimation for a military airplane program. An example for a commercial airplane program is given in Section 5.4.

Figure 2.4 shows example cost histories for two airplane programs. Note that the operating cost source is much larger than the acquisition cost source. The latter in turn is much larger than the research, development, test and evaluation cost source. The cost histories of Figure 2.4 are schematically represented in Figure 2.5. It is seen that:

$$C_{OPS} >> C_{ACQ} >> C_{RDTE} \qquad (2.4)$$

What emerges from Figures 2.3 - 2.5 is the following important conclusion:

<u>THE CONCEPTUAL AND PRELIMINARY DESIGN PHASES ARE RESPONSIBLE FOR LOCKING IN MOST OF THE LIFE CYCLE COST OF AN AIRPLANE!!</u>

The implication for airplane design engineers and for airplane program managers is that:

<u>SIGNIFICANT LEVERAGE AFFECTING LIFE CYCLE COST EXISTS ONLY IN THE CONCEPTUAL AND PRELIMINARY DESIGN PHASES!!</u>

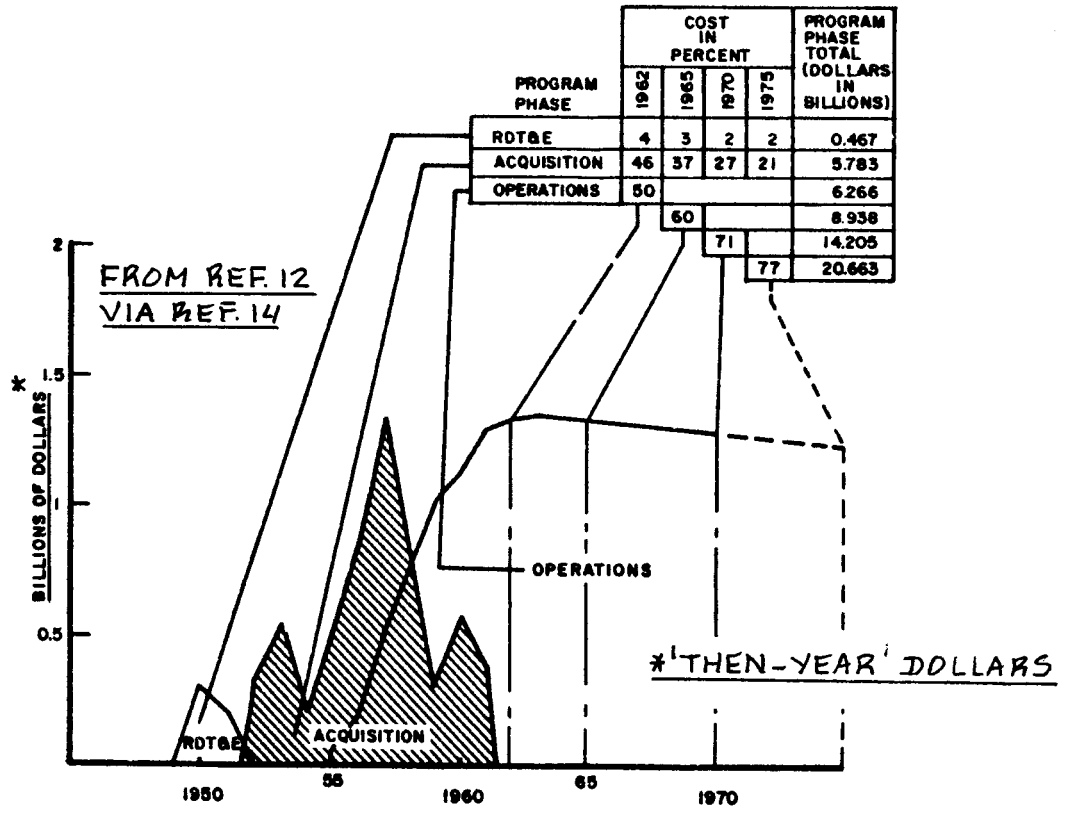

Figure 2.4a Life Cycle Cost History of the B-52 Program

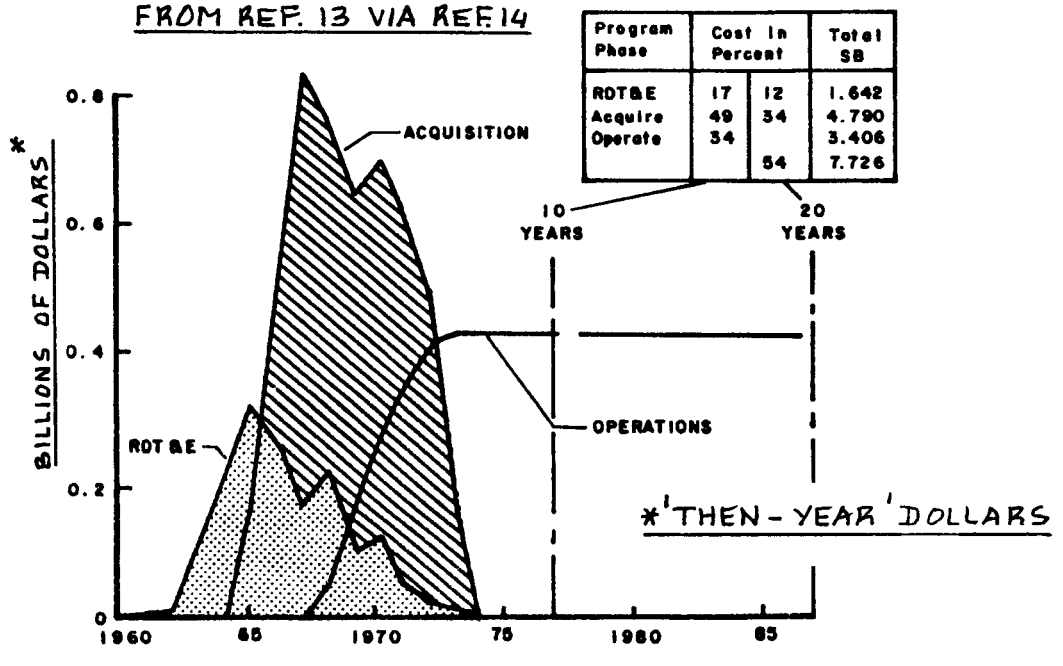

Figure 2.4b Life Cycle Cost History of the F-111 Program

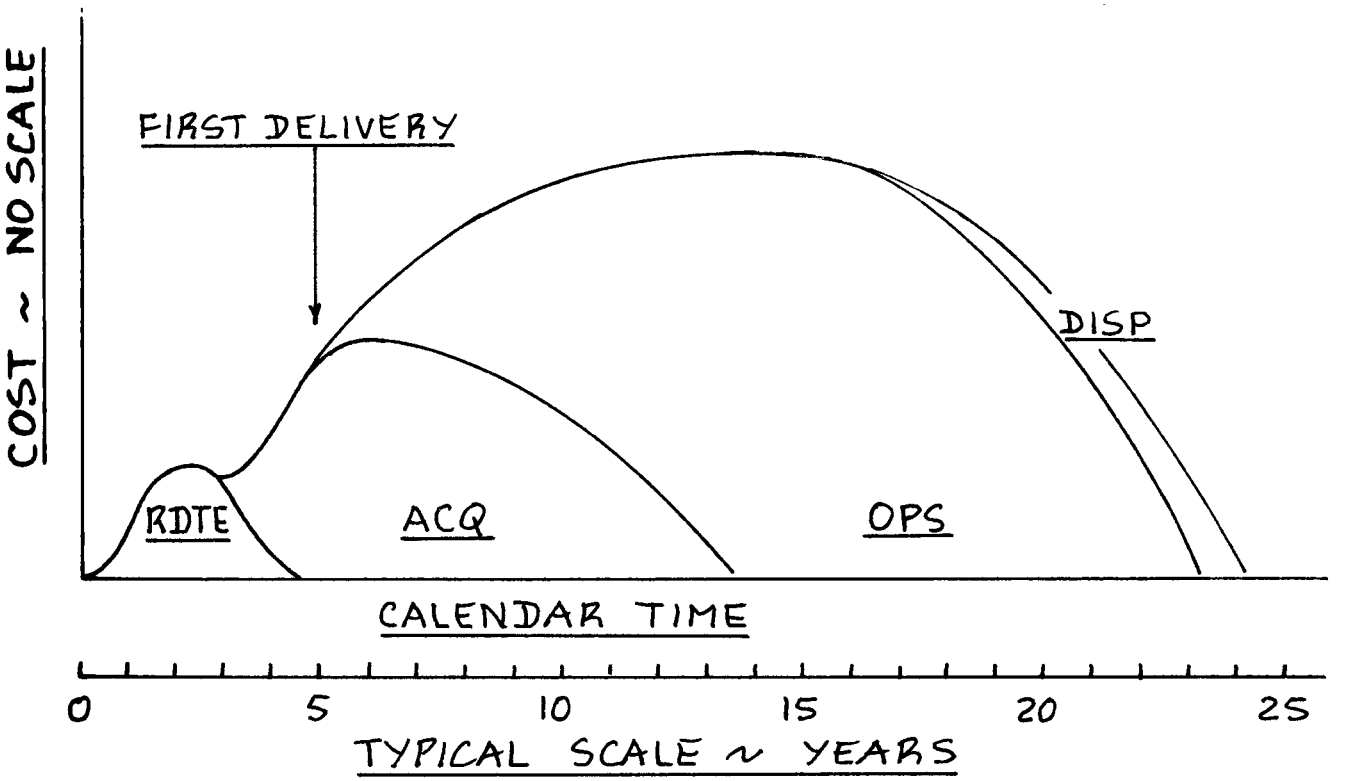

Figure 2.5 Schematic Representation of Life Cycle Cost History of Typical Airplane Programs

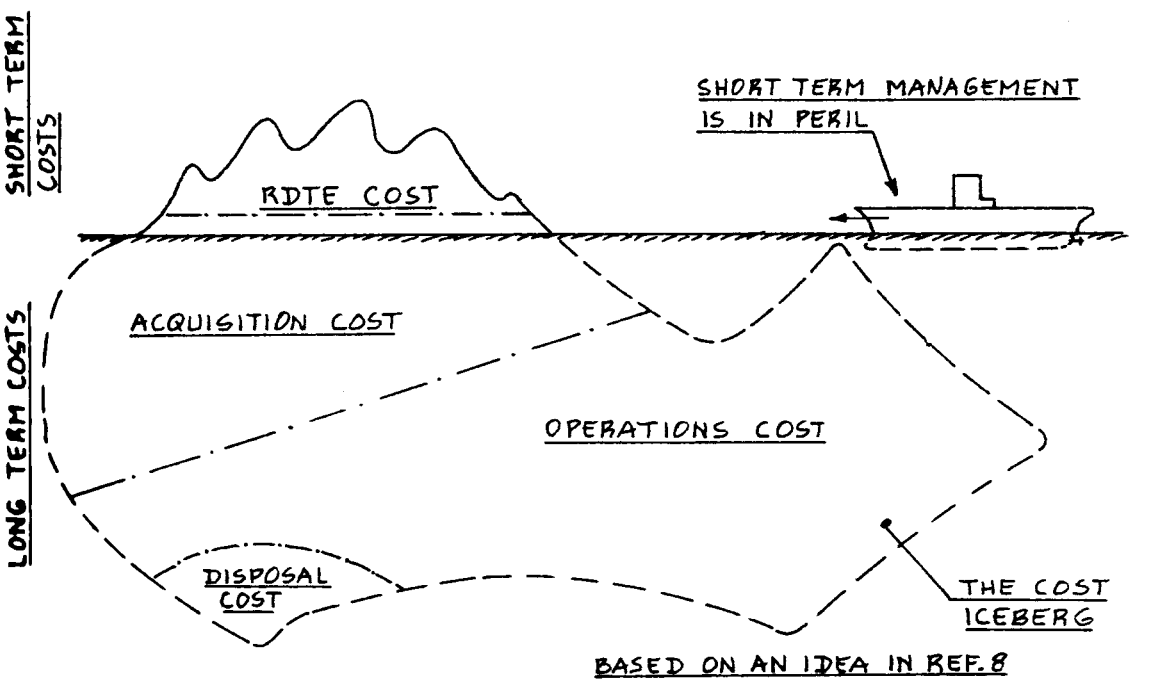

Figure 2.6 The Iceberg Effect in Airplane Program Management

Another way of illustrating these facts is found in Figure 2.6. The airplane program manager is like the captain of a ship navigating close to an iceberg. The program manager has many pressures upon him to lower RDTE costs (the short term outlook). Yielding to these pressures may in fact increase LCC! Performing more RDTE work, when directed at designing to minimize LCC, can result in significant savings to the customer and therefore to society as a whole. It takes courage and wisdom to purposely increase RDTE costs so that LCC will be lower.

During the preliminary airplane design process as described in Parts I through VII many design decisions are made which have a significant effect on airplane life cycle cost. Airplane designers must be aware of these effects if their designs are to be 'cost-effective'.

Step 36 in the preliminary design process (See Part II, page 23) requires the designer to perform a preliminary cost analysis for the new airplane. This in turn means that designers must have available a systematic method for estimating LCC. Chapters 3 through 7 present methods for estimating the major LCC sources of Eqn.2.3.

In addition to having a method for estimating LCC, the designer must have an understanding of how either total LCC or any of its cost sources can be minimized. Several important principles in the areas of DESIGN OPTIMIZATION, DESIGN-TO-COST and DESIGN-TO-PRICE are discussed in Chapter 8.

Finally, it is necessary to have an understanding of various factors (in addition to cost) which may affect an airplane program decision. That subject is taken up in Chapter 9.

Because it is hard for aeronautical engineering students to 'find' hard data on prices, the author has included price data for airplanes, engines, propellers and avionics systems in the form of several appendices. It is hoped that these data (even though they will become obsolete rather rapidly) will be useful to the reader.

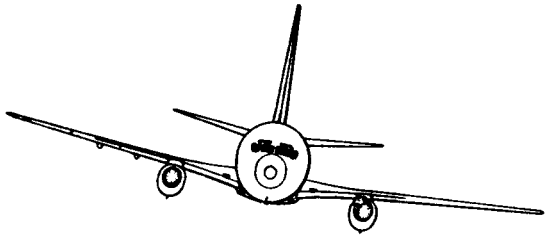

2.3 EXAMPLES OF AERONAUTICAL ENTERPRISES

Aeronautical engineering students should be aware of the various types of aeronautical enterprises which exist. After all, these enterprises are most likely to be their future employers.

From an ownership point of view there are three types of aeronautical enterprises:

1. Privately owned.

2. Government owned (country, state, local).

3. Part private and part government owned.

In the following, some selected examples of each are given. There is no implication of importance, relative or absolute, to be attached to these examples. They are merely what came to the author's mind while developing this text. An extensive list of aeronautical enterprises can be found in Reference 9. When consulting Ref.9 the reader will come to the conclusion that aeronautics is very much an international affair! Aeronautics is expected to become even more international in the future.

1. Examples of privately owned aeronautical enterprises are:

Manufacturers of airplanes:

In the USA:

Boeing, McDonnell-Douglas, Lockheed, General Dynamics (including Cessna), Grumman, Raytheon-Beech, Piper and Learjet Corp.

Foreign:

Robin, Grob, Reims-Aviation, Pilatus, Mudry.

Operators of airplanes:

In the USA:

American Airlines, United Airlines, Federal Express, US Air, TWA , Northwest and Southwest Airlines.

Foreign:

British Airways, Martin Air, Cross Air and Tyrolean.

2. Examples of government owned aeronautical enterprises are:

Manufacturers of airplanes:

In the USA: none. But: the U.S. government owns several plants which it leases to private companies.

Foreign:

Fabrica Militar de Aviones, Embraer, CASA, IPTN, Antonov, Ilyushin, PZL, Airbus GmbH and Aeritalia.

Operators of airplanes:

In the USA:

USAF, USNavy, U.S.M.C., US Coast Guard and FAA.

Foreign:

Aeroflot, SAS, Garuda Indonesian and Air France.

3. Examples of part private and part government owned aeronautical enterprises are:

Manufacturers of airplanes:

In the USA: none.

Foreign:

SIAI-Marchetti, Piaggio, Partenavia, Dassault-Breguet, MBB and Fokker.

Operators of airplanes:

In the USA: none.

Foreign:

KLM (Royal Dutch Airlines), Lufthansa, and UTA.

There are many other aeronautical enterprises which supply parts, systems and engines. To save space, these were not included as examples. Nevertheless, these supplier enterprises are important. For an airplane manufacturing industry to be viable, a network of parts and system suppliers (the aeronautics infra-structure) must exist! Airplanes cannot be built without:

* Materials such as: aluminum, steel and titanium alloys, composites, etc.
* Wheels, brakes and tires
* Engines and APU's
* Avionics systems and instruments
* Pumps, lines, sensors, cables and fasteners
* Interiors, including insulating materials

Reference 9 provides an annual listing of airplane operators, manufacturers and suppliers with details about their corporate structure. This reference deals with foreign as well as domestic enterprises.

Last (and not least!) a healthy aeronautics industry requires very long term research capabilities. In most countries such long term research facilities are owned by the government. NASA in the USA is an example.

2.4 SOME OBSERVATIONS ON PROFIT AND COST

In general, the objective of a privately owned aeronautical enterprise is to make a profit. The profit made before taxes is sometimes referred to as the operating margin. Examples of operating margins for several aeronautical enterprises is presented in Table 2.1. Since the tax situation of a company can vary from year to year and from country to country, the operating margin of a company is not the same as its profit. In day-to-day use of these terms they are frequently interchanged.

In the case of military, government owned enterprises, profit is not an objective. Instead, getting the 'best' defense or offense per dollar paid ('biggest bang per buck') is usually the objective.

In the case of civilian, government owned enterprises, profit may not be an immediate objective. Significant participation in some market segment to generate jobs and general prosperity is an important objective of many government owned enterprises.

In the case of part private and part government owned aeronautical enterprises the objective is usually to make a profit albeit not necessarily each year.

Another objective which can play a role in privately owned enterprises is: to 'have fun at building airplanes and not lose money'.

It is expected that the manner in which an aeronautical enterprise is managed will depend on its objective.

Table 2.1 Operating Margins in Percentage of Sales for the Period 1985 - 1988

Aerospace Manufacturers	1985	1986	1987	1988
Boeing Commercial	4.7	4.2	3.6	5.1
Boeing Military	8.0	7.5	1.5	-2.6
Chrysler (Gulfstream)	N/A	9.0	12.9	11.7
General Dynamics Convair	13.3	12.5	10.1	9.3
General Dynamics Cessna	N/A	-82.5	1.7	5.5
General Electric Engines	14.3	14.5	13.9	15.4
G.M. (Hughes)	N/A	7.8	8.6	8.8
Grumman Aerospace	4.4	3.3	1.6	5.3
Honeywell/Sperry	3.4	6.1	6.3	-7.7
Kaman	7.9	7.8	8.2	8.1
Learjet	N/A	N/A	0.0	0.0
Litton Adv. Electronics	11.3	5.7	8.0	7.8
Lockheed Aeronautical	10.6	10.4	8.1	6.3
Loral (Goodyear)	N/A	20.0	18.7	N/A
LTV Aircraft Products	12.3	8.8	9.4	3.4
McDonnell Douglas				
Combat Aircraft	8.7	6.7	5.7	6.6
Transport Aircraft	3.7	3.0	2.7	2.6
Moog (Hydr. Actuators)	15.2	13.8	11.4	-1.0
Northrop Aircraft	9.0	1.6	4.5	1.9
Northrop Electronics	9.0	8.0	6.2	3.6
Raytheon Beech	-2.3	1.4	-1.3	3.0
Rockwell North American	9.3	10.3	13.8	12.4
Teledyne (aviation, electronics)	8.6	6.9	10.2	9.4
United Tech (P and W)	7.6	6.1	12.0	10.8
U.T. (Sikorsky, Hamilton)	9.8	-8.8	3.0	-0.4

Data from: Flight International, June 10, 1989

Airlines	1985	1986	1987	1988
American Airlines	8.7	6.8	6.4	9.1
USAir	9.5	9.2	10.6	7.6
United Airlines	-4.5*	1.3	3.0	7.4
Delta Airlines	7.8	0.8	7.6	7.2
Northwest Airlines	2.9	4.6	3.8	3.6

*Strike

Data from: Aviation Week and Space Techn., June 19, 1989

NOTE: Operating margin is the profit before taxes.

When profit is the primary objective, the temptation is for management decisions to focus on the short term: 'maximizing profit this quarter'. This can lead to the iceberg disaster depicted in Figure 2.6.

When profit is not the immediate objective, management decision making tends to focus on the long term.

The time required for development and certification of an airplane does affect management decision making. Because of the long time it takes to develop and certify airplanes, management decision making in the airplane industry should focus on the long term.

Whatever management objectives are, the cost of developing, certifying, producing and operating an airplane must be known with some certainty before a decision to 'launch' an airplane program is made.

Because airplane programs take many years to evolve through the phases shown in Figure 2.3, inflation (= cost escalation) plays an important role in estimating program cost. So does interest on investment: the cost of money.

Estimates for cost magnitudes are usually given in 'then-year' dollars. It is customary to scale cost data from one 'then-year' to another with a cost escalation factor: CEF. Figure 2.7 shows how this CEF has varied with calendar time since 1965. In Figure 2.7 the CEF has been arbitrarily normalized to a value of 1.0 for 1970. Cost from one year to another may be 'scaled' as follows:

$$\text{Cost}_{19XX} = \text{Cost}_{19YY}(\text{CEF}_{19XX}/\text{CEF}_{19YY}) \qquad (2.5)$$

where: the ratio $(\text{CEF}_{19XX}/\text{CEF}_{19YY})$ is the CEF-ratio.

The reader is referred to References 8 and 10 for a detailed discussion and development of the ideas of airplane program cost. Chapters 3 through 7 present rapid methods for estimating airplane program costs. These methods are aimed strictly at Phases 1 and 2 as depicted in Figure 2.3. They should be used for preliminary cost estimating purposes only.

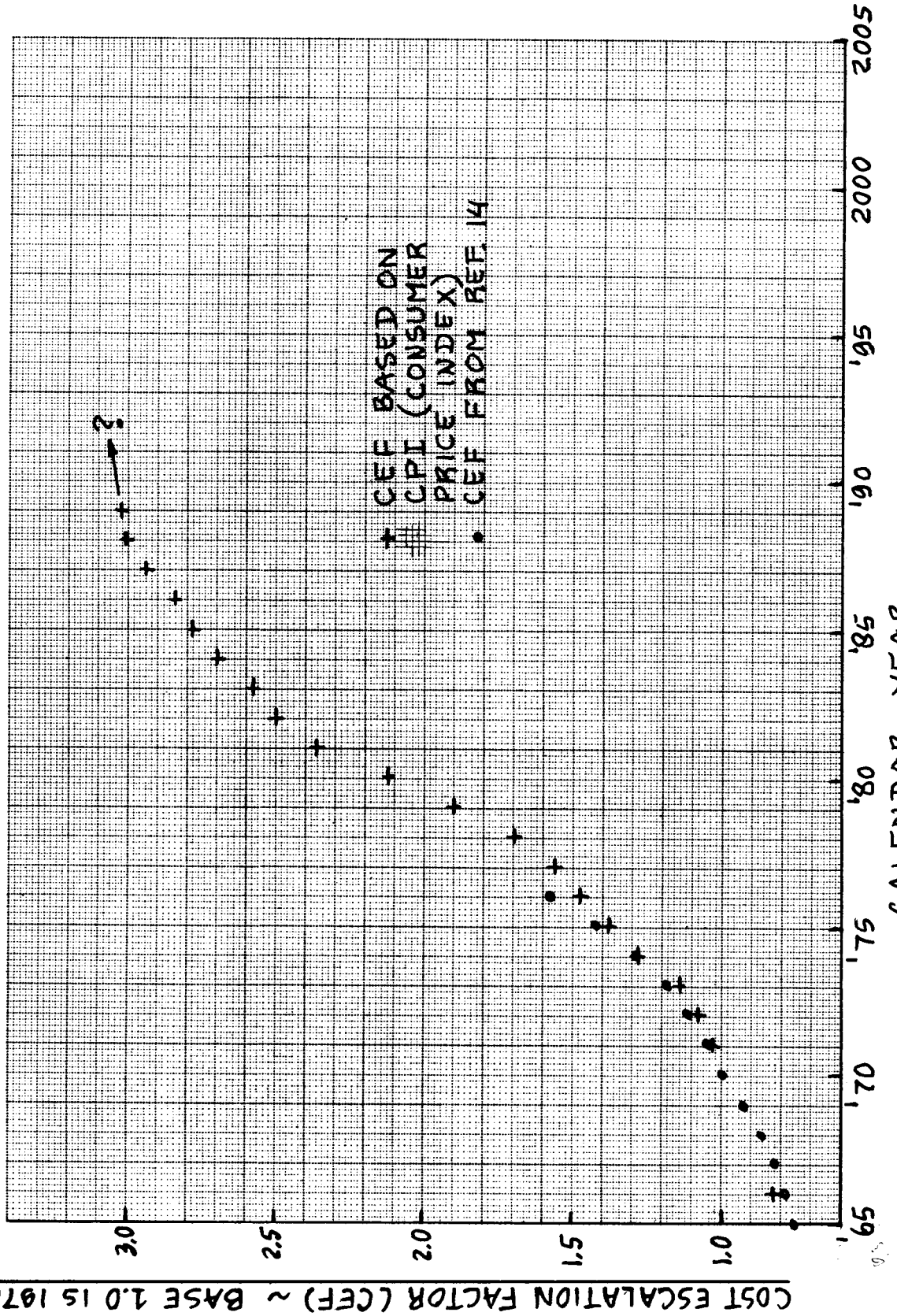

Figure 2.7 Variation of Cost Escalation Factor with Time

3. METHOD FOR ESTIMATING RESEARCH, DEVELOPMENT, TEST AND EVALUATION COST AND A METHOD FOR ESTIMATING PROTOTYPING COST

The purpose of this chapter is to present:

1) A method for estimating research, development, test and evaluation cost (C_{RDTE}) for airplanes.

2) A method for estimating prototyping cost (C_{PROT}) for airplanes.

The RDTE cost, C_{RDTE}, is the first cost source seen in Eqn.(2.3). RDTE cost is accumulated during Phases 1-3 in Figure 2.3. Phases 1-3 involve those activities which take a new airplane all the way from the planning and conceptual design stage to certification. This applies not only to military, but also to commercial airplanes. Phases 1-3 normally include the design, construction, ground and flight testing of a number of static and flight test airplanes. Figure 2.3 shows how the RDTE activities of Phases 1-3 fit into an airplane program.

The method for estimating RDTE cost is based on that of Ref.11. It should be used for preliminary cost estimation purposes only. The method can be applied to military as well as to commercial airplane programs.

RDTE costs are normally broken down into seven cost categories:

3.1 Airframe Engineering and Design Cost: C_{aed_r}

3.2 Development Support and Testing Cost: C_{dst_r}

3.3 Flight Test Airplanes Cost: C_{fta_r}

3.4 Flight Test Operations Cost: C_{fto_r}

3.5 Test and Simulation Facilities Cost: C_{tsf_r}

3.6 RDTE Profit: C_{pro_r}

3.7 Cost to finance the RDTE phases: C_{fin_r}

The total RDTE cost for a new airplane program may be estimated from:

$$C_{RDTE} = C_{aed_r} + C_{dst_r} + C_{fta_r} + C_{fto_r} + C_{tsf_r} + C_{pro_r} + C_{fin_r} \quad (3.1)$$

Expressions for estimating these seven categories of RDTE cost are presented in Sections 3.1 through 3.7. An example application is given in Section 3.8.

Not all airplane programs are aimed at eventual production. Some are started for reasons of developing and/or demonstrating some aspect of advanced technology: the X-29 and X-31 programs are typical examples. A method for estimating the cost of such 'experimental' or 'prototyping' programs, together with an application is given in Section 3.9.

3.1 AIRFRAME ENGINEERING AND DESIGN COST: C_{aed_r}

Airframe engineering and design activities typically break down as follows:

1. Planning, conceptual design and associated cost studies (Phase 1 activities of Figures 2.1 and 2.3).

2. Preliminary design and system integration studies, including any associated cost studies (Phase 2 activities of Figures 2.2 and 2.3).

3. Engineering for windtunnel models, mock-ups and engine tests.

4. Design of windtunnel models and mock-ups.

   Note: Figure 3.1 records the number of windtunnel test hours needed in the past for several airplane programs.

5. Design and construction of dedicated test facilities, conduct of developmental tests and static tests including systems tests.

   Note: Items 3-5 are normally part of Phases 1 and 2 of Figures 2.1 through 2.3.

6. Detail design and development (This is represented by Phase 3 in Figure 2.3).

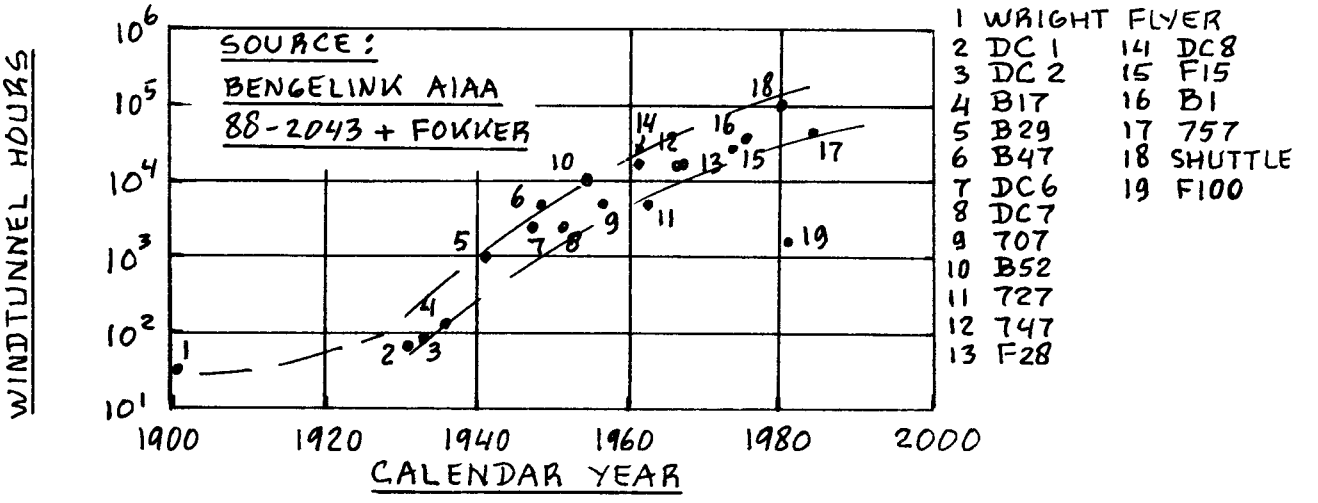

Figure 3.1 Windtunnel Hours Required in Typical Airplane Programs

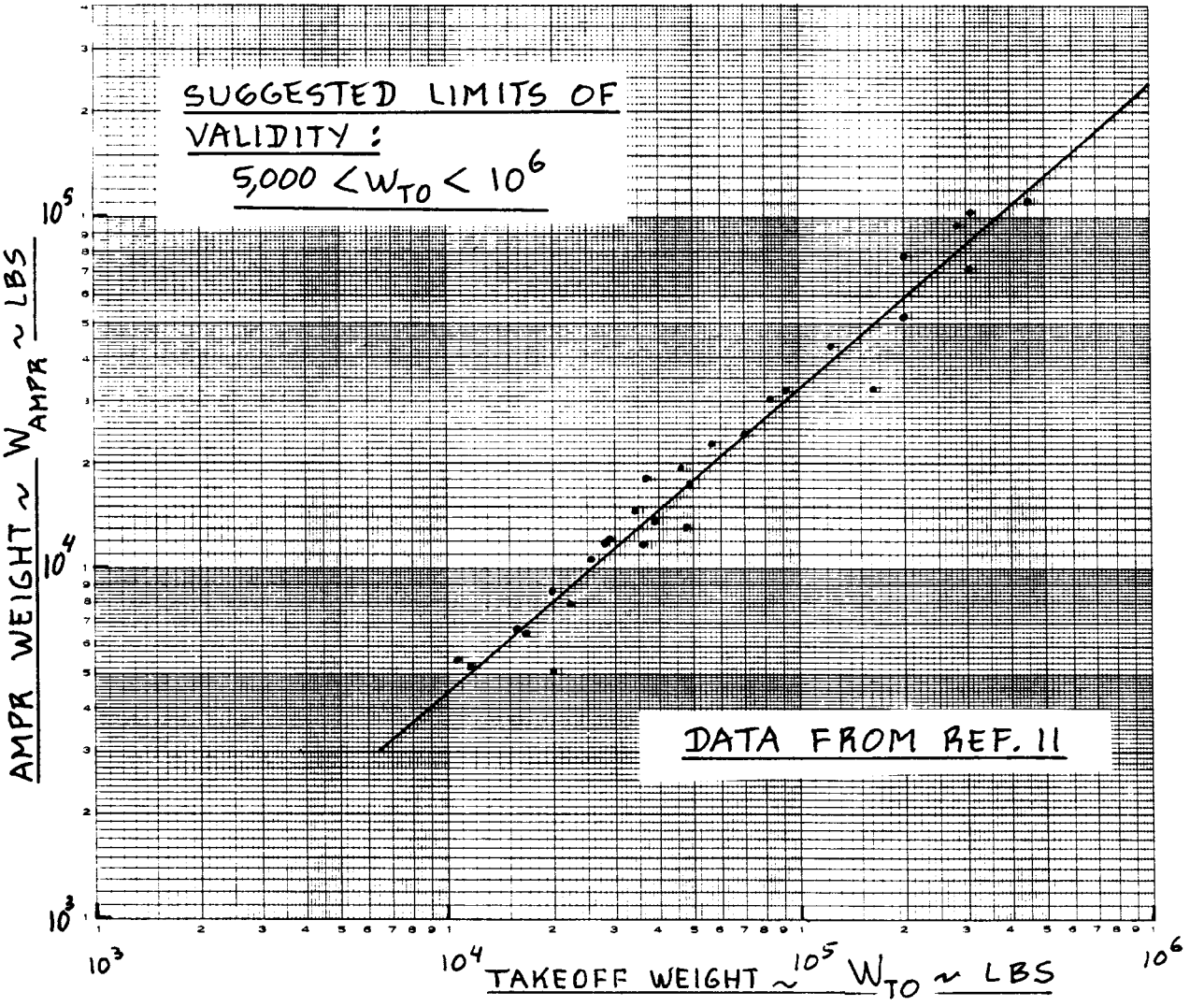

Figure 3.2 Data and Trend Line of AMPR Weight as Related to Takeoff Weight

7. Release and maintenance of drawings and specifications. It is of interest to mention that the first Boeing 747 required 75,000 drawings.

   Note: During the last ten years most companies have switched from 'hand-drafting' to CAD (Computer Aided Drafting). The effect of this on airframe engineering and design cost, C_{aed_r} is to reduce this cost. By how much, varies from one manufacturer to another.

8. Liaison with manufacturing and with vendors.

9. Incorporation and analysis of design changes.

10. Development of specifications for materials, processes and for items purchased from vendors.

11. Analysis of reliability.

12. Analysis of maintainability and accessibility.

    Note: items 6-12 are normally part of Phase 3 of Figure 2.3.

The total engineering manhours required to complete Phases 1-3 of Figure 2.3 may be estimated from:

$$MHR_{aed_r} = 0.0396(W_{ampr})^{0.791}(V_{max})^{1.526}(N_{rdte})^{0.183}(F_{diff})(F_{cad}) \quad (3.2)$$

The airframe engineering and design cost associated with Phases 1-3 of Figure 2.3 can be computed from:

$$C_{aed_r} = (MHR_{aed_r})(R_{e_r}) \quad (3.3)$$

The various terms in Equations (3.2) and (3.3) are defined as follows:

W_{ampr} is the so-called AMPR weight of the airplane. AMPR stands for: Aeronautical Manufacturers Planning Report. This weight is also referred to as the DCPR weight, where DCPR stands for: Defense Contractors Planning Report. The AMPR weight is defined by:

$$W_{ampr} = W_E - (\text{SUM } W_i)_{i=1}^{i=11} \qquad (3.4)$$

with:

W_E = airplane empty weight. A preliminary method for estimating airplane empty weight is given in Part I. A more detailed method for estimating empty weight and airplane component weights is given in Part V.

W_1 = weight of wheels, brakes, tires and tubes. Note: this is NOT the total landing gear weight, W_g of Part V.

$W_2 = W_e$, weight of engines (See Part V)

$W_3 = W_{ess}$, weight of starter (See Part V)

W_4 = weight of cooling fluid (Cooling fluid weight should be based on recommendations from the engine manufacturer)

W_5 = weight of rubber or nylon fuel cells (See Part V)

$W_6 = W_{els}$, weight of batteries, electrical power supply and electrical power conversion equipment (See Pt V)

$W_7 = W_{iae}$, weight of instruments, avionics and electronic equipment (See Pt V)

$W_8 = W_{arm}$, weight of armament and fire-control system (See Part V)

$W_9 = W_{api}$, weight of airconditioning units and fluid (See Part V)

$W_{10} = W_{apu}$, weight of APU (See Part V)

$W_{11} = W_{tfo}$, weight of trapped fuel and oil (See Parts I and V)

Many of the weight items 1-11 are often purchased from vendors. These items are NOT normally manufactured by the airframer.

IMPORTANT NOTES:

1. Lacking detailed knowledge of airplane component weights, an alternate (but less accurate) way of finding W_{ampr} is to use

Figure 3.2 which translates into:

$$W_{ampr} = \text{invlog}\{0.1936 + 0.8645(\log W_{TO})\} \quad (3.5)$$

where: W_{TO} is the takeoff weight. Methods for determining airplane takeoff weight are given in Parts I and V.

2. The cost of 'engineering' weight items W_i into the airframe is included in Eqn(3.1) despite the fact that W_{ampr} excludes these items!

V_{max} = V_C for civil airplanes (keas)

= V_H for military airplanes (keas)

For a definition of these speeds, see Section 4.2 in Part V of this text.

N_{rdte} is the number of airplanes produced for the RDTE phase. This number includes flight test airplanes as well as airframes used for static testing.

For military programs use: N_{RDTE} = 6 - 20

For commercial programs use: N_{RDTE} = 2 - 8

F_{diff} is a judgement factor which accounts for the difficulty (i.e. complexity) of a new airplane program. It is suggested to use:

F_{diff} = 1.0 for programs involving fairly conventional airplanes. Airplanes of the 1970 era fall in this class of relative difficulty.

F_{diff} = 1.5 for programs involving moderately aggressive use of advanced technology.

F_{diff} = 2.0 for programs involving very aggressive use of advanced technology. Examples would be: the X-29 and a laminar flow transport.

NOTE: The reader should not try to 'lowball' this difficulty factor. As a general rule, airplane development tends to be more difficult than anticipated.

F_{cad} is a judgement factor which accounts for the effect of computer aided design capability on airframe engineering and design cost. The following values are suggested:

F_{cad} = 1.2 for manufacturers which are in a CAD learning mode.

F_{cad} = 1.0 for manufacturers which are using 'manual' drafting techniques.

F_{cad} = 0.8 for manufacturers which are experienced in the use of CAD.

R_{e_r} is the engineering dollar rate per hour charged for the airframe engineering activity. It is preferred to use currently hourly rates. However, such information is often not available. Lacking data on current rates, the rates shown in Figure 3.3 may be used. Engineering manhour rates vary with factors such as: local cost-of--living, number of engineers in the job market, union contracts etc.

NOTES: 1. The engineering dollar rate per hour includes the following cost items:

*direct engineering labor
*overhead
*general and administrative costs
*miscellaneous direct charges such as: overtime premiums, travel, per diem, miscellaneous taxes, etc.

2. For airplane programs with a significant security requirement (such as 'black' programs) the hourly rates should be assumed to be 25 percent higher! Security measures add a lot of extra cost to a program.

For future estimates it is suggested to use:

$$(R_{e_r})_{\text{then year}} = (R_{e_r})_{1989}\{(CEF_{\text{then year}})/(CEF_{1989})\} \quad (3.6)$$

where: $(R_{e_r})_{1989}$ is the engineering manhour rate for 1989 as found from Figure 3.3 or from actual data.

$\{(CEF_{\text{then year}})/(CEF_{1989})\}$ is the CEF-ratio as found from Fig.2.7.

NOTE: Equation (3.6), suitably modified, can also be used to adjust the manufacturing and tooling manhour rates of Section 3.3.

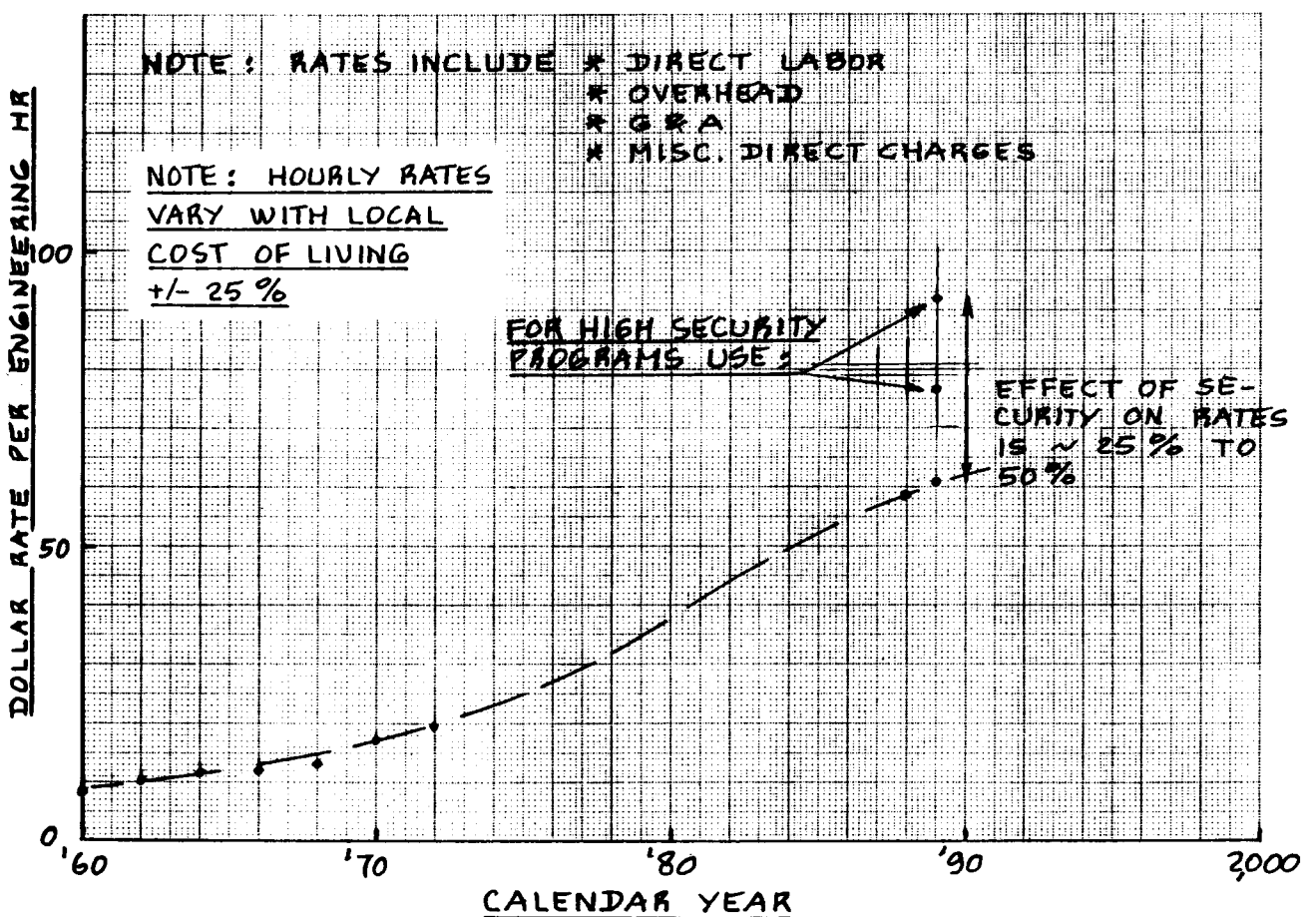

Figure 3.3 Variation of Engineering Manhour Rates with Calendar Time

3.2 DEVELOPMENT SUPPORT AND TESTING COST: C_{dst_r}

Typical activities which are responsible for this cost category are:

1. Windtunnel testing
2. Systems testing (for example the iron bird mentioned in Part IV)
3. Structural testing (strength, fatigue and materials testing)
4. Propulsion testing
5. Simulation for development support testing

The total cost of the above named activities is called C_{dst_r} and may be estimated from:

$$C_{dst_r} = 0.008325(W_{ampr})^{0.873}(V_{max})^{1.890}(N_{rdte})^{0.346}(CEF)(F_{diff}) \quad (3.7)$$

where: CEF is the cost escalation factor of Figure 2.7. Note that the value of CEF is 1.0 for 1970.

All other quantities are defined in Section 3.1.

3.3 FLIGHT TEST AIRPLANES COST: C_{fta_r}

This cost category is normally broken down into the following cost components:

1. Cost of engine and avionics as acquired from vendors: $C_{(e + a)_r}$
2. Manufacturing labor cost: C_{man_r}
3. Manufacturing material cost: C_{mat_r}
4. Tooling cost: C_{tool_r}
5. Quality control cost: C_{qc_r}

To estimate C_{fta_r} it is suggested to use:

$$C_{fta_r} = C_{(e + a)_r} + C_{man_r} + C_{mat_r} + C_{tool_r} + C_{qc_r} \quad (3.8)$$

where: $C_{(e + a)_r}$ is the cost of engines and avionics for the airplanes and airframes required for the RDTE phases. It can be found from:

$$C_{(e + a)_r} = \quad (3.9)$$

$$(C_{e_r} N_e + C_{p_r} N_p + C_{avionics_r})(N_{rdte} - N_{st})$$

where: C_{e_r} is the cost per engine. This may be estimated with the help of Appendix B.

N_e is the number of engines per airplane.

C_{p_r} is the cost per propeller. This may be found with the help of Appendix B.

N_p is the number of propellers per airplane. Note that N_p is not necessarily the same as N_e!

$C_{avionics_r}$ is the cost of avionics equipment per airplane. This equipment normally consists of: radar(s), navigation equipment, automatic flight control systems and computers, maintenance and fault detection equipment.

For military airplanes the following may also be included: fire control equipment, missile guidance equipment and other items required for the mission of that particular airplane.

After preparing a listing of all avionics systems required for the mission of the airplane, an individual cost estimate of each such system may be obtained with the help of Appendix C. This appendix also contains a 'short-cut' method for estimating avionics cost.

N_{rdte} is defined in Section 3.1.

N_{st} is the number of static test airplanes. These are NOT normally equipped with engines, propellers or avionics systems.

C_{man_r} is the manufacturing cost of the flight test airplanes. It may be estimated from:

$$C_{man_r} = (MHR_{man_r})(R_{m_r}) \qquad (3.10)$$

where: (MHR_{man_r}) is the number of manufacturing manhours required in Phases 1-3 of Figure 2.3. This may be found from:

$$MHR_{man_r} = \qquad (3.11)$$

$$28.984(W_{ampr})^{0.740}(V_{max})^{0.543}(N_{rdte})^{0.524}(F_{diff})$$

R_{m_r} is the manufacturing labor rate in dollars per manhour: see Figure 3.4. Also: read the note after Eqn. (3.6).

Other factors are defined in Section 3.1.

C_{mat_r} is the cost of materials to manufacture the flight test airplanes. It is found from:

$$C_{mat_r} = 37.632(F_{mat})(W_{ampr})^{0.689} *$$

$$*(V_{max})^{0.624}(N_{rdte})^{0.792}(CEF) \qquad (3.12)$$

where: F_{mat} is a correction factor which depends on the type of materials used in the construction of the airplane:

F_{mat} = 1.0 for airframes made primarily of conventional aluminum alloys

= 1.5 for stainless steel airframes

= 2.0 - 2.5 for airplanes where the primary structure is made with 'conventional' composite materials, Li/Al alloys and/or ARAL

= 3.0 for carbon composite airframes

In most cases, the reader will have to 'estimate' his own 'correction' factor F_{mat}.

All other quantities in Eqn (3.12) are defined in Section 3.1.

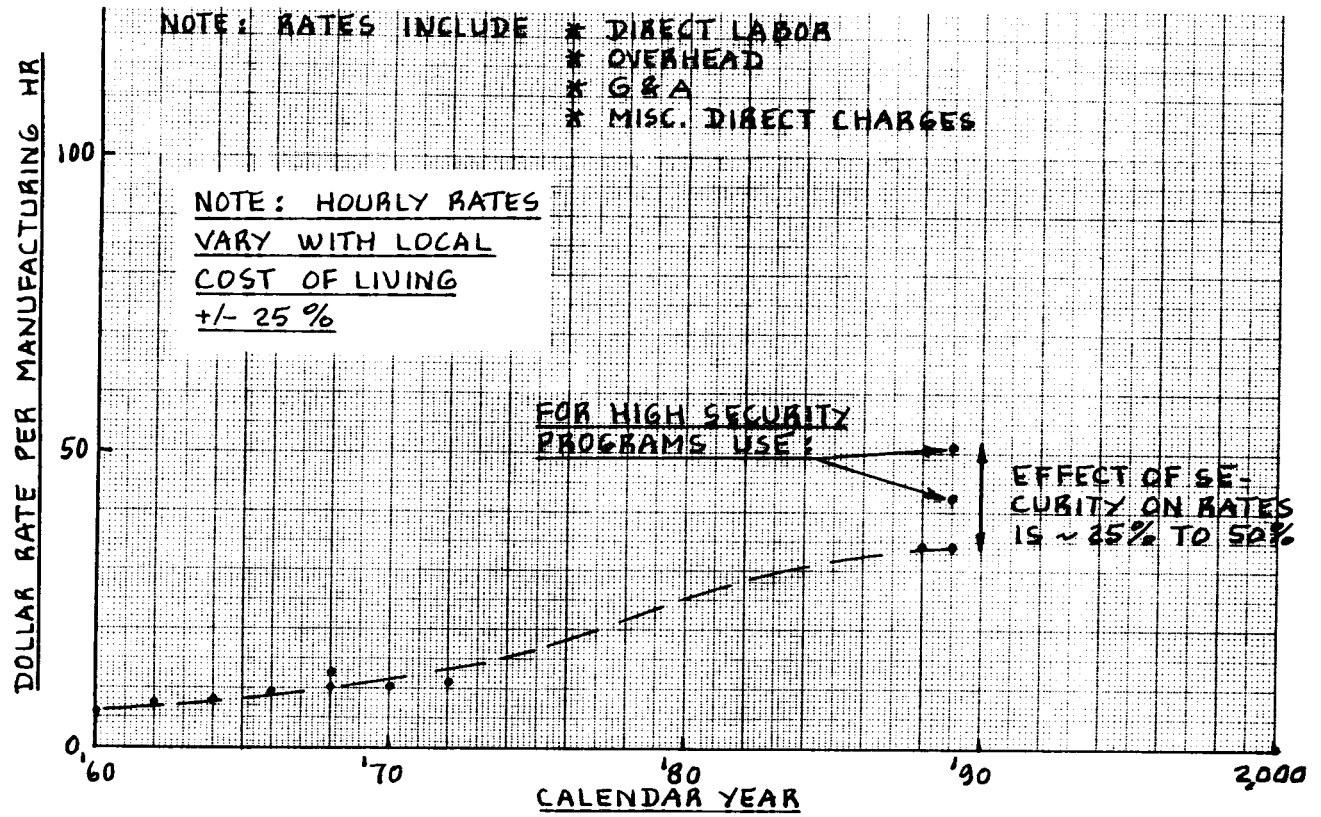

Figure 3.4 Variation of Manufacturing Manhour Rates with Calendar Time

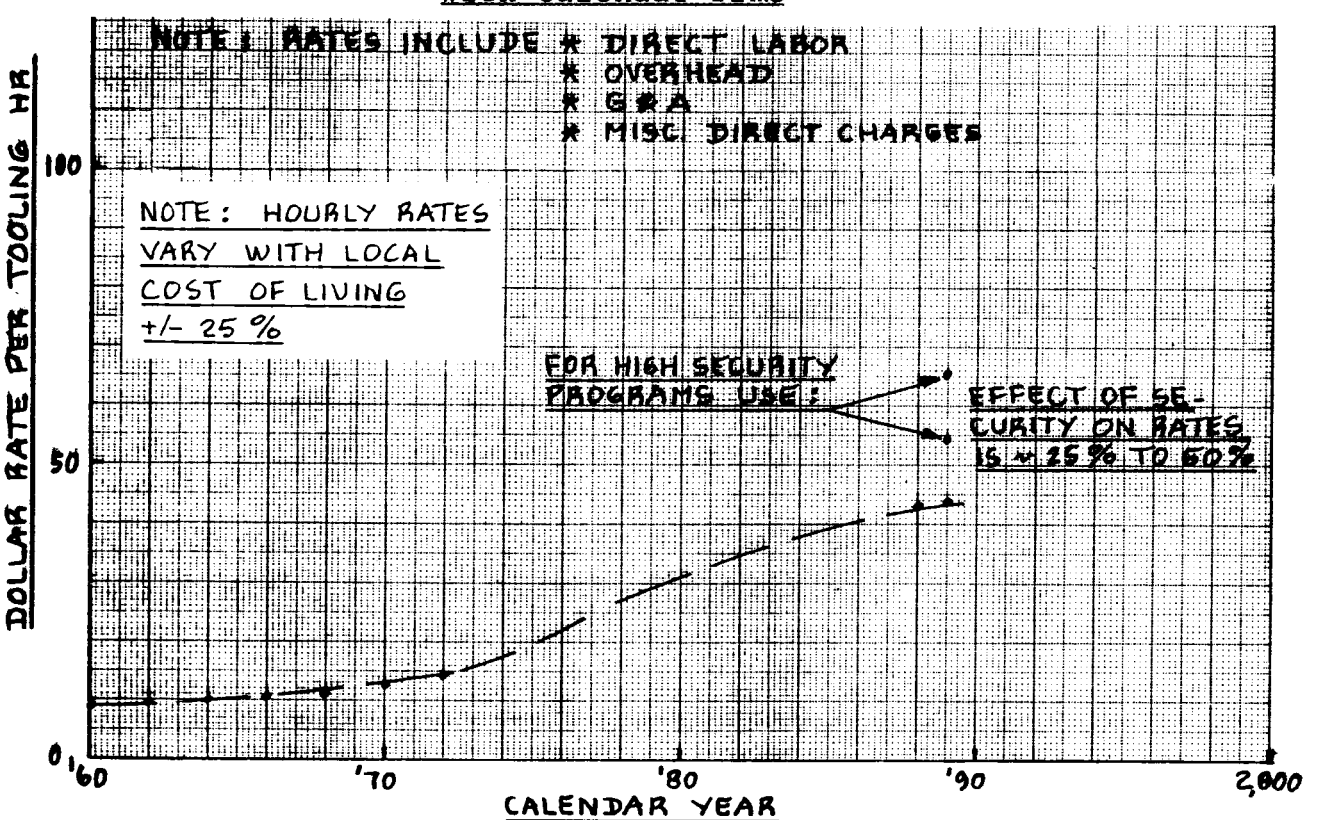

Figure 3.5 Variation of Tooling Manhour Rates with Calendar Time

C_{tool_r} is the tooling cost associated with the manufacturing of flight test airplanes. It can be estimated from:

$$C_{tool_r} = (MHR_{tool_r})(R_{t_r}) \quad (3.13)$$

where: (MHR_{tool_r}) represents the tooling manhours needed in Phases 1-3 of Fig.2.3. This may be found from:

$$MHR_{tool_r} = 4.0127(W_{ampr})^{0.764}(V_{max})^{0.899} *$$

$$*(N_{rdte})^{0.178}(N_{r_r})^{0.066}(F_{diff}) \quad (3.14)$$

R_{t_r} is the tooling labor rate in dollars per manhour which can be found from Figure 3.5. Also: read the comment after Eqn.(3.6).

N_{r_r} is the RDTE production rate in units per month. For RDTE a typical rate is 0.33 units per month.

Other factors are defined in Section 3.1.

C_{qc_r} is the quality control cost associated with manufacturing of the flight test airplanes. It may be estimated from:

$$C_{qc_r} = 0.13(C_{man_r}) \quad (3.15)$$

where: (C_{man_r}) is found from Eqn.(3.10)

NOTE: The manufacturing and tooling manhour rates depend on the same factors listed for the engineering manhour rates on page 27. In addition, if the manufacturing and tooling processes involve toxic materials, special facilities may be required. This would tend to increase the overhead component of the hourly rates. The designer must somehow account for this in any cost estimates.

3.4 FLIGHT TEST OPERATIONS COST: C_{fto_r}

The following activities are normally responsible for this cost category:

1. Flight testing of flight test airplanes. As an example, the Boeing 747 required 1,400 flight test hours before reaching its first 'type' certification.

2. Simulation activities associated with flight testing. This type of activity becomes very significant in the development of inherently unstable airplanes.

3. If the 'observables' of an airplane are important a significant amount of flight test time will have to be dedicated to the determination of the various 'signatures' of the airplane such as:

   * radar cross section

   * infrared signature

   * acoustic signature

   * optical signature

The total cost for these activities may be estimated from:

$$C_{fto_r} = 0.001244(W_{ampr})^{1.160}(V_{max})^{1.371} *$$

$$*(N_{rdte} - N_{st})^{1.281}(CEF)(F_{diff})(F_{obs}) \qquad (3.16)$$

where: F_{obs} is a factor which depends on the importance of having 'low' observables. Based on the author's judgement it is suggested to use:

For commercial airplanes and for military airplanes without a 'stealth' requirement: $F_{obs} = 1.0$

For 'stealthy' airplanes: $F_{obs} = 3.0$

All other terms are as previously defined.

3.5 TEST AND SIMULATION FACILITIES COST: C_{tsf_r}

In many airplane programs it will be found necessary to build new, dedicated test facilities. For example, in the case of a fly-by-wire, inherently unstable airplane a simulation facility will be required which couples the flight control software to the actual flight control hardware and which includes a sophisticated moving base cab with realistic displays. In addition, extensive software validation tests may be required.

There are not sufficient data in the literature to predict this type of cost. It is the responsibility of the designer to understand the facilities available to him during the development of the airplane. If, because of the special nature of the airplane new facilities must be constructed, an estimate of these costs must be made with the help of facilities people.

For preliminary cost estimating purposes it is suggested to use:

$$C_{tsf_r} = (F_{tsf})(C_{RDTE}) \qquad (3.17)$$

where: C_{RDTE} is found from Eqn. (3.1)

F_{tsf} is a cost adjustment factor which depends on judgement. The author suggests to use:

F_{tsf} = 0.00 if no extra facilities are required

= 0.20 if extensive test and simulation facilities are required. The X-29, ATF and B-2 programs are examples of this.

3.6 RDTE PROFIT: C_{pro_r}

In most cases a privately held enterprise will want to make a profit on RDTE activities. The total cost of RDTE activities can be a very substantial amount and it can also take many years. The profit cost category may be estimated from:

$$C_{pro_r} = (F_{pro_r})(C_{RDTE}) \qquad (3.18)$$

where: F_{pro_r} = 0.10 for a suggested profit of 10 percent.

C_{RDTE} is found from Equation (3.1).

NOTE: The actual profits vary significantly with politics (military), with market conditions (civilian) and with management strategy. Table 2.1 presents examples of profits made by various enterprises during the 1985-1988 time period. The reader should note that these profit figures are for the corporate entities listed. The profit made on a specific RDTE program may be more or it may be less. Many military programs have a fixed profit clause built in.

3.7 COST TO FINANCE THE RDTE PHASES: C_{fin_r}

In many instances a manufacturer will borrow money to finance the RDTE phases depicted in Figure 2.3. Borrowing money in turn costs money. However, even if internally generated cash is used for RDTE financing, there are costs associated with this: the money used could have earned interest!

Methods for estimating these financing costs are judged to be beyond the scope of this text. To estimate financing costs the calendar time element associated with an airplane program becomes of critical importance. A very general discussion of the calendar time factor is included in Chapter 9.

For a fundamental discussion of the cost of money the reader is referred to Reference 8, Section 2.4.4.

Lacking better information on the cost of financing the RDTE phase it is suggested to use:

$$C_{fin_r} = (F_{fin_r})(C_{RDTE}) \qquad (3.19)$$

where: F_{fin_r} = 0.1 to 0.2, depending on the interest rates which are available.

C_{RDTE} is found from Equation (3.1).

3.8 EXAMPLE APPLICATION OF ESTIMATING RDTE COST

In this section an example application of the method for estimating RDTE costs is given. The example applies to the Ourania jet transport of Parts I, II and V of this text. Assume that it is required to estimate RDTE costs for the Ourania program for the year 1992.

The material is organized as follows:

3.8.1 RDTE Cost Input Data

The following input data are required to estimate RDTE costs with the method of Sections 3.1 through 3.7.

W_{TO} = 123,683 lbs from p.11, Part V. This assumes that the airframe will be made mostly from Li/Al alloys.

The AMPR weight, W_{ampr} is determined from Eqn.(3.5):

W_{ampr} = invlog{0.1936 + 0.8645(log123,683)} =

= 39,437 lbs

$V_{max} = V_C$ = 295 kts from p.43, Part V. Note that this speed is in KEAS, at sea level!

N_{rdte} = 5, consisting of 3 flying prototypes and 2 airframes for structural testing. Because of the decision to use Li/Al alloys, it is prudent to perform a detailed structural evaluation! One airframe will be used for static testing (which includes watertank pressurization testing of the fuselage), the other for dynamic testing to determine the fatigue life. Therefore:

N_{st} = 2

CEF = 3.10, extrapolated from Figure 2.7 for 1992.

F_{diff} = 1.8 from page 26/27. This is based on the judgement that the combined use of Li/Al alloys and relaxed static stability (See Part II, p.272) represents a fairly aggressive use of new technology.

F_{cad} = 0.90 from page 27. This assumes moderate experience in the use of computer aided design methods.

N_e = 2 (number of engines per airplane: Pt I, p.55)

C_{e_r} = the cost per engine. This depends on the takeoff thrust of the engine, according to Appendix B. From Part I, p.184: T_{TO} = 47,625 lbs., therefore, the design takeoff thrust per engine is: 47,625/2 = 23,813 lbs.

The engine cost to the manufacturer is the price, EP, charged by the engine manufacturer. From Eqn(B9):

$$EP_{1989} = \text{invlog}\{2.3044 + 0.8858(\log 23,813)\} =$$

$$= \text{USD } 1,518,385$$

This price must be modified with the 1992 to 1989 CEF-ratio according to Eqn (B1). The CEF-ratio is found from Figure 2.7. The result is:

C_{e_r} = (3.10/3.02)1,518,385 = USD 1,558,607

N_p = 0 since the Ourania has no propellers.

$C_{avionics_r}$ = the cost of avionics per RDTE airplane.

If a detailed list of required avionics equipment were available, a reliable estimate of this cost contribution could be made. As a shortcut, it will be assumed that the installed avionics cost for the RDTE airplanes will be roughly 10 percent of the airplane market price, AMP_{1992}. The latter is found from Eqns (A14) and (A1):

$$AMP_{1992} = \{(3.10)/(3.02)\}[\text{invlog}\{3.3191 +$$

$$+ 0.8043(\log 123,683)\}] = \text{USD } 26,680,852$$

Therefore, ten percent of this amounts to roughly:

$C_{avionics_r}$ = USD 2,670,000 per RDTE airplane

R_{e_r} = (3.10/3.02)62.00 = 63.64 USD/mhr for the engineering manhour rate in 1992 as estimated with the help of Eqn.(3.6) and Figure 3.3.

CEF is the cost escalation factor obtained from Figure 2.7. For 1992:

$CEF_{1992} = 3.10$

$R_{m_r} = (3.10/3.02)34.44 = 35.35$ USD/mhr for the manufacturing manhour rate in 1992 as estimated with the help of Eqn.(3.6) and Figure 3.4.

$F_{mat} = 2.3$ from page 31. This is because of the decision to use Li/Al alloys.

$R_{t_r} = (3.10/3.02)43.06 = 44.20$ USD/mhr for the tooling manhour rate in 1992 as estimated with the help of Eqn.(3.6) and Figure 3.5.

$N_{r_r} = 0.33$ units per month (assumed).

$F_{obs} = 1.0$, according to page 34.

F_{tsf} = an adjustment factor which depends on the extra test and simulation facilities required for a new airplane program. Because of the relaxed stability decision made on the Ourania program, page 35 suggests:

$F_{tsf} = 0.2$

$F_{pro_r} = 0.10$, assumed from p.35.

$F_{fin_r} = 0.10$, assumed from p.36.

This completes the list of input requirements for estimating RDTE cost. The RDTE cost calculations are presented in sub-section 3.8.2.

3.8.2 RDTE Cost Calculations

With the input data from sub-section 3.8.1 the following RDTE cost component estimates can be made:

From Eqns (3.3) and (3.2):

$$C_{aed_r} = 0.0396(39,437)^{0.791}(295)^{1.526}(5)^{0.183} * \\ *(1.8)(0.9)(63.64) = \text{USD } 139,046,557$$

From Eqn (3.7):

$$C_{dst_r} = 0.008325(39,437)^{0.873}(295)^{1.890}(5)^{0.346}*$$
$$*(3.1)(1.8) = \text{USD } 38,819,483$$

From Eqn (3.9):

$$C_{(e+a)_r} = \{(1,558,607)(2) + (2,670,000)\}*(3) =$$
$$= \text{USD } 17,361,642$$

From Eqns (3.10) and (3.11):

$$C_{man_r} = 28.984(39,437)^{0.740}(295)^{0.543}(5)^{0.524}*$$
$$*(1.8)(35.35) = \text{USD } 236,680,646$$

From Eqn (3.12):

$$C_{mat_r} = 37.632(2.3)(39,437)^{0.689}(295)^{0.624}(5)^{0.792}*$$
$$*(3.1) = \text{USD } 48,975,376$$

From Eqns (3.13) and (3.14):

$$C_{tool_r} = 4.0127(39,437)^{0.764}(295)^{0.899}(5)^{0.178}*$$
$$*(0.33)^{0.066}(1.8)(44.20) = \text{USD } 213,015,201$$

From Eqn (3.15):

$$C_{qc_r} = 0.13(236,680,646) = \text{USD } 30,768,484$$

From Eqn (3.8):

$$C_{fta_r} = 17,361,642 + 236,680,646 + 48,975,376 +$$
$$+ 213,015,201 + 30,768,484 = \text{USD } 546,801,349$$

From Eqn (3.16):

$$C_{fto_r} = 0.001244(39,437)^{1.160}(295)^{1.371}(3)^{1.281}*$$
$$*(3.1)(1.8) = \text{USD } 14,791,812$$

From Eqn (3.17):

$$C_{tsf_r} = 0.20(C_{RDTE})$$

From Eqn(3.18):

$$C_{pro_r} = 0.10(C_{RDTE})$$

From Eqn.(3.19):

$$C_{fin_r} = 0.10(C_{RDTE})$$

From Eqn (3.1):

$$C_{RDTE} = 139,046,557 + 38,819,483 + 546,801,349 +$$

$$+ 14,791,812 + 0.20(C_{RDTE}) + 0.10(C_{RDTE}) + 0.10(C_{RDTE})$$

from which it follows that:

C_{RDTE} = USD 739,459,201/(0.6) = USD 1,232,432,002 or rounding off to next highest million:

C_{RDTE} = <u>USD 1,232,000,000</u>

This represents the estimated 1992 cost of the entire RDTE part of the Ourania jet transport program.

Figure 3.6 shows the contribution of this RDTE cost to the unit cost of the Ourania transport. Note, that this type of RDTE program makes financial sense only if more than, say 250 transports can be expected to be sold.

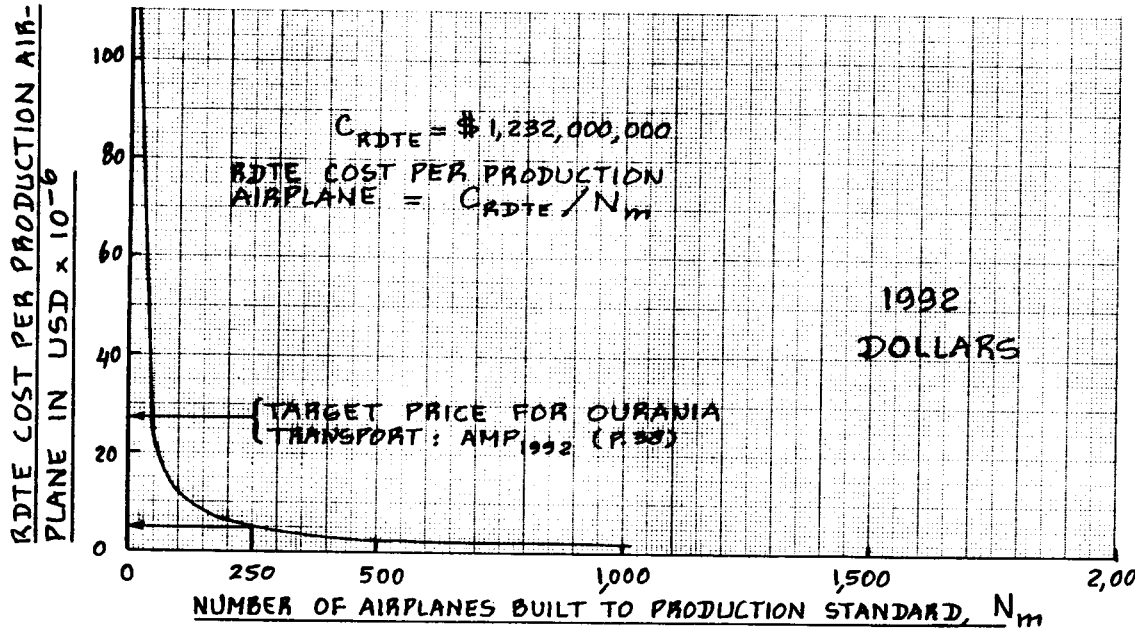

Figure 3.6 Effect of Number of Airplanes Produced on the RDTE Cost Contribution per Airplane

3.9 METHOD FOR ESTIMATING PROTOTYPE PROGRAM COST WITH AN EXAMPLE APPLICATION

The purpose of this section is to present a method for estimating the cost of developing, manufacturing and flight testing prototypes. Prototypes are usually built rather quickly and without provisions required for a follow-on production program.

Nevertheless, many prototype programs do lead to a follow-on production program. Examples are the F-104, T-38, B-47, B-52, C-130 and KC-135 programs.

In many cases a prototype program is conducted mainly for the purpose of evaluating certain technologies: the NASA X-planes, such as the X-29 and the X-31 are good examples of this.

The method presented here should be applied ONLY to prototype programs where 1-4 airplanes are constructed. If more than 4 prototypes are to be constructed the RDTE method of Chapter 3 should be used instead. The method is based on Reference 23.

The prototype program cost may be estimated from:

$$C_{PROT} = (1115.4)(10^3)(W_{ampr})^{0.35}(N_{prot})^{0.99} * \\ *(CEF_{\text{then year}})/(CEF_{1973}) \qquad (3.20)$$

where: W_{ampr} is found from Eqn.(3.4) or from Eqn.(3.5).

N_{prot} is the number of prototypes to be built. This number should not exceed 4. When it does, the RDTE method of Chapter 3 should be used.

$CEF_{\text{then year}}$ is the Cost Escalation Factor (CEF) of Fig. 2.7 for a given 'then year'.

CEF_{1973} is the CEF for 1973 as obtained from Figure 2.7: $CEF_{1973} = 1.14$.

To illustrate the use of the method it will now be applied to the Grumman X-29 prototype program. A three-view of the X-29 is shown in Figure 3.7. The X-29 program was funded by DARPA (Defense Advanced Research Projects Agency). Grumman was awarded the X-29 contract in

December of 1981 for a total of USD 80,000,000. An anonymous source has indicated that Grumman invested a total of USD 20,000,000 of its own money on top of the DARPA funding. The total cost of the X-29 program (until delivery to NASA) was thus estimated at USD 100,000,000.

The following data are found in the 1985-1986 issue of Jane's All the World Aircraft:

W_{TO} = 17,800 lbs

N_{prot} = 2

Using Eqn.(3.5) it is found that:

W_{ampr} = 7,380 lbs

The 1982 CEF value is found from Figure 2.7 as:

CEF_{1982} = 2.5

With Eqn.(3.20): C_{PROT} =

$(1115.4)(10^3)(7,380)^{0.35}(2)^{0.99}(2.5)/(1.14)$ =

= USD 109,724,907

This is in good agreement with the actual cost which was quoted before.

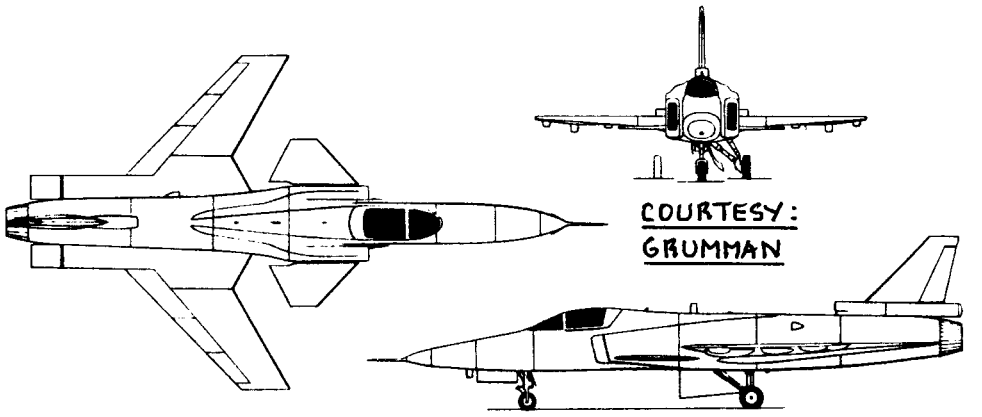

Figure 3.7 Three-view of the Grumman X-29

SIAI - MARCHETTI S.211 AVIONIC SYSTEM

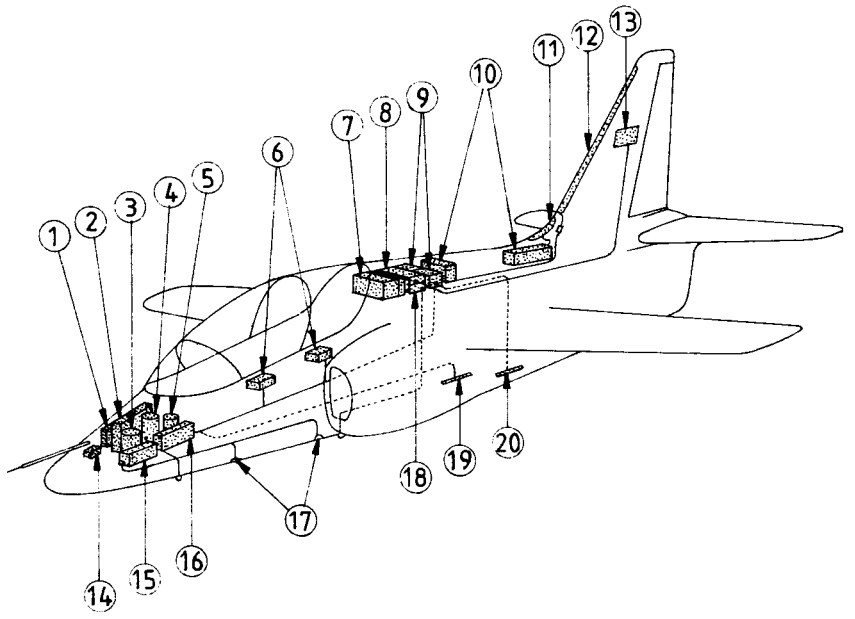

KEY

1. FLIGHT DIRECTOR COMPUTER
2. ADF
3. VERTICAL GYRO
4. DIRECTIONAL GYRO
5. RATE GYRO
6. AVIONIC CONTROL UNIT
7. TACAN
8. DME
9. V/UHF
10. HF
11. UHF ANTENNA
12. V/UHF ANTENNA
13. VOR/ILS ANTENNA
14. ALTITUDE SENSOR
15. R/ALTIMETER
16. IFF
17. R/ALTIMETER ANTENNA
18. VOR/ILS
19. ADF LOOP ANTENNA
20. MARKER BEACON ANTENNA

4. METHOD FOR ESTIMATING MANUFACTURING AND ACQUISITION COST

The purpose of this chapter is to present a method for estimating manufacturing cost: C_{MAN} and acquisition cost: C_{ACQ} for airplane programs. These costs are incurred during Phase 4 of an airplane program as shown in Figure 2.3. The acquisition cost represents the second cost source of the life cycle cost defined in Eqn.(2.3).

The following definitions are important:

Definition 1: The number of airplanes produced during an airplane program is $N_{program}$.

Definition 2: The number of airplanes produced to production standard during an airplane program is N_m.

Definition 3: The number of airplanes produced during the RDTE phases of an airplane program is: N_{rdte}.

Consequently: $N_{program} = N_m + N_{rdte}$ (4.1)

Table 4.1 shows examples of the total number of airplanes built in several airplane programs.

Definition 4: The total manufacturing cost associated with an airplane program is: C_{MAN}.

Definition 5: The total acquisition cost associated with an airplane program is: C_{ACQ}.

The difference between acquisition cost and manufacturing cost is the profit made by the manufacturer: C_{PRO}, so that:

$$C_{ACQ} = C_{MAN} + C_{PRO} \quad (4.2)$$

Again, the costs mentioned sofar represent program costs. The price paid by the user of an airplane (which is his acquisition cost) depends on a number of factors:

Table 4.1 Examples of Airplane Program Production Runs

Note: No. Produced equals $N_{program}$ of Eqn.(4.1).

Fighters

Type	No. Produced
Gen.Dyn. F-111	563
Gen.Dyn. F-16	>3,000
Gloster Meteor	3,545
Gloster Javelin	435
Grumman F9F2-5	1,325
Grumman F9F6-8	1,985
Grumman F11F	201
Grumman F14	> 900
Lockheed F-94	387
Lockheed F-80	1,732
Lockheed T-33	5,691
Lockheed F-104	2,578
McDonnell F-4	>5,000
McDD F-15	>2,000
McDD F-18	>1,500
SAAB JA37	329
SAAB J35A	604

Commercial Transports

Type	No. Produced
Douglas DC-7	338
Douglas DC-8	556
McDD DC-9, MD-80+	>1,000
Boeing 707	870
Boeing 727	1,834
Boeing 737	>2,600
Boeing 747	> 750

General Aviation

Type	No. Produced
Beech Duke	471
Beech Duchess	437
Beech Model 18	8,000
Cessna 140	5,429
Cessna 150	23,839
Cessna 310	5,447
Cessna 421	> 1,900
Cessna 500/501	315

Mil. Trainers/Liaison

Type	No. Produced
Cessna L-19	3,399
Beech T-34B	423
Beech T-34C	> 300
Cessna T-37	1,838
Fokker S-14	20
NAA T2C	521
Northrop T-38	1,189

Mil. Transports/Bombers

Type	No. Produced
Northrop C-125	23
Fairchild C-132	300
Lockheed C-130	>2,000
Lockheed C-141	285
Boeing B-47	2,004
Boeing B-52	742
Boeing KC-135	760
Douglas C-133	50

Regional Transports

Type	No. Produced
Beech M-99	234
Beech 1900	> 100
Fairchild Merlin/ Metroliner	> 800
Embraer-110	> 500
Embraer-120	> 150
DHC-6	> 832
DHC-7	> 115
DHC-8	> 137
Dornier 228	> 133
Fokker F-27	786
Fokker F-28	241
Fokker F-100	> 300
BAC-146	> 100
Pilatus B/N-2B	>1,077
Shorts 330	> 165
Shorts Skyvan	150

1. the total number of airplanes built by the manufacturer: $N_{program}$

2. the number of airplanes acquired: N_{acq}. In commercial programs this number tends to be only a fraction of $N_{program}$. For example, an airplane program may see 1,000 transports built. One airline customer may buy (acquire) 60 airplanes.

   In military programs (discounting foreign sales) N_{acq} is usually the same as N_m.

3. the manufacturers profit which can be negotiated: for large fleet buys a manufacturer often offers a lower profit to enhance his market share.

4. the cost of the RDTE program: C_{RDTE} (See Ch.3)

An estimate of the unit price per airplane can be obtained from:

$$AEP = \{(C_{MAN} + C_{PRO} + C_{RDTE})/N_m\} \qquad (4.3)$$

This assumes that the RDTE airplanes are not sold during the program. The effect of RDTE cost on the unit cost of an airplane was shown in Figure 3.6.

Another assumption made in Eqn.(4.3) is that no spare parts are bought by the user. In most cases commercial and military customers will want to buy a certain number of spare parts. The cost of spare parts is discussed in Chapters 5 and 6.

Having stated these fundamentals, the remainder of this chapter deals with the development of a method for estimating manufacturing cost: C_{MAN} and manufacturer's profit: C_{PRO}.

The method is a modified version of the methods of References 11 and 14. It should be used for preliminary cost estimation purposes only. The method can be applied to military as well as to commercial airplane programs.

The total airplane program manufacturing cost can be broken down into the following cost categories:

4.1 Airframe Engineering and Design Cost: C_{aed_m}

4.2 Airplane Production Cost: C_{apc_m}

4.3 Production Flight Test Operations Cost: C_{fto_m}

4.4 Cost of financing the manufacturing program: C_{fin_m}

The total manufacturing cost may be estimated from:

$$C_{MAN} = C_{aed_m} + C_{apc_m} + C_{fto_m} + C_{fin_m} \quad (4.4)$$

Expressions for estimating the first three cost categories of the manufacturing cost are presented in Sections 4.1 through 4.3. The cost of financing the manufacturing part of the program is briefly discussed in Section 4.4. In Section 4.5 an equation is presented for estimating the manufacturer's profit. An example application is developed in Section 4.6. A discussion of the effect of several design and production parameters on the estimated price of an airplane is given in Section 4.7.

4.1 AIRFRAME ENGINEERING AND DESIGN COST: C_{aed_m}

Airframe engineering and design typically consists of the following activities:

1. Engineering design work necessitated by problems uncovered during RDTE phases 1-3 (Figure 2.3).
2. Design studies and integration studies associated with special customer requests.
3. Sustaining engineering associated with:
   * errors made in the manufacturing process
   * changes made in manufacturing of components
4. Release and maintenance of drawings and specifications.
   NOTE: during the last ten years most companies have switched from 'hand-drafting' to CAD (Computer Aided Design). The effect of this on C_{aed_m} is to reduce these costs.

   By how much, varies from one manufacturer to another.
5. Liaison engineering with manufacturing and with vendors.
6. Incorporation and analysis of design changes.
7. Development of specifications for materials and processes.
8. Analysis of reliability.
9. Analysis of maintainability and accessibility.

The total (= program) cost of the above named activities is called: C_{aed_m} and may be estimated from:

$$C_{aed_m} = (MHR_{aed_{program}})(R_{e_m}) - (MHR_{aed_r})(R_{e_r}) \qquad (4.5a)$$

or, with Eqn.(3.3):

$$C_{aed_m} = (MHR_{aed_{program}})(R_{e_m}) - C_{aed_r} \qquad (4.5b)$$

where: $MHR_{aed_{program}}$ is the total amount of engineering manhours required for the entire airplane program, that is for <u>all</u> $N_{program}$ airplanes. These manhours may be estimated from:

$$MHR_{aed_{program}} = 0.0396(W_{ampr})^{0.791}(V_{max})^{1.526} *$$

$$*(N_{program})^{0.183}(F_{diff})(F_{cad}) \qquad (4.6)$$

C_{aed_r} is computed with Eqn.(3.3).

R_{e_m} is the engineering manhour rate in dollars per hour for the entire airplane program. It may be assumed equal to R_{e_r} which in turn is obtained from Figure 3.3.

$N_{program}$ is the total number of airplanes produced: See Eqn.(4.1).

Other symbols are defined in Section 3.1.

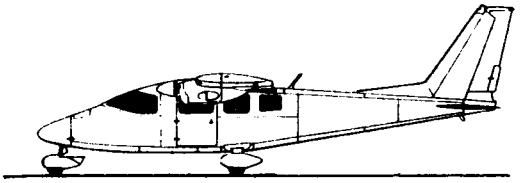

4.2 AIRPLANE PROGRAM PRODUCTION COST: C_{apc_m}

The airplane (program) production cost category, C_{apc_m}, normally consists of the following cost components:

1. Cost of engine and avionics as acquired from vendors: $C_{(e + a)_m}$
2. Cost of interior: C_{int_m}
3. Manufacturing labor cost: C_{man_m}
4. Manufacturing material cost: C_{mat_m}
5. Tooling cost: C_{tool_m}
6. Quality control cost: C_{qc_m}

The following equation is suggested for estimating airplane program production cost, C_{apc_m}:

$$C_{apc_m} = C_{(e + a)_m} + C_{int_m} + C_{man_m} + C_{mat_m} + C_{tool_m} + C_{qc_m} \quad (4.7)$$

where: $C_{(e + a)_m}$ is the cost of engines and avionics equipment as paid to vendors. This can be estimated from:

$$C_{(e + a)_m} = (C_{e_m} N_e + C_{p_m} N_p + C_{avionics_m})(N_m) \quad (4.8)$$

where: C_{e_m} is the cost per engine during the manufacturing phase. This cost can differ from the cost per engine incurred in the RDTE phases: C_{e_r}.

Lacking better information, the method of Appendix B may be used to estimate the cost of production engines.

N_e is the number of engines per airplane.

C_{p_m} is the cost per propeller during the manufacturing phase. This cost can differ from the cost per propeller incurred in the RDTE phases: C_{p_r}.

Lacking better information, the method of Appendix B may be used to estimate the cost of production propellers.

N_p is the number of propellers per airplane. Note that N_p may not be the same as N_e!

$C_{avionics_m}$ is the cost of avionics equipment per airplane. This cost may differ from the avionics cost associated with the RDTE airplanes. Lacking better information, the method of Appendix C may be used.

Note: in civilian airplanes the total cost of avionics typically is 5 to 15 percent of the airplane cost without avionics.

in military airplanes the total cost of avionics, depending on the mission of the airplane, may range from 10 to 100 percent of the airplane cost without avionics.

C_{int_m} is the cost of the airplane interior.

Note: The cost estimating methods of References 11 and 14 do not account for interior cost as a separate cost component. In military airplanes, for which these methods were primarily derived, this is acceptable because their interior cost is included in the statistical equations used for estimating cost. This includes items like passenger seats, ejection seats, insulating materials, etc.

The cost of interiors in commercial airplanes can be substantial and must be accounted for as a separate item. In commercial airplanes the cost of the interior includes items such as:

seats, partitions, cabin sidewall, ceiling and floor materials, galleys, lavatories, closets, storage bins, entertainment systems, lighting systems, insulating materials, etc.

The reader will have observed that interior cost was NOT accounted for in Eqn.(3.8) for the RDTE part of the airplane program. The reason is that flight test airplanes are normally NOT equipped with anything approaching a production interior.

To account for the interior cost component it is suggested to use:

$$C_{int_m} = (F_{int})(N_{pax})(N_m)* \\ *(CEF_{then\ year})/(CEF_{1990}) \qquad (4.9)$$

where: F_{int} is the interior cost factor expressed in USD/pax. The following values are suggested for calendar year 1990:

F_{int} = 0 USD/pax for military airplanes

= 500 USD/pax for light general aviation airplanes

= 1,000 USD/pax for regional transport airplanes

= 2,000 USD/pax for jet transports

= 3,000 USD/pax for business jets

N_{pax} is the number of passengers.

CEF values are obtained from Figure 2.7.

C_{man_m} is the labor cost incurred in manufacturing N_m airplanes to production standard. It may be estimated from:

$$C_{man_m} = \qquad (4.10a)$$

$$(MHR_{man_{program}})R_{m_m} - (MHR_{man_r})R_{m_r}$$

or, with Eqn.(3.10):

$$C_{man_m} = (MHR_{man\ program})R_{m_m} - C_{man_r} \qquad (4.10b)$$

where: $MHR_{man}{}_{program}$ represents the total number of manhours required for the manufacturing of $N_{program}$ airplanes. It can be found from:

$$MHR_{man}{}_{program} = 28.984(W_{ampr})^{0.740}(V_{max})^{0.543} * *(N_{program})^{0.524}(F_{diff}) \quad (4.11)$$

$R_{m}{}_{m}$ is the manufacturing labor rate per hour for the entire program. This may be assumed to be equal to $R_{m}{}_{r}$ which in turn is determined from Figure 3.4.

Other symbols are as defined before.

$C_{mat}{}_{m}$ is the materials cost incurred while manufacturing N_{m} airplanes to production standard. It may be found from:

$$C_{mat}{}_{m} = C_{mat}{}_{program} - C_{mat}{}_{r} \quad (4.12)$$

where: $C_{mat}{}_{program}$ is the total materials cost associated with building $N_{program}$ airplanes. It follows from:

$$C_{mat}{}_{program} = 37.632F_{mat}(W_{ampr})^{0.689}(V_{max})^{0.624} * *(N_{program})^{0.792}(CEF) \quad (4.13)$$

$C_{mat}{}_{r}$ is found from Eqn.(3.12).

All other symbols are as defined before.

$C_{tool}{}_{m}$ is the tooling cost to produce N_{m} airplanes. It may be estimated from:

$$C_{tool_m} = \quad (4.14a)$$

$$(MHR_{tool_{program}})R_{t_m} - (MHR_{tool_r})R_{t_r}$$

or, with Eqn.(3.13):

$$C_{tool_m} = (MHR_{tool_{program}})R_{t_m} - C_{tool_r} \quad (4.14b)$$

where: $MHR_{tool_{program}}$ is the total number of tooling manhours required to build $N_{program}$ airplanes.

It can be estimated from:

$$MHR_{tool_{program}} = 4.0127(W_{ampr})^{0.764}(V_{max})^{0.899} *$$

$$*(N_{program})^{0.178}(N_{r_m})^{0.066}(F_{diff}) \quad (4.15)$$

R_{t_m} is the tooling labor rate in dollars per manhour as found from Figure 3.5. Note: R_{t_m} may differ from R_{t_r}. It is suggested to ignore this difference in preliminary cost estimations.

N_{r_m} is the airplane manufacturing rate in units per month.

Other symbols are as defined before.

C_{qc_m} is the quality control cost associated with building N_m airplanes. It may be found from:

$$C_{qc_m} = 0.13(C_{man_m}) \quad (4.16)$$

where: C_{man_m} is found from Eqn.(4.10)

4.3 PRODUCTION FLIGHT TEST OPERATIONS COST: C_{fto_m}

This cost category is normally neglected in preliminary cost estimating calculations. Depending on the airplane program it may not be negligible. The following equation is suggested for estimating C_{fto_m}:

$$C_{fto_m} = N_m(C_{ops/hr})(t_{pft})(F_{ftoh}) \qquad (4.17)$$

where: N_m is the number of airplane built to production standard.

$C_{ops/hr}$ is the airplane operating cost per hour as computed with the method of Chapter 5 (commercial airplanes) or Chapter 6 (military airplanes).

t_{pft} is the number of flight test hours flown by the manufacturer before airplane delivery to the customer. It is suggested to use:

t_{pft} = 2 hrs for general aviation airplanes
10 hrs for jet transports
20 hrs for military airplanes

F_{ftoh} is the overhead factor associated with the production flight test activities. Lacking actual overhead data it is suggested to use:

$F_{ftoh} = 4.0$

4.4 COST TO FINANCE THE MANUFACTURING PHASE: C_{fin_m}

Usually a manufacturer will borrow money to finance the manufacturing phase (Phase 4 in Figure 2.3) of an airplane program. Borrowing money in turn costs money. However, even if internally generated cash would be used for production financing, there are costs associated with this: the money used could have been earning interest!

Methods for estimating these financing costs are judged to be beyond the scope of this text. To estimate financing costs, the calendar time element associated with an airplane program becomes critically important. A discussion of the effect of calendar time on interest is also beyond the scope of this text.

For a fundamental discussion of the cost of money the reader should consult Reference 8.

For preliminary cost estimating purposes it is suggested to use:

$$C_{fin_m} = (F_{fin_m})(C_{MAN}) \qquad (4.18)$$

where: F_{fin_m} = 0.1 to 0.2, depending on the interest rates which are available.

C_{MAN} is found from Equation (4.4).

4.5 PROFIT: C_{PRO}

As indicated in Chapter 2, privately held aeronautical enterprises will want to make a profit on airplane manufacturing activities. This profit, which is part of the cost of airplane acquisition (Eqn.4.2), may be estimated from:

$$C_{PRO} = (F_{pro_m})(C_{MAN}) \qquad (4.19)$$

where: F_{pro_m} = 0.10 for a suggested profit of 10 percent.

C_{MAN} is found from Equation (4.4).

NOTE: Profits can vary significantly with politics (military) and with market conditions (civilian). Table 2.1 presents examples of profits made by various manufacturers during the 1985-1988 time period. The reader must keep in mind that these profit figures are for the corporate entities listed. The profit made on any given manufacturing program may be more or less.

4.6 EXAMPLE APPLICATION OF ESTIMATING MANUFACTURING AND ACQUISITION COST

The purpose of this section is to present an example application of the method for estimating the manufacturing and acquisition costs of an airplane program. In addition, an estimate for the unit price of the airplane will be determined. The example applies to the Ourania jet transport of Parts I, II and V of this text.

Since cost and price are tied to calendar time, it will be assumed that the cost and price estimates are required for the year 1992.

The material is organized as follows:

4.6.1 Manufacturing and Acquisition Cost Input Data

4.6.2 Manufacturing and Acquisition Cost Calculations

4.6.3 Determination of Estimated Unit Price

4.6.1 Manufacturing and Acquisition Cost Input Data

The following input data are required to estimate the manufacturing and acquisition cost for the Ourania program with the method of Sections 4.1 through 4.5.

W_{TO} = 123,683 lbs from p.11, Part V. This assumes that the airframe will be made mostly from Li/Al alloys.

The AMPR weight, W_{ampr}, is determined from Eqn.(3.5):

W_{ampr} = invlog{0.1936 + 0.8645(log123,683)} =

= 39,437 lbs

$V_{max} = V_C$ = 295 kts from p.43, Part V. Note that this speed is in KEAS, at sealevel!

N_{rdte} = 5 (see p.37)

The number of airplanes produced to production standard, N_m, must be assumed at this point. The assumption is made that a marketing analysis has shown that 500 airplanes can be sold, so that:

N_m = 500

With Eqn.(4.1):

$N_{program}$ = 5 + 500 = 505

F_{diff} = 1.8, according to p.37

F_{cad} = 0.90, according to p.38

R_{e_m} = 63.64 USD/mhr (Set equal to R_{e_r} of p.38)

C_{e_m} = the cost per engine during the production program. Lacking better information at this point, this cost will be assumed equal to the engine price paid in the RDTE program: C_{e_r} of p.38:

C_{e_m} = USD 1,558,607

N_e = 2 (number of engines per airplane: Pt I, p.55)

N_p = 0 since the Ourania has no propellers

$C_{avionics_m}$ = the cost of avionics per airplane in the production phase of the program. At this point it will be assumed that the avionics cost for production airplanes is the same as that for the RDTE airplanes: $C_{avionics_r}$. For the reasons stated on p.38:

$C_{avionics_m}$ = USD 2,670,000 per airplane

F_{int} = 2,000 USD/pax from p.52

N_{pax} = 150 from p.55, Part I.

R_{m_m} = 35.35 USD/mhr (Set equal to R_{m_r} of p.39)

F_{mat} = 2.3 from p.31

CEF_{1992} = 3.10 from p.20

CEF_{1990} = 3.05 from p.20

R_{t_m} = 44.20 USD/mhr (Set equal to R_{t_r} of p.39)

N_{r_m} = the unit production rate per month. It is assumed that the Ourania delivery rate will be 5 per month:

N_{r_m} = 5 units per month

$C_{ops/hr}$ = the total operating cost per block hour for the Ourania. This cost includes the direct and indirect cost of the manufacturer to operate this airplane during production flight testing. Operating cost can be computed with the method of Chapter 5. At this point it will be assumed that this cost for 1992 is USD 2,500 per block hour:

$C_{ops/hr}$ = USD 2,500 per block hour

t_{pft} = the number of flight test hours flown by the manufacturer before delivery to the customer. From Section 4.3:

t_{pft} = 10 hours

The flight test overhead factor (p.55) is set at:

F_{ftoh} = 4.0

The following data from the RDTE cost calculations are also needed:

C_{aed_r} = USD 139,046,557, from p.39

C_{man_r} = USD 236,680,646, from p.40

C_{mat_r} = USD 48,975,376, from p.40

C_{tool_r} = USD 213,015,201, from p.40

F_{fin_m} = 0.10 (assumed from p.56)

F_{pro_m} = 0.10 (assumed from p.56)

C_{RDTE} = USD 1,232,000,000, from p.41

4.6.2 Manufacturing and Acquisition Cost Calculations

With the input from sub-section 4.6.1 the following manufacturing cost categories can now be determined:

From Eqns (4.5) and (4.6):

$$C_{aed_m} = 0.0396(39,437)^{0.791}(295)^{1.526}(505)^{0.183}*$$

$$*(1.8)(0.90)(63.64) - 139,046,557 =$$

$$= 323,557,187 - 139,046,557 = \text{USD } 184,510,630$$

From Eqn.(4.8):

$$C_{(e + a)_m} = \{(1,558,607)(2) + 2,670,000\}(500) =$$

$$= \text{USD } 2,893,607,000$$

From Eqn.(4.9):

$$C_{int_m} = (2,000)(150)(500)(3.10/3.05) =$$

$$= \text{USD } 152,459,016$$

From Eqns (4.10) and (4.11):

$$C_{man_m} = 28.984(39,437)^{0.740}(295)^{0.543}(505)^{0.524}*$$

$$*(35.35)(1.8) - 236,680,646 =$$

$$= 2,657,217,752 - 236,680,646 =$$

$$= \text{USD } 2,420,537,106$$

From Eqns (4.12) and (4.13):

$$C_{mat_m} = 37.632(2.3)(39,437)^{0.689}(295)^{0.624}*$$

$$*(505)^{0.792}(3.1) - 48,975,376 =$$

$$= 1,894,088,669 - 48,975,376 =$$

$$= \text{USD } 1,845,113,293$$

From Eqns (4.14) and (4.15):

$$C_{tool_m} = 4.0127(39,437)^{0.764}(295)^{0.899}(505)^{0.178}*$$

$$*(5)^{0.066}(1.8)(44.20) - 213,015,201 =$$

$$= 579,548,654 - 213,015,201 = \text{USD } 366,533,453$$

From Eqn.(4.16):

$$C_{qc_m} = 0.13(2,420,537,106) = \text{USD } 314,669,824$$

With Eqn.(4.7):

$$C_{apc_m} = 2,893,607,000 + 152,459,016 +$$

$$+ 2,420,537,106 + 1,845,113,293 +$$

$$+ 366,533,453 + 314,669,824 =$$

$$= \text{USD } 7,992,919,692$$

From Eqn.(4.17):

$$C_{fto_m} = 500(2,500)(10)(4) = \text{USD } 50,000,000$$

The financing cost, C_{fin_m}, will be determined from Eqn.(4.18) with $F_{fin_m} = 0.10$ so that:

$$C_{MAN} = (184,510,630 + 7,992,919,692 +$$

$$+ 50,000,000)/(0.9) = \text{USD } 9,141,589,247$$

From Eqns (4.2) and (4.19):

$C_{ACQ} = (1.1)(9,141,589,247) = \text{USD } 10,055,748,000$, or rounding off to the next highest million:

$C_{ACQ} = \text{USD } 10,056,000,000$

4.6.3 Determination of Estimated Unit Price

The price per airplane may now be estimated from Eqn.(4.3) as:

$$AEP_{1992} = (10,056,000,000 + 1,232,000,000)/500 =$$

$$= \text{USD } 22,576,000$$

This price should be checked for realism by comparison to the statistical market price data in Appendix A. Eqn.(A14) with Eqn.(A1) yields:

$$AMP_{1992} = \{(3.10)/(3.02)\}[\text{invlog}\{3.3191 +$$

$$+ 0.8043(\log 123,683)\}] = \text{USD } 26,680,852$$

The estimated price, AEP, is in fair agreement with the market price, AMP. A discussion of various factors which affect the airplane estimated price is presented in section 4.7.

4.7 EFFECT OF SEVERAL DESIGN AND PRODUCTION PARAMETERS ON AIRPLANE ESTIMATED PRICE: AEP

When inspecting the cost estimating equations in Sections 4.1 through 4.5 it is clear that the following parameters play a role in determining the program manufacturing cost and thereby in determining airplane price:

1. Airplane takeoff weight, W_{TO}, because of its effect on W_{ampr} which appears in Eqns.(4.6), (4.11), (4.13) and (4.15).
2. Airplane design cruise speed, V_{max}, which appears in the same equations as W_{ampr}.
3. Total number of airplanes built, $N_{program}$ which appears in the same equations as W_{ampr}.
4. Airplane production rate, N_{r_m}, which appears in Eqn.(4.15) for the tooling cost.
5. Airplane RDTE cost and the number of airplanes (N_m) over which this cost is to be recovered.

The purpose of this section is to show the results of some trade studies conducted to illustrate the effect of these design and production parameters on airplane estimated price. The author gratefully acknowledges the the work of Mr. Larry Bellmard who conducted these trade studies for the Ourania program of Sections 3.8 and 4.6.

Figure 4.1 shows the effect of the following parameters on the airplane estimated price, AEP:

* Total number of airplanes built, $N_{program} = 5 + N_m$

* Takeoff weight, W_{TO}

Observe that for the first 1,000 airplanes the airplane unit price is strongly affected by the number of airplanes built. After the 1,000 mark is reached there is still some price reduction to be seen but the effect is much less dramatic. There are two reasons for the rapid initial unit price reduction:

1) the so-called 'learning curve' effect

2) the RDTE cost contribution per airplane decreases hyperbolically with the total number of airplanes produced. This was already observed in Figure 3.6.

Figure 4.2 illustrates the 'learning curve' effect for three airplane programs: B-727, B-737 and McDD F-15. Note that the number of manhours required per airplane per pound decreases linearly when plotted on a log-log scale. This learning curve effect can be mathematically expressed as follows:

$$(\text{MHRS per unit}) = (\text{MHRS})_1/(N_{program})^n \qquad (4.20)$$

where: $MHRS_1$ is the number of manhours required to produce unit (= airplane) number 1.

$N_{program}$ is the total number of airplanes built.

n is the learning curve exponent. The meaning of n is best illustrated with a graphical example. This is done in Figure 4.3. Note that for a so-called 80 percent learning curve the exponent value is: n = 0.322. For a P percent learning curve the exponent n may be found from:

$$P = 100/(2^n) \qquad (4.21)$$

The learning curves shown in Figure 4.2 represent a 73 percent learning curve. Learning curves of 73 to 80 percent are fairly typical for the airframe manufacturing industry. The 'learning curve' effect noted here is already 'built' into the statistical cost equations of Sections 4.1 through 4.5.

The effect of airplane takeoff weight, W_{TO}, on airplane price is also shown in Figure 4.1. It is seen that the effect of weight on price is important when the number of airplanes produced is small.

Figure 4.4 illustrates the effect of airplane speed, V_{max}, on airplane price. It may be seen that increased speed requirements would increase airplane price rather significantly, when not many airplanes are produced.

Finally, Figure 4.5 shows that airplane production rate has a minor effect on airplane price except for the case where very small numbers are produced.

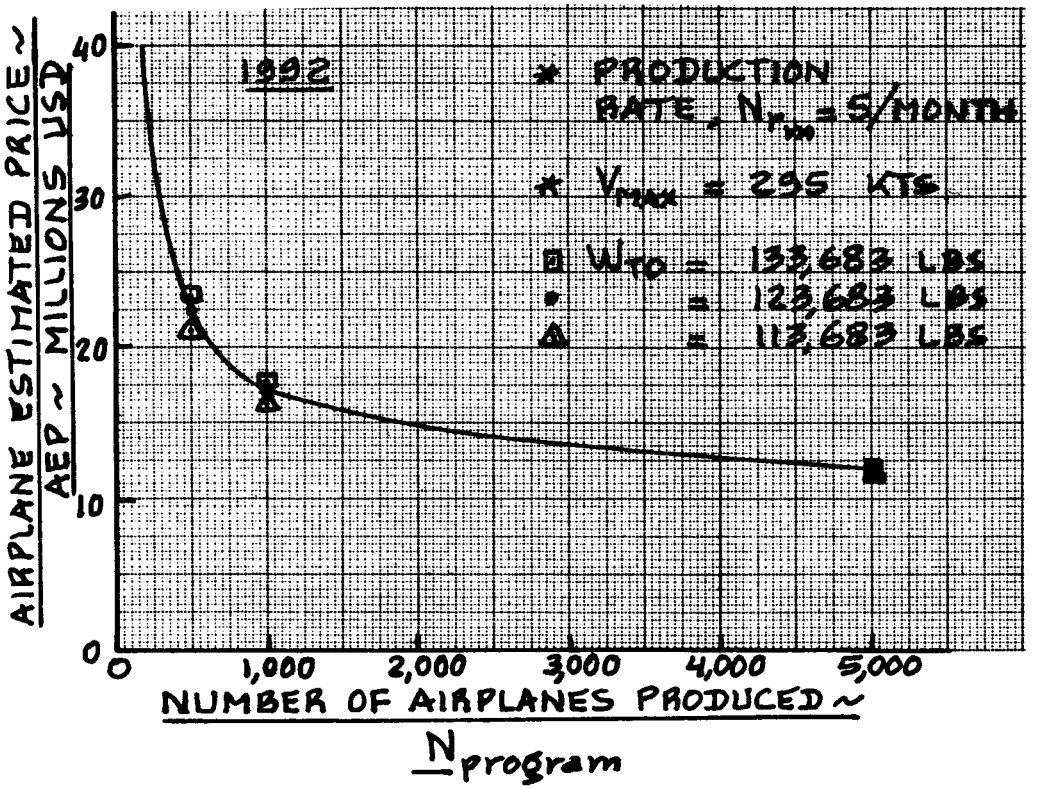

Figure 4.1 Effect of Number of Airplanes Produced and of Takeoff Weight on Airplane Estimated Price

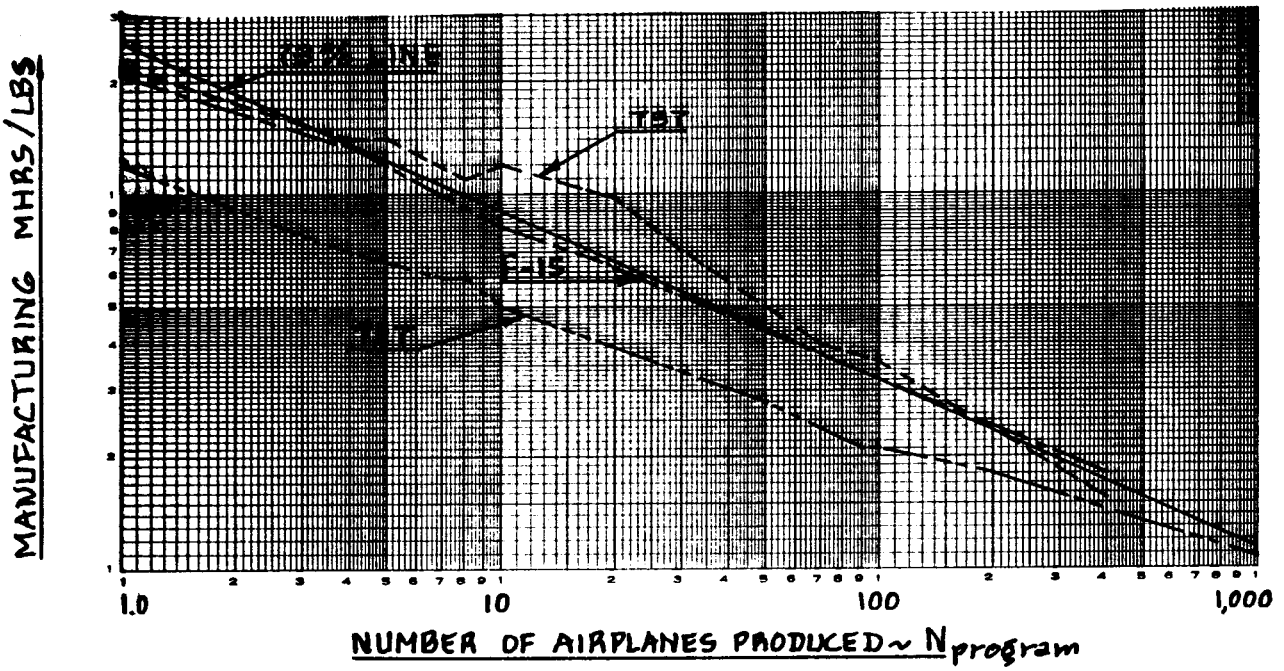

Figure 4.2 Learning Curves for Three Airplane Programs

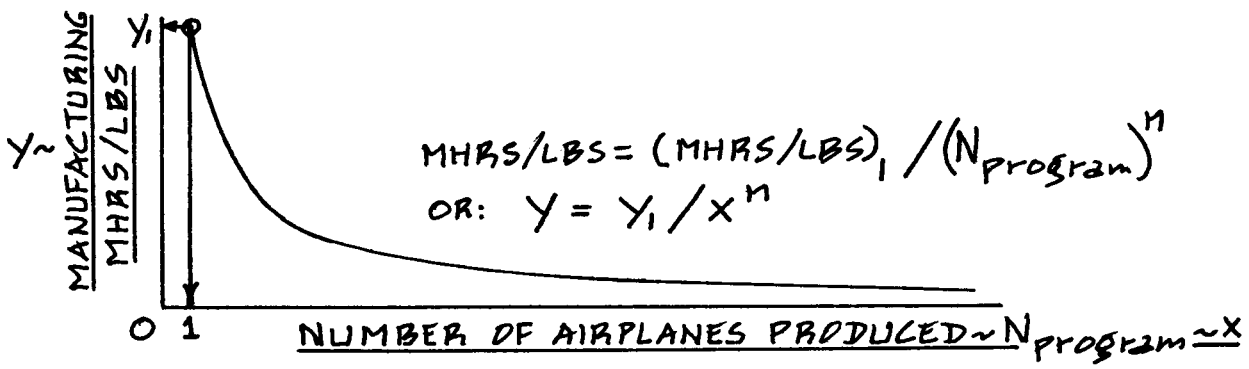

Figure 4.3a Reduction of Manhours with Units Produced

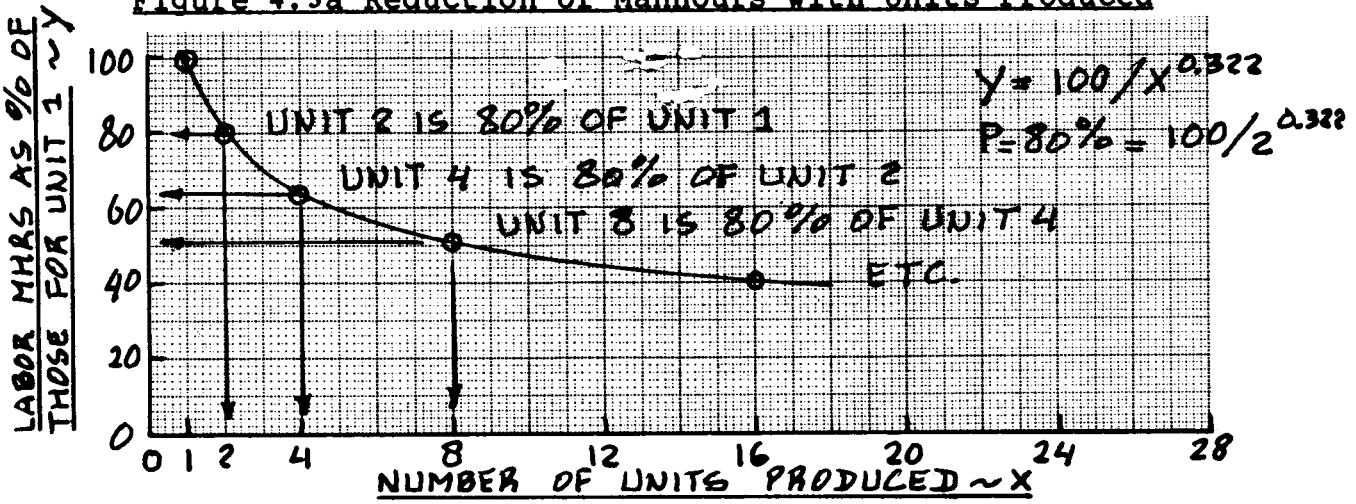

Figure 4.3b Percentage Reduction of Manhours with Units Produced

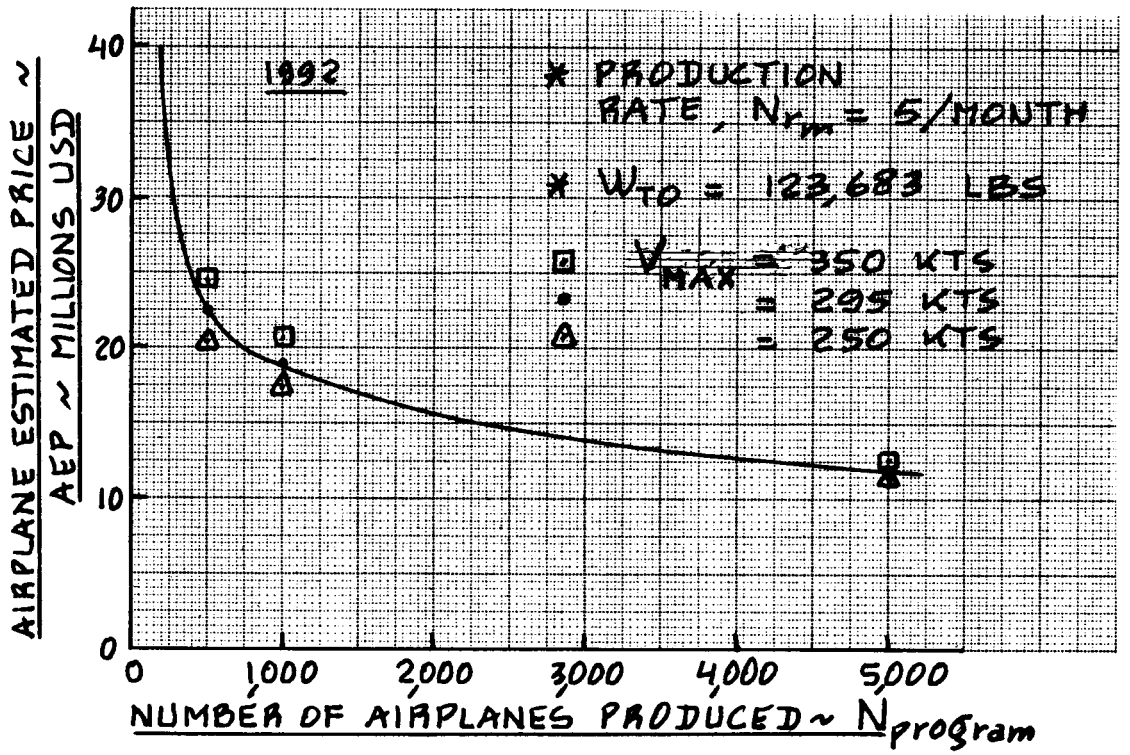

Figure 4.4 Effect of Number of Airplanes Produced and of Cruise Speed on Airplane Estimated Price

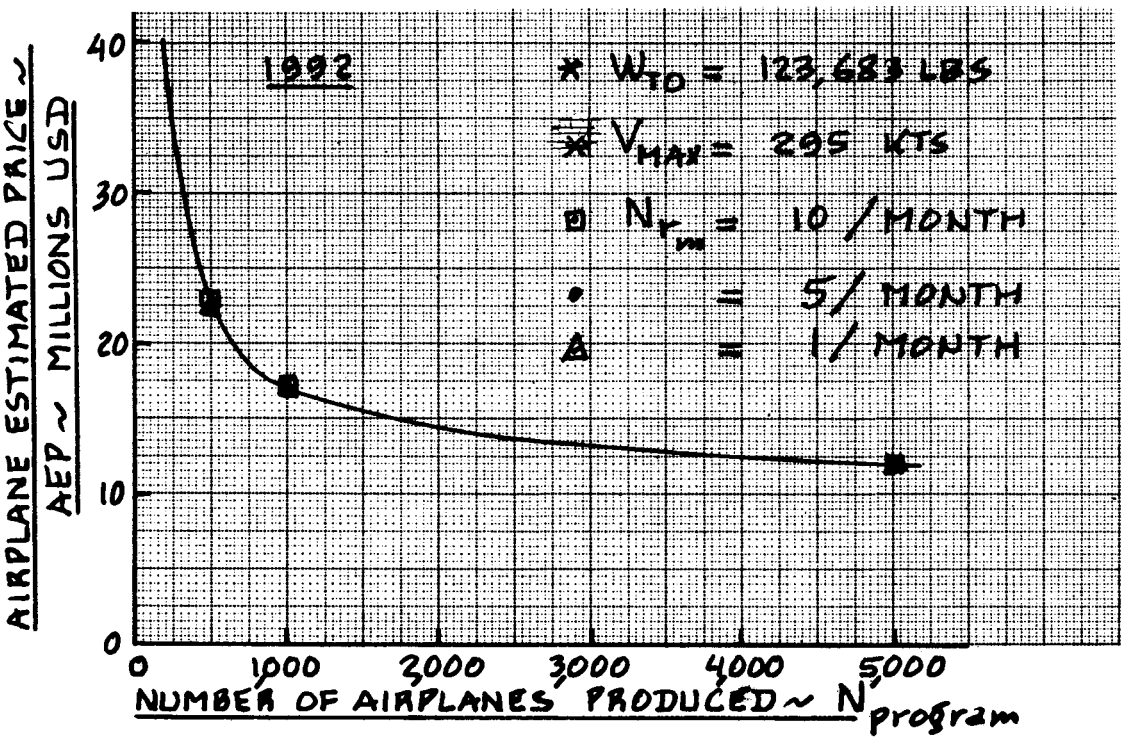

Figure 4.5 Effect of Number of Airplanes Produced and of Production Rate on Airplane Estimated Price

5. METHOD FOR ESTIMATING OPERATING COST OF COMMERCIAL AIRPLANES

The purpose of this chapter is to present a method for estimating the operating cost of commercial airplanes. A commercial airplane is defined as any non-military airplane. The method applies to airliners (all types), corporate airplanes and personal airplanes. A method for estimating the operating cost of military airplanes is presented in Chapter 6.

IMPORTANT ASSUMPTION:

Commercial operators acquire airplanes over many calendar years. As a result, commercial airplane production may vary considerably from year to year. The effect of all this on operating cost is difficult to model. It will therefore be ignored. Instead, the assumption is made that whatever numbers of airplanes are acquired by various operators, are acquired in one particular year and at one particular price.

The methodology presented in this chapter is based on methods and data presented in References 15 - 21. The material in this chapter is organized as follows:

5.1 Method for Estimating the Program Operating Cost of Commercial Airplanes: C_{OPS}

5.2 Method for Estimating the Direct Operating Cost of Commercial Airplanes: DOC

5.3 Method for Estimating the Indirect Operating Cost of Commercial Airplanes: IOC

5.4 Example Application

5.5 Some Important Observations about Commercial Airplane Operating Cost

5.1 METHOD FOR ESTIMATING THE PROGRAM OPERATING COST OF COMMERCIAL AIRPLANES: C_{OPS}

The total (or program) operating cost of commercial airplanes, C_{OPS}, is shown in relationship to other life cycle cost (LCC) sources in Eqn.(2.3) and in Figure 2.3.

The operating cost source is divided into the following two cost categories:

$$C_{OPS} = \sum_{i=1}^{i=n} (C_{ops_{dir}})_i (N_{acq})_i + \sum_{i=1}^{i=n} (C_{ops_{ind}})_i (N_{acq})_i \quad (5.1)$$

where: C_{OPS} is the program operating cost source of Eqn.(2.3). It is expressed in USD.

$(C_{ops_{dir}})_i$ is the program direct operating cost for the i^{th} airplane customer, expressed in USD/airplane.

$(N_{acq})_i$ is the number of airplanes acquired by the i^{th} customer. Table 5.1 shows examples of fleet sizes acquired by various customers.

Note: because commercial loss rates due to accidents are relatively small, the effect of this on the number of active airplanes will be ignored.

$(C_{ops_{ind}})_i$ is the program indirect operating cost for the i^{th} airplane customer, expressed in USD/airplane.

The airplane program direct and indirect operating costs (per operator and per airplane) as defined by Equation (5.1) may be estimated from:

$$(C_{ops_{dir}})_i = (DOC)_i (R_{bl_{ann}})_i (N_{yr})_i \quad (5.2)$$

and:

$$(C_{ops_{ind}})_i = (IOC)_i (R_{bl_{ann}})_i (N_{yr})_i \quad (5.3)$$

where: $(DOC)_i$ is the direct operating cost per nautical mile of the airplane as flown by the i^{th} customer and expressed in USD/nm (per airplane). A method for estimating DOC is presented in Section 5.2.

Table 5.1 Typical Fleet Sizes in 1989

Airline	Boeing					McDonnell Douglas			Lockheed	Airbus
	727	737	747	757	767	DC-9	DC-10	MD80-82	L-1011	A300-310
Domestic										
American	164	24	2		45		63	153		13
Continental	96	97	8			48	15	65		12
Delta	130	74		50	30	36		40	40	
Eastern	116			25		81	2		20	20
Fed.Express	118		21				24			
Northwest	209		40	33		139	20	8		
Pan Am	70		34							31
TWA	70		19		11	48		33	35	
United	145	134	31		19		56			
US Air	44	201			6	74		31		
Foreign										
KLM		16	21				5			10
SAS					5	60	7	31		
British Airways		49	40	35			8		17	
Air France	24	16	35							22
Lufthansa	24	58	25				11			19
Alitalia			12			43		42		16

$(R_{bl_{ann}})_i$ is the total annual block miles flown by the i^{th} customer, expressed in nautical miles (nm) per airplane. This is related to block speed and to annual utilization as shown in Eqn.(5.4).

$(N_{yr})_i$ is the number of years during which the airplane is operated by the i^{th} customer. It must be recognized that airplanes are sold and resold during their operational lives. For the purpose of program cost estimating it is suggested to use:

For transport airplanes: N_{yr} = 20 years

For corporate airplanes: N_{yr} = 20 years

For personal owner airplanes: N_{yr} = 20 - 40 years

$(IOC)_i$ is the indirect operating cost per nautical mile of the airplane as flown by the i^{th} customer and expressed in USD/nm per airplane. A method for estimating IOC is presented in Section 5.3.

The reason for using the nautical mile (as opposed to the statute mile) as the operating cost basis is an arbitrary one. The reader will find that both mile types are used in the reference literature.

The reason for expressing the program cost, C_{OPS}, as a sum over i customers is the fact that direct and indirect operating costs vary considerably from one customer to another. However, there are no reliable methods for predicting what the cost variations among various customers will be. For the reader who wishes to actually calculate C_{OPS} for any given airplane program it is suggested to use 'reasonable averages' for $(C_{ops_{dir}})_i$ and for $(C_{ops_{ind}})_i$ while setting $(N_{acq})_i$ equal to N_m, the total number of airplanes built to production standard. For the remainder of this chapter the subscript i can therefore be omitted without ambiguity.

The total annual block miles, $R_{bl_{ann}}$, (now without subscript i) in Eqns (5.2) and (5.3) can be expressed as:

$$(R_{bl_{ann}}) = (V_{bl})(U_{ann_{bl}}) \qquad (5.4)$$

where: V_{bl} is the block speed in nm/hr. The concept of block speed is illustrated in Figure 5.1. V_{bl} may be calculated with Eqn.(5.5).

$U_{ann_{bl}}$ is the annual utilization in block hours. This depends on airplane type and on routes flown: see the discussion on page 76.

For zero wind, the block speed, V_{bl}, is found from:

$$V_{bl} = (R_{bl})/t_{bl} \qquad (5.5)$$

where: R_{bl} is the block distance measured in nm. It is defined in Figure 5.1. The block distance depends on the routes flown. It is suggested to use the 'great circle' distance between city pairs for R_{bl}. Table 5.2 gives examples of block distances between typical city pairs.

t_{bl} is the block time in hours. Figure 5.1 shows how t_{bl} is defined. It may be found from:

$$t_{bl} = t_{gm} + t_{cl} + t_{cr} + t_{de} \qquad (5.6)$$

where: t_{gm} is the time spent in ground maneuvers, such as pulling away from the gate, taxiing to the active runway, takeoff run, landing ground run and taxiing to the gate at the point of final destination. It is expressed in hours. The ground maneuver time may be estimated from:

$$t_{gm} = 0.51(10)^{-6}(W_{TO}) + 0.125 \qquad (5.7)$$

where: W_{TO} is the takeoff weight of the airplane as found with the methods of Part I, Chapter 2 or, more accurately with those of Part V, Chapters 2 and 4.

Note: Eqn.(5.7) includes an allowance of one minute for the takeoff run.

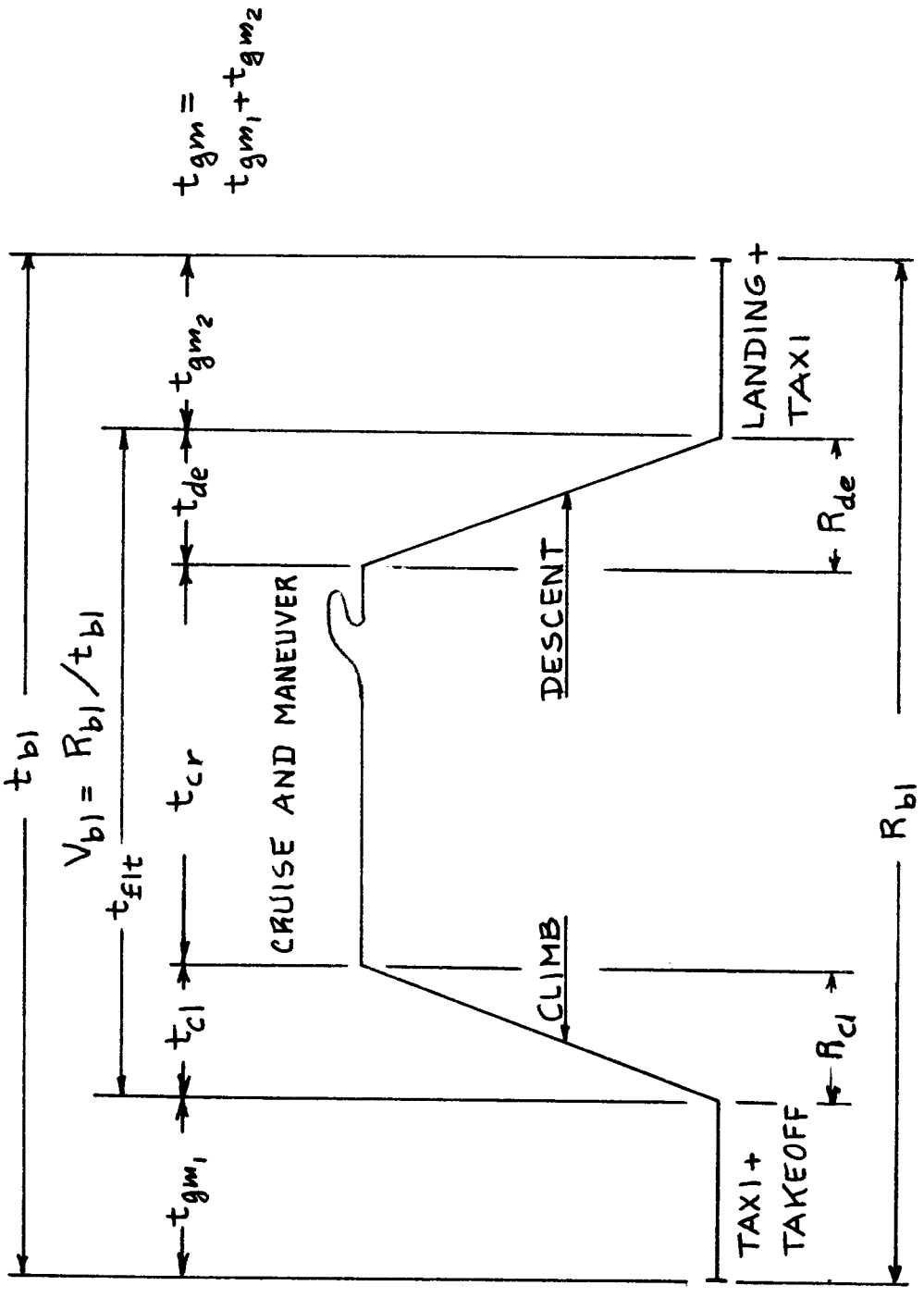

Figure 5.1 Mission Profile Definitions

Table 5.2 Example Block Distances, R_{bl}, Between City Pairs

City-Pairs Under 500 nm		R_{bl} (nm)			R_{bl} (nm)
Detroit	- Chicago	220	Wash. DC*	- Columbus	301
Buffalo	- Wash. DC*	270	Chicago	- Pittsburg	380
Chicago	- Cleveland	274	Reno	- Portland	424
Rochester	- Wash. DC*	283	Omaha	- Denver	430
Chicago	- Des Moines	288	Atlanta	- Pittsburg	487
City Pairs From 500 - 1,000 nm		R_{bl} (nm)			R_{bl} (nm)
Oakland	- Portland	501	Boise	- Denver	572
S.L. City	- S.Francisco	551	Seattle	- S.Francisco	669
Chicago	- Wash. DC**	555	N.Y.***	- Chicago	719
Huntsville	- Wash. DC*	558	Cleveland	- Ft.Lauderd.	972
Las Vegas	- Denver	561	Rochester	- Tampa	960
City Pairs From 1,000 - 1,700 nm		R_{bl} (nm)			R_{bl} (nm)
Denver	- Cleveland	1,066	Chicago	- Seattle	1,522
S.L. City	- Chicago	1,104	Los Ang.	- Chicago	1,538
Chicago	- Boise	1,264	Birmingh.	- Los Ang.	1,589
Memphis	- Los Ang.	1,430	Huntsville	- Los Ang.	1,610
Chicago	- Reno	1,469	S.Francis.	- Chicago	1,644
City Pairs From 1,700 - 2,300 nm		R_{bl} (nm)			R_{bl} (nm)
Los Ang.	- Detroit	1,749	N.Y.***	- Los Ang.	2,190
S.Francis.	- Detroit	1,846	N.Y.***	- S.Francis.	2,284
Los Ang.	- Wash. DC**	2,016			

* National Airport ** Dulles *** JFK

Chicago as listed here is O'Hare.

Data based on United Airlines Information, Ref.20.

t_{cl} is the time required to climb and to accelerate to the cruise speed, expressed in hours. A rapid method for predicting t_{cl} is presented in Part VII, pages 127-128.

t_{cr} is the time spent in cruise, expressed in hrs. It is suggested to use for:

Domestic operations:

$$t_{cr} = (1.06R_{bl} - R_{cl} - R_{de} + R_{man})/V_{cr} \quad (5.8a)$$

International operations:

$$t_{cr} = (1.01R_{bl} - R_{cl} - R_{de} + R_{man})/V_{cr} \quad (5.8b)$$

where: the factors 1.06 and 1.01 account for the fact that great circle distances cannot usually be flown for a variety of reasons.

R_{cl} is the distance to climb and to accelerate to cruise speed, in nm. It can be estimated from:

$$R_{cl} = (V_{cl})(t_{cl}) \quad (5.9)$$

where: V_{cl} is the projected horizontal speed of the airplane during the climb, in kts. For shallow climbs this may be assumed to be the same as the true airspeed in the climb. This speed is a by-product of the climb rate calculations for finding t_{cl}.

The reader is referred to pages 124-128 in Part VII.

R_{de} is the distance covered during the descent, in nm. It can be estimated from:

$$R_{de} = (V_{de})(t_{de}) \quad (5.10)$$

where: V_{de} is the projected horizontal speed of the airplane during the descent, in kts.

Note: For shallow descents this is roughly the same as the true airspeed during the

descent. This speed is a by-product of the descent rate calculations of pages 159-161 in Part VII.

t_{de} as used in Eqns (5.6) and (5.10), is the time taken to descend. It may be computed with the method of p.159-161 in Part VII.

R_{man} is the distance covered while maneuvering due to ATC (air traffic control) constraints (in nm), with:

$$R_{man} = (V_{man})(t_{man}) \qquad (5.11)$$

where: V_{man} is the speed while maneuvering as required by ATC constraints. It is suggested to use:

below 10,000 ft: $V_{man} = 250$ kts

above 10,000 ft: $V_{man} = V_{cr}$ (kts)

t_{man} is the time spent in ATC maneuvering. It can be found from:

$$t_{man} = 0.25(10)^{-6}W_{TO} + 0.0625 \qquad (5.12)$$

V_{cr} is the airplane cruise speed in kts. Different operators cruise airplanes at different speeds. For preliminary costing it is recommended to use:

$$V_{cr} = V_C \qquad (5.13)$$

where: V_C is the design cruise speed of an airplane in <u>nautical miles</u> per hour (kts).

<u>NOTE:</u> V_C is normally a 'given' in the mission specification of an airplane. Examples are found on pages 50 and 55 in Part I. The reader should ascertain that V_C of Eqn.(5.13) is consistent with the V_C defined in his V-n diagram calculations of Ch.4, Part V. However, note that V_C in the V-n diagram is expressed in KEAS and not in kts.

The annual utilization in block hours, $U_{ann_{bl}}$, as defined in Equation (5.4) depends on the type of airplane and on the routes flown. The weekly magazine Aviation Week and Space Technology publishes utilization data on a quarterly basis for passenger transports. The monthly magazine Business and Commercial Aviation publishes data on the utilization of other commercial airplanes. The reader will find representative utilization data for several types of airplanes in Table 5.3.

Lacking more detailed information it suggested to determine $U_{ann_{bl}}$ as follows:

<u>For passenger transports:</u>

$$U_{ann_{bl}} = (10^3)[3.4546(t_{bl}) + 2.994 + \quad (5.14a)$$

$$- \{12.289(t_{bl})^2 - 5.6626(t_{bl}) + 8.964\}^{1/2}]$$

<u>For cargo transports:</u>

$$U_{ann_{bl}} = (10^3)[6.053(t_{bl}) + 5.70 + \quad (5.14b)$$

$$- \{37.771(t_{bl})^2 + 13.494(t_{bl}) + 32.490\}^{1/2}]$$

where: t_{bl} is determined from Equation (5.6).

Eqns (5.14) are shown graphically in Figure 5.2.

<u>For All Other Types of Airplanes:</u> see Table 5.3.

Observe that annual airplane utilization so far has been expressed in terms of block hours. It is sometimes desirable (for a variety of reasons) to express the annual utilization in terms of flight hours: $U_{ann_{flt}}$. This can be done as follows:

$$U_{ann_{flt}} = (U_{ann_{bl}})(V_{bl})/(V_{flt}) \quad (5.15)$$

where: V_{flt} is the average flight speed at which the airplane is operated, in kts. It is noted that the average flight speed is always greater than the block speed. In turn, the average

Table 5.3 Utilization of Commercial Airplanes

Operator	1988 Airplane Utilization of Narrow-Body Jets in Block Hours per Day				
	727-200	737	757	MD-80	DC-9
American	7.8	9.2	NA	8.8	NA
United	9.2	7.9	NA	NA	NA
Delta	8.9	7.9	8.4	8.0	7.3
US Air/Piedmont	8.2	7.6	NA	NA	7.9
TWA	6.6	NA	NA	8.7	6.0

	1988 Airplane Utilization of Wide-Body Jets in Block Hours per Day				
	747	767	A300	DC-10	L-1011
American	10.2	11.1	NA	9.0	NA
Pan American	11.0	NA	8.4	NA	NA
United	12.0	10.8	NA	10.0	10.2
TWA	11.0	10.8	NA	NA	10.0
Continental	8.0	NA	7.0	10.0	NA

The following data are representative annual-utilization numbers in block hours for various types of airplanes:

Type of Operation:	Long Haul Block Time: $t_{bl} > 5$	Medium Haul Block Time: $2 < t_{bl} < 5$	Short Haul Block Time: $0.5 < t_{bl} < 2$
Airplane Type			
Jet Transports	3,600-4,400	2,100-3,300	1,000-3,000
Regional Transports	NA	2,000-3,000	1,000-2,500
Corporate Transp.	500-1,500	400-1,200	300-1,000
Personal Transp.	NA	200-800	200-800
Agricultural	NA	NA	500-1,000
Trainers	NA	NA	1,000-2,500

NA = Not Applicable

Data Sources: Various issues of 'Aviation Week and Space Technology' and 'Business and Commercial Aviation'.

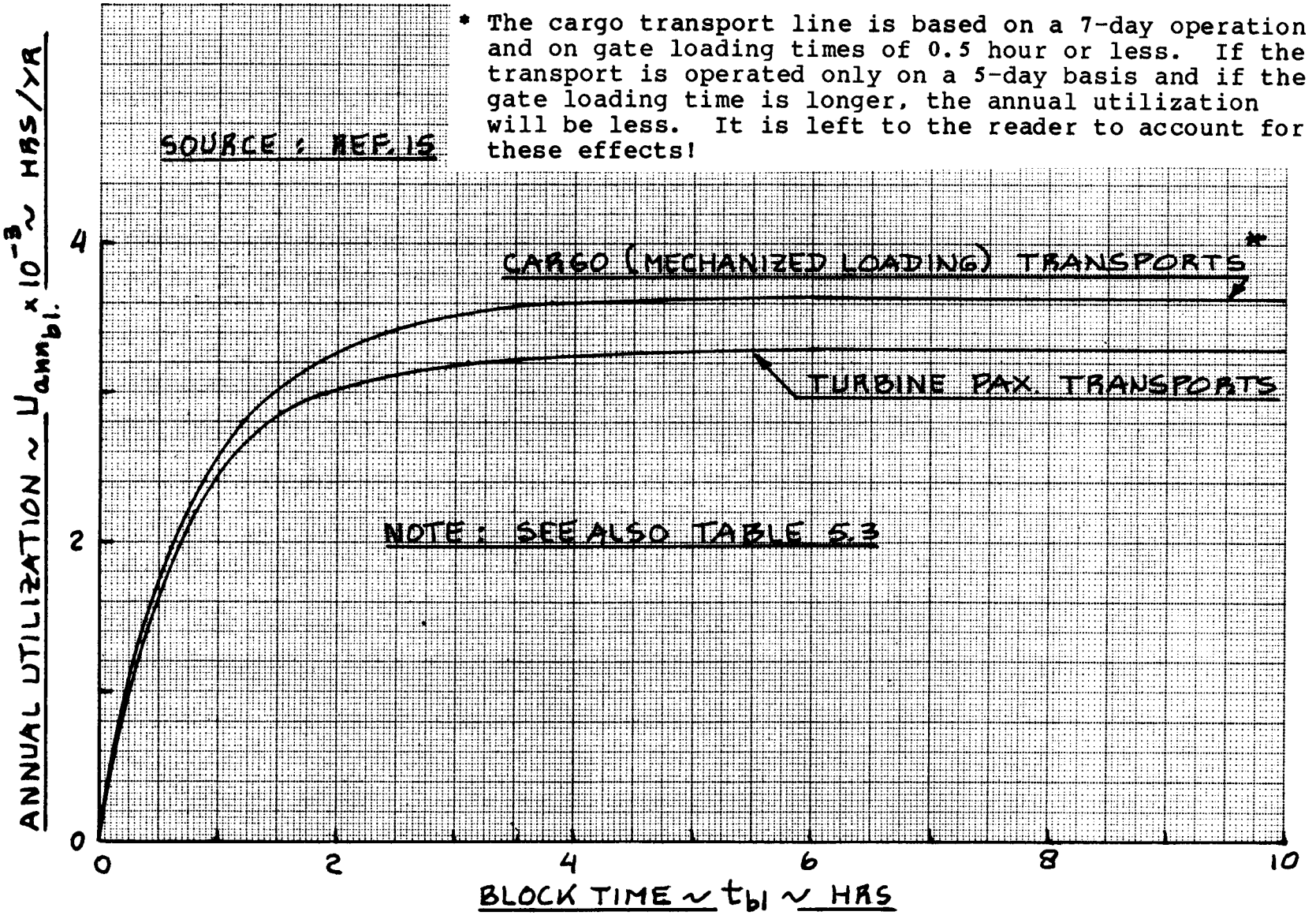

Figure 5.2 Effect of Block Time on Annual Utilization

flight speed is always less than the design cruise speed. This leads to the inequality:

$$V_{cr} > V_{fl} > V_{bl} \quad (5.16)$$

The average flight speed may be found from:

$$V_{flt} = V_{cr}(t_{cr}/t_{flt}) \quad (5.17)$$

where: t_{cr} is found from Equations (5.8)

t_{flt} is the average flight time which can be computed from:

$$t_{flt} = t_{cl} + t_{cr} + t_{de} \quad (5.18)$$

where: t_{cl} and t_{de} are defined on pages 74 and 75, respectively.

Note: it is observed that t_{man} of Eqn.(5.11) is already included in the definition of t_{cr} via the term R_{man} in Eqn.(5.8)!

Remember, that C_{OPS} in Equation (5.1) represents one of four program cost sources of Life Cycle Cost (LCC) as expressed by Equation (2.3). This cost source as such is normally NOT of any particular interest to a commercial airplane operator. However, the following cost categories are VERY IMPORTANT to typical airplane operators:

1a) Direct operating cost per nautical mile: (DOC)

and:

1b) Direct operating cost per block hour: $\{(DOC)(V_{bl})\}$

2a) Indirect operating cost per nautical mile: (IOC)

and:

2b) Indirect operating cost per block hour: $\{(IOC)(V_{bl})\}$

Sections 5.2 and 5.3 present methods for estimating DOC and IOC respectively. An example application is provided in Section 5.4. Finally, a number of important observations regarding DOC and IOC are made in Section 5.5.

5.2 METHOD FOR ESTIMATING THE DIRECT OPERATING COST OF COMMERCIAL AIRPLANES: DOC

The purpose of this section is to present a method for estimating the direct operating cost (DOC) in USD/nm incurred while operating commercial airplanes.

The method which is presented here is an adaptation of the so-called ATA-method of References 15 and 16 with various inputs from References 17-21. The ATA-method, as such, applies only to passenger and cargo transport airplanes. With the adaptation given here the method can be applied to any type of commercial airplane.

Table 5.4 presents an overview of cost components and cost elements which contribute to direct operating cost per nautical mile: DOC, which is broken down as:

$$DOC = DOC_{flt} + DOC_{maint} + DOC_{depr} + DOC_{lnr} + DOC_{fin} \quad (5.19)$$

where: DOC_{flt} is the direct operating cost of flying in USD/nm: see Sub-section 5.2.1

DOC_{maint} is the direct operating cost of maintenance in USD/nm: see Sub-section 5.2.2

DOC_{depr} is the direct operating cost of depreciation in USD/nm: see Sub-section 5.2.3

DOC_{lnr} is the direct operating cost of landing fees, navigation fees and registry taxes in USD/nm: see Sub-section 5.2.4

DOC_{fin} is the direct operating cost of financing in USD/nm: see Sub-section 5.2.5

NOTE: The right hand side of Table 5.4 indicates which DOC elements apply to various airplane types.

5.2.1 Direct Operating Cost of Flying: DOC_{flt}

The direct operating cost of flying (in USD/nm) is broken down into the following flying cost elements:

$$DOC_{flt} = C_{crew} + C_{pol} + C_{ins} \quad (5.20)$$

Table 5.4 Overview of Direct Operating Cost (DOC)

DIRECT OPERATING COST ~ DOC ~ USD/nm		AIRLINE	CORPORATE	PERSONAL
DOC COMPONENTS	DOC ELEMENTS			
FLYING ~ DOC_{flt} (5.20)	CREW ~ C_{crew} (5.21)	✓	✓	NO
	FUEL+ ~ C_{pol} (5.25)	✓	✓	✓
	INSURANCE ~ C_{ins} (5.31)	✓	✓	✓
MAINTENANCE ~ DOC_{maint} (5.33)	AIRFRAME LABOR ~ $C_{lab/ap}$ (5.34)	✓	✓	✓
	ENGINE LABOR ~ $C_{lab/eng}$ (5.36)	✓	✓	✓
	AIRFRAME MATERIALS ~ $C_{mat/ap}$ (5.37)	✓	✓	✓
	ENGINE MATERIALS ~ $C_{mat/eng}$ (5.38)	✓	✓	✓
	APPLIED MAINTENANCE BURDEN ~ C_{amb} (5.39)	✓	✓	NO
DEPRECIATION ~ DOC_{depr} (5.40)	AIRFRAME ~ C_{dap} (5.41)	✓	✓	✓
	ENGINE(S) ~ C_{deng} (5.42)	✓	✓	✓
	PROP(S) ~ C_{dprp} (5.43)	✓	✓	✓
	AVIONICS ~ C_{dav} (5.44)	✓	✓	✓
	AIRFRAME SPARE PARTS ~ C_{dapsp} (5.45)	✓	✓	NO
	ENGINE SPARE PARTS ~ C_{dengsp} (5.46)	✓	✓	NO
LANDING & NAVIG. FEES, REGISTRY TAXES ~ DOC_{lnr} (5.47)	LANDING FEES ~ C_{lf} (5.48)	✓	✓	NO
	NAVIGATION FEES ~ C_{nf} (5.52)	✓	✓	NO
	REGISTRY TAXES ~ C_{rt} (5.53)	✓	✓	✓
FINANCE ~ DOC_{fin} (5.55)		✓	✓	✓

where: C_{crew} is the crew cost in USD/nm

C_{pol} is the fuel and oil (pol means: petroleum, oil and lubricants) cost in USD/nm

C_{ins} is the airframe insurance cost in USD/nm

Methods for estimating these cost elements are presented in sub-sub-sections 5.2.1.1 through 5.2.1.3.

5.2.1.1 Crew cost per nautical mile: C_{crew}

The crew cost per nautical mile, C_{crew}, can be found from:

$$C_{crew} = \sum_{j=1}^{j=4} \left[(n_{c_j}) \{ (1 + K_j)/V_{bl} \} (SAL_j/AH_j) + (TEF_j/V_{bl}) \right] \quad (5.21)$$

where: For transport airplanes:

n_{c_j} is the number of crew members of each type, j.

j indicates the type of crew member. The following distinctions are normally made:

n_{c_1} stands for captain.

n_{c_2} stands for co-pilot.

n_{c_3} stands for flight engineer.

Note: the cost of the cabin crew (flight attendants) is accounted for in the indirect operating cost, see Section 5.3.

The number of crew members which must be carried depends on government regulations (FARs), company rules and union rules. Lacking precise information the following numbers are suggested:

n_{c_1} = 1 for scheduled block times < 10 hours
= 2 for scheduled block times > 10 hours

n_{c_2} = as for n_{c_1}

n_{c_3} = 0 for airplanes with a 2-man cockpit

= as for n_{c_1} for airplanes with a 3-man cockpit

For personal owner type airplanes:

It is common NOT to count the cost of the pilot, so that:

n_{c_j} = 0 and j=1 only.

For agricultural airplanes:

n_{c_j} = 1 and j=1 only.

K_j is a factor which accounts for such items as: vacation pay, cost of training, crew premium, crew insurance, and payroll tax. This factor varies from one operator to another. Lacking more detailed data on operator work rules and benefits, it is suggested to use: K_j = 0.26.

V_{bl} is the airplane block speed in nautical miles per hour. The block speed may be found from:

$$V_{bl} = R_{bl}/t_{bl} \qquad (5.22)$$

where: R_{bl} is the block distance in nautical miles. It is defined in Figure 5.1.

t_{bl} is the block time in hours: see Fig.5.1 and Equation (5.6).

SAL_j is the annual salary paid to a crew member of type j. Crew member salaries depend on the following factors:

*equipment flown: salaries tend to increase with airplane weight and with airplane speed
*seniority
*union and company rules

References 15 and 16 contain formulas which relate crew salaries to airplane weight and speed. These formulas applied reasonably well in the sixties because the airline industry was heavily regulated by the CAB:

Civil Aeronautics Board. The author believes that these salary relations can no longer be used. Table 5.5 contains recent data on crew salary ranges. The reader must decide which salaries apply to his airplane.

To estimate crew salaries for future years it is suggested to use:

$$SAL_{\text{then year}} = \qquad (5.23)$$

$$= SAL_{1989}\{(CEF_{\text{then year}})/(CEF_{1989})\}$$

where: the CEF values are found from Fig.2.7.

AH_j is the number of flight hours per year for a crew member of type j. Lacking actual data, the following numbers are suggested as applicable to all flight crew members:

<u>For domestic operations:</u>

AH_j = 800 hrs for jets
= 900 hrs for props

<u>For international operations:</u>

AH_j = 750 hrs for jets
= 850 hrs for props

TEF_j is the travel expense factor associated with each type of crew member. Since flight crews normally stay in the same hotel it is not necessary to vary the TEF from one crew member to another. It is suggested to use for calendar year 1990:

<u>Domestic routes:</u> TEF = USD 7.0/bl.hr

<u>International routes:</u> TEF = USD 11.0/bl.hr

For future years use:

$$TEF_{\text{then year}} = \qquad (5.24)$$

$$= TEF_{1990}(CEF_{\text{then year}})/(CEF_{1990})$$

where: the CEF values are found from Fig.2.7.

Table 5.5 Salaries and Wages Paid by Operators in 1989

Cockpit Crew:	Salary Range in USD/year		
Airplane Type:	Captain	First Officer	Flight Engineer
Jet Transport BAC 111 - B747	35,000- 144,000	24,000- 67,000	20,000- 62,000
Corp. Jet Transp. Learjet M23 - Gulfstr.III	30,000- 72,000	22,000- 52,000	NA
Corp. Turboprops MU-2 - King Air 300	25,000- 52,000	20,000- 32,000	NA
Regional Turboprops DHC-6 - F-27	20,000- 52,000	11,000- 21,000	NA
Corporate Recips Single - Twin	20,000- 47,000	19,000- 26,000	NA

Cabin Crew:	Salary Range in USD/year	
	Purser	Cabin Attendant
All airplane types	25,000-47,000	19,000-32,000

Maintenance Personnel:	Hourly Wage Range, USD/hr	
	Fixed Base Operators (FBO)	Airlines
Avionics specialist	6.60 - 15.60	8.00 - 20.60
Dispatcher	5.00 - 10.40	7.00 - 15.50
Inspector	5.00 - 16.60	10.00 - 22.60
Line Personnel	3.35 - 12.80	5.00 - 10.30
Mechanic with A/P	5.00 - 18.40	10.00 - 22.60
Mechanic without A/P	5.00 - 11.30	8.00 - 15.50
Stock Clerk	3.35 - 7.20	5.00 - 10.30

NOTES: 1. For years other than 1989 use:

$$(\text{SAL or Wage})_{\text{then year}} =$$

$$= (\text{SAL or Wage})_{1989}\{(CEF_{\text{then year}})/(CEF_{1989})\}$$

where: the CEF data are obtained from Fig.2.7.

2. Salary and wage data do NOT include overhead!
3. Sources: Professional Pilot, Discussions with industry people and CEF data, Fig.2.7.
4. NA = Not Applicable

5.2.1.2 Fuel and oil cost per nautical mile: C_{pol}

The fuel and oil cost per nautical mile, C_{pol}, can be estimated from:

$$C_{pol} = (W_{F_{bl}}/R_{bl})(FP/FD) + (W_{ol_{bl}}/R_{bl})(OLP/OD) \quad (5.25)$$

where: $W_{F_{bl}}$ is the block fuel used in lbs. This amount of fuel is the same as the mission fuel used, $W_{F_{used}}$:

$$W_{F_{bl}} = W_{F_{used}} \quad (5.26)$$

A preliminary method for computing $W_{F_{used}}$ is presented as Eqn.(2.14) of page 16, Part I. More accurate methods to compute $W_{F_{used}}$ are given in Sections 5.4 and 5.5 of Part VII.

NOTE: Reference 20 shows that airline experience indicates that the mission fuel consumption of an airplane tends to increase with calendar time for the following reasons:

* engine deterioration
* airframe surface deterioration (seals, finish)

If the reader wishes to account for this, 0.5 percent increase in fuel consumption per year of service seems to be the industry average.

R_{bl} is the block distance in nautical miles as defined in Figure 5.1.

FP is the price of fuel in USD/gallon

Figure 5.3 shows how fuel prices have varied with calendar time. There is no accurate way to predict how fuel prices will vary in the future. The reader is encouraged to call a local fixed base operator (FBO) to determine actual fuel prices.

NOTE: in this text 'gallon' means 'US gallon'!

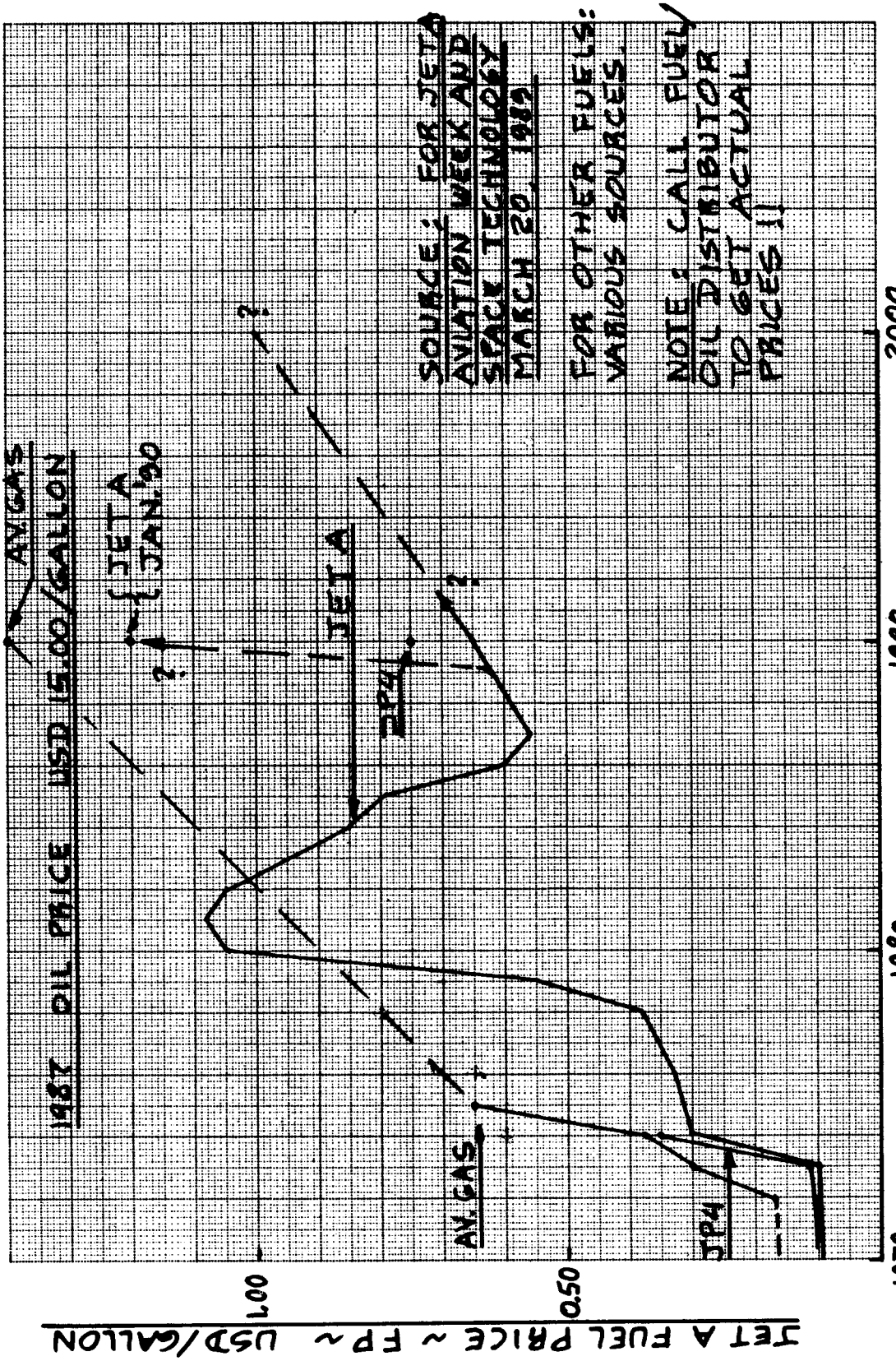

Figure 5.3 Variation of Fuel Prices with Calendar Year

FD is the fuel density in lbs/gallon. The following values are suggested:

Aviation Gasoline:

grades 100/130: FD = 6.0 lbs/gallon
grades 108/135: FD = 5.9 lbs/gallon
grades 115/145: FD = 5.8 lbs/gallon

Aviation Petroleum:

Kerosene:	FD = 6.7 lbs/gallon
JP-1:	FD = 6.65 lbs/gallon
JP-3:	FD = 6.45 lbs/gallon
JP-4:	FD = 6.55 lbs/gallon
JP-5:	FD = 6.82 lbs/gallon
Jet A	FD = 6.74 lbs/gallon

$W_{ol_{bl}}$ is the weight of oil and lubricants used, in lbs. It depends strongly on the type of powerplants and systems in need of lubricants. Manufacturers of engines and systems normally specify the hourly consumption of oil and lubricants. Lacking such specific information, it is suggested to use:

for reciprocating engines:

$$W_{ol_{bl}} = (W_{F_{used}})/70 \qquad (5.27)$$

for turbine engines:

$$W_{ol_{bl}} = (0.70)(N_e)(t_{bl}) \qquad (5.28)$$

where: N_e is the number of engines

t_{bl} is the block time in hours as found from:

$$t_{bl} = R_{bl}/V_{bl} \qquad (5.29)$$

Note that Eqn.(5.29) is a modification of Eqn.(5.5).

Eqns (5.27) and (5.28) may be assumed to account for consumption of oil and lubricants together.

OD is the oil density in lbs/gallon. The following values are suggested:

Oil (MIL-6082B, grade 1100): OD = 7.40 lbs/gallon
Synthetic oil (MIL-L-7808-1): OD = 7.74 lbs/gallon

OLP is the price of oil and lubricants in USD/gallon.

Figure 5.3 also shows the price of oil. Just like is the case for fuel prices, there is no accurate way to predict oil prices in the future.

An alternate method to account for the direct operating cost of oil and lubricants is to assume that it is 5 percent of the direct operating cost of fuel. This leads to:

$$C_{pol} = 1.05(W_{F_{bl}}/R_{bl})(FP/FD) \qquad (5.30)$$

5.2.1.3 Cost of airframe insurance per nautical mile: C_{ins}

Airplane operators carry airframe insurance for the following reasons:

1. ground and flight risk of experiencing airframe damage or total loss
2. passenger liability in case of injury or death
3. third party liability in case of injury or death
4. cargo damage risk

Most airplane operators will want to carry airframe damage insurance (to cover item 1) to an amount equal to the replacement value of the airplane. Although some operators will prefer to 'carry' a certain amount of the insurance themselves, there is a cost associated with that as well: a reserve will have to be created and the interest cost on the reserve can be thought of as part of the cost of insurance.

NOTE WELL: In references 15-20 the convention has been adopted to consider item 1 above as part of the DOC while items 2-4 are considered as part of the IOC (Section 5.3). This convention is followed here also!

Insurance rates for hull damage or loss depends on the so-called hull loss rate. Figure 5.4 gives historic insight into the hull losses of jet transports. Note that the annual hull loss rate on the average is about 2.0 per 1,000,000 departures.

For details on insurance rates the reader should consult an aviation underwriter. Lacking such precise information it is suggested to use:

$$C_{ins} = (f_{ins_{hull}})(AMP)/\{(U_{ann_{bl}})(V_{bl})\} \qquad (5.31)$$

where: $f_{ins_{hull}}$ is the annual hull insurance rate in USD per USD airplane price, per airplane and per year. Typical values for this hull insurance rate range from:

$$f_{ins_{hull}} = 0.005 \text{ to } 0.030 \text{ USD/USD/airplane/year}$$

AMP is the airplane market price in USD. AMP may be estimated rapidly with the method given in Appendix A. A more detailed method for computing AMP is presented in Sub-section 4.6.3.

$U_{ann_{bl}}$ is the annual block hour utilization as determined from the discussion on p.76.

V_{bl} is the block speed in nm/hr (kts) as defined by Eqn.(5.5).

An alternate method to account for hull insurance is to set:

$$C_{ins} = 0.02(DOC) \qquad (5.32)$$

where: DOC is found from Eqn.(5.19).

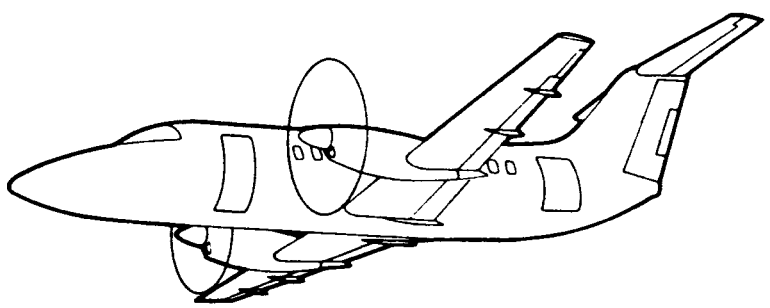

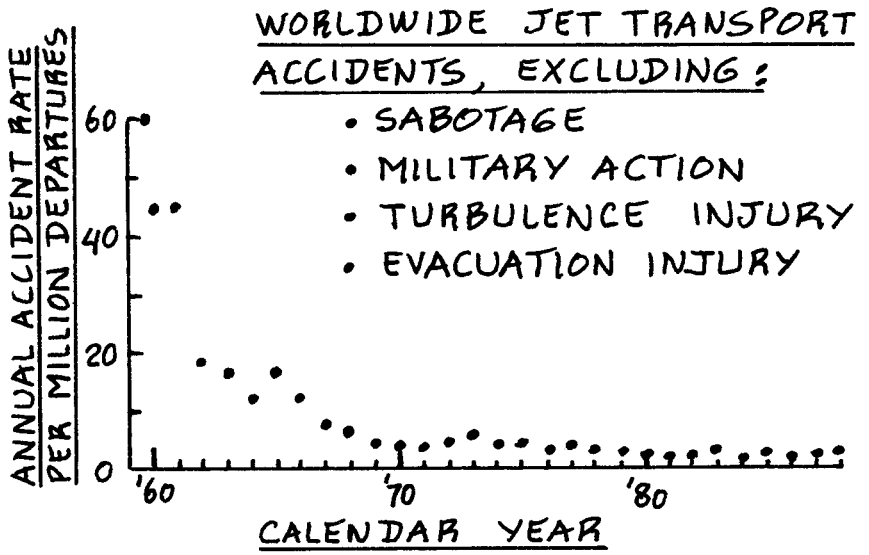

SOURCE: AVIATION WEEK AND SPACE TECHNOLOGY JULY 24, 1989

WORLDWIDE HULL LOSS RATES 1959-1988

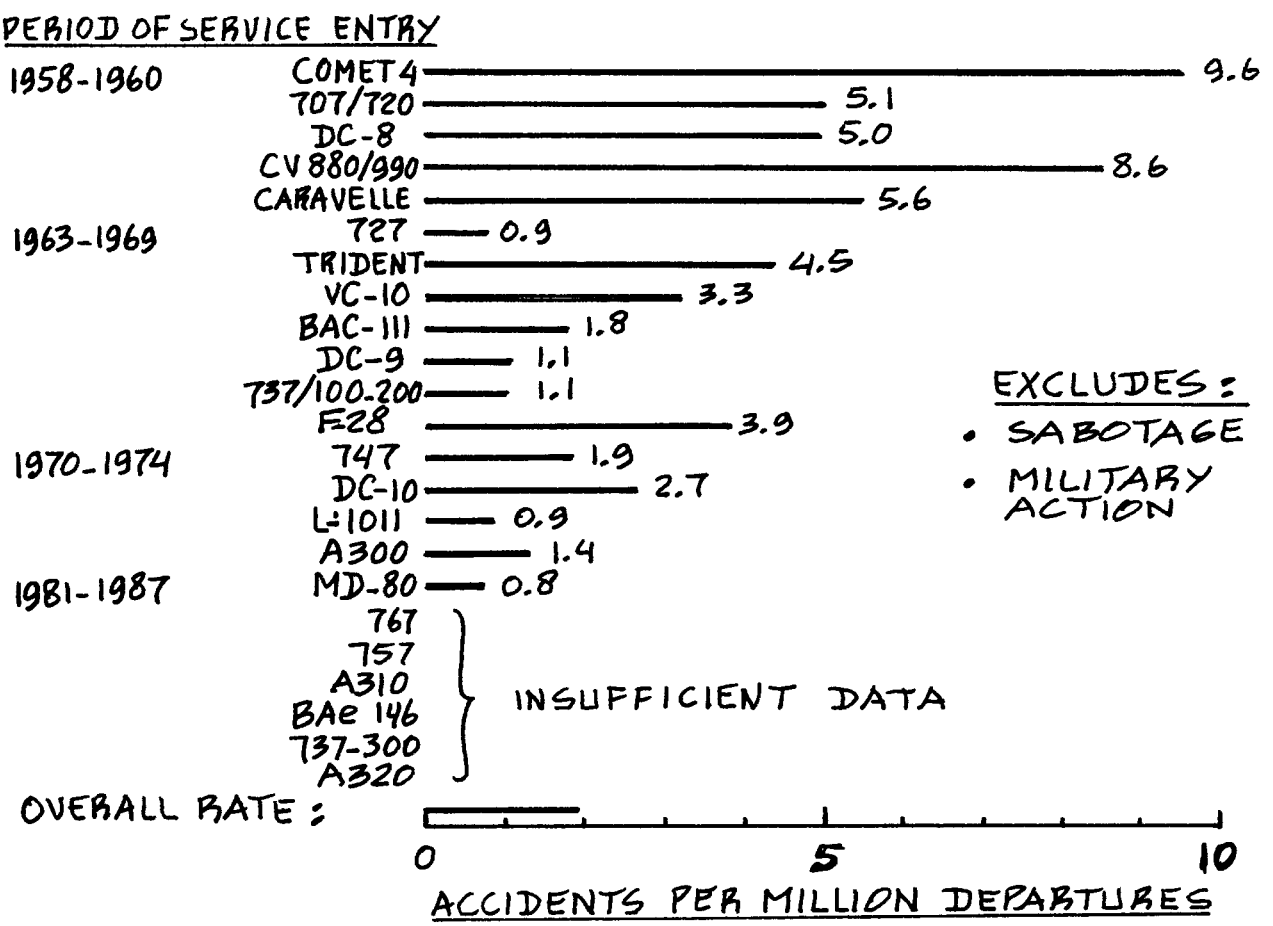

Figure 5.4 Worldwide Accident and Hull Loss Rates

5.2.2 Direct Operating Cost of Maintenance: DOC_{maint}

The direct operating cost of maintenance is broken down as follows:

$$DOC_{maint} = C_{lab/ap} + C_{lab/eng} + C_{mat/ap} + C_{mat/eng} + C_{amb} \quad (5.33)$$

where: $C_{lab/ap}$ is the labor cost of airframe and systems (other than the engines) maintenance in USD/nm. See: Eqn.(5.34).

$C_{lab/eng}$ is the labor cost of engine(s) maintenance in USD/nm. See: Eqn.(5.36).

$C_{mat/ap}$ is the cost of maintenance materials for the airframe and systems (other than the engines) in USD/nm. See: Eqn.(5.37).

$C_{mat/eng}$ is the cost of maintenance materials for the engines in USD/nm. See Eqn.(5.38).

C_{amb} is the applied maintenance burden in USD/nm. See Eqn.(5.39).

The maintenance labor cost per nautical mile of airframe and systems, $C_{lab/ap}$, can be estimated from:

$$C_{lab/ap} = 1.03(MHR_{map_{bl}})(R_{l_{ap}})/(V_{bl}) \quad (5.34)$$

where: 1.03 is called a non-revenue factor. It accounts for extra maintenance costs incurred due to flight delays.

$MHR_{map_{bl}}$ is the number of <u>airframe and systems</u> maintenance man hours needed per block hour. This is related to the number of maintenance man hours per flight hour, $MHR_{map_{flt}}$ as follows:

$$MHR_{map_{bl}} = (MHR_{map_{flt}})(t_{flt}/t_{bl}) \quad (5.35)$$

where: t_{bl} is found from Eqn.(5.6)

t_{flt} is found from Eqn.(5.18)

It is desirable to use actual man hour data where possible. Lacking such information the data of Table 5.6 (given per flight hour) and/or Fig. 5.5 (given per block hour) may be used as a guide.

NOTE WELL: Aviation Week and Space Technology publishes data on airframe and systems maintenance on a regular basis. The reader should check the latest issues for updated information. Ref.20 contains detailed maintenance data for United Airlines airplanes for the year 1975.

$R_{l_{ap}}$ is the airplane maintenance labor rate per manhour in USD/hr. It is desirable to use actual labor rate data. Lacking such information, Table 5.5 may be used: use the 'mechanic with A/P' data.

V_{bl} is the block speed as found from Eqn.(5.5).

The maintenance labor cost per nautical mile of engines, $C_{lab/eng}$ can be estimated from:

$$C_{lab/eng} = 1.03(1.3)(N_e)(MHR_{meng_{bl}})(R_{l_{eng}})/(V_{bl}) \quad (5.36)$$

where: the factor 1.3 accounts for cycle-dependent labor as opposed to cycle-independent labor.

N_e is the number of engines per airplane.

$MHR_{meng_{bl}}$ is the number of engine maintenance hours needed per block hour per engine. Whenever possible, it is desirable to use actual manhour data. Lacking such information the data of Table 5.6 and/or Figures 5.6 and 5.7 may be used.

$R_{l_{eng}}$ is the engine maintenance labor rate per man hour in USD/hr. It may be found from Table 5.5: use the 'mechanic with A/P' data.

The cost of maintenance materials for airframe and systems (other than the engines) per nautical mile may be estimated from:

$$C_{mat/ap} = 1.03(C_{mat/apblhr})/V_{bl} \quad (5.37)$$

where: $C_{mat/apblhr}$ is the airframe and systems maintenance materials cost per airplane block

Table 5.6 Maintenance Manhour Data for Commercial Airplanes

Airplane Type	Annual Utilization in flight hours, $U_{ann_{flt}}$	Maintenance Manhours* per flight hour, MHR_{flthr}	Data from year
Cessna 150	250	0.3	1974
Cessna Skywagon	250	0.5	1974
Beech Kingair 90	350	1.0	1974
Cessna Citation I	400	3.0	1974
McDD DC-9-30	2,900	6.4	1973
B-707-300	3,196	8.4	1973
B-727-100	2,670	7.9	1973
B-727-200	2,800	6.5	1973
B-737-200	2,200	6.6	1973
B-747-100	3,525	14.5	1973
L-1011	1,870	14.1	1974
McDD DC-10-10	2,450	10.9	1973

Data Source: Nicolai, Ref.14

* sum of airframe (+ systems) and engine maintenance hrs:

$$MHR_{flthr} = MHR_{map_{flt}} + MHR_{meng_{flt}}$$

For additional data, see Ref.20 (1976). The distribution between airframe (+ systems) and engine maintenance manhours varies considerably with airplane and engine type, and in particular with engine 'maturity'.

Engine maintenance manhours have been reported anywhere from 10 to 50 percent of the total maintenance manhours per flight hour. For modern jet transports with highly mature engines, the trend is for the engine maintenance manhours to constitute about 10 percent of the total maintenance manhours per flight hour.

Lacking the specific information given in Ref.20 it is suggested to split the total maintenance manhours per flight hour evenly between the airframe (+ systems) and the engine(s).

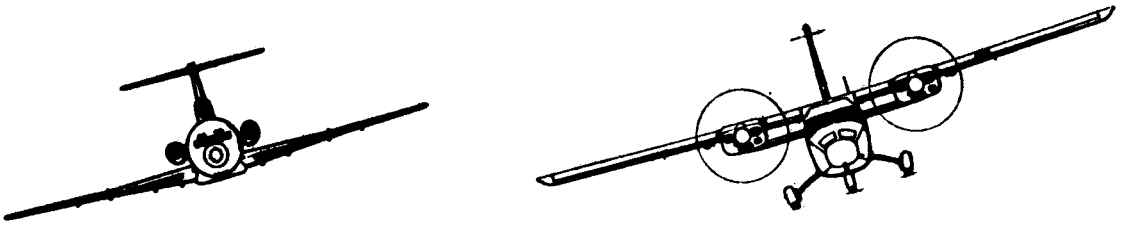

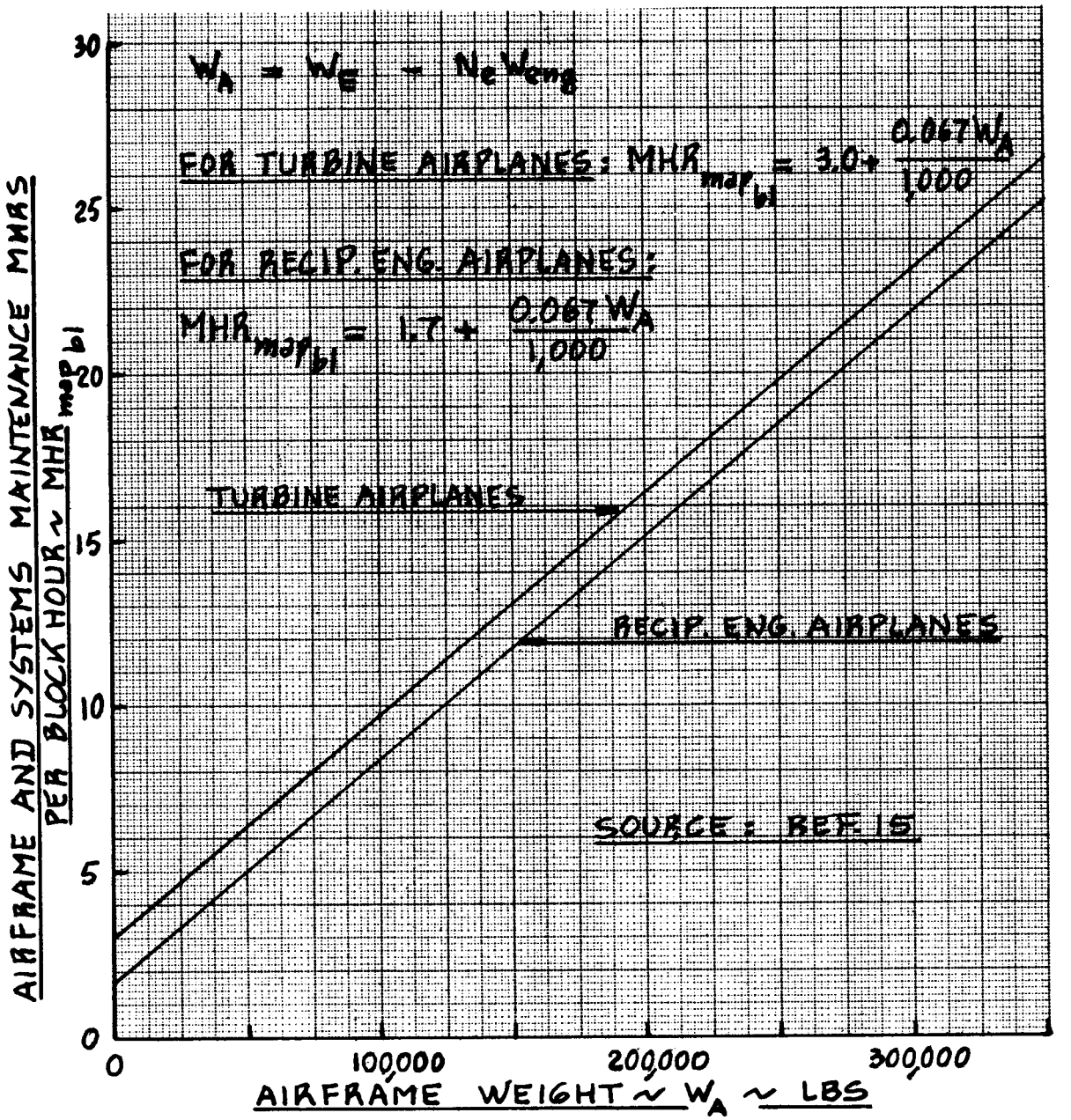

Figure 5.5 Effect of Airframe Weight on Airframe and Systems Maintenance Man Hours

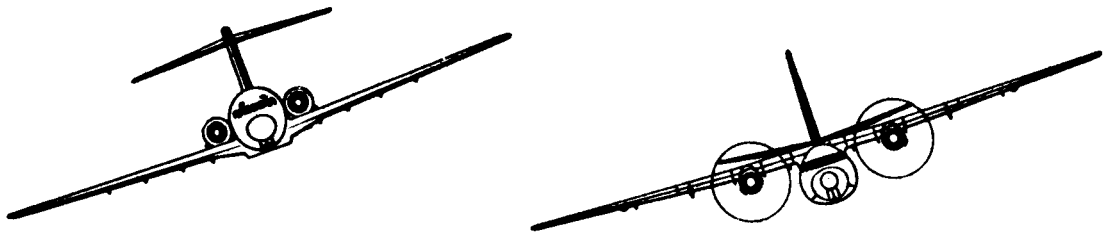

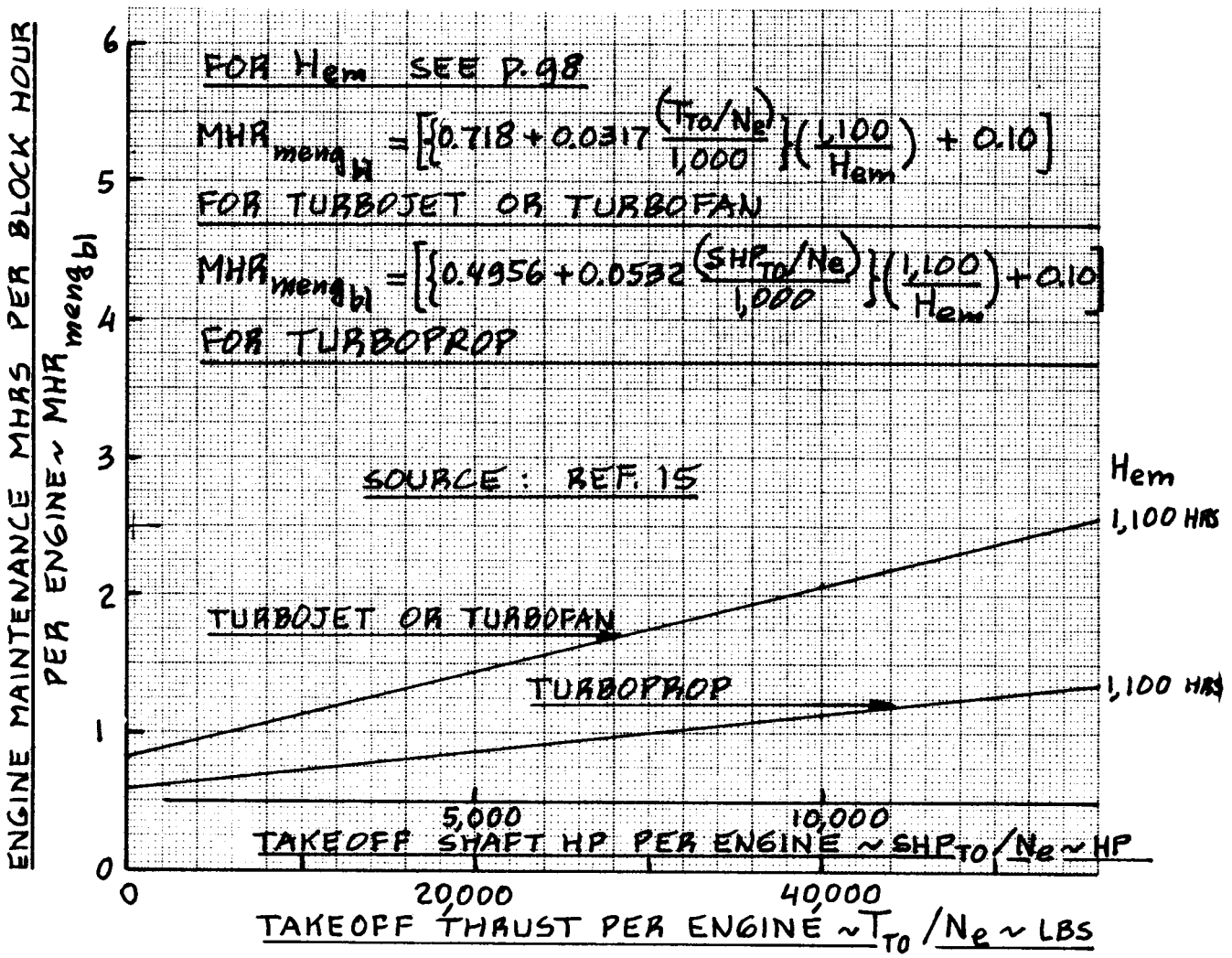

Figure 5.6 Effect of Takeoff Thrust and Takeoff Shaft Horsepower on Turbine Engine Maintenance Manhours

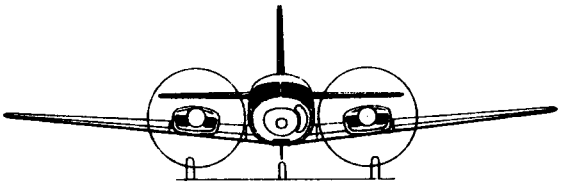

$$MHR_{meng_{bl}} = \left\{0.0765\left(\frac{W_{eng}}{1{,}000}\right)^2 + 0.2495\left(\frac{W_{eng}}{1{,}000}\right)\right\} \times \left\{\frac{0.70}{K_{H_{em}}} + 0.30\right\}$$

NOTES: 1) FOR W_{eng} SEE CH.6 PART V

2) FOR $K_{H_{em}}$ SEE FIG. 5.11

$K_{H_{em}} = 1.0$

SOURCE: REF. 15

ENGINE MAINTENANCE MHRS PER BLOCK HOUR PER ENGINE ~ $MHR_{meng_{bl}}$

0 1 2 3 4 5 6

0 2,000 4,000 6,000

WEIGHT PER ENGINE ~ W_{eng} ~ LBS

Figure 5.7 Effect of Engine Weight on Reciprocating Engine Maintenance Man Hours

hour in USD/hr. It may be found from Figure 5.8.

The cost of maintenance materials for the engine(s) per nautical mile may be estimated from:

$$C_{mat/eng} = 1.03(1.3)(N_e)(C_{mat/engblhr})/V_{bl} \quad (5.38)$$

where: the factor 1.3 accounts for cycle-dependent as opposed to cycle-independent material.

$C_{mat/engblhr}$ is the engine maintenance materials cost per engine per airplane block hour in USD/hr. It may be found from Figures 5.9-5.11. Note that one factor which must be decided on is H_{em},

the attained number of hours between engine overhauls. That number depends on the 'maturity' of the engine in question. Lacking data based on actual operating experience, use:

For turbine engines: H_{em} = 3,000 - 5,000 hrs

For recipr. engines: H_{em} = 1,000 - 2,000 hrs

The cost of the applied maintenance burden per nautical mile, C_{amb}, may be estimated from:

$$C_{amb} = 1.03[(f_{amb/lab})\{(MHR_{map_{bl}})(R_{l_{ap}}) + (N_e)(MHR_{eng_{bl}})(R_{l_{eng}})\} + (f_{amb/mat})\{C_{mat/apblhr} + (N_e)C_{mat/engblhr}\}]/(V_{bl}) \quad (5.39)$$

where: $f_{amb/lab}$ and $f_{amb/mat}$ are overhead distribution factors for labor and for material cost, respectively. These overhead factors are intended to cover such costs as: building, lighting, heating as well as administrative costs associated with airplane maintenance. Lacking actual overhead data it is suggested to use (see top of p.102):

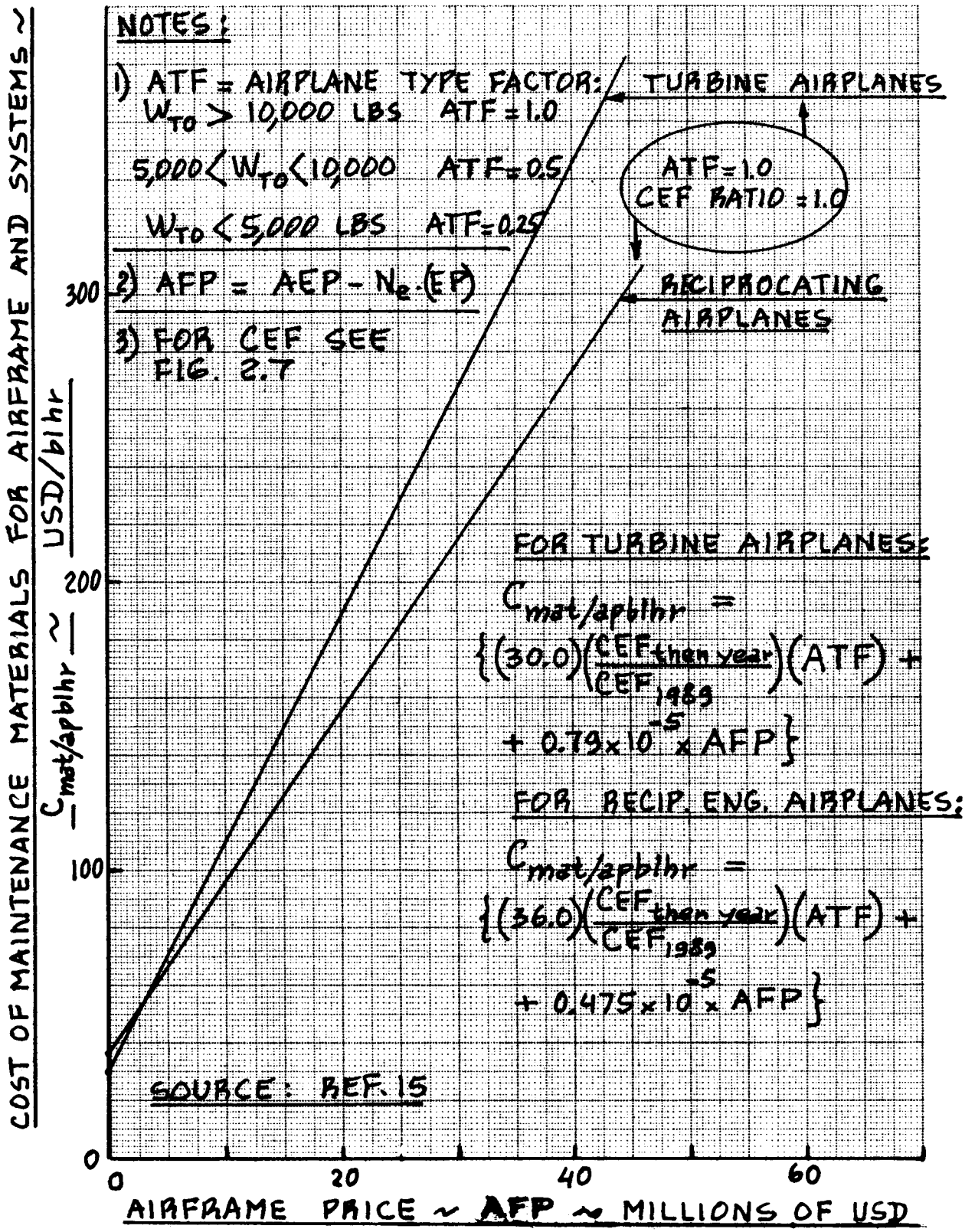

Figure 5.8 Effect of Airframe Price on Airframe and Systems Maintenance Materials Cost

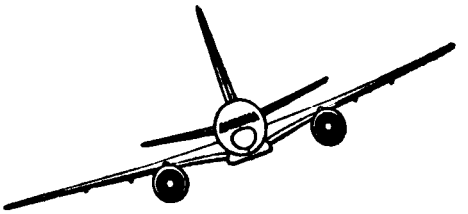

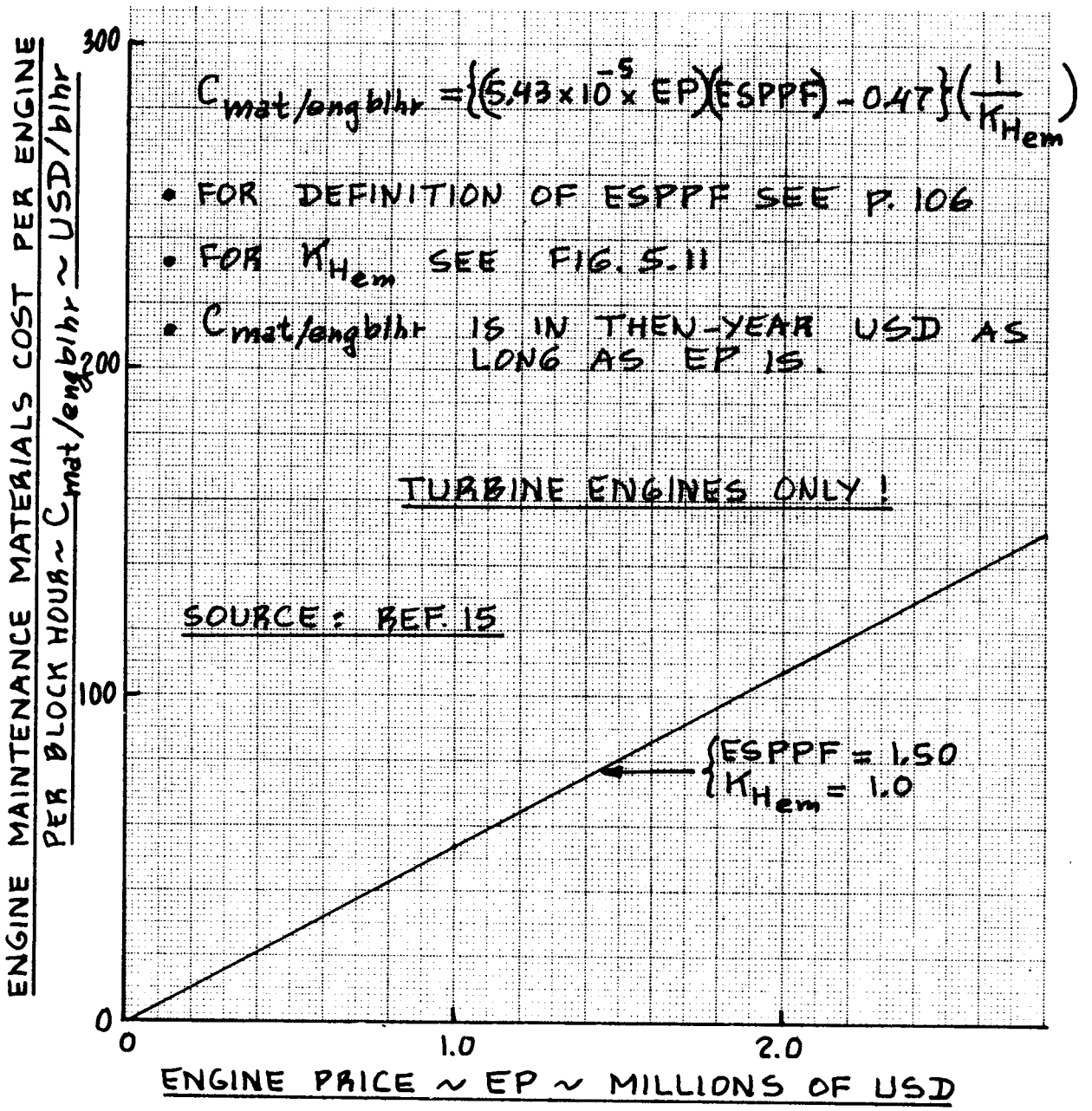

Figure 5.9 Effect of Engine Price on Turbine Engine Maintenance Materials Cost

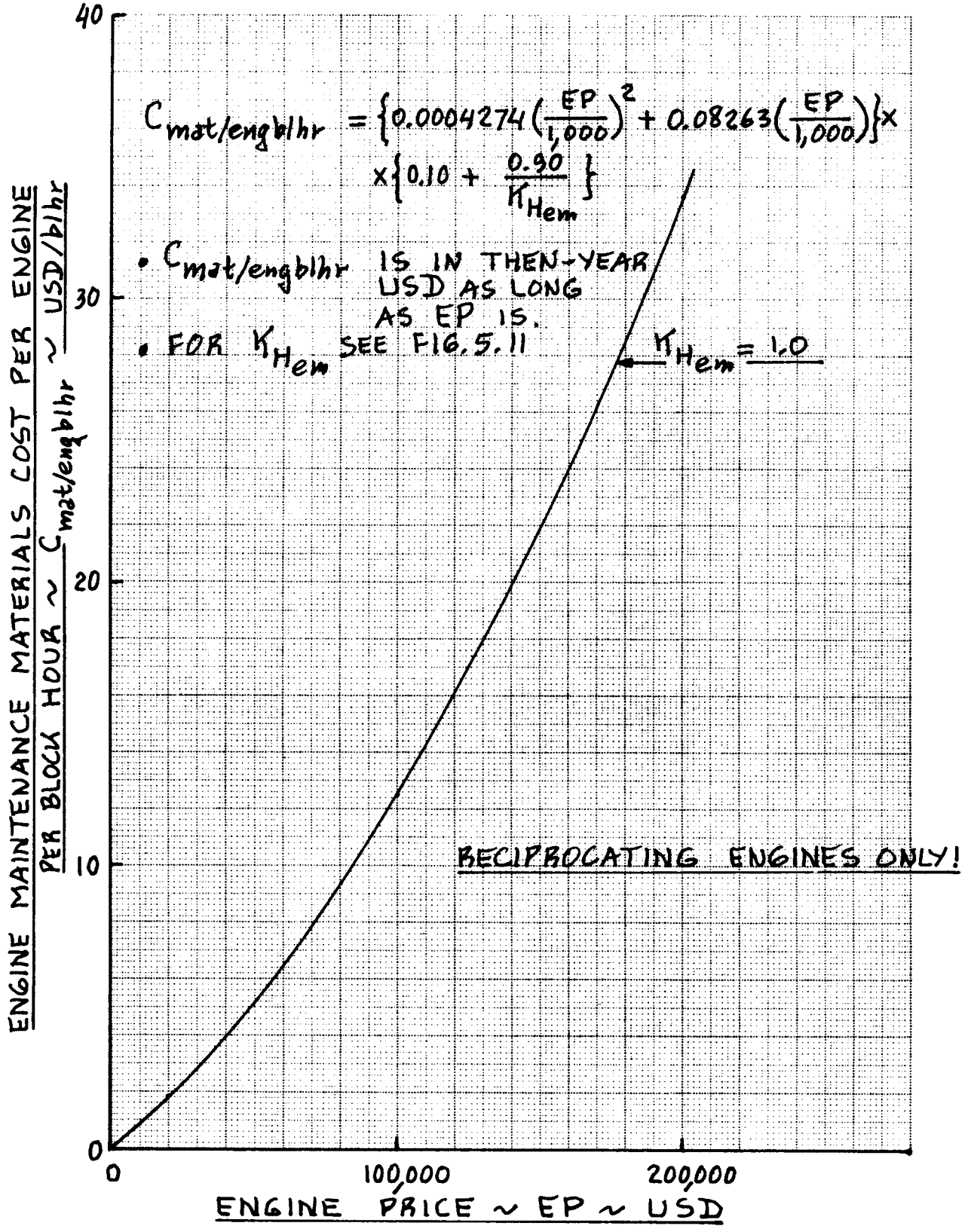

Figure 5.10 Effect of Engine Price on Reciprocating Engine Maintenance Materials Cost

	Personal	Corporate	Airlines
$f_{amb/lab}$ =	0.80-0.90	0.90-1.00	1.00-1.40
$f_{amb/mat}$ =	0.20-0.30	0.30-0.40	0.40-0.70

The other terms in Eqn.(5.39) were defined before.

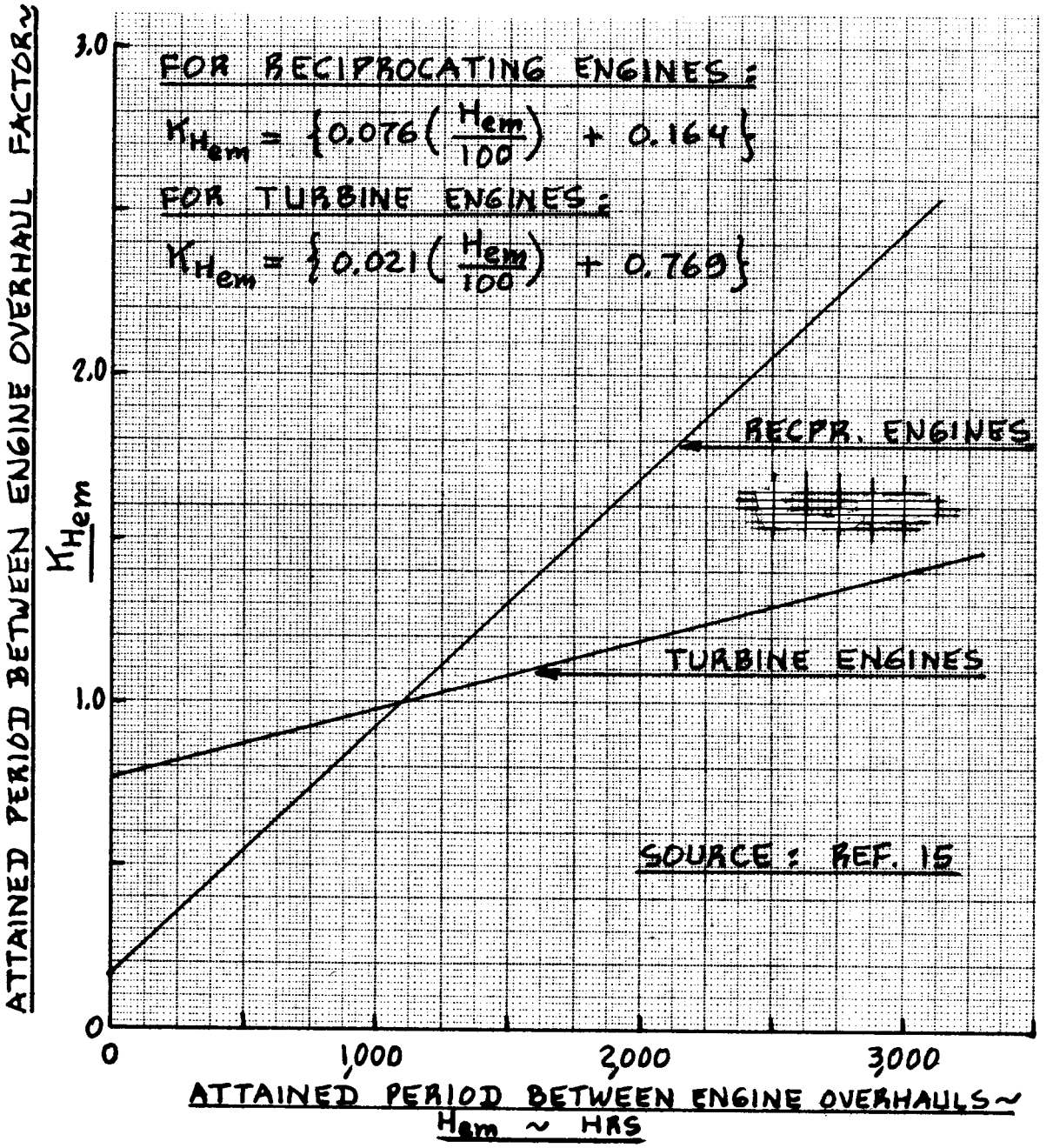

Figure 5.11 Factor Depending on Attained Engine Period Between Engine Overhauls

5.2.3 Direct Operating Cost of Depreciation: DOC_{depr}

The direct operating cost of depreciation is broken down as follows:

$$DOC_{depr} = C_{dap} + C_{deng} + C_{dprp} + C_{dav} + C_{dapsp} + C_{dengsp} \quad (5.40)$$

where: C_{dap} is the cost of airplane depreciation without engines and without propellers, avionics systems and spares (= airframe), in USD/nm. See Eqn.(5.41).

C_{deng} is the cost of engine depreciation (as mounted on the airplane but without propellers), in USD/nm. See Eqn.(5.42).

C_{dprp} is the cost of depreciation of propellers, in USD/nm. See Eqn.(5.43).

C_{dav} is the cost of depreciation of avionics systems in USD/nm. See Eqn.(5.44).

C_{dapsp} is the cost of depreciation of airplane spare parts in USD/nm. See Eqn.(5.45).

C_{dengsp} is the cost of depreciation of engine spare parts in USD/nm. See Eqn.(5.46).

The cost of airframe depreciation per nautical mile, C_{dap}, can be estimated from:

$$C_{dap} = \frac{(F_{dap})\{(AEP) - (N_e)(EP) - (N_p)(PP) - (ASP)\}}{(DP_{ap})(U_{ann_{bl}})(V_{bl})} \quad (5.41)$$

where: F_{dap} is an airframe depreciation factor. This factor depends on the perceived resale value of the airplane: see Table 5.7, p.107.

AEP is the airplane estimated price in USD. It can be estimated with the methods of Ch.4 or Appendix A.

N_e is the number of engines per airplane.

EP is the engine price (per engine) in USD. It can be found from Appendix B.

N_p is the number of propellers per airplane.

PP is the price per propeller in USD. It can be determined from Appendix B.

ASP is the avionics systems price per airplane in USD. This can be found from Appendix C.

DP_{ap} is the airplane depreciation period. This depends on the operator's business strategy. Table 5.7 may be used as a guide.

$U_{ann_{bl}}$ is the annual utilization in block hours. It may be found from page 76.

V_{bl} is the block speed in nm/hr as found from Equation (5.5).

The cost of engine depreciation per nautical mile, C_{deng}, may be determined from:

$$C_{deng} = \frac{(F_{deng})(N_e)(EP)}{(DP_{eng})(U_{ann_{bl}})(V_{bl})} \qquad (5.42)$$

where: F_{deng} is the engine depreciation factor. This factor depends on the perceived resale value of each engine: see Table 5.7, p.107.

DP_{eng} is the engine depreciation period. This depends on the operator's business strategy. The data of Table 5.7 may serve as a guide.

The cost of depreciation of propellers, C_{dprp}, in USD/nm can be found from:

$$C_{dprp} = \frac{(F_{dprp})(N_p)(PP)}{(DP_{prp})(U_{ann_{bl}})(V_{bl})} \qquad (5.43)$$

where: F_{dprp} is the propeller depreciation factor. This factor depends on the perceived resale value of each propeller: see Table 5.7, p.107.

DP_{prp} is the propeller depreciation period. This depends on the operator's business strategy. The data of Table 5.7 may serve as a guide.

The cost of depreciation of avionics systems, C_{dav}, in USD/nm may be estimated from:

$$C_{dav} = \frac{(F_{dav})(ASP)}{(DP_{av})(U_{ann_{bl}})(V_{bl})} \qquad (5.44)$$

where: F_{dav} is the avionics systems depreciation factor. This factor depends on the perceived resale value of the avionics systems. Experience has indicated little or no resale value as shown in Table 5.7, p.107.

DP_{av} is the avionics systems depreciation period. This depends on the operator's business strategy AND on federal regulations (in terms of requiring new types of equipment: TCAS is an example). The data of Table 5.7, p.107 may serve as a guide.

The cost of depreciation of airplane spare parts, C_{dapsp}, in USD/nm may be estimated from:

$$C_{dapsp} = \frac{(F_{dapsp})(F_{apsp})\{(AEP) - (N_e)(EP)\}}{(DP_{apsp})(U_{ann_{bl}})(V_{bl})} \qquad (5.45)$$

where: F_{dapsp} is the airplane spare parts depreciation factor. This factor depends on the perceived resale value of the airplane spare parts. The data of Table 5.7, p.107 may serve as a guide.

F_{apsp} is the airplane spare parts factor. It is equal to the ratio of airplane spare parts cost to the cost of the airplane minus engines. This factor depends on repair and maintenance operating experience with the airplane. Lacking actual data it is suggested to use: $F_{apsp} = 0.10$.

DP_{apsp} is the airplane spare parts depreciation period. This depends on the operator's business strategy. The data in Table 5.7 may serve as a guide.

Note: the airplane spare parts factor may be assumed to account also for spare parts needs for propellers and avionics systems.

The cost of engine spare parts depreciation, C_{dengsp}, in USD/nm can be estimated from:

$$C_{dengsp} = \frac{(F_{dengsp})(F_{engsp})(N_e)(EP)(ESPPF)}{(DP_{engsp})(U_{ann_{bl}})(V_{bl})} \qquad (5.46)$$

where: F_{dengsp} is the engine spare parts depreciation factor. It depends on the perceived resale value of the engine spare parts. The data of Table 5.7 should serve as a guide.

F_{engsp} is the engine spare parts factor. It is equal to the ratio of the cost of engine spare parts to the cost of one engine. The engine manufacturer usually recommends a ratio for each given engine depending on experience in the field. For preliminary cost estimating purposes it is suggested to use: $F_{engsp} = 0.50$.

ESPPF is the engine spare parts price factor. It depends on the engine manufacturer's policy in pricing spare parts. If all engine components could be purchased at the same price as a fully assembled engine, the value of ESPPF would be 1.0. It is suggested to use: ESPPF = 1.50.

DP_{engsp} is the depreciation period for engine spare parts. It depends on the operator's business strategy. The data of Table 5.7 may be used as a guide.

Table 5.7 Suggested Depreciation Periods and Depreciation Factors for Airframe and Equipment

Item	Suggested Depreciation Period		Residual Value in Percent	Depreciation Factor*	
Airframe	DP_{ap}	= 10	15	F_{dap}	= 0.85
Engines	DP_{eng}	= 7	15	F_{deng}	= 0.85
Propellers	DP_{prp}	= 7	15	F_{dprp}	= 0.85
Avionics	DP_{av}	= 5	0	F_{dav}	= 1.00
Airplane Spares	DP_{apsp}	= 10	15	F_{dapsp}	= 0.85
Engine Spares	DP_{engsp}	= 7	15	F_{dengsp}	= 0.85

* Depreciation factor =

= {1 - (Residual Value)/(Original Price)}

5.2.4 Direct Operating Cost of Landing Fees, Navigation Fees and Registry Taxes: DOC_{lnr}

There is no uniform agreement whether the operating costs caused by landing fees, navigation fees and registry taxes are to be considered direct or indirect operating costs. In this text the decision has been made to include them as direct operating costs.

The direct operating cost of landing fees, navigation fees and various taxes can be broken down in the following manner:

$$DOC_{lnr} = C_{lf} + C_{nf} + C_{rt} \qquad (5.47)$$

where: C_{lf} is the direct operating cost due to landing fees in USD/nm. This can be found from:

$$C_{lf} = (C_{aplf})/\{(V_{bl})(t_{bl})\} \qquad (5.48)$$

where: C_{aplf} is the airplane landing fee per landing. This is a function of

airplane takeoff weight (it is assumed, that after landing, it will take off again!) AND of local airport authority policy. Lacking actual landing fee data it is suggested to use:

$$C_{aplf} = 0.002W_{TO} \text{ USD/lbs} \quad (5.49)$$

V_{bl} is the block speed in nm/hr as found from Eqn.(5.5).

t_{bl} is the block time as defined by Equation (5.6).

An alternate method is to consider C_{lf} to be a simple fraction of the DOC. Based on data from Ref.20 it is suggested to use:

$$C_{lf} = (f_{lf})(DOC) \quad (5.50)$$

where: f_{lf} is a factor which depends on airplane size. This factor depends on local airport authorities which set these landing fees. Lacking actual data it is suggested to use:

$$f_{lf} = 0.036 + 4(10^{-8})W_{TO} \quad (5.51)$$

where: W_{TO} is the airplane takeoff weight in lbs.

C_{nf} is the cost of navigation fees in USD/nm. It may be estimated from:

$$C_{nf} = (C_{apnf})/\{(V_{bl})(t_{bl})\} \quad (5.52)$$

where: C_{apnf} is the navigation fee charged per airplane per flight, expressed in USD/flight. This fee varies from route to route and from country to country.

Lacking actual data it is suggested to use:

For operations in the USA:

C_{apnf} = 0 USD/flight

For operations outside the USA:

C_{apnf} = 10.00 USD/flight

C_{rt} is the direct cost of registry taxes expressed in USD/nm. Based on data from Ref.20 it is suggested to use:

$$C_{rt} = (f_{rt})(DOC) \qquad (5.53)$$

where: f_{rt} is a factor which depends on airplane size. This factor depends on state and country governments which set these registry taxes. Lacking actual data it is suggested to use:

$$f_{rt} = 0.001 + (10^{-8})W_{TO} \qquad (5.54)$$

where: W_{TO} is the airplane takeoff weight in lbs.

5.2.5 Direct Operating Cost of Financing: DOC_{fin}

The direct operating cost of financing the airplane in USD/nm, DOC_{fin}, depends on how an operator is financing his fleet of airplanes. Operators can elect to borrow money to pay for airplane(s) and spare parts as well as to finance their operation. They frequently elect to lease part or all of their flying equipment.

Even when an operator decides to use his own money to finance the airplanes and their operation, there is a cost associated with that: interest.

Methods for estimating financing cost are judged to be beyond the scope of this text. However, the reader may wish to account for financing costs by the following simple 'rule-of-thumb':

$$DOC_{fin} = 0.07(DOC) \qquad (5.55)$$

This 'rule-of-thumb' is based on the observation that financing costs typically run to 7 percent of the total DOC as found from Eqn.(5.19).

5.3 METHOD FOR ESTIMATING THE INDIRECT OPERATING COST OF COMMERCIAL AIRPLANES: IOC

The purpose of this section is to provide a method for estimating the indirect operating cost (IOC) in USD/nm, incurred while operating commercial airplanes.

Table 5.8 presents an overview of cost components and cost elements which contribute to the indirect operating cost per nautical mile.

NOTE: The right hand side of Table 5.8 indicates which IOC elements apply to various airplane types.

The indirect cost associated with airplane operations vary significantly from one operator to another. Also, as will be seen, the airplane designer has very little influence over this cost category. The method proposed here to estimate the indirect operating cost assumes that the IOC can be expressed as a simple fraction of DOC:

$$IOC = f_{ioc}(DOC) \qquad (5.56)$$

where: f_{ioc} is the fraction of DOC by which IOC is estimated. When reviewing published data on the relationship between IOC and DOC, it is found that f_{ioc} is strongly dependent on block distance, R_{bl}, as well as on the type of airplane. Figure 5.12 provides some data for this fraction.

Lacking actual IOC data it is suggested to use:

For transport operations: f_{ioc} as in Fig.5.12

For personal owner and for corporate airplanes: $f_{ioc} = 0.$

As will be seen, airplane designers have very little design leverage over the magnitude of the indirect operating costs of an airplane operator. Despite this fact, the author believes that it is desirable for aeronautical engineering students to develop at least a basic understanding of those factors which determine IOC. For that reason a discussion of IOC breakdown is presented next. For a discussion of IOC trends, see Section 5.5.

Table 5.8 Overview of Indirect Operating Cost (IOC)

INDIRECT OPERATING COST ~ IOC ~ USD/nm		AIRLINE	CORPORATE	PERSONAL
IOC COMPONENTS	IOC ELEMENTS			
PASSENGERS ~ IOC_{pax} (5.58)	MEALS ~ C_{mls}	✓	✓	NO
	INSURANCE ~ $C_{pax/ins}$	✓	✓	✓
	CABIN ATTENDANTS ~ C_{cat}	✓	✓	NO
	PASSENGER HANDLING, BAGGAGE HANDLING, SALES & RESERVATIONS, SECURITY, MISC ~ $C_{pax/gen}$	✓	NO	NO
STATION ~ IOC_{sta} (5.59)	MAINTENANCE OF GROUND EQUIPM'T & FACILITIES ~ C_{mgef}	✓	✓	NO
	DEPRECIATION OF GROUND EQUIPM'T & FACILITIES ~ C_{dgef}	✓	✓	NO
AIRPLANE SERVICE, CONTROL AND FREIGHT ~ IOC_{ascf} (5.60)	AIRPLANE SERVICE ~ C_{aps}	✓	✓	✓
	AIRPLANE CONTROL ~ C_{apc}	✓	✓	NO
	FREIGHT HANDLING ~ C_{frt}	✓	NO	NO
PROMOTION, SALES AND ENTERTAINMENT ~ IOC_{pse} (SUB-SECT. 5.3.4)	COMMISSIONS TO TRAVEL AGENCIES,	✓	NO	NO
	PUBLICITY AND ADVERTISING,	✓	NO	NO
	ENTERTAINMENT	✓	NO	NO
GENERAL AND ADMINISTRATIVE ~ IOC_{gaa} (SUB-SECT. 5.3.5)	ADMINISTRATIVE, ACCOUNTING AND CORPORATE STAFF + FACILITIES	✓	✓	NO

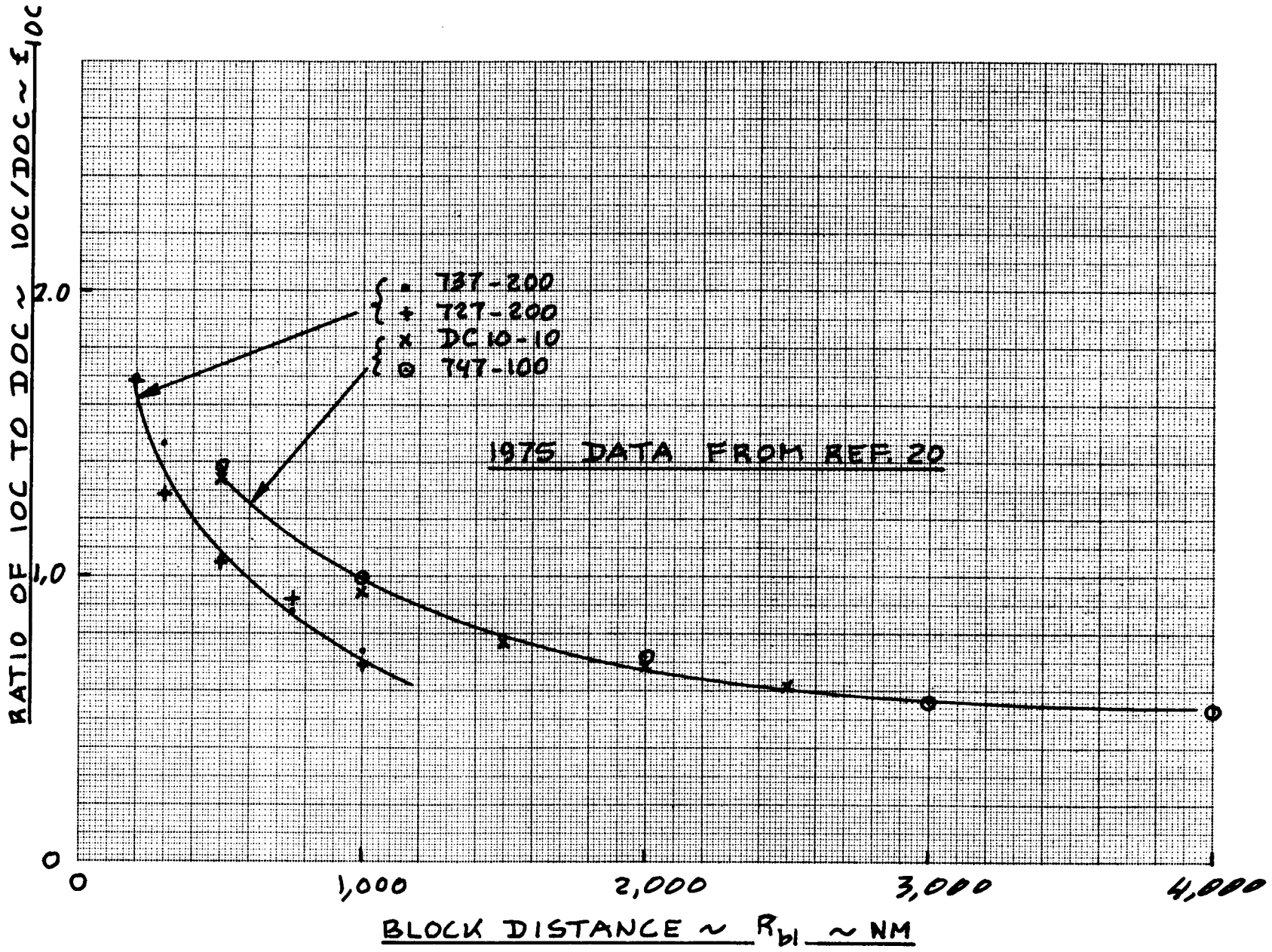

Figure 5.12 Effect of Block Distance on the Ratio of IOC to DOC

The indirect operating cost per nautical mile for a commercial airplane is broken down into the following IOC cost components:

$$IOC = IOC_{pax} + IOC_{sta} + IOC_{ascf} + IOC_{pse} + IOC_{gaa} \quad (5.57)$$

where: IOC_{pax} is the indirect operating cost for passenger services, expressed in USD/nm: see Sub-section 5.3.1.

IOC_{sta} is the indirect cost for maintaining and depreciating ground equipment and ground facilities, expressed in USD/nm: see Sub-section 5.3.2.

IOC_{ascf} is the indirect operating cost for airplane and traffic servicing, control and for freight, expressed in USD/nm: see Sub-section 5.3.3.

IOC_{pse} is the indirect operating cost for promotion, sales and entertainment, expressed in USD/nm: see Sub-section 5.3.4.

IOC_{gaa} is the indirect operating cost for general administrative expenses, expressed in USD/nm: see Sub-section 5.3.5.

Sub-sections 5.3.1 through 5.3.5 contain breakdowns for these indirect operating cost components.

5.3.1 Indirect Operating Cost for Passenger Service: IOC_{pax}

The indirect operating cost for passenger services may be broken down as follows:

$$IOC_{pax} = C_{mls} + C_{pax/ins} + C_{cat} + C_{pax/gen} \quad (5.58)$$

where: C_{mls} is the cost for meal service. This depends on the routes flown and on the level of service which the operator wants to provide for his passengers.

The airplane designer has minor leverage over this cost item. The design of the airplane

galleys constitutes this leverage. No quantitative method for estimating this leverage is available.

$C_{pax/ins}$ is the cost for passenger insurance. There exists an international agreement between airline operators on the amount of passenger insurance that must be carried: the so-called Warsaw Convention. The cost of this insurance to an airline varies with the underwriter of that insurance and with the accident history of the airline.

Other than designing the airplane to be safer than previous airplanes, the airplane designer has no design leverage over this cost element.

C_{cat} is the cost for cabin attendants. The number of cabin attendants which must be carried aboard an airplane is regulated by the FAA. Part III, p.59 shows how many cabin attendants are required. By using salary data from Table 5.5 it is possible to determine the actual cost of flight attendants.

The designer has no leverage over this cost element.

$C_{pax/gen}$ is the cost associated with the following items:

* Passenger handling
* Passenger baggage handling
* Sales and reservations
* Security
* Miscellaneous passenger costs

No reliable quantitative method is available for estimating this cost element. The designer of the airplane does have some design leverage over the following items:

* design of baggage space and the ease of access to baggage handling personnel or equipment

* boarding and unboarding of passengers is affected significantly by the interior cabin layout.

5.3.2 Indirect Operating Costs for Station Operation: IOC_{sta}

The indirect operating cost for station operation can be broken down as follows:

$$IOC_{sta} = C_{mgef} + C_{dgef} \quad (5.59)$$

where: C_{mgef} is the cost of maintaining ground equipment and facilities

C_{dgef} is the cost of depreciation of ground equipment and facilities

The designer has some leverage over these cost elements: requirements for ground facilities and for ground equipment are dependent on the type of systems which need to be accessed for servicing while the airplane is at the gate. No quantative method is available to estimate this cost element.

5.3.3 Indirect Operating Cost for Airplane Service, Airplane Control and Freight: IOC_{ascf}

The indirect operating cost for aircraft service, control and freight is broken down into the following cost elements:

$$IOC_{ascf} = C_{aps} + C_{apctrl} + C_{frt} \quad (5.60)$$

where: C_{aps} is the cost of airplane service. It depends on how well the airplane was designed from a gate servicing viewpoint: see Part III, pages 82-83.

If all required service vehicles cannot have simultaneous access to the airplane then the cost of servicing will increase.

C_{apctrl} is the cost of airplane control. It depends on the amount of equipment and personnel needed to push (or maneuver) the airplane away from the gate or help it approach the gate.

C_{frt} is the cost associated with handling freight. This freight is NOT passenger baggage. Many airlines will try to carry extra freight when possible to bring in additional revenue.

Depending on how this freight must be handled (people, containers, handling equipment) this cost component can be high or low. The airplane designer has definite design leverage over this cost element. Sub-section 3.3.5 in Part III provides details on the layout of cargo/baggage holds.

5.3.4 Indirect Operating Cost for Promotion, Sales and Entertainment: IOC_{pse}

The following activities contribute to this indirect cost component:

* Commissions to travel agencies
* Publicity and advertising campaigns
* Entertainment

The airplane designer has no leverage over this item unless there is something about the appearance or public appeal of the airplane that causes this cost to increase.

No quantitative method for estimating this cost component is avalable.

5.3.5 Indirect Operating Cost for General and Administrative Cost: IOC_{gaa}

The following activities contribute to this indirect cost component:

* requirements for administrative and accounting personnel as well as for their facilities
* requirements for corporate staffers and their facilities

The mentality of upper level management has a major effect on the magnitude of this cost item: the degree of fanciness in the corporate offices and the various perks associated with company officers all influence this cost item. No quantitative method is available for estimating this cost component. The airplane designer certainly has no design leverage over this cost component.

5.4 EXAMPLE APPLICATION

The purpose of this section is to present an example application of the methods for estimating program operating cost, C_{OPS}, direct operating cost, DOC, and indirect operating cost, IOC, of Sections 5.1, 5.2 and 5.3 respectively. The example has been constructed around the Ourania jet transport, to be consistent with the examples given in Sections 3.8 and 4.6. The data will be computed for calendar year 1990.

The material is organized as follows:

5.4.1 Ourania Mission Data

5.4.2 Calculation of Direct Operating Cost: DOC

5.4.3 Calculation of Indirect Operating Cost: IOC

5.4.4 Calculation of Program Operating Cost: C_{OPS}

5.4.5 Discussion of Results

5.4.1 Ourania Mission Data

Before operating costs can be determined, some baseline data about the airplane mission are needed. These baseline data are essentially those dealing with block distance, block speed and block times. Definitions and formulas for these factors were given in Section 5.1.

The block distance for the Ourania will be assumed to be equal to the 1,500 nm range requirement specified in Table 2.18 of Part I: R_{bl} = 1,500 nm.

Block time, t_{bl}, is determined from Eqn.(5.6). This in turn requires the ground maneuvering time, t_{gm}, the time-to-climb, t_{cl}, the time to cruise, t_{cr}, and the time to descend, t_{de}. These times will be found next.

The ground maneuvering time, t_{gm}, is obtained from Eqn.(5.7). This in turn requires the takeoff weight, W_{TO}, which is: W_{TO} = 123,683 from p.11, Part V.

Therefore: $t_{gm} = 0.51(0.123683) + 0.125 = 0.19$ hrs

The time-to-climb, t_{cl}, is found from p.56 of Part I as: $t_{cl} = 14$ min. $= 0.23$ hrs

The time-to-cruise, t_{cr}, is found from Eqn.(5.8a). This in turn requires the block distance, R_{bl}, the distance-to-climb, R_{cl}, the distance-to-descend, R_{de}, the maneuvering distance, R_{man}, and the cruise speed, V_{cr}. These distances will be found next.

The distance-to-climb is found from p.56, Part I as: $R_{cl} = 64$ nm.

The distance-to-descend is found from Eqn.(5.10). The average speed during the descent will be assumed to be 250 kts. For the Ourania it will also be assumed that the average descent rate from 35,000 ft is 2,500 ft/min so that:

$t_{de} = 35{,}000/2{,}500 = 14$ min $= 0.23$ hrs. Therefore:

$R_{de} = 250(0.23) = 58$ nm

The maneuvering distance, R_{man}, is determined from Eqn.(5.11). The maneuvering speed is set equal to the cruise speed: $V_{man} = V_{cr} = 473$ kts (p.56, Part I). The maneuvering time, t_{man}, follows from Eqn.(5.12):

$t_{man} = 0.25(0.123683) + 0.0625 = 0.093$ hrs

Therefore:

$R_{man} = 473(0.093) = 44$ nm

The cruise time now follows from Eqn.(5.8a):

$t_{cr} = \{1.06(1{,}500) - 64 - 58 + 44\}/473 =$

$= 1{,}512/473 = 3.20$ hrs

The block time now follows from Eqn.(5.6):

$t_{bl} = 0.19 + 0.23 + 3.20 + 0.23 = 3.85$ hrs

The block speed can now be found from Eqn.(5.5) as:

$V_{bl} = 1,500/3.85 = 390$ kts

The annual utilization in block hours may be computed from Eqn.(5.14a) as:

$$U_{ann_{bl}} = (10)^3[3.4546(3.85) + 2.994 +$$

$$- \{12.289(3.85)^2 - 5.6626(3.85) + 8.964\}^{1/2}] = 3,282 \text{ hrs}$$

NOTE: this annual utilization amounts to an average daily utilization of about 9 hours. For a well run airline, on 1,500 nm stage lengths, this is a reasonable number. Table 5.3 also substantiates this.

5.4.2 Calculation of Direct Operating Cost: DOC

The Ourania direct operating cost in USD/nm is computed with Eqn.(5.19). The five cost components of DOC are detailed in sub-sections 5.2.1 through 5.2.5. The calculations for these cost components are presented in sub-sub-sections 5.4.2.1 through 5.4.2.5. The DOC is computed in sub-sub-section 5.4.2.6.

5.4.2.1 Direct operating cost of flying: DOC_{flt}

This cost is found with Eqn.(5.20).

Crew Cost: C_{crew}

This cost may be estimated with Eqn.(5.21).

The mission specification for the Ourania jet transport of Table 2.18, Part I, p.55 specifies a crew of two. Therefore, in Eqn.(5.21):

$n_{c_1} = 1$ and also: $n_{c_2} = 1$

From page 83: $K_j = 0.26$

The crew salaries for the captain (n_{c_1}) and for the first officer (n_{c_2}) are determined from Table 5.5. The annual flight hours for each are found from p.84:

$SAL_1 = 85,000$ USD/yr $\qquad AH_1 = 800$ hrs

$SAL_2 = 50,000$ USD/yr $\qquad AH_2 = 800$ hrs

These data are assumed to be applicable for 1990.

The travel expense factor, TEF, according to p.84 is:

$$TEF_1 = TEF_2 = 7 \text{ USD/blhr}$$

The crew cost per nautical mile can now be estimated from Eqn.(5.21) as:

$$C_{crew} = \{(1.26/390)(85,000/800) + 7/390\} +$$

$$+ \{(1.26/390)(50,000/800) + 7/390\} =$$

$$= 0.361 + 0.220 = 0.581 \text{ USD/nm}$$

Fuel and oil cost: C_{pol}

This cost is determined with Eqn.(5.30)

The block fuel used, $W_{F_{bl}}$, is the same as the mission fuel used, $W_{F_{used}}$, which in turn is given by Eqn.(2.14) of Part I. Reference is made to the example calculation for fuel used in sub-section 2.6.2 of Part I. Note that mission phases 6 and 8 as depicted in the mission profile of Table 2.18 (Part I) should not be counted as normal operational fuel used. Therefore, the M_{ff} calculation of p.58 of Part I must be modified to:

$$M_{ff} = (0.992)(1)(0.990)(1)(0.909)(0.980)(0.995)*$$

Mission Phase: 9 8 7 6 5 4 3

$$*(0.990)(0.990) = 0.853$$

Mission Phase: 2 1

The mission phase numbers refer to Table 2.18 in Part I. This yields for the operational mission fuel used, $W_{F_{used}}$, with Eqn.(2.14) of Part I:

$$W_{F_{bl}} = (1 - 0.853)(123,683) = 18,181 \text{ lbs}$$

The 1990 price of Jet A fuel will be assumed to be 0.65 USD/gallon (Figure 5.3), while the density (p.88) is

6.74 lbs/gallon. Therefore, with Eqn.(5.30):

$$C_{pol} = (1.05)(18,181/1,500)(0.65/6.74) =$$

$$= 1.227 \text{ USD/nm}$$

Insurance cost: C_{ins}

This cost is found from Eqn.(5.32):

$$C_{ins} = 0.02(DOC)$$

The direct operating cost of flying may now be computed from Eqn.(5.20) as:

$$DOC_{flt} = 0.581 + 1.227 + 0.02(DOC) =$$

$$= 1.808 + 0.02(DOC) \text{ USD/nm}$$

5.4.2.2 Direct operating cost of maintenance: DOC_{maint}

This cost is found from Eqn.(5.33).

Maintenance labor cost for airframe and systems: $C_{lab/ap}$

This cost may be calculated from Eqn.(5.34). The number of maintenance manhours per blockhour for airframe and systems, $MHR_{map_{bl}}$, may be found from Figure 5.5. This is seen to depend on the airframe weight, W_A, defined as:

$$W_A = W_E - W_{pwrplt} = 65,133 - 9,891 = 55,242 \text{ lbs},$$

where the weight data were found on p.11 of Part V.

Figure 5.5 now yields:

$$MHR_{map_{bl}} = 3.0 + 0.067(55.242) = 6.7 \text{ mhrs/blhr}$$

The airplane maintenance labor rate per manhour is assumed from Table 5.5 to be: $R_{l_{ap}} = 16$ USD/mhr.

Therefore, with Eqn.(5.34):

$$C_{lab/ap} = 1.03(6.7)(16)/390 = 0.283 \text{ USD/nm}$$

Maintenance labor cost for engines: $C_{lab/eng}$

This cost is found from Eqn.(5.36). The number of engine maintenance hours per engine, per block hour, $MHR_{meng_{bl}}$, may be determined from Figure 5.6. It is seen

to depend on the takeoff thrust per engine, (T_{TO}/N_e), and on the attained period between engine overhauls, H_{em}.

The takeoff thrust per engine is found from page 184 in Part I as:

$$(T_{TO}/N_e) = 47,625/2 = 23,813 \text{ lbs}$$

The attained overhaul period for the engine, H_{em}, is assumed to be 3,000 hrs (see p.98). For a new engine, this is not an unreasonably high number. Therefore, from the equation in Figure 5.6:

$$MHR_{meng_{bl}} = [\{0.718 + 0.0317(23.813)\}*$$
$$*(1,100/3,000) + 0.10] = 0.64 \text{ mhrs/blhr}$$

The hourly labor rate for engine maintenance will be assumed to be the same as that for the airframe:

$R_{l_{eng}} = 16$ USD/hr so that with Eqn.(5.36):

$$C_{lab/eng} = 1.03(1.3)(2)(0.64)(16)/390 = 0.070 \text{ USD/nm}$$

NOTE: it is of interest to 'check' whether the total manhours for maintenance are reasonable. This total is: 6.7 + 2(0.64) = 7.98 mhrs/blhr. This can be translated into mhrs/flthr with Eqn.(5.35). The value for t_{flt} is found from Eqn.(5.18) as:

$$t_{flt} = 0.23 + 3.20 + 0.23 = 3.66 \text{ hrs}$$

The block time, t_{bl}, was found to be 3.85 hours, so that the maintenance manhours per flight hour follow from Eqn.(5.35) as:

$$\text{MHR per flt hour} = (\text{MHR per bl hour})(t_{bl})/(t_{flt}) =$$
$$= 7.98(3.85/3.66) = 8.4 \text{ mhrs/flthr.}$$

This number appears reasonable when compared with the data in Table 5.6.

Maintenance materials cost for airplane and systems: $C_{mat/ap}$

This cost can be found from Eqn.(5.37). The cost of airplane maintenance materials per blockhour, $C_{mat/apblhr}$, is determined from Figure 5.8. It depends on the airframe price, AFP:

$$AFP = AEP - N_e(EP) =$$

$$= 22,576,000 - 2(1,558,607) = \text{USD } 19,458,786$$

where: the airplane and engine prices are found from pages 62 and 58 (Section 4.6), respectively.

With Figure 5.8:

$$C_{mat/apblhr} = 30.0 + 0.79(194.58786) =$$

$$= 183.72 \text{ USD/blhr}$$

where: the 1990 to 1989 CEF ratio has been assumed to be equal to 1.0.

Therefore, with Eqn.(5.37):

$$C_{mat/ap} = 1.03(183.72)/390 = 0.485 \text{ USD/nm}$$

Maintenance materials cost for engines: $C_{mat/eng}$

This cost is computed from Eqn.(5.38). The cost of engine maintenance materials per blockhour, $C_{mat/engblhr}$, may be found from Figures 5.9 and 5.11. It was already assumed that the attained overhaul period for the engines is H_{em} = 3,000 hrs (See p.122). Thus, from Figure 5.11:

$K_{H_{em}} = 1.40.$

Then, with the equation in Figure 5.9:

$$C_{mat/engblhr} = \{0.0543(1,558.607)(1.5) +$$

$$- 0.47\}/1.40 = 90.34 \text{ USD/blhr}$$

Thus, with Eqn.(5.38):

$$C_{mat/eng} = 1.03(1.3)(2)(90.34)/390 = 0.620 \text{ USD/nm}$$

Applied maintenance burden cost: C_{amb}

This cost may be found from Eqn.(5.39). The overhead distribution factors are selected from the top of page 102 as:

$f_{amb/lab} = 1.30$ $\qquad$ $f_{amb/mat} = 0.60$

Therefore from Eqn.(5.39):

$$C_{amb} = 1.03[1.30\{(6.7)(16) + 2(0.64)(16)\} +$$

$$+ 0.60\{183.72 + 2(90.34)\}]/390 = 1.016 \text{ USD/nm}$$

Total direct maintenance cost: DOC_{maint}

The total direct cost for maintenance now follows with Eqn.(5.33) as:

$$DOC_{maint} = 0.283 + 0.070 + 0.485 + 0.620 + 1.016 =$$

$$= 2.474 \text{ USD/nm}$$

5.4.2.3 Direct operating cost of depreciation: DOC_{depr}

This cost is found with Eqn.(5.40).

Airplane Depreciation Cost: C_{dap}

This cost may be computed with Eqn.(5.41).

The following terms are found in Table 5.7:

Airframe depreciation factor: $F_{dap} = 0.85$

Airplane depreciation period: $DP_{ap} = 10$ yrs

The following price terms were found in Section 4.6:

Airplane estimated price: AEP = USD 22,576,000
Engine price: EP = USD 1,558,607
Avionics systems price: ASP = USD 2,670,000

Number of propellers: $N_p = 0$. Now, with Eqn.(5.41):

$$C_{dap} = \frac{0.85\{22,576,000 - 2(1,558,607) - 2,670,000\}}{10(3,282)(390)} =$$

$$= 1.115 \text{ USD/nm}$$

Engine Depreciation Cost: C_{deng}

This cost is determined with Eqn.(5.42).

The following terms are found in Table 5.7:

Engine price depreciation factor: $F_{deng} = 0.85$

Engine depreciation period: $DP_{eng} = 7$ yrs

With Eqn.(5.42):

$C_{deng} = \{0.85(2)(1,558,607)\}/\{7(3,282)(390)\} =$

$= 0.296$ USD/nm

Propeller Depreciation Cost: C_{dprp}

This cost is zero: the Ourania has no propellers.

Avionics Systems Depreciation Cost: C_{dav}

This cost may be found with Eqn.(5.44).

The following terms are found in Table 5.7:

Avionics systems depreciation factor: $F_{dav} = 1.00$

Avionics systems depreciation period: $DP_{av} = 5$ yrs

With Eqn.(5.44):

$C_{dav} = \{1.0(2,670,000)\}/\{5(3,282)(390)\} =$

$= 0.417$ USD/nm

Airplane Spare Parts Depreciation Cost: C_{dapsp}

This cost may be found with Eqn.(5.45).

The following terms are found from Table 5.7:

Airplane spare parts depreciation factor:

$F_{dapsp} = 0.85$

Airplane spare parts depreciation period:

$DP_{apsp} = 10$ yrs

The airplane spare parts factor, F_{apsp}, is assumed to have the value 0.10: see p.105.

With Eqn.(5.45):

$$C_{dapsp} = \{0.85(0.1)(19,458,786)\}/\{10(3,282)(390)\} =$$

$$= 0.129 \text{ USD/nm}$$

Engine Spare Parts Depreciation Cost: C_{dengsp}

This cost may be estimated from Eqn.(5.46).

The following terms are found in Table 5.7:

Engine spare parts depreciation factor:

$$F_{dengsp} = 0.85$$

Engine spare parts depreciation period:

$$DP_{engsp} = 7 \text{ yrs}$$

The engine spare parts factor, F_{engsp}, will be set equal to 0.50 as suggested on p.106. The engine spare parts price factor, ESPPF will be set equal to 1.50 as suggested on page 106. Therefore, with Eqn.(5.46):

$$C_{dengsp} = \{0.85(0.50)(2)(1,558,607)*$$

$$*(1.5)\}/\{7(3,282)(390)\} = 0.222 \text{ USD/nm}$$

Total Direct Operating Cost of Depreciation: DOC_{depr}

From Eqn.(5.40):

$$DOC_{depr} = 1.115 + 0.296 + 0 + 0.417 + 0.129 +$$

$$+ 0.222 = 2.181 \text{ USD/nm}$$

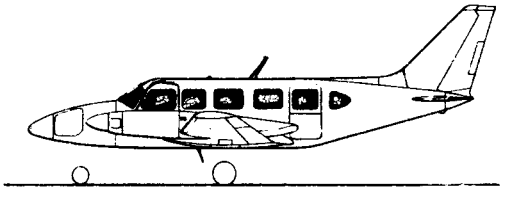

5.4.2.4 Direct operating cost of landing fees, navigation fees and registry taxes: DOC_{lnr}

This cost may be determined with Eqn.(5.47).

Cost of Landing Fees: C_{lf}

This cost is estimated with Eqn.(5.48).

The landing fee per landing, C_{aplf}, is determined from Eqn.(5.49) as:

$$C_{aplf} = 0.002(123,683) = \text{USD } 247.37$$

Therefore, with Eqn.(5.48):

$$C_{lf} = 247.37/\{(390)(3.85)\} = 0.165 \text{ USD/nm}$$

Cost of Navigation Fees: C_{nf}

According to Eqn.(5.52) and p.109, for domestic operations:

$$C_{nf} = 0$$

Cost of Registry Taxes: C_{rt}

This cost is estimated with Eqn.(5.53).

The factor f_{rt} is determined from Eqn.(5.54) as:

$$f_{rt} = 0.001 + 0.00123683 = 0.00224$$

Therefore, with Eqn.(5.53):

$$C_{rt} = 0.00224(DOC)$$

Total Direct Operating Cost of Landing Fees, Navigation and Registry Taxes: DOC_{lnr}

With Eqn.(5.47):

$$DOC_{lnr} = 0.165 + 0 + 0.00224(DOC) =$$

$$= 0.165 + 0.00224(DOC) \text{ USD/nm}$$

5.4.2.5 Direct operating cost of financing: DOC_{fin}

Lacking better information, Eqn.(5.55) will be used:

$$DOC_{fin} = 0.07(DOC)$$

5.4.2.6 Total direct operating cost: DOC

The DOC cost components of sub-sub-sections 5.4.2.1 through 5.4.2.5 can be combined with Eqn.(5.19) to yield:

$$DOC = 1.808 + 0.02(DOC) + 2.474 + 2.180 + 0.165 +$$

$$+ 0.00224(DOC) + 0.07(DOC) =$$

$$= 6.627 + 0.09224(DOC) \text{ USD/nm}$$

or: $DOC = 7.300$ USD/nm

5.4.3 Calculation of Indirect Operating Cost: IOC

The Ourania indirect operating cost may be estimated with Eqn.(5.56) where the factor f_{ioc} is extrapolated from Figure 5.12 as:

$$f_{ioc} = 0.50$$

Therefore: $IOC = 0.50(DOC) = 0.5(7.300) =$

$$= 3.650 \text{ USD/nm}$$

5.4.4 Calculation of Program Operating Cost: C_{OPS}

The Ourania program operating cost may be estimated from Eqns (5.1) - (5.3).

It will be assumed that a total of 500 airplanes will be acquired and that all operators have the same route system:

$$N_{acq} = 500$$

The total annual block miles per airplane, $R_{bl_{ann}}$, may be found from Eqn.(5.4):

$$R_{bl_{ann}} = (390)(3,282) = 1,279,980 \text{ nm}$$

The number of years during which the airplane is being operated will be assumed to be equal to the airframe depreciation period, which is 10 years:

$$N_{yr} = 10 \text{ yrs}$$

Therefore, with Eqns (5.1) - (5.3):

$$C_{OPS} = (7.300)(1,279,980)(10)(500) +$$

$$+ (3.650)(1,279,980)(10)(500) =$$

$$= \text{USD } 70,078,905,000$$

5.4.5 Discussion of Results

The significance of the numerical results which were obtained in this section are discussed as follows:

5.4.5.1 Discussion of DOC results
5.4.5.2 Discussion of Program Cost results
5.4.5.3 Discussion of DOC trade studies

5.4.5.1 Discussion of DOC results

To determine the realism of the DOC predictions for the Ourania transport, several of its DOC components will be compared with DOC data of existing airplanes.

Table 5.9 provides the information. Aviation Week and Space Technology publishes DOC data regularly. The data in Table 5.9 were published in the August 28, 1989 issue, however: these data are for the year 1988.

Note that the data in Table 5.9 are given in USD per block hour. The Ourania DOC predictions of sub-section 5.4.2 are in USD per nautical mile. To convert it was necessary to multiply by the block speed: 390 kts.

The Ourania data are for the year 1990. The CEF-ratio from 1990 to 1988 is 1.003 according to Figure 2.7. This is so close to 1.0 that the Ourania data may be compared with the 1988 data for comparable airplanes.

The Ourania estimates in Table 5.9 appear to be very reasonable when compared to the data for comparable airplanes. However, the following question should be asked:

'Can a new design, such as the Ourania, be viable if its total DOC is not significantly better than that of existing airplanes?'

To address this question, the following point should be made: the DOC total for the Ourania is inflated by the selection of a 10 year depreciation period. Figure 5.13 presents the results of a trade study which shows the effect of the depreciation period on DOC. The depreciation period used by the airlines in conjunction with the data in Table 5.9 is not known. The author believes that this

Table 5.9 Direct Operating Cost Data in USD/blhr for Several Jet Transports

Source of airline data: Aviation Week and Space Technology, August 28, 1989*

Type No. of Airlines No. of Airplanes	Relative Cost	Crew	POL	Total Flight DOC	Airplane Maint.	Engine Maint.	Total Maint.	Total DOC
Boeing 727-200	High	568	834	1,633	266	195	539	2,306
11 airlines	Low	217	674	1,091	108	49	341	1,711
809 airplanes	Average	442	711	1,286	182	118	445	1,891
Boeing 737	High	449	549	1,707	269	178	484	2,250
13 airlines	Low	165	399	749	43	14	159	1,159
661 airplanes	Average	282	446	1,104	152	84	318	1,540
Boeing 757	High	547	574	1,546	152	241	415	2,136
4 airlines	Low	187	509	1,075	80	11	190	1,681
98 airplanes	Average	410	549	1,301	106	157	334	1,933
McDD MD-80	High	561	782	1,525	321	859	1,411	3,377
8 airlines	Low	196	455	1,028	44	32	124	1,380
305 airplanes	Average	405	530	1,245	127	203	416	1,884
McDD DC-9	High	485	781	1,953	311	337	773	2,749
8 airlines	Low	181	272	777	52	53	225	1,268
445 airplanes	Average	366	478	1,044	181	143	423	1,569
Ourania** 500 airplanes	Estimated in 5.4.2***	227	479	766****	300	269	965	2,847

* 1988 Data ** 1990 Estimates

*** The data in 5.4.2 are in USD/nm. They must be multiplied by the block speed of 390 kts to obtain the data for this table.

**** Includes 0.02DOC for insurance

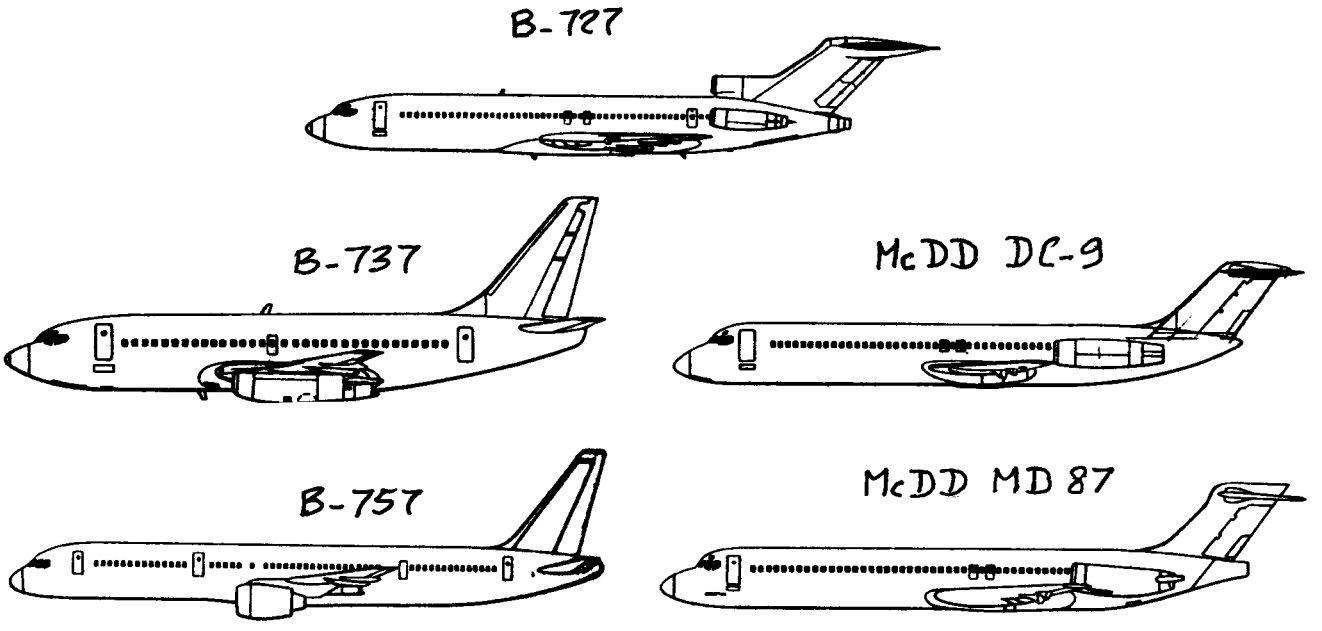

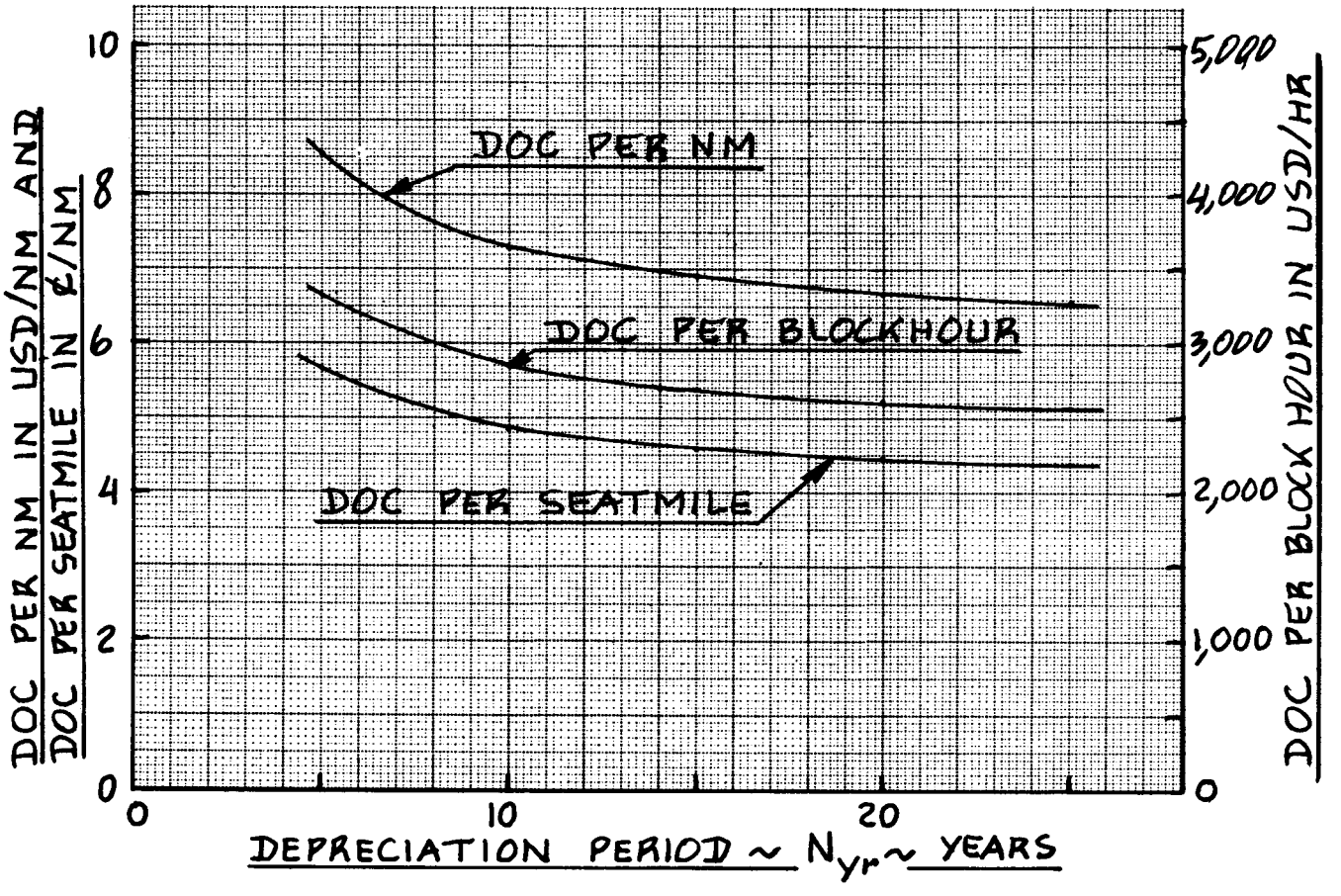

Figure 5.13 Effect of Depreciation Period on the Direct Operating Cost of the Ourania Transport

period is much longer than 10 years! If a 20 year period of depreciation is used, the Ourania data look better!

One final comment on the data in Table 5.9: the wide gap between the 'high' and the 'low' data is caused by a number of factors:

* differences in route structure
* differences in pay scales
* differences in depreciation strategies
* differences in age of airplanes

5.4.5.2 Discussion of program cost results

It is now possible to compare the three program cost sources of Eqn.(2.3) for the Ourania program with each other. The fourth cost source, C_{DISP}, was not considered because the expected life of the airplane is considerably longer than the 10 year depreciation period used in finding the program operating cost data.

The three program cost sources are as follows:

1.) Research, development, test and evaluation program cost, from Section 3.8:

C_{RDTE} = USD 1,232,000,000

2.) The acquisition program cost, from Section 4.6:

C_{ACQ} = USD 10,056,000,000

3.) The operating program cost, from Section 5.4:

C_{OPS} = USD 70,078,905,000

What is clear from all this is that the trends of Figure 2.5 and therefore inequality (2.4) are indeed correct:

$$C_{OPS} \gg C_{ACQ} \gg C_{RDTE}$$

There appears to be roughly an order of magnitude (i.e. a factor of 10) difference between the three major program cost sources. This should emphasize further the points made by Figure 2.3: early design decision making has a large impact on the ultimate cost of an airplane program!

5.4.5.3 Discussion of DOC trade studies

The purpose of this sub-sub-section is to present and discuss the results of several trade studies which show how DOC is affected by the following parameters:

1) Block distance, R_{bl}

2) Crew salary, SAL

3) Fuel Price, FP

4) Specific fuel consumption, c_j

5) Airframe and systems maintenance manhours per block hour, $MHR_{map_{bl}}$

6) Take-off weight, W_{TO}

The results of these trade studies are presented in Figures 5.14 through 5.19.

Figure 5.14 shows the strong effect of block distance on DOC: decreasing the block distance below 1,000 nm has a very inflationary effect on DOC.

The effect of crew salary on DOC is seen to be very weak in Figure 5.15: doubling the crew salary has only a marginal effect on DOC.

Figure 5.16 indicates the very strong effect of fuel price on DOC. Figure 5.17 shows that specific fuel consumption also has a strong effect on DOC. If fuel prices rise too much, there will be strong pressure on airplane designers to seek ways to:

1) reduce fuel consumption: lower drag!

and

2) decrease specific fuel consumption: more advanced engine technology!

It is seen from Figure 5.18 that the number of airplane maintenance manhours per block hour is a strong factor in determining airplane DOC. Anything that the designer can do to lower the need for maintenance will be benificial. However, read the caution notes below!

Finally, Figure 5.19 shows that an increase in take-off weight (as caused by an increase in empty weight) also drives up the DOC of an airplane. Thus, designing for low empty weight helps to keep the DOC down.

NOTES OF CAUTION:

I. If a reduction in takeoff weight is achieved by use of more expensive materials or manufacturing techniques,

and:

If a reduction in drag or engine specifics is achieved by higher cost in manufacturing of airframe and/or engine,

then it will be necessary to evaluate the net benefit on DOC. The data presented here assume that ALL ELSE is kept constant. That is hardly ever the case!

II. Several cost contributions in this chapter were expressed as a fraction of DOC. One example is the IOC of sub-section 5.4.3. There is no reason why IOC should change if parameters such as takeoff weight, fuel price, engine specific fuel consumption, etc. are changed. The effect of these parameters on the total operating cost (TOC) should therefore be evaluated with the help of a baseline IOC. This baseline IOC must be kept constant while parameters which do not affect IOC are being varied.

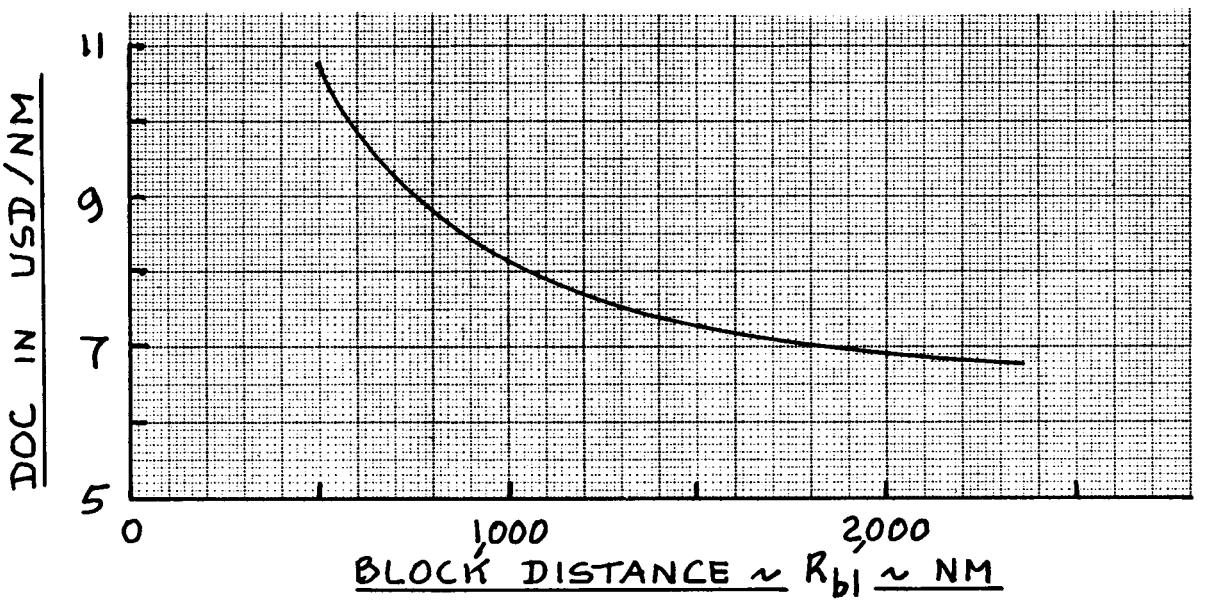

Figure 5.14 Effect of Block Distance on the Direct Operating Cost of the Ourania Transport

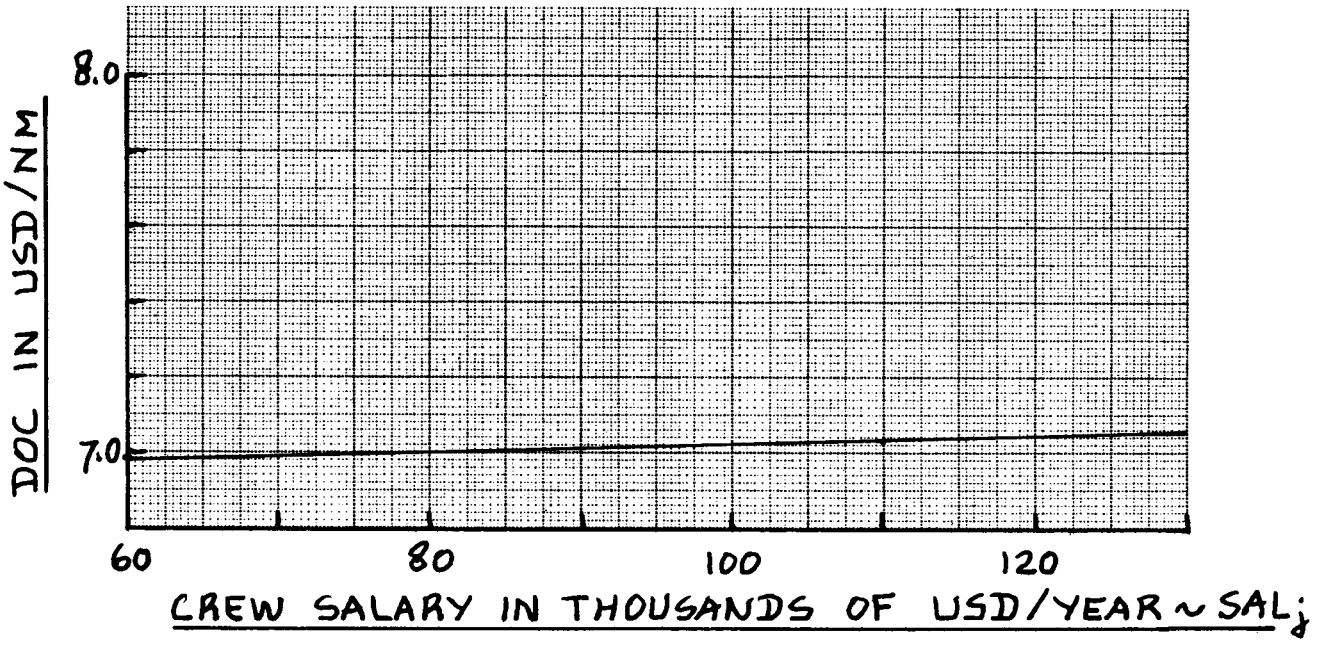

Figure 5.15 Effect of Crew Salary on the Direct Operating Cost of the Ourania Transport

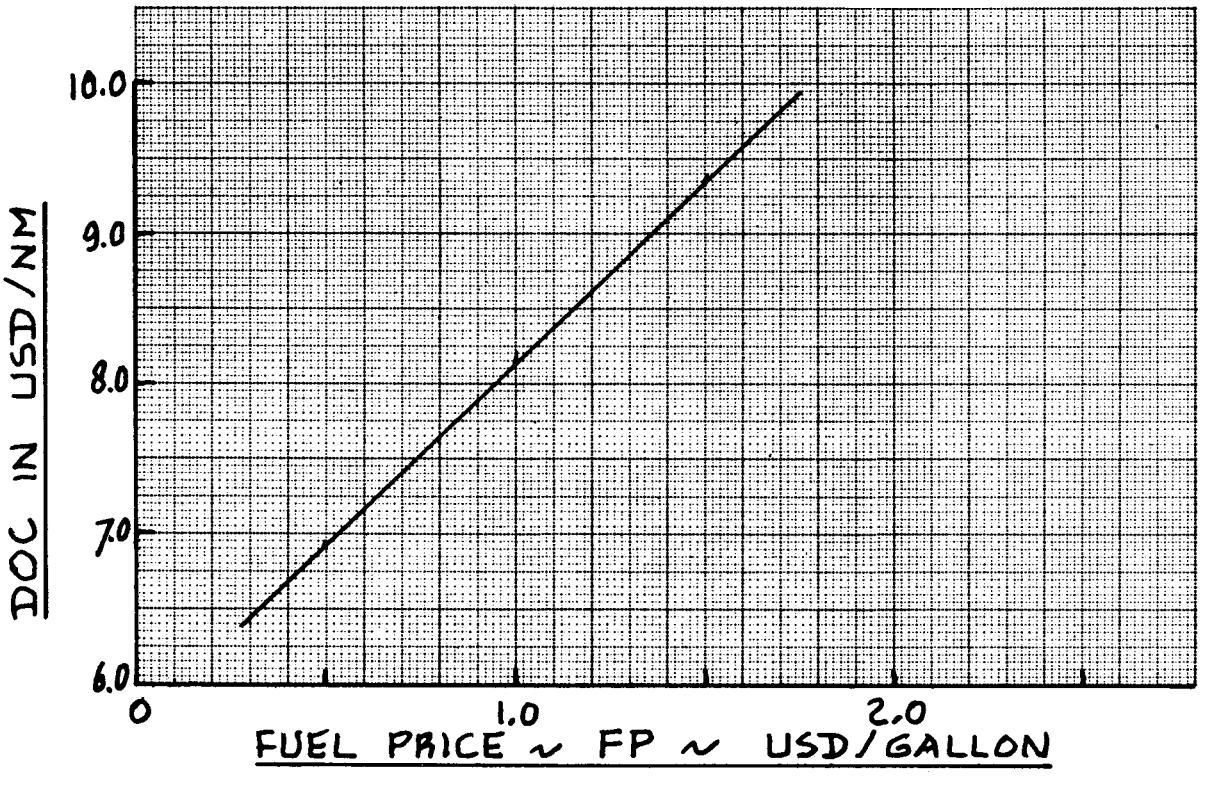

Figure 5.16 Effect of Fuel Price on the Direct Operating Cost of the Ourania Transport

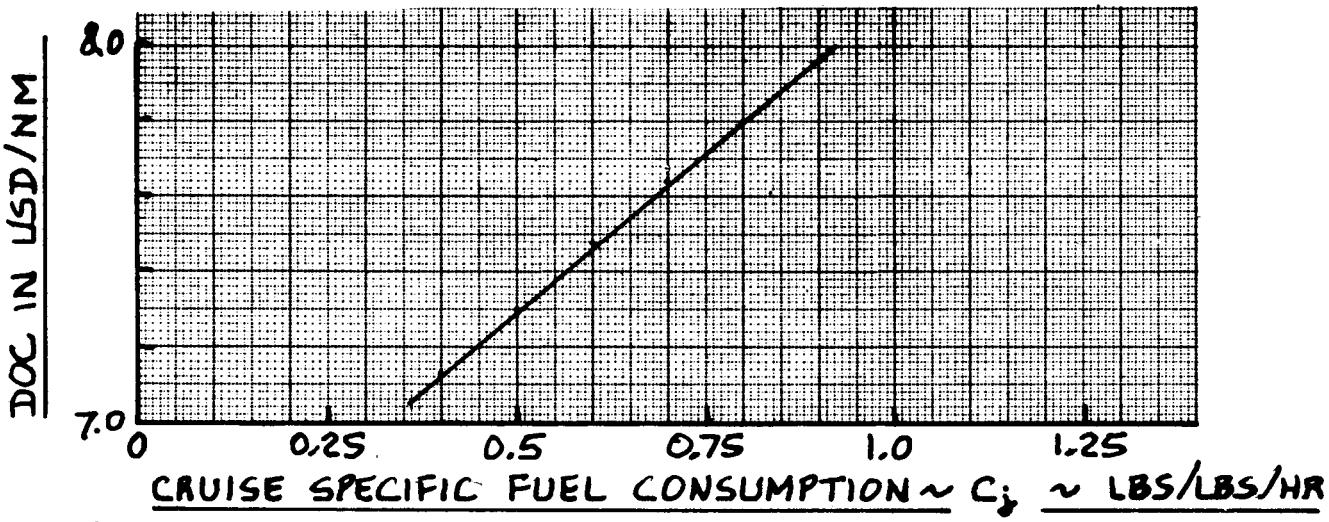

Figure 5.17 Effect of Specific Fuel Consumption on the Direct Operating Cost of the Ourania Transport

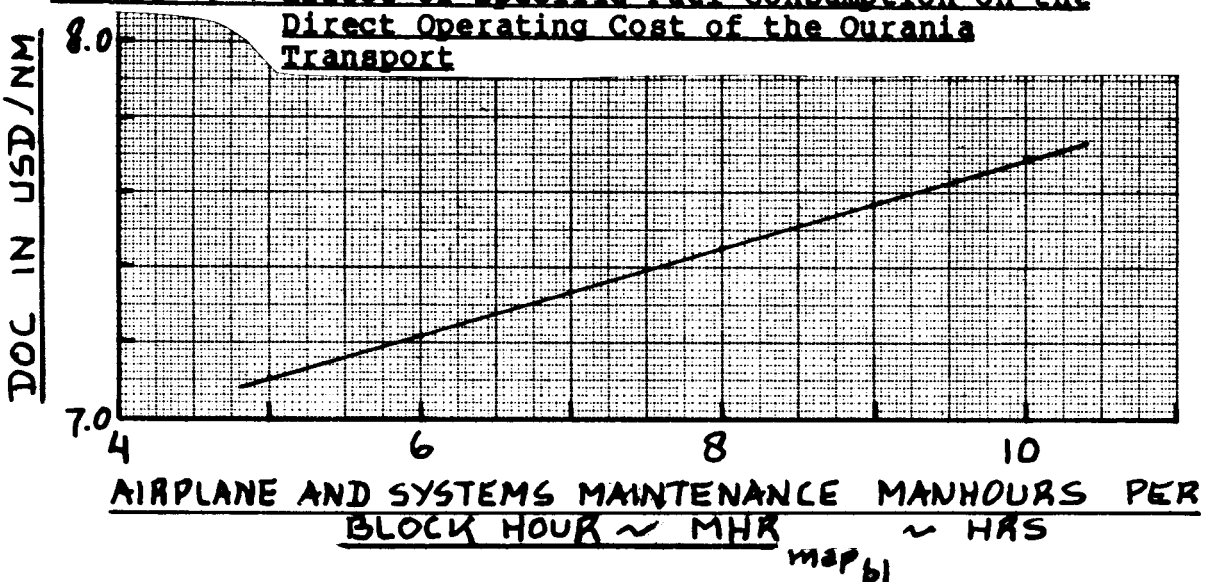

Figure 5.18 Effect of Maintenance Manhours per Block Hour on the Direct Operating Cost of the Ourania Transport

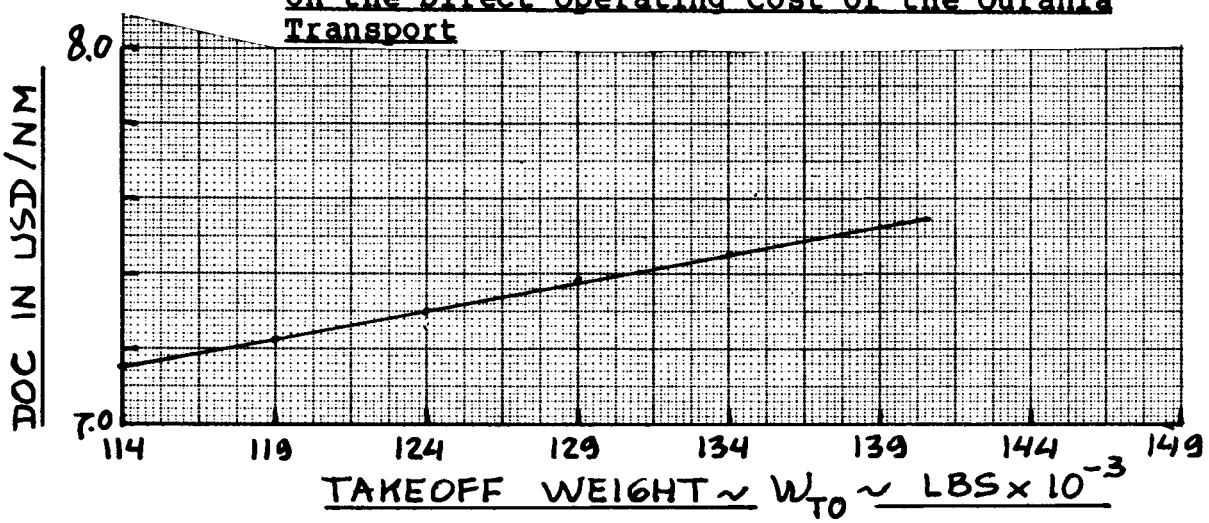

Figure 5.19 Effect of Takeoff Weight on the Direct Operating Cost of the Ourania Transport

5.5 SOME IMPORTANT OBSERVATIONS ABOUT COMMERCIAL AIRPLANE OPERATING COST

The purpose of this section is to discuss a number of important aspects of airplane operating costs: direct (DOC), indirect (IOC) and total (TOC). The total operating cost, TOC, is related to the direct (DOC) and indirect (IOC) operating costs by:

$$TOC = DOC + IOC \tag{5.61}$$

Table 5.10 shows some historical trends of the operating cost components as defined by Equations (5.19) and (5.57). Note that the financing cost is not included because this is not normally disclosed by airlines.

Note that the DOC over the last decade has gradually decreased from 56 percent to 53 percent of TOC, while the IOC has increased from 44 percent to 47 percent of TOC. The reason for these changes is not known. Based on the data, it seems reasonable to assume for the year 1985:

$$DOC = 0.53(TOC) \tag{5.62}$$

$$IOC = 0.47(TOC) \tag{5.63}$$

Note also from Table 5.10 that the fuel and oil cost fraction of TOC has increased from 19 percent to 23 percent, despite a decrease in fuel prices (Fig.5.3) from 1981 to 1985! Also, the flight crew cost as a fraction of TOC has decreased from 9 percent to 7 percent. This may be because during this period:

1) inflation was brought under reasonable control
2) average crew salaries have decreased.

It is useful to keep the orders of magnitude of the various operating cost contributions in mind. The 1985 data suggest the following tabulation of TOC components:

$$DOC_{flt} = 0.33(TOC) \tag{5.64}$$

where:

$$C_{crew} = 0.07(TOC) \tag{5.64a}$$

$$C_{pol} = 0.23(TOC) \tag{5.64b}$$

$$C_{ins++} = 0.03(TOC) \tag{5.64c}$$

$$DOC_{maint} = 0.10(TOC) \tag{5.65}$$

Table 5.10 Trends in Airline Total (= DOC + IOC) Operating Cost Components

Cost Item	1976	1981	1982	1983	1984	1985
Direct Operating Cost (DOC)						
Flight crew, C_{crew}	0.086	0.072	0.072	0.072	0.069	0.068
Fuel, oil and lub., C_{pol}	0.193	0.292	0.272	0.245	0.233	0.232
Hull insurance, rentals and training, C_{ins++}	0.039	0.027	0.025	0.027	0.031	0.034
DOC_{flt}	0.318	0.391	0.370	0.344	0.333	0.333
DOC_{maint}	0.125	0.103	0.100	0.100	0.101	0.100
DOC_{depr}	0.080	0.064	0.068	0.072	0.072	0.071
DOC_{lnr}	0.037	0.035	0.033	0.033	0.030	0.030
DOC Total	0.560	0.593	0.571	0.549	0.536	0.534
Indirect Operating Cost (IOC)						
IOC_{pax}	0.094	0.086	0.091	0.092	0.092	0.092
IOC_{sta}	0.133	0.113	0.122	0.126	0.130	0.130
IOC_{pse}	0.149	0.147	0.155	0.164	0.166	0.165
IOC_{gaa}	0.064	0.061	0.061	0.069	0.076	0.079
IOC Total	0.440	0.407	0.429	0.451	0.464	0.466
TOC = DOC + IOC	1.000	1.000	1.000	1.000	1.000	1.000

Notes: 1) IOC_{frt} is included in IOC_{sta} 2) Source: Interavia, Feb.1987

$$DOC_{depr} = 0.07(TOC) \quad (5.66)$$

$$DOC_{lnr} = 0.03(TOC) \quad (5.67)$$

$$IOC_{pax} = 0.09(TOC) \quad (5.68)$$

$$IOC_{sta} = 0.13(TOC) \quad (5.69)$$

$$IOC_{pse} = 0.17(TOC) \quad (5.70)$$

$$IOC_{gaa} = 0.08(TOC) \quad (5.71)$$

It is of interest to consider the effect of block distance, R_{bl}, and of airplane type on the various contributions to TOC.

Figures 5.20 and 5.21 provide this information for four types of airplane for the four major DOC components. It is noted from Fig.5.20 that block distance has essentially no effect on the fractions of DOC_{flt} and DOC_{depr} of total DOC. However, airplane type has a significant effect on their relative contributions.

It is noted from Figure 5.21 that block distance and type of airplane both have a significant influence on the magnitudes of DOC_{maint} and DOC_{lnr} relative to total DOC.

Figures 5.22 - 5.24 provide similar information for the five major IOC components. It is noted from Fig.5.22 that neither the type of airplane nor block distance have much effect on the magnitudes of IOC_{pax} and IOC_{gaa} relative to total IOC.

However, as is seen in Figures 5.23 and 5.24, both airplane type and block distance have a considerable effect on IOC_{sta}, IOC_{pse} and IOC_{ascf} as a fraction of total IOC.

The author believes that even though the data in Figures 5.20 - 5.24 are from 1975, they can be expected to apply to 1990 (and perhaps beyond) because of the fact that (as Table 5.10 indicates) calendar time had only a minor effect on the distribution of TOC components.

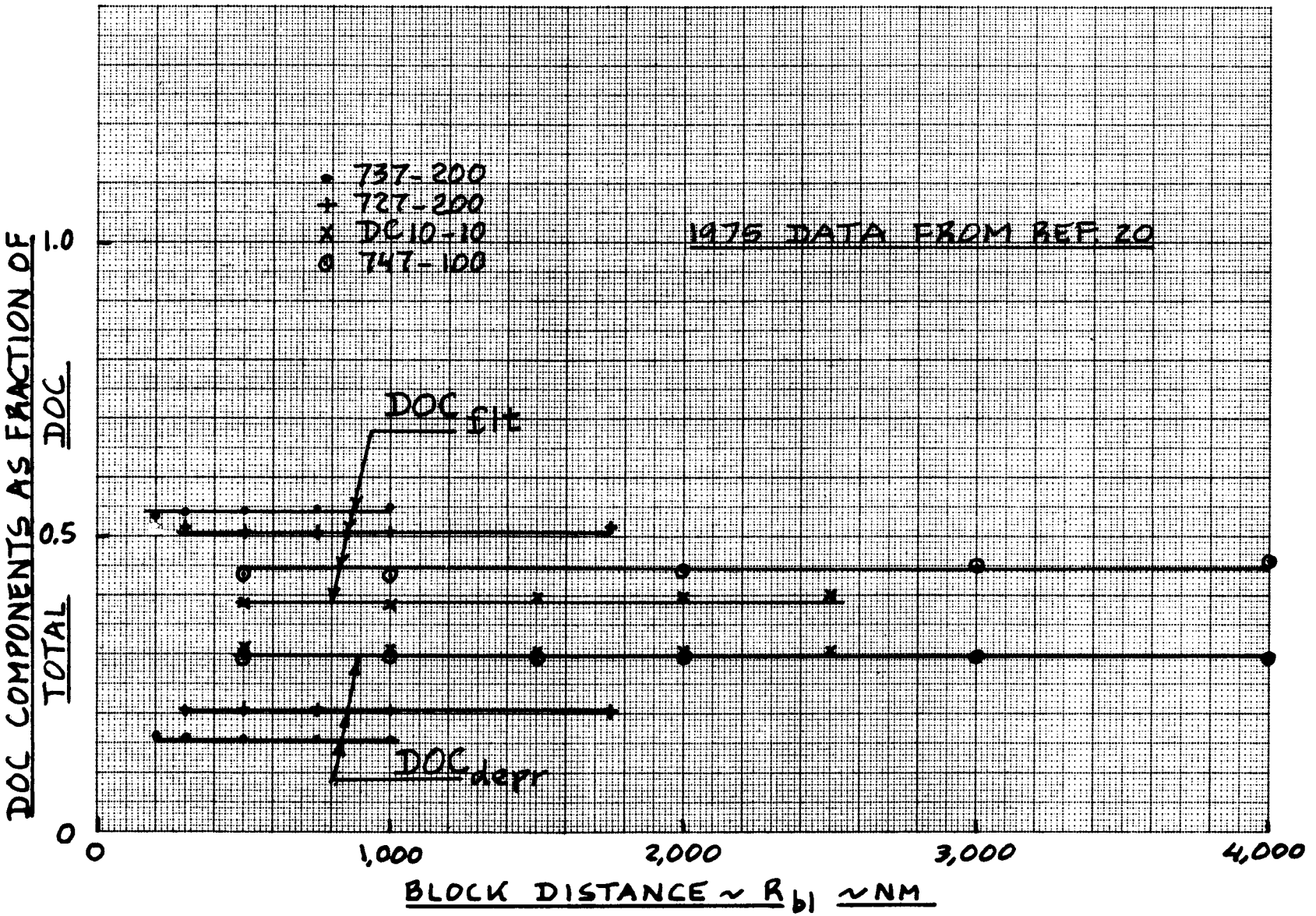

Figure 5.20 Effect of Block Distance and Airplane Type on the Direct Operating Cost for Flight and Depreciation as a Fraction of Total DOC

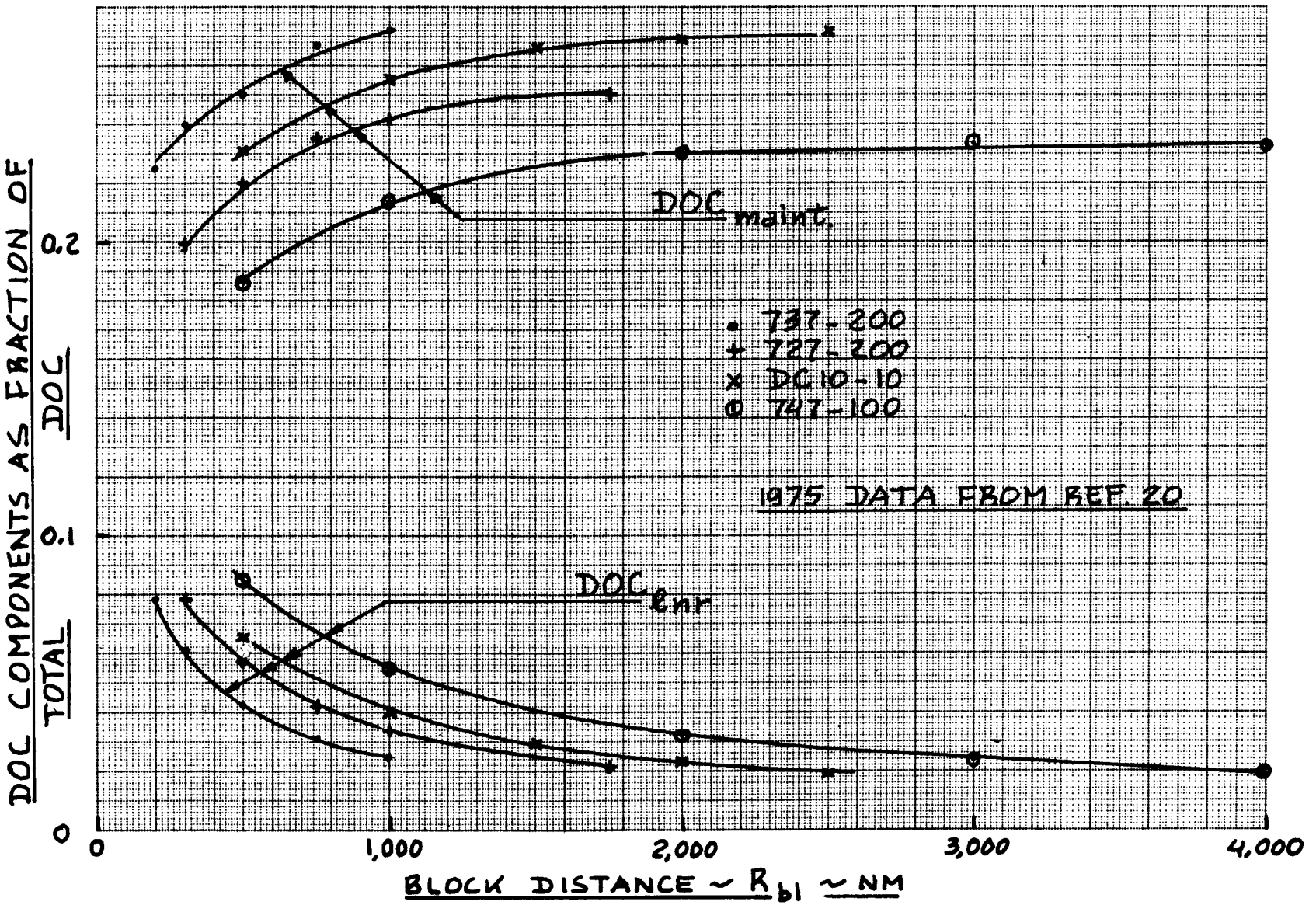

Figure 5.21 Effect of Block Distance and Airplane Type on the Direct Operating Cost for Maintenance and Landing, Navigation and Registration as a Fraction of Total DOC

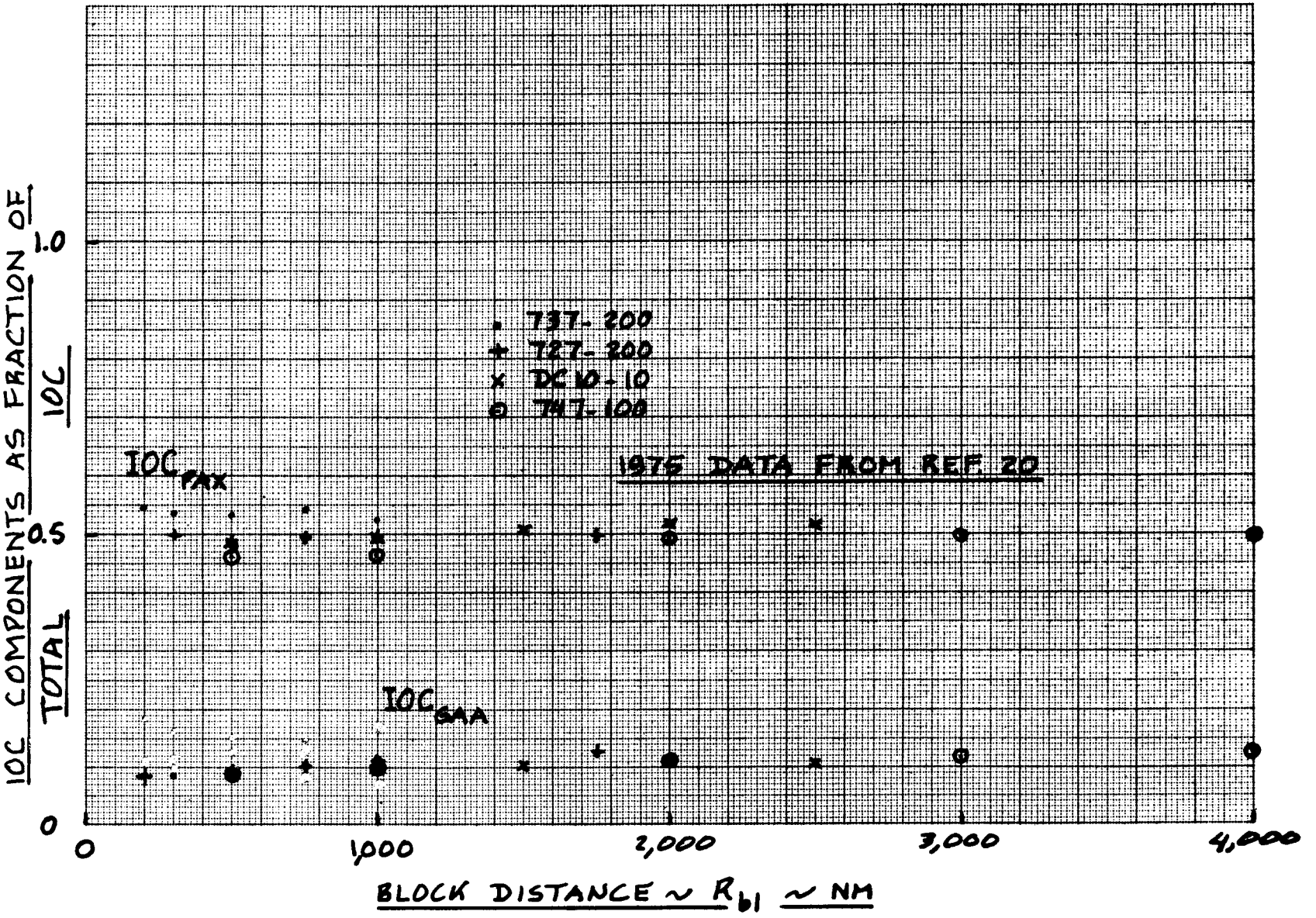

Figure 5.22 Effect of Block Distance and Airplane Type on the Indirect Operating Cost for Passengers and General Administrative Expenses as a Fraction of Total IOC

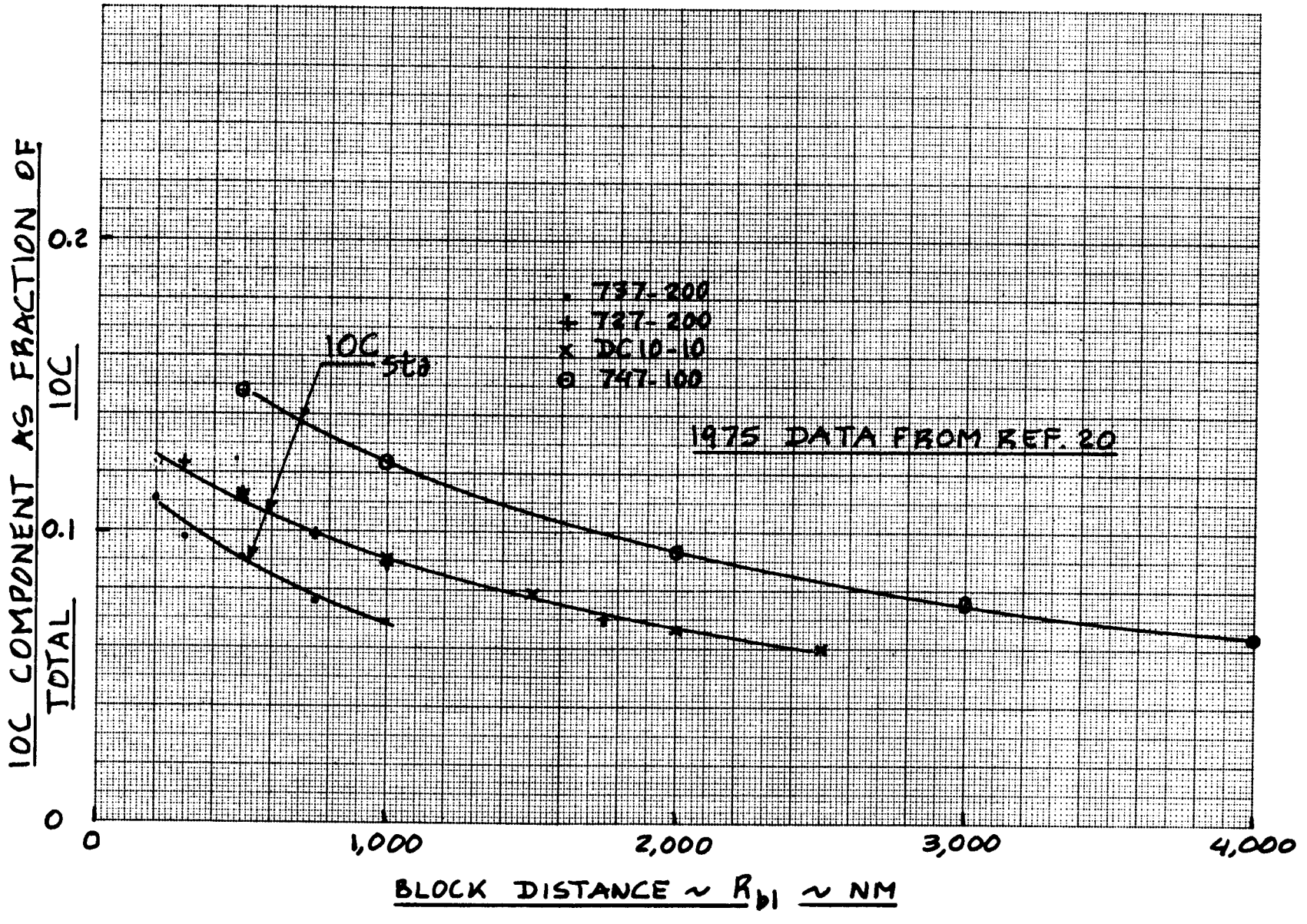

Figure 5.23 Effect of Block Distance and Airplane Type on the Indirect Operating Cost for Station Operation as a Fraction of Total IOC

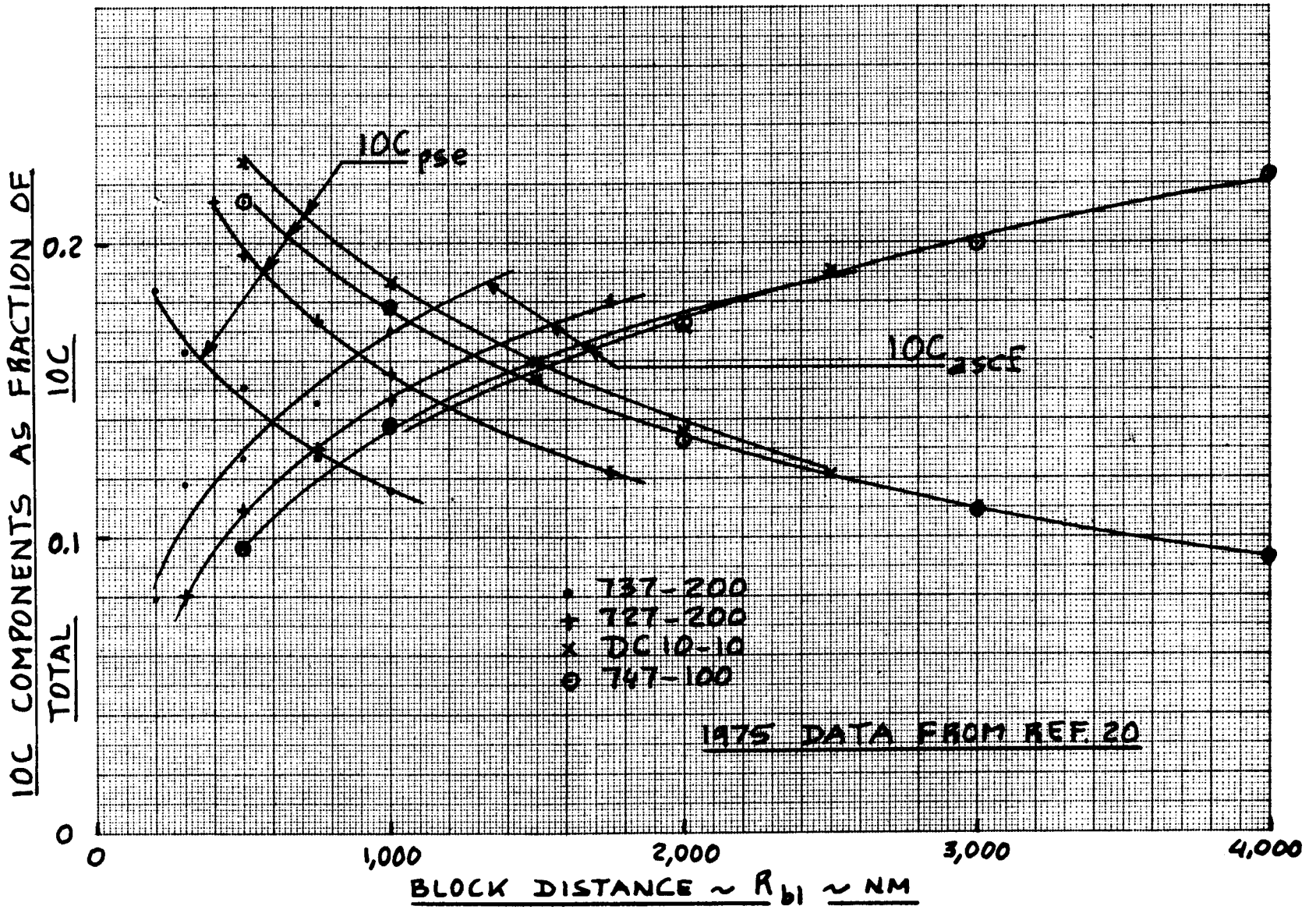

Figure 5.24 Effect of Block Distance and Airplane Type on the Indirect Operating Cost for Promotion, Sales and Entertainment and for Airplane Service, Control and Freight as a Fraction of Total IOC

6. METHOD FOR ESTIMATING OPERATING COST OF MILITARY AIRPLANES

The purpose of this chapter is to present a method for estimating the operating cost of military airplanes in peace time. A method for estimating the operating cost of commercial airplanes is presented in Chapter 5.

A detailed method for estimating operating cost for military airplanes is provided in Ref.10. Despite the level of detail given in Ref.10, it is not sufficient to give the preliminary designer specific insight into what can be done (from a design viewpoint) to lower operating cost of military airplanes. Therefore, the author has decided to combine the methods, ideas and data given in Refs 10 and 14 into a simpler method. This method should be used only for preliminary cost estimating purposes.

IMPORTANT ASSUMPTION:

Military airplanes are acquired in a manner depending considerably on budgetary and political constraints. It is not possible to translate such constraints into any rational format. Therefore, no attempt will be made to represent program operating cost as a summation over a number of calendar years. Instead, the assumption will be made that the number of airplanes to be acquired, N_{acq}, have indeed been acquired by the military service. Furthermore, the assumption will be made that deliveries have been made to ONE military service only so that cost differences between services need not be accounted for.

The program operating cost of military airplanes can be broken down as follows:

$$C_{OPS} = C_{POL} + C_{PERSDIR} + C_{PERSIND} + C_{CONMAT} + C_{SPARES} + C_{DEPOT} + C_{MISC} \quad (6.1)$$

where: C_{POL} is the program fuel, oil and lubricants cost: see Section 6.1

$C_{PERSDIR}$ is the program cost of direct personnel (that is aircrew and maintenance): see Section 6.2

$C_{PERSIND}$ is the program cost of indirect personnel: see Section 6.3

C_{CONMAT} is the program cost of consumable materials used in conjunction with maintenance: see Section 6.4

C_{SPARES} is the program cost of spares: see Section 6.5

C_{DEPOT} is the program cost associated with depots: see Section 6.6

C_{MISC} is the program miscellaneous cost: see Section 6.7

The total (or program) operating cost of military airplanes, C_{OPS}, is shown in relationship to other life cycle cost (LCC) sources in Eqn.(2.3) and in Figure 2.3.

A summary for the determination of the program operating cost for a military airplane, C_{OPS}, is presented in Section 6.8. An example application of the method is given in Section 6.9. Some important observations on the subject of military airplane operating cost are included in Section 6.10.

6.1 PROGRAM COST OF FUEL, OIL AND LUBRICANTS: C_{POL}

The program cost of fuel, oil and lubricants depends on the following:

* type of airplane
* mission of the airplane
* annual utilization
* number of airplanes in active service

The program cost for fuel, oil and lubricants can be estimated from:

$$C_{POL} = [(F_{OL})(W_{F_{used}})\{(FP)/(FD)\}* *(N_{mission})(N_{serv})](N_{yr}) \qquad (6.2)$$

where: F_{OL} is a factor which accounts for the cost of oil and lubricants. According to Ref.14 it is acceptable to use: $F_{OL} = 1.005$

$W_{F_{used}}$ is the mission fuel used in lbs. per mission. This can be found from Eqn. (2.14) in Part I or from the more detailed method of Section 5.4, Part VII.

FP is the price of fuel in USD per gallon. This is obtained from Figure 5.3. In most instances the price of JP-4 can be used.

FD is the fuel density in lbs per gallon. This may be obtained from p. 88. In most instances the density of JP-4 can be used.

$N_{mission}$ is the number of missions flown per year. This can be estimated from:

$$N_{mission} = (U_{ann_{flt}})/(t_{mis}) \qquad (6.3)$$

where: $U_{ann_{flt}}$ is the annual utilization in flight hours. Table 6.1 provides typical data for military airplane utilization in peace time.

t_{mis} is the average mission time in hours. Figure 6.1 shows how this is defined.

NOTE: in the case of multi-mission airplanes, a scenario of typical 'mission mixes' per year must be predicted.

N_{serv} is the number of airplanes of the type in actual service. This number is averaged as:

$$N_{serv} = N_{acq} - N_{res} - 0.5(N_{loss}) \qquad (6.4)$$

where: N_{acq} is the number of airplanes which are acquired

N_{res} is the number of airplanes held in active reserve

N_{loss} is the number of airplanes lost through accidents over the service life, N_{yr}

How to determine these three airplane quantities is discussed next.

TABLE 6.1 MILITARY AIRPLANE UTILIZATION IN FLIGHT HOURS PER YEAR AND MILITARY CREW TO AIRPLANE RATIOS

Airplane Type	Flight Hours per airplane per year, $U_{ann_{flt}}$	Crew Ratio per airplane, R_{cr}	Number in crew N_{crew}
Trainers	600 - 1,000	-	2
Fighters	250 - 400	1.1	1 - 2
Bombers	300 - 600	1.5	2 - 5
Tankers	300 - 600	1.5	4 - 6
Transports	< 1,200	1.5	4 - 8
	1,200 - 2,400	2.5	4 - 8
	2,400 - 3,600	3.5	4 - 8

NOTE: average annual utilization for military airplanes is 350 hours

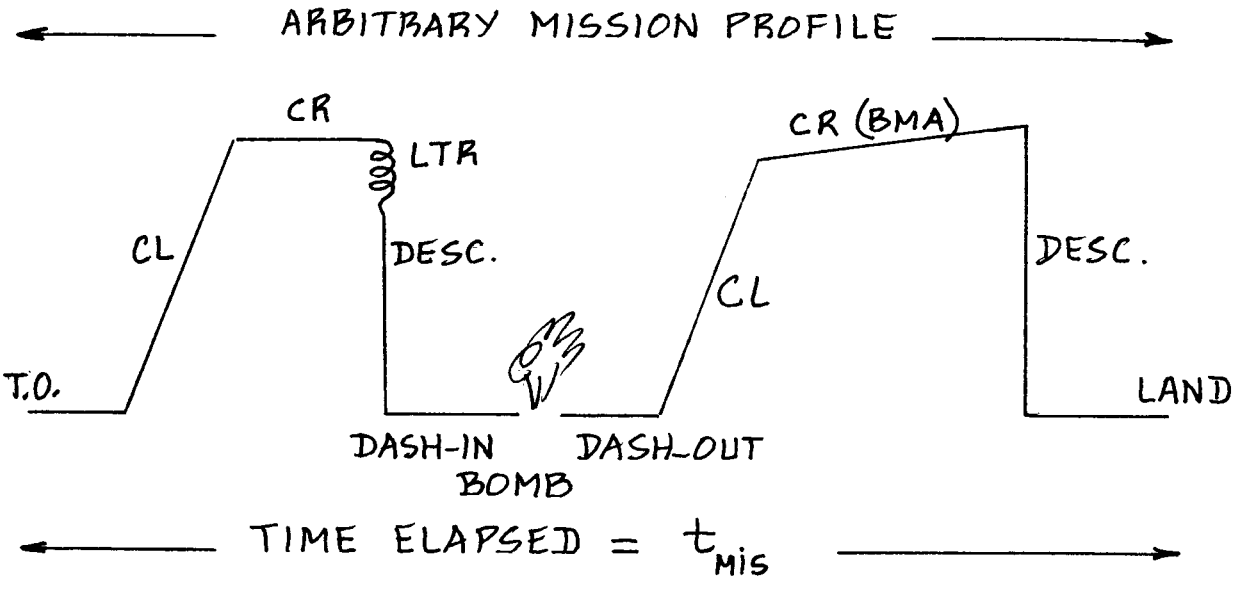

NOTE: FOR EXAMPLE MISSION PROFILES, SEE: P.61 IN PART I AND PAGES 244-248, AND 280-284 IN PART VII.

Figure 6.1 Definition of Mission Time, t_{mis}

The number of airplanes acquired, N_{acq}, is assumed to be equal to the number of airplanes built to production standards, N_m. This in turn is related to the total number of airplanes built, $N_{program}$ by:

$$N_{program} = N_m + N_{rdte} \quad (6.5)$$

where: N_{rdte} is the number of airplanes built during the research, development, technology and evaluation phase. For military programs this number is in the following range:

$$N_{rdte} = 6 \text{ to } 20 \quad (6.6)$$

NOTE: Table 4.1 gives examples of airplane program production runs for several military programs.

The number of airplanes held in reserve, N_{res}, depends on factors such as: politics and estimated loss rates in peace time. For preliminary cost estimating purposes it is suggested to use:

$$N_{res} = 0.10(N_{acq}) \quad (6.7)$$

The total number of airplanes lost due to accidents in peace time, N_{loss}, is estimated from:

$$N_{loss} = (L_R)(N_{serv})(U_{ann_{flt}})(N_{yr}) \quad (6.8)$$

where: L_R is the annual loss rate expressed in airplanes lost per 10^5 flying hours. Table 6.2 shows typical loss rates for USAF and for USN/USMC.

For the reader interested in loss rate data in times of military conflict, reference is made to Section 13.3 in Part IV. Methods to predict combat loss rates are given in Ref.22.

N_{yr} is the number of years the airplane is in active service. In peace time this number may be assumed to range from 20 to 40 years. Table 6.3 provides 1987 data for the average age of several U.S. military airplanes.

All other quantities were previously defined.

Table 6.2 Military Airplane Accident Summaries for 1984 and 1986

Type	1984 Number of Accidents	1984 Total Flight Hours (Fleet)	1984 Accident Rate, L_R	1986 Number of Accidents	1986 Total Flight Hours (Fleet)	1986 Accident Rate, L_R
USAF:						
T-37	1	333,000	0.3	1	333,300	0.3
T-38	3	375,000	0.8	4	363,600	1.1
F-4	11	275,000	4.0	12	245,000	4.9
RF-4	1	77,000	1.3	5	78,000	6.4
F-5	2	29,000	6.9	6	26,500	22.6
F-15	3	176,000	1.7	7	194,400	3.6
F-16	10	200,000	5.0	11	250,000	4.4
F-111	3	79,000	3.8			
A-7	6	86,000	7.0	1	83,300	1.2
A-10	6	222,000	2.7	3	214,300	1.4
C-130	3	375,000	0.8	2	400,000	0.5
C-135				1	250,000	0.4
C-141	1	333,000	0.3	1	333,300	0.3
B-52	2	105,000	1.9			
Totals:	52	2,665,000	2.0	54	2,771,700	1.9
USN and USMC:						
T-34C	1	179,597	0.6	2	180,900	1.1
T2-J	2	84,734	2.4	2	14,300	14.0
TA-4	9	102,739	8.8	6	118,300	5.1
F-4	4	86,331	4.6	5	54,400	9.2
F-14	4	110,727	3.6	10	120,600	8.3
F-18	1	47,256	2.1	2	107,500	1.9
A-4	4	49,472	8.1	3	59,200	5.1
A-6	7	106,637	6.6	6	104,900	5.7
EA-6	3	26,778	11.2	3	29,800	10.0
A-7	13	146,547	11.3	9	126,400	7.1
AV-8	1	18,297	5.5	3	25,400	13.1
Totals:	49	960,000	5.1	51	941,700	5.4

Data from: Aviation Week and Space Technology, March 11, 1985 and June 8, 1987
Note: Accident Rate = Loss Rate = L_R in airplanes per 100,000 flying hours

TABLE 6.3 SOME AIR FORCE AIRPLANES AND THEIR AGE (1987)

Airplane Type	USAF No. in Service	USAF Ave. Age (yrs)	ANG No. in Service	ANG Ave. Age (yrs)	AF Reserve No. in Service	AF Reserve Ave. Age (yrs)
T-33	54	29.4	21	31.7		
T-37	609	25.3				
T-38	810	21.5				
F-4	596	17.1	602	20.5	119	21.0
F-5	96	11.7				
F-15	732	6.9	66	11.4		
F-16	943	3.7	132	5.5	49	5.0
F-100	10	29.4				
F-106	5	28.1	33	27.9		
F-111	334	16.4				
A-7	31	15.9	342	14.1		
A-10	451	6.9	106	8.0	97	9.0
A-37	22	13.8	60	14.7		
C-5	76	12.1	5	16.9	15	17.0
C-9	23	16.5				
C-10	56	2.9				
C-12	75	6.2	6	1.9		
C-20	13	1.1				
C-21	79	2.7	3	0.1		
C-22	1	3.6	4	2.7		
C-23	18	2.4				
C-130	354	19.3	210	19.8	168	23.4
C-135	608	26.2	104	28.6	24	29.0
C-140	5	24.7				
C-141	255	21.0	8	21.3	8	22.0
E-3	33	7.9				
B-1	60	0.8				
B-52	263	27.0				
FB-111	62	17.1				

Data from: Air Force Magazine, May 1987

NOTE: This table may be used to estimate N_{yr} for a new military airplane program.

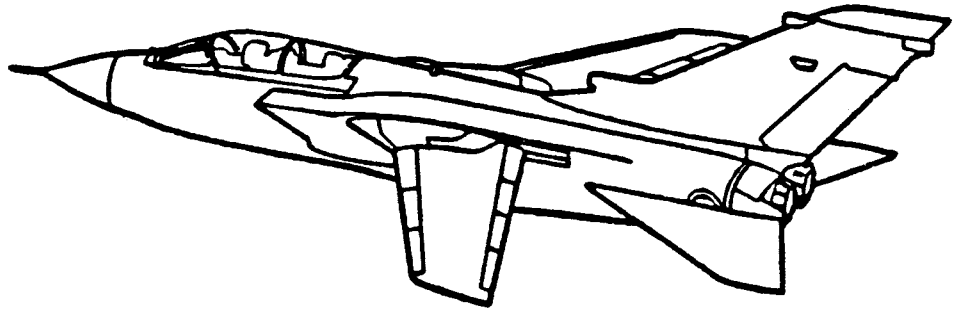

6.2 PROGRAM COST OF DIRECT PERSONNEL: $C_{PERSDIR}$

The program cost component of direct personnel can be split into two elements:

$$C_{PERSDIR} = C_{crewpr} + C_{mpersdir} \quad (6.9)$$

where: C_{crewpr} is the program cost for aircrews: see sub-section 6.2.1

$C_{mpersdir}$ is the program cost for direct maintenance personnel: see sub-section 6.2.2

6.2.1 Program Cost of Aircrews: C_{crewpr}

The program cost for aircrews may be estimated from:

$$C_{crewpr} = \quad (6.10)$$

$$= (N_{serv})(N_{crew})(R_{cr})(Pay_{crew})(OHR_{crew})(N_{yr})$$

where: N_{serv} is found from Eqn. (6.4)

N_{crew} is the number of crew members required for the airplane: see Table 6.1.

R_{cr} is the crew ratio per airplane. This may be determined with the help of Table 6.1.

Pay_{crew} is the annual pay in USD per year. The annual pay depends on:

* pay grade
* years of service

Table 6.4 gives military pay data applicable to the calendar years 1989 and 1990. To determine Pay_{crew}, several assumptions must be made about crew composition in terms of grade and years in service. For preliminary cost estimating purposes it is suggested to assume:

For trainers: average crew member is a 1st Lt. with 5 years of military service.

For fighters: average crew member has the rank of captain with 8 years of military service.

Table 6.4 1989 Military Pay Data for Aircrews*

Years in Service	Basic Pay in USD/year — Rank: Col/Capt	LtCol/Cmdr	Maj/LtCmdr	Capt/Lt	1stLt/LtJG	2ndLt/Ens
4	38,099	32,677	28,488	26,964	24,109	19,418
6	38,099	32,677	29,027	28,253	24,617	19,418
8	38,099	32,677	30,308	29,268	24,617	19,418
10	38,099	33,667	32,375	30,857	24,617	19,418
12	38,099	35,474	34,196	32,375	24,617	19,418
14	39,391	37,854	35,759	33,174	24,617	19,418
16	45,619	40,687	37,325	33,174	24,617	19,418
18	47,952	43,020	38,358	33,174	24,617	19,418
20	48,996	44,323	38,358	33,174	24,617	19,418
22	51,836	45,871	38,358	33,174	24,617	19,418

Aviation Career Incentive Pay (ACIP), excl.' Hazardous Duty Pay' in USD/month

Years of Aviation Officer Service	<or =2	>2	>3	>4	>6	>18	>20	>22
Monthly Rate	125	156	188	206	400	370	340	310

Aviation Continuation Pay (Re-up Bonus) in USD/year

Years of Active Federal Commissioned Service	6	7	8	9	10	11	12
1989 Bonus	9,000	9,000	8,250	8,250	7,125	6,000	4,875
Subsequent annual bonus	12,000	12,000	11,000	11,000	9,500	8,000	6,500

* Source: Professional Pilot Magazine, April, 1989

For bombers: average crew member has the rank of major with 12 years of military service.

For transports: average crew member has the rank of 1st Lt. with 5 years of military service. Note: transports often carry non-commissioned personnel!

IMPORTANT NOTE: the ranks given are for 'average' crew members in the USAF and the USMC only. For the USN use the 'equivalent' ranks of Table 6.4.

An example military pay calculation will now be given. For this example it is assumed that the crew pay needs to be found for a USAF fighter:

Page 152 suggests that for preliminary costing purposes it may be assumed that for a fighter the average crew member has the rank of captain with 8 years of military service. In that case, it is seen from Table 6.4 that:

$$Pay_{crew} = (29{,}268 + 12*400 + 12{,}000) =$$

$$= 46{,}068 \text{ USD/year}$$

The 12,000 pay factor assumes 1990 and beyond aviation continuation pay.

NOTE: Military pay scales are subject to congressional action. For years beyond 1990, the reader should check whether these pay scales are valid!

OHR_{crew} is an overhead rate factor, associated with the actual crew pay. Lacking actual military overhead data, it is suggested to use: $OHR_{crew} = 3.0$. This overhead rate factor is similar in magnitude to industry overhead rates.

N_{yr} is the number of years the airplane is in active service. This quantity may be estimated with the help of Table 6.3.

6.2.2 Program Cost of Direct Maintenance Personnel: $C_{mpersdir}$

The program cost of direct maintenance may be estimated from:

$$C_{mpersdir} = (N_{serv})(N_{yr})(U_{ann_{flt}})* \\ *(MHR_{flthr})(R_{m_{ml}}) \qquad (6.11)$$

where: N_{serv} is found from Eqn.(6.4)

N_{yr} is found from Table 6.3.

$U_{ann_{flt}}$ is found from Table 6.1

MHR_{flthr} is the number of maintenance manhours required per flight hour. This depends on the following factors:

* number of years in service
* equipment density (this affects accessibility)
* maturity of the technologies used in the airplane systems: propulsion, avionics, flight controls, brakes, wheels and tires.

Table 6.5 provides some historical data on the effect of 'years in service' on MHR_{flthr} for a number of military airplanes. Figure 6.2 shows some data based on actual USNavy experience for A4 type airplanes.

Figure 6.3 illustrates how equipment density affects the maintenance hours per flight hour.

The cost analyst should not attemp to arbitrarily 'lowball' a number for MHR_{flthr}. Instead, a list should be prepared of all factors which affect maintenance and which compare the new design with a comparable existing design for which MHR_{flt} is known. Only then can an educated estimate for MHR_{flthr} be made.

Nicolai (in Ref.14) implies that the number of maintenance manhours per flight hour is related

Table 6.5 Maintenance Man-Hours per Flight Hour for Military Airplanes

Type	1973	1974	1975	1976	1977	1978	1979	1980	1981	1982	1983
T-37	7.8										
T-38	10.0		8.8	11.6	8.7	9.0	12.2	9.0	10.3	6.8	10.9
F-100			19.8	17.1	17.1	16.1					
F-4D			55.6	41.9	54.2	56.2	47.7	44.8	28.4	26.9	42.0
F-4E	33.0										
RF-4C			39.6	31.9	33.8	34.2	32.8	31.1	22.9	18.2	36.1
F-5	17.0										
FB-111A			57.2	47.7	36.4	58.2	47.6	45.8	60.8	49.0	56.0
F-111D	40.0		19.8	17.1	17.1	16.1					
F-15		20.0	29.1	27.8	26.0	30.6	31.9	28.6	36.9	30.5	44.1
F-15C								13.6	24.3	22.3	32.8
F-16A	25.0						25.4	22.6	11.2	14.6	21.8
F-16B								18.4	13.9	15.3	30.6
A-7D	25.0										
A-10		13.0				7.2	11.8	12.0	11.2	8.9	13.9
C-130	20.0			25.1	37.1	22.4	19.6	19.8	21.6	19.7	24.7
C-141	21.0		17.5	18.6	18.2	17.3	15.0	15.0	20.7	19.3	25.2
C-5A	40.0		107.9	89.4	48.2	41.9	53.4	47.3	52.5	37.0	64.9
C-9	12.0										
KC-135	26.6		32.8	31.6	34.0	26.6	21.2	23.2	20.2	17.5	24.2
B-52D	37.0										
B-52G	49.0		46.5	46.9	44.9	45.5	42.1	40.6	39.6	34.0	50.7
B-52H			45.5	48.9	47.6	49.3	39.5	33.9	34.6	30.2	42.9

The following ranges are suggested for preliminary cost estimating purposes:

For Trainers: 6 - 10 For Fighters: 15 - 35
For Bombers: 25 - 50 For Transports: 25 - 60

Data from: Refs 14, 24 and Air Force Magazine, September 1983.

to the total area (in square feet) of all access panels in an airplane!

$R_{m_{ml}}$ is the military maintenance labor rate in USD/hr. This depends on many factors, including the ratio of civilian versus military personnel used in maintenance functions. For 1989, this labor rate, <u>including all overhead</u> contributions may be assumed to be:

$$(R_{m_{ml}})_{1989} = 45 \text{ USD/hr}$$

For future years it is suggested to use:

$$(R_{m_{ml}})_{\text{then year}} = (R_{m_{ml}})_{1989} * (CEF_{\text{then year}})/(CEF_{1989}) \qquad (6.12)$$

where: the CEF-values are found from Figure 2.7.

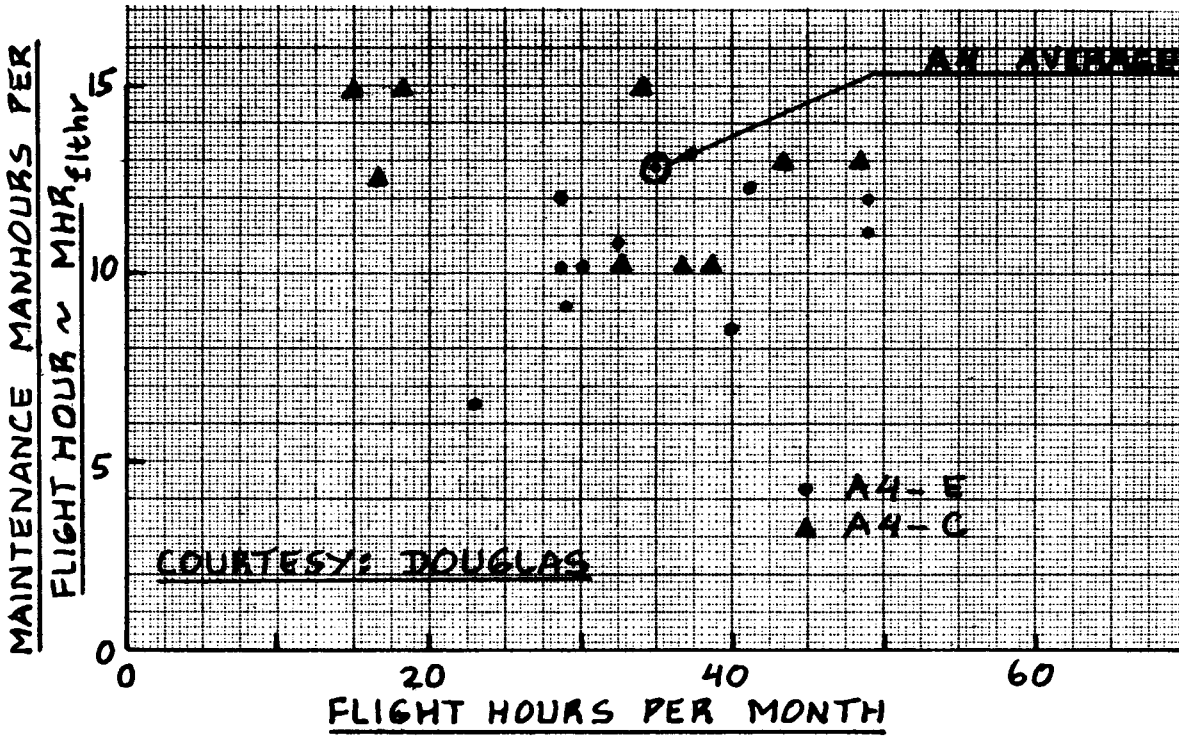

Figure 6.2 Effect of Flying Hours per Month on Maintenance Manhours per Flight Hour

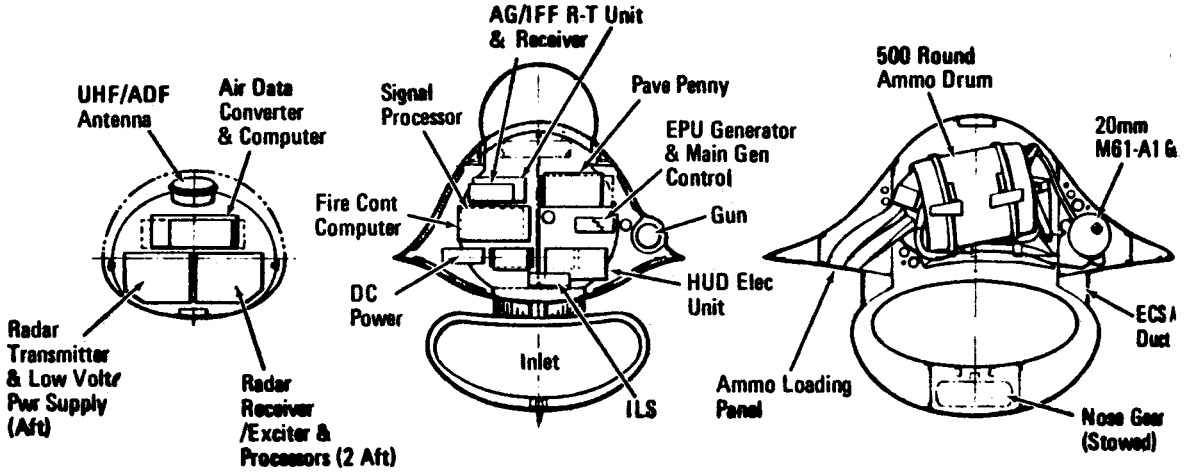

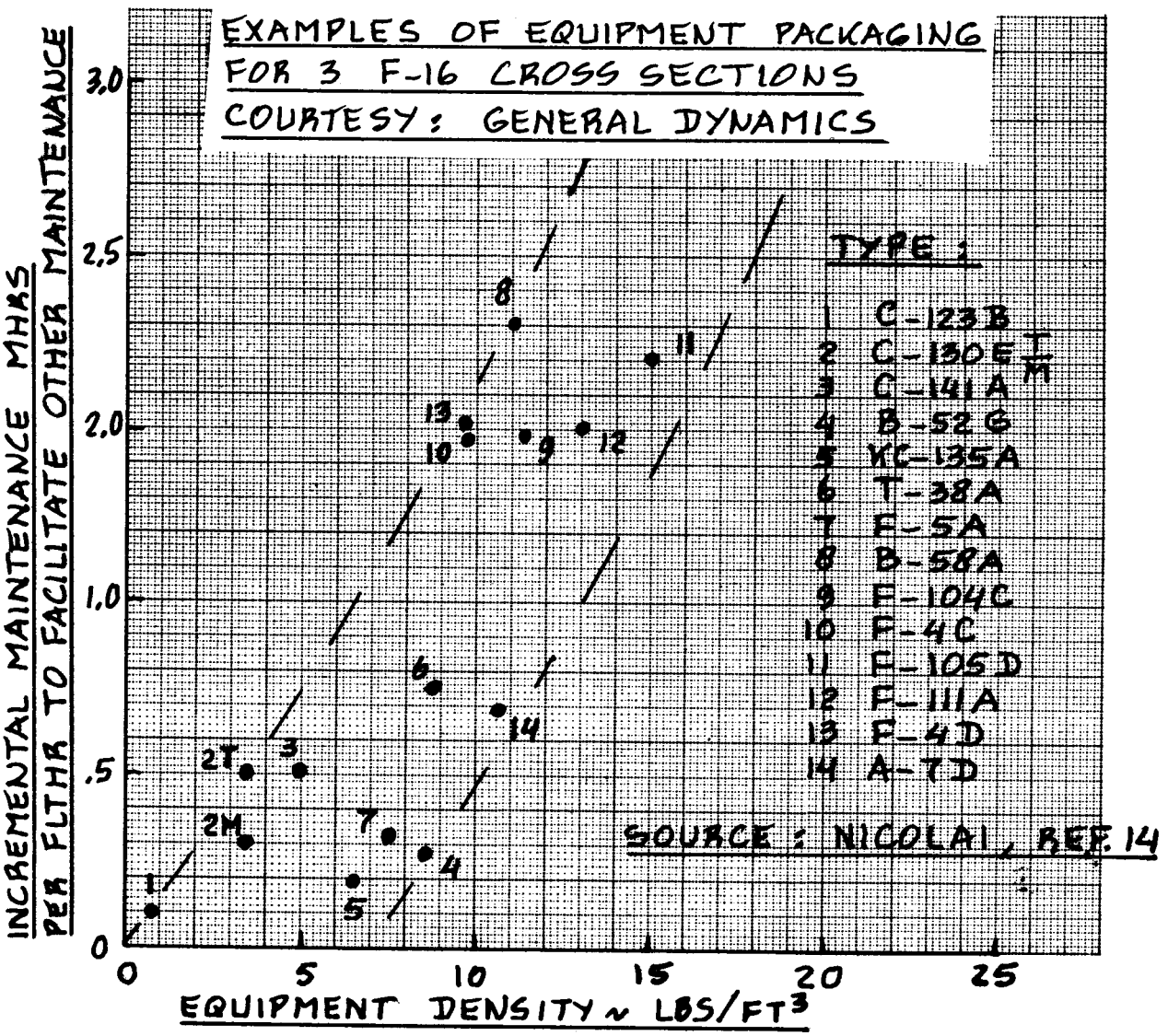

Figure 6.3 Effect of Equipment Density on Maintenance Manhours per Flight Hour

6.3 PROGRAM COST OF INDIRECT PERSONNEL: $C_{PERSIND}$

This cost component covers the cost of all squadron level personnel which are not directly involved in flight operations or airplane maintenance. This cost component may be estimated from:

$$C_{PERSIND} = (f_{persind})(C_{OPS}) \qquad (6.13)$$

where: C_{OPS} is given by Eqn. (6.1)

$f_{persind}$ may be estimated with the help of Table 6.6

6.4 PROGRAM COST OF CONSUMABLE MATERIALS: C_{CONMAT}

This cost component covers the cost of consumable materials used in conjunction with military airplane maintenance functions. This cost component may be found as follows:

$$C_{CONMAT} = (N_{serv})(N_{yr})(U_{ann_{flt}})*$$

$$*(MHR_{flthr})(R_{conmat}) \qquad (6.14)$$

where: R_{conmat} is the average cost in USD/hr (USD per maint. hour) for consumable materials. Lacking specific information it is suggested to use:

$$R_{conmat} = (6.50)(CEF_{then\ year})/(CEF_{1989}) \qquad (6.15)$$

where: the factor 6.50 is the 1989 cost of consumable materials in USD per maintenance hour.

All other terms were previously defined.

6.5 PROGRAM COST OF SPARES: C_{SPARES}

The program cost of spares may be estimated from:

$$C_{SPARES} = (f_{spares})(C_{OPS}) \qquad (6.16)$$

Table 6.6 Multipliers for Program Operating Cost of Military Airplanes

Operating Cost Component	Operating Cost Fraction (=Multiplier)	Fraction of Total Program Operating Cost For Each Airplane Type				
		B52G	C-141	F-111	F-4	A-7D
C_{POL}	f_{pol}	0.14	0.23	0.05	0.10	0.04
$C_{PERSDIR}$	$f_{persdir}$	0.34	0.32	0.28	0.38	0.38
$C_{PERSIND}$	$f_{persind}$	0.16	0.13	0.14	0.20	0.20
C_{SPARES}	f_{spares}	0.13	0.16	0.27	0.12	0.16
C_{DEPOT}	f_{depot}	0.20	0.15	0.22	0.13	0.16
C_{MISC}	f_{misc}	0.03	0.01	0.04	0.07	0.06
Totals:		1.00	1.00	1.00	1.00	1.00

Source: Ref.14, Figure 24.1

NOTES: 1) The fractional contribution of consumable materials cost, C_{CONMAT}, is included in the miscellaneous cost item in this table.

2) The following assumption may be made: $C_{CONMAT} = 0.25(C_{MISC})$

where: C_{OPS} is given by Eqn.(6.1)

f_{spares} may be estimated with the help of Table 6.6

6.6 PROGRAM COST OF DEPOT: C_{DEPOT}

Many overhaul and maintenance actions on military airplanes are not carried out at the squadron or wing level. Instead, these are carried out at so-called depots. The program depot cost associated with the operation of a given airplane type may be estimated from:

$$C_{DEPOT} = (f_{depot})(C_{OPS}) \qquad (6.17)$$

where: C_{OPS} is given by Eqn.(6.1)

f_{depot} may be estimated with the help of Table 6.6

6.7 PROGRAM COST OF MISCELLANEOUS ITEMS: C_{MISC}

The following miscellaneous cost elements contribute to the operating cost of military airplanes:

* requirements for technical data to support maintenance functions
* requirements for training, training data and training equipment
* requirements for support equipment

Reference 10 provides detailed cost estimating relations for these items. For the purpose of preliminary cost estimating it is suggested to use:

$$C_{MISC} = (f_{misc})(C_{OPS}) \qquad (6.18)$$

where: C_{OPS} is given by Eqn.(6.1)

f_{misc} may be estimated with the help of Table 6.6

Using the assumption made at the bottom of Table 6.6, it is possible to write C_{MISC} alternatively as:

$$C_{MISC} = {}^{4}C_{CONMAT} \qquad (6.19)$$

6.8 SUMMARY FOR THE DETERMINATION OF THE PROGRAM OPERATING COST OF MILITARY AIRPLANES : C_{OPS}

The program operating cost of military airplanes, with the help of equations (6.1), (6.2), (6.9) and (6.13) through (6.18) may now be found from:

$$C_{OPS} = \frac{C_{POL} + C_{PERSDIR} + C_{CONMAT}}{(1 - f_{persind} - f_{spares} - f_{depot} - f_{misc})} \qquad (6.20)$$

By using Equation (6.19) it is also possible to cast Equation (6.20) in the following form:

$$C_{OPS} = \frac{C_{POL} + C_{PERSDIR} + C_{CONMAT} + C_{MISC}}{(1 - f_{persind} - f_{spares} - f_{depot})} \qquad (6.21)$$

or:

$$C_{OPS} = \frac{C_{POL} + C_{PERSDIR} + {}^{5}C_{CONMAT}}{(1 - f_{persind} - f_{spares} - f_{depot})} \qquad (6.22)$$

In comparing the program operating costs from one airplane to another it is often desirable to do this on the basis of their so-called program operating cost per hour: $C_{OPS/HR}$.

This program operating cost per flight hour may be obtained from:

$$C_{OPS/HR} = (C_{OPS})/\{(N_{serv})(N_{yr})(U_{ann_{flt}})\} \qquad (6.23)$$

where: C_{OPS} follows from Equations (6.20), (6.21) or (6.22).

All other terms were previously defined.

6.9 EXAMPLE APPLICATION

The purpose of this section is to present an example application of the method for determining the program operating cost of military airplanes. The material is organized in the following manner:

6.9.1 Program Operating Cost Components

6.9.2 Program Operating Cost Total

6.9.3 Program Operating Cost per Flight Hour

6.9.1 Program Operating Cost Components

The example will be constructed around the ground attack fighter airplane of Parts I and II (called Eris). The mission specification for this fighter is found in Table 2.19 of Part I.

The assumption will be made that all costs must be computed for the year 1990.

Program Fuel, Oil and Lubricants Cost: C_{POL}

These costs are computed with Eqn.(6.2).

The input requirements for Eqn.(6.2) are:

F_{OL} = 1.005, according to page 146.

$W_{F_{used}}$ = 18,500lbs, according to p.67 of Part I.

The assumption will be made that JP-4 is the fuel of choice for this ground attack fighter airplane.

FP = 0.75 USD/gallon (assumed from Fig.5.3, p.87).

FD = 6.55 lbs/gallon, from p.88.

$N_{mission}$ is computed from Eqn.(6.3) as:

$N_{mission}$ = 350/2.67 = 131 missions per year

This assumes an annual utilization of $U_{ann_{flt}}$ = 350 flight hours (see Table 6.1) and a mission duration of t_{mis} = 2.67 hours. The latter is pieced together with the help of Table 2.19 in Part I.

The following data are assumed for the number of airplanes involved in the Eris development, production and acquisition program:

$N_{program} = 750$ $N_{rdte} = 10$ $N_m = 740$

With the assumption made on page 145:

$N_{acq} = 740$ units

Next, the number of airplanes in active service will be determined from Eqn.(6.4).

It will be assumed that 10 percent of the Eris fleet will be held in active reserve: $N_{res} = 74$ units

The loss rate per 100,000 flight hours will be assumed to be: $L_R = 2$, which is an optimistic projection, based on Table 6.2.

The number of years during which the Eris will be in active service is assumed to be: $N_{yr} = 25$ years.

With Eqns (6.8) and (6.4):

$N_{serv} = 740 - 74 - [\{(0.5)(2)(350)(25)\}/100,000]N_{serv} =$

$= 740 - 74 - 0.0875N_{serv}$, so that:

$N_{serv} = 666/1.0875 = 612$ units

Now with Eqn.(6.2):

$C_{POL} =$ USD 4,266,978,750

Program Cost of Direct Personnel: $C_{PERSDIR}$

This cost may be determined with Eqn.(6.9).

The program cost for aircrews is found with the help of Equation (6.10). In this equation the following input data remain to be determined:

Since the Eris requires only one pilot:

$N_{crew} = 1.0$

The crew ratio, $R_{cr} = 1.1$ from Table 6.1.

The crew pay is assumed to be that of the example of page 154, so that:

$$Pay_{crew} = 46,068 \text{ USD/year}$$

The crew overhead factor, OHR_{crew} is assumed to be:

$$OHR_{crew} = 3.0 \text{ (p.154)}.$$

With these data, the program cost for aircrews can be found from Eqn.(6.10) to be:

$$C_{crewpr} = (612)(1)(1.1)(46,068)(3)(25) =$$

$$= \text{USD } 2,325,973,320$$

The program cost for direct maintenance personnel is found with Eqn.(6.11). In this equation the following input data remain to be determined:

For maintenance manhours per flight hour, Table 6.5 has been used to project the following number:

$$MHR_{flthr} = 12$$

The maintenance labor rate per manhour for 1990 (including overhead) will be determined from Eqn.(6.12) as:

$$R_{m_{ml}} = 45(3.04)/(3.02) = \text{USD } 45.30$$

The program cost for direct maintenance personnel can now be computed:

$$C_{persdir} = (612)(25)(350)(12)(45.30) =$$

$$= \text{USD } 2,910,978,000$$

The program cost of direct personnel, aircrews and maintenance personnel is found with Eqn.(6.9) as:

$$C_{PERSDIR} = 2,325,973,320 + 2,910,978,000 =$$

$$= \text{USD } 5,236,951,320$$

Program Cost of Indirect Personnel: $C_{PERSIND}$

This cost component may be determined from Eqn.(6.13) and Table 6.6 as:

$$C_{PERSIND} = (0.20)(C_{OPS}), \text{ where } f_{persind} = 0.20$$

Program Cost of Consumable Materials: C_{CONMAT}

This cost is determined with Eqn.(6.14). The following input data remain to be determined:

With Eqn.(6.15):

$R_{conmat} = 6.50(3.04)/(3.02) =$

$= 6.54$ USD per maint.hour

With Eqn.(6.14):

$C_{CONMAT} = (612)(25)(350)(12)(6.54) =$

$=$ USD 420,260,400

Program Cost of Spares: C_{SPARES}

This cost is found with Eqn.(6.16) and Table 6.6 as:

$C_{SPARES} = (0.14)(C_{OPS})$, where $f_{spares} = 0.14$

Program Cost of Depot: C_{DEPOT}

This cost is found from Eqn.(6.17) and Table 6.6 as:

$C_{DEPOT} = (0.15)(C_{OPS})$, where $f_{depot} = 0.15$

Program Cost of Miscellaneous Costs: C_{MISC}

This cost component is found from Eqn.(6.19) as:

$C_{MISC} = {}^{4}C_{CONMAT} = 4(420,260,400) =$

$=$ USD 1,681,041,600

6.9.2 Program Operating Cost Total

The program operating cost total may now be computed with Equation (6.21) as follows:

$$C_{OPS} = \frac{(4,266,978,750 + 5,236,951,320 + 420,260,400 + 1,681,041,600)}{(1 - 0.20 - 0.14 - 0.15)} =$$

$$= 11,605,232,070/0.51 = \text{USD } 22,755,000,000,$$

which has been rounded off to the nearest million.

6.9.3 Program Operating Cost per Flight Hour

The program operating cost per flight hour may be determined with Equation (6.23) as:

$$C_{ops/hr} = 22,755,000,000/\{(612)(25)(350)\} =$$

$$= 4,249 \text{ USD/hour}$$

The reader will have observed the fact that neither cost of depreciation nor cost of financing is included in the military program operating cost per flight hour.

Since military airplanes 'belong' to the tax payers, they are not depreciated in any commercial sense of the word. Also, the cost of financing is not included, because military operating costs are deferred out of annual budgets alotted by the congress.

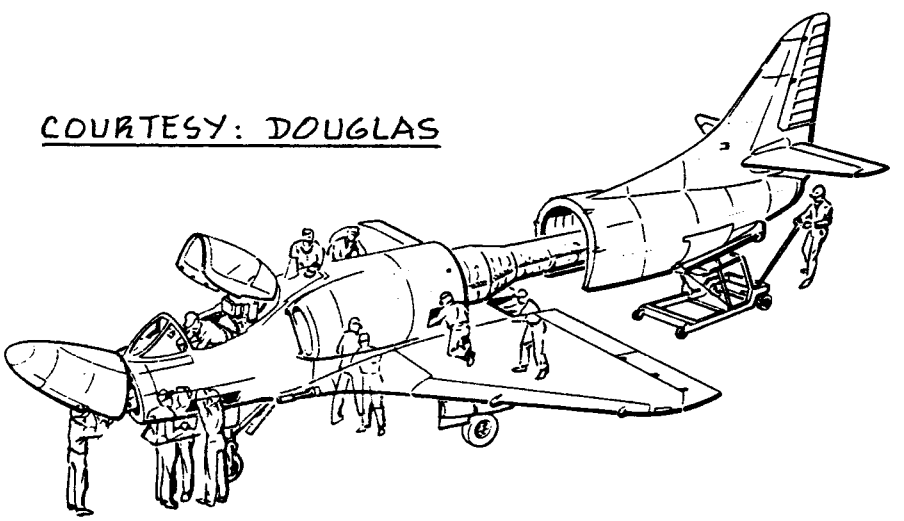

6.10 SOME OBSERVATIONS ON OPERATING COST OF MILITARY AIRPLANES

The purpose of this section is to provide the reader with additional insight and with additional references relative to the operating cost of military airplanes. The material is organized as follows:

6.10.1 Military Service Organization, Typical Airplane Numbers in Service and Reasons for High Operating Cost

6.10.2 Discussion of Operating Cost Distribution

6.10.3 Examples of System Maintainability and Reliability

6.10.1 Military Service Organization, Typical Airplane Numbers in Service and Reasons for High Operating Cost

Most military airplane operations are conducted at the squadron or wing level. The number of airplanes per squadron, the number of squadrons per wing and the number of wings per Air Force or per Navy Group depends on many tactical, strategic and political considerations which are beyond the scope of this text. For the interested reader, Air Force Magazine and the United States Naval Institute Proceedings (both are monthly magazines) publish annual details about USAF, USN and USMC service organizations. Although the US Army does operate several fixed wing airplane types, this service concentrates on rotary wing airplanes for combat roles. Since this text deals only with fixed wing airplanes, USArmy airplanes have not been considered.

Next, some examples are given of how military airplanes are distributed numerically at the squadron level. The examples given apply to the USAF. Table 6.7 shows how many airplanes are typically assigned to a squadron. Table 6.8 indicates the number of squadrons dedicated to specific operational tasks. Table 6.9 shows the number of active airplanes and the annual flying hours produced by each for recent years.

Because military forces have to be able to operate relatively independently of large fixed bases during war times, a certain amount of duplication in support and infrastructure is inevitable. This in turn implies that the operation of military airplanes cannot be conducted

TABLE 6.7 NUMBER OF AIRPLANES PER SQUADRON

Airplane Type	Number per Squadron	Airplane Type	Number per Squadron
A-10	18 or 24	B-1	16
F-4	12 or 24	B-52	13 - 19
RF-4	18	C-5	15 or 16
F-5	11, 18 or 20	C-9	3 or 11
F-15	15, 18 or 24	C-130	16
F-16	18 or 24	AC-130	10
F-106	15	KC-10	19
F-111	12, 18 or 24	KC-135	13 - 25
FB-111	8 or 11	C-141	13 - 17
		E-3	2, 4 or 16

Source: Air Force Magazine, May 1988

TABLE 6.8 USAF FLYING SQUADRONS BY MISSION TYPE

Active Forces	FY'85	FY'87	FY'89*
Strategic Bomber	22	22	25
Air Refueling	35	36	35
Strategic Comm. and Ctrl	6	6	6
Intelligence	3	3	3
Strategic Reconnaissance	1	1	1
Strategic Interceptor	4	3	2
Fighter	78	81	79
Tactical Reconnaissance	8	7	5
Tactical Electr. Warfare	3	4	4
Special Operations Forces	5	5	5
Tact. Air Comm. Ctrl Syst.	3	3	3
Tactical Air Ctrl Syst.	7	7	7
Weather	2	2	1
Rescue	8	9	7
Tactical Airlift	14	13	12
Strategic Airlift	17	17	18
Special Mission	1	1	1
Aeromedical Airlift	3	3	3
Total Active Forces	220	223	217
Reserve Forces:			
ANG Selected Reserve	91	91	91
Air Force Reserve	56	57	58
Total Squadrons	367	371	366

Source: Air Force Magazine, May 1988 * Estimated

TABLE 6.9 NUMBER OF ACTIVE AIRPLANES AND FLYING HOURS

Airplane Type	Number of Active Airplanes in: FY'85	FY'87	FY'89*
Strategic Bomber	330	393	420
Tanker	559	576	566
Fighter/Interceptor/Attack	3,057	3,033	2,998
Recon./Electronic Warfare	418	432	438
Cargo/Transport	859	848	852
Search and Rescue (fixed wing only)	37	35	31
Helicopter (incl. rescue)	234	191	171
Trainer	1,613	1,595	1,515
Utility/Observation/Other	180	110	112
Total USAF	7,287	7,213	7,103
Air National Guard Total	1,688	1,732	1,736
Air Force Reserve Total	468	502	514
Total Active USAF, ANG and USAF Reserve	9,443	9,447	9,353
	Flying Hours in Thousands:		
USAF	2,914	2,837	2,770
ANG	423	435	447
AF Reserve	140	153	156
Total Fl. Hrs in Thousands	3,477	3,425	3,373
Average Flying Hours per year, per airplane:	368	363	361

Source: Air Force Magazine, May 1988 * Estimated

COURTESY: SAAB

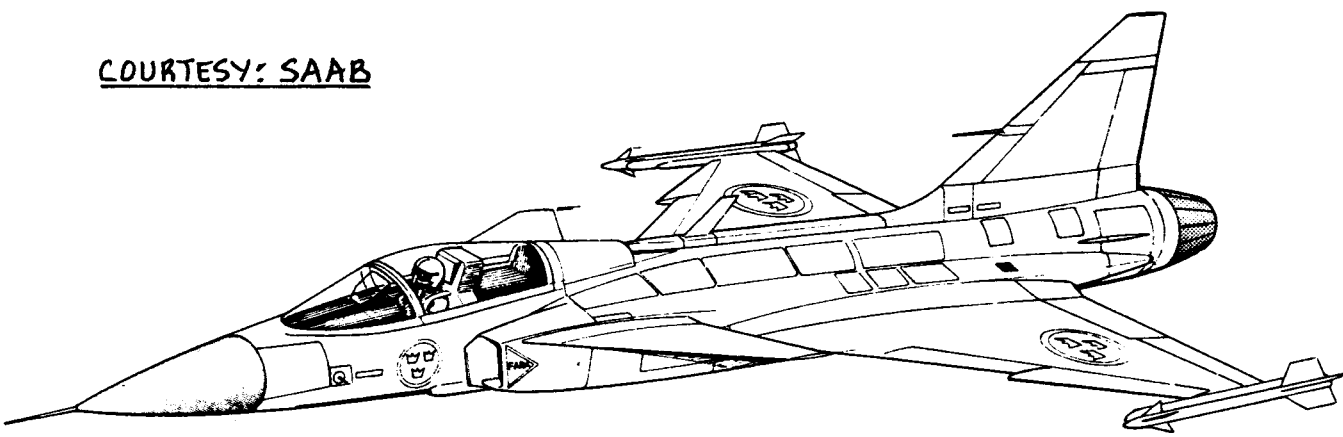

at levels of efficiency comparable to commercial airplane operations. This is one reason why the operating cost per hour for airplanes such as the Eris ground attack fighter is predicted to be rather high: USD 4,249 per flight hour as determined on page 167.

The challenge to the airplane designer is to design military airplanes and their systems layout in such a way that their mission can be accomplished at an affordable cost to the taxpayers.

The following subsections present observations on several aspects of operating cost distribution as well as on system reliability and maintainability.

6.10.2 Discussion of Operating Cost Distribution

Figure 6.4 shows the contribution to total operating cost of each cost component considered in Equation (6.1) for the Eris fighter. The cost data were calculated in Section 6.9. The percentage contribution of the seven operating cost components can be summarized as follows:

1)	C_{POL} (Fuel, oil and lubricants):	19
2)	$C_{PERSDIR}$ (Direct personnel): aircrew 10, maintenance 13	23
3)	C_{SPARES} (Spares):	14
4)	C_{CONMAT} (Consumable materials):	2
5)	$C_{PERSIND}$ (Indirect personnel):	20
6)	C_{DEPOT} (Depot):	15
7)	C_{MISC} (Miscellaneous):	7
	C_{OPS} (Total operating cost percentage)	100

The following operating cost items are directly affected by the airplane designer and the design decisions he makes, mostly those in the early phases of preliminary design:

* Fuel, oil and lubricants (see Parts I and VII, specifically for what governs W_F and W_{fto})

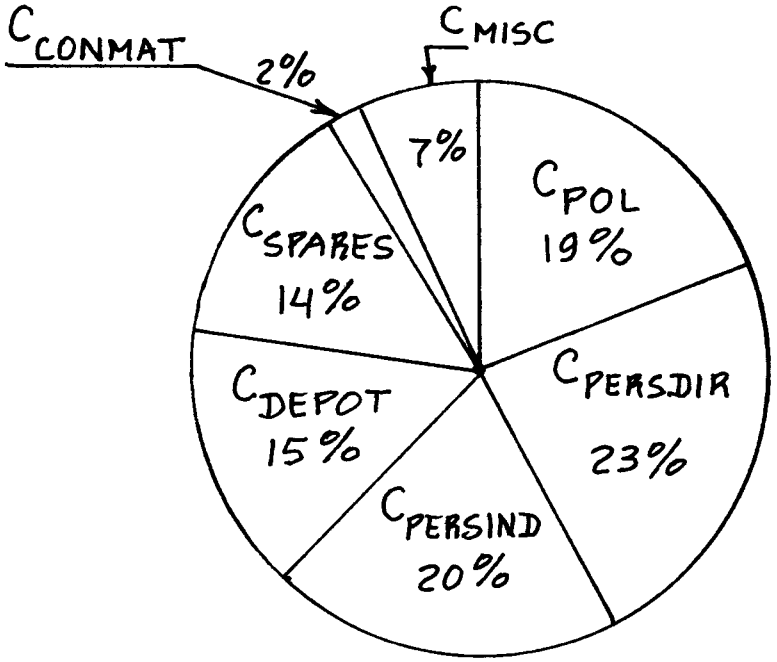

Figure 6.4 Distribution of Program Operating Cost Components for the Eris Fighter Program

Table 6.10 CLASSICAL EXAMPLES OF POOR DESIGN PRACTICES

EXAMPLE 1: In the F-4 fighter, the radio was a high failure rate item. It was installed underneath the rear ejection seat. To remove and to replace this radio this ejection seat had to be removed first. This made radio removal and replacement very expensive.

EXAMPLE 2: In the AV-8B V/STOL fighter, it is required to remove the wing before the engine can be removed. This adds significantly to the cost and time of engine removal.

EXAMPLE 3: In the B-1B bomber, a 'quick access' port was installed to allow for rapid checking and adding of engine oil levels. However, the oil gauge itself was hidden behind the very panel which included the 'quick access' panel. Maintenance personnel had to remove that entire panel before they could access the oil gage. That defeated the entire purpose of the 'quick access' port.

* Aircrew and maintenance (see Parts II, III and IV, for details on configuration, cockpit, structure and system layout design practices)

From the tabulation on page 171 it is clear that the designer has direct leverage over 58 percent of the operating cost of a typical ground attack fighter. Two examples illustrate this:

EXAMPLE 1: Maintenance Manhours

In Section 6.9 it was shown that the program operating cost for the Eris fighter is USD 22,755,000,000 over a projected 25 year life. The maintenance manhours per flight hour were assumed to be 12.

Through careless design it is conceivable that this number could increase to 24 maintenance manhours per flight hour. Table 6.5 shows that this can indeed occur. In such a case, the program operating cost increases by:

USD 1.2x2x2,910,978,000 (see p.165) = USD 6,986,347,200.

This means an increase of 31 percent of the total program operating cost!

If, on the other hand, by careful design the maintenance manhours per flight hour could be decreased from 12 to 6, a program operating cost savings of:

USD 1.2x0.5x2,910,978,000 (see p.165) = USD 1,746,586,800

would be the result. That is a savings of 8 percent!

EXAMPLE 2: Mission Fuel Used

It was shown on p.164 that the Eris program operating cost for fuel, oil and lubricants is approximately: USD 4,300,000,000. The designer should be able to reduce this cost by paying careful attention to details of:

* engine inlet design
* nozzle and boattail design
* aerodynamic design
* c.g. excursion diagram

A ten percent reduction in this cost item should be within reach: this shaves USD 430,000,000 off the program operating cost!

A thoughtless designer can needlessly increase operating cost. Table 6.10 gives three classic examples of poor design decisions from a maintenance viewpoint.

Chapter 8 contains a tabulation of specific design guidelines aimed at reducing cost.

NOTE OF CAUTION:

On p.171 all seven of the operating cost contributions are expressed as a fraction of the total operating cost. Whenever fundamental airplane design parameters are changed, there is no intrinsic reason why the cost items 4-7 should change as the fractions would dictate.

Therefore, whenever a cost trade study is conducted, a baseline should be established for the cost items 4-7. These baseline costs should then be kept constant while the effect of certain design parameters which affect cost items 1-3 is being investigated.

6.10.3 Observations on System Maintainability and Reliability

Chapter 8 and References 25-28 are recommended for further reading about ways to improve airplane maintainability and reliability.

Many military missions require the use of very complex avionics systems. Such systems are required to allow the airplane to function as a weapon system rather than merely as a gunnery or bombing platform.

Also, the nature of military missions, particularly in terms of speed, altitude and weather capability often dictates the use of very advanced technology. This is inherently expensive, risky and to some extent can cause frequent breakdowns.

As a result of poor system and component reliability as well as poor accessibility of those components which require frequent attention, the operational readiness of military airplanes has tended to be poor: see Table 6.11! Table 6.12 indicates how various avionics components affect the time between maintenance. Recollecting that, on the average, military airplanes fly about 350 hours per year, the need for maintenance occasions per year is very high, as shown in Table 6.13. Airplane designers should be able to straighten out their act! Again, Chapter 8 contains some tabulated guidelines which can be helpful in reducing cost.

Table 6.11 EXAMPLES OF FIGHTER READINESS

Airplane Type	Airplane Complexity	Not Mission Capable in percentage	Mean Flight Hours between Failure	Maintenance Events per Sortie	Maintenance Manhours per Sortie
USAF					
A-10	Low	32.6	1.2	1.6	18.4
A-7D	Medium	38.6	0.9	1.9	23.8
F-4E	Medium	34.1	0.4	3.6	38.0
F-15	High	44.3	0.5	2.8	33.6
F-111F	High	36.9	0.3	9.2	74.7
F-111D	High	65.6	0.2	10.2	98.4
USN					
A-4M	Low	27.7	0.7	2.4	28.5
AV-8A	Low	39.7	0.4	3.0	43.5
A-7E	Medium	36.7	0.4	3.7	53.0
F-4J	Medium	34.2	0.3	5.9	82.7
A-6E	High	39.3	0.3	4.8	71.3
F-14A	High	47.1	0.3	6.0	97.8

Source: Aviation Week and Space Technology, October 6, 1980

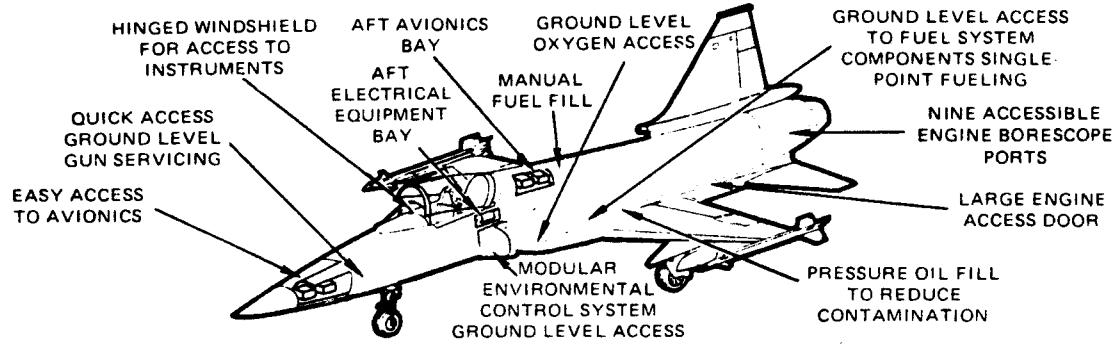

COURTESY: NORTHROP

ACCESSIBILITY FEATURES

TABLE 6.12 AVIONICS SYSTEM OPERATIONAL TIME BETWEEN MAINTENANCE, IN FLIGHT HOURS

Avionics System	F-111	F-4	F-16	A-7	F-15
Instruments	15	17	60	45	32
Autopilot	13	43	NA	NA	61
UHF	42	22	57	64	24
IFF	35	NA	44	89	15
Navigation	66	4	172	59	18
Fire Control	71	3	9	26	6
ECM	7	7	25	20	22

NA = not available
Source: Aerospace America, August 1985

TABLE 6.13 AVIONICS SYSTEM DOWN OCCURRENCES PER YEAR
BASED ON 350 FLIGHT HOURS PER YEAR

Avionics System	F-111	F-4	F-16	A-7	F-15
Instruments	23	21	6	8	11
Autopilot	27	8	NA	NA	6
UHF	8	16	6	5	15
IFF	10	NA	8	8	23
Navigation	5	88	2	6	19
Fire Control	5	117	39	13	58
ECM	50	50	14	18	16

NA = not available Source: Table 6.12

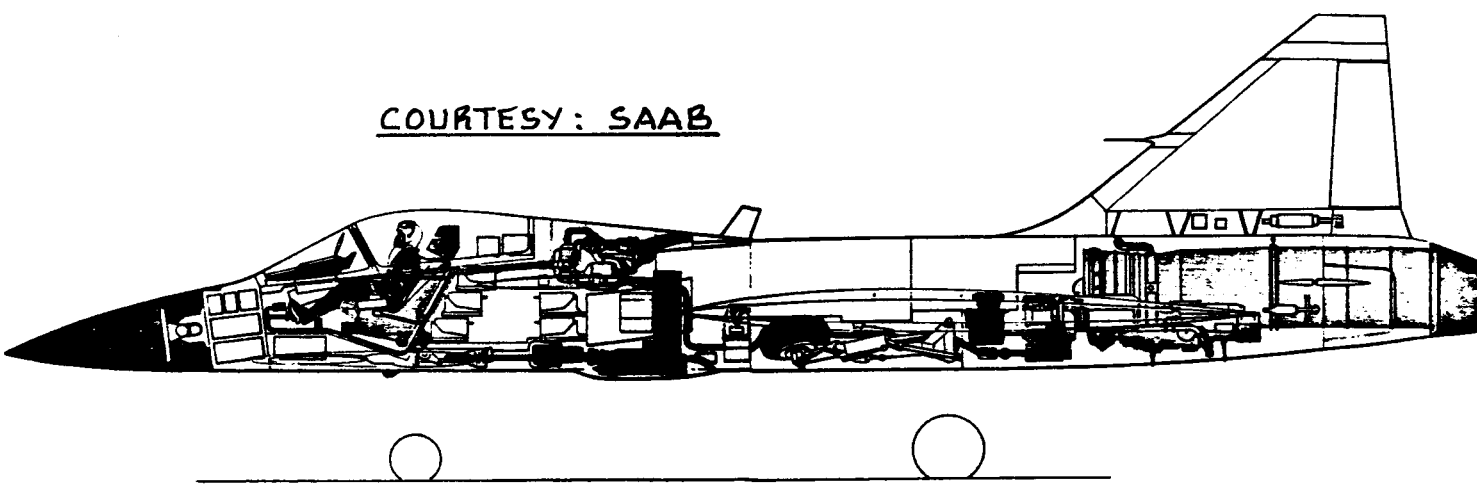

7. EXAMPLE OF LIFE CYCLE COST CALCULATION FOR A MILITARY AIRPLANE

The purpose of this chapter is to present an example of the calculation of life cycle cost (LCC) of a military airplane. The example has been constructed for the Eris ground attack fighter of Parts I and II. An equation for life cycle cost (LCC) was given in Ch.2, as Eqn.(2.3):

$$LCC = C_{RDTE} + C_{ACQ} + C_{OPS} + C_{DISP} \qquad (7.1)$$

where: C_{RDTE} is the total cost of research, development, test and evaluation

C_{ACQ} is the program acquisition cost

C_{OPS} is the program operating cost

C_{DISP} is the program disposal cost

More detailed definitions of these cost sources are provided in Chapter 2, pages 9 - 11. Methods for determining the first three sources of LCC are developed in Chapters 3 - 6. Applications of these methods to the Eris fighter program are given in Sections 7.1 - 7.3. An approach to the determination of disposal cost (C_{DISP}) is given in Section 7.4. The life cycle cost of the Eris fighter is computed in Section 7.5. Definitions for airplane unit cost are given and illustrated in Section 7.6. The material is organized as follows:

7.1 RESEARCH, DEVELOPMENT, TEST AND EVALUATION COST OF THE ERIS GROUND ATTACK FIGHTER

In this section the research, development, test and evaluation cost, C_{RDTE}, will be estimated for the Eris ground attack fighter. The mission specification for this fighter is stated in Table 2.19 of Part I. The assumption will be made that the cost estimates are needed for calendar year 1990. The method used is that of Ch.3. To use the method the following input data are needed:

W_{TO} = 64,905 lbs from p.14, Part V.

W_E = 33,500 lbs from p.14, Part V.

V_{max} = 450 kts from p.45, Part V.

N_{rdte} = 10 assumed from p.26.

N_{st} = 2. However, it will be assumed that even the two static test airplanes will be fully equipped with engines and avionics.

F_{diff} = 2.0 assumed from p.26 as well as the design decision to use 'de-facto' stability, which was made in sub-section 11.4.3 of Part II.

F_{cad} = 0.8 assumed from p.27.

From Eqn.(3.5):

$$W_{ampr} = \text{invlog}\{0.1936 + 0.8645(\log 64{,}905)\} =$$

$$= 22{,}585 \text{ lbs}$$

Airframe Engineering and Design Cost: C_{aed_r}

From Equation(3.2):

$$MHR_{aed_r} = 0.0396(22{,}585)^{0.791}(450)^{1.526}(10)^{0.183} *$$

$$*(2.0)(0.8) = 3{,}002{,}542 \text{ hrs}$$

R_{e_r} = 62.00 USD/hr from Figure 3.3, which assumes that the Eris program does not require a high level of security.

From Eqn.(3.3):

C_{aed_r} = 3,002,542(62.00) = USD 186,157,604

Development Support and Test Cost: C_{dst_r}

CEF for 1990 is 3.03 as determined from Figure 2.7.

From Eqn.(3.7):

$C_{dst_r} = 0.008325(22,585)^{0.873}(450)^{1.890}(10)^{0.346}*$

$*(3.03)(2.0)$ = USD 73,166,699

Flight Test Airplanes Cost: C_{fta_r}

This follows from Eqn.(3.8). First, all five cost components in this equation will be determined.

Cost of engine and avionics: $C_{(e + a)_r}$

The required takeoff thrust per engine, T_{TO_e}, follows from p.191, Part I:

T_{TO_e} = 29,670/2 = 14,835 lbs

From Eqn.(B9) in Appendix B, the 1990 engine price may be estimated as follows:

EP_{1990} = [invlog{2.3044 + 0.8858log(14,835)}]*

$*(3.03/3.02)$ = USD 1,001,757

The avionics cost, $C_{avionics}$, will be assumed to be 25 percent of the Eris unit flyaway cost, AMP_{1990}. The latter is estimated from Eqn.(A14) in Appendix A:

AMP_{1990} = (3.03/3.02)*

*[invlog{2.3341 + 1.0586(log64,905)}] =

= USD 26,903,782

Thus, $C_{avionics}$ = 26,903,782/4 = USD 6,725,946

From Eqn.(3.9):

$$C_{(e + a)_r} = \{2(1,001,757) + 6,725,946\}(10) =$$

$$= \text{USD } 87,294,600$$

where it has been assumed that all 10 prototypes, including the 2 used for static testing, will be fully equipped with engines and avionics.

Manufacturing cost of flight test airplanes: C_{man_r}

From Eqn.(3.11):

$$MHR_{man_r} = 28.984(22,585)^{0.740}(450)^{0.543}(10)^{0.524})*$$

$$*(2) = \text{USD } 8,906,551 \text{ hrs}$$

R_{m_r} = 35 USD/hr from Figure 3.4

From Eqn.(3.10):

$$C_{man_r} = 35(8,906,551) = \text{USD } 311,729,285$$

Materials cost for the flight test airplanes: C_{mat_r}

From Eqn.(3.12):

$$C_{mat_r} = 37.632(1.0)(22,585)^{0.689}(450)^{0.624}*$$

$$*(10)^{0.792}(3.03) = \text{USD } 31,943,800$$

In this application it is assumed that the Eris is manufactured with primarily conventional materials (so that F_{mat} = 1.0) and that the 1990 CEF value is 3.03.

Tooling cost for the flight test airplanes: C_{tool_r}

From Eqn.(3.14):

$$MHR_{tool_r} = 4.0127(22,585)^{0.764}(450)^{0.899}*$$

$$*(10)^{0.178}(0.33)^{0.066}(2.0) =$$

$$= 5,784,225 \text{ hrs}$$

where the factor 0.33 represents the assumed manufacturing rate per month for the prototype phase, see p.33.

The tooling hourly rate is assumed to be:

R_{t_r} = 44 USD/hr from Figure 3.5.

From Eqn.(3.13):

$$C_{tool_r} = 44(5,784,225) = \text{USD } 254,505,900$$

Quality control cost for the flight test airplanes: C_{qc_r}

From Eqn.(3.15):

$$C_{qc_r} = 0.13(311,729,285) = \text{USD } 40,524,807$$

Finally, from Eqn.(3.8):

$$C_{fta_r} = 87,294,600 + 311,729,285 + 31,943,800 +$$

$$+ 254,505,900 + 40,524,807 = \text{USD } 725,998,392$$

Flight Test Operations Cost: C_{fto_r}

From Eqn.(3.16):

$$C_{fto_r} = 0.001244(22,585)^{1.160}(450)^{1.371}(8)^{1.281}*$$

$$*(3.03)(2) = \text{USD } 52,739,614$$

Test and Simulation Facilities Cost: C_{tsf_r}

In sub-section 11.4.3 of Part II the decision was made to use 'de-facto' stability in the Eris design. Therefore, from Eqn.(3.17):

$C_{tsf_r} = 0.20(C_{RDTE})$ as suggested on p.35.

Profit over Flight Test Airplanes: C_{pro_r}

From Eqn.(3.18):

$$C_{pro_r} = 0.1(C_{RDTE})$$

Cost to Finance the Flight Test Airplanes: C_{fin_r}

It will be assumed that the manufacturer will have to arrange for the financing of the Eris fighter program. Consistent with Section 3.7, the financing rate will be assumed to be 0.10 (p.36) so that, with Eqn.(3.19):

$$C_{fin_r} = 0.1(C_{RDTE})$$

Total Research, Development, Test and Evaluation Cost: C_{RDTE}

From Eqn.(3.1):

$$C_{RDTE} = (186,157,604 + 73,166,699 + 725,998,392 + 52,739,614)/(1 - 0.2 - 0.1 - 0.1) =$$

$$= 1,038,062,309/0.6 = \text{USD } 1,730,103,848$$

Rounding this off:

$$C_{RDTE} = 1,730,000,000$$

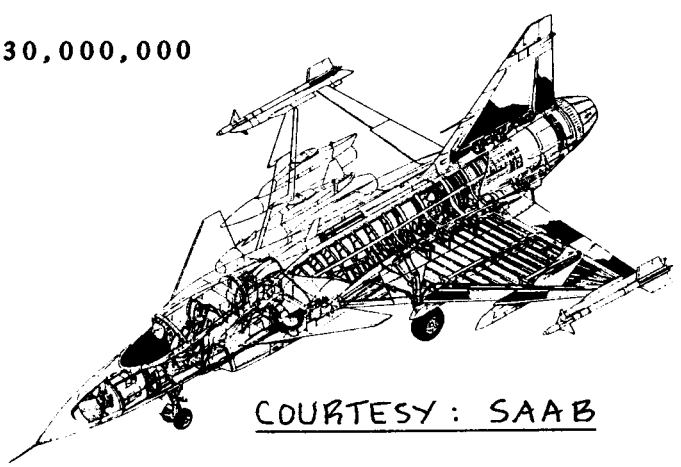

COURTESY: SAAB

7.2 MANUFACTURING AND ACQUISITION COST OF THE ERIS GROUND ATTACK FIGHTER

In this sub-section the manufacturing and acquisition costs, C_{MAN} and C_{ACQ}, will be estimated for the Eris ground attack fighter. The mission specification for this fighter is stated in Table 2.19 of Part I. The assumption will be made that the cost estimates are needed for calendar year 1990. The method used is that of Ch.4. To use the method the input data for Section 7.1 as well as the following input data are needed:

$N_{program}$ = 750 airplanes will be assumed.

N_{rdte} = 10 from page 178.

This yields with Eqn.(4.1):

N_m = 740

The Eris will be assumed to be manufactured with rather conventional materials, thus: F_{mat} = 1.0 as was also assumed on page 180.

Airframe Engineering and Design Cost of Production Airplanes: C_{aed_m}

This will be determined from Eqn.(4.5b). First, the engineering manhours for the Eris program are found from Eqn.(4.6):

$$MHR_{aed_{program}} = 0.0396(22,585)^{0.791}(450)^{1.526}*$$

$$*(750)^{0.183}(2.0)(0.8) =$$

$$= 6,616,455 \text{ hrs}$$

The engineering hourly rate will be assumed to be 62.00 USD/hr, as on p.178. Next, with Eqn.(4.5b) and with the C_{aed_r} of p.179:

$$C_{aed_m} = (6,616,455)(62.00) - 186,157,604 =$$

$$= 410,220,210 - 186,157,604 = \text{USD } 224,062,606$$

Airplane Program Production Cost: C_{apc_m}

This cost will be computed with Eqn.(4.7). First, all six cost components in this equation will be found.

Cost of engine and avionics of production airplanes: $C_{(e + a)_m}$

This follows from Eqn.(4.8). It will be assumed that the engine and avionics cost for the production version of the Eris fighter is the same as that for the RDTE version. With the cost data from pages 179 and 180:

$$C_{(e + a)_m} = \{(2)(1,001,757 + 6,725,946)\}(740) =$$

$$= (8,729,460)(740) = \text{USD } 6,459,800,400$$

Cost of the interiors of production airplanes: C_{int_m}

This cost is determined from Eqn.(4.9) with $F_{int} = 0$ for military airplanes:

$$C_{int_m} = 0$$

Manufacturing cost of production airplanes: C_{man_m}

Equation (4.10b) will be used to estimate this cost item. First, the program manufacturing manhours are computed from Eqn.(4.11):

$$MHR_{man_{program}} = 28.984(22,585)^{0.740}(450)^{0.543} *$$

$$*(750)^{0.524}(2) = 85,554,269 \text{ hrs}$$

The manufacturing labor rate will be assumed to be the same as that used in the RDTE phase on p.180:

R_{m_m} = 35 USD/hr. Thus, with Eqn.(4.10b) and with the data of p.180:

$$C_{man_m} = (85,554,269)(35.00) - 311,729,285 =$$

$$= 2,994,399,415 - 311,729,285 = \text{USD } 2,682,670,130$$

Materials cost for production airplanes: C_{mat_m}

The materials cost of the production program is determined with Equation (4.12). First, the materials cost of the entire program is found from Eqn.(4.13):

$$C_{mat_{program}} = 37.632(1.0)(22,585)^{0.689}(450)^{0.624}*$$

$$*(750)^{0.792}(3.03) = \text{USD } 975,966,932$$

where $F_{mat} = 1.0$ and $CEF_{1990} = 3.03$ were obtained from page 180.

Next, the cost of materials for the production program follows from Eqn.(4.12) as:

$$C_{mat_m} = 975,966,932 - 31,943,800 = \text{USD } 944,023,132$$

Tooling cost for production airplanes: C_{tool_m}

This cost item will be calculated with Eqn.(4.14b). First, the program tooling manhours are determined with Eqn.(4.15):

$$MHR_{tool_{program}} = 4.0127(22,585)^{0.764}(450)^{0.899}*$$

$$*(750)^{0.178}(10)^{0.066}(2) =$$

$$= 15,623,711 \text{ hrs}$$

In this calculation it was assumed that the Eris will be manufactured at a rate of $N_{r_m} = 10$ airplanes per month. For a production program of 740 units, this represents a 6 year program. That is quite reasonable for this type of airplane.

The tooling hourly rate will be assumed to be equal to that used in the RDTE phase on p.181:

$$R_{t_m} = 44.00 \text{ USD/hr}$$

Now, with Eqn.(4.14b) and the data from p.181:

$$C_{tool_m} = (15,623,711)(44.00) - 254,505,900 =$$

$$= 687,443,284 - 254,505,900 = \text{USD } 432,937,384$$

Quality control cost for production airplanes: C_{qc_m}

This cost will be found with Eqn.(4.16):

$$C_{qc_m} = 0.13(2,682,670,130) = \text{USD } 348,747,117$$

It is now possible to determine the entire airplane production cost from Eqn.(4.7) as follows:

$$C_{apc_m} = 6,459,800,400 + 0 + 2,682,670,130 +$$

$$+ 944,023,132 + 432,937,384 + 348,747,117 =$$

$$= \text{USD } 10,868,178,163$$

Cost of Flight Test Operations for Production Airplanes: C_{fto_m}

This cost is estimated with Eqn.(4.17). On p.167 it was found that for the Eris: $C_{ops/hr} = 4,249$ USD/hr.

However, this operating cost includes the effects of military overhead, depot, spares and other factors. It is necessary to eliminate these factors from the p.167 operating cost before Eqn.(4.17) can be applied. Instead of doing this, it is assumed here that the operating cost per hour to the manufacturer is roughly 2,000 USD/hr.

Production airplane flight test hours per airplane are assumed to be:

$t_{pft} = 20$ hrs/airplane as stated on p.55.

The manufacturers flight test overhead factor is assumed to be: $F_{ftoh} = 4.0$ (on p.55). So, with Eqn.(4.17):

$$C_{fto_m} = (740)(2,000)(20)(4.0) = \text{USD } 118,400,000$$

Manufacturing Program Financing Cost: C_{fin_m}

The assumption will be made that the financing cost

for the manufacturing phase of the Eris program will be carried by the manufacturer and/or his lenders. A rate of 10 percent will be assumed. Thus, with Eqn.(4.18):

$$C_{fin_m} = 0.10(C_{MAN})$$

Program Manufacturing Cost: C_{MAN}

This cost can now be found from Eqn.(4.4) and the data determined in this section:

$$C_{MAN} = (224,062,606 + 10,868,178,163 +$$

$$+ 118,400,000)/(1 - 0.1) = 11,210,640,769/0.9 =$$

$$= \text{USD } 12,456,000,000 \text{ after some rounding off.}$$

Profit over the manufacturing phase: C_{pro_m}

According to the suggestion made on p.56, a 10 percent profit for the manufacturing phase is reasonable. Therefore, with Eqn.(4.19):

$$C_{PRO} = (0.10)(C_{MAN}) = \text{USD } 1,245,600,000$$

Program Acquisition Cost: C_{ACQ}

The total Eris program acquisition cost is estimated from Eqn.(4.2) as:

$$C_{ACQ} = 12,456,000,000 + 1,245,600,000 =$$

$$= \text{USD } 13,701,600,000$$

or, after rounding off:

$$C_{ACQ} = \text{USD } 13,702,000,000$$

7.3 OPERATING COST OF THE ERIS GROUND ATTACK FIGHTER

The program operating cost of the Eris fighter was determined with the method of Chapter 6 in Section 6.9. The result from p.167 is:

$$C_{OPS} = \text{USD } 22,755,000,000$$

7.4 DISPOSAL COST OF THE ERIS GROUND ATTACK FIGHTER

There comes a point in time when any airplane no longer has commercial or military value. That point is normally reached when:

1. The airplane has reached the end of its safe structural life and structural repairs are judged to be not economical.

2. The airplane has reached the end of its economic life: it can no longer compete effectively in the face of more modern airplanes.

3. The airplane ceases to have military value. This can occur if either its mission is no longer a viable one, or improvements in technology have rendered it obsolete.

4. It has been damaged beyond repair (such as in certain crashes or by damage caused by weather).

Whenever an airplane ceases to have commercial or military value it needs to be disposed of. The cost associated with such disposal is referred to as the disposal cost. The cost of disposing of airplanes depends on the types of materials used in construction and/or in operation. Disposal usually consists of:

1. Temporary storage

2. Draining of liquids and disposal thereof

3. Disassembly of engines and certain systems (such as computers and instruments)

4. Cutting up of the airframe and disposal of the resulting materials

There are costs associated with each of these actions. However, it is quite possible that there is a salvage value associated with actions 2-3. Examples are: resale value of engines, instruments, scrap metals (for re-cycling) and other materials. Any disposal costs are therefore partially offset by these resale values.

In some airplanes, materials and liquids are used which pose a problem for the environment if they are not disposed of with care. Examples are:

* Beryllium alloys
* Most composites (because they are not inherently degradable)
* Many oils and liquids (such as hydraulic fluids)

The author believes that it should be the responsibility of designers to include in their design decision making some serious thinking (and actions) about disposal problems. It is not ethical to assume that future generations will be able to 'take care' of problems created by design decisions of today.

To responsibly account for future disposal problems will require that designers enlist the help of chemical and environmental engineers in the design decision making process. Only that way can the cost of disposal be estimated with credibility.

One of the reasons that the earth environment is in serious trouble today is the fact that disposal problems are not included in design thinking and design decision making at most levels of industrial activity today.

Examples of potential problems which were caused by the lack of disposal considerations in design thinking are given in Table 7.1.

The author is not aware of any reliable methods for the estimation of airplane disposal costs. Reference 8 mentions disposal cost but provides no guidelines for its estimation.

In view of this sad state of affairs, it is suggested to use the following 'fudge' factor to account for the disposal of airplanes:

$$C_{DISP} = 0.01(LCC) \qquad (7.2)$$

Whether or not this accounts fairly for the actual balance between resale values and disposal costs is very much an open question.

7.5 LIFE CYCLE COST OF THE ERIS GROUND ATTACK FIGHTER

The life cycle cost of the Eris fighter program will now be determined with Equation (7.1). The cost sources in this equation have the following magnitudes for the Eris fighter program:

TABLE 7.1 EXAMPLES OF POTENTIAL ENVIRONMENTAL PROBLEMS

Item	Problem
Nuclear waste	Insufficiently considered in the original decision to move ahead with fission power generation.
Lithium batteries	Used in thousands of personal computers. What will happen to this hazardous waste when personal computers are discarded?
Americium	This hazardous material is used in many smoke detectors. What will happen to this material when smoke detectors are discarded?
Non-biodegradables	These materials are used in nearly all 'fast food' containers today. Their disposal is creating massive waste piles in the environment.
Composites in airplanes and cars	The use of various types of composites is rapidly increasing. What will happen to these materials when disposal time comes around?

Source: This table is based on ideas by Mr. Ben Williams of the Air Force Institute of Technology.

C_{RDTE} = USD 1,730,000,000 (from p.182)

C_{ACQ} = USD 13,702,000,000 (from p.187)

C_{OPS} = USD 22,755,000,000 (from p.187)

C_{DISP} = USD 386,000,000 (with Eqn.(7.2))

With Equation (7.1) this yields:

$LCC_{Eris\ program}$ = USD 38,573,000,000

Observe, that for the Eris program:

$C_{OPS} \gg C_{ACQ} \gg C_{RDTE}$

This was also noted on p.11 in Chapter 2. It was further substantiated by the Ourania jet transport cost calculations which are summarized on p.132 in Ch.5.

The reason why the operating cost of the Eris program is 'only' twice that of the acquisition cost is that Eris is a relatively small airplane. The Eris has a crew of only one and consumes much less fuel per mission than bomber or transport airplanes. Also, the annual utilization of the Eris is much less than that of typical civil transports.

The relative magnitudes of the first three cost sources in the LCC equation do suggest one more time:

THE PRELIMINARY DESIGN PHASE (PART OF RDTE) LOCKS IN MOST OF THE LIFE CYCLE COST OF AN AIRPLANE!

This lesson should not be lost on designers nor on design managers.

7.6 UNIT COST OF THE ERIS GROUND ATTACK FIGHTER

The problem with determining the unit cost of military airplanes is largely one of definition. The author has decided to use the following definitions:

1) The manufacturing unit cost is defined as:

$$C_{muc} = (C_{MAN})/(N_m) \qquad (7.3)$$

2) The acquisition unit cost is defined as:

$$C_{auc} = (C_{ACQ})/(N_m) \qquad (7.4)$$

3) The program unit cost is defined as:

$$C_{puc} = (C_{ACQ} + C_{RDTE})/(N_m) \qquad (7.5)$$

4) The life cycle unit cost is defined as:

$$C_{lcuc} = (LCC)/(N_m) \qquad (7.6)$$

The reader will observe that the third definition corresponds to what for commercial airplanes was called the airplane estimated price, AEP, in Equation (4.3).

In the popular press the concept 'unit flyaway cost' is often used. However, the definition of this 'unit flyaway cost' is usually omitted, leaving the reader to guess how it is defined. The author believes that the definitions 1), 2) and 3) are useful in comparing unit

costs of airplanes with similar missions. Airplane designers should keep in mind the fact that only the fourth definition reflects the actual unit cost to the taxpayer!

It is instructive to use the Eris fighter as an example of what these unit costs actually are.

With Eqn.(7.3) and p.187, the manufacturing unit cost is estimated as:

$$C_{muc} = 12,456,000,000/740 = \text{USD } 16,832,432$$

or, rounded off:

$$C_{muc} = \text{USD } 17,000,000$$

With Eqn.(7.4) and p.187, the acquisition unit cost is estimated as:

$$C_{auc} = 13,702,000,000/740 = \text{USD } 18,516,216$$

or, rounded off:

$$C_{auc} = \text{USD } 19,000,999$$

With Eqn.(7.5), p.187 and p.182, the program unit cost is estimated as:

$$C_{puc} = (13,702,000,000 + 1,730,000,000)/740 =$$

$$= \text{USD } 20,854,054$$

or, rounded off:

$$C_{puc} = \text{USD } 21,000,000$$

With Eqn.(7.6) and p.191, the life cycle unit cost is estimated as:

$$C_{lcuc} = (38,573,000,000)/740 = \text{USD } 52,125,676$$

or, rounded off:

$$C_{lcuc} = 52,000,000$$

Note that the airplane market price estimate for 1990 as obtained from Equation (A14) in Appendix A (see p.179) represents an over-estimate! Since the avionics price estimate of p.180 is based on a percentage of AMP the actual Eris cost estimates should be revised downward accordingly. This was not done in this text.

8. AIRPLANE DESIGN OPTIMIZATION AND DESIGN-TO-COST

A major question which every airplane designer asks himself at one time or another is: 'How can airplanes be designed so that they are the best possible?'

The problem with the use of the word 'best' is that it is not immediately clear what is meant by it. Therefore, it is 'better' to ask the following questions:

A) How can airplanes be designed so that their performance is maximized?

B) How can airplanes be designed so that their empty weight is minimized?

C) How can airplanes be designed so that their cost is minimized?

D) How can airplanes be designed to a given cost?

In mathematics, the words MAXIMUM and MINIMUM are both related to the concept: OPTIMUM. Maxima or minima arise by attempts to optimize certain functions of independent variables. Such functions are given the generic name: cost functions. The mathematical theory of optimization of cost functions is well developed and documented: References 29 and 30 are typical examples.

In airplane design, examples of cost functions are:

* Range
* Endurance
* Fuel consumption
* Empty weight
* Operating cost
* Return on investment

Before these cost functions can be optimized it will be necessary to express them functionally in terms of a finite set of design variables. After reviewing the material in Parts I through VII it will be agreed that the number of airplane design variables is very large indeed. Also, many of these variables are not truly independent, AND their interrelationship is not always definable.

That is why the airplane design process in Parts I and II was referred to as non-unique and iterative. It is useful to review these terms before returning to the idea of design optimization.

The airplane design process is non-unique because:

1. It is possible that more than one configuration approach results in an acceptable airplane. This is clearly illustrated by Figure 1.1 in Part II!

2. It is possible that more than one approach to the interior layout design and systems design leads to an acceptable airplane. Parts II, III and IV contain many examples of this.

The airplane design process is iterative because:

1. Most design decisions made early in the airplane design process turn out to have major (and often not foreseen) impact on design decisions which are made later. If that impact is unfavorable, many earlier decisions have to be reconsidered: i.e. the design has to be iterated*.

2. Except for a relatively small number of design variables (to be discussed later), it has not yet been found possible to relate design variables to each other in a mathematically unique manner. Besides, many airplane design variables are not even independent in the mathematical sense.

To arrive at an acceptable airplane design solution, many design decisions are therefore made on the basis of experience or intuition. This in turn makes it necessary to iterate through previous design decisions. The need for this was amply illustrated in Parts I, II and V. The iterative nature of the design decision-making process is 'formalized' through the step-by-step design procedures called: Design Sequences I and II as outlined in Part II.

It should be clear from Parts I - VII and also from Chapters 3 - 7 in this volume that it is nearly always desirable to keep the takeoff weight of an airplane (for a given mission) as low as possible. It is therefore essential that the designer understand the sensitivity of his design to those mission parameters and those design variables which have been found by experience to have a major impact on the takeoff weight of a new airplane. The problem of takeoff weight sensitivity was dealt with in some detail in Part I, Chapter 2. Applications and interpretations of the takeoff weight sensitivity of a new airplane are presented in Section 8.1.

---

* The process of arriving at a satisfactory weight and balance situation (Part II, Chapter 10) is one example!

Note the use of the word 'acceptable' (not optimum) in previous paragraphs. To find a true optimum design solution, the following steps must be completed:

1) One or more cost functions must be defined. These cost functions must be consistent with the mission objectives of the airplane AND they must not conflict with each other.

2) Mathematical relationships between each cost function and certain design variables must be formulated.

3) A rule must be formulated which makes clear how the cost function(s) is (are) to be evaluated: maximum or minimum AND whether or not design constraints are to be accounted for.

4) Design constraints and their relationship to certain design variables must be identified.

5) A theory (mathematical procedure) by which the optimum will be found must be agreed upon.

It depends on the specifics of a particular design problem how these steps are to be taken. Sections 8.2 through 8.6 contain suggestions and guidelines to help airplane design students find their way through the maze called: design optimization. Several examples of design optimization studies are discussed in Section 8.7.

Decisions to go ahead with an airplane program are rarely made without economic considerations. Minimizing economic cost is therefore a 'driver' in many airplane design and airplane program decisions.

More and more, cost itself is being viewed as a constraint. In the design and development of military airplanes, budget limitations are playing an increasingly important role. Such budget limitations must be viewed by the designer as a constraint.

Similarly, in the design and development of commercial airplanes, the acquisition cost (cost of ownership) as well as the direct operating cost are being viewed as design constraints.

This raises the question of how to design airplanes within certain cost constraints: design-to-cost. An introduction to this subject is given in Section 8.8.

Assume that the 'best' of all available design optimization tools have been employed in the design of a new airplane. There still are many aspects of the design which were untouched by the process of optimization, if only because the number of variables accounted for in any formal design optimization procedure is relatively small.

Examples of design variables left untouched by most design optimization processes are found in areas such as:

* interior layout design
* systems design and integration
* materials selection
* application of new, maturing technologies

It is in these areas where the experience and the intuition of the designer are the only method to keep cost down. Therefore, it is useful for the designer to have available a list of 'detail design guidelines' which have been found helpful in lowering airplane cost. Such guidelines are given in Section 8.9.

The material in this chapter is therefore organized as follows:

8.1 TAKEOFF WEIGHT SENSITIVITY

It was shown in Chapters 3 - 7 that airplane takeoff weight plays an almost dominant role in determining cost. For that reason it is essential that airplane designers understand what 'drives' the takeoff weight. The purpose of this section is to review and discuss the sensitivity of airplane takeoff weight to mission performance parameters and to airframe design parameters.

A mathematical derivation of the sensitivity of airplane takeoff weight to such parameters can be found in Chapter 2 of Part I. In that chapter, the takeoff weight sensitivity to certain design parameters is expressed as the partial derivative: $\partial W_{TO}/\partial y$, where: y is any one of the following parameters:

* Empty weight, W_E
* Payload weight, W_{PL}

and, for any given mission phase i*:

* Range, R_i
* Endurance, E_i
* Lift-to-drag ratio, $(L/D)_i$
* Specific fuel consumption, c_{j_i} or c_{p_i}
* Propeller efficiency, η_{p_i}

The validity of these takeoff weight sensitivities depends on the validity of a statistical relationship between airplane takeoff weight and airplane empty weight which can be written as:

$$\log W_{TO} = A + B \log W_E \qquad (8.1)$$

where: W_{TO} is the takeoff weight in lbs

W_E is the empty weight in lbs

A and B are regression coefficients determined from weight data on existing airplanes

It was shown in Chapter 2 of Part I that this type of relationship exists for airplanes with similar mission orientation. The scatter of actual takeoff weight and empty weight values relative to Eqn.(8.1) was shown to be

---

*For a definition of what is meant by mission phases, see Chapter 2 in Part I.

small. Numerical values for the regression coefficients A and B are given in Table 2.15 of Part I for twelve types of airplanes with similar mission orientation.

Whenever new, lighter structural materials are used in a new design, the validity of Eqn.(8.1) is in doubt. A method to account for the use of advanced materials is given in Appendix B of Part I.

Anytime a statistical method is employed it might be expected that the method becomes highly suspect whenever new, untried configurations are proposed. A discussion of circumstances which can 'drive' a designer toward new and untried configurations is presented in Reference 31.

The significance of takeoff weight sensitivities to an airplane designer is best illustrated with an example. For this example an airplane designed to fill the market void identified as Void I in Figure 9.4 (next chapter!) will be used. A preliminary mission specification for such an airplane is given in Table 8.1. For lack of a better name the airplane will be referred to as the SLRT: Small Long Range Transport.

The takeoff weight sensitivities for the SLRT are determined with the help of a user-friendly, preliminary design computer program called AAA: Advanced Aircraft Analysis program. The main features of this program are described in Reference 32. The takeoff weight sensitivities of the SLRT are determined in three steps:

Step 1: Calculation of the regression coefficients A and B in Eqn.(8.1).

Figure 8.1 shows a 'screendump' of the AAA program after entering takeoff weight and empty weight data for the 23 jet transports identified in Table 8.2. Note the following values for A and B:

$$A = 0.15 \qquad B = 1.02$$

Figure 8.2 shows a logarithmic plot of the weight data from Table 8.2. Note the small amount of scatter, thus supporting the validity of using Equation 8.1.

The mission specification of Table 8.1 is a very aggressive one: there is no such airplane in existence in 1990! It can be expected that to design a workable SLRT, use of more advanced structural materials (compared to those used in the 23 airplanes of Table 8.2) will be required. For that reason, Equation (B2) of Appendix B

Table 8.1 Mission Specification for the Small, Long Range Transport (SLRT)

Passengers:	125 (175 lbs each plus 40 lbs baggage)
Crew:	2 + 4 = 6 (175 lbs each plus 40 lbs baggage)
Range:	5,000 nm still air range
Average cruise altitude:	45,000 ft
Design cruise speed:	450 kts
Fuel reserves:	10 percent of mission fuel used

Table 8.2 Transport Jet Data Used in Obtaining the Regression Coefficients for Eqn.(8.1)

No.	Type	Takeoff Weight (lbs)	Empty Weight (lbs)
1.	Canadair 600	41,100	22,650
2.	601	43,100	23,940
3.	Airbus A300-600	363,765	188,291
4.	600R	375,885	187,251
5.	Airbus A310-200	305,560	166,742
6.	300	330,695	167,477
7.	Airbus A320-100	145,505	83,062
8.	-200	158,730	84,586
9.	Fokker F-100-A	95,000	51,720
10.	Yakovlev 42	124,560	76,180
11.	Tupolev 204	206,130	124,780
12.	British Aerospace 146-100	84,000	48,150
13.	-200	93,000	49,505
14.	Boeing 737-200	124,500	59,738
15.		115,500	59,500
16.	737-400	138,500	71,578
17.		150,000	72,520
18.	757-LR	250,000	124,380
19.	767	300,000	176,470
20.		400,000	195,770
21.	Gulfstream GIV	71,700	40,312
22.	McDonnell Douglas MD-81-A	140,000	77,291
23.	-C	160,000	79,333

Source: Jane's All the Worlds Aircraft, 1989

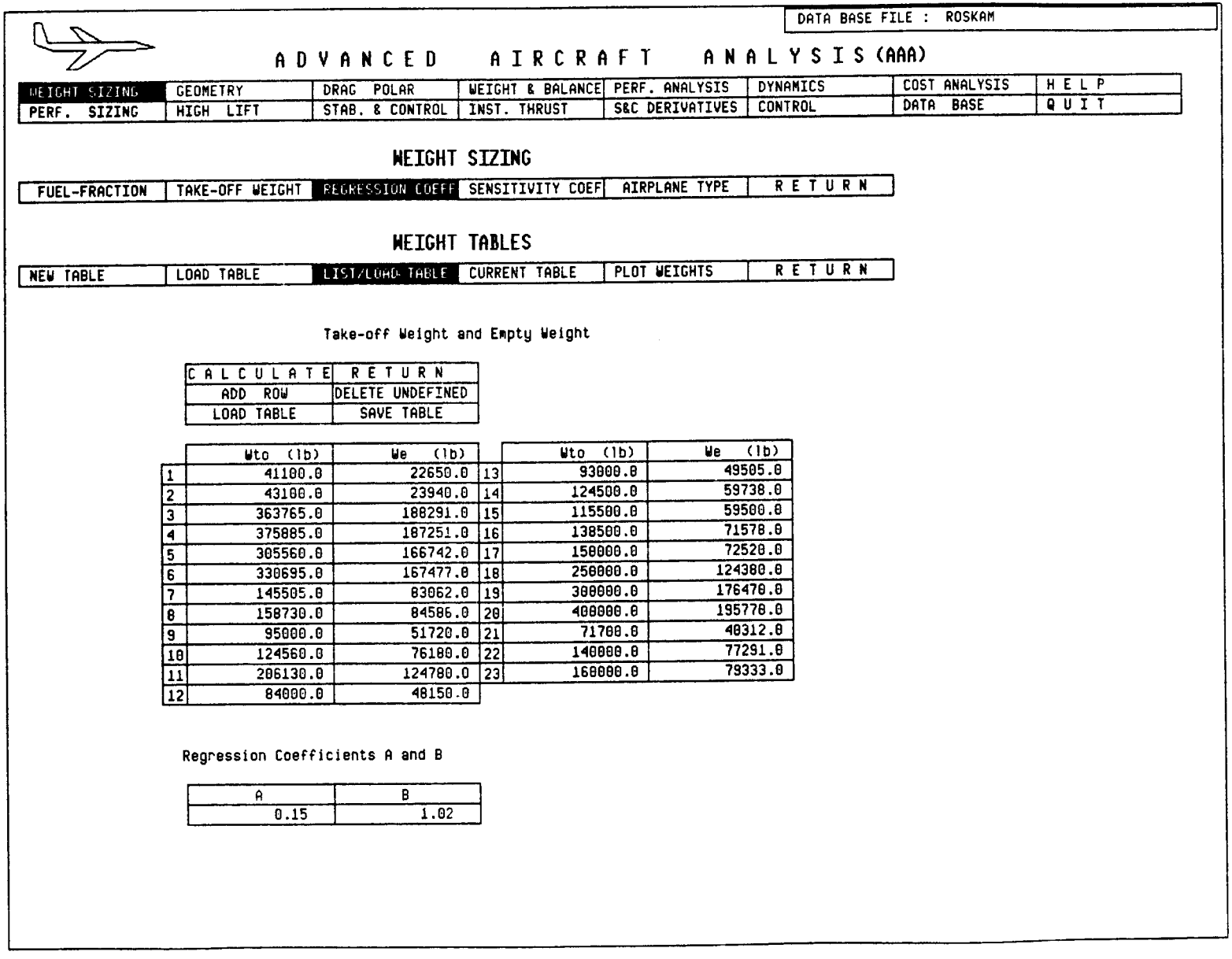

	Wto (lb)	We (lb)		Wto (lb)	We (lb)
1	41100.0	22650.0	13	93000.0	49505.0
2	43100.0	23940.0	14	124500.0	59738.0
3	363765.0	188291.0	15	115500.0	59500.0
4	375885.0	187251.0	16	138500.0	71578.0
5	305560.0	166742.0	17	150000.0	72520.0
6	330695.0	167477.0	18	250000.0	124380.0
7	145505.0	83062.0	19	300000.0	176470.0
8	158730.0	84586.0	20	400000.0	195770.0
9	95000.0	51720.0	21	71700.0	40312.0
10	124560.0	76180.0	22	140000.0	77291.0
11	206130.0	124780.0	23	160000.0	79333.0
12	84000.0	48150.0			

Figure 8.1 AAA Screendump of Takeoff Versus Empty Weight Regression Analysis

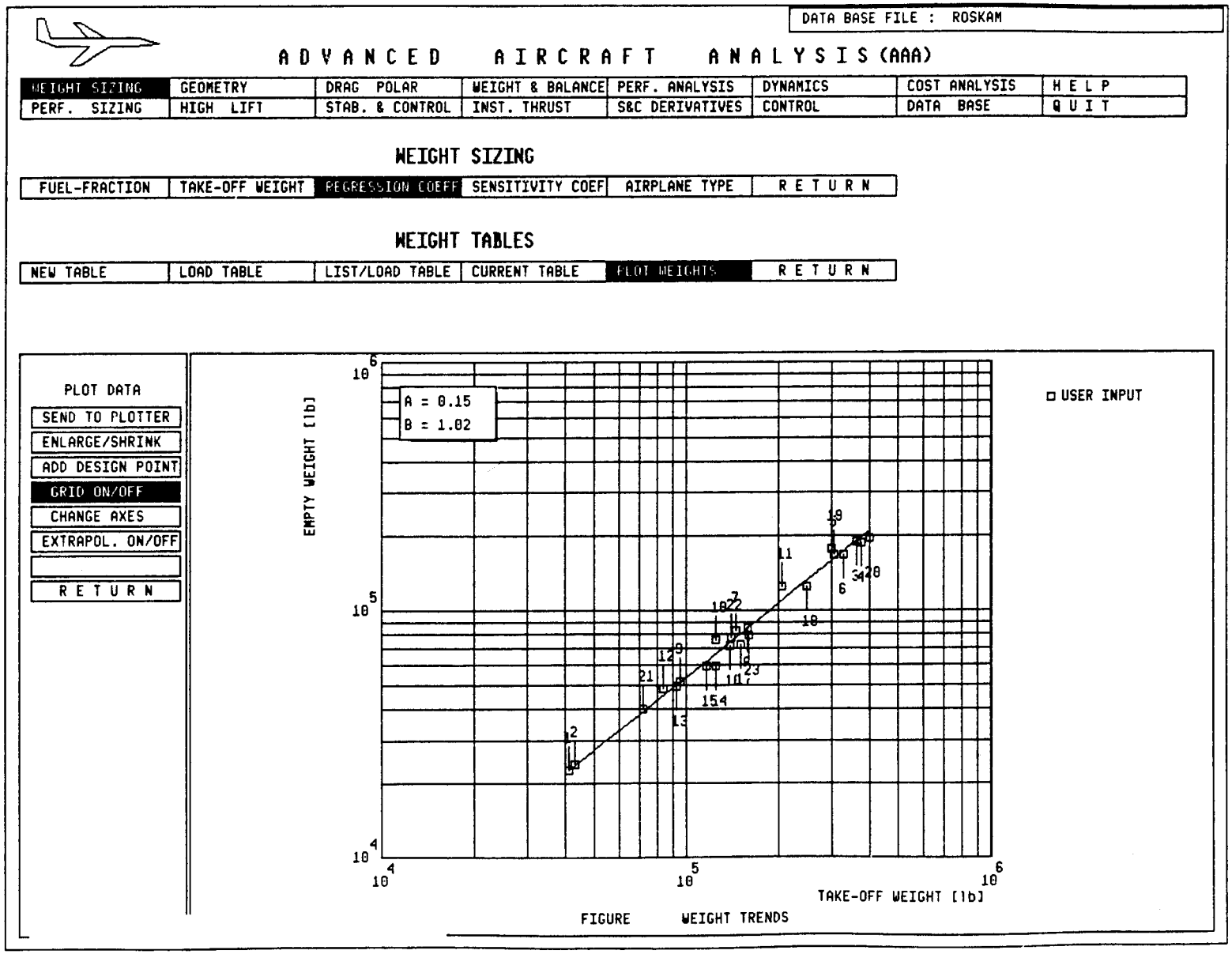

Figure 8.2 AAA Screendump of Logarithmic Plot of Takeoff Weight Versus Empty Weight

in Part I is used to find an 'improved' value for the regression coefficient A. The assumption is made that by judicious use of composites and Li-Al alloys a 5 percent reduction in empty weight is achievable: $\eta = 0.95$, thus:

$$A_{new} = 0.15 - 1.02\log(0.95) = 0.173$$

The assumption has been made here that the regression coefficient B is NOT affected by the choice of new structural materials.

Step 2: Calculation of takeoff weight for the SLRT.

The takeoff weight of the SLRT can be estimated from Equation (2.24) in Part I, which is:

$$\log W_{TO} = A + B\log(CW_{TO} - D) \qquad (8.2)$$

where: $$C = \{1 - (1 + M_{res})(1 - M_{ff}) - M_{tfo}\} \qquad (8.3)$$

with: M_{res} the reserve mission fuel fraction, specified in Table 8.1: $M_{res} = 0.10$.

M_{ff} the overall mission (used) fuel fraction, see Eqn.(2.13), p.16, Part I.

M_{tfo} = trapped fuel and oil fraction, see p.69, Part I. Use: $M_{tfo} = 0.005$.

$$D = W_{PL} + W_{crew} \qquad (8.4)$$

where: W_{PL} is the payload weight in lbs

W_{crew} is the crew weight in lbs

Next, the AAA program of Ref.32 is used to compute the overall mission fuel fraction, M_{ff}. The critical mission phase for M_{ff} is the one corresponding to the extreme range requirement of Table 8.1. Figure 8.3 shows the input data needed to find the cruise fuel fraction: $(W_{i+1}/W_i)_{cruise}$. Note the aggressive use of:

aerodynamics technology: $(L/D)_{average} = 21.0$ and of

engine technology: $c_j = 0.5$ lbs/lbs/hr

Figure 8.4 shows the result of the takeoff weight calculation: $W_{TO} = 152{,}548$ lbs.

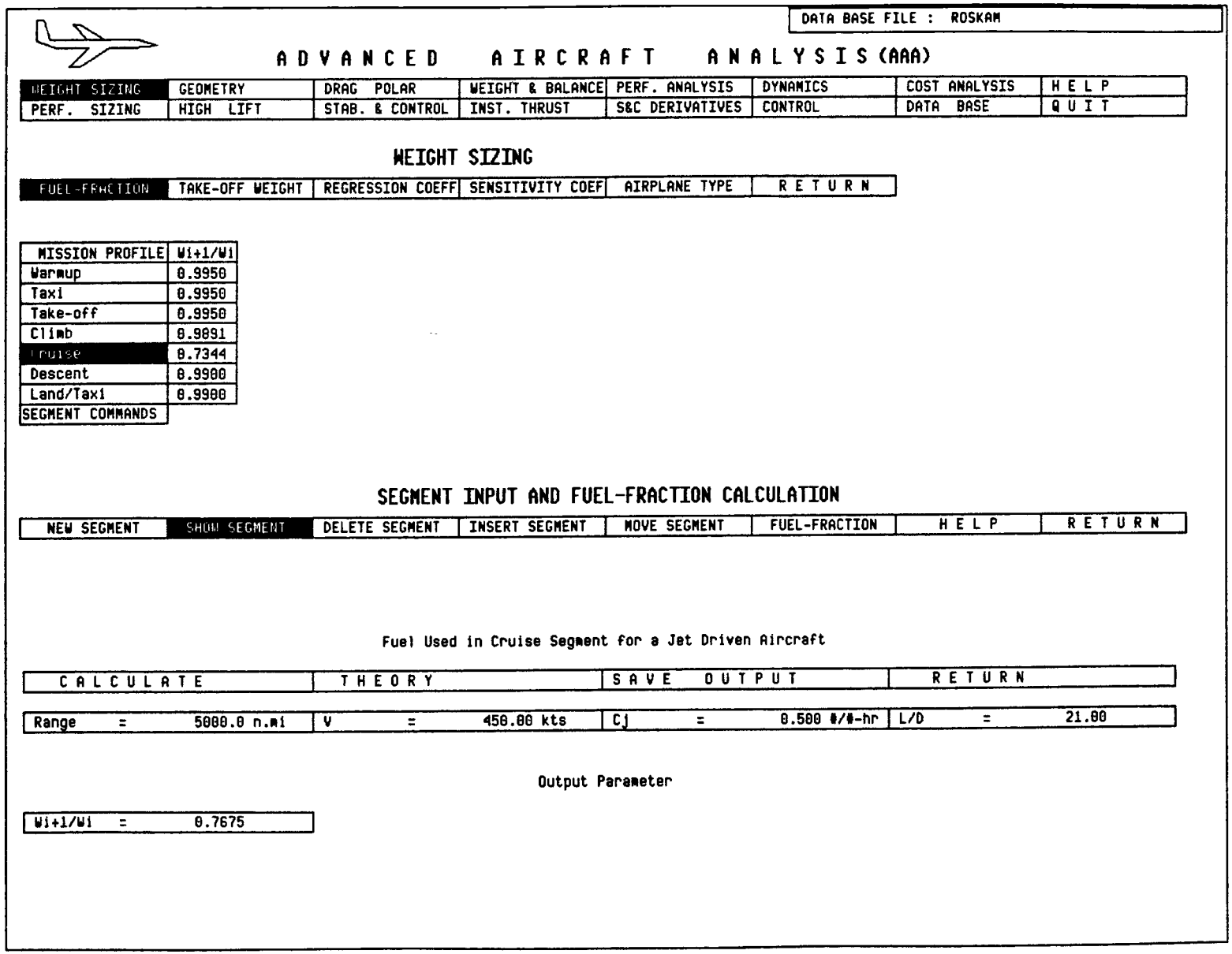

Figure 8.3 AAA Screendump of Fuel Fraction Calculation for a Cruise Mission Phase

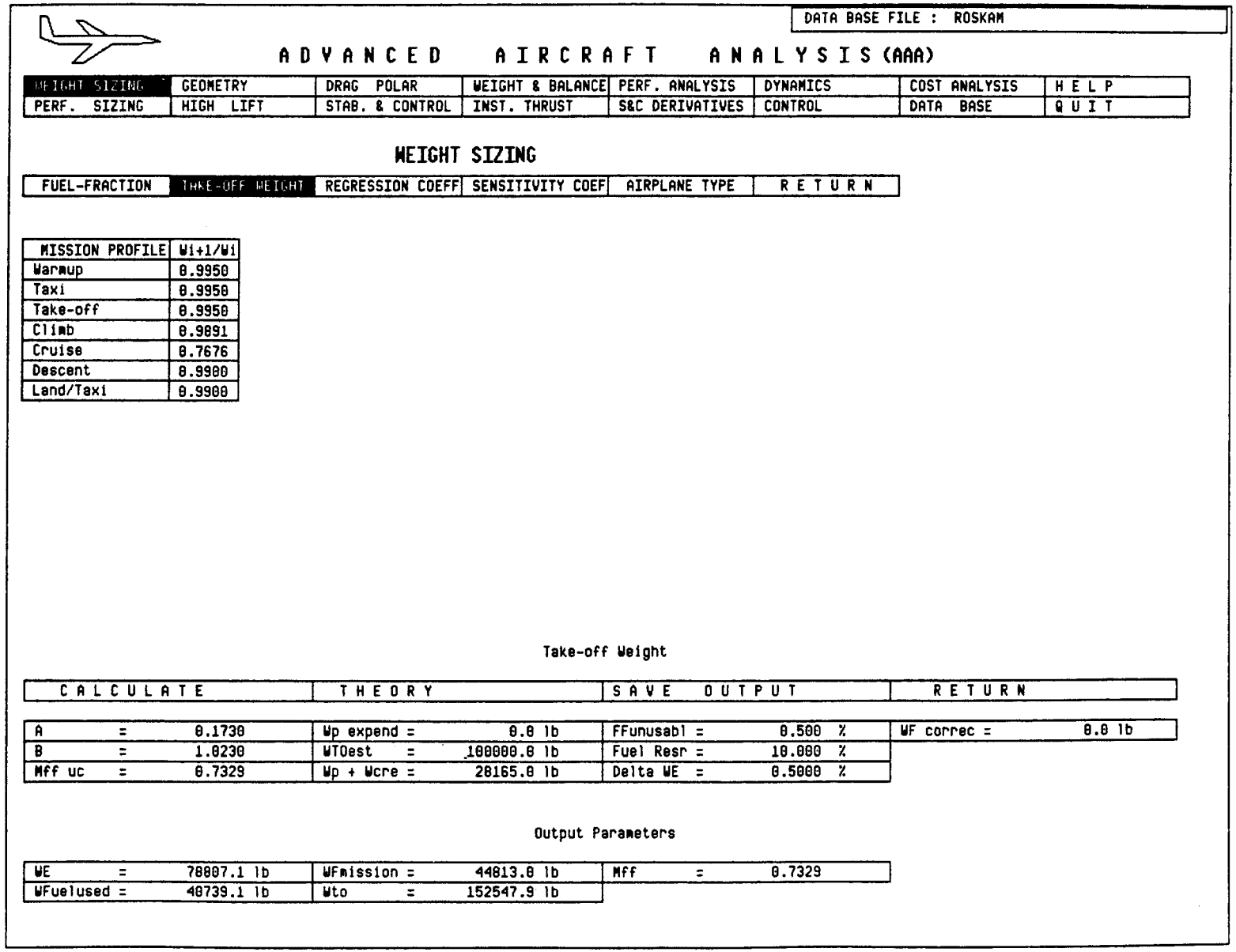

Figure 8.4 AAA Screendump of Overall Mission Fuel Fraction and Takeoff Weight Calculation

Step 3: Calculation of takeoff weight sensitivities.

Formulas for $\partial W_{TO}/\partial y$ were derived in Section 2.7 of Part I. Because of the proposed aggressive use of the following technologies:

* materials: A * aerodynamics: L/D * engine: c_j

it is particularly important that the sensitivity of takeoff weight to these three parameters be understood.

Figure 8.5 shows a AAA screendump of the relevant sensitivity calculations. An interpretation of these results is now given:

1) Sensitivity of takeoff weight to empty weight: W_E

   From Figure 8.5:

   $\partial W_{TO}/\partial W_E = 1.98$ (2.0 rounded off)

   This signifies that for each extra pound of empty weight, the takeoff weight grows by 2 lbs. Such growth in weight might occur as a result of not being able to achieve the assumed 5 percent empty weight reduction and/or by careless structural design. Management should exercise extra careful weight control during the detail design phase!

2) Sensitivity of takeoff weight to cruise specific fuel consumption: c_j

   From Figure 8.5:

   $\partial W_{TO}/\partial c_j = 331,591$ (332,000 lbs/lbs/hr/lbs, rounded off)

   This signifies that if the engine s.f.c is not 0.5, but say 0.55, the takeoff weight would increase by $\Delta W_{TO} = 0.05 \times 332,000 = 16,600$ lbs!

   Management has to watch out that the engine manufacturer can indeed achieve the promised levels of cruise specific fuel consumption!

3) Sensitivity of takeoff weight to cruise lift-to-drag ratio: L/D

   From Figure 8.5:

DATA BASE FILE : ROSKAM

A D V A N C E D A I R C R A F T A N A L Y S I S (AAA)

WEIGHT SIZING	GEOMETRY	DRAG POLAR	WEIGHT & BALANCE	PERF. ANALYSIS	DYNAMICS	COST ANALYSIS	H E L P
PERF. SIZING	HIGH LIFT	STAB. & CONTROL	INST. THRUST	S&C DERIVATIVES	CONTROL	DATA BASE	Q U I T

WEIGHT SIZING

FUEL-FRACTION	TAKE-OFF WEIGHT	REGRESSION COEFF	SENSITIVITY COEF	AIRPLANE TYPE	R E T U R N

SENSITIVITY STUDY AND GROWTH FACTORS : INPUT

C A L C U L A T E	T H E O R Y	N E X T P A G E	R E T U R N

B =	1.0230	Mff uc =	0.7329	Wp expend =	0.0 lb	Wp + Wcre =	28165.0 lb
FFunusabl =	0.500 %	Fuel Resr =	10.000 %	WF correc =	0.0 lb	Wto =	152547.9 lb
WE =	78807.1 lb						

SENSITIVITY : OUTPUT

dWto/dWpl =	5.09	dWto/dWe =	1.98

MISSION PROFILE	dWto/dWpExp	dWto/dCj lb*hr	dWto/dR lb/nm	dWto/dLD lb	dWto/dE lb/hr
Warmup					
Taxi					
Take-off					
Climb		12534.1		-459.5	22979.2
Cruise		331590.9	33.1	-7895.0	
Descent					
Land/Taxi					

Figure 8.5 AAA Screendump of Calculation of Takeoff Weight Sensitivity to Mission and Technology Parameters

$\partial W_{TO}/\partial(L/D) = -7895.0$ (-7,900 lbs per unit L/D, rounded off)

This signifies that if the average cruise L/D is not 21.0, but say 19.0, the takeoff weight would increase by $\Delta W_{TO} = 2x7,900 = 15,800$ lbs!

Management has to exercise careful control over the aerodynamics department to ensure that the projected high cruise L/D can indeed be achieved!

4) Sensitivity of takeoff weight to a change in the required minimum fuel reserves of 10 percent as stipulated in Table 8.1.

Suppose that the airworthiness authorities would stipulate an increase in minimum fuel reserves from 10 percent to 15 percent. This increase can be interpreted as a change in the requirement for cruise range from 5,000 nm to 5,250 nm while keeping the old ten percent reserve number.

From Figure 8.5:

$\partial W_{TO}/\partial R = 33.1$ (33.0 lbs/nm rounded off)

This signifies that an increase of 250 nm range due to an increase in fuel reserve minimums would force an increase in takeoff weight of:

$\Delta W_{TO} = 250x33.0 = 8,250$ lbs

Before launching a project such as the SLRT it is essential that the designer assures himself that critical fuel reserve rules are accepted by all parties concerned!

It should be clear from this discussion that takeoff weight is critically dependent on several design parameters. The prelimininary designer should determine the sensitivity of takeoff weight to these parameters early in the design process. In this manner, management can be guided to take the appropriate action with regard to the establishment of controls on critical design parameters.

Having thusly established the sensitivity of a new design to critical design parameters the designer should initiate studies of airplane design optimization. The first step on the road to optimization studies is the identification of cost functions. Section 8.2 presents a discussion of potential airplane design cost functions.

8.2 EXAMPLE COST FUNCTIONS IN AIRPLANE DESIGN

Airplane designers are confronted with a wide range of cost functions which are potential candidates for optimization. Cost functions in airplane design can be generically classified as follows:

1) Performance Cost Functions
2) Weight Cost Functions
3) Economic Cost Functions

Sub-sections 8.2.1 through 8.2.3 provide several examples of each. A major problem in the conduct of airplane design optimization studies is the very selection of cost functions. Cost functions, to be useful, must be consistent with the mission objective of an airplane, AND they must not conflict with each other. A brief discussion of this problem is given in sub-section 8.2.4.

8.2.1 Examples of Performance Cost Functions

The reader should review the example mission specifications of Tables 2.17 through 2.19 in Part I. It is seen that in these mission specifications, several performance characteristics appear repeatedly:

1. Cruise speed, V_{cr}
2. Time-to-climb to altitude, t_{cl}
3. Cruise range, R_{cr}
4. Loiter time (or endurance), E

As long as everything else is the same, performance cost functions 1, 3 and 4 beg to be maximized while cost function 2 begs to be minimized, particularly in the case of fighter interceptors.

Before these cost functions can be optimized it is necessary to relate them to a set of design parameters. How to relate typical cost functions to airplane design parameters is discussed in Section 8.3.

8.2.2 Examples of Weight Cost Functions

The reader is referred again to the mission specifications of Tables 2.17 through 2.19 in Part I. Payload is seen to be a prominent requirement in all. Furthermore, from the performance sizing procedures outlined in Part I, it is obvious that takeoff weight, empty weight and fuel weight all play an important role. Therefore, the following weights suggest themselves as potential candidates for weight cost functions:

1. Payload weight, W_{PL} 2. Takeoff weight, W_{TO}

3. Empty weight, W_E 4. Fuel weight, W_F

It is clear that weight cost functions 2 and 3 beg to be minimized. In any given airplane, the sum of payload weight and fuel weight is referred to as the useful load:

$$W_{US} = W_{PL} + W_F \tag{8.5}$$

It is the useful load (sum of the cost functions 1 and 4) which beg to be maximized.

In Part V, page 26, Eqn.(4.2), the empty weight, W_E, was expressed as:

$$W_E = W_{struct} + W_{pwr} + W_{feq} \tag{8.6}$$

where: W_{struct} is the airplane structural weight

W_{pwr} is the powerplant weight

W_{feq} is the fixed equipment weight

Each of these three empty weight components can be viewed as a weight cost function: their minimization is certainly desirable.

Before any optimization can take place, a mathematical relation between the weight cost functions and a set of design variables will have to be developed. That is discussed in Section 8.3.

8.2.3 Examples of Economic Cost Functions

For airplane operators the economic aspects of airplanes is of prime importance. This is certainly so for commercial operators. However it is true to a large extent even for military operators. Therefore, cost must be made as low as possible. From discussions in Chapters 2 through 7 it follows that candidates for economic cost functions could be:

1. Manufacturing cost, C_{MAN} 2. RDTE cost, C_{RDTE}

3. Direct operating cost, DOC 4. Life cycle cost, LCC

In addition, the following economic cost functions suggest themselves:

5. Return on investment, ROI 6. Profit potential, P_{pot}

Before any of these cost functions can be used in an optimization study it is necessary to relate them to airplane design variables. Examples of how some of these economic cost functions are related to design variables are discussed in Section 8.3.

8.2.4 Consistency of, and Conflict Between Cost Functions

For any airplane design cost function to be useful, it must satisfy two criteria:

1. It must be consistent with the mission objectives of the airplane.

2. It must not conflict with another cost function that has already been selected.

An example of a cost function which is not consistent with a mission objective would be:

Minimizing wave drag in an airplane that spends only a small amount of time in supersonic flight conditions.

Examples of cost functions which conflict with each other are:

A) Optimize lift-to-drag ratio, L/D with wing aspect ratio, A, as a variable, while also minimizing wing structural weight with A as a variable.

B) Minimizing structural weight with properties of structural materials as a variable, while also minimizing manufacturing cost with only materials weight as a variable. It may be, that the cost of advanced materials 'outweighs' their weight advantage!

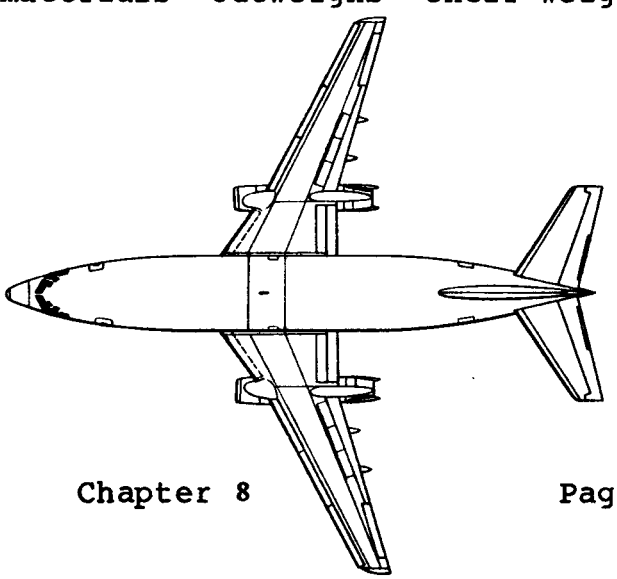

8.3 RELATION BETWEEN COST FUNCTIONS AND AIRPLANE DESIGN VARIABLES

In this section, some of the example cost functions of Section 8.2 will be expressed in terms of appropriate airplane design variables. Finding such expressions for other example cost functions is left as an exercise for the reader. In addition, a discussion is presented on how some of these design variables themselves depend on or relate to each other. The material is organized as follows:

8.3.1 Performance Cost Functions
8.3.2 Weight Cost Functions
8.3.3 Economic Cost Functions

8.3.1 Performance Cost Functions

The following two performance cost functions of subsection 8.2.1 will be discussed:

* Cruise speed, V_{cr} * Cruise Range, R_{cr}

8.3.1.1 Cruise speed as a cost function

It will be assumed that the classical parabolic drag polar format is applicable:

$$C_D = C_{D_o} + (C_L)^2/(\pi Ae) \qquad (8.7)$$

Below the absolute ceiling, each airplane can fly level at two speeds: a low speed and a high speed. The high speed is referred to as the cruise speed. All this applies at cruise thrust settings only! It may be seen from Equation (3.60) in Part I that airplane cruise speed, V_{cr}, can be written as follows:

$$V_{cr} = \qquad (8.8)$$

$$= \left[(W/S)_{cr} \frac{(T/W)_{cr} + \{\{(T/W)_{cr}\}^2 - (4C_{D_o})/(\pi Ae)\}^{1/2}}{(\rho C_{D_o})}\right]^{1/2}$$

where: $(W/S)_{cr}$ is the wing loading for the cruise flight condition being considered

$(T/W)_{cr}$ is the thrust-to-weight ratio for the cruise flight condition being considered

C_{D_o} is the zero lift drag coefficient

A is the wing aspect ratio

e is Oswald's efficiency factor

If these five parameters are viewed as independent design variables (which, as will be shown, they are NOT), and cruise speed is seen as a cost function which should be maximized, four conclusions can be drawn. V_{cr}:

1) increases with increasing wing loading,
2) increases with increasing thrust-to-weight ratio,
3) increases with decreasing zero lift drag coefficient,
4) increases with increasing product Ae

In other words, a maximum cruise speed value does not exist. There are several flaws in this reasoning:

Flaw 1: Wing loading cannot be increased independently.

NOTES: 1. The cruise wing loading differs from the takeoff wing loading because fuel has been used between takeoff and cruise.

2. The takeoff wing loading is constrained by a number of performance constraints as was shown in Chapter 3 of Part I.

Therefore: The cruise wing loading, $(W/S)_{cr}$, cannot be varied independently.

Flaw 2: Thrust-to-weight ratio cannot be increased independently.

NOTES: 1. The cruise thrust-to-weight ratio differs from takeoff thrust-to-weight ratio because of differences in thrust (throttle) setting and also because of altitude effects on engine output.

2. The takeoff thrust-to-weight ratio is constrained on its low side by performance considerations as shown in Chapter 3 of Part I.

3. Selecting a high thrust-to-weight ratio to attain a high cruise speed is probably self defeating: engine weight and cost will increase, as will engine fuel specifics.

Thus: the cruise thrust-to-weight ratio, $(T/W)_{cr}$, cannot be varied independently.

Flaw 3: The zero lift drag coefficient cannot be independently decreased. See Chapter 4 in Part VI for methods to compute C_{D_o} for airplanes.

NOTES: 1. At low subsonic speeds, C_{D_o} depends on:

a) airplane wetted area, S_{wet}. Wetted area in turn depends on the overall layout of the configuration and on the wing area: see Chapter 12 in Part II.

The reader is reminded of the fact that wetted area tends to correlate in a logarithmic manner with airplane takeoff weight for airplanes with similar mission orientation. See Part I, Figures 3.22.

b) skin friction coefficient, c_f. This in turn depends on Reynolds Number, Mach Number and on the smoothness of the exterior surfaces.

c) airplane interference drag and separation drag. These factors depend on the detailed layout of the external surfaces.

2. At high subsonic speeds, C_{D_o} depends on all previous factors AND on the dragrise behavior of an airplane. The dragrise depends on such detail design variables as: thickness ratio, sweep angle and aspect ratio of wing and empennage as well as on the overall progression of crosssectional areas: area ruling!

3. At supersonic speeds, C_{D_o} depends on all previous factors AND on lift induced wave drag.

Therefore: the zero-lift drag coefficient, C_{D_o}, can not be varied independently.

Flaw 4: The product Ae cannot be increased independently.

NOTES: 1. Increasing wing aspect ratio has the following consequences:

a) wing weight increases (This is seen from the wing weight equations in Ch.5 of Part V).

b) aeroelastic effects may become unacceptable. Examples of aeroelastic effects are:

* aileron reversal
* flutter
* aeroelastically induced shift of the wing aerodynamic center

Aeroelastic effects depend on:

* structural arrangement
* properties of structural materials
* aerodynamic load distribution
* mass distribution
* dynamic pressure of the flight condition

Reference 33 is an excellent introduction to the theory of aeroelasticity.

c) wing span may become too large because of operational considerations.

2. Oswald's efficiency factor, e, depends on the following variables:

* wing aspect ratio
* wing sweep angle
* airfoil leading edge radius
* wing lift curve slope (the latter also is a function of aeroelastic effects)

Chapter 4 of Part VI contains a method for estimating 'e'.

Therefore: the product Ae cannot be varied independently.

The cruise speed of the airplane therefore depends not on four variables (which are not independent), but on many more. Most of these additional design variables or design factors are not easily related to each other, certainly not during the early design phases.

8.3.1.2 Cruise range as a cost function

It is shown in Chapter 5 of Part VII that the cruise range depends on how the cruising flight is carried out: cruise at constant altitude, cruise at constant Mach number or some combination of these. Eqns (5.33) through (5.36) in Part VII provide simplified analytical formulas for cruise range under either scenario. Only the case of constant speed cruise of a jet airplane will be taken up here. From Equation (5.36) in Part VII:

$$R_{cr} = (U_1/c_j)_{cr}(L/D)_{cr}\ln(W_{initial}/W_{end}) \qquad (8.9)$$

where: U_1 is the true airspeed in kts

c_j is the engine specific fuel consumption in (lbs/hr)/lbs

L/D is the lift-to-drag ratio

NOTE: all of these quantities are for the cruise flight condition

$W_{initial}$ is the airplane weight at the start of cruise in lbs

W_{end} is the airplane weight at the end of cruise in lbs

Observe that:

$$U_1 = M_1 a \qquad (8.10)$$

where: M_1 is the steady state (cruise) Mach number

a is the speed of sound at the cruise altitude in kts

Substituting Eqn.(8.10) into Eqn.(8.9) yields:

$$R_{cr} = (a/c_j)_{cr}\{M(L/D)\}_{cr}\ln(W_{initial}/W_{end}) \qquad (8.11)$$

It is clear from this equation that for:

* a given cruise altitude (which defines a)
* a given engine cruise thrust setting (which, with the given altitude and known engine inlet conditions, defines c_j)

* a given weight ratio, $W_{initial}/W_{end}$

the cruise range is maximized for maximum {M(L/D)}.

Figure 8.6 illustrates how L/D of a typical transport jet varies with Mach number. Note that {M(L/D)} becomes maximum at a Mach number different from that at which (L/D) becomes a maximum. All of this must be tempered by the fact that the airplane also must be flying at a lift coefficient which is consistent with the L/D at $\{M(L/D)\}_{max}$. From Table 3.1 in Part VI:

$$C_{L_{cr}} = W/\bar{q}S = f\{C_{D_o}(\pi Ae)\}^{1/2} \qquad (8.12)$$

where: f is a factor, such that $0<f<1.0$, which accounts for the fact that $C_{L_{cr}}$ is not the same as the value C_L takes on at maximum L/D.

For a discussion of the design variables which are determinant for C_{D_o}, A and e, the reader should read sub-sub-section 8.3.1.1. The reader should also appreciate the fact that the weight ratio, $W_{initial}/W_{end}$, in Eqn.(8.11) is itself not an independent variable. Values for this ratio, typical for transport jets, are shown in Table 8.3. The actually available weight ratio depends on the overall configuration of the design, in particular on the general structural arrangement and on materials used in the structure.

TABLE 8.3 TYPICAL CRUISE WEIGHT RATIOS, $W_{initial}/W_{end}$
FOR JET TRANSPORTS

Transport Type	W_{TO}(lbs)	W_F(max, lbs)	$W_{initial}/W_{end}$
Boeing 747-400	800,000	387,000	1.70
Boeing 767-200ER	300,000	113,000	1.47
Boeing 757	250,000	75,000	1.34
McD.D. MD81A	140,000	39,000	1.31
McD.D. DC-10-30	572,000	246,000	1.58
Airbus A320-100	150,000	28,000	1.19
Airbus A320-200	162,000	42,000	1.28

Note: data assume that 15 percent of the fuel is used for reserves and for conditions other than cruise.

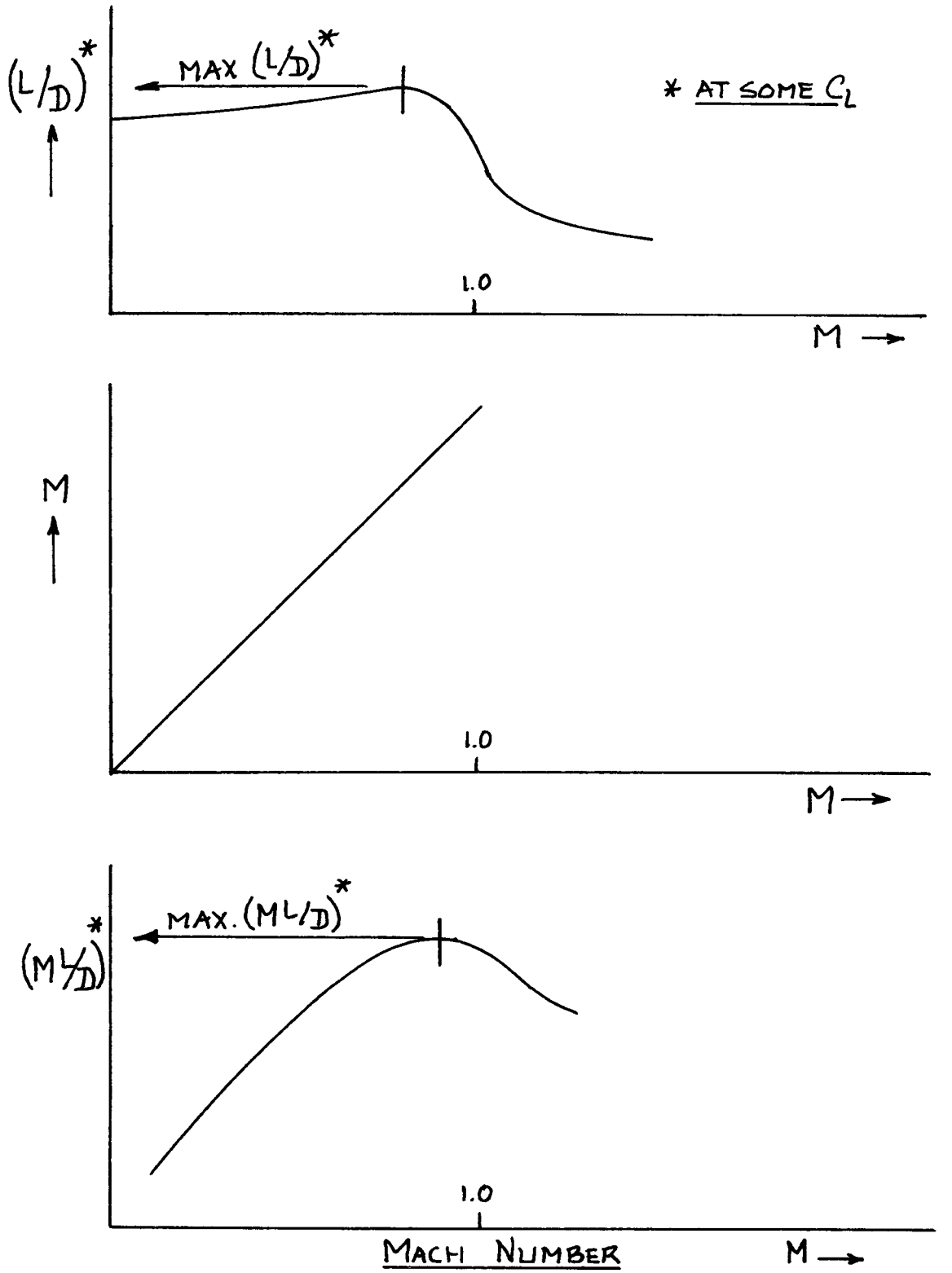

Figure 8.6 Effect of Mach Number on L/D and on M(L/D)

8.3.2 Weight Cost Functions

The following two weight cost functions of sub-section 8.2.2 will be discussed:

* Empty weight
* Useful load

8.3.2.1 Empty weight as a cost function

From Equation (8.6):

$$W_E = W_{struct} + W_{pwr} + W_{feq} \qquad (8.13)$$

Minimizing any one of these empty weight contributions is clearly desirable. A problem with this statement is that in many instances attempts to reduce weight can be costly (in terms of dollars!). Thus, a balance must be struck between weight decrease and cost increase.

The Class II weight estimation formulas of Chapters 5, 6 and 7 of Part V can be used to relate airplane empty weight to fundamental design variables. The Class II weight equations are derived from a data base which consists primarily of airplane structures made from aluminum alloy types of materials. When more advanced materials are planned, downward adjustments have to be made.

There are no simple methods to account for the effect of advanced materials and/or manufacturing processes on dollar cost. To do justice to the effect of dollar cost, much more detailed knowledge about the design of the airplane must be available than is normally the case in advanced design. An interesting approach to the problem of dollar-cost-weight trades in airplane design is found in Reference 34.

The reader should observe that many of the component weight equations in Chapter 5 of Part V require the limit load factor as an input. The limit load factor itself is not an independent variable! The V-n diagrams of Ch.4 of Part V show the design load factor to be a function of:

* the takeoff weight
* the flight envelope
* the gust response behavior

It is clear from this discussion that the relationship between empty weight and design variables is a very complicated one.

8.3.2.2 Useful load as a cost function

The useful load of an airplane is defined in Eqn.(8.5) as:

$$W_{US} = W_{PL} + W_F \qquad (8.14)$$

where: W_{PL} is the payload weight

W_F is the fuel weight

Payload weight and payload type are normally defined in the mission specification of an airplane. It turns out that payload weight and payload type both have a significant effect on airplane empty weight. Examples which illustrate this effect are:

1) In a passenger jet transport, the number of passengers carried, the class of service offered and the requirements for on-board meals and other services have a major impact on the weight of cabin interior amenities.

2) In a cargo jet transport, the type of cargo has a major effect on the structural design and layout of the cargo hold:

* if containers are to be carried, roller-rails and tie-down provisions are required

* if concentrated loads are to be carried (any type of roadable or off-highway type vehicle), major floor reinforcements are required

* if front, rear and/or side loading of the payload is/are required, major structural provisions for these features will be required

* if weapons have to be carried and launched, major provisions in the structure to take the various weapons loads will be required

The reader is referred to Parts III and IV for more detailed discussions of these effects.

The point to be made here is that payload itself can be a complex function of design variables involved in the empty weight of an airplane, mostly in the structural and fixed equipment part of this weight.

8.3.3 Economic Cost Functions

The following three economic cost functions of subsection 8.2.3 will be discussed:

* Manufacturing cost (C_{MAN}
* Direct operating cost (DOC)
* Return on investment (ROI)

8.3.3.1 Manufacturing cost as a cost function

A method for determining airplane manufacturing cost was presented in Chapter 4. The method, as reflected by Equations (4.4), (4.5), (4.7), (4.17) and (4.18), shows that airplane manufacturing cost depends on the following design parameters:

1) Takeoff weight, W_{TO} (through the AMPR weight of Equation (3.4) or (3.5))
2) Maximum design speed, V_{max}, as defined on p.26
3) Number of airplanes produced to manufacturing standard, N_m
4) Labor rates for engineering, manufacturing and tooling, R_{e_m}, R_{m_m} and R_{t_m}
5) Number of passengers, N_{pax} (only for commercial airplanes
6) Manufacturing rate, N_{r_m}
7) Various judgement factors, F_{diff}, F_{cad}, F_{int}, F_{mat}, F_{ftoh} and F_{fin_m}
8) Cost escalation factor, CEF
9) Operating cost per hour, $C_{ops/hr}$, and number of production flight test hours, t_{pft}
10) Cost of engines and avionics

Design variables 1) and 2) are the most important ones. It turns out that the engine cost is related to the takeoff weight.

8.3.3.2 Direct operating cost (DOC) as a cost function

A method for determining airplane direct operating cost is presented in Chapters 5 and 6. The DOC of an airplane depends (according to Equations (5.19) and (6.1) and their components) on the following design variables:

1) Takeoff weight, W_{TO}, because many of the DOC component costs are expressed in terms of the takeoff weight

2) Cockpit crew requirements: this is determined by the mission of the airplane

3) Fuel used: this depends on lift-to-drag ratios and on engine efficiencies

4) Accessibility and ease of maintenance

For a discussion of the relative significance of DOC component contributions, see Chapters 5 and 6.

It turns out that takeoff weight, aerodynamic and fuel efficiency are normally the 'driving' factors behind the DOC of commercial and military airplanes.

8.3.3.3 Return-on-investment (ROI) as a cost function

The following definition of return-on-investment (ROI) will be used:

$$ROI = \{\frac{(REV - DOC - IOC)V_{bl}}{(AEP)(1 - tx_{inv})}\}(1 - tx_{rev})U_{ann_{bl}}(100) \quad (8.15)$$

where: REV is the revenue in USD per nm

DOC is the direct operating cost in USD per nm

IOC is the indirect operating cost in USD per nm

V_{bl} is the block speed in nm/hr

AEP is the airplane estimated price in USD (See page 62)

tx_{inv} is the investment tax credit rate extended by the government to the operator. For preliminary design purposes it is suggested to use: $tx_{inv} = 0.10$ (ten percent).

tx_{rev} is the 'income' or 'revenue' tax rate paid to the government. For preliminary design studies, use: $tx_{rev} = 0.20$.

Note: tax rates are determined by the congress and therefore are a variable over which the designer has little control!

$U_{ann_{bl}}$ is the annual airplane utilization in hours

Note that ROI as defined in Eqn.(8.15) comes out as a percentage.

It is obviously desirable to maximize ROI. However, there are a number of problems:

* The ticket price charged per nautical mile, REV, must be competitive or no passengers will be willing to pay the price

* The ticket price will influence market demand to some extent: the demand for passenger miles is elastic

* DOC and IOC should be kept as low as possible. Methods for computing DOC and IOC are given in Chapters 5 and 6 of this volume. Note the very large number of airplane design and operating variables which enter the picture!

* Annual utilization should be kept as high as possible. There are several limitations to this:

  a) if annual utilization goes above some number, maintenance and repairs become a problem

  b) the route structure of the airline may not make it feasible to have high annual utilization

8.4 DESIGN CONSTRAINTS IN AIRPLANE DESIGN

Aeronautics is one of the most heavily regulated activities of mankind. The reason for this is: SAFETY. To ensure minimum standards of safety in airplane design and in airplane operation, governments adopt and enforce minimum standards of airworthiness and operating safety.

These standards have been referred to as the 'regulations' in this series of books. Many aspects of these regulations were covered in Parts I through VII. Copies of those regulations which directly impact airplane performance, stability and control (and thereby the configuration design) are included as appendices to Part VII.

From a design optimization viewpoint, these regulations should be interpreted as: design constraints. Design constraints limit the numerical ranges of design parameters which are available to the designer.

In addition to regulatory design constraints, there are many other examples of design constraints. Airplane design constraints are generically classified as follows:

1. Design constraints related to airworthiness
2. Design constraints related to operational safety
3. Design constraints related to operational factors other than safety
4. Design constraints related to economics
5. Design constraints related to the infra-structure
6. Design constraints related to typical military requirements
7. Design constraints related to the environment

There is no implied priority in the listing of these design constraints. They can all play important roles in arriving at key design decisions. Examples of airplane design constraints and the role played in design decision making are provided in sub-sections 8.4.1 through 8.4.7.

8.4.1 Design Constraints Related to Airworthiness

Civilian and military airworthiness is ensured by specifying minimum standards of:

1. Airplane performance with and without all engines operating

2. Airplane handling qualities with and without all engines operating

3. Structural integrity in the presence of extreme atmospheric and/or other operational loads

4. Reliability and/or redundancy of flight crucial systems

Parts I through VII contain many examples of the impact of airworthiness regulations on airplane design. In the following, one example of each of these airworthiness constraints will be given.

8.4.1.1 Example of a performance constraint

It was shown in Chapter 3 of Part I that takeoff and landing distances are regulated by certain definitions of fieldlength: ground distance, air distance and obstacle height. Also, factors such as air density, temperature and humidity must be acounted for. If an airplane is to safely operate from a field with a given minimum fieldlength, then the result of these fieldlength constraints is to limit the available choices of wing loading and of thrust-to-weight ratio. This was shown in Chapter 3 of Part I in the form of a plot of takeoff thrust-to-weight ratio, $(T/W)_{TO}$, versus takeoff wing loading, $(W/S)_{TO}$.

Figure 8.7 is an example of this. The range of design parameter values which are denied by the fieldlength constraints is clearly indicated. A complicating factor is that the size of the 'denied' ranges is a function of the flap capability of the airplane, as expressed through the maximum lift coefficients: $C_{L_{max_{TO}}}$ and $C_{L_{max_L}}$.

Table 3.1 in Part I gives ranges of numerical magnitudes for these maximum lift coefficients for mechanical flaps. There are various forms of augmentation (blowing is one example) which can be used to attain significantly higher values of maximum lift coefficient. In any case, there are limits to attainable maximum lift coefficients. These limits can have a number of causes: aerodynamic, flap weight, flap system complexity and flap system cost are only a few of these.

It is possible to formulate these maximum lift coef-

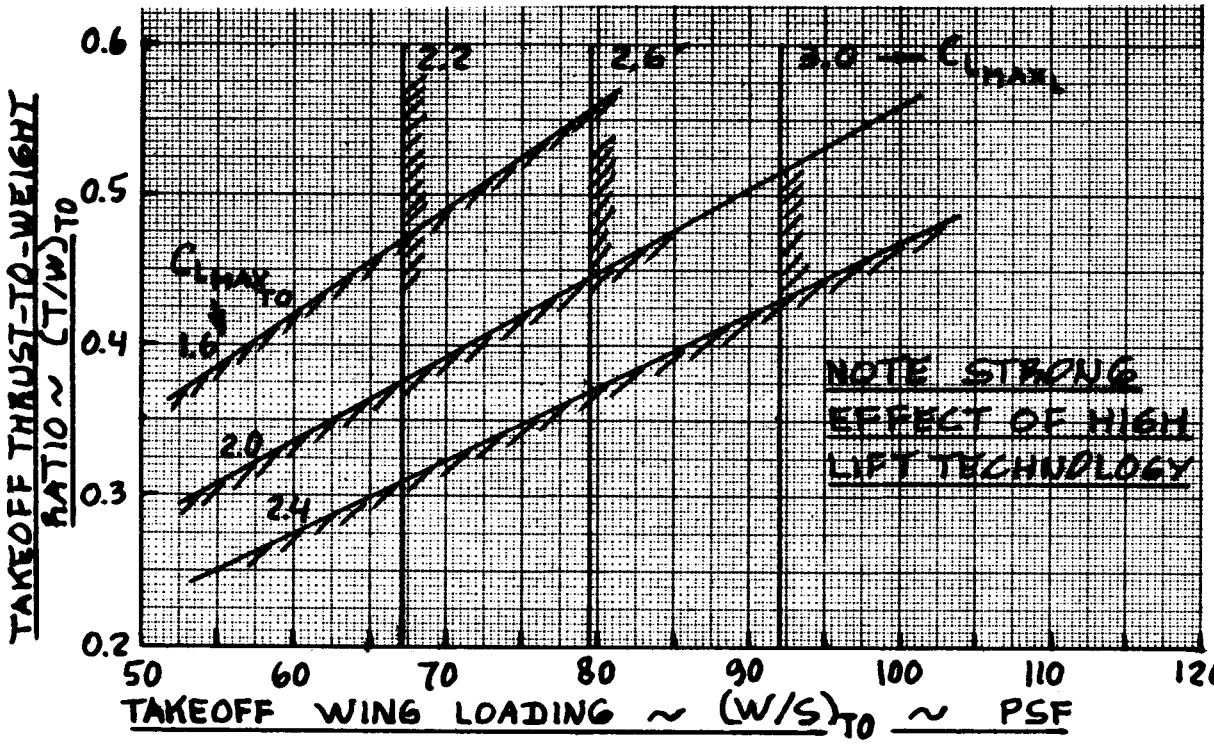

Figure 8.7 Example of Fieldlength Constraints on Wing Loading and Thrust-to-Weight Ratio

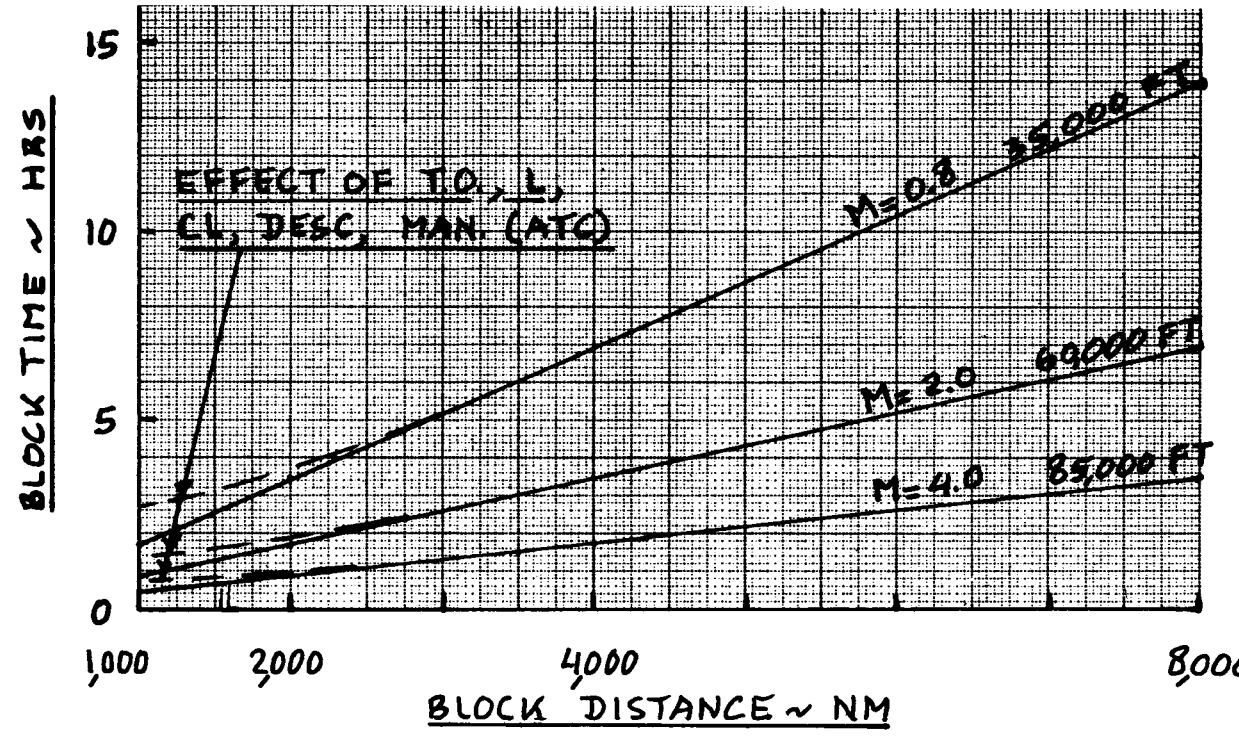

Figure 8.8 Effect of Cruise Mach Number and Block Distance on Block Time

ficient limits in a suitable mathematical format. This is most easily done for the case of mechanical flaps. The lift prediction methods of Part VI are examples of how this can be done. Considerations involving calendar time and money restrictions make it difficult to arrive at similar formulations for items such as: flap weight, flap system complexity and flap system dollar cost.

Here is an example of a case where design intuition and design experience will enter the picture. An experienced designer will not hesitate to make a flap design decision based on intuition. However, this makes the design process no longer optimizable in the rational sense of the word.

8.4.1.2 Example of a handling quality constraint

Minimum requirements for safe handling qualities are discussed briefly in Part II and in Part VII. Analytical methods for determining handling quality parameters are presented in References 35 and 36. It can be shown that each requirement for handling qualities translates into some form of design constraint. One example will be discussed: the minimum control speed problem.

In multi-engine airplanes, with one engine inoperative, it is required that the pilot be able to maintain control down to the so-called minimum control speed, V_{mc}. The airworthiness requirements (see Appendices A and B in Part VII) stipulate the following relationship between the minimum control speed, V_{mc}, and the stall speed, V_s:

$$V_{mc} < 1.2V_s \tag{8.16}$$

The stall speed itself is related to the wing loading and the maximum lift coefficient (clean, flaps up and flaps down!):

$$V_s = \{2(W/S)/(\rho C_{L_{max}})\}^{1/2} \tag{8.17}$$

The minimum control speed (in a takeoff flight condition) for a twin engine airplane can be approximated as follows:

$$V_{mc} = [\{(2T_{TO_e})(y_T)\}/\{(C_{n_{\delta_R}})_{max}(Sb\rho)\}]^{1/2} \tag{8.18}$$

where: T_{TO_e} is the take-off thrust of the most critical engine in lbs

y_T is the lateral moment arm of the most critical engine in ft

$C_{n_{\delta_R}}$ is the rudder control power derivative in rad^{-1}

$\delta_{r_{max}}$ is the maximum allowable rudder deflection in rad

S is the wing area in ft^2

b is the wing span in ft

ρ is the atmospheric density in $slugs/ft^3$

Each design parameter in Equation (8.18) itself may depend on a number of other design parameters. For example, the control power derivative, $C_{n_{\delta_R}}$, is a function of:

* vertical tail size
* vertical tail geometry (aspect ratio, sweep angle, taper ratio and airfoil)
* vertical tail location on the configuration
* rudder size, shape and location

The maximum allowable rudder deflection, $\delta_{R_{max}}$, is a function of:

* Vertical tail stall behavior and Reynolds Number
* Rudder geometry
* Vertical tail location on the configuration

When all these design parameters have been decided upon, the V_{mc} constraint defines a minimum allowable vertical tail size. This in turn has an impact on overall airplane drag, weight and center of gravity location. The latter will also impact the stability and control of the airplane!

8.4.1.3 Examples of structural integrity constraints

Examples of structural design constraints are all those factors which impact on the airloads and other loads which act on an airplane as it operates in the air or on the ground. In the preliminary design phase the structural integrity requirements impact the design decision making process through factors such as:

* specified limit load factor

  This has an impact on structural weight and thus on overall weight, center of gravity locations and on cost.

* specified design touchdown velocity

  This has an impact on the design of the landing gear which in turn impacts airplane takeoff weight and the volumetric requirement of the gear upon retraction. The latter can also have an economic impact if the retracted landing gear volume limits payload or fuel carrying capability.

8.4.1.4 Examples of system reliability and redundancy constraints

Whenever the failure of an airplane system is considered to have a major impact on safety, it is called a flight crucial system. The hydraulic system is a flight crucial system if it is the only source of control in flight. That is the case in many transports today.

Whenever a system is defined as flight crucial it must satisfy certain standards of reliability and redundancy. For more information on the subject of safety and redundancy, see Chapters 6 and 13 in Part IV and also Appendix C in Part VII.

Flight crucial systems are 'allowed' to fail in a catastrophic manner at the rate of once per 10^9 flight hours (or sometimes flights). One task of the designer is to estimate the reliability of each such system, in terms of catastrophic failure rate per X flight hours. Once this estimate is available it is easy to compute how many independent systems are required to satisfy the 10^9 requirement. It is not difficult to see that the outcome of these system design considerations can have an impact on airplane weight, airplane layout (signal and power

path redundancy!!), airplane complexity, airplane maintenance requirements and airplane cost.

Casting these constraints in mathematical formats suitable for use in optimization is a formidable task.

8.4.2 Design Constraints Related to Operational Safety

Examples of this type of design constraint are:

* Airplane ceiling

  Each airplane has an altitude-weight combination beyond which it is unsafe to operate. The reason for this limit is the proximity of stall speed, buffet limit and maximum allowable Mach number. There are also cases where airplane handling qualities are compromised beyond certain combinations of airplane weight and altitude.

* Airplane operating speed and/or Mach number

  At each altitude, airplanes are limited in minimum and maximum allowable speed for a variety of reasons having to do with engine or airframe limitations or with handling quality limitations.

* Fuel reserves

  When airplanes are flown on a given route, there exist regulations (FAR 135) which specify that flight to alternate airports must be possible in case of weather limitations at the airport of destination. This leads to requirements for fuel reserves. These fuel reserves increase the weight of the airplane. They also require that enough fuel volume is available on board to store it.

* Emergency and evacuation constraints

  These constraints require certain airplanes to be equipped with:

  a) emergency exits of prescribed size and location
  b) evacuation slides
  c) life rafts and floatation equipment
  d) fire safety equipment

  All these requirements translate into weight and volume needs which should be viewed as constraints on the design decision-making process.

These constraints must be translated into functional relations between various airplane design variables. This cannot (in general) be done until detailed data on the aerodynamic and the structural design are available.

8.4.3 Design Constraints Related to Operational Factors Other than Safety

Examples of this type of design constraint are:

* Servicing requirements: commercial

  A jet transport, when arriving at the gate, needs to be serviced by a wide variety of servicing vehicles. Critical here is the so-called 'gate turn-around time' which must be kept to a minimum. Airplanes parked at the gate do not earn money! A discussion of this problem is given in Part III, Chapter 3 (page 82).

  This design constraint implies that there must be sufficient access to various systems of the airplane to make simultaneous servicing possible. This in turn puts constraints on the location of equipment in the airplane and on the size and location of access doors and access covers. These considerations tend to have a significant impact on structural design (strength and fatigue life) and therefore on weight and cost.

* Servicing requirements: military

  A military airplane returning from a combat mission needs te be turned around and readied for its next mission in as short a time as possible.

  This design constraint is similar to that of the jet transport at the gate. However, in the case of military airplanes these functions may have to be carried out by personnel wearing polar and/or chemical warfare clothing. This makes the design of access doors and covers very critical: they tend to be large!

* Landing gear constraints

  The reader is asked to review the landing gear design and disposition criteria of Ch.9 in Part II and in Ch.2 of Part IV. Most of these gear design criteria should be viewed as design constraints.

No attempt has been made here to derive functional relations between these design constraints and the appropriate airplane design variables.

8.4.4 Design Constraints Related to Economics

Examples of design constraints related to economics are:

* Revenue
* Program Cost
* Acquisition cost
* Travel time

A brief discussion of each follows.

* Revenue as a constraint

In certain markets the customer may not be willing to pay more than a certain amount of USD per nm. It is essential that airplane designers understand such limits and incorporate them into their design trade studies to determine the economic viability of a proposed design. Such limits on 'extractable' revenue should be viewed as design constraints.

* Acquisition cost as a constraint

The acquisition cost of an airplane translates into the cost of ownership. There are limitations on the allowable cost of ownership for commercial as well as for military airplanes. Again, such limitations should be viewed as design constraints.

* Program cost as a constraint

In military programs in particular the total allowable program cost should be seen as a design constraint.

These three cost constraints all bear a relation to the 'design-to-cost' problem which is discussed briefly in Section 8.8.

* Travel time as a constraint

Figure 8.8 shows how trip time relates to block-speed for various triplengths (block distances). It is seen that for transpacific distances there is not much payoff, in terms of time gained, for flying beyond Mach 4.0. This design constraint is caused by the 'smallness' of the earth.

8.4.5 Design Constraints Related to the Infra-structure

Examples of design constraints which are related to the infra-structure are:

* Gate space at airports of intended operation

  This may limit the designer to a given wing span. One example of this is the Boeing 747-400. Winglets were added to this airplane largely to avoid greater wing span. In future designs, folding wing tips may have to be considered as well!

* Hangar size

  Airplanes may have to fit into existing hangars. Construction of new hangars is expensive. Some operators may not be willing to spend money to build a new hangar just because the airframer decided to build an airplane which does not 'fit'. This constraint can therefore dictate the outside dimensions of the airplane regardless of any aerodynamic or other considerations!

  Such size constraints are common in the design of carrier based airplanes for the navy: deck spotting, elevator spotting and hangar deck spotting considerations all impose size constraints on the airplane designer.

* Width of existing taxiways

  Construction of airport taxiways involves major expenses. If an airplane manufacturer designs an airplane with a (landing gear) configuration which is not compatible with existing taxiways he may find no buyers for that airplane!

8.4.6 Design Constraints Related to Typical Military Requirements

Examples of such design constraints are:

* Gun integration constraints

  Guns impose a number of serious constraints on the design of an airplane. For a discussion of these, see Chapter 3, Part IV.

* Missile integration constraints

  This may dictate internal and/or external space requirements. It may also dictate a range of design parameters related to aerodynamics, weights and flight controls. For a discussion of weapon integration, see Chapter 3, Part IV.

* Stealth requirements

  Requirements for stealth may dictate the external shape of the airplane and/or the structural arrangement, quite apart from any conventional aerodynamic and/or structural design considerations.

  Prominent examples of such airplanes are the B-2 and the F-117A.

8.4.7 Design Constraints Related to the Environment

Examples of this type of design constraint are:

* Noise

  This design constraint may dictate the size, location and type of powerplant installation. In turn, this has a significant impact on weight, complexity and fuel consumption.

* Fuel dumping

  If a requirement would be formulated against fuel dumping, airplane landing gears would have to be designed for considerably greater weight at touchdown. This would impact airplane weight and landing gear retraction volume requirements.

* Atmospheric pollution

  Requirements to minimize 'visible' atmospheric pollution have already resulted in a redesign of burner systems in jet engines.

  Depending on the outcome of on-going research of potential ozone destruction by high flying supersonic transports, their burner systems may have to be tailored specifically to the prevention of releasing certain combustion products. The effect of these considerations on engine performance is still subject to question.

8.5 RULES FOR EVALUATING COST FUNCTIONS

It will be assumed that at this point the following steps have been taken:

1. One or more cost functions have been selected for optimization. These cost functions must be consistent with the required mission performance of the airplane.

2. The cost functions selected under 1. have been expressed functionally in terms of a range of airplane design variables.

3. Airplane design constraints have been cast in a format which relates them clearly to airplane design variables.

Next, a decision has to be made which of the cost functions are to be maximized or minimized while at the same time observing specific constraints.

NOTE WELL:

A) It is just as important to keep in mind which potential cost functions and which potential design constraints have NOT been considered. Doing this avoids the pitfall of believing that the results of optimization procedures (constrained or not) are somehow absolute.

B) Probably the most difficult aspect of the design optimization process is to decide which cost functions and which constraints should be used.

8.6 METHODS FOR DESIGN OPTIMIZATION

The purpose of this section is to acqaint the reader with reference material in the area of airplane design optimization. A detailed treatment of methods for design optimization is considered beyond the scope of this text.

There exists an impressive amount of literature on the subject of airplane design optimization. References 37 and 38 are recommended as excellent introductions to this subject. Both references contain many citations of other literature pertinent to design optimization.

Optimization methods can be broadly classified as:

1. Optimization within a given discipline

2. Multidisciplinary optimization

In each case, the optimization methods may or may not consider effects of design constraints: constrained or unconstrained optimization.

Most of the early design optimization methods dealt with optimization problems related to a particular design discipline, usually without accounting for constraints.

Examples are methods for optimizing airplane performance and/or aerodynamic parameters. References 39, 40 and 41 fit this category. Typical of the design conclusions drawn from these methods is Kuchemann's conclusion in Ref.39, that the best lift-to-drag ratio which is achievable in supersonic cruise is:

$$(L/D)_{max} = 4(M + 3)/M \qquad (8.19)$$

A problem with optimization within any discipline is that it can result in unrealistic design solutions. For example: induced drag is reduced by allowing the wing aspect ratio to assume very large values. This runs into problems with wing structural weight. Therefore, it is necessary to account for the disciplines of structural and aerodynamic analysis together whenever one impacts the other.

A problem with design optimization without proper regard of constraints is that it also can lead to unrealistic design solutions. Consider the following example:

A supersonic fighter has a requirement for a long subsonic mission leg, followed by a short supersonic dash requirement, followed again by a long subsonic leg to home base.

It is possible, by the application of area-ruling methods, to minimize the supersonic wave drag of this airplane. However, it may be that a result of minimizing wave drag is an increase in wetted area over that needed for efficient subsonic flight. If the fuel used in the short supersonic dash is significantly less than that used during the long subsonic legs, it may be that wave drag minimization makes no sense.

In this case, wave drag should have been minimized subject to the constraint that total mission fuel consumption (subsonic + supersonic) is kept to a minimum.

The subject of airplane design optimization in the presence of design constraints is extensively discussed in References 37 and 38.

Recently, research in airplane design optimization has moved in the direction of multidisciplinary design optimization subject to a multitude of constraints. To become familiar with recent trends in design optimization methods References 42 through 46 should be consulted.

The next section presents some examples of the end product of typical design optimization studies.

8.7 EXAMPLES OF DESIGN OPTIMIZATION STUDIES

The purpose of this section is to present a brief discussion of results of potential design optimization studies. For more details on how to perform such studies references 42 - 46 should be consulted.

Example 1: The economic value of blockspeed

For a given airplane, operated over a given stage length (block distance) and at a given altitude, the question can be asked: at what speed is the operator's profit margin the highest possible?

In this case, a solution can be found by plotting the various operating cost components as a function of blockspeed. Figure 8.9 shows an unscaled example of such a plot. Note the behavior of the fuel cost contribution:

* at low block speeds, fuel usage increases because of the increase in induced drag

* at high block speeds, fuel usage increases because zero-lift drag and compressibility drag increases

Figure 8.9 shows various 'optima' which correspond to different block speeds:

* block speed for minimum fuel cost
* block speed for minimum fuel used per nm per hr
* block speed for minimum DOC
* block speed for maximum profit margin

It is of interest to observe that the block speed for the lowest DOC is lower than the blockspeed for the greatest profit margin!

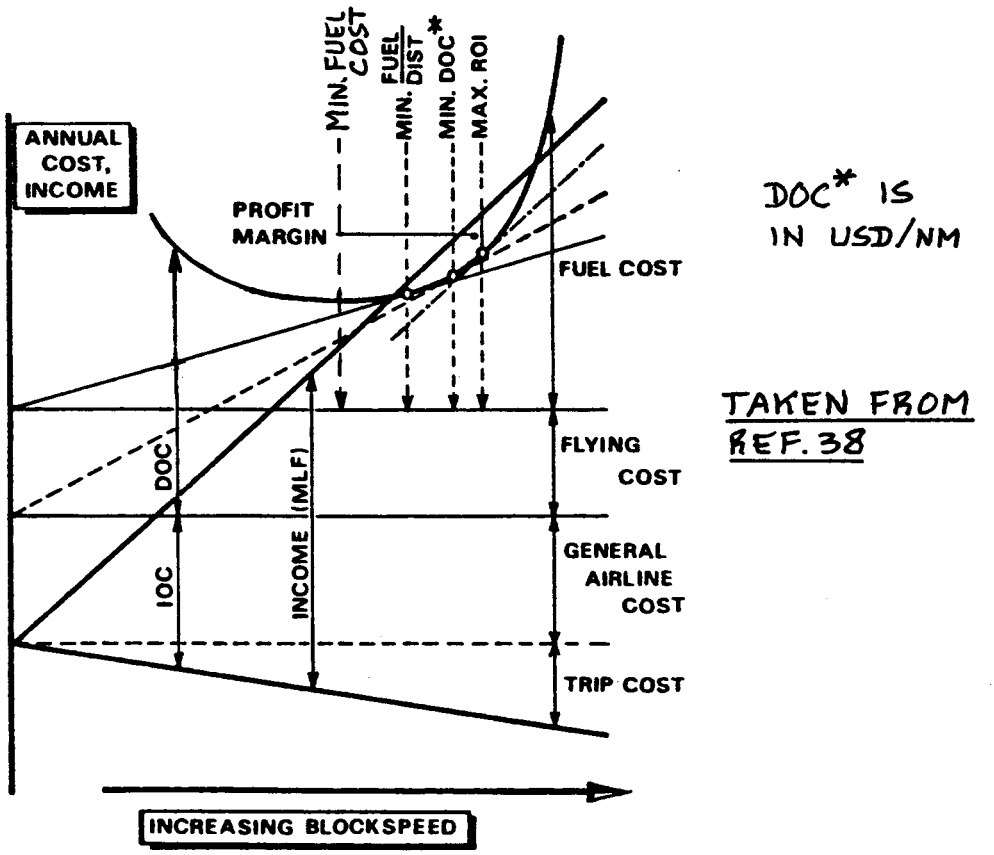

Figure 8.9 The Economic Consequence of Blockspeed

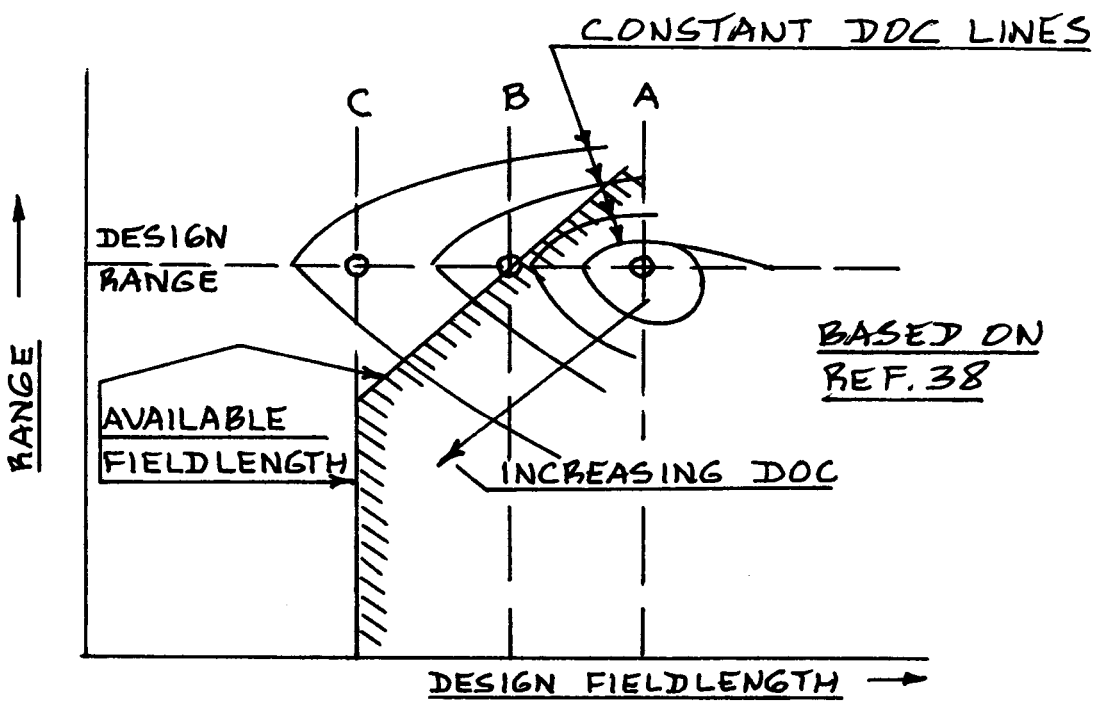

Figure 8.10 Effect of Fieldlength Constraints on Direct Operating Cost (DOC)

Note that in Figure 8.9 various factors were kept constant. The validity of the study results are subject to question if these factors are allowed to vary!

Example 2: Effect of fieldlength constraints on DOC

The reader is reminded of the various fieldlength constraints placed on commercial aircraft. This topic was extensively covered in Chapter 3 of Part I.

For a given airplane, operated over a given range, the takeoff weight allowed is limited by fieldlength considerations. At any given takeoff weight, the useful load (sum of payload weight and fuel weight) is fixed: for long ranges payload must be off-loaded!

Figure 8.10 shows an unscaled example of the effect of fieldlength on DOC, with range as a second parameter. The 'design field length' is defined as that takeoff distance required with maximum passengers and maximum takeoff weight under critical atmospheric conditions and one engine failing.

Point A reflects an airplane which has been 'optimized' for minimum DOC in cruise: it does not meet the fieldlength constraint. Point B represents an airplane which meets the fieldlength constraint exactly, but at slightly greater DOC. Point C reflects an airplane which meets the fieldlength requirement at any range, but at higher DOC yet.

The lesson from this study is that designing for extreme fieldlength requirements may result in serious compromises in DOC. It may be better to design to Point B AND to offer versions of the airplane with slightly different wings and/or high lift devices to operators with extreme fieldlength requirements.

The airplane design process as described in Parts I and II is a sequential process. If design optimization studies are conducted at each step along the way, it is argued in Reference 47 that the result is a sub-optimal design solution. An example of this is given next.

Example 3: Minimizing wing structural weight in a sequential manner

This example is based on Reference 46. Suppose wing structural weight needs to be minimized subject to some performance measure, PM. This performance measure, PM,

could be the payload for a given range. Constraints C_1 and C_2 (C_1 could be a fieldlength constraint and C_2 could be an engine-out, rate-of-climb constraint) are also imposed on the problem.

Figure 8.11 shows a possible result where the wing aspect ratio is used as an independent variable. The point P_1 is the constrained optimum for this case study. Suppose that, as a result of this type of study, the wing aspect ratio is frozen at a value A_1. Also suppose that at some later point in the design process a flutter study has been conducted which results in an added constraint, reflected by C_3 in Figure 8.12. As a result, the wing structural weight has to be increased to a value corresponding to point P_2. However, if the flutter study had been conducted earlier, point P_3 might have been selected as the desirable design point!

It is worthwhile to end with an observation first made in Reference 47. The reader is asked to refer to Figure 8.13. Observe that as the time into the design process increases, the knowledge about the design also increases. However, this increasing knowledge about the design implies that more and more design variables are 'frozen'. That in turn limits the potential design freedom. Therefore, the ability to act on the results of design optimization studies gradually disappears as time into the design process increases. Reference 47 refers to this state of affairs as the paradox of sequential design decision making. This 'peril' can be avoided by careful selection of design cost functions and judicious application of design optimization studies.

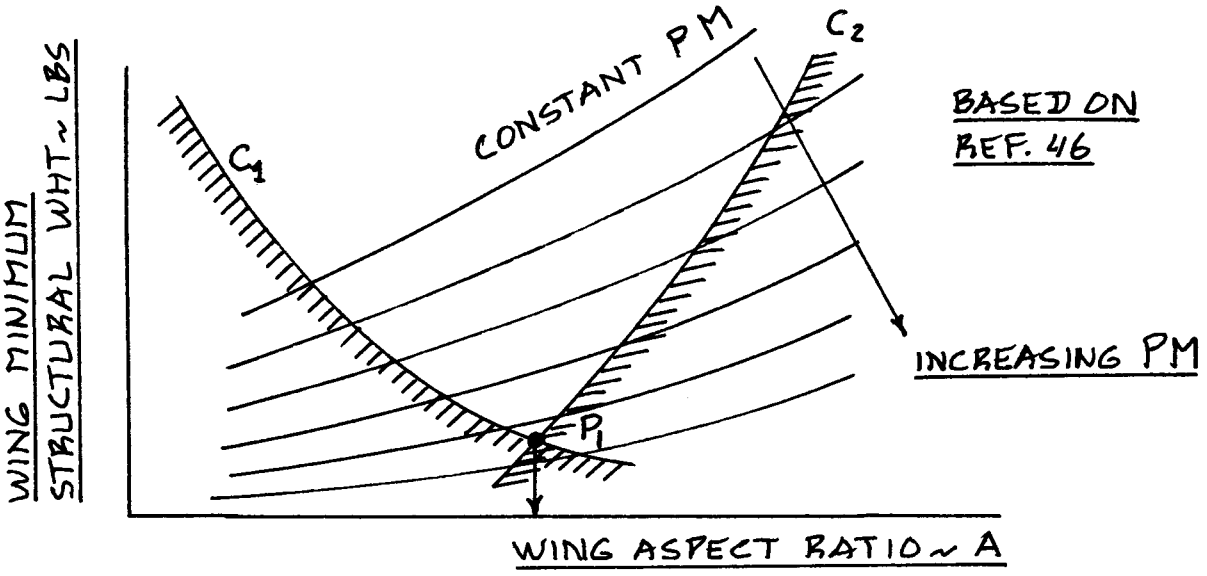

Figure 8.11 Optimization of Wing Weight with Aspect Ratio Subject to Two Constraints

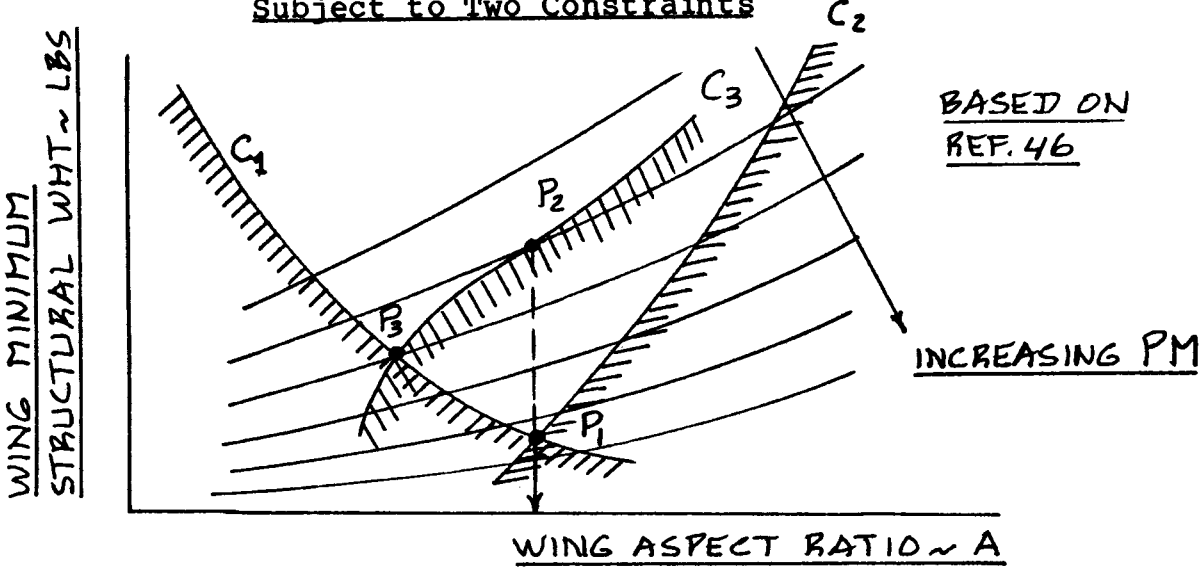

Figure 8.12 Optimization of Wing Weight with Aspect Ratio Subject to an Additional (Later Discovered) Constraint

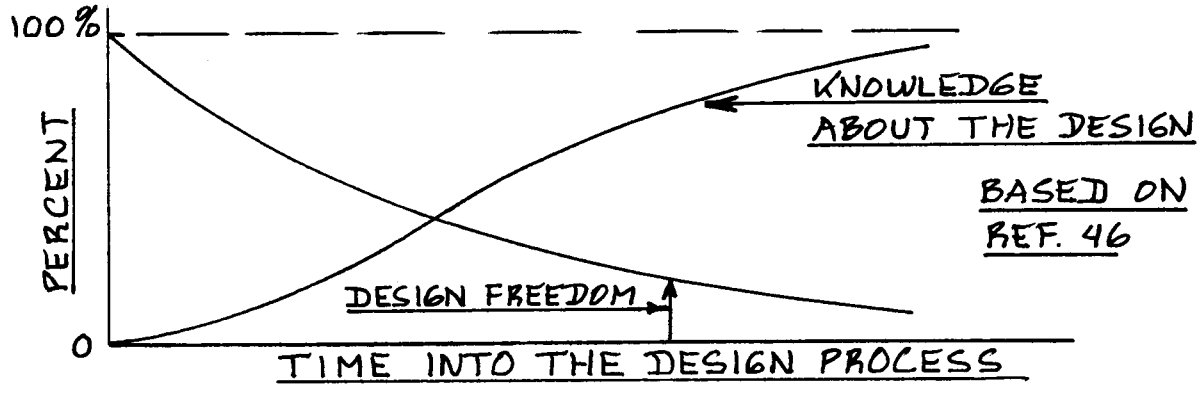

Figure 8.13 Illustration of the Paradox of Sequential Design

8.8 INTRODUCTION TO THE DESIGN-TO-COST PROBLEM

Budgets for airplane programs are always limited. Also, airplane operators cannot afford airplanes if they are too expensive. Interesting questions therefore are the following:

1. Assume that an airplane has been designed to some mission specification. How much is that airplane worth to the operator?

2. Given a certain net worth and given the need for a certain number of airplanes, can a manufacturer design, develop and manufacture such an airplane and make a profit?

The first question is referred to as the so-called 'net worth' problem. Sub-sections 8.8.1 and 8.8.2 give an approach to estimating airplane net worth.

The second question is referred to as the so-called 'design-to-cost' or the 'design-to-price' problem. An approach to this problem is given in sub-section 8.8.3.

8.8.1 The Commercial Airplane Net Worth Problem

Definition: The net worth of an airplane is the price an operator is willing to pay for an airplane because the potential for profit (Return-on-investment, or ROI) is demonstrable.

The net worth of an airplane can be determined via an operational market analysis. Such a market analysis should result in the following data:

* definition of routes, frequencies, passenger demand and/or cargo demand

* definition of sustainable revenue factors such as USD/paxnm and/or USD/tonnm

A preliminary estimate of the sustainable revenues can be obtained from the literature. Figure 8.14 is just one example. From such data it is possible to estimate the annual revenue which can be obtained per airplane. Assuming a desired return-on-investment percentage, the allowable airplane price (net worth) can be recovered from Equation (8.15) by solving it for AEP, the airplane estimated price.

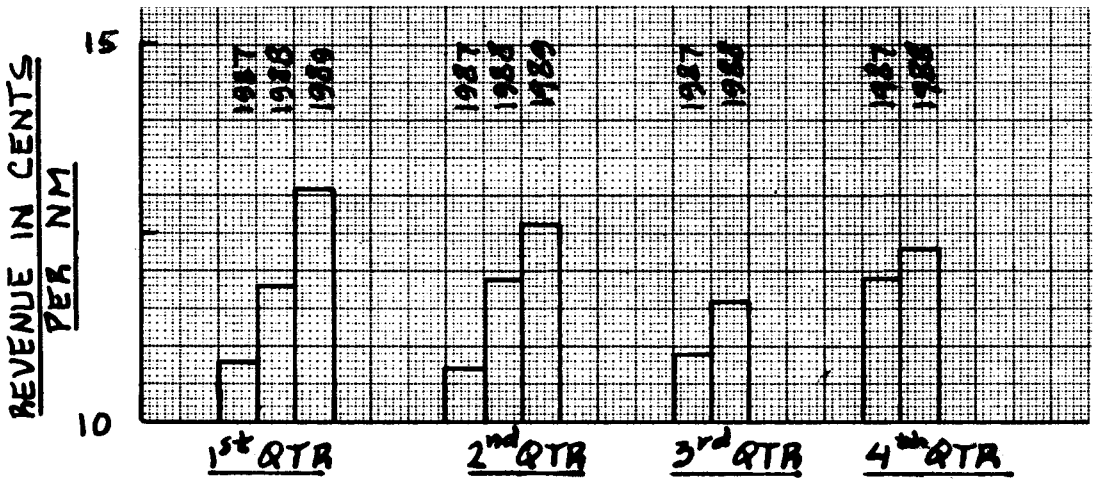

Figure 8.14 Example of Airline Revenues

A problem with this procedure is that the direct operating cost, DOC, itself is a function of AEP, as shown in Chapter 5, Eqns (5.19), (5.40) and (5.41). Solving for AEP is therefore a complicated matter.

The IOC (indirect operating cost in Eqn.(8.15)) can be assumed to be some constant fraction of DOC as suggested in Section 5.3.

8.8.2 The Military Airplane Net Worth Problem

Estimating the net worth of a military airplane is a tricky proposition. For combat airplanes one approach is to estimate the worth of potential targets which have to be destroyed by the airplane in question. At least in theory, it would not make economic sense to develop an airplane which costs considerably more than the targets it is supposed to destroy. This line of thinking thus sets an upper bound on the allowable airplane cost. Reference 48 can be helpful in this regard.

For military training airplanes the problem is a lot simpler. It is not too difficult to determine the cost of training pilots. Knowing the number of pilots which have to be trained an estimate can be made of the allowable cost of the airplane: its net worth. Reference 49 provides more detailed insight into this problem.

8.8.3 The Design-to-Cost Problem

It will be assumed that as a result of the solution to the net worth problem in sub-sections 8.1.1 or 8.8.2, the following information is available:

* Airplane mission specification

* Airplane net worth, ANW (usually assumed to be the same as airplane estimated price, AEP)

* Number of airplanes required in a market, N_{market}

Assuming that the number of airplanes to be built to production standard, N_m, is equal to:

$$N_m = F_m(N_{market}) \tag{8.20}$$

where: F_m is a factor (> 1.0) which reflects the level of optimism about additional markets for that airplane.

The estimated revenue from this airplane program to the manufacturer is:

$$R_{man} = (N_m)(ANW) \tag{8.21}$$

If the airplane manufacturer is to make a profit on this airplane program, the amount R_{Man} must equal the sum of airplane acquisition cost, C_{ACQ} (Eqn.(4.2)) and airplane RDTE cost, C_{RDTE}:

$$R_{man} = C_{ACQ} + C_{RDTE} \tag{8.22}$$

With Eqns (4.2) and (4.19) this yields:

$$R_{man} = C_{MAN}(1 + F_{pro}) + C_{RDTE} \tag{8.23}$$

Thus, equating (8.21) and (8.23):

$$(N_m)(ANW) = C_{RDTE} + C_{MAN}(1 + F_{pro}) \tag{8.24}$$

By assuming that C_{RDTE} is a constant fraction of C_{MAN} it is now possible to determine the 'allowable' cost of development and manufacturing. Figure 8.15 shows a typical example of the breakdown of various costs in a commercial jet transport program. Similar data can be extracted from the literature or can be estimated with the methods of Chapters 3 - 7.

Knowing the 'allowable' cost of airplane development and manufacturing, the next problem is to decide if it is feasible to design an airplane which can be profitably built within these cost constraints. This problem can be solved iteratively by using the methods of Chapter 4.

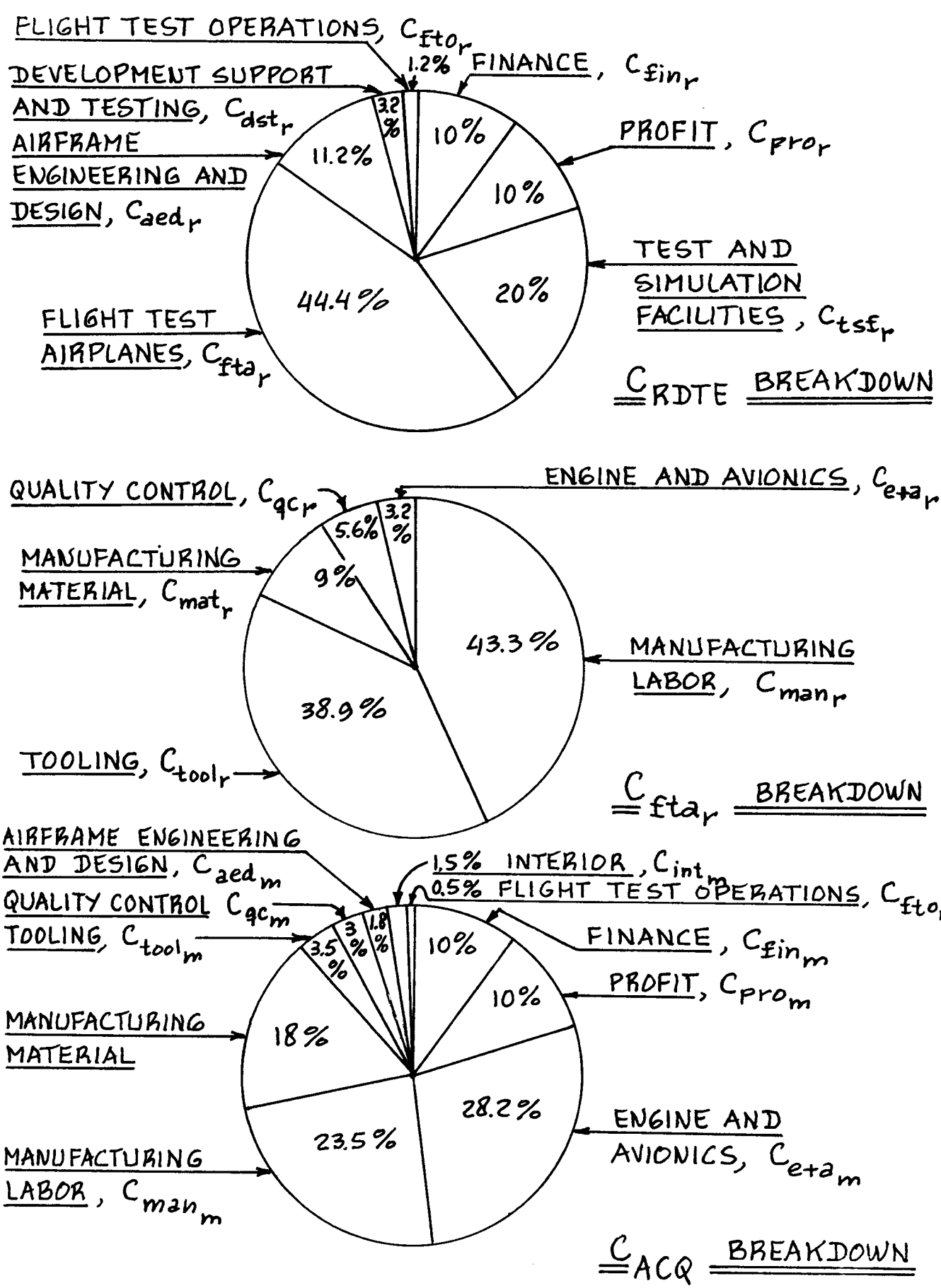

Figure 8.15 Breakdown of Costs in a Jet Transport Program

8.9 DESIGN GUIDELINES FOR LOWERING COST

Even after applying the most thorough of preliminary design methods, including design optimization procedures, many aspects of the detail design of the airplane remain to be decided. Particularly at the system design and at the system design integration level, those detail design decisions can have a significant impact on airplane cost, especially the manufacturing and operating costs.

The purpose of this section is to present a series of design guidelines which, when followed, tend to reduce airplane cost. These guidelines should be carefully considered in any new design.

The 88 design guidelines as presented in Tables 8.4 are the direct result of problems encountered with airplanes designed without the benefit of these guidelines. The author acknowledges the fact that the majority of the 88 guidelines come from research done by Mr. B. Williams, Director of the Center for Reliability, Maintainability and Quality, Air Force Institute of Technology, WPAFB.

SIAI-MARCHETTI S.211 FUEL SYSTEM

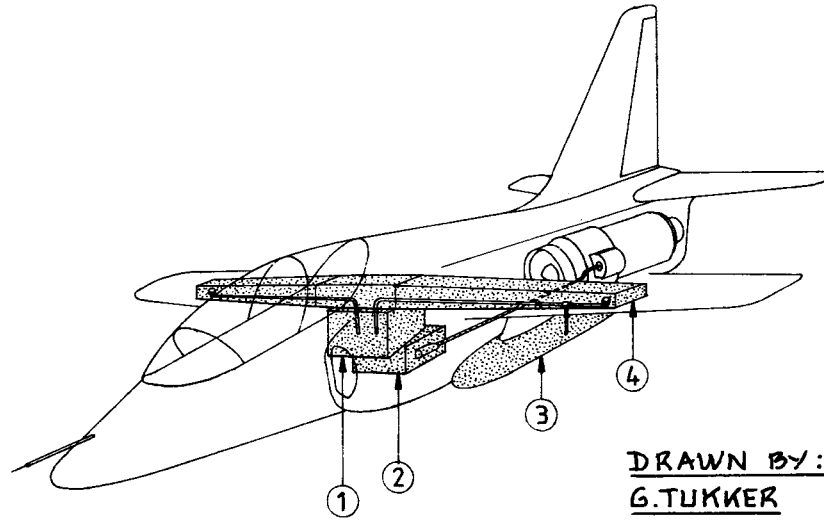

DRAWN BY:
G.TUKKER

KEY

1. FUSELAGE TANK
2. HOPPER
3. DROP TANK
4. WING TANK

Table 8.4 DESIGN GUIDELINES FOR LOW COST

Guideline	Applicability Commercial	Military
SYSTEMS		
1. Minimize complexity and number of parts associated with all items which require frequent servicing and/or access.	x	x
2. Keep ALL plumbing away from heat sources.	x	x
3. Make most components accessible to people while they stand on the ground. Access step-ups, ladders and platforms are sources of trouble and accidents.	x	x
4. Design so that simultaneous refueling and rearming is possible with the engines running.		x
5. Design so that all required servicing vehicles can access the airplane simultaneously while parked at the gate.	x	
6. Design ALL flight crucial systems with redundant drive and with redundant signal path systems.	x	x
7. Design the installation of identical components for complete interchangeability: no installation should be unique.	x	x
8. Design wire bundles so they will 'fit' only one way, avoiding the possibility of miswiring.	x	x
9. If reversed installation of a component can cause malfunctioning, design the installation for a one way fit.	x	x
10. Design all access panels with CAPTIVE fasteners and with retaining devices.	x	x

Table 8.4 (CONT'D) DESIGN GUIDELINES FOR LOW COST

Guideline	Applicability Commercial	Applicability Military
SYSTEMS (Cont'd)		
11. Design access to units which require servicing during turn-arounds so that personnel wearing winter clothing AND gloves can service them.	x	x
12. Design all systems which contain liquids (oil, hydraulics, fuel, glycol and water) so that these liquids can be easily poured in when necessary.	x	x
13. Design oil and hydraulic systems so that they can be completely replenished by ONE person in 5 minutes.	x	x
14. Put servicing instructions on placards in easy to read letters.	x	x
15. Size fluid reservoirs for one full day of operation.	x	x
16. Design avionics systems for fit in integrated, easily removable racks.	x	x
17. Locate avionics racks so that exposure to vibration is minimized.	x	x
18. Locate airplane rate and acceleration sensors so they cannot read false signals due to gun induced vibrations.		x
19. Standardize all micro-integrated circuits.	x	x
20. Design APU systems to provide for adequate cooling on the ground in a hot day environment.	x	x

Table 8.4 (CONT'D) DESIGN GUIDELINES FOR LOW COST

Guideline	Applicability Commercial	Applicability Military
SOFTWARE		
21. Establish rigid control over software design AND over software modifications.	x	x
22. Design digital systems so that in-flight computing resources use only HALF of the total system capability (i.e. processing capacity, execution time and memory).	x	x
23. Design software to be compatible with ground systems and with test stations.	x	x
24. Design data management systems to be modular: one update input to update all systems.	x	x
AIRFRAME		
25. Design access doors and panels which require frequent opening with quick opening latches.	x	x
26. Design access doors and panels so that they are easy to close AND so that unlocked doors and panels are easily spotted.	x	x
27. Design door hinges so that if they break, they cannot tear into other primary structure(s).	x	x
28. Design the airframe so that NO structural components have to be removed in order to remove the engine.	x	x
29. Structural areas with a high probability of failure, fatigue or corrosion SHALL be visible and inspectable.	x	x

Table 8.4 (CONT'D) DESIGN GUIDELINES FOR LOW COST

Guideline	Applicability Commercial	Applicability Military
AIRFRAME (Cont'd)		
30. Design airframe jack points so they do not interfere with gear operation, flap operation and other check-out procedures with the airplane on the jacks.	x	x
31. Provide adequate access to integral fuel tanks so that resealing is made possible.	x	x
32. Design for access to all crew station equipment without having to remove a seat.	x	x
33. Ejection seats must be removable without having to disassemble the canopy.		x
34. Install drag chutes in a pre-container to facilitate re-installation.		x
35. All seat components must be inspectable with the seat installed in the airplane.		x
36. Design the nosegear so that the airplane can be towed without having to disconnect steering power and so that the airplane can be towed within the design steering range.	x	x
37. Design landing gear door actuation system as simple as possible.	x	x
38. Wheel and brake assemblies should be separately removable.	x	x
39. Design landing gear so that jacking is NOT needed for scheduled maintenance and inspection events.	x	x

Table 8.4 (CONT'D) DESIGN GUIDELINES FOR LOW COST

Guideline	Applicability Commercial	Military
FLIGHT CONTROLS		
40. Design control surfaces so that they can be replaced without re-rigging the flight control system.	x	x
41. Provide and design for rigging pins with the cockpit controls in the neutral position.	x	x
42. ALL flight control system components must be accessible for all types of maintenance.	x	x
43. Where possible, LIMIT the autopilot authority.	x	x
ENGINES AND INSTALLATION		
44. All engine driven accessories and their electronic controls should be airframe mounted.	x	x
45. Design engine mountings so that each engine can be removed AND replaced within 1.5 hours.	x	x
46. Some engines require access to the top of the engine. Provide easy access in such cases.	x	x
47. Any engine mounted accessories shall be replaceable with the engine installed.	x	x
48. Engine removal shall be possible without jacking or otherwise supporting the airframe.	x	x
49. Design the engine-to-airframe interfaces so they are all located in one area.	x	x

Table 8.4 (CONT'D) DESIGN GUIDELINES FOR LOW COST

Guideline	Applicability Commercial	Applicability Military
ENGINES AND INSTALLATION (Cont'd)		
50. All engine performance sensors must be replaceable within 10 minutes.	x	x
51. Design engine throttle controls so that rigging is not required.	x	x
52. The engine oil system must be designed for operation at prolonged negative 'g's.		x
AUXILIARY POWER UNIT		
53. Ground checkout of the APU must be possible with one access panel.	x	x
54. Design airframe hardpoints to enable quick APU removal and replacement.	x	x
55. It must be possible to operate the APU via an external panel when the airplane is on the ground.	x	x
ELECTRONIC COUNTERMEASURES SYSTEM		
56. Failure of the automatic temperature control system shall NOT preclude manual operation of the system.		x
57. If ECS cooling ducts are located in inaccessible areas DON'T use duct material which deteriorates with age.		x
58. ECS lubrication systems shall be designed so that operation in extreme cold is possible.		x

Table 8.4 (CONT'D) DESIGN GUIDELINES FOR LOW COST

Guideline	Applicability Commercial	Applicability Military
ELECTRICAL POWER SYSTEM		
59. Design for over current protection from any single failure.	x	x
60. Design wire bundles for easy removal for modifications.	x	x
61. Design to prevent wire chafing through holes and hinges in the case of long wire bundles.	x	x
62. Keep wire bundles away from heat sources.	x	x
63. Locate the power distribution panel in a non-hazardous area with the engine(s) running on the ground.	x	x
64. All flight station panels must be connected via pendant cables to allow for removal without disturbing ANY adjacent equipment.	x	x
65. Incorporate service loops in the case of sliding chassis or hinged doors.	x	x
66. All grounding receptacles must be in accessible areas AND must be replaceable.	x	x
67. Design the power generation and main battery system so that the main battery is fully charged after one mission.	x	x

Table 8.4 (CONT'D) DESIGN GUIDELINES FOR LOW COST

Guideline	Applicability Commercial	Military
LIGHTING		
68. Incorporate lights in the wheelwells for maintenance.	x	x
69. Isolate lights from vibration.	x	x
70. All external lights must be rapidly replaceable.	x	x
71. Design strobe light location to avoid disoreintation of flight crew.	x	x
72. Minimize the use of retractable lights and/or use highly reliable retraction/extension mechanisms.	x	x
HYDRAULIC SYSTEMS		
73. Design hydraulic line and hose runs to prevent the inadvertent cross-connection of systems.	x	x
74. Identify the required fluid type CLEARLY at all fluid filler points.	x	x
75. Design all filters, shut-off valves, pressure switches and sub-components for separate removal.	x	x
76. Incorporate isolation valves in each sub-system to allow for maintenance, bleeding, etc.	x	x
77. Incorporate quick disconnect fittings for ground servicing and for connecting to a maintenance cart.	x	x
78. Incorporate a central hydraulic system control panel for maintenance personnel.	x	x

Table 8.4 (CONT'D) DESIGN GUIDELINES FOR LOW COST

Guideline	Applicability Commercial	Applicability Military
FUEL SYSTEM		
79. Fuel quantity transmitters should be mounted to accept high 'g' maneuvers.		x
80. Fuel quantity indicators should indicate remaining fuel in a proportional manner.	x	x
81. Design ALL fuel system components so they can be removed WITHOUT draining the fuel tanks.	x	x
82. Any motor operated shut-off valve shall have the motor removable while the valve is in the fuel system.	x	x
83. Design fuel system with common valves and common pumps.	x	x
84. Incorporate a single point refueling and control panel.	x	x
FAULT DETECTION SYSTEM		
85. All individual fault detection systems should report to a master system.	x	x
86. Failure status should be reported to pilot for manual selection of a backup system.	x	x
87. All in-flight failures must be data linked to the ground for maintenance preparations.	x	x
88. The crew station must have a 'mission capability' panel.	x	x

9. FACTORS IN AIRPLANE PROGRAM DECISION MAKING

The purpose of this chapter is to discuss several factors which must be considered before making an airplane 'program-go-ahead' decision. Much of the material included in this chapter is based on ideas which are developed in the series: 'Case Studies in Aircraft Design', published by the American Institute of Aeronautics and Astronautics (AIAA) as References 50 through 53. An excellent overview of the airplane program decision making process is presented by J.E.Steiner in Ref.54. Finally, the reader is urged to familiarize himself with Ref.25 which provides insight into military airplane programs.

The following factors can play a role in a decision to 'launch' or 'not launch' an airplane development and/or an airplane production program:

9.1 FACTORS INVOLVING COMMERCIAL AND/OR FINANCIAL FEASIBILITY

Before embarking on a new airplane program it is necessary to investigate the following commercial feasibility factors:

These factors are discussed next.

9.1.1 Market Potential

Market research is an essential component of the decision making process leading to an airplane program go-ahead. The following elements deserve attention:

9.1.1.1 Understand the customer and his organization
9.1.1.2 Identify and compare with the competition
9.1.1.3 Identify voids in the market
9.1.1.4 Forecast the size of the market
9.1.1.5 Forecast the net worth of the airplane
9.1.1.6 Decide on ability to produce at a cost below the airplane net worth
9.1.1.7 Identify and contact customer decision makers

9.1.1.1 Understand the customer and his organization

First, it is necessary to recognize the fundamental differences between commercial and military customers. Figure 9.1 shows the overall relationship between the manufacturer, the customer and the regulator for:

* Commercial Airplane Programs
* Military Airplane Programs

Second, it is essential that those involved in the airplane design decision making process understand the individual customer, his organization and his needs. In the early phases of the design it is of particular importance to know and understand those persons working for potential customers who are in charge of 'technical decision makers'. It should be noted that the technical decision makers are often not the financial decision makers and vice versa. Frequent contact between the customer and the manufacturer is essential, particularly during the early phases of the design.

9.1.1.2 Identify and compare with the competition

Identification of the competition is an essential ingredient in any competitive enterprise. It was also made part of the configuration design development procedures on page 11 of Part II.

The following reference material has been found very useful in identification of competitive designs:

* Jane's All the World Aircraft (British, Annually)
* Business and Commercial Aviation (U.S., Monthly)
* Aviation Week and Space Technology (U.S., Weekly)
* Interavia (Swiss, Monthly)
* Flight International (British, Weekly)
* Sales brochures from competitors

There are many ways to study comparative strengths and weaknesses of competing designs. Table 9.1 and Figures 9.2 and 9.3 show typical presentations from which

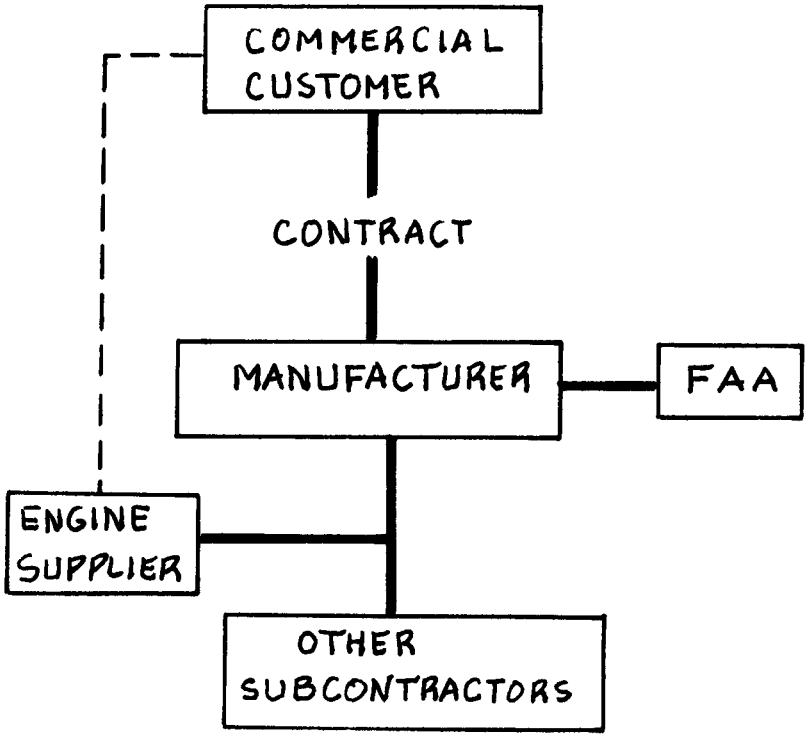

Figure 9.1a Relation Between Manufacturer, Customer and Regulators: Commercial

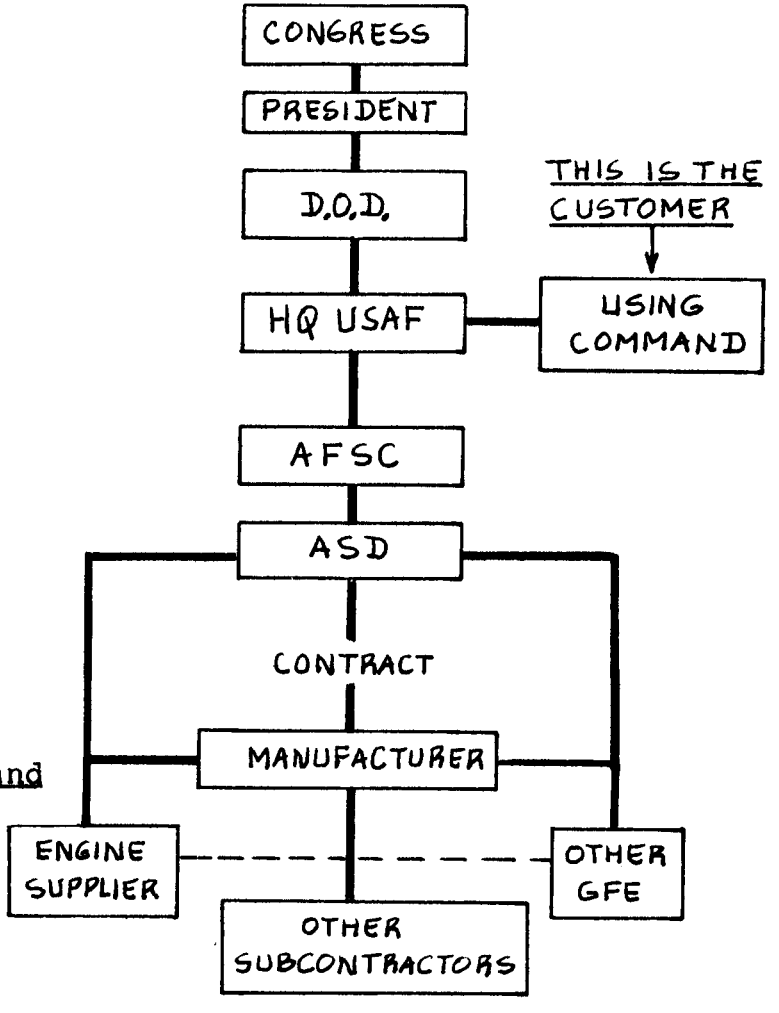

Figure 9.1b Relation Between Manufacturer, Customer and Regulators: Military

TABLE 9.1 COMPARISON OF SIMILAR AIRPLANE DESIGNS

Types:	SAAB 340	Boeing/DH Dash 8	Embraer Brasilia
Specifications			
Max. seating capacity	35	36	30
Power plants (2 each)	CT7-5A2	PW120	PW115
Shp per engine	1,735	1,800	1,600
Max seating capacity	5+35	3+40	3+30
Dimensions			
Length (ft)	64.9	73.0	65.6
Span (ft)	70.3	85.0	64.9
Height (ft)	22.5	24.6	20.8
Wing area (ft^2)	450	585	424.4
Wing aspect ratio	11.0	12.4	9.9
Weights			
Max. takeoff wht (lbs)	27,275	33,000	25,353
Std. empty wht (lbs)	17,415	21,590	15,586
Max. useful load (lbs)	9,860	11,410	9,767
Max. usable fuel (lbs)	5,690	10,160	5,862
(gallons)	843	1,451	875
Max landing wht (lbs)	26,500	32,400	24,802
Max. wing loading (psf)	60.6	56.4	59.8
Performance			
Takeoff fieldlength (ft) (SLS, ISA)	3,960	3,370	4,560
Max. climb rate (ft/min)			
AEO	1,850	1,660	2,250
OEI	500	450	630
Best climb rate speed, AEO (kts)	139	117	NA
Stall speed (kts)	82	72	86
Serv. ceiling AEO (ft)	25,000	25,000	31,000
Serv. ceiling OEI (ft)	16,200	13,400	18,500
Normal cruise speed (kts)	277	265	285
At altitude of (ft)	26,000	15,000	25,000
High speed cruise (kts)	281	265	300
At altitude of (ft)	15,000	15,000	20,000
Fuel flow for:			
Normal cruise (lbs/hr)	948	1,244	832
High sp. cruise (lbs/hr)	1,098	1,244	1,080
Turbulent air penetration speed (kts)	190	180	182
Max IFR range, ISA (nm)*	1,345	1,270	1,240
Range, 4,000 lbs payload	581	1,180	615

*Includes 100 nm diversion plus 45 minute hold

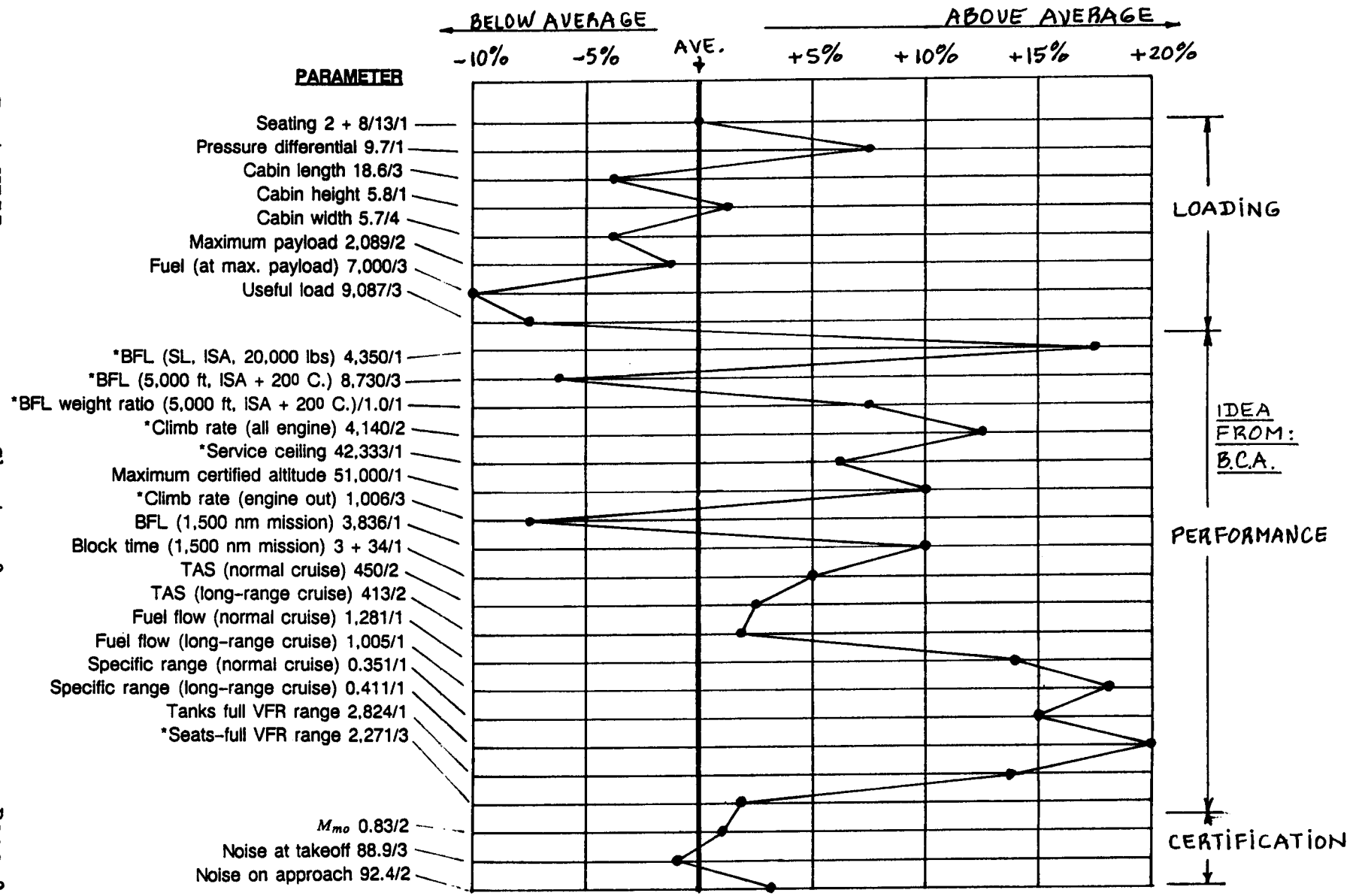

Figure 9.2 Comparison of Similar Airplane Designs

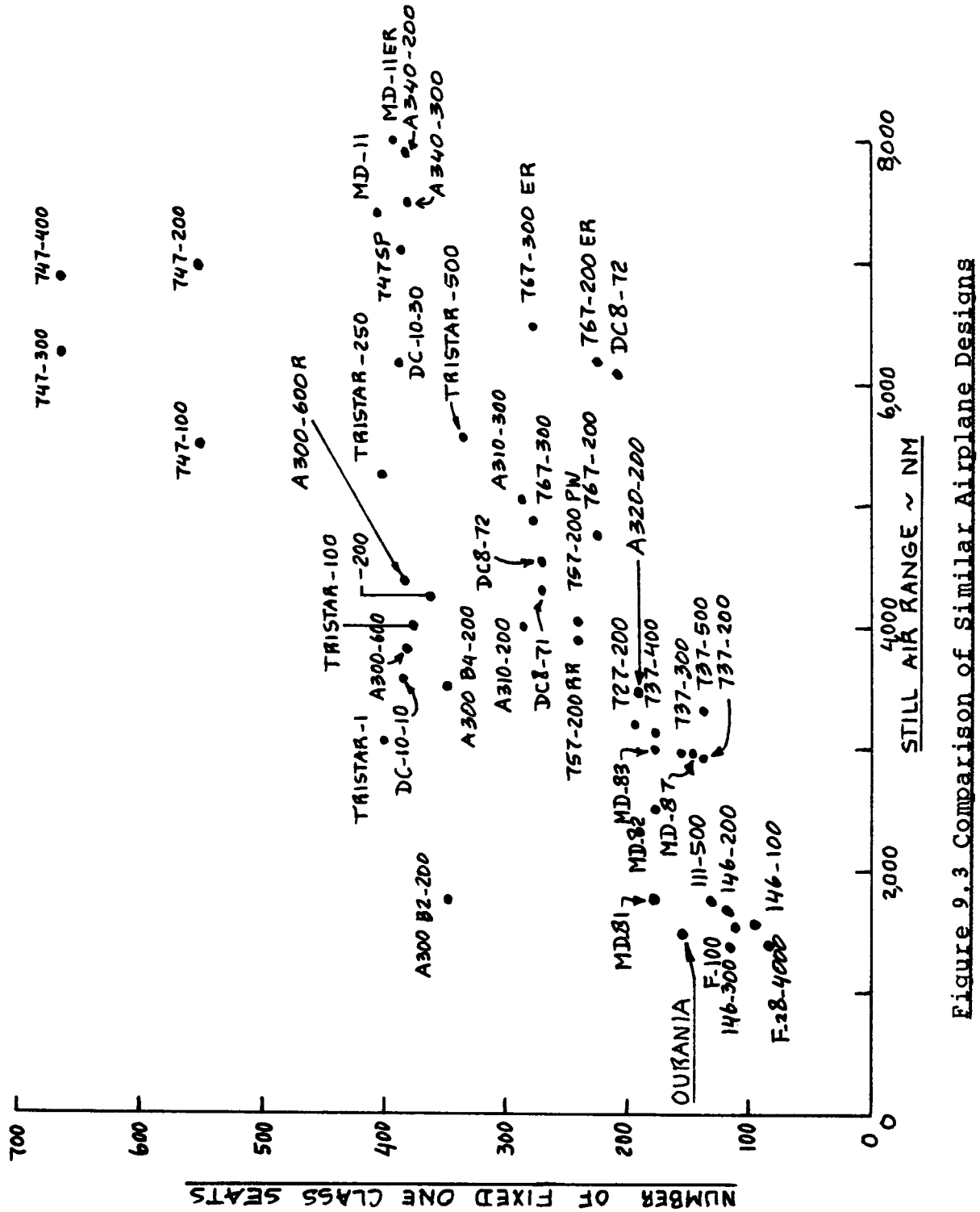

Figure 9.3 Comparison of Similar Airplane Designs

the nature of the competition can be discerned.

When comparing a new design to existing competitive airplanes, ALWAYS assume that the competititon will NOT sit still! Instead, try to imagine various scenarios for the competition to respond. Possible responses from the competition might be:

* Launching of a derivative design

  This could be very cost effective and may be hard to beat with a new design!

* Launching of a competitive new design

  Depending on the cost structure of the competition and on the technology level employed, this may or may not be a threat.

9.1.1.3 Identify voids in the market

Figure 9.3 shows a seat-range diagram for existing jet transports. Figure 9.4 shows that same information but with the airplane identifications left off. It is seen that there are several voids in the diagram. The following questions should be asked:

1.) Are there technical or economic reasons for the voids?

2.) If so, can these reasons be removed by clever and new design approaches?

Take for example the void labeled I in Figure 9.4. Void I would suggest an airplane capable of flying 125-175 passengers over a still air range of 4,000-5,000 nm. The question is: what might be the market for such an airplane? The answer could be: very long but very thin international routes.

* Long means: large distances between city pairs.

* Thin means: passenger demand is relatively small and does not justify the deployment of large wide body airliners.

Table 9.2 shows a list of such city pairs. What must be determined next is how many people might want to travel these routes and what prices might they be willing to pay for their tickets. Market research studies can be conducted to find the answers.

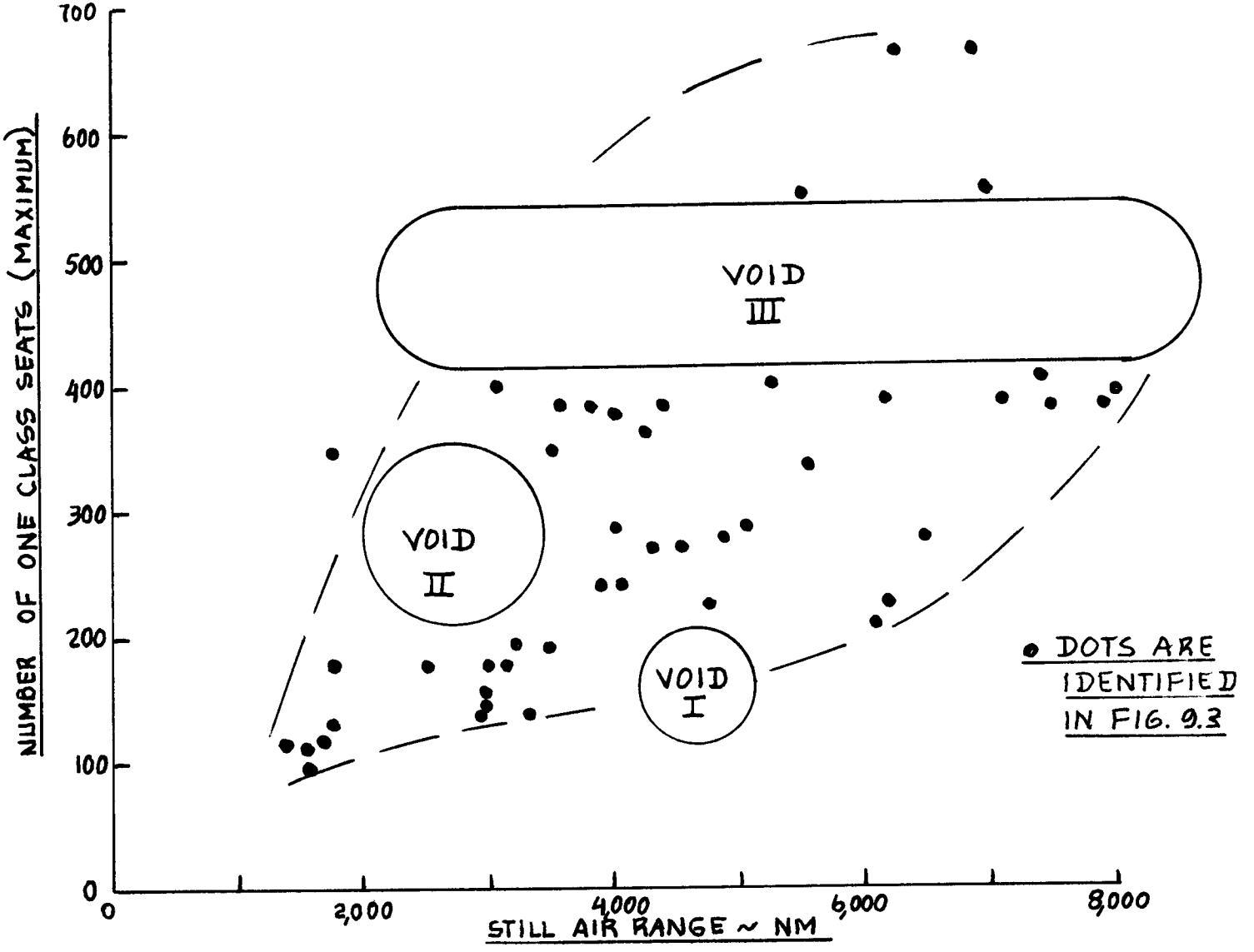

Figure 9.4 Identification of Market Voids

TABLE 9.2 CITY PAIRS WHICH FIT VOID I IN FIGURE 9.4

City Pairs		Great Circle Distance
Kansas City, MO, USA	- Amsterdam, Holland	4,700 nm
Sevastopol, USSR	- Trenton, N.J., USA	5,000 nm
Helena, Montana, USA	- Glasgow, UK	4,200 nm
Baton Rouge, LA, USA	- Rio de Janeiro, Brazil	4,900 nm
Norfolk, VA, USA	- Lima, Peru	3,500 nm
Hamburg, W.Germany	- Dar es Salaam, Tangan.	4,500 nm
Vienna, Austria	- Recife, Brazil	4,900 nm
Osaka, Japan	- Surabaja, Indonesia	3,500 nm
Seattle, WA, USA	- Amsterdam, Holland	4,800 nm
Montreal, Canada	- Abidjan, Ivory Coast	4,800 nm

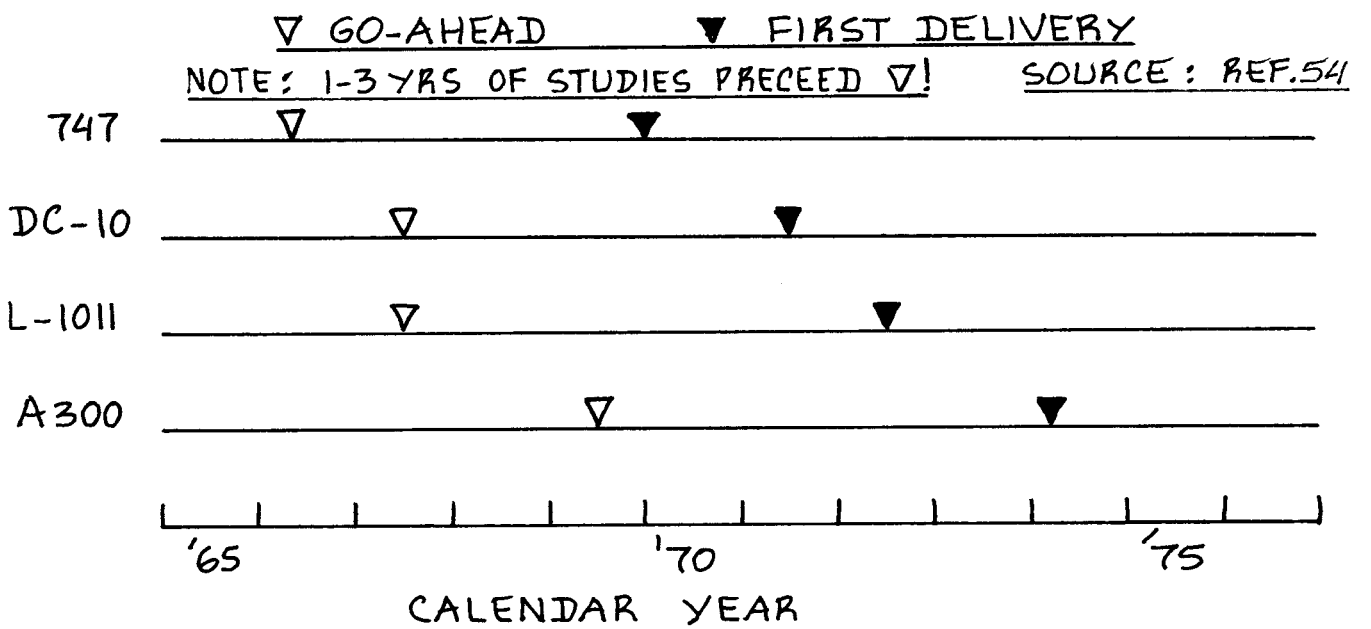

Figure 9.5 Development Times for Four Transport Programs

9.1.1.4 Forecast the size of the market

To make a credible estimate of the size of the market for the new airplane, the information developed in 9.1.1.3 needs to be translated into flight frequencies required to serve example city pairs. Some growth rate is normally accounted for. Typical growth scenarios will postulate that 5 to 10 percent growth occurs annually.

This way the number of airplanes required to serve these new markets can be estimated. With that done, the market share must be estimated. A cautious approach is to assume that a new design might 'catch' 1/3 of the estimated total market.

9.1.1.5 Forecast the net worth of the airplane

The definition of net worth of an airplane is given in Chapter 8 (p.241): it is the price the customer may be willing to pay if there is reasonable assurance of an acceptable return-on-investment (ROI).

A method for determining net worth was also outlined in Chapter 8.

9.1.1.6 Decide on ability to produce at a cost below the airplane net worth

It makes no sense to initiate serious marketing of an airplane until it has been determined that it is possible to manufacture it at a cost well below the airplane net worth. The methods of Chapter 4 should be used to obtain an estimate of the manufacturing cost.

9.1.1.7 Identify and contact customer decision makers

With most of the marketing homework completed, the final step is to try to 'convince' the financial decision makers of one or more customers to commit to ordering the airplane. It should be noted that the financial decision makers are usually not the technical decision makers and vice versa. This tends to be so for commercial as well as for military airplanes.

9.1.2 Development Cost and Time

New airplane development programs can take a very long time. Figure 9.5 illustrates this for several jet transport programs. Also, as shown by the RDTE cost estimation examples of Chapters 3 and 7, the cost of a new airplane development program is extremely high. Management must be prepared to 'sink' a lot of money into the project for many years before any signs of financial returns occur. Figure 9.6 is an illustration of this for the Ourania transport program used in earlier examples.

9.1.3 Availability of a Skilled Work Force

It should not be taken for granted that a skilled work force will always be available to carry out a new airplane development and production program. Historically, aircraft manufacturing employment has gone through many peaks and valleys. Figure 9.7 is an example.

Following major layoffs of production workers, many of these workers will move elsewhere or change job types. Most of these workers may then be 'lost' from that area.

Training of new workers is very expensive but may have to be considered as part of the start-up costs of a new airplane program.

9.1.4 Required Production Investment

Examples of methods for predicting manufacturing costs were given in Chapters 4 and 7. The amount of money involved is usually beyond the capability of an airframer to raise without borrowing money from one or more financial institutions.

The following numbers are recalled:

For the Ourania (150 passenger, medium range jet transport) the estimated program manufacturing cost is:

USD 9,142,000,000 (rounded off from p.61.)

The 'up-front' investment in tooling and engineering cost associated with this manufacturing program is:

USD 552,000,000 (rounded off from pages 60 and 61.)

In addition to these investment needs, there are those for materials, various facilities, engines and avionics. It is true that some of these costs can be

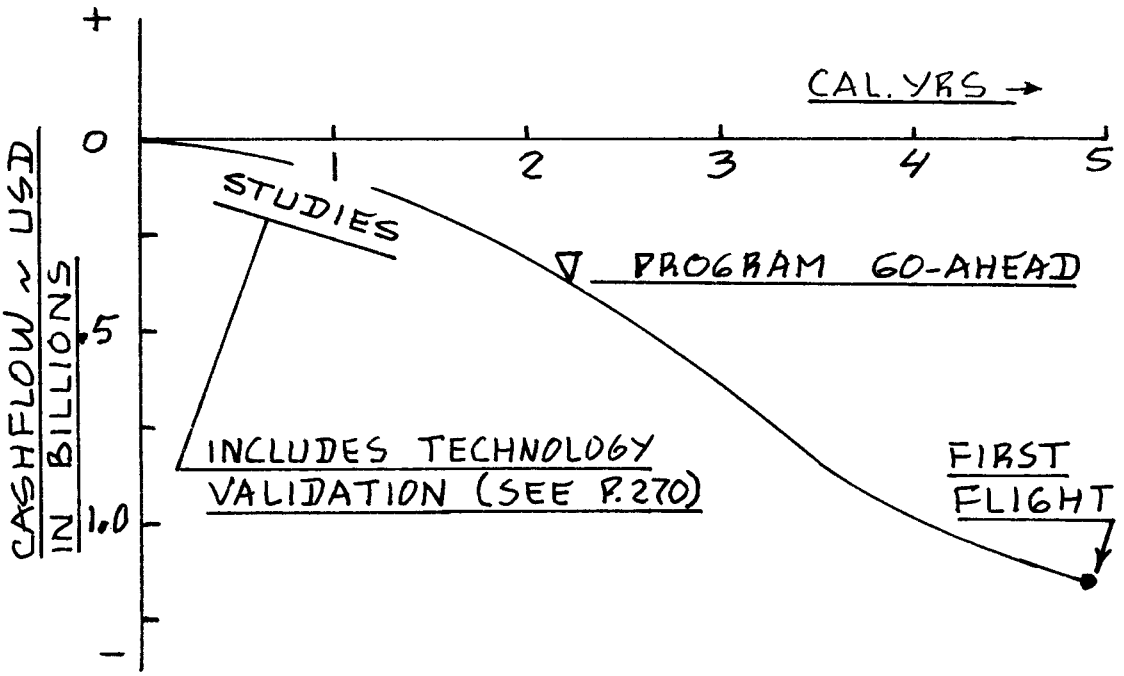

Figure 9.6 Example Cash Sink in a Transport Program

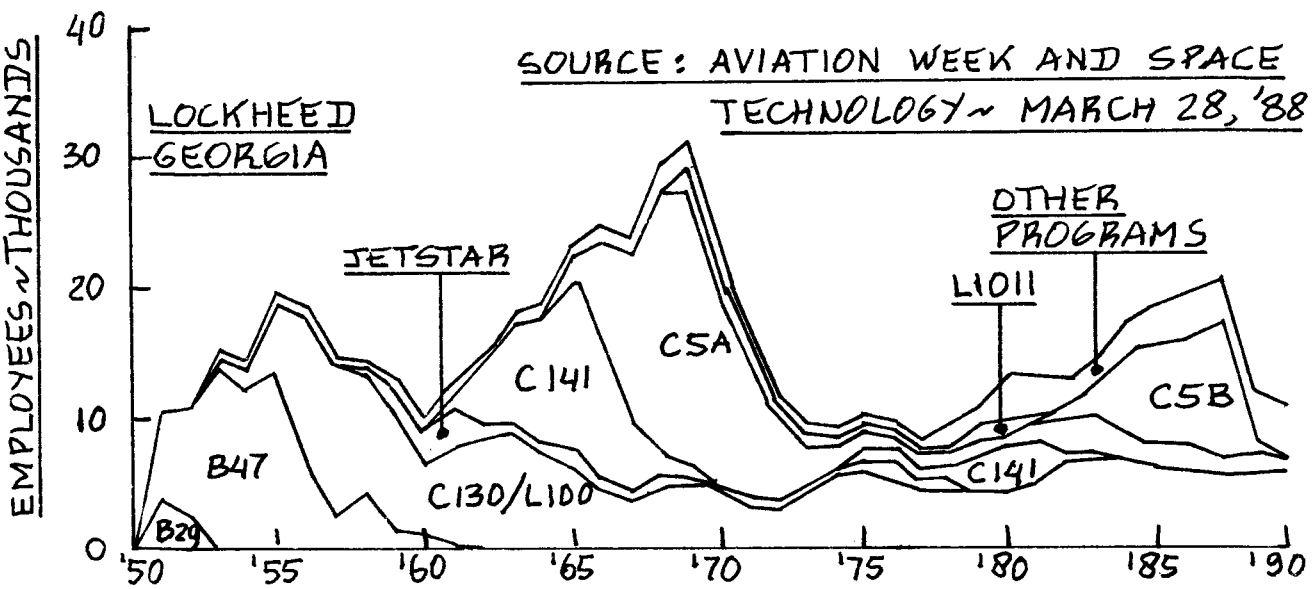

Figure 9.7 Typical Employment Fluctuation in an Airplane Manufacturing Operation

spread out over the duration of the manufacturing program. However, a considerable part has to be invested 'up-front'. The interest over that 'up-front' investment must also be accounted for. If only the tooling and engineering are 'counted' as part of this 'up-front' investment and if the annual interest rate is, say 10 percent, this represents an annual interest payment of USD 55,000,000!!

The need for 'up-front' manufacturing investment money may be so great that risk-sharing arrangements have to be sought with other companies in the USA or abroad.

9.1.5 Potential for Return on Investment (ROI)

At some point well before first deliveries take place, it is customary in the 'airplane business' that the customer begins to make 'progress' payments toward his airplane(s). As a result, some money will start flowing back into the manufacturer's coffers. The difference between program expenditures and program receipts is called the program cash-flow. Figure 9.8 illustrates the cash-flow associated with a typical commercial transport program. Note that the cash-flow does not become positive until 10 years after initiation of the program! However, receipts start coming in after year 3 or 4.

The ultimate profitibility of the program (Return on Investment, or ROI) is determined by the behavior of the cash-flow with time. As it turns out, many airplane programs are viable over the long run ONLY if the manufacturer is willing to adjust his design to new market conditions. This normally results in many 'derivatives' of the original design. However, the design, development, testing and certification of these derivatives is not without cost. Figure 9.9 illustrates the effect of such derivative programs on total program cash-flow.

NOTE TO DESIGNERS: It is important to design the original airplane in such a way that derivatives are in fact possible. For example, if an airplane cannot be grown by lengthening the fuselage because of a landing gear or takeoff rotation limitation it should not have been designed that way in the first place!

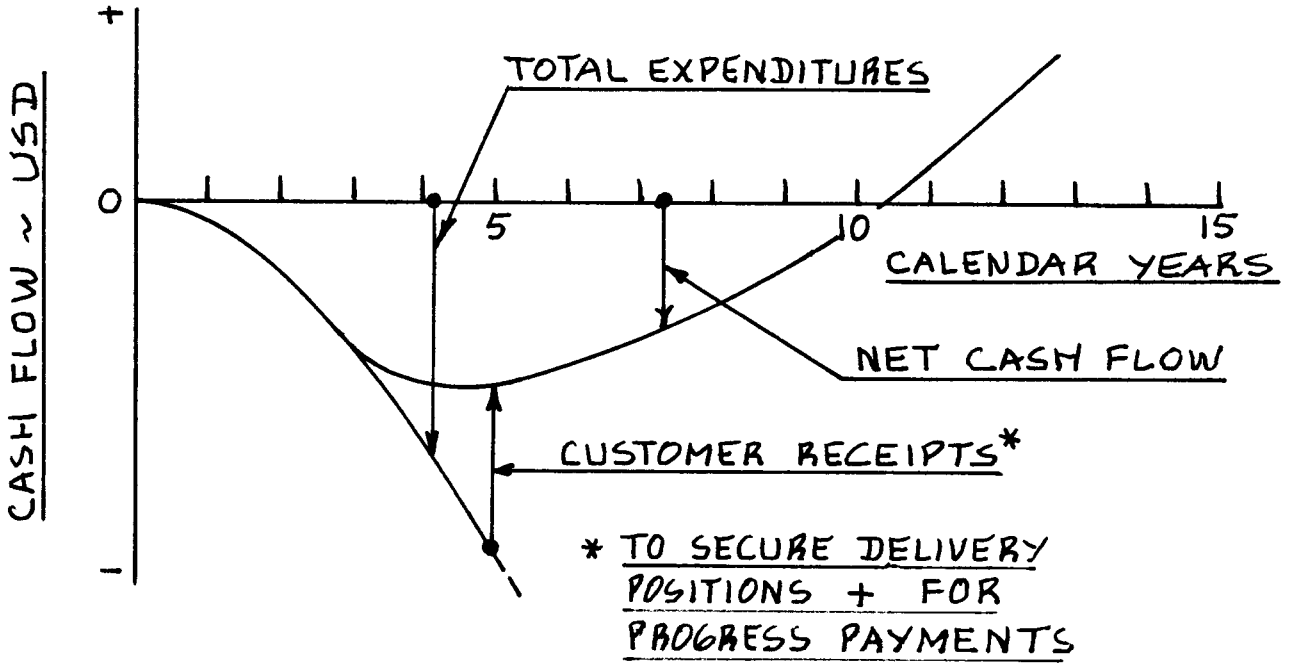

Figure 9.8 Example of Cash Flow in a Commercial Jet Transport Program

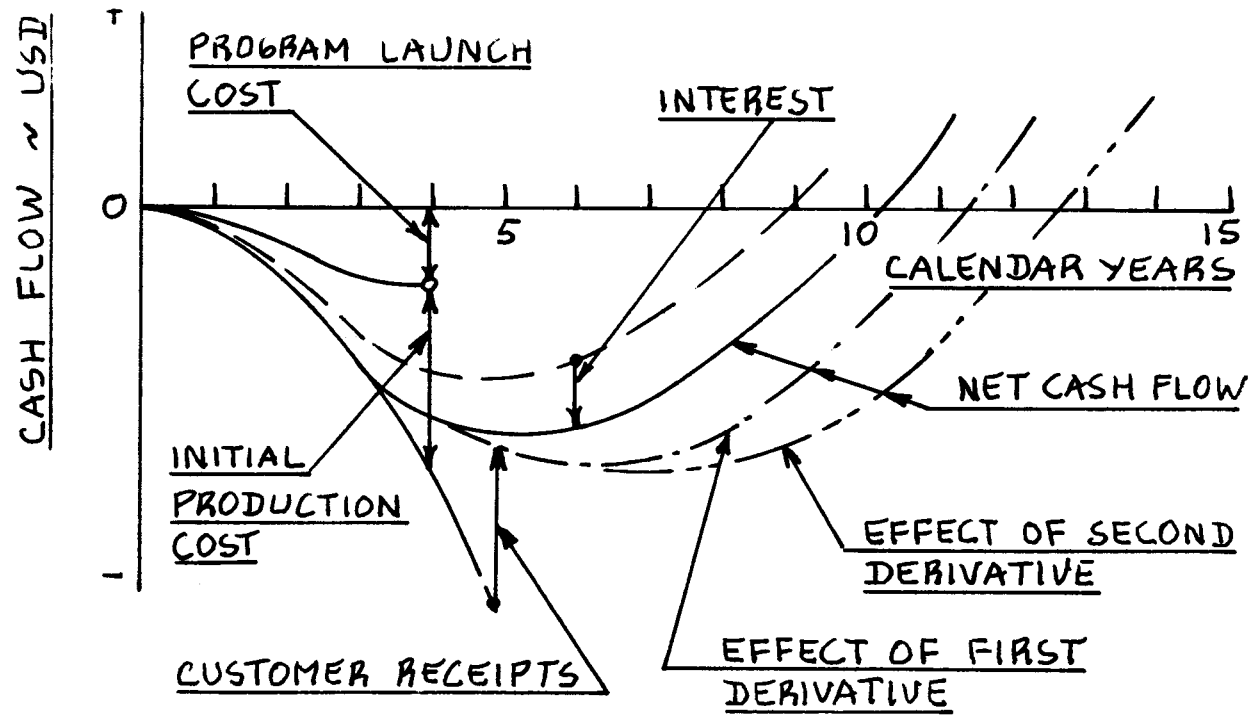

Figure 9.9 Effect of Derivatives on the Cash Flow of a Commercial Jet Transport Program

9.2 FACTORS INVOLVING TECHNOLOGICAL FEASIBILITY

It makes little sense to proceed with new airplane development and/or manufacturing plans without first determining the technological feasibility of the program.

Technological feasibility (or lack thereof) has many facets. To name a few:

* Configuration selection
* Structures
* Flight controls
* Materials
* Aerodynamics
* Propulsion
* Systems
* Manufacturing

The preliminary design methods outlined in Parts I through VII are aimed at establishing the technological feasibility of a new design. Fundamental flaws in the design are supposed to be 'smoked out' as a result of the two preliminary design sequences: P.D. Sequence I and P.D. Sequence II described in Part II.

However, if major advances (innovations) over past airplane designs are to be achieved, it is often required of the preliminary designer to take a risk in one or more of the technological facets mentioned before. Taking a risk implies the extrapolation of currently available and VALIDATED technologies. Examples are:

* Configuration selection: proposing a new configuration which is radically different from existing design practice

* Aerodynamics: assuming that the lift-to-drag ratio in cruise is significantly above that of existing design practice

* Structures: assuming that a new material with much greater strength-to-weight ratio (compared to current design practice) will work out

* Propulsion: assuming that a new engine with much lower s.f.c. (specific fuel consumption) will materialize

* Flight Controls: assuming that a new approach to flight control system design will work and will be certifiable

* Systems: assuming that a new approach to the design of one or more airplane systems will work out

The emphasis in all this is on the word VALIDATED.

NOTE 1: There is nothing wrong with assuming that major advances in technology can be made AND to integrate these advances in a new design during the preliminary design phases.

NOTE 2: There is much wrong with NOT doing the research, development and test work needed to VALIDATE any of these 'extrapolated' technologies.

NOTE 3: It is foolhardy to decide to proceed with the integration of UNVALIDATED technology into the detail design development phase of an airplane.

There are many historical examples of airplane programs which were launched without adequate VALIDATION of one or more aspects of technology used in the design. The consequences of launching an airplane program without technology validation can range from:

* mere embarrassment to a fatal crash, or from:

* minor cost overruns to bankruptcy.

Any unvalidated technology when used in a new airplane design can therefore become a 'profit suppressor' or even a 'show stopper'. It is essential that designers acquaint themselves with all technology factors which may become either a profit suppressor or a show stopper. The purpose of this section therefore is to provide airplane designers with a discussion of a number of technology factors which in past airplane programs have proven to be a profit suppressor or a show stopper. The material is organized as follows:

9.2.1	Drag prediction	9.2.2	Loads prediction
9.2.3	Laminar flow	9.2.4	Range prediction
9.2.5	Maximum speed prediction	9.2.6	VTOL capability
9.2.7	New materials	9.2.8	New engines
9.2.9	Manufacturing processes	9.2.10	De-facto stability
9.2.11	Summary		

This list of possible show stoppers is far from complete. However, it serves to illustrate problems which manufacturers have stumbled into because of excessive optimism or because of insufficient testing.

Examples of each are given without naming the manufacturer or the program involved.

9.2.1 Drag Prediction

Drag prediction is still a 'troublesome' aspect of aeronautical technology, despite all the advances made in computational aerodynamics as well as in wind-tunnel testing techniques. Drag was under-predicted on several recent military airplane programs. The results were:

a) on a military transport program performance was compromised and costly modifications were made

b) on a tactical fighter program performance was compromised to the point where even after costly modifications the effectiveness of the airplane was significantly reduced

c) a military jet trainer program was cancelled well into the flight test program

9.2.2 Loads Prediction

Airframe airload prediction can be a major headache in the transonic speed regime. On a recent military jet transport program the inboard wing airloads were under-predicted. This led to reduced wing fatigue life and costly modifications to the airframe.

9.2.3 Laminar Flow

Laminar flow has the potential to reduce friction drag very considerably. However, the stability of laminar boundary layers is tenuous. Therefore, those factors which are known to affect laminar boundary layer stability must be completely understood. For example, it is well known that high leading edge sweep angles tend to lead to rapid laminar boundary layer transition to turbulent flow which increases friction drag by a considerable amount. Therefore, it might not make sense to use high leading edge sweep if laminar flow is essential to attain the predicted operating speed of a new airplane.

This has resulted in significant downward revision of the cruise speed of a business airplane.

9.2.4 Range Prediction

If an airplane must have very long range capability, the Breguet range equations of page 15, Pt I show that three factors are essential:

1) High average lift-to-drag ratio: $(L/D)_{cr}$

2) Low weight ratio: W_{end}/W_{begin}

3) Low engine fuel specifics: c_p or c_j

The technical program decision makers had better assure themselves that none of these factors are very sensitive to optimism in their prediction. If they are, a directed research program aimed at obtaining these optimistics values may have to be financed.

An early jet transport program ran into this type of a problem resulting in not meeting transatlantic range predictions.

9.2.5 Maximum Speed Prediction

If an airplane must attain very high speed at sea-level, a number of factors bear watching:

1) Drag, including compressibility drag

2) Aeroelastic deformations which affect drag and controllability

3) Flutter, particularly in not yet encountered modal combinations

It takes a major engineering effort up-front to determine whether or not all technical risks in these three areas have been lowered sufficiently to justify launching the program. A number of jet fighter programs were launched without sufficient validation in these areas. The result was either early cancellation or a significant reduction in operational capability.

9.2.6 VTOL Capability

The following factors must be solidly researched and tested before launching a VTOL program:

* Suckdown effects of the configuration

* Adequacy of the reaction controls in hover

* Efficiency of ejectors used

* Reingestion of high temperature gasses

* Foreign object damage

Several VTOL programs of the past failed because one or more of these factors were not adequately researched. In all cases major cost overruns caused the program to be cancelled. In one case a test pilot also lost his life.

9.2.7 New Materials

On several occasions new materials have been introduced without adequate testing. Examples are:

1) Introduction of 7075-ST aluminum in areas of the wing structure where corrosion/crack induced fatigue led to very low structural life.

In a commercial jet transport program this forced the manufacturer into a very costly re-skinning program.

2) Introduction of composites which were found to be subject to (difficult-to-detect) delaminations resulting in compromises to the integrity of the structure.

This caused the manufacturer to use significantly thicker skins than planned. As a result the airplane 'gained' a lot of unplanned weight which reduced the useful load.

3) Introduction of composites without proper manufacturing control over weight. This led to unpredictable weight variability from one production airplane to the next.

This caused the termination of the program and bankruptcy of the manufacturer.

9.2.8 New Engines

History is full of examples of airplanes which did not succeed because the engines around which they were designed never reached either acceptable performance or acceptable reliability.

There are also many programs where engine problems caused major cost overruns, delays in deliveries and corresponding financial headaches for the manufacturer.

9.2.9 Manufacturing Processes

Consider the following case histories:

1) As part of the manufacturing process, a given airplane component may have to be quelched in water. The water used comes from the city water supply. During one season, the city puts some chlorine compounds in their water. The chlorine alters the structural characteristics of that airplane component.

   It took a lot of 'detective' work by engineers to identify this problem.

2) A manufacturer introduces metal-to-metal bonding in small radius skin structures, such as a horizontal tail. Say that in the analysis of the flutter behavior of the tail, all bonding was assumed to be complete. Suppose that as a consequence of local disbonding, the tail develops flutter which causes inflight airframe failure. Now the probability of a minor flaw in manufacturing has major consequences!

9.2.10 De-facto Stability

A new airplane requires a certain inherent static instability to meet certain mission demands. The manufacturer decides to employ a digital flight control system. However, the manufacturer engages a sub-contractor to assist in the development of the flight control laws. Somehow, inadequate provisions are made to simulate the control laws before first flight. The first prototype crashes, causing major program delays and cost overruns.

9.2.11 Summary

There are several lessons in all these examples:

1. PLAY THE 'WHAT-IF' GAME AT ALL LEVELS OF DESIGN DECISION MAKING.

2. LEARN FROM MISTAKES MADE ON PAST PROGRAMS. DO SO BY READING THE TECHNICAL LITERATURE.

3. THERE IS NO SUBSTITUTE FOR THOROUGH ENGINEERING RESEARCH AND TESTING: IN OTHER WORDS, VALIDATE THE TECHNOLOGY

9.3 FACTORS INVOLVING MANUFACTURING FACILITIES

The following examples are offered as illustrations of the importance of considering requirements for manufecturing facilities in early design decision making.

Example 1

Sometimes, to assure technological feasibility, new manufacturing methods and processes must be worked out. There is no guarantee that these will work. Therefore, a certain amount of manufacturing research may have to be performed to ensure that the product will perform as advertised.

Examples of programs where a very intensive program of manufacturing research was carried out are the F-27 and the F-28 transport programs and the SR-71 reconnaissance airplane program.

Example 2

It is desirable from a structural weight viewpoint to have as few joints in any structure as possible. In wing design this may lead to a requirement for very long wing skin panels. If it is not possible to manufacture these panels on existing milling machines new facilities may have to be acquired. The cost of this must be taken into account. An example of this is the 747 program.

Example 3

If laminar flow must be maintained over a large part of the wing chord it is essential that very tight surface tolerances be maintained. This has been found relatively easy to accomplish when using composite skins because of their inherent high degree of stiffness.

In metallic structures, maintaining large laminar flow runs is critically dependent on the number of joints and fasteners used. Two methods are used to minimize the number of joints and fasteners:

A) Manufacturing the wing torque box out of two sections which are joined on the neutral axis. Figure 9.10 shows an example of that method. This method requires the availability of sophisticated machining equipment.

B) Manufacturing external surfaces with 'outside-in' instead of the more conventional 'inside-out' method.

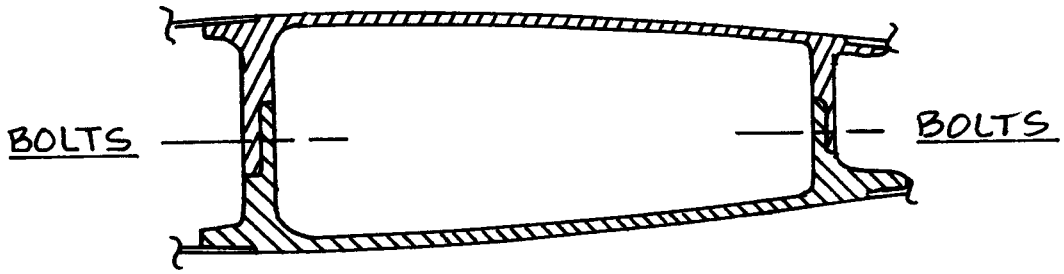

Figure 9.10 Manufacturing a Wing Torquebox in Two Pieces

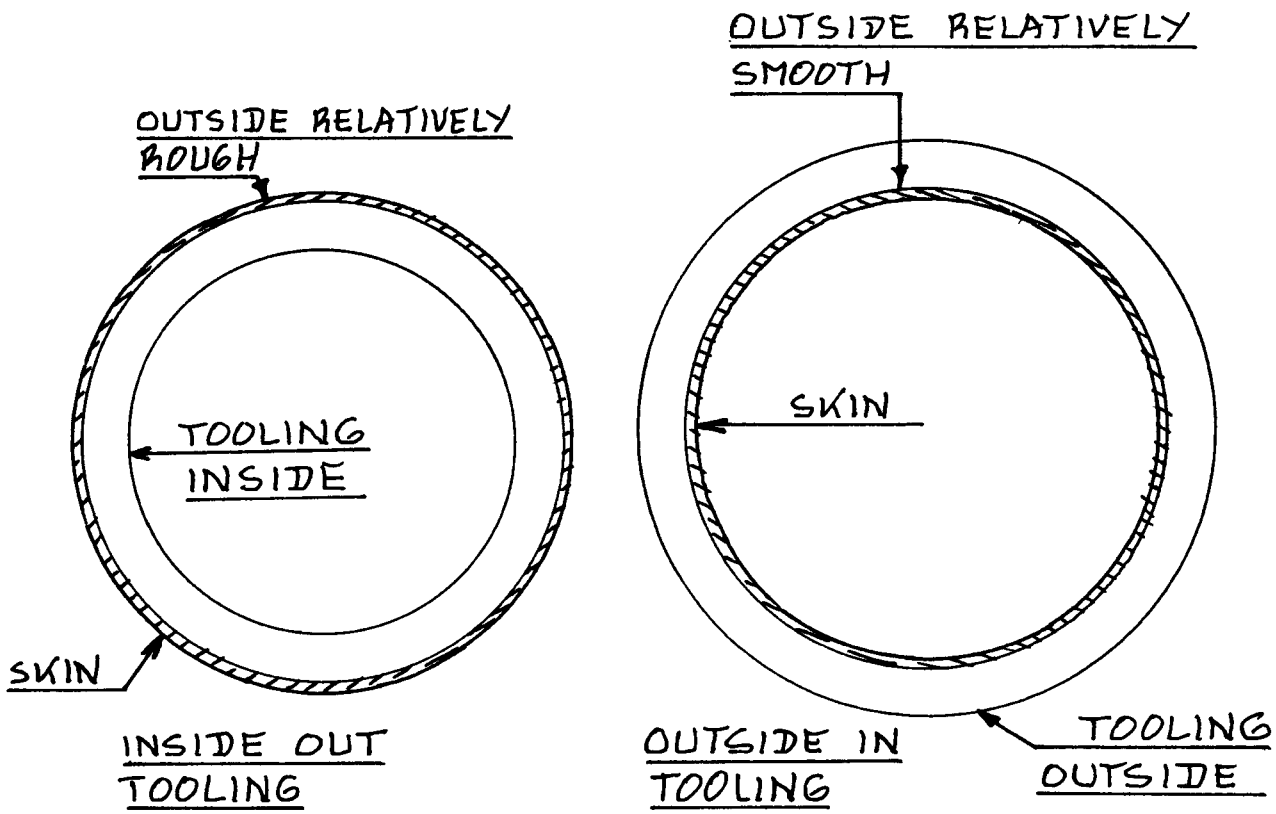

Figure 9.11 Inside-out (Old Style) and Outside-in Method (New Style) of Airframe Manufacturing

Figure 9.11 shows an example of this method. It is also possible to manufacture wings in that manner. This method requires a new approach to tooling design.

All this emphasizes the need for preliminary design organizations to discuss their designs with manufacturing experts at the earliest possible time. In this manner it is possible to prevent poor design decisions to go unchallenged before it is too late. In addition, this can help to identify the need for new manufacturing equipment and new manufacturing facilities early in the design program. This way, the cost consequences of design decisions which affect manufacturing receive early scrutiny.

9.4 FACTORS INVOLVING POLITICAL AND/OR ENVIRONMENTAL FEASIBILITY

There are situations where political and/or environmental pressures cause airplane programs to be terminated or altered. The purpose of this section is to acquaint the reader with some of these pressures. Three examples will be discussed.

Example 1: Nuclear Power

In the fifties, major studies were conducted to determine the technological and financial feasibility of using nuclear power for the propulsion of large intercontinental bombers and transports. Flight tests of at least one small nuclear reactor were in fact carried out in a B-36 airframe. This program was eventually terminated for a number of reasons. Questions were raised relative to the technological and financial feasibility (i.e. the projected high cost).

But there were other questions such as: what happens in the case of a crash with perhaps an explosion and/or a fire? How much nuclear contamination of the environment will occur? How many people might get killed due to the radiation effects? What is the probability of such a crash occurring?

These questions all beg for answers because they affect political and environmental issues.

It is the lack of acceptable answers to these questions which, probably more than any technical or financial issue, led to the termination of this and other nuclear aircraft propulsion projects.

But there is another issue here: ETHICS.

Should engineers push for starting a flight hardware project if there are serious questions about safety and about the environment?

The author believes that engineers SHOULD NOT DO SO! Engineers have an ethical commitment to society not to engage in activities which lead to major safety problems and/or problems with the environment.

Example 2: Supersonic Transports

Consider the following question: Do large fleets of supersonic transports have the potential of causing significant damage to the earth's ozone layer?

Major study programs of the chemical interactions between engine exhausts and the upper atmosphere are now being conducted by NASA to determine the answer to this question.

Until the answer to this question is available and widely accepted by the scientific and political community there SHOULD NOT be a commercial supersonic transport program.

The reader will remember the cancellation of the US-SST program in the late sixties. That program was cancelled mostly because of environmental pressures. These pressures prevailed because the aeronautical community failed to come up with scientifically sound arguments to defuse them.

The reader may ask: what about military supersonic flights? The answer has to do with relative levels of pollution. Consider the following argument.

Assume that there are, worlwide, 5,000 military airplanes able to sustain supersonic cruising flight. These airplanes fly on the average 350 hours per year. However, of those 350 hours, they probably spend less than 10 percent of their flying time in supersonic, high altitude flight conditions. This represents 175,000 hours of flight in the ozone layer.

Now consider a worldwide fleet of 1,000 commercial supersonic transports. This fleet could consist of a mixture of business jets and airliners. Say that these airplanes fly an average of 3,000 hours per year. About 70 percent of this time will be spent in a supersonic

flight condition. The average takeoff weight of this fleet of airplanes will probably be about 500,000 lbs, compared to at most 50,000 lbs for their military counterparts. The reason why takeoff weight is important has to do with the fact that the cruise thrust (and thus the engine massflow) is proportional to takeoff weight. This represents a factor 10 difference.

This commercial fleet of SST's will therefore produce the military equivalent of (1,000)(0.7)(3,000)(10) = 21,000,000 hours of flight in the ozone layer. This represents a factor of 120 difference. That is more than TWO ORDERS OF MAGNITUDE!! That is why commercial supersonic flying might be a problem whereas military supersonic flying is thought to be insignificant in terms of ozone destruction.

Example 3: Noise

During the late sixties and early seventies serious questions were raised about airplane noise, particularly the following types of noise:

1) Airport and community noise caused by takeoff operations

2) Airport and community noise caused by approach and landing operations

3) Community noise and damage caused by sonic booms from supersonic overflights

The noise levels in many instances had become intolerable to many people. Political action followed. This in turn resulted eventually in legislation under which:

1) Takeoff noise is regulated in FAR 36

2) Approach and landing noise is regulated in FAR 36

3) Supersonic overflight (other than in certain restricted, military areas) is prohibited by law

As a result, airplane propulsion systems must all be designed so that they meet the minimum noise standards of FAR 36. Many older transport jets were (and are still) being phased out because their modification to the latest FAR 36 standards is not economical.

9.5 LESSONS LEARNED FROM PAST AIRPLANE PROGRAMS

The purpose of this section is to present a listing of lessons learned (the hard way) on past airplane programs. The 19 lessons were taken from Reference 54 with minor revisions.

Lesson 1: Engines

Engines usually take at least a year longer for development than airplanes. In planning an airplane program this must be accounted for.

It is advisable to design the airframe around at least two engines from different engine manufacturers. If not, one knowingly takes a large degree of program risk. Figure 9.12 shows the engine options available on the 747 in 1982.

Lesson 2: Being there First

Being the first manufacturer to go ahead with a new, advanced airplane does not assure success. History shows that the eventual prize may go to the manufacturer who is second, provided that one is fast on his feet and is technically and financially sound.

Lesson 3: Losing a Competition

A competitive loss can motivate the loser more than the winner. This possibility should be carefully considered by management!

Lesson 4: Validated Technology

Generally speaking, the highest VALIDATED state of technology has produced the longest term, and thus, the most financially rewarding production program. Note the emphasis on the word VALIDATED.

Management should always weigh the risks and unanticipated costs associated with advanced technology. It should be ready to take program actions to minimize these.

Lesson 5: Hidden Conservatisms

Engineering should not be allowed to make conservative design assumptions AND keep these hidden from program management.

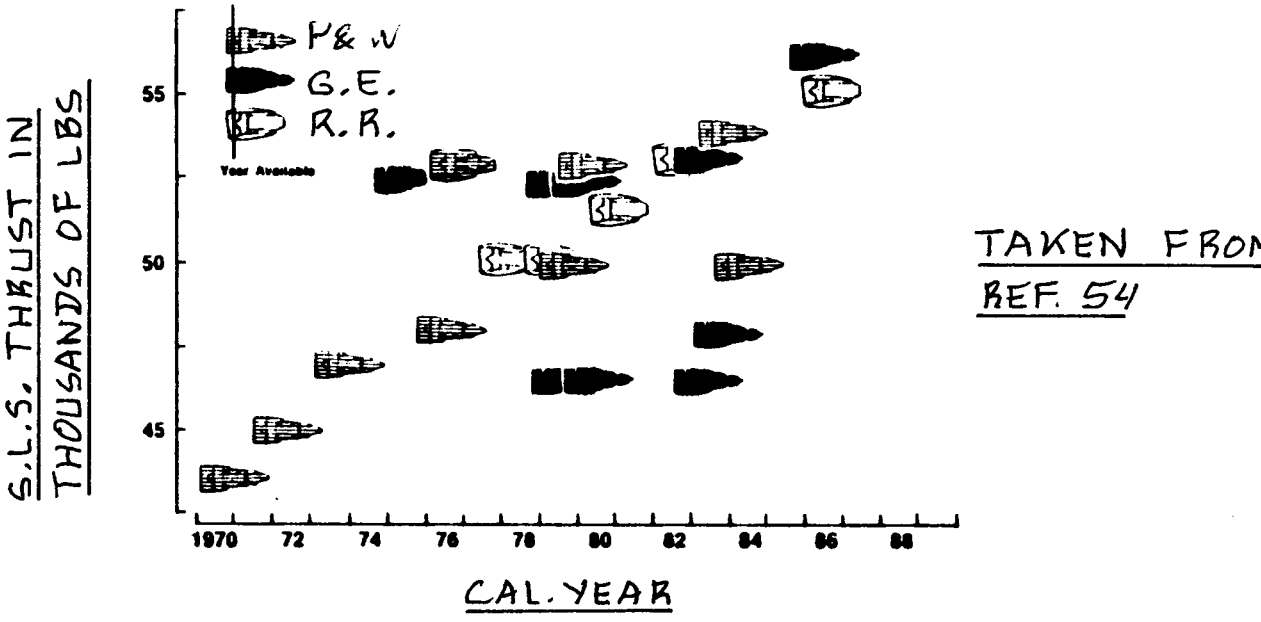

Figure 9.12 Engine Options Available in the 747 Program

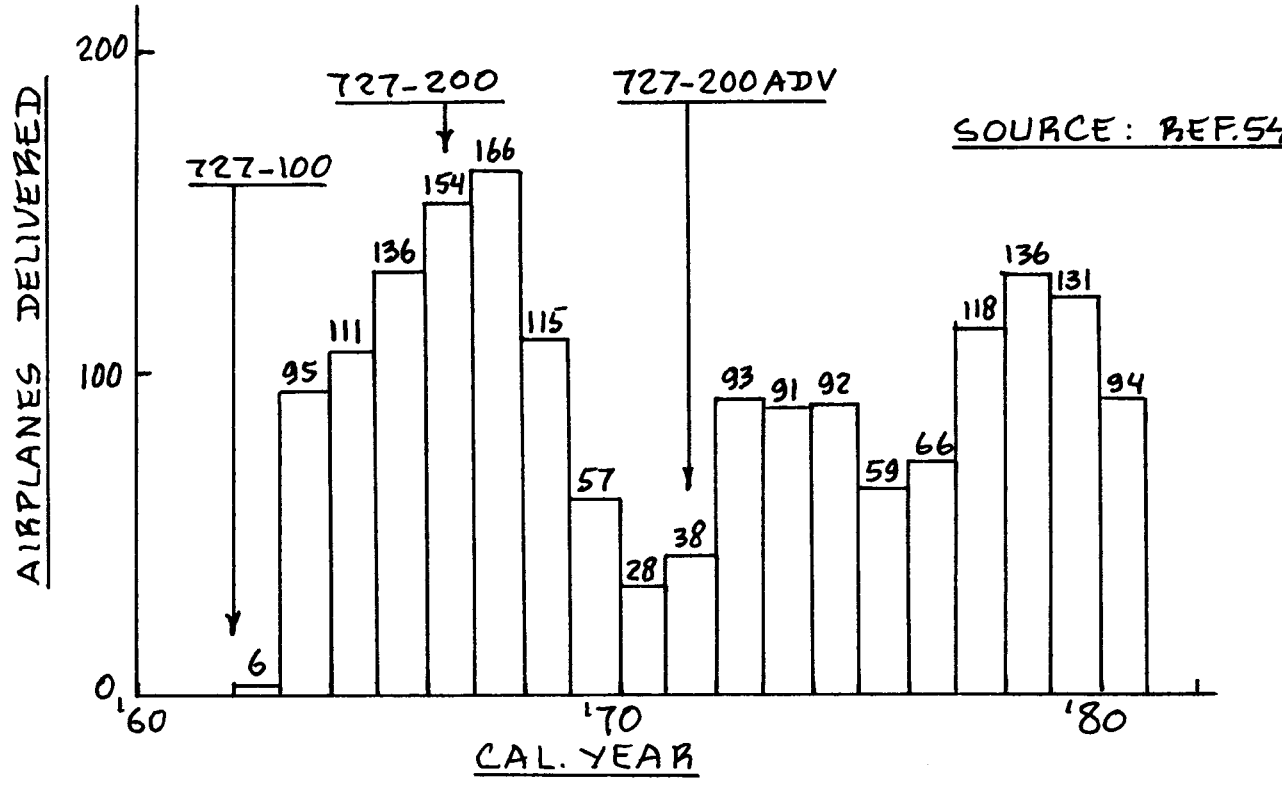

Figure 9.13 Early Delivery History of the 727 Program

A consequence of not heeding this lesson may be that the design is invalidated and/or that growth is not felt to be possible. This could stop an actually promising design from being launched!

Lesson 6: Non-recurring Investment

The RDTE cost associated with airplane development programs is also referred to as a 'non-recurring' cost. If a company wants to be in the commercial airplane market it should be prepared for investments of roughly twice the original RDTE investment cost. These costs may cover a period of 3-10 years.

Lesson 7: Staying power

Commercial airplane programs require that the manufacturers have 'staying power' to carry them over temporary market depressions or unexpected actions taken by the government.

Figure 9.13 shows the early delivery history of the Boeing 727, clearly indicating the need for staying power.

Lesson 8: Red-White-and-Blue Team Approach

To arrive at the 'best possible' design solution for a given mission it has been found to be cost effective to deploy two or three design teams. Each team should be given access to the same budget and talent pools as well as other required resources. This way, two to three different design approaches to a given mission can be compared and the 'best' one selected for full scale development.

It is vital that all three teams know and understand the rules by which what is 'best' will be decided.

Lesson 9: Up-Front Investment

To get a truly good airplane requires a large 'up-front' investment. This investment is to cover cost for new technology development, new machinery which may be required, training and equipment.

In commercial developments, management is free to decide on such investments AND to implement such decisions.

In U.S. government acquisition procedures there is no provision to adequately accommodate this.

Lesson 10: Producing Paper Airplanes

Government paper competitions which start airplane production programs without prototypes MAY result in selection of the bravest and least informed winner, with uncorrectable consequences.

Lesson 11: Readying Technology

Readying new technology developments for application to a production program can be a long and very expensive process. This process will frequently warrant funding stimulation. The payoff, when the need and technology readiness match, can be enormous.

Lesson 12: Sizing a New Airplane

Past decisions that have resulted in airplanes which were improperly sized indicate that designers should moderate their thinking to find a middle ground between 'highs' and 'lows' in projected market growth, competitor proliferation and airport constraints.

Lesson 13: Need for Maturation

A good airplane program requires at least two years of concentrated 'pre go-ahead' study and planning.

The penalty for omitting this phase is greater exposure to large changes late in the development program.

Lesson 14: Understanding Real Customer Needs

There is no substitute for understanding the real needs of a customer. This applies to commercial as well as to military programs. The job of the airplane designer is to design the airplane which the customer wants WHILE still meeting or providing for product capabilities the customer will want five years after all the basic design decisions have been made.

Lesson 15: Definition of Program Success

Management should clearly have in mind what is meant by ultimate program success. Designing two (or even more) airplanes 'head on' for the same market may

result in financial failure of one manufacturer unless the market is very large or segmented.

Lesson 16: Catering a Design to One Customer

Most good airplanes are designed to meet a broad spectrum of market requirements. Therefore, design compromises are ESSENTIAL. In the commercial market case, designing to the detailed requirements of one customer can result in an unsatisfactory program. Starting a program with one customer, while designing to a broader market need, can be satisfactory.

Lesson 17: Product Support

Product support after delivery is just as important as is successful design. Product support represents a growing financial burden with time in a successful airplane program. Without it, a manufacturer will soon find himself losing customers.

Lesson 18: World Competition

The airplane business is an international business.

In the race to acquire the most rewarding aeronautical technology, the prize will go to the nation and/or to the manufacturer who runs the fastest. The nation and/or the manufacturer who stops running will lose, regardless of lead or government protection.

Lesson 19: Design Emphasis

In future designs, the most constructive emphasis is to build a superior product at the lowest manufacturing cost.

10. REFERENCES

1. Roskam, J., Airplane Design: Part I, Preliminary Sizing of Airplanes.

2. Roskam, J., Airplane Design: Part II, Preliminary Configuration Design and Integration of the Propulsion System.

3. Roskam, J., Airplane Design: Part III, Layout Design of Cockpit, Fuselage, Wing and Empennage: Cutaways and Inboard Profiles.

4. Roskam, J., Airplane Design: Part IV, Layout Design of Landing Gear and Systems.

5. Roskam, J., Airplane Design: Part V, Component Weight Estimation.

6. Roskam, J., Airplane Design: Part VI, Preliminary Calculation of Aerodynamic, Thrust and Power Characteristics.

7. Roskam, J., Airplane Design: Part VII, Determination of Stability, Control and Performance Characteristics: FAR and Military Requirements.

Note: These books are all published by: Roskam Aviation and Engineering Corporation, Rt4, Box 274, Ottawa, Kansas, 66067, Tel. 913-2421624.

8. Blanchard, B.S., Design and Manage to Life Cycle Cost, M/A Press, Portland, Oregon, 1978.

9. Anon., World Aviation Directory, Published annually by Ziff-Davis Publishing Company, Washington, D.C.

10. Earles, M.E., Factors, Formulas and Structures for Life Cycle Costing, Eddins-Earles, 89 Lee Drive, Concord, Mass, 01742.

11. Levenson, G.S., Boren, H.E., Tihansky, D.P. and Timson, F., Cost Estimating Relationships for Aircraft Airframes, Rand Report R-761-PR, February 1972, The Rand Corporation, Santa Monica, California.

12. Reel, R.E., Totey, C.E. and Johnson, W.L., Weapon System Support Cost Reduction Study (U), ASD/XR Report 72-49, ASD/XRG, WPAFB, Ohio, June 1972.

13. Johnson, W.L. and Reel, R.E., Maintainability/Reliability Impact on System Support Costs, AFFDL-TR-73-152, AFFDL/PTC, WPAFB, Ohio, December 1973.

14. Nicolai, L.M., Fundamentals of Aircraft Design, METS Inc., 6520 Kingsland Court, California, 95120.

15. Anon., Standard Method of Estimating Comparative Direct Operating Costs of Transport Airplanes, Air Transport Association of America report, June 1960.

16. Anon., Standard Method of Estimating Comparative Direct Operating Cost of Turbine Powered Transports, Air Transport Association of America report, December 1967.

17. Anon., Standard Method for the Estimation of Direct Operating Costs of Aircraft, Society of British Aircraft Constructors report, November 1959.

18. Maddalon, D.V., Estimating Airline Operating Costs, p.849-870, CTOL Transport Technology, NASA N78-29046, 1978.

19. Anderson, J.L. and Andrastek, D.A., Operating Cost Model for Local Service Airlines, SAWE Paper 1098, Society of Allied Weight Engineers, 1976.

20. Coykendall, R.E. et al, Study of Cost/Benefit Tradeoffs for Reducing the Energy Consumption of the Commercial Air Transportation System, NASA CR-137891, 1976.

21. Vos, R. et al, United States Air Transportation 1980, NASA/WVU Summer Predoctoral Program in Engineering Systems Design, West Virginia University, Morgantown, West Virginia, 1980.

22. Ball, R.E., The Fundamentals of Aircraft Combat Survivability and Design, AIAA Education Series, 1985, American Institute of Aeronautics and Astronautics, Washington, D.C.

23. Large, J.P., Campbell, H.G. and Cates, D., Parametric Equations for Estimating Airframe Costs, Rand Report R-1693-1-PA and E, February 1976, The Rand Corp., Santa Monica, California.

24. Raymer, D.P., Aircraft Design: A Conceptual Approach, AIAA Education Series, 1989, American Institute of

Aeronautics and Astronautics, Washington, D.C.

25. Augustine, N., Augustine's Laws, American Institute of Aeronautics and Astronautics, Wash., D.C., 1983.

26. Gebman, J., Avionics Maintainability: More Important Than Reliability, AIAA Paper 89-2096, 1989.

27. Kemp, A.H., Effective Integration of Supportability Design Criteria into Computer Aided Design for the Conceptual Design Phase, AIAA Paper 88-4473, 1988.

28. Lerner, E.J., Avionics Unreliability Turns Fighters into Shop Queens, Aerospace America, August 1985.

29. Weinstock, R., Calculus of Variations, McGraw Hill, N.Y., 1952.

30. Leitmann, G., Optimization Techniques with Applications to Aerospace Systems, Academic Press, N.Y., 1962.

31. Roskam, J., What Drives Unique Configurations?, SAE Paper 881353, Aerospace Technology Conference and Exposition, Anaheim, CA, Oct.3-6, 1988.

32. Roskam, J. and Malaek, S., Automated Aircraft Configuration Design and Analysis, SAE Paper 891072, General Aviation Aircraft Meeting and Exposition, Wichita, KS, April 11-13, 1989.

33. Bisplinghof, R.L., Ashley, H. and Halfman, R., Aeroelasticity, Addison Wesley, 1955.

34. Kenyon, R.E. and Mueller, R.N., Cost-Weight Interface in Aircraft Design, Paper No.969, 32nd Annual Conference of the Society of Allied Weight Engineers, London, England, June, 1973.

35. Roskam, J., Airplane Flight Dynamics and Automatic Flight Controls, Pt.I, Roskam Aviation and Engineering Corp., Rt.4, Box 274, Ottawa, KS, 66067, 1982.

36. Roskam, J., Airplane Flight Dynamics and Automatic Flight Controls, Pt.II, Roskam Aviation and Engineering Corp., Rt.4, Box 274, Ottawa, KS, 66067, 1982.

37. Sliwa, S.M., Use of Constrained Optimization in the Conceptual Design of a Medium-Range Subsonic Transport, NASA Technical Paper 1762, December 1980.

38. Torenbeek, E., Fundamentals of Conceptual Design Optimization of Subsonic Transport Aircraft, Report LR-292, Delft University of Technology, The Netherlands, August, 1980.

39. Küchemann, D., The Aerodynamic Design of Aircraft, Pergamon Press, Oxford, England, 1978.

40. Sears, W.R., On Projectiles of Minimum Wave Drag, Quarterly of Applied Mathematics, Vol.4, No.4, 1947.

41. Jones, R.T., The Minimum Drag of Wings in Frictionless Flow, Jornal of the Aeronautical Sciences, No.18, pp 75-81, 1951.

42. Sliwa, S.M. and Arbuckle, D., OPDOT: A Computer Program for the Optimum Preliminary Design of a Transport Airplane, NASA TM 81857, September, 1981.

43. Sobieszczanski-Sobieski, J., Berthelemy, J.F. and Riley, K.M., Sensitivity of Optimum Solutions to Problem Parameters, AIAA Journal, Volume 20, No.9, p.1291, September 1982.

44. Wrenn, G.A. and Dovi, A.R., Multilevel Decomposition Approach to the Preliminary Sizing of a Transport Aircraft Wing, Journal of Aircraft, Volume 25, No.7, pp 632-638, July, 1988.

45. Sobieszczanski-Sobieski, J., On the Sensitivity of Complex, Internally Coupled Systems, AIAA Paper 88-2378, 29th Structures, Structural Dynamics and Materials Meeting, April 18-20, Williamsburg, VA, 1988.

46. Sobieszczanski-Sobieski, J., Multidisciplinary Optimization for Engineering Systems: Achievements and Potential, DFVLR Symposium on Optimization, Bonn, West Germany, June 1989.

47. Sobieszczanski-Sobieski, J., Barthelemy, J.F. and Giles, G.L., Aerospace Engineering Design by Systematic Decomposition and Multilevel Optimization, Int'l Council of Aeronautical Sciences, 14th Congress, Toulouse, France, September 1984, ICAS-84-4.7.3.

48. Bennett, J.H., Kills, Sorties and Dollars, AIAA Paper 89-2073, AIAA/AHS/ASEE Aircraft Design, Systems and Operations Conf., Seattle, WA, July 31 - Aug.2, 1989.

49. Bach, D., United States Air Force Trainer Masterplan, SAE Paper 881466, Aerospace Technology Conference and

Exposition, Anaheim, CA, October 3-6, 1988.

50. Steiner, J.E. et al, Case Study in Aircraft Design: The Boeing 727, AIAA Professional Study Series, September, 1978.

51. Fozard, J.W., Case Study in Aircraft Design: The British Aerospace Harrier, AIAA Professional Study Series, July, 1978.

52. Stuart, W.G., Case Study in Aircraft Design, The Northrop F-5, AIAA Professional Study Series, September, 1978.

53. Garrard, W.C., Case Study in Aircraft Design: The Lockheed C-5, AIAA Professional Study Series, not dated.

54. Steiner, J.E., How Decisions Are Made: Major Considerations for Aircraft Programs, AIAA 1982 Wright Brothers Lectureship in Aeronautics, Seattle, WA, 1982.

55. Anderson, J.L., A Parametric Determination of Transport Aircraft Price, SAWE Paper 1071, 34th Annual Conference of the Society of Allied Weight Engineers, Seattle, Washington, May 5-7, 1975.

56. Muehlbauer, J.C. et al, Turboprop Cargo Aircraft Systems Study, Phase I, NASA CR 159355, Lockheed Georgia Company, November 1980.

57. Lays, E.J. and Murray, D.L., General Aviation Turbine Engine (GATE) Study, Final Report, NASA CR 159603, Williams Research Corporation, June, 1979.

58. Renze, P.P. and Terry, J.E., Application of Advanced Technologies to Derivatives of Current Small Transport Aircraft, Final Report, NASA CR 166197, Beech Aircraft Corporation, July, 1981.

59. Keiter, I.D., Advanced Propeller Technology Examined, Automotive Engineering, Volume 89, Number 7, 1981.

60. Anon., Cost Trends for Fighter Avionics, Advertisement in: Aviation Week and Space Technology, p.132, December 2, 1985.

61. Spearman, L., Some Fighter Aircraft Trends, AIAA Paper 84-2503, AIAA Aircraft Design, Systems and Operations Meeting, Oct./Nov. 1988, San Diego, CA.

Airplane Servicing Arrangement 757

Flight Turnaround

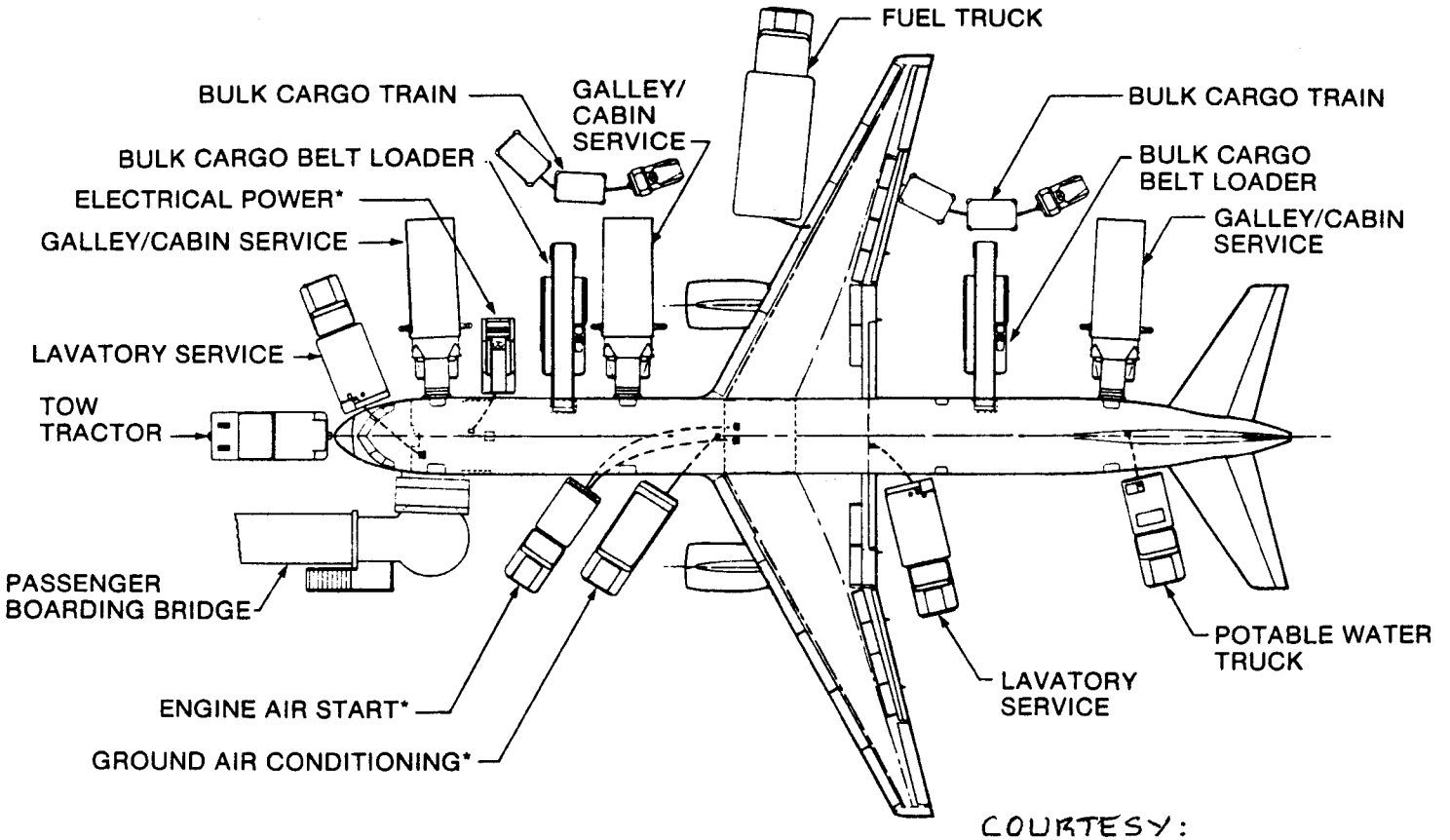

*ONLY REQUIRED WHEN APU IS NOT BEING USED

COURTESY:
BOEING

11. INDEX

Nacelle Installation 757

CF6-32C

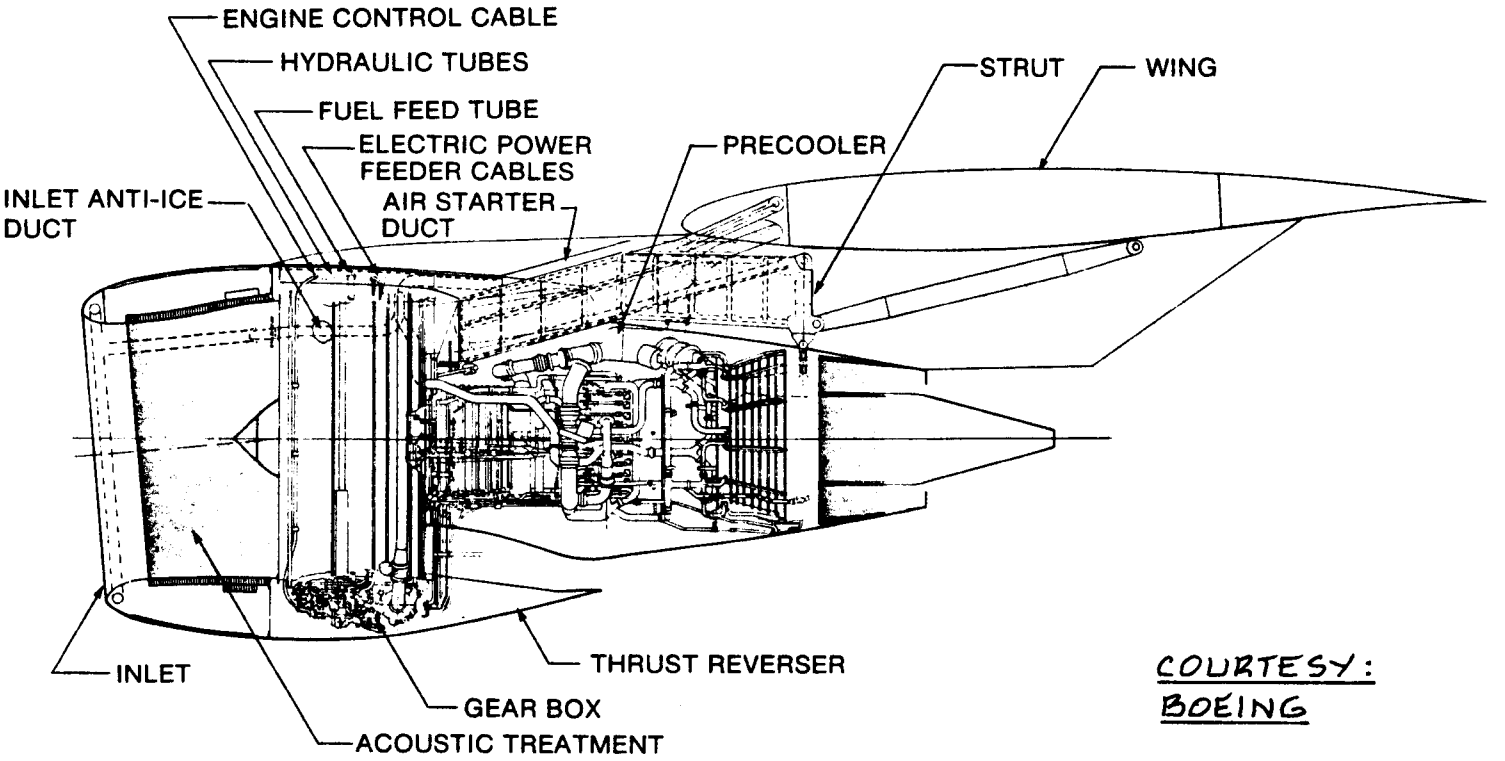

COURTESY: BOEING

ACOUSTIC TREATMENT

APPENDIX A: AIRPLANE PRICE DATA

The purpose of this appendix is to provide airplane price data as well as a rapid method for 'ball-parking' airplane prices for future designs. Most of the information presented was obtained from the following sources:

1. Business and Commercial Aviation: this monthly magazine publishes an annual Planning and Purchasing Handbook, usually as part of the April or May issue.

2. Aviation Week and Space Technology: this weekly magazine publishes an annual Aerospace Forecast and Inventory issue, usually as part of the March issue.

3. Flight International: this British weekly magazine publishes regular overviews of airplane price data.

4. AOPA Pilot: this monthly magazine publishes a general aviation aircraft directory usually as part of its March issue.

5. Professional Pilot Magazine: this monthly magazine publishes regular listings of airplane prices.

6. Interavia: this Swiss monthly magazine contains regular overviews of airplane price data.

Definition: The amount of dollars charged to an airplane operator to acquire that airplane is called the airplane market price: AMP.

Airplane prices vary with the following factors:

* Takeoff weight
* Performance
* Technology features
* Manufacturing cost
* Calendar time (if only because of cost escalation)
* Market conditions (demand and competition)
* Manufacturer sales strategies
* Government rules and regulations (certification standards, politics)
* Legal issues (product liability)

Except for the effect of cost escalation, no easy

rules for predicting the effect of these factors on airplane price can be given. Since all airplane price data are 'dated' by calendar year, the following equation is suggested to allow for cost escalation:

$$AMP_{19XX} = AMP_{\text{then year}}(CEF_{19XX}/CEF_{\text{then year}}) \qquad (A1)$$

where: AMP_{19XX} is the desired airplane price in 19XX

$AMP_{\text{then year}}$ is the given airplane price in 'then year' dollars

CEF is the cost escalation factor obtained from Figure 2.7. The ratio $(CEF_{19XX}/CEF_{\text{then year}})$ is called the CEF-ratio.

Sources 1-6 provide price data for many different calendar years. Therefore, Eqn.(A1) was used to 'correct' all data to 1989 dollars.

Airplane prices can be correlated with many factors. The most common factors used are the takeoff weight and the number of seats. In this appendix airplane prices are correlated with takeoff weight only. A brief discussion of other price parameters is given in Section A11. The airplane price data are organized as follows:

A1 SAILPLANE PRICE DATA

A2 ULTRALIGHT AIRPLANE PRICE DATA

A3 AGRICULTURAL AIRPLANE PRICE DATA

A4 SINGLE ENGINE PISTON AIRPLANE PRICE DATA

A5 MULTIENGINE PISTON AIRPLANE PRICE DATA

A6 MULTIENGINE TURBOPROP AIRPLANE PRICE DATA

A7 BUSINESS JET AIRPLANE PRICE DATA

A8 TURBOPROP COMMUTER AIRPLANE PRICE DATA

A9 COMMERCIAL TRANSPORT PRICE DATA

A10 MILITARY AIRPLANE PRICE DATA

A11 A GENERAL LOOK AT AIRPLANE PRICE DATA

A1 SAILPLANE PRICE DATA

Sailplane prices are plotted as a function of their takeoff weight in Figure A1. These data are based on information from the March, 1985 issue of AOPA Pilot Magazine. The data were adjusted to 1989 dollars with Equation (A1) and a CEF ratio of 1.082 obtained from Fig.2.7.

It is seen that there is a large spread in the data. The trend line is seen to 'fit' the data (+/- 25 percent) for unpowered as well as powered sailplanes. Based on this trend line the following equation is suggested for 'ballparking' sailplane prices:

$$AMP_{1989} = \text{invlog}\{1.1592 + 1.0705(\log W_{TO})\} \qquad (A2)$$

where: AMP_{1989} is the predicted market price for sailplanes in 1989 dollars.

This equation applies to the following range of takeoff weights: 600 lbs $< W_{TO} <$ 2,000 lbs and should NOT be used outside that range.

A2 ULTRALIGHT AIRPLANE PRICE DATA

The March, 1985 issue of AOPA Pilot Magazine contains a lengthy listing of ultralight prices. Because these aircraft are usually delivered in the form of a kit (raw materials or pre-cut) most prices apply to the unassembled vehicle. There did not seem to be a reasonable correlation between prices and takeoff weights. Based on the aforementioned data, the following ranges are suggested for 'ballparking' ultralight airplane prices in 1989 dollars:

Pre-cut kits: $AMP_{1989} = 5(W_{TO})$ to $10(W_{TO})$ (A3)

Raw material kits: $AMP_{1989} = 3(W_{TO})$ to $10(W_{TO})$ (A4)

According to the data, ultralight takeoff weights range from 400 to 800 lbs. Note: ultralights are not certified to FAR standards.

A3. AGRICULTURAL AIRPLANE PRICE DATA

Prices for agricultural airplanes are plotted as a function of takeoff weight in Figure A2. These data are based on information from the March, 1984 issue of AOPA Pilot Magazine and from the October, 1984 issue of Agricultural Aviation Magazine. The data were adjusted to 1989 dollars using Equation (A1). The CEF ratio of 1.119 was obtained from Figure 2.1.

Some of the price data were judged to be unrealistically low by the author. These 'suspect' data are identified in Figure A2. After disregarding these data, a regression analysis was performed. This resulted in the following formula for 'ballparking' prices of agricultural airplanes:

$$AMP_{1989} = \text{invlog}\{-0.6681 + 1.5799\log(W_{TO})\} \qquad (A5)$$

where: AMP_{1989} is the predicted market price for agricultural airplanes in 1989 dollars.

This equation applies to the following range of takeoff weights: 3,000 lbs $< W_{TO} <$ 15,000 lbs and should NOT be used outside that range.

It is interesting to observe that engine type does not seem to have a significant effect on agricultural airplane price trends.

A4. SINGLE ENGINE PISTON AIRPLANE PRICE DATA

The price of single engine piston airplanes depends on the following factors:

* engine aspiration: normal or turbocharged
* cabin pressurization (most are not!)
* takeoff weight and performance
* product liability insurance

Figure A3 shows the calendar time history of a single engine piston training airplane compared to the CEF. The price of this airplane compares reasonably with CEF trends until about 1982 when product liability became a major factor in airplane pricing. In 1985 Cessna decided to discontinue the production of this type: the price had become unreasonably high!

Price data for single engine piston airplanes were taken from the March, 1989 Planning and Purchasing Handbook issue of Business and Commercial Aviation Magazine. The data are plotted in Figure A4. Two trend lines suggest themselves: one for airplanes with normally aspirated engines and the other for airplanes with turbocharged engines. Note, that the pressurized Piper Malibu follows the latter trend line. Also note, that the only (in 1989) certified single engine turboprop airplane (the Cessna Caravan I) follows the normally aspirated trend line.

Note: the Lake-4 amphibian and the Beech BE-A36 were excluded from the data base because of the 'specialty nature of these airplanes. The Piper Super Cub was added to the data as follows: W_{TO} = 1,750 lbs at USD 45,000.

A regression analysis was performed to determine the trend line equations which may be used for 'ballparking' single engine piston and single engine turboprop prices.

For single engine airplanes with normally aspirated piston engine or with a turboprop engine:

$$AMP_{1989} = \text{invlog}\{-1.2435 + 1.8459(\log W_{TO})\} \qquad (A6)$$

For single engine airplanes with turbocharged piston engines (with and without cabin pressurization):

$$AMP_{1989} = \text{invlog}\{-1.1174 + 1.8459(\log W_{TO})\} \qquad (A7)$$

where: AMP_{1989} is the predicted airplane market price for single engine airplanes in 1989 dollars.

These equations apply inside the following range of takeoff weights: $1{,}500 < W_{TO} < 10{,}000$ and should NOT be used outside that range.

A5. MULTIENGINE PISTON AIRPLANE PRICE DATA

Airplane price data for 1989 and 1980 were obtained from the Planning and Purchasing Handbook (March issue of Business and Commercial Aviation Magazine). The data for 1980 were adjusted to 1989 with a CEF-ratio of 2.045 obtained from Figure 2.7. The resulting price data are plotted in Figure A5. Observe that the effect on price of turbocharging (over normally aspirated engines) and of cabin pressurization (over unpressurized) is negligible.

The author decided to eliminate the relatively very

highly priced Partenavia airplanes from the data before determining the trend line (See Figure A5) with a regression analysis. As a result, the following equation can be used for 'ballparking' prices for multiengine piston airplanes:

$$AMP_{1989} = \text{invlog}\{-0.8526 + 1.7413(\log W_{TO})\} \qquad (A8)$$

where: AMP_{1989} is the predicted market price for multiengine piston airplanes in 1989 dollars.

This equation applies to the following range of takeoff weights: 3,000 lbs $< W_{TO} <$ 8,000 lbs and should NOT be used outside that range.

A6. MULTIENGINE TURBOPROP BUSINESS AIRPLANE PRICE DATA

This airplane category consists of airplanes which are configured for business and NOT for airline use. The 1989 Planning and Purchasing Handbook of Business and Commercial Aviation Magazine (March issue) was used to plot the price data of Figure A6. A regression analysis was performed on these data. From this, the following equation was derived, which may be used for 'ballparking' airplane prices:

$$AMP_{1989} = \text{invlog}\{1.9153 + 1.1115(\log W_{TO})\} \qquad (A9)$$

where: AMP_{1989} is the predicted airplane market price for multiengine turboprop business airplanes in 1989 dollars.

This equation applies to the following range of takeoff weights: 8,000 lbs $< W_{TO} <$ 50,000 lbs and should NOT be used outside this range.

A7 BUSINESS JET AIRPLANE PRICE DATA

This airplane category consists of business airplanes, NOT airline configured airplanes. Price data were taken from the March 1989 issue of the Planning and Purchasing Handbook of Business and Commercial Aviation Magazine. Figure A7 shows a plot of these data. As seen, prices of the Gulfstream GIV and several Boeing airplane adaptations for business usage do not fit a linear trend. After eliminating these airplanes from the data a regression analysis was performed. The result is the following

equation which may be used to 'ballpark' airplane prices for this category:

$$AMP_{1989} = \text{invlog}\{0.6570 + 1.4133\log(W_{TO})\} \qquad (A10)$$

where: AMP_{1989} is the predicted airplane market price for business jets in 1989 dollars.

This equation applies to the following range of takeoff weights: 10,000 lbs $< W_{TO} <$ 60,000 lbs and should NOT be used outside this range.

A8 TURBOPROP COMMUTER AIRPLANE PRICE DATA

Price data for turboprop commuter airplanes were obtained from the March 1989 issue of the Planning and Purchasing Handbook of Business and Commercial Aviation Magazine. The data are plotted in Figure A8. A regression analysis was performed on the data. This resulted in the following equation, which can be used to 'ballpark' airplane prices for this category:

$$AMP_{1989} = \text{invlog}\{1.1846 + 1.2625(\log W_{TO})\} \qquad (A11)$$

where: AMP_{1989} is the predicted airplane market price for turboprop commuters in 1989 dollars.

These equations apply to the following range of takeoff weights: 6,000 lbs $< W_{TO}$ 50,000 lbs and should NOT be used outside these ranges.

A9 COMMERCIAL JET TRANSPORT PRICE DATA

Commercial jet transport price data were taken from the October 10, 1987 issue of Flight International (British weekly aviation magazine). A CEF ratio of 1.0237 was applied to adjust the data to 1989 dollars. The adjusted data are plotted in Figure A9. The trend line was determined with a regression analysis which yielded the following equation:

$$AMP_{1989} = \text{invlog}\{3.3191 + 0.8043(\log W_{TO})\} \qquad (A12)$$

where: AMP_{1989} is the predicted airplane market price for jet transports in 1989 dollars.

This equation can be used to obtain a 'ballpark' es-

timate of jet transport prices. The equation applies to the following range of takeoff weights:

60,000 lbs < W_{TO} < 1,000,000 lbs and should NOT be used outside this range.

A10 MILITARY AIRPLANE PRICE DATA

Prices for military airplanes vary with the following factors:

* takeoff weight and performance
* types of technology included
* mission orientation (weapons capability)
* procurement politics

Price data for military airplanes are published on occasion in sources such as magazines number 2, 3 and 6 mentioned on page 297. The author has collected price data (in the form of unit fly-away prices without spares) from these sources and applied the appropriate CEF-ratio to adjust these data to 1989 dollars. Figure A10 represents a plot of these data. It is noted that military airplane prices vary 'all over the lot' when plotted in this manner. After eliminating the price data for what the author considers 'old technology' fighters, a regression analysis was performed and a trend line established. Except for the T-45 (which appears to be extremely expensive) the trend line follows the data rather well. Thus, the following equation is suggested for 'ballparking' prices for military airplanes:

$$AMP_{1989} = \text{invlog}\{2.3341 + 1.0586(\log W_{TO})\} \qquad (A13)$$

where: AMP_{1989} is the predicted airplane market price for military airplanes in 1989 dollars.

This equation applies within the following range of takeoff weights: 2,500 lbs < W_{TO} < 1,000,000 lbs and should NOT be used outside that range.

A11 A GENERAL LOOK AT AIRPLANE PRICE DATA

Figure A11 presents a plot of all price-versus-takeoff-weight equations discussed in Sections A1 - A10. The suggested ranges of takeoff weight values are indicated with large dots. Note the two overall trend lines drawn in Figure A11. As seen, business jets and military air-

planes differ from these trend lines significantly. It seems that, roughly speaking, the business jets and the military airplanes are 2 to 3.5 times as expensive as all other types of airplane.

An interesting question is: How have airplane prices varied with calendar years in 'then yaer' dollars? The answer may be found in Figures 9, 10 and 15 of Ref.25. The author has taken the trend lines from Figures 9, 10 and 15 of Ref.25 and derived the following equations:

For tactical airplanes (Fig.9, Ref.25):

$$(AMP_{\text{then year}}) = \qquad \text{(A14)}$$

$$= \text{invlog}\{-104.8212 + 0.056604(19XX)\}$$

For bombers (Fig.15, Ref.25):

$$(AMP_{\text{then year}} = \qquad \text{(A15)}$$

$$= \text{invlog}\{-138.4443 + 0.074074(19XX)\}$$

For commercial transports (Fig.10, Ref.25):

$$(AMP_{\text{then year}}) = \qquad \text{(A16)}$$

$$= \text{invlog}\{-99.2972 + 0.054054(19XX)\}$$

where: $(AMP_{\text{then year}})$ is the airplane market price in 'then year' dollars.

19XX is a calendar year anywhere between 1910 and 1990.

Figure A12 presents plots for each equation. Plots of the U.S. annual defense budget and the gross national product are superimposed. Note the following:

I. All airplane prices tend to increase with calendar time. The logarithmic slope of the price trends is larger than a similar slope of economic trends. If that trend is not reversed, airplanes will become unaffordable!

II. The logarithmic slope of bomber price trends is 50 percent greater than that of commercial transports!

In comparing airplane prices with one another, the following parameters are often used:

* Dollars price per pound of takeoff weight
* Dollar price per seat (civilian airplanes only)

Table A1 tabulates the prices per lbs of takeoff weight for all types of airplanes considered in this appendix. Note that, except for the commercial jet transports, the price per lbs increases for all types of airplanes with increasing takeoff weight. The slope constant in Eqns (A2) through (A11) and Eqn.(A13) are all larger than 1.0, but the slope constant for commercial transports (see Eqn.(A12)) is less than 1.0! An explanation for this may be that commercial transports represent a relatively 'mature' technology.

Note again that business jets and military aircraft at the high end of their weight ranges cost about the same in terms of dollars per lbs of takeoff weight!

Table A2 shows the cost per seat for civilian airplanes. It is of interest to observe that the price per seat for transport type airplanes falls in a relatively narrow range: 160,000 to 360,000 dollars/seat. Also note the very high price per seat for the upper end of the business jets!

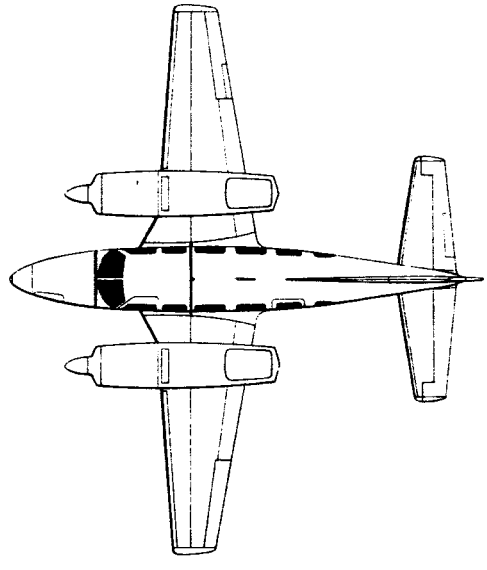

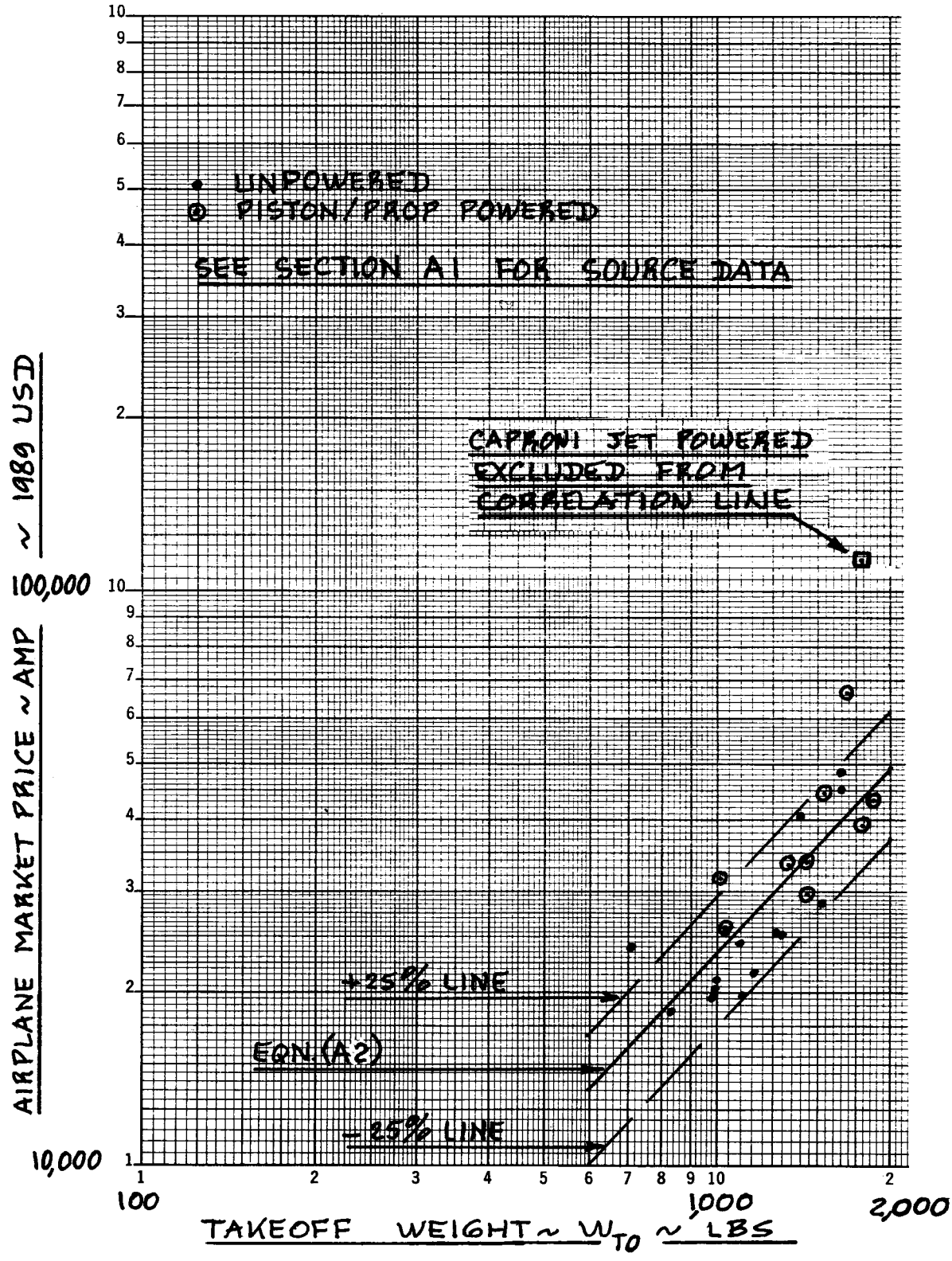

Figure A1 Effect of Takeoff Weight on the Price of Sailplanes

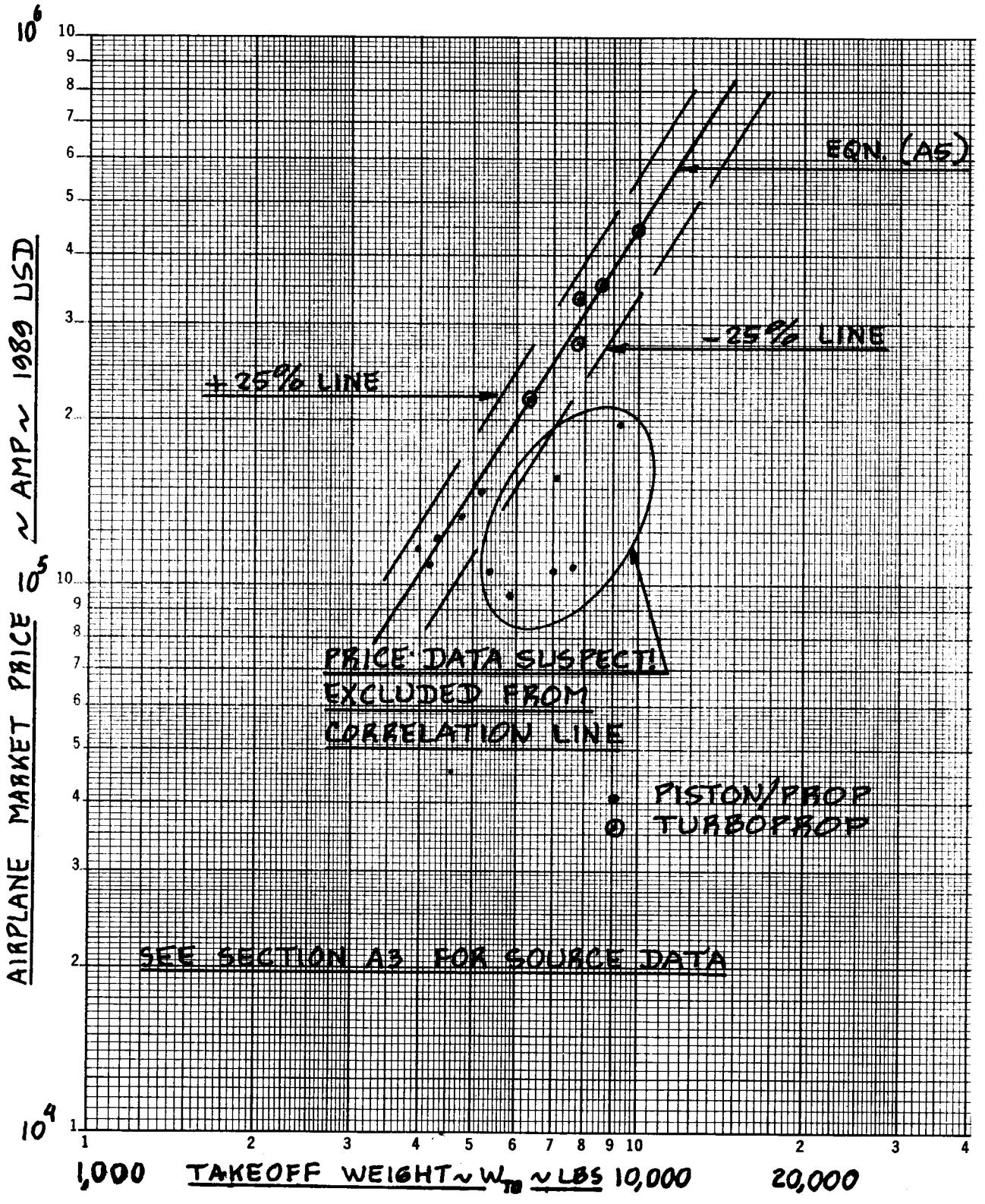

Figure A2 Effect of Takeoff Weight on the Price of Agricultural Airplanes

Figure A3 Variation of the Price of a Light Trainer Airplane with Calendar Year

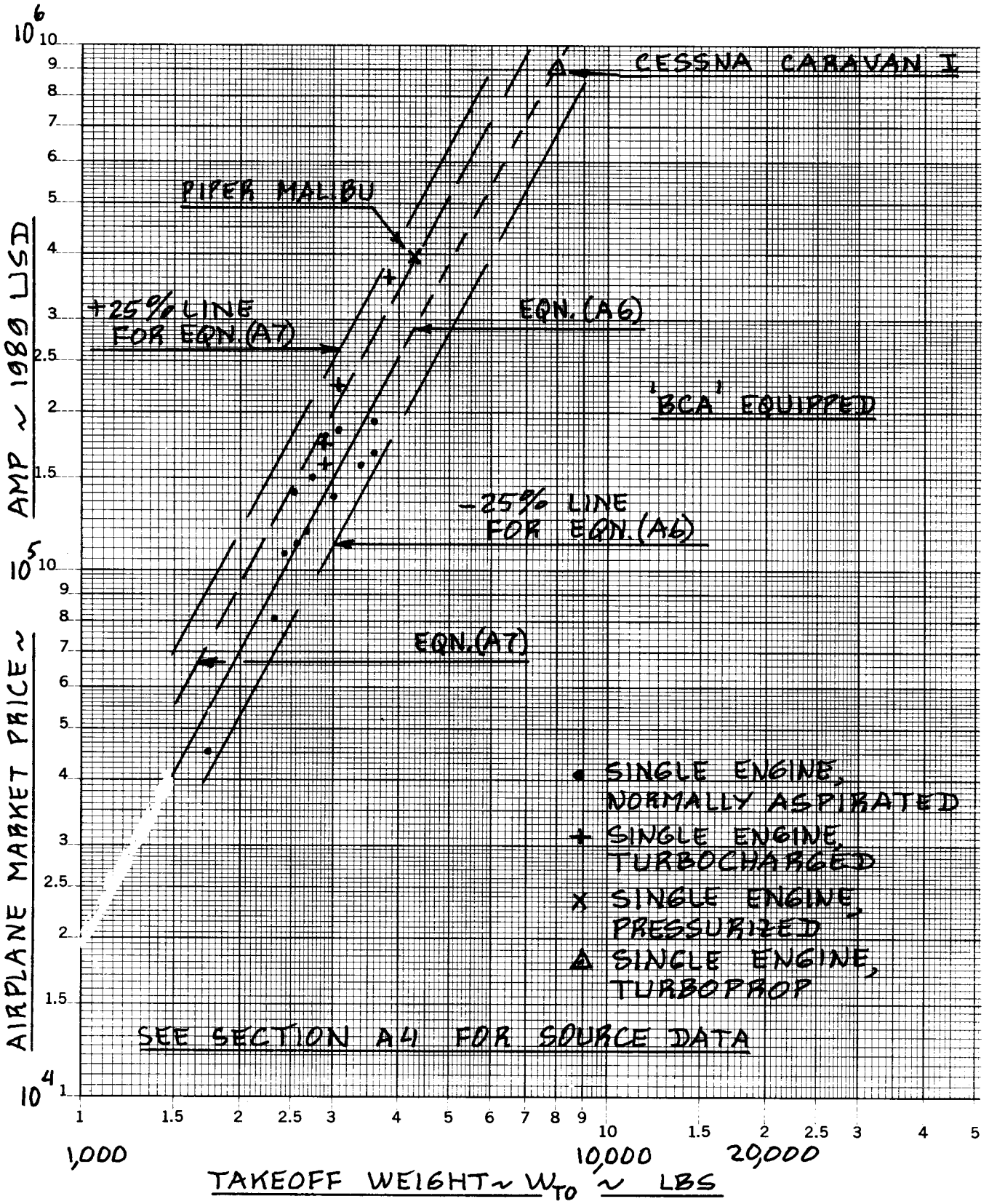

Figure A4 Effect of Takeoff Weight on the Price of Single Engine Piston Airplanes

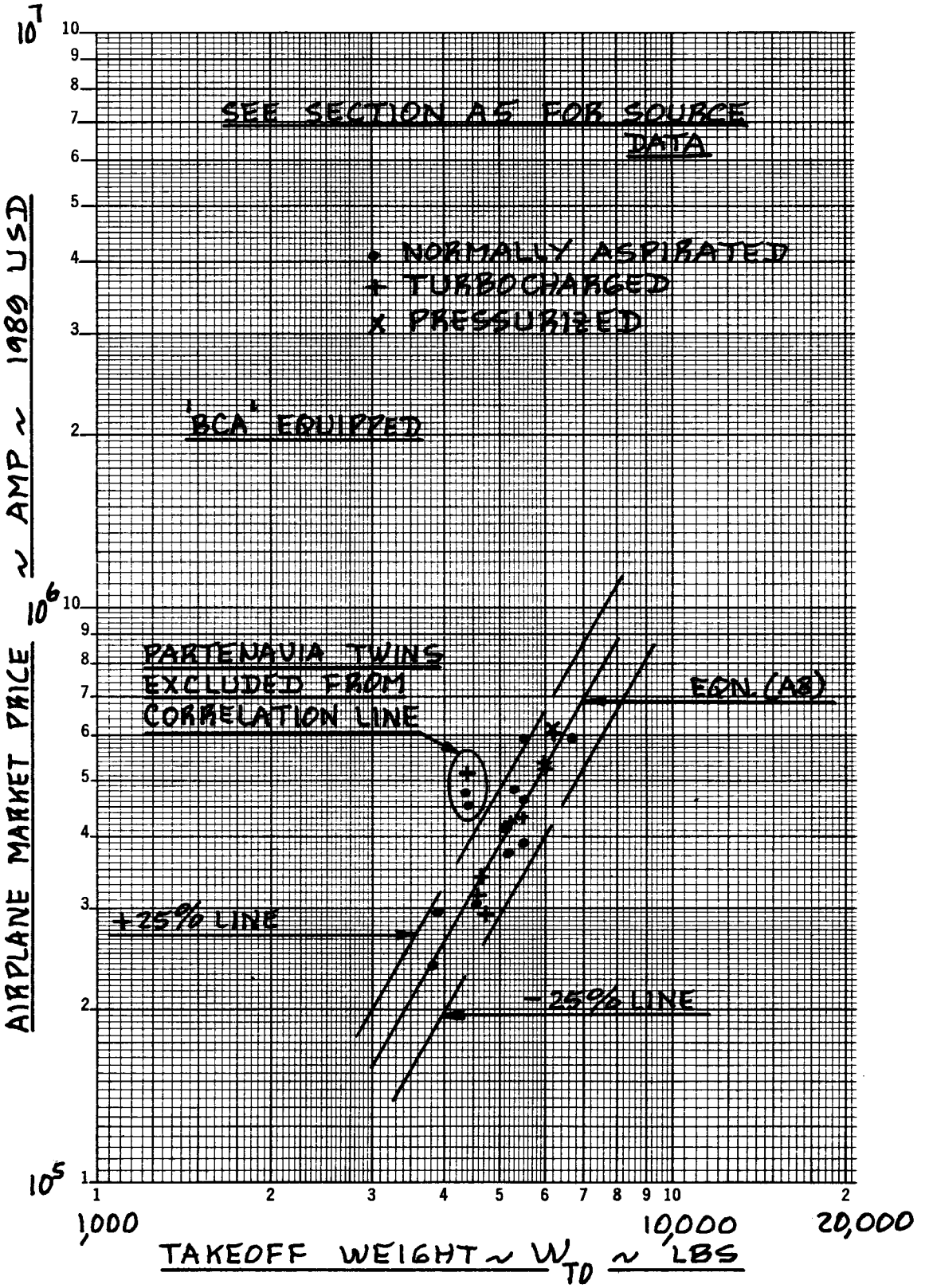

Figure A5 Effect of Takeoff Weight on the Price of Multiengine Piston Airplanes

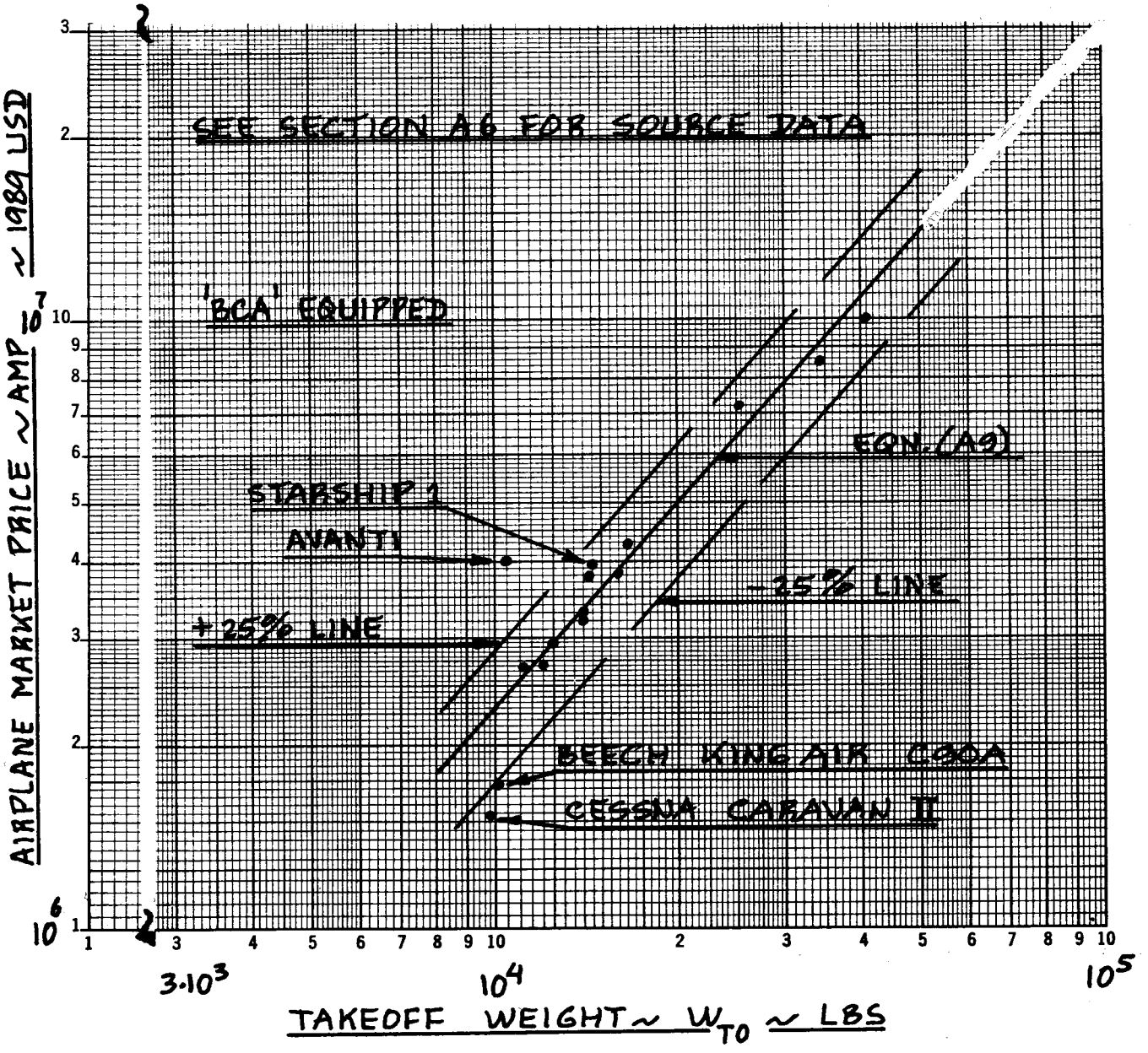

Figure A6 Effect of Takeoff Weight on the Price of Multiengine Turboprop Business Airplanes

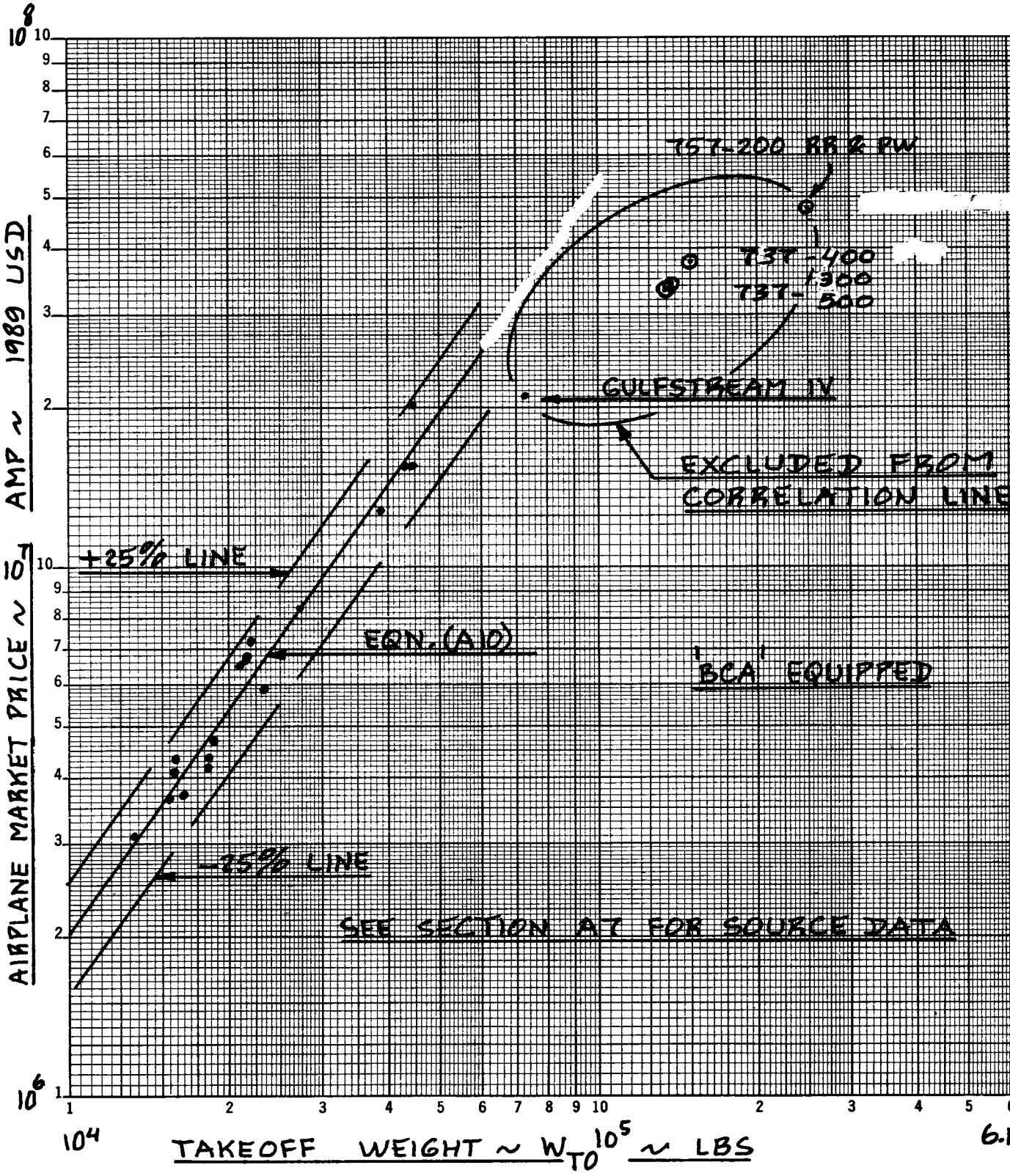

Figure A7 Effect of Takeoff Weight on the Price of Business Jets

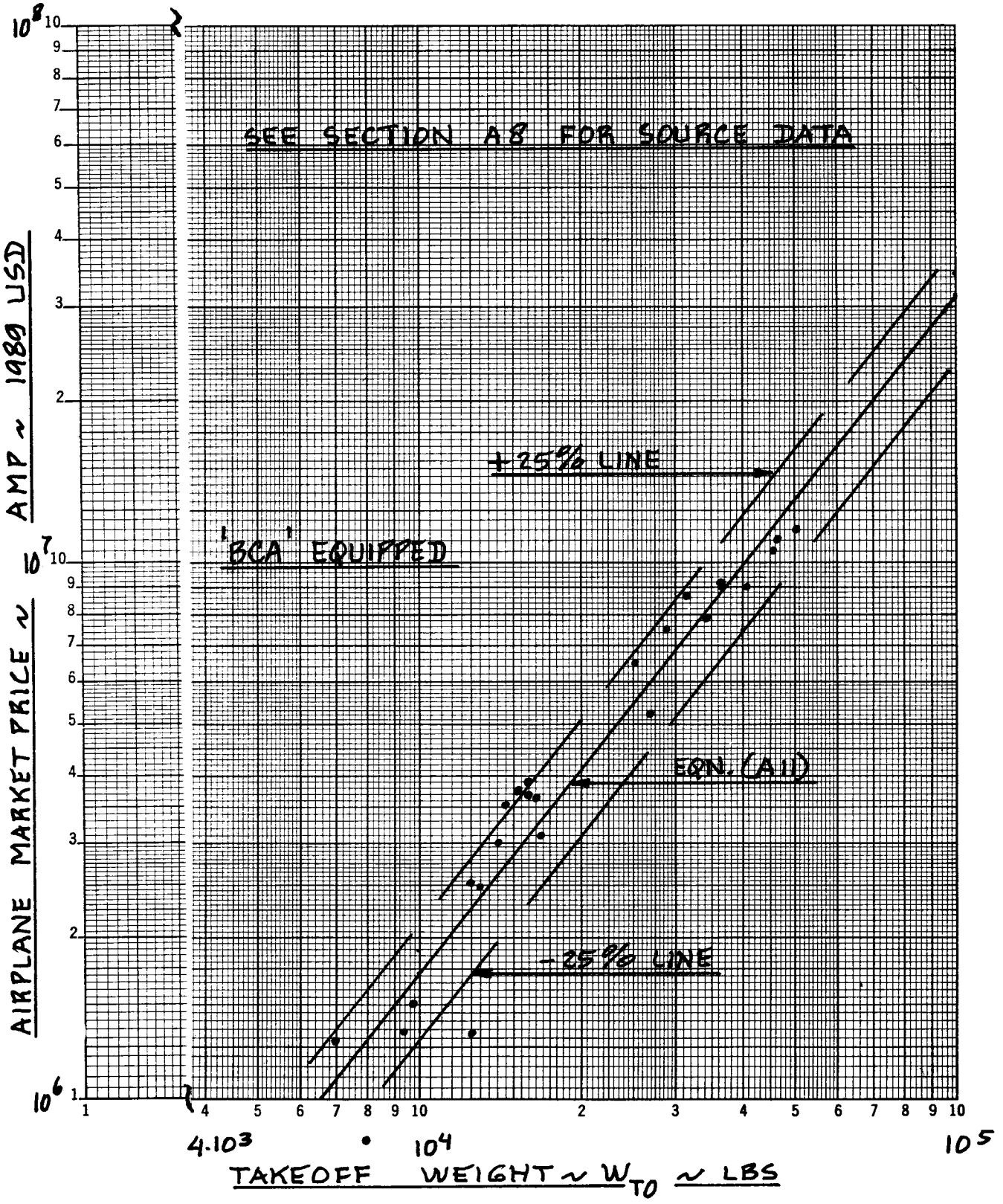

Figure A8 Effect of Takeoff Weight on the Price of Turboprop Commuter Airplanes

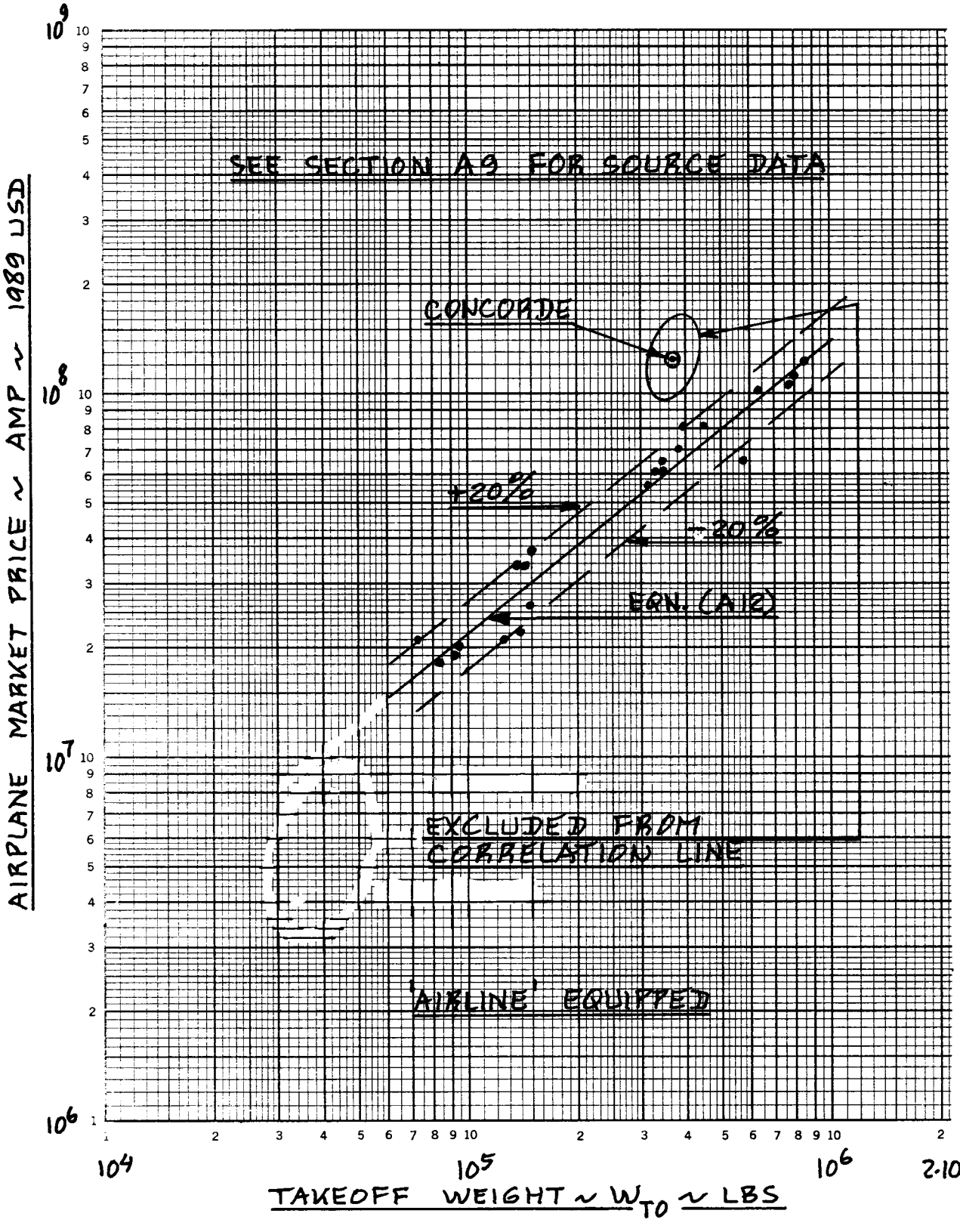

Figure A9 Effect of Takeoff Weight on the Price of Commercial Jet Transports

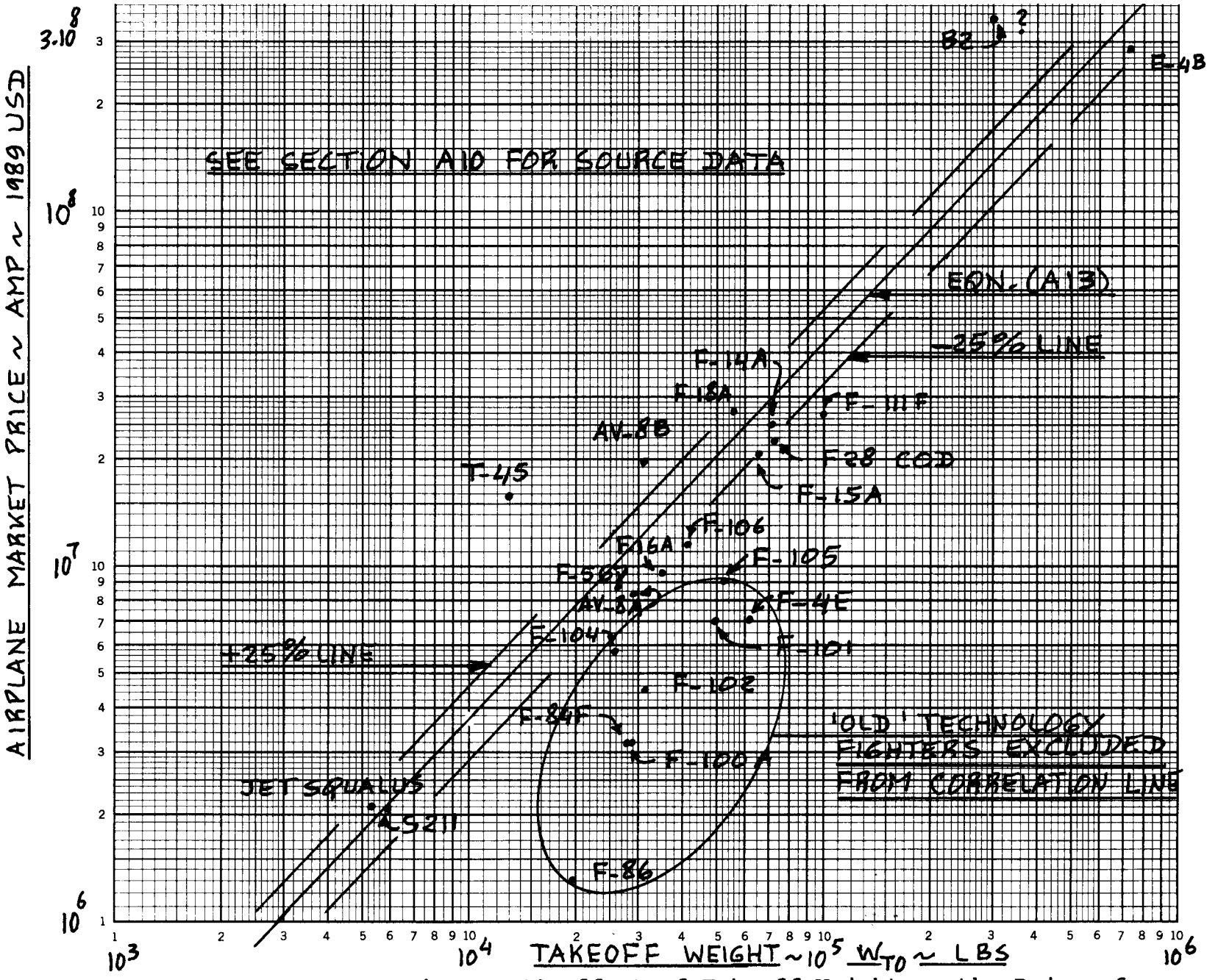

Figure A10 Effect of Takeoff Weight on the Price of Military Airplanes

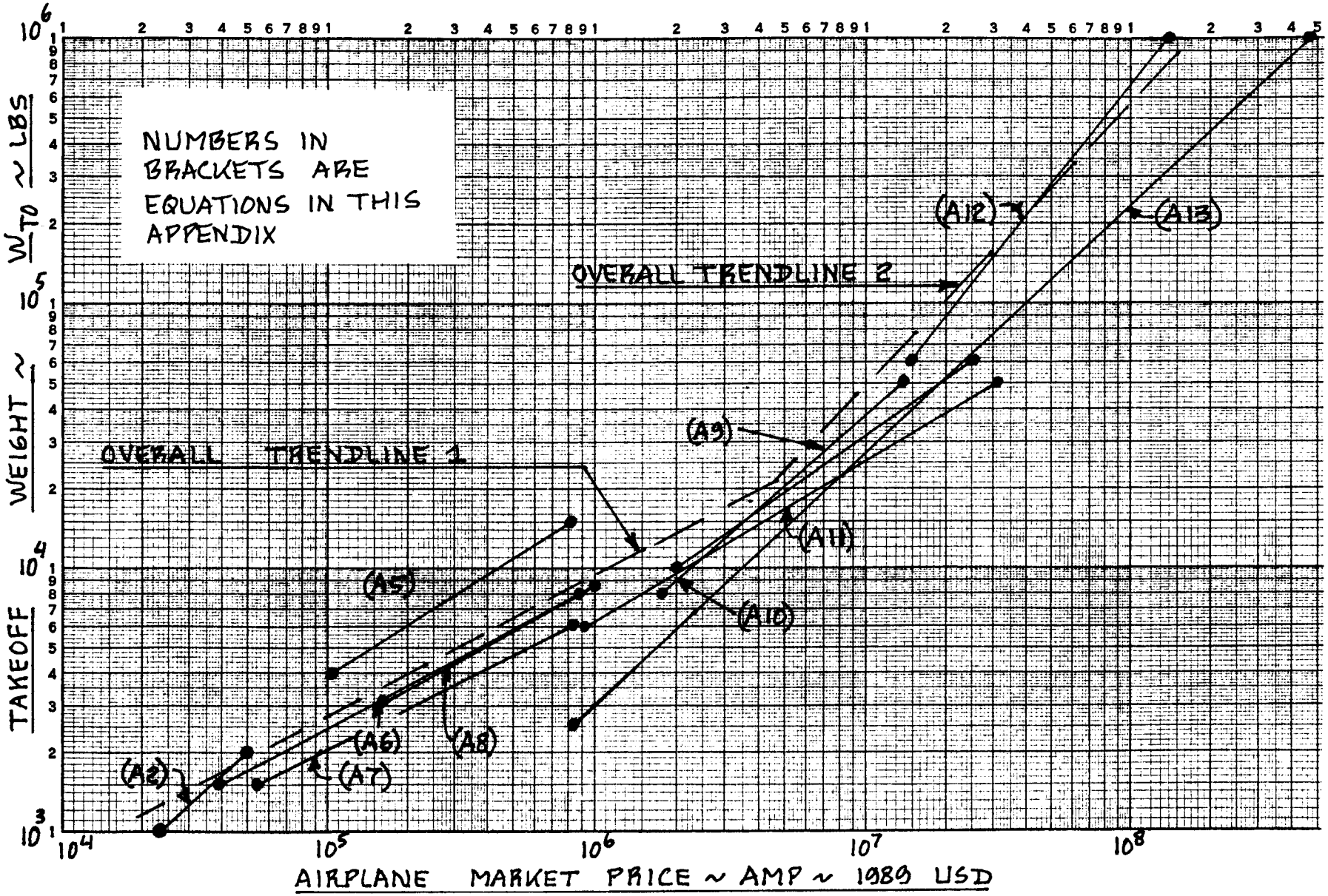

Figure A11 Composite Plot of Price Versus Takeoff Weight of all Airplane Types

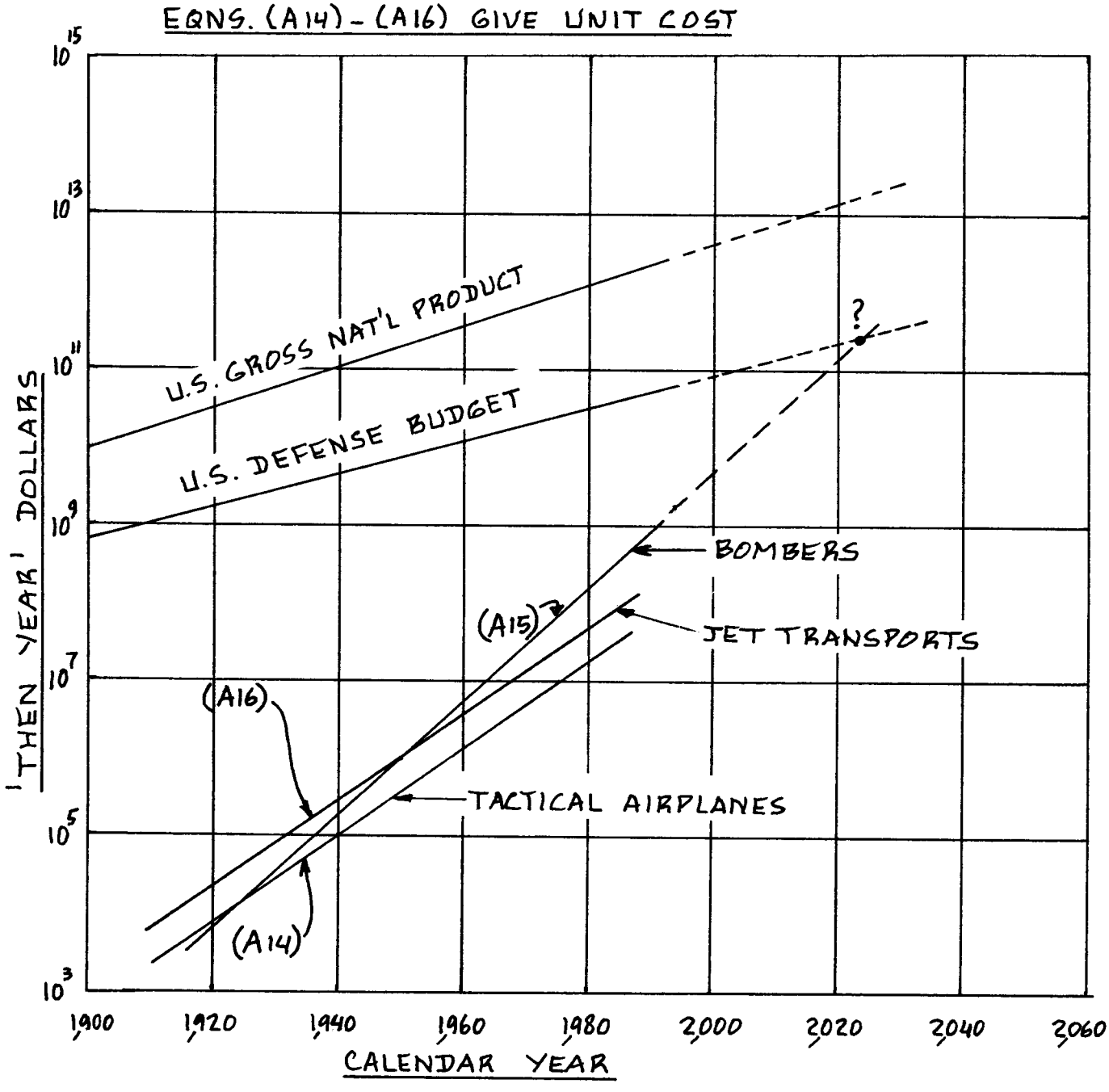

Figure A12 Effect of Calendar Year on the Price of Three Airplane Types

Table A1 Ranges of Airplane Price per Pound for 1989

Airplane Type	Range of Takeoff Weights in Lbs Range of Prices in Dollars/Lbs		
Sailplanes	600	to	2,000
Eqn.(A2)	23	to	25
Ultralight Airplane Kits	400	to	800
Eqns (A3 and A4)	3	to	10
Agricultural Airplanes	3,000	to	15,000
Eqn.(A5)	22	to	57
Single Engine Piston Airplanes			
Normally Aspirated	1,500	to	10,000
Eqn.(A6)	28	to	138
Turbocharged	1,500	to	10,000
Eqn.(A7)	37		185
Multieng. Piston Airpl.	3,000	to	8,000
Eqn.(A8)	53	to	110
Multieng. TBP Airplanes	8,000	to	50,000
(Business), Eqn.(A9)	224	to	275
Business Jets	10,000	to	60,000
Eqn.(A10)	204	to	428
Turboprop Commuter Airplanes	6,000	to	50,000
Eqn.(A11)	150		262
Commercial Transp. Jets	60,000	to	1,000,000
Eqn.(12)	242		140
Military Airplanes	2,500	to	1,000,000
Eqn.(A13)	341		485

Table A2 Ranges of Airplane Price per Seat for 1989

Airplane Type	Range of Price per Seat in Dollars/Seat		
Sailplanes	16,000	to	80,000
Single Engine Piston Airplanes	20,000	to	50,000
Multiengine Piston Airplanes	33,000	to	70,000
Multiengine Turboprop Airplanes (Business)	115,000	to	450,000
Business Jets	320,000	to	1,600,000
Turboprop Commuter Airplanes	160,000	to	360,000
Commercial Transport Jets	170,000	to	250,000

APPENDIX B ENGINE AND PROPELLER PRICE DATA

The purpose of this appendix is to provide engine and propeller price data as well as a rapid method for 'ball-parking' such prices for future designs. The sources listed in Appendix A for airplane price data (which, by the way INCLUDE the cost of the engine to the airframe manufacturer) publish engine and propeller price data only sparingly. The data presented in this appendix were primarily taken from References 55 through 59.

Propulsion system prices are affected by:

* Uninstalled engine thrust or horsepower
* Turbine and compressor technology
* Calendar time (if only because of cost escalation)
* Market conditions (demand and competition)
* Manufacturer sales strategies
* Government rules and regulations (Certification requirements, specifications and politics)

Except for the effect of cost escalation, no easy rules for predicting the effect of these factors on propulsion system prices can be given. Since all engine and propeller price data are 'dated' by calendar year, the following equation is suggested to allow for cost escalation:

$$PSP_{19XX} = PSP_{\text{then year}}(CEF_{19XX}/CEF_{\text{then year}}) \qquad \text{(B1)}$$

where: PSP_{19XX} is the desired propulsion system price in 19XX

$PSP_{\text{then year}}$ is the given propulsion system price in 'then year' dollars

CEF is the cost escalation factor obtained from Fig.2.7. The ratio $(CEF_{19XX}/CEF_{\text{then year}})$ is called the CEF-ratio

Equation (B1) may be applied to adjust prices for engines (EP) and/or propellers (PP) from one year to another. Because the price data in References 55 - 59 are in various 'then year' dollars, Equation (B1) was used frequently to adjust price data to 1989 dollars.

IMPORTANT NOTE: In chapters 4 - 7 the symbols used for engine and/or propeller cost to the airframe manufac-

were C_e and C_p respectively. In this appendix, the symbols used for engine and/or propeller price are EP and PP respectively. For practical purposes it is acceptable to assume:

$$EP = C_e \qquad \text{AND:} \qquad PP = C_p \qquad \text{(B2)}$$

The engine and propeller price data in this appendix are organized as follows:

B1 PISTON ENGINE PRICE DATA

B2 TURBOPROP ENGINE PRICE DATA

B3 PROPELLER PRICE DATA

B4 JET ENGINE PRICE DATA

B1 PISTON ENGINE PRICE DATA

Piston engine price data were taken from Ref.55 and adjusted to 1989 dollars with Eqn.(B1). The prices do NOT include the price of the propeller. Price data for propellers are given in Section B3.

Piston engine price data are plotted versus engine shaft horsepower at takeoff (SLS), SHP_{TO_e} in Figure B1. The solid line represents the trend line obtained from a regression analysis on all data points. The trend line does not represent the data very well. To improve this, the horsepower range was split in two ranges:

80 - 200 shp AND: 200 - 500 shp.

Separate correlation lines were determined for each range. From this, the following formulas were derived for 'ballparking' piston engine prices:

For the shaft horsepower range of 80 - 200 shp:

$$EP_{1989} = \text{invlog}\{2.9923 + 0.4536(\log SHP_{TO_e})\} \qquad \text{(B3a)}$$

For the shaft horsepower range of 200 - 500 shp:

$$EP_{1989} = \text{invlog}\{-0.7770 + 2.0917(\log SHP_{TO_e})\} \qquad \text{(B3b)}$$

where: SHP_{TO_e} is the takeoff shaft horsepower per engine at sealevel standard (SLS) conditions.

Do NOT use these equations outside the ranges of shaft horsepower indicated.

B2 TURBOPROP ENGINE PRICE DATA

Price data for turbopropeller engines (NOT including the price of the propeller) were obtained from Refs 55 - 58. These 1975 data were adjusted to 1989 dollars with the help of Eqn.(B1). The data are plotted in Figure B2. A trend line was determined with a regression analysis. The trend line is seen to represent the data very well. This leads to the following equation for 'ballparking' turbopropeller engine prices:

$$EP_{1989} = \text{invlog}\{2.5262 + 0.9465(\log SHP_{TO_e})\} \qquad (B4)$$

This equation applies to a shaft horsepower range of 400 to 5,000 shp. It should NOT be used outside that range. For larger engines, Ref.56 suggests the following equations:

$$EP_{1989} = (1.418)(2{,}160{,}000)\{0.4(SF) + 0.600\} \qquad (B5)$$

for $SF > 1.0$ and:

$$EP_{1989} = (1.418)(2{,}160{,}000)\{0.533(SF) + 0.467\} \qquad (B6)$$

for $SF < 1.0$

where: the factor 1.418 is the 1989 to 1980 CEF-ratio

2,160,000 is the 1980 base price in US dollars for a turboprop engine with 20,424 shp

SF is an engine shp scale factor determined from:

$$SF = SHP_{TO_e}/20{,}424 \qquad (B7)$$

NOTE: the price data in this Section INCLUDE the engine gearbox, but NOT the propeller.

B3 PROPELLER PRICE DATA

Price data for propellers were obtained from Refer-

ences 56 through 59 and adjusted to 1989 dollars. The data are plotted in Figure B3. It is seen that there are not enough data points to establish the effect of number of blades on propeller cost. A trend line was drawn by performing a regression analysis on all METAL propeller data. This line has the following equation which may be used to 'ballpark' METAL propeller prices:

$$PP_{1989} = \text{invlog}\{0.6119 + 1.1432(\log SHP_{TO_e})\} \qquad (B8)$$

For COMPOSITE propellers the following equation may be used:

$$PP_{1989} = \text{invlog}\{0.7746 + 1.1432(\log SHP_{TO_e})\} \qquad (B9)$$

These equations should NOT be used outside a range of 100 - 20,000 shp.

B4 JET ENGINE PRICE DATA

Jet engine price data were taken from Ref.55 and plotted versus maximum sealevel static thrust, T_{TO_e} in Figure B4. The data do NOT indicate a systematically higher price for turbofans than for turbojets. That is why only one regression analysis was performed, resulting in the solid line in Figure B4. The data straddle the trend line within a +/- 20 percent band. Using Eqn.(B1) to correct the jet engine price data from 1975 to 1989, the line labelled 'suggested for 1989' was obtained. The equation which represents this line is:

$$EP_{1989} = \text{invlog}\{2.3044 + 0.8858(\log T_{TO_e})\} \qquad (B10)$$

This equation may be used to 'ballpark' new engine prices. It should NOT be used outside the takeoff thrust range of 1,000 to 50,000 lbs per engine.

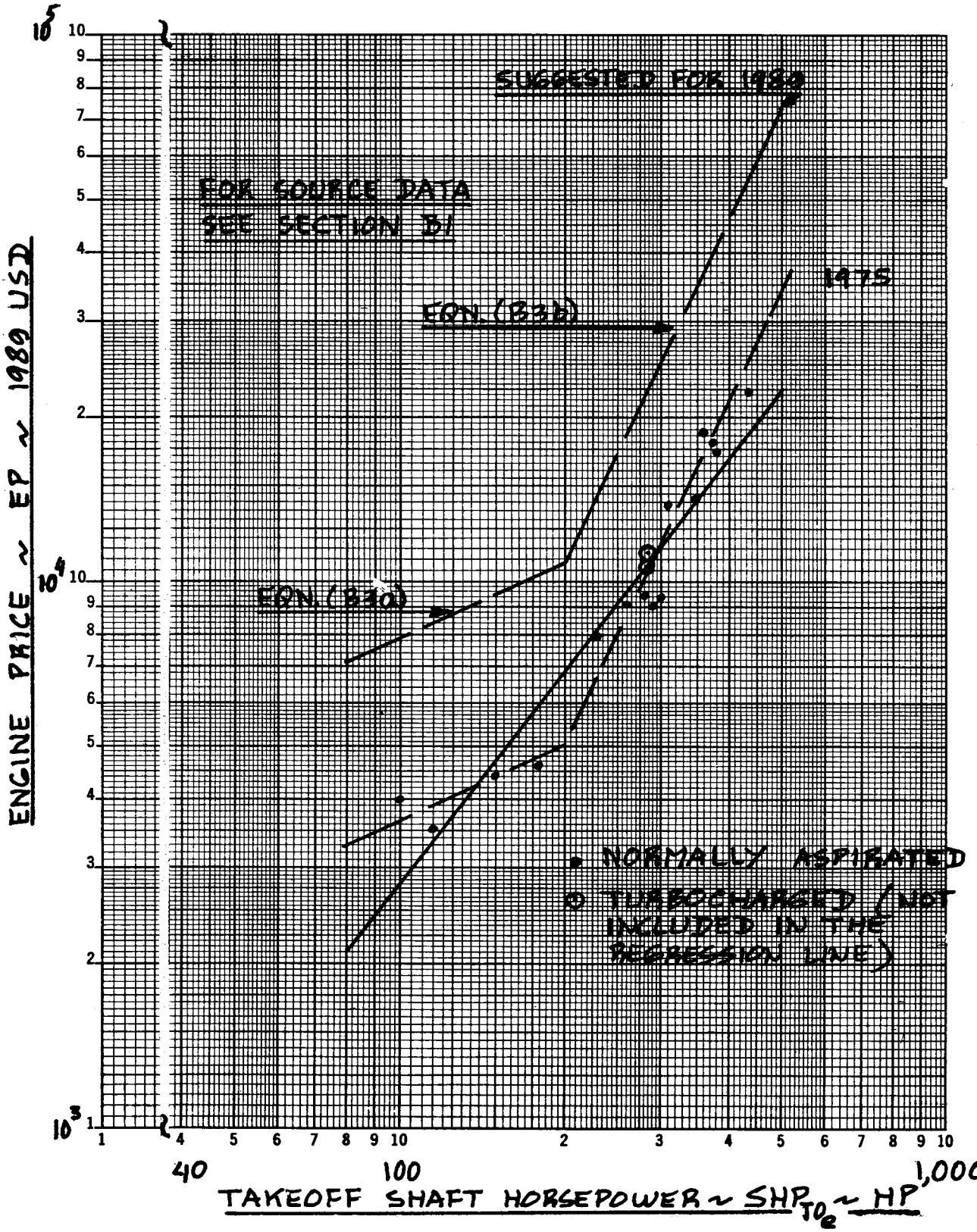

Figure B1 Effect of Shaft Horse Power on the Price of Piston Engines

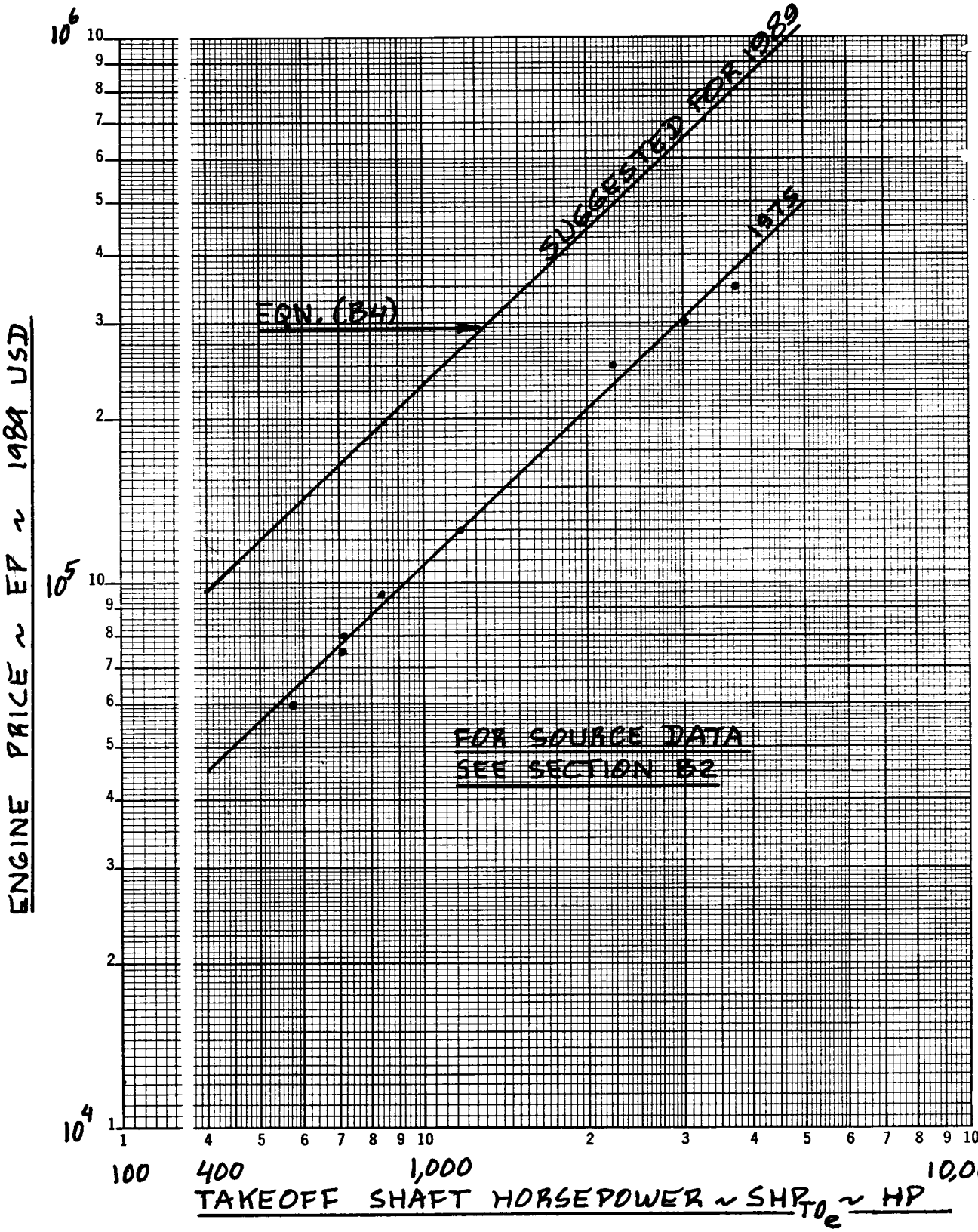

Figure B2 Effect of Shaft Horse Power on the Price of Turboprop Engines

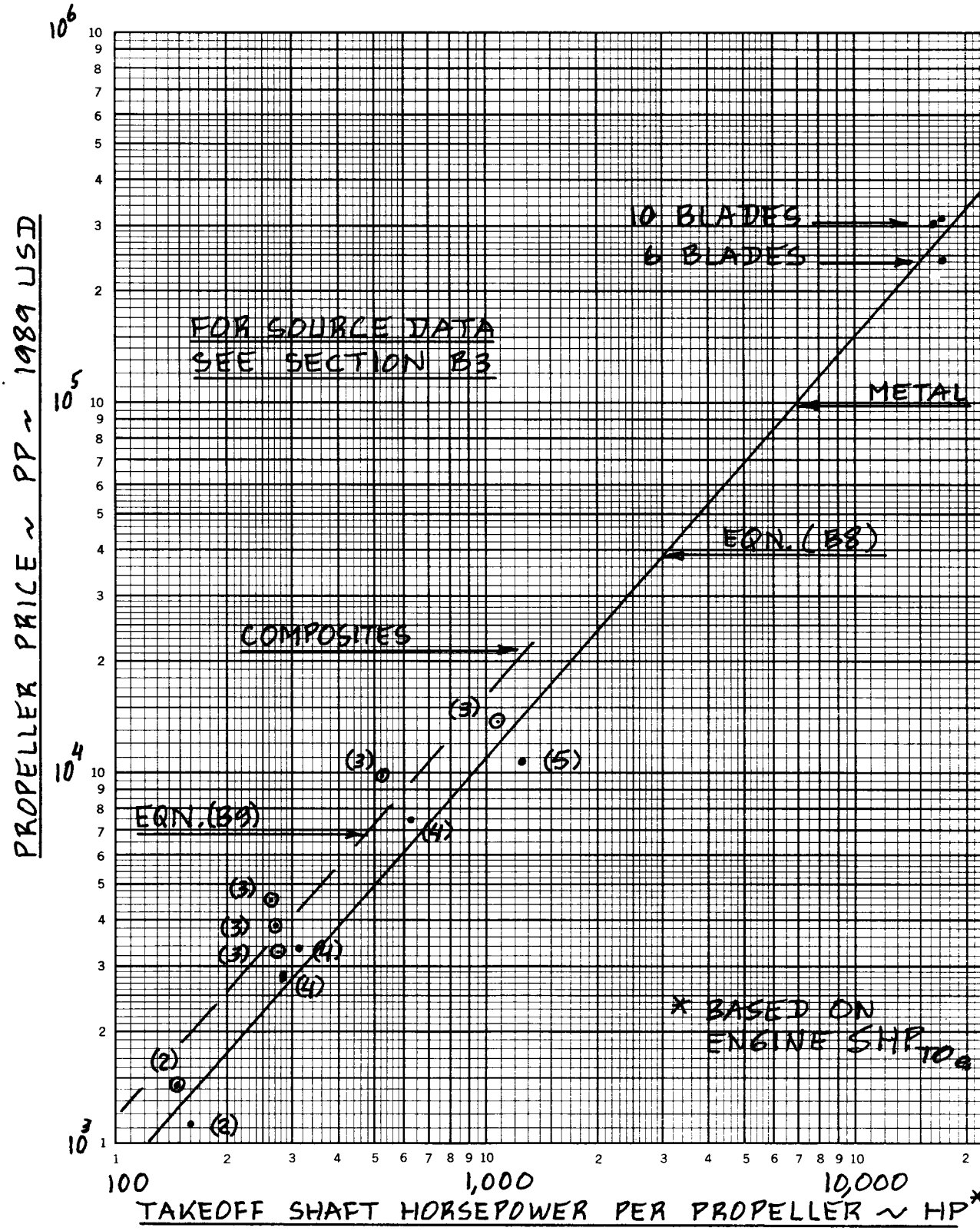

Figure B3 Effect of Shaft Horse Power on the Price of Propellers

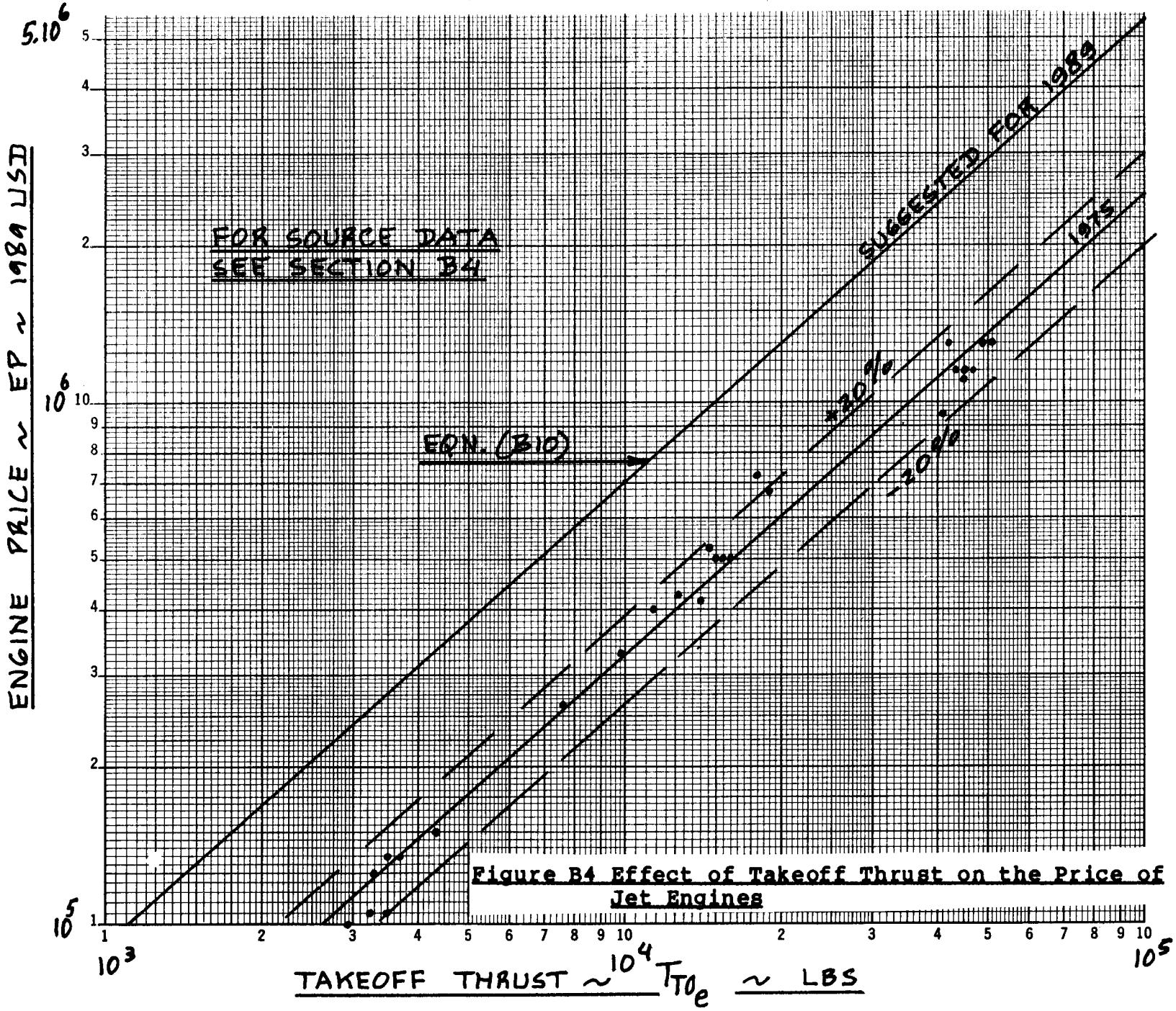

Figure B4 Effect of Takeoff Thrust on the Price of Jet Engines

APPENDIX C AVIONICS SYSTEMS PRICE DATA

The purpose of this appendix is to provide price data for airplane avionics systems.

The material is organized as follows:

C1 COMMERCIAL AVIONICS SYSTEMS PRICE DATA

C2 MILITARY AVIONICS SYSTEMS PRICE DATA

C1 COMMERCIAL AVIONICS SYSTEMS PRICE DATA

The author is grateful to Business and Commercial Aviation Magazine for their permission to copy the Avionics Section of the 1989 Planning and Purchasing Handbook. The material presented in this Section is an exact copy of the following pages of the May 1989 issue of Business and Commercial Aviation: pages 151, 152, 154, 156, 158, 160, 161, 162, 164, 166, 168, 170, 172, 174, 176, 178 and 182 through 202. These pages appear here as pages 330 through 366.

The reader should realize that any price data will vary with time and with marketing strategies of manufacturers. Whenever possible, actual and recent price data should be used. Lacking such information, the price of any avionics system listed in this appendix for 'then years' other than 1989 may be estimated from:

$$(\text{Avionics System Price})_{\text{then year}} = \qquad \text{(C1)}$$

$$= (\text{Avionics System Price})_{1989}(\text{CEF}_{\text{then year}}/\text{CEF}_{1989})$$

where: $(\text{Avionics System Price})_{1989}$ may be found from the data in pp. 330 - 366.

CEF is the cost-escalation-factor of Figure 2.7 in Chapter 2.

IMPORTANT NOTE: The symbol used for total avionics cost in Chapters 4 - 7 is: $C_{avionics}$. This cost is intended to be the SUM of the individual avionics system prices obtained from this section.

INTRODUCTION 1989 AVIONICS

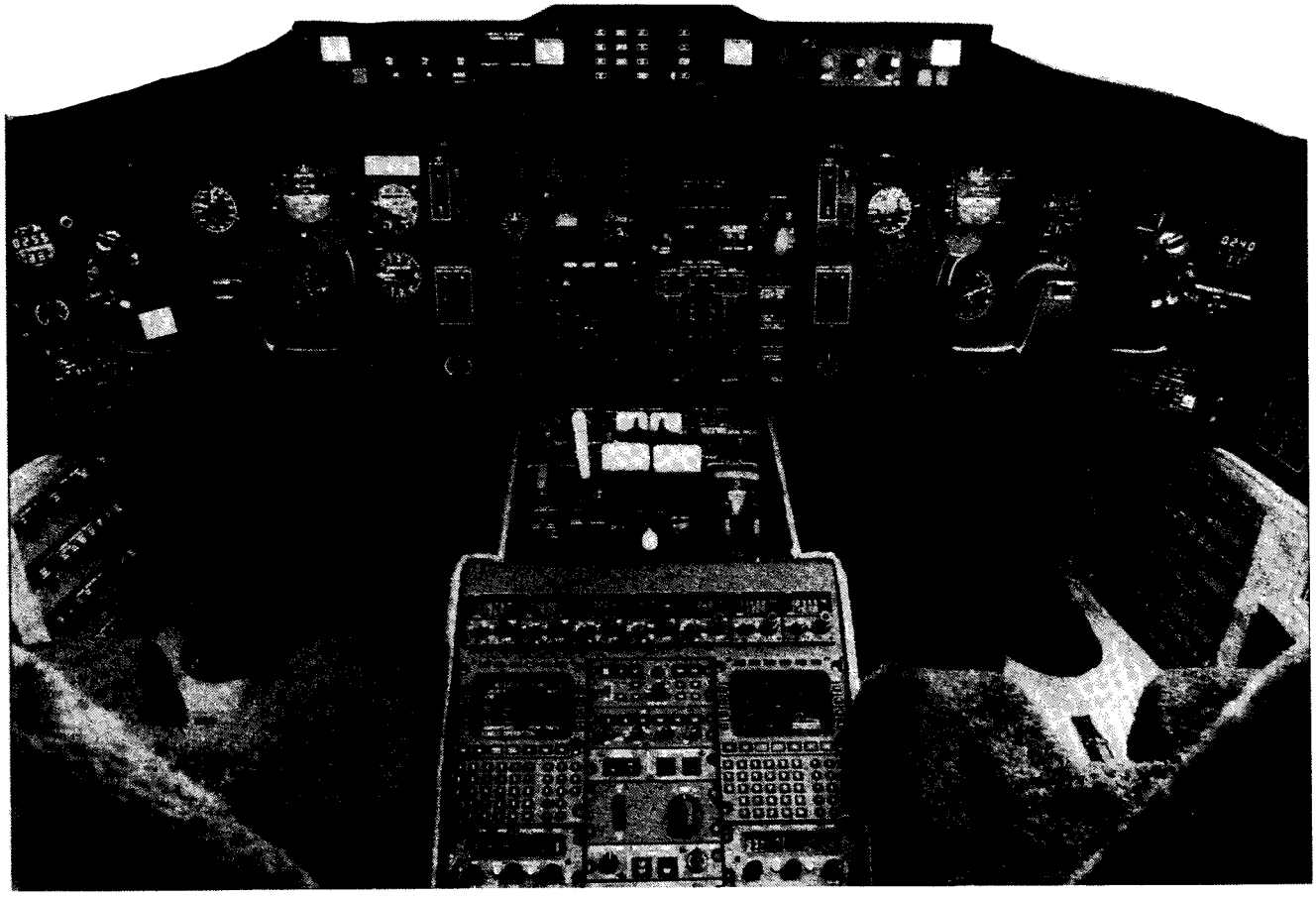

Canadair's Challenger 601-3A cockpit utilizes quiet/dark design principles.

Business aircraft operators will remember the last decade of the 20th century as being the period during which digital avionics became dominant on business aircraft. Looking at the array of digital equipment in today's business aircraft, it's hard to remember that little over a decade ago, digital comm/nav/pulse radios were just being introduced. Electronic flight instrument systems (EFIS) were rarely seen in business aircraft prior to the mid-1980s. The proliferation of navigation management systems (NMS) is an even more recent phenomenon.

Integration is the single most prominent development in digital avionics today. The big three avionics houses—Bendix/King, Honeywell and Rockwell/Collins—are placing great emphasis on integrated avionics packages. For example, comprehensive Bendix/King or Honeywell installations may include EFIS, NMS, digital air data computers, comm/nav/pulse radios and weather avoidance radar—all manufactured by one company. Rockwell/Collins packages feature virtually the same broad line-up of equipment except that the firm relies on outside manufacturers for NMS such as Universal Navigation Corporation.

In late 1988, Collins announced its Pro Line 4 fully integrated avionics system that upped the ante for all competitors (see *EFIS* elsewhere in this B/CA *Planning and Purchasing Handbook*). This brand-new design features EFIS, an engine instrument and crew alerting system (EICAS) and cockpit control display units (CDUs)—all branching out from a central computer that constitutes the heart of the system. Left- and right-side navigation computer modules, radios, sensors and data concentrators are all contained in just one remote-mount computer, greatly reducing the volume, weight and number of components in the avionics bay.

Pro Line 4 accelerates the acceptance of Arinc 429 as the digital interface of choice in business aircraft. Other digital and analog interface formats will persist for many years, owing to preferences of individual avionics manufacturers, but Arinc 429 (or possibly GAMA 429) is becoming about as commonplace as the RS 232 serial digital interface used by desktop computers.

Multi-sensor NMS have all but squeezed out single-sensor navigation

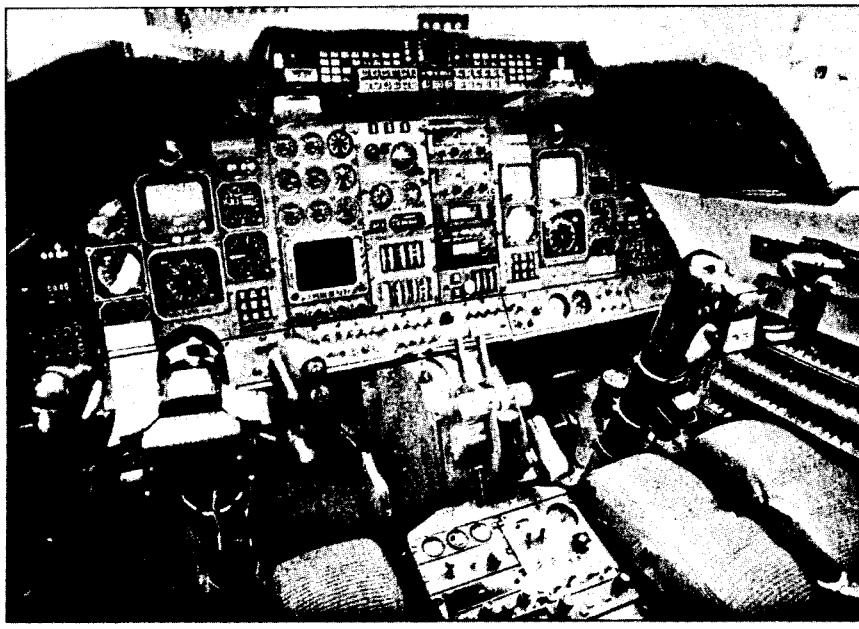

The Learjet 55's flight deck boasts an impressive array of standard avionics including five-tube Collins EFIS, Bendix/King HF, Universal UNS-1 navigation management system with VLF/Omega sensor, SELCAL and a Global Wulfsberg Flitefone VI. Digital avionic designs are becoming increasingly prevalent.

systems in the more sophisticated business aircraft. Multi-sensor NMS units are able to take advantage of reliable and accurate short-range DME and VOR signals when in line-of-sight reception range of ground stations. Some systems, such as the Foster LNS 616B, are capable of using UHF TACAN bearing and distance information, thereby escaping the radial scalloping signal distortion associated with some VOR signals.

NMS provide exceptional flexibility in the choice of long-range nav sensors. Some aircraft operators may need Omega/VLF receivers for extended over-water operations. Others may opt for Loran-C sensors, a popular choice for continental U.S. operations. For frequent international operations, it's hard to beat the current generation of laser inertial reference sensors that have achieved drift rates well under the one-nautical-mile-per-hour variation design criteria.

While the launch of Navstar global positioning satellites has resumed (there were eight of a planned 21 satellites in orbit at press time), the cost of putting operational and spare satellites into orbit could be a hot topic on Capitol Hill with today's emphasis on federal budget deficit reduction. If funding constraints delay the launch of additional GPS vehicles, multi-sensor NMS designers may be forced to look at inter-operable multi-sensor technology.

An inter-operable system is quite different from an NMS that simply uses inputs from several independent long-range navigation sensors. Such a system actually combines inputs from many sources to compute the aircraft's position. For example, GPS might be used for an extremely accurate time check. One line of position might be computed from signals received from Omega or VLF stations, while a second line of position might be obtained from a pair of Loran-C transmitters. And eventually all Loran-C stations may be synchronized, permitting a Loran-C receiver to plot lines of position from any two stations in any GRI chain—without the need to receive the master station.

As for ease-of-use features, virtually all long-range and nav management systems now come equipped with comprehensive databases. Operators can expect to find airports and navaids stored in almost all of these systems, with the better units having intersections and even arrival and departure procedures.

Most manufacturers now are making database updating easy. Rather than pulling a unit out of the avionics bay or changing internal components, such as programmable read-only memory chips, many systems may be equipped with optional diskette data-loaders. One innovative approach to updating is the use of database cartridges so compact that they easily fit into a shirt pocket.

Panel-mounted Loran-C receivers will be found in the flight decks of many business aircraft for which nav management systems represent too large an investment; however, the number of active manufacturers of such systems may stabilize at about a half-dozen strong firms.

Manufacturers' top of the line systems such as ARNAV Systems' R-50, Foster Airdata Systems' F4 Phoenix, Northstar's M1 and II-Morrow's 618 SuperBandit, have airport, navaid and special-use airspace databases. Most of these units are certified for VFR operations only, except for the IFR-certified Foster F4 Phoenix. Bendix/King will enter the panel-mount Loran-C market later this year when the firm introduces its cross-chain, IFR-certifiable unit. This innovative product should prove highly capable for a panel-mount Loran-C receiver because of its reception range, its impressive database and its wide selection of features. But don't anticipate existing Loran-C manufacturers to stand still in the face of this new competitor.

By the year's end, we also anticipate that at least one manufacturer will announce a panel-mount NMS, complete with a short-range VOR/DME navigation capability as well as an internal Loran-C receiver. It is not unreasonable to conclude that a GPS sensor will find a home in compact, panel-mount nav systems in the future, right alongside the internal Loran-C sensor.

We also can look forward to the expanded use of EFIS in business aircraft because of the variety and sophistication of information that can be displayed on a single tube. In addition, reversion modes reduce the odds of being grounded by a single tube or component failure.

Growing in importance is the increasing time and cost associated with repairing aging electro-mechanical instruments. The reliability of EFIS units has increased substantially in the last several years, reducing the overall cost of ownership to a level that is becoming competitive with

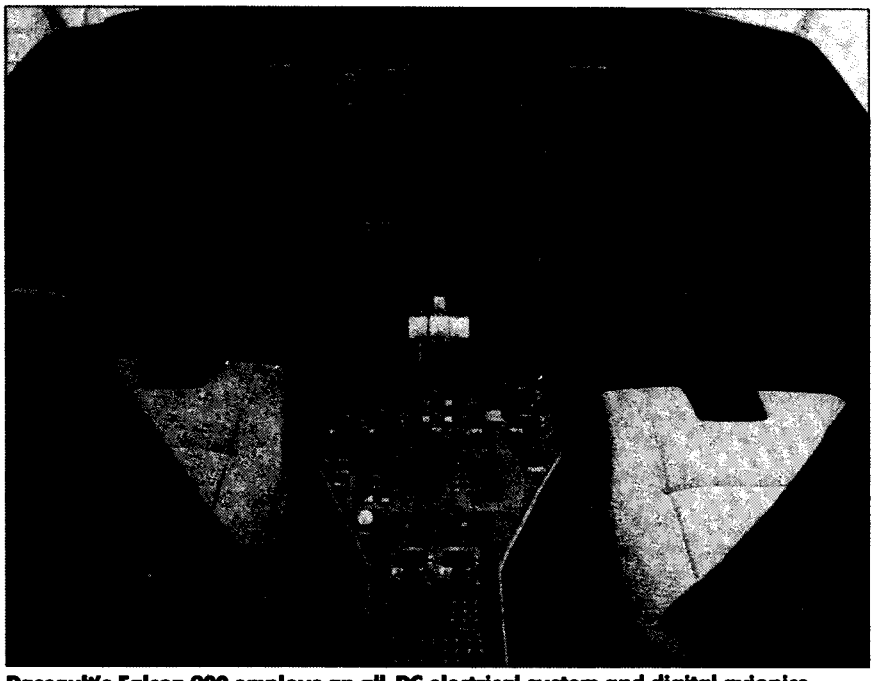

Dassault's Falcon 900 employs an all-DC electrical system and digital avionics throughout its spacious cockpit. Honeywell furnishes the aircraft's radar, dual laser IRSes, EFIS and dual Flight management systems. Collins Pro Line II Navcomm is standard on the aircraft.

conventional "clocks and dials." In recent years, we've witnessed a great deal of research and development activity, accompanied by subtle but effective publicity, regarding flat panel displays. However, we will need to wait beyond 1989 before seeing flat panel displays offered for business aviation.

The trend in EFIS is toward parts commonality. The number and variety of displays, instruments, dials and annunciators is declining in instrument panels. This decline is accompanied by a reduction in shop spares. Ultimately, fleet operators that have equipped all their various aircraft with the same brand of EFIS/EICAS may find their parts shelves bare of all flight and engine instruments, plus annunciators, save one common replacement display tube and maybe one spare generic symbol generator.

TCAS, the traffic alert and collision avoidance system that has been mandated for the air carriers and air taxi operators of larger aircraft, continues to be a popular topic discussed by business aircraft operators. Many industry officials believe that such operators would quickly purchase TCAS units if they were certified and in dealer inventory.

Legitimate concern exists on the part of some observers that active TCAS installed on host aircraft may overload the reply capacity of the conventional ATCRBS transponders on intruder aircraft. Such a limitation may heighten the need for development of passive collision avoidance systems, such as Avion Systems' Sentinel II (B/CA, March 1989, page 49).

Nevertheless, there is little doubt that any future derivative collision avoidance system will rely on conventional transponders as the key cooperative avionics unit needed to identify intruder aircraft.

The arrival of active TCAS is putting pressure on Mode S transponder development. Mode S transponders are used by TCAS systems in two approaching host aircraft to coordinate traffic avoidance maneuvers.

Activity associated with microwave landing systems (MLS) continues to be decidedly flat as a result of the stalemate between the FAA and its MLS ground station supplier, Hazeltine. Delivery delays, cost overruns and organizational problems have plagued the MLS program for more than three years and many business aircraft operators simply have lost interest in buying MLS avionics.

But, it should be noted that the Europeans are going ahead with their

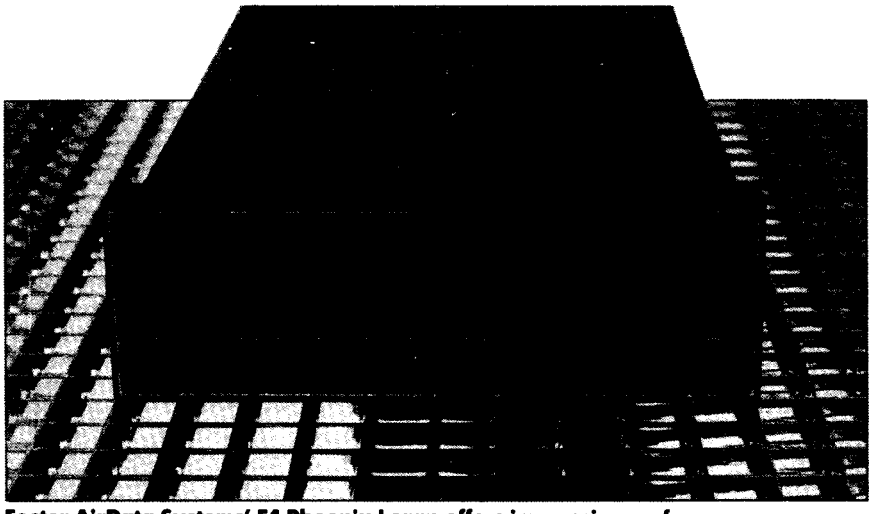

Foster AirData Systems' F4 Phoenix Loran offers impressive performance, operating features, all-lighting readability and relatively low-cost.

MLS installation plans. On the Continent, MLS deployment is being mandated by the success of commercial FM broadcasters that are legally climbing up the frequency band into the lower end of frequencies formerly allocated to ILS localizers. Also, the rock-solid, stable signal characteristics of MLS represent a genuine improvement compared to ILS at airports subject to terrain interference or ground-plane variations caused by snow drifts or tidal changes.

In the United States, MLS deployment is likely to occur first at military and federal government airports plus a few private installations. Because of these developments, business aircraft owners that operate internationally will find a greater need for MLS avionics in the immediate future than operators that fly within the confines of North America.

The next 12 months will be exciting ones in the avionics market. While it's not likely that a third crew seat will be added to business aircraft, the intelligent functions, decision-making assistance and help in controlling the aircraft provided by today's advanced avionics may just make two pilots think that there's an extra crewmember somewhere in the cockpit.

AVIONICS GLOSSARY

ADF—Automatic direction finder, a navigation receiver providing bearing to a nondirectional beacon.
ADI—Attitude deviation indicator.
AHRS—Attitude-heading reference system, a sensor deriving aircraft attitude from a strapdown gyro or other position sensor, accelerometers, and heading from a flux valve; replaces the conventional gyro set.
Air Data—Values computed from pitot, static and temperature measurements, usually by means of a digital computer; Arinc 575 defines outputs.
AM—Amplitude modulation.
AOA—Angle of attack.
Arinc—Acronym for Aeronautical Radio, Incorporated, a nonprofit corporation owned by member airlines to define form, fit and function of avionics equipment and to provide radio communication services.
Arinc 419—A compendium of digital information transfer characteristics as applied in Arinc 500-series equipment specifications.
Arinc 429—A standard for broadcast digital information transfer systems for general applications.
Arinc 561—Inertial navigation system specifications.
Arinc 571—Inertial sensor attitude-heading reference system specifications.
Arinc 575—Digital air-data system specifications.
Arinc 600-series—Equipment specifications.
Arinc 700-series—All digital equipment specifications for new-generation transport category aircraft.
ASCB—Avionics Standard Communication Bus, a digital electronic bus developed by Sperry that provides bidirectional "broadcasting" of data between aircraft systems by means of a "ring network"; similar to, but slower than the MIL-S 1553 network.
ATI and ATR—Arinc form factors (see "Arinc Form Factor" chart).
BCD—Binary coded decimal.
Beam Width—The included angle of a weather radar interrogation signal as defined by the antenna characteristic.
BRG—Bearing.
CDI—Course deviation indicator.
CDP—Counter-drum-pointer, a type of altimeter display that uses a combination of a rotating drum with numerals and a pointer.
CDU—Control-display unit.
Coherent Detection—A technique used in certain ADF receivers to improve useful range by providing better definition of weak signals.
Composite Video—Analog VOR receiver output before processing.
Contact Digitizer—A mechanical device that converts analog information to digital codes by means of electrical contacts.
CRT—Cathode ray tube, similar to a "TV" picture tube.
CW—Continuous wave, a radio carrier broadcast that does not have modulation.
DA—Drift angle.
DG—Directional gyro.
DH—Decision height.
Digitizer—Any electronic device capable of converting information to a digital format; usually refers to encoding devices that convert sensed altitude into a transponder code.
DR—Dead reckoning.
DTK—Desired track.
Duplex—Separate channels for transmission and receiving.
E- (as a prefix)—Used with "ADI"or "HSI," to designate an electronic display using a CRT.
EAROM—Electrically alterable read-only memory, a type of digital memory device.
ECDI—Electronic course deviation indicator.
EFIS—Electronic flight instrumentation system.
EEPROM—Electrically erasable programmable read-only-memory.
Gas discharge—A type of luminescent digital display, usually seven-segment and driven by a high-voltage source; characterized by low heat generation.
FM—Frequency modulation.
GCR—Ground clutter rejection.

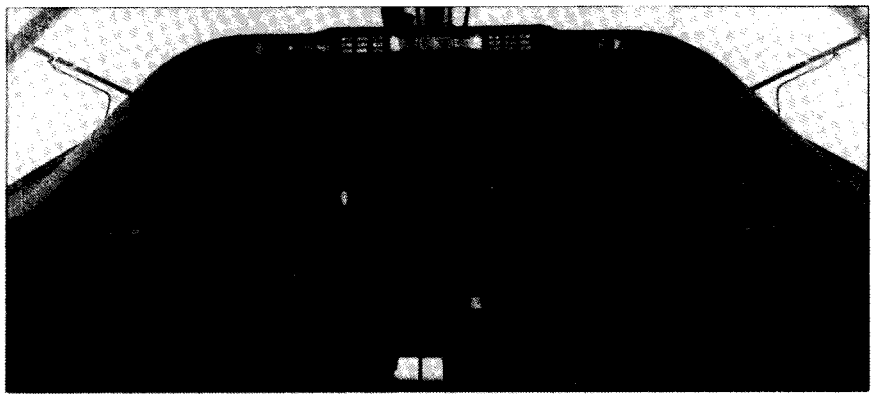

The Beechjet 400 cockpit will be the first to be equipped with Collins Pro Line 4 EFIS, an advanced integrated display system that could grow into an all-glass panel.

GMT—Greenwich Mean Time, used in navigation systems.
GS—Groundspeed.
Hot Wire—Any method for providing some continuous electrical power to a memory device from the airplane's primary battery.
HSI—Horizontal situation indicator.
Hz or Hertz—Cycles per second, used to describe radio frequencies; usually with the prefix *k* for kilo (thousands) or*M* for mega (millions).
ILS—Instrument landing system, a precision approach system using a localizer, glideslope, an outer marker beacon, middle marker beacon and approach lights.
INS/IRS—Inertial navigation system/inertial reference system.
ITU—International Telephone Union, refers to certain HF channels.
Laser IRS—An inertial reference system deriving angular rate information by measuring doppler shift between two contra-rotating light beams.
LCD or LC—Liquid crystal display.
LED—Light-emitting diode.
LOC—Localizer, the course guidance component of an ILS.
Looks per minute—Scanning or sweep rate of a weather radar antenna.
Loran-C—Hyperbolic grid navigation system that is based upon measured time differences (TD) from pulse transmissions.
Mid-Continent Gap—A lapse in Loran-C signal coverage roughly spanning the United States and Canada, east of the Rocky Mountains and west of the Mississippi River.
MFD—Multifunction display, the "third or fifth tube" in an EFIS, replaces the weather radar and displays radar data, navigation maps, checklists, and other information.
MS—Military specifications, which define the size of a standard three-inch instrument panel cutout for such mechanical displays as altimeters and airspeed indicators.
N/A—Not applicable.
NDB—Nondirectional beacon.
NMS—Navigation management system.
Nonvolatile—Describes a digital memory that retains information through system shutdown.
Omega—A very-low-frequency navigation system.
Optical Digitizer—Any device using a photosensor to read a light beam through slots or cutouts and thereby to convert analog information to digital codes.
Peak power output—The maximum transmitter power output measured over a very short time period; usually used to rate pulse transmissions.
PEP—Peak envelope power, a standard electronic rating of any AC source, including a radio transmitter.
Pulse—A transmission of very brief duration used to carry information by using time measurement or as a series of pulses representing code.
RA—Radio altitude.
RAM—Random access memory.
RMI—Radio magnetic indicator.
RMS—Root mean square.
RNAV—Area navigation.
ROM—Read-only memory.
RS-232—A serial digital format used in data transmission.
RT—Receiver-transmitter combined in a single line-replaceable unit.
SAR—Search and rescue, usually pertaining to weather radars and navigation systems.
SI—Slip indicator or inclinometer, usually a ball within a tube containing fluid.
Simplex—Single frequency for both transmitting and receiving in communications; generally implies a push-to-talk function and verbal procedures.
Slaving Rate—The rate, in degrees per minute, a compass system can adjust for gyro precession; a "fast-slave" mode is used to align a compass system when first turned on.
SSB—Single sideband, a highly efficient form of radio transmission wherein information is carried on a sideband instead of the center carrier in order to gain range performance; usually used in HF communication transceivers.
STC—(1) Sensitivity-time compensation, in weather radar a technique and circuit for calibrating a display; (2) supplemental type certificate.
Synchro—Any device capable of converting mechanical position into an (analog) electronic signal.
Synthesizer—Frequency synthesizer, an electronic circuit capable of generating multiple frequencies from a single crystal oscillator.
TAS—True airspeed.
TD—Time difference, in Loran-C navigation measurements.
3P—Three-pointer altimeter display.
TKE—Track error.
TRK—Track, or path over the ground.
TSO—Technical standard order, a performance specification and production compliance criteria applied to avionics and defined by FARs and the Radio Technical Commission for Aeronautics.
TTG, TTS or TTW—Time to go, time to station, time to waypoint.
Turbulence Mode—Flight control system mode in which a "softer" response to gust upsets is programmed.
2 X 5—Two-out-of-five, an electronic radio tuning code.
USB—Upper sideband.
VAC—Volts alternating current.
VDC—Volts direct current.
VLF—Very low frequency, refers to Navy VLF transmissions used in long-range navigation systems in combination with Omega.
VNAV—Vertical navigation, or the capability to compute pitch-axis maneuvers and altitude-related points in space.
VOR—Very high frequency omni range.
X-band—Frequency range in which most general aviation weather radars operate.
XTK—Cross track; cross track error.

ARINC FORM FACTOR

The standard air transport radio (ATR) case is shown with all optional projections included. Volumes are given, except for the forward-facing projections called "doghouses."

Not shown on this chart is the short, low-profile (SLP) case used in the Collins Pro Line. All Pro Line remote units are about 3.25 inches high and 14 inches long and vary in width.

Panel-mounted avionics are built to the "mark width," which is about 6.25 inches. Widths will vary beyond the 6.25 inches because of flanges that extend beyond the radio mounting tray.

In the avionics tables, a case size is shown as 2 ATI, 3 ATI, up through 4 ATI. Arinc 600 conversion factors: As a rule of thumb, divide Minimum Configuration Units (MCU) by eight for ATR size:

1 MCU = 1/8 ATR*
2 MCU = 1/4 ATR
3 MCU = 3/8 ATR
4 MCU = 1/2 ATR
5 MCU = 5/8 ATR*
6 MCU = 3/4 ATR
7 MCU = 7/8 ATR*
8 MCU = 1 ATR

AIR TRANSPORT INDICATOR (ATI) CASE SIZES

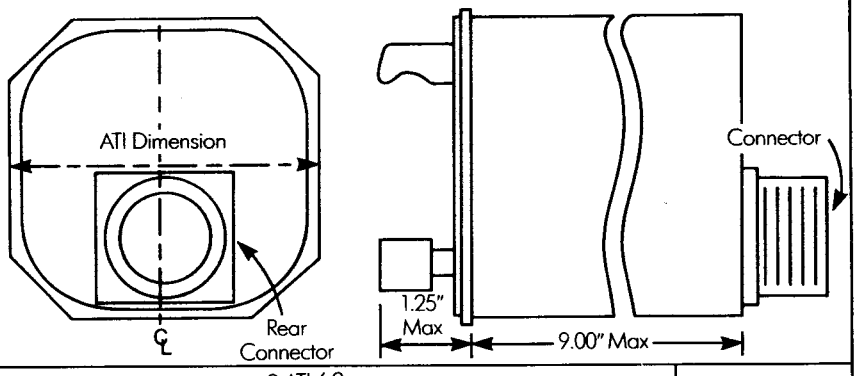

3 ATI 6.2				
Case Size Nominal	Case Size Actual	Air Transport Indicator	Length	Max Weight (lb)
2	2.175"		Expressed to nearest 10th of an inch.	3
3	3.175"			5
4	3.975"			9
5	4.975"			14
6	5.975"			20

STANDARD ATR CASE DIMENSIONS

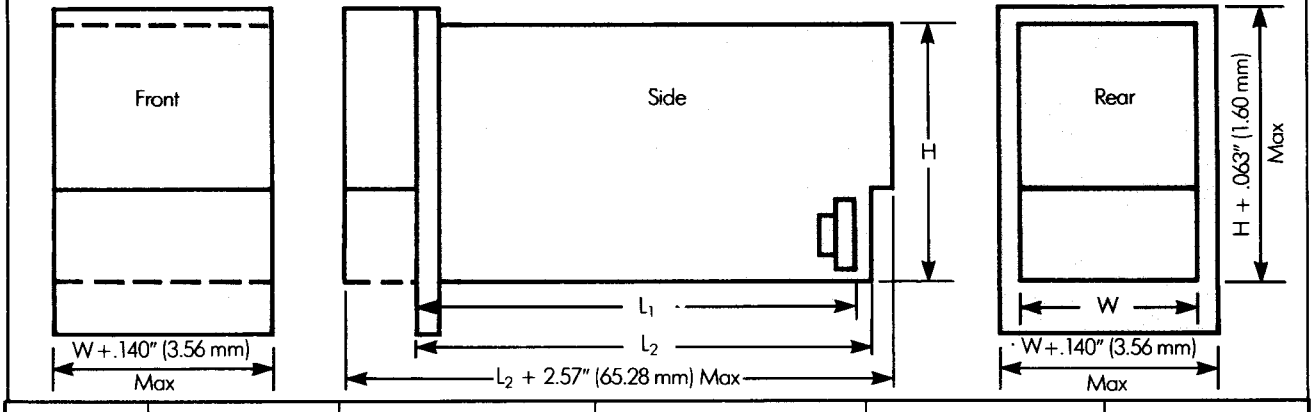

ATR Size	Approx. Vol.		W		L_1		L_2 (Max)		H (Max)	
	In^3	Liter	±.03 In	±.76 mm	±.04 In	±1.0 mm	In	mm	In	mm
Dwarf	95	1.56	2.25	57.15	12.52	318.0	12.62	320.5	3.38	85.8
¼ Short	215	3.52	2.25	57.15	12.52	318.0	12.62	320.5	7.62	193.5
¼ Long	335	5.49	2.25	57.15	19.52	495.8	19.62	498.3	7.62	193.5
⅜ Short	340	5.57	3.56	90.41	12.52	318.0	12.62	320.5	7.62	193.5
⅜ Long	530	8.69	3.56	90.41	19.52	495.8	19.62	498.3	7.62	193.5
½ Short	470	7.70	4.88	123.95	12.52	318.0	12.62	320.5	7.62	193.5
½ Long	725	11.88	4.88	123.95	19.52	495.8	19.62	498.3	7.62	193.5
¾ Short	720	11.80	7.50	190.50	12.52	318.0	12.62	320.5	7.62	193.5
¾ Long	1,120	18.36	7.50	190.50	19.52	495.8	19.62	498.3	7.62	193.5
1 Short	975	15.98	10.12	257.05	12.52	318.0	12.62	320.5	7.62	193.5
1 Long	1,510	24.75	10.12	257.05	19.52	495.8	19.62	498.3	7.62	193.5
1½	2,295	37.62	15.38	390.65	19.52	318.0	19.62	498.3	7.62	193.5

B/CA Art Dept.

AUTOMATIC DIRECTION FINDERS

MANUFACTURER	MODEL TSO	MEMORY CAPACITY FREQ. (kHz) DISPLAY	POWER INPUT MEMORY TYPE	UNITS/ WEIGHT (lb) SIZE	PRICE (uninstalled)	REMARKS
Bendix/King Avionics 400 N. Rogers Rd. Olathe, KS 66062 (913) 782-0400	KR 86 none	N/A 200-1750 mechanical	14 or 28 VDC none	2/6.3 6.25 x 2.6 x 9.05	$2,760	Panel-mounted; automatic band switching; self-contained indicator; no RMI capability; KA 42B combined loop-sense antenna available at same price
	KR 87 C41c	2 200-1799 gas discharge	11 to 33 VDC EAROM nonvolatile	3/6.7 6.25 x 1.3 x 11.23	$3,855	Panel-mounted; times flight and approaches; coherent detection; includes slaved KI 227 indicator; KI 228 dual pointer indicator available, KI 229/KNI 582 RMIs available as options
	KDF 806 C41c	2/9* 190-1799 gas discharge	28 VDC EAROM non-volatile	3/7.4 5.0 x 2.0 x 10	$8,935	Digital control head displays both active/standby frequency; coherent detection; flag circuitry; strappable for 2182 kHz, Gables control optional; combined loop-sense antenna included; remote flip-flop optional; *nine-frequency pilot-programmable "A" control head optional; night vision goggle compatible "A"control head optional; two-year warranty
	DFS-43 C41c	2 190-1860* (0.5 kHz) LCD or dichroic	28 VDC non-volatile	3/8.4 4.0 x 4.0 x 12.62	$12,926	ADF left-right steering to HSI; *2182 kHz intl. distress freq std; combined antenna; 0.5 kHz spacing, analog and Arinc 429 interfaces; two-year warranty
Collins Avionics Group Rockwell International 400 Collins Rd. NE Cedar Rapids, IA 52498 (319) 395-4085	ADF-650A C41c	N/A 200-1799 mechanical	14 VDC* none	3/6.0 6.25 x 1.75 x 10.8	$4,425	Panel-mounted; includes ANT-650A combined loop-sense antenna and IND-650A indicator *28 to 14 VDC adapter — $120
	ADF-462 C41d	6 190-1799 gas discharge	28 VDC nonvolatile	3/8.0 ⅜ ATR-SL	$10,105	Built-in diagnostics; compatible only with CSDB or Arinc 429 controls, digital signal processing; 2182 KHz emergency frequency; includes CTL-62 CSDB control and ANT-462A antenna; ANT-462B dual antenna optional
	ADF-60A C41c	2/6 190-1750 (½-kHz steps) gas discharge	28 VDC nonvolatile	3/8.7 ⅜ ATR-SL	$10,630	Remote-mounted; coherent detection; combined loop-sense antenna; dual antenna optional; three-wire or sine/cosine RMI output available; includes CTL-60 electronic control and ANT-60A; optional CTL-62 with CAD-62 adapter provides serial digital tuning and six stored frequencies
	DF-206 C41b	N/A 190-1750 (0.5-kHz steps) none	28 VDC none	6/15.1 ¼ ATR-S	$20,816	Remote-mounted; azimuth card driven by compass system; automatic pointer stow in receive position; coherent detection; includes flush fixed loop and sense antennas, antenna cable, control head, antenna coupler; Arinc 570

AUTOMATIC DIRECTION FINDERS

MANUFACTURER	MODEL TSO	MEMORY CAPACITY FREQ. (kHz) DISPLAY	POWER INPUT MEMORY TYPE	UNITS/ WEIGHT (lb) SIZE	PRICE (uninstalled)	REMARKS
Narco Avionics Inc. P.O. Box 1807 Laguna Beach, CA 92652-1807 (714) 497-5077	ADF 841 C41c	2 200-1799 gas discharge	11-32 VDC hot-wire nonvolatile	3/5.7 6.25 x 1.5 x 11.0	$3,022	Digital ADF with dual-frequency, flip-flop capability; elapsed- and flight-timers; includes combined loop-sense antenna and indicator
Terra Corp. 3250 Pan American Freeway NE Albuquerque, NM 87107 (505) 884-2321	TDF 100 none	N/A 200-1799 mechanical	11 to 33 VDC N/A	3/6.8 3.2 x 1.6 x 11.5	$1,895	

LONG-RANGE NAVIGATION SYSTEMS

MANUFACTURER	MODEL	SYSTEM TYPE DISPLAY	NUMBER WAYPOINTS DATABASE	OUTPUTS	INPUTS	POWER INPUT MEMORY	UNITS/ WEIGHT (lb)	PRICE (uninstalled)	REMARKS
Advanced Navigation, Inc. 61 Thomas Johnson Dr. Frederick, MD 21701 (301) 695-4040	ANI-7000 Sensor	Loran-C sensor only	N/A N/A	Arinc 419/ 429 pos., GS, track, circular error probability computation	N/A	18 to 32 VDC —	2/14.6	$8,640	TSO C60a; software identical to ANI-7000; a Loran-C sensor for use with KNS 660, Tracor 7880 and other navigation management computer systems
	ANI-7000	Loran-C incandescent filament	200 nonvolatile internal battery	Lat/long and all nav data, with four analog steering signals standard; CDI / HSI; autopilot data; ARINC 429, 561, 568; EFIS, RMI, RS-232; GMT clock	HDG, TAS optional for automatic wind calculation	18 to 32 VDC (60 watts) —	3/19.6	$11,448	TSO C60a full continental US airspace IFR-approved including mid-continent area, limited non-precision approach approval AC 90-45A; AC 20-121
ARNAV Systems 16100 SW 72nd Ave. P.O. Box 23939 Portland, OR 97223 (503) 684-1600	R-25	Loran-C LED	1150 nonvolatile RAM	Waypoint alert; CDI; HSI; autopilot; RS-232	FC-10 Fuel computer; manual input of TAS & HDG for wind calculations altitude for VNAV gph, fuel remaining for fuel range	10 to 35 VDC —	2/4.0	$2,495	Plain language alphanumeric display; antenna included

LONG-RANGE NAVIGATION SYSTEMS

MANUFACTURER	MODEL	SYSTEM TYPE / DISPLAY	NUMBER WAYPOINTS / DATABASE	OUTPUTS	INPUTS	POWER INPUT / MEMORY	UNITS/ WEIGHT (lb)	PRICE (uninstalled)	REMARKS
ARNAV Systems 16100 SW 72nd Ave. P.O. Box 23939 Portland, OR 97223 (503) 684-1600	R-50 Database	Loran-C LED	150 nonvolatile RAM	Waypoint alert warnings; PTK & APR annunciator; CDI; HSI; autopilot; RS-232	FC-10 Fuel Computer; manual input of TAS & HDG for wind calculations; altitude for VNAV advisories	10 to 35 VDC —	2/4.0	$3,995	Plain language alphanumeric display; 20 route legs; auto extended range; CDI nav bearing; nearest 6 airports; nearest 6 VORs; TCA Alert
	R-40	Loran-C LED	200 nonvolatile RAM	Waypoint alert warnings; PTK & APR annunciator; CDI; HSI; autopilot; RS-232	None	10 to 35 VDC —	1/4.5	$4,495	Plain language alphanumeric display; 20 route legs; Omni (pseudo VOR) extended range; CDI scaling; TSO C60a
	R-40 Database	Loran-C LED	150 nonvolatile RAM	Waypoint alert warnings; PTK & APR; annunciator; CDI; HSI; autopilot RS-232	Manual input of TAS & HDG for wind calculations altitude for VNAV	10 to 35 VDC —	1/4.5	$4,995	IFR in compliance with AC 20-121; 10,000+ waypoint database with emergency nearest airport search; min. safe altitude; auto extended range; 20 route legs; Omni (pseudo VOR); optional aerial survey configuration (VFR certification); available with grid/nav aerial survey software — no database: $4,745
	R-60 Database	Loran-C LED	200 nonvolatile RAM	Waypoint alert warnings; PTK & APR; annunciator; CDI; HSI; autopilot; RS-232	Manual input of TAS & HDG for wind calculations altitude for VNAV	10 to 35 VDC —	2/7.7	$9,495	Designed specifically for pedestal installations; TAS & winds aloft; VNAV; extended range; 20 route legs; Omni (pseudo VOR); available with grid/nav aerial survey software — VFR configuration without database
AZURE Technology San Jose Jet Center 1250 Aviation Ave. San Jose, CA 95110 (408) 947-2070	Long Ranger F/P	Loran-C fixed panel or portable	99 none	RS-232	None	12 VDC —	2/4.2	$1,095	automatic chainswitching and station management; four flight plans up to 10 waypoints each. Antenna and mounting options avail.
Canadian Marconi 2442 Trenton Ave. Montreal, Quebec, Canada H3P 1Y9 (514) 341-7630	CMA-734 OSS (sensor) Mk II	Omega/VLF —	891 non-volatile RAM	Position, status, stations used, GS	synchro heading, air data (optional)	28 VDC —	2/15.0	$23,833	Arinc 429; optional LCD CDU completes system for back-up long-range nav capability; TSO C94; three-year warranty
	CMA-764 OSS (sensor)	Omega/VLF —	891 non-volatile RAM	position, status, station used, GS	Arinc 429, heading air data	28 VDC —	2/8.7	$23,962	Optionall LCD CDU completes system for back-up long-range nav capability; TSO C94; three-year warranty

LONG-RANGE NAVIGATION SYSTEMS

MANUFACTURER	MODEL	SYSTEM TYPE / DISPLAY	NUMBER WAYPOINTS / DATABASE	OUTPUTS	INPUTS	POWER INPUT / MEMORY	UNITS/ WEIGHT (lb)	PRICE (uninstalled)	REMARKS
Canadian Marconi 2442 Trenton Ave. Montreal, Quebec, Canada H3P 1Y9 (514) 341-7630	CMA-734 "Arrow" Mk II	Omega/VLF liquid crystal	891 non-volatile RAM	Pos, steering, nav data, HSI, autopilot	synchro, heading, TAS	28 VDC —	3/17.2	$27,250	Lightweight system, tracks three Omega and one VLF frequency; TSO C94; three-year warranty
	CMA-734 Alpha Mk II	Omega/VLF incan-descent filament	4,000 non-volatile RAM	Position, steering, nav data, HSI, autopilot	synchro, heading, TAS	28 VDC —	3/20.0	$37,507	CMA-734 with alphanumeric CDU; three-year warranty
	CMA-771 Alpha Mk III	Omega/VLF incan-descent filament	4,000 non-volatile RAM	Pos, steering, nav data, HSI, autopilot, digital	synchro, heading, TAS	115 VAC, 400 Hz —	3/33.0	$54,207	Standard CMA-771 but with alphanumeric CDU; optional HSI synchro outputs; Arinc 599 analog, Arinc 429 digital interfaces; compatible with Global-Wulfsberg NDB-2; three-year warranty
Foster Airdata Systems, Inc. 7020 Huntley Rd. Columbus, OH 43229 (614) 888-9502	LRN 500	Loran-C LCD	234 non-volatile RAM	L6R-3, 1K ohm loads; T/F-2, 200 ohm loads; Flag-3, low-level 1K ohm loads; parallel track and WPT alert annun-ciation	none	10 to 32 VDC —	1/3.1	$1,695	TSO C60a; IFR — AC 20-121; includes panel unit, 5,400 waypoint pilot-changeable database cartridge, antenna and preamp; VNAV advisories, nearby airport locater; "Demo Mode" allows removal from aircraft; carrying case $50
	F-4 Phoenix	Loran-C LED dot matrix	234 nonvolatile RAM	see LRN 500	none	10 to 32 VDC —	1/3.1	$2,595	See LRN 500
	LNS 616B	Loran C/ auto Tacan LED	400 non-volatile RAM	HSI, EFIS, RS-232, Arinc 561, RMI, RS-232 Tacan channeling	VOR composite, Arinc 568, Foster serial	18 to 32 VDC —	3/12.75	$22,800	TSO C60a; provides channeling to Foster DME 670 for automatic navigation; includes NY-153 antenna; optional DME-670 $11,900
Global Systems 2144 Michelson Dr. Irvine, CA 92715 (714) 851-0119	GNS-500A Series 4A	VLF/ Omega CRT	127 NDB-2 interface	Arinc 561 and 571 to EFIS; radar; INS; including Pos; TK; DTK; DA; GS; TTW; flight plan waypoints wind; dist. mag. var.	Heading; TAS; Arinc 571; Pos from INS; EFIS; radar; Arinc 561; joystick from EFIS; AFIS performance data	28 VDC at 7.5 amp —	3/39.0	$64,025	GPS compatible; stores 127 waypoints defined by five letters, nine flight plans up to 20 waypoints each; digital datalink with AFIS; sunlight readable, full-alphanumeric CRT CDU; Interfaces with FD, EFIS and autopilots; auto GMT and date; active flight plan capacity 50 waypoints; GNS 500A Series 1 - 3 may be converted to Series 4 configuration

LONG-RANGE NAVIGATION SYSTEMS

MANUFACTURER	MODEL	SYSTEM TYPE / DISPLAY	NUMBER WAYPOINTS / DATABASE	OUTPUTS	INPUTS	POWER INPUT / MEMORY	UNITS/ WEIGHT (lb)	PRICE (uninstalled)	REMARKS
Global Systems 2144 Michelson Dr. Irvine, Ca. 92715 (714) 851-0119	GNS-500A Series 4M special mission navigation system	VLF/ Omega CRT	127 NDB-2 interface	Arinc 561 and 571 to EFIS; radar; INS; including Pos; TK; DTK; DA; GS; TTW; flight plan waypoints wind; dist. mag. var.; flight data recorder	Heading; TAS; Arinc 571; Pos from INS; EFIS; radar; Arinc 561; joystick from EFIS; AFIS performance data; forward looking infra-red sensor	28 VDC at 7.5 amp —	3/39.0	$66,525	same capabilities as Series 4A + quick-initialization for scramble launch; special search / surveillance flight patterns; law enforcement, military configuration
Honeywell Inc. P. O. Box 29000 Phoenix, AZ 85039 (602) 863-8000	LASEREF	Laser IRS —	none none	Arinc 429, Arinc 419, Arinc 561 Incl: attitude, heading (mag & true), GS, wind, track, present position	TAS Alt. V. Spd.	115 VAC, 400 Hz or 28 VDC backup —	2/48	$146,742	Price includes installation kit; primarily analog interfaces to flight director (EFIS or EM), autopilot, radar, NMS:GNS-1000, UNS-1, KNS-660; fast align; no pressurization required
	LASEREF II	Laser IRS —	none none	ASCB, Arinc 429, Arinc 419 Incl: attitude, heading (mag & true); GS, wind, track, present, position	TAS Alt V. Spd.	115 VAC, 400 Hz or 28 VDC back-up —	2/48.0	$149,563	Primarily digital interfaces to Honeywell FMS, EFIS, autopilot; fast align; no pressurization required
Internav Box 1261 Sydney, Nova Scotia B1P 6J9 Canada (902) 564-2043	LC1210 (sensor)	Loran-C none	— —	Position	—	12/28 VDC, 20W —	2/10.0	$8,000	Loran-C sensor for navigation computer systems; continuous dual-chain operation; Output/ Control via Arinc 429 (dual input, triple output)
	LC1200	Loran-C vacuum fluorescent	200 nonvolatile RAM and EPROM	Pos; track error; TTW; GS; HSI; wind; digital interface	Heading; TAS, VOR-DME	12/28 VDC, 40W —	3/15.0	$12,000	Continuous dual chain operation, Arinc format CDU; 1,200 programmed waypoint database; multiroute storage, optional VOR/DME back-up mode; five character alphanumeric waypoint identifiers position output for air-ground datalink; D/R mode usable outside Loran signal areas; optional SAR program

LONG-RANGE NAVIGATION SYSTEMS

MANUFACTURER	MODEL	SYSTEM TYPE / DISPLAY	NUMBER WAYPOINTS / DATABASE	OUTPUTS	INPUTS	POWER INPUTS / MEMORY	UNITS/ WEIGHT (lb)	PRICE (uninstalled)	REMARKS
Litton Aero Products 6101 Condor Road Moorpark, CA 93021 (805) 378-2000	LTN-311	VLF/Omega 8-line LED	99 none	Digital pos; track; GS; TTG, HSI; Wind; XTD; TAE; DA; TH	Heading; TAS; ADC valid	115 VAC, 400 Hz —	3/41.0	$44,190	Direct ARINC replacement for LTN-211; integrated GPS optional; ACARS route entry with OAT option; AC/DC noninterruptible P.S.; XTK discrete; Digital Air Data (575/429); std ARINC 599; BITE/STATUS in English language; pre-heated oscillator for rapid start; 1 year warranty
	LTN-211	Omega —	9 none	Pos; track error; TTW; GS; HSI; wind	Heading; TAS	115 VAC, 400 Hz —	3/34.0	$44,580	HSI synchro and digital outputs standard; Arinc 599; optional VLF receiver available; 1 year warranty
	LTN-710	GPS LED matrix	— —	Digital ARINC 429; pos; track; vert track; velocity; acceleration Time (> 100 ns); course steering	Altimeter precise clock	115 VAC, 60-400 Hz —	3/20.0	$50,000	Designed for aerial survey; present position display only; operates over entire range of signal levels; fixed freq. signals; single correlator; two IF freqs.; phase sampler; time accuracy to 900 nanoseconds; operational worldwide; 24 hr. all-weather coverage; pos. accuracy 40 SEP 3-D; 1 year warranty
	LTN-72	INS —	9 none	Pos; track error; TTW; GS; HSI; wind	TAS	115 VAC, 400 Hz 28 VDC back-up —	3/62.0	$172,285	Expandable memory; may be transverse-mounted; standby battery optional; Arinc 561; 1 year warranty
	LTN-92	Laser INS 5-line LED matrix	99 none	Arinc 561 digital & analog Arinc 704 digital	VOR/DME; Tacan; Arinc 429; autopilot; steering; EFIS, PMS; Radar; pos; trk error; TTW; GS; HSI; wind	115 VAC / 400 Hz 28 VDC back-up —	3/63.6	$174,360	Pin for pin replacement for gymbaled-gyro inertial nav systems — Arinc 561 in 1 ATR configuration; accommodates Omega/VLF acceleration advisory or GPS; interfaces with bulk storage units; solid-state design; 3 year warranty
	LTN-72R	INS/ RNAV —	9 none none	Pos; track error; TTW; GS; HSI; wind	TAS; VOR-DME	115 VAC, 400 Hz 28 VDC back-up —	3/62.0	$175,090	Combined INS andvortac-based RNAV; compatible with Global-Wulfsberg NDB-2; meets requirements for enroute, terminal and approach; may be transverse-mounted; standby battery optional; Arinc 561; 1 year warranty

LONG-RANGE NAVIGATION SYSTEMS

MANUFACTURER	MODEL	SYSTEM TYPE / DISPLAY	NUMBER WAYPOINTS / DATABASE	OUTPUTS	INPUTS	POWER INPUTS / MEMORY	UNITS/ WEIGHT (lb)	PRICE (uninstalled)	REMARKS
Litton Aero Products 6101 Condor Road Moorpark, Ca. 93021 (805) 378-2000	LTN-90 -100	Laser IRS sensor	N/A N/A	Arinc 429; Pos; attitude; heading; angular rates; acceler-ations; drift angle; VS; GS; flight path angle, wind track	Arinc 429 air data	115 VAC, 400 Hz 28 VDC back-up —	2/43.0	$190,030	Optional control display unit; primary inertial sensor for navigation management computer systems; complies with Arinc 704 spec for IRS; growth capability to ADIRS; 10 MCU size; for digital applications; 3 year warranty
	LTN-72RL	INS/ RNAV —	99 none	Pos; track error; TTW; GS; HSI; wind	TAS; VOR-DME	115 VAC, 400 Hz 28 VDC back-up —	3/62.0	$192,070	Combined INS and VORTAC-based RNAV; compatible with Global-Wulfsberg NDB-2; meets requirements for enroute, terminal and approach; transverse-mounted; standby battery optional; bulk storage with five-line alphanumeric LED display; Arinc 561; 1 year warranty
	LTN-91	Laser IRS sensor	N/A N/A	Arinc 429; Pos; attitude; heading; angular rates; acceler-ations; drift angle; VS; GS; flight path angle, wind track	Arinc 429 air data	115 VAC, 400 Hz 28 VDC back-up —	2/43.0	$196,030	Optional control display unit; primary inertial sensor for navigation management computer systems; complies with Arinc 704 spec for IRS; growth capability to ADIRS; 10 MCU size; additional analog outputs; 3 year warranty
Northstar Avionics 30 Sudbury Rd. Acton, MA 01720 (617) 897-6600	M1	Loran-C LED	250 non-volatile RAM	analog	rotary knob	10 to 30 VDC EPROM	2/4.5	$3,995	Great ergonomics; VFR-only; no TSO; 20,000+ waypoint database; update with 8 EPROM chips — $75, dealer replaceable; first update included in purchase price; all 6,500 US public airports, 1,150 VORs, 1,600 NDBs and 4,800 low-altitude intersections; 20 waypoint flight plan; 3 year warranty
Narco Avionics Inc. P.O. Box 1807 Laguna Beach, CA 92652-1807 (714) 497-5077	LRN 840	Loran-C LCD	200 non-volatile RAM	External CDI autopilot	RS-232	11 to 32 VDC RAM with five yr. battery	2/4.0	$1,050	Automatic selection of GRI; secondaries MAG VAR; database available with airports, VORs, other fixes; database update cartridge — $75, plugs in back of unit
STS Avionic Products, Inc. 11600 Lilburn Park Road St. Louis, MO 63146 (314) 567-0304	120MC	Loran-C LCD	120 non-volatile RAM	analog, CDI	encoded altitude, heading, air data	10 to 32 VDC —	2/5.0	$1,995	Cross-chain, master-independent operation; concentric knob controls; 15,000 waypoint database; database updates with unit installed; includes antenna, coupler and mounting hardware; new super-twist LCD; 3 year warranty

LONG-RANGE NAVIGATION SYSTEMS

MANUFACTURER	MODEL	SYSTEM TYPE / DISPLAY	NUMBER WAYPOINTS / DATABASE	OUTPUTS	INPUTS	POWER INPUTS / MEMORY	UNITS/ WEIGHT (lb)	PRICE (uninstalled)	REMARKS
Terra Corp. 3520 Pan American Freeway NE Albuquerque, NM 87107 (505) 884-2321	TLC 120 none	Loran-C gas discharge	120 none	CDI autopilot	rotary knob	10 to 40 VDC —	2/2.5	$1,595	2.0-in high by 6.25-in wide by 11.0-in long; panel-mounted; includes whip antenna with CT6 preamp
Tracor, Inc. Avionics Products 6500 Tracor Lane MD 27-23 Austin, TX 78725 (512) 929-2233 Exclusive Distributor: DAC International Inc. 6702 McNeal Dr. Austin, TX 78729 (512) 331-5323	TA-7880	Omega/ VLF color CRT	2,480 30,000 waypoints optional	Pos; track error; TTW; GS; HSI; winds; CDI; autopilot roll steering; radar; cabin display	heading; TAS	21.5 VDC to 36 VDC —	3/17.0	$29,583*	*base price; 2,480 pilot-defined waypoints, 170 flight plans with up to 96 waypoints each, alphanumeric identifiers; optional outputs: analog — HSI, autopilot, synchro and roll steering; digital — Arinc 429, 561; EFIS compatible; Jeppesen world-wide database optional — $11,275; TA-2000 3½" disk database loader — $3,360; TA-7900 large CDU ¢6,797, exchange; includes E-field antenna and installation kit; optional DME/DME nav, GPS
	TA-7900	Omega/VLF color CRT	2,480 30,000 waypoints optional	Pos; track error TTW; GS; HSI; winds; CDI; autopilot roll steering; radar; cabin display	heading; TAS	21.5 VDC to 36 VDC or 115 AC, 400 Hz —	3/23.0	$44,973*	*base price; Arinc 599 spec'n Omega/VLF; price includes ADF coupler; 2,480 pilot-defined waypoints; 170 flight plans with up to 96 waypoints each, alphanumeric identifiers; standard outputs: analog — HSI, autopilot, synchro and roll steering; digital — Arinc 419, 429, 561; EFIS compatible; 60,000 waypoint Jeppesen database optional — $11,275; TA-2000 3½" disk database loader — $3,360
II Morrow, Inc. P.O. Box 13549 Salem, OR 97309 (503) 581-8101	604	Loran-C LED	200 —	CDI, HSI, autopilot, RS-232	concentric knobs, push buttons	6.5-48 VDC RAM with five-year battery	1/3.68	$1,795	VFR only; TSO C60a; panel-mounted; 6.25W x 2.0H; 350 KTAS A-16 antenna with preamp included; manual magnetic variation input; world-wide coverage — 14 station chains; manual secondary selection; upgradable to 604TCA configuration; includes installation kit; 26-month warranty

LONG-RANGE NAVIGATION SYSTEMS

MANUFACTURER	MODEL	SYSTEM TYPE / DISPLAY	NUMBER WAYPOINTS / DATABASE	OUTPUTS	INPUTS	POWER INPUTS / MEMORY	UNITS/ WEIGHT (lb)	PRICE (uninstalled)	REMARKS
II Morrow, Inc. P.O. Box 13549 Salem, OR 97309 (503) 581-8101	612B	Loran-C LEC	100 EPROM	CDI, HSI, autopilot RS-232	concentric knobs, push buttons	6.5-48 VDC RAM with five-year battery	1/3.75	$2,695	VFR only; 6.25in. wide by 2.0-in high; panel-mounted; includes A-16 antenna with preamp; TSO C60a; standard database for 48 United States and Alaska; optional database includes 620 Canadian airports; dealer-installed EPROM database updates — $75; alphamatic sort; offset waypoint mode; non-volatile two-leg flight plan; couples to Shadin fuel management system, Glatzer ELT; VNAV option; Model 612C also available in 3 ATI package — $2,995; includes installation kit; 26-month warranty
	604TCAep	Loran-C LED	100 cartridge	CDI, HSI, autopilot, external annunicators, RS-232	concentric knobs, push buttons	6.5-48 VDC RAM with five-year battery	1/3.75	$2,995	VFR only; 6.25-in wide by 2.0-in high; includes A-16 antenna with preamp; all 19 Loran-C chains; database cartridge user-installed in rear panel — includes 7,000 airports, VORs, VORTACs and NDBs in US, Canada and Alaska; update cartridges available every 56 days, each — $75, annual subscription — $200; couples to Shadin fuel management system, Glatzer ELT; 26-month warranty
	618	Loran-C LED	100 EPROM	CDI, HSI autopilot, external annunciators RS-232	concentric knobs, push buttons	6.5-48 VDC RAM with five-year battery	2/3.75	$3,295	VFR only; 6.25W x 2.0H; panel-mounted; A-16 antenna with preamp included; 20,000+ WP database for lower-48 US; updates — $75; auto secondary search; emergency airport search; couples to Shadin fuel management system, Glatzer ELT; comprehensive special use airspace intrusion feature; 26-month warranty
	612	Loran-C LED	100 EPROM	CDI, HSI autopilot, external annunciators RS-232	concentric knobs, push buttons	6.5-48 VDC RAM with five-year battery	2/3.75	$3,295	TSO C60a; 6.25W x 2.0H; panel-mounted; A-16 antenna with preamp included; IFR — AC 20-121; 2,600 WP database for lower-48 US; updates — $75; auto secondary search; emergency airport search; couples to Shadin fuel management system, Glatzer ELT; NPA software available; 26-month warranty

LONG-RANGE NAVIGATION SYSTEMS

MANUFACTURER	MODEL	SYSTEM TYPE DISPLAY	NUMBER WAYPOINTS DATABASE	OUTPUTS	INPUTS	POWER INPUTS MEMORY	UNITS/ WEIGHT (lb)	PRICE (uninstalled)	REMARKS
II Morrow, Inc. P.O. Box 13549 Salem, Or. 97309 (503) 581-8101	614R	Loran-C LED	100 EPROM	CDI, HSI, autopilot RS-232	N/A	6.5-48 VDC RAM with five-year battery	2/4.75	$6,995	IFR — AC 20-121; IFR demo approach certification; remote, standard Dzus rail mount for CDU; includes 521 KTAS-rated, A-17 antenna with preamp; TSO C60a; 0 — 50,000' MSL; VNAV standard; all other specifications same as 612IFR

VHF NAVCOMS

MANUFACTURER	MODEL TSO	DISPLAY MEMORY CHANNELS STORABLE	VOR OUTPUT	POWER OUTPUT (watts)	POWER INPUT	UNITS/ WEIGHT (lb) SIZE	PRICE (uninstalled)	REMARKS
Aire-Sciences, Inc. 216 Passaic Ave. Fairfield, NJ 07006 (201) 228-1880	RT-553A none	mechanical none none	CDI/HSI	6	14 VDC*	1/5.5 6.5 x 3.25 x 10.9	$2,175	Built-in converter-indicator; output for remote converter-indicator; built-in intercom; *28 to 14 VDC adapter, $145
	RT-563A none	mechanical none none	CDI/HSI	5	14 VDC*	1/7.8 6.5 x 3.25 x 10.9	$2,995	Automatic omni; built-in converter-indicator; output for remote converter-indicator optional *28 to 14 VDC adapter, $145
Bendix/King Avionics 400 N. Rogers Rd. Olathe, KS 66062 (913) 782-0400	KX 155 C34c C36c C37b C38b C40a	gas discharge EAROM non-volatile 2	CDI/RMI	10	14 or 28 VDC	2/7.0 6.25 x 2.5 x 10.25	$3,240	Auto squelch; includes KI 209 VOR/ LOC/ GS converter-indicator; price includes built-in 40-channel GS receiver; optional audio amplifier; 760 channel;
	KX 165 C34c C36c C37b C38b C40a	gas discharge EAROM non-volatile 2	CDI/RMI HSI	10	14 or 28 VDC	2/7.0 6.25 x 2.0 x 10.25	$7,225	Auto squelch; includes KI 206 VOR/LOC/ GS indicator; price includes built-in VOR converter and GS receiver; price less GS with indicator $6,350; digital radial readout
Narco Avionics Inc. P.O. Box 1807 Laguna Beach, CA 92652-1807 (714) 497-5077	Escort IIA none	gas discharge none none	none	5	14 VDC,	1/3.0 3.25 x 3.25 x 10.75	$1,149	Auto omni, digital OBS, ECDI, and digital bearing; 28 VDC configuration — $1,229

Footnote: All prices and weights, unless noted in Remarks, include a nav indicator.

VHF NAVCOMS

MANUFACTURER	MODEL TSO	DISPLAY MEMORY CHANNELS STORABLE	VOR OUTPUT	POWER OUTPUT (watts)	POWER INPUT	UNITS/ WEIGHT (lb) SIZE	PRICE (uninstalled)	REMARKS
Narco Avionics Inc. P.O. Box 1807 Laguna Beach, CA 92652-1807 (714) 497-5077	MK-12D C34c C37b C38b C40a	gas discharge hot-wire non-volatile 2/2	CDI/HSI	8	14 or 28 VDC	2/4.4 6.25 x 2.5 x 11.0	$3,569	Includes GS receiver and separate ID-825 VOR/LOC/GS indicator; $2,955 without GS and with ID-824 VOR/LOC indicator; includes 2x5 DME channeling; 8-watt transmitter; 720 channels; Cessna ARC form factor,direct-replacement design — $1,795
	MK-12E C34c C37b C38b C40a	gas discharge hot-wire non-volatile 2/2	CDI/HSI	8	14 or 28 VDC	2/5.4 6.25 x 2.5 x 11.0	$3,955	Includes GS receiver and separate ID-825 VOR/LOC/GS indicator; $3,343 without GS and with ID-824 VOR/LOC indicator; includes 2x5 DME channeling; 8-watt transmitter; 760 channels
	NCS-812 C34c C37b C38b C40a	gas discharge hot-wire non-volatile 2/2	CDI/HSI	8	14 or 28 VDC	2/5.4 6.25 x 2.5 x 11.0	$5,510	Includes separate 25-watt IDME-895 DME/ VOR/LOC/GS indicator and GS receiver; 8-watt VHF comm transmitter; 760 channels
Terra Corp. 3520 Pan American Freeway NE Albuquerque, NM 87107 (505) 884-2321	TXN 920 none	mechanical/ ECDI none none	CDI	6	14 VDC*	2/2.5 6.25 x 1.6 x 10.0	$1,795	Pushbutton tuning; manual or auto squelch; with GS — $2,195; 2x5 DME channeling; *28 to 14 VDC adapter — $85
	TXN 960 none	mechanical/ ECDI none none	built-in	6	14 VDC*	1/3.7 6.25 x 3.3 x 10.0	$1,795	Pushbutton tuning; auto squelch, manual override; with GS — $2,195; 2x5 DME channeling: *28 to 14 VDC adapter — $85

Footnote: All prices and weights, unless noted in Remarks, include a nav indicator.

VHF PANEL-MOUNTED NAV RECEIVERS

MANUFACTURER	MODEL TSO	DISPLAY MEMORY CHANNELS STORABLE	INCLUDES GS MB	POWER INPUT VOR OUTPUT	UNITS/ WEIGHT (lb) SIZE	PRICE (uninstalled)	REMARKS
Aire-Sciences, Inc. 216 Passaic Ave. Fairfield, NJ 07006 (201) 228-1880	R-662 C36c C40a	mechanical none none	no no	14 or 28 VDC DC to CDI	2/4.9 3.25 x 2.62 x 11.4	$945	interfaces with ECDI-541 converter-indicator — $995; glideslope and 2x5 DME channeling optional
	R-552 none	mechanical none none	no no	14 or 28 VDC DC to CDI	2/5.0 3.2 x 2.62 x 11.44	$1,745	Includes converter-indicator; glideslope and 2x5 DME channeling optional; includes ECDI-554A display

VHF PANEL-MOUNTED NAV RECEIVERS

MANUFACTURER	MODEL TSO	DISPLAY MEMORY CHANNELS STORABLE	INCLUDES GS MB	POWER INPUT VOR OUTPUT	UNITS/ WEIGHT (lb) SIZE	PRICE (uninstalled)	REMARKS
Aire-Sciences, Inc. 216 Passaic Ave. Fairfield, N.J. 07006 (201) 228-1880	R-554 none	mechanical none none	yes no	14 or 28 VDC DC to CDI	2/5.4 3.25 x 2.62 x 11.44	$2,620	Includes indicator; 2x5 DME channeling
	R-664 C34c C36b C40a	mechanical none none	yes no	14 or 28 VDC DC to CDI	2/5.4 3.25 x 2.62 x 11.44	$2,885	Interfaces with OBS indicator; 2x5 DME channeling
Bendix/King Avionics 400 N. Rogers Rd. Olathe, KS 66062 (913) 782-0400	KN 53 C34c C36c C40a	gas discharge EAROM non-volatile 2	no no	11 to 33 VDC CDI*	2/4.7 6.25 x 1.3 x 10.5	$4,250	Displays both active and preset frequency; price includes *KI 203 indicator; $5,100 with GS and *KI 204 indicator
Collins Avionics Div. Rockwell International 400 Collins Rd. NE Cedar Rapids, IA 52498 (319) 395-4085	VIR-351 C36c C40a	incandescent filament none none	no no	14 VDC* OBS resolver ORZ'd at 300° 0.05 Vrms to RNAV	2/4.2 3.12 x 2.6 x 12.45	$4,925	Displays either frequency or to/from bearing; electronic frequency readout; includes IND-350A indicator; includes glideslope and DME channeling; Arinc 547 *28 to 14 VDC adapter — $120
Narco Avionics Inc. P.O. Box 1807 Laguna Beach, CA 92652-1807 (714) 497-5077	NAV-824 C36c C40a	gas discharge hot-wire non-volatile 2	no no	11 to 32 VDC Arinc: .5 Vms at 0°	1/3.3 6.25 x 1.5 x 11.0	$2,132	RMI function; ID 824 indicator included in price; 2x5 DME channeling
	NAV-825 C34c C36c C40a	gas discharge hot-wire non-volatile 2	yes no	11 to 32 VDC N/A	1/3.3 6.25 x 1.5 x 11.0	$2,625	RMI function; ID 825 indicator included in price; 2x5 DME channeling
Terra Corp. 3520 Pan American Freeway, NE Albuquerque, NM 87107 (505) 884-2321	TN 200 none	mechanical none none	optional no	14 VDC* N/A	1/1.5 3.2 x 1.6 x 9.0	$695	2x5 DME channeling; with GS option $995; *28 to 14 VDC adapter — $85

VHF REMOTE-MOUNTED NAV RECEIVERS

MANUFACTURER	MODEL TSO	DISPLAY MEMORY CHANNELS STORABLE	INCLUDES GS MB	POWER INPUT VOR OUTPUT	UNITS/ WEIGHT (lb) SIZE	PRICE (uninstalled)	REMARKS
Bendix/King Avionics 400 N. Rogers Rd. Olathe, KS 66062 (913) 782-0400	VNS-41 C40b C36c C34c C35d	LCD or dichroic non-volatile 2	yes yes	28 VDC analog, Arinc 429	2/5.5 4.0 x 4.0 x 12.62	$12,695	Digital RMI readout, analog or Arinc 429 interface; includes LCD control head; two-year warranty
	KNR 634 C40a C36c C34c C35d	gas discharge EAROM non-volatile 2*	yes yes	28 VDC CDI, RMI, HSI	2/5.8 2.0 x 5.0 x 10.0	$13,310	Includes GS and MB receivers; self-contained converter; price includes KFS 564 with simultaneous digital display of active and standby frequency; Gables control option; King Serial Data tuning; also available without GS or MB; requires 26 VAC for sine/cosine output; night vision compatible "A" control head available; *optional control head with 9 programmable frequencies
	KNR 634A C40a C36c C34c C35d	gas discharge EAROM non-volatile 2*	yes yes	28 VDC Arinc 429 CDI, RMI, HSI	2/6.5 3.0 x 5.0 x 10.0	$17,485	synchro-interface RMI optional; price includes GS and MB receivers, control head; night vision compatible "A" control head available; *optional control head with 9 programmable channels; two-year warranty
	KTU 709 C66a	252 gas discharge EAROM non-volatile none	no no	28 VDC CDI, RMI	2/6.6 3.0 x 5.0 x 10.0	$18,425	Tacan: includes DME; bearing information derived from DME signal; price includes KDI 572 DME indicator; King serial data tuning; control head optional; night vision compatible "A" control head available; two-year warranty
Collins Avionics Div. Rockwell International 400 Collins Rd. NE Cedar Rapids, IA 52498 (319) 395-4085	VIR-32 C34c C35d C36d C40b	gas discharge non-volatile 6	yes yes	28 VDC, 26 VAC, 400 Hz sine/cosine serial digital	2/5.7 ⅜ ATR-SL	$13,390	RMI compatible; replaces VIR-30A directly; includes CTL-32 serial digital control; digital signal processing; built-in diagnostics; rotor modulation filter optional (strap)
	VIR-432 C34d C35d C36d C40b	gas discharge non-volatile 6	yes yes	28 VDC, 26 VAC, 400 Hz serial digital	2/5.7 ⅜ ATR-SL	$15,055	Built-in diagnostics; compatible only with CSDB or Arinc 429 controls; includes CTL-32 CSDB control; digital signal processing; auto instrumentation for use with RMI; rotor modulation filter optional (strap)
	51RV-4 C34c C36c C40a	mech. synchro none none	yes no	28 VDC, 26 VAC, 400 Hz electronic synchro driver	1/9.9 ½ ATR-S	$17,184	Self-contained converter; RMI capability; RNAV compatibility; options for glideslope receiver and monitoring of any or all functions; digital circuitry, output and tuning; coherent detector in receiver; Arinc 547; 2x5 DME channeling

VHF REMOTE-MOUNTED NAV RECEIVERS

MANUFACTURER	MODEL TSO	DISPLAY MEMORY CHANNELS STORABLE	INCLUDES GS MB	POWER INPUT VOR OUTPUT	UNITS/ WEIGHT (lb) SIZE	PRICE (uninstalled)	REMARKS
	VIR-31A C34c C35d C36c C40a	gas discharge non-volatile 2	yes yes	28 VDC; 26 VAC, 400 Hz three-wire synchro	2/8.0 ½ ATR-SL	$18,425	RMI compatibility; includes CTL-30 electronic control; 2x5 DME channeling; three-wire synchro VOR output; rotor modulation filtering optional
Collins Avionics Div. Rockwell International 400 Collins Rd. NE Cedar Rapids, IA 52498 (319) 395-4085	VIR-30A C34c C35d C36c C40a	gas discharge nonvolatile 2	yes yes	28 VDC; 26 VAC, 400 Hz sine/cosine	2/6.8 ⅜ ATR-SL	$18,840	RMI compatibility; superflag output; includes CTL-30 electronic control; 2x5 DME channeling; four-wire sine-cosine VOR output
Honeywell Inc. P. O. Box 29000 Phoenix, AZ 85038 (602) 863-8000	RNZ-850 C34d C35d C36d C40b C41d C66b	Color CRT non-volatile RAM 1 to 12	yes yes	28 VDC, 26 VAC 400 Hz serial digital, analog	2/—	—	Nav subsystem of SRZ-850 Primus II integrated, digital radio system; full dual system price — $128,427; includes RM-850 color CRT radio management unit, digital audio system, NV-850 VHF nav receiver, DF-850 ADF with AT-860 combined loop sense antenna, DM-850 precision format compatible DME (+/–100-ft) with station ID display and 6 channel scanning; built-in diagnostics, maintenance log; 1 to 12 stored channels depending on function; self-contained converter; digital signal processing; RTCA DO-160B environmental, DO-178A software

VHF PANEL-MOUNTED TRANSCEIVERS

MANUFACTURER	MODEL TSO	DISPLAY	MEMORY CHANNELS STORABLE	NOMINAL POWER OUTPUT (watts)	POWER INPUT	UNITS/ WEIGHT (lb) SIZE	PRICE (uninstalled)	REMARKS
Aire-Sciences, Inc. 216 Passaic Ave. Fairfield, NJ 07006 (201) 228-1880	RT-551A none	mechanical	none none	6	14 VDC*	1/2.7 3.25 x 2.62 x 10.66	$2,050	Manual squelch; portable version available *28 to 14 VDC adapter, $145
	RT-661A C37b C38b	mechanical	N/A N/A	6	14 or 28 VDC*	1/2.7 3.25 x 2.62 x 11.44	$2,250	Manual squelch; portable version available *Adapter, $145

VHF PANEL-MOUNTED TRANSCEIVERS

MANUFACTURER	MODEL TSO	DISPLAY	MEMORY CHANNELS STORABLE	NOMINAL POWER OUTPUT (watts)	POWER INPUT	UNITS/ WEIGHT (lb) SIZE	PRICE (uninstalled)	REMARKS
Bendix/King Avionics 400 N. Rogers Rd. Olathe, KS 66062 (913) 782-0400	KY 96A C37c C38c	LCD	EEPROM 9	7	28 VDC	1/2.9 6.25 x 1.3 x 10.5	$1,140	Auto leveling; auto squelch; stuck mike protection; remote mike keying and channel call-up; 760 channel
	KY 97A C37c C38c	LCD	EEPROM 9	7	14 VDC	1/2.9 6.25 x 1.3 x 10.5	$1,140	Auto leveling; auto squelch; stuck mike protection; remote mike keying and channel call-up; 760 channel
Bendix/King Avionics 400 N. Rogers Rd. Olathe, KS 66062 (913) 782-0400	KY 92 C37b C38b	mechanical	none none	7	14 VDC*	1/3.2 6.25 x 1.5 x 10.5	$2,160	Auto squelch; self-test *28 to 14 VDC adapter, $300; 760 channel
	KY 196A C37b C38b	gas discharge	EAROM non-volatile 9	16	28 VDC	1/3.2 6.25 x 1.3 x 10.5	$3,060	Auto squelch; displays active and standby frequency; remote flip-flop; optional remote call-up; 760 channel; optional extended frequency range available
	KY 197A C37b C38b	gas discharge	EAROM non-volatile 9	7	14 VDC	1/3.2 6.25 x 1.3 x 10.5	$3,060	Same as KY 196A, but 14 VDC power input
Collins Avionics Div. Rockwell International 400 Collins Rd. NE Cedar Rapids, IA 52498 (319) 395-4085	VHF-253 C37b Class II; C38b	LCD	EAROM non-volatile 6	10	10 to 32 VDC	1/2.7 6.3 x 1.3 x 12.1	$3,910	Remote frequency management; visible active and standby frequencies plus four stored presets; liquid-crystal displays; optional broadband version (VHF-253S) $4,440
General Aviation Electronics, Inc. 8284 E. 250th Hampton, MN 55031 (507) 263-4002	Alpha 720 none	incandescent filament	none none	5	14 VDC	1/4.0 6.5 x 2.5 x 10.0	$1,000	Vehicle- or ground-station versions available; 25kHz spacing; 10-watt carrier option — $200
Narco Avionics Inc. P.O. Box 1807 Laguna Beach, CA 92652-1807 (714) 497-5077	COM-810/ 811 C38b Class C	gas discharge	volatile (.2mA hotwire) 2	8	14 or 28 VDC	1/3.6 6.25 x 1.5 x 11.0	$1,295	Auto squelch; audio leveling: speaker, mike; 10-watt amp included
Terra Corp. 3520 Pan Am Freeway NE Albuquerque, NM 87107 (505) 884-2321	TX 720 none	mechanical	none none	5	14 VDC*	1/1.2 3.2 x 1.6 x 9.0	$945	Auto squelch; lighted; intercom; portable, vehicle or ground station version available *28 to 14 VDC adapter — $85

VHF REMOTE-MOUNTED TRANSCEIVERS

MANUFACTURER	MODEL TSO	DISPLAY	MEMORY CHANNELS STORABLE	POWER OUTPUT (watts)	POWER INPUT	UNITS/ WEIGHT (lb) SIZE	PRICE (uninstalled)	REMARKS
Bendix/King Avionics 400 N. Rogers Rd. Olathe, KS 66062 (913) 782-0400	KTR 908 C37b C38b	gas discharge	EAROM 2*	20	28 VDC	2/4.3 1.8 x 5.0 x 10.0	$8,310	Includes KFS 598 control with digital display of active and standby frequencies; Gables control option; remote flip-flop *optional control head with 9 programmable frequencies and remote frequency call-up function; 760 channel; 118.0 - 151.975 MHz option; night vision compatible "A" control head available; 2-year warranty
	VCS-40 C37c C38c	LCD or dichroic	non-volatile 2	20	28 VDC	2/5.5 4.0 x 4.0 x 12.62	$10,775	Arinc 429 or analog interface; continuous transmit capable; SELCAL and ACARS compatible; 760 channel; 118.0 - 151.975MHz option; 2-year warranty
Collins Avionics Div. Rockwell International 400 Collins Rd. NE Cedar Rapids, IA 52498 (319) 395-4085	VHF-21A C37c C38c	gas discharge	non-volatile 8	20	28 VDC	2/5.8 ⅜ ATR-SL	$8,900	Directly replaces VHF-20A; built-in diagnostics; 2x5 serial tuning; includes CTL-22 serial tuning control; VHF-21B, 118.0 - 151.975 MHz — $11,635
	VHF-22A C37c C38c	gas discharge	non-volatile 8	20	28 VDC	2/5.8 ⅜ ATR-SL	$8,900	Built-in diagnostics; 2x5 serial digital tuning — includes CTL-22 serial tuning control; VHF-22B, 118.0-151.975MHz — $11,635
	618M-3 C37b C38b	none	none none	25	28 VDC	1/10.1 ½ ATR-S	$9,748	Arinc 566A
	VHF-422A C37c C38c	gas discharge	non-volatile 8	20	28 VDC	2/5.8 ⅜ ATR-SL	$9,895	Built-in diagnostics; compatible only with CSDB or Arinc 429 controls; includes CTL-22 CSDB control; VHF-422B, 118-151.975 MHz — $12,795
	VHF-20A C37b C38b	gas discharge	non-volatile 2	20	28 VDC	2/6.8 ⅜ ATR-SL	$10,705	CTL-20 electronic control included; VHF-20B, 118 - 151.975 MHz — $13,635
Global-Wulfsberg Systems 2144 Michelson Dr. Irvine, CA 92715 (714) 851-0119	WT-200B C37b C38b	mechanical	none none	20	28 VDC	1/5.6 2.9 x 5.2 x 13.28	$7,982	Arinc and VHF 20A conversion mount available; 1,360 channels at 25 KHz spacing from 118.000 to 151.975 MHz; narrow or wide IF bandwidth models available; all solid state

Footnote: Arinc form factor is shown in the Units/Weight/Size columns. (See Form Factor explanation at the front of the Avionics section.)

VHF REMOTE-MOUNTED TRANSCEIVERS

MANUFACTURER	MODEL TSO	DISPLAY	MEMORY STORABLE CHANNELS	POWER OUTPUT (watts)	VOLTS INPUT	UNITS/ WEIGHT (lb) SIZE	PRICE (uninstalled)	REMARKS
Honeywell Inc. P. O. Box 29000 Phoenix, AZ 85038 (602) 863-8000	RCZ-850 C37c C38c C112	color CRT	non-volatile RAM 2 to 12	20, 500*	28 VDC	2/— 14.0 x 6.8 x 3.36	—	Comm subsystem of SRZ-850 Primus II integrated, digital radio system; full dual system price — $128,427; includes RM-850 color CRT radio management unit, 20-channel AV-850 or -851 digital audio system, TR-850 VHF transceiver with 118.0 - 151.975MHz range, XS-850 500-Watt Mode S transponder; built-in diagnostics, maintenance log; 2 to 12 stored channels depending on function; digital signal processing; RTCA DO-160B environmental, DO-178A software

Footnote: Arinc form factor is shown in the Units/Weight/Size columns. (See Form Factor explanation at the front of the Avionics section.)

HF TRANSCEIVERS

MANUFACTURER	MODEL TSO	CHANNELS FREQ CONTROL	FREQ. RANGE (MHz)	POWER OUTPUT (watts)	POWER INPUT	UNITS/ WEIGHT (lb)	PRICE COUPLER	REMARKS
Aircom Electronics, Ltd 9501 Ryan Ave. Dorval, Quebec H9P 1A2 Canada (514) 636-3874	SSB 10/20 none	10 crystal	2-29.999 SSB/AM	100 PEP	28 VDC	1/7.3	$10,080* $1,344*	*$12,000 Canadian, $1,600 Canadian; remote-, panel- and direct- (side) mount configurations available; 14 - 28 VDC remote coupler, fully compatible with other HF radios;
Bendix/King Avionics 400 N. Rogers Rd. Olathe, KS 66062 (913) 782-0400	KHF 950 C31c C32c	280,000 synthesizer	2-29.9999 SSB/AM	150 PEP (SSB) 35 (AM)	28 VDC	3/20.2	$16,860 —	Automatic antenna coupler included; 99 operator programmable, 176 ITU radiotelephone channels with standard, KCU 951 control head; optional, space saving KFS 594 control head provides 19 operator programmable, 176 ITU radiotelephone channels; optional dual HF shunt antenna; optional SELCAL compatibility; optional speech processing; explosion proof; two-year warranty
	KHF 990 C31c C32c	280,000 synthesizer	2-29.9999 SSB/AM	150 PEP (SSB) 35 (AM)	28 VDC	3/22.5	$19,270 —	Designed for helicopter use; includes digital antenna coupler/ probe antenna in single unit; 19 preset, 176 ITU radiotelephone channels with standard KFS 594 control head; explosion proof, salt-spray proof; two-year warranty

HF TRANSCEIVERS

MANUFACTURER	MODEL TSO	CHANNELS FREQ. CONTROL	FREQ. RANGE (MHz)	POWER OUTPUT (watts)	POWER INPUT	UNITS/ WEIGHT (lb)	PRICE COUPLER	REMARKS
Collins Avionics Div. Rockwell International 400 Collins Rd. NE Cedar Rapids, IA 52498 (319) 395-4085	HF-230 C31c C32c	280,000 synthesizer	2-29.9999 SSB/AM AM	100 PEP (SSB)	28 VDC	4/24.4	$16,640 —	Half-duplex; compatible with maritime radiotelephone network; additional channels: 40 operator programmable, 176 ITU radiotelephone preprogrammed channels; optional SELCAL; PAC-230 antenna coupler for helicopters, $17,710 system price; weight 23.2 lbs.
	HF-9000 C31d C32d	280,000 synthesizer	2-29.9999 SSB/AM AM data	175 PEP,	28 VDC	3/27.5	$28,200 —	Fiber-optic interface; 99 operator programmable, 176 ITU radiotelephone programmed channels; selectable power output — 10, 50, 175-Watt PEP; rapid-tune antenna coupler (40 msec computer tuning); BITE
	628T-3A C31c C32c	280,000 synthesizer	2-29.9999 SSB/ AM/CW	400 PEP (SSB) 125 (AM) 25 (CW)	28 VDC; 115 VAC, 400 Hz	3/26.0	$30,336 —	Panel-mounted control; remote-mounted ½ ATR-S transceiver and antenna coupler; power amplifier coupler; shock mounts included; frequencies automatically tuned in 0.1-kHz increments; Arinc 533, 404; Varies with installation
Sunair Electronics 3101 S.W. 3rd Ave. Fort Lauderdale, FL 33315 (305) 525-1505	ASB-500 C31c C32c	32,000 synthesizer	2-17.999 SSB/AM	100 PEP (SSB)	28 VDC	2/36.8	$9,495* —	*Factory dealer price; panel-mounted LED control unit; remote-mounted transceiver; SELCAL compatibility; includes automatic, full HF range ACU-150D microprocessor controlled antenna coupler
	ASB-850 C31c C32c	284,000 synthesizer	2-29.9999 SSB/AM	100 PEP (SSB)	28 VDC	3/30.0	$11,850 —	Integrated package including SCU-80 control-display unit, RE-800 remote-mounted HF transceiver and ACU-810 microprocessor-controlled antenna coupler; SELCAL compatibility

DISTANCE MEASURING EQUIPMENT

MANUFACTURER	MODEL TSO	CHANNELS OUTPUT	DISPLAY	QUANTITIES DISPLAYED	PEAK POWER OUTPUT (watts)	VOLTS INPUT	UNITS/ WEIGHT (lb) SIZE	PRICE (uninstalled)	REMARKS
Bendix/King Avionics 400 N. Rogers Rd. Olathe, KS 66062 (913) 782-0400	KN 64 none	200 King serial data	gas discharge	dist.: 0-389 nm gnd. spd.: 0-999 kt TTS: 0-99 m.i.n.	35	11 to 33 VDC	1/2.4 6.25 x 1.3 x 12.2	$2,085	Distance accuracy: ±0.1 nm nominal to 99 nm, ±1.0 nm 100 to 200 nm; panel-mounted; includes antenna and installation kit; accepts remote nav channeling

Footnote: Arinc form factor is shown in the Units/Weight/Size columns. (See Form Factor explanation at the front of the Avionics section.)

DISTANCE MEASURING EQUIPMENT

MANUFACTURER	MODEL TSO	CHANNELS OUTPUT	DISPLAY	QUANTITIES DISPLAYED	PEAK POWER OUTPUT (watts)	VOLTS INPUT	UNITS/ WEIGHT (lb) SIZE	PRICE (uninstalled)	REMARKS
Bendix/King Avionics 400 N. Rogers Rd. Olathe, KS 66062 (913) 782-0400	KN 62A C66a	200 King serial data	gas discharge	dist.: 0-389 nm gnd. spd.: 0-999 kt TTS: 0-99 min	100	11 to 33 VDC	1/2.4 6.25 x 1.3 x 12.2	$4,515	Distance accuracy: ±0.1 nm nominal to 99 nm, ±1.0 nm 100 to 200 nm; panel-mounted; includes antenna and installation kit; accepts remote channeling
	KN 63 C66a	200 King serial data	gas discharge	dist.: 0-389 nm gnd. spd.: 0-999 kt TTS: 0-99 min	100	11 to 30 VDC	2/3.6 6.5 x 1.9 x 11.55	$6,850	Distance accuracy: ±0.1 nm nominal to 99 nm, ±1.0 nm 100 to 200 nm; includes KDI 572 indicator; optional slaved indicator
	KDM 706 C66a	252 King serial data	gas discharge	dist.: 0-389 nm gnd. spd.: 0-999 kt TTS: 0-99 min	250	28 VDC	2/5.5 2.5 x 5.25 x 11.8	$11,295	Distance accuracy: ±0.1 nm to 99 nm, ± 100 to 200 nm; includes KDI 572 indicator; optional slaved indicators; remotely mounted; 2-year warranty
	KDM 706A C66b	252 Arinc 429, 568	gas discharge	dist.: 0-389 nm gnd. spd.: 0-999 kt TTS: 0-99 min	250	28 VDC	2/6.3 5.0 x 3.0 x 10.0	$13,385	KDM 706 with Arinc 429, 568 interface; KDI 572 included; optional slaved indicators; remotely-mounted; night vision compatible "A" control head available; 2-year warranty
	DMS-44 C66	252 2 x Arinc 568 2 x 40mv/nm Arinc 429 40-bit serial	LCD or dichroic	dist.: 0-300 nm gnd. spd.: 0-999 kt TTS: 0-19:59 min	325	28 VDC	2/6.6 5.0 x 4.0 x 12.62	$15,690	Triple scanning DME, displays Nav 1 and Nav 2 distance simultaneously; Arinc 429 or analog interface; displays RNAV distance; remotely-mounted; 2-year warranty
	KTU 709 C66a	252 King serial	gas discharge	dist.: 0-389 nm gnd. spd.: 0-999 kt TTS: 0-99 min	250	11 to 33 VDC	6.6 5.0 x 3.0 x 10.0	$17,260	Tacan (DME with Tacan-based bearing independent of VOR); optional KFS-579A control head — $4,180; KDI 572 indicator included; night vision compatible "A" control head available; 2-year warranty
Collins Avionics Div. Rockwell International 400 Collins Rd. NE Cedar Rapids, IA 52498 (319) 395-4085	DME-450 C66a	200 40 mv/nm	incandescent filament	dist.: 0-199.9 nm gnd. spd.: 0-399 kt TTS: 0-120 min	100	14 or 28 VDC	3/6.1 3.5 x 5.0 x 11.0	$7,605	Distance accuracy: ±0.1 nm or 1%; includes ANT-451 antenna and IND-450 indicator
	DME-451 C66a	200 40 mv/nm	incandescent filament	dist.: 0-199.9 nm gnd. spd.: 0-399 kt TTS: 0-120 min	100	14 or 28 VDC	3/6.4 3.5 x 5.0 x 11.0	$9,215	Distance accuracy: ±0.1 nm or 1%; built-in timer based on GMT clock; includes ANT-451 antenna and IND-451 indicator

Footnote: Arinc form factor is shown in the Units/Size/Weight column. (See Form Factor explanation in the front of the Avionics section.)

DISTANCE MEASURING EQUIPMENT

MANUFACTURER	MODEL TSO	CHANNELS OUTPUT	DISPLAY	QUANTITIES DISPLAYED	PEAK POWER OUTPUT (watts)	VOLTS INPUT	UNITS/ WEIGHT (lb) SIZE	PRICE (uninstalled)	REMARKS
Collins Avionics Div. Rockwell International 400 Collins Rd. NE Cedar Rapids, IA 52498 (319) 395-4085	DME-42 C66b	252 40 mv/nm Arinc 568B serial digital	gas discharge	dist.: 0-300 nm gnd. spd.: 0-999 kt TTS: 0-120 min ID: 2,3,4 letters	300	28 VDC	2/6.2 ½ ATR-SL	$12,935	Includes two-digit-code diagnostics; directly replaces DME-40; tracks three channels simultaneously when used with CTL-32 and IND-42A (CTL-32 controls nav receiver); serial digital, 2 x 5 tuning; digital signal processing; echo monitor; includes IND-42A indicator
	DME-442 C66b	252 40 mv/nm Arinc 568B serial digital	gas discharge	dist.: 0-300 nm gnd. spd.: 0-999 kt TTS: 0-120 min ID: 2,3,4 letters	300	28 VDC	2/6.2 ½ ATR-SL	$14,510	Tracks three channels simultaneously when linked to CTL-32, IND-42A; decodes / displays station ident; compatible interfaces: Collins Serial Data Bus (CSDB) or ARINC 429, only; digital signal processing; echo monitor; built-in diagnostics; includes IND-42A
	DME-40 C66a	252 40 mv/nm Arinc 568 pulse pair	gas discharge	dist.: 0-250 nm gnd. spd.: 0-999 kt TTS: 0-99 min	300	28 VDC	2/8.1 ½ ATR-SL	$15,950	Distance accuracy: ±0.1 nm or 0.01%; includes IND-40 indicator
	860E-5 C66a	252 Arinc 568B	N/A	dist.: 0-390 nm	700	115 VAC, 400 Hz	1/16.0 ½ ATR-SL	$26,016	Distance accuracy: ±0.1 nm nominal; indicator not included
	860E-4 C66a	252 Arinc 521D	N/A	dist.: 0-390 nm	700	115 VAC, 400 Hz	1/20.0 ½ ATR	$30,080	Distance accuracy: ±0.2 nm; channeling and lock-on less than 2.5 seconds; indicator not included
Foster Airdata Systems, Inc. 7020 Huntley Rd. Columbus, OH 43229 (614) 888-9502	DME 670 C66b	252 RS-422, Arinc 568, DME pulse pair, 40 mv/nm, 400 HzAC	LED dot matrix	dist.: 0-400 nm gnd. spd.: 0-720 kt TTS: 0-99 min. bearing: (Tacan) 0-359° ID: 3, 4 letter Morse	250	28 VDC	2/6.8 10.25 x 3.25 x 5.0 1/2-3ATI x 6.5	$11,900	Tracks up to four stations; displays distance and ident or Tacan radial from two stations; distance, ident, Tacan radial and speed from single station; also available with ARINC 429 output for interface with long-range navigation systems
Narco Avionics Inc. P.O. Box 1807 Laguna Beach, CA 92652-1807 (714) 497-5077	DME 890 none	200 Narco digital	gas discharge	dist.: 0-160 nm gnd. spd.: 44-600 kt TTS: 0-99 min	25	11 to 32 VDC	1/3.3 6.25 x 1.5 x 11.0	$1,949	Microprocessor controlled; meets all minimum operating characteristics; Narco RNAV 860, NS-801 compatible
	IDME 891 none	200 Narco digital	LED	dist: 0-160 nm gnd. spd.: 44-600 kt	25	11 to 32 VDC	1/26 three-inch cutout	$2,639	Requires MK 12D; package with GS, $3,650; includes VOR/LOC indicator and marker lights; compatible with Mark 12D, NAV 825, RNAV 860, NS-801

Footnote: Arinc form factor is shown in the Units/Weight/Size column. (See Form Factor explanation in the front of the Avionics section.)

TRANSPONDERS

MANUFACTURER	MODEL TSO	INTERRO-GATION MODES	POWER OUTPUT (watts)	VOLTS INPUT	UNITS/ WEIGHT (lb) SIZE	PRICE (uninstalled)	REMARKS
Aire-Sciences, Inc. 216 Passaic Ave. Fairfield, NJ 07006 (201) 228-1880	RT-787 C74c Class 1A	A,C	500	14 VDC*	2/3.4 6.5 x 1.8 x 9.9	$1,495	Manual reply-light dimmer *28 to 14 VDC adapter, $95
	RT-887 C74c Class 1A	A,C	500	14 VDC*	2/4.0 3.25 x 3.25 x 10.12	$1,795	Manual reply-light dimmer; electronic digit display; mounts into 3.25-inch instrument cutout *28 to 14 VDC adapter, $95
Bendix/King Avionics 400 N. Rogers Rd. Olathe, KS 66062 (913) 782-0400	KT 76A C74c Class 1A	A,C	250	14 or 28 VDC*	1/3.1 6.25 x 1.6 x 10.0	$1,225	Automatic reply-light dimmer; system test; remote ident capability *Adapter, $30
	KT 79 C74c Class 1A	A,C	250	11 to 33 VDC	1/3.4 6.25 x 1.3 x 10.5	$3,315	Auto 1200 select; displays encoded altitude; all solid-state, no cavity tube; remote ident capability
	KXP 756 C74c Class 1A	A,C	250	28 VDC	2/4.7 5.0 x 1.75 x 10.0	$6,975	Includes KFS 576 digital control head with auto 1200 select; test displays encoded altitude; solid-state; no cavity tube; Gables control optional; remote ident capability; night vision compatible "A" control head available; 2-year warranty
	TRS-42 C74c	A,B,C	325	28 VDC	2/5.8 4.0 x 4.0 x 12.62	$10,125	Analog or Arinc 429; controls two RTs; auto 1200 select; digital Mode C altitude readout; 2-year warranty
Collins Avionics Div. Rockwell International 400 Collins Rd. NE Cedar Rapids, IA 52498 (319) 395-4085	TDR-950 C74c Class 1A	A,C	250	14 VDC*	2/2.0 6.3 x 1.6 x 8.2	$2,010	Manual reply-light dimmer; optional remote ident *28 to 14 VDC adapter, $125
	TDR-90 C74b C74c	A,C	500	28 VDC	2/4.9 ¼ ATR-SL	$8,045	Remote-mounted; manual reply-light dimmer; includes CTL-90 electronic control; optional CTL-92 with CAD-62 adapter provides serial digital tuning, two stored codes
	621A-6A C74a	A,B,C (D opt.)	700	115 VAC, 400 Hz	3/15.0 ⅜ ATR-S	$17,808	Remote-mounted; must add control head with reply-light; Arinc 572
	TPR-720 C74c C112	A,C,S	250-631	115 VAC, 400 Hz	1/12.0 ½ ATR	$19,348	Mode S transponder; 4 MCU package (approx. ½ ATR); LCD CDU — 5.0 lbs

ENCODING ALTIMETERS/DIGITIZERS

MANUFACTURER	MODEL TSO	INTERRO-GATION MODES	POWER OUTPUT (watts)	VOLTS INPUT	UNITS/ WEIGHT (lb) SIZE	PRICE (uninstalled)	REMARKS
Narco Avionics Inc. P.O. Box 1807 Laguna Beach, CA 92652-1807 (714) 497-5077	AT-150 C74C Class 1A	A, C	250	14 or 28 VDC*	1/2.3 6.25 x 1.75 x 11.3	$1,249	Manual reply-light dimmer; remote ident available *Adapter; $27
Terra Corp. 3520 Pan American Freeway, NE Albuquerque, NM 87107 (505) 884-2321	TRT 250 C74C Class 2a	A,C	200	10 to 30 VDC	1/1.7 3.2 x 1.6 x 10.0	$1,195	All solid-state; no cavity tube; remote ident capability; push-button code selection; 3" ATI configuration available

ENCODING ALTIMETERS/DIGITIZERS

MANUFACTURER	MODEL TYPE	RANGE (x 100 ft)	DISPLAY CASE	LENGTH WEIGHT	DIGITIZER DESIGN	POWER INPUT	PRICE (uninstalled)	REMARKS
ACK Technologies 424 W. Julian St. San Jose, CA 95110 (408) 287-8021	A-30 altitude digitizer	–10+307	— —	6.0 .45	solid state	10 to 32 VDC	$325	TSO C88a; remotely mounted
Aero Mechanism 20327 Nordhoff St. Chatsworth, CA 91311-6161 (818) 709-2851	8141B-35LW —	–10+350	CDP 3" ATI	6.26 .75	optical	14 or 28 VDC	$4,743	Millibar baro setting optional; mating connector included; internal lighting: 5, 14, 28 VDC available; TSO C10b, C88
Aerosonic Corp. P.O. Box 4627 Clearwater, FL 33515 (813) 461-3000	102200 -01812 —	–10+200	3P 3 ATI	5.3 2.0	optical	14 or 28 VDC	$1,391	Millibar baro setting, dual scale, internal lighting and altitude alerter optional; TSO C10b, C88
	102200 -01818 —	–10+350	3P 3 ATI	5.1 2.0	optical	14 or 28 VDC	$1,470	Millibar baro setting, dual scale, internal lighting and altitude alerter optional; TSO C10b, C88
	102200 -01831 —	–10+350	CDP 3 ATI	6.4 2.4	optical	14 or 28 VDC	$2,531	Millibar baro setting, dual scale, internal lighting and altitude alerter optional; TSO C10b, C88
	101400- 01235 —	–10+500	CDP 3 ATI	5.2 7.7	optical	14 or 28 VDC	$2,575	Millibar baro setting, dual scale, internal lighting and altitude alerter optional; other configurations available; TSO C10b, C88

ENCODING ALTIMETERS/DIGITIZERS

MANUFACTURER	MODEL TYPE	RANGE (x 100 ft)	DISPLAY CASE	LENGTH WEIGHT	DIGITIZER DESIGN	POWER INPUT	PRICE (uninstalled)	REMARKS
Bendix/King Avionics 400 N. Rogers Rd. Olathe, KS 66062 (913) 782-0400	KE 127 altitude digitizer	–10+200	— —	3.25 1.00	optical	14 or 28 VDC	$1,075	Digitizer only; remotely-mounted;
	KEA 129 encoding altimeter	–10+2000	3P MS	5.57 1.90	optical	14 or 28 VDC	$2,585	Millibar / inches baro setting; kit and rack included; internally lighted
	KEA 130 encoding altimeter	–10+350	3P MS	5.57 1.90	optical	14 or 28 VDC	$2,850	Millibar / inches baro setting; internally lighted; kit and rack included; KEA 130A with altitude pre-select / alerter compatibility $3,035
	KEA 346 servoed encoding altimeter	–10+500	CDP 3 ATI	8.94 2.90	optical	28 VDC	$8,800	Internal lighting; altitude-alert outputs; DH annunciation; dual baro set in millibars or inches
Kollsman Avionics Division 220 Daniel Webster Hwy. Merrimack, NH 03054 (603) 889-2500	B4515 Alti-coder	–10+200	CDP MS	4.75 2.50	optical	28 VDC + 115 VAC	N/A	Price dependent on specific aircraft; internal white or red lighting; three-digit display; 35,000-ft model available
	B4450 Alti-coder II	–10+350	3P MS	5.30 2.50	optical	14 or 28 VDC	N/A	Price dependent on specific aircraft; optional internal lighting and failure warning flag
	24929 encoding altimeter	–10+200	CDP 3 ATI	6.9 2.9	optical	14 or 28 VDC	$14,400*	* base price; red, white or blue lighting; 35,000-ft / 50,000-ft models available
	28007 encoding altimeter	–10+500	CDP 3 ATI	8.3 3.5	contact	26 VAC 400 Hz	$15,504*	* base price;,above options, features; includes altitude alert, altitude rate outputs
	28702 encoding altimeter	–10+350	CDP 3 ATI	7.0 3.5	contact	28 VDC	$16,044*	* base price; above options, features
	29007 encoding altimeter	–10+50	CDP 3 ATI	8.0 3.8	contact	26 VAC 400 Hz	$17,536*	* base price; above options, features; includes radio altimeter (RA) display; links to GPWS; requires separate RA receiver/transmitter
	29702	–10+350	CDP 3 ATI	8.0 3.8	contact	28 VDC	$18,512*	* base price; optional altitude alert light; extended baro range; above options, features
Narco Avionics Inc. P.O. Box 1807 Laguna Beach, CA 92652-1807 (714) 497-5077	AR-850 altitude digitizer	–10+250 –10+307 altitude digitizers	— —	6.15 0.7	solid state	11 to 32 VDC	$260 $300	–10;250 model TSO C88a –10;307 model not TSOed

ENCODING ALTIMETERS/DIGITIZERS

MANUFACTURER	MODEL TYPE	RANGE (x 100 ft)	DISPLAY CASE	LENGTH WEIGHT	DIGITIZER DESIGN	POWER INPUT	PRICE (uninstalled)	REMARKS
Pointer, Inc. 1027 N. Stadem Dr. Tempe, AZ 85281 (602) 966-1674	L115 altitude digitizer	–10+200	— —	7.3 1.1	solid state	14 or 28 VDC	$575	tentative price; remotely mounted; installation kit included
Terra Corp 3520 Pan American Freeway, N.E. Albuquerque, NM 87107 (505) 884-2321	AT 3000 blind encoder	–10+300	— —	6.2 0.5	solid state	14 or 28 VDC	$495	Digitizer only; remote-mounted
Trans-Cal Industries, Inc. 16141 Cohasset Street Van Nuys, CA 91406 (818) 787-1221	D120P2-T D125P2-T D130P2-T D135P2-T D150P2-T altitude digitizers	–10+200 –10+250 –10+300 –10+350 –10+500	— —	3.75 1.0	optical	14 or 28 VDC	$765 $850 $850 $925 $1,700	replaceable electronic module for ease of repair; uses generic aneroid designed for sensitive baro altimeters
United Instruments 3625 Comotara Ave. Wichita, KS 67226 (316) 685-9203	5035 encoding altimeter	–10+200 –10+350	3P MS	5.50 1.80	optical	14 or 28 VDC	$1,617 $1,760	Optional white or blue-white lighting

HORIZONTAL SITUATION INDICATORS/COMPASS SYSTEMS

MANUFACTURER	MODEL TSO	DISPLAY CASE GYRO	SLAVING RATE (norm. fast)	VOLTS INPUT AUTOPILOT OUTPUT	UNITS/ WEIGHT (lb)	PRICE (uninstalled)	REMARKS
Aeronetics 455 Keho Blvd. Carol Stream, IL 60188 (312) 668-3040	8000 C6c, C34c C36c, C40b	3 ATI remote	3 degrees/min 150 degrees/ min	28 VDC Arinc analog	3/6.7	$7,370	Arinc format; automatic emergency mode function (flux valve input); autopilot outputs; with bearing pointer — $8,460; 3 wire synchro boot strap output to RMI; two-year warranty
	421 Series C6c, C34c C36c, C40b	4 ATI remote	3 degrees/min 300 degrees/ min (nominal)	28 VDC Arinc analog	3/7.5	$7,800	Arinc format; with bearing needle — $8,480; with bearing needle and digital distance and course readout — $10,080; individual components available; Arinc 568 or King Serial Digital; 40 mv/nm optional; two-year warranty
Bendix/King Avionics 400 N. Rogers Rd. Olathe, KS 66062 (913) 782-0400	KCS 305 C6c	4 ATI remote	3 degrees/min 240 degrees/ min	115 VAC 400 Hz Hdg. 393 mv AC/ degree Course: 393 mv AC/ degree	4/10.4	$5,755*	*base price; includes autopilot outputs; many options available; includes boot strap heading in HSI; night vision goggle compatible instruments available; 2-year warranty

HORIZONTAL SITUATION INDICATORS/COMPASS SYSTEMS

MANUFACTURER	MODEL	DISPLAY CASE TYPE GYRO	SLAVING RATE (norm. fast)	VOLTS INPUT AUTOPILOT OUTPUT	UNITS/ WEIGHT (lb)	PRICE (uninstalled)	REMARKS
Bendix/King Avionics 400 N. Rogers Rd. Olathe, KS 66062 (913) 782-0400	KCS 55A C6c	3 ATI remote	3 degrees/min 180 degrees/ min	14 or 28 VDC Hdg.±550 mv DC/ deg.: max. ±12.5v Course: ±220 mv DC/deg.: max ±12.5v	4/9.4	$7,750	Includes autopilot outputs; RMI output $815 additional; night vision goggle compatible instruments available
Century Flight Systems Mineral Wells, TX 76067 (817) 325-2517	NSD-360A-15 C5c C9c C52a	3 ATI panel mounted	non-slaved	14 or 28 VDC potentiometer	1/4.5	$3,805	Includes autopilot outputs; requires 5-in vacuum
	NSD-360A (S) -26 C6c C9c C52a	3 ATI panel mounted	2 degrees to 3 degrees/min N/A	14 or 28 VDC potentiometer	4/5.1	$5,525	Includes autopilot outputs; requires 5-in vacuum; NSD-360A-35(S) provides RMI output, requires 26 VAC, 400 Hz power — $6,135
Collins Avionics Div. Rockwell International 400 Colli28,375ns Rd. NE Cedar Rapids, IA 52498 (319) 395-4085	MCS-65 C6c	— remote	2 degrees/min 7 degrees/sec	28 VDC three-wire synchro	3/6.7	$9,055	Includes autopilot outputs; digital interface with EHSI-74
	PN-101 C6c	3 ATI remote,	3 degrees/min 300 degrees/ min	14 or 28 VDC three-wire synchro	4/12.7	$24,520	Includes autopilot outputs, slaving accessory and 331A-3G course indicator

Footnote: Arinc form factor is shown in the Units/Weight/Size column. (See Form Factor explanation in the front of the Avionics section.)

RADIO ALTIMETERS

MANUFACTURER	MODEL TSO	ALTITUDE RANGE PITCH/ROLL LIMITS	ACCURACY	UNITS SIZE/WEIGHT	DISPLAY	PRICE (uninstalled)	REMARKS
Bendix/King Avionics 400 N. Rogers Rd. Olathe, KS 66062 (913) 782-0400	KRA 10A FM/CW none	-20-2,000 ft ±20 degrees/20 degrees	40-500 ft ±5 ft or 5%; 500-2,000 ft ±7%	rcvr./xmtr. 3.1 x 3.5 x 8 in; ind. 3 ATI; 1 ant. 3.8 lb	pointer and dial type; linear scale expanded from 0-500 ft	$4,635*	*28 VDC system; continuous DH set; "skewed" antenna optional for mounting on angled aircraft surface; 14 VDC configuration — $4,807
	KRA 405 FM/CW C87	-20-2,000 ft ±20 degrees/ ±25 degrees	-20-500 ft ±3 ft or 3%; 500-2,000 ft ±5%	rcvr./xmtr. 11.5 x 5 x 3 in; ind. 3 ATI; 2 ant.; 10.7 lb	pointer and dial type; linear scale expanded from 0-500 ft	$11,490	Continuous DH set; tracking to 2,500 ft; expanded helicopter version available; night vision goggle compatible version available; 2-year warranty
Collins Avionics Div. Rockwell International 400 Collins Rd. NE Cedar Rapids, IA 52498 (319) 395-4085	ALT-50A CW C87	-0+2,000 ft ±40 degrees/ ±50 degrees	±2 ft or 2%;	rcvr./xmtr. ⅜ ATR-SL; indicator, .83 x 3.38 in two antennas; 6.7 lb	digital	$11,935	DH light and four trips settable over entire range; includes DRI-55 indicator and two ANT-52 antennas
	ALT-55B CW C87	-0+2,500 ft ±40 degrees/ ±50 degrees	±2 ft or 2%;	rcvr./xmtr. ⅜ ATR-SL; indicator, .83 x 3.38 in two antennas; 6.7 lb	digital	$14,010	DH light and four trips settable over entire range; includes DRI-55 indicator and two ANT-52 antennas
	AL101 FM/CW C87	-20+2,500 ft ±40 degrees/ ±50 degrees	-20+500 ft ±2 ft or 2%; 500-2,500 ft ±5%	rcvr./xmtr. ½ ATR-S; ind. 3 ATI; 2 ant. 7-in dia. x 2.75 in; 22.5 lb	pointer and dial type; linear -20+500 ft; logarithmic 500-2,500 ft	$39,236	ARINC 552, 552A specification design, includes vertical tape instrument
Honeywell Inc. P.O. Box 29000 Phoenix, AZ 85038 (602) 863-8000	AA-300 pulse C87	0-2,500 ft ±45 degrees/ ±45 degrees	0-100 ft ±5ft; 100-500 ft ±5%; 500-2,500 ft ±7%	rcvr./xmtr. 10.7 x 4 x 7.5 in; ind. 3.3-in dia. x 4 in; 2 ant. 8.25 lb	pointer and dial type; linear scale expanded from 0-500 ft or 0-200 ft	$14,307	Altitude rate optional; continuous DH set; tracking to 3,000 ft; includes RT-300 receiver/transmitter, RA-315 indicator and AT-300 antenna
Terra Corp. 3520 Pan American Freeway NE Albuquerque, NM 87107 (505) 884-2321	TRA 3000 FM/CW none	40-2,500 ft ±20 degrees/ ±30 degrees	40-100 ft ±5 ft; 100-500 ft ±5%; 500-2,500 ft ±7%	rcvr./xmtr. 1.0 x 5.0 x 7.6 in; indicator 3.5 x 3.25 x 4.0 in. antenna built into R/T unit; 2.5 lb	—	see remarks	*Prices: with TRI 20 LED indicator — $2,395; with TRI 30 analog indicator — $2,995; with TRI 40 LED indicator, with 100' AGL gear warning — $3,295; continuous DH set; aux analog output and STWT
	TRA 3500 FM/CW none	0-2,500 ft ± 20 degrees/ ± 30 degress	0-10 ft ± 1 ft; 10-100 ft ± 5 ft; 100-2,500 ft ± 5-7%	rcvr./xmtr. 3.0 x 3.0 x 6.9 in; indicator: 3.5 x 3.25 x 4.0 in; —	pointer and dial type; linear 40-2,500 ft; (enlarged linear 40-500 ft)	$5,495	Price includes TRI 40 LED indicator, including 100 ft gear warning; TSO C87 pending; anti-hover circuit design

Footnote: Arinc form factor is shown in the Units/Size/Weight column. (See Form Factor explanation in the front of the Avionics section.)

THUNDERSTORM DETECTION SYSTEMS

MANUFACTURER	MODEL	RANGE (nm)	DISPLAY SIZE / VIEWING ANGLE	DISPLAY TYPE	UNITS/ WEIGHT (lb)	PRICE (uninstalled)	REMARKS
Honeywell Inc. P.O. Box 29000 Phoenix, AZ 85038 (602)863-8000	LSZ-850	Same as radar display to 100 nm	Interfaces on radar display 120 or 360 degrees	Quantitative electrical discharge activity displayed on CRT	3 11.0	$19,703	Frequency of lightning discharge causes one of three unique symbols to be displayed at the relative location of such activity; integrated radar & lightning system sensor controls available
3M Stormscope Systems 6530 Singletree Dr. Columbus, OH 43229 (614) 885-3310	WX-8	100	3-in dia. 135 degrees	liquid-crystal display	1 + ant. 4.0	$3,975	Panel-mounted unit/display; three-color liquid-crystal display range resolution; storm intensity enhancing; 10 - 30 VDC
	WX-1000 Stormscope Series II	25 50 100 200	3-in ATI 120 or 360 degrees	vertical electrical discharge activity on CRT	2 + ant. 10.9	$8,995	Displays only vertical electrical discharge activity associated with thunderstorms; up to six checklists; clock/calendar mode with elapsed and flight time; built-in test and error code display; future expansion capability; 10.5 - 32 VDC; 28 Watts; TSO C110
	WX-1000+ Stormscope Series II	25 50 100 200	3 in. ATI 120 or 360 degrees	vertical electrical discharge activity on CRT	2 + ant. 10.9	$9,995	Heading stabilized — 5 to 50 VAC, 400 Hz; displays only vertical electrical discharge activity associated with thunderstorms; up to six checklists; clock/calendar mode with elapsed and flight time; built-in test and error code display; future expansion capability; 10.5 - 32 VDC; 28 Watts; TSO C110

MLS RECEIVERS

MANUFACTURER	MODEL TSO	CHANNELS CONTROL/ DISPLAY	SIZE/WEIGHT	POWER	PRICE (uninstalled)	REMARKS
Bendix/King Avionics 400 N. Rogers Rd. Olathe, KS 66062 (913) 782-0400	MLS-21 C104	200 ICAO standard rotary knob LCD	receiver: 11.75 x 5 x 3.9 in. control: 2.5 x 3.125 x 2.5 in. (2) antenna: flush-mount system weight: 8.7 lbs	28 VDC/ .75 amps	$20,162	Arinc 429 compatible; ICAO magnetic course reference; price includes installation tray, kit and two antennas; PDME compatible & EFIS compatible; night vision goggle compatible control head available; two-year warranty
Canadian Marconi 2442 Trenton Ave. Montreal, Quebec, Canada H3P 1Y9 (514) 341-7630	CMA-2000 NA	200 ICAO standard rotary knob LCD	receiver: 3 MCU control: 3.75 x 5.75 x 2.375 in. (3) antenna system weight: 11.5 lbs	115 VAC 400 Hz, 75 VA max	$31,040	In full compliance with Arinc 727 and ICAO specifications; analog and Arinc 429 interfaces; manual and fully automatic self-test; auto/manual angle modes; three-year warranty
Honeywell Inc. P.O. Box 29000 Phoenix, AZ 95038 (602) 863-8000	MLZ-850 C104	200 ICAO standard rotary knob LED	receiver: 13.9 x 3.3 x 3.9 in. control: 2.375 x 2.625 x 5.5 in. (2) antenna: 1.2 x 2.5 in. flush aperture system weight: 6.6 lbs	28 VDC	$23,033	Price includes tray and installation kits; analog output to ADI, HSI, FCS; CSDB digital interface; 2x5 DME channeling; updatable to future ICAO magnetic course reference; Primus II MLS sensor configuration, 5.5 lbs — $19,520

NAVIGATION MANAGEMENT SYSTEMS

MANUFACTURER	MODEL TSO	TOTAL WAYPOINTS FLIGHT PLANS / WAYPOINTS DATA ENTRY	PRIMARY SENSOR(S) ADDITIONAL SENSORS	INPUTS OUTPUTS	POWER INPUT COOLING	ATR SIZE / WEIGHT / UNITS	PRICE	REMARKS
Bendix / King Avionics 400 N. Rogers Rd. Olathe, KS 66062 (913) 782-0400	KNS 660 C40b C90a	3,000 400 / 25 keyboard (non-volatile)	DME/DME VOR/DME Omega/VLF TACAN GPS Loran C IRS	analog digital analog digital	28 VDC 26 VAC / 400 Hz forced air required	2/20.2 —	$28,570*	*47,995 with optional Omega/VLF sensor; world-wide database: VORs, TACANs, airports, intersections, airport data, SIDs, STARs, with updating every 28 days with Bendix / King supplied diskette; monochrome CRT; VNAV advisory; optional full-alpha keyboard; coupled VNAV with KFC 400; compatible with Bendix / King GPS sensor; direct interface with Bendix EFIS; radar mapping available through Bendix / King weather radar with optional GC 360A radar graphics unit; optional rubidium frequency standard; night vision compatible CDU available; special packages may be available; two-year warranty

NAVIGATION MANAGEMENT SYSTEMS

MANUFACTURER	MODEL TSO	TOTAL WAYPOINTS FLIGHT PLANS / WAYPOINTS DATA ENTRY	PRIMARY SENSOR(S) ADDITIONAL SENSORS	INPUTS OUTPUTS	POWER INPUT COOLING	ATR SIZE / WEIGHT / UNITS	PRICE	REMARKS
Canadian Marconi 2442 Trenton Ave. Montreal, Quebec, Canada H3P 1Y9 (514) 341-7630	CMA-900 pending	35,000 400 / 99 keyboard disk data loader	DME / DME Omega/VLF IRS MLS GPS Loran-C DADC	analog Arinc 429 analog Arinc 429 Arinc 561	28 VDC / 60 Watts or 115 VAC / 80 VA no external cooling required	Color CDU: 5.75 x 6.8 x 7.8; 8 lbs. NMU: 2 MCU; 10 lbs.	$50,000	price varies with number and type of interfaces and optional long-range sensors; internal Omega/VLF included, may be replacedwith optional, internal GPS; external Omega/VLF sensor available;10 Arinc 429 input ports; fuel computer optional; frequency management optional; 3.5" diskette data loader optional; ColorCDU capable of controlling other sub-systems
Global-Wulfsberg Systems 2144 Michelson Dr. Irvine, CA 92715 (714) 851-0119	GNS X C115	256 49 / 30* keyboard	DME/DME VOR/DME Loran C VLF/Omega IRS	Arinc 429 Arinc 571 CSDB analog Arinc 429 Arinc 561 Arinc 571 CSDB analog	28 VDC / 1.8 Amps 26 VAC / 400 Hz** no external cooling required	Computer: ¼ATR-S / 8.4 lbs CDU: 4.5 x 5.75 x 6.5 / 5.5 lbs	$41,852	*up to 50 route waypoints on active flight plans; **AC power for analog interfaces only; price includes installation kit, Loran C sensor board, 50,000 waypoint, worldwide internal database, fuel flow interface, full alpha keyboard CDU; no VNAV; frequency management system standard; AFIS compatible, optional Data Management Unit — $26,700, first year subscription included; 3.5" diskette Data Transfer Unit — $2,800; with AFIS option, flight plans and messages can be interchanged via datalink; optional VLF/Omega RPU — $22,500
	GNS 1000 C115 C109 C94a	256 49 / 30* keyboard	DME/DME VLF/Omega VOR/DME IRS	Arinc 429 Arinc 571 CSDB analog Arinc 429 Arinc 561 Arinc 571 CSDB analog	28 VDC / 5.2 Amps 26 VAC / 400 Hz** no external cooling required	Computer: ½ATR-S / 15.0 lbs Receiver / Processor: ½ATR-S / 16.0 lbs NDB-2: ¼ATR-S / 9.1 lbs CDU: 4.5 x 5.75 x 6.5 / 5.5 lbs	$88,143	*up to 50 route waypoints on active flight plans; ** AC power for analog interfaces only; price includes installation kit, H-field antenna; dual systems — $159,177; monochrome CRT; optional full alpha keyboard — $1,220; no VNAV; frequency management system standard; AFIS compatible, optional Data Management Unit — $26,700, includes first year subscription; 3.5" diskette Data Transfer Unit — $2,800; with AFIS option, flight plans and messages can be interchanged via datalink; compatible with almost all fuel flow sensors or indicators; 25,000 waypoint NDB-2 database includes North American / European or world-wide data; remove database from aircraft every 28 days to update; VLF/Omega Receiver Processor Unit included in price, but may be deleted for credit

NAVIGATION MANAGEMENT SYSTEMS

MANUFACTURER	MODEL TSO	TOTAL WAYPOINTS FLIGHT PLANS / WAYPOINTS DATA ENTRY	PRIMARY SENSOR(S) ADDITIONAL SENSORS	INPUTS OUTPUTS	POWER INPUT COOLING	ATR SIZE / WEIGHT / UNITS	PRICE	REMARKS
Honeywell Inc. P.O. Box 29000 Phoenix, AZ 85038 (602) 863-8000	LASERNAV II —	255 20 / 20 keyboard	Laser IRS VOR DME VLF/Omega	Arinc 429 Arinc 419 Arinc 429 Arinc 561 Arinc 571 CSDB	28 VDC / 5 VDC or 115 VAC / 400 Hz no external cooling required	INU: modified 10 MCU / 48.5 lbs CDU: Arinc 704-4 / 7.0 lbs	$163,214	certificated as a primary sole-source, long-range navigation system; supplies attitude and heading reference to flight instruments; ring-laser-gyros used for inertial reference; monochrome display; NDB-2 database, updated with Honeywell-supplied tape; accommodates 2 x VORs, 2 x DMEs, 2 x VLF/Omega sensors; compliance with RTCA DO-160A
	FMZ-800 C115	1,400 100 / 50 3.5" disk data loader	DME/DME VOR Omega/VLF IRS AHRS (MLS) (GPS) air data	2 x ASCB 3 x Arinc 429 6 x CSDB ASCB Arinc 429 CSDB	28 VDC / 2.7 Amps no external cooling required	Color CDU: 5.4 x 7.5 x 10.0; 9.4 lbs Computer: ½ATR-S; 14.3 lbs	$92,326	system "learns" operating characteristics of aircraft from previous flights; 200 pilot-defined waypoints in addition to those listed; non-volatile EEPROM memory; flight plans computed by Lockheed JetPlan and down loaded via 3.5" diskette; mono display also available; 3-D navigation with full VNAV; linked J-route / V-airway mode; radial intercept mode; full-autothrottle growth mode; ACARS / datalink growth mode; Loran-C capability — TBA; no TACAN; USIFR-RNAV, NAT MNPS, RNAV Approach, sole-source over-water nav approvals; full Jeppesen database, updated with 3.5" diskette data loader; standard equipment on Canadair 601-3A, Gulfstream IV and Falcon 900 aircraft; 30,000 waypoint database standard; optional 1.25-Mbyte NZ-910 international nav database including 4,000+ paved airports, airways, SIDs/ STARs; 28-day updates take less than 8 minutes; 1-year warranty
Universal Navigation Corporation 3260 East Lerdo Rd. Tucson, AZ 85706 (602) 741-2300	UNS-1 NMS C115 C66b C94a C60a	3,000 200 / 98 keyboard alpha or line-item selection (3.5" disk data loader)	DME/DME VOR IRS Omega/VLF Loran-C GPS TACAN DADC	analog Arinc 429 Arinc 575 CSDB analog Arinc 429 Arinc 561 Arinc 571 Arinc 575 ASCB	28 VDC / 1.8 Amps 26 VAC / 400 Hz no external cooling required	CDU: 5.75 x 4.5 x 6.75, 4.5 lbs NCU: 2 MCU, 7.0 lbs 5.75W x	$30,000	price varies with up to three optional long-range sensors; 40,000 waypoint worldwide database; auto-scanning DME / DME / DME; diskette data loader — $3,600; advisory VNAV; direct-to key; two engine fuel management — DC-analog inputs; optional Super CDU to upgrade to UNS-1A configuration — mono CRT, adds 3.0 lbs and $7,000, color CRT, adds 3.0 ibs and $12,000; direct-to key; 3-D approach mode; direct-to mode; optional frequency management system; multi-chain Loran-C sensor — $12,000; UNS-RRS DME/VOR/ TACAN sensor — $16,000; optional UNS-764 VLF/Omega sensor — $22,000; three-year warranty includes sensors

NAVIGATION MANAGEMENT SYSTEMS

MANUFACTURER	MODEL TSO	TOTAL WAYPOINTS FLIGHT PLANS / WAYPOINTS DATA ENTRY	PRIMARY SENSOR(S) ADDITIONAL SENSORS	INPUTS OUTPUTS	POWER INPUT COOLING	ATR SIZE / WEIGHT / UNITS	PRICE	REMARKS
Universal Navigation Corporation 3260 East Lerdo Rd. Tucson, Az. 85706 (602) 741-2300	UNS-1A Compact FMS C115 C66b C94a C60a	3,000 200 / 98 keyboard alpha or line item select (3.5" disk data loader)	DME / DME VOR IRS Omega/VLF Loran-C TACAN GPS DADC	analog Arinc 429 Arinc 575 CSDB analog Arinc 429 Arinc 561 Arinc 571 Arinc 575 ASCB	28 VDC / 2.1 Amps 26 VAC / 400 Hz no external cooling required	SuperCDU: 5.75 x 6.4 x 7.88 7.6 lbs NCU: 2 MCU, 7.8 lbs	$55,000	price varies with CDU and up to five long-range sensors; 40,000 waypoint worldwide database; auto-scanning DME/DME/DME and VOR/DME; monochrome super CDU, deduct $5,000; frequency management unit — $10,000; dual system data cross-talk mode; off-line flight planning; diskette data loader — $4,500; plus all features and options of UNS-1 NMS above; three-year warranty includes sensors
	UNS-1A FMS C115 C66b C94a C60a	3,000 200 / 98 keyboard alpha or line item select (3.5" disk data loader)	DME / DME VOR IRS Omega/VLF Loran-C TACAN GPS DADC	analog Arinc 429 Arinc 575 CSDB analog Arinc 429 Arinc 561 Arinc 571 Arinc 575 ASCB	28 VDC / 2.3 Amps 26 VAC / 400 Hz no external cooling required	SuperCDU: 5.75 x 6.4 x 7.88 7.6 lbs NCU: 2 MCU, 11.0	$72,500	price varies with CDU and up to five optional long-range sensors; includes color Super CDU; optional SID/STAR/Approach database — $10,000; fuel management with up to four inputs; all features and options of UNS 1A Compact FMS listed above; three-year warranty includes sensors

AIRBORNE TELEPHONE SYSTEMS

MANUFACTURER	MODEL COLORS	MODE OF OPERATION	POWER OUTPUT (watts) MAX ALT	POWER INPUT	UNITS/ WEIGHT (lb)	PRICE (uninstalled)	REMARKS
Global-Wulfsberg Systems 2144 Michelson Dr. Irvine, CA 92715 (714) 851-0119	Flitefone VI 7	full duplex, HF optional	10 51,000 ft	28 VDC	2/9.5	$7,664	Remote handsets and controls available; direct-dial capable
Terra Corp. 3520 Pan American Freeway, N.E. Albuquerque, NM 87107 (505) 884-2321	Jetfone II 4	full duplex	8 40,000 ft	28 VDC	1/4.25	$3,000	Self-contained; panel-mounted unit; includes handset
	TD-3000 N/A	full duplex, AGRAS	10 55,000 ft	28 VDC	2/6.8	$7,500	Direct dial compatible; automatic channel selection, operator alert; additional handsets, $535; digital channel readout; includes cockpit control unit

C2 MILITARY AVIONICS SYSTEMS PRICE DATA

The prices of military avionics systems depend strongly on the following factors:

* Requested performance
* Operational environment (particularly high 'g' levels and extreme temperatures)
* Frequency of modifications requested by various military services
* Number of systems procured

In some cases the military will purchase 'off-the-shelf' commercial avionics equipment. In that case the price data of Section C1 might be applicable.

In most cases military avionics systems are developed for specific military purposes. Since prices of such equipment are not published regularly in the open literature, another approach is recommended. That approach is to use fractional cost data based on published information.

Figures C1 - C3 are examples of such fractional data. It appears from these data that military avionics costs typically range from:

$$C_{avionics/military} = 0.05(AEP) \qquad (C1)$$

to:

$$C_{avionics/military} = 0.40(AEP) \qquad (C2)$$

where: AEP is the airplane estimated price as estimated from Equation (4.3)

The reader has to apply 'judgment' to determine the magnitude of the fraction (0.05 to 0.40) which applies to a new design.

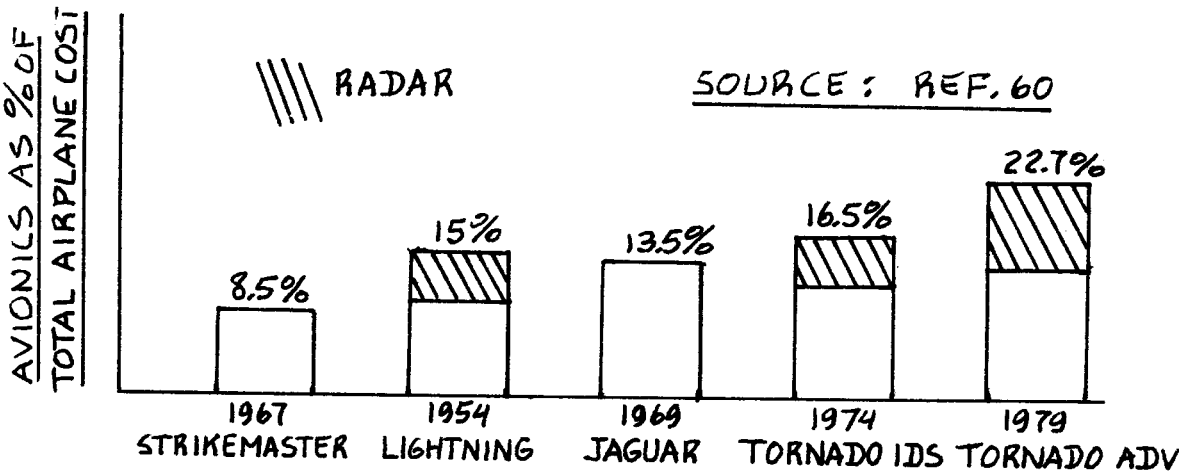

Figure C1 Avionics as a Percentage of Total Airplane Cost

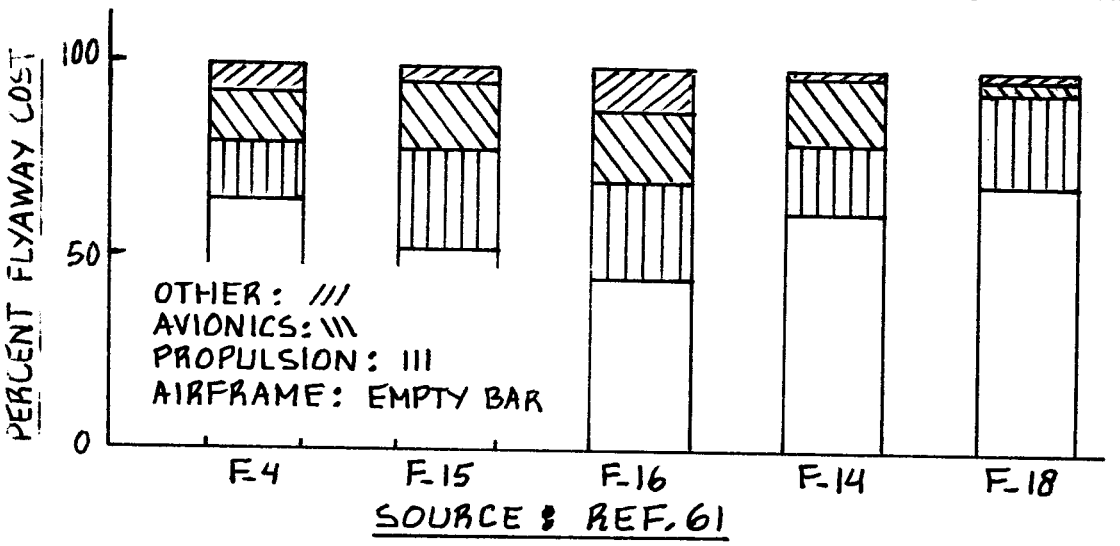

Figure C2 Avionics and Other Equipment as a Percentage of Flyaway Cost

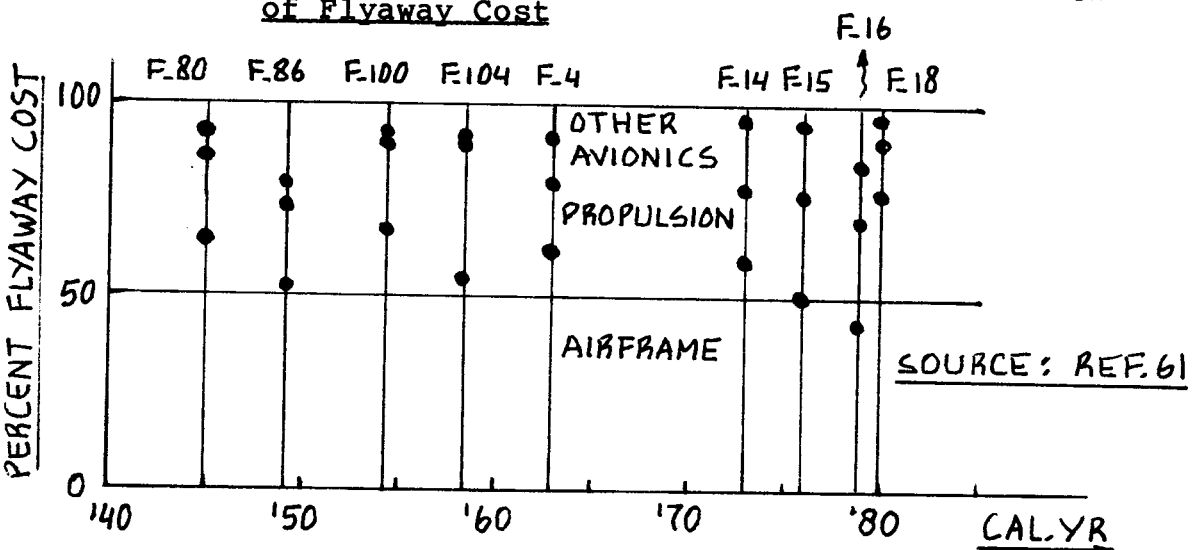

Figure C3 Historical Distribution of Avionics and Other Equipment as a Percentage of Flyaway Cost

DESIGN, ANALYSIS AND RESEARCH CORPORATION

ERRATA: AIRPLANE DESIGN PART I

Copyright © 1985-89 by Dr. Jan Roskam
Year of Print, 1985, 1989
(Revised June 11, 1997)

page 51, Eqn. (2.9) units for c_P= (lbs/hr)/hp

line 6 from bottom replace 1,000 nm with 1,000 sm

page 52, line 3 1000 is standard miles

page 61, Table 2.19 Take-off and Landing: groundrun of less than 2,400 ft.

page 64, line 3 and 5 W is the take-off weight: W_{TO}

page 69, Eqn. (2.23) $D = (W_{PL} + W_{CREW}) + W_{p_{\exp}}$
Where $W_{p_{\exp}}$ is the weight of the expended payload.
(i.e., Missles, bombs, etc.)

page 95, line 14 from bottom remove “range of”

page 98, line 8 from bottom replace $C_{L_{TO_{\max}}}$ by $C_{L_{\max_{TO}}}$

page 106, line 2 replace four factors: with five factors:

page 115, Eqn. (3.18) $V_A = 1.1 V_{s_{PA}}$

page 132, 4th line delete “an”

page 150, Eqn. (3.32) $RC_h = RC_0(1 - h / h_{abs})$

page 152, Eqn. (3.38) $$\sin\gamma = \frac{T}{W}\left[P_{dl} - \sqrt{P_{dl}^2 - P_{dl} + \left(1 + \left(\frac{L}{D}\right)^2\right)^{-1}\left(\frac{T}{W}\right)^{-2}}\right]$$

page 186, Section 3.7.4.2

line 3 ...groundrun as < 2,400 ft.

line 7 S_L = 1.9 x 2,400 =
= 4,500 ft.

From Figure 3.16 S_L = 4,500/0.6 = 7,500 ft.

From Figure 3.17 this yields: V_A^2 = 25,000 kts^2.

$$V_A = \left\{21{,}200(1.3/1.2)^2\right\}^{1/2} = 158\,kts$$ should be

$$V_A = \{25{,}000\}^{1/2} = 158\,kts$$

DESIGN, ANALYSIS AND RESEARCH CORPORATION

ERRATA: AIRPLANE DESIGN PART II

Copyright © 1985-89 by Dr. Jan Roskam
Year of Print, 1985, 1989
(Revised June 11, 1997)

page 102, Step 3.1, 2nd line ...falls into one of the eight catagories...

page 158, Step 6.10 *Eqn. (6.1) should be Eqn. (6.2)*

page 170, Eqn (7.8) and (7.11-18) C_l should be c_l

pages 176 to 185 The example problems of Section 7.2 are incorrect. The K_Λ factor was multiplied instead of divided to yield the $C_{l_{max}}$ values for Step 7.4 of 7.2.1, 7.2.2, and 7.2.3. Each example will be addressed below.

Section 7.2.1 Twin Engine Propeller Driven Airplane

The results of step 7.4 should be:

	Take-off flaps		Landing flaps	
$\frac{S_{wf}}{S}$	0.3	0.6	0.3	0.6
$\Delta C_{l_{max}}$	0.58	0.29	2.32	1.16

Z_{fh} should be $\frac{Z_{fh}}{c}$.

For Step 7.5, the referenced equations and figures are wrong:

Eqn. (7.15) should be Eqn. (7.16).
Eqn. (7.14) should be Eqn. (7.15).
Eqn. (7.13) should be Eqn. (7.14).
Figure 7.7 should be Figure 7.8.
Figure 7.3b should be Figure 7.4.
Eqn. (7.10) should be Eqn. (7.11).

Section 7.2.2 Jet Transport

The results of step 7.4 should be:

	Take-off flaps		Landing flaps	
$\frac{S_{wf}}{S}$	0.6	0.8	0.6	0.8
$\Delta C_{l_{max}}$	3.00	2.24	3.84	2.88

For Step 7.5, the referenced equations and figures are wrong:
Eqn. (7.10) should be Eqn. (7.11)
Figure 7.3b should be Figure 7.4

Section 7.2.3 Fighter

The results of Step 7.4 should be:

	Take-off flaps		
$\frac{S_{wf}}{S}$	0.4	0.8	1.0
$\Delta C_{l_{max}}$	4.00	2.000	1.60

These corrections will affect the results of each sample problem. It is left to the reader to complete the sample problems using the correct results of Step 7.4. The summary and referenced drawings of Step 7.6 may change due to these corrections.

pages 178, 181, and 184

Under Step 7.4, K_{Δ} should be K_{Λ}

page 267

Eqn (11.13)

$N_D = 0.75 N_{t_{crit}}$ should be $N_D = 0.25 N_{t_{crit}}$

Eqn (11.14)

$N_D = 0.25 N_{t_{crit}}$ should be $N_D = 0.10 N_{t_{crit}}$

DESIGN, ANALYSIS AND RESEARCH CORPORATION

ERRATA: AIRPLANE DESIGN PART III

Copyright ©1986-89 by Dr. Jan Roskam
Year of Print, 1986, 1989
(Revised March 15, 1999)

page 15, Table 2.3	Switch values for β_1 and β_2
page 194, 8th line from top	replace “stability” with “Stability”.

DESIGN, ANALYSIS AND RESEARCH CORPORATION

ERRATA: AIRPLANE DESIGN PART IV

Copyright © 1986-89 by Dr. Jan Roskam
Year of Print, 1986, 1989
(Revised December 14, 1999)

page 54, Table 2.18	For fighters and trainers, the details are in Figure 2.26, not Figure 2.25.
page 380, 7th line from top	replace “is” with “are”

DESIGN, ANALYSIS AND RESEARCH CORPORATION

ERRATA: AIRPLANE DESIGN PART V

Copyright © 1985-89 by Dr. Jan Roskam
Year of Print: 1985, 1989
(Revised December 14, 1999)

page 34, Eqn (4.13) $n_{\lim pos} \geq 2.1 + 24{,}000 / (GW + 10{,}000)$

page 43, 12th line from top V_A should be *217 kts.*

page 45, 8th line Change *Selene* to *Eris*

page 61, under Step 6 n_{ult} = 7.33 should read n_{lim} = *7.33*

page 71
Eqn (5.12) *57.5* should be *174.04*

Eqn (5.13) *15.6* should be *639.95*
Replace exponent *1.249* with *0.1249*

page 72
6th line replace 'ib' with 'in'

13th line replace $1/4_V$ by $\Lambda_{1/4_V}$

page 72 - 74 All comments about the canard weight should reference 5.2.1.1.

page 74
Eqn (5.19) Replace $1/2_H$ by $\Lambda_{1/2_H}$

Eqn (5.20) $W_v = K_v S_v \left[3.81 \left(S_v^{0.2} V_D \right) \Big/ \left(1000 \sqrt{\cos \Lambda_{c/2_v}} \right) - 0.287 \right]$
Replace $1/2_V$ by $\Lambda_{1/2_V}$

page 75, Eqn (5.23) $W_f = 0.04682 (W_{TO})^{0.692} (P_{\max})^{0.374} (l_{f-n})^{0.590}$
where P_{max} is the maximum fuselage perimeter expressed in feet.

page 76
Eqn (5.24) N_{pax} is the number of passengers including the pilot.

Eqn (5.26) Replace 2 x 10.43 by 10.43

page 77, Eqn (5.27) l_h = distance from wing root c/4 to horizontal tail root c/4 in ft

page 78, Eqn (5.29) $W_n = K_n W_{TO}$ should be $W_n = K_n P_{TO}$

page 79
2nd line — Eliminate and replace by "P_{TO} = Take-off power in HP"

Eqn (5.32) — $$W_n = 0.045(P_{TO})^{5/4}(N_e)^{-1/4}$$

page 81

Eqn (5.38) — $$W_g = 0.013W_{TO} + 0.362(W_L)^{0.417}(n_{ult.l})^{0.950}(l_{s_m})^{0.183} + 6.2 + + 0.0013W_{TO} + 0.007157(W_L)^{0.749}(n_{ult.l})(l_{s_n})^{0.788}$$

7th line from bottom — Replace $N_{ult.l}$ by $n_{ult.l}$

4th line from bottom — Replace 62.61 by 62.21

page 85
Section 6.1.2, 9th line — Should read: *Equations (6.4) and (6.6) may also be used...*

page 87, Eqn (6.8) — $$W_{ai} + W_p = 1.03(N_e)^{0.3}(P_{TO})^{0.7}$$

page 90, Eqn (6.14) — Method assumes that the number of engines equals the number of propellers

page 92, Eqn (6.23) — $$W_{fs} = 1.6\left[\frac{W_f}{K_{fsp}}\right]^{0.727}$$

See the associated insert for the comparison of Torenbeek and GD methods.

page 93, — Add an increment of 5 to all equation numbers throughout Chapter 6 (i.e., Eqn. (6.22) becomes Eqn. (6.27)).

page 95, Eqn (6.34b) — $$W_{apsi} = 0.4K_b(N_e)^{0.2}(P_{TO})^{0.8}$$

page 98, — Add an increment of 1 to all equation numbers throughout Chapter 7.

page 99, Eqn (7.4) — $$W_{fc} = 0.33(W_{TO})^{2/3}$$

page 108, — Eqn (7.44) Remove the (before N_{pax} in the cabin windows weight component.

page 109, Eqn (7.46) — K_{st} = 0 for no ejection seat

page 111,
3rd line of Section 7.12 — Should read: *Part IV, Chapter 3.*

DESIGN, ANALYSIS AND RESEARCH CORPORATION

ERRATA: AIRPLANE DESIGN PART VI

Copyright © 1987-90 by Dr. Jan Roskam
Year of Print, 1987, 1990
(Revised December 14, 1999)

page xx $\bar{x}_{ac_h} = x_{ac_h} / \bar{c}$

page 27, Eqn (4.9) $C_{L_w} = C_L - C_{L_c} \frac{S_c}{S} - C_{L_h} \frac{S_h}{S}$

page 46, Eqn (4.33) $C_{D_{L_{fus}}} = 2\alpha^2 \frac{S_{b_{fus}}}{S} + \eta c_{d_c} |\alpha|^3 \frac{S_{plf_{fus}}}{S}$

page 47, Figure 4.20 $M_c = M \sin|\alpha|$

page 49

Eqn (4.39) $C_{D_{L_{fus}}} = \alpha^2 \left(S_{b_{fus}} \right) / S$

Eqn. (4.41) $C_{D_{o_{fus}}} = \left(C_{f_{fus}} \left(\frac{S_{wet_{fus}}}{S_{fus}} \right) + C_{D_{N_2}} + C_{D_A} + C_{D_{A(NC)}} + C_{D_{b_{fus}}} \right) \frac{S_{fus}}{S}$

page 52, Eqn (4.43) $C_{D_{L_{fus}}} = F \left\{ 2\alpha^2 \frac{S_{b_{fus}}}{S} + c_{d_c} \frac{S_{plf_{fus}}}{S} |\alpha|^3 \right\}$

page 70, 9th line Should read "... of 4.2.2.1 but with the appropriate..."

page 73
Eqn. (4.60) Add: $\varepsilon_n > 0$ *for upwash and* $\varepsilon_n < 0$ *for downwash*

Last line Should read: *Chapter 8.*

page 77, Eqn. (4.63) $\Delta c_{l_2} = +0.056(i_n)$ with i_n expressed in degrees

page 86
3rd line Should read: ... *from Eqn. (4.6)*

Eqn. (4.74) '*Chapter 9*' should be '*Chapter 8*'

page 105, Eqn (4.84)

$$\Delta C_{D_{trim_{prof}}} = \left(\Delta C_{D_p} \right)_{\Lambda_{c/4_h}=0} \cos\Lambda_{c/4_h} \left(\frac{S_{ef}}{S_h} \right) \left(\frac{S_h}{S} \right) + \left(\Delta C_{D_p} \right)_{\Lambda_{c/4_c}=0} \cos\Lambda_{c/4_c} \left(\frac{S_{cf}}{S_c} \right) \left(\frac{S_c}{S} \right)$$

page 142 The reference to Chapter 6 in Part IV should be Chapter 7

page 171, Eqn. (6.25) Replace $\dot{m}_{gas}$ with $\dot{m}_a$

Where $\dot{m}_a$ follows from Eqn. (6.19)

page 177, 22nd line Section on supersonic jet inlets should be Section 6.2.3.4

page 181, Eqn. (6.44)
$$F_{inl} = 1 + 1.75 \left\{ \left(\frac{\mu_{inl} - 1}{\mu_{inl}} \right) \left(\frac{1}{\frac{A_m}{A_c} - 1} \right) \right\}$$

page 229, Eqn. (8.7)
$$\Delta c_l = \eta_1 \left(c_{l_{\delta f_1}} \right) \left(\delta_{f_1} \right) \left\{ (c + c_1)/c \right\} + \eta_2 \left(c_{l_{\delta f_2}} \right) \left(\delta_{f_2} \right) (c'/c)$$

page 233, Eqn. (8.10)
$$\Phi_{TE_{UPPER}} = arctan\{10 \frac{y_{90} - y_{100}}{c}\}$$

page 245, Eqn. (8.20)
$$\alpha_w = \alpha + i_w$$

page 268, Eqn. (8.32) Should be
$$C_{L_o} = C_{L_{o_{wf}}} + C_{L_{\alpha_h}} \eta_h (S_h/S) \left(-\varepsilon_{o_h} - \alpha_{o_{L_h}} \right) + C_{L_{\alpha_c}} \eta_c (S_c/S) \left(\varepsilon_{o_c} - \alpha_{o_{L_c}} \right)$$

where: $\alpha_{o_{L_h}}$ and $\alpha_{o_{L_c}}$ can be found using the method of Section 8.1.3.1.

page 269, Eqn (8.37) For jet airplanes, the horizontal tail dynamic pressure should be calculated from:

$$\eta_h = 1 - \frac{2.42 \sqrt{C_{D_{o_w}}} \cos^2 \left(\frac{\pi z_{h_{wake}}}{2 \Delta z_{wake}} \right)}{\frac{x_{h_{wake}}}{\bar{c}} + 0.30}$$

where:

$C_{D_{o_w}}$ is the wing zero-lift drag coefficient as found from 4.2.1.1.

$$z_{h_{wake}} = a \sin \left(\gamma_h - \alpha - i_w + \varepsilon_h \right)$$

$$x_{h_{wake}} = a \cos \left(\gamma_h - \alpha - i_w + \varepsilon_h \right)$$

$$\Delta z_{wake} = 0.68 \bar{c} \sqrt{C_{D_{o_w}} \left(\frac{x_{h_{wake}}}{\bar{c}} + 0.15 \right)}$$

page 269, Eqn (8.37) (Cont.)

with:

a and γ_h shown in Figure 8.63;
$\bar{c}$ as the wing mean geometric chord;
α as the airplane angle of attack;
i_w as the wing incidence angle; and

$$\varepsilon_{cl} = \frac{1.62 C_{L_w}}{\pi A}$$

page 270, Figure 8.63 Should be

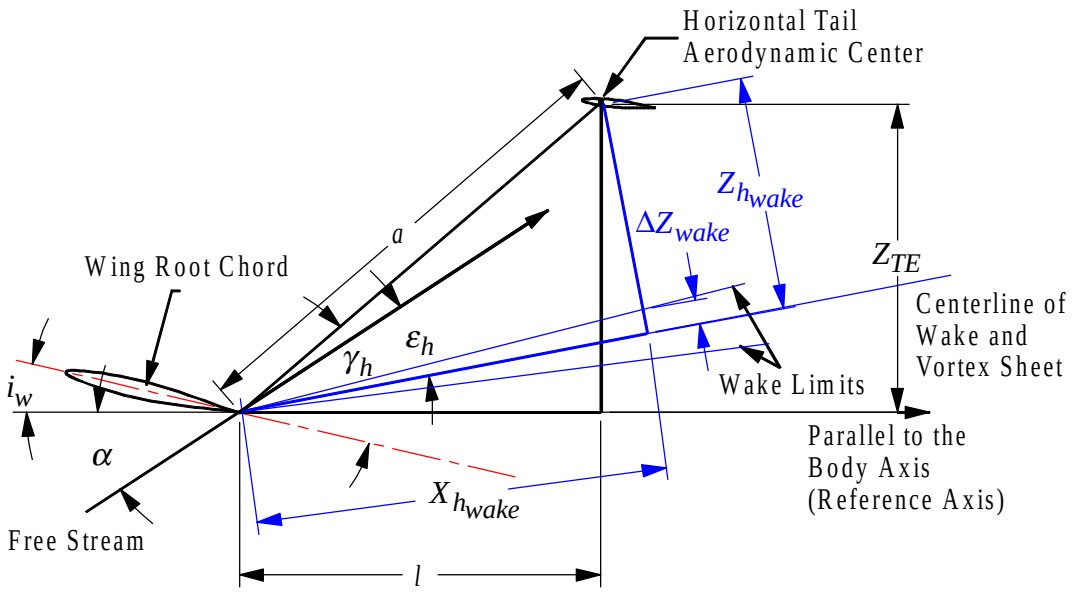

page 275, Eqn. (8.50) Parenthesis after ε_{0h} should be moved to after $d\varepsilon/d\alpha$.

page 279, Fig. (8.70) Units for $\dfrac{\left(\dfrac{\Delta\varepsilon_f A b_f}{b}\right)}{\Delta C_{L_w}}$ should be *degrees*

page 280, Eqn. (8.54)

$$\Delta C_{L_{max}} = K_{cw}\Delta C_{L_{max_w}} - \left(C_{L_{\alpha_w}}\right)_\delta \Delta\alpha_{w/c} + (S_c/S)\Delta C_{L_{max_c}} + (S_h/S) C_{L_{\alpha_h}} \left(-\Delta\varepsilon_f\right)$$

page 305, Eqn (8.73) The bar over the 2 should be over the c.

page 311, Eqn (8.74) The first term on the r.h.s. should read: $\left(\bar{x}_{ref} - 0.25\right)\Delta C_{L_w}$

where: ΔC_{L_w} is the wing lift increment due to flaps.

page 320, Eqn (8.78) Replace 'i_w' with '$-i_w$'.

page 323, 1st line Should read *airplane zero angle of attack. . .*

page 333, Eqn. (8.97) $\varepsilon = \varepsilon_{o_h} + \alpha\left(\frac{d\varepsilon_h}{d\alpha}\right)$

page 333, Eqn. (8.97) $\varepsilon = \varepsilon_{o_c} + \alpha\left(\frac{d\varepsilon_c}{d\alpha}\right)$

page 340, Eqn. (8.107) $K_{T_i} = \frac{550 SHP_{AV_i}\sqrt{\rho}}{\left(2W/S\right)^{3/2} D_{P_i}{}^2}$

page 342, Eqn. (8.108) $\left(dC_m/dC_L\right)_N = \sum_{i=1}^{n}\left[\frac{\left(dC_N/d\alpha\right)_{P_i}\left(d\bar{\varepsilon}_{P_i}/d\alpha\right)\left(l_{P_i}\right)(0.79)\left(D_{P_i}\right)^2}{S\bar{c}C_{L_{\alpha_w}}}\right]$

page 374, Eqn. (10.8) $C_{T_{X_1}} = C_{D_1}$

page 375, Last Line $\partial C_D/\partial C_m$ should be $\partial C_D/\partial M$.

page 377
Eqn. (10.12) $C_{m_u} = -C_{L_1}\left(\partial \overline{X}_{ac_a}/\partial M\right)M$

Eqn. (10.13) $C_{T_{x_u}} = (1/\bar{q}S)\left(\partial P_{reqd}/\partial u\right) - 3C_{T_{x_1}}$

Eqn. (10.15) $C_{T_{X_u}} = (M_1/\bar{q}S)(\partial T_{reqd}/\partial M) - 3C_{T_{X_1}}$

page 382,
Eqn (10.24) Add a ‘)’ to the end of Equation 10.24

2nd line below Eqn (10.24) Equation ‘(10.23)’ should be equation ‘(10.22)’.

page 390, Fig. (10.16) z_h should be ‘the vertical distance between the horizontal tail aerodynamic center to the fuselage center line’.

page 397,
6th line from bottom Replace C_{y_β} by $C_{y_{\beta_v}}$

page 398, *Eqn (10.44)* $C_{n_{T_\beta}} = -\underset{i=1}{\overset{i=n}{Sum}}\left[\left\{\left(dC_N/d\alpha\right)_{p_i}(0.79)\left(D_{P_i}\right)^2\left(l_{p_i}\right)\right\}\Big/ Sb\right]$

page 401~415, Fig.30~33 $z_v = z_p\cos\alpha_f - l_p\cos\alpha_f$

page 417, Eqn (10.50)

$$C_{y_p} = 2C_{y_{\beta_v}}\left(\frac{z_v \cos\alpha - l_v \sin\alpha - z_v}{b}\right) + 3\sin\Gamma\left(1 - \frac{4z}{b}\sin\Gamma\right)\left(C_{l_p}\right)_{\substack{\Gamma=0 \\ C_L=0}}$$

where: z - is the vertical distance between the cg and the wing root quarter-chord point.

$$\left(C_{l_p}\right)_{\substack{\Gamma=0 \\ C_L=0}} = \frac{k}{\beta}\left(\frac{\beta C_{l_p}}{k}\right)_{C_L=0}$$

page 418, Figure 10.35

Replace $\frac{\beta C_{l_p}}{k}$ with $\left(\frac{\beta C_{l_p}}{k}\right)_{C_L=0}$

page 419, Eqn. (10.55)

$$\frac{\left(C_{l_p}\right)_\Gamma}{\left(C_{l_p}\right)_{\Gamma=0}} = 1 - \frac{4z_w}{b}\sin\Gamma + 12\left(\frac{z_w}{b}\sin\Gamma\right)^2$$

page 421, Eqn.(10.62)

$$C_{n_{p_w}} = \left\{\left(C_{n_p}/C_L\right)_{\substack{C_L=0 \\ M}}\right\}C_{L_w} + \left(C_{n_p}/\varepsilon_t\right)\varepsilon_t + \left[\Delta C_{n_p}\Big/\left(\alpha_{\delta_f}\delta_f\right)\right]\alpha_{\delta_f}\delta_f$$

page 422, Eqn. (10.66)

$$\alpha_{\delta_f} = \Delta c_l / \left(c_{l_\alpha}\delta_f\right)$$

page 424, Eqn. (10.71)

$$\left(C_{L_{q_w}}\right)_{M=0} = \left(0.5 + 2\frac{x_w}{\bar{c}}\right)C_{L_{\alpha_w}}$$

page 435, Eqn. (10.89)

$$C_{D_{i_h}} = \frac{2C_L}{\pi A e}C_{L_{\alpha_h}}\eta_h\frac{S_h}{S}$$

page 439,

Eqn. (10.97)

$$C_{D_{i_c}} = \frac{2C_L}{\pi A e}C_{L_{\alpha_c}}\eta_c\frac{S_c}{S}$$

Eqn. (10.100)

$$C_{m_{i_c}} = C_{L_{\alpha_c}}\eta_c\bar{V}_c$$

page 440, Eqn (10.102)

Replace $c_{l_{\alpha_h}}$ with $c_{l_{\alpha_c}}$

page 446, Eqn (10.110)

$$c_{l_\delta} = \frac{c_{l_\delta}}{\left(c_{l_\delta}\right)_{theory}}\left(c_{l_\delta}\right)_{theory}k'$$

where k' is found from Figure 8.13

page 447,

Eqns. (10.111) & (10.113) It is assumed that: $\left(C_{l_\delta}\right)_{left} = \left(C_{l_\delta}\right)_{right}$

page 461, Eqn. (10.123) Should read:

$$C_{y_{\delta_r}} = K_\delta C_{L_{\alpha_v}} \frac{S_v}{S}\left\{\frac{c_{l_\delta}}{\left(c_{l_\delta}\right)_{theory}}\right\}\left(c_{l_\delta}\right)_{theory}\left(\frac{k'}{c_{l_{\alpha_v}}}\right)\left\{\frac{\left(\alpha_\delta\right)_{C_L}}{\left(\alpha_\delta\right)_{c_l}}\right\}$$

Eqn (10.123) is correct for a single vertical tail only. For a twin vertical tail:

$$C_{y_{\delta_r}} = 2\left(\frac{C_{y_{\beta_{v_{(wfh)}}}}}{C_{y_{\beta_{v_{eff}}}}}\right)K_b C_{L_{\alpha_v}} \frac{S_v}{S}\left\{\frac{c_{l_\delta}}{\left(c_{l_\delta}\right)_{theory}}\right\}\left(c_{l_\delta}\right)_{theory}\left(\frac{k'}{c_{l_{\alpha_v}}}\right)\left\{\frac{\left(\alpha_\delta\right)_{C_L}}{\left(\alpha_\delta\right)_{c_l}}\right\}$$

where: $\left(\frac{C_{y_{\beta_{v_{(wfh)}}}}}{C_{y_{\beta_{v_{eff}}}}}\right)$ is found from Figure 10.17.

All other parameters are the same.

page 467, Eqn. (10.129) $\left(c_{h_\alpha}\right)_{theory}$ is found from Figure 10.63b. The parameter $\frac{c_{l_\alpha}}{\left(c_{l_\alpha}\right)_{theory}}$ in Figure 10.63b is itself found from Figure 10.64a with the assumption that $\tan\frac{\Phi'_{TE}}{2} = \frac{t}{c}$.

page 470,
1st line (10.126) should be (10.128).

Eqn. (10.130) $\frac{c_{l_\alpha}}{\left(c_{l_\alpha}\right)_{theory}}$ is obtained from Figure 10.64a with the assumption that $\tan\frac{\Phi'_{TE}}{2} = \frac{t}{c}$.

page 484, Eqn (10.145) Replace 'α_δ' with '$-\alpha_\delta$'.

page 521, (Pratt and Whitney handbook errors)
Pressure (psia) for 200,000 ft should be 0.002655 psia
Pressure (psia) for 200,131 ft should be 0.002641 psia
Pressure Ratio, δ, for 154,199 ft should be 0.001095

DESIGN, ANALYSIS AND RESEARCH CORPORATION

ERRATA: AIRPLANE DESIGN PART VII

Copyright © 1988-91 by Dr. Jan Roskam
Year of Print: 1988, 1991
(Revised December 14, 1999)

page 11,
last sentence of 3rd para. Typical numerical values for gearing ratios are given in Table 4.1 of Part IV, not Part VI.

page 39, Figure 2.5 z_T should be negative as shown

page 44, Eqn. (2.39) Should read:

$$S_h = \frac{-z_T T + z_D D + W\left(x_{mg} - x_{cg} + \mu_g z_{mg}\right) - L_{wf}\left(x_{mg} - x_{ac_{wf}} + \mu_g z_{mg}\right) - C_{m_{ac_{wf_g}}} \bar{q}_{rot} S\bar{c} + I_{yy_{mg}} \ddot{\Theta}}{\bar{q}_{rot}\left(x_{mg} - x_{ac_h} + \mu_g z_{mg}\right) C_{L_{h_{\max}}}}$$

page 49, Eqn. (2.54) The 4th term on the left hand side should read:
'+ $Y_{ng}\left(x_{ng} + x_{cg}\right)$ - ...'

page 50, Eqn. (2.57) The 4th term on the left hand side should read:
$0.025\left(\Psi_A + \Psi_{steer}\right) P_{ng}\left(x_{ng} + x_{cg}\right)$

page 98, 1st sentence Should read, "Civil: FAR 23.201, 23.203, 23.205, ..."

page 152, Eqn. (5.59) $T\sin\left(\alpha + \phi_t\right) + C_L \bar{q} S - W\cos\phi - (W/g) U_1 Q_1 \sin\phi = 0$

page 159,
Last sentence of 1st para. Should read, "See Section 5.3."

page 161, Eqn. (5.77) $RD = \left\{(W/S)(2/\rho)\left(C_D^2 / C_L^3\right)(\cos\gamma)^3\right\}^{1/2}$

page 164, AS-5263 thrust required for level flight at $1.15V_s$, not $1.15V_{s_{PA}}$.